

8.º Congresso Internacional de Química do Cimento

8th International Congress on the Chemistry of Cement

8e Congrès International de la Chimie des Ciments

22-27 de setembro de 1986
Rio de Janeiro — Brasil



8.º Congresso Internacional de Química do Cimento

8th International Congress on the Chemistry of Cement

8e Congrès International de la Chimie des Ciments

Special Reports/Principal Reports
Rapports Spéciaux/Rapports Principaux
Volume I

22-27 de setembro de 1986
Rio de Janeiro — Brasil



8.º Congresso Internacional de Química do Cimento

8th International Congress on the Chemistry of Cement

8e Congrès International de la Chimie des Ciments

Special Reports/Principal Reports
Rapports Spéciaux/Rapports Principaux
Volume I

22-27 de setembro de 1986
Rio de Janeiro — Brasil

Não é permitida a reprodução dos Anais sem prévia autorização da Comissão Organizadora do Congresso.

The Proceedings are not to be reprinted without a previous permission of the Organizing Commission of the Congress.

La reproduction des Annales est interdite sans, au-devant, l'autorisation de la Commission d'Organisation du Congrès.

• • •

A substância e a forma de apresentação dos trabalhos que compõem os Anais do Congresso são de exclusiva responsabilidade de seus autores.

The substance and the form of presentation of the papers that compound the Proceedings of the Congress are exclusive responsability of their authors.

Le fond et la forme de publier les travaux qui composent les Annales du Congrès sont d'exclusive responsabilité de leur auteurs.

Secretaria Geral do 8º CIQC:
Rua da Assembléia, 10 - 40º and. - Gr. 4001
Tel.: 221-6562 – Telex: (021) 33191
20011 Rio de Janeiro – RJ – Brasil

Apoio financeiro da

finep FINANCIADORA DE ESTUDOS E PROJETOS

ORGANIZING COMMISION:

PRESIDENT:	JOSÉ ERMÍRIO DE MORAES FILHO	BRASIL
EXECUTIVE VICE-PRESIDENT:	PAULO MÁRIO FREIRE	BRASIL
TECHNICAL DIRECTOR:	FRANCISCO DE ASSIS BASÍLIO	BRASIL
ADMINISTRATIVE DIRECTOR:	JOÃO BATISTA MENESCAL FIUZA	BRASIL
DIRECTORS:	ALBERTO LUIZ GONÇALVES SOARES	BRASIL
	ENRIQUE GUNTHER DREWES	BRASIL
	EPAMINONDAS MELO DO AMARAL FILHO	BRASIL
	MARCÍLIO DE BRITO	BRASIL
	NEWTON GOULART	BRASIL

SCIENTIFIC COMMITTEES:

– SOUTH AMERICA:		
• PRESIDENT:	FRANCISCO DE ASSIS BASÍLIO	BRASIL
	ALVARO AUGUSTO ALVES PINTO	BRASIL
	DANTE E.J. VERONELLI	ARGENTINA
	FLEMING OEST	BRASIL
	HANS BUCHER	BRASIL
	JOÃO GASPAR DJANIKIAN	BRASIL
	LUIZ ROBERTO MARTINS DE MIRANDA	BRASIL
	MARIA DAS GRAÇAS JAQUÁ	BRASIL
	MARIA LUIZA MOREIRA DE MORAES	BRASIL
	NEY JOSÉ DE SOUZA E SILVA	BRASIL
	PABLO KITTL D.	CHILE
	PAULO RODRIGUES	BRASIL
	ROBERTO R. COELHO	BRASIL
	YASUKO TESUKA	BRASIL
	YUSHIRO KIHARA	BRASIL
– NORTH AND CENTRAL AMERICA, AND FAR EAST:		
• PRESIDENT:	JAN P. SKALNY	U.S.A.
MEMBERS:	DELLA M. ROY	U.S.A.
	GEOFFREY FROHNSDORFF	U.S.A.
	GERARD G. LITVAN	CANADA
	HIROSHI UCHIKAWA	JAPAN
	J. FRANCIS YOUNG	U.S.A
	JORGE MARIO VILLASENOR	MEXICO
	R.E. OBERHOLSTER	SOUTH AFRICA
	SIDNEY DIAMOND	U.S.A.
	S.W. TRESOUTHICK	U.S.A.
	WU ZHONG-WEI	CHINA
– EUROPE, ASIA AND AFRICA:		
• PRESIDENT:	JEAN PAUL MERIC	FRANCE
MEMBERS:	C. CHARRETON	FRANCE
	FRANCO MASSAZZA	ITALY
	FRANÇOIS LE BEL	FRANCE
	FRIEDRICH W. LOCHER	WEST GERMANY
	F. YAGIZ	TURKEY
	H.W.W. POLLITT	ENGLAND, U.K.
	JOSE CALLEJA	SPAIN
	J. TALLABER	HUNGARY
	LABO KADA ABOUBACAR	NIGERIA
	O.P. MTCHEDLOV-PETROSSIAN	U.S.S.R.
	P. DUTRON	FRANCE
	RENATO BUCCHI	ITALY
	S.K. CHOPRA	INDIA
	T.V. KOUZNETSOVA	U.S.S.R.
	WIESLAW KURDOWSKI	POLAND

CONTENTS/TABLE DE MATIÈRES

THEME/THÈME 1: Pages

– **Clinker formation and properties/Formation et proprietés du clinker.**
- Chairman/Président: C.D. POMEROY (England, U.K.)
- Secrétaire: M.S. MARINHO (Brasil)

SUB-THEME/SOUS-THÈME 1.1.

– **Kinetic of clinker formation/Cinétique de la formation du clinker.**
- Chairman/Président: O.P. MTCHEDLOV-PETROSSIAN (U.S.S.R.) 11
- Principal Reporter/Rapporteur Principal: F.P. GLASSER (Scotland, U.K.) *

* *The Report of F.P. Glasser was not received in time. It will be published in Volume VI.*

SUB-THEME/SOUS-THÈME 1.2:

– **Relationship of processing parameters to clinker properties; Influence of minor components/ Rapport entre les paramètres du processus et les proprietés du clinker; Influence des éléments mineurs.**
- Chairwoman/Président: A.I. BOIKOVA (U.S.S.R.) 19
- Principal Reporter/Rapporteur Principal: I. MAKI (Japan) 34

SUB-THEME/SOUS-THÈME 1.3:

– **Low energy clinker formation/Formation d'un clinker consommant peu d'énergie.**
- Chairman/Président: J.P. MERIC (France) 51
- Principal Reporter/Rapporteur Principal: F.W. LOCHER (West Germany) 57

THEME/THÈME 2:

– **Hydration of clinker components individually and in cements/Hydratation des composants du clinker et des ciments.**
- Chairman/Président: G. FRONHSDORFF (U.S.A.)
- Secrétaire: P.J.M. MONTEIRO (Brasil)

SUB-THEME/SOUS-THÈME 2.1:

– **Physical chemistry of hydration process; Influence of minor components and admixtures/ Physico-chimie du processus d'hydratation; Influence des éléments mineurs et des matières d'additions.**
- Chairman/Président: A.M. DMITRIEV (U.S.S.R.) 73
- Principal Reporter/Rapporteur Principal: H.F.W. TAYLOR (Scotland, U.K.) 82

SUB-THEME/SOUS-THÈME 2.2:

– **Microstructure of hardened cement paste and its effects on its behaviour/Microstructure de la pâte de ciment hydraté et ses effets dans son comportement.**
- Chairman/Président: P.K. MEHTA (U.S.A.) 113
- Principal Reporter/Rapporteur Principal: S. DIAMOND (U.S.A.) 122

SUB-THEME/SOUS-THÈME 2.3:

– **Bond: paste-aggreagate, paste-reinforcement and paste-fibres/Adhrérence: pâte-granulat, pâte-armature et patê-fibres.**
- Chairman/Président: J.P. SKALNY (U.S.A.) 151
- Principal Reporter/Rapporteur Principal: F. MASSAZZA (Italy) 158

THEME/THÈME 3:

–**Blended and special cements/Ciments spéciaux et ciments avec additions.**
- Chairman/Président: V.I.KUSCHIDI (U.S.S.R.)
- Secrétaire: Y. KIHARA (Brasil)

SUB-THEME/SOUS-THÈME 3.1:
- **Characteristics and activation of blending components/Caractéristiques et activation des composants des matières d'addition.**
  - Chairman/Président: R. BUCCHI (Italy) 185
  - Principal Reporter/Rapporteur Principal: M. REGOURD (France) 199

SUB-THEME/SOUS-THÈME 3.2:
- **Effect of blending components on hydration and structure formation/Effets des composants des matières d'additions dans l'hydratation et dans la formation de la structure.**
  - Chairman/Président: J. CALLEJA (Spain) 233
  - Principal Reporter/Rapporteur Principal: H. UCHIKAWA (Japan) 249

SUB-THEME/SOUS-THÈME 3.3:
- **Special cements. Calcium aluminate and other no-silicate cements/Ciments spéciaux. Ciments à base d'aluminates calciques et autres ciments sans silicates.**
  - Chairwoman/Président: T.V. KOUZNETSOVA (U.S.S.R.) 283
  - Principal Reporter/Rapporteur Principal: W. KURDOWSKI (Poland) 292

THEME/THÈME 4:
- **Influence of cement in the durability of concrete/Influence du ciment dans la durabilité du béton.**
  - Chairman/President: G.WISCHERS (West Germany)
  - Secrétaire: H.R.E. BUCHER (Brasil)

SUB-THEME/SOUS THÈME 4.1:
- **Pore structure, permeability and diffusivity as related to durability/Structure des pores, perméabilité et diffusibilité en liaison avec la durabilité.**
  - Chairman/Président: R.E. OBERHOLSTER (South Africa) 323
  - Principal Reporter/Rapporteur Principal: R.F. FELDMAN (Canada) 336

SUB-THEME/SOUS-THÈME 4.2:
- **Mechanism of cement paste degradation due to chemical and physical processes/Mécanisme de la dégradation de la pâte de ciment due aux processus chimiques et physiques.**
  - Chairman/Président: G.G. LITVAN (Canada) 359
  - Principal Reporter/Rapporteur Principal: D.M. ROY (Canada) 362

SUB-THEME/SOUS-THÈME 4.3:
- **Compatibility of cement paste with aggregate and reinforcements, including electrochemical corrosion/Compatibilité de la pâte de ciment avec les armatures, y compris la corrosion électrochimique.**
  - Chairman/Président: R. CIGNA (Italy) 383
  - Principal Reporter/Rapporteur Principal: R. TURRIZIANI (Italy) 388

THEME/THÈME 1

Clinker formation and properties. Formation et proprietés du clinker.

Chairman/Président
C.D. Pomeroy
Cement & Concrete Association
England, U.K.

Secretary / Secrétaire
M.S. Marinho
ICI — Brasil S/A
São Paulo, Brasil

SUB-THEME/SOUS-THÈME 1.1

Kinetic of clinker formation.
Cinétique de la formation du clinker.

Chairman/Président
O.P. Mtchedlov-Petrossian
Cement Research Institute
Kharkov, U.S.S.R.

Principal Reporter/Rapporteur Principal
F.P. Glasser
University of Aberdeen
Scotland, U.K.

O.P. MCHEDLOV-PETROSSYAN, Cement Research Institute, Moscow

KINETICS OF CLINKERING

1.1

Cement manufacturing today is a highly efficient technology both in respect of the amount of raw materials handled and in respect of the processing methods. Nevertheless, the industry often comes under criticism for the relatively high consumption of energy. Another crucial aspect intrinsic to the industry concerns improvement in the cement technology, which is not only economic but also ecological problem.

Profound alterations in the manufacturing equipment are possible theoretically, but cannot be expected in the foreseable future. Therefore an improvement-oriented analysis of cement technology should be focused on the processes of clinker formation whose physico-chemical fundamentals should be reinvestigated, specifically chemical thermodynamics and kinetics. Unfortunately, for all importance of this fact, thus far this field is reported fairly unadequately /1, 2/. One should not overlook that a change in manufacturing equipment unavoidably entails corrections to the process introduced on the basis of thermodynamic and kinetical data.

The kinetics of clinker formation is a function of a number of chemical processes between the interacting components of raw mix and depends primarily on the nature of the components, their preparation, temperature condition, and the procedure and duration of temperature treatment. The reactivity of the mix components depends on their thermodynamic properties, so to control the kinetics of clinker formation one has to evaluate the structure and energy characteristics of the pertinent compounds. The following ways could be set out for clinkering kinetics control:

1. differential approach to traditional raw materials with account of the nature of the major and minor contributors
2. use of new sources of raw materials
3. evaluation of the effects of burning conditions (atmosphere in the calcination kiln, heating rate, etc.)
4. utilization of mineralizers and calcination temperature lowering components
5. use of activating effects
6. introduction of technogenic products
7. modification of equipment involved in calcination processes
8. package application of the aforementioned means

About one report in ten presented to the Congress is concerned with one of the above topics, and this review will take up each of them in succession.

1. Differential Approach to Traditional Raw Materials with Account of Minor Components

Calcium carbonate used for cement production offers, depending on its structure and water content, a profound influence on the calcination process. This effect is comparable with that of the type of silicate component /3/.

A thorough investigation into calcium carbonate properties /4/ has indicated that the presence of aragonite in place of calcite lowers the initiation temperature of the interaction with the argillaceous component by 50°C and even more, while the degree of limestone mergelization changes quality of the clinker owing to different rates of mineral formation at the final stages of burning.

There are only a few systematic studies into the effect of minor constituents that have been reported so far /5/. Obviously the time is ripe for such investigations to be conducted on a wider scale, especially in view of new sources of raw materials coming into use.

2. Use of New Sources of Raw Materials

A gradual decline in the capacity of the traditional sources of raw materials necessitates that a substitution be devised and introduced on a fractional basis. Utilization of ingenious rocks of the basis group, for example basalts, and also silicious

rock, shales, open pit soils, and such, has been reported /6, 7/. Some of these materials result in fuel savings, and reductions in burning temperature and duration. Another interesting feature concerns new type of product, so the utilization of labradorite resulted in agrillaceous belite cement which places itself in between portland cement and agrillaceous cement /8/.

3. Evaluation of the Effects of Burning Conditions

According to the classical scheme of calcination, a number of factors influence the process kinetics. They include the formation of lining, the ring formation phenomenon, dust generation, and the like. Depending on the type of kiln, it takes from 40 minutes to 5 hours to heat up a clinkering charge /9/. This fact obviously governs the process kinetics, specifically, it conditions the state and assimilation of calcium oxide.

4. Utilization of Mineralizers

Because the formation of tricalcium silicate from bicalcium silicate and calcium oxide occurs only in the presence of the melt phase, the process kinetics is under considerable influence of mineralizers which, even in small amounts, accelerate the process of clinkering. The choice of mineralizers is normally conditioned by harmful effects they can cause in the cement. Most suitable therefore are fluorine compounds /10/ such as fluorides of alkali and alkali earth metals and salts of siliconeous acid. Chlorine compounds are far less desirable. Phosphogypsum may be used to advantage.

Of the intrinsic components of the charge, the more effective mineralizer is iron oxide which facilitates a "movable" melt production and its better penetration into the charge bulk thus providing the adhesion necessary for granulation.

5. Use of Activating Effects

This area is poorly developed whatsoever. Whereas multiple publications have been devoted to the effects on cement paste and concrete, this aspect in the cement raw material charge is elucidated only weakly. The existing experience leaves no doubt whatsoever that a **preprocessing** activation of minerals by suitable means will influence the calcination kinetics.

A cement production technology has been reported with preburning activation of the charge by radiation /11/. The activation can be effected by a beam of light, protons, ions, or X-rays of various irradiance, and results in lesser energy requirements for clinkering.

Some recent works deal with the utilization of nuclear wastes in cement manufacture /12/. Although there is certain confusion about the process technology, one cannot overlook that such admixtures could activate the burning kinetics.

6. Use of Technogenic Products

As a result of the technological revolution the amount of industrial wastes piles up at a catastrophic rate. The proportion of nonindustrial and houshold wastes is also increasing.

Of more than 70 million tons of ferrous slags that are yielded annually by the Soviet iron and steel industry, about 30 million tons is consumed in the cement industry. More specifically, utilization covers 70% of blast-furnace slags, more than 40% of ferroalloy slags, and more than 20% of steelmaking slags.

Kushchidy /13/ has indicated that the proportion of wastes utilizable in the industry can be markedly increased. Technogenic products can be utilized in many various ways as burning intensifiers, grinding aids, reactive admixtures, **plasticizers**,

etc. /14/.

Significant amount of environmentally deleterious flyashes, formerly rejected into the air by thermal power plants, is also utilized in the cement industry. This component calls for appropriate raw-mix compositions, but it is beyond doubt that flyash is energetically advantageous due to its unburnt fuel content.

In many cases technogenic products are used to advantage as hydraulic admixtures.

Analysis of process exergy (utilizable energy) /15/ indicates that it is worth using technogenic products as energy saving component, while the charging of crushed slag through the cold end of the kiln favorably affects the kinetics of clinkering /16/.

7. Modification of Burning Process Equipment

Two principal ways may be envisaged here: (i) hardware modification keeping traditional sources of energy and (ii) search for and use of new sources of energy.

(i) After the Second World War, clinkering technology experienced a jump-wise development period /17/. Novel calcination schemes were devised that brought decarbonation beyond the kiln and research in this direction is continuing. New arrangements have been introduced for double-end and combined feed of kilns, and for charging industrial wastes and burning semiproducts.

(ii) The earlier suggestion to alter the traditional clinkering technology was connected with the production of energoclinker (fused portlandcement clinker), first experimented with by V. Mikhaelis at the end of the last century. Later, in attempts to overcome technical difficulties, burning was carried out in blast furnaces, electric furnaces, steelmaking convertors, cyclon melting chambers, and plasma furnaces.

In the plasma burning technology, calcination is effected in low temperature plasma with particle energy below 1 eV. The plasmochemical processes are realized at temperatures of 1000 to 10 000 K generated by an electric arc or a hf or microwave discharge in any atmosphere suitable for the chemical reactions. This technology drastically reduces process duration, cuts down the number of stages involved, decreases the equipment size and lends itself well for complete automation of the process.

A nevel clinkering technology of plasma burning has been developed and introduced in Great Britain /18/. Reportedly, it has improved the cost-effectiveness of cement manufacture by 25%. The initial costs of the set-up are lower than that of a traditional kiln, and its energy requirements are also diminished due to technogenic products utilized (mining soils, shales).

At the 5th International Symposium on Plasma Chemistry in Edinburg, 1981, French researchers reported a three-phase rotating plasma kiln for hydraulic cementitious materials. Its specific energy consumption was 2 to 4 kWh/kg clinker, with no account of furnace gases and clinker heat.

Another advantage of plasma treatment is that it profoundly changes physico-chemical properties of the products.

Attempts at radiation-chemical processing, attractive from the fuel economy standpoint, have faced the need for considerable funds and equipment sophistication due to the radiation hazard. Thus far there exist no radiation-chemical apparatus of appropriate power and fast-electron generators which could handle actual industrial outputs. Apart from that, estimates predict low efficiencies for such plants.

8. Package Application of Aforementioned Factors

Summing up, the further refinement of burning kinetics must be supported by a combined utilization of the aforementioned factors. This solution package may be variously combined according to the economi-

cal viability of the particular production environment.

This approach appears to be most suitable for the refinement of clinkering kinetics with account of performance indices of the component processes such as the rate of heating, decarbonation and recrystallization of calcium oxide, melting temperature and melt properties, ultimate burning temperature, and cooling rate. Mathematical treatment of an input package of such data yields a program of process kinetics optimization.

The implication of new raw materials and technogenic products in such a refinement is highly advisable, though simultaneous account is in order as to the amounts of introduced sulfur and chlorine and such volatile elements as tin, lead, chromium, nickel, cadmium, selenium, and thallium /9/.

Mathematical modeling of clinkering reactions in burning /20/, and studies into burning conditions and temperature /21/ also contribute to the better understanding of the clinker formation process.

References

1. V.I. Babushkin, G.M. Matveyev, O.P. Mchedlov-Petrossyan. Thermodynamics of Silicates. Springer Verlag, Heidelberg, 1985.
2. F.P. Glasser. Kinetics of some Cement Burning and Hydration Reactions. Characterisation and Performance Prediction of Cement and Concrete, Ed. J.F. Young, Urbana, 1982.
3. О.П.Мчедлов-Петросян, А.П.Николаев, Т.Ю.Щеткина. Влияние химического и минерального состава сырьевого компонентов на динамику клинкерообразования. В кн.: "Краткие тезисы докладов на VI Всесоюзном научно-техническом совещании по химии и технологии цемента. Москва, 1982, стр. 102-107.
4. Т.Ю.Щеткина, А.П.Николаев, Е.В.Николаев Влияние физико-химических свойств извести на процесс клинкерообразования. "Цемент", 1984, № 3, стр. 11-13.
5. R. Bucchi. Features of the Role of Minor Compounds of Cement Clinker. Part 1 a. 2 World Cement Technol. 12 (5) 210 - 232, 258-274 (1981).
6. А.А.Пащенко, Е.А.Мяникова и др. Цементы из базальтов. Киев, Наукова думка, 1983, 190 стр.
7. С.Д.Макашев. Влияние физико-химических свойств сырья на реакционную способность сырьевой смеси и процесс минералообразования клинкера. Труды VI Международного конгресса по химии цемента.М., Стройиздат, 1976, т. I, стр. 156-162.
8. Л.А.Захаров. Глиноземисто-белитовый цемент. Изд. Айастан, Ереван, 1969, 213 с.
9. F. Locher. Zement. Ullmanns Encyclopädie der technischen Chemie. Verlag Chemie, Weinheim, 1983, S. 545-574.
10. Б.В.Волконский, П.Ф.Коновалов, С.Д.Макашев. Минерализаторы в цементной промышленности. М., Стройиздат, 1964.
11. И.Г.Абрамсон и др. Радиоционно-технический способ получения портландцементного клинкера. Цемент, № 9,1976,с. 6-7.
12. C.M. Jantzen, F.G. Glasser, E.E. Lachowski. Structalisation of Nuclear waste Continuously in Portland Cement J. Am. Ceram. Soc., 67, No. 10, pp. 638-704.
13. В.И.Кущиди. Полнее использовать в отрасли отходы и побочные продукты. Цемент, № 2, 1982, стр. 1-3.
14. Л.Я.Гольдштейн. Комплексные способы производства цемента. Ленинград, Стройиздат, 1985, 159 стр.
15. Н.М.Жаворонков и др. Теоретическое обоснование применения новых видов сырья в цементной промышленности. ДАН СССР, 1979, т. 245, № 3, стр. 666-669.
16. Н.П.Коган, О.П.Мчедлов-Петросян, А.И.Здоров, А.И.Дрепин. Интенсификация процесса получения цементного клинкера за счет обжига шихты, состоящей из независимых исходных физико-химических систем. ДАН СССР, 1978, т. 238, № 2,

стр. 408-4II.

17. М.М.Сычев. Тенденции развития цементной промышленности за рубежом. М., Обзорная информация ВНИИЭСМ,1977, 40 стр.
18. Cemplas Process Ind. Eng., 1 878, 10, No. 3.
19. S. Sprung. Technologische Probleme beim Brennen des Zement-klinkers, Ursache und Lösung. Habilitationsschrift, Aachen, 1982.
20. O.P. Mchedlov-Petrossyan, T.Y. Shchetkina, N.I. Sapozhnikova, j. Talaber and K. Bocsi. Connection between Solid State Clinkerization Reactions with the Mineralogical Composition and Heat Treatment Conditions of Raw Mixes. Epitoanyag, 1981, v. 33, No. 3, p. 81-84.
21. D. Bürger, U. Ludwig. Zur Reaktivität von im Niedrigtemperaturbereich hergestellten Calciumsilicaten. Tagunsbericht, 9. Internationale Baustoff- und Silikattagung. Weimar, 1985, S. 27-32.

SUB-THEME/SOUS-THÈME 1.2

Relationship of processing parameters to clinker properties; influence of minor components.

Rapport entre les paramètres du processus et les proprietés du clinker, influence des éléments mineurs.

Chairman/Président:

A.I. Boikova
Academy of Sciences of the U.S.S.R.
Leningrad, U.S.S.R.

Principal Reporter/Rapporteur Principal:

I. Maki
Nagoya Institute of Technology
Nagoya, Japan

A.I. BOIKOVA, Dr. Chem. Sc., Senior Research Scientist, Institute of Silicate Chemistry of the USSR Acad. Sci., Leningrad, USSR

Chemical Composition of Raw Materials as the Main Factor Responsible for the Composition, Structure and Properties of Clinker Phases

INTRODUCTION

At the 7th International Congress on the Chemistry of Cement Bucchi /1/, Sprung /2/, Timashev /3/ and Meric /4/ considered in detail the influence of the main factors - the nature of raw materials, their preparation, heat-treatment schedule and the fuel - on the formation and properties of clinker. The analysis of the clinker formation kinetics was also given. At the present Congress the information reported in those papers can hardly be significantly changed or supplemented by new data different in principle.

However, an ever growing need in Portland cement clinker throughout the world, on the one hand, and the high energy capacity of its production and hence the necessity to decrease the costs of this process, on the other hand, make us to reexamine each of the parameters influencing the formation process and properties of clinker.

In particular, a perspective possibility for the development of new technological procedures is the chemical activation. The same idea was expressed in the conclusion of Bucchi's paper. It makes possible the logical continuation of the discussion at this Congress.

At the preceding Congress one aspect of the problem of chemical activation was dealt with, namely: the intensification of clinker formation process at the stage of the liquid phase by influence of various elements and their combinations on the structure and properties of the melt /3,5/.

There is, however, another aspect of the chemical activation problem - the use of the crystal-chemical features of clinker compounds for the influence of impurities on their structure and properties and consequently on the structure and properties of clinker as a whole. The knowledge of the mechanism of influence of various impurities on the separate clinker phases will undoubtedly permit us to decrease power consumption.

These data are of importance in connection with the increase of the variety of chemical elements - constituents of the batch for clinker production. A set of compounds to be used for chemical activation has recently widened owing to both the necessity of exploiting new deposits and the utilization of wastes.

It is worth noting that at present there are some data concerning the use of such unusual materials as rare-earth compounds and radioactive wastes. They will be dealt with in a separate paragraph.

This report is not, however, a review of papers devoted to some or other problem. It outlines some concepts mainly concerned with the capability of clinker phases to distribute various impurity elements in the lattices and the possibility of activation of the phases by impurities (chemical activation) and by heat treatment (thermal activation).

To make an idea about the capabilities of atomic structures of clinker compounds ($3CaO.SiO_2$, $3CaO.Al_2O_3$, $2CaO.SiO_2$, $2CaO.(Al,Fe)_2O_3$) to distribute various impurity elements in their lattices, we shall remind of the peculiarities of isomorphism in the real clinker phases which determine their practical properties. The chemical activation is attained first of all owing to isomorphous substitutions.

The isomorphous substitutions of atoms in crystals (or formation of solid solutions) are a widespread phenomenon in both natural and artificial minerals. It provides practically important physical-chemical and physical-mechanical properties of many materials.

PECULIARITIES OF ISOMORPHISM IN CLINKER PHASES

1. The main crystal-chemical feature of the atomic structure of clinker compounds which is of great practical importance is their capability of the distribution in the lattice of numerous and various impurities (Na, K, Mg, Mn, Cr, Ti, P, S a.o.) which isomorphously substitute the main structural elements. An explanation for this should be sought first of all in the similarity of the chemical nature and sizes of atoms, constituents of the structure of clinker minerals, with other atoms. Clinker minerals are composed of such elements (Ca, Al, Fe, Si) which possess the greatest (compared to other elements of the Periodic system) capability of various substitutions.

Among the families (pleiads) of isomorphous elements (Table 1), the one with Ca is most numerous. Those with Al, Fe, Si are also numerous. The table has been composed on the base of a large body of data on the isomorphism of various elements in natural minerals.

Each of the chemical elements in the table as structural element of the mineral or compound considered can be isomorphously substituted by the surrounding elements. The table was proposed in 1969 at the 2nd All-Union Symposium on Isomorphism held in Moscow /6/.

Although this table does not provide us with ample information about isomorphism of individual elements, it can be regarded as a basis for the consideration of isomorphism in both natural and synthetic minerals and for further discussion.

The isomorphous substitutions in clinker and natural minerals have much in common as in both of them the main "rock-forming" (petrogenic) elements are Ca, Si, Al, Fe.

When considering the isomorphism in clinker minerals we proceed from the well-known concept regarding isomorphism as the phenomenon of atomic order, i.e. as substitution of lattice atoms of the host crystal by impurity atoms. In this case the consideration of isomorphism between equivolume radicals (e.g. between $/SiO_4/^{4-} \rightleftharpoons /GeO_4/^{4-}$) or between molecules (e.g. $3CaO.SiO_2$ and $3CaO.GeO_2$) does not contradict this point.

It should be emphasized that in considering the isomorphism in clinker minerals one usually identifies two concepts: isomorphous substitutions of atoms in crystals and formation of solid solutions of substitution (clinker phases).

These two concepts imply two approaches to the understanding of the phenomenon of isomorphous substitution: physicochemical (solid solutions) and crystal-chemical (isomorphous mixtures).

In analysis of the reason of isomorphism (the formation of solid solutions), among many other factors /6-9/, we first of all take into consideration "the size" factor, i.e. the effective atomic and ionic radii. The capability of Ca, Al, Fe, Si of being substituted by numerous and different elements is of great importance. Practically all impurities of the raw mixtures and wastes can be distributed in a certain amount among the clinker minerals.

2. However, it should always be taken into consideration that each of the minerals can arrange in its lattice only a certain quantity of impurities due to the peculiarities of its atomic structure. Such a set of oxides is usually called either the limiting solubility of the solid solution or the isomorphous capacity.

As was shown at 7th Congress, the greatest quantity of impurities are concentrated in the aluminate (≈ 12-13 wt% when calculated for the same amount of oxides) and aluminoferrite (≈ 10-11 wt%) phases of clinker owing to the peculiarities of their structures. Thus the C_3A lattice contains large holes of a radius of 1.47 Å which promote heterovalent isomorphous substitutions and the distribution of compensating atoms (free charges). The calcium aluminoferrite lattice contains convenient positions for such atoms as Mg, Mn, Si, Ti. These are octahedral and tetrahedral positions for Fe^{3+} and Al^{3+}. Mg and Mn occupy the Fe^{3+} and Al^{3+} octahedral positions, whereas Si and Ti occupy tetrahedral positions by sub-

TABLE 1

Pleiads of isomorphous elements

		I	II	III	IV	V	VI	VII	VIII			0
1	I	1 H						(H)				2 He
2	II	3 Li Mg Na Al Mn Fe	4 Be Li Al Si	5 B Al Si	6 C P S Ge	7 N	8 O Cl S	9 F Cl				10 Ne
3	III	11 Ca Sr Na K Li Ag Pb Y TR Zr	12 Fe Mn Mg Al Sc Li Zn Tl Ca Cd Cu Ni Co Cr	13 Ca Si B Cr Mg Al Fe Tl In Li Be Sc Mn V Mo	14 Al Si Ge Be B Ti Fe P S	15 As V P Si S C Cr Sb	16 Cl As S Sc Sb Te Si P	17 F Cl Br I S				18 Ar
4	IV	19 Rb Na K Tl Ba Sr Ca Cs Pb	20 Mn Sr Mg Ca Y TR Fe Zn Cu Sc Ba Pb Mn Zr Th U	21 Y Sc Zr Ca Mn TR (Y)	22 Fe Ti Nb Ta V Si Mn Cr Zr W Al	23 Fe Ti V Cr Mo As P Mn Re	24 Al Fe Cr V Mn Ti Tc	25 Fe Mg Mn Zn Al Ti Ca Sr Tl V Sc Re	26 Li Mg Ca Ni Rh Cs Ag Cr Pd Fe Sc Th Cr Y Ti Tl Hg Zn Cu Sn Ga Ge Zr Nb Ta Cd	27 Fe Co Ni Cu Pb	28 Fe Ni Cu Pt Rh Pd Ag Zn	
	V	29 Ag Au Fe Cu Co Zn Ni Tl Pb Cd Sn	30 Fe Cd Mn Zn In Gd Ag Au Tl Hg	31 Fe Ga Zn Al Ge In	32 Ga Zn Fe Ge Sc Si Tl As	33 Sb S Bi As P V	34 S Se Te As	35 Cl Br I				36 Kr
5	VI	37 K Rb Ca Tl	38 Ca Ba Sr Y TR Na Pb	39 TR Y Ca Th U	40 Hf Zr Np TR Ca Fe Tl Th U Ta Sc	41 Ta Nb Zr Fe W Mo Sn U Sc	42 W Mo Re Ti Nb	43 Tc	44 Rh Ru Ir Os Pd Fe Pt	45 Ru Rh Fe Ir Os Pt Au	46 Rh Pd Hg Pt Au Fe Ni	
	VII	47 Cu Tl Ag Au	48 Zn Cd Hg Mn Fe Cu In	49 In Zn Sn Pb	50 In Sn Nb Ta Tl Fe Zn Ga Ge W Cu	51 As Sb Bi S Te	52 Se Te S Sb	53 Br I Cl				54 Xe
6	VIII	55 K Rb Cs Tl Na	56 Sr Ba Ra Pb Ca	57 Ce La TR Sc Na Al Y Zr Mn	72 Zr Hf Sc Ti Y Nb Ca Ta	73 Nb Ti Ta Zr Sn W Fe	74 Mo W Nb Ta Sc Zr Ti Fe Sn	75 Mo Re Mn Fe Os Ir Pt	76 Ru Rh Os Ir Pt Fe Au	77 Os Ir Pt Au Fe Ru Rh	78 Rh Pd Pt Ir Fe Cu Au Os Ni	
	IX	79 Ag Au Cu Pt Fe Ir	80 Cd Hg Fe Zn Cu Ag In Au Tl Pb	81 Cu Tl Ag	82 Ag Pb Cd Ir Bi Eu Cu Tl Zn Sn	83 Sb Bi As Au Fe Cu Pb S	84 Po	85 At				86 Rn
7	X	87 Fr	88 Ra Ba Pb	89 Ac	90 U Th TR (Ce) Ca Fe Y Zr Sc	91 Pa	92 Y Zr U Th TR (Y) Tl Sc Nb					

Lanthanoids

58 Ce Ca Sr TR (Sc) Th Na Tl Zr U Sc	59 Pr	60 Nd	61 Pm	62 Sm	63 Eu Pb	64 Gd Y TR (Y)	65 Tb	66 Dy	67 Ho	68 Er	69 Tm	70 Yb	71 Lu

TABLE 2

Chemical composition of alinite clinker phases

Phase \ Composition (wt%)	CaO	MgO	Al_2O_3	SiO_2	Cl	Na_2O	K_2O	Mn_2O_3	Fe_2O_3	TiO_2
Alinite	65.2	3.9	3.8	21.9	3.1	0.2	0.1	0.0	1.5	0.4
	61.7	2.5	3.2	27.0	3.0	0.2	0.3	0.0	1.9	0.3
	64.2	3.4	2.5	25.7	3.0	0.0	0.1	0.0	0.5	0.6
Corroded grains of alinite	70.1	1.2	1.0	26.4	0.1	0.2	0.1	0.0	0.7	0.2
	71.8	1.3	0.9	24.7	0.1	0.1	0.0	0.0	0.8	0.2
	64.4	1.2	2.0	29.4	1.1	0.3	0.3	0.0	1.5	0.4
Belite	62.3	0.5	1.1	34.5	0.2	0.2	0.4	0.0	0.4	0.3
	60.8	1.3	0.8	36.4	0.1	0.0	0.2	0.0	0.4	0.1
	61.8	0.2	0.9	35.4	0.0	0.4	0.7	0.0	1.3	0.0
Aluminate	47.2	0.0	41.8	0.3	4.0	0.3	0.0	0.0	6.3	0.1
	47.2	0.0	41.7	1.3	4.0	0.0	0.0	0.0	5.7	0.1
	50.7	0.1	42.8	0.8	3.9	0.0	0.0	0.0	1.6	0.0
Calcium aluminoferrite	47.2	2.3	10.1	1.4	0.3	0.0	0.1	2.2	35.4	1.2
	47.0	2.0	9.0	2.3	0.0	0.0	0.1	0.9	37.2	1.5
	48.1	3.2	8.6	2.1	0.1	0.1	0.0	1.6	34.3	1.8

stituting for Fe^{3+} and Al^{3+}.

The C_2S and C_3S (especially the latter) are less capable of adopting isomorphous impurities. The isomorphous capacity of C_2S is $\sim$6 wt%. The least quantity of impurities ($\sim$4 wt%) is distributed in the C_3S lattice. This allows us to assume that the C_3S lattice is rather dense, without large holes between the structure polyhedra.

It is well known that the formation of clinker minerals proceeds under extremely non-equilibrium conditions. The change of the latter (chemical composition of raw materials, thermal schedule of burning) can lead to both the qualitative and some quantitative changes of the elemental phase composition. As an example, the chemical composition of the phases of one of the alinite clinkers is given in Table 2. Attention is drawn to the fact that both the amount of impurities and their set in belite and calcium aluminoferrite are different from those in the same phases of portland cement clinkers.

It is of interest that manganese enters only the aluminoferrite phase; the same is observed with titanium. As usual, the aluminoferrite phase also contains a considerable amount of magnesium and silicon. The total amount of impurities in belite and calcium aluminoferrite of the alinite clinker is less than in the same phases of portland cement clinker.

The different composition of phases is observed in white clinkers (see our paper presented at this Congress). Two types of β-belite differ in impurity content which is higher in belite crystallized from the liquid phase.

3. The solubilities of components in clinker minerals are interdependent. If, for example, in formation of a solid solution between C_3A and Na_2O the limiting saturation occurs at 6 wt% Na_2O, then for the solid solution of C_3A with Na_2O+K_2O the limiting amount of Na_2O in the solid solution will be less than 6 wt% as here the same role will be played by K_2O.

For charge compensation the additional Na^+ (K^+) are distributed in the lattice holes. Such an interdependence is valid for any isomorphous element pretending to the same positions (e.g. Al^{3+} and Fe^{3+} in alite and belite).

4. For clinker and natural minerals the heterovalent type of isomorphism is most widespread. This type of substitutions is most advantageous for clinker phases as it causes significant lattice distortions. The necessary condition for heterovalent substitutions is the compensation of a free charge which can be realized in different ways.

For heterovalent isomorphism it is essential that the structure contained holes convenient for charge-compensating ions (C_3A) to locate in them. For more dense structures the heterovalent substitutions can take place but they are very limited and cause great distortions of the structure (C_3S).

The most clear example of heterovalent isomorphism is the Ca^{2+}—Na^+ substitution in solid solutions of C_3A with Na_2O. The free charge compensation proceeds here according to a simple scheme: $Ca^{2+} \rightleftharpoons 2Na^+$. One Na atom occupies Ca sites; another, compensating atom, is located in the holes of C_3A lattice. By changing the chemical composition of starting mixtures, for example, by introducing K^+, the latter, along with Na^+, can isomor-

phously substitute for Ca^{2+} and play the role of a compensating ion. If the reaction mixtures contains Si^{4+}, the appearance of $Na^{+}(K^{+})$ in the C_3A lattice can also proceed some other way owing to another compensation scheme, namely: $Ca^{2+}Al^{3+} \rightleftharpoons Na^{+}K^{+})Si^{4+}$.

The analysis of both the schemes of heterovalent substitutions leads us to understand that each of them brings about its own distortions in the C_3A structure and consequently the changes in properties. This example has been given to emphasize the fact that the compensation schemes can be chosen by changing the chemical composition of the reaction mixtures.

It is of interest to illustrate the heterovalent isomorphism between the elements in a natural mineral. Thus, the $Be^{2+} \rightleftharpoons Li^{+}$ isomorphous substitution is characteristic of beryll $Al_2Be_2/Si_6O_8/$. It is accompanied by entering the beryll structure canals of large $Na^{+}(K^{+})$ atoms, sometimes Cs^{+}, more seldom Rb^{+} and (OH). Beryll can contain up to 5-7 wt% Na, Li, K and to 3 wt% Cs. Besides, part of Al^{3+} can be substituted by Mg and Fe with charge compensations by alkali elements located in the structure canals. As a result, cesium beryll (vorobyevite) has the composition $Al_{2-x}(Mg,Fe^{2+})_xBe_3Si_6O_{18}(Cs,Na)_x \cdot H_2O$

If one takes into account that each clinker mineral contains a set of isomorphous impurities, then it can be assumed that the solid solution structure is far from being an "ideal" structure of the host mineral free of impurities. The greater the number of pairs of heterovalent isomorphous substitutions taking place in the clinker phase structure, the greater are the structure distortions. Owing to this the activity of minerals can be increased and the properties of materials (activity, grinding capability) improved on the whole.

Among clinker minerals, belite and calcium aluminoferrite undergo the strongest structure distortions due to the presence of a set of impurities. Thus, in the lattice of a complex polycomponent solid solution of $6CaO.2Al_2O_3.Fe_2O_3$ with $MgO+Mn_2O_3+SiO_2+TiO_2$ ($\sim$7 wt% in the whole) there are several heterovalent substitutions requiring charge compensation, breaking the electrostatics and microsymmetry of the structure. The distortion is caused by different valence states and ionic sizes of isomorphous pairs: $Al^{3+}—Mg^{2+}$, $Fe^{3+}—Mg^{2+}$, $Al^{3+}—Si^{4+}$, $Fe^{3+}—Si^{4+}$, $Al^{3+}—Ti^{4+}$, $Fe^{3+}—Ti^{4+}$. The structure distortions are so strong that calcium aluminoferrite of complex composition can be partly amorphous. Fig.1 demonstrates "consequencies" of isomorphism in the aluminoferrite phase containing as isomorphous impurities Na, K, Mg, Mn, Si, Ti, P (the total content of impurities calculated for the same amount of oxides is $\sim$ 12 wt%, these are mainly MgO, SiO_2, TiO_2). The X-ray diffraction pattern for this phase shows that many reflections bear a strongly diffused character (2θ of 58-62°, 48-51°) and are each non-uniformly shifted with respect to the other (2θ of 32-35°, 45-50°, 58-61°). Reflection 022 moves sharply to 200, reflection 141 merges with 200, reflection 080 strongly shifts to the region of small angles and 202 to that of large angles. The form of the whole diffractogram is similar to that for $6CaO.2Al_2O_3.Fe_2O_3$ without impurities.

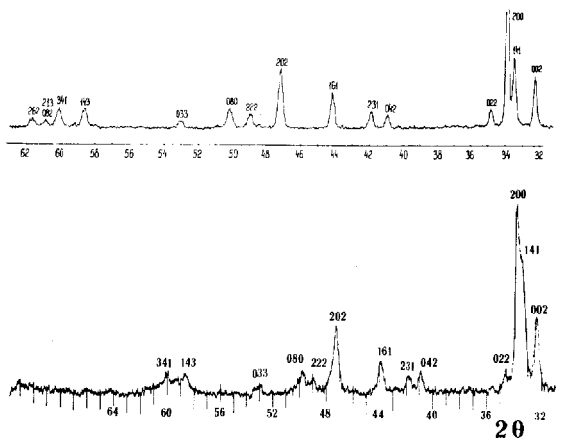

Fig.1 - X-ray diffraction pattern of calcium aluminoferrites:
I - $6CaO.2Al_2O_3.Fe_2O_3$;
II - $(Ca_{2.06}{}^{Na}{}_{0.06}{}^{K}{}_{0.01})(Al_{0.89}{}^{Fe}{}_{0.58}{}^{Mg}{}_{0.15}{}^{Mn}{}_{0.02}{}^{Si}{}_{0.23}{}^{Ti}{}_{0.04}{}^{P}{}_{0.01})\,O_5$

The "consequencies" of isomorphous substitutions influence the hydration properties as well. The hydration kinetic curves for the aluminoferrite phases of complex composition (Fig.2) show a higher activity in all stages compared to $6CaO.2Al_2O_3.Fe_2O_3$. Table 3 gives the chemical composition (wt%) of the synthesized aluminoferrite phases of complex composition (solid solutions based on $6CaO.2Al_2O_3.Fe_2O_3$); Table 4 gives unit cell parameters and densities for these phases.

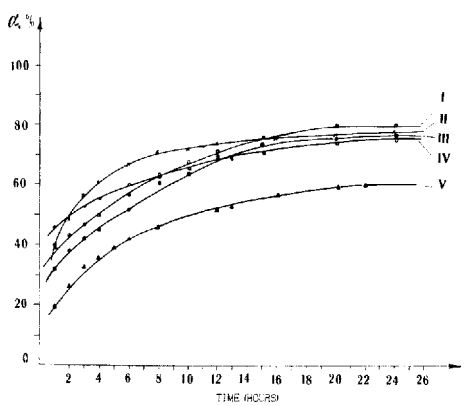

Fig.2 - Hydration kinetic curves for calcium aluminoferrites of complex composition. I-AF-1; II-AF-2; III-AF-3; IV-AF-4; V-C_6A_2F.

TABLE 3

Oxides \ Samples	AF-1	AF-2	AF-3	AF-4
CaO	49.92	47.45	49.61	48.62
Al_2O_3	19.34	19.56	19.38	20.06
Fe_2O_3	19.69	22.19	19.81	21.38
Na_2O	0.10	0.13	0.08	0.13
K_2O	0.11	0.18	0.18	0.09
MgO	2.54	2.65	2.53	2.66
Mn_2O_3	0.58	0.95	0.51	0.97
SiO_2	5.43	4.47	6.01	3.71
TiO_2	1.42	1.81	1.41	1.85
P_2O_5	0.25	0.07	0.27	0.09
L.O.I.	-	0.05	0.21	-
Σ	99.38	99.51	100.00	99.56
Σ imp.	10.43	10.26	10.99	9.50

TABLE 4

Samples	Unit cell parameters			Densities (g/cm^3)
	a, Å	b, Å	c, Å	
AF-1	5.288	14.566	5.554	3.67
AF-2	5.331	14.492	5.550	3.64
AF-3	5.333	14.505	5.553	3.60
AF-4	5.328	14.642	5.535	3.51

It should be emphasized in conclusion that the mechanism of heterovalent isomorphous substitutions in clinker phases has been insufficiently studied.

5. The necessity of the free charge compensation by heterovalent isomorphous substitutions leads to one of the most important "consequencies" of isomorphism in clinker phases: the variation of stoichiometry of oxides and the presence of excess calcium in solid solutions. The CaO excess was found in C_2S and C_3S solid solutions and in the real alite, belite and aluminate clinker phases. As an example we give the compositions (by EPMA) of alite, belite and aluminate phases:

$(3.04CaO \cdot 0.009Na_2O \cdot 0.004K_2O \cdot 0.054MgO)(SiO_2 \cdot 0.029Al_2O_3 \cdot 0.014Fe_2O_3 \cdot 0.009TiO_2 \cdot 0.004P_2O_5)$;

$(2.11CaO \cdot 0.03Na_2O \cdot 0.015K_2O \cdot 0.02MgO \cdot 0.001 Mn_2O_3)(SiO_2 \cdot 0.027Al_2O_3 \cdot 0.023Fe_2O_3 \cdot 0,006TiO_2)$;

$(3.52CaO \cdot 0.03Na_2O \cdot 0.02K_2O \cdot 0.06MgO)(Al_2O_3 \cdot 0.12Fe_2O_3 \cdot 0.34SiO_2 \cdot 0.005TiO_2 \cdot 0.002P_2O_5)$.

The excess of CaO was found in solid solutions of C_3S ($Ca3O/SiO_4$/) with Y_2O/SiO_4/, La_2O/SiO_4/ and Sc_2O/SiO_4/ /10-12/.

In formation of such solid solutions the heterovalent isomorphous substitutions $3Ca^{2+} \rightleftharpoons 2La(Y,Sc)^{3+}$ take place. The two trivalent La(Y,Sc) ions occupy positions of two divalent Ca ions. In this case the charge compensation can be attained by distribution in the lattice of additional calcium ions. In other words, the formation of solid solutions between tricalcium silicate and orthosilicates of yttrium and rare-earth elements took place with participation of additionally introduced CaO. Table 5 gives the chemical composition of the solid solutions of C_3S with $Y_2O_3 \cdot SiO_2$, $La_2O_3 \cdot SiO_2$ and $Sc_2O_3 \cdot SiO_2$, according to chemical analysis (wt%).

6. An important result of isomorphism in clinker phases is as follows. The above indicated capability of clinker minerals to distribute in their structure a significant amount of impurities together with excess CaO in the solid solutions evidences unambiguously for the inaccuracy of calculation of the quantity of minerals in the clinker according to chemical analysis for C_3S, C_2S, C_3A and C_4AF free of impurities.

Furthermore, the EPMA data on the composition of clinker phases of different manufactures showed that in the ratio of oxides $CaO:Al_2O_3:Fe_2O_3$ the aluminoferrite phase is close to the 6:2:1 and not 4:1:1 composition. The difference in Fe_2O_3 content between these phases is rather high.

7. The crystal chemistry of the real clinker phases with a set of impurities in the lattice is related not only with the peculiarities of static isomorphism in clinker minerals considered above but also deals with the dynamics of isomorphism - the distribution mechanism of impurities among clinker phases.

In formation of polycomponent solid solutions impurities are distributed not accidentally but, as experiment shows, they prefer the lattices of crystals with crystallographically convenient positions. This would seem to be natural but the experimental finding of this fact for clinker phases has a peculiar sense of practical importance /13/.

Actually, knowing the formation mechanism of clinker polycomponent solid solutions and taking into account a set of the main and secondary impurity elements characteristic of each phase, one can predict from the

TABLE 5

Composition of raw mixtures	Chemical composition (wt%)					Combined CaO (wt%)	CaO:SiO_2	CaO excess
	CaO	SiO_2	TR_2O_3	LOI	Σ			
93 wt% $3CaO.SiO_2$+7 wt% $Y_2O_3.SiO_2$	68.89	25.61	5.39	-	99.89	-	3.05 :1	1.20
90 wt% $3CaO.SiO_2$+10 wt% $Y_2O_3.SiO_2$	66.79	24.99	7.80	0.23	99.81	-	3.12 :1	2.86
97 wt% $3CaO.SiO_2$+3 wt% $La_2O_3.SiO_2$	71.48	24.79	2.03	1.91	100.21	1.3	3.07 :1	1.68
96 wt% $3CaO.SiO_2$+4 wt% $La_2O_3.SiO_2$	71.38	24.95	2.78	1.12	100.23	0.5	3.10 :1	2.40
99 wt% $3CaO.SiO_2$+1 wt% $Sc_2O_3.SiO_2$	73.52	25.60	0.74	0.27	100.13	0.59	3.088:1	2.11
97 wt% $3CaO.SiO_2$+3 wt% $Sc_2O_3.SiO_2$	72.14	25.60	1.42	0.73	99.89	-	3.09 :1	2.16

chemical composition of raw materials the preferential distribution of each impurity in the phases.
Thus, Mg^{2+}, Mn^{3+}, Ti^{4+}, Si^{4+} are mainly concentrated in calcium aluminoferrites owing to Fe^{3+} and Al^{3+} octahedral and tetrahedral positions favourable to them. The quantity of these elements in calcium aluminoferrites is greater than in any other clinker mineral.

As mentioned above, a clear example of the dependence of impurity distribution on the convenient crystal-chemical positions is the lattice of tricalcium aluminate. The presence of large holes in the C_3A structure in combination with the large Ca^{2+} cations create favourable conditions for both the distribution of other large cations and realization of various heterovalent isomorphous substitutions. As a result, sodium (potassium) of the starting material enters mainly the tricalcium aluminate and together with Na(K) silicon also enters the latter. The Al^{3+} octahedral positions in the C_3A lattice are favourable for Fe^{3+} as well. In this way a set of impurities for C_3A can be selected.

C_2S also has its own set of impurities. Thus, P^{5+} and S^{6+} are located mainly in C_2S substituting for Si^{4+} in tetrahedral positions. From EPMA Mg, Al, Fe are the main isomorphous impurities in C_2S although the amount of Mg concentrated in belite is less than in calcium aluminoferrite.

The main clinker silicate C_3S does not possess such an original set of isomorphous impurities as C_2S, C_3A, C_6A_2F(C_4AF). From the percentage the main impurities in alite are Mg, Al, Fe. Their amount in alite is almost the same as in belite. The lowest isomorphous capacity of C_3S compared to other clinker phases can be indicative of rather a dense structure of this silicate.

The groups of the main and secondary (in brackets) isomorphous impurities present in clinker phases are as follows (the main estimating factor is the quantity of impurities):
C_3S - Mg,Al,Fe (Na,K,Cr,Ti,P,S a.o.);
C_2S - Mg,Al,Fe,P,S (Na,K,Mn,Cr a.o.);
C_3A - Na(K),Fe,Si (Mg,Mn,Cr,Ti a.o.);
C_6A_2F(C_4AF) - Mg,Mn,Si,Ti (Na,K,Cr a.o.).

From the physicochemical point of view the phases with a set of impurities in the lattice can be regarded as polycomponent solid solutions whose main constituents are $3CaO.SiO_2$, $2CaO.SiO_2$, $3CaO.Al_2O_3$, $6CaO.2Al_2O_3.Fe_2O_3$($4CaO.Al_2O_3.Fe_2O_3$) and the impurity components Na_2O, K_2O, Mn_2O_3, MgO, Cr_2O_3, TiO_2, P_2O_5 and others.

The main conclusion to be drawn from the analysis of the chemical composition of real clinker phases is that the peculiarities of impurity distribution and those of isomorphism in clinker minerals are the basis of control over the structure and properties of phases and consequently clinkers and cements on the whole.

ONCE MORE ON THE COMPOSITION OF CLINKER PHASES

At present there are many papers concerned with the EPMA study of the composition of real clinker phases. Nevertheless these data do not and cannot contain ample information as the impurity composition of raw materials of various cement factories in different countries changes in both the variety of chemical elements and their amounts. The variety of impurities in the raw material increases due to the use of wastes. Apart from the most widespread impurities (Na,K, Mg,Mn,Cr,Ti,P,S), some others can appear in the raw materials, namely: Sr,Ba,Zn,Ni,Co, Pb,Y, rare-earth elements, radioactive wastes /14-16/ etc.

Of great interest are papers which report the results of studies of all phase compositions of clinkers produced by different manufacturers of one and the same country. Such systematic investigations provide statistical material as the source of new information.

Thus, by investigation of the chemical composition of the phases of clinkers of 20 cement plants, a special role played by MgO was revealed /17/. All clinkers contained impurities Na,K,Mg,Ti, some contained P, others - S. The quantities of these elements in clinkers, when calculated for the same amount of oxides, were within the ranges (wt%): Na_2O - 0.2-1.2; K_2O - 0.3-1.8; MgO - 0.3-5.0; TiO_2 - 0.1-0.4; P_2O_5 - 0.1-0.4; SO_3 - 0.1-0.8. The contents of the main phase-forming oxides were in the limits restricted by saturation coefficients and by the silicate and alumina moduli.

The phase compositions of the clinkers were determined by X-ray, microscopic and EPMA methods. The clinkers contained as a rule the monoclinic alite, β-belite, aluminoferrite phase mainly based on C_6A_2F (some clinkers contained also C_4AF, the cubic and tetragonal aluminate phases. Several clinkers contained periclas (the main maximum in the X-ray patterns at 2θ of 43°). Some clinkers contained both the cubic and tetragonal aluminate phases.

Fig.3 shows X-ray diffraction patterns of two commercial clinkers. Clinker 1 contains the cubic and tetragonal aluminates, clinker 2 - only a cubic aluminate. Both the clinkers contain various amounts of periclas, the greatest amount is contained in clinker2 ($\sim$ 4 wt%).

Table 6 gives the chemical compositions (wt%) of the clinker phases according to EPMA (concentration ranges are represented).

To establish the relation between the chemical composition of the phases and the chemical composition of the clinkers, we determined the coefficients representing the ratio of the mean element concentration in the phase studied to its total content in the clinker.

TABLE 6

Oxides, wt% / Phases	CaO	Al_2O_3	Fe_2O_3	SiO_2	Na_2O	K_2O	MgO	TiO_2
Alite	69.34-73.30	0.60-1.14	0.63-1.52	24.20-26.64	0.02-0.25	0.10-0.34	0.46-2.05	0.05-0.17
Belite	59.70-64.20	0.96-1.92	0.93-1.74	30.90-35.20	0.06-0.35	0.53-2.86	0.23-1.10	0.07-0.27
Aluminate	48.10-61.20	21.65-34.20	4.30-6.60	3.67-6.60	1.10-2.25	1.40-3.85	0.55-1.15	0.03-0.40
Alumino-ferrite	45. 95-51.75	13.70-23.16	18.67-30.63	2.50-4.55	0.05-0.20	0.05-0.85	1.60-3.30	0.40-1.73

TABLE 7

Oxides, wt% / Phases	CaO	Al_2O_3	Fe_2O_3	SiO_2	Na_2O	K_2O	MgO	TiO_2
Alite	1.05-1.15	0.09-0.23	0.17-0.36	1.07-1.24	0.02-0.36	0.11-0.53	0.34-0.82	0.13-0.82
Belite	0.92-1.00	0.21-0.38	0.27-0.48	1.36-1.68	0.09-0.87	0.59-3.06	0.08-0.42	0.38-1.25
Aluminate	0.74-0.95	4.04-8.14	0.91-1.75	0.16-0.30	1.65-6.68	1.40-8.00	0.11-0.97	0.13-0.61
Alumino-ferrite	0.71-0.80	3.00-5.20	4.55-7.86	0.09-0.26	0.04-0.50	0.07-0.83	0.58-3.00	2.25-8.67

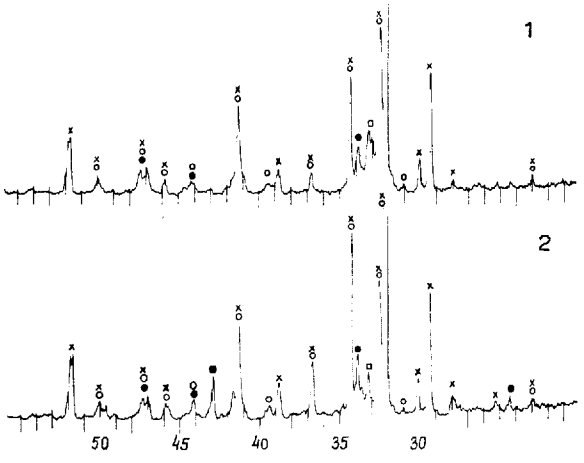

Fig.3 - X-ray diffraction patterns of commercial clinkers; × - alite, o - belite, □ - aluminate, ● - aluminoferrite, ■ - periclas.

The intervals of the coefficients change are given in Table 7 with their minimum and maximum values. The data of Table 7 show that these intervals are rather large. The distribution of Fe and Al in the alite and belite phases seemed to be most stable. Based on the data of measurements and calculations one can deduce:

Fe_2O_3(of alite)=(0.17-0.36)Fe_2O_3(of clinker)
Fe_2O_3(of belite)=(0.27-0.48)Fe_2O_3(of clinker)
Al_2O_3(of alite)=(0.09-0.23)Al_2O_3(of clinker)
Al_2O_3(of belite)=(0.21-0.38)Al_2O_3(of clinker).

Based on the data on the average chemical composition of clinker phases and chemical composition of all clinkers, the quantitative phase composition of the clinkers has been calculated /17/. The results of these calculations showed that none of the clinkers contained such a total amount of phases which could reach 100%. This evidences for the presence in clinker, apart from the main phases (C_3S, C_2S, C_3A, C_6A_2F), also of some quantity of the probable secondary phases (MgO, CaO, K_2SO_4, Na_2SO_4, glassy phase).

The data on the average chemical composition of the phases and their amount in clinkers and the data on the clinker chemical composition were used to determine the fraction of each element (oxide) with respect to its total content in the clinker which is spent on the formation of each clinker phase. Thus, for the alite phase to form the following quantities of oxides (of the total content in clinker) are needed: 60-90 wt% CaO, 60-86 wt% SiO_2 (main oxides) and 15-40 wt% Na_2O etc. (impurity oxides) (Table 8).

Special attention is drawn to the distribution of MgO. From 30 to 87 wt% MgO are spent on the main clinker phases to form. Consequently, 13-70 wt% MgO form periclas. The quantity of periclas was calculated for all clinkers studied. Fig.4 shows the dependence of quantity of the periclas on the MgO content in clinkers. Using this curve, one can determine the quantity of periclas in the clinkers.

The role of MgO in the formation of clinker silicate phases was also mentioned. The amounts of impurities in the alite and belite phases were found to increase with increasing amount of MgO in clinker. This tendency is shown in Figs.5 and 6. The explanation for this fact comes from the decrease of viscosity of clinker liquid phase with increasing MgO quantity /3,5/ which makes easier the diffusion of impurity com-

TABLE 8

Phases \ Oxides (wt%)	CaO	Al_2O_3	Fe_2O_3	SiO_2	Na_2O	K_2O	MgO	TiO_2
Alite	60-90	9-17	12-20	60-86	15-40	10-40	20-60	6-10
Belite	9-25	1- 7	3- 5	10-30	2- 8	8-45	2- 3	2-10
Aluminate	3-12	20-40	6-15	1- 3	25-70	20-80	1- 2	1- 3
Aluminoferrite	6-12	40-60	60-80	1- 4	2- 3	1- 2	7-30	70-90

ponents in the lattices of the minerals. Such a capability was found in none of the other components.

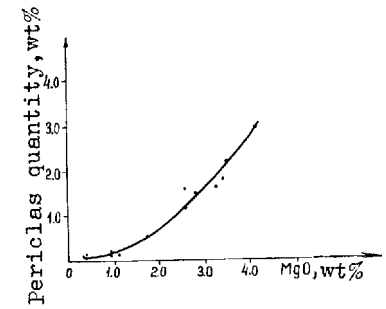

Fig.4 - Amount of periclas in clinkers vs. total MgO content in clinkers.

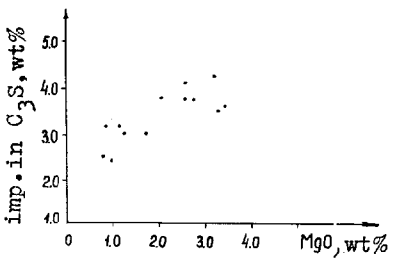

Fig.5 - Amount of impurities in alite vs. total MgO content in clinkers.

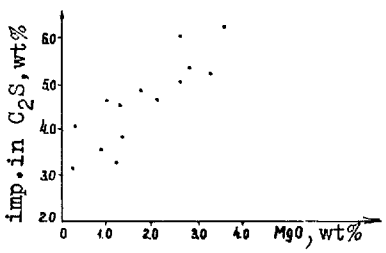

Fig.6 - Amount of impurities in belite vs. total MgO content in clinkers.

ON THE CHEMICAL COMPOSITION OF NATURAL ANALOGS OF CLINKER PHASES

Hatrurite /18/, larnite /19/, bredigite /20/, nagelschmidtite /18/, brownmillerite /21/, mayenite /21/ are natural analogs of alite, β-, α'-, α - belite, brownmillerite, aluminate $C_{12}A_7$. The analog of C_3A is not yet known.

Hatrurite, the analog of C_3S was found in the larnite-brownmillerite-mayenite rock. The mineral was called by the name of its deposits - Hatrurim. It is of interest that the hatrurite-larnite-brownmillerite rock is almost analogous in mineralogical composition to Portland cement clinker. The chemical composition of hatrurite, according to EPMA, is as follows (wt%): SiO_2-26.1; CaO-72.8; Al_2O_3-0.4; TiO_2-0.3; Fe_2O_3-0.2; traces of MgO, Σ =99.8; its formula is $Ca_{2.97}Al_{0.01}Ti_{0.01}SiO_5$.

The chemical composition of nagelschmidtite, bredigite and larnite of the Hatrurim deposits determined by EPMA is given in Table 9 /18/.

TABLE 9

Oxides (wt%) \ Mineral	Nagelschmidtite (α - C_2S)	Bredigite (α' - C_2S)	Larnite (β - C_2S)
CaO	62.06	62.32	64.31
SiO_2	27.88	30.45	32.12
Al_2O_3	0.03	0.04	0.02
Fe_2O_3	0.02	0.02	0.02
MgO	0.05	0.05	neg.
SO_3	0.12	0.06	0.25
P_2O_5	8.27	4.63	2.67
Cr_2O_3	0.03	0.01	0.01
K_2O	0.84	1.16	0.19
Na_2O	0.82	0.68	0.77
MnO	0.03	0.02	0.02
Total	100.15	99.44	100.38
Σ imp.	10.21	6.67	3.95

It is known that on stabilization of C_2S various polymorphic forms the high temperature forms "require" a greater amount of impurities than the low-temperature forms. In natural analogs this regularity is retained. It is also interesting that natural analogs may have the same set of isomorphous impurities as the phases of industrial clinkers. The composition of natural analogs can change the same way as that of the clin-

ker minerals, i.e. depending on the composition of the formation medium (chemical composition of the raw material). Thus some different data on the chemical composition of larnite and bredigite are given in /22,23/.

According to /22/the formulae of larnite and bredigite are as follows:
larnite - $(Ca_{2.01}Na_{0.01})(Si_{0.97}S_{0.03}P_{0.01})$
bredigite -
$(Ca_{1.76}Mg_{0.26}Na_{0.01})(Si_{0.95}S_{0.02}P_{0.01})$.
These two minerals differ in MgO content. The β-modification of C_2S, larnite, is reported to be stabilized by 1% of impurities by cationic substitutions. The investigation also showed that larnite and bredigite can coexist and larnite is not formed by conversion of the high-temperature form - bredigite.

The following formulae for larnite and bredigite are suggested according to EPMA of natural minerals /23/:
larnite - $Ca_2Si_{1-y}Al_yO_{4-y/2}$ (traces of Na, Mg, P, S have been found); bredigite - $Ca_{2-x}Mg_xSiO_4$(x=0.22) (traces of Na, Al, P, S have been found).

Tables 10 and 11 give the chemical composition of natural brownmillerite and mayenite from different deposits, respectively /18/.

TABLE 10

Oxide	1*	2*	3*	4*	5*	6*
CaO	44.8	46.6	47.7	46.8	43.7	46.2
MgO	n.d.	n.d.	1.6	1.4	n.d.	n.d.
Al_2O_3	22.3	19.8	19.7	22.7	13.1	17.2
Fe_2O_3	27.6	32.5	28.6	25.5	41.9	30.5
TiO_2	1.5	2.8	1.9	3.0	1.9	
Cr_2O_3	0.1	0.3	n.d.	0.3	n.d.	
ins.res.	4.0					
Total	100.3	102.0	99.5	99.7	100.6	93.9

1*. Brownmillerite from a calcite-gypsum rock. 2*. From a weathered rock. 3*. From an altered larnite rock. 4*. From a larnite rock rich in mayenite. 5*. From a spurrite-marble. 6*. From Mayen.

TABLE 11

Deposit / Oxide	Mayenite from Hatrurim	Mayenite from Mayen
CaO	47.0	45.7
Al_2O_3	49.5	45.2
Fe_2O_3	1.5	2.0
MnO	1.4	-
SiO_2	0.4	-
TiO_2	traces	-
L.O.I.	-	2.2
Total	99.8	95.1

RADIOACTIVE AND RARE EARTH ELEMENTS IN CLINKER PHASES

Of special interest are recent papers /14-16/ in which the possibility of utilization of radioactive wastes has been considered from the point of view of crystal chemistry and phase equilibria.
The use of radioactive wastes is possible owing to crystal chemical stabilization of isotopes during clinkering of usual portland cement clinker. It is assumed that 20-30 wt% of such wastes can be used due to the formation of diluted solid solutions and distribution of radioactive elements in crystal lattices of host-matrix cement compounds C_3S, C_2S, C_4AF, (C_6A_2F). C_3A is not a matrix for dilute solid solutions to form.

Table 12 gives the possible waste compositions. Crystal chemical stabilization can be achieved in the following way /16/:
1. Elements of groups A,D,E,H (i.e. Ln,Sr, Ba,Ni,Mg,Zn,Cs) substitute for Ca.
2. Elements of groups B,C (i.e. Fe,Cr,Al, Mo) substitute for Si.
3. Elements of groups B,C,F,G,I,Y (i.e. Cr, Al,Mo,U,Ru,Ce,Zr) substitute for Fe.

It is also mentioned that Ln,Fe,Cr,Al,Sr, Ba,Ni,Mg,Zn are mainly distributed in C_2S, whereas Mo,Cs are mainly located in C_3S, C_4AF can contain elements of all groups.

TABLE 12

Group code	Oxides	Amount present in waste form(mol%) PW-4b	MAGNOX
A	Ln_2O_3	13.45	2.89
B	$Fe_2O_3+Cr_2O_3$	5.30	
	$Fe_2O_3+Cr_2O_3+Al_2O_3$		23.90
C	MoO_3	16.36	4.08
D	SrO+BaO	9.38	2.26
E	NiO	6.30	
	NiO+MgO+ZnO		56.55
F	UO_3	3.37	0.06
G	RuO_2	10.20	1.76
H	Cs_2O	4.69	1.29
I	CeO_2	8.85	2.44
J	ZrO_2	22.12	4.79

Clinkering at 1000 °C of raw mixtures containing more than 20-30 wt% various radioactive wastes does not result in full radionuclide partitioning. At 1200 °C volatilization may occur. That is why the burning of mixtures containing radioactive wastes should be carried out at 1100 °C. This is an optimum temperature to prevent volatilization and activation during clinkering.

It is worth noting that as reported in paper /16/ the distribution of radioactive isotopes in non-aqueous clinker phases will also take place in hydration products.

Another fact should also be mentioned. Although the observed distribution of radio-

active elements has been described in the context of established phase equilibria for commercial waste-cement systems, it is applicable to transuranic, medium- and low-level wastes.

Of great interest is the isomorphism between Ca^{2+} and rare-earth elements and Y^{3+} in clinker phases, owing to the possible practical utilization of wastes with TR /14-16/. The effective use of wastes containing elements unusual for clinker phases, such as radioactive and rare-earth elements is first of all related with the distribution of these elements in lattices of matrix compounds as the result of isomorphous substitution and with the formation of dilute solid solutions.

Isomorphism between Ca^{2+} and rare-earth elements (TR^{3+}) as well as yttrium (Y^{3+}) is a common phenomenon among natural minerals. Thus, fluoroapatite $Ca_2Ca_3/PO_4/F$ was found to contain up to 12 wt% TR_2O_3 and about 10.6 wt% Y_2O_3 /24/; (apatite can contain about 30 varieties of impurity elements); titanite (sphen) $CaTi/SiO_4/O$ contains up to 12 wt% TR_2O_3; eudialite $Na_4Ca_2Zr/Si_3O_9/_2$ to 8 wt% TR_2O_3 (La,Ce,Pr a.o.); andradite $Ca_3Fe_2/SiO_4/_3$ - 12 wt% TR_2O_3 (La,Ce,Pr,Nd, Sm,Eu,Gd,Tb,Dy,Ho,Er,Tm,Yb,Lu and Y were found); vesuviane $Ca_{19}Mg_3Al_{10}/Si_2O_7/_4$ $/SiO_4/_{10}O_2(OH)_6$ - to 16.7 wt% TR_2O_3 /24/. A lot of examples can be given.

Isomorphous substitutions of TR for Ca are due to similar ionic radii of these elements and the same structure of the outer electron shells. This fact is related to both natural and synthetic materials.

The substitution of rare-earth elements and yttrium for Ca in C_3S and C_2S was known earlier. The solid solutions of $3CaO.SiO_2$ with oxyorthosilicates of yttrium, lanthanum and scandium were studied /10-12/. The selection of these compounds as solid solution components was due to several factors: crystal-chemical similarity between them (tricalcium silicate as an oxyorthocompound $Ca_3O/SiO_4/$, on the one hand, and $Y_2O/SiO_4/$ and $La(Sc)_2O/SiO_4/$, on the other), similarity in sizes of Ca^{2+} and TR^{3+}, similarity of chemical properties (configuration of the outer electron shells).

The formation of solid solutions was established by X-ray, microscopic and DTA methods. The compositions of solid solutions were determined by chemical analysis. The samples of $3CaO.SiO_2$ containing 7 wt% $Y_2O_3.SiO_2$, 5 wt% $La_2O_3.SiO_2$, 10 wt% $Gd_2O_3.SiO_2$, 3 wt% $Sc_2O_3.SiO_2$, 7 wt% $Nd_2O_3.SiO_2$ represented a homogeneous phase - solid solution.

The chemical compositions of the solid solutions have been given above (Table 5). Fig.7 shows the fragments of X-ray diffraction pattern of triclinic, monoclinic and rhombohedral solid solutions of C_3S with La_2O_3. Only the use of lanthanum permitted the stabilization of all modifications of solid solutions. The use of yttrium and gadolinium yielded the formation of triclinic and monoclinic solid solutions, scandium led to the triclinic solid solutions to form.

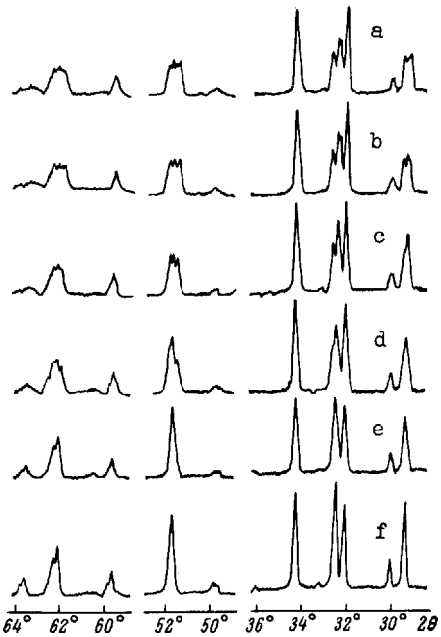

Fig.7 - X-ray diffraction patterns of triclinic (a,b,c), monoclinic (d) and rhombohedral (e,f) solid solutions of C_3S with La_2O_3.
La_2O_3 content (wt%): a - 0.2; b - 0.5; c - 1.0; d - 1.5; e - 2.0; f - 4.0.

Fig.8 gives the DTA curves for quenched (a) and annealed (b) solid solutions of C_3S with $Y_2O_3.SiO_2$, $La_2O_3.SiO_2$, $Sc_2O_3.SiO_2$. Only two transformations have been analyzed: at 920 and 980 °C. The DTA showed that endothermic transformations depend not only on the kind of impurity element (Y,La,Sc) and its concentration in the solid solution but also on the thermal treatment of the samples. Thus, yttrium not only decreases the temperature of polymorphic transformations of the solid solution compared to C_3S but also leads to the merging of two endothermic minima at a 5 wt% $Y_2O_3.SiO_2$ concentration in the solid solution (Fig.8, a).

The annealed solid solutions of C_3S with 5 wt% $Y_2O_3.SiO_2$ again show two endothermic effects within the temperature range 900-1000 °C. A similar thermal behaviour is observed in the solid solutions of C_3S with $Gd_2O_3.SiO_2$.

The solid solution of C_3S with lanthanum in the lattice shows a different character of thermal behaviour. At 3 wt% $La_2O_3.SiO_2$ and more in the solid solutions the DTA curve for the solid solution (quenched sample) shows the splitting of the endothermic effect (Fig.8, a, curves 6,7). In the DTA curve for the solid solution of C_3S with 5 wt% $La_2O_3.SiO_2$ the splitting deepens to

separate the effect into two endothermics. The annealed solid solutions with such amounts of $La_2O_3.SiO_2$ show two usual endothermic transformations in the DTA curve within the considered temperature interval. The appearance of the additional effect is due to the strong distortion of the C_3S lattice influenced by lanthanum and to the disordering of the distribution of elements in the C_3S lattice. The C_3S lattice with a Sc impurity undergoes the least changes (Fig.8, curve 8).

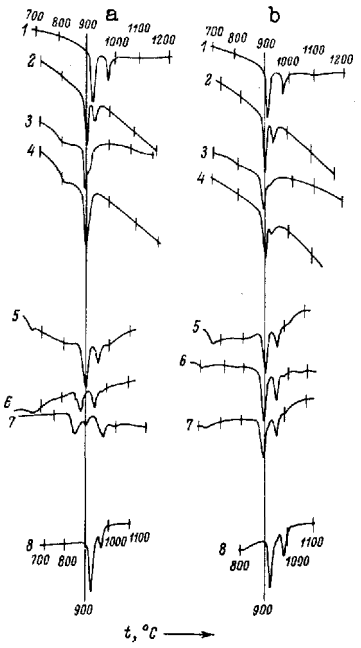

Fig.8 - DTA curves for quenched (a) and annealed (b) C_3S (curve 1) and solid solutions of C_3S with $Y_2O_3.SiO_2$ (curves 2-4), $La_2O_3.SiO_2$ (curves 5-7), $Sc_2O_3.SiO_2$ (curve 8).
Content (wt%):
2,3,4 - C_3S with 3.0,4.0,5.0 % $Y_2O_3.SiO_2$, respectively;
5,6,7 - with 2.0,3.0,5.0 % $La_2O_3.SiO_2$, respectively;
8 - with 1.0 % $Sc_2O_3.SiO_2$.

It is worth noting that the presence of lanthanum in the C_3S lattice permitted us to reveal in the DTA curve the transformation at 1050 °C as well.

As seen from IR spectra (Fig.9), the absorption bands characteristic of C_3S decrease significantly their intensity in the spectra of solid solutions and diffuse with increasing content of oxyorthosilicate in them.

The DTA data were used to construct hypothetic diagrams of the regions of solid solutions in the systems $CaO.SiO_2$-$Y_2O_3.SiO_2$ and $3CaO.SiO_2$-$La_2O_3.SiO_2$ (Fig.10).

Attention is drawn to the fragment of the X-ray pattern for the solid solution of C_3S with 5 wt% $La_2O_3.SiO_2$. The quenched solid solution is rhombohedral, when annealed it is triclinic.

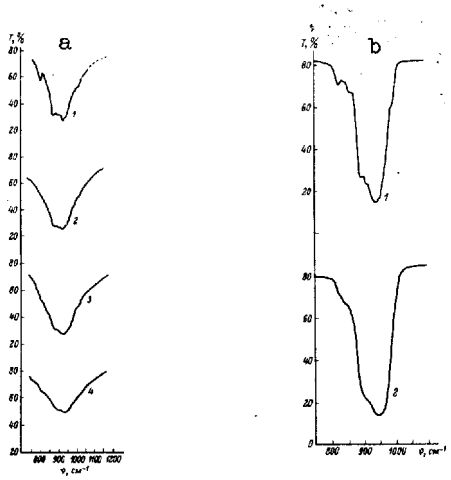

Fig.9 - IR spectra of $3CaO.SiO_2$ (curve 1) and solid solutions:
a - with $Y_2O_3.SiO_2$ (3,6,12 (in batch) wt%)
b - with $Sc_2O_3.SiO_2$ (1 wt%)

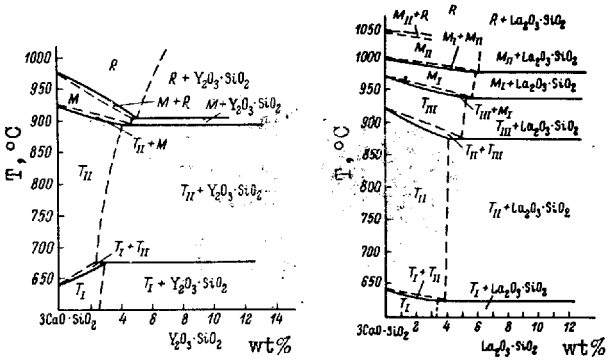

Fig.10 - Regions of solid solutions in the systems $3CaO.SiO_2$-$Y_2O_3.SiO_2$ and $3CaO.SiO_2$-$La_2O_3.SiO_2$.
T - triclinic, M - monoclinic, R - rhombohedral modifications.

In conclusion of this study the following should be noted . Rare earth elements can be used as specific crystal chemical indicators allowing to reveal the peculiarities of structure and the properties of host matrix minerals. Owing to the calcium isomorphism in the solid solutions of C_3S with rare-earth elements we managed to establish the fact of practical importance - the supersaturation of solid solutions with calcium oxide. Only the DTA curves for solid solutions of C_3S with lanthanum showed all polymorphic transformations of triclinic solid solutions analogous to triclinic tricalcium silicate. In the solid solutions of C_3S with yttrium and rare-earth elements we observed a disorder phenomenon (quali-

tatively) in the distribution of structural elements of the lattice characteristic of the solid solutions of substitution. The disorder was fixed based on the diffused character of the IR-spectra, the change of index Δ (index of lattice distortion) /25/ and the splitting of effects in the DTA curves.

Triclinic, monoclinic and rhombohedral polymorphic modifications of C_3S stabilized, respectively, by 0.75, 1.50 and 4.50 wt% La_2O_3 were obtained also by other investigators /26,27/. Their data coincide with the results of the above investigations of solid solutions of C_3S with La_2O_3 and $La_2O_3.SiO_2$. But the presence in the C_3S solid solution of 7.27 wt% La_2O_3 seems to be increased /27/.

There are also papers concerned with the substitution of TR^{3+} and Y^{3+} for Ca^{2+} in C_2S, the solid solutions of C_2S with yttrium, lanthanum and neodymium orthosilicates being studied /28,29/. It was shown that in the Ca_2SiO_4-$Y_4(SiO_4)_3$ system the region of homogeneity exists up to 35 wt% $Y_4(SiO_4)_3$, in the Ca_2SiO_4-$La_4(SiO_4)_3$ - up to 35 wt% $La_4(SiO_4)_3$ and in the Ca_2SiO_4-$Nd_4(SiO_4)_3$ up to 40 wt% $Nd_4(SiO_4)_3$. The formation of solid solutions leads to successive stabilization of β -, α' -, α -C_2S. In the Ca_2SiO_4-$Y_4(SiO_4)_3$ system β-, α'-, α - C_2S are stabilized in the solid solutions at $Y_4(SiO_4)_3$ concentrations of up to 7.5, 12-25 and 30-35 wt%, respectively. In the Ca_2SiO_4-$La_4(SiO_4)_3$ system these modifications are stabilized at $La_4(SiO_4)_3$ contents of up to 5, 15-20 and 25-35 wt%. In the Ca_2SiO_4-$Nd_4(SiO_4)_3$ system they are stabilized at $Nd_4(SiO_4)_3$ contents of up to 7.5, 17.5-27.5 and 32.5-40 wt%.

The above mentioned results give us grounds to assume that firstly, all other rare-earth elements can also isomorphously substitute for Ca^{2+} in C_3S and C_2S. Secondly, an important practical result follows: rare earth elements which can be present in the wastes utilized will be "adopted" by the clinker silicate phases. A greater amount of rare-earth elements can be distributed in C_2S than in C_3S.

Investigations under laboratory conditions showed that La_2O_3 not only accelerates the clinker formation process but improves the technical properties of cement /30/.

ON IMPERFECTION OF CLINKER PHASES AS A RESULT OF THE PRESENCE OF IMPURITIES IN THE LATTICE

One of the results of isomorphous substitutions in crystals is their imperfection. In practice, each solid solution is defective. Classification of defects has been made in /31/.

We studied the interrelation between composition, structure, defects and hydration activity of solid solutions of C_3S with ZnO /32/.

Selection of ZnO as a solid solution component was due to the fact that this oxide allows stabilization of a whole series of C_3S modifications (triclinic, monoclinic, rhombohedral) and also due to its practical importance.

The phases were identified using X-ray and microscopic methods, DTA and IR-spectroscopy. The composition was determined by chemical analysis. ZnO concentration in various modifications was as follows (here and further percent by weight): T_I up to 1%; T_{II}, T_{III} from 1.0 to 2.0%; M_I from 2.0 to 2.5%; M_{II} from 2.5 to 4.0%; R from 4.0 to 5.0%. The limiting solid solution contained $\sim$ 5% ZnO. The X-ray patterns of these solid solutions are similar to the ones of solid solutions with La_2O_3.

The formation of solid solutions accompanied by substituting Zn^{2+} for Ca^{2+} is related with a considerable change of $3CaO.SiO_2$ matrix structure, disordering in the distribution of crystal lattice elements and defect formation. As an example of $3CaO.SiO_2$ structure distortion influenced by Zn impurity we show the IR-spectra of triclinic, monoclinic and rhombohedral modifications of the solid solutions (Fig.11).

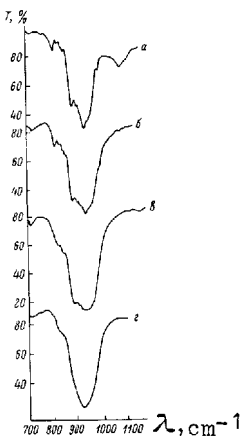

Fig.11 - IR-spectra of $3CaO.SiO_2$ (a) and solid solutions with ZnO: b - triclinic, c - monoclinic, d - rhombohedral.

The defective state of the lattice depends on the chemical nature and amount of impurity /33/. Imperfection of solid solutions of C_3S with ZnO and its dependence on the impurity concentration was characterized using the data of an electron-microscopic study of the etching picture of crystal surfaces.

The character of formation, distribution and orientation of etching figures is an indication of various defects. Three types of etching figures were distinguished: triangular with an average size of 0.3-0.5 μm,

pointlike (0.01 μm) and rounded (0.7-1.0 μm) On the surface of crystals of pure C_3S mainly the triangular and pointlike etching figures were observed. The surface part free of etching figures occupied 60%. With inreasing ZnO content in the solid solution it decreased rapidly and at ∿ 1.5% ZnO practically disappeared. The appearance of etching figures on the overall crystal surface evidences for the fact that it is the impurity component that causes lattice defectness.

A comparative consideration of the etching picture of pure $3CaO.SiO_2$ and the one with ZnO permitted us to find that the presence of impurity leads to the formation of etching figures of the rounded form. Similar etching figures were also observed on crystals of C_3S solid solutions with other impurities, for example, with MgO, Al_2O_3, Cr_2O_3 and P_2O_5 /33/.

The pointlike and triangular etching figures were called "structural" (they probably are of dislocation nature) and rounded - as "impurity" etching figures according to their origin.

To estimate quantitatively the relations of various etching figures, we calculated their densities which are as follows (figures/cm^2): $1\text{-}80\cdot10^4$, $40\cdot10^7\text{-}100\cdot10^7$ and $0\text{-}90\cdot10^4$ for triangular, pointlike and rounded figures, respectively.

Figure 12 is graphic representation of the dependence of impurity ($\rho_{imp.}$) and structural ($\rho_{str.}$) etching figures on ZnO concentration in the solid solution using density values of pointlike figures.

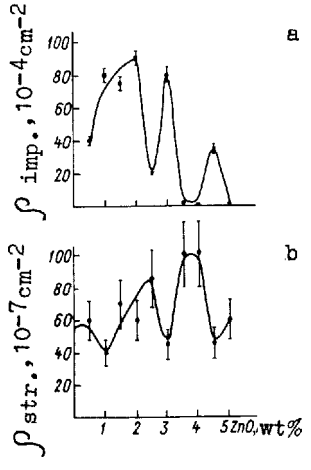

Fig.12 - Densities $\rho_{imp.}$ and $\rho_{str.}$ as a function of ZnO content in the solid solution.

Analysis of the ρ values as well as the etching figures allowed us to reveal the redistribution of densities with changing ZnO concentration. As is seen, the course of the curve is complicated. In a general case the change of direction of each curve coincides with rearrangement of one solid solution modification to the other. Actually the extrema in both the curves corresponding to ∿ 1% ZnO coincide with the T_I—T_{II} rearrangement; those at ∿ 2% ZnO - with the T_{II}—M_I and the ones at ∿ 2.5% ZnO with the M_I—M_{II}. A prolonged concentration interval of 3.0-4.0% ZnO covers the formation region of rhombohedral modification.

Comparison of curves $\rho_{imp.}$ and $\rho_{str.}$ shows that they are a mirror reflection of one another: the maximum in the curve $\rho_{imp.}$ corresponds to the minimum in $\rho_{str.}$ The study of the etching picture and the form of the curves leads to the assumption that the mechanism of the primary entering of an impurity into the matrix crystal lattice implies its concentration on the active parts of the crystal, i.e. on the ready defects.

The $\rho_{imp.}$ maxima coincide with impurity aggregates in the lattices of the modifications formed. The rearrangement of the lattice by formation of the next modification is connected with the impurity concentration on the ready defects by the distribution of this impurity among structural positions during $Ca^{2+} \rightleftharpoons Zn^{2+}$ isomorphous substitution. The new polymorphic modification formed is characterized by increased density of structural defects (Fig.12). A great amount of pointlike etching figures are on the surface of crystals undergoing the given transformation stage. The formation of the next modification starts with the impurity concentration on the ready defects of the lattice of the preceding polymorphic modification formed etc.

Rearrangement of the lattice due to the change of crystal system (e.g. in a triclinic - monoclinic - rhombohedral series) is accompanied by a sharper structural change than the one of the T_I—T_{II} or M_I—M_{II} types. Actually, the largest impurity concentration was observed in the sample with 2% ZnO, which is a boundary concentration between triclinic and monoclinic forms. The greatest density of structural defects was observed for the monoclinic form being in the stage of rearragement into the rhombohedral modification.

The relation between imperfection and hydration activity was considered. The curves for the dependence of the degree of hydration of solid solutions on ZnO content (Fig.13) are of complicated character (with maxima and minima) which is also due to the structural rearrangement of polymorphic modifications.

It should be particularly mentioned that the maximum values of the degree of hydration of the samples with 2 and 4% ZnO correspond to the maximally defective state of the lattice of solid solutions; the first maximum corresponds to a maximum value of $\rho_{imp.}$ and the second to that of $\rho_{str.}$. The greatest hydration activity has been observed for a solid solution containing

4% ZnO and being in the stage of rearrangement to the rhombohedral modification. This solid solution has the maximum amount of structural defects.

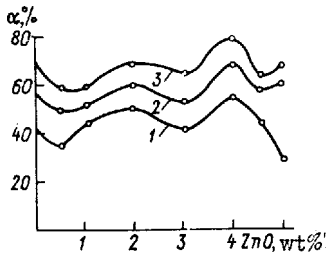

Fig.13 - Degree of hydration of solid solutions C_3S with ZnO. 1 - after 1 day; 2 - after 3 days; 3 - after 28 days.

It is worth noting in conclusion that solid solutions being in the state of structural rearrangement and formation of new modifications are most active. They possess the maximum density of impurity and structural defects and the highest degree of hydration.

CONCLUSION

Two main crystal chemical features of clinker matrix minerals - C_3S, C_2S, C_3A, C_6A_2F, C_4AF -
(1) the tendency to the distribution of various impurities in the lattices instead of the main structural elements (isomorphism) and
(2) the capability of the formation of various crystal forms (polymorphism)
are a basis of the chemical and thermal activation of the phases, a base for for further development of the chemistry and technology of cement, for new economical technological prosedures.

Thus, these two peculiarities of C_2S structure underlie the basis of technology of belite clinkers (more economical compared to that of portland cement clinker) developed at present.

The chemical varieties of impurities and their combinations as well as various burning and cooling schedules are in their essence practical ways of controlling the structure and properties of crystals. They also provide both the different imperfection of crystals and the quality of crystallinity and in some cases their partial amorphization. The properties of the crystals and material on the whole can be changed in the desired direction.

However, the activation processes of separate clinker phases for the purpose of improvement of their properties have been studied insufficiently.

At present the problems of the composition complication and sharp quenching are of actual importance for clinker phases as well as for many other materials of modern engineering.

Complication of the composition of clinker phases is inevitable to a certain degree because of widening the kinds of raw materials utilized. It is the influence of impurities and heat treatment schedule on the structure of clinker compounds that makes possible the development of economically advantageous technologies.

ACKNOWLEDGMENTS

The author is deeply grateful to Mrs. I.G. Labetskaya for having translated the paper into English and to Mr. V.S. Marinichev for his help in preparation of the manuscript.

REFERENCES

1.- R. BUCCHI (1980), "Influence of the nature and preparation of raw materials on the reactivity of raw mix", Proc. 7th Int. Congr. Chem. Cement, Paris, vol. I, Principal reports, I-1/3-1/43.

2.- S. SPRUNG (1980), "Effect of the burning process on the formation and properties of the clinker", Ibid., I-2/1-2/17.

3.- V.V. TIMASHEV (1980), "The kinetics of clinker formation. The structure and composition of clinker and its phases", Ibid., I-3/1-3/20.

4.- J.-P. MERIC (1980), "Influence of grinding and storage conditions of clinker", Ibid., I-4/1-4/16.

5.- V.V. TIMASHEV, A.P. OSOKIN, V.G. AKIMOV and E.N. POTAPOVA (1983), "Alite formation in oxide-salt melts", Chemistry and Chemical Technology of Silicate Materials, Trudy MKhTI im. Mendeleeva (Proceedings of the Mendeleev Moscow Chemical Technological Institute N 128, 90-98.

6.- The Second All-Union Symposium on the Problem of Isomorphism (1969), Abstracts of Papers, Moscow.

7.- E.S. MAKAROV (1973), "Isomorphism of atoms in crystals", "Nauka", Moscow, 288 p.

8.- V.S. URUSOV (1975), "Energetic Crystal Chemistry", "Nauka", Moscow, 395 p.

9.- N.L. SMIRNOVA and N.V. BELOV (1969), "Isomorphism and Similar Concepts in the Light of Crystal Chemistry", Geokhimiya N 11, 1291-1301.

10.- N.A. TOROPOV and A.I.BOIKOVA (1963), "Solid solutions of tricalcium silicate with yttrium oxyorthosilicate", Dokl. AN SSSR 151, 5, 1114-1117.

11.- A.I. BOIKOVA, N.A. TOROPOV and A.K. KUZNETSOV (1964), "Rare earth silicates as crystal-chemical indicators", Solid solutions of tricalcium silicate with lanthanum oxyorthosilicate", Dokl. AN SSSR 156, 4, 865-868.

12.- A.I. BOIKOVA and N.A. TOROPOV (1966), "Study of solid solutions of tricalcium ilicates with rare-earth oxyorthos icates", Experiment in Technical Mineralogy and Petrography, Moscow, 25-30.

13.- A.I. BOIKOVA (1982), "Crystal chemistry of solid solutions of cement clinker minerals", Tsement N 9, 6-9.

14.- C.M. JANTZEN and F.P. GLASSER (1979), "Stabilization of nuclear waste constituents in portland cement", Am. Cer. Soc. Bull., vol. 58, N 4, 459-466.

15.- C.M. JANTZEN, F.P. GLASSER and E.E. LACHOWSKI (1982), "Solid-state reactions of sintered commercial radwaste ceramics: I. PUREX and MAGNOX wastes without additives", Mat. Res. Bull., vol. 17, N 1, 77-87.

16.- C.M. JANTZEN, F.P. GLASSER and E.E. LACHOWSKI (1984), "Radioactive waste-portland cement systems: I, Radionuclide distribution", Journ. Amer. Cer. Soc. vol. 67, N 10, 668-673.

17.- O.I. FOMICHEVA and A.I. BOIKOVA (1986), "Quantitative regularities of distribution of impurities among the phases of portland cement clinker", Tsement N 5 (in press).

18.- SH. GROSS (1977), "The mineralogy of the Hatrurim formation, Israel", Bull. Geol. Survey Israel N 70, 1-80.

19. C.E. TILLEY (1929), "Larnite (calcium orthosilicate, a new mineral) and its associated minerals from the limestone contact-zone of Scawt Hill, Country Antrim", Mineral. Mag. vol. 22, N 125, 77-86.

20.- C.E. TILLEY (and H.C.G. VINCENT (1948), "Occurence of an orthorombic high-temperature form of Ca_2SiO_4(bredigite) in the Scawt Hill contact zone and as a constituent of slags", Mineral. Mag. vol. 28, N 200, 255-273.

21.- G. HENTSCHEL (1964), "Mayenit, $12CaO \cdot 7Al_2O_3$, und brownmillerit, $2CaO \cdot (Al,Fe)_2O_3$, zwei neue minerale in den kalksteineinschlussen der lava des ettringer bellerberges", Neues Jharb. f. Mineral, Mh., N 1, 22-29.

22.- H.G. MIDGLEY and M. BENNET (1971), "A microprobe analysis of larnite and bredigite from Scawt Hill, Larne, Northern Ireland", Cem. Concr. Res. v. 1, N 4, 413-418.

23.- S.L. SARKAR and J.W. JEFFERY (1978), "Electron microprobe analysis of Scawt Hill bredigite-larnite rock", J. Am. Ceram. Soc. vol. 61, NN 3-4, 177-178.

24.- A.S. POVARENNYKH (1966), "Crystal chemical classification of the mineral kinds", Nauk. Dumka, Kiev, 547 p.

25.- A. MIYASHIRO (1957), "Cordierite-indialite relations", Amer. Journ. Sci. vol. 255, N 1, 43-62.

26.- L. STEVULA and J. PETROVICH (1981), "Hydration of polymorphic modifications of C_3S", Cem. Concr. Res. v. 11, N 2, 183-190.

27.- W. SINCLAIR and G.W. GROVES (1984), "Transmission Electron Microscopy and X-ray Diffraction of Doped Tricalcium Silicate", J. Amer. Ceram. Soc. v. 67, N 5, 325-330.

28.- N.A. TOROPOV and N.F. FEDOROV (1962), "Stabilization of high-temperature forms of dicalcium silicates by orthosilicates of lanthanoids", Zhurn. Prikl. Khim. vol. 35, N 10, 2156-2161.

29.- N.A. TOROPOV and N.F. FEDOROV (1962) "Solid solutions of lanthanum orthosilicate in dicalcium silicate", Zhurn. Prikl. Khimii vol. 35, N 11, 2548-2550.

30.- P.F. RUMJANTSEV and Z.I. SKOTNIKOVA (1970), "Influence of lanthanum oxide on the formation kinetics and properties of cement clinker", Cementitious Materials of Siberia and Far East, Nauka, Novosibirsk, 112-115.

31.- M. REGOURD and A. GUINIER (1974), "Crystal chemistry of the constituents of portland cement clinker", Moscow, VNIIESM, 63 p.

32.- A.I. BOIKOVA, M.G. DEGEN, V.A. PARAMONOVA and V.V. SUDINA (1978), "Defectness and hydration activity of the solid solutions of C_3S with ZnO", Tsement, N 5, 3-5.

33.- N.A. TOROPOV, M.G. DEGEN, A.I. BOIKOVA (1971), "Elektronenmikroskopische Untersuchung fester Lösungen mit Tricalciumsilicat", Silikattechnik v. 22, N 12, 400-402.

Relationship of processing parameters to clinker properties; influence of minor components 1.2

1 Introduction

The fine crystalline textures of the portland clinker constituent minerals, inclusive of the chemical composition, reflect sensitively their growth environments during clinkering and thus may provide a wealth of information as to the actual processing conditions of clinker in the kiln. With regard to belite and the interstitial materials, calcium aluminate and calcium aluminoferrite, those relations have already been made clear to a certain extent especially in connection with the condition of cooling. This report, therefore, lays emphasis exclusively on alite as such an information carrier. The fine textures of alite have been discussed in terms of the parameters relevant to crystal growth with special reference to the environments peculiar to portland clinker. The processing parameters in manufacturing clinkers, inclusive of the preparation of raw mixes, are significant, in this context, in connection with their influence on the environmental conditions of crystal growth. The relation between the fine textures of alite and the resultant hydraulic properties of cements produced, the materials characterization in the true sense of the word (1), is a problem separate from the present theme though important and will not be dealt with here.

The crystal structures of the R and M_3 forms of C_3S, which are respectively the highest-temperature modification and the most common constituent of alite in works portland clinker, have been reviewed with regard to the origin of the complex polymorphism of C_3S.

2 Characteristic aspects of crystal growth of alite in portland clinker

2.1 Growth from HTS

The crystal growth of alite in portland clinker is essentially the growth from a high temperature solution - usually abbreviated as HTS (2,3). In the HTS growth the constituents of the material to be crystallized are dissolved in a suitable solvent and crystallization occurs as the solution becomes critically supersaturated. The supersaturation may be promoted by evaporation of the solvent, by cooling the solution or by a transport process between dissolving and growth zones due to temperature or concentration gradient.

With alite in portland clinker the interstitial melt, which appears at around 1300°C and reaches about twenty percent by weight, acts as HTS. C_3S, which melts incongruently at 2070°C, is extremely difficult to be grown from the pure melt. The presence of the interstitial melt in portland clinker significantly lowers the temperature of C_3S formation and encourages its growth. The dissolution of CaO and C_2S into the interstitial melt creates the supersaturation necessary for nucleation and growth. The reaction process to form C_3S was illustrated, for simplicity, on the phase diagram of the system $CaO-C_2S-C_4AF$ by Kondo and Choi (4) and more elaborately by Christensen et al. (5,6) on the ternary system $CaO-Al_2O_3-SiO_2$.

The HTS growth, on the other hand, necessarily introduces various sorts of defects into the crystal such as substitutional or interstitial incorporation of solvent ions, microscopic and macroscopic inclusions of solvent or impurities, nonuniform doping of elements added etc. Such circumstances are essentially the same with alite in portland clinker. The inherent heterogeneity of nucleation and growth environments in clinker further gives rise to increasing complexities in the characters of the resultant crystals.

The chemical and physical properties of the interstitial melt in clinker, as a matter of course, exert great influence on the growth mode of alite. With regard to the characterization of the interstitial melt and its interaction with CaO and C_2S, the contributions of Russian scientists are significant (7,8).

2.2 Nucleation

The rate of nucleation has a pronounced influence on the average crystal size of alite obtained. In the homogeneous nucleation the free energy ΔG^* for producing spherical nuclei of critical radius $r^* = 2\gamma v/\Delta\mu$ is given by

$$\Delta G^* = 16\pi\gamma^3 v^2/3(\Delta\mu)^2 \qquad (1)$$

where γ is the interfacial surface energy of the solid phase, v is the molecular volume of the solute, and $\Delta\mu$ is the free energy difference per molecule between the solid and the liquid phases. In the solution growth the driving force for crystal growth, $\Delta\mu$, can be expressed in terms of the actual concentration C and the equilibrium concentration C_e by

$$\Delta\mu = kT\log(C/C_e) = kT\log(1+\sigma) \qquad (2)$$

where k is the Boltzmann constant, T is temperature and $\sigma = (C - C_e)/C_e$ defines the supersaturation.
When $\sigma \ll 1$, $\Delta\mu \cong kT\sigma$. Hence

$$\Delta G^* = 16\pi\gamma^3 v^2/3k^2T^2\sigma^2 \qquad (3)$$

The rate equation for the formation of critical nuclei is

$$R = c\cdot\exp(-\Delta G^*/kT) \qquad (4)$$

This thermodynamic factor must be modified by the rate at which molecules can diffuse to such nucleation sites. Since the diffusion rate is inversely proportional to the viscosity η, the nucleation rate I, taking both thermodynamic and kinetic factors into account, is given by

$$I = K\cdot\exp(-\Delta G^*/kT)/\eta \qquad (5)$$

or from eqn.(1)

$$I = K \cdot \exp\{-16\pi\gamma^3 v^2 / 3kT(\Delta\mu)^2\}/\eta \qquad (6)$$

Eqn.(6) shows that I varies rapidly with the driving force $\Delta\mu$ or the supersaturation $\Delta\mu/kT$ mainly through the exponential term. In actual clinker processing conditions the state of supersaturation is by no means steady but varies to a considerable extent with resultant wide change in the rate of nucleation during clinkering. In general, nucleation is favored both kinetically and thermodynamically at elevated temperatures. For the same nucleation rate much higher supersaturation is required at lower temperatures.

Heterogeneous nucleation on a solid surface or other available center increases the nucleation rate because of a reduction in the interfacial free energy. An expression for the rate of heterogeneous nucleation may be obtained by replacing ΔG^* in eqn.(5) by $\phi\Delta G^*$, where the factor ϕ varies from 1 to 0 as a function of the contact angle θ, which is indicative of the affinity between the nucleus and the substrate. The heterogeneous nucleation of alite may therefore occur, e.g. on the preexisting belite grains at an early stage of clinker formation when the supersaturation is relatively low. But the subsequent rise in supersaturation as well as the fall in viscosity with increasing firing temperature necessarily promotes the homogeneous nucleation in conformity with the eqns. (5) and (6), though truly homogeneous nucleation will never be achieved in portland clinker. The crystallization centers thus formed, when brought in zones of undersaturation, dissolve and become nutrients of neighboring growing crystal individuals.

With regard to the second nucleation, conceivable under the vigorous agitation of clinker particles in the kiln, there are no substantial data available at present.

2.3 Growth instability

2.3.1 Morphological instability

The equilibrium form of alite is usually made up of three special forms, one pedion and two rhombohedra(Fig.1). However, the growth forms of alite in portland clinker are not always faceted but show a wide variety of morphological instability from cellular, skeletal to dendritic according to the environmental conditions of growth during clinkering. Some typical examples of morphological irregularity were shown for the fluorine-bearing alite grown from a fused cement clinker (Figs.2 and 3)(9). Fig.2 gives an example of a periodic array of cellular protrusions on (0001). Such corrugated surface appears in connection with the formation of constitutionally supersaturated regions due to the segregation of the solvent rejected by the solid interface growing at high rates. Capillarity effect, interface kinetics of crystal growth and surface diffusion of solute reduce or extinguish such perturbations (10,11). The cellular protrusion is commonly observed for alite in portland clinker as well. In the later stages of clinkering the alite crystal generally shows a marked trend toward faceting, despite the preexisting morphological irregularity, due to the much lower growth rate resulting from the decrease in supersaturation.

2.3.2 Growth instability as defined by the entrapment of the interstitial melt

At high growth rates the crystal grows with the entrapment of solvent inclusions. This defines growth instability in the HTS growth; or in stable growth the crystal grows without entrapping solvent inclusions. This criterion of growth stability is useful especially in discussing the fine crystalline textures of alite in portland clinker because of its pronounced capability of explaining many other distinctive features of alite (3). The inclusions of the interstitial melt are concentrated normally in the core of the crystal, suggesting the considerably high growth rate at the initial stage of crystallization when the supersaturation is relatively high. The melt inclusion, usually 2 - 3 μm in diameter, is characterized distinctly under the microscope by a small pore existing inside due to solidification.

Trapping of the interstitial melt results from any loss of stability by the crystal growth form, as exemplified in Fig.4. The melt inclusions may also occur, when the growth front as a whole is stable, at regions on the crystal surface where the supersaturation is zero or very low, due to overgrowth by layers spreading successively from regions where the supersaturation is relatively high (12). Under similar conditions the crystal of alite can entrap fine grains of belite and free lime as well.

Bubbles are also entrapped in quantities during this stage of crystal growth. The gas dissolved in the interstitial melt behaves, during growth, like impurities of the segregation coefficient $k < 1$, and will be rejected at the solid-liquid interface as the crystal grows. When the interstitial melt is saturated with gas, the layer in the melt just ahead of the advancing interface will soon become supersaturated with the gas. In case there is no free surface available in the melt within the diffusion limit of the gas, bubbles are nucleated, which provide sinks for the gas diffusing from neighboring supersaturated regions in the melt. The bubbles, normally entrapped densely in the core of the crystal, are mostly less than 0.5 μm in diameter. The dark field illumination discloses most clearly the distribution of the bubbles in the crystal (Fig.5). The alite crystals in laboratory-made clinkers are free from such minute submicroscopic bubbles. This indicates that the nucleation of bubbles may be promoted by the mechanical shock due to the vigorous agitation of clinker particles in the rotary kiln.

The unstable growth, if prolonged, gives rise to remarkable morphological irregularity of the crystal produced. The cores of the alite

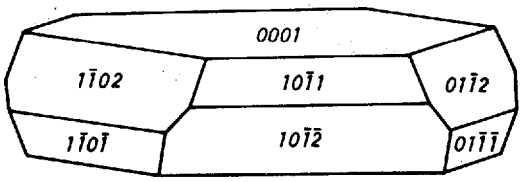

Fig. 1- Equilibrium form of alite.

crystals in Fig.6, disclosed by etching with the aqueous solution of ammonium chloride and characterized by the presence of melt inclusions, are mostly skeletal or dendritic in appearance and seldom surrounded by facets. The skeletal growth is a specific case of non-uniform growth resulting from the supersaturation higher at the corners and edges of a crystal than at the centers of the crystal faces. A progressively increasing degree of constitutional supersaturation in those regions leads to dendritic formation with projections in the direction of rapid growth. Because of its high rate of growth the unstable growth, in general, produces M_1 at ambient temperature provided MgO content in clinker is low to moderate, i.e. the regions characterized by the presence of melt inclusions practically coincide with those made up of M_1 (Fig.6).

At low growth rates the crystal of alite grows without entrapping inclusions appreciably; that is, the stable growth. The desupersaturation with the progress of alite precipitation, noticeable in the later stages of clinkering, lowers the growth rate in favor of the occurrence of stable growth. It is M_3 that is formed predominantly in this stage of crystal growth. The crystal appears smooth with a scarcity of entrapped materials under the microscope and shows a marked trend toward faceting. Fig.6 shows how M_3 thus formed overgrows the core consisting of M_1 to give a well-faceted zoned crystal of alite. The prolonged growth instability is a prerequisite for the occurrence of the apparent zonal structures of alite. In short, a decrease in growth rate makes the growth mode of alite change from unstable to stable with the corresponding change in phase composition from M_1 with or without liquid inclusions to M_3. However, the phase constitution of alite, depending primarily on the concentration of MgO in solid solution, is not to be relied upon exclusively for judging the growth conditions during clinkering.

Concerning the growth rate of alite in portland clinker, there are no reliable data availale at present to specify the critical growth rate which divides the unstable growth from the stable growth. However, from a number of typical HTS growh experiments it has been found that the growth rate for stable growth seldom exceeds widely the value of 5×10^{-6} cm $\cdot$ sec^{-1}(13). The critical growth rate of this order is probably imposed by such surface-kinetic processes as desolvation, integration at kinks, and the removal of solvent molecules from the surface. In the later stages of clinker formation, therefore, the surface kinetic process plays a much more important role than the bulk diffusion process in the crystal growth of alite. Faceting of the crystal is also promoted in spite of the pronounced preexisting morphological irregularity due to the unstable growth.

In general, the core of the crystal initially formed unstably is defective in every respect as compared with the periphery grown stably. The density of dislocations as revealed by etching, for example, is much more higher in the core than in the periphery (14). Screw-like dislocations can be introduced during skeletal growth of a crystal (15). Solid and liquid inclusions entrapped in quantities in the core may also produce dislocations because of imperfect lattice closure around them. The plane defect, though not characterized in details yet, has been found to

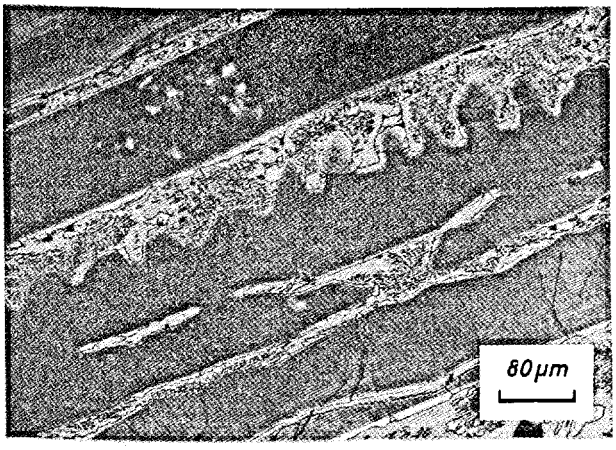

Fig. 2- Cellular protrusions on (0001). Section perpendicular to (0001). Reflected light.

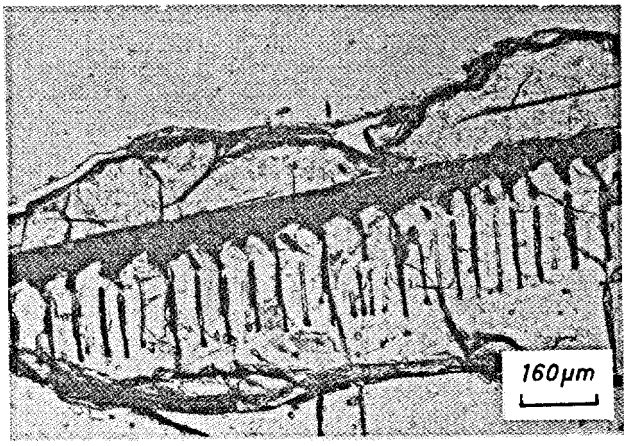

Fig. 3- Cellular projections with faceted tips. Section parallel to (0001). Transmitted light. Open polar.

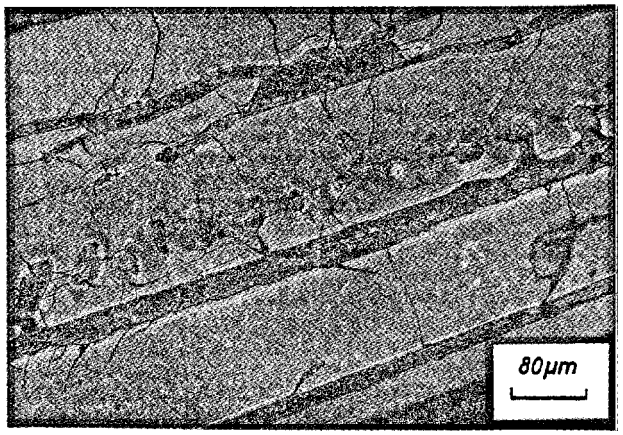

Fig. 4- Periodic solvent inclusions due to cellular perturbations.

exist in alite crystals (16).

2.4 Recrystallization - Ostwald ripening

Recrystallization of alite, prevalent in the later stages of clinker formation, also changes its crystalline textures to a considerable extent (17). This is remarkable when clinkers are kept long at fairly high temperatures and preexisting crystals are small in size. The modified Gibbs-Thomson equation holds for recrystallization in the presence of liquid - Ostwald ripening.

$$C_r = C_\infty \exp(2\gamma M/RTdr)$$

C_∞: concentration of the saturated solution in equilibrium with a large crystal
C_r: concentration of the saturated solution in equilibrium with a crystal of radius r
γ : specific surface energy of the equilibrium form of the crystal
d : density of the crystal
M : molecular weight of the dissolved substance
T : absolute temperature
R : gas constant

This equation indicates that for a certain concentration of the solution there corresponds a definite crystal size in equilibrium with this solution. If an aggregate consisting of crystals of various sizes is introduced into a solution of a given concentration, those crystals smaller in size than the corresponding critical radius will dissolve; whereas the larger ones continue to grow at the expense of the dissolved substance as the solution is supersaturated with respect to them. Concerning alite in clinker such conditions may favorably be attained toward the end of clinker formation when CaO is almost exhausted with a pronounced drop in supersaturation with respect to C_3S. The rate of recrystallization is promoted with increasing firing temperature.

The crystal form of alite apparently changes, during recrystallization, from tablets on {0001} to massive granules with the pyramidal faces, $\{10\bar{1}1\}$ and $\{1\bar{1}02\}$, well-developed (17). This suggests that with a decrease in supersaturation the growth comes to predominate along the c-axis rather than in the direction perpendicular to it. Therefore, the ratio l/w of the crystal, where l is the length parallel to (0001) and w the width perpendicular to it, is indicative of the environment during growth.

Generally M_3 is formed as the recrystallization product with a decrease in impurity in solid solution (18). The decrease in impurity content is such that without much MgO in clinker the recrystallization product occasionally appears as T_2. T_2, characterized by its low birefringence (<0.003), oblique extinction and polysynthetic twinning, overgrows preexisting M_3 to give reversely zoned alite crystals (in contrast with the normal zonation in which the peri-

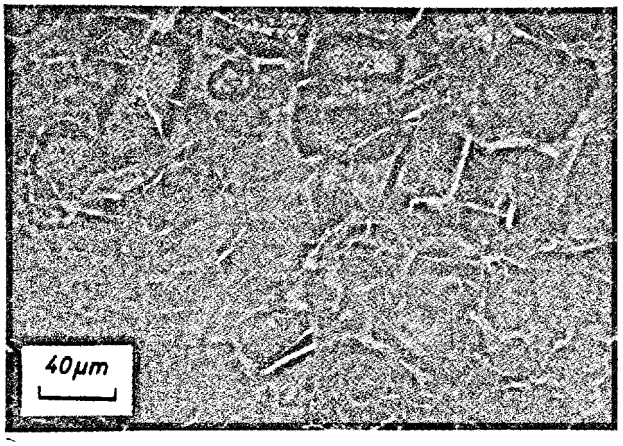

Fig. 5- Distributions of bubbles in alite crystals. Dark field image. Transmitted light. Works portland clinker.

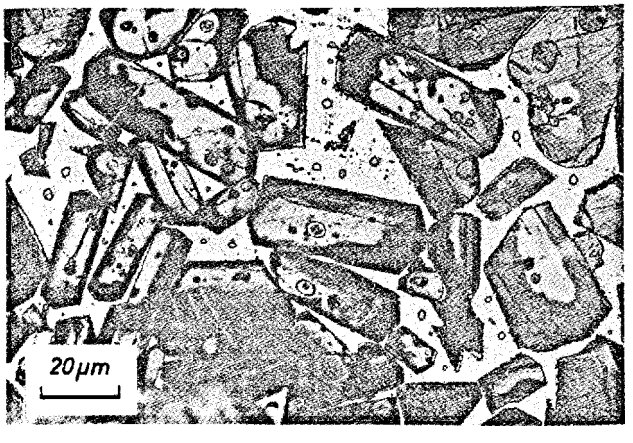

Fig. 6- Zonal structure with M_3 overgrowing M_1 as disclosed by etching with NH_4Claq. Laboratory clinker. Reflected light.

phery is higher in birefringence than the core). The homogenization of chemical composition with time due to bulk diffusion eventually gives alite crystals made up uniformly of T_2.

3 Processing of portland clinker and crystalline texture of alite

3.1 General consideration

The crystallization as a whole comprises two processes, nucleation and growth. Widely different crystalline textures of alite result according to which of these two processes predominates over the other.

Generally the nucleation process becomes predominant when the supersaturation attained is so high that the crystallization occurs far from equilibrium conditions. A number of isothermal clinker burning experiments proved that the rate of nucleation, in general, becomes increasingly high with a rise in firing temperature. Upon nucleation at high rate remarkable desupersaturation follows because of the limited growth environments in clinker, encouraging the formation of numerous small faceted crystal individuals consisting practically of M_3. Usually they are poor in melt inclusions and appear short prismatic in thin or polished sections under the microscope. The l/w ratios of the crystals range for the most part between 2 and 3. The crystals are usually mixed, more or less, with zoned crystals whose cores are made up of M_1 with apparent traces of unstable growth. Presumably such cores may be grown in the initial stage of clinker formation, when the growth rate of the crystal is relatively high in comparison with the nucleation rate. The zoned crystals, in spite of M_3 growing thick on (0001), give much higher l/w ratios ranging between 3 and 4 and appear long prismatic under the microscope.

Under those conditions in which the growth process continues to predominate over the nucleation process, the unstable growth persists with a pronounced development of crystal individuals. In actual clinker processing such circumstances may be achieved most favorably at relatively low temperatures, where the occurrence of new crystallization centers is depressed while the growth of crystal individuals proceeds at fairly high rates. In the early stages of clinker formation, therefore, there exists a general trend of alite crystals occurring as M_1 with or without the entrapment of melt inclusions according to the rate of growth.

Usually the maximum supersaturation or growth rate for stable growth decreases with an increase in crystal size, i.e. despite the decrease in supersaturation the unstable growth tends to persist once the crystal has developed large. The morphological stability also tends to decrease with increasing crystal size (9). Anomalously large grains of alite are liable to occur due to the coalescence of crystal individuals in the same crystallographic orientations.

The decrease in supersaturation consequent on the progress of clinkering reaction at elevated temperatures gives rise to the occurrence of M_3, which overgrows the cores made up of M_1 to produce zoned alite crystals. New crystallization centers consisting uniformly of M_3 continue to nucleate though low in frequency.

When the rise in supersaturation is depressed to a considrable degree or the rate of C_3S formation remains rather low all through the clinkering reaction, the crystal grows stably throughout with a scarcity of entrapped materials. M_1 is formed in abundance in the early stages of clinker formation. Because of the close similarity in growth environment between M_1 and M_3 there exists an increasing trend, with the progress of clinkering at elevated temperatures, toward the occurrence of hybrid crystals of both phases existing in patches rather than in zones. They are usually well-faceted.

3.2 Effect of processing parameters on the fine textures of alite

3.2.1 Heating rate

The rate of dissolution of both CaO and C_2S into the interstitial melt rises exponentially with temperature (7); so that fast heating of the raw mix to significantly high temperatures promotes their dissolution into the melt, leading to the predominance of the nucleation process. Definite heating rates or maximum firing temperatures necessary for such high rates of nucleation depend largely on the characteristics or burnability of the raw mix and cannot be predicted without specifying them in details. Generally speaking, lower heating rates and firing temperatures suffice with increasing burnability of the raw mix. The high supersaturation necessary for such enhanced rate of nucleation may be created most favorably by the strong interaction of low density CaO and C_2S with the interstitial melt, probably with the change in the mechanism of dissolution from diffusive to molecular-dispersive (7). Ono, in his method of estimating the burning condition and the quality of clinkers (19), also specified the rate of heating as the major processing factor that determines the grain size of alite.

With decreasing heating rate or firing temperature the growth process comes to predominate, with a systematic change in the fine textures of alite as described in the preceding section. Apparent zonal structures result when clinker is subsequently burnt long enough at high temperatures. Much slower heating tends to produce well-faceted crystals with M_1 and M_3 intergrown in patches, which, however, occur uniformly as M_3 in the presence of much MgO in clinker.

3.2.2 Maximum firing temperature and retention time

These two factors are significant in relation to their influence on the rate of recrystallization as well as the fine textures of alite. Generally, high growth rate of alite, in comparison with the rate of nucleation, can be attained at relatively low firing temperatures in favor of the growth instability and the occurrence of M_1 in preference to M_3 at ambient temperature. M_3, on the other hand, is formed favorably at much lower growth rates. This occurs when alite is precipitated most quickly at elevated temperatures or when the supersaturation is lowered considerably in the later stages of normal clinker formation.

This trend of phase differentiation can be compared with the formulation in the Ono's method (19) that the higher the maxiumum firing temperature the greater is the birefringence of alite produced, though the relation between the birefringence and the phase constitution of alite is not mentioned explicitly.

When clinker is retained long at elevated temperatures after the virtual completion of alite preciptation, Ostwald ripening occurs appreciably to produce M_3 in plenty, giving well-faceted large crystals of alite. In the absence of much MgO in clinker T_2 may occur as the result of recrystallization. The low birefringence and the polysynthetic twinning are characteristic of T_2. The reverse zonation is liable to be observed when a raw mix of high burnability is fired and kept long at elevated temperatures (2).

3.2.3 Calcination

The calcination of a raw mix below the liquid formation temperature (ca. 1300°C) has large influence on the fine textures of alite resulting from the subsequent burning at higher temperatures (2). The calcination, in general, encourages the growth process of alite precipitation at firing temperatures and, when prolonged, tends to produce zoned crystals in spite of such high heating rate employed as otherwise leads to the predominance of nucleation over growth (Fig.7). The calcination is detrimental to the burnability of the raw mix, due probably to the densification of CaO crystal grains during heating.

3.2.4 Preparation of raw mixes

Inhomogeneity inherent in the preparation of raw mixes necessarily leads to wide local variations of the fine textures of alite, according to the appreciably different growth environments in the clinker particle, as well as the change in mineralogical and interstitial melt composition (20). These relations may be predicted to a certain extent from what has been hitherto mentioned. Incorporation of coarse-grained or low reactivity starting raw materials in the raw mix, as a whole, favors the prevalence of growth over nucleation even if the raw mix is quickly heated, without being calcined, to significantly high temperatures.

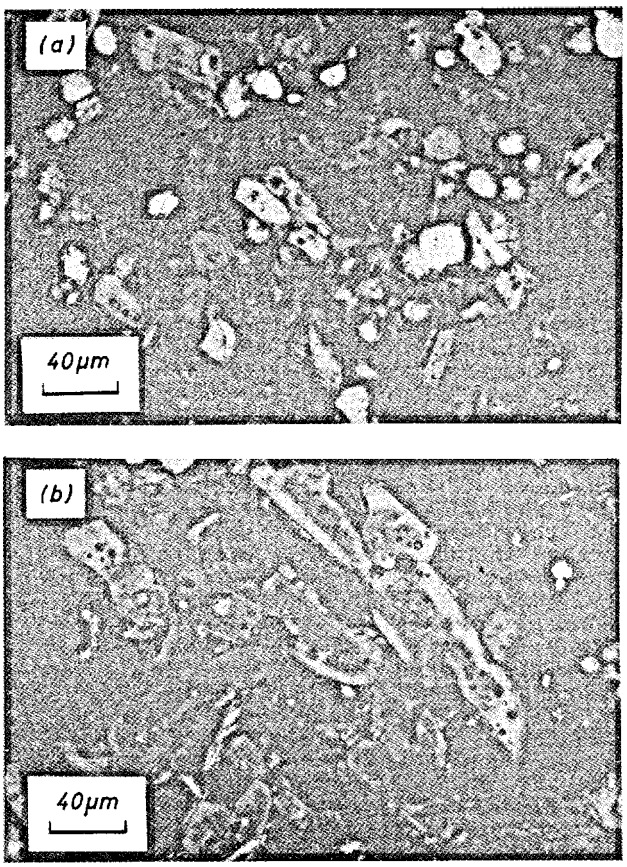

Fig. 7- Laboratory-made clinker. Transmitted light. Crossed polars. (a) Heated at 100°C/min from 1000 up to 1600°C, then cooled at 50°C/min down to 1400°C and quenched in air. (b) Preheated at 5°C/min from 1000 up to 1200°C. The same heating and cooling program except for retention for 5 min at 1600°C.

Such moduli of the raw mix as H.M., S.M., I.M. and L.S.F. significantly change the burnability of the raw mix and, in this connection, exert great influence on the resultant fine textures of alite. The A/F ratio (I.M.), in particular, has a pronounced influence on the viscosity of the interstitial melt and thus causes a definite change in the growth mode of alite (14).

The effect of minor components in the raw mix, whether intentionally added or not, will be discussed in details in the following section.

4 Influence of minor components

4.1 Underlying principles

The minor component in clinker changes the physical properties of the interstitial melt and consequently the rate of dissolution of both CaO and C_2S to a considerable extent.

Such effects have been reviewed extensively by Timashev et al. on the high temperature solution of the system $CaO-SiO_2-Al_2O_3-Fe_2O_3$ on the acid-base concept (7,8). The quaternary solution, analogous in composition and structure to the interstitial melt in portland clinker, is an ionic HTS with a skeleton structure comprising silicate anions of low degree of polymerization, as evidenced by its low viscosity of the order of 0.1 Pa.s.

In the structure of such high temperature solutions the following acid-base equilibrium holds for amphoteric elements as Al and Fe.

$$MeO_4^{5-} \rightleftarrows Me^{3+} + 4O^{2-} \qquad (1)$$

$$K = \frac{[Me^{3+}]\ [O^{2-}]^4}{[MeO_4^{5-}]} \qquad (2)$$

A decrease in viscosity results when the minor addition of a foreign component shifts the equilibrium of the eqn.(1) to the right and increases the concentration of Me^{3+} ions which is highly mobile in comparison with MeO_4^{5-}. The viscosity increases when the reverse process occurs. It is to be expected that the viscosity change depends largely on the field strength of cation added or the attractive force between cation and oxygen. The higher the value of the field strength, the more covalent or less ionic becomes the bond. Thus the field strength can be correlated with the ionicity of the bond, which is expressed in terms of the difference in electronegativity χ_A and χ_B of cation and anion, e.g. by the formula $1 - \exp\{-(\chi_A - \chi_B)^2/4\}$ (Pauling). In view of oxygen being the only electronegative element in the melt the effect of the minor addition of a foreign element on the viscosity of the melt can be discussed in terms of its electronegativity associated with its electron configuration in the outermost shell. For the s-elements of basic character the viscosity of the liquid decreases linearly with increasing electronegativity or decreasing basicity of the element added, provided the temperature and the concentration are kept constant (in the order of K→Ba→Na→Sr→Ca→Mg). The similar trend exists also for the p-elements of acidic character (Al→P→B→S→Cl→F). For the d-elements the viscosity decreases, as expected, with increasing Me - O bond strength. These relations hold so far as the concentration of a foreign oxide added does not exceed 2 - 3 percent. The surface tension of the melt increases for the s-elements with increasing electronegativity but decreases for the p-elements.

Butt and Timashev showed under isothermal burning conditions that the viscosity of the melt is of primary importance to the dissolution of CaO and C_2S in the liquid (7). High surface tension also favors the dissolution through encouraging the dispersion of CaO and C_2S grains in the liquid, though it has no effect on the kinetics of dissolving high density CaO grains (7). Usually the rate of dissolution of C_2S is high enough, especially in the presence of alkalies, in comparison with the relatively low diffusion rate of silicate ions produced. The formation of alite is normally governed by the dissolution of CaO, which is diffusion-controlled. Intensification of CaO dissolution and resultant rapid precipitation of alite can be achieved by the interaction of low density CaO grains with the liquid of low viscosity and high surface tension. Minor components can therefore influence the burnability of the raw mix as evaluated by the amount of CaO left uncombined under a certain fixed condition of burning. In this connection it is noteworthy that the burnability of the raw mix also increases systematically with the value of field strength of the basic element added (K→Na→Li→Ba→Ca→Mg)(21).

4.2 Effect of MgO

MgO enters the C_3S lattice replacing CaO up to about 2% by weight. An increase in MgO content in the raw mix, therefore, leads to an apparent increase in L.S.F.; in this connection, Christensen proposed a modified LSF-formula taking the role of MgO into account (22). Nevertheless, the burnability of the raw mix can be improved remarkably by introducing a small amount of MgO, especially at relatively low temperatures (7,22). MgO in the interstitial melt promotes the dissolution of CaO by appreciably increasing the surface tension as well as decreasing the viscosity of the melt, especially in the presence of alkalies which lower the surface tension and increase the viscosity to a considerable degree.

It is by promoting the nucleation process of alite precipitation that MgO improve the burnability or accelerate the formation of C_3S. With an increment of MgO in the raw mix, for example, large zoned crystals of alite can be replaced completely by small faceted crystals consisting practically of M_3 with a scarcity of inclusions. The amount of CaO left uncombined decreases definitely with the increase in MgO content in the raw mix. With plenty of MgO in clinker prolonged calcination followed by fairly rapid heating to the maximum firing temperature is absolutely necessary for producing zoned alite crystals in quantities.

4.3 Effect of SO_3

SO_3, in contrast with MgO, obviously promotes the growth process of alite precipitation in favor of the occurrence of large crystal individuals. The much higher growth rate in the presence of SO_3 comes from a pronounced drop in the viscosity of the interstitial melt. Under normal conditions of clinker processing incorporation of a small amount of SO_3 in clinker favors to produce zoned crystals, which otherwise occur uniformly of M_3. With more than one percent of SO_3 in clinker alite crystals are developed anomalously large, consisting practically of M_1. They are usually highly irregular in shape, skeletal to dendritic. and seldom faceted com-

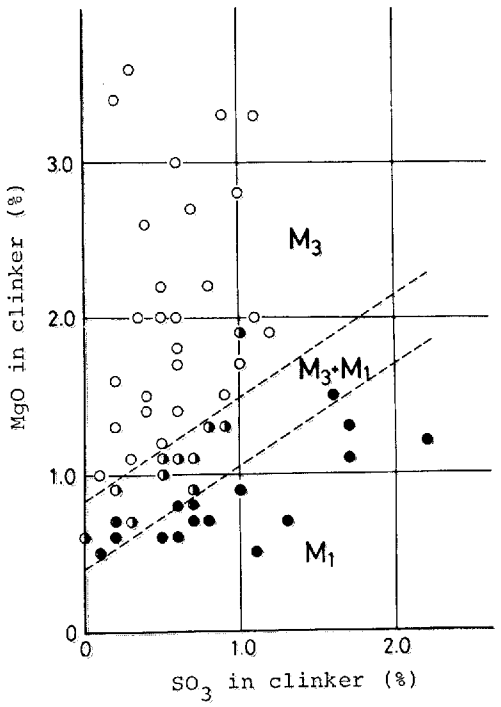

Fig. 8- Phase constitution of alite against MgO and SO_3 contents in works portland clinker.

pletely. The interstitial melt is normally entrapped in quantities in the core. The crystal grows entrapping small grains of belite and free lime as well. An improvement in burnability may result, in the presence of SO_3 in an appropriate content, from the enhanced growth rate of alite. Excess addition, however, leads to an appreciable drop in the amount of alite produced (7). The similar trend is observed when P_2O_5 is added in the raw mix.

The effect of SO_3 on the dissolution of CaO or C_2S is not straightforward. Sulfate ions in the interstitial melt remarkably lowers its viscosity in favor of the dissolution of CaO; whereas the decrease in surface tension, which slows down the dispersion of CaO grains and promotes the grain growth due to recrystallization, may reduce the former effect.

The formation of two liquids in the presence of alkalies and SO_3 in large quantity changes the physical properties of the melt to a considerable degree and thus influences the crystallization mode of alite. In fact the effect of SO_3 on the fine textures of alite can be reduced considerably by introducing alkalies in high concentration.

4.4 Interaction of MgO and SO_3

The high MgO content in the raw mix favors the stabilization of M_3 at ambient temperature due not only to the intensification of the nucleation process but also to the high MgO concentration to be distributed to alite during growth. The incorporation of SO_3 in clinker, on the other hand, promotes the growth process of alite precipitation in favor of the stabilization of M_1 at ambient temperature. Thus SO_3 acts in opposition to MgO with respect to the crystallization mode and the resultant phase constitution of alite, and vice versa. This explains the relation in Fig.8, in which the constituent phase of alite is plotted against the amounts of MgO and SO_3 in the clinker (2). The phase state of alite is transformed from M_1 to M_3 via the hybrid state of both phases with increasing amount of MgO. With an increase in SO_3 content in clinker much more MgO is required to produce alite entirely as M_3. A wide change in alkali content in clinker will modify the relation because of the strong affiniy of alkalies for SO_3 to form compounds. A completely different phase relation diagram may be obtained when the processing conditions of clinker are thoroughly changed.

4.5 Distribution of minor components

When the crystal with the impurity concentration C_S is growing from the solution the concentration of which with respect to the impurity is C_L, the ratio $C_S/C_L = k$ defines the distribution coefficient. The effective distribution coefficient k_e in actual growth conditions differs, more or less, from the equilibrium distribution coefficient k_o as derived from the phase equilibrium diagram, due to the segregation of the impurity at the growing solid-liquid interface.

Burton, Prim and Slichter (23) obtained a simple relation between k_e and k_o.

$$k_e = \frac{k_o}{k_o + (1 - k_o)\exp(-v\delta/D)}$$

where v is the growth rate, δ is the thickness of diffusion boundary layer formed by segregation and D the diffusion coefficient. The effective distribution coefficient k_e varies between k_o and 1 as a function of $v\delta/D$. Increase in growth rate leads to the depletion or enrichment of impurity component in the solid according to whether $k>1$ or $k<1$. It is to be noted, however, that the BPS model is for the growth in the steady state and that this condition will never be met with the crystal growth in portland clinker.

The MgO content of alite as determined by EPMA varies approximately linearly with that of the clinker, though the reported slopes are varied to a certain extent from one another (24-27). This shows the distribution relation existing between alite and the melt during growth in view of MgO being concentrated in the interstitial melt (27). The similar trend exists also for Fe_2O_3 (24-26). No such clear relation can be observed for Al_2O_3 according to the data by Kristmann (26), though there is the evidence, on the other hand, for the correlated incorporation of Al_2O_3 with Fe_2O_3 (18,27).

1.2

Electron microprobe analysis was made separately for the core and the periphery of the zoned crystal in view of the different growth modes between them (14). Fig.9 illustrates the difference in chemical composition for both parts. Considering practically the same MgO content, the (Al_2O_3 + Fe_2O_3) content much higher in the core than in the periphery may contribute primarily to the stabilization of M_1 at ambient temperature in accordance with the phase relation diagram by Woermann et al. (28). The high (Al + Fe) concentration in the core may come from the higher rate of growth at the initial stage of crystallization. No appreciable difference in chemical composition can be found between M_1 and M_3 grown in patches, suggesting close similarities in growth environments between the two phases. The redistribution of impurities during recrystallization under the condition very close to equilibrium results in a remarkable decrease in impurity content (18).

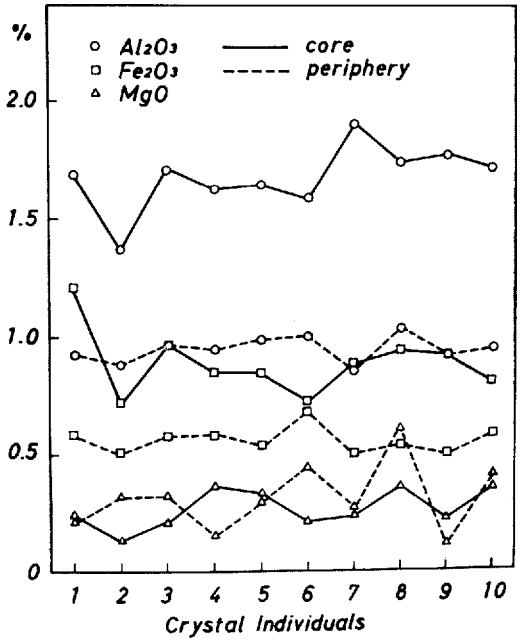

Fig. 9- Distinction of chemical composition between the core and periphery of zoned alite crystals.

The chemical composition is by no means homogeneous throughout the crystal individual, being greatly influenced by the growth rate and its anisotropy. It is absolutely necessary, therefore, to take into account carefully the fine textures of the crystal in exactly interpreting the result of various microprobe analyses.

5 The crystal structure of alite

5.1 R form at 1200°C

Nishi and Takéuchi (29) has refined the crystal structure of C_3S at 1200°C to R = 10% for 159 reflections employed.

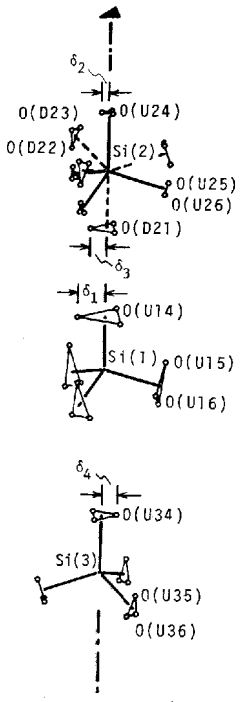

Fig.10- Three independent tetrahedra on the threefold axis in the rhombohedral structure at 1200°C. $\delta_1 = 0.7$ Å, $\delta_2 = 0.2$ Å, $\delta_3 = 0.4$ Å, $\delta_4 = 0.4$ Å.

Crystal data at 1200°C: $\underline{a} = 7.153(6)$, $\underline{c} = 25.586(15)$Å, space group R3m, unit cell contents $9 \times Ca_{2.98}Si_{0.98}Al_{0.04}O_5$.

The structure obtained is significantly different from the average structure proposed by Jeffery (30) in the following points.

(1) Of the three independent tetrahedra on the 3-fold axis, the one about Si(1) is 60° different in orientation around the axis from the corresponding tetrahedron in the Jeffery's structure (Fig.10).
(2) The tetrahedron about Si(2) statistically points upward (U-orientation) and downward (D-orientation). The fraction of the D-orientation is 70 % at 1200°C.
(3) All the tetrahedra are tilted in such a way that their apical bonds slightly swing away from the 3-fold axes with Si atoms being kept on the axes (denoted by δ in Fig.10).

Fig.11 shows the silicate tetrahedra and the coordination polyhedra around Ca ions in the mirror plane parallel to (110) and passing through the origin. In view of the statistical orientation of the Si(2) tetrahedra this figure illustarates the case in which the Si(2) tetrahedron has the D-orientation. The coordination for Ca(1) and Ca(2) is sixfold as in the Jeffery's model, while that of Ca(3) is sevenfold. In the case of polyhedra around Ca(3), however, two of the seven Ca - O

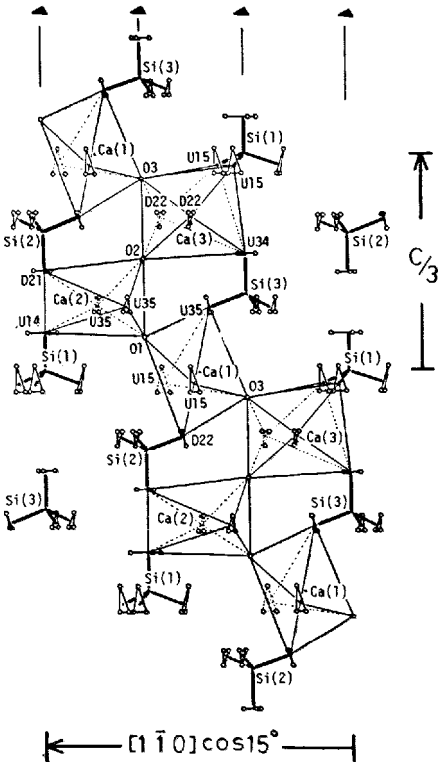

Fig.11- The structure of the rhombohedral phase of tricalcium silicate at 1200°C, showing the silicate tetrahedra and the polyhedra about the Ca atoms in the mirror plane parallel to (110) and passing through the origin. Si(2) tetrahedra point downward in this figure. Viewed down [110] but rotated by 15° around the c-axis.

bonds have a distance as long as 2.96Å. In this respect the coordination of Ca(3) may be regarded basically as fivefold. The mean coordination number may then be 5.66 in the rhombohedral structure. An overall average of the Ca - O bond lengths at 1200°C gives a value of 2.51Å, which is 5% longer than in the Jeffery's structure at ambient temperature.

5.2 M_3 form

Crystal data: $a = 33.083(8)$, $b = 7.027(2)$, $c = 18.499(4)$Å, $\beta = 94.12(2)°$, Unit cell contents $36 \times Ca_{2.89}Mg_{0.11}SiO_5$, $V = 4289Å^3$, space group Cm.

This large monoclinic cell characterized by complicated supercell reflections was first reported by Jeffery (30) and later proved to correspond to that of the M_3 modification (31). The supercell structure of this form has been determined and refined to R = 9.9% by Nishi, Takéuchi and Maki (13.6% for 2818 superstructure reflections and 5.9% for average structure) (32).

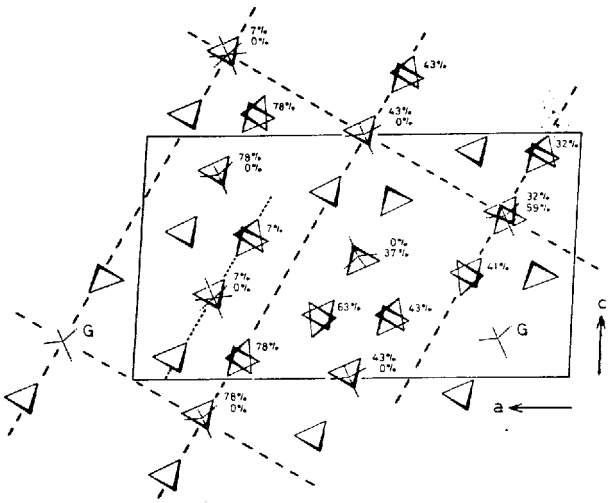

Fig.12- Orientational disorder of the silicate tetrahedra at y=0. The broken lines trace the cell of the rhombohedral average structure. For tetrahedra with U-D disorder fractions of U are indicated. For those with U-D-G disorder fractions of U and D are indicated in this order. No figures for those having fixed orientation.

Fig.12 shows the arrangement of the silicate tetrahedra at y=0. The broken lines trace the rhombohedral cell. The mode of orientational disorder of the silicate tetrahedra is different from that of the corresponding tetrahedra in the rhombohedral structure.

The silicate tetrahedra can be classified into three categories with regard to the c-axis of the rhombohedral subcell.

(1) those having fixed orientation (either U or D).
(2) those showing disorder in two orientations U and D (U-D disorder).
(3) those showing U-D-G disorder, where G represents a new type of orientation of neither U nor D.

Among eighteen silicate tetrahedra in Fig.12 six belong to the category (1). The remaining twelve tetrahedra show statistical orientations, each being defined in terms of U, D and G orientations.

The thirty six Ca atoms in the unit cell can be classified into two groups; eighteen Ca's on the mirror plane and eighteen Ca's lying approximately on a plane close to y=1/4. Most of the Ca's show positional splittings. This effect is small for Ca's in the first group, while it is significant for Ca's in the second group. The coordination numbers of the Ca atoms, taking into account the occupancies of the oxygen atoms smaller than unity because of the orientational disorder of tetrahedra, were found to be 6.0 - 7.12,

with the mean of 6.15. This value lies between 6.21, the average coordination number calculated by the authors for T_1 (33), and 5.66 for R. Besides, as regards the orientational order-disorder of silicate tetrahedra, M_3 shares the feature with both R and T_1; all the tetrahedra are ordered in orientation in the triclinic structure. The complex polymorphism of C_3S, therefore, may arise from the orientational disorder of silicate tetrahedra associated with the consequent change in coordination about Ca atoms.

5.3 Phase identification of alite

As regards the polymorphism of C_3S seven modifications have been confirmed to exist by means of XRD, DTA and optical microscopy (34,35).

$$T_1 \overset{620}{\longleftrightarrow} T_2 \overset{920}{\longleftrightarrow} T_3 \overset{980}{\longleftrightarrow} M_1 \overset{990}{\longleftrightarrow} M_2 \overset{1060}{\longleftrightarrow} M_3 \overset{1070}{\longleftrightarrow} R$$

(T: Triclinic, M: Monoclinic, R: Trigonal)

In works portland clinker alite normally occurs as M_1 or M_3 at ambient temperature (36,37). When heated, alite in clinker first reverts to T_2 at around 700°C irrespective of its initial phase constitution (31,38,39). The corresponding exothermic peak, which is clearly recognized for synthetic C_3S solid solutions, cannot usually be found on the DTA diagram, being masked by the pronounced endothermic peak due to the $\beta \rightarrow \alpha_L'$ transition of belite at around this temperature. Upon reversion M_3 shows a sharp decrease in birefringence. After the reversion to T_2 alite undergoes phase transitions regularly according to the normal polymorphic sequence of C_3S. It seems that M_2, as well as T_3, can no longer exist as a constituent phase of alite in portland clinker because of the high impurity content in solid solution (31). The direct transition from T_2 to M_1 occurs at 790 - 850°C with an endothermic effect, which was previously ascribed to the monoclinic to trigonal transition (40). M_1 is then transformed directly into M_3 at around 950°C with an abrupt rise in birefringence. In spite of these alite made up completely of M_3 in clinker rich in MgO usually gives no indication of phase change until the direct transition to R above 1000°C.

M_{1b}, a variety of M_1 distinct from M_{1a} in cell geometry (34), has been proved to be M_3 (31). M_1 (= M_{1a}) was formerly misinterpreted as R because of an apparent trigonal character of its cell, which is noticeable, in particular, with alite in clinker rich in SO_3.

Still there seem to be some difficulties in identifying unequivocally the phase state of C_3S solid solutions. Sinclair and Groves (41) proved by means of electron diffraction that C_3S solid solutions doped with Zn(34, 42), La(43), Al+F(44,45) and Al+Mg+F(46) and identified as R by XRD are in reality monoclinic or triclinic in symmetry. Then the high hydraulic activity and strength development reported for "rhombohedral" alite can no longer be explained in terms of its structural peculiarity, i.e. the highest-temperature modification or the highest crystal symmetry. The supercell nature is characteristic of each lower temperature modification of C_3S. It is ordinarily the geometry of subcell and neither the true supercell nor the diffraction symmetry including supercell reflections that we can derive from the X-ray powder diagram. The coalescence of subcell lines on the powder diffraction diagram does not necessarily lead to the higher symmetry of the structure. In this respect it is encouraged to use jointly other available means than XRD. More reliable and systematic procedures must be developed for unequivocal phase identification of C_3S solid solutions.

6 Conclusive remarks

A number of processing parameters involved in clinker manufacturing, when viewed from their influence on the fine textures or characters of the clinker constituent minerals, are so closely related with one another that it occasionally leads to insignificant conclusions to combine each of them directly, without the consideration of other parameters, with a certain specific character of the constituent mineral. For example, the heating rate or maximum firing temperature necessary for the occurrence of growth instability of alite depends largely on the precalcination or preparation, inclusive of minor components, of a raw mix. For unequivocal correspondence the processing parameters must be interpreted in terms of their influence on the fundamental parameters of crystal growth or the environmental conditions of nucleation and growth.

In the proceeding of the last symposium in Paris in 1980 Skalny and Young raised a question if two plants (or even laboratories) can produce cements with exactly the same properties (47). In other words, this question manifests the poor reproducibility in the manufacturing of cements. In the light of what has been hitherto mentioned, the difficulty lies, so far as the clinker manufacturing is concerned, in the accurate control and reproduction of the crystallization process of each of the clinker constituent minerals, especially that of alite from the interstitial melt. The fine textures or characters of the clinker minerals are so widely variable according to their process of crystallization as to make the unique correspondence to their hydraulic properties extremely difficult. On the other hand, such situation, when viewed from another angle, may leave plenty of room for further improvement and diversification in the quality and production of cements in future. Accurate evaluation as well as detailed reproduction of the fine textures of the clinker minerals will stimulate the study of hydration in this light and lead to the elucidation of their relation to the hydraulic properties of cements produced. Further it is to be noted that the fine textures of the clinker minerals can provide a reasonable means for evaluating the burnability of a raw mix in association with the quality of cement.

References

1.- "Characterization of Materials", The Materials Advisory Board Publication MAB-229-M, National Academy of Sciences-National Academy of Engineering, Washington, D.C., March, 1967.

2.- I. MAKI and K. GOTO (1982) "Factors Influencing the Phase Constitution of Alite in Portland Cement Clinker", Cement Concr. Res. 12, 301-8.

3.- I. MAKI (1984) "Growth Instability and Crystalline Textures of Alite in Cement Clinker", Il Cemento 81, 165-74.

4.- R. KONDO and S. CHOI (1968) "Mechanisms and Kinetics of Portland Cement Clinker Formation for an Example of the Solid State Reaction in the Presence of a Liquid Phase", Proc. 5th Int. Symp. Chem. Cement, Tokyo, Vol.I, 163-71.

5.- N.H. CHRISTENSEN and K.A. SIMONSEN (1970) "Diffusion in Portland Cement Clinker", J. Am. Ceram. Soc. 53, 361-64.

6.- N.H. CHRISTENSEN and O.L. JEPSEN (1971) "Diffusion in Three-Component Cement Clinkers", J. Am. Ceram. Soc. 54, 208-10.

7.- Y.M. BUTT and V.V. TIMASHEV (1974) "The Mechanism of Clinker Formation. Processes and Ways of Modification of Clinker Structure", Proc. 6th Int. Symp. Chem. Cement, Moscow, PP.

8.- V.V. TIMASHEV (1980) "The Kinetics of Clinker Formation. The Structure and Composition of Clinker and its Phases", Proc.7th Int. Symp. Chem. Cement, Paris, I-3/1-20.

9.- I. MAKI, K. NAKAGAWA, K. HIRAIWA and T. NONAMI (1984) "Characterization of Fluorine-bearing Alite in Rapid-Hardening High Strength Cement Clinker Manufactured by Fusion", Il Cemento 81, 3-12.

10.- A. OKAWA (1982) Crystal Growth (in Japanese), Shokabo, Tokyo, p.192.

11.- R.T. DELVES (1975) Crystal Growth (International Series of Monographs on the Science of the Solid State, Vol.6, Ed. B.R. PAMPLIN), Pergamon Press, Oxford, p.40.

12.- A.E. CARLSON (1959) Growth and Perfection of Crystals (Ed. DOREMUS et al.), Wiley, N.Y., p.421.

13.- D.E. ELWELL and H.J. SCHEEL (1975) Crystal Growth from High Temperature Solutions, Academic Press, N.Y., p.255.

14.- I. MAKI et al. Unpublished data.

15.- A.A. CHERNOV (1984) Crystal Growth (Modern Crystallography III), Springer Verlag, Berlin, pp.150, 256.

16.- K.E. HUDSON and G.W. GROVES (1982) "The Structure of Alite in Portland Cement Clinker, TEM evidence", Cement Concr. Res. 12, 61-8.

17.- I. MAKI, H. HABA and S. TAKAHASHI (1983) "Effect of Recrystallization on the Characters of Alite in Portland Cement Clinker", ibid. 13, 689-95.

18.- I. MAKI and S. TAKAHASHI (1984) "Redistribution of Impurity during Recrystallization of Alite in Portland Cement Clinker", ibid. 14, 413-8.

19.- Y. ONO (1980) "Microscopical Estimation of Burning Condition and Quality of Clinker", Proc. 7th Int. Symp. Chem. Cement, Vol.I, I-206-11; (1981) "Microscopical Observation of Clinker, for the Estimation of Burning Condition, Grindability and Hydraulic Activity", Proc. 3rd Int. Conf. Cement Microscopy, Houston, 198-210.

20.- V. JOHANSEN (1973) "Model for Reaction Between CaO Particles and Portland Cement Clinker", J. Am. Ceram. Soc. 56, 450-4.

21.- I. TEORENAU and T.V. HUYNH (1970) "Wechselbeziehungen zwischen der mineralisierenden Workung der Stoffe auf die Portlandzementklinkerbildung und dem periodischen System der Elemente", Silicates Industriels 35, 281.

22.- N.H. CHRISTENSEN (1978) "The Effects of Magnesia on Lime Combination in Clinker", World Cement Techn. 223-6.

23.- J.A. BURTON, R.C. PRIM and W.P. SLICHTER (1953) "The Distribution of Solute in Crystals Grown from the Melt. Part I. Theoretical", J. Chem. Phys. 21, 1987-91.

24.- G. YAMAGUCHI and S. TAKAGI (1968) "The Analysis of Portland Cement Clinker", Proc. 5th Int. Symp. Chem. Cement, Tokyo, Vol.I, 181-218.

25.- P. TERRIER (1968) ibid. Written Discussion, 218-9.

26.- M. KRISTMANN (1977) "Portland Cement Clinker: Mineralogical and Chemical Investigations, Part I, Microscopy, X-Ray Fluorescence and X-Ray Diffraction", Cement Concr. Res. 7, 649-58; (1978) "Part II, Electron Microprobe Analysis", ibid. 8, 93-102.

27.- A. GHOSE and P. BARNES (1980) "Distribution of Minor Elements in Cement Clinkers - Macroscopic and Microscopic Variations", World Cement Techn. 441-3.

28.- E. WOERMANN, W. EYSEL and TH. HAHN (1969) "Chemical and Structural Inves-

tigations of Solid solutions of Tricalcium Silicate, Part 5", Z-K-G 22, 414-22.

29.- F. NISHI and Y. TAKEUCHI (1984) "The Rhombohedral Structure of Tricalcium Silicate at 1200°C", Zeit. Krist. 168, 197-212.

30.- J.W. JEFFERY (1952) "The Crystal Structure of Tricalcium Silicate", Acta. Cryst. 5, 26-35.

31.- I. MAKI and K. KATO (1982) "Phase Identification of Alite in Portland Cement Clinker", Cement Concr. Res. 12, 93-100.

32.- F. NISHI, Y. TAKEUCHI and I. MAKI (1985) "The Tricalcium Silicate $Ca_3O[SiO_4]$: The Monoclinic Superstructure", Zeit. Krist. In Press.; Y. TAKEUCHI, F. NISHI and I. MAKI (1984) "Structural Aspects of the Phase Transitions in Tricalcium Silicate Ca_3SiO_5 (C_3S)", Acta Cryst. A40, C215.

33.- R. GOLOVASTIKOV, R.G. MATVEEVA and N.V. BELOV (1975) "Crystal Structure of the Tricalcium Silicate $3CaO \cdot SiO_2$ = C_3S", Sov. Phys. Crystallogr. 20, 441-5.

34.- M. BIGARE, A. GUINIER, C. MAZIERES, M. REGOURD, N. YANNAQUIS, W. EYSEL, Th. HAHN and E. WOERMANN (1967) "Polymorphism of Tricalcium Silicate and its Solid Solutions", J. Am. Ceram. Soc. 50, 609-19.

35.- I. MAKI and S. CHROMY (1978) "Microscopic Study on the Polymorphism of Ca_3SiO_5", Cement Concr. Res. 8, 407-14.

36.- I. MAKI and S. CHROMY (1978) "Characterization of the Alite Phase in Portland Cement Clinker by Microscopy", Il Cemento 75, 247-52.

37.- I. MAKI (1979) "Phase Constitution of the Alite in Portland Cement Clinker from Modern Manufacturing Processes", Il Cemento 76, 167-76.

38.- G. MASCOLO, W. EYSEL and TH. HAHN (1974) "Thermal Behavior of Synthetic Alites", Proc. 6th Int. Symp. Chem. Cement, Moscow, Suppl. Paper.

39.- I. MAKI, T. OGIWARA and S. CHROMY (1981) "Differential Thermal Analysis of Portland Cement Clinker and Phase Constitution of Alite", Il Cemento 78, 53-60.

40.- J.W. JEFFERY (1952) "The Tricalcium Silicate", Proc. 3rd Int. Symp. Chem. Cement, London, p.45.

41.- W. SINCLAIR and G.W. GROVES (1984) "Transmission Electron Microscopy and X-Ray Diffraction of Doped Tricalcium Silicate", J. Am. Ceram. Soc. 67, 325-30.

42.- I. ODLER and S. ABDUL-MAULA (1983) "Polymorphism and Hydration of C_3S Doped with ZnO", J. Am. Ceram. Soc. 66, 1-4.

43.- L. STEVULA and J. PETROVIC (1981) "Hydration of Polymorphic Modification C_3S", Cement Concr. Res. 11, 183-90.

44.- Y. ONO, T. UNO and Y. KANAI (1965) "Synthesis of Five Polymorphic Modifications of C_3S", Rev. 19th Gen. Meeting Cement Assoc. Japan 36-41 (1965); Semento Gijutsu Nenpo 19, 33-37.

45.- R.T.H. ALDOUS (1983) "The Hydraulic Behavior of Rhombohedral Alite", Cement Concr. Res. 13, 89-96.

46.- R. KONDO and K. YOSHIDA (1968) "Miscibility of Special Elements in Tricalcium Silicate and Alite and the Hydration Properties of C_3S Solid Solutions", Proc. 5th Int. Symp. Chem. Cement, Tokyo, Vol.I, 262-74.

47.- J. SKALNY and J.F. YOUNG (1980) "Mechanisms of Portland Cement Hydration", Proc. 7th Int. Symp. Chem. Cement, Paris, Vol.I, II-1/1-35.

Acknowledgment

Part of the work by the author in this report was supported financially by the Grant-in-Aid for Scientific Research from the Japanese Ministry of Education, Science and Culture (No.60430017).

SUB-THEME/SOUS-THÈME 1.3

Low energy clinker formation.
Formation d'un clinker consommant peu d'énergie.

Chairman/Président
J.P. Meric
Societé des Ciments Français
Paris, France

Principal Reporter/Rapporteur Principal
F.W. Locher
Forschungsinstitut der Zementindustrie
Dusseldorf, West Germany

J.P. MERIC - STE DES CIMENTS FRANCAIS - Tour Générale - Cedex 22 -
92088 - PARIS LA DEFENSE (FRANCE)

FORMATION D'UN CLINKER CONSOMMANT PEU D'ENERGIE.
LOW ENERGY CLINKER FORMATION

Dans l'Industrie du Ciment l'énergie thermique et mécanique a toujours représenté un élément très important du prix de revient que les Ingénieurs ont de tout temps cherché à réduire. La mobilisation de grandes quantités d'énergie est cependant dans la nature même de cette Industrie qui consiste à activer des matériaux naturels stables en les portant à un potentiel énergétique suffisamment élevé pour les rendre instables en présence d'eau. C'est de cette instabilité que le ciment tire sa capacité à former des liaisons en retombant dans un état stable et en libérant une partie de l'énergie qui lui a été communiquée. Une comparaison de l'énergie mise en jeu pour assurer la cohésion d'un béton avec celle qui est effectivement dépensée pour la fabrication du ciment donnerait sans doute une idée de la limite ultime que la consommation énergétique pour la fabrication d'un liant pourrait atteindre. L'objet du Thème 1.3 de ce huitième Congrès de la Chimie du Ciment se limite à une étape seulement dans l'enchaînement des phénomènes qui conduisent des matériaux naturels aux liaisons dans le béton : la consommation d'énergie dans la fabrication du clinker qui est le matériau de base de presque tous les ciments fabriqués dans le monde entier.
L'enjeu des travaux consacrés à ce Thème est considérable puisque dans le monde l'on fabrique actuellement aux environs de 820 millions de tonnes de clinker au prix d'une consommation énergétique de près de 100 millions de tonnes équivalent pétrole et de 60 milliards de kilowattheures électriques.
Les retombées des économies réalisées dans la consommation énergétique pour la fabrication du clinker atteignent une dimension exceptionnelle; il s'agit donc d'un objectif de première importance pour tous les Organismes de Recherche qui travaillent sur le ciment.

Na indústria do Cimento a energia térmica e mecânica sempre representou um elemento muito importante do preço de custo, que os Engenheiros procuram ao longo do tempo reduzir. A mobilização de grandes quantidades de energia é, entretanto, inerente a própria natureza dessa Indústria que consiste em ativar materiais naturais estáveis levando-os a um potencial energético suficientemente elevado para torná-los instáveis em presença d'água. É desta instabilidade que o cimento tira sua capacidade de formar ligações recaindo em um estado estável e liberando uma parte da energia que lhe foi fornecida. Uma comparação da energia posta em fogo para assegurar a coesão com aquela que é efetivamente gasta para a fabricação do cimento daria sem dúvida uma indéia do limite urbano que o consumo energético para a fabricação de um aglomerante poderia atingir. O objetivo do Tema 1.3 deste 8º Congresso Internacional de Química do Cimento se limita somente a uma etapa no encadeiamento dos fenômenos que conduzem dos materiais naturais às ligações no concreto: o consumo de energia na fabricação do clínquer que é o material de base de quase todos os cimentos fabricados no mundo inteiro.

O interesse dos trabalhos consagrados a esse Tema é considerável pois, no mundo, fabrica-se atualmente cerca de 820 milhões de toneladas de clínquer com preço de consumo energético de perto de 100 milhões de toneladas equivalentes de petróleo e de 60 bilhões de Kilowats-hora de eletricidade.

As economias realizadas no consumo energético na fabricação do clínquer atingem uma dimensão excepcional; trata se portanto de um objetivo de alta importância pàra todos os organismos de pesquisa que trabalham em cimento.

J.P. MERIC - STE DES CIMENTS FRANCAIS - Tour Générale - Cedex 22 -
92088 - PARIS LA DEFENSE (FRANCE)

FORMATION D'UN CLINKER CONSOMMANT PEU D'ENERGIE
LOW ENERGY CLINKER FORMATION

1. LA CONSOMMATION D'ENERGIE DANS LES FOURS A CLINKER.

Le clinker est obtenu en général à partir de matériaux naturels qui sont le calcaire d'argile et le sable, on leur ajoute souvent une faible quantité de matériaux d'origine industrielle. Ces matériaux étaient jadis introduits dans le four à l'état humide et c'est presque uniquement le taux d'humidité du matériau qui déterminait la consommation d'énergie. Dans ce système dénommé voie humide la consommation d'énergie thermique par tonne de clinker pouvait s'élever à 6500 MJ.

L'Industrie Cimentière a pu très rapidement faire des économies d'énergie en alimentant ses fours par des matériaux secs. Il a été nécessaire de concevoir des échangeurs spéciaux pouvant recevoir une farine sèche et broyée. La consommation de ce procédé dénommé voie sèche a pu tomber aux environs de 3100 MJ par tonne de clinker, il faut toutefois ajouter à ces chiffres l'énergie nécessaire au séchage des matériaux. Ce séchage s'effectue maintenant à l'extérieur du four mais en utilisant ses pertes thermiques sous forme de gaz chauds. Lorsque l'humidité des matières ne dépasse pas quelques pour cent ces pertes sont suffisantes pour sécher les matériaux sans aucun appoint thermique extérieur , sinon un appoint est nécessaire mais le bilan global est toujours positif.

C'est par ce changement de procédé que l'Industrie Cimentière a obtenu ses principales économies d'énergie.

Maintenant est-il possible d'aller plus loin et comment ? telle est la question que se posent les Services de Recherche.

Les réponses apportées à ces questions peuvent être examinées à la lumière d'une analyse détaillée de la consommation thermique d'un four en voie sèche.

Cette consommation est la somme de trois termes :

1. L'énergie consommée pour le séchage.
2. L'enthalpie théorique de formation du clinker à partir de matériaux secs.
3. Les pertes thermiques du four à ciment.

Le séchage des matières premières a été évoqué et on n'insistera pas davantage sur ce sujet qui est un problème technologique certes important, mais qui n'est pas spécifique de la chimie du clinker. Il est manifeste que pour réduire ce poste de dépense énergétique, il convient de choisir des matières premières aussi sèches que possible et utiliser d'une manière optimale les pertes du four pour l'évaporation de l'eau. Il importe donc que ces pertes soient obtenues à un potentiel thermique aussi élevé que possible pour intensifier l'effet de séchage. Tel n'est pas le cas par exemple du four en voie semi sèche où le potentiel de gaz d'exhaure est abaissé par l'eau de granulation.

Les mêmes considérations s'appliquent lorsque les pertes sont utilisées pour produire de l'énergie électrique; il importe là aussi de conserver l'exergie des pertes.

Les efforts actuels des chercheurs portent sur la réduction de l'enthalpie de formation et sur la réduction des pertes.

2. L'ENTHALPIE DE FORMATION DES CLINKERS

La thermodynamique nous donne un moyen de calculer l'enthalpie de formation en fonction de la composition. Les chercheurs savent donc quelle composition choisir pour diminuer cette enthalpie. Ils ont aussi vu que l'on pouvait agir sur la saturation du clinker, former préférentiellement du C_2S, utiliser la chaleur latente de certains matériaux naturels ou industriels et également modifier très profondément la composition des clinkers pour obtenir des produits réactifs à faible contenu énergétique.

Ces différents points sont passés en revue.

2.1. La saturation du clinker.

L'enthalpie de formation du clinker en fonction de sa composition a été étudiée par ZUR STRASSEN.

Dans la composition l'élément le plus important est la chaux qui est obtenue en général par décarbonatation du calcaire. Cette réaction est très endothermique et absorbe 3125 MJ par tonne de CaO alors que la chaleur de formation théorique d'une tonne de clinker courant n'est que de 1800 MJ/T de clinker. Cette différence provient du caractère exothermique de la réaction $2C + S \rightarrow C_2S$ qui contribue heureusement à abaisser le bilan de formation du clinker. Il est à noter que la réaction $C_2S + C \rightarrow C_3S$ est à nouveau endothermique, et que de plus elle se produit à haute température alors que le C_2S est susceptible de se former à température plus basse. En outre, la formation de C_3S exige un surcroît de chaux qu'il est nécessaire de décarbonater. La formation du C_3S est donc plus coûteuse en énergie que celle de C_2S, il en résulte que le taux de saturation en chaux du clinker a une influence directe sur l'enthalpie de formation.

Cette influence peut se résumer de la manière suivante :

J.P. MERIC - STE DES CIMENTS FRANCAIS - Tour Générale - Cedex 22 -
92088 - PARIS LA DEFENSE (FRANCE)

FORMATION D'UN CLINKER CONSOMMANT PEU D'ENERGIE.
LOW ENERGY CLINKER FORMATION.

TAUX DE SATURATION	CONSOMMATION THEORIQUE MJ/T
100	1800
95	1750
92	1715
90	1690
88	1670
85	1640
82	1600
80	1570

L'abaissement du taux de saturation entraîne en général une réduction de la réactivité du clinker. Cette réduction est plus ou moins accusée suivant la nature des matières premières et du profil thermique du four. Elle doit faire l'objet d'une étude de cas par cas pour tenir compte des facteurs spécifiques précédents ainsi que des caractéristiques du produit souhaitées par les utilisateurs. Cette étude ne peut souvent être entreprise que directement sur l'installation industrielle tant les paramètres liés au procédé sont déterminants et difficiles à simuler en laboratoire. Les effets sur le produit lui-même ne se révèlent pas toujours au niveau du mortier normalisé, et très souvent il faut aller jusqu' aux utilisations sous forme de béton pour juger de tous les effets d'une modification des paramètres de fabrication. Cependant il est possible de tracer en laboratoire les lignes générales de l'influence de ces modifications sur le produit, ce sont ces lignes générales qui guident les expériences en grandeur réelle.

2.2. Le C_2S réactif.

Lorsque le facteur de saturation est réduit aux environs de 0.7 on ne fabrique plus que du C_2S. Sa chaleur de formation est particulièrement basse puisqu'elle se situe aux environs de 1335 MJ/T. Malheureusement ce matériau présente une réactivité beaucoup plus faible que le C_3S et ne lui est donc pas substituable directement. De nombreux chercheurs ont essayé de l'activer et dans ce domaine les différentes voies possibles continuent à être étudiées.

Il semble qu'il soit nécessaire, ou bien de former ce corps à basse température, et donc de s'accommoder de cinétiques de formation assez médiocres, ou alors, de le former à haute température en le trempant d'une manière très énergique. L'on introduit ainsi des irréversibilités qui dégradent le rendement de la récupération thermique et qui risquent de pénaliser le bilan global de l'opération. Nul doute que si un jour le C_2S réactif est mis en fabrication, il faudra inventer de nouveaux procédés de cuisson adaptés au traitement particulier qui lui sera nécessaire.

2.3. L'utilisation de chaleurs latentes.

Il est possible de baisser la chaleur de formation du clinker en partant de produits ou naturels ou industriels présentant une énergie latente qui vient en déduction du bilan normal. Tel est le cas lorsque dans la matière se trouvent des matières carbonées ou des sulfures. Il faut alors trouver le meilleur moyen de les utiliser. L'introduction avec la matière en amont peut conduire à une combustion prématurée et une augmentation des pertes, alors qu'en aval on risque un mélange trop tardif avec les autres matériaux et donc une hétérogénéité préjudiciable à la qualité des matériaux. L'introduction au milieu du four dans un précalcinateur est une solution qui résout élégamment ce problème, mais qui ne peut être appliquée dans tous les cas.

Certains résidus industriels peuvent contenir de la chaux non carbonatée, comme les laitiers de haut fourneau par exemple. Dans ces conditions l'enthalpie de formation du clinker peut diminuer dans certains cas de 130 MJ par tonne, soit de près de 7%. Cette diminution est entièrement répercutée sur la consommation du four contrairement à celle qui résulte de la présence de matières combustibles dans le cru.

L'ajout de laitier à la matière crue présente un intérêt indiscutable sur le plan de l'énergie, son utilisation n'est freinée que par des questions de disponibilité de laitier et de coût de broyage.

2.4. L'introduction de nouveaux éléments dans le clinker.

Plusieurs chercheurs ont essayé de fabriquer des clinkers en modifiant considérablement sa phase fondue. L'on obtient toujours des ciments contenant un certain type de bélite avec l'objectif d'aboutir à une réactivité aussi élevée que possible.

Dès le début du siècle FERRARI en Italie a étudié les ciments très riches en Fe_2O_3 qui portent son nom. Récemment aux USA MEHTA a réexaminé la fabrication de ciments riches en SO_3 contenant $C_4A_3\bar{S}$. En URSS NUDELMAN a étudié puis fabriqué des ciments contenant jusqu'à 3 % de chlore. L'addition de nitrates a été examinée en France par ARNOULD pour la fabrication de nouveaux clinkers. Tous les produits ainsi obtenus présentent une enthalpie de formation plus faible que le clinker classique et qui se rapproche de celle du C_2S (1335 MJ/T). En outre ces produits sont en général obtenus à des températures plus basses que les clinkers courants; on peut donc espérer une réduction des pertes thermiques du four. Ces aspects positifs sont toutefois pénalisés par la nécessité de maîtriser les tendances à la fusion et à la volatilisation de la matière .L'approvisionnement en nitrates, chlorures et sulfates peut dans certaines circonstances se révéler

J.P. MERIC - STE DES CIMENTS FRANCAIS - Tour Générale - Cedex 22 -
92088 - PARIS LA DEFENSE (FRANCE)

FORMATION D'UN CLINKER CONSOMMANT PEU D'ENERGIE
LOW ENERGY CLINKER FORMATION

coûteux et un recyclage de ces éléments après volatilisation entraînera toujours une dégradation énergétique pénalisante pour le bilan global. On constate également que les propriétés des ciments fabriqués avec ces clinkers sont souvent très éloignées de celles dont le marché a l'expérience. Ces ciments se trouvent ainsi cantonnés à des utilisations spéciales et n'ont pas encore connu de véritable généralisation malgré leur potentiel d'économies d'énergie.

3. LA REDUCTION DES PERTES DU FOUR A CIMENT.

La consommation réelle du four à ciment est la somme de la consommation théorique qui a été détaillée dans les paragraphes précédents et des pertes. Dans un four moderne les pertes sont de l'ordre de 1330 MJ par tonne de clinker. Elles résultent du rayonnement des parois (250 MJ/T) du rejet de gaz de combustion chauds (660 MJ/T) et de la chaleur du clinker non récupérée pour réchauffer l'air de combustion (420 MJ/T), cette chaleur est en général évacuée par l'air d'exhaure du refroidisseur. Le rendement d'une telle installation est ainsi de 57 % ce qui est déjà élevé;on a néanmoins cherché à l'améliorer encore par la mise au point d'échangeurs perfectionnés. Les performances précédentes ne peuvent être observées sur une longue période que si le four est en fonctionnement stable , c'est-à-dire que l'équilibre entre les pertes amont et aval est durablement maintenu. Toute instabilité ou tout incident se traduit en effet par une augmentation de la consommation thermique; ainsi un mauvais fonctionnement du refroidisseur entraîne une diminution des entrées thermiques dans le four qu'il faut compenser par un surcroît de combustible qui entraîne à son tour une augmentation du volume des gaz de combustion et donc une augmentation des pertes amont. Il se manifeste donc un effet cumulatif entre les sources de pertes, les pertes se cumulant et entraînant une détérioration brusque de rendement. La conduite d'un four exige donc une grande vigilance, elle est facilitée par l'utilisation d'ordinateurs et de méthodes de contrôle commande modernes qui maintiennent les installations dans un état de fonctionnement proche de l'optimum. Le précalcinateur qui ne conduit pas directement à des économies d'énergie facilite la stabilisation du four, et par la régularité de marche induit des économies indirectes.

3.1. Le four idéal.

Quelle marge d'amélioration présente encore le four à ciment ? Telle est la question que se posent les Ingénieurs chargés de concevoir les équipements de demain.

Les équations des transferts thermiques permettent de calculer la consommation d'un four dont les échangeurs fonctionnent dans des conditions idéales. Ainsi, en partant d'un clinker dont l'enthalpie de formation est de 1800 MJ/T, s'il était possible de réduire à zéro le rayonnement du four par une isolation complète, d'épuiser les fumées de sortie jusqu'à la température de condensation de l'eau et de disposer d'un refroidisseur suffisamment perfectionné pour porter les gaz d'entrée du four à la même température que la matière, la consommation thermique pourrait tomber à 2260 MJ par tonne de clinker. Si dans les mêmes conditions le rendement du refroidisseur pouvait être porté à 100 % et si tous les gaz chauds étaient envoyés dans le four, la consommation tomberait à 1920 MJ par tonne de clinker, ce qui constitue le minimum envisageable avec un four alimenté par un foyer classique; ce minimum est très proche de la consommation théorique de 1800 MJ par tonne.

Si la consommation thermique d'un four à ciment peut être calculée avec précision, la consommation électrique en revanche se révèle plus difficile à estimer. L'on peut simplement constater que toute augmentation du rendement thermique s'obtient par une activation des échanges donc un brassage plus énergique des gaz et de la matière, celui-ci exigeant davantage d'énergie électrique. Ainsi le passage de la voie humide à la voie sèche s'est accompagné d'une dépense électrique accrue. L'expérience a cependant montré que cet accroissement était largement inférieur à la réduction de l'énergie thermique en termes équivalents.

Les hypothèses précédentes supposent que des technologies appropriées soient mises au point pour faire fonctionner les échangeurs perfectionnés qui sont nécessaires pour atteindre des rendements élevés. Des projets à ce sujet existent, mais la difficulté des travaux de recherche-développement s'accroît au fur et à mesure que l'on s'approche des limites théoriques, or celles-ci sont déjà très proches.

Par ailleurs, dans les fours actuels les rejets thermiques sont souvent utilisés pour le séchage des matériaux et accessoirement pour la production de courant électrique. Augmenter le rendement du four reviendrait à supprimer ces rejets et pour le séchage, il faudrait alors consommer un surcroît de combustible aux foyers auxiliaires. L intérêt d'une augmentation du rendement du four est donc surtout manifeste pour les installations qui disposent de matières premières parfaitement sèches; c'est dans ce type d'installations que les prochains progrès des fours trouveront leurs premières applications.

Des tentatives en ce sens ont été faites. On a réalisé un échangeur plus proche de la réversibilité que les échangeurs à grille qui sont actuellement utilisés. Il comportait une cuve destinée à assurer un contact très étroit des gaz et de la matière. Le rendement de récupération passait alors de 70 % à 80 %, mais la matière n'était plus trempée à la sortie du four ce qui n'est pas favorable à la réactivité du clinker, et d'autre part, le clinker chaud présentait une tendance à l'agglomération,ce qui bloquait le fonctionne-

J.P. MERIC - STE DES CIMENTS FRANCAIS - Tour Générale Cedex 22 -
92088 - PARIS LA DEFENSE (FRANCE)

1.3

FORMATION D'UN CLINKER CONSOMMANT PEU D'ENERGIE
LOW ENERGY CLINKER FORMATION

ment de l'échangeur.

En ce qui concerne les échangeurs amont, l'amélioration des échanges a été obtenue par une augmentation du nombre de cyclones; on s'est ainsi rapproché des conditions de reversibilité qui ont été évoquées plus haut.

Ces échangeurs plus poussés ne donneront de résultats satisfaisants que si l'état physique de la matière est bien maîtrisé, c'est-à-dire que si les chimistes trouvent le moyen d'éviter les agglomérations et les collages intempestifs.

3.2. Les minéralisateurs.

L'effet minéralisateur du fluor et de différents autres ions est bien connu depuis longtemps. Il se traduit par une accélération des réactions de clinkérisation à température donnée ou par une diminution de la température de clinkérisation pour une durée fixée. Ce même effet peut être obtenu par une diminution de la saturation en chaux. L'influence de ces modifications sur la consommation du four et sur le niveau des pertes est moins bien connue. L'expérience cimentière permet cependant de dire que la différence de consommation thermique entre un cru facile à combiner et un cru difficile à combiner est de l'ordre de 200 MJ par tonne de clinker, ce qui représente près de 5 % de la consommation du four. L'enjeu d'une amélioration est donc particulièrement important. Comment expliquer l'influence de l'aptitude à la combinaison des composants du clinker sur le rendement du four ?

Il est manifeste que l'abaissement de la température conduit à une réduction des pertes par rayonnement. D'autre part, l'examen du diagramme Q,T de l'échange entre les gaz et la matière montre que la diminution des seuils de décarbonatation exerce une influence favorable sur le niveau des rejets thermiques par les gaz. En revanche, le clinker arrivant plus froid sur le refroidisseur aval, le rendement de l'échange qui se produit sur la grille diminue.

Au total cependant le bilan est positif et se traduit par l'économie signalée plus haut. Cette économie ne peut cependant s'observer dans la réalité que si le réglage du four peut être adapté au nouveau profil de température de la matière et que si l'on évite toute surcuisson.

Il faut souligner qu'une amélioration de l'aptitude à la cuisson peut également être obtenue par un broyage approprié des matières crues et particulièrement des composants les plus difficiles à combiner comme le sable.

Un broyage très poussé exigera sans doute plusieurs Kwh/tonne de clinker qui dans chaque cas devront être comparés aux MJ par tonne de clinker économisés. Pour chaque four il existe un optimum entre broyage et aptitude à la cuisson qui devra être redéfini lorsque les minéralisateurs sont utilisés.

3.3. Le soutirage des alcalis et des chlorures.

Les crus de cimenterie peuvent contenir des alcalis ou des chlorures qui sont indésirables dans le clinker pour assurer le respect des normes en vigueur dans certains pays. L'élimination de ces produits est effectuée par un soutirage de gaz de fours dans un endroit où les températures sont supérieures à leur température de condensation. De cette manière on est conduit à augmenter les pertes thermiques du four en mettant à l'atmosphère des gaz aux environs de 1000°C. La perte thermique qui en résulte est très élevée, d'autant plus élevée que l'on cherche à pousser l'élimination des alcalis ou des chlorures. Les fours à précalcinateurs présentent un avantage important à cet égard puisque le volume des gaz de four est très réduit par rapport au four classique, ceux-ci sont donc davantage enrichis en produits volatils et on peut donc se contenter d'un soutirage réduit, ce qui limite les dépenses thermiques. Celles-ci n'en restent pas moins très élevées comme le montre l'exemple suivant :

Consommation sans by pass :..... 3360 MJ/T
Consommation avec 50% de by pass : 3720 MJ/T
Consommation avec 100% de by pass : 4180 MJ/T

Il apparaît ainsi que certaines exigences des normes peuvent avoir un effet pénalisant sur les consommations énergétiques. Il est donc nécessaire de vérifier très précisément leur bien-fondé avant de les adopter, car bien souvent il est difficile de concilier des contraintes chimiques pointues imposées par des considérations de qualité du béton (réaction alcali granulat, résistance à l'eau de mer, résistance aux eaux sulfatées) et d'obtenir une consommation d'énergie optimale sur le four à ciment.

4. CONCLUSION.

Les différentes possibilités pour économiser l'énergie dans la fabrication du clinker qui ont été passées en revue peuvent se diviser en deux catégories :d'une part, les améliorations qu'il est possible d'entreprendre immédiatement en utilisant les connaissances disponibles, et, d'autre part, les recherches à plus long terme pour l'amélioration des échangeurs et la fabrication de nouveaux clinkers.

Les améliorations qu'il est possible d'apporter immédiatement à la fabrication du clinker consistent essentiellement à optimiser la composition chimique du ciment. Cette optimisation doit tenir compte non seulement de l'énergie dépensée au four, mais également de celle qu'il est nécessaire de fournir au broyeur. Ainsi l'influence bénéfique d'un abaissement du taux de saturation du clinker sur la consommation théorique et sur l'aptitude à la cuisson se traduit en général par des économies de combustible, mais aussi par une diminution de la réactivité du clinker. Il est alors nécessaire de compenser cette diminution par un broyage

J.P. MERIC - STE DES CIMENTS FRANCAIS - Tour Générale - Cedex 22
92088 - PARIS LA DEFENSE (FRANCE)

1.3

FORMATION D'UN CLINKER CONSOMMANT PEU D'ENERGIE
LOW ENERGY CLINKER FORMATION.

plus poussé ou par une réduction des constituants secondaires ajoutés au ciment; c'est-à-dire par des dépenses qui vont à l'encontre des économies escomptées.

Un bilan global alors s'impose pour trouver les points de consigne les plus appropriés; le cimentier étend en général ce bilan jusqu'au béton car l'utilisateur final n'est pas seulement sensible à la réactivité du ciment, mais également à d'autres caractéristiques qui influencent la rhéologie, le ressuage, la couleur, l'aptitude à l'étuvage, la compatibilité avec les adjuvants, la durabilité, etc...

Le problème qui se pose au chimiste est donc d'établir les relations entre le choix des matériaux crus, les caractéristiques du ciment et les propriétés du béton, c'est dans ce cadre qu'il doit chercher les points de consigne qui assurent la consommation énergétique la plus faible possible. Ce problème fait donc intervenir de nombreux paramètres, et il est d'autant plus complexe qu'il s'y ajoute en général des contraintes sur les investissements, sur la disponibilité en matières premières et sur la préservation de l'environnement. Tous les jours les cimentiers affrontent cette complexité et lui apportent des solutions; celles-ci sont rendues plus efficaces encore au fur et à mesure que de nouveaux progrès sont obtenus dans la connaissance des phénomènes chimiques qui se déroulent dans les fours et les broyeurs.

Que faut-il attendre à plus long terme compte tenu des progrès déjà accomplis dans la fabrication du ciment ? On peut prévoir que toute amélioration qui rapprocherait les performances des outils actuels de leur limite asymptotique sera très coûteuse, qu'il s'agisse de mettre au point de nouveaux échangeurs pour les fours ou de concevoir de nouveaux ciments. Il faut alors se demander si les coûts énergétiques futurs justifieront de tels investissements en recherche-développement, et il faut reconnaître que les fluctuations actuelles des coûts de l'énergie ne permettent pas de faire une prévision indiscutable.

Tout projet à très long terme devrait s'appuyer sur une base économique solide constituée par le prix d'équilibre de l'énergie, c'est-à-dire le prix qui permet de valoriser les ressources marginales nécessaires à la satisfaction de la demande. Ce prix est difficile à connaître, mais l'on sait que son accroissement est fatal en raison de l'épuisement progressif des ressources énergétiques d'accès facile. Les experts prévoient ainsi un doublement du prix d'équilibre entre 1986 et l'an 2000; il est de plus probable que cette évolution ne s'arrêtera pas là. Ceci signifie que les recherches à long terme sur les consommations énergétiques dans l'Industrie du ciment, même si elles sont coûteuses ne constituent pas seulement un exercice intellectuel pour le chercheur, mais représentent un investissement judicieux pour le futur.

F. W. Locher Research Institute of the Cement Industry
Dusseldorf, Federal Republic of Germany

Low energy clinker
Formation d'un clinker consommant peu d'énergie

Summary Cement clinker can be produced in the dry process with an energy consumption of under 3100 kJ/kg of clinker (740 kcal/kg). The greater part of this energy is consumed in the dissociation of the calcium carbonate in the feed material and in maintaining the high burning temperature of 1450°C. Fuel energy can therefore be saved by lowering the calcium carbonate content in the feed material and/or lowering the burning temperature needed for clinker formation.

The burning temperature can be brought down to about 1300°C by the addition of mineralizers and/or fluxes. The energy saving effected by such means is probably not much more than 5%.

If the calcium carbonate content of the raw mix is reduced, the content of dicalcium silicate in the clinker increases at the expense of the tricalcium silicate. The early strength of cement made from belite clinker of this kind becomes higher if the clinker is cooled very rapidly or if it contains, besides dicalcium silicate, more vigorously reactive compounds poorer in CaO, e.g., calcium aluminate, calcium aluminoferrite, calcium aluminosulphate and/or alinite.

With rapid clinker cooling the energy saving is limited because the heat losses of the cooler are greater. With cements containing calcium aluminate, calcium aluminoferrite and/or calcium aluminosulphate it is probably possible to effect energy savings of about 25% in comparison with portland cement. It should be considered, however, that the strength development - at least at the start of the hardening process - is due chiefly to the formation of ettringite, calcium aluminate hydrate and calcium aluminoferrite hydrate, and to a less extent to the formation of calcium silicate hydrate. An energy saving of up to 30% is claimed for the production of alinite cement. However, this cement contains about 1% chloride and is therefore in many countries unacceptable as a binder for making reinforced concrete.

In general, cements produced from low energy clinker harden at a notably slower rate than ordinary standard cements. Concrete made from low energy clinker cements must therefore be kept moist for appreciably longer periods. On the other hand, it does indeed attain the required strength, but not the low permeability in the surface layers which is essential to durability.

Alternatives to low energy clinker cements are, among others, slag cements, pozzolanic cements and fly-ash cements, the production of which likewise requires less energy. As they have proved satisfactory in practice for many years now, and have been standardized in many countries, they continue to enjoy preference.

O clinquer de cimento pode ser produzido pelo processo seco com um consumo de energia inferior a 3.100 kJ/kg de clinquer (740 kcal/kg). A maior parte desta energia é gasta na dissociação do carbonato de cálcio no material de alimentação, e na manutenção da elevada temperatura de queima de 1.450°C. Portanto, a energia do combustível pode ser economizada pela redução do teor de carbonato de cálcio no material de alimentação e/ou pela redução da temperatura de queima necessária para a formação do clinquer.

A temperatura de queima pode ser baixada para cerca de 1.300°C pela adição de mineralizadores e/ou fundentes. A economia de energia obtida por estes meios provavelmente não é muito mais que 5%.

Se o teor de carbonato de cálcio na mistura crua for reduzido, o teor de silicato bicálcico no clinquer aumenta à custa do silicato tricálcico. A resistência inicial do cimento feito do clinquer de belita deste tipo torna-se mais alta se o clinquer tiver sido resfriado muito rapidamente ou se contiver, além do silicato bicálcico, compostos mais intensamente reativos, mas pobres em CaO, por exemplo, aluminato de cálcio, ferroaluminato de cálcio, sulfoaluminato de cálcio e/ou alinita.

Com o resfriamento rápido do clinquer a economia de energia é limitada, porque as perdas de calor do resfriador são maiores. Com cimentos contendo aluminato de cálcio, ferroaluminato de cálcio e/ou sulfoaluminato de cálcio provavelmente é possível fazer economias de energia de cerca de 25% em comparação com o cimento portland. Dever-se-ia considerar, entretanto, que o desenvolvimento da resistência - pelo menos no início do processo de endurecimento - se deve principalmente à formação de etringita, hidrato de aluminato de cálcio e hidrato de ferroaluminato de cálcio, e em menor extensão à formação de hidrato de silicato de cálcio. Admite-se uma economia de até 30% com a produção de cimento de alinita. Todavia, este cimento contém cerca de 1% de cloreto e é, portanto, inaceitável em muitos países como um ligante para fabricação de concreto reforçado.

Em geral, os cimentos produzidos com clinquer de baixa energia endurecem com velocidade marcantemente mais baixa do que os cimentos comuns padrão. Por isso concreto feito com cimentos de clinquer de baixa energia devem ser mantidos úmidos por períodos apreciavelmente mais longos. Por outro lado, ele sem dúvida atinge a resistência exigida, mas não a baixa permeabilidade nas camadas de superfície, que é essencial para a durabilidade.

Alternativas para os cimentos de clinquer de baixa energia são, entre outras, cimentos de escória, cimentos pozolânicos e cimentos de cinza volante, cuja produção igualmente requer menos energia. Como agora eles já foram satisfatoriamente provados na prática, e já foram padronizados em muitos países, continuam a atrair a preferência.

1. Introduction

Cement manufacture requires a relatively high input of energy, namely, fuel energy for burning the cement clinker and electric energy for cement grinding. Since the steep rise in the cost of energy, which began in 1973, efforts have therefore increasingly been directed at reducing energy consumption in the production of cement. In this context, attention is focused particularly on fuel energy saving.

One possibility, which is already being utilized to a greater or lesser extent in many countries, is the use of latently hydraulic or pozzolanic materials as ingredients of cement. These materials are either obtained unavoidably as wastes from other industrial processes, e.g., blastfurnace slag or fly-ash, or are won as natural rock products. In general, therefore, they require only thermal energy for drying them. These materials and the cements made from them will be dealt with in other principal papers. The present paper is concerned solely with clinkers which can be burned with reduced input of fuel energy.

2. Fundamental aspects

In modern cyclone preheater kilns portland cement clinker can be produced with a fuel energy consumption of under 3100 kJ/kg (740 kcal/kg) (1). In the wet process, on the other hand, a fuel energy consumption of at least 5000 kJ/kg (1200 kcal/kg) must be reckoned with.

The fuel energy input to the dry-process cement kiln serves essentially to dissociate the calcium carbonate which is the chief component of the raw mix and to heat the feed to the temperature of around 1450 °C necessary for clinker formation. The additional energy demanded by the wet process is required for evaporating the water. Therefore a saving in fuel energy can be effected more particularly by reducing the proportion of calcium carbonate in the raw mix and/or lowering the clinkering temperature.

If the calcium carbonate content of the raw mix is reduced, a clinker with lower tricalcium silicate and higher dicalcium silicate content is obtained, with correspondingly very slow hardening. That is why the literature comprises many reports of research aiming to improve the hardening capacity of cements made from such clinkers. Some of these investigations were concerned with increasing the hydraulic reactivity of the dicalcium silicate constituent by applying certain measures in burning and cooling the clinker. In many cases it was investigated whether tricalcium silicate can at least partly be replaced by other compounds which, though having a lower CaO content, have a similarly rapid hardening behaviour. Such compounds containing less CaO are calcium aluminates, calcium aluminoferrite, calcium aluminosulphate and alinite.

There are as yet no reports indicating whether cements produced from such clinkers have already been used for making concrete, especially reinforced concrete, and how successful they have proved if they have indeed been so used. In this connection the durability of the concrete, which is becoming an increasingly important consideration with regard to concrete structures, is more particularly of interest.

3. Burning at low temperature

Normal raw mixes with a lime saturation factor above about 0.95 are generally burned at clinkering temperatures of around 1450 °C. In particularly favourable cases lower temperatures, down to about 1300 °C, may suffice. Even lower clinkering temperatures are possible if mineralizers and/or fluxes are used, which are sometimes added in amounts of up to about 3 % by weight to the raw mix. Mineralizers are substances which, even when present in small amounts, promote formation of the clinker compounds, especially the formation of tricalcium silicate. Fluxes

are substances which lower the temperature at which the formation of liquid phase commences, and decrease the viscosity of the clinker melt. It is usually not possible to draw a clear-cut distinction because many substances have both a mineralizing and a fluxing action.

The literature contains many publications indicating to what extent various substances promote clinker formation. A comprehensive review of the literature has been given by W. A. Klemm and J. Skalny (2). In comparative investigations (3, 4) it was found that clinker formation is promoted particularly by fluorides and silicofluorides. According to I. Odler and S. Abdul-Maula (3) the heavy metals zinc, copper and cobalt are also effective. If these metals are added as fluorides or silicofluorides, an additive effect is obtained.

The addition of such substances enables the clinkering temperature in an industrial cement kiln to be lowered by about 200 K. There is divergence of opinion as to how much fuel energy can be saved in this way. From their literature review W. A. Klemm and J. Skalny (2) come to the conclusion that a fuel energy saving of about 150 kcal/kg of clinker (625 kJ/kg) is attainable as a result of lowering the clinkering temperature by 100 - 200 K. According to N. H. Christensen and V. Johansen (5), however, a lowering of the clinkering temperature by 150 K will effect a saving of probably not more than 25 kcal/kg (105 kJ/kg).

With regard to such estimates it must be taken into account that although the heat losses of the kiln are greatly reduced due to a lowering of the clinkering temperature, with less fuel energy input there is also less energy to be recovered from the clinker cooler for the benefit of the burning process. With kilns characterized by high fuel energy consumption and correspondingly high heat losses, e.g., wet-process kilns, the saving may be substantially greater than with much more economical kilns such as those equipped with grate preheaters or cyclone preheaters. For a modern kiln with cyclone preheater and precalcining it has been estimated by H. O. Gardeik (6) on the basis of model calculations that a 200 K lowering of the clinkering temperature would result in a 5 % fuel energy saving, i.e., a reduction from, say, 3140 kJ/kg (750 kcal/kg) to 2985 kJ/kg (715 kcal/kg). These values are in agreement with those indicated by N. H. Christensen and V. Johansen (5).

In making this estimate, however, H. O. Gardeik presupposes that the added mineralizer does not change the temperature level of the calcining process. On the other hand, R. Pöhlmann (7) found in his research that an addition of 0.5 and 1.0 % by weight of calcium fluoride also lowers the calcining temperature by about 80 K. According to H. O. Gardeik the fuel energy saving is thereby increased to about 6 %, i.e., the fuel energy consumption would be reduced from, say, 3140 kJ/kg (750 kcal/kg) to 2950 kJ/kg (705 kcal/kg).

4. Belite cement

The reactions of clinker formation theoretically require an energy input of between 1590 and 1850 kJ/kg of clinker (380 - 440 kcal/kg), on average 1750 kJ/kg (420 kcal/kg). The major part of this input is due to the dissociation enthalpy of calcium carbonate. The energy requirement for the decomposition of the clay minerals is only quite low, and the formation of the clinker compounds from the oxides is an exothermic reaction. The theoretical heat requirement therefore decreases considerably if the calcium carbonate content of the raw mix and, in consequence, the tricalcium silicate content of the clinker is reduced and the dicalcium silicate content increased.

Dicalcium silicate-rich cements generally harden so slowly that their usefulness as binding agents for structural concrete is

limited or indeed inadequate. That is why the literature comprises so many publications on investigations undertaken with the object of improving the hydraulic hardening capacity of such cements. U. Ludwig and co-workers (7-11) found that an addition of ground clinker of normal composition substantially accelerates the hardening of belite cement. This is in agreement with the results of research conducted by I. Odler and J. Schüppstuhl (12), which indicates that pure tricalcium silicate as an activator promotes rapid hardening of ß-dicalcium silicate. Besides, the hydraulic properties of belite clinker can be improved by alkalies, which should be added to the raw mix before burning (13).

Various investigations are concerned with the possibility of enhancing the hydraulic hardening capacity of belite by very rapid cooling of the clinker (14-19). In this way not only the high-temperature modifications of dicalcium silicate are stabilized, but their reactivity is also increased (17). Detailed investigations have shown that such belite cements with lime saturation factors between about 0.78 and 0.85, dicalcium silicate contents according to Bogue between about 40 and 60 % and tricalcium silicate contents between 40 and 20 % attain higher standard strengths if the clinker is very rapidly cooled in the temperature range from 1300 to 900 °C (17). As a result of such cooling, however, the 28-day strength is increased considerably more than the 3-day early strength. From the diagrams contained in the publication it is apparent that the cement made from the rapidly cooled clinker with a lime saturation factor of 0.85 attains standard strengths of 17.5 N/mm² at 3 days and 60 N/mm² at 28 days for a specific surface of 3200 cm²/g (Blaine). By extrapolation, using the procedure given by G. Sadran and R. Dellyes (20), the corresponding 2-day standard strength is found to be about 12 N/mm². Normal portland cements, ground to the same fineness, attain on average about 22 N/mm² at 2 days and 50 N/mm² at 28 days when tested by this method.

A cooling rate of at least 1000 up to about 3000 K/minute is to be regarded as sufficiently rapid. The rate of cooling achieved in the usual industrial clinker coolers is about 150 - 300 K/minute. More rapid cooling requires special equipment. It is therefore proposed that the conventional clinker cooler be preceded by cooling in a fluidizing trough cooler, preferably in conjunction with prior comminution of the clinker (18).

The saving in fuel energy that would be effected by burning belite clinker can be estimated with the aid of the model calculations of H. Rosemann (21). The basis for these calculations is provided by investigations on various industrial kiln plants, which revealed that a reduction of the reaction enthalpy for clinker formation will, for otherwise unchanged conditions, affect the overall fuel energy requirement of the kiln plant by approximately a factor of 1.5. The thermal efficiency of the clinker cooler is similarly important, however. If the heat losses of the clinker cooler are decreased or increased, the heat losses of the kiln plant as a whole will likewise decrease or increase by a factor of 1.5. These results of the model calculation are represented in Fig. 1. For this

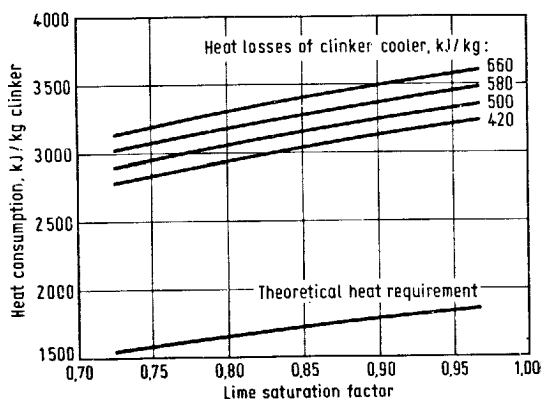

Fig. 1: Influence of the lime saturation factor and the efficiency of the cooler on the fuel energy requirement of a cyclone preheater kiln

purpose it has been assumed that, for a clinker composition calculated according to Bogue with unvaryingly 11 % tricalcium aluminate, 9 % calcium aluminoferrite and 1 % MgO, only the contents of tricalcium silicate and dicalcium silicate can vary. Furthermore, in conformity with (17), it has been presupposed that the required temperature for clinker formation is lowered from 1450 °C to 1300 °C with the lowering of the lime saturation factor from 0.97 to 0.80.

The shape of the curves shows that the reaction enthalpy of clinker formation decreases from about 1850 kJ/kg of clinker (440 kcal/kg) to 1640 kJ/kg (390 kcal/kg) if the lime saturation factor is reduced from 0.97 to 0.80, i.e., a decrease of 210 kJ/kg (50 kcal/kg). If the heat losses of the clinker cooler remain unchanged, the fuel energy requirement of the kiln plant decreases by 300 kJ/kg (70 kcal/kg). Efficient clinker coolers have heat losses of about 450 kJ/kg of clinker (110 kcal/kg). But if cooling is accomplished more rapidly in a given clinker cooler, the heat losses increase considerably, e.g., from 450 kJ/kg of clinker (110 kcal/kg) to 650 kJ/kg (155 kcal/kg). As a consequence, the overall consumption of fuel energy undergoes practically no further change. Energy savings would be possible only if, by means of design modifications to the clinker cooler, the heat losses could be reduced to their original values.

5. Modified belite cements

The hydraulic hardening capacity of cements consisting predominantly of dicalcium silicate can be improved by compounds which harden more rapidly and which may also accelerate the hydration of the dicalcium silicate. Among other authors, P. K. Mehta (22) has presented an overview of such modified belite cements.

Compounds which promote hardening are more particularly the constituents of high-alumina cement, namely, monocalcium aluminate and "$12CaO \cdot 7Al_2O_3$" as also the compounds $3CaO \cdot 3Al_2O_3 \cdot CaSO_4$. Cements based on these substances are alumina-belite cement (23, 24) and Porsal cement (25, 26). Both these cements contain 60 - 65 % of dicalcium silicate, but differ from each other in their content of the compounds $3CaO \cdot 3Al_2O_3 \cdot CaSO_4$, "$12CaO \cdot 7Al_2O_3$" and $CaSO_4$. The clinker is burned from raw mixes of suitable composition at temperatures between 1250 and 1300 °C. Fuel energy consumption is probably of the same order of magnitude as that for belite cement. The cements are ground to finenesses above 4000 cm²/g, i.e., they are somewhat more finely ground than normal portland cements, for otherwise they would set too slowly. Their standard strengths are reported to be approximately equal to those of normal portland cements. It can be presumed that the early strength is due more particularly to the formation of ettringite and calcium aluminate hydrates and that the calcium silicate hydrate formed from dicalcium silicate contributes only at a substantially later stage to structure and strength development, so far as the water needed for hydration is then still available.

The high iron oxide cement described by P. K. Mehta (27, 28) can also be classed among the belite cements. The clinker, which consists on average of 35 % dicalcium silicate, 30 % calcium aluminoferrite, 20 % $3CaO \cdot 3Al_2O_3 \cdot CaSO_4$, and 15 % $CaSO_4$, can be burned at 1200 °C. At this low temperature a clinker is formed which is likely to be easily grindable and in which the calcium aluminoferrite content is not present in fused form, so that it reacts quickly with water and contributes to strength development. For finenesses of 3500 cm²/g the standard strengths are comparable to those of normal portland cements. The saving in energy is stated to be 25 % (27).

6. Alinite cement

Alinite cement has been developed in the USSR, where it has been patented since May 1977 and is also already produced industri-

ally. B. I. Nudelman and others are named as the inventors. Protection by patent has existed also in many other countries since May 1977.

From the German patent specifications (29-32) and from the literature (33-39) it appears that the raw mix for making the alinite clinker contains between 6 and 23 % by weight of calcium chloride. The other raw material components are present in approximately the same mix proportions as are typical of portland cement clinker manufacture. It would seem, however, that the MgO content has to be increased a little in order to stabilize the alinite.

Since calcium chloride melts at 772 °C, a salt melt (eutectic $CaCl_2$-$CaCO_3$ or $CaCl_2$-CaO) is formed already at relatively low temperatures, which promotes the chemical reaction between the components of the raw mix. But even at temperatures below that of melt formation there occur solid reactions in which calcium chloride participates or which are promoted by calcium chloride.

The following phase composition is stated for the product of the burning process, alinite clinker:

alinite	60 - 80 % by weight
belite	10 - 30 % by weight
calcium aluminochloride	5 - 10 % by weight
calcium aluminoferrite	2 - 10 % by weight

According to A. Boikova (36) the phase composition is a good deal more complicated, however. It would appear that particularly also the distribution of the chloride among the various compounds is not yet known. The formula ascribed to alinite is $Ca_{11}(Si_{0.75}\ Al_{0.25})_4\ O_{18}\ Cl$ (33, 34) or $3(0.875CaO \cdot 0.070MgO \cdot 0.055CaCl_2) \cdot (0.885SiO_2 \cdot 0.115Al_2O_3)$ (40) or, less exactly, $21CaO \cdot 6SiO_2 \cdot Al_2O_3 \cdot CaCl_2$. According to the formula, alinite clinker therefore contains, because of its alinite and calcium aluminochloride content, between 3 and 4 % by weight of chloride. Usually, 3 % by weight of Cl^- is stated in the literature.

As information contained in the patent specifications indicates, between 6 and 23 % by weight of calcium chloride is added to the raw mix for making alinite clinker. It would seem that the calcium chloride can in part be replaced by sodium chloride and/or potassium chloride. If it is presumed that 10 % by weight of calcium chloride added to the mix is sufficient and that for alinite clinker, as for normal cement clinker, a raw meal/clinker factor of 1.55 is applicable, the amount of calcium chloride needed can be put at about 150 kg per ton of alinite clinker.

The burning temperature for alinite clinker is stated to be 1000 - 1100 °C. Also, its reaction enthalpy is reportedly about 545 kJ/kg (130 kcal/kg) lower than that of normal cement clinker. This would mean that the production of alinite clinker requires about 1250 kJ/kg (300 kcal/kg) less fuel energy input, and since it is also appreciably more easily grindable than normal portland cement clinker, electric energy consumption for cement grinding is lower, too. Overall a saving in fuel and electric energy of up to 30 % and a reduction in the cost of production of 10 - 12 % in comparison with normal portland cement are claimed.

Even at the lower burning temperature of 1000 - 1100 °C the chloride already vaporizes considerably and gives rise to cyclic processes which may upset plant operation. Conceivably, such upsets may be substantially less in the wet than in the dry process.

According to the patent literature, the chloride content of alinite clinker is lowered after the burning process by exposing the clinker to the action of a gas-vapour-air mixture. It is hardly likely, however, that contents of Cl^- below 1 % by weight can be attained in this way. Chloride contents of between 1 and 5 % by weight of Cl^- are mentioned in the patent literature. This means that alinite cement contains chloride in such

amounts as to make its use in reinforced concrete questionable for reasons of corrosion protection.

It can be presumed that alinite reacts with water in much the same way that tricalcium silicate does, forms similar hydration products and therefore attains comparable strengths. Quite probably, alinite has an even higher reactivity, while the chloride content may well have an accelerating effect.

When alinite cement undergoes hydration, hydration products are formed from its compounds. As a result, the chloride initially present in combined form in the alinite and in the calcium aluminochloride is released and can then promote corrosion of steel reinforcement. In investigations on these aspects which were carried out in the Research Institute of the German Cement Industry it was found that steel bars embedded axially in 4 cm x 4 cm x 16 cm mortar prisms had become completely corroded at the surface after 5 years' storage in the open air. It follows that alinite cement is not suitable as a binder for making reinforced concrete.

Such problems of steel corrosion would not arise if fluorine alinite - as described by, among others, U. Ludwig, A. Wolter, D. Bürger and R. Pöhlmann (7-10) - which is formed at temperatures of 1000 - 1100 °C were suitable as the basis for making low energy clinker. It has only a relatively slow rate of hardening, however.

7. Structural properties of cements made from low energy clinker

In general, the only criterion applied to the serviceability of cements produced from low energy clinker is the standard strength of the cement, which is tested in accordance with the relevant national standards and determines the allocation of cements to particular strength classes. In various investigations the water demand of the cement is additionally taken into account. Even so, it is by no means certain that concrete made from such cement according to the established rules will possess the same working properties as concrete with cements that have long proved dependable.

Concrete structural components must have the required strength and be durable. For external construction units this means, among other criteria, that the concrete must be weather-resistant and, where relevant, also frost-resistant and that it must protect the reinforcing steel from corrosion. For concrete made from conventional cements these properties are guaranteed by virtue of their compliance with the relevant cement and concrete standards. For cements with different composition and different properties such assurance cannot be presumed as a matter of course.

The loadbearing capacity of a concrete component depends primarily on the strength of the concrete in its core, i.e., in the volume enclosed within the reinforcement. The imperviousness and thickness of the concrete cover to the reinforcing steel are factors governing corrosion protection, i.e., this depends essentially on the more or less thick surface layer of concrete. For a given concrete mix composition both the strength of the concrete core and the imperviousness of the concrete cover increase as hydration of the cement progresses, because the hydration products of the cement more and more completely fill the voids previously filled with mix water.

However, it would seem that the cement hydration products can occupy only those voids which still contain water. Whereas the concrete core remains saturated with water for quite a long time, the zones close to the surface, i.e., the concrete cover to the reinforcement, dry out relatively quickly if they are not kept adequately moist. It may be that the drying of the capillary pores near the concrete surface is also promoted by chemical shrinkage, i.e., the reduction in volume which occurs during hydration because the hydration products of the cement occupy

less space than the cement and water before hydration. As a result, an underpressure develops which, if not enough moisture is available, causes ambient air to be drawn by suction into the capillary pores of the concrete. These pores can then no longer be filled with hydration products. In consequence of this the capillary porosity of the surface layer does not decrease any further, although the strength of the concrete in the still saturated core continues to increase.

The essential requirement for durability of the concrete and corrosion protection of the reinforcing steel is, first and foremost, an impervious and dense surface layer. To make concrete possessing these properties it is, in conjunction with a sufficiently high cement content, necessary to have an appropriately low water/cement ratio and to ensure that the degree of hydration of the cement is as high as possible also in the surface layer of the concrete. The governing influence of the water/cement ratio and degree of hydration on the permeability of hardened portland cement paste is represented in Fig. 2. This diagram is based on the relationship between permeability and capillary porosity - as measured by T. C. Powers (41) - and on the calculated relationship between the capillary porosity, water/cement ratio and degree of hydration (42, 43). For a water/cement ratio of 0.55 a sufficiently low permeability is attained only for a degree of hydration in excess of 80 %.

On the construction site it is usually not possible to protect concrete for more than a short time against drying out. In order to ensure that the surface layer is nevertheless of low porosity and sufficiently impervious, it is essential that the cement achieves the highest possible degree of hydration in this short time and supplies a sufficient amount of hydration products to reduce the capillary porosity. The concrete with a composition that satisfies this requirement will attain a strength well above the required

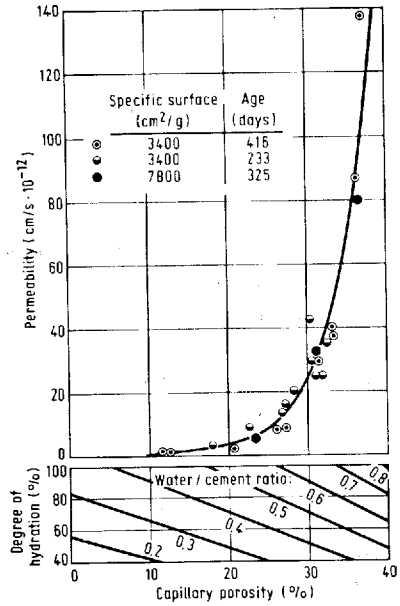

Fig. 2: Permeability of hardened cement paste in relation to the capillary porosity, the water/cement ratio and the degree of hydration of the cement

minimum strength. In making concrete for external structural components the aim, besides strength, should therefore more particularly be: durability.

The rules for making concrete are geared to standard cements which, with regard to durability, have long proved satisfactory in actual practice. Cements produced from low energy clinker cannot as a matter of course be expected to achieve the same behaviour if it has merely been shown that they attain the minimum strengths laid down in the cement standards. Because of their composition their hydration proceeds appreciably more slowly than that of standard cements. Although the 28-day standard strengths of low energy clinker cements are about equal to those of standard cements and are usually even distinctly higher after storage in water for even longer periods, their early strengths are always considerably lower. This indicates that at the start of hardening the amount of hydration products formed is less and that

the capillary porosity of the concrete is therefore appreciably greater than when standard cements are used.

These considerations show that the standard strength at 7 days or at 28 days is not an adequate criterion for judging that concrete made from new cements of this type will, under the conditions of curing and hardening encountered in practice, be just as durable as concrete made from standard cements. Further tests are therefore necessary which take account also of the permeability of the hardened cement paste. In this context it is especially important that the test specimens should harden under humidity conditions similar to those to which the surface layer of concrete will be exposed in practice. The diffusion of oxygen can be adopted as a measure of imperviousness. Such measurements were performed already quite a long time ago by H. E. Schwiete, H. J. Böhme and U. Ludwig (44, 45, 46).

8. Economy

In general, it will have to be presumed that a cement plant cannot switch its entire production to cements made from low energy clinker. High-early-strength cements, which can presumably not be manufactured from low energy clinker, will always claim a by no means negligible share of the market. The production of low energy clinker means therefore that an additional type of clinker has to be made, requiring the preparation and burning of a special raw mix. For this it will be necessary to provide adequate grinding capacity and special facilities for at least the separate storage of the raw mix, clinker and cement. The manufacture of belite cement will presumably also require modifications to the clinker cooler, which can then not be used for the cooling of normal clinker.

Alternatives to cements made from low energy clinker are cements which, besides clinker, also contain other substances as their major constituents, more particularly those which are available as waste materials or can be produced without any considerable input of energy. Such materials are, in the first place, glassy blastfurnace slag, natural pozzolanas (e.g., certain volcanic rocks), artificial pozzolanas (e.g., fly-ash), and inert or almost inert materials (e.g., limestone). The energy saving effected by using these materials is probably at least of the same order of magnitude as the energy saving attainable with cements made from low energy clinker.

Cements comprising several major constituents have been manufactured and used in many countries for a long time now. They have proved satisfactory in practice and have been standardized in many countries. So it is understandable that these cements have enjoyed preference over cements made from low energy clinker.

References

(1) Bonn, W., and Lang, Th.: Brennverfahren; Generalbericht zum VDZ-Kongreß '85 "Verfahrenstechnik der Zementherstellung". Zement-Kalk-Gips 39 (1986) No. 3.

(2) Klemm, W. A., and Skalny, J.: Mineralizers and fluxes in the clinkering process. Cements Research Progress 1976, pp. 259-291; Am. Ceram. Soc., Columbus, Ohio, 1977.

(3) Odler, I., and Abdul-Maula, S.: Einfluß von Mineralisatoren auf das Brennen des Portlandzementklinkers. Zement-Kalk-Gips 33 (1980) No. 3, pp. 132-136 and 278-282.

(4) Toropov, N. A., Luginina, I. G., and Luginin, A. N.: Über den chemischen Einfluß von Zusätzen auf die der Klinkerbildung vorangehenden Prozesse - Zur Beschleunigung der Klinkerbildung durch Zusatz von Mineralisatoren. Silikattechn. 22 (1971) No. 7, pp. 220-222.

(5) Christensen, N. H., and Johansen, V.: Role of liquid phase and mineralizers. J. Skalny (Editor): Cement Production and Use. Engineering Foundation, US Army Research Office, 1979, pp. 55-69.

(6) Gardeik, H. O.: Einfluß der Sintertemperatur auf den spezifischen Energieverbrauch beim Brennen von Zementklinker. Zement-Kalk-Gips 34 (1981) No. 4, pp. 169-174.

(7) Pöhlmann, R.: Zur Brennbarkeit von Portlandzementrohmehlen in Abhängigkeit von Kalkstandard sowie Zusätzen und der hydraulischen Reaktivität beim Übergang von kalkreichen zu kalkarmen Portlandzementen. Dissertation RWTH Aachen (1986).

(8) Ludwig, U., and Wolter, A.: Zur Bildung und Stabilität von Tricalciumsilikat und Aliten. Zement-Kalk-Gips 32 (1979) No. 9, pp. 455-459.

(9) Wolter, A.: Zur Bildung und Stabilität von Tricalciumsilikat und Aliten. Forschungsbericht des Landes NRW, No. 3092, Westdeutscher Verlag, Opladen (1982).

(10) Bürger, D.: Beitrag zur Synthese und Reaktivität von bei niedrigen Temperaturen hergestellten Calciumsilikaten. Dissertation RWTH Aachen (1985).

(11) Bei, R.: Untersuchungen zur Reaktivität von Portlandzementen in Abhängigkeit vom Kalkstandard, Brenngrad und Sinterhilfsmittel beim Klinkerbrand. Dipl.-Arbeit RWTH Aachen (1985).

(12) Odler, I., and Schüppstuhl, J.: Combined hydration of tricalcium silicate and β-dicalcium silicate. Cem. Concr. Res. 12 (1982) No. 1, pp. 13-20.

(13) Gies, A., Töpfer, P., and Knöfel, D.: Alkaliaktivierter Belitzement. German Patent 05 34 14 196 (1984).

(14) Stark, J., Müller, A., Rümpler, K., and Dahm, B.: Über aktiven Belit-Zement. Teil I: Zielstellung, Versuchsprogramm, erste Ergebnisse. Silikattechn. 30 (1979) No. 12, pp. 357-362.

(15) Stark, J., Rümpler, K., Schrader, R., Müller A., Dahm B., and Rudolph, R.: Über aktiven Belit-Zement. Teil II: Einfluß des Kühlregimes auf die Zementfestigkeit. Silikattechn. 31 (1980) No. 2, pp. 50-52.

(16) Stark, J., Müller, A., Schrader, R., and Rümpler, K.: Über aktiven Belit-Zement. Teil III: Abgrenzung des Existenzgebietes von aktivem Belit-Zement. Silikattechn. 31 (1980) No. 6, pp. 168-171.

(17) Stark, J., Müller A., Schrader, R., and Rümpler, K.: Existenzbedingungen von hydraulisch aktivem Belit-Zement. Zement-Kalk-Gips 34 (1981) No. 9, pp. 476-481.

(18) Müller, A., Stark, J., and Rümpler, K.: Zum Stand der Entwicklung eines aktiven Belit-Zementes. Zement-Kalk-Gips 38 (1985) No. 6, pp. 303-304.

(19) Ghosh, S. N., Mathur, V. K., and Chopra, S. K.: Low temperature OPC-type cement containing superhydraulic C_2S-phase. Cem. Concr. Res. 14 (1984) No. 3, pp. 437-438.

(20) Sadran, G., and Dellyes, R.: Représentation linéaire de la résistance mécanique des ciments en fonction du temps. Application à la normalisation. Rev. Matér. (1966) No. 606, pp. 93-106.

(21) Rosemann, H.: Brennstoffenergiebedarf von Zementdrehofenanlagen mit Vorcalcinierung. Publication is being prepared.

(22) Mehta, P. K.: Investigations on energy-saving cements. World Cem. Technol. 11 (1980) No. 4, pp. 166-177.

(23) Sacharow, L. A.: Tonerde-Belitzement. Silikattechn. 22 (1971) No. 11, pp. 374-376.

(24) Zakharov, L. A.: Alumina-belite cement. 6. Intern. Congr. Chem. Cem., Moscow (1974), Sec. III-4.

(25) Viswanathan, V. N., Raina, S. J., and Chatterjee, A. K.: An explanatory investigation on Porsal Cement. World Cem. Technol. 9 (1978) No. 4, pp. 109-118.

(26) Raina, S. J., Viswanathan, V. N., and Chatterjee, A. K.: Der Hydratationsverlauf von Porsal-Zement. Zement-Kalk-Gips 31 (1978) No. 10, pp. 516-518.

(27) Mehta, P. K.: Energy, resources and the environment - a review of the US cement industry. World Cem. Technol. 9 (1978) No. 5, pp. 144-160.

(28) Mehta, P. K.: High iron oxide hydraulic cement. US Patent 4, 036, 657 (1977).

(29) Nudelman, B. J., et al: Verfahren zur Herstellung von Zementklinker aus einer chlorhaltigen Rohmischung. German Patent 27 22 635 (1977).

(30) Nudelman, B. J., et al: Rohmischung zur Herstellung von Zement. German Patent 27 22 641 (1977).

(31) Nudelman, B. J., et al: Zement und dessen Herstellungsverfahren. German Patent 27 22 642 (1977).

(32) Nudelman, B. J., et al: Verfahren zur Herstellung von Zement. German Patent 27 47 732 (1977).

(33) Ilyukhin, V. V., Nevsky, N. N., Bickbau, M. J., and Howie, R. A.: Crystal structure of alinite. Nature 269 (1977) No. 5627, pp. 397-398.

(34) Ilyukhin, V. V., Nevsky, N. N., Howie, R. A., Bickbau, M. J., and Below, N. V.: Crystal structure of alinite. Doklad. Akad. Nauk. URSS 237 (1977) No. 4, pp. 834-836.

(35) Noudelman, B., Bikbaou, M., Sventsitski, A., and Ilukhine, V.: Structure et propriêtê de l'alynite et du ciment d'alynite. 7. Intern. Congr. Chem. Cem., Paris (1980) Vol. III, pp. V 169 - V 174.

(36) Boikova, A.: Remarks on alinite (Contribution to the discussion). 7. Intern. Congr. Chem. Cem., Paris (1980) Vol. IV, pp. 44-45.

(37) Bikbaou, M.: Processus de formation des minêraux et composition de phase du clinker d'alinite. 7. Intern. Congr. Chem. Cem., Paris (1980) Vol. IV, pp. 371-376.

(38) Noudelman, B.: Fabrication de ciment d'alinite à basse température. Ciments, bêtons, platres, chaux (1982) No. 735, pp. 111-112.

(39) Author is not mentioned. Le ciment d'alinite, une innovation à confirmer. Ciments et Chaux (1982) No. 722, p. 21.

(40) Massazza, F., and Gillioli, C.: Contribution to the alinite knowledge. il Cemento 80 (1983) No. 2, pp. 101-106.

(41) Powers, T. C.: The physical structure and engineering properties of concrete. Portl. Cem. Assoc. Res. Dept. Bull 90 (1958).

(42) Locher, F. W.: Volumenänderungen bei der Zementerhärtung. Zement und Beton (1975) No. 85/86, pp. 22-25.

(43) Locher, F. W.: Die Festigkeit des Zements. beton 26 (1976) No. 7, pp. 247-249; No. 8, pp. 283-286.

(44) Schwiete, H. E., and Ludwig, U.: Über die Bestimmung der offenen Porosität im Zementstein. Tonind.-Ztg. 90 (1966) No. 12, pp. 562-574.

(45) Schwiete, H. E., Böhme, H. J., and Ludwig, U.: Messungen der Gasdiffusion zur Beurteilung der offenen Porosität von Mörteln und Betonen. Beton-Informationen (1968) No. 2, pp. 22-26.

(46) Schwiete, H. E., and Böhme, H. J.: Bestimmung der effektiven Porosität von Beton durch Gasdiffusionsmessungen. Zement-Kalk-Gips 23 (1970) No. 3, pp. 125-134.

THEME/THÈME 2

Hydration of clinker components individually and in cements.

Hydratation des composants du clinker et des ciments.

Chairman/Président:

G. Fronhsdorff
National Bureau of Standards
Gaithersburg, MD, U. S. A.

Secretary/Secrétaire:

P. J. M. Monteiro
Companhia de Cimento Portland
Paraiso
Rio de Janeiro, Brasil

SUB-THEME/SOUS-THÈME 2.1

Physical chemistry of hydration process, influence of minor components and admixtures.

Physico-chimie du processus d'hydratation; influence des éléments mineurs et des matières d'additions.

Chairman/Président:

A. M. Dmitriev
Institute Niicement
Moscow, U.S.S.R.

Principal Reporter/Rapporteur Principal:

H.F.W. Taylor
Department of Chemistry University of Aberdeen
Scotland, U. K.

A.M. DMITRIEV, NIICement, Moscou, URSS

CHIMIE PHYSIQUE DU PROCESSUS D'HYDRATION. INFLUENCE DES ELEMENTS MINEURS ET DES MATIERES D'ADDITIONS

L'hydration du ciment est un processus de l'interaction chimique entre le ciment et l'eau ayant comme résultat une structure assurant la résistance mécanique et les autres propriétés de la pierre de ciment.

La formation de structure est déterminée par des propriétés des phases hydratées et par des conditions de leur formation.

D'après les travaux de T.C. Powers, R. Brounjard, H.E.W. Taylor, A.V. Voljensky et autres, les propriétés du ciment durci dépendent essentiellement des propriétés physiques et physico-chimiques des liants et des hydrates se formant lors du durcissement.

La conaissance des aspects différents du processus de la formation de la structure de la pierre de ciment permettrait le contrôler et obtenir des matériaux à propriétés prédéterminées.

Dans l'ouvrage de J.P. Meric (1) il est noté que le béton n'a pas encore épuisé ses possibilités, c'est pourquoi le progrès considérable y peut être atteint. En tenant compte de cela le domaine de la chimie du ciment qui étudie des procédés de l'hydratation, doit occuper une situation prédominante dans les années à venir, car l'amélioration des propriétés techniques de la pierre de ciment ainsi que des bétons est liée avec l'action sur le processus de l'hydratation du ciment.

1. Influence des particularités de la morphologie, de la structure et de la composition des minéraux de clinker sur le processus de leur hydratation

1.1. Facteurs structuraux de la phase solide

Les années précédentes on a fait publier des ouvrages dans lesquels la structure était apréciée au niveau moléculaire et électronique, où on a attiré l'attention aux facteurs cristallochimiques (types de liaison chimique, leur longueur, des angles de valence, des nombres de coordination).

Ainsi, dans l'ouvrage (2) on propose d'utiliser en qualité de critérium de l'hydrolicité de la phase solide, le rapport des rayons ioniques de l'anion et du cation, la différence entre les négativités et le produit de ces valeurs. On a démontré que l'augmentation de la fraction de liaisons covalentes fait croître le taux de la polymérisation de la phase solide.

Dans certains cas, la rupture de liaison chimique dans la structure de la phase anhydre est probable en conséquence de la polarisation lors de l'interaction des phases solide et liquide.

On a établi (3) que dans les systèmes $CaO-Al_2O_3$, $CaO-SiO_2$, $CaO-P_2O_5$, $CaO-SO_3$, l'hydraulicité des phases solides diminue au fur et à mesure que le taux de covalence de la liaison E - O augmente. Ainsi, on fait apparaître la nécessité de l'analyse plus détaillée de la liaison chimique et son influence sur la réactivité de la phase solide.

L'aspect cristallochimique n'est pas moins important, il est développé dans les ouvrages de L.G. Chpynova et al., qui ont montré que le déficit d'électrons valents sur des atomes d'oxygène appartenant à la structure des combinaisons anhydres, favorise la réactivité hydraulique (4; 5). Il est bien connu que β-C_2S est une modification de la bélite à la plus basse réactivité. L'analyse de causes de ce phénomène a mis en évidence que l'anisotropie de liaisons énergétiques dans la structure de β-C_2S est minimum (169-206 kJ), et quant aux atomes d'oxygène, c'est la saturation complète des valences qu'y est propre, détermine ainsi l'inertie de la phase mentionnée.

Aussi, l'espèce de la structure électronique des phases anhydres a-t-elle ne grande importance parce que la présence et la distribution d'électrons dans les anions de celles-ci fait varier leur réactivité. L'un des mécanismes réels de l'interaction de la phase solide avec l'eau est celui de

donneur-accepteur. Le rôle de ligands est joué par les molécules d'eau, tandis que des anions de la phase solide ayant des orbitales vacantes au niveau extérieur sont des donneurs. Si on considère la structure électronique d'anions des phases actives à éléments du II période du tableau Mendéléev (aluminates, silicates, phosphates, sulphates de calcium), on voit ces anions avoir la quantité variable d'électrons inapparies ce qui mène à l'apparition de quantités variables d'orbitales vacantes sous l'action du champ de ligands, lesdites quantités diminuent de Al_4^{5-} à SO_4^{2-}. La réactivité hydraulique s'abaisse dans le même sens.

Il est à souligner encore un aspect cristallochimique du processus d'hydration. Il s'agit du caractère de combinaison des motifs principaux du réseau cristallin de la phase anhydre. Il est connu que l'augmentation de la température de cuisson de certains minéraux réactifs mène à l'abaissement de la vitesse de leur interaction à l'égard de l'eau (6). Il y arrive une amorphisation partielle de la structure, l'augmentation du taux de son interliaison pour le compte de l'apparition d'atomes-ponts d'oxygène dans la structure de la phase anhydre. Par exemple, en substitution aux liaisons Al(Fe) - O - Ca - O - Al(Fe) liant des motifs $Al(Fe)O_4$ et $Al(Fe)O_6$, on voit des liaisons Al(Fe) - O - Al(Fe) beaucoup plus covalentes et, par conséquence, plus fortes. Ce fait se traduit par ce qu'il se forme lors de l'hydration une grande énergie pour la polarisation et la rupture de ces liaisons influant sur la vitesse du processus de l'hydration.

Ainsi, l'aspect cristallochimique de l'hydration des liants mérite la plus grande attention et exige que des chimistes et des physiciens y prennent part.

1.2. Influence des impuretés des minéraux de clinker sur le processus de leur hydration

La réaction d'hydration de minéraux de clinker se déroule sur l'interphase "solide-solution de l'électrolyte". Le chargement de la surface de semi-conducteurs, y compris des minéraux de clinker, peut être contrôler en y introduisant des s-, p-, d- élements.

Il est universellement admis (7) que l'influence des éléments mineurs sur le processus d'hydration des minéraux n'est pas à un chiffre. Il arrive souvent que des résultats contradictoires ne laissent pas sûrement définir l'influence de telle ou autre impureté sur les propriétés des phases de clinkers. Les réactions d'hydration du ciment sont de n-type sur des semi-conducteurs (8), donc la distribution d'électrons selon les zones des semi-conducteurs et les valeurs de la zone interdite joue un rôle important. Comme il est connu, il est possible que les zones valentes et conductrices soient recouvertes ce qui a comme résultat une zone commune (comme dans les métaux) et les électrons reçoivent la possibilite de se déplacer dans les limites de cette zone. A son tour, ce fait favorise l'échange des électrons de cette phase avec les molécules d'eau ce qui mène à l'apparition de paires communes d'électrons, c'est-à-dire à la condensation du système. Ainsi, la contraction, par telle ou outre manière, de la largeur de la zone interdite active les minéraux de point de vue de leur interaction avec l'eau.

On montre dans les travaux (9; 10) que la concentration de défauts, l'énergie Fermi, la largeur de la zone interdite, la concentration de porteurs de charge peuvent évidement servir d'objets de contrôle des propriétés des systèmes liants. Ce point de vue est confirmé par les données du travail (11) dont les auteurs modifiaient C_2S à l'aide d'additions différentes. Dans les échantillons de C_2S modifié, on calculait la largeur de la zone interdite et déterminait la quantité de l'eau combinée chimiquement (Tableau).

Les résultats des recherches sur la réactivité hydraulique des minéraux de clin-

2.1

Tableau

Modificateur	Largeur de la zone interdite, eV	Quantité de l'eau combinée chimiquement, %			
		1j	3j	7j	28j
FeO	2,65	5,34	6,77	7,14	9,90
TiO_2	3,01	5,27	6,72	7,05	9,30
Fe_2O_3	3,19	0,78	3,08	4,33	6,61

ker montrent que la présence de l'addition-accepteur menant à l'apparition de vacances positives, c'est-à-dire au charge positif de la surface, a pour effet l'augmentation plus considérable de la réactivité par rapport à l'addition-donneur. Il s'en suit que les recherches dans le domaine de la chimie du processus de l'hydratation doivent être orientées sur la possibilité de l'activation de mineraux par les additions correspondantes. Il est aussi nécessaire d'étudier plus détaillement le chimisme des actes élementaires de l'interaction hétérogène sur la surface de la phase solide active en tenant compte de la composition ionique de l'eau.

1.3. Rôle des phénomènes superficiels dans le processus d'hydratation de minéraux de ciment

Dans le stade initial de l'hydratation, il se déroule la sorption de molécules H_2O sur les centres actifs de la surface. L'adsorption dissociative est une particularité de ce processus qui est accompagné par la variation considérable de pH dans les limites de la double couche électrique et par la formation d'un hydrocomplexe de calcium se dissolvant et par le passage de ce dernier dans la solution sous forme d'ions $CaOOH^-$ (12). Il s'en suit l'apparition d'un centre actif secondaire, c'est-à-dire d'un défaut dans la couche superficielle hydratée. On suppose que les élements structuraux principaux du film sont les suivants: $Ca(OH)^+$, $SiO_2(OH)^{2-}$, $SiO_3(OH)^{3-}$.

Cette considération laisse isoler 3 groupes de centre actifs (13): primaires, secondaires et"temporels" dont la provenance est dûe au défauts biographiques. Cette manière d'aborder le problème des positions des phénomènes électroniques dans la couche superficielle permet de tracer les voies de contrôle du processus d'hydratation.

Les questions de l'état de la surface du solide méritent d'être étudiées sérieusement, aussi que la régulation de ses propriétés par la variation du régime de la synthèse de la phase solide active.

La conception de phénomènes électroniques dans la couche superficielle lors de l'hydratation des liants (14; 15) mène à la nécessité de la considération de la théorie de la catalyse hétérogène pour comprendre le fond des processus d'hydratation.

Tenant compte du rôle considérable des centres actifs lors du processus d'hydratation, le nouveau domaine de recherches devient possible: introduction d'activateurs de durcissement ayant lesdits centres ou favorisant leur apparition. Par exemple, l'introduction de matériaux thermoactivés dans le système "ciment-eau" contribue à l'augmentation de la quantité de centres actifs superficiels et à l'accélération du processus d'hydratation (16). L'introduction dans le système en durcissement d'oxydants ou d'accepteurs d'électrons créant des centres positifs, accélère aussi le processus d'hydratation (17).

En liaison avec des conceptions ci-dessus citées, le rôle considérable des actes élementaires chimiques est mis en évidence, parce que se sont ces actes qui déterminent le mécanisme du procédé. A présent, des renseignements à ce sujet sont peu nombreux.

Dans l'ouvrage (18) les auteurs donnent une succession suivante des actes élementaires de l'interaction entre l'eau et C_3S: a) sorption de H_2O sur la surface de C_3S; b) chimisorption avec la formation de la liaison électrostatique Ca-OH; c) formation de OH à partir du proton de la molécule d'eau et d'ion d'oxygène de surface et

l'apparition de liaisons Ca ← OH, OH...OH; d) formation de germes C_3SH_x et $Ca(OH)_2$ sur les zones de dislocation de la surface.

Ainsi, il se produit une hydroxilation de la surface avec la formation de liaisons Si-OH et Ca-OH.

Les données analogiques sur l'hydratation de ß-C_2S sont présentées dans l'ouvrage (19).

En tout cas, la formation du groupe Si-OH est nécessaire, pour le compte du quel il se produit le procédé de polycondensation menant à l'apparition dans la structure de la pierre de ciment du réseau continu dû aux liaisons Si-O-Si. Il en résulte une tendance possible de recherches concernant la favorisation des liaisons Si-O-Si, l'introduction d'additions redistribuant l'entourage oxygéné de gros cations dans les structures de phase anhydre , ce qui laisse les tetraèdres SiO_4^- se réunir en diorthogroupes Si_2O_7 commensurables avec de octaèdres de calcium (20).

2. Rôle de la phase liquide dans le procéssus d'hydratation du ciment et de ses composants

2.1. Importance de la structure de l'eau

Jusqu'à présent, on attirait une attention insuffisante à la question des propriétés de la phase liquide.

Une particularité de la structure de l'eau consiste dans la présence des liaisons d'hydrogène assurant sa composition tetraédrique et l'agrégation des molécules H_2O.

Tenant compte de l'interaction donneur-accepteur lors d'hydratation des liants, ayant aussi en vue l'apparition de contacts de cohésion sur les centres actifs de la surface due aux liaisons d'hydrogène et donneur-accepteur, on doit conclure que l'association anomale des molécules de l'eau lors de la transition phasique à 50-55°C environ (21), diminue la dissolution de SiO_2 et CaO ce qui mène, selon Mayants M.M., à la formation de la structure à superficie spécifique basse (22). Pendant l'augmentation ultérieure de la température cette anomalie disparaît ce qui met en évidence le phénomène connu de l'accélération du processus d'hydratation dans les conditions hydrothermales.

Ayant en vue des données sur le procèssus d'hydratation des minéraux de ciment, il est à affornier que la structure de l'eau est un des facteurs pouvant être utilisé dans le contrôle de la vitesse du processus en l'influençant.

2.2. Rôle de la composition ionique de la phase liquide

L'introduction dans la phase liquide de différents électrolytes change fortement ses propriétés (24), ce qu'on utilise largement dans la production du béton.

Pourtant, il est à remarquer que dans la plus grande majorité de recherches des différents auteurs on ne trouve pas de l'information concernant le mécanisme de l'action des additions bien qu'il soit nécessaire d'y attirer une attention spéciale.

D'aprés son action, toutes les additions chimiques faisant partie de l'eau de gâchage peuvent être divisées en deux gros groupes: celles agissant avec de minéraux de clinker lors de l'hydratation et celles qui n'agissent pas mais changent leur solubilité. Les additions du 1er groupe réagissent avec $Ca(OH)_2$ en le mettant hors de réaction et déplaçant l'équilibre de dissolution incongruente de C_3S ou réagissent avec la phase alumineuse en accélérant la formation de l'ettringite et formant des complexes hydroalumineux.

Les additions du 2me groupe exercent une influence sur la structure de l'eau, favorisant sa destructuration ou, au contraire, renforçant la liaison des molécules dans les agrégats $(H_2O)_x$. Dans le premier cas la solubilité s'abaisse, dans le deuxième elle s'augmente. En même temps une série d'additions a un effet complexe.

A titre d'exemple de l'interprétation

2.1

differente des résultats obtenus pour la même addition il est utile d'examiner des données sur $CaCl_2$. Tous les chercheurs notent l'accélération de l'hydratation des silicates de calcium en présence de $CaCl_2$.

Dans le travail (24) on constate que $CaCl_2$ réagit avec $Ca(OH)_2$ et avec la phase hydroalumineuse formant des complexes, ce qui accélere la dissolution du liant de départ.

Ainsi, dans (25) il est nettement établi la formation de CSH dans une heure en présence de $CaCl_2$. Des résultats analogues sont expliqués dans l'ouvrage (26) par ce que les ions de Cl^- diffusent vite à travers une membrane osmotique faisant naître une surpression qui détruit ladite membrane et libèrent les surfaces de grains pour l'accès d'eau.

Selon les données de l'ouvrage (27), l'influence de $CaCl_2$ se traduit par la diminution de la solubilité du gypse, par l'augmentation de la sursaturation et intensification de la synthèse d'hydrosulfoaluminates de calcium, c'est-à-dire $CaCl_2$ exerce une influence sur la partie alumineuse du clinker et pas sur la partie siliceuse.

Le point de vue bien intéressant est présenté dans les ouvrages (28; 29) dont les auteurs comptent que l'introduction de $CaCl_2$ favorise l'intensification des procédés de polycondensation et de la formation des liaisons Si-O-Si dans la pierre de ciment.

Ainsi, il n'y a pas de clarté dans les problèmes du mécanisme de l'action d'additions sur le processus d'hydratation. Il en résulte la nécessité des recherches approfondies aux niveaux moléculaire et électronique. C'est pourquoi des recherches sur la structure de l'eau additionnée sont d'une grande actualité. La question est en ce que certaines additions favorisent la structuration de l'eau, les autres ont une action contraire. Il en résulte la différence des propriétés de la pierre de ciment avec additions car ces dernières en variant la structure de la phase liquide, varient le déroulement des processus chimiques colloïdes.

2.3. Rôle de pH dans le processus d'hydratation des liants

Comme on l'a déjà noté, la question de priorité de l'influence de telles ou autres particules d'eau (ions H_3O^+ ou OH^-) est bien litigieuse. Et, en même temps, il a une importance principale. Sa résolution peut influer sur la voie de contrôle des propriétés des surfaces.

Par exemple, si on traite en facteur décisif la protonisation de la surface de ciment par les ions H_3O^+ quand le ciment est gâché par des acides (pH < 4), il faut chercher à ce que les centres actifs sur la surface de la phase solide aient la charge négative, autrement dit il faut contrôler les propriétés de la phase solide en y introduisant des additions de type donneur.

Et, au contraire, l'avouement de la présence decisive d'ions OH^- (pH $> 10,5$) fait introduire dans la phase solide des additions de type accepteur qui charge négativement la surface. Les références pour le domaine pH = $5 \div 8$ sont bien contradictoires. Ainsi, le problème de pH dans le processus d'hydratation exige sa résolution ultérieure. Et, en même temps, en contrôlant pH du milieu de gâchage ou peut contrôler les propriétés physico-chimiques de la pierre de ciment (30).

2.4. Possibilités de l'activation de la phase liquide

Les propriétés de la phase liquide jouent un grand rôle dans l'hydratation, c'est pourquoi il faut suivre la voie de destructuration de l'eau en diminuant la quantité de liaisons hydrogéniques. Les moyens en peuvent être différents: introduction d'additions chimiques dans l'eau, son traitement magnétique, oultrasonique, le traitement par l'oxygène et, enfin, l'introduction de tensio-actifs ou d'enveloppes impolaires sur des particules de ciments.

Donc, nous avons bésoin de la théorie

qui expliquerait l'action des propriétés de l'eau sur l'hydratation, aussi que des méthodes du traitement de l'eau.

2.5. Rôle des phases liquides "extérieure" et "intérieure" dans la pierre de ciment

Lors du processus d'hydratation, dans les néoformations du ciment et sur la frontière de leur couche avec les grains initiaux du ciment, des couches intermédiaires aqueuses et des cavités apparaissent dans les zones intercouches des néoformations à structure lamellaire, ainsi que dans les cavités des fibres hydrosiliceuses (voir fig.) et dans la zone de passage du grain de ciment à la couche hydratée (selon A.E. Cheykin).

Ces zones de la phase liquide peuvent être traitées en "zones intérieures" car elles se trouvent à l'intérieur du volume des néoformations hydratées et sont liées au milieu extérieur à travers des membranes semi-conductrices composées de phases solides finement dispersées ou lamellaires.

La saturation en $Ca(OH)_2$ et en autres constituants de la phase liquide intérieure s'effectue apparément vite comme cela est montré en cas de systèmes - modèles (31).

Tout le reste du volume de la phase liquide formant, en particulier, des pores capillaires peut être nomé "phase extérieure."

Selon (32), la saturation de cette phase s'effectue pendant 45 min - 2 heures. Ce fait explique l'existence d'une période d'induction dans le processus d'hydratation et de formation de structure.

Il est à noter que dans les recherches (32) dont le développement est presenté également à ce Congrès, les mesures du taux de saturation s'effectuait à l'aide des électrodes sélectives pour CaO et Al_2O_3 directement dans la pierre de ciment sans en extraire la phase liquide, cette extraction perturberait considérablement la structure de la pierre et modifierait la composition

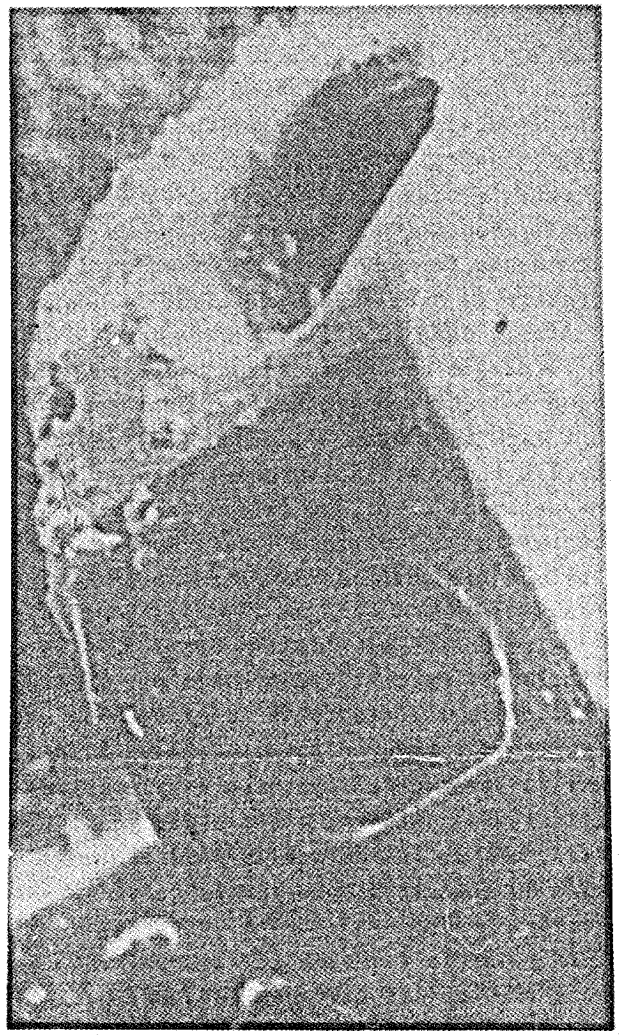

Fibres tubulaires de $C_6S_3H_n$ synthétisées dans l'autoclave

du liquide.

Des adjuvants introduits dans le clinker modifient dans une grande mesure tout d'abord des propriétés de la phase liquide intérieure, et ceux introduits dans l'eau de gâchage modifient des propriétés de la phase liquide extérieure.

Ce ne sont que des adjuvants tensioactifs et CO_2 de l'air qui exercent une influence égale sur les deux zones de la phase liquide. Ainsi, on a montré que des covités dans des fibres hydrosiliceuses l'existence desquelles a été prédites en 1957 par S. Brunauer (33) et observées par V. Timachev et al. (voir fig.), se cicatrisent

en présence de CO_2 de l'air (34) ce qui ralentit considérablement le processus d'hydratation.

Il a été montré (35) que la phase liquide intérieure est mobile dans la plus grande mesure dans les hydrosilicates et les hydroaluminates de calcium.

De plus, il existe des bases expérimentales pour conclure que la phase liquide intérieure de toutes les néoformations hydratées est un système interlié (36) dans lequel une mobilité des molécules dans une de ses parties augmente la mobilité du système tout entier.

Des considérations pareilles ont amené I.D. Birchall et al. (37) à conclure qu'une sousalimentation des fibres tubulaires des hydrosilicates et leur croissance sont effectuées et contrôlées de l'interieur qu'en cas d'organismes végétaux. C'est pourquoi, la croissance des néoformations peut être égalée aux "jardins siliceux".

Cette conclusion fait immédiatement lier les phases "interieure" et "extérieure" dans le système ciment - eau en vue d'activer le durcissement. En cas trivial, aux grands rapports E/C (>1) la liaison de telles zones de la phase liquide ne présente pas d'intérêt. En cas de basses valeurs de E/C (0,1-0,2) cette liaison par trituration dans un malaxeur spécial à deux cylindres a permit à Birchall et al (38) d'obtenir de nouveaux matériaux inorganiques à base de ciment (New Inorganical Materials - IM). Ces matériaux ont une résistance à traction et à flexion à un ordre plusélevée et celle à compession à 30-50% plus haute que des ciments ordinaires.

Ces travaux sont continués en URSS avec des autres systèmes analogiques, dont les résultats sont pareils

A présent ces recherches se développe activement, étant un premier résultat réel de la théorie de l'hydratation proprement dite, son application pratique.

Le problème consiste en interaction entre les parties inorganique, organique et aqueuse de ces nouveaux matériaux; cette interaction doit être optimisée ayant pour but de diminuer des pressions nécessaires pour mélanger et former. Evidement, il faudra apprendre à utiliser des analogies imprévues avec des matériaux biogènes pour comprendre comment peut-on distribuer le minimum de la matière organique à l'effet maximal pour la résistance du système de ciment.

Ainsi, toutes les données citées ci-dessus témoignent la nécessité de prendre en compte des interactions fines, c'est-à-dire des interactions aux niveaux moléculaires et électroniques.

Il faut aussi faire attention avant tout aux phénomènes superficiels, à la formation de complexes lors de l'hydratation, à l'électrophysique, aux procédés d'échange d'ions et catalytiques, dont l'étude doit être complexe et se baser sur les résultats récents de la chime et de la physique du corps solide, sur la théorie des solutions.

La connaissance des lois profondes du processus d'hydratation des liants met entre les mains des technologues un levier puissant. En l'utilisant, ils pourront contrôler le processus de la synthèse des phases anhydres et celui de leur hydratation et obtenir des matériaux à propriétés prédéterminées, y compris à propriétés uniques.

Bibliographie

1. J.P. Meric. Les ciments et les bétons d'aujourd'hui et de demain. Ciments, bétons, plâtres, Chaux. No. 752-1185.
2. Л.Б. Сватовская, М.М. Сычев. Проявление вяжущих свойств и особенности химической связи и структуры соединений.- Тр.5-го Всесоюзного научно-технического совещания по химии цемента. М., 1980, 140-142.
3. В.Е. Каушанский. Структурно-химическая характеристика элементов, образующих гидратационно ативные фазы.- Краткие тезисы докладов на УІ Всесоюзном науч-

но-техническом совещании по химии и технологии цемента. М., 1982, 38-43.

4. Л.Г. Шпынова, В.В. Илюхин, М.А. Саницкий. Кристаллохимические факторы гидратационной активности цементных минералов. - Доклады АН УССР, серия "Б", №2, 1983, 53-55.
5. Л.Г. Шпынова, М.А. Саницкий. Гидратационная ативность ферритов и алюмоферритов кальция.- Украинский хим. журнал, 1983, т.49, вып.11, 1138-1142
6. П.П. Гайджуров, Г.С. Зубарь, И.В. Уварова. Влияние температуры синтеза на процесс гидратации двухкальциевого феррита.- Известия ВУЗов. "Химия и химическая технология", 1982, 25, №9, 1124-1126.
7. А.И. Бойкова. Цементные минералы сложного состава.- "Химия силикатов и оксидов", Л.,1982, 255-274.
8. A.K. Chatterji, T.C. Phatak, K.D. Dharijal. Reaction bytwin Portland Cement Clinker and water. "Nature", v. 203, No. 4941, 1964, 138-139.
9. В.В. Тимашев, В.Г. Акимов и др. Влияние точечных дефектов на гидратационную активность твердых растворов двухкальциевого силиката с хромом.- Труды Московского химико-технологического института им. Д.И. Менделеева, 1980, №116, 106-109.
10. Л.И. Туркина, М.М. Сычев, Л.Г. Судакас, Связь электрических свойств цементных минералов с их активностью в вяжущих системах.- Журнал прикладной химии, 1981, 54, №6, 1315-1321.
11. М.М. Сычев. Роль электронных явлений при твердении цементов.- Цемент, 1984, №7, 10-13.
12. В.В. Данилов. О механизме гидратации в цементном тесте. VI Международный конг. по химии цемента,т.2,кн.1,73-74.
13. М.М. Сычев. Способ повышения активности клинкера и цемента."Цем-т",1985
14. P.W. Brown, J. Pommersheim, G. Frohnsdorff - A kinetic model for the hydration of tricalcium silicate. Cem. and Concr. Res., 1985, v. 15, 35-41.
15. В.П. Касперчик, В.С. Солдатов. Эффект "отравления" при гидратации трехкальциевого силиката, предварительно обработанного растворами нитроновых солей.- Докл. АН БССР,1984, 28, № 10, 908-910.
16. М.М. Сычев. Химическая активация твердения цементных и бетонных смесей отходами и горными породами.- Труды НИИцемента, 1982,№69, 25-31.
17. Л.Е. Сватовская, М.М. Сычев и др. Электронные явления при твердении цементных смесей.- "Цемент", 1980, №7, 6-8.
18. И.В. Кравченко, Г.М. Тарнаруцкий и др. Об элементарных актах гидратации C_3S . Сб."Гидратация и твердение вяжущих" Львов, 1981, 97-100.
19. D. Menetrier, I. Jawed, T.S. Sun, J. Skalny-Surface studies of hydrated β-C_2S - Cem. and Cancr. Res., 1980, 10; No. 3, 425-432.
20. В.Е. Каушанский. Роль свойств жидкой фазы в процессе гидратации вяжущих материалов.- Журнал прикл. химии, 1982, 55, №9, 1934-1940.
21. М.С. Мецик, В.Д. Переверзев. Известия ВУЗов, сер."Физика",№2,1964, 27.
22. М.М. Маянц. Исследование особенностей физико-химических процессов гидратации портландцемента в условиях тепловлажностной обработки до 100°С. Автореф. канд. диссертации,М., 1965.
23. R. Sierra. Reparation des differentes formes d'eau dans la structure des pâtes pures de C_3S et de ciment portland Bull. liai-s Lab. ponts et Chaussées, 1982, No. 117, 77-81, 132, 134, 136.
24. В.Б. Ратинов, Г.И. Розенберг. Добавки в бетон. М., 1973, 62-76.
25. J. Bensted. Early Hydration behaviour of portland cement in water, calcium

chloride and calcium formiate solutions. Part IV, Effects of intergrinding the calcium chloride and formiate. - Silicat., ing., 1980, 45, No. 3, 67-69.

26. N.B. Singh, P.N. Ojha - Effect of $CaCl_2$ on the hydration of tricalcium silicate - J. Mater. Sci., 1981, 16, No. 10, 2675-2681.
27. Е.Ф. Шаров. Анализ состава жидкой фазы портландцемента при его гидратации в присутствии хлористого кальция.- Изв. ВУЗов, Химия и хим.технология, 1982, 25, №3, 345-347.
28. F. Tamas, K. Kovacs, A. Sok, K. Sarkar, D.M. Roy- Effect of calcium chloride upon the oligomerisation of calcium silicates and cement. - Silicat, ing., 1979, 44, No. 9, 205-211.
29. С.И. Евтюхова, Е.П. Андреева. Влияние хлористого кальция на состав метастабильных растворов при гидратации двух- и трехкальциевого силикатов.- Коллоидный журнал, 1984, 44, №3, 442-449.
30. Г.С. Кальчик, Е.Н. Булатова и др. Ионизированная вода в технологии приготовления бетона.- Строит. материалы и конструкции, 1982,№3,30-31.
31. Dauble D.D. New development in understanding the chemistry of cement hydration. "Philosophical transactions of Royal Society"(London), 1983, v. A 310, No. 1, 53-66.
32. Кошмай А.С., Мчедлов-Петросян О.П. Электрохимическая интерпретация процесса схватывания цементных паст. "Цемент", 1980, №7, 4-5.
33. Brunauer S. Some questions of the Physic and the Chemistry of Cement Surface. II Internat. Congress Surface Activity. Proceeding, v. 2, London, HMSO, 1957, 17-35.
34. Батутина Л.С. Интенсификация твердения цемента предварительной гидратацией. Автореферат канд. диссертации, М., НИИцемент, 1984.
35. Габуда С.П. Связанная вода. Факты и гипотезы. Новосибирск,"Наука",1982,159
36. Kuznetzova T.V., Kravtchenko, I.V., Yudovich B.E. Dielectric Constant of Water and Differential Thermal Analysis of Cement Hydration Products. - Proceedings of 6-th International Conference for Thermal Analysis (ICTA-80), Boyreit (BRD), 1980, p. 338GL.
37. Birchall I.D., Howard A.I., Bailly I.E. On the hydration of Portland Cement. Proceedings of Royal Society (London), 1978, v. A 360, No. 1702, pp. 445-453.
38. Birchall I.D., Howand A.I., Kondell K. Flexrul Strengs and Porosity of Cements. "Nature", 1981, v. 289, No. 5796, 388--390.

H.F.W. Taylor, Department of Chemistry, University of Aberdeen,
Meston Walk, Old Aberdeen AB9 2UE, Scotland, United Kingdom

Chemistry of Cement Hydration

Chimie d'Hydratation du Ciment

SUMMARY: Recent advances in the chemistry of hydration of portland cement without extenders are critically reviewed under the following headings. 1, Introduction. 2, C-S-H gel: electron optical studies of composition, silicate anion structure, water content, density, thermal behaviour, structure at the nanometre level. 3, Other hydration products: AFm, AFt and hydrogarnet phases, hydration products of the ferrite phase, calcium hydroxide. 4, Quantitative phase determinations, mass balance, indirect determinations of C-S-H composition, volume fractions. 5, Microstructural development: early, middle and late periods of reaction. 6, Hydration reactions: aluminate and ferrite phases, action of gypsum, theories of the induction period, reaction mechanism in the late period. 7, Reactivities of clinker phases. 8, Solution compositions and equilibria: $CaO-SiO_2-H_2O$ system, aluminate and sulphate systems, pore solutions in cement pastes. 9, Admixtures: inorganic admixtures, organic retarders. 10, Kinetics and modelling of the hydration process.

SUMÁRIO: Avanços recentes na química de hidratação do cimento portland sem adições são revistos criticamente nas seguintes seções: 1. Introdução. 2. Gel do C-S-H: estudos eletro-ópticos da composição, estrutura iônica dos silicatos, conteúdo de água, densidade, comportamento térmico, estrutura ao nível nanômetro. 3. Outros produtos de hidratação: AFm, AFt e fase hydrogarnetos, produtos de hidratação da fase férrica, hidróxido de cálcio. 4. Determinações quantitativas das fases, balanço de massa, determinações indiretas da composição do C-S-H, frações volumétricos. 5. Desenvolvimento microestrutural: períodos iniciais, médios e finais da reação. 6. Reações de hidração: fases de aluminato e férricas, ação do gesso, teorias do período de indução, mecanismo de reação no período posterior. 7. Reatividades das fases do clínquer. 8. Composição e equilíbrio das soluções: o sistema $CaO-SiO_2-H_2O$, sistema de aluminatos e sulfatos, solução nos poros das pastas de cimento. 9. Aditivos: aditivos inorgânicos, retardadores orgânicos. 10. Cinética e modelo do processo de hidratação.

1 INTRODUCTION

This paper critically reviews investigations into the chemistry of cement hydration since the Paris Congress in 1980. The early sections deal with the products, excluding those formed during the first hours of reaction, and the later ones with reaction processes, including early products and effects of admixtures. Microstructural development is considered only to the extent needed to understand reaction mechanisms, as other aspects are dealt with in another Principal Report. Other topics omitted for the same reason include gel structure above the nanometre scale, pastes containing fly ash or other extenders, and effects of aggregates on hydration reactions or products. Investigations discussed relate to pastes with w:c ratios of 0.3 - 0.7 and hydrated at 15° - 25°C unless otherwise stated.

2 C-S-H GEL

2.1 ELECTRON-OPTICAL STUDIES OF COMPOSITION

2.1.1 TECHNIQUES: EPMA AND SEM MICROANALYSIS

The techniques of microanalysis with the electron probe (EPMA) or scanning electron microscope (SEM) differ from each other only in minor respects. In both cases, the electron beam is properly directed at a polished surface. The volume analyzed is 1 - 10 μm^3 and increases with the accelerating voltage. Analyses of fracture surfaces by this method are, except possibly under very special conditions, only semi quantitative (1) and will not be discussed. Interpretation of results for the C-S-H of cement or calcium silicate pastes is complicated by two effects. First, observed Ca/Si ratios increase with the accelerating voltage (2,3). Second, the spread of ratios in individual analyses for a given specimen and accelerating voltage is considerably greater than is found for more normal substances, such as anhydrous clinker phases; in a typical case, for the C-S-H of a C_3S paste, examined at 10 kV, the range of Ca/Si ratios was approximately 1.5 - 2.0, with a mean of 1.72 (3).

Rayment and Majumdar (2) considered that the increase in apparent Ca/Si ratio with accelerating voltage occurred because, as the latter increased, it became progressively more likely that the region analyzed would contain unreacted C_3S (in a paste of that compound), or CH, or both. They concluded that the best estimate of the true mean value was that obtained at the lowest possible voltage, which they considered to be 6 kV. Employing similar reasoning, Chatterji (4) and Chatterji and Thaulow (5) concluded that, for analyses at 15 kV, the best estimate of the true mean ratio was near to the bottom end of the observed range. Both these methods gave values of 1.4 - 1.6 for C_3S pastes.

EPMA and SEM analyses can give absolute contents of elements and not merely ratios; for a pure calcium silicate paste, if oxygen equivalent to the Ca and Si is added, the deficiency from 100 % should, in theory, be attributable to water. From data for pastes dried by heating or under reduced pressure, the H_2O/Ca ratio under the conditions of an electron optical analysis is most unlikely to exceed about 0.85; this corresponds to an anhydrous oxide total of 86 %. The observed totals are almost always less than this (2,3,6-9). Taylor and Newbury (3) found that the totals of individual analyses tended to increase with the Ca/Si ratios, from ca. 60 % at Ca/Si = 1.5 to ca. 80 % at Ca/Si = 1.9.

Taylor and Newbury (3) accepted the possibility that Ca/Si ratios above 1.5 in C_3S pastes arose from mixtures with C_3S or CH, but noted two objections to this hypothesis. First, the majority of indirect determinations of Ca/Si ratio (i.e., from the contents of CH and unreacted C_3S, if any) have given values of 1.7 - 1.8. Second, the existence of CH intimately mixed with the C-S-H has been convincingly demonstrated only in cement pastes of unusually low w:c ratio (10). Replying to a comment by Chatterji (11), they pointed out that admixture with phases of higher Ca/Si ratio was not the only possible source of error; more specifically, there could be errors tending to make the observed ratio low. Any effect that retarded the incident electrons and was not fully corrected for would do this, as it would decrease the output of Ca X-rays more than that of Si X-rays; the observed ratios would decrease with decreasing voltage, and low ratios would be associated with low totals. They considered it likely that some such effect operated, and that the true value of the mean Ca/Si ratio in C_3S pastes was 1.7 - 1.8, both higher and lower values in individual analyses being explainable as artifacts. Compositional variability on a sub micrometre scale was not excluded.

The transport of electrons through highly microporous materials, such as C-S-H gel, is not well understood, and various effects might cause unexpectedly great retardation of the incident beam. One arises from the possible presence in the pores of carbonaceous matter originating either from pump oil vapour or from organic liquids used in drying, sawing or polishing; at 6 kV, very little on or immediately below the surface would markedly lower the output of Ca X-rays. Internal charging is another possibility. The best compromise in voltage for analyses of pure calcium silicate pastes is probably 10 kV; for cement pastes, if heavier elements are being analyzed for, 15 kV may be preferable. The observed deficiencies in the totals are unlikely to be due solely to water. Further study of sources of error in EPMA or SEM analysis of such materials is needed.

2.1.2 TECHNIQUES: ANALYTICAL ELECTRON MICROSCOPY

In this method (AEM), the specimen is examined in transmission. The volume analyzed is much smaller than in EPMA or SEM analysis and is not primarily affected by the accelerating voltage. The specimen thickness must not exceed 20 to 30 nm; this can be achieved by grinding and redispersing, or by ion thinning. All results yet reported for hydrated cements are for redispersed samples. The method gives atomic ratios, but it is normally impracticable to obtain absolute contents of elements.

Even wider variations in composition between individual analyses from the same specimen have been observed than in EPMA or SEM analyses, e.g., Ca/Si ratios of 1.2 - 2.0 for the C-S-H of C_3S pastes (12). Lachowski and Diamond (13) found such variations, not only between particles, but also between points ca. 2 μm apart, within particles. There has been some discussion of possible sources of error in the analysis of C-S-H gel and other cement hydration products by this method (11,14-17). Provided the (stringent) conditions for analysis are met, individual analyses are probably reliable, but the possibility of sampling errors cannot be ignored, because of the small size of the specimen (<< 1 μg) and the way in which it is isolated by grinding and redispersing. It is impossible to tell which part of the grosser microstructure a given particle comes from. Because of the extreme compositional variation, Lachowski and Diamond (13) concluded that earlier studies may have concentrated unduly on mean values, and the writer agrees. Attempts to prepare analyzable specimens by ion thinning have so far been rather discouraging,

and the method would not necessarily yield any more representative a sample, as the areas thinned are small and thinning may be selective.

2.1.3 RESULTS: CALCIUM SILICATE PASTES

For the C-S-H of C_3S pastes, recent EPMA and SEM analyses have given reported Ca/Si ratios of 1.5 - 2.0 (2-5,18). Taking into account the accelerating voltages used, and the possible sources of error discussed above, the most probable mean value appears on present evidence to be ca. 1.7. The only such analysis of a β-C_2S paste (3) gave a ratio of 1.78. The earlier AEM studies gave mean values of 1.43 - 1.66 for C_3S pastes (12,19) and 1.37 - 1.41 for β-C_2S pastes (20), but later work on C_3S pastes gave 1.7 - 1.8 (21). The earlier results are probably too low. The EPMA, SEM and AEM results together cover a range of w:s ratios, and hydration times from 1 day to 30 years, and neither of these variables appears to have any marked effect on the Ca/Si ratio.

2.1.4 RESULTS: CEMENT PASTES

EPMA and SEM analyses of the C-S-H in cement pastes have been reported (6-9,22,23). In some, distinction was made between "inner" and "outer" products, where "inner" product denotes either rims around partly reacted cement grains, or relicts of fully reacted grains, and "outer" product denotes material formed in what was originally water filled space. At the resolution available in X-ray microanalysis, it is probably impossible to distinguish outer product from inner product of the smaller cement grains, and "undesignated" product would be a better description. The inner product of alite and belite appears to be pure C-S-H; mean or median Ca/Si ratios of 1.7 (6,8, 22), 1.7 - 2.0 (7) and 1.9 - 2.0 (9), and a bimodal distribution with centroids at 1.75 and 1.95 (23), have been reported for it. Ratios of other elements to Ca found for this product have been: Na, ca. 0.01; Mg, 0.01 - 0.08; Al, 0.04 - 0.08; S, 0.01 - 0.03; K, 0.01 - 0.02; Fe, 0.01 - 0.03 (6-9,23). The pastes to which the above data refer were made from cements of various compositions, at w:c ratios of 0.3 - 0.6, and hydrated for times from 3 days to 23 years. Taken as a whole, the results suggest that the composition does not vary greatly with either time or w:c ratio within these limits, apart from a possible decrease with time in the S/Ca ratio. The composition probably depends to some extent on that of the cement, or perhaps more directly on that of the alite and belite it contains. This is especially true of the Mg/Ca ratio, which appears to reflect that of the alite, and in turn, that of the cement.

Rayment and Majumdar (7) could distinguish inner and outer products only in cements containing unreacted alite. In cases where distinction was possible, the outer or undesignated product had a mean Ca/Si ratio of 2.6 - 2.7, and Al/Ca and S/Ca ratios higher than those of the inner product. The authors regarded the outer product as C-S-H, and, noting that the (Ca + Mg)/(Si + Al + S + Fe) ratio was less variable than the Ca/Si ratio, concluded that Mg could replace Ca and that Al, S and Fe could replace Si in the C-S-H structure. By using X-ray images, Taylor and Newbury (8) distinguished inner and outer products in an essentially fully reacted, 23 year old paste. They obtained results similar to those of Rayment and Majumdar (7), but interpreted them differently. Plotting (Al + Fe)/Ca ratios against Si/Ca ratios for individual analyses, they noted that the great majority of points lay within a triangle whose apices represented the compositions of C-S-H, CH and hydrogarnet, which was the principal hydrated aluminate phase (Fig. 1). They concluded that points not lying near the corners of this triangle represented mixtures. Harrisson et al. (9) obtained similar results for younger pastes, in which the major hydrated aluminate phase was AFm. Neither of the last two investigations indicated that the inner and outer product C-S-H differ in Ca/Si ratio if the presence of other phases in the outer product is allowed for. There were indications that they differ in contents of minor elements; notably, Mg appears to be low or absent in the outer product.

AEM analyses of C-S-H from cement pastes have given somewhat erratic results for the mean Ca/Si ratio, values of which have ranged from 1.4 to 2.7 (13,19,24, 25). An early observation that this ratio decreases markedly with time (19) was not confirmed in later work (25). A comparison study of EPMA and SEM results for the same pastes gave good agreement between the two methods, with mean Ca/Si ratios by AEM of 1.75 - 1.85 (23). The ratios of minor elements to Ca, for which data were first obtained by AEM (24), agree reasonably well with those found from EPMA and SEM analyses. As with the C-S-H of calcium silicate pastes, the mean Ca/Si ratios are of uncertain reliability, and values below about 1.7 are probably incorrect. The results of individual analyses may be more significant.

Lachowski and Diamond (13), studying compositional variation within particles at the micrometre level by AEM, reported Ca/Si ratios varying locally between 0.89 and just over 3. Ratios of other elements to Ca also varied widely, and, in agreement with Rayment and Majumdar (7), the authors found the ratio of (Ca + Mg) to (Si + Al + S + Fe) less variable than that of Ca to Si. Examination of their individual analyses shows that the higher Ca/Si ratios, where not attributable to presence of CH, are usually associated with high Al/Ca and S/Ca ratios. As with the EPMA and SEM results described earlier, these compositions probably arise from mixtures of C-S-H with AFm phase, supporting the conclusion that this can occur at or below a micrometre level. Both C-S-H and AFm phase have layer structures, and a close mixture within the gel is structurally reasonable.

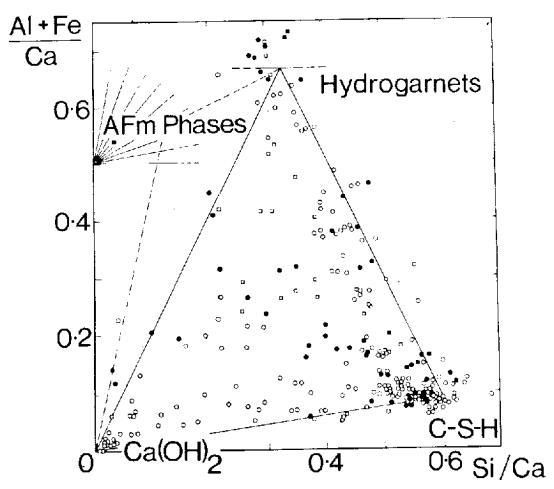

Fig. 1. Results of SEM microanalyses for a 23-year old cement paste (8).
Open circles: Mg/Ca < 0.20, S/Ca < 0.04.
Filled circles: Mg/Ca < 0.20, S/Ca ⩾ 0.04.
Open squares: Mg/Ca ⩾ 0.20, S/Ca < 0.04.
Filled squares: Mg/Ca ⩾ 0.20, S/Ca ⩾ 0.04.

2.2 SILICATE ANION STRUCTURE

2.2.1 NATURE OF THE ANIONS

By the time of the Paris Congress, a number of conclusions about the silicate anions in C_3S pastes appeared to have been established, based largely on results of trimethylsilylation (TMS) studies. The contents of monomer (SiO_4) were largely or wholly attributable to unreacted C_3S. The C-S-H contained substantial amounts of dimer (Si_2O_7) and of larger species, collectively if loosely called polymer, but little or no trimer or cyclic tetramer. The average anion size increased with time. Some information existed about the nature of the polymeric ions, based largely on gel permeation chromatography (GPC) of their TMS derivatives; at all ages, the most important single component was a relatively small one, possibly a tetramer or pentamer, but the precise nature of these ions was not established. For cement pastes, the data were less detailed. In general, the position appeared similar to that for C_3S pastes, but there were indications that the hydration products included monomer and that the proportion of the Si present in polymeric ions was less than for comparable C_3S or β-C_2S pastes.

Several subsequent studies have dealt primarily with TMS techniques (26-29). Dent Glasser et al. (29) examined the TMS derivatives of the C-S-H of cement pastes by high pressure liquid chromatography, thin layer chromatography, mass spectrometry and IR spectrometry. The results showed that the major low molecular weight anion larger than dimer was linear pentamer (Si_5O_{16}). Various larger species were found, but could have been artifacts.

A major advance has come from the use of ^{29}Si NMR (30-33), which complements the TMS approach in two respects. First, it is a purely physical method, in which there is no possibility of altering the anion structure through chemical side reaction. Second, it gives slightly different information, relating directly, not to the specific anions present, but to the environments of the Si atoms. The terms Q^0, $Q^1 \ldots Q^4$ denote the connectivites of the silicate tetrahedra, i.e., the numbers of other such tetrahedra with which they share oxygen atoms. For C_3S and cement alike, the results showed that, after a few hours, the content of Q^0 begins to decrease, and that Q^1 begins to form, accompanied later by Q^2; neither Q^3 nor Q^4 has been detected. Q^0 can only be monomer, Q^1 without Q^2, Q^3 or Q^4 can only be dimer, and Q^1 plus Q^2 in the absence of Q^3 and Q^4 can only occur in single chains, possibly including dimer, or in a mixture of these with single rings. Most importantly, the absence of Q^3 and Q^4 shows that three dimensional clusters or other highly connected species are absent. Clayden et al. (32) found high correlations between estimates of the degree of hydration from the relative intensities of the Q^0 and Q^1 peaks in the NMR spectrum, the amount of CH, and the cumulative heat evolution.

These results made possible a more detailed interpretation of the results of TMS/GPC studies. For alite pastes, Hirljac et al. (34) showed that the chromatograms could be accounted for if the major species in the C-S-H were dimer, linear pentamer, and linear octamer; at late ages, especially in pastes cured much above room temperature (65° - 70°C), larger species were also present. This suggests that the anions in the C-S-H of C_3S pastes are chains with 2, 5, 8...(3n-1) tetrahedra.

Data for cement pastes continue to be less detailed than those for C_3S or alite pastes, but recent studies (35,36) confirm that the silicate anions are closely similar to those in C_3S pastes. The similarity between the GPC curves for the TMS derivatives shows that the sequences of anion sizes are the same, at least from dimer upwards. So far as either the TMS or the NMR method is concerned, atoms replacing Si are not parts of the anion. It follows that, if other atoms replace Si, they can not do so at all of the Si sites, as this would cause the purely silicate parts of the chain to include sections not belonging to the (3n-1) series. Substitution permissible only in every third site is not excluded.

Another interpretation of TMS results has recently been proposed (37), involving formation of three dimensional cluster ions. This is incompatible with both the NMR evidence (30-33) and the observed mean connectivities of 1.6 - 2.0 that have been found by the TMS method for the polymer ions (35,36). If derivatives of such anions are formed, they presumably result from side reactions.

Opinions have differed as to whether the hydration products contain monomer, for both C_3S and cement pastes. Stade et al. (38) concluded that the C_3S hydration product contained substantial amounts, even after 28 days at ordinary temperature. In contrast, several groups of workers using TMS have concluded that, for C_3S or alite pastes, the amounts of monomer found could be largely or wholly attributed to unreacted starting material (34,35 39,40). Wu et al. (39) considered that the monomer content could be used to determine the degree of hydration. Neither TMS nor molybdate methods are sufficiently accurate to show whether monomer is completely absent in the products, especially at low degrees of hydration. Cross polarization NMR, which can distinguish between Si atoms near to H atoms and ones that are not, shows that, in C_3S pastes, the product formed up to the end of the induction period contains only monomeric silicate, and that dimer begins to form only after the induction period is over; large amounts of monomer are never present in the product (33).

2.2.2 QUANTITATIVE STUDIES

Detailed, quantitative interpretation of TMS results is rendered somewhat uncertain by the fact that total recoveries of Si are typically only 80 - 90 %, and because it is probably impossible to completely eliminate interconversion of anionic species through side reactions. For tricalcium silicate or alite pastes hydrated for 28 days at 20° - 25°C, estimates of the fractions of the total Si recovered, based on results of several TMS studies (35,36,41), are: monomer, 0.25 - 0.30; dimer, 0.30 - 0.45; polymer ($\geqslant$ 5 Si), 0.15 - 0.25. Corresponding data for 180 days are: monomer, 0.10 - 0.15; dimer, 0.40 - 0.60; polymer, 0.25 - 0.35. Another investigation (34) gave similar results for dimer and polymer, but higher ones for monomer (0.44 at 28 days, 0.32 at 180 days). The amount of dimer passes through a maximum at about 180 days, but even after 30 years, this species accounts for about 40 % of the total Si (35). A study using the molybdate method for times up to 28 days gave relatively larger amounts of polymer (38).

The amounts of different anionic species within the polymer have been determined, from GPC of the TMS derivatives. For alite pastes, Hirljac et al. (34) found that pentamer accounted for about 75 % of the Si in the polymeric ions at 7 days, 60 % at 28 days, and 45 % at 180 days. At ordinary temperatures, anions containing more than 11 Si atoms were formed in appreciable quantities only after 1 year. Mohan and Taylor (35) and Uchikawa and Furuta (41) gave

results as number average and weight average sizes, which appear to indicate somewhat higher proportions of the larger species. After 22 years, the proportions of these species are considerable, but pentamer is still an important component (35).

Results for cement are not very different from those for C_3S. Massazza and Testolin (36) found that the amount of Si present as polymer relative to that present as dimer increases less rapidly in cement than in C_3S pastes. For a 28 day old cement paste, they recovered about 36 % of the total Si as dimer and 20 % as polymer; for a corresponding C_3S paste, the respective values were about 31 % and 26 %. In cement pastes, the amounts of Si present as dimer and as polymer are about equal at 1 year (35,36). β-C_2S pastes have also been studied (36,42).

2.2.3 EFFECTS OF TEMPERATURE AND OTHER VARIABLES

The rate of polymerization increases markedly with temperature (34,38,43). For an alite paste hydrated for 100 days at 5°C, Hirljac et al. (34) recovered about 53 % of the total Si as dimer and 15 % as polymer. At 25°C, the corresponding recoveries were dimer, 42 %, and polymer, 24 %, while at 65°C, they were dimer, 34 % and polymer, 31 %. The distribution within the polymer is also markedly displaced to larger sizes with increase in temperature. Comparison of the TMS/GPC results for alite pastes hydrated for 1 year at 65°C (34) with those of pastes hydrated for up to 30 years at ordinary temperatures (35) suggests that the ultimate distribution of anion size may not vary greatly with temperature in the 5°C - 65°C range for which data are available.

The effects of accelerators and retarders have been studied. Changes in the nature of the products have been claimed (44), but neither Hirljac et al. (34), using TMS, nor Clayden et al. (31), using NMR, could find any effect other than that on the rate of reaction. Prolonged drying, and change in w:c ratio, are reported to have only minor effects on the course of polymerization (45). Polymerization is reported to be increased if the paste is heated before being loaded mechanically, while loading itself is reported to increase polymerization in young specimens and to decrease it in mature specimens (46).

2.3 WATER CONTENT, DENSITY AND THERMAL BEHAVIOUR

2.3.1 GENERAL

The literature shows some confusion regarding the density of C-S-H gel, and also regarding the porosity, which is a closely related quantity. The following considerations are relevant.

First, the density depends on the water content, which in turn depends on how the specimen has been equilibrated or dried. For any meaningful discussion of density in relation to structure at a chemical level, it is essential to know the total water content of the material in the state to which the density value relates. By "total water content" is meant the total amount of water lost up to ca. 1000°C, corrected for contributions from other phases. So long as this point is recognized, a wide range of density values can be equally meaningful for the same sample. Data in the literature, beginning with those of Powers and Brownyard (47) and of Feldman (48), indicate densities of C-S-H gel, corrected for other phases, in the region of 1900 - 2000 kg m^{-3} for saturated material, 2300 - 2400 kg m^{-3} for material equilibrated at 11 % rh, and 2500 - 2700 kg m^{-3} for material dried at 110°C or D-dried. The corresponding H_2O/Ca ratios, similarly corrected, are approximately 2.3 - 2.5, 1.3 - 1.4, and 0.8 - 0.9, respectively.

Second, the density of a solid material is a meaningful concept only to the extent that there is a sufficiently well defined boundary between it and the surrounding medium. Any fluid (liquid or gas) in which the solid is immersed in order to measure the density must itself be of known and uniform density, penetrate at all points up to but not beyond the boundary, and not alter the solid volume of the material when brought into contact with it. These conditions are normally easily met for non porous, solid bodies of macroscopic dimensions, but for a material such as C-S-H gel, the position is more complex. Atoms do not have sharp boundaries; if this cannot be ignored, the density may depend on the properties of the surrounding medium, and the densities of separated layers may differ from those of the same layers in contact with each other. These considerations are especially relevant to C-S-H gel that has been dried at humidities below about 11 % rh, or at temperatures much above ambient, and may explain observations that observed values depend on the fluid used to determine them.

2.3.2 NEW DETERMINATIONS

Relis and Soroka (49) reported that the densities of cement hydration products increased with the degree of hydration; for a typical cement, values of ca. 2550 kg m^{-3} at 20 % hydration and 2650 kg m^{-3} at 40 % hydration were obtained, and by extrapolation, a value of 2720 kg m^{-3} for complete hydration was suggested. There was discussion as to the validity of these conclusions (50).

Feldman and Ramachandran (51) determined the densities of mature cement pastes from which the CH had been leached. Using He on pastes that had been equilibrated at 11 % rh, and allowing time for the gas to flow in, a value of 2350 kg m^{-3}, uncorrected for other phases, was obtained. Data were also obtained for pastes that had been further dried. The results showed that removal of the CH did not alter the properties of the C-S-H, but that with further leaching, the structure was partly destroyed.

Juhász (52) followed changes in dielectric constant and other properties of pastes heated at temperatures up to 1000°C as a method of studying water binding. Parrott et al. (53) reported a study of alite pastes that included density and TG determinations. For pastes that had been treated with methanol to replace the pore water and then dried over silica gel, the density, corrected for other phases, was 2375 kg m^{-3}. It did not change with hydration time between 1 and 203 days. "Bound water", defined as that lost on TG between 100°C and 750°C, was 0.235 g per g of C_3S for a fully reacted paste; this value is not corrected for CH. The authors found 0.39 g of CH to be formed per g of C_3S on complete reaction. These data imply that the C-S-H has a Ca/Si ratio of 1.8 and an H_2O/Ca ratio of 1.0; its water content can also be expressed as 0.14 g per g of tricalcium silicate reacted. It was also found that the loss on TG at 100°C to 200°C was proportional to that at 200°C to 400°C throughout hydration, providing further evidence that the product does not change. The 100°C to 200°C loss was about 15 % greater than that at 200°C to 400°C.

Taylor (54) and Taylor et al. (25) calculated various quantities for cement pastes, including porosities and amounts and specific volumes of non evaporable and gel water, from estimates of quantitative phase composition. In order to obtain results agreeing with ones in the literature for broadly similar pastes, the following values for the density and water content of the C-S-H were assumed

in the later and more definitive work (25): Saturated conditions, density, 1950 kg m^{-3}, H_2O/Ca, 2.5; Equilibrated at 11 % rh, density, 2300 kg m^{-3}, H_2O/Ca, 1.4; Dried at 110°C, density, 2650 kg m^{-3}, H_2O/Ca, 0.85. A standard TG curve was given for the C-S-H gel. The data were expressed as molar ratios of H_2O retained in the C-S-H to Ca in the C-S-H for each of a series of temperatures, some typical values being 0.28 at 425°C (immediately below the CH step), 0.70 at 200°C, and 1.00 at 150°C. There were indications that the C-S-H in cement pastes retains some of its water on TG to higher temperatures than that of C_3S pastes, perhaps because substituents impede the crystallization of anhydrous phases. The results of Parrott et al. (53) appear to indicate a somewhat greater loss of water between 200°C and 400°C, but this could depend on the TG conditions used.

2.4 C-S-H AND RELATED PHASES FORMED OTHER THAN IN CEMENT OR CALCIUM SILICATE PASTES

Of the various studies reported, we shall consider only a few that are especially relevant to cement hydration. Some others, concerned chiefly with solution compositions or equilibria, are considered later.

Stade et al. (55,56) studied the incorporation of Al^{3+} and Fe^{3+} into C-S-H preparations made in suspension. NMR studies showed that preparations with Ca/Si ratios of 1.0 - 1.5 and Al/Si ratios of ca. 0.07 contained both tetrahedrally and octahedrally coordinated Al, the proportion of the latter increasing with Ca/Si ratio; at a ratio of 1.5, all the Al was octahedrally coordinated. Electron spin resonance and Mössbauer studies showed that Fe, which could be incorporated up to a level of at least 0.18 atoms per atom of Si, was almost all octahedrally coordinated. Neither Al nor Fe substitution had much effect on the distribution of silicate anion size, and it was concluded that these elements do not replace Si in the structure. As noted elsewhere in this review, there are indications that part of the AFm phase in cement pastes is closely mixed with the C-S-H. A similar explanation could perhaps account for the above results.

A new crystal structure determination of 1.1 nm tobermorite ($C_5S_6H_5$ approx.) is reported (57). The results confirm those of Megaw and Kelsey (58) and provide some additional detail. Jennite ($C_9S_6H_{11}$) has been synthesized in suspensions at 80°C from CH and either fumed silica, silica glass, or volcanic glass (59,60). An Al-bearing jennite was also prepared, which had slightly different cell parameters, behaved differently on heating, and was less crystalline.

2.5 C-S-H GEL STRUCTURE AT THE NANOMETRE LEVEL

The term "nanometre level" is preferred to "crystal structural level" because of the low degree of crystallinity. We shall assume that, at the coarser pore structural level, the structure is adequately described by the model of Feldman and Sereda (61), perhaps as modified by Daimon et al. (62). The question to be addressed concerns the nature of the individual layers. Early XRD work, reviewed by Bernal (63), indicated a layer structure and further suggested that this was closely related to that of 1.1 nm tobermorite. The name "tobermorite gel" was widely used for some years, but later rightly fell into disuse because of lack of evidence together with marked differences in composition, degree of crystallinity and silicate anion structure. Structural relationships to jennite were also suggested (64).

Recently, Taylor (65) has suggested that many properties of C-S-H gel can be accounted for if most of the layers are structurally imperfect ones of jennite, and a smaller proportion are similarly related to the more highly hydrated, 1.4 nm form of tobermorite ($C_5S_6H_9$). Both jennite and 1.4 nm tobermorite have structures that can be described in terms of alternating main layers and interlayers. The constitutional formula of 1.4 nm tobermorite, somewhat idealized, is $[Ca_4Si_6O_{18}H_2].Ca\ 8H_2O$, where square brackets enclose the contents of the main layer. The latter is based on a central, Ca-O sub layer, all the O atoms of which are shared with silicate chains of empirical formula Si_3O_9H. The constitutional formula of jennite, similarly expressed, is $[Ca_8Si_6O_{18}H_2(OH)_8].Ca\ 6H_2O$. The main layers are again based on central, Ca-O portions, but in this case only some of the O atoms are shared with Si_3O_9H chains, the rest being parts of OH groups. The layers differ sufficiently in structure that it is unlikely that one structure could merge into the other within a single layer, but layers of both types might well coexist within a poorly ordered structure.

Taylor (65) suggested that, in C-S-H gel, numerous silicate tetrahedra were missing from both types of layer, in a way that would fragment the chains into lengths containing 2,5,8...(3n-1) tetrahedra. In the tobermorite type layers, one third of the Si and an equivalent amount of O was missing, giving them the formula $Ca_5Si_4O_{14}H_2.8H_2O$; in the jennite type layers, up to one third was missing, giving the formula $Ca_9Si_{4+n}O_{14+2n}H_2(OH)_8.6H_2O$, where $0 \leq n \leq 2$. For each type of layer, it was possible to calculate the Ca/Si ratio for a given chain length (Fig. 2). A jennite type layer with an average chain length of 5 would have a Ca/Si ratio of 1.8; this is approximately that of C-S-H gel, and would account for the high proportion of pentamer formed in the material.

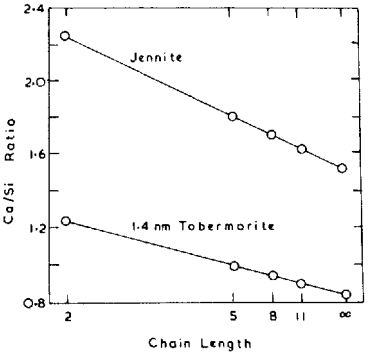

Fig. 2. Calculated Ca/Si ratio as a function of chain length in the jennite and tobermorite structures (65).

The evidence cited comprised conditions of formation, silicate anion structure, H_2O/Ca ratios and densities for three different drying conditions, TG curves, XRD pattern, selected area electron diffraction patterns, and the range of Ca/Si ratios observed in AEM analyses. The observed mean Ca/Si ratio of 1.7 - 2.0 could arise in various ways. At early ages, a mixture of tobermorite type and jennite type layers was formed, both with purely dimeric anions, and having Ca/Si ratios of 1.25 and 2.25, respectively. At later ages, jennite type layers containing larger anions, especially pentamer, became increasingly important. Since they contained fewer missing tetrahedra, these were thermodynamically more stable;

this could explain the occurrence of the polymerization process.

It was suggested that, in C-S-H gel equilibrated at 11 % rh, the layers had the H_2O/Ca ratios of jennite and 1.4 nm tobermorite. In material that had been dried at 110°C or D-dried, they were similarly related to the known dehydration products of these phases, namely metajennite ($C_9S_6H_7$) and 1.1 nm tobermorite. In saturated material, they had the H_2O/Ca ratios of jennite and 1.4 nm tobermorite, and the micropores described by Daimon et al. (62) and others were full of water. In each case, this explained the observed H_2O/Ca ratio and density. Attention was drawn to the early work of McConnell (66) on a naturally occurring C-S-H gel, known as plombierite; this had some close similarities to the material in cement pastes, including the H_2O/Ca ratio both under saturated conditions and at lower humidities.

Two other structures for C-S-H gel at the nanometre level have recently been proposed. Grudemo (67) suggested a structure, based on XRD evidence, closely related to that of CH. The silicate ions were separate tetrahedra, and the structure is thus incompatible with the TMS and NMR evidence. In a long series of papers, Shebl et al. (68) developed the hypothesis that the final product of hydration of C_3S or β-C_2S is 1.1 nm tobermorite, "identical with the natural and synthetic mineral." This conclusion was largely based on extraction experiments using a modified Franke solvent, supported by IR evidence. The CaO extracted was categorized as "free", "interlayer" and "bound"; for 1 mole of fully reacted C_3S, the amounts of these were 1.0, 0.5 and 0.67 moles, respectively. The conclusion that the product is identical with 1.1 nm tobermorite is untenable; it does not give a tobermorite XRD pattern, and differs in anion structure and other respects. Moreover, the work of Feldman and Ramachandran (51) shows that major damage to the structure occurs well before a Ca/Si ratio equal to that of tobermorite has been reached. The results, nevertheless, provide much data on the progressive breakdown of the C-S-H structure, and are of interest from this point of view.

3 OTHER HYDRATION PRODUCTS

3.1 AFm PHASES IN CEMENT PASTES

3.1.1 ELECTRON OPTICAL ANALYSES

The first electron optical analyses of AFm phases in cement pastes were obtained using AEM and were reported at the Paris Congress (69). Later studies by the same method (24,25) have given substantially similar results. Marked compositional variations between crystals from the same specimen were found; significant amounts of Si were present, and mean S/Ca ratios were well below that of monosulphate. The deficiencies in sulphate were not compensated by the contents of silicate, and it was assumed that some of the interlayer anion sites were occupied by hydroxide; hydroxoaluminate was also believed to be present, to an extent that increased as hydration proceeded. These substitutions are equivalent to solid solution with C_4AH_X and C_2AH_X, respectively.

Harrisson et al. (9) have reported SEM microanalyses of AFm phases in cement pastes elsewhere in these Proceedings. In pure portland cement pastes, regions of AFm phase free from other phases had, typically, Al/Ca ratios near 0.5 and Si/Ca ratios near 0.05. S/Ca was rather variable and, most commonly, 0.10 - 0.15. They were low in other elements, including Fe. AFm phase closely mixed with C-S-H, occurring in the outer product, was similar in composition to the above, but tended to have a higher S/Ca ratio, which was sometimes as high as 0.25, the theoretical value for monosulphate. In a very few cases, AFm phase containing little or no S was found. There was no positive evidence that any of the AFm phase contained much Fe, or that its Al/Ca ratio deviated far from 0.5, the latter indicating that little or no hydroxoaluminate was present in the interlayer sites. As noted earlier, some of Rayment and Majumdar's results (7) of outer product can also be interpreted as being of mixtures of C-S-H with AFm phase, and this is also true of some AEM analyses, which relate to much smaller volumes of material.

3.1.2 COMPARISON WITH XRD AND IR EVIDENCE

XRD evidence, beginning with that of Copeland et al. (70), shows that typical cement pastes more than a few days old, that have not been strongly dried and that have been protected from carbon dioxide before and during examination, give peaks corresponding to AFm phases with layer thicknesses of approximately 0.89 nm and 0.78 nm. Several studies on the pure C-A-$\bar{S}$-H system have shown that a miscibility gap exists in the C_4AH_n-$C_4A\bar{S}H_n$ series: Roberts (71) concluded that it extended from S/Ca = 0 to S/Ca = 0.125, and reported layer thicknesses for the solid solution varying from 0.877 nm at S/Ca = 0.125 to 0.896 nm at S/Ca = 0.25 (monosulphate). Substantial replacement of the SO_4 in monosulphate by 2 OH can thus occur with only minor effect on the layer thickness. Substitution of silicate for sulphate probably has little effect on the layer thickness (72). The peak at 0.78 nm can reasonably be assigned to C_4AH_X; this assignment is supported by the fact that mild attack by CO_2 causes a peak at about 0.82 nm to appear. The XRD evidence thus indicates the presence in typical portland cement pastes of two kinds of AFm phase, one of which is C_4AH_n, and the other having a S/Ca ratio that could be anywhere between 0.125 and 0.25, with possible partial replacement of sulphate by silicate.

From IR evidence, Bensted (73) concluded that the AFm phase in cement pastes differed from pure monosulphate. It was less crystalline, and its sulphate content decreased as hydration proceeded.

The SEM analytical results (9) are, in the main, compatible with these results. If replacement of sulphate by silicate is assumed, the compositions mostly fall into the range that would be expected to give an X-ray peak at about 0.89 nm. One might, however, have expected to have found more particles containing little or no S, to account for the peak at 0.78 nm. The close admixture of much of the AFm phase with C-S-H could well explain the IR evidence of poor crystallinity.

It is more difficult to reconcile some of the AEM results with the other evidence. This applies most strongly to those analyses giving Al/Ca ratios well above 0.5, which imply presence of interlayer hydroxoaluminate, and to the finding by AEM of occasional crystals relatively high in Fe. As with AEM analyses of C-S-H, the individual analyses may be valid, but sampling may present a serious problem, and the significance of mean ratios found by this method must be considered uncertain.

3.2 AFt AND HYDROGARNET PHASES IN CEMENT PASTES

The electron optical analysis of AFt phases is especially difficult because of the ease with which decomposition and probable loss of material occur in the electron beam. As with the AFm phases, AEM analyses were reported at the Paris Congress (69); they indicated compositions significantly different

from that of ettringite, notably in showing lower S/Ca ratios and significant contents of Si. Later studies by the same method have given broadly similar results (24,25,74); the most recent (74) showed that deficiencies in both S and Al were common, but were usually though not always balanced by Si. Fe/Ca ratios were usually below 0.01. No EPMA or SEM analyses have been reported. Bensted (73) concluded from IR evidence that the AFt phase in cement pastes, like the AFm phase, was relatively poorly crystalline.

Taylor and Newbury (8) reported EPMA analyses of the hydrogarnet which was the principal hydrated aluminate phase in a 23 year old cement paste. The mean composition was near to $Ca_3Al_{1.2}Fe_{0.8}SiO_{12}H_8$, but Mg was also present, and it was not clear how much, if any, was in the hydrogarnet. This composition is near to that suggested by Copeland et al. (70) from XRD evidence.

3.3 AFm, AFt AND HYDROGARNET PHASES FORMED OTHER THAN IN CEMENT PASTES

As with C-S-H, we shall only consider studies that are particularly relevant to cement hydration; some dealing mainly with solution compositions or equilibria will be discussed later. Fischer and Kuzel (75) reexamined phases in the system C_4AH_n-$C_4A\bar{C}H_n$ system, using single crystal and powder XRD. The phases were:

C_4AH_n with n = 19 (2 polytypes), 13, 11 and 7;

$C_4A\bar{C}_{0.5}H_n$ with n = 12, 11.25, 10.5, and 6.5;

$C_4A\bar{C}H_n$ with n = 11, 9 - 9.95, and 6.

C_4AH_{13} was shown to have a 12-layer structure and its unit cell was determined. New XRD, thermal and IR data were given for many of the phases. Fischer et al. (76) described two naturally occurring specimens of hydrocalumite.

Gessner et al. (77) studied C_2AH_8 by NMR; they found that all the Al was octahedrally coordinated. This does not support the interlayer anion structure proposed by Scheller and Kuzel (78), and the constitution $[Ca_2Al(OH)_6][Al(OH)_3(H_2O)_3]OH$ was suggested. An AFm phase containing sulphite was described (79), but an attempt to prepare one containing sulphide was unsuccessful, though a compound with S/Ca = 2 was obtained (80).

Several studies on the formation, stability or thermal dehydration and rehydration of ettringite have been reported (81-83). Others, dealing mainly with ettringite morphology or with the possible existence of amorphous or quasi crystalline precursors to AFm or AFt phases, are considered later. Other studies on AFt phases concern refinement of the thaumasite crystal structure (84,85), thermal decomposition of thaumasite (86) and naturally occurring AFt phases containing Cr(III) or borate (87-89). Among studies on hydrogarnets (90-93) is one that includes a crystal structure refinement and a formula relating cell parameter to composition (91). Murat (94) reviewed thermal properties (mainly DTA) of hydrated calcium aluminate phases.

3.4 HYDRATION PRODUCTS OF THE FERRITE PHASE

Uncertainty persists as to the hydration products of the ferrite phase in cement pastes. Copeland et al. (70) concluded from careful XRD studies that it yielded a hydrogarnet phase, but subsequent XRD studies on pastes of other cements do not appear to have shown this, except with cements hydrated for long times or at elevated temperatures. In agreement with several earlier workers, Teoreanu et al. (95) found that hydration of C_4AF or C_2F by itself gave an iron hydroxide, together with AFm and hydrogarnet phases. Fortune and Coey (96) similarly concluded from a Mössbauer and XRD study that hydration of C_4AF by itself at 72°C gave a hydrogarnet and an FH_x gel, the latter giving a weak, broad X-ray band centred at 0.44 nm. Relatively little of the iron entered the hydrogarnet, and none at all if gypsum was present. In contrast, Harchand et al. (97,98) concluded from Mössbauer and IR studies on cement pastes that no FH_x gel was formed, and that the Fe entered the AFm phase. Bensted (99) agreed, and considered it unlikely that FH_x would form in presence of CH. Evidence from X-ray images in the SEM indicates that, when the interstitial phases hydrate, the Fe does not migrate away from the resulting relicts (8), and this conclusion is supported by results at higher resolution obtained from backscattered electron images (100). Mass balance calculations suggest that the amounts of Fe present in the AFm phase and C-S-H are insufficient to account for all the Fe supplied by the clinker phases that have reacted (25). SEM microanalyses of pastes by Harrisson et al. (9) showed no regions high in Fe that were not also high in Ca, Al, Si and, sometimes also, in Mg, and could be interpreted as indicating that the Fe was present in a separate phase that was mixed at or below the micrometre scale with C-S-H, AFm phase low in Fe and, sometimes, a phase high in Mg. Several other studies have been reported (101-103).

The problem is not solved, though the balance of the existing evidence seems to favour the view that, when the ferrite phase hydrates in a cement, the space it occupied is filled with a close mixture of C-S-H, AFm phase low in Fe, a hydrated phase high in Fe, and often, another one high in Mg. Such a mixture can have a bulk composition quite close to that of the hydrogarnet that has sometimes been found (8,70), which could thus readily form from or instead of it under favourable conditions. More work is, however, needed. Studies on C_4AF by itself are only of background relevance, even if CH and gypsum are added, because the ferrite phase in cement is normally closely mixed with aluminate phase, hydrates in an environment dominated by the silicate phases, and has a composition that is not even close to the C_2A-C_2F series, but is typically near to $Ca_2AlFe_{0.6}Mg_{0.2}Si_{0.15}Ti_{0.05}O_5$ (104). X-ray microanalysis in the EPMA or SEM probably does not give sufficient resolution, but backscattered electron imaging may provide further useful data.

3.5 CALCIUM HYDROXIDE

The existence, or otherwise, of amorphous or cryptocrystalline CH has received attention. Marchese (105) could detect CH in some 12th century lime mortars by thermal methods but not by XRD, and concluded that it was amorphous. Neal and Stanger (106) reported that CH occurred in nature in both crystalline and amorphous forms. Vitkovskii (107) considered that the CH in cement pastes included amorphous material. Groves (10) examined cement pastes of low w:c ratio (0.15) by TEM of ion thinned sections. He found parallel clusters of CH platelets about 10 nm thick, rotated through various angles around their common c-axis and embedded in gel; the larger crystals common in normal pastes were not observed. Abo-El-Wafa and Al-Wakeel (108) concluded from IR evidence that the CH in alite pastes was poorly crystalline, especially at low w:s ratios. On the other hand, Rayment and Majumdar (7) concluded from their EPMA study that microcrystalline CH was not present in cement pastes of normal w:c ratio.

The possibility of ionic substitutions in CH has been examined. AEM results (24) supported earlier conclusions that the CH in cement pastes contained

significant amounts of foreign ions, especially silicate and sulphate. Shpynova et al. (109,110) calculated the effects that substitutions in interlayer sites, balanced by omission of H, would have on the XRD powder pattern, and concluded from experimental observations that CH modified by such substitutions could be prepared. The C-S-H structure suggested by Grudemo (67) is based on a similar concept. In contrast, some other studies, summarized by Barker (111), suggest that CH largely avoids incorporating foreign ions, and the AEM evidence could possibly be explained by the existence of inclusions.

Barker et al. (112) made an XRD study of strain in CH crystals, including ones grown in presence of colloidal silica. Brindley and Kao (113) discussed crystal structures and IR spectra of brucite type hydroxides, including CH. Barker (111) and Barker and Barnes (114) reviewed aspects of the growth of CH in cement pastes and its role in the development of strength.

4 QUANTITATIVE PHASE DETERMINATIONS, MASS BALANCE AND VOLUME FRACTIONS

4.1 EXPERIMENTAL METHODS OF PHASE DETERMINATION

4.1.1 UNREACTED CLINKER PHASES

Quantitative X-ray diffraction analysis (QXDA) is probably the only practicable method at present for determining the unreacted clinker phases individually in a cement paste. The problem is similar to, though more complex than, that of determining the phases in an unreacted clinker, and will not be discussed here. Gutteridge (115) recently described a least squares procedure and applications to anhydrous cement systems. Determinations in pastes are of low precision; Odler and Dörr (116) estimated the precision at not better than ±3 % for unreacted alite in alite pastes, and for cement pastes, even this would be difficult to achieve (25). Analysis of backscattered electron images obtained in the SEM is a rapidly developing technique, and may prove a more effective method, both for unreacted clinker phases and for CH (117).

4.1.2 CALCIUM HYDROXIDE

Many recent papers have dealt with determination of CH in cement or calcium silicate pastes. Thermal methods used have included thermogravimetry (TG) or differential thermogravimetry (DTG; 25,53,54,116, 118-123), semi isothermal DTG (124), thermal evolved gas analysis (TEGA; 124,125) and differential thermal analysis (DTA) or differential scanning calorimetry (DSC; 118,125-128). QXDA has been used (54,67,116, 118-121,125,126), as has IR (129). Chemical extraction methods have included the use of aqueous $CaCl_2$ (4) or aqueous CH (126), and of Franke solvent or related organic media (68,116,118,125). Some of the investigators have found significant differences between the results of thermal methods and QXDA, with QXDA usually giving lower results (116,118,119,125, 126), but others have reported no differences outside experimental error (25,120). There is broad agreement that extraction methods give higher results than either thermal methods or QXDA (116,118,125,126). It has been suggested that QXDA gives low results due to presence of amorphous CH (126); some workers consider that this may also apply to thermal methods, either for the same reason (116), or because of CH that is adsorbed on the C-S-H (125) or present as interlayer CH (68). Sources of error in the determination of CH by TG have been discussed (54).

The following conclusions are suggested. First, adsorbed or interlayer Ca^{2+} and OH^- are not CH, but parts of the C-S-H. Second, part of the CH in some or all cement pastes could be intimately mixed with C-S-H. There is no convincing evidence for the presence in cement pastes of amorphous CH, or, except in pastes of unusually low w:c ratio (10), of cryptocrystalline CH, but the present evidence probably does not exclude the possibility of mixture within the gel at or approaching a single layer level. Ultimately, the differences may be ones of how C-S-H is defined. CH mixed with C-S-H at or near a single layer level would not be recognized as a separate phase by EPMA or SEM analysis, and possibly not by QXDA or thermal methods, but it might well be counted as CH by extraction methods or AEM. Further investigation is needed; structural and analytical studies of ion-thinned sections probably offer the best hope of providing definitive evidence.

Day (130) found that if either cement paste or CH was soaked in methanol, an increase in weight loss occurred on DTG in nitrogen in the 700°C region. He considered that methanol, or some reaction product, was retained in the paste and reacted with CH to produce a carbonate like material. This conclusion, which is of much interest because methanol or other organic liquids are often used to stop hydration, was challenged (131), but nevertheless appears worthy of further investigation. It is not inconceivable that small organic molecules could be strongly sorbed and then pyrolise giving CO, which in the presence of active CaO could yield $CaCO_3$ and C. If such a process does, in fact, occur, it has important implications for the determination of CH by TG, and might also account for an observation (25,54) that the loss on TG above the CH step exceeds the CO_2 content found in a separate, chemical determination, as the samples studied had previously been soaked in acetone, which might have a similar effect.

4.1.3 HYDRATED SILICATE AND ALUMINATE PHASES

The literature is conflicting as to the possibility of determining the hydrated aluminate phases in cement pastes by thermal or X-ray methods. Uchikawa et al. (128) found it possible using DSC to determine monosulphate, C_4AH_x and C_3AH_6, but not ettringite or C-S-H. Later, however, they reported ettringite contents determined by a modified TG-DSC method (132). Millet et al. (133) found that QXDA gave false results for ettringite due to effects of grinding; DTA was better in this respect, but the need for grinding still caused problems. Ogawa and Roy (82) found it possible to determine ettringite either by QXDA or by DSC, and Bensted (134-137) reported ettringite contents determined by DTA. Crammond (138) determined ettringite, thaumasite and gypsum by QXDA. Odler and Abdul-Maula (139) found that AFt phase could best be determined by DTA, as the peak area scarcely depended on composition or crystallinity, though care was needed to avoid interference from C-S-H. For AFm phase, QXDA was probably the best method; however, though very sensitive, it gave only semi quantitative results. Grudemo (67) reported C-S-H contents found by QXDA.

From the foregoing results, it appears that thermal methods and possibly QXDA may be used for determining AFt phase, but it is doubtful whether the direct determination of either C-S-H or AFm phase in pastes has been successfully achieved. The very close admixture of much of the AFm phase with C-S-H, together with its variable composition and imperfect crystallinity, explains the difficulty. Least squares fitting of observed and calculated TG curves probably offers the best possibility, but better standard data and a fuller understanding of AFm compositions and how they affect the thermal behaviour are required.

4.2 MASS BALANCE AND INDIRECT DETERMINATION OF C-S-H COMPOSITION

4.2.1 CALCIUM SILICATE PASTES

Many studies have been reported over a long period with the object of determining the Ca/Si ratio of the C-S-H in calcium silicate pastes indirectly, from the contents of unreacted starting material, if any, and of CH. Some indicated marked changes in this ratio as hydration proceeds. The most recent studies do not confirm this, except perhaps for the very early stage of reaction. Odler and Dörr (116) reported Ca/Si ratios in C_3S pastes of 1.60 using an extraction method for CH, or of 1.99 using TG, with an uncertain but lower value for the product of the first 1 - 2 % of reaction. LeSueur et al. (120) reported values of 1.7±0.1 and 1.8±0.2 for C_3S pastes made with and without $CaCl_2$, respectively, both substantially independent of the degree of reaction. The difference between these values was not considered significant. Parrott et al. (53) obtained closely similar results, discussed in Section 2.3.2, which gave a value of 1.8 for an alite paste. For β-C_2S pastes, the results of Kantro and Weise (140) and of Fujii and Kondo (141) indicate values around 1.8 at complete hydration. Shibata et al. (142) described the preparation and hydration of an unstabilized β-C_2S that gave virtually no detectable CH on hydration, and which thus gave C-S-H with a Ca/Si ratio close to 2.0.

Taken as a whole, these results agree well with the conclusions derived from electron optical analyses, discussed earlier. There are several indications that β-C_2S tends to give a product with a slightly higher Ca/Si ratio than that formed from C_3S, and the results of Shibata et al. (142) provide an extreme example of this. Small experimental errors have a disproportionate effect on Ca/Si ratios determined indirectly, especially at low degrees of reaction. It is now reasonably certain that the Ca/Si ratio of the C-S-H reaches its final value not later than the end of the induction period.

4.2.2 CEMENT PASTES

For typical portland cements, CH contents, referenced to the ignited weights, are typically 18 - 25 % after times of 3 - 12 months (25,118,122,126). Contents of AFt phases appear to have been determined only for short hydration times; Uchikawa et al. (128) and Bensted (134 - 137) quote values of, typically, 2 - 4 % for normal cements at 4 h.

Taylor et al. (25) reported contents of C-S-H and hydrated aluminate phases determined by a difference method. The amounts of unreacted clinker phases, CH and $CaCO_3$ were determined by approximate QXDA, TG and a chemical method, respectively; the compositions of the clinker phases were known from SEM microanalyses; the nature of the hydrated aluminate phases (AFm or AFt or both) was established by XRD; their mean compositions and that of the C-S-H were determined by AEM. Knowing also the bulk composition of the cement, the amounts of CaO, SiO_2, Al_2O_3 and SO_3 present in the hydrated silicate and aluminate phases were obtained by difference. A linear, simultaneous equation was set up for each of the oxides mentioned, having the compositions of the hydrated phases as coefficients, the amounts of those phases as unknowns, and the quantity of the oxide to be accounted for as the right hand side. These equations were then solved by least squares to find the most probable amounts of the hydrated silicate and aluminate phases. The results were tested in three ways. First, using standard data for each phase, a simulated TG curve was calculated and compared with the observed one. Second, quantities such as porosities were calculated, which could be compared with typical data from the literature for comparable cements. Third, the discrepancies between the total amounts of all the oxides present, both major and minor, were compared with those accounted for by all the anhydrous and hydrated phases.

The results of the first two of these tests were reasonably satisfactory, but the mass balance test showed some systematic discrepancies: on the average, 2.5 % of CaO (referenced to the ignited weight) and 0.7 % of Fe_2O_3 were unaccounted for, and the calculated content of SiO_2 was 1.1 % too high. Suspicion fell on the C-S-H compositions, determined by AEM, which were mostly between 1.6 and 1.7; higher values would have improved the agreement. It was also suggested that the presence of an iron rich gel, perhaps containing some Ca, could account for the discrepancy for Fe_2O_3 and contribute to that for CaO. Subsequently, SEM analyses of the hydration products of one of the same cements were carried out (9), and gave a Ca/Si ratio of ca. 2.0 for the C-S-H. Substitution of this value in the calculations greatly improves the agreement for CaO.

The effect on mass balance of varying the Ca/Si ratio assumed for the C-S-H is shown by the following hypothetical calculation for a fully reacted cement:

(i) Assume the cement composition to be: Na_2O, 0.2; MgO, 1.3; Al_2O_3, 5.4; SiO_2, 20.6; SO_3, 2.7; K_2O, 0.4; CaO, 65.3; TiO_2, 0.3; Fe_2O_3, 3.0; Misc., 0.7; Total, 99.9 %.
(ii) Assume the CH content, referenced to the ignited weight, to be 23.8 %; this is at the upper end of the probable range.
(iii) Assume the atom ratios in the C-S-H, relative to Ca, to be: Mg, 0.02; Al, 0.05; Si, 0.50; S, 0.01; Fe, 0.015 (Ca/Si = 2.0).
(iv) Assume those in the AFm phase to be: Mg, 0.02; Al, 0.50; Si, 0.02; S, 0.18; Fe, 0.03.
(v) Assume 0.9 % of CO_2, present as calcite.
(vi) Set up and solve two simultaneous equations to determine C-S-H and AFm phase, using the contents of Al_2O_3 and SiO_2, and thus making the mass balance complete for these components and concentrating the principal discrepancies into the result for CaO.

This gives a calculated total of 65.3 % for CaO, in excellent agreement with the amount present in the cement; other totals are: MgO, 0.7 %; SO_3, 2.6 %; Fe_2O_3, 1.2 %. If the calculation is repeated assuming a Ca/Si ratio of 1.7 for the C-S-H, the calculated total for the CaO is 60.1 %, which is 5.2 % below the amount in the cement. If a lower content of CH is assumed, it is necessary to assume that the C-S-H has a Ca/Si ratio greater than 2.0 if balance for the CaO is to be obtained. These results support the view that, for some cements at least, the Ca/Si ratio of the C-S-H is closer to 2.0 than to 1.7. They also indicate that not all the Fe_2O_3 in the hydration products is present in the AFm phase and C-S-H, and the same is probably true of the MgO.

4.3 VOLUME FRACTIONS

Volume fractions in pastes depend on drying conditions and are subject to the same considerations as densities and water contents, discussed in Section 2.3.1. For an alite paste with w:s 0.6, treated with methanol and then dried over silica gel, Parrott et al. (53) reported experimental data which, extrapolated to complete reaction, give: CH 0.20; C-S-H, 0.35; pores $\ll$ 50 nm, 0.25; pores > 50 nm, 0.20. For

cement pastes, Taylor et al. (25) calculated volume fractions and some related quantities from the amounts and densities of phases, using procedures and data quoted in Sections 2.3.2 and 4.2.2. Porosities were obtained by difference. For a paste with w:c = 0.5, hydrated for 1 year and equilibrated at 11 % rh, the volume fractions were: Unreacted clinker phases, 0.05; CH, 0.11; $CaCO_3$, 0.01; C-S-H, 0.37; AFm, 0.15; micropores ($\lesssim$ 5 nm), 0.13; capillary pores, 0.18. Interlayer space was counted as part of the C-S-H. The Ca/Si ratio assumed for the C-S-H in such calculations has little effect on the resulting porosities, but the volume fraction of C-S-H is liable to change by up to 0.04, with corresponding change in that of AFm phase. These two sets of results are approximately compatible if due allowance is made for differences in composition, w:s ratio and divisions between C-S-H, micropores and larger pores.

5 MICROSTRUCTURAL DEVELOPMENT

5.1 INTRODUCTION

Knowledge of microstructural development in cement pastes has greatly increased since the Paris Congress. The contributions of P.L. Pratt and his co-workers at Imperial College, London, have been especially important, and the writer is much indebted to him and to Dr. K.L. Scrivener for helpful discussions, on which this section is largely based. The advances were possible because several techniques were used. With any one technique for studying cement paste microstructure, there are inevitably questions concerning the representative nature, or otherwise, of the fields examined, and the extent to which the microstructure has been altered during specimen preparation or examination. No one method is likely to answer all such questions satisfactorily but from the use of several methods and critical comparison of the results, a reasonably clear picture has begun to emerge.

The most important, relatively new methods are high voltage transmission electron microscopy (HVEM) with environmental or "wet" cells to reduce water loss (143-145), scanning transmission electron microscopy (STEM) of ion thinned sections (146), and backscattered electron imaging (BEI) of polished sections in the SEM using detectors designed to maximize contrast due to compositional differences and to minimize that associated with topography (117). Scrivener and Pratt (147) have concisely described the uses of these techniques. Other methods have included X-ray imaging in EPMA (8), SEM examination of matched fracture surfaces (148), and SEM using a cryo stage to avoid dehydration (149). Microstructural development in C_3S or alite pastes differs in important respects from that in cement pastes, and we shall consider it separately. Following Jennings et al. (150), we shall refer to the early, middle and late periods of microstructural development, with boundaries at $\approx$3 h and 20-30 h for typical cements at 20°C, and to the corresponding products.

Unless a wet cell or cryo stage is used, extreme dehydration occurs in any electron optical investigation, and it has been shown (100,150) that this can have drastic effects on the fine microstructure. However, drying begins as soon as the rh falls below saturation, and any paste at lower humidities will contain regions in which water is in varying degrees deficient. The water is lost initially from the wider pores, which appear in electron micrographs as the most open parts of the structure. One would expect them to be disproportionately represented on fracture surfaces.

5.2 CEMENT: THE EARLY PERIOD

The period up to 3 h comprises the pre induction and induction periods. The anhydrous cement has a wide particle size distribution, with, typically, 15 % < 5 μm and 10 % > 50 μm (151). BEI indicates that most grains are polymineralic (Fig. 3a; 100,117). If surface active admixtures are absent, the grains tend to flocculate in water. HVEM with wet cells shows that, at high dilutions, a gelatinous layer or membrane forms over the grain surfaces soon after mixing (143,145). A product of similar appearance, though not necessarily of the same composition, has been observed on the surfaces of C_3A hydrated in presence of gypsum (152). There appears to be no unequivocal, direct evidence for the formation of a gel layer during the first minutes of hydration in cement pastes of realistic w:c ratio, but the observed behaviour of C_3A plus gypsum, together with evidence from concentrations in solution, strongly suggests that one is formed, and that it is probably amorphous, colloidal, and rich in Al and Si but also contains significant amounts of Ca and SO_4 (100).

Dalgleish et al. found that, after 1 h, stubby rods of AFt phase, typically 250 nm long and 100 nm thick, were formed (153-155). Later studies by Scrivener and Pratt (100,147,152), using both wet cells in the HVEM and ion thinned sections in the STEM, showed that these can occur at some distance from the cement grains, suggesting that they have nucleated either in the solution, or on the outer surface of a thin layer of gel (Fig. 3b). On drying, they fall back on to the grain surfaces, on which they are unevenly distributed, possibly reflecting compositional differences in the underlying grains.

The first study using a wet cell, made at high w:c ratios, showed tubular growths radiating from the cement grains, which were believed to have formed by a "silicate garden" mechanism (143). It was later shown that they were rich in Ca, Al and S, and were not formed if C_3S was substituted for cement (156). They have not been observed in the more recent studies made at normal w:c ratios, and do not appear to be a significant feature of normal cement hydration.

5.3 CEMENT: THE MIDDLE PERIOD

5.3.1 FORMATION OF C-S-H AND CH

The period from 3 h to 20-30 h comprises the acceleratory and early deceleratory periods, during which some 30 % of the cement reacts. It is characterised by the rapid formation of C-S-H and CH. Many observers studying fracture surfaces have reported the formation during this period of C-S-H as fibres apparently radiating from cement grains (Type I of Diamond, 157). Honeycombs or reticular networks (Diamond Type II) have also often been seen. Rosettes of fibres $\approx$2μm in diameter forming bulges on larger surfaces could result from reaction of small cement grains adhering to larger ones (100). There are several indications that the C-S-H when wet consists of foils, and that the fibres or honeycombs are, at least in part, produced on drying (100,147,158).

The C-S-H forms a thickening layer or shell around the cement grains (154,158); which engulfs and possibly nucleates on the framework of AFt rods (Fig. 3c; 152). A significant amount has formed in 3 h, and the particle surfaces are entirely covered by 4 h (154). The shells grow outwards; by about 12h, they are 0.5-1.0 μm thick, and inter shell cohesion is sufficient that fracture sometimes occurs through the shells and not between them. This stage, which corresponds approximately to the maximum in heat evolution rate, was termed the cohesion point; the structure of

interconnected shells around the larger grains was considered to play an important part in determining the mechanical and other properties, which thus depend on the particle size distribution (154,158).

From studies using wet cells, BEI and ion thinned sections, Scrivener and Pratt (100,147,152) showed that spaces develop between the shells and the anhydrous grains; they are detectable at 5 h in ion thinned sections, and by 12 h are up to 0.5 μm wide. They were believed to contain solutions with high concentration gradients and possibly colloidal material. Initially, therefore, the shell grows outwards and by becoming less porous, rather than inwards, and the spaces widen as the anhydrous material, primarily alite and C_3A, is consumed. The mode of growth shows that the shells are, at this stage, permeable and that reaction occurs through solution. This last conclusion is reinforced by the observation that C-S-H also grows on fly ash surfaces, if present, before any detectable reaction of the fly ash has taken place (159).

The same studies showed that, before the end of the middle period, C-S-H begins to deposit also on the inner surfaces of the shells, and that the spaces between the latter and the anhydrous cores begin to fill up (Fig. 3d). Cement grains were shown to differ in behaviour depending on their size, phase composition, and internal microstructure. Ones smaller than ≈3 μm dissolved completely by the end of the acceleratory period, giving almost entirely outer product, which was often absorbed in the shells surrounding larger grains. Grains containing high proportions of C_3A might develop larger spaces within their shells. The behaviour of the larger grains is considered in Section 5.4.

Partly or completely empty shells, called "Hadley grains" and up to at least 10 μm across, were first observed on fracture surfaces (160). Pratt and Ghose (158) noted that it would be difficult to reconcile any widespread occurrence of such cavities in a mature paste with the density of the material, and concluded that they were temporary phenomena. The separations between shell and core observed in BEI or ion thinned sections are typically ≲ 3 μm, but can be larger around C_3A (100,158). Scrivener (100) observed that large, empty shells often result from cores having fallen out on fracture.

CH forms during the middle period, as hexagonal plates in the water filled space, and makes a major contribution to the filling of space between the shells (158).

5.3.2 FORMATION OF AFm AND AFt PHASES

Many observers have reported the outward growth of long, thin needles of AFt phase in pastes about 1 day old. Their formation, which is a renewed one of this phase, was shown to occur at 16 h and to coincide with a shoulder on the downward slope of the main heat evolution peak (Fig. 3d; 153,158). The length of the needles is, typically, 1-2 μm, but can reach 10 μm. The heat evolution may well be associated chiefly with the renewed dissolution of C_3A, and perhaps also of ferrite phase. Both AFt and AFm phase can also form inside the shells. The latter become less permeable as more product is formed, causing the solution inside them to become isolated and low in sulphate; AFm phase therefore tends to form inside, and AFt phase outside the shells (100, 152,158).

Locher (161) considered that recrystallization of ettringite played a major part in setting. The

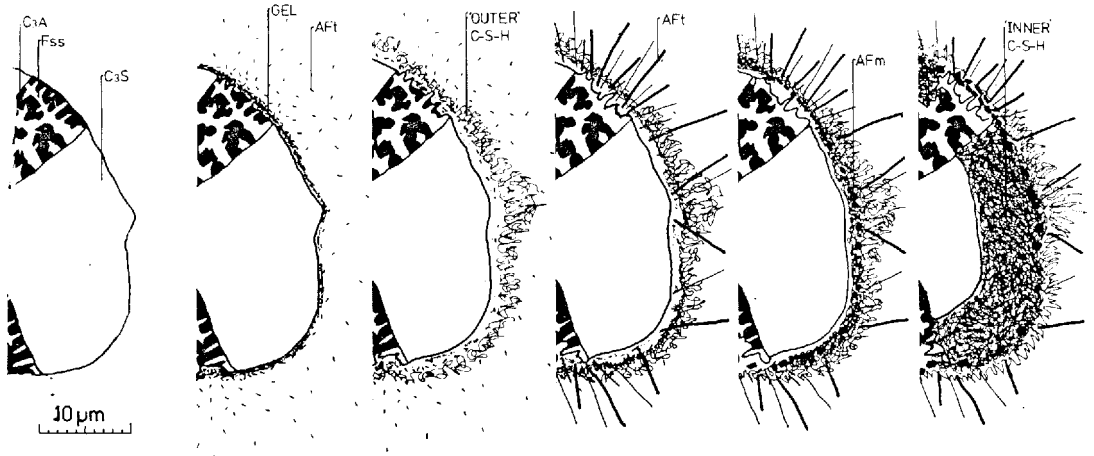

c) Unhydrated Section of polymineralic grain. (scale of interstitial phase is slightly exaggerated)

b) ~10 min Some C_3A (&/or Fss) reacts with calcium sulphate in solution. Amorphous, aluminate rich gel forms on the surface and short AFt rods nucleate at edge of gel and in solution.

c) ~10hrs Reaction of C_3S to produce 'outer' product C-S-H on AFt rod network leaving ~½μm between grain surface and hydrated shell.

d) ~18hrs Secondary hydration of C_3A (&/or Fss) producing long rods of AFt. C-S-H 'inner' product starts to form on inside of shell from continuing hydration of C_3S.

e) 1-3days C_3A reacts with any AFt inside shell forming hexagonal plates of AFm. Continuing formation of 'inner' product reduces separation of anhydrous grain and hydrated shell.

f) ~14days Sufficient 'inner' C-S-H has formed to fill in the space between grain and shell. The 'outer' C-S-H has become more fibrous.

Fig. 3. Microstructural development during the hydration of portland cement (Scrivener, 100).

observations described in the previous sections do not support this view, the early formation of AFt phase occurring before initial set, and the later formation after final set. From quantitative determinations of ettringite with parallel ones of setting times, Bensted (137) concluded that setting was directly associated with loss of mobility of water, and that in normal setting, this in turn was primarily caused by formation of C-S-H. In agreement with this view, Dalgleish et al. (155) considered that initial set was associated with the beginning of rapid C-S-H formation, and final set with completion of coverage of the cement grains by C-S-H.

5.4 CEMENT: THE LATE PERIOD

5.4.1 FORMATION OF C-S-H

The late period is one of increasingly slow reaction, beginning at 20-30 h. In it, C-S-H forms by three, distinct mechanisms, the first two of which have started earlier (100,152,158). In the first, the shells grow outwards and become less porous, adding to the outer product. SEM of fracture surfaces (158) and BEI of polished surfaces (100) showed that their thickness reaches 8-10 μm in 7-14 d. In the second, they grow inwards. The anhydrous phases meanwhile dissolve, and the spaces between them and the surrounding shells continue to grow at first, until at 4 d those around the silicates are up to ≈3 μm wide. Gradually, the growth of C-S-H overtakes the retreat of the anhydrous surface, and the gaps close up; in the larger grains, they disappear by 7-14 d (Fig. 3e and f; 100). Grains smaller than 15-20 μm hydrate completely before the space has been entirely filled, leaving cavities up to 5 μm in diameter that have been observed on fracture surfaces (158) and even on polished surfaces of pastes up to 23 years old (100).

Both the above mechanisms occur through solution. The third probably does not. After the spaces have been filled, the alite continues to react, and the interface between it and the surrounding C-S-H moves slowly inwards. Reaction of the belite is undetectable by electron microscopy at 7 d (100), but by 28 d, about 25 % has reacted, and an advancing interface is observed as with the alite. Ultimately, in pastes of sufficiently high w:c ratio, completely reacted relicts of both alite and belite can be observed either by X-ray imaging (8) or by BEI (100), in each case of polished surfaces. X-ray microanalyses show that both have been completely converted into C-S-H (8,9), and BEI shows that, in the belite relicts, the lines of the original twin lamellae are preserved (100).

If inner product is defined as that formed in space initially occupied by solid, it comprises two types: that deposited from solution on the insides of the shells, and that formed by the third, or topochemical mechanism. BEI of a 23 year old paste (100) that had also been examined by EPMA, including X-ray imaging (8), showed three zones of C-S-H, possibly corresponding to the three modes of formation. The "inner product" defined by X-ray imaging or EPMA or SEM spot analyses corresponds, at least approximately, to that formed topochemically. The "outer product" defined by these methods corresponds, again approximately, to the material of the shells. As has been seen, the topochemical product is formed only from the larger grains, the shells around which include the space originally occupied by smaller grains; this reinforces the conclusion (Section 2.1.4) that "undesignated product" would be a more exact desciption. Jennings et al. (150) suggested that "late product" was a term preferable to "inner product", and a good case can be made for this. It is uncertain whether the C-S-H deposited inside the shells from solution is compositionally identical with that formed topochemically, i.e., pure C-S-H, or with the outer product, which consists of C-S-H often closely mixed with AFm phase. The spacial resolution of X-ray microanalysis is probably inadequate to settle this question.

The topochemical product can possibly be identified with Diamond's (157) Type IV C-S-H. His Type III C-S-H (equant grains) presumably includes all but the most porous parts of the shell material, and possibly also that deposited on the insides of the shells. The microstructure of Type III C-S-H was clarified by the work of Jennings et al. (150), who showed that material that fitted this description when examined in reflection appeared when examined by STEM of ion thinned sections to consist of interleaved and interlocked thin foils. These and other morphological varieties of C-S-H gel are, almost certainly, not distinct categories, but points in a continuum of forms, all derived from sheets which tend to roll, crumple or shred in a preferred direction. The way in which they do this, and the extent, appear to depend largely on the amount of space available, perhaps together with such other factors as the mechanism or rate of formation, or the presence of admixtures, and can be further modified by drying, fracture, or other processes after formation.

5.4.2 FORMATION OF CH

CH continues to form in the water filled space during the late period of reaction, and is readily observed on fracture surfaces (157), X-ray images (8), or BEI (117). The thin plates seen earlier give place to large crystals or dense masses up to tens of μm in size that can engulf other phases. This change presumably results from the decrease in available space.

Scrivener and Pratt (152) suggested that the continued hydration of alite in the enclosed regions within the shells must lead to formation there of microcrystalline CH. EPMA and SEM analyses (Section 2.1.4) show that the inner or late product has a Ca/Si ratio of 1.7-2.0, indicating that most of the CH escapes. It may, nevertheless, be significant that the Ca/Si ratio tends to be higher than in C_3S pastes, in which a shell structure does not form, though partial replacement of Si by Al may also be partly or wholly responsible.

5.4.3 FORMATION OF Al- OR Fe-CONTAINING PHASES

During the late period, AFm phase has been observed to form inside the shells (100); it could result from reaction of water with aluminate or ferrite phase, together with decomposition of AFt phase, if present (Fig. 3e) The analytical evidence shows that AFm phase also forms outside the shells, where it is normally closely mixed with C-S-H (9), and may result, in whole or in part, from decomposition of AFt phase; however, in some white cements, relatively large plates have been observed (100). Areas high in Fe, forming relicts of the interstitial material, were observed by X-ray imaging (8). The higher resolution obtainable with BEI shows them to be, more specifically, relicts of the ferrite phase, and to have a zoned structure (100). An outer zone, about 1 μm wide, possibly consisted of an iron hydroxide phase, and an inner zone was believed to consist of unreacted ferrite.

5.5 TRICALCIUM AND β-DICALCIUM SILICATES

5.5.1 C_3S AND β-C_2S : EARLY PRODUCTS

Menétrier et al. (162-164) and Jawed and Skalny (165) extended earlier studies using high resolution SEM,

ESCA and solution analyses, in which pellets of C_3S or β-C_2S were dipped in water or aqueous solutions. No protective coatings were observed; the surfaces of the crystals were attacked unevenly, and within a few minutes, minute particles of product were deposited. Subsequently, films, honeycombs or fibres of C-S-H, and later also CH, were observed. Several other workers have reported broadly similar results. Groves (166), studying ion thinned specimens of C_3S that had been dipped in water or aqueous solutions, found that at 3-6 h, a layer of amorphous material had been formed. Jennings et al. (150), using a wet cell with HVEM, observed the formation during the induction period of thin flakes or foils, which they called "Type E" C-S-H. Scrivener (100) made a similar observation, and noted that on drying, the foils either collapsed or crumpled to form fibres. Le Sueur et al. (120), in an SEM study of C_3S pastes, reported that after 30 m, an amorphous looking layer had been formed. Stewart and Bailey (167) found the first substantial product of C_3S hydration visible in an SEM examination to consist of thin flakes or foils. Possibly all these observations are consistent with the hypothesis that the first product consists of foils or flakes exfoliating from the surface, which can change in various ways on drying.

Ings et al. (168) placed single crystals of C_3S in an alite slurry (w:s = 2), later removing them for SEM examination. A layer of apparently structureless product built up to a thickness of 5 μm in 30 m, together with cryptocrystalline CH; later, it shrank, with formation of acicular outgrowths. Calorimetric evidence showed that the single crystals were highly reactive, but the product layer contained Al, and had thus formed in part also from the alite. The authors concluded that an initial, transient hydrate was formed, which served as a barrier layer, and that its subsequent transformation ended the induction period.

5.5.2 C_3S AND β-C_2S: MIDDLE AND LATE PRODUCTS

As with cement, the middle period is that of rapid formation of C-S-H and CH, and several early studies showed the formation of Diamond Type I material, together in the outer product with massive CH (157). Jennings et al. (150), using a wet cell, found that the period began with the formation of an apparently structureless layer of gel, which they called "Type 0" C-S-H, and which grew to a thickness of ≈0.5 μm over several days. It changed, rather slowly, to give acicular particles where space was freely available, or crumpled and interlocked foils where it was not. As noted in Section 5.4.1, the latter product, when seen in reflection, resembled Diamond Type III C-S-H, and a less porous component, which could have been the inner or late product, was also present. These changes were encouraged by drying or ageing.

Stewart and Bailey (167), in the SEM examination reported earlier, obtained results varying with the structural modification of the C_3S. With a monoclinic modification, the foils that had grown previously lifted and peeled, giving crumpled sheets, but with triclinic or rhombohedral preparations, needle like outgrowths were formed. All three specimens eventually gave similar structures, in which needle like outgrowths were bridged by crumpled foils. Studies using a cryo stage indicated that the outgrowths were not an artifact of drying (149).

Scrivener (100), studying alite pastes with HVEM and a wet cell, found that the product at 1 d consisted of crumpled foils in places where it was thin enough for the structure to be observed, with no evidence of fibrillar outgrowths. Fibrils were, however, produced if the paste was allowed to dry; in a paste not cured in water, this could apparently happen through local exhaustion of water. There was no indication of more than the one, basic morphological type of C-S-H, though the inner or late product would not have been observed. Pastes of C_3S mixed with C_3A were studied by BEI (100,152); with the C_3A particles, large spaces developed between the anhydrous cores and the surrounding hydration products, but with those of C_3S, no spaces were observed. This contrasted markedly with the behaviour of the alite in cement, and supported the view that the spaces and shell structure in cement pastes are caused by the presence of the aluminate phase.

5.5.3 C_3S AND β-C_2S : CONCLUSIONS

The following conclusions are suggested from the above observations. On mixing, the C_3S begins to dissolve, and C-S-H precipitates as foils, which peel off or exfoliate. The resulting layer becomes progressively thicker and more tightly packed, but at no stage is there convincing evidence of any continuous film or membrane. The foils very readily change into acicular forms or honeycombs on drying, which is bound to occur locally under any conditions other than saturated. As noted by Pratt and Ghose (158), the absence of a shell structure and of spaces between the anhydrous material and the product are very important differences from cement, for which C_3S is therefore of limited value as a model. CH is deposited in the outer product, as with cement.

5.6 COHESION AND THE EFFECT OF WET CURING

In both C_3S and cement pastes, cohesion probably results primarily from the coming together of foils, which transforms an essentially particulate gel into a continuous one, but in the more open parts of the structure, where local drying would be most likely to occur, this process might be confined to the crossing points of foils rolled or shredded into fibres and thus barely if at all distinguishable from an interlocking process. An effect of wet curing is to prevent or at least minimize the changes in C-S-H morphology that occur on drying. These changes are probably, at least in part, irreversible.

5.7 TRICALCIUM ALUMINATE AND THE FERRITE PHASE

Scrivener and Pratt (152) studied the paste hydration of these phases using a wet cell with HVEM. In the absence of calcium sulphate, C_3A yielded initially a filmy, amorphous looking product, similar to that seem earlier in SEM by Breval (169). The films appeared crumpled and sometimes peeling from the surface, and it was thought unlikely that they could inhibit reaction. Later, hexagonal plates and icositetrahedra were seen. If gypsum was present, an amorphous layer was again formed, but it appeared denser and more coherent. Its formation was followed by that of rods of AFt phase on the outer edge of the layer and in the solution; they were easily damaged by the beam. If the sample was dried, the rods remained, but the amorphous layer could no longer clearly be seen. If hemihydrate was substituted for gypsum, the early microstructure was dominated by secondary gypsum, which made it impossible to see whether an amorphous layer had been formed; AFt crystals again formed, and were shorter and thicker than those formed in the paste made up with gypsum. The difference in morphology was attributed to the higher degree of supersaturation obtained with hemihydrate. Pastes of C_4AF with gypsum or hemihydrate behaved in a way broadly similar to those of C_3A with the same admixtures, but the amorphous layer seems to have been less evident. The two samples of C4AF used differed greatly in reactivity.

6 HYDRATION REACTIONS

6.1 C_3A AND C_4AF IN THE EARLY AND MIDDLE PERIODS

6.1.1 C_3A

Jawed and Skalny (170) studied the early hydration of C_3A using electron spectroscopy for chemical analysis (ESCA). The Ca/Al ratio in the surface layer increased to ≈2.0 in 2 s and then decreased to ≈1.7 in several minutes, thereafter remaining steady for several hours. These results suggest that calcium aluminate hydrates, and not an Al rich layer, are being formed. In contrast, Glasser and Marinho (171) found that the Ca/Al ratio in solution was >1.5 after 30 s, and concluded that an Al rich layer was formed. They, and also Shin and Glasser (172), made similar studies on Na doped forms of C_3A.

Hampson and Bailey (173,174) found from SEM and TEM studies that the first product of C_3A hydration in presence of gypsum was a disordered phase with an irregular platelet morphology similar to that of the calcium aluminate hydrate observed by Breval (169). At high pH values (≈12.5) of the surrounding medium, short rods of a structurally imperfect AFt phase were produced, and could form a coherent coating on the C_3A grains; in the presence of CH, this coating was eventually ruptured, and longer rods of ettringite, which had grown at lower pH beneath the coating, were observed. From solubility data, the authors concluded that the ionic activity products of synthetic ettringite preparations varied with the pH. This was attributed to the existence of major structural defects in the crystals formed at the higher pH values, which also accounted for their morphology. Initially, these defects were believed to be vacancies in Al sites, balanced by additional H (173), but it was later considered more likely that they were Ca and SO_4 vacancies (175). Vacancies of this latter type were also considered to exist in the larger crystals precipitated at lower pH values, when these were first formed. Tubular particles of ettringite, formation of which had been reported in cement suspensions (143,176), were not observed; their formation from cement was attributed to the presence of alkalis in the aluminate phase in the latter case. Scrivener (100) found that reaction of Na-doped C_3A in presence of gypsum gave a dense mass of tangled, irregular rods, which tended to bubble under the electron beam. This suggests that hollow fibrils could result from dehydration.

Brown et al. (177) studied the kinetics of reaction of C_3A with solutions containing various combinations of Ca, Na, SO_4 and OH ions. Four C_3A samples differing in specific surface area were used. The rates of loss of Ca and SO_4 from the solution depended on the initial composition of the solution, but the rate of sulphate uptake per unit surface area of C_3A was constant. Ca and SO_4 were not consumed in equimolar proportions, and it was concluded that formation of ettringite was accompanied by that of C_4AH_x. This interpretation was preferred to that assuming formation of an AFt phase in which SO_4 was partially replaced by OH because attempts to prepare such products had failed. It was also consistent with phase equilibrium evidence, which indicated that ettringite could not exist in direct contact with C_3A, but that an AFm phase should occur in the interfacial zone. The authors considered that, because of its needle like morphology, ettringite by itself was unlikely to be an effective diffusion barrier, but that in a composite, each would enhance the effect of the other, thus producing a barrier effect.

As noted in Section 5.7, Scrivener and Pratt (152) found that the ettringite crystals formed from C_3A in presence of hemihydrate were shorter and stubbier than those formed with gypsum. They attributed the morphological difference to the higher degree of supersaturation which was obtained with hemihydrate.

6.1.2 C4AF AND MIXED INTERSTITIAL MATERIAL

Fukuhara et al. (178) studied the kinetics of the hydration of C_4AF in presence of gypsum and CH in pastes with w:s = 0.5. They concluded that the retarding effect of gypsum was inversely proportional to the surface area of the C_4AF; if the amounts of gypsum per unit area in two experiments were the same, the heat liberation curves were also the same. From calorimetric data, they concluded that the products of the reaction were ettringite with minor replacement of Al by Fe, and an amorphous iron(III) hydroxide. They also found the enthalpy of the hydration reaction to be 173 cal g^{-1} (352 kJ $mole^{-1}$) of C_4AF and found the rate to be diffusion controlled until the depth of reaction had reached 0.6 μm.

Plowman and Cabrera (179) studied the hydration of a paste (w:s = 0.7) of interstitial material (a mixture of the ferrite and aluminate phases) that had been isolated from a cement. The reaction was followed by continuously monitoring the material in an X-ray diffractometer, in a carbon dioxide free atmosphere. In contrast to Locher (161), they found that both phases were consumed much more rapidly if gypsum was absent than if it was present. The rate constant for the aluminate was about 6 times as great as that for the ferrite. From their results, they concluded that retardation was due to a protective coating of AFm phase together with withdrawal of water caused by ettringite formation, and that the reaction was diffusion controlled. The maximum proportion of gypsum that they used was 56 mg to 700 mg of the interstitial starting material; this is much lower than the proportion in a typical cement, which is about 56 mg to 200 mg of interstitial material, much of which, moreover, is not accessible in the early stages of reaction.

6.1.3 SET CONTROL BY GYPSUM - DISCUSSION

The explanations of the set controlling action of gypsum given by the above investigators (173-179) agree in the conclusion that a protective layer is formed. The layer consists of short, stubby rods of AFt phase, probably together with an underlying sub stratum, and, as suggested by Brown et al. (177), both these components may play a part. It may be considered doubtful whether even poorly formed AFt crystals would, by themselves, be effective. With pure C_3A, the sub stratum appears to be of AFm composition; with cement, it probably is not, and appears to be gelatinous, though it may well have an underlying foil like morphology. Hampson and Bailey (173,174) predicted that gypsum could be effective in controlling set if the surrounding solution had a pH in the approximate range 12.3-12.8, and that admixtures shifting the pH out of this range would render gypsum ineffective; further work is probably needed to test this hypothesis. There is disagreement as to what controls the morphology of the AFt phase; Hampson and Bailey found that the short, stubby rods were produced if the pH was high, but Scrivener and Pratt's (152) observations using hemihydrate show that they can also result from a higher level of supersaturation.

Many portland cements contain small proportions of calcite, either added deliberately or present as an impurity in the gypsum. Bensted (180) found that, if gypsum was replaced by limestone, AFm and AFt phases containing carbonate ions were formed.

6.1.4 SECOND STAGE FORMATION OF ETTRINGITE

The delay of approximately 16 h before the second stage of AFt formation takes place has to be explained. Scrivener (100) noted that it occurred after the major middle period reaction giving C-S-H and CH, and suggested two possibilities. One was that the reaction of the alite rendered the gel layer unstable. The other was that a decrease in Ca concentration, caused by precipitation of CH, increased the rates of dissolution of gypsum and of C_3A. Yet another possibility is that the dissolution of the alite makes available additional surfaces of the interstitial phases.

6.2 C_3S AND β-C_2S IN THE EARLY AND MIDDLE PERIODS

6.2.1 ESCA, SURFACE AREA AND SIMS STUDIES

ESCA studies of the early hydration of C_3S (181,182) and β-C_2S (183) were reported. All show, in broad agreement with earlier results, an initial, rapid fall in surface Ca/Si ratio, followed by a rapid increase and a subsequent, slower decrease to values of 1.5-2.0. Regourd et al. (181) attributed the initial decrease to formation of a Primary Hydrate, with Ca/Si << 3. Assuming a Ca/Si ratio of 1, the layer of hydrate at this stage was 0.8 nm thick. The increase in Ca/Si ratio that followed was attributed to formation of a Secondary Hydrate, which persisted throughout the induction period; as the product layer thickened, the contribution of the underlying C_3S to the signal decreased, and with it the surface Ca/Si ratio. The Secondary Hydrate had a Ca/Si ratio of 2.0. At 4h, well after the contribution from the C_3S had disappeared, the shape of the Si_{2p} peak changed, indicating a major change in the structure of the Secondary Hydrate. This coincided with the end of the induction period, and consequent formation of Diamond Type I C-S-H, with dimeric silicate anions.

The results of Ménétrier et al. (183) for β-C_2S indicated that the thickness of the hydrate layer was ≈5 nm after 15 s and ≈15 nm after 6 h, both at 25°C. Stadelman et al. (182) made studies on C_3S with times of up to 8 h. For a pellet immersed in water at w:s = 10, results similar to those of Regourd et al. were obtained, but a second maximum in the surface Ca/Si ratio was observed, and was attributed to formation of CH. Parallel studies of surface area by Kr sorption showed that the surface area passed through a sharp maximum corresponding to the initial sharp minimum in surface Ca/Si ratio; the product after this stage, which had a relatively high Ca/Si ratio and relatively low specific surface area, was considered to act as a protective layer during the induction period. A second, broader maximum in the surface area curve was attributed to formation of CH, initially finely divided. Early hydration of cement has also been studied using secondary ion mass spectrometry (SIMS), which indicated a depth of reaction of 10-20 nm in 10 minutes (184).

6.2.2 THEORIES OF THE INDUCTION PERIOD

The mechanism and products of C_3S hydration have been reviewed in a collaborative paper (185), which includes a discussion of theories of the induction period. In one group of hypotheses, it is assumed that the initial or first stage product does not act as a barrier layer; its presence may affect the kinetics, but the ending of the induction period does not depend on its destruction. In these hypotheses, the induction period occurs because of a delay in the nucleation or growth of a second stage or major product; some workers consider that this is the CH (Hypothesis No. 1), and others that it is the C-S-H (Hypothesis No. 2). In the second group of hypotheses, the first stage product acts as a barrier, and the induction period ends when it is destroyed because of a phase transformation or ageing process (Hypothesis No. 3), or by osmotic bursting or some related effect (Hypothesis No. 4).

We shall consider only a few recent contributions. Support for Hypothesis No. 4 rested largely on early wet cell observations at high w:c ratios (143), which have not been confirmed in the more recent studies on pastes discussed in Section 5. Ings et al. (168) considered that their results using single crystals of C_3S, described in Section 5.5.1, supported Hypothesis No. 3; however, they appear to show that a change occurs in the C-S-H, but not necessarily that this change corresponds to the destruction of a barrier layer. Other recent reports in which destruction of a barrier layer was assumed are those of Stadelman et al. (182), Ball (186), and Pommersheim et al. (187), who constructed a mathematical model of the hydration of tricalcium silicate on this basis.

An argument against any barrier layer hypothesis was advanced by Odler and Schüppstuhl (188), who confirmed and extended earlier studies showing that the length of the induction period for C_3S was affected by, among other things, the concentration of defects in the C_3S. They pointed out that there was no reason to believe that this could affect the quality of the hydration product as a barrier layer.

Wu and Young (189) determined Ca and OH concentrations as a function of time in suspensions of C_3S in water or various salt solutions. The results supported previous indications that the CH nuclei are poisoned by silicate ions, with the result that CH does not precipitate until a relatively high degree of supersaturation has been reached.

Brown et al. (190) reported studies in which the precipitation of CH from supersaturated solutions obtained from C_3S hydration was followed conductimetrically. Seeding with CH, itself also obtained from hydration of C_3S, greatly accelerated the precipitation of CH, seeding with C-S-H being much less effective; however, separate experiments using conduction calorimetry showed that addition of solid CH had no detectable effect on the length of the induction period. Earlier experiments by Odler and Dörr (191) had also shown that the induction period was not significantly affected by seeding with CH, but that it was shortened by seeding with C-S-H.

Brown et al. (192) concluded that the kinetics of C_3S hydration can be explained if it is assumed that an initial hydrate forms a layer surrounding the C_3S grains, that the final product nucleates in this layer and that the kinetics during the middle period of reaction are controlled by the growth of C-S-H. This evidence, together with that in the previous paragraph, supports Hypothesis No. 2.

Jennings (193) showed that the concentrations in the bulk solution are controlled by transient equilibia with the layers of product surrounding the C_3S grains, and concluded that these layers acted as barriers that allowed high concentration gradients to exist near to the C_3S surfaces.

The evidence appears to the writer to favour the view, proposed by Sierra (194) and others, that the induction period is caused by a delay in either the nucleation or the growth of the C-S-H. The early product is a barrier in the sense that it allows high concentration gradients to exist, but the induction

period does not end because it is destroyed. It is not a necessary part of this hypothesis that more than one type of C-S-H should be involved, but there are several indications that this is the case; these include the evidence from cross polarization NMR (33) and ESCA (181), the observations of Ings et al. (168) using single crystals, and the kinetic arguments of Brown et al. (192), all of which suggest that a change occurs at the end of the induction period.

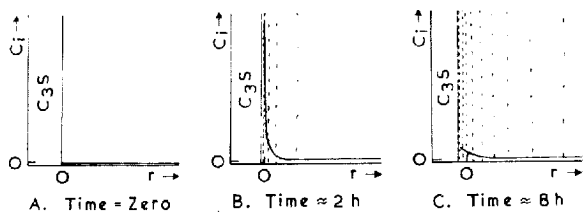

Fig. 4. Schematic plots of the analytical or total concentrations (C_i) of either CaO or SiO_2 against distance from the original position of the C_3S surface (r). Stippling represents reaction product (195).

The following discussion (195) relates to the reaction during the early and middle periods in a C_3S paste, but is applicable with some modifications to β-C_2S or to the silicate phases in cement. The immediate factors controlling the rate at which the C_3S dissolves are its inherent reactivity and the CaO and SiO_2 concentrations close to its surface. These latter depend on the rates at which the ions are supplied and removed. Initially, both concentrations are zero, and the rate of dissolution is high (Fig. 4a). This diagram is purely schematic, and the curves serve for both oxide components. Steep concentration gradients build up close to the surface, and the rate decreases (Fig. 4b). Relatively little product is deposited at this stage, but what there is limits the rate at which ions diffuse away into the solution. The rate at which the product (at this stage, almost entirely C-S-H) is deposited increases with the amount already formed, according to a law of growth, and after a time the increased rate at which ions are removed causes the concentration gradients near to the C_3S surface to weaken, so that the rate of dissolution increases (Fig. 4c). The consequent increase in CaO concentration in the bulk solution leads to precipitation of CH. After some 12 h, the increasing quantity of product causes the concentrations near the surface to increase again, and the rate of dissolution once more decreases.

During the induction period, and also in the later part of the middle period of reaction, the concentrations close to the C_3S surface must be very much higher than those in the bulk solution; if they were not, they would have no significant effect on the rate of dissolution. One should not, therefore, necessarily expect to find any close relationships between the concentrations in the bulk solution, which alone can be measured by existing techniques, and the rate of consumption of the C_3S.

This hypothesis could readily be modified, and would indeed be strengthened, if it was shown that the type of C-S-H that forms the major product only begins to form at the end of the induction period. It applies to cement paste, with modifications arising from the shell structures surrounding the grains, from the fact that the C-S-H is, initially, deposited close to the C_3S surface, and possibly also because the composition of the bulk solution differs greatly from that in a C_3S paste.

6.3 REACTIONS IN THE LATE PERIOD

During the late period, the anhydrous phases remaining in the larger grains are no longer in contact with water molecules other than those contained in the surrounding product, mainly in its micropores and interlayer spaces. Under these conditions, a through solution mechanism, if possible at all, is likely to be even slower than an 'in situ' or topochemical one. Many years ago, McConnell (66) found naturally occurring crystals of β-C_2S and of a related mineral, bredigite, that had been partially converted into plombierite (C-S-H gel), apparently by an in situ mechanism. The plombierite was sufficiently crystalline that it was possible to show that it had been formed in a definite crystallographic orientation relative to the starting material. Funk (196) showed that, under certain conditions, β-C_2S prepared in the laboratory behaved in the same way.

Extending an argument of McConnell (66), Taylor (197) calculated the numbers of atoms of each element in a specified volume of starting material or product (Table I). It was assumed that the product included the micropores but no capillary pores, and that it was saturated; these assumptions are consistent with the results of Powers and Brownyard (47) and with the density and water content of plombierite (66). The C-S-H composition was assumed to be $1.7CaO.SiO_2.4H_2O$. The numbers of oxygen atoms are the same to within 10 % in all the phases considered, but in order to replace C_3S or β-C_2S by C-S-H, many Ca and Si atoms must be lost and H atoms gained.

TABLE I. Numbers of Atoms in $1000/N_o$ cm^3 (197)

Phase	Density ($g\ cm^{-3}$)	Ca	Si	H	O
C_3S	3.21	42.2	14.1		70.3
β-C_2S	3.30	38.3	19.2		76.6
C-S-H	2.07	15.5	9.1	72.8	70.1

A mechanism was suggested by which this could occur (197). It is shown in Fig. 5 for C_3S; a similar mechanism is possible for β-C_2S. The microstructural evidence shows that an interface advances into the grain as reaction proceeds. There is no diffusion of water molecules through the inner or late product; H ions are transferred from one O atom (probably water

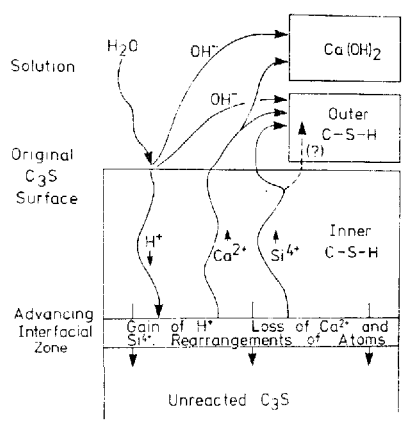

Fig. 5. Suggested mechanism for the hydration of C_3S during the late period of reaction (197).

molecule) to another within the late product, until they reach the C_3S surface, which is attacked much as if it were in contact with an aqueous solution. A narrow zone is assumed to exist at the interface, in which the substantial rearrangements of atoms needed to convert the C_3S into C-S-H take place. The Ca and Si atoms that are lost migrate outwards through the late product, and ultimately pass into the CH or outer product C-S-H. There is little or no long range movement of O atoms. It was suggested that the Si migrated by a series of movements through the faces of tetrahedra, from ones initially filled to ones initially empty, and that this same mechanism could also permit the changes in silicate anion type both during and after C-S-H formation. The movement of Si was possibly rate controlling in this stage of reaction.

Jennings (198) suggested that the porosity of the late product may be lower than assumed above. This may be so, and is indeed suggested by the results of Relis and Soroka (49). If it is, the microporosity associated with the C-S-H elsewhere in the paste would have to be greater, in order to account for the observation (47) that complete hydration is not possible at w:c ratios below about 0.38. A lower porosity in the late product would mean that less Si had to migrate, but even if this product contained no micropores at all, some Si would still have to be lost from the C_3S, and much more from the β-C_2S.

As noted earlier, C-S-H formed in situ from β-C_2S tends to adopt a preferred crystallographic orientation relative to the starting material (66,196). This may explain the persistence of relicts of twin boundaries in reacted belite grains. The numbers of Mg and of Al atoms per unit volume are roughly the same in typical alites, belites and C-S-H of cement pastes, and probably little migration of these elements occurs during the late period of reaction.

7 REACTIVITIES OF CLINKER PHASES

Barret et al. (199) suggested a mechanism for the dissolution of C_3S, based on a repeating sequence of three steps. In the first, H ions are transferred from water molecules to oxygen atoms in the C_3S surface, producing OH and hydrogen silicate ions. In the second, calcium ions pass into solution to the extent needed to cancel the unbalance of charge in both solid and solution resulting from the previous step. In the third, the remaining ions from the part of the structure already affected are dissolved. This is the most difficult process, because the cations and anions cannot move independently, and the transfer of hydrogen silicate ions was regarded as limiting the rate. A new area of surface was thus exposed, and the sequence repeated.

In this mechanism, the initial attack is by water molecules acting as Brønsted acids. This concept goes a long way towards explaining the differing reactivities of the anhydrous clinker phases. It suggests that a major factor governing reactivity is the average basicity of the oxygen atoms, i.e., the real (as opposed to formal) charges that they carry. This is greater for C_3S than for β-C_2S, because it contains oxide ions, and is greater for β-C_2S than for the less basic calcium silicates, because the latter contain oxygen atoms linked to two silicons. For a given degree of condensation, one would also predict that calcium aluminates would be more reactive than calcium silicates; this is, in fact, the case, as is shown by the very differing reactivities of C_3A and α-$CaSiO_3$, in both of which the anions are rings. The argument could be extended to explain the inertness of granulated slag to this form of attack, and its relative susceptibilty to basic attack.

The above theory does not explain the differing reactivities of β- and γ-C_2S. Jost and Ziemer (200) proposed a different hypothesis, in which they assumed that phases in which Ca-O polyhedra shared faces were reactive and those that did not were not. They showed that some earlier theories of reactivity, in which the latter was related to coordination number, distortion of polyhedra, or openness of structure did not accord with modern knowledge of the crystal structures. The calcium silicates that were hydraulically active, including β-C_2S, contained face sharing Ca-O polyhedra, and the inactive ones, including γ-C_2S, did not.

This theory is of much interest because it explains the differing reactivities of β- and γ-C_2S. However, it cannot be the main factor controlling reactivity: CaO, with no sharing of faces, is highly reactive, while corundum, in which faces are shared, is inert. It is more likely that oxygen basicity is the main factor and that this is a subsidiary one. Jost and Ziemer also considered some other crystal chemical influences on reactivity, such as twinning. These may provide a basis for understanding the many and often seemingly contradictory observations in the literature on the effects of polymorphism and ionic substitution on reactivity, especially for belites.

8 SOLUTION COMPOSITIONS AND EQUILIBRIA

8.1 THE CaO-SiO_2-H_2O SYSTEM

Barret et al. (199) described the results of experiments in which C_3S was extracted with a rapid flow of water saturated with C-S-H. These showed that the process was one of congruent dissolution followed by precipitation of a product with Ca/Si 1. The ESCA evidence (Section 6.2.1) was interpreted in terms of removal of atoms from the C_3S structure by the mechanism described in Section 7, as opposed to precipitation of a hydrate and change in its composition as suggested by Regourd et al. (181).

Fujii and Kondo (201) studied poorly crystalline calcium silicate hydrates formed by mixing solutions of calcium nitrate and sodium silicate. Freshly precipitated C-S-H of low Ca/Si ratio, giving the XRD pattern of C-S-H(I) (quasi-crystalline tobermorite) took up CaO from solution at 20°C only until the Ca/Si ratio reached 1.5, but precipitates aged at 20°-50°C could have Ca/Si ratios up to 1.87. Solubility data at 30°C were determined, and agreed substantially with results of previous investigators. Using the Gibbs-Duhem equation, Ca/Si ratios were calculated from them; they agreed with those found experimentally. The same authors also calculated thermochemical data for C-S-H from the solubility data (202). The material was treated as a solid solution of composition $(0.833 + x)Ca(OH)_2.SiO_2.0.917H_2O$ and for Ca/Si = 1.7, the values obtained, all for 298 K, were ΔH_f° = = -2890 kJ /mol, ΔG_f° = 2630 kJ/mol, and S^* = 200 J/mol.K.

Brown et al. (203) determined the concentrations of calcium and silica in solution during the first 4 hours of hydration of C_3S at 24°C. Two samples of C_3S, differing in specific surface area, and w:s ratios of 0.7 to 20 were used. For all of the experiments, some of which were obtained at times as short as 30 s, the concentrations in the filtered solutions lay on the same curve, which was close to that found by Fujii and Kondo (201) and several other previous investigators for C-S-H preparations made in other ways. An equilibrium between the C-S-H and the

solution was thus rapidly established. For the early period, in which it was assumed that no CH had precipitated, fractions of C_3S reacted were calculated from the concentrations in solution, assuming Ca/Si ratios for the solid derived from equilibrium data in the literature; this indicated that at a w:s ratio of 0.7, about 0.3 % of the C_3S had reacted at the end of the induction period. The rate of hydration thus calculated increased markedly with w:s ratio, but was almost independent of the surface area of the C_3S.

The method of calculating the degree of reaction described above may give low results, because it ignores the probable existence of high concentration gradients close to the C_3S surface; significant amounts of material may be contained in the solution in this region, and some CH may be precipitated.

Several other recent studies have yielded plots of the analytical concentration of CaO against time in C_3S hydration (164,189,204,205). All show the concentration reaching supersaturation in CH during the induction period, but the curves vary in shape, and one (205) is unusual in showing no subsequent decrease towards saturation within 3 months.

Jennings (193) critically examined the many sets of data in the literature for the concentrations of CaO and SiO_2 in solutions in contact with C-S-H. He showed that, with few exceptions, the data points lay on one or other of two, distinct curves. Those lying on the lower of these curves (Fig. 6, Curve A) had, with few exceptions, been obtained using material prepared, not from C_3S, but by mixing solutions of sodium silicate and of a soluble calcium salt or from calcium oxide or hydroxide and silicic acid. XRD evidence for some of these preparations indicated that this curve was the metastable solubility curve of C-S-H(I) or material of similar structural type but lower crystallinity. Those lying on the upper curve, B, had all been obtained from experiments similar in principle to those of Brown et al. (203), whose results were thus among the few exceptions. Barret et al. (199) had regarded a curve close to Curve B as a "supersolubility curve" of C-S-H, but this was improbable; supersaturation would be expected to produce a scatter of points and not a distinct curve. The concentrations were much too low for it to be the metastable solubility curve of C_3S. Jennings concluded that it was the metastable solubility curve of a form of C-S-H that was produced from C_3S, which was metastable relative to C-S-H(I), but not readily converted into it. Probably without exception, the points on Curve B relate to solutions undersaturated in CH. Jennings (198) pointed out that they therefore relate to the form of C-S-H existing before the end of the induction period. As noted in Section 6.2.2, he also observed that the maintenance of metastable equilibrium conditions between the solution and the hydration product showed that the latter forms a barrier which allows high concentration gradients to be maintained near to the C_3S surface.

8.2 SULPHATE AND ALUMINATE SYSTEMS

Bailey and Hampson (206) discussed ionic and neutral species present in aqueous solutions in the part of this system relevant to the early and middle periods of cement hydration. The complex species (or ion pairs) liable to occur in significant proportions, with stability constants in square brackets, are $CaOH^+$ [25], $CaSO_4$ [204], $NaSO_4^-$ [5] and KSO_4^- [10]. Aluminate ions occur as $Al(OH)_4^-$. Solubility products given were: CH, 6.46×10^{-6}; $CaSO_4.2H_2O$, 2.6×10^{-6}; gibbsite, 5×10^{-35}. These data refer to activities. An extension of the Debye-Hückel equation was used to calculate activity coefficients for the ionic species; for the neutral species, $CaSO_4$, a different expression was used. An iterative procedure was outlined, by which it was possible to calculate the concentration and activity of each species from the analytical concentrations. Table II gives typical results for a liquid phase analysis from cement, using data of Thomas et al. (207). The concentrations of Al_2O_3 and SiO_2 were very low.

Table II. Analytical and Species Concentrations and Activity Coefficients (f) for the Aqueous Phase in a Cement Paste. [Concentrations in m mol l^{-1}; K denotes (K+Na); Ref. 206]

	Ca^{2+}	SO_4^{2-}	OH^-	K^+	$CaOH^+$	$CaSO_4$	KSO_4^-
Analytical	57	58	35	15	-	-	-
Species	24.5	30.7	27.9	13.7	7.0	25.8	1.3
f	0.42	0.35	0.76	0.77	0.77	0.87	0.77

Due apparently to errors in the data, the positive and negative charges do not balance, but the importance of the corrections is clear. The uncorrected data indicate an ionic product of 7×10^{-5} for CH, which is much above saturation; the corrected data indicate an activity product of 4.6×10^{-6}, which is below saturation. Bailey and Hampson also concluded that an early decrease in the concentrations of Ca^{2+} and SO_4^{2-} was due, not to precipitation of a calcium aluminosulphate hydrate, but to conversion of a more soluble form of calcium sulphate into gypsum.

Rechenberg and Sprung (208) presented concentration data for the $CH-CaSO_4-H_2O$ system in presence of alkali hydroxides and sulphates, and for cement pore solutions. They concluded that increases in Ca concentrations in presence of sulphates were due, not to oversaturation in CH, but to the higher solubility of calcium sulphate. Neither the presence of complex species, nor deviations of activity coefficients from unity were explicitly considered, and it would be of interest to reexamine these results by the method used by Bailey and Hampson.

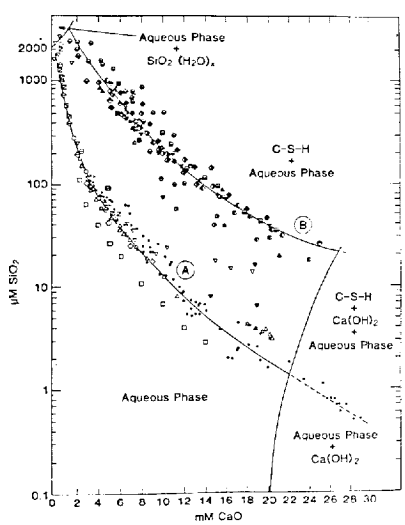

Fig. 6. Concentration data for C-S-H from various investigations; phase fields are only roughly delineated (Jennings,193).

Barret et al. (209) discussed equilibria in the $CaO-Al_2O_3-CO_2-H_2O$ system with reference to the formation of $C_4A\bar{C}_{0.5}H_{12}$ in cement systems.

8.3 PORE SOLUTIONS IN CEMENT PASTES

Since the Paris Congress, the compositions of cement pore solutions have been studied either by filtration or centrifugation at early ages and relatively high w:c ratios or by using "squezeers" to cause outflow of liquid under pressure (207,208,210-215). The results confirm and extend those of earlier workers, beginning with Lawrence (216) and Longuet et al. (217). For typical cements and normal w:c ratios, the concentrations of Na^+, K^+, Ca^{2+}, SO_4^{2-} and OH^- reach levels above 0.01 M within 1 h. Those of Ca and SO_4 subsequently fall, and are typically below 5 mM by 1 d, but those of Na, K and OH remain high, so that the solutions become ones essentially of alkali hydroxides. The concentrations change relatively little after a few days. Typical concentrations for pastes more than a few days old are Na, 0.05-0.2 M; K, 0.2-0.5 M; pH, 13.4-13.8. Other concentrations, including those of silica and alumina, are extremely low, even during the first few minutes (210).

Diamond (212) reported on pastes of a moderate alkali cement (0.32 % Na_2O, 0.60 % K_2O) at w:c = 0.4. The Na and K concentrations were compared with those that would have existed had all the alkalis in the cement dissolved and stayed in solution. Corrections were applied for the water bound in the products, which was assumed to be that retained at 105° (211), corresponding to 0.21 g/g cement for complete hydration. On this basis, about 80 % of the K and 60 % of the Na were found to remain in solution indefinitely.

The above correction for bound water appears too small, as much interlayer water in C-S-H and AFm phases, and water in AFt phases, is lost below 105°C. Recalculation assuming a more realistic bound water content of 0.32 g/g for complete hydration indicates that only about 55 % of the K and 45 % of the Na remain in solution indefinitely. Glasser and Marr (213,214), using a correction similar to the above, studied two cements, one high and the other low in alkalis. They found that about one third of the Na was in solution at 14 months, and their results indicate that about 60 % of the K is also in the solution. They stressed the difference in behaviour between Na and K, and the desirability of considering them separately; Na was much more readily accommodated in the solid products than was K.

Electron optical analyses do not distinguish material present in the pore solution from that in the hydration products, because the pore solution evaporates on drying and the dissolved material is deposited. Recent SEM analyses on pure portland cement pastes (9) show Na and K contents in the products agreeing to within experimental error with those not accounted for by unreacted clinker phases.

Concentrations during the first hour were studied by Thomas and Double (210), using a cement containing 0.19 % Na_2O and 0.42 % K_2O at w:s = 2. The Ca and SO_4 concentrations increased rapidly in the first 2 m to peak values around 60 mM and then dropped in 20 m to 30 mM. The authors attributed this to dissolution of gypsum and precipitation of ettringite or a sulphoaluminate gel; as noted earlier, Bailey and Hampson (206) attributed it to dissolution of a more soluble form of calcium sulphate and precipitation of secondary gypsum. The Na, K and OH concentrations also rose rapidly in the first few minutes, Na and K becoming constant at 5 mM and 20 mM, respectively, after 10 m. Studies from 1 h onwards were reported by Luke and Glasser (215), using a squeezer with pastes of high and low alkali cements at w:c = 0.6. For a cement similar in composition to that studied by Thomas and Double (210), Ca was relatively constant at 22-24 mM and SO_4 at 35 mM during the period from 1 to 6 h, both falling sharply during the acceleratory period that followed. Comparison with the results of Thomas and Double is difficult because of the difference in w:c ratios, but there are suggestions that both Ca and SO_4 concentrations may pass through more than one maximum during the first 6 h. Early hydration has also been followed by electrical conductivity (218).

All the concentrations result from balance between dissolution and precipitation effects. During the early period, Na and K are supplied mainly by alkali sulphates and C_3A, SO_4 by gypsum, hemihydrate, and alkali sulphates, OH by C_3A and alite, and Ca by alite, C_3A and the calcium sulphate phases. The phases most likely to be precipitated are secondary gypsum and other sulphates, C-S-H, AFt phase, and probably amorphous initial products. A full explanation of the changes in concentrations requires knowlege of the phases present at each stage, and of the appropriate solubility products, activity coefficients and stability constants of complex species. The approach described by Bailey and Hampson (206) is appropriate. The distribution of alkalis between individual phases in the unreacted cement, and especially between alkali sulphates and major clinker phases, should be taken into account.

9 ADMIXTURES

9.1 INORGANIC ADMIXTURES

Many inorganic salts accelerate the hydration, both of cement and of C_3S; a smaller number retard it. Previous investigations giving systematic information on the basic chemistry were summarized by Double (219) and by Wilding et al. (220), who also reported new data for cement. They noted that, in general, both the length of the induction period and the rate of the subsequent reaction were affected, a plot of the height of the main heat peak against the time after mixing at which it occurred giving a linear relationship with high positive correlation.

Unless added in very high concentrations, relatively few inorganic salts retard hydration. With most of those that do, precipitates are formed, and in some such cases, it has been shown that protective coatings are formed around the cement grains (207, 221,222); this may apply to the others also. The formation of a precipitate does not necessarily cause retardation, however; $MgCl_2$, for instance, is an accelerator.

For C_3S and cement alike, accelerating effects are approximately additive properties to which both anion and cation contribute. They are so widespread as to suggest that some generic property of electrolytes is involved, which may however be augmented or counteracted by specific effects (185). Compared with such organic retarders as sucrose, relatively high concentrations are needed. Very broadly, the effectiveness of an ion increases with its charge and decreases with its size, though a rank order is more clearly established for cations than for anions (220), and Ca is apparently more effective than would be expected from its charge and size. The situation is complicated by the fact that many ions are present partly as complexes, such as $CaOH^+$ (220). As was noted in a paper by Double (219), the ranking of ions shows

similarities to the Hofmeister series, which relates to the coagulation of hydrophilic colloids. The basis of this series is that particles of such colloids are kept apart by water molecules, for which the added ions compete. Wilding et al. (220) considered that the rate of hydration was controlled by diffusion of water and solutes through protective layers of C-S-H formed at a very early age around the cement grains, and that flocculation rendered these more porous. It is very probable that flocculation or coagulation of the C-S-H is the major effect, though, as was noted in Section 6.2.2, the rate of hydration in the induction and acceleratory periods, both for cement and for C_3S, is probably controlled more by nucleation and growth of the product than by its ability to act as a diffusion barrier. Jennings (198) suggested that the C-S-H particles grow by aggregation or accretion of smaller particles, possibly under 10 nm in size. This is precisely the type of process to which flocculation processes of the kind discussed above apply.

NMR evidence and CH determinations (Sections 2.2.3 and 4.2.1) show that the addition of $CaCl_2$ does not alter the Ca/Si ratio or silicate anion structure of the C-S-H formed from C_3S. Differences in late strengths are probably due to ones at the microstructural level, which have been observed on fracture surfaces (120,157), and which, in turn, can probably be attributed to ones in the rate and other conditions under which the C-S-H is formed.

The study by Wu and Young (189) on Ca and OH concentrations in C_3S suspensions containing various admixtures was mentioned in Section 6.2.2. The authors found that the times at which maximum supersaturation in CH was attained were in all cases shorter than for C_3S mixed with water; with the salts, the rates at which the C_3S supplied ions to the solution were nearly always greater, but the level of maximum supersaturation was essentially unaffected. In a similar study by aqueous solution analyses and calorimetry, Brown et al. (223) found that, in presence of $CaCl_2$ or $CaSO_4$ (≈0.02 M), acceleration began only after CH precipitation had started. They reasoned that acceleration by Ca salts was partly due to depression of the OH concentration through the common ion effect; however, this did not account for the fact that the accelerating effect depended on the nature of the anion, and some other effect, possibly flocculation of a colloid or alteration in the product microstructure, was probably also operative.

From calorimetry, combined water determinations and SEM studies, Odler and Wonnemann (224) concluded that addition of alkali sulphates to cement does not affect the progress of C_3S or C_3A hydration. The setting time is shortened, especially with K_2SO_4 due to formation of syngenite, $K_2Ca(SO_4)_2.2H_2O$.

9.2 ORGANIC ADMIXTURES

In contrast to inorganic admixtures, many organic substances retard the hydration of both cement and pure C_3S, and are often effective at very low concentrations. Double (219) and Wilding et al. (220) included a number of organic admixtures in the plots of calorimetric data mentioned in the previous section. As with inorganic admixtures, both the maximum rate of heat evolution and the time taken to reach it are in general affected, and approximately the same relationship between these two quantities was found to apply in the two cases. They noted that sucrose and raffinose are especially good retarders.

Thomas and Double (225) studied the hydration of cement, C_3S and β-C_2S in the presence of the disodium salt of ethylene diamine tetraacetic acid (EDTA) at w:s ratios of 2-10. In contrast to what happened in the absence of the admixture, for which Si concentrations in the solution were < 50 μM even by 20 s, an initial flush of Si into the solution occurred, but the concentrations decreased in 10 m to approximately the levels found for the controls. This effect was attributed to complexing of Ca by EDTA, making it unable to precipitate the silicate. This situation could only continue until all the EDTA had been used up; one EDTA anion is required to complex one Ca ion. Separate experiments confirmed that EDTA could prevent precipitation of C-S-H. EDTA is only moderately effective as a retarder. Its action was attributed to increase in the amount of C-S-H formed after the EDTA had been used up, and decrease in its Ca/Si ratio, which affected its morphology; both factors made it more effective as a protective coating.

Thomas and Birchall (226) and Birchall and Thomas (227) examined the mechanism of retardation by sugars. They determined concentrations during the first few hours of hydration in cement slurries with w:s = 2 and usually 50 mM in sucrose. As with EDTA, Si concentrations reached much higher values than in the absence of admixtures, though more slowly. In contrast to what occurred with EDTA, they did not decrease again, but remained high for at least 5 h, the longest time studied. The analytical concentrations of other elements were also high; at 1 h, at a sucrose concentration of 50 mM, they were, approximately, Ca, 125; Si, 21; Fe, 7; Al, 5; OH, 250, all in mM/l. Hydroxide was determined by titration to phenolphthalein, and includes the sucrose anion. Studies using ^{13}C NMR and ^{29}Si NMR gave no evidence that Si-sucrose complexes were formed in solution, and it was concluded that the high concentrations existed in solution because sucrose was adsorbed on nuclei of hydration products, which it thus poisoned and prevented from growing. This hypothesis was previously suggested, in relation to CH, by Young (228).

Birchall and Thomas (227) supported this conclusion with further evidence. Experiments using sucrose and either CaO or CH confirmed that sucrose inhibited nucleation of CH and showed that the solutions contained a 1:1 Ca-sucrose complex of formula $R\text{-}O^{-}\text{--}Ca^{+}\text{-}OH$, where $R\text{-}O^{-}$ is the sucrose anion. The important difference in behaviour from EDTA (226) was that the latter complexed Ca in the solution, but the Ca-sucrose complex was also adsorbed on the surface of the CH. The non-precipitation of C-S-H might be explained (226) by assuming that formation of a layer of C-S-H began with its CH-like central part, to which the silicate ions were later added, thus making it possible for poisoning by the Ca-sucrose complex to occur. One may add a further argument for supposing that the Ca-O part of the structure in any local region is formed before the Si-O part: a CH layer can exist without being condensed with silicate anions, but the manner in which the silicate ions condense is peculiar to the Ca compounds, and is entirely different from that found, e.g., with Mg. It is however, not necessary for an entire layer of a metal hydroxide structure to be pre-formed before the silicate anions are added to it.

In reply to a comment by Chatterji, Thomas and Birchall (229) considered that the Al and Fe were present in the strongly alkaline, sucrose-containing solutions as hydroxo complexes. They also (226) related the retarding properties of a number of other sugars to their structures and chemical behaviour

with cement. Sucrose and raffinose were especially good retarders because they were non-reducing sugars and contained 5-membered rings. These characteristics favoured the formation of complexes having pendant -CaOH groups, which were the actual retarding species. Sucrose and raffinose acted as monodentate ligands; some other compounds, e.g., reducing sugars and hydroxycarboxylic acids, were probably bidentate. Like the sexadentate EDTA anion, they tended to complex the Ca in solution, but were not readily adsorbed on a growing CH or C-S-H surface.

Other important classes of organic admixtures include air entraining agents and superplasticizers. Apart from incidental retarding effects, no major effects on the chemistry of the hydration process, as opposed to the rheology, seem to have been reported, and these classes of admixture will not be considered here. There is, however, evidence that superplasticizers may be adsorbed preferentially on particular clinker phases, and this may be expected to affect the early hydration reactions; also, the different dispersion of the cement grains in the mixing water may affect the microstructure of the mature product. There is as yet little systematic information on the pastes of low w:c ratio that can be prepared with their use; Groves's (10) study of CH in such pastes has already been mentioned.

10 KINETICS AND MODELLING

The modelling of hydration kinetics has recently been reviewed (230), and only a few aspects and investigations will be discussed. Parrott and Killoh (231) outlined a method for modelling the degree of hydration, heat evolution and bound water content in cement pastes. They began by summarizing data from the literature, and adding some new data (232), for the percentages of individual clinker phases consumed as a function of time. For alite, the ranges of observed values were, approximately, < 10, 40-60, 70-80 and 85-95 % at 0.1, 1, 10 and 100 d, respectively. The corresponding ranges for belite were < 5, 10-20, 30-50 and 60-95 %. For the aluminate phase, they were 5-20, 25-40, 75 and 90 %, and for the ferrite phase, zero, 20, 60 and 90 %. The data for the aluminate and ferrite phases, and also for alite and belite at low degrees of reaction, were scanty. The large spread of values for alite and belite is probably as much a result of the low precision of the available experimental methods (Section 4.1.1) as of real differences between cements.

Parrott and Killoh constructed a fitted curve for each phase from these data on a semi empirical basis. It was then assumed that the phases could be treated as hydrating independently and that the behaviour of each did not change during the course of hydration. Values were assumed for the bound water content of the products formed from each, and for the heat evolved from each, on complete hydration. It was thus possible to calculate the cumulative heat evolution, bound water content and degree of reaction for the cement as a whole, which was defined as the weight mean for the four phases. In these calculations, which gave satisfactory agreement with a range of data from the literature, account was taken of the specific surface area of the cement, w:c ratio and relative humidity (rh). New calorimetric data suggested that in the early stages of reaction, hydration rates for all four phases were proportional to the specific surface area, and that later, this variable had little effect. An equation was given relating hydration rate to rh, and a correction was introduced that lowered the assumed hydration rates if the degree of hydration exceeded 1.333 x (w:c).

The effect of particle size distribution has received attention. Knudsen (233,234) described what he termed the "dispersion model" of cement hydration. He assumed that the degree of hydration, α, could be obtained by integrating the contributions from particles of different sizes, each of which was represented by an equivalent radius, r, and that for a given time, t, an equation could be written in which some function of $\alpha(r,t)$ was equal to either kt/r or kt/r^2, where k was a constant. These two types of equation represented linear and parabolic kinetics, respectively. Knudsen showed that, after the integration had been carried out for realistic particle size distributions, a wide range of functions of α could be used with little effect on the results; it was, however, possible to distinguish whether the underlying kinetic law was linear or parabolic. He concluded that the effects of particle size distribution swamped most of the other factors affecting the kinetics, and that the possibility of establishing any detailed kinetic law from the experimental data were accordingly limited. The results did not support the widely held view that a change to diffusion control occurs after the acceleratory period; depending on the cement, and possibly on the conditions of hydration, either a linear or a parabolic law appeared to be followed throughout. The pre induction and induction periods were excluded from the analysis.

The assumptions underlying this approach require careful investigation. The importance of particle size distribution, especially at low degrees of hydration, is not in doubt, but it is difficult to reconcile the conclusions noted at the end of the previous paragraph with the experimental data on microstructural development described in Section 5.

Bezjak (235) adopted a different approach to the problem of particle size distribution. He allowed that the kinetic law governing hydration for each particle changed as hydration proceeded, but considered that the times at which these changes took place depended on the size of the particle; as a result, different kinetic laws operated simultaneously, for particles of different sizes. The assumptions in this approach, too, require careful scrutiny in the light of the microstructural evidence.

As noted by Brown et al. (230), a number of workers have represented the kinetics of C_3S or cement hydration by the Avrami-Erofeyev equation, $-\ln(1 - \alpha) = kt^m$, where k and m are constants. As these reviewers noted, the justification for its use in this context is questionable. The derivation of the left hand side of the equation assumes that nucleation of the product occurs at random within the volume initially occupied by the starting material to which α relates, and that the product also forms within this volume; this is not what happens on hydration of cement. The significance of the right hand side of the equation, which relates to nucleation and growth, is less questionable, and the values of m obtained by applying the equation may be meaningful. It must nevertheless be noted that this approach can take no account of particle size distribution, and that it is all too easy to obtain a linear relationship in the double logarithmic plots that are used in applying the equation.

The hydration of cement is a complex process, and the factors governing its kinetics are very imperfectly understood. For these reasons, the most practical attempts to model it have been those with

a high proportion of empirical content. To exploit to the maximum the high degree of predictive capacity that such approaches can provide, a broad base of experimental data is needed. This does not appear to exist at present, and its aquisition is probably the most important prerequisite for advances in the modelling of hydration kinetics. Kinetic data are needed for (a), otherwise identical cements differing in particle size distribution hydrated under identical conditions; (b), different cements of as nearly as possible the same particle size distribution hydrated under the same conditions; and (c), the same cements hydrated at different temperatures, w:c ratios and relative humidities, and under realistic conditions in which temperature and relative humidity are not constant. These data need to include determinations of the fractions of each of the individual clinker phases reacted, obtained, e.g., from QXDA; overall estimates of the degree of hydration, obtained, e.g., from "bound water" determinations, are not sufficient. The particle size distributions of the cements, bulk chemical compositions, and quantitative phase compositions, determined, e.g., by QXDA, as opposed to Bogue compositions, need to be known. Given a basis of data of this type, an approach along the lines followed by Parrott and Killoh (231) probably offers the greatest possibility of further development. It may be possible to combine it with that of Knudsen (233,234) to take greater account of the effects of particle size distribution.

ACKNOWLEDGMENTS

Many of the ideas expressed in this review owe much to discussions with others. Especially, I thank Dr. P.W. Brown and Dr. H.M. Jennings (National Bureau of Standards, USA) and Professor P.L. Pratt and Dr. K.L. Scrivener (Imperial College, London) for many helpful discussions and for making available the results of work in course of publication, and Dr. J. Cahn (National Bureau of Standards) and Professor M. Soustelle (École Nationale Supérieure des Mines, St-Étienne, France) for helpful clarifications of specific points.

REFERENCES

1. J.I. GOLDSTEIN, D.E. NEWBURY, P. ECHLIN, D.C. JOY, C. FIORI and E. LIFSHIN (1981) "Scanning Electron Microscopy and X-Ray Microanalysis", 673 pp. Plenum Press, New York.
2. D.L. RAYMENT and A.J. MAJUMDAR (1980) "The Composition of CSH Phase(s) in Hydrated C_3S Paste"; pp. II-64/II-70 in Vol. 2. of Proc. 7th. Int. Congr. Chem. Cement, Paris, 1980. Editions Septima, Paris.
3. H.F.W. TAYLOR and D.E. NEWBURY (1984) "Calcium Hydroxide Distribution and Calcium Silicate Hydrate Composition in Tricalcium Silicate and β-Dicalcium Silicate Pastes", Cem. Concr. Res. 14 (1) 93-98.
4. S. CHATTERJI (1980) "CaO/SiO_2 Mole Ratio of Calcium Silicate Hydrate in Fully Hydrated Tricalcium Silicate Paste", Cem. Concr. Res. 10 (6) 783-787.
5. S. CHATTERJI and N. THAULOW (1980) "Estimation of the Chemical Composition of Precipitated Phase by the Electron Beam Microanalytical Technique", X-Ray Spectrometry 9 (1) 5-7.
6. P.L. RAYMENT (1982) "The Effect of Pulverised Fuel Ash on the C/S Molar Ratio and Alkali Content of Calcium Silicate Hydrates in Cement", Cem. Concr. Res. 12 (2) 133-140.
7. D.L. RAYMENT and A.J. MAJUMDAR (1982) "The Composition of the C-S-H Phases in Portland Cement Pastes", Cem. Concr. Res. 12 (6) 753-764.
8. H.F.W. TAYLOR and D.E. NEWBURY (1984) "An Electron Microprobe Study of a Mature Cement Paste", Cem. Concr. Res. 14 (4) 565-573.
9. A. HARRISSON, N.B. WINTER and H.F.W. TAYLOR (1986) "An Examination of Some Portland Cement Pastes With and Without Extenders Using Scanning Electron Microscopy With X-Ray Microanalysis Capability", These proceedings, submitted.
10. G.W. GROVES (1981) "Microcrystalline Calcium Hydroxide in Portland Cement Pastes of Low Water-Cement Ratio", Cem. Concr. Res. 11 (5-6) 713-718.
11. S. CHATTERJI (1984) "A Discussion of [Ref. 3]", Cem. Concr. Res. 15 (4) 740; Reply, ibid. pp. 741-743.
12. J.A. GARD, K. MOHAN, H.F.W. TAYLOR and G. CLIFF (1981) "Analytical Electron Microscopy of Cement Pastes. I, Tricalcium Silicate Pastes", J. Am. Ceram. Soc. 63 (5-6) 336-337.
13. E.E. LACHOWSKI and S. DIAMOND (1983) "Investigation of the Composition and Morphology of Individual Particles of Portland Cement Paste. 1. C-S-H Gel and Calcium Hydroxide Particles", Cem. Concr. Res. 13 (2) 177-185.
14. S. CHATTERJI (1981) "Comment on [Ref. 12]", J. Am. Ceram. Soc. 64 (2) C39-C40; Reply, ibid. p. C40.
15. A. GHOSE and P. BARNES (1982) "Analytical Transmission Electron Microscopy of Portland Cement and Its Hydration Products", Cement (Bombay) 15 (1) 15-20; Chem. Abstr. 97 27681, 1982.
16. D. CHESCOE (1980) "Analysis of Cement Hydration Products at 100 and 200 kV", Proc. 7th. Eur. Congr. Electron Microscopy 3 54-55.
17. D. CHESCOE and P.J. GOODHEW (1981) "Optimization of Instrumental Conditions for TEM Analysis of Hydrated Cement", pp. 119-124 in Proc. Conf. Quant. Microanalysis with High Spacial Resolution, London; Chem. Abstr. 97 114261, 1982.
18. K. OGAWA, H. UCHIKAWA, K. TAKEMOTO and I. YASUI (1980) "The Mechanism of the Hydration in the System C_3S-Pozzolana", Cem. Concr. Res. 10 (5) 683-696.
19. E.E. LACHOWSKI, K. MOHAN, H.F.W. TAYLOR, C.D. LAWRENCE and A.E. MOORE (1981) "Analytical Electron Microscopy of Cement Pastes: III, Pastes Hydrated for Long Times", J. Am. Ceram. Soc. 64 (6) 319-321.
20. K. MOHAN and H.F.W. TAYLOR (1981) "Analytical Electron Microscopy of Cement Pastes: IV, β-Dicalcium Silicate Pastes", J. Am. Ceram. Soc. 64 (12) 717-719.
21. E.E. LACHOWSKI and K. MOHAN (1985) Unpublished work quoted in Ref. 11.
22. M. REGOURD, B. MORTUREUX and H. HORNAIN (1983) "Use of Condensed Silica Fume as Filler in Blended Cements"; pp. 847-865 in Vol. 2 of Proc. 1st. Int. Conf. Use of Fly Ash, Silica Fume and Other Mineral By-Products in Concrete, Montebello. Amer. Concrete Institute Sp. Publ. SP 79.
23. D.L. RAYMENT and E.E. LACHOWSKI (1984) "The Analysis of OPC Pastes: A Comparison Between Analytical Electron Microscopy and Electron Probe Microanalysis", Cem. Concr. Res. 14 (1) 43-48.
24. E.E. LACHOWSKI, K. MOHAN, H.F.W. TAYLOR and A.E. MOORE (1980) "Analytical Electron Microscopy of Cement Pastes: II, Pastes of Portland Cements and Clinkers", J. Am. Ceram. Soc. 63 (7-8) 447-452.
25. H.F.W. TAYLOR, K. MOHAN and G.K. MOIR (1985) "Analytical Study of Pure and Extended Portland Cement Pastes: I, Pure Portland Cement Pastes", J. Am. Ceram. Soc. 68 in the press.
26. A.K. SARKAR and D.M. ROY (1980) "Studies of the Trimethylsilyl Derivatives of Unhydrated Cement and Hydrated Cement Pastes by Fourier Transform Infrared Spectroscopy", J. Chem. Technol. Biotechnol. 30 (9) 485-490.

27. A. BENTUR and J.F. YOUNG (1981) "Simplified Method for Determining the Polysilicate Content in Cementitious Pastes Using Trimethylsilyl Derivatives", Cem. Concr. Res. 11 (2) 287-290.
28. N. YANG, Z. WANG, W. JIANG and Y. YIANG (1983) "Determination of the State of Calcium Silicates by the Trimethylsilylation Method", Guisuanyan Xuebao, 11 (1) 112-119; Chem. Abstr. 99 42548, 1983.
29. L.S. DENT GLASSER, E.E. LACHOWSKI, M.Y. QURESHI, H.P. CALHOUN, D.J. EMBREE, W.D. JAMIESON and C.R. MASSON (1981) "Identification of Some of the Polysilicate Components of Trimethylsilylated Cement Paste", Cem. Concr. Res. 11 (5-6) 775-780.
30. E. LIPMAA, M.MÄGI, M. TARMAK, W. WIEKER and A.-R. GRIMMER (1982) "A High Resolution ^{29}Si NMR Study of the Hydration of Tricalcium Silicate", Cem. Concr. Res. 12 (5) 597-602.
31. N.J. CLAYDEN, C.M. DOBSON, G.W. GROVES, C.J. HAYES and S.A. RODGER (1984) "Solid State NMR Studies of Cement Hydration", Proc. Brit. Ceram. Soc. (35) 55-64.
32. N.J. CLAYDEN, C.M. DOBSON, C.J. HAYES and S.A. RODGER (1984) "Hydration of Tricalcium Silicate Followed by Solid State ^{29}Si NMR Spectroscopy", Chem. Comm. (21) 1396-1397
33. N.J. CLAYDEN, C.M. DOBSON, C.J. HAYES and S.A. RODGER (1984) "Hydration Reactions of Tricalcium Silicate by ^{29}Si NMR"; pp. 370-371 in Proc. 22nd. Ampère Conf. Magnetic Resonance and Related Phenomena, Zurich, 1984. Schippert & Co., Zurich.
34. J. HIRLJAC, Z.-Q. WU and J.F. YOUNG (1983) "Silicate Polymerization During the Hydration of Alite", Cem. Concr. Res. 13 (6) 877-886.
35. K. MOHAN and H.F.W. Taylor (1982) "A Trimethylsilylation Study of Tricalcium Silicate Pastes", Cem. Concr. Res. 12 (1) 25-31.
36. F. MASSAZZA and M. TESTOLIN (1983), "Trimethyl silylation in the Study of Pozzolana-Containing Pastes", Cemento 80 (1) 49-62.
37. B.R. CURRELL, H.G. MIDGLEY, M. MONTECINOS and J.R. PARSONAGE (1985) "A Study of Portland Cement Hydration by Trimethylsilylation Techniques", Cem. Concr. Res. 15 (5) 889-900.
38. H. STADE, W. WIEKER and G. GARZO (1983) "On the Formation of Ill-Crystallized Calcium Silicates. IV. Anion Composition of the Hydration Products of Tricalcium Silicate", Z. Anorg. Allg. Chem. 500 123-131.
39. Z.-Q. WU, J. HRILJAC, C.-L. HWANG and J.F. YOUNG (1983) "Orthosilicate Analysis: A Measure of Hydration in Pastes of Alite and Portland Cement", J. Am. Ceram. Soc. 66 (5) C86-C87.
40. M. MICHAUX, D. MÉNÉTRIER and P. BARRET (1983) "Study by Trimethylsilylation of the Degree of Condensation of Silicate Ions in Calcium Hydrosilicate", C. R. Hebd. Acad. Sci. Paris, Ser. 2, 296 (14) 1043-1046.
41. H. UCHIKAWA and R. FURUTA (1981) "Hydration of C_3S-Pozzolana Paste Estimated by Trimethylsilylation", Cem. Concr. Res. 11 (1) 65-78.
42. V.V. TIMASHEV, E.V. CHEKUNOVA and N.S. NIKONOVA (1980) "Structure of Silicate Anions of Tricalcium Silicate and β-Dicalcium Silicate Hydration Products", Tr. Mosk. Khim.-Tekhnol. Inst. im. D.I. Mendeleeva 116 122-125; Chem. Abstr. 97 10947, 1982.
43. L.J. PARROTT (1981) "An Examination of the Silicate Structure of Tricalcium Silicate Hydrated at Elevated Temperature", Cem. Concr. Res. 11 (3) 415-420.
44. S.I. EVTYUKHOVA and E.P. ANDREEVA (1982), "Effect of Calcium Chloride on Polycondensation in the Isolation of Calcium Hydrosilicates as a New Phase", Vestn. Mosk. Univ., Ser. 2: Khim. 23 (2) 153-159; Chem. Abstr. 97 59925, 1982.
45. L.J. PARROTT and J.F. YOUNG (1981) "Effect of Prolonged Drying Upon the Silicate Structure of Hydrated Alite Pastes", Cem. Concr. Res. 11 (1) 11-17.
46. R.L. DAY and B.R. GAMBLE (1983) "The Effect of Thermal Pretreatment on the Creep of Hardened Cement Paste", Cem. Concr. Res. 13 (5) 638-648.
47. T.C. POWERS and T.L. BROWNYARD (1948) "Studies of the Physical Properties of Hardened Portland Cement Paste", Bull. 22, 992 pp. Portland Cement Assoc., Chicago.
48. R.F. FELDMAN (1972) "Density and Porosity Studies of Hydrated Portland Cement", Cement Technol. 3 (1) 5-14.
49. M. RELIS and J. SOROKA (1980) "Limiting Values for Density, Expansion and Intrinsic Shrinkage in Hydrated Portland Cement", Cem. Concr. Res. 10 (4) 499-508.
50. T. KNUDSEN (1982) "A Discussion of [Ref. 49]", Cem. Concr. Res. 12 (1) 123-124; Reply, ibid. p. 125.
51. R.F. FELDMAN and V.S. RAMACHANDRAN (1982) "Microstructure of Calcium Hydroxide Depleted Cement Paste. I. Density and Helium Flow Measurements," Cem. Concr. Res. 12 (2) 179-189.
52. Z.A. JUHÁSZ (1984) "Degree of Depolarization, An Indicator for Water Bonding in Hydrated Cement Pastes", Cem. Concr. Res. 14 (1) 142-144.
53. L.J. PARROTT, R.G. PATEL, D.C. KILLOH and H.M. JENNINGS (1984) "Effect of Age on Diffusion in Hardened Alite Cement", J. Am. Ceram. Soc. 67 (4) 233-237.
54. H.F.W. TAYLOR (1984) "Studies on the Chemistry and Microstructure of Cement Pastes", Proc. Brit. Ceram. Soc. (35) 65-82.
55. H. STADE, D. MÜLLER and G. SCHELER (1984) "On the Structure of Ill-Crystallized Calcium Hydrogen Silicates. V. Studies on the Coordination of Al in C-S-H-(Di, Poly) by ^{27}Al NMR Spectroscopy", Z. Anorg. Allg. Chem. 510 16-24.
56. H. STADE, K. ULBRICHT and H. MEHNER (1984) "On the Structure of Ill-Crystallized Calcium Hydrogen Silicates. VI. Chemical, ESR and Mossbauer-Spectroscopic Investigations on the Incorporation of Fe^{3+} into C-S-H (Di,Poly)", Z. Anorg. Allg. Chem. 514 149-163.
57. S.A. HAMID (1981) "The Crystal Structure of the 11Å Natural Tobermorite $Ca_{2.25}[Si_3O_{7.5}(OH)_{1.5}]$.<< >> $1H_2O$", Z. Krist. 154 (3-4) 189-198.
58. H.D. MEGAW and C.H. KELSEY (1956) "Crystal Structure of Tobermorite", Nature (London) 177 (4504) 390-391.
59. N. HARA and N. INOUE (1980), "Formation of Jennite from Fumed Silica", Cem. Concr. Res. 10 (5) 677-682.
60. N. HARA and N. INOUE (1982), "Formation of Jennite and Its Thermal Behaviour"; pp. 849-858 in Proc. 1st. Int. Symp. Hydrothermal Reactions, Tokyo, 1982. Assoc. for Sci. Doc. Infom., Tokyo Institute of Technology.
61. R.F. FELDMAN and P.J. SEREDA (1970) "A New Model for Hydrated Portland Cement and Its Practical Implications", Engnrg. J. 53 (8-9) 53-59.
62. M. DAIMON, S.A. ABO-EL-ENEIN, G. HOSAKA, S. GOTO and R. KONDO (1977) "Pore Structure of Calcium Silicate Hydrate in Hydrated Calcium Silicate", J. Am. Ceram. Soc. 60 (3-4) 110-114.
63. J.D. BERNAL (1954) "The Structures of Cement Hydration Compounds"; pp. 216-236 in Proc. 3rd. Int. Symp. Chem. Cement, London, 1952. Cement and Concrete Assoc., London.
64. H.F.W. TAYLOR (1969) "The Calcium Silicate Hydrates"; pp. 1-26 in Vol. 2 of Proc. 5th. Int. Symp. Chem. Cement, Tokyo, 1968. Cement Assoc. of Japan.

65. H.F.W. TAYLOR (1986) "Proposed Structure for C-S-H Gel", J. Am. Ceram. Soc., in the press.
66. J.D.C. McCONNELL (1955) "The Hydration of Larnite (β-Ca_2SiO_4) and Bredigite (α_1-Ca_2SiO_4) and the Properties of the Resulting Gelatinous Mineral Plombierite", Mineral. Mag. 30 (229) 672-680.
67. Å. GRUDEMO (1984) "Variation with Solid Phase Concentration of Composition, Structure and Strength of Cement Pastes of High Age", Cem. Concr. Res. 14 (1) 123-132.
68. F.A. SHEBL, F.M. HELMY and U. LUDWIG (1985) "A New Approach on the Hydration Mechanism of Tricalcium Silicate", Cem. Concr. Res. 15 (5) 747-757, and 12 other references therein.
69. H.F.W. TAYLOR and D.M. ROY (1980) "Structure and Composition of Hydrates"; pp. II-2/1 to II-2-13 in Vol. 1 of Proc. 7th. Int. Congr. Chem. Cement, Paris, 1980. Editions Septima, Paris.
70. L.E. COPELAND, D.L. KANTRO and G. VERBECK (1962) "Chemistry of Hydration of Portland Cement"; pp. 429-465 in Vol. 1 of Proc. 4th. Int. Symp. Chem. Cement, Washington, 1960. NBS Monograph 43, US Dept. of Commerce.
71. M.H. ROBERTS (1969) "Calcium Aluminate Hydrates and Related Basic Salts"; pp. 104-117 in Vol. 2 of Proc. 5th. Int. Symp. Chem. Cement, Tokyo, 1968. Cement Assoc. of Japan.
72. M. REGOURD, H. HORNAIN and B. MORTUREUX (1976), "Evidence of Calcium Silicoaluminates in Hydrated Mixtures of Tricalcium Silicate and Tricalcium Aluminate", Cem. Concr. Res. 6 (6) 733-740.
73. J. BENSTED (1982) "An Infrared Spectral Examination of Calcium Aluminate Sulphate Hydrates Encountered in Portland Cement Hydration"; pp. 85-96 in Proc. Int. Sem. Calcium Aluminates, Turin, 1982. Polytecnico di Torino.
74. S. DIAMOND and E.E. LACHOWSKI (1983) "Investigations of the Composition and Morphology of Individual Particles of Portland Cement Paste : 2. Calcium Sulfoaluminates", Cem. Concr. Res. 13 (3) 335-340.
75. R. FISCHER and H.-J. KUZEL (1982) "Reinvestigation of the System $C_4A.nH_2O$-$C_4A.CO_2.nH_2O$", Cem. Concr. Res. 12 (4) 517-526.
76. R. FISCHER, H.-J. KUZEL and H. SCHELLHORN (1980) "Hydrocalumite : Solid Solution of 'Friedel Salt' $3CaO.Al_2O_3.CaCl_2.10H_2O$ and Tetracalcium Aluminate Hydrate $3CaO.Al_2O_3.Ca(OH)_2.12H_2O$?", Neues Jahrb. Min., Monatsh. (7) 322-334.
77. W. GESSNER, D. MÜLLER, H.-J. BEHRENS and G. SCHELER (1982) "On the Coordination of the Aluminium in the Calcium Aluminate Hydrates $2CaO.Al_2O_3.8H_2O$ and $CaO.Al_2O_3.10H_2O$", Z. Anorg. Allg. Chem. 486 193-199.
78. T. SCHELLER and H.-J. KUZEL (1976) "Studies on Dicalcium Aluminate Hydrates"; pp. 217-220 in Vol. 2 (1) of Proc. 6th. Int. Congr. Chem. Cement, Moscow, 1974. Stroizdat, Moscow.
79. T. YASUE, M. MIHARA and Y. ARAI (1981) "Synthesis and Characteristics of a New Compound in the System CaO-Al_2O_3-$CaSO_3$-nH_2O", Sekko To Sekki (173) 5-15; Ceram. Abstr. 61 05696A, 1981.
80. C. VERNET (1982) "Behavior of the Sulfide(2-) Ion in the Hydration of Slag-Rich Cements. Formation of Sulfide(2-) Solid Solutions in Hexagonal Aluminate Hydrates", Silicates Ind. 47 (3) 85-89.
81. K. KIRA, Y. MAKINO and Y. MURATA (1981) "Dehydration and Rehydration of Ettringite", Gypsum and Lime, 170 7-13; Chem. Abstr. 95 66720, 1981.
82. K. OGAWA and D.M. ROY (1981) "$C_4A_3\bar{S}$ Hydration Ettringite Formation, and Its Expansion Mechanism: I. Ettringite Stability", Cem. Concr. Res. 11 (5-6) 741-750.
83. N. YANG, B. ZHONG, P. DONG and J. WANG (1984) Formation and Stability Conditions for Ettringite", Guisuanyan Xuebao 12 (2) 155-165; Chem. Abstr. 101 156478, 1984.
84. J. ZEMANN and E. ZOBETZ (1981) "Does the Carbonate Group in Thaumasite Have an Anomalously Large Deviation from Planarity?", Kristallografiya, 26 (6) 1215-1217; Sov. Phys. Cryst. 26 (6) 689-690.
85. H. EFFENBERGER, A. KIRFEL, G. WILL and E. ZOBETZ (1983) "A Further Refinement of the Crystal Structure of Thaumasite, $Ca_3Si(OH)_6CO_3SO_4.12H_2O$", Neues Jahrb. Min., Monatsh. (2) 49-59.
86. P. KRESTEN (1983) "Kinetics of the Thermal Decomposition of Thaumasite from Långban (Sweden)", Geolog. Föreningens. Stockholm Förhandl. 104 (1) 10; Chem. Abstr. 98 19621, 1983.
87. S. GROSS (1980) "Bentorite, a New Mineral from the Hatrurim Area, West of the Dead Sea, Israel", Israel J. Earth Sci. 29 81-84.
88. P.J. DUNN, D.R. PEACOR, P.B. LEAVENS and J.L. BAUM (1983) "Charlesite, a New Mineral of the Ettringite Group from Franklin, New Jersey", Am. Mineral. 68 (9-10) 1033-1037.
89. D.R. PEACOR, P.J. DUNN and M. DUGGAN (1983) "Sturmanite, a Ferric Iron, Boron Analog of Ettringite" (1983), Canad. Min. 21 (4) 705-709.
90. E. PASSAGLIA and R. RINALDI (1984), "Katoite, a New Member of the $Ca_3Al_2(SiO_4)_3$-$Ca_3Al_2(OH)_{12}$ Series and a New Nomenclature of the Hydrogrossular Group of Minerals", Bull. Minéralogie (Paris) 107 (5) 605-618.
91. R. BASSO, A. DELLA GIUSTA and L. ZEFIRO (1983) "Crystal Structure Refinement of Plazolite : A Highly Hydrated Natural Hydrogrossular", Neues Jahrb. Min., Monatsh. (6) 241-250.
92. A.I. ALEKSEEV and V. Ya. ABRAMOV (1981) "Syntheses of Calcium Hydrogarnets of $3CaO.Al_2O_3.xSiO_2(6-2x)H_2O$ Compositions", Zh. Prikl. Khim. (Leningrad) 54 (7) 1460-1464; Chem. Abstr. 95 208402, 1981.
93. R. BASSO, F. CIMMINO and B. MESSIGA (1984) "Crystal Chemical and Petrological Study of Hydrogarnets from a Fe-Gabbro Metarodingite (Gruppo di Voltri, Western Liguria, Italy)", Neues Jahrb. Min., Abhandl. 150 (3) 247-258.
94. M. MURAT (1982) "Thermal Stability of the Hydrated Calcium Aluminates and Related Phases. Characterization by Thermoanalytical Methods"; pp. 59-84 in Proc. Int. Sem. Calcium Aluminates, Turin, 1982. Polytechnico di Torino.
95. I. TEOREANU, C. HRITCU, N. BUTUCESCU and L. BUCEA (1981) "Electron Microscopic and Thermal Analysis Studies on the Hydration of 4Calcium Oxide.Alumina.Iron(III) Oxide and 2Calcium Oxide.Iron(III) Oxide", Rev. Roum. Chim. 26 (9-10) 1213-1220; Chem. Abstr. 96 39769, 1982.
96. J.M. FORTUNE and J.M.D. COEY (1983) "Hydration Reactions of Calcium Aluminoferrite", Cem. Concr. Res. 13 (5) 696-702.
97. K.S. HARCHAND, VISHWAMITTAR and K. CHANDRA (1980) "Infrared and Mössbauer Study of Two Indian Cements", Cem. Concr. Res. 10 (2) 243-252.
98. K.S. HARCHAND, R. KUMAR and K. CHANDRA (1984) "Mössbauer and X-Ray Investigations of Some Portland Cements", Cem. Concr. Res. 14 (2) 170-176.
99. J. BENSTED (1980) "A Discussion of [Ref. 97]", Cem. Concr. Res. 10 (5) 719-721.
100. K.L. SCRIVENER (1984) "The Development of Microstructure During the Hydration of Portland Cement", Thesis, University of London.
101. N.A. EISSA, H.A. SALLAM, S.H. SALAH, S.A. ABO-EL-ENEIN, M.Y. HASSAAN and A. GASSIM (1982) "Follow-Up of the Iron States in Cement Paste During the Hydration Process by Using Mössbauer Effect", Tonind. Zeit. 106 (9) 994-665.

102. L. STAFFERI (1982) "Influence of Gypsum on the C_2F Hydration at Short Periods", Cemento 79 (3) 159-168.
103. M. MUNTIGAN and M. GEORGIU-RADULESCU (1983) "Hydration of Tetracalcium Aluminoferrite ($4CaO.Al_2O_3.Fe_2O_3$) and Dicalcium Ferrite ($2CaO.Fe_2O_3$)", Stroit. Mater. Silik. Prom-St. 24 (3) 3-5; Chem. Abstr. 99 92783, 1983.
104. A. HARRISSON, H.F.W. TAYLOR and N. WINTER (1985) "Electron Optical Analyses of the Phases in a Portland Cement Clinker, with Some Observations on the Calculation of Quantitative Phase Compositions", Cem. Concr. Res. 15 (5) 775-780.
105. B. MARCHESE (1980) "Non-Crystalline $Ca(OH)_2$ in Ancient Non-Hydraulic Lime Mortars", Cem. Concr. Res. 10 (6) 861-864.
106. C. NEAL and G. STANGER (1984) "Calcium and Magnesium Hydroxide Precipitation from Alkaline Groundwaters in Oman, and Their Significance to the Process of Serpentinization", Miner. Mag. 48 (2) 237-241.
107. R.E. VITKOVSKII (1984) "Effect of Calcium Hydroxide Dehydration Determined on DTA Patterns of Cement Stone", Zh. Prikl. Khim. (Leningrad) 57 (6) 1295-1298; Chem. Abstr. 101 156487, 1984.
108. O. ABO-EL-WAFA and E.J. AL-WAKEEL (1984) "Infrared Spectroscopic Study of the Paste Hydration of Alite", TIZ-Fachber. 108 (6) 398-399.
109. I.G. SHPYNOVA, N.V. BELOV and S.K. MEL'NIK (1980) "The Possibility of Isomorphism in Portlandite", Kristallografiya 25 (5) 967-971; Sov. Phys. Cryst. 25 (5) 555-558.
110. I.G. SHPYNOVA, N.V. BELOV and S.K. MEL'NIK (1980) "The Role of the Structure of Portlandite in the Formation of Cement Stone", Kristallografiya, 25 (6) 1188-1193; Sov. Phys. Cryst. 25 (6) 680-683.
111. A.P. BARKER (1984), "Structural and Mechanical Characterization of Calcium Hydroxide in Set Cement and the Influence of Various Additives", World Cement 15 (1) 25-31.
112. A.P. BARKER, N.H. BRETT, and J.H. SHARP (1981) "An X-Ray Investigation of Strain in Calcium Hydroxide Powders", Sci. Ceram. 11 375-383.
113. G.W. BRINDLEY and C.-C. KAO (1984), "Structural and IR Relations Among Brucite Like Divalent Metal Hydroxides", Phys. Chem. Minerals 10 (4) 187-191.
114. A.P. BARKER and P. BARNES (1984) "Characterization of Calcium Hydroxide in Set Cements Using Some Established and Novel Techniques", Proc. Brit. Ceram. Soc. (35) 25-40.
115. W.A. GUTTERIDGE (1984) "Quantitative X-Ray Powder Diffraction in the Study of Some Cementive Materials", Proc. Brit. Ceram. Soc. (35) 11-23.
116. I. ODLER and H. DÖRR (1979) "Early Hydration of Tricalcium Silicate. I. Kinetics of the Hydration Process and the Stoichiometry of the Hydration Products", Cem. Concr. Res. 9 (2) 239-248.
117. K.L. SCRIVENER and P.L. PRATT (1984) "Backscattered Electron Images of Polished Cement Sections in the Scanning Electron Microscope"; pp. 145-155 in Proc. 6th. Int. Conf. Cement Microsc., Albuquerque, NM, USA, 1984. Internat. Cement Microscopy Assoc., Duncanville, TX, USA.
118. H.G. MIDGLEY (1979) "The Determination of Calcium Hydroxide in Set Cements", Cem. Concr. Res. 9 (1) 77-82.
119. J.A. DALZIELL and W.A. GUTTERIDGE (1984) Unpubl. work quoted in Ref. 115.
120. P.J. LeSUEUR, D.D. DOUBLE and G.W. GROVES (1984) "Chemical and Morphological Studies of the Hydration of Tricalcium Silicate", Proc. Brit. Ceram. Soc. (35) 177-191.
121. A. KUMAR and D.M. ROY (1984) "Effect of Fineness on Properties of Classified Cements", Cem. Concr. Aggr. 6 (1) 47-51.
122. Y. HALSE, D.J. GOULT and P.L. PRATT (1984) "Calorimetry and Microscopy of Flyash and Silica Fume Cement Blends", Proc. Brit. Ceram. Soc. (35) 403-417.
123. C.J. FORDHAM and I.J. SMALLEY (1985) "A Simple Thermogravimetric Study of Hydrated Cement", Cem. Concr. Res. 15 (1) 141-144.
124. B. EL-JAZAIRI and J.M. ILLSTON (1980) "The Hydration of Cement Paste Using the Semi-Isothermal Method of Derivative Thermogravimetry", Cem. Concr. Res. 10 (3) 361-366.
125. A. BENTUR and R.L. BERGER (1979) "Chemical Composition of C-S-H Gel Formed in the Hydration of Calcium Silicate Pastes", J. Am. Ceram. Soc. 62 (3-4) 117-120.
126. V.S. RAMACHANDRAN (1979) "Differential Thermal Method of Estimating Calcium Hydroxide in Calcium Silicate and Cement Pastes", Cem. Concr. Res. 9 (6) 677-684.
127. V.S. RAMACHANDRAN (1982) "Estimation of $Ca(OH)_2$ and $Mg(OH)_2$ - Implications in Cement Chemistry", Israel J. Chem. 22 240-246 (1982).
128. H. UCHIKAWA, S. UCHIDA and Y. MIHARA (1980) "Determination of Hydration Products in Hardened Cement Paste by Thermogravimetry and Differential Scanning Calorimetry", Sem. Gijutsu Nenpo (34) 58-62; Chem. Abstr. 95 119940, 1981.
129. S. GRZESCZYK (1982) "Study of Calcium Hydroxide Content in Hydrated Clinker by Infrared Vibrational Spectroscopy", Cem.-Wapno-Gips. (10) 151-153; Chem. Abstr. 98 203390, 1983.
130. R.L. DAY (1981) "Reaction Between Methanol and Cement Paste", Cem. Concr. Res. 11 (3) 341-349.
131. S. CHANDRA and P. FLODIN (1982) "Discussion of [Ref. 130]", Cem. Concr. Res. 12 (2) 261-262; Reply, ibid. p.263.
132. H. UCHIKAWA, S. UCHIDA, K. OGAWA and S. HANEHARA (1984) "Influence of $CaSO_4.2H_2O$, $CaSO_4.1/2H_2O$ and CaSO4 on the Initial Hydration of Clinker Having Different Burning Degree", Cem. Concr. Res. 14 (5) 645-656.
133. J. MILLET, A. BERNARD, R. HOMMEY, A. POINDEFERT and I.A. VOINOVITCH (1980) "The Determination of Ettringite in Cement and Mortar Pastes", Bull. Liaison Lab. Ponts Chaussees 109 91-95; Chem. Abstr. 94 179577, 1981.
134. J. BENSTED (1981) "An Examination of the Early Hydration Characteristics of Ultrarapid Hardening Portland Cement", Cemento 78 (2) 81-92.
135. J. BENSTED (1982) "Effects of the Clinker-Gypsum Grinding Temperature upon Early Hydration of Portland Cement", Cem. Concr. Res. 12 (3) 341-348.
136. J. BENSTED (1983) "Early Hydration of Portland Cement - Effects of Water/Cement Ratio", Cem. Concr. Res. 13 (4) 493-498.
137. J. BENSTED (1983) "Chemical Aspects of Setting of Normal Portland Cement"; pp. 69-86 in Proc. Conf. Characterization and Performance Prediction of Cement and Concrete, Henniker, NH, USA, 1982. Engineering Foundation, NY.
138. N.J. CRAMMOND (1985) "Quantitative X-Ray Diffraction Analysis of Ettringite, Thaumasite and Gypsum in Concretes and Mortars", Cem. Concr. Res. 15 (3) 431-441.
139. I. ODLER and S. ABDUL-MAULA (1984) "Possibilities of Quantitative Determination of the AFt-(Ettringite) and AFm-(Monosulphate) Phases in Hydrated Cement", Cem. Concr. Res. 14 (1) 133-141.
140. D.L. KANTRO and C.H. WEISE (1979) "Hydration of Various Beta-Dicalcium Silicate Preparations", J. Am. Ceram. Soc. 62 (11-12) 621-626.

141. K. FUJII and W. KONDO (1979) "Rate and Mechanism of Hydration of β-Dicalcium Silicate", J. Am. Ceram. Soc. 62 (3-4) 161-167.
142. S. SHIBATA, K. KISHI, K. ASAGA, M. DAIMON and P.R. SHRESTHA (1984) "Preparation and Hydration of β-C_2S Without Stabilizer", Cem. Concr. Res. 14 (3) 323-328.
143. D.D. DOUBLE, A. HELLAWELL and S.J. PERRY (1978) "The Hydration of Portland Cement", Proc. Roy. Soc. (London) A359 (1699) 435-451.
144. H.M. JENNINGS and P.L. PRATT (1980) "The Use of a High-Voltage Electron Microscope and Gas Reaction Cell for the Microscopical Examination of Wet Portland Cement", J. Mater. Sci. Lett. 15 (1) 250-252.
145. G.W. GROVES (1981) "Portland Cement Clinker Viewed by Transmission Electron Microscopy", J. Mater. Sci. 16 (4) 1063-1070.
146. B.J. DALGLEISH and K. IBE (1981) "Thin-Foil Studies of Hydrated Portland Cement", Cem. Concr. Res. 11 (5-6) 729-739.
147. K.L. SCRIVENER and P.L. PRATT (1984) "Characterisation of Portland Cement Hydration by Electron Optical Techniques", Proc. Mater. Res. Symp. 31 351-356. Elsevier Sci. Publishing Co.
148. B.MARCHESE (1983) "A Scanning Electron Microscopy Contribution to the Study on Cement Pastes. Note IV: A SEM-EDXRA Combination of Fracture Surfaces of Ordinary Portland and Blast-Furnace Cement Pastes", Cemento 80 (2) 107-120.
149. J.E. BAILEY and H.R. STEWART (1984) "C_3S Hydration Products Viewed Using a Cryo Stage in SEM", J. Mater. Sci. Lett. 3 (5) 411-414.
150. H.M. JENNINGS, B.J. DALGLEISH and P.L. PRATT (1981) "Morphological Development of Hydrating Tricalcium Silicate as Examined by Electron Microscopy Techniques", J. Am. Ceram. Soc. 64 (10) 567-572.
151. G.C. BYE (1983) "Portland Cement. Composition, Production and Properties", 149 pp. Pergamon Press, Oxford.
152. K.L. SCRIVENER and P.L. PRATT (1984) "Microstructural Studies of the Hydration of C_3A and C_4AF Independently and in Cement Paste", Proc. Brit. Ceram. Soc. (35) 207-219.
153. B.J. DALGLEISH, P.L. PRATT and E. TOULSON (1982) "Fractographic Studies of Microstructural Development in Hydrated Portland Cement", J. Mater. Sci. 17 (8) 2199-2207.
154. B.J. DALGLEISH, A. GHOSE, H.M. JENNINGS and P.L. PRATT (1982) "The Correlation of Microstructure with Setting and Hardening in Cement Paste"; pp. 137-143 in Proc. Int. Conf. Concrete at Early Ages, Paris, 1982. RILEM, Paris.
155. B.J. DALGLEISH, A. GHOSE, H.M. JENNINGS and P.L. PRATT (1982) "The Early Reaction Between Portland Cement and Water", Sci. Ceram. 11 297-302.
156. P. BARNES, A. GHOSE and A.L. MACKAY (1980) "Cement Tubules - Another Look", Cem. Concr. Res. 10 (5) 639-645; Discussions by J.D. Birchall, with Reply, and by D.D. Double, ibid. (1981) 11 (2) 299-304.
157. S. DIAMOND (1976) "Cement Paste Microstructure - An Overview at Several Levels"; pp. 2-30 in Hydraulic Cement Pastes : Their Structure and Properties. Cement and Concr. Assoc., Slough,UK.
158. P.L. PRATT and A. GHOSE (1983) "Electron Microscope Studies of Portland Cement Microstructure During Setting and Hardening", Phil. Trans. R. Soc. Lond. A310 (1511) 93-103.
159. S. DIAMOND, D. RAVINA and J. LOVELL (1980) "The Occurrence of Duplex Films on Flyash Surfaces", Cem. Concr. Res. 10 (3) 297-300.
160. B.D. BARNES, S. DIAMOND and W.L. DOLCH (1978) "Hollow Shell Hydration of Cement Particles in Bulk Cement Paste", Cem. Concr. Res. 8 (3) 263-272.
161. F.W. LOCHER (1980) "Hydration of Pure Portland Cements"; pp. 49-55 in Vol. 4 of Proc. 7th. Int. Congr. Chem. Cement, Paris, 1980. Editions Septima, Paris.
162. D. MÉNÉTRIER, D.K. McNAMARA, I. JAWED and J. SKALNY (1980) "Early Hydration of β-C_2S: Surface Morphology", Cem. Concr. Res. 10 (1) 107-110.
163. D. MÉNÉTRIER, I. JAWED and J. SKALNY (1980) "Effect of Gypsum on C_3S Hydration", Cem. Concr. Res. 10 (5) 697-701.
164. D. MÉNÉTRIER, I. JAWED and J. SKALNY (1980) "Hydration of Tricalcium Silicate - A Study by High Resolution Scanning Electron Microscopy", Silicates Ind. 45 (12) 243-248.
165. I. JAWED and J. SKALNY (1982) "Surface Phenomena During Tricalcium Silicate Hydration", J. Colloid Interface Sci. 85 (1) 235-243).
166. G.W. GROVES (1983) "T.E.M. Studies of Cement Clinker Compounds, Their Hydration and Strong Cement Pastes", Phil. Trans. R. Soc. Lond. A310 (1511) 79-83.
167. H.R. STEWART and J.E. BAILEY (1983) "Microstructural Studies of the Hydration Products of Three Tricalcium Silicate Polymorphs", J. Mater. Sci. 18 (12) 3686-3694
168. J.B. INGS, P.W. BROWN and G. FROHNSDORFF (1983) "Early Hydration of Large Single Crystals of Tricalcium Silicate", Cem. Concr. Res. 10 (6) 843-848.
169. E. BREVAL (1976) "C_3A Hydration", Cem. Concr. Res. 6 (1) 129-138.
170. I. JAWED and J. SKALNY (1982) "Surface Phenomena During Early Hydration of Tricalcium Aluminate"; pp. 125-129 in Proc. Int. Sem. Calcium Aluminates, Turin, 1982. Polytechnico di Torino.
171. F.P. GLASSER and M.B. MARINHO (1984) "Early Stages of the Hydration of Tricalcium Aluminate and Its Sodium-Containing Solid Solutions", Proc. Brit. Ceram. Soc. (35) 221-236.
172. G.Y. SHIN and F.P. GLASSER (1983) "Chemistry of Cement Pore Fluids. I. Suspension Reactions of $Ca_{3-x}Na_{2x}Al_2O_6$ Solid Solutions With and Without Gypsum Additions", Cem. Concr. Res. 13 (3) 366-376.
173. C.J. HAMPSON and J.E. BAILEY (1982) "On the Structure of Some Precipitated Calcium Alumino-Sulphate Hydrates", J. Mater. Sci. 17 (11) 3341-3346.
174. C.J. HAMPSON and J.E. BAILEY (1983) "The Micro-Structure of the Hydration Products of Tri-Calcium Aluminate in the Presence of Gypsum", J. Mater. Sci. 18 (2) 402-410.
175. J.E. BAILEY and C.E. HAMPSON (1983) "The Microstructure and Chemistry of Tricalcium Aluminate Hydration", Phil. Trans. R. Soc. London, A310 (1511) 105-111.
176. J.E. BAILEY and D. CHESCOE (1981) "A Progress Report on Analytical Electron Microscopy of the Hydration of Tricalcium Aluminate"; pp. 595-606 in Vol. 4 of Proc. 7th. Int. Congr. Chem. Cement, Paris, 1980. Editions Septima, Paris.
177. P.W. BROWN, L.O. LIBERMANN and G. FROHNSDORFF (1984) "Early Hydration of Tricalcium Aluminate in Solutions Containing Calcium Sulfate", J. Am. Ceram. Soc. 67 (12) 793-799.
178. M. FUKUHARA, S. GOTO, K. ASAGA, M. DAIMON and R. KONDO (1984) "Mechanisms and Kinetics of C_4AF Hydration with Gypsum", Cem. Concr. Res. 11 (3) 407-414.

179. C. PLOWMAN and J.G. CABRERA (1984) "Mechanism and Kinetics of Hydration of C_3A and C_4AF, Extracted from Cement", Cem. Concr. Res. 14 (2) 238-248.
180. J. BENSTED (1983) "Further Hydration Investigations Involving Portland Cement and the Substitution of Limestone for Gypsum", World Cement 14 (10) 383-392.
181. M. REGOURD, J.H. THOMASSIN, P. BAILLIF and J.C. TOURAY (1980) "Study of the Early Hydration of Ca_3Si0_5 by X-Ray Photoelectron Spectrometry", Cem. Concr. Res. 10 (2) 223-230.
182. C. STADELMANN, R. TRETTIN, W. WIEKER and M. RAMM (1985) "Studies of the Hydration of Ca_3Si0_5 by ESCA- and Krypton-Adsorption-Measurements", Cem. Concr. Res. 15 (1) 145-150.
183. D. MÉNÉTRIER, I. JAWED, T.S. SUN and J. SKALNY (1980) "Surface Studies of Hydrated β-C_2S", Cem. Concr. Res. 10 (3) 425-432.
184. W. GERHARD and E. NÄGELE (1983) "The Hydration of Cement Studied by Secondary Ion Mass Spectrometry (SIMS)", Cem. Concr. Res. 13 (6) 849-859.
185. H.F.W. TAYLOR, P. BARRET, P.W. BROWN, D.D. DOUBLE, G. FROHNSDORFF, V. JOHANSEN, D. MÉNÉTRIER-SORRENTINO, I. ODLER, L.J. PARROTT, J.M. POMMERSHEIM, M. REGOURD and J.F. YOUNG (1984) "The Hydration of Tricalcium Silicate [RILEM Committee 68-MMH, Task Group 3]", Mater. Constr. (Paris) 17 (102) 457-468.
186. M.C. BALL (1983) "Stress as a Factor in the Hydration of C_3S", Cem. Concr. Res. 13 (5) 744-746.
187. J.M. POMMERSHEIM, J.R. CLIFTON and G.J. FROHNSDORFF (1982) "Mathematical Modeling of Tricalcium Silicate Hydration. II. Hydration Sub-Models and the Effect of Model Parameters", Cem. Concr. Res. 12 (6) 765-772.
188. I. ODLER and J. SCHÜPPSTUHL (1981) "Early Hydration of Tricalcium Silicate. III. Control of the Induction Period", Cem. Concr. Res. 11 (5-6) 765-774.
189. J.Q. WU and J.F. YOUNG (1984) "Formation of Calcium Hydroxide from Aqueous Suspensions of Tricalcium Silicate", J. Am. Ceram. Soc. 67 (1) 48-51.
190. P.W. BROWN, K. GALUK and G. FROHNSDORFF (1984) "The Rate of Calcium Hydroxide Precipitation Measured by Electrical Conductance", Cem. Concr. Res. 14 (6) 843-846.
192. I. ODLER and H. DÖRR (1979) "Early Hydration of Tricalcium Silicate. II. The Induction Period", Cem. Concr. Res. 9 (3) 277-284.
193. P.W. BROWN, J. POMMERSHEIM and G. FROHNSDORFF (1985) "A Kinetic Model for the Hydration of Tricalcium Silicate", Cem. Concr. Res. 15 (1) 35-41.
193. H.M. JENNINGS (1986) "Equilibria Between Aqueous Phase and Two Types of Calcium Silicate Hydrate", J. Am. Ceram. Soc., in press.
194. R. SIERRA (1976) "Contribution to the Kinetic Study of Hydration of Tricalcium Silicate"; pp. 138-143 in Vol. 2, Part 1 of Proc. 6th. Int. Congr. Chem. Cement, Moscow, 1974. Stroizdat, Moscow.
195. H.F.W. TAYLOR (1986) "Some Aspects of Cement Hydration Mechanisms"; in Proc. Conf. Cement Manufacture and Use, Henniker, NH, 1985, in the press. Engineering Foundation, NY.
196. H. FUNK (1962) "Two Different Ways of Hydration in the Reaction of β-Ca_2SiO_4 with Water at 25 to 120°C; pp. 291-295 in Vol. 1 of Proc. 4th. Int. Symp. Chem. Cement, Washington, 1960. NBS Monograph 43, US Dept. of Commerce.
197. H.F.W. TAYLOR (1985) "The Reactions of Cement Compounds with Water"; in Proc. 10th. Int. Symp. Reactivity of Solids, Dijon, 1984, in the press. Elsevier Science Publishers, Amsterdam.
198. H.M. JENNINGS (1985) Private Communication.
199. P. BARRET, D. MÉNÉTRIER and D. BERTRANDIE (1983) "Mechanism of C_3S Dissolution and Problem of the Congruency in the Very Initial Period and Later On", Cem. Concr. Res. 13 (5) 728-738.
200. K.H. JOST and B. ZIEMER (1984) "Relations Between the Crystal Structures of Calcium Silicates and Their Reactivity Against Water", Cem. Concr. Res. 14 (2) 177-184.
201. K. FUJII and W. KONDO (1981) "Heterogeneous Equilibrium of Calcium Silicate Hydrate in Water at 30°C", J. Chem. Soc. Dalton Trans. (2) 645-651.
202. K. FUJII and W. KONDO (1983) "Estimation of Thermochemical Data for Calcium Silicate Hydrate (C-S-H)", J. Am. Ceram. Soc. 66 (12) C220-C221.
203. P.W. BROWN, E. FRANZ, G. FROHNSDORFF and H.F.W. TAYLOR (1984) "Analyses of the Aqueous Phase During Early C_3S Hydration", Cem. Concr. Res. 14 (1) 257-262.
204. K. SUZUKI, T. NICHIKAWA, K. KATA, H. HAYASHI and S. ITO (1981) "Approach by Zeta-Potential Measurement on the Surface Change of Hydrating C_3S", Cem. Concr. Res. 11 (5-6) 759-764.
205. I. ODLER and E.N. STASSINOPOULOS (1982) "On the Composition of the Pore Liquid of Hydrated Cement Pastes", TIZ-Fachber. 106 (6) 394-401.
206. J.E. BAILEY and C.J. HAMPSON (1982) "The Chemistry of the Aqueous Phase of Portland Cement", Cem. Concr. Res. 12 (2) 227-236.
207. N.L. THOMAS, D.A. JAMESON and D.D. DOUBLE (1981) "The Effect of Lead Nitrate on the Early Hydration of Portland Cement", Cem. Concr. Res. 11 (1) 143-153.
208. W. RECHENBERG and S. SPRUNG (1983) "Composition of the Solution in the Hydration of Cement", Cem. Concr. Res. 13 (1) 119-126.
209. P. BARRET, D. BERTRANDIE and D. BEAU (1983) "Calcium Hydrocarboaluminate, Carbonate, Alumina Gel and Hydrated Aluminates Solubility Diagram Calculated in Equilibrium with CO_{2g} and with Na_{aq} Ions", Cem. Concr. Res. 13 (6) 789-800.
210. N.L. THOMAS and D.D. DOUBLE (1981) "Calcium and Silicon Concentrations in Solution During the Early Hydration of Portland Cement and Tricalcium Silicate", Cem. Concr. Res. 11 (5-6) 675-687.
211. R.S. BARNEYBACK and S. DIAMOND (1981) "Expression and Analysis of Pore Fluids from Hardened Cement Pastes and Mortars", Cem. Concr. Res. 11 (2) 279-285.
212. S. DIAMOND (1981) "Effect of Two Danish Flyashes on Alkali Contents of Pore Solutions of Cement-Flyash Pastes", Cem. Concr. Res. 11 (3) 383-394.
213. F.P. GLASSER and J. MARR (1984) TThe Effect of Mineral Additives on the Composition of Cement Pore Fluids", Proc. Brit. Ceram. Soc. (35) 419-429.
214. F.P. GLASSER and J. MARR (1985) "The Alkali Binding Potential of OPC and Blended Cements", Cemento 82 (2) 85-94.
215. K. LUKE and F.P. GLASSER (1986) "Chemical Changes Occurring During the Early Hydration of PFA-OPC Mixtures"; in Proc. Conf. Materials Research Soc., Boston, 1985, in press.
216. C.D. LAWRENCE (1966) "Changes in Composition of the Aqueous Phase During Hydration of Cement Paste and Suspensions"; pp. 378-391 in Symp. Structure Portland Cement Paste and Concrete". Sp. Rep. 90, Highway Res. Board, Washington.

217. P. LONGUET, L. BURGLEN and A. ZELWER (1973). "The Liquid Phase of Hydrated Cement", Rev. Mater. Constr. (676) 35-41.
218. F.D. TAMÁS, E. FARKAS and D.M. ROY (1983) "Electrical Conductivity of Pastes Made of Clinker + Gypsum", Proc. Brit. Ceram. Soc. (35) 237-248.
219. D.D. DOUBLE (1983) "New Developments in Understanding the Chemistry of Cement Hydration", Phil. Trans. R. Soc. Lond. A310 (1511) 53-66.
220. C.R. WILDING, A. WALTER and D.D. DOUBLE (1984) "A Classification of Inorganic and Organic Admixtures by Conduction Calorimetry", Cem. Concr. Res. 14 (2) 185-194.
221. G. ARLIGUIE, J.P. OLLIVIER and J. GRANDET (1982) "Study of the Retarding Effect of Zinc on the Hydration of Portland Cement Paste", Cem. Concr. Res. 12 (1) 79-86.
222. G. ARLIGUIE and J. GRANDET (1985) "Calorimetric Study of the Hydration of Portland Cement in Presence of Zinc", Cem. Concr. Res. 15 (5) 825-832.
223. P.W. BROWN, C.L. HARNER and E.J. PROSEN (1986) "The Effect of Inorganic Salts on Tricalcium Silicate Hydration", Cem. Concr. Res. in press.
224. I. ODLER and R. WONNEMANN (1983) "Effect of Alkalies on Portland Cement Hydration. II. Alkalies Present in Form of Sulphates", Cem. Concr. Res. 13 (6) 771-777.
225. N.L. THOMAS and D.D. DOUBLE (1983) "The Hydration of Portland Cement, C_3S and C_2S in the Presence of a Calcium Complexing Admixture (EDTA)", Cem. Concr. Res. 13 (3) 391-400.
226. N.L. THOMAS and J.D. BIRCHALL (1983) "The Retarding Effect of Sugars on Cement Hydration", Cem. Concr. Res. 13 (6) 830-842.
227. J.D. BIRCHALL and N.L. THOMAS (1984) "The Mechanism of Retardation of Setting of OPC by Sugars", Proc. Brit. Ceram. Soc. (35) 305-315.
228. J.F. YOUNG (1972) "A Review of the Mechanisms of Set-Retardation in Portland Cement Pastes Containing Organic Admixtures", Cem. Concr. Res. 2 (4) 415-433.
229. S. CHATTERJI (1984) "A Discussion of [Ref. 226]", Cem. Concr. Res. 14 (5) 759-760; Reply, ibid., pp. 761-762.
230. P.W. BROWN, J.M. POMMERSHEIM and G. FROHNSDORFF (1984) "Kinetic Modeling of Hydration Processes", Cements Research Progress 1983, 245-260.
231. L.J. PARROTT and D.C. KILLOH (1984) "Prediction of Cement Hydration", Proc. Brit. Ceram. Soc. (35) 41-53.
232. J. DALZIELL and W. GUTTERIDGE (1984) Unpublished data quoted in Ref. 231.
233. T. KNUDSEN (1983) "Modeling Hydration of Portlan Cement. The Effect of Particle Size Distribution"; pp. 125-149 in Proc. Conf. Characterization and Performance Prediction of Cement and Concrete, Henniker, NH, 1982. Engineering Foundation, NY.
234. T. KNUDSEN (1984) "The Dispersion Model for Hydration of Portland Cement. I. General Concepts", Cem. Concr. Res. 14 (5) 622-630.
235. A. BEZJAK (1983) "Kinetics Analysis of Cement Hydration Including Various Mechanistic Concepts. I. Theoretical Development", Cem. Concr. Res. 13 (3) 305-318.

SUB-THEME/SOUS-THÈME 2.2

Microstructure of hardened cement paste and its effects on its behaviour.

Microstructure de la pâte de ciment hydraté et ses effets dans son comportement.

Chairman/Président:

P. K. Mehta
Civil Engineering Department
University of California, Berkeley
Berkeley, CA, U.S.A.

Principal Reporter/Rapporteur Principal:

S. Diamond
School of Civil Engineering
Purdue University
West Lafayette, IN, U.S.A.

HARDENED CEMENT PASTE - MICROSTRUCTURE AND ITS RELATIONSHIP TO PROPERTIES

P. K. Mehta
Civil Engineering Department
University of California, Berkeley, USA

Summary

The intent of this report is to highlight the research needs that are important in the near future for the advancement of the present state of our knowledge on the microstructure and structure-property relationships in hardened cement paste. For this purpose, an overview of both the known and the unknown aspects of the microstructural components, namely the types of solid phases, voids, and water, is given.

The difficulties underlying the characterization of the microstructure are discussed because a complete characterization is essential if usable models of structure-property relationship are to be developed. Some of the problems are attributable to the inherent characteristics of the component phases; others are artifacts of testing and may be overcome by development and use of new tools of research.

Even more important than new research tools is the need for new ways of thinking. It seems that we have reached a turning point in cement research, when hardened cement paste and concrete should no longer be treated as composed of independent parts that need to be individually and thoroughly characterized. For meaningful research, such complex materials need to be approached as if consisting of intricate and interconnected systems, with interdependent relationships.

Sumário

A intenção deste relatório é enfocar as necessidades de pesquisas que são importantes em um futuro próximo para o avanço do estudo do nosso conhecimento em microestrutura e em relações estrutura-propriedade na pasta de cimento endurecida.

Com esta finalidade, é fornecida uma revisão tanto de aspectos conhecidos como de aspectos desconhecidos referentes aos componentes microestruturais, em particular aos tipos de fases sólidas, vazios e água.

As dificuldades relacionadas à caracterização da microestrutura são discutidas porque uma completa caracterização é essencial se modelos usáveis da relação estrutura-propriedade forem a ser desenvolvidos. Alguns dos problemas são atribuídos às características inerentes às fases componentes, outras são artefatos do teste e devem ser eliminados pelo desenvolvimento e uso de novas aparelhagens para pesquisa.

Mesmo mais importante que novas aparelhagens para pesquisas é a necessidade de novas maneiras de pensar. Parece que chegamos a um ponto de mudança na pesquisa do cimento, quando a pasta de cimento endurecida e concreto deverão não mais serem tratados como compostos de partes independentes que necessitem serem individualmente e completamente caracterizados. Para uma pesquisa significativa, tais materiais complexos devem ser enfocados como se constituídos de intrincados e interligados sistemas, com relações interdependentes.

INTRODUCTION

There is no doubt that many important developments in structural materals have resulted from the recognition that properties of a solid are derived from its microstructure. Hardened portland cement paste is a porous solid containing voids that may be wholly or partially filled with water. Since the complete characterization of microstructure involves making a determination of the types, amounts, and distributions of all the component phases present, hardened cement paste in concrete represents one of the most complex systems among the manufactured materials.

Since the pioneering studies of Powers (1,2) first published about 40 years ago, considerable research effort has been devoted to the characterization of microstructure of hardened cement paste, and to develop usuable structure-property relationships. The intent of this report is not to present a review of the current research on the subject. Instead, for the purpose of highlighting the future research needs, an overview of the present state of our knowledge on microstructure and structure-property relationships in hardened cement paste, is given. The limitations in the knowledge are discussed and new directions for research are proposed.

MICROSTRUCTURE OF HARDENED CEMENT PASTE

Portland cement is composed of particles with a wide size distribution range, from < 1 μm to 100 μm. Most particles are multimineralic and contain a heterogeneous distribution of compounds that vary in chemical composition and crystal structure. The hydration mechanisms are very complex (3) and, therefore, representative models of the cement hydration process and products are difficult to construct. However, it is generally agreed that hardened cement paste structure is composed of a highly heterogeneous system of several kinds of solids, voids, and water. Both the known and unknown aspects of the individual components of the structure are discussed next.

Solids in Hardened Cement Paste

In addition to residual unhydrated cement particles, depending on the degree of hydration, the solid phases in hardened cement paste consist essentially of the C-S-H phase, the AF_t and AF_m phases, and CH.

Regarding the chemical composition, crystal structure, and morphology of the C-S-H, which is the principle product of portland cement hydration, studies on hydration of pure C_3S and C_2S by many researchers including Brunauer and Kantro (4) showed that the C-S-H phase is poorly crystalline, and varible in composition and morphology. From direct studies on hardened portland cement pastes, using Analytical Electron Microscopy, Moore (5) reported that the Ca/Si ratio of the C-S-H varied between 1.25 and 4.0 during the course of hydration. The content of bound water in the C-S-H is also found to vary, and is greatly influenced by the method of testing. Moore also confirmed the findings of earlier researchers that the C-S-H phase contains significant and variable amounts of foreign ions, such as Aℓ, Fe, Mg, and $\bar{S}$.

The published literature seems to contain conflicting data on average composition of the C-S-H in hardened cement paste. This is not only due to differences in the cement composition and curing conditions but also to a serious limitation of the electron optical methods, which permit the analysis of a very small size of the specimen area from a system noted for a high degree of heterogeneity. Nevertheless, there is general agreement that the chemical composition of the C-S-H in hardened cement paste shows considerable variations, not only between different cement samples but also within the same cement sample.

More important than the chemical composition is the crystal structure of the C-S-H, because the atomic structure determines the bonding forces both within a C-S-H crystal and the surrounding products in contact with it. X-ray and other diffraction techniques for structural investigation have failed to provide details of the internal structure of the C-S-H in cement pastes cured at ordinary temperature, except that the material is almost amorphous or poorly crystalline.

Bernal (6) hypothesized that the crystal structure of the C-S-H in hardened portland cement paste resembles the natural mineral, 1.1 nm tobermorite ($C_5S_6H_5$). The main structural elements of tobermorite are silicate tetrahedra chains which are believed to be responsible for the layer structure. Taylor (7) initially suggested a structural resemblence of the C-S-H to the mineral jenite ($C_9S_6H_{11}$), but later revised his opinion. Recently (8) he has proposed that most of the structural elements in the C-S-H consist of an imperfect jenite with many silicate tetrahedra missing from the chain, and that some portions of the structure resemble 1.4 nm tobermorite. Moore (5) believes that the structure does not contain layers and silicate chains but contains roughly equidimensional clusters. Grudemo (9) suggested that there are short order, hydrogen-bonded, silicate chains arranged in a square fashion, with calcium ions and water molecules between. In short, there is no agreement yet on the exact crystal structure of the C-S-H in hardened cement paste.

Among the difficulties inherent in the characterization of internal structure of poorly crystalline solids is the fact that the structural order frequently gets destroyed during the investigation, for instance specimen preparation techniques disturbing the structure. Another problem is the likelihood of the structure itself changing with time. There is evidence that some monomeric silicate tetrahedra initially present in the C-S-H are gradually replaced by dimeric components.

In regard to morphology of the C-S-H, until recently reliable techniques to characterize the size and shape of crystals in poorly crystalline solids were not available. Using transmission and scanning electron microscopic techniques, researchers have found that the arrangement of the C-S-H crystals in hardened cement paste varies from a loose network to densely agglomerated fibrils. Like the chemical composition and the crystal structure, the morphology of individual C-S-H crystals seems to vary greatly within the same paste and also with time. It is

also sensitive to specimen preparation techniques. Since the size and shape of crystals determine the surface area and interparticle bonding forces, the inability to completely characterize the C-S-H morphology presents another obstacle in the way of modelling structure-property relations in hardened cement paste.

Many of the above described limitations in the characterization of the C-S-H phase are applicable to other solid phases in hardened portland cement pastes. Both the AF_t and AF_m show highly variable chemical composition and contain substantial amounts of foreign ions (5). Although the degree of structural order in the AF_t and AF_m crystals in cement paste is far better than the C-S-H, the crystal structures and therefore the interatomic and the intercrystalline bonding forces are not precisely known. Typically, AF_t crystals are needle-shaped and AF_m crystals have hexagonal-plate morphology, and are larger than the C-S-H fibrils. However, as with the C-S-H, the size and morphology of both AF_t and AF_m crystals can vary widely within the same cement paste and also with time.

Calcium hydroxide is the only solid phase in hardened portland cement paste that occurs in a relatively pure form with only small amounts of foreign ions present (5). In young cement pastes, well-defined euhedral crystals of CH, with hexagonal-plate morphology, can be easily observed in large voids. In mature pastes, the fracture surface generally contains unusually large areas of compacted calcium hydroxide crystals. Due to the large crystal size and therefore a low surface area, the interparticle bonding force between CH crystals or between a CH crystal and other solids in the cement paste are weak.

Due to local differences in water/cement ratio, type and concentration of ions present, and curing conditions, the morphology and the size of calcium hydroxide crystals is also known to vary considerably within the same cement paste. In fact, on the basis of observed differences between the CH contents determined by quantitative X-ray diffraction and by thermal gravimetric analysis, some researchers believe in the existence of a non-crystalline or amorphous CH. The effect of changes in the crystal structure and morphology of CH on the strength and other properties of hardened cement paste are not well understood.

Voids in Hardened Cement Paste

Hardened portland cement paste contains voids of numerous shapes and sizes, the exact size distribution in a given specimen being dependent on the original water/cement ratio and degree of hydration. Typically, the size range varies from extremely small interlayer space (0.5 to 3 nm), which is conceived to be a part of the internal structure of the C-S-H, to large cavities on the order of 1 μm, occurring at the site of originally water-filled space that has not yet been filled by the solid products of cement hydration reactions.

Adsorption techniques using nitrogen, methanol, or water vapor have been widely used for measurements of pore size distribution in hardened cement pastes. Mercury intrusion porosimetry has also been effectively used but published reports (10) show that every technique suffers from one limitation or the other. This is because most of the currently used methods of determining the pore size distribution require predrying of the paste, which tends to alter the pore structure. Low-temperature calorimetry and back-scattered electron imaging techniques are being investigated to study the amounts and distribution of porous as well as solid phases, without the necessity of predrying. It is too early to present an evaluation of these techniques.

Water in Hardened Cement Paste

Depending on the environmental relative humidity to which a hardened cement paste has been exposed, there may be several types of water present in the system. The categorization of voids based on their size is particularly useful because it helps to classify the types of water in hardened cement paste according to the degree of difficulty of its removal. For instance, the interlayer space (0.5 to 3 nm) in the C-S-H crystal structure contains rigidly bonded water molecules which cannot be removed by ordinary drying. At the other extreme are the large cavities, of the order of 100 nm and more, in which water can exist in its normal (partially hydrogen-bonded) form. This free or bulk water, can be easily removed.

The intercrystallite spaces of the order of 3 to 10 nm voids, which exist within the aggregations of poorly crystalline solids such as the C-S-H, hold a type of water called the adsorbed water that exists in a relatively more ordered form than the bulk water. However, it is less rigidly bonded than the interlayer water in the C-S-H. The degree of difficulty with which the adsorbed water can be removed decreases as one moves away from the solid surface. Presumably, a similar situation exists for the other poorly crystalline phases in hardened cement paste.

Although volume changes in hardened cement paste can be related to the types of water present, researchers find it difficult to determine accurately the amounts of water associated with each type. This is because in desorption-sorption experiments it is difficult to attain equilibrium as the bonding energy of the adsorbed water held in intercrystallite pores overlaps that of the bound water associated with the C-S-H structure. Also, it should be noted that it is not possible to separate the adsorbed water contribution of the C-S-H from the other poorly crystalline phases in the system.

STRUCTURE-PROPERTY RELATIONS

In cementitious materials, strength, drying shrinkage, creep, and permeability are among the important properties that are influenced by the microstructure of hardened cement paste. However, for several reasons it has not been possible to develop usable structure-property relationships. The data from quntitative measurement tests for the properties are greatly affected by the specimen size and testing conditions. Also, in complex heterogenous system, it is not the micro-level structure aspects of the individual components but their macro-level interactions that determine the behavior of the system as a whole. Subject to these limitations, a

brief review of the structure-property relationship in hardened cement paste is presented next.

Strength

In porous solids, the indirect relationship between strength and porosity can be effectively used to determine the strength of a material from the total porosity, provided the pores are of more or less a uniform size. However, the pores or voids in hardened cement paste are not of a uniform size. Since the forces of attraction across the intercrystallite spaces in the aggregations of the C-S-H and other poorly crystalline solids are stronger than those across the large (capillary) cavities, it seems that the volume of capillary voids rather than total porosity should be strength limiting. This in fact was confirmed from the experimental data of Powers (2) who found the following exponential relationship between the compressive strength (S) and capillary porosity (P):

$$S = k(1 - P)^n$$

where k and n are constants, the value of which depends on the intrinsic strength of the cement paste at zero capillary porosity. From his experimental study Powers found the numerical values of n and k to be 3, and 34000 (psi units), respectively. Using different casting and curing conditions, other researchers have reported different values for n and k, which is to be expected due to possible changes in the intracrystallite and intercrystallite bonding forces. Numerous modified relationships between strength and capillary porosity have appeared in the published literature, but the basic idea remains the same.

From standpoint of modelling the strength-porosity relationship, thus there seem to be several unsurmountable difficulties. First, the intrinsic nature of the bonding forces, both between the several hydration products and within each remains variable and therefore indeterminate. Second, although from standpoint of strength it seems reasonable to subdivide the pore size distribution into two categories namely the pores that adversely affect the strength and the pores that do not, this task is not easy because there is no consensus about a clear dividing line between the two classes of pores; besides it is difficult to make an accurate determination of pore sizes with currently available research techniques.

Third, not much information is available about the stress concentrations and microcracks at regions of inhomogeneity (for example, at the interface between the C-S-H and CH crystals). Such microcracks arise due to environmental effects, viz. changes in humidity and temperature. In homogeneous brittle materials, under a tensile stress a crack would propagate catastrophically once the stress has reached a critical value. But in heterogeneous materials, with complex and unpredictable microcrack patterns such as hardened cement paste, the process of crack propagation can be very complicated and cannot be modelled in a realistic manner.

Drying Shrinkage and Creep

Saturated cement paste is not a dimensionally stable material. Due to moisture movements, it undergoes substantial strain when subjected to drying conditions (drying shrinkage) or sustained loading (creep). Both creep and drying shrinkage strains are generally associated with the removal of adsorbed water from intercrystallite pores (3 to 10 nm). The simple relationship between the loss of adsorbed water and drying shrinkage from a saturated cement paste is illustrated by Fig. 1 (11). However, causes of drying shrinkage and creep are not fully understood. A probable mechanism for drying shrinkage is that when confined to narrow spaces between two solid surfaces the adsorbed water causes a disjoing pressure (i.e., oriented water molecules need more space than randomly occurring molecules of bulk water), however its removal relieves the disjoining pressure thus causing the shrinkage of the system (12). Others believe that the water held in small capillaries (< 50 nm) exerts hydrostatic tension and its removal induces compression of the solid structure, thus also contributing to the shrinkage of the system.

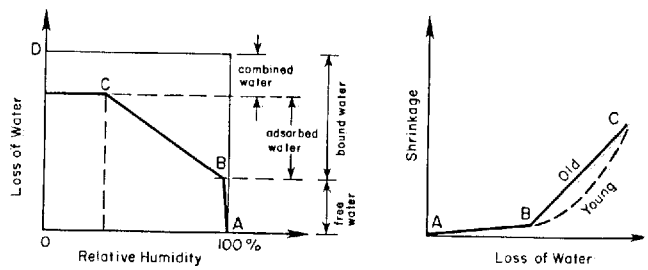

Fig. 1 Relationship Between the Drying Shrinkage and the Types of Water Present in Hardened Cement Paste (11)

There seems to be a general agreement that the bulk water in large capillary voids has essentially no effect on the drying shrinkage and creep phenomena. The published literature contains numerous constitutive relationships for prediction of drying shrinkage or creep in hardened cement paste but their validity is questionable. Among other factors, in actual practice both the drying shrinkage and creep are influenced by conditions that are difficult to model, such as the tortuosity of the water transport path through the capillary network, and the environmental humidity and temperature variations. From standpoint of modelling structure-property relations in hardened cement paste, the situation is further complicated by the fact that both drying shrinkage and creep in turn affect the structure, which leads to a highly complex situation (13).

The practical significance of the drying shrinkage and creep data for hardened cement paste is also limited by the fact that dimensional changes in concrete are largely determined by the aggregate type and content, and by the structure of the transition zone between aggregate and cement paste. In fact, several additional causes of creep in concrete, such as propagation of microcracks in the transition zone and delayed elastic strain in aggregate are not even considered in creep studies on hardened cement paste.

The mechanism of creep of hardened cement paste itself may be even more complex than proposed above. Elaborating this point, Illston (14) says, "The physical and chemical happenings that are associated with creep are on a molecular scale, and there is no convincing direct evidence of what actually goes on; so the explanation of creep has, perforce, consisted of interpreting engineering level observations in terms of likely physical and chemical phenomena. This is the way that the creep mechanism game is played, and many research workers in this field have indulged themselves and enjoyed the game."

In conclusion, as with strength-structure relationships, it is difficult to develop realistic and usable relations between the microstructure and drying shrinkage or creep in hardened cement paste. The difficulties include the great deal of inherent ambiguity in the microstructure of the paste itself, the absence of reliable methods to characterize the structure completely and to measure the properties accurately, and the complicated mechanisms underlying the phenomena.

Permeability and Durability

Since the hydration products of portland cement consist of alkaline compounds of calcium, hardened cement paste is subject to chemical deterioration when exposed to acidic environment. The rate of chemical deterioration depends on whether the chemical attack is confined to the surface, or whether it is also at work within the interior of the material. In porous solids this is determined by permeability, which is controlled by the continuity of the pore system. In addition to chemical attack from aggressive fluids permeating from the surface to the interior of the hardened cement paste, it may be noted that many other physical-chemical processes of deterioration associated with the movement of water are controlled by permeability or the state of interconnections existing between the network of pores.

That total porosity of hardened cement paste cannot be directly related to permeability has been known for some time. For instance, Powers (2) observed that the coefficient of permeability of a freshly mixed (0.7 water/cement ratio) paste was of the order of 10^{-4} to 10^{-5} cm/sec and with the progress of hydration as the capillary porosity decreased so did the coefficient of permeability, but there was no direct proportionality between the two. For a small decrease in capillary porosity during the 5- to 24-day hydration period, the coefficient of permeability dropped from 4000×10^{-11} to 10×10^{-11} cm/sec.

Attempts have been made to determine the relationship between permeability and pore size distribution obtained by mercury intrusion porosimetry. It has been reported (15,16) that the threshold pore diameter, i.e., the largest pore diameter at which mercury intrusion becomes continuous, is related to permeability. Although the validity of constitutive relationships is usually limited to the materials and test conditions used, it is possible to conclude that the permeability, like the strength of hardened cement paste, is more influenced by the volume and size of large pores than small pores. This point is illustrated by Fig. 2 (17) where P stands for the volume fraction of large pores of an arbitrary size. Again, the dividing line between the large and the small pores has to be resolved. Contrary to 4 nm proposed by Parrott (18), Mehta and Manmohan (16) found that permeability was related to the volume of pores larger than about 100 nm.

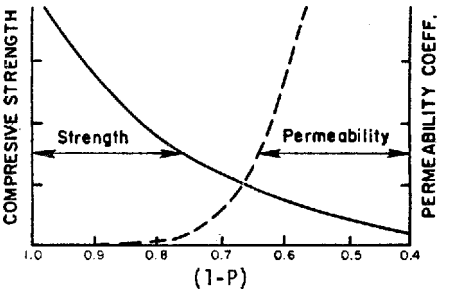

Fig. 2 Relationship Between Large Pores (P) and Strength or Permeability (17)

From standpoint of developing usable relationships between pore size distribution and permeability, it may not be enough to resolve the controversy about the minimum pore size and volume that are necessary to cause a significant amount of fluid flow in hardened cement paste. This is because in the course of time environmental interactions on the hardened cement paste are capable of altering the microstructure and, therefore, the permeability. In heterogeneous systems, internal stresses due to drying or thermal shrinkage, frost action, and expansive chemical reactions, frequently lead to microcracking. The occurrence of microcracks tends to enhance the coefficient of permeability considerably. On the other hand, as a result of attack by an aggressive fluid on hardened cement paste, the crystallization of insoluble reaction products into capillary voids may cause pore blockage and thus reduce the permeability of the system.

From given environmental conditions and microstructure of hardened cement paste, attempts have been made to predict the performance of cementitious systems to various phenomena that effect durability adversely. Examples of these phenomena are the alkali-silica reactions, sulfate attack, frost action, and corrosion of embedded steel. In this area of research, a serious gap in our knowledge is the lack of reliable information on the mechanism that lead to failure. There has been a tendency in the durability research to confuse the cause for the effect. This is because the causes of distress are often subtle and not so obvious, whereas the effects are gross and more easily observable. For instance, in the case of sulfate attack large crystals of ettringite are found in microcracks. Does the crystal growth cause the initial distress and microcracking, or does the formation of microcracks by any other process provide adequate space for the ettringite crystals to grow? Another example is the cracking-corrosion interaction in reinforced concrete structures exposed to sea water. For example, it is illustrated by Fig. 3 (19) that rather than corrosion initiating the microcracks - an assumption commonly made in corrosion research - it is the presence of microcracks in concrete which initiates the corrosion phenomenon.

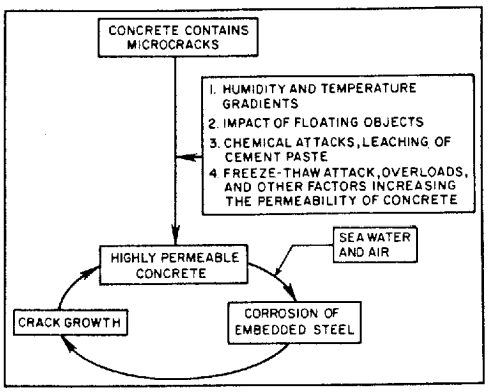

Fig. 3 Cracking-corrosion Interaction in Reinforced Concrete Exposed to Sea Water (19)

MODELLING OF STRUCTURE-PROPERTY RELATIONSHIPS

Mathematical modeling of structure-property relationships in hardened cement paste is not well advanced due to unavoidable imperfections in generalized models as a result of ambiguities in our knowlege about the solid hydration products, pore size distribution, and moisture states. In a recently published report, Parrott (18) presented a critical evaluation of the underlying problems. He observed that the inherent reactivity of cement compounds, the resulting pore fluid compositions, and the geometry of formation of the products of hydration are not understood well enough for building a general model of the reaction rates of cement compounds to be formulated. Recognizing that the variability of cement composition is a major problem, the author suggested that advances in this field are likely to depend upon the availability of cements of controlled composition and particle size, and upon the parallel use of several experimental techniques. However, the expectation that portland cements with a more uniform composition than available today will be available in the future, appears to be unrealistic. This is because due to variations in processing conditions and natural raw materials for making portland cement clinker, each clinker nodule represents a unique experiment in high-temperature phase relations.

Some researchers believe that a complete characterization of the pore structure may not be necessary for an assessment of the important engineering properties. Powers (2) suggested that many properties of the hardened cement paste can be successfully described by dividing the total pore volume into small and large pores. For the purpose of modelling the structure-property relations, Parrott (18) seems to favor the idea. This author (17) has also suggested that the compressive strength and permeability of hardened cement paste seem to be influenced more by the volume of pores larger than 50 or 100 nm, whereas the drying shrinkage and creep are influenced more by the volume of pores smaller than 10 nm. More work is needed to confirm this, and to determine the role of pores in the intermediate size range, 10-50 nm.

Further according to Parrott (18), since the properties of hardened cement paste vary considerably with the moisture state of the hydration products, the inadequate characterization of the moisture state is another shortcoming in our existing structure-property relationship models. In desorption-sorption isotherms, equilibrium is rarely achieved; again cyclic moisture conditions cause hysteresis and irrecoverable changes in pore structure during drying. Parrott says, "When we consider changes in microstructure due to hydration, carbonation, anisotropy, irreversibility, and hysteresis, the task of modelling becomes formidable. For microstructural modelling to develop and gain acceptance, it will probably be necessary to build sub-models of limited scope such that they can be combined when proven."

Recognizing that the microstructure of hardened cement paste is sensitive not only to the cement composition, water/cement ratio, and curing temperature but also to subsequent changes in hydration conditions, Parrott (18) has introduced the idea of a progressively changing rather than a static model of the structure in terms of input parameters and mathematical logic steps required to obtain specific microstructure and property outputs. These steps include calculations of cement compound reactions, volume of hydration products, bound water, heat evolution, pore structure, moisture state and mass transport, and engineering properties.

Based on the approach suggested by Parrott (18), Jennings and Johnson (20) described the results of an investigation on simulation of the microstructure development during the hydration of a cement compound, such as C_3S. According to the authors, "The core of the model is a data file which contains numerical information about the size of the volume in which hydration occurs and about all the materials contained within the volume. This file can be operated on by any of a number of subroutines, each of which represents some aspects of the hydration process. After one subroutine has effected a change, another is called on to make appropriate adjustments to other aspects of the system. This process continues until no further changes are necessary to account for all material and energy in the system. When all particles have been hydrated a specified small amount, one hydration cycle has been completed. Hydration calculations continue in this *cyclic* and stepwise manner until either a predetermined number of cycles is completed or all the anhydrous material is consumed."

A functional flow chart from the Jennings and Johnson's model (20), which simulates development of microstructure and bulk properties in hydrating cementitious systems is shown in Fig. 4. Each box

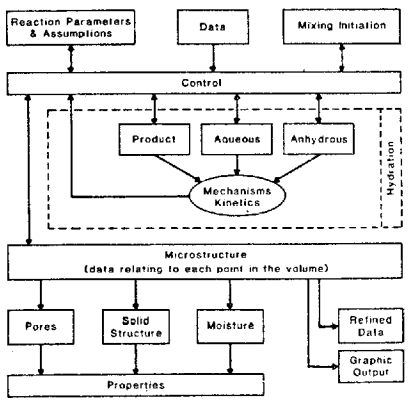

Fig. 4 Flow Chart for Simulating Hydration (20)

represents a number of subroutines, each of which performs a particular function; arrows indicate the direction of information flow. If there is controversy about a particular mechanism, several subroutines, each representing a different hypothesis may be used for trial runs. This would allow for improvements in the model as hypotheses are refined and algorithms are developed. According to the authors, any new knowledge in the form of new mechanisms and new understanding of the various processes can be easily incorporated into the model. This feature of the model is very useful because interactions between the hydration reactions of individual cement compounds are highly complex. Also, it should be possible to incorporate into the model cause-effect relationships between subtle and observable changes in the microstructure of hardened cement paste, such as the ones which occur during physical-chemical processes of deterioration.

NEW DIRECTIONS

Researchers engaged in the characterization and control of the microstructure of hardened cement paste, with the object of helping concrete technologists produce a material of improved or predictable performance characteristics, would do well to take note of a subtle paradigm shift in other fields of science. The attitude of reductionism in science is no longer considered adequate in understanding the behavior of complex systems. According to reductionists, any system can be understood from a mere sum of its parts and, therefore, all one needs to do is to reduce the system to its constituent parts, learn about the properties of each part, and then integrate the knowledge.

Commenting on the paradigm shift from the reductionist to the systems view in biological materials, Capra (21) says, "The systems view looks at the world in terms of relationships and integration. Systems are integrated wholes whose properties cannot be reduced to those of smaller units. Instead of concentrating on basic building blocks, the systems approach emphasizes basic principles of organization. Examples of systems abound in nature. Every organism - from the smallest bacterium through the wide range of plants and animals to humans - is an integrated whole. Systemic properties are destroyed when a system is dissected, either physically or theoretically, into isolated elements. Although we can discern individual parts in any system, the nature of the whole is always different from the mere sum of its parts. Another important aspect of systems is their intrinsically dynamic nature. Their forms are not rigid structures but are flexible yet stable manifestations of underlying processes."

It seems that a similar shift from the reductionist approach to the systems approach will be necessary for understanding and improving the behavior of other complex materials, such as hardened cement paste and concrete. With hardened cement paste, a great deal of ongoing research effort as well as work during the last forty years has been on the development of knowledge about the chemical composition and hydration reactions of individual cement compounds, and about the properties of solid hydration products. Yet the goal of tailoring the microstructure to produce a material with improved performance characteristics has remained elusive because in complex systems meaningful relationships do not exist between the structures at the micro-level and the properties at the macro-level.

Nevertheless, some progress has been made in the field of high strength and highly impermeable cementitious products by using superplasticizing and pozzolanic admixtures, which cause pore-size and grain-size refinements (17). These advancements have resulted from empirical studies, rather than from research on microstructure and structure-property relationship models of hardened cement paste. We seem to have exhausted the usefulness of research on the characteristics of individual constituent phases in hardened cement paste. The future research must now focus on the interconnections and interdependencies between the constituents, i.e. each of the constituent phases should be defined not by what it is by itself, but by its relationship to others.

CONCLUSION AND RECOMMENDATIONS

1. Hardened portland cement paste is a heterogeneous and complex material comprising of several types of solids, voids, and water. The chemical composition, crystal structure, and morphology of the solid phases differs markedly not only from one cement paste to another but also within the same cement paste. These characteristics of hardened cement paste are a direct result of unavoidable differences in the compound composition of cements, and the changes which occur in hydration products with curing time, temperature, and humidity.

2. Due to several limitations, complete characterization of the microstructure of hardened cement paste is very difficult. The solid products of hydration occur in a wide variety of crystalline forms ranging from amorphous to well crystallized particles of various sizes and shapes. Since several hydration products are poorly crystalline and unstable under most testing conditions, the crystal structures and the associated bonding forces are unknown. Similarly, the pore size distributions cannot be accurately known because the commonly used methods of characterization of the pore structure require predrying of the specimen, which alters the microstructure. For better characterization of porosity and solid phases, the techniques which do not require predrying, such as low temperature calorimetry and back scatter electron imaging, need to be fully investigated.

3. Structure-property relationships that may be *generally* applicable to hardened cement paste cannot be easily developed. This is because not only the microstructural characteristics of the paste but also the measured values for properties, such as strength, drying shrinkage, creep, and permeability, are greatly influenced by the specimen preparation techniques and testing conditions. Also, most available data tend to relate the behavior at the macroscopic level to hypothetical processes assumed to be occurring at the atomic or the micro levels. This is inappropriate and therefore leads to questionable relationships.

4. For reasons given above, although a large body of knowledge on the microstructure and properties of hardened cement paste has been developed since the pioneering studies of Powers on the subject about 40 years ago, very little of this knowledge has found application in actual practice. This shows that more attention than perhaps necessary has been paid by researchers to the individual parts of the system, such as chemical composition of cement compounds, hydration mechanisms, and physical-chemical characteristics of hydration products - and less attention has been paid to the validity of the knowledge produced, to the system as a whole. It follows therefore, that in order to advance the state of the art, more important than new techniques of microstructural analysis will be new ways of characterizing the system.

   For instance, instead of determining the amounts of C-S-H, AF_t, AF_m, and CH present in a hardened cement paste, it may be useful to categorize the solid phases into more cementitious (viz., C-S-H, AF_t, AF_m) and less cementitious (viz., crystalline CH) components based on surface area, and to determine the relative proportions of each component. Similarly, instead of the present arbitrary classification between gel and capillary porosity, pore size distribution should be classified into small and large pores, based on the relationship of each class to strength, drying shrinkage, and other properties of hardened cement paste.

5. For dealing with complex systems, it would help to keep abreast of developments in other disciplines. Recent advancements in theoretical physics occurred when the physicists changed their world view from reductionist to holistic. That is instead of looking at the world as a machine made up of isolated and independent parts, the physicists now see the world as a web of interconnected and therefore interdependent relationships that are intrinsically dynamic. The more we know about the world of hardened cement paste and concrete, the more it appears to be a microcosm of the human world. Therefore, for research on hardened cement paste to be applicable to concrete practice, the reductionist approach to structure-property relationships must be replaced with a holistic approach (pertaining to the whole).

6. Cement researchers must not lose sight of the fact that the bulk cement paste in concrete seldom becomes strength or permeability limiting. These and other important properties of concrete are more influenced by the microstructure of the cement paste in the transition zone which is present between coarse aggregate and bulk cement paste. Obviously, the validity of knowledge on the structure and properties of bulk cement paste will remain limited unless this knowledge is extended to understand and control the structure and properties of cement paste in the transition zone. Only new and enlarged concepts of how things are, will make it possible for us to interact with them in meaningful ways.

REFERENCES

1. T. C. Powers and T. L. Brownyard, "Studies of the Physical Properties of Hardened Portland Cement Paste," J. Amer. Concr. Inst. Proc., Vol. 43, Oct. 46 - Apr. 47, (1947).

2. T. C. Powers, "Structure and Physical Properties of Hardened Portland Cement Paste," J. Amer. Ceram. Soc., Vol. 41, No. 1, 1-6 (1958).

3. J. P. Skalny and J. F. Young, "Mechanisms of Portland Cement Hydration," Proc. Seventh Intl. Congress on the Chemistry of Cements, Paris, Vol. 1, Section II-1, 1-45 (1980).

4. S. Brunauer and D. L. Kantro, "The Hydration of Tricalcium Silicates and β Dicalcium Silicate from 5°C to 50°C," The Chemistry of Cements, Vol. 1, ed: H. F. W. Taylor, Academic Press (1964).

5. A. E. Moore, "Structure and Composition of Compounds in Hydrated Cement Pastes," Proc. Seventh Intl. Congress on the Chemistry of Cements, Paris, Vol. 3, Section VI, 93-102 (1980).

6. J. D. Bernal, "The Structure of Cement Hydration Compounds," Proc. Third Intl. Symp. on the Chemistry of Cements, London, 216-236 (1952).

7. H. F. W. Taylor, "The Calcium Silicate Hydrates," Proc. Fifth Intl. Symp. on the Chemistry of Cements, Tokyo, Vol. 2, 1-26 (1968).

8. H. F. W. Taylor, "Jennite, 1.4 nm Tobermorite, and C-S-H Gel," Paper presented at the 87th Annual Meeting of the Amer. Ceram. Soc., Cincinnati (1985).

9. A. Grudemo, "The Crystal Structure of Cement Hydration Products," Nordic Concrete Research, Oslo, Publication No. 3, 49-62 (1984).

10. P. J. Sereda, R. F. Feldman, and V. S. Ramachandra, "Structure Formation and Development in Hardened Cement Paste," Proc. Seventh Intl. Congress on the Chemistry of Cements, Paris, Vol. 1, Section VI-1, 1-44 (1980).

11. L'Hermite, "Volume Changes of Concrete," Proc. Fourth Intl. Symp. on the Chemistry of Cement, Washington, D.C., 659-694 (1960).

12. F. H. Wittman, "Interrelationship Between Structure and Properties," Proc. Conf. on Hydraulic Cement Pastes: Their Structure and Properties, Cement and Concrete Assoc., U.K., 96-117 (1976).

13. S. Diamond, "Cement Paste: Rheology and Evolution of Properties and Structures," Proc. Seventh Intl. Congress on the Chemistry of Cements, Paris, Vol. 4, 113-123 (1980).

14. J. M. Illston, J. M. Dinwoodie, and A. A. Smith, Concrete, Timber, and Metals, Van Nostrand Rheinhold Co., p. 293 (1979).

15. B. K. Nyme and J. M. Illston, "Capillary Pore Structure and Permeability of Hardened Cement Paste," Proc. Seventh Intl. Congress on the Chemistry of Cements, Paris, Vol. 3, Section VI, 182-185 (1980).

16. P. K. Mehta and D. Manmohan, "Pore Size Distribution and Permeability of Hardened Cement Pastes," ibid., Vol. 3, Section VII, 1-5 (1980).

17. P. K. Mehta, Concrete: Structure, Properties and Materials, Prentice-Hall, Inc., p. 27-34, 202 (1986).

18. L. J. Parrott, "Critical Questions in Modelling the Development of Microstructure of Hardened Cement Paste," Cement and Concrete Association, London, Report No. PP/416 (1985).

19. P. K. Mehta and B. C. Gerwick, "Cracking-Corrosion Interaction in Concrete Exposed to Marine Environment," Concrete International, Vol. 4, No. 10, 45-52 (1982).

20. H. M. Jennings and S. K. Johnson, "Simulation of Microstructure Development During the Hydration of a Cement Compound," Paper presented at the 87th Annual Meeting of the Amer. Ceram. Soc., Cincinnati (1985).

21. F. Capra, The Turning Point - Science, Society, and the Rising Culture, Bantam Books (1983).

SIDNEY DIAMOND

THE MICROSTRUCTURES OF CEMENT PASTE IN CONCRETE

SUMMARY

A review and interpretation is provided of the current state of knowledge with respect to microstructures developed in Portland cement concrete under various conditions. Current developments in techniques for studying the microstructure are described. The microstructural elements in ordinary portland cement paste are illustrated, and the details of the developing processes of cement hydration are discussed. The early formation of shells around cement grains is illustrated, and the status of hollow hydration shells described. Because of their present widespread use in concrete, the influences on microstructure of incorporation of fly ash, silica fume, and slag are stressed. The special microstructures of the interfacial zones formed around aggregates and around steel and glass fibers in concretes are explored in detail in view of the importance of these special zones to concrete performance.

FOREWARD

The present paper constitutes a review and personal interpretation by the writer of the progress made in the general area of hydrated cement paste microstructure since the preceding 7th International Congress in Paris in 1980.

At that Congress there was no specific principal report devoted to the microstructure of paste per se: rather, the subject was covered in part by Taylor and Roy (1) in their principal paper on "Structure and Composition of Hydrates" and in part by Sereda, Feldman, and Ramachandran in their principal paper on "Structure Formation and Development in Hardened Cement Pastes" (2). While both treatments provided significant microstructural coverage, both were primarily concerned with other, albeit related, aspects of cement paste. Contributions to the Paris Congress relating to paste microstructure were summarized by the writer in his General Report (3); there were comparatively few of these.

In the intervening years there has been a major increase in the availability of scanning electron microscopes, which continue as the primary tool for microstructural investigation in cement systems. In consequence, many more laboratories have facilities available for studies in this area, and there has been a corresponding increase in the number of papers published. The present review is not intended to be exhaustive, and because of the increased activity in this area a number of excellent papers will not be discussed.

In addition to the formally published literature, the writer is aware of two excellent recent Ph. D. theses devoted largely to paste microstructure, one by Scrivener (4) dealing primarily with cement paste per se, and one by Monteiro (5) dealing mostly with microstructural effects on concrete properties.

Despite this rise in research activity in the area, microstructures of cement paste systems are still not well understood by the general technical community. The difficulty of selecting the pertinent aspects of the microstructure of even a particular cement paste under investigation remains formidable; describing it in a publication so that it may readily be understood is even more difficult. A discussion the nature and magnitude of some of these difficulties was presented by the present writer in a recent treatment (6).

In that paper it was calculated that a set of 10 of the usual SEM micrographs taken in various places on a 1 cm square cement paste sample surface at 10,000x (a normal magnification for studying cement paste) provides a sampling of only 0.001% of the surface of that specimen. If the microstructure varies appreciably from place to place, as it ordinarily does, it is difficult to be sure that this limited sampling is adequate to insure that a proper representation of the structure has been secured.

Furthermore, each individual micrograph may reveal several different microstructural features. Picking out the pertinent points for discussion and then describing the structures verbally is something of an art.

It is hoped that despite these difficulties the present paper may help to contribute to a more general understanding of cement paste as a material, as well as to an appreciation of the present state of knowledge of its microstructure.

It seems appropriate that before entering into the details, the writer specifically indicate something of his own biases concerning the subject. They include the following judgements:

1. The present writer feels strongly that the cement paste microstructures of primary importance are not those of laboratory mixed cement pastes but rather those microstructures actually present between sand grains and aggregates in concrete in service. The two may be similar, but they are certainly not identical.

2. Most of the lessons that can readily be learned from the study of the microstructures developed in pastes of pure cement minerals (e.g. C_3S) have by and large already been established, and future work on the development of microstructures should more heavily concentrate on cement, rather than C_3S, pastes. This is especially so in view of the fact that the cement hydration processes in concrete are strongly affected by chemical and other features not present in laboratory-mixed C_3S pastes.

3. There has also been something of a major change in concrete practice since 1980 in that "pure" portland cement concrete has become almost a rarity in many countries, most concrete now containing fly ash, slag, silica fume, or pozzolans of one type or another. Accordingly, the microstructures of cement pastes developed in the presence of these supplementary cementitious components are no longer a peripheral matter of interest primarily to specialists, but have become matters of central concern.

4. Cement paste microstructure needs to be understood primarily because of its influence on the behavior and properties of the concretes and other cement systems in which it is incorporated. However, the behavior may often be controlled by special microstructures that arise in specific locations in the system, rather than by the general or most prevalent microstructure. Illustrations in concrete include the special areas adjacent to aggregate interfaces, for example, or zones surrounding embedded steel reinforcement or prestressing cables. Another example is the special microstructure that wet exposure develops between individual glass fibers in strands of alkali-resistant glass fibers in GFRC (glass fiber reinforced concrete).

The remainder of the present paper will be devoted to a synthesis and interpretation of cement paste microstructures in the light of the extensive developments that have been recorded in the past six years.

INTRODUCTION

Hardened cement paste is a relatively inhomogeneous assemblage of particles, films, microcrystals, and other solid structural elements bonded together in a porous mass, and in its native state

containing pore solution and some empty (air-filled) spaces. The non-solid components may be as important as the solid elements in some contexts.

On drying, much of the pore solution evaporates, shrinkage usually occurs, and ultrastructural details in certain particles may change irreversibly.

The air-filled spaces in the cement paste of partially dried concretes consist of two distinct classes of space: relatively large, mostly spherical entrained and entrapped air voids, usually lined with a smooth layer of calcium hydroxide; and smaller, geometrically complex "capillary" pores representing the residue of space between the original cement grains. "Capillary" pores resaturate readily; air voids do not. To avoid confusion, it is prudent to keep the distinction between the two classes clearly in mind, a caution that has not been universally adhered to in the literature.

"Capillary" pores tend to fill up to a greater or lesser degree with solid hydration products on continued hydration, and give way to still finer pores between hydration product particles and to some extent to "gel" pores within them. The boundary between ultrafine pores "between" and "within" C-S-H gel particles has never been conclusively established. Indeed, in a recent paper Taylor (7) stressed the point that the term gel porosity is a misnomer, because the water supposedly present in gel pores is in reality present in the hydrated phases. The subject remains an area of much controversy and confusion.

In concrete, cement pastes exist as relatively thin ribbons of material surrounding and separating sand grains and coarse aggregate pieces. As published measurements have indicated (8), in representative concretes the average spacing between adjacent sand grains at their narrowest separation is only of the order of 100 μm, about the magnitude usually ascribed to the sum of the two "aureoles de transition" thought to surround each aggregate grain.

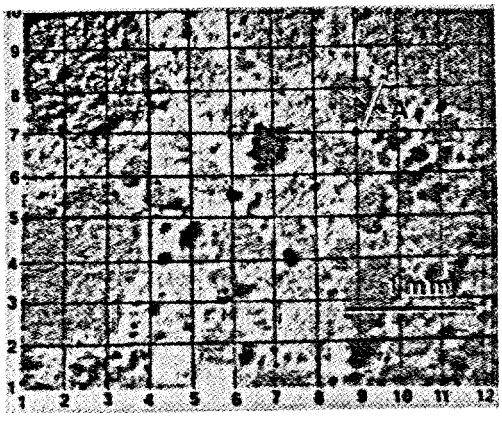

Fig. 1. Illustration of narrowness of paste ribbons in concrete.

Fig. 1, from (8), shows an area on a plane surface of a typical concrete; widths of the paste ribbons were measured on a statistical basis as controlled by the superimposed grid. The position marked "A" shows a typical measurement.

Although the ribbons of paste are narrow, individual cement paste particles are two orders of magnitude smaller yet, ranging in size from a fraction of a μm to several μm. Hence the term "microstructure" and the need for electron-based microscopes to investigate the details.

Cement paste arises as a direct result of the hydration of portland cement with a restricted amount of water. The microstructure varies greatly with the amount of water (more conventionally, with the water:cement ratio) used. The importance of this feature cannot be stressed too highly, both in terms of microstructure itself and in terms of the effects produced on many technical properties (strength, permeability, resistance to service-induced degradation) of the material in service.

The microstructure in a given system is also a function of time. Early age microstructural features develop rapidly on contact of the cement with water. These change with time on a scale of minutes or hours at first, and then more slowly over the first week or so after mixing. The hydration processes in most cement systems are rarely quite completed in practice; as hydration processes continue over periods of months or years, concomitant slow changes in microstructure may occur from deposition of late hydration products. Changes may also come about by solution and reprecipitation of certain previously-existing components independently of additional hydration.

Thus a specific cement paste or concrete hydrating under specific conditions generates not a single microstructure but a successive set of microstructures at progressive stages of development. To add to the complication, any given paste at a given age will be found to vary in microstructural details from place to place, reflecting variations in the local assemblage of the clinker grains that gave rise to the paste in each vicinity.

As a practical matter, the local variations may be adequately described by reference to only two or three typical local assemblages, which after a few days may not change very much with time. However, zones near aggregate interfaces and other special areas always require additional specific investigation to describe their pertinent features.

The writer considers that a proper microstructural description should consist of at least (a) a description of the various kinds of structural elements (particles, films, crystals, entrained air voids, etc.) that are present, together with some indication of their sizes and proportions, and (b) a description of their juxtapositions and mutual arrangements in space within the volume of the system. There may be several different typical assemblages of particles co-existing in different places within the cement paste; this fact should be duly noted, and the relative proportions of each estimated. Unfortunately, few, if any, "proper" microstructural studies meeting this standard have yet been published.

In the present state of the art, microstructural descriptions are ordinarily qualitative, and are necessarily quite subjective. However it appears

that computer-based image analysis techniques may soon make quantitative descriptions more generally available.

Such computer-based image analysis programs should not be confused with more ambitious computer modelling programs. In the latter quantitative descriptions are derived by algorithms based on specific assumptions for successive periods of hydration under specified conditions. Such hydration modeling programs are currently being developed at several institutions, and the concepts involved have been discussed in some detail by Jennings et al. (9). A remarkable illustration of what can be done along these lines with current technology was presented by Jennings and Johnson (10), in terms of a simulation of the hydration processes and microstructural development in a C_3S paste.

Fig. 2, kindly supplied by H. M. Jennings, represents one output of such a program. The figure is a computer-drawn microstructural image in which the circles represent the original C_3S grains and the hexagons precipitating calcium hydroxide crystals. The original boundaries of the C_3 grains are depicted by the narrow white circles; the gray areas represent C-S-H gel deposited both within and external to the original grain boundaries. The figure represents the state of the system at a specific hydration time, and sequences of such figures can be produced to image the calculated microstructure at any desired age.

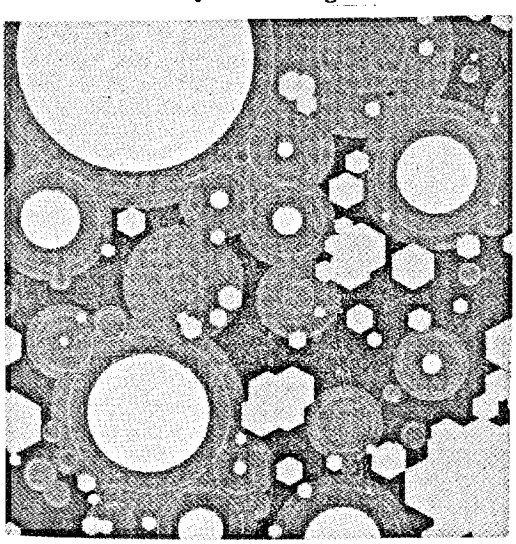

Fig. 2. Computer-drawn representation of a stage in C_3S hydration (H. M. Jennings).

While the concept and some of the specifics of such modelling of microstructural development can be extended to portland cement paste, such extension is extremely difficult because of the much greater complexity of the cement system, and success should not be expected in the near future.

Properly speaking, pore size distributions elements should logically form a part of a microstructural picture of a cement paste. However, historically such distributions have been developed using techniques (such as mercury intrusion porosimetry) that are separate from and do not correlate readily with microscopic studies. Furthermore, a number of controversies have arisen relative to their interpretation. Because of these difficulties, pore size distributions will not be treated in detail in this review.

TECHNIQUES OF INVESTIGATION

The sizes of the structural features in cement paste are such that the magnification capability of optical microscopes, however refined, are of little applicability, and electron microscopes of one kind or another are required.

Early work in the area was done by transmission electron microscopy (TEM), but long before the Paris Congress scanning electron microscopy (SEM) had effectively displaced TEM techniques for this purpose. The latter has major advantages in ability to handle large samples conveniently, and in ability to permit one to visualize depth and topography; this has more than made up for the more limited resolution offered by most SEM instruments.

Dalgleish and Ibe (11) developed effective procedures for ion-beam thinning sections of hardened cement paste for use in then newly-developed scanning transmission electron microscopy (STEM). In STEM examinations the image is formed by a raster technique, but is derived from electrons transmitted through very thin sections or films of materials, as in TEM. A combination of conventional fracture-surface SEM and ion-beam thinned STEM micrographs were used to provide a more definitive picture of the types of structures present.

Among the several possible imaging modes available in SEM is one in which the backscattered electrons are used to form the raster image. While the resolution is ordinarily not as high as the usual secondary electron images available from the same instrument, Scrivener and Pratt (12) have taken advantage of the differential element contrast capability available in this mode to produce extremely useful and informative backscatter electron image (BEI) micrographs of polished cement paste surfaces. These clearly delineate, for example, areas of calcium hydroxide crystals from areas of C-S-H gel, or areas of hydration product from areas of unhydrated clinker compounds. They can readily be used with image analysis techniques to produce quantitative estimates of the contents of specific components in the paste.

Barker at al. (13) illustrated the potential applicability for cement paste of a number of unusual microscopic technologies, including synchrotron topography and scanning acoustic microscopy, as well as BEI. At the same conference Barker and Barnes (14) reviewed and illustrated a variety of techniques for distinguishing phase composition of microstructural features within the SEM.

The continued utility of transmission electron microscopy, particularly if ion-beam thinned specimens, has been demonstrated by Groves (15).

All of the techniques mentioned so far necessarily involve drying of the paste specimen and exposure to high vacuum. The drying procedure itself may have unwanted effects, especially at very early ages. Orr (16) described a freeze-drying proce-

dure designed to minimize such difficulties. Possible effects of drying cement pastes on their microstructural characteristics were also emphasized by Parrott (17), who proposed a solvent replacement procedure followed by evaporation of the low surface tension replacement fluid used.

It is also possible to avoid drying, by imaging wet cement pastes in special wet cells using high voltage (transmission) electron microscopy (HVEM); instruments capable of doing this ordinarily operate at ca. 1 million electron volts and are available only in a few centers. Jennings et al. (18) combined HVEM observations with both conventional SEM and STEM observations of ion-beam thinned specimens, but unfortunately, only studied hydrating C_3S pastes. While the HVEM images are provided at high magnifications, their crispness and the ability to define detail are limited.

Use of a "wet cell" of an entirely different type within a standard SEM was reported by Diamond et al. (19). In this system the image is formed by backscattered electrons detected by a Robinson detector; the specimens themselves are completely saturated and are kept wet by a stream of water-saturated air pumped through the specimen chamber, which is isolated from the high vacuum electron column. The system was developed primarily for detection and observation of crack formation on paste and mortar specimens loaded in tension (20 - 22) and subsequently, in compression (23) within the SEM; its use and characteristic operating parameters were described in some detail by Diamond et al. (24).

Resolution in this system is adequate for observations of cracking and crack propagation, but not for proper study of microstructural details in cement paste. Micrographs taken at much more than 1,000x suffered from loss of resolution. A somewhat different kind of wet cell has recently been developed by Jennings et al. at the National Bureau of Standards for which a patent has been applied for (25); this device is said to be capable of securing useful micrographs of wet pastes at up to about 5,000x magnification, and thus does have the potential for study of cement paste microstructure.

MICROSTRUCTURAL ELEMENTS IN ORDINARY CEMENT PASTES

As is well known, portland cements hydrating under ordinary conditions give rise to several morphological forms of calcium silicate hydrate gel (usually abbreviated as C-S-H gel or even CSH); to calcium hydroxide; to ettringite or ettringite-like AFt phases; to calcium aluminate monosulfate hydrate or related AFm phases; and occasionally to small amounts of other phases, notably hydrogarnets. These, combined with residues of unhydrated clinker components and the pore spaces between (and possibly within) the solid particles comprise the microstructural elements making up cement paste.

It is usually considered that C-S-H gel makes up the largest proportion of the system, with calcium hydroxide of somewhat lesser importance, and the AFt and AFm phases being of relatively minor account. The total of these phases naturally increases with degree of hydration, as the proportion of residual unhydrated cement diminishes. The relative volume of pore space also diminishes, but the degree to which the original water-filled space between the cement grains is filled depends strongly on the water:cement ratio.

Taylor (7) has recently calculated from experimental measurements the weight and volume proportions of each of the phases in several specific portland and portland-fly ash pastes. A w:c 0.5 portland cement paste hydrated for 3 months was found to have, in its saturated state, volume percentages of 40% C-S-H gel, 16% AFm product, 12% calcium hydroxide (plus 1% calcium carbonate carbonation product), a total of 8% of residual unhydrated cement, and a total of 24% of pore space. No attempt was made to define the relative proportions of the different C-S-H gel types. However, weight percentages in the saturated state, and volume and weight percentages in the dried condition were also estimated. The unexpectedly high content of AFm phase and the apparent absence of AFt product was not commented on.

The hydration processes, even if carried to completion, do not completely efface all traces of the original cement grains. As indicated by Taylor and Newbury (26) the original outlines of the clinker grains are substantially preserved and can be traced by Mg and Fe x-ray imaging.

Besides being the major component of the hydrated cement paste system, C-S-H gel is notorious for the variability of its morphological development. Approximately 10 years ago the present writer (27) proposed a rough classification of C-S-H gel particles observable in portland cement pastes into four morphological types. This classification seems to have held up reasonably well. Illustrations of Type I (acicular or lath-shaped), Type II (reticulated or honeycomb) and Type III (small disks or spheres) structures are common in current literature and are too numerous to cite individually. Various authors have also identified local regions of very dense "inner product" CSH as corresponding to the Type IV hydration product. This is more commonly seen when using specimen preparation techniques other than simple fracturing.

Illustrations of the several types are provided below. These are taken at relatively low magnifications to attempt to preserve an impression of the cement grain context in which they develop.

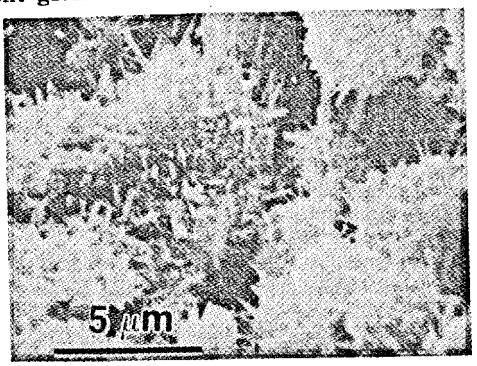

Fig. 3. Type I C-S-H gel particles growing radially around cement grains.

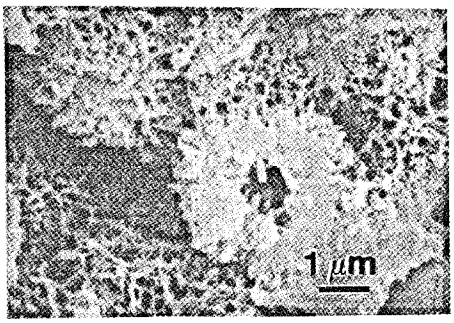

Fig. 4. Type II C-S-H gel network; note the submicron size of the mesh, and the hollow hydration shell (early hydration).

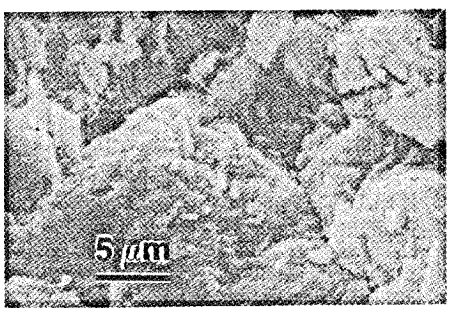

Fig. 5. Fine textured, almost featureless Type III C-S-H gel (late hydration).

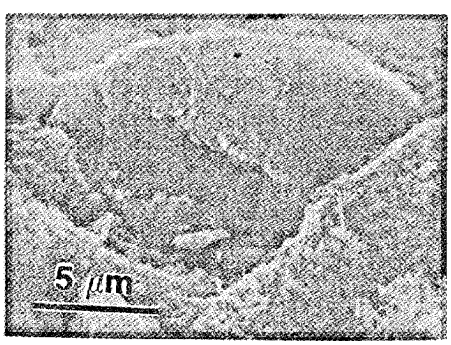

Fig. 6. An "inner" hydration product cement grain residue showing dense Type IV morphology.

One of the peculiarities of portland cement paste is the degree to which the microstructure developed varies with relative amount of water-filled space in which the hydration processes take place, and also with chemical components that may dissolved in the water. The four C-S-H gel morphological types described by the present writer were meant to categorize the hydration product on conventional cement paste, and are certainly not the only morphologies that can be produced. This was illustrated profusely by Odler and Lin (28) who hydrated polished clinker surfaces in a various free solution exposures, and produced a variety of well developed morphological types not usually seen in cement pastes.

A somewhat different classification of C-S-H gel morphological types, especially formulated to describe the sequential development of microstructural features in the early stages of C_3S (rather than cement) hydration, has been developed by Jennings et al. (29). The later stages described in this scheme correspond in substance, although not in nomenclature, to three of the four C-S-H gel types described by the present writer. Type III C-S-H gel was not observed in these studies.

The C-S-H gel types defined by the present writer were meant as shorthand descriptions of C-S-H gel morphologies as seen in scanning (or transmission) electron microscopy. These techniques ordinarily require that the cement pastes observed be predried and evacuated before observations can be made. It has been suggested that Type I or fibrous particles, especially those produced in the earliest stages of hydration, may to some degree be artifacts of drying. These are said to be produced from preexisting colloidal or gelatinous crumpled films or foils which roll up or otherwise assume a fibrous morphology. Evidences for this point of view in the form of high-voltage transmission electron microscope pictures of wet C_3S pastes were published by Jennings et al. (18) and subsequently for both C_3S and C_2S pastes by Scrivener (4). The concept has been reviewed and restated by Jennings (29) in a recent review of cement microstructure development.

In these works as published, it is not exactly clear whether the authors ascribed such genesis to all Type I particles in hydrating C_3S pastes or only to those formed in the earliest stages of hydration. Jennings (30) indicated that the latter was the case in his experience; he considered that most of the Type I material formed in hydrated C_3S and in cement paste was not due to changes induced on drying, but preexisted as such in the undried pastes.

Lachowski and Diamond (31) made a study of fragments of cement pastes ground and examined in an analytical electron microscope and in an SEM. Composition was determined on appropriate very thin spots on the fragments, each of which was subsequently mounted for SEM work. It was hoped that information might be obtained on possible differences in composition between particles of C-S-H gel showing the different characteristic morphological types, but unfortunately, all of the C-S-H gel particles obtained for study were classifiable as Type III C-S-H gel. The compositional parameters still showed considerable variation, even from thin spot to thin spot on the same particle.

The work did provide an opportunity to image characteristic Type III gel at high resolution, and Diamond and Lachowski published several of such micrographs taken at up to 80,000x (32). Little additional detail could be gained, but it was clear that this gel consists of rounded nodules of the order of 0.2 μm, fused together to make up more massive particles.

C-S-H gel is not the only component in cement

paste with a variable morphology. A considerable variation in morphology of calcium hydroxide is also present, although it has not been formally divided into classes and thus not always appreciated. Thin amorphous-appearing films that are flat or sometimes curved in complex fashions, thin linings of pores and coatings developed on foreign substances included within pastes, thin plates without specific recognizable interplanar angles, thin but clearly hexagonal plates, thick plates, massive layered structures incorporating CSH gel and other particles, and oriented multi-particulate deposits of several different morphologies have been seen by various investigators in cement pastes. This point has been recently emphasized by Shpynova et al.(33), who studied the range of variation of calcium hydroxide morphologies derived from CaO hydration under various conditions.

A few of these types are illustrated in Fig. 7 below, taken from the water-rich region of a four day old w:c 0.5 paste cast against a glass substrate. A thin film is visible to the right of "A", and thin hexagonal platy crystals ("B") and a large, euhedral hexagonal crystal ("C") are also visible. Micrographs showing other well-formed calcium hydroxide morphologies, developed especially near interfaces, will be presented later.

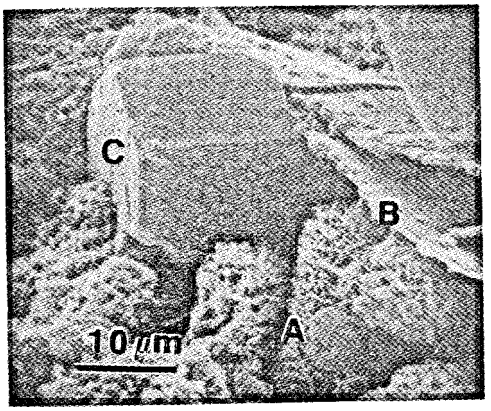

Fig. 7. Illustration of several $Ca(OH)_2$ morphologies

Much more representative of the usual status of most of the calcium hydroxide in mature pastes are the micrographs of Figs. 8 and 9 below. A "mature" paste microstructure is characterized by an intimate intermingling of layered deposits of calcium hydroxide and Type III C-S-H gel; indeed many instances of the layered calcium hydroxide crystals growing around and encapsulating pockets of gel (and other paste components) have been observed. The usual presentation of the layers in fractured pastes is approximately normal to the fracture surface, as in Fig. 8, but occasional fractures run along the layers, as seen in Fig. 9.

Of great interest is the demonstration by Groves (34) using TEM of ion-beam thinned specimens of low water:cement ratio cement pastes that embedded in the dense Type III C-S-H gel structure are very small microcrystalline clusters of calcium hydroxide, only about 100 A thick and stacked normal to the local c-axis direction but in a two-dimensionally random array. Such very small stacks are not generally observed using SEM,

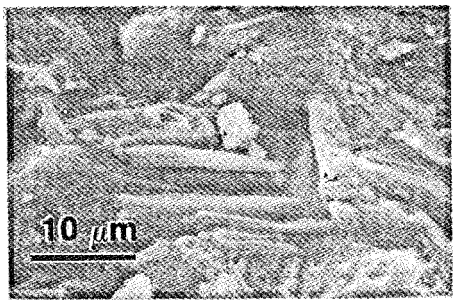

Fig. 8. Typical intermingling of layered calcium hydroxide with Type III C-S-H gel.

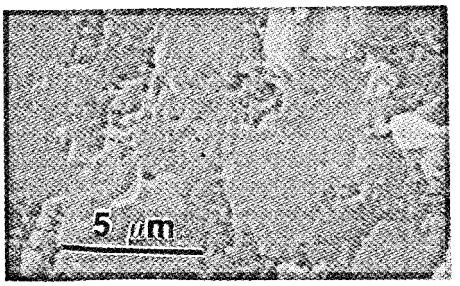

Fig. 9. Exposure of calcium hydroxide along the layer, showing the intermingling.

The interspersion of calcium hydroxide in much larger crystals with C-S-H gel on a much coarser scale was a feature in the investigation of Marchese (35); this author examined fracture surfaces of old, but higher water content cement pastes using EDXRA and paired examination of each matching side of the fracture surfaces produced.

Calcium aluminate hydration products, while quantitatively less important and geometrically less complex, may be important features in the development of microstructure in certain types of cement pastes, notably expansive cement; and of course are of major concern in sulfate attack and perhaps in other secondary degradation processes.

Ettringite-type (AFt) crystals are usually elongated particles, sometimes roughly circular in cross section, sometimes bounded by plane surfaces. Hollow or partly hollow particles have been observed. Ettringite particles show some variation in size and may show considerable variation in aspect ratio, short, stubby rods being reported to occur under some conditions. Monosulfate-type (AFm) crystals are almost invariably small thin hexagonal plates, found in local clusters of relatively few particles, with a characteristic edge-to-face contact between adjacent plates.

Fig. 10 provides some indication of the morphologies of these phases, although the figure itself was taken from a paste composed entirely of high-calcium fly ash and water, rather than a cement paste. The spheres are obviously fly ash particles, the rods are ettringite, and the thin plate ("A") is an AFm phase.

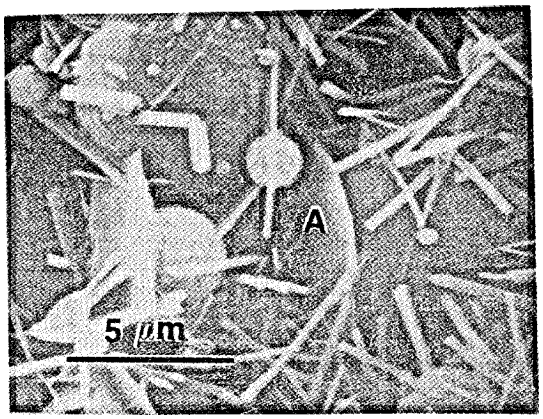

Fig. 10. Morphologies of AFt and AFm phases developed in a fly ash paste.

The development of C_3A and C_4AF products independently with and without sulfate, and in cement pastes were studied using a wet cell in a HVEM by Scrivener and Pratt (36); the importance of the solution sulfate concentration at the time of hydration in determining the product morphology was stressed. Of possibly greater importance were the observations of the influence of the presence of C_3A in the development of hollow shell hydration grains, as discussed subsequently.

Ettringite is of course much more important as a microstructural element in expansive cement than in conventional portland cement systems. Ogawa and Roy (37) studied the formation and morphology of ettringite produced in pastes whose main component was the type K expansive compound, C_4A_3S; early ettringite seemed to occur as small irregular particles; later deposition occurred as a radial zone of elongated crystals around the hydrating grains, with expansion said to commence when these zones intersected each other.

All of these microstructural units exist in and are characteristic of cement paste in concrete that has been hydrated under ambient conditions. As is well known, high temperature curing and especially autoclaving, can result in substantial changes in the compositions and microstructures of the products formed. Autoclaving, especially, generates an entirely different class of hydration product, comprising well crystallized calcium silicate hydrates and other compounds. The details of microstructures developed under these conditions are not considered further in this review.

UTRASTRUCTURE OF CEMENT PASTE STRUCTURAL ELEMENTS

The crystal structures of calcium hydroxide, ettringite, and calcium monosulfate hydrate components of cement paste are well established, and while the latter two are subject to significant atomic substitution, there is little fundamental uncertainty as to their structure on a scale below that visible in conventional scanning or transmission electron microscopy.

This is of course not true for C-S-H gel; the degree of crystallinity in this material is so poor that conventional structural analysis procedures are useless. Indeed, it is not at all clear whether the different C-S-H gel morphological types represent materials with significant ultrastructural (or even compositional) differences, or whether they are different morphological forms of quite the same substance.

The chemistry, water content, and internal structures of C-S-H gel particles have been reviewed intensively by Taylor in the 1980 Paris Congress (1) along with similar treatments of the AFt and AFm phases. A more recent summary (38) was provided by this author as part of a series of instructional modules in cement science. The chemical composition of C-S-H gel particles is found to be variable, with mean Ca:Si ratio of 1.4 to 1.6 in different mature cement pastes; individual analyses may depart fairly widely from these mean values. Substantial, but variable amounts of aluminum, iron, and sulfate ions are also usually found. The ascertainable water content of the solid hydration product particles is significant, but varies with type of drying. As mentioned previously, crystallinity is very badly expressed, with only two or three weak x-ray diffraction peaks discernable. The silicate anions are partly polymerized in the structure of the C-S-H gel, the degree of polymerization increasing with age.

Very recently, Taylor (39) has presented evidence for a proposed C-S-H gel ultrastructure consisting of disordered layers, most of which are structurally imperfect jennite and others structurally imperfect 1.4nm tobermorite.

In addition to the above characteristics and others enumerated by Taylor (38), it is well established by a variety of techniques that C-S-H gel particles possess a large internal surface. While the geometrical details of the internal surface are not, in the present writer's opinion, adequately understood, Winslow (40) has recently shown that the fractal surface dimensions of cement pastes are very high (2.95 to 3.09 in his measurements), indicating a very rough and irregular arrangement of this internal surface structure.

In the absence of hard structural information, a number of so-called "models" of C-S-H gel based on inferences from measured properties have been proposed, illustrated repeatedly in review publications, and discussed frequently. The writer does not feel that any of these are sufficiently well based to be of serious consequence to the present microstructural treatment, and they will not be considered further.

ORIGIN AND ARRANGEMENT OF MICROSTRUCTURES IN CEMENT PASTES

In this section the writer hopes to convey some picture of the microstructural patterns observed in cement paste, and an indication of the current state of efforts to understand its origin and development.

Cement paste arises as a result of hydration reactions taking place in cement mixed with a limited amount of water. Hydration reactions begin almost immediately, but ordinarily slow down though a period of only minor activity, during which mutual adjustments of the arrangements of cement grains

and other particles can take place. A surge in rate of hydration is then ordinarily experienced, which is shortly followed by setting; the mobility of the system is then essentially lost.

The development of the hydration product structure can conveniently be divided into three parts: (1) the earliest stages of hydration in which the focus of activity is confined to the actual surfaces and near-surface mix water surrounding the individual cement grains; (2) a later stage, in which hydration products project into or are deposited within the solution-filled space between the cement grains, meet, and start to form a coherent skeletal structure which then stabilizes grain-to-grain arrangements and results in setting; and finally (3) the remainder of the hydration processes, during which the skeletal structure fills in with additional hydration product generated from within the original outlines of the cement grains. The first two stages occur during the first hours of hydration, with the third stage comprising most of the actual period of active hydration.

The details of the first stage are perhaps little influenced by the water:cement (w:c) ratio, but the morphology produced in the second and third stages are to a large extent dominated by this parameter. The same cement can produce distinctly different microstructural assemblages depending on the amount of water-filled space available. The point was illustrated with respect to a "low porosity" cement by Diamond (41), and has been more recently re-expressed with respect to C_3S paste by Abo-el-Enien (42). Even compaction of an already-mixed paste followed by vacuum removal of excess water squeezed out of the system was found by Bajza (43) to change the character of the hydration products that were subsequently deposited; after effective compaction little of the usual massive calcium hydroxide crystal deposition could be detected.

In discussing the initial hydration stages, the floc structure of fresh cement paste should not be ignored. As is well known, ordinary portland cement mixed with water, in the absence of superplasticizers or special dispersants, invariably forms floc structures. Visible sedimentation of these flocs can be seen in diluted pastes; the counterpart of this in concrete is bleeding. The individual flocs may range up to several hundred μm in size, and may be composed of many individual clinker particles. They involve relatively close contacts between some portions of the clinker grains, but contain substantial pocket of empty (water-filled) space; additional water filled spaces occur between adjacent flocs. On setting, these spaces become "capillary" pores. In typical concretes batched at high water:cement ratios, these subdivide but remain incompletely filled despite long-continued hydration.

The nature of the surfaces of ground cement grains undoubtedly influences early hydration profoundly. Little is known about these surfaces. They would be expected to be comprised more or less randomly of patches C_3S and C_2S, with occasional narrower exposures of zones of the smaller interstitial C_3A - ferrite assemblages, depending on how the specific clinker fractures in the grinding process. It is expected that many surfaces may be contaminated with smeared deposits of gypsum or hemihydrate because of the universal interginding of this softer component. Dalgleish et al.(44) reported the existence of smeared surfaces on the particles of as-received cement of one type of the three examined, but not on another. They were not able to determine the nature of the smearing material. Gypsum is known to dissolve only slowly in mix water, and smeared surface deposits, if present, may remain for some hours.

The local availability of gypsum smeared onto some cement surfaces combined with surface exposure of at least local areas of interstitial C_3A may account for recent observations that suggest that one of the earliest recognizable hydration responses is the formation of an amorphous or gelatinous film around some grains with a composition approaching that of AFt (45). Indeed, hollow sacs and hollow tubules of gelatinous material having such composition have been observed to form by several authors, including Barnes et al. (46) and Pratt and Jennings (45). The "glutinous films" reported as the earliest products by Orr (47) may fall into this category, although no chemical information was provided by this author.

On the other hand, Dalgleish et al.(44) reported etch pitting on clean surfaces of a cement that did not have a smeared deposit as its earliest hydration response, followed by subsequent development of deeper pitting and deposition of possible hydration products on some areas; other areas remained smooth and seemingly unaffected in the same period. There is no indication, in this detailed description of the earliest hydration morphology, of any "glutinous film" formation, nor of crinkled films and foils that have been variously reported. This may be a consequence of the specimen preparation procedure used, which involved freeze drying.

After a few hours Dalgleish et al. reported that small regular individual particles of "calcium hydroxide and/or AFt" morphology appeared widespread over the surface of one cement, followed by generation of a fibrous deposit of C-S-H appearing to arise from a filmy layer on the surface. AFt products seemed more plentiful in the initial deposits around grains of the other two cements examined, but by four hours "all of the cements...showed particle surfaces entirely covered by product."

The next step in the sequence seems clear, and has been remarked as an important step in the hydration process since its first clear description by Hadley (48) as early as 1972. A micrograph taken from this work is provided as Fig. 11. It was evident from Hadley's results that by 1 day many grains in near-aggregate surface zones investigated by him had formed thin (1 μm thick) shells, and that the enclosed clinker grains had subsequently dissolved away, leaving a large gap or in some cases a completely hollow shell.

In 1978 Barnes, Diamond and Dolch (49) concluded that hollow shell grains occur in bulk paste as well as that formed in aggregate-influenced zones, and that such grains constituted the vast majority of grains so fractured that the interior was visible. The paper concluded with the implication that the formation of such grains was an intrinsic part of

the normal cement hydration process that should not be overlooked in modelling the hydration process. The present writer is gratified that this is finally being recognized.

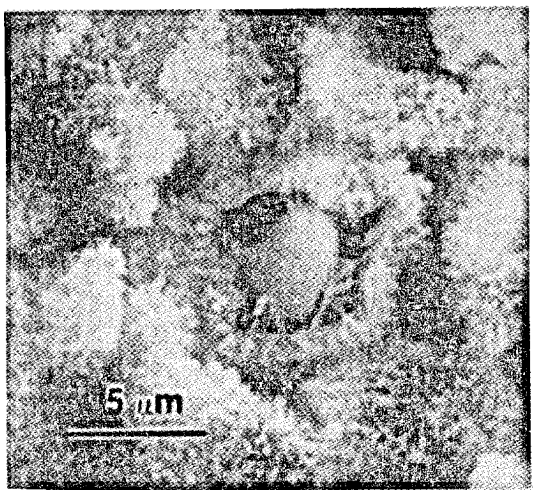

Fig. 11. Hydration shell and remnant grain (w:c 0.5 paste cast on glass slide, 1 day). Fig. 13 from the thesis of Hadley, 1972 (48).

Hadley originally considered the structure of the shell to consist of an inner layer of oriented and stacked platelets of calcium hydroxide deposited first on the cement grain, with an outer shell of C-S-H gel. He found AFt rods and platelets of AFm projecting inward from the shells into the empty space formerly occupied by cement grains, and occasionally rods projecting outward.

Subsequent work suggests that the shell structure is less regular than Hadley supposed, and is principally C-S-H rather than calcium hydroxide. However, the local composition and to some extent the local appearance at high magnification may vary from place to place around the perimeter of a given shell. Many shells seem to be slightly incomplete, in that small holes or thin spots can be detected through which solutions can apparently diffuse easily.

In recent work, the formation of such shells starting around 12 hours after the beginning of hydration was clearly described by Dalgleish et al.(44), with a micrograph taken at this time showing detachment of the shell from the hydrating cement core. The feature was even more prominent at 18 hours, and a STEM micrograph of an ion-beam thinned specimen taken normal to the shell at this time showed an apparent thickness of approximately 0.5 µm, and a gap of almost this extent.

Further details of such shells were provided recently by Pratt and Ghose (50), along with confirmation of their status as intrinsic features of the normal cement hydration process.

On further hydration it was proposed by Pratt and Ghose (50) that there is a progressive inward thickening of most shells, from an early thickness of the order of 1-2 µm at ca. 12 hours, to up to 5 µm at 4 days, and possibly exceeding 10 µm after 7 days. This does not seem to have been the usual case in the writer's experience and that of his colleagues.

For example, none of the shells rescorded in the original work of Hadley (29) much exceeded 2 µm in thickness, and the pastes examined were up to 14 days old. In the Ph. D. thesis of Barnes (51) cement mortar specimens were examined after a 14-day hydration period; residual shell thicknesses observed in hollow shell grains (for example in his Figs. 266 and 267) did not appear to appreciably exceed 2 µm.

With the recognition that definite shells of hydration product surround individual cement grains after a few hours of hydration, the subsequent processes of hydration and microstructural formation can be subdivided; attention should be paid separately to what happens on further hydration within the shell, and what happens to the space between shells. Attention to the latter will be postponed.

It is evident that the shells do not constitute impenetrable barriers to the outward flow of dissolved clinker components, since as hydration proceeds the outside capillary space progressively fills up with freshly-deposited hydration product. Thus residual clinker cores necessarily get smaller as hydrations continues, and many disappear.

There seems to be some difference of opinion, however, on what else happens within the perimeter of the shell.

It is worth restating at this point that according to Taylor and Newbury (26) the original boundaries of the cement grains in old pastes can be established by electron probe microanalysis imaging of the distribution of Mg. Thus one can establish the inner boundary of the original shell as deposited around a given clinker grain.

Once the shell has been deposited, some cement grains empty out their contents quickly and become fully hollow. Other hydrating grains do not; instead hydration is accompanied by deposition of dense hydration product just inside of, and contiguous with, the inside of the shell. Various workers report that in such grains the shell plus dense hydration product thus gets thicker as the core gets smaller, with only a small gap being observed between the augmented shell and the core.

According to Pratt and Ghose (50) this narrow gap as observed by conventional SEM procedures may be an artifact of drying. In any event, these authors have clearly depicted the formation of the dense inner deposit of hydration product within the shell. This interior hydration product is apparently C-S-H gel without visible particulate structure, presumably the Type IV gel.

Scrivener and Pratt (52) suggested that if the shell is tight, calcium hydroxide necessarily formed by the C_3S hydration reaction will be dispersed in microcrystalline form through this dense inner CSH product. The hydration product in any case may not be homogeneous; zones of iron-rich material interpreted as relicts of interstitial material almost unmoved from their original locations within

cement grains have been reported by Taylor and Newbury (26).

Some uncertainty exists in understanding why some clinker grains hydrate in the first mode, i.e. so as to form hollow shells, and others in the second, so as to form dense inner product. Scrivener (4, p. 155) suggested that it is only the smaller clinker grains that form completely hollow shells, with hollow grains larger than 5 μm never being observed. The basis for the distinction is thus suggested as being the size of the individual grain; some subsequent authors have accepted this as a working criterion. This may not be correct. Hollow grains have been observed in the writer's laboratory by Hadley (29) and by Barnes (51) in the 10 to 15 μm size range, without any attempt to select or look for especially large hollow shells. Indeed, the stereo pair of a completely hollow shell grain published as Fig. 3 of (49) is about 12 μm. in diameter.

A fairly revealing hollow shell micrograph taken from Barnes (51) is reproduced as Fig. 12 below. The paste had a w:c ratio of 0.65 and was hydrated 1 day. Energy-dispersive x-ray analysis of the residual core at Point 1 indicated that it was C_3S (Ca:Si atom ratio 2.88). Point No. 2 on the smooth area of the shell yielded a Ca:Si of 4.36, with some sulfur being detected (Ca:S 0.22) The shell at this point is thus mostly C-S-H gel with a little bit of $Ca(OH)_2$.

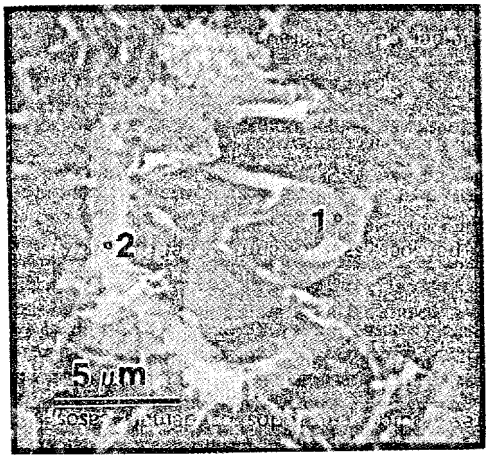

Fig. 12. Partly hydrated hollow-shell grain (w:c 0.65 cement paste, 1 day).

Instead of hollow-shell hydration being a mode restricted to small grains, our interpretation in the past has been that it is a function of local space external to the grains, i.e. local water:cement ratio. Hollow-shell grains were first located in connection with studies of the aggregate cement interfacial zones, where high local water contents are common. In a small casual experiment carried out some years ago the writer found that pastes mixed at very high water contents, such as w:c 0.7, produced large numbers of hollow-shell grains easily visible on fracture surfaces; in contrast pastes mixed at very low water contents were almost entirely unproductive of such observations.

If this concept is correct, the implication is that clinker grains hydrating in wet environments will tend to "leak" dissolved material which precipitates as hydration product in the external spaces if such spaces are plentiful; if they are scarce, i.e. the cement grains are closely packed, this becomes progressively more difficult, and precipitation of hydration product necessarily tends to ensue within the shells as inner product.

Fig. 13 below provides an illustration of hollow shell development in a very wet paste.

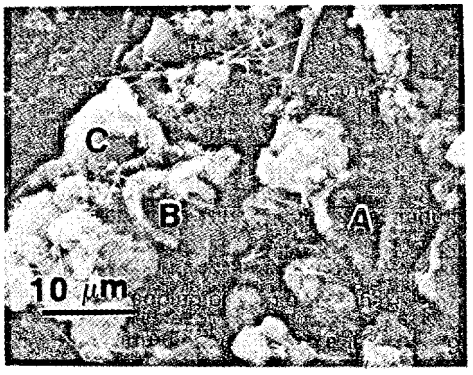

Fig. 13. W:C 0.70 cement paste, 1 day, showing three nearby hollow shell grains.

It is also possible that the effectiveness of the shells as a partial barrier may depend in part on the individual layout of the clinker compounds on the surfaces of each grain; for example, if the shall requires a film of calcium aluminate sulfate to deposit on, as seems possible, grains with little C_3A exposure on the surface may not form a complete film and hence give rise to "leaky" shells.

It may be useful at this point to remark that the hollow shell mode of hydration apparently depends on the presence of calcium aluminates and gypsum, and is not found, for example, in C_3S-water pastes. Classical studies of C_3S hydration have thus been misleading indicators of what to expect with cement hydration.

It is now appropriate to return to consideration of that part of microstructure development that concerns deposition of hydration products in the "capillary" spaces between the clinker grains. This has been more easily followed in microstructural studies, and generally more familiar.

The scenario is approximately as follows. Early C-S-H Type I fibers and ettringite rods are supplemented rapidly by calcium hydroxide deposition; reticulated (Type II) C-S-H zones appear, and adjacent shells start to become tied together. Thin calcium hydroxide plates grow and then thicken and the characteristic layered $Ca(OH)_{23}$ morphology starts to be seen; deposition of fine-particle Type III C-S-H gel starts to overlay and obscure some of the earlier deposits; now-massive deposits of calcium hydroxide continue to grow and start to intrude around and encapsulate local regions of C-S-H gel, and the particle outlines start to become more difficult to see, especially in low water:cement pastes.

The processes naturally vary in detail from place to place in a given paste, and the rate of deposi-

tion of product is naturally conditioned by the cement used and by the local environment.

Illustrations by the writer of the mature product morphology have appeared in Refs. 6, 27, and various other places, and by many other authors in a variety of publications.

The extent to which the morphology attains maturity is frequently not uniform over the entire paste or concrete system. In consequence several different local morphologies may simultaneously persist. As indicated in (6), a generally dense paste marked by extensive infilling of Type III C-S-H gel and massive intergrown calcium hydroxide deposits may often contain pockets of entirely different and "looser-textured" morphology. In these pockets individually discernable Type I particles and ettringite rods persist, patches of the Type II network structure remain, and visual space between particles makes their individual identifications easy. Broken hollow-shell (Hadley) grains may be seen in such pockets, and local clusters of thin AFm plates may occasionally be detected. Few of these features can be seen in the denser, more mature regions of the same paste.

This localization of the microstructural development pattern is perhaps a consequence of the restriction of movement of dissolved cement components before they precipitate as hydration products as emphasized by Taylor and Newbury (26); the generalization they arrived at was that "a substantial proportion of the precipitation occurs within distances below a few μm or even a few nm" from the staring site in a clinker grain.

PASTE MICROSTRUCTURE IN THE PRESENCE OF SUPPLEMENTARY CEMENTITIOUS COMPONENTS

Supplementary cementitious components or mineral admixtures include, but are not restricted to such substances as slag, silica fume, fly ash (pfa), and ground natural pozzolans incorporated in concrete either as factory blended cements or as materials batched separately into the concrete. These components by their mere physical presence naturally affect the development of paste microstructure; most also enter into chemical responses with the developing hydration product system.

As a general principle the writer considers that microstructure-forming processes respond to all aspects of the internal environment during hydration. Many of these may be changed by the incorporation of supplementary components.

A number of effects are possible, which may conveniently be grouped as follows:

(a) Physical effects accompanying the introduction of the particles of the supplementary component. These are mostly in the same size range as cement grains, except for silica fume. The typical particle size of most silica fumes is perhaps two orders of magnitude smaller than that of cement grains. The numbers of such particles added in any real application are thus immense compared to the number of cement grains, and so-called "filler effects" have been extensively discussed in the technical literature.

(b) Physicochemical effects are possible, especially manifesting themselves in modifications of the floc structure. As an illustration, Helmuth (54) recently proposed that many fly ashes reduce water demand by a deflocculating effect resulting from their finest particles becoming adsorbed on or stuck to large cement grains.

(c) Chemical effects, which may take place directly or indirectly. For example, species such as alkali sulfates present as coatings on a few fly ashes dissolve quickly and greatly modify the alkalinity and sulfate content of the mix water and thus the pattern of early hydration (55). Acceleration of the early hydration of several cement components by seemingly "inert" low calcium fly ashes has been reported (56). Chemical effects may be indirect, in that they can involve reactions with hydration products rather than with the hydrating cement grains. An obvious examples is late stage "pozzolanic" reaction with previously deposited calcium hydroxide.

On a somewhat different level are effects produced by chemical admixtures used, sometimes at a high dosage level, together with a supplementary component. The obvious examples are the effects resulting from high dosages of superplasticizer in silica fume concrete or in certain high strength fly ash bearing concretes. It appears that certain combinations together produce major effects on the microstructure that would not be present if either were used independently.

Microstructural Effects Of Fly Ash Incorporation

Fly ash or pfa, unlike many other supplementary components, is a highly inhomogeneous material. It is composed of individual particles that are collected, rather than being ground from a larger mass, and these particles are not alike. Rather, each particle is derived independently from an individual ground fragment of coal being carried on an air stream, isolated from its neighbors. Its composition, and thus to some extent its behavior in cement systems, may be different from its neighbor. This tends to make microscopic interpretations of the general effect of adding a given fly ash to cement rather difficult; different particles do different things.

Different fly ashes also vary considerably from one source to another, depending both on the coal being burned and the details of the power plant operating system.

A distinction is customarily made between low-calcium content fly ashes derived mostly from bituminous coals and high-calcium ashes from subbituminous and lignite coals. This is operationally (if not by definition) the distinction between the "Class F" and "Class C" pozzolans of ASTM C 618. The microstructural implications of this dichotomy are not yet clear. Much work has been done over the years with low calcium fly ashes, but the effects of the high calcium fly ashes on cement paste microstructure have only recently begun to be documented.

The apparent physicochemical effect of some fly ashes on the floc structure of cement paste has already been mentioned.

With respect to what happens to the fly ash particles themselves, a considerable body of information has developed. It appears that one of the first recognizable responses is the deposition of a thin duplex film of calcium hydroxide topped by a sparse layer of C-S-H gel on their surfaces. This seems morphologically and compositionally identical to the duplex film known to be characteristically deposited on other inert components (glass, aggregates, etc.) incorporated in cement paste or concrete.

Diamond et al (57) provided micrographs showing almost complete early coverage of fly ash particles by such films; similar coverage on some particles but not on others was reported by Ghose and Pratt (58) and Pratt (50). An interesting paired TEM and SEM view of such a structure was provided recently by Blaschke (59) in his Fig. 12.

The next stage in the response seems to be a densification and modification of this early duplex film into a fairly tight and dense shell, apparently by continued deposition of both C-S-H gel and calcium hydroxide. The latter sometimes deposits in a particular "stacked plate" morphology. A clear illustration of this phenomenon is present in the micrographs of Halse et al. (60). The thin film covering the large fly ash sphere in their Fig. 4 (taken at one day of hydration) is peeled back exposing the duplex film laterally; in Fig. 6, after 7 days, the film has densified into a clearly-defined shell visible particularly clearly around the bright fly ash sphere in the upper part of the figure. Another clear illustration of shell formation was provided in Fig. 7 of the paper by Montgomery et al (61).

Sometimes the original duplex film persists without appreciable densification into a shell; such lack of densification seems evident in the persistence of the duplex film appearance in Figs. 14 at 3 days, and 15 at 14 days in the pastes of Ghose and Pratt (58).

Meanwhile, the usual processes of cement hydration occur on the cement grains, including the development of shells around them and the formation of Hadley grains, as seen for example in Fig. 9 of Ghose and Pratt (58). An interpretation relating occurrences of these microstructural development in fly ash cement pastes with calorimetric responses was recently provided by Halse et al. (62).

Replacement of a significant proportion of cement with fly ash entails a practical risk that unless the fly ash itself contains a quickly available source of calcium sulfate, the gypsum balance in the system may be affected. This may influence both setting and the early hydration responses. It is possible to add gypsum along with the fly ash, and Huang (63) has explored the microstructural and other consequences of so doing. He found evidences of earlier production of gel around fly ash spheres when gypsum was added, and a general appearance of enhanced pozzolanic reactions at intermediate ages.

Whether gypsum is added or not, sooner or later reaction commences on the glass-rich surfaces of some, but not all of the fly ash spheres; this is despite the fact that they are covered by a duplex film or a shell. The reaction is evidenced first by light etching, and as the etching progresses the outlines of crystals of mullite and quartz embedded within the fly ash glass start to become visible. The progressive development of this process of removal of glass and exposure of embedded unreactive crystals is very clearly illustrated in the micrographs constituting Fig. 7 of Halse et al.(60).

It should be mentioned that some fly ash spheres are of radically different composition than most. Many fly ashes contain some content of iron-rich spheres contain extensive embedded magnetite-type iron oxides and only a little glass. The glass may also be iron rich. Such glass reacts only very slowly, but eventually exposes crystals of embedded iron oxides quite different in appearance from the usual mullite or mullite and quartz crystals uncovered in the majority of spheres. Other iron-rich spheres seem not to react at all.

As cement hydration processes proceed and additional hydration products are laid down, the formerly isolated shells surrounding the fly ash spheres tend to become bound together in the developing interconnected structure of the densifying cement paste. Calcium hydroxide may be locally deposited, and sometimes is seen to partly surround and specifically encapsulate fly ash spheres within their shells. A striking illustration of this was provided by Montgomery et al. (61) in their Fig. 4.

This tieing in of shells to the densifying cement paste skeletal structure seems to occur at the same time that progressive dissolution occurs from reactions at the fly ash surfaces within the shells. At least in some cases this leads to gaps developing between the progressively reacting fly ash grain and its surrounding shell, seemingly analogous to gaps developing in hollow-shell hydration of cement grains. Pratt (56) reported that such hollow-shell development in fly ash grains seemed particularly prominent where fly ash spheres had been surrounded by massive layers of calcium hydroxide.

The presence of gaps is also evident in results of Jawed and Skalny (64) and Chanda and Bailey (65).

In a rather unusual study by Montgomery and Diamond (66), the propagation of cracks induced by mechanical loading was studied in the SEM for special pastes in which large fly ash cenospheres were prominent components. Despite the relatively thin walls of the hollow cenospheres, the advancing cracks almost inevitably went around them rather than thorough them. The paths were clearly between the cenospheres and the lime-rich shells that surrounded them. This may have been due to the existence of such gaps, which were evident once the crack had passed.

Away from the fly ash grains themselves, it appears that the general cement paste microstructure that develops when fly ash particles are used is not dissimilar to that of plain cement paste. However the partly-reacted (and occasional completely unreacted) fly ash particles are a prominent feature, particularly obvious because of their characteristic spherical shape.

It is generally appreciated that the presence of fly ash both limits the amount of calcium hydroxide that deposits in the early stages of hydration and subsequently results in removal of some of the previously deposited calcium hydroxide. The locations and microstructural features of the removal process, that is, the pozzolanic reaction per se, have not to the writer's knowledge been adequately documented.

As mentioned previously, the specific effects of high calcium fly ashes on the microstructure of cement systems has received attention only recently, in part because they have only recently come into general use. A considerable body of information is now developing.

Grutzeck et al.(67) reported unusual shell formations observed on incorporating high calcium fly ash with an oil-well cement hydrated at 38° C. The shells were dense, radially oriented bundles of C-S-H gel. It is not certain whether these and other observations would be reproduced using their fly ash with ordinary cement under a more conventional hydration regime.

Scheetz et al. (68) studied a number of unusual combinations of materials, including one that involved a high calcium fly ash, with a Class H oil-well cement in the joint presence of an expansive additive, NaCl, and a superplasticizer. Several unusual microstructural features were observed, including extensive development of ettringite both inside of and outside of the separated outer shells around the fly ash spheres. Again the relevance of these features to conventional cement paste morphologies with high calcium fly ashes remains to be established.

Somewhat more conventional fly ash concretes containing high calcium fly ashes were studied by Baker and Laguros (69). They confirmed that duplex films deposit and are evident on fracture surfaces early in the hydration processes with high-calcium fly ashes as well as with low-calcium ashes. They found that after 7 days many smooth-surfaced spheres were observed to be projecting upward from the general fracture surface, with corresponding empty sockets observable on the opposite fracture surface. This is presumably due to the development of a gap between the sphere and its shell, similar to those reported for low-calcium fly ash pastes.

Pistilli (70) provided a number of micrographs of the paste structure in concretes batched with a high content of high calcium fly ash with and without water reducer. While the focus of the investigation was on the air-entrainment characteristics of the various mixes, enough detail can be seen in the micrographs to suggest that the microstructure developed did not differ radically from that customarily seen with low-calcium ashes.

Very recently Mills (71) examined cement hydration products incorporating high-calcium fly ash and found results similar to those previously discussed; that is, development of thin reaction shells around the fly ash spheres, opening up of a gap between these shells and the underlying spheres, and the eventual envelopment of some of the fly ash grains in calcium hydroxide. Mills called attention specifically to the very prominent early precipitation of ettringite near the fly ash particles, and on a more general note, to the possible unbalancing of the C_3A and gypsum characteristic of portland cements by uncontrolled addition of fly ash as a mineral admixture.

The papers cited above, and others, represent a response to the growing importance of the use of fly ash in concrete. However, many details remain to be unravelled. The writer was disappointed in the almost complete lack of study of microstructure among the reports presented at the just-concluded 2nd International Conference on Fly Ash, Silica Fume, Slag, and Natural Pozzolans in Concrete in Madrid. Of the many papers on fly ash in concrete, only that of Tenoutasse and Marion (72) on Belgian fly ashes, provided information on microstructure.

In addition to their influences on the microstructures of "bulk" cement pastes, fly ashes also influence the special microstructures developed at such critical locations as cement-aggregate interfacial zones. Consideration of these effects will be found in the section of this paper dealing with such special microstructures.

Microstructural Effects of Silica Fume

While the volume of concrete produced with silica fume is very much less than that produced with fly ash, the modification and potential improvement of properties is so great that silica fume concrete commands great international interest.

The microstructural effects to be expected depend on the relative amount of silica fume used with the cement, and more importantly, with whether or not the silica fume is accompanied by an effective dosage of superplasticizer or water reducer. Such accompaniment produces a synergistic deflocculating and dispersing effect, which results in fluidity at very low water contents, and which changes the structure of the resulting paste significantly. In the absence of a dispersing agent, silica fume adds significantly to the cement water demand so that high water contents must be used, and a very different microstructure develops.

A number of workers have documented the dense final structure that develops when silica fume is used with effective superplasticizers, but only a little information is available on the early stages of cement hydration with silica fume under these conditions. Grutzeck et al.(73) investigated the response of silica fume itself to immersion in dilute (but saturated) solutions of calcium hydroxide. They found that some silica dissolves quickly and reprecipitates as a silica-rich gel layer on the surfaces of the remaining undissolved fume particles, which then become agglomerated. With time, this layer of reprecipitated silica reacts further to produce C-S-H gel.

Subsequently Grutzeck et al. (74) studied early microstructural development in pastes made with Class F (oil well) cement and several varieties of silica fume or ferrosilicon dust. Agglomerations of remnant fume were identified after some weeks similar to the gel-bound fume agglomerations that had been described earlier (73), but not in all cases. C-S-H gel similar in appearance to Type III gel in ordinary cement pastes were observed

growing on agglomerated spheres. Only a trace of calcium hydroxide was left unreacted in these cement pastes at 28 days; at higher temperatures of hydration no calcium hydroxide was seen even at 7 days.

The mature paste structure produced in low water content pastes batched with silica fume and superplasticizers has been studied by a number of authors. Essentially the same picture is presented by all of these, including Aitcin et al. (75), Dingsoyr et al. (76), Marusin (77), Regourd (78, 79), and Regourd et al. (80). Where more than a minor amount of silica fume is used, the paste microstructure developed is completely different from that of ordinary cement paste. The structure is variously described as "dense", "amorphous", "of high compacity", etc. The basic structure appears to be that of Type III C-S-H gel particles but packed into an unusually dense array, with only rare and isolated small gaps. Type I elongated and Type II network or reticulated C-S-H gel morphologies are never seen. Large masses of layered calcium hydroxide intergrowing around and encapsulating C-S-H gel, a prominent feature of ordinary mature cement paste, are rarely seen, although in systems with smaller amounts of silica fume x-ray diffraction usually indicates that some $Ca(OH)_2$ persists. The boundaries between individual small Type III C-S-H gel particles are indistinct, as though the particles have partly fused, and in many systems a bright sheen seems to overly some or all of the fracture surface. This could perhaps represent residual "silica gel" of the type described by Grutzeck et al. (73,74).

The microstructure may be affected by surprisingly small amounts of silica fume. Regourd et al. (81) investigated the microstructure of mortars with 30% of slag, fly ash, or pozzolanic component, and 5% silica fume incorporated as a supplementary admixture to improve the strengths and mechanical properties of these systems. Only slight changes in the microstructure were observed with the slag system, which was already dense; with pozzolans and fly ash, some densification of the structure was observed; with inert components such as quartz and crystalline slag, a considerable benefit was realized, and the paste structure was significantly densified.

In addition to the major effects of silica fume on "bulk" microstructure, significant effects are reported on the microstructure of the interfacial regions surrounding aggregates; these will be discussed later.

There is a tendency to ascribe the rather strong effects on bulk microstructure described above to a specific response induced by the silica fume, rather than to the combined effects of silica fume and the superplasticizer. This tendency is reinforced by the results of studies like that of Marusin (82) which show negligible microstructural effects by superplasticizers alone. However, the writer is not sure that the structure induced by the silica fume-superplasticizer combination is specifically attributable to the silica fume, or indeed is uniquely dependent on the presence of the fume.

For a number of years the writer and other investigators have been examining the properties of gypsum free "low porosity" concretes, which are formulated at low water contents using conventional ground portland cement clinker without gypsum addition. Paste w:c ratios of around 0.20, and concrete w:c ratios of around 0.25 can be effectively batched in the resulting highly deflocculated system. The deflocculation (and control of set) are effected by a combination of admixtures, usually including a lignosulfonate and an alkali carbonate or bicarbonate. These systems achieve strengths and technical properties similar to those obtained with silica fume-superplasticizer combinations but involve no necessary supplementary cementitious component; fly ash is sometimes used to improve rheology, but it is not necessary.

Investigations of the microstructure of mature paste in these systems have been carried out by Diamond and Gomez-Toledo (83), and more recently by Coleman (84), Skvara and Zbuzek (85,86), and Subba Rao et al.(87), among others. The characteristic microstructure developed in these systems on maturity is extremely similar to that reported for dense silica fume concretes; the same dense, apparently partly fused Type III C-S-H gel morphology, the same absence of layered calcium hydroxide masses, and as documented by Coleman (84), a similar sheen over at least some regions of the fracture surface examined.

In (83) it was shown that the same ground clinker-admixture combination that produces this dense microstructure when hydrated at low water contents, produced normal cement hydration product microstructures in the agglomerations developed on bottle hydration (w:c 10). The bottle hydration provides a large volume of available space to deposit hydration products; paste hydration at low water contents provides only a minimum of such space, and indeed hydration usually stops short of completion for lack of space. These considerations suggest that the dense microstructure produced in low porosity concrete, so similar to that produced in silica fume-superplasticized concrete, might be a normal response to the restricted hydration space conditions rather than to specific chemical features of the hydration system.

Very recently a new but related gypsum-free low porosity system consisting of ground clinker treated with polyphenol sulfonate and alkali carbonate was described by Skvara and Rybinova (88); this appears to develop the same type of dense microstructure as the previous systems described.

MICROSTRUCTURAL EFFECTS OF SLAG

Slag, more specifically ground granulated blast furnace slag, has been used for many years as a supplementary cementitious material with generally excellent results. The percentage of slag ordinarily used is much higher than used for fly ash or silica fume; a significant portion of the C-S-H gel generated in such concretes made with slag cement or separately-batched slag must be due to hydration of the slag component itself.

Regourd (89) provided some information on paste microstructure in her principal paper on the structure and behavior of slag-portland cement hydrates at the Paris Congress. An early development of large amounts of ettringite, widely dispersed and derived from the alumina in the slag was noted;

phases. The C-S-H gel developed was described as compact, well-crystallized, and dense.

Recent microstructural studies of slag-containing systems include that of Tanaka et al. (90), a study by Marchese (91), and a previously-mentioned study by Regourd et al. (81).

Tanaka et al. (90) depicted the development of a skeleton hydrated layer rich in MgO on the surfaces of the slag grains: at a later stage this layer converts to a denser "inner hydrated layer" which remained distinct from the bulk paste deposited by the cement.

The differing mature microstructures developed by plain portland cement and slag cement were compared by Marchese (91); the denser character of the slag-containing system was apparent.

Regourd et al. (81) studied a 30% slag system and a corresponding 25% slag - 5% silica fume system. At 28 days the slag system appeared to show a fairly dense microstructure, but some open voids and some zones could be seen of less dense C-S-H material in a pattern resembling Type II gel. Around residual slag grains a 1-μm thick rim or zone consisting of very small "tangled thin plates" were observed, with an unremarked but extremely obvious gap of about the same thickness separated this from the residual slag particle. When silica fume was incorporated with the slag the rim zone was found to be denser and the general C-S-H gel appeared to be significantly denser as well.

In general it appears that slag cements do indeed generate a significantly more compact paste microstructure than do plain portland cements, but more porous local patches of what appears to be fine-textured Type II C-S-H gel may be found, as well as some other residual open space. The microstructure is definitely less compact than that occurring in dense superplasticized silica fume or gypsum-free low porosity systems.

MICROSTRUCTURE OF SPECIAL "MDF" SYSTEMS

The microstructure of special ultrastrong MDF systems developed by Birchall and associates and described in a number of publications, has been investigated by Groves (92) and by Sinclair and Groves (93). These systems are hardly cement pastes in the conventional sense. They are characterized by an extremely limited extent of hydration, and by the fact that the hydration products are embedded in and entwined with a continuous polymer matrix. MDF pastes made with portland cement show no fibrous C-S-H gel products, and the calcium hydroxide generated is microcrystalline; those made with calcium aluminate cement generate an amorphous hydration product said to have a $CaO:Al_2O_3$ ratio of about 1.

MICROSTRUCTURE IN SPECIAL ZONES

Without doubt the most important special zone of cement paste microstructure is that of the zone near the surface of contact with aggregates and sand grains in concrete. The influence of this zone on the behavior of concrete is considerable, and significant work has been done toward defining it and describing its characteristics. Other special zones of importance include the region around included steel (fibers, strands, or reinforcement) in concrete, and the special local zone developed within and around glass fiber strands in glass fiber reinforced concretes.

THE AGGREGATE INTERFACIAL REGION AND THE "AUREOLE DE TRANSITION"

The concept that the cement paste developed around coarse aggregate pieces in concrete is somewhat different in structure than bulk cement paste has been held for many years. Early work defined the transition zone, or as viewed in two dimensions on a section, the "aureole de transition", as a region extending radially outward from the aggregate surface and gradually merging into the bulk paste microstructure over a distance of perhaps 50 μm.

The prevalence of calcium hydroxide in this region was observed many years ago. Maso and his associates at Toulouse early established by x-ray diffraction that the apparent amount of calcium hydroxide and its degree of preferred orientation (with c-axis normal to the surface) diminishes with distance from the aggregate surface. The thickness of the zone through which calcium hydroxide preferred orientation can be measured is customarily taken as the size of the aureole de transition and the limit of the region of paste affected by the aggregate.

However, detailed studies have shown that the special microstructure developed in paste within the affected zone is complex (and variable). Differences between the microstructure of such zones and "bulk" cement paste microstructure are more extensive and profound than simply the presence of extra, well oriented calcium hydroxide in the former.

Pertinent developments in this area prior to 1980 were appropriately reviewed in the Paris Congress principal paper by Maso (94). Another review to 1980 was provided by Struble et al. (95). Subsequently a considerable body of work was reported at the Colloque International "Liaisons Pates de Ciment Materiaux Associes" held at Toulouse in 1982. A spate of recent papers and the previously mentioned thesis of Monteiro (5) have been produced since then.

Early work at Purdue University included theses by Hadley (49) and Barnes (51). This work and its extensions, taken together with the steady progress of developments by members of the Toulouse group and others, provide a reasonably consistent and well-documented picture of the details of the processes of microstructural development near an aggregate interface for conventional flocculated fresh cement paste. The following summarizes the present writer's understanding of the general effects encountered.

(1) Fresh cement paste is ordinarily flocculated, and consists of multi-particle flocs that are often up to several hundred μm in extent and roughly spherical in shape. The flocs, held together by VanderWaals' (dispersion) forces at points of close contact between adjacent clinker grains, are strong enough to resist dispersion by

mechanical agitation while concrete is mixed, and to some extent to resist changes in shape on consolidation. In consequence, cement grains pack against aggregate surfaces poorly, leaving extensive areas of high local water content both between grains within flocs, and between adjacent flocs.

(2) As a result of early calcium hydroxide supersaturation in the mix water, there is a tendency to rapidly precipitate a layer of calcium hydroxide, ca. 0.5 μm thick, on aggregate surfaces exposed to the mix water; this layer is in the form of a film that is crystalline to x-ray diffraction but without visible crystalline boundaries along its surface.

(3) Due perhaps to poisoning by dissolved silica, this film does not increase in thickness appreciably with time. Instead a thin single layer of short fibrous C-S-H gel in open parallel array develops on its paste-facing surface, with the fibers extending roughly normal to the film. The thickness of the combined or "duplex" film so created is usually no more than 1 μm. The C-S-H layer may densify somewhat with time with the individual fibers becoming more closely spaced, or the fibers may join at apices to create a layer with a morphology approaching that of network (Type II) C-S-H gel.

(4) The film may not form over all areas of aggregate surface in contact with the fresh paste; the proportion of areas covered with pastes of lowered calcium hydroxide producing capacity, e. g. slag cements, may be significantly reduced.

(5) Depending on age, nature of the aggregate, and circumstances of fracture, if fracture takes place at or near the original interface the film may be mostly retained by the aggregate or it may remain mostly bonded to the paste side. Even if it follows the latter mode, its adhesion to the aggregate may be sufficiently strong that it may carry some of the aggregate with it.

(6) This duplex film has been seen to deposit on aggregates of a variety of compositions, on silica glass, on alkali-resistant glass fibers, on steel, on polytetrafluoroethylene ("Teflon") , plastic, etc. Thus its deposition is not a consequence of any reaction with a particular kind of surface, but rather is the normal result of nucleation on any surface in contact with a supersaturated liquid.

(7) This thin duplex film is not the "aureole de transition" or the interfacial zone, which typically is 40 or 50 μm thick; rather it constitutes only the thin boundary element in closest contact with actual aggregate surface.

(8) On the cement paste side of the duplex film is the volume of space of high local water content described previously. The relatively sparsely packed cement grains in the flocs in this volume of space hydrate so as to produce large populations of hollow shell grains; thus most of the hydration products deposit in the water-filled space between the shells rather than within the shells.

(9) After a day or two have elapsed, a new thin secondary layer of calcium hydroxide, typically about 3 μm thick, develops immediately under the duplex film, that is, on the paste side. This is seen as a layer of thin, closely stacked calcium hydroxide crystals in parallel array, with their faces oriented at an acute angle with the duplex film. This layer is usually incomplete, but it serves as something of an intermediate layer between the very thin duplex film and the sparsely populated region below.

(10) Larger, individual, euhedral tabular-shaped crystals of calcium hydroxide may also develop at about the same time below this secondary layer, and many of these crystals may be oriented so that the c-axis is parallel, rather than normal to the surface.

(11) Despite the fact that the clinker grains in the sparsely-populated zone below the secondary calcium hydroxide layer are depositing their hydration product largely into the empty spaces between the shells, the local volume of such space is so great that much of it remains empty even after nearly all of the cement hydration has taken place. This sparsely-occupied space subsequently "attracts" further deposits of calcium hydroxide in various forms, and of ettringite. The process of accumulating these later deposits extends over a period of weeks rather than days. The mass of calcium hydroxide accumulated seems far greater than the mass of ettringite, which is only occasionally encountered.

(12) These late calcium hydroxide deposits often appear as arrays of layered crystals, tens of μm long, and quite thick. They surround and encompass previously deposited hydration products. They may extend fairly deep into the paste, and only gradually give way to the usual C-S-H gel - $Ca(OH)_2$ bulk paste microstructure.

(13) These late calcium hydroxide deposits are not rigorously oriented with their c-axis normal to the interface. Arrays of large crystals locally parallel to each other are usually seen, but they vary in orientation with respect to the surface, some even having their c-axis parallel to rather than normal to the surface.

There is seeming conflict between the statements above and the usual picture, based on x-ray diffraction, of preferential calcium hydroxide orientation with c-axis normal to the surface. This apparent conflict is resolvable by attention to x-ray diffraction theory. The SEM results show the presence of increased numbers of large calcium hydroxide crystals near the interface, occurring locally parallel to each other but at varying orientations. Only those crystals which happen to be oriented with c-axis normal to the surface of a specimen (assumed parallel to the aggregate) can contribute to the enhanced basal x-ray diffraction peak; the others simply do not register. Thus while there are extra crystals oriented parallel to the aggregate surface, there are also extra crystals oriented in other by directions as well.

(14) Smaller interfacial zones of similar structure may be expected to surround smaller coarse aggregate pieces and sand grains. The mutual orientations of these zones to each other and to that of any large aggregate piece in the vicinity may be complex.

While some of the statements above reflect the current general consensus, others may be controversial or poorly understood. It seems appropriate here to provide at least some visual indications of the basis for these generalizations.

Fig. 14 below, taken from the thesis of Barnes (51) shows the paste-facing surface of a duplex film formed when a cement paste specimen was cast against a glass microscope slide. The film remained attached to the glass slide on parting, and the view is looking down on the glass slide and its attached film. The sparse layer of short, fibrous C-S-H gel is immediately visible, and the underside of the film of calcium hydroxide may be seen in spots where the gel is particularly sparse.

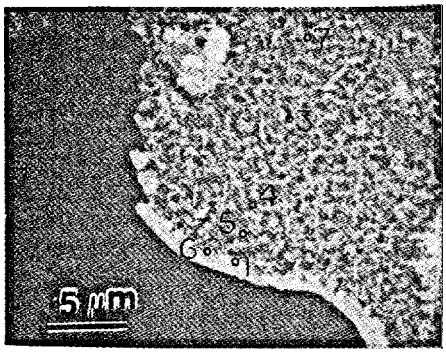

Fig. 14. Duplex film, C-S-H side upward. Paste cast against glass at w:c 0.65, 1 day.

The paste side uncovered by removal of the duplex film is shown, also for a 1-day old w:c 0.65 paste, in Fig. 15 below. The calcium hydroxide side of a portion of the duplex film is visible as the gray area marked "1" in the upper left of the figure. The exposed paste underneath is sparsely occupied by hydrating cement grains. Partly hollow hydration shells are visible at "A and "B", and in various other places, and "C" seems to mark a very large and fully hollow shell.

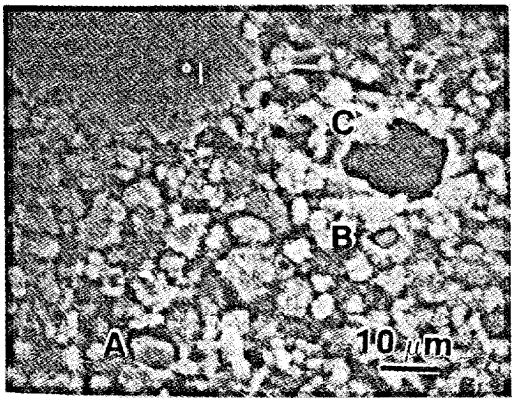

Fig. 15. Poorly-populated zone of paste immediately underneath a duplex film. (w:c 0.65 paste, 1 day, cast against glass).

Fig. 16, taken of a w:c 0.5 paste hydrated for 4 days, reflects the subsequent formation of the layer of secondary calcium hydroxide under the duplex film. The calcium hydroxide side of the duplex film is the uniform gray surface present over the upper and leftmost parts of the micrograph. Where it has been stripped away the underlying structure of the paste is visible. The layer of secondary calcium hydroxide referred to previously is the bright region marked "A". The area marked "B" represents still sparcely-filled space at levels below the secondary calcium hydroxide deposit, starting perhaps 2 or 3 μm below the surface.

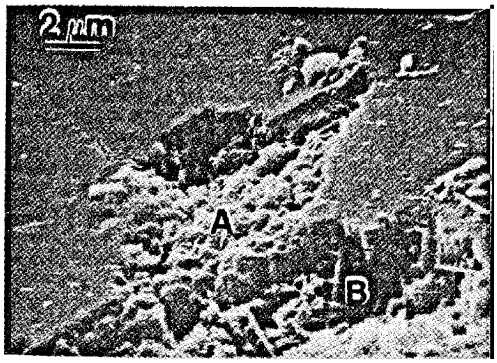

Fig. 16. Detail of secondary calcium hydroxide layer in paste cast against glass (w:c 0.5, 4 days)

A better view of the secondary calcium hydroxide layer ("A") and of the extent of empty space in the paste below it ("B") can be seen in Fig. 17 below.

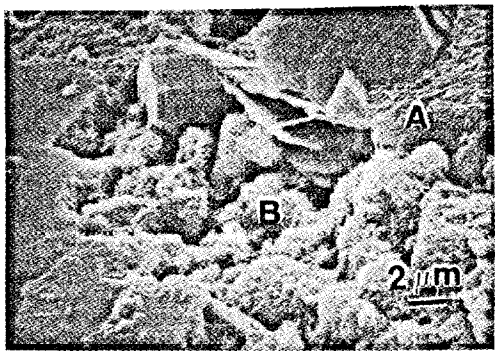

Fig. 17. Another view of a paste immediately below the duplex film.

An idea of the eventual deposition of calcium hydroxide in this sparsely-filled zone, and indications of the differing orientations of the calcium hydroxide that may develop are provided in Figs. 18 and 19.

Variations in the general pattern described above may be expected depending on various factors including the specific characteristics (and possible chemical reactivity) of the aggregate itself, the water:cement ratio, the effects of superplasticizers or superplasticizer-silica fume combinations in deflocculating the paste, the nature and amount of supplementary cementitious components or inert fillers used, and many others.

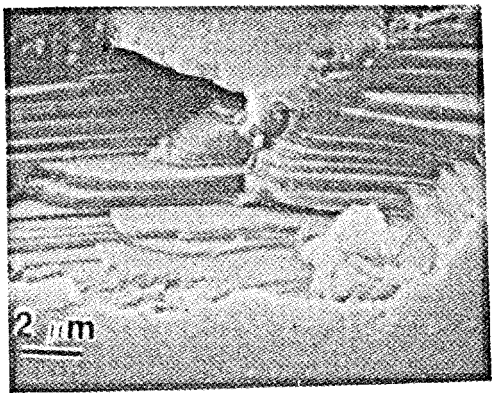

Fig. 18. W:C 0.5 paste cast against glass, 30 days old.

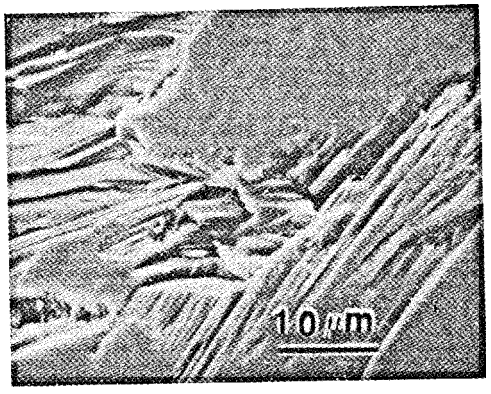

Fig. 19. W:C 0.5 paste cast against glass, 30 days old.

The study of the interfacial zone has involved a number of specialized techniques, including applications of both x-ray diffraction and scanning electron microscopy. An exposition of the special x-ray diffraction technique developed at Toulouse was provided at the Paris Congress by Grandet and Ollivier (96) and a more general review of applicable techniques was provided by Carles-Gibergues et al. (97).

The sequence of events that constitute the steps taking place in the formation of the interfacial zone were reviewed by Ollivier and Grandet (98). Their synthesis is different in some details from that provided above by the present writer. The importance of the influence of the early hydration reactions, especially the C_3A reactions that produce early deposition of ettringite, was stressed by them. They considered that there is a competition of sorts between radial ettringite growth around nuclei, and oriented calcium hydroxide development in the near-aggregate region of the interfacial zone.

Subsequently Monteiro and Mehta (99) studied the variation of ettringite concentration with distance from a granite aggregate surface as a function of time. They found that early (1-day) ettringite deposition is pronounced in the region closest to the aggregate; the content appeared to reduce linearly with distance over a zone of about 100 μm, where its content became negligible. At later ages a substantial and uniform concentration developed in the region beyond about 35 μm from the aggregate, but the region closer to the aggregate continued to be somewhat enriched with ettringite in comparison.

The influence of seepage of the mixing water in practical concrete on the development of the interfacial zones around aggregate pieces was stressed by Hoshino and Tomabechi (100).

A number of recent studies have documented various departures and variations from the general pattern of the duplex film and the features of the interfacial zone as described above.

The special effects that may mark the interfacial zone developed with limestone aggregates are of major importance, in view of the widespread use of limestone aggregate in concrete. Early reports of stronger bond formation and local chemical reaction were summarized by Monteiro and Mehta (101). Some of these involve local formation of calcium carboaluminate at the interface; for example Grandet and Ollivier (102) demonstrated such formation from previously-formed hemicarboaluminate in the zone adjacent to the aggregate surface, and corresponding etching of the aggregate.

Such reactions might readily disturb either previously deposited interfacial features or modify those that would develop subsequently. This may provide an explanation for the failure of Struble and Mindess (103) to find any trace of the expected duplex film between the paste and limestone aggregate that they investigated; rather, these authors found "a somewhat continuous layer, several microns thick, of apparently parallel calcium hydroxide crystals at the interface." This is apparently the secondary calcium hydroxide layer pictured in Figs. 16 and 17 above.

As mentioned by these authors, both Langton and Roy (104), and Conjeaud et al (105) had previously found duplex films at interfaces with limestone. Subsequently Monteiro and Mehta (106) clearly documented the early development of such films by cement pastes surrounding limestone aggregate, although the films may have been discontinuous and incomplete. Subsequent severe chemical etching of the underlying calcite was shown to take place, presumably destroying the duplex film in the process.

Monteiro and Mehta then duplicated these observations using a C_3S paste rather than a cement paste; this led to their suggestion that the etching reaction is not due to carboaluminate formation, aluminum being absent in this case. Rather they tentatively attributed it to the formation of an unusual basic calcium carbonate with a variable composition approximating $CaCO_3$-$Ca(OH)_2$-H_2O. It appears to the present writer that the duplex film might be the prime local source of the $Ca(OH)_2$ for such a reaction, if it occurs.

A contribution toward the understanding of the

geometry of interfacial zones in real concrete has been provided recently by Monteiro et al. (107). Following up the early indication by Barnes et al. (108) that interfacial zone features do develop around sand grains, and the more recent measurements of Diamond et al. (8) which disclosed the likelihood that the interfacial zones of adjacent sand grains in concrete overlapped, these authors confirmed that sand grains as well as coarse aggregate pieces create interfacial zones around themselves. They indicated that the mutual intersections of zones around adjacent particles might interfere with the orientation of calcium hydroxide around any given grain. This might modify the measured size of the zone, if calcium hydroxide orientation is used as the measurement criterion for size.

Other recent studies of "normal" interfacial zone development and properties were reported by Zimbelman (109), Xie (110), and Skalny and Mindess (111).

The properties of the zone naturally reflect the specific physico-chemical regime under which it develops. Massazza (112) demonstrated that on autoclaving at 180°C, quartz, feldspars, and several varieties of glass aggregate react with the cement paste and develop an interfacial structure dominated by 1.1nm tobermorite laths; this interfacial zone is harder (and stronger) than the bulk autoclaved paste. In some systems the initial interfacial product is hydroxyellastadite, which then transforms to tobermorite. Limestone aggregates apparently do not develop such a zone.

Somewhat less drastic changes accompany the substitution of Type K expansive cement for ordinary portland cement, as reported by Monteiro and Mehta (113). The duplex film formed is discontinuous, and large tabular hexagonal crystals of calcium hydroxide with a nearly random orientation develop adjacent to it. A concentration of ettringite near the actual interface was demonstrated, but the apparent amount of ettringite formed here seems somewhat less than might have been expected.

Changes are also expected to accompany replacement of some of the portland cement with supplementary cementitious components. Carles-Gibergues et al. (114) described various effects of different systems. Fly ash containing many plerospheres absorbed enough mix water to lower fluidity of the paste near the aggregate surface and reduce the thickness of the measured aureole de transition; high calcium fly ashes, acting as plasticizers, increased fluidity and thus increased the thickness of the zone. Silica fume, used by itself, decreased fluidity and reduced the thickness. Somewhat surprisingly to the writer, but in accord with results obtained by Barnes (51), blends with slag behaved little differently than unmodified portland cements. Silica fume was found to cause progressive replacement, with time, of the calcium hydroxide in the interfacial zone with secondary C-S-H gel derived from the pozzolanic reaction; in consequence, the calcium hydroxide-rich layer was reduced to a narrow zone extending only a few μm from the aggregate.

Recently Huang and Feldman (115) indicated that with time, mortars containing silica fume showed an unexpected increase in mercury-intruded pore volume attributed to pores of 100 to 1000 nm. The time involved was commensurate with the time over which the pozzolanic reaction might proceed. These authors attributed the increased pore space in this size range to space generated by consumption of some of the lime deposited in the interfacial zone, presumably to form C-S-H gel with a coarse ("discontinuous") pore structure. Similar results were subsequently reported by Feldman (116).

The results cited above with respect to silica fume refer to systems of relatively high water content without the dispersive effect of the high dosage of superplasticizer ordinarily used in practice. In contrast to these modest effects, dispersed, superplasticized silica fume systems develop an entirely variant local structure near the interface. As shown clearly by Aitcin et al. (75), Dingsoyr et al. (76), Regourd et al. (80), and others, in such systems, while there may have been a duplex film or a thin layer rich in calcium hydroxide at early ages, after appreciable hydration the paste is fully dense and tight right up to the true interface, and neither calcium hydroxide, ettringite, nor empty space can be seen.

MICROSTRUCTURE OF PASTE ZONE SURROUNDING STEEL AND OTHER METALS

Steel is incorporated in concrete as reinforcement, as prestressing cable, and occasionally as steel fibers. Galvanized steel (presenting a zinc surface to the concrete) and other metals are occasionally used in concrete for special purposes. The interfacial structures developed next to such surfaces are of interest both for their effects of bond and mechanical properties, and for their possible influences on corrosion behavior.

The microstructure of the interfacial zones formed around steel fibers was profusely illustrated by Bentur et al. (117) and shown to have features in common with zones around aggregate particles. The usual duplex film was found, but this was surrounded by a zone of 10 to 30 μm thickness occupied by massive calcium hydroxide. This massive calcium hydroxide layer was not continuous parallel to the fiber, but was interrupted at intervals by more porous areas.

Beyond this massive calcium hydroxide layer, these authors found a highly porous layer of loose C-S-H deposits, through which induced cracks usually preferred to travel. The pattern of crack propagation induced in steel-fiber reinforced pastes was separately reported by Bentur et al. (118) and Bentur and Diamond (119), and shown to be in part a consequence of this microstructural development.

The interfacial zone around steel fibers in mortar was investigated by Sun et al. (120) using microhardness measurements. They concluded, in excellent agreement with the pattern described by Bentur et al. (117), that the thickness of the transition zone was approximately 40 μm, and that the weakest layer was about 25 to 35 μm from the steel surface.

Monteiro et al (121) investigated the reinforcing steel - cement paste interface from the corrosion point of view, in the presence of added chloride.

Pastes with and without silica fume were compared, with the pastes examined being spontaneously parted from the steel by drying shrinkage. The duplex films were clearly evident, although these authors suggest that "the interfacial film consists of large CH crystals", rather a contradiction in terms. The silica fume appeared to make little visible difference in the microstructure, but apparently induced greater corrosion.

The formation of the transition zone developed around galvanized steel was studied by Arliguie and Grandet (122). A relatively thick chemically-perturbed zone was found to develop, with crystalline calcium hydrozincate formed close to the zinc interface, a layer containing zinc hydroxide further away, and a still further layer deficient in calcium hydroxide. The pattern is modified somewhat if calcium chloride is present, due to the prior formation of zinc hydroxychloride at the zinc surface (123).

Microstructural responses induced in pastes of C_3A (124) and C_3S (125) to incorporation of iron, copper, or zinc wires were studied by Tashiro and co-workers.

MICROSTRUCTURE WITHIN AND AROUND GLASS FIBER STRANDS IN GLASS FIBER REINFORCED CONCRETE SYSTEMS

Glass fiber reinforced concretes (or more properly, mortars) have been increasing used for special purposes, notably architectural panels and other thin-sheet applications. A major limitation on their even wider use has been the reduction in ductility and strength accompanying exposure to wet conditions in service, despite use of alkali-resistant glass compositions. This special durability problem was the subject of a recent international symposium in Chicago (126).

It appears from results of Bentur (127), Bartos (128), and others, that while alkali attack on the glass may in fact take place to some degree over prolonged periods, the basic problem is microstructurally related. Glass fibers are customarily provided in strands of about 200 individual 10 to 12 μm-thick fibers, which are chopped to short lengths and incorporated in the cementitious product mix. The narrow spaces between the parallel fibers, typically no more than a μm or two in width, do not admit cement particles, but become sites for deposition of massive calcium hydroxide and sometimes C-S-H gel. Mills (129) has shown that calcium hydroxide seems to show a marked preference for deposition such fibers rather than on other available surfaces.

As a result of this deposition within the strands, individual fibers become tightly bound to each other and locked to the surrounding cement paste. This results in loss of strain capacity; the individual fibers can no longer pull out independently, nor can they bend individually to accept off-axis stresses.

Fig. 20 depicts the empty space between the individual fibers in GFRC that has not become embrittled; Fig. 21, the appearance of typical calcium hydroxide deposits that surround the glass fibers after long exposure to wet conditions.

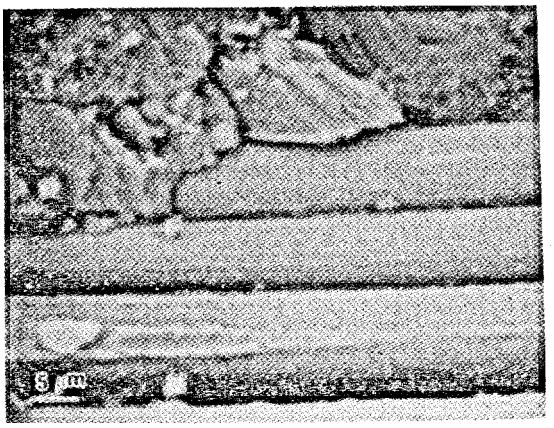

Fig. 20. View showing empty space between glass fibers in GFRC that has not been embrittled.

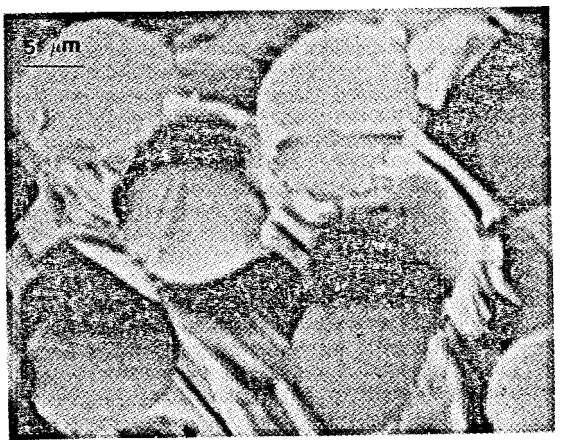

Fig. 21. Morphology of calcium hydroxide deposits surrounding glass fibers in weathered GFRC.

Bentur and Diamond (130) have studied the details of the response of the fibers in cement paste to a crack induced by compact tensile loading within the SEM. The details of the pullout and subsequent fracture of the fibers are clearly conditioned by the pre-existing microstructure of the region surrounding the strand and of the spaces within it.

A number of systems to reduce this effect have been proposed. Majumdar and Stucke (131) have reported details of the microstructural development in and around the strands when supersulfated cement is used instead of portland cement. Ettringite deposited early in this system eventually carbonates, and the spaces become filled with deposits of gypsum and calcite.

Microstructural details of another system for improving the durability of GFRC developed by Bentur and Diamond (132) were recently described. This system involves direct incorporation of a dispersed slurry of silica fume by wicking action into the inter-fiber spaces before the strands are included in the GFRC product. The prior presence of the silica fume appears to pre-

vent the subsequent deposition of calcium hydroxide in these spaces, and beneficially modifies the microstructure of the hydration products immediately surrounding the strand.

The GFRC symposium proceedings also include microstructural characterizations by Kumar and Roy (133) of glass fiber strands incorporated in several blended cements and subsequently autoclaved, and a study by Cohen and Constantiner (134) of microstructural effects accompanying use of cements with additions of alkali sulfate and of silica fume to the matrix mixture.

CONCLUSION

It is evident from the great mass of information cited that significant progress has been made in understanding the development of the microstructure of cement paste in concrete, including pastes incorporating fly ash, silica fume, and other supplementary components, and including the special microstructures developed near aggregate interfaces, around steel, and in other special zones. The application of such understanding for the production of stronger and more durable structures and concrete products offers a further challenge that is just beginning to be met. Perhaps by the time of the next Congress it may be appropriate to provide for a review on the applications of microstructural knowledge to practice, rather than on microstructure per se.

REFERENCES

1. Taylor, H. F. W. and Roy, D. M., "Structure and Composition of Hydrates, Proc. 7th Congr. Chem. Cement, Paris v. I pp. II-2/1 to II-2/13 (1980).

2. Sereda, P. J., Feldman, R. F., and Ramachandran, V. S., "Structure Formation and Development in Hardened Cement Paste," Proc. 7th Congr. Chem. Cement, Paris v. I pp. VI-1/3 to VI-1/44 (1980).

3. Diamond, S., "Cement Pastes: Rheology, Evolution of the Properties, and Structures," Proc. 7th Congr. Chem. Cement, Paris, v. IV pp. 113-123 (1980).

4. Scrivener, K. L., "The Development of Microstructure During the Hydration of Portland Cement," Ph. D. thesis, Dept. of Matall. and Matls. Sci., Imperial College, London (1984).

5. Monteiro, P. J. M., "Microstrucuture of Concrete and its Influence on Mechanical Properties," Ph. D. thesis, Dept. of Civil Eng., University of California, Berkeley (1985).

6. Diamond, S., "On the Microstructure of Solids in Hardened Cement Paste," Proc. Engr. Found. Conf. on Cement Manufacture and Use, Henniker, N. H. (1985); in press.

7. Taylor, H. F. W., "Studies on the Chemistry and Microstructure of Cement Pastes," Proc. Brit. Ceram. Soc. v. 35, pp. 65-82 (1984).

8. Diamond, S., Mindess, S., and Lovell, J, "On the Spacing Between Aggregate Grains in Concrete and the Dimensions of the Aureole de Transition," in "Liaisons Pates de Ciment Mater. Assoc.", Proc. RILEM Colloq., Toulouse, pp. C-42 to C-46 (1982).

9. Jennings, H. M., Clifton, J., Frohnsdorff, G., and Johnson, S. K., "On Establishing Functional Relationships Between Reaction Mechanisms and Engineering Properties of Cement-Based Systems," Proc. Eng. Found. Conf. on Cement Manufacture and Use, Henniker, N. H. (1985); in press.

10. Jennings, H. M. and Johnson, S. K., "Simulation of Microstructure Development During the Hydration of a Cement Compound," accepted for publication, Amer. Ceram. Soc. (1986).

11. Dalgleish, B. J. and Ibe, K. "Thin Foil Studies of Hydrated Portland Cement," Cem. Concr. Res. v. 11 pp. 729-740 (1981).

12. Scrivener, K. L. and Pratt, P. L., "Backscattered Electron Images of Polished Cement Sections in the Scanning Electron Microscope," Proc. 6th Conf. Cement Microscopy, Albuquerque, pp. 145-155 (1984).

13. Barker, A. P., Barnes, P., Fisher, G. R., and Hennings, H. M., "Novel Microscopy Techniques for Studying the Microstructure of Clinkers and Hydrated Cements - Some Preliminary Results," ibid. pp. 5-19 (1984).

14. Barker, A. P. and Barnes, P., "A Review of Techniques for Phase Delineation Within cement in the SEM," ibid. pp. 156-172 (1984).

15. Groves, G. W., "TEM Studies of Cement Clinker Compounds , their Hydration, and Strong Cement Pastes," Phil. Trans. R. Soc. London A - 310 pp. 79-83 (1983).

16. Orr, D. M. F., "Application of the SEM to the Study of the Intiail Hydration of Portland Cement Paste," Cem. Concr. Res. v. 13 pp. 146-148 (1983).

17. Parrott, L. J., "Novel Methods of Processing Cement Gel to Examine and Control Microstructure and Properties," Phil. Trans. R. Soc. London, A - 310 pp. 155-166 (1983).

18. Jennings, H. M., Dalgleish, B. J., and Pratt, P. L., "Morphological Development of Hydrating Tricalcium Silicate as Examined by Electron Microscopy Techniques," J. Amer. Ceram. Soc. v. 64 pp. 567-572 (1981)

19. Diamond, S., Mindess, S., and Lovell, J., "Use of a Robinson Backscatter Detector and "Wet Cell" for Examination of Wet Cement Paste and Mortar Specimens Under Load," Cem. Concr. Res. v. 13 pp. 107-113 (1983).

20. Diamond, S. and Mindess, S., "Scanning electron Microscopic Observations of Cracking in Portland Cement Paste," Proc. 7th Congr. Chem. Cement, Paris, v. III pp. VI-114 to VI-119 (1980).

21. Mindess, S. and Diamond, S. "A Preliminary SEM Study of Crack Propagation in Mortar," Cem. Concr. Res. v. 10 pp. 509-519 (1980).

22. Mindess, S. and Diamond, S., "The Cracking and Fracture of Mortar," Mater. and Struct. (Paris) n. 86 pp. 107-113 March-Apr. (1982).

23. Mindess, S. and Diamond, S., "A Device for Direct Observation of Cracking of Cement Paste or Mortar Under Compressive Loading Within the SEM," Cem. Concr. Res. v. 12 pp. 569-576 (1982).

24. Diamond, S., Lovell, J., Mindess, S., and Bentur, A., "Development and Applications of Devices to Study Cracking Within the SEM," Proc. 6th Conf. Cement Microscopy, Albuquerque, pp. 438-452 (1984).

25. Jennings, H. M., Grimes, J., and Brown, P. L., "Wet Cell for Use With Scanning Electron Microscope," U. S. Patent Application (1986).

26. Taylor, H. F. W. and Newbury, D.,"An Electron Microprobe Study of a Mature Cement Paste," Cem. Concr. Res. v. 14 pp. 565-573 (1984).

27. Diamond, S., "Cement Paste Microstructure: An Overview at Several Levels," in Proc. Conf. on Hydraulic Cement Pastes: Their Structure and Properties, Sheffield pp. 2-30 (1976).

28. Odler, I. and Lin, S., "SEM Studies on Polished Clinker Surfaces," Proc. 7th Conf. Cement Microscopy, Fort Worth, pp. 382-395 (1985).

29. Jennings, H. M., "The Developing Microstructure in Portland Cement," in Advances in Cement Technology, S. N. Ghosh, ed., Pergamon Press, pp. 349-396 (1983).

30. Jennings, H. N., personal communication, July 1986.

31. Lachowski, E.E. and Diamond, S., "Investigation of the Composition and Morphology of Individual Particles of Portland Cement Paste: 1. C-S-H gel and Calcium Hydroxide Particles," Cem. Concr. Res. v. 13 pp. 177-185 (1983).

32. Diamond, S. and Lachowski, E. E., "On the Morphology of Type III C-S-H Gel," Cem. Concr. Res. v. 10 pp. 703-705 (1980).

33. Shpnova, L. G., Belov, N. V., and Mel'nik, S. K., "Role of Calcium Hydroxide Crystal Structure in the Formation of Limestone and Cement Stone," Dokl. Akad. Nauk SSSR, v. 257 pp. 178-181 (1981); Chem. Abstr. v. 95 102002 (1981).

34. Groves, G. W., "Microcrystalline Calcium Hydroxide in Portland Cement Pastes of Low Water:Cement Ratio," Cem. Concr. Res. v. 11 pp. 713-718 (1981).

35. Marchese, B., "Morphology and Composition of Twin Fracture Surfaces of a Crack in Portland Cement Paste," Cem. Concr. Res. v. 13 pp. 435-440 (1983).

36. Scrivener, K. L. and Pratt, P. L., "Microstrucutural Studies of the Hydration of C_3A and C_4AF Independently and in Cement Paste," Proc. Br. Ceram. Soc. v. 35, pp. 207-219 (1984).

37. Ogawa, K. and Roy, D. M., "C_4A_3S Hydration, Ettringite Formation, and Its Expansion Mechanism: II. Microscopic Observation of Expansion," Cem. Concr. Res. v. 12 pp. 101-110 (1982).

38. Taylor, H. F. W., "Portland Cement:Hydration Products," in "Instructional Modules in Cement Science, D. M. Roy, ed., Matls. Educ. Council, Penn. State Univ., University Park, PA, pp. 29-45 (1985).

39. Taylor, H. F. W., "Proposed Structure for Calcium Silicate Hydrate Gel," J. Amer. Ceram. Soc. v. 69 pp. 464-466 (1986).

40. Winslow, D. N., "The Fractal Nature of the Surface of Cement Paste," Cem. Concr. Res. v. 15 pp. 817-824 (1985).

41. Diamond, S., "An Alternative to Gypsum Set Regulation for Portland Cements," World Cement Techn. v. 11 pp 116-121 (1980).

42. Abo-el-Enein, S. A., "Physicochemical and Microstructural Characteristics of Hardened Alite Pastes," Proc. 5th Conf. Cement Microscopy, Nashville, pp. 15-163 (1983).

43. Bajza, A., "Structure of Compacted Cement Pastes," Cem. Concr. Res. v. 13 pp. 239-246 (1983).

44. Dalgleish, B. J., Ghose, A., Jennings, H. M., and Pratt, P. L., "The Correlation of Microstructure With Setting and Hardening in Cement Paste," Proc. RILEM Conf. Concrete at Early Ages, Paris, v. I pp. 137-143 (1982).

45. Pratt, P. L. and Jennings, H. M., "The Microchemistry and Microstructure of Portland Cement," Ann. Rev. Mater. Sci. v. 11 pp. 123-149 (1981).

46. Barnes, P., Ghose, A., and Mackay, A. L., "Cement Tubules - Another Look," Cem. Concr. Res. v. 10 pp. 639-646 (1980).

47. Orr, D. M. F., "Structure and Strength of Portland Cement Mixes at Early Ages," Proc. RILEM Conf. Concrete at Early Ages, Paris, v. I pp. 57-61 (1982).

48. Hadley, D. N., "The Nature of the Paste-Aggregate Interface," Ph. D. thesis, School of Civil Eng., Purdue Univ. (1972).

49. Barnes, B. L., Diamond, S., and Dolch, W. L., "Hollow Shell Hydration Particles in Bulk Cement Paste," Cem. Concr. Res. v. 8 pp. 263-271 (1978).

50. Pratt, P. L. and Ghose, A., "Electron Microscope Studies of Portland Cement Microstructures During Setting and Hardening," Phil. Trans. R. Soc. Lond. A-310 pp. 93-103 (1983).

54. Helmuth, R. A., "Water-Reducing Properties of Fly Ash in Cement Pastes, Mortars, and Concretes: Causes and Test Methods," Proc. 2nd Conf. Fly Ash, Silica Fume, Slag, and Nat. Pozzolans in Concrete, Madrid, v. 1 pp. 723-740 (1986).

55. Diamond, S. and Lopez-Flores, F., "Comparative Studies of the Effects of Lignitic and Bituminous Fly Ashes in Hydrated Cement Systems," Proc. Symp. Effects of Flyash in Cement and Concrete, Mater. Res. Soc., pp. 112-123 (1981).

56. Pratt, P. L., "The Influence of PFA on the Hydration of Cement and Concrete," Proc. Symp. Use of PFA in Concrete, Leeds, v.2 pp. 29-52 (1982).

57. Diamond, S., Ravina, D., and Lovell, J., "The Occurrence of Duplex Films on Flyash Surfaces," Cem. Concr. Res. v. 10 pp. 297-300 (1980).

58. Ghose, A. and Pratt, P. L., "Studies of the Hydration Reactions and Microstructure of Cement Flyash Pastes," Proc. Symp. Effects of Flyash in Cement and Concrete, Mater. Res. Soc., pp. 82-91 (1981).

59. Blaschke, R., "The Matrix and Its Resistance of Fly Ash Concrete," Proc. 7th Conf. Cement Microscopy, Fort Worth, pp. 288-304 (1985).

60. Halse, Y., Pratt, P. L., Dalziel, J. A., and Gutteridge, W. A., "Development of Microstructure and Other Properties in Flyash OPC Systems," Cem. Concr. Res. v. 14 pp. 491-498 (1984).

61. Montgomery, D. G., Hughes, D. C., and Williams, R. I. T., "Fly Ash in Concrete - A Microstructural Study," Cem. Concr. Res. v. 11 pp. 591-604 (1981).

62. Halse, Y., Gault, D, and Pratt, P. L., "Calorimetry and Microscopy of Fly Ash and Silica Fume Cement Blends," Proc. Br. Ceram. Soc. v. 35 pp. 403-417 (1984).

63. Huang, S., "The Effect of Addition of Gypsum on the Hydration of Fly Ash Cement," Proc. Symp. Use of PFA in Concrete, Leeds, v. 2 pp. 55-66 (1982).

64. Jawed, I. and Skalny, J., "Hydration of Tricalcium Silicate in the Presence of Fly Ash," Proc. Symp. Effects of Flyash in Cement and Concrete, Mater. Res. Soc. pp. 60-70 (1981).

65. Chanda, S. and Bailey, J. E., "Flexural Strength and Fracture Properties of Fly Ash Blended Cement," Mat. Res. Soc. Proc. v. 43, pp. 107-118 (1985).

66. Montgomery, D. G. and Diamond, S., "The Influence of Fly Ash Cenospheres on the Details of Cracking in Flyash-Bearing Cement Pastes,", Cem. Concr. Res. v. 14 pp. 767-775 (1984).

67. Grutzeck, M.W., Roy, D. M., and Scheetz, B.E., "Microstructure of High-Lime Fly Ash in Cementitious Mixes," Cem. Concr. Res. v. 11 pp. 291-294 (1981)

68. Scheetz, B. E., Grutzeck, M. W., Strickler, D., and Roy, D. M., Effect of Composition of Additives Upon Microstructures of Hydrated Portland Cement Composites," Proc. 3rd Conf. Cement Microscopy, Houston, pp. 307-318 (1981).

69. Baker, M. D. and Laguros, J. G., Reaction Products in Fly Ash Concrete," Mater. Res. Soc. Proc. v. 43 pp. 73-83 (1985).

70. Pistilli, M. F., "The Effect of Several Air-Entraining Agents on Concrete Containing a Higher Than Normal Amount of Class C Fly Ash," Proc. 3rd Conf. Cement Microscopy, Houston, pp. 331-346 (1981).

71. Mills, R. H., "Characterization of Fly Ash Hydration Reactions From Microstructure," Proc. Mat. Res. Soc. v. 65, pp. 207-217 (1986).

72. Tenoutasse, N. and Marion, M., "Characterization of Belgian Fly Ashes and Their Behavior in Cement Paste," Proc. 2nd. Conf. Fly Ash, Silica Fume, Slag, and Nat. Pozzolans in Concrete, Madrid, v. 1 pp. 51-76 (1986).

73. Grutzeck, M. W., Atkinson, S., and Roy, D. M., "Mechanism of Hydration of Condensed Silica Fume in Calcium Hydroxide Solutions, Proc. 1st Conf. Fly Ash, Silica Fume, Slag, and Nat. Pozzolans in Concrete, Montebello, v. 2 pp. 643-664 (1983).

74. Grutzeck, M. W., Roy, D. M., and Wolfe-Confer, D., "Mechanism of Hydration of Portland Cement Composites Containing Ferrosilicon Dust," Proc. 4th Conf. Cement Microscopy, Las Vegas, pp. 193-202 (1982).

75. Aitcin, P. C., Regourd, M., and Bedard, C., "Microstructural Study of a 135 MPa (19,500 psi) Ready Mix Concrete," Proc. 5th Conf. Cement Microscopy, Nashville, pp. 164-179 (1983).

76. Dingsoyr, E., Mosberg, T., and Young, J. F., "Influence of Aggregates on the Strength and Elastic Modulus of High Strength Mortars Containing Microsilica," Mat. Res. Soc. Proc., v. 42 pp. 211-218 (1985).

77. Marusin, S., "Microstructure and Pore Characteristics of Concrete Containing Condensed Silica Fume With A Superplasticizer," Proc. 8th Conf. Cement Microscopy, Orlando, pp. 327-335 (1986).

78. Regourd, M., "Pozzolanic Reactivity of Condensed Silica Fume," in Condensed Silica Fume, P. C. Aitcin, ed., les Editions de'l Universite de Sherbrooke, pp. 20-24 (1983).

79. Regourd, M., "Microstructure of High Strength Cement Based Systems," Mat. Res. Soc. Proc. v. 42. pp. 3-17 (1985).

80. Regourd, M., Mortureux, B,, Aitcin, P. C., and Pinsonneault, P., "Microstructures of Concretes Containing Silica Fume," Proc. 4th Conf.Cement Microscopy, Las Vegas, pp. 249-260, (1982).

81. Regourd, M., Mortureux, B., and Hornain, H., "Use of Condensed Silica Fume as Filler in Blended Cements," Proc. 1st Conf. Fly Ash, Silica Fume, Slag, and Nat. Pozzolans in Concrete, Montebello, v. 2 pp. 847-869 (1983).

82. Marusin, S., "Microstructure and Pore Characteristics of Conventional Portland Cement Concrete Vs. Concrete Containing HRWR," Proc. 7th Conf. Cement Microscopy, Ft. Worth, pp. 419-425

(1985).

83. Diamond, S. and Gomez-Toledo, F., "The Microstructure of Low-Porosity Portland Cement Paste," Il Cemento, v. 75 pp.189-194 (1978).

84. S. E. Coleman, "Low Porosity High Strength Concrete for Bridge Decks," Ph. D. Thesis, School of Civil Eng., Purdue Univ. (1981).

85. Skvara, F. and Zbuzek, B., "Microstructure of Hardened Gypsum-Free Portland Cement," Tonind. Ztg. v. 104 pp. 823-827 (1980).

86. Skvara, F. and Zbuzeck, B., "The Morphology and Composition of Hardened Pastes of Gypsum-Free Cement," Silikaty, v. 27 pp. 215-223 (1983).

87. Subba Rao, V. V., Sharma, K., Jain, N. K., Syal, S. K., and Chopra, S. K., "SEM Studies on Clinker and Cement Pastes Containing Superplasticizer Based on Paper Plant Black Liquor and alkali Carbonates," Proc. 6th Conf. Cement Microscopy, Albuquerque, pp. 182-194 (1984).

88. Skvara, F. and Rybinova, M., "The System Ground Clinker-Polyphenol Sulfate-Alkali Metal Salts," Cem. Concr. Res. v. 15 pp. 1013-1021 (1985).

89. Regourd, M., "Structure and Behavior of Slag Portland Cement," Proc. 7th Congr. Chem. Cement, Paris, v. I pp. III-2/10 to III-2/26 (1980).

90. Tanaka, H., Totani, Y., and Saito, Y., "Structure of Hydrated Glassy Blast Furnace Slag in Concrete," Proc. 1st. Conf. Fly Ash, Silica Fume, Slag, and Nat. Pozzolans in Concrete, Montebello, v. 2 pp. 963-977 (1983).

91. Marchese, B., "An SEM Contribution to the Study on Cement Pastes: Note IV," Il Cemento, v. 80 pp. 107-120 (1983).

92. Groves, G. W., "TEM Studies of Cement Clinker Compounds - Their Hydration, and Strong Cement Pastes," Phil. Trans. R. Soc. Lond., A-310pp. 79-83 (1983).

93. Sinclair, W. and Groves, G. W., "The Microstructure of High Strength Cement Pastes," Mat. Res. Soc. Proc. v. 42, pp. 31-37 (1985).

94. Maso, J. C., "The Bond Between Aggregates and Hydrated Cement Paste," Proc. 7th Congr. Chem. Cement, Paris, v. I pp. VII-1/3 to VII-1/15 (1980).

95. Struble, L., Skalny, J.,and Mindess, S., "A Review of the Cement Aggregate Bond," Cem. Concr. Res. v. 10 pp. 277-286 (1980).

96. Grandet, J. and Ollivier, J. P., "New Method for the Study of Cement-Aggregate Interfaces," Proc. 7th Congr. Chem. Cement, Paris, v. III pp 85-89 (1980).

97. Carles-Gibergues, A., Grandet, J., and Ollivier, J. P., "The Techniques of investigation on the Contact Zone Between Cement Paste and Aggregate," Proc. RILEM Colloq. Liaisons Pates de Ciment Materiaux Associes, Toulouse, pp. D-9 to D-13 (1982).

98. Ollivier, J. P. and Grandet, J., "Sequence of Formation of the Aureole of Transition," ibid. pp. A-14 to A-22 (1982).

99. Monteiro, P. J. M. and Mehta, P. K., "Ettringite Formation on the Aggregate-Cement Paste Interface, " Cem. Concr. Res. v. 15 pp. 378-380 (1985).

100. Hoshino, M. and Tomabechi, T., "Microscopic Study on Hardening Process and Structural Defect at the Boundary Between Cement Paste and Aggregate," Zairyo, v. 32 pp. 716-722 (1983); Chem. Abstr. v. 99 145032 (1983).

101. Monteiro, P. J. M, and Mehta, P. K., "Transition Zone Between Aggregate and Type K Expansive Cement," Cem. Concr. Res. v. 16 pp. 111-114 (1986).

102. Grandet, J. and Ollivier, J. P., "Etude de la Formation du Monocarboaluminatede Calcium Hydrate Au Contact d'Un Granulat Calcaire Dans Un Pate de Ciment Portland," Cem. Concr. Res. v. 10 pp. 759-770 (1980).

103. Struble, L. and Mindess, S., "Morphology of the Cement Aggregate Bond," Int. J. Cement Comp. and Lightweight Concrete v. 5. pp.79-86 (1983).

104. Langton, C. A. and Roy, D. M., "Morphology and Microstructure of Cement Paste - Rock Interfacial Regions," Proc. 7th Congr. Chem. Cement, Paris, v. III pp. VII-127 to VII-132 (1980).

105. Conjeaud, M., Lelong. B., and Cariou, B., "Liaison Pate de Ciment Portland-Granulats Naturals," ibid. v. III pp. VII-6 to VII-11 (1980).

106. Monteiro, P. J. M. and Mehta, P. K., "Interaction Between Carbonate Rock and Cement Paste," Cem. Concr. Res. v. 16 pp. 127-134 (1986).

107. Monteiro, P.J.M., Maso, J. C., and Ollivier, J. P., "The Aggregate-Mortar Interface," Cem. Concr. Res. v. 15 pp. 953-958 (1985).

108. Barnes, B. D., Diamond, S., and Dolch, W. L., "Micromorphology of the Interfacial Zone Around Aggregates in Portland Cement Mortar," J. Amer. Ceram. Soc. v. 62 pp. 21-24 (1979).

109. Zimbelman, R, "A Contribution to the Problem of Cement Aggregate Bond, Cem. Concr. Res. v. 15 pp. 801-808 (1985).

110. Xie, , S., "Study of the Interfacial Bonding in Cement-Based Composite Materials," Guisuanyan Xuebao, v. 11 pp. 489-497 (1983); Chem. Abstr. v. 100 161023 (1984).

111. Skalny. J. and Mindess, S., "Physico-Chemical Phenomena at the Cement Paste-Aggregate Interface," Mater. Sci. Monographs, v. 28A (React. Solids, A) pp. 517-521 (1985).

112. Massazza, F, "Interface Reactions Between Cement Paste and Aggregates in Autoclaved Mor-

tar," Proc. RILEM Colloq. Liaisons Pates de Ciment Materiaux Associes, Toulouse, pp. A-45 to A-54 (1982).

113. Monteiro, P. J. M. and Mehta, P. K., "Transition Zone Between Aggregate and Type K Cement Paste," Cem. Concr. Res. v. 16 pp. 111-114 (1986).

114. Carles-Gibergues, A, Grandet, J., and Ollivier, J. P., "Evolution of the "Aureole de Transition" on Aging in BlendedCement Pastes," Proc. RILEM Colloq. Liaisons Pates de Ciment Materiaux Associes, Toulouse, pp. B-11 to B-16 (1982).

115. Huang, Chen-Yi and Feldman, R. F, "Influence of Silica Fume on the Microstructural Development in Cement Mortars," Cem. Concr. Res. v. 15 pp. 285-294 (1985).

116. Feldman, R. F., "The Effect of Sand/Cement Ratio and Silica Fume on the Microstructure of Mortars," Cem. Concr. Res. v. 16 pp. 31-39 (1986).

117. Bentur, A., Diamond, S., and Mindess, S., "The Microstructure of the Steel Fibre-Cement Interface," J. Matls. Sci. v. 20 pp. 3610-3620 (1985).

118. Bentur, A., Diamond, S., and Mindess, S., "Cracking Processes in Steel Fiber Reinforced Cement Pastes," Cem. Concr. Res. v. 15 pp. 331-342 (1985).

119. Bentur A. and Diamond, S., "Crack Patterns in Steel Fiber Reinforced Cement Paste," Mater. and Struct. (Paris) v. 18 pp. 49-55 (1985).

120. Sun, W., Gao, J., and Qin, H., "Bond Strength of the Interface Between Fiber and Matric in Steel Fiber-Reinforced Concrete," Guisuanyan Xuebao v. 13 pp. 292-300 (1985); Chem. Abstr. v. 104 55314 (1986).

121. Monteiro, P. J. M., Gjorv, O., and Mehta, P. K., "Microstructure of the Steel-Cement Paste Interface," ibid. v. 15. pp. 378-380 (1985).

122. Arliguie, A. and Grandet,J., "Formation of "Aureole de Transition" Between Portland Cement Paste and Zinc," Proc. RILEM Colloq. Liaisons Pates de Ciment Materiaux Associes, Toulouse, pp. A-33 to A-38 (1982).

123. Arliguie, A. and Grandet, J., "Influence of Calcium Chloride on the Contact Zone Between Portland Cement Paste and Zinc," ibid. pp. A-39 to A-44 (1982).

124. Tashiro, C. and Ueoka, K., "Bond Strength Between C_3A Paste and Iron, Copper, or Zinc Wire, and Microstructure of the Interface," Cem. Concr. Res. v. 11 pp. 619-624 (1981).

125. Tashiro, C. and Tatibana, S., "Bond Strength Between C_3S Paste and Iron, Copper, and Zinc Wire and Microstructure of Interface," ibid. v. 13 pp. 377-382 (1983).

126. Proc. Symp. Durability of Glass Fiber Reinforced Concrete, Chicago, S. Diamond, ed., Prestressed Concr. Inst., 356 pp. (1986).

127. Bentur, A., "Mechanisms of Potential Embrittlement and Strength Loss of Glass Fiber Reinforced Cement Composites, ibid." pp. 109-123 (1986).

128. Bartos, P., "Effects of Changes in Fibre Strength and Bond Characteristics Due to Ageing on Fracture Mechanisms of GFRC," ibid. pp.136-146 (1986).

129. Mills, R. H., "Preferential Precipitation of Calcium Hydroxide on Alkali-Resistant Glass Fibres," Cem. Concr. Res. v. 11 pp. 689-698 (1981).

130. Bentur, A. and Diamond, S., "Fracture of Glass Fiber Reinforced Cement," Cem. Concr. Res. v. 14 pp. 31-42 (1984).

131. Majumdar, A. J. and Stucke, M. S., "Microstructure of Glass Fibre-Reinforced Supersulphated Cement," Cem. Concr. Res. v. 11 pp. 781-788 (1981).

132. Bentur, A. and Diamond, S., "Effects of Direct Incorporation of Microsilica into GFRC Composites on Retention of Mechanical Properties After Ageing," Proc. Symp. Durability of Glass Fiber Reinforced Concrete, Chicago, pp. 337-351 (1986).

133. Kumar, A. and Roy, D. M., "Microstructure of Glass Fiber/Cement Paste Interface in Admixture Blended Portland Cement Pastes," ibid. pp. 147-157 (1986).

134. Cohen, M. D. and Constantiner, D., "Morphological Developments of High and Low Alkali Cement Paste at the Glass Fiber-Cement Paste interface," ibid. pp. 158-173 (1986).

Sidney Mindess, University of British Columbia, Vancouver, Canada; Ivan Odler, Technical University Clausthal, Federal Republic of Germany; and Jan Skalny, W. R. Grace & Co., Research Division, Columbia, Maryland, U.S.A.

SIGNIFICANCE TO CONCRETE PERFORMANCE OF INTERFACES AND BOND: CHALLENGES OF THE FUTURE

SUMMARY: Interfacial regions and bond characteristics play an important role in all types of cementitious composites. In modern concrete, three types of interfaces must be considered: cement-aggregate, mortar-fiber, and mortar-reinforcing steel. All three types are important in determining not only the mechanical properties, but also the durability of concrete. This contribution analyzes the significance of these complex interfaces to the performance of concrete. Present problems are summarized, future challenges and needs are discussed, and suggestions are put forward as to the methodologies and experimental approaches to be taken to permit a systematic alteration in interfacial behavior.

As regiões interfaciais e as características da aderência exercem um papel importante em todos os tipos de compostos cimentosos. No concreto moderno devem ser considerados três tipos de interfaces: cimento-agregado, argamassa-fibra, e argamassa-aço da armadura. Os três tipos são importantes na determinação não só das propriedades mecânicas, mas também para a durabilidade do concreto. Esta contribuição analisa a importância destas interfaces complexas para a performance do concreto. São resumidos os problemas atuais, e se discutem os desafios e necessidades futuros, sendo apresentadas sugestões tais como metodologias e melhoras experimentais a serem adotadas para permitir uma alteração sistemática no comportamento interfacial.

INTRODUCTION

Concrete may be modelled as consisting of aggregate particles dispersed in a matrix of hardened cement paste (hcp). The performance of plain concrete must therefore be governed by the properties of the hcp and of the aggregate, and by the nature of the interface between them. When fibers or steel reinforcement are used, the bond between the mortar phase and these reinforcing materials is also very important. There is ample evidence that the structure of the cement matrix in the vicinity of the aggregate surface, or in the vicinity of fibers or steel reinforcement, is distinctly different from that in the bulk hcp. However, the detailed structure of the interfacial zone is variable; it depends upon the nature of the cement, the type of aggregate, the presence of admixtures, the type of reinforcement, curing conditions, and so on.

In general, the interfacial zone contains more calcium hydroxide (CH) than does the bulk hcp. Moreover, the CH crystals in the interfacial zone are not randomly oriented; they exhibit a preferred orientation with regard to the surface of the aggregate or the reinforcement. The thickness of the interfacial zone, as determined by measurements of the orientation of CH crystals (1, 2) is about 50-100 μm. It appears that only the first 10-20 μm are significantly different in mechanical properties from the bulk hcp. Nonetheless, in typical concrete mixes, the volume of hcp constituting the interfacial zone represents a significant fraction of the total volume of the cement matrix (3).

The relative importance of mechanical interlocking, van der Waals forces, epitaxial crystal growth phenomena, or other factors in contributing to the bond between hcp and either aggregate particles or reinforcement is still unknown. It is generally accepted that the interfacial zone represents the "weak link" in cementitious systems, since it appears to be the region of highest porosity and lowest strength. However, there is at the present time no way of predicting how much improvement can be made in the overall performance of concrete through improvements in bonding. Indeed, in some cases an increase in bond strength may be detrimental to the behavior of concrete.

In the past, a great deal of research has been directed towards improving the properties of hcp, aggregates, and reinforcing materials. Very little, however, has been done explicitly to try to alter the interfacial region itself. The purpose of this paper is to attempt to analyze the significance of interfacial effects to the performance of concrete, in terms of strength, ductility, and durability. The focus will be on future challenges and needs, with emphasis on the approaches which might be taken to permit systematic alterations to interfacial characteristics, and hence to the behavior of concrete.

THE NATURE OF THE INTERFACE

(a) Cement-Aggregate Interface. In the region of the cement-aggregate interface, there is a higher w/c ratio than in the bulk hcp, due to bleeding effects and to the surface effects of the aggregate face. This results in a region of higher porosity. There is also a higher concentration of CH at the interface than in the bulk hcp. Some researchers have found that there is a "duplex film" at the interface: plates of CH oriented parallel to the aggregate surface, and backed by a layer of C-S-H (4-7). Others, however, have found little evidence for such a duplex layer; they have found only a localized increase in CH crystals, but with no preferred orientation (8, 9). Still others have found a definite layer of oriented CH crystals on the surface of the aggregate, but without the C-S-H backing (10).

(b) Cement-Steel Interface. The cement-steel interface is similar to the cement-aggregate interface, probably because it too has a higher w/c ratio than does the bulk hcp. For instance, Bentur, Diamond and Mindess (11) have reported that the interfacial zone in well-hydrated systems consists of (Fig. 1):

i) a 1-2 μm thick duplex film in contact with the (fibrous) reinforcement;

ii) outside of this, a zone of 10-30 μm thickness, largely occupied by relatively massive CH crystals, and

iii) outside of this, a highly porous layer parallel to the interface.

Other investigators have reported similar findings, though the same sort of differences in observations as reported above for the cement-aggregate interface exist in the literature. In addition, some investigators (12, 13) have also found ettringite in the open spaces around the interfaces.

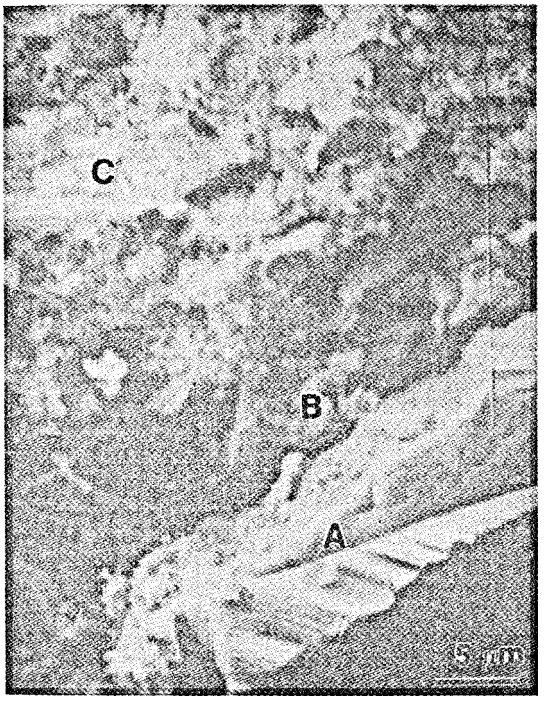

Figure 1: Interfacial zone exposed on fracturing perpendicular to the fiber axis showing the CH layer (A), a porous layer backing this layer (B), and the bulk cement paste (C), from Ref. 11.

(c) Cement-Glass Fiber Interface. Here again, there is disagreement in the literature as to whether there is a duplex film at the cement-glass interface. Some investigations have reported a duplex film (14-16). On the other hand, Bentur (17) has reported that when the spacing between the filaments making up the fiber is large (>10μm), there are large platy crystals of CH approximately perpendicular to the filament surface, along with clusters of C-S-H and occasional long needles of ettringite. When the spaces between filaments are small (<3μm), little or no material penetrates into these spaces. The structure of the hcp in the interfacial region is in general very porous, again due to a higher w/c ratio.

(d) Nature of the Bond. In all of the cases discussed above, it remains uncertain as to whether the bond is primarily due to mechanical interlocking, or whether there is some component of chemical bonding. While a few studies have suggested evidence of a chemical reaction between aggregates and hydrating cement paste (e.g., 18-21), it is not clear to what extent such reactions would contribute to bond strength. It would appear, based on the available evidence, that the major component of cement-aggregate bond strength is due to mechanical interlocking, perhaps assisted by epitaxial growth of some hydration products on aggregate surfaces.

The case of bonding between hcp and steel is much clearer, as there is no evidence of any chemical reaction. The bond is entirely mechanical.

EFFECT OF BOND ON CONCRETE PROPERTIES

(a) Strength. The effect of cement-aggregate bond strength on the strength of concrete is not clear. Some investigators (22-24) report little or no relationship between bond strength and concrete strength. On the other hand, others do find such a relationship. For instance, Alexander and Taplin (25) reported a linear correlation between concrete strength and the hcp and bond strengths, in which the coefficient for bond strength was one-half that for the hcp strength. The equation has the form

$$y = b_0 + b_1 m_1 + b_2 m_2$$

where y = modulus of rupture of concrete

m_1 = modulus of rupture of paste

m_2 = modulus of rupture of cement-aggregate bond

b_0, b_1, b_2 = linear regression coefficients

(b) Ductility. It is generally observed that, as concrete strength (and therefore perhaps bond strength) increases, the brittleness of the concrete also increases. There is evidence of considerable microcracking at the hcp-aggregate interface during loading of concrete (e.g., 26, 27). It has been suggested (23, 24) that increasing the bond strength increases the stress level at which extensive microcracking begins, which might explain the increase in brittleness with higher strengths.

The only real way to bring about a significant increase in concrete "ductility" is to incorporate fibers into the mix. In the practical range of fiber reinforced concrete, the fibers fail by pull-out rather than by fracture. In this case, the fiber-matrix bond controls the apparent ductility. The pull-out of a straight fiber is shown in Fig. 2, showing some separation and apparent interlocking at the interface (28).

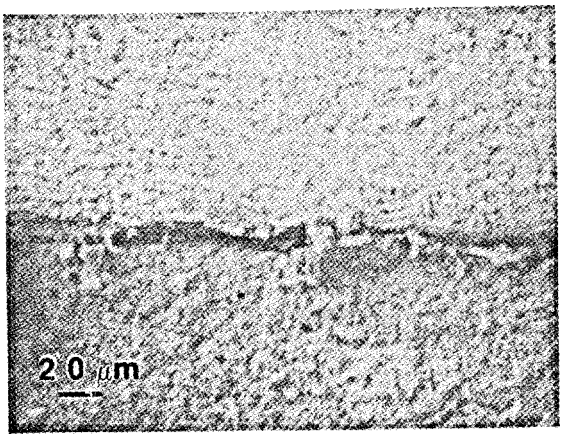

Figure 2: Pull-out of a straight fiber, showing some separation and apparent interlocking at the interface (28).

(c). Durability. There is very little published work on the effect of the interfacial region on concrete durability. There is no clear dependence of durability on bond strength, or on other interfacial properties. The aggregate-hcp interface does not appear to play a major role in determining the permeability of concrete (29, 30), and hence probably does not play much of a role in determining concrete durability. Valenta (31, 32), however, has reported some contrary findings.

CHALLENGES FOR THE FUTURE

In principle, a number of techniques might be employed to alter the hcp-aggregate (or fiber, or reinforcing steel) bond:

i) Suitable cement-aggregate combinations, considering the chemistry of the aggregate and the chemistry of the cement, including the minor compounds.

ii) Surface treatment of the aggregate (or reinforcing materials).

iii) Use of chemical admixtures.

iv) Use of mineral admixtures such as silica fume, which combine with CH, or additives which control the crystal growth.

v) Choosing appropriate curing conditions.

vi) Changes in the geometry of reinforcing materials to improve the pull-out resistance.

vii) Use of polymer impregnation.

It is fairly certain that these techniques, either singly or in conjunction with each other, could indeed increase the bond strength between hcp and other materials, and could bring about alterations in the chemistry and morphology of the interfacial region. The real questions are:

1. Under what circumstances do we want to improve the bond strength?

2. Are there cases in which improving the bond strength may be detrimental to concrete behavior?

3. Does the interface have any significant effect on durability?

(a) Benefits of Improving the Bond Strength. Increasing the hcp-aggregate bond strength, for ordinary concrete, is likely to increase the strength and elastic modulus of the concrete, and to increase the stress level at which extensive microcracking begins to take place. However, there are real limitations to the effectiveness of this approach. First, concrete strength is only moderately dependent (if at all) upon the bond strength. Moreover, it is well known that in high strength concretes, cracks tend to propagate through, rather than around, aggregate particles, Fig. 3. Thus, for high strength concretes, improvements in bond strength alone are likely to be of little benefit.

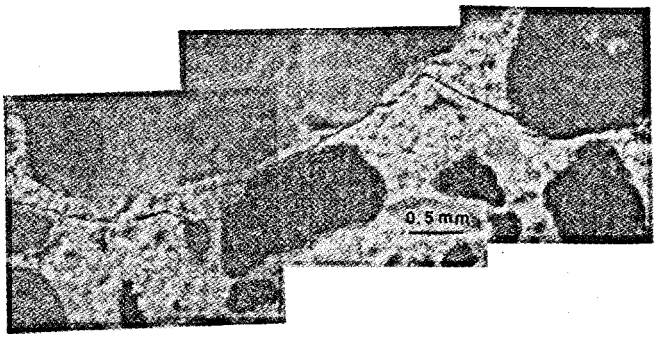

Figure 3: (a) Crack propagating around aggregate particles in normal strength concrete.

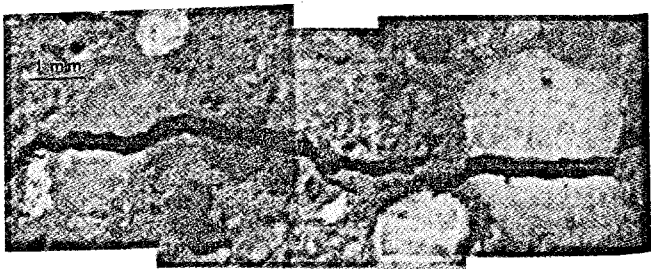

(b) Crack propagating through aggregate particles in high strength concrete.

For reinforced concrete, improvements in bond strength are likely to be more beneficial. In order for a composite material such as reinforced concrete to be effective, there must be adequate bond between the concrete and the steel. However, while it may be possible to improve the bond strength by optimizing the pattern of ribs on deformed reinforcing bars, the potential improvements in concrete behavior are not great, since it appears to be relatively easy to provide sufficient bond for current design practice by using existing construction technology.

It is for fiber reinforced concrete (frc) that improvements in the matrix-fiber bond strength are likely to be most beneficial. Optimizing the geometry and stiffness of the fibers, combined with the use of appropriate admixtures and consolidation techniques, could significantly improve the bond. This should lead to the production of materials with both higher strengths and greater ductility. Even in this case, however, there is a limit on how much the bond should be improved. Fibers are more effective in terms of ductility of frc when they fail by pulling out of the matrix rather than by fracturing, and this must be considered when increases in bond strength are contemplated. The pull-out of two different types of deformed fibers is shown in Fig. 4 (28).

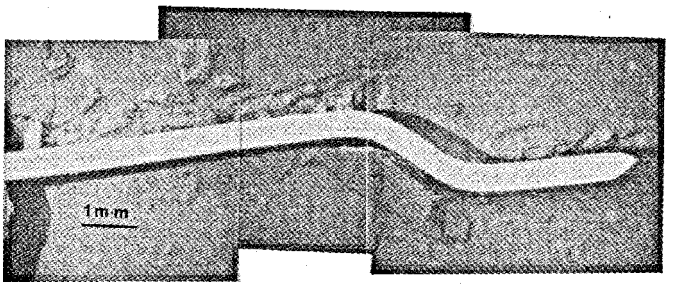

Figure 4:(a) Pull-out of a hooked fiber, showing local matrix crushing and fiber-matrix debonding (28).

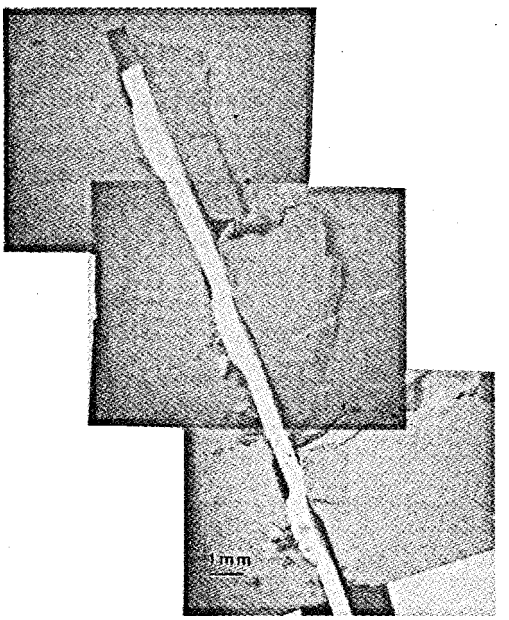

Figure 4:(b) Pull-out of a ribbed fiber, showing damage in the matrix (28).

(b) Possible Disadvantages of Improved Bond Strength. There are several cases in which improvements in bond strength could be detrimental to concrete behavior. In terms of the cement-aggregate bond, an increase in bond strength could increase the elastic modulus. However, it is also likely to decrease the energy required for fracture, i.e., it will make the concrete more brittle. For normal concrete, cracks tend to propagate along the cement-aggregate interfaces. This introduces a great deal of tortuosity to the crack path, thereby increasing the fracture energy. However, with improved bond, cracks will propagate more directly through the aggregate particles themselves, thus likely reducing the fracture toughness. In addition, since the elastic constants for hcp and aggregate are quite different, improved bond might lead to more severe stress concentrations under load in the interfacial region, again increasing the possibility of brittle behavior.

With fibers, improvements in bond strength are most likely to be achieved by changing the geometry of the fibers, rather than by the use of admixtures or chemical treatment. Again, improvements

in bond strength may be of limited value if they promote fracture of the fibers rather than pull-out.

For steel reinforcement, the matter is more complex. Bond strength may be the limiting factor in certain cases, such as beam-column connections under cyclic loading. However, improvements in bond strength will increase the likelihood of shear cracking, due to high localized stresses. There would also be an increase in the frequency of bond cracks perpendicular to the normal flexural cracks. Indeed, for reinforced concrete to "work" properly, there must be some slip between the steel and the concrete. Therefore, improvements in bond strength should be approached with caution. One recent example of this problem is the behavior of reinforced concrete under impact loading. It was found (33) that increasing the bond strength increased the probability that the steel reinforcing bars themselves would fail under impact loading, leading to catastrophic failure of the beams. Failure of a smooth reinforcing bar in a concrete beam under impact loading is shown in Fig. 5 (33).

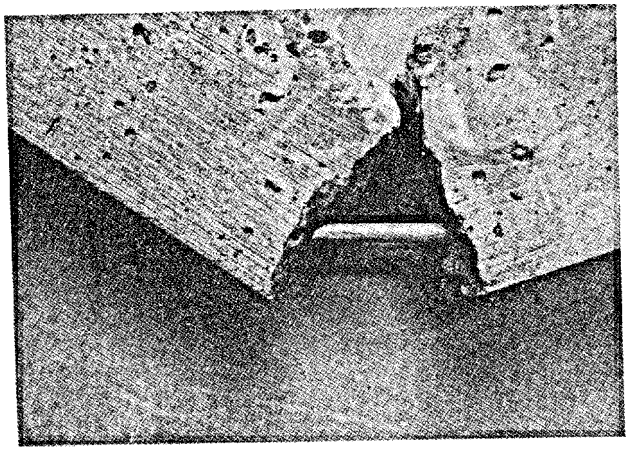

Figure 5: Failure of a smooth steel reinforcing bar in a concrete beam subject to impact loading (33).

(c) Effects of the Interfacial Region on Durability. As has been indicated above, there is no clear evidence that improving the interfacial region in concrete will improve durability. Durability appears to be much more strongly a function of the aggregate and hcp properties. Improvements in the matrix will, as well as improving durability, in general also lead to improvements in the cement-aggregate or cement-steel bond, but the improvements in bond will be secondary effects not directly influencing the durability.

METHODS OF STUDYING INTERFACIAL PHENOMENA

We still do not really understand the fundamental mechanisms which control interfacial phenomena, and until we do, it is difficult to imagine any systematic way in which to optimize the interfacial structure for different applications. In order to try and solve this basic problem, a much more comprehensive study of the interface will have to be undertaken, employing a large number of different techniques, each of which might provide some clues. We believe that one of the avenues to increasing our capabilities for engineering microstructures is wider use of knowledge developed in other fields of materials science, primarily metallurgy and ceramics (e.g., 34, 35). Such knowledge is generated by intelligent exploitation of basic chemical and physical principles.

Apart from measurements of the bond strength, and the standard mineralogical studies of the aggregate and chemical analysis of the cement, the following methods might be employed: ion beam etching, wet cell TEM, radioactive tracer techniques, EDXA line scanning, ESCA, and SIMS. Since the interfacial phenomena seem to have a large influence on the crack path that develops during the fracture process, a fracture mechanics approach to describing failure in terms of fracture energies and surface energies should also be considered.

CONCLUSIONS

We would expect that a heightened interest, an increase in research activity, and the introduction of additional experimental methods would extend our knowledge of the cement-aggregate and cement-reinforcement interfaces. In a very few cases, this might lead to marked increases in concrete quality. In most cases, however, we would expect, at best, only moderate increases in concrete quality. It would be useful, as one technique for matching the performance of concrete more closely to its structural requirements, to be able to modify the bond. However, the influence of the interfacial bond on concrete performance should not be over-emphasized. Particularly for high strength or high performance concretes, the available literature suggests that changing the interface could only bring about second-order modification in concrete behavior. For major changes, the cement paste, the aggregate, and the reinforcing materials themselves must be modified.

REFERENCES

1. J. Grandet, J.P. Ollivier, 7th Inter. Congress on the Chemistry of Cement, Paris, Vol. III, VII-85 (1980).

2. J.P. Ollivier, Contribution a l'Etude de L'hydration de la Pate de Ciment Portland au Vorsinage des Granulats, Ph.D. Thesis, Toulouse (1981).

3. S. Diamond, S. Mindess, J. Lovell, Colloque International, Liaisons Pates de Ciment Materiaux Associes, Toulouse, France, C. 42 (1982).

4. P.J.M. Monteiro, J.C. Maso, J.P. Ollivier, Cement and Concrete Research, 15, 953 (1985).

5. A. Carles-Gibergues, J. Grandet, J.P. Ollivier, in P. Bartos (ed.), Bond in Concrete, Applied Science Publishers, 24 (1982).

6. B.D. Barnes, S. Diamond, W.L. Dolch, J. American Ceramic Society, 62, 21 (1979).

7. C.A. Langton, D.M. Roy, 7th Inter. Congress on the Chemistry of Cement, Paris, Vol. III, VII-127 (1980).

8. M. Conjeaud, B. Lelong, B. Cariou, 7th Inter. Congress on the Chemistry of Cement, Paris, Vol. III, VIII-6 (1980).

9. J. Skalny, S. Mindess, in P. Barret and L.-C. Dufour (eds.), Reactivity in Solids, Elsevier Science Publishers, Amsterdam, 517 (1985).

10. L. Struble, S. Mindess, Int. J. Cement Composites and Lightweight Concrete, 5, 79 (1983).

11. A. Bentur, S. Diamond, S. Mindess, J. Materials Science, 20, 3610 (1985).

12. D.W. Hadley, Ph.D. Thesis, School of Civil Engineering, Purdue University (1972).

13. D.J. Pinchin, D. Tabor, Cement and Concrete Research, 8, 15 (1978).

14. B.D. Barnes, S. Diamond, W.L. Dolch, Cement and Concrete Research, 8, 233 (1978).

15. M.S. Stucke, A.J. Majumdar, J. Materials Science, 11, 1019 (1976).

16. E.B. Cohen, S. Diamond, in Fibre Reinforced Cement and Concrete, Proc. RILEM Symposium, The Construction Press, 315 (1975).

17. A. Bentur, private communication.

18. M. Suzuki, M. Mizukami, Review of the 29th General Meeting, Cement Association of Japan, 94 (1975).

19. B.J.F. Patten, UNICIV Report No. 2-82, University of New South Wales, Australia (1972).

20. H.E. Schwiete, U. Ludwig, J. Albeck, Wiss. Z. Tech. Univ. Dresden, 17, 1587 (1968).

21. S. Chatterji, J.W. Jeffery, Indian Concrete J., 45, 346 (1971).

22. G. Fagerlund, Proceedings of the International Symposium on Pore Structure and Properties of Materials, RILEM/IUPAC, Prague, D51 (1973).

23. T.T.C. Hsu, F.O. Slate, G.M. Sturman, G. Winter, J. American Concrete Institute, 60, 209 (1963).

24. C. Perry, J.E. Gillott, Cement and Concrete Research, 7, 553 (1977).

25. K.M. Alexander, J.H. Taplin, Australian Journal of Applied Science, 15, 160 (1964).

26. S. Mindess, S. Diamond, Materiaux et Constructions, 15, 107 (1982).

27. S. Mindess, S. Diamond, Cement and Concrete Research, 12, 569 (1982).

28. A. Bentur, S. Mindess, S. Diamond, Int. J. Cement Composites and Lightweight Concrete, 7, 29 (1985).

29. S. Mindess, R.J. Gray, J. Skalny, ACI-RILEM Seminar on Technology of Concrete, Mexico City, 121 (1984).

30. L.D. Wakely, D.M. Roy, Cement and Concrete Research, 12, 533 (1982).

31. O. Valenta, International Symposium on the Durability of Concrete, Preliminary Report, Prague, 53 (1981).

32. O. Valenta, Proceedings, Fifth International Symposium on the Chemistry of Cement, Tokyo, Vol. 3, 193 (1960).

33. A. Bentur, S. Mindess, N. Banthia, in Cement-Based Composites, Strain Rate Effects on Fracture, Materials Research Society Symposia Proceedings, Vol. 64, 193 (1960).

34. R.W. Rice, in Ceramic Engineering and Science Proceedings, 2, The American Ceramic Society (1981).

35. J.D. Venables, in Proceedings of 12th Natl. SAMPE Technical Conference, Society for the Advancement of Material and Process Engineering, 909 (1980).

F. MASSAZZA, *Professor of Applied Chemistry - Italcementi, Laboratorio Chimico Centrale, Bergamo, Italy* 1

U. COSTA, *Dr. of Chemistry - Italcementi, Laboratorio Chimico Centrale, Bergamo, Italy*

2.3

BOND: PASTE-AGGREGATE, PASTE-REINFORCEMENT AND PASTE-FIBRES
ADHERENCE: PATE-GRANULAT, PATE-ARMATURE ET PATE-FIBRES

1. INTRODUCTION

Strength of good concretes ranges between about 30 and 40 $N \cdot mm^{-2}$ but these values can be doubled if aggregates and cement are carefully chosen, the w/c ratio is reduced (in case by using superplasticizers)and a vigorous compaction is applied (1). In any case,the strength of concrete is much lower than that of its two components, cement paste and aggregate.

Cement pastes made with w/c ratios ≤ 0.30, anhyway such that they guarantee a good workability, have compressive strength exceeding 100 $N \cdot mm^{-2}$ after 28 days' curing (2)(3)(4)(5)(6). In their turn good aggregates attain 200 $N \cdot mm^{-2}$ without any difficulty (7)(8).

Based on an unanimous acknowledgement, the lower concrete strength is attributed to the relative weakness of the paste-aggregate interface (9)(10). In other words, the adhesion is lower than the cohesion of aggregates and paste. The same problem is found in paste-reinforcement and paste-fibre systems.

Several conferences, some of which are mentioned in the bibliographic references (11)(12)(13)(14), have been devoted to this specific subject which is very important from both the practical and theoretical points of view.

2. AGGREGATE-CEMENT PASTE BOND

2.1 Chemical reactions at the interface

Chemical reactions can occur between aggregate and cement paste. Depending on the cases they can improve or worsen the bond between the two components.

Among the particularly studied positive reactions there are those involving C_3A (or CA) present in the cement with the calcite present in calcareous aggregate and the hydrolysis lime with the siliceous aggregate quartz.

By examining polished marble samples covered with a portland cement paste (w/c = 0.5), it was observed that carboaluminate hydrate $C_3A \cdot CaCO_3 \cdot 11H_2O$ forms in the interface area. The amount of this compound in the paste decreases quickly as the distance from the interface increases (fig. 1). Its formation is slowed down by low w/c ratios. Monocarboaluminate is not the product of a direct reaction but it is the result of the reaction between the aggregate calcite and the partially carbonated aluminate hydrate $C_4A \cdot \frac{1}{2}CO_2 \cdot 12H_2O$.

The cement paste creates in limestone some attack patterns that are already visible under the optical microscope after one day. The attack intensity depends on the orientation of the calcite crystals(15). A portlandite film having the crystals oriented with c-axis, perpendicular to the interface, forms on the marble polished surface (16)(17). Also the grains of a calcareous monodimensional sand (d = 4-5 mm) show the signs of a reaction with the portland cement C_3A, which forms calcium monocarboaluminate $C_3A \cdot CaCO_3 \cdot 12H_2O$ (18). In filler cements, a hydrated zone of carboaluminate forms with time around the carbonate grains. This fact is accompanied by the disappearance of 20-25% calcite. The reaction of $CaCO_3$ with aluminates prevents ettringite from transforming into monosulphate (19).

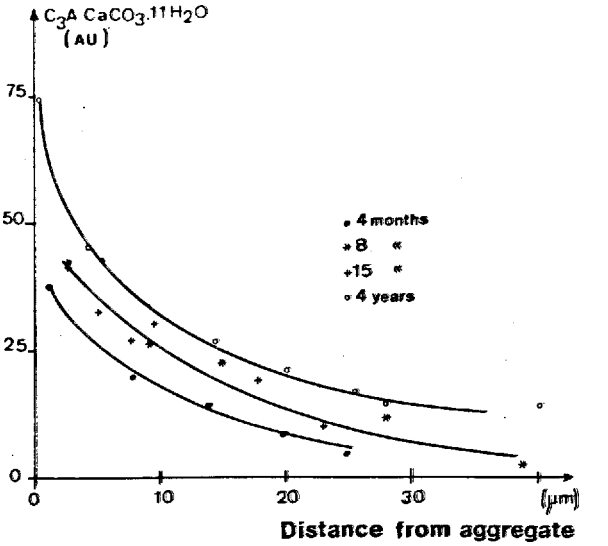

FIG. 1: Evolution of carboaluminate hydrate in the cement paste starting from the interface (w/c = 0.29) (15)

In mixes 1:1 of portland cement and calcareous filler $C_3A \cdot CaCO_3 \cdot 11H_2O$ can be found already after three days' hydration and the increase is appreciable after a week. Also in this case its formation occurs at the detriment of $C_4A \cdot \frac{1}{2}CO_2 \cdot 12H_2O$ which forms quickly owing to the reaction of $CaCO_3$ with aluminate hydrates. The mechanism of its formation is analogous to that due to the action of the atmospheric carbon dioxide (15).

At room temperature there is no evidence of the occurence of chemical reactions between quartz and cement paste (20)(21), however at 60°C the quartz surface is attacked (21). If the hydration is performed at 80°C with saturated vapour, the situation changes. In fact, by mixing the cement with seven different powdered materials (quartz, microcline, albite, anorthite, horneblende, augite and olivine), it was observed that the first four materials react progressively with the cement paste till 180 days, whereas the three others remain inactive (22).

The paste-siliceous aggregate reactions are enhanced if curing occurs under hydrothermal conditions. Quartz, for example, reacts in autoclave at 190°C with the cement paste and forms at the interface a tobermorite crystal layer that grows topochemically on the aggregate crystals (23). A similar hydrothermal reaction also occurs with other crystalline or vitrous silicates, if the free reaction energy ΔG is negative (24). Nevertheless these reactions can be overlooked if the investigation methods are not sufficiently so-

phisticated (25).

In the presence of calcium carbonate the monocal - cium aluminate hydration is considerably accelerated (26)(27). The thermal flow developed during the hydra tion reaction always appears with a single peak. This leads to think that carboaluminate and aluminate hy - drates form simultaneously, even though with diffe - rent kinetics depending on the nature and percenta g e of calcium carbonate, and temperature (28). Dolomite behaves like calcium carbonate whereas magnesite, as quartz, causes no reaction (28).

The presence of carboaluminate instead of hexago - nal calcium aluminate hydrates justifies the behaviour of aluminous cement mortars and concretes which, when they contain suitable amounts of calcareous filler, show no strength decrease related to the hexagonal a- luminate conversion to the cubic form. Conversely,the strength retrogradation is not hindered if the filler is siliceous, since silicates do not react with alumi nates (29).

When flexural breaking tests are performed on two concretes made with aluminous cement and containing an aluminous aggregate, with the same composition of ce- ment, and a siliceous aggregate respectively, t h e cracks follow different patterns. In fact, SEM obser- vations showed that in the former case cracks cross paste and aggregate indiscriminately and in the lat - ter they mainly spread at the paste-aggregate interfa- ce (30). Although it must be consider that SEM obser- vations demand the sample drying and this operati o n unavoidably causes the formation of microcracks, the differences between the two concretes lead to assume that a chemical bond forms between aluminous aggrega- te and cement paste. This conclusion is supported by that after 45 days the paste-aggregate interface can- not visibly be distinguished and only the X-ray image analysis enables the boundary of the two components to be distinguished (30).

A reaction generally considered as harmful is that occurring on the surface of some siliceous aggregates (opal chalcedony, glasses, a.s.o.) capable of react - ing with the alkalis in cement. It causes expansions, cracks in concrete and after all a decrease in the bond strength at the interface (31).

Tests performed by casting a mortar on polished sur faces of reactive aggregates showed that the interfa- ce bond decreases with time, as shown in fig. 2.

Reactions between aggregate and cement paste that led to important deteriorations in concretes were al- so noticed with aggregates other than those usually considered as dangerous, such as gneiss and mica - shists. Kaolinite and hydromica form at the interface in contact with the aggregate grains, whereas a gel composed of sodium calcium silicate is noticed in the paste side. Conversely, in a concrete made with ser - pentine, the cause of deterioration was related to the formation of brucite that resulted in a disconti- nuity between paste and aggregate (32). On the other hand, the dedolomitization phenomenon was observed in a concrete 30 years old but no sign of deterioration was noticed (32).

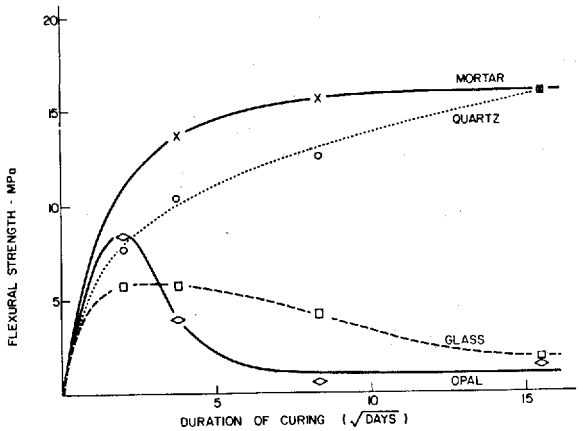

FIG. 2: Change in bond strength of glass, opal and quartz over an eight month period (Curing conditions: 95-100% relative humi- dity and 23°C) (31)

It is not always possible to attribute with cer - tainty the strength decrease in the aggregate-cement paste bond to the alkali-aggregate reaction. For in - stance, at the interface between quartzite grains and mortar, the presence of dark spots due do the iron mi- gration from the aggregate was observed. For this rea- son it was impossible to abscribe the strength decrea se to the formation of alkaline calcium silicate hy - drate (typical product of the alkali-aggregate reac - tion), to that of iron hydroxide gel or to that of both (31). The alkali-aggregate reaction cannot result in the typical displays of the phenomen. For example, with natural sand formed of quartz diorites, only a decohesion of the bond between grains and cement pa - ste was observed. In this case it was noticed that the aggregate surface was covered with a film of reac tive opal produced by a slow natural weathering (33).

If the reactive material is highly subdivided, the alkali-aggregate reaction causes a disgregation of the siliceous particles but not a concrete expansion. Indeed, the reaction has positive effects since it re sults in the combination of free lime which forms dur ing the cement hydration. If the aggregate is reacti- ve towards cement but contains Al_2O_3, Fe_2O_3 and CaO, such as fly ashes and slags, compounds form which do not absorb water and therefore do not increase their volume (34).

The subject of the alkali-aggregate reaction has widely been developed in the latest years and a great deal of information about the matter can be found in the proceedings of the meetings devoted to this speci fic topic (35)(36)(37)(38)(39)(40).

2.2 Interface morphology

2.2.1 Portland cements

It is by now accepted that near the aggregate-cement paste interface the cement paste has a structure different from the bulk paste, also in the absence of chemical reactions. This indicates that the process of the hydrate formation and crystallization is troubled in some way by the aggregate presence and, therefore, the aggregate-matrix bond also depends on physical factors. In the interface area there is an enrichment in portlandite which forms, in contact with the aggregate, a thin film in its turn covered with a thin C-S-H layer one particle thick. This layer (duplex film) is about 1 μm thick **(41)(42)**. However, this two-layered area only forms on unreactive aggregates, four different layers having been detected on the reactive ones (for ex. opal) **(43)**.

Not all Authors observed the presence of this duplex film **(44)**, but there is a general agreement on that the portlandite crystals are preferably arranged with c-axis perpendicular to the interface **(16) (41) (42)**. In any case it must be reminded that well defined hexagonal crystals are unusual at the interface **(45)**.

The duplex film is followed by a very porous interface zone, the "transition aura" **(46)** containing large differently oriented crystals, clusters of C-S-H and ettringite. This zone is about 50 μm thick.

Portlandite present in this area shows two typologies:

a) relatively large (10-30 μm) and well formed crystals, with c-axis roughly parallel to the interface, developed in the wide spaces available at the beginning of hydration;

b) stacked plates which fill the residual pores, present in the aged pastes, and with c-axis roughly normal to the interface.

The preferential orientation of portlandite is determined in a sample called double specimen, shown in fig. 3 **(20)**.

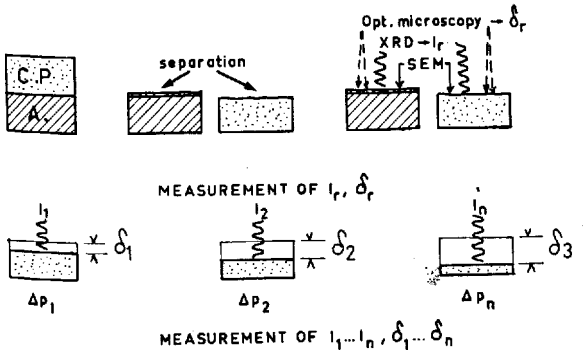

FIG. 3: Determination of orientation index I and transition aura thickness δ_0 **(20)**

The aura thickness δ_0 is measured by the reflected light microscope, that is the thickness which remains adherent to the aggregate after separation, whereas the orientation index I is determined by X-ray diffraction analysis **(26)**.

The orientation index I is obtained by the expression:

$$I = \frac{i'_{(001)}}{i'_{(101)}} \cdot \frac{i^\circ_{(101)}}{i^\circ_{(001)}} \qquad 1)$$

where $i_{(001)}$ and $i_{(101)}$ are the intensities of the diffraction peaks of planes (001) and (101), measured on both the examined sample (i') and a pulverized cement paste (i°) having quite disordered crystals **(17)**. In the cement pastes $\frac{i^\circ(001)}{i^\circ(101)} = 0.74$ and therefore 1) becomes

$$I = \frac{i'_{(001)}}{i'_{(101)}} \cdot 1.35 \qquad 2)$$

After the paste has been separated from the aggregate by bending rupture of the samples, successive layers of the paste remained adherent to the aggregate are removed by abrasion and the $i'(001)/i'(101)$ ratio is determined for each level.

The obtained results lead to determine the orientation index within the transition aura. The orientation index I (fig. 4) **(20)** attains the highest values on the film adherent to the aggregate and decreases as the distance σ from the interface increases, as far as to become equal to 1 when $\delta_0 \simeq 40\,\mu$m (orientation limit) **(17)**.

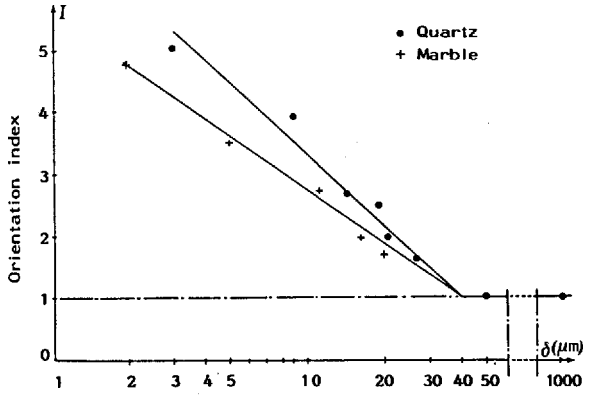

FIG. 4: Index of orientation I vs. nature of aggregate **(20)**

The thickness δ_0 of the transition aura does not practically change as the time varies, since it only depends on the thickness of the liquid film that initially wetted the aggregate. On the contrary, the orientation index increased continuously at least till 180 days, owing to the crystallization of additional portlandite **(47)**.

The nature of the aggregate and the curing time do

not affect δ_0 but only the tendency to orient the portlandite crystals, that is the derivate of curve $I = f(\log \delta)$. Conversely the orientation limit δ_0 varies as the w/c ratio increases **(16)**.

The preferential orientation of portlandite increases with the w/c ratio as far as the latter attains the value 0.33, however it decreases when the ratio is higher, for example 0.50. Under these conditions also appreciable amounts of aluminate hydrates, which hinder the regularity in the portlandite crystal growth, cristallize in a disordered manner on the aggregate **(30)**. A $Ca(OH)_2$ film deposited on the aggregate is covered with elongated particles of C-S-H gel projecting normally to the interface. This C-S-H structure evolves with time towards a reticulated structure **(41)**.

It was also observed that at 60°C partially hydrated cement grains and fine needle-shaped C-S-H structures were adherent to the aggregate surface **(43)**.

Among the factors hampering the orientation of portlandite crystals there are the aggregate roughness (unevenness of the same order of magnitude as the $Ca(OH)_2$ crystal sizes), the formation of aluminate hydrates and ettringite, low w/c ratios, extremely short setting times. Generally, the characteristics of the transition aura are fixed during the setting-preceding period **(48)**.

The regularity of portlandite crystallization worsens when the aggregate is calcareous **(49)**. In fact, aluminate hydrates react with marble whose surface is corroded,so giving the calcium hydroxide crystallization a rough surface that reduces the regularity of portlandite growth.

Similarly the addition of finely subdivided calcium hydroxide to cement gives portlandite, which crystallizes from the solution, manifold germs where the $Ca(OH)_2$ crystals can develop in all the directions. As a consequence, the portlandite amount depositing on the aggregate grains reduces. This assumption finds an indirect confirmation in the improvement of the mortar mechanical strengths when 2% $Ca(OH)_2$ was added **(49)**.

Other differences in composition exist between interface and bulk paste. In fact it was found that in the transition aura, besides the different orientation of portlandite, the AFt phase content decreases quickly as the distance from the aggregate-cement paste interface increases. From this point of view the behaviours of a portland and a calcium sulphoaluminate cements are not different **(50)**. The ettringite content decreases regularly as far as an asymptotic value at a distance from the interface which decreases with time **(45)(51)** (fig. 5).

The cement paste is much more affected by the nearness to the surface of the aggregate grain that it can be expected by the research performed on specimens of pastes cast on polished surfaces of aggregates **(52)**. In fact the average minimum distance separating two sand grains ranges between 100 μm and 75 μm with respect to the mix ratios. Therefore each crack which forms under load is forced to pass in primis within the transition aura whose thickness is about 50 μm **(52)**. Hence most concrete ought to be affected by the interface area, so leaving very little room to the development of the "bulk" cement paste **(52)**.

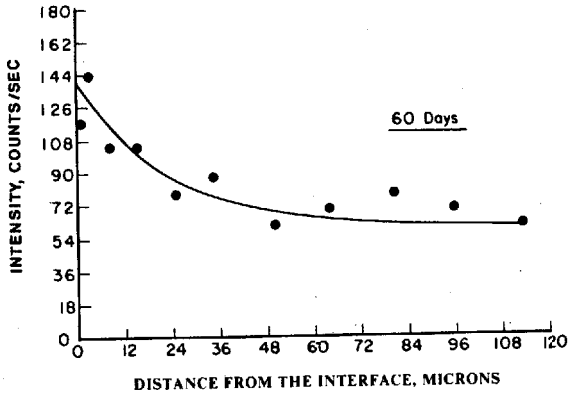

FIG. 5: Variation in the ettringite concentration in the interfacial zone **(51)**

The examination under the optical microscope of polished sections showed an enrichment in fine cement particles around the aggregate grains. This phenomenon can have a steric as well as electrostatic explication. Anyway this enrichment in fine particles can explain the fact observed by X-ray that, in contact with the aggregate, the hydration is a little quicker than that occurring in the bulk paste **(18)**.

When slag is used as an aggregate, the slag hydration does not modify the original shape of the grain but gives rise to a hydrated layer that becomes deeper and thicker as curing proceeds **(53)**. If curing is made in the air instead of in water, the boundary between the reacted and unaltered parts of the slag becomes porous, owing to drying, and many microcracks between the slag particles and the cement paste form **(54)**.

2.2.2 Blended cements

In blended cements, that is containing slag, fly ashes, silica fumes a.s.o., the paste structure around the aggregate is different. With slag-containing cements δ_0 is higher than with Portland cements, probably because at the beginning of hydration there is a higher availability of water; on the contrary the orientation index is lower. Also with fly ashes the δ_0 and I values deviate appreciably from those measured on portland cement paste **(47)**. A great deal of research mentioned in Moscow **(55)** indicated that the ash grains, at least the largest ones, behave as a microaggregate around which a local increase in the w/c ratio takes place. In this way they become preferential sites on which the portlandite and ettringite crystals form tangentially.It results that the amount of portlandite crystals available on the aggregate sam

ple is lower and this explains why, with fly ashes, the orientation index does not change with curing **(47)**.

In the cements containing silica fumes, which have a much stronger pozzolanic activity than fly ashes, δ_0 and I are much lower than pure portland cement. Portlandite disappears with time, except near the aggregate surface where it remains longer in the form of an oriented crystal film. Therefore the pozzolanic activity of the addition does not modify the interface structure, weak point of concrete, except at long term. On the contrary, it increases the paste strength and eliminates the discontinuities created by the $Ca(OH)_2$ crystals **(47)**.

2.2.3 Aluminous cement

The particular morphology of the aluminous cement-calcareous aggregate interface is explained by admitting that a chemical reaction occurs between the two components. In fact, in mortars and concretes containing limestone the microcracks are present in the cement paste, whereas in those made with siliceous aggregate they are observed at the grain surface **(30) (56)**. Crystalline concretions like those covering the pore walls were observed on the enucleation niches of the siliceous aggregate **(56)**.

The interface is no longer visually distinguishable **(30)** in 45 day-aged mortars containing an artificial aluminous aggregate (ALAG) and an aluminous cement.

2.3 Mechanical properties

2.3.1 Strength

The mechanical properties of concrete depends on those of its components and, to a determining extent, on the bond between cement matrix and aggregate grains.

2.3.1.1 Ordinary curing

From the mechanical point of view, the transition aura is much more anisotropic than the bulk cement paste **(30)**. The higher the orientation index I of portlandite crystals in the aura the easier the crack propagation according to the hydroxide planes (001), and therefore the lower the mechanical strength **(16)**.

The adhesion between paste and aggregate essentially depends on the aggregate roughness, whereas the reaction of the hydrated aluminate with the calcareous aggregate only plays a secondary role **(18)**. For this reason by using limestone and quartz grains(both roundish) the same results are obtained (see table 1) **(18)**. Vice versa, by increasing the surface roughness of a calcareous aggregate,that is by passing from smooth to chemically attacked to crushed grains, the mechanical properties as well as the flexural/compressive strength ratio (R_f/R_c) improve (see table 2)**(18) (57)**. In other terms the increase in the paste adhesion to the aggregate favours more the tensile strength than the compressive one **(58)**.

TABLE 1: Flexural strength and percentage of broken aggregates in mortars (1:1; w/c=0.30) of portland cements **(18)**

Cement with	Aggregate	2 days		90 days	
		flexural MPa	%broken aggreg.	flexural MPa	%broken aggreg.
3% C_3A	limestone	5.4	3	9.1	22
	quartz	5.8	5	9.1	18
13% C_3A	limestone	8.0	13	9.3	14
	quartz	7.9	9	8.7	15

An exception is represented by reactive aggregates, such as blastfurnace slags, which give considerably higher strengths than those obtained with calcareous aggregate. With slags, compressive strengths regularly increase with curing whereas flexural strengths tend to reach a peak at 28 days and to decrease at 90 days. This behaviour was observed with both crushed and roundish aggregates **(57)**. In flexural tests the percentage of broken grains was always much higher when the grains were crushed and this clearly proves that in this case the mechanical adhesion was better **(57)**.

TABLE 2: Strength and percentage of broken aggregates in mortars (1:1.5; w/c = 0.28) containing aggregates of different surface morphology **(57)**

With aggregates	Age (days)	2	7	28	90
Polished	% broken aggregates	7	17	11	11
	flexur.MPa	7.5	8.0	7.9	8.3
	compress.MPa	46.6	61.4	73.4	76.8
	compressive/ flexural	6.2	7.7	9.3	9.3
Acid-etched	% broken aggregates	28	32	33	27
	flexur.MPa	7.9	8.5	8.1	8.6
	compress.MPa	51.9	61.5	75.7	77.9
	compressive/ flexural	6.6	7.2	9.3	9.1
Broken	% broken aggregates	39	52	57	62
	flexur.MPa	8.2	9.8	10.7	11.3
	compress.MPa	55.4	68.9	81.4	94.1
	compressive/ flexural	6.8	7.0	7.6	8.3

Drying causes in mortars some microcracks (0.1 μm) along the interface between hydrated layer of mortars and cement paste. Drying lowers the dynamic modulus of elasticity of concretes, but the effect is stronger for those containing slag than natural sand **(53)**. The specific creep of mortars with slag sand is higher than that of mortars with river sand owing to, at least partly, the plasticity of the aura of the hydrated material covering the grains **(53)**.

The use of an aggregate (ALAG) and an aluminous cement of similar chemical composition, led to higher compressive strengths than those obtained with two aggregates formed of siliceous material (SiO_2 = 96%)and a steel slag. The concrete containing ALAG, water-cured at 38°C, exceeded the strength of 120 $N \cdot mm^{-2}$ after 3 years. Another important property this aggregate gives to concrete is the flexural/compressive strength ratio which is twice that of the concrete containing the siliceous aggregate **(30)**. This fact can only be interpreted by assuming that a stronger paste-aggregate bond is established.

2.3.1.2 Autoclaving

Autoclaving little increases the strength of concretes with calcareous and basaltic aggregate (18 and 28% respectively) but enhances it considerably when the aggregate consists of granite, jasper and quartz. In these cases strength increases of the order of 64, 107 and 129% were obtained **(59)**.

The rises are the consequence of the chemical reaction occurring between quartz and cement paste and of the epitaxic growth on the quartz grains of the hydrated phases that strengthen the paste-aggregate bond.

The formation of a reaction layer having an intermediate strength between aggregate and paste (cement plus silica powder) was pointed out by microhardness measurements given in table 3 **(24)**.

TABLE 3: *Microhardness of aggregates and cement paste in autoclaved mortars* **(24)**

Aggregate	Microhardness - $N \cdot mm^{-2}$		
	aggregate	Cement paste	
		near the aggregate	far from aggregate
Quartzite	56	15	6
Quartz glass	59	12	6
Pink feldspar	41	13	5
Milk-white feldpar	45	13	5.5
Wollastonite	14* / 31*	7.5	6
Wollast. glass	43	14	6
Limestone	14	6.5	6
Granite	-	-	-

*) according to the crystal orientation

However the formation of an interface layer having a higher strength than the paste is only one of the factors determining the high strength of autoclaved concretes or mortars. In fact the strength increase of the interface can be made useless by a low compressive strength of the aggregate, even if the latter has a high microhardness (table 4)**(24)**.

TABLE 4: *Compressive strength of autoclaved mortar microcubes ($N \cdot mm^{-2}$)(side= 1.7 mm)* **(24)**

Aggregate	Strength	St. dev.
Quartzite	110	7
Quartz glass	69	6
Pink feldspar	71	4
Milk-white feldspar	-	-
Wollastonite	70	9
Wollastonite glass	-	-
Limestone	77	8
Granite	74	4

Autoclaving increases the secant modulus of elasticity of the concretes containing siliceous aggregates and decreases it in those containing a calcareous one. Autoclaving reduces the hysteresis loops formed by loading and unloading curves. This effect is particularly significant with quartz aggregates (fig.6)**(59)**.

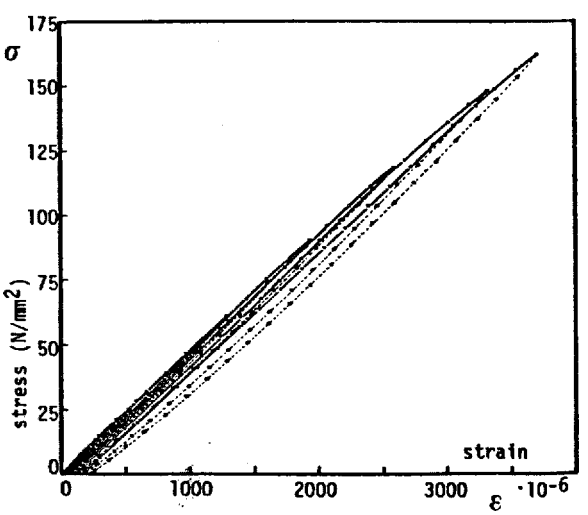

FIG. 6: *$\sigma - \varepsilon$ curves in subsequent loading and unloading cycles for autoclaved concrete containing quartz aggregate* **(59)**

2.3.2 Theoretical limit strength

The mechanical strength of a material measures its capacity to oppose forces that tend to break the bond existing between the crystals or the atoms forming it. The real strength depends on many factors, that would

be pointless to know, together with the highest strength values that theoretically belong to a certain material.

During the studies performed on the interface morphology and the cement-aggregate bond the following points were ascertained:

- *in ordinary concretes the aggregate-cement paste interface is, for several reasons, the weakest point of the system and the place where cracking begins, whereas the aggregate is the strongest component.*
- *If interfacial reactions occurs at room temperature, they increase the mechanical strength only because they enhance the aggregate roughness, and therefore facilitate the mechanical adhesion of pastes.*
- *The chemical reactions occurring in autoclave between siliceous aggregates (acid) and cement paste (basic) make the interface layer stronger than the cement pastes, only if they are accompanied by an epitaxic growth of the hydrated phases on the aggregate grains. In this case it is the cement paste that represents the weak point of concrete.*
- *On the contrary, in concretes containing light-weigth aggregates, it is the aggregate that shows the lowest strength.*

Therefore, the concrete strength depends on the cohesion of the cement paste and the aggregate, as well as the adhesion between the former and the latter and it is determined by the weakest value.

2.3.2.1 Cement paste

Many researchers, by considering that porosity is determining for mechanical strength, prepared pastes (or wet powders) characterized by lower and lower porosities. A short summary of these works, made before the 8th Congress on the Chemistry of Cement in Paris, is found in **(60)**. To correlate the mechanical strength with the capillary porosity, several formulas were proposed which fit the experimental data rather well (fig. 7)**(5)**.

However, when they are extrapolated at zero porosity, they lead to rather discordant values of the limit strength.

By hot-compacting under pressure a slightly wet cement powder (w/c $\simeq$ 0.1), very low porosities (1.78%) and very high compressive strengths (650 $N \cdot mm^{-2}$) were attained. Strength $\sigma_{c,0}$ extrapolated at zero porosity gave a value above 700 $N \cdot mm^{-2}$ **(61)**. Since tensile strength is equal to about 1/20 of the compressive one, tensile strength σ_t obtainable with a zero porosity paste should be about 35 $N \cdot mm^{-2}$.

This value clearly exceeds that obtained with ordinary pastes (σ_t = 4-8 $N \cdot mm^{-2}$)**(62)(63)(64)**, but it only represents a fraction of the paste theoretical strength that can be calculated from Griffith's **(65)** and Orowan's **(66)** formulas respectively:

$$\sigma_t = \sqrt{\frac{2\gamma \cdot E}{\pi c}} \quad 3) \qquad \sigma_t = \sqrt{\frac{\gamma \cdot E}{2c}} \quad 4)$$

where:

γ = surface energy
E = modulus of elasticity
c = half-length of an elliptical section microcrack.

However, if these formulas are used, some considerations need to be made. The energy amount used to produce a fracture surface is higher than γ and therefore 3) and 4) must contain the real value of the fracture work **W** that, besides the surface energy, also includes the plastic work associated to the crack propagation:

$$\sigma_t = \sqrt{\frac{2W \cdot E}{\pi c}} \quad 5) \qquad \sigma_t = \sqrt{\frac{W \cdot E}{2c}} \quad 6)$$

W is equal to 2.3 $J \cdot m^{-2}$ **(67)** or, according to latest works, it ranges between 7 and 14 $J \cdot m^{-2}$**(68)**.

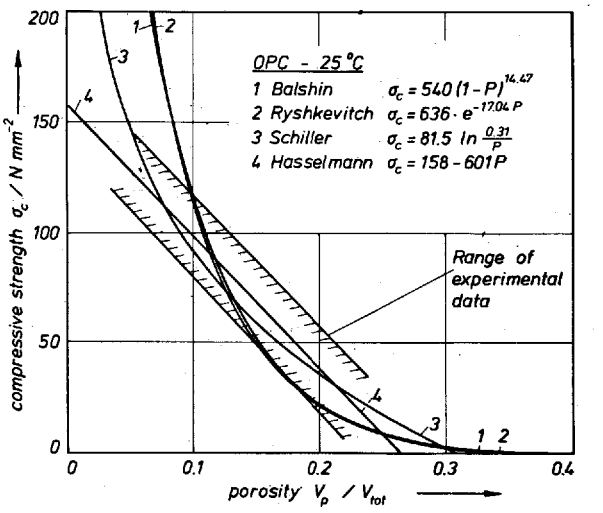

FIG. 7: Relationships between porosity and compressive strength **(5)**

To calculate σ_t it is not necessary to know W, since it is enough to determine experimentally the critical stress intensity factor K_{IC} = W·E. This is a measurement of the magnitude of the stress concentration existing in front of the crack tip when the crack begins to propagate quickly. This factor ranges between 0.4 and 0.5 $MN \cdot m^{-3/2}$ **(69)(70)(71)(72)(73)(74)** and it increases as curing lengthens, the more quickly the paste hardens **(70)**.

Now, by assuming that the cement paste is without capillary pores and the radius of the largest pores (equal to about 10 nm) represents the half-magnitude

of the maximum cracks, the theoretical tensile strength from 5) should be $\simeq 900$ N·mm^{-2} **(75)**.

Conversely, by introducing the experimentally measured tensile strength $\sigma_t \simeq 4$ into 5), **c** should be 6 mm. However, cracks of this magnitude have never been observed in ordinary cement pastes.

The discrepancies between experimental results and theoretical deductions have not been explained yet, probably because the terms of the fracture mechanics depend on different and not always well known factors. For example, the appreciable flexural strength improvement obtained with cement pastes containing water soluble resins was explained by the elimination of the macrodefects and by considering the cracks of Griffith's theory **(76)**. However, this assumption is in disagreement with the fact that the vacuum removal of air bubbles did not improve strength appreciably **(77)**.

The fracture work W and the critical stress intensity factor K_{IC} depend on the paste porosity according to a relation qualitatively indicated in fig. 8 **(74)**. The two values also depend on the relative humidity and the drying history. The dependence is rather complex since the relative curves show some peaks and a clear hysteresis in drying and wetting cycles. In fact, when the relative humidity lowers down from 100 to 0, W increases from 7 to 14 J·m^{-2} and K_{IC} from 0.20 to 0.46 MN·m$^{-3/2}$ **(74)**.

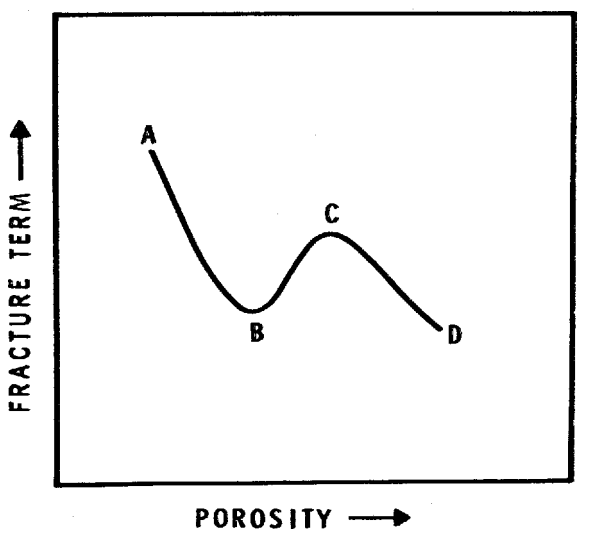

FIG. 8: Schematic of generalized fracture term-porosity curve **(74)**

The apparent values of the stress intensity factor also depend on the sizes of the tested specimen **(73)-(78)**. This dependence of the cement paste mechanical behaviour on humidity has a practical important implication, since the cement paste drying doubles compressive strength **(79)(80)**. This result seems in conflict with the experimental evidence that drying produces many microcracks that should lower strength. As a matter of fact drying is accompanied by other phenomena acting on the grain separation surfaces and, therefore, on bond. In particular, drying decreases the disjoining pressure acting on the crack tips, whereas wetting produces the opposite effect.

In fact, let us consider a crack in a dried cement paste. Van der Waals' forces act to the crack tip, assumed to be wedge-shaped and of atomic sharpness. These forces tend to join the crack borders and therefore they contribute to the material strength. If now the cement paste adsorbs water, the crack tips will fill with water. As a consequence, Van der Waals' forces will decrease and this will produce expansion and mechanical strength lowering.

According to another model the impact of the adsorbed water molecules on the crack faces creates a pressure which opposes Van der Waals' forces, makes the cement expand **(80)(81)** and decreases strength. This mechanism corresponds to Banghan's model proposed to explain the behaviour of the porous solids which expand when they adsorb water **(82)**.

The theory is supported by that, when the dried pastes are saturated with other organic solvent, strength does not decrease appreciably. In fact, their large molecules cannot enter the finest cracks, as the water ones do, and therefore they are unable to produce the disjoining pressure as well as to weaken the solid-solid bond. The water action is enhanced by the electrolytes dissolved in the pore water, which exert a weakening effect **(80)**. The disjoining pressure created by the surface water adsorption is not an assumption to justify certain behaviours of concrete but it is a real and experimentally determined value **(83)**.

A factor which plays an important role in determining strength is the cement paste heterogeneity that can be clearly observed by examining the fracture surface under the microscope **(60)**. Several weakening causes can be recognized also in the absence of capillary pores, such as the hydrated crystal interfaces, the different size of crystals, stress state a.s.o.

For example, portlandite crystals, which constitute 20-25 wt.% of portland cement pastes **(84)(85)**, are discontinuity areas because they have bigger sizes than those of the other hydrated phases. Generally the tabular hexagonal crystals of $Ca(OH)_2$ do not exceed 0.020 mm **(43)**, but in some cases the parallel association of several crystals extends for about 0.1 mm, as figure 9 shows **(60)**. Also higher diameters ($\sim$0.2 mm) **(86)** of crystals were observed in C_3S pastes, thereby it cannot be excluded that in the cement paste, and above all in concrete, larger plates than the above-mentioned ones can form. Since the tensile strength of portlandite crystals along c-axis (about 1 N·mm^{-2}) is much lower than that of the paste **(68)**, it can reasonably be assumed that these relatively large crystals behave as microcracks **(60)**.

The parallel associations of portlandite plates

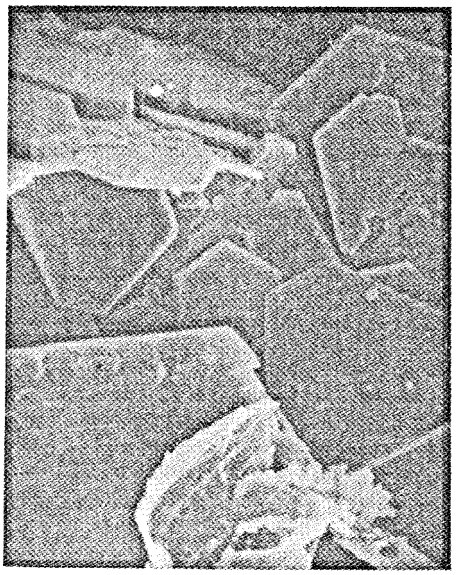

FIG. 9: Parallel association of portlandite lamel - lar crystals. Magnification 1400 X **(60)**

can be deformed, as figure 10 **(87)** shows, and therefo re stress states combined with deformations can likely favour the crack formation and propagation under load.

The strength increase in the dried pastes was also attributed to portlandite precipitation from the pore solution **(80)**. However, this assumption does not seem consistent, since it was proved **(88)(89)(90)** that the pore solution has very little lime and mainly contains alkaline hydroxides. Obviously it cannot be excluded that it is the crystallization of these hydroxides that improves the dried paste strength.

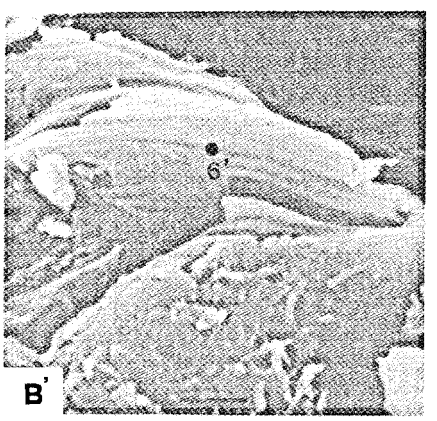

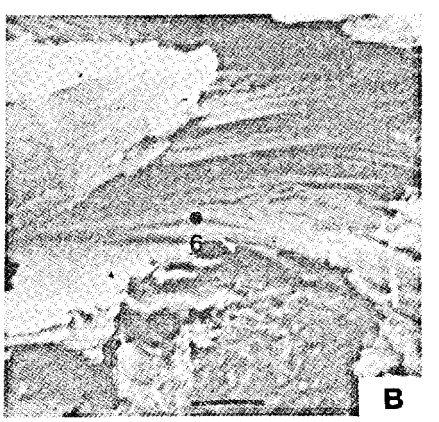

FIG. 10: Specular fracture surfaces of cement pastes showing deformed portlandite plates. Magnification 1000 X **(87)**

A contribution to eliminate the discrepancies between theory and experimental results can be obtained by considering the fractal nature of the cement paste surface. In fact, it has lately been proved that the roughness of the cement paste surface is such that the range of scale over which the surface if fractal in character extends, at least, between about 15 and 700 Å **(91)**.

This means that the cracks present in the cement paste and where the failure under load begins have not smooth walls. These have a complex orography, since they are formed of smaller and smaller valleys which finally reach atomic sizes. This means that the cracks, present or forming under load in pastes and concretes, have a much larger surface than that can be determined by the common methods of microscopic investigation.

2.3.2.2 Aggregate

Generally compressive strength of the more commun rocks do not exceed 250 $N \cdot mm^{-2}$ **(7)(8) (92) (93) (94)(95)**, nevertheless it is possible to find samples with higher values. There are few data on tensile strength but, in any case, they are rather low and generally range between 3 and 10 $N \cdot mm^{-2}$ **(7)**. The cohesion of stony materials is therefore poor and of the same order of magnitude as cement pastes. It must be noticed that the rock strength increases quickly as the sample sizes decrease, since the natural occurring crack sizes reduce **(8)**. Anyway, in the common aggregates reduced to about 10 mm, the residual microcracks have sizes (>1 mm) justifying their poor tensile strength.

2.3.2.3 Cement paste-aggregate interface

In ordinary concretes the bond between aggregate and cement paste of mortar is weaker than the cohesion of the two constituents, indeed the interface tensile strength is 10-50% that of pastes **(9)(10)**. The causes are different and related to chemical and structural differences existing near the paste-aggregate interface, described in the previous sections.

Figure 11 shows how the bond strength depends on the aggregate nature and its surface state and how it increases with time. Anyway it remains considerably lower than the common tensile strength values for pastes (4-5 $N \cdot mm^{-2}$) and mortars (3-4 $N \cdot mm^{-2}$) **(64)**.

It is obvious that, to increase the concrete strength, the bond strength at the paste-aggregate interface needs to be enhanced. This aim can be achiev-

ed by improving the mechanical adhesion of the paste (however the strength increases are poor) or causing a true chemical reaction between paste and aggregate.

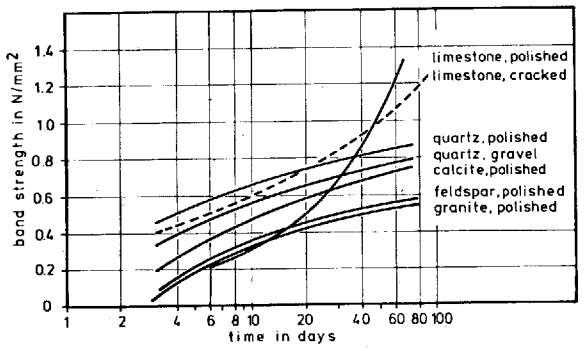

FIG. 11: Bond strength between portland cement stone and different aggregates with coarse or polished surface. w/c = 0.35 **(64)**

Another system to improve the strength of cement pastes as well as mortars and concretes is to impregnate them with resins. The fundamental results of this procedure, published in 1968 **(100)** and largely confirmed later on, proved that strength is multiplied by 4-5 times.

2.3.3 Brittleness

The strength is the most common parameter for the evaluation of the building materials, above all for the security of construction. However, its determination gives no indications about the failure process. A parameter describing the fracture behaviour is brittleness or its inverse, toughness.

All the stony materials, and therefore also cement pastes, mortars and concretes, are brittle. As known, a material is defined as brittle when the fracture occurs with little or no preventive plastic deformation.

In many cases the absence or reduction of brittleness can constitute an important requisite for the use of cementicious materials. This fact explains why many works have lately been devoted to the study of this property. It is worth emphasizing that also brittleness depends on the bonds acting inside the concrete and its constituents.

According to Griffith **(65)** there is in each solid a critical crack length beyond which the crack propagates in an explosive manner. As long as the cracks have a length lower than the critical one, nothing happens, however high the stress may be at the crack tip. Equation 5) shows that the critical length is the longest the greatest the fracture work **W**.

In the last few year many attempts have been made to apply the concepts of the linear elastic fracture mechanics and the elastic plastic fracture mechanics to cementitious materials. Among the studied fracture parameters there are the fracture work, the critical stress intensity factor of fracture toughness (K_{IC}), the strain energy release rate (G_{IC}), the J-integral. The latter, expressed by the formula $J = \frac{1}{b}\frac{du}{da}$, is defined as the change in potential energy **u** when the crack is extended by an infinitesimal amount "**da**". **b** is the specimen thickness.

The following relation refers to materials having linear elastic behaviour

$$J_{IC} = G_{IC} = K_{IC} = \frac{(1-\nu^2)}{E} \qquad 7)$$

where ν is Poisson's ratio and E is the modulus of elasticity. However, unfortunately, the many studies have not yet found a fracture mechanics parameter that can by itself quantify the concrete resistance to the crack propagation **(96)**.

2.3.3.1 Cement pastes

In the cement pastes the fracture work **W** is about 2.3 $J \cdot m^{-2}$ **(67)** or, according to more recent works, 7-14 $J \cdot m^{-2}$ **(74)**, whereas in metals it attains 10^4-10^6 $J \cdot m^{-2}$. The difference is appreciable and this explains why cement is brittle, unlike steel.

It was assumed that anhydrous cement grains, portlandite crystals and pores can act as crack arrestors **(74)**. The subject deserves to be studied more thoroughly by suitable research, however, as far as the $Ca(OH)_2$ is concerned, it must be reminded that the lowest the portlandite content (for example, in pozzolanic cements) the highest the flexural-compressive strength ratio and that this is attributed to a better cohesion of the paste.

The stress intensity factor varies in autoclaved cement pastes as a function of porosity, microhardness and silica content, but the values are still included between 0.20-0.50 $MN \cdot m^{-2/3}$, that is within those observed for the pastes cured under ordinary conditions **(97)**. This means that brittleness does not undergo important variations with the hydrothermal treatment.

To increase the fracture work and therefore to slow down or stop the crack propagation, it has been a common practice for a long time to add fibres to the cement paste **(96)**. The gains in fracture energy and strength can be evaluated by examining the data of table 5 **(98)**.

They remain significant also if the inaccuracies of the the calculated values of toughness K_{IC} are considered **(99)**. The strength increase obtained by impregnating concrete with resins was attributed to the porosity decrease and the cement-aggregate bond strengthening **(101)(102)**. Nevertheless, it was proved that the polymer impregnation does not cause significant improvements in the interface bond strength in PIC(Polymer Impregnated Concrete), but only in the matrix strength **(103)**.

Latest research lead to think that this is due to the fracture energy increase, that is from 9.1 to 75 $J \cdot m^{-2}$ **(104)**.

The fracture energy of polymerized methyl methacrylate is about 600 $J \cdot m^{-2}$ **(105)** thereby, if the polymer percentage in the paste is known, a simple calculation shows that the fracture energy of the impregnated pastes is almost exclusively due to the polymer fracture **(104)**.

TABLE 5: Mechanical property data for unreinforced and reinforced ceramics **(98)**

	Young's modulus $GN \cdot m^{-2}$	Bond strength $MN \cdot m^{-2}$	Work of fracture $kJ \cdot m^{-2}$
Unreinforced Pyrex	60	100	0.004
Pyrex composite (50v/o type I carbon fibre)	193	700	5
Unreinforced cement paste	13	10	0.02
Cement composite (9v/o type II carbon fibre)	34	170	7.5

2.3.3.2 Aggregates

The common aggregates obtained by natural or artificial comminution of rocks are brittle. Nevertheless their toughness is considerably higher than that of the cement paste and concrete. The few available data have recently been summarized in a review devoted to the fracture mechanics parameters **(106)**. Toughness, expressed by the stress intensity factor, varies around 2.0 $MN \cdot m^{-3/2}$ for marble and 3.3 $MN \cdot m^{-3/2}$ for quartz. Therefore the K_{IC} value measured for marble and quartz is of a higher order of magnitude than for a cement paste with w/c ratio = 0.4, aged for 7 days **(72)**.

2.3.3.3 Interface

Also as regards the matrix-aggregate interface the data relevant to the fracture mechanics parameters are very limited **(106)**. Toughnesses K_{IC} of 0.16 ± 0.04 $MN \cdot m^{-3/2}$ and 0.21 ± 0.04 $MN \cdot m^{-3/2}$ were measured for the cement paste-limestone interface and the cement paste-quartzite interface respectively **(107)**. Previously, specimens with slightly different sizes gave 0.1 $MN \cdot m^{-3/2}$ for the interface with quartz **(72)**. It can be noticed that these values are considerably lower than those relevant to paste and aggregate.

2.3.3.4 Concretes

The values of the critical stress intensity factor obtained by different Authors have been collected and compared recently **(96)**. K_{IC} varies from 0.07 to 0.87 and, although the measurement difficulties justify a certain scattering, the variation is too large to be only attributed to this cause. Indeed the reasons of this variability are many and among these there are: the non-inclusion of the slow crack growth in the analysis, the tortuosity and irregularities of cracks in concrete, the effect of the aggregate **(108)** and sample **(78)** sizes. Moreover, it must not be neglected that the tensile strength σ_t varies appreciably as the typical parameters for concrete change. For example σ_t increases from 2.2 to 4.5 $N \cdot mm^{-2}$ by using crushed limestone instead of expanded clay. Tensile strength decreases as the w/c ratio and the maximum aggregate diameter increase and it rises, of course, as curing proceeds **(109)**.

The fracture toughness of autoclaved air-entrained concretes increases proportionally to compressive strength and load rate. According to the type of material K_{IC} ranged between 0.05 and 0.08 $MN \cdot m^{-3/2}$ **(110)**.

In any case, without considering the fracture mechanics which is beyond the subject of this review, the available data confirm the concrete brittleness and the extreme variability of the K_{IC} value. These data are likely to be adversely affected by the low values of the stress intensity factor relevant to the interface.

3. REINFORCEMENT-CEMENT PASTE BOND

3.1 Chemical reactions at the interface

As known, the reinforcement steel in contact with the alkaline solution existing in the cement paste pores (pH $\simeq$ 13.5) is covered with an oxide protective layer which hampers the metal corrosion. Other interactions do not seem to occur between reinforcement and paste, and the bond between the two components remains weak.

By replacing mild by stainless steel, the situation does not change but, if copper and brass reinforcement are used, a bond of chemical origin is supposed to form since the interface bond increases **(111)**. By contrast, a real chemical reaction occurs between the cement paste and the zinc covering the galvanized steel reinforcement. This reaction causes strongly negative effects since the $Zn(OH)_2$ formation on the cement grain surface produces an appreciable setting delay. Only when zinc hydroxide is transformed by the cement calcium hydroxide into calcium hydroxizincate, the setting and hardening of cement can resume their normal course **(112)**. However the calcium hydroxizincate formation has also a positive action since it improves the mechanical bond between cement paste and galvanized steel **(113)**. The $CaCl_2$ addition does not prevent setting and hardening delays occurring near the galvanized reinforcement, even if the reaction trend is different, since zinc hydroxichloride forms instead of zinc hydroxide. In the long run also zinc hydroxichloride transforms into calcium hydroxizincate. The reaction is strongly accelerated by the presence of calcium hydroxide **(114)**.

By studying the interaction between tricalcium alu

minate pastes and reinforcement it was noticed that the nature of the C_3A hydration products changes depending on the used metal. After 28 days C_3AH_6 forms on iron and copper wires whereas hexagonal aluminates, C_4AH_{13} and C_2AH_8, together with cubic C_3AH_6, are observed on the zinc ones **(115)**.

3.2 Interface morphology

The bond between paste or mortar and mild steel was studied by cylindric samples, obtained by casting pastes or mortars on the circular upper face of steel. The samples were broken under tensile strength **(63) (111)**. The fracture forms in the paste very near to the interface in young samples, and at the interface in the older ones. The examination of the fracture surfaces reveals that the material in contact with steel largely, but not exclusively, consists of portlandite. The thickness of this layer is varying but not less than 1 μm. It consists of tabular $Ca(OH)_2$ crystals with c-axis aligned roughly normal to the steel **(111)**.

The portlandite layer is not continuous since also isolated C-S-H areas and regions, where the gel engulfs portlandite crystals, are observed on the steel. The presence of C-S-H in direct contact with steel is significant since it indicates that silicate hydrates can form also through a mechanism of dissolution and precipitation **(111)**.

If the steel is oxidized, portlandite deposits on a surface troubled by corrosion and the crystal growth occurs in a disorderly way; in fact after a curing day the orientation index is rather low ($I \simeq 1.7$)**(116)**.

3.3 Mechanical properties

The adhesion between reinforcement and concrete, or cement paste, enables stresses to be transferred through the interface. The bond strength that joints the two materials and allows the stress transfer consists of two components: tensile and shear bond. The former opposes the action of forces acting normally to the interface, the latter opposes the stresses acting along the interface and tending to cause a mutual slip of steel and concrete. Two kinds of shear bond are active: elastic and frictional.

Finally the use of deformed steel bars gives a mechanical anchorage to concrete. The mechanism of stress transfer and failure becomes very complex in this case, also in connection with the variety of the reinforcement profile.

The tensile bond between mild steel and cement paste, measured by direct tensile tests, attains similar values to those obtained between ordinary unreactive aggregates and paste. In fact, tensile strengths of about 5 $N \cdot mm^{-2}$ for pastes and about 4 $N \cdot mm^{-2}$ for mortars were obtained after 28 days' curing **(63)**.

Bond strength increases as the w/c ratio decreases, curing proceeds and the compaction duration lengthens. Moreover it is higher when the interface is horizontal instead of vertical during casting and curing**(63)**.

The failure surfaces tend to localize at the cement paste-steel interface. In fact, the number of cases when this kind of failure occurred was 73.3% for mild steel and 80.3% for stainless steel after 7 days' curing. However, with copper and brass, the percentage of these interface fractures was 3.3 and 3.2% respectively. This proves the existence of a better adhesion, likely of chemical origin. This improved bond affects the interface tensile strength as it is shown in fig.12**(111)**.

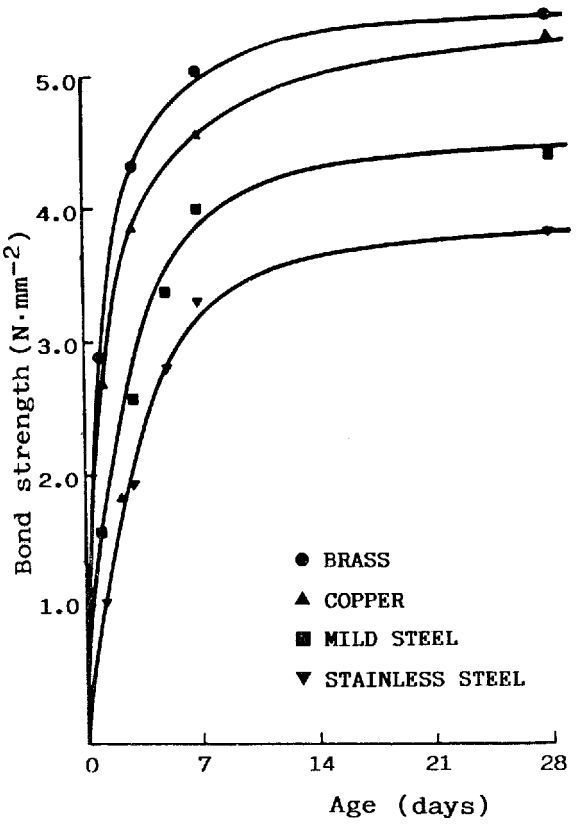

FIG. 12: Bond strengths between various substrates and cement paste of w/c 0.3 **(111)**

When a steel bar embedded in concrete is submitted to a pull-out test, that is when it is tensioned, a tensile stress occurs at the interface since the roughnesses of the two materials oppose sliding. If the stress is lower than certain values, deformations are elastic and cease as the load is removed **(117) (118) (119)**. By contrast, if the stress is higher, roughnesses will failure and only the frictional component will remain active **(117)**.

The repeated loading and unloading cycles progressively deteriorate the steel-concrete bond (fig. 13). Especially under cyclic loadings (for ex. earthquakes), an appreciable degradation of the load-transfer mechanism is noticed after a small number of cycles **(120)**.

The joint effect of superplasticizer and silica fume enabled the increase in the bond stress corresponding to a slip of 0.1 mm. By optimizing the admixture content and the w/c ratio, it was possible to quadruple the paste bond stress, more than double the mortar bond (by 2.5) and nearly quadruple the concrete one (by 3.6) **(121)**. The improvement was attributed to the decreased porosity since the steel-concrete bond had increased in a similar ratio to the porosity reduction **(121)**.

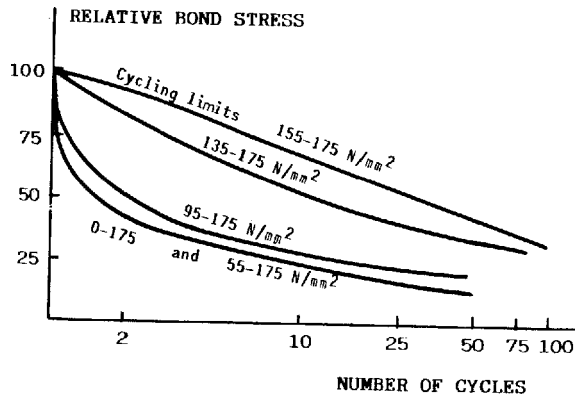

FIG. 13: Deterioration of bond under repeated loading **(117)**

The bond strength attained after 28 days between C_3A pastes and zinc wires is higher than with steel and copper wires **(115)**.

A characteristic of the concrete-reinforcement bond concerns its dependence on temperature. The adhesion loss as temperature rises is higher (in percent) with polished steel than with rusted and cold-deformed steel **(122)**. The bond properties are more adversely affected by temperatures than the concrete mechanical properties. The decrease with temperature in the bond strength of ribbed bars is of the same order of magnitude as the decrease in the concrete compressive strength.

Reinforcing bars covered with resin have lately been used to prevent the reinforcement corrosion under aggressive conditions. The pull-out tests showed that the reinforcement-concrete bond was satisfactory with an epoxy-resin covering, but unsatisfactory with a vinyl chloride resin one. Nevertheless not all the epoxy resins showed a good resistance to creep **(123)**. For more detailed information reference is made to the proceedings of a recent congress where the mechanical features of the reinforcement-concrete bond were submitted to an accurate analysis **(124)**.

4. *FIBRE-CEMENT PASTE BOND*

4.1 *General properties*

The cementitious products have low tensile strength and toughness. To improve these characteristics, it has been a common practice for some time to strengthen the cement matrix with fibres. The fibre function is to inhibit or retard the crack propagation in the cementitious material submitted to stress and to transform the unstable and uncontrolled growth of a crack into a slow and controlled one. Fibres give the material a certain tensile strength also after breaking (post-cracking strength) and increase the deformation capacity as well as the absorbed energy. The practical advantages of incorporating fibres into the cementitious composites are however limited by the low fibre volume that can be included, owing to workability requirements **(125)**.

The most known and common fibre is asbestos but others, both natural and artificial, have lately been added to this material: glass, resin, carbon, cellulose and steel.

However, the fibre-reinforced products have not always had the desired applicative success. One of the most important reasons is that the properties of some fibre-reinforced composites worsen with time. Important, if not exclusive, cause of this behaviour seems to be the changes occurring at the matrix-fibre interface **(126)**.

A great deal of research has recently been undertaken to try to understand the mechanism through which fibres reinforce the cement paste and to characterize the factors contributing to the composite properties. Nevertheless, even if progress was made, a final model interpreting the experimental data has not been established so far. In fact, many Authors expressed some doubts about the possibility that the linear elastic fracture mechanics (LEFM) can be applied to fibre-reinforced cements. They also suggested to use elatoplastic concepts to interpret the properties of these materials.

For this reason many studies were carried out to determine the J-integral, the critical stress intensity factor K_{IC}, the strain energy release rate G_{IC}. However, the use of these parameters as fracture criterion has not generally produced final results. For example the J-integral, calculated at the maximum load, decreases considerably with the depth of the initial notch of the samples. Therefore, it cannot be considered as a geometry-independent material fracture toughness parameter **(96)(127)**, even it is more sensitive to the fibre content **(127)**. Similarly K_{IC} varies appreciably since it depends on the sample sizes, the type of load, the type of adopted tests a.s.o. **(99)** **(128)**. Moreover, there is uncertainty on the exact crack length at the moment of instability **(99)**.

A promising method is that of R-curve analysis which characterizes the resistance to fracture of materials during incremental slow stable crack extension. If the stress intensity factor is expressed as a function of depth Δa of the crack created by stress, and not by the sum of the notch length and the crack $(a + \Delta a)$, there exist a relation independent of the notch depth and very sensitive to the fibre content in cement (fi-

gure 14) (96). Analogous results were obtained by flexural testing concretes containing steel, glass and polypropylene fibres (99).

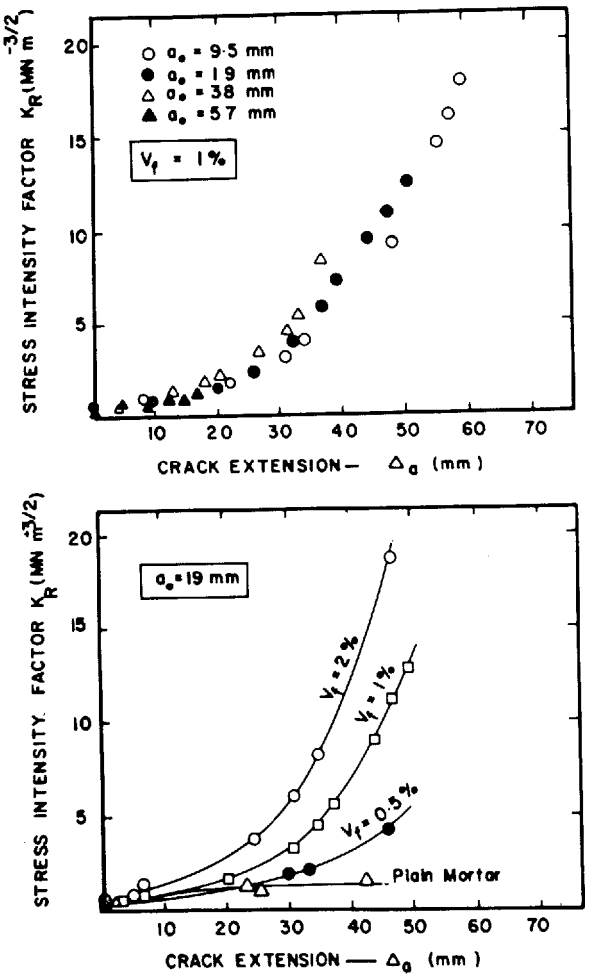

FIG. 14: R-curves for different initial notch depth and fibre volume (96)

The curves of K_a (apparent fracture toughness) as a function of the crack growth Δa can be subdivided into two parts. In the former, corresponding to small loads, K_a increases slowly with almost linear trends, in the latter the apparent toughness grows very quickly.

The difficulties met by several researchers in applying the fracture mechanics to the analysis of the fibre-reinforced cement composites are likely to be due to that the crack extension and patterns are not simple but more or less complex with linearity deviations and formation of secondary branches (99) (129) (130).

Selected bibliographic references on the problems of the fracture mechanics in fibre-reinforced cementitious materials are found in some recently published reviews (96)(131)(132).

4.2 Interface

Among the factors contributing to determine the properties of fibre-reinforced cement products the interface between fibres and cement paste is of primary importance. Therefore it is clear why the tensile stress-strain curve shape, the composite strength and its ability fo absorb energy critically depend on the stress transfer mechanism between reinforcement and matrix.

An increase in tensile strength is obtained by strengthening the interface bond of fibre-reinforced composites. Nevertheless a strong bond seemsto be the cause of brittleness (126). A weaker bond can offer several advantages since it favours the crack tip blunting by interface delamination and it increases the fracture work by fibre pull-out after failure(133).

The interface bond is made up of two main components: tensile bond τ_t and shear bond τ_s. In its turn, it can be subdivided into elastic shear bond τ_e and frictional shear bond τ_f (99). For completeness'sake, another bond should be considered, that is the mechanical anchorage due to the deformed fibres, which adds to the shear bond (126).

The interface bond is expressed by the sum of the chemical and cohesive bond τ_c and the frictional bond τ_i (134):

$$\tau_s = \tau_c + \tau_i \qquad 8)$$

An exact determination of the tensile bond in fibre-reinforced composites is very difficult (134), also owing to the irregular section of many fibres and their random distribution (126). The largest information concern the iron fibres that consist of elements with fixed and reproducible sizes and unreactive towards the cement paste.

Therefore the bond characteristics in the cement-fibre composites are still relatively unexplored because, in spite of the indubitable progress made in the knowledge of the mechanism of the bond failure,sure numerical values are missing.

The most common method to determine the bond strength is the pull-put test that enables the average bond strength to be calculated. Several recentworks (99)(126)(134) show many bibliographic references useful to master the working modes used in the pull-out tests and other methods and to interpret the results.

The interface and frictional bonds can be calculated from the pull-out test data for a rather large range of fibre length embedment (135). When the fibre embedment in the matrix is short, τ approaches τ_s (interface bond) and when it is long it approaches τ_i (frictional bond) (134).

The values of τ_s, τ_c and τ_i have recently been calculated by using previous data (136) obtained on cement pastes containing bright high tensile strength

steel wires (see table 6 **(134)**).

TABLE 6: Calculated values of $\bar{\tau}$, τ_s, τ_i, *and* τ_c *(N·mm^{-2})* ***(134)***

	$\bar{\tau}$	τ_s	τ_i	$\tau_c = \tau_s - \tau_i$
Rusty HT wire in air	10.4	22.0	8	14
Bright HT wire in air	11.0	15.5	7.7	7.7
Bright HT wire in air	5.5	7.4	4.9	2.5

$\bar{\tau}$ = average bond strength
τ_s = total interface bond
τ_i = frictional bond
τ_c = cohesive or chemical bond

The same calculation applied to data relevant to polypropylene fibres led to very uncertain values, especially because fibres had broken in many cases. Anyway the following limits were calculated **(134)** from the literature data **(116)**:

$$0.6 < \tau_s < 0.98 \quad N\cdot mm^{-2} \qquad 9)$$

$$0 < \tau_i < 0.34 \quad N\cdot mm^{-2} \qquad 10)$$

An analogous tentative calculation was made on a single fibre, but without success **(134)**.

4.3 Asbestos fibres

A still important role in improving the flexural strength of cement materials is played by asbestos fibres. In fact these fibres have high mechanical strength and high resistance to fire and chemical attack. Moreover their easy wetting facilitates the dispersion in water and the adhesion to the cement paste.

Differently from what observed with the aggregates and steel reinforcement no enrichment in portlandite, always associated to a bond weakening, was observed at the asbestos fibre-cement paste interface. Portlandite crystals are noticed on fibres but they are isolated and do not create structurally weaker areas **(133)**.

By pulling-out the fibre bundles from the cement matrix, it is found that a thin hydrated cement film sticks to the fibres **(137)**. This means that the bond between fibre and matrix is higher than the matrix cohesion **(133)**. A contribution to the strength increase is given by the fine asbestos fibrils. In fact fibres are defiberized by the mechanical working of the asbestos-cement mixture and twist with the C-S-H silicate hydrate fibres **(133)**.

4.4 Steel fibres

The pull-out that causes the steel fibre-reinforced cement materials to fail occurs with much lower loads than those demanded for the fibre breaking. This leads to search for systems able to improve the metal-cement paste bond.

Among the adopted solutions there are the fibre deformation to improve the mechanical anchorage, some surface chemical treatments and the fibre covering with other materials in order to increase adhesion. In fact, the mortar flexural strength increases progressively by passing from stainless steel to mild steel to brass-coated steel fibres. However the improvement is relatively poor and anyhow much lower than the most appreciable one caused by an increase in the fibre content. Conversely compressive strength does not depend on the fibre nature **(138)**.

The use of brass-coated steel instead of mild steel fibres had the advantage to improve the composite rupture work (expressed by the area under the load-deformation curve) by one order of magnitude.

The stress intensity factor K_a increases as the fibre content rises, as shown in fig. 14 **(96)**. The stress intensity factor or apparent fracture toughness of mortars containing steel fibres is about twice that obtained with glass fibres **(99)**.

The fact that after the steel fibre debonding no traces of cement paste were observed let assume that no chemical bonds form between the two materials **(139)**. However, the microscopic examination and the electron microanalysis pointed out that the pulled-out wires are widely covered with a thin layer of hydrated cement **(130)(140)**. The mistake can arise from that, when the crack in the cement paste runs parallely to the fibre, its distance from the interface is small, 10-40 μm, and therefore a pseudodebonding forms **(130)**.

The microscopic examination of the fibre-reinforced composites submitted to failure has recently allowed important progress to be obtained on the knowledge of the behaviour of these materials. The cement hydration causes the formation, around the steel fibres, of a hydrated cement layer where composition, pore structure and morphology have different characteristics from those of the bulk cement matrix **(141)**. A thick layer mostly consisting of hexagonal portlandite crystals, with c-axis perpendicular to the steel surface, form in contact with the metal surface **(141)**. More precisely, the fibre appears to be covered with a duplex film about 1 μm thick made up of, in the order, $Ca(OH)_2$ and C-S-H in its turn covered with a layer 10-20 μm thick of dense portlandite **(130)**. The interface zone also includes areas where $Ca(OH)_2$ did not deposit and it contains a rather porous mass of C-S-H, ettringite and individual crystals of $Ca(OH)_2$ in contact with the duplex film **(142)**. Portlandite is followed by a zone having a relatively great porosity and finally by the bulk cement paste **(130)(141)**. The portlandite percentage and its preferential orientation decrease gradually as the distance from fibre lengthens **(141)**. In the interface zone the $Ca(OH)_2$ content is higher by 20-40% than that of the bulk cement paste **(143)**. Microhardness measurements showed that the high-porosity transitional zone can extend as far as 100 μm **(144)**.

The presence of the fibre placed perpendicularly to the notch generally modifies the crack propagation which occurs according to four different ways. Only in one of these the crack overtakes the fibre without deviating, whereas in the others displacements and branches are observed **(129)**. After overtaking the fibre, the crack generally moves sideways and runs, for a given stretch, some ten μm fr , the steel surface **(130)**.

It was already previously observed **(144)** that with stainless steel fibres the locus of failure lay in the cement paste at the distance of several microns from the wire surface. The fact that the crack preferably runs at a certain distance from the reinforcement can explain why an increase in the interface bond is not often accompanied by an increase in the composite mechanical properties **(130)**.

Cracks meeting inclined fibres undergo a deviation and propagate parallely to the fibre at a given distance. This course means that the inclined fibres do not contribute to the post-cracking load-carrying capacity of the composite **(130)**.

The peculiar microstructure of the interface zone fits with the course of cracks obtained by tension (schematized in fig. 15 **(130)**) and with the crack arrest mechanism proposed by Cook and Gordon **(145)**(fig. 16) for cracks which during propagation meet weak interfaces formed, for example, of scaling planes.

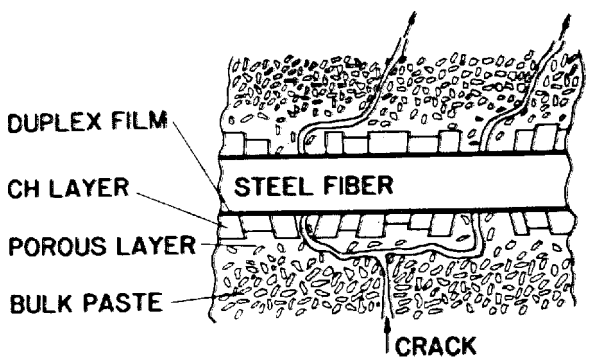

FIG. 15: Schematic description of the propagation of a crack across (under) a steel fiber embedded in cement paste, showing crack arrest and branching **(130)**

The winding path of cracks, their separation and branching, as well as their partial debonding at the interface contribute to the energy adsorption during the fibre-reinforced composite fracture **(146)** and make the modeling of the cracking process more difficult.

4.5 Glass fibres

In the last few years many studies have been oriented to the development of glass-reinforcement cements (GRC) above all to improve tensile strength and toughness of the cementitious materials. Nevertheless, although these products show excellent mechanical properties, their uses are very limited since the properties worsen with time. This worsening is unanimously attributed to the deterioration undergone by glass fibres owing to the strong alkalinity of the cement paste which embeds them. This phenomenon concerns both common glasses (for example glass E and borosilicate glass) and special glasses (alkali-resistantglass).

By using a special arrangement it was possible to observe under SEM the crack formation and propagation in the samples submitted to tensile tests **(147)**. The tests were carried out on cement paste containing glass fibres. The 13x24x32 mm specimens had a notch to favour the fracture.

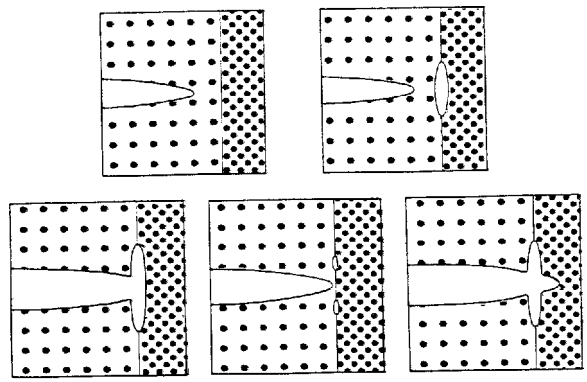

FIG. 16: Interaction between an advancing crack and a plane of weakness under various conditions **(145)**

When fibres are oriented normally to the direction of crack propagation, the most common fracture pattern is with a single laterally displaced crack (type III)**(129)**. A typical load-displacement curve obtained in pull-out tests is shown in fig. 17.

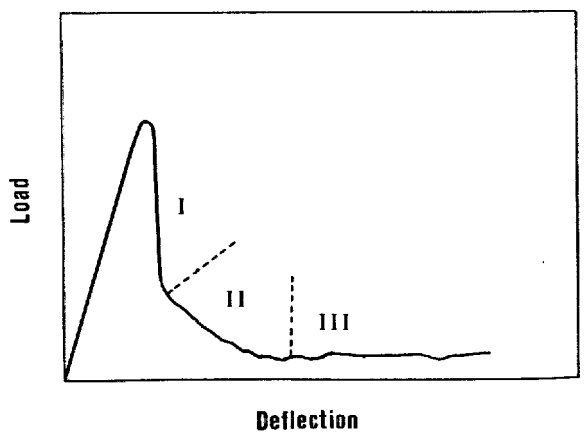

FIG. 17: Typical load-time curve **(129)**

The crack appears after reaching the peak load and therefore it propagates quickly (stage I). In stages II and III a crack widening is observed but fibres maintain their continuity and still bridge the crack.

The cracks, observed in macroscale, appear to go straight on but under the microscope they have a zig-zag course and move sideways by 0.5-2.5 mm, after overtaking the fibre **(129)**.

Also in glass-reinforced cements (GRC) the interface plays a primary role in determining the composite mechanical properties. The contact between peripheral fibres of the glass strand and matrix is not continuous owing to many voids in the cement matrix at the interface **(148)**. The preferential precipitation of portlandite crystals was observed on glass fibre strands AR. These crystals form an extremely dense layer with a strong axis normal to the longitudinal axis of fibres **(149)**. It was previously noticed that, after five years' ageing, the glass fibres were mostly wound with $Ca(OH)_2$ **(150)**. The same work emphasized that in the interface area the residual porosity was almost null and the glass fibre surface examined under the scanning electron microscope appeared clean, without particles adhering to the matrix **(150)**, in agreement with other Authors **(129)**.

SEM observations on fibre-reinforced pastes showed that between the glass fibres forming a strand there is little material, probably because their distance is too small (3 μm) to allow the cement grains to penetrate between them. This interface structure is confirmed by that the AR glass threads pulled-out of the matrix during the tensile tests are clean. The clean fibre surface is in its turn an index of adhesive failure and suggests that the chemical bond is little effective **(129)**.

For this reason the tensile bond is often neglected and only the shear bond is considered. The latter appears to be varying if it is considered both in its whole and in its components, elastic and frictional **(148)**. The presence of the frictional bond is proved by that the interface is untouched beyond the cracking area, also when the crack opening exceeds 100 μm **(129)**.

The tensile, flexural, impact strength decrease with time represents the greatest technical difficulty in the large use of glass fibre-reinforced cements. The decrease in the composite properties is generally attributed to the fibre strength reduction, owing to the alkalinity of the environment where fibres are embedded.

However, alkalinity is not the main factor for the deterioration of the fibre performances since the same phenomenon, even if to a slightly less extent, was observed in supersulphated and aluminous cements which are known to be little basic **(151)**. Perhaps it is more correct to maintain that the environment created by the cement involves the glass fibres in some chemical reactions **(152)**. After ten years the strengths of specimens water-cured for 7 days decrease by passing from the specimens aged in air (20°C, 40% R.H.) to those in water (20°C) and natural environment **(153)**.

Anyway, starting from the assumption that portland cement alkalinity is the main reason of retrograda - tion in GRS strength, several attempts were made to use less basic cements. A not decisive improvement is obtained with supersulphated **(151)(154)** and aluminous **(151)** cements. Also the addition of pozzolanic materials improves the resistance to corrosion of glass fibres (both borosilicate and zirconic glass) the more the lower the amount of free calcium hydroxide remaining in the paste **(155)**.

The filler addition to portland cement does not modify the GRC behaviour to the action of time, whereas the addition of an Italian pozzolana improves it slightly. In this case, the interface appeared to be less dense than that obtainable with ordinary portland cement and, consequently, the impact strength at long term is higher than ordinary GRC **(156)**.

4.6 Polypropylene fibres

The polypropylene fibres have a high tensile strength and a high rupture elongation, good chemical resistance and insensitivity to moisture. Additions to cement or concrete increase considerably its flexural and impact strength. Polypropylene fibres occur as single, relatively big filaments ($\emptyset$ = 150 μm), fibrillated or not, ribbons, fibrillated films. The bond of the fibre bundles with the cement paste is low, 0.1 $N \cdot mm^{-2}$, but this is likely an underestimated value since a portion of the filament surface does not come into contact with the cement paste and, therefore, does not participate in bond **(157)**.

It was previously observed that the bond strengths calculated with polypropylene fibre-reinforced composites were not true bond strengths, owing to the great number of broken fibres **(158)**.

The composite fracture work increases with the fibre content and triples for a volume content of 3% **(159)**.

4.7 Miscellaneous fibres

In wooden fibre-reinforced composites cracks follow winding courses and failure mainly occurs for the fibre pull-out, even if broken fibres are observed **(160)(161)**.

The wetting of wooden fibre-reinforced cements causes a flexural strength reduction by 10-20% **(161)** or by 20-40% **(162)** with respect to dry samples. By contrast water increases the material toughness **(161)(163)(164)** (fig. 18).

This behaviour was explained with two models. In the former **(163)** it is assumed that in a dry environment cellulose fibres are strong and brittle and firmly adherent to the cement matrix. For this reason the

composite strength is high, but toughness is low owing to the small pull-out length of fibres. In a wet environment cellulose fibres are ductile and, owing to stretching and unravelling, they are pulled-out more easily. Therefore they produce a strength decrease and a toughness increase.

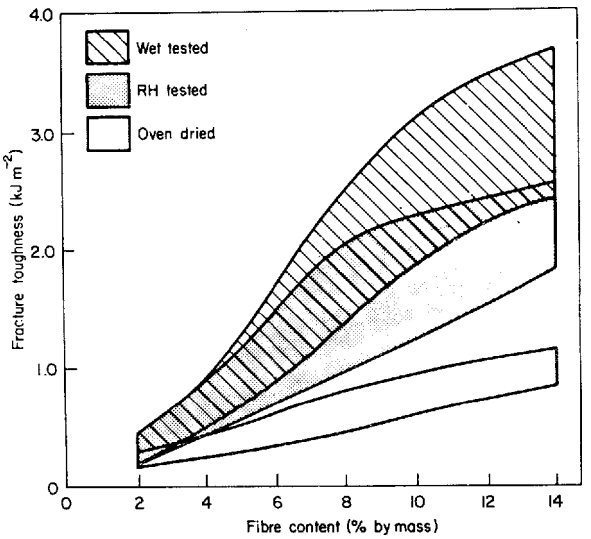

FIG. 18: Effect of fibre content on fracture toughness following various preconditioning treatments **(164)**

The latter model **(162)** assumes that the fibre-cement paste bond is due to the variation in the hydrogen bonds and hydroxide bridges. Furthermore it is based on that the tensile strength of dry fibres is equal to that of wet fibres, whereas their stiffness is ten times higher. In any case, as SEM shows, the fibres are firmly anchored to the cement matrix.

In a dry environment the hydrogen bonds and the hydroxide bridges are active and contribute to give a high mechanical strength. However the fibre stiffness penalizes toughness. Vice versa, in a wet environment the hydrogen bonds are destroyed by the disjoining pressure of the water molecules penetrating between the two materials. At the same time fibres become more ductile and expand. The maximum pull-out length increases but appreciable frictional forces develop.

It results that strength decreases and toughness increases. The technical advantages obtained by fibres suggested to prepare mineral fibres, different from the traditional ones and having better performances. Through hydrothermal reactions between $Ca(OH)_2$, $CaCO_3$ and quartz in the presence of alkali, pectolite and tobermorite fibres with a maximum length of 140 μm and 200 μm respectively were obtained **(164)**.

5. *CONCLUSIONS*

All experiences agree in maintaining that the aggregate/cement paste bond strength is generally weak. Improvements are obtained when the aggregate surface is rough or made as such by a mechanical treatment or a chemical attack.

Similar results are obtained with fibres (asbestos, steel wires, glass fibres).

In any case the weakest zone, that is where fracture occurs, is not generally the cement paste-aggregate (or fibre) interface but a zone in paste far from the interface some tenths of μm. It is inferred that, to increase the mechanical strength of the cement materials, it is necessary to enhance the characteristics of this zone, the so-called transition aura.

An improvement can be obtained by reducing the porosity of the paste, and therefore of the interface, or else, with clearly higher results, by causing the chemical reaction between paste and aggregate to form an intermediate layer made up of C-S-H crystals growing epitaxycally on the aggregate.

The best results are obtained by autoclaving a/c low-ratio concretes containing quartz aggregates.

In this case the paste/aggregate bond strengthening appears with an appreciable increase in compressive strength which attains about 180 N·mm^{-2}. Whatever the strength reached by concrete may be, the latter does not lose its brittleness. This is a typical property of the material which was the object of many and detailed studies to check whether the cement materials comply with the concepts of the linear elastic fracture mechanics and to determine its use characteristics.

A gradual and significant increase in the cement material toughness can be obtained by introducing increasing amounts of fibres. In fact, the latter cause an increase in the fracture work by two orders of magnitude. Unfortunately there are technological limits to the content of fibres that are allowed to be introduced into a cement material.

The results of the experimental studies aiming at clarifying the mechanism of beginning and continuation of the fracture cannot be defined as final. However, they let foresee the possibility of improving the bonds existing between the components of the cement materials and, therefore, to improve the performances of these products.

REFERENCES

(1) **L.J. PARROTT,** *C.A.C.A. - Techn.Report TRA 417, 1969, pp. 13*

(2) **T.C. POWERS, T.L. BROWNYARD,** *J. Am.Concr. Inst. 1947, 18, 845*

(3) **G. WISCHERS,** *Schriftenr. Zementind. 1961,(28) pp. 117*

(4) *Internal Report of Central Chemical Laboratory Italcementi*

(5) M. RÖSSLER, I. ODLER, *Cem. Concr. Res. 1985, 15 (2), 320*

(6) S. DIAMOND, C. GOMEZ-TOLEDO, *Cem. Concr. Res.1978, 8 (5), 613*

(7) J.A. TALOBRE, *La Mécanique des Roches et ses Applications, Dunod, Paris, 1967*

(8) M.M. SINGH, *Physical Properties of Rocks and Minerals, vol. II, Y.S. Touloukian, Mc Graw-Hill Book Co., N.Y., 1981, 83*

(9) T.T.C. HSU, F.O. SLATE, G.M. STURMAN, G. WINTER, *J. Am. Concr. Inst. 1963, 60 (2), 209*

(10) S.P. SHAH, F.O. SLATE, *The Structure of Concrete and its Behaviour under Load(London, 28-30 Sept. 1965), 1968, 82*

(11) *The Structure of Concrete and its Behaviour under Load (London, 28-30 Sept. 1965),1968*

(12) *Colloque International Liaisons Pâtes de Ciment Matériaux Associés (Toulouse, 17-19 Nov. 1982)*

(13) *Liaison de Contact dans les Matériaux Composites utilisés en Genie Civil, Colloque RILEM-INSA (Toulouse, 22-24 Nov. 1972)*

(14) *7th Int. Congr. on the Chem. of Cement (Paris, 30 June-5 July 1980)*

(15) J. GRANDET, J.P. OLLIVIER, *Cem.Concr.Res. 1980, 10 (6), 759*

(16) J. GRANDET, J.P. OLLIVIER, *7th Int.Congr. on the Chem. of Cement (Paris, 30 June - 5 July 1980), vol. III, VII-63*

(17) J. GRANDET, J.P. OLLIVIER, *7th Int.Congr. on the Chem. of Cement (Paris, 30 June-5 July 1980), vol. III, VII-85*

(18) M. CONJEAUD, B. LELONG, B. CARIOU, *7th Int. Congr. on the Chem. of Cement (Paris, 30 June-5 July 1980), vol. III, VII-6*

(19) B. MORTUREUX, H. HORNAIN, M. REGOURD, *Coll. Int. Liaisons Pâtes de Ciment Matériaux Associés (Toulouse, 17-19 Nov. 1982), A.64*

(20) A. CARLES-GIBERGUES, J. GRANDET, J.P. OLLIVIER, *Bond in Concrete (Paisley, 14-16 June 1982), 24*

(21) F. MASSAZZA, M. PEZZUOLI, *Internal Report of Central Chemical Laboratory Italcementi*

(22) Y. HAGIWARA, M. HARADA, *The Cem. Ass. of Japan - Review of the 37th Gen. Meet. (Tokyo, May 1983), 82*

(23) F. MASSAZZA, M. PEZZUOLI, *7th Int. Congr. on the Chem. of Cement (Paris, 30 June - 5 July 1980), vol. III, VII-16*

(24) F. MASSAZZA, M. PEZZUOLI, *Coll. Int. Liaisons Pâtes de Ciment Matériaux Associés(Toulouse, 17-19 Nov. 1982), A.45*

(25) C.A. LANGTON, M.W. GRUTZECK, D.M. ROY, *Cem. Concr. Res. 1980, 10 (3), 449*

(26) M. MURAT, A. NEGRO, A. BACHIORRINI, *C.R. Seances Acad. Sci. - Ser. C 1980, 291 (13), 287*

(27) A. NEGRO, A. BACHIORRINI, M. MURAT, *Il Cemento 1981, (2), 71*

(28) A. BACHIORRINI, M. MURAT, A. NEGRO, *Coll. Int. Liaisons Pâtes de Ciment Matériaux Associés (Toulouse, 17-19 Nov. 1982), A.1*

(29) L. CUSSINO, A. NEGRO, *7th Int. Congr. on the Chem. of Cement (Paris, 30 June-5 July 1980), vol. III, V-62*

(30) M. CONJEAUD, A. BONIN, C.M. GEORGE, R. MONTGOMERY, F.P. SORRENTINO, *Coll. Int. Liaisons Pâtes de Ciment Matériaux Associés (Toulouse, 17-19 Nov. 1982), C.12*

(31) C. PERRY, J.E. GILLOTT, *Durability of Building Materials 1983, 1 (4), 305*

(32) F.X. DELOYE, A. LE ROUX, R. LESAGE, *Coll. Int. Liaisons Pâtes de Ciment Matériaux Associés (Toulouse, 17-19 Nov. 1982), B.1*

(33) M. REGOURD, H. HORNAIN, B. MORTUREUX, P. POITEVIN, H. PEUPORTIER, *Coll. Int. Liaisons Pâtes de Ciment Matériaux Associés(Toulouse, 17-19 Nov. 1982), B.17*

(34) TANG MING-SHU, ZHEN SHI-HUA, HAN SU-FEN, *Coll. Int. Liaisons Pâtes de Ciment Matériaux Associés (Toulouse, 17-19 Nov. 1982), A.10*

(35) *Seminar on Alkali-Silica Reaction (Køge Denmark, 20-21 May 1974)*

(36) *Symposium on Alkali-Aggregate Reaction - Preventive Measures (Reykjavik, 11-14 August, 1975)*

(37) *Symposium on The Effect of Alkalies on the Properties of Concrete (London, 6-9 Sept. 1976)*

(38) *Fourth Int. Conf. on the Effects of Alkalies in Cement and Concrete (Purdue University, 4-8 June 1978)*

(39) *Proc. of the Fifth Int. Conf. on Alkali-Aggregate Reaction in Concrete (Città del Capo, 30 March-3 April 1981)*

(40) *6th Int. Conf. "Alkalis in Concrete: Research and Practice" (Copenhagen, 22-25 June 1983)*

(41) B.D. BARNES, S. DIAMOND, W.L. DOLCH, *Cem. Concr. Res. 1978, 8 (2), 233*

(42) B.D. BARNES, S. DIAMOND, W.L. DOLCH, *J.*

Am. Cer. Soc. 1979, 62 (1-2), 21

(43) **C.A. LANGTON, D.M. ROY,** *7th Int. Congr. on the Chem. of Cement (Paris, 30 June-5 July 1980), vol. III, VII-127*

(44) **L. STRUBLE, S. MINDESS,** *Int. J. Cem.Compos. Lightweight Concr. 1983, 5 (2), 79*

(45) **P.J.M. MONTEIRO, J.C. MASO, J.P. OLLIVIER,** *Cem. Concr. Res. 1985, 15 (6), 953*

(46) **J. FARRAN, R. JAVELAS, J.C. MASO, B. PERRIN,** *Coll. Int. RILEM-INSA: Liaisons de Contact dans Ies Matériaux Composites utilisés en Génie Civil (Toulouse, 22-24 Nov. 1972), vol. I, 60*

(47) **A. CARLES-GIBERGUES, J. GRANDET, J.P. OLLIVIER,** *Coll. Int. Liaisons Pâtes de Ciment Matériaux Associés (Toulouse, 17-19 Nov. 1982), B.11*

(48) **J.P. OLLIVIER, J. GRANDET,** *Coll. Int. Liaisons Pâtes de Ciment Matériaux Associés (Toulouse, 17-19 Nov. 1982), A.14*

(49) **J.P. OLLIVIER, J. GRANDET,** *Coll. Int. Liaisons Pâtes de Ciment Matériaux Associés (Toulouse, 17-19 Nov. 1982), A.23*

(50) **WU ZHONG-WEI, LIU BAO-YUAN, XIE SONG-SHAN,** *Coll. Int. Liaisons Pâtes de Ciment Matériaux Associés (Toulouse, 17-19 Nov. 1982), A.28*

(51) **P.J.M. MONTEIRO, P.K. MEHTA,** *Cem. Concr. Res. 1985, 15 (2), 378*

(52) **S. DIAMOND, S. MINDESS, J. LOVELL,** *Coll. Int. Liaisons Pâtes de Ciment Matériaux Associés (Toulouse, 17-19 Nov. 1982), C.42*

(53) **S. NAGATAKI, M. TAKADA,** *7th Int. Congr.on the Chem. of Cement (Paris, 30 June-5 July 1980), vol. III, VII-90*

(54) **S. NAGATAKI, M. TAKADA, H. KAMEDA,** *The Cem. Ass. of Japan - Review of the 33th Gen. Meet. (Tokyo, June 1979), 104*

(55) **M. KOKUBU, J. YAMADA,** *The VI Int. Congr. on the Chem. of Cement (Moscow, Sept.1974)*

(56) **A. BACHIORRINI, L. CUSSINO,** *Il Cemento 1980, (3), 183*

(57) **B. COTTIN, S. MARCDARGENT, B. CARIOU,** *Coll. Int. Liaisons Pâtes de Ciment Matériaux Associés (Toulouse, 17-19 Nov. 1982), C.20*

(58) **J.C. MASO,** *7th Int. Congr. on the Chem. of Cement (Paris, 30 June-5 July 1980), vol. I, VII-1/3*

(59) **G.P. TOGNON, P. URSELLA, G. COPPETTI,** *7th Int. Congr. on the Chem. of Cement (Paris, 30 June-5 July 1980), vol. III, VII-75*

(60) **F. MASSAZZA,** *25° Convegno AITEC: Il Cemento e il Calcestruzzo negli anni'80 (Parma, 17 - 18 Oct. 1985)*

(61) **D.M. ROY, G.R. GOUDA,** *J. Am. Cer. Soc. 1973, 56 (10), 549*

(62) **T.T.C. HSU, F.O. SLATE,** *J. Am. Concr.Inst. 1963, 60 (4), 465*

(63) **C.L. PAGE, M.N. AL KHALAF, A.G.B.RITCHIE,** *Cem. Concr. Res. 1978, 8 (4), 481*

(64) **R. ZIMBELMANN,** *Cem. Concr. Res. 1985, 15 (5), 801*

(65) **A.A. GRIFFITH,** *Phil. Trans. Roy. Soc. (London) 1920, A221, 163*

(66) **E. OROWAN,** *Z. Krist. 1934, A89, 327*

(67) **F. MOAVENZADEH, R. KUGUEL,** *J. Mater.1969, 4 (3), 497*

(68) **H.M. JENNING,** *quoted by Mindess in "Fracture Mechanics of Concrete" ed. by F.H. Wittmann, 1983, 104*

(69) **D.J. NAUS, J.L. LOTT,** *J. Am. Concr. Inst. 1969, 66 (6), 481*

(70) **H. HORNAIN, B. MORTUREUX, M. REGOURD,** *Coll. Int. Liaisons Pâtes de Ciment Matériaux Associés (Toulouse, 17-19 Nov. 1982), C-56*

(71) **J.H. BROWN, C.O. POMEROY,** *Cem. Concr.Res. 1973, 3 (4), 475*

(72) **B. HILLEMEIER, H.K. HILSDORF,** *Cem. Concr. Res. 1977, 7 (5), 523*

(73) **D.D. HIGGINS, J.E. BAILEY,** *J. Mat. Sci.1976, 11, 1995*

(74) **J.J. BEAUDOIN,** *Cem. Concr. Res. 1982, 12 (6), 705*

(75) **F. MASSAZZA, U. COSTA,** *Sandro Dei Poli 1985 - Testimonianze e Note Scientifiche in Onore del 70° Compleanno, Politecnico di Milano, 1985, 417*

(76) **J. BIRCHALL, A.L. HOWARD, K. KENDALL,** *Nature 1981, 289 (5796), 388*

(77) **N.B. EDEN, J.E. BAILEY,** *J. Mat. Sci. 1984, 19 (1), 150*

(78) **S. ZIEGELDORF, H.S. MÜLLER, H.K. HILSDORF,** *Cem. Concr. Res. 1980, 10 (5), 589*

(79) **F. WITTMANN,** *Mat. Constr. 1968, 1 (6),547*

(80) **B. ROBERTSON, R.H. MILLS,** *Cem. Concr.Res. 1985, 15 (2), 225*

(81) **F. WITTMANN,** *Deutscher Ausschuss für Stahlbeton 1977 (290)*

(82) **D.H. BANGHAN,** *Symp. Soc. Chem. Ind. (London, May 1946)*

(83) **N. STOCKHAUSEN,** *Hydraulic Cement Pastes: their Structure and Properties (Sheffield,8-9 April 1976), 219*

(84) **A.P. BARKER,** *World Cement 1985, 15 (1), 25*

(85) **R.L. BERGER, D.S. CAHN, J.D. McGREGOR,** *J. Am. Cer. Soc. 1970, 53 (1), 57*

(86) **R.L. BERGER, J.D. McGREGOR,** *Cem. Concr. Res. 1972, 2 (1), 43*

(87) **B. MARCHESE,** *Cem. Concr. Res. 1983, 13(3), 435*

(88) **P. LONGUET, L. BURGLEN, A. ZELWER,** *Rev. Mat. Constr. 1973, (676), 35*

(89) **P. LONGUET,** *Silicates Industriels 1976, 41 (7/8), 321*

(90) **S. DIAMOND,** *Il Cemento 1977, (4), 149*

(91) **D.N. WINSLOW,** *Cem. Concr. Res. 1985, 15 (5), 817*

(92) **M. PIERI,** *I Marmi d'Italia - Graniti e Pietre Ornamentali, U. Hoepli ed., Milano 1950*

(93) **D.O. WOOLF,** *ASTM STP 169, 1956, 314*

(94) **A.M. NEVILLE,** *Properties of Concrete, I.Pitman & Sons Ltd., London 1973*

(95) **G. COPPETTI, G.P. TOGNON,** *Tribol. Lubr. 1973, vol. VIII, 190*

(96) **G. VELAZCO, K. VISALVANICH, S.P. SHAH,** *Cem. Concr. Res. 1980, 10 (1), 41*

(97) **J.J. BEAUDOIN,** *Cem. Concr. Res. 1983,13 (1), 81*

(98) **R.W. DAVIDGE,** *Bull. Phys. Soc. 1972,23, 649*

(99) **R.N. SWAMY,** *Int. J. Cem. Compos. Light - weight Congr. 1980, 2 (1), 43*

(100) **M. STEINBERG, L.E. KUKACKA, P. COLOMBO, J.J. KELSCH, B. MANOWITZ, J.T. DIKEOU, J. E. BACKSTROM, S. RUBENSTEIN,** *Concrete-Polymer Materials, First Topical Report, BNL 50134, Dec. 1968*

(101) **A. AUSKERN, W. HORN,** *J. Am. Cer. Soc.1971, 54 (6), 282*

(102) **A. AUSKERN, W. HORN,** *Polymers in Concrete, ACI Publication SP-40, American Concrete Institute, Detroit 1973, 223*

(103) **N.J. CARINO,** *Cem. Concr. Res. 1977, 7 (4), 439*

(104) **A. AUSKERN, W. HORN,** *Cem. Concr. Res. 1974, 4 (5), 785*

(105) **R.H. DAVIDGE, G. TAPPIN,** *J. Mat. Sci. 1968, 3, 165*

(106) **S. ZIEGELDORF,** *Fracture Mechanics of Con - crete,ed. by F.H. Wittmann, 1983, 371*

(107) **S. ZIEGELDORF,** *10 Forschungskoll.des DAfStb, Karlsruhe 1979, 43*

(108) **S.P. SHAH,** *Fracture Mechanics of Concrete: Material Characterization and Testing,ed. by A. Carpinteri & A.R. Ingraffea, 1984, 111*

(109) **P.E. PETERSSON,** *Cem. Concr. Res. 1980, 10 (1), 91*

(110) **F.H. WITTMANN, I. GHEORGHITA,** *Cem. Concr. Res. 1984, 14 (3), 369*

(111) **M.N. AL KHALAF, C.L. PAGE,** *Cem.Concr.Res. 1979, 9 (2), 197*

(112) **G. ARLIGUIE, J. GRANDET, R. DUVAL,** *7th Int. Congr. on the Chem. of Cement (Paris, 30 June-5 July 1980), vol. III, VII-22*

(113) **G. ARLIGUIE, J. GRANDET,** *Coll. Int. Liai - sons Pâtes de Ciment Matériaux Associés (Toulouse, 17-19 Nov. 1982), A.33*

(114) **G. ARLIGUIE, J. GRANDET,** *Coll. Int. Liai - sons Pâtes de Ciment Matériaux Associés (Toulouse, 17-19 Nov. 1982), A.39*

(115) **C. TASHIRO, K. UEOKA,** *Cem. Concr. Res. 1981, 11 (4), 619*

(116) **G. ARLIGUIE, J. GRANDET, J.P. OLLIVIER,** *Mat. Constr. 1985, 18 (106), 263*

(117) **E.W. BENNETT, I.G. SNOUNOU,** *Bond in Concrete (Paisley, 14-16 June 1982), 140*

(118) **E. VOS, H.W. REINHARDT,** *Bond in Concrete, (Paisley, 14-16 June 1982), 173*

(119) **M. ARNAUD, M. BOURABRAB, M. LORRAIN,** *Bond in Concrete (Paisley, 14-16 June 1982), 162*

(120) **P. PLAINES, T. TASSIOS, E. VINTZELEOU,** *Bond in Concrete (Paisley, 14-16 June 1982), 193*

(121) **T.A. BURGE,** *Bond in Concrete (Paisley, 14- -16 June 1982), 273*

(122) **U. DIEDERICHS, U. SCHNEIDER,** *Mag. Concr. Res. 1981, 33 (115), 75*

(123) **J.R. CLIFTON, R.G. MATHEY,** *J. Am. Concr. Inst. 1983, 80 (4), 288*

(124) *Bond in Concrete (Paisley, 14-16 June 1982), ed. by P. Bartos*

(125) **H. NAYEB HASHEMI, M.D. COHEN,** *Cem. Concr. Res. 1985, 15 (5), 879*

(126) **P. BARTOS,** *Int. J. Cem. Compos. Lightweight Concr. 1981, 3 (3), 159*

(127) **S. MINDESS, F.V. LAWRENCE, C.E. KESLER,** *Cem. Concr. Res. 1977, 7 (6), 731*

(128) **S. MINDESS,** *Cem. Concr. Res. 1984, 14 (3), 431*

(129) **A. BENTUR, S. DIAMOND,** *Cem. Concr. Res. 1984, 14 (1), 31*

(130) A. BENTUR, S. DIAMOND, S. MINDESS, *Cem. Concr. Res. 1985, 15 (2), 331*

(131) S. MINDESS, *Int. J. Cem. Compos. Light - weight Concr. 1980, 2 (1), 3*

(132) S. MINDESS, *Fracture Mechanics of Concrete ed. by F.H. Wittmann, 1983, 481*

(133) S.A.S. AKERS, G.G. GARRETT, *J. Mat. Sci. 1983, 18 (7), 2200*

(134) V. LAWS, *Composites 1982, 13 (2), 145*

(135) C.D. LAWRENCE, *J. Mat. Sci. 1972, 7*

(136) R.C. DE VEKEY, A.J. MAJUMDAR, *Mag. Concr. Res. 1968, 20 (65), 229*

(137) A.J. MAJUMDAR, *RILEM Symp. on Fibre Reinforced Cement and Concrete (London, 14-17 Sept. 1975), 1976, 279*

(138) M.N. AL KHALAF, C.L. PAGE, A.G.B.RITCHIE, *Cem. Concr. Res. 1980, 10 (1), 71*

(139) J. POTRZEBOWSKI, *Bond in Concrete (Paisley, 14-16 June 1982), 51*

(140) D.J. PINCHIN, D. TABOR, *Cem. Concr. Res. 1978, 8 (2), 139*

(141) C.L. PAGE, *Composites 1982, 13 (2), 140*

(142) A. BENTUR, S. DIAMOND, S. MINDESS, *J.Mat. Sci. 1985, 20 (10), 3610*

(143) D.J. PINCHIN, D. TABOR, *Cem. Concr. Res. 1978, 8 (1), 15*

(144) D.J. PINCHIN, D. TABOR, *RILEM Symp. on Fibre Reinforced Cement and Concrete (London, 14-17 Sept. 1975), 1976, 521*

(145) J. COOK, J.E. GORDON, *Proc. Roy. Soc.1964, 282 A, 508*

(146) A. BENTUR, S. DIAMOND, *Mat. Constr. 1985, 18 (103), 49*

(147) S. MINDESS, S. DIAMOND, *Cem. Concr. Res. 1980, 10 (4), 509*

(148) P. BARTOS, *Bond in Concrete (Paisley, 14-16 June 1982), 60*

(149) R.H. MILLS, *Advances in Cement-Matrix Composites (Boston, Nov. 1980), 229*

(150) M.S. STUCKE, A.J. MAJUMDAR, *J. Mat. Sci. 1976, 11, 1019*

(151) A.J. MAJUMDAR, *Advances in Cement-Matrix Composites (Boston, Nov. 1980), 37*

(152) K. LITHERLAND, D.R. OAKLEY, B.A.PROCTOR, *Advances in Cement-Matrix Composites (Boston, Nov. 1980), 61*

(153) B. SING, A.J. MAJUMDAR, *J. Mat. Sci. Letters 1985, 4 (8) 967*

(154) A.J.MAJUMDAR, B. SINGH, T.J. EVANS, *Composites 1981, 12 (3), 177*

(155) S. OHSAWA, R. KONDO, *7th Int. Congr. on the Chem. of Cement (Paris, 30 June-5 July 1980), vol. III, VII-69*

(156) B. SINGH, A.J.MAJUMDAR, *Int. J. Cem. Comp. Lightweight Concr. 1981, 3 (2), 93*

(157) N.J. DAVE, D.G. ELLIS, *Int. J. Cem. Comp. Lightweigth Concr. 1979, 1 (1), 19*

(158) P.L. WALTON, A.J.MAJUMDAR, *Composites 1975, 6 (5), 209*

(159) T. KOIZUMI, S. HASABA, S. SUKEDA, *The Cem. Ass. of Japan - Review of the 37th Gen. Meet. (Tokyo, May 1983), 217*

(160) R. ANDONIAN, Y.W. MAI, B. COTTERELL, *Int. J. Cem. Comp. Lightweight Concr. 1979, 1 (4), 151*

(161) S. MINDESS, A. BENTUR, *Int. J. Cem. Comp. Lightweight Concr. 1982, 4 (4), 245*

(162) R.S.P. COUTTS, P. KIGHTLY, *J. Mat. Sci. 1984, 19 (10), 3355*

(163) Y. W. MAI, M.I. HAKEEM, B. COTTERELL, *J. Mat. Sci. 1983, 18 (7), 2156*

(164) R.S.P. COUTTS, *Composites 1984, 15 (2), 139*

THEME/THÈME 3

Blended and special cements. Ciments spéciaux et ciments avec additions.

Chairman/Président :

V. I. Kuschidi
Institute Niicement
Moscow, U.S.S.R.

Secretary/Secrétaire :

Y.Kihara
Associação Brasileira de Cimento Portland, São Paulo, Brasil

SUB-THEME/SOUS-THÈME 3.1

Characteristics and activation of blending components.

Caractéristiques et activation des composants des matières d'addition.

Chairman/Président :

R. Bucchi
Italcementi, S.p.A.
Bergamo, Italy.

Principal Reporter/Rapporteur Principal:

M. Regourd
C.E.R.I.L.H.
Paris, France

R. BUCCHI, Italcementi S.p.A., ITALIA.

APERCUS SUR LES AJOUTS ET LES CIMENTS COMPOSES DU POINT DE VUE DE L'INDUSTRIE.
OUTLINES ON ADDITIONS AND COMPOSITE CEMENTS. POINT OF VIEW OF INDUSTRY.

RESUME. On estime qu'aujourd'hui à peu près 90 millions de tonnes par an d'ajouts sont employées dans le monde entier pour produire au moins 280 millions de tonnes de ciments composés. On dispose dans le monde de 500 millions de tonnes par an de laitiers de haut fourneau (granulés et non) et de cendres volantes.
Cependant, à partir de cette constatation, il n'est certainement pas possible de prévoir que la production de ciments composés soit nécessairement appelée à augmenter dans un proche avenir.
Pour que ceci se réalise, il faudrait en effet que les utilisateurs acquièrent des connaissances et une expérience dont ils ne disposent pas encore à présent. Il faudrait aussi que l'industrie sélectionne plus rigoureusement la qualité des ajouts qu'elle ne le fait aujourd'hui, et qu'elle dispose de procédés et de moyens pour les valoriser.
Cette sélection et cette valorisation ne peuvent se faire de manière efficace qu'en cimenterie, ce qui exclut que les laitiers broyés ou les cendres volantes soient employées de manière efficace directement à la bétonnière.
Toute référence aux aspects économiques de la production de ciments composés a été ici évitée intentionnellement.

SUMMARY. It is estimated that about 90 milion t per year of additions are used today to produce not less than 280 milion t of composite cements. The only availability of (granulated or not) blastfurnace slags and fly ash attains 500 milion per year on the whole.
This favourable situation does not justify the forecast that the production of composite cements will necessarily increase in the near future.
As a matter of fact this can only happen if users acquire the knowledge and the skill which, at present, they are lacking in. Moreover, it is necessary for the industry to select the quality of the additions more strictly than today and to be placed in a position to use them better by processes and means. Anyhow ground slags and fly ash should never be added directly to the concrete mixer.
Any reference to the economic features of the composite cement production was intentionally avoided.

R. BUCCHI, Italcementi S.p.A., ITALIA.

1. DEFINITIONS ET CLASSIFICATION.

1.1 Dans ce travail on appelle ciments composés (ou ciments aux ajouts) les ciments contenant moins de 95% de clinker portland (constituant principal) et des quantités variables, dans des limites définies, d'un ou plusieurs ajouts (ou constituants secondaires) par rapport au total clinker + ajouts (donc, sulfate de calcium et adjuvants exclus).
Cette définition comprend tous les ciments autres que ceux de catégorie I du projet de norme européenne EN 197-1 (1,2,3,4) (tableau I). Seulement 20 normes de 24 Pays - sur 64 normes au total appliquées dans 96 Pays - ne prévoient pas de ciments composés (5). Néammoins la production de ciment de ces 24 Pays ne concerne que 59 millions de t par an (6) correspondant à un peu plus de 6% de la production mondiale (tableau II).

1.2 Metha (7) a récemment proposé une classification des sous-produits siliceux d'origine industrielle utilisables comme ajouts (ou comme ingrédients des bétons), qui constituera la base de la classification RILEM (8).
La classification donnée par Sersale (9) comprend aussi les pouzzolanes, les tufs lithiques et les diatomites. Le premier arrangement taxonomique de ces matières naturelles est dû à Turriziani (10).

2. PRODUCTION DE CIMENTS COMPOSES.

2.1 Les ciments composés ne sont pas une nouveauté 11). Les ciments pouzzolaniques ont été normalisés en Italie depuis 1929 (12); les ciments contenant du laitier sont produits en Allemagne, France, Luxembourg, Belgique, ecc. depuis plus d'un demi-siècle. Les ciments aux cendres volantes ont été développés en France vers la fin des années '50. Seuls les ci-

TAB. I. PROJET DE NORME CEN[(a)]: pr EN 197-1. DEFINITIONS ET TERMINOLOGIE DES CIMENTS (1, 2, 3, 4).

catégorie	designation	teneur en masse en %[(b)] de				
		clinker K	laitier[(c)] S	pouzzolane naturelle Z	cendres volantes Z	filler F
I	ciment portland	$95 \leq K \leq 100$		$0 \leq S, Z, F, \leq 5$		
II-S	ciment portland au laitier	$65 \leq K \leq 90$	$10 \leq S \leq 35$	$0 \leq Z, F \leq 5$		
II-Z	ciment portland à la pouzzolane	$65 \leq K \leq 90$	$0 \leq S \leq 5$[(d)]	$10 \leq Z \leq 35$		$0 \leq F \leq 5$[(d)]
II-S/Z	ciment portland composé	$65 \leq K \leq 88$	$6 \leq S \leq 29$	$6 \leq Z \leq 29$		$0 \leq F \leq 5$
III	ciment de haut fourneau	$20 \leq K \leq 64$	$36 \leq S \leq 80$[(e)]	$0 \leq Z, F \leq 5$		
IV	ciment pouzzolanique[(f)]	$K \geq 60$	$0 \leq S \leq 5$[(d)]	$Z \leq 40$		$0 \leq F \leq 5$[(d)]

(a) Dans l'introduction du projet on fait état d'une quatrième sous-catégorie II, relative au ciment portland au filler II-F, dont la teneur en filler peut être supérieure à 5% (1,4).
(b) Les valeurs numériques se réfèrent à clinker + constituants secondaires et excluent sulfate de calcium et adjuvants (4).
(c) Granulé ou bouleté de haut fourneau.
(d) La teneur totale en laitier et/ou filler ne peut pas excéder 5%.
(e) Une mention doit indiquer le cas où la teneur en laitier dépasse 65%.
(f) Le ciment pouzzolanique doit satisfaire à l'essai de pouzzolanicité EN 196-5.

R. BUCCHI, Italcementi S.p.A., ITALIA.

ments contenant de la poudre de silice sont relativement récents (13,14). Les tableaux III et IV donnent la répartition par catégorie des ciments produits ou vendus dans les principaux Pays. Les valeurs de ces tableaux ont été élaborées à partir des données publiées par CEMBUREAU (6), par Dutron (1,2) ainsi qu'à partir de diverses autres sources (15,16, 17). Les principaux producteurs de ciments composés sont l'URSS, les Pays du CEMBUREAU(*), la Chine et l'Inde. Au sein du CEMBUREAU se distinguent l'Espagne, la France, l'Italie et la Grèce. Depuis quelques années en Belgique et en Hollande les ciments de classe de résistance ordinaire ne sont que des ciments composés (18). En Inde la production de ces ciments a été triplée en quatre ans (19,20).
Des Pays importants, au contraire, comme les Etats Unis, le Royaume Uni, l'Afrique du Sud, le Canada et la Suisse, dont certains ont de larges disponibilités en ajouts d'origine industrielle, ne produisent aujourd'hui encore que du ciment ne contenant que du clinker. Il faut probablement chercher l'origine de cette situation assez particulière dans des traditions très anciennes.

TAB. II. PRODUCTION DE CIMENT DES PAYS DONT LES NORMES NE PREVOIENT PAS DE CIMENTS COMPOSES (5, 6).

	année 1983	
	production 10^6 t/a	% production mondiale
Egypte	5,50	0,60
Nigéria	3,00	0,33
Zambie	0,34	0,04
Gana	0,28	0,03
Colombie	4,84	0,53
Venezuela	4,44	0,48
Amérique C.le (a)	2,05	0,22
Uruguay	0,41	0,04
Jamaïque	0,28	0,03
Paraguay	0,15	0,02
Irak	9,50	1,04
Thaïlande	7,23	0,79
Philippines	4,56	0,50
Pakistan	4,18	0,46
Singapour	3,00	0,33
Israël	2,20	0,24
Sri Lanka	0,48	0,05
Suisse	4,02	0,44
Irlande	1,48	0,16
Nouvelle Zélande	0,96	0,10
Total	58,90	6,43

(a) Normalisation unique pour Costa Rica, El Salvador, Guatémal, Honduras, Nicaragua.

(*) Font partie du CEMBUREAU les industries cimentières des 19 Pays suivants de l'Europe Occidentale: Autriche, Belgique, Danemark, Finlande, France, Allemagne, Grèce, Irlande, Islande, Italie, Luxembourg, Norvège, Hollande, Portugal, Royaume Uni, Espagne, Suède, Suisse, Turquie.

2.2 Etant donnée l'étendue des intervalles de teneur en ajouts prévus par plusieurs normes des différents Pays, il est difficile d'évaluer le volume de constituants secondaires utilisés aujourd'hui. Pour surmonter cet obstacle CEMBUREAU (21,2) a fait une enquête auprès des Associations des Fabricants de ciment des Pays d'OCDE et a obtenu les résultats donnés par le tableau V.

3. DISPONIBILITE D'AJOUTS D'ORIGINE INDUSTRIELLE.

3.1 Dire que dans le monde entier on produit 250 millions de t par an de laitiers (22), 300 millions de t par an de cendres volantes (23,24) et plus d'1 million de t par an de poudre de silice (25,24) est peu significatif du point de vue pratique tant qu'on ne tient pas compte de la distribution géographique relative des approvisionnements en constituants secondaires et des usines à ciment. Par ailleurs, les informations au sujet de la nature des constituants secondaires sont souvent imprécises, bien que très abondantes, et font la confusion parmi les différentes qualités de laitiers (de haut fourneau et sidérurgiques, granulés et non) et de cendres volantes, bottom ashes et boiler slags. Il n'est pas donc facile de se faire une idée précise.

3.2 Pour élaborer les valeurs du tableau VI on a interprété critiquement les données disponibles concernant, lorsqu'il a été possible, plusieurs années. Pour chaque valeur on a mentionné la référence à la source utilisée.
On a indiqué dans le tableau les disponibilités annuelles de laitiers de haut fourneau, soit granulés, soit bouletés, soit refroidis lentement; pour les cendres, par contre, on n'a donné que les quantités emportées par les gaz de combustion hors de la chaudière et recueillies à l'état sec.
Il fait remarquer que, malgré tout le soin qui a été apporté au traitement de ces données, quelques unes des valeurs du tableau peuvent ne pas correspondre exactement à la réalité.

R. BUCCHI, Italcementi S.p.A., ITALIA.

4. ASPECTS ECOLOGIQUES.

4.1 L'industrie cimentière de la plupart des pays n'utilise qu'en partie les laitiers et les cendres disponibles; l'industrie du bâtiment n'est pas à même d'en absorber la totalité.
Il se pose donc le problème de la mise en décharge des tonnages inutilisés, problème qu'une augmentation de la production des ciments composés serait capable de résoudre en partie. D'autre part la diminution de la production de clinker portland entraînerait une réduction de la consommation de matériaux de carrière (qui pour chaque t de clinker montent à 0,7 m^3 environ) et une plus faible pollution atmosphérique. Cette dernière - pour un four moderne avec broyage du cru en ligne, et avec une consommation de 3.800 MJ/t de clinker - représente en moyenne 0,2 kg de poussières et 1,3 kg de NO_x (sous forme de NO_2) pour chaque t de clinker produit (39). Les émissions de SO_2 peuvent être évaluées à 0,3 kg environ par t de clinker produit (40).
Les avantages écologiques du remplacement d'1 t de ciment portland par 1 t de ciment composé sont calculés au tableau VII pour ce qui concerne les matériaux.

4.2 En ce qui concerne l'énergie, les évaluations du tableau VIII se fondent sur une demande d'énergie thermique de 3.800 MJ et d'énergie électrique de 80 kWh par t de clinker produit. En termes d'énergie primaire - 1 kWh équivaut à 9,096 MJ (41) - la demande totale est 4.528 MJ par t de clinker.
De plus on suppose que le broyage, le transfer dans les silos et l'extraction demandent 30 kWh (273 MJ) et 38 kWh (346 MJ) respectivement par t de ciment portland et par t de ciment composé. Dans les calculs on a négligé l'énergie dépensée pour le transport en usine des constituants secondaires (qu'on aurait dû calculer de toute façon au déduction de l'énergie de transport des matières premières correspondant au clinker remplacé). L'erreur qu'on fait, pour des distances comprises dans un rayon de 200 km avec voyage de retour à vide, varie entre 6 et 60 MJ par t de ciment, selon la distance et le type de transport. La différence de demande d'énergie des deux types de ciment est peu moins de 1.000 MJ/t et le rapport est d'à peu près 0,78. Ces valeurs sont en bon accord avec celles publiées précedemment (36,35, 33,2,42,43,21, 30), si l'on tient compte de la composition du ciment aux ajouts qu'on a ici considéré.

TAB. III. DISTRIBUTION EN % DE LA PRODUCTION DES DIFFERENTES CATEGORIES DE CIMENT. ELABORATION DES STATISTIQUES CEMBUREAU (6) ET D'AUTRES SOURCES (1, 2, 13, 14).

pays (a)	production 10^6 t	% ciment cat.I			% ciment cat.II			% ciment cat.III			% ciment cat.IV		
	1984	1980	1981	1982	1980	1981	1982	1980	1981	1982	1980	1981	1982
Cembureau	191,4		53,0	52,0		25,0	27,5		7,0	7,5		13,0	13,0
URSS	130,0	30,0			44,5			25,5			-		
Chine	121,0	9,1		8,5	46,0		46,5	38,4		37,1	1,5		1,7
Japon	82,0	92,1	90,5	89,4	2,0	2,0	2,0	5,8	7,2	8,4	0,1	0,1	0,1
USA	71,0	99,0	99,0	99,0	1,0	1,0	1,0	-	-	-	-	-	-
Inde	30,0	35,4	35,5	23,5	47,2	47,0	59,0	17,4	17,5	17,5	-	-	-
Brésil	19,5	80,9	84,0	78,5	-	-	-	11,3	10,0	9,0	7,5	6,0	12,5
Mexique	18,0	76,0	67,2	62,0	-	-	-	-	-	-	22,9	30,4	37,6
Pologne	16,5	14,9	10,7	31,0	61,0	64,4	47,0	23,8	24,9	22,0	0,3	-	-
Yougoslavie	9,3		7,5	8,0		92,0	89,0		0,5	3,0		-	-
Afrique du Sud	8,2	92,8	93,0	92,5	4,0	4,5	5,0	3,2	2,5	2,5	-	-	-
Canada	8,4	100,0	100,0	99,0	-	-	1,0	-	-	-	-	-	-
Argentine	5,2		95,5			4,5			-			-	

(a) Principaux pays producteurs en ordre décroissant de production.
Les espaces en blanc indiquent des données non disponibles.

R. BUCCHI, Italcementi S.p.A., ITALIA.

5. QUALITE DES AJOUTS. VARIABILITE.

5.1 Le laitier granulé de haut fourneau est l'ajout le plus connu (22) et le plus fiable pour la qualité (44). Son activité dépend du degré de polymérisation des groupes SiO_4^{-4} et de l'énergie de liaison Me-O des cations dépolymérisateurs du verre (4,5,46). Ces paramètres ne sont pas contrôlés par les déterminations de routine de l'usine. Cependant les laitiers bien trempés d'une même origine ont des propriétés suffisamment constantes, comme il est démontré par les valeurs du tableau IX (40).

5.2 La qualité des cendres récupérées, sèches, à la sortie de la chaudière d'une installation thermoélectrique est au contraire très variable (48,49,50, 35,51,52). La connaissance des paramètres qui influencent leur activité et leur comportement est récente et peut-être encore incomplète. On juge, d'ailleurs, que les propriétés les plus variables - et malheureusement les plus importantes pour la qualité du ciment - sont celles qui influencent l'ouvrabilité et l'absorption des adjuvants.
Beaucoup de cendres améliorent l'ouvrabilité (53,54, 55,58), d'autres la détériorent (48,56,57,58). Presque toutes augmentent la consommation d'adjuvants du béton; ceci dans une proportion différente qui dépend de la structure moléculaire de l'adjuvant (56,58).

TAB. IV. DISTRIBUTION EN % DES VENTES INTERIEURES DES DIFFERENTES CATEGORIES DE CIMENT DANS LA CEE ET LES PAYS DU CEMBUREAU. ELABORATION DES STATISTIQUES CEMBUREAU (6) ET D'AUTRES SOURCES (16, 17).

pays (a)	production 10^3t 1984	% ciment cat.I			% ciment cat.II			% ciment cat.III			% ciment cat.IV		
		1982	1983	1984	1982	1983	1984	1982	1983	1984	1982	1983	1984
CEE	160.962	52,0	52,1	53,5	27,7	27,6	26,9	7,4	7,2	7,2	12,9	13,1	12,4
CEMBUREAU:													
Italie	38.891	51,5	50,1	53,1	-	-	-	5,0	5,1	5,1	41,5	42,4	39,3
Espagne	26.643	18,5	19,8	17,7	75,6	73,0	74,5	1,2	2,0	2,0	4,6	5,2	5,7
RFA	26.224	75,8	75,3	76,7	8,6	7,9	7,2	14,7	14,5	13,6	0,5	0,5	0,6
France	24.025	26,9	27,4	26,2	71,9	71,8	67,8	0,9	0,6	0,8	-	-	-
Turquie	15.735												
Royaume Uni	13.552	90,5	91,0	90,8	-	-	-	0,3	0,4	1,8	-	-	-
Grèce	13.460	9,0	10,2	11,6	91,0	89,8	88,4	-	-	-	-	-	-
Belgique	5.708	49,1	30,8	30,8	12,0	27,5	26,4	36,9	38,6	39,1	-	-	-
Portugal	5.483	91,0	92,7	99,0	2,0	6,0	-	7,0	1,3	1,0	-	-	-
Autriche	4.852	21,0	24,0	6,5	78,0	75,0	92,4	1,0	1,0	0,9	-	-	-
Suisse	4.297	100,0	100,0	100,0	-	-	-	-	-	-	-	-	-
Hollande	3.176	37,4	29,1	28,5	0,5	5,7	7,5	62,1	65,2	63,9	-	-	-
Suède	2.360	98,0	89,0	89,0	2,0	11,0	11,0	-	-	-	-	-	-
Finlande	1.645	21,0	18,0	23,9	78,0	81,0	75,3	1,0	1,0	0,4	-	-	-
Norvège	1.459	97,0	42,0	26,0	-	56,0	70,7	-	-	-	-	-	-
Danemark	1.450	70,0	68,0	61,2	23,0	32,0	38,8	-	-	-	-	-	-
Irlande	1.377	100,0	100,0	100,0	-	-	-	-	-	-	-	-	-
Luxembourg	973	6,0	7,6	6,0	41,9	40,1	46,4	52,1	52,3	47,6	-	-	-
Islande	114	11,0	12,0	-	83,0	84,0	100,0	-	-	-	6,0	4,0	-

(a) En ordre decroissant de production.
Les espaces en blanc indiquent des données non disponibles.

La corrélation entre l'activité pouzzolanique (chaux combinée) et la résistance mécanique est très faible, voire inexistante (56,59,62).

Bien que dans plusieurs Pays des normes spécifiques (37,60,62,63,64,65) d'une certaine manière définissent la qualité des cendres destinées au béton ou

TAB. V. PROPORTIONS (% EN MASSE) DE CONSTITUANTS SECONDAIRES DANS LES CIMENTS, SEL. (21, 2).

	1980	1983	1990	2000
Europe Occidentale	15	17	23	30
Amérique du Nord	1	3	10	20
Japon	3	5	12	20
OCDE	9	11	16	25

au ciment, on reconnaît souvent que les paramètres retenus sont inappropriés et que les limites fixées sont incertaines (56,62,24,66, 67).
En effet les propriétés d'une cendre dépendent non seulement de la teneur en carbone et du refus à 45 µm (paramètres qui se répètent dans la plupart des normes) mais aussi du spectre granulaire, du facteur de forme des particules (48), de leur porosité, de la rugosité de la surface (67,68), de la nature et quantité d'éventuels revêtements en sulfate, hématite, magnétite (68), de la présence de P_2O_5 (56) et de V_2O_5 (40), etc. Ces variables sont à leur tour reliées à des paramètres de procédé qui peuvent changer fréquemment, comme la qualité et la finesse du charbon, la conduite de la combustion et la charge de la chaudière (57,67,68,36).
Ce type de situation peut justifier les contradictions de la littérature sur les propriétés des cendres et permet de comprendre les échecs observés sur certains bétons où une partie du ciment a été remplacée par de la cendre directement à la bétonnière.

L'emploi de cendres volantes comme liant demande beaucoup de prudence. Elles ne doivent être traitées que dans les usines à ciment, selon les méthodes et les procédés propres à la fabrication du ciment (4, 35,36,56).
Le tableau X donne les caractéristiques de cendres volantes selectionnées provenant de centrales thermoélectriques italiennes (40).

5.3 La poudre de silice ("condensed silica fume")

TAB. VI. EVALUATION DES DISPONIBILITES ANNUELLES D'AJOUTS D'ORIGINE INDUSTRIELLE DANS LES PAYS PRINCIPAUX. ANNEES 1980-1985.

pays[a]	production ciment'84 10^6t	laitiers[b]		cendre volante[c]		poudre de silice	
		10^6t/a	réf.	10^6t/a	réf.	10^3t/a	réf.
Cembureau	191,4	45[d]	(2)	33[e]	(2)		
URSS	130,0	27	(26)	80[e]	(27,28)	150	(29,13)
Chine	121,0	25	(2,8)	27-80[e]	(29,27)		
Japon	82,0	25	(2,8)	2-3	(2,8,27)	70	(29)
USA	71,0	27-30	(2,30,7)	50-60	(31,32,23)	300	(29,13)
Italie	38,9	3	(33)	1,2	(34)	10	(29)
Inde	30,0	4-6	(8,19)	8	(19)		
Espagne	26,6			5	(27)	30	(29)
RFA	26,2	11	(8,33)	2-3	(8,35,36)	6-25	(29,8)
France	24,0	8	(8)	5	(8,23)	20-60	(29,8)
Brésil	19,5					13	(29)
Pologne	16,5			12-15	(27,28,23)		
Royaume Uni	13,6	6	(33,8)	10	(37,38)		
Yougoslavie	9,3			5	(27)		
Canada	8,4	3	(7,8)	3	(8,27)	15	(29)

(a) En ordre décroissant de production de ciment.
(b) Laitiers de haut fourneau granulés, bouletés et refroidis lentement.
(c) Bottom ashes et boiler slags exclus.
(d) Seulement laitier granulé.
(e) Il s'agit évidemment de cendres totales.
Les espaces en blanc indiquent des données non disponibles.

est connue depuis longtemps comme ingrédient des bétons; elle est aussi employée comme ajout des ciments. Les microsphères de verre dont elle est constituée doivent leurs propriétés exceptionnelles à leur extrême finesse (jusqu'à 7.000 $m^2 kg^{-1}$ et plus) (69) et à une activité pouzzolanique très élevée (25,70).
Jahren (71) a montré que la teneur en SiO_2 peut varier entre des limites plutôt larges (63-98%), selon le procédé de production (silicium métallique ou alliages Fe-Si de titre différent) et selon les matières premières employées. La finesse est ainsi assez variable (69).
Cette matière est relativement peu abondante et elle est devenue, aujourd'hui, assez chère (29). En outre, elle présente la propriété très gênante d'augmenter considérablement la demande en eau des ciments. Son intérêt comme constituant secondaire des ciments composés est, donc, très limité.

TAB. VII. AVANTAGES ECOLOGIQUES DE LA PRODUCTION D'UNE t DE CIMENT COMPOSE(a) (CLINKER 0,70) AU LIEU D'UNE t DE CIMENT PORTLAND (CLINKER 0,93).

Diminution de mouvement de matière dans le territoire	extraite en moins clinker 0,7 (0,93-0,70) filler 0,03 : 2,2 ajouts déchargés en moins: 0,26 : 1,3 total	= 0,16 m^3/t = 0,01 " = 0,20 " = 0,37 m^3/t
Diminution de pollution atmosphérique(b)	poussières en moins (39) 0,20 (0,93-0,70) NO_x en moins (39) 1,30 (0,93-0,70) SO_2 en moins (40) 0,30 (0,93-0,70)	= 0,04 kg/t = 0,30 " = 0,07 "

(a) On suppose que les constituants sécondaires sont laitier et cendre volante dans la proportion 1:1 et que 0,13 t de laitier par t de ciment composé sont sechés par la chaleur enthalpique de l'air en excès du refroidisseur à grille.
(b) Produite par les fumées du four et de l'air en excès du refroidisseur à grille.

5.4 Les pouzzolanes et les tufs lithiques sont des roches pyroclastiques (9) de bonne constance qualitative. Les variations dans le même gisement, ou dans des gisements de la même origine, concernent des stratifications différentes qui peuvent se distinguer par leur teneur en verre, le degré de diagénisation ou présence de matières étrangères déposées entre deux explosions du volcan.
Au contraire, pour les argiles et les marnes diatomitiques (9) - dites aussi, improprement, pouzzolanes sédimentaires - les variations de composition et

TAB. VIII. ENERGIE DEMANDEE POUR LA PRODUCTION DE CIMENT PORTLAND ET DE CIMENT COMPOSE(a).

ciment portland: clinker 93% ciment composé: 70%K+13%S+13%Z		énergie demandée MJ/t de ciment	
		portland	composé
clinker	0,93·4528	4.211	
	0,70·4528		3.170
constituants secondaires:			
traitement laitier(b)	0,13·36		5
traitement c. volantes	0,13·18		2
ciments (broyage, ensilage et extraction):			
portland		273	
composé			346
	total	4.484	3.523

(a) Sauf quantité d'énergie nécessaire pour le transport des constituants secondaires de source de production à cimenterie.
(b) On suppose que le laitier est seché par la chaleur enthalpique de l'air en excès du refroidisseur à grille.

TAB. IX. VARIABILITE DES CARACTERISTIQUES DE LAITIERS GRANULES DE HAUT FOURNEAU DE PRODUCTION ITALIENNE. ANNEES 1984 ET 1985 (40).

échantillons examinés		TAR 16	PIO 15	SER 9
$\frac{C+M+A}{S}$	extrêmes	1,63-1,87	1,50-1,85	1,32-1,56
	moyenne	1,78	1,67	1,44
	s	0,07	0,12	0,07
teneur en verre(a),%	extrêmes	85-95	85-95	70-90
	moyenne	92	92	82
	s	3,7	2,8	9,0
eau pour consistance norm.,(b) %	extrêmes	26,3-27,0	26,3-27,4	25,6-27,4
	moyenne	26,7	26,6	26,6
	s	0,5	0,5	0,3

(a) Déterminée par voie microscopique sel. Padilla (47).
(b) Melange 30% laitier broyé à 300 $m^2 \cdot kg^{-1}$ (Blaine) et 70% de ciment portland de référence (42,5 $N \cdot mm^{-2}$).

de structure peuvent être considérables. A cause de leur teneur en argile ces matières ne devraient pas être utilisées pour produire des ciments à la pouzzolane ou pouzzolaniques. Ainsi qu'il a été observé pour les cendres volantes, les pouzzolanes ne presentent pas davantage de corrélation entre l'activité (chaux combinée) et la résistance des mortiers (72).

5.5 Le filler calcaire est un constituant secondaire des ciments composés français (5) et - pour des teneurs limitées à 5% - des ciments européens de la norme EN 197-1 (*).
Les fillers ne sont pas tout à fait inertes. Leur activité peut être expliquée:

- par un "effet microfiller", c'est-à-dire de dispersion des particules de clinker et de remplissage des vides intergranulaires (4, 68);
- par un effet épitaxique sur les hydrates C-S-H de la pâte (4,74);
- par les réactions avec les produits d'hydratation des aluminates du clinker (75,73,4).

Tous les calcaires ne conviennent pas en tant que fillers (4). Les meilleurs résultats sont obtenus par des roches à teneur élevée en $CaCO_3$ (>80%), exemptes, ou presque, de matière argileuse et ayant une structure particulière (vérifiable indirectement pour l'absence de matières organiques). Il est vraisemblable que les calcaires anciens, profondement diagénisés, compacts et non poreux (calcaires micritiques) se prêtent bien à cet usage.

TAB. X. VARIABILITE DES CARACTERISTIQUES DE CENDRES VOLANTES SELECTIONNEES DE PRODUCTION ITALIENNE 1985 (40).

			VAD	LAS	FUS	MFL
échantillons examinés			16	11	11	11
P.ä.F. , % en masse		extrêmes moyenne s	4,0-9,5 7,0 1,2	1,6-15,4 5,7 4,3	6,4-10,6 8,4 1,5	7,1-11,1 9,2 1,3
P_2O_5 tot., % en masse		extrêmes moyenne s	0,11-0,53 0,24 0,12	0,24-1,54 0,93 0,55	0,60-2,24 0,97 0,48	0,54-1,42 1,20 0,30
résidus, % en masse sur	40 µm	extrêmes moyenne s	23,5-36,3 28,5 3,1	8,1-26,0 19,0 4,9	13,0-27,0 21,0 4,2	13,5-18,8 16,8 2
	63 µm	extrêmes moyenne s	16,2-27,5 20,4 3,1	5,0-20,6 13,1 4,3	7,4-19,8 14,3 3,4	8,0-12,3 10,5 1,7
	90 µm	extrêmes moyenne s	9,1-19,0 12,5 2,6	3,0-16,3 7,6 3,9	3,7-13,0 8,6 2,8	4,2-6,7 5,7 1,0
eau pour consistance normale (a), %en masse		extrêmes moyenne s	26,4-30,3 28,4 0,8	27,4-33,6 29,7 2,1	30,8-33,4 32,0 1,0	34,0-35,8 35,1 0,7

(a) Mélange 30% cendre volante telle quelle et 70% de ciment portland de référence (42,5 $N \cdot mm^{-2}$).

(*) On envisage que cette norme comprendra aussi des ciments de catégorie II-F, avec plus de 5% de filler, probablement jusqu'à 20%.

R. BUCCHI, Italcementi S.p.A., ITALIA.

Le filler doit être broyé à des finesses très poussées.

6. QUALITE DES CIMENTS.

6.1 Dans tous les ciments composés une partie de clinker est remplacée par une quantité égale d'ajouts ayant une activité moins prompte et une finesse en général plus élevée. Ce remplacement entraîne un certain nombre de conséquences.
La première concerne la progressivité du développement des résistances mécaniques, à finesse du clinker égale. Aux brèves échéances elles sont toujours inférieures à celles d'un portland de classe égale (56,76) (FIG. 1). Le phénomène s'aggrave pendant la saison froide (57) et cause toujours une impression mauvaise, surtout par les utilisateurs les moins expérimentés.

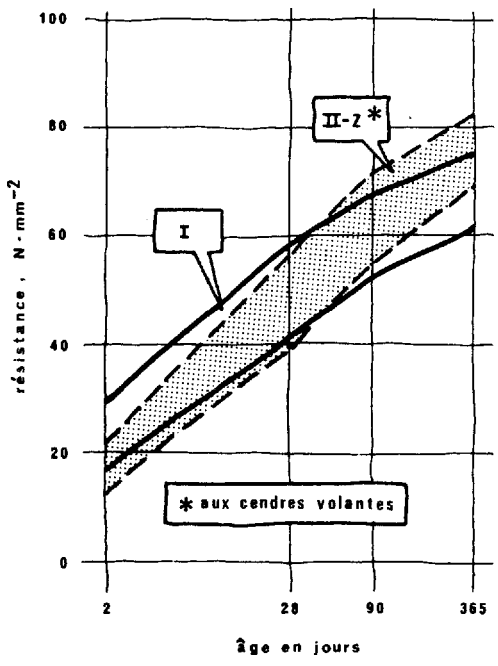

FIG. 1. EVOLUTION DES RESISTANCES DES CIMENTS PORTLAND ET AUX CENDRES VOLANTES EN MORTIER ISO. SEL. BRAUN ET GEBAUER (56).

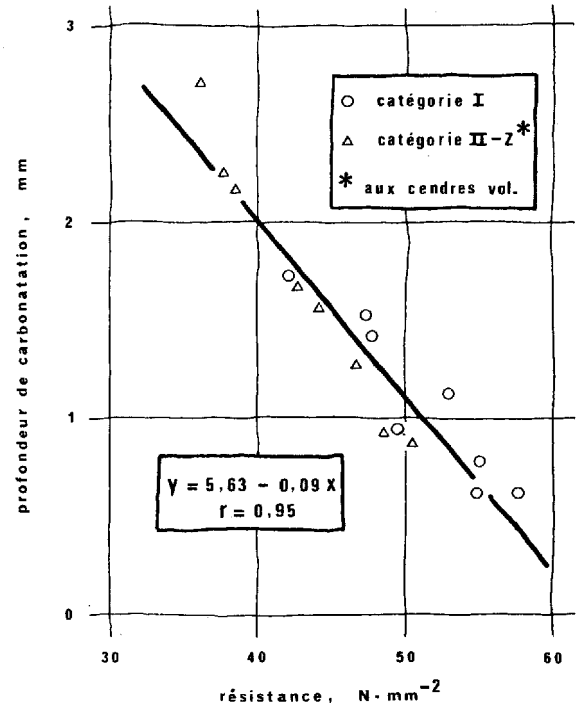

FIG. 2. RELATION ENTRE RESISTANCE DU BETON ET PROFONDEUR DE CARBONATATION. SEL. BRAUN ET GEBAUER (56).

La deuxième conséquence a la même origine que la première (activité retardée de l'ajout) mais elle peut produire des effets favorables, si l'on veille à eviter les pertes d'eau par évaporation par la surface (56, 68). Elle provient de la précipitation des hydrates des ajouts dans la solution des pores ou ils remplacent l'eau qui les remplit (55,76). Les pores de la pâte se transforment en pores du gel; leur distribution dimensionnelle subit un glissement vers les valeurs les plus petites (25,58,77,78,79, 80). Ce mécanisme exige un environnement humide pendant plusieurs jours.
L'absence de portlandite dans la pâte des ciments pouzzolaniques n'est plus considérée comme un facteur essentiel. Le remplacement du clinker par l'ajout a d'autres conséquences qui ne sont pas moins importantes, notamment son action de microfiller (4, 68,74) et une teneur plus élevée en C-S-H dans la pâte, au détriment des hydrates de C_3A (9,23,81). On explique ainsi pourquoi la matrice des bétons de ciment composé - pour des rapports peu élevés de E/C et une conservation en milieu humide - est plus uniforme, plus dense, moins perméable, et s'oppose à la

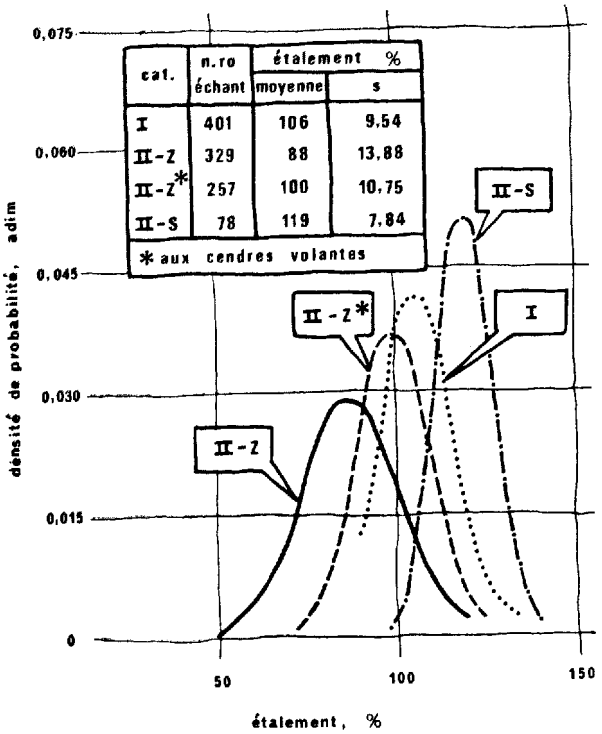

FIG. 3. CONSISTANCE DU MORTIER (E : C = 0,5) DE DIFFERENTS CIMENTS 32,5 N·mm^{-2}. TABLE A SECOUSSES SELON UNI 7044 (1972) (40).

diffusion des ions agressifs, en résumé elle est plus durable que celle qui est obtenue avec les ciments portland (25,81,82,83, 84,85,86). Elle protège de la corrosion les armatures en acier aussi bien que la pâte de portland (56,84,87) (FIG. 2) et elle paraît moins sujète à la réaction alcalis-granulat siliceux (7,9,23, 29,67).

6.2 Ces résultats - on le répète - sont conditionnés par l'emploi de rapports E/C suffisamment bas. Le problème de l'ouvrabilité est, donc, capital.
Aux FIG. 3 et 4 on compare les ouvrabilités de mortiers et bétons de trois catégories de ciments composés avec celles d'un portland ordinaire (40). Les ciments de laitier de haut fourneau présentent, comme on sait, les ouvrabilités les meilleures. Pour les emplois les plus difficiles des pouzzolaniques on conseille l'utilisation modérée de plastifiants. Les ciments contenant de la poudre de silice doivent être toujours employés avec des dosages adéquats de superplastifiants. Toutes ces catégories de ciment se comportent avec les entraîneurs d'air aussi bien que le portland.
Comme il a déjà été dit au paragraphe 5.2, les ciments aux cendres volantes présentent un comportement ambigu, qui dépend de la teneur variable en particules sphéroïdales présentes dans la cendre, ainsi que quelques Auteurs l'ont indiqué (36,48,55, 56) (Fig. 5); il dépend aussi de la teneur, en général variable, en particules très fines, comme d'Autres suggèrent (62,68). Les ciments des FIG. 3 et 4 ont une demande en eau plus élevé que le portland. D'une manière générale, les ciments aux cendres qui demandent plus d'eau sont les mêmes que ceux qui absorbent davantage les adjuvants en en rendant l'action moins efficace.

7. CONCLUSIONS.

7.1 Le problème du développement des ciments composés se réduit à celui de la maîtrise de la qualité des ajouts et à celui du mode de préparation et conservation des bétons.

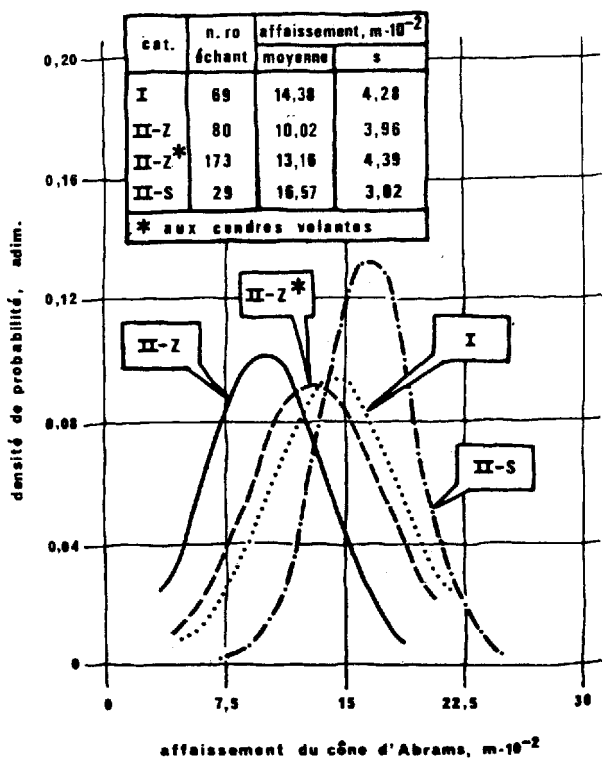

FIG. 4. CONSISTANCE DU BETON SELON UNI 7163 (1979) CIMENTS 32,5 N·mm^{-2}. DOSAGE 350 kg·m^{-3}, E:C = 0,6. GRANULOMETRIE GRAVIER TYPE FULLER $D_{max.}$ = 0,022 m (40).

R. BUCCHI, Italcementi S.p.A., ITALIA.

Il est certainement plus facile de produire un ciment portland contenant uniquement du clinker qu'un ciment composé de qualité, du fait que les critères par lesquels on sélectionne aujourd'hui les ajouts ne sont pas tout à fait adéquats et les procédés technologiques utilisés dans les usines ne sont pas les plus efficaces.
Ces défauts sont particulièrement nets pour les ciments aux cendres.
Il est également plus facile d'utiliser un ciment portland que des ciments composés. Ces derniers, en effet, sont des produits quelque peu sophistiqués, qui donnent des bétons meilleurs que ceux de portland - surtout vis à vis de la durabilité - pourvu qu'ils soient gâchés avec des rapports E/C suffisamment bas et soient conservés en milieu humide pour plusieurs jours.

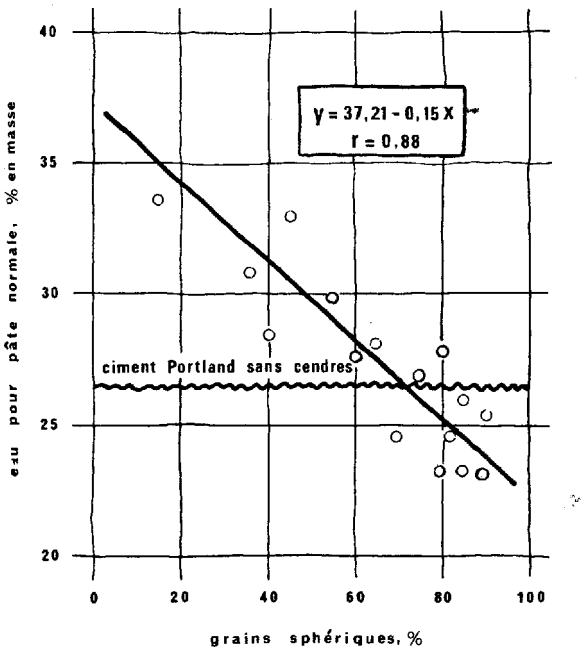

FIG. 5. INFLUENCE DE LA TENEUR EN GRAINS SPHERIQUES DES CENDRES VOLANTES SUR LA DEMANDE D'EAU DE LA PATE NORMALE (MELANGE 70 % CIMENT PORTLAND ET 30 % CENDRES VOLANTES). SEL. BRAUN ET GEBAUER (56).

7.2 L'activité des ajouts est tributaire du procédé par lequel ils sont obtenus et l'on ne peut pas penser qu'un haut fourneau ou bien une centrale thermoélectrique puissent être conduits en visant la qualité de leurs sous-produits. Pour améliorer l'activité et la qualité des ajouts il est donc nécessaire de suivre des voies différentes.
Avant tout il faut entreprendre une sévère sélection à l'origine. Elle devrait être effectuée sur la base de critères beaucoup plus efficaces que ceux disponibles aujourd'hui et, surtout, avec une attitude différente de l'attitude actuelle. La recherche devra éclaircir les paramètres qui sont décisifs pour le contrôle complet du comportement hydraulique d'un ajout.

Les traitements en usine des ajouts sont l'autre moyen pour obtenir des produits finis de qualité.
La seule homogénéisation de quantités même considérables peut être insuffisante. Chaque matière d'addition, soit artificielle soit naturelle, est constituée d'une partie active par sa structure ou sa finesse, et d'une partie indésirable. L'idéal serait de faire suivre la sélection à l'origine d'une sélection plus poussée, réalisée au cours d'une phase de comminution et de séparation.

La technologie doit donc s'enrichir de procédés et de méthodes permettant de broyer selectivement les matières et de séparer les fractions obtenues avec une efficacité et une précision meilleures que celles que nous connaissons actuellement. Le progrès des connaissances devra nous conduire à combiner rationnellement ces fractions pour obtenir le meilleur ciment composé possible (88).

7.3 L'avenir des ciments composés n'est pas donc seulement fonction de la disponibilité des ajouts ou des implications écologiques liées à leur production ou leur utilisation. Il depend aussi étroitement du progrès des connaissances de leur utilisation, des perfectionnements de la technologie et de l'accumulation de l'expérience de leur utilisation.

BIBLIOGRAPHIE.

1. DUTRON,P. (1984) "Les ciments d'aujourd'hui et de demain au service du béton manufacturé. 1ère Partie: les ciments d'aujourd'hui" Proc. 11ème Congr. Int. Ind. Béton, 82, Brussels.

2. DUTRON,P. (1983) "Standardized cements and manufactured cements. Present situation and prospects" Cembureau Seminar with 7th Int. Ready Mixed Concrete Congr. I 1, London.

3. DUTRON,P. (1983) "Normes internationales et européennes pour les ciments" 7th Int. Ready Mixed Concr. Congr. G5 (2), London.

4. CALLEJA,J. (1983) "Adiciones y cementos con adiciones" Cemento y Horm. 54, 439.

5. CEMBUREAU (EUROPEAN CEMENT ASSOCIATION) (1985) "Cement standards of the world", Paris.

6. CEMBUREAU (EUROPEAN CEMENT ASSOCIATION) (1980--1984) "World statistical review", Paris.

7. METHA,P.K. (1983) "Pozzolanic and cementious by products as mineral admixtures for concrete. A critical review" Proc. CANMET/ACI 1st Int. Conf. ACI Publ. SP-79, I 1, Montebello.

8. CEMBUREAU (EUROPEAN CEMENT ASSOCIATION) (1985) "Technical newsletter TN 1/1985, 28 th jan.", Paris.

9. SERSALE,R. (1983) "Aspects of the chemistry of additions" Advances in cement technology edt. by S.N. Gosh, 537. Pergamon Press, Oxford.

10. TURRIZIANI,R. (1964) "Aspects of the chemistry of pozzolanas" The chemistry of cements edt. by H.F.W. Taylor Vol.2,69. Academic Press, London.

11. DUTRON,P. (1981) "La réponse de l'industrie cimentière aux problèmes économiques et techniques d'aujourd'hui" Silicates Ind. 46, 255. Cemento y Horm. 53, 211 (1982).

12. PARISSI, F. et MAROTTA,R. (1969) "Sessanta anni di norme italiane sui leganti idraulici" Ind. Ital. Cem. 39, 417.

13. LEWANDOWSKI,R. (1984) "Verwendung mineralischer Nebenprodukte zur Betonherstellung" Beton + Fertigt. 50 H.1, 36.

14. HJORTH,L. (1983) "Development and application of high-density cement-based materials" Phil. Trans. Roy. Soc. A 310, 167, London.

15. THE CEMENT ASSOCIATION OF JAPAN (1981, 1982, 1983) "Cement statistics in Japan", Tokyo.

16. CEMBUREAU (EUROPEAN CEMENT ASSOCIATION) (1985) "Comunications privées", Paris.

17. BUNDESVERBAND DER DEUTSCHEN ZEMENTINDUSTRIE (1985) "Zahlen aus der Zementindustrie", Köln.

18. ROCK PRODUCTS EDITORS (1984) "Trends" Rock Pro. 87, n. 11, 31.

19. CHOPRA,S.K. et NARANG,K.C. (1981) "Blended cements. Raw materials including industrial wastes" Papers of All India Seminar on Cement, III, 493, New Delhi.

20. CHOPRA,S.K. et NARANG,K.C. (1981) "Blended cements. Manufacturing process and technologies" Papers of All India Seminar on Cement, III, 561, New Dehli.

21. GRUNER,H., COLLIS,H., RYDAHL,S. et MAGEL,P. (1981) "Rapport sur la consommation d'energie du secteur du ciment dans les Pays de l'OCDE à l'horizon 2000" Cembureau, Paris.

22. SMOLCZYK,H.G. (1980) "Structure et caractérisation des laitiers" 7e Congr. Int. Chimie Ciments Vol. I, III-1/3, Paris.

23. IDORN,G.M. (1981) "International aspects of development of the uses of fly ash with cement" Proc. Symp. N Mat. Res. Soc. 244, Boston.

24. MALHOTRA,V.M. (1983) "The use of fly ash, silica fume, slag and other mineral by-products in concrete" 7th Int. Ready Mixed Concrete Congr. G6 (1), London.

25. HJORTH,L. (1982) "Microsilica in concrete" Nordic Concr. Res. Publ. n. 1, 9-1 The Nordic Concrete Federation, Oslo.

26. KOUCHIDI,V.I. (1981) "Fabrication et utilisation des ciments mixtes" Silicates Ind. 46, 251.

27. KOVACS,R. (1982) "Verwentung von Flugaschen in der Zementindustrie, T.II" TIZ-Fachberichte 106, 803.

28. KOVACS,R. et TALABER,J. (1984) "State of the utilisation of fly ash for cement production in eastern-european and some other countries" Silicates Ind. 49, 31.

29 MALHOTRA,V.M. et CARETTE,G.G. (1983) "Silica fume concrete. Properties, applications and limitations" Concrete Int. 5, n. 5,40.

30. PORTLAND CEMENT ASSOCIATION (1976) "Energy conservation in the cement industry" Federal Energy Admin. Conservation Paper n. 29, Washington.

31. FABER,J.H. et BABCOCK,A.W. (1984) "Ash marketing and quality control practices in the United States including the affects of the EPA's guideline for the federal procurement of ash" Ash Tech'84. Proc. 2nd Int. Conf. Ash Technol. and Marketing 1, London.

32. HARNBY,H., BURNET,G. et MURTHA,M. (1984) "Mineral recovery from coal conversion solid wastes" Ash Tech'84. Proc. 2nd Int. Conf. Ash Technol. and Marketing 279, London.

33. ENVIRONMENTAL RESOURCES LIMITED (1983) "Clean technologies in the EEC cement industry" CEC EUR 8394 EN, Brussels.

34. ENTE NAZIONALE PER L'ENERGIA ELETTRICA (ENEL)

(1985) "Comunicazione privata 12.11.1985", Roma.

35. MAGEL,P. (1983) "Flugasche. Chance und Herausforderung für die deutsche Zementindustrie" Zement-Kalk-Gips 36, 249.

36. HEUFERS,H. et MAGEL,P. (1984)" Flugaschezement. Herstellungsverfahren, Qualitat und Wirtschaftlichkeit" Zement-Kalk-Gips 37, 55.

37. SMITH,M.A. (1977) "Seven national standards for pulverized fuel ash compared" Precast Concrete 8, 191.

38. STAMP,R.J et SMITH,I.E. (1984) "Pulverized fuel ash. Waste material or mineral resource?" Ash Tech'84. Proc. 2nd Int. Conf. Ash Technol. and Marketing 67, London.

39. BYE,G.C., HEILESEN,S. et SPRUNG,S. (1985) "Memorandum to EC Commission on proposal directive COM (83) 704 final" 18.02. 1985.

40. ITALCEMENTI S.p.A. (1984-1985) "Statistiche interne", Bergamo.

41. ENTE NAZIONALE PER L'ENERGIA ELETTRICA (ENEL) (1983) "Produzione e consumo di energia elettrica in Italia 1983" 6, Roma.

42. JACOBS,J. (1982) "Einsatz von Flugstaub aus Steinkohlefeuerungen im Betonbau" VGB Kraftwerkstechn. 62, 1099.

43. AGUANELL,M., BARAGANO,J., GOMA,F., GONZALEZ VILA,V., LOPEZ SOLER,R., MARTINEZ YNZENGA,J.I., PEREZ ALONSO,J. et REZOLA IZAGUIRRE,J. (1982) "Investigacion industrial sobre ahorro de energia en la fabricacion de nuevos cementos compuestos espanoles" Cemento y Horm. 53, 5.

44. DAIMON,M. (1980) "Mécanisme et cinétique de l'hydratation du ciment au laitier" 7e Congr. Int. Chimie Ciments. Vol. I, III-2/1, Paris.

45. SATARIN,V.I. (1974) "Slag portland cement" Principal Paper. 6th Int. Congr. Chemistry of Cement, Moscow.

46. ROJAK,S.M., SHKOLNIK,J.S. et ORLOW,W.W. (1975) "Crystallochemical structure and hydraulic properties of blastfurnace slags" Cem. Wap. Gips 12, 355.

47. PADILLA,E. (1952) "Détermination microscopique du poursantage de verre dans les laitiers de haut fourneau" Silicates Ind. 17, 163.

48. HOPKINS,C.J. et CABRERA,J.G. (1984) "The influence of pulverized fuel ash on the workability of concrete" Ash Tech'84. Proc. 2nd Int. Conf. Ash Technol. and Marketing 393, London.

49. CABRERA,J.G., WOOLLEY,G.R., HOPKINS,C.J., LEE, R.E., PLOWMAN,C. et FOX,H. (1984) "The relevance of pulverized fuel ash properties on the strength of concrete" Ash Tech'84. Proc. 2nd Int. Conf. Ash Technol. and Marketing 303, London.

50. GRAHAM,J. et BRINKWORTH,D.C. (1984) "Characteristics of pulverized fuel ash from different power stations and dust collection points" Ash Tech'84. Proc. 2nd Int. Conf. Ash Technol. and Marketing 23, London.

51. LEWANDOWSKI,R. (1983) "Einfluss unterschiedlicher Flugasche - qualitaten und - zugabemengen auf die Betoneigenschaften" Beton + Fertigt. 49, H. 1-3, 11, 105, 152.

52. DUTRON,P. (1977) "El ahorro de energia por adiciones al cemento" Materiales de Constr. n. 166-167, 103.

53. BERRY,E.E. et MALHOTRA,V.M. (1980) "Fly ash for use in concrete. A critical review" J. Am. Concr. Inst. 77, 59.

54. JARRIGE,A. (1971) "Les cendres volantes" Eyrolles, Paris.

55. KOKUBU,M. (1968) "Fly ash and fly ash cement" Principal Paper Proc. 5th Int. Symp. Chemistry of Cement, Vol. IV, 75, Tokyo.

56. BRAUN,H. e GEBAUER,J. (1983) "Möglichkeiten und Grenzen der Verwendung von Flugaschen im Zement" Zement-Kalk-Gips 36, 254.

57. MEININGER,R.C. (1982) "Use of fly ash in cement and concrete" Concrete Int. 4, n. 7, 52.

58. UCHIKAWA,H, UCHIDA,S. et OGAWA,K. (1982) "Influence of characterers of fly ash on the fluidity and structure of fly ash cement paste" J. Res. Onoda Cement Co. 34, n. 107,7.

59. CLIFTON,J.R., BROWN,P.W. et FROHNSDORFF,G. (1977) "Reactivity of fly ashes with cement" Cement Research Progress Cap. 15,321. Am. Ceramic Soc., Columbus.

60. BUTLER,W.B. (1982) "A critical look at ASTM C 618 and C 311" Cem. Concr. Aggr. 4, n. 2, 68.

61. BRADBURY,H.W. (1982) "The use of fly ash in pre-blended cements" Silicates Ind. 47, 283.

62. HELMUTH,R. (1983) "Some questions concerning

ASTM standards and methods of testing fly ash for use with portland cement" Cem. Concr. Aggr. 5, 103.

63. MANZ,O.E. (1983) "Review of international specifications for use of fly ash in portland cement concrete" Proc. CANMET/ACI 1st Int. Conf. ACI Publ. SP-79, I 187, Montebello.

64. BROWN,P.W., CLIFTON,J.R. et FROHNSDORFF (1976) "Energy conservation through the facilitation of increased blended cement use" NBS IR 76-1008, Energy Research and Development Administration, Washington.

65. ROSSOUW,E. et KRUGER,J. (1983) "Review of specifications for additions for use in concrete" Proc. CANMET/ACI 1st Int. Conf. ACI Publ. SP-79, I 201, Montebello.

66. MATHER,B. (1983) "Cements users'expectations with regard to blended cements" Proc. CANMET/-ACI 1st Int. Conf. ACI Publ. SP-79, I 255, Montebello.

67. PLOWMAN,C. (1984) "The chemistry of PFA in concrete. A review of current knowledge" Ash Tech'84. Proc. 2nd Int. Conf. Ash Technol. and Marketing 437, London.

68. RICHARTZ,W. (1984) "Zusammensetzung und Eigenschaften Von Flugaschen" Zement-Kalk-Gips 37, 62.

69. PISTILLI,M.F., WINTERSTEEN,R. et CECHNER,R. (1984) "The uniformity and influence of silica fume from a US source on the properties of portland cement concrete" Cem. Concr. Aggr. 6, 120.

70. AITCIN,P.C. et VEZINA,D. (1984) "Resistence to freezing and thawing of silica fume concrete" Cem. Concr. Aggr. 6, 38.

71. JAHREN,P. (1983) "Use of silica fume in concrete" Proc. CANMET/ACI 1st Int. Conf. ACI Publ. SP-79, II 625, Montebello.

72. MASSAZZA,F. (1983) "Cementi clinker/pozzolana" Cembureau Seminar with 7th Int. Ready Mixed Concrete Congr. II d, London.

73. MERIC,J.P. (1984) "Les ciments d'aujourd'hui et de demain au service du béton manufacturé. 2ème Partie: les ciments de demain" Proc. 11ème Congr. Int. Ind. Béton, 103, Brussels.

74. CALLEJA,J. (1982) "Apostillas al trabajo de P. Dutron titulado la rispuesta de la industria cementera a los problemas economicos y técnicos actuales" Cemento y Horm. 53, 227.

75. SPOHN,E. et LIEBER,W. (1965) "Reaktionen zwischen Calcium carbonate und Portlandzement" Zement-Kalk-Gips 18, 483.

76. KOVACS,R. (1982) "Verwentung von Flugaschen in der Zementindustrie T.I" TIZ-Fachberichte 106, 658.

77. FELDMAN,R.F. (1981) "Pore structure formation during hydratation of fly ash and slag cement blends" Proc. Symp. N Mat. Res. Soc. 124, Boston.

78. MANMOHAN,D. et METHA,P.K. (1981) "Influence of pozzolanic, slag, and chemical admixtures on pore size distribution and permeability of hardened cement pastes" Cem. Concr. Aggr. 3, 63.

79. METHA,P.K. et GJORV,O.E. (1982) "Properties of portland cement concrete containing fly ash and condensed silica fume" Cem. Concr. Res. 12, 587.

80. ROY,D.M. et PARKER,K.M. (1983) "Microstructures and properties of granulated slag-portland cement blends at normal and elevated temperatures" Proc. CANMET/ACI 1st Int. Conf. ACI Publ. SP-79, I 397, Montebello.

81. FRIGIONE,G. et SERSALE,R. (1983) "Gypsum in blast-furnace cements" Am. Cer. Soc. Bull. 62, 1275.

82. AITCIN P.C., PINSONNEAULT,P. et RAU,G. (1981) "The use of condensed silica fume in concrete" Proc. Symp. N Mat. Res. Soc. 316, Boston.

83. BACHE,H.H. (1981) "Densified cement/ultra-fine particle-based materials" 2nd Int. Conf. Superplast. Concr., Ottawa.

84. SHORT,N.R. et PAGE,C.L. (1982) "The diffusion of chloride ions through portalnd and blended cement pastes" Silicates Ind. 47, 237.

85. GJORV,O.E. et VANNESLAND,O. (1979) "Diffusion of chloride ions from seawater into concrete" Cem. Concr. Res. 9, 229.

86. PAGE,C.L., SHORT,N.R. et EL TARRAS,A. (1981) "Diffusion of chloride ions in hardened cement pastes" Cem. Concr. Res. 11, 395.

87. GEBAUER,J. (1982) "Some observations on the carbonatation of fly ash concrete" Silicates Ind. 47, 155.

88. MERIC,J.P. (1980) "Influence du broyage et du mode de conservation du clinker" 7ème Congr. Int. Chimie Ciments Vol I, IV-4/2, Paris.

THEME 3. CIMENTS SPECIAUX ET CIMENTS AVEC ADDITIONS

SOUS - THEMÈ 3.1.

CARACTERISTIQUES ET ACTIVATION DES PRODUITS D'ADDITION

M. REGOURD
C.E.R.I.L.H.
PARIS, FRANCE

1. INTRODUCTION

Les caractéristiques et les différents moyens d'activer les produits ajoutés au ciment Portland ont été présentés dans les thèmes III et IV du précédent Congrès à Paris en 1980. Les cinq rapports principaux (1, 2, 3, 4, 5), les deux rapports généraux (6, 7) et les "panels" (8, 9) ont traité séparément les laitiers, essentiellement de haut fourneau donc hydrauliques et les pouzzolanes, roches naturelles ou cendres volantes. En conclusion, il est apparu que laitiers et pouzzolanes ne devaient plus être considérés comme de simples produits d'addition mais comme des ajouts réactifs, et précoces pour certains d'entre eux.

Depuis le Congrès de Paris, les efforts des chercheurs ont porté plus particulièrement sur la caractérisation et la réactivité de matériaux pouzzolaniques très diversifiés comme les cendres volantes et les fumées de silice. Trois quarts des communications leur ont été consacrés lors de la première conférence internationale sur l'utilisation des cendres volantes, fumées de silice, laitiers et autres sous-produits minéraux dans le béton à Montebello (Canada) en 1983. La MRS "Materials Research Society" organise tous les ans à Boston un symposium sur les cendres volantes. Outre les cendres et les fumées de silice, de nouveaux produits sont dès à présent utilisés à l'échelle industrielle. Ce sont par exemple les fillers calcaires entrant dans la composition des ciments CPJ fabriqués en France.

Ce rapport tentera de faire le point sur l'apport des techniques ou des méthodes nouvelles dans la caractérisation et l'activation des laitiers, des pouzzolanes et des fillers, tous matériaux qui peuvent en premier lieu être localisés sur le diagramme ternaire CaO, SiO_2, Al_2O_3 (fig. 1).

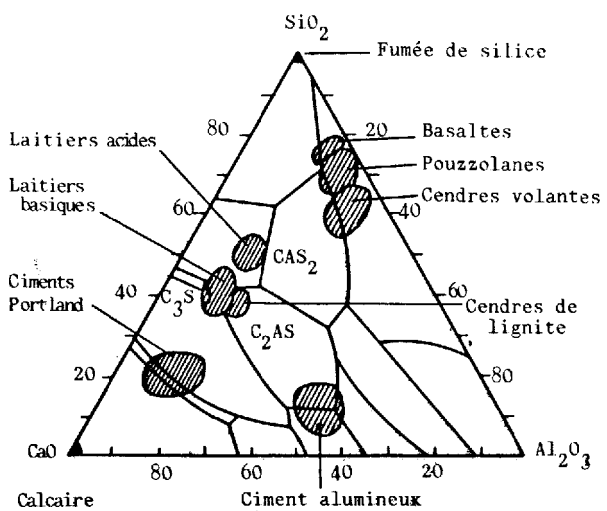

Fig 1 - Diagramme ternaire $CaO-Al_2O_3-SiO_2$. Position des différents produits d'addition par rapport aux oxydes et au Ciment Portland.

2. LES LAITIERS DE HAUT FOURNEAU

Dans son rapport principal au Congrès de Paris, HG. SMOLCZYK (1) a rappelé la formation du laitier fondu surnageant la fonte et sa trempe soit par granulation, soit par bouletage. En moyenne, le laitier contient 35 % SiO_2, 40 % CaO, 8 % MgO, 12 % Al_2O_3. Un refroidissement lent entraîne la cristallisation de silicates d'aluminium et de magnésium dont les plus courants sont la mélilite (solution solide entre la gehlénite C_2AS et l'akermanite C_2MS_2) et la merwinite C_3MS_2. le laitier trempé est vitreux. Sa structure a été affinée par R. DRON (10).

2.1. Structure des laitiers vitreux

La trempe fige à la température ambiante une configuration instantanée de la structure désordonnée du laitier fondu apparenté à la famille des silicates liquides. La structure d'un verre de silicate se déduit de celle de la silice vitreuse par la coupure de certaines liaisons Si-O-Si et la neutralisation des charges négatives, créées par des cations métalliques appelés modificateurs de structure.

La première approche de la structure fondée sur les modèles de G.N. TOOP et C.S. SAMIS (11) et C.R. MASSON (12) faisait intervenir des ions oxygène pontants O^o et non pontants O^- (13). La nouvelle conception utilise l'ion O^{2-} et le niveau de basicité du milieu caractérisé par le p_F (grandeur analogue au pH des solutions aqueuses) qui détermine le taux de neutralisation de la silice et l'activité des oxydes MO. Le p_F est déduit des spectres Raman à excitation laser dont les bandes spectrales caractérisent les éléments structuraux :

SiO_4, $-SiO_3$, $= SiO_2$, $\equiv SiO$, $= Si =$ (14)

S , Z , E , Y , X (10)

Q = 0, Q = 1, Q = 2, Q = 3, Q = 4 (15)

Q = connectivité des tétraèdres SiO_4.

Un spectre Raman de laitiers industriels ou de verres de silicate présente (fig. 2) un massif entre 800 et 1100 cm^{-1} et deux bandes à 680 et 580 cm^{-1}. En se fondant sur les travaux de B. PIRIOU et P. Mc MILLAN (16), R. DRON (10) a attribué la bande :

- 580 cm^{-1} à la vibration Al-O-Al
- 680 cm^{-1} aux espèces silicates E(Q=2) et Z (Q=1)
- 800 - 1100 cm^{-2} aux espèces silicatées Y (Q=3), E(Q=2), Z(Q=1), S(Q=0)

La décomposition du massif à partir des bandes caractéristiques de SiO, SiO_2, SiO_3, SiO_4 (respectivement à 1050, 980, 910 et 850 cm^{-1}) considérées comme Gaussiennes, donne la position, la largeur et la hauteur des pics de chacune des espèces silicatées, estimant ainsi leur proportion dans le matériau et permettant la détermination du p_F. Si $p_F > 1$, il y a tendance à la ségrégation d'espèces basiques comme les orthosilicates, le domaine d'idéalité se situant entre $p_F = -1$ et $p_F = 1$. Le tableau I regroupe quelques cas typiques.

Tableau I - Intensité des composantes du massif haute fréquence du spectre Raman normalisé à 100 et valeurs du p_F (10).

Echantillons	I_Y Q = 3	I_E Q = 2	I_Z Q = 1	I_S Q = 0	p_F
Verres synthétiques					
CS	30.7	45.0	7.2	17.1	0
C_2AS	11.1	20.1	45.6	23.2	1.150
C_6MAS_5	10.0	28.1	34.7	27.2	0.884
Laitiers industriels					
n° 1	10.5	26.4	34.5	28.6	0.910
n° 2	7.7	15.8	39.9	36.5	1.247

Les éléments structuraux de la silice sont, en dehors des tétraèdres SiO_4 isolés, des groupes anioniques condensés dont les charges négatives sont neutralisées par des cations comme Ca^{2+} et Mg^{2+} . Le fait que les spectres des verres dont le magnésium s'est substitué au calcium soient superposables aux spectres des verres purement calciques tend à attribuer le même rôle à CaO et MgO, tous deux pouvant être considérés comme des bases fortes. Le même traitement théorique appliqué aux systèmes acide-base de l'aluminium identifie l'espèce cationique complexe AlO^{+} et l'ion Al^{3+} . L'aluminium se place, quant à sa configuration ionique, entre le silicium covalent et le calcium ionique. Il joue le rôle d'une base faible. La structure du laitier peut être assimilée à celle d'un filet dont l'ossature est formée du réseau silicaté covalent et dont certaines mailles ont été sectionnées aux points les plus faibles (fig. 3). La réactivité hydraulique du laitier est liée au caractère cationique de l'aluminium qui se dissout en premier, le réseau silicaté et calcique étant hydrolysé en un second temps.

La coordination des ions Al et Mg et le degré de polymérisation ont été étudiés par ailleurs dans des verres synthétiques de composition proche de celle des laitiers de haut fourneau. S. GOTO, T. YOSHU et M. DAIMON (17) ont mesuré, par spectroscopie de fluorescence X, les déplacements chimiques de AlKα par rapport au pic AlKα du métal. Les déplacements sont de l'ordre de 0,22eV, mais les largeurs à mi-hauteur des raies sont comparables à celles des Al tétracoordonnés. D'après le calcul de l'orbitale moléculaire, le niveau d'énergie du spectre de Al peut varier mais le profil du spectre reste le même. Donc, les Al sont trétracoordonnés à l'oxygène et l'histoire thermique ne modifie pas la coordination de l'aluminium dans ces verres synthétiques.

Y. RUN-ZHANG, O. SHI-XI et G. GIANG-YING (18) ont déduit la coordination des ions Al et Mg dans des verres du système $CaO-MgO-Al_2O_3-SiO_2$, de la comparaison des spectres de fluorescence X de minéraux connus. Des mélanges de kaolinite (Al octaédrique) et feldspath potassique (Al tétraédrique) d'une part, de forstérite

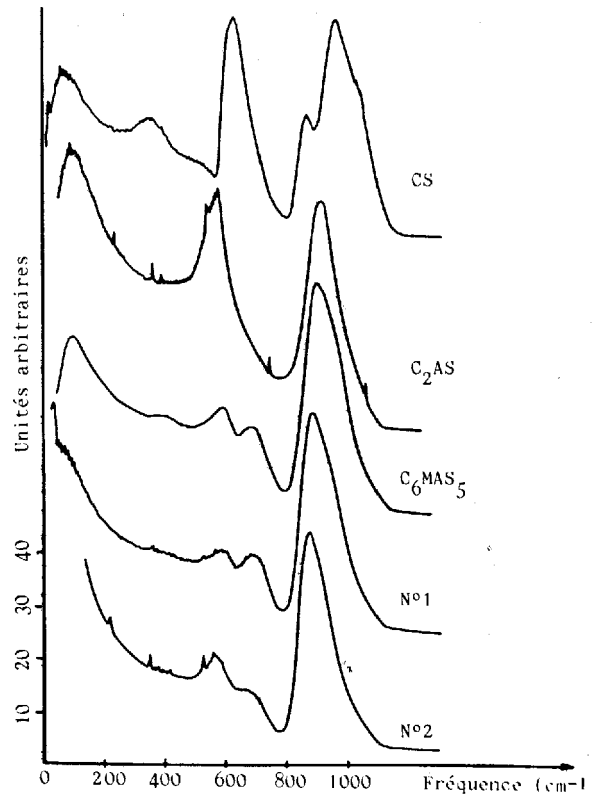

Fig. 2 - Spectres Raman de différents silicates, aluminosilicates et laitiers de haut fourneau (10)

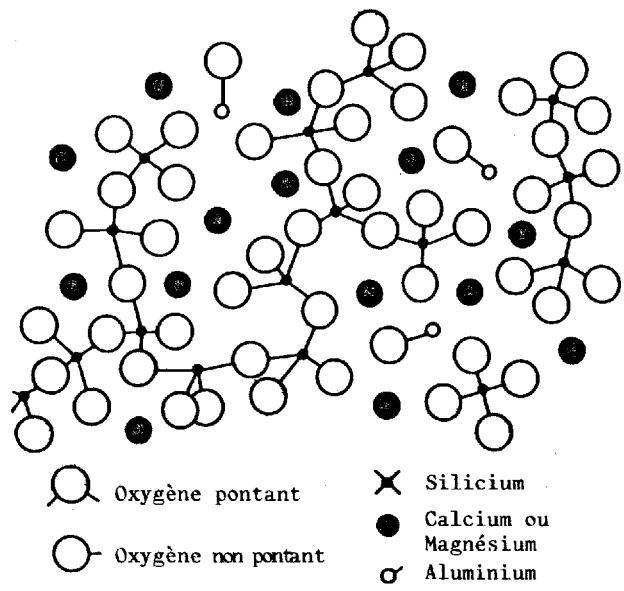

Fig 3 - Représentation schématique de la structure vitreuse d'un laitier (10)

(Mg octaédrique) et de picotite (Mg tétraédrique) ont été utilisés comme témoins. Les rapports MeO6/MeO4 varient de 0,14 à 2,13 dans les laitiers considérés. Les meilleures performances mécaniques des ciments contenant 50 % de ces laitiers ont été atteintes quend le rapport MeO6/MeO4 était égal à 0.5.

S.M ROIAK et J. Ch. CHKOLNIK (19) étudiant la liaison Me-O ont, par résonance paramagnétique électronique et spectrométrie d'absorption infra rouge, trouvé que Al est en coordinance 6 et qu'il joue un rôle important dans la dépolymérisation des espèces silicatées et l'activité hydraulique du laitier.

Le degré de polymérisation de la silice a été estimé par spectrométrie infra rouge dans des verres du système $CaO-SiO_2-Al_2O_3-Fe_2O_3-MgO$ (20). L'activité hydraulique croît dans le même sens que celui des liaisons ioniques, mais jusqu'à une certaine limite qui correspond à la cristallisation de silicates dont la réactivité décroît dans l'ordre suivant : $C_2S > C_2AS > C_3S_2 > CS$.

Des défauts de structure ont été mis en évidence, dans des verres de gehlénite et de laitier synthétique par P. FIERENS et P. POSWICK (21). La thermoluminescence et l'exoémission électronique révèlent l'influence de la trempe sur les caractéristiques énergétiques et entropiques des défauts de l'état vitreux et en conséquence sur la vitesse d'hydratation.

2.2 Structure et composition des laitiers industriels

Les laitiers industriels vitreux présentent en diffraction des Rayons X, un halo large et diffus centré à 3 Å (fig. 4). Ce halo est l'image du degré d'ordre local qui existait dans le liquide et qui a été figé par la trempe. Par contre, il n'existe aucun ordre à grande distance comme dans les cristaux. Une analyse à la microsonde électronique des éléments Ca, Al, Si, Mg révèle dans certains cas une distribution homogène d'un grain à l'autre et à l'intérieur de chaque grain, ce à l'échelle du micron. Une composition de verre correspondant à la formule $C_{5,6}AM_{0,73}S_4$ (22) a donné après dévitrification par chauffage à 1000°C, une mélilite dont la composition élémentaire est celle du verre d'origine. En fait, les laitiers totalement vitreux et de composition homogène sont rares. Des hétérogénéités de composition sont aisément décelables.

Les laitiers qui ne sont que partiellement vitreux se caractérisent en diffraction des Rayons X par une superposition à l'anneau de corps aniorphe, de raies bien définies (fig. 4). Les minéraux ainsi identifiés sont essentiellement une mélilite, la merwinite et accessoirement du quartz, de la calcite, de l'oldhamite et des oxydes de fer. L'observation au microscope électronique à balayage montre que certains grains contiennent des domaines orientés de microcristaux le plus souvent sous forme dendritique (23). Ces domaines correspondent à un stade précoce de cristallisation dans lequel seuls se sont développés les arêtes et les sommets des cristallites (24) (fig. 5). L'analyse élémentaire à l'aide du spectromètre X en dispersion d'énergie ou à la microsonde électronique révèle des hétérogénéités dans la répartition des principaux éléments. E. DEMOULIAN, P. GOURDIN, F. HAWTHORN et C. VERNET (23) ont trouvé un enrichissement du verre en alumine et éléments mineurs dans un laitier contenant 35 % de merwinite (Tableau II). Les corrélations simples ou multiples entre la composition de ce verre et les résistances mécaniques des mortiers de ciments contenant 76 % de laitier permettent de déduire que le verre est plus réactif que le laitier de composition moyenne. En conclusion de cette étude, une vitrification parfaite n'est pas le critère d'une réactivité maximale. Les cristaux de merwinite (de 0 à 5 %) accroissent les résistances mécaniques. Au-delà de 5 % de C_3MS_2 et jusqu'à 35 %, les baisses de résistances ne sont que de faible amplitude. Ce résultat important a été depuis confirmé par J.P.H FREARSON, et J.M. UREN (25) qui ont observé au microscope électronique à balayage des zones hydratées plus larges autour des grains de laitier vitreux contenant en inclusions des cristaux dendritiqus de merwinite que celles des particules totalement vitreuses.

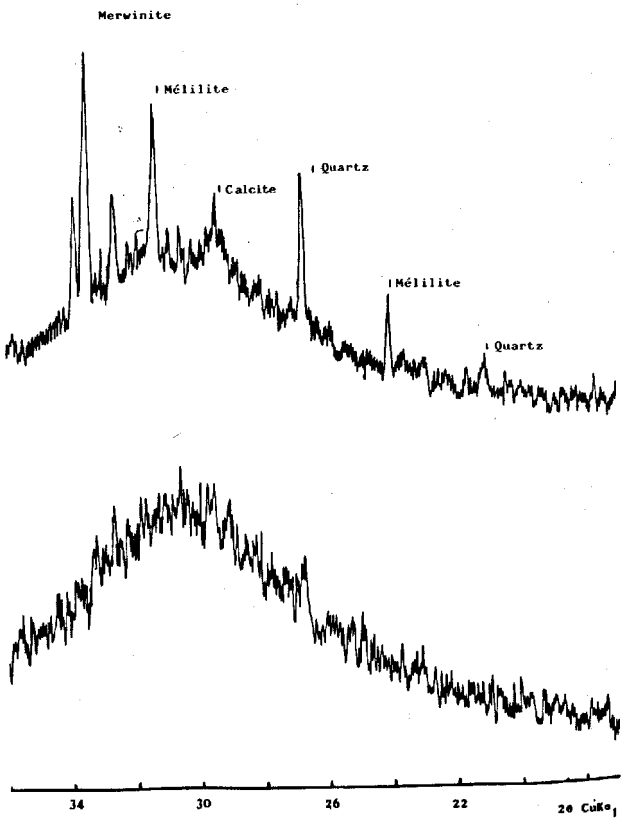

Fig 4 - Diagrammes de diffraction des Rayons X d'un laitier totalement vitreux (halo de corps amorphe) et d'un laitier partiellement cristallisé.

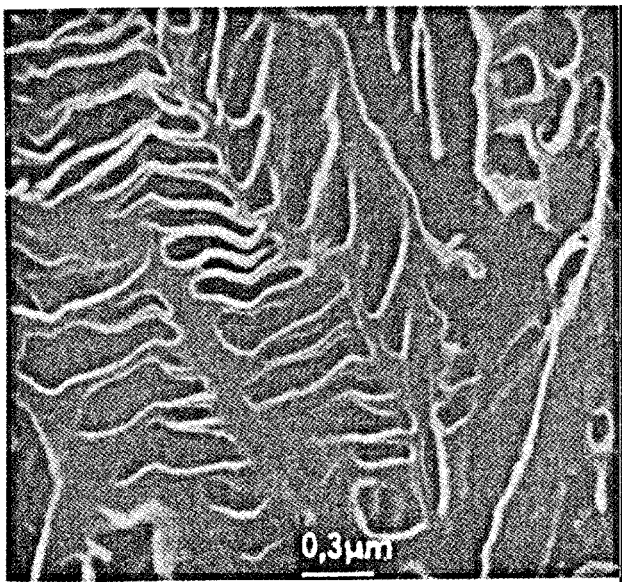

Fig 5 - Cristallisation dendritique de la merwinite dans un laitier vitreux (24).
Section polie attaquée par NH_4Cl.

Tableau II - Analyse chimique globale d'un laitier contenant 35 % de merwinite et analyse élémentaire à la microsonde de la fraction vitreuse (23).

	laitier	verre
SiO_2	33.6	32.0
Al_2O_3	11.1	17.0
FeO	0.89	1.37
MnO	0.64	0.98
TiO_2	0.55	0.85
CaO	42.1	37.2
MgO	8.7	6.7
Na_2O	0.38	0.58
K_2O	0.81	1.25
S^-	1.10	1.69
F^-	0.09	0.14
Cl^-	0.044	0.068

P.W SCOTT, S.R. CRITCHLEY et F.C.F. VILKINSON (26), analysant des laitiers granulés et bouletés, vitreux à plus de 95 % ont trouvé, en général, une composition du verre proche de celle du laitier. Cependant, des différences systématiques ont été mises en évidence dans les laitiers les plus riches en alumine. Dans ce cas, les cristaux de mélilite sont proches de la gehlénite et le verre contient plus de silicium et moins d'aluminium que la composition globale. Malgré la présence de cristaux d'oldhamite CaS, le verre n'est pas appauvri en soufre relativement à la composition globale.

H. ROPER (27) a également observé une certaine hétérogénéité dans le verre de laitiers trempés à l'eau ou à l'air ou encore bouletés. Ces laitiers sont considérés comme des liquides de Stuart étant donnée leur grande facilité à cristalliser en particules aciculaires.

A une échelle plus fine que celle du microscope électronique à balayage, la diffusion des Rayons X a identifié des microhétérogénéités de 300 à 900 Å (28) et la thermoluminescence ou l'émission d'exoélectrons, des défauts superficiels (29). Microhétérogénéités et défauts superficiels modifient l'état énergétique du système et infuencent favorablement l'hydratation. La spectrométrie de photoélectrons XPS aussi appelée ESCA (Electron Spectroscopy for Chemical Analysis) donne la composition élémentaire superficielle des grains de laitier (fig. 6) . Le suivi de l'hydratation par la mesure de la variation des rapports caractéristiques Ca/Si et Al/Si dans la couche superficielle de 60 Å d'épaisseur prouve que le laitier réagit dès son contact avec l'eau et se dissout d'une manière incongruente.

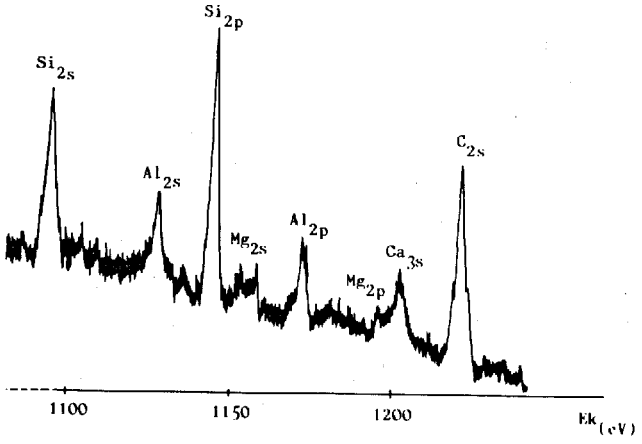

Fig. 6 - Spectre XPS d'un laitier granulé vitreux contenant 44,5 % CaO, 33,9 % SiO_2 , 14,6 % Al_2O_3 et 4,7 % MgO (30). Le carbone C_{2S} sert de témoin.

La spectrométrie de masse quadripolaire a identifié et dosé les gaz occlus (31). Ce sont dans les huit laitiers étudiés et par ordre d'importance décroissante H_2, N_2, CO, H_2O, A, CO_2.

La composition minéralogique potentielle des laitiers vitreux a été calculée par P. GOURDIN (32) à partir des principaux oxydes SiO_2 , Al_2O_3, CaO, MgO déterminés par analyse chimique et des phases cristallisées susceptibles d'apparaître au cours de la dévitrification i.e. C_2AS, C_2MS_2, CS, C_3S_2 , C_3MS_2 , C_2S. Les équations établies conduisent à conclure que les laitiers de haut fourneau utilisés en cimenterie sont potentiellement constitués de C_3S_2 , C_2AS et C_2MS_2 pour 95 %, de CS ou C_3MS_2 ou C_2S pour 5 %. La composition ainsi définie, a été retrouvée par diffraction des Rayons X après dévitrification des laitiers par un traitement à 1000°C pendant 24 heures et un refroidissement lent.

Un traitement à 850°C de différents laitiers entraîne la cristallisation d'une mélilite et dans certains cas, de la merwinite. Celle-ci disparaît après un traitement à 1000°C (24). Les mélilites de recristallisation différent par leurs paramètres cristallins, intermédiaires entre ceux de la gehlénite et de l'akermanite, et par la largeur des raies de diffraction des Rayons qui peut être considérée comme un paramètre d'ordre. Les thermogrammes en analyse thermique différentielle présentent plusieurs signaux, le premier est attribué à la merwinite, les suivants à la structuration de la mélilite.

2.3. Caractérisation des laitiers

L'analyse chimique et structurale des laitiers industriels tente de relier les caractéristiques des produits anhydres à leur réactivité hydraulique et en conséquence aux performances des ciments au laitier.

- Des *indices ou modules d'hydraulicité* ont été établis à partir des principaux oxydes CaO, MgO, Al_2O_3, SiO_2. Le plus utilisé est $\frac{C+M+A}{S}$. Il entre dans les spécifications de certains pays comme la République Fédérale d'Allemagne i.e. DIN 1164 : $\frac{C+M+A}{S} > 1$ (valeur également adoptée par la Grande-Bretagne) et le Japon où $\frac{C+M+A}{S} > 1.4$. Il n'existe cependant aucun module simplifié unique pouvant prévoir par exemple la résistance mécanique d'un ciment au laitier à 2, 7, 28 jours. En prenant en compte l'analyse chimique complète et plus particulièrement les éléments mineurs Fe, Ti, Mn, S, K, Na, F, Cl et le taux de vitrification, E. DEMOULIAN et al (23) ont obtenu des coefficients de corrélation multiples de 0,97 , 0,94 et 0,93 respectivement à 2,7;28 jours (résistances de mortiers ISO, ciment contenant 76 % de laitier) à comparer aux meilleures corrélations simples 0,91 , 0,82 , 0.84 données dans les mêmes conditions par l'indice $\frac{C+M+A}{S}$. Ces résultats montrent l'importance d'une part des éléments mineurs le titane par exemple déjà étudié par S.M. ROIAK et J. Ch. CHIKOLNIK (19), le fluor, le sodium, le chlore, d'autre part du degré de cristallisation.

- L'estimation du *degré de cristallisation* du laitier ou de son complément le *taux de vitrification* peut être atteinte par deux méthodes, la diffraction des Rayons X et la microscopie optique. Parce qu'il existait des différences dans les données de ces méthodes, une optimisation des procédures a été entreprise (33 - 34 - 35). R.D. HOOTON et J.J. EMERY (33) pratiquent la méthode de l'étalon interne (10 % CaF_2) et des témoins synthétiques (C_2MS, 50 % C_2MS_2 - 50 % C_2AS, C_3MS_2, CMS_2 et CMS) dans l'analyse quantitative par diffraction des Rayons X. Leur méthode microscopique (Méthode Mc Master modifiée) utilise la lumière transmise polarisée et une lamelle de gypse qui colore en rose les particules vitreuses et en jaune ou bleu les particules cristallisées. Le comptage de 150 particules, de taille comprise entre 45 et 63 μm range les grains non biréfringents mais d'éclat laiteux en nicols croisés, dans la fraction cristalline. Il existe une bonne corrélation entre les résultats de la diffraction des Rayons X et le comptage microscopique. Différents indices d'hydraulicité ont été testés dans la prévision des résistances mécaniques. Celui incluant le pourcentage de verre, de CaO, SiO_2 et Mn donne les meilleures corrélations à 7 jours soit: R = 0.688 (verre) + 3.03 (CaO) - 7.97 (SiO_2) - 14.24 (Mn) + 177.1 avec r = 0.943, pour 37 laitiers de nature différente et des résistances mécaniques mesurées sur des cubes de mortier.

Les résultats d'une analyse quantitative réalisée au CERILH (34), en collaboration avec J.P.H.FREARSON, I. SIMS et J.M. UREN (35), sur des laitiers de provenances diverses, en utilisant la méthode microscopique BS 81/12794 DC et la diffraction des Rayons X sont groupés dans le tableau III.

Le comptage microscopique effectué sur 1000 grains ne tient compte que des particules biréfringentes. La diffraction des Rayons X, méthode de l'étalon interne s'appuie sur les témoins que sont les produits de recristallisation des laitiers après une heure à 900°C et un refroidissement lent. La microscopie optique surestime systématiquement la part cristallisée par rapport à la DRX. probablement en raison de la cristallisation dentritique et de l'enrichissement en verre de la fraction fine bien trempée.

Tableau III - Dosage de la fraction cristalline par DRX et microscopie optique. Le minéral est C_3MS_2.

laitier	DRX: échantillon tout venant broyé % de merwinite	Microscope optique fraction 40-63μm % de cristaux
1	2	3,5
2	3	7
3	6	13,5
4	7	14
5	17	26

J.P.H. FREARSON, I. SIMS et J.M. UREN (35) ont mis au point une méthode de dosage par microscopie optique par réflexion. Les échantillons sont des sections polies attaquées par une solution d'acide nitrique dans l'éthanol. Le microscope métallurgique de haute résolution distingue:

. le verre : brun clair.

. les cristaux : aciculaires, globulaires, dendritiques bleuâtres de merwinite ou à section carrée sans couleur et au relief prononcé de mélilite.

. les particules de fer: éclat métallique.

. la résine d'enrobage très uniforme.

Le comptage s'effectue sur 500 points. Les résultats de l'analyse de sept échantillons, comparés à ceux de la DRX apparaissent dans le tableau IV. Il existe une excellente corrélation pour les laitiers A, B, G. Les différences observées dans les autres échantillons sont à relier à la difficulté d'estimation du verre dans un grain partiellement dévitrifié. Au contraire, la microscopie optique caractérise le type de cristallisation des particules dévitrifiées, ce que ne fait pas la diffraction des Rayons X.

Tableau IV - Estimation du taux de verre dans des laitiers, par microscopie optique et DRX (% en poids)

Laitier	Microscopie optique	DRX
A	70	70
B	65	66
C	70	74
D	61	68
E	79	75
F	51	44
G	90	90

E. DEMOULIAN, C. VERNET, F. HAWTHORN et P.GOURDIN (36) ont élaboré une méthode de détermination de la teneur en laitier dans un ciment, par dissolutions sélectives. Une solution contenant de l'EDTA (Acide éthylénediamine tétraacétique) de la triethanolamine et de la soude dissout complètement à pH = 11,5 le clinker et le sulfate de calcium. La soude évite la précipitation de la silice ou des hydroxydes. Le laitier se retrouve dans le résidu et peut être examiné au microscope. C'est une méthode plus rapide que la séparation par liqueurs denses ou la microscopie optique.

2.4. Activation des laitiers

Le laitier est hydraulique. Bien qu'il puisse réagir dès les premiers instants, comme l'ont montré les courbes de chaleur d'hydratation (24), de spectrométrie de photoélectrons (30), de conductance (37), ou de dissolution (38), le laitier s'hydrate plus lentement que le ciment Portland. Il peut cependant être activé par différentes voies: chimique, mécanique, thermique.

- Activation chimique

Comme M. VON EUW l'a rappelé dans son rapport général au Congrès de Paris (6), activer chimiquement le laitier, c'est le maintenir dans un milieu à pH suffisamment élevé par addition de soude, de chaux, de silicate ou de carbonate de soude. Les sulfates de calcium, le gypse, l'hémihydrate, l'anhydrite, le phosphogypse et le chlorure de calcium sont aussi des activants bien connus.

De nouveaux ciments au laitier sont apparus:

. le silicociment (39), mélange de laitier broyé, de métasilicate de soude, de gypse (naturel ou phosphogypse) et éventuellement de filler calcaire.

. le ciment F (40), mélange de laitier broyé et d'adjuvants chimiques (5 à 8 %) qui sont un activant alcalin et un plastifiant réducteur d'eau lignosulfonate. Le ciment F se présente sous forme de poudre ou de solution. Utilisé dans le béton, l'effet d'entraînement d'air du lignosulfonate peut être réduit par l'utilisation d'un produit anti-moussant (41).

. le ciment avec addition de SAS (42)
Le SAS est un produit polyminéral sulfoalumino-siliceux qui confère au ciment de laitier des performances mécaniques aussi élevées que celles d'un ciment Portland.

Dans les ciments au laitier plus traditionnels, l'activant est le clinker de ciment Portland.

L. VERNET et al (37) ayant mis en évidence les couplages chimiques entre le clinker et le laitier qui se dissolvent simultanément mais à des vitesses différentes (6), F. HAWTHORN et al (43) ont étudié les influences réciproques laitiers-clinkers dans des ciments contenant 80 % de laitier. Le clinker active le laitier mais les résistances à 1 jour du ciment, sont beaucoup plus fonction de la qualité du laitier que de la nature du clinker. A 28 jours, la composition du clinker intervient i.e. les meilleures performances sont obtenues avec des clinkers riches en C_3S et en C_3A orthorhombique (contenant des alcalins dans son réseau cristallin) pour des laitiers broyés finement. Les résistances à un an sont en relation avec la finesse du laitier.

J. METSO et E. KAJAUS (44) ont comparé l'activation de laitiers de haut fourneau (contenant de la gehlénite et de la merwinite) par différents produits minéraux : clinker, NaOH, $Ca(OH)_2$, Na_2CO_3. Na_2SiO_3 ciment alumineux, phosphogypse, cendres volantes + NaOH, Na_2CO_3 + NaOH.La meilleure activation est obtenue avec le clinker de ciment Portland. L'adjuvant F (lignosulfonate + sels de sodium) a un effet activant aussi important que celui du clinker.

- Activation mécanique

La finesse de broyage du laitier intervient dans son couplage avec le clinker (43) et joue un rôle très positif dans les résistances finales (45). V.A. DIMITRIEV et al (46) activent mécano-chimiquement les ciments au laitier par broyage dans un broyeur à jet qui détruit le squelette du réseau silicaté et active les ions oxygène.

- Activation thermique

R.D. HOOTON et J.J. EMERY (47) ont autoclavé différents laitiers bouletés dans des mélanges avec du clinker de ciment Portland et de silice fine (farine de silice). Le principal hydrate formé est la tobermorite. A.A. GOVOROV, E.V. DJONSS et F.D. OVTCHARENKO (48) ont traité à l'autoclave pendant 48 heures à 250°C des coulis préparés à partir de 17 verres dont la composition chimique varie de 20-45 % CaO, 5-30 % Al_2O_3, 5-70 % SiO_2, à teneur en MgO constante, soit 5 %. Les laitiers les plus performants se situent dans deux zones particulières du diagramme $CaO-MgO-Al_2O_3-SiO_2$ (à 5 % MgO) i.e.domaine de cristallisation de la pseudowollastonite et du pyroxène et domaine de cristallisation de l'anorthite. Les résistances élevées ont été attribuées à la formation de la gyrolite et de la tobermorite dans le premier cas, de la tobermorite et de l'anorthite hexagonale, dans le second. L'accroissement de MgO (17 à 18 %) dans des laitiers acides (Al_2O_3 13-17 %) a entraîné des résistances initiales plus élevées des coulis autoclavés (49).

3. LES LAITIERS D'ACIERIE

Les laitiers d'aciérie provenant de convertisseurs à oxygène contiennent de la chaux et de la magnésie libres, des oxydes de fer qui, bien que phases mineures, risquent d'entraîner une expansion des ciments.

La teneur maximale en chaux libre a été fixée à 3 % dans des laitiers chinois, hydrauliques par la présence de C_3S, d'après Y.J. WANG ET G.X. XIE (50). La magnésie peut être de l'ordre

de 18 %. Elle est partiellement combinée dans les silicates ou en solution solide avec FeO et MnO. La teneur optimale en MgO a été fixée par le rapport $\frac{MgO}{FeO + MnO}$ qui doit rester inférieur à l'unité. Le périclase MgO responsable des expansions a pu être annihilé par L. SHONSUN (51) grâce à l'addition de laitier de haut fourneau de cendres volantes, de sulfate de magnésium, ou par un traitement préalable de carbonatation.

Une modification de la composition d'un laitier LD produit par le procédé BOP (Basic Oxygen Process) a été obtenue par M. CONJEAUD, C.M. GEORGE et F. SORRENTINO (52) en ajoutant pendant l'affinage de l'acier, un produit synthétique contenant $CaO-Al_2O_3-MgO-Fe_2O_3$ appelé CAM FLUX, en proportions calculées d'après les diagrammes de phase. L'addition d'alumine (entre 6 et 15 % du produit final) conduit à un laitier hydraulique cristallisé contenant 43 % C_2S, 23 % d'une solution solide (Ca, Fe, Mn), 0,29 % C_4AF et 4 % $3CaO\ P_2O_5$.

Une tentative d'utilisation de laitiers BOF (Basic oxygen Furnace) comme granulats dans un béton a montré la formation d'hydrates de C_2S et C_2F à la surface des grains de laitier qui sous l'action du CO_2 atmosphérique se carbonatent en calcite et carboaluminate hydraté. Une chute des résistances mécaniques en fonction du temps a été attribuée par M. KAWAMURA et al (53) à une faible liaison ciment-laitier.

4. LES LAITIERS DE METAUX NON FERREUX

Parmi les laitiers de métaux non ferreux figurent le laitier de magnésium qui a des propriétés hydrauliques et les laitiers de nickel, de cuivre et de plomb qui sont des produits pouzzolaniques.

. *laitier de magnésium*

Le laitier de magnésium produit en France à partir de dolomites décarbonatées réduites par le silicium, se présente sous deux formes (54). Le matériau refroidi à l'air est pulvérulent, constitué de $\gamma\ C_2S$ principalement, et de $C_{12}A_7$. Le matériau trempé à l'eau est granulé. Partiellement vitreux, il contient $\beta\ C_2S$ et C_3AH_6 cristallisés. Les deux formes s'hydratent en C_2ASH_8 et $C_4AH_{13} - C_3AH_6$ cristallisés, la première réagissant plus rapidement que la seconde. Un mélange des deux variétés a conduit A. CARLES-GIBERGUES, B. THENOZ et A. VAQUIER (54) à optimiser un liant alumineux dans lequel les deux laitiers réagissent mutuellement.

. *laitiers de cuivre, de nickel et de plomb*

Les laitiers de cuivre étudiés séparément par J.R. BARAGNO et P. REY (55) et H. ROPER, K. KAM et G.J. AULD (56) sont constitués d'une matrice vitreuse partiellement cristallisée en fayalite Fe_3SiO_4 et oxydes de fer Fe_3O_4, Cr_2O_3FeO. Ce sont des produits pouzzolaniques qui réagissent avec $Ca(OH)_2$ donnant des CSH amorphes ou alvéolaires et peuvent donc être utilisés dans les ciments.

Le laitier de nickel granulé est après broyage, plus réactif qu'une cendre volante d'après le test de pouzzonalicité ASTM C595 effectué par J. LANEUVILLE (57). Neuf laitiers canadiens de cuivre, de nickel et de plomb testés par E. DOUGLAS, V.M. MALHOTRA et J.J. EMERY (58) ont développé des résistances mécaniques proportionnellement à leur degré de vitrification. E. DOUGLAS et P.R. MAINWARING (59) ont caractérisé et hydraté deux laitiers de cuivre provenant d'un four à réverbère. Le premier laitier trempé à l'air, contient 41 % de verre, 57 % de fayalite, 5 % de spinelle. Le second laitier trempé à l'eau est composé suivant les échantillons de 75 à 95 % de verre, 15 à 5 % de fayalite, 10 à 0 % de spinelle. Le verre analysé à la microsonde électronique est plus riche en Al_2O_3, SiO_2, K_2O, CaO dans le laitier trempé à l'air que dans le laitier trempé à l'eau. Ce dernier renferme plus d'oxyde de fer que le premier. Tous deux pourraient être utilisés dans un ciment composé.

5. LES "LAITIERS" DE GAZEIFICATION DU CHARBON

Les "laitiers" de gazéification du charbon se présentent sous l'aspect d'une gangue noire et vitreuse qui, liquide à la température de combustion (1500 - 1700°C), a été trempée à l'eau. Il existe différents procédés de production de ces laitiers dans lesquels une fraction du résidu peut se retrouver sous la forme de cendres volatiles. Ces procédés ont été décrits par D. RAVINA (60), P.L. OWENS (61), P.J. NIXON, G.J. OSBORNE et C.N. SHEPPERD (62). L'observation microscopique sur lames minces confirme l'isotropie à plus de 95 % du matériau. Sur cinq laitiers étudiés par P.J. NIXON et al (62), quatre contenaient 21 à 34 % CaO, 33 à 38 % SiO_2, 18 à 23 % Al_2O_3, 5 à 21 % Fe_2O_3 et pouvaient être considérés comme des produits pouzzolaniques. Le cinquième avec 4 % CaO, 33 % SiO_2, 15 % Al_2O_3 et 6 % Fe_2O_3 était un produit hydraulique.

6. LES CENDRES VOLANTES

Les cendres volantes sont collectées dans les dépoussièreurs électrostatiques ou mécaniques des centrales thermiques à charbon. Dans le procédé de combustion sèche, le charbon est brûlé à une température variant de 1100 à 1400°C. La caractérisation des sous-produits de la combustion et de la gazéification du charbon a été largement traitée depuis le Congrès de Paris (4, 5, 7, 9) et en particulier au cours des Symposia de la Materials Research Society présidés par S. DIAMOND en 1981 et G.J. Mc CARTHY en 1984 et 1985. Un groupe de travail créé dans le cadre de la commission RILEM 67 FAB (Fly Ash in Building) présidée par K. WESCHE a rédigé sous la direction de J.L. ALONSO (63) un rapport très complet qui sera présenté à la seconde conférence internationale sur les additions minérales en Avril 1986 à Madrid. De même, la Commission RILEM 73 SBC (Siliceous by Products used in Cements) présidée par P.K. MEHTA rendra compte des spécifications et de l'utilisation des cendres volantes.

6.1. Caractérisation chimique des cendres volantes

Les cendres volantes sont classées par l'ASTM C618 en deux catégories suivant la provenance du charbon et la teneur en $SiO_2 + Al_2O_3 + Fe_2O_3$ (64), soit :

. *cendres de classe F* : anthracite ou charbon bitumineux, $SiO_2 + Al_2O_3 + Fe_2O_3 > 70$ %.

. *cendres de classe C* : lignite ou charbon

subbitumineux, $SiO_2 + Al_2O_3 + Fe_2O_3 > 50$ %.

Le tableau V dû à G. FROHNSDORFF et J.R. CLIFTON (65) donne les domaines de composition des cendres américaines.

Tableau V - Composition de différentes cendres volantes en fonction de la provenance du charbon (65).

Oxyde % en poids	Anthracite	Bitumineux	Subbitumineux
SiO_2	47 - 68	7 - 68	17 - 58
Al_2O_3	25 - 43	4 - 39	4 - 35
Fe_2O_3	2 - 10	2 - 44	3 - 19
CaO	0 - 4	1 - 36	2 - 45
MgO	0 - 1	0 - 4	0,5 - 8
Na_2O	-	0 - 3	-
K_2O	-	0 - 4	-
SO_2	0 - 1	0 - 32	3 - 16
TiO_2	1 - 2	0 - 4	0 - 2
P_2O_5	0 - 4	0 - 3	0 - 3

L'ASTM C 618 limite la teneur en SO_3 à 5 % et recommande un taux de Na_2O inférieur à 1,5 %.

La France n'a pas une classification aussi distincte que celle de l'ASTM. Les cendres, suivant leur teneur en CaO et SO_3, sont identifiées comme silicoalumineuses, silicocalciques ou sulfocalciques. Le tableau VI établi par P.C. AITCIN, F. AUTEFAGE, A. CARLES-GIBERGUES et A. VAQUIER (66) montre que :

- la cendre silicoalumineuse correspond à une cendre de classe F.
- la cendre silicocalcique est une cendre de classe C.
- la cendre sulfocalcique n'entre pas dans la classification ASTM.

Tableaux VI - Composition de trois cendres françaises typiques (66).

Oxyde % en poids	Silico-alumineuse	Silico-calcique	Sulfo-calcique
SiO_2	59.4	24.0	13.5
Al_2O_3	22.4	18.5	5.5
Fe_2O_3	8.9	17.0	3.5
CaO	2.6	24.0	59.0
MgO	1.3	1.0	1.8
SO_3	2.4	8.0	15.1
Na_2Oeq	2.2	0.8	-
$SiO_2+Al_2O_3+Fe_2O_3$	90.7	59.5	22.5

La composition chimique globale de la cendre reflète celle du charbon (64), soit :

- *chimique* qui varie dans un large domaine: SiO_2 : 10 à 70 %, Fe_2O_3 : 2 - 50 %, CaO : 0,5 à 30 %.
- *minéralogique:* argiles kaolinite et illite, micas muscovite et biotite, feldspaths orthoclase et albite, oxydes de fer hématite et magnétite, carbonates calcite, dolomite, sidérite, chlorures halite et sylvite, quartz, pyrite, rutile.

Au cours de la combustion du charbon, si les matières organiques brûlent rapidement, la transformation des minéraux est par contre, complexe. Les réactions sont de déshydratation, décarbonatation, désulfuration, volatilisation. Les résidus des particules les plus grossières fondent, s'agglomèrent et se déposent. Les particules les plus fines restent dans le courant d'air où elles sont en suspension sous forme de gouttelettes. Refroidies rapidement elles se figent en sphères vitreuses, les plus grosses d'entre elles contenant une fraction cristallisée. Au cours du refroidissement, les sulfates alcalins de la phase vapeur se déposent à la surface des particules ou cristallisent entre les particules. Le produit final qu'est la cendre volante est par conséquent un matériau hétérogène dont la caractérisation exige une analyse de phase du solide.

6.2. Caractérisation minéralogique des cendres volantes :

Les cendres volantes silicoalumineuses, de classe F sont essentiellement vitreuses. Les cendres silicocalciques, de classe C, sont partiellement vitreuses et la composition du verre est différente de celle des précédentes (67).

- *phase vitreuse*

Une étude détaillée des halos de diffraction des Rayons X a permis à S. DIAMOND (68-69) de différencier la phase vitreuse des cendres suivant leur teneur en CaO (fig. 7). Une relation linéaire entre le pourcentage de chaux de la cendre et le maximum du halo, avec un coefficient de régression r = 0,90, a été établie jusqu'à 20 % CaO (fig. 8). Au-delà de 20 % CaO, la position angulaire du halo ne varie plus.

La phase vitreuse des cendres de classe F s'apparente à la structure des verres siliceux. Le verre des cendres de classe C contenant plus de 20 % CaO est proche de la structure des verres d'aluminate de calcium comme le $C_{12}A_7$. D'après P.K. MEHTA (67), le verre reste un aluminosilicate vitreux qui se rapproche de celui des laitiers de haut fourneau.

Quatre cendres siliceuses ont été observées, sous microscope optique, par B. MATHER (70) qui a considéré les particules isotropes transparentes comme vitreuses. La plupart d'entre elles étaient des sphères de 1 à 2 μm dont environ 10 % contenaient cependant des inclusions cristallines de mullite. Le verre était alors coloré en jaune vert et son indice de réfraction était le plus élevé. La teneur en silice d'un verre peut être estimée à partir de son indice de réfraction. Une relation linéaire inverse a été trouvée entre la teneur en silice de la cendre et l'indice de réfraction des particules vitreuses. Le tableau VII résume les caractéristiques des quatre cendres étudiées.

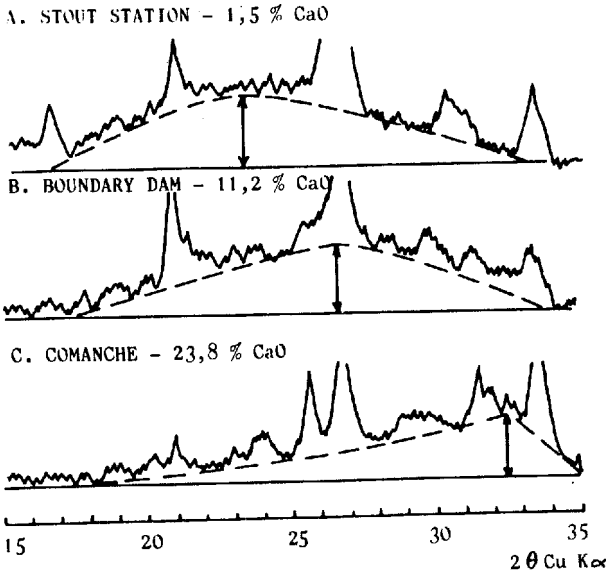

Fig. 7 - Diagrammes de diffraction des rayons X de trois cendres à teneur croissante en CaO. Déplacement du halo caractéristique de la phase vitreuse (69)

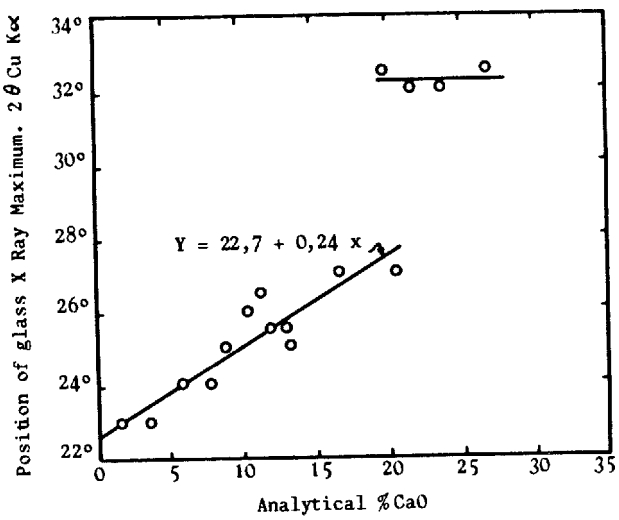

Fig. 8 - Variation de la position du maximum du halo de diffraction des Rayons X en fonction du pourcentage en chaux de la cendre (69)

Les éléments traces qui peuvent se concentrer à la surface des particules de cendre ont été dosés par spectrométrie de masse d'ions secondaires. R.W. LINTON, S.R. BRYAN, B. COX et D.P. GRIFFIS (71) se sont attachés à la détection et à la distribution d'éléments lourds toxiques comme Tl, Pb, U. L'équipement SIMS (Secondary Ion Mass spectrometer) Cameca IMS - 3 f permet, grâce au traitement informatique des images, de tracer le profil de concentration d'un élément en profondeur et de reconstituer sa distribution spatiale dont la résolution dans un plan X - Y est de 1 à 2 μm et en profondeur le long de l'axe Z, de 0,1μm. Le thallium, le plomb, le thorium et l'uranium dont les concentrations sont, dans les cendres, respectivement 3, 54, 39 et 9 ppm en poids ne sont pas répartis uniformément. Les profils de concentration (fig. 9) révèlent un enrichissement superficiel des ions Tl^+, Pb^+ et U^+. Au contraire le thorium et le titane sont répartis dans toute la masse, avec toutefois une hétérogénéité intra et interparticulaire.

Tableau VII - Analyse du verre de quatre cendres siliceuses (70)

Caractéristiques	Cendres de charbon bitumineux			
	A	B	C	D
composition de la cendre				
SiO_2 % en poids	47,2	47,4	38,2	44,9
CaO	5,3	2,3	3,9	2,3
% de verre dans les fractions :				
150 - 75 μm	60	55	35	60
< 75 μm	82	76	52	72
Indice de réfraction des particules vitreuses				
moyenne	1.546	1.557	1.568	1.565
étendue	1,48-1,64	1,52-1,64	1,50-1,68	1,52-1,64

La radioactivité naturelle des cendres volantes australiennes a été mesurée par spectroscopie des Rayons X par J. BERETKA et P.J. MATHEW (72). L'activité de ^{226}Ra, ^{232}Th et ^{40}K ne dépasse pas, en général, la limite spécifiée par les pays de l'OCDE soit 370 Bq/kg ou 10^{-8} curie/kg. La répartition du radium et du thorium diffère suivant la taille des particules de cendres : l'activité est plus élevée dans la fraction fine. Le potassium radioactif est en général distribué uniformément dans les différentes tranches granulométriques.

Les cendres sont considérées par A.R. REID (73) comme biologiquement inertes. Des études cliniques des employés de la CEGB (Central Electricity Generating Board) n'ont révélé aucune lésion pathologique. La limite admise de 10 mg de cendre par m3 de poussière reste valable.

. *phases cristallisées*

Les diagrammes de diffraction des Rayons X des cendres comportent des pics de phases cristallisées qui se superposent à l'anneau de corps amorphe (fig.7) Une étude détaillée de la minéralogie des cendres de lignite et de charbons subbitumineux a été publiée par G.J. Mc CARTHY et ses collaborateurs (74, 75). Une comparaison entre les cendres d'anthracite, de charbons bitumieux et subbitumineux réalisée par B.E. SCHEETZ, D.W. STRICKLER, M.W. GRUTZECK et D.M. ROY (76) et S. DIAMOND (64) indique que les phases cristallisées ne sont pas, à quelques exceptions près, comme le quartz, les minéraux présents dans le charbon mais des constituants secondaires formés dans la zone de combustion. Les minéraux majeurs sont le quartz, la mullite $3Al_2O_3 \cdot 2SiO_2$, la

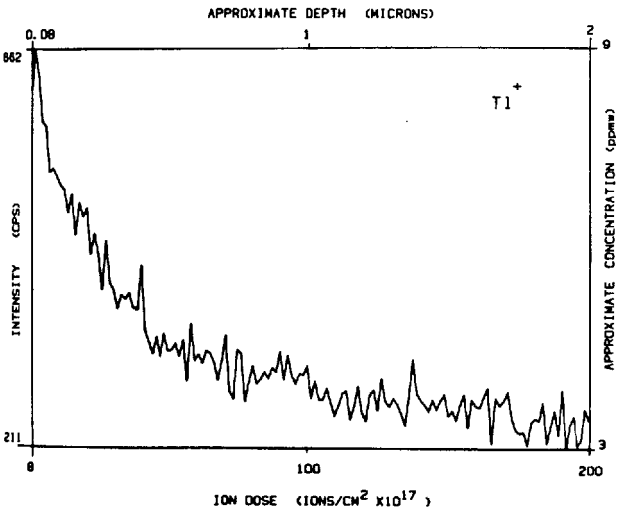

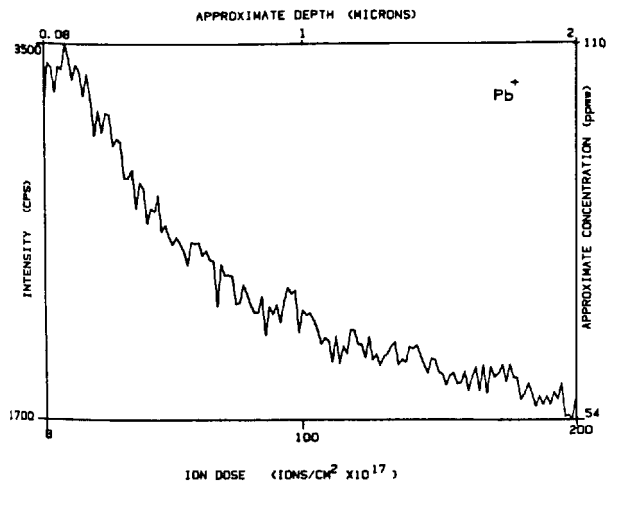

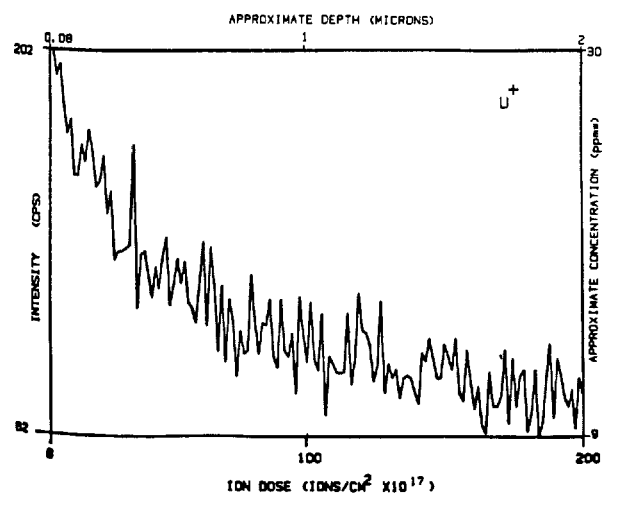

Fig. 9 - Profils SIMS de concentration en profondeur pour les ions Tl^+, Pb^+, U^+ (71)

géhlénite $Ca_2 Al_2 SiO_7$, l'hématite Fe_2O_3, des spinelles proches de la magnétite Fe_3O_4, la périclase MgO, la mervinite $3CaO, MgO, 2SiO_2$, l'anhydrite $NaSO_4$ III l'aphthalite $(Na,K)_2SO4$. Les minéraux mineurs ou les constituants cristallisés n'apparaissant que dans un type de cendre sont la chaux CaO, l'aluminate tricalcique C_3A, les silicates C_3S et C_2S et la phase C_4A_3S dans les cendres silicocalciques.

A l'observation microscopique, les minéraux apparaissent soit en inclusions, soit en dépôts à la surface des particules de cendre. Les cristaux sont caractérisés par leur morphologie et leur analyse élémentaire par spectrométrie X en dispersion d'énergie EDAX sur des surfaces de fracture observées au microscope électronique à balayage par W. RICHARTZ (77). Le quartz (fig.10) et la mullite se sont révélés après dissolution du verre d'une cendre silicoalumineuse dans l'acide fluorhydrique. Les mêmes photos ont été publiées par Y. HALSE, P.L. PRATT, J.A. DALZIEL et W.A. GUTTERIDGE (78) dans le cas de ciments aux cendres hydratés. La découverte de ces cristaux, inaltérés après 28, 90 et 275 jours, prouve leur inertie hydraulique.

Dans une cendre de lignite les principales phases, analysées quantitativement sur sections polies par R.J. STEVENSON (79), sont des silicates de Ca - Mg - Na - Al (mélilite, merwinite, C_2S, néphéline, hématite, périclase). Les phases secondaires (calcite, portlandite, brucite, thénardite, ettringite, gypse, goèthite) se sont probablement formées par réaction avec l'eau ou par précipitation à partir des solutions utilisées dans la manutention des cendres. Les particules de cendre, prises individuellement, varient en composition chimique et minéralogique.

6.3. Morphologie et composition modale des cendres volantes

Les cendres volantes se présentent généralement sous la forme de particules sphériques, pleines ou creuses. Les sphères creuses sont appelées cénosphères (fig. 17). Les sphères qui contiennent des particules de taille variable sont les plérosphères. Le nombre des particules encapsulées peut varier de 10 à 200.

Dans les cendres provenant de charbons insuffisamment brûlés, les fractions résiduelles de charbon sont soit sphériques (fig. 18), soit anguleuses (80) soit poreuses, soit stratifiées (fig.18)

Elles peuvent atteindre 12 % en poids de la cendre siliceuse de classe F et constituent la part la plus importante de la perte au feu.

La composition modale de cendres de charbon bitumineux (cendres PFA: Pulverized Fuel Ash) a été calculée par F.H. HUBBARD, R.K. DHUR et M.S. ELLIS (81) à partir de la diffraction des Rayons X pour le dosage des phases cristallisées mullite, quartz, magnétite, hématite et de la fluorescence X pour l'analyse chimique globale. La phase vitreuse apparaît sous la forme de cénosphères dont la génération résulte de la fusion partielle de l'illite dans la potasse. La mullite provient du métamorphisme de la kaolinite. La proportion de phase vitreuse est essentiellement une fonction de rapport molaire K_2O/Al_2O_3 qui sera

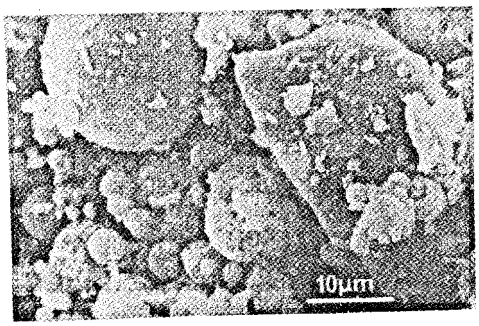

Fig. 10 - Particule irrégulière de quartz après traitement de la cendre à l'acide fluorhydrique (77)

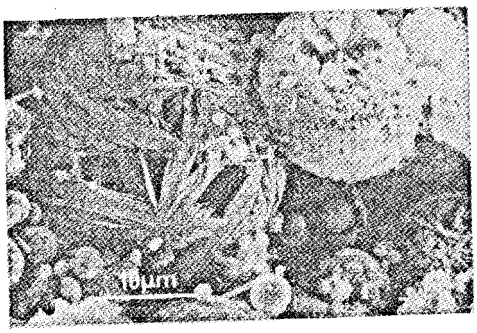

Fig. 11 - Lames de mullite 3 Al_2O_3. $2SiO_2$ après traitement à l'acide fluorhydrique (77)

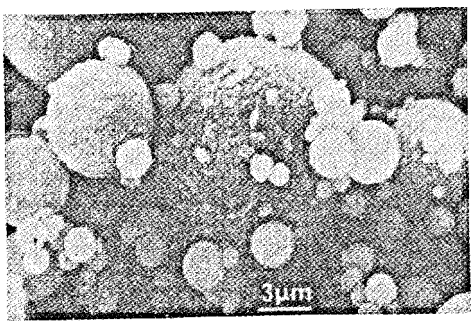

Fig. 12 - K_2SO_4 finement divisé déposé à la surface des grains de cendre (77)

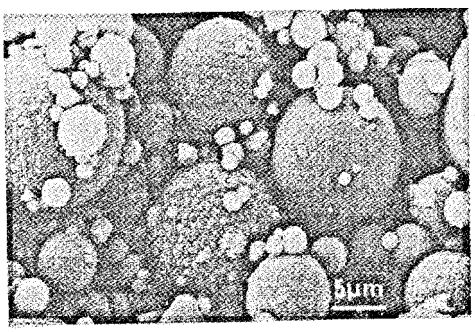

Fig. 13 - $CaSO_4$ finement divisé déposé à la surface des grains de cendre (77)

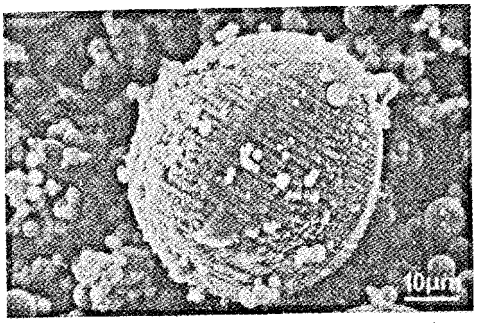

Fig. 14 - F_2O_3 finement divisé à la surface d'un grain de cendre (77)

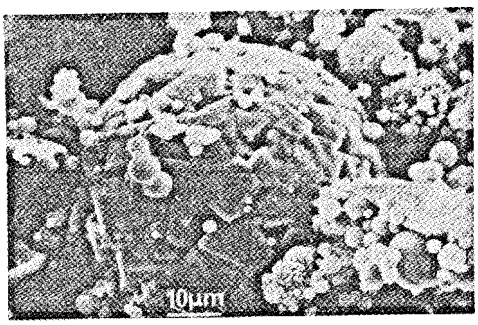

Fig. 15 - Fe_3O_4 cristallisé à la surface d'un grain de cendre

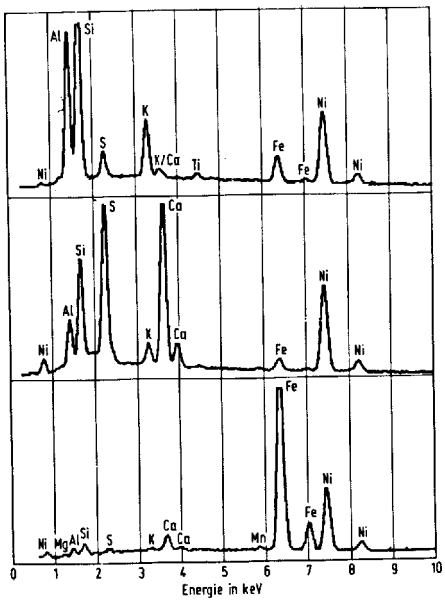

Fig. 16 - Analyse X en dispersion d'énergie de la surface des particules de cendres (77).
Du haut vers le bas:

1. Surface des cendres de la figure 12 : K_2SO_4
2. Surface des cendres de la figure 13 : $CaSO_4$
3. Surface de la cendre de la figure 14 : Fe_2O_3

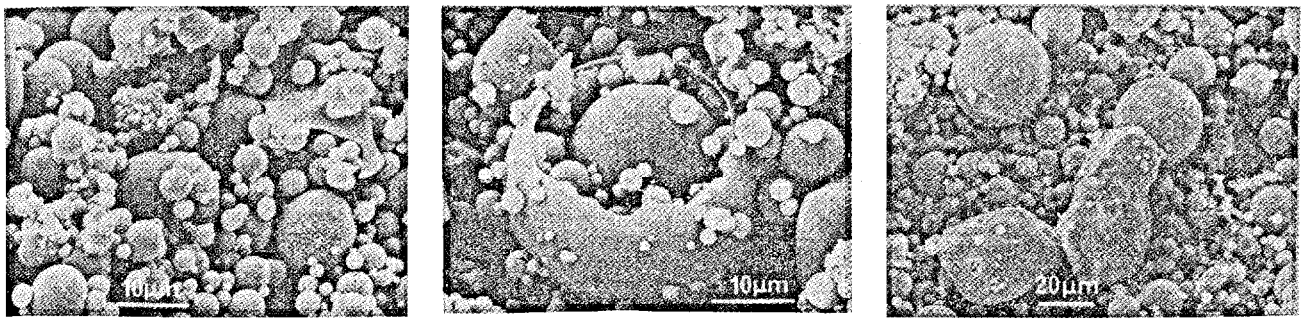

Fig. 17 - Morphologie typique des cendres volantes (1) sphères à surface lisse,(2) plérosphères, (3) grains allongés (77)

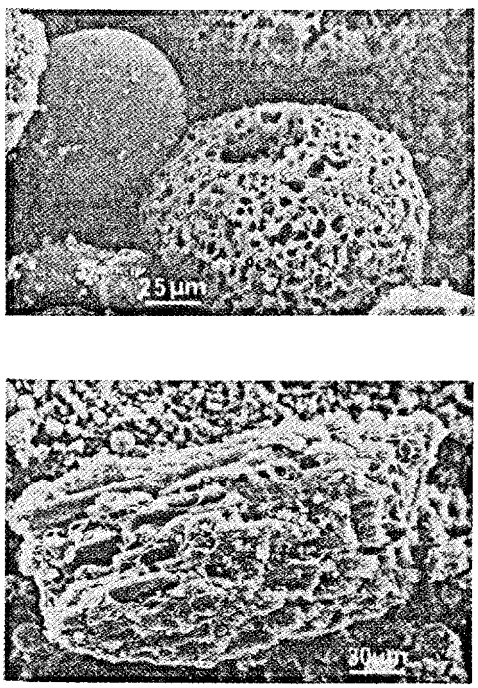

Fig. 18 - Particules de charbon résiduel (77)

utilisé comme un indice de pouzzolanicité potentielle.

6.4. Granularité et surface spécifique des cendres volantes

La spécification ASTM C 618 exige d'une cendre moins de 34 % en poids de particules ne passant pas au tamis n° 325 (45µm). Or, la distribution granulométrique peut être très large et influencer à la fois la réactivité chimique et la demande en eau de la cendre dans un ciment. S. DIAMOND (82) présente la granulométrie des cendres sous forme d'histogrammes. Six tranches ont été retenues i.e. 0 - 5 µm, 5-13, 13 - 26, 26 - 45, 45 - 75, 75 - 115 µm. La largeur de chaque classe, obtenue par la méthode classique de la pipette d'Andreasen, est approximativement 1,6 fois celle de la classe précédente. Quartorze cendres en provenance de l'Indiana ont été comparées à une cendre type de taille moyenne 19 µm avec 12 % des grains >45 µm et 10 % <5 µm. La cendre la plus fine contenait 75 % des grains <5 µm et la plus grossière 75 % >45 µm (fig. 19).

Les cendres de charbon bitumineux en provenance du Canada offrent, d'après R.T. HEMMINGS (83)une distribution de taille assez étendue mais en général, 15 % des grains sont inférieurs à 10 µm. L'observation au microscope électronique à balayage montre que le quartz se trouve plutôt dans les gros grains et la mullite dans la fraction fine.

Une cendre siliceuse française a été broyée par A. CARLES-GIBERGUES et A. VAQUIER (84). La cendre brute contenait 11,5 % de quartz, 4 % de magnétite et 21 % de mullite, proportions de phases cristallisées qui se retrouvent dans différentes tranches granulométriques (de 200 à 1,5 µm) telles que le révèle l'analyse quantitative par diffraction des Rayons X. Le broyage semble essentiellement désagglomérer les particules de cendres entraînant une fluidification du matériau et une demande en eau moindre dans la rhéologie des ciments, mortiers et bétons frais.

Les cendres des centrales américaines modernes ont une distribution de taille de particules qui se déplace vers les faibles dimensions i.e. 40 à 50 % sont inférieures à 10 µm et moins de 20 % sont supérieures à 45 µm. La surface spécifique mesurée par adsorption d'azote est plus élevée que la surface spécifique Blaine. P.K. MEHTA (85) suggère que les très fines particules de chaux et de sulfates alcalins déposés à la surface des sphères contribuent largement à la valeur mesurée, dans le cas des cendres calciques.

Il est préférable, d'après D. RAVINA (86) d'utiliser la méthode de la perméabilité à l'air plutôt que l'analyse granulométrique, dans l'estimation de la finesse des cendres. Les centrales thermiques modernes produisant des cendres fines, la surface spécifique devrait figurer dans la norme ASTM. L'importance de la surface spécifique a aussi été soulignée par K. TUUTTI et G. FAGERLUND (87) qui ont montré que certaines sphères de cendres n'ont qu'une couche vitreuse très superficielle, le centre étant constitué de phases cristallines inertes (quartz et mullite). La surface spécifique Blaine de la cendre est fonction de la finesse de broyage du charbon (88). Les imbrûlés n'ont par contre qu'un effet négligeable.

La densité des cendres mesurée par picnométrie

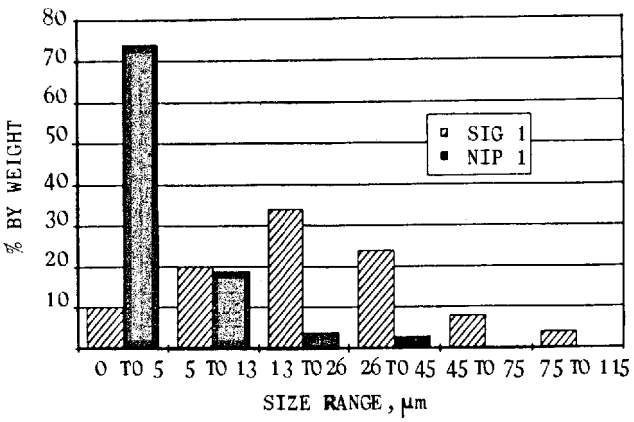

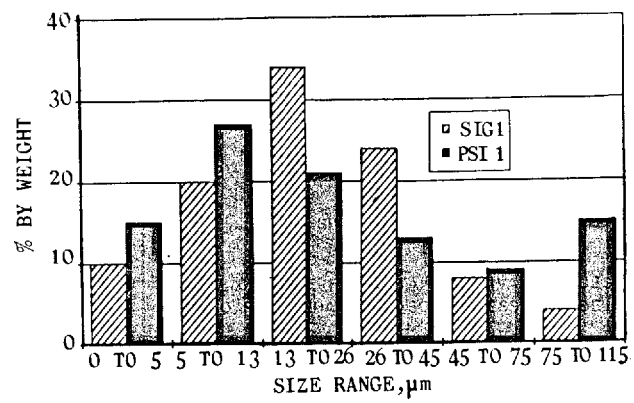

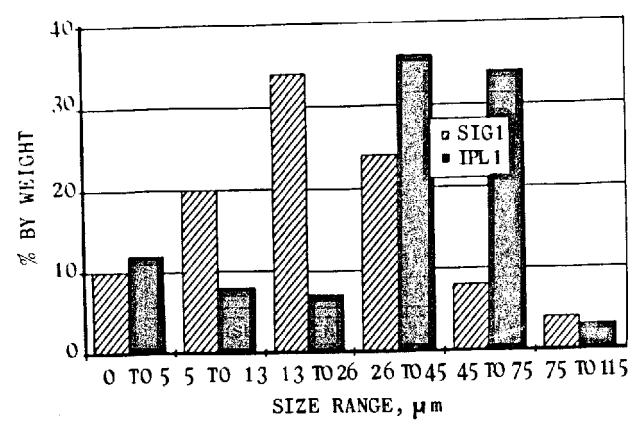

Fig. 19 – Distribution de la taille des particules de trois cendres siliceuses, de la plus fine à la plus grossière comparée à une distribution moyenne (82)

à l'hélium ou à l'azote varie de 2,2 à 2,8 g/cm^3. Quand la densité augmente l'anneau de corps amorphe dans le diagramme de diffraction des Rayons X se déplace vers les petits angles, en relation avec un enrichissement en silice (83).

6.5. Pouzzolanicité et activation des cendres volantes

Les cendres volantes sont des produits d'addition aux ciments et bétons qui agissent :

- en premier lieu, *physiquement* par la forme et la taille de leurs particules sur la rhéologie du matériau frais,

- en second lieu, *chimiquement* par leur pouzzolanicité (cendres siliceuses) ou leur hydraulicité (cendres calciques) sur le développement des résistances mécaniques et la durabilité du matériau durci.

Les caractéristiques d'une pouzzolane concernent son aptitude à d'abord réagir avec la chaux en présence d'eau puis à former des hydrates liants. Les tests de pouzzolanicité sont nombreux (63).

• *chimiques*, ils mesurent soit le taux de dissolution de la silice dans une solution d'acide fluorhydrique à 0,1 mole (89) ou la combinaison avec $Ca(OH)_2$ dans l'eau au voisinage de l'ébullition sous agitation magnétique (90), soit la concentration en ions Ca^{2+} et l'alcalinité de la solution de la chaux en contact avec la cendre.

• *mécaniques*, ils évaluent le rapport de la résistance en compression sur cubes de mortier de ciment aux cendres à la résistance du ciment Portland (norme ASTM C 311).

Tous ces tests sont contestés, à savoir :

* la chaux fixée par la cendre n'est pas toujours corrélée à la résistance du ciment aux cendres (93).

* la nature de $Ca(OH)_2$, pure ou commerciale (contenant des impuretés) influe sur l'indice de pouzzolanicité chimique (92).

* deux cendres de même indice ASTM C 311 peuvent dans un ciment commercial développer des résistances différentes (85).

Aussi O.E. MANZ (94), E. ROUSSOUW et J. KRUGER (95) ont-ils souhaité la mise au point de tests et de spécifications qui seraient utilisés uniformément à l'échelle internationale. Il semble que la mesure des résistances mécaniques de mortiers accélérés par la température (85, 91) soit un élément de réponse. Dans sa revue critique des produits d'addition, hydrauliques et pouzzolaniques, P.K.MEHTA (67) avait conclu que la composition minéralogique (et non la composition chimique) gouverne le comportement de ces sous-produits minéraux. C'est par cette approche que F.H. HUBBARD (81, 96) a proposé un nouvel indice appelé PPI (Pozzolanic Potential Index) qui prédit le potentiel de réaction d'une cendre à se combiner aux ions calcium de la pâte

de ciment et à participer aux résistances à long terme.

Le PPI est le rapport molaire $\frac{K_2O}{Al_2O_3}$. 10, directement relié à la concentration de cénosphères vitreuses. Trois classes de cendres britanniques ont été répertoriées. Elles correspondent à la :

- classe 1 : $(K/A).10 > 1.0$, haute réactivité.

- classe 2 : $0,5 < (K/A).10 < 1.0$, réactivité moyenne.

- classe 3 : $(K/A).10 < 0,5$, faible réactivité.

L'activation des cendres volantes siliceuses dans un ciment peut être obtenue par l'intermédiaire de la finesse qui libère la phase vitreuse. Le broyage peut aussi entraîner des microcontraintes dans les particules vitreuses (97) qui deviennent plus réactives. La température est l'activant le plus utilisé. Les cendres traitées à 80° C (91), 73° C (98), 60° C (99), 50° C (100), 40°C (101) peuvent être utilisées telles quelles sans nécessité d'un pourcentage élevé en fines particules.

6.6. Spécifications nécessaires à une plus large utilisation des cendres volantes

Chimie, minéralogie, granularité sont les trois caractéristiques les plus imporrantes des cendres (76, 97, 102). Les spécifications ASTM actuelles classant les cendres par leur teneur en $SiO_2 + Al_2O_3 + Fe_2O_3$ (classes F et C) et par leur pourcentage de particules passant au tamis de 45 μm apparaissent insuffisantes ou demandent à être affinées (67, 85, 97, 103). Dans sa revue détaillée de la nécessité d'une recherche approfondie sur la caractérisation des cendres et leur utilisation dans les ciments et bétons, S. DIAMOND (104) a dégagé les points suivants qu'il considère comme fondamentaux :

1 - distinction entre cendres bien brûlées (0 à 3 % carbone), mal brûlées (3 à 6 % carbone) et très mal brûlées (> 6 % carbone) ceci en raison des interférences entre le carbone résiduel et les adjuvants dans le béton.

2 - distinction entre cendres à faible teneur en chaux (< 5 % CaO), à teneur moyenne (5 % < CaO < 15 %) et à forte teneur (> 15 % CaO), plutôt que la classification ASTM, classe F et classe C.

3 - nécessité de considérer la teneur en sulfates alcalins qui, rapidement solubles, modifient la composition de l'eau de gâchage et l'hydratation précoce du ciment. Proposition de trois catégories, correspondant à des teneurs 0,5 % - de 0,5 à 1,5 %, > 1,5 %.

4 - nécessité de considérer également la teneur totale en sulfate qui peut modifier le temps de prise. D'où trois classes : 1 %, 1 à 3 %, > 3 %.

5 - importance de la quantité de particules creuses (cénosphères et plérosphères) déterminée par microscopie optique. Trois possibilités: 5 % (cendres à "particules solides"), 5 à 10 %, > 10 %.

A titre d'exemple, une cendre pourrait être bien brûlée, à teneur modérée en calcium, à particules solides avec une bonne distribution de taille des particules, à faible teneur en sulfates alcalins mais à pourcentage intermédiaire en sulfate total. A partir de ces caractéristiques bien définies, il devrait être possible d'interpréter les effets que produit une telle cendre dans le béton et en conséquence de prévoir le comportement d'une cendre similaire.

La commission RILEM 73 SBC, présidée par P.K.MEHTA fera le point de ses travaux à la 2ème Conférence Internationale sur les cendres volantes, fumées de silice, laitiers et pouzzolanes naturelles en avril 1986. Seront présentés un schéma des spécifications ne retenant que la teneur en $SO_3 < 5$ %, la perte au feu < 6 % et le remplacement de l'essai pouzzolanique ASTM C 618 par une mesure de résistances mécaniques à 7 jours et à 50 - 70°C. La teneur maximale de particules passant au tamis de 45 μm serait fixée à 20 %. Il reste à mettre au point un test permettant de caractériser les cendres pouzzolaniques et les cendres hydrauliques.

Aux cendres de charbon bitumineux ou de lignite se sont ajoutés récemment deux autres produits : la cendre de tourbe (105) et la cendre SDA (106) qui demandent toutes deux à être optimisées. La composition chimique et surtout la perte au feu de la cendre de tourbe varient dans un large domaine en fonction du type de marais et de la centrale thermique. La cendre SDA (Spray Drying Absorption) recueillie dans les systèmes d'épuration des gaz des centrales de plus de 8000 MW de puissance est formée de 75 % de cendre volante, 20 % de sulfite de calcium hémihydraté, 5 % de gypse + chlorure de calcium + chaux hydratée. Des études à long terme sont nécessaires étant donnée la teneur inhabituelle en sulfite et en chlorure.

7. LES FUMEES DE SILICE

Les fumées de silice ont pris un essor considérable depuis le Congrès de Paris. R. SERSALE (4) les avait citées dans son Rapport Principal comme des silices réactives. Ce matériau, généralement de haute pouzzolanicité, a été utilisé en Norvège dès 1950, puis en Islande et au Canada en 1970, et dans de nombreux pays à partir de 1980.

La fumée de silice entre à présent dans la composition de ciments industriels et dans des bétons dont elle accroît très favorablement les résistances mécaniques, la légèreté et la durabilité.

7.1. Production des fumées de silice

Les fumées de silice sont générées au cours de la fabrication du silicium métallique ou de divers ferroalliages de silicium dans des fours à arc électrique (107 - 108 - 109). Le métal ou l'alliage sont produits par réduction d'un mélange de quartz, de charbon, de copeaux de bois, de minerai (fer, chrome, manganèse). La charge chauffée par le courant électrique se dissocie en métal (ou alliage) liquide et vapeur de SiO qui s'oxyde à l'air et se condense en microsphères de SiO_2 qui sont collectées dans des filtres. La figure 20 due à L.HJORTH (107) donne le schéma du four et des réactions chimiques de la formation de la fumée de silice. Celle-ci peut provenir des alliages (109):

. Fe-Si 50, 75, 90 % contenant respectivement 43 à 50 %, 72 à 78 %, 87 à 96 % Si.

. Fe-Cr-Si.

. Si-Mn avec $15 < Si < 25$ %.

. Ca-Si résultant du traitement d'un mélange quartz-chaux.

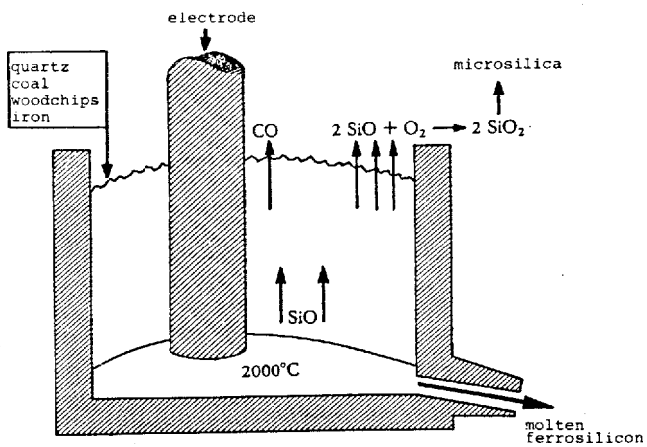

Fig. 20 : Schéma de la production des fumées de silice (107)

7.2. Composition chimique des fumées de silice

La composition chimique des fumées de silice dépend du type de four (avec ou sans récupérateur de chaleur) de la constitution de la charge (avec ou sans copeaux de bois, avec ou sans minerai métallique) et de la nature du charbon.

Le tableau VIII publié par G. RAU et P.C.AITCIN (109) groupe les analyses chimiques des différentes fumées de silice.

Les teneurs en carbone et à un degré moindre, en fer, colorent en gris sombre la fumée de silice. Celle-ci est blanche quand le four est équipé d'un récupérateur de chaleur. La régularité de la composition de la fumée de silice est assurée pour un four donné et une charge donnée.

Pour un même type d'alliage, la composition varie cependant d'un pays à l'autre mais la teneur en silice reste toujours très élevée (excepté pour CaSi et SiMn).

7.3. Structure des fumées de silice

Les fumées de silice se présentent sous la forme de particules sphériques et vitreuses dont la taille moyenne se situe entre 0,1 et 0,2 μm. Si les photos prises au microscope électronique en transmission (fig. 21) montrent une multitude de microsphères après dispersion dans l'acétone (110), les fumées de silice collectées dans les récupérateurs de poussière apparaissent d'après H. KOLDERUP (111) comme des agglomérats dont la taille peut atteindre quelques microns.

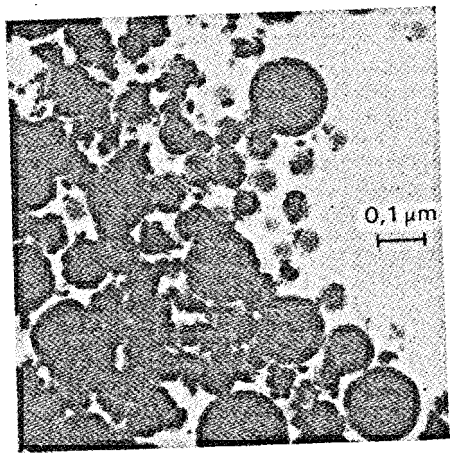

Fig. 21 - Particules de fumée de silice observées au microscope électronique par transmission (110)

Tableau VIII Composition chimique de différentes fumées de silice (109)

Alliage	Si	Fe-Si 90 %	Fe-Si 75 %	Fe-Si 50 % Fumée blanche	Fe-Si 50 %	Fe Cr Si	Ca Si	Si Mn
SiO_2	94 - 98	90 - 96	86 - 90	90	84,1	83	53,7	19
Fe_2O_3	0,02 - 0,15	0,2 - 0,8	0,3 - 5,0	2,9	8,0	1,0	0,7	3,9
Al_2O_3	0,1 - 0,4	0,5 - 3,0	0,2 - 1,7	1,0	0,8	2,5	0,9	5,5
CaO	0,1 - 0,3	0,1 - 0,5	0,2 - 0,5	0,1	1,0	0,8	23,2	12,4
MgO	0,2 - 0,9	0,5 - 1,5	1,0 - 3,5	0,2	0,8	7,0	3,3	2,4
Na_2O	0,1 - 0,4	0,2 - 0,7	0,3 - 1,8	0,9	-	1,0	0,6	1,1
K_2O	0,2 - 0,7	0,4 - 1,0	0,5 - 3,5	1,3	-	1,8	2,4	8,7
C	0,2 - 1,3	0,5 - 1,4	0,8 - 2,3	0,6	1,8	1,6	3,4	3,7
S	0,1 - 0,3	0,1 - 0,4	0,2 - 0,4	0,1	-	-	-	-
MnO	0,1	0,1 - 0,2	0 - 0,2	-	-	-	-	-
Perte au feu	0,8 - 1,5	0,7 - 2,5	2,0 - 4,0	-	3,9	2,2	7,9	7,5

La densité est proche de celle de la silice vitreuse. Elle diffère d'une fumée d'alliage à une autre, restant toutefois dans le domaine 2,10 à 2,25 (Tableau IX). La surface spécifique varie de 13 à 23 m^2/g, quelle soit calculée ou mesurée par adsorption d'azote. Elle est donc beaucoup plus élevée que celle du ciment Portland ou des cendres volantes (1 à 1,5 m^2/g). Les différences entre surface spécifique et densité se reflètent dans les courbes de distribution de la taille des particules (fig. 22).

Tableau IX - Densité de différentes fumées de silice (110)

Si	Fe-Si 75%	Fe-Si 50%	Fe-Si 75% blanche	Fe Cr Si	Ca Si	Si Mn
2,23	2,21	2,30	2,33	2,42	2,55	3,13

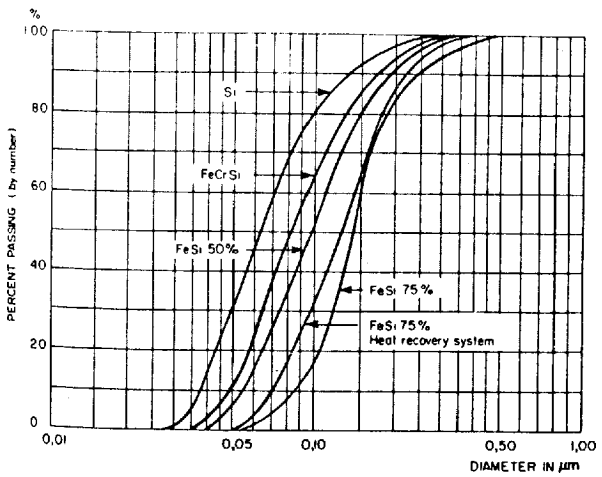

Fig. 22 - Distribution de la taille des particules dans différentes fumées de silie (109)

L'extrême finesse des fumées de silice et leur faible densité posent un problème de manutention et de transport. Un camion transportant 35 tonnes de ciment Portland ne pourra véhiculer que 7 à 9 tonnes de fumée de silice. Aussi des procédés de granulation à l'air ont-ils été mis au point (110). La fumée de silice peut aussi se présenter sous forme de coulis à 50 % d'eau.

Dans les ciments et bétons, les particules de silice sont dispersées par un malaxage énergique et l'emploi d'adjuvants fluidifiants. Les microsphères se répartissent entre les grains de ciment jouant un rôle physique de filler (fig. 23 et 24).

Les fumées de silice sont caractérisées par un anneau de corps amorphe dans les diagrammes de diffraction des Rayons X (fig. 25). Portées à 1100°C, elles se dévitrifient en cristobalite. Seule la silice Fe - Si 50 cristallise en enstatite (Fe, Mg) SiO_3 (fig. 26).

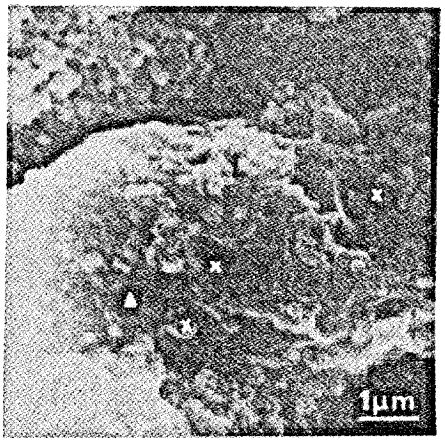

Fig. 23 - Ciment Portland à la fumée de silice. Les particules de silice (x) comblent les vides entre les grains de clinker (▲) de 50 à 100 fois plus gros (112)

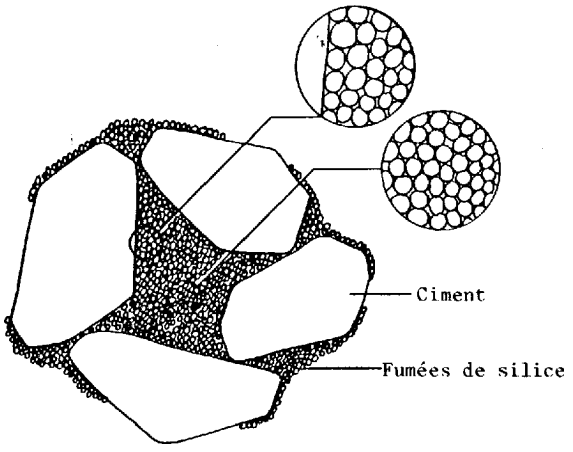

Fig. 24 - Schématisation d'une pâte de ciment Portland contenant de la fumée de silice dispersée par un fluidifiant (113)

7.4. Pouzzolanicité des fumées de silice

Les fumées de silice sont des produits hautement pouzzolaniques (114, 115, 116, 117, 118). Quatre échantillons de silice Si, Fe-Si 50 %, Fe Cr Si, Ca Si, étudiés par diffraction des Rayons X, se sont classés, à 2 et 7 jours, quant à la combinaison avec la chaux, dans l'ordre décroissant suivant (119):

Si>Fe Si>Fe Cr Si>Ca Si

A 28 jours, les trois premières silices se retrouvent au même rang mais la quatrième reste moins réactive que les autres. Ce manque de réactivité peut être relié à une teneur plus faible en silice, à une taille de particules plus grossière et à la présence de carbone. Si la silice est utilisée en produit d'addition dans le ciment Portland ou de substitution dans le béton, il est donc important de connaître son origine et sa composition ceci

d'autant plus que certaines usines électrométallurgiques mélangent les fumées récupérées dans des fours différents ou provenant d'alliages différents. Si les fumées de silice sont considérées comme des produits pouzzolaniques, elles doivent d'après P.C. AITCIN (120) répondre aux spécifications ASTM. Or :

- Ca Si et Si Mn contiennent moins de 70 % de $Si_2O + Al_2O_3 + Fe_2O_3$ (ASTM C 618).

- Fe Cr Si dépasse la limite de 5 % MgO admise par l'ASTM C 618.

- Ca Si peut inclure du carbure de calcium qui produit de l'acétylène au contact de l'eau.

Les publications ne mentionnent pas toujours le type de fumée de silice mais à l'examen de l'analyse chimique donnée, les produits les plus utilisés semblent les silices Si, Fe Si - 90 % ou Fe Si - 75 %.

Le second volet de la réaction pouzzolanique c'est-à-dire la formation d'hydrates liants est clairement démontré par le développement des résistances mécaniques. La fumée de silice, *produit d'addition au ciment Portland* accroît nettement les résistances en compression à partir du dixième jour. Cet accroissement est fonction de la nature du ciment Portland et du dosage en fumée de silice. Il semble que l'optimum se place entre 5 et 15 % du poids du ciment. Une étude sur l'influence de la fumée de silice utilisée dans un ciment aux cendres volantes a été présentée au colloque international de Montebello séparément par G.G. CARETTE et V.M. MALHOTRA (121) et M. REGOURD B. MORTUREUX et H. HORNAIN (122). Les deux communications arrivent à la même conclusion, à savoir l'intérêt de l'action conjuguée de la fumée de silice et de la cendre volante, la première agissant aux jeunes âges, la seconde prenant le relais à long terme. Les mêmes résultats ont été obtenus avec des laitiers et des pouzzolanes naturelles, peu réactifs. Un ciment à faible chaleur d'hydratation a pu être mis au point en ajoutant 15 % de fumée de silice à 35 % de laitier peu réactif et 50 % de ciment Portland ASTM type II. Le nombre de Kjoules mesuré est 30 % inférieur à celui du ciment Portland bien que les résistances mécaniques à 28 jours soient les mêmes (123). Par contre il existe une compétition entre fumée de silice et laitier réactif relative à la combinaison avec la chaux, compétition qui est défavorable à la résistance à 28 jours (122). Il est donc recommandé d'utiliser la fumée de silice à bon escient. Sa production limitée (1,2 millions de tonnes par an dont un tiers produit par les Etats-Unis, la Norvège et le Japon) la destine à des matériaux spécifiques (124).

Le béton de fumée de silice est moins résistant au jeune âge que le béton de ciment Portland de même classe à 28 jours. Il est cependant possible d'optimiser un béton de fumée de silice par le choix judicieux du ciment Portland et du fluidifiant. D'après AITCIN, BEDARD, PLUMAT et HADDAD (125), certains ciments se comportent mieux que d'autres dans un béton destiné à atteindre 100 MPa. Un béton de très haute résistance, facile à mettre en oeuvre, serait celui préparé avec un ciment de haute résistance.

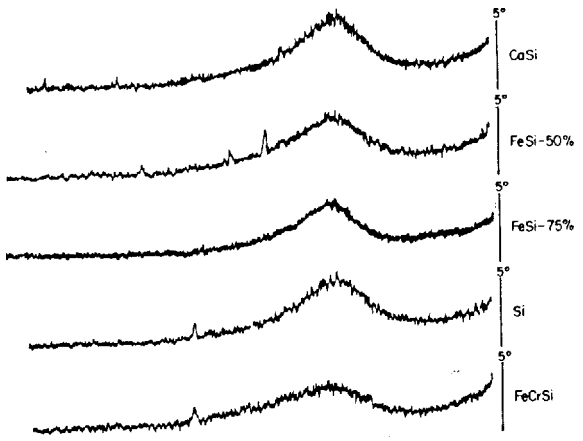

Fig. 25 - Diffraction des Rayons X. Anneau de corps amorphe centré à 4 Å de différentes fumées de silice (109).

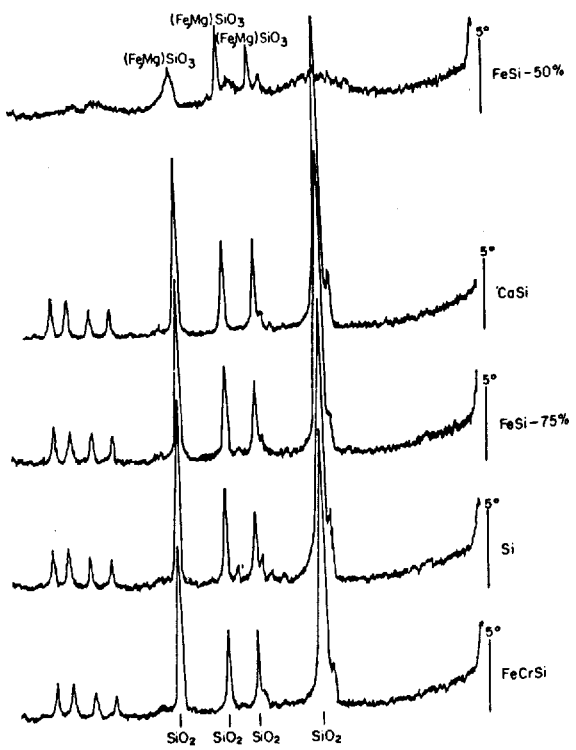

Fig. 26 - Dévitrification des fumées de silice portées à 1100°C. Apparition des pics de diffraction des Rayons X de la cristobalite SiO_2 et de l'enstatite Fe Mg SiO_3 (109).

7.5. Innocuité des fumées de silice

Parce que les fumées de silice sont amorphes et se présentent sous la forme de microsphères, elles diffèrent totalement du quartz cristallisé en grains anguleux, responsable de la silicose. Aucun cas de cette malade professionnelle n'a été diagnostiqué après presque 30 ans de production de silice précipitée vitreuse.

Si le recul concernant la fumée de silice est moins important que le précédent K. JAHR (126) estime que le risque de silicose est très faible étant donné l'inexistence de quartz et l'innocuité des éléments mineurs. La limite acceptable de fumée respirable serait de 3 mg/m^3.

7.6. Spécifications de la fumée de silice

La commission RILEM 73 BSC présidée par P.K.MEHTA recommande :

- de n'utiliser que des fumées de silice contenant au moins 80 % de SiO_2.

- de mesurer les résistances mécaniques d'un béton à 10 % de fumée de silice en poids du ciment (rapport E/C = 0,7) et de le comparer, aux mêmes échéances, à celles d'un béton témoin (norme norvégienne NS 3474 du 1981).

8. LA BIOSILICE

Les cendres d'écorce de riz sont, comme les fumées de silice, des pouzzolanes hautement réactives. Toutes deux constituées essentiellement de silice amorphe, elles diffèrent cependant par la morphologie de leurs particules (67) et leur réactivité initiale. La cendre d'écorce de riz est cellulaire, de grande surface spécifique 50 à 60 m^2/g. Si elle réagit plus rapidement que la fumée de silice, i.e. dès le premier jour dans les ciments, son activité a cessé à 28 jours.

Les écorces de riz ne doivent pas être calcinées à plus de 600°C, température à partir de laquelle, la silice amorphe cristallise, d'abord en cristobalite, ensuite en tridymite. La température de 400°C a été suggérée comme optimale par P. NIMITYONGSKUL, M.W.J.A de SILVA et P. KARASUDHI (127). Un nouveau procédé de calcination a été présenté par P.C.KAPUR (128). Il s'agit du brûleur TIB (Tube - in - Basket) dans lequel la température entre 350 et 600°C, donne des cendres de surface BET de 60 à 80 m^2/g, sans carbone résiduel et avec une structure très poreuse.

Une étude des propriétés de mélanges cendres-chaux par D.J. COOK et P.SUWANVITAYA (129) montre que l'optimum du rapport chaux-cendres est égal à l'unité quant au développement des résistances mécaniques. Le taux de carbone ne devrait pas dépasser 20 %.

9. LES POUZZOLANES NATURELLES

Les pouzzolanes naturelles ont été largement traitées au Congrès de Paris dans les rapports principaux de R. SERSALE (4), de K. TAKEMOTO et H.UCHIKAWA (5) et dans le rapport général de F. MASSAZZA (7).

9.1. Classification des pouzzolanes naturelles

La classification des pouzzolanes prête toujours à discussion tant sont grandes les différences dans la composition chimique et minéralogique des roches. Les pouzzolanes sont soit volcaniques, soit sédimentaires, vitreuses ou zéolitiques. Parmi ces dernières se placent les tufs type herschélite et les trass type chabasite. La "terre blanche" d'Italie, la gaize des Ardennes françaises, l'opale du Maroc, l'argile blanche Beppu du Japon sont presqu'exclusivement constituées de silice hydratée amorphe. Dans toutes ces pouzzolanes coexistent des minéraux cristallisés comme le quartz, les feldspaths, l'argile, la dolomie, la magnétite, les pyroxènes, la calcite, la cristobalite (91, 134, 131). F. MASSAZZA et U. COSTA (132) classent les constituants des pouzzolanes du point de vue de leur réactivité en trois catégories :

- les *constituants actifs* : phases vitreuses (fig. 27) plus ou moins altérées, l'opale, des terres à diatomées, les zéolites cristallisées.

- les *constituants inertes* : phases cristallisées autres que les zéolites.

- les *constituants nocifs* : substances organiques et argiles gonflantes.

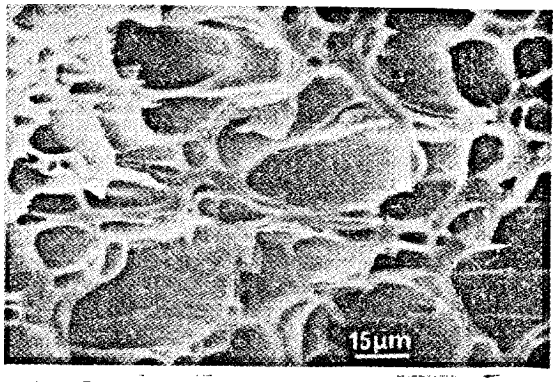

Fig. 27 - Phase vitreuse vacuolaire d'une pouzzolane naturelle (132).

La composition chimique de la fraction active de différentes pouzzolanes a été déterminée par trois méthodes (132) :

. analyse chimique indirecte : attaque par HCl et KOH, analyse de la solution et du résidu (méthode a)

. analyse chimique des fractions séparées par liqueurs denses (méthode b).

. analyse élémentaire à la microsonde électronique (méthode c).

L'analyse des pouzzolanes vitreuses ne pose pas de problème particulier. Il n'en est pas de même pour les pouzzolanes à phase vitreuse altérée contenant des minéraux cristallisés en inclusions. Dans ce cas, les trois méthodes ont donné des résultats très discordants. Seule la première (méthode a) semble se rapprocher le plus de la réalité.

Les facteurs responsables de la réactivité de la pouzzolane avec la chaux sont entre autres, sa composition chimique (silice et alumine) et sa surface spécifique BET. Le coefficient de corrélation

entre la chaux consommée à 7 jours et la surface BET a été trouvé égal à 0,95 (132).

9.2. Les argiles activées

Les argiles considérées comme matériau pouzzolanique peuvent être utilisées :

- telles quelles : elles sont alors activées par la chaux.

- traitées thermiquement entre 600 et 900°C. Les argiles "cuites" étaient auparavant classées dans les pouzzolanes artificielles, classification contestée par R. SERSALE (4) au Congrès de Paris.

Les argiles sont des alumino-silicates à structure feuilletée ou lamellaire construite à partir de tétraèdres SiO_4 et d'octaèdres AlO_6. Les ions divalents tels Mg^{2+} sont en coordination octoaédrique. La caractéristique des argiles est l'épaisseur des feuillets : i.e. 7 Å pour la kaolinite, 10 Å pour l'illite, 14 Å pour la chlorite. Certaines argiles comme la sépiolite ou l'attapulgite sont fibreuses.

. *Les argiles stabilisées à froid* par la chaux ou le clinker sont utilisées :

- dans la préfabrication d'éléments de bâtiments tels que cloisons et planchers ou de briques et carreaux (133, 134).

- dans la stabilisation de sols tropicaux latéritiques riches en kaolinites (135).

La réactivité des argiles dans les mélanges argile-chaux et argile-ciment est mise en évidence par les courbes de dégagement de chaleur, de captation des ions Ca^{2+}, de variation de pH. Les résultats obtenus par ces différentes méthodes confirment le rôle de la nature minéralogique de l'argile. La réactivité de sept argiles (montmorillonites, illites, kaolinites) décroit de la montmorillonite à la kaolinite (133). Cependant, la réaction des argiles avec la chaux n'entraîne pas systématiquement la formation d'hydrates liants, second volet de la pouzzolanicité. C'est le cas de la montmorillonite. Par contre, les mélanges à base d'argile illitiques calcaires ou kaolino-illitiques calcaires et siliceuses donnent des matériaux compacts. La stabilisation à froid des argiles peut conduire au développement de matériaux de bâtiment bon marché et à faible taux énergétique incorporé. Ces réalisations restent cependant limitées, l'activation des argiles pouzzolaniques étant essentiellement thermique.

. *Les argiles traitées thermiquement* entre 600 et 900°C doivent leur réactivité à la désorganisation de leur structure cristalline par déshydroxylation.

M. MURAT (136, 137, 138) a trouvé l'optimum de la réactivité du métakaolin et de l'illite après calcination à 800°C. Les mélanges chaux-métakaolin développent des résistances mécaniques plus élevées que celles des ciments à pouzzolanes naturelles J. AMBROISE (139) a obtenu des résistances de 23 à 27 MPa à 28 jours pour des ciments fabriqués à partir des sols tropicaux du Mali et de la latérite de Yaoundé.

10. LES FILLERS CALCAIRES

Les fillers calcaires, produits d'addition au ciment Portland sont de génération récente. Ils n'avaient pas été traités en tant que tels au Congrès de Paris. La normalisation française autorise l'utilisation; jusqu'à concurrence de 35 %, de fillers qu'elle définit comme des "Produits obtenus par broyage fin ou par pulvérisation de certaines roches (calcaire, basalte, laitiers, kieselguhr, bentonite, cendres volantes,....) naturelles ou non, agissant principalement, grâce à une granulométrie appropriée, par leurs propriétés physiques sur certaines qualités du ciment (accroissement de maniabilité, diminution de perméabilité et de capillarité, réduction de la fissurabilité,...). Les fillers sont inertes s'ils n'ont aucune action chimique sur les ciments en présence d'eau; ils sont actifs s'ils ont, même partiellement, des propriétés hydrauliques ou pouzzolaniques en présence de ciment et d'eau".

Les fillers entrant dans la composition des ciments composés français appelés CPJ, sont essentiellement constitués de calcite.

10.1. Minéralogie des fillers calcaires industriels

Les fillers calcaires peuvent être analysés par diffraction des Rayons X, microscopie optique, spectrométrie d'absorption infrarouge.

- *La diffraction des Rayons X* révèle que les fillers calcaires industriels ne sont pas très différents de la calcite avec toutefois des raies plus ou moins élargies (fig. 28). Cet élargissement du profil des raies peut être relié à une grande finesse des grains ou à une distorsion du réseau cristallin (140)

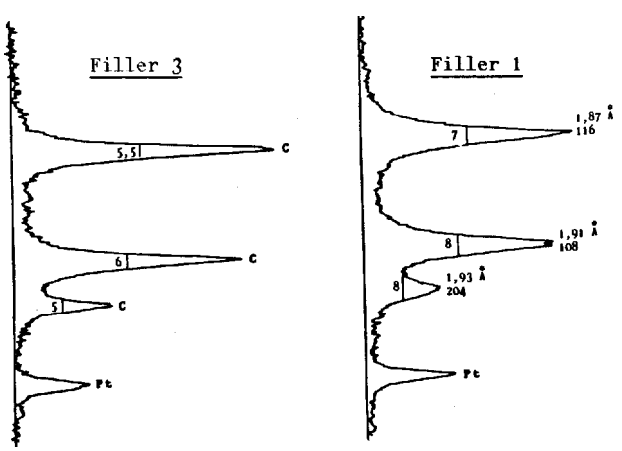

Fig. 28 - Diagramme de diffraction de Rayons X de deux fillers calcaires industriels.
C = calcite, Pt = étalon interne.

- *L'observation microscopique* des roches sur lames minces, en lumière polarisée, montre une différence de texture. Les fillers se présentent soit en gros cristaux, soit en grains très fins, soit en gros

3.1

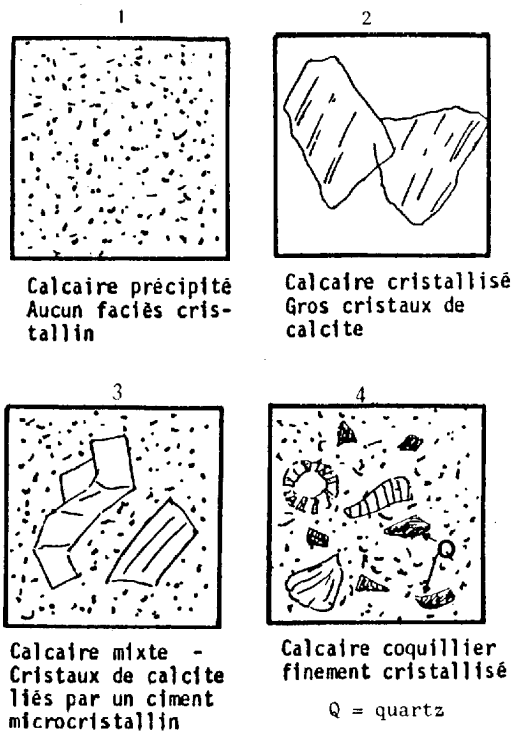

Fig. 29 - Caractéristiques morphologiques des fillers calcaires (140)

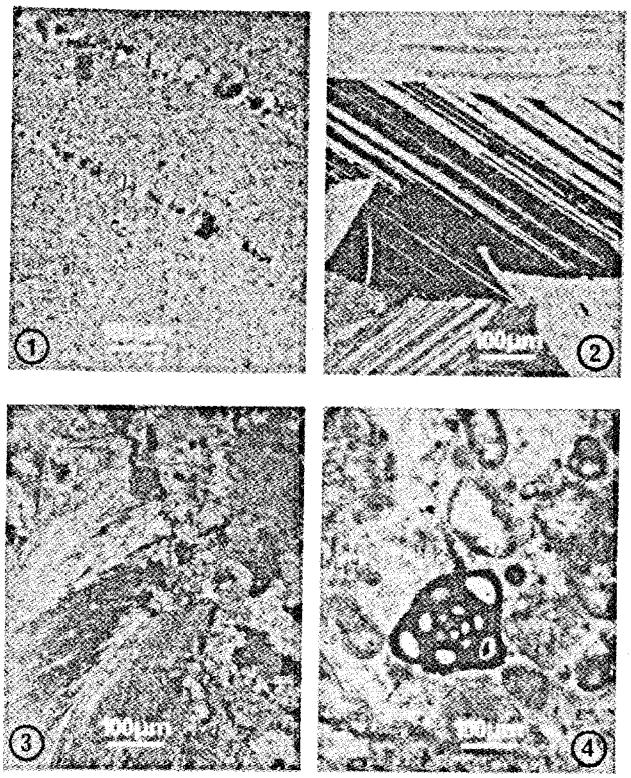

Fig. 30 - Microtexture des fillers calcaires telle qu'observée en microscopie optique en lumière polarisée (1, 2, 4) et transmise (3)

grains dans une matrice microcristallisée (fig.29 et 30). Quatre de ces fillers ont été étudiés plus particulièrement :

. Le filler n° 1 est un calcaire à 90 % de calcite microcristallisée (raies DRX élargies fig. 28). Examiné en lumière polarisée, la teinte est beige uniforme avec seulement quelques veines de cristaux plus gros (fig. 30). En lumière naturelle transmise, la lame mince est constituée d'éléments en forme de pelotes liés par un ciment spathique. La silice y apparaît soit amorphe, soit microcristallisée fibreuse (calcédoine), soit bien cristallisée (quartz). Les autres minéraux mineurs, sont la glauconie (mica potassique) et quelques particules ferrugineuses.

. Le filler n°2 est un calcaire dur, très pur, à plus de 95 % de calcite. Les cristaux sont bien développés (0,2 à 1 mm). La dolomie n'y existe qu'à l'état de traces. Dans les fractions les plus fines du concassé la calcite est en grains monocristallins, les assemblages polycristallins ayant été rompus.

. Le filler n°3 est un calcaire de cristallisation mixte : dans la roche gris-bleu alternent de la calcite microcristallisée et des macro-cristaux réfléchissants de couleur claire. Sur lame mince (fig. 30), la calcite et la dolomie en gros cristaux mosaïque sont liés par $CaCO_3$ microcristallisé contenant de la pyrite de fer en inclusions.

La teneur en dolomie $MgCa(CO_3)_2$ dosée par diffraction des Rayons X est de l'ordre de 9 %. Les raies de la calcite sont fines (fig. 28).

. Le filler n°4 est de texture hétérogène. Sur lames minces en lumière transmise, il se révèle constitué de débris de milioles, organismes marins, liés par de la calcite macro-cristalline de recristallisation. Il s'agirait donc d'une calcarénite à bioclastes ou biocalcarénite à ciment spathique.

La calcite recristallisée est pure. Dans la fraction microscristallisée coexistent des pyrites associées parfois à des oxydes de fer. Le taux de calcite est supérieur à 90 %.

- *La spectrométrie d'absorption infrarouge* a été utilisée par A. BACHIORRINI (141) pour estimer le désordre cristallin de différents carbonates, synthétiques et naturels. Un "coefficient de désordre" Cd exprimant le rapport de la diffusion d'une bande à sa densité optique a été défini dans le but de comparer les carbonates entre eux.

Les calcites des spectres a, b, d, de la figure 31 correspondent à un Cd respectivement égal à 56, 31, 53. Les deux premiers échantillons étaient des produits purs pour analyse (calcite 99 %), le troisième un calcaire oolithique. Une calcite bien cristallisée servant de témoin donne un Cd = 25. Deux autres formes du carbonate de calcium $CaCO_3$, une vatérite synthétique et une aragonite naturelle, répondent à Cd = 49 et Cd = 33.

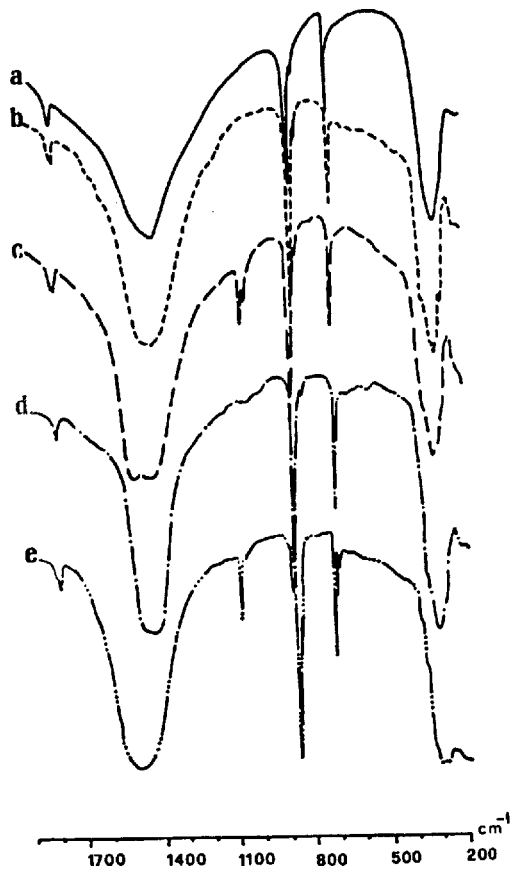

Fig.31 - Spectres d'absorption infrarouge de calcaires (141)

a, b = calcite pure, d = calcaire oolithique
c = vatérite synthétique, e = aragonite naturelle

10.1. Réactivité du filler calcaire

Les fillers calcaires jouent un rôle physique dans la compacité du CPJ mais ils sont également réactifs. La disparition de la calcite, la formation de carboaluminates, l'accélération de l'hydratation de C_3A et C_3S dans les ciments Portland (140, 142, 143, 144) ou de CA dans les ciments alumineux (141 - 145), la modification des C-S-H, la création d'une "auréole de transition" entre le filler et la pâte de ciment, la compétition entre carbonate et gypse dans l'hydratation de C_3A sont autant de facteurs propres à la réactivité du filler calcaire. Ces facteurs n'ont pas été décelés dans l'étude des mêmes échantillons contenant du quartz finement broyé qui est considéré comme un filler inerte (140-141).

Les résistances mécaniques de mélanges expérimentaux à 75 % de ciment Portland CPA et 25 % filler (nos 1, 2, 3 - 4 précédemment étudiés) sont groupées dans le tableau X. Elles montrent que la présence de calcite à réseau cristallin désorganisé entraîne un développement plus rapide des performances mécaniques que la présence d'une calcite bien cristallisée. Cependant, tous les fillers calcaires restent supérieurs au quartz broyé à la même finesse.

Tableau X - Résistances en compression (MPa)

mélange expérimental { 75 % CPA 55, 3200 $cm^2.g^{-1}$; 25 % filler, 4700 $cm^2.g^{-1}$; Pâtes pures: E/C = 0,30 (140)

Echéance	CPA témoin	C P J				
		Filler calcaire				Quartz
		1	2	3	4	
28 jours	105	87	83	85	81	74
3 mois	122	102 *	98 *	93 ×	91 ×	88

×: Calcite bien cristallisée,
*: Calcite à réseau cristallin désorganisé.

A. BACHIORRINI (141) arrive aux mêmes conclusions en présence d'aluminate monocalcique qui se dissout d'autant plus rapidement que le coefficient de désordre du calcaire est plus élevé dans le mélange $CaCO_3$ + CA. La cinétique d'hydratation du CA n'est pas modifiée en présence de quartz.

Les données du tableau X concernent des mélanges expérimentaux dans lesquels seule variait la nature du filler calcaire. Or, ces fillers sont utilisés industriellement pour la production de CPJ. Les ciments composés industriels proviennent d'usines différentes donc de clinkers différents et sont broyés à des surfaces spécifiques variées (tableau XI). Un ciment CPJ est caractérisé par sa classe de résistance c'est-à-dire sa résistance moyenne à 28 jours.

Tableau XI - Composition et surface specifique Blaine de sept CPJ fillérisés industriels

Classe du CPJ*	type de filler (fig.30)	Teneur en filler %	Surface spécifique Blaine $cm^2.g^{-1}$
45 R**	1	10	3450
35	1	25	3100
55 R	2	15	4200
45 R	2	25	4200
45	1	9	3925
45	3	15	3550
45	4	10	3810

*Résistance à 28 jours en mortier ISO (MPa)

**R = rapide { 45 R = 15 MPa à 2 jours ; 55 R = 22,5 MPa à 2 jours

Le tableau XI montre que le filler type n°1 donne à raison de 10 % un CPJ 45 R (R = rapide) pour une surface spécifique Blaine de 3450 cm^2/g et à raison de 9 %, un CPJ 45 pour une surface spécifique Blaine

de 3925 cm^2/g. Dans ces conditions, c'est la nature du clinker qui intervient dans le développement des résistances mécaniques. Des résistances aussi élevées que 55 MPa à 28 jours et 22,5 MPa à 2 jours pour le CPJ 55 R à 15 % de filler sont le résultat d'une optimisation de la qualité du calcaire, de sa finesse et de sa compatibilité avec le clinker. Les résistances mécaniques ne sont cependant pas les seules performances à prendre en compte. Un béton de CPJ doit être aussi maniable qu'un béton de ciment Portland CPA.

10.2. Choix du filler calcaire

Un calcaire peut être caractérisé par sa composition chimique et minéralogique, sa broyabilité, sa porosité, sa surface BET. La calcite peut être friable ou dure à broyer suivant qu'elle se présente sous la forme microcristallisée ou en macrocristaux:

composition chimique et minéralogique

Une étude réalisée par R. GUYOT et R. RANC (146) sur des bétons de CPJ à même taux de fillers, d'origines diverses et de caractéristiques différentes, telles que:

- densité : 2,2 à 2,7
- porosité : 0,3 à 18,4 %
- BET : 2,1 à 4,2 m^2/g
- absorption capillaire : 1 à 12 g/100 cc,

montre que, à maniabilité constante, le rapport E/C reste inchangé pour six fillers à teneur élevée en carbonate (tableau XII).

Au contraire, la présence d'argiles dans les fillers, identifiées par leur teneur en alumine et en silice, influe sur la rhéologie du béton. Dans les mêmes conditions que celles du tableau XII, deux fillers contenant :

- le premier : 0,45 % SiO_2 et 0,3 % Al_2O_3.
- le second : 19,8 % SiO_2 et 5,98 % Al_2O_3,

demanderont respectivement à maniabilité égale, un rapport E/C de 0,53 à 0,57.

Aussi les critères de choix d'un filler se sont-ils fixés sur une teneur minimale en argile. Celle-ci peut être dosée par la capacité d'absorption du bleu de méthylène. La limite supérieure acceptable serait de 1,5 grammes de bleu pour 100 grammes de filler dont la taille des grains est inférieure à 80 µm. La teneur en matières organiques ne devrait pas dépasser 0,5 %.

· *finesse*

La surface spécifique du calcaire qui peut atteindre 7000 cm^2/g n'a pas d'influence marquée sur la rhéologie du béton (146). Les CPJ industriels sont obtenus par cobroyage du clinker et du filler, deux constituants dont la broyabilité peut être très différente. La figure 31 donne d'un mélange expérimental constitué de 75 % clinker gypsé et 25 % calcaire cobroyés à une surface spécifique Blaine de 4200 cm^2/g, les courbes de répartition granulaire de chacun des constituants.

Tableau XII - Caractéristiques des fillers calcaires et des bétons dosés à 350 kg de CPJ à 15 % de fillers par m^3 (143)

Caractéristiques des fillers		Calcaire industriel					
		1	2	3	4	5	6
composition chimique	SiO_2	5,3	2,3	1,55	0,9	0,5	2,5
	Al_2O_3	0,6	1,5	0,5	0,4	0,3	0,8
	Fe_2O_3	0,4	0,7	0,4	0,1	0,2	0,6
	CaO	52,2	52,6	50,1	54,7	55,0	52,5
	MgO	0,1	0,2	3,5	0,4	0,2	0,6
caractéristiques physiques	Densité	2,20	2,66	2,55	2,70	2,72	2,40
	Porosité %	18,4	0,6	8,6	0,4	0,3	11,3
	BET m^2/g	2,1	3,9	3,0	2,19	2,07	4,23
	Absorption capillaire g/100cc	12,9	1,1	8,0	0,6	0,2	9,6
Caractéristiques des bétons : slump 10 cm							
E/C		0,54	0,55	0,54	0,54	0,53	0,54
Rc à 28 j MPa		39,8	39,0	37,3	42,0	40,8	40,9

La distribution des grains de clinker et des grains de filler a été déterminée par analyse quantitative par diffraction des Rayons X de différentes tranches séparées par sédimentométrie à la pipette d'Andreasen (147). Le filler de broyabilité 160 cm^2/joule est plus fin que le clinker de broyabilité 70 cm^2/joule. L'aire massique calculée par J.P. BOMBLED, G. BELLINA et B. MORTUREUX (147) est de 7370 cm^2/g pour le filler et le gypse, 3 190 cm^2/g pour le clinker.

10.3. Compatibilité clinker-filler

Les ciments composés CPJ représentent 62 % de la production francaise. La moitié de ces CPJ sont des ciments aux fillers calcaires. Si pour un CPJ 45 la résistance de 45 MPa est toujours atteinte à 28 jours les résistances aux courtes échéances peuvent être différentes d'un mélange filler-clinker à un autre. C'est ce que montre le tableau XIII dans lequel les ciments Portland CPA et les ciments composés CPJ, sont de résistance égale à 48 MPa à 28 jours (146).

Le tableau XIII révèle également que le CPJ 45 a, dans les trois cas, une résistance à 1 jour plus élevée que celle du CPA. Cet accroissement de la résistance précoce, favorable à un démoulage plus rapide du béton de CPJ, peut être attribué à la fois à la finesse plus grande du clinker et au rôle physique de remplissage du filler.

Un broyage séparé clinker-filler a permis la production, dans une même cimenterie, d'un CPJ 55 et d'un CPJ 45 contenant respectivement 15 et 27 % de calcaire. C'est ce que montre le tableau XIV.

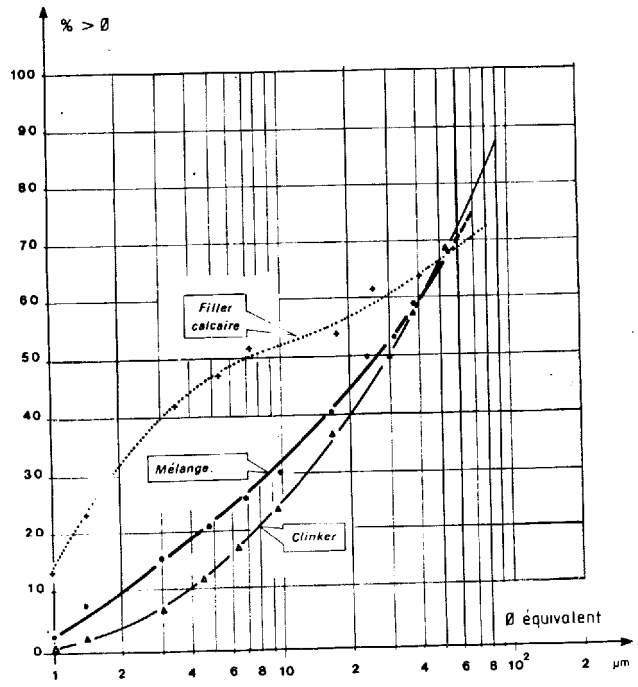

Fig. 32 - Répartition granulaire du clinker et du calcaire cobroyés en laboratoire dans un mélange 75 % clinker + 25 % filler de surface spécifique Blaine 4200 cm^2/g (147)

Tableau XIII - Résistance en compression de mortiers ISO, à 1 jour et 28 jours (141)

Type de ciment	Surface spécifique du clinker $cm^2.g^{-1}$	Rc (MPa) 1 j	28 j
Clinker A			
. CPA : ciment Portland	2700	15,5	48
. CPJ : CPA + 15% filler	4500	18,4	48
Clinker B			
. CPA : ciment Portland	2500	10	48
. CPJ : CPA + 15% filler	4100	15,4	48
Clinker C			
. CPA : ciment Portland	1900	4	48
. CPJ : CPA + 15% filler	3500	9	48

Les compositions minéralogiques des clinkers des CPJ industriels sont assez proches, les unes des autres. L'analyse quantitative des phases par diffraction des Rayons X donne des teneurs de C_3S variant entre 54 et 63 % et de C_3A entre 8 et 10 % (140).

En conclusion, une usine peut à partir d'un même clinker, préparer différents CPJ en jouant sur la finesse du clinker. Le filler doit être relativement pur sans teneur excessive en argile et en matières organiques.

Tableau XIV - Résistances en compression de mortiers ISO à 1 jour et 28 jours. Le clinker et le filler des CPJ ont été broyés séparément (146)

Type de ciment	Surface Spécifique du clinker	Rc (MPa)	
	(cm^2/g^{-1})	1 j	28 j
CPA 55	3340	15,1	58,3
CPJ 55 15 % filler calcaire	3970	18,5	57,5
CPA 45	2550	11,2	49,9
CPJ 45 27 % filler calcaire	3970	15,0	49,0

Un projet de norme européenne sur les ciments composés aux fillers calcaires est en cours de discussion. Les spécifications tiendront compte:

- du pourcentage maximal de filler ajouté au clinker de ciment Portland.

- de la composition du filler : taux maximal en calcite, teneur minimale en argile et en matières organiques.

11. LES CIMENTS COMPOSES D'AUJOURD'HUI

Les laitiers, cendres volantes, pouzzolanes naturelles, fillers calcaires, en remplaçant le clinker dans les ciments composés, entrent dans le cadre des économies d'énergie (148). Considérés comme produits hydrauliques, pouzzolaniques ou fillers, ils participent aux performances des ciments qu'elles soient rhéologiques, mécaniques ou de durabilité. Seule la fumée de silice (ou microsilice) partage les chercheurs. Pour bon nombre d'entre eux elle est un filler pouzzolanique. Pour d'autres, son action se limite à celle d'un filler (149).

Les ciments composés, optimisés par les producteurs, sont assurés d'une régularité de fabrication et d'homogénéisation. A titre d'exemple, la France a une longue expérience dans la production des ciments au laitier soient:

- ciment CPJ : $\leq$ 35 % laitier.
- ciment de haut fourneau CHF : 60 à 75 % laitier.
- ciment de laitier au clinker CLK : $>$ 80 % laitier.

Depuis 1979 elle utilise, dans les CPJ, les fillers calcaires qu'ils soient seuls ou qu'ils coexistent avec des laitiers ou des cendres, à savoir:

- CPJ 55 R : 8 à 27 % filler.
- CPJ 45 R, 45 : 15 à 27 % filler.
- CPJ 45 : 17 % laitier, 5 % cendre, 8 % filler.

Cendres et laitier apparaissent également dans le ciment CLC.

- CLC 45 : 26 % laitier, 21 % cendres.

Le tableau XV donne la répartition de ces différents ciments dans la production de 1984 qui s'élevait à 22,7 millions de tonnes.

Tableau XV - Répartition des différents ciments produits en France en 1984, définis par leur classe de résistance. Norme Française NF P 15.301.

	% en tonnage
- Ciment Portland CPA	
• HP : hautes performances (30 MPa à 2 jours)	5,9
• 55 R et 55	14,9
• 45 R et 45	2,8
- Ciments composés CPJ	
• 55 R et 55	2,9
• 45 R et 45	57,1
• 35	2,8
- Ciment composé CLC 45	
• L = laitier, C = cendre	1,0
- Ciments au laitier	
• CHF : HF, 55, 45	0,8
• CLK : 45 R et 45	4
- Divers (ciments à maçonner, ciments spéciaux, chaux hydrauliques)	7,8

Les normes nationales diffèrent largement d'un pays à l'autre quant aux domaines de composition des ciments Portland avec additions minérales. Le défi des années 1990, serait d'après G. FROHNSDORFF et J.P. SKALNY (150), l'uniformisation des ciments composés. Un développement rapide de nouvelles spécifications qui seraient rédigées en termes de performances permettrait une prévision de comportement, dans le temps et dans les environnements agressifs, des matériaux comme le béton.

12. CIMENTS COMPOSITES FUTURISTES

Une génération de matériaux de très hautes performances est récemment apparue sur le marché. Ces produits qui offrent un avenir nouveau aux ciments et bétons, ont été présentés et discutés lors de deux réunions internationales, la première, organisée par la Royal Society à Londres en 1983 sur le développement des ciments, dans la technologie des années 1990, la seconde par la Materials Research Society à Boston en 1984 sur les matériaux de très hautes résistances, à base de ciments.

Des résistances en compression de 100 MPa atteintes par des bétons traditionnels sont le résultat d'une sélection judicieuse de constituants incluant des ciments à 20-35 % de cendres volantes (151).

Des mortiers de ciment contenant 50 à 65 % de laitier de haut fourneau et étuvés de 27 à 175°C ont donné des résistances de 95 à 240 MPa (152).

En dehors des ciments composés d'aujourd'hui sont nés des matériaux futuristes comme le DSP et le ciment MDF :

- le DSP (Densified System containing homogeneously arranged ultrafine Particles) constitué de ciment Portland, de microsilice et de fluidifiant, est gâché avec un faible rapport eau/(ciment + silice), de 0,12 à 0,22. Sa résistance en compression s'élève à 270 MPa (153). Matériau fragile, il devient ductile quand il est renforcé de fibres. Des fibres de polypropylène de 6 mm utilisées par L. HJORTH (153) ont multiplié par 9.000 l'énergie de rupture d'un DSP extrudé (9 kJ/m^2).

- le ciment MDF (Macro Defect Free) mis au point par J.D. BIRCHALL (154) est constitué soit de ciment Portland, soit de ciment alumineux dont la dispersion et la lubrification des grains sont obtenues par l'utilisation de polymères organiques solubles dans l'eau (hydroxypropylméthyl cellulose, polyacrylamide polyvinylacétate). Un malaxage énergique du mélange, 6 % (en masse) de polymère, 9 % d'eau et 85 % de ciment, donne une pâte plastique qui peut être moulée, laminée, extrudée. Le matériau se présente comme une céramique de très faible porosité (1 % en volume) et de résistance en flexion très élevée (150 MPa). Le ciment MDF peut être fillérisé par des particules traditionnelles comme les cendres volantes mais aussi par l'alumine, le carbure de silicium, la poudre d'acier. Il peut également être renforcé de fibres. Son énergie de rupture passe de 0,2 à 100 kJ/m^2 pour 9 % en volume de fibres de kevlar.

Le DSP et le ciment MDF matériaux organo-minéraux, doués de hautes caractéristiques mécaniques offrent des voies nouvelles à l'utilisation des liants hydrauliques (155). Ces composites à base de ciment ont été testés avec succès dans des domaines aussi inhabituels que la cryogénie, l'electromagnétisme, l'acoustique, la balistique (156). Leur aptitude au moulage et leur légèreté les destinent à l'aérospatiale (157) où ils peuvent concurrencer les céramiques et les métaux. Leur développement signifie que les ciments traditionnels n'ont pas été exploités dans la totalité de leur potentiel. Se substituer au bois, au métal, à la matière plastique, à la céramique, est le défi que lancent aux chercheurs les matériaux composites à base de ciment: beau programme pour le 9ème Congrès International de la Chimie des Ciments.

Remerciements

L'auteur remercie vivement tous les chercheurs qui l'ont aidée dans la rédaction de ce rapport. Elle est plus particulièrement reconnaissante aux Prof. P.C. AITCIN, A. CARLES-GIBERGUES, S. DIAMOND, aux Dr J.P.H. FREARSON, R.W. LINTON, P.W. SCOTT, I. SIMS, J.M. UREN, de lui avoir communiqué leurs résultats avant qu'ils ne soient publiés et à Mr. J. VOLANT de s'être chargé de la recherche bibliographique.

REFERENCES

Les références relatives au 7ème Congrès International de la Chiime des Ciments, Edition Septima seront abrégées en VII CICC PARIS. Celles de la première conférence internationale sur l'utilisation des cendres volantes, fumées de silice, laitiers et autres sous-produits minéraux dans le béton de Montébello (Canada) apparaîtront comme 1rst International Conference Montebello.

1.- H.G. SMOLCZYK (1980), "Structure and Characterization of Slags". Principal Report. VII CICC Paris. Vol I, Thème III-1, 1-16.

2.- M. DAIMON (1980) "Mechanism and Kinetics of Slag Cement Hydration. "Principal Report VII CICC Paris. Vol I, Thème III-2, 1-8.

3.- M. REGOURD (1980) "Structure and Behavior of Slag Cement Hydrates". Principal Report. VV CICC Paris. Vol. I, Thème III-2, 9-26.

4.- R. SERSALE (1980) "Structure and characterization of Pozzolanas and Fly Ashes". Principal Report VII CICC Paris. Vol I, Thème IV-1, 1-21.

5.- K. TAKEMOTO and H. UCHIKAWA (1980). "Hydration of Pozzolanic Cements". Principal Report. VII CICC Paris. Vol I, Thème IV-2, 1-29.

6.- M. VON EUW (1980). "Structure des laitiers et hydratation des ciments de laitier". Rapport général. VII CICC Paris. Vol IV, Thème III, 63-70.

7.- F. MASSAZZA (1980). "Structure of Pozzolana and Fly Ash and The Hydration of Pozzolanic and Fly Ash Cements". General Report. VII CICC Paris. Vol IV, Thème IV, 85-90.

8.- M. VON EUW, M. DAIMON, R. DRON, B. ENTINE, P. FIERENS, L. SHOUSUN, M. REGOURD, H.G. SMOLCZYK (1980). Discussion du Panel, Thème III, VII CICC Paris, Vol. IV, 71-84.

9.- F. MASSAZZA, R. SERSALE, K. TAKEMOTO, A.M. DIMITRIEV, P. LONGUET, R. MAGNAN, J. SKALNY (1980) Panel Discussion. Thème IV, VII CICC Paris, Vol IV 91-96.

10.- R. DRON (1984). "Structure et réactivité des laitiers vitreux". Thèse de Doctorat ès Sciences. Paris VI, 11 janvier 1984.

11.- G.W. TOOP and G.S. SAMIS (1962) "Activities of ions in silicate melts". Trans. Met. Soc. Aime; 224, 5, 878-887.

12.- C.R. MASSON (1968) "Ionic equilibria in liquid silicates. J. Amer . Ceram. Soc. Vol 51, nº 3, 134-143.

13.- R. DRON (1979) "Structure des silicates fondus. Interprétation statistique de la théorie de Masson". CR Acad Sci. Paris. t 28q Série C 397-400.

14.- P.F. Mac MILLAN (1981) "A Structural Study of Aluminosilicate Glasses by Raman Spectroscopy PhD. Arizona State University.

15.- M. REGOURD (1983) "Slag and Slag Cements". Journal of Educational Modules for Materials Science and Engineering. Vol 5, nº 5, 688-714.

16.- B. PIRIOU et P.Mc MILLAN (1983) "Ordre et spectroscopie vibrationnelle des silicates". Bull Miner 106, 23-32.

17.- S. GOTO, T. YOSHII and M. DAIMON (1985) "Effects of the Thermal History on the Hydraulic Properties of Slags". Cem. Concr. Res. Vol 15, 964-968.

18.- Y. RUN-ZHANG, O. SHI-XI and G. QIONG-YING (1983). "Structure and Hydraulic Activity of Slags in the System $CaO-MgO-Al_2O_3-SiO_2$" Silicates Industriels 1, 3-6.

19.- S.M. ROIAK et J. Ch CHKOLNIK (1980) "Influence des particularités physiques et chimiques des laitiers de haut fournau sur leur activité hydraulique". VII CICC Paris, Vol III, 74-77.

20.- Y. RUN-ZHANG and G. QIONG-YING (1982). "Influenc of Structural Features of Slags on their Hydraulic Activity". Silicates Industriels 12, 279-281.

21.- P. FIERENS et P. POSWICK (1977) "Etude cinétique de l'hydratation de laitiers synthétiques". Silic. Industriels 42, 4-5, 235-45.

22.- M. REGOURD, H. HORNAIN et B. MORTUREUX (1976) "Microstructure des ciments au laitier Rev. Mater. Constr. nº 699, 83-86.

23.- E. DEMOULIAN, P. GOURDIN, F. HAWTHORN et C. VERNET (1980) "Influence de la composition chimique et de la texture des laitiers sur leur hydraulicité" VII CICC Paris, Vol II, III-89.

24.- M. REGOURD, B. MORTUREUX, E. GAUTIER, H. HORNAIN et J. VOLANT (1980) "Caractérisation et activation thermique des ciments au laitier" VII CICC Paris, Vol II, III-105.

25.- J.P.H. FREARSON and J.M. UREN (1986) "investigations of a Ground Granulated Blast-Furnace Slag Containing Merwinitic Crystallisation". To be presented at the 2nd Int. Conf. on the Use of Fly Ash, Silica Fume, Slag and Natural Pozzolans in Concrete. Madrid April 21-26.

26.- P.W. SCOTT, S.R. CRITCHLEY and F.C.F. WILKINSON (1985) "Microstructure and Phase Relations of Some Granulated and Pelletised Blastfurnace Slags". Seminar on Slags. York GB. Oct. 1985. To appear in Mineralogical Magazine.

27.- H. ROPER (1980) "Composition, Morphology, Hydration and Bond Characteristics of Some Granulated Slags" VII ICCC Paris, Vol II, III-13.

28.- C. VERNET, E. DEMOULIAN, P. GOURDIN et F. HAWTHORN (1980) "Cinétique de l'hydratation des ciments au laitier". VII ICCC Paris

Vol II, III-128.

29.- P. FIERENS et P. POSWICK (1980) "Nouveaux aspects de l'hydratation des laitiers industriels". VII ICCC Paris Vol II, III-112.

30.- M. REGOURD, J.H. THOMASSIN, P. BAILLIF and J.C. TOURAY (1983) "Blast Furnace Slag Hydration. Surface Analysis". Cem Concr Res 13, 549-556.

31.- B. COURTAULT (1980) "Etude des gaz des laitiers granulés de haut fourneau". VII ICCC Paris Vol II, III-117.

32.- P. GOURDIN (1980) "Composition minéralogique potentielle des laitiers vitrifiés de haut fourneau". Ciments-Bétons-Plâtres-Chaux n° 727, 6, 363-65.

33.- R.E. HOOTON and J.J. EMERY (1983) "Glass Content Determination and Strength Development Predictions for Vitrified Blast Furnace Slag". 1rst International Conference Montebello Vol II 943-962.

34.- M. REGOURD (1985) "Application of XRD to Some Problems of the Cement Industry". Seminar on Advances in Powder Diffraction Crystallography". Stockholm, May 7-9. To appear in Chemica Scripta.

35.- J.P.H. FREARSON, I. SIMS and J.M. UREN (1986) "Development of Test Procedures to Determine The Glass Content of Ground Granulated Blast Furnace Slag". To be presented at the 2nd International Conference on the Use of Fly Ash, Silica Fume, Slag and Natural Pozzolans in Concrete. Madrid April 21-25.

36.- E. DEMOULIAN, C. VERNET, F. HAWTHORN et P. GOURDIN (1980) "Détermination de la teneur en laitier dans les ciments par dissolutions sélectives". VII CICC, Paris Vol II, III-151.

37.- C. VERNET, E. DEMOULIAN, P. GOURDIN et F. HAWTHORN (1980) "Cinétique de l'hydratation des ciments au laitier". VII CICC Paris, Vol II, III-128.

38.- R. DRON et F. BRIVOT (1980) "Approche du problème de la réactivité du laitier granulé". VII CICC Paris, Vol II, III-134.

39.- I VOINOVITCH, M. RAVERDY et R. DRON "Ciment de laitier sans clinker" VII CICC Paris, Vol II, III-122.

40.- B. FORSS (1982) "F. Cement a Low Porosity Slag Cement for the Precasting Industry". International Conference on Slag and Blended Cements, Feb 12-19, Univ. of Alabama, Birmingham.

41.- H. KUKKO and R. MANNONEN (1982) "Chemical and Mechanical Properties of Alkali-Activated Blast Furnace Slag F. Concrete". Nordic Concrete Research The Nordic Concrete Federation. Publication n° 1. Oslo, 16.

42.- VI SATARINE, S.VCHESTOPEROV, Y.M. SYRKINE, B.G. CHOKOTOVA, A.I. ZDOROV, L.A. FEDWER, (1980) "Intensification des processus de durcissement du ciment Portland de laitier et perfectionnement de la structure du ciment durci". VII CICC Paris, Vol II, III-69.

43.- F. HAWTHORN, E. DEMOULIAN, P. GOURDIN et C. VERNET (1980) "Laitiers et clinkers. Influences réciproques ". VII CICC Paris, Vol II, III-145.

44.- J. METSO and E. KAJAUS (1983) "Activation of Blast Furnace Slag by Some Inorganic Materials". 1rst International Conference Montebello. Vol II, 1059-1073.

45.- V.I. SATARINE (1974) "Slag Portland Cement". VIth International Conference Chemistry of Cement. Moscow Principal Paper.

46.- V.A. DIMITRIEV, V.I. AKUNOV, V.M. ALBAC, S.D. MAKASHEV et N.V. CUKANOVA (1981). "Activation mécanochimique des ciments composés". C.R. 10, 18-19.

47.- R.D. HOOTON and J.J. EMERY (1980) "Pelletized Slag Cement : Autoclave Reactivity". VII CICC Paris, Vol II, III-43.

48.- A.A. GOVOROV, E.V. DJOUSS et F.C. OVTCHARENKO (1983). "Le durcissement hydrothermal des coulis de verres $CaO-MgO-Al_2O_3-SiO_2$ ". CR. Acad Sci Ukraine, Série B, n° 9 30-32.

49.- A.A. GOVOROV, N.V. BABOUGHINA, J.Ch. CHKOLNIK et F.D. OVTCHARENKO (1984) "L'influence de la teneur en MgO des laitiers sur leur activité hydraulique en milieu hydrothermal". CR. Acad. Sci. Ukraine. Série B n° 10, 29-32.

50.- WANG YU-JI and XIE GONG-XIN (1980) "Research on the Main Mineral Phase and Its Cementitious Properties of Oxygen Converter Slag (O.C.S.)". VII CICC Paris, Vol II, III-19.

51.- LUO SHOUSUN (1980) "Effect of MgO in Steel Slag on Soundness of Cement" VII CICC Paris, Vol II, III-25.

52.- M. CONJEAUD, C.M. GEORGE and F.P. SORRENTINO (1981). "A new Steel Slag for Cement Manufacture: Mineralogy and Hydraulicity". J Cem. Concr.. Res. 11, 1, 85-102.

53.- M. KAWAMURA, K. TORII, S. HASABA, N. NICHO and K. ODA. (1983) "Applicability of Basic Oxygen Furnace Slag as a Concrete Aggregate". 1rst International Conference Montebello Vol II, 1123- 1141.

54.- A. CARLES-GIBERGUES, B. THENOZ et A. VAQUIER (1980) "Utilisation d'un laitier de magnésium comme liant alumineux". VII CICC Paris, Vol II, III-78.

55.- J.R. BARAGANO and P. REY (1980) "The Study of a Non Traditional Pozzolan : Copper Slag". VII CICC Paris, Vol II, III-37.

56.- H. ROPER, F. KAM and G.JAULD (1983)" Characterization of a Copper Slag Used in Mine Fill Operations". 1rst International Conference Montebello. Vol II, 1091-1109.

57.- J. LANEUVILLE (1980) "The Hardening of Nickel Slags". VII CICC Paris-Vol II, III-52.

58.- E. DOUGLAS, V.M. MALHOTRA and J.J. EMERY (1985) "Cementitious Properties of Non Ferrous Slags from Canadian Sources". Cement Concrete and Aggregates. ASTM.0149-612318510006, 3-14.

59.- E. DOUGLAS and P.R. MAINWARING (1985). "Hydration and Pozzolanic Activity of Non Ferrous Slag". Ceram. Bull. Vol 64, n° 5, 700-706.

60.- D. RAVINA (1981) "Production and Collection of Fly Ash for Use in Concrete". Fall Meeting MRS. Symposium N.S. Diamond Ed. 2-11.

61.- P.L. OWENS (1980) "Pulverised Fuel Ash". Concrete n° 54, 35-36 July.

62.- P.J. NIXON, G.J. OSBORNE and C.N. SHEPPERD (1983) "Cementitious Properties of Slags from the British Gas/Lurgi Slagging Gasiper". Silicates Industriels, 12, 253-262.

63.- J.L. ALONSO (1986) "Characterization of Fly Ash". Report Task Group n° 1, RILEM Committee 67 FAB.

64.- S. DIAMOND (1981) "The Characterization of Fly Ashes". Symposium N. Annual MRS meeting. Ed. S. Diamond, 12-23.

65.- G. FROHNSDORFF and J.R. CLIFTON (1981). "Fly Ash in Cements and Concretes : Technical Needs and Opportunities". U.S. Dept Commerce. NBSIR, 81-2239. 27 pages.

66.- P.C. AITCIN, F. AUTEFAGE, A. CARLES-GIBERGUES and A. VAQUIER (1986) "Comparative Study of the Cementitious Properties of Different Fly Ash to be presented at the second International Conference on Fly Ash" Madrid 21-26 Avril 1985.

67.- P.K. MELITA (1983) "Pozzolanic and Cementitious by products as Mineral Admixture for Concrete. A critical Review. 1rst International Conference Montebello, Vol I, 1-46.

68.- S. DIAMOND and F. LOPEZ-FORES (1981) "On the Distinction in Physical and Chemical Characteristics Between Lignitic and Bituminous Flyashes". Symposium N. Materials Research Society. S. Diamond Ed 34-44.

69.- S. DIAMOND (1983) "On the Glass Present in Low-Calcium and in High-Calcium Fly Ashes. Cem. Concr. Res. 13, 459-464.

70.- B. MATHER (1984) "The Glass in Low Calcium Fly Ash. "Cem. Concr. Res. 14, 887-890.

71.- R.W. LINTON, S.R. BRYAN, X.B. COX, D.P. GRIFFIS (1986) "3D Chemical Characterization of Micron-Sized Coal Fly Ash Particles". MRS Annual Meeting Dec. 1985. To appear in MRS Vol 65.

72.- J. BERETKA and P.J. MATHEW (1984) "Natural Radioactivity of Anstralian Fly Ashes". 2nd International Conference on Ash Technology and Marketing. London 16-21 Sept, 719-724.

73.- A.R. REID (1984) "A Review of Toxicological Testing of Pulverised Fuel Ash". Ibid Ref. 72, 725-728.

74.- G.J. Mc CARTHY, K.D. JWANSON, L.P. KELLER and W.C. BLATTER (1984). Seminar K, MRS Meeting 1983, Cem. Concr. Res 14, 471-478.

75.- G.J. Mc CARTHY, L.P. KELLER, P.J. JCHIELDS, M.P. ELLES and K.C. GALBREATH (1984) "Mineralogical Characterization of a Lignite Gasification Ash From a Low-BTU Fixed-Bed Gasifier 1.X-Ray Phase Analysis. Seminar K, MRS Meeting 1983, Cem. Concr. Res. 14, 479-484.

76.- B.E. SCHEETZ, D.W. STRICKLER, M.W. GRUTZECK and D.M. ROY (1981) "Physical and Chemical Behavior of Selectively Etched Fly Ashes". Symposium N-MRS Meeting. S. Diamond Ed. 24-33.

77.- W. RICHARTZ (1984) "Composition et Propriétés des cendres volantes (Zusammensetzung und Eigenschaften von Flugaschen)". Zement, Kalk, Cips 2, 62-71.

78.- Y. HALSE, P.L. PRATT, J.A. DALZIEL and W.A. GUTTERDGE (1984). "Development of Microstructure and Other Properties in Flyash OPC Systems" Seminar N, MRS Meeting (1983). Cem. Concr. Res, 14, 491-498.

79.- R.J. STEVENSON (1984) "Mineralogical Characterization of a Lignite Gasification Ash from a Low-BTU Fixed-Bed Gasifer II. Scanning Electron Microscope "Phase Analysis" Seminar N. MRS Meeting 1983, Cem. Concr. Res. 14, 485-490.

80.- S. DIAMOND (1982) "Intimate Association of Coal Particles and Inorganic Spheres in Fly Ash". Cem. Concr. Res. 12, 405-407.

81.- F.H. HUBBARD, R.K. DHIR et M.S. ELLIS (1985) "Pulverized-Fuel Ash For Concrete" : Compositional Characterization of United Kingdom PFA". Cem. Concr. Res. 15, 185-198.

82.- S. DIAMOND (1986). A Procedure for the Interpretation of Fly Ash Particle Size Data". Symposium T MRS Meeting 1985. To appear in Vol. 65. Joint Highway Research Report FHWA/IN/JHRP.

83.- R.T. HEMMINGS (1986) "Characterization of Size and Density Fractions of a Canadian Fly Ash". Symposium T. MRS Meeting 1985 To appear in Vol 65.

84.- A. CARLES-GIBERGUES et A. VAQUIER (1985). "Influence du broyage sur la réactivité d'une cendre volante". Ciments, Bétons, Plâtres, Chaux, 752, 1/85, 46-50.

85.- P.K. MEHTA (1985) "Influence of Fly Ash Characteristics on the Strength of Portland. Fly Ash Mixtures". Cem. Concr. Res. 15, 669-674.

86.- D. RAVINA (1980) "Optimized determination of PFA (Fly Ash) fineness with Reference to Pozzolanic Activity". Cem. Concr. Res. 10, 573-580.

87.- K. TUUTTI and G. FAGERLUND (1985). "Fly Ash. Its properties and Fields of Application in the Cement Industry". Technology of Concrete when Pozzolans, Slags and Chemicial Admixtures are used". Rilem and ACI Symp. Monterrey N.L Mexico 103-119.

88.- Y. EFES (1980) "Etude des facteurs influençant la surface Blaine des cendres de charbon et des effets de la surface Blaine sur les autres propriétés". (Untersuchungen über Einflüsse auf die spezifische Oberfläche nach Blaine von Steinkohlenflugaschen une über Auswirkungen des Blaine-Wertes aud andere Eigenschaften). TAZ-Fachberichte Rohstoff-Engineering. 1/80-104, 20-29.

89.- E. RAASK (1980) "Utilization of Pozzolanic and Cenospheric Ashes". VII CICC Paris, Vol II, IV-1.

90.- M. RAVERDY, F. BRIVOT, A.M. PAILLERE et R. DRON (1980) "Appréciation de l'activité pouzzolanique des constituants secondaires". VII CICC Paris, Vol II, IV-36.

91.- B. MORTUREUX, H. HORNAIN, E. GAUTIER et M. REGOURD (1980) "Comparaison de la réactivité de différentes pouzzolanes". VII CICC Paris. Vol III, IV-110.

92.- S. SCHLORHOLTZ, T. DEMIREL and J.M. PITT (1984). "An Examination of the ASTM Lime Pozzolanic Activity Test for Class C Fly Ashes". Symposium K. MRS meeting 1983. Cem. Concr. Res, 14, 499-504.

93.- U. COSTA and F. MASSAZZA (1983) "Some Properties of Pozzolanic Cements Containing Fly Ashes". 1rst International Conference Montebello Vol I, 235-254.

94.- O.E. MANZ (1983) "Review of International Specifications for Use of Fly Ash in Portland Cement Concrete". IIrd Ref 93, 187-200.

95.- E. ROUSSOUW and J. KRUGER (1983) "Review of Specifications for Additions for Use in Concrete Ibid Ref 93, 201-220.

96.- F.H. HUBBARD (1984) "A compositional Index of The Pozzolanic Potential of Pulverized Fuel Ash". J. Mater Sci Letters 3, n° 11, 958-960.

97.- R.C. JOSHI, R.L. DAY, V.M. MALHOTRA and G.G. CARETTE (1986). "Relationship Between Pozzolanic Activity and Mineralogy, Morphology and Chemical Properties of Fly Ashes". Symposium T. MRS meeting 1985. To appear in MRS Vol 65.

98.- D. RAVINA (1981) "Efficient Utilization of Coarse and Fine Fly Ash in Precast Concrete by Incorporating Thermal Curing". J. AMER Conc. Inst. 78, n° 3, 194-200.

99.- A. CARLES-GIBERGUES, B. THENOZ et A. VAQUIER (1980). "Mécanisme d'hydratation d'une cendre de lignite calcaire". VII CICC Paris, Vol II, IV-53.

100.- E. VAZQUEZ, J. ROVIRA, R. AVRIN and A. ROCA (1985) "Effects of Accelerated Curing in Mortar and concrete with Fly-Ash Addition". Technology of Concrete when Pozzolans, Slags and Chemical Admixtures are used". Rilem and ACI Symp. Monterrey N.L. Mexico, 415-444.

101.- D.G. MONTGOMERY, D.C. HUGUES and R.I.T. WILLIAMS (1981) "Fly Ash in Concrete. A Microstructure Study" Cem. Concr. Res. 11, 4, 591-603.

102.- G.M. IDORN and N. THAULOW (1985) "Effectiveness of Research on Fly Ash in Concrete". Cem. Concr. Res. 15, n° 3, 535-544.

103.- D. MATHER (1983) "Cement Users' Expectations with Regard to Blended Cements". 1rst International Conference Montebello. Vol I, 255-266.

104.- S. DIAMOND (1982) "Rand D Needs to Stimulate Use of Fly Ash in Cement and Concrete : Long-Term R and D Requirements". Workshop at Electric Power Research Institute. Palo Alto California. W.T. Bakker Ed. 4, 34-44.

105.- J. METSO (1984) "Utilization of Finnish Peat Fuel Ash in Making Concrete". Silicates industriels, 6, 115-119.

106.- E. JONS (1985) "Sda-Ash as the only Residue from Flue Gas Cleaning" Technology of Concrete when Pozzolans, Slags and Chemical Admixtures are used. Rilem and ACI Symposium Monterrey NL Mexico 19-34.

107.- L. HJORTH (1982) "Microsilica in Concrete" Nordic Concrete Research Publication n° 1, Paper 9, 1-18, Oslo.

108.- G. RATH (1983) "The Operation and Design of Electric Reduction Furnaces for the Production of Ferrosilicon and Silicon Metal" Condensed Silica Fume Ed. P.C. Aitcin - Université de Sherbrooke Canada, 15.

109.- G. RAU and P.C. AITCIN (1983) "Different Types of Condensed Silica Fume". Ibid Ref 108, 9-14.

110.- P.C. AITCIN (1983) "Physico-Chemical Characteristics of Condensed Silica Fume" Ibid Ref 107, 16-19.

111.- H. KOLDERUP (1977) "Particle Size Distribution of Fumes Formed by "Ferrosilicon" Production". Air Pollution Control Association Journal. Vol 27n° 2, 127-130.

112.- M. REGOURD, B. MORTUREUX, P.C. AITCIN and P. PINSONNEAULT (1982) "Microstructure of Field Concretes Containing Silica Fume". Las Vegas, 249-260.

113.- H.H. BACHE (1981) "Densified Cement/Ultrafine Particle Based Materials". 2nd International Conference on Superplasticizers in Concrete Ottawa 1-35.

114.- A. TRAETTEBERG (1978) "Silica Fumes as a Pozzolanic Material". Il Cemento 5, 3, 369-376 (1978).

115.- H. ASGEIRSSON and G.GUDMUNDSSON (1979) "Pozzolanic Activity of Silica Dust". Cem. Concr. Res. 9, 2, 249-252.

116.- M. REGOURD, B. MORTUREUX and E. GAUTIER (1981) "Reactivity of Various Pozzolanes". Vth International Symposium Use of Pozzolanas-Monterey-Mexico, 1-14.

117.- A.D. BUCK and J.P. BURKES (1981) "Characterization and Reactivity of Silica Fume". Proc. of the 3rd International Conference Cement Microscopy, Houston, 279-285.

118.- M.W. GRUTZECK, D.M. ROY and D. WOLFE (1982) "Mechanism of Hydration of Portland Cement Composites Containing Ferrosilicon Dust". Proceedings of the 4th International Conference Cement Microscopy. Las Vegas, 193-202.

119.- M. REGOURD (1983) "Pozzolanic Reactivity of Condensed Silica Fume". Condensed Silica Fume. Ed. P.C. Aitcin, University Sherbrooke Canada, 20-24.

120.- P.C. AITCIN (1983) "Influence of Condensed Silica Fumeon the Properties of Fresh and Hardened Concrete". Ibid Ref. 119, 25-27.

121.- G.G. CARETTE and V.M. MALHOTRA (1983) "Early-Age Strength Development of Concrete Incorporating Fly Ash and Condensed Silica Fume". 1rst International Conference Montebello, Vol II, 765-784.

122.- M. REGOURD, B. MORTUREUX and H. HORNAIN (1983). "Use of Condensed Silica Fume in Blended Cements". Ibid Ref. 121, 847-866.

123.- S. LESSARD, P.C. AITCIN and M. REGOURD (1983) "Development of a Low Heat of Hydration Blended Cement". 1rst International Conference Montebello, Vol II, 747-764.

124.- V.M. MALHOTRA and G.G. CARETTE (1982) "Silica Fume. A Pozzolan of New Interest for Use in Some Concretes". Concrete Construction, 5, 443-446.

125.- P.C. AITCIN, C. BEDARD and M. PLUMAT (1980). "Very High Strength for Very High Strength Concrete". Seminar L. MRS 1984, Vol 42, 201, 210.

126.- J. JAHR (1983) "Possible Health Hazards from Different Types of Amorphous Silicas. Suggested Threshold Limit Values". Condensed Silica Fume. Ed P.C. Aitcin Univ Sherbrooke Canada 28-33.

127.- P. WIMITYONGSKUL, M.W.J.A. de SILVA and P. KARASUDHI (1981) "Current Stage of Research and Reactivity of Rice Husk Ash Cement". Vth International Symposium Use of Pozzolanas in Concrete. Monterrey NL Mexico.

128.- P.C. KAPUR (1985) "Production of Reactive Bio-Silica from the Combustion of Rice Husk in a Tube-in-Basket (TIB) Burner". Powder Technology 44, 63-67.

129.- D.J. COOK and P. SUWANVITAYA (1983) "Properties and Behaviour of Lime-Rice Husk Ash Cements". 1rst International Conference Montebello, Vol II, 831-846.

130.- J. GRZYMEK, W. ROSZCZYNIALSKI and K. GUSTAW (1980) "Hydration of Cements with Pozzolanic Additions". VII CICC Paris, Vol III, 66-71.

131.- V. GRBA, N. BLAZEVIC, Z. SOLJIC (1982) "Propriétés chimiques et physico-chimiques des systèmes de silicates pouzzolaniques. 1. Recherches Chimiques, Structurales et Techniques" (proprietades quimicas y fisico-quimicas de los sistemas de silicatos con activadad puzolanica. A. Investigaciones quimicas, estructurales y technicas) Cemento Hormigon. 53, 588, 973-986.

132.- F. MASSAZZA and U. COSTA (1979) "Aspects of the Pozzolanic Activity and Properties of Pozzolanic Cements". Il Cemento 1, 3-18.

133.- M. ALBENQUE, L. COLLON, S. LOREC, J.P. BOMBLED, B. MORTUREUX, M. REGOURD et J. VOLANT (1982). "Etude et mise au point de produits en argile stabilisée par le ciment". Ciments Bétons Plâtres Chaux n° 737, 4, n° 738, 5, 16 pages.

134.- J.P. BOMBLED (1983). "Evaluation technique d'un certain nombre de matériaux adaptés aux ressources des pays en voie de développement". Colloque UNESCO sur l'habitat des pays en voie de développement. Paris. 245-251.

135.- C. WEBER et J. BACOT (1983) "Faisabilité des parpaings en latérite-ciment" Ibid Ref 134, 55-59.

136.- M. MURAT et A. BACHIORRINI (1982) "Corrélation entre l'état d'amorphisation et l'hydraulicité du métakaolin". Colloque cristallochimie des kaolintes et applications. Paris Nov. 1981, Bull Muner Crist 105, 543-555.

137.- M. MURAT (1982). "Activation des argiles en réacteur solaire. Etude des ciments de métakaolin". Rapport final de recherche PIRDES-CNRS. Paris, 78 pages et Entropie (1983), 110, 82-85.

138.- M. MURAT (1983) "Hydration Reaction and Hardening of Calcinated Clays and Related Minerals" Cem. Concr. Res 13 (2) 259-266, 13(4), 511-518, 13(5), 631-637.

139.- J. AMBROISE (1984) "Elaboration de liants pouzzolaniques à moyenne température et étude de leurs propriétés physico-chimiques et mécaniques". Thèse Doctorat d'Etat-Lyon-2 juillet.

140.- B. MORTUREUX, H. HORNAIN et M. REGOURD (1982) "Liaison pâte de ciment-filler dans les ciments composés. Colloque International

Liaison Pâte de Ciment-Matériaux Associés. A 64. Toulouse (France).

141.- A. BACHIORRINI (1985) "Interactions physico-chimiques entre l'aluminate monocalcique et différents carbonates au cours de la réaction d'hydratation". Thèse Doctorat. Université Lyon.

142.- J. JAMBOR (1980) "L'influence de $3CaO.Al_2O_3.CaCO_3.nH_2O$ sur la structure de la pâte de ciment". VII CICC Paris 1980. Seminaire A, Vol IV, 487-492.

143.- J.P. OLLIVIER (1981) "Contribution à l'étude de l'hydratation de la pâte de ciment Portland au voisinage des granulats. Thèse Doctorat. Toulouse.

144.- M. CONJEAUD, B. LELONG et B. CARIOU (1980) "Liaison pâte de ciment Portland-granulats naturels" VII CICC Paris, Vol III, VII-6.

145.- A. BACHIORRINI, M. MURAT et A. NEGRO (1981). "Influence des ajouts calcaires sur l'hydratation de l'aluminate monocalcique". Colloque international. Liaisons pâtes de ciment-matériaux associés. Toulouse. A.1.

146.- R. GUYOT et R. RANC (1983) "La Maîtrise des propriétés du béton par le choix et la qualité des ciments avec ajouts calcaires". 1rst International Conference Montebello. Session scientifique.

147.- J.P. BOMBLED, G. BELLINA et B. MORTUREUX (1986) "Détermination des courbes granulométriques et des aires massiques des constituants de mélanges cobroyés : applications aux fillers et laitiers" Communication au 8ème Congrès International de la Chimie des Ciments. Rio de Janeiro.

148.- P.K. MEHTA (1980) "Investigations on Energy Saving Cements". World Cement Technology, 11, n° 4, 166-177.

149.- S. CHATTERJI, W. THAULOW and P. CHRISTENSEN (1982). "Pozzolanic Activity of byproduct Silica-Fume from Ferro silicon Production". Cem. Concr. Res. 12, 6, 781-784.

150.- G. FROHNSDORFF and J.P. SKALNY (1983). "Cement in the 1990s : Challenges and Opportunities" Phil. Trans. R. Soc. Lond. A 310, 17-30.

151.- R.L. CARRASQUILLO (1985) "Production of High Strength Pastes, Mortars and Concretes". Materials Research Society, Vol 42, 151-168.

152.- D.M. ROY and G.M. IDORN (1985) "Relation between Strength Pore Structure and Associated Properties of Slag-Containing Cementitions Materials". Materials Research Society, Vol.II 2, 133-142.

153.- L. HJORTH (1983) "Development and Application of High Density Cement-Based Materials". Phil. Trans. R. Soc. Lond A 310, 167-173.

154.- J.D. BIRCHALL (1983). "Cement in the Context of New Materials for an Energy-Expensive Future". Phil Trans. R. Soc. Lond. A 310, 31-42.

155.- S. DIAMOND (1985) "Very High Strength Cement-Based Materials. A Prospective". Materials Research Society. Vol 42, 233-243.

156.- N. ALFORD and J.D. BIRCHALL (1985). "The Properties and Potential Applications of Macro Defect Free Cement". Materials Research Society, Vol 42, 265-276.

157.- S. WISE, J.A. SATKOWSKI, B. SCHEETZ, J.M. RIZER, M.L. MACKENZIE and D.D. DOUBLE (1985) "The Development of a High Strength Cementitious Tooling/Molding Material". Materials Research Society. Vol. 42, 253-263.

SUB-THEME/SOUS-THÈME 3.2

Effect of blending components on hydration and structure formation.

Effets des composants des matières d'additions dans l'hydratation et dans la formation de la structure.

Chairman/Président :

J. Calleja
Instituto Español del Cemento y sus Aplicaciones (IECA)
Madrid, Spain

Principal Reporter/Rapporteur Principal:

H. Uchikawa
Onoda Cement CO., Ltd.
Tokyo, Japan

FUTURE TRENDS IN THE RESEARCH OF THE STRUCTURE, PROPERTIES AND BEHAVIOUR OF BLENDED CEMENTS

TENDENCES FUTURES DANS LA RECHERCHE DE LA STRUCTURE, LES PROPRIETES ET LE COMPORTEMENT DES CIMENTS AUX AJOUTS

J. CALLEJA. Professor, Instituto Español del Cemento y sus Aplicaciones (IECA).Madrid. Spain

SUMMARY: Any attempt to foresee the future of the cement research must be based on previous achievements and on the present knowledge in this field.

The most direct object of research in cement should be the applicability of its results to the solution of practical questions related to technological needs.

Consequently, any tendency on studies looking at the future must take into account the gaps in knowledge, the controversial aspects, the questions not enough clear, and more particularly the aim to solve specific problems in the area of cement and concrete technology.

The technological properties of cement derivatives greately depend, on the other hand, on their structure -macro and micro- in terms of porosity, permeability, stability and durability against physical and/or chemical actions; on the other hand, the behaviour of fresh and hardened concrete - rheology, water demand and retention, workability, setting and hardening mechanism and kinetics,shrinkage, creep, expansion, swelling, etc. -, depend on the structure of the cement derivatives as well.

Moreover, cements today and even more tomorrow may and must contain a certain proportion of addtions of more or less active natural materials or waste products for economical, technological and ecological reasons - energy and resources saving -. These materials present in - cements or in concretes may modify substantially the structure, properties an behaviour of - pastes, mortars and concretes.

The present Special Report attempts to show a partial and personal view of some possible and prioritary trends in the near future research in cement, taking into account the foregoing - considerations.

Qualquer tentativa de previsão do futuro da pesquisa do cimento deve basear-se nos conhecimentos anteriores e atuais adquiridos neste campo.

O objetivo mais direto da pesquisa sobre cimento deverá ser a aplicabilidade dos seus resultados para a solução de questões práticas relacionadas com as necessidades tecnológicas.

Consequentemente, qualquer tendência dos estudos voltados para o futuro deve levar em consideração as lacunas de conhecimento, os aspectos controvertidos, as questões ainda não bastante claras e, mais particularmente, o propósito de resolver problemas específicos na área da tecnologia do cimento e do concreto.

As propriedades tecnológicas dos derivados do cimento dependem, por outro lado, da sua estrutura - macro e micro - em termos de porosidade, permeabilidade, estabilidade e durabilidade contra ações físicas e/ou químicas; por outro lado, o comportamento do concreto fresco ou endurecido - reologia, necessidade e retenção de água, trabalhabilidade, mecanismo e cinética de pega e endurecimento, retração, fluência, expansão, inchação, etc. - também depende da estrutura dos derivados do cimento.

Além disso, os cimentos atuais e mais ainda no futuro podem e devem conter uma certa proporção de adições de materiais naturais ou de produtos de rejeito, mais ou menos ativos, por razões econômicas, tecnológicas e ecológicas - economia de energia e de recursos -.

Estes materiais, presentes nos cimentos ou nos concretos, podem modificar substancialmente a estrutura, as propriedades e o comportamento de pastas, argamassas e concretos.

Este Relatório Especial tenta mostrar uma visão parcial e pessoal de algumas tendências possíveis e prioritárias no futuro próximo da pesquisa do cimento, levando em conta as considerações anteriores.

FOREWORD

The task ascribed to this author consists in making an attempt to forecast the near future trends in the research dealing with hydration and structure of blended cements.

Obviously any future must be based on the present and on the past. Past and present have lead to a given level of knowledge, but they have also been able to show the existence of gaps in this knowledge, and the need of a more complete understanding of certain aspects of problems not yet solved, the solution of which being of the greatest interest for technological purposes.

Consequently, the need of more deep knowledge and the urgency to solve actual problems, and new problems continuously arising in the fields of theory and practice, are questions to be taken into account in a prospective of the future research in cement.

On the other hand, the task proposed may offer the possibility to use to some extent the imagination, as well as to provoke questions and answers on some of the yet controversial aspects of the item treated.

The author's aim has then to be manifold: to show the most outstanding items of the theme treated; to point out gaps, insuficiences and deficiences in the knowledge of it; to mention unsolved problems existing, and to put questions to get answers, all in the field of the future research trends on the structure, properties and behaviour of blended cements.

INTRODUCTION

Macroscipic properties and technological behaviour of cement pastes, mortars and concretes as factors conditioing their efficient employ in practice, depend basically upon the texture and microstructure of the cement matrix. This is formed by an homogeneous mixture of anhydrous cement and water, and serves to link together the other components of the conglomerates, i. e., the aggregates. The properties and behaviour of the conglomerates also depend upon the aggregates themselves

The texture and microstructure of the contact zones between cement matrix -paste- and aggregates, the so-called interfaces, also influence to a great extent the technological behaviour of mortars and concretes.

It is obvious that the microstructure of the cement paste depends in turn on the nature of the anhydrous cement, i. e. on its chemical composition and physical charactetistics (mainly upon its fineness -specific surface; particle size distribution-, shape and surface condition of the particles, etc.).

It is also evident that the structure of the interphase paste/aggregate is determined by the nature of the cement paste -ultimately by that of the anhydrous cement-, by that of the aggregate (physical, chemical and mineralogical characteristics of its surface), and by their mutual interactions.

All these factors so far mentioned are referred to the materials forming the conglomerates. But in addition to them there must be also be taken into account other factors dealing with the proportions of the materials, as for instance the w/c ratio in the cement paste and the amount of cement per unit volume or weight in mortars and concretes. Moreover, the way in which these materials are manipulated, i. e., the concrete technology affects the final result, as far as the conglomerate properties and performance are concerned.

The nature of the anhydrous cement and its behaviour in hydration, as well as the nature of the hydrated products formed are determined by the main cement components: clinker, setting regulator and additions ; among the latter, potentially or latent hydraulic products such as basic granulated blast-furnace slags; natural or artificial pozzolanic materials such as some volcanic rocks and fly ashes; and more or less "inert" materials such as fillers - mainly calcareous in nature: limestones-

The chemical composition of the mentioned components, their activity and reciprocal interactions, their relative proportions and their particle size distribution and specific surface, as well as those of the cements resulting from their blending, are decisive in determining the texture and microstructure of the cement paste and matrix, its internal cohesion and external adherence to the aggregates through the interphases formed, as well as in conditioning the corresponding macroscopic properties and behaviour of the conglomerates.

These properties, as referred to mortars and concretes, may be very simply grouped, from a practical point of view, in three main aspects: mechanical strength, stability (soundness) and durability.

The mechanical strenght of the conglomerates depends on that of the cement matrix and the aggregates, and on the bonding forces and lindkages between them. The stability or soundness is related to the constancy of volume in terms of shrinkage or in terms of expansion or swelling, all of them considered as potential causes of concrete cracking and failure.

Durability is a very wide concept which must be defined and limited to its correct context in each specific and particular instance. In most general terms it could be defined as the capability of the concrete to maintain a sufficiently acceptable security level all along its foreseable service life, in the forecasted actual service conditions. More restrictively considered, durability could be defined as the capability of the concrete to withstand any attack of external origin derived from its service conditions. In this respect durability could be considered as equivalent to chemical resistance, and in this sense the concept is usually and widely employed.

Mechanical resistance, stability and durability are closely related to each other, for the strength may decay as a consequence of instability or unsoundness, and this may in turn be produced either by internal actions of the concrete components or between them, or by external attacks caused by aggressive chemical agents - or by both together-.

Strength, stability and durability are conditioned by the physical texture and by the chemical and mineralogical structure of the cement paste. As far as the physical texture of the paste is concerned, porosity, permeability to fluids and penetrability to ions are concepts and measurable magnitudes of the greatest importance. In turn, porosity is a global concept which requires further precision, for in the case of the cement paste it is necessary to distinguish between total, capillary and gel porosity, in relation in each case with the shape and size of the pores, with their more or less extended open or closed character and interconnections,with the accesibility of fluids to them, with - their ability to develop capillary forces causing capillary suction and rise, etc.

Obviously porosity is more or less closely related to permeability and penetrability to ions and consequently is a decisive factor as far as durability is concerned.
Finally porosity, either considered as a - whole or considered in each of its particular aspects, depends and is conditioned (as well as its evolution) by the physical, chemical and mineralogical characteristics of the cement pastes, which in turn depend on the nature and properties of the anhydrous cement, other things being equal.

All the above mentioned relationships are - particularly important and show how decisive they may be when dealing with blended cements containing different proportions of additions more or less "active", such as those mentioned above.

SYSTEMS IN HYDRATED CEMENT PASTES

In cement pastes are three main different systems: one corresponding to the solid phases formed by the crystalline and gel-like products resulting from hydration(together with the not yet completely hydrated material); other corresponding to the spaces remaining between the solid phases, totally or partially void or occupied by the liquid phase of the paste; and the third one corresponding to the liquid phase itself. The - three systems evolve with time from the very beginning of the hydration. The structure and properties of the paste, as well as the perfomance of mortars and concretes, greately depend on the final characteristics of the paste, as a result of the nature and evolution of solid, liquid and voids systems.

Moreover, the evolution of the three systems are mutually affected, the changes in each of them being closely related to the changes of the other two. A manifestation of the parallel and interconnected evolutions of these systems is the controversial aspect concerning the increase of CSH density with the degree of hydration (time) (1) (2).

The nature and evolution of the systems are different depending mainly on the type of cement. Hence the differences existing between pastes of pure portland cements and pastes of blended cements.

Most studies on solid and void systems have been devoted preferently to pure portland cement pastes, but few of them deal with the pastes or the more complex cements. It is obvious because if the study of pure portland cement pastes is enough complicated, as several authors using many different techniques have shown, much more so must be the research on pastes of the so many old and new blended cements (containing blast-furnace slags,slags of metallurgies other than siderurgy,natural pozzolans, fly ashes, silica fume, thermically activated clays, rice husk ashes,brick flour, etc.). Consequently much scientific and technological papers have been published on the - former subject, but few of them on the latter In addition, no much comparative studies on both subjects are available

SOLID SYSTEM

The solid system of the hydrated cement paste is formed by all the hydration products from the anhydrous clinker phases, by those of the blended materials -if any- and by the products formed by mutual interactions between hydrated phases each other or with anhydrous phases. All the hydrating products-and then the solid system as a whole -evolve with time and external conditions.

In the case of portland cements the main hydration products which determine the morphology, structure and properties of the paste are those derived from the main clinker components, i. e., the anhydrous calcium silicates: tobermorite-like compounds CSH, portlandite CH resulting from partial hydrolysis of them, together with calcium sulfoaluminate hydrates and other more or less complex aluminate (ferrite) hydrates (AFt and AFm phases in general).The shapes and ways in which - these compounds are formed and evolve to their final state determine the nature and characteristics of the cement paste.

In the following but few mentions will be made - except if necesary or convenient- to pastes of pure single phases of the clinker; major attention will be paid to pastes of - different portland and blended cement types, as they are more directly related to the - technological behaviour and performance of mortars and concretes in practice.

CSH composition,morphology and anion structure

Many types of CSH have been mentioned by - different authors depending on the research methods used and the conditions involved. Among the characteristics determined for the better knowledge of CSH properties are the chemical composition -particularly the C/S

ratio, the presence of other elements such as Si, Al, Fe. Mg, alkalies, and the anion structure (degree of polymerization)-, the crystallinity,the size of the formations,etc i.e., the morphology. All this has lead to describe several types of products in different degrees of evolution according to the circumstances.

It must be remembered that generally speaking CSH in fully hydrated portland cement pastes is different from that of C_3S pastes,in that the former contains an appreciable amount of monomer (with dimer and polymer also present), small amounts of linear trimer and but little or no cyclic trimer and tetramer (3) (4).

In the same line other observations by several techniques show differences between hydration mechanisms and hydration products of C_3S and portland cement. It still remains - the question of the distinction between - "inner" and "outer" products, as well as - that between "early" and "late" products,as the latter may be considerer as those formed beneath the "early" products and pushing - them into the void spaces (5) (6).

These are the reasons why extrapolation of - what happens with C_3S hydration to the - hydration of portland cements is not advisable. For example, the early product of the portland cement hydration,according to some opinions, is not a "type E CSH" as in the - case of C_3S hydration, presented with the - appearance of foils or flakes formed on the surface of the C_3S (7); it is a gelatinous membrane coating the grains and approaching the phase AFt in composition, which is formed from aluminate phases and may cover all the cement particles (8). Moreover, there are also significant differences between the middle and late products, which in the case of C_3S ("type O CSH") - start from an initial viscous gel formed below the "type E CSH" and evolving to other varieties (similar to "type I CSH") or to "type III CSH", or even to other types depending on circumstances -available space- and in the case of portland cement are products of different nature (7) (8).

It is also foreseable that much more differences will also exist between CSH (primary and secondary) in blended cement pastes -particularly those of pozzolanic cements-with respect to pastes of a reference portland cement; as well as that these and other - differences in the structure of the pastes could explain differences in properties and behaviour of concretes from portland and - blended cements. This is a point which could be the objective for further research directed to induce in the cement paste the structure most favourable for given technological purposes.

As to the C/S ratio in CSH, the following considerations may be made. In ordinary - portland cement pastes (9) - in this case in agreement with C_3S pastes (10) (11)- there are substantial compositional variations between different CSH particles, as far as the C/S ratio and the amounts of A, S and F included in them are concerned.

C/S ratio in CSH ist most usually between 1,5 and 2,5. C in CSH can be partially substituted by M (for instance coming from slags or fly ashes) giving CMSH which contributes to strength in opposition to the CMSH coming - from attack of CSH by magnesium salts, with simultaneous formation of MH (12).

Differences also exist between CSH from C_3S pastes with and without pozzolans. For the latter (13) the ratio decreases from 3 - within the unreacted grain, to 2 at a distance of less than 1 μm from the grain surface, with ratios of 2,5-3 in between; this is more evident in older pastes. For the C_3S-pozzolan pastes the results are similar in the neighbourghood of the C_3S grain surfaces, but the C/S ratio decreases gradually when approaching the surface of the pozzolan particles; this proofs that Ca penetrates into the pozzolan grains. For higher alkali pozzolans voids can be developped between the surfaces of the pozzolan particles and the hydrated products (13).

Different values of the C/S ratio have been found in function of age and conditions. For instance, between 1 and 21 days the mean C/S value of type I and fibrous CSH is 1,88,higher as compared with the corresponding value 1,56 for C_3S (14) (15).

According to other data, in pastes of ordinary portland cement the mean C/S ratio decreases from about 2 to about 1,6; in addition, - significant amounts of A, S and F have been detected in CSH with higher C/S ratios, and even in the AFm phase (9).

C/S ratios decrease with time from 1,9 at 1 day to 1,4-1,6 after 2-3 years; in the same way the mean A/C+M and F/C+M ratios increase, and the mean S/C+M ratio decreases after several years (16).

As far as CSH compounds are concerned, it is well know that their types I to IV including their compositions -C/S ratio; presence of M which may replace C; presence pf A,F and even $\bar{S}$ which may replace S; $(C+M)/(S+A+F+\bar{S})$ ratio (17) -, as well as their forms: fibrous,foil-like, rolled foils, lamellar, tubular (solid or hollow), etc. and their anion structure (degree of polymerization of their silicate anions) may have a great influence in the micromorphology of the paste. For instance, in a pure portland cement paste the C/S in the CSH coming from alite was about 1,7, whereas in the paste of a cement containing fly ash the corresponding C/S was about 1,5 due to higher S values and to the presence of K in CSH. The increasing proportion of K in the CSH structure does not explain the reducing expansion effects caused by alkali-aggregate (silica) reaction (18). Other more general explanation of it is available, as will be exposed later on. (19)

Fly ashes accelerates C_3S and cement hydration reducing both CH and C/S ratio in CSH hydrated silicates, incorporating A, F and S in them, irrespective of the ash composition

(20) (21) due to the faster dissolution of C_3S caused by Ca^{2+} adsorption and CSH precipitation on the fly ash surface (20). Opposite results and explanations have also been reported (22) so that this is a controversial point

The microstructure of CSH fibers forming radiating bundles arranged in a honeycomb network substituting the glass of the cenospheres attacked by the pore solution is typical of portland cement and fly ash pozzolanic reaction; radial growing CSH is formed by both - topochemical nad through-solution mechanisms (23).

With much more active pozzolanic materials, as for instance silica fume, the C/S ratio in CSH may be as low as 1,2, all the CH formed being consumed by pozzolanic reaction. Nevertheless, the faster reaction of the cement takes place even with finelly divided inert fillers without pozzolanic activity (24).

On the other hand, the amount of reactive silica in pozzolanic materials increases the extent and the degree of condensation of the polymeric silicate anions to form double - chains, when reacting with C_3S (25).

Moreover, the composition of CSH varies from the outer part of the hydrating alite grains, more in the younger than in the older pastes, so that the mean C/S values oscilate between 1,7 and 2,7 and (C+M)/(S+A+F+S) values - between 1,4 and 1,7 (17), somewhat below those of pure C_3S pastes.

All this, as referred to cements containing highly active pozzolanic materials, indicates that anion polymerization takes places more rapidly in the presence of such materials (20), so that different types of - additions present in cement do in fact influence the above mentioned values and consequently the composition and maybe the microstructure and morphology of CSH hydrates.

Correspondingly to the faster reaction of cement alite in the presence of fly ash and silica fume in portland cement, the CH content of the pastes is much lower than in the case of pure cement pastes (21).

This behaviour corresponds mainly to low C fly ashes (class F); high C fly ashes (class C) having C/S ratios able to form directly CSH compounds (i.e., ashes having own - hydraulic properties) form CSH in radial - fibrous bundles on the surface of the consuming cenospheres(23).

It has been recently developed a method to study the distribution of alkalies -particularly K- between solid and liquid phases in the cement paste. It has been found that CSH gels with high C/S ratios do not significantly absorb K, and that absorption - rapidly increases as C/S decreases, which is explained in terms of colloidal particle charges: the charge is positive in high C/S surfaces, with no absorption; whereas the charge is neutral or negative as C/S decreases then acting van der Waals forces or - chemisorption, respectively, with the corresponding increase in K sorption (26).

The conclusion of the foregoing is that there may be substantial differences in the composition and structure of the CSH compounds, depending on the type of cement and on the presence (nature and amount) of blending additions to clinker.

As far as the anion structure of the CSH hydrated phases, as well as other characteristcs of their solid and void systems are concerned, they may determine certain particular behaviours of the hardened pastes, as for instance the - creep. Creep seems to depend more particularly on the degree of silicate polymerization (27), though there are many deficiences in the understanding of creep and on creep prediction (28).

The degree of polymerization of the silicate anions in CSH from C_3S, as studied by techniques based on the formation of trimethylsilylation derivatives (TMS), increases by causes not attributable to progressing hydration. On the other hand, drying processes and ageing may seriously influence the results(29).

Different techniques have shown that in the separation of linear from monocyclic or bicyclic species of polymeric TMS derivatives the major low molecular weight anion larger than dimer is probably the linear pentamer, and - that the most abundant anionic species larger than this, could be cyclic and bicyclic nonamer (30).

On the other hand, it is also to be expected differences as far as CSH in pastes of blended cements are concerned, as compared with - those of C_3S and portland cement. In fact (at least in the case of C_3S with natural - pozzolans, fly ashes and blast-furnace slags) the blended pastes show higher contents of dimer, trimer and polymer, as referred to the quantities of Si afforded by C_3S: this really demonstrates the existence of reactions due to the presence of blended materials (31), in the same way that other results (not dealt with here) have shown the influence of admixtures and treatments on the size of the tobermorite (11 Å or 14 Å) and on the composition, anionic size and structure -double chains, single chains- of the CSH gel formed (32).

As to the morphology of CSH, the microstructure of cement pastes at 8 months of hydration shows fibers of CSH emerging from a sublayer which borders zones of fine grained product. Both, fibers, and fine grained product contain traces of F and S, the C/S ratio being higher withing the fine grained material (33).

It must be considered the fact that in agreement with what has been exposed in dealing with methods (as referred to the structure of CSH), the nature of the cement pastes, as far as their morphology is concerned, is a matter of almost permanent controversy in many aspects. particularly in those related to hydration models of the silicate phases and their greater or smaller similarity with the models described for other systems in which the same forms of

precipitation have been observed - hollow tubes formation and tubular growths in silicate and aluminate systems, "silicate garden" effects in various systems including aluminates, etc. (34) (35) (36).

A macroscopic aspect of the morphology and structure of the cement paste largely affecting to its properties, and particularly to one of the main of them, the strength, is an uniform and homogeneous distribution of the hydrated compounds -especially the silicates- as well as an ordered and regular disposal of the boundary zones between different hydrates (37). The same is valid as to the distribution of voids and the pore size distribution in the cement paste.

It has been recently found that with an adequate use of "crents" (=crystallization components or agents) it is favoured the formation of highly basic calcium silicate hydrates (38).

Portlandite CH

As for CH, it seems that more than one kind of it exists in hydrated cement pastes(39).

Theoretical calculations and experimental studies have respectively considered and shown that isomorphous replacements of H by Si and other atoms may take place in interlayer sites under various conditions, provoking very variable morphologies in the CH, which in turn plays a decisive part as a matrix for gel formation in the hardening cement pastes (40) (41) (42).

It is possible that depending on the variable morphologies of the CH, its reaction with the acidic components of the blended materials in cements may differ, as far as the rate and completeness of the reaction are concerned. This may also be in connection with the nature of the products formed in different conditions -amount, shape and size of the crystals of CH in the case of C_3S hydration (43)-,which may affect the nature of the cement paste in mortars and concretes. In fact, it has already been reported that the CH formed in pastes of blended cement reinforced with alkali-resistant glass fibers show a higher affinity for the fiber surfaces than for the surface of fly ash or granulated slag particles which normally act as deposition areas for CH (44),

Though it has been said that the major contribution to the formation of the morphology and microstructure of the cement paste corresponds to the hydrated silicates, this does not mean that other phases (aluminate and ferrite simple and complex phases) do not participate. On the contrary, they take also part and what is much more important, their interaction and complementary contribution with the hydrated silicate phases determine the properties of the cement pastes, as will be seen in dealing briefly with aluminate phases.

Aluminate phases

Though less studied in relation with the structure and properties of the cement paste as compared with silicate phases, it can be said that in a similar way to what happens with the silicates, the presence of pozzolans and CH influences the transformation of hexagonal hydrated phases (AFm) into cubic phases, and that of ettringite (AFt) to monosulfate phase (AFm) -at least in C_4AF pastes-(45).

As far as ettringite is concerned, it may appear in the morphology of the cement pastes forming small angular rods in discontinuous layers on the surface of anhydrous particles. Probably CSH is formed thereafter in the discontinuities leaved by ettrigite, followed by the formation of CH around the previously formed particles and by the rolling up of the CSH (I) foils to form fibers which finally evolve to become CSH (III) (46). In this way there is a simultaneity-continuity between hydration of aluminate and silicate phases, both contributing to conform the microstructure and morphology of the cement paste.

Other cements form larger ettringite crystals much earlier (47). Normally the ettringite content in pure cement pastes decreases after a period of about 1 day, while in pastes of cements containing medium to high $\bar{S}$ contents the ettringite increases during 28 days and more -this may also occur in portland cements containing fly ashes- (21).

In such cases it is clear that the contribution of ettringite to the structure of the cement paste is even more important.

But not only the amount of ettringite formed influences the structure and morphology of the cement paste; its crystallinity also plays an outstanding role, being in turn influenced by the availability of Al atoms, SO_4^{2-} groups and the pH value in its formation, so that the lack or scarcity of Al atoms reduces the average length of the columns, and high pH values cause the loss of fibrous habit of the ettringite, giving place to products poorly crystalline, which form coherent coatings (48).

In this respect the presence of blended additions in cements may have in general a great importance in determining the final structure and morphology of the pastes, depending on the ettringite formation, as is the case mentioned for fly ash cements(21).

Ettringite expansion -mainly in the case of expansive cements- is still a controversial point as to wether the cause of expansion is due to water adsorption by the poorly crystalline material, or to crystall growth, or both (49). In this respect the knowledge of the influence of blended materials in cements would also be of value.

Ahother interesting point would be that of the conditions in which ettringite formation

takes place, either by through-solution or by topochemical mechanisms, or both sucesively in this order (50).

Finally, the use of "crents" (=crystallization agents or components) to induce the hydration and hardening of C_3A in such a way as to obtain much more stable forms of high sulfate calcium sulfoaluminates and sulfoferrites is being practiced with succes (38).

VOIDS SYSTEM (POROSITY)

The void space system condition the density (compactness), porosity, permeability, penetrability to ions, as well as the capillary and colloidal properties of the cement paste (capillary suction and capillary raise, osmotic membranes and cells formation, etc.)

But the characteristics of the voids system (pore structure of the paste) as far as size and pore size distribution are concerned are, as mentioned, determined by the own evolution of the solid system, through an interlocking dependence (1) (2).

Not only the properties mentioned, but particularly the perhaps most appreciated of them in concrete, i.e. the strength, is largely influenced by the porosity and its characteristics, and hence by the nature of the voids system.

The strength seems to depend on the pore size distribution rather than on the total pore volume of the void system (51) (52), so that it is convenient to distinguish between macropores, mesopores, micropores, capillary pores and gel pores, and to consider their relative proportions and variations when dealing with cement paste properties, such as strength, permeability and penetrability to ions, factors all of them determining and conditioning the durability.

The strength seems to be controlled by the largest pores and not by the total porosity, for the largest deffects, faults and flaws in structures condition their strength. A proof of it seems to be that the decrease of such largest flaws increases the strength (53). This increase could not be correlated with total porosity, but with the maximum pore size, according to the GRIFFITH theory (54), at least on a quantitative point of view(55).

Moreover it seems to exist an optimum ratio between larger and smaller pores which determines a maximum fracture toughness in pastes (56). Furthermore creep of cement pastes is affected by the widening of small pores, due to reduction of interactions between particles (57).

When artificial modifications are created in the structure of pastes and morters, so that a progressive closing of non saturated pores and a pressurizing of the free pore water are induced -for instance by cyclic loading-, the observed non linearity of the σ-ε curve is to be attributed to the closing of pores rather than to microcracking. (58).

The relationships between strenght and porosity, including the influence of the chemical composition of the cements and the strength developing capacity of the hydration products, have been interpreted with the aid of a model (59).

The pore structure of the hardened cement paste is such that the porosity is shifted towards the smaller pore sizes, which aids to a better resistance to chemical attack, and particularly to the effects of alkali-aggregate expansive reaction with cements containing very high amounts of alkalies(60).

In a broad sense, increases in strength have been attributed to decreasing in both macropososity and gel porosity, i.e.,to total porosity, as well as to an uniform distribution of hydrated silicates and to an orderly disposal of the contact zones between hydrated products.

The decreasing capillary porosity and the increasing thickness of the diffuse double layer on the pore surface with increasing slag content in cement causes a decrease in the Cl^- and SO_4^{2-} ionic diffusion coefficients, and a corresponding increase in corrosion resistance of concrete by chemical attacks. The permeability of blast-furnace-slag cements to Cl^- ion has been found to be greater than that to SO_4^{2-} ion (61) - perhaps due to the differences in their respective ionic radii and charges.

Microporosity, mesoporosity and macroporosity, as well as total porosity influence in very different ways the various properties and behaviour of the hardened cement pastes. For instance, mccroporosity and mesoporosity seem to be correlated to shrinkage rather than total porosity (27), as well as with the mineralogical composition of the cement -C_3A content- (62).

There have been presented arguments favouring the idea that the strength is largely influenced by the volume of the largest pores in the paste, in such a way that any correlation with total porosity is casual (63). Moreover and consequently an elimination or reduction of the largest pores naturally occuring in cement pastes would increase their strength (64). Not only the strengths are affected by the presence of larger pores in the paste, but also its permeability, which in turn affects the durability (65).

This may explain why pastes of blended cements containing materials able to form and to afford secondary tobermorite (for instance, blasf-furnace slags, natural pozzolans, fly ashes and other artificial pozzolans) show lower total and larger pores, lower permeability and penetrability to ions - also due to higher ion exchange capacity(66) and higher final strength and durability. In fact, the pore size structure of slag cement mortars differs very much from that of mortars made with ordinary portland cement (67).

total porosity, pore size distribution and other properties of cement paste and concretes is that the depths of carbonation in specimens of portland fly ash cements are essentially independent of the fly ash cement, though the speed of carbonation is influenced by the total amount of cementitious material per unit volume of concrete (as a consequence of its influence on the total porosity and on the larger-to smaller pores ratio). It also conditions the absence of steel rusting in the more compact and impervious concretes (68). Furthermore it has been found in the same line that diffusion of chloride ions within cement pastes is greatly influenced by the cement composition, and less by the w/c ratio (69)(70).

The influence of the pore size distribution -as far as the ratio of larger to smaller pores is concerned- is such that although the volume of pores in hydrated pastes is higher the higher the w/c ratio and the slag content in cement the differences due to w/c ratio decrease with the higher slag content in the cement paste(71).

If the foregoing is of general application to the pastes of any type of cement, in the case of pastes from blended cement containing natural pozzolans, fly ashes, calcined rice husk and hulls, as well in the case of cements containing granulated blasf-furnace slags, there is a useful correlation between pore size distribution and strength, permeability and sulfate resisting characteristics. The analysis of the pore size distribution seems to proof that the (simultaneous) enhancement of strength and chemical resistance is directly related to an important reduction of the total volume of the larger pores greater than 1000 Å (72) (73).

Porosity of blended cements containing fly ash or slag have higher total porosity but finer pores than pastes of reference portland cement for almost equal compressive strengths. In this respect hydration at higher temperatures benefits to the blended cements more than to the plain portland cement (74).

The influence of blending in the pore structure of the paste causes a different behaviour as far as permeability, penetrability to ions and durability against frost action and chemical attack are concerned which is more favourable to blended cements. A proof that properties of pastes such as porosity and strength of different cements containing or not fly ashes or slags are determined by their different pore size distribution is that mechanical properties at zero porosity are generally improved at ordinary temperatures and impaired at higher temperatures in blended cements containing slags or fly ashes.

Blended cements, as stated, have much finer pore structure and, evidently, a lower CH content than pure portland cements (75). In autoclaved materials the pore size distribution changes from coarse to fine with increasing contents of fly ash, and CH dissapears in the paste if the ash content is high enough (76). The influence of the pozzolanic action in modifying the pore structure of the paste sometimes explained by the filling of voids with the ettringite formed, is not only attributable to natural pozzolans and fly ashes, but also to clays activated by calcination with similar results, as far as sulfate resistance is concerned. This behaviour is maintained -as usually occurs-while voids are not completely filled and there is space available for the crystallization of ettringite without exerting expansive pressure(77).

Similarly and owing to the mentioned finer voids system in the case of blended -slag- cements, their pastes show a lower diffusivity to chloride ions, so that the salt scaling resistance of their concretes greately increases with the increasing slag content (78).

Permeability

Permeability of cement pastes is, as known, a decisive factor in concrete durability. The permeability coefficient of the pastes is a function, not only of the porosity,but also of the surface area of the hydration products and of the free energy for flow (79). Moreover, cement pastes with high especific surface areas can retain large amounts of water in a state of equilibrium, so that the migration of moisture is slower than in pastes having a high capillary porosity (80).

The decreasing capillary porosity and the increasing thickness of the diffuse double layer on the pore surface with increasing slag content in cement causes a decrease in the Cl^- ans SO_4^{2-} ionic diffusion coefficients, and a corresponding increase in the corrosion resistance of concrete to chemical attacks. The permeability of portland slag cements to Cl^- ion is greater than that to SO_4^{2-} ion - dependence between diffusivity and ionic radius- (61).

Moreover, the relationship between pore size distribution, permeability and slag content in blast-furnace slag cements is such that the permeability coefficient of a cement paste with 70% of slag is considerably lower than that of a cement paste with 30% of slag, despite the much higher total porosity of the former. The explanation is that the total porosity of the 70% slag paste is formed by 45 to 150 Å pores, more difficult to penetrate than the porosity of the 30% slag cement paste (72).

The mechanisms involved in the strength development of portland cement fly ash pastes (81) may explain the different structure and properties of the pastes from other different points of view, such as imperviousness and higher chemical resistance. Assuming that the particles of fly ash provide points within the paste which facilitates the easy and rapid nucleation of the cement hydration products

on them, these products may cover and occlude the individual fly ash cenospheres. As a consequence the strength and the porosity change from earlier to later ages, so that the former increases and the latter decreases as a result of the pozzolanic reactions.

Penetration of ions

Penetration of ions such as Cl^- and SO_4^{2-} in concretes is decisive for their chemical resistance to attacks. Ionic penetrability is different from permeability to gazes and liquids through cement pastes, though indirectly related to it. Diffusion of Cl^- ions into concrete is affected by w/c ratio (porosity, permeability) only in the surface layer and at short time of contact, whereas at longer times of exposure the main influencing factor in the depth of penetration is the cement composition. Moreover, it has been argued that Cl^- ion diffusion through pastes is largely determined by the cement composition and less by the w/c ratio (69) (70).

In this respect the blended cements may show substantially much less penetration than pure portland cement, as the Cl^- ion diffusion not only depends on permeability, but also on the ionic exchange capacity of the cement paste system in each case. This capacity is higher for blended cement according to their composition (66). In a different way the higher chemical resistance - particularly to $MgSO_4$ solutions and sea water- of blended cements, as compared with that of ordinary portland cements could be partially explained by a much more scarce substitution of Mg^{2+} for Ca^{2+} in CH and/or in CSH to form MH and secondary gypsum, to give in turn expansive secondary ettringite poorly crystallized (82). The major difficulty for substitution in the case of blended cement might be ascribed to: a lower amount of clinker and therefore of C_3S; a much less CH formed; a fixation of CH in the form of secondary tobermorite; a lower C/S ratio in the tobermoritic compounds formed, either primary or secondary (porosity, permeability and diffusion of anions are not accounted for here).

PORE LIQUID SYSTEM

Liquid phase in pores is the third component submitted to parallel evolution together with solid and voids systems. It is obvious that the evolutions of all the three systems are very closely linked to one another. Liquid phase is the vehicle through which dissolution, precipitation and crystallization processes take place, depending on solubilities, saturation or oversaturation conditions for the hydrating and hydrated products, according to their common presence and mutual interactions in it.

The clinker components which more rapidly pass into solution are obviously the more soluble: alkali sulfates and alkali hidroxides, giving to the liquid phase the corresponding pH-value and concentrations in the different cations and anions. These concentrations and pH values evolve as the hydration processes progress.

Studies on composition of the liquid phase in the pores must be done under equilibrium conditions, which not always is easy or possible.

Pore liquid analysis of cement pastes show high total alkali concentrations which reveals major differences between results of laboratory studies and the actual cement hydration in practice due to the high alkali content of the commercial cements -not common in laboratory cements-, which reduces the solubility of Ca, rendering it practically insoluble. This lowers the importance of the calcium transport involved in hydration mechanisms carried out through the liquid phase (26).

It is thought that taking into account the hight alkali content in the liquid phase, the presence of added blending materials in cement -slags, pozzolans, fly ashes- may be important as to the distribution of alkalies between solid and liquid phases.

The progress of the reactions between additions and cement could be followed by analysis of the liquid phase, though much time is required to attain a final state of equilibrium, particularly in the case of certain more slowly reacting addtions.

The similarity between K and Cs adsorption has permitted the use of radio-Cs to make accelerated studies of the foreseable long term adsorption of K by CSH. It has been found that high C/S tobermoritic gels do not significantly adsorb Cs, and that adsorption rapidly increases as C/S decreases, so that the uptake of Cs (K) by the solid phase CSH and the decrease of Cs (K) in the pore liquid, in relation with the C/S ratio, show, for instance, that silica fume reacts rapidly with CH, followed by high-silica fly ashes (26).

These studies, based on high pressure squeezing of cement pastes to separate the liquid phase, seem to have a promishing future.

BLENDED CEMENTS

As a matter of fact R&D on the field of blended cements containing blast-surface slags, nctural pozzolans and fly ashes - as the main blending materials -, as well as silica fume, rice husk, thermically activated clays, slags from metallurgies other than siderurgy, etc. continue to increase more and more, by obvious reasons already mentioned.

In this respect further increases are to be expected in the future, particularly when the European CEN standards on cement will be adopted in the EEC

The possibility of ternary and quaternary cements containing slags and/or pozzolans/fly ashes, and/or limestone filler as additions blended with clinker and setting regu

lator is already oblidgeing to much research in this field.

It must be thought that not only economical reasons of different order (ecology, spare of energy and material resources, profit of waste materials, reduction of energy consumption in cement manufacture) are involved, but also technological reasons (more resistant and durable cements as far as chemical resistance to sulfates and sea water attack, to Cl^- and SO_4^{2-} penetration, to alkali-aggregate expansive reactions, etc.)

Slag cements

Much of the questions related to the structure of blast-furnace slag cements pastes have been dealt with under other topics, particularly under the item "Fineness".

Nevertheless, it must be said here that, as far as other aspects are concerned, no similar unanimity of criteria exits as in the case of fineness.

For example, it has been argued that in normally ground slag cements the mineralogy of the clinker has an influence on the properties greater than that of the fineness (83). It has been also exposed that the chemistry and glass content of the slag has litle effect on certain behaviours of the slag cements, as for instance in hydrothermal treatments (84), though on the other hand other opinions show that minor components - among them the crystalline fraction-present in slags influence their hydraulicity, so that the presence of 3-5% of crystalline matter, rather than the total absence of it (as in completely vitrified slags) gives optimum results as far as reactivity is concerned (85).

In spite of these and other not fully concordant results -whose explanation would be worth while to clarify- the need to spare energy, to preserve resources of raw materials and to profit mass and energy of waste products have induced to study and test the possibility to use slags other than basic granulated blast-furnace slags, such as electrothermal-phosphorous slags (86), copper metallurgy slags (87), nickel metallurgy slags (88) in cement manufacture. The results so far obtained seem to be acceptable in each case, as compared with those of comparable portland-pozzolan cements, as far as strength and sulfate and sea water resistance are concerned.

All these new materials and the corresponding derived cements are requiring now and will require new studies and research in the future to adquire enough knowledge of them.

Blended cements containing 40 to 65% of pulverized granulated blast furnace slags may show higher strengths from 7 days onwards, better sulfate resistance and lower alkali-aggregate reactivity than the reference - portland cements (89), probably due to the fact that cements containing high enough slag contents give pastes with much smaller volume of pores greater than 500 Å; this is not the case for cements with lower contents (30%) or slag(90).

It has been recently found that it is possible to increase the hydraulic activity of blast-furnace slag cements acting on their hydration mechanism and on the formation conditions of their hydrated phases through a directed crystallization of their anhydrous active phases and through the chemical and thermical depolymerization of the vitreous structures of their active components(91).

Pozzolan cements

As in the case of slag cements many toppics related to natural pozzolan and fly ash cements have been treated in other parts of this paper, for instance in those dealing with the composition and morphology of CSH. However, other items will be deal with here, in relation with the already mentioned trend to spare mass of raw materials, to reduce energy consumption and to profit mass and potential energy of waste materials.

Among the natural materials, some of them with higher, lower or even no pozzolanic activity -diatomite, calcareous gaze and even pulverized limestone - may give cements with different behaviour as far as strength and durability are concerned. The mentioned materials give 28 days strengths and reductions in the CH available at 90 days decreasing in the order exposed. The resistance to sulfate attack was in the three cases higher than that of a reference portland cement(due to the decrease of CH in the two former cases and to formation of calcium carboaluminate hydrate in the latter (92).

Among pozzolanic cements with artificial products(waste products, sub-products, by-products), those made with burnt clay and waste roofing tiles give better sulfate resistance (though lower strengths) than pure portland cements (93).

A sub-product used successfully as pozzolanic material is silica fume. The reaction product formed by silica fume with a high content of amorphous silica very finely grained and with a great surface area, showing a high degree of pozzolanicity, seems to be CSH(1) with a C/S ratio of about I, which causes an improved development of strengths (60), particularly if combined with a portland clinker rich in alkalies(94).

Ash ofcalcined rice hulls or husk (another product rich in amorphous silica) used as pozzolanic material in proportions higher than the usual in pozzolanic cements provide high strength cements (95). Their pastes - should have a structure similar to that of the silica fume cements, i. e., less porous (smaller pores), more impervious and resistant to chemical attacks.

The lime content of fly ash mixed with portland cements seems to be in favour of an increase in strength and a reduction in the porosity of the pastes, due to a certain hydraulicity, perhaps as compared with the strength and porosity of pastes from portland cements mixed

with silica flour -exempt of lime- (96). This shows that not all the siliceous materials with pozzolanic activity react in the same way and lead to similar results. On the other hand the mutual interactions between clinker components and fly ash components is such that for instance, in the system formed by C_3A and fly ash the hydration is quite - different, depending on the origin of the C_3A -or on that of the clinker- (laboratory produced or kiln produced(97).

Care must be taken with respect to the possibility of expansions due to higher free lime contents in certain fly ashes. On the other hand the temperature contributes to accelerate the lime-fly ash reaction, to increase the adherence between fly ash grains and the surrounding hydration products and to achieve higher compacity and lower porosity and permeability in the cement pastes(98).

A relationship has been established between the chemical composition of the fly ash and the sulfate resisting behaviour of the concrete containing it, in function of the C and F contents and their ratio in the fly ash; the lower the C and the higher the F contents, the better the sulfate resistance (99).

For instance, sulfate expansion is greatly reduced for blended cements with low calcium fly ashes, irrespective of the ash content, and sometimes even with some high calcium fly ashes at contents higher than 10% (100), so that portland fly ash cement and also slag cement derived from an ASTM type I portland cement high in C_3A may behave like an ASTM type V portland cement with a C_3A content five times lower, as far as sulfate resistance is concerned (101).

Not only sulfate resistance, but also the resistance against alkali aggregate expansive damage and strengths are improved with blended materials, either fly ashes (18), natural pozzolans (102) or blastfurnace slags(103) and even with calcium and magnesium carbonates in small amounts -3%-(104), the explanation of it being the denser microstructure of the cement paste caused by crystallization of higly polymerized silicate anions (103) (104) and -partially at least- the chemical binding of alkalies in the structure of CSH (18) (103).

In fact, the contribution to strength (and probably some other benefits of the pozzolanic materials) have been attributed in some cases (105) to additional CSH formation -as mentioned elsewhere in this paper-, as well as to an increase in the degree of polymerization of the calcium silicate hydrates.

In this respect, the polymerization degree and the structure of the gel phases are very - important factors in determining the properties of concretes in dependence on the reactivity and amount of silica in the pozzolanic materials. Anyway this is a point not yet sufficiently studied (31) as data lacks which would be crucial to evaluate the reactivity of pozzolans and particularly that of fly ashes(106).

However, it has also been established that the difference in the pore size distribution of hidrated cements rather than their chemical composition plays a predominant role in the texture of the paste and consequently in the sulfate resistance, when ASTM type F fly ash and rice husk are used as pozzolanic materials (90). No controversy seems to exist in principle, as chemical composition and pore size distribution may be closely related each other, though it cannot yet be concluded on the influence of fly ash in the pore structure as to give an structure model of general validity (107), but the general consensus is that it reduces the proportion of total and large pores as a consequence of the pozzolanic reaction progress with increase of the amount of hydration products formed and reduction of permeability to fluids and penetrability to ions.

Though there is a general agreement in that pozzolanic cements show much better durability properties as compared with other cements, it seems to be clear that all the causes of it are not yet satisfactorily explained. For instance, questions such as the reduction to acceptable levels of the expansive reaction of active aggregates with high-alkali cements, by substitutiong a part of the cement by natural pozzolans (108) require futher study, although some -at least partial- explanations have been given for it (19). For example, a more general explanation is that the finer fly ash - like other pozzolans and slags which, in turn, are siliceous materials highly reactive with alkalies -, react with alkalies in the way that the overall expansion, instead of being the result of a set of few but very intense, localized and anisotropic actions, is the result of a set of many dispersed, isotropic and individually much weaker actions. Consequently extension, isotropy and weakness sustitutes to intensity, anisotropy and strengthness so that the expansive forces may be more easyly withstood, without damage or with much lees damage (19) . By the way, it must be said that this same principle of general application has also been invoked later to explain the influence of admixtures in expansive cements (109).

Much more recently it has been expressed that there where a cement matrix includes a large number of microparticles bonded to hydrates the capacity of the matrix to absorb volume changes -provoking stresses - without impairing concrete by cracking is very probably improved. This could be another similar principle of - more general application (110).

Nevertheless there is no a clear idea on the paper of fly ashes in the chemical mechanism of alkali-silica reactions (81). though it is assumed that ash particles act as nucleation points for hydrates and perhaps may contribute to stress relieving mechanisms tending to reduce microcrackning (81).

Moreover, as far as alkali aggregate reaction is concerned, the much better behaviour of the fly ash pozzolanic cements as compared with ordinary portland cements even low in alkalies, is not affected by a substantial alkali content

in fly ashes (even as "available alkalies") as they do not contribute to the alkali content of the pore solution(111). Perhaps this same explanation would be valid for alkali-trachytic natural pozzolans, but in any case other explanations not involving alkalies themselves may be afforded (19).

A more complete knowledge of the chemical and mineralogical composition, as well as of the petrography and diagenesis of pozzolans is necessary to overcome the lack of certitude in some aspects; to this lack contribute the difficulties involved in the evaluation of properties and behaviour of pozzolanic materials, which do not permit to explain - differences between them (112). As in the case of the new slag cements, further studies will be required to know better all the new pozzolanic cements.

In both cases of new slag cements and new pozzolan cements, as in some other cases, the technology has preceeded to the science, i.e. the pragmatism and the empiricism (for the moment) have advantage over the theoretical aspects. Nevertheless, it is foreseable that if such cements as the mentioned have to be developed, a major and deeper knowledge of them will be necessary, and surely the future research will be able to afford it.

Cements with limestone filler

Much attention is being recently paid to the use of limestone in certain proportions as blending material in cements, in order to reduce the fuel consumption in cement manufacture, without impairing the performance of the resulting cements.

Limestone has been considered as an additive not only for pure portland cements, but also for blast-furnace slag cements and pozzolanic cements. An example of it is the project of new European cement standards CEN.

In fact, small amounts of limestone up to 10% in portland blast-furnace slag cements improve the grindability, particularly if impure limestones are added. A 5% of limestone gives maximum bending strengths (15% higher than control) up to 91 days, but compressive - strengths at this time decrease almost proportionally to the limestone content. Drying shrinkage and sulfate resistance are improved (113). Even 2% of limestone addtion enhances the bending strength at much shorter times(114). The positive effect of small amounts of carbonate components in the grindability of clinker has recently been confirmed (115).

It is well know that limestone has been used in some countries instead of gypsum as setting regulator, because of the scarcity of gypsum and gypsum-like waste products or sub-products. This means that at the fineness of the cement -perhaps higher- the limestone reacts with calcium aluminates to form calcium carboaluminate hydrate, as in the case of the interfacial zones between calcareous aggregates and cement paste (116).
The presence of finely ground limestone in - cement pastes may alter the interfacial composition between limestone grains and the hydration products, as is the case between calcareous aggregates and cement paste. The bond between calcareous grains and hydrated cement paste is achieved through the formation of $C_4A\bar{C}H_{10}$, but no further contribution to - strength is afforded by limestone, as it does not form its own hydration products as in the case of slags, for instance.

In the case of quartz even an initial reaction is absent (12).

It would be worth while deeper research on this matter to clarify the action and influence of the blended cements containing, in addition, finelly ground limestone (117).

CONCLUSIONS AND FUTURE TRENDS

The follpwing conclusions could be drawn from the foregoing exposition:

1. As stated elsewhere, in reviewing the scientific and technical literature on cement it can be noticed that from year to year the research is widely repeated with minor or no variations. This fact has been attributed to the great number of researchers working in many different countries and to a not enough close examination of the literature(118).

2. However, there still exist many gaps in the scientific knowledge of several problems, the solution of which should be decisive to achieve advancements and developments in cement and concrete technology.

3. The so many technologies, methods, equipments and tools in general at disposal for research work in cement chemistry, physics, mineralogy and technology are often individually insufficient to solve the problems of knowledge put by the scientific and technological needs.

4. The isolated individual work, or the work done sporadically by small groups of researchers is not sufficient to gain a knowledge deep enough in the main questions of the fundamental problems.

5. As a consequence of the foregoing conclusions it should be advisable the previous - communication, as well as the coordination and the cooperation between research workers on cement, all over the world and to a much larger extent than up to now, in order to plonify in commom their more or less similar - researches and to save time and to spare costs and efforts in achieving more reliable results of general interest leading to more complete, clear and useful knowledge and understanding of the problems studied.

6. One way to do it could be the simultaneous focussing of as many research techniques as possible (successively on one and the same from several problems ordered prioritarily according with needs and general interest) by various experts especialized in the different fields of the research work, as those mentioned in conclusion 3.

7. It is to be expected that in the near future new techniques for study will arise and that some of those already established will be

improved or adequeately modified in order to overcome some of their present insuficiences or deficiences.

8. Among the gaps, or incertitudes mentioned in the foregoing -and consequently among the controversial aspects on the knowledge on the structure of the hydration products in cement pastes, dealt with in the preceeding exposition-, the following may be recapitulated:

- A not sufficiently clear definition and differentiation of the so many varieties of CSH compounds and forms, in relation with - the so many variables influencing them, particularly in the much less studied cases of - blended cement pastes.

- In connection with the foregoing, micromorphology of cement pastes in general-and that of blended cement pastes in particular, as less known - is a matter of almost permanent controversy, mainly in the aspect of hydration models for silicate phases, in comparison with models described for other systems and phases. This point should be more deeply considered and clarified.

- Another still controversial point refers to the conditions and mechanism of ettringite formation and expansion: topochemical/through--solution?; crystalline growth/water adsorption?; both?. Which would be the influence of blended materials in it?.

No total unanimity of criteria exists as to the relative influence of clinker mineralogy, glass content and crystalline fraction in slags, minor elements and fineness, as far as the hydraulicity and behaviour of blast-furnace slag are concerned.

- No much knowledge and experience is still available on slag of different metallurgies already used in slag cement manufacture, and on the corresponding cements.
- Not enought physico-chemical crucial data are available (in opposition to what happens for instance in the case of blast-furnace slags) to evaluate the activity of pozzolanic materials and more specificaly of fly ashes.

- In a similar sense no clear or complete ideas are yet formed either on the paper of fly ashes as regards the mechanisms of alkali-silica expansive reactions, or in the pore structure of the paste, so that in this latter case an explanation of general validity could be expressed.

These are some -certainly not all-the trends in future research on blended cements, from the point of view of the author. Theoretical aspects of the knowledge on the physics, chemistry and mineralogy of the cement pastes are combined in them with technological problems and needs, as related to concrete, which actually constitute the background of the cements.

1. T.KNUDSEN."A discussion of the paper 'Limiting values for the density, expansion, and intrinsic shrinkage in hydrated portland cement' by M.RELIS and I.SOROKA". Cem. Concr. Res. 12 (3) 123-124 (1982).
2. M.RELIS and I.SOROKA. "A reply to ref. 1. Cem. Concr. Res. 12 (1) 125 (1982).
3. A.K.SARKAR and D.M.ROY. "A new characterization technique for trimethylsilylated products of old cement pastes". Cem. Concr. Res. 9 343-352 (1979).
4. E.E.LACHOWSKI. "Trimethylsilylation as a tool for the study of cement pastes (2). Quantitative analysis of the silicate fraction of portland cement pastes". Cem. Concr. Res. 9 337-342 (1979).
5. H.M.JENNINGS and P.L.PRATT. "The use of a high voltage electron microscope and gas reaction cell for the microstructural investigation of wet portland cement". J.Mater. Sci. 15 (1) 250-235 (1980).
6. H.M.JENNINGS and P.L.PRATT. "On the reactions leading to calcium silicate hydrate, calcium hydroxide and ettringite during the hydration of cement". Proc. Paris Congr. 1980 Vol.II pp. 11-141/146.
7. H.M.JENNINGS, B.J.DALGLEISH and P.L.PRATT. "Morphological development of hydrating tricalcium silicate as examined by electron microscopy techniques". J. Amer.Cerem. Soc. 64 (10) 567-572 (1981).
8. P.L.PRATT and M.JENNINGS. "The microchemistry and microstructure of portland cement". Ann. Rev. Mater. Sci. 11 123-149 (1981).
9. A.E.MOORE. "Structure and composition of compounds in some fully hydrated cement pastes". Proc. Paris Congr. Vol.III pp.VI-97/ /102 (1980).
10. S.CHATTERJI and N.THAULOW. "Estimation of the chemical composition of precipitated phase by the electron beam-microanalytical technique". X-Ray Spectrometry 9 (1) 5-7 (1980).
11. S.CHATTERJI. "CaO/SiO_2 mole ratio of calcium silicate hydrate in fully hydrated tricalcium silicate paste". Cem. Concr. Res. 10 (6) 783-787 (1980).
12. G.WISCHERS and W.RICHARTZ. "Einfluss der Bestandteile und der Granulometrie des Zementes auf das Gefüge der Zementsteine". Beton Verlag GmbH, Düsseldorf, 35 p. (1982).
13. K.OGAWA, H.UCHIKAWA, K.TAKEMOTO and I.YASUI. "The mechanism of the hydration in the system C_3S-pozzolana". Cem. Concr. Res. 10 (5) 683-696 (1980).
14. H.F.W.TAYLOR. "Mineralogy, microstructure and mechanical properties of cements". Proc. Brit. Ceram. Soc. (28) 147-163 (1979).
15. J.E.BAILEY and D.CHESCOE. "Microstructure and mechanical properties of cement". Proc. Brit. Ceram. Soc. (28) 165-177 (1979).
16. E.E.LACHOWSKI, K.MOHAN, H.F.W.TAYLOR, C.D. LAWRENCE and A.E.MOORE. "Analytical electron microscopy of cement pastes: III pastes hydrated for long time". J. Amer. Ceram. Soc. 64 (6) 319-321 (1981).
17. P.L.RAYMENT and A.J.MAJUMDAR. "The composition of the CSH phases in portland cement pastes". Cem.Concr.Res. 12 (6) 753-764 (1982)
18. P.L.RAYMENT. "The effect of pulverised fuel ash on the C/S molar ratio and alkali content of calcium silicate hydrates in cement". Cem.Concr.Res. 12 (2) 133-140 (1982).
19. J.CALLEJA. "Quelques considérations fondamentales sur le problème de la durabilité du bèton. Application aux réactions alkali

granulat". Séminaire sur 'La Durabilité des Bétons et des Pierres'. Saint-Remy lès Chevreuse (France) pp. 1-36 Série FNB. Collège International des Sciences de la Construction (1981).
20. K.MOHAN and H.F.W.TAYLOR. "Pastes of tri calcium silicate with fly ash. Analytical electron microscope, trimethylsilylation and other studies". Proc.Symp. 'Effects of Fly Ash Incorporation in Cement and Concrete', Boston 1981 pp 54-59 (Mat.Res.Soc. Univ.Park, PA, 1982).
21. S.ABDUL-MAULA and I.ODLER. "Hydration reaction in fly ash portland cements". Ibid. (ref. 20) pp 102-111.
22. I.JAVĚD and J.SKALNY. "Hydration of tricalcium silicate in the presence of fly ash". Ibid. (ref. 20) pp. 60-70.
23. N.W.GRUTZEK, D.M.ROY and B.E.SCHEETZ. "Hydration mechanisms of high-lime fly ash in portland cement compsites". Ibid. (ref. 20) pp 92-101.
24. E.J.SELLEVOLD, D.H.BAGER, E.K.JENSEN and T.KNUDSEN. "Silica fume cement pastes: hydration and structure". Proc.Nordisk Minisеminar on Silica in Concrete, Trondheim (Norway) 1981).
25. R.SIERRA. "Distribution of the different forms of water in the structure of pure pastes of C_3S and portland cement". Proc.Paris Congr. Vol.III pp. VI-201/206 (1980).
26. F.P.GLASSER and J,MARR. "The alkali binding potencial of OPC and blended cements". Il Cemento 82 (2) 85-93 (1985).
27. A.BENTUR, J.H.KUNG, R.L.BERGER, J.F.YOUNG, N.B.MILLESTONE, S.MINDESS and F.V.LAWRENCE. "Influence of microstructure on the creep and drying shinkage of calcium silicate pastes". Proc.Paris Congr. Vol.II pp. -26/31 (1980).
28. B.R.GAMBLE. "Creep: problems and approaches involving the metastability of hardened cement paste". F.D.LYDON ed. 'Developments in Concrete Technology 1', pp. 163-171, Appl. Sci.Publ.Ltd. London 1979.
29. N.B.MILLESTONE. "Ageing and drying of tri calcium silicate pastes". Proc.Paris Congr. Vol. III pp. VI-131/134 (1980).
30. L.S.DENT GLASSER, E.E.LACHOWSKI,M.Y.QURESHI, H.P.CALHOUN, E.E.EMBREE, W.D.JAMIESON and C.R.MASON. "Identification of some of the polysilicate components of trimethylsilylated cement paste". Cem.Concr.Res. 11 (5-6) 775-780 (1981).
31. H.UCHIKAWA and R.FURUTA. "Hydration of C_3S-pozzolan paste estimated by trimethylsilylation". Cem.Concr.Res. 11 (1) 65-78 (1981).
32. V.HORVATH and J.PETROVIC. "A contribution on the determination of anionic structures of silicates". Silikaty 25 (4) 347-357 (1981).
33. B.J.DALGLEISCH and K.IBE. "Thin foil studies of hydrated portland cement". Cem. Concr.Res. 11 (5-6) 729-739 (1981).
34. J.D.BIRCHALL. "A discussion of the paper 'Cement tubules-another look' by P.BARNES, A.GHOSE and A.L.MACKAY". Cem.Concr.Res. 11 (2) 299-300 (1981); further discussion by D.D.DOUBLE, ibid. pp. 303-304; reply to J.D. BIRCHALL by P.BARNES et al., ibid. p. 301.
35. R.D.COATMAN, N.L.THOMAS and D.D.DOUBLE. "Studies of the growth of silicate gardens and related phenomena". J.Mater.Sci. 15 (8) 2017-2026 (1980).
36. W.WIEKER and H.STADE. "Silicate gardens - only a curiosity?. Spectrum (Berlin) (4) 18-21 (1981); Chem.Abstr. 95 208394 (1981).
37. N.N.KRUGLITSKII and R.G.VAGNER. "Effect of physical and chemical activation on the coagulation structure of cement dispersions and the microstructure of stone". Proc. 13th Conf.Silic.Sc.Silic.Ind. V.3 pp. 139-144 (1981); Chem.Abstr. 97 149602 (1982).
38. A.K.ZAPOLSKY, B.E.YUDOVICH et al. "Hydration in the C_3A-krent-gypsum-water system". Tsement (1) 16-17 (1985).
39. J.BENSTEDT. "Some instrumental investigations of portland cement hydration. Part II: Differential Thermal Analysis (DTA)". Il Cemento 76 117-126 (1979).
40. L.G.SHPYNOVA, N.V.BELOV and S.K.MELHNIK. "The role of the structure of portlandite in the formation of cement stone". Krystallogr. 25 (6) 1188-1193 (1980); Sov.Phys. Cryst. 25 (6) 680-683 (1980).
41. L.G.SHPYNOVA, N.V.BELOV and S.K.MELHNIK. "The possibility of isomorphism in portlandite". Krystallogr. 25 (5) 967-971 (1980); Sov.Phys. Cryst. 25 (5) 555-558 (1980).
42. L.G.SHPYNOVA, N.V.BELOV and S.K.MELHNIK. "Role of calcium hydroxide crystal structure in the formation of limestone and cement stone". Dokl.Akad.Nauk SSSR 257 (1) 178-181 (1981); Chem.Abstr. 95 102002 (1981).
43. J.P.BOYER and R.L.BERGER. "Influence of the temperature increased during the induction period of C_3S hydration on the microstructure and strength of C_3S mortars". J.Amer. Ceram.Soc. 63 (11-12) 675-680 (1981).
44. R.H.MILLS. "Preferential precipitation of calcium hydroxide on alkali-resistant glass fibres". Cem.Concr.Res. 11 (5-6) 689-697 (1981).
45. S.MONOSI, G.MORICONI and M.COLLEPARDI. "The effect of pozzolans on the tetracalcium aluminoferrite hydration". Il Cemento 77 (4) 229-236 (1980).
46. B.J.DALGLEISH, P.L.PRATT and E.TOULSON. "Fractographic sudies of microstructural development in hydrated portland cement". J. Mater.Sci. 17 (8) 2199-2207 (1982).
47. B.J.DALGLEISH, A.GHOSE, H.M.JENNINGS and P. L.PRATT. "The correlation of microstructure with setting and hardening in cement paste", Proc.Int.Conf. on Concrete at Early Ages 1 137-143 (1982), Paris, Presse P.& Ch.
48. C.J.H.HAMPSON and J.E.BAILEY. "On the structure of some precipitated calcium aluminosulfate hydrates". J.Mater.Sci. 17 (11) 3341-3346 (1982).
49. P.K.MEHTA. Introduction to Chap. 9 "Blended or Modified Portland Cements and High Alumina Cements". Cem.Res.Progr. p. 164 (1982).
50. M.M.ERKENOV. "Ettringite formation mechanism in the early periods of portland cement

hydration". Tsement (2) 16-17 (1985).
51. A.BAJZA. "Properties of cement pastes and mortars cured under different experimental conditions". Cem.Concr.Res. 12 (1) 39-50 (1982).
52. N.M.ALFORD and D.D.DOUBLE. "Determination of porosity in hardened cement pastes in relation to stregth". Stud.Surf.Sci.Catal. 10, 259-268 (1982); Chem.Abstr. 97 132406 (1982).
53. J.D.BIRCHALL, A.J.HOWARD and K.KENDALL. "Strong hydraulic cements". Proc.Brit.Ceram. Soc. 32 25-32 (1982).
54. N.M.ALFORD, G.W.GROVES and D.D.DOUBLE. "Physical properties of high strength cement pastes". Cem.Concr.Res. 12 (3) 349-358 (1982).
55. L.I.KNAB, J.R.CLIFTON and J.B.INGS. "Effect of maximum void size and aggregate characteristics on the strength of mortar". Liaisons Pâtes de Ciment Matériaux Associés, pp. C27-C32. Comm.Colloq.Int.Toulouse (France) Nov. (1982).
56. J.J.BEAUDOUIN. "Effect of humidity and porosity on fracture of hardened portland cement". Cem.Concr.Res. 12 (6) 705-716 (1982).
57. M.J.SETZER. "A model of hardened cement paste for linking shrinkage and creep phenomena", in 'Fundamental Research on Creep and Shrinkage of Concrete', pp. 47-57, F.H.WITTMAN ed., Martinus Neihoff Publ. The Hague, Netherlands (1982).
58. G.PONS and J.C.MASO. "Comportement méchanique d'éprouvettes de mortier soumisses à des chargements cyclique de faible fréquence: Influence du durcissement initial du mortier au moment de la mise en charge". Mat.Constr. (Paris) 15 (90) 539-547 (1982).
59. E.S.JONS and B.OSBAECK. "The effect of cement composition on strength described by a strength-porosity model". Cem.Concr.Res. 12 (2) 167-178 (1982).
60. H.ASGEIRSSON and G.GUDMUNDSSON. "Pozzolanic activity of silica dust". Cem.Concr.Res. 9 (2) 249-252 (1979).
61. E.G.LEVIT and S.S.OLYACHENKO. "Diffusion, permeability and corrosion resistance of portland slag cement in corrosive media". Izv.Sev. Kauk.Nauchn.Tsentra Vyss Shk (4) 90-93 (1980); Chem.Abstr. 94 213166 (1981).
62. V.DORKIN and Yu.ZAIRSEV. "Effect of cement kind in chemical and drying shrinkage". Proc. Paris Congr. Vol.III pp.VI-57/60 (1980).
63. N.M.ALFORD. "A theoretical argument for the existence of high strength cement pastes". Cem.Concr.Res. 11 (4) 605-610 (1981).
64. J.D.HOWARD and A.J.KENDALL. "Flexural strength and porosity of cements". Nature 289 388-390 (1981).
65. S.GOTO and D.M.ROY. "The effect of w/c ratio and curing temperature on the permeability of hardened cement paste". Cem.Concr.Res. 11 (4) 574-579 (1981).
66. O.E.GJORV and O.VENNESLAND. "Diffusion of chloride ions from sea water into concrete". Cem.Concr.Res. 9 (2) 229-238 (1979).
67. Y.SUZUKAWA, W.KOBAYASHI and S.OKABAYASHI. "Physical properties of portland blast-furnace slag cement mortars cured in air". Sekko To Sekkai (154) 2-10 (1978); Ceram. Abstr. 58 (1-2) 8f (1979).
68. Y.SUZUKAWA, M.MINAMI, S.SUZUKAWA and K. FUKUDA. "Twenty years test on concrete using fly ash cement". Rev. 33th Meet.Cem.Assoc. Japan, Paper 63 (1979).
69. S.GOTO and D.M.ROY. "Diffusion of ions through hardened cement pastes". Cem.Concr. Res. 11 (5-6) 751-757 (1981).
70. C.L.PAGE, N.R.SHORT and A.EL TARRAS. "Diffussion of chloride ions in hardened cement pastes". Cem.Concr.Res. 11 (3) 395-406 (1981).
71. Y.EFES. "Effect of cement with varying content of granulated blast-furnace slag on chloride diffusión in concrete". Betonwerk Fertigteil Tech. 46 302-306 (1980).
72. D.MANMOHAN and P.K.MEHTA. "Influence of pozzolana, slag and chemical admixtures on pore size distribution and permeability of hardened cement pastes". Cem.Concr.Res. 3 63-67 (1981).
73. P.K.MEHTA. "Studies on blended portland cements containing Santorin earth". Cem.Concr. Res. 11 507-518 (1981).
74. R.F.FELDMAN. "Durability of blended cements to high concentration of chloride solutions" Proc. 5th Int.Symp.Concrete Technology, pp. 263-288, Univ.Nuevo León, Monterrey, N.L. Mexico (1981).
75. R.F.FELDMAN. "Pore structure formation during hydration of fly ash and slag cements blends". Proc.Symp. 'Effects of Fly Ash Incorporation in Cement and Concrete' 1981. pp. 124-133 Ed.S.DIAMOND Mat.Res.Soc., Univ. Park, PA 1982.
76. S.NAGATAKI, E.SAKAI and T.TAKEUCHI. "The hydrothermal reaction of fly ash cement system and properties of autoclaved concrete with fly ash and superplasticiser". Rev. 35th Meet.Assoc. Japan p. 158 (1981).
77. C.SAMANTA and M.K.CHATTERJEE. "Sulfate resistance of portland pozzolanic cement in relation to strength". Cem.Concr.Res. 12 (6) 726-734 (1982).
78. G.FAGERLUND. "The influence of slag cement on the frost resistance of the hardened concrete". Swedish Cem.Concr.Res.Inst.Res. Report No.1 (1982).
79. T.C.POWERS. "The specific surface area of hydrated cement obtained from permeability data". Mater.Constr. (Paris) 12 (69) 159-168 (1979).
80. C.L.D.HUANG, H.H.SIANG and C.H.BEST. "Heat and moisture transfer in concrete slabs". Int.J.Heat Mass Transfer 22 (2) 257-266 (1979); Chem.Abstr. 91 78214 (1979).
81. D.G.MONTGOMERY, D.C.HUGHES and R.I.T. WILLIAMS. "Fly ash in concrete: a microstructural study". Cem.Concr.Res. 11 591-603 (1981).
82. M.REGOURD. "Phisico-chemical studies of cement pastes, mortars and concretes exposed to sea water. Performance of concrete in marine environment". Amer.Concr.Inst.Specc. Publ. SP-65 63-82 (1980).
83. P.HAWTHORN, E.DEMOULIAN, P.GOURDIN and C. VERNET. "Blast-furnace slags and clinkers mutual influences". Proc.Paris Congr. Vol. II pp. III-145/150 (1980).

84. R.D.HOOTEN and J.J.EMERY. "Pelletized slag cement: autoclave reactivity". Proc.Paris Congr. Vol.II pp. III-43/47 (1980).
85. E.DEMOULIAN, P.GOURDIN, F.HAWTHORN and C. VERNET. "Influence of slags chemical composition and texture on their hydraulicity". Proc. Paris Congr. Vol.II pp.III-89/94 (1980).
86. I.A.KRYZHANOVSKAYA. "Sulfate resistance slag portland cements based on electrophos phorus slags". Kompleksn.Ispolz.Miner.Syrya Vol.II 62-68 (1979); Chem.Abstr. 93 136993 (1980).
87. J.R.BARAGAÑO and P.REY. "The study of a non-traditional pozzolan: copper slags". Proc.Paris Congr.Vol.II pp.III-37/42 (1980).
88. J.LANEVILLE. "The hardening of nickel slags". Proc. Paris Congr. Vol.II pp.III-52/57 (1980).
89. F.J.HOGAN and J.W.MEUSEL. "Evaluation of durability and strength development of a ground granulated blast-furnace slag". Cem. Concr.Aggr. 3 40-52 (1981).
90. P.K.MEHTA. "Sulfate resistance of blended portland cements containing pozzolans and granulated blast-furnace slags". Proc. 5th Int.Symp.Concrete Technology, Univ. Nuevo León, Monterrey, N.L.México (1981).
91. Ya.Sh.SKOLNIK. "Possible increase of blast-furnace slag hydraulic activity". Tsement (2) pp. 14-15 (1985).
92. J.GRZYMEK, W.ROSZCZYNIALSKY and K.GUSTAW. "Hydration of cements with pozzolanic additions". Proc.Paris Congr. Vol.III, pp. IV-66/71 (1980).
93. A.THEVARASH, V.PERAMPALAM and M.SELVARATRAM. "Some studies in pozzolanic cements". J.Natl. Sci.Counc. Sri Lanka 7 (1) 57-64 (1979); Chem.Abstr. 93 30823 (1980).
94. A.TRAETTEBERG. "Silica fumes as a pozzolanic material". Cemento 75(3)369-376 (1979).
95. P.K.MEHTA. "Siliceous ashes and hydraulic cements prepared therefrom". U.S.Patent 4, 105, 459 Aug. 8 (1978).
96. B.B.HOPE. "Autoclaved concrete containing fly ash". Cem.Concr.Res. 11 227-233 (1981).
97. C.PLOWMAN and J.G.CABRERA. Cem.Concr.Res. 14 238-248 (1984).
98. H.SHIYUAN. "Hydration of fly ash cement at elevated temperature".Proc. 5th Int.Symp.Concrete Technology, pp. 15-34, Univ.Nuevo León, Monterrey, N.L.México (1981).
99. E.R.DUNSTAN. "A possible method for identifying fly ash that will improve the sulfate resistance of concrete". Cem.Concr.Aggr. 2 20-30 (1980).
100. J.C.ROSNERL, J.G.CHEHOVITS and R.G.WARBURTON. "Sulfate resistance of mortars using fly ash as partial replacement for portland cement". Proc. 6th Int.Ash Utiliz.Symp.Vol. I pp. 37-56 Reno, Nevada (1982).
101. N.P.MAILVAGANAM, R.S.BHAGRATH and K.L.SHAW. "Sulfate resistance of mortars containing superplastic sers with fly ash or blast-furnace slags". Developments in the Use of Superplasticisers, ACI SP-68 pp. 535-556, A. Concr.Inst. (1981).
102. D.H.CAMPBELL, C.H.WEISE and H.LOWE. "Mount St. Helena's volcanic ash in concrete". Concr.Intern. 4 (7) 24-31 (1982).
103. D.M.ROY and G.IDORN. "Hydration, structure and properties of blast-furnace slag cements, mortars and concretes". J.Amer.Concr.Inst. 79 (6) 444-457 (1982).
104. V.V.TIMASHEV and P.G.KOZHEMYAKIN. "Effect of calcium and magnesium carbonates as additives on hydration of portland slag cements". Tr.Mosk.Khim. (SSSR) (118) 70-78 (1981); Chem.Abstr. 97 16918 (1982).
105. P.HERR, W.WIENER and G.PRIEM. "The use of silica residue as admixture of pozzolan portland cements". Cim.Bét.Plât.Chaux (740) 169-171 (1981).
106. G.M.IDORN. EPRI Workshop Proc,Special Report CS 2616 SR (1982).
107. G.M.IDORN. Symp.N.Materials Research Soc. Annual Meeting, Boston pp.244-259 Nov.(1981).
108. R.POO. "Inhibition of the alkali-aggregate reaction using Mexican natural pozzolans". Proc. 5th Int.Symp.Concrete Technology, Univ. Nuevo León, Monterrey, N.L.México (1981).
109. M.D.COHEN and C.W.RICHARDS. "Effects of the particle sizes of expansive clinker on strength-expansion characteristics of type K expansive cements". Cem.Concr.Res. 12 (6) 717-725 (1982).
110. C.PLOWMAN. "The chemistry of PFA in concrete-A review of current knowledge". Ash Tech '84, Proc. 2nd Int.Conf. on Ash Technol. and Marketting, Barbican Centre, London, Sept. (1984).
111. S.DIAMOND. "Effect of the Danish fly ashes on alkali contents of pore solutions of cement-fly ash pastes". Cem.Concr.Res. 11 383-394 (1981).
112. F.MASSAZZA and U.COSTA. "Aspects of the pozzolanic Cements". Il Cemento 76 (11) 3-18 (1979).
113. I.OHARA, T.IWABUCHI, I.OKAWE and S.TEKEUCHI. "Effect of limestone on the properties of portland blast-furnace slag cements". Rev. 32nd Meet.Cem.Assoc. Japan 60-62 (1978).
114. H.MYARI and R:FURUKAWA. "Cement with high bending strength". Chem.Abstr. 90 108904 (1979).
115. M.PUCHYR and T.TABORSKY. "Properties of cements with carbonates as admixtures". Stavivo (7/8) 306-307 (1985).
116. J.GRANDET and P.OLLIVIER. "Etude de la formation du monocarboaluminate de calcium hydraté au contact d'un granulat calcaire dans une pâte de ciment portland". Cem.Concr.Res. 10 (6) 759-770 (1980).
117. C.A.LANGTON and D.M.ROY. "Morphology and microstructure of cement paste/rock interfacial region". Proc.Paris Congr. Vol.III pp. VII-127/132 (1980).
118. S.MINDESS. "Introduction to Chapter 7 "Properties of fresh and hardened pastes"". Cements Research Progress Chap. 7 p. 152 (1980).

THEME III - BLENDED AND SPECIAL CEMENTS

3.2 EFFECT OF BLENDING COMPONENTS ON HYDRATION AND STRUCTURE FORMATION

by **Hiroshi UCHIKAWA**, Dr. Eng., ONODA Cement Co. Ltd., JAPAN

1. INTRODUCTION

The blending component has been traditionally used for improving the properties of fresh and hardened cement as well as saving resource and energy. The qualities and role of it have been considerably varied as the social and economical environments have changed.

The characters of blending components have extremely changed by lowering the basicity of granulated blastfurnace slag caused by the progress of iron manufacturing technology and by increasing of the unburnt carbon and lime contents of fly ash by exhaust gas circulation, two step combustion and lime stone injection in the coal combustion furnace for lowering NOx and SOx. Besides, the characters of fly ash have remarkably varied by the combustion process of coal. Silica fume byproduced in the manufacturing process of metallic silicon and ferrosilicon has gained recognition for application as the blending component with growing of the semiconductor industry and of the production of steel. Since these blending components have been accompanied by natural pozzolana, the kinds of them are being increased.

Mechanical placing of concrete and shortening of the construction term have become possible by the progress of construction technology. As a result, the water reducing agent, AE agent and superplasticizer have been commonly used and curing always has been insufficient, so the demands for improving the properties such as workability, its time dependency and setting of fresh concrete and strength and durability of hardened concrete are becoming increasingly severe.

Since the characters of blending component have been changed and varied, and the application of blended cement has been diversified, it is necessary to clarify the effect of the characters of blending component on the high stable properties and performance of blended cement. It is essential, therefore, to make clear the relationship of flocculation structure of fresh cement paste and the structure of hardened cement paste with the characters of blending component by characterizing the blending component sufficiently and reviewed the effects of the characters of blending component on the hydration of blended cement based on the equilibrium theory and kinetics.

From these viewpoints, this paper reviews based on the research reports published since the 7th International Congress on the Chemistry of Cement held in 1980 to collect new knowledge.

2. CHARACTER OF BLENDING COMPONENTS

2.1 Slag

2.1.1 Origin and classification of slag

Slag is a byproduct which is separated from molten metals as a low melting point substance by adding agents such as limestone in the process of refining metal oxide in ore under reducing atmosphere. It is divided into two category, that is, ferrous slag which occupies large part of slag and nonferrous slag. The former is corresponding to blastfurnace slag and converter slag byproduced in steel making process, while the latter, to nickel slag, copper slag, lead slag and so on. Slag as a blending component for cement is characterized by high latent hydraulic property and granulated blastfurnace slag is well known. Recently, several papers (1)(2)(3) have been reported on the hydraulic property of nonferrous slag and converter slag. These slags have, however, poor hydraulic property and often contain substance hampering the hydration of cement, so their uses are rather limited. As for blastfurnace slag, it is classified into quenched slag and slow cooled slag. The latter is slowly cooled in air, which is rich in crystalline phase with poor hydraulic property, therefore it is not used as a blending component for cement. On the other hand, the former has high latent hydraulic property so that it is used extensively as blending component. Quenched one is called as granulated, pelletized or rapid air-blowed blastfurnace slag, depending on their cooling methods. Although these slags contain various amounts of glass phase, there is no remarkable difference on the kinds of crystalline phase.

2.1.2 Chemical composition of granulated blastfunace slag

The chemical composition of slag changes corresponding to impurities in iron ore, limestone or dolomite added and ash in cokes used as the reducing agent. The main constituents of SiO_2, Al_2O_3, CaO and MgO are in the range of 27-40, 5-33, 30-50 and 1-21%, respectively (4). It contains less than 1% of Fe_2O_3, 0.003-0.007% of Cr_2O_3, less than 3% of TiO_2, less than 2% of MnO, less than 3% of S, 1-3% of Na_2O+K_2O, 0.02-0.09% of P_2O_5, 0.19-0.26% of Cl and 0.09-0.23% of F (4)(5). Overall chemical composition is almost the same as melilite which is a solid solution of gehlenite (C_2AS) and akermanite (C_2MS_2).

According to the improvement of iron refining processes, chemical composition of the slag byproduced tends to increase in SiO_2 and MgO content while Al_2O_3 remains same. **Fig. 1** shows the position of each blending component in the ternary $CaO-Al_2O_3-SiO_2$ system. Slag is richer in CaO and MgO than the other blending components.

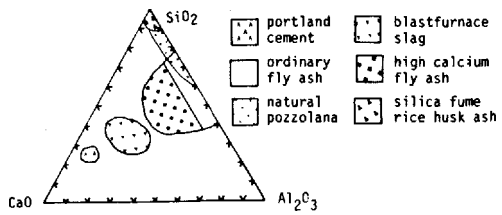

Fig. 1 The position of each blending component in the ternary $CaO-Al_2O_3-SiO_2$ system

Many studies (5)(6) pointed out that the basicity defined as the ratio of basic to acid element is not necessary suitable index for the evaluation of reactivity of slag. They are still, however, one of the reliable index at present and it is recommended to keep CaO/SiO_2 and $(CaO+MgO+Al_2O_3)/SiO_2$ more than 1.0 and 1.4, respectively.

In a pure water, Ca and Si ions are dissolved depending on C/S ratio of slag and the solution reaches pH of about 10. On the other hand, in an alkaline solution of pH 13, the amount of Ca, Al and Si ions dissolved is increased up to 8-10, 1-2, 3-4 ppm, respectively in about 10 minutes (7). These amounts, however, decrease after hydrates precipitated and change with the chemical compositions and the condition of slag produced.

2.1.3 Glass phase content and crystalline phase of granulated blastfurnace slag

The content of glass phase in slag varies with chemical composition, initiation temperature of cooling and cooling method. With the increasing ratio of $(CaO+MgO)/(SiO_2+Al_2O_3)$ of slag in the range of more than 1.15, glass phase content of slag decreases because network former of glass such as SiO_2 and Al_2O_3 is reduced (8). Slag melts completely at 1713°K and more, begins to crystallize melilite below 1673°K and perfectly crystallizes below 1593°K.

From the phase diagram in the system $CaO-Al_2O_3-SiO_2$ with 10% MgO by Osborn et al (9), the overall chemical composition of slag lies in the range of initial crystallization area of melilite, therefore the amount of melilite in crystallized phase occupies over 70%. Melilite has gehlenite side composition at first, but gradually moves to akermanite side with crystallization. Accordingly, crystal is generally zoned rectangular plate or cubic with the size of 50 to 500 μm. Subsequently crystallized materials are the two of seven phases of merwinite (C_3MS_2), larnite (C_2S), rankinite (C_3S_2), wollastnite (CS), pyroxene (CMS_2), forsterite (M_2S) and monticelite (CMS) which lie in adjacent to each other in the surrounding initial crystallization area of melilite (9). Composition of slag lies generally in the range satisfying two equation, $CaO+2.78MgO-1.86SiO_2>0$ and $SiO_2-0.59Al_2O_3-2.98\ MgO>0$. Merwinite and larnite are crystallized after melilite with decreasing temperatures Small size larnite is crystallized at eutetic point when melt is cooled very slowly.

The glass content in slag is one of the most valuable indexes for evaluating hydraulic property of slag (4) (6). As glass phase has internal energy of 200 J/g, it shows higher reactivity than crystal phase (4). Although granulated blastfurnace slag used for blended cement contains 70% or more glass in general, but it usually exceeds over 95% in Japan (5).

2.1.4 Composition and structure of amorphous phase

The difference in chemical composition between glass phase and overall slag itself is considered to be slight based on the results of electron probe microanalysis (EPMA) of glass phase (7). Glass phase tends to have lower Al_2O_3 and higher MgO with the decreasing of glass content. This phenomenon is caused by variation of local chemical composition of crystallized phase as shown in **Fig. 2.** In general, chemical composition of slags with high glass phase content is microscopically homogeneous but that of slag rich in crystalline phase is heterogeneous.

The structure of amorphous phase is classified into two group, that is, structure of atomic level and structure of texture level which ranges from several to tens nm. Glass phase consists of the network former such as SiO_4^{4-} and the network modifier such as six coordinated Ca^{2+} existing in the gaps of network formers to balance the electrical charges. **Table 1** shows the kinds and coordination numbers of molecular groups in amorphous phase from the results of previous papers. It has found that Al and Mg act not only network former but also network modifier.

The condensation degree of silicate ion in slag measured by IR is smaller than that of other blending components as shown in **Fig. 3,** which consists mainly of monomer and dimer. A result is supported by



	Al_2O_3 content	basicity ((C+M+A)/S)
white	more than 65%	more than 2.2
pink	30-	2.0 -
red	15-	1.9 -
yellow	10-	1.85-
green	7-	1.8 -
light blue	5-	1.75-
blue	3-	1.65-
black	less than 3%	less than 1.65

Fig. 2 X-ray map of Al and $(CaO+MgO+Al_2O_3)/SiO_2$ ratio on the polished surface of slag grain rich in crystalline phase by EPMA with ultra-high speed wide area multianalyser (7).

Table 1 Kind of network former and network modifier

	coordination number	kind of ion and ion group
Network former	4	SiO_4^{4-}, AlO_4^{5-}, MgO_4^{6-}
Network modifier	6	Ca^{2+}, Al^{3+}, Mg^{2+}, Na^{+}, K^{+}

the data of ^{29}Si chemical shift on the number of bridged and nonbridged oxygen in SiO_4 tetrahedron by nuclear magnetic resonance with fourier transformer (FT-NMR) (7). Namely, the number of bridged oxygen ranges 0.5 to 0.8 and silicate ion consists mainly dimer $Si_2O_7^{6-}$, and monomer SiO_4^{4-}.

Measurement by trimethyl sililation method (TMS) indicates that monomer and dimer of silicate in slag increase with increase of glass content regardless of thermal treatment and chemical composition of slag (7). In general, condensation degree of silicate ion in slag decreases with increase of the C/S ratio, A/S ratio, amount of MgO and content of minor constituents which can take fourfold coordination. **Fig. 4** shows one example of the kind and amount of silicate ion in slags measured by TMS in comparison with the other blending components.

Although Al had previously been considered to be in sixfold coordination, both sixfold and fourfold coordinations are recently proved to exist. Al trends to change from fourfold to sixfold coordination as the content of CaO and MgO, C/S and A/S ratio increases (10). Al of fourfold coordination increases in the crystallized slag. In plant slag having 5% of MgO, 0.45 of A/S ratio and 1.2 to 1.3 of C/S ratio, the rate of fourfold and sixfold coordination is found to be 2:3.

As for structure of amorphous phase, irregular network structure of Si-O chain of silicate and agglomerated structure of very minute crystal are proposed from two different stand points. No x-ray small angle scatter-

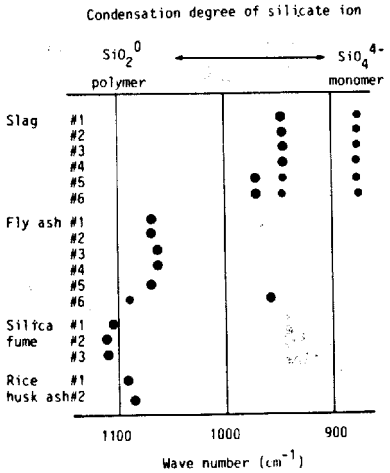

Fig. 3

Peak position of infra-red absorption spectrum of blending component (7)

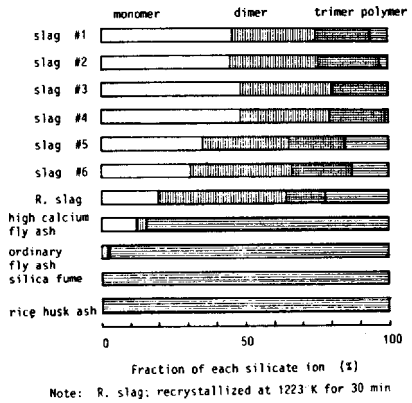

Fig. 4

The kind and amount of silicate ion in blending component measured by TMS (7)

ing of quenched slag, however, recognized (7). Electron emission by photoexcitation suggests that structure defect of slag varies by it cooling condition (11).

2.1.5 Shape and fineness of slag

Blastfurnace slag is a sharp-pointed and irregular shaped sandy material having particle size of a few mm. It is used by separate grinding or intergrinding with portland cement clinker. In separate grinding, it is ground to a Blaine specific surface area of about 3,000-6,000cm^2/g according to the desired quality of blastfurnace slag cement. It is well known that hydraulic activity are improved when slag is ground to 43μm or less in particle diameter (8), so it is ground to finer particle size than ordinary portland cement.

2.2 Fly ash

2.2.1 Origin and classification

Fly ash is a coal ash recovered from boiler exhaust gas which is produced by ground coal firing in power station, and consists of spherical fine particle of certain size. Character of fly ash depend upon the kinds of coal and combustion temperature at boiler. Crystalline phase in fly ash varies with the CaO content in coal. The higher the burning temperature, the more it contains amorphous phase and spherical particles. Fly ashes produced by cyclone furnace operating at high burning temperature (2073-1773°K) and by fine ground coal firing furnace (1773-1273°K) are suitable for blending component for cement.

In this paper, fly ash with small amount of CaO having basicity ($(CaO+MgO+Al_2O_3)/SiO_2$) of 0.2 to 0.7 is called ordinary fly ash and much amount of it having basicity of 1.0 to 1.8 is named high calcium fly ash.

2.2.2 Chemical composition

The chemical composition of fly ash depends on the composition of original coal ash. Ash obtained from anthracite and bituminous coal is known as ordinary fly ash and one from sub-bituminous and lignite coal is named as high calcium fly ash. As shown in **Fig. 1**, ordinary fly ash is poor in CaO and MgO and rich in SiO_2 and Al_2O_3 compared with blastfurnace slag. On the other hand, composition of high calcium fly ash is similar to that of slag. Main chemical composition of ordinary fly ash and high calcium fly ash is SiO_2: 34-60%, 25-40%, Al_2O_3: 17-31%, 8-17%, Fe_2O_3: 2-25%, 5-10%, CaO: 0.5-10%, 10-38% and MgO: 1-5%, 1-3%, respectively. These chemical compositions varies depending on the kinds of fly ash as well as on each fly ash particle itself and position of particle (7)(12). In general, the smaller the particle size become, the larger the amounts of CaO, alkalies and SO_3 is, and the larger the particle size, the richer the Al_2O_3 content. It contains P_2O_5, TiO_2, MnO, BaO and SrO less than 3, 3.5, 1, 1 and 0.5%, respectively (13)(14)(15). Unburnt carbon content generally ranges in 2-4%, but some cases it reaches 10%. Crystalline and amorphous carbon in fly ash has irregular or spherical shape with a specific surface area of a few to hundreds m^2/g and amount of which is increased in case of low temperature and reduced atmosphere combustion to reduce nitrogen oxide in exhaust gas (21).

CaO, SiO_2, Al_2O_3, Na_2O, K_2O, SO_3 and P_2O_5 in fly ash dissolve into water. The amount of dissolved ranges 30-750, 0.5-10, 0.4-30, 1.7-10, 1.0-35, 0.5-1,400 and less than 0.5ppm, respectively.

2.2.3 Glass phase content and crystalline phase

The content of glass phase in fly ash depends on its chemical composition and the combustion temperature of coal. The melting point of ash in the system SiO_2-Al_2O_3 is 1573-1773°K and that in the system CaO-SiO_2-Al_2O_3 is 1373-1573°K. When quenched from higher temperature than these, fly ash is vitrified.

Ordinary fly ash exposed to high temperature contains small amount of crystalline quartz and mullite. As shown in **Fig. 5**, mullite forms radially developed texture suggesting crystallization from molten glass phase. As exposed temperature is decreased, magnetite (Fe_3O_4), hematite (Fe_2O_3) and anhydrite coexist with quartz and mullite. Metallic iron film is occationally observed on the surface of magnetite and hematite. As ash does not melt below 1273°K, mullite is not produced and clay mineral in coal remains partly without being dehydrated and decomposed (16).

High calcium fly ash exposed to high temperature contains mullite, quartz and C_3A. When exposed to lower temperature, hauyne ($C_3A_3 \cdot CaSO_4$) and in some cases a small amount of free lime coexists with the crystalline phases mentioned above (17). In addition, C_4AF, C_3S, C_2AS, MgO, alsilite, ($K_2O \cdot Al_2O_3 \cdot SiO_2$), alkaline sulphate ($(K,Na)_2SO_4$), silimanite (AS) and so on are occasionally existed (12)(15)(17).

Fly ash with high glass content is favourable for blended cement (7). Unstable fly ash produced at low temperature is unsuitable especially in high calcium fly ash. Average glass content determined by x-ray diffraction analysis (XRD) is generally 60% or more (7)(12). Small fly ash particle is rich in glass phase while large particle contains much crystal due to slow cooling rate. **Fig. 6** shows typical powder x-ray diffraction patterns of blending components.

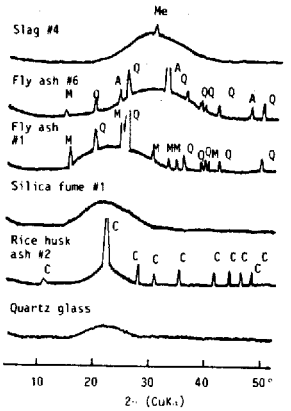

Fig. 6 Typical powder x-ray diffraction pattern of blending component (7).

(note; Me: melilite
Q : quartz
A : C_3A
M : mullite
C : cristobalite)

2.2.4 Composition and structure of amorphous phase

According to EPMA analysis, chemical composition of glass phase in ordinary fly ash is 27.1-70% for SiO_2, 7.1-31.2 for Al_2O_3, 0.5-29.8 for Fe_2O_3 and 1.0-34.7 for CaO and the basicity lies in the range of 0.45 to 0.9 (7). On the other hand, glass phase in high calcium fly ash have the basicity of about 1.65 similar to that of slag (7).

As shown in **Fig. 6**, the position of halo lies at 18-30°(2θ of CuKα) in ordinary fly ash, which is the same position as that of quartz glass responsible to the (111) reflection of α-cristobalite. Regarding high calcium fly ash, halo position of SiO_2-Al_2O_3 glass shifts continuously from 23 to 28° by the addition of CaO up to 20% but it appears at 32° corresponding to that of $C_{12}A_7$ when CaO added exceeds 20% (18). On the other hand, halo of high calcium fly ash and granulated blastfurnace slag appeared at 32° is considered to be due to the (211) reflection of melilite (7). From this result, it may be said that structure of glass phase in ordinary fly ash has similar structure to α-cristobalite and that in high calcium fly ash has similar structure of melilite. Judging from IR spectra shown in **Fig. 3**, condensation degree of silicate in ordinary fly ash glass phase is large and in high calcium fly ash it is small but same level to slag.

Few papers have reported on the coordination number of aluminium existing in glass phase of fly ash. It may, however, be 4, considering the fact that weight ratio of SiO_2/Al_2O_3 exceeds 2.6.

2.2.5 Shape and fineness of fly ash

The shape and surface of fly ash is sphere and smooth when it produced from coal with homogeneous ash composition under high temperature. As the combustion temperature becomes lower, the irregular quartz remained as a original shape, sphere coated by Fe_2O_3, $CaSO_4$ and alkali sulphate depositing particle on its surface are often observed (16). Fly ash consists of single sphere and multi sphere containing smaller spheres in it. About 20% of fly ash particles is hollow. The particle size and specific surface area of Blaine and BET is ranged between less than several hundreds μm, 2,000-4,000cm^2/g and 0.4-1.0m^2/g, respecctively.

2.3 Silica fume

2.3.1 Origin and classification

Silica fume, sometimes known as silica dust, silica flour, fused silica, volatilized silica or microsilica is a byproduct formed in the production process of metallic silicon and ferrosilicon by reducing the quartzite with carbon electrode or open arc electric furnace at about 2273°K. Gasified SiO at high temperature is deposited as SiO_2 by the oxidation during cooling. Therefore, the chemical composition of silica fume changes with the purity of silicon product (19).

2.3.2 Chemical composition

The chemical composition of silica fume depends not only upon the raw material such as silica sand, quartzite, iron and chromium, but also upon the quality of electrode and coal. SiO_2 in silica fume is usually over 80% and its compositional variation is small and is less than 1.3% of daily variation for 28 days' operation (20)(21) though SiO_2 content is higher in silicon manufacturing and low in ferrosilicon manufacturing. Minor components in silica fume are 0.1-0.5% of Al_2O_3, 0.1-5% of Fe_2O_3, less than 0.12% of CaO, less than 0.1% of TiO_2, less than 0.07% of P_2O_5, less than 1% of alkalies, 2-5% of carbon and 0.1-0.2 of S.



carbon (12) Q: quartz (12) mullite

Fig. 5 Transmisson electron micrograph, back scattering image and scanning micrograph of materials in fly ash

Silica fume dissolves rapidly within 30 minutes after contacting with saturated $Ca(OH)_2$ solution and the concentration of SiO_2 in the solution reaches 5-6ppm, then it decreases 1-2ppm accompanying with formation of hydrate. Silica fume hardly dissolves into conc. HCl. About 70% of it is, however, dissolved into 10% Na_2CO_3 solution after treated by hot conc. HCl (7).

2.3.3 Content of amorphous phase and kinds of crystalline phase

Silica fume produced by gas-gas reaction in air consists mainly of amorphous phase and is a fine particle. It sometimes includes a few percent of quartz which may be brought from recovered raw materials.

2.3.4 Composition and structure of amorphous phase

In narrow sense, glass is defined as a inorganic substance consists of quenched melt without crystallization. Under this definition, amorphous phase existing in slag and fly ash is a glass. On the contrary, amorphous phase in silica fume is not a glass because it is produced by gas-gas reaction. Structure of amorphous phase in silica fume is similar to that of quartz glass and condensation degree of silicate ion in amorphous phase is deduced to be high as shown in **Fig. 3** and **4** and number of bridged oxygen is four from FT-NMR measurement (7).

2.3.5 Shape and fineness

Silica fume has an spherical shape, and its particle size distribution lies below 0.1μm which is finer one-hundredth than that of slag and fly ash. BET specific surface area measured by nitrogen adsorption is high. It ranges over 20 to 200m^2/g. Porosity of silica fume powder packed is about 82%. Compactability of silica fume powder are smaller than other blending components in spite of having spherical shape.

3 HYDRATION

3.1 Classification of hydration process

The hydration reaction of cement compounds and cement are varied according to the elementary reaction mechanism corresponding to each reaction process and the kind of hydrates produced in the process of hydration is also complicatedly varied. Although it is debatable how to classify the hydration process with time, the paper classifies the initial hydration process into three stages, stages I, II and III, based on the heat evolution curve in the hydration as shown in **Fig. 7** for the convenience of further discussion. The addition of a third component such as the blending component changes the hydration of cement compounds and cement.

The stage I for C_3S is the gently heat evolution period immediately after mixing with water, corresponding to the pre-induction and induction periods. The hydrate produced is mainly composed of C-S-H. The stage II is the period of hydration with vivid heat evolution, corresponding to the acceleration and deceleration periods. The hydrates produced are mainly Type I and II of C-S-H and $Ca(OH)_2$. The stage III is the period during which the hydration is determined by the ion diffusing through the layer of C-S-H precipitated around the unhydrated C_3S particle and the hydration rate is lowered. The hydrates produced are mainly composed of Type I and III of C-S-H.

The stage I for C_3A is the period during which the remarkable heat development immediately after mixing water is gradually reduced. At this period hexagonal hydrates (C_2AH_8 and C_4AH_{19}) are vigorously produced and the hexagonal hydrates convert partially to cubic hydrate (C_3AH_6). The stages II and III are the periods of slow reaction.

The stage I for the mixture of C_3A with $CaSO_4$ and that of C_3A with $CaSO_4$ and $Ca(OH)_2$ is the period of the formation of ettringite accompanied by a large amount of heat evolution. The heat evolution peak shown in the stage II indicates the conversion of ettringite to monosulphate hydrate.

The heat evolution curve in the hydration of cement contains the additional curve of belite and ferrite solid solution besides alite and tricalcium aluminate. It is divided into stage I including the heat evolution peak by the formation of ettringite, the stage II including the vivid hydration of alite and conversion of ettringite to monosulphate hydrate and the stage III including the slow hydration process controlled by the successive diffusion.

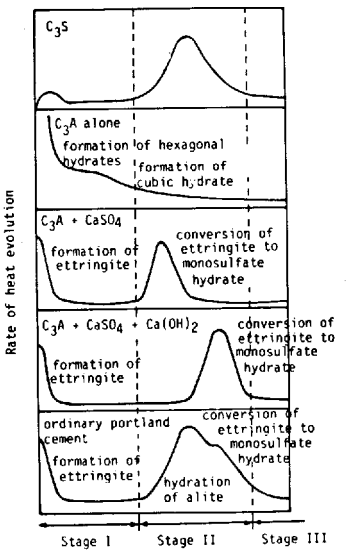

Fig. 7

Classification of initial hydration process based on heat evolution curve

3.2 Hydration of granulated blastfurnace slag and blastfurnace slag cement

3.2.1 Hydration of granulated blastfurnace slag

3.2.1.1 Effect of activator

A low penetrable pseudomorphiric layer is formed on the surface of slag immediately after mixing with water and it inhibits the water penetration to the slag particle and the dissolution of ion from the slag. It is inevitable, therefore, for keeping up the hydration of slag to add an activator. Alkalies, gypsum, $Ca(OH)_2$ and portland cement are known as the activator. The mixture of alumina cement, $Ca(OH)_2$ and K_2SO_4, and hauyne clinker as well as the effects of heat treatment of slag itself and regulation of the fineness of it on the acceleration of hydration of slag have been presented at the 7th International Congress held in Paris (6)(22).

Although a small quantity of $Ca(OH)_2$ accelerates the

hydration of slag, the addition more than the requirements has little effect. NaOH has a large effect with increasing the addition, but the hydration is hardly proceeded with age. Gypsum accelerates the hydration still more with increasing of addition and with age though it has a little effect as the activator. The mixture of gypsum and a small quantity (about 1%) of $Ca(OH)_2$ is a good activator (6).

The alkaline activator has the effects of accelerating the elution of Si and Al ion by breaking the glass structure of slag and of depositing the hydrate by increasing the ionic concentration in the liquid phase. When gypsum exists, the concentrations of Ca and Al ion are kept low because ettringite is produced. When pH is enhanced regardless of the presence of gypsum, the elution of Al ion is especially accelerated. This is the initiator for hydration. When pH of the liquid phase is approximately 12, the equivalent point of the production of ettringite, the hydration is accelerated the best.

There is the optimum amount, though a little, of lime based activator in the hydration of slag with gypsum. In order to develop the high strength, it is important to keep the concentrations of Ca^{2+}, SO_4^{2-} and Al^{3+} in the liquid phase of paste so as to produce only ettringite (6).

The results of the effect of activator added below 10% evaluated by 7 days' strength indicate that portland cement and clinker have the highest effect, Na_2CO_3-NaOH mixture is the second highest, sulphide sludge ash, gypsum-cement mixture and fly ash-NaOH mixture have the medium effect and fly ash, Na_2CO_3-$NaSiO_3$ mixture, alumina cement, HCl, $CaCl_2 \cdot 2H_2O$ and gypsum have little effect (23). Since the ground fresh slag is active, it develops the high strength without activator. Although the ground slag stored in a silo loses the activity in a month, pelletized slag preserves it for long time.

The hydration of slag is generally based on the elution of the chain structure of SiO_4 and AlO_4 in slag by the attack of OH^-. In order to maintain the vivid hydration of slag, it is necessary to supply externally OH^- because Ca^{2+} and OH^- alone eluted from the slag are not enough. It is also necessary to form the appropriate structure of hydrate on the surface of slag. The forming conditions and crystallinity of hydrate largely depend upon the concentration of OH^-. When pH of the liquid phase is kept at approximately 12 and SO_4^{2-} coexists, well crystallized hydrate containing aluminium can be produced. There is the optimum SO_3 content according to the slag content in blastfurnace slag cement (24).

3.2.1.2 Hydrates produced

When alkali and its salt are used as the activator, C-S-H with low C/S ratio, C_4AHx and C_2ASH_8 are produced. C_4AHx is converted to hydrogarnet with age. It is said that alkaline ions act as the catalyser. A small amount of $Ca(OH)_2$ used as the activator produces the same hydrates as alkali salt do, while a large amount of it produces no C_2ASH_8. When sulphate is added, ettringite and monosulphate hydrate or solid solution of monosulphate hydrate and C_4AHx and $Al(OH)_3$ are produced. C-S-H has the lower C/S ratio (25) and contains larger amount of MgO and Al_2O_3 than C-S-H of portland cement. When a large amount of MgO is contained in the slag, C_4AHx-C_4MHx solid solution and $Mg_6Al_2CO_3(OH)_{16} \cdot 4H_2O$ are produced (26).

The kind and composition of the hydrates produced from slag depend upon the chemical composition of slag and kinds of activator. These hydrates are generally the same as those from portland cement though the content of MgO is a little larger.

The formation of low C/S C-S-H largely depended upon the concentration of Ca^{2+} in the liquid phase.

3.2.2 Influence of slag on the hydration of cement compounds

3.2.2.1 Influence of slag on the hydration of C_3S

Few studies on the influence of slag on the hydration of cement compounds have been reported so far because it is generally considered that slag is inert without activator. When blastfurnace slag is added to C_3S, the peak of heat evolution curve appeared in ten hours after mixing with water based on the vivid hydration of C_3S is generally delayed a little, but the hydration degree of C_3S determined by XRD increases at the age of 1 to 3 days, and thereafter it is the same as that without slag and lower than that in case of adding fly ash or white clay (27). The value of pH in the liquid phase of paste is lower by adding slag immediately after mixing with water and the concentration of Ca^{2+} is lower than that without slag but it recovers gradually. Thus, the addition of slag delays a little the hydration of C_3S in the stages I and II as shown in **Fig. 13**, while it accelerates the hydration in the stage III or later because the slag particles become the depositing site for C-S-H produced by the hydration of C_3S (27). The hydration of C_3S in the stages I and II is affected by the water soluble components of slag, ion adsorbing capacity, and in the stage III it depends upon the surface potential and surface roughness of slag in paste, pozzolanic reactivity and state of deposited hydrate.

3.2.2.2 Influence of slag on the hydration of C_3A and C_4AF

There have been few researches on the influence of slag on the hydration of C_3A and C_4AF. Slag does not vary so much the concentration of Ca^{2+}, Al^{3+} and SO_4^{2-} in the liquid phase of paste which affects the hydrationof C_3A and C_4AF. Ettringite and calcium aluminate hydrate produced have good crystallinity to form the relatively porous structures, which is different from C-S-H precipitating densely on the surface of unhydrated particle in the hydration of C_3S. It is, therefore, considered that slag acts as retarder rather than accelerator in the hydration of C_3A and C_4AF at stages I and II even if it acts as the precipitating site (28). Although the early stage hydration of C_3A and C_4AF are delayed in the gypsum-$Ca(OH)_2$ coexisting system, they are not delayed so much in the stages I and II of the system containing slag because $Ca(OH)_2$ and $CaSO_4$ are adsorbed on the surface of slag and part of them are consumed by pozzolanic reaction. The hydration of cement compounds in the diffusion controlling process is accelerated by adding a blending component because the hydration space is increased.

3.2.2.3 Hydration of clinker minerals in blastfurnace slag cement

As shown in the heat evolution curves in the early stage of blastfurnace slag cement illustrated in **Fig. 8**, the second peak based on the vivid hydration of alite is delayed by adding blastfurnace slag at 288°K,

but it is slightly advanced at a temperature above room temperature (29).

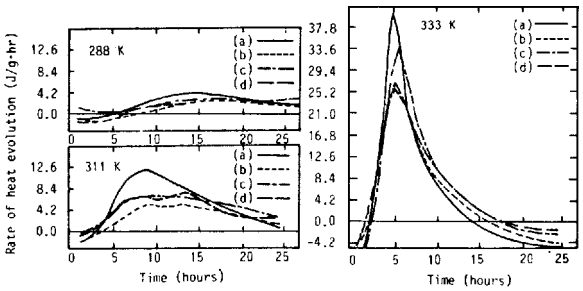

Fig. 8 Rate of heat evolution with time of cement hydrated at 288, 311 and 333°K (29)

The measurements of heat of hydration of blastfurnace slag cement concrete containing 30% of slag are the same as those mentioned before. The temperature rise of the concrete caused by the vivid hydration of alite in the stage II is approximately one hour behind that of portland cement at 295°K (30).

A paper (31) reported that the hydration of alite is accelerated in the range of larger content of slag. It is elucidated that the hydration of alite in the stage III and later is accelerated by the effect of precipitating site of slag and the increase of hydration space.

The hydration in the stages I and II for the blastfurnace slag cement with fine slag is accelerated as shown in **Fig. 9.**

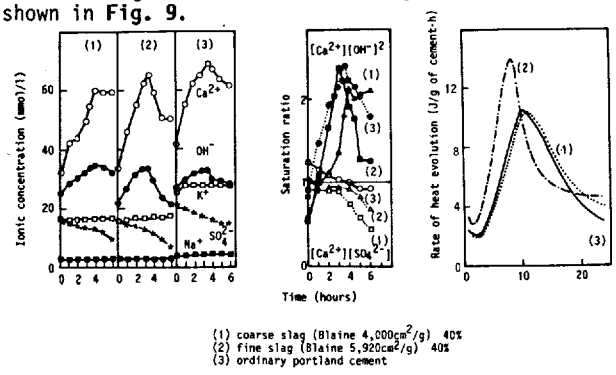

Fig. 9 Ionic concentration and saturation ratio of $Ca(OH)_2$ and $CaSO_4$ in liquid phase of fresh paste and heat evolution curve of the hydration of blastfurnace slag cement at 293°K (32)

Acceleration of hydration of alite by fine slags added is considered to be caused by shifting of the peak of $Ca(OH)_2$ saturation ratio (ratio of the solubility product of $[Ca^{2+}]$ and $[OH^-]^2$ calculated from the measurements of the liquid phase to the solubility product of $[Ca^{2+}]$ and $[OH^-]^2$ in equilibrium at the same ionic strength) in the liquid phase corresponding to the rising point of vivid hydration of alite toward the shorter time and by increasing of precipitating site of hydrate. The reason for the acceleration of hydration of alite at stage I by increase of hydration temperature and adding fine slag seems to be caused by the consumption of Ca^{2+} in the liquid phase by slag and promotion of dissolution of Ca^{2+} from alite. This fact is corresponded to the change of the surface structure of alite observed with scanning electron microscope (SEM). Since Ca^{2+} and SO_4^{2-} are also fixed by slag, the saturation ratio of $Ca(OH)_2$ and of $CaSO_4$ (defined same as $Ca(OH)_2$) become lower to accelerate the hydration of interstitial phase in the presence of Ca^{2+} and SO_4^{2-}.

3.2.3 Pozzolanic reactivity and reaction rate of granulated blastfurnace slag

3.2.3.1 Pozzolanic reactivity of granulated blastfurnace slag

Although pozzolanic activity is generally evaluated by the correlation of the factors such as the amount of glass phase and acid soluble part, basicity and specific surface area with the developed strength of blended cement mortar or concrete, the coefficient of correlation is not always high. It has been proposed, therefore, that the quality of pozzolanic material should be evaluated by the defined value such as pozzolanic reactivity instead of the ambiguous concept like the hydration activity expressed by strength (33).

The reactivity of slag must be defined substantially by the chemically reacted amount. Since the glass phase has higher level of free energy than the crystalline phase, it is suggested that the glass phase is corresponded with the reactivity of slag more deeply than the other factors. It is useful, therefore, for understanding the reactivity of slag to clarify the contributions of the amount, chemical composition, structure, active site and chemical and physical defects of glass phase as the useful indices.

The magnitude of structural defect of glass in the fused slag produced by various quenching conditions is expressed as the number of electrons radiated by photoexcitation. The strength and combined water content of the mixture kneaded with NaOH solution at the W/C ratio of 0.11 are determined. The results indicate that the structural defect is correlated closely with the compressive strength, but the combined water content is not correlated with the compressive strength. Namely, the structural defect of glass affects the texture formed by the hydrates produced rather than the reacted amount of slag (20). Heat of hydration is widely varied according to the kinds of slag though they have almost the same glass content, hydraulic modulus and chemical composition. This variation seems to be caused by the structural difference of glass. Most of Al^{3+} ions in the glass phase tend to be 4 coordination number estimating from the chemical shift by fluorescent X-ray analysis and the hydration activity is enhanced by the increase of content of Al_2O_3 and basicity (31).

The amount of slag dissolved in the solution of pH 12.6 the same as the saturated solution of $Ca(OH)_2$ was determined (34). The results indicated that the more the sum of dissolved amounts of Ca, Al and Si, the higher the reactivity of slag is. Assuming, therefore, that only the initial dissolution of slag in the alkaline solution is related to the reactivity of slag, it can be evaluated by determining the dissolved amount. The dissolved amount is increased with increasing of the amount of Al_2O_3 in the slag. The group of AlO_4 in the glass structure greatly contributes to the dissolved amount (34) which is decreased by partially replacing CaO with MgO. The more the percent of monomer of silicate in the slag, the more the sum total of CaO, SiO_2 and Al_2O_3 dissolved from

the slag in the alkaline solution (7).

In short, the slag with high content of Al_2O_3, high basicity, high content of silicate monomer and high content of glass phase is highly reactive. Due to lack of appropriate analytical method, it has not been clarified yet how the factors such as active site and chemical and physical defects affect the change in the reactivity of slag with time.

3.2.3.2 Pozzolanic reaction rate of granulated blastfurnace slag

The reaction rate of slag is varied according to temperature, ratio to water and kind and amount of activator as well as the character of slag. The hydration of slag is slower than that of C_3S. The hydrated layer begins to be formed on the surface of slag particles in about six hours after mixing with water and the hydration becomes vivid in 12 hours to 3 days after that.

It was reported (35) that the hydration degree of the mixture of C_3S and 40% of slag with 5,680 cm^2/g of Blaine specific surface area at 293°K at the W/C ratio of 0.40 is about 10% at 1 day, about 20% at 3 days, about 45% at 28 days, which the hydration rate of the blastfurnace slag cement containing 40% of slag with 4,000 cm^2/g of Blaine specific surface area at 293°K at the W/C ratio of 0.40 is about 28% at 1 day, about 38% at 28 days and about 52% at 180 days and the hydration of slag proceeds in two stages.

There is almost no study in which the reaction degree of slag in cement was systematically investigated varying the character of slag. Summarizing the preceding results of researches on the reaction rate of slag, the hydration rate of slag in blastfurnace slag cement containing slag of 4,000 to 5,000 cm^2/g of Blaine specific surface area at 293°K is estimated 10 to 20% at 1 day, 30 to 40 % at 28 days and 50 to 60% at 180 days.

The apparent activation energy of blended cement with separately ground slag in hydration is 49 kJ/mol calculating from the heat of hydration, which is larger than 44 kJ/mol of portland cement alone (29). This indicates the hydration of blastfurnace slag in blastfurnace slag cement largely depends upon the temperature.

The appearance time of the third peak caused by the hydration of slag is not so much varied with increase of amount of slag added as shown in the heat evolution curve of hydration in **Fig. 8.** It shifts, however, toward the shorter time with raising the temperature and at 333°K both peaks corresponding to the hydration of alite and slag fold together. The heat of hydration of the blastfurnace slag cement with 50% of slag at 300°K is smaller than that of portland cement alone, while that at 333°K is larger than this as shown in **Fig. 10.** These phenomena support the above-mentioned view that the hydration of slag in blastfurnace slag cement is remarkably affected by the temperature.

The heat of hydration of blastfurnace slag cement is essentially lower than that ordinary portland cement, but that containing a smaller quantity of slag is sometimes higher at the early age than ordinary portland cement. This is caused by the heat of hydration of slag and the acceleration of hydration of cement at age of 1 day and later. The high strength-developing cement with low heat of hydration can be manufactured by adding the optimum, larger quantity of slag with the proper fineness and particle size distribution.

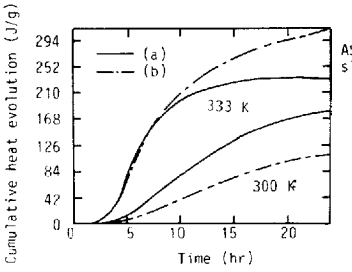

ASTM Type II cement with 0% slag (a), 50% slag (b)

Fig. 10

Cumulative heat evolution of cement at 330°K and 333°K (29).

3.2.4 Hydration process of blastfurnace slag cement

There has been few report on the hydration mechanism of blastfurnace slag cement essentially different from the principal report presented by Takemoto and Uchikawa at the 7th International Congress on the Chemistry of Cement.

From the viewpoint of reaction rate, the hydration process of slag can be divided into the dissolution period immediately after mixing with water, first dormant period, primary accelerating period, latter dormant period, secondary accelerating period and diffusion-controlling period.

Slag begins to dissolve into water immediately after mixing with it. The measurements by X-ray photoelectron spectroscopy (XPS) indicate that the C/S ratio on the surface of slag reaches the constant value in approximately five minutes after mixing with water regardless of the original composition of slag (36). The higher the original C/S ratio is, the more Ca ion is easily dissolved in the liquid phase and the C/S ratio on the surface of slag is lowered after mixing with water in the presence of alkali (36). Ca^{2+} is dissolved from the slag according to its C/S ratio to from C-S-H on the surface in a short time after mixing with water and soon the reaction changes to the dormant period. The hydration degree of slag is 2% or less in this period.

The vivid hydration of alite in blastfurnace slag cement precedes the active hydration of slag in it and the surface of slag is covered with hydrates of cement. The hydration of slag proceeds with supersaturated Ca^{2+} and alkali ions attack. At this time, Ca^{2+} ions are incorporated through the layer of hydrate from the liquid phase. The degree of supersaturation in the liquid phase is gradually lowered by the precipitation of $Ca(OH)_2$ and the concentration of Ca^{2+} becomes stable to form well crystallized inner hydrated layer. Part of Ca^{2+} and Al^{3+} actively dissolved from the particles of unhydrated slag react with the inner hydrated layer and the rest is transferred through it to the liquid phase. At the traces of slag from which the ions is eluted the skeleton hydrated layer with shell structure is often formed. The hydration of slag is slow down in 3 days and later and then the skeleton hydrated layer changes to the inner hydrated layer as the reaction proceeds (37).

3.3 Hydration of fly ash and fly ash cement

3.3.1 Hydration of fly ash

3.3.1.1 Hydration of high calcium fly ash

High calcium fly ash is mainly composed of glass phase and other crystalline phases including C_2S, C_3A, free CaO, $CaSO_4$, $C_4A_3\bar{S}$ and MgO. Since it has self-hardening properties, ettringite, monosulphate hydrate and C-S-H are produced and hardened by free CaO acting as the activator when mixing with water. Although the behaviour of hydration of C_3A and C_2S in fly ash is the same as that in cement, the formation rate of C-S-H from the glass phase is relatively slow (38). The formation of ettringite increases at the temperature up to 313°K and it is decomposed at 333°K (39).

3.3.1.2 Hydration of ordinary fly ash

Ordinary fly ash is not hydrated by itself, but it is hydrated by adding alkalies and $Ca(OH)_2$. The hydrates such as C-S-H, $C_3A \cdot CaCO_3 \cdot H_{12}$ (C_4AH_{13}) and C_2ASH_8 are produced and hydrogarnet is formed at later stage. Although the hydrates produced in fly ash cement are almost the same as those in ordinary portland cement, the C/S ratio of C-S-H produced is generally lower than those of portland cement and blastfurnace slag cement.

The more $Ca(OH)_2$ is supplied, the more it is fixed by SiO_2 and Al_2O_3 in fly ash and the higher the calcium content in the hydrate produced is. When the less $Ca(OH)_2$ is supplied, these trend reverses (33)(40). The more $Ca(OH)_2$ is added, the faster it is consumed (41). The reaction degree of fly ash is increased by adding $CaSO_4 \cdot 2H_2O$ in the same manner as that of slag, because the surface area is increased by destructing the structure of glass and crystalline phases due to the dissociation of Al_2O_3 reacting with SO_4^{2-}. The reaction of glass phase in fly ash with Ca^{2+} is generally as slow as it is initiated from one to three days at the room temperature. Since the particle size distribution of fly ash is broad and its chemical composition is varied according to different particle group, it is difficult to divide clearly the reaction process into steps. It is possible, however, to divide it into six steps in the same way as slag.

3.3.2 Influence of fly ash on the hydration of cement compounds and fly ash cement

3.3.2.1 Influence of fly ash on the hydration of C_3S

Similarly to slag, fly ash retards the hydration of C_3S in the stages I and II, and accelerates that in the stage III and later.

Since Al ion eluted from fly ash takes part deeply in the rate of hydration of C_3S and the nucleation and growth of C-S-H and $Ca(OH)_2$, the hydration of C_3S in the stage I is the more retarded the more Al ion is eluted in the alkaline solution (42). The influence of the concentration of Ca^{2+} in the liquid phase on the early hydration of C_3S is varied according to the form of C_3S (43). The higher the concentration of Ca^{2+} is, the more the hydration of pure C_3S alone is retarded, while the more those of C_3S solid solution with Al_2O_3 and the Fe_2O_3 and pure C_3S in the mixture with C_3A and C_4AF are accelerated (44). This fact shows, therefore, that the concentration of Ca^{2+}, nucleation rate of hydrate and form of hydrates produced are affected by the coexisting ions.

C_3S with and without 30% of the fly ash which has Blaine specific surface area of 3,730cm²/g containing small quantities of quartz and mullite as well as the glass phase was hydrated at 298°K with the W/C ratio of 0.50 and the hydration degree of C_3S was determined by XRD. The results indicate that the hydration degree of C_3S alone at the age of one day is 35%, while that of the mixture is 45% (45). The fact indicates hydration of C_3S in the stage III is accelerated by adding fly ash. These results coincide with those of the preceding researchers (27).

There are few difference on the effects of fly ash on the hydration of C_3S in the stage III. The easier the adsorption of Ca^{2+} onto the surface of fly ash; the negatively higher the surface potential; the lower the smoothness of surface; the higher the fineness of fly ash, the better it functions as the precipitating site for hydration; and the effect of accelerating the hydration at the stage III and later is large.

3.3.2.2 Influence of ordinary fly ash on the hydration of C_3A and C_4AF

Fly ash frequently retards the hydration of C_3A. The degree of retardation mainly depends upon the content of SO_3 in the fly ash as well as the amount of alkalies dissolved and calcium adsorption capacity (47). Ca^{2+} and SO_4^{2-} such as compositional ratio of gypsum are dissolved from some kinds of fly ash. Ca^{2+} dissolved is adsorbed onto the Al-rich surface produced by non-stoichiometric dissolution to lower the hydration activity and furthermore SO_4^{2-} is also adsorbed to retard the hydration of C_3A (46). SO_3 in fly ash retards the hydration more than the equivalent amount of gypsum, because the effect of fly ash may be promoted by the other ions dissolved from it.

In the mixture of C_3A and $CaSO_4 \cdot 2H_2O$, when blending components with few dissolve alkalies, large calcium adsorption capacity and 7 or less pH of the suspension are added to the mixture, the hydration of C_3A and the conversion of produced ettringite to monosulphate hydrate are generally accelerated. On the other hand, when a blending components with considerable amounts of free CaO and alkalies and with 12 or more pH of the suspension are added, the hydration of C_3A is inhibited and the conversion of ettringite to monosulphate hydrate is retarded. Most of fly ash is similar to the latter case though being varied according to the kind of it. When the fly ash with high calcium adsorption capacity and high pozzolanic reactivity is added to the mixture, the hydration rate in each stage is often increased and the conversion of ettringite to monosulphate hydrate is accelerated (28). The increase of hydration space by adding fly ash is also caused by accelerating the hydration in the stage III and later. It has almost the same effects on the hydration of C_4AF.

3.3.2.3 Hydration of clinker minerals in fly ash cement

The heat evolution peak based on the hydration of alite in fly ash cement is appeared in several to twenty hours after mixing with water and later than that for ordinary portland cement (38)(48). But the hydration degree of alite at 1 day and later is higher than that of ordinary portland cement(12)(33). This is also confirmed by the experiment of synthesized cement (49). It is concluded, therefore, that the addition of fly ashgenerally retards the hydration of alite in the stages I and II but accelerates it in the stage III.

The start of vivid hydration of alite in ordinary portland cement coincides with the period which maximum $Ca(OH)_2$ saturation ratio in the liquid phase of paste is attained. If appearance of the maximum is

delayed, the vivid hydration of alite is also late. Since the rising curve of the $Ca(OH)_2$ saturation ratio for fly ash cement is gentle and the maximum is developed late as shown in **Fig. 11**, the vivid hydration of alite is also late. Considering that the addition of fly ash with small calcium adsorption capacity, high contents of Ca^{2+} and alkalies dissolved (12)(50) and high content of unburnt carbon (12) retards the hydration of alite, alkalies, Ca^{2+}, hydroxyl group and organic compounds inhibit the consumption of $Ca(OH)_2$ in the liquid phase, so the delay of dissolution of Ca^{2+} from alite hinders the saturation ratio of $Ca(OH)_2$ in the liquid phase of fresh paste from increasing.

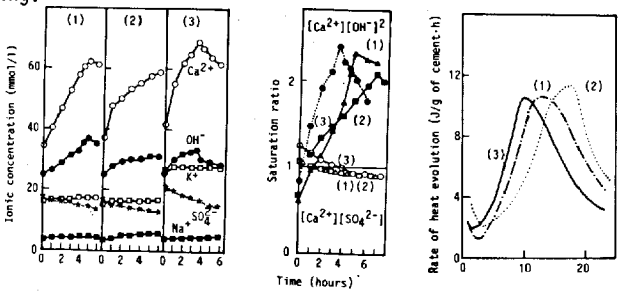

(1) fly ash cement with 40% of ordinary fly ash
(2) fly ash cement with 40% of high calcium fly ash
(3) ordinary portland cement

Fig. 11 Ionic concentration and saturation ratio of $Ca(OH)_2$ and $CaSO_4$ in liquid phase of fresh paste and heat evolution curve of the hydration of fly ash cement at 293°K (32)

The hydration degree of alite is high in the stage III in the same manner as that of slag. It is probably because the dissolution of alite is accelerated by the precipitation of part of C-S-H on the surface of fly ash grains. When fly ash is coarse, the hydration degree of alite is sometimes small even in the stage III. Fly ash accelerates the hydration more than slag in the stage III unless their fineness are much different from each other.

There are two reports showing apparently different results on the effect of blending fly ash on the hydration of interstitial phase. One is that fly ash accelerates the hydration and the other is that fly ash retards the hydration. It is generally known that the hydration rate of interstitial phase is inhibited and the formation of ettringite depressed in the stage I of ordinary portland cement as the $Ca(OH)_2$ saturation ratio in the liquid phase of cement paste is increased. It has been concluded that the hydration of amorphous or crystalline calcium aluminate of fly ash and portland cement is more inhibited and the formation of ettringite is lowered in the presence of SO_4^{2-} in fly ash cement at their CaO/Al_2O_3 molar ratio of 3.0 or more with increasing of the $Ca(OH)_2$ saturation ratio, while the production of ettringite is increased at the their CaO/Al_2O_3 ratio below 3.0 with increasing of the $Ca(OH)_2$ saturation ratio (13). This is because the hydration of interstitial phase depends upon the composition of it as well as the variation of the composition of liquid phase of fresh paste by the addition of fly ash.

Monosulphate hydrate is more produced in the hardened fly ash cement paste than in hardened ordinary portland cement paste as shown in **Fig. 12**. Since it is difficult to determine directly the hydration degree of interstitial phase which exists a little in fly ash cement, the hydration rate is generally estimated from the production of ettringite or monosulphate hydrate. It is suggested that the hydration of C_3A and C_4AF in cement after one day is accelerated by the addition of fly ash.

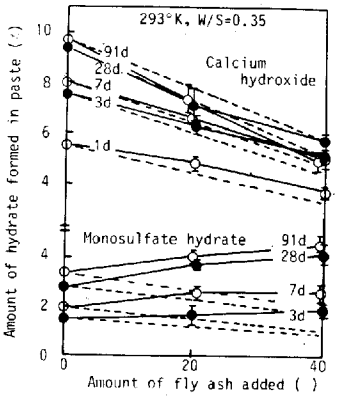

Fig. 12

Amount of monosulfate hydrate and $Ca(OH)_2$ in fly ash cement with age at 298°K (12)

3.3.3 Pozzolanic reactivity and reaction rate of fly ash

3.3.3.1 Pozzolanic reactivity of high calcium fly ash

High calcium fly ash composed of the same minerals as contained in cement or slag such as C_3A, $C_4A_3\bar{S}$, $C_{12}A_7$, C_2F and $CaSO_4$, glass phase and free CaO. The composition of glass phase varies between CaO-rich and ordinary fly ash like. The fly ash rich in CaO and Al_2O_3 has high pozzolanic reactivity.

The reaction rate of fly ash cement containing high-calcium fly ash estimated from the amount of combined water is higher than that of the fly ash cement containing ordinary fly ash (49).

3.3.3.2 Pozzolanic reactivity and reaction rate of ordinary fly ash

The pozzolanic reactivity of a blending component is mainly expressed as the amount of combined $Ca(OH)_2$ or the reaction degree of blending component itself. The glass phase largely affects the pozzolanic reactivity of fly ash in general. The reactivity is enhanced with increasing of strain of glass phase and the amount of CaO in it, but the reactivity is lowered with increasing of Fe_2O_3 (51). The crystalline phase such as mullite, quartz, hematite and magnetite are inert.

Among the correlations of the amount of combined $Ca(OH)_2$ (g/100g of pozzolana) as the index of pozzolanic reactivity with specific surface area (m^2/g), acid-soluble part (%), SiO_2/Al_2O_3 ratio in acid soluble part and content of glass phase (%) of fly ash, the coefficient of correlation with the amount of glass and acid soluble part are relatively high (33). Since the most part of fly ash is composed of glass phase, fly ash with the glass phase containing a lot of acid soluble part is suggested to have surely high pozzolanic reactivity.

The mean degree of condensation of silicate in the glass phase of fly ash is larger than that of slag (7). The dissociation rate of SiO_2 from the glass phase reacting with OH^- is generally lower than that of slag and the reactivity is also lower than that of slag. The reactivity of fly ash is enhanced with increasing of the amount of glass and the basicity of glass phase and with decreasing of the degree of con-

densation of silicate. The reactivity closely correlates with the acid soluble amounts of SiO_2 Al_2O_3 (7). In the case of containing a lot of reactive Al_2O_3, fly ash has much combined water and large consumption of $Ca(OH)_2$ (7). In such a case the reaction degree of fly ash is not necessarily related to them.

The more $Ca(OH)_2$ is added or available, the higher the reactivity is at the later age. The reactivity of fly ash mixed with $Ca(OH)_2$ is higher than that mixed with cement. This is considered to be because the surface of fly ash is covered with the hydrate produced by hydration of cement prior to the pozzolanic reaction, so the diffusion of Ca^{2+} to the particles of fly ash is inhibited.

Pozzolanic reaction rate of fly ash are summarized in **Table 2.**

Table 2 Hydration rate of fly ash

(1)	(2)	(3)	(4)	(5)	(6)	(7)
S=44.2%, A=22.6%, F=10.4% C=7.7%, i.l=5.0%(C'=4.2%) Blaine=3,590cm²/g	$Ca(OH)_2$	10% 60%	298°K W/S= 12.5	$Ca(OH)_2$ (Franke method)	4d:4%, 60d:9% 13% 26%	(41)
S=49.0%, A=28.8%, F= 5.5% C=9.0%, i.l=7.0%(C'=6.1%) Blaine=3,900cm²/g	$Ca(OH)_2$	10% 60%	298°K W/S= 12.5	$Ca(OH)_2$ (Franke method)	4d:1%, 60d:3% 3%, 13%	(41)
S=49.1%, A=24.4%, F= 4.2% C=6.2%, i.l=4.6%, G=86% Blaine=3,590cm²/g	$Ca(OH)_2$	25%	298°K -	$Ca(OH)_2$ (DSC, XRD)	28d:20% 91d:33%	(33)
S=55.2%, A=27.5%, F= 9.5% C=1.8%, i.l=3.0% Blaine=4,050cm²/g	$Ca(OH)_2$	20-60%	303°K W/S= 0.5-1.2	$Ca(OH)_2$ (TGA)	1d: 4-5% 91d:20-50%	(40)
S=51.2%, A=27.3%, F= 9.3% C=1.3%, i.l=2.6%(C'=1.5%) Blaine=3,730cm²/g	C_3S	33.3%	298°K W/S= 0.5	fly ash (S.M. method)	1d: 2%, 28d:14%, 1y:47%	(45)
S=49.1%, A=24.4%, F= 4.2% C=1.3%, i.l=2.6%, G=86% Blaine=3,590cm²/g	C_3S	40%	293°K W/S= 0.4	fly ash (TMS)	7d: 4%, 28d:10%, 180d:18%	(53)
S=59.3%, A=25.0%, F= 4.3% C=2.8%, i.l=1.5%, G=64% Blaine=3,910cm²/g	cement	20% 40%	293°K W/C= 0.35	fly ash (TMS)	28d:3%, 91d:5% 28d:3%, 91d:4%	(12)
S=58.8%, A=25.8%, F= 4.1% C=2.7%, i.l=1.7%, G=80% Blaine=2,990cm²/g	cement	20% 40%	293°K W/C= 0.35	fly ash (TMS)	28d;4%, 91d:11% 28d:5%, 91d:12%	(12)
S=49.1%, A=24.4%, F= 4.2 C=6.2%, i.l=4.6%, G=86% Blaine=3,590cm²/g	cement	40%	293°K W/C= 0.30	$Ca(OH)_2$ alite (XRD)	28d:0.8g $Ca(OH)_2$ /100g pfa 91d:4.5g "	(33)
S=58.2%, A=21.9%, F= 4.0% C=2.0%, i.l=4.4%,	cement	20% 20%+4% gypsum, 20% 20%+4% gypsum,	-	$Ca(OH)_2$ alite (XRD)	28d: 5g " 15g " 1y:13g " 21 "	(52)

note; (1); character of fly ash,
S: SiO_2, A: Al_2O_3, F: Fe_2O_3, C: CaO, i.l: ig. loss, C': carbon
G: glass phase
(2); blended material
(3); mixing ratio
(4); hydration temperature
(5); determined material and method
S.M. method: salicylic acid-methanol solvent method
(6); hydration degree
(7); reference

3.3.4 Hydration process of fly ash cement

There has been few other opinion on the hydration mechanism of fly ash cement essentially different from the principal report presented at the Paris' Congress (33).

Small quantities of soluble Ca, Si, Al and alkalies ions are dissolved from ordinary fly ash in cement paste and the hydrates produced from the cement are precipitated on the negatively charged surface on fly ash particles. Since the fly ash retards the increasing of $Ca(OH)_2$ saturation ratio brought by the hydration of alite and lowers $CaSO_4$ saturation ratio in the liquid phase of cement paste in the stages I and II, the hydration of interstitial phase is accelerated but that of alite is retarded. $Ca(OH)_2$, ettringite and granular hydrated product, C-S-H, are observed on the surface of fly ash in four hours after mixing with water. The hydrations of alite and interstitial phase are more accelerated in the stage III and later than in portland cement alone and duplex coating is made uniformly on the surface of fly ash (54). Rod like ettringite grows on the surface of fly ash at the age of one day to form Hadley grain (38). Etching of the surface of fly ash by the pore solution at around one day proves that initial reaction takes place on the surface. At the age of three days, the surface of fly ash is thickly coated with the hydrate some of which breaks off from fly ash particles. The structure of hardened paste becomes dense from 14 days on and Hadley grain disappears.

In case of high calcium fly ash, the hydration mechanism is essentially the same as that of ordinary fly ash and C-S-H grows toward the outside of the glass phase of high calcium fly ash (55). The hardened cement paste with the fly ash and additional quantity of gypsum shows the typical structure based on the pozzolanic reaction at 3 days and later.

3.4 Hydration of cement containing silica fume and rice husk ash

3.4.1 Hydration of silica fume and rice husk ash with $Ca(OH)_2$

Rice husk ash bears many resemblances to silica fume though the former is of fine irregular shape and the latter is spherical. Both are x-ray crystallographically amorphous, but some of them contain cristobalite and quartz as crystalline phase.

Since silica fume contains particles as fine as 0.1μm or less and it has large surface energy, it dissolves in saturated $Ca(OH)_2$ solution in a time as early as 5 to 15 minutes and SiO_2 rich hydrate is deposited in layers on the particles of silica fume. C-S-H with the C/S ratio of 1 is remarkably produced at 293°K in 24 hours after mixing with water and at 311°K in 8 hours (56). Rice husk ash actively reacts with $Ca(OH)_2$ and the reaction is relatively fast terminated. When the rice husk ash with the specific surface area of 152m²/g and 80% of SiO_2 is mixed with $Ca(OH)_2$ at the ratio of $Ca(OH)_2$/rice husk ash of 1/4 and 1/1.5, the reaction with $Ca(OH)_2$ is almost completed until final setting (57). Even when the mixing ratio is higher, the amount of combined $Ca(OH)_2$ after 3 to 7 days is extremely low. The reactivity of the rice husk ash containing 20% or more carbon is low.

The reaction of silica fume and rice husk ash with $Ca(OH)_2$ is affected by the specific surface area, particle size distribution and surface energy caused by a small strain of structure of SiO_2. C-S-H produced has lower C/S ratio than that of slag and fly ash. In the relationships between the mixing ratio of rice husk ash, the amount of combined $Ca(OH)_2$ and C/S ratio of C-S-H based on the previous work (57), the less the amount of $Ca(OH)_2$ mixed, the less the combined amount of $Ca(OH)_2$ of rice husk ash is and the less the C/S ratio of C-S-H produced is. Since C-S-H with the C/S ratio of less than 0.8 is considered to be impossible to exist, calcium silicate hydrate once produced is converted to lower C/S C-S-H to produce

$Ca(OH)_2$ in case of insufficient $Ca(OH)_2$ and another C-S-H is formed. When SiO_2 exists excessively, C-S-H with the C/S ratio of more than 0.8 seems to coexist together with SiO_2.

3.4.2 Influence of silica fume and rice husk ash on the hydration of cement compounds and silica cement

3.4.2.1 Influence of silica fume and rice husk ash on the hydration of C_3S

According to the experimental results on the hydration of the mixture of C_3S having the specific surface area of 3,000 cm^2/g and amorphous silica "aerosil" at 293°K (58), the first peak in stage I is enlarged by adding a small amount of amorphous SiO_2; the first peak becomes smaller and the second peak in stage II shift towards the shorter time by increasing the addition of SiO_2; and the dormant period disappears by adding further more SiO_2 up to the C_3S/SiO_2 ratio of 0.67 or less. The reason why the hydration of C_3S is accelerated is as follows: Ca^{2+} in the liquid phase produced by dissolution of C_3S is adsorbed by active silica, so the concentration of Ca^{2+} is lowered; metastable supersaturated layer is hardly formed around the particles of C_3S; and C-S-H with a low C/S ratio which make easily the diffusion of Ca^{2+}, is produced (58).

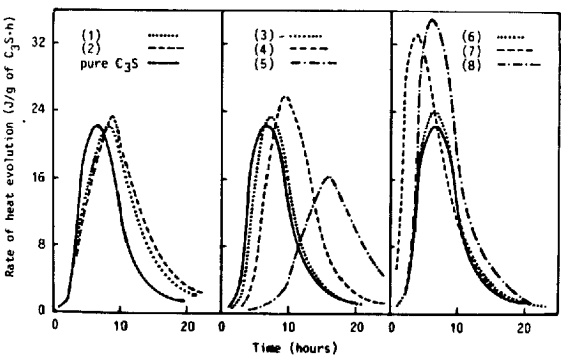

No	blending component	content	BET	Blaine	calcium adsorption capacity	Zeta potential
(1)	coarse slag	20	2.67	4,000	0.055	-18
(2)	fine slag	20	2.86	5,900	0.053	- 9
(3)	ordinary fly ash	20	0.44	3,840	-0.026	- 8
(4)	ordinary fly ash ground	20	1.91	8,400	-0.005	-14
(5)	high calcium fly ash	20	0.57	3,730	-0.005	10
(6)	rice husk ash	20	0.75	-	0.027	-20
(7)	silica fume	20	20.91	-	0.203	-33
(8)	aerosil	5	167	-	0.326	-

note; content: (%), BET: m^2/g, Blaine: cm^2/g, calcium adsorption capacity: mmol Ca/g, Zeta potential: mV (water suspension)

Fig. 13 Heat evolution curve of the hydration of C_3S with each blending component (32).

Examples of hydration of pure C_3S with each of slag, fly ash, silica fume, rice husk ash and aerosil made at the W/S ratio of 1.0 at 293°K are shown in Fig. 13. The hydration of C_3S is accelerated by adding a pozzolanic material with the calcium adsorption capacity (obtained from the difference of Ca ion concentrations between before and after suspending it in the $Ca(OH)_2$ saturated solution for 3 hours) of approximately more than 0.1 (mmol/g of pozzolana), but it is hardly changed or retarded by adding the pozzolanic material with that below 0.1 mmol/g. The calcium adsorption capacity of silica fume and rice husk ash is 0.02 to 0.4 mmol/g. The hydration of C_3S containing silica fume with the calcium adsorption capacity of 0.1 mmol/g or more and large specific surface area is accelerated in each stage.

3.4.2.2 Influence of silica fume and rice husk ash on the hydration of C_3A and C_4AF

There has been almost few studies on this systems. It is considered that the hydration of C_3A and C_4AF without $CaSO_4 \cdot 2H_2O$ is extremely accelerated immediately after mixing with water because the concentration of Ca^{2+} in the liquid phase of paste is markedly lowered by adding silica fume and rice husk ash, but the hydration is retarded when the unhydrated particle are covered with Al_2O_3-rich layer. Since $Ca(OH)_2$ is consumed by pozzolanic reaction of silica fume and rice husk ash, the retarding effect of $CaSO_4$ on the hydration of C_3A and C_4AF is lowered. Although ettringite is vigorously produced immediately after mixing with water even in the system containing $CaSO_4 \cdot 2H_2O$, hydration precedes as the same as that of system without $CaSO_4 \cdot 2H_2O$ after $CaSO_4 \cdot 2H_2O$ is consumed

3.4.2.3 Hydration of clinker minerals in silica cement

The heat evolution curve of silica cement containing the silica fume (SiO_2=94.5%, Fe_2O_3=0.25%, Al_2O_3=3.40% and BET specific surface area=17m^2/g) is shown in **Fig. 14**. The hydration of alite in the stage I, II and III of the early hydration is accelerated by adding the

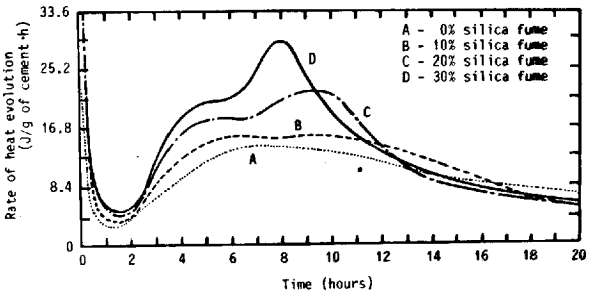

Fig. 14 Heat evolution curve of the hydration of cement with silica fume (59)

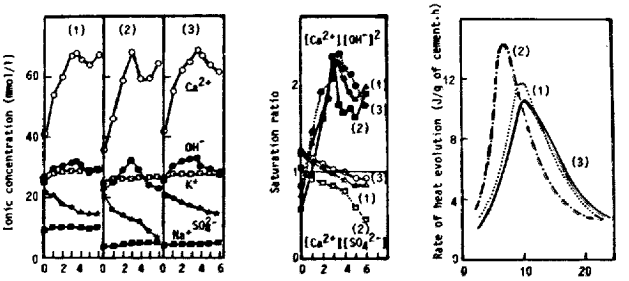

Fig. 15 Ionic concentration and saturation ratio of $Ca(OH)_2$ and $CaSO_4$ in liquid phase of fresh paste and heat evolution curve of the hydration of silica cement at 293°K (32)

silica fume. The hydration of interstitial phase is also accelerated and the appearance of the third peak based on the conversion of ettringite to monosulphate hydrate is advanced. The $Ca(OH)_2$ saturation ratio in

the liquid phase of paste with each of silica fume and aerosil is low immediately after mixing with water and subsequently sharply raised to the maximum earlier than that of cement without blending component as shown in **Fig. 15.** The $CaSO_4$ saturation ratio is also remarkably decreased with time.

3.4.3 Pozzolanic reactivity and pozzolanic reaction rate of silica fume and rice husk ash

3.4.3.1 Pozzolanic reactivity

The pozzolanic reactivities of silica fume and rice husk ash were investigated from the variations of consumption of $Ca(OH)_2$ and amount of SiO_2 reacted in the system blended with $Ca(OH)_2$. The results are as follows: reactivities of them depend upon the amount and specific surface area of amorphous phase; the larger the specific surface area, the higher the reactivities are; and pozzolanic reactivity well corresponds to the amount of acid soluble SiO_2 so that the amounts of acid soluble SiO_2 per specific surface area of both blending components are almost equal to each other (7). The reactivities of silica fume and rice husk ash are closely related to surface energy connected with the amount, particle size distribution, structural strain and specific surface area of amorphous phase.

3.4.3.2 Pozzolanic reaction rate

When $Ca(OH)_2$ is mixed with the rice husk ash having the specific surface area of 152 m^2/g, it is consumed at a rate of 20 to 120 (g/100g of rice husk ash) at 293°K for 3 hours (57). When $Ca(OH)_2$ mixed with rice husk ash having the specific surface area of 1-7 (m^2/g) at mixing ratio of around 1.0, it is consumed at 318°K at a rate of 5 to 20 (g/100g of rice husk ash) and 20 to 55 at age of one day and seven days, respectively. The reaction degree of silica fume with the specific surface area of 4-22 m^2/g is 40-65% and 85-90% at age of one day and seven days, respectively (7).

Pozzolanic reaction rate of silica fume and rice husk ash added to C_3S and cement become remarkably lower than that added to $Ca(OH)_2$ similar to that in the case of slag and fly ash. An experimental result indicates that the amount of $Ca(OH)_2$ combined in the cement mixed with 30% silica fume is 3 (g/100g of silica fume) in 10 hours, 6.6 (g/100g of silica fume) in 1 day and 13 (g/100g of silica fume) in 3 days (59). The reaction degree of silica fume and rice husk ash ranges from the same degree as slag to fairly higher degree than it though no accurate measurements have been reported.

3.4.4 Hydration process of silica cement containing silica fume and rice husk ash

Silica fume and rice husk ash adsorb Ca ion in the liquid phase of fresh phase in early stage after mixing with water and form the germ of C-S-H on the surface (56). Ca ion is actively dissolved from alite with lowering of Ca ion concentration in the liquid phase and the hydration of alite in the early stage is accelerated. At this time, the $CaSO_4$ saturation ratio is also lowered and the hydration of interstitial phase such as C_3A and C_4AF is accelerated. Ettringite produced in the stage I has a shape with a larger aspect ratio. C-S-H production by pozzolanic reaction is initiated at around ten hours and it proceeds during 1 and 7 days. The amount of remaining $Ca(OH)_2$ in the hardened paste is decreased with the production of C-S-H which has low C/S ratio.

4. RHEOLOGICAL PROPERTIES AND FLOCCULATION STRUCTURE OF FRESH BLENDED CEMENT PASTE

In this chapter, the formation process of flocculation structure of fresh cement paste was grasped relating to the changes in amount and morphology of the hydrates, specific surface area, surface potential and thickness of water film of the paste corresponded to the change of rheological properties and the flocculation structure of fresh cement paste was discussed from data observed directly by SEM based on the sample freezing method.

4.1 Rheological properties of cement paste

4.1.1 Definition and measuring method

The definition of shear stress, shear strain, shear rate, Newtonian fluid, non-Newtonian fluid, Bingham body, thixotropy, rheopexy and dilatancy are the same as explained before (60).

A typical flow curve of cement paste has a straight line as the shear rate is increased or decreased as shown in **Fig. 16.** Cement paste is approximated to a Bingham fluid (62). In this case, the intersection of the extension of straight line and the axis of shear stress is the yield value and the inclination of the line is plastic viscosity. There are, however, many problems from the viewpoint of the reliability of measurements (63). Considering convenient analysis for determining the rheological properties, the method determining the yield value and plastic viscosity by the rotational viscometer is superior to the one-point test method determining the flow, amount of water for the standard consistency and slump. It is difficult, however, to compare the data with each other because the testing method by viscometer is not standardized. Since the rheological properties of cement paste is extremely sensitive to the experimental conditions, it has been indicated that the mixing method must be standardized first of all (64). It has been proposed (65) that the rotor of rotational viscometer must be exchanged according to the water cement ratio of the sample to lessen the error caused by the agglomeration of sample as much as possible. The rheological properties depend largely upon the surface of cylinder and rotor of the rotational viscometer (66), the experimental conditions including shear rate and the kind of cement (61). Since the hysteresis loop of flow curve greatly varies according to the recycle time, it is desirable to make the measurement within the short time such as two minutes to keep the reproducibility.

Since the rheological properties of cement paste varies continuously in the measuring period with proceeding of the hydration, it is difficult to measure flow curve continuously. Therefore, the measuring method of the variation of the apparent viscosity at the constant shear rate (67), the measuring method of the apparent yield value of the intermittent, extraordinarily low shear rate (68) and the test of generating the continuous flow curve by continuously varying the shear rate (69) have been used. Mortar grout show the properties of non-Newtonian fluid in general (70), while concrete show the flow behaviour like Bingham flow.

The rheological properties of the mortar and concrete with high content of cement are controlled by those of paste, while those of the mortar and concrete with low content of cement, by those of aggregate (71). The more the content of cement, the lower the yield value is in general. It has been tried to estimate the rheological properties of concrete from those of paste (72). There is the relationship among the yield value, slump and compacting factor of concrete as shown in **Table 3**, but the plastic viscosity relates remotely to the slump and compacting factor.

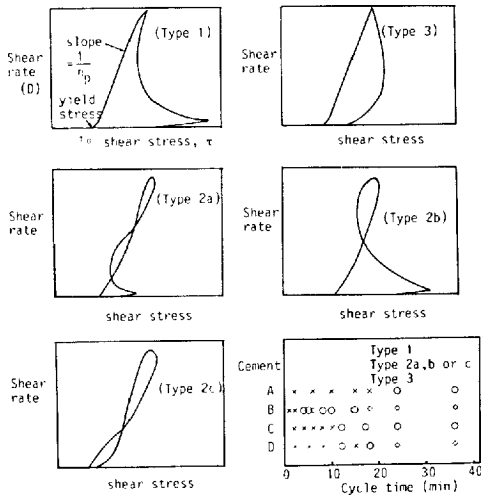

Fig. 16 A typical flow curve of fresh cement paste (61)

Table 3 Correlation coefficient between workability test parameters for ordinary portland cement replacement with pulverized fuel ash by equal volume and equal weight (73)

	slump	VeBe	Comp. factor	g	h
	Replacement by equal weight				
slump	1.00	-0.75	0.95	-0.93	-0.26
Ve Be	-0.84	1.00	-0.64	0.84	-0.31
Comp. factor	0.85	-0.87	1.00	-0.96	-0.45
g	-0.97	0.93	-0.98	1.00	0.14
h	-0.69	0.85	-0.88	0.84	1.00
	Replacement by equal volume				

g; measured value relating to yield value
h; measured value relating to viscosity

4.1.2 Relationship between rheological properties and setting of fresh ordinary portland cement paste

According to the measurement of the variation of apparent viscosity of the clinker paste under the constant shear rate in 0, 30, 60 and 90 minutes after mixing with water, time depending characteristics all of them are the same regardless of addition of the organic admixture. The time dependency of the apparent viscosity is caused by the rheopectic features developed by the change of flocculation structure with applying the shearing force and it is hardly affected by the hydration (67). While the other paper points out that the viscosity is caused by agglomeration of cement particles and the agglomerative force relates to the frictional force in proportion to the 2/3rd power of the number of contact points (74).

On the other hand, the rheological properties of fresh cement paste depend upon the thickness of water film around the cement particle. The viscosity increases as the thickness of water film decreases. Since the latter is inversely proportioned to the specific surface area, it is thought that the viscosity increases in general as the specific surface area increases for the same content of water. The same specific surface area gives the same thickness of water film. In this case, the viscosity is increased as the particle size distribution of cement becomes narrow and ordinary portland cement containing 15% of the particles as fine as 5μm or less shows the minimum viscosity (75). It is probably considered that water film with the uniform thickness is formed around the different sized cement particles packed closely which move easily by the bearing effect. Since a proper amount of superplasticizer makes similarly the dispersion of cement particles well to pack the smaller particles into the gap between the larger particles, the plastic viscosity is exponentially decreased and the yield value is linearly decreased (76). The thickness of water film of 1.2μm around the cement particles with Blaine specific surface area of 4,300cm^2/g in the fresh paste of 0.5 of water cement ratio goes down to 0.5μm by ettringite formation from the hydration of several percent of C_3A for a few minutes after mixing with water. The viscosity is, therefore, increased.

The more the amount of potassium in C_3A solid solution , the higher the activity of C_3A is. The viscosity depends upon the quantity and morphology of the hydrate produced from the aluminate phase (77). As either the specific surface area of cement or the volume concentration of the solid in the paste is increased, the yield value is especially remarkably raised, though the plastic viscosity also is increased (78).

Summarizing these results, Uchikawa (79)(80) illustrated the setting of cement rheologically and chemically as follows: The viscosity of cement paste mixed with a proper amount of water increases up to hardening through setting with the lapse of time. The viscosity increases rapidly at the initial stage, slowly at the middle stage and rapidly again at later stage as shown in **Fig. 17.** The initial and final setting are the critical points during the variation of viscosity of cement paste and they are the values of penetration resistance of the cement paste with the standard consistency against the constant load of the standard needle.

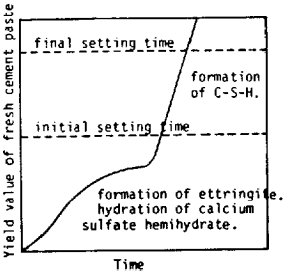

Fig. 17

Schematic diagram explaining the change of yield value of fresh paste until final setting (79)

The initial viscosity increase is mainly caused by the three dimensional network structure formed by gypsum produced by hydration of hemihydrate contained in the cement and ettringite produced by hydration of tricalcium aluminate solid solution (C_3Ass) and ferrite solid solution (C_4AFss) contained in the cement. The

trend at the middle stage is caused by temporarily inhibiting the hydration of cement due to short supply of Ca^{2+} to the liquid phase because the cement particles are covered with the above mentioned rod like crystals and C-S-H, so the transfer of water and ions is limited to the diffusion through the layers of these hydrates. When the concentration of Ca^{2+} in the liquid phase reaches a certain level of the $Ca(OH)_2$ saturation degree at the hydration temperature, C-S-H is rapidly precipitated around the existing nucleation seeds and the balance of ionic concentrations inside and outside the protective layer of the hydrates covering the unhydrated particle is lost, so the osmotic pressure is increased to break the protective layer and water comes to directly contact with the fresh surface of cement particles. When C-S-H is vividly produced in this manner, the viscosity of cement paste is sharply increased again.

In the normal setting, the viscosity corresponding to the initial and final settings reaches during the vivid production of C-S-H.

4.2 Rheological properties of blended cement paste, mortar and concrete

4.2.1 Viscosity of blending component

The viscosity of the suspension of nonreactive particles in water depends upon the volumetric ratio of water to particle, number of contact points between particles and adhesiveness. The sample is prepared in such a way that quartz as a nonreactive material is mixed with 50% of slag, 25% of fly ash and 10% of silica fume in inner percentage according to the usual usage and water is added to the mixture to make up 0.35 of the water solid ratio. The time dependency of the viscosity of sample determined by the rotational viscometer with double cylinder is shown in **Fig. 18.** The viscosity is expressed by the yield value calculated from the torque of the sample stirred by the intermittent rotation at the rate of 0.1 rotation every 12 seconds.

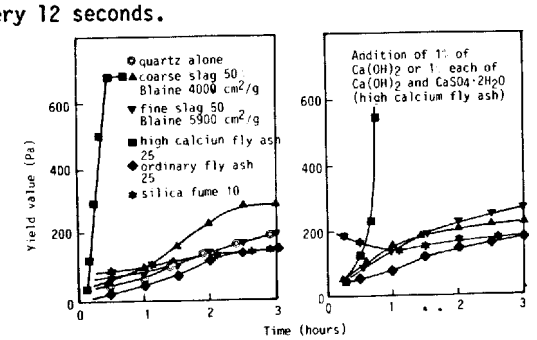

Fig. 18 Time dependency of the viscosity of the quartz powder with blending component by the rotational viscometer with double cylinder (W/S=0.35, 293°K) (82)

In the suspension of quartz alone, the quartz particles settle down as the time passes and they are densely packed on the bottom of vessel. Therefore the yield value varies from 50 to 200 Pa for three hours after mixing with water. The coarser granulated blastfurnace slag gives larger variation of the yield value with time than the finer one. Although the ordinary fly ash shows the variation of the yield value at a little lower level, the yield value for the high calcium fly ash is sharply increased by hydration of C_3A in it. The yield value for silica fume is high immediately after mixing with water but the time dependendency is small.

When 1% of $Ca(OH)_2$ is added to these blending components and 1% each of $Ca(OH)_2$ and $CaSO_2 \cdot 2H_2O$ are added to high calcium fly ash, the yield value for silica fume immediately after mixing with water is increased because of the adsorption of Ca^{2+} and dissolution of it into $Ca(OH)_2$ solution, and the rising of yield value for high calcium fly ash is delayed by the inhibition of hydration of C_3A.

The time dependency of the viscosity of blended cement paste with portland cement (Blaine specific surface area : 3,240 cm^2/g) instead of quartz particles is shown in **Fig. 19.** The yield value immediately after mixing with water is increased by adding any blending component without exception and then it is increased by hydration after approximately two hours successively followed by the rapid increase. The increasing process of yield value of fresh paste is divided two step of 2 hours after mixed with water and later.

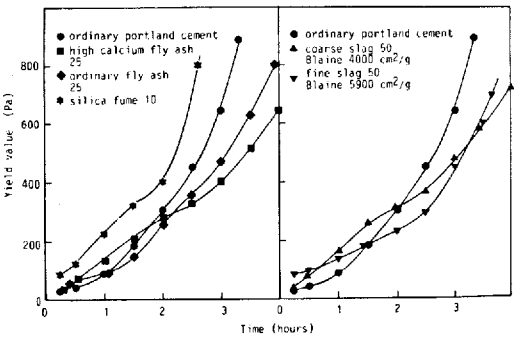

Fig. 19 Time dependency of the viscosity of cement paste with blending component (W/S=0.35, 293°K) (82)

As for particle shape, when same kind of cement is used, the relationship between the yield value, τ_0, of the paste of a certain kind of cement and the volume concentration of solid, v, is as follows:

$$\tau_0 = P_f \cdot e^{P_s(v-0.5)} \qquad -(3)$$

where P_f is constant regarding the fineness of particles, and P_s is constant regarding the plasticity of solid and the shape of particle. **Fig. 20** shows the relationship in various blended cements between the volume concentration of solid and the yield value. In this figure, the inclination of the straight line is expressed as P_s and the shape of particle approaches sphere with decreasing P_s. The value of P_s is increased by adding coarse slag to ordinary portland cement, while it is decreased by adding fine slag to it. Although P_s is also generally decreased by adding fly ash or silica fume, it is increased by adding fly ash with coarse grain fineness and high content of irregular particles. The effect of addition of 25% of fly ash on the value P_s is almost the same as that of 10% of silica fume.

4.2.2 Blastfurnace slag cement

Many papers (83) reported that the fluidity of paste, mortar and concrete is improved in proportion to the volume of the slag substituted for part of cement. The degree of improvement by the irregular shaped slag is generally lower than that by fly ash with spherical particles. The rheological properties of blastfurnace

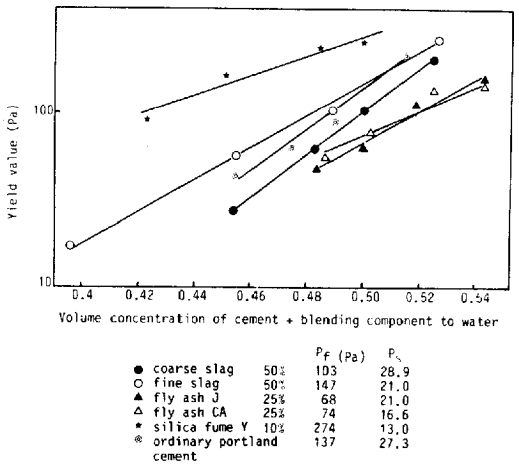

Fig. 20 The relationship in various blending component between the volume concentration of solid and the yield value (293°K)(82).

slag cement varies according to the grinding method. For addition of separately ground slag as shown in **Fig. 21**, the slump of concrete is increased with increasing the blending of slag regardless of the water cement ratio and the amount of water required for obtaining the same slump in 50% mixture can be decreased by approximately 5%. Although the slump of concrete is uneffected by the slag with the fineness as wide as Blaine specific surface area of approximately 5,000cm²/g, it is decreased by the slag with fineness higher than that (84). Generally, the plastic viscosity is slightly decreased by blending slag, while the yield value is remarkably decreased. When slag is interground with cement clinker, both plastic viscosity and yield value are increased by adding slag. It is considered that the fluidity of blastfurnace slag cement interground is decreased by the coarse blastfurnace slag particle in it because slag has lower grindability than clinker.

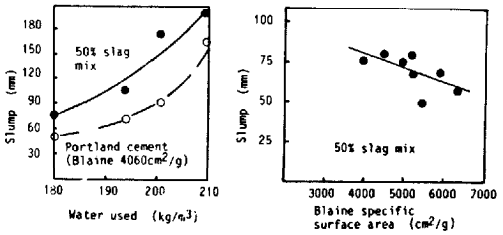

Fig. 21 The relationship between slump of concrete and content of water used, and Blaine specific surface area (84)

The final setting of blastfurnace slag cement is generally 45 to 90 minutes behind that of ordinary portland cement. There is, however, a report (84) that there is no clear relationship between the setting time and the change of slump with elapsed time, because there is no difference in the change of slump loss beginning from the same slump conditions between them.

4.2.3 Fly ash cement

The fluidities of paste and concrete of fly ash cement which is produced by substituting fly ash for part of cement are much improved compared with that of ordinary portland cement. The fluidity of concrete is much more improved than that of paste because of the increase of paste volume in concrete in addition to the improvement of fluidity of the paste. It is known (68)(73)(85) that there is an optimum substitution ratio for improving the fluidity, but the equivalent substitution in volume is different from that in weight. The substitution ratio of approximately 10% in weight shows the maximum of slump within actual fly ash cement composition as shown in **Fig. 22**. Since the specific gravity of fly ash is lower than that of ordinary portland cement and both of them have the same specific surface area, the specific surface area per unit volume of fly ash cement is decreased as the substitution ratio of fly ash by the equivalent substitution in volume is increased.

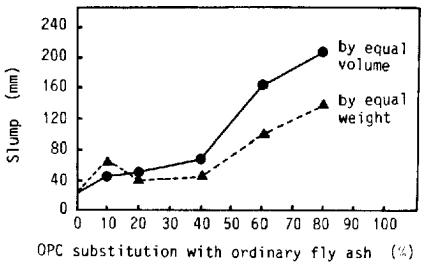

Fig. 22 The relationship between the slump of concrete and the amount of fly ash substituted. (85)

Since the fluidization of concrete is facilitated by the bearing effect of the spherical particles of fly ash, the amount of water required for the specified workability can be reduced. Although the volume concentrations of water and aggregate are decreased by the equivalent substitution in weight and the workability is slightly lowered, it is improved by the increase of spherical fly ash particle content when those materials are added more than certain limits (98).

The yield value of fresh concrete is decreased by substituting fly ash for a part of cement, but the plastic viscosity of it remains unchanged in the same manner as in blastfurnace slag. Considering that the fluidity of fly ash cement concrete containing the fly ash with 45μm or over in diameter is hardly improved, it is necessary that the particle diameter is below the specified value. It is probably because the coarser particles include a lot of irregular particles. Actual yield value is inapplicable to any relationships (78) of τ_0 with the specific surface area and the volume concentration of solid. It is required, therefore, to consider the shape factor and particle size distribution of fly ash particles.

The fluidity of fly ash cement paste immediately after mixing with water is evaluated by the evaluation index of fluidity of fly ash defined by the following equation (13). The larger this value, the larger the fluidity of fly ash cement.

$$\text{Fluidity evaluation index} = (\text{sp.gr.} \times \text{shape factor}) / (\text{sp.surface area} \times \text{porosity}) \quad -(3)$$

The variation of viscosity for two hours after mixing with water depends upon the amount and shape of ettringite precipitated. When $Ca(OH)_2$ saturation ratio of liquid phase in the paste is decreased by adding fly ash, the production of ettringite is raised and the aspect ratio of the formed hydrate is increased.

The viscosity after mixing with water is raised rapidly in this case.

When a highly acidic lignin sulphonate-based superplasticizer is used, the abnormal increase of yield value and decrease of slump are frequently observed. This is because a lot of needle ettringites with high aspect ratio are rapidly produced as the degree of $Ca(OH)_2$ saturation of liquid phase in the paste is further lowered (68).

There are two kinds of carbon in fly ashes. The one is amorphous carbon with a specific surface area as high as several hundred m^2/g and the other is the crystalline one with low specific surface area. The adsorption of organic admixture is especially high in the concrete using the fly ash containing the former.

4.2.4 Silica cement blended with silica fume

In order to keep specified fluidity of the blended cement with a small amount of silica fume, much more water must be added. When the same amount of water is added to the blended cement paste containing silica fume, the yield value is increased as shown in **Fig. 19** and the value P_f become large, while the value P_s become small as shown in **Fig. 20.** The increase of yield value is mainly caused by the increase of specific surface area. In order to get the same slump of the concrete containing 30% of silica fume, the amount of water must be increased by 30%.

Review on "Effect of blending material on the rheology of cement paste and concrete" (83) says that a water reducing admixture or a superplasticizer is inevitably used for silica fume blended cement because the yield value of paste is much increased and the plastic viscosity is enhanced. It is necessary for concrete containing the same amount of water to use 5 to 10 wt% of a water reducing admixture depending upon the amount of silica fume added (86) in order to obtain the same workability as ordinary portland cement. It has been indicated that the workability of concrete with low amount of cement is improved by the addition of silica fume, but concrete as much as 450kg/m^3 of cement sets rapidly by it. When a water reducing agent is used, silica fume is applied to filling up the void between the aggregate and the paste in the concrete containing silica fume as much as 20%. There is no necessity, therefore, to increase the amount of water. No bleeding is observed at all even in the concrete showing 10 to 20 cm slump (15).

4.3 Setting of blended cement

Setting time of blastfurnace slag cement is delayed at a rate of 10 to 20 minutes per 10% of mixing of slag compared with that of ordinary portland cement (87). By using lignin sulphonate as a superplasticizer, the setting time is lengthened at the rate of 2 hours for 0.25% addition and 6 or more hours for 0.5% addition (88). The setting time is delayed with increasing of the content of particles 10μm or under in slag though the effect of the fineness of slag is small. As the chemical composition of slag is converted from gehlenite (C_2AS) side to akermanite (C_2MS_2) side, the setting time is lengthened. When extremely 90 to 100 %of slag is composed of gehlenite, the flash setting often takes place.

Fly ash lengthens the setting time of fly ash cement more than slag. It is delayed approximately 20 minutes by adding 10% of ordinary fly ash (85). The larger the carbon content in fly ash, the more the amount of water required for the standard consistency is and the longer the setting time is (89). A paper reports that the setting time is hardly affected even though the carbon content in high calcium fly ash is increased (89), while the other paper reports the contrary result (90).

Although both initial and final setting times are shortened in silica fume blended cement, generally the setting is considerably delayed by using a lot of superplasticizer for improving the workability.

4.4 Factors influencing on the formation of flocculation structure

4.4.1 Amount of hydrates and their morphology

The hydrate participating in the early flocculation structure of blended cement paste is ettringite in the same way as in portland cement. The amount and morphology of it takes part in formation of skeleton structure.

Although amount of ettringite formed per unit weight of blended cement paste varies according to the kind and content of the blending component, it is always increased by adding the blending component, considering the amount of ettringite formed per unit weight of ordinary portland cement (dash line in **Fig. 23**) calculated from mixing ratio of it (82).

On the other hand, the content of $Ca(OH)_2$ in the blended cement paste is less than the amount of $Ca(OH)_2$ calculated from mixing ratio of ordinary portland cement. This phenomenon shows the adsorption by the blending component or the consumption by the pozzolanic reaction with it.

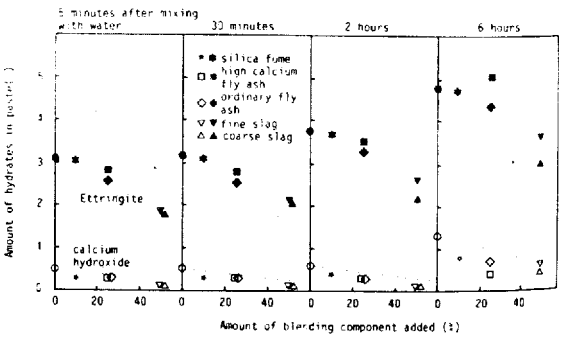

Fig. 23 Amount of ettringite and $Ca(OH)_2$ formed in the initial hydration of blended cement (82)

Ettringite produced in initial hydration is locally precipitated and its morphology varies in equant, short rod or needle type depending upon saturation ratio of $Ca(OH)_2$ and $CaSO_4$ of liquid phase in the paste (91). The diameter of the crystal of ettringite is almost 0.1 to 1.0μm, but some of the crystals grow up to 5μm by recrystallization at final setting (91). Since the saturation ratio of $Ca(OH)_2$ of liquid phase in the paste is lowered by adding the blending component and the hydration space is extended, the aspect ratio of the ettringite is generally increased (13). The trend is remarkable in fly ash and silica fume with high calcium adsorption capacity and it is much more marked as the addition of them is increased. On the other hand, C-S-H produced first by hydration of alite is mainly Type I C-S-H of needle

0.1 to 1μm and it forms sometimes network. Although the hydrate precipitated on the surface of blending component is fewer than on the surface of cement particles at the earlier stage, the hydrate is more easily precipitated on fly ash and silica fume than on slag, as for as the blending component is concerned.

4.4.2 Specific surface area of fresh paste

The specific surface area of fresh paste hardly increased in dormant period of hydration of cement. The specific surface area of paste up to four hours after mixing with water determined by the nitrogen adsorption and Blaine specific surface area methods are shown in **Fig. 24.** The results indicate that the specific surface area increases a little in five minutes after mixed with water and is kept constant for two hours, followed by the rapid rise. Since the decrease of specific surface area by the dissolution of cement particle is offset by the increase of surface area of fine hydrate produced immediately after mixing with water, the increase of specific surface area of fresh paste is not proportional to the formation of hydrate. The increase of specific surface area in the earlier stage of hydration is caused by the production of ettringite, while the subsequent increase is mainly caused by the vivid hydration of alite.

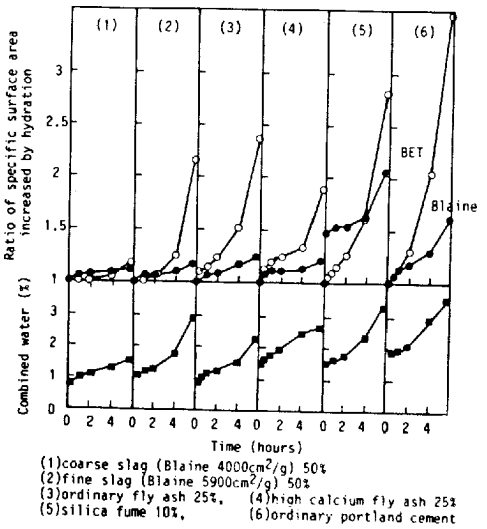

Fig. 24 The time dependency of combined water and ratio of specific surface area increased by the initial hydration of blended cement (W/C=0.35, 293°K)(82)

Both specific surface areas in ordinary portland cement show the same variation for a while after mixing with water, but the BET specific surface area is more remarkably increased than Blaine specific surface area two hours later. This indicates that the increase of specific surface area by fine C-S-H precipitated on the surface of cement particles is larger than that by the decrease of unhydrated cement particles by hydration. The specific surface area of blastfurnace slag cement with coarse slag is slightly increased. But silica fume blended cement shows remarkable increase in specific surface area immediately after mixing with water. This is probably caused by the dispersion effect of silica fume and the gelation accompanied by dissolution of it.

4.4.3 Zeta potential of fresh cement paste

The potential of the cement and blending component particles electrically charged in water varies with proceeding of hydration. Zeta potential is useful for examining the relative variation of potential though the measured values vary sometimes according to the measuring methods.

In fresh cement paste, Ca ions with high potential and rich in quantity greatly affects the charge of stern layer, so zeta potential of paste depends upon the ionic concentration of Ca ions (13). Although cement particles show the negative or low positive charge in the dilute solution, the potential of positive charge is raised in the paste solution with the normal water cement ratio as $Ca(OH)_2$ saturation ratio of liquid phase increases. The measurements of zeta potential of the blending component by the streaming potential method show the high negative potential in distilled water or dilute calcium ionic solution and these potential generally turn to positive as the concentration of calcium ion is increased. The variations of zeta potential of ordinary portland cement and blended cement paste with proceeding hydration are shown in **Fig. 25.** It reveals that the time dependency of zeta potential is smaller than the increase of yield value of paste, the amount and the surface area of hydrate formed. The measured value of zeta potential is the mean value of the potentials of each particle in the paste and not the variation of local potential of each particle. On the contrary, the hydration is microscopically the sum of local reaction degree proceeding from the active center of the reaction particle and the reaction degree varies locally. It is appropriate, therefore, to consider that zeta potential on the surface of particle in the paste practically differ remarkably with individual particle.

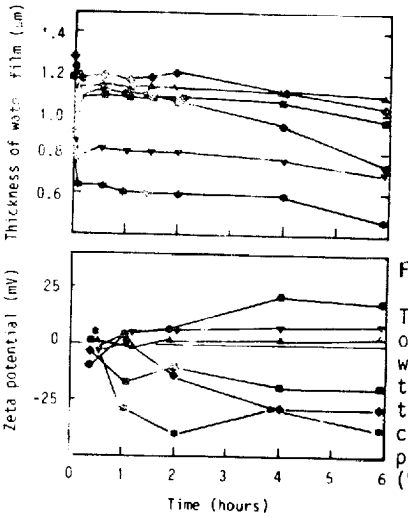

Fig. 25 The time dependency of thickness of water film calculated and zeta potential of blended cement paste with proceeding hydration (W/C=0.35, 293°K)(82)

Zeta potentials of slag particle alone vary with the kinds of slag, ranging from -15 to -23mV. Zeta potential of blastfurnace slag cement is increased in negative value as slag is more added (81). This is generally considered to be depending upon selective dissolution of metallic ion of the network modifier in the glass phase predominating in the slag into the mixing water.

Zeta potential of fly ash dispersed in distilled water shows generally negative, ranging from -10 to -21mV, but that of some kinds of fly ash shows positive, ranging from 10 to 20mV. That of silica fume shows negative as high as -30mV.

4.4.4 Thickness of water film between particles in fresh cement paste

Although 20 to 30 wt% of water is ought to be theoretically fixed by hydration as combined water, only approximately one tenth of it is fixed till the setting. When the hydration of cement is stopped by acetone and it is dried under the humidity of RH 11%, only free water is evaporated and the combined water of the hydrates including ettringite and C-S-H remain. The time tendency of the amount of combined water of fresh blended cement paste is shown in **Fig. 24.** That of each cement corresponds closely to the variation of specific surface area, increasing immediately after mixing with water and increasing again two hours later.

Assuming that the thickness of water film on the surface of each particle in cement paste is constant regardless of the size of particle, the thickness of water film on the surface of particle is calculated from (W/S)/M. W/S is weight ratio of water to particle, M is Blaine specific surface area.

The time dependency of the thickness of water film of ordinary portland cement paste and blended cement paste estimated from change in Blaine specific surface area of paste are shown in **Fig. 25.** The thickness of water film of paste and the time dependency of it are decreased by adding a blending component. Since the variation of the thickness of water film is not necessarily corresponding to that of the viscosity of paste as shown in **Fig. 19**, it is necessary to consider that the viscosity of paste is controlled by considering the shape and surface potential of particle, content and morphology of hydrate in early stage and variation of specific surface area in addition to the thickness of water film.

4.5 Flocculation structure of fresh blended cement paste

The flocculation structure of fresh cement paste with free water cannot be observed as it is by the usual way because the sample has been dewatered for drying under high vacuum in the sample chamber of electron microscope. The concentrated suspension of fresh paste is able to be directly observed by rapidly freezing the water using liquid nitrogen. This freezing method is an epoch-making technique for directly observing the flocculation structure of fresh cement paste. Back scattering electron image was used to distinguish the cement, blending component and hydrate from the free water filling the gap between them. Since each constitution and particle presents a contrast corresponding to its average atomic number by this method, the frozen free water is seen darkest and cement, blending component and hydrate particle can be distinguished from each other according to the brightness. The results are shown in **Fig. 26.**

In the fresh paste of ordinary portland cement, only coarse particles approximately 10μm in diameter with fine particles 2 to 3μm or less are dispersed in the free water and besides, few single fine particles and further coarse particles which are agglomerated directly observed. The cement particles most of which are angular are unevenly dispersed. The average thickness of water film around the particle is 3μm and it is several times thicker than that of 0.9μm calculated assuming that the solid particles are same sized spheres. The discrepancy is considered to be derived from that fine particles stick to coarse ones and the shape of particles is much different from sphere. C-S-H as well as ettringite begin to be precipitated and then the cement particles begin to agglomerate through the medium of C-S-H and ettringite in two hours after mixing with water. In this stage, several particles stick together at most and these coarse particles agglomerate further through the medium of the fine particles existing between them. In six hours corresponding to final setting stage, the hydrate is increasingly deposited on the surface of cement particles and the particles are three-dimensionally connected to each other by the locally, thickly deposited layers of hydrates. The thickness of water film is, therefore, slightly decreased in this stage as shown in **Fig. 26.** This fact supports the before mentioned estimation (79)(80) of the formation process of flocculation structure. It is considered that the dispersion of solid particles immediately after mixing with water is closely related to the average physical properties such as specific surface area and shape of the solid particle, and the local surface potential and hydration activity of the particles of cement and blending component and the production and growth of hydrate largely affect the formation of flocculation structure with hydration.

Substituting a blending component with the equal weight of cement generally decreases the thickness of water film around the particles. The decreasing degree varies according to the shape, specific surface area and amount of blending component added. The average thicknesses of water film immediately after mixing with water to coarse slag, fine slag and fly ash are 1.5 to 2, 1 and 1 to 1.5μm, respectively. These values are a little larger than those calculated by the above mentioned method, 1.1, 0.8, 1.1μm, respectively. The discrepancy between the actual value and calculated one for blended cement is smaller than that for ordinary portland cement, because slag or fly ash seems to be well dispersed due to sticking of few fine particles to the surface of blending component particles. Although the thickness of water film around blended cement particles is relatively uniform compared with that around ordinary portland cement particles, water film around blending component particles is a little thicker than the latter. Although the gap between the solid particles blended with coarse slag is larger than that between the solid particles blended with fine slag, the solid particles blended with fly ash is more uniformly dispersed than those blended with these slags. The hydrate is deposited on the surface of blending component particles as well as that of cement particles as the hydration proceeds and the flocculation structure is formed a little late in the same way as that of ordinary portland cement. Silica fume sticks to the whole surface of cement particles.

Adding a naphtalenesulphonic acid-formaldehyde condensate-based superplasticizer improves the dispersion of solid particles of any kinds of cement, so that fine particles hardly stick to coarse particles. The free water in which microfine particles are well dispersed shows the behaviour as if the thickness of water film between coarse particle is increased. Since the superplasticizer is adsorbed onto the surface of solid particles, they are negatively charged in

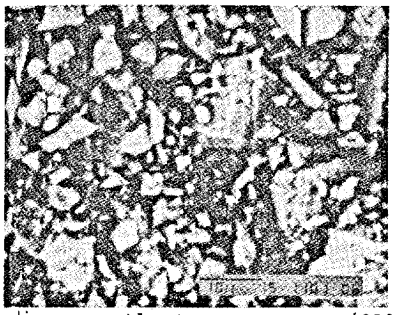

ordinary portland cement paste (OPC) at 5 minutes after mixing with water



OPC at 2 hours



OPC at 6 hours

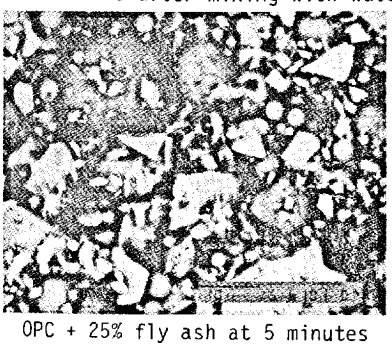

OPC + 25% fly ash at 5 minutes

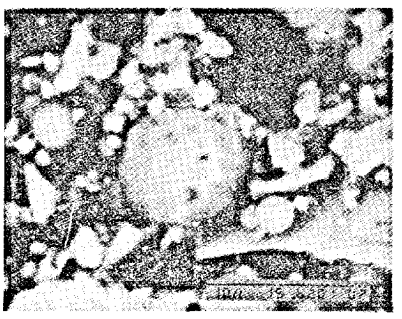

OPC + 25% fly ash at 2 hours



OPC + 25% fly ash at 6 hours

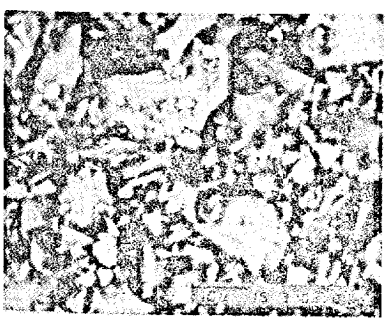

OPC + 50% coarse slag at 5 minutes

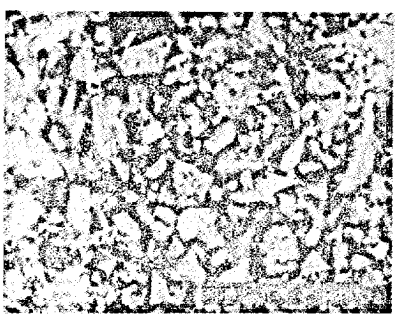

OPC + 50% fine slag at 5 minutes

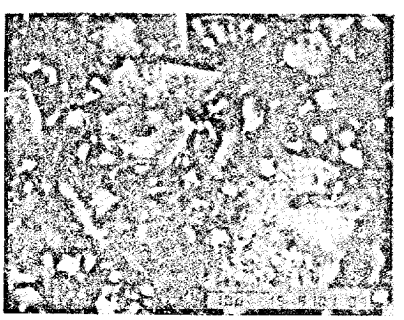

OPC + 10% silica fume at 5 minutes



OPC + superplasticizer at 5 minutes

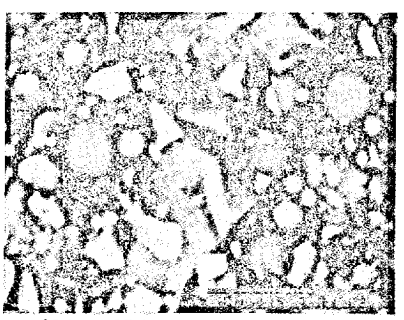

OPC + 25% fly ash superplasticizer at 2 hours

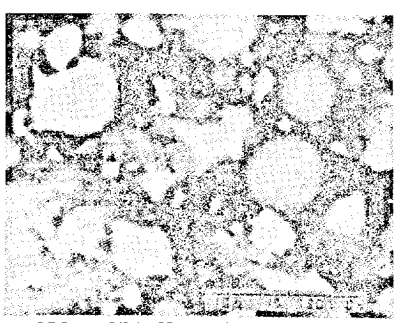

OPC + 25% fly ash superplasticizer at 6 hours

Fig. 26 Back scattered image of fresh cement paste with and without blending component and organic admixture by SEM based on the sample freezing method (W/C=0.35, 293°K)(82)

general. Although the particles are dispersed by the electrostatic repulsion, the microfine particles dispersed in the free water are hydrated and deposited on the surface of microfine particles as if the hydrate is deposited directly from the free water, so that these particles forms characteristic conjugated texture. Although the cement paste, especially ordinary fly ash blended, in addition of a lignin-sulphonate-based superplasticizer is dispersed in the same manner as that with a naphtalenesulphonic acid-formaldehyde condensate-based superplasticizer in 20 minutes after mixing with water, the concentration of Ca ion in the liquid phase of paste is decreased and the production of ettringite is accelerated as the hydration pro-

ceeds. The flocculation structure is similar to that without superplasticizer.

5. PROPERTIES AND STRUCTURE OF HARDENED CEMENT PASTE

5.1 Relationship between mechanical strength and structure of hardened blended cement paste

The strength of hardened cement paste could be determined essentially by its composition and structure. However, hydrates and unhydrate existing in hardened paste are very heterogeneous, which have the specific strength of themselves and they have complicated binding each other. In addition, the strength is also dependent on the pore containing more than 10% of the total volume in hardened paste as well as the kind and ratio of fluids in these pores.

The pore structure of hardened paste is explained mainly by porosity and pore size distribution. Finer pore in capillary pore space up to 3 nm in diameter can now be measured by modified penetration porosimeter with well reproducibility. The pore size measured is, however, corresponded to pore entry diameter but not exact pore diameter. Also, there are generally unfavourable problems such as lost porosity which mercury can not penetrate into finer pore, uncertain contact angle, damage of specimen in measuring procedure (92). It is, therefore, necessary to ensure higher reliability for measured value comparing with the data of adsorption method.

The chemical composition of C-S-H formed in blended hardened cement paste and ordinary portland cement paste measured by EPMA is shown in **Table 4.** The C/S ratio of C-S-H in hardened paste become lower in the order of ordinary portland cement, blastfurnace slag cement, fly ash cement. The amount of Al_2O_3 incorporated into C-S-H increases in the order of ordinary portland cement, fly ash cement and blastfurnace slag cement, and both amounts of Na_2O and K_2O in C-S-H increase in the order of ordinary portland cement, blastfurnace slag cement and fly ash cement. **Fig. 27** shows x-ray image map of K, Al, C/S and C/S+A ratio on polished surface of hardened paste with and without blending component by EPMA with high speed wide-area multi-analyser. The micrographs observed well coincide with that above mentioned. Silica cement paste with silica fume contains lower C/S C-S-H according to increase of amount added and is poor in Al bearing hydrates (93).

Table 4 Chemical composition of C-S-H in the hardened cement paste with 40% and without blending component (W/C=0.40, 293°K, age 4 years)(94)

	C/S	A/C	C/(S+A)	Na_2O	K_2O (%)
OPC	2.03	0.06	1.81	0.03	0.11
fly ash cement	1.01	0.21	0.84	0.24	0.33
blastfurnace slag cement	1.62	0.44	0.96	0.23	0.30

Fig. 28 shows pore size distribution of gel pore space in hardened cement paste with blastfurnace slag and fly ash measured by N_2 adsorption method. Maximum peak at about 2 nm in diameter, which corresponds to average distance between C-S-H solid surface decreases in fly ash cement but it is enhanced in blastfurnace slag cement. It is probably due to the formation of more dence structure by low C/S C-S-H in former and the increase in amount of C-S-H in latter.

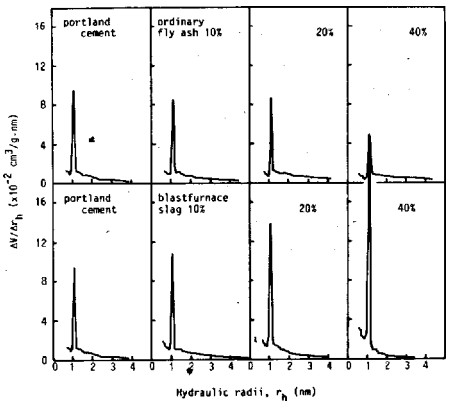

Fig. 28 pore size distribution of gel pore space in the hardened cement paste with blastfurnace slag and fly ash measured by N_2 adsorption method (W/C=0.40, 318°K)(96)

The pore size distribution of hardened blastfurnace slag cement paste in the early age is almost the same as that of ordinary portland cement paste. The total pore volume trend to be equal or slightly smaller. However, the pore volume of 3 to 5 nm become larger in the later as the pozzolanic reaction proceeds. There are difference in pore distribution between two kind of hardened cement paste. A relatively sharp peak of pore size distribution is observed at radius of about 12.5 nm for ordinary portland cement, while a broad peak was noticed at about 3.5 nm for blastfurnace slag cement (95). This is because blastfurnace slag cement has little $Ca(OH)_2$ and ettringite which make coarse nonuniform texture with weak bond C-S-H and forms dense structure producing spherical hydrates such as C-S-H and hydrogarnet which are main hydrates (95). A typical volume ratio of each capillary pore size in hardened blended cement paste is shown in **Fig. 29.**

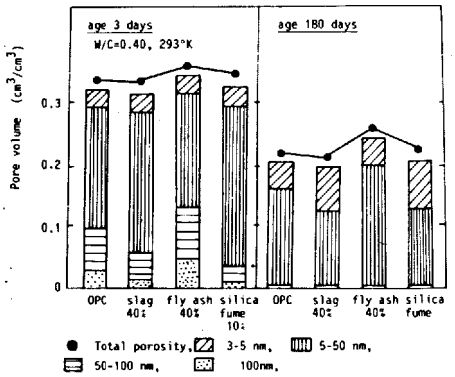

Fig. 29 Typical volume ratio of each capillary pore size in hardened blended cement paste

The porosity of hardened fly ash cement paste in early age become larger than that of ordinary portland cement and the volume of large pores of over 100 nm in size is far larger compared with ordinary portland cement. Although the pore size distribution peak shifts toward smaller pore size with age, total porosity is still larger even at 180 days. The large pore volume in early age is considered to result in the voids around fly ash particles or in the pores inside fly ash particles (100).



OPC, K

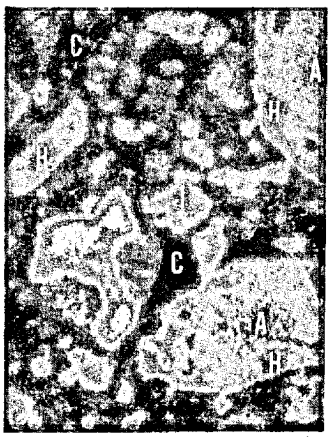

OPC, Mg

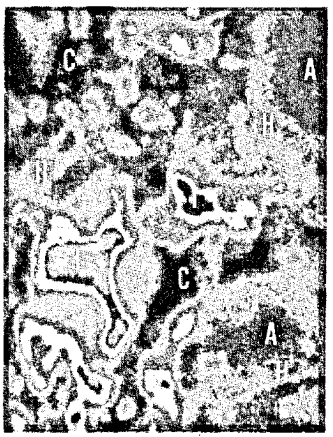

OPC, Al



OPC, C/S ratio

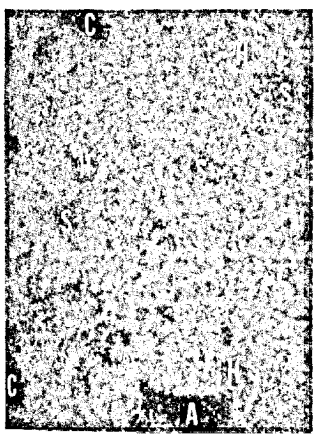

Slag 40%, K

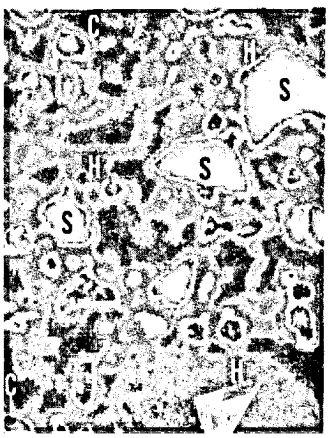

Slag 40%, Mg

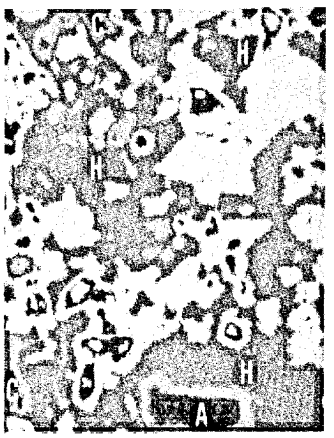

Slag 40%, Al



Slag 40%, C/S+A ratio



Silica fume 10%, Al

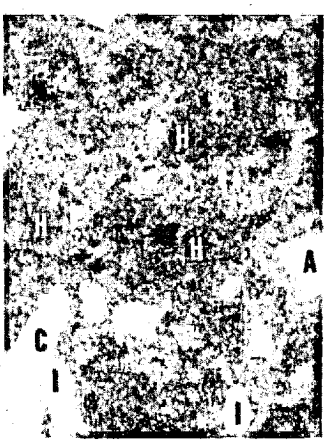

Silica fume 10%, C/S ratio



Fly ash 40%, Al



Fly ash 40%, C/S ratio

	K_2O	MgO	Al_2O_3	C/S	C/A+S
white	>2.9%	>9.0%	>18.0%	>3.0	>3.0
red	1.5	7.0	14.0	2.5	2.5
yellow	1.0	5.0	10.0	1.8	1.8
green	0.7	3.0	5.0	1.6	1.6
light blue	0.5	1.0	2.0	1.4	1.4
blue	0.3	0.6	1.0	1.2	1.2
black	<0.3	<0.6	<1.0	<1.2	<1.2

H: C-S-H, A: Alite, S: Slag grain
F: Fly ash grain, I: Interstitial phase
C: $Ca(OH)_2$

Fig. 27 X-ray image map of K, Al, C/S and C/S+A ratio on the polished surface of hardened paste with and without blending component by EPMA with high speed wide area multianalyser (W/C=0.40, 318°K) (93)

The volume of large pore size in hardened silica cement paste in which 30% of cement is replaced with the same volume of silica fume, is small compared with that of ordinary portland cement paste even at early age of 7 days In 28 days, though the total porosity is nearly same, silica cement paste hardly contains pore larger than 0.1μm. This tendency is more marked in 90 days (97). Reduction of capillary pore space and threshold pore diameter in silica cement paste with silica fume in early age is considered to be caused by filler effect of fine particle and rapid initiation of pozzolanic reaction.

The relationship between porosity and strength of hardened cement paste has been reviewed in detail (101), of which typical equations are as follow.

$$\sigma = \sigma_0(1 - P)^A \quad \text{(Bal'shin's formula)} \quad \text{--- 3)}$$

$$\sigma = \sigma_0 e^{-BP} \quad \text{(Ryshkewitch's formula)} \quad \text{--- 4)}$$

$$\sigma = C\ln(P_{cr}/P) \quad \text{(Schiller's formula)} \quad \text{--- 5)}$$

(σ : strength, σ_0 : strength for porosity 0,
P : porosity, P_{cr}: porosity at strength 0,
A, B, C: constants)

The strength estimated from these equations well coincides with practically measured one in early age, but the deviation between measured and estimated one becomes greater at later ages if the change in strength of hydrates such as C-S-H with age not taken into consideration (97). This indicates that the strength of cement is affected by qualitative factors such as the type of hydrates produced, the adhesive force between hydrates or between hydrates and unhydrates, and the shape of pores as well as quantitative factors such as pore volume and amount of hydrates.

In hardened fly ash cement paste with relatively large cenosphere grains, cracks developed under load propagate from one fly ash grain to another and more than 90% of them pass around the cenosphere-paste interface. Cenosphere grain itself rarely breaks. On the other hand, when an air entraining agent is added to give the same voids as cenosphere, cracks pass through air voids at their center and the air voids shows no resistance against cracking (98). Namely, it is apparent that a cenosphere grain of fly ash unlike air voids, however its wall may be thin, serves to relax stresses.

5.2 Durability and structure of hardened blended cement concrete

5.2.1 Relationship between freezing-thawing stability and structure of hardened concrete

The freezing-thawing stability of concrete correlates well with air-void spacing factor (ASTM C457-80). In order to enhance freezing-thawing stability, it is necessary to decrease the volume of pores less than several nm in size which are unstable at 273 to 253°K, and to increase the volume of relatively large pores about several tens of micrometers in size which can be observed under an usual optical microscope, that is, to decrease the air void spacing factor. The stability can be enhanced by increasing the volume of air voids 10 to 90μm in diameter (99).

When silica fume is added to portland cement, the volume of pores larger than 100 nm in size is decreased, while the volume of pore of 5 to 50 nm in size increases compared with plain concrete, and this enhances the capacity against damage from freezing-thawing cycles, thus improving freezing-thawing stability. On the other hand, when fly ash is used, the freezing-thawing stability tends to lower with increasing amount of fly ash in spite of decrease of decrease in amount of pore less than 5 nm in diameter, especially, that of fly ash cement with more than 30% of fly ash is remarkably lower. This is mainly depended upon the increase of capillary pore space (100), especially from 100 to 1000 nm.

The soluble alkali in fly ash serves to increase alkali content in mixing water, resulting in lowered freezing-thawing stability. It is known that high calcium fly ash contains this kind of alkali in larger amounts. The content of soluble alkali sometimes reaches to 0.5-1.5%. When 30% of such high calcium fly ash is added to portland cement, content of soluble alkali in mixing water becomes 1.4% (102).

The amount of air-entraining agent which is used to obtain a certain level of air void volume in fresh concrete has higher correlation with the content of organic materials in fly ash than the amount of unburnt carbon. The more amount of organic material in fly ash, the more amount of the agent added. High calcium fly ash generally has higher air holding capacity than ordinary fly ash.

5.2.2. Relationship between permeability and structure of hardened paste

Permeability (K_1) increases exponentially with increasing W/C ratio and drops sharply with the progress of hydration and with age. Higher W/C ratio increases total porosity and the threshold diameter, but causes little change in volume of pores less than 132 nm in size. Permeability correlates well with the volume of pore larger than 132 nm, and can be estimated from four factors of volume of pores larger than 132 nm in size (V_1), volume of pores between 132 and 29 nm in size (V_2), threshold diameter (TD) and modified porosity (MTP = total porosity/degree of hydration) as shown in **Fig. 30.**

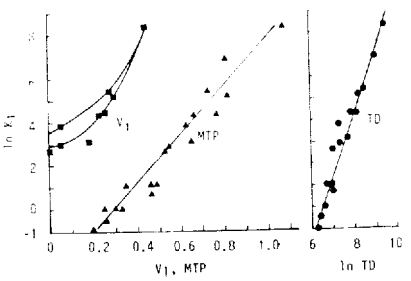

Fig. 30 Relationship between V_1, MTP, TD and permeability (103)

Permeability of hardened cement paste generally decreases with the progress of hydration, and the degree of this reduction in permeability has no direct relation to the amount of gel (hydrates produced) and is correlated with the sites where gel formation occurs. Permeability decreases when gel is formed at such a site as to block properly capillary pores. $Ca(OH)_2$ formed in hydration of ordinary portland cement, which precipitates in pores, have no such blocking effect. On the other hand, C-S-H and C_4AH_{19} formed as a result of pozzolanic reaction tend to block capillary pores, thereby decreasing permeability of hardened

blended cement paste (105).

Permeability of water or air has high correlation with volume of pore larger than a certain level, rather than with total porosity (106)(107). It is , therefore important whether a pore is continuous or discontinous (108). It seems reasonable to consider that pores with an inlet diameter larger than 100 nm are continuous inside the paste structure with a high probability and that many of the smaller pores less than 100 nm are closed.

Volume of pore larger than 100 nm in hardened blastfurnace slag cement paste is small even at the early age, while hardened fly ash cement paste has larger pore at early age and the volume of large pore tends to diminish in the later age. In silica fume cement, the volume of these large pores decreases very sharply. Permeability of blended cement paste at each age may be determined by such changes of pores.

5.2.3 Relationship between permeability of ions and structure of hardened paste

When discussing on permeability of ions such as Cl and alkalies through hardened cement paste, it is necessary to consider the electrostatic interactions between the ions and the walls of diffusion passes, and to their chemical reactions with hydrates and unhydrates present in the system as well as the pore size distribution.

The diffusion coefficient of Cl ions through hardened cement paste increases with increasing W/C ratio as shown in **Fig. 31**, which shows a sharp rise at W/C ratio of 0.6 where the volume of continuous pores larger than 100 nm begins to increase. The diffusion coefficient increases with rising temperature and Arrhenius plot become a single straight line. It is, therefore, suggested that this type of diffusion is of a single dormant activated process. Cl^- diffusion co- efficients for various kinds of cement are large in the order of sulphate resisting cement, ordinary portland cement, fly ash cement with 30% of fly ash, blastfurnace slag cement with 65% of slag. The highest coefficient of sulphate resisting cement is due mainly to the large pore volume, while both diffusion coefficients of fly ash cement and blastfurnace slag cement paste are small in spite of their high porosity, therefore this phenomenon is considered to be caused by other factors except porosity (109).

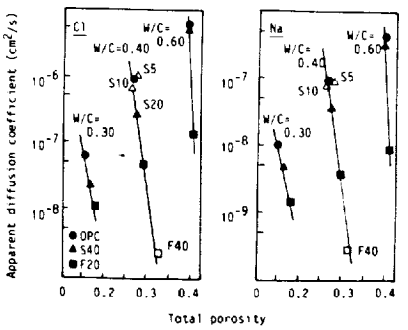

Fig. 31 Relationship between total porosity of hardened paste cured at 318°K and diffusion coefficient of Cl and Na ions (94)(96)

A study (94) states that diffusion and movement of alkali ions are affected by the pore structure in hardened cement paste. When the same kind of cement was used, diffusion of alkali ions becomes increasingly difficult as the total porosity decreases and the pore size distribution curve shifts towards smaller size. Capillary pore has more contribution than gel pore to the reduction of diffusion coefficient. The diffusion coefficient of alkali ions through hardened ordinary portland cement paste is the highest, followed by hardened blastfurnace slag cement and fly ash cement paste. Accompanying to formation of low C/S C-S-H by addition of pozzolanic material, average distance between solid surface of C-S-H produced become shorter. This fact is considered to relate with reduction of diffusion coefficient. The inclination of alkali concentration gradient from the alkali solution side toward the distilled water side, observed in hardened paste after a diffusion test, is larger in the order of portland cement, blastfurnace slag cement and fly ash cement. The alkali concentration of alkali solution side become higher in that order and that of the distilled water side become lower in that order. Such a difference in resistance of diffusion of alkali ions could not be explained by the difference in pore structure. It is, therefore necessary to consider other factors such as the composition, structure and interfacial characteristics of hydrates. Zeta potential of hardened cement paste powder measured by streaming 1N NaOH solution is high in the order of fly ash cement, blastfurnace slag cement and ordinary portland cement, turning from negative to positive values with time in the latter two and also showing high positive values in fly ash cement immediately after contacting with the solution. This indicates that the hydrates produced in fly ash cement paste prevents the most diffusion of alkalies by electric repulsion, followed by those of blastfurnace slag cement. The C/S ratio of C-S-H in hardened cement paste become lower in the order of portland cement, blastfurnace slag cement and fly ash cement. This trend reverses the order of the amount of alkalies in hardened paste after diffusion test. The high resistance against diffusion of alkalies of hardened fly ash cement paste is probably due to the low C/S C-S-H with a relatively large specific surface area and capable of adsorbing much alkalies. The amounts of slag and fly ash added to portland cement in order to suppress the progress of alkali aggregate reaction is 50% and 25%, respectively, based on vast experience and experimental data in the past. The validity of these figures is supported by the experimental results described above.

5.2.4 Depression of alkali aggregate reaction by addition of pozzolanic material

The reasons for the suppression of alkali aggregate reaction by addition of pozzolanic materials is summarized as follows: (a) pozzolanic reaction forms low C/S C-S-H, which fixes alkalies through adsorption or solid solution, thereby decreasing alkali ion concentrations in the pore solution; (b) the C-S-H formed by pozzolanic reaction fills up the pores in hardened cement paste, thus making the structure denser and depressing the movement of pore solution; (c) adsorption of alkali ions on the surface of pozzolanic materials and pozzolanic reaction with $Ca(OH)_2$, lower OH ion concentration in the pore solution; (d) addition of pozzolana turns the zeta potential on the surface of pores in hardened cement paste positive, thereby depressing the movement and diffusion of alkali ions in liquid pores; and (e) the increase in unit weight of water as a result of addition of pozzolanic materials causes a change in porosity, thus relaxing local expansion pressure. In addition, it is also postula-

ted that addition of pozzolana serves to lower OH^- and Ca^{2+} concentrations, to increase the alkali ion/Ca ion concentration ratio in pore solution, and to enhance the alkali ion/Si ion ratio in alkali silica gel produced, thus increasing the fluidity of gel and creating such condition that depresses development of pressure in hardened concrete (110).

Although it is true that addition of pozzolanic materials is effective in depressing alkali aggregate reaction, addition of a small amount of pozzolanic materials such as fly ash sometimes leads to large expansion. If a small amount of blending component is added, the amount of alkali released by its reaction with $Ca(OH)_2$ in early age is larger than the amount of alkali in the liquid phase absorbed by it (111). This has been considered to be as one of the reason. This assumption, however, must be demonstrated on the basis of experimental facts.

5.2.5 Relationship between durability and shape of pore in hardened cement paste

Mercury penetration or gas-adsorption technique has been chiefly used to measure porosity and pore size distribution for analysis of pore structure in hardened cement paste. Either of these techniques give only pore size distribution and could not tell how a pore changes in sectional area of longitudinal direction. A new attempt was made in recent years to determine the difference in pore shape between hardened ordinary portland cement and blended cement paste and to grasp its correlation with the properties, by utilizing a novel analytical method.

Pore structure in hardened ordinary portland cement and fly ash cement paste were analysed by the methanol-immersion, helium-picnometer and mercury penetration methods, and the data obtained were discussed with hydration degree and $Ca(OH)_2$ content to give a insight into the structure of hardened paste (108). This study reveals that pores in blended cement paste are discontinuous, while pores in ordinary portland cement paste are continuous, though having very narrow sections. It is also pointed out in this paper that there is a possibility of overestimating the porosity of blended cement paste as a result of destruction of fine pores during pore size distribution measurement by the mercury penetration method.

6. CONCLUSION

The effects of various blending components on the hydration and structure formation have been reviewed mainly based on the results of studies reported after the 7th international congress on the chemistry of cement held in Paris in 1980.

(1) Hydration, flocculation structure of fresh paste, hardened paste structure and physical properties developed by these factors are affected by the characters of the blending component. Granulated blastfurnace slag is the most common blending component consisting of sharp-pointed and irregular shaped sandy material. It is mainly composed of SiO_2, Al_2O_3, CaO and MgO and it has melilite composition with gehlenite and akermanite as end members. Although most part of it is glass phase, the melilite formed is changed from gehlenite composition to akermanite with proceeding of crystallization. The crystal shows, therefore, zonal structure depending on the change of composition. The average composition of glass phase is practically equal to that of crystalline phase which has a little higher Al_2O_3 and lower MgO. The glass phase consists of monomer and dimer mainly composed of $Si_2O_7^{6-}$ and $SiAlO_7^{7-}$. The higher glass phase content is, the higher the contents of dimer and monomer are. The more the C/S ratio, A/S ratio, MgO content and small quantities of components with 4 coordination are, the lower the condensation degree is.

(2) Fly ash consists of single sphere and multi sphere containing smaller spheres. About 20 percent of fly ash particles is hollow. The particle size and specific surface area is ranged between 100-0.3μm and 2,500 - 4,000cm^2/g, respectively. It is mainly composed of SiO_2, Al_2O_3, Fe_2O_3 and CaO depending on the kinds of coal and classified into ordinary fly ash (basicity: 0.2 to 0.7) and high calcium fly ash (basicity: 1.0 to 1.8) according to the composition. Glass phase ranges from 55 to 85 % depending on the combustion temperature of coal. Ordinary fly ash has the more CaO, alkalies and SO_3, the smaller the diameter is, while it has the more Al_2O_3, the larger the diameter is. The crystalline phase contains sometimes magnetite, hematite and anhydrite in case of low combustion temperature as well as quartz and mullite. Unburnt carbon comprises microcrystalline and amorphous carbons as well as crystalline carbon, and their contents are varied according to the combustion atmosphere. The degree of condensation of silicate ion in the glass phase is larger than that in granulated blastfurnace slag and the structure is close to that of quartz glass (α-cristobalite). High calcium fly ash contains C_3A, quartz and mullite as crystalline phase, and some low temperature calcined products contain hauyne, but it cannot be used due to instability. The degree of condensation of silicate ion in the glass phase is the same as that in slag and the structure is similar to $C_{12}A_7$ glass or melilite glass. Basicity of crystalline phase is slightly lower than that of glass phase.

(3) Silica fume deposited from gaseous phase produced by the oxidation of SiO vaporized at high temperature consists of spherical microfine particles of 0.1μm or less in diameter. Specific surface area is 20 to 200 m^2/g. Most part of it is amorphous and the crystalline phase mainly composed of quartz is several percent or less. The compactability is so poor that the porosity of powder packed is 80%. Silica fume contains 80% or more of SiO_2 and several percent of Fe_2O_3, Al_2O_3 and C. SiO_2 content in the byproduct of silicon is high, while that in the byproduct of ferro-silicon is low. The amorphous phase comprises high degree silicate ion condensate which has the similar structure to that of quartz glass.

(4) The hydration process of cement is divided into early and later stages. The early stage is further divided into stages I, II and III based on the heat evolution curve of hydration. The stage I has an heat evolution peak derived from the contact of cement with water and the production of ettringite. The stage II has a heat evolution peak derived from the vivid hydration of alite and the conversion of ettringite to monosulphate hydrate. The stage III has a gentle heat evolution process derived from the gradual hydration by the diffusion of ions through the layer of hydrate produced on the surface of unhydrates.

(5) The hydration process of granulated blastfurnace slag, ordinary fly ash and silica fume proceeds in such a manner that -Si-Si- chain or -Al-Al- chain is attacked by OH^- ion in the aqueous solution and part

of it is eluted. The hydration is exceedingly accelerated when the concentration of OH^- ion is equal to the concentration of ettringite formation in granulated blastfurnace slag and ordinary fly ash and when that is sufficiently high in silica fume.

(6) Although the kinds of hydrated products from blended cement are not basically different from those from portland cement, C/S ratio of precipitated C-S-H of blended cement is less than 2 to 1.7 of C-S-H from ordinary portland cement, that of blast furnace slag cement is 1.7 to 1.4, that of fly ash cement is 1.6 to 1 and that of silica cement is 1.6 to 0.8 depending upon amount added. C-S-H from slag cement contains particularly much solid solution of Al_2O_3 and MgO and that of fly ash cement contains much Na_2O and K_2O as solid solution. In case of calcium aluminate hydrates, when a blending component containing much MgO is added, C_4AHx-C_4MHx based solid solution and $Mg_6Al_2CO_3(OH)16{\cdot}4H_2O$ are produced. When the concentration of calcium ion is low in the liquid phase, C_2ASH_8 is also produced.

(7) Adding granulated blastfurnace slag or fly ash retards the hydration of C_3S, C_3A and alite in cement in the stages I and II but accelerates that of interstitial phase in cement in the stages I and II. The effect is more remarkable in fly ash than in blastfurnace slag. Although the hydration of C_3S, C_3A, alite and interstitial phase in cement is accelerated at stage III and later, the effect of accelerating hydration in the further later stage is not so clear. Although the effects of blending components on the hydration rate of the cement compounds and cement have been a controversial matter so far, it has become possible to be systematically explainable by dividing the hydration process as mentioned before and by characterizing the blending component.

(8) The pozzolanic reactivity of slag, fly ash and silica fume is enhanced with increasing of basicity, content of acid soluble SiO_2 and Al_2O_3, structural strain and CaO content and decreasing of degree of condensation of silicate ion in the glass phase, while that is lowered with increasing of Fe_2O_3 content in the glass phase. The specific surface area and particle size distribution of the blending component affect also the pozzolanic reactivity. The degree of pozzolanic reaction of blending component mixed with cement is lower than that with $Ca(OH)_2$, because the former supplies less $Ca(OH)_2$ than the latter. The pozzolanic reaction rate is decreased in the order of silica fume, slag and fly ash. Probably the reasons are as follows: the specific surface area of silica fume is the largest; the glass phase in slag contains more CaO than that in fly ash; and the condensation degree of silicate ion in the glass phase of slag is lower than that in the glass phase of fly ash. The pozzolanic reaction rate of slag largely depends on the temperature.

(9) The rheological properties of fresh cement paste, mortar and concrete containing a large amount of cement are determined by those of paste, while those containing a small amount of cement are determined by the rheological properties of aggregate. The rheological properties of fresh blended cement paste depend on the kinds of blending component.

(10) The rheological properties of fresh cement paste immediately after mixing with water are affected by the particle size distribution of cement and blending component and the thickness of water film around the particles as well as the concentration of solids. The thickness of film around the particles is related to the fineness of cement. Free water is fixed in the hydrate as combined water and the thickness of film is decreased as the hydration proceeds. The rheological properties are, therefore, affected by the contents and morphology of the hydrate deposited on the surface of particles of cement and blending component. There is the structure of packing of particles which minimizes the plastic viscosity and the yield value. A superplasticizer has so high dispersion effect that the structure of packing is optimized while the plastic viscosity and yield value are lowered.

(11) Since the flow curve of fresh cement is varied according to the measuring conditions, it is necessary to keep the surface of cylinder, shape of rotor, shear rate and cycle time of the rotational viscometer constant. It is difficult, however, to directly compare the measurements under different conditions with each other. The slump and compacting factor of fresh concrete are hardly related to the plastic viscosity of fresh concrete.

(12) Adding slag and fly ash to cement improves the fluidity lowering the plastic viscosity and yield value. The effect of lowering the yield value is generally higher. The addition of silica fume remarkably raises the yield value. The plastic viscosity is markedly increased in the blastfurnace slag cement produced by intergrinding because of coarse particles of slag. The concrete of fly ash cement which is produced by replacing 10% of cement by the equal weight of fly ash comprised of spherical particles has the highest fluidity and the improving effect of fluidity in concrete is higher than that in paste. Since silica fume consists of fine particles, a large amount of water is required to obtain a certain workability, so it is essential to use a superplasticizer.

(13) Setting is generally retarded by replacing portland cement by slag or fly ash. It is retarded by 10 and 20 minutes on the average replacing 10% of portland cement by slag and fly ash, respectively. The retardation of setting is larger with increasing of the amount of particles as fine as 10μm or under and of chemical composition shifted to akermanite (flash setting occurs for 90 to 100% of gehlenite) in slag and with increasing of the contents of organic materials and carbon in fly ash. Although setting is remarkably accelerated by replacing cement by silica fume, the addition of a large amount of superplasticizer sometimes retards the setting.

(14) The results of flocculation structure of fresh cement paste observed by the sample freezing-back scattering electron image method indicate as follows: angular coarse particles approximately 10μm in diameter with fine particles of 2 to 3μm are unevenly dispersed immediately after mixing with water; the thickness of water film is nearly 3μm which is several times thicker than the calculated value; several cement particles begin to agglomerate through the medium of ettringite and C-S-H in two hours after mixing with water; the thickness of hydrate deposited on the surface of cement particles is increased in the final setting stage; and these particles continue to agglomerate three dimensionally through the locally, thickly deposited layers of hydrate. The thickness of water film around the solid particles of blended cement is lower than that for ordinary portland cement as the blending component is well dispersed. The thickness of water film around the surface of blending

component particles is thicker than that around the cement particles though the thickness is relatively uniform. When 50% of coarse and fine slag and 25% of fly ash are added to cement, the thicknesses of water film are 1.5 to 2, 1 and 1 to 1.5μm, respectively, which are close to the calculated values. The formation of flocculation structure of blended cement proceeds practically equally to that of ordinary portland cement though a little late. Adding a naphtalenesulphonic acid-formaldehyde condensate-based superplasticizer to the cement paste, the microfine particles are well dispersed in the free water, so that the hydrate is deposited on the surface of particles as if the hydrate is deposited directly from the free water. The characteristic flocculation structure is formed through the medium of the hydrate. Although the particle are well dispersed in the cement paste blended with a ligninsulphonate-based superplasticizer, the flocculation structure makes little difference from that without superplasticizer.

(15) The strength of hardened cement paste is affected by the qualitative factors such as the strength of unhydrated product and hydrate itself, bond strength between them, pore size distribution and shape and continuity of pore, external factors such as temperature and humidity as well as the quantitative factors such as the quantity of hydrate and porosity. The hardened paste strength of blended cement is higher than that of ordinary portland cement paste at the later age because of low porosity and low amount of continuous pore, production of low C/S ratio of C-S-H with large specific surface area and few $Ca(OH)_2$ which makes coarse nonuniform texture with weak bond to C-S-H. The pores over 100nm in diameter in the fly ash cement are increased at early age, while those 100 nm or over in diameter in the silica fume blended cement mostly disappear. A large amount of Al-bearing hydrate is produced in the cement blended with granulated blastfurnace slag or high calcium fly ash, while the hydrated products in the silica fume blended cement is mainly composed of C-S-H. Since pore structure and hardened paste texture at each age are varied accord-ing to the kinds and characters of blending component, the strength of the hardened cement paste is varied accordingly.

(16) The pore size distribution of hardened cement paste can be classified based on the durability into: (a) pores as large as 2μm or over in diameter and those as small as several nm or under in diameter relating to freezing and thawing resistance, (b) pores tens to hundreds nm in diameter relating to the gas and water permeabilities affecting neutralization by carbonation, and (c) pores tens nm or under in diameter relating to the diffusion and transfer of ion affecting chemical resistance, resistance to seawater, resistance to sulphate and chloride attack and resistance to alkali aggregate reaction.

(17) Since the pores a few nm or under in diameter lowering the stability of the hardened cement paste at 273 to 253°K are decreased and those tens nm in diameter is increased by adding granulated blastfurnace slag or silica fume, the stress caused by freezing and thawing is absorbed to alleviate damages. Since the pores several μm in diameter are also increased in blastfurnace slag cement concrete, the air void spacing factor is lowered, so the freezing and thawing resistance for the same amount of air is increased. Since the addition of fly ash increases the capillary pore space of hundreds nm or over in diameter depending upon the amount of addition, the freezing and thawing resistance is lowered. When the addition exceeds 30%, it is remarkably decreased.

(18) The gas and water permeabilities depend upon the continuity of pore in hardened cement paste. Since the pores 100 nm or over in diameter are probably interconnected, the permeabilities are positively correlated with the amount of these pores. The pores 100nm or over in diameter in blastfurnace slag cement and silica cement are less than those in ordinary portland cement throughout the whole hydration age. At the early age, those pores in fly ash cement are more than those in ordinary portland cement. The amount of those pores at the later age are larger in the order of portland cement, fly ash cement, silica cement and blastfurnace slag cement, especially those pores in silica cement are extremely decreased with age.

(19) The diffusion and movement of alkalies and chlorine ions are reduced with decreasing of the amount of pores and shifting of the pore size distribution to the smaller side in the same kind of cement. The capillary pore space contributes to decreasing the diffusion coefficient more than gel pore space. When the data are compared at the same level of blending component added, the diffusion coefficient of alkalies and Cl ions is large in the order of ordinary portland cement, blastfurnace slag cement, fly ash cement and silica cement paste. These orders do not necessarily coincide with those of total pore space and of the pore size distribution of tens nm or under in diameter. It is necessary, therefore, to consider that the diffusion and movement of ion are affected by the composition, structure and interfacial properties of hydrates as well as pore structure in the hardened cement paste.

The author would like to express the sincerest thanks to Mr. S. Uchida, Mr. K. Ogawa and Mr. S. Hanehara for their assistance of preparing of the report.

7. REFERENCE

1.- WANG YU-JI and XIE GONG-XIN (1980), "Research on the main mineral phase and its cementituous properties", 7th Int. Cong. Chem. Cem., Paris, II, III- 19-24.

2.- J.R. BARAGANO and P. REY (1980), "The study of a nontraditional pozzolan; copper slag", 7th Int. Cong. Chem. Cem., Paris, II, III- 37-42.

3.- J. LANEUBILLE (1980), "The hydration of nickel slag", 7th Int. Cong. Chem. Cem., Paris, II, III- 52-57.

4.- H.G. SMOLCZYK (1980), "Slag structure and identification of slag", 7th Int. Cong. Chem. Cem. Paris, I, III- 1/3-1/17.

5.- Y. ONO, S. KAWAMURA and T. ITO (1983), "Strength of slag cement and contribution of basicity and vitrification degree", Semento gijyutsu nenpo (in Japanese), 37, 77-80.

6.- M. DAIMON (1980), "Mechanism and kinetics of slag cement hydration", 7th Int. Cong. Chem. Cem. Paris, I, III- 2/1-2/9.

7.- H. UCHIKAWA, S. UCHIDA and S. HANEHARA (1986), "Effect of character of amorphous phase in blending

components on their reactivity in calcium hydroixde mixture" , 8th Int. Cong. Chem. Cem., Rio de Janeiro.

8- K.E. DAUGHERTY, B. SAAD, C. WEIRICH and A. EBERENDU (1983), "The glass content of slag and hydraulic activity", Silicates Industriels, (4-5), 107-110.

9.- E.F. OSBORN, R.C. DEVRIES, K.H. GEE and H.M. KRANER (1954), "Optimum composition of blastfurnace slag as deduced from liquidus data for the quaterary system CaO-MgO-Al_2O_3-SiO_2", Journal of metals, (January), 33-45.

10.- H. TANAKA, Y. TOYA and Y. SAITO (1982), "Relationship between hydraulic activity and coordination state of Al^{3+} ion in artificial slag glass", Semento gijyutsu nenpo (in Japanese), **36**, 73-76.

11.- P. FIERENCE and P. POSWICK (1980), "New aspects of industrial slag hydration", 7th Int. Cong. Chem. Cem. Paris, **II**, III- 112-116.

12.- H. UCHIKAWA, S. UCHIDA and K. OGAWA (1982), " Influence of the properties of fly ash on the fluidity and structure of fly ash cement paste", Int. Sym., The use of PFA in concrete, Leeds, 83-94.

13.- H. UCHIKAWA, S. UCHIDA and K. OGAWA (1982), "Influence of fly ash characteristics on the rheological properties of fresh fly ash cement paste", Proc. Ann. Mtg of Material Research Society, M4.4, Boston, Concrete rheology, 203-214.

14.- S. DIAMOND (1981), "The characterization of flyashes", Proc. Ann. Mtg of Material Research Society, Boston, Effect of fly ash incorporation in cement and concrete, 12-23.

15.- B.E. SCHEETZ, D.W. STRICKLER and M.W. GRUTZECH, D.M. ROY (1981), "Physical and chemical behavior of selectively etched fly ash", Proc. Ann. Mtg of Material Research Society, Boston, Effect of fly ash incorporation in cement and concrete, 24-33.

16.- W. RICHARTZ (1984), "Composition and properties of fly ashes", Zement-kalk-gips, **37**, 62-71.

17.- S. DIAMOND and F. LOPEZ-FLORES (1981), "On the distinction in physical and chemical characteristics between lignitic and bituminous fly ashes", Proc. Ann. Mtg of Material Research Society, Boston, Effect of fly ash incorporation in cement and concrete, 34-44.

18.- S. DIAMOND (1983), "On the glass present in low calcium and in high calcium fly ashes", Cem. Conc. Res., **13**(4), 459-464.

19.- P.C. AITCIN, P. PISONNEAUT and G. RAW (1981), "The use of condensed silica fume in concrete", Proc. Ann. Mtg of Material Research Society, Boston, Effect of fly ash incorporation in cement and concrete, 316-325.

20.- M.F. PISTILLE, G. RAU and R. CECHNER (1984), "The variation of condensed silica fume from a Canadian source and its influence on the properties of portland cement concrete", Cem. Conc. Agg., **6**, 33-37.

21.- M.F. PISTILLE, R. WINTERSTEEN and R. CECHNER (1985), "The uniformity and influence of silica fume from a US source on the properties of portland cement concrete", Cem. Conc. Agg., **7**, 120-124.

22.- M. REGOURD (1980), "Structure and behaviour of slag cement hydration", 7th Int. Cong. Chem. Cem. Paris, I, III- 2/10-2/26.

23.- J. METSO, E. KAJAUS (1983), "Activation of blast furnace slag by some inorganic materials", 1st Int. Conf. The use of fly ash, silica fume, slag and other mineral by-products in concrete, Montebello, I, 519-537.

24.- H. EI-DIDAMONY, A.S. TAHA and H.A. AMER (1983), "The role of $CaSO_4$ content in the hardening of slag rich cement", Zement-Kalk-Gips, **36**, 241-243.

25.-M. REGOURD, B. MARTUREUX and H. HORNAIN (1982), "Use of condensed silica fume as filler in blended cement", 1st Int. Conf. The use of fly ash, silica fume, slag and other mineral by-products in concrete, Montebello, **II**, 831-845.

26.- G. MASCOLO and D. MARINO (1980), "MgO-bearing phase in the hydration products of slag cement", 7TH Int. Cong. Chem. Cem., Paris, **II**, III- 59-62.

27.- K. OGAWA, H. UCHIKAWA, K. TAKEMOTO and I. YASUI, "The mechanism of the hydration in the system C_3S-pozzo-lana", Cem. Con. Res., **10**(5), 683-696.

28.- H. UCHIKAWA and S. UCHIDA (1980), "Influence of pozzolana on the hydration of C3A", 7th Intn. Cong. Chem. Cem., Paris, **III**, IV- 23-29.

29.- X. WU, D.M. ROY and C.A. LANGTON (1983), "Early stage hydration of slag cement", Cem. Con. Res., **13**(2), 227-286.

30.- N.P. MAILVAGANAM and R.S. BHAGRATH (1983), "Effects of admixtures on portland cement concrete incorporating blastfurnace slag and fly ash", 1st Int. Conf. The use of fly ash, silica fume, slag and other mineral by-products in concrete, Montebello, I, 519-537.

31.- Y. TOTANI, Y. SAITOH, M. KAGEYAMA and H. TANAKA (1980), "The hydration of blastfurnace cement", 7th Int. Cong. Chem. Cem. Paris, **II**, III- 95-98.

32.- H. UCHIKAWA, S. UCHIDA and T. OKAMURA (1986), "Influence of blending component on the hydration of cement compound and blended cement", submitted to Cem. Conc. Res.

33.- K. TAKEMOTO and H. UCHIKAWA (1980), "Hydration of pozzolanic cement", 7th Int. Cong. Chem. Cem. Paris, I, IV- 2/1-2/29.

34.- R. DRON (1983), "Fracteurs chinimues et structuraux de la reactivite des laitiers", Silicate Industriels **47**(6), 143-147.

35.- S.A. ABO-El-ENEIN, A.A. ATA and A. HASSANIEN (1983), "Kinetics and Mechanism of slag cement hydration", Silicate Industriels, (6), 115-120.

36.- M. REGOURD, J.H. THOASSIN AND J.C. TOURAY (1983), "blastfurnace slag hydration. surface analysis", Cem. Con. Res., **13**(4), 549-556.

37.- H. TANAKA, Y. TOTANI and Y. SAITOH (1983), "Structure of hydrated glassy blast furnace slag in concrete", 1st Int. Conf. The use of fly ash, silica fume, slag and other mineral by-products in concrete,

Montebello, II, 963-977.

38.- A. GHOSE and P. L. PRATT (1981), "Studies of the hydration reaction and microstructure of cement-fly ash paste", Proc. Ann. Mtg of Material Research Society, Boston, Effect of fly ash incorporation in cement and concrete, 82-91.

39.- A. CARRLES-GIBERGUES, B. THENOZ and A. VJAQUIER (1980), "Hydration mechanism of a flyash produced from calcareous lignite", 7th Int. Cong. Chem. Cem. Paris, III, IV- 53-59.

40.- F.G. BUTTER and E.J. WALKER (1982), "The rate and extent of reaction between calcium hydroxide and pulverized fuel ash", Int. Sym., The use of PFA in concrete, Leeds, 111-120.

41.- G. TOGNON and P. URSELLA (1981), "Combined lime and specific surface area of hydration products of lime-fly ash mixes", Proc. Ann. Mtg of Material Research Society, Boston, Effect of fly ash incorporation in cement and concrete, 145-154.

42.- I. JAWED and J. SKALNY (1981), "Hydration of tricalcium silicate in the presence of fly ash", Proc. Ann. Mtg of Material Research Society, Boston, Effect of fly ash incorporation in cement and concrete, 60-70.

43.- H. UCHIKAWA (1984), "The role of free lime in early hydration of alite - retarder or accelerator?", Ceramic bulletin, **63**(9), 1143-1146.

44.- H. UCHIKAWA, S. UCHIDA, K. OGAWA and T. OKAMURA (1985), "Influence of intergrinding of CaO on setting time and initial hydration process of cement", J. Cerm. Soc. Japan (in Japanese), **93**(4), 201-208.

45.- K. MOHAN and H.F.W. TAYLAR (1981), "Paste of tricalcium silicate with fly ash analytical electron microscopy, trimethylsililation and other studies", Proc. Ann. Mtg of Material Research Society, Boston, Effect of fly ash incorporation in cement and concrete, 54-59.

46.- J. SKALNY and J.F. YOUNG (1980), "Mechanisum of portland cement hydration", 7th Int. Cong. Chem. Cem. Paris, I, II- 1/3-1/45

47.- C. PLOWMAN and J.G. CABRERA (1981), "The hydration reaction of calcium aluminate", Cement and concrete, proceed. symp. ann. meet., 71-81.

48.- I. MELAND (1983), "Influence of condenced silica fume and fly ash on the heat evolution in concrete", 1st Int. Conf. The use of fly ash, silica fume, slag and other mineral by-products in concrete, Montebello, II, 665-676.

49.- S.A. MAULA and I. ODLER (1981), "Hydration reactions in fly ash-portland cements", Proc. Ann. Mtg of Material Research Society, Boston, Effect of fly ash incorporation in cement and concrete, 102-111.

50.- W. FAJUN, M.W. GRUTZECK and D.M. ROY (1985), "The retarding effects of fly ash upon the hydration of cement paste: The first 24 hours", Cem. Conc. Res., **15**(1), 174-184.

51.- R. SERSALE (1980), "Structure and characterization of pozzolanas and of fly ash", 7th Int. Cong. Chem. Cem. Paris, I, IV- 1/3-1/18.

52.- H. SHIYUAN (1982), "The effect of addition of gypsum on the hydration of fly ash cement", Int. Sym., The use of PFA in concrete, Leeds, 53-66.

53.- H. UCHIKAWA and R. FURUTA (1981), "Hydration of C_3S-pozzolana paste estimated by trimethylsilylation", Cem. Conc. Res., **11**(1), 65-78.

54.- S. DIAMOND, D. RAVINA and J. LOVELL (1980), "The occurence of duplex film on fly ash surface", Cem. Conc. Res., **10**(2) 297-300.

55.- M.W. GRUTZECK, D.M. ROY and B.E. SHEETZ (1981), "Hydration mechanism of fly ash in portland cement composite", Proc. Ann. Mtg of Material Research Society, Boston, Effect of fly ash incorporation in cement and concrete, 92-101.

56.- M. MICHAEL, W. GRUTZECK, S. ATRINSKON and D.M. ROY (1983), "Mechanism of hydration of condensed silica fume in calcium hydroxide solution", 1st Int. Conf. The use of fly ash, silica fume, slag and other mineral by-products in concrete, Montebello, **II**, 643-664.

57.- D.J. COOK and P. SUWANVITAYA (1983), "Propertes and behavior of lime-rice husk ash cement", 1st Int. Conf. The use of fly ash, silica fume, slag and other mineral by-products in concrete, Montebello, **II**, 831-845.

58.- W. KURDOWSKI and W. NOCUN-WCZELIK (1983), "The tricalcium silicate hydration in the presence of active silica", Cem. Conc. Res., **13**(3), 341-348.

59.- H. CHENG-YI and R.F. FELDMAN (1985), "Hydration reaction in portland cement-silica fume blends", Cem. Conc. Res., **15**(4) 585-592.

60.- H. UCHIKAWA (1982), "Modern methods of characterization of materials related to cement", Lectured at the conference held on september 24th, 1984 in San Paulo, Brasil under sponsoredship of ABCP and IPT., J. Res. Onoda Cement co., **34**(108), 64-100.

61.- P.F.G. BANFILL and D.C. SAUNDERS (1981), "On the viscometric examination", Cem. Conc. Res., **11**(3), 363-370.

62.- F. MASSAZZA and U. COSTA (1982), "Rheological probrem related to the use of cement", il Cemento, **79**(4), 217-242.

63.- R.A. HELMUTH (1980), "Structure and rheology of fresh cement paste", 7th Int. Cong. Chem. Cem. Paris, **III**, IV- 0/16-0/30.

64.- J.F. YOUNG (1982), "Effect of chemical admixtures on the rheological properties of fresh concrete", Proc. Ann. Mtg of Material Research Society, M4.4, Boston, Concrete rheology, 120-138.

65.- R. LAPASIN (1983), "Rheology of cement paste", il Cemento, **79**(4), 234-260

66.- J.I. BHATTY and P.F.G. BANFILL (1982), "Sedimentation behavior in cement paste subjected to continuous shear in rotational viscometers", Cem. Conc. Res., **12**(1), 69-78.

67.- Y. OTSUBO, S. MIYAI and K. UMEYA (1980), "Time dependent flow of cement", Cem. Conc. Res., **10**(5), 631-638.

68.- H. UCHIKAWA, K. OGAWA and S. UCHIDA (1982), "Influence of organic additives in the rheological properties of fly ash cement paste", Proc. Ann. Mtg of Material Research Society, M4.4, Boston, Concrete rheology, 192-202.

69.- D.S. CAO and S. DIAMOND (1982), "Cement paste rheology - an attempt at clarification", Proc. Ann. Mtg of Material Research Society, M4.4, Boston, Concrete rheology, 139-151.

70.- E.L. WHITE and D.M. ROY (1983), "Rheological behaviour of cement slurries, mortars and grouts", Advance in cement technology, 120-138.

71.- P.F.G. BANFILL (1982), "An experimental study of the effect of PFA on the rheology of fresh concrete and cement paste", Int. Sym., The use of PFA in concrete, Leeds, 161-171.

72.- D.W. HOBBS (1980), "The effects of pulverized fuel ash upon the workability of cement paste and concrete", Mag. Conc. Res., **32**, 219-226.

73.- C. ELLIS (1982), "The application of the two point workability test and British standard test to OPC/PFA concrete" Int. Sym., The use of PFA in concrete, Leeds, 289-306.

74.- K. HATTORI and K. IZUMI (1982), "New rheological theory of concentrated suspension", Proc. Ann. Mtg of Material Research Society, M4.4, Boston, Concrete rheology, 14-29.

75.- F. SKVARA, K. KOLAR, J. NOVOTNY and Z. ZADAK (1981), "The effect of cement particle size distribution upon properties of paste and mortars with low water-to-cement ratio", Cem. Conc. Res., **11**(2), 247-255.

76.- P.F.G. BANFILL (1981), " A viscometric study of cement past containing superplasticizers with a note on experimental technique", Mag. Conc. Res., **33**(114), 37-47.

77.- F.W. LOCHER, W. RICHARDZ, S. SPRUNG and H.M. SYLLA (1982), "Setting of cement: part III. influence of clinker manufacture", Zement-kalk-gips, **35**, 669-676.

78.- W. vom BERG (1979), "Influence of specific surface and concentration of solids upon the flow behaviour of cement paste", Mag. Conc. Res., **31**(109), 211-216.

79.- H. UCHIKAWA (1984), "Materials desigh of cement", Ceramics (in Japanese), **19**(5), 394-403.

80.- H. UCHIKAWA (1984), "Review on the rheological properties of fresh fly ash cement paste based on the knowledge of chemistry of cement hydrate", Cem. Conc. (in Japanese), (445), 7-17.

81.- X. WU and D.M. ROY (1982), "Zeta potential investigations during hydration of slag cement", Proc. Ann. Mtg of Material Research Society, M4.4, Boston, Concrete rheology, 215-222.

82.- H. UCHIKAWA, S. UCHIDA and S. HANEHARA (1986), "Flocculation structure of fresh cement paste determined by sample freezing-back scattering electron image method", submitted to il cemento.

83.- D.M. ROY, J. SKALNY and S. DIAMOND (1982), "Effect of blending material on the rheology of cment paste and concrete", Proc. Ann. Mtg of Material Research Society, M4.4, Boston, Concrete rheology, 152-173.

84.- J.W. MEYSEL and J.H. ROSE (1983), " Production of granulated blastfurnace slag at Spallow Points, and the workability and strength potential of concrete incorporating the slag", 1st Int. Conf. The use of fly ash, silica fume, slag and other mineral by-products in concrete, Montebello, **II**, 867-890.

85.- R.Z. YAUN, S.X. JIN and J.C. QUAN (1982), "Effects of fly ash on rheology of fresh cement paste", Proc. Ann. Mtg of Material Research Society, M4.4, Boston, Concrete rheology, 182-191.

86.- E.J. SELLEVOID and F.F. RADJY (1983)," Condensed silica fume (microsilica) in concrete: water demand and strength developments", 1st Int. Conf. The use of fly ash, silica fume, slag and other mineral by-products in concrete, Montebello, **II**, 667-695.

87.- F.J. HOGEN and J.W. MEUSEL (1981), "Evaluation for durability and strength development of a ground granulated blastfurnace slag", Cem. Conc. Agg., **3**(1), 40-52

88.- X. WU and D.M. ROY (1984), "Slag cement utilization: rheological properties and related characterization", Cem. Conc. Res., **14**(4). 521-528

89.- R.O. LANES and J.F. BEST (1982), "Properties and use of fly ash in portland cement concrete", Conc. Inter., **4**(7), 81-92.

90.- S. DIAMOND and F. LOPEZ-FLORES (1981), "Comparative studies of the effect of lignightic and bituminous flyash in hydrated cement systems", Proc. Ann. Mtg of Material Research Society, Boston, Effect of fly ash incorporation in cement and concrete, 112-123

91.- H. UCHIKAWA, S. UCHIDA, K. OGAWA and S. HANEHARA (1984), "Influence of $CaSO_4 \cdot 2H_2O$, $CaSO_4 \cdot 1/2H_2O$ and $CaSO_4$ on the initial hydration of clinker having different burning degree", Cem. Conc. Res., **14**(5), 645-656.

92.- N.McN. ALFORD and A.A. RARMAN (1981), "An assesment of porosity and pore sizes in hardened cement paste", J.Mat. Sci., 16, 3105-3114.

93.- H. UHCIKAWA, S. UCHIDA and S. HANEHARA (1986), "Element distribution on the polished surface of hardened cement paste estimated by EPMA with high speed wide area multianalyser", submitted to il cemento.

94.- H. UCHIKAWA (1985), "Effect of blastfurnace slag and fly ash blending on the alkali ions through hardened cement paste", Cem. Conc. (in Japanese), (460) 20-27.

95.- D.M. ROY and K.M. PARKER (1983), "Microstructures and properties of granulated slag-portland cement blends at normal and elevated temperatures", 1st Int. Conf. The use of fly ash, silica fume, slag and other mineral by-products in concrete, Montebello, I, 397-411.

96.- H. UCHIKAWA, S. UCHIDA and K. OGAWA (1986),

paste", 8th Int. Cong. Chem. Cem., Rio de Janeiro.

97.- M. RELIS and I. SOROKA (1980), "Compressive strength of low-porosity hydrated portland cement", J. Amer. Ceram. Soc., **63**, 690-694.

98.- D. MONTGOMERY and S. DIAMOND (1984), "The influence of fly ash cenospheres on the details of cracking in fly ash-bearing cement pastes", Cem. Conc. Res., **14**(6), 765-775.

99.- J. MURATA, M. KAWASAKI, T. SAKAI and T. KAWAI (1983), "Resistance to freezing and thawing of concrete using ground blast-furnace slag", 1st Int. Conf. The use of fly ash, silica fume, slag and other mineral by-products in concrete, Montebello, **II**, 999-1011.

100.- I. TEOREANU and L.D. NICOLESCU (1982), "The properties of power station fly-ash concrete", Int. Sym., The use of PFA in concrete, Leeds, 231-241.

101.- P.J. SEREDA, R.F. FELDMAN and V.S. RAMACHANDRAN (1980), "Structure formation and development in hardened cement paste", 7th Int. Cong. Chem. Cem. Paris, **I**, VI- 1/3-1/44.

102.- M.F. PISTILLI (1983), "Air-void parameters developed by air-entraining admixtures, as influenced by soluble alkalis from fly ash and portland cement", J. ACI, **80**, 217-222.

103.- P.K. MEHTA and D. MANMOHAN (1980), "Pore size distribution and permeability of hardened paste", 7th Int. Cong. Chem. Cem. Paris, **III**, VII-1 VII-5.

105.- R.F.M. BAKKER (1983), "Permeability of blended cement concrete", 1st Int. Conf. The use of fly ash, silica fume, slag and other mineral by-products in concrete, Montebello, **I**, 591-605.

106.- S. GOTO, D.M. ROY (1981), "The effect of W/C ratio and curing temperature on the permeability of hardened cement paste", Cem. Conc. Res., **11**(4), 575-579.

107.- P.K. MEHTA (1981), "Studies on blended portland cements containing santorin earth", Cem. Conc. Res., **11**(4), 507-518.

108.- R.F. FELDMAN (1983), "Significance of porosity measurements on blended cement performance", 1st Int. Conf. The use of fly ash, silica fume, slag and other mineral by-products in concrete, Montebello, **I**, 415-433.

109.- N.R. SHORT, C.L. PAGE (1982), "The diffusion of chloride ions through ortland and blended cement pastes", Silicate industriels, **47**, 237-240.

110.- W. GUTT, P.J. NIXON, M.E. GAZE (1980), "Fly ash and alkali aggregate reaction", 7th Int. Cong. Chem. Cem., Paris, **III**, VII- 110-113

111.- T. MING-SHU, Y. YU-FENG, Y. MEI-GI and Z. SHI-HUA (1983), "The preventive effect of mineral admixtures on alkali-silica reaction and its mechanism", Cem. Conc. Res., **13**(2), 171-176.

SUB-THEME/SOUS-THÈME 3.3

Special cements. Calcium aluminate and other no-silicate cements.

Ciments spéciaux. Ciments à base d'aluminates calciques et autres ciments sans silicates.

Chairman/Président :

T. V. Kouznetsova
Mendeleyev Institute of Chemical Technology, Moscow, U.S.S.R.

Principal Reporter/Rapporteur Principal:

W.Kursdowski
Academy of Mining and Metallurgy Institute of Building Materials and Refractories, Krakow, Poland

T.V. KUZNETSOVA, Mendeleyev Institute of Chemical Technology, Moscow USSR

STATE OF THE ART AND PROSPECTS OF SPECIAL CEMENTS

Diversity of the constructions projects and items specific engineering and service conditions invarious industrial structures motivated the creation of special cements with appropriate engineering properties. Today these cements and widely used in precast, ordinary and prestressed reinforced concrete structures. They are also useful for the construction projects exploited in corrosive media. These are sea and river piers, docks, wharfs, highways and air fields. Special cements do a variety of jobs in water proofing and radiation shielding, in drilling wells and in construction works under various klimatic conditions and seasons.

Development and Diversification of Special Cements. The early research efforts in the field were aimed of designing cements which were resistant corrosive media, wind and water erosion, especially that by sea and ground waters, containing considerable amounts of soluble salts. Interaction of salts with the concrete results in premature failure.

At the turn of the century this problem was attacked by minerous researches in many countries. It was generally recognized that the percolation of sea water into the bulk of concrete can cause its failure. This phenomenon was observed more frequently in warm seas than in northern seas where the main causes of failure are alternate freezing and thawing of the concrete as well as ice attrition. It was, however, very difficult to determine which factors are of major importance: physical or chemical.

A great deal of attention has been devoted to the production of dense concrete which resists the penetration of water and leaching of lime. Lime used to be bound by hydraulically active materials. Thus the trass cements (pozzolona) have been devised. The investigation of pozzolane cements revealed the influence of the mineral composition of clinker on the concrete corrosion resistance. The optimal proportion has been established for C_3S and C_2S content on one hand and calcium silicates, aluminates and alumoferrites of the other. Years of research have shed light on the character of physical and chemical processes causing corrosion of portland cement so that one may select the cement composition in accordance with the type of corrosion, corrosive action of water and its inflow rate to the surface of the structure.

Investigations of hydration and hardening of portland cement have led to the development of early-strength and high-strength cements. Extensive research in this area has been motivated by extensive construction based on the use of precast concrete which revolutionized the construction technology by replacing the bricklaying operations with mechanized processes of assembly. High productivity of concrete construction plants was achieved with early-strength cement. The use of high-strength cement resulted in decreasing the structural weight. Appealing and aesthetic appearance of buildings and structures required decorative cements. This need had motivated the development of the plasticized cements.

Penetration of portland cement into ever new fields has stimulated the development of the oil-well cements. The technology has been devised to manufacture cements for cold and hot wells as well as for light weighted and gel cements.

Investigations into early hydration phases resulted in compositions for the production of asbestos cement. Studies into the hydrodynamic phenomena that take place in dehydrating and compressing asbestos cement films formed the basis for the optimization of the asbestos cement technology.

Alumina cement evolved from the studies of $CaO-Al_2O_3-SiO_2$ systems. The chemical and mineral compositions of this cement as well as the hydration processes and properties have been reported by Gorge (1). The need for low shrinkage concretes stimulated the development of expanding cements. These we-

re proposed for using to tension the concrete reinforcement. The respective cements and concretes were defined as stressing and self-stressing.

Each of the mentioned cements deserves attention, but report is focused on the most promising cements which have been intensively developed after the 7th International Congress on the Chemistry of Cement.

The composition of portland cement remains the same as 135 years ago. In comparison with other materials changing their properties virtually every day portland cement is an old and durable product. Therefore portland cement production is likely to be carried out in the same way for as many years in the future. One should not overlooked that the basic components of portland cement, such as silicon, aluminium, calcium, sulphur and iron, are the major elements of the earth's crust.

It is unlikely that any other binding materials involving rare and trace elements can compete with portland cement in the near future.

It would be instructive to notice that the mentioned elements occupy even positions in the periodical table. According to one of the basic laws of geochemistry, derived by Fersman, these elements must form huge deposits which can be easily exploited. This is why portland cement is such an attractive product.

The only exclusion is the odd aluminous of at No. 13. The very number of this element suggests that this is an unreliable element. However as it is well known from geochemistry that being combined with suitable even elements aluminium can form extremely strong and durable compounds. The combinations formed within raw materials with oxygen and silicon as well as within portland cement with oxygen and calcium are so streng that can exist over the geological period. This fact is also for portland element.

Thus, it is quite clear that portland cement has very good perspectives and will dominate among binding materials for a long time. Hence we should not spare our efforts to improve its technology, quality of composition and properties. However, now mankind takes urgent problems which must be solved immediately. These include saving fuel and energy, and pollution control. Many researchers are concerned with these problems all-throughout the world. In this connection aluminium compounds which provides portland cement with new and inimitable properties are the subject of great attention. Being incorporated into portland cement these compounds increase its compressive strength by 5-10 MPa (2). High-strength portland cement reaches 50-60 MPa after 28 days, and abreminate cements reach this figure after only 3 days of hardening. Changes within calcium aluminate composition make the cement and refractories expansive

The intensive development of new technology and improvement of the present production processes have required the creation of reliable materials to be used under conditions where ordinary cement fail or become completely useless. Specifically, at high pressures and temperatures, steam and gas mixtures contain oxygen and hydrogen oxides. These interact with cement iron oxides and form Fe_3C $Si(OH)_4$ and $Si(OH)$. The formation of these hydrates and the crystalization of Fe_3C is accompanied by the concrete expansion which results in considerable stresses and failure. This problem necessitated the creation of cements containing minimum amounts of ferrous and cilicon oxides.

High Alumina Heat Cement. This cement is characterized by high strength, refractoriness, and resistance corrosive media and melted metal. Concrete strength is known to depend on the mineralogical and granulometric composition.

Monoaluminate cement (CA) has relatively high strength during early hardening ages without considerable increase in the course of hardening.

Calcium exhibits low strength dialuminate

in early ages reaches high values at long hardening terms. By regulating the CA/CA_2 ratio and the degree of dispersion one can obtain cements with uniform strength development rate over the ensire hardening period.

To optimize the condition of calcination of alumina cement containing generally monacalcium aluminate the phase diagrams of the CaO - mineral admixture system were investigated. The mineralizer was one of the following compounds: chlorides ($CaCl_2$, NaCl and KCl), fluorides (CaF_2, NaF and KF), borates (metroborate, metaborate and calcium borate bicalcium, the troborate and metaborate Na and K), and chromates with chromium valency of III and VI (chromate Ca and Na, Cr oxide). The mechanism of interaction of Al_2O_3 and CaO in the presence these mineralizators was described and the possibility of changing of mineralogical composition of high alumina cement was reported.

The compound $12CaO \cdot 7Al_2O_3 (C_{12}A_I)$ considerably affects the properties of high alumina cements so this phase has attracted much interest.

Reference (4) pays much attention to the content of oxygen within $C_{12}A_7$ which was obtained by firing at temperature of 900°C in air $C_{12}A_7$ always contains excessive amount of oxygen which can be lately determined analytically. $C_{12}A_7$ synthesized in the air at temperatures of 1250--1350°C contains 0,10-0,12% of excessive oxygen. The contents of excess oxygen increases for decreasing water content or hydroxyl groups, especially at firing of the material in dry air or oxygen atmosphere. The maximum content of excess oxygen (0,56%) was found in $C_{12}A_2$ specimens synthesized in dry oxygen atmosphere at 1300°C, thus the synthesized material had the formula $C_{11}A_7 \cdot CaO_{1,49}$. In phases $C_{11} \cdot A_7 \cdot Ca(OH)_2$, $C_{11}A_7 \cdot CaF_2$ and $C_{11}A_7 \cdot CaCl_2$, no excess oxygen was observed. These findings show that $C_{12}A_7$ has the ultimate formula $C_{11}A_7 \cdot CaO_2$ in which two oxygen atoms can be replaced with two atoms of fluorine or chromium atoms or with two hydroxyl groups. The $C_{12}A_7$ structure remains even with complete absence of excess oxygen.

Similar investigations have been carried out in our laboratory (5). X-ray analysis, and chemical and microscopic methods indicated that the sequence of phase formation in the $CaO-Al_2O_3$ system, irrespective of admixtures is arranged in the order $C_{12}A_7 \rightarrow CA \rightarrow CA_2$. Depending on the amount of fluorine-chlorine-ions the system yields different chlorine-bearing. When the cake contains about 1% of fluorine and chlorine, $C_{11}A_7CaF_2$ and $C_{11}A_7CaCl_2$ are present together with CA.

If the percentage of fluorine and chlorine is higher, the formation of $C_3A_3CaF_2$ and $C_3A_3 \cdot CaCl_2$ is also observed.

It has been recognized that the strength of concrete acquired in hydrating high alumina cement containing fluorine and chlorine is lower at early ages (up to 14 days) than that of ordinary cements, but later on a continuous increase of strength is observed. The heat-resistance properties of high alumina cements such as residual strength, fire resistance, deformability at high temperatures and thermal resistance were investigated on concrete specimens using brick bats of refractory high alumina bricks and crushed synthetic corundum as aggregates. The cement samples used contained mainly CA_2 and technical alumina. The same strength development was observed for concretes made of various cements. A sharp decrease in strength was evident at heating from 200° to 400°C. The decrease was lower for the concrete made of cement containing technical alumina. Heated from 200°C to 400°C, the concrete made of unblended cement experiences a decrease in strength by 30-33%; and heated up to 900°C, down to 50-52%. At the same heating conditions, the strength of the concrete made of cement with an admixture of technical alumina decreases from by 20 and 30% respectively.

The presence of SiO_2 and Fe_2O_2 admixtures in cement gives a somewhat higher decrease of strength of concrete at heating. It has been established 6 that increasing the content of $SiO_2+Fe_2O_3$ in cement from 0,3 to 2,2% decreases the concrete heat resistance from 1750 to 1520°C and the temperature of deformation from 1660 to 1360°C. Hence, the presence of alumina and ferrous oxide impurities in courent considerably deteriorates the properties of refractory concretes. Taking into account the mentioned decrease in strength of concrete in heating it would pay to give it an opportunity to reach such a strength that would remain relatively high upon heating. Targetted studies into the problem have shown that allowance for higher setting times from 3 to 10 days enables an increase of residual strength, which even upon heating remains higher by absolute value than the strength of the 3-day concrete.

To reveal the effect we performed studies steam awing, of cements containing 70% calcium aluminates ($CA+CA_2$) and 30% technical alumina. One group of specimens was immersed in water, another group after conditioning in moist air for 3 days was brought to open air, and a third group was steam curred.

The tests indicated Table 1 that after stern curing the compressive strength remains practically at the 3 day level of hardening under ordinary conditions. The character of strength development at drying and further heating of the concrete subjected to steam curing does not differ from that of the cements hardened in water and in open air. Consequently, it is advantageous that to steam cure concrete products made of high alumina cement.

The heat resistance observed is 1740--1770°C, deformation starts at 1420°C, and 4% strain is within 1540°C to 1620°C. In heating a small voluminous expansion is observed within 0,65 to 0,8. The thermal resistance is from 45 to 60 thermal cycle.

According to Yasno at al. (7), the cement refractoriness can be altered by changing the grain size analysis and the shape of cement particles. We designed an alumina cement of certain mineral and grain comositron which ensures for the conctere a high workability, high strength and refractoriness after setting. The cement comprises 40-60% of a compound including $CaO \cdot Al_2O_3$ with $Ca \cdot 2Al_2O_3$, $12CaO \cdot 7Al_2O_3$, $4CaO \cdot Al_2O \cdot Fe_2O_3$ and $2CaO \cdot Al_2O_3 \cdot SiO_2$, and 40-60% of Al_2O_3. The size of nonspherical alumina cement particles must be 30 um, and the specific surface 0,5-1,2 m^2/g. The recomended proportion of particles below 5 μ size is 10-35%.

Table 1

Effect of Setting Conditions on the Concrete Strength at Elevated Temperatures

Setting conditions	Setting age, days	Compressive strength, MPa		
		Reference	After drying at 100 100°C	at 800°C
Immersed in water	3	52	84	59
	7	69	90	67
	28	87	105	77
On air	3	52	80	52
	7	59	85	61
	28	73	87	63
Steam curing	4.5 hours	55	86	64

The resistance of concretes made of high alumina cement to corrosion was investigated with the aim of using it for linings which are in contact with melted metals and operate as in reducing media. The resistance was determined by the quantity of concrete dissolved in the melt. The solubility was determined by the changing content of Al_2O_3 in the molten slag. Analysis indicated that the amount of Al_2O_3 in the slag decreased by 0,2% abs. i.e. the concrete is highly resistant to the attack by molten slag.

Drozdr at al. (8) have suggested a method for the production of refractory aluminium silicate concrete which resists liquid metal and slags and is intended for metal-melting linings. The concrete composition is a mixture of refractory aggregates and alumina cement with carbon filler additive (preferably graphite). The latter is added in quantities of 5-30% by weight. This concrete has not only high refractory properties, but resists well the attack of melted slag and metal.

Modification of high alumina cements is carried out by producing barium and strontium aluminates (9) whose application range is limited by the temperature 1800°C. For higher temperatures, irconium-bearing cements (10) must be used. These cements include barium zirconium aluminate, calcium zirconium aluminate and strontium zirconium aluminate brands. The basic components of these elements are barium zirconates, calcium aluminates and zirconates as well as strontium aluminates and zirconates. These cements exhibit a high heat resistance (2050-2400°C) compressive strength (43-65 MPa), and low shrinkage (1%). Spinel-bearing cements include spinel and alkali aluminates. Depending on the spinel composition, these cements relate to two types: with alumomagnesia spinel $MgO \cdot Al_2O_3$ and with chrom-magnesia spinel $MgO \cdot Cr_2O_3$. These cements relate to high heat resistant, early setting, and high strength cementitious materials because they contain calcium aluminates in addition to spinels.

High early-strength cements. In spite of unquestionable progress in the application of aluminate cements the use of these cements is limited by two factors: the shortage of raw materials and phase transformation at hardening accompanied by a decrease in concrete strength. This necessitated the development of cements possessing high rate of strength development similar to that of aluminate cements and durability which is characteristic of cements containing calcium silicate. The investigations into the $CaO-Al_2O_3-CaSO_4$ (11, 12, 13) system evaluated the components of initial phases, intermediate compounds their temperature interval of stability, the components of final firing products, the sequence of minerals formation and process kinetics and the activation energy of phase formation. A sulphaluminate clinker composition was developed as follows: calcium sulphoaluminate $3Ca \cdot Al_2O_2CuSO_4$ (C_4A_3S), calcium aluminate $12CaO \cdot 7Al_2O_3$ ($C_{12}A_7$) or $CaO \cdot Al_2O_3$(CA) and high temperature bicalcium silicate $2CaO \cdot SiO_2$(C_2S). The investigation of the hydration process of C_4A_3S has shown that its hydration rate is close to $C_{12}A_7$ but as for composition and morphology of hydrate compounds it is close to CA_2 (14).

- the structure of cement stone is represented by stretched crystals which form a mesh structure with cells filled by gel phase, thus providing high density and strength.
- ettringite, calcium hydroaluminates CAH_{10} and C_2AH_8, aluminuous hydroxide formed at the early hydration stages have been preserved in concrete for a long time.

In contrast to $C_{12}A_7$, there is no recrystalization of hydrate compounds when hydrating and hardening C_4A_3S and concrete is characterized by strength increase. The presence of C_2S in clinker intensifies the cement hydration process binding $Ca(OH)_2$ which is given off thus providing the formation of calcium hydrosilicates. The concrete strength during 10 hours from the early hydration process reaches 10/15 MPa.

The high strength sulphur aluminate cements react to water quite rapidly. The chemical reaction proceeded allows to maintain the high temperature of concrete during 3-4 hours thus in some cases it is possible completely to avoid the steam curing of concrete. The above concreate is characterized by high water and sulphur resistance. In general it is an interesting and perspective direction in chemistry of cement.

That's why the compounds forming on the base of calcium orthosilicate, calcium monoaluminate and fugaceous components containing fluorine, chlorine and sulphur: $2(2CaOSiO_2)\cdot CaSO_4$, $2(2CaOSiO_2)\cdot CaF_2$, $2CaOSiO_2\cdot CaCl_2$, $3CaO\cdot 3Al_2O_3\cdot CaSO_4$, $3CaO\cdot 3Al_2O_3\cdot CaF_2$, $3CaO\cdot 3Fe_2O_3\cdot CaSO_4$, II $CaO\cdot 7Al_2O_3\cdot CaF_2$, II $CaO\cdot 7Al_2O_3\cdot CaCl_2$ are the subject of intensive and detailed investigation. The synthesis of some of them have been carried out by P.P. Budnikov and S.M. Rogosina long ago. Unfortunately nowadays the studies on synthesis of new compounds are carried out within the limited interval of consentrations without drawing corresponding condition diagrams this the researchers came to the repeated conclusions. The partial invistigations of the $CaO-Al_2O_2-CaF_2$ 15,16 triple system have been carried out.

The high fugacity of fluorine, chlorine and sulphur causes the inconstancy of these compounds. In this case the structure and properties must be specified. It is required to investigate the structure of these compounds as well as the possibility of synthesis at low temperature.

The most investigated compound was mentioned to be C_4A_3S. Sulphur aluminate clinker is used for producing the various types of cements. The interaction of sulphoaluminate cement containing $3(CA)\cdot CaSO_4$, C_2S, free CaO and $CaSO_4$ with heavy metal compounds K_2CrO_4, $Pb(NO_3)_2$, $CaCl_2\cdot 2H_2O$ and Al_2O_3. The above compounds were mixed with cement paste in the form of water solution at the ratio of the solution and paste equal to I. The prepared mixture was placed into the matrix and kept during 3 days at 20°C and relative humidity of 90%. The efficiancy of heavy metal binding by cement paste was determined by quantity of unbinding compounds of heavy metals. It was revealed that the ions of chromium and cadmium are fully bound but the binding of lead and arsenic is considerably weak.

The formation of ettringite chromium derivitive as a result of interaction between cement paste and K_2CrO_4 was obtained by using the method of X-ray diffractometry. As a result of reaction of $CdCl_2$ the solid solution of $CdCl_2$ and $CaSO_4$ is formed. Lead is bound mainly in the form of sulphate. In general calcium sulphur aluminate is considered as expanding additive for production of noncontracting expanding and stressing cements (17).

Expanding cements. The industrial application of C_4A_3S as expanding additive when producing cements in the USA have been proposed for the first timein the sixties by A. Clain. The investigations in this field are constantly being increased. Before the Congress the Chemistry of Cement held in Paris the expanding cements have been produced mainly in the USSR, USA and Japan.

The publications released during the part several years give an evidence that investigations of the above cements are carried out in many countries. So in Rumania (18) the possibilities of production of energy saving noncontracting, expanding sulphur aluminate cements using belit slag, phosphogypsum, limestone and boxite, are considered. The initial mixtures had molar ratio of C/S equal to 1,83-3,26 and S/(A + F) equal to 0,52 - 1,24. The clinkers being produced contained 2,5 - 31,3% of C_4A_3S. Clinkers was milled up to specific surface by Blaine equal to 2500-2700 cm^2/g. After being kept in humid space during 28 days the samples had a compressive strength of 300-510 kgf/cm^2 and on expantion strength of 0,025-1,37%.

The publications of chinese scientists (19) give information about the use of $C_4A_3\bar{S}$ for production of noncontracting and expanding cements. The idea to create the clinker capable of being base for expanding cement without additives has been proposed at the 5th international Congress on the Chemistry of Cement held in Tokyo as for back as 1968 by Holsted (20). This can allow to stabilize its quality.

The above clinker containing simultaneously C_3S and $C_4A_3\bar{S}$ (21) and being used

for production not only of expanding cement but also for production of stressing one has been produced in the USSR. The similar information has been given in (22).

The raw material blend contained (%): 71-7,5 of limestone, 19-20,9 of fly ash, 6-6,7 gypsum and 1,5-1,6 of CaF_2; the contents of SO_3 in the blend was 1/3-1/4 of Al_2O_3 contents. The blend was subjected to firing in the laboratory by means of rotary kiln of semifactory and factory type. The clinker produced contained 50-60% of C_3S and consederable amount of C_4A_3S. The cement made of the such clinker had the initial setting time of 12 to 48 min and the final setting time of 17 to 145 min. The strength at age of 3 days was equal to 20-40 MPa. A great deal of attention is devoted to the problem of durability of the cements.

The corrosion resistance of expanding and stressing cements was investigated under conditions modifying the service of concrete as an isolating layer when affected by saturated solutions of $MgCl_2$ and $CaCl_2$. The investigations of the concrete structure made of expanding and stressing cements revealed that the structure is characterized by much higher density to compare with the porosity of concrete made on the base of ordinary sulphate resistant portland cement. The ratio of micro and macropores is also changed in concrete. The quantity of micropores having the radius from 100 to 1000 A is increased but that of macropores ($>10\ \mu$) is decreased thus the law penetrance (Table 2) and high corrosion resistance of concrete made of expanding and stressing cements within the solution of MgCl containing 400 mg/l of magnesium ions are provided. The composition, structure and properties of concrete made of ordinary portland cement and expanding cement hardening at 20°C during 10 23 years have been investigated by the methods of X-ray diffractional analysis and scanning electrone microscopy as well as by physical and chemical tests. Expanding cement contained 89% of portland cement and 11% of expanding additive which was calcium surphur aluminate. After the manufacturing the samples were kept during 24 hours in the space with humidity of 100%, subsequently they were kept in water or in the open air (at relative humidity of 60%). It was revealed that the samples of concrete made of expanding cement after 10 years of hardening were provided with the same durability as those made of portland cement.

Table 2

Waterproofing and corrosion resistance of concrete

Cement type	Penetrance factor		Resistance factors Kc
	0.5 MPa	1.0 MPa	
Portland cement	$2.1 \cdot 10^{-5}$	$2.8 \cdot 10^{-5}$	0.74
Expanding cement	$2 \cdot 10^{-8}$	$1.8 \cdot 10^{-8}$	0
Stressing cement	$2.15 \cdot 10^{-8}$	$1.73 \cdot 10^{-8}$	

Thus the cements with composition of $3CaO \cdot 3Al_2O_3 \cdot CaSO_4$ as well as the mixture of the latter with portland cement represent the type of cements suitable for producing concretes resistable to attack by sulphate and magnesium medium. In our opinion these cements in future will be of great importance.

Other kinds of cement. There are some reasons for limiting the maximum strength developed by calcium cements. The latter include:

- unordered fibrous structure of the concrete which basic characteristics were only the subject of intensive investigations being carried out during the past five years by means of inspecting and raster electron microscopes.
- internal stresses being developed at intergrowth of the hydrate new formation when aggregating.
- disbalance between the number of active centers on the initial grain surface of cement and number of nucleus of the crys-

tals capable of decrystalizing from solution when mixing cement ingredients with water.

In case of the lack of nucleus, the strength starts growing slowely and developes within the late terms thus the effective application of the cement in construction products is infavourable. The special interest is devoted to solving the problem of elimination of the concrete basis defect-the law tensile strength. The polymerization methods being used at present related to filling the pores by the elastic material. In this case no law chemical bond with concrete is occured. The pores are filled only partially. The fulfilment of the above methods is very complicated and gives a little effect. The need is required for inorganic polymers which can be used as concrete component enables sharply improve the relationship between the compession strength and tensile strength of the cement components. It is known that the fiberous-gellike structure at concrete receives a mechanical load depending on the fibre geometrical characteristics, their spacial displacement when aggregating modulus of elasticity as well as in connection with the intergrowth character. The results of production investigations show that sizes of individual fibres and aggregation geometrical characteristics can be changeable when affecting the cement composition and milling conditions. However the need is required for mathematic theory of the fibreous-gellike structure strength which can explain which sizes of fibres and ways of arrangement in the aggregation are better thus to approach the optimum characteristics. Phosphate binders are defined as the composites formed by means of chemical reaction between the solid powderlike component (fillers) and liquid phosphate compound (binder). The ratio of solid and liquid depends on the powder specific surface, specific weight, chemical activity of components and the way of formation. In general the ratio is determined by the required elasticity of the mass after mixing with water.

During the interaction process of initial components the nonorganic phosphate polymers with the certain degree of polymerization and acting as the product cement phase are formed (24).

The brief summary of development of special cement chemistry allows to suppose that in the near future (up to 2000 year) aluminate, sulphur aluminate, expending and modified silicate cements will remain to be the basic products which are used for the production of various types of concrete provided with special construction and technical properties.

Deep theoretical researches, development of chemistry and physics will show in future the ways of development of special cements on the basis of application of large number of waste products.

REFERENCES

1. George C.M. Industrial Aluminat Cements. - Structure of cements and Construction. - New York, 1983, 210-260.
2. Дмитриев А.М., Кузнецова Т.В., Юдович Б.Э., Запольский А.К. Гидратационное легирование цементов крентами. - Труды УI Всесоюзного научно-технического совещания по химии и технологии цемента. М., 1982, с. 94-98.
3. Packter A., Zaidi S.A. - Silicat. ind., 1983, v. 48, No. 7-8, p. 139-146.
4. Brisi Cesare, Lucco Boriete Maria. - Cemento, 1983, v. 80, No. 3, p. 155-164.
5. Кузнецова Т.В., Лыткина Т.А., Шишкина Л.Д. Высокоглиноземистый цемент из промышленных отходов. - Труды УI Всесоюзного научно-технического совещания по химии и технологии цемента. М., 1982, с. 98-102.
6. Dolezsaik K., Vörös T., Reuter O. - Epitőanyag, 1983, v. 35, No. 10, p. 361-364.

7. Юкихира Ясуо, Сато Масатака, Исимару Тосиаки. Дэнки кагаку когё к.к.Заявка 58-36953, Япония, Заявл.25.08.8I, № 56-I32I85.
8. Mieczyslaw Drozdz, Wanda Wolek, Kazimierz Tkaczyk, Jozef Pilch, Leon Madejski, Andrzej Kozlowski. Institut Materialow Ogniotwalych. -
9. Вълков В. - Строителни матер.и силикат. пром-ст, I983, т.24, № I0, с.7-I0
10. Мельник М.Т., Илюха Н.Г., Шаповалова Н.Н. Огнеупорные цементы. Киев, Высшая школа, I984, I2I с.
11. Mehta Povindar Kumar. - Cement. Wapno. G Gips, 1982, v. 35, No. 7, p. 79-84, 66-67.
12. Онок К., Накамура С., Сайн Т. - У Международный конгресс по химии цемента. М., Стройиздат, I973, 459-460.
13. Кузнецова Т.В. Физико-химические основы технологии расширяющихся и напрягающих цементов. - Труды НИИцемента, I976, № 38, с. 77-85
14. Румянцев П.Ф., Мариничев В.С. Тезисы докладов 2-го Сов.-Чехосл.симпозиума по строению и свойствам силикатных и оксидных систем. Ленинград, I98I, с. 7I-72
15. Massazza F. Je Cemento, 1983, No. 3, p. 127-141.
16. Marut Toshinisa, Uchida Ikuo, Kato Kazumi. - Rev. 32 Cen. Meet. Cem., Assoc. Jap. Techn. Secc. - Tokyo, 1978, 65-68.
17. Кузнецова Т.В., Марко В.И. Безрукова С.Г. - Цемент, I978, № I, с. I2-I4
18. Teoreanu Jon, Muntean Marcela. - Cem. and Concr. Res., 1983, v. 13, No. 5, p. 711-720.
19. Wu zhongwei and wang Yansen. - 7 Intern. Congr. Chem. Cem., Paris, 1980, v. 3, p. 27-32.
20. Холстед П.Э. Расширяющиеся и напрягающие цементы. - Химия цемента по ред. Х.Ф.У.Тейлора, I969, с. 367-375.
21. Кравченко И.В., Кузнецова Т.В., Хлусов В.Б. Алитосульфоалюминатный клинкер и цементы на его основе. - Цемент, I978, № 8, с. 7-9.
22. Wei Jen-Zhao, Wang V.E. - Silicat. Ind., 1983, v. 48, No. 4-5, p.93-97.
23. Jsogai Jun, Nakaya Selichi, Nakagawe Koji. - Rev. 34 Gen. Meet. Cem. Assoc. Jap. Techn., Sess. - Tokyo, 1980, p. 177-178.
24. Копейкин В.А., Петрова А.П., Рашкович И.А. Материалы на основе металлофосфатов. - М., Химия, I976, I96 с.

SPECIAL CEMENTS

W.KURDOWSKI , C.M. GEORGE , F.P. SORRENTINO

Professor W.KURDOWSKI is Director of the Institute of Buildings Materials and Refractories of Academy of Mining and Metallurgy (KRAKOW/POLAND)

Doctor C.M. GEORGE is technical Director at Lafarge Calcium Aluminate Inc. (NORFOLK /U.S.A)

Doctor F.P SORRENTINO is Principal Scientist at Lafarge Coppee Research (VIVIERS/ FRANCE)

1) GENERAL INTRODUCTION

Preliminary remarks

In reviewing progress in this field for the 8 th international Congress on the Chemistry of cements the authors are again conscious that full justice cannot be done to all the publications that have appeared in the last six years.A selective review has been chosen in preference to a purely bibliographical approach The basis for selection has involved the inter play of several criteria:

- a desire to maximise the international content (papers from more than 20 countries are included)
- priority given to papers concerned with chemical aspects.
- condensation of multiple publications on the same topic by the the same or closely associated research groups.
- emphasis given to divergent views expressed on a given subject
- the pragmatic implications of both predominantly scientific contributions and those of a primarely empirical nature.

In this manner the following review has been restricted to some 300 publications.The authors extend their sincere apologies to all those work has not been mentioned.

definitions:

Special cements are binders used for specific applications ,requiring materials whose characteristics are outside the limits standardised for portland cement or manufactured from raw material ,by means of process differents from those of portland cement.

This proposed definition , based on preparation and use of cement is restrictive ,because it does not take into account the fact that it is possible to obtain special properties with ordinary Portland cement, by using admixtures ,or by special treatment (autoclaving .....) .On the other hand ,a definition based on the fundamental concept of the nature of liaison developed by the binders to insure its cohesion or its adhesion to aggregates does not allow a conclusive distinction because such types of hydraulic bond can lead to a special or a conventional cement. This is the reason why ,in spite of its weakness ,we shall use this definition at least as starting point of our paper.

The special cements present a scientific and industrial interest:

— the increase of the knowledge of Portland cement obtained during half of a century leads to an increase of the difficulties of research in this field and requires more and more complicated experimental procedures .The study of new systems of binder could allow a better understanding of the mechanism of the conventional cements.

—industrially,the production of Portland cement is increasing in the low GNP countries and decreasing in the high GNP countries where conversely the production of special cements is increasing . Consequently there exists in these countries an increasing interest to invest in high added value binders used for applications different from construction.

The difficulty in classifying these special cements (as has been noted earlier) is due to their permanent evolu tion in time and space.In the books or publications trea ting cements, the works concerning special cements are found in the chapters "unclassified binders , other binders, miscellaneous ,..... " The logical and ideal evolution of a special cement is to become standard or con ventional ,as has been shown by their evolution through the international conferences of chemistry of cement. At the Stockholm congress in 1938 (1a), two types of cements , somewhat differents of portland cement occur : aluminous and pouzolanic cement.

At London (1960),(1b) the idea of special use is highlighted with the aluminous , expansive , oil well ,masonry cements. and *M.A. Swayse* identifies the idea of special cements and special uses.

At Washington (1960) (1c) "High strength cements" occur beside aluminous, slag and pozzolan cements.

At Tokyo (1968) (1d) a special chapter is devoted to fly ash cements.

At Moscov (1974) , (1e) the congress entails a theme concerning polymer cements, beside additives cements (fly ash, pozzolanic, slag expansive, aluminous, or high early strength cement .A need of classification occurs (*N.E.Fyodorov*) "Binders , classed as special cements are mainly derivatives,differing from common Portland cement ,by higher absolute strengths,and rates of its development, resistance to aggressive environments and also by such properties as specific gravity ,color, etc.."

At Paris (1980) we notice that additive cements (slag ,pozzolan, fly ash ..) do not belong any more to special cements and a new development of binders , being special by their manufacturing process (active belite, alinite cements ..),this evolution becoming necessary for saving energy during the crisis.(1f)

Since1980,few general works (2 /3/4) have been published , particularly in "CEMENT RESEARCH PROGRESS ", (5) where the authors establish a distinction between modified portland cements and "other binders " (5a/5b) *(M Collepardi* in his chapter "CEMENTI SPECIALI "treats together, additives cements ,colored cements , aluminous etc .. . .(6) . The chapter "SPECIAL CEMENTITIOUS SYSTEM " writte n by *V.S Ramachandran et al* (7) concerns the phosphate bound , the aluminous and Reg Set cements .

The Chapter "SPECIAL CEMENT " published by the others (8) ,reviews the literature published on the subject un til 1982 and proposes a definition allowing the idea of special use and unconventional process from special raw material to be taken into consideration.
This definition includes some types of special cements which have not yet found the position they occupy in scientific or patents literature concerning the binders they are very fast setting cements or chemically bound cements (magnesian, phosphatic, dental ,water glass cements ...
Conversely this definition excludes Portland cement with admixtures or with additives (slags, fly ash .....)

The litterature published since 1980 allows us the development of the following topics:

- aluminous cements
- expansive cements
- fast setting and hardening cements
- very high strengths cements
- low energy cements
- chemically bound cements

..(Phosphates cement, Magnesia cement, Dental cement, Water glass cements)

From this analysis two tendencies concentrate the research activities:

- .....The will ,already expressed during the last congress to produce clinker or cements less costly , by using either special process , or special raw material
- .....The use of cements for other applications than construction; this involves cements with special properties (density, strengths, etc ...) The studies aimed to characterise theses properties and to industrialize the products.

2)ALUMINOUS CEMENTS

SYNTHESIS PHASE COMPOSITION of ANHYDROUS CALCIUM ALUMINATES

Thirty percent of the papers reviewed concern this topic. There is substantial agreement amongst various authors on the equilibrium conditions of formation of C_5A_3 and $C_{12}A_7$,the latter being stabilized by the absorption of O_2 or H_2O. Other researchers emphasize the extreme precautions needed to synthesize individual aluminates by sintering: under industrial conditions it is evident that equilibrium is not attained. Several papers describe the use of Mossbauer Spectroscopy to characterise calcium aluminoferrites and the distribution of iron in cements

G.I. Zhmoidin et al (18) report a study of the conditions of formation and stability of $C_{12}A_7$, C_5A_3 and the glassy phase of equivalent composition . Previous work is reviewed and data presented on the effect of time,temperature and atmosphere in this system in the solid and liquid state. $C_{12}A_7$ crystallises when molten material absorbes oxygen containing gases which create short range structural nuclei in the liquid state at 1500° or below .This is accompanied by an abrupt increase in melt viscosity, thus providing a convenient experimental investigation method. Strongly reducing atmospheres and longer ,higher, soak temperatures favor C_5A_3 and glass formation on quenching. Formation of $C_{12}A_7$ derivates of the type $C_{11}A_7.CX_n$ (where X=F, Cl,S,SO_4,CO_2) are alternative methods of stabilising the structure. In a further publication , these authors describe a mass spectrometer study of the sorption of H_2O, CO/CO_2 and O_2 (air) by molten and solid $C_{12}A_7$

Comparison of measured gas composition with those calculated for thermodynamic equilibrium lead the authors to conclude that all gases other H_2O are picked up only in the molten state ,and provide nuclei for the development of zeolitic polycrystalline $C_{12}A_7$ during solidification . By contrast water molecules can also enter the solid structure during cooling due to their smaller size.
Measurements of gas compositions during heating in vacuum are also used to estimate the isosteric heats of desorption. The value for H_2O is in the range typical of physical bonding, whereas of the other gases are nearly on order of magnitude greater indicating the breaking of chemical bonds . It is concluded that the desorption of the larger diameter gas molecules can occur only by disruption of the crystal structure of the $C_{12}A_7$ itself. The total amount of gases absorbed in the molten state at 1500° where similar to the previously reported values for $C_{12}A_7$ stabilised in the presence of dry O_2

Three papers by *C.Brisi et al* (19/20) also discuss conditions of formation and equilibrium relationships for various calcium aluminates.Heating $C_{12}A_7$ of mixtures of CA and C_3A between 1000° and 1280° in very low partial pressures of oxygen and water produces C_5A_3 and C_3A . Above 1280° the stable product is $C_{12}A_7$,despite the absence of oxygen ,and also of water ,except perhaps in very minute quantities,to stabilise the structure .Thus both C_5A_3 and $C_{12}A_7$ are seen as equilibrium products in the $CaO-Al_2O_3$ system .

In the temperature range from 1100° to about 1500°, CA and CaF_2 react to produce C_3A_3f .In the presence of air ,some fluorine is lost as volatile fluorides leading to the appearance of $C_{12}A7.CaF_2$ at the partial or com

plete expense of C_3A_3f . $C_{12}A_7$ quenched in air from temperatures above 900° contains excess oxygen in quantities that increase as the quantity of H_2O in the system is lowered. Compounds of the type $C_{12}A_7.CX_n$,where X is H_2O, F_2 or O_2 contain no excess oxygen.No excess oxygen was detected when heating $C_{12}A_7$ in dry hydrogen, but it was not certain that hydroxyl groups where totally absent .An amorphous mixture of CaO and Al_2O_3 obtained by stepwise drying up to 700° of the coprecipitated nitrates, formed C_5A_3 ,with traces or residual CaO when subsequently treated in air to 900° Prolonged soaking formed some CA and eventually C_3A and $C_{12}A_7$. At 1200° the effects were accelerated,but , under dry hydrogen C_5A_3 remained the only phase.

By contrast, calcining the nitrates at 1000° without preliminary drying produced predominantly C_3A and CA.

Other intimately mixed amorphous starting materials produced by different precipitation techniques gave similar results.It is concluded that C_5A_3 is a true equi librium reaction product of the reaction between stœchiometric mixtures of CaO and Al_2O_3. (20)

The reaction between molten CA and solid ∞ alumina has been studied by *L.C. Dejonghe et al* (21) ,using transmission electron microscopy of thin sections prepared from the reaction zone between two adjacent polycrystalline α alumina interfaces containing the melt at 1530°. The alumina contained 4% SiO_2 as a separate alumino-silicate phase.With CaO as the mobile species ,CA_6 plate like crystals ,oriented in the direction of the diffusion path were formed .Porosity at the interface increased with degree of reaction , weakening the bond between CA and A after solidification. Limitation of reaction by diffusion through the CA_6 was alleviated by the formation of liquid channels, accommodating the SiO_2 as calcium alumino silicate in which transport of CaO is enhanced .Beyond the CA_6 layer ,which did not accomodate silica , CA_2 was formed .When essentially silica free corundum monocrystal were substitued,reaction rate was greatly reduced .Polycrystalline pure alumina produced an intermediate effect.In an other publication (22) these authors present evidence of a wider range of non stœchiometry in calcium aluminates than has been generally proposed hi herto. *V.K. Singh et al*(23) has published studies of the reaction between $CaCO_3$ and CaO to form CA , CA_2 ,and of the sintering of synthetic CA, CA_2 and mixture of the two.The kinetics of CA formation by solid state reaction (1200°C < 0 <1380°) of CaO and Al_2O_3 gave an activation energy of 38 Kcal/mole. With particles of the reactants in contact C_3A forms first on the CaO side followed by $C_{12}A_7$.On the alumina side CA, CA_2, and CA_6 are detected . Synthetic CA prepared by repeated firing and grinding of $CaCO_3$ -Al_2O_3 mixes was sintered at 1350° to 1460°.From the densification curves the diffusion coefficient calculated was similar to that reported for the self diffusion of Ca in CaO (24)

.Sintering mixtures of synthetic CA and CA_2 led to cal culated activation energies (91-99 Kcal/mole) which were lower than those reported for either CA (120/ 125 Kcal/mole) or CA (134Kcal/mole)alone.The acti vation energies for the mixtures increase with the starting CA_2/CA ratio .Complementary microstructural studies ,(25) show evidence of grain growth accompanying densification.The sintering of CA is volume diffu sion dependent and kinetics are strongly affected by initial particle size. A further studies of sintering Al_2O_3 and $CaCO_3$ at 1450° is reported by *A.Mathieu.* (9) A pure natural carbonate was used together with aluminas prepared by calcining Bayer hydrate at various temperatures . Great care was taken with homogenizing the raw materials with a target A/C ratio of 1.02. Despite this actual values ranged from 1.012 to 1.028 and values of combined A/C in the sintered pellets from 0.94 to 1.01 .As a consequence ,the mineralogy and hydraulicity of the resulting clin kers varied considerably. MC analysis detected some highly significant relationship between raw materials proper ties and the properties of the clinkers.Thus $C_{12}A_7$ strongly affects the size of the initial calorimetric heat of wetting and the timing of the main exothermic hydration peak.The size of this peak ,however ,depends primarily on the Ca contents of the clinker,this phase always forming at the expense of $C_{12}A_7$ and CA_2. Degree of sintering was very strongly dependent on the fineness of the of the starting alumina but not its temperature of preparation nor fineness of the limes tone .The author emphasises the extreme difficulty of controlling the degree of sintering. *T.V Kuznetsova et al* (26) have also studied calcium aluminate formation by sintering .They recommend double firing and long, high soak temperatures to produce a single mine ral composition from lime and alumina.In the presence of SiO_2 ,mineralizers can be used to prevent gehlenite formation and modify early strength development .Particular attention was focussed on additions of cal cium sulphate and calcium sulphoaluminate formation .The hydration kinetics and SEM structure of hydrates produced from these clinkers was also investigated .

This work was a basis for development of rapid harde ning,sulphate resistant and self stressing cements. A kinetic study of the formation of CA and C_3A from $CaCO_3$ and Al_2O_3 powders has been published by *K.S. Chou et al* (27) at temperatures of 1200° to 1300° using XRD . Results fit models for diffusion of CaO and calculated activation energies agree with previously published values for the diffusion of CaO through C_3A .Transport through the product layer is thus considered to be the rate determining step.

.In the alumina rich part of the CaO ,Al_2O_3 diagram new measurements of the activity of CaO by e.m.f. measurements using a solid electrolyte are reported (28) .The free energy enthalpy and entropy of formation of CA_2 and CA_6 are calculated. *A.Bachiorrini* (29) used I.R. spectroscopy to study the transformation of amor phous CA into the metastable orthorhombic form and ultimately to the stable monoclinic form under the inf luence of heat . I.R. appears to be a useful alternative to XRD studies. *C.L. Honeybourne* has studied the Moss bauer spectra of aluminous cement of the fondu type ,at 4.2° K (30).This follows a previous study at room temperature .The total iron content of the cement ,exp ressed as Fe_2O_3 was 17.2% . 45% of this was present in magnetically ordered C_4AF clusters ,22% as wustite while iron ions ,present individually or in very small clusters ,made up 12 % and 21 % of $Fe^{2+}$and Fe^{3+} res pectively .Magnetite was present in only very small quantities which is consistent with the rapid cooling to which the cement clinker is subjected in manufac ture. *S Chandra* (31) has studied the kinetics of forma tion by sintering of BA and BA_6 ,in the presence and absence of $BaCl_2$.$2H_2O$ using Al_2O_3 and $BaCO_3$ or $BaSO_4$ as starting materials .Reaction of compressed powder compacts in air was studied by XRD at tempe- rature between 800° and 1500°. Reaction rates were faster with $BaSO_4$ than $BaCO_3$ and completed earlier.In both cases the addition of 25% of $BaCl_2.2H_2O$ caused significant acceleration and reduced the sintering tem peratures by up to 250°.This is attributed to liquid phase formation facilitating transport phenomena.The chemical composition and the mineralogical composi- tion (determined by QXRD and microscopy)of 30 sam- ples of Fondu type aluminous cement clinker are discu- ssed by *F.P. Glasser et al* (9).Based on their previous phase diagram studies ,mineralogical compositions based on chemical analyses are compared with the experimentally determined phase compositions. The system is considerably more complicated than the case of portland cement clinkers since the production of aluminous cement clinkers by fusion usually gives rise to five components:CaO,Al_2O_3,SiO_2,Fe_2O_3, and FeO.It is also evident that equilibrium crystalization is not fully achieved during cooling -a glassy phase is almost invariably present and C_2AS and $C_{12}A_7$ frequently coexist whereas they are incompatible at equilibrium. Despite these complications ,the CA content of the clinker ,(the main hydraulic component)can be fairly accurately predicted if due to allowance is made for the role of FeO .(allowance is also made for the pre sence of MgO but it is normally only at very low con centrations).The solubility of these two components in the the liquid is in practice about 3.7% .Above this level allowance has to be made for pleochroite forma tion,for which the authors estimate the formula $C_{22}A_{13}f_3S_4$ .On this basis the average calculated CA content for MgO+FeO<3.7 is 51.1% compared with a measured value of 49.6 . No calculated values differed from the measured values by more than 20% and 2/3 of the calculations were within 10% .For MgO +FeO >3.7% the average calculated CA content was 40.5 % com- pared to an experimental value of 43.5% with 90% of all calculations within 20% of the measured value and 1/3 within 10%. This is considerably better than any previous attempts to predict the CA contentof this type of aluminous cement from its chemical composi- tion. A further three papers (32/33) describe investi gations of calcium aluminoferite $CF_{(1-x)}A_x$ in alumi nous cement using Mossbauer spectroscopy at room temperature and at 20° K,and XRD. Both CF and CA are present simultaneously and the concentration of CA increase with X.Fe atoms occupy two differents sites in CF and only one in CA.Aluminous slags obtained from the alumino thermal manufacture of chromium show cementitious properties. Although the chemical compo sition favours CA_2 formation with which *G.I.Zaldat et al* (10) associates high strength potential these authors observed poor binder performance in certain slags .Studying this phenomenon led to the identifica tion and synthesis at 1400° of a new phase in the Na_2O-CaO-Al_2O_3 system in which Cr_2O_3 can substi- tute for Al_2O_3 up to 6.4% .By raising the temperature above 1500° this phase decomposes ,releasing Na_2O and forming CA2 .The cementitious properties of these slags improve as the Na2O content is reduced . *S.DOU,* (34) presents a theoretical study of molten alkaline earth aluminates (MO.Al_2O_3) using polymer theory , taking AlO_3^{3-} as the monomer .the activity of MO can then be expressed in terms of composition (mole frac- tion of Al_2O_3)and the equilibrium constant for the polycondensation. K11 for the reaction $2\,Al_2O_3^{3-} \longrightarrow Al_2O_5^{4-} + O^{2-}$ is used. Activities

calculated from this linear chain polymer model agree with experimental values in the litterature .The application of polymer theory to silicates and phosphates can thus be extended to aluminates.

HYDRATION of CALCIUM ALUMINATES

Nearly sixty percent of the publications discussed deal with the aspects of hydration. Inthe C-A-H system both synthetic CA and CA2 and industrial cements are studied .The effects of granulometry ,stœchiometry and temperature on kinetics are investigated .Extensive thermodynamic analyses of equilibrium hydrate formation and solution phase metastability are presented ,extending the work of these authors prior to 1980 ,including the effect of some foreign ions.These models ,based on experimental studies provide a coherent and extensive explanation of the hydration of calcium aluminates ,even when equilibrium is not fully achieved ,which is frequently the case in practice.New work is reported on the link between hydration, microstructure and mechanical properties and the importance of thermal history is stressed. ljterature on carbonation is abundant including the action of CO_2 and the effects of powdered $CaCO_3$ on hydrate formation and decomposition . Some papers continue to advocate the use of CaCO3 to overcome the effects of conversion, which was such a dominant preoccupation of the period 1974 /1979 (C.M. George see reference 1f and 8 in "general introduction") .Other work is ambivalent while one paper is decisively negative.This reviewer considers that conversion should always be presumed in practice -the pricipal interest in industrial aluminous cements (apart from their temperature properties) resides in their ability to develop within hours substantial strength which is retained long term irrespective of conversion. Diverse papers treat the effect of chemical additives on cement rheology and strengths ,including some discussion of chemical mechanisms involved ,an aspect which warrants much further study.A number of useful papers describe experimental methods of studying hydration.

The System C-A-H *A RETTEL et al*(35) used a combination of differential calorimetry and NMR to study the hydration of synthetic CA at various temperatures. XRD and SEM were also used. NMR allows distinguishing quantitatively between Al ^{IV} present in CA and Al ^{VI} in the hydration products. The NMR spin lattice relaxation time of protons is also observed to decrease corresponding to progressive crystallisation of hydrates . By taking account of both the Al coordination and the spin relaxation times the nature and extent of hydration can be followed ,including formation of amorphous products inaccessible to XRD. Below about 30° hydration assymptotes to 40% ,while at 70° and above hydration approaches 100% .Between these temperatures there is a gradual transition with a temporary plateau at 40% hydration .The authors attribute this pattern to protection of residual CA at lower temperature by precipitated hexagonal hydrates and alumina gel ,and conversion to cubic hydrate and crystallisation of gibbsite removing that protection at high temperatures.

An investigation of the microstructure of calcium aluminate hydrate using XRD and SEM has been published by *W.Wolek et al* (36) . 60 % and 70 % alumina were used. At low water/cement ratio (W/C) , 0.26 and normal temperature CA hydrate about 5 times faster than CA_2 At W/C =0.5 the ratio had dropped to 2 and at W/C =1 both aluminates hydrated completely. CAH_{10} formed in all cases . At the highest W/C under humid storage long ,hexagonal needles were observed.When humidity is decreased ,fibrous CAH_{10} appears ,together with plate like C_2AH_8 crystals .At higher temperatures with W/C >0.5 trapezoidal C_3AH_6 and AH_3 are formed.

Several interesting paper (37/38) describe the effects of stœchiometry and granulometry on the hydration kinetics of monocalcium aluminate ,as studied by isothermal calorimetry and electrical conductivity. The latter techniques proves both simple and sensitive. CA with C/A ratios of 0.96 to 1.04 was prepared by solid state sintering of pure Al203 and $CaCO_3$ powders. Despite careful homogenization and repeated firing and grinding cycles mixtures of CA and CA_2 could only be obtained below C/A=0.97 and mixtures of CA and $C_{12}A_7$ only above C/A =1.01 .Otherwise,all three phases were present.The initial conductivity of water in contact with the powdered product increased faster as the C/A ratio was raised , and precipitation of hydrate occured earlier.This corresponds to the well known accelerating effect of $C_{12}A_7$.Complementary thermoluminescence measurements indicated a concomittant increase in lattice defects. The accelerating influence of powder fineness was also demonstrated and it was shown that vibromilling is more efficient than ballmilling in reducing particle size and creating lattice vacancies.

B.Cottin et al (9) report several experimental studies aimed at explaining anomalies in the temperature dependence of setting of certain aluminous cements. Portland cements and the substanstially pure (white) aluminous cements show a progressive acceleration of setting time with increasing temperature (0 to 40°). By contrast ,aluminous cements containing C_2S show an increase in setting time at temperatures approaching 30° .Fondu cement is the most widely quoted exemple: an initial set of 3 1/2 hours at 20° is approximately doubled at 30°,whether or not the system is precured for up to 3 hours at 20°C.The same is observed with

synthetic cements composed of CA and C_2S or CA +C_2S +$C_{12}A_7$ setting times are approximately doubled although the absolute value of setting time is substantially reduced in the presence of $C_{12}A_7$ .The principal hydrate at 20° is CAH_{10},while at 30° it is C_2AH_8 the letter precipitates more slowly than the former .This observation alone however cannot explain the phenomenon since the pure cements exhibit no retardation. The role of SiO_2 covering the CA grains at 30° could not be demonstrated experimentally and is not consistent with the same retadation occuring when Fondu cement is precured at 20°.There is marginal evedence that the accelerating effect of $C_{12}A_7$ at 20° may be diminished at 30°C.An adequate explaination remains to be found. Papers by *M.Soustelle et al* (39) present thermodynamic studies of equilibrium and supersaturation in the hydration of calcium aluminates from which the shape of conductimetry curves can be simulated and explained .Since conductimetry measures only the total ionic concentration of a solution ,the results cannot be interpreted without a knowledge of the equilibrium constants for the reactants involved or complementary chemical analysis .The authors conclude that at 21° ,CAH_{10} is the only stable calcium aluminate that can precipitate and that the appearance of C_2AH_8 and $C_4A.CO_2.11H_2O$ (in the presence of CO_2) is dependent on achieving solution supersaturation with respect to CAH_{10}.*P.Barret et al* complete their previously published studies of the C-A-H (and C-S-H)diagram with a treatment of solubility diagrams for hydrated calcium aluminates,carboaluminates and carbonate, and alumina gel in equilibrium with atmospheric CO_2 and sodium ions in solution (40/41).Supersaturation in the C-A-H diagram existes in an area bounded by curves for C_2AH_8 and AH_3 within which immediate precipitation may not occur and for which a curve of minimum instability can be calculated thermodynamically.These curves are PH dependent and are displaced from their locations in the pure C-A-H diagram by the presence of carbonate and alkali ions in solution.These authors consider both carbonate dissociation and dissolution of CO_2 as sources of carbonate ions .They also point out that the equilibriuml conditions defined will not occur in cement pastes or concretes where access of CO_2 is limited.Calculation for these conditions based on experimental work are to be presented.These modified solubility diagrams offer a more realistic description of cement hydration than the equilibrium curves for the C-A-H diagram alone. *P.Barret* (40) also provides a useful review of models of the hydration of calcium sulphate hemihydrate,monocalcium aluminate and tricalcium silicate.The effect of curing conditions on strength development of aluminous cement of the Fondu type is examined in some detail by *B.Cottin et al* (9) The conversion of the low density hydrates formed at room temperatures into denser C_3AH_6 and alumina hydrates is accompanied by a strength reversion to a minimum value beyond which strength increases once more.Curing at higher temperature (eg 50° and above) C_3AH_6 forms directly and the strength development is monotonic.Deliberate or involontary changes in curing temperature induce intermediate effects .The combined effect of time and temperature on strength thus gives rise to a complicated pattern (8) which can only be interpreted in any given case through a proper record of the thermal history.Furthermore ,the absolute level of strength depends also on the W/C ratio as is well known.Strength development is particularly sensitive to temperature changes occuring in the time period corresponding to the initial precipitation of hydrates (setting time). This analysis shows that the apparently complex hardening characteristics of aluminous cement pastes and concrete are nevertheless predictable and controllable.*H.G. Midgley* , using Fondu cement with a typical CA content measured by QXRD of 45 % calculated the compresssive strength of pastes and concretes from hydrate contents determined by DTA (9).Curing temperatures from 18 to 60) ages from 1 day to 3 years, and W/C ratios from 0.25 to 0.40 were employed. The correlation coefficients between calculated and measured strengths were greater than 0.9.the hydrates detected were CAH_{10},C_2AH_8,C_3AH_6,C_2ASH_8 and crystalline alumina hydrate.At low W/C ratios ,normal temperature and early ages the specific strength contribution from CAH_{10} ,C_3AH_6,and AH_3 are approximately the same.At higher curing temperatures and /or at later ages C_2ASH_8 plays a dominant role .The strength contribution of C_3AH_6 decreases to zero when crystal size increases to greater than 1 micron .This occurs at high curing temperatures and high W/C ratio. At low W/C ratios and normal curing temperatures the crystal size of C_3AH_6 is about 0.01 µm. Under these conditions the cubic hydrate appears to contribute equal strength to the low density CAH_{10} hydrate.

J.J.Beaudoin(42) has published valuable information on microhardness and fracture mechanics of aluminous cement pastes. After normal curing for 3 days ,samples with a cast-in notch ,were stored for a minimum of 2 weeks at11% RH to eliminate variations in strengths due to humidity.Some samples were then heat treated to provide a series of specimens in which the ratio of

hexagonal to cubic hydrates ,determined by DSC spanned a wide range.Load deflection curves and microhardness were then measured.Relationship between fracture parameters and microhardness were then determined by regression analysis and showed a high degree of correlation.This implies that microhardness can be used to predict fracture behaviour .Hydrate morphology (hexagonal or cubic) affects fracture ,a mixture of the two types of hydrate showing greater fracture toughness than the CAH_{10} hydrate alone.The same has also examined the effect of high aspect ratio mica flake distributed in the cement paste matrix (42).Flexural strength and fracture toughness are considerably enhanced : there is some concommitant loss in compressive strength.Matrix porosity and volume concentration of the mica determines the strengths obtained. Reviewing the use of calcium aluminate cements in refractories, *S.Maczura et al*(43) comment on the effect of W/C and curing temperature on strength development before and after firing .Elevated curing temperatures are recommended to achieve maximum hydration.

Carbonation CO_2. A further investigation by *R.Fischer et al* of the system $C_4A\ nH_2O$- $C_4A.CO_2.nH_2O$ is reported (44),using X ray and electron diffraction, IR and Raman spectroscopy,TGA and DTA ,at 22° and 100% RH In the absence of carbonate ,the hydrate $C_4A.19H_2O$ was obtained. As carbonate was added (atmospheric CO_2 was excluded) C_4A 1/2 CO_2 H_2O began to form until $C_4A.19H_2O$ dissapeared at CO_2/Al_2O_3 =0.5 .Further addition of carbonate developed $C_4A.CO_2.11H_2O$ Exposing $C_4A.19H_2O$ solutions top gaseous CO_2 caused rapid superficial conversion to C_4A $1/2CO_2.12\ H_2O$ suggesting a diffusion controlled process.Continued exposure did not advance the reaction measureably but some $CaCO_3$ and $Al(OH)_3$ eventually formed.There appears to be very little solid solution in this system. *V.LACH et al*describe the CO_2 carbonation of CAH_{10} and C_3AH6 in aluminous cements (9). A through solution mechanism is given for decomposition of CAH_{10} producing vaterite, aragonite and calcite. Carbonation of C_3AH_6 is considered to be topochemical.At high W/C ratios $C_3A.CaCO_3$ $11H_2O$ first forms and subsequently decomposes to the various forms of $CaCO_3$.The gaseous carbonation ofC_3AH_6 to aragonite appears to be rever -sible with intermediate composition corresponding to CO_2 hydrogarnets. The authors give results for the temperature dependence of CO_2 absorption by aluminous cement concrete and the increase in strength due to carbonation in the absence of soluble alkalis.Rapid carbonation takes place only when liquid water is present in the pores of the concrete.The reaction between CO_2 and CAH_{10} is faster than the conversion of CAH_{10} to C_3AH_6 in the absence of CO_2.On this basis the authors regard CO_2 as a catalyst or accelerator of conversion.Carbonation in the presence of alkalis causes a decrease in strength and ultimate disintegration of the concrete if sufficient water,alkalis and CO_2 are continually accessible.This can be prevented by using low water content highly impermeable concrete or by protecting the surface of the concrete from the ingress of CO_2. Under these circumstances excellent durability results.

M.Perez et al have studied the carbonation of alumi nous cement mortars hydrated at 40,60 and 80° (45) .W/C ratios of 0.42,0.40,0.38 were used ,the lower values being obtained with a superplasticiser. Examination of the reaction products using XRD and IR spectroscopy showed that this did not affect the nature of the reaction involved.Treatment with CO_2 at the same temperatures led to the formation of $CaCO_3$ and alumina hydrates.The presence of α Al_2O_3 is also reported.The degree of reaction increased with tempe rature. Although the extent of reaction increases with time ,the rate of reaction is greatest for short periods of initial hydration . This appears to imply that the degree of crystallization of C_3AH_6 improves with age while its reactivity diminishes in consequence ..Carbonation with CO_2 increases strength. The authors present regression equations relating strength to treatment temperature and allowing a calculation of strength changes when carbonation takes places. Partial substitution of the sand used in the mortars studied by limestone also increases strength. Both these observations are in agreement with a number of other authors *P.Soukatchoff* reports (46) tests on durability of 1/2 cement sand mortars exposed to pure agressive mountain water (free CO_2 content ,13-15 mg/l).Exposure was over 15 years with an ambient temperature of 0-10° .Portland cement,Portland slag cement ,and aluminous cement were compared. A W/C ratio of 0.45 was used ,which is higher than normally recommended for aluminous cement in corrosive environment 0.40 or 0.35 is generally preferred .Despite this ,the aluminous cement was little attacked while the other cements were considerably corroded. A reference sample of aluminous cement/sand mortar stored in normal water at 20° was virtually fully converted with a porosity of 16.5% . The mortar

in the aggressive water showed a porosity of 18.2 % with carbonation and no evidence of conversion .Two papers by *R.D. Blinkinsop et al* (47) deal with the reactions in aqqueous solution between both synthetic C_3AH_6 and the hydration products of aluminous cement ,and alkali carbonates or water containing CO_2. In the first paper,lithium,sodium,potassium,and ammonium carbonate solutions were shaken with synthetic C_3AH_6 and with material obtained from old, substan tially converted aluminous cement concrete.The reac tion with the carbonates begins rapidly in all cases and is accelerated by increasing temperature. Calcium carbonate and alkali aluminates are formed. $CaCO_3$ pre cipitates within minutes. The other reaction product is alkali aluminate hydrate. When CO_2 is freely available they are decomposed to alumina hydrates and alkali carbonate is regenerated. The alumina hydrate precipitates slowly and this ,in conjunction with the $CaCO_3$ is postulated to form a protective layer on C_3AH_6. reactant creating a diffusion controlled system in which reaction rate is progressively diminished.The effect is more pronouced in converted cement paste which contains hydrated calcium alumino ferrite as well as C_3AH_3.Decomposition of the alumino ferrite could lead to early precipitation of iron hydroxide gel thus strengthening the diffusion barrier. There is evidence that reaction in the of CO_2 does not go to completion.This is attributed to the much larger effec tive ionic radius of solvated lithium ions and their cor responding lower mobility. In the second paper cylin ders of neat cement Fondu paste hydrated at 20° and at 40° were stored in Na_2CO_3 and Li_2CO_3 solutions.Depth of penetration was found to be proportional to time of immersion ,concentration of carbonate and permeabi lity (determined by the W/C ratio and the degree of conversion of cylinders)..reaction was much slower with lithium than with sodium and the surface skin formed by precipitation of reaction products was much harder.Storing the cylinders in water containing CO_2 also produced carbonation of the paste but in the absen ce of alkali carbonates,calcium bicarbonate can be for med first and precipitation of calcium carbonate is delayed .Also the alumina hydrates formed by hydra tion of the cement can dissolve and will diffuse out of the paste microstructure before again to solid precipi tates in the storage vessel .The diffusion barriers to continued reaction are significantly reduced. It is interesting to note in connection with these two papers that experimental evidence exists showing a cri tical level of W/C ratio (hence porosity and permeabi lity) in aluminous cement pastes below which carbo nation reactions redu ced to very low values (unpubli shed work)

$CaCO_3$: Using isothermal calorimetry, conductivity measurement, XRD and SEM , *A.Negro et al*(48) have stu died the effect of various powdered CaCO3 materials on the hydration of synthetic CA .The time taken to reach the maximum in the main exothermic hydration peak de creases as the proportion of $CaCO_3$ is increa sed from 0 to 50% by weigth ,and hydration is carried out at 21 °c. The extent of the effect varies according to the type of carbonate employed .Whenever carbonate is present $C_4A_{11}H_2O$ is formed as well as CAH_{10} ,and since only one hydration peak is observed even with substœchiometric additions it is concluded that calcium carbo aluminate hydrate acts as a precipitator of calcium aluminate hydrate.Initial attempts to con firm this hypothesis by electron microprobe analysis of deposits formed on the surface of calcite crystals suspended in a solution in contact with excess CA have not been successful and further studies are in progress. In conjunction with the studies by *A.Negro et al* , *F.Indelicato* has investigated the creep and elasticity of aluminous cement concretes made from calcareous and siliceous aggregates (9).His studies were carried out at 20° for ages up to 250 days .The mechanical properties are distinctly improved by the use of calcareous aggregates.In a complementary study of aluminous cement - limestone aggregate interac tions reported at the 1980 international Congress of cement (9). *A.Negro et al* further support the use of this type of cement to improve the durabitity of this type of aluminous cement concrete in load bearing and corrosion resistant applications.

A.Bachiorinni et al(49) have also published a paper dealing specifically with the SEM study of aluminous cement hydration in the presence of siliceous and of calcareous aggregates.With limestone both normal cal cium aluminate hydrates and calcium carboaluminate hydrate are formed and porosity gradually diminishes with ageing as hydration progresses. Maximum pore dia meters of 500 µm at 28 days diminish to a few 10'S of microns and open pores are gradually eliminated. These effects are obviously favourable to concrete perfor mance. In the presence of siliceous aggregates total porosity does not change markedly with age although average pore diameter appear to increase. Crack propa gation concentrates at the cement aggregate interface whereas transgranular cracking occurs even at 28 days with limestone and after 3 months aggregate and paste become virtually indistinguishable.*A.Bachiorinni et a*(49) have extended the study of the interaction between aluminous cement :carbonate mixtures to include $MgCO_3$. At room temperature magnesium carbo nate forms much less carcoaluminate hydrate than cal cium carbonate.At higher temperatures ,40° the reac tion proceeds rapidly producing $C_4A\,CO_2\,11H_2O$ preci

pitate with virtually no Mg incorporated.In an investiga tion of the formation of monocarboaluminate hydrate *J.Grandet et al* (50) find that the reaction rate increases with W/C cement ratio.Dissolution of $CaCO_3$ is slow and ionic mobility in the liquid phase is low,so that the reaction product is confined to the interfacial zone. C_4A $1/2CO_2$ $12H_2O$ forms first rapidly and is then converted more slowly to C_4A CO_2 $11H_2O$ .The interfacial reaction increase the surface roughness of the grains thus enhancing the strength of the cement grain bound.Mention may also be made here of a study by *A.Bonin et al*(11).The authors examined the micro structure and mechanical properties of aluminous cement bonded to an angular calcium aluminate aggre gate or to smooth silica grains.The interfacial region of lower density between cement and silica persisted to long ages and fracture surfaces showed cracking occurred in the interface. By contrast the calcium alu minate aggregate developed high strength very rapidly with extensive intragranular fracture the interface again became indistinguished after short hydration times.Clearly both mechanical and chemical factors contribute significantly to the mechanical properties of concrete. *C. Fentiman* (51) using XRD and strength measurements to compare the behavior of aluminous cement (Fondu) mortars made from silica sand, limes tone and mixture of the two.Curing below 25° led to the formation of CAH_{10} in all cases which converted to C_3AH_6 and AH_3 when heated ,with the expected strength reduction .Curing above 25° led to the increa sing formation of $C_4ACO_2 11H_2O$ in the presence of limestone up to about 40°c ,beyond which C_3AH_6 gra dually became the dominant hydrate .After 24 hours curing in the neighborhood of 40° the main hydrate present in the absence of carbonate is C_3AH_6 while in the presence of carbonate it is $C_4A.CO_2.112H_2O$ .This hydrate was stable for up to 7 days it is unfortunate that the authors meassurement do not extend longer ages .Thus while it is clear that the incorporation of limeston in aluminous cements does not prevent con version the long term stability of a cement hydrated directly to monocarboaluminate remains in question. *H.G.Midgley*(52) has studied the hydration of Fondu pas tes mixed with pure calcium carbonate powder ,and the compressive strengths obtained as a function of curing temperature and time .Curing temperatures from 20° to 80° were used under water with a W/C ratio of 0.27. Hydrate development was followed by DTA .At 20° a 7:3 mix of cement and carbonate showed initial for mation of CAH_{10} then a reduction in its rate of forma tion as carbo aluminate began to appear.Both phases continued to develop beyond 24 hours reaching stable levels after 7 days. No C_2AH_8 was detected .At 50° carboaluminate appeared within 2 hours and developed up to 1 day .After 10 days the amount of carboalumi nate had not changed significantly.At 60°more carbo aluminate was present after 2 hours but was not fur ther increased up to 10 days when the amount present was substantially less than for curing at 50° and 20° at 65 to 70° carbo aluminate was present beyond 6 hours. At 50° and above C_3AH_6 and gibbsite replace CAH_{10} .from this it is concluded that carbo aluminate is thermodynamically unstable above about 60°.

Strength measurement were confined to curing 8:2 cement carbonate pastes at 20°c and 50°C.Neat cement (no carbonate additions) was also tested .Cubes were tested at ages from 1 to 90 days.At both temperatures and all ages the carbonate additions resulted in lower strengths than the neat paste alone.After 1 day at 20° carbonate addition caused a 10% reduction in strength which is less than migth be expected from the increa sed W/C ratio (the same W/C ratio was used in both cases so that the W/C ratios were 0.27 for the neat paste and 0.34 when the carbonate was added). At 50°C after 1 day the carbonate mix was about 35% lower in strength.After 90 days strengths were lower at 50° than at 20° C due to conversion while the presence of carbonate caused a 25 to 35 % lower strength than in absence .These differences could well be explained by W/C ratio differences. Furthermore if strength changes reported by Midgley are compared with the nature and amounts of the different hydrates present there is no evidence for any strength enhancement from carboalu minate formation even making large allowance for the W/C ratio effect.The most dramatic comparison is pro vided by the data for 7 days curing at 50° as shown in table 1.

Hydrate content and comparative strengths of aluminous cement pastes with and without $CaCO_3$ additions

(*interpolated from graphs published by Midgley* (52)

7 days hydration under water at 50°

cement %	100	80
CaCO3 %	nil	20
Water %	27	27
CAH10 %	16	1
C4ACO2.12 H2O %	nil	16
C3AH6 %	10	9
AH3%	8	13
CCS Mpa	158.6	40.7

TABLE 1

Chemical additions: A study of acceleration and retardation of aluminous cement hydration at room temperature ,with particular focus on lithium salts and citric acid is reported by *S.A Rodger et al* (53) .Experimental techniques were XRD ,calorimetry and chemical analysis of the solution phase ,with Lafarge Fondu Cement. In the presence of lithium ions supersaturation is moved from the CAH_{10} field of the metastable C-A-H diagram to the C_2AH_8 field. However as C_2AH_8 begins to precipitate more anhydrous cement ,(CA) dissolves and solution chemistry moves back to supersaturation.The authors conclude that the acceleration effect of lithium is due to the rapid formation of lithium acetate acting as nucleation sites for hydrate precipitation, or to the intrinsically homogeneous nucleation of C_2AH_8 compared to CAH_{10}.The former explaination is preferred.The retarding effect of citric acid is difficult to explain.The experimental results show no evidence of inhibition of hydrate nucleation nor of absorption on the cement grains impeding dissolution. It is suggested that initially the acid complexes Ca ions in solution causing precipitation of alumina gel and that subsequently it is precipitated with the calcium aluminate hydrates ,again in an amorphous form which coats the cement particles and and slows down their passage into solution.An other study of the effect of chemical additions on the setting time of Fondu is by *B.R. Currell et al* (54) .Neat pastes were used at 18°C gauged with water in which the chemicals had been previously dissolved .Set was measured with a cone penetrometer and heat evolution followed by calorimetry. Conductimetry and DTA were also employed. Taking the CA content of the cement as 55% it was shown that set occurs most rapidly at a W/CA ratio by weigth of unity.In subsequent experiments a ratio of 0.5was maintained.The effects of a variety of cations and anions were examined .These affected the rates of the reactions leading to heat evolution ,hydrate precipitation and set. Overall the effects may be summarized as follows: Li<< Na < no additives < K < Ca < NH4 < Sr

OH< no additives <Cl < NO3 < Br < acetate

acceleration **retardation**

As has been noted many times ,the effect of Li is far greater than for any otheer cation. A further observation from this work is that there is an optimum concentration of Li which causes the fastest set ,the value depending on the nature of the associated anion. The mechanism of acceleration is taken to be bringing together of OH groups bonded to the solvated Al ions by interaction with cations leading to the formation of OXO bridges with the elimination of water.This condensation reaction then precipitates CAH_{10} .Of cations examined Li is the only one which is tetrahedrally coordinated and this would facilitate its role in the formation of OXO bridges. By contrast ,anion penetration (exept OH-) can replace -OH groups coordinated to Al thus preventing bridge formation.When sufficient cement has dissolved to use up the anions in solution ,hydrate formation and set can take place .Thus the retarding effect of the anions would be proportional to the amount added as is generally observed. *S.Fujimoto et al* have reviewed the rheology of aluminous cement -refractory oxide mixtures controlled by the use of defloculating agents (55) In the absence of deflocu lents Ca^{2+} and Al^{3+} dissolve from the cement. producing a floculated system in which the cement is poorly dispersed and thus inefficiently used .Defloculents suchas salts of phosporic acid delay dissolution of Ca^{2+} favouring dispersion of cement and allowing good workability for installation.Later dissolution of cement becomes dominant leading to set and strength development .

Different phosphates show different levels of effectiveness.The influence of organic additives on CA/CA_2 refractory cement concretes has also been studied by *I.Teoreanu et al* (56) ,who demonstrate the retarding and defloculating effects which lead to better cement distribution and thus improved properties at lower cement content. These authors also measured the degree of hydration of the cement and the BET surface area of the hydrated pastes which was doubled by the chemical addition in the most favourable case.This did not affect CA_2 hydration but CA hydration was decreased by about 10% The most effective additive was a naphtalene -formaldehyde.The hydration of calcium aluminates in aqueous phosphoric acid solutions at 35° has been studied (57) using SEM XRD and IR spectroscopy.Phosphoric acid behaves as a retarder and prevents all reaction above a certain phosphate /aluminate limit which is different and characteristic for each type of aluminate .This appears to be due to absorption on the anhydrous grains of phosphate ions acting as a barrier to water.A further publication concerning the effect of chemical admixtures is given by *F.Massaza et al* (58). These authors compare the action of lignosulphonate with sulphonate formaldehyde superplasticisers on C_4AH_{13} and C_3AH_6 .Both are absorbed on these hydrates from lime water solutions but only C_4AH_{13} when dissolved in dimethyl sulphoxide.The absorption isotherms for the superplasticisers are different from the lignosulphonate reflecting their very different molecular structures.Zeta potential of the suspended hydrates is reduced to constant negative values by absorption while viscosity apparently passes through a maximum as admixture concentra

tion is increased.This effect is attributed to a competi tion between repulsive ionic forces and bridging bet ween the suspended solids.A paper by *H.A. Van straten et al*(59) although not directly concerning calcium alu minates,is mentioned for its bearing on hydration che mistry.These authors investigated the effect of Li ,Na and K ions on precipitation from supersaturated alumi nate solutions.In the absence of Li an amorphous preci pitate first forms followed by pseudo boehmite and ultimately bayerite.In the presence of Li ,bayerite pre cipitates preferentially and rapidly.At low supersatu ration and high Li/Al ratios in solution ,lithium alumi nate is detected.

Techniques: *M.Murat* has very extensively and usefully reviewed the published data available from the thermo analytical characterisation of both calcium aluminate hydrates and those containing sulfate ,carbonate and chloride (9) DTA is a particularly valuable technique. The clearest results are obtained if allowance is made for the effect of sample size on peak temperature ,as recommended by Midgley (60) The interpretation of thermograms remains difficult when many different hydrates are present simultaneously due to local variations in the water vapour pressure in equilibrium with the sample. *A.B. Afshar et al* have used measure ments of electrical resistivity ,dielectric constant and heat evolution to study the hydration of aluminous cement/portland mixes,(61) .Once again Lafarge Fondu Cement was used and these authors report its CA content as 18%. Dielectric constant peaks after 40 minutes of hydration at room temperature while resis tivity is at a minimum.The subsequent decrease in die lectric constant is considered to be due to alumina gel formation while resistivity increase reflects ionic concentrations in solution. After a dormant period dielectric constant again increases as the gel coating is disrupted increasing surface polarizability ,while solution concentrations change little .A second peak in dielectric constant coincides with maximum tempera ture rise which is normally associated with hydrate precipitation.In the case of aluminous cement/portland cement mixtures the effects are greatly accelerated and it is proposed that the techniques described could be used to control formulations to a desired rate of set. I.R detection of calcium aluminate hydrates in samples which had also been examined by DTA ,shows that IR is a valid alternative method for estimating the degree of conversion in samples of aluminous cement concrete.In reporting his work *J.Bensted*(62) points out that the technique offers a semi quantita tive analysis of conversion as low medium of high. *A.Bachiorrini et al* have studied various techniques for arresting the hydration of aluminous cement ,aiming at maximum reproductibility. Washing in ethyl alcohol and rinsing with an alcohol /ether mixture followed by drying is recommended (63) .This work is confined to the pre-setting period, and the drying technique was not found to be critical .For studies of more advanced hydration this would clearly not be the case. The use of heat evolution measurement as an alternative to pene trometry for determining initial set is reported by *C.H. Fentiman et al*(64) .For normal setting the proportio nality constant is unity. False set is not accompanied by heat evolution so that practical use of this simple technique is a reliable method of determining demoul ding times.Restriction of penetrometer tests to fine ,fairly cement rich mortars does not apply to the heat evolution test.

SOME APPLICATIONS:

Many publications and patents have continued to appear representating widespread and diversifying uses of calcium aluminates.Only few are reviewed here. Long term tests of glass fibre reinforced cement show the distinct advantage of the lower alkalinity of aluminous compared to portland cements. Macro defect free cements represent an emerging potential for which aluminous cements appear to be the preferred material .The specific corrosion resistant advantages of aluminous cements are reconfirmed .One paper ref lects the growing interest in rapid setting mixtures of Portland and aluminous cements.Other papers discuss the use of chemical additions to enhance the performan ce of aluminous cement in refractory concrete. Research on refractory applications -a major indus trial use of aluminous cements could benefit more from the international Congress on the the chemistry of Cement than has been the case hitherto.

A.J. Majumdar et al report the results of a 10 years test of the mechanical properties of glass fiber reinforced Lafarge Fondu cement pastes (65) .Storage conditions were in air and under water at 18 to 20° C and outdoor exposure.Dry storage at 35° and wet sto rage at 25 to 60° C was also used .With alkali resis tant glass fibre ,MOR and impact resistance were inc reased compared to the unreinforced matrix and this improvement was maintained when stored in air at 20°C and 40%RH .Stored under water or outdoors ,the initial improvement was substantially reduced after 10 years but remained considerably better than when OPC was used.Reinforcement with E-glass is also effec tive at early ages but in wet storage deterioration is greater and more rapid than with alkali resistant fibres .the decrease in strengths can be related to con version of the cement hydrates and corrosion of the fibres by hydroxyl ions. The better performance of aluminous cement compared to Portland cement may be attributed to the higher ph developed in the latter case .The authors suggest that the reduction in failure

strength due to conversion of calcium aluminate hydra tes is of the order of 15 to 20%. Failure strains at 10 years under water at 20° were also higher in the alumi nous cement composites and was no evidence of fibre corrosion in the fracture surfaces. *J.D. Birchall et a.* (15/122:) have described the exceptional properties of aluminous cements pastes specially processed to eliminate large pores (called MDF macro defect free cement) - see the chapter "very high strength cement". *M.Balsevics et al*(12) report the development of two rapid setting ,rapid hardening cements based on mixtures of portland and aluminous cement , -see the chapter "fast setting and hardening cement ". *H.G.Midgley* has published recommendations for con crete quality required for sulphated soils (13) In the most severe conditions (SO_3 in excess of 2.0%) alumi nous cement concrete with very high cement content and low W/C ratio is the preferred type .Aluminous cement concretes are also resistant to dilute mineral acids which attack Portland cement .These recommen dations are based of both laboratory and field case studies. Three papers from Brazil describe various aspect of calcium aluminate cement technology Bauxites used in cement manufacture and the chemical composition of a range of cements from a number of countries are compared,and manufacturing techniques used in Brazil are described (66).The effect of cement content on the density ,porosity ,firing shrinkage and compressive strength of concretes made from electro fused alumina and a 60% Al_2O_3 cement is reported in detail . Cement contents ranging from 15% to 25% are recommended.The third paper by *G.W.Cortes et al*(66) reports the effects of various chemical additions to the ement on the water demand, density and strength of a 60% Al_2O_3 cement brown fused alumina concrete after curing,drying and firing.It is concluded that the accelerators,retarders,and plasticisers studied tend to reduce the concrete compressive strengths particular ly in the critical refractories temperature range where hydraulic bonding is little advanced.These papers are not primarily concerned with cement chemistry.The use of chemicaladmixtures to modify the properties of refractory concretes containing aluminous cement is also discussed by *D.R.Lankard et al*(67).Low interme diate and high purity cements were used with calcined fire clay and with tabular alumina for the high purity cement. Sulphonate formaldehyde condensates ,hydroxy carboxylic acids ,lignosulphonate and sodium citrate were used as water reducers or plasticisers , these materials also exhibiting a set retardation.Wood and vinsol resins were employed as air entrainers.The plasticisers ,by reducing W/C ratio ,improving workability and extending working time of low and medium duty concretes considerably improved performance without affecting refractoriness.The same admixtures had virtually no effect on the high purity material material which is probably due to the fact that the high purity cement itself already contains chemical additives.The resins were effective in all concrete to improve dryout properties but strengths were decreased.The nature of the chemical reactions between admixtures and cement is not discussed. Mention should be made of a recent growing interest in a non cementitious application of calcium aluminates .Premelted compositions approximating to $C_{12}A_7$ and with low levels of iron oxides and silica are seeing increasing use for clean steel practices as cover slag and for ladle desulphurization of steel. These materials are molten at steel temperatures .B.Ozturk et al (68) have studied the high temperature S partition coefficient between Al killed and CaS-$CaO-Al_2O_3$ melts .CaS solubility in the slag increases with temperature and with the CaO/Al_2O_3 ratio.

A broad summary of application of calcium aluminate cements has recently been prepared (69)

3)EXPANSIVE CEMENTS

INTRODUCTION

The chemistry of expansive cements was comprehensi vely discussed on the congresses in Moscow and in Paris (1e/1f) . Recently appeared a further ,systematic review of these problems (8).In this connection we will present only the latest attainments and give the newest literature,referring the interested to bibliogra phic surveys, given in these reviews. In order to present the cements manufactured in industrial scale ,their composition is given in table 2.

As can be inferred from this review,the cements being based on the expansive reaction of ettringite forma tion show an emphatic predominance. However, the cements utilizing the hydration of CaO are worthy of notice,all the more so as recently numerous patents for these cements have been appeared (70a). Also MgO excites larger and larger interest (70 b). A mixture of dolomitic and a siliceous material fired at 1300° -1900° has been likewise suggested (71). Finally the CA_2 phase as an expansive addition is proposed (72).

Also other non conventional sources of alumina are searched.(73/74)

In the period elapsed since the Parisian Congress the expansion mechanism and the factors influencing the extent of ettringite expansion continued to be the main object of notice. Also new field of application of expan sive cements have been recorded.

TABLE 2

TYPE of CEMENT	TYPE of MATRIX	ADDITIONS		
		alumina phase	sulphates phases	lime
M *SSSR**	Portland cement	aluminous cement	Gypsum	
M *SSSR*	Portland cement	alumina slag	Gypsum	lime
K *USA*	Portland cement	$C_4A_3\bar{S}$ **	Gypsum or Gypsum + anhydrite	
K *Japan*	Portland cement	$C_4A_3\bar{S}$	Gypsum or Gypsum + anhydrite	
S *USA*	Portland cement (with high % C_3A)		Gypsum	
AEC*** *SSSR*	Aluminous cement	$C_4A_3H_{13}$	Gypsum	
AEC *SSSR*	Aluminous cement		Gypsum	
AEC **** *China*	Aluminous cement		Gypsum	
AEC *SSSR Bulgaria*	Portland cement	alunite	Gypsum	
AEC *SSSR*	Portland cement	$Al_2(SO_4)_3$		
AEC *Japan*	Portland cement CaO inclusions C_3S/ or $CaSO_4$ matrix			lime
The components are mixed during cement grinding				

* Expansive cements in SSSR are divided into 3 grades 20/40/60 because the expansive potential generated in the cements is about 20/40/60 Kg/cm ^{2} respectively

**Expansive clinker containing C_4A_3S ,clinker phases ,free lime and anhydrite

*** AEC = Aluminous expansive cement

**** very similar to the old Lafarge patent (see reference 8)

MECHANISM OF EXPANSION

Most often two hypotheses:crystallisation pressure and water adsorption continue to be mentioned.

In the last period .,several works supporting the occurence of expansion as a result of crystallisation pressure appeared .*K. Ogawa et al* (75) found ,basing on systematic microstructural observation ,that during the early hydration, irregularly located ettringite crystals were produced around the $C_4A_3\bar{S}$ grains .At the later stage ,however ,the ettringite crystals were arranged radially around the $C_4A_3\bar{S}$ particles.Moreover, the reaction zone appeared to be more compact than the same zone at the early stage .This change from irregularly oriented to radially arranged ettringite is considered by the authors to be the first important step in causing the expansion. These results support the cristallisation hypothesis.

V. Alunno-Rossetti et al (76) investigated the com pacts composed of a mix of C_4ASH_{12} and CS :they explain the expansion of these compacts as resulting from simultaneous action of the crystallisation pres sure ,water adsorption and interparticle repulsion due to a high zeta potential.Around the monohydrate grains a felt- like layer of ettringite crystals is formed ,the thickness of which increases.They fill free spaces and start to jostle causing the expansion to occur.This exp lanation is identical with the model proposed previous ly by *A. Bentur et al* (77) and by *Chatterji et al* (78) The saturation of the liquid phase in calcium ions ,due to CH addition increases considerably the zeta poten tial .This results in the presence of lime in a new expansion mechanism,based on a simultaneous develop ment of the cristallisation pressure and water adsorp tion with the formation of a diffuse ionic layer around the particles and with the generation of repulsion for ces due to a fairly high zeta potential value. A high value of zeta potential was found also by *S.Chen et a.* (79) .This explain the advantageous effect of lime on the increase of expansion, observed by other authors. (80) .

The expansion increase also with the amount of ettringite formed ,which was recently supported by *Negro et al*(81) .*P.K.Mehta* (82) confirmed ,once more that colloidal ettringite gives a greater expansion with which other authors agree also (*Zhao Yu Pin* (1f))

Wang Shanba et al (17) investigating various mix tures in which the ettringite is formed ,arrived at the conclusion that the cristazllisation presssure related to the growth of ettringite crystals is decisive for this process.

Ettringite formed either in saturated or unsaturated CaO solution reveals this expansive action .A model to explain the mechanism and the kinetics of expansion process in K- type expansive cements has been propo sed by *M.D.Cohen* (83) .The model is able to explain ,why the S-type expansive cements are less effective than the K-type ones. *S.Viti et al*(84) also elaborated the model of expansion of C_3A mixtures with gypsum and quartz, allowing the anticipation of the dimensio nal changes of samples during the hydration process.

Clastres et al (9) report very interesting results. They found a very close correlation between the expansion of expansive cement pastes and the inten- sity of peak of ettringite on the DTA curves.On the other hand the expansion occurs when the total amount of calcium sulfate is consumed. No traces of monosul

fate was detected. In the authors opinion these data support the Mehta expansion mechanism based on changing of water content of ettringite.

EXPENSION INFLUENCING FACTORS

M.Collepardi (85) investigated the effect of superplasticizers on the behavior of expansive cements taking into account that they allow lowering the W/C ratio they are desirable as they give the possibility of reducing the addition of the expansive component to cement

Cohen et al (86) studied the effect of the fineness of $C_4A_3\bar{S}$ .They stated in agreement with expectation ,that an increase in fineness accelarates the expansion process ,though an excessive fineness reduces its extent the extent of expansion is inversely proportional to the fineness. (figure 1)

It seems to be necessary to add ,that an important effect will be exerted by the matrix ,namely by its strength growth rate .

The problem of the fineness was also studied by *Kuznetsova et a* (87) They found that the most important factor was the content of the grain below 20 microns.In an other work ,Kuznetsova also examined the influence of the microstructure of the clinker ,which seems to be important.

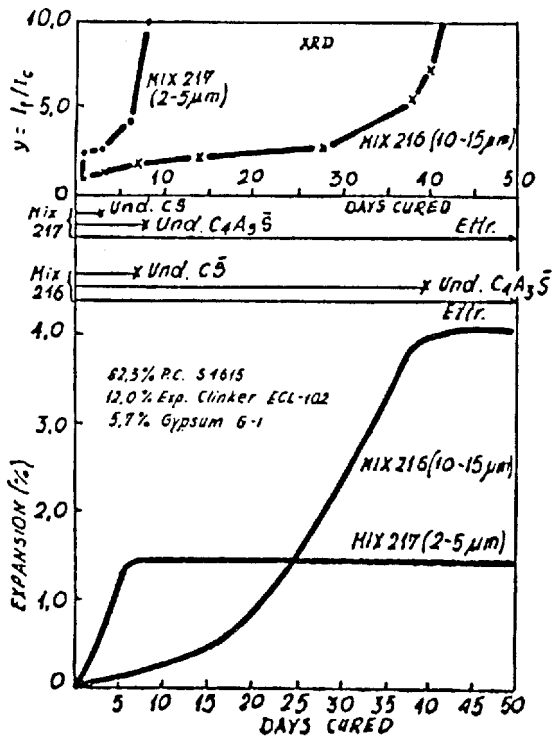

FIGURE 1

A. Negro et al (81) investigated the effect of temperature and ascertained that in the range from 20° to 40° the expansion increases with temperature.

On the other hand in the range from 50° to 60° the increase of expansion is more rapid ,but it stabilizes at a lower level .They explain this observation with the increase in the size of ettringite crystals.

The effect of temperature was also studied by *K.Togawa et al* (88) .Higher curing temperatures increase the rate of expansion ,but the ultimate expansion at 14 days is greatest for curing at 10° or 20°.*K Ogawa et al* (89) followed the effect of CaO ,NaOH and NaCl .They found that the absence of CaO modifies both the size and the morphology of ettringite crystals ,reducing the expansion. Their investigations showed a great importance of the microstructure.'at the present time of Nacl an other expansion mechanism takes place ,and the stability of ettringite becomes lowered .Probably a part of SO_4 ions in its structure is substituted by Cl ,modifying the morphology of ettringite ,which forms thick ,stubby crystals instead of usual elongated ones.

SPECIAL APPLICATION OF EXPANSIVE CEMENTS

Apart from traditional applications of portland cements ,the use of which considerably developed since the Paris congress ,series of non typical directions of utilization of expansive cement have appeared.

Already at the Paris congress ,various special applications were mentioned. *C.H. Dowding et al* (90) studied the processs of rock comminution with cement of high expansivity . Many recent work concerning a rather special application of expansive cement and concrete appeared in SSSR. An expansive cement with the addition of high calcium fly ash for water wells was investigated.(91) . *A.N. Savitskii et a.* (92) proposes an expansive concrete for underground storage of liquified methane and ethylene.

V. Timashev et al (93) demonstrated the purpose fullness of expansive cement utilization for manufacturing asbestos cements board , which allow considerably better products to be obtained .

L.K. Upolovnikova et al (94) proposed a new type of expansive polymer cement ,which can be used as thightening products in construction works.

Also *B.I. Smirnov et al.* (95) elaborated the utilisation of expansive cement for manufacturing of sealing insulation linings . *Y.N. Titov et al* (96) presented their experiences in constructing and exploitation of concrete pavements used in airports . *V.V. Mikhajlov et al* (97) report the use of expansive cements at low temperatures with the addition of sodium nitrite.

4)FAST SETTING and FAST HARDENING CEMENT
HIGH EARLY STRENGTHS CEMENTS

INTRODUCTION

The conventional cements do not give an answer to the specific uses such as: __ rapid demolding of molded pieces (a) __ highway repair during the traffic (b) (rapid repair of concrete paving) __ sealling of sanitary ,electrical,woodworking, devices .(c) __ entrapment of spring water in cellar, underground ...(d) __ cement rendering in water ,instantaneous space filling (caulking of boats) (d) __ positionning of stops, temporary marks or mechanical supports (d)

These applications do not require exactly the same properties of the binder and , to satisfy them the cement must have :

(a) a normal setting time (60/90 mns), high early strengths and normal long term strengths for structural pieces.

(b) a setting time of 15 mns and compressive strengths of 15 mPa at 45 mns (these figures are an order of magnitude)

(c) a short setting time (8 to 15 mns) and high strengths

(d) a very short setting time (< 3mns) but no specially high strengths

All of these characteristics concerns the hydraulic activity of the cements and can be obtained for example:

1) from conventionnal cements (OPC-Ordinary Portland Cement) or industrial special cements (HAC-High Alumina Cement)

11) by modification of the phase percentages

12) increasing the fineness or a better particles size distribution

13) addition of admixtures

2)From mixtures of cements such as OPC and HAC

21) binary mixture

22) binary mixture and small addition of inorganic or organic products

23)ternary or multicomponents mixtures (OPC/GYPSUM/HAC .....)

3)from new system of binders such as

31)chemical bound cements (magnesium phosphates)

32) binders based on, $C_4A_3\overline{S}$ or $C_{11}A_7CaX_2$

In the case of industrial cements (case N°1), the improvement of one property has, most of the time , a deleterious consequence on the other properties and constrained properties such as workability, durability, long term strengths ,reliabitity of the properties or economic conditions limit this kind of solutions.These problems as well as the proposed solutions have been discussed in the chapter "fast setting cement " (8) and the chemical cements will be discussed in a special paragraph, .The following chapter describes the new tendencies that have occured since 1980 to decrease the setting time and increase high early strengths

CEMENTS BASED ON A MIXTURE OF ALUMINOUS AND PORTLAND CEMENT

The main objective of the studies concerning this kind of cement is the control of the setting time by addition of calcium components (0.5 /5% for 6mns of setting time) in the manufacture of molded products (98) ,or addition of calcium anhydride ,sodium sulfate or citric acid _ *M.Balsevics et al*(12) , *Y. Efes*(99)_

The ternary mixture OPC/HAC/GYPSUM allows early strengths by formation of ettringite (100/101) .In other cases more complex systems with resins (PVA) and sodium salts allow a settting time of 2 mns used to fill holes and cracks (102) Self-levelling cements (103) have been obtained by addition of pozzolans ,urea ,and caseine. Aluminous cements ,based on CA,can be replaced by alumino-belites cements (104) or $C_{12}A_7$ or $C_{11}A_7CaX_2$ (X being a halogen (105) : it is possible to reinforce a cement based on OPC +active silica + $C_{11}A_7CaX_2$ with glass fibres (106).

Portland cement can be replaced by a JET SET CEMENT which bring C_3A instead of CA (107). The coumpond $C_{11}A_7CaX_2$ can be used independently or with gypsum (108/109) and admixture (110).

CEMENTS BASED ON $C_4A_3\overline{S}$

First of all, this compound was used in the composition of expansive cements :later further researchs highlighted the property of this coumpond to form rapidly ettringite and thus to obtain high early strengths. The cements ,based on $C_4A_3\overline{S}$,C_2S and free lime are prepared by burning a raw material containing SO_3 /Al_2O_3 in a ratio of 1.3/1.9 .The strengths are 27 mPa at 3 hours and 59 mPa at 28 days _ *G.Sudoh et al*(1f)

A high early strength cement (15/24 mPa at 4hrs) ,based on $C_4A_3\overline{S}$,C_2S and CS (111a) is obtained by burning at 1200°/1300° a raw material of ratio SO_3/Al_2O_3 =0.4/1.7 moles and C/A =0.5 /1.2 moles.It can be used mixed with portland cement.The variation of setting time are due to the free lime ,according to the authors (111a) and are minimised in this case.

The cements ,based on $C_2S/C_4A_3\overline{S}$ (111 b) require less energy to be manufactured than OPC and give higher strengths (13 mPa at 2 hrs ,81 mPa at 28 days) (112)

During the process of clinkering $C_4A_3\bar{S}$ based cement ,care must be taken to prevent the $C\bar{S}$ decomposition to obtain a stable clinker and avoid the SO_3 volatilisa tion (113) .The strengths will depend on C_2S /$C_4A_3\bar{S}$ and free lime._ *I. Teoreanu et al*(12)

The addition of admixture (citric acid ,dextrose,) allows a regulation of the setting time at 20 mns with good compressive strengths (114) .High strength cements have been produced by firing bauxite, limes tone and chemical gypsum: they are based on $C_4A_3\bar{S}$ 31% C_4AF 33% C_2S 36% and provide 82 mPa strengths at 3 days .(115) The use of a mortar of cement ,based on $C_4A_3\bar{S}$ (43 %) C_2S (16%) $C\bar{S}$ (26 %) C_4AF (4%) , reinforced with glass fibres (5%) allows flexural strengths of 25 mPa at 24 hrs and good long term strengths (116) . By autoclaving ,belite cements containing 34.5% C_2S and 15.5 % $C_4A_3\bar{S}$ give 135.6 mPa compresssive strengths at 185° for 18 hrs. (117)

MECHANISM OF SETTING AND HARDENING :

Very few fundamental studies have been published on this topic-,but we may distinguish 3 types of process.

1)acceleration of the hydration kinetics of the cement phases by the action of fineness(118) or admixtures :in this cases the hydration products are the same as in conventional cement or slightly modified (morphology, C/S ..).

2)Setting and hardening by ettringite formation .It is known from the laboratory experiments that a clinker containing differents proportions of $C_4A_3\bar{S}$,CaO ,$C\bar{S}$, have a different behavior during the hydration (119)

The mechanism and speed of ettringite formation in presence of $SO_4^=$ or Ca^{++} ions is developed in the chapter devoted to expansive cements.The formation of hydrates (calcium aluminate, or silico aluminate) by simultaneous dissolution in defined proportions of specific ions and precipitation as been studied by *B. Cottin et al*(120)

5)VERY HIGH STRENGTH CEMENTS

INTRODUCTION

The properties of mortars and concrete depend on the rate of hydration reactions ,the microstructure and the morphologie of the hydrates ,the porosity of the pastes and its distribution (size and shape of the pores) in the hardened cement paste,the properties of the aggre gates,and quality of the bond between the paste and the aggregates.These parameters are functions of the chemical and mineralogical composition of the cement ,the fineness,the particle size distribution , the quali ty of the aggregate the proportion of cement ,water, aggregates and the method of mixing and curing .

The normal evolution of the products and the industrial techniques leads to a continuous increase of the com pressive strengths and often of the ratio flexural /com pressive strengths. In 1950 a concrete of 34 mPa was taken as high strength concrete: in 1960 a 42/52 mPa concrete was usual :In 1970 62 mPa concrete was produced .Presently ,a compressive strength of 70 mPa is considered as high although 110 mpa concrete have been industrially realised.

Independently of these improvments of the mechanical properties ,fundamental studies leads to the produc tion of materials based on cements ,with properties similar to these of plastics.A congress held in Boston in 1984 (15) highligths these new developments :two types of material can be separated:

— those using conventional hydraulic binders (types of OPC) and classical way of placing :these material are used for the construction industry

—those using a special process of shaping (hot pres sing, extrusion, autoclaving ..) and whose the applica tion is different from the construction industry : this sort of application is less developed than the other because they are in competition with of plastic ,or other materials..

HIGH STRENGTH CONCRETE

A review of the state of the art has been published by the committe A.C.I. in 1984 (14).the adopted definition is :"concrete having specified compressive strengths for design of 6000 psi (41 mPa) or greater , but ..... considerations shall not include concrete using exotic material or techniques i.e. polymer impregnated con- crete , epoxy concrete with artificial or heavy weight aggregates ".

The conditions of obtaining high strength materials are connected to the quality of materials (cements, admixtures,aggregates,fine filler,water,...) the process (weighing, mixing ,transport ,placing ,curing) and to the procedures of control of the products and the process.

The standard deviation is the main parameter to consider in the choice of cement (the variation compo sition must be less than 4 % for C_3S ,0.2% for SO_3 and 0.5 % for the loss of ignition : the fineness must be defined at less than 375 cm2/g. The rise of tempera ture in the concrete is an other important parameter which leads to the choice of the cement.As exemple in the square column (1.2 m of side) of THE WATER TOWER PLACE in Chicago ,the temperature rose from 24° to 66° for a concrete containing 500Kg /m2 of cement. The admixtures used , essentially intended to get a better workability (consequently the strengths increase by diminishing the water /cement ratio) ,a better control of the hydration and an increased durabi lity (air entraining agent):the recommended additives are lignosulfonates, carboxylates ,and condensats of melamines and sulfonic naphtalene.

The weight and the particle size distribution of the fine aggregates is determined more by its effect on the water demand than on the possibility of the maxi mum compaction .A sand with a finess modulus of 3 gives the best results as workability and compres sive strengths. The coarse aggregates must have a mini mum size of 9.5/12.7 mm and a maximum of 19/25.4 mm:they must be clean, angular, and crushed (100%), with a minimum of plates or long particles.

The concrete must contain 392/557 kg /m3 of cement and the water cement ratio can be 0.27/0.33. A 100 mPa concrete has been realised from a type 1 cement __ 500 kg /m3 of cement ,30 kg of fine silica ,1100Kg of coarse aggregates __,a water/cement ratio of 0.25__20 l/m3 of superplastisizer (based on sulfonic naphtalene) and 1.5/1.8 of retarding agent is added.

After placing ,a water curing is recommended because it allows the hydration reaction to occur at a controled moisture and temperature. Control tests are necessary most of the time because it is difficult to predict the properties of high strength concretes from the data used for the conventional concretes. The high strength concretes normally have an high percentage of cement, a low water cement ratio,an usual quantity of aggregates, admixtures, and inorganic addition: they find their economic advantages in the reduction of the size of the structural work and the weight of reinfor ced steel bars.

HIGH STRENGTH CEMENTS PASTES

introduction

The strength of hardened cement take their origin from:

__the interatomic strength ,existing inside the molecu es of hydrates :they depend on the nature ,composition of the hydrates ,and their quantity. (rate of the reaction)

__the interparticular strength between the hydrates or the interfacial strengths between hydrates or anhy drous grains.They depend on the size, morphology of the hydrated parti cles, on the way they are put together and consequently total porosity, the distribution of this porosity or the size of the large pores.

The ways of modification of the strength ,or the brit tleness of the materials are __ modifications of the nature and structure of the hydrates (autoclave, or organo-mineral bond)

__ reduction of the porosity or optimis ation of its distribution by different techniques such as mechanical treatment of the pastes by vibration or pressing ,or high pressure compaction or high shear mixing.

__ the use of dispersing or fluidifying agent to decrease the quantity of water

__ the impregnation by resins or sulfur

__the use of well defined granulometry powder

Although these methods have been initiated before 1980 ,they are presently being studied at the labo ratory level (morphology studies, ...) and developed industrially : among them, the autoclave techniques,the use of superplasticizers ,fume silica ,(D.S.P.) and the use of high shear mixing are the most important:

autoclave

This process involves the use of a temperature of 150°/250° and a water vapor pressure of 0.6 to 2 mPa The mixtures of cement, sand , lime and quartz form hydrates whose the structure cover a wide range from amorphous to well cristallised , alfa C_2SH ,tobermo rite,C_5S_6H , xonotlite C_6S_6H etc.. the high strengths seem to be associated to the formation of cristallised phases analogous to tobermorite with a fine porous structure.

The microstructure of the autoclaved cement pastes show the formation of a continuous lattice of dense particles, which participate to the strengths ,by their internal strengths ,but also by interparticular forces.

D.S.P. materials

The material called D.S.P. (densified system containing homogeneously arranged ultrafine particles) (121) is produced by mixing portland cement ,ultra fine silica (0.1 micron _ byproduct of ferro alloys industry) ,a superplasticizer and water ('W/C=0.12 to 0.22). The grains of cements during the hydration ,react with sili ca to form 'C'S'H ' of low C/S ratio and shell shape which gives the cohesion of the mass.The homogeneity of the material is obtained by means of the defloculent properties of the superplasticizers wich ,associated to an high energy mixing allows to reach a low ratio W/C and compressive strengths of 350/400 mPa.

Other additions such as propylene fiber ,or steel fiber ,increase the flexural strengths or the conductivity. A composite ,known commercially under the name of DASH 47 is produced by mixing in a planetary grinder, different sorts of stainless steel (53.5 %) OPC class H (24.3%), fine quartz(11.8),pure silica (33%) water (6.2%) and anti foaming plus superplastiscizer admix tures:this effect is probably due to the combination of portlandite to the amorphous silica to give well cris tallised silica.

MDF material

The MDF material (macrodefect free cement) (122 to 126)is obtained by high shear mixing a cement paste and a water soluble polymer. The MDF material can reach 100 mPa flexural strengths ;this effect is due to the the reduction of the porosity and the size of the largest pores.The strengths are predicted by the Griffith's equation which involves the surface energy the elastic modulus and the size of the defects.

In order to obtain these strengths ,it is necessary to have a W/C =0.12 ratio and thus to use an special equipment such as a rolling mill to make the paste and remove the largest defects.To help the paste formation it is also necessary to add polymers whose role is more important than simply a rheological aid . Two sys tems have been particularly studied — a high alumina cement and a polyvynilic alcohol acetate (PVA) hydro lysed at 79% or a portland cement with a polyacryla mide. In the first case PVA hydrolyses completly in basic media and the alumina ions Al(OH)- bond the poly mers chains :the material becomes rubbery and later more rigid by dehydration of polymer and formation of small quantity of amorphous hydrates.The mechanism of hardening between portland cement and polyacryla mide is similar to those of dental cements (ionomeric cements).the difference concerns the setting time which is increased in the case of MDF by the use of polyacrylamide instead of polyalkenoic acid.The special properties of these material find applications in the field of acoustic,cryogenic,protection(armour) or anti electro magnetic radiation screens

6)LOW ENERGY CEMENTS

INTRODUCTION

The production of cement at a minimum energy has certainly become the main objective of the cement producer since the oil crisis.The first solution in this way has been realised by a modification of the process

— change of wet to dry process, use of precalciner

— or by the use of second quality combustible (low grade fuel, tyres, ..).

The good results given by these solutions are now limited by the physico chemistry of the cement or by the local economic conditions..The production of the clinker of portland cement requires energy (1700 Kj/Kg of clinker) to decarbonate $CaCO_3$ and to reach the temperature of formation of C_3S.

In order to reduce the energy consumption it is thus necessary

1) to decrease the temperature of formation of C_3S

— this objective is reached by using mineralizers

2) and /or to diminish the quantity of calcite :this lead to a cement containing a large proportion of belite and little or no C_3S

To compensate the loss of reactivity (strengths) of this cement ,due to the low C_3S content several solutions have been proposed:

—increase the reactivity of the belite

—formation ,beside the belite of active phases : the role of alite in the increase of strengths is then pla- yed by ettringite developed during the first step of the hydration by the aluminate phases and the sulfates ions.(127)

MINERALISERS

The principle of adding to the raw material substances which facilitate the reaction of sintering in the rotary kiln has been known for a long time, but its indus trial application has been slowed down because of eco nomic problems.In spite of the decrease of the clinke ring temperature of 200° ,when we consider the heat recovered and the necessity of by passing the gas, the gain of energy is small (5%) and does not compensate the price of the mineralizer. (128) .The solutions have been to find mineralizers or mixture of mineralizers allowing not only a gain of energy but also an increase of the strengths of the cement :positive results have been reached by *G.K. Moir*(129)with a mixture of fluo rine and gypsum .

ALINITE CEMENTS

Calcium chloride acts as mineralizer by formation of intermediate compounds (Calcium chlorosilicates) (130 / 131)) .By addition of a larger quantity of calcium chloride ,a phase called alinite occurs at low temperature

$(C_{11}(SiO2_{0.75}Al_{0.25})_4 O_{18}Cl$ .Its low temperature of formation (1000° /1100°)and its capability of develo ping bond has lead to an industrial development of this product (10/132/133)

The chemical composition of alinite and specially the influence of MgO in its structure ,the conditions of its formation are still an unsolved problem.

.Several formula have been proposed (134)

$21\,CaO\,6SiO_2\,Al_2O_3CaCl_2$

$3(Ca0_{0.88}Mg0_{0.0065}CaCl2_{0.055})Si02_{0.885}Al203_{0.115}$

$3(Ca0_{0.875}Mg0_{0.007}CaCl2_{0.0055})Si02_{0.885}Al203_{0.115}$

$3(Ca0_{0.89}Mg0_{0.055}CaCL2_{0.055})(Si02_{0.91}AL203_{0.007}Fe203_{0.002}$

The presence of chloride ions in solution leads to advantages such as concreting in cold weather,but to disadvantages such as corroding the reinforced bars. Some tentatives has been tried to prevent the chloride ion release (addition of slag, alumina ...or increasing the sintering temperature to produce alite and alinite together) (135/136) .At this time from an industrial point of view,the presence of chloride ions in solution during the hydration of alinite cement or Cl- minerali zed cement , limits their development to very special use

BELITE CEMENTS

The reactivity of belite depends on the size of the cris tals,the impurities included ,and the polymorphic form of the belite.To increase this reactivity it is possible to stabilize the most hydraulic form of the belite or to create defect by thermal shock (cooling in air or water at more than 500°/mns). (137 to 141)

The Figure 2 (139) shows the influence of the cooling rate on the compressive strength at 28 days:

Some other authors claim to have obtained a reactive clinker without water quenching ,but only by control ling the raw material and the burning process.(142)

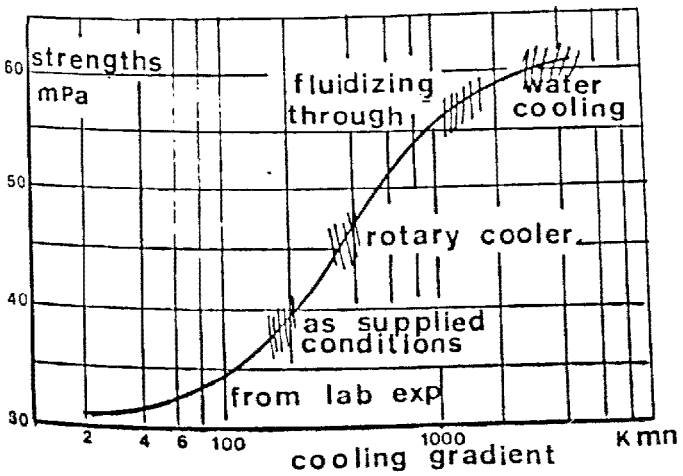

FIGURE 2

7)CHEMICALLY BOUND CEMENTS

MAGNESIA CEMENTS

The magnesium oxychloride cements,also known as Sorel cements are formed as a result of mixing mag nesium oxide powder with a solution of magnesium chloride. In this chapter we include also the cements formed with other salts such as sulfate.These cements have high early strength and are suitable for use with all kinds of aggregates (including glass fibers, asbes tos , wood,and expanded clays) in large quantities.

They find applications in building field :

__for industrial floor because of their elastic proper ties and their resistance to accumulate static charges (143/144)

__ insulation lightweight wall (145 to 148)

__ Wood cement board or interior building panel (149/ 150)

__decorative coating (because of their ressemblance to marble,they are used for rendering panel (151/152 /153)

__fire resistant panel (154 to 168)

and in many other fields such as sealent in salt and coal mines (169) ,metal coating molds (170), molded products (171/172) grinding wheels (173/174) or fil tration plates (for replacing asbestos in food and beve rage processing) (175), or as heat reflecting layer for metal halides vapoor lampe (176) or for immobilizing tritium containing waste water (177)

In spite of standart conditions of practice these cements have great disadvantages such as dimension nal instability and lack of resistance to atmo pheric agents (they are water soluble ,releasing corrosive solution)

In order to overcome these disadvantages research has been undertaken to develop a better understanding of the setting and hardening properties and to experiment with additives to improve their performance in the presence of water.

Studies of relative reaction rates shows that the phase called 5-1-8 e.g. $5\,Mg(OH)_2,MgCl_2,8\,H_2O$ cristallises more rapidly than the phase 3-1-8 e.g. ($3\,Mg(OH)_2,MgCl_2,8\,H_2O$) and that cements near 3-1-8 compositions react more rapidly with atmos pheric CO_2 to form chlorocarbonate phases (178).

The influence of sodium ion on the phases formation has been studied by potentiometric, coulometric and XRD analysis.The phase distribution relative to the ph of the solution and concentration of Cl^- and Mg^+ ions are defined by equilibrium diagram (179/180).The har dened cements reach their best strengths and stability when the phase 5-1-8 is the main final product. (181)

The setting time of the cement paste has been corre lated to the crystalline phases detected by XRD (182). The reaction appeared to proceed through 4 steps : __dissolution of MgO in MgCl2 solution ,__hydrate nucleation,__rapid precipitation of hydrates __ slow evolution to the equilibrium state .(183/184)
4 hydrates exist at 25 ° Mg(OH)2 ,5-1-8, 3-1-8, and $MgCl_2$,$6H_2O$.

The lack of water resistance of the cement is related to the presence of 5-1-8- phase the reactivity of MgO and its degree of burning are related to the setting time and to the strength (magnesite,calcined at 600/ 750° gives a normal setting time)(185/186)
The difficulty of mixing a powder with a corrosive liquid seems to have been solved by storage conditions (187)The powder Mg(OH)2/ MgCl2,6H2O/MgO is placed in sealed bag to be mixed with water when used .the setting time is 190/270 mns and the 28 days comp resive strength 36 mPa.
The addition of autoclaved phosphogypsum,dolomite ..increases the strength and shortens the setting time (188).the use of asbestos waste (189/190) or ascha rite byproducts allows the preparation of cheap mag nesia cements (191)
Several solutions have been proposed to improve the water resistance such as : __treating MgO by phosphoric acid (192)
__impregnating by molten sulfur or bitumen emulsion (193)
__addition of organic compound (194/195)
__addition of phosphorus containing fiber (196)
__special treatment (hydrothermal,thermal ,CO2 .)(197/198/199)
Most of these applications have been studied by the company SEKISUI chemical which has published more than 50 patents ,difficult to describe completly here because of the lack of spac

PHOSPHATE CEMENTS

The Phosphate Cements find applications in the refrac tory industry (phosphate bonded bricks,flame resistant coating) or in road construction (highway patching ,or repairs of preformed concrete products (200) or soil stabilizer (201).
The phosphate bond can be produced in different ways:
__a mixture of oxides Al_2O_3 ,Cr_2O_3, MgO ..... and phos phoric acid or aluminum phosphate $Al(H_2PO_4)$ (202 to 206)
A mortar containing a proportion of 5/12 of MgO and aluminum phosphate plus sand and gravel set in 10 mns with an high release of heat and a compressive stren gth of 18 mPa at 1 hour (207)
__a solution of ammonium polyphosphate $(NH_4)_2HPO_4$ mixed with MgO gives a setting time of 3 minutes and a compressive strength of 14 mPa at 1 hour :the cris talline phases NH_4MgPO_4 6 H_2O and $Mg_3(PO_4)_3$ $4H_2O$ have been detected. (208)
Commercial magnesia-phosphate cement consists of a powder of MgO, $NH_4H_2PO_4$,$Na_5P_3O_{10}$ and inert filler .It is mixed with water and after 2 minutes an exother mic reaction takes place leading to asetting after 10 /15 mns and hardening after 30/60 mns. The principal product of the reaction is $MgNH_4PO_4$ $6H_2O$.(209/210)
__the dissolution of calcium silicates (CS, glass .....) in phosphoric acid solution lead to interesting strengths (211).
The systematic studies undertaken in this field con cern the following problems: Control of setting time (212/213)
Extension of the phosphatic bond to other oxides (Cr,Pb, Ti,) (214/220)
Increases of strength by addition of polymers (221/222/223) or
Thermal treatment (224/225)

DENTAL CEMENTS

Dental cements are produced by mixing a powder (MgO ,ZnO,calcium silicates,apatites, glass,.....) and a liquid which can be carboxylic acid (mono or polymers of acry lic,methacrylic,itaconic acid ....) or phosphoric acid. (226 to 239) the association of glass and carboxylic acid is called glass ionomer or polyalkénoate cements: the glass is formed by melting a mixture of CaO/SiO2/ CaF_2/Cryolithe/NaF/ ....and quenching the liquid .This type of glass has the property of being ion leachable i.e. to be able to release calcium or/and aluminum ions at a controlled rate during the reaction with the acid allowing a control of the setting. These cements are used for sealing crown ,prothesis,or for filling (tooth ,and roots canals).
Many problems occur during the use of these cements :
__ storage stability (the carboxylic acid polymerise in the pot during the storage leading to an increase of the viscosity during the mixing)
__control of the viscosity ,and the set ting time of the paste
__ adhesion to the dentine and the ena mel of the tooth
__ hardness and resistance to corrosive solution in the mouth
__ biocompatibitlity with gum and pain less (relieves patient from pain when applied in mouth for cementing or filling treatment) The tentatives of solutions concern either the solid (240/241),the liquid (242 to 250) or the liquid and the solid together (251 to 259)

WATER GLASS CEMENTS

The waterglass cements are composed from sodium silicates (260/261/262) of ratio SiO_2/Na_2O =3.9/4.1 and are produced by the same process as ordinary glass by melting a mixture of silica and sodium carbonate (263 to 268) The world production of this type of binder is 3.3 Mt/y.They are used in different type of applications:

— preparation of foundry molds or clay bonded sand (269 to 271)
—molded construction panel (272) foam material for thermal insulation composition (273 to 276)
— asbestos cement (277)
—inorganic silicate pain (278/279)
—Strengthening weak foundation or ground cement or soil stabilization (280 to 288)

The studies undertaken aim to improve the binders pro perties and the water resistence. : several systems are proposed by addition of polymers phosphates ,Na_2SiF_6, $CaCl_2$ .....(289 to 300)

REFERENCES:

a)General introduction ,Conferences, Books

1) International Congress on the chemistry of cement
a) 1st STOCKHOLM **(1938)**
b) 3d LONDON **(1952)**
c) 4 WASHINGTON **(1960)**
d) 5 TOKIO **(1968)**
e) 6 MOSCOV **(1974)**
f) 7 PARIS **(1980)**

2) MALISCH (W.R.) conc.construction 26 (4) 331 **(1981)**
3)Technology in the 1990 :development in hydrated cement . Royal society of London **(1983)**
4) GLASSER (F.P.) the chemistry and chemically related properties of cement :British ceramic society **(1984)**
5) Cement Research progress : published by the american ceramic society **(1983/1984)**
a) MEHTA (P.K.) high alumina cements and modified portland cements
b) CARTZ(L). miscellaneous binders and coatings
6) COLLEPARDI (M.) Scienza e technologia del calcestruzo ; ed. Ulrico Hoegh MILAN **(1980)**
7) RAMACHANDRAN (V.S.) et al Concrete science ed. Heyden § son **(1981)**
8) BARNES (P.) Structure and performance of cements ed. Applied science publishers ltd **(1984)**
9) International symposium on calcium aluminates TORINO (Italy) september **(1982)**
10) 6th National scientific and technical meeting. on cement chemistry. and technology . Report book 139/143 MOSCOV (SSSR) **(1983)**
11)International symposium on bonds between cements pastes and other materials TOULOUSE (France) **(1982)**
12)International Baustoff and Silicattagung (IBAUSIL) WEIMAR (RDA) **(1985)**
13)Annual symposium institut of concrete technology University of WARWICK (U.K) **(1981)**
14)State of the art :report on high strength cement Committee report A.C.I. 363 R. **(1984)**
15) YOUNG (J.F.) Very High Strengths cements based material : Symposium BOSTON (U.S.A.) **(1984)**
16) Material engin. conference LEEDS (U.K) **(1984)**
17) Symposium of cement and concrete BEIJING (China) China acad. publication 161 **(1985)**

b) specific references

aluminous cements

18) ZHMOIDIN (G.I) et al : cem. conc. res. 14 ,386/96 **(1984)** cem. conc. res. 15, 442/452 ,**(1985)**
19)BORLERA (M.L.) et al : Il cemento 1 ,13/20, **(1984)**
20)BRISI (C) et al : il cemento 1 , 3/14, **(1983)** Il cemento 3,155/164 ,**(1983)**, 4 ,187/195 **(1984)**
21) DEJONGHE (L.C.) et al : J.amer.ceram. soc. (65) ,2, 27/30 **(1984)**
22) SCHMID (H.) et al : phil.mag. A. (48),2, 287/297 **(1983)**

23)SINGH V.K. et al : trans. J. Brit. ceram. soc. (79) 112/114, (1980)
24) MANDAL (U.K). et al : science of sinter. (16) ,3 , 187/193 (1984)
25) ALI (M.M) et al : ibid. (27) ,3, 271/3 (1985)
26)KUZNETSOVA (T.V.) et al :Tsement 9 ,17/8 , (1982)
27) CHOU (K.S.) et al : cem. conc. res. (11) 167/74, (1981)
28) SKOLIS (Y.Y). et al : Rus. J. phys. chem. 55 (1) 25/27 (1981)
29) BACHIORRINI (A.) : cem. conc. res. (15) 167/173, (1985)
30)HONEYBOURNE (C.L.) : Can. J. spect. (27) 4 ,117/122 (1982) cem. conc. res. (10) ,35 ,(1980)
31)CHANDRA (S.) : cer. bull. (64) 8, 1120/28 , (1985)
32)KUMAR (R.) et al : cem. conc. res. (15) 520/524, (1985)
33)HARCHAND (H.S.) et al : cem. conc. res. (13) 465 (1983) . (14) 19/24 , (1983)
34)DOU S.: Silicates indusriels 4,5, 101/106, (1984)
35)RETTEL (A.) et al : Brit. ceram. trans. J. 84 25/28, (1985)
36)WOLEK (W.) et al : Mater. Ognlot. , 32 ,75/9 (1980)
37) FOURNIER (A.A) et al : cem. conc. res. (15) 151/158 (1985) , (15) 269/275 (1985)
38) GALTIER (P) et al : cem. conc. res. (14), 679/685 (1984)
39)SOUSTELLE (M.) et al : cem. conc. res. (15) 655/661 ,(1985) (15) ,421/430 ,(1985)
40)BARRET (P.) et al : cem. conc. res. (13) 789:800, (1983)
41) BARRET (P) ciments platres et chaux 755-A 237/244 ,(1985)
42)BEAUDOIN (J.J.) : cem. conc. res. (12) 289/299 , (1982) (12) ,157/166, (1982)
43) MACZURA (G.) et al : cer. eng. sci. proc. , jan/feb/ 46/67 ,(1983)
44) FISHER R. et al : cem. conc. res. (12) 517/526 , (1982)
45) PEREZ (M.) et al : cem. conc. res. (13) 759/770 ,(1983) (14) ,161/169, (1984) (14) 1/10, (1984)
46) SOUKATCHOFF (P.): mater. et const. (18) 104, 115/122, (1985)
47) BLENKINSOP (R.D.) et al : cem. conc. res. (15) 276/284 (1985) , (15) 385/390, (1985)
48) NEGRO (A.): bull. min. (105) 284/290 (1982)
49)BACHIORRINI (A.) et al : Il cemento 3 , 183/190 (1980) C.R. acad. sc. Paris (294) 963/65 , (1982)
50) GRANDET (J.) et al : cem. conc. res. (10) 759/770, (1980)
51) FENTIMAN (C.H.) : cem conc. res (15) 622/630 (1985)
52) MIDGLEY (H.G.) :clay mineral (19) 857/864, (1984)
53)RODGER (S.A) et al : cem. conc. res. (14) 73/82, (1984)
54)CURRELL (B.R.) et al : in Press
55)FUJIMOTO (S.) et al : Taikabutsu overseas (2) 55/60 (1983)
56) TEOREANU I. et al : Interceram (5) 49/50 (1985)
57) YAMAZAKI (K) : J. ceram. soc. Jpn. (89) 31/40, (1981)
58)MASSAZA (F.) et al : J.amer ceram. soc. (65) 4,203/7,(1982)
59) VAN STRATEN (H.A.) et al : J.col. interf. sc. (103) 2, 493/507, (1985)
60)MIDGLEY (H.G.) : thermo. acta (27) 281/4, (1985)
61) AFSHAR (A.B.) et al: J. mater. sci. let. 4, 851/854, (1985)
62) BENSTED (J.) : World cem. 117/120 , (1982)
63) BACHIORRINI (A.) et al :cem.conc. res. (12) 559/567 (1982)
64)FENTIMAN (C.H.) et al : J. Inst. ref. engrs. 3/5 (1984)
65)MAJUMDAR (A.J.) et al : J. mater. sci. (16) 2597/ 2607 (1981)
66) KERR DE PAIVA CORTES et al : Ceramica (26) ,121, 9/16 , (1980) , (26), 223/231, (1980) ,(26), 271/280, (1980)
67) LANKARD (D.R.) et al :Ceram. bull. (62) , 9 , 1019/35, (1983)
68) B.OZTURK (B.) et al : metal sci. (18), 299/305, (1984)
69)GEORGE (C.M.) et al : ind. min. in the press

b) expansive cements

70) CHICHIBU CEM. COMP. :a) J.P. 82135748 (08/1982) *C.A 97 221836 1982*
b) J.P. 82 135749 (08/1982) *C.A 97 221837 1982*
71) NIHON CEM COMP. : J.P. 575330 (11/1982) *C.A. 98 220847 1983*
72) GOLDSCHMIDT(E.M.) et al : SSSR P. 71100025 (01/1980) *C.A 92 1520252 1980*
73) AVDYUKOV V.I. et al : Tsement 8 12 (1982)
74) EL-DIDAMONY (H.) et al : Zement Kalk Gips 35 8 435
75) OGAWA(K). et al : Cem. conc. res. 12 101 (1982)
76) ALUNNO-ROSETTI (V.) et al :Cem. conc. res. 12 577 /667 (1982)
77) BENTUR (A.) et al : cem. conc. res. 4 709 (1974) 5 139 (1975)
78) CHATTERJEE (S.) et al : Mag. conc. res. 15 83 (1963)
79) CHEN (S.) et al : Cem. conc. res. 12 257 (1982)
80) KURDOWSKI (W.) et al : Cem. conc. res. 11 29 (1981)

81) NEGRO (A.) et al :Cem. conc. res. 12 677 **(1982)**
82) MEHTA(P.K.) et al Cem .Conc. res. 12 121 **(1982)**
83) COHEN (M.D.) : Cem. Conc. res. 13 519 **(1983)**
84) VITI (S.) et al : il cemento 79 101 (**1982)**
85) COLLEPARDI (M.) et al : ACI SP 68 159/171 Amer. Conc. inst. Detroit **(1981)**
86) COHEN (M.D.) et al cem. conc. res. 12 6 717**(1982)**
87) KUZNETSOVA (T.V.) et al : Tsement 3 20 **(1983)** Tsement 6 8 **(1983)**
88) TOGAWA (K). et al : rev. 35 th gen. cem. assoc. Japan 145 **(1981)**
89) OGAWA(K) et al : Cem. Conc. res. 12 247 **(1982)**
90) DOWDING (C.H.)et al Proc. am. Soc. civ. eng. 108 GT 10 1288 **(1982)**
91) BAHKATOV (D.N). et al Izv. Vyssh. Ucheb. Zaved gel. Razved (26) 5 114 **(1983)**
92) SAVISKII (A.N). et al :Stoik. Zhel agr. Sred 52 **(1981)**
93) TIMASHEV (V.V). et al Stroit Mater. 7 19 **(1981)**
94) UPOLOVNIKOVA L.K. et al Tsement 11 18 **(1981)**
95) SMIRNOV (B.I.) et al Beton i Zhelezobeton 4 23 **(1981)**
96) TITOV (Y.N). et al : Beton i Zhelezobeton 4 17 **(1981)**
97) MIKHAJLOV (V.V). et al Beton i Zhelezobeton 4 13 **(1981)**

fast setting and fast hardening cements
high early strengths cements

98) IND.MIJ.VELDHOEN BV(VELD) : Dutsch P. 004468 **(29/12/1983)**
99) EFES (Y) : Betonwerk fertigkeit technik 8 503/505 **(1980)**
100) VOLZHENSKI (A.V.) et al : SSSR P. 742403 **(29/06/1980)**
101) GALER(R.E.) et al :USP 4488909 **(01/12/1984)** USP 4350533 (**21/09/1982)**
102) AGUIARI (G) : B.P 2050342 **(07/01/1981)**
103) DENKI KAGAKU KOGYO : J.P. N° 59146958 **(23/08/1984)**
104) BATRAK (A.I.) et al : SSSR P. 808418 **(28/02/1981)**
105) ONODA CEMENT KK : J.P. N°57149852 **(16/09/1982)**
106) NIPPON SHEET GLASS : J.P. N° 58176156 **(15/10/1983)**
107) SUMITOMO CEMENT KK : J.P. 59182261 **(17/10/1984)**
108) DENKI KAGAKU KOGYO : J.P. N°83044801 **(05/10/1983)**
109) TOYOTA CENT RES : J.P. 57011859 **(21/01/1982)**
110) DENKI KAGAKU KOGYO KK : J.P. N° 213128 **(12/11/1983)**
111) NIPPON CEMENT KK : J.P. :N° 57200252 **(08/12/1982)** J.P. 571566347 (**27/09/1982)**
112) KRAVTCHENKO et al ; SILICONF Budapest **(1981)**
113) NIPPON CEMENT KK : J.P. N° 56014459 **(12/02/1981)**
114) GALER R.E.et al : USP N°4286991 **(01/09/1981)**
115) KULIKOVA T.G. et al ,:Tsement (7) 11/12 **(1983)**
116) FURUHASHI E.et al : Rev. 36 th mtg. Cem assoc Japan 63/64 **(1982)**
117) MAJLING J.et al Stavivo 61 2 66/67 **(1983)**
118) BENSTED J : il cemento 2 81 **(1981)**
119) ATAKUZIEV et al Izv. Vyssh .Uchebn. Zaved. Khim. technol. 26 /9 1143/1146 **(1983)**
120) COTTIN B. et al : Amer. ceram. soc. Cincinnati **(1982)**

very high strength cements

121) HJORTH (L) : Phil. Trans. R. London A 310 163/173 **(1983)**
122) BIRCHALL (J.D.) : ibid A 310 31/42 **(1983)** J . of material science letter 1 125/6 **(1982)** annual meet. inst. ceram. EXETER july **(1984)**
123) KENDALL (K) et al : ibid A.310 139/153 **(1983)**
124) ALFORD (N.McN) : J. of mat .sci. 20 374 **(1985)** *(ref. 16)*
125) SINCLAIR (W) et al : J. of material science 20 2846/52/60 (**1985)**
126) BEAUDOIN (J) et al : Cem. conc. res.15 105/6 **(1985)**

low energy cements

127) KURDOWSKI (W.) et al Cement wapno gips 10 271/3 **(1983)**
128) GARDIEK (H.) Zement Kalk Gips vol 4 169 **(1981)**
129) MOIR (G.K.) World cement technology 374 **(1982)** Phil.trans.Brit.Soc. London A 310 123**(1983)**
130) GARBACIK (A) Cement Wapno Gips 7 73 **(1982)**
131) Importance of calcium chlorosilicate for the cement chemistry .Conference Krakov **(1985)**
132) NUDELMAN (B.) : F. P. N° 2351923 **(1981)** see ref 10
133) SIMMA I. (YA.) et al (see ref 10)
134) MASSAZA (F.) et al il cemento 2 101 **(1983)**
135) ALEKSEEV (S.N) et al Beton i zhelezobeton 8 13 **(1982)**
136) STEPANOVA (V.F.) Prom. Stroit SSSR 8 26 (**1983)**
137) VEB ZEMENTBAU DESSAU G.P. 258326 **(21/12/1983)**
138) STARK (J) et al Zement Kalk Gips 11 476 **(1981)** see ref 12 , Silikattechnick 31 50 **(1982)**

139) MULLER (A) et al :Zement Kalk Gips 6 303 **(1985)**
Vortrag 1.2.8.8. IBAUSIL Weimar **(1982)**
140) SHUBIN (V.I.) et al see ref 10
141) SCHRADER (R.) et al F.P. 258373 **(12/09/1983)**
142) GHOSH (S.N.) et al : Cem. conc. res. 14 437/8 **(1984)**

magnesia cements

143) KOLOTUSHKIN (W.N). et al SSSR P. 1025687 **(30/06/1984)**
SSSR P. 730648 **(30/04/1980)**
144) DE ZWAAN (J.) Swed P. 435711 **(15/10/1984)**
145) BECKERICH (P) F.P. 2499550 **(13/08/1982)**
146)CAR(M.) G.P. 3304033 **(9/08/1984)**
147) PREEDY (J.) B.P. 2079811 **(27/01/1982)**
148) UBE INDUSTRY J.P. 58130150 **(03/08/1983)**
149) CHU NIPPON KAKOHAN SEYZO K.K. J.P. 58110458 **(17.07/1983)**
150) NAKA NIPPON KAKOBAN J.P. 58110458 **(01/07/1983)**
151) EIDA Co Ltd J.P. 5711888 **(21/01/1985)**
152) ASAHI CHEMICAL INDUSTRY J.P. 5755674 **(25/11/1982)**
153) BECKERICH (P.à F.P. 2479182 **(20/10/1981)**
154) EDWARDS (A.G). et al B.P.1590384 **(03/06/1981)**
155) PHALEN (T.E). Mater. technol. 6 1 93/97 **(1980)**
156) CARSON (J.W.) et al G.P. 3006163 **(20/08/1981)**
157) MABIN (J.E) B.P. 1601948 **(04/11/1981)**
158) REPKA (P). et al Czech.P. 216253 **(15/05/1984)**
159) LEONOV (A.A.) et al : SSSR P. 1143725 **(07/03/1985)**
160) VUZDUGAN (S.F). Eur. P. appl. 82910 **(06/07/1983)**
161) DRINKUTH (F.) et al Eur. P. appl. 19180 **(26/11/1980)**
162) PRIOR (W.L). et al U.S.P 117540 **(1/02/1980)**
163) GRATZEL (O.K). et al ASTM spec. tech. publ. 68/93 **(1983)**
164) HERRERA(M.E.) ASTM spec. tech. publ. 94/101 **(1983)**
165) EIDA Co ltd J.P. 57104761 **(29/06/1982)**
57011889 **(21/01/1982)**
166) SMITH (M.A.) B.P. 1604584 **(09/12/1981)**
167) SHAPLAND ltd B.P. 2036832 **(02/07/1980)**
168) QUANT(H.) G.P. 3046405 **(09/09/1982)**
169) POLESZAK (M). Cement Wapno gips 11,12, 371/4 **(1984)**
170) HUGHES (G.A). B.P. 2073728 **(21/10/1981)**
171) BECKERICH (P). et al U.S. P. 4419196 **(06/12/1983)**
F.P. 2487816 **(05/02/1982)**
172) SHANNON (R.F). U.S.P. 4362675 **(07/12/1982)**
173) SHIMIZU (K). Yogyo Kyokaishi 91 (1) 42/9 **(1983)**
Kure Kogyo Shikenjohokoku 24 37/41 **(1981)**
174) ONODA (K). J.P. 5571658 **(29/05/1980)**
175) PRIMELSKI (F). G.P. 3042157 **(19/05/1982)**
176) EGYESULT (,) B.P. 2085221 **(19/05/1982)**
177) THIELE (D). B.P. 2842475 **(3/04/1980)**
178) URWONGSEE(L).et al J.amer. Ceram. Soc 63 9,10, 501/4 **(1980)**
179) MAZURANIC (C) et al J. Amer Ceram. Soc. 65 10,523/4 **(1982)**
180) BILINSKI (H.)et al J. Amer. Ceram. Soc. 67 4, 266/9 **(1984)**
181) MATKOVIC (B.) report FHWA /RD-80/128 **(1981)**
182) MATHUR (R). et al Res. Ind. 29 ,3, 195/2021 **(1984)**
183) MENETRIER(D.) et al Mat. sci. Mono. 28A (react. solids Pt A) 541 **(1985)**
184) SAQOUT(S.) Ph.D. thesis DIJON **(1983)**
185) LOPEZ-GOMEZ (P.) Cem. Hormigon 52 569 329/49 **(1981)** 52 570 444/73 **(1981)** 52 571 579/92 **(1981)** 52 572 659/86 **(1981)**
186) ALEGRET (S). et al J. Amer. ceram. Soc. 67 9 579/82 ,**(1984)**
187) DUYSTER (H.) et al G.P. 2921245 **(1980)**
188) KUBRAKOV (M.S.) SSSR P. 1106800 **(1984)**
189) NAGAMORI (M.) et al Can..P. 1130537 **(1982)**
190) ZHU (P.) Huaxue Shijie 23 ,5 152/4 **(1982)**
191) SIJKOV (S.P.) et al Tr. Mosk. Khim. Tekhnol. inst. iml. D.I. Mendeleva 123 85/8 **(1982)**
192) SMITH-JOHANNSEN (R. U.S. P .4352694 **(5/10/1982)** B.P. 2023619 **(3/01/1980)**
193) SRIVASTAVA R.S. Res. Ind. 28 3 203/6 **(1983)**
194) SHUSHARIN (V.I.) et al SSSR P. 767052 **(30/09/1980)**
195) BOBUSKI(W.G.) et al ind. Eng. chem. Prod. Res. Dev. 21 4 531/3 **(1982)**
196) ERMOLENKO (I.N).et al Vestsi Akad. Navuk SSSR Ser Khim. Navuk 3 111/5 **(1984)**
197) PASCHENKO (A.A) et al Stroit Mater. izdeliya sanit. teckh. 5 25/6 **(1982)**
C.A. 100196819 1984
198) TEMPLE(C.S.) U.S.P. 4185066 **(22/01/1980)**
199) TEOREANU(I.)et al Mater.const. Bucharest 14 4 172/5 **(1984)**

phosphate cements

200) SHERIFF(F.G.) et al U.S.P. 4487632 **(11/12/1984)**
U.S.P. 4505752 **(19/03/1985)**
201) TOKUYAMA SODA K.K. J.P. 60055076 **(29/03/1985)**
202) APPELT (R.) Sprechsaal 116 9 765/773 **(1983)**

203)IOVKOV (G.) Stroit. mater. silik. prom-st 23 9/10 11/15 **(1982)**

C.A. 98 184394 1983

204)SEMENOV (G.M.) et al Deposited doc./ VINITI 4313 82 **(1982)**

C.A. 99217582 1983

205)TIMASHEV (V.V) et al Tr. Mosk. Khim. techn. 128 134/143 **(1983)**

C.A. 101 77766 (1984)

206)TOMIC (E.A.) U.S.P. 4394174 **(19/07/1983)**

207)HEYMAN (J.E.) et al Swedisch P. 7907738 **(27/04/1981)**

208)SUGAMA (T.) et al Cem. concr. res. 13 4 499/506 **(1983)**
Cem. concr. res. 13 3 407/416 **(1983)**

209)EL-JAZAIRI (B.) Concrete 12 **(1982)**

210)ABDELRAZIG (B.E.I) et al see ref 4

211)PROSSER (H.J.)et al J. Dent. res. 62 5 598/600 **(1983)**

212)SHANNON (R.F.) U.S.P. 4362675 **(07/12/1982)**

213)STEPANOVA (I.N.) et al Izv. Akad .Nauk. SSSR Neorg. Mater. 19/9 1598/99 **(1983)**

C.A. 10038715 1984

214)ZHENZHURIST (A.I.) et al Izv. Vyssh. Uchebn. Zaved., Khim. Khim. tekhnol. 25 &à 1163/68 **(1982)**

C.A. 98 10661 1983

deposited doc. SPSTL 387 Khp-D81 **(1981)**

C.A. 98112625 1983

215)MASLIKOVA (M.A.) Deposited doc. SPSTL 1258 Khp D 82 **(1982)**

C.A. 101 598201 1984

216)BUTYLIN (A.B.) et al Steklo Sitally i Silicaty Minsk 12 93/95 **(1983)**

C.A. 101 27452 1984

217)SUDAKAS(G.L.) et al Izv. Akad. Nauk. SSSR. Neorg. Mater. 18 1 140/144 **(1982)**

C.A. 97 202472 1982

218)PETROVA(A.P.) et al Khim. Prom. st. Ser. Fosfornaya Prom. st. 4 10/11 **(1981)**

C.A. 96 204484 1982

219)IVOKOV (G.) et al Stroit. mater. Silik. Prom-st. 22 8 9/14 **(1981**

220)SYCHEV (M.M.) et al Izv. Akad Nauk. SSSR. Neorg. Mater. 18 2 318/22 **(1982)**

C.A. 96 222252 1982

221)VASHKEVICH (N.V.) et al Zh. Prikl. Khim. (Leningrad) 54 9 2048/2052 **(1981)**

C.A. 96 23921 1982

222)REICHARDT (R.) Stomatol DDR 32 7 476/483 **(1982)**

C.A. 97 168793 1982

223)VASHKEVITCH (N.V). et al deposited doc VINITI 3846 81 **(1981)**

C.A. 98 94606 1983

224)STALEGO (J.P.) et al U.S.P. 4312674 **(26/01/1982)**

225)YAMAZASKI (K.) et al Yogyo kyokaishi 89 12 661/668 **(1981)**

C.A. 96109038 1982

dental cements

226) MAROLF (R.) Schweiz. monatsch. Zahmed. 94 117/133 **(1984)**

227)KAJIWARA(M.) J.mater. Sci. lett. 3 7 617/9 **(1984)**

228)COOK (W.D.) J.Biomed. mater. res. 17 6 1015/27 **(1983)**

229)IRIC (M.)et al Shika Zaizyo Kikai 2 6 820/23 **(1983)**

C.A. 100 215481 1983

230)HODD (K.A.) et al. Adhesion (London) 8 153/67 **(1984)**

231)KUBOTA (T. et al Zairo Kagaku 19 4 217/222 **(1982)**

232)COOK (.D.) Biomaterial 4 1 21/24 **(1983)**
4 2 85/88 **(1983)**
J. Biomed. Mater. Res. 17 2 283/291 **(1983)**

233)WIEGHAM (H.)et al J.Dent. Res. 62 2 105/108 **(1983)**

234)OEILO (G.) et al. J.Dent. Res. 62 8 937/39 **(1983)**

235)MATSUYA (S.)et al. Dent .Mater. J. 2 1 76/85 **(1983)**
2 1 68/75 **(1983)**

236)TSUKIBOSHI (M.) et al J.Prothet. Dent. 51 4 503/508 **(1984)**

237)BRANCO (R.) et al. Acta Odontol. Scand. 41 6 349/49 **(1983)**

238)BRUNE (D.)et al Scand. J; Dent. res. 92 2 156/160 **(1984)**

239)BAGNALL (R.D. et al. J. dent. 12 2 135/38 **(1984)**

240)SMYTH (H.T.) U.S.P. 4452622 **(05/06/1984)**

241)BRADEN (M.) B.P. 2108132 **(11/05/1984)**

242)AKAHANE (S.) et al F.P. 2550088 **(08/02/1985)**

243)SHIMOKOBE (H.et al U.S.P. 4524824 **(08/02/1985)**

244)SHIKA KOGYO K.K. J.P. 57126407 **(06/08/1982)**
J.P. 57126406 **(06/06/1982)**
J.P. 57002209 **(07/01/1982)**
J.P. 57002209 **(07/01/1982)**
U.S.P. 4342677 **(03/08/1982)**
U.S.P. 4374936 **(22/02/1983)**

245)HIGO (M.) et al U.S.P. 4383052 **(10/05/1983)**

246)SUN STAR HAMIGAKI J.P. 57021308 **(04/02/1982)**

247)TSUNEKAWA (M.) et al U.S.P. 4404150 **(13/091983)**

248)DE GROOT(K). et al. G.P. 3024944 **(11/02/1982)**

249)DEWHIRST (F.E.) U.S. P. 4280842 **(28/07/1981)**

250)PURRMANN (R.) et al U.S.P. 430605 **(23/11/1982)**

251)TOKUYAMA SODA K.K. J.P. 56110606 **(01/09/1981)**
J.P. 59122411 **(14/07/1984)**
J.P. 59122410 **(14/07/1984)**
J.P. 60081115 **(09/05/1985)**
J.P. 6007890 **(04/05/1985)**

252)MIRAI KAGAKU K.K. J.P. 60036404 **(25/02/1985)**

253)BRAUER (G.M.) U.S.P. 6582759 **(14/08/1984)**
J.Dent. Res. 63 2 137/140 **(1984)**

254)Mc LEAN (J.W). et al U.S.P. 4527979 **(09/07/1985)**

255)ISHIBASHI (T). J.P. 58083605 **(19/05/1983)**

256)SANKIN KOGYO K.K. J.P. 57075908 **(12/05/1982)**

257)SANSTAR J.P. 57046908 **(17/03/1982)**

258)MITSUBISHI MINING CEMENT J.P. 56026808 **(16/03/1981)**

259)KAWAHARA (H.) J.P. 57134407 **(19/08/1982)**

water glass cements

260) VON LAUFENBERG (J.)et al Glastech. Ber. 56 11 294/8 **(1983)**

261)SCHELER (H)et al Mitteilungsbl. chem. ges. D.D.R. 29 7 149/53 **(1983)**

262)TEPLYAKOV (S.K.) Liteinoe Proizv 5 18/20 **(1984)**

263)AFANAS'EVA (V.A.) Steklo Keram. 3 18/19 **(1983)**

264)SHOKUBAI KASEI KOGYO J.P. 57027922 **(15/02/1982)**

265)DOKAI KAGAKU KOGYO J.P. 57 111 227/228/ 230/ 231 **(10/07/1982)**

266)FLEMMING (E)) G.P. 158101 **(29/12/1982)**

267)HENKEL (K.G). et al G.P. 3012073 **(08/10/1981)**

268)CARLIN (W.W.) et al U.S.P. 4303487 **(03/07/1981)**

269)DOROSHENKO (S.P). Lit. Proisvod 1 14/15 **(1983)**

270)SITARAMAJAH (D.) Founderya Ital. 31 6 175/83 **(1982)**

271)IVANOV (A.A.) et al Liteinoe Proizvod 7 13/14 **(1984)**

272)DAVIDOVITS (J.)et al U.S.P. 4509985 **(09/04/1985)**

273)SAVCHENKAV (V.I.) et al SSSR P. 10004324 **(15/03/1983)**

274)NISSHIN KOGYO K.K. J.P. 60016878 **(28/01/1985)**

275)BRODSKII (V.P.) SSSR P. 887554 **(07/12/1981)**

276)MARKAN (I.F.)et al Beton Zhelezobeton (Moscow) 9 18/19 **(1983)**

277)PACH (L.) et al Stavivo 60 6 248/50 **(1982)**

278)NEEBY (J.E.) et al U.S.P. 4312673 **(26/01/1982)**

279)TOKUDA(S.) et al Kagaku to Kogyo (OSAKA) 57 5 183/187 **(1983)**

280)LOPEZ RUIZ(A.) Quim. Ind. (Madrid) 29 7 8 493/503 **(1983)**

281)TOSHIMA KENSETSU KO J.P. 57172975 **(25/10/1982)**

282)ASASHI DENKA KOGYO J.P. 58037079 **(04/03/1983)**

283)SHIMODA GIJITSU KEN J.P. 58029882 **(22/02/1983)**

284)NISSAN CHEM.IND. K.K. J.P. 58047082 **(18/03/1983)**

285)SHIMODA GIJITSU KEN J.P. 58047081/2 **(18/03/1983)**

286)NITTO CHEM. IND. . K.K. J.P. 57100213 **(22/06/1982)**
J.P. 57158284 **(30/09/1982)**
J.P. 57195786 /7 **(01/12/1982)**
J.P. 58195787 **(01/12/1982)**

287)MITSUI TOATSU CHEM. IND. J.P. 57174381 **(27/10/1982)**

288)KYOKADO ENG.K.K. J.P. 57094082 **(11/06/1982)**
J.P. 57109889 **(08/07/1982)**
J.P. 58065786 **(19/04/1983)**
J.P. 58074780 **(06/05/1983)**
J.P. 58079082 **(12/05/1983)**

289)TEOREANU (I.) et al Zement Kalk Gips B 37 8 427/31 **(1984)**
Mater. const. 14 1 14/18 **(1984)**

290)ROENSCH (E.)et al Z. chem. 24 4 129/130 **(1984)**

291)BELOBROV (B.A.) et al Liteinoe Proizvod 5 16/17 **(1984)**

292)YAKOVLEVA (L.A.) et al Izv. Vyssh. uchebu Zaved Khim. Khim. Tekhnol. 27 1 83/88 **(1984)**

C.A. 100144013 1984

293)SHEVCHUK (V.V). et al Elektron obrat. mater. 6 47/50 **(1983)**

294)SAEKI (T.) et al Bull. chem. soc. Jap. 57 1571/95 **(1984)**

295)SANGO (K.) et al. Ind. Eng. chem. prod. res. dev. 23 2 315/317 **(1984)**

296)YOSHIDA (A. et al Kogyo Gijutsu Shikensho Hokoku 31 2047/52 **(1983)**

C.A. 10073042 (1984)

297)SCHMITT (H.)et al J. Phys. Colloq. 69 275/8 **(1982)**

298)INOUE (H). et al J.appl. polym. sci. 28 8 2499/2508 **(1983)**

299)TOA GOSEI CHEM. IND. Ltd J.P. 57034019 **(15/02/1983)**

300)NAITO H. et al U.S.P 4415364 **(15/11/1983)**

THEME/THÈME 4

Influence of cement in the durability of concrete. Influence du ciment dans la durabilité du béton.

Chairman/Président:

G. Wischers
Forschungsinstitut der Zementindustrie Dusseldorf, West Germany.

Secretary/Secrétaire:

H. R. E. Bucher
Associação Brasileira de Cimento Portland, São Paulo, Brasil

SUB-THEME/SOUS-THÈME 4.1

Pore structure, permeability and diffusivity as related to durability.

Structure des pores, perméabilité et diffusibilité en liaison avec la durabilité.

Chairman/Président:

R. E. Oberholster
National Building Research Institute
Pretoria, South Africa

Principal Reporter/Rapporteur Principal:

R. F. Feldman
Division of Building Research
National Research Council
Ottawa, Ontario, Canada

SUB-THEME 4.1

PORE STRUCTURE, PERMEABILITY AND DIFFUSIVITY OF HARDENED CEMENT PASTE AND CONCRETE IN RELATION TO DURABILITY : STATUS AND PROSPECTS

R E OBERHOLSTER

National Building Research Institute
Council for Scientific and Industrial Research
Pretoria
South Africa

1. INTRODUCTION

This document deals with aspects of the porosity, permeability and diffusivity of hardened cement paste (hcp) which are currently considered important in relation to the durability of concrete. The views expressed are not only, or necessarily, mine, but generally those expressed in publications by researchers in this field.

The references used may not be the only references on the subject, but merely those I have selected to illustrate a specific point.

Hardened cement paste has been studied intensively for many years in respect of its physical properties, morphology and mineralogy. A better understanding of hcp will ultimately lead to a better understanding of concrete.

Concrete is a composite material consisting of hcp and, normally, sand (fine aggregate) and gravel or crushed rock (coarse aggregate). Other, less conventional, materials may also be used with the cement - such as lightweight aggregate, asbestos-, glass- or other fibre. Furthermore, part of the portland cement may be replaced by mineral admixtures such as milled granulated blast-furnace slag, fly ash or silica fume; workability aids or air entrainers may also be added. In contrast to hcp therefore, concrete is a heterogeneous multicomponent material, whose properties are an integration of the properties of the individual constituents and their interactions with one another.

An understanding of the properties of hcp and aggregates helps to explain the nature of concrete, but whether a bridge has been established between research material and its application by the practising engineer and the concrete technologist, is a moot point.

2. DURABILITY

During the past few years there has been great interest in, and discussion of, the durability of building materials in general and of concrete in particular (1). In Japan, for example, the number of papers on durability and service life has increased rapidly since about 1955 and papers on reinforced concrete almost doubled between 1956 and 1976 (2). Wiegler ascribes the increase in deterioration of concrete structures exposed to outdoor conditions to the higher aggressivity of the environment, and to the slenderness of modern concrete structures which makes them more prone to this problem (3).

In the past, information on the durability of building materials was obtained from long-term observations, from case studies and from the comparison of the behaviour of materials under both similar and different conditions. During the past decade, however, the aim has been to analyse the performance of materials and to design experiments to facilitate prediction of service life, under a range of service conditions, through mathematical analysis (2,4).

The establishment of data bases such as AEPIC for international use, to record the performance of building materials, including durability performance, aims at providing better-documented information on the causes of durability-related defects in buildings and other structures, and at providing easier access to new findings relating to durability (5).

The development of computer-based expert systems, such as DURCON, (5) to assist in making decisions on the durability of concrete mixtures - both to aid mixture design and to assess the durability of existing concrete - has obvious potential.

However, systematic scientific research, based on carefully designed experiments, is still required to provide the technical background for the mathematical prediction of service life. In this respect it is important to define the system (concrete) properly, as well as to establish the significance, the extent and the kinds of degradation factors, characterise any products and establish each kind of degradation mechanism. It is further necessary to determine a quantitative indicator of degradation, establish how it can be measured, devise an accelerated test to simulate the degradation mechanism and, finally, relate the laboratory test data to field test data and put the findings into practice (6).

In the case of concrete, its properties are determined by its constituents and the manufacturing process:

$$C = f(c,ca,s,w,v,x_1....x_n) \quad (1)$$

where

C = concrete;
f = function of;
c = cement;
ca = coarse aggregate*;
s = sand*;
w = mix water;
v = mixing, placement, curing; and
$x_1....x_n$ = mineral admixtures, chemical admixtures, reinforcement, etc.

Any property, P (such as for example porosity, permeability, diffusivity), of concrete is particular to that specific concrete. Therefore,

$$P = f(C) = F(c,ca,s,w,v,x_1....x_n) \quad (2)$$

By keeping all but one variable constant in laboratory experiments, the effect of each on a particular property of concrete can be studied, for example:

$$P = f(c)_{ca,s,w,v,x_1....x_n} \quad (3)$$

The degradation of a concrete can be caused by a property of any one of its constituents, reaction between constituents, poor manufacturing techniques, exposure to aggressive environments or a combination of the above. If linear expansion, E, of a concrete is taken as an indication of the deterioration due to, for example, exposure to a sulphate environment, e, then:

$$E = f(C,e) \quad (4)$$

and

$$E = f(C)_e \quad (5)$$

---

* The coarse and fine aggregates are indicated separately although in some definitions they are referred to collectively and as an inert material, bound together by the cement paste.

for different concretes exposed to the same sulphate environment, or

$$E = f(e)_C \quad \ldots\ldots\ldots\ldots\ldots\ldots\ldots\ldots\ldots\ldots \quad (6)$$

for the same concrete exposed to different sulphate environments.

The above approach should form the basis of systematic accelerated tests as well as of long-term tests to predict the performance of concrete made with certain materials or of concrete exposed to certain environmental conditions and to establish the relationship between an accelerated test and long-term exposure tests performed under natural exposure conditions. An example of linear expansion data obtained for five different test procedures involving the same aggregate is shown in figure 1. Figure 2 shows data obtained for the same concrete exposed at four different sites with widely different climates. All the data are in respect of the alkali reactivity of concrete.

In respect of porosity, permeability and diffusivity, the above approach should be followed to obtain and evaluate data on:

(i) the effect of each of the variables in equation 1 on the porosity, permeability and diffusivity of concrete;

(ii) the effect of porosity on permeability and diffusivity;

(iii) the relationship between the durability of concrete and porosity, permeability and diffusivity, in respect of, for example, each of the following:

(a) freezing and thawing;
(b) salt crystallisation;
(c) chloride penetration;
(d) carbonation;
(e) corrosion;
(f) sulphate attack;
(g) soft water attack;
(h) alkali-silica and alkali-carbonate rock reaction;
(i) mechanical loading or abrasion.

3. POROSITY

3.1 Cement paste

The work of Powers and Brownyard (7) on the structure and properties of cement pastes led to the proposal of models for the structure of cement gel (8), the distinction between gel pores and capillary pores and the classification of total water in hcp as (i) water of constitution (water of crystallisation or otherwise chemically bound); (ii) adsorbed water, bound by surface forces; and (iii) capillary water (water in the pores, not bound by surface forces).

The gel consists of colloidal C-S-H particles of up to two or three layers, arranged randomly and bonded together by surface forces, as in clay, with occasional strong ionic-covalent bonds linking adjacent particles. There is not sufficient long-range order to consider the material crystalline. Water vapour can penetrate all the

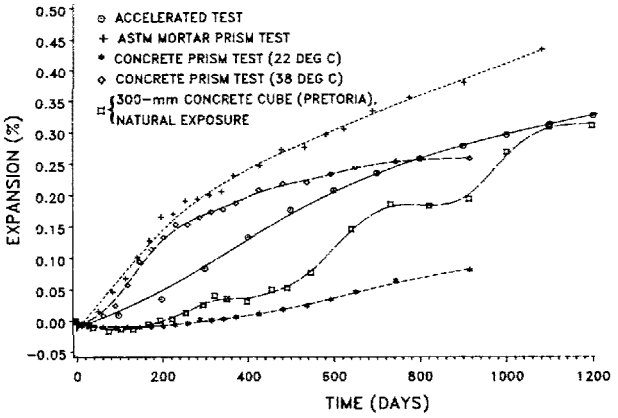

FIGURE 1: Comparison of results of five tests for potential alkali reactivity of a greywacke/hornfels aggregate under different test conditions. For the accelerated test the days must be divided by 100

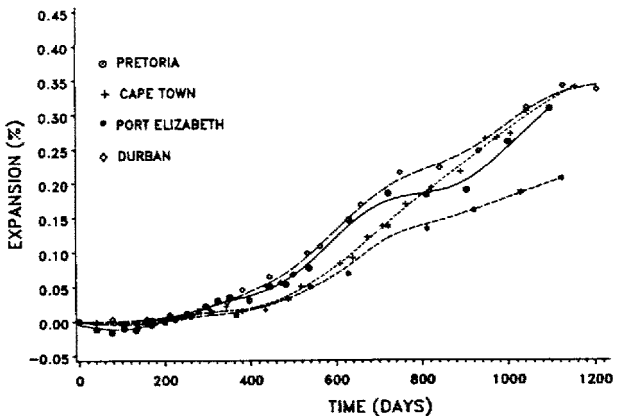

FIGURE 2: Comparison of expansion of 300-mm concrete cubes due to alkali-silica reaction under natural exposure conditions in four different climatic areas. Na_2O equivalent of cement is 1.1 per cent and cement content of concrete 350 kg/m³

spaces between the particles to provide a measure of their surface area, whereas nitrogen can only penetrate larger spaces and does not measure the whole surface area. The water between the layers is held until strong drying occurs, when it is lost irreversibly. The gel itself has a porosity of about 28 per cent.

In the Feldman-Sereda model (9) the C-S-H structure is presented as an irregular array of single layers which may come together randomly to create interlayer space, as is observed in clay minerals, but in no regular ordered way. Bonding between layers is considered to be through solid-solid contacts which are visualised as bonds intermediate in character between weak van der Waals' and strong ionic-covalent bonds. The solid-solid contacts form on drying but are disrupted by wetting. Interlayer bonding is a special kind of chemical

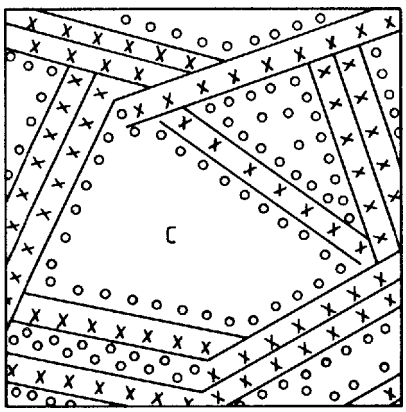

(a)

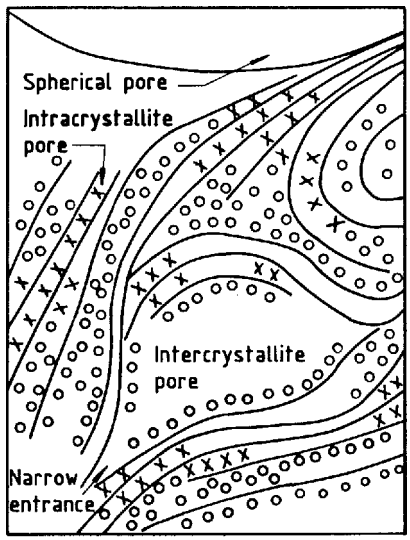

(b)

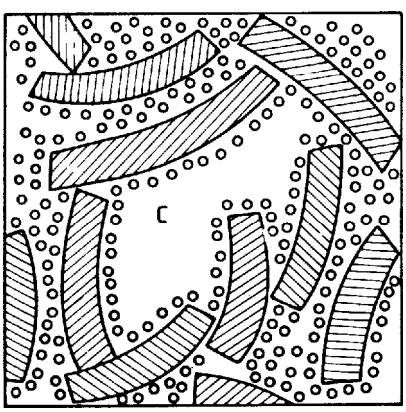

(c)

LEGEND

x	Water in interlayer regions
o	Water adsorbed on surfaces
C	Capillary pore
———	C-S-H sheets
▨	C-S-H particles

FIGURE 3: Schematic presentation of various models of C-S-H (a) Powers and Brunauer adapted from (7); (b) Feldman-Sereda (9) successively modified by Daimon et al (10) and Rahman (14); (c) Munich, adapted from Wittman (15); based on the schematic presentations of Mindess and Young (17)

bonding and cannot be considered as resulting from interactions between free surfaces. Water can move reversibly in and out of the interlayer space. Thus, nitrogen adsorption most closely measures the surface area of pores within the material, since adsorption of water molecules within the interlayer region distorts the measurements made with water vapour.

Based on adsorption studies on hydrated C_3S paste after the removal of $Ca(OH)_2$, Daimon et al (10) modified the Feldman-Sereda model because, according to them, only then was the true pore structure revealed. Adsorption measurements indicated the existence of two kinds of pores: a wider inter gel-particle pore which can be seen even in the inner C-S-H by SEM, and a smaller intragel pore existing within the gel particles which cannot be observed by SEM. The intragel pores are further classified into an intercrystallite pore similar to the micropore reported by Brunauer et al (11), but which may enlarge in the presence of water, and intracrystallite pores corresponding to the interlayer space mentioned by Feldman (12). Alford and Rahman (13) concluded that closed spherical voids, or macropores, that cannot be intruded by mercury, contribute significantly to the total porosity of hcp, affect the pore size distribution, modify surface areas determined by mercury intrusion porosimetry (MIP) and thus contribute to "lost" porosity. The macropores greatly affect the tensile strength of the hcp. Such spherical macropores are therefore incorporated in the modified Feldman-Sereda pore model (14).

The Munich model discussed by Wittman (15, 16) is essentially a physical model based on sorption measurements. With the help of this model, the behaviour of hcp under different moisture conditions is explained. Van der Waals' forces contribute to the binding energy between particles, but strong ionic-covalent bonding still predominates.

In all the models the relationship between solid phase, pores and water is presented. Three of the models are shown in Figure 3.

TABLE 1: Classification of pore sizes in hydrated cement paste after Mindess & Young (17)

Designation	Diameter	Description (Name of corresponding pore)	Role of water	Paste properties affected
Macropores	1 000 - 15 μm	Large spherical voids (13, 14)	Behaves as bulk water	Strength, permeability
Capillary pores	15 - 0.05 μm	Large capillaries	Behaves as bulk water	Strength, permeability
	50 - 10 nm	Medium capillaries Capillary cavity (7) Inter gel-particle pores (10)	Moderate surface tension forces generated	Strength, permeability, shrinkage at high humidities
Gel pores	10 - 2.5 nm	Small (gel) capillaries	Strong surface tension forces generated	Shrinkage to 50% RH
	2.5 - 0.5 nm	Micropores Gel pores (7) Inter-crystallite pores (10)	Strongly adsorbed water, no menisci form	Shrinkage, creep
	< ca. 0.5 nm	Micropores "interlayer" (Interlayer space (9)) Intra-crystallite pores (10)	Structural water involved in bonding	Shrinkage, creep

A classification of pore sizes in hydrated cement paste according to Mindess and Young (17) but incorporating the macropores of Alford and Rahman (13) and indicating the corresponding pore designations of Powers and Brownyard (7), Feldman and Sereda (9) and Daimon et al (10) is given in Table 1. Such a classification of pores into size ranges is merely convenient and does not imply that the size distribution of pores is not continuous.

The techniques that are used to determine porosity are:

- mercury intrusion porosimetry (MIP) which enables the widest range of pore size distribution to be measured (ca. 1000 μm to 3 nm);
- the capillary condensation method which uses several different adsorbates (mainly nitrogen and water) on cement pastes in the limited range of about 50 to 4 nm (18);
- the helium inflow and helium pycnometric technique (19); and
- the quasi-elastic or inelastic neutron scattering method (20).

With the first two methods, the pore sizes recorded are not necessarily the true diameters but the pore-entry diameters. Water always gives a higher porosity and surface area for hcp than, for example, nitrogen (18). Several workers (21, 22, 23, 24) have discussed the reasons for differences in results obtained by the different techniques. Winslow and Diamond (21) ascribed the "lost porosity" - that is, the fraction of the total pore space unintruded by mercury - to pores which were too fine to be measured by MIP. Diamond (22) later suggested that the lost porosity might be in the ultrafine pores, in encapsulated pockets of gel, which would be unintrudable to mercury at any pressure. Beaudoin (23) suggested that the reason why mercury cannot enter all the pore space accessible to helium is the existence of microspace between aggregates of C-S-H sheets which are inaccessible to mercury. Alford and Rahman (13) and Rahman (14) ascribed the lost porosity mainly to the presence of large voids (macropores ca. 1 000 to 0.1 μm diameter) enclosed by gel with pores too fine to be recorded by MIP.

Porosity influences the physical and mechanical properties of hcp, such as compressive and flexural strength, hardness, fracture toughness, Young's modulus, shrinkage, creep, diffusion and permeability. Powers and Brownyard (7) realised this and they expressed the dependence of strength on porosity in terms of the gel:space ratio i.e. the ratio of the volume of hydrated cement paste to the sum of the volumes of the hydrated cement and the capillary pores. Later workers expressed porosity in terms of volume of pores relative to the total volume of the specimen. The relationship between porosity and strength is expressed indirectly in the equation of Feret, where compressive strength σ_c is connected with the volumes V_c of cement, V_w of water and V_a of air (25):

$\sigma_c = A[V_c/(V_c + V_w + V_a)]^2$ and A is a constant.

The porosity of hcp incorporates the effect of both the initial water:cement ratio and curing (hydration). The correlation of porosity with mechanical properties of materials has led to three types of equation, mainly semi-empirical, namely:

$\sigma = \sigma_0(1-p)^A$ derived by Balshin (26);

$\sigma = \sigma_0 e^{-Bp}$ derived by Ryshkewitch (27)

where σ_0 is the strength at zero porosity, p is porosity and A and B are constants. A third equation:

$\sigma = D \ln \frac{P_{cr}}{p}$ was derived by Schiller (28)

where p_{cr} is zero strength porosity, and p is a constant. Similar equations have been derived and applied for Young's modulus and for fracture energy of cementitious materials, namely (29,30)

$E = E_0(1-p)^s$ and (31):

$R = R_0 e^{-kp}$

where E_0 and R_0 are Young's modulus and fracture energy respectively, at zero porosity and k is a constant (28).

Experimental data relating porosity to the strength properties of hcp are presented by Verbeck and Helmuth (32), Sereda et al (24) and Kendall et al (25), among others. From their data it is clear that porosity is a major factor limiting the strength of hcp. Mix parameters, especially the water:cement ratio, greatly influence the porosity of hcp (33). Techniques to limit the porosity of hcp include pressing (34), hot pressing (35, 36, 37), the use of chemical admixtures to aid grinding and to enable the use of lower water:cement ratios in mixing of pastes (38-42) and impregnation (43,44).

A characteristic of hcp is its low flexural strength, typically between 3 and 10 MPa. Birchall et al (45), Alford (46) and Kendall et al (25) have demonstrated that the commonly observed flexural weakness of hcp is due to the presence of large voids (>100 μm) which are largely undetected by conventional methods of pore analysis, such as gas adsorption and MIP. The low flexural strengths normally found are associated with macroscopic flaws rather than microscopic or mineralogical features of the gel, and the conventional strength-total porosity relationship is largely fortuitous. It appears that the principal reason for an increase in strength with a reduced total porosity is that the methods used to reduce porosity, such as compaction or hot pressing, also reduce the size of the largest pore. By the addition of polymer to make the mix plastic, the employment of high-shear mixers and the removal of air bubbles by press moulding at 5 MPa, a macro-defect free (MDF) cement product, with a high bending strength of 70 MPa, can be produced even though the porosity volume remains at a high level (46, 47). The large increase in flexural strength of the MDF cement paste is attributed to a reduction in maximum void size and is explained on the basis of Griffith's theory:

$$\sigma = \sqrt{\frac{2ER}{\pi c}}$$

where c is half the flaw length.

It is, however, uncertain whether macropores in poorly compacted pastes with a low w:c ratio, which contain large amounts of unhydrated cement, can be considered as flaws in the Griffith sense (48).

3.2 Aggregate

Less attention has been given to the morphology and physical properties of aggregates than to hcp. However, in the light of the semi-empirical relationships mentioned in the previous section, it can be stated that various properties of aggregate are influenced by the volume and dimensions of the internal pore system. These include density, strength, permeability, modulus of elasticity, Poisson's ratio and durability (in respect of mechanisms of deterioration such as freeze-thaw resistance and alkali-silica reaction).

Dolch (49) has referred briefly to work done on the porosity of aggregates and has given a short discussion on methods of measuring the porosity of aggregates. The methods are optical microscopy (to a minimum diameter of ca. 1 μm), pycnometric methods, the McLeod gauge porosimeter (the latter two methods measure the effective porosity) permeability measurement, absorptivity measurement, and the vapour adsorption method as well as MIP to determine equivalent pore size and pore size distribution.

Much attention has been given to the effect of the porosity of aggregates on the freeze-thaw durability of concrete. Some of the earliest work was done by Sweet (50), Dolch (51) and Verbeck and Landgren (52). Non-durable aggregates are characterised by a large volume of small pores which rapidly acquire a high degree of saturation but will not let the water drain out easily when it expands on freezing; most of the pores in non-durable aggregates are smaller than 200 nm (53). Kaneuji (quoted in Ref. 54) developed the following relationship between the pore characteristics of an aggregate and its frost resistance in concrete:

$$EDF = 0.579/PV + 6.12\ (MD) + 3.40$$

where

EDF = expected durability factor
PV = intruded volume of pores larger than 4.5 nm in diameter, cm^3
MD = median diameter of pores larger than 4.5 nm in diameter, measured by a mercury porosimeter.

An objection to MIP for predicting aggregate durability is the very small sample (2 to 5 g) that can be tested.

Equations similar to the one above, for freeze-thaw durability and porosity, have apparently not been established for aggregate properties such as strength, modulus of elasticity, Poisson's ratio and shrinkage. It appears also that no attention at all has yet been given to the presence of macro defects in aggregates, such as the micro fractures which are commonly observed in many aggregates. Although there are many tests to assess the suitability and potential durability of aggregates for use in concrete, such as for aggregate crushing value, Los Angeles abrasion resistance, magnesium sulphate soundness and drying shrinkage (which are all adversely influenced by increased porosity), I am not aware of experimental data relating porosity to the above properties of aggregates.

3.3 Concrete

Hardened concrete that is properly proportioned, mixed and placed consists of hcp, aggregate and, inevitably, entrapped voids. Voids can also be purposely entrained by the use of an air-entraining agent. The hcp is composed of remnants of cement grains, cement gel and space not filled with cement gel; these spaces are the capillary pores. The cement gel has a porosity of at least 28 per cent (7, 54). Porosity in the aggregate is most commonly between 1 and 5 per cent (55) but can be between 2 and 24 per cent, for example in limestone rocks used by Dolch (49) in freeze-thaw durability studies.

The pores in concrete therefore, can consist of gel pores, capillary pores, entrapped pores, entrained pores and pores in the aggregate. Such pores are inherent to concrete.

However, poor mixture design, placement or compaction can result in bleeding channels and pockets, cavities under aggregates and reinforcing bars, and honeycombing. Such voids are largely due to poor practice and are to a greater or lesser extent always present in concrete; however, such pores should not occur, provided concreting materials are chosen correctly and proper care is taken in manufacture.

In the short term, plastic settlement, plastic shrinkage and thermal contraction may cause cracks in concrete while, in the long term, cracks may be caused by reversible and irreversible drying shrinkage, carbonation, sulphate attack, alkali-aggregate reaction and structural movement, any of which will increase the porosity of the concrete. These cracks should not occur, provided proper care is taken.

As mentioned, cement gel has a porosity of not less than 28 per cent and it usually is higher (54). The capillary space is initially determined by the water:cement ratio and if it is about 0.35 by mass, the bulk volume of the gel will eventually be sufficient to fill this space and produce a paste free of capillary pores (55). At higher w:c ratios, a paste having a large volume of capillaries that are almost continuous will be produced, but which may, with continued curing, become filled and isolated provided that the original w:c ratio was small enough. At w:c ratios above 0.70 no amount of curing will fill capillary space.

Although only about 25 to 40 per cent by volume (15 to 30 per cent by mass) of concrete is cement paste, the strength and elasticity of the concrete is affected to a great extent by the strength of the cement paste, which is intimately related to its own porosity (51, 55). Except when aggregates are very weak, the upper limit of concrete strength tends to be determined by the strength of the cement paste and the strength of the cement-aggregate bond. However, none of the equations which relate porosity to the strength and fracture energy of the hcp can be applied directly to concrete. Fagerlund (56), therefore, suggested a strength-porosity relationship in which the effect of the aggregate is considered, as well as an equation for the calculation of the modulus of elasticity of a concrete as a function of the concrete's constituents and age (57).

4. PERMEABILITY AND DIFFUSIVITY

4.1 General aspects

The relevance of molecular transport processes in hcp and concrete has been reviewed and their relevance to durability discussed by Lawrence (58). Among the different transport processes, data on permeability are apparently the simplest to obtain. Therefore, permeability determination is the preferred test to relate to concrete durability, although diffusivity is theoretically more useful. Fortunately, results of the simpler permeability test appear to be readily convertible to diffusivity (59). A fair amount of data on the relationship between permeability and diffusivity, and other parameters such as concrete mix composition and curing has been collected by Lawrence (59).

Powers and Brownyard (7) established that there is a relationship between the capillary porosity of hcp and its permeability. Their results were analysed by Fagerlund (60), and excellent agreement was found. Fagerlund also studied the kinetics of water absorption in concrete and found that water absorption is a simple function of the capillary porosity but that the air pores larger than about 5 to 10 μm seem to take no part in the absorption at all.

Grube and Lawrence (61) reported the initial results of a co-operative investigation undertaken by seven laboratories into the permeability of concrete to oxygen. Values lay in the range of 0.001 to 30×10^{-16} m². Different laboratories reported large differences for similar mixes, amounting in extreme cases to a factor of 17 times. This large variation is ascribed to differences in casting and curing. The oxygen permeability is very sensitive to small changes in mix design and degree of curing. Initial curing is most important and for a cement content of 300 kg/m³, increasing the curing from 1 to 3 days reduced permeability by a factor of 5, on average, and by a further factor of 9 when curing was increased to 28 days. Changing the w:c ratio has a lesser but still important effect: for example, reducing the w:c ratio by 0.05 reduced permeability on average 1.6x. Increasing the cement content from 240 to 300 kg/m³ and keeping the w:c ratio 0.7, increased permeability by a factor of 2.1 on average. Similar results were obtained by Mills (62) for cement content.

The different results obtained for portland cement with additions may appear to be contradictory, unless properly interpreted. Fagerlund (60) found that increasing slag content to 65 per cent increased the resistance of concrete to water penetration. The concrete had been pre-treated for the equivalent of 91 days wet-curing when the tests were started and were dried at 50 °C for a week prior to the test. Gräf and Grube (63) found that portland blast-furnace cement (PBFC) concretes had a higher oxygen permeability than portland cement concrete, but that after prolonged sealed curing, the PBFC concrete may become more impervious. Hillsdorf et al (64) in comparing the freeze-thaw durability of portland cement concrete with PBFC concrete, both air-entrained, after exposure to carbonation, found a poorer durability for the PBFC concrete. This is ascribed to the increased capillary porosity of the PBFC concrete, because of carbonation. The effect of carbonation is much less pronounced if the surface layers are moist-cured for several weeks prior to carbonation.

For portland cement concretes containing 20 per cent fly ash, Gräf and Grube report greater permeability for one fly ash and less for another, when compared with portland cement alone, when curing has been poor. Mortars of portland cement and fly ash have higher diffusion coefficients than mortars of portland cement alone, because of the coarser pore structure of the former according to Bager (65).

Plasticisers and superplasticisers may change the pore structure of concrete detrimentally, resulting in slightly greater permeability to air, than that

of concrete made without these additives (66). In contrast, Collepardi and Massidda (67) found increased strength and decreased capillary porosity, pore diameter and permeability for concrete in which water-reducing additives were used. Resistance to sulphate attack was increased. However, it is possible that the slight differences recorded by Huovinen (66) were not significant.

4.2 Corrosion of reinforcing steel

The corrosion of reinforcing steel is the most frequent source of distress in concrete, not only in countries where de-icing salts are used, but also in arid regions, especially in coastal areas. Carbonation or reaction with SO_2 causes a drop in pH of the pore solution from 12.5 or higher to less than 9, thus destroying the passivating effect of calcium hydroxide. Chloride ions produce soluble products at the anodic site, causing a breakdown in the passivity of the steel, and oxygen consumes electrons at the cathodic site (this last reaction is rate-controlling). It is therefore natural that studies of gaseous diffusion of oxygen and carbon dioxide, and the ionic diffusion of chloride ions through concrete, should receive wide attention in an attempt to obtain critical data for the prediction of the service life of reinforced concrete.

Lawrence (59) details steel reinforcement cover requirements under different climatic conditions for different w:c ratios, based on the oxygen diffusivity in the different climatic conditions.

4.3 Carbonation

The depth of carbonation follows a square root of time law and is a function of the permeability of the concrete, the relative humidity of the concrete and the concentration of CO_2 in the environment. The depth of carbonation may vary between 19.5 mm and 0.05 mm in the first year for the worst and best situations respectively, in respect of the diffusivity of concrete (58). For low w:c ratio concrete, the depth of carbonation in the first year will typically be in the order of 1 to 2 mm and should pose no serious threat of initiation of steel corrosion except with very poor quality concrete or very shallow covers (68). Carbonation affects the pore structure of the cement paste. Total porosity is reduced, the mode of the pore size distribution being shifted towards larger diameters. The larger pores seem to be unaffected but the volume of smaller pores is reduced by a factor of 2. Carbonation reduces both the diffusivity and the permeability of especially low w:c ratio mortars. However, carbonation causes an increase in the capillary porosity of mortars made with PBFC with a slag content of 75 per cent (64). The depth of carbonation is greater where fly ash replaces part of the portland cement (69).

4.4 Chloride

Sorenson and Maahn (70) studied chloride penetration in 15- to 20-year-old concrete in Denmark. Chloride penetration can be approximated by a semifinite diffusion system which follows the square root of time law and is a function of the initial concentration of chloride in the concrete, the effective surface concentration of chloride, the permeability and the humidity of the concrete. The reaction of chloride with certain cement constituents, affects the diffusion coefficient. If 0.06 per cent chloride in concrete, by mass, is considered the threshhold concentration in respect of steel corrosion, then within 15 to 20 years this value is attained 30 to 120 mm below the concrete surface (the depth of the outermost reinforcement). Because some of the chloride is bound as Friedel's salt, it would be desirable to have a measure of the critical chloride concentration based on pore solution or water-soluble chloride.

For concrete immersed in sea water (0.9 per cent chloride; diffusion coefficient of chloride ion $D = 5 \times 10^{-12}$ m²/s for NaCl), Lawrence (58) gives a chloride concentration of about 0.009 per cent in 1.3 years and 0.3 per cent in 9 years, at a depth of 50 mm. Doubling the depth of cover quadruples the time required for a certain concentration of chloride to be reached. The pore size distribution of hcp is altered by chloride penetration and the greater the amount of chloride present, the smaller the pores found; consequently the permeability to water will be reduced (71).

The diffusion coefficients of chloride ion into hcp vary from 3 to 7 x 10^{-12} m²/s for the monovalent cations Li^+, Na^+ and K^+ but increase to 10 to 18 x 10^{-12} m²/s when the accompanying cations are Ca^{++} or Mg^{++}. The diffusion coefficient of chloride decreases in the order $MgCl_2$>$CaCl_2$>LiCl>KCl>NaCl. The diffusion coefficients of the alkali metal cations are somewhat less than those of chloride and vary between 2 to 3 x 10^{-12} m²/s (72).

Hansson et al (73) report that for the same quantity of chloride added to ordinary portland cement mortar as $CaCl_2$, NaCl or KCl, the corrosion rate is strongly dependent on the cation, $CaCl_2$, having a much more deleterious effect than either NaCl or KCl. The addition of $CaCl_2$ creates a more open pore structure which allows easier diffusion and a higher electrical conductivity, and it reduces the pH of the pore solution. NaCl and KCl increase the porosity to a lesser extent and they increase the pH of the pore solution.

4.5 Sulphate

The diffusion of sulphate into hcp gives diffusion coefficients between 2 and 30 x 10^{-14} m²/s, which is 10 to 100 times slower than for chloride (74). Lawrence (58) calculated the maximum and minimum depths of penetration of sulphate ions ($D = 10^{-13}$ m²/s) into concrete for combinations of 200 and 500 kg cement per m³, and SO_4 concentrations of 0.1 and 1 per cent, to be 3.8 and 0.6 mm after 3 years.

4.6 Drying and wetting

Equations for the movement of liquid water or aqueous solution into dried concrete and their application are explained by Lawrence (58). According to Bažant and Najjar (75), the drying of concrete is a nonlinear diffusion function. The diffusion coefficient decreases sharply from 2.2 x 10^{-6} to 5.5 x 10^{-11} m²/s as the pore humidity drops from 0.9 to 0.6 while below 0.6 it appears to be approximately constant. Kalimeris and Hall (76) applied the unsaturated water-flow theory developed mainly by soil physicists to water-flow processes in porous building materials,

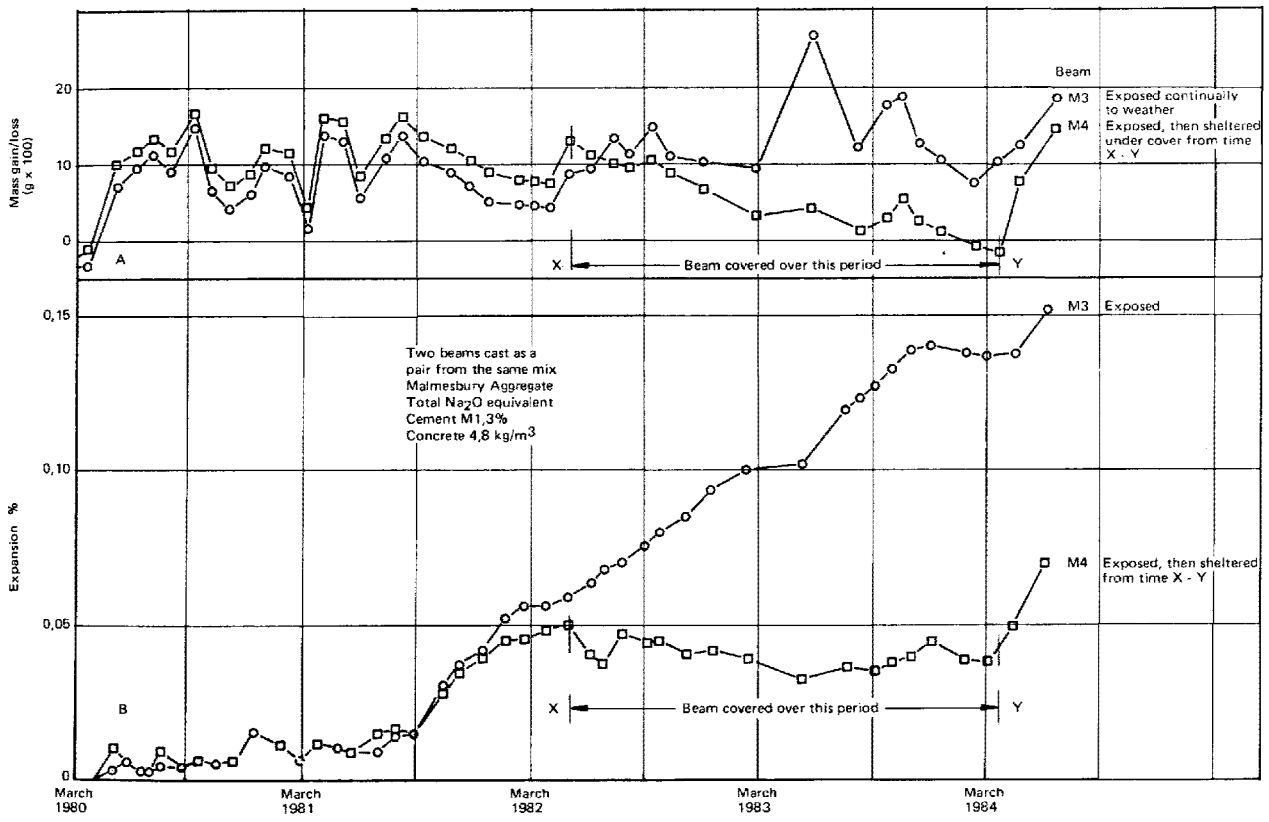

FIGURE 4: The effect of exposure conditions on mass gain and loss and the expansion caused by alkali-silica reaction in concrete beams, 1 000 mm x 350 mm x 400 mm (77)

but did not extend the theory to include systems where soluble salts are present, in other words, where there are osmotic and other solute-dependent effects. Clearly, more work is required to relate unsaturated water flow to both pore structure and durability of cementitious systems.

4.7 Frost durability

The susceptibility of concrete to frost damage depends on the permeability of the cement paste, the degree of saturation, the amount of freezable water, the rate of freezing and the average maximum distance from any point in the paste to a free water surface where ice can form safely. An air content of at least 3 per cent by volume of the concrete is required to provide the bubble spacing not exceeding 0.2 mm and void size between 0.05 and 1.25 mm which are necessary to ensure frost durability. A strength loss of 10 to 20 per cent due to 2 to 4 per cent air entrainment can be anticipated if the water content is not reduced, and careful control of concrete mix parameters is therefore required to achieve both the required volume of bubbles and permeability of the paste, to ensure frost durability without affecting the concrete strength detrimentally (8,17).

4.8 Alkali-aggregate reaction

Very few quantitative data are available on molecular transport processes in concrete and their effect on alkali-aggregate reaction. It is, however, known that moisture plays a very important role. The curves in Figure 4 show that expansion caused by alkali-silica reaction, under natural exposure conditions, stops if the concrete is sheltered and starts again when the cover is removed. The interruption in expansion is followed by a loss in mass of the concrete. A similar effect is obtained if the concrete is coated with a solvent-based silicone (77).

5. CEMENT PROPERTIES, CONCRETE TECHNOLOGY AND DURABILITY

Exhaustive research has been done on porosity and its influence on the mechanical, physical and morphological properties of hcp, and the influence of factors such as w:c ratio on porosity. It appears, however, that the concrete industry is either unaware of such research, or not applying it. Corish and Jackson (78) and a working group of the British Concrete Society (79), recently showed

TABLE 2: Changing strengths of Portland cement concrete in Great Britain. Cement content ca. 300 kg/m³, w:c ratio 0.60 (80)

Period	28-day-strength in N/mm²
1945 - 1947	25.0
1948 - 1953	29.0
1954 - 1958	33.0
1959 - 1965	36.5
1966 - 1974	39.5
1975 - 1980	43.5

TABLE 3: Changing cement contents and maximum w:c ratios for concretes in Great Britain, achieving a 28-day strength of 33 MPa, all with the same workability (80)

Period	Minimum Cement content	Maximum water:cement
1945 - 1947	380 kg/m³	0.47
1948 - 1953	325 kg/m³	0.55
1954 - 1958	300 kg/m³	0.60
1959 - 1965	280 kg/m³	0.64
1966 - 1974	265 kg/m³	0.67
1975 - 1980	250 kg/m³	0.72

that the major differences in British cements through the years, have been an increase in the ratio of C_3S to C_2S, while the proportion of silicates has remained about constant. The proportions of the other compounds in cement have also remained constant and cement has not become significantly finer. There has been a marked increase in the strength of concrete with a given quantity of cement, most noticeably at an early age. As strengths went up, cement contents dropped and w:c ratios increased. The changes in concrete mix proportions and strength are reflected in Tables 2 and 3 from Wischers (80).

In the United States, cement strengths have more than tripled since 1916, mainly owing to finer grinding. During this period the cement content of the same class of concrete has decreased by 40 per cent, from about 380 to 230 kg/m³ (w:c ratio about 0.45) (81).

The above changes in properties of cement, and the resultant changes in concrete design parameters, naturally cause concern about the durability of the concrete. Parrot (82) has developed a predictive model which utilises research data to assess the effect of such changes on the properties of concrete. The input variables are mass fractions of the cement phases, surface area, w:c ratio, maximum days cured, curing conditions and temperature. The main output data are relative volumes of C_2S, C_3S, C_3A, C_4AF, gypsum and fly ash; relative volumes of calcium hydroxide and calcium silicate; relative volumes of C_3A and C_4AF hydrates; total porosity, porosity larger than 4 nm, and porosity smaller than 4 nm; relative humidity, both evaporable and chemically bound water; the heat evolved, the rate of heat evolution, compressive strength, paste density and permeability to water.

Parrot's model indicates that modern cements have disadvantages that may outweigh their advantages; for higher strength concrete, modern cements still require shorter curing times to achieve a given permeability, but for lower strength concrete, longer curing times are required. The longer curing times required at lower strengths to achieve low permeability, are impractical, regardless of the cement composition. Modern, high early strength cements enable less cement and higher w:c ratios to be used to achieve the required strength; this results in more porous concrete with a higher permeability and lower durability than previously. It is therefore imperative, when specifying a grade of concrete, to provide for durability by specifying a minimum cement content and a maximum w:c ratio. Minimum cement contents should, however, be realistic and due regard must be given to unfavourable effects of unnecessarily high cement contents, such as shrinkage, thermal cracking and possible high alkali content.

6. PROSPECTS

During the past 15 years attention has been given to the development of low-porosity cementitious products. More recently, there has been a coordinated effort to test the permeability and diffusivity of hcp and concrete as well as an attempt to relate the results to problems of durability.

The foregoing discussion indicates that future research should be directed in the directions outlined below:

(i) It is imperative to capture all details of construction projects in data bases, to establish computerised management systems for the maintenance, repair and rehabilitation of structures, to record information on the durability of concrete materials and to feed the data to researchers.

(ii) Efforts to develop models for the prediction of service life at the initial stage of planning of a structure, and to aid mix design for maximum durability under particular exposure conditions, should be intensified and results applied.

(iii) A greater number of reliable accelerated tests, properly correlated to long-term tests and performance in practice, are required to test the constituents of concrete and to use the data in predictive service-life models.

(iv) Models of hcp need to be refined since they assist in the interpretation of test results for properties such as specific surface, pore structure, state of water, permeability and diffusivity. The techniques used to determine these properties also need refinement.

(v) Continued research is required into the methods of characterising pore structure of hcp, aggregate and concrete to attempt to eliminate, or at least explain different results obtained by different methods.

(vi) Procedures for permeability and diffusivity determinations must be standardised to eliminate large differences obtained by different laboratories.

(vii) The results of the mathematical modelling of cement hydration, pore structure and permeability have been successfully applied to concrete design. Such modelling needs to be continued and improved.

(viii) The application of theory and technology to produce low-porosity cement systems needs more attention.

(ix) Overall, it appears that the durability of concrete can be expressed in terms of either porosity or one of the related parameters - permeability or diffusivity. The knowledge to design durable concrete under most environmental and exposure conditions, exists. A major effort is, however, required to impart this knowledge to the construction sector and to produce durable concrete under a diversity of field conditions.

7. ACKNOWLEDGEMENTS

The useful comments of Dr D Davis, retired Executive Director of the Portland Cement Institute of South Africa, Mr J van Dijk of the NBRI and the plotting of the graphs by Dr G Davies of the NBRI, are gratefully acknowledged.

8. REFERENCES

1. H J Wierig (1984). Foreword. Proceedings of the RILEM seminar on The Durability of Concrete Structures Under Normal Outdoor Exposure, Hannover.

2. K Shirayama (1985). Research activities and administrative measures on durability of buildings. State of the art in Japan. Materiaux et Constructions, 18, No 105, 215-221.

3. H Wiegler (1984). Recommended practice in Germany (FRG) for improved durability of concrete structures under outdoor exposure conditions. Proceedings of the RILEM seminar on The Durability of Concrete Structures Under Normal Outdoor Exposure, Hannover, 19-25.

4. J W Martin (1984). Service life prediction from accelerated ageing test results using reliability theory and life testing analysis. Quoted from Reference 5.

5. J R Wright and G Frohnsdorff (1985). Durability of building materials: durability research in the United States and the influence of RILEM on durability research. Materiaux et Constructions, 18, No 105, 205-214.

6. R E Oberholster, J H P van Aardt and M P Brandt (1983). Durability of cementitious systems in Structure and Performance of Cements. Edited by P Barnes. Applied Science Publishers, London and New York, 365-413.

7. T C Powers and T L Brownyard (1946, 1947). Studies of the physical properties of hardened portland cement paste. J Amer Concr Inst, Vol 18, Nos 2 to 8.

8. T C Powers (1958). The physical structure and engineering properties of concrete. PCA Bulletin. No 'C, Chicago, 28 pp.

9. R F Feldman and P J Sereda (1970). A new model for hydrated portland cement and its practical implications. Eng. Jour (Canada) 53, 53-59.

10. M Daimon, S A Abo-El-Enein, G Hosaka, S Goto and R Kondo (1977). Pore structure of calcium silicate hydrate in hydrated tricalcium silicate. Jour Amer Ceram Soc, 60, 110-114.

11. S Brunauer, J Skalny and I Odler (1973). Pore structure and properties of materials. Proc RILEM/IUPAC Int Symp Pore Structure and Properties of Materials, Prague, C3-26.

12. R F Feldman (1968). Sorption and length-change scanning isotherms of methanol and water on hydrated portland cement paste. Proceedings Fifth International Congress on the Chemistry of Cement, Tokyo, Japan, 53-66.

13. N McN Alford and A A Rahman (1981). An assessment of porosity and pore sizes in hardened cement pastes. J Mater Sci 16, 3105-3114.

14. A A Rahman (1984). Characterisation of the porosity of hydrated cement pastes. British Ceramic Proceedings, No 35. The Chemistry and Chemically Related Properties of Cement, 249-266.

15. F H Wittman (1979). Trends in research on creep and shrinkage of concrete. Publication No 79-08, Cement Production and Use. Engineering Foundation, New York, pp 143-161.

16. F H Wittman (1980). Properties of hardened cement paste. Proceedings Seventh International Congress on the Chemistry of Cement, Paris, V1-2, pp 1-14.

17. S Mindess and J F Young (1981). Concrete. Prentice-Hall Inc, New Jersey.

18. D Winslow (1978). The validity of high pressure mercury intrusion porosimetry. J Colloid and Interface Sci 67, 42-47.

19. R F Feldman (1973). Volume change, porosity and helium flow studies of hydrated portland cement. Proceedings RILEM/IUPAC Int Symp Pore Structure and Properties of Materials, Prague, C101-116.

20. D H C Harris, C G Windsor and C D Lawrence (1974). Free and bound water in cement pastes. Mag Concr Res 26 (87), 65-72.

21. D N Winslow and S Diamond (1970). A mercury porosimetry study of the evaluation of porosity in portland cement. ASTM J Mater 5, 564-585.

22. S Diamond (1971). A critical comparison of mercury porosimetry and capillary condensation pore size distributions of portland cement pastes. Cem Concr Res 1, 531-545.

23. J J Beaudoin (1979). Porosity measurements of some hydrated cementitious systems by high pressure mercury intrusion - microstructural limitations. Cem Concr Res 9, 771-781.

24. P J Sereda, R F Feldman and V S Ramachandran (1980). Structure formation and development in hardened cement pastes. Proceedings Sixth International Congress on the Chemistry of Cement, Paris, Sub-theme V1-7, 3-44.

25. K Kendall, A J Howard and J D Birchall (1983). The relation between porosity, microstructure and strength, and the approach to advanced cement-based materials. Phil Trans R Soc London. A310, 139-153.

26. M Y Balshin (1949). Relation of mechanical properties of powdered metals and their porosity and the ultimate properties of porous metal. Dokl Akad Nauk SSSR, 67, 831-834, quoted from Reference 24.

27. E Ryshkewitch (1953). Compression strength of porous sintered alumina and zirconia. J Amer Ceram Soc. 36, 65-68.

28. K K Schiller (1971). Strength of porous materials. Cem Concr Res 1, 419-422.

29. T C Hansen (1965). Influence of aggregates and voids on modulus of elasticity of concrete, cement mortar and cement paste. J Amer Concr Inst 62, 193-215.

30. R H Helmuth and D H Turk (1966). Elastic moduli of hardened portland cement and tricalcium silicate pastes: Effect of porosity. Symposium on Structure of Portland Cement Paste and Concrete, No 90, 135-144. Washington: Highway Research Board.

31. R W Rice. S W Freeman, R C Pahanka, J J Mechalsky, Jr, and C CM Wu (1977). Microstructural dependence of fracture mechanics parameters in ceramics. Symposium on Fracture Mechanics of Ceramics, Vol 4, 849-876.

32. G Verbeck and R A Helmuth (1968). Structures and physical properties of cement pastes. Proceedings Fifth International Symposium on the Chemistry of Cement, Tokyo, Vol III, 1-31.

33. T C Powers (1960). Physical properties of cement paste. Proceedings Fourth International Symposium on the Chemistry of Cement, Washington, Vol II, 577-613.

34. I Soroka and P J Sereda (1968). The structure of cement-stone and the use of compacts as structural models. Proceedings Fifth International Symposium on the Chemistry of Cement, Tokyo, Vol III, 67-73.

35. D M Roy, G R Gouda and A Bobrowsky (1972). Very high strength cement paste prepared by hot pressing and other high pressure techniques. Cem Concr Res 2, 349-366.

36. D M Roy and G R Gouda (1973). High strength generation in cement pastes. Cem Concr Res 3, 807-820.

37. D M Roy and G R Gouda (1975). Optimisation of strength in cement pastes. Cem Concr Res 5, 153-162.

38. M Yudenfreund, I Odler and S Brunauer (1972). Hardened Portland cement pastes of low porosity. I. Materials and experimental methods. Cem Concr Res 2, 313-330.

39. M Yudenfreund, J Skalny, R Sh Mikhail, S Brunauer (1972). Hardened portland cement pastes of low porosity. II. Exploratory studies. Dimensional changes. Cem Concr Res 2, 331-348.

40. I Odler, M Yudenfreund, J Skalny and S Brunauer (1972). Hardened portland cement pastes of low porosity. III. Degree of hydration. Expansion of paste. Total porosity. Cem Concr Res 2, 463-480.

41. I Odler, J Hagymassy, Jr, E E Bodor, M Yudenfreund and S Brunauer (1972). Hardened portland cement pastes of low porosity. IV. Surface area and pore structure. Cem Concr Res 2, 577-589.

42. M Yudenfreund, K M Hanna, J Skalny, I Odler and S Brunauer (1972). Hardened portland cement paste of low porosity. V. Compressive strength. Cem Concr Res 2, 731-743.

43. R F Feldman and J J Beaudoin (1976). Structure and properties of porous cement systems and their modification by impregnants. Proceedings Conf on Hydraulic Cement Pastes: Their Structure and Properties, Sheffield, 150-165.

44. R N Swamy (1979). Review. Polymer reinforcement of cement systems. J Mater Sci 14 1521-1553.

45. J D Birchall, A J Howard and K Kendall (1981). Flexural strength and porosity of cements. Nature Vol 289, 388-390.

46. N McN Alford (1981). A theoretical argument for the existence of high strength cement pastes. Cem Concr Res 11, 605-610.

47. J D Birchall (1983). Cement in the context of new materials for an energy-expensive future. Phil Trans R Soc Lond A310, 31-42.

48. J J Beaudoin and R F Feldman (1985). High strength cement pastes - a critical appraisal. Cem Concr Res 15, 105-116.

49. Dolch, W L (1959). Studies of limestone aggregates by fluid-flow methods. Proceedings Amer Soc for Testing and Materials (ASTM) Vol 59, 1204-1215.

50. Sweet, H S (1948). Research on concrete durability as affected by coarse aggregate. Proceedings Amer Soc for Testing and Materials (ASTM) Vol 48, 988-1016.

51. W L Dolch (1978). Porosity. ASTM STP 169B: Significance of Tests and Properties of Concrete and Concrete-Making Materials, 646-655.

52. Verbeck, G J and R Landgren (1960). Influence of physical characteristics of aggregates on frost resistance of concrete. Proceedings Amer Soc for Testing and Materials, Vol 60, 1063-1079.

53. A Shakoor and C F Scholer (1985). Comparison of aggregate pore characteristics as measured by mercury intrusion porosimeter and Iowa pore index results. ACI Journal, 82, No 4, 453-458.

54. T C Powers 1978. The nature of concrete. ASTM STP 169B: Significance of Tests and Properties of Concrete and Concrete-Making Materials, 59-73.

55. G Verbeck (1978). Pore structure. ASTM STP 169B: Significance of Tests and Properties of Concrete and Concrete-Making Materials, 262-274.

56. G Fagerlund (1973). Strength and porosity of concrete. Proceedings RILEM/IUPAC International Symposium on Pore Structure and Properties of Materials, Prague, D51-73.

57. G Fagerlund (1973). The elastic moduli of concrete. Ibid, D129-141.

58. C D Lawrence (1981). Durability of concrete: molecular transport processes and test methods. C & CA Technical Report 544, 25 pp.

59. C D Lawrence (1984). Transport of oxygen through concrete. British Ceramic Proceedings, No 35, Chemistry and Chemically-Related Properties of Cement, 277-293.

60. G Fagerlund (1982). On the capillarity of concrete. Nordic Concrete Research, Publication No 1, Oslo, 6.1-6.20.

61. H Grube and C D Lawrence (1984). Permeability of concrete to oxygen. Proceedings of the RILEM Seminar on the Durability of Concrete Structures under Normal Outdoor Exposure, Hannover, 68-79.

62. R H Mills (1985). Mass transfer of water vapour through concrete. Cem Concr Res 15, 74-82.

63. H Gräf and H Grube (1984). The influence of curing on the gas permeability of concrete with different compositions. Proceedings of the RILEM Seminar on the Durability of Concrete Structures under Normal Outdoor Exposure, Hannover, 80-89.

64. H K Hilsdorf, J Kropp and M Günter. Carbonation, pore structure and permeability. Ibid 182-196.

65. H Bager (1984). Effect of curing on the pore structure and permeability of cement-fly ash mortars. Ibid, 102-115.

66. P Huovinen (1982). Air permeability of concrete. Nordic Concrete Research, Publication No 1, Oslo, 10.1-10.17.

67. M Collepardi and L Massidda (1976). The influence of water-reducing admixtures on the cement paste and concrete properties. Proceedings Conf on Hydraulic Cement Pastes: Their Structure and Properties, Sheffield, 256-267.

68. D G Manning (1985). Debate: Crack width, cover and corrosion. Concrete International, 7, No 5, 20-21.

69. R G Patel, L J Parrot, J A Martin and D C Killoh (1985). Gradients of microstructure and diffusion properties in cement paste caused by drying. Cem Concr Res 15, 343-356.

70. B Sorenson and E Maahn (1982). Penetration rate of chloride in marine concrete structures. Nordic Concrete Research, Publication No 1, Oslo, 24.1 - 24.18.

71. H Midgley and J M Illston (1984). The penetration of chlorides into hardened cement paste. Cem and Concr Res, 41, 546-558.

72. H Ushiyama and S Goto (1974). Diffusion of various ions in hardened portland cement paste. Sixth International Symposium on the Chemistry of Cement, Moscow, pp 23.

73. C M Hansson, Th Frølund and J B Markussen (1985). The effect of chloride cation type on the corrosion of steel in concrete by chloride salts. Cem Concr Res 15, 65-73.

74. J W T Spinks, H W Baldwin and T Thorvaldson (1952). Tracer studies of diffusion in set portland cement. Canadian Journal of Technology, 30, 20-28.

75. Z P Bažant and L U Najjar (1971). Drying of concrete as a nonlinear diffusion problem. Cem Concr Res 1, 461-473.

76. N Kalimeris and C Hall (1983). Absorption and desorption of water by porous building materials. Proceedings International Conference on Materials Science and Restoration, Esslingen, 57-66.

77. K E Putterill and R E Oberholster (1985). Investigation of the different variables that influence the expansion of concrete caused by alkali-aggregate reaction under natural environmental conditions. CSIR Research Report BRR 626, Pretoria, South Africa, 31pp.

78. A T Corish and P J Jackson (1982). Portland cement properties - past and present. Concrete 16, No 7, 16-18.

79. British Concrete Society (1984). Changes in cement properties and their effects on concrete. London, 22 pp.

80. G Wischers (1984). The impact of the quality of concrete constructions on the cement market. Holderbank Management and Consulting Ltd. Group Meeting Aug 1984. Report No DIR 84/8448/4, p4.

81. E Munro (1985). Concrete durability in a free market system. Cementimagination, Sept, 2pp.

82. L J Parrot and D C Killoh (1984). Prediction of cement hydration. British Ceramic Proceedings, No 35, The Chemistry and Chemically-Related Properties of Cement, 41-53.

R.F. Feldman, Division of Building Research, National Research Council Canada

PORE STRUCTURE, PERMEABILITY AND DIFFUSIVITY AS RELATED TO DURABILITY
INFLUENCE DE LA STRUCTURE DES PORES, DE LA PERMÉABILITÉ ET DE LA DIFFUSIVITÉ SUR LA DURABILITÉ

SUMMARY: This paper discusses permeability measurements made by fluids, water and oxygen, on both normal and blended hydrated portland cements. Sample preparation and experimental procedure are vital considerations. Pore structure determinations by several procedures are discussed together with work relating it to permeability.

Methods of diffusion measurements of both ions and oxygen are presented and related to the protection of reinforcing steel by the concrete matrix. Counter-diffusion methods of water replacement by different fluids are compared. The relevance of several techniques to giving information with regard to resistance of concrete to various forms of attack is debated.

R.F. Feldman, Division of Building Research, National Research Council Canada

INTRODUCTION

Most physical and engineering properties of hardened cement pastes and concretes depend on their microstructure. Relationships between compressive strength and porosity have been researched greatly and have been adequately reviewed (1). However, several studies on durability have indicated that permeability is probably the most important factor in relation to durability (2-9).

The objective of durability studies is to predict performance in various environments. Some of these environments cause chemical changes in concrete which depend on the permeation of the reacting species (10). The permeation may be in the liquid state, e.g., water containing various ions, or in the gaseous state, such as oxygen or carbon dioxide (11,12). In many instances the transport mechanism may involve diffusion, such as in the case of the penetration of chloride or sulfate ions (7,13,14), but the diffusivity of a body may be related to similar pore structure parameters, as is permeability (11).

Accurate measurement of permeability is important for characterizing materials in nuclear waste isolation and other applications (15-19), and this has led to a renewed effort in understanding permeability-pore structure relationships (20-25).

Recently, there has been increasing concern over the factors that control the durability of exposed, reinforced concrete structures (6,8,26-33). Whereas it is recognized that good quality concrete provides adequate protection under normal circumstances, it is also clear that in certain structures, such as bridges and parking garages, and some in contact with sea water, where chloride ions are present in sufficient quantity, new approaches are needed (34-44).

Specifications for concrete have often been based on its 28-day strengths, but it is now apparent that quantitative information is required on the effect of a range of parameters such as the water/cement ratio, the binder content, curing conditions, effect of cement additives and replacements on the durability and thus permeability of concrete (44-45).

New studies have revealed that durability of cement and concrete can be improved by the incorporation of materials such as pulverized fuel ash (fly-ash), condensed silica fume, rice husk ash, and other pozzolanic materials (34-44). Although it is known that these materials react with calcium hydroxide produced by portland cement hydration, little is known about the changes in structure brought about by this interaction. Similar results with regard to the permeability of mixtures of portland cement and ground granulated blast furnace slag have been observed (36,46). Some workers have correlated these properties with the $Ca(OH)_2$-CSH interface (37,47) and others with the apparent increased volume of small pores (36).

Despite several investigations of the effects of supplementary cementing materials on permeability and the relation of these to pore structure, the factors controlling permeability are still not clearly understood (24,36,44). This is partly due to the methods of obtaining pore-size distribution data. Several investigations have shown that the pore-size distribution curves obtained from mercury intrusion porosimetry (the main method for obtaining pore-size distribution data) are subject to details of the specimen preparation prior to the experiments (48-50).

In recent years, investigators have used different methods of drying specimens before making pore structure measurements (51-55). These methods include the use of solvents, such as methanol, which has recently been shown to react with $Ca(OH)_2$ and possibly CSH (56-58), and isopropanol (50), which appears to show more promise since it is relatively non-reactive. Some of these methods have been compared with direct oven drying, and differences in porosity have been used to develop explanations for permeabilities of both blended and plain pastes (25,49,53).

Permeability and diffusivity related to durability of mortars and concretes involve more parameters than those involving paste, such as the nature of the aggregate paste bonds and interfaces. Greater difficulties than with pastes may also exist with cracking on drying, due to the restraint of the aggregate.

The objective of this review is to identify the basic factors relating pore structure to permeability (and diffusivity) and how they affect durability.

EQUATIONS USED TO CALCULATE PERMEABILITY

Permeability to Water

The permeability coefficient is most commonly calculated through a modified D'Arcy equation:

$$Q = KA \frac{dh}{dx} \qquad (1)$$

where

- Q = flow through the specimen (m^3/s)
- K = permeability of medium (m/s)
- A = cross-sectional area through which flow is occurring (m^2)
- $\frac{dh}{dx}$ = hydraulic gradient across the specimen and is equal to $P/\rho g \ell$
- ℓ = thickness of the specimen, P is the applied pressure and ρ is the density.

Permeability to Oxygen

Contrary to the case of water, oxygen is compressible and the pressure gradient through the concrete or cement paste pores will be considerable; the mass flow rate of gas, however, must be the same through the concrete specimen length when a steady flow has been achieved.

During experimental determination, gas flow rate, R (cm^3/s) is measured at an absolute pressure of P_1 bar, with an input pressure of P_2 bar. Thus, in the D'Arcy equation, the flow rate is taken at the average pressure $(P_2 + P_1)/2$, while the pressure gradient across the specimen of thickness L is $P_2 - P_1$. Assuming the viscosity of oxygen to be

2.02×10^{-5} Ns/m^2 at 20°C, the permeability coefficient is calculated as:

$$K = \frac{4.04 \cdot R \cdot P_1 \cdot L \cdot 10^{-16}}{A \cdot (P_2^2 - P_1^2)} \quad m^2/s \qquad (2)$$

Diffusion of Water Vapour

When saturated specimens of paste or concrete are dried under controlled conditions, the simple measurement of weight loss with time can give an estimate of the diffusion constant "D" (m^2/s), as shown in the following equation for small-to-moderate times:

$$\frac{W_t}{W_\infty} = 1.127 \sqrt{\frac{Dt}{L^2}} \qquad (3)$$

where W_t is the weight loss at time, t(s), and W_∞ is the ultimate weight loss. L(m) is half the thickness of the specimen.

Diffusion of Oxygen Through Saturated Specimens

A simple diffusion equation based on Fick's law is usually employed in calculating D_N, the average effective diffusivity (m^2/s).

$$Q_A = \frac{D_N \times S \times (C_1 - C_2) \times P}{L \times R \times T} \qquad (4)$$

where

Q_A = molecular flow of oxygen (mol/s)
L = thickness of the specimen (m)
S = cross-sectional area (m^2)
R = gas constant (m^3 atm/K mol) = 8.206×10^{-5}
T = absolute temperature
C_1 and C_2 are the mole fractions of oxygen in the gaseous phases in contact with opposing faces of the specimen.

Diffusion of Ions Through Saturated Cement Pastes

If a specimen of cement paste of thickness "ℓ" and area "A" separates two compartments where in one an ionic species has concentration C_1 and in the other a concentration C_2, where $C_1 >> C_2$, C_1 is effectively constant and C_2 increases linearly, then a quasi-steady state exists and the activity of chloride ion does not change at all points in the specimen.

Thus,
$$C_2 = \frac{DA\,C_1\,(t - t_o)}{V \times \ell} \qquad (5)$$

where

V = volume of compartment 2
t_o = time taken for steady-state conditions to occur
D(cm^2/g) = effective diffusivity of the ion.

This diffusivity is also called the intrinsic diffusivity (D_i) and experimentally it is easier to work in terms of the average flux per unit area of the medium rather than the liquid. However,

$$D_i = D_f \frac{\varepsilon\delta}{\tau^2} \qquad (6)$$

where

D_f = diffusivity in free liquid
ε = volume of pore fraction
τ = tortusity
δ = constrictivity, which depends both on the porous medium and the diffusion species

$\varepsilon\delta/\tau^2$ is known as the diffusibility of the medium.

Diffusion Coefficient of Chloride Ions from Non-Steady State Values

The diffusion coefficients may be calculated for chloride ions by measuring the quantity of chloride penetrated at various distances within the specimen:

$$D_{C\ell} = \frac{-1}{2t} \cdot \frac{dx}{dc} \int_o^{C_1} x\,dc \qquad (7)$$

where

$D_{C\ell}$(cm^2/s) = diffusion coefficient
x = distance (cm) from the boundary
t = time (s)

dx/dc is calculated from the slope of the chloride concentration vs. distance plot and $\int_o^{C_1} x\,dc$ is calculated from the area under the curve.

SAMPLE PREPARATION FOR MEASUREMENT OF PERMEABILITY

Water Permeability

Many researchers have commented upon the length of time taken for steady-state flow conditions to be established when water at high pressure is forced through the pores of concrete or pastes (25,35,45,48,49). In fact, in some instances a reverse flow has been observed.

Many explanations have been offered: a) continued hydration during the test; b) calcium hydroxide transport and crystallization in larger pores, causing blocking; c) formation of calcite in pores; d) changing composition of pore solution; e) lack of initial saturation of the concrete; f) effect of water pressure on stability of pore structures. Day et al. questioned whether total steady state would, in fact, be attained, and defined steady state as the change of permeability coefficient in one day, being less than 0.1×10^{-12} m/s (48). Most workers have emphasized the need to vacuum saturate specimens before the test; Day et al. (48) reported results in which vacuum saturation procedures were performed over a period of 20 days without an appreciable change in weight, but the permeability test resulted in an increase in sample weight of 25 to 50% of the weight of water which flowed through the concrete. It is apparent that satisfactory results cannot be obtained on unsaturated specimens, and to saturate specimens by vacuum is difficult.

Care must be taken to avoid cracks in the concrete due to drying or to have ruptures occurring at the seal (the side of the specimen where it is held in the apparatus). Leaks also will give totally erroneous values.

TABLE 1. Summary of Results from Oxygen Permeability Tests (48)

Concrete Type	No. of Samples	Sat. Moist Content, % of SSD	Drying Method	Total Days	Moisture Loss, % of SSD	Perm. to Oxygen (E-9 m/s) (+/- stand. dev.)	Perm. After 105°C Drying (E-9 m/s) (+/- stand. dev.)
Plain Concrete Mix I	6	4.8	Vacuum @ 20°C	62	3.6	54+/-25	151+/-41
	5	4.8	50% rh @ 20°C	58	3.2	63+/-23	171+/-22
	8	4.7	Isoprop.+ 38°C Oven	60	3.8	27+/-8	91+/-37
Fly-ash Concrete Mix II	6	5.4	Vacuum @ 20°C	73	3.8	22+/-1	55+/-19
	5	5.3	50% rh @ 20°C	56	3.6	35+/-7	86+/-25
	9	5.3	Isoprop.+ 38°C Oven	59	3.2	13+/-5	38+/-18

Oxygen Permeability

Oxygen permeability measurements are quick since reliable steady-state values are attained rapidly, and applied pressures can be low (11). However, in order to make a measurement, the specimen must be dried, and changes in the pore structure with respect to saturated conditions will probably result. The results of oxygen permeability experiments performed by Day et al. (48) on concrete are presented in Table 1. Three procedures of drying were used: (i) vacuum drying at 20°C; (ii) drying at 53% RH at 20°C in a gloved box; (iii) isopropanol solvent replacement followed by drying in an oven at 38°C.

After permeability measurements were made, all specimens were oven dried at 105°C and permeability to oxygen was again measured. The results indicate that the drying method had a large influence, with the isopropanol replacement yielding the lowest permeabilities. Oven drying in every case increased the permeabilities considerably but it is possible that part of this may be due to microcracking of the concrete. The other differences are thought to be due to pore structure collapse and coarsening of the pores leading to higher permeabilities. It has been suggested by Day et al. (48) and Marsh (25) that the isopropanol drying causes the least disruption to the pore structure. Work by Parrot, using methanol and other organic solvents, leads to the same conclusion (51).

PORE STRUCTURE DETERMINATIONS

Permeability has been shown to be dependent not so much upon porosity, as are some mechanical properties, but on pore-size distributions (20,21). Three methods are mainly used for measuring pore-size distribution: (A) mercury intrusion porosimetry; (B) gas adsorption-desorption, usually performed with nitrogen or butane; (C) electron microscopy and image analysis; there is a fourth method, (D) Wood's metal intrusion, which is similar to A.

A - In order to measure the pore-size distribution of a body, the sample must be dried, and microstructural properties of cement paste are highly dependent upon the details of drying. Marsh et al. (50) have measured pore-size distributions for propan-2-ol-dried specimens and for identical specimens dried directly in the oven at 105°C. The results for ordinary portland cement paste and a fly-ash blend are presented in Figs. 1 and 2, respectively, each for the two drying procedures. The thickness of the specimens used in these drying procedures was not reported.

For the ordinary cement, after two months hydration, there is a reduced slope for oven-dried specimens below 80 Å pore radius, but overall the distribution curves are not largely different. However, for the one-day specimen (Fig. 1) and the fly-ash blends (Fig. 2) there are large differences, as there are also for the threshold diameters, R_t, in Fig. 2. Pore volumes at pore radii equal to and greater than 350 Å and two months hydration are not too different for the ordinary cement, but differences are greater for the blended paste; this suggests that drying might affect the permeability of blended pastes but not that of ordinary pastes.

Feldman (37,38,47) measured pore-size distributions of ordinary portland cement, fly-ash, slag and silica fume blends. Drying in these cases was done by evacuating thin specimens (1 mm thick) for 15-24 hours before heating to 105°C. Results are shown in Figs. 3 and 4. In the case of ordinary portland cement, intrusion curves are of decreasing slope (concave to the pore-size axis), while for the blends of slag and fly-ash the curves become convex to the pore-size axis (increasing slope) between 28 days and three months hydration. In the case of silica fume, the blends become concave between seven and fourteen days hydration (Fig. 4), depending on the concentration of silica fume. The fly-ash samples of Marsh and Day, dried by solvent replacement, also show this feature (50). This result has been related to the $Ca(OH)_2$ content of the body (37) (Fig. 5a). The slope of the distribution curve at maximum intruded pressure was plotted against hydration time in Fig. 5b. The

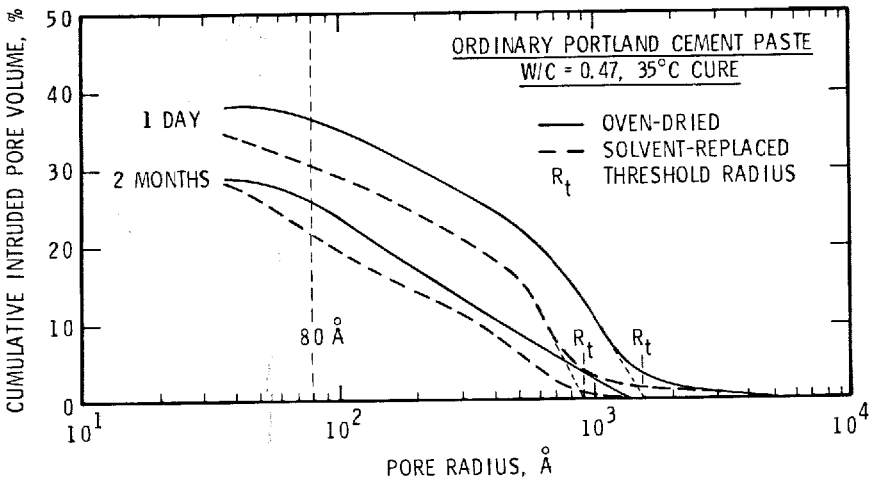

FIGURE 1

TYPICAL MERCURY POROSIMETRY RESULTS FOR OVEN-DRIED AND SOLVENT-REPLACED ORDINARY PORTLAND CEMENT PASTE

BR 6779-1

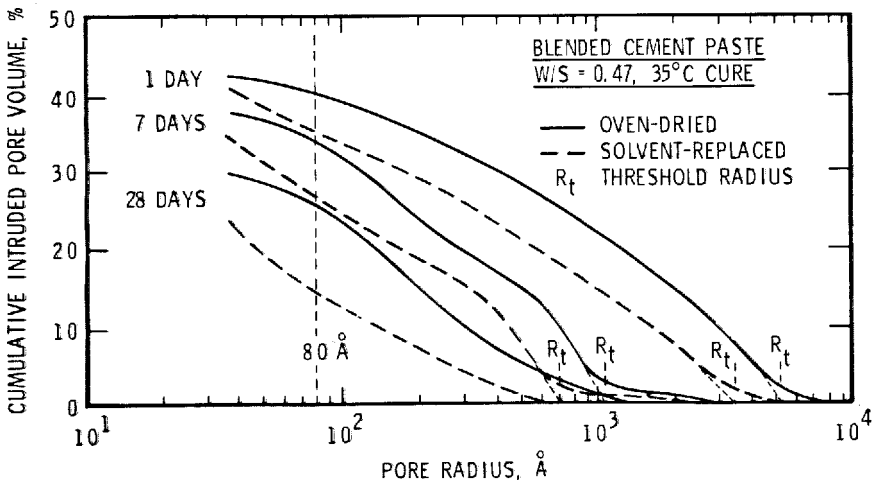

FIGURE 2

TYPICAL MERCURY POROSIMETRY RESULTS FOR OVEN-DRIED AND SOLVENT-REPLACED BLENDED CEMENT PASTE

BR 6779-2

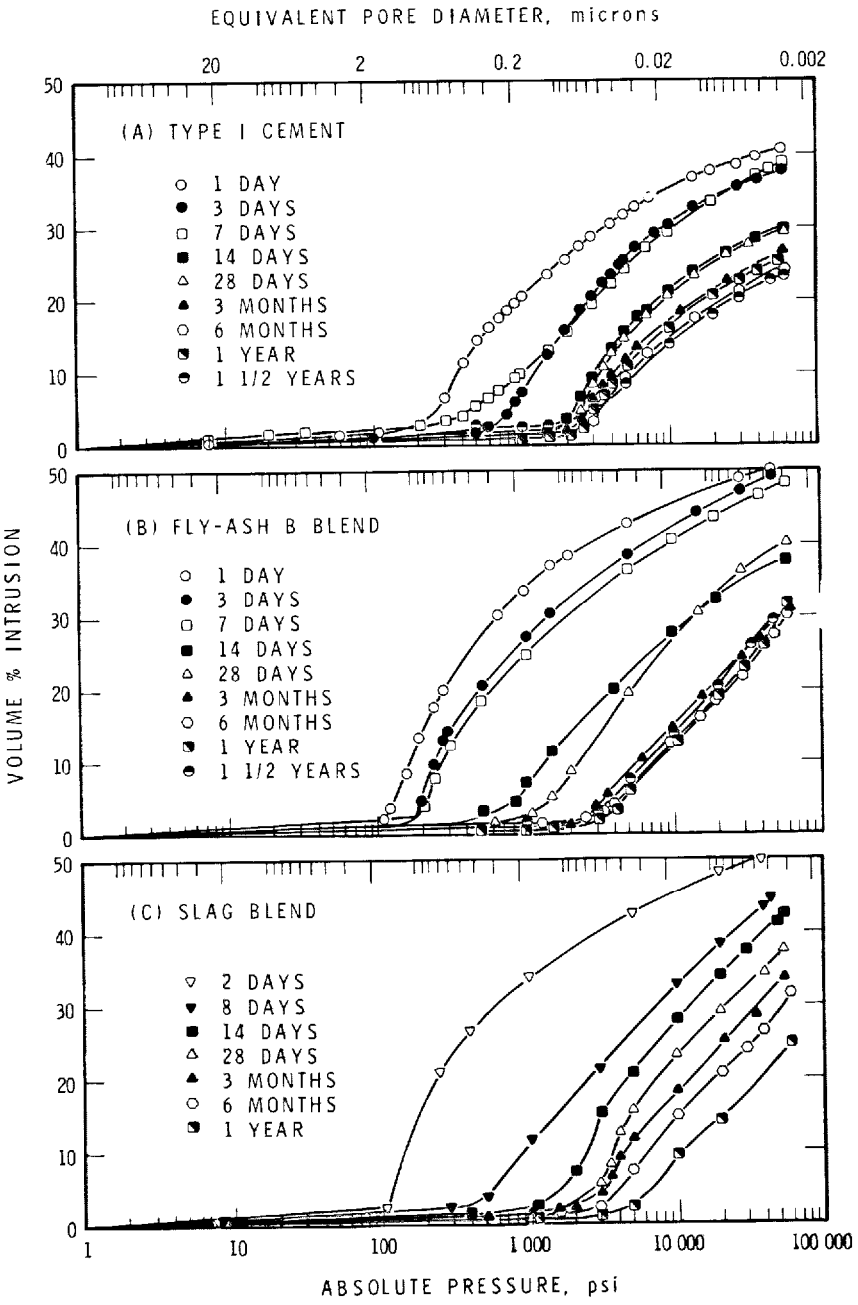

FIGURE 3

CHANGE IN PORE-SIZE DISTRIBUTION OF CEMENT PASTE AND CEMENT BLENDS WITH HYDRATION TIME AT 21°C

BR 6188-6

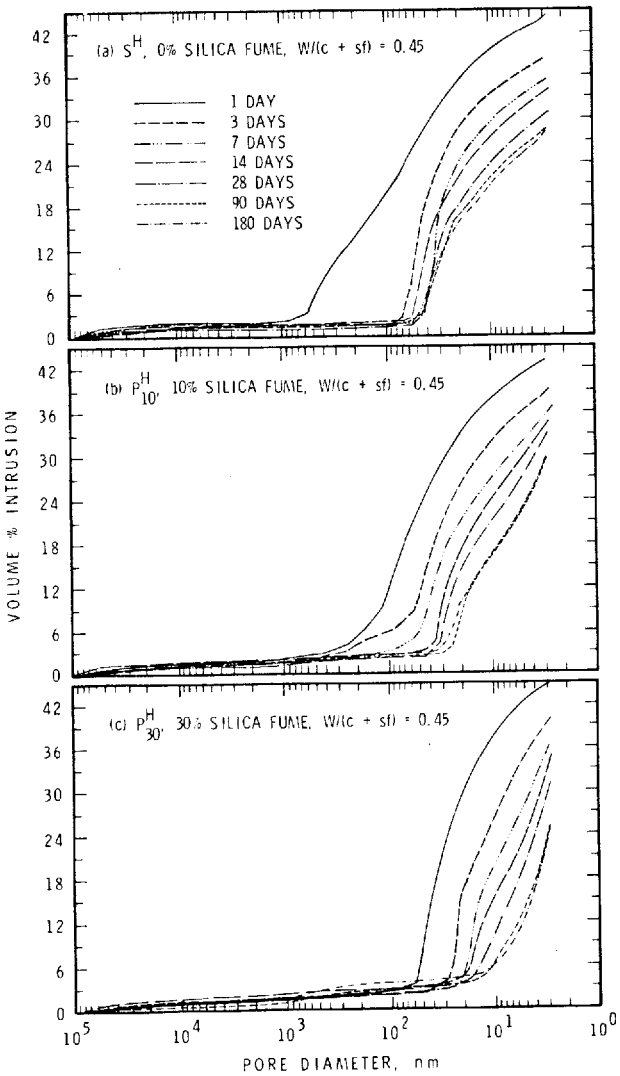

FIGURE 4

CHANGE IN PORE-SIZE DISTRIBUTION FOR CEMENT PASTE WITH AND WITHOUT SILICA FUME

BR 6779-16

$Ca(OH)_2$ content is also plotted against hydration time (Fig. 5a). It may be observed that where the $Ca(OH)_2$ content is low or decreasing, the slope is high or increasing. This is for the cases of the blended cements.

The effect of the mercury intrusion process on the microstructure has been investigated (60). Specimens that have been intruded with mercury were reintruded. This was performed by removing the mercury by extended distillation. The repeated intrusion showed that, in most samples of plain portland cement paste, the pore-size distribution did not change much but for all the blends major differences occurred. The result shown in Fig. 6 is a change in character of the curve from convex to concave to the pore diameter axes, and an intrusion threshold at a much higher pore diameter. This was explained (60) on the basis that the hydrated blended cement pore structure was made up of relatively large, but discontinuous, thin-walled pores. During mercury intrusion, these pores were disrupted at high pressure and intruded. Repeat intrusion would result in these pores being filled at much lower pressures. The harsher technique of direct oven drying might result, in some instances, in the same damage that occurred during mercury intrusion. This was shown to be the case by Marsh and Day (49); they compared helium porosities measured for ordinary or blended portland cement pastes dried by direct oven heating and by propan-2-ol treatment. Results in Fig. 7 show that higher porosities are obtained for the blends by the direct oven-drying technique.

The presence of $Ca(OH)_2$ in hydrated ordinary portland cement pastes has been used by Feldman (37) to explain the relative continuity of this pore structure as compared to that of blends. The work of Marsh et al. (50) has shown greater similarity in their pore-size distribution (Figs. 1 and 2) when solvent or direct oven dried.

Roy and Parker (36) prepared cements, Type II and 60:40 blend of slag with the cement, for mercury intrusion. They dried them by three different methods: freeze-dried, vacuum dried at 80°C for 2 hours, and dried with acetone followed by room temperature vacuum drying. Samples from the three methods were reported to show little difference in pore structures. These authors also found that the critical radius (radius at maximum dV/dP) of a cement paste may correspond with the microstructure of the material. In the pastes made with a w/c of 0.5 and 0.6, they found that the critical radius may be resolved by microscope. In well-developed gels, the critical diameter was about the distance between the fibers observed in SEM micrographs. Slag-cement pastes were concluded to have a finer structure than portland cement pastes from the observation of a smaller critical pore radius.

Midgley and Illston (53) dried pastes for mercury intrusion measurements in vacuum at 105°C and for electron microscopy by solvent replacement with ether. Comparisons made of pore radii by these techniques found surprising equivalence of pores above 100 Å radius, suggesting that different drying techniques may mainly affect pores less than 100 Å radius.

Total porosities measured by mercury intrusion are also indicative of the microstructure of hydrated pastes. As discussed above, the fine pore structure is sensitive to drying techniques and the pressure used in the mercury porosimeters. Several workers (47,49,61) have found that the porosities of plain pastes measured by mercury porosimetry and by helium pycnometry give similar values. Marsh and Day (49) have found that this is true for directly oven-dried specimens and for those which were solvent-replaced (propan-2-ol) and then oven dried (Fig. 8). However, for mature oven-dried fly-ash pastes, the helium porosity is as much as 10% by volume less than mercury porosity (47,49,61) and for solvent-replaced specimens this difference is as much as 20% less (48). Other results by Marsh and Day (49) showed that helium porosities of oven-dried

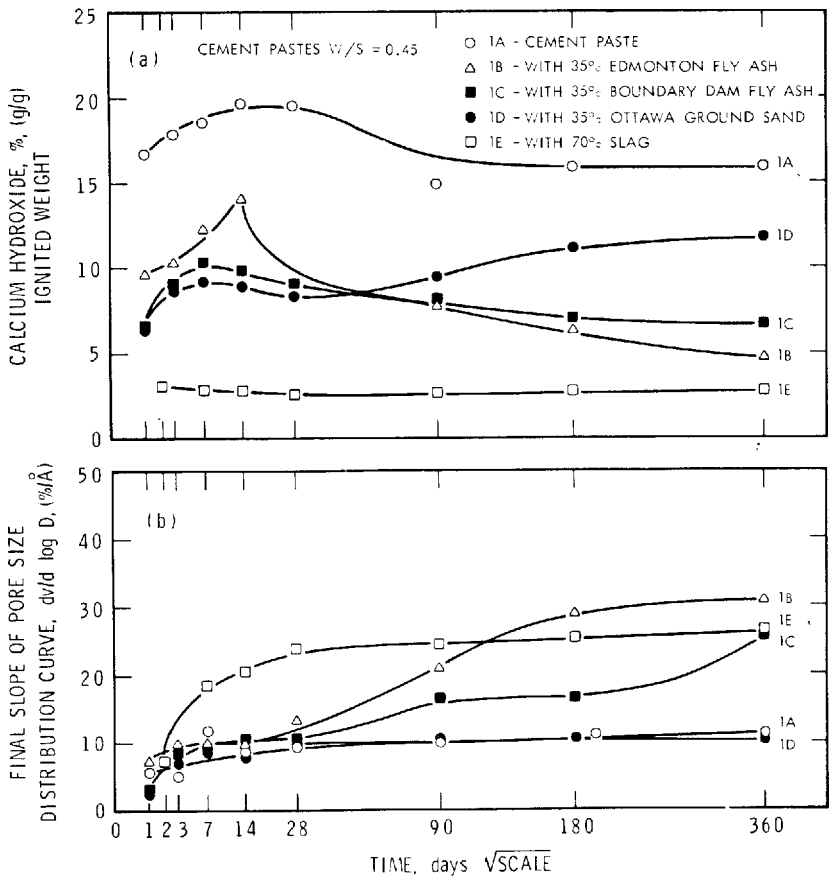

FIGURE 5
CHANGE IN (a) $Ca(OH)_2$ CONTENT AND (b) SLOPE AT MAXIMUM MERCURY INTRUSION PRESSURE FOR VARIOUS PORTLAND CEMENT BLENDS

BR 6779-17

specimens, especially for blended cements, are much higher than helium porosities for propan-2-ol-replaced specimens (Fig. 7).

Marsh and Day (49) considered the measure of total porosity of propan-2-ol-replaced specimens as a good indicator of accessible porosity and thus related to permeability (25). A plot of this porosity vs. the permeability of water-saturated paste specimens is presented in Fig. 9. Despite the wide scatter, there appears to be a correlation.

B - Nitrogen adsorption has been used much in the past but systematic variation in drying procedures and comparison with a molecule involving purely physical interactions have not been previously done. Lawrence (62,63) has concluded that nitrogen and butane interactions are physical in nature. In addition, he concluded that hardened pastes, when rapidly dried, contain slit-shaped pores with widths that vary in size from micro to macro. Average pore slit widths lie between 2 and 4 nm, while the hydration products approximate to platy aggregations with overall average thicknesses between 30 and 1000 nm. Slowly dried pastes have much reduced surface areas and wider, more symmetrical pores. Pore analysis of the mesopore surface for rapidly dried pastes has yielded surface areas well below BET values, indicating that a considerable fraction of the surface area was contained in micropores. Evidence also exists of restricted adsorption at relative pressures above 0.6, indicating a preponderance of slit-shaped pores. Methanol drying appears to shift the pore-size distribution of specimens to smaller radii as compared with D-drying.

More research is needed on the relationship between the change in the micro pores with a given drying technique to the change in the macro pores, since the latter pores are more relevant to properties dependent on permeability of the material.

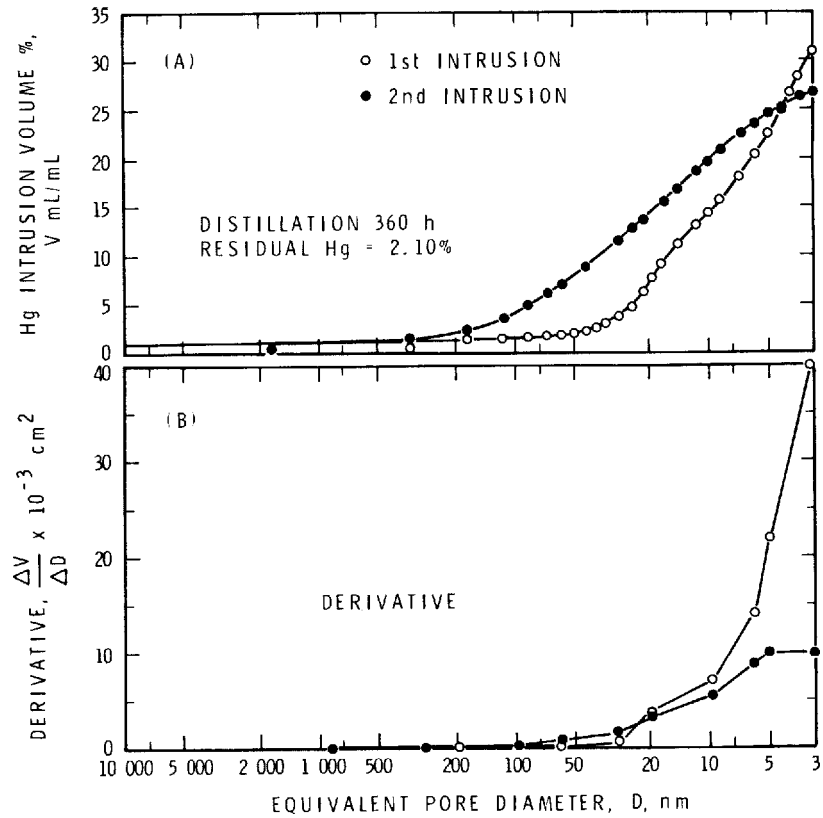

FIGURE 6

Hg INTRUSION AND DERIVATIVE FOR FLY-ASH AND CEMENT BLEND HYDRATED FOR 2 YEARS AT 35°C

BR 6382-5

C - A method for large pore analysis has been developed by Jennings, Parrott and co-workers (54). Samples are dried by solvent replacement and vacuum treatment at room temperature. These samples are then impregnated under vacuum with a low-viscosity epoxy resin; after the resin hardened, the impregnated samples were ground flat and polished. They were then etched with 50% hydrochloric acid + 50% water to yield a resin replica of the impregnated pores. The polished surface of the resin replica was viewed with a scanning electron microscope and fields of about 10^{-8} m^2 were photographed. These two-dimensional representations of the pore structure were analyzed, using an image analyzer. The areas analyzed were selected to be representative of a larger field of view. Some subjective decisions were required in deciding where a pore-solid interface should be drawn, but differences between individuals were not great. Porosity maps were constructed and some results are illustrated in Table 2. The open porosity determined from microscopy was estimated by excluding isolated and single-entrance pores that were thought not to be able to contribute to flow through the channels in the two-dimensional image. This is extremely speculative since in three dimensions the situation may be entirely different. The impregnated porosity from the microscopy measurement is shown to be similar to large pores >50 nm diameter obtained from volumetric measurements (difference between total porosity determined by water or methanol and the volume of pores penetrated by butane at a relative pressure of 0.95). However, it appears as if the estimate of the small pores by butane determined on dried samples would be considerably less than those occupied by water or methanol from the wet state, since they both occupy interlayer positions. Thus, this method of determining pores >50 nm diameter should lead to a considerable overestimate. The technique of helium pycnometry would be a better method to determine the volume of larger, continuous pores.

Despite the fact that some of the assumptions in this technique may be difficult to confirm, it does seem to show that the decrease of larger, continuous pores with degree of hydration is much more abrupt than merely the decrease of large pores (Table 2).

D - Wood's metal intrusion. Recently, several workers have claimed that cement paste has low-tensional strength due to the presence of large

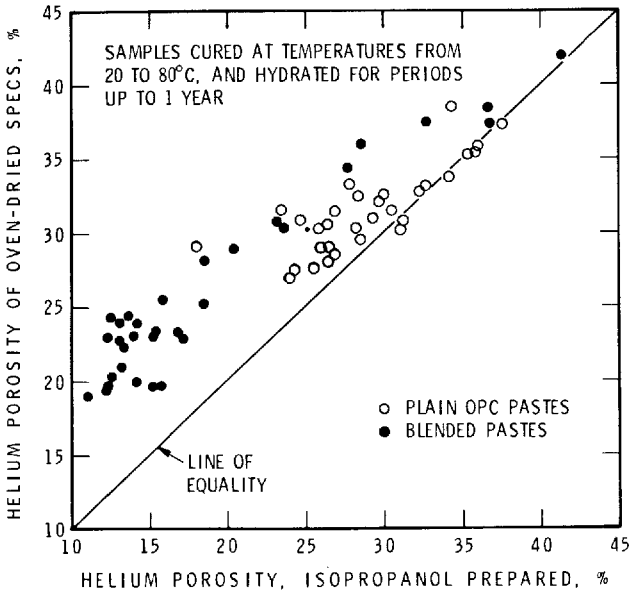

FIGURE 7

COMPARISON OF MEASURED HELIUM POROSITIES FOR DIFFERENT SPECIMEN DRYING METHODS

BR 6779-3

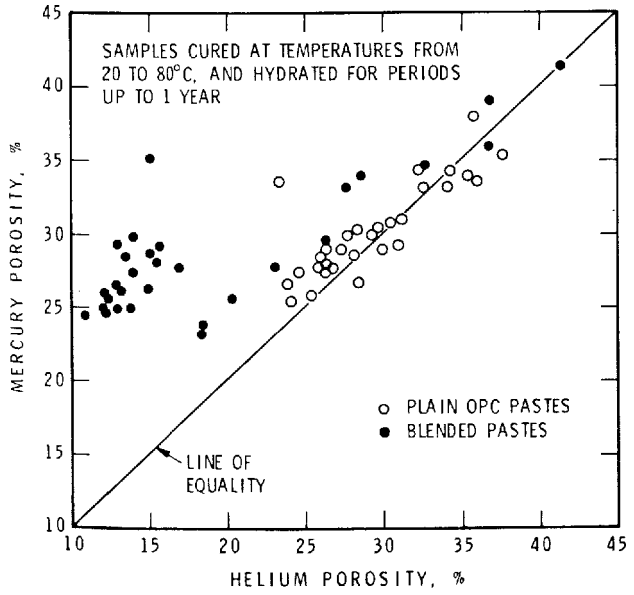

FIGURE 8

COMPARISON OF MERCURY AND HELIUM POROSITIES FOR SPECIMENS PREPARED BY THE SOLVENT-REPLACEMENT METHOD

BR 6779-4

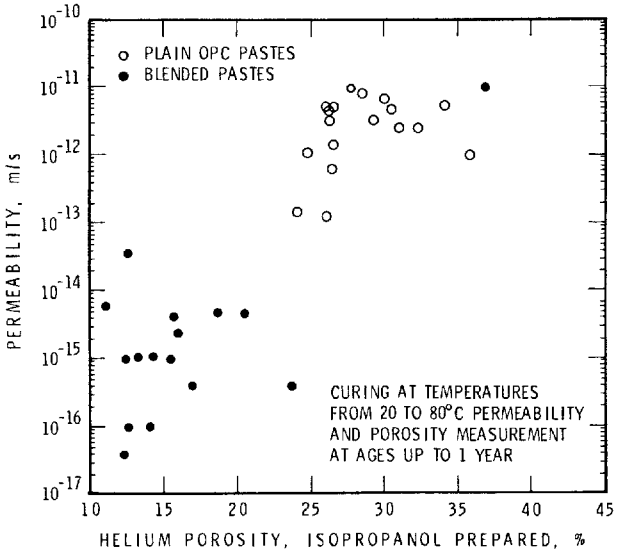

FIGURE 9

PLOT OF HELIUM POROSITY vs PERMEABILITY OF WATER-SATURATED PASTES

BR 6779-5

TABLE 2. Results of Diffusivity and Porosity Properties for Alite Hydrated at Various Times (54)

Hydration time (days)	1	3	10	28
Degree of hydration	0.22	0.30	0.50	0.83
Diffusion time, $et_{\frac{1}{2}}$ (min)	30	34	74	142
Miscroscopy results				
Impregnated porosity	0.50	0.42	0.26	0.25
Open porosity	0.44	0.38	0.15	0.12
Open pores (%)	88	90	58	48
Volumetric estimates				
Total porosity	0.61	0.58	0.55	0.49
Porosity >50 nm wide	0.51	0.44	0.34	0.27

spherical pores which act as critical flaws (64,65). These pores are stated to be greater than 15 μm and as large as 1000 μm. In addition, it has been emphasized that these pores cannot be observed by mercury intrusion because entrance into these pores may be limited by the fact that their entrances are smaller than can be entered by mercury at the maximum pressure. Wood's metal is a four-component fusible alloy which melts at 70°C, the composition being bismuth 50%, cadmium 10%, tin 13.3%, and lead 26.7%. It has a contact angle of 102° with cement paste. Rahman (66) used Wood's metal as a porosimetric fluid and after impregnating at pressures of 0.92 and 40 MPa (400 and 10.6 nm pore diameters, respectively) and allowed any intruded metal to freeze within pores. Rahman (66) examined fractured surfaces and found that there was very little intrusion of Wood's metal at a pressure of 0.92 MPa, even though pores of about 100 μm diameter existed. At the higher pressure, some of these pores became filled with Wood's metal.

Rahman (66) concludes that these macropores contribute significantly to the total porosity and affect pore-size distribution. Other work (47,59,60), especially on blended cements, indicated that some of these pores do exist and, in fact, density measurements by helium pycnometry confirm this but, on the other hand, on plain pastes with w/c of 0.4 or higher, helium and mercury intrusion porosities are similar and density values are consistent. Nevertheless, these pores, if present in significant proportion, could eventually affect the permeability of a body if continuity between these and other large pores occurred due to cracks formed by drying or other harsh treatment.

PERMEABILITY MEASUREMENTS

Water as Fluid in Plain Pastes

The design of equipment to measure the permeability of paste or concrete to liquid water has a long history (16,35). It is clear that the critical element was the prevention of leakage around the specimen. Many workers (18,35,48) cast an epoxy ring around the specimen with the seal dependent upon the epoxy-concrete bond. Other workers have used a conical specimen with a silicone rubber seal (25). More recently, Lawrence, Day and co-workers have used a system whereby a transverse pressure, greater than that of the permeating fluid, could be applied to a sealing membrane (45,48). With such a system, Mills found a strong dependence of permeability on confining pressure on concrete (16). This effect may be attributed to opening and closing of cracks in the specimen, and illustrated the difficulties involved with this measurement.

Marsh (25) measured water permeability of ordinary portland cement paste prepared at w/c of 0.47 and cured at 20, 35, 50 and 65°C. The 28-day and 3-month specimens cured at 20°C yielded values of approximately 1.5×10^{-13} m/s, whereas the 35, 50 and 65°C pastes had values of between 4 and 9×10^{-12} m/s. Hooton (35), using a sulfate-resisting cement mixed at w/c of 0.36, found decreases from 340×10^{-13} to 1×10^{-13} m/s during hydration from 7 to 180 days. Goto and Roy (23) compared pastes cured for 28 days at different w/c's and temperatures. At 27°C and w/c of 0.35 the permeability was 0.6×10^{-13} m/s, while at 60°C, at the same w/c, the permeability was 1×10^{-12} m/s. Nyame and Illston (21,22) and Mehta and Manmohan (20) also measured permeabilities of ordinary portland cement at several w/c and curing times; values obtained by Nyame and Illston (21,22) varied from 5×10^{-6} m/s at 2 days hydration and w/c of 1.0 to 5×10^{-15} m/s at 10 months hydration and w/c of 0.23 (Fig. 10). These authors found a relatively small but significant decrease in permeability with increasing pressure applied during the experiment and attributed this to some clogging of pores by the increase of pressure in addition to continued hydration.

Water as Fluid in Blended Pastes

Marsh (25) and co-workers (49) measured permeabilities of pastes where 30% of cement was replaced with fly-ash. Significant decreases in permeability were observed. However, at a

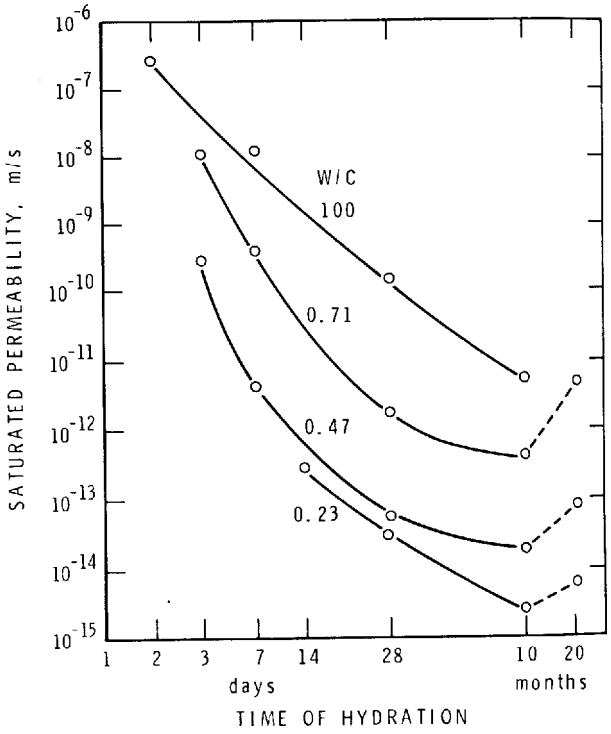

FIGURE 10

EFFECTS OF HYDRATION ON PERMEABILITY OF HARDENED CEMENT PASTES OF DIFFERENT W/C RATIOS

BR 6779-6

temperature of 20°C, decreases in permeability relative to ordinary cement were not observed until after 28 days hydration; permeabilities fall from 7×10^{-12} m/s at 28 days to 6×10^{-15} m/s after 3 months hydration. Similar reductions in permeability were observed at 35°C between 7 and 28 days hydration, while at 50 and 65°C the blended pastes achieved low permeability by 7 days. Hooton (35) observed decreased permeability with silica fume addition and Manmohan and Mehta (2) observed similar trends with additions such as rice husk ash, fly-ash and blast furnace slag. Roy and Parker (36) also found permeabilities of slag-cement blend pastes to be considerably lower than ordinary portland cement pastes. Samples were made at w/c's of 0.30, 0.40, 0.50 and 0.60 and were cured at 27, 45, 60 and 90°C for periods from 14 to 28 days. Permeabilities increased with curing temperature and w/c ratio.

Permeabilities of blended cement concretes were measured by Lawrence (44). He found that mature concretes containing 35% replacement of cement by fly-ash were two to five times less permeable than ordinary portland cement or slag-cement concrete when compared at the same 28-day cube strength. Mills (16) also observed that permeability of concrete was significantly decreased by partial substitution of portland cement with fly-ash.

Oxygen as Fluid

Gas flows much more readily through concrete samples than does water, and so pressures are much lower and time needed to attain steady state is much less. However, to measure permeabilities, the specimen must be dried. Results in Table 1 (48) show that for a concrete of w/c of 0.47, the methods of drying are very important. These have been discussed in section 3b. Grube and Lawrence (67) reported initial results of permeability measurement from a cooperative program undertaken by seven laboratories (8). Oxygen permeabilities lay in the range 0.001 to 30 x 10^{-16} m^2. Specimens were dried between 50 and 65% RH. Considering mixes containing 300 kg cement/m^3, it was found that increasing curing time from one to three days reduced permeability by an average of five times, while a further increase in curing time to 28 days resulted in a further decrease in permeability by nine times. Change in w/c ratio, on the other hand, has a lesser though still important effect; reducing w/c ratio by 0.05 reduced permeability 1.6 times on average. Other works obtained similar results (68). Lawrence (44) extended his study to blended cements and found that concrete specimens that had 35% replacement of cement with fly-ash and that were dried to 55% RH had permeabilities about five times less than ordinary cement or slag. Similar results had previously been reported for undried specimens using water as fluid (2,25).

White et al. (19) and McDaniel (4) measured permeability of mortars using nitrogen gas. Specimens were pre-dried to constant weight at 110°C. Using the Klinkenberg correction, they found that values obtained by water and those by nitrogen were comparable.

DIFFUSION MEASUREMENT

A major problem of concrete durability is the corrosion of reinforcement steel. The steel is normally in a passive state, but this may change as a result of the diffusion of carbon dioxide or chloride ions. Rates of subsequent steel corrosion may depend on the rate of diffusion of oxygen to the steel, as well as diffusion of various ions. Knowledge of the parameters controlling diffusion rates are thus very important.

Oxygen Diffusion

Relatively few studies of gas diffusion in concrete have been carried out. Some earlier, comprehensive work was carried out by Zagar (69) and Darr and Ludwig (70), and others have provided interesting data (71). Darr et al. (70) calculated an ordinary effective diffusion constant, while Lawrence (11) calculated an average diffusion constant, which is an approximation of the value given by Darr and Ludwig (70). Grube and Lawrence (72) extended previous work by using a wider range of mixes and different curing conditions (20 hours or 28 days) followed by drying to 55% RH. They observed that once a certain degree of drying had been achieved, the diffusivity of oxygen remained reasonably unaffected by further drying. Tuutti has shown that diffusivity is very sensitive to drying humidity (12). In his work, Lawrence showed that oxygen diffusivity and permeability are related

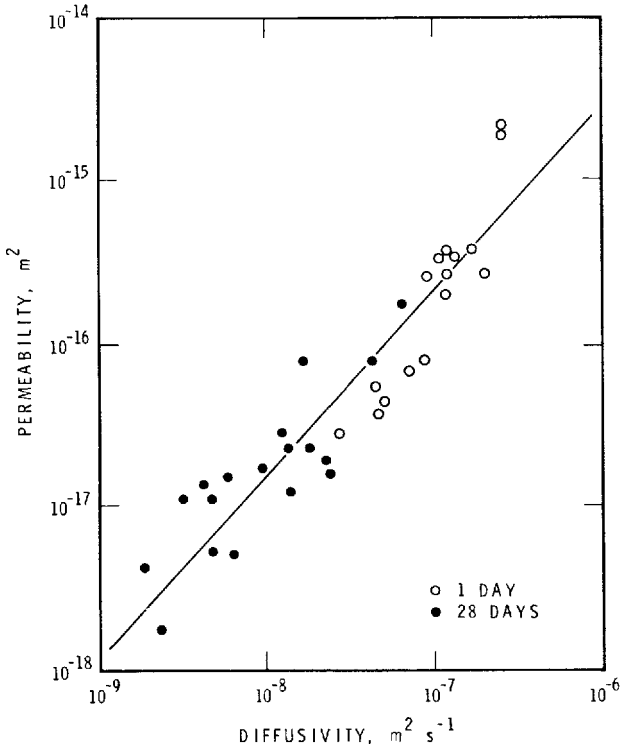

FIGURE 11

RELATION BETWEEN OXYGEN DIFFUSIVITY AND PERMEABILITY

BR 6779-7

linearly (Fig. 11) (11). He felt that this relationship may be useful in developing a simpler technique for testing durability. He also showed that the diffusion rate of CO_2 in fully carbonated concrete can be estimated from the diffusion rate of oxygen.

Calculations by Lawrence (11) using expressions derived by Crank (73) for diffusion plus reaction have been given (10). A linear increase of carbonation depths with square root of time is predicted and observed.

As discussed above, the relative humidity or the degree of filling of the pore structure within the concrete with aqueous solution will greatly affect diffusion processes and this state is one that often exists. De Wind (74) has suggested that for a given concrete, the ratio of oxygen diffusivity in the dried state to that in the saturated state should approximate to the ratio of the bulk diffusivities of oxygen in air and liquid water and would be about 10^6. This contention involves many assumptions. Previous measurements (11,12) of diffusivity on concrete dried to 50-60% RH were about 10^{-8} m^2/s, thus oxygen diffusivities through saturated concretes should be of the order of 10^{-14} m^2/s. Further work by Lawrence (75) on a variety of saturated concretes obtained values the majority of which fell between 1 and 8 x 10^{-13} m^2/s. These are considerably smaller than those reported by Tuutti (12) and suggest that concrete offers a much more resistant barrier to the passage of oxygen

than does liquid water. This is contrary to the conclusions of some other workers (70).

Assuming Lawrence's measurements are accurate (75), a state of active corrosion is possible for reinforcing steel in good quality, saturated concrete since too little oxygen will penetrate to form a passivating layer on anodic areas. However, a low rate of corrosion due to the low rate of oxygen reduction at the cathode also results, but the overall effect is beneficial.

Ionic Diffusion

The factors controlling corrosion of reinforcing steel in concrete have been investigated by several workers recently (6-8,12,26-33). Hansson et al. (8) have concluded that the important factors are: (i) the $C\ell^-$ and OH^- content of the pore solution; (ii) the porosity and pore-size distribution of the matrix material; (iii) the resistivity of the matrix. The corrosion rate, in addition to the above factors, is controlled by the availability of oxygen.

Work by Page et al. (19,27,28) and by Treadaway et al. (29), using pastes with micro-silica replacement, measured corrosion behaviour of embedded steel. Corrosion potential and linear polarization measurements were made; pore solutions were analyzed. This work showed that levels of corrosion protection cannot be accurately predicted solely on the basis of data related to the pore solution composition, such as the ratios of free chloride to hydroxyl ion concentrations. This is significant because a number of investigations (12,76) in simulated concrete pore solutions containing dissolved oxygen and various levels of chloride and hydroxyl ions has suggested that a critical ratio for $C\ell^-/OH^-$ of 0.6 exists. Knowledge of the relative diffusivities of chloride and other ions in the various matrices is also required. Hansson et al. (8) have shown that the same quantity of $C\ell^-$ added to ordinary portland cement mortar has different effects when added as $CaC\ell_2$, $NaC\ell$, or $KC\ell$. The corrosion rate is strongly dependent on the cation, $CaC\ell_2$ having a much more deleterious effect than either $NaC\ell$ or $KC\ell$. These workers (8) observed a coarsening of the pore structure in the 100 to 1000 nm range by mercury porosimetry and suggested that the increased severity of $CaC\ell_2$ addition is due to a combination of the pore structure change and decrease in the pH, but is not related to the concentration of $C\ell^-$ remaining in the pore solution. Preece (33) showed that a cement-slag mortar with a significantly finer pore structure than normal cement mortar had an electrical resistivity ten times higher and chloride diffusivity ten times lower than the normal cement mortar; in addition, the initiation of chloride-induced corrosion and the subsequent rates of corrosion were both lower in theslag mortar.

There have been only a few studies of the diffusion of ions through water-saturated cement reported in the literature. Kondo et al. (77) measured effective diffusion coefficients by placing solution saturated with $Ca(OH)_2$ on one side of a specimen in a diffusion cell, and a chloride solution saturated with $Ca(OH)_2$ on the other. Coefficients were determined for ions when $LiC\ell$, $NaC\ell$, $KC\ell$, $CaC\ell_2$ and $MgC\ell_2$ were used. Mixed solutions were also used. Fifty to one hundred hours were required before a steady-state condition was attained. The diffusion of $C\ell^-$ ion combined with divalent cation was greater than that combined with monovalent cations and it decreased in the order of $DC\ell^-$ ($MgC\ell_2$) > $DC\ell^-$ ($CaC\ell_2$) > $DC\ell^-$ ($LiC\ell$) > $DC\ell^-$ ($KC\ell$) > $DC\ell^-$ ($NaC\ell$). These values varied from 18.3 to 6.25 $\times 10^{-12}$ m^2/s, while values for Na^+, K^+ and Li^+ were 1.70, 2.95 and 1.70 $\times 10^{-12}$ m^2/s, respectively. Kondo et al. (77) pointed out that the cement paste behaved as an electro-positive, semi-permeable membrane. The fact that $CaC\ell_2$ and $MgC\ell_2$ react physically and chemically with the cement paste probably has some influence on the high coefficient values for $C\ell^-$ when these salts are used. Ushiyama et al. (78) investigated the diffusion rates of $SO_4^=$ and found that $C\ell^-$ diffuses 10 to 100 times faster than that of $SO_4^=$ but the value of the latter was dependent on the pH of the solution and appeared to be affected by ettringite formation. Goto et al. (79) measured the effective diffusion coefficient from the penetration depth of $C\ell^-$ and obtained a value of 3.4 $\times 10^{-12}$ m^2/s. It was suggested that corrections should be made for the chloride reaction with aluminate phases and a value of 230 $\times 10^{-12}$ m^2/s was given. These workers also pointed out that the diffusion of $C\ell^-$ ion was faster with Mg^{++} than in Na^+. Midgley and Illston (80) also measured the chloride diffusion coefficients by measuring chloride concentrations in specimens that were soaked in $NaC\ell$ solution for six months or one year. Results were obtained for w/c ratios of 0.23, 0.47 and 0.71. Values after one year were 0.56, 0.85 and 2.17 $\times 10^{-12}$ m^2/s, respectively. Goto and Roy (80) used a diffusion cell to measure the diffusion coefficient of both Na^+ and $C\ell^-$ as a function of temperature and w/c ratio. Deionized water was in the other side of the cell. They found no pronounced effects of w/c ratio or curing conditions, and they found that the $C\ell^-$ had a higher diffusion coefficient than Na^+, about 6.9 $\times 10^{-12}$ m^2/s and 1.5 $\times 10^{-12}$ m^2/s, respectively, at a w/c ratio of 0.4 for a Type I cement at 27°C. However, activation energies for the diffusion of Na^+ and $C\ell^-$ were 20 and 12 kcal mol^{-1}, respectively. Bakker (46) also measured coefficients of diffusion of Na^+ and K^+ ions. These were measured for a mortar of w/c ratio of 0.5 and sand/cement ratio of 2.0, using both ordinary portland and blast furnace slag cement. Values after 14 days for the ordinary portland cement are similar to those obtained by Goto and Roy (81); values for portland and blast furnace mortars for Na^+ ions after 14 days hydration were 2.38 and 0.10 $\times 10^{-12}$ m^2/s, respectively.

Page et al. (7,13,82,83) measured effective diffusivities of $C\ell^-$ using 1M $NaC\ell$ in saturated $Ca(OH)_2$ and saturated $Ca(OH)_2$ in the other compartment. They measured values as a function of temperature and w/c ratio. An Arrhenius plot for ordinary portland cement of different w/c ratios is shown in Fig. 12 (82). Results of Collepardi (84) are also plotted. Activation energies at w/c of 0.4 are 10 kcal/mole in a similar range as Goto and Roy (81). Values of effective diffusivities of $C\ell^-$ in other cement pastes were also measured by Page et al. (83) and are shown in Table 3. These authors (57,13,82,83) measured pore distributions by mercury intrusion and were not able to observe significant differences in the microstructure; porosities were, in fact, larger for the fly-ash paste. However, since recent data (60) have shown that pores of

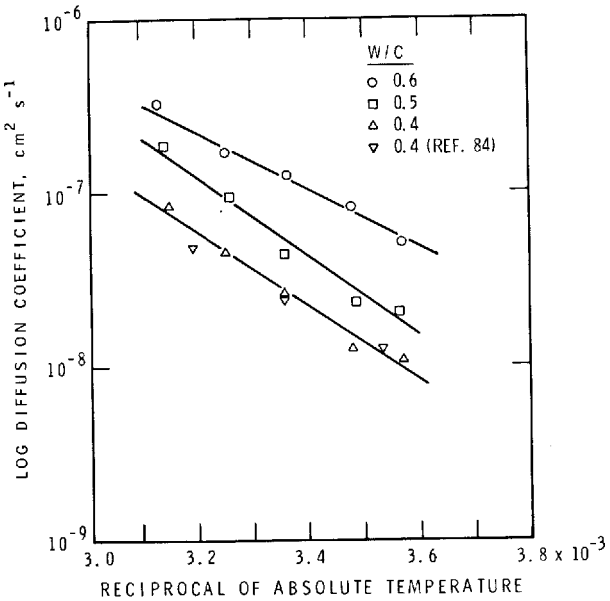

FIGURE 12

ARRHENIUS PLOTS FOR EFFECTIVE DIFFUSION COEFFICIENTS OF Cl^- IN PORTLAND CEMENT PASTE AT VARIOUS W/C RATIOS

BR 6779-8

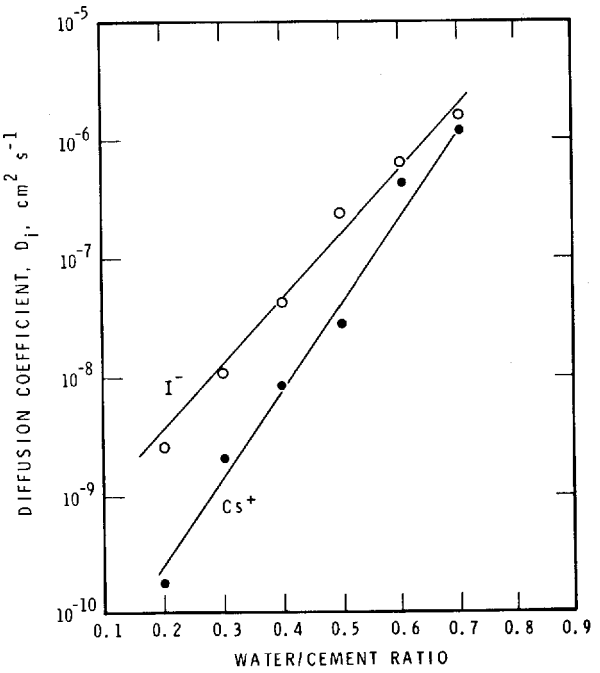

FIGURE 13

INTRINSIC DIFFUSION COEFFICIENT FOR I^- AND $^{137}Cs^+$ MEASURED AT 30°C AS A FUNCTION OF W/C RATIO

BR 6779-9

TABLE 3. Effective Diffusivity of Chloride Ions at 25°C in Various Cement Pastes of w/c 0.5 (82)

Type of Cement	D x 10^9 cm^{2}s^{-1}
OPC	44.7
OPC/30% PFA	14.7
OPC/65% BFS	4.1
SRPC	100.0

slags and fly-ash pastes are relatively discontinuous, despite larger values for porosity and pore-size distribution, this result is not unexpected.

Shigeru et al. (85) also drew attention to the importance of pore structure and correlated diffusion coefficient with volume of pores with radius under 20 Å. Atkinson et al. (14) considered studies where diffusion cells have concentrated NaCℓ solution on one side without Na^+ ions on the other side as dubious, since there may be osmotic flow effects from the low to the high concentration side of the cell. To get around this problem these authors (14) measured interdiffusion and employed KI and KCℓ on opposite sides of the cell. These have approximately the same osmotic coefficients. In another experiment, the authors (14) utilized CsCℓ in the whole diffusion cell, using the ^{137}Cs radioisotope to follow the diffusion. Results for ions I^- and Cs^+ are presented in Fig. 13 (14). It is shown that the intrinsic coefficient of diffusion is a strong function of w/c ratio, which is approximately exponential. The results for I^- diffusion through a single specimen as a function of the inverse of temperature are plotted in Fig. 14 (14) for w/c of 0.4. These results are in good agreement with those of Page et al. (82) for $C\ell^-$, which indicates that osmotic influences were not major. However, Atkinson et al. (14) measured a temperature cycle, from 20 to 60°C and then down to 10°C and then back to 20°C. Irreversible effects which tend to increase the diffusion coefficient occur. Included in Fig. 14 are results for the electrical conductivity for I^- ion at infinite dilution $\lambda°$, which is indicative of the expected temperature dependence of diffusion in the free liquid. These experiments led Atkinson et al. (14) to conclude that the apparent temperature dependence of the diffusion has at least two contributions; one is temperature-induced changes in the pore structure and the other is the basic temperature dependence of the diffusion mechanism. The apparent activation energy from the increasing temperature part of the cycle is 11 kcal/mol and is in reasonable agreement with the other workers (81,83). However, the decreasing temperature part of the cycle yields a value of 4.6 kcal/mol which is closer to the apparent activation energy of $\lambda°$ for the free aqueous I^- ion at infinite dilution (3.2 kcal/mol). Atkinson et al. (14) concluded that the model that best explains the pore structure is one in which relatively large pores are interconnected by much finer ones.

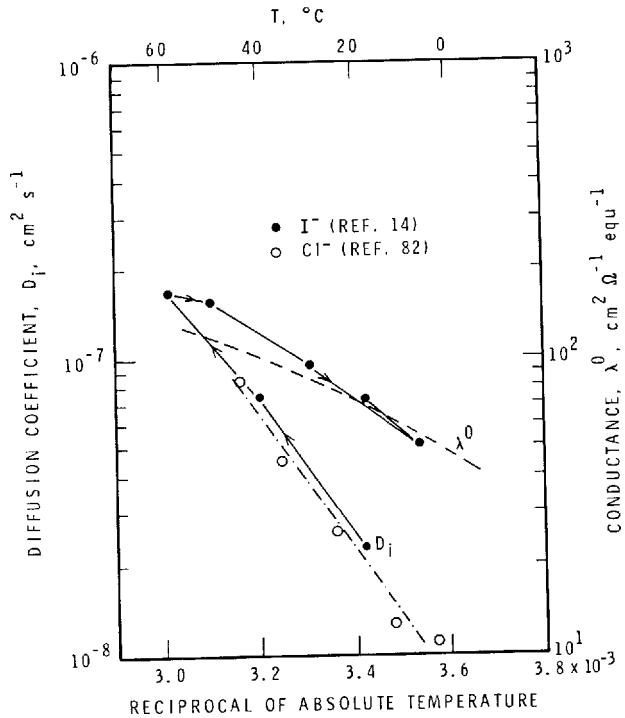

FIGURE 14

EFFECT OF TEMPERATURE ON THE DIFFUSION OF I^- IONS THROUGH A SINGLE SPECIMEN OF W/C RATIO OF 0.4

BR 6779-10

Counter Diffusion-replacement of Water by Different Fluids

Fluid exchange involves the immersion of a water-saturated specimen of hydrated paste or concrete with a water miscible fluid. Much work has been done in this regard with the use of organic solvents (51,52,54,86,87). Parrott (51) has used 3-mm thick slices of hydrated paste. This counter diffusion process follows a standard equation for non-steady-state diffusion, from which it is possible to calculate an intrinsic diffusion coefficient. Parrott (52) has shown that the time taken for replacement of half the evaporable water in hydrated alite, $e\tau_{\frac{1}{2}}$, or half the pore water in porous glass, is approximately a linear function of the viscosity of the fluid. Parrott used a series of organic solvents: methanol, ethanol, propan-1-ol, propan-2-ol, n-pentane and benzene, and concluded that the process of exchange was a simple, physical process of counter diffusion. Table 4 by Parrott (52) illustrates the effect of age upon $e\tau_{\frac{1}{2}}$ and porosity obtained by methanol for moist-cured samples of alite having an original w/c ratio of 0.59. The effect of alite hydration increases the time required for half of the methanol exchange to take place as the pore system becomes finer.

Feldman (88) measured coefficients of diffusion for mature, normal cement paste prepared at a w/c ratio of 0.8, using propan-2-ol and methanol. He obtained values of 1.67×10^{-15} m^2/s and 7.39×10^{-15} m^2/s, respectively. These values may be compared with the diffusion coefficients for water vapour (2×10^{-10} to 5×10^{-11} m^2/s) reported by Lawrence (45) and the values of ionic diffusion of Cl^-, Na^+ ions, etc. discussed earlier.

TABLE 4. Diffusivity and porosity values for methanol exchange in hydrated alite cured to different ages (w/c ratio of 0.59) (86)

Age (days)	1	3	10	28	203
$e\tau_{\frac{1}{2}}$ (min)	30	32	74	142	271
Porosity water	0.613	0.583	0.554	0.532	0.495
Porosity methanol	0.612	0.566	0.551	0.523	0.479

Parrott (52) measured diffusion rates of water from alite specimens which had been pre-dried to various relative humidities and re-wetted. Specimens were measured by solvent replacement in a water-resaturated state, using methanol, and the effect of the pre-drying on the structure could be detected by comparing $e\tau_{\frac{1}{2}}$ values. These results are shown in Fig. 15 (52). Values of $e\tau_{\frac{1}{2}}$ vary by a maximum of six times for different humidities of initial drying. These results were compared with those obtained by measuring $s\tau_{\frac{1}{2}}$, half the time

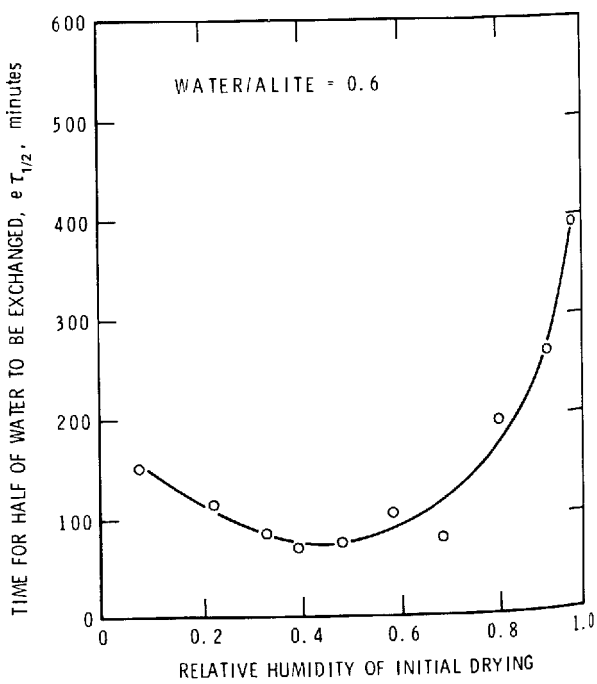

FIGURE 15

EFFECT OF PREVIOUS DRYING UPON RATE OF EXCHANGE OF WATER WITH METHANOL IN HYDRATED C_3S, W/C RATIO OF 0.6

BR 6779-11

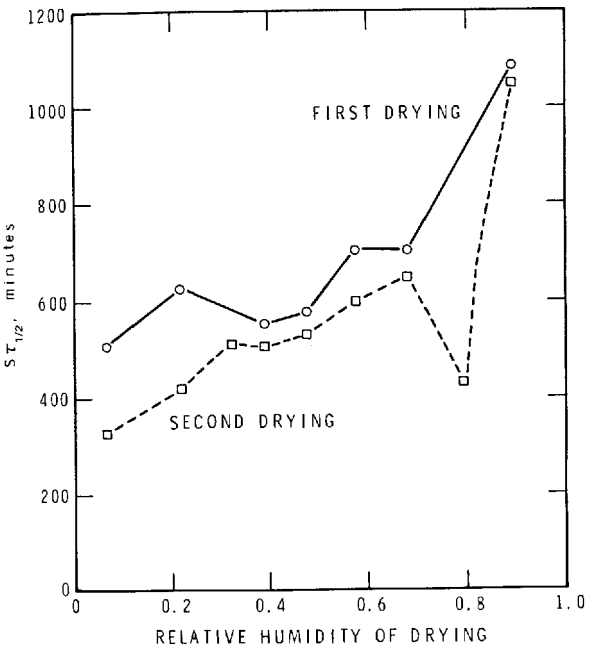

FIGURE 16

$S\tau_{1/2}$ PLOTTED AGAINST RELATIVE HUMIDITY OF DRYING FOR HYDRATED C_3S, W/C RATIO OF 0.6

BR 6779-12

taken to dry from saturation to a selected relative humidity in a single step; re-saturation and then second drying were also measured. Observed differences imposed by drying on subsequent rates (Fig. 16) (86) are not as great as those observed from the methanol exchange data (Fig. 15). Day and Illston (89) found that the rate of drying had little effect on subsequent swelling vs. time and swelling vs. moisture gain relationships, while Feldman (88) found that diffusion coefficients for replacement by propan-2-ol varied by a maximum factor of only about 2.50 between no pre-drying and other humidities of pre-drying.

Although the solvent replacement technique appears to be useful in measuring relative diffusion rates in cement and concrete and even the quality of concrete in the field (87), the choice of methanol as the solvent appears to be questionable. Several workers have suggested (56-58) that methanol reacts with both $Ca(OH)_2$ and CSH in hydrated paste to form calcium methoxide or a methylated complex. Beaudoin (56), using many techniques such as conduction calorimetry, X-ray diffraction, infrared spectroscopy, and thermal analysis, has found that there is immediate reaction when methanol is placed in contact with $Ca(OH)_2$ or hydrated cement paste and considerable reaction product is formed; microstructures of the cement systems studied were modified after treatment. Feldman (88) observed considerable swelling on treating hydrated cement pastes (w/c ratio = 0.8) with methanol; after 14 days, expansion exceeded 0.10% (1000 microstrain) and diffusion rate measurements indicated that most of the expansion occurred only after 85% of the methanol had entered the structure. In addition, modulus of elasticity measurements made after methanol treatment showed that there was a considerable decrease in this property. On the other hand, when porous silica glass is solvent-replaced by methanol, the expansion observed was less than 0.01%.

Reactions between cement paste or $Ca(OH)_2$ and propan-2-ol were not observed by any of the above workers, although Feldman (88) observed a shrinkage of about 0.14% during solvent replacement of water with propan-2-ol. This shrinkage is at least partly due to the difference in surface interactions between water and hydrated cement and propan-2-ol and hydrated cement. The difference between water and methanol surface interactions are not great, as indicated from the results with porous glass, and the considerable swelling observed during the water replacement by methanol may be due to further separation of the CSH sheets by the penetration of the methanol molecule and/or the formation of calcium methoxide. Results obtained by low-angle X-ray scattering (90) have indicated that sheets are sufficiently separated at high relative humidities to register as surface area (ca 650 m^2/g) during these experiments. The ability of methanol to enter the layered structure may explain the swelling and the very high surface areas (ca 330 m^2/g) calculated by Parrott (52) from methanol adsorption. In this work (52), the fact that a methanol molecule may interact with two opposite surfaces, simultaneously, in a confined space, has not been considered.

The use of propan-2-ol as a solvent for drying (as discussed in a previous section) and for measuring diffusion rates in counter diffusion experiments appears to be more appropriate than the use of methanol; the very pertinent results on the effect of drying history by Parrott (52) should be repeated with this solvent. The solvent-replacement technique to measure the effect of drying on pore structure and other gradients, as shown by Parrott (86) is a promising technique.

PORE STRUCTURE - PERMEABILITY RELATIONSHIPS

Nyame and Illston (21) studied the relationship between permeability of hardened cement paste to liquid water and the pore structure. They defined a term, the maximum continuous pore radius (r_∞) as the maximum slope from a plot of intruded volume versus pore radius obtained from a mercury intrusion porosimetry (the mode of drying was not indicated) and proposed an equation relating this parameter and the permeability:

$$K = 1.684\ r_\infty^{3.284} \times 10^{-22} \qquad (8)$$

where K is the permeability with correlation coefficient of 0.96. However, for pores of radius less than 1000 Å, the scatter of data is great. At 350 Å radius permeability varies from 10^{-12} to 10^{-15} m^2/s. These authors (21,22) also showed, as expected, that there was no unique relationship between total porosity and permeability, since specimens of similar porosity may have totally different pore-size distributions. This non-unique behaviour was also found for permeability versus surface area relationships but a better relationship

was found relating permeability and total porosity and hydraulic radius:

$$\log K = 38.45 + 4.08 \log (\varepsilon r_h^2) \qquad (9)$$

with a correlation coefficient of 0.895, where ε cm^3/g is the total porosity, and r_h is the hydraulic radius. Figure 17 shows a very broad scatter at the low permeability end of the curve.

Mehta and Manmohan (20) correlated permeability data obtained using water as fluid to four parameters: the volume of pores > 1320 Å diameter divided by the total mercury intruded porosity (V_1), the volume of pores in the 1320 - 290 Å range also divided by the intruded porosity (V_2), the threshold diameter (TD) (the largest pore diameter at which the intrusion of mercury is established) and the modified total porosity (MTP), the total pore volume (mL/g) divided by the degree of hydration. Using data for pastes prepared at w/c ratios from 0.3 to 0.9, hydrated for 25, 90 days and one year, they obtained the following empirical relation:

$$K = \exp(3.84\ V_1 + 0.2\ V_2 + 0.56 \times 10^{-6}\ TD + 8.09\ MTP - 2.53) \qquad (10)$$

with a correlation coefficient of 0.95.

Marsh (25) found no distinct relationship between permeability and derivative of pore-size distribution curves. However, the derivative distributions obtained from their oven-dried specimens of high permeability (defined as $>10^{-13}$ m/s) portland cement-fly-ash blends all show a large but reasonably narrow peak in the large pore region (700-1100 Å radius). This peak is absent or very small for the pastes known to have low permeability (defined as $<10^{-14}$ m/s). In addition, the low permeability pastes show a larger frequency of occurrence of pores of radius of approximately 100-300 Å. Propan-2-ol-dried specimens differed from oven-dried, mainly in the region of pores less than 350 Å, while in the region of large pores the peak moved from 700-1100 Å to approximately 500-700 Å (Fig. 18) (25). However, the presence or absence of this peak, regardless of the method of drying, corresponds to a high or low permeability specimen. All ordinary portland cement pastes, whether oven-dried or propan-2-ol-replaced, showed a substantial peak in the large pore region.

Marsh and Day (49) state that porosity values obtained by helium pycnometry for propan-2-ol-dried blended pastes represent the accessible porosity. This porosity can thus be related to the permeability, as shown in Fig. 9. However, as shown by several workers (37,49) this porosity is only a portion of the total porosity (Fig..7) (49), whereas the ordinary portland cement pastes show close agreement in porosities obtained by mercury intrusion or by helium pycnometry. Propan-2-ol replacement and helium pycnometry are gentle enough techniques to preserve the discontinuous structure of the blended cements, while mercury intrusion breaks into the discontinuous structure which partly forms during the secondary reaction of the pozzolan and the $Ca(OH)_2$.

Feldman (37,47,60) found the discontinuous structure to form not only through pozzolanic

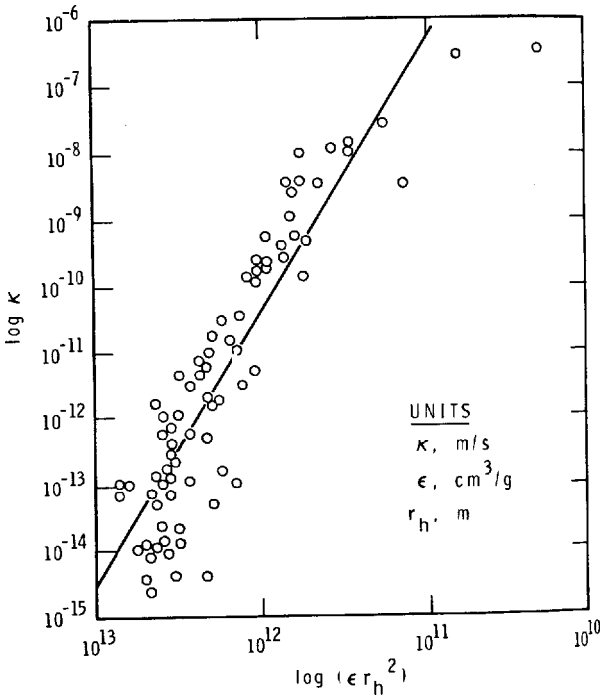

FIGURE 17

A COMPARISON OF LOG PERMEABILITY FOR HARDENED CEMENT PASTE WITH FACTOR LOG (εr_h^2)

BR 6779-13

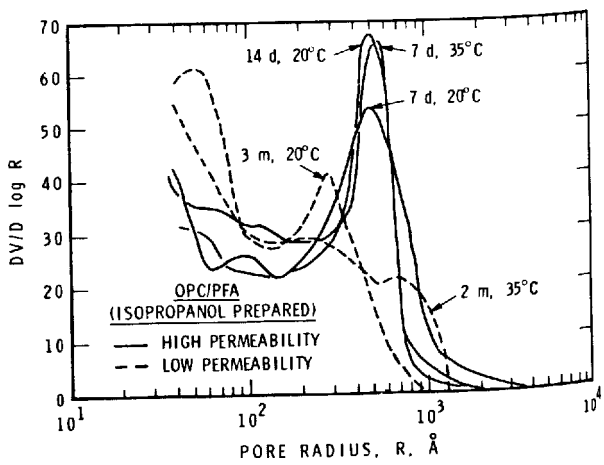

FIGURE 18

RELATIONSHIP OF DERIVATIVE FROM PORE DISTRIBUTION OF ISOPROPANOL PREPARED PORTLAND CEMENT-FLY-ASH BLEND AND PERMEABILITY

BR 6779-14

reactions but with blends containing high quantities of blast furnace slag. He related the structure to the $Ca(OH)_2$ content remaining in the specimen and not to the product formed during the consumption of $Ca(OH)_2$ in the pozzolanic reaction. He considered that a large amount of $Ca(OH)_2$ in the specimen would result in many deficient $Ca(OH)_2$-CSH interfaces contributing to a continuous pore path. The $Ca(OH)_2$ is present in large quantities in ordinary portland cement but not in the hydrated blends. When the $Ca(OH)_2$ content in the paste matrix is less than about 7 percent, the slope of the distribution curve at "maximum intrusion pressure", plotted in Fig. 5b for the fly-ash blend, increases to values similar to those of the slag blend.

Parrot et al. (54) plotted the diffusion parameter $e\tau_{\frac{1}{2}}$, obtained by replacement of water with methanol, against porosity for pores greater than 500 Å wide. These results are presented in Fig. 19. An abrupt transition in diffusion behaviour occurs and the authors (54) state that open channels are blocked by relatively small quantities of hydration products.

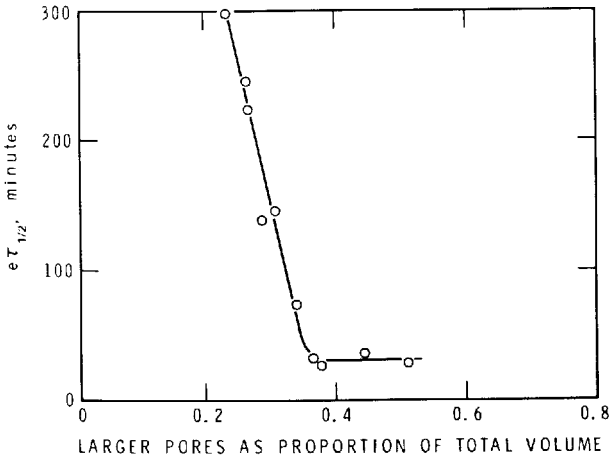

FIGURE 19
DIFFUSION PARAMETER $e\tau_{1/2}$ vs VOLUME OF LARGER PORES AS A FRACTION OF TOTAL VOLUME

BR 6779-15

DURABILITY AND RELEVANT METHOD OF MEASURING PERMEABILITY OR DIFFUSIVITY

Several techniques for measuring permeability or diffusivity have been discussed in this paper. Although many of these techniques can be similarly related to parameters of pore structures, each technique may be more applicable to a particular form of material breakdown. In the case of corrosion of reinforcing steel, both oxygen or chloride diffusion measurements may be the most apt, while in the case of water permeation under high pressures a high pressure technique should, perhaps, be applied since these pressures may change the pore structure. Other factors such as the chemical composition of the cement may be particularly relevant to $C\ell^-$ ion diffusion rates; this may make it necessary to use diffusion data obtained only from direct $C\ell^-$ ion diffusion measurements. Techniques which involve severe treatment, such as fairly extensive drying, heating or chemical treatment such as the use of methanol, may not be applicable to the general situation.

It is clear that more laboratory work using several techniques should be performed on materials with a broad range of pore structures, and these materials should be submitted to specific forms of long-term field exposure. Results may show that more simple techniques can give valid results.

This paper is a contribution from the Division of Building Research, National Research Council of Canada.

REFERENCES

1. V.S. Ramachandran, R.F. Feldman and J.J. Beaudoin, "Concrete Science", Heyden-Wiley, London-Philadelphia, 427 p. (1981).

2. S.E. Pihlajavaara and H. Paroll, "On the Correlation between Permeability Properties and Strength of Concrete", Cem. Concr. Res., 5, pp. 321-328 (1975).

3. R.A. Helmuth, "Effects of Mineral Admixtures on the Durability of Concrete", Engineering Foundation Conference, Henniker, NH, U.S.A. (1985).

4. E.W. McDaniel, "Constant Technology for Bore Hole Plugging: An Interim Report on Permeability Measurements of Cementitious Solids". Oak Ridge National Laboratory, Contract No. W-7405-eng-26, with U.S. Dept. of Energy (1980).

5. C.D. Lawrence, "Durability of Concrete: Molecular Transport Processes and Test Methods", Cem. Concrete Assoc., U.K., Technical Report 544 (July 1981).

6. K.W.J. Treadaway, "Research into Durability of Reinforcement in Concrete Structures under Normal Exposure Conditions", Proc. RILEM Seminar on the "Durability of Concrete Structures under Normal Outdoor Exposure", Hannover, Germany, pp. 202-209 (1984).

7. W.R. Holden, C.L. Page and N.R. Short, "The Influence of Chlorides and Sulphates on Durability", Ch. 9 In "The Corrosion of Reinforcement in Concrete Construction", pp. 143-150, London (June 1983) (Ed. A.P. Crane) Pub. Ellis Horwood, Chichester.

8. C.M. Hansson, Th. Frolund and J.B. Markussen, "The Effect of Chloride Cation Type on the Corrosion of Steel in Concrete by Chloride Salts", Cem. Concr. Res. 15(1), pp. 65-73 (1985).

9. C.D. Pomeroy, "Requirements for Durable Concrete", Cem. Concrete Assoc., 15 p. (PP/403) (1985).

10. C.L. Page and Ø. Vennesland, "Pore Solution Composition and Chloride Binding Capacity of Silica-Fume Cement Pastes", Materials and Structures, 16 (91), pp. 19-25 (1983).

11. C.D. Lawrence, "Transport of Oxygen through Concrete", British Ceramic Soc. Meeting, "Chemistry and Chemically-Related Properties of Concrete" (Ed. F.P. Glasser), London (April 1984).

12. K. Tuutti, "Corrosion of Steel in Concrete", Swedish Cement and Concrete Research Inst., ISSN 0346-6906 (1982).

13. P. Lambert, C.L. Page and N.R. Short, "Diffusion of Chloride Ions in Hardened Cement Pastes Containing Pure Cement Minerals", British Ceramic Soc. Meeting, Chemistry and Chemically Related Properties of Cement", (Ed. F.P. Glasser) pp. 267-275, London (Sept. 1984).

14. A. Atkinson and A.K. Nickerson, "The Diffusion of Ions Through Water-Saturated Cement", Matls. Sci., 19(9), 3068-3078 (1984).

15. R.D. Hooton and N.C. Burnett, "Development of a Highly Durable Concrete for the Storage, Transport and Disposal of Irradiated Fuel", Presented at ACI Symp. on Concrete and Cementitious Materials for Radioactive Waste Management (Nov. 1984).

16. R.H. Mills, "The Permeability of Concrete for Reactor Containment Vessels", a research report prepared for the Atomic Energy Control Board, Ottawa, 74 p. (July 1983).

17. A.J. Watson and C.C. Oyeka, "Oil Permeability of Hardened Cement Pastes and Concretes", Mag. Concr. R. 33(115), 85-95 (1981).

18. B.B. Hope and V.M. Malhotra, "The Measurement of Concrete Permeability", Can. J. Civ. Eng., 11(2), 287-292 (1984).

19. E.L. White, B.E. Scheetz, D.M. Roy, K.G. Zimmerman and M.W. Grutzek, "Permeability Measurements on Cementitious Materials for Nuclear Waste Isolation", Symposium on "Science underlying radioactive waste management", Vol. 1, pp. 471-478, Boston (1978).

20. P.K. Mehta and C. Manmohan, "Pore Distribution and Permeability of Hardened Cement Pastes", 7th Int. Symp. on Chemistry of Cement, Paris, Vol. III, pp. VII-1 - VII-5, 1980.

21. B.K. Nyame and J.M. Illston, "Capillary Pore Structure and Permeability of Hardened Cement Paste", 7th Int. Symp. on Chemistry of Cement, Paris, Vol. III, pp. VI-181 - VI-186 (1980).

22. B.K. Nyame and J.M. Illston, "Relationships between Permeability and Pore Structure of Hardened Cement Paste", Mag. Concr. Res., 33 (116), 139-146 (1981).

23. S. Goto and D. Roy, "The Effect of w/c Ratio and Curing Temperature on the Permeability of Hardened Cement Pastes", Cem. Concr. Res., 11, pp. 575-579 (1981).

24. D. Manmohan and P.K. Mehta, "Influence of Pozzolan, Slag, and Chemical Admixtures on Pore-size Distribution and Permeability of Hardened Cement Pastes", Cement, Concrete and Aggregate, 3(1), 63-67 (1981).

25. B.K. Marsh, "Relationships between Engineering Properties and Microstructural Characteristics of Hardened Paste Containing PFA as a Partial Cement Replacement", Ph.D. Thesis, Hatfield Polytechnic and Cem. Concrete Assoc.

26. P. Schiessl, "Some Aspects of Corrosion Protection of Reinforcement Embedded in Outdoor Structural Members", Proc. RILEM Seminar on the "Durability of Concrete Structures under Normal Outdoor Exposure", Hannover, Germany, pp. 197-201 (1984).

27. C.L. Page and K.W.J. Treadaway, "Aspects of the Electro-chemistry of Steel in Concrete", Nature, 297(5862), 109-115 (1982).

28. C.L. Page and J. Havdahl, "Electro-chemical Monitoring of Corrosion of Steel on Microsilica Cement Pastes", Materials and Structures, 18 (103), 41-47 (1985).

29. K.W.J. Treadaway and C.L. Page, "The Durability of Steel in Concrete", BRE News, 64, pp. 4-5 (1984).

30. B. Hope, A. Ip and D. Manning, "Corrosion and Electrical Impedance in Concrete", Cem. Concr. Res., 15(3), 525-534 (1985).

31. C.M. Preece, H. Arup and I. Frolund, "Electro-chemical Behaviour of Steel in Dense Silica-Cement", SP 79, Proc. 1st Int. Conf. on the Use of Fly-ash, Silica Fume, Slag and Other Mineral By-Products in Concrete, Montebello, Que., Can., Vol. II, pp. 785-796 (1983).

32. C.M. Hansson, "Comments on Electro-chemical Measurements of the Rate of Corrosion of Steel in Concrete", Cem. Concr. Res., 14(4), 574-584 (1984).

33. C.M. Preece, "Corrosion of Steel in Concrete", KBS Rapport 82-19 (1982).

34. N.R. Short and C.L. Page, "The Diffusion of Chloride Ions through Portland and Blended Cement Pastes", Silicates Indus., 47(10), 237-240 (1982).

35. R.D. Hooton, "Permeability and Pore Structure of Cement Pastes Containing Fly Ash, Slag and Silica Fume", ASTM Symposium, Denver, CO (1984). To be published.

36. D.M. Roy and K.M. Parker, "Microstructure and Properties of Granulated Slag-Portland Cement Blends at Normal and Elevated Temperatures, SP 79, Proc. 1st Int. Conf. on the Use of Fly-ash, Silica Fume, Slag and Other Mineral By-products in Concrete, Montebello, Que., Can., Vol. 1, pp. 397-414 (1983).

37. R.F Feldman, "Significance of Porosity Measurements on Blended Cement Performance", Proc. 1st Int. Conf. on the Use of Fly-ash, Silica Fume, Slag and Other Mineral By-products in Concrete, Montebello, Que., Can., SP 79, Vol. 1, pp. 415-434 (1983).

38. R.F. Feldman and Huang Cheng-yi, "Microstructural Properties of Blended Cement Mortars and Their Relation to Durability", Proc. RILEM Seminar on "Durability of Concrete Structures under Normal Outdoor Exposure", Hannover, Germany, pp. 133-140 (1984).

39. R.F. Feldman and Huang Cheng-yi, "Resistance to Mortars Containing Silica Fume to Attack by a Solution Containing Chlorides", Cem. Concr. Res., 15(3), 411-420 (1985).

40. P.K. Mehta and O.E. Gjorv, "Properties of Portland Cement Concrete Containing Fly Ash and Condensed Silica Fume", Cem. Concr. Res., 12(5), 587-595 (1982).

41. A. Mor and P.K. Mehta, "Effect of Superplasticizing Admixtures on Cement Hydration", Cem. Concr. Res., 14(5), 754-756 (1984).

42. P.K. Mehta, "Studies on Blended Cements Containing Santorin Earth", Cem. Concr. Res., 11(4), 507-518 (1981).

43. P.K. Mehta, "Properties of Blended Cements Made from Rice Husk Ash", Am. Concrete Inst. J., 74(9), 440-442 (1977).

44. C.D. Lawrence, "Permeability Measurements on Blended Cement Concretes", Cem. Concrete Assoc., DN/4044 (1985).

45. C.D. Lawrence, "Permeability Measurements on Concretes", Cem. Concrete Assoc., DN/4038 (1982).

46. R.F.M. Bakker, "About the Cause of the Resistance of Blast Furnace Cement Concrete to the Alkali-Silica Reaction", Proc. Cape Town Conf., "Alkali-Aggregate Reaction in Concrete", pp. 279-285 (1981).

47. R.F. Feldman, "Pore Structure Formation during Hydration of Fly-ash and Slag Cement Blends", Mat. Res. Soc. Symp., pp. 124-133 (1981).

48. R.L. Day, R.C. Joshi, B.W. Langan and M.A. Ward, "Measurement of the Permeability of Concretes Containing Fly Ash", Proc. 7th Int. Ash Utilization Symp., Orlando, FL, U.S.A., Vol. 2, pp. 811-827 (1985).

49. B.K. Marsh and R.L. Day, "Some Difficulties in the Assessment of Pore Structure of High Performance Blended Cement Pastes", Mat. Res. Soc. Symp. Proc., "Very High Strength Cement-based Materials", 42(1), 113-122 (1985).

50. B.K. Marsh, R.L. Day, D.G. Bonner and J.M. Illston, "The Effect of Solvent Replacement Upon the Pore Structure Characterization of Portland Cement Paste", RILEM Symp. on Principles and Applications of Pore Structural Characterization, Milan, 1983.

51. L.J. Parrott, "Novel Methods of Processing Cement Gel to Examine and Control Microstructure and Properties", Roy. Soc. of London Philos. Trans. A310, pp. 155-166 (1983).

52. L.J. Parrott, "Effect of Drying History upon the Exchange of Pore Water with Methanol and upon Subsequent Methanol Sorption Behaviour in Hydrated Alite Paste", Cem. Concr. Res., 11(5), 651-658 (1981).

53. H.G. Midgley and J.M. Illston, "Some Comments on the Microstructure of Hardened Cement Pastes", Cem. Concr. Res., 13(2), 197-206 (1983).

54. L.J. Parrott, R.G. Patel, D.C. Killoh and H.M. Jennings, "Effect of Age on Diffusion in Hydrated Alite Cement", J. Amer. Ceram. Soc., 67(4), 233-237 (1984).

55. F.G.R. Gimblett, Z. Mohd Amin and K.S.W. Sing, "Influence of Pre-treatment on the Microstructure of Calcium Silicate Hydrate Gels", 7th Int. Symp. on Chemistry of Cement, Paris, Vol. II, pp. 225-231 (1980).

56. J.J. Beaudoin, "Validity of Using Methanol for Studying the Microstructure of Cement Paste. In press. To be submitted to J. of Materials and Structures.

57. J.J. Beaudoin, "Interaction of Aliphatic Alcohols with Cement Systems". In press. To be submitted to Il Cemento.

58. R. Day, "Reactions between Methanol and Portland Cement Paste", Cem. Concr. Res., 11(3), 341-349 (1981).

59. R.F. Feldman and Huang Cheng-yi, "Properties of Portland Cement-Silica Fume Pastes I. Porosity and Surface Properties", Cem. Concr. Res., 15(5), 765-774 (1985).

60. R.F. Feldman, "Pore Structure Damage in Blended Cements Caused by Mercury Intrusion", J. Amer. Ceram. Soc., 62(1), 30-33 (1984).

61. J.J. Beaudoin, "Porosity Measurement of Some Hydrated Cementitious Systems By High Pressure Mercury Intrusion - Microstructural Limitations", Cem. Concr. Res., 9(6), 771-781 (1979).

62. C.D. Lawrence, "Sorption Studies of the Microstructure of Hydrated Cement", Cem. Concrete Assoc., PP/352 (1983).

63. C.D. Lawrence, "Hardened Cement Paste Pore Structures from N_2 and Butane Adsorption Isotherms", RILEM Symp. on Principles and Applications of Pore Structural Characterization, Milan (1983).

64. K. Kendall, A.J. Howard and J.D. Birchall, "The Relation between Porosity, Microstructure and Strength, and the Approach to Advanced

Cement-based Materials", Roy. Soc. of London Philos. Trans. A310, pp. 139-153 (1983).

65. J.D. Birchall, "Shells, Cements and Ceramics", J. Por. Cem. Soc., 83(6), 158-165 (1984).

66. A.A. Rahmain, "Characterization of the Porosity of Hydrated Cement Pastes", Proc. British Ceramic Soc., 35, pp. 249-266 (1984).

67. M. Grube and C.D. Lawrence, "Permeability of Concrete to Oxygen", Proc. RILEM Seminar on "Durability of Concrete Structures under Normal Outdoor Exposure", Hannover, Germany, pp. 68-79, (1984).

68. M. Gräf and H. Grube, "The Influence of Curing on the Gas Permeability of Concrete with Different Compositions", Proc. RILEM Seminar on "Durability of Concrete Structures under Normal Outdoor Exposure, Hannover, Germany, pp. 80-87, (1984).

69. L. Zagar, "Methods of Determination of Pore Structure, Permeability and Diffusion", RILEM/Inpac. Symposium, "Pore Structure and Properties of Materials", Vol. 4, C-249 to C-277, Prague (1973).

70. G.M. Darr and U. Ludwig, "Determination of Permeable Porosity", Materials and Structures, 6, pp. 185-190 (1973).

71. M. Hurling, "Oxygen Permeability of Concrete", Proc. RILEM Seminar on "Durability of Concrete Structures Under Normal Outdoor Exposure", Hannover, Germany, pp. 91-101 (1984).

72. M. Grube and C.D. Lawrence, "Permeability of Concretes to Oxygen", Draft Report for Cambureau (confidential), January (1985).

73. J. Crank, "The Mathematics of Diffusion", Oxford Clarendon Press, 414 p. (1975).

74. G. de Wind, "Discussion of K. Tuutti "Corrosion of Steel in Concrete" (ref. 12), Technical High School, Delft (1983).

75. C.D. Lawrence, "Diffusion of Oxygen Through Saturated Concrete", Cement and Concrete Assoc., England, PP/397, Seminar at Oxford University 13-14 Sept. (1984).

76. D.A. Hausmann, "Steel Corrosion in Concrete", Mater. Prot., 6, pp. 19-23 (1967).

77. R. Kondo, M. Satake and H. Ushiyama, "Ionic Diffusion Measurements in Hardened Cement Paste", Semento Gijutso henpo, 28, pp. 41-44 (1974).

78. H. Ushiyama, H. Iwakura and T. Fukunaga, "Diffusion of Sulphate Ion in Blended Portland Cement", Review, Cement Association of Japan, 30, pp. 47-49 (1976).

79. S. Goto, M. Tsunetani, H. Yanagida and R. Kondo, "Diffusion of Chloride Ion in Hardened Cement Paste", Yogyo Kyokaishi, 87(3), pp. 126-133 (1979).

80. H.G. Midgley and J.M. Illston, "The Penetration of Chloride Into Cement Paste", Cem. Concr. Res., 14(4), 546-558 (1984).

81. S. Goto and D.M. Roy, "Diffusion of Ions Through Hardened Cement Paste", Cem. Concr. Res., 11(5), 751-757 (1981).

82. C.L. Page, N.R. Short and A. El Tarras, "Diffusion of Chloride Ions in Hardened Cement Pastes", Cem. Concr. Res., 11(3), 395-406 (1981).

83. N.R. Short and C.L. Page, "The Diffusion of Chloride Ions Through Portland and Blended Cement Pastes", Silicates Indust., 47(10), 237-240 (1982).

84. M. Collepardi, A. Marcialis and R. Tunizlani, "Penetration of Chloride Ions into Cement Pastes and Concretes", J. Amer. Ceram. Soc., 55(10), 534-535 (1972).

85. K. Shigeru, T. Takagi, S. Goto and M. Diamon, "Diffusion of Ions Through Hardened Paste of Various Cements", CAJ Review, pp. 75-77 (1983).

86. L.J. Parrott, "An Examination of Two Methods for Studying Diffusion Kinetics in Hydrated Cements", Materials and Structures, 17(98), 131-137 (1984).

87. R.G. Patel, L.J. Parrott, J.A. Martin and D.C. Killoh, "Gradients of Microstructure and Diffusion Properties in Cement Paste Caused by Drying", Cem. Concr. Res. (1985). In press.

88. R.F. Feldman - unpublished work.

89. R.L. Day and J.M. Illston, "The Effect of Drying on the Drying-Wetting Behaviour of Hardened Cement Paste", Cem. Concr. Res., 13(1), 7-17 (1983).

90. D.N. Winslow and S. Diamond, "Specific Surface of Hardened Portland Cement Pastes as Determined by Small-Angle X-Ray Scattering", J. Amer. Ceram. Soc., 57(5), 193-197 (1974).

SUB-THEME/SOUS-THÈME 4.2

Mechanism of cement paste degradation due to chemical and physical processes.

Mécanisme de la dégradation de la pâte de ciment due aux processus chimiques et physiques.

Chairman/Président:

G. G. Litvan
Division of Building Research
National Research Council
Ottawa, Ontario, Canada

Principal Reporter/Rapporteur Principal:

D. M. Roy
Materials Research Laboratory the
Pennsylvania State University
University Park, PA, U.S.A.

G.G. Litvan, Division of Building Research, National Research Council Canada

MECHANISM OF CEMENT PASTE DEGRADATION DUE TO CHEMICAL AND PHYSICAL PROCESSES
MÉCANISME DE DÉGRADATION DE LA PÂTE DE CIMENT CAUSÉE PAR DES PROCESSUS CHIMIQUES ET PHYSIQUES

SUMMARY: Two areas of research are discussed; namely, clarifying the reasons for volume instability that accompanies all degradation processes and establishing the relationship between the characteristics of the pore system and freeze-thaw resistance of concrete. Studies in these areas are needed, and promise to yield significant progress in improving durability of concrete.

São discutidas duas áreas de pesquisa: ou seja, esclarecimento das razões para a instabilidade de volume que acompanha todos os processos de degradação, e estabelecimento da relação entre as características do sistema de poro e a resistência ao congelamento-descongelamento do concreto. São necessários estudos nesta área, e prometem resultar em progresso significativo na melhora da durabilidade do concreto.

G.G. Litvan, Division of Building Research, National Research Council Canada

INTRODUCTION

The durability of cement paste is a most topical field now that economic restraint and conservation are, and will remain, the rule of the day. My task as special reporter is to discuss future research trends in cement paste degradation; that is, what will probably be developed, and what has not but should be the subject of future research. The very nature of the task thus compels me to go beyond the scientifically proven facts and engage in an expression of personal views and in some speculation which, I hope, will prompt some discussion.

The degradation process has a variety of causes:

- undesirable reactions between a constituent of the cement paste and a substance originating from the surrounding environment (CO_2, SO_4^{--}, $C\ell^-$, seawater, various chemicals);
- undesirable reactions between a constituent of the cement paste and the aggregate (alkali-aggregate reaction);
- freezing and thawing;
- abrasion.

The term "degradation" means that the paste fails to serve the intended purpose for the length of time expected. It should be noted that, normally, cement paste or concrete can and often does have an essentially indefinite life span, in the absence of degradation processes.

Volume Instability

The performance of cement paste is deemed to be unsatisfactory usually because of loss of structural integrity. Concrete as a construction material is used almost solely for structural purposes.

Why are volume instability and loss of mechanical strength associated with certain chemical and physical processes in cement paste? This is then the central question in research on degradation to which we are seeking an answer. Most theories are in agreement concerning the primary causes of the various deterioration processes; for example, the reaction of lime and calcium silicate hydrate with carbon dioxide causes carbonation shrinkage, the reaction of sodium and potassium hydroxide with silica or carbonate causes major cracking in alkali-aggregate reaction, and exposure to below-freezing temperatures causes freeze-thaw damage. The reasons for the volume instability, cracking and loss of strength, however, are less well understood, as evidenced by the multitude of explanations existing for almost every process.

The possibility that all or many degradation processes have a common mechanism has not been considered, to my knowledge; yet we know that in nature valid explanations are usually simple and universal.

Chemical degradation processes usually consist of dissolution of matter and formation of a new phase; for example, in alkali-aggregate reactions the dissolution of silica and the formation of silica gel. These reactions involve breakage of bonds; in the cited example, those between the aggregate and the paste.

Cement paste is a composite system with built-in stresses caused by drying shrinkage, moisture and temperature gradients, and chemical reactions, such as hydrations or ageing. The process of degradation thus results in a change of the level and distribution of stresses that will manifest themselves in volume changes leading, in extreme cases, to cracking and destruction of the entire solid.

It has been shown that removing a constituent of the hardened paste; for example, leaching lime, results in expansion (1). It was observed that partial dissolution of the paste by $HC\ell$ causes an increase of the volume of the remainder of the paste (1). Sulfate attack and rusting of reinforcing steel are a variation of the same mechanism.

Carbonation of lime in the paste in situ does not involve breakage of the bond between the lime granules and the rest of the paste. In this process, the addition of CO_2 onto the $Ca(OH)_2$ exposed on the surface and the elimination of H_2O occur, which may even increase bond strength. Addition reactions or adsorption occurring on the surface have been found to result in contraction (2) and that, of course, is the volume change accompanying carbonation.

Exploring the relationship between bond breakage, surface compound formation and volume changes appears to be a promising area of research.

Freezing and Thawing

Air entrainment has made possible the use of concrete in northern countries. The still unacceptably high rate of failure due to freeze-thaw action clearly indicates, however, that in practice the problem has not yet been solved satisfactorily. Sensitivity of the air-entraining process to a host of material, process and environmental factors seems to render the method far less reliable than is required.

One solution to the problem is to entrain air using pre-formed voids; that is, to add granules of solids having pores of the required size (3). The reason for discussing this approach here is the finding made in the course of its development that, while in conventional air entrainment only air voids larger than 10 μm in diameter are believed to be beneficial, particulates which had smaller pores, mainly 0.3 to 2 μm in diameter, were the most effective in protecting cement from freeze-thaw damage. In fact, granules with large pores primarily between 7 and 10 μm in diameter proved to be ineffective. It was also found that air-entrained cement-paste specimens containing a high-range water reducer had very good freeze-thaw resistance if mainly smaller pores (0.3 to 2 μm in diameter) were present (4). These observations suggest that a review of the relationship between pore characteristics and freeze-thaw durability of concrete in general, and the role of the large entrained air voids in particular, could be rewarding. A number of workers investigated the relationship between the pore characteristics and

the frost resistance of aggregates (5-8). It is probable that the relationships between pore characteristics and frost resistance will prove to be the same for most porous solids.

Once determined, the critical pore characteristics can serve as the basis for predicting frost resistance, making it possible to use material properties instead of performance under accelerated conditions that are seldom representative of the real environment. Also, the loss in mechanical properties caused by conventional air entrainment can be reduced, or avoided altogether. It may also be possible to find a chemical admixture that will entrain pores of only the required small sizes.

Prediction of Performance

Our understanding of the mechanism of the various degradation processes has been insufficient to solve problems such as prediction of performance of cement paste under specified conditions.

Assessment of the resistance of cement paste to carbonation, chemical attack, alkali-aggregate reaction and freeze-thaw resistance is currently based on performance in accelerated tests. This approach suffers from the inherent contradiction of the objectives: to speed up testing in order to obtain results as soon as possible, and to test for a long enough time to ensure the creation of representative conditions. Most of the current tests are not very reliable, presumably because the conditions of the accelerated test differ in a qualitative sense from those in the field. As mentioned earlier, the best solution is to base prediction on material characteristics, but to do so the mechanism of degradation needs to be better understood.

Prediction of performance is also hampered by the lack of knowledge about the effect of various factors and the combination of such factors on the overall degradation process. For example, it makes little sense to talk about frost-resistant cement paste without specifying the environment in which such a paste is expected to perform without degradation. Although moisture content, rate of cooling, and wall thickness are recognized to be factors, their effect is seldom known in quantitative terms. Performance can obviously not be predicted on the basis of only one side of the equation; that is, the material properties, without knowledge of the characteristics of the environment and their influence on the process. Perhaps more than ever before, this knowledge is now required. For example, cement is being used for the construction of drilling platforms, liquefied-gas storage tanks and chemical plants, often located in hostile environments.

* * *

Blended cements are already widely used, but their utilization will continue on a larger scale along with new types of additives. The era of pure ordinary portland cement concrete will come to an end. The effect of composition on durability is far from being satisfactorily understood, and knowledge of long-term behaviour of pastes made of blended cements is even more uncertain.

Although many questions remain to be answered, there is little doubt that the know-how to produce cement paste with good durability will be developed.

This paper is a contribution of the Division of Building Research, National Research Council of Canada.

REFERENCES

1. G.G. Litvan, "Volume Instability of Porous Solids I". 7th International Congress on the Chemistry of Cement, Vol. III, Paris, 1980, pp. VII.46-VII.50.

2. G.G. Litvan, "Volume Instability of Porous Solids II. Dissolution of Porous Silica Glass in Sodium Hydroxide". J. Materials Science 19, No. 8, 1984, pp. 2473-2780.

3. G.G. Litvan and P.J. Sereda, "Particulate Admixture for Enhanced Freeze-Thaw Resistance of Concrete". Cement and Concrete Research 8, No. 1, 1978, pp. 53-60.

4. G.G. Litvan, "Air Entrainment in the Presence of Superplasticizers". J. American Concrete Institute, July/August 1983, pp. 326-331.

5. R.D. Walker and Tai-Chou Hsieh, "Relationship between Aggregate Pore Characteristics and the Durability of Concrete Exposed to Freezing and Thawing". Highway Research Record No. 226, Highway Research Board, Washington, D.C., 1968, pp. 41-49.

6. Y. Koh and E. Kamada, "The Influence of Pore Structure of Concrete Made with Absorptive Aggregates on the Frost Durability of Concrete". Proceedings RILEM/IUPAC International Symposium on Pore Structure and Properties of Materials, Prague, Sept. 1973, ARTIA, Prague, 1973, Vol. II, pp. F-45-F-62.

7. H. Lange and S. Modry, "Determination of the Frost Resistance of Limestone Aggregates in the Light of Porosity Investigation". Proceedings RILEM Symposium on Durability of Concrete, Prague, Sept. 1969, Building Research Institute, 1969, pp. B-129-B-138.

8. M. Kaneuji, D.N. Winslow and W.L. Dolch, "The Relationship between an Aggregate's Pore Size Distribution and Its Freeze-Thaw Durability in Concrete". Cement and Concrete Research 10, No. 3, 1980, pp. 433-441.

D.M. Roy
Materials Research Laboratory, The Pennsylvania State University, University Park, PA 16802, USA

MECHANISMS OF CEMENT PASTE DEGRADATION DUE TO CHEMICAL AND PHYSICAL FACTORS

SUMMARY

The resistance of hardened cement paste to chemical attack and physical degradation is the result of combined composition and microstructural factors with environmental exposure conditions. Factors controlling the initial microstructure development and its effect on the operation of forces of degradation are discussed briefly. Alkali-silica reactions and means for minimizing their harmful effects are treated briefly (the addition of pozzolans, ground granulated blast furnace slag, silica fume, or fly ash, which develop a finer pore structure, reduce hydroxyl (and alkali) contents of the paste pore solutions and reduce calcium hydroxide which may later serve to replenish the pore solutions and enhance the alkali-silica reaction). Sulfate attack (forming expansive ettringite, gypsum, brucite, and sometimes associated with calcite formation) may also be controlled by pozzolanic additions, which develop fine microstructures, and minimize expansion. Chloride transport mechanisms and reactions and their implications for corrosion are reviewed. The diffusion rates of chloride ions in pastes with blast furnace slag and silica fume additions are several times lower than for portland cement at an early age. Pozzolans or fly ash take longer to develop their preventive effects. Chlorides are 'fixed' in the solid or on the pore surfaces of blended cement pastes. Excessive carbonation of portland or blended pastes is usually the result of too high w/c, improper or insufficient curing, and exposure to low-intermediate (50-65%) R.H. environments at an early age. Free energy changes favor carbonation of cement paste at atmospheric CO_2 pressures, accelerated by an open pore structure and low relative humidity; high-$Ca(OH)_2$ content pastes carbonate most readily, other factors being equal. Additional degradation mechanisms include leaching (with implications for radioactive and toxic element release); Na, K, Cs, Cl ions are released by diffusion, while Ca, silicate and aluminate species have different release mechanisms. Effects of freezing and thawing, the role of air entrainment, the interaction of organic species with blended cements, their effects on bubble spacing, and on durability are treated briefly. Cooperative physical and chemical effects are important, and not fully understood.

A resistência da pasta endurecida de cimento ao ataque químico e à degradação física é resultado de fatores combinados da composição e da microestrutura com as condições de exposição ambiental. São discutidos resumidamente os fatores que controlam o desenvolvimento inicial da microestrutura e seu efeito sobre a atuação de forças de degradação. Resumidamente se trata das reações álcali-sílica e dos meios para minimizar seus efeitos prejudiciais (a adição de pozolanas, escória de alto forno granulada moída, microsílica, ou cinza volante, que desenvolvem uma estrutura mais fina de poro, reduzem os teores de hidroxil (e álcali) das soluções de poro da pasta e reduzem o hidróxido de cálcio que pode, mais tarde, servir para reencher as soluções de poro e favorecer a reação álcali-sílica). O ataque de sulfato (formando etringita expansiva, gesso, brucita, e algumas vezes associado com formação de calcita) pode também ser controlado por adições pozolânicas, que desenvolvem microestruturas finas, e minimizam a expansão. São revistos os mecanismos e reações de transporte do cloreto e suas implicações na corrosão. As velocidades de difusão dos íons de cloreto nas pastas com escória de alto forno e microsílica adicionados são várias vezes mais baixas do que no cimento portland na idade inicial. Pozolanas e cinza volante demoram mais a desenvolver seus efeitos preventivos. Os cloretos são "fixados" no sólido ou sobre as superfícies do poro das pastas de cimento aditivado. Carbonatação excessiva das pastas de cimento portland ou aditivado é resultado de relação água/cimento muito alta, cura inadequada ou insuficiente, ou exposição a ambientes com umidade relativa baixa-intermediária (50 - 65%) na idade inicial. Mudanças na energia livre favorecem a carbonatação da pasta de cimento sob pressões atmosférias de CO_2, acelerada por uma estrutura aberta de poro e baixa umidade relativa; pastas com alto teor de $Ca(OH)_2$ se carbonatam mais prontamente, sendo iguais os outros fatores. Mecanismos adicionais de degradação incluem lixiviação (com implicações de liberação de elemento radioativo e tóxico); íons de Na, K, Cs, Cl são liberados por difusão, enquanto Ca, espécies de silicato e aluminato têm mecanismos diferentes de liberação. São tratados resumidamente os efeitos de congelamento e descongelamento, o papel do ar entranhado, a interação de espécies orgânicas com cimentos aditivados, seus efeitos sobre o espaçamento de bolha, e sobre a durabilidade. Os efeitos físicos e químicos cooperativos são importantes, e não entendidos totalmente.

INTRODUCTION: FACTORS INVOLVED IN CEMENT PASTE DEGRADATION

The resistance of hardened cement paste to chemical attack and physical degradation when exposed to an aggressive environment, or when interaction takes place between potentially reactive internal components and the external environment is not related strictly to the mechanical strength of the material; i.e., strong materials do not always resist attack and disintegrative forces in any environment in which they are placed. Nevertheless, it is true that higher strength cement pastes are generally less permeable, and thereby will provide better resistance to chemical attack and physical degradation than low strength materials. It is a truism that water content (and w/c ratio) of a cement paste is probably the most important single factor in determining the subsequent porosity and permeability of the hardened paste, and that decreasing water content serves to decrease porosity and usually increases strength.

The porosity and pore structure of cement pastes exert major control on the ingress of potentially deleterious substances. This should be stated early although a detailed treatment of these factors is the subject of other papers in this Symposium* (65). Nevertheless, the pore structure and microstructure constitute major rate-controlling factors for potentially harmful transport processes, whether the species being transported is water (to give rise to alkali-silica expansion), sulfate ions (causing sulfate attack), chloride ions (to depassivate the protective layer on reinforcing steel), acids, or oxygen or carbon dioxide.

The factors controlling microstructure and pore structure have not been immediately obvious or totally predictable from past knowledge, because, e.g., certain mineral admixtures, substituents (supplementary cementing materials), or pozzolanas promote development of a fine pore structure and cause lower permeability (and diffusivity of potentially deleterious species) far beyond that which would be predicted on the basis of the water/cementitious solids ratio alone.

Concerning the predictability of properties, there are two stages in the preparation of cementitious materials which should be carefully controlled for they are critical for affecting their ultimate resistance to forces of degradation: 1) the fresh state, during mixing, placing and consolidation; and 2) the curing stage. Beyond the chemistry of the cementitious materials, factors which influence early stage rheological properties can significantly affect the physical properties of the hardened paste which control their ultimate durability. Poor mixing, inadequate dispersion, bleeding and related phenomena can give rise to inhomogeneities in the hardened paste microstructure, which can provide pathways for rapid transport of harmful species. There are certain limits beyond which water cannot be reduced, and maintain adequate workability. Plasticizers and superplasticizers are commonly used to improve fluidity, but their use also affects the course of hydration, and their effects on the resistance to environmental attack are not fully known, although in general harmful effects have not been reported.

A combination of chemical and physical factors are influential in the curing stage: e.g., changing the chemistry, as by partial substitution of pozzolanas, granulated blast furnace slag or silica fume for cement can prevent excessive heat evolution which would result in micro-cracking. This is above and beyond their effect in generating a finer pore structure. On the other hand, when the rate of heat evolution is low, it may be necessary to pay greater attention to adequate curing so that an acceptable degree of maturity of the paste is reached before it is exposed to adverse conditions.

The chemical, physical, and microstructural properties of hardened cement pastes are critically interrelated with respect to their effects on degradation. This paper attempts to review recent knowledge on the degradation of hardened cement pastes in several areas: alkali-silica reaction/expansion, sulfate attack, chloride penetration and relevance to corrosion, and carbonation and oxygen penetration, and set it within the context of the above general framework. Freezing and thawing mechanisms are also treated briefly.

ALKALI-SILICA REACTION

General

This type of degradation is considered first because the components for deleterious reaction are mostly contained within the cement paste itself (along with the aggregate), and only the introduction of water from the outside is necessary to cause distress. Alkali-aggregate reaction, and more particularly the formation of an expansive gel is an increasingly widespread phenomenon. It has been studied recently both in simplified systems and in mortars and concretes (1,2). The reaction of silica in concrete may be expressed as a process activated by the presence of hydroxyl ions in cement paste associated with alkalis and is represented [somewhat adapted from Powers and Steinour (3)] as:

$$-Si-OH + Na^+ + OH^- \rightarrow -Si-O^- Na^+ + H_2O$$

where the hydroxyl reacts first with the silanol (Si-OH) groups. At high hydroxyl concentrations this attacks the much stronger siloxane bridging bonds (Si-O-Si) and the result is:

$$-Si-O-Si- + 2NaOH \rightarrow -Si-O^- Na^+ + Na^+O^- -Si- + H_2O$$

The open structure of amorphous or glassy silica is much more readily attacked by the OH^- than is dense crystalline silica, particularly quartz, with SiO_2 strongly bound in orderly crystal structures. The product of the reaction with amorphous silicates is alkali-silica gel, a poorly defined colloidal isotropic coagulate (4-6). Dent-Glasser and Kataoka (4,5) calculated imbibition pressures close to 50 kg/cm^2 (5 MPa) in systems with poorly crystalline silica and NaOH solution. The maximum pressure was found to correspond to a SiO_2/Na_2O ratio between 3 and 5, thus defining a 'pessimum content'.

*R.F. Feldman, 'Pore Structure, Permeability and Diffusivity as Related to Durability,' Theme 4.1.

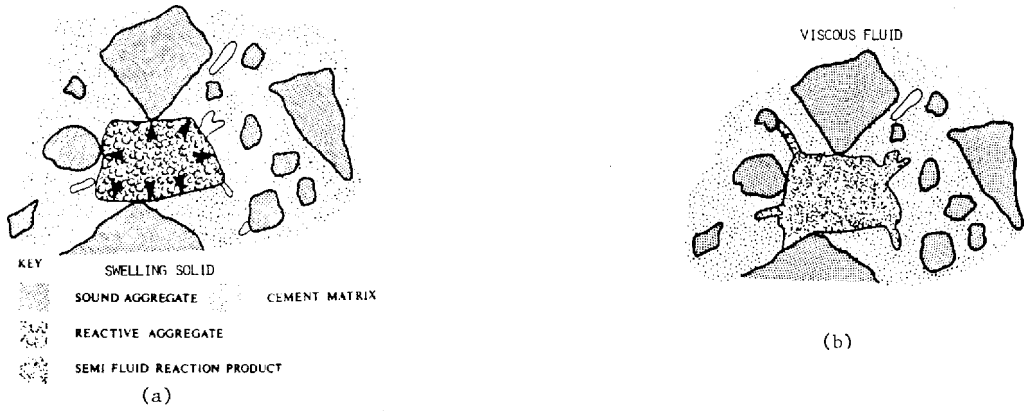

Fig. 1. (a) Swelling solid exerts pressure on adjacent solid material. (b) viscous fluid exerts pressure after pore space is filled. Adapted from Ref. (4).

Figure 1 shows schematically the relative effects of a swelling solid and liquid (4,5).

Swelling pressures in synthetic soda-silica gels were measured by Diamond and co-workers (7,8) who identified the existence of two types: a high swelling pressure (4-11 MPa) gel and a low swelling pressure (0.5 MPa) gel. There was no strict correlation of swelling pressure with chemical composition of gels. They found that large free swelling expansion did not necessarily result in a high swelling pressure, and observed that Ca-containing gels expanded modestly.

Dent-Glasser and Kataoka (9) further studied the role of calcium in alkali-aggregate reaction. They found that Ca^{2+} ions were adsorbed and reacted with the solid silica surface to form C-S-H on the surface of the silica gel. Although the layer appeared to behave as a semi-permeable membrane, it is possible that this apparent selectivity arises from a continuing chemical reaction in or on the layer between different species.

Tang Ming Shu (10) observed that expansion took place before the reaction products became fluid, concluding that the expansion is not compatible with the formation of a semi-permeable membrane. Ludwig (11) described a dynamic osmotic equilibrium, in which elevated temperatures accelerated the reaction but led to lower damage at long term. Gillott and Beddoes (12) concluded that osmosis is the driving force requiring preferential diffusion of water into the silica particles to generate swelling pressure. These authors used an interesting combination of Fourier shape and surface texture analysis microscopy and osmotic pressure results. Figg (13) agreed that osmotic pressure developed due to the inward diffusion of alkalies and OH^- ions, followed by the imbibition of water and the softening of glass aggregates. An alkaline silica gel was formed and the absorption of water by the gel was the second stage of the reaction identified by Kawamura et al. (14) by means of EDX and microhardness measurements. The diffusion of calcium ions into opal grains was observed to lag behind the intrusion of alkali.

In concrete, the alkali-aggregate reaction depends on maintaining a critical balance between free moisture, temperature, and wet/dry cycles; however, results of Diamond, Barneyback and Struble (7) suggest that expansion is not necessarily dependent on external water, but may occur as a consequence of the sorption of the pore solution into the gels formed. Regourd, Hornain and Poitevin (15) performed a microstructural (SEM and EPMA) study of deteriorated concretes which indicated the formation of gels of high SiO_2 content (C/S* ~0.2 to 0.4) around the aggregates, and richer calcium gels (C/S ~1.3) in the cement paste. A secondary formation of silicate crystals was observed on the aggregates in contact with the gel; while massive deposits of ettringite and calcium hydroxide were also observed in contact with the aggregates. The latter type of ettringite crystals are believed by St. John (16) to be the result of the movement of fluids through the concrete, which apparently are not harmful.

Tang et al. (17) have contrasted the microstructure of mortar samples (1x1x4 cm) made with 30 different rocks, which were treated briefly in NaOH solutions, and then autoclaved. Wilsson and Peterson (18) attributed pop-outs in concrete floors of moist indoor structures to a cement high in alkalies and a moisture problem. They discussed the moisture pessimum, which was close to 90% RH at room temperature. Both humidity and temperature are responsible for the gel viscosity. Cole and Lancucki (19) examined 30-year-old concrete with reaction rims around siltstone and sandstone aggregates, identifying okenite (CS_2H_2) and its precursor, in which some Ca was replaced by K and Na. XRD reflections occurred at 10.6Å and 8.85Å for okenite, and 12Å for its precursor phases. Deloye et al. (21) reported that in some cases of alkali-aggregate reaction the source of alkalis was the aggregates themselves: e.g., gneiss, granite, and serpentine. The gel is found to coexist with other compounds in some deteriorated structures.

Since the use of low alkali cement is not

*Cement abbreviations: C = CaO, S = SiO_2, H = H_2O, A = Al_2O_3, F = Fe_2O_3, w/c = water/cement.

always appropriate (21), the addition of slags, fly ash and pozzolanic materials to cements and concretes can be very beneficial (11,22-36). The effect of additives is reported to give hydrates with low permeability which reduces the mobility of the OH^- ions in the pore fluid (30). This is despite the fact that the admixtures may themselves have high alkali contents (30b). For a given proportion of 'pozzolan', those with highest silica contents usually gave the greatest reduction in expansion. The reduction in expansion achieved by blending reactive additives with a high alkali cement is generally greater than the dilution effect (27,28), where significant reductions in expansion have occurred in cements using both fly ash and slag (27). Good pozzolanic fly ash can be used at 30 to 40% replacement, or slag at 70% (22,27,28,35). For cements containing more than 65% slags, Bakker recommends that the alkali content be <2% equivalent Na_2O (22). He further concluded (23,24) that the expansion resistance of blast-furnace cement concretes is due to the formation of additional hydrates closing the porous system, rather than the fixation of calcium or alkali ions. Metso (25) found that the susceptibility to alkali-aggregate reaction depends on the sodium concentration in the blast-furnace slag-based binding agent and the amount of opal used as a very reactive aggregate, while Hobbs (26) suggests that water-soluble alkali content from all sources should not be greater than 2.5 kg/m^3 of concrete. He also showed (37) that a 40% replacement of a high-alkali cement by fly ash or granulated blast-furnace slag reduced the alkali silica reaction. Both materials act to reduce alkalis, blast-furnace slag being more effective in reducing damage. The effect of the temperature in modern concretes is also important where the early curing temperature is more than 20°C (27).

Blended cements, blast furnace slag cements, and pozzolanic cements have been used for many years (38-44) in the presence of potentially reactive aggregates to mitigate their effects. More recent suggestions have been that the amount of slag or fly ash must be as high as 50-60% and 25-30% respectively. The difference in resistance to alkali-aggregate attack between Portland cement and blast furnace cement is reported to be due to a major extent to the difference in permeability of the paste to alkali ions and water (45-47).

Grattan-Bellew (48,49) in his re-evaluation of standard mortar and concrete prisms used to monitor the alkali-aggregate reaction, stated that the petrographic examination of aggregates is a preliminary stage in the evaluation of their potential reactivity and that the expansion of concretes is directly related to the alkalinity of the interstitial solution. Thus it is necessary to determine soluble alkalis. The acceptable aqueous, alkali content for concrete in a moist environment, and in the presence of reactive aggregates, is reported to be 3 kg/m^3 (50,51). This limit assumes that all alkalies from Portland cement are available to go through solution.

Rayment (52) used EPMA to measure the C/S ratio of C-S-H in cement pastes containing 20% of fly ash and found a lower C/S and a higher amount of potassium than in ordinary pastes (1.71 to 1.55).

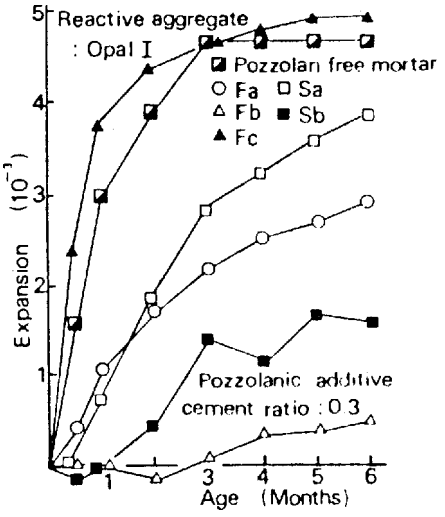

Fig. 2. Expansion curves, ASTM 227 test for opal-containing mortars (0.75 A/C, 0.4 w/c, with A = 10% opal, 90% sand). Additives as indicated in Table 1 [adapted from Ref. (54)].

Table 1
Total Alkali Contents of Pozzolanic Additives.*

Fly ash A	: Fa	2.00%
Fly ash B	: Fb	1.04
Fly ash C	: Fc	4.70
Silica fume	: SF	2.39
Blast furnace slag A	: Sa	0.59
Blast furnace slag B	: Sb	0.51

Adapted from Ref. (54).

Gudmundsson and Aisgeirsson (53) and Kawamura et al. (54) have shown the effectiveness of silica fume and other pozzolans substitution in high alkali cements for reducing expansion of alkali reaction aggregates. Figure 2 shows the effectiveness of pozzolanic additives from Table 1 in reducing expansion. Only the fly ash with 4% alkali was not effective. Additional studies have been reported in ref. (55) on the effects of fly ash, slag and silica fume on the relevant properties, while Oberholster (56) has elaborated preventive measures against alkali-silica reactions and given some examples. He discussed work of Van Aardt and Visser in which gel reaction products contained, in addition to 3.07Å C-S-H, a sodium phase, N-C-S-H with a basal x-ray diffraction spacing of 12.6Å, the latter said to be a swelling gel. Aitcin and Regourd (57) presented some field evidence of sidewalks using reactive aggregates and a palliative measure of 10-40% substituted silica fume, which was successful in controlling reaction for up to 4 years.

Alkalis in Pore Solutions: Mechanisms

Techniques developed first by Longuet et al. (58) to express pore solutions from hardened cement

pastes have recently been investigated extensively (7,8,31) in order to develop further understanding of the hydration process. Diamond (59) reported that in ordinary portland cement pastes the alkali and hydroxyl ion concentrations reached a steady state after a few days (in one instance ~0.8N) in the absence of alkali-silica reaction and remained relatively constant with time. In the presence of a pessimum proportion of opal, the concentration dropped to reach a steady state of ~0.35N. He reported that fly ash was somewhat variable in its effect on the alkali and hydroxyl ion pore solution concentrations, either diminishing or increasing it depending on the fly ash characteristics, while 5 or 10% fume (microsilica) added to a moderate alkali cement was effective in decreasing the concentration by 1 to 2-1/2 times, by 80 days. The effectiveness of silica fume was confirmed by Page and Vennesland (60). Malek and Roy (47) found that saturated $Ca(OH)_2$ solutions in contact with blast furnace slag-cement pastes and opal would lose their Ca ions first before the alkali ions. Glasser and Marr (61,62) found that silica fume is more effective in removing alkali and hydroxyl ions from solution than are blast furnace slag, fly ash or a natural pozzolan when all are present at 15% replacement level; while at 65% replacement level of high-alkali (1.02%) cement, Silsbee et al. (63) found that blast furnace slag by 28 days had reduced the pore solution alkali content by ~3 times (dropping from ~0.78N to ~0.25N), after passing through a slight maximum at ~12 days. Roy et al. (64) found that 30% cement replacement with a high alkali Class F fly ash caused the alkali concentration to go through a much higher delayed maximum at ~3 months, dropping by ~20% by 6 months.

The reactivity of glass fibers with alkalis in cement pore solutions in glass fiber reinforced cement (grc) is a special case of alkali-silica reaction. Majumdar et al. (66) observed a reduction of bending, tensile, and impact strengths after 5 years of water storage or natural weathering, while little change occurred in relatively dry conditions. Kondo and Ohsawa (67) studied the rate of pozzolanic reaction between various silicates and $Ca(OH)_2$ or portland cement and identified highly reactive siliceous materials which can prevent alkali-aggregate reaction and deterioration of glass-fiber reinforcement cement. As indicated, Diamond has shown that reduced alkali levels exist in cement paste pore solutions containing silica fume (59), while Silsbee et al. (63) have shown similar effects with ground granulated blast-furnace slag. Figure 3 shows the concentration of ions at an early age in pore solutions (59), while Fig. 4 shows those expressed from later age solutions, showing the much lower concentrations when slag is present. Experiments were carried out at elevated temperatures to accelerate the reactions (and produce possibly more stable phases), as well as to simulate very long time reactions under ambient conditions (68). Twenty percent silica fume substituted for cement appears to be effective in reducing $Ca(OH)_2$, alkali hydroxide and, apparently surface corrosion. Sixty-five percent blast furnace slag was shown to be also relatively effective but not as highly so as the silica fume. Bentur (69) reported similar findings with grc treated at atmospheric pressure, where apparently less adhesion (or reaction) existed between paste and fiber in the presence of silica fume, and higher strength was found. Additional discussion of alkali-silica reactions in grc is given in ref. (70,71).

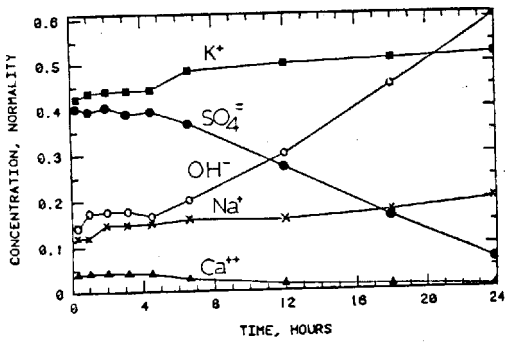

Fig. 3. Concentrations of ions in pore solutions, early age [adapted from Ref. (59)].

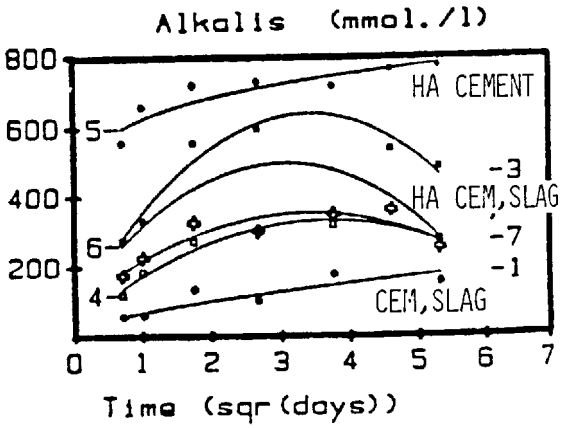

Fig. 4. Alkali level in pore solutions [after Ref. (63)]. #5 = high alkali cement; #6 = HA cement, slag 50:50; #1 = normal cement, slag 50:50.

Clearly, blast-furnace slag (high replacement levels) and silica fume are more effective than fly ash or pozzolans in lowering the alkali content of the solutions, when they are used at the appropriate replacement levels. Silica fume and granulated blast-furnace slag, it would seem, would compete effectively with reactive aggregate to minimize the alkalis available for reaction. Fly ash appears somewhat more variable in its properties; it is assumed that at later ages its major effectiveness will be in reducing the permeability and hence inhibition of water penetration which could cause swelling.

SULFATE ATTACK (SULFATE-RICH WATER, GROUND WATER, OR SEA WATER)

Introduction

Frequently the degradation of cementitious materials is due not to a single cause but arises

from the combined action of numerous potentially destructive forces, among them the action of sulfate attack. Soluble sulfates may react with some of the compounds in hydrated cement which, depending on the circumstances, can lead to disruptive expansion, strength loss, and/or disintegration. The usual chemical reactions concerned are given in idealized form as follows:

a) Ettringite formation:

$$4CaO\cdot Al_2O_3\cdot xH_2O + 3CaSO_4\cdot 2H_2O + H_2O \rightarrow$$

$$3CaO\cdot Al_2O_3\cdot 3CaSO_4\ 32H_2O + Ca(OH)_2 \qquad (1)$$

[The gypsum may be derived from reaction 2a) or 3); also, reaction may take place with the monosulfate to form the trisulfate, ettringite]

b) Gypsum and ettringite formation:

$$Ca(OH)_2 + MgSO_4 + 2H_2O$$

$$\rightarrow CaSO_4\cdot 2H_2O + Mg(OH)_2 \qquad (2a)$$

$$3CaO\cdot Al_2O_3\cdot 6H_2O + 3CaSO_4\cdot 2H_2O + H_2O \rightarrow$$

$$3CaO\cdot Al_2O_3\cdot 3CaSO_4\cdot 32H_2O \qquad (2b)$$

c) Gypsum formation:

$$Ca(OH)_2 + Na_2SO_4 + 2H_2O \rightarrow$$

$$CaSO_4\cdot 2H_2O + 2NaOH \qquad (3)$$

d) Brucite and gypsum formation:

$$C\text{-}S\text{-}H\ [xCaO\cdot ySiO_2] + MgSO_4 + H_2O \rightarrow$$

$$CaSO_4\cdot 2H_2O + Mg(OH)_2 + SiO_2 \qquad (4)$$

e) Additionally, the less common reaction with ammonium sulfate forms gypsum and ammonia, which can be quite harmful because the release of ammonia drives the reaction (72):

$$(NH_4)_2SO_4 + Ca(OH)_2 \rightarrow CaSO_4\cdot 2H_2O + 2NH_4OH\uparrow$$

To the above reactions, Chatterji added the growth of large $Ca(OH)_2$ crystals catalyzed by sulfate solutions (73,74).

Thus each of the major components of hydrated cements can react with sulfate to produce an expansive or deleterious reaction, although the C-S-H is believed to react primarily with $MgSO_4$. The formation of either gypsum or ettringite can produce

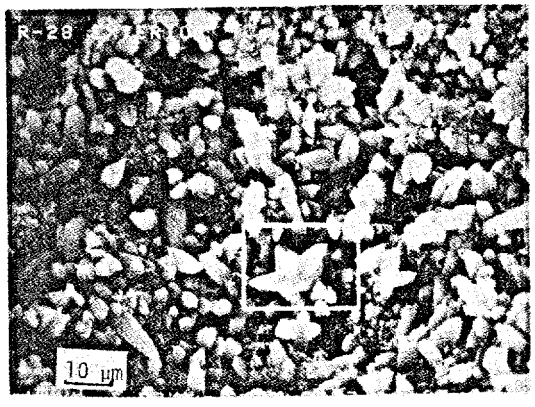

(a)

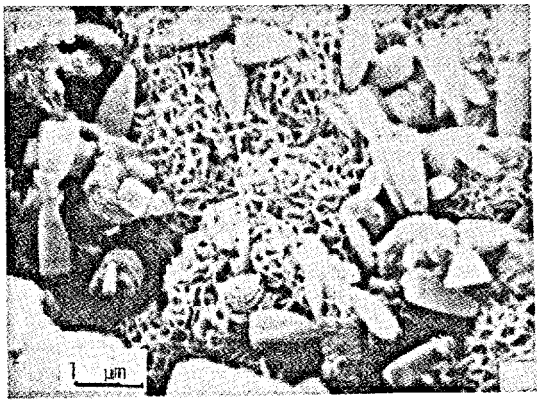

(b)

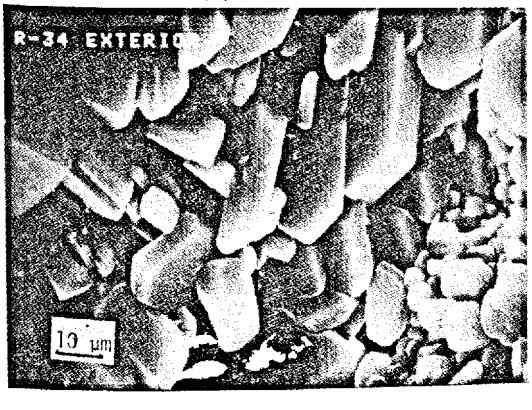

(c)

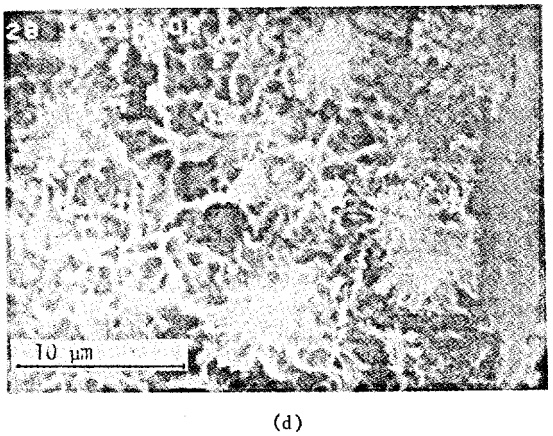

(d)

Fig. 5. (a,b) SEM images of typical reaction products on surface of mortar exposed to Na_2SO_4: a) Calcite dominant. b) calcite (distorted) large crystals, layered brucite plates and coarse C-S-H network. c) Exposed to 1:1 Na_2SO_4:$MgSO_4$, gypsum prisms dominant. d) Interior of a bar exposed to Na_2SO_4 after 9 months showing dense C-S-H.

expansion, although the expansion is usually much greater with ettringite than the former.

Examples are shown in Fig. 5 of some surface reaction products of mortar bars exposed to Na_2SO_4 and $MgSO_4$ solutions; these have undamaged interiors.

Recent Studies of Degradation

Resistance of cement and concrete to this kind of attack may be considered on the basis of the above reactions. When it became clear that the tricalcium aluminate content of portland cement greatly affected its sulfate resistance, a sulfate-resisting cement was developed in which the Al_2O_3 content was reduced. The degree of resistance of such cements varies, and the normal practice of increasing sulfate resistance by using low C_3A cements (75) is often replaced with the more recent practice of preparing low permeability, low $Ca(OH)_2$ concrete. The resistance of portland cement concrete to sulfate attack can be increased by the substitution of a pozzolana in the mixture. A partial explanation of the action of such materials is that the reactive SiO_2 in the pozzolana reacts with the free $Ca(OH)_2$ in concrete to produce additional C-S-H binder. It also diminishes the $Ca(OH)_2$ in hardened portland cement paste, reducing the amount of expansion through the reaction of calcium hydroxide with SO_4^{2-} ions (to produce $CaSO_4 \cdot 2H_2O$), and also plays a part in the reactions by which aluminates expand to cause deterioration.

ACI Committee 201 on Durability of Concrete organized a one-day symposium on sulfate resistance (76) which included work by Brown (77) who determined that experiments at a controlled pH and sulfate concentration accelerated the sulfate attack over that in normal laboratory experiments (see Fig. 6). Dunstan (78) described an approach to predicting sulfate resistance of a concrete from chemical composition, w/c and percentage pozzolana or

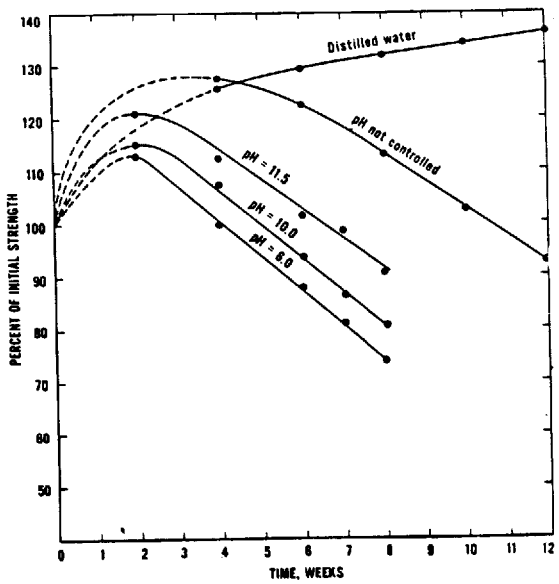

Fig. 6. Variation of cube strength with pH in 0.35 M Na_2SO_4 solution [adapted from Ref. (77)].

blended material. A scheme for the assessment of sulfate resistance was developed by Visvesvaraya et al. (79), while Tikhomirova (80) compared the corrosiveness of sulfate solutions of the various cations belonging in groups I and II of the periodic table and those of the transition metals, finding a relationship.

Mehta (81) reviewed the durability of concrete in a marine environment (82), and concluded that even high-C_3A cement can have excellent sulfate resistance if the permeability is low enough. Conjeaud (83) studied cement mortars exposed to artificial sea water and indicated that after an initial rapid diffusion of $SO_4^{=}$ (and presumably Mg^{2+}) an almost impermeable brucite layer or aragonite layer was formed. Based on laboratory experiments with artificial sea water, Regourd (84) discussed degradation of $Ca(OH)_2$ and C-S-H through the action of $SO_4^{=}$ and Mg^{2+} to form $Mg(OH)_2$, $CaSO_4 \cdot 2H_2O$, ettringite and thaumasite [$CaSiO_3 \cdot CaSO_4 \cdot CaCO_3 \cdot 15H_2O$], similarly stating that chemical attack from sea water only occurs with permeable concretes. She also indicated that cements containing more than 65% slag have the greatest resistance to the sea. Bensted (85) briefly discussed chemical considerations of sulfate attack and considered the effect of slag, pozzolanic, and high alumina cements.

Mehta (87,88) continued the studies of blended cements, measuring the porosity of such cements in sulfate solutions. He related the differences in pore size distribution, rather than chemical composition of the paste to the resistance to aggressive solutions, indicating that the behavior is controlled by the degree of the pozzolanic reactions before the exposure to sulfate containing solutions, which was confirmed also by Medgyesi (88) and Philleo (89).

The use of pelletized blast-furnace slag was found by Mills (90) to provide a great advantage in guarding against the danger of sulfate attack. Al-Rawi and Sarsam (91) found a very significant improvement in the resistance of concrete to sulfate attack, by a partial replacement of sulfate resisting cement by pozzolan, which alleviates a critical situation, especially when high sulfate content sand is used. A portland cement produced from nepheline slurry base was found (92) to be sulfate resisting, presumably in part due to a lower calcium hydroxide content.

The sulfate resistance of pozzolanic cements with calcined clays has been deduced from their flexural strengths (93) measured after immersion in 5% $MgSO_4$ solution. Strength improves at first but is followed by a later decrease in strength, attributed to the formation of expansive ettringite after the voids of cement paste have been filled. El Didamony et al. (94) have found that the addition of 20% of interground burnt Nile silt improves the resistance of portland cement to sulfate attack, as does the addition of 20% amorphous silica with superplasticizer (95). Frigione and Sersale (96) demonstrated in their study of the influence of gypsum content on the volume stability of blast furnace slag cements, that there was an optimum sulfate content with an expansion taking place above this limit. Wang and Li (97) used cements blended

with steel slag solely, or in conjunction with granulated slags. The steel slag was shown to enhance the impermeability and improve the resistance to mechanical and chemical corrosion of cements. However, the presence of too large an amount of free calcium hydroxide can cause expansion. The resistance of slag-portland cements to sulfates depends on the Al_2O_3 content of the cement (98), but also on the nature of hydrates; i.e., there is less ettringite than in portland cements. Massazza (99) after extensive studies of concrete in a marine environment concluded that pozzolanic and blast furnace cements were highly beneficial because they reduced CH and C_3A, while increasing the amount of C-S-H. He also recommended good curing. His precautions for making durable concrete are summarized in Table 2.

Table 2
Sea Water (and Sulfate-Resistant) Concrete Rules.

1. Cement content ≥ 320-360 kgm^{-3}
2. w/c < 0.40-0.45
3. Compr. strength $\geq$ 40 MPa
4. Use pozzolanic or blast furnace slag cements
5. Use a (reinforcement) bar cover $\geq$ 60 mm
6. Wet cure a long time

A very low porosity slag cement (F cement), highly resistant to sulfates, has been developed by Forss (100). The formation of expansive ettringite has been observed by Braga Reis (101) in samples containing ground weathered granites in sulfate solutions saturated with $Ca(OH)_2$, indicating the potential for this type of reactive aggregate (i.e., granite containing kaolinite) to contribute to a variety of types of sulfate attack. Rock fragments after 9 months of immersion showed significant cracking.

At the International Seminar on Calcium Aluminates held in Torino (Italy) (73), the role of ettringite in expansion, among other topics, was discussed. The expansion of ettringite has been attributed to water absorption by Mehta and Wang (102), not influenced particularly by the origin of the ettringite, whether precipitated from a solution, formed by paste hydration of a C_3A and gypsum mixture, or formed from $C_4A_3\bar{S}$, gypsum and $Ca(OH)_2$ mixtures.

Chen and Mehta (103) have measured a negative zeta potential of -11.6 mV at the surface of ettringite crystals, while Alunno-Rossetti et al. (104) measured zeta potential at the surface of ettringite crystals equal to +30mV in saturated lime solution. Other causes of expansion reported include the increase in volume of solids and the crystallization pressure, the conversion of monosulfate into ettringite (104) corresponding to a 77% increase in the volume of the solid. A slightly impervious felt of small ettringite crystals formed in calcium hydroxide solution. Teoreanu and Dumitrescu (105) suggested that ettringite can crystallize both topochemically and from solution, while others (106) suggested it was topochemical.

Ogawa and Roy (107) found that the crystals of ettringite around $C_4A_3\bar{S}$ grains were at first unoriented or flat but later on the crystals arranged radially and the expansion began when the reaction zones intersected (see Fig. 7), developing pressure during their progressive growth, apparently along a preferential growth direction, the needle axis. Colloidal expansive ettringite has been identified by XRD and DTA (108,109) and its formation was related to length changes. Mixtures of C_3A, $CaSO_4 \cdot 2H_2O$, $Ca(OH)_2$, and quartz hydrated at 22, 30, 40, 50, 60°C expanded, again correlated with the formation of colloidal ettringite; while monosulfoaluminate appeared when the expansion ended. Temperature increase favored the formation of colloidal ettringite. Finally, Mehta (110) re-examined the mechanism of sulfate attack on portland cement, concluding that studies on ettringite alone were inadequate for a complete understanding. A proper understanding of the mechanisms of deterioration

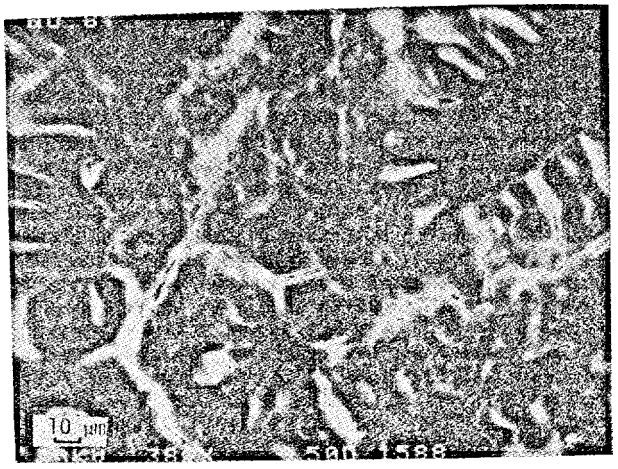

Fig. 7. SEM/EBS polished section of $C_4A_3\bar{S}$ reacting to form ettringite showing anhydrous core and radial ettringite which causes expansion.

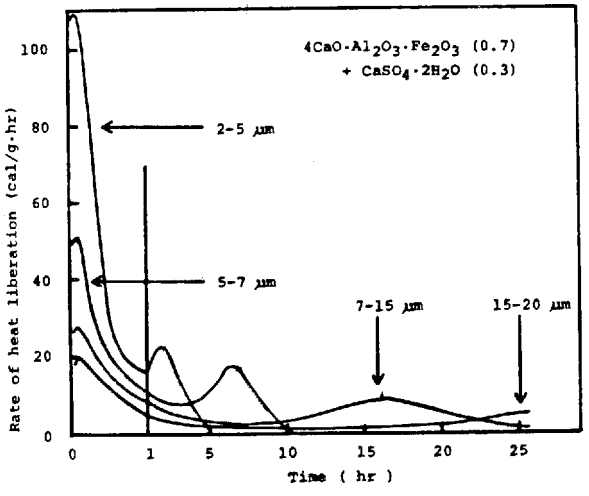

Fig. 8. Effect of particle size on rate of reaction of C_4AF with gypsum and water [adapted from Ref. (112)].

should employ considerations of all possible physical-chemical effects of SO_4^{2-} ions on all the constituents of the cement paste. He indicated that only poorly crystalline ettringite seems to expand due to water adsorption. The role of evaporation was identified by St. John (111) in sulfate attack on concrete in tunnels, where a concentration of Na_2SO_4 solution built up due to the evaporation of ground water by the ventilation. The sodium sulfate crystals deposited slowly over a 30-year period causing exfoliation of the concrete, resulting in the need for costly repairs.

Fukuhara et al. (112) have shown that there is extensive reaction between C_4AF and gypsum (see Fig. 8); hence its role in sulfate attack must be further considered. Roy et al. (113) observed a hydrotalcite-like phase (Mg,Al,OH,CO_2-containing layer structure phase) formed in slag-cement mortars exposed to magnesium sulfate solutions. This apparently innocuous phase may form from the Mg in slag in the absence of $MgSO_4$ solution; it is a Mg equivalent of C_4AH_x.

There is some controversy regarding the effectiveness of fly ash in sulfate resistance. Hughes (114) showed that prolonged curing of OPC/fly ash mixtures was necessary to induce sulfate resistance to 0.7M Na_2SO_4 solutions. Guyot et al. (115) indicated that 15-20% of slag, fly ash or pozzolan has been used for many years in France and imparted reasonable sulfate resistance; however, the utilization of cements containing a high amount of slag is much more effective and is justified for stuctures exposed to sulfates. Galchineckafa et al. (116) reported that cements with electrothermophosphoric slags were resistant to sulfates and contained less secondary gypsum and ettringite than portland cements. Recently van Aardt and Wisser (117) found on the basis of limited tests with enhanced levels of NaOH, that the alkali level in proportion to the C_3A and SO_4 content was important in sulfate degradation. A suggestion was made that the following relationship should apply in order to limit expansion:

$$\frac{C_3A}{SO_3 + Na_2O \text{ eq.}} < 3 \text{ and } \frac{SO_3}{Na_2O} < 3.5 > 1$$

CHLORIDE REACTIONS

Chlorides and Implications for Corrosion

Concern with chlorides in cement paste is primarily because of corrosion of steel in reinforced concrete, an electrochemical process, which is implemented by an electrolyte (particularly as present in corrosive groundwater and sea water) which may induce the establishment of an electric potential. Steel in concrete is usually protected by a film of oxidized iron, FeO·OH or Fe_2O_3 which normally causes passivation; however, this protective layer may be destroyed if the pH falls below ~11.5. In hydrated cement the pH of the pore fluid is approximately 13, which stabilizes these oxide layers. However, a decrease in pH can be brought about by carbonation from the atmosphere or neutralization of the $Ca(OH)_2$ pore solutions (118) particularly under the influence of chloride ion in groundwaters or sea water (119,120). Thus, investigation of the penetration rate of chloride into concretes is a relative measure which may be used for prediction of concrete durability (65,121-124). Hansson and Hansson (125) have discussed the major factors which control electrical conduction in cement-based materials: the concentration and mobility of the ions in the pore solution, and the porosity and pore size distribution.

Although in the absence of steel reinforcement, which is the major emphasis of this paper, solutions of sodium and potassium chlorides in themselves are believed to have minor effects on mature portland cement concrete, if their solutions are concentrated, they are reported to cause disintegration. The formation of tetra-calcium aluminate dichloride-10 hydrate (Friedel's salt) is probably an important factor in understanding the disintegration process, but increased solubility of $Ca(OH)_2$ in $CaCl_2$ solutions is also believed to be a contributing factor. Other factors such as changing the pore structure and reducing the pH are significant and will be discussed.

Chloride Transport and Reaction

As a key to the factors influencing the rate of penetration of chloride ions into hardened cementitious materials, and their consequent effects, the diffusion of Cl^- ions through hardened cement pastes has been studied by Page et al. (126) and by Goto and Roy (127). The activation energy for the ionic diffusion was calculated as 42 $kJ \cdot mol^{-1}$ (126) and 50 $kJ \cdot mol^{-1}$ (127) for a mature portland cement paste (w/c = 0.4); diffusion of Cl^- ions is strongly influenced by the type of cement, and blended cement pastes with 30% fly ash or 65% slag gave lower diffusion than portland cement pastes (126). The durability of blended cements to highly concentrated chloride solution (27.5% $CaCl_2$ + 3.9% $MgCl_2$ + 1.8% NaCl) is another matter, as was reported by Feldman (128). He found that blends with 35% fly ash or 70% slag had a finer pore size distribution than Type I portland cement and a lower $Ca(OH)_2$ content, which improved their durability.

When both Cl^- and $SO_4^=$ are present (as in sea water) there is a competition between chloride and sulfate ions as found by Ogawa and Roy (107). Friedel's salt is formed as a decomposition product of ettringite in 20% NaCl solution above 100°C; while at lower temperatures Cl^- is detected in the ettringite, which then is less expansive.

The gradient of chloride and sulfate ions diffusing in concretes, from 0.27 M $CaCl_2$ and 1 M Na_2SO_4 solutions, has been studied by Rio and Turriziani (129) for three types of cement: a ferric portland cement resistant to sulfates (low-C_3A), a pozzolanic cement, and a slag cement. Concrete permeability was in the order pozzolanic cement > slag cement > ferric portland cement.

Later longer term studies (130) (up to 15 months) showed the trend, that Cl^- and $SO_4^=$ penetrations in portland cement were similar, and that the penetration order was: portland cement (w/c = 0.50) > SO_4-resistant cement (w/c = 0.50) > slag cement

(w/c = 0.52) > pozzolanic cement (w/c = 0.53), with the first two relatively close and the latter two relatively close. The chloride penetration depth was about double that of the $SO_4^=$. This is consistent with diffusivity data of Barnes and Roy (131) who found in salt-containing mixtures (containing fly ash and/or slag) consistently lower diffusion rates by a factor of 2-5 times for $SO_4^=$ than Na^+, and others (121), (123) who found that the chloride anion diffusion was considerably faster than the cations, Na^+, K^+ or Cs^+.

Chloride diffusion follows Fick's law (65,121,122,124,132-134) and is lower in blast furnace slag cements than in portland cements. The reduction in diffusion rate in fly ash cements is significant (65,122,124,135) though variable, while sulfate-resistant portland cements may have higher diffusion rates. Silica fume has been shown to decrease the diffusivity (65,123), even at relatively high w/c (65,123,124). Page et al. (122) found effective diffusivities as follows for chloride ions at 25°C following 60 days of curing:

Table 3

cement	$Dx10^9$ cm^2s^{-1}
OPC	44.7
OPC/30% PFA	14.7
OPC/65% BFS	4.1
SRPC	100.0

Mortars with w/c = 0.45 and 0.60 (SiO_2 fume = 10 and 30%) when exposed to a Mg, Ca, and Na mixed chloride solution showed substantially increased resistance to Cl^- penetration and attack, as evidenced in flexural tests and decreased pore size (136). Kumar and Roy (65,123,124) showed similar trends and low chloride diffusivities with slag and silica fume additions (Table 4).

Table 4
Chloride Diffusion Coefficients with CsCl Diffusion, w/c = 0.35.

Cement % Blend	$Dx10^9$ cm^2 S^{-1} 28 days	90 days
OPC	75.1	57.2
Slag 65	9.62	4.87
Si Fume 10*	2.9	1.12
Fine Quartz 25	---	67.7
Fly Ash 30	55.8	---

The formation of Friedel's salt resulting from the reaction between chlorides and the aluminates of the cement paste has been reported by several investigators (137-141). Grutzeck and Roy (138) have shown that Friedel's salt is abundant in salt-saturated grouts and mortars, where it sometimes suppresses ettringite formation. Conjeaud (141) detected chloro-ettringite in the study of portland cement pastes and mortars attacked by a concentrated $CaCl_2$ solution (300 g/L), as a secondary reaction product, since the main degradation parameter was found to be the dissolution of $Ca(OH)_2$ and the formation of calcium oxychloride [$CaCl_2 \cdot Ca(OH)_2 \cdot H_2O$], which is expansive. Hofmann (142) reported formation of the salt $CaCl_2 \cdot 4H_2O$. Midgley and Illston (143) suggested that the higher the content of Friedel's salt, the less chloride penetration because it will become tied up in the low solubility salt. Smolczyk (144) also reported Friedel's salt formation. Ivanov and Janbykh (145) reported a long term study of concretes exposed to $MgCl_2$ and $CaCl_2$ solutions, showing that $CaCl_2$ forms both $CaO \cdot CaCl_2 \cdot H_2O$ and Friedel's salt. These reactions occurred slowly, while with NaCl the concrete was finally degraded after 8 years. Kishitani et al. (146) found that penetration of Cl^- was major in concrete made with OPC and sulfate-resistant cement after 5 years, while it was much less with blast furnace slag cement.

Pereira and Hegedus (147) developed a diffusion-reaction-equilibration model in which Langmuir adsorption and Fickian diffusion were coupled in attempt to predict time-Cl^- penetration depth plots in concrete. Uchikawa et al. (148) showed that Na^+ diffusion was markedly decreased in slag and fly ash-containing pastes, which they related to the zeta-potential.

Pore solution compositions provide a key to transport inhibition mechanisms and enable comparisons among the effectiveness of various materials. Free and bound chlorides have been determined by Tuuti (149) who analyzed four solutions and found that the amount of bound chloride was dependent on the kind of chloride salt, e.g., $CaCl_2$ gave more bound chloride than did KCl. Roy et al. (150,151) found that the chloride content of pore solutions of fly ash-containing and slag-containing cement pastes are diminished by up to 80% over a 3-month period, compared with ~40% reduction in a pure portland cement pastes (152,153). Ramachandran et al. (154) found that pore solution chloride content increased in proportion to the $CaCl_2$ added to the initial mixture, and that a mixture of C_3A-gypsum immobilized much more chloride than did C_3S (see Fig. 9). Page and Vennesland (60) measured the OH^-, Cl^-, SO_4^{2-}, Na^+, K^+ and Ca^{2+} contents of pore solutions of pastes with different proportions of silica fume, and found a reduction in the chloride binding capacity. Shigeru et al. (155) measured apparent diffusion coefficients for Na^+ and Cl^- ions, and found penetration as follows: sulfate-resistant cement > portland cement > slag cement. Finally, Hansson et

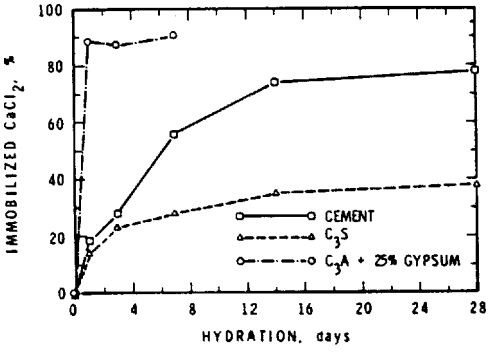

Fig. 9. Immobilized $CaCl_2$ in pastes as determined from pressure extraction [adapted from Ref. (154)].

al. (156) determined the effect of chloride cation type on the corrosion of steel in concrete. $CaCl_2$ was found to have a much more deleterious effect than KCl or NaCl, related to coarsening pore structure and pore solution pH, not directly related to the chloride content of the pore solution.

CARBONATION

Introduction

At room temperature the main stable phases in the system hydrated cement-CO_2 are $CaCO_3$ (calcite), quartz (although hydrous silica is usually the identified reaction product) and aluminum hydroxide (gibbsite). When stored in normal atmosphere, hardened cement pastes and concretes develop an outer region of carbonated material which has a reduced pH.

Babuskin et al. (157) have calculated the equilibrium CO_2 pressures for the carbonation of various hydrated cement phases (Table 5). It is seen that the equilibrium values are much lower than atmospheric CO_2 pressure (~3.2×10^{-4} atm.). Instead of C-S-H, tobermorite is given in the table, but high-Ca C-S-H should require an even lower P_{CO2} in order to carbonate (158,159), since the carbonation reaction of $Ca(OH)_2$ has the most negative free energy change. Thus, ultimately with adequate access to CO_2, all cement minerals should carbonate, as would many natural minerals (158).

In view of the free energy changes strongly favoring carbonation, Lawrence (160) has pointed out the high importance of molecular and other transport properties.

Carbonation Reactions and Degradation

Lach and Matousek (161) have found in their study of the carbonation of C_3AH_6 and high alumina cement that $C_3A \cdot CaCO_3 \cdot 11H_2O$ ($C_4A\bar{C}H_{11}$) is formed first and later decomposes into $Al(OH)_3$ and $CaCO_3$ (vaterite or aragonite initially, and ultimately calcite). They indicated that carbonation could be divided into four stages characterized by changes of the microstructure. Jungermann (162) concluded that the damage of reinforced and pre-stressed concretes by carbonation occurs in three stages as a result of: (i) CO_2 diffusion in the finest capillary pores; (ii) dissolution of CO_2 in the water film; and (iii) neutralization of $Ca(OH)_2$ by the carbonic acid. Majumdar and Stucke (163) observed in carbonated samples of glass fiber reinforced super-sulfated cement, that ettringite and C-S-H were altered by the action of CO_2. In general, modification of a relatively small amount of ettringite leads to an appreciable loss in strength in super-sulfated cement, where carbonation was often found to take place more readily in the composite cement where glass fibers increased the porosity and the permeability.

Favorable effects of carbonation on the other hand, were shown in some instances: Komarneni and Roy (164) showed that carbonation could be used to immobilize Cs, Sr, and Ba from nuclear waste in cements and mortars. In this case the action of CO_2 helped to form a chemical barrier for the migration of nuclear elements, and formed insoluble hydroxy-carbonate compounds. The cement content, cement composition, w/c ratio, and strength were shown in some long term studies (50 years) of steel reinforced concrete slabs of different composition (165) to affect resistance to carbonation. High quality concretes made with either portland or portland-fly ash cement behave satisfactorily, but in lean mixes (low cement content and high w/c ratio) portland cement concretes are reported to be superior. The strength increase of portland cement concretes due to carbonation is greater the lower the w/c ratio (166), since calcium carbonate occupies a higher volume, partly filling up the pores of the cement paste. Some blast-furnace slag cement concretes, which are poorer in calcium hydroxide than are portland cement concretes have been reported to show reduction in strength after carbonation.

DeSitter (167), Trub (168), and Friede and Schubert (169) have measured the depth of carbonation in concrete. This depth was 2 mm after 10 years and 7 mm after 50 years (167), and was dependent on the type of cement and on the moisture distribution (170). Silica fume reduced the rate of carbonation of concretes (171) (Table 6) but the depth of carbonation in foamed or cellular concretes is greater (172-174) than that in normal concretes. The simultaneous action of CO_2 and Cl^- has been studied by Beckett (175) and DeSitter (167): a maximum of $CaCl_2$, between 1.8 and 2.3%, was located at depths between 15 and 25 mm, while the super-

Table 5

Calculated Results of the Carbonation Reactions of the Constituents of Cement Paste.

No. of Reactions	Equations of Reactions	ΔG^0_{298} of reactions [kcal/ml]	P_{CO2} equilibrium values [atm]
1	$1/5\ (5CaO \cdot 6SiO_2 \cdot 5.5H_2O) + (sol) + CO_2\ (gas) = CaCO_3\ (sol) + 6/5\ SiO_2\ (sol) + 1.1\ H_2O\ (liq)$	-11.29	$10^{-8.28}$
2	$1/4\ (4CaO \cdot Al_2O_3 \cdot 19H_2O)\ (sol) + CO_2\ (gas) = CaCO_3 (sol) + 1/2\ Al(OH)_3\ (am) + 4H_2O\ (liq)$	-14.70	$10^{-10.78}$
3	$1/3\ (3CaO \cdot Al_2O_3 \cdot 3CaSO_4 \cdot 32H_2O)\ (sol) + CO_2\ (gas) = CaCO_3\ (sol) + CaSO_4 \cdot 2H_2O\ (sol)$	-10.26	$10^{-7.52}$
4	$1/3\ (3CaO \cdot Fe_2O_3 \cdot 3CaSO_4 \cdot 32H_2O) + CO_2 = CaCO_3 + CaSO_4 \cdot 2H_2O + 2/3\ Fe(OH)_3 + 23/3\ H_2O$	-14.07	$10^{-10.31}$
5	$Ca(OH)_2\ (sol) + CO_2\ (gas) = CaCO_3\ (sol) + H_2O\ (liq)$	-17.82	$10^{-13.1}$

+assumed tobermorite (147). sol = solid, am = amorphous. After Ref. (157).

Table 6
Effect of SiO_2 Fume on Carbonation Depth in Concretes+ with 100, 250, and 400 kgm^{-3} Cement.

CEM	SiO_2	P*	Depth mm
100	0	0	25.4
100	10	0	18.2
100	20	2	11.3
250	0	0	6.8
250	20	2	3.4
400	0	0	3.7
400	10	0	3.8
400	20	2	1.2

*Plasticizer +10 mm slump

ficial layer (7 to 8 mm) contained less $CaCl_2$, 1 to 1.6% (167). Weber (176) presented a mathematical model for calculating the progress of carbonation as a function of time, showing that a carbonation coefficient can be calculated using the diffusion laws as in the case of water adsorption.

Barret et al. (177) presented new solubility curves for AH_3, CAH_{10}, C_2AH_8, C_3AH_6, C_4AH_{13}, $CaCO_3$ (calcite), and $C_4A\bar{C}H_{11}$ in equilibrium with different p_{CO2} values, where it was indicated that calcite or monocarboaluminate alternately could be stable depending on p_{CO2}. Soustelle et al. (178) presented saturation and supersaturation curves for the same, and discussed the relation of conductometric curves to the latter, and also the implications for real cement pastes. Suzuki et al. (179) calculated a k_{sp} for C-S-H of $5.5x10^{-49}$, for material precipitated from solution, and in turn discussed the conditions under which carbonation could take place (Fig. 10).

Discussion

As mentioned above, complete carbonation of hydrated portland cement paste, to $CaCO_3$, hydrated silica, alumina and ferric oxide, is chemically possible, though well-made concrete after prolonged exposure usually shows little carbonation. Similarly, sulphoaluminates theoretically carbonate to yield $CaSO_4 \cdot 2H_2O$, vaterite (eventually calcite) and hydrous alumina. The greater part of the CO_2 taken up by specimens of mortar and calcium silicate hydrate exposed to the atmosphere is held as poorly crystallized vaterite, aragonite or calcite; a high pH favors the formation of vaterite.

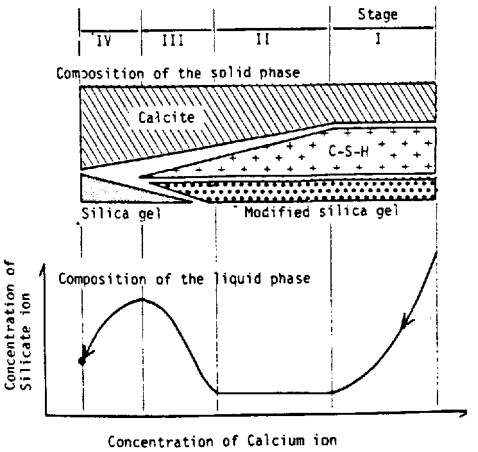

Fig. 10. Carbonation stages (schematic) of C-S-H, prepared from solution [adapted from Ref. (179)].

Carbonation is not a straightforward process. For instance, the theoretical maximum percentage of carbonation observed is dependent on environmental humidity, reaching a maximum at 50% R.H. Diffusion of gases (O_2 and CO_2) takes place at orders of magnitude higher rates through air than in the liquid state. Specimens may shrink considerably at 50% relative humidity during carbonation, due to carbonation of $Ca(OH)_2$ and C-S-H, while at a relative humidity of 25%, little carbonation shrinkage occurs, probably due to the carbonation of only the $Ca(OH)_2$. The uptake of CO_2 by crushed cement paste particles is dependent on the relative humidity.

Lawrence (160) has quoted work describing the depth of carbonation after increasing times and for different concretes (where diffusion constants lie between $2x10^{-7}$ and $2x20^{-11}$ m^2/s), calculated for the a) worst and b) best situations:

$$a) \quad X_1 = 2 \times 0.004 \times \sqrt{2x10^{-7}t}$$

and

$$b) \quad X_2 = 2 \times 0.001 \times \sqrt{2x10^{-11}t}$$

After 1 year ($3x10^7$ s) depths of carbonation were reported to be 19.5 mm and $4.9x10^{-2}$ mm. Hobbs (180) quoted some worst case data after only 1 day curing followed by exposure to 65% R.H. He gave the formula

$$d_c = 18\sqrt{t}\ [W/(C+0.3p) - 0.18]$$

(p = slag, t = time, yrs., d = mm) to relate depth of carbonation in portland and slag-substituted concretes for these materials. Roberts (181) earlier confirmed a square root of time/carbonation dependency for slag-containing concretes. Osborne (182) indicated that there was a good correlation between depth of carbonation and compressive strength at 28 days. Implications are that adequate curing is necessary to prevent carbonation, especially of fly ash containing materials. It could be inferred from his report that ground granulated slag-containing concretes have the same carbonation degree as portland cement concretes of similar strength. Lower permeabilities will no doubt decrease the carbonation rates.

OTHER DEGRADATION MECHANISMS

Leaching

The reverse of the transport of ions or chemical species into a cement paste is the movement of water through the paste and removal of species, leaching, which depends on the pore structure and water permeability of the paste (183-185,65,121). As water permeation involves the transport of a liquid through a porous medium under a pressure gradient, leaching involves the transport of species under a concentration gradient, e.g., in the case with very pure water in contact with cement paste,

which provides a negative concentration gradient compared with the paste pore water (63) to generate the potential for leaching, particularly of hydroxyl, calcium and sulfate ions (186-188,131). The extent of leaching depends on the initial cement composition, the concentration gradient in the respective fluids, the cement paste permeability, solubilities of the species concerned, and temperature.

The subject of leaching has been addressed recently in connection with the potential use of cementitious materials in the isolation and disposal of nuclear waste (131,137,139,183-207). A cementitious matrix is considered both as an encapsulant to solidify low to intermediate level nuclear waste to prevent release of harmful radionuclides to the environment (190,191,186,204) or simply to control release of soluble salts to the environment (197,131). It also provides a favored method for the control of release of other toxic substances (207-209).

Most of the above studies related to nuclear waste isolation are concerned with the release of trace species or radionuclides present in small concentrations, in attempt to control release of toxic species, but a number are concerned with the release of major elements as well (186-188,191-198, 200,201,204,207,208,210). In addition, the leaching of major elements is of concern for the sealing of geologic repositories for radioactive waste, where the cementitious sealing materials should maintain low permeability (137-140,183,188,196,207) for prolonged periods.

Soluble cations such as Cs have been found to leach and be released by a diffusion mechanism (65,123,186) although their release may be inhibited by their incorporation in the cement paste as insoluble phases (191-193,195,198,199). The sodium cation (and presumably K^+) similarly is leached by a diffusion mechanism (191-200,121) as is the chloride anion, although the release of both may be somewhat inhibited by the formation of relatively insoluble phases (186,124) or by surface adsorption (185). Nevertheless, the pore solutions of cement pastes will ordinarily contain relatively high concentrations of alkalis (31,63) and also of chlorides (64) which are potentially available for leaching. The existence of a very fine pore structure then will serve to inhibit the leaching process.

Table 7
Typical Leach Rates of Species in Cementitious Materials.
$(g\ m^{-2}d^{-1})^{++}$

	OPC/Pollucite*	OPC/SiO_2/+ Powellite	CsZP-** Slag/SiO_2/OPC
Ca	1.4	1.9	
Cs	1.7		0.14-2.0
Na	5.8		
Si	1.5		
Al	0.08	0.41	
Sr		0.29	
Mo		0.15	
I		13	

*Ref. (193). +Ref. (194). **Ref. (198).
++Rationalized to % species in initial product.

Sr and Ba are also released by a diffusion mechanism, while other ions such as aluminate, rare earth, and uranium species are relatively insoluble in cements, their release is not primarily diffusion controlled, and they are released at a very slow rate. Even the silicate anion is released slowly (192-196). Sulfate ions are released at about an order of magnitude slower rate than sodium, chloride and nitrate ions (131).

Calcium is released at a slower rate, about one-fourth that of sodium (193) (see Table 7). There are also indications that the calcium release and particularly strontium release may be slowed by partial carbonation (211). Zamorini et al. (208) recently have determined release rates of calcium ions from different size cement specimens, and found no significant size effect in experiments up to 28 days at 50°C. They confirmed the non-diffusion nature of the release mechanism. They presented a relationship between leached fraction of calcium and time as follows:

$$F = B\ t^n$$

where F is the leached fraction, t = time in days and B is a constant. This was found to apply to different size specimens as long as the geometric surface of the solid to volume liquid was kept constant. The exponent n was ~1/3.

Barnes and Roy (196) have discussed the thermodynamic control of stability in the release of ions from cement paste by leaching, implying that once the calcium hydroxide is completely leached, the calcium silicate hydrate (C-S-H) will be the rate-controlling substance. A high-calcium C-S-H is presumably more leachable than one with lower Ca content, or indeed than crystalline tobermorite.

Atkinson et al. (186) have also discussed leaching mechanisms of radio ions, and confirmed that Cs^+ is released primarily by a diffusion mechanism from cement pastes, while Sr is not.

Freezing and Thawing

The degradation of cementitious materials due to freezing and thawing is a complex subject, which involves the interaction of the cement paste microstructure, any aggregate contained, the action of salts present in pore solutions, the humidity of the environment, and the types of temperature cycles. Dry concrete may withstand freezing and thawing indefinitely, whereas saturated concrete, even if properly air entrained, may be seriously damaged by a few cycles of freezing and thawing (212). High degrees of saturation and rapid cooling are both detrimental, whereas air entrainment with proper bubble spacing can be effective in providing reservoirs to accommodate otherwise destructive ice crystal expansion. We attempt to summarize here briefly some of the relevant current findings.

Dorner and Setzer (213) investigated the hydration of fresh cement pastes with low temperature DTA. They concluded from the freezing behavior that

during hydration the volume of the larger pores decreases and the volume of the medium sized gel pores increases. Grubl and Sotkin (214) studied rapid ice formation on cooling of hardened paste, finding that the first freezing peak in DTA thermograms related to specimen size, water content, and change in length.

Buil and co-workers (215,216) have studied the ice-supercooled water system in order to understand the frost action upon porous media. They used a physical model for the experimental study of the equilibrium, the two phases being subjected to the same temperature but different pressures. The results agreed with the macroscopic thermodynamic law giving the ice pressure as a function of the temperature of the system.

Pigeon and Lachance (217) submitted non-air-entrained and air-entrained concretes to 300 freeze-thaw cycles in air at 100 percent relative humidity and at a freezing rate of 2°C/h. They determined the critical air void spacing (the value below which concrete was damaged), to be 680 μm for a w/c ratio of 0.5, agreeing well with that expected from Powers' hydraulic pressure theory.

Numerous studies have been made of concretes with fly ash, slag and silica fume. Fly ash and ground granulated blast-furnace slag additions have been used successfully in frost resistant concrete. Whether the concrete was only air entrained, or air entrained and superplasticized, slag cements performed satisfactorily in the ASTM freeze-thaw test (218). However, repeated dosages of superplasticizers like sulfonated melamine or naphthalene formaldehyde condensates led to a loss of the air entrained and had a negative effect on the freeze-thaw resistance; while lignosulfonates performed better in this regard (219). Fundamental aspects of the paste microstructure and its porosity seem to be the most important factors overall in frost resistance (220).

Grasenick and Soretz (221) through EM observations of hardened cement pastes have shown the short term localization of deicing salts. The increasing porosity, and the formation of ice crystals and the crystal deposits in pores have been followed together with the measurement of created pressures.

Bache (222) described materials called Densified Cement/Ultrafine Particle-Based Materials (DSP) which contain much silica fume. These materials (DSP concretes) were said to offer a high resistance to frost action, since the amount of freezable water is very low. Because of this low content and small pore size, freezing was said to occur at lower temperatures than in normal cement concrete, and the drying-resaturation process apparently does not operate. Concretes made with silica fume have been reported to be frost resistant without air entrainment (223). However, Jahren also reported (224) that silica fume concrete gives better resistance to frost action if it is combined with superplasticizer and a w/c ratio greater than 0.5.

Zaman, Ridgway and Ritchie (225) caution that visual estimation of damage due to freezing and thawing may be misleading, and propose flexural strength tests, emphasizing that flexural strengths are more sensitive to damage than are compressive strengths. Despite the fact that scaling and spalling occurred, the minimum loss in mechanical properties was found with a 4% NaCl solution.

Fly ash, silica fume, and slag have been shown by Yuan and Cook (226) to improve the frost resistance of concrete. After 1200 freeze-thaw cycles, concretes with a 20% replacement of Class C (high-calcium) fly ash from sub-bituminous coal, were stronger than the control portland cement concrete (226). Samarin et al. (227) reported that the durability of fly ash concretes in which fly ash was used either as a component of blended cement or as an addition to the concrete has been demonstrated with field concretes, over a period of 20 years. Carbon content of fly ash has been of concern; but Sturrup et al. (228) found that if it is less than 12% it does not deleteriously affect the frost resistance of concretes, provided the carbon content is known so that the dosage of air entraining agent can be increased appropriately.

Slag additions improve the frost resistance of concrete better than fly ash (229) when strength and air content are kept constant. Pigeon and Regourd (230) related the good performance of slag cements to low bubble spacing factors and to a very dense and homogeneous microstructure of the paste. Murata et al. (231) improved the frost resistance of non-air entrained concretes using blast furnace slag, which resulted in a larger porosity in the range of 10-90 μm radius. According to Pistilli, the bubble spacing factor depends on the type of admixture and amount of soluble alkalies from fly ash and portland cement (233). Superplasticizers are reported to have a more beneficial effect than water reducing agents (234).

Olsen (235) used a two-dimensional finite element computer model to predict frost penetration in saturated porous media. The temperature, water and ice content, frost penetration and generated pore water pressures can be predicted as a function of freezing time and given boundary conditions.

Dorner (236) used DSC to investigate phase changes between 20°C and -60°C in the supercooling of water. Chlorides were found to affect the phase change, even after the specimen had been previously freeze-dried (Fig. 11). Chatterji (237) investigated the freezing of autoclaved porous material containing various air-entraining solutions, followed by a study of mixed air-entraining agents and water reducers. Chatterji et al. (238) found that the minimum solution content needed for a sustained expansion varied from agent to agent. Whiting (239) found that low water/cement ratio concrete (0.30-0.32) required up to 10 times as much air entraining agent to produce the same air content and air void characteristics as normal.

DISCUSSION

The degradation of hardened cement paste has been discussed, and has been shown to involve numerous chemical and physical factors, both as inherent in the cement paste composition and microstructure and as interacting with the

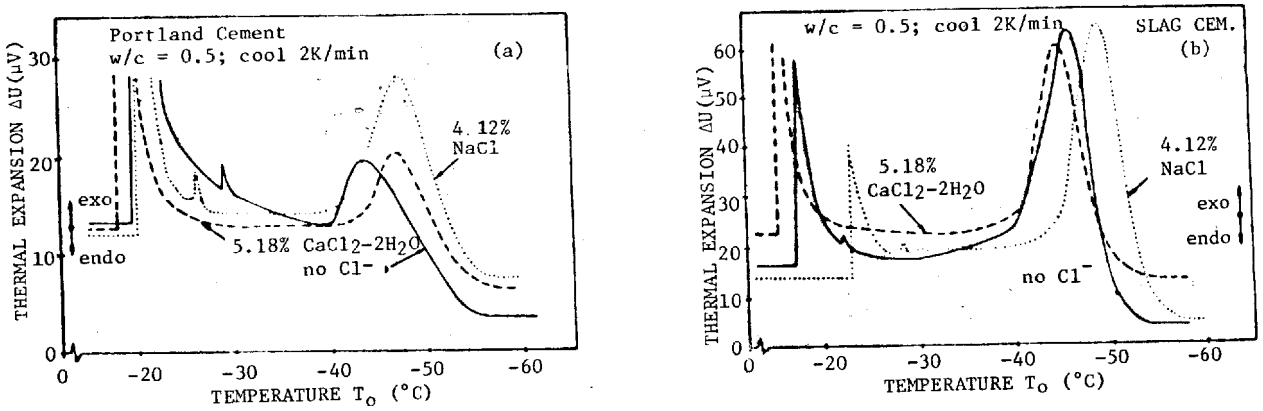

Fig. 11. Phase change of the pore water in 4-month-old water-saturated pastes from (a) portland cement and (b) slag-cement (HOZ35) [adapted from Ref. (236)].

environmental exposure conditions. To predict the performance of cement paste in different environments, it is necessary to consider the development of the cement paste structure beginning with the fresh state, mixing, placing and consolidation, and through the curing period, before being able to determine the probable effects of long-term exposure (240-244). A number of authors have emphasized that it is necessary when making durable concrete to develop a dense and well-homogenized microstructure, and establish that the concrete is well cured (99,244). The effects of undesirable cracking developed as a result of thermal stresses (244), resulting from uncontrolled excess heat evolved during hydration are critical as they influence long term durability. The mechanisms of molecular transport (160) and ionic transport (60,65,121) are important in the operation of disruptive forces of degradation, whether drying shrinkage, freezing and thawing, carbonation, or intrusion of undesirable chloride, sulfate, or other salts or chemicals; or leaching or release of undesirable encapsulated toxic or radioactive waste species (192,197) to the environment. The pore structure is critical in transport processes (65,123).

These mechanisms then act as cooperative phenomena interacting with chemical features either inherent in the cement paste composition itself, e.g., excess C_3A for potential interaction with sulfate or chloride; potentially reactive silica in the aggregate to interact with high alkali cement; or chloride ions followed by oxygen penetrating to depassivate improperly covered reinforcing bars. The investigation of the chemistry of pore solutions (31,63) along with studying the solids, is becoming a better established means of monitoring chemical changes taking place, combining the effects of the initial paste nature and its response to changes from the environment. The thermodynamic stability of phases is important in controlling degradation processes (157-159,179), as, e.g., the free-energy change to produce carbonated products is much greater with high-calcium hydroxide compositions than with lower content (157,159). Free energy changes were favorable to 'pozzolanic' reactions of portland cement with siliceous (and alumino-silicate) pozzolans, producing more chemically stable C-S-H, which is part of the reason for the enhanced durability of pastes containing such admixtures (137,157-159), along with their relative stability in the presence of other intruding chemical species. Alumina may also be important (47,199b).

Considerable advances have been made in understanding mechanisms of degradation; however, much remains to be determined, particularly concerning the cooperative phenomena, i.e, the interaction of the numerous early-stage developmental controlling factors, the consequent physical and chemical characteristics of the hardened cement paste and its microstructure, and the potentially disruptive physical and chemical forces of degradation.

ACKNOWLEDGEMENT

The author acknowledges financial support of the National Science Foundation, Blue Circle (Atlantic), Inc., Oy Lohja, Civil and Marine, Ltd., and Frodingham, Ltd.

REFERENCES

1. G.M. Idorn and Steen Rostam, Eds., Alkalis in Concrete; Research and Practice, Danish Concrete Assn., Copenhagen (1983).
2. Proc. Fifth Int. Conf. Alkali-Aggregate Reaction in Concrete, Cape Town, S. Africa (March 1981).
3. T.C. Powers and H.H. Steinour, Proc. ACI 51, 491-541 and 785-810 (1955).
4. L.S. Dent Glasser and N. Kataoka, Ref. (2), S252/23.
5. L.S. Dent Glasser and N. Kataoka, Cem. Concr. Res. 11 (1), 1-10 (1981).

6. D.M. Roy, Proc., Eng. Found. Conf., Henniker, NH (1985, in press).
7. S. Diamond, R.S. Barneyback, Jr., and L.J. Strubble, Ref. (2), paper S252/22.
8. L.J. Strubble and S. Diamond, Cem. Concr. Res. 11 (4), 611-618 (1981).
9. L.S. Dent-Glasser and N. Kataoka, Cem. Concr. Res. 12 (3), 321-331 (1982).
10. Tang Ming Shu, Cem. Concr. Res. 11 (3), 477-478 (1981).
11. U. Ludwig, Ref. (2), paper S525/24.
12. J.E. Gillott and R.J. Beddoes, Ref. (2), paper S525/25.
13. J.W. Figg, Ref. (2), paper S252/7.
14. M. Kawamura, K. Takemoto, and S. Hasaba, Trans. Japan Concr. Inst. 4, 1-8 (Dec. 1982).
15. M. Regourd, H. Hornain, and P. Poitevin, Ref. (2), paper S252/35.
16. D.A. St. John, Cem. Concr. Res. 11 (5/6), 801-802 (1981).
17. M.-S. Tang, S.-F. Han, and S.-H. Zien, Cem. Concr. Res. 13 (3), 417-422 (1983).
18. L.D. Wilsson and O. Peterson, Rep. JVBM-3014, Div. Bldg. Mater., Lund Inst. Technol. (1983).
19. W.F. Cole and C.J. Lancucki, Cem. Concr. Res. 13 (5), 611-618 (1983).
20. F.X. Deloye, A. Le Roux, and R. Lesage, Bull. Liason Lab. Pont. Chauss. 126, 37-44 (1983).
21. G.M. Idorn, Ref. (2), paper S252/16 (1981).
22. R.F.M. Bakker, Ref. (2), paper S252/29 (1981).
23. R.F.M. Bakker, Cim., Betons, Platres Chaux (734), 49-53 (1982).
24. R.F.M. Bakker, a) Silicates Ind. 47 (3), 91-95 (1982); b) Ref. (54), Vol. I, 589-606.
25. J. Metso, Silicates Ind. 47 (4-5), 123-127 (1982).
26. D.W. Hobbs, Ref. (2), paper S252/30 (1981).
27. R.E. Oberholster and W.B. Westra, Ref. (2), paper S252/31 (1981).
28. P.J. Nixon and M.E. Graze, Ref. (2), paper S252/31 (1981).
29. B.D.G. Johnson, Ref. (2), paper S252/33 (1981).
30. (a) F.G. Buttler, S.R. Morgan, and E.J. Walker, Ref. (2), paper S252/38 (1981).
(b) L. Boswell, E.C. Robert, F.G. Buttler, and S.R. Morgan, Ref. (1), 231-238 (1983).
31. S. Diamond, Cem. Concr. Res. 11 (3), 383-394(1981).
32. Proc. Fifth Int. Symp. Technol. Concrete, Monterrey, Mexico, Sept. 1981, Univ. N. Leon, Monterrey, Mexico.
33. R. Poo Ulibarri, Ref. (28), 545-556 (1981).
34. C.J. Mendoza, Ref. (28), 557-582 (1981).
35. G. Frigione and R. Marotta, World Cem. Technol. 12 (2), 73-78 (1981).
36. W. Kordina and W. Schwick, Betonwerk-Fertigteil-Technik. 47 (6), 328-331 (1981).
37. D.W. Hobbs, Mag. Concr. Res. 34 (119), 82-94 (1982).
38. M.E. Gaze and P.J. Nixon, Mag. Concr. Res. 35 (123), 107-110 (1983).
39. M.-S. Tang, Y.-F. Ye, H.-Q. Yuang, and S.-H. Zhen, Cem. Concr. Res. 13 (2), 171-176 (1983).
40. J. Calleja, Cem. Hormigon 54 (598), 827-850 (1983).
41. R.C. Mielenz, Concr. Intern. 5 (8), 34-42 (1983).
42. D.W. Hobbs, Mag. Concr. Res. 35 (122), 55-58 (1983).
43. P. Poitevin and M. Regourd, Ann. ITBTP. Ser. Mater. 59 (413), 109-143 (1983).
44. M. Regourd, Travaux (577), 62-67 (1983)
45. Workshop on Blast-Furnace Slag Cements and Concretes, York, England, 14-17 Oct. (1985).
46. R.F.M. Bakker, in Ref. (45), paper 24 (1985).
47. R.I.A. Malek and D.M. Roy, in Ref. (1), 223-232 (1983).
48. P.E. Grattan-Bellew, Durability Build. Mater. 1, 363-376 (1983).
49. P.E. Grattan-Bellew, Mater. Struct. (Paris) 16 (94), 243-250 (1983).
50. Minimizing the Risk of Alkali-Silica Reaction, Guidance Notes, Cem. Concr. Assoc., No. 97.304 (1983).
51. M.P. Brandt and R.E. Oberholster, Rep. NBRI-CSIR-BRR580, 96 pp. (1983) (Natl. Bldg. Res. Inst. CSIR, Pretoria, S. Africa).
52. P.L. Rayment, Cem. Concr. Res. 12 (2), 133-140 (1982).
53. (a) H. Aisgeirsson and G. Gudmunsson, Cem. Concr. Res. 9, 249-252 (1979).
(b) G. Gudmunsson and H. Aisgeirsson, Ref. (1), 217-222.
54. M. Kawamura, K. Takemoto, and S. Hasaba, CAJ Review (1984), 92-95.
55. Proc. First Int. Conf. on the Use of Fly Ash, Silica Fume, and Other Mineral By-Products in Concrete, Montebello (ACI SP-79) (1983).
56. R.E. Oberholster, Ref. (1), 419-434 (1983).
57. P.-C. Aitcin and M. Regourd, Cem. Concr. Res. 15, 711 (1985).
58. P. Longuet, P. Burglen, and A. Zellwer, Rev. des. Mater. 1, 35-81 (1973).
59. S. Diamond, Ref. (1), 155-166 (1983).
60. C.L. Page and O. Vennesland, Mat. Structures (RILEM) 16, 19-25 (1983).
61. F.P. Glasser and J. Marr, British Ceramic Proc. 35, 419-419 (1984).
62. F.P. Glasser and J. Marr. Il Cemento, 85-94 (1985).
63. M. Silsbee, R.I.A. Malek, and D.M. Roy (this Symposium, 1986).
64. D.M. Roy, R.I.A. Malek, M. Rattanussorn, and M.W. Grutzeck, in Fly Ash and Coal Conversion By-Products: Characterization, Utilization and Disposal II, Materials Res. Soc. Proc., Eds. G.J. McCarthy, D.M. Roy, and F.P. Glasser (in press, 1986).
65. A. Kumar and D.M. Roy (this Symposium, 1986).
66. A.J. Majumdar, B. Singh, A.A. Langley, and M.A. Ali, J. Mater. Sci. 15, 1085-1096 (1980).
67. (a) R. Kondo and S. Ohsawa, J. Amer. Ceram. Soc. 62 (9-10), 447-449 (1980).
(b) Sh. Ohsawa and R. Kondo, Ceram. Bull. 59 (11), 1147-1150 (1980).
68. A. Kumar and D.M. Roy, Proc. Symposium on Durability of Glass Fiber Reinforced Concrete, Ed. S. Diamond, PCI, Chicago, IL (1986, in press).
69. A. Bentur, Eng. Found. Conf., Henniker, NH (Aug. 1985).
70. D.M. Roy, A.J. Majumdar, S.P. Shah, and J.A. Manson, Eds., Advances in Cement-Matrix Composites, Proc., Mat. Res. Soc., 102 Materials Research Laboratory, University Park, PA (1980).
71. D.J. Hannant, Fibre Cements and Fibre Concretes, John Wiley and Sons, NY (1978).
72. R.E. Oberholster, J.H.P. van Aardt, and M.P. Brandt, pp. 365-414 in Structure and

Performance of Cements, Ed. P. Barnes, Applied Science, London (1983).
73. M. Murat et al., Eds., Calcium Aluminates, Internatinal Seminar, 14-16 September (1982), Torino, Italy.
74. S.Chatterji, Ref. (73), 325-333 (1982).
75. M. Regourd, H. Hornain, P. Levy, and B. Mortureux, 7th Intl. Cong. Chem. Cem. Vol. IV, pp. 129-147 (1980); Vol. III, pp. 104-109 (1980).
76. The Verbeck Memorial Symposium Sulfate Resistance, ACI SP-77 (1982), Detroit, MI.
77. P.W. Brown, Ref. (72), 83-91 (1982).
78. E. Dunstan, Jr., Ref. (76), 41-62 (1982).
79. H.C. Visvesvaraya and A.K. Mullick, Quality Control Concr. Struc. (RILEM Symp.), Vol. 1, pp. 303-310 (1979) (Swedish Cem. Concr. Res. Inst., Stockholm).
80. M.F. Tikhomirova, Zh. Prikl. Khim. 52 (7), 1475-1479 (1979); Chem. Abstr. 92, 98479 (1980).
81. P.K. Mehta, Ref. (82), 1-20.
82. Performance of Concrete in Marine Environment, ACI SP-65, Detroit (1980).
83. M.L. Conjeaud, Ref. (82), 39-62.
84. M. Regourd, Ref. (82), 63-82.
85. J. Bensted, World Cem. Technol. 12 (5), 178-184 (1981).
86. P.K. Mehta, Ref. (32), 35-50.
87. P.K. Mehta, Cem. Concr. Res. 11 (4), 507-518 (1981).
88. I. Medgyesi, Ref. (32), 351-368 (1981).
89. R. Philleo, Ref. (32), 145-158.
90. R.H. Mills, Ref. (32), 84-116.
91. R.S. Al-Rawi and J.B. Sarsam, Ref. (32), 237-260.
92. T. Ja Galperina, S.N. Bykova, L.A. Grechko, V. Ja Ostrovljanckik, and N.F. Jankov, Tsement, (7), 9-10 (1981).
93. C. Samanta and M.K. Chatterjee, Cem. Concr. Res. 12(6), 726-734 (1982).
94. H. El-Didamony, A.S. Taha, S.A. Abo-El-Enein, and H.A. Amer., Zem.-Kalk-Gips 35 (7), 378-381 (1982).
95. P.H. Perkins, Concrete 16 (8), 29-30 (1982).
96. G. Frigione and R. Sersale, Il Cemento 80 (1), 15-28 (1983).
97. Y.-J. Wang and D.-L. Li, Silicates Ind. 48 (6), 121-126 (1983).
98. A.I. Zdorov, I.A. Kryzhanovskaja, Ja. M. Syrkin, E.E. Kirjaeva, Z.B. Entine, and A.A. Batalina, Tsement, (5), 4-5 (1983).
99. F. Massazza, Il Cemento 82, 3-26 (1985).
100. B. Forss, Silicates Ind. 48 (3), 79-82 (1983).
101. M.O. Braga Reis, Cem. Concr. Res. 11 (4), 541-547 (1981).
102. P.K. Mehta and S. Wang, Cem. Concr. Res.12 (1), 121-122 (1982).
103. S.S. Chen and P.K. Mehta, Cem. Concr. Res. 12 (2), 257-259 (1982).
104. V. Alunno-Rossetti, G. Chiocchio, and A.E. Paolini, Cem. Concr. Res. 12 (5), 577-585 (1982); Cem. Concr. Res. 12 (6), 667-676 (1982).
105. I. Teoreanu and C. Dumitrescu, Cem. Concr. Res. 12 (2), 141-155 (1982).
106. M.D. Cohen, Proc. Fourth Int. Conf. Cement Microsc., Las Vegas, Nevada, pp. 202-224 (March 1982); Cement Microsc. Assoc., Duncanville, TX.
107. K. Ogawa and D.M. Roy, Cem. Concr. Res. 12 (1), 101-109 (1982).
108. P. Clastres and M. Murat, Ref. (75), paper III.14 (1982).
109. A. Negro and A. Bachiorrini, Cem. Concr. Res. 12 (6), 677-684 (1982).
110. P.K. Mehta, Cem. Concr. Res. 13 (3), 401-406 (1983).
111. St. John, Cem. Concr. Res. 12 (5), 633-639 (1982).
112. M. Fukuhara, S. Goto, K. Asaga, M. Daimon, and R. Kondo, Cem. Concr. Res. 11, 407-414 (1981).
113. D.M. Roy, E. Sonnenthal, and R. Prave, Cem. Concr. Res. 15, 914-916 (1985).
114. D.C. Hughes, Cem. Concr. Res. 15, 1003-1012 (1985).
115. R. Guyot, R. Ranc, and A. Varizat, Ref. (55), 453-470 (1983).
116. Ju.L. Galchineckaja, I.A. Kryzhanovskaja, Ja.M. Syrkine, and A.I. Zdorov, Tsement(9), 18-19 (1983).
117. J.H.P. van Aardt and S. Visser, Cem. Concr. Res. 15, 485-494 (1985).
118. P. Kumar Mehta and Ben C. Gerwick, Jr., Concr. Intl., 45-51 (Oct. 1982).
119. O.E. Gjorv and O. Vennesland, Cem. Concr. Res. 9 (2) (1979).
120. W.G. Hime and E. Bernard, Concr. Construct. 26 (9), 768-769 (1981).
121. S. Goto and D.M. Roy, Cem. Concr. Res. 11 (5), 575-581 (1981).
122. C.L. Page, N.R. Short, and A. El Tarras, Cem. Concr. Res. 11, 395-406 (1981).
123. A. Kumar, Diffusion and Pore Structure Studies in Cementitious Materials, PhD Thesis in Solid State Science, The Pennsylvania State University, University Park, PA 16802 (1985).
124. D.M. Roy, A. Kumar, and J.P. Rhodes, ACI (Madrid Conf., 1986).
125. I.L.H. Hansson and C.M. Hansson, Cem. Concr. Res. 15, 201-212 (1985).
126. C.L. Page, N.R. Short, and A. El Tarras, Cem. Concr. Res. 11 (3), 395-406 (1981).
127. S. Goto and D.M. Roy, Cem. Concr. Res. 11 (5/6), pp. 751-758 (1981).
128. R.F. Feldman, Ref. (32), 261-288 (1981).
129. A. Rio and R. Turriziani, Il Cemento 79, 45-58 (1982).
130. A. Rio and R. Turriziani, Il Cemento 80 (1) 37-48 (1983).
131. M. Barnes and D.M. Roy, Leaching of Saltstones Containing Fly Ash and Slag, Internal Report (1985).
132. H. Weigler, Ed., Verein Oesterreich. Zementfabrik., 43-53 (Int. Colloq. Corrosion by Chlorides, Vienna, Austria, 1983).
133. K.P. Grosskurth and W. Malorny, Ref. (29), 22-40 (1983).
134. P. Shiessl, Ref. (19), 131-143 (1983).
135. C.L. Page, N.R. Short, and W.R. Holden, Cem. Concr. Res. 1, 79-86 (1986).
136. R.F. Feldman and Huang Cheng-yi, Cem. Concr. Res. 15, 411-420 (1985).
137. D.M. Roy and F.L. Burns, Scientific Basis for Nuclear Waste Management, Vol. 11, 631-640, Ed. W.L. Lutze, North-Holland, NY (1982); Symp. Proc., Materials Research Society.
138. M.W. Grutzeck and D.M. Roy, Experimental Characterization and Stability of Salt- and Nonsalt-Containing Grouts and Mortars, BMI/ONWI-568, ONWI, Battelle Memorial Inst.,

Columbus, OH (1985).
139. D.M. Roy, M.W. Grutzeck, and L.D. Wakeley, Salt Repository Seal Materials: A Synopsis of Early Cementitious Materials Development, BMI/ONWI-536, ONWI, Battelle Memorial Inst., Columbus, OH (1985).
140. L.D. Wakeley, B.E. Scheetz, M.W. Grutzeck, and D.M. Roy, Cem. Concr. Res. 11 (1), 131-142 (1981).
141. M. Conjeaud, Ref. (73), paper III.1 (1982).
142. D.W. Hofmann, Cem. Concr. Res. 14, 49-56 (1984).
143. H.G. Midgley and J.M. Illston, Cem. Concr. Res. 14, 546-558 (1984).
144. H.G. Smolczyk, Ref. (132), 60-62 (1983); Betonwerk und Fertigteil-Technik, Heft. 12 (7 pp.) (1984).
145. F.M. Ivanov and N.N. Janbykh, Beton Zelezobeton. (6), 26-27 (1982).
146. K. Kishitani, T. Sawada, W. Kobayashi, and M. Minanin, C.A.J Review (1981), 176-178.
147. C.J. Pereira and L.L. Hegedus, I. Chem. E. Symp. Series #87, 427-438 (1984).
148. H. Uchikawa, S. Uchida, and K. Ogawa, C.A.J. review (1984), 56-59.
149. K. Tutti, Ref. (132), 79-91 (1983).
150. D.M. Roy. R.I.A. Malek, and M. Silsbee, Workshop on Blast Furnace Slag Cements and Concretes, Oct. 14-17 (1985), York, England.
151. D.M. Roy, R.I.A. Malek, and M. Silsbee, Fly Ash Symposium, Mat. Res. Soc. Proc. (1986), Mat. Res. Soc., Pittsburgh, PA.
152. C.L. Page and O. Vennesland, Mater. Struct. (Paris) 16 (91), 19-25 (1983).
153. S. Diamond and F. Lopez-Flores, Am. Cer. Soc. Communications, C-162 - C-164 (1981).
154. V.S. Ramachandran, R.C. Seeley, and G.M. Polomark, Materiaux et Constructions 17, 285-289 (1984).
155. V. Shigeru, T. Takagi, S. Goto, and M. Daimon, C.A.J. Review (1983), 76-77.
156. C.M. Hansson, Th. Frolund, and J.B. Markussen, Cem. Concr. Res. 15, 65-73 (1985).
157. V.I. Babushkin, G.M. Matveyev, and O.P. Mchedlov-Petrossyan, Thermodynamics of Silicates (Transl. of Thermodynamika Silikatov, 4th Edn.), Springer-Verlag, NY (1985).
158. W.P. Freeborn and D.M. Roy, Low Temperature Phase Equilibria in the System Concrete-Tuff: Thermodynamic Calculations, Experimental Studies, and Natural Assemblages, Report to Los Alamos Natl. Lab., Los Alamos, NM (1983).
159. S.L. Sarkar, ONWI-201 (DOE) Battelle Memorial Institute, Columbus, OH (1982).
160. C.D. Lawrence, Durability of Concretes: Molecular Transport Processes and Test Methods, Technical Report 544, Cement and Concrete Assn., Wexham Springs, U.K. (1981).
161. V. Lach and M. Matousek, Ref. (61), Paper III.11 (1982).
162. B. Jungermann, Betonwerk, Fertigteil-Tech. 48 (6), 358-362 (1982).
163. A.J. Majumdar and M.S. Stucke, Cem. Concr. Res. 11 (5/6), 781-788 (1981).
164. S. Komarneni and D.M. Roy, Cem. Concr. Res. 11 (5/6), 789-794 (1981).
165. J. Gebauer, Silicates Ind. 47 (6), 155-159 (1982).
166. R. Frey and H.J. Goerke, Tonind. Ztg. 106 (3), 184-187 (1982).
167. W.R. DeSitter, Cement (Netherlands) 35 (3), 188-193 (1983).
168. V.A. Trub, Bull. Cim. 51 (22), 6 pp. (1983).
169. H. Friede and P. Schubert, Tonind.-Ztg. 107 (1), 38-43 (1983).
170. T. Uomoto and K. Kobayashi, Ref. (55), Vol. II, 1013-1038 (1983).
171. O. Vennesland and O.E. Gjorv, Ref. (55), Vol. II, 719-730 (1983).
172. G.A. Dapkus and V.Ju. Stankjavichjus, Beton Zelezobeton. (5), 35 (1983).
173. B.D. Bagrov, Beton Zelezobeton. (5), 36 (1983).
174. P. Nischer, Betonwerk, Fertigteil, Technik. 49 (3), 148-151 (1983).
175. D. Beckett, Concrete (London) 17 (2), 16-18 (1983).
176. H. Weber, Betonwerk, Fertigteil, Technik. 49 (8), 508-514 (1983).
177. P. Barret, D. Bertrandie, and D. Beau, Cem. Concr. Res. 13, 789-800 (1983).
178. M. Soustelle, B. Guilhot, A.A. Fournier, M. Murat, and A. Negro, Cem. Concr. Res. 15, 655-661 (1985).
179. K. Suzuki, T. Nishikawa, and S. Ito, Cem. Concr. Res. 15, 213-224 (1985).
180. D.W. Hobbs, Ref. (45) (1985).
181. M.H. Roberts, BRE Information Paper, IP 6/81 (Apr. 1981).
182. G.J. Osborne, Ref. (45) (1985). To be published in Durability of Building Materials.
183. E.L. White, B.E. Scheetz, D.M. Roy, K.G. Zimmerman, and M.W. Grutzeck, pp. 47-478 in Scientific Basis for Nuclear Waste Management, Vol. 1; Proc., Materials Research Society, Ed. G.J. McCarthy, Plenum, NY (1979).
184. C.S. Poon, A.I. Clark, R. Perry, A.P. Barker, and P. Barnes, Cem. Concr. Res. 16 (2), 161-172 (1986).
185. A. Kumar, S. Komarneni, and D.M. Roy, Diffusion of Cs^+ and Cl Through Sealing Materials, Waste Management 86, Am. Nucl. Soc. (1986).
186. A. Atkinson, A.K. Nickerson, and T.M. Valentine, Radioactive Waste Management and the Nuclear Fuel Cycle 4, 357-378 (1984).
187. A. Atkinson, ibid. 3, 371-386 (1983).
188. D.M. Roy, Borehole and Shaft Plugging Proceedings, OECD/USDOE, Columbus, OH (7-9 May 1980), 369-384, OECD, Paris, France (1980).
189. J.E. Mendel, BNWL 1765, Battelle Pacific Northwest Laboratories, Richland, WA (1973).
190. J.G. Moore, H.W. Godbee, and A. Kibbey, Nucl. Technol. 32, 39 (1977).
191. D.M. Roy, Proc., Conf. on High-Level Radioactive Solid Waste Forms, U.S. Nucl. Regulatory Commission (18-21 Dec. 1978), Denver, CO, pp. 479-516; NUREG/CP-0005, Ed. L. Casey (Apr. 1979).
192. D.M. Roy, B.E. Scheetz, M.W. Grutzeck, A.K. Sarkar, and S.D. Atkinson, Proc., Intl. Symp. Ceramics in Nuclear Waste Management, Cincinnati, OH, pp. 136-142, Eds. T.D. Chikalla and J.E. Mendel, Nucl. Div., Am. Ceram. Soc. and U.S.D.O.E., Conf.-790420 (1979).
193. D.M. Roy, B.E. Scheetz, L.D. Wakeley, and M.R. Barnes, Nucl. and Chem. Waste Mgt. 3, 35-42 (1982).
194. M.W. Barnes, B.E. Scheetz, L.D. Wakeley, S.D. Atkinson, and D.M. Roy, Scientific Basis for Nuclear Waste Management, Vol. 6, pp. 147-154, Ed. S.V. Topp, North-Holland, NY (1982);

Materials Research Society Symposium Proceedings.
195. B.E. Scheetz, D.M. Roy, C. Tanner, M.W. Barnes, M.W. Grutzeck, and S.D. Atkinson, Am. Ceram. Soc. Bull. 64, 687-690 (1985).
196. M.W. Barnes and D.M. Roy, Scientific Basis for Nuclear Waste Management, Vol VI, pp. 159-166, Ed. Douglas C. Brookins, North-Holland, NY (1983); Materials Research Society Symposium Proceedings.
197. M.W. Barnes, D.M.Roy, and C.A. Langton, Scientific Basis for Nuclear Waste Management, VIII, pp. 865-874, Eds. C.M. Jantzen, J.A. Stone, and R.C. Ewing (1985); Materials Research Society Symposium Proceedings, Vol. 44.
198. Wei Fajun, M.W. Grutzeck, and D.M. Roy, Scientific Basis for Nuclear Waste Management,V VIII, pp. 899-902, Eds. C.M. Jantzen, J.A. Stone, and R.C. Ewing (1985); Materials Research Society Symposium Proceedings, Vol. 44.
199. (a) D.M. Roy, Wei Fajun, and M.W. Grutzeck, Advances in Ceramics, Nuclear Waste Management 8, 401-405, Am. Ceram. Soc., Columbus, OH (1984).
(b) S. Komarneni and D.M. Roy, Science 221, 647-648 (1983).
200. M.W. Barnes, D.M. Roy, and L.D. Wakeley, Ref. (199), 406-412 (1984).
201. C.E. McCulloch, M.J. Angus, F.P. Glasser, and A.A. Rahman, Ref. (199), 413-418 (1984).
202. V.W. Schneider and F.W. Ledebrink, Ref. (199), 394-400 (1984).
203. P.C. Picalo, M.S. Davis, and J.W. Adams, Ref. (198), 919-926 (1985).
204. L.R. Dole, in Waste Management 85, Vol. 2, 455-462, American Nuclear Soc., Chicago, IL (1985).
205. a. R. Koster, Ref. (199), 487-491 (1985).
b. B. Kienzler, E. Karthaus, and R. Koster, KFK-3612 (Nov. 1983).
206. C.W. Forsberg, Environ. Sci. Technol. 18, 2, 564 (Feb. 1984).
207. B.E. Scheetz and D.M. Roy, Cer. Bull. 64 (32), 452 (1985).
208. E. Zamorani, G. Serrini, and H. Blanchard, Cem. Concr. Res. 16 (3) (1986).
209. I.P. Murarka, Scientific Basis for Effective Fly Ash Disposal, Fly and Coal Combustion By-Products, Characterization, Utilization and Disposal, Eds. G.J. McCarthy, F.P. Glasser, and D.M. Roy, Materials Research Society Proceedings (1986), Pittsburgh.
210. R.I.A. Malek, P.H. Licastro, and D.M. Roy, Ref. (209) (1986).
211. S. Komarneni and D.M. Roy, Cem. Concr. Res. 11, 759-764 (1981).
212. V.S. Ramachandran, R.F. Feldman, and J.J. Beaudoin, Concrete Science, Heyden and Son, Ltd., London (1981).
213. H.W. Dorner and M.J. Setzer, Cem. Concr. Res. 10 (3), 403-411 (1980).
214. P. Grubl and A. Sotkin, Cem. Concr. Res. 10 (3), 333-345 (1980).
215. M. Buil, J. Aguirre-Puente, and A. Soisson, C.R. Acad. Sci. Paris 293 (Serie II), 653-656 (1981).
216. M. Buil and J. Aguirre-Puente, Amer. Soc. Mech. Eng. Winter Ann. Mtg. Abstr. No. 81-WA/HT-69 (Nov. 1981).
217. M. Pigeon and M. Lachance, J. Amer. Concr. Inst. 78, 282-291 (1981).
218. V.M. Malhotra, Ref. (32), 159-184.
219. V.M. Malhotra, Mater. Struct. (Paris) 14 (80), 79-89 (1981).
220. F.D. Lydon, Precast Concr. 12 (5), 228-231 (1981).
221. F. Grasenick and S. Soretz, Zem. Beton. 27 (3), 120-122 (1982).
222. H.H. Bache, Densified Cement/Ultra-Fine Particle-Based Materials, Aalborg Portland (Denmark), Rep. (1981) (Presented at Second Int. Conf. Superplasticizers in Concr., Ottawa, Canada, 1981).
223. E.V. Sorensen, Ref. (55), Vol. II, 709-718 (1983).
224. P. Jahren, Ref. (55), Vol. II, 625-642 (1983).
225. M.S. Zaman, P. Ridgway, and A.G.B. Ritchie, J. Amer. Concr. Inst. 79 (1), 56-58 (1982).
226. R.L. Yuan and J.E. Cook, Ref. (55), Vol. I, 307-320 (1983).
227. A. Samarin, R.L. Munn, and J.B. Ashby, Ref. (55), Vol. I, 143-172 (1983).
228. V.R. Sturrup, R.D. Hooton, and T.G. Clendenning, Ref. (55), Vol. I, 71-86 (1983).
229. J. Virtanen, Ref. (55), Vol. II, 923-942 (1983).
230. M. Pigeon and M. Regourd, Ref. (55), Vol. II, 979-998 (1983).
231. J. Murata, M. Kawasaki, T. Sakai, and T. Kawasi, Ref. (55), Vol. II, 999-1012 (1983).
232. K. Hirai, Ref. (55), Vol. II, 1039-1058 (1983).
233. M.F. Pistilli, J. Amer. Concr. Inst. 80 (3), 217-222 (1983).
234. M.H. Roberts and B.W. Adderson, Mag. Concr. Res 35 (123), 86-98 (1983).
235. M.P.J. Olsen, Cem. Concr. Res. 14, 113-122 (1984).
236. H.W. Dorner, Cem. Concr. Res. 14, 807-815 (1984).
237. S. Chatterji, Cem. Concr. Res. 15, 13-20 (1985).
238. S. Chatterji, A. Jensen, N. Thaulow, and P. Christensen, Cem. Concr. Res. 15, 729-734 (1984).
239. D. Whiting, J. Am. Concr. Inst. 82, 716-723 (1985).
240. D.M. Roy and G.M. Idorn, ACI Journal 79-43, 444-457 (Nov.-Dec. 1982).
241. D.M. Roy, S. Diamond, and J.P. Skalny, Concrete Rheology, Ed. Jan Skalny, pp. 152-173; Proc., Symposium M, Materials Research Society (1982).
242. G.M. Idorn and D.M. Roy, Cem., Concr. and Aggregates 6 (1), 3-10 (1984).
243. D.M. Roy and G.M. Idorn, Very High Strength Concrete-Based Materials, Ed. J.F. Young, pp. 133-142; Mat. Res. Soc. Symp. Proc. (1984).
244. G.M. Idorn, Concrete International (Feb. 1984), 13-20.

SUB-THEME/SOUS-THÈME 4.3

Compatibility of cement paste with aggregate and reinforcements, including electrochemical corrosion.

Compatibilité de la pâte de ciment avec les granulats et les armatures, y compris la corrosion électrochimique.

Chairman/Président:

R. Cigna
Facoltà di Ingegneria
Università di Roma
Roma, Italy

Principal Reporter/Rapporteur Principal:

R. Turriziani
Facoltà di Ingegneria
Università di Roma
Roma, Italy

Durability of Reinforced Concrete - Needed Research

Ranieri Cigna
University of Rome, Italy

Many years ago, in Canada, there was a sudden failure of a prestressed, reinforced concrete pipeline, which occurred even before it began operation. This event led to an extensive series of studies and research into both the causes of the damage and the precautions to be taken during manufacture in order to prevent future failures (1-4).

The alarm raised by this case resulted in thorough examinations being carried out also on numerous other cases of failure of prestressed reinforced concrete structures in the hypothesis that the state of tension of the wires could in some way influence their tendency to corrode and consequently affect the durability of structures (5)(6)(7).

On that occasion, interdisciplinary research groups were formed where corrosion experts worked alongside cement and structural engineering experts. At about the same time it was noted that conventional reinforced concrete could also fail due to corrosion, when previously the reinforcement was considered unassailable in the favourable environment in which it was situated. Thus, also in this sector, there was a considerable impulse for applied research.

Moreover, from the beginning of the Seventies, the enormous increase in the utilization of concrete in marine and tropical environments brought to light very serious corrosion problems.

As a consequence, numerous national and international bodies began, and still continue, research for a greater understanding of the mechanisms which initiate the corrosive processes and for specifying design and installation regulations aimed at protecting the reinforcement (8)(9).

The report presented by prof. Turriziani at this Congress reviews the results obtained by researchers from various parts of the world in the specific sector of reinforcement corrosion; therefore, this paper will give only an outline of the problems still being debated and show what lines of research seem appropriate for further investigation.

Tropical and sub-tropical environments

Geymayr, Treadaway et al. have recently pointed out the particular features which distinguish and condition the behaviour of corrosion in reinforced concrete structures in tropical and sub-tropical countries (10)(11).

This topic, as it relates to the Middle East, was also dealt with by a special section of the First Arabian Conference on Corrosion held in Kuwait in February 1984 (12)(13)(14). The problems which emerged can be summarized as follows:

a) Aggregates
River aggregates are scarce. Aggregates from mines are dirty with silt and contaminated with chlorides and sulphates.
Washing is difficult and too costly.

b) High temperature and humidity
The high temperature increases water-demand, accelerates setting time, increases cement content for a given water/cement ratio, increases carbonation rate. High humidity accelerates corrosion of steel, favours cement hydration during storage.

c) Environment salinity
Depending on the distance from the sea, the chloride content in the atmosphere has a certain influence on the resistance to corrosion of reinforcement, when this factor has not been taken into account during the design stage.

The research suggested in this instance should be directed to the study of alternative cements to Portland, and especially of a pozzolanic or blast-furnace type, as well as the influence of curing methods.

Bridge decks

The economic repercussions due to the damage suffered by road bridges in the United States have had a

considerable impact on research in this sector(15).

If it is admitted that there is no substitution for chlorides such as deicing salts, and if it is agreed that the design and installation of these structures are acceptable, researchers must concentrate on ways and means of preventing corrosion.

The prevention method most often suggested is cathodic protection with impressed current of the reinforcement. However, even this technique does not appear perfectly reliable, especially with regard to:

a) choice, positioning and distribution of auxiliary anodes;

b) choice and positioning of reference electrodes;

c) determination of the protection potential and consequently of the current to maintain the structure in non-corrodible conditions;

d) influence of dynamic stresses to which the concrete is subjected, particularly in relation to the formation of cracks and the consequent infiltration of water and salts.

Of the four points listed above, the potential necessary to achieve cathodic protection merits brief examination.

It is important to observe that whenever a pitting phenomenon begins in very localized areas, a considerable acidification can occur with self-stimulating effects and propagation even without oxygen replenishment.

Cathodic protection of reinforcement steel constitutes a rather special example of the application of this technique, which recalls that of stainless steels subject to pitting. In both cases the metal is not kept at a potential below that of thermodynamic equilibrium (immunity zone), but must be kept in the narrow range of values in which there is passivity for alkaline pH and immunity for acid pH (16)(17).

Fig. 1 shows the trend of the steel polarization curve in an alkaline environment, with and without start of pitting due to the presence of chlorides: the range of potentials in which the steel is kept in passive conditions is shown, as well as the range corresponding to the normal state of non-corrosion (immunity). In the immunity zone there is hydrogen evolution; this phenomenon is not normally harmful, provided that pH is not too low. Besides at low pHs and low protection potentials the steel-concrete bond may be damaged.

Fig. 2 gives a potential-pH diagram of the steel at 25 °C, and clearly shows the situation which would occur with and without the cathodic protection. It

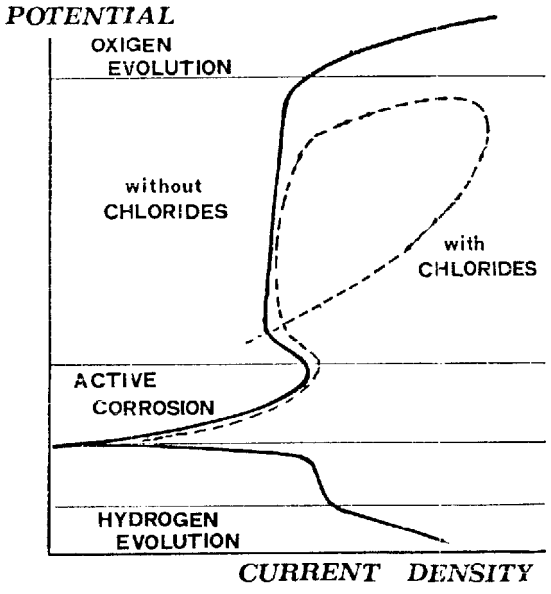

Fig. 1 - Polarization curve of iron in alkaline environment

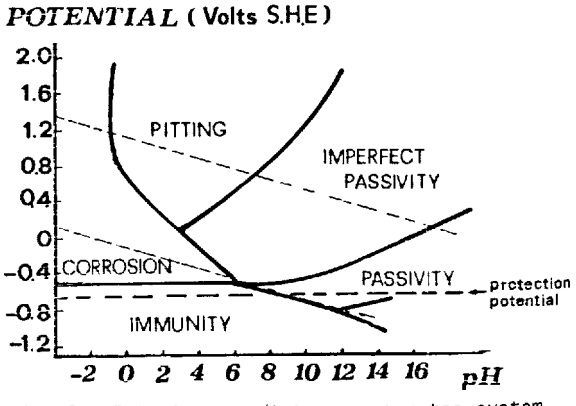

Fig. 2 - Potential - pH diagram for the system Fe - H_2O in presence of chlorides

can be observed that, since the protection potential lies just below the equilibrium potential, the very slight hydrogen evolution inside the pits cannot harm the iron-concrete bond, due precisely to its limitation. Moreover in a short time the hydrogen ions concentration is lowered and the re-alkalinization of the solution adjoining the metallic surface leads to the consequent passive protection.

This hypothesis needs to be supported by further experimental research which must not be carried out in an aqueous solution, and which requires the use of mortar or concrete specimens and up-dated and qualified electrochemical techniques and instruments.

Another subject to be investigated more deeply in the cathodic protection sector is the influence of interruptions in the energy supply: it should be useful to determine the maximum time during which the structure does not suffer excessive corrosion attack without electrical protection. This data would be most important when solar batteries are used, since the costs of the energy accumulation are quite high.

Electrochemical characterization of concrete

Given that concrete can be considered to all intents and purposes a second species conductor, since it has its own electrolytical conductivity and is the site of ionic diffusion processes, it is important that a more profound knowledge of its electrochemical characteristics is acquired in the years to come.

A promising way of reaching conclusive knowledge of the composition of the pore solution, which also constitutes the environment in which the reinforcement can become passive, or corrode, is by the expression of cement paste and mortar (18)(19)(20).

Fig.3 shows a diagram of the device which has been used up to now for research of the type suggested.

The pressures currently used for the pressing operation are in the order of 350 MPa and the specimen volumes in the order of 50 ml.

The adoption of this technique can, in a short time, provide important information on the nature of the electrolyte in contact with the reinforcement according to numerous parameters. Among those most worthy of consideration are: the type of cement used, the type of curing, the age, the presence of additives, and the exposure environment.

The study, carried out following this technique, of the reactivity of chlorides with some of the constituents of the clinker has demonstrated that there is a considerable difference between the "free chlorides" and those bound in chemical compounds, and therefore not dangerous from a corrosion aspect (19)(21).

However, other techniques can also be adopted. For example to study the diffusivity of chlorides and oxygen inside the concrete, electrochemical measurements could be taken of the potential assumed by suitable chosen metal specimens, embedded in the conglomerate at appropriate distances from the external surface.

Another study which undoubtedly merits adequate investigation is that of the role played by oxygen in the corrosive processes of the reinforcement.

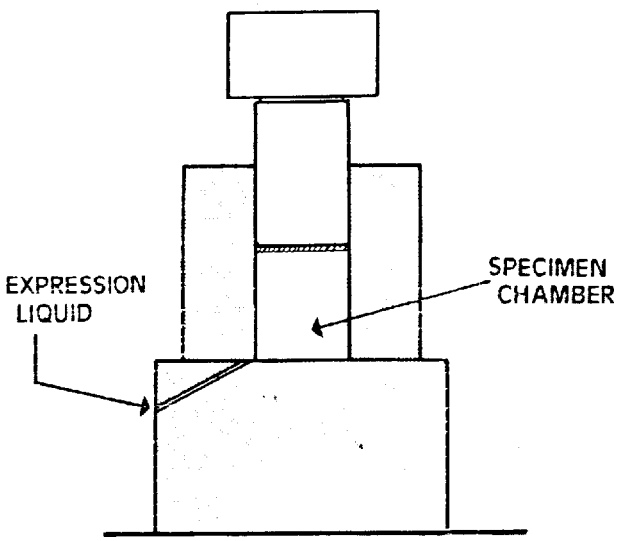

Fig. 3 - Apparatus for expression of pore solution from cement pastes

It is often affirmed that in the absence of oxygen any attack is blocked because the cathodic reaction is not nourished, and this appears very plausible when taking into account the high pH of the pore solution and consequently the weak oxidizing power of the hydrogen ions which are present in a very small quantity. This assessment seems to be confirmed by the observation made by many researchers on the non-corrodibility of reinforcement in concrete situated at a great depth in the sea. In this instance, when the oxygen present in the mix has been consumed, its replenishement is clearly negligible and steel is taken to active zone potential values, which correspond to an extremely low corrosion rate in the order of a few micrometres/year.

It has, however, been ascertained that when a pitting phenomenon starts up on the metal, enough acidity is created locally to allow evolvment of the phenomenon even without an additional supply of oxygen.

Finally, the very important role which macrocell action plays in the corrosion process should be further investigated (15).

Protection methods

One method proposed for preventing reinforcement corrosion is by coating the surface with various kinds of materials, in order to constitute a real barrier against water, oxygen, chlorides, carbon dioxide, or any other substance which can provoke aggression of the steel.

In order to yield high performance, considerable care is required both in the preparation of the surface and in the application of the coatings.

It is considered that studies on this protective technique must be suitably extended, with particular reference to the following points:

a) choice of the product to apply;

b) methods for anchoring the coating to the concrete;

c) sealing porosity with finishing coatings;

d) assessment of any dangers inherent in the total blockage of respiration of the concrete beneath the coating.

As far as the other proposed protection methods are concerned, further long-term exposure tests are needed in order to evaluate the goodness of the use of calcium nitrite as a corrosion inhibitor in chloride containing concrete, especially when chlorides come from the environment and when cracking may occur.

Monitoring methods

During the last decade, considerable impetus has been given to studies on techniques for monitoring the state of the reinforcement under the aspect of its tendency to corrode. In particular, the adoption of electrochemical methodologies has been suggested, such as surveying the polarization resistance, the a.c. impedance, and electrochemical noise. Of these three techniques, more extensive studies have been made on the first, and some consider it the most suitable both for laboratory studies and for in situ measurements(22).

However, despite the fact that experiments conducted on metallic structures with polarization resistance measurements have always been positive, this technique is considered difficult to apply on reinforced concrete. This is because the measuring electrodes need to be arranged in the structure while it is being cast and their position has to simulate that of the reinforcement itself, and also because the resistivity of concrete is very high.

The first two observations also apply to impedance measurements, which are not influenced by the resistivity. Impedance measurements appear particularly suitable for laboratory research on passivation and depassivation of reinforcement in mortar or concrete specimens.

Still to be considered is the electrochemical noise monitoring technique, which is known to be based on the evaluation of fluctuations in the potential over time. This method has already been applied to installed structures with some results (23). It is therefore considered that greater attention should be paid to the possibility of adopting this method of monitoring, particularly for detecting corrosive attacks from pitting due to chlorides.

REFERENCES

1) R. E. Bald "Regina Prestressed Concrete Pipe Failure", Corr. Tech., Aug., 217 (1962)

2) G. E. Monfore, G. J. Verbeck "Corrosion of Prestressed Wire in Concrete", J. Am. Concr. Inst., Proc., 57, 491 (1960)

3) R.H.Evans "Use of Calcium Chloride in Prestressed Concrete", Proc. World Conf. on Prestressed Concrete, paper A 31 (1957)

4) R. Cigna, M. Maraghini, and G. Schippa " Sulla corrosione delle armature nei calcestruzzi precompressi" Ind. Ital. Cemento 35(12), 801 (1965)

5) M. H. Roberts " Effect of Calcium Chloride on the Durability of Pretensioned Wire in Prestressed Concrete", Mag. Concr. Res. 14, 143 (1962)

6) R. F. Stratfull " Effect on Reinforced Concrete in Sodium Chloride and Sodium Sulfate Environments" Mat. Protection 3, 74 (1964)

7) D. A. Lewis " Some Aspects of the Corrosion of Steel in Concrete", First Int. Congr. on Metallic Corrosion, London 1961, p. 547

8) B. C. Gerwick Jr. "Research Requirements for Concrete in Marine Environments", ACI SP 65-31, American Concrete Institute, Chicago MI, 577 (1980)

9) M. B. Leeming Mice "The Durability of Reinforced Concrete in Seawater - An Outline of Results from the UK Concrete in the Oceans Programme", Int. Symp. "Behaviour of Offshore Concrete Structures", Brest, Oct. 1980, I-6, C.N.E.X.O.

10) G. W. Geymayr " Repairs of Concrete in Tropical Marine Environment", ACI SP 65-29, American Concrete Institute, Chicago MI, 527 (1980)

11) K. W. J. Treadaway, G. Mac Millan, P. Hawkins,

and C. Fontanay "The Influence of Concrete Quality on Carbonation in Middle Eastern Copnditions - A Preliminary Study", in A. P. Crane "Corrosion of Reinforcement in Concrete Construction", Ellis Horwood ed., Chichester, 101 (1983)

12) M. T. Ayoub "Stress Corrosion of Concrete Reinforcement in Hot Climates", Proc. First Arabian Conf. on Corrosion, Kuwait Feb. 1984, p. 788

13) A. A. Jeragh, N. Ismael "Corrosion of Reinforced Concrete Foundations in Kuwait", Proc. First Arabian Conf. on Corrosion, Kuwait Feb. 1984, p. 801

14) H. M. Shalaby, H. Al-Mazeedi "The Corrosion Behaviour of Reinforcing Steel in the Aggressive Components of Seawater", Proc. First Arabian Conf. on Corrosion, Kuwait Feb. 1984, p. 819

15) J. E. Slater " Corrosion of Metals in Association with Concrete", ASTM STP 818, American Society for Testing and Materials, Philadelphia (1983)

16) R. Cigna, O. Fumei " Sulla protezione catodica dei ferri del calcestruzzo armato" Ind. Ital. Cemento 42(11), 855 (1982)

17) N. S. Berke " The Use of Anodic Polarization to Determine the Effectiveness of Calcium Nitrite as an Anodic Inhibitor", ASTM STP 906, V. Chaker ed., Philadelphia, 78 (1986)

18) P. Longuet, L. Burglen, and A. Zelwer "La Phase Liquide du Ciment Hydrate", Rev. Mater. Constr. 676, 35 (1973)

19) P. Lambert, C.L. Page, and N. R. Short "Pore Solution Chemistry of the Hydrated System Tricalcium Silicate/Sodium Chloride/Water", Cem. Concr. Res. 15, 675 (1985)

20) C. Andrade and C.L. Page "Pore Solution Chemistry and Corrosion in Hydrated Cement Systems Containing Chloride Salts: A Study of Cation Specific Effects", Br. Corros. J. 21(1), 49 (1986)

21) V. S. Ramachandran, R. C. Seeley, and G. M. Polomark "Free and Combined Chloride in Hydrating Cement and Cement Components", Mat. Constr. 17(100), 285 (1984)

22) J. L. Dawson "Corrosion Monitoring of Steel in Concrete", in A. P. Crane "Corrosion of Reinforcement in Concrete Construction", Ellis Horwood ed., Chichester, 175 (1983)

23) D. G. John, J. Lomas, J. Dawson, and P. Searson "Electrochemical Techniques for the Investigation and Monitoring of the Corrosion of Reinforcing Steel in Concrete", Proc. First Arabian Conf. on Corrosion, Kuwait Feb. 1984, p.755

R. TURRIZIANI (University of Rome, Italy)

4.3 INTERNAL DEGRADATION OF CONCRETE: ALKALI-AGGREGATE REACTION, REINFORCEMENT STEEL CORROSION

The internal degradation mechanisms which can induce premature deterioration of concrete are forms of alkali-aggregate reactivity and corrosion of the reinforcement.

The deterioration is caused by the generation of expansive forces within the concrete. Consequently, tensile stresses develop which are too great to be supported by the limited plastic deformation of the concrete. The result is the formation of cracks reaching the surface of concrete.

If nothing else interferes, the process manifests itself by crack systems and other features which are characteristic of the particular deterioration mechanism involved.

In unrestrained concrete, the cracks caused by the alkali-aggregate reaction have a random distribution which takes the form of a mapwork crack pattern.

In conventional reinforced concrete the pattern of cracking is modified. The effective development of the crack is influenced by the nature and level of stress, the geometry of the structure and detailing of the reinforcement.

The type of crack pattern consistent with the corrosion of reinforcing steel shows straight cracks directly related to the position of the reinforcement. The cracks can develop up to substantial widths of several mm. Subsequently, spalling will occur to large areas of the cover exposing the reinforcement underneath. The corner bars are almost always more corroded than the rest.

Numerous factors can give the degradation mechanisms the opportunity to operate at a rate which compromises the reputation of the concrete for permanency.

The occurrence of alkali-aggregate reaction forms has been attributed to limited and inaccurate study of the source of aggregates, as well as to unsuitable aggregate-cement combinations, introduction of alkalis from external sources and concentrations of alkalis by moisture migration through the concrete.

With regard to alkali-aggregate reaction an inaccurate survey of aggregates can be due to many causes. This includes inappropriate choice of test methods, procedures for evaluating the test results which are unsuitable for the aggregates under examination, and lack of time for carrying out long-term tests.

The occurrence of corrosion of steel in concrete has been attributed to poor design, inadequate quality of concrete, incorrect construction practice, presence of chlorides and, occasionally, to stray currents.

Poor design will lead to corrosion induced by unexpected cracking of the concrete. The greater width of the surface cracks can be due to the fact that the concrete has not reached the expected resistance or because the tensile stresses are more than expected.

If the chloride content does not exceed the safety level, the reason for active corrosion of reinforcing steel lies in the area of the mix design and workmanship. Inadequate cover, poor compaction, high water-cement ratio are factors which determine the rate of corrosion.

The chloride ions can derive from the surrounding environment (as in marine constructions, or where concrete is exposed to de-icing salts) or from the addition to the mix of an excessive quantity of set-accelerators containing chloride.

Properly designed and constructed reinforced-concrete structures should therefore rarely experience corrosion damage.

No structure has ever collapsed because of the alkali-aggregate reaction, just as no sudden catastrophic failure due to steel corrosion has been observed in conventional reinforced-concrete structures.

In many cases the structures affected by alkali-aggregate reaction have only remained under

observation within minimum maintenance, but there are cases of repair involving the replacement of structural parts. The interventions are often dictated by aesthetic requirements, as in the case of building facades, or concern for future structural soundness.

The control of the effect of corrosion on the performance of a component is governed by different criteria. The two internal degradation mechanisms differentiate in an important respect: the alkali-aggregate reaction terminates when the reactive aggregate is consumed or the alkali concentration in the pore solution which permeates the cement matrix falls below a given level, while the reinforcement corrosion can in theory continue until the metal is consumed. It is a fortunate coincidence that in conventional reinforced concrete involved in corrosion phenomena of the reinforcing steel, the deterioration of the concrete manifests itself much before the reduction in the resistance of the bar has reached a structurally meaningful level. Present knowledge indicates that the reported cases of structural damages have only involved the destruction of the concrete. The low rate of corrosion and the visible signs of its progression permit the problem of control to be referred to maintenance rather than to safety.

In the area of pre-stressed concrete, the problem is not cracking but the influence of the corrosive environment on the mechanical strength of the pre-stressed steel. In this case, sudden structural failure can occur.

Over the past six years, important advances have been made in understanding the mechanisms of reaction and the micro-structural aspects of the alkali-aggregate reaction.

With regard to the reaction mechanism, the majority of the work has been undertaken in the area of alkali-silica. It is noted that the chemical attack and the physical process of expansion are divided into two distinct stages. Initially,an alkaline silicate gel is formed which then increases in volume by absorbing the pore solution. The dimensional variations resulting from this swelling of the gel generate expansive pressure if the increase in volume cannot be accomodated in any surrounding porous space. The expansive deterioration proceeds as long as the gel keeps its rigidity and can thus exercise a directional pressure.

Present evidence demonstrates that while the imbibition process is related to osmosis, the presence of a semi-permeable membrane to separate the regions with different chemical potential is unnecessary.
Much information on the microstructure of alkali-silica and alkali polycrystalline-aggregate reaction products has been obtained through SEM, supplemented by local chemical information from EDXA and EMPA.

The intrusion of alkalis and calcium in opal has been studied on opal cylinders and in mortar containing opaline sand. The alkalis penetrate deeply while the calcium is concentrated on the periphery.

There is convincing evidence that the reactivity of polycrystalline rocks to alkalis is associated with the presence in the rock of amorphous and cryptocrystalline silica, strained quartz, degraded feldspars and clay-like materials. In concrete sampled from deteriorated structures, amorphous and crystalline products have been found to co-exist around the majority of polycrystalline rock aggregates. The crystalline phase is stable only in a very wet environment. When dried it is transformed into poorly crystallized okenite. There are indications that the crystalline phase is produced by the gel transformation.

Considerable research and development has been undertaken in the area of corrective measures. These measures should prevent the problem of alkali-aggregate reaction during initial concrete mix design.

Where it is not possible to use low-alkali cement, an alternative method for reducing the risk of expansion is to limit the quantity of reactive alkalis available in the concrete mix by lowering the cement content. The safety level, with a given source of aggregates, is determined by experiments.The use of natural and artificial pozzolanic materials and blast-furnace slag to reduce the expansion from alkali-aggregate reaction has been discussed in numerous papers with emphasis on fly ashes and microsilica. The action mechanism of the mineral admixtures in preventing the alkali-aggregate reaction has not been completely understood. The preventive action has been attributed to alkali sorption, to low ionic diffusivity and reduced permeability,as well as to improved distribution of the calcium hydroxide released by hydrolysis.

In all the areas of information development, a considerable contribution has emerged from greater knowledge of the pore fluid chemistry, made possible by the application of the technique of expressing liquid under high pressure from hardened cement pastes and mortars.

Efforts have been focussed on accelerated test methods and on the revision of methods for evaluating results of standard tests.

In recent years constant attention has been paid to the corrosion of steel in concrete due to its widespread occurrence in certain types of structures and

the high costs of repair. A review of literature shows that the greatest problems of deterioration occur on the abutments of bridges due to an increase in the use of de-icing chemicals (chlorides) necessitated by the bare pavement policy. Damage to conventional and pre-stressed reinforced concrete pipelines and buildings exposed to marine environment appears less serious.

Prestressed concrete offshore structures for production and storage of oil have been developed in Europe after the discovery of oil fields in the North Sea. Extensive research work was undertaken in the 70's to support their construction. The results of this research work permitted a greater understanding of the electrochemical and diffusion mechanism, related to steel reinforcement corrosion, to take place, not even for this kind of structures, but also for a generalized application.

Concrete normally provides embedded steel with a high degree of protection against corrosion. This is because the high alkalinity of the pore solution in the cement paste and the oxygen dissolved in the solution produce a passive film on the surface of the steel which acts as a barrier against corrosion.

The rupture of the passive film can occur when the alkalinity is lowered by carbonation to the point in which the protective film is no longer stabilized or when the concentration of chlorides in the pore solution exceeds the threshold level. The threshold concentration depends on the pH value.

Carbonation is normally a slow process and is unlikely to penetrate a good concrete more than about 30 mm.

The reasons for the effect of the chlorides are not completely understood. It seems probable that chloride ions are incorporated in the oxide layer, making it permeable to the ferrous ions. However it is also possible that the chlorides react with the passive film allowing the formation of a soluble iron oxychloride to occur.

A further effect is that the chlorides reduce the electrical resistance of the pore solution, thus increasing the corrosion current and therefore the corrosion rate.
Yet, another notable effect of the presence of chlorides is the probability that the corrosion will be accompanied by pitting.

Results of field observations as well as laboratory studies show that the corrosion of reinforcement in concrete is electrochemical.
After the passive film ruptures, active-passive cells or concentration cells, or both, develop.
Due to the high pH and the presence of oxygen, the controlling cathodic reaction is the reduction of oxygen:

$$1/2\ O_2 + H_2O + 2\ e \ \text{---}> \ 2\ OH^-$$

while in the areas where the passive film is ruptured, the anodic reaction of metal dissolution occurs:

$$Fe \ \text{---}> \ Fe^{+2} + 2\ e$$

The Fe^{+2} ions are subsequently transformed into iron oxides through a certain number of complex reactions. The corrosion product occupies a greater volume than that of the metal removed. It is not possible to estimate exactly the greater volume of the reaction product with respect to the volume of the metal. The increase varies with the conditions of the process, but the consensus of opinion indicates that a reasonable value lies in the 2-3 ratio. At the start,the reaction product is accumulated within the concrete pores close to the surface of the metal,and only after all the surrounding space has been occupied do tensile stresses develop which produce cracks in the concrete.

The rate of corrosion probably depends on two factors: the electrical resistance of the electrolyte which occupies the porous system of the concrete, and the ability of the oxygen to reach the cathodic areas. The resistance between anode and cathode decreases as the moisture and salt concentration increase . The replenishment of oxygen is not a limiting factor for structures exposed to air, but it is probably the greatest controlling factor in submerged structures. In this latter case the corrosion depends on the oxygen dissolved in the water and on the rate of diffusion of the oxygen through the liquid which permeates the concrete.

With regard to reinforcement corrosion, concrete permeability is of critical concern.

For a concrete with low permeability,the rate at which water, chloride ions, oxygen and carbon dioxide can diffuse to the iron-paste interface will be very low, as will the rate at which the alkalinity at the interface can be reduced by leaching.

Obviously, the thickness of the cover over the steel is another important factor in preserving the reinforcement from the exposure environment.

The content and type of cement have a significant influence on the presence of chlorides. The chlorides react with the aluminates and alumino-ferrites to form solid chloroaluminates and chloroferrites, thus reducing the concentration of chlorides in the pore fluid.

Numerous mix design modifications, the use of inhibitors, new construction techniques and special additives have been proposed to decrease the chloride

permeability of bridge deck concrete. Work to date has indicated that several methods affect the penetration rate of chlorides into concrete. However, little information exists regarding long-term results.

Depending upon the cause, type and extent of corrosion, preventive measures may involve cathodic protection,coated rebars,external additional coating for the concrete or replacement of the surface concrete with a more adequate cover of dense, well-compacted relatively impermeable concrete.
Polymer impregnation and internal sealing by adding wax beads to the mix are other methods developed to greatly reduce the permeability of concrete.

Since it is difficult and costly to repair concrete which has reached advanced stage of deterioration due to corrosion of reinforcing steel, much work has been done to develop techniques capable of detecting the corrosion at an early stage.

I. ALKALI-AGGREGATE REACTION

I.1. Alkali-Silica Reaction

I.1.1. The Mechanism of Reaction and Expansion in Alkali-Silica Interaction.The subject is discussed by Dent Glasser (1) and Dent Glasser and Kataoka (2). The Authors appear to hold the view that the expansive pressure is sufficiently explained by imbibition of pore solution into gel as reaction with alkali proceeds.

When some kinds of poorly crystallized hydrous silica are placed in contact with a suitable solution of alkali hydroxides, two reactions occur (2). One is a typical acid-base reaction which consists of the neutralization of the acidic silanol groups (Fig.1):

$$\equiv Si\text{-}OH + OH^- = \equiv SiO^- + H_2O$$

the other leads to the formation of polyelectrolyte units through the rupture of the siloxane bridges (Fig.2):

$$\equiv Si\text{-}O\text{-}Si\equiv + 2OH^- = 2\ \equiv SiO^- + H_2O$$

The negative charges on the terminal oxygen atoms are balanced by alkaline cations. If a sufficient reserve of alkali hydroxide is available the attack of Si-O-Si bonds proceeds. The number of cross-linkages decreases while the number of polyelectrolyte units able to reorient and extend themselves increases as swelling agent is imbibed. In other words, the attack of the siloxane bridges loosens the network which becomes progressively less rigid. The final product is an alkaline silicate solution containing monomeric and polymerized species.

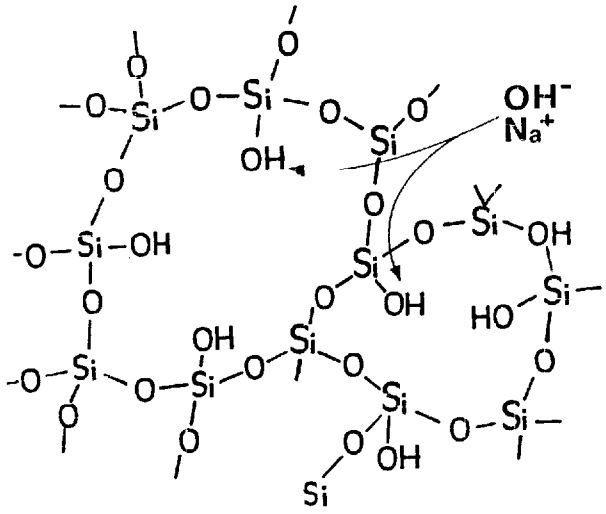

Fig. 1 - Acidic silanol groups in the gel are neutralised by the alkali. (ref. 2)

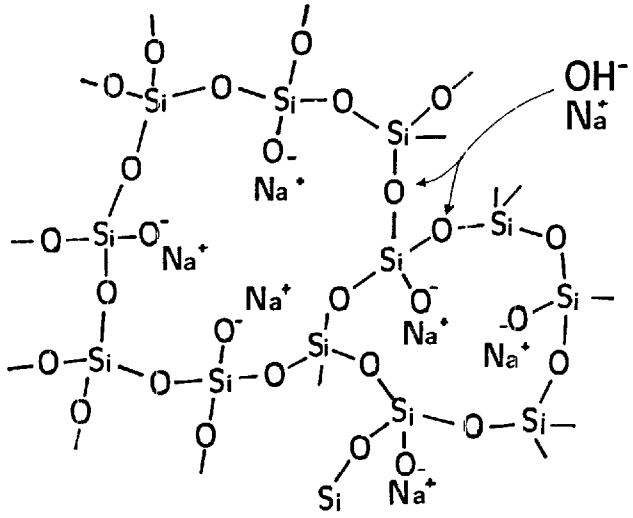

Fig. 2 - Furtner supplies of alkali attack siloxane bridges. (ref.2)

The damaging phase of reaction is the attraction of aqueous solution by the gel through an imbibition process which causes swelling.

The swelling on contact with a liquid can be seen as a manifestation of the tendency of the material attacked to dissolve, or at least to peptize, to the colloidal solution state.

The progressive decrease in rigidity of the particle portion penetrated and attacked by the alkaline solution, and the hydration spheres of the alkaline cations which maintain the electric neutrality of the polyelectrolyte units,support the imbibition process. Thus,other OH^- ions can penetrate increasingly deeper into the structure of the reactive particle. The liquid moves spontaneously towards the inside of the reactive particle where its chemical potential is lowest, i.e. in the region containing the highest concentration of polyelectrolyte units. Dent Glasser (1) observes that the imbibition process does not require the presence of a semipermeable membrane to separate the regions with different chemical potentials. The gel itself can behave as a semi-permeable membrane without the need for supposing this function to be met by a reacted coating.

When the reactive particle is enclosed in the hydrated cement matrix, as in concrete and mortar, the tendency of the attacked portion to swell is resisted by the surrounding material. The swelling pressure which develops is therefore the force which must be just able to prevent the solution from entering the gel. Certainly the swelling is partially opposed by elastic forces. If the decomposition reaches the point in which the gel becomes viscous liquid able to ooze and be absorbed into the surrounding matrix, the pressure is only exercised when the porous space is completely filled or if the imbibition rate is greater than the rate with which the viscous gel oozes (2).

Dent Glasser and Kataoka (2) conclude: "such a swelling solid...may well be the most disruptive item that a set concrete could contain since it can exert pressure on any neighbouring rigid bodies..."

The decrease in total expansion observed when the alkali-silica reaction is made to occur at temperatures above normal room temperature has also been explained by Vivian (3) in terms of rigidity of the silicate alkaline gel: since the effect of the temperature is to accelerate the attacking process, the quantity of gel that is sufficiently rigid to exert directional swelling pressure on the mortar and thus to widen cracks declines rapidly.

The effectiveness of the alkaline attack and its evolution depends on the structural features of the silica and on the reaction conditions. Gutteridge and Hobbs (4) have analysed in terms of its mineral constituents Beltane opal and an Australian opaline rock designated V17 which was used by Vivian in many of his experiments.Beltane opal rock contains approximately 82% by weight of reactive siliceous material which is identified as a mixture of opal-A, opal-C and tridymite according to the criteria suggested by Jones and Segnit (5).
The reactive constituent of opaline V17 rock is cristobalite and disordered tridymite and can be classified as opal-CT (5). Gutteridge and Hobbs (4) have also carried out experiments on the dissolution of Beltane opal constituents using a 3 M sodium hydroxide solution. It is found that in the 20-80 °C range opal-A dissolves more rapidly than opal-C and in turn more opal-C dissolves than tridymite. The results indicate that the expansive deterioration observed in mortar bars containing Beltane opal as an aggregate is due mainly to the attack of opal-A when the bars are stored at 20 °C and due to attack of opal-A and opal-C when stored at 35 °C and over.

The quantity of aggregate dissolved appears to greatly depend upon the accessibility of the silica structure to the alkaline hydroxide solution. Thus the reaction between hydroxyl ions and well-crystallized silica or other relatively dense forms of silica takes place only on the surface (6). The reaction is slow and produces discrete silicate ions which pass directly into solution.

Over the last years, pore fluid chemistry has become a promising area of information development, making possible significant new insights into the course of alkali-silica reaction. The development occurred through adopting the technique of expressing liquid under high pressures from hardened pastes and mortars of cement. This technique was conceived by Longuet et al. (7) and refined by Barneyback and Diamond (8).

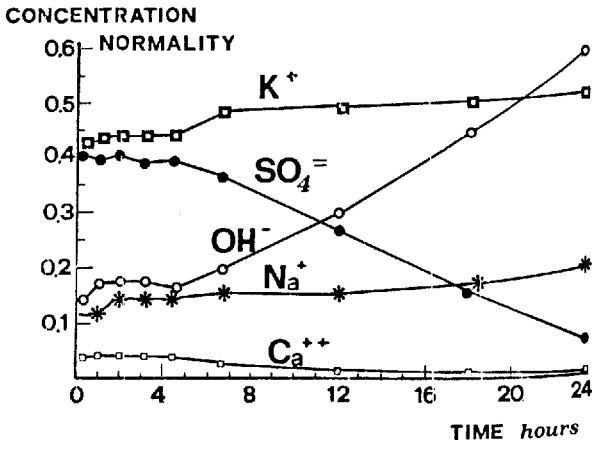

Fig. 3 - Concentrations of Calcium, Sodium, Potassium, Sulfate and Hydroxyl Ions in Pore Solutions Expressed From Cement Pastes at Ages Up To 1 Day. (ref. 10)

Results from work by the Diamond Laboratory are particularly valuable for following the evolution of the reaction. The position is illustrated in the Figures 3 to 6 and in Table 1 (9)(10). Figure 3 represents the early evolution of the pore solution chemistry,

the data of Table 1 the long-term evolution. Portland cement used was an ASTM Type I with an alkali content of 0.91% Na_2O equivalent, but the values plotted in Figure 3 refer to solutions expressed from pastes while the data in Table 1 refer to solutions from mortar with quartz sand.

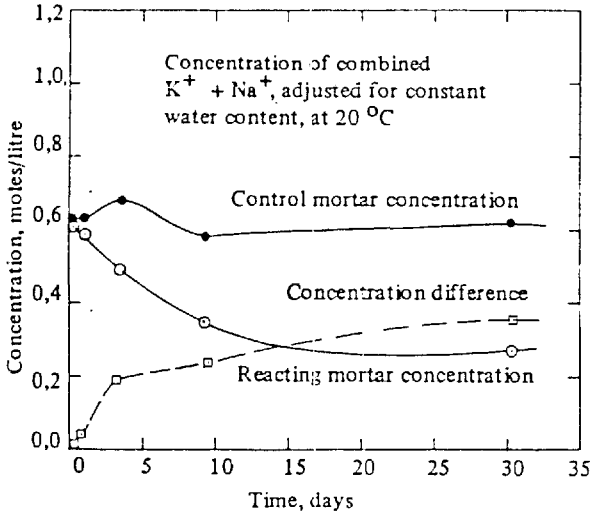

Fig. 4 - Comparison of the combined alkali concentrations (adjusted for bound water) of reacting and of control mortars as functions of time at 20°C. (ref. 9)

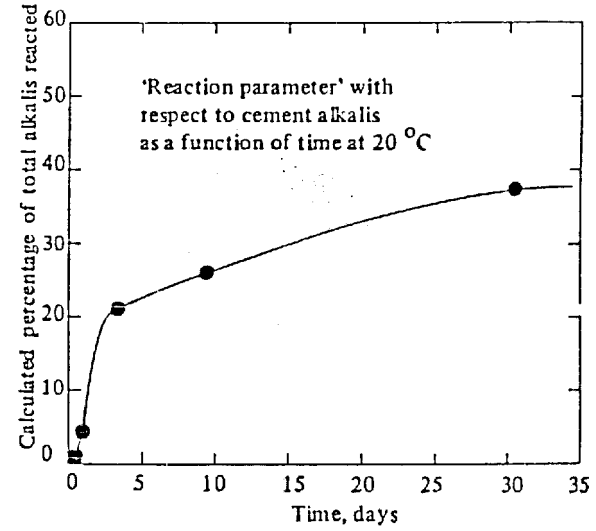

Fig. 5 - Calculated reaction parameter with respect to cement alkalis as a function of time at 20°C for a series of reacting mortars. (ref. 9)

Generally, after a day or two,the pore fluid is converted into a concentrated solution of alkaline hydroxides containing little more than a trace of calcium (0.001 N).

In the long term, the alkali content of the pore fluid usually reaches 70-80% of the alkalis contained in the cement in the long term. It is suggested (10) that in the absence of severe drying out or other special circumstances,the concentrations of alkalis in the pore fluid of the concrete can be expected to vary from 0.35 N for a concrete made with low-alkali cement and low cement factor,to a little more than 1 N for a rich concrete made with a high-alkali cement and low water content.

Table 1

Analyses of Pore Solutions Expressed from High-Alkali Cement Mortars

Age (Days)	Concentration (equivalents/liter) Ca^{+2}	Na^+	K^+	OH^-
15	0.001	0.22	0.55	0.73
49	0.002	0.22	0.59	0.77
70	0.000	0.24	0.57	0.75
149	0.002	0.23	0.60	0.80
585	0.000	0.24	0.58	0.78

Ref.(10).

Factors affecting the final alkali concentration in pastes or mortars,which are kept sealed (so that no extra water is available during the course of hydration), include: the alkali content of the cement, the cement content, the rate with which the cement gives up the alkalis, the w/c ratio of the mix, and the hydration rate of the cement.

Consensus of opinion suggests that the alkali uptake in the cement hydration products has no significant influence if compared with the other factors listed above.

When siliceous reactive aggregate is present, alkaline hydroxide is removed from the pore fluid and the reduction is ascribed to the formation of solid reaction products. Figures 4 and 5 illustrate this point. The control mortar contains un-reactive quartz sand. In the reacting mortar, part of the quartz sand is replaced with Beltane opal. The cement used contains 1.31% Na_2O equivalent, the water/cement ratio is 0.5 and the aggregate/cement ratio is 2. The concentrations plotted in Figure 4 are adjusted to those they would have been,if the water consumed in the cement hydration process had been returned to the pore solution.

The curve of Figure 5 represents the alkalis taken from the pore fluid in the reacting mortar (values for the difference curve of Figure 4),and standardized at the reference level of 0.845 M which represents the combined concentration of alkalis in the

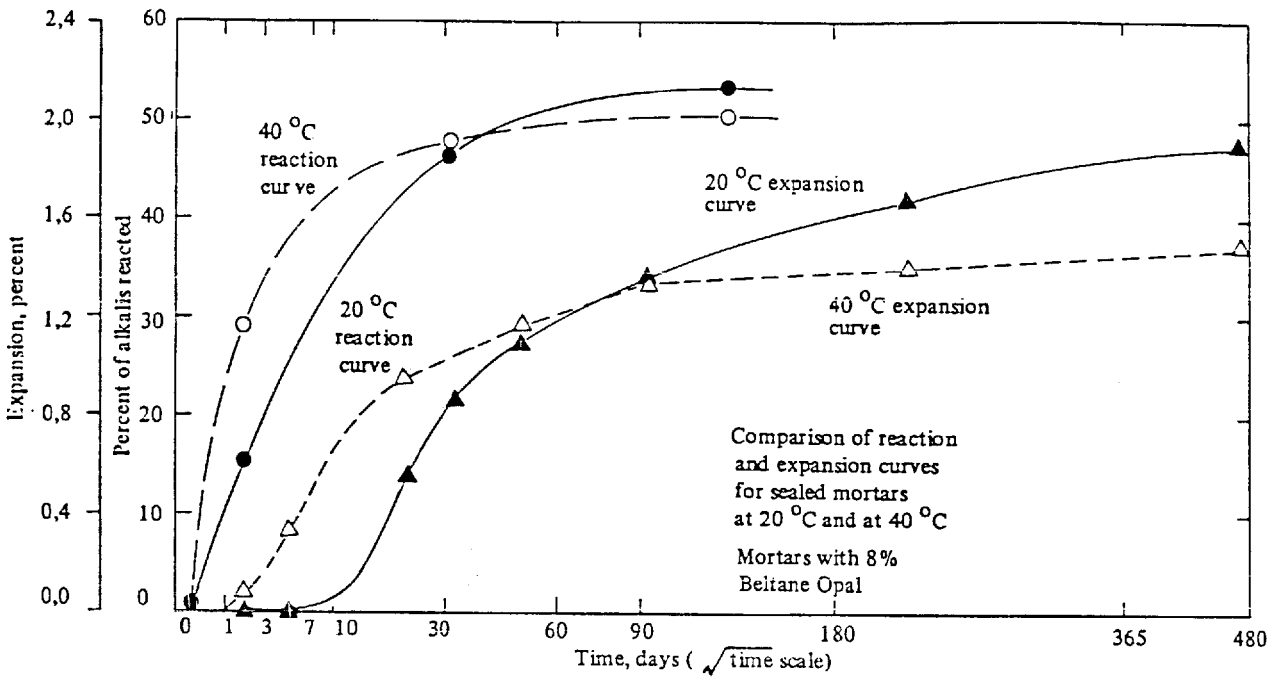

Fig. 6 - Comparison of reaction parameter curves vs, expansion curves for sealed mortar specimens at 20°C and at 40°C. (ref. 9)

paste water if the total load of alkalis in the cement completely dissolves. The curve in Figure 5 indicates that an almost stationary state seems to have been reached at about one month at a reaction parameter of not much more than 35% .However, in the control mortars (Fig. 4) after 1.5 days the alkalis in solution are about 70% of the reference concentration and this level is maintained indefinitely.

The effect of temperature on the reaction kinetics and on the development of the expansion is illustrated in Figure 6 (9). The mortar composition is identical that first mentioned, except that the cement used has a lower alkali content, 0.9% Na_2O equivalent.

In order to overcome the reproducibility problems arising from normal test methods, the expansion measurements are carried out according to a procedure developed by Barneyback (9). Short mortar cylinders are incorporated into thin, flexible butyl rubber sheaths so that neither extra water is gained, nor pore solution leached, during the course of the reaction.

The flexibility of the sheath ensures that there will be no appreciable resistance to the expansion.

The effect of an increased storage temperature for Beltane opal is that, while the initial rate of expansion of the mortar is increased, the total long-term expansion is less.

The temperature markedly accelerates the reaction speed and the results at 40 °C indicate that already within a week the reaction parameter has almost reached the maximum level.

Diamond et al. (9) consider that the results given in Fig. 6 are interesting for various reasons:

(i) The chemical attack and the physical process of expansion are separated into two distinct stages.
(ii) The expansion is produced in complete absence of water sorption from outside and therefore the fluid absorbed by the alkaline silicate gel can only be supplied by the pore solution.
(iii) Since the concentration of alkalis in the pore fluid remains at an almost stationary level during the test period, Diamond et al.(9) conclude that the flow of liquid in the gel consists of a mass transfer from the solution.

Hobbs (11) has discussed a model for predicting the time to cracking and the expansion of mortar prisms which contain Beltane opal and are stored underwater at 20 °C.

The model is based on the assumption that the alkali-silica reaction is a two-stage process. In the first stage, if a sufficient reserve of alkalis is available, the siliceous material rapidly reacts with the alkaline hydroxide. In the second stage,the first reaction product absorbs water molecules and OH^- ions

to form an alkaline silicate gel. The rate of the conversion to gel is proportional both to the concentration in volume, v, of the first reaction product remaining at time t, and to a simple power function of the alkali concentration in the pore water, A, at the time in which the first reaction is complete:

$$\frac{dv}{dt} = k_2 A^{k_3} v$$

A is given by:

$$A = (Na_2O)_{eq} \left[1 - \frac{0.02\, R\, a/c}{(Na_2O)_{eq}} \right] \Big/ w/c$$

where R is the content of Beltane opal in weight of the total aggregate and (Na_2O) eq. is the water-soluble alkali content of the cement. It has been observed that 0.02 is the ratio of the water-soluble alkali content to the Beltane opal content at which cracking due to alkali-silica reaction does not occur.

The expansion of the mortar after cracking is given by:

$$k_4 \{ V_R [\exp(-1.5\, k_2 A^{k_3}) - \exp(-k_2 A^{k_3} t)] - k_5 \}$$

The time at the first cracking is obtained from:

$$t_c = \frac{-\ln[\exp(-1.5 k_2 A^{k_3}) - 0.004/V_R]}{k_2 A^{k_3}}$$

where V_R is the concentration in volume of Beltane opal in the mortar. The constants k_2, k_3, k_5 are calculated by experimental data and found to be 1×10^6, 5 and 0.004 in order. The value of k_4 (0.715) is chosen so that the model correctly predicts the expansion at 200 days of the mortar bars tested. The predictions arising from this model are reasonably compatible with the observed expansive behaviour of the mortars. The model is not applicable to mortars containing a reactive constituent in the aggregate which is not easily accessible to OH^- ions.

I.1.2. Swelling Properties of Synthetic Alkali-Silica Gels. Recent studies by various Authors concerning chemical and physical aspects of the swelling phenomenon are described in this section. The preferred approach has been to undertake testing on ternary (Na_2O-SiO_2-H_2O) and quaternary (Na_2O-CaO-SiO_2-H_2O) synthetic gels prepared as model-systems of gels which form in concrete containing a reactive aggregate with alkali-silica reaction. Following this approach, Struble (12) prepared gels by converting silicic acid sols to sodium silica sols by the addition of controlled amounts of sodium hydroxide solutions, sometimes containing calcium hydroxide. The ternary and quaternary sols thus obtained are transformed into gels by vacuum evaporation over a dry ice trap.

The swelling properties of synthetic gels (9) (13) (14) have been examined in three different types of experiments:

(i) the gels were allowed to swell freely, without applying any confining force
(ii) the confining force was determined according to the requirements to prevent swelling
(iii) the water absorption was made to occur against a constant applied load less than the swelling pressure as measured at point (ii).

The swelling agent used in these experiments was water and the water-gel contact occurred via a porous frit, filter paper and semipermeable membrane.

No clear relation was found between Na_2O/SiO_2 molar ratio of the gel, extent of expansion at free swelling and swelling pressure. The gels with a large expansion at free swelling did not necessarily develop high swelling pressures.

The gels which showed high swelling (60-80%) vary in Na_2O/SiO_2 molar ratio from 0.27 to 0.53, the low-swelling gels (less than 4%) from 0.28 to 0.46%.

The swelling pressures measured fell into two distinct categories: gels which develop pressures from 2 to 10.9 MPa and gels with less than 0.5 MPa.

The 0.27 Na_2O/SiO_2 gel, yielding the greatest free expansion (82%), develops a swelling pressure less than 0.5 MPa.

Conversely, the 0.34 Na_2O/SiO_2 gel, which develops a swelling pressure of 10.9 MPa, the highest measurement in synthetic gels examined to date, shows only 1.7% of expansion at free swelling. Surprising behaviour is observed in swelling tests under a constant applied load. In general, it is to be expected that maximum expansion is reached in free swelling conditions. When the water uptake occurs under a load less than the swelling pressure, the expansion should be less than at free swelling. However, if the load applied is greater than the swelling pressure, the gel should shrink. Many gels demonstrate the condition described (Fig.7), others instead do not follow the expected pattern (Fig.8,9). Thus the gel in Fig.8 (Na_2O/SiO_2 = 0.34; swelling pressure 10.9 MPa) shrinks initially and then abruptly liquefies if the water absorption occurs under an applied load of 2.2 MPa. However, it swells more than it does without a load if the water absorption occurs under an applied load of 9.9 MPa. The gel in Fig.9 has a Na_2O/SiO_2 molar ratio of 0.42, a swelling pressure of a little over 3 MPa and a free swelling of 63%. In the tests under load the gel initially expands more

than without the load and then suddenly liquefies.

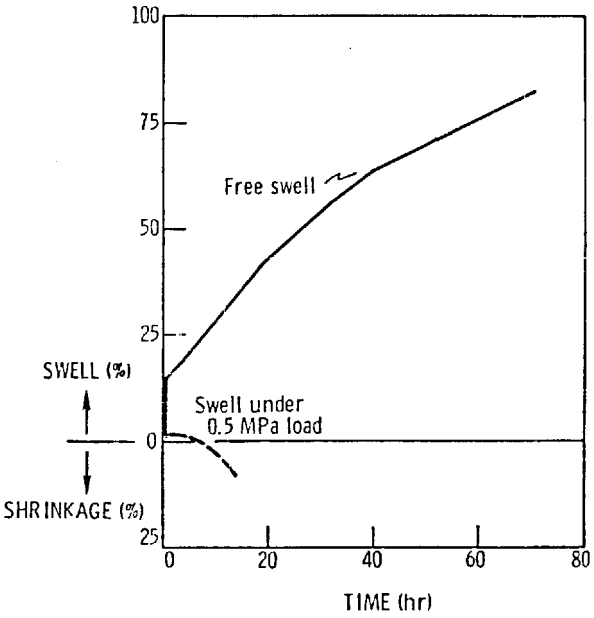

Fig. 7 - Measured swell under zero load (free swell) and under 0.5 MPa load for a gel of molar composition Na_2O 0.27, SiO_2 1.00, H_2O 1.93, whose measured swell pressure was 0.42 MPa. (ref. 14)

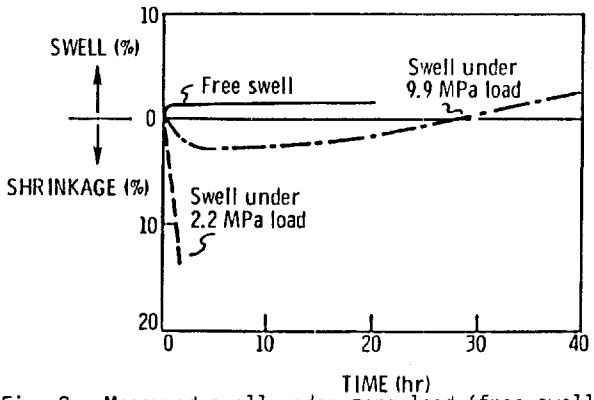

Fig. 8 - Measured swell under zero load (free swell) and swell under 2.2 MPa and 9.9 MPa loads for a gel of molar composition Na_2O 0.34, SiO_2 1.00, H_2O 2.24, whose measured swell pressure was 10.9 MPa (ref. 14)

The great variability in behaviour observed in the three types of experiments is attributed by Authors (14) to variations in the molecular structures of the gels. It is hypothesized, on the basis of the results given by Dent-Glasser et al. (15) that the synthetic gels studied consist on highly polymerized species, of polymeric groups with low molecular weight and of monomerical units. It is considered that the system has not yet reached structural balance and therefore

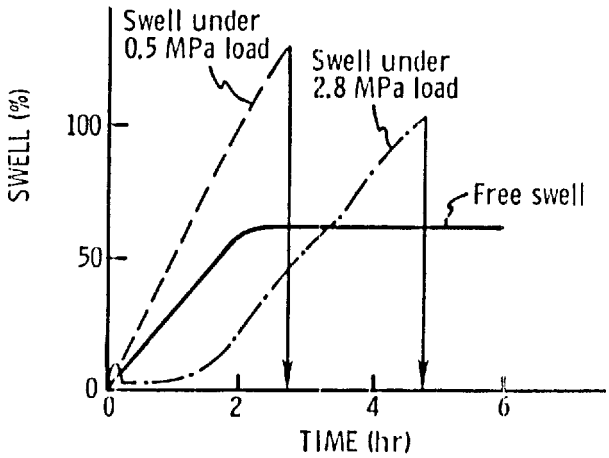

Fig. 9 - Measured swell under zero load (free swell) and swell under 0.5 MPa and 2.8 MPa loads for a gel of molar composition Na_2O 0.42, SiO_2 1.00, H_2O 1.57, whose measured swell pressure was 3.1 MPa (ref. 14)

when the water absorption is made to occur under a constant applied load, the complex molecular structure of the gel can undergo variations which produce unexpected behaviour (14).

The structural instability of gels seems confirmed by the ageing effect. In a single test (14) it was found that, after 4 months, the free expansion drops from 63 to only 2% and the swelling pressure from 3.1 MPa to 0.08 MPa.

The presence of calcium in the gel does not seem to have a significant effect either on the free swelling or on its capacity to develop pressure (9). The two gels tested containing calcium can be classified as moderately active. One (0.27 Na_2O - 0.17 CaO - 1 SiO_2 - 1.16 H_2O) yields an expansion of 3.1% and develops a pressure of 0.51 MPa, the other (0.35 Na_2O - 0.18 CaO - 1 SiO_2 - 1.57 H_2O) an expansion of 8% and a pressure of 0.3 MPa.
These values, when compared with those relevant to purely sodium-silica gels of similar Na_2O/SiO_2 ratio indicate no special effect of the calcium.
However, in one respect the two quaternary gels differ from the ternary gels. The first preserve the condition of granular solid after exposure to the various types of test procedure, while the others generally become fluid.

Further knowledge of the relationship between free swelling and chemical composition of the Na_2O-SiO_2-H_2O synthetic gels was acquired from a different type of experiment (2) (6). Silica gel was left in contact, i.e. without stirring, with a sodium hydroxide solution until it reached a state of equilibrium or near equilibrium. The reaction rate was con-

trolled by diffusion of the solution through the mass of silica gel and thus the reaction conditions appeared similar to those in concrete.

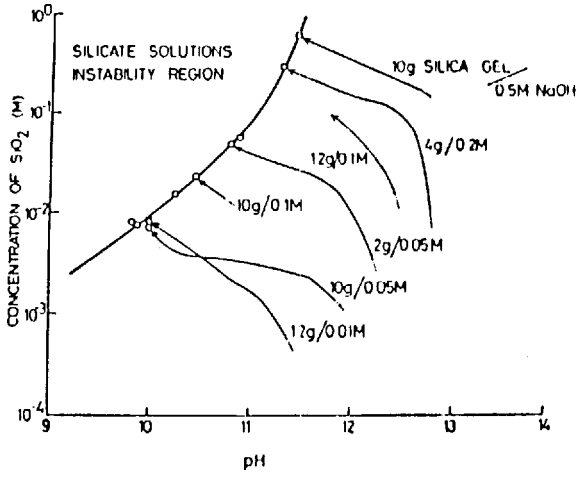

Fig. 10 - The final concentration of dissolved silica against pH (heavy line) and the paths by which individual solutions approach it (light lines). (ref. 6)

The curve in Fig. 10 represents the separation between stable and unstable regions of the alkaline silicate solutions. When the silica gel comes into contact with an alkaline hydroxide solution, the pH of the solution drops and the silica concentration in solution, $[SiO_2]$, rises. In Fig.10 it can be seen that when a dissolution path reaches the curve, the dissolution ceases. If insufficient silica gel is taken, the solubility curve is never reached, while if the gel exceeds the quantity of sodium hydroxide in solution, the pH of the liquid rapidly falls and the dissolution path reaches the solubility curve at lower pH and hence at a lower final $[SiO_2]$. Thus the maximum value of SiO_2 is attained at an intermediate total SiO_2/Na_2O molar ratio around 3-4 (Fig.11), depending on NaOH concentration.

The dotted line refers to dissolution tests with stirring. It is worth noting that the free swelling and the imbibition pressure both vary in the same way in function of the SiO_2/Na_2O molar ratio of the initial mixture (Fig.12).

The swelling is measured after 30 minutes of contact between gel and solution while the osmotic pressure is calculated by the final concentration of the species in solution. It is but a short step from osmotic pressure to imbibition pressure. Since the final state of the gel-solution system of alkaline hydroxide is a siliceous alkaline solution, formally speaking the swelling of the gel can be called osmotic, and therefore Dent Glasser and Kataoka (2) assume that the imbibition pressure of the gel can be considered equal to the osmotic pressure of the surrounding solution. Following this view, the osmotic pressure values in Fig. 12 represent the

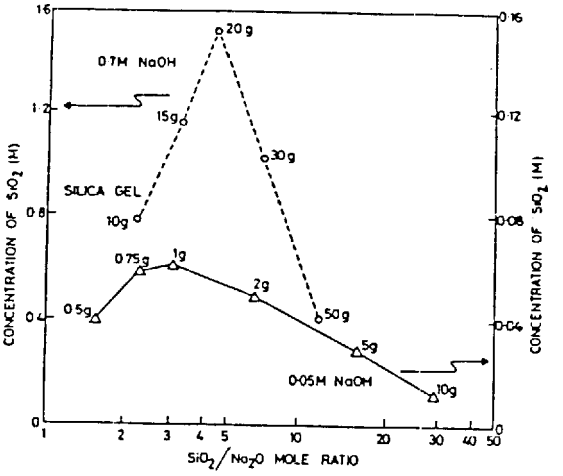

Fig. 11 - The relationship of the final concentration of dissolved silica with total SiO_2/Na_2O mole ratio.
solid line: dissolution in 0.05 M NaOH solution without stirring.
dashed line: dissolution in 0.7 M NaOH solution with stirring.
(ref. 6)

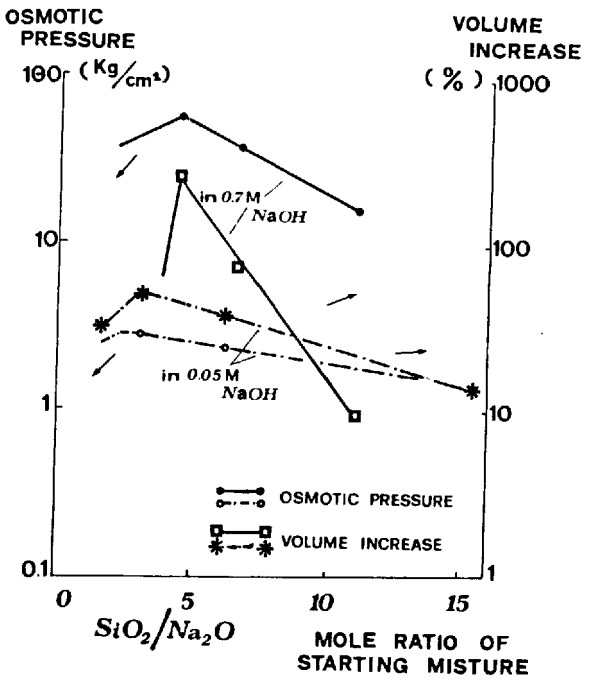

Fig. 12 - Free swell of solids and osmotic pressure of solutions plotted against SiO_2/Na_2O ratios of the starting mixtures. (ref. 2)

imbibition pressures of the remaining gel when the system has reached the state of equilibrium or near equilibrium.

The imbibition pressures rise rapidly as the sodium hydroxide content of the solution increases and the maximum value calculated is 55 kg/cm^2. There are no estimates of imbibition pressure available for SiO_2/Na_2O molar ratios lower than 3, because the fluidity and the solubility rise rapidly below this value. The crosses on the curves of the osmotic pressure correspond to solutions in which no solid remained.
The presence of peaks within narrow interval of SiO_2/Na_2O molar ratios between 3 and 5 appears compatible with the existence of a "pessimum" concentration of reactive aggregate (6).

I.2. Microstructural Aspects of Alkali-Aggregate Reaction.

Useful information on the microstructural aspects of the alkali-aggregate reaction has been obtained by means of scanning electron microscopy (SEM) supplemented by local chemical information derived from EDXA and EPMA.
SEM based methods have been applied on mortar containing opal or industrial glass, on specimens of opal and on concrete containing polyphase siliceous aggregates,sampled from deteriorated structures.
The intrusion of alkalis and calcium in opal has been studied in mortars containing opaline sand and on opal cylinders 1 cm in diameter surrounded by a mixed bed of quartz sand and solid $Ca(OH)_2$. The mixed bed was soaked with a 1 N KOH solution to fill the pores. In mortars cured at room temperature for 33 days, Diamond et al. (9) have found that the opal granules were deeply penetrated by K^+ ions (sodium was not detected by the instrument used). Calcium also penetrates the grains, but it is concentrated in the peripheral layer.The Ca/Si ratio rapidly decreases, falling from 0.14 at the edge to 0.006 about 45 μm inside . Instead, the K/Si ratio inside the grain is practically constant and equal to 0.021.

Penetration in opal cylinders (9) occurs with the same features. The K^+ ions penetrate deeper and in a considerably greater proportion than the Ca^{+2} ions (Fig.13). However, the calcium intrusion is meaningful because its concentration in the solution which soaks the mixed-bed is only 0.001 N. In addition, the surface of the cylinder is not in contact either with CSH or with crystallizations of $Ca(OH)_2$ as happens with opal granules in mortar.

Kawamura et al. (16) have measured variations in microhardness within a reacting grain (5-2.5 mm).The microhardness measurements were made at about 20 μm spaces.The local chemical composition was detected inside the microhardness measurement/spots and elsewhere by EDAX.

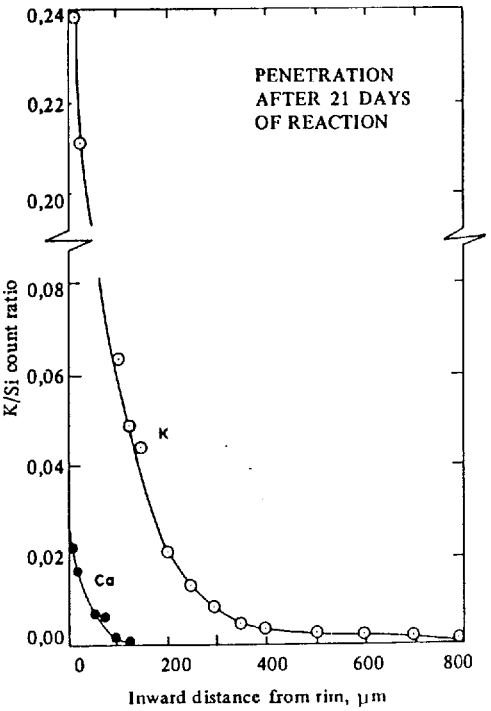

Fig. 13 - EDXA analysis of penetration of K and Ca into cylindrical opal specimen surrounded by 1M KOH and Solid $Ca(OH)_2$ particles. (ref. 9)

The mortar bar (25x25x250 mm), prepared using ordinary Portland cement(0.78% equiv. Na_2O) and Akase opaline rock (Ishikawa Prefecture), was stored at 38 °C and 100% RH. In some mortars, 1% of NaOH by weight of cement was added. Initially, a rapid increase is observed in the alkali concentration within the peripheral layer of the grain and a decrease in microhardness.The soft region increases in thickness as the attack proceeds and the hardness decreases as increasing amounts of water penetrate.The alkali intrusion is followed by that of Ca^{+2} In an opal grain the hardness at the edge, after 28 days, is greater than at 50 μm inside.The Authors suggest that the recovery of hardness could be related to the increased concentration of Ca^{+2} ions at the edge of the grain.The opinion has also been expressed (9)(16) that the penetration of Ca^{+2} ions occurs because of a surface diffusion process, according to Powers and Steinour's hypothesis (17).

In the absence of additional NaOH, the thickness of the soft region decreases at all ages.

A considerable number of pat tests have been carried out in the examination of UK aggregates from various sources.Poole et al. (18) have examined with SEM and

EPMA the gels produced by pats stored in a lime saturated mixture of NaOH and KOH, at 20 °C, 30 °C, 40 °C and 50 °G for periods up to 56 days.
The Na_2O/K_2O ratio of the gels and their morphology vary with temperature. The potassium proportion increases as the temperature rises but the total quantity of alkalis is extremely variable and cannot be related to the reaction temperature.

The morphological variation from nodule to crumpled foil gel as the formation temperature rises is explained by assuming that the gel/solution interface behaves like an elastic osmotic membrane. At higher temperatures, . under the thrust of the rapidly formed reaction product, the membrane frequently splits allowing the gel to spill out as a sheet or foil around which a new membrane is formed. The final result of repeated disruptions in the osmotic membrane is a mass of plates and foils.

There is convincing evidence (19)(20)(21)(22) that, besides more or less instable silica combinations, certain kinds of siliceous polycrystallized rocks are also likely to prove reactive with alkalis and may lead to disruptive expansion.Regourd et al. (19) have examined two South African concretes with rock aggregates of similar mineralogical nature.

Concrete A, prepared in the NBRI (Pretoria) Laboratories, was kept at 40 °C and 100% RH for one year. Concrete B was sampled by core drilling from a 20-year-old deteriorated structure.The mineral content of the aggregates in the two concretes is mainly quartz, feldspars and phyllosilicates (biotite mica, chlorites and/or vermiculite).

In both concretes, around the greater part of the aggregates fractured along a cleavage plane, there are rims of dark gel and an inner white zone of crystalline material. In the larger pores of the cement paste there is gel with a molar ratio of CaO/SiO_2 1.3-1.4. Ettringite has been found surrounding the aggregates, and $Ca(OH)_2$ found in contact with them, both in large crystals. Thaumasite is also present in concrete A.

The crystalline material inside the aggregates is characterized by 10 X-ray diffraction peaks with the two strongest at 12.3 and 8.6 Å.

According to the Authors the reactive phases contained in the aggregates are finely crystallized quartz (whose state of strain probably brings together the more reactive forms of silica as amorphous silica, opal),the phyllitic minerals (i.e. chlorite, vermiculite) and the feldspar and mica alteration products.

The alkali-aggregate reaction, studied by Cole et al. (21)(23)(24) in concrete specimens from a dam built 30 years ago in Australia, shows analogous features.

The coarse aggregate is made up of 64% sandstone and 36% siltstone. The two rocks contain different proportions of quartz, chlorite and mica combined with lesser quantities of feldspar and organic matter. The quartz grains are embedded in a matrix of fine clay and mica minerals.Also in this case there are pronounced reaction rims around the majority of the aggregates, inside which there is a white, crystalline material. Pores and cavities in the cement matrix are lined with hardened transparent gel and subsequently filled with a white opaque deposit. Occasionally some pores contain a white, soft material similar to that found in the aggregate. A fine mesh of interlocking needles of trona ($NaHCO_3 . Na_2CO_3 . 2H_2O$), $Ca(OH)_2$ and calcite has been observed in a void together with the gel.

The crystalline material which is formed inside the reaction rims of the aggregate and the loose deposit of some pores have similar X-ray patterns. When the concrete is very wet, a common feature of all patterns is the strong spacing (I = 100) at 12.2 Å. By heating the crystalline material to 110 °C for 2 hours and storing it in air for 12 days, a new pattern appears, characterized by spacings at 10.6 and 8.85 Å (21). The same transformation is observed when the material is dried naturally for some years (24). The 10.6 and 8.85 Å phase is identified (23) (24) as hardly crystallized okenite, $CaO. 2SiO_2. 2H_2O$ in which some Ca is replaced by K and Na. The 12.2 Å phase is assigned the role of hydrated precursor ($4H_2O$) of okenite (24).

The 12.2 Å phase is only stable in a wet environment. When it is dried and its water content falls below 2 moles,okenite is formed and the transformation cannot be reversed by wetting the sample. The precursor of okenite was initially described (21) as a "material like zeolite A". Subsequently, a re-examination of the data led to the conviction (24) that there is no convincing evidence as to why the precursor can be identified with any of the known compounds.

The products of alkali-aggregate reaction from a certain number of concrete dams in the US, one 50 years old, have also been found to contain crystalline material (25) (26). The patterns in the X-rays are characterized by spacings which are close to those listed by Cole et al. (21) (24). It is probable that the differences observed are to be attributed to different hydration states.

There are also indications that the crystalline material is the product of the gel transformation.Apart from the similar chemical composition, it has been observed (19) that there is a zone with a semi-crystalline intermediate texture between the white material inside the aggregate and the dark rims. Moreover, it has also been found (21) that samples of gels contained in the pores of the cement matrix, amorphous in X-rays (at the most they show a calcite

pattern), when re-examined one year later in the laboratory, show an analcite pattern.

A crystalline calcium-potassium-silicate has been identified by Oberholster (22) in concretes containing orthoquartzite from badly-cracked structures in the Eastern Cape (South Africa) and in a concrete containing greywacke and hornfels from the Lansdowne bridge in the South-Western Cape. The age of the structures ranges from 10 to 25 years. The mean C/S and K/S ratios, calculated by EPMA data, agree with the values of Regourd et al. (19) but less so with the values of Cole et al. (21)(24). The X-ray diffraction patterns of the crystalline reaction products in concrete from six structures have close similarities to those featured by Cole et al. (21)(24) for concrete from a dam in Australia. Some of the variations observed between X-ray patterns of the 6 samples examined are probably due to different states of hydration. Thus, the main line of diffraction at 12.2 Å, found only for the reaction product in the concrete containing greywacke and hornfels, shifts to about 11.1 Å if the recording was done with Guinier camera with vacuum applied. In the other patterns, there is a medium intensity line between 10.99 to 10.74 Å instead of the 12.2 Å line. This confirms the findings of Cole et al. (21) (24) and could indicate that the crystalline product has lost water due to exposure at a moderately high temperature.

A last example (27) concerns concrete from a structure built 5 years ago in a hot and humid country. The aggregates used in the concrete contained reactive rocks made up of granodiorites and quartzites. The granodiorites included strained quartz (undulatory extinction angle from 31° to 39°) together with plagioclases and feldspars, both altered. In the quartzites, amorphous silica (opal) and microcrystalline silica (calcedony) embedded quartz grains. The reaction products are a gel at the cement matrix - quartzite aggregate interface and a lamellar crystalline material richer in potassium and poorer in calcium with respect to gel. This latter is deposited in the cracks of the aggregates or between the cleavage planes. Massive deposits of ettringite are found close to aggregates or in pores and cavities of the cement matrix.

Two crystalline products of a 0.25 Na_2O . 0.8 - 1.0 CaO . SiO_2 . x H_2O (main X-ray diffraction peaks at 12.6 and 3.06 Å) and 0.33 Na_2O . 0.67 CaO . SiO_2. x H_2O (main line 16 Å) have been identified by van Aardt and Visser (28) in reaction systems at 80 °C and in 1 N NaOH solution or greater concentration. In a subsequent report (29) the same Authors state that the 12.6 Å compound, although poorly crystalline, is also formed when Portland cement and 2N NaOH solution react at 22 °C for two months. Diamond (10) consider this last result interesting because it implies that the expanding alkali-calcium silica gel, produced in the alkali-silica reaction at ambient temperatures, can be regarded as a disordered form of a crystalline compound, in agreement with that found in references (19),(21),(22),(25) and (26).

To date, the EDXA and EPMA results indicate that calcium is an ordinary component of expansive gel.

There are differing opinions about the mechanism by which the calcium is transferred from the cement paste to an alkali-silica reaction product.

Regourd et al. (19) suggest that the sol alkali-silica moves outside the reaction site and attacks the phases rich in calcium, $Ca(OH)_2$ and CSH, freeing Ca^{+2} ions which penetrate the reaction rim by diffusion. Once the $Ca(OH)_2$ in contact with the reacting aggregate has been worn away, the sol spreads into the cement matrix where it mainly interacts with CSH.

The arguments supporting the hypothesized mechanism are: a) the decrease, and sometimes the disappearance, of $Ca(OH)_2$ crystallizations on the aggregate; b) a partial gelification of the cement paste particularly evident in the layer close to the aggregate, and c) the mobility of the sol which is demonstrated by the existence, in some of the pores of the cement matrix, of a calcium-alkali-silica gel richer in calcium (C/S = 1.3-1.4) than the gel in pores far from the alkali-aggregate reaction site. The gelification of the cement paste is indicative of CSH releasing calcium.

Diamond (10) agrees on the mobility of the sol and on the penetration of the calcium in the reaction rim by diffusion and hypothesizes that the release of Ca^{+2} ions is to be attributed to a decrease of pH in the liquid phase of the pores below 12.45. His hypothesis is based on the fact that the pH of stability of the alkali-silica sol is less than the pH of the saturated $Ca(OH)_2$ solution. Consequently, where the sol is present, there will be a release of calcium from the phases containing it. The experiments with opal cylinders seem to support this hypothesis.

I.3. Corrective Measures.

Where it is not possible to avoid the use of an aggregate containing reactive constituents, a remedy for preventing or minimizing the risk of alkali-aggregate reaction can be found in the most appropriate of the following options:

- low-alkali cement
- total quantity of alkalis in the concrete mix below a specified limit
- replacement of part of the Portland cement with finely ground pozzolanic materials.

I.3.1. Low-Alkali Cement. American work has indicated

that deleterious expansion from alkali-aggregate reaction is not likely to occur provided the alkali content of Portland cement is not greater than the equivalent of 0.6% Na_2O.

Since the publication of Stanton's paper (30), a few sporadic cases have been pointed out in which Portland cements with a quantity of alkalis even lower than 0.6% Na_2O have given rise to harmful expansion. The reasons for failure were the pessimum effect and the release of soluble alkalis from the aggregate. Other possible causes are considered to be the introduction of alkaline salts by external sources or the concentration of alkalis by the migration of humidity through the concrete.

Stark (31)(32) has documented a case where the use of low-alkali cement was not shown to be effective in preventing the field concrete from cracking. The aggregates involved contained from 1 to 10% in weight of volcanic reactive material, consisting of glass of andesitic to rhyolitic composition. Cracking was observed 5 to 8 years after construction. In a few cases, the first cracks were noticed after 2 years.

The deterioration was ascribed to soluble alkalis contributed by the aggregate. The results of laboratory investigations in accordance with ASTM C227 showed that the mortars made with low-alkali cement give deleterious expansion similar to field concrete.

The rate of expansion of the mortar prisms is low and it is therefore necessary to extend the testing time up to 12 months. Typical results are shown in Fig.14, where the cement-alkali level is plotted against an 0.05% expansion time. This expansion level was chosen because it is the approximate limit above which microcracking was found to extend from reactive particles into surrounding mortar.

The plot in Fig.14 indicates that a single level of alkalis, such as 0.6%, cannot be considered meaningful for all aggregates even under the same storage conditions. Stark (32) recommends simultaneous tests with a range of both high and low alkali cement to be carried out when the reactive aggregate is suspected to cause the release of alkalis.

Way and Cole (33) have investigated the relative reactivities of nineteen Australian rocks, all containing varying quantities of feldspars, in $Ca(OH)_2$ solution. The digestion procedures were the same as those used by Van Aardt and Visser (34). The only difference concerns the test temperature: the reaction was carried out at 50 °C instead of 95 °C.
In the digestion of the powdered rocks (- 75 μm), basalt and granite release large quantities of alkalis as a result of the breakdown of feldspars in the rock. The siltstones are the least reactive of the rock types and the sandstones are markedly less reactive than granites and basalts.

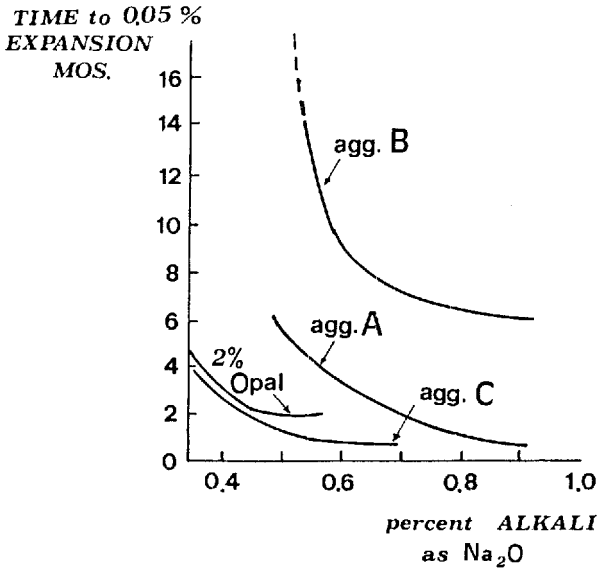

Fig. 14 - Plot of ASTM C227 test results showing time to 0.05% expansion. (ref. 32)

The quantity of alkalis released in the digestion of small pieces of rock are insignificant if compared with the quantities liberated from the powdered rocks.
No relationship was found between the quantities of alkalis released in test conditions and the performance of the various types of rocks as concrete aggregates. Basalts and granites have good service records in Australian experience, while the deleteriously reactive sedimentary rock samples, included in the list of rocks studied, did not distinguish themselves for the quantity of alkalis released.

Malek and Roy (35) suggest that the presence of feldspars in a rock contributes, through giving up alumina, to making the reaction of the rock with the alkalis innocuous. These Authors have examined the effect of the type of aggregate on the alkali-aggregate reaction. Beltane opal and a partially vitreous feldspar rock (basalt) were used. The basalt resulted deleteriously reactive in the chemical test (ASTM C289) and innocuous in the mortar bar test modified in agreement with Brotschi and Mehta (36).
In dissolution experiments with 1 N NaOH solution at 43 °C, it was found that the basalt released, beside silica, a significant quantity of alumina. The expansion tests show that the reaction with the alkalis shifts from deleterious to innocuous when the total molar ratio Al_2O_3/SiO_2 of the used mixes, including both cement and aggregate, is increased.
The result of the expansion tests is ascribed to the formation of calcium hydrated aluminates in which 7 OH^- per one Al atom can be incorporated.
Malek and Roy hypothesize that this consumption of OH^- ions could reduce the attack on the Si-O-Si bridges of the Beltane opal and promote the formation

of siliceous gel with a high Ca/alkali ratio.

Grattan-Bellew and Beaudoin (37) have studied the effect of the addition of phlogopite mica flakes on the expansion of concrete prisms made with reactive aggregate and high and low-alkali cements. Flakes of phlogopite mica of a high aspect ratio are used to improve the tensile strength and fracture toughness of Portland cement pastes. In the phlogopite mica, one of the four silicon atoms in the tetrahedral sheet is substituted by one aluminium atom and the defect of one positive charge is compensated by one potassium ion which is located on the layer surface. It is known that some potassium can be exchanged for other cations. The addition of 1.3% by volume of mica to concrete made with a carbonate reactive aggregate (dolomitic limestone from Kingston, Ontario) causes a small growth in the rate of expansion. The results indicate that the effect is less with high alkali-cement, probably because the percentage increase of total soluble alkalis would be smaller. The Authors finally emphasized the need for caution only in the case of concrete in which the alkali-aggregate reaction is suspected and a larger volume of flakes is added.

I.3.2. Alkali Content of Concrete Mix. Field and laboratory studies over the past years have shown that an alternative method for reducing the risk of expansion is to restrict the quantity of reactive alkalis available in the concrete mix by limiting the cement content. The method is based on the fact that the alkalinity of the pore fluid in the concrete is controlled both by the level of alkalis in the cement and by the cement contained in the mix.

The expansion potential is a function of the reactivity of the aggregate and of the total quantity of reactive alkalis available per m^3 of concrete. Consequently, the safe level for the content of reactive alkalis available in the concrete, applicable with a given source of reactive aggregate, must be determined by experiment.

When alkali sources other than cement are absent, the reactive alkalis available in a Portland cement concrete are normally calculated by (38):

$$A = (C \times a)/100$$

where: A = alkali content of concrete (kg/m^3),
C = cement content of concrete (kg/m^3),
a = acid-soluble alkali content of Portland cement expressed as a percentage in weight of Na_2O equiv.

In practice, any calculation relating to the reactive alkali content of the concrete should consider the variation of both the cement content in concrete and the alkali content in cement (38).
Proper consideration has also to be made for alkalis introduced into the mix by sources other than cement. Alkalis can arise from the aggregate, additives and seawater if used as mixing water. The aggregates can contribute either because of alkali salts contamination or because of soluble alkalis release, but the latter event is not very frequent.

Alkalis can be absorbed by hardened concrete exposed to brackish water, seawater or de-icing salts. It is suggested that alkali sulphate and chloride solutions introduced from outside may cause an enhanced hydroxyl ion concentration, provided free $Ca(OH)_2$ is available in the cement paste (39),(40),(41) At present, there is not enough information to estimate the effects of these exposure conditions and to translate them into specifications (42). In these cases, the use of a blended cement obtained with pozzolana of proved effectiveness should be the only option.

In Great Britain, experiences with aggregates containing opaline silica have indicated a safe level of 3 kg/m^3 (38),(43).
For reactive aggregates in New Zealand, the lower limit proposed is 3.5 kg/m^3 (44). Oberholster (22), in the case of concretes made with different Malmesbury aggregates (south-western Cape), has reported the following limits (Fig.15):

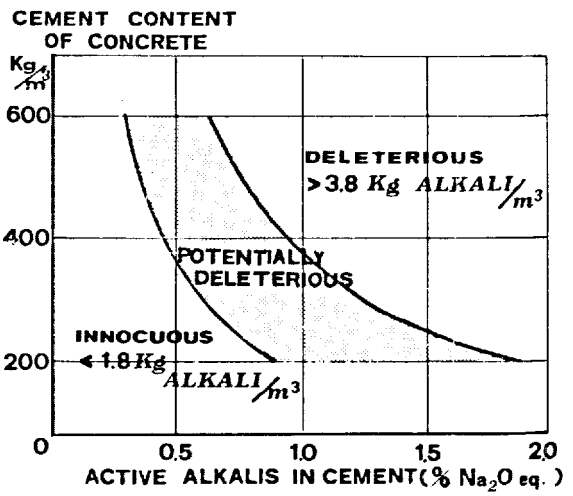

Fig. 15 - Relationship between the active alkali content of cement, the cement content of concrete and the resultant potential of the concrete for alkali-aggregate reaction. (ref. 22)

(i) above an active alkali content of 3.8 kg Na_2O equiv. per m^3, deleterious expansion will occur;

(ii) below 1.8 kg Na_2O equiv. per m^3, the expansion damage is avoided;

(iii) between 3.8 and 1.8 kg Na_2O equiv. per m^3, the

degree of expansion depends on the reactivity of the aggregate and the active alkali content of the concrete;

With the orthoquartzites of the Table Mountain Group, the lower and upper limits are respectively 2.5 and 4.5 kg active Na_2O equiv. per m^3 of concrete (22).

The figures given by Oberholster are referred to concrete containing 350 kg/m^3 of cement and stored under ASTM C227 conditions. The aggregate is considered deleteriously expansive if the concrete expands more than 0.05% at one year of age.

I.3.3. Replacement with Pozzolanic Materials . Experiences in the US and elsewhere have shown that a great variety of natural and artificial pozzolanas are effective in reducing to an acceptable level expansion due to alkali-aggregate reaction. The list includes various natural materials, most of which are of volcanic origin, and artificial materials such as calcined shale, burnt clays, fly ashes (also pulverized fuel ash = pfa), ground granulated blastfurnace slags (ggbfs) and microsilica (also known as condensed silica fume). At present, fly ashes and granulated slags (ggbfs) are of greater interest because they are widely available.

The quantity of pozzolana to be used as a corrective depends on the reactivity of the aggregate and on the quality and composition of the pozzolana itself. Consequently, many investigations have been made to ascertain the optimal minimum addition of pozzolana to highly reactive aggregates such as opal and Pyrex glass.

With few exceptions, pozzolanas contain alkali levels comparable to, or above, those of Portland cement. Most of these alkalis are combined in the glassy structure of the pozzolana and only a very small part is soluble in water. The water-soluble alkali content of flyash is usually less than 0.1 % as Na_2O equiv.

In past and recent literature much data is given to demonstrate that the alkalis combined in vitreous structures are involved in the hydration reaction of the pozzolana.

Buttler et al. (45) have found in pastes of pfa and $Ca(OH)_2$ that there is a close relationship between the rate of dissolution of the pfa and the release of alkali metal ions to the solution.

However, the quantity of alkalis which participate in the pozzolanic reaction remains unknown. Furthermore, it is not known how the alkalis released distribute themselves between the hydrated solid phases and the pore fluid, or whether the alkalis liberated by the pozzolanic reaction are to be associated with an equivalent quantity of OH^- ions.

Boswell et al. (46) are of the opinion that the extra alkalis liberated by the acid-base or pozzolanic reaction of the pfa do not have to be directly related to an equivalent concentration of OH^- ions. This opinion is based on the observation that the mortar prisms made using pfa as a blending agent, and which show a marked reduction in expansion compared to control prisms, can contain alkalis far in excess of that calculated by the clinker content within the blended cement.

However,the prevalent opinion is that the alkalis from pozzolana can be ignored because the material reacts slowly and the alkalis released are not rapidly available to promote the alkali-aggregate reaction, like those deriving from Portland cement.

At the most it is suggested (38) that the water-soluble alkali content of the pozzolana be included in any calculation relating to the reactive alkali content of the concrete. This is because the water-soluble alkalis are rapidly available and contribute to the alkalinity of the pore solution in the early stages of the cement hydration process.

Hobbs (43) proposes a procedure for calculating the reactive alkali content of concrete in which partial account is made of the alkalis in pfa. This Author has considered the effect of pfas in preventing the expansion due to the alkali-aggregate reaction and has pointed out that his observations support the view that pfa acts like a cement with an alkali content of 0.2% by weight.

Limits are also placed on the alkali content of slags for use in low alkali slag cements. In accordance with German Standard DIN 1164, when the blended cement contains at least 50% of slag, the acid-soluble alkali content of the blend must be less than 1.1 percent equivalent Na_2O. When the blended cement contains at least 65% of slag, the DIN limit is 2 percent equivalent Na_2O.
A limit is also suggested in reference (38) where it is reported in section 4.5.2 that : "A combination of ggbfs and any UK Portland cement which contains 50% or more ggbfs may be considered equivalent to a Portland cement with 0.6% maximum alkali content, provided that the acid soluble alkali contents of both Portland cement and the ggbfs are less than 1.1%".

I.3.3.1. Mechanisms of Preventive Action . The following mechanisms have been suggested to explain the preventive action exerted by different types of pozzolanic materials in the alkali-aggregate reaction:

1) Alkali sorption from the pore solution;
2) Low ionic diffusivity and reduced permeability in

the blended cement pastes;
3) Uniform distribution of the $Ca(OH)_2$ released by hydrolysis.

The work that has been described in literature dealing with the preventive action of pozzolana gives reasonable evidence for assuming that all the mechanisms listed are in operation, but their relative importance can vary according to the specific pozzolana under consideration.

Alkali Sorption - The preventive mechanism based on alkali sorption necessarily requires a minimum concentration of alkaline hydroxides in the concrete pore solution in order to initiate and sustain the alkali-aggregate reaction. The pozzolana added in partial replacement of the cement must be able to remove alkalis from the pore solution, so that their concentration falls below the threshold value.

The consensus of opinion suggests that the pozzolana is helped to react with the alkalis more quickly than the reactive aggregate by its greater fineness and it is agreed that no deleterious expansion is associated with the alkali-pozzolana reaction.

It is reasonable to expect the threshold concentration to vary with the particular system considered, but, according to Diamond (10), it is unlikely to be lower than 0.25 N, a concentration for which a pH of 13.4 is calculated.

Support for the sorption mechanism results from an increased knowledge of the pore fluid chemistry.

Diamond (10), Page and Vennesland (47) have found that the use of microsilica as a partial replacement for Portland cement causes remarkable changes in the composition of the pore fluid. The results in Table 2 indicate that substitution of increasing proportions of the cement by microsilica brings about a regular reduction in the OH^- ion concentration of the solution. The reduction in the OH^- ion concentration is accompanied by a corresponding reduction in the total available alkaline ion percentage which remains in solution. The results in Table 2 also indicate that the microsilica possesses a remarkable ability to remove potassium ions.

Figure 16 shows the influence of the microsilica content on the pH of the pore solution. In the case of pastes made with cement containing 30% of microsilica, the pH value is less than the equilibrium value of the saturated $Ca(OH)_2$ solution.

However, at the present time, it is not possible to predict how the other types of mineral admixtures influence the pore solution chemistry, nor is it known what significance to attribute to opposite observations.
The results obtained using various commercial fly

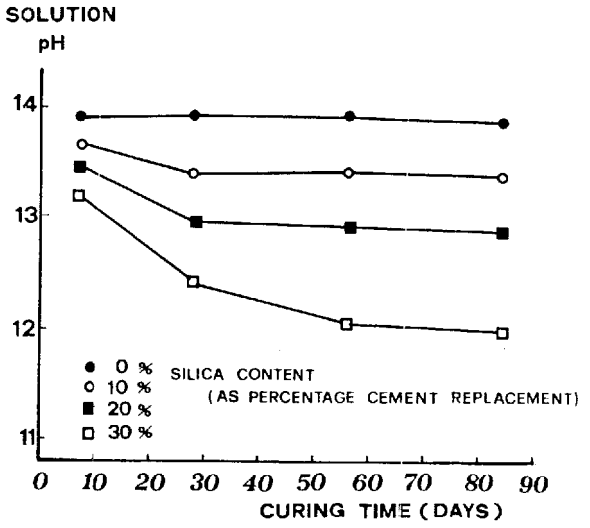

Fig. 16 - Influence of silica content on pH values of cement pastes at different stages of curing. (ref. 47)

Table 2

Analyses of Pore Solutions

Mix Proportions (% weight) Silica fume / Cement+silica	Curing Time (days)	Ionic Concentration (mmoles/l) Na^+	K^+	Ca^{+2}	OH^-	SO_4^{-2}
0	7	263	613	1	788	23
	28	271	629	1	834	31
	56	322	695	3	839	44
	84	323	639	2	743	27
10	7	161	388	1	486	20
	28	101	209	0	241	40
	56	117	218	1	233	30
	84	107	192	2	228	27
20	7	109	231	1	290	23
	28	59	109	1	91	33
	56	54	77	2	81	34
	84	51	69	2	78	25
30	7	75	143	1	152	33
	28	35	53	2	26.1	35
	56	40	39	5	11.4	36
	84	30	30	7	9.8	32

Ref. (47).

ashes and cement of varying alkali content, indicate that the blending agent can leave the OH^- ion concentration level more or less stationary (48), act efficiently by reducing it, or cause an appreciable increase. The figures in Table 3 , which illustrate this, were obtained by the Diamond laboratory (10).

The effect of adding volcanic pozzolana to Portland

Table 3

Measured OH^- Ion Concentration of Expressed Pore Solutions (Equivalents/liter)*

Age Days	OPC Paste	Paste With Flyash D	Paste With Flyash C
1	0.35	0.26	0.68
7	0.43	0.31	0.83
28	0.45	0.28	0.98
90	0.43	0.27	1.04
180	0.41	0.24	0.99

* Ref.(10).

cement on pore solution alkalinity has only been studied (49) in the case of a pozzolana widely used in south-west US. The pore solutions were expressed from mortars made of high-alkali Portland cement. When 25% in weight of sand was replaced by pozzolana, the alkalinity of the solution was more than halved (0.33 N) as compared to that of the only Portland cement mortar (0.78 N).

There is no direct evidence of the ability of blast-furnace granulated slag to remove alkaline hydroxide from the pore fluids.
Glasser and Marr (50) have determined the distribution of sodium and potassium between pore fluid and hydrated solid phases in pastes made using low-alkali Portland cement (approx. 0.5% Na_2O equiv.) and various blending agents. 15% of the Portland cement was replaced by an equal weight of mineral admixture. The pastes were kept for 14 months at 18-20 °C and at 90-100% RH.

Table 4

OPC or OPC-blend	Sodium moles/l	Potassium moles/l
neat- 100% OPC	0.054	0.209
15% F.H.S.	0.075	0.089
15% silica fume	0.021	0.050
15% pfa	0.075	0.213
15% pfa	0.045	0.154
15% ggbfs	0.072	0.196
15% pozzolan	0.082	0.293

Ref.(50).

The results of the analyses of the pore solution shown in Table 4 indicate that the mineral additions, although only present at a level of 15%, influence the potential alkali content. However, if one considers the relative reactivity of the blending agents examined, 14 months at 18-20 °C can be insufficient to reach a steady-state chemical balance in all the blended cement pastes. The Authors suggest that the microsilica has completely reacted, that a considerable amount of reaction has occurred for flame hydrolysis silica (F.H.S.) and for the volcanic pozzolana, but that the extent of the reaction of the two pfas is far from being complete.

The view on the microsilica reactivity is consistent with the suggestion of Sellevold et al. (51), according to which all the $Ca(OH)_2$ available in Portland cement pastes should be consumed with the addition of silica in excess of some 24% by weight of cement.

The figures of the thermogravimetric analyses (50) show that the slag has not reacted with a significant quantity of $Ca(OH)_2$ in accordance with the fact that, in slag cement pastes, $Ca(OH)_2$ can only be entirely consumed when the Portland cement is substituted with a large quantity of reactive slag. It is assumed (50) that the hydration of the slag is also incomplete, but that the hydration quantity exceeds 50%.

The possible implication of the above discussion regarding the relative reactivity of the blending agents is that a stationary chemical balance was only attained in the pastes containing microsilica. In the other cases, not all the alkalis available were released. Therefore, when considering the balance after the 14 months, it can be expected that the additional alkalis will still be released to the pore fluid and/or the hydration products. Glasser and Marr (50) calculate the sodium and potassium balance by assuming that all the alkalis of the cement and the mineral addition are available for release into the pore fluid. The calculation procedure is discussed in reference (52). The results of the distribution of alkalis between solid and aqueous phases, plotted separately for sodium and potassium, indicate, in agreement with the figures of Diamond (10) and Page and Vennesland (47),that the microsilica causes substantial variations in the composition of the pore fluid, encouraging in particular distribution of potassium in the hydrated solid phases. Slag and volcanic pozzolana have a neutral behaviour as regards their ability to influence the distribution of sodium and are relatively inefficient in increasing the potassium content in the hydration products. Due to its high potassium content, the volcanic pozzolana causes a significant increase of the potassium content in the pore fluid. F.H.S. has a neutral behaviour with both Na and K. The two pfas demonstrate a tendency to modify the distribution of Na and K. The Authors (50) consider that in the long term pfas will produce a significant effect,although they will be less effective than the microsilica, because they contain less reactive silica and release alkalis as

they hydrate.

The analysis of data presently to hand appears to suggest that the preventive action exerted by the pozzolanas with an activity mainly due to a $Ca(OH)_2$-SiO_2 reaction should be in relation with the ability of the pozzolanic material to produce CSH gel with a low C/S molar ratio right from the first stages of hydration. In other words, the effectiveness of the preventive action is linked to the use of finely ground pozzolana containing substantial quantities of a siliceous component with a high degree of structural disorder. If an adequate quantity of pozzolana which responds to these features is used, the composition of CSH produced by the anhydrous silicates of clinker will also be altered.

Experimental facts and observations indicate that the CSH gel with a low C/S molar ratio is able to incorporate alkalis, in particular potassium.
Rayment (53) has studied with EPMA the effect of fly ash on the C/S molar ratio and alkali content of CSH gel in hardened pastes at 8 days of age. The 20% replacement of high-alkali Portland cement by a low-alkali fly ash (0.75% Na_2O equiv.), classified as a good pozzolana by the Lea test, lowered the C/S molar ratio of the inner hydrates around the alite grains from 1.71 to 1.55. At the same time, the potassium content rose from 0.58 to 0.76%. The change in the C/S molar ratio was produced not by a reduction in the calcium content but by an increase in the silicon quantity. It was not possible to detect reaction rims around the fly ash spheres.

Poitevin and Regourd (54) have found that the K_2O content in CSH gel in 70-30 OPC-microsilica pastes is much higher than in CSH gel of the corresponding paste of only Portland cement. The figures in Table 2 and 4 show that microsilica is also the pozzolanic material which more than any other helps K ions to pass from the pore fluid to the hydrated solid.

CSH Composition *

	neat-100%OPC	70%OPC-30%microsilica
C/S	1.55	0.9
$\%K_2O$	0.1 %	1.1 %

*as determined by EPMA

Glasser and Marr (50) explain the different ability of CSH gels to incorporate potassium ions on the basis of the charge of colloidal particles. The sign of the charge depends on the relative availability of cations and anions. At a high C/S ratio the charge is positive, at a low C/S ratio it is negative. At some intermediate ratios the gel is not charged, leaving Van der Waals forces to operate. The Authors, in support of their interpretation, cite the CSH absorption figures for radiocesium (55), which is chemically similar to potassium.

The significant role played by the reaction between $Ca(OH)_2$ and silica of the pozzolana in preventing the expansion of mortar prisms is discussed in references (40)(41)(56).

Tang Ming Shu et al. (56) suggest a mechanism mainly based on two assumptions:

1) the pozzolana initially incorporates alkalis from the pore fluid;

2) the incorporated alkalis, and possibly those released by the pozzolana which reacts with $Ca(OH)_2$, could afterwards pass into the pore solution depending on the ratio between $Ca(OH)_2$ available and the reactive silica content of the pozzolana.

In support of the last assumption, the results are given of the expansion tests made with a variety of blended cements using high alkali OPC and opaline sand as reactive aggregate. In some tests, finely ground CaO, calcined at moderate temperature has been added. If CaO is not added, the expansions measured were invariably proportional to the pozzolana content. Particular attention was paid to the expansion, over time, of the mortars made using pozzolanic tufa at 10% replacement level. The expansion was not significant up to 6 months (0.042%) but became 0.197% at two years of age. The delayed increase is ascribed to a release of already incorporated alkalis, caused by the increase in the C/S in CSH ratio, due to a deficit of reactive silica.

All the mortars containing added CaO expanded more than the control mortars and the increase was greater the lower the reactivity of the blending agent.

On the basis of petrographic studies in concrete specimens from structures which had given trouble by alkali-silica reaction, Chatterji (40) has suggested, firstly, that the presence of free $Ca(OH)_2$ is a necessary prerequisite for the development of deleterious expansion due to alkali-aggregate reaction and, secondly, that a complete removal of $Ca(OH)_2$ by addition of a suitable quantity of siliceous pozzolana will stop the expansive development even in conditions of unlimited supply of alkaline salts. To establish the validity of these assertions, Chatterji et al. (41) carried out expansion tests on mortar bars made using Portland cement mixed with various quantities of diatomite of Danish origin (moler). The aggregate was opaline sand and the mortar bars were tested for their expansivity by means of the hot NaCl solution method (T.I. Test: Teknologisk Institute Byggeteknic Gregersensvey, Taastrup, Denmark), following the 8 week evaluation standard. An addition of

20% or more moler stopped expansion.

The petrographic examinations and XRDA both showed that the mortar specimens containing 20% moler had no crystalline $Ca(OH)_2$.

Ionic Diffusivity and Permeability . The involvement of the permeability and ionic diffusion in the prevention factors is consistent with the following observations:

(i) the examination of various concrete structures which have failed due to the alkali-aggregate reaction has demonstrated that damage can only occur when the concrete is wet;

(ii) the progress of the alkali-aggregate reaction depends on the rate with which the alkalis migrate to the reaction site;

(iii) the development of the expansion requires that an adequate transport of liquid be guaranteed;

(iv) the main technical benefits deriving from the use of pozzolanic materials in concrete are mostly related to a decreased permeability. The improvement is due to the denser, microporous structure with low capillary porosity of the hardened pastes of blended cement. It has been found (59) that as long as a hydrated paste of cement do not contain pores > 1320 Å, the coefficient of permeability remains insignificantly low.

A considerable amount of information about the features of microporosity, permeability and ionic diffusion was gained mainly from the case of blast furnace cement pastes.

The features of the microporous structure of the hydration product of blastfurnace cements has been discussed in numerous papers.
Smolczyk (60), Gjorv and Vennesland (61), Parker and Roy (62) have found that in the blastfurnace cement pastes a structure with very fine pores had developed. In a mix of 80-20 of slag-cement paste, 2/3 of the total porosity is made up of the smallest pores of 200 Å (61). The corresponding fraction in the mix of only Portland cement paste drops to less than 1/3.

Regourd (63) stated that CSH in blastfurnace cement is more compact and lower in calcium of CSH in OPC and that the dimensional distribution of the pores is less coarse.

Bakker (64) has demonstrated that the ionic diffusion rate and the transport of water in 75% slag-cement mortars (w/c = 0.45, a/c = 2) are markedly reduced with respect to corresponding mortars of Portland cement. The diffusion coefficients measured according to Kondo et al.'s method (65) are 5 to 20 times less, while the transport of water is almost entirely blocked as the ageing progresses. Bakker (64) concludes that the preventive action exerted by the blastfurnace cement with a high slag content can, to a great extent, be ascribed to the reduced permeability and diffusion rate of the hydrated matrix of the cement. He excludes that the sorption of alkalis by CSH can play a significant role.

In this last respect, however, not all are of the same opinion. Smolczyk (66), Diamond (10), Roy and Idorn (67) retain that the hydration product of cement can incorporate alkalis. The two last Authors, when discussing a short and long-term model of the hydration process of slag cements, stated that: "the Portland cement fraction releases alkalis and lime during the hydration, while the slag fraction retains alkalis and lime in its hydration products, presumably CSH phases incorporating alkalis in their structure".
Chatterji and Clausson-Kaas (68) do not give much credit to sorption. They find that, also in the case of blastfurnace cement, the determinant factor of prevention is the removal of $Ca(OH)_2$ from the cement matrix. When this aim is achieved, the expansion is blocked even if there is unlimited supply of alkalis from an outside source. Chatterji and Clausson-Kaas provide data on expansion of mortar prisms tested by bathing them in a saturated NaCl solution at 50 °C. The mortars are made using opaline sand as reactive aggregate and blastfurnace cements with a > 65% slag content. Two cements were used, chosen by the preliminary screening of a certain number of commercial samples of German origin.

The choice method was the absence of free $Ca(OH)_2$ in 28-day-old paste as determined by X-ray diffraction. The formation of a meaningful quantity of monochloroaluminate, both in the control prisms with only OPC and in those of blastfurnace cement mortar, is considered indicative of the migration of NaCl and of replenishment of OH^- ions. Consequently:

(i) any possible sorption of alkalis is balanced by the migration of the bath solution;

(ii) the absence of expansion cannot be attributed to the lack of OH^- ions, because these are released during the monochloroaluminate formation process.

The Authors (68) conclude by asserting that their results are not influenced by the ability of the reaction product to incorporate alkalis. If the relation between absence of free $Ca(OH)_2$ and the absence of expansion is confirmed, the high slag content required to render the preventive action of the blastfurnace cement efficient would be explained by the low $Ca(OH)_2$ demand on the part of the slag.

$Ca(OH)_2$ Distribution . The mechanism is discussed by Kawamura et al. (16) who carried out tests with opal embedded in cement and cement/fly ash pastes. It has been found that the alkali-opal reaction in the presence of fly ash is not inhibited but, unlike what occurs in cement-only pastes, the alkaline silicate keeps a considerably greater quantity of calcium. The result is regarded as particularly interesting, since:

1) it supports the suggestion of Verbeck and Gramlich (57) according to which the progress of the alkali-silica reaction mainly depends on the availability of Ca^{+2} ions on the surface of the reactive siliceous aggregate particle. In other words, the quantity of $Ca(OH)_2$ contained in the cement matrix is not so important as its uniform distribution;

2) it is consistent with the observation that, in blended cement pastes, $Ca(OH)_2$ is preferentially absorbed on the surface of the fly ash particles and this should promote the mobilization and distribution of the calcium. .

On the basis of these considerations, the Authors hypothesize that the expansion reduction due to fly ash is to be attributed to the fact that the alkaline silicate formed in the alkali-aggregate reaction can rapidly transform itself into rigid, non-expansive alkali-silica-calcium gel. If this is the case, it can be expected that a preventive action can also be exercised to some extent by a filler. In fact, it has been found (58) that finely ground quartz, calcite or dolomite reduce the alkali-opal expansion, but its effectiveness was shown to be very modest. The tests were carried out with a constant alkali content in order to cancel the effect of the dilution.

I.3.3.2. Microsilica. It is an ultrafine powder consisting of spherical particles of mainly amorphous SiO_2, with an average diameter of about 0.1 μm, obtained as a by-product of the silicon and ferrosilicon smelting industries.

The addition of microsilica to concrete improves significantly both strength and durability and has shown that it prevents alkali-silica reaction. Microsilica has not been much tested for this latter aim, but the results obtained to date indicate that the material is very active and that the minimum optimal addition is markedly lower than that of other pozzolanic materials (69) (70) (71). It has been found that microsilica acts through alkali sorption of CSH with a low C/S ratio (10) (27) (47) (50).

In Iceland (70) where the Portland cement produced is very high in alkalis (1.3% equiv. Na_2O) and it is not possible to avoid the use of reactive aggregates, the severe deterioration problems observed during the Seventies in concrete houses have been successfully resolved by using Portland cement substituted with 5-7.5% of microsilica for the new buildings. In order for full advantage to be taken of the pozzolanic addition, it is recommended to wash the aggregate if dredged from the sea; this will prevent additional alkalis and Cl^- ions being introduced into the mix. It seems that Cl^- ions have a catalytic action on the alkali-silica reaction and that the accelerating effect is relatively greater at lower temperatures.

The pozzolanic action of microsilica was also effective in the case of aerated concretes on which large quantities of de-icing salts have been applied (71). In the construction of an experimental sidewalk at S.K.W. Canada Plant in Becancour, Quebec, different concrete mixes were used made with varying amounts of high-alkali cement (1.15% equiv. Na_2O) and microsilica. The reactive mineral is contained in the coarse aggregate and it is fine vitreous silica. About 4 years after construction, there is no evidence of deterioration from alkali-silica expansive reaction. Only in the mix richest in cement (OPC factor 415 kg/m^3) and with the lowest microsilica addition (15%) has some potassium silicate gel been found, but it must be considered quite exceptional.

I.3.3.3. Pulverized Fuel Ashes. Despite the considerable attention given to the use of pfa as a means for preventing expansion due to alkali-aggregate reaction, it is still debatable whether pfa acts only as a diluter of alkalis in the cement or whether the benefit is greater than that expected from dilution only.

Typical works undertaken in this area are those by Hobbs (43) (72) (73), Nixon and Gaze (74) (75), Oberholster and Westra (69) and Gaze and Nixon (76). Hobbs describes results of expansion tests at 20 °C, on the basis of which he reaches the conclusion that pfa acts as a diluter of alkalis in the cement. Gaze and Nixon give results of expansions tests at 38 °C which revealed suitable in supporting the opinion that low-alkali pfa has a specific action against the alkali-silica reaction.
Oberholster and Westra found out that a number of mineral admixtures, including pfa, reduced the expansion of mortar prisms more than could be attributed to the effect of dilution.
Hobbs (43) carried out a series of expansion tests using 7 pfa and 6 Portland cements, both with variable alkali content. Mortars of 1:2, 1:2.75, 1:3.5 and 1:4.25 have been made with variable quantities of pfa which replace the Portland cements. The reactive aggregate was Beltane opal in the 150-300 μm size range and the proportion of opal in the mortars was adjusted so that the ratio of water-soluble alkalis to opal is close to the "critical value" of 0.067. The linear expansions were measured at 20 °C. Only

five of the mixes examined produced mortars which did not crack and did not expand. In the remaining cases the expansive strain at which the cracking occurred was generally less than 300 x 10^{-6}. A number of blended mortars cracked earlier than the Portland cement mortar with similar alkali content. The expansion rate after cracking is frequently greater in mortars containing pfa, so that the expansion at early ages can be greater. Hobbs (43) suggests that the increased initial expansion and the early cracking of these mortars could be attributed to a late development of the mechanical resistance or to the release of additional alkalis to the pore fluid.

All the pfas were shown to be effective in reducing long-term expansion and the Author attributes this to a possible significant pozzolanic action. The smaller final expansion is a consequence of the abrupt reduction in the expansion rate which usually becomes negligible within 50 days. The Fig. 17 gives an example of the expansion-age relation.

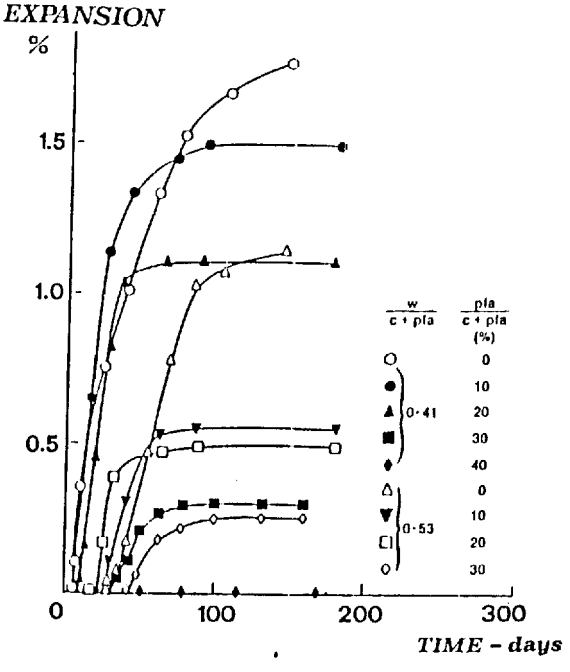

Fig. 17 - Variation of expansion with age. pfa 7, cement C. (ref. 43)

The effectiveness of the pfas in reducing long-term expansion varies greatly. For the mortars with a pfa/(c+pfa) replacement ratio ranging between 0.4 and 0.3, the 200-day expansions can vary by a factor of around 3. Hobbs (43) suggests that the variations can be related to the fineness and/or the alkali content of the pfa. The greatest expansion occurs with the greatest alkali-content and lowest specific surface pfa.

The lowest alkali content of the blended cement mortar in which cracking has been observed is 2.85 kg/m^3. This value is calculated by only taking account of the acid-soluble alkalis of the clinker and is compared with the 3.5 kg/m^3 value observed for a Portland cement mortar. The difference between the two values is almost entirely annulled if it is assumed that pfa acts like a cement with a 0.2% alkali content. In this assumption the lowest alkali content of the blended cement mortar in which cracking is observed becomes 3.4 kg/m^3.

On the basis of the similarity of the two values, Hobbs (43) considers that pfa at 20 °C mainly behaves as a diluter of the alkalis in the cement. He concludes that it is unlikely that deleterious expansion due to alkali-silica reaction in concrete containing a reactive aggregate, exposed to external humidity, will occur if the acid-soluble Na_2O equivalent of the concrete is lower than 3 kg/m^3.

Hobbs (73) has also studied the effects of replacing 5% in weight of Portland cement with pfa or limestone flour on the expansion of mortar bars tested at their critical alkali/reactive silica ratio and stored in water at 20 °C. The reactive aggregate is Beltane opal. In agreement with results given by other Authors (77) (78), the small additions of secondary material increase the expansion when the alkalis contributed by Portland cement are 5.3 kg/m^3, and slightly reduce it at a 4.3 kg/m^3 level. Since the 200-day expansion measured on mortar prisms with a 3.6 and 3.4 kg/m^3 alkali content from Portland cement is not higher than 0.024%, it is concluded that the safety limit of 3 kg equivalent Na_2O per m^3 of concrete can be also considered valid for concretes in which up to 5% in weight of the cement is replaced by pfa or limestone flour.

Nixon and Gaze (74) (75) have presented the results of an extensive work on the effectiveness of 12 pfas in reducing expansion due to alkali-aggregate reaction. The investigations involved mortar bar expansion tests in which Pyrex glass, Beltane opal or chert were used as reactive aggregate and expansion tests on concrete prisms containing reactive sand from the Thames Valley. The reactive constituent of this sand is flint in the coarser size fractions. Only one, high-alkali Portland cement (1.06% equiv. Na_2O) was used for the control mixes and for those with blended cement. The test bars were stored at 100% RH and at temperatures of either 38, 20 or 5 °C. In the mortar bars with chert, the total alkali level of the cement rose to 2.5% equiv. Na_2O by adding NaOH to the mixing water (74). The cement factor of concrete prisms with reactive sand from the Thames Valley is 740 kg/m^3.

All the test methods demonstrate that the expansion is significantly reduced if a sufficient quantity of pfa (about 30%) is used (Fig.18,19,20).

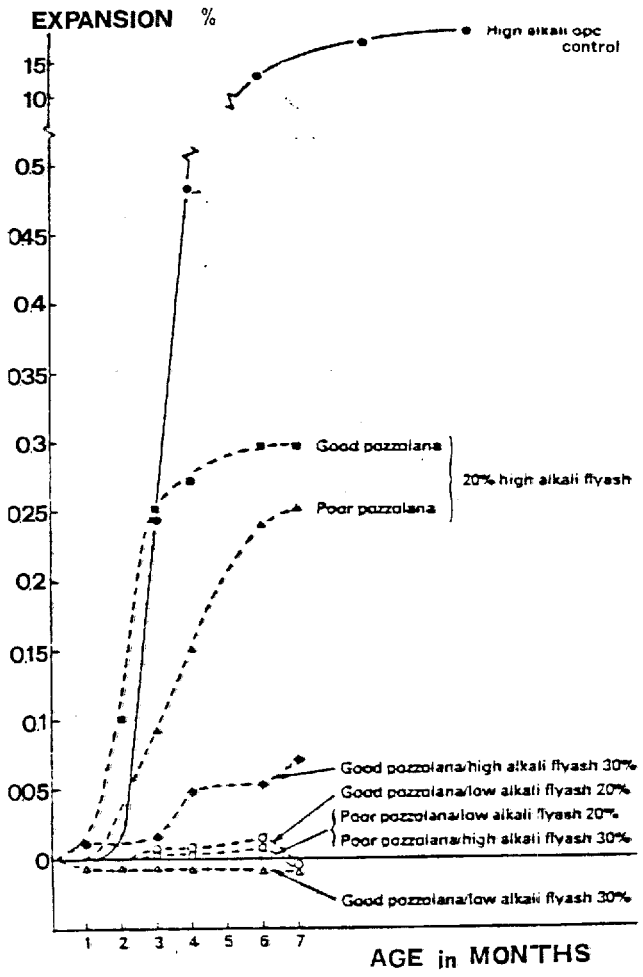

Fig 18 - Effect of flyash properties on expansion of mortar bars containing 12 g opal/100 g cement. 20°C (ref. 75)

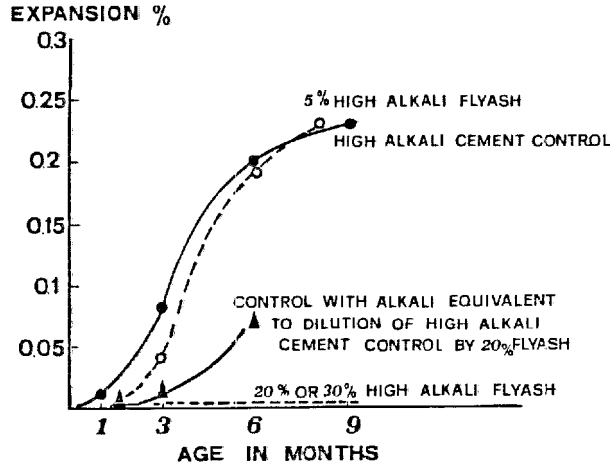

Fig. 19 - Concrete prisms containing high alkali OPC/hign alkali flyash with 30% flint/quartz fine aggregate; curing at 38°C. (ref. 75)

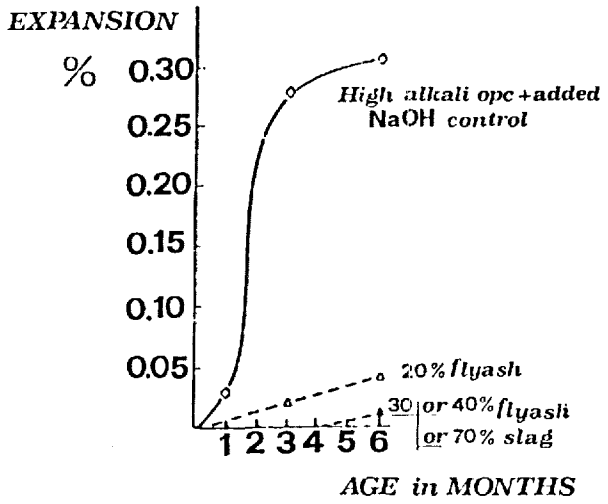

Fig. 20 - Expansion of mortar bars containing chert aggregate with high alkali opc +added NaOH (total of 2.5% equiv. Na_2O) and 20, 30 or 40% flyash or 70% slag. Curing at 38°C. (ref. 74)

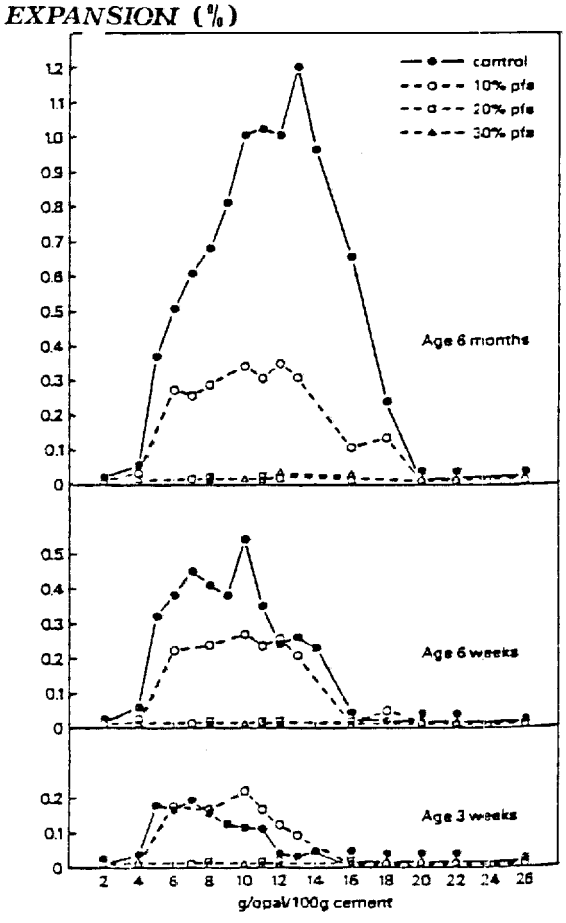

Fig. 21 - Mortar bars containing high alkali opc/high alkali flyash with beltane opal aggregate. 38°C (ref. 75)

The action of the pfas at a 20 °C storage temperature is less efficient than at 38 °C (Fig. 21,22). Nixon and Gaze (75) suggest that the different behaviour is to be ascribed to the effect the temperture has on the pozzolanic activity of the blending agent.

At 38 °C (Fig. 21), using Beltane opal as reactive aggregate, there are mortars where 10% replacement of the Portland cement with high-alkali pfa produces a greater expansion than the control one up to an age of between 3 to 6 weeks. At 20 °C (Fig.22) the mixes with 20% of high-alkali pfa also expand more rapidly than the control one and only at ages of over six months does the expansion of the control mixes become greater in most cases.

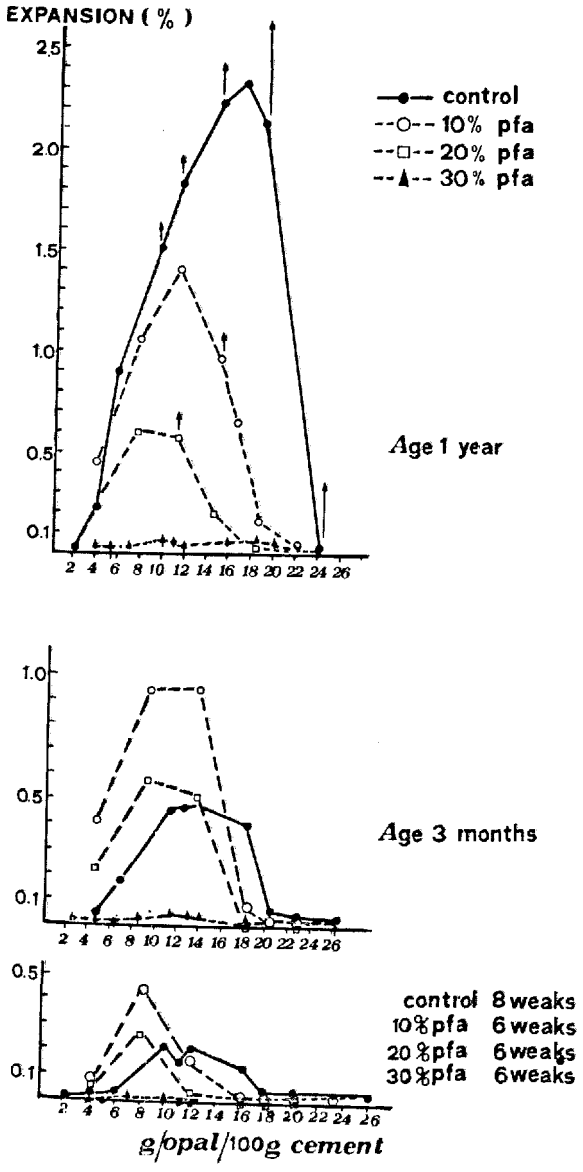

Fig. 22 - Mortar bars containing high alkali opc/high alkali flyash with beltane opal aggregate. 20°C (ref. 75)

In agreement with Hobbs' results, Nixon and Gaze (75) also find that the quantity of total alkalis of pfa is important for determining the relative efficiency of different pfas in reducing the expansion when the reactive aggregate is opal. The low-alkali fly ashes are more efficient than high-alkali fly ashes. This is not the case with Pyrex glass, with chert or with the reactive sand of the Thames Valley.

In order to show that pfa really possesses a specific action against alkali-aggregate reaction, Gaze and Nixon (76) have carried out expansion tests at 38 °C in mortar bars with a constant alkali content, in which, however, the effect of the dilution was annulled. The constant alkali level was adjusted by adding the appropriate amounts of K_2SO_4 to the mixing water. The reactive aggregate is Beltane opal and the 12 g per 100 g of cement proportion is close to that which gives the maximum expansion at the chosen alkali level of 1.18 equiv. Na_2O (Fig. 21). Only one low-alkali pfa, classified as good pozzolana, was used. The aggregate/cement ratio was 2.75, and the storage temperature of the mortar prisms was 38 °C. The results are plotted in Figures 23 and 24. They show that the expansions at 10 1/2 months are reduced at all pfa replacement levels, so that pfa cannot be seen just as a diluter without a specific action. At 20 and 30% replacement, the expansion becomes very small.

However, in Fig. 24 it can be seen that the effect of the dilution also plays a significant role in reducing the expansions and, since in practice both dilution and specific action occur, the Authors conclude that the use of sufficient pfa should be an efficient means for controlling alkali-aggregate reaction.

The greater final expansion caused by the reduction of alkalis from 1.18% to 1.08% Na_2O (Fig.24) confirms the existence of a critical alkali/silica ratio in reactions involving opaline aggregates.

Although the results in Fig.23 give valuable evidence for supporting the thesis that pfa exercises a specific action against alkali-silica reaction, Gaze and Nixon (76) still consider that more information is required for the result to be accepted from a practical point of view. There are two reasons for caution. First, the fact that the efficiency of a pfa depends on its alkali content could mean that the beneficial action can be cancelled out by the alkalis released by the pfa.Second, at ordinary temperature the pozzolanic activity, as deduced from the expansion tests (Fig. 21,22), is markedly reduced and this could signify that the specific action has less influence than the dilution effect which remains unchanged. These reasons for caution have found acceptance in "Minimizing the Risk of Alkali-Silica Reaction-Guidance Notes" (38). At section 4.5.3 it is established that "it is improbable that damage to the concrete will occur if an ordinary Portland cement is

replaced by 30% or more of pfa, as long as the alkali content of the concrete provided by the Portland cement is no more than 3.0 kg/m^3".

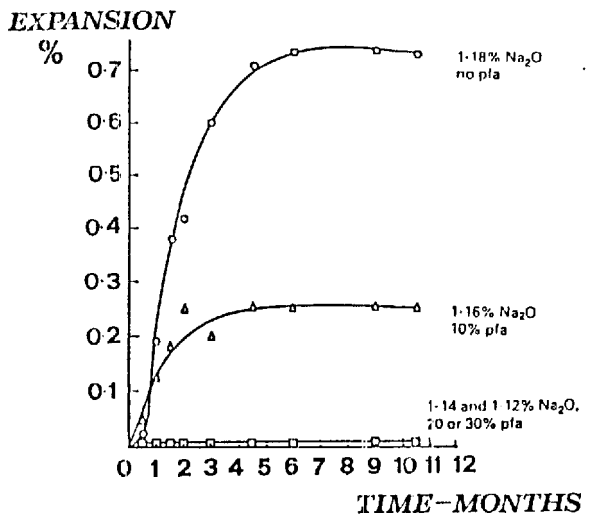

Fig. 23 - Effect of pfa upon expansion at constant alkali content.
12 g opal per 100 g cement. Specimens stored at 38°C. (ref. 76)

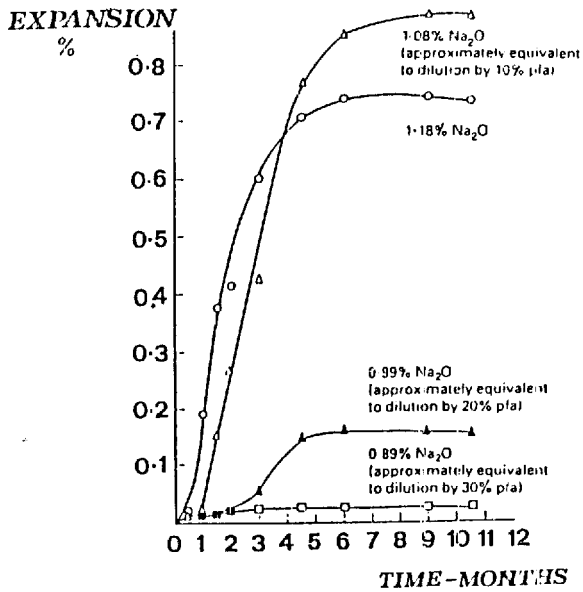

Fig. 24 - Effect of alkali dilution upon expansion.
12 g opal per 100 g cement. Specimens stored at 38°C. (ref. 76)

Oberholster and Westra (69) have considered the effect on the expansion of mortar prisms of a number of blending agents, including pfa, slag, moler and silica flour. Malmesbury aggregate from the Tygerberg Formation, showing no pessimum effect, was used with high-alkali Portland cement (0.97% Na_2O equiv.). The mortar prisms were made and preserved in accordance with ASTM C227, except that an aggregate/cement ratio of 1.5 was used in the majority of mixes. As may be expected, increasing richness of the mortar led to greater reactivity, that is a great rate of reaction.

The relative effectiveness of the various mineral admixtures in reducing the expansion after 55 days of preservation in a wet environment is shown in Fig.25. The upper curve indicates the effect of replacing high-alkali cement (0.97%) with increasing amounts of cement containing 0.16% Na_2O equiv.

In other words, this curve shows the reduction in expansion produced when the high-alkali cement is diluted.

The conclusion, which appears evident from the Figure (25), is that the reduction in expansion obtained by blending mineral admixtures into high-alkali cement is greater than can be ascribed to the dilution effect. Since the amount of expansion calculated by extrapolation (dotted curve) for mortar bars made with cement at 0.6% Na_2O equiv. is 0.13% if a maximum expansion of 0.1% is taken as acceptable, then the curves in Fig.25 suggest that the following percentages of blending agents are necessary to effectively reduce the expansion.

Data from Oberholster and Westra (69)

Admixture	Percent m/m cement replaced	Per cement m/m* admixture added
Calcined shale	25	21
pfa	20	14
Silica flour	10	7
Kieselguhr	15	10
Molererde	15	9
Slagment	30	27

* The amount in this column is equal to the mass of cement replaced.

The effectiveness of a number of pfas has been examined in accordance with ASTM C441 by Dunstan (79). The average expansion at 14 days of mortar bars from the control mixture is 0.421%. No pfa produced a minimum value of 75% at 14 days for reduction of mortar expansion as required by the test specifications. With the sole exception of two pfas which did not produce any reduction in expansion, in the remaining 22 the greatest reduction was 68% and the smal-

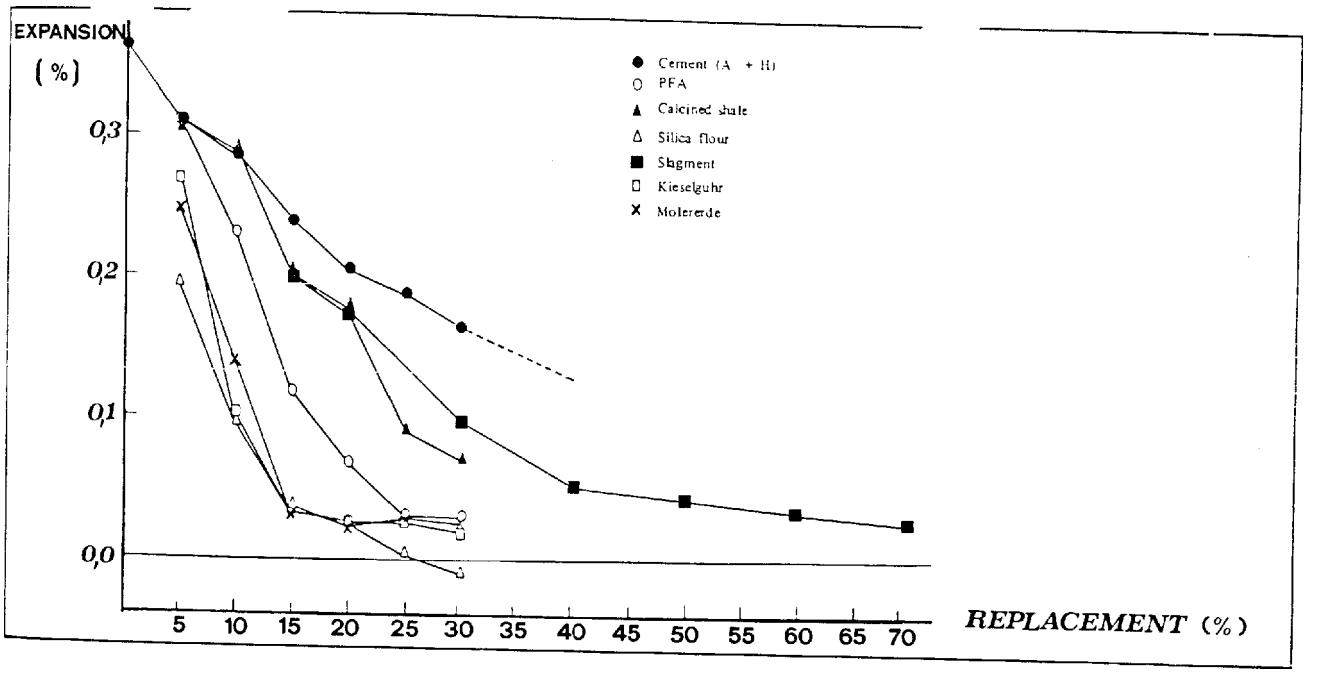

Fig. 25 - Effect of replacing cement H(0.97) with increasing amounts of cement A(0.16) or various mineral admixtures, on the linear expansion of mortar prisms stored over water in sealed containers at 38°C for 555 days. Aggregate, hornfels PS_2. a/c ratio 1.5. (ref. 69)

lest 12%. The results suggest that there is a relation between the CaO content of pfas and expansivity of mortar prisms at 14 days. Ashes with a high CaO content are less efficient than low CaO ashes. The minimum replacement percentage to reduce expansion due to the alkali-aggregate reaction may be very close to the CaO percentage of pfa (79).

In agreement with the results of Nixon and Gaze (75), the alkalis of the pfas seem to have little effect on the extent of the expansion. Dunstan has also found that the pfas showing the best improvement of concrete sulphate resistance when used at 25% replacement of Portland cement, show lower expansions of mortars bars when used at 20% replacement.

Boswell et al. (46) carried out expansion tests with Beltane opal (ASTM C227) and with Pyrex glass (ASTM C441) using a high alkali pfa and a Portland cement containing 1.17% equiv. Na_2O. At the end of 6 months, one of the prisms and the solutions at the bottom of the expansion containers were analysed to determine the distribution between dilute acid soluble alkali content of the mortars and leached alkalis.

While the expansion of the prisms containing Pyrex glass is markedly reduced when pfa is used at 45% replacement of Portland cement, the use of pfa at the same replacement level with opal as a reactive aggregate increases the expansion to a small extent with the sole exception of the mortar containing the pessimum concentration of opal. For this latter the expansion in microstrain is 268 against 528 of the control prisms. It is suggested that the inefficiency demonstrated by the blended cement when used in mixes at high concentrations of opal could be due to the fact that opal acts as a pozzolana in competition with pfa. Thus the beneficial effect of pfa does not wholly appear. Boswell et al. (46) also found that the mortar prisms made with blended cements generally contain greater quantities of dilute acid-soluble alkalis than the control prisms. But, despite the fact that more soluble alkalis are present in the mortars containing pfa, the quantity of leached alkalis decreases when the reactive aggregate is Pyrex glass, and remains almost unchanged if the aggregate is opal. The ability of blended cement mortars to retain alkalis is considered to arise from the low permeability of the hydrated matrix which hinders the ionic migration.

I.4. Testing Methods

The research was concerned with the need to shorten the testing times and improve the current methods of evaluating the results of the expansion tests, in mortar and concrete, and chemical test.

According to Grattan-Bellew (100),at the present time there is little chance of shortening the testing times by developing new and rapid methods able to clearly demonstrate if an aggregate is expansively

reactive or not. At the most the Author sees the possibility of combining the petrographic analysis and chemical method in order to supply a suitable indication of aggregate reactivity, but this development also requires time before it can be implemented. Thus many papers have dealt with the development of methods aiming at accelerating the procedures of existing tests. The work is in progress. On the basis of the evidence available, more time is requireded in order to establish which of the accelerated methods proposed are entirely satisfactory.

Data in recent literature indicates that there is little possibility of adopting general methods for evaluating the results of standard tests. In order to apply successfully the same tests to geological formations of different regions it is however necessary to choose local evaluation methods based upon the essential correlation with field experience.

I.4.1. Petrographic Examination. ASTM C295-85 (80) is utilized to determine the mineralogical composition of aggregates and to detect the presence of minerals noted in practice for their reactivity with alkalis. The method is also used to examine the microstructure of damaged concretes (27)(81).

The analysis is accomplished by means of optical microscopy, generally supplemented by other techniques such as the X-ray diffraction analysis (XRD), scanning electron microscopy (SEM),energy-dispersive X-ray analysis (EDXA), electron probe microanalysis (EPMA) or wavelength dispersive spectrometry (WES).

The petrographic examination is a very valuable test which gives a preliminary indication of possible deleterious reaction to identifies the most appropriate form of subsequent testing. The petrographic examination also recognizes in advance the presence of constituents that may mislead results, or produce results that are difficult to interpret reliably in subsequent chemical or physical tests.

In the case of aggregates containing quartz, it is considered possible to transform the petrographic examination into a semi-quantitative reactivity test, by measuring the undulatory extinction angle (82). Extinction angles of less than 15° would be characteristic of non-reactive aggregates. This correlation seems to be confirmed by some extinction-angle measurements on South African aggregates, noted for their expansivity (83).

I.4.2. Chemical Methods . ASTM C289-81 (84) is the chemical test most widely used to evaluate the potential reactivity of silica-bearing aggregates. Briefly, the test is performed as follows. The aggregate is crushed to pass a no. 50 screen. The 50-100 mesh sieve fraction is retained and immersed in a 1 N NaOH solution (25 g aggregate - 25 ml NaOH) at 80 ^{o}C for 24 hours. The method estimates the amount of SiO_2 dissolved (Sc) and the reduction of alkalinity (Rc). Sc is plotted on a logarithmic abscissa against Rc on a linear ordinate. The results are interpreted on the basis of standard curves which divide the diagram into three regions corresponding to innocuous, potentially deleterious and deleterious aggregates, respectively. The test is attractive because the results can be obtained within 2-3 days and only small quantities of sample are required.

In the majority of cases, the results correlate well with aggregate behaviour in mortar-bar expansion tests, but they are not suitable for predicting the degree of expansion caused by the aggregate in concrete nor to determine the comparative orders of reactivity between different types of aggregates. The chemical test should be regarded as an aggregate reactivity acceptance test (85). Various Authors (83) (85)(86) have expressed reservations on the experimental procedure.

The values of Sc and Rc are substantially affected if the sample to be treated contains a significant amount of material of less than 150 μm. Sc will increase due to the silica contributed by innocuous minerals (e.g.quartz) attacked by the alkaline solution because of their fine subdivision state (83) and the relatively high test temperature (85).Misleading readings are also obtained if magnesium carbonate, iron carbonate or serpentine are present in the aggregate. These substances promote large reduction in alkalinity (87). Difficulties in evaluating the results have also been experienced with samples of trachitic tuff containing gypsum. These samples exhibited Rc values from 73 mmoles/l to 900 mmoles/l and Sc values from about 71 mmoles to zero, varying the gypsum content (as SO_3) from 0.4 to 12%.

The use of phenolphthalein as an indicator is not considered very satisfactory since the end-point is rather undefined and is a function of the quantity of silica dissolved (86). Moreover, the value of Rc,as currently determined, would include both the reduction in concentration of the OH^- ions and that of the Na^+ ions. More reliable results could be obtained by separately determining the reduction in concentration of the OH^- ions (with a pH-meter) and Na^+ ions (by spectroscopy) (86).

As is well-known, the ASTM graph curve (84) is constructed by the results of tests with US rocks containing opal, flint, chalcedony or volcanic glass as reactive components. The extension of the method to aggregates of other geological areas has not changed the significance of the test but has led to the following observations: 1) the evaluation methods quantified by the standard curve are not universally applicable; 2) the test conditions might not reflect

the innocuous character of an aggregate at an ordinary temperature and 3) for some aggregates, Sc may be used as the only classification parameter.

The fact that the ASTM standards are not applicable to all aggregates independently of their geological history, is not surprising if it is considered that the degree of reactivity of a rock in a certain set of test conditions is related to the rock features which are peculiar to the originating geological area. These features include the quantity, type and location of impurities, the degree of crystallization, the extent and frequency of lattice defects, the fineness of the crystal grain, the porosity, average radius and degree of interconnection of the pore system.

Thus, in the case of late-expansive aggregates (5 hornfels and 4 greywackes) of the Tygerberg Formation in the Cape Peninsula of South Africa, it has been found that the ASTM 289 test does not permit the reactivity of these aggregates to be differentiated (89).

The Sc values are low and the Sc/Rc ratios are located near the innocuous-potentially deleterious curve. Subsequently, it was found (90) that, by increasing the test time from 3 to 7 days, there was a satisfactory correlation between the Sc values and the mortar prism expansions. The criterion proposed for potentially reactive aggregates of Tygerberg Formation is 1% of dissolved silica after 3 days or more than 2% after 7 days.
However, it has been suggested (83) that a satisfactory correlation between Sc and the mortar prism expansion could be obtained in a similar way by considering that the dividing line between reactive and non reactive aggregates must lie at a value of Sc between 35 and 50 mmoles/l.

The reactive aggregates of the Malmesbury Formation in the same region are instead classifiable by ASTM C289 criteria.

For the South African aggregates a modified chemical test has also been proposed (29): 10g of the fraction passing at 600 μm and retained on 300 μm is treated in 25 ml of 1 N NaOH solution with 1g of $Ca(OH)_2$ at 80 °C for seven days. Poorly defined XRD peaks between 12 Å and 16 Å for the gel separated from the mixture is a sure indication of excessively expanding aggregate.
The ASTM criteria are instead effective for differentiating the reactivity of New Zealand andesite rocks (44).
In the case of 14 Icelandic and 15 Danish sands, the results of the ASTM C289 test correlate with those of both ASTM C227 expansion test (91) and Teknologisk Institute Byggeteknic Gregersensvey method (92), by assuming Sc = 100 mmoles/l as the value indicative of potentially harmful behaviour. For Danish gravels the corresponding value is Sc = 50 mmoles/l. For both sands and gravels a value of Sc = 200 mmoles/l is indicative of the separation between potentially reactive and reactive aggregates (83).

A large number of British aggregates is classified as deleterious or potentially deleterious by the chemical test (Sc > 100 mmoles/l) (42). The result, however, is considered excessively pessimistic because the grouping includes materials used for years and found to be unaffected by deleterious reactions (42)(88). A less pessimistic test for these aggregates is the gel pat test (88), (93). This test consists of immersing a smoothed, sawn surface of the mortar containing the reactive aggregate in a 1 N NaOH solution at 38 °C for three days. The formation of gel is an indication of the reactivity of the aggregate.

A similar test is used also in Czechoslovakia (94).

For German reactive aggregates from the Schleswig-Holstein region, a modified chemical test has been developed (95). The aggregate is divided into two fractions of 1-2 and 2-4 mm. A sample of each fraction is digested in NaOH solution at 90 °C for 60 min. The digested samples are filtered, washed, dried and weighed. The weight loss of the samples is called "part soluble to alkalis" and is considered a measure of the potential reactivity of the aggregate. The limitations of this test have been discussed in reference (96).

I.4.3. Mortar Bar Expansion Test . The mortar-bar test, ASTM C227-81 (91),measures the linear expansion of 25x25x285 mm mortar prisms, stored at 37.8 ± 1.7 °C and 100% RH . The test is carried out using high-alkali cement (preferably above 0.8% as Na_2O equiv.) or the particular cement used for field concrete and sand of specified grading. The method recommended for evaluating the potential reactivity of an aggregate is given in ASTM C33-85 Appendix XI (97). A linear expansion greater than 0.05% at three months or 0.1% at six months is to be considered as excessive. If an expansion greater than 0.05% at three months does not correspond to an expansion greater than 0.1% at 6 months, the cement-aggregate combination is to be considered as non-deleterious.

The expansion values at the times indicated are suitable for opal-bearing aggregates which have a time - expansion curve with a short period of initiation followed by a fast rate of expansion.

In many other cases, the waiting time required to obtain a reliable response exceeds the 6-month limit and can also be a few years. Therefore, the guidelines given in ASTM C33-85 should not be considered mandatory (83) (88), otherwise one runs the

risk of classifying as non-reactive an aggregate which could be deleterious in field applications. Recommendations based on values of harmful expansions not referred to a definite time interval are given in references (98) and (99). The rationale of the various criteria is discussed in (100).

Markedly long test times are typical of late-expansive siliceous aggregates. New Zealand aggregates (44), reactive or potentially reactive to chemical test, do not give meaningful expansions at 6 and 12 months, while for longer times they reach unacceptable expansions. For these aggregates a suitable criterion could be 0.1% at 2 years (44).

For the aggregates of the Tygerberg Formation (89) the 0.05% limit at 3 months does not allow the innocuous materials to be differentiated from the deleterious ones. The standard (0.05% at 72 or 120 weeks) proposed for the aggregates of Nova Scotia (101), similar to those of the Tygerberg Formation, is also considered un-acceptable because it is not certain that an expansion of 0.05% after about 17 months of storage can be solely attributed to the alkali-aggregate reaction.

In the case of aggregates from the UK, the results of ASTM C227 test do not correspond with those observed in field concrete (88) (102). The principal reactive mineral of the UK aggregates involved in alkali-silica reaction is cryptocrystalline quartz in flint and chert. Only if the alkali content of the cement is increased to 2.4% as Na_2O equiv. by adding KOH to mixing water, definite differences in reactivity between aggregates of different origin may be observed (102). It has also been found (88) that a quartz sand of the Himalayas and an Icelandic metaquartzite, both classified as deleterious by the chemical test, have given a linear expansion of 0.05% at 15 months and 0.1% at 12 months, respectively. Despite the limitations listed, the mortar-bar test is, at present, the most widely-used expansion test.

The assumption of standards on a local basis eliminates the risk of erroneous reactivity classifications, but does not resolve the problem of long waiting times.

In order to satisfy the obvious necessity for a timely response, modifications to the test procedure have been proposed (70) (96) (103) (104) (105), as well as a method for calculating the long-term expansivity based on the early expansion data (83) (106).

The cross-section of mortar or concrete bar seems to have a marked influence on the extent of expansion (104). If the height (160 mm) is kept constant and the base of the specimens is varied from 20 to 100 mm, the linear expansion increases. It is recommended (104) that the cross-section of ASTM prisms is brought to 40x40 mm (measurement also recommended by RILEM (107)) in order to decrease the risk of missing reactive aggregates.

On the basis of preliminary results indicating a catalytic effect of Cl^- ions on the alkali-silica reaction, especially at low temperatures, it is suggested (70) that the test ASTM C227 could be accelerated by using mixing water with 0.7% of NaCl.

An accelerated version of the test C227 has been developed in Denmark by the Teknologisk Institut Byggeteknik Gregersensvey, Taastrup (T.I. method)(96) (103). Mortar prisms (40x40x160 mm) are cured in water at 23 °C for 27 days, then stored in a saturated NaCl solution at 50 °C. By comparing the results observed on 14 Icelandic, 15 Danish and one Swedish sands (92), a good correlation is found between the test C227 (>0.1% at 1 year) and both the T.I. (>0.1% at 20 weeks), and C289 (Sc >100 mmoles/l) methods. In the brackets are the criteria according to which a sand is considered as harmful. The T.I. method with the 8-week standard is found to be unsuitable because the majority of the Icelandic sands and some Danish ones are still expanding at this age. The T.I. method is reported to be satisfactory for relating the mineralogical composition and the time-expansion features of over 100 Danish sands (108), as well as for evaluating the potential reactivity of Danish coarse aggregates (8/16 and 16/32 mm fractions) separated by heavy-media-separation technique (109).

The T.I. method has also been adopted to evaluate the effect of air-entrainment on mortar prisms expansion (110). Opaline sand is used as reactive aggregate and the changes in the length of the prisms are measured up to 8 weeks. It is found that the introduction of about 4% air decreases the expansion on average by about 40%.

The petrographic examination of 8-week-old mortars has demonstrated that, in the case of opaline sand, the air bubbles are at least partially filled with isotropic gel, while the air bubbles in the control mortars remain empty.

The Authors suggest that air-entrainment may be used as an additional safeguard whenever alkali-aggregate reaction is suspected. However, the filling of the air bubbles naturally reduces the effectiveness of the entrained air-void system in a freeze-thaw environment.

The effectiveness of mineral admixtures in preventing alkali-silica reaction has also been evaluated with the T.I. method (41) (68).

Another accelerated version of the test ASTM C227 is the "Chinese" autoclaved mortar bar test (105). In this test, mortar prisms (10x10x40 mm) are stored for 24 h in a fog room, then steam cured at 100 °C for 4 h

and finally autoclaved at 150 °C for 6 h in a 10% KOH solution.The expansion is measured between treatments. The curing temperature in the autoclave is determined by taking into account the fact that the control prisms with quartz sand expand to an appreciable extent (0.02%) only when the temperature exceeds 150 °C. Data is given on 28 aggregates, including 9 reactive ones; some of the latter already expanding more than 0.05% after the steam curing. The expansions in autoclave ranged between 1.3% for opaline aggregate and 0.23% for a volcanic glass. The results of the accelerated test are largely consistent with those of the ASTM test. The autoclave method was also used successfully to compare the effectiveness of volcanic tuff, fly ash and slag in preventing alkali-silica reaction (56) (58).

An accelerated version of the test ASTM C227 has also been developed in South Africa (29). Mortar prisms made with low alkali cement are stored in 1 N NaOH solution at 80 °C. Specimen expansions are measured daily for 14 days. It has been suggested (22) that >0.08% but <0.2% expansions indicate late-expansive siliceous rock. An expansion of 0.2% or more is typical of early-expansive siliceous rock.

With regard to accelerated tests, it must be borne in mind that they do not always modify the rates of aggregate reaction and specimen expansion consistently (83),(85).

In some cases, these tests can reduce the amount of expansion while in other circumstances they can promote reactions which do not progress under ordinary conditions. Based upon the observation that an acceleration in the alkali-silica reaction produces less deterioration in the concrete structures (111), a "decelerated" test method has been developed at Aachen in West Germany. This method differs from the ASTM C227 test in the mortar composition (less cement content),in the aggregate particle size (absence of coarser aggregate fractions),in the specimen dimensions (40x40x160 mm) and in the curing temperature (18-23 °C). A comparison between the two tests was made using as reactive aggregates opaline sandstone, aggregate from Bultwisch quarry, Malmesbury aggregate and feldspatic greywacke from Nova Scotia (112). For the more reactive aggregates (opaline sandstone) it is confirmed that, with respect to the Aachen method, the test ASTM C227 accelerates the alkali-aggregate reaction (due to the higher cement content and the greater curing temperature) but reduces the deterioration of the specimens. For less reactive aggregates (greywacke, Malmesbury and Bultwisch) the results of the comparison are not yet known because longer testing times are required (2-3 years).

The mortar bar expansion test can also be used to evaluate the reactivity of Portland cements. Pyrex glass (113-114) or opal (36) are generally used as reactive aggregate, but it has been shown that better results could be obtained using hornfels of the Malmesbury Formation as reactive aggregate (115). With this type of aggregate there is a satisfactory relationship between expansion of specimens and available alkali content of the cement, the latter being determined according to the ASTM C311-85 procedure (116).

The effect of the w/c ratio on the expansion in mortar bars has been investigated by Lenzner (117).

The bars were obtained by using mortar with mix proportions of the aggregate-cement ratio equal to 3 and with an increasing water-cement ratio, varying from 0.4 to 0.7. The mortar was prepared with standard sand and a 4% substitution with a 0.09-0.5 mm fraction of opaline sand. The mortar prisms were kept at room temperature in a humid atmosphere.

The damage caused by the reactivity of the aggregate is estimated by measuring the expansion and variations in the natural resonance frequency. The results indicate that the maximum expansion is obtained at a w/c ratio of 0.6. The "pessimum" ratio is related to the kind of mix.

Vivian (118) has examined the effect of repeated drying and wetting on the expansion of mortar bars containing opal V17 as reactive aggregate. If the water is removed from the mortar at an early age, the alkali-opal reaction is inhibited and the expansion can be arrested. When a sufficiently large quantity of water or water vapour is reabsorbed, the alkaline attack takes place again and expansion and cracking follow the reaction.

The drying of an expanded and cracked mortar bar has no effect on the degree of expansion. The expansion is caused by the development and enlargement of the cracks which produce marked displacements and which become partially filled with incompletely deformable, mobile reaction product. Also in this case the expansion process is arrested but reacted aggregate particles resume their swelling tendencies as water or vapour is reabsorbed.

I.4.4. Concrete Expansion Test . The undoubted advantage of the concrete prism test permits conditions which best reflect the field situation , in particular, proportions of ingredients and grading of aggregates. Therefore, some Authors (83) claim that the concrete prism test may be the most reliable method for testing all types of aggregates. In fact , this is the only satisfactory test for aggregates such as late-expansive siliceous rocks and reactive carbonate rocks, whose expansivity has been shown to increase by larger grain size.

For aggregates which display the classical alkali-

silica reaction, the test C227 runs shorter because the deleterious process is accelerated when the fineness and surface area of the aggregate are greater.

The concrete prism test is adopted as Canadian Standard (CSA A 23.22 - 14 A)(99). The evaluation methods are specified in CSA A 23.1 M 77, Appendix B 3.5 (99). Changes in length are measured in a concrete prism with dimensions not less than 75x75x300 mm. The concrete is made with 310 kg/m^3 of cement and 80± 10 mm slump; the prisms are stored at 23 °C in a wet environment. Linear expansions of 0.03% at any age indicate a potentially deleterious aggregate.

It is now widely recognized that the use of concrete specimens is compulsory (102) when conducting laboratory expansion tests in order to demonstrate the reactivity of UK aggregates. The test conditions found to be appropriate are : high alkali cement (1.05% as Na_2O eq.), high cement content (740 or 560 kg/m^3), low water/cement ratio, and curing at 38 °C. The procedure also ascertains the existence of a pessimum effect for a Thames Valley flint aggregate (102).

No explanation has yet been given for the expansion and cracking found in concrete prisms and not in mortar prisms, despite the fact that both mixes contained similar quantities of alkalis, were made with the same water/cement and aggregate/cement ratios and were stored under the same conditions (102).

Nixon and Bollinghaus (119) have examined the effect of the alkali-aggregate reaction on the tensile and compressive strengths of concrete made with UK aggregates containing flint and high-alkali cement. On the basis of the results in reference (102) the mix composition is chosen to give an alkali content in the concrete of about 6.3 kg Na_2O equivalent per cubic metre, corresponding to a 600 kg/m^3 cement factor.
Tensile strengths are measured on 100 x 200 mm cylinders, compressive strengths on 100 mm cubes. The cylinders were stored at 38 °C in 100% RH, the cubes were cured at 20°C in water. Two cylinders, first intended for the tensile strength measurement, were instead tested for compressive strength.
The development of the alkali-aggregate reaction was evaluated through the expansion of 75 x 75 x 200 mm concrete prisms, some stored in water at 20 °C, some in 100% RH at 38 °C.
The results of the mechanical and expansion tests, monitored up to 1 year, are shown in Fig.26 . A substantial decrease in the tensile strength is observed before the concrete expands and cracks. The loss in strength occurs after 2 months, while significant expansion and cracking of prisms develop after 6 months.
The two compressive strength values at 30 °C indicate only some decrease at 1 year, by which time the concrete prisms have severely deteriorated. The compressive strength at 20 °C does not appear affected and this corresponds with the insignificant development of the expansion.

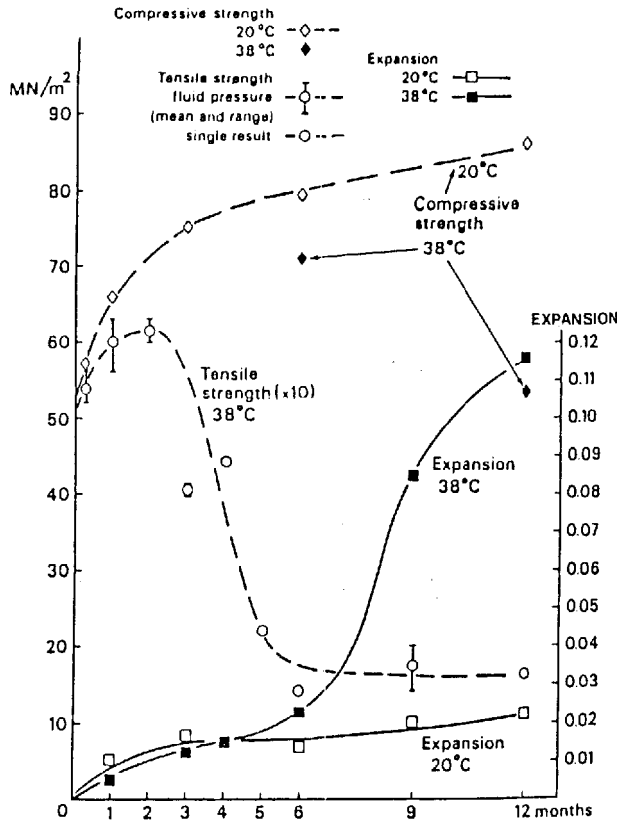

Fig. 26 - Tensile and compressive strength development and expansion of concrete stored at 20 or 38°C. (ref. 118)

Measurements of concrete samples from structures affected by alkali-aggregate reaction confirm the trend of the laboratory data.

Even though the concrete prism method appears reliable under many circumstances, a generalized use of this method is considered unlikely (88)(120). In fact, some practical aspects, such as the collection of large-sized aggregate, the preparation of a great number of mixes, the long storage period, the quantity of aggregate required and storage room, are considered unfavourable for the diffusion of the method .

The problem of the long testing time is still unresolved. Moreover, it is likely to happen that the test procedure could require adjustments related to the reactivity of the particular aggregate. Attempts to accelerate the expansion by dipping the prisms in saturated NaCl solution at 50 °C were not very successful (83). These are preliminary tests and more work has to be undertaken before a definitive asses-

sment can be given. In order to reduce the testing time, and consequently the drawbacks, greater attention might be paid to the possibilities offered by the expansion rate method (100) (106).
The concrete cube test is another method used to evaluate the potential reactivity of the cement-aggregate combinations. This is a qualitative test since the reactivity of the system is evaluated on the basis of the formation of visible cracks in concrete specimens.

In the original version (121), 30 cm concrete cubes are stored in a fog room at 40 °C. In a second version, 10 cm cubes are cured at 65% RH with the base of the specimens (1 cm) immersed in water at 20 °C. Under these conditions, the presence of reactive aggregate produces notable cracks in the specimens right above the water level. The most recent version of the test (83) consists of immersing the 10 cm concrete cubes in a water bath at 23 °C. This temperature is considered as optimum for solubility of silica.

Although the test is quite simple, and is also suitable for use in field conditions, it appears troublesome in the case of late-expansive aggregates, because of the excessively long test times required for the formation of conspicuous cracks in the specimens.

I.4.5. Rock Expansion Test. The rock cylinder test ASTM C586-69 (122) is a method specifically designed to detect potential expansivity of reactive carbonate rocks. This method measures the changes in length of cylinders (35 mm height and 9 mm diameter) of the same rock. The expansion is produced by soaking in 1 N NaOH solution at room temperature. Expansions greater than 0.1% are indicative of reactivity. Usually, the expansive phenomenon appears within 28 days except in the case of carbonate rocks, known as late-expanders (123) (124). It is recommended that rock-cylinder expansion be verified by additional expansion tests, preferably in concrete, because it is not yet possible to relate the results of ASTM C586 test with the expansive behaviour of field concrete.
The applicability of the test C586 to carbonate rocks from the Middle East and North Africa has been discussed in references (88) (125). The case of three Libyan rocks is examined (125): a dolomitic rock with acid-insoluble residue formed of quartz, kaolinite and muscovite, and two carbonate rocks taken from different sides of the same quarry, one impure limestone and the other dolomitic limestone. The last two rocks have an acid-insoluble residue formed of quartz, palygorskite and chamosite.

The dolomitic rock is late-expansive; it first contracts up to two months, after which it starts to expand. Expansion at 4 months exceeds 0.1% and stops at 9 months (0.24%). The other two rocks show only contractions. For dolomitic rock cylinders, the variations in length can be related to variations in weight. For the other two rocks, however, there is no relationship. Criteria for the interpretation of data are also discussed (125).

A modified version of the test ASTM C586 is the miniature rock prism test (126). It uses small-dimension prisms (3x6x30 mm or even 3x6x15 mm) to accelerate the saturation of the rock with alkalis and thus the expansive phenomenon. This test could be useful for evaluating gravels (88). However, it has been suggested that small-dimension prisms cored from the same rock sample could expand differently since they are not equally representative of the composition of the rock (127).
Another accelerated version of the test ASTM C586 has been developed in Czechoslovakia (128) and adopted as a test standard in that country (CSN 72 1160). Basically, the method measures the variation in length of carbonate rock prisms (10x10x30 mm) autoclaved in a NaOH solution at 215 °C and 2.1 MPa for 6 hours.

The three tests (ASTM C 586, CSN 72 1160 and Miniature Prism) have also been used to evaluate the potential reactivity of late-expansive siliceous aggregates. The results were not very satisfactory since the expansions of the rock cylinder (101) or miniature rock prism tests (129) could not be easily related with those of the concrete prism test. In the case of the Czechoslovakian test, the expansions were accompanied by the formation of phases which did not occur in ordinary conditions (83).

Neither the test ASTM C586 nor the miniature prism method is suitable for evaluating the potential expansivity of aggregates with a classic alkali-silica reaction. The specimens either dissolve completely or break up due to the dissolution of the bonds between the grains (106) (129).

I.4.6. Osmotic Cell Test. This test was developed about 30 years ago to study the expansion mechanism related to the alkali-silica reaction (57). Recently, the method has been reproposed to evaluate the potential reactivity of late-, and early-expansive siliceous aggregates (130).

An osmotic cell is used which consists of two chambers, one for reaction and one for reserve. Both are filled with 1 N NaOH solution and separated by a cement paste membrane (w/c = 0.55). The test involves introducing a sample of aggregate (the fraction between screens no. 50 and 100) into the reaction chamber and then measuring the flow rate of the liquid through the membrane. Reactive aggregates cause a positive flow which remains constant for some weeks, and whose extent depends on the reactivity of the aggregate. Preliminary tests showed that the

criterion for differentiating a reactive from a non-reactive aggregate is a flow rate greater than 1.5 to 2.0 mm/day. With this test it is also possible to detect the potential reactivity of some late-expansive aggregates for which the test ASTM C227 is unsuitable. The test appears to be promising for its relative simplicity and rapidity.

II. COMPATIBILITY BETWEEN CONCRETE AND REINFORCEMENT

It is generally agreed that concrete is a material of considerable durability in that it provides the reinforcement embedded in it with an environment particularly suitable for preventing corrosion.

However, in the past there have been numerous cases of inadequate behaviour of structures in reinforced concrete.

In this regard much study and research has been undertaken on the behaviour of the reinforcement as a function of its mix features and the environment in which it is situated.

A far-ranging and in-depth survey of this subject, sponsored by the American Society for Testing and Materials, was carried out by Slater in 1983 (131).

Here, and also elsewhere (132), major importance is given to the problems connected with the economic implications of corrosive phenomena on concrete reinforcement which in many countries, particularly in the United States, have reached impressive levels. More recently, in Great Britain, the extremely high level of deterioration of buildings to be accounted for in present and future years has been stressed (133). An even more recent survey has been conducted by the American Concrete Institute (134).

In this brief and concise report an attempt was made to include a selection of more recent publications by authors from various parts of the world. Inevitably however, some citations of equally important scientific weight may be lacking; it must also be remembered that this particular subject is presented at the Congress on Cement for the first time.

II.1. Mechanism of corrosion behaviour of iron in concrete.

II.1.1. Electrochemical Behaviour of Iron in Concrete. Iron, like the majority of metals, can undergo oxidation as a result of the environment in which it is situated on the basis of two different phenomena which are normally defined as dry corrosion and wet corrosion. In the case of reinforcement of concrete, there is no doubt that this latter must be considered as an electrolytic conductor (135); therefore the phenomena relevant to the behaviour of metals in contact with it fall within the category of wet corrosion, also called electrochemical corrosion (136)(137)(138).

As is known, iron is a metal with an active-passive behaviour. Pourbaix's diagram on the iron-water system describes the thermodynamic behaviour of the metal: it clearly shows that in the pH interval typical of the solution present in the pores of the concrete, iron is normally passive (Fig.27) (139)(140)(141).

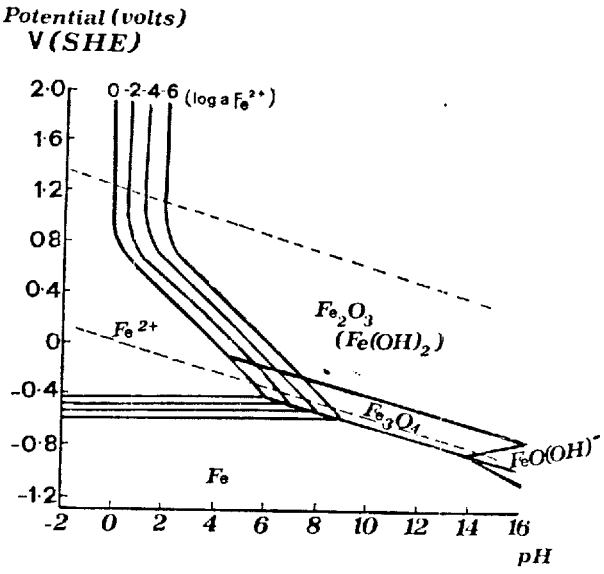

Fig. 27 - Potential-pH equilibrium diagram for system Fe-H_2O at 25°C (After Pourbaix)

Passivity is due to the formation of a thick impervious superficial film (20-200 Å of highly protective iron oxides Fe_3O_4 and Fe_2O_3) (142). From a kinetic point of view, the curve which describes the course of the current density as a function of the assumed or imposed potential polarization curve is that given in Fig. 28 (141)(143)(144). It can be seen that the critical current necessary to pass from the active to passive state is around 1-10 mA/m^2 and corresponds to a corrosion rate of a few μm/y, while the current density necessary to maintain the passive stage, is about 0.1 mA/m^2 and corresponds to tenths of μm/y. The use of polarization curves for characterizing the electrochemical phenomena which govern the behaviour of the reinforcement, dates back more than twenty years (145)(146) and is very useful for explaining corrosion mechanisms in the presence of chlorides.

Since concrete reinforcement is normally in a state of passivity, it can only be attacked by corrosion when the passive layer deteriorates. This can occur when the corrosion agents present in the environment

surrounding the concrete come into contact with the reinforcement. Therefore the layer of concrete which covers the reinforcement, namely the concrete cover, plays an extremely important role.

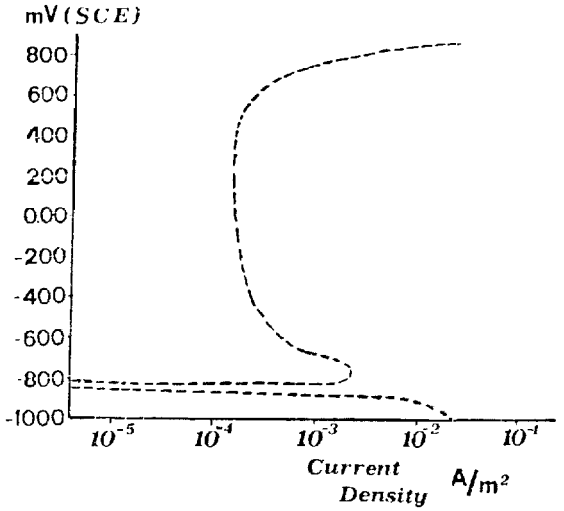

Fig. 28 - Experimental potentiostatic polarization curves for steel in OPC mortar (w/c=0.5)

Just as a good-quality paint can constitute a reliable protective barrier against a metal being attacked by the surrounding environment, so the concrete cover constitutes, independently of the electrochemical action on the iron, a real physical barrier which limits the passage of corrosive agents and water (143)(147)(148). The efficiency of the barrier is obviously linked to certain properties of the concrete, the most important being porosity and permeability.

Another property which has a considerable influence on the evolution of the corrosive phenomena of the reinforcement and which is electrochemical is the resistivity of the concrete (136). It depends to a great extent on the composition of the admixture, the workmanship, the humidity, the quality and quantity of the ions present as well as the temperature (149)(150). Freshly-made concrete can have a resistivity of around 150-300 ohm x cm, which rises to 3000-20000 ohm x cm and even higher after it has been exposed to the air for a few days (151)(152). The presence of chlorides has a considerable effect on the resistivity, halving it for example if it is equal to 0.6% of the weight of the concrete (153). Although concrete is a very composite material, it is possible to take the resistivity values apparent on the surface as indication of the state of corrosion of the reinforcement (154).

The depassivation of iron in concrete is often, but not always, concomitant with the deterioration of the cover (143)(155)(156)(157). The most widespread causes of reinforcement corrosion are to be attributed to the phenomenon of carbonation and also to the presence of chloride ions; although in different ways, both causes lead to the lowering of the pH in the environment close to the iron and to the subsequent loss of passivity (143)(158)(159).

Naturally, the presence of cracks in the cover facilitates the penetration of aggressive agents and therefore the danger due to their presence has been suitably studied (160). The presence of stray currents and differential aeration cells can also cause corrosion in the reinforcement, provided Cl^- ions are also present(161).

II.1.2. Carbonation. Carbon dioxide contained in the environment surrounding the concrete, be it air or water, can penetrate it with a speed which greatly depends on certain properties of the concrete.

Carbonation kinetics for various types of concrete in different environments follow the general relation:

$$dx/dt = K\sqrt{t}$$

in which the proportionality constant K depends on various parameters relevant both to the quality of the concrete (w/c ratio, type of cement, porosity, etc.) and to the type of environment (temperature, relative humidity, etc), as well as obviously to the presence of cracks in the concrete (143)(162-165). Tuutti (166), in order to calculate the thickness of the concrete in which neutralization had occurred as a result of carbonation, used as an analogy the oxygen diffusion figures obtained from other authors (Fig.29) (167). He found, as was foreseeable, that there is a greater carbon dioxide penetration in environments with less relative humidity; evidently, in this case, pores are easily permeated by air. Nevertheless, except in special cases, the time needed to carbonate 2 cm of cover is in the order of some tens of years, as reported by Page (143) and Locke (168), according to whom the penetration rate of carbon dioxide falls well below a mm/year not long after the structure has been completed.

In these conditions, the danger of the decreasing of the pH of the electrolyte in contact with the reinforcement, due to carbonation of the concrete can be recognized even in the design stage. Therefore it is possible to take appropriate precautions, by establishing the concrete mix, the w/c ratio and the curing conditions, a means to prevent defects due to particular environments. Despite the fact that it is possible to predict the entity of the carbonation with a certain precision, and therefore also the danger of corrosion of the reinforcement over time, precocious deterioration phenomena have occurred in recent years in reinforced concrete structures in Middle East countries (169)(170)(171).

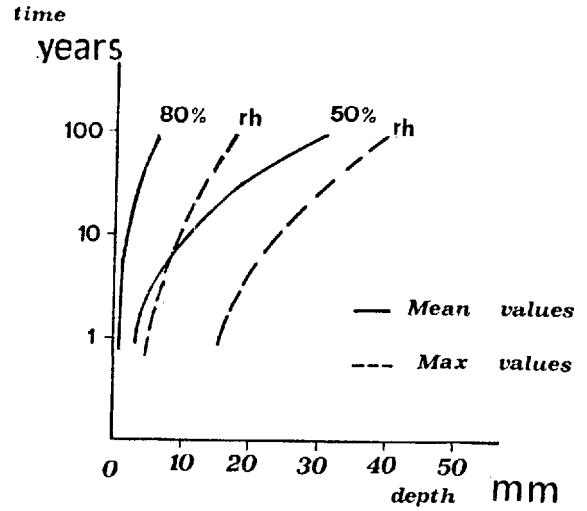

Fig. 29 - Calculated depths of carbonation in varying relative humidity. Cement content 400 kg/m^3, w/c=0.5 (ref. 166)

It is evident that this phenomenon is to be attributed to the high atmospheric temperatures, as well as to the workmanship and the traditional curing methods. Moreover, it has been observed that there is an additional negative factor due to the presence of chlorides, although modest, from the use of inert substances which contain them as impurities.

II.1.3. Chlorides. Chlorides, as is known, can be found in concrete either in the manufacturing stage or they can derive from the external environment.

In the first case, their presence may be discovered and consequently the resulting problems can be evaluated beforehand; chlorides can be contained in the mixture water, in the impurities of the aggregates, in the additives, or can be deliberately added to the cement to accelerate the hardening phenomena.

In the second case it is possible for the chloride ions to transfer themselves from the external environment to the inside of the concrete but it is less easy to foresee their penetration rate and concentration at a given depth; it is therefore much more difficult to evaluate the consequences of their entry at the design stage. The chlorides can originate from saline water, or from the atmosphere, or from salt which is spread on roads to prevent ice during the winter. The mechanism which regulates the attack of Cl^- ions on reinforcement is the one which normally governs the iron pitting phenomenon in an alkaline environment. The theories which can explain the pitting phenomenon are very clearly expounded by Foley (172) and discussed by Dehghanian and Locke (173)(174); the final result however is that of an acid attack on the iron, in some small, well-defined areas of the reinforcement, which is self-stimulating due to the hydrolysis of the soluble compound which is formed as follows:

$$FeCl_2 + 2H_2O \rightarrow Fe(OH)_2 + 2HCl$$

From the point of view of kinetic behaviour of iron in an alkaline environment in the presence of chlorides, the comparison of the relevant polarization curve (Fig.30) with that obtained in the absence of chlorides can be very useful (141)(143)(175).

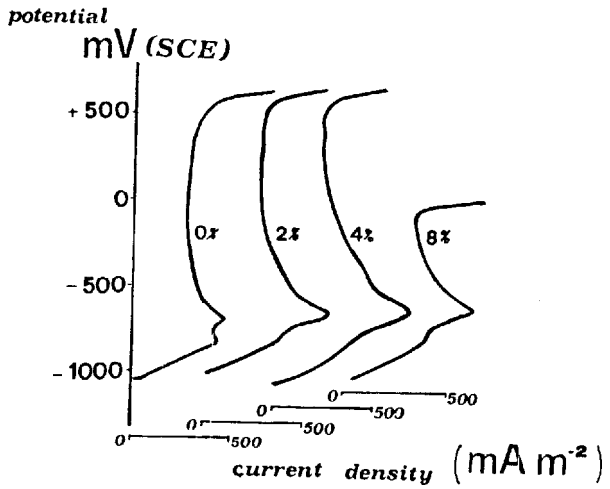

Fig. 30 - Potentiodynamic anodic polarization of mild steel in hydrated OPC pastes of w/c=0.4 containing various percentages of calcium chloride hydrate by weight of cement (sweep rate=1 mV/s) (ref.143)

It is thus possible to show that a drop in the spontaneous potential of the iron in the presence of Cl^- corresponds to the start of an anodic reaction of dissolution which makes the pit develop.

What is instead difficult to determine, and therefore to prescribe, is the maximum admissable chloride content in concrete without the pitting phenomenon taking place; this uncertainty is mainly due to the unknown amount of free chlorides, i.e. of those able to attack the passive layer; the limit concentration value which determines the corrosion possibility depends on many factors including the origin of the chlorides and the accompanying cation (176). In particular, as regards the chlorides which are present right from the moment of mixing, they are bound together due to a greater or lesser degree which results in the formation of insoluble chloraluminates (173)(174)(177-181).

It has also been hypothesized that other constituents of the clinker can react with the Cl^-, decreasing its

danger, but this is open to discussion (179).

The ratio between free and bound chlorides has also not been agreed upon by researchers. This is not surprising if one considers that the parameters which influence this figure are numerous (sulphate content, w/c ratio, curing conditions, nature of cement, nature of cation linked to Cl^-, ect.).It almost appears superfluous to stress that the penetration rate of chlorides is also influenced by temperature.

The use of high-pressure extraction techniques proposed by Longuet (7) and recently applied in the study of this problem (182)(183)(184), could give a definitive response to this controversial question in the near future.

When chlorides only emanate from the environment surrounding the structures the possibility that they will depassivate the reinforcement is strictly linked to their diffusion rate inside the concrete. Various attempts have been made to quantify the rate at which chlorides enter the concrete (185)(186)(187) and pastes of hardened cement (188), by assessing the time required to create a concentration of chlorides exceeding the well known 0.6 value of the Cl^-/OH^- ratio, proposed as the maximum limit for not having corrosion (189)(190).

As regards the quantity of chlorides this is expressed as a weight percentage with respect to the cement and is considered dangerous for the corrosion behaviour of the reinforcement. A frame of reference is given in Table 5 (168)(191)(192).

Table 5

Chloride limits for Portland Cement Mixes (ACI)

Structure	Cl % weight, based on cement weight
Prestressed	0.06
Reinforced structure wet, exposed to Cl environment	0.10
Reinforced structure wet, not Cl in environment	0.15 *
Above ground, dry	no limit

* Also recommended by FHA

II.1.4. Oxygen. A widely-held opinion is that when oxygen is lacking around the reinforcement any possibility of corrosion ceases to exist. This derives from the belief that it is only oxygen which feeds the cathodic reaction in an environment with such a high pH. An indirect demonstration of this hypothesis lies in the experimental observation that the reinforcement of structures completely immersed in seawater has very low corrosion rates (less than 10 μm/y. This is because of the difficulty of the oxygen to diffuse in water-saturated concrete, despite the very negative potentials, peculiar of activity conditions (193). The values of the diffusion rate of oxygen, expressed in mA/m^2, determined by various authors and reported in Table 6, confirm the aforesaid observation (194). The possible presence of static or dynamic loads does not aggravate the situation (195).

Table 6

Oxygen fluxes through saturated concrete. Concretethickness from 20 to 70 mm

Reference	Oxygen flux (mA/m^2)
Wilkins (1979)	< 0.8
Tuutti (1982)	0.5
Vennesland (1981)	< 0.7
Vennesland (1982)	0.3 - 1.5
Gjørv (1976)	0.1 - 2.5
VERITAS	0 - 0.5

However, it must be remembered that if the pH in the environment close to the reinforcement falls to values in the field of acidity, either due to carbonation or, as some authors suggest, to hydrolysis of the iron chloride, the corrosive attack can be considerable even in the absence of oxygen (159).

II.1.5. Influence of Cracks. The determination of the maximum size of cracks which can form on the visible surface of the concrete has been the subject of numerous studies and analyses (196-200), as well as a special research programme (160).

It is naturally necessary to realize that, once again, there are numerous parameters which influence the choice of the maximum acceptable value: origin of the cracks, their static or dynamic nature, type of environment in contact with the structures, longitudinal or transversal position of the cracks with respect to the rods, etc.

These uncertainties are reflected by the fact that the maximum amplitude values which are recommended

vary from 0.1-0.2 mm (201)(202) to 0.4 mm (203) and up to 0.5 mm (194).

II.1.6. Influence of Macro-Cells. Since concrete is a macro-heterogeneous material there may exist within it quite different concentrations of oxygen and chlorides, and even pH; as a consequence macro-cells are formed with a distance of some meters between the anodic and cathodic zones (204)(205)(206).

The worst conditions are to be found when a small, scarcely aerated zone (anode) is combined with a vast area, rich in oxygen (cathode) in the presence of chlorides; in fact in this case a large potential difference between the two areas forms and therefore a high current may flow. The cracks encourage the formation of macro-cells.

II.1.7. Stray Currents. The idea that the presence of stray currents, either direct or alternating, can induce corrosion in concrete reinforcements, finds confirmation in literature (206): corrosion problems are often attributed to the presence of stray electrical current which can result from adjacent electrical facilities.

Moreover, the negative role which, in the long term, the current sent by means of the cathodic protection systems can play on the adhesive force of the concrete on the reinforcement, has been pointed out (207).

II.1.8. Service Time. Taking into account the variables in force and the many approximations, a complex mathematical model was set up a few years ago which allows thw corrosion rate of the reinforcement to be established and the service life of a structure to be forecast (208)(209).
A more realistic approach to the assessement of the "useful life" period of a structure in reinforced concrete has been made by Tuutti (186) and adopted by Schiessl (210), who propose defining this period on the basis of two stages. During the first stage, of t_{in} duration, conditions are created in which the corrosive attack begins; during the second stage, of t_{pr} duration, the attack proceeds and exposes the structure to precarious conditions. Once the period

$$t_{tot} = t_{in} + t_{pr} \text{ (service time)}$$

has passed it is necessary to perform the repairs and reconstruction considered necessary (Fig.31).

Naturally, the preliminary calculation of the times t_{in} and t_{pr} is rather uncertain since it depends on a great many parameters.
Browne, on his side, in order to assess the service time of structures, proposes the following procedure (185).

a. Dust samples are taken at various depths from the surface and chloride ion contents determined.

b. Using the equation

$$C(xt) = C_o \left[1 - \text{erf}\,(x/(2\,D_c\sqrt{t}))\right]$$

where C(xt) = the chloride level at distance, x, after time, t, for an equilibrium chloride level, C_o, at the surface.
D_c = the chloride diffusion coefficient
erf = the error function (obtained from standard tables)

and employing a computer programme, values of C_o and D_c are derived.

c. Having obtained C_o and D_c from samples taken from an actual structure, the chloride level with depth from the surface at any age can be calculated and plotted.

d. To calculate the time to activate the steel, a critical chloride level of 0.4% chloride by weight of cement is taken.

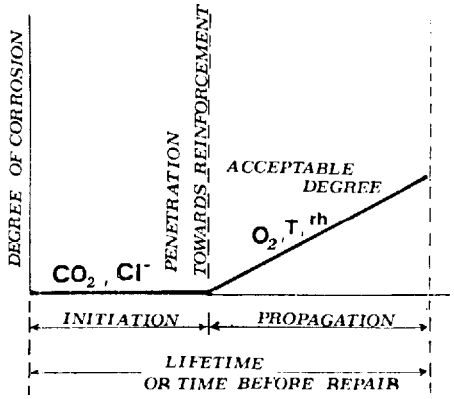

Fig. 31 - Schematic drawing of the corrosion process of steel in concrete.

II.2. Measures Against Premature Deterioration.
As seen in the previous paragraph, reinforcement is normally found in conditions of passivity and thus does not undergo corrosion.

Therefore, in order to prevent the ingress of carbon dioxide and chlorides during initial design and installation preventive measures must be taken.

These measures, as various recent surveys have suggested (194)(211-221), concern both the fabrication methods and the use of techniques belonging to the vast sector of anticorrosion (cathodic protection, use of inhibitors, protective coatings, etc).

In many cases it is advisable to consider the use of both measures.

II.2.1. Executive Process. The parameters influencing

the protective properties of concrete with regards to the reinforcement are: the quality of the water and of the aggregates, the use of additives, the type of cement, the cement content, the water-cement ratio, the thickness of the cover, the working methods and the curing conditions.

The majority of these parameters determine the degreee of porosity and compaction of the concrete and therefore its resistance to diffusion of aggressive agents. The various national organizations responsible for issuing standars have therefore established specifications in this regard, which also take account of the atmospheric environment of the structures to be built. CEB, Comite' Eurointernational du Beton, has undertaken a survey on the standards in use in various countries, as well as the recommendations put forward by European experts (191)(203). Therefore data can be found on the optimal choices regarding parameters during the design stage with a view to adequate prevention of corrosive phenomena concerning reinforcement.

Attention should be paid to the cement quality: a recent survey (222) shows that the use of pozzolanic materials (blast furnace cement, flying ash, highly dense microsilica cement), although in some cases causing an increase in passive current density, give a greater resistance to corrosion due to chlorides with respect to the use of ordinary Portland. Moreover, in recent literature (47)(222-228) results are reported which identify the role played by silica in improving corrosion prevention.

With regard to chlorides the use of sulphur-infiltrated cement has also been suggested to improve the anticorrosion features (229).

II.2.2. Anti-Corrosion Techniques.

II.2.2.1. Coating of Concrete. In environments where it is foreseeable that aggressive substances, and especially chlorides, can penetrate the concrete, it is possible to improve the impermeability by coating the exposed surface. The types of coatings studied are numerous and are listed in various surveys (230)(231)(232).

The main property which a good coating should possess is the low permeation offered to corrosive agents (water, steam, salts). At the same time the coating must have a good bond with the concrete, resistance to abrasion, UV rays stability, and chemical inertia as regards the constituents of the concrete.

It should be stressed that besides the nature of the binder, the choice of fillers and solvents as well as the application methods, are very important. The use of epoxy and urethane resins for coatings appears particularly effective.

On the other hand, the use of sheet-type membranes, suggested as a result of research into the protection of bridge decks, is debatable (233). Such membranes can, in fact, develop problems such as blistering, poor curb sealing and pinholing.

As an alternative to a coating, it is possible to modify a thin surface layer of concrete by impregnation with organic substances such as linseed oil, methyl methacrylate, silanes. The major drawback appears to be the techniqùe of heating which must be carried out with suitable precautions in order no to provoke the formation of cracks (234)(235).
Experiments have been made on wax bead impregnation in the concrete mix; after placement the structure is heated and the wax melts, coating the pores. Problems of heating are similar to those of the organic substances impregnation.

II.2.2.2. Coating of Iron. This is a classic protection method in general industrial practice. As regards concrete reinforcement, two types of coatings have been specially studied: epoxy painting and galvanizing, the use of which is debatable.

A little over ten years have passed since the first widescale use of reinforcements coated with epoxy resins (236). The types of resins which can be used have been thoroughly studied and data on the behaviour of coated rods as regards corrosion is promising (237)(238). Recommended epoxy coating thickness to guarantee a good adherence to concrete are in the order of 5-10 mils. Cement-slurried wires have also shown a good behaviour with regard to corrosion (239). Tests conducted on iron deliberately painted with very defective coatings still denote a considerable improvement in resistance to corrosion (211).

The use of zinc coatings on reinforcement rods, achieved by hot immersion,has been widely studied (240-249) and is also the subject of an ASTM standard (250).

Even today there is no unanimity of views on the effectiveness of such a coating; in particular it seems that the good results obtained in the US over the last decades, which have led to the use of galvanized rods in more than 2% of reinforced concrete structures, have not already had positive confirmation in Europe (240) nor in Japan (221).

The main reason for this difference in behaviour could lie in the lower alkaline content required by American specifications, and consequently in the lower pH value of the solutions contained in the pores (243)(244).

Attempts to prevent zinc corrosion with chrome treatment or with the addition of chromates to the mixture during the stage in which the cement is still fresh have not given appreciable results (221)(240).

In addition, doubts have been raised about the soundness of the adhesion between the galvanized rods and the concrete (241).

II.2.2.3. Use of Inhibitors. Until the early Seventies, research into the use of possible inhibitors to add to the concrete in order to decrease the corrosion tendency of the reinforcement, mainly due to chlorides, was directed to oxidants as chromates, phosphates, nitrites, benzoates, used for corrosive waters. Subsequently, efforts were almost totally concentrated on the study of inhibitive properties of one product: calcium nitrite. This product, unlike sodium nitrite which is equally effective in inhibiting corrosion, does not have deleterious effects on concrete strength, and also acts as an accelerator (251-255).

The mechanism proposed to explain the passivating features of calcium nitrite is the same as that put forward to explain its functioning in an aqueous solution; it should however be pointed out that its capacity to delay the start of corrosive phenomena in the presence of chlorides is limited to a chloride/nitrite molar ratio of 1.5, above which the additive is no longer effective. The water/cement ratio, and therefore the use of water reducers, also play a considerable role, so much so that it seems certain that for w/c > 0.5 the presence of nitrite in the mixture becomes useless(255).

II.2.3. Electrochemical Methods.

II.2.3.1. Electrochemical Removal of Chlorides. A series of tests conducted by Slater demonstrate that, by applying an electric field to the reinforced concrete structure which already contains a dangerous amount of chlorides, one can, with a few devices, remove a considerable percentage of them, thus ensuring that their concentration drops to levels which will not induce corrosion (256). This method still requires further testing and, moreover, its economic feasibility must be demonstrated.

II.2.3.2. Cathodic Protection. Cathodic protection of reinforcement was first applied in the field in the early sixties and has always had difficulty in achieving wide acceptance, despite growing development in the bridge deck sector.

A few years ago the ASTM organized a convention on steel corrosion in the presence of chlorides at which were greatly emphasized attempts made prior to W.W.II to apply cathodic protection methods to reinforcement to prevent corrosion (257)(258).

There are evidently no great difficulties to overcome in the case of reinforced concrete structures in contact with electrolytes (buried pipes, tank interiors, offshore platforms, etc.) since the design criteria of traditional cathodic protection systems can be applied to them (259).

There is instead, given the particular nature of the configuration of aerial reinforced concrete structures, a salient fact in designing a cathodic protection system for reinforcement rods, which is that it has to be carried out when the structure is being designed. In fact, it is necessary to prepare in advance, at the appropriate time, both the short circuit connection of the entire steel rod network and the arrangement of the auxiliary and references electrodes which permit the protective electric circuit to be closed, an arrangement which causes some problems. Much has already been done, but much still remains to be done, precisely in relation to the solution of these practical problems. In addition, the electrochemical criteria which govern cathodic protection in concrete are still today being discussed.

A study by Haussmann in 1969 (260) gives as voltage values for rod protection -0.50 volt and -0.71 volt respectively (vs. copper-copper sulphate reference electrode) for steel reinforcement uncorroded and for reinforcement already corroded.

Subsequent experiments, in particular those conducted in the presence of chlorides and therefore in an environment in which steel passivation can be less, advise values of -0.77 (261)(262) or even less negative (263)(264) or values to be established on a case by case basis (265)(266)(267)(268).

For protection with impressed currents as auxiliary electrodes, besides the traditional ones in graphite and iron silicon usable for buried or immersed structures, the use of conductive layers or conductor concretes with embedded metallic wires are suggested for aerial structures (269)(270).

Given the relatively modest power consumption required for cathodic protection of concrete reinforcement, the use of solar energy generators has been tested in recent times (271)(272). Not being competitive where there is the possibility of using mains current these have found applications in the protection of off-shore platforms and in bridge decks situated in isolated areas. Given the discontinuity of the power supply of photovoltaic generators, the influence of the decrease or cancellation of the power was studied in order to decrease the accumulators capacity (273)(274). The results were conflicting, even though the hypothesis of Fromm and Wilson (275) appears promising and reveal that the duration of the non-corrosion of the concrete reinforcement left to itself after a long period of cathodic protection is about 160 hours.

For sacrificial anode protection systems, magnesium, zinc and Al-Zn-In alloy anodes have been used with

success (276)(277). The latter seem to be preferred because magnesium when embedded in concrete gives voluminous corrosion products which crack the structure and zinc does not give a sufficient potential difference between it and steel.

II.3. Corrosion Monitoring of Concrete Reinforcement. In the case of reinforced concrete it is possible to visibly ascertain a state of corrosion of the rods only when the corrosive phenomena are already well advanced.

Over the past years, besides the well-tested, if debatable, evaluation method based on measuring the potential with respect to a reference electrode, various other instrumental measurement methods have been proposed: electrical resistance, linear polarization resistance, electrochemical potential noise, AC impedance.

Two recent surveys on the evaluation of the state of corrosion of reinforcements are those of Perenchio (278) and Dawson (279): the first is directed more towards the examination of already collapsed structures, while the second discusses investigation methods which can possibly be adopted in situ. A summary of the main electrochemical detection research, with particular reference to reinforced concrete is given in (280) and (281).

Obviously, the case of laboratory studies is different, since the corrosion tendency of iron controlled as a function of various experimental parameters can be considerably facilitated by adopting methods which are not easily extended to field measurements.

II.3.1. Electrical and Electrochemical Tests.

II.3.1.1. Corrosion Potential. It is very easy to measure the spontaneous potential, or free corrosion or half-cell potential of reinforcement, when the reinforcement is entirely short-circuited (which does not always occur in reality) (282-287). The technique is described in an ASTM specification (288) and can be summarized as follows: the measuring circuit given in Fig. 32 is set up, taking care that the contact between the concrete surface and the reference electrode is made by inserting a sponge soaked in a solution with a high electric conductivity.

The electric contact with the reinforcement must be obtained on any rod emanating from the structure or with the external metal parts, as long as it is ensured that they are in turn short-circuited with the reinforcement.

The reference electrode is usually copper-saturated copper sulphate, but it can also be a saturated calomel. The results obtained are normally represented by a map on which equipotential lines are given: it can be equally just as useful to construct a potential graph of halfcell vs cumulative frequency.

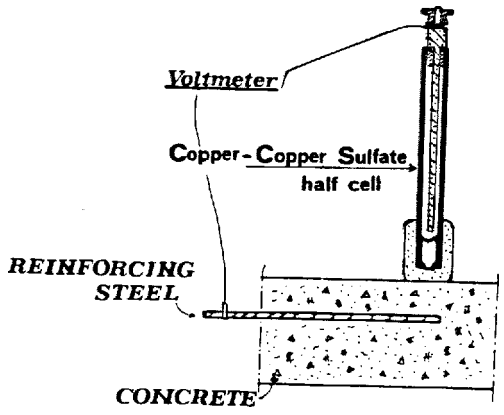

Fig. 32 - Copper-Copper Sulfate Half Cell Circuitry.

The state of corrosion of the different portions of the reinforcement in relation to the potential values measured (referred to the electrode $Cu/CuSO_4$) is the following:

$E > -0.20$ V 90% probability of absence of corrosion
$E > -0.35$ V 90% probability of corrosion
$-0.35 < E < -0.20$ V uncertain situation

Recently, the use of the reference electrode $Cu/CuSO_4$ for measurements on concrete has been advised against, since relatively high-value diffusion potentials could form on the contact surface between the solution contained in the electrode and the alkaline solution contained in the pores of the concrete (289).

When considering old structures, another source of uncertainty in the measurement could be given by a surface layer of concrete with high resistivity; in this case it is advisable to locally remove this layer before measuring.

As regards the significance of the measurements obtained, there are two trends. According to some authors (290)(291) a certain relation can be found between the potential values and the corresponding corrosion rate. Other authors (134)(279)(292) give more importance to the differences in potential found between different points than in the absolute values of the measurements; if one considers, for example, the case of water-saturated structures, the potential is very negative due to the lack of oxygen, but the corrosion rate is very low, contrary to what the ASTM standard would lead one to suppose. In these cases it is proposed to give greater importance to the diffe-

rences in potential between different points of the reinforcement or to the gradients between the isopotential curves.

II.3.1.2. Electrochemical Noise. This probably represents the most interesting novelty of the last years in the field of corrosion monitoring and, although still at an early stage, could lead to interesting developments, especially for identifying localized forms of corrosion such as pitting and crevices.

The measuring technique consists of finding the spontaneous fluctuations of the corrosion potential by means of a highly sensitive voltmeter with a data logger; the signal is then transformed from the time domain to the frequency one using an algorithm based on FFT (Fast Fourier Transform) or MEM (Maximum Entropy Method). The duration of the measurement depends on the frequency fields concerned and varies from 15' to 2h.

The experiments which have already been conducted both in the laboratory and on installed structures seem to give the following indications: in the absence of corrosion a slight variation of the potential is observed accompanied by random fluctuations; in the presence of pitting, a series of sudden falls and rises of the potential is recorded followed by a relatively slow exponential recovery; the slope of the noise/frequency curve is less than that noticed in the absence of corrosion; the standard deviation of the noise is proportional to the corrosion rate (279)(292)(293).

II.3.1.3. Electrical Resistance. This method is based on the obvious consideration that the thinning of a sheet or the diminution of the diameter of a filament due to corrosion leads to an increase of electrical resistance. It is widely used for the corrosion rate determination in fluids with low conductivity, especially in petroleum liquids. In the case of reinforced concrete, the electrolyte is the concrete itself, and the probe containing the filament or sheet must be inserted into the structures either during installation (new structures) or during reparation (old structures); in both cases, the position of the test element must be similar to that of the rods and several probes should be inserted so that the results represent the state of the entire reinforcement. The slope of the electrical resistance-time curves allows, when the dimensions of the starting element are known, the generalized corrosion rate to be calculated in terms of annual peretration(294).

This type of measurement does not allow a situation of localized attack (pitting) to be recognized at the moment it takes place. However, it may be adopted to control the functioning of the cathodic protection (257).

II.3.1.4. Polarization Resistance. For some years the measurement technique for linear polarization resistance (LPR) has ben applied in many sectors of the industry and has been thoroughly investigated both in theoretical studies and by means of practical applications.

The measurement is based on the Stern and Geary equation, which relates the corrosion current density, i, (due to the functioning of local cells) with the variation in potential to which the material under examination is submitted following the passage of imposed current:

$$I_{corr} = \left[ba.bc/2.3(ba+bc)\right] i/\Delta V$$

where ba and bc are the coefficients of Tafel's equations relevant to oxidation and reduction reactions respectively. The term $\Delta V/i$ is given the name of polarization resistance and is measured in ohm x cm^2 (i is a current density) (295). For practical reasons it must be ensured that the variation in potential is always the same (for example 5 or 10 mV), taking into account that the coefficients ba and bc do not vary very much as long as the ervironment is the same (for example concrete); if the environmental conditions vary (oxygen content, pH, presence of chlorides), the expression becomes:

$$I_{corr} = B \cdot i$$

Moreover, taking Faraday's laws into account, one has:

$$v_{corr} = k \cdot i$$

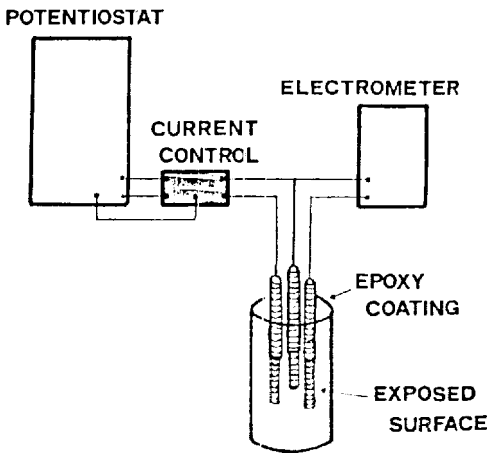

Fig. 33 - Galvanostatic polarization set up using rebars as reference, working and counter electrode (ref. 297)

The practical implementation of the measurement is obtained by using a circuit of the type illustrated in Fig.33. In order to determine the corrosion beha-

viour over time, the three electrodes are normally equal and made of the same material as the reinforcement (in the case of reinforced concrete, three pieces of bars); the electrode which functions as a reference, can also be of another material but for practicality, and especially for concrete, it is usually the same as the other two.

Sometimes only two electrodes are used, and in this case they are both subjected to polarization, one cathodic and the other anodic; it is considered that this method is less precise than the previous one, since the result can be affected by considerable errors due to the fact that the polarization phenomena in both directions (anodic and cathodic) are very different.

For several years the measurements of the corrosion rate of reinforcement rods by surveying the polarization resistance has been carried out (296)(297) on laboratory test pieces. When this method is used on structures, it is necessary to place a suitable number of probes in selected positions at the time of construction in order to follow the corrosion progress over time.

Unlike the electrical resistance method, that of polarization resistance allows the actual corrosion rate to be determined at any given moment. However in the case of reinforced concrete structures this does not constitute a preferential element since concrete characteristics are not subject to sudden variations and consequently neither is the corrosion rate.

Among the limitations in the use of this technique there is the poor conductivity of some concretes: if the resistivity of the electrolyte reaches 10^6 ohm . cm (per 3-electrode probe) or even only 10^5 ohm . cm (per 2-electrode probe) the ohmic drop in the electrodes must be considered too high and the values obtained are extremely inaccurate. Also, in this case, as for measurements based on electrical resistance variations, it is not possible to obtain reliable indications of the occurrence of pitting attacks.

The values of the B constant suggested for calculating the corrosion current density are 26 mV for rods in an active state and 52 mV for those in the passive state (296), but very different values have also been calculated and employed (298)(299).

Over and above the uncertainties and limitations introduced both by the choice of coefficient B and resistivity of the concrete, the tests conducted to date appear to demonstrate that the corrosion rate measurements based on the determination of the polarization resistance are sufficiently reliable.

II.3.1.5. Alternating Current Impedance. Electrochemical impedance is a term which refers to the interface response of an electrochemical system, of the type to be found between an electrode which corrodes and the surrounding environment, with an electrochemical disturbance transmitted from outside.

Obviously the electrochemical interface does not behave like a simple resistance but like a combination of various elements: the simplest equivalent circuit includes the resistance of the electrolyte, the capacitance of the double electrochemical layer and the resistance of the charge transfer. This last term is equal to the polarization resistance and is therefore inversely proportional to the corrosion rate.

Impedance measurements can be carried out in the domain of the frequencies by applying a small-amplitude disturbance (10-20 mV) as a sinusoidal wave of known frequency and observing the phase displacement and the impedance module, and then repeating the measurement at different frequencies in a chosen field (between 10 kHz and 1 mHz for concrete) (152)(259)(300).

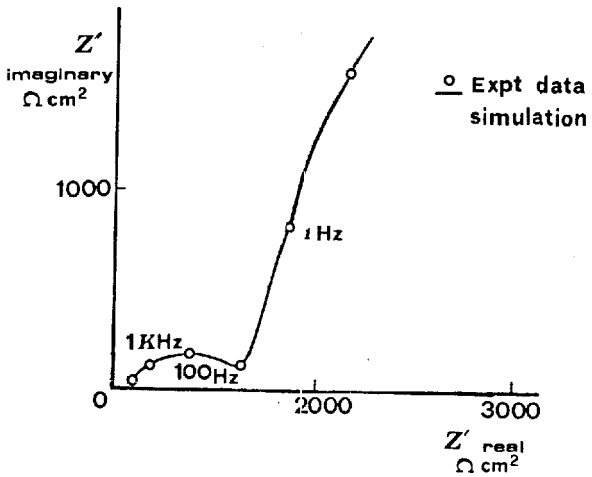

Fig. 34 - Impedance plot from steel in concrete

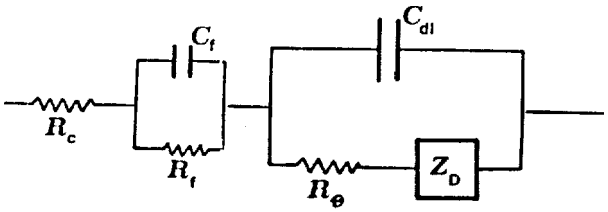

FIG. 35 - Equivalent circuit used for computer simulation of impedance data (ref. 303)

The measurement is normally done with a digital instrument known as a frequency response analyser (FRA) or transfer function analyser (TFA). The data

are then processed by a computer equipped with suitable programs and a graph is obtained of the type given in Fig. 34. For concrete reinforcement, Dawson and his collaborators (301) propose the equivalent circuit of Fig. 35, in which the charge transfer resistance is in series with a Warburg diffusion term and both are in parallel with the capacitance of the double layer. In this way it is possible to calculate the resistance of the electrolyte and of the corrosion products, as well as the resistance of the charge transfer which corresponds to the polarization resistance. It is also possible to have indications on the reaction mechanisms, if that is the system under activation and diffusion control and if the phenomena of absorption, etc. intervene (152)(302)(303)(304).

The technique has thus been applied both for studying the corrosion mechanisms of rods in concrete and for finding real values for the polarization resistance not influenced by the concrete resistance. Rp can be directly employed in Stern and Geary's equation for calculating the corrosion rate. However, for evaluating the state of the reinforcement, some authors consider that given the uncertainty about the real value of coefficient B, the measurement technique based on the electrochemical impedance does not lead to any substantial improvements (305)(306).

II.3.2. Other Types of Tests. The visual inspection of a damaged structure can supply a certain amount of information (278)(279).

Cracking patterns can indicate the presence of structural problems, drying shrinkage, corrosion of reinforcement, etc. In addition, if freezing-thawing phenomena have caused the external layer of the concrete to become rubble, there is the clear indication that this layer can act as a sponge, encouraging the absorption of salt water and therefore corrosion. Finally, it is possible to note if there are conditions which facilitate the corrosive attack at the poorly-made patches perimeters.

A structure which has undergone a delamination which is not yet perceptible from the outside produces a different sound from that of a healthy structure when submitted to a mechanical blow.

This observation is the basis of mechanical survey methods, often used as a first test by the American Highway Research and Department of Transportation. It involves dragging a length of chain over the surface and examining the sound obtained: the delaminated areas respond with a hollow sound.
An analogous comparative test can be conducted with Schimdt's hammer: any presence of voids formed by delamination give a response similar to that obtained with concrete which has a lower compression resistance.

The infrared thermography detection of concrete delamination, mainly due to corrosion phenomena, is based on the difference in surface temperature which exists between sound and unsound concrete. This technique has been succesfully applied to concrete bridge decks (307).

Moreover samples can be removed in order to determine the condition of the concrete and the state of corrosion of the reinforcement. The depth of the carbonation can be demonstrated by means of a phenolphthalein indicator. A purple stain indicates the areas where the basicity of the concrete has remained high.

Core sampling permits the concentration of chloride and sulphate ions present at various depths to be evaluated by chemical analysis, as well as the measurement of some physical characteristics such as porosity, permeability, etc. Mechanical resistance tests can be carried out on the cores.

Before coring and after the appropriate calibration, it is useful to detect the thickness of the cover by means of a Pachometer.
The instrument is based on a transitorized oscillator which provokes the formation of an electromagnetic field in a coil, which is distorted by the presence of the reinforcement rod.

The detection of the acoustic emission i.e. of the little noise resulting from the concrete subjected to loads due to embedded metal corrosion, is considered by some Authors to be very important for laboratory studies, and can also be successfully extended to field situations in substitution for those listed above (308)(309).

REFERENCES

1) L.S.Dent Glasser "Osmotic Pressure and the Swelling of Gels". Cem. Concr. Res., 9, 515-517 (1979).

2) L.S. Dent Glasser, and N. Kataoka "The Chemistry of Alkali-Aggregate Reactions". Proc. 5th Int. Conf. on "Alkali-Aggregate Reaction in Concrete", Cape Town, March 30- April 3, 1981, S252/23, 8 pp.

3) H.E. Vivian "Some Effects of Temperature on Mortar Expansion". Austr. J. Appl. Sci., 2, 114-122 (1951).

4) W.A. Gutteridge, and D.W. Hobbs "Some Chemical and Physical Properties of Beltane Opal Rock and Its Gelatinous Alkali-Silica Reaction Product". Cem. Concr. Res., 10, 183-193 (1980).

5) J.B. Jones, and E.R Segnit "Nature of Opal. I. Nomenclature and Constituent Phases" J. Geol. Soc. Austr., 18(1), 57-68 (1971).

6) L.S. Dent Glasser, and N. Kataoka "The Chemistry

of Alkali-Aggregate Reaction". Cem. Concr. Res., 11, 1-9 (1981).

7) P. Longuet, L. Burglen and A. Zelwer "La Phase Liquide du Cement Hydrate". Rev. Mater. Constr., 1, 35-41 (1973).

8) R.S.Barneyback Jr, and S.Diamond "Expression and Analysis of Pore Fluids from Hardened Cement Pastes and Mortars". Cem. Concr. Res., 11, 279-285 (1981).

9) S. Diamond, R.S. Barneyback, Jr, and L.J. Struble "On the Physics and Chemistry of Alkali-Silica Reaction". Proc. 5th Int. Conf. on "Alkali-Aggregate Reaction in Concrete". Cape Town, March 30-April 3, 1981, S252/22, 10 pp.

10) S. Diamond "Alkali Reaction in Concrete-Pore Solutions Effects". Proc. 6th Int. Conf. on "Alkalis in Concrete", Copenhagen, June 22-25, 1983, 155-166.

11) D.W. Hobbs "The Alkali-Silica Reaction- A Model for Predicting Expansion in Mortar", Mag. Concr. Res., 33, 208-219 (1981).

12) L.S. Struble "Swell and Other Properties of Synthetic Alkali-Silica Gels". M.S. Thesis, School of Civil Engineering, Purdue Univ., 150 pp. (1979).

13) L.J. Struble, and S. Diamond "Swelling Properties of Synthetic Alkali-Silica Gels". J. Am. Cer. Soc., 64, 652-655 (1981).

14) L.J. Struble, and S.Diamond "Unstable Swelling Behaviour of Alkali-Silica Reaction". Cem. Concr. Res., 11, 611-617 (1981).

15) L.S. Dent Glasser, E.E. Lachowski, and G.G. Cameron "Studies on Sodium Silicate Solutions by the Method of Trimethylsilation". J. Appl. Chem. Biotechnol., 27, 39-47 (1977).

16) M. Kawamura, K. Takemoto, and S. Hasaba "Application of Quantitative EDXA Analyses and Microhardness Measurements to the Study of Alkali-Silica Reaction Mechanisms". Proc. 6th Int. Conf. on "Alkalis in Concrete", Copenhagen, June 22-25, 1983, 167-174.

17) T.C. Powers, and H.H. Steinour "An Interpretation on Some Published Researches on the Alkali-Aggregate Reaction". ACI J.,51, 781-811 (1955).

18) A.B. Poole, and I. Al-Dabbagh "Reactive Aggregates and the Products of Alkali-Silica Reaction in Concretes". Proc. 6th Int. Conf. on "Alkalis in Concrete", Copenhagen, June 22-25,1983, 175-184.

19) M. Regourd, H. Hornain, and P. Poitevin "The Alkali-Aggregate Reaction-Concrete Microstructural Evolution". Proc. 5th Int. Conf. on "Alkali-Aggregate Reaction in Concrete", Cape Town, March 30-April 3, 1981, S252/35, 9 pp.

20) M. Regourd, H. Hornain, B. Mortureux, P. Poitevin. and H. Peuportier "Alterations de la Liaison de Ciment-Granulats dans le Béton. La Réaction Alcalis-Granulats". Colloque International "Liaisons Pates de Ciment-Materiaux Associés". Toulose, Nov. 1982, B.17.

21) W.F. Cole, C.J. Lancucki, and M.J. Sandy "Products Formed in an Aged Concrete". Cem. Concr. Res., 11, 443-454 (1981).

22) R.E. Oberholster "Alkali Reactivity of Siliceous Rock Aggregates: Diagnosis of the Reaction, Testing of Cement and Aggregate and Prescription of Preventive Measures". Proc. 6th Int. Conf. on "Alkalis in Concrete", Copenhagen, June 22-25, 1983, 419-433.

23) W.F. Cole, C.J. Lancucki, and M.J. Sandy "A Replay to the Discussion by Alan D. Buck and Katharine Mather of the Paper "Products Formed in an Aged Concrete".Cem.Concr.Res.,12,129-130 (1982).

24) W.F. Cole, and C.J. Lancucki "Products Formed in an Aged Concrete - The Occurrence of Okenite". Cem. Concr. Res., 13, 611-619 (1983).

25) A.D. Buck, and K. Mather "Alkali-Silica Reaction Products from Several Concretes: Optical, Chemical, and X-Ray Diffraction Data". Proc. 4th Int. Conf. on "Effects of Alkalies in Cement and Concrete", Purdue University, June 4-7, 1978, 73-85.

26) K. Mather "Condition of Concrete in Martin Dam after 50 Years of Service". Cem. Concr. Aggregates, 3, 53-62 (1981).

27) M. Regourd "Methods of Examination". Proc. 6th Int. Conf. on "Alkalis in Concrete", Copenhagen,June 22-25, 1983, 275-289.

28) J.H.P. Van Aardt, and S. Visser "Reaction between Rocks and the Hydroxides of Calcium, Sodium and Potassium: Progress Report No. 1". National Building Research Institute, Pretoria, 14 pp. (1982).

29) J.H.P. Van Aardt, and S. Visser "Reaction between Rocks and the Hydroxides of Calcium, Sodium and Potassium: Progress Report No. 2". National Building Research Institute, Pretoria, 34 pp. (1982).

30) T.E. Stanton "Expansion of Concrete through Reaction between Cement and Aggregate". ASCE Proc., 66, 1781-1811 (1940).

31) D. Stark "Alkali-Aggregate Reactivity in the Rocky Mountain Region". Proc. 4th Int. Conf. on "Effects of Alkalies in Cement and Concrete", Purdue University, June 4-7, 1978, 235-243.

32) D. Stark "Alkali-Silica Reactivity:Some Reconsi-

derations". Cem.Concr.Aggregates, 2,92-94 (1980).

33) S.J. Way and W.F. Cole "Calcium Hydroxide Attack on Rocks". Cem. Concr. Res., 12, 611-617 (1982).

34) J.H.P. Van Aardt, and S. Visser "Calcium Hydroxide Attack on Feldspars and Clays: Possible Relevance to Cement-Aggregate Reactions". Cem. Concr. Res., 7, 643-648 (1977).

35) R.I.A. Malek, and D.M. Roy "Effect of Slag Cements and Aggregaem Type on Alkali-Aggregate Reaction and Its Mechanisms". Proc. 6th Int. Conf. on "Alkalis in Concrete", Copenhagen, June 22-25, 1983, 223-230.

36) J. Brotschi, and P.K. Mehta "Test Methods for Determining Potential Alkali-Silica Reactivity in Cement". Cem. Concr. Res., 8, 191-199 (1978).

37) P.E. Grattan-Bellew, and J.J. Beaudoin "Effect of Phlogopite Mica on Alkali-Aggregate Expansion in Concrete". Cem. Concr. Res., 10, 789-797 (1980).

38) "Minimizing the Risk of Alkali-Silica Reaction-Guidance Notes". Available from the Cement Concrete Association, Oct. 1985.

39) W. Pettifer, and P.J. Nixon "Alkali Metal Sulphate- A Factor Common to both Alkali-Aggregate Reaction and Sulphate Attack on Concrete". Cem. Concr. Res., 10, 173-181 (1980).

40) S. Chatterji "The Role of $Ca(OH)_2$ in the Breakdown of Portland Cement Concrete Due to Alkali-Silica Reaction". Cem. Concr. Res., 9, 185-188 (1979).

41) S. Chatterji, N. Thaulow, P. Christensen, and A.D. Jensen "Studies of Alkali-Silica Reaction with Special Reference to Prevention of Damage in Concrete, a Preliminary Study". Proc. 6th Int. Conf. on "Alkalis in Concrete", Copenhagen, June 22-25, 1983, 253-260.

42) Department of the Environment, Building Research Establishment "Alkali-Aggregate Reactions in Concrete". Her Majesty's Stationery Office, London, BRE Digest 258, 8 pp. (1982).

43) D.W. Hobbs "Influence of Pulverized-Fuel Ash and Granulated Blastfurnace Slag upon Expansion Caused by the Alkali-Silica Reaction". Mag. Concr. Res., 34, (119), 83-94 (1982).

44) R.A. Kennerley, D.A. St John, and L.H. Smith "A Review of Thirty Years of Investigation of the Alkali-Aggregate Reaction in New Zealand". Proc. 5th Int. Conf. on "Alkali-Aggregate Reaction in Concrete", Cape Town, March 30-April 3, 1981, S252/12, 9 pp.

45) F.G. Buttler, S.R. Morgan, and E.J. Walker "Studies on the Rate and Extent of Reaction between Calcium Hydroxide and Pulverised Fuel Ash". Proc. 5th Int. Conf. on "Alkali-Aggregate Reaction in Concrete", Cape Town,March 30-April 3,1981,S252/38,9 pp.

46) L. Boswell, E.C. Roberts, F.C. Buttler, and S.R. Morgan "Alkali Content and Expansion of Mortars Containing Pulverized Fuel Ash". Proc. 6th Int. Conf. on "Alkalis in Concrete", Copenhagen, June 22-25, 1983, 231-238.

47) C.L. Page, and D. Vennesland "Pore Solution Composition and Chloride Binding Capacity of Silica-Fume Cement Pastes". Mater. Constr. (Paris), 16, (91), 19-24 (1983).

48) S. Diamond "Effects of Two Danish Flyashes on Alkali Contents of Pore Solutions of Cement-Flyash Pastes". Cem. Concr. Res., 11, 383-394 (1981).

49) R.S. Barneyback, Jr. "Alkali-Silica Reactions in Portland Cement Concrete". Ph. D. Thesis, Purdue University, 352 pp. (1983).

50) F.P. Glasser, and J. Marr "The Alkali Binding Potential of OPC and Blended Cements". Il Cemento, 82, 85-94 (1985).

51) E.J. Sellevold, D.H. Bager, E. Klitgaard Jensen, and T. Knudsen "Silica Fume-Cement Pastes: Hydration and Pore Structure". Proc. Nordisk Mini-Seminar on "Silica in Concrete", Trondheim, Dec. 10, 1981, 32 pp.

52) F.P. Glasser, M.J. Angus, C.E. McCulloch, D. MacPhee, and A.A. Rahman "The Chemical Environment in Cements". Scientific Basis for Nuclear Waste Management VIII. Mater. Res. Soc., Pittsburg PA, 44, 849-858 (1985).

53) P.L. Rayment "The Effect of Pulverized-Fuel Ash on the C/S Molar Ratio and Alkali Content of Calcium Silicate Hydrates in Cement". Cem. Concr. Res.,12,133-140 (1982).

54) P. Poitevin, and M. Regourd "Durabilité des Bétons: Cas des Granulats Réactifs". Annales de l'ITBTP Série:Matériaux, 59, (413), 110-140 (1983).

55) F.P. Glasser, A.A. Rahman, C.E. McCulloch, M.J. Angus, and D. MacPhee "Immobilization Potential of Cements for Soluble and Insoluble Radwaste Constituents". Proc. Am. Concr. Inst. Symp. (in press).

56) Tang Ming-shu, Ye Yu-feng, Yuan Mei-qi, and Zen Shi-hua "The Preventive Effect of Mineral Admixtures on Alkali-Silica Reaction and Its Mechanism". Cem. Concr. Res., 13, 171-176 (1983).

57) G.J. Verbeck, and C. Gramlich "Osmotic Studies

and Hypothesis Concerning Alkali-Aggregate Reaction". ASTM Proc., 55, 1110-1131 (1955).

58) Tang Ming-shu, and Han Su-fen "Rapid Method for Determining the Preventive Effect of Mineral Admixtures on Alkali-Silica Reaction". Proc. 6th Int. Conf. on "Alkalis in Concrete", Copenhagen, June 22-25, 1983, 383-386.

59) P.K. Mehta "Performance of Concrete in Marine Environment". SP-65 American Concrete Institute, Detroit, 1-20.

60) H.G.S. Smolczyk "Slag Structure and Identification of Slags". Proc. 7th Int. Congress on "The Chemistry of Cement", Paris, 1980, Vol. 1, III-1/3-III-1/11.

61) E.O. Gjorv, and O. Vennesland "Diffusion of Chloride Ion from Sea Water" Cem. Concr. Res., 9, 229-238 (1979).

62) K.M. Parker, and D.M. Roy "Porosity, Permeability and Microstructure of Portland-Blastfurnace Slag Cement Pastes". Am. Cer. Soc. Bull., 61, 345- 357 (1982).

63) M. Regourd " Discussion on Paper S252/29". Proc. 5th Int. Conf. on "Alkali-Aggregate Reaction in Concrete", Cape Town, March 30-April 3, 1981.

64) R.F.M. Bakker "About the Cause of the Resistance of Blastfurnace Cement Concrete to the Alkali-Silica Reaction". Proc. 5th Int. Conf. on "Alkali-Aggregate Reaction in Concrete", Cape Town, March 30-April 3, 1981, S252/29, 6 pp.

65) R. Kondo, M. Satake, and H. Ushiyama "Diffusion of Various Ions in Hardened Portland Cement". Cem. Assoc. of Japan, 28th Gen. Meet., Tokyo, May 1974, 41-43.

66) H.G.S. Smolczyk "Investigation on the Diffusion of Na Ion in Concrete". Symp. on "Alkali-Aggregate Reaction", Reykjavik, 1975, 183-188.

67) D.M. Roy, and G.M. Idorn "Hydration, Structure and Properties of Blastfurnace Slag Cements, Mortars and Concrete". ACI J., 79, (43), 444-457 (1982).

68) S. Chatterji, and N.F. Clausson-Kaas "Prevention of Alkali-Silica Expansion by Using Slag-Portland Cement". Cem. Concr. Res., 14, 816-818 (1984).

69) R.E. Oberholster, and W.B. Westra "The Effectiveness of Mineral Admixtures in Reducing Expansion Due to Alkali-Aggregate Reaction with Malmesbury Group Aggregates". Proc. 5th Int. Conf. on "Alkali-Aggregate Reaction in Concrete", Cape Town, March 30-April3, 1981, S252/31, 6 pp.

70) G. Gudmundsson, and H. Asgeirsson "Parameters Affecting Alkali Expansion in Icelandic Concretes". Proc. 6th Int. Conf. on "Alkalis in Concrete", Copenhagen, June 22-25, 1983, 217-221.

71) P.C. Aitcin, and M. Regourd "The Use of Condensed Silica Fume to Control Alkali-Silica Reaction. A Field Case Study". Cem. Concr. Res.,15, 711-719 (1985).

72) D.W. Hobbs "Expansion Due to Alkali-Silica Reaction and the Influence of Pulverized Fuel Ash". Proc. 5th Int. Conf. on "Alkali-Aggregate Reaction in Concrete", Cape Town, March 30-April 3, 1981, S252/30, 10 pp.

73) D.W. Hobbs "Possible Influence of Small Additions of Pfa, Ggbf and Limestone Flour upon Expansion Caused by the Alkali-Silica Reaction". Mag. Concr. Res., 35, (122), 55-58 (1983).

74) P.J. Nixon, and M.E. Gaze "The Use of Flyash and Granulated Blastfurnace Slag to Reduce Expansion Due to Alkali-Aggregate Reaction". Proc. 5th Int. Conf. on "Alkali-Aggregate Reaction in Concrete", Cape Town, March 30-April 3, 1981, S252/32, 10 pp.

75) P.J. Nixon, and M.E. Gaze "The Effectiveness of Flyashes and Granulated Blastfurnace Slags in Preventing AAR". Proc. 6th Int. Conf. on "Alkalis in Concrete", Copenhagen, June 22-25, 1983, 61-68.

76) M.E. Gaze, and P.J. Nixon "The Effect of Pfa upon Alkali-Aggregate Reaction". Mag. Concr. Res., 35, (123), 107-110 (1983).

77) L.C. Porter "Small Proportions of Pozzolan May Produce Detrimental Reactive Expansion in Mortar". Denver, U.S. Dept. of the Interior, Bureau of Reclamation, July 1964, Report No. C-113, 22 pp.

78) L. Pepper, and B. Mather " Effectiveness of Mineral Admixtures in Preventing Excessive Expansion of Concrete Due to Alkali-Aggregate Reaction". ASTM Proc., 59, 1178-1202 (1959).

79) E.R. Dunstan "The Effect of Flyash on Concrete Alkali-Aggregate Reaction". Cem. Concr. Aggregates, 3, (2), 101-104 (1981).

80) ASTM C295-85 "Standard Practice for Petrographic Examination of Aggregates for Concrete". Annual Book of ASTM Standards, Vol. 04.02, Sect. 4, 220-230 (1985).

81) G. Samuel, A.K. Mullick, S.P. Ghosh, and R.C. Wason "Alkali-Silica Reaction in Concrete - SEM and EDAX Analyses". Proc. 6th Int. Conf. Cem. Microsc., 276-291 (1984).

82) L.M.M. Dolar-Mantuani "Undulatory Extinction in

Quartz Used for Identifying Potentially Alkali-Reactive Rocks". Proc. 5th Int. Conf. on "Alkali-Aggregate Reaction in Concrete", Cape Town, March 30-April 3, 1981, S252/36, 6 pp.

83) P.E. Grattan-Bellew "Evaluation of Test Methods for Alkali-Aggregate Reactivity". Proc. 6th Int. Conf. on "Alkalis in Concrete", Copenhagen, June 22-25, 1983, 303-314.

84) ASTM C289-81 "Potential Reactivity of Aggregates (Chemical Method)" Annual Book of ASTM Standards, Vol. 04.02, Sect. 4, 200-207 (1985).

85) H.E. Vivian "Assessment of Aggregate-Reactivity Tests and Significance of Test Results". Proc. 6th Int. Conf. on "Alkalis in Concrete", Copenhagen, June 22-25, 1983, 365-368.

86) L.S. Dent Glasser, and N. Kataoka "Some Observations on the Rapid Chemical Test for Potentially Reactive Aggregate". Cem. Concr. Res., 11, 191-196 (1981).

87) V.S. Ramachandran, R.F. Feldman, and J.J. Beaudoin "Concrete Science", Heyden & Sons Ltd., Chapt. 10, p. 349 (1981).

88) I. Sims " The Application and Reliability of Standard Testing Procedures for Potential Alkali-Reactivity". Proc. 5th Int. Conf. on "Alkali-Aggregate Reaction in Concrete", Cape Town, March 30-April 3, 1981, S252/13, 12 pp.

89) M.P. Brandt, R.E. Oberholster, and W.B. Westra "A Contribution to the Determination of the Potential Alkali Reactivity of Tygerberg Formation Aggregates". Proc. 5th Int. Conf. on "Alkali-Aggregate Reaction in Concrete", Cape Town, March 30-April 3, 1981, S252/11, 6 pp.

90) M.P. Brandt, and R.E. Oberholster "Study of Tygerberg Formation Aggregate for Potential Alkali Reactivity, Implications of Test Methods and Application of the Findings in Practice". CSIR Res. Rep., 580, 96 pp. (1983).

91) ASTM C227-81 "Potential Alkali Reactivity of Cement-Aggregate Combinations (Mortar Bar Method)". Annual Book of ASTM Standards, Vol. 04.02, Sect. 4, 156-161 (1985).

92) N. Thaulow, and H. Olafsson "Alkali-Silica Reactivity of Sands, Comparison of Various Test Methods. Nordtest Project". Proc. 6th Int. Conf. on "Alkalis in Concrete", Copenhagen, June 22-25, 1983, 359-364.

93) F. E. Jones and R. D. Tarleton "Reaction between Aggregates and Cement. Part VI. Alkali-Aggregate Interaction: Experience with Some Forms of Rapid and Accelerated Tests for Alkali-Aggregate Reactivity. Recommended Test Procedures". NBS Res. Pap. No. 25, Her Majesty's Stationery Office, London (1958).

94) CSN72 1162 "Stanovenie Odolnostri Prirodneho Stavebneho Kamena Proti Silicifikach". MTD 691.2.620.1 679.682.1, Ceskoslovenska Statna Norma Schvalena, 24.10 (1981).

95)"Vorbeunge Massnahemen Gegen Schadigende Alkalireaktion im Beton" Beton, 24, (5), 179-185 (1974).

96) A.D. Jensen, S. Chatterji, P. Christensen, N. Thaulow, and H. Gudmundsson "Studies of Alkali-Silica Reaction. Part 1. A Comparison of Two Accelerated Test Methods". Cem. Concr. Res., 12, 641-647 (1982).

97) ASTM C33-85 Appendix XI "Methods for Evaluating Potential Reactivity of an Aggregate (Par. 1.3)". Annual Book of ASTM Standards, Vol. 04.02, Sect. 4, 20 (1985).

98) Engineer Manual EM 1110-2-2000 "Engineering and Design Standard Practice for Concrete (Appendix B.3C)". Dept. of the Army, Office of the Chief of Engineers, Washington, D.C. (1971).

99) CSA CAN3-A23.1-M77, Appendix B3 "Tests for Alkali-Aggregate Reactivity (3.4, ASTM Standard C227, Potential Alkali Reactivity of Cement-Aggregate Combinations (Mortar Bar Method). 3.5, CSA Test Method A23.2-14A, Alkali-Aggregate Reaction, National Standard of Canada); CAN3 A23.2-M77, Concrete Materials and Methods of Concrete Construction, Methods of Tests for Concrete. Canadian Standards Assoc., Canada, 122-123 (1977).

100) P.E Grattan-Bellew "Re-evaluation of Standard Mortar Bar and Concrete Prism Tests for Alkali-Aggregate Reactivity". Mater. Constr. (Paris), 16, 243-250 (1983).

101) M.A.G. Duncan, E.G. Swenson, and J.E. Gillott "Alkali-Aggregate Reaction in Nova Scotia. Part III. Laboratory Studies of Volume Change". Cem. Concr. Res., 3, 233-245 (1973).

102) P.J. Nixon, and R. Bollinghaus " Testing for Alkali Reactive Aggregates in the UK". Proc. 6th Int. Conf. on "Alkalis in Concrete", Copenhagen, June 22-25, 1983, 329-336.

103) S. Chatterji "An Accelerated Method for the Detection of Alkali-Aggregate Reactivities of Aggregates". Cem. Concr. R es., 8, 647-650 (1978).

104) R.F.M. Bakker " The Influence of Test Specimen Dimension's on the Expansion of Alkali Reactive Aggregate in Concrete". Proc. 6th Int. Conf. on "Alkalis in Concrete", Copenhagen, June 22-25, 1983, 369-376.

105) Tang Ming-shu, Han Sun-fen, and Zhen Shi-hua "A Rapid Method for Identification of Alkali Reactivity of Aggregate". Cem. Concr. Res., 13, 417-422 (1983).

106) P.E. Grattan-Bellew "A Review of Test Methods for Alkali-Expansivity of Concrete Aggregates". Proc. 5th Int. Conf. on "Alkali-Aggregate Reaction in Concrete", Cape Town,March 30-April 3,1981,S252/9,13 pp.

107) Rilem "Final Report on Aggregates". Mater. Constr. (Paris), 15, 205-258 (1982).

108) P. Christensen, S. Chatterji, N. Thaulow, and A.D. Jensen "Alkali-Silica Reactivity of Various Danish Flint Types". Proc. 6th Int. Conf. on "Alkalis in Concrete", Copenhagen, June 22-25, 1983, 315-320.

109) P. Christensen, S. Chatterji, A.D. Jensen, and N. Thaulow " Preliminary Investigation on Alkali-Silica Reactivity of Density Separated Coarse Aggregate". Proc. 6th Int. Conf. on "Alkalis in Concrete", Copenhagen, June 22-25, 1983, 105-109.

110) A.D. Jensen, S. Chatterji, P. Christensen, and N. Thaulow "Studies of Alkali-Silica Reaction- Part II. Effect of Air Entrainment on Expansion". Cem. Concr. Res., 14, 311-314 (1984).

111) D. Lenzner, and U. Ludwig "The Alkali-Aggregate Reaction with Opaline Sandstone from Schleswig-Holstein". Proc. 4th Int. Conf. on "Alkalies in Concrete", Purdue University., West Lafayette, June 4-7, 1978, 11-34.

112) D. Lenzner "Comparative Laboratory Tests on the Alkali-Silica Reaction". Proc. 6th Int. Conf. on "Alkalis in Concrete", Copenhagen, June 22-25, 1983, 321-327.

113) S. Sprung "Einfluss von Zement und Zusatsen auf die Alkalireaktion". Schriftenr. Zementind., 40, 69-78 (1973).

114) M. Berra "Performance of Some Italian Cements Tested for Alkali-Silica Reaction". Proc. 6th Int. Conf. on "Alkalis in Concrete", Copenhagen, June 22-25, 1983, 377-382.

115) M.P. Brandt, R.E. Oberholster, and W.B. Westra "The Alkali-Aggregate Reaction: a Contribution Concerning the Determination of the Reactivity of Portland Cements". Proc. 5th Int. Conf. on "Alkali-Aggregate Reaction in Concrete", Cape Town, March 30-April 3, 1981, S252/10, 7 pp.

116) ASTM C311-85 "Standard Methods for Sampling and Testing Fly Ash or Natural Pozzolans for Use as a Mineral Admixture in Portland Cement Concrete". Annual Book of ASTM Standards, Vol. 04.02, Sect. 4, (1985).

117) D. Lenzner "Influence of the Amount of Mixing Water on the Alkali-Silica Reaction". Proc. 5th Int. Conf. on "Alkali-Aggregate Reaction in Concrete", Cape Town, March 30 - April 3 , 1981, S252/26, 5 pp.

118) H. E. Vivian "The Effect of Drying on Reactive Aggregate and Mortar Expansions". Proc. 5th Int. Conf. on "Alkali-Aggregate Reaction in Concrete", Cape Town, March 30 - April 3, 1981, S252/28, 5 pp.

119) P. J. Nixon, and R. Bollinghaus "The Effect of Alkali-Aggregate Reaction on the Tensile and Compressive Strength of Concrete". Durability of Building Materials, 2, 243-248 (1985).

120) V.S. Ramachandran, R.F. Feldman, and J.J. Beaudoin "Concrete Science", Heyden & Sons Ltd., Chapt. 10, p. 351 (1981).

121) J. Von Bonzel, and J. Dahms "Alkalireaktion im Beton". Herstellung Verwendung, 23, H.11, S495/500 und H.12, S547/554 (1973).

122) ASTM C586-69 "Standard Test Method for Potential Alkali Reactivity of Carbonate Rocks for Concrete Aggregates (Rock Cylinder Method)". Annual Book of ASTM Standards, Vol. 04.02, Sect. 4, 360-363 (1985).

123) L.M.M. Dolar-Mantuani Symp. on "Alkali-Carbonate Reaction", Record No. 45, Highway Res. Board, 178-195 (1964).

124) L.M.M. Dolar-Mantuani "Mineral Aggregates". Record No. 353, Highway Res. Board, 1-14 (1971).

125) I. Sims, and P. Sotiropoulos "Standard Alkali-Reactivity Testing for Carbonate Rocks from the Middle East and North Africa". Proc. 6th Int. Conf. on "Alkalis in Concrete", Copenhagen, June 22-25, 1983, 337-349.

126) P.E. Grattan-Bellew, and G.G. Litvan Symp. on "The Effect of Alkalies on the Properties of Concrete", Cem. Concr. Assoc., London, 227-245 (1976).

127) V.S. Ramachandran, R.F. Feldman, and J.J. Beaudoin "Concrete Science", Heyden & Sons Ltd., Chapt. 10, p. 352 (1981).

128) J. Kazimir "Moznosc Skratenia Skusky Rozpinania Dolomitovych Hornin s Alkaliami". Staveb. Cas. 25, cs. Veda Bratislava, 413-432 (1977).

129) P.E. Grattan-Bellew "Evaluation of Miniature Rock Prism Test for Determining the Potential Alkali-Expansivity of Aggregates". Cem. Concr. Res., 11, 699-711 (1981).

130) D. Stark "Osmotic Cell Test for Identifying Potential for Alkali-Aggregate Reactivity". Proc. 6th Int. Conf. on "Alkalis in Concrete", Copenhagen, June

22-25, 1983, 351-357.

131) J.E.Slater "Corrosion of Metals in Association with Concrete". ASTM STP 818,American Society for Testing and Materials,Philadelphia (1983).

132) B.Husock,R.M.Wilson,and W.H.Hooker "Overview of the Rebar Corrosion Problem". Proc. Seminar on "Solving Rebar Corrosion Problems in Concrete", Paper n.1, Chicago Sept. 1982, NACE, Houston TX (1982).

133) C.J.F.P.Jones " Maintenance Problems and Economics". Proc. Seminar on "Corrosion and Degradation of Building Materials and System Building",London Oct.1985,Oyez (1985).

134) ACI Commitee 222 "Corrosion of Metals in Concrete". ACI J., 82, 3-32 (1985).

135) M.Arpaia,and G.Trisciuoglio " Rilievi sperimentali per la caratterizzazione del calcestruzzo come conduttore elettrolitico". Energia Elettrica,(5), 219-225 (1982).

136) P.Wittekind " A Review of Steel Corrosion in Concrete". Concrete,17,(6),13-15 (1983).

137) J.W.Figg " Rusting Reinforcement,The n.1 Problem of Concrete Durability". Concrete, 14,(5),34-36 (1980).

138) K.W.J. Treadaway "The Durability of Steel in Concrete". BRE News, 61,4-5 (1984).

139) M.Pourbaix "Atlas of Electrochemical Equilibria in Aqueous Solutions". Pergamon Press,Oxford (1966).

140) N.S.M.Wilkins, and P.F.Lawrence "Mechanism of Corrosion of Steel Reinforcements in Concrete". Proc. Symp. on "Corrosion Steel Reinforcement in Concrete Construction". Society of Chemical Industry,London, 105-118 (1978).

141) C.M.Hansson "Comments on Electrochemical Measurements of Rate of Corrosion of Steel in Concrete". Cem.Concr.Res.,14, 574-584 (1984).

142) R.J.Vetter "Electrochemical Kinetics". Academic Press,New York (1967).

143) C.L.Page,and K.W.J. Treadaway "Aspects of the Electrochemistry of Steel in Concrete". Nature 297, 109-115 (1982).

144) P.Pedeferri "La corrosione degli acciai nelle strutture:fenomenologia e prevenzione". Atti Sem. "Normativa e Controllo dei Materiali dell'Ingegneria Strutturale", ISMES,Bergamo,Maggio 1985.

145) H.Kaesche "Die Prufung der Korrosionsgefahrdung von Stahlarmierungen durch Betonzusatzmittel". Zement Kalk Gips,12,(7),289-294 (1959).

146) H.J.Engell,and A.Baumel "Korrosion van Stahl in Beton". Archiv.Eisenhuttenwesen,30, 417 (1959).

147) BRE "The Durability of Steel in Concrete:Part I Mechanism of Protection and Corrosion". Digest 263,Garston (1982).

148) A.Neville "Corrosion of Reinforcement" Concrete, 17,(6),48-50 (1983).

149) I.L.H.Hansson "Electrical Resistivity Measurements of Portland Cement Based Materials". Cem. Concr. Res.,13, 675-683 (1983).

150) I.L.H.Hansson,and C.M.Hansson "Ion Conduction in Cement-based Materials". Cem.Concr.Res., 15, 201-212 (1985).

151) W.J.McCarter, M.C.Forde, and H.W.Whittington "Resistivity Characteristics of Concrete". Proc. Instn. Civ. Engrs. Part2,71, 107-117 (1981).

152) M.Arpaia,and G.Trisciuoglio "Contributo alla caratterizzazione dell'elettrodo metallo-calcestruzzo". Atti 1.Conv.Naz.ASMI,Milano, Oct.1983,Ed.Pitagora,Bologna, 223.

153) D.G.Moore, D.T.Klodt, and R.J.Hense "Protection of Steel in Prestressed Concrete Bridges". NCHRP Report 90, Highway Res. Board, Washington DC (1970).

154) N.J.M.Wilkins "Resistivity of Concrete", Material Development Division,AERE Harwell,Jan. 1982,AERE-M 3232.

155) H.Arup "Corrosion of Reinforcing Steel in Concrete,An Overview". Proc.2nd Eur.Sem.Failure and Repair of Corroded Reinforced Concrete Structures, London Press Centre,Oct 1984,Oyez.

156) N. Wilkins "International Seminar Electrochemistry and Corrosion of Steel in Concrete,A State-of-the Art Summary".Mat.Performance,19,(5),52-54 (1983).

157) H.Arup "The Mechanisms of the Protection of Steel by Concrete", in A.P.Crane "Corrosion of Reinforcement in Concrete Construction",Ellis Horwood,Chichester,151-157 (1983).

158) P.Pedeferri "Corrosione e protezione dei materiali metallici", Clup,Milano (1978).

159) J.F.Henriksen "The Corrosion and Protection of Steel in Saturated Ca(OH)2 Contaminated with NaCl". Corrosion Sci.,20, 1241-1249 (1980).

160) A.W.Beeby "Cracking and Corrosion" Concrete with Oceans Technical Report n.1, Cement and Concrete Association (1978).

161) M.Arpaia "Corrosione delle armature in acciaio dei manufatti in calcestruzzo". Rend. 8.Congr.Intern. Manufatto in Cemento,Stresa,May 1975.

162) M.Matousek "Influence des Caracteristiques du Ciment sur les Proprietes du Beton et de sa Resistance a la Corrosion Atmospherique". Proc.7th Int.Symp. on Chemistry of Cements,Paris,vol.4,764-765 (1980).

163) M.Hamada "Neutralization of Concrete and Corrosion of Reinforcing Steel". Proc. 5th Int. Symp. on Chemistry of Cement,Tokyo,vol.3,343-369 (1968).

164) A.Meyer "Investigation on the Carbonation of Concrete". Proc.5th Int.Symp.on Chemistry of Cement, Tokyo.vol.3,394-401 (1968).

165) R.Kondo, M.Damon,and T.Akiba " Mechanisms and Kinetics on Carbonation of Hardened Cement". Proc.5th Int.Symp.on Chemistry of Cement,Tokyo,vol.3,402-409 (1968).

166) K. Tuutti "Corrosion of Steel in Concrete". Proc.6th Eur.Congress on Metallic Corrosion, London, Sept.1977,655-661.

167) O.E.Gjorv, O.Vennesland A.H.S. El-Busaidy "Diffusion of Dissolved Oxygen through Concrete". Corrosion 76,NACE,Houston,Paper no.17 (1976).

168) C.E.Locke "Mechanism of Corrosion of Steel in Concrete". Proc. Sem. on "Solving Rebar Corrosion Problems in Concrete", Paper n.2, Chicago Sept. 1982, NACE, Houston TX.

169) K.W.J. Treadaway, G.McMillan, P.Hawkins, and C.Fontenay " The Influence of Concrete Quality on Carbonation in Middle Eastern Conditions-A Preliminary Study", in A.P.Crane "Corrosion of Reinforcement in Concrete Construction",Ellis Horwood,Chichester, 101-118 (1983).

170) E.A. Kay, P.G. Fookes, and D.J. Pollock " Middle East Concrete 3.Deterioration Related to Chloride Ingress". Concrete(London),15,(11),22-28 (1981).

171) P.G.Fookes,D.J.Pollock, and E.A.Kay "Middle East Concrete 2.Rates of Deterioration". Concrete (London), 15,(9), 12-19 (1981).

172) R.T.Foley "Role of Chloride Ion in Iron Corrosion". Corrosion,26,(2),58-70 (1970).

173) C.Dehghanian,and C.E.Locke "Electrochemical Behavior of Steel in Salt Contaminated Concrete; Part 1". Corrosion,39,(8), 299-305 (1983).

174) C.Dehghanian,and C.E.Locke "Electrochemical Behavior of Steel in Salt Contaminated Concrete; Part 2". Corrosion,38,(9), 494-499 (1982).

175) N.J.M.Wilkins,and P.F.Lawrence "The Corrosion of Steel Reinforcements in Concrete Immersed in Seawater", in A.P.Crane "Corrosion of Reinforcement in Concrete Construction",Ellis Horwood,Chichester, 119 (1983).

176) C.M.Hansson,Th.Frolund,and J.B.Markussen "The Effect of Chloride Cation Type on the Corrosion of Steel Concrete by Chloride Salts". Cem. Concr. Res., 15, 65-73 (1985).

177) P.K.Mehta "Effect of Cement Composition on Corrosion of Reinforcing Steel in Concrete", ASTM STP629, D.E.Tonini, S.W.Dean Jr.Eds,American Society for Testing and Materials,12-19 (1977).

178) W.Richartz "Die Bindung von Chlorid bei der Zementerhartung". Zement-Kalk-Gips,22,(10), 447-456 (1969).

179) V.S. Ramachandran, R.C.Seeley, and G.M.Polamark "Free and Combined Chloride in Hydrating Cement and Cement Components". Mater. Constr.17,(100),285-289 (1984).

180) P.Lambert,C.L.Page,and N.R.Short "Pore Solution Chemistry of the Hydrated System Tricalcium Silicate/Sodium Chloride/Water". Cem. Concr. Res.,15,675-681 (1985).

181) P.Rechberger "Elektrochemische Modellversuche zur Frage der Chloridinduzierten BetonstahlKorrosion". Zement Kalk Gips,36,(10),582-590 (1983).

182) S.Diamond,and L.F.Federico "Fate of Calcium Chloride Dissolved in Concrete Mix Water". J.Am. Ceramic.Soc.,64,162 (1981).

183) I.I.Kurbatova,and V.G.Abramkina "Kinetics of Crystallization of Products Formed in Cement Pastes with Additions of Calcium Chloride". J.Appl.Chem. (USSR),49,1064 (1976).

184) W.R.Holden,C.L.Page,and N.R.Short "The Influence of Chlorides and Sulphates on Durability", in A.P. Crane "Corrosion of Reinforcement in Concrete Construction", Ellis Horwood, Chichester, 143-150 (1983).

185) R.D.Browne "Mechanisms of Corrosion of Steel in Concrete in Relation to Design, Inspection,and Repair of Offshore and Coastal Structures". ACI SP-65, American Concrete Institute, Chicago, 169-204 (1980).

186) K.Tuutti "Service Life of Structures with Regard to Corrosion of Embedded Steel", ACI SP-65, American Concrete Institute,Chicago,223-236 (1980).

187) M. Collepardi, A. Marcialis, and R. Turriziani "Penetration of Chloride Ions into Cement Pastes and Concretes".J. Am. Ceramic Soc.,55,(10),534-535 (1972)

188) C.L.Page,N.R.Short,and A.El Tarras "Diffusion of Chloride Ions in Hardened Cement Pastes". Cem. Concr. Res.,11, 395-406 (1981).

189) D.A.Hausmann "Steel Corrosion in Concrete". Mat. Protection,6,(11), 19 (1967).

190) G.J.Verbeck "Mechanism of Corrosion of Steel in Concrete". ACI SP-49, American Concrete Institute,21 (1975).

191) CEB "Durability of Concrete Structures-State of the Art Report". Bulletin d'Information,n.148,Comite Eurointernational du Beton (1982).

192) R.E. West, and W.G. Hime "Field Test of Reinforcement Corrosion in Concrete". Mat. Performance, 24,(7),29-36 (1985).

193) P.Fidjestol, and N. Nielsen "Field Test of Reinforcement Corrosion in Concrete". ACI SP-65, American Concrete Institute,Chicago MI,305-321 (1980).

194) P.Fidjestol,B.Ronning.and B.T.Roland "Revised Criteria for Prevention of Corrosion in Offshore Concrete Structures". Corrosion 85, Boston, Paper no. 262 (1985).

195) N.Nielsen,and B. Espelid "Corrosion Behavior of Reinforced Concrete under Dynamic Loading". Mat. Performance,24,(7), 44-50 (1985).

196) BRE "The Durability of Steel in Concrete: Part 2,Diagnosis and Assessment of Corrosion-Cracked Concrete". Digest 264,Garston (1982).

197) A.W.Beeby "Corrosion of Reinforcement and Crack Widths". Proc. Int. Symp.on "Offshore Structures",Rio de Janeiro,vol.1-3 (1979).

198) K.Okada, W.Koyanagi, and T.Miyagawa "Chloride Corrosion of Reinforcing Steel in Cracked Concrete". Proc. Int. Symp. on "Offshore Structures",Rio de Janeiro, vol.1-4 (1979).

199) O.Vennesland,and O.E.Gjorv "Effect of Cracks in Submerged Concrete Sea Structures on Steel Corrosion". Mat. Performance,20,(8), 49-51 (1981).

200) T.Uomoto,K.Kobayashi,and K.Tsuji "Deterioration of Concrete Beams and Columns Caused by Corrosion of Reinforcing Steel Bars". Proc.4th Asian-Pacific Corrosion Control Conf., Tokyo, [illegible] 1985, 700-707.

201) M. Makita, Y. Mori, and K. Katawaki "Marine Corrosion Behavior of Reinforced Concrete Exposed at Tokyo Bay". ACI SP-65, American Concrete Institute, Chicago MI,271-289 (1980).

202) K.Okada,and T.Miyagawa "Chloride Corrosion of Reinforcing Steel in Cracked Concrete". ACI SP-65, American Concrete Institute, Chicago MI, 236-255 (1980).

203) CEB "Draft CEB-Guide to Durable Concrete Structures". Bulletin d'Information n.166,Comite International du Beton (1985).

204) V.K.Gouda,and H.M.Mourad "Galvanic Cells Encountered in the Corrosion of Steel Reinforcement I. Differential pH Cells". Corrosion Sci.,14, 681-690 (1974).

205) V.K.Gouda,and H.M.Mourad "Galvanic Cells Encountered in the Corrosion of Steel Reinforcement II. Differential Salt Concentration Cells". Corrosion Sci.,15, 307-336 (1975).

206) R.L.Miller,W.H.Hartt,and R.P.Brown "Stray Current and Galvanic Corrosion of Reinforcing Steel in Concrete". Mat. Performance,15,(5), 20-27 (1976).

207) C.E.Locke,C.Dehghanian,and L.Gibbs " Effect of Impressed Cement on Bond Strength between Steel Rebar and Concrete". Corrosion 83, Anaheim, Paper no. 178 (1983).

208) Z.P.Bazant "Physical Model for Steel Corrosion in Concrete Sea Structures - Theory". ASCE J., Structural Division, Proc. 105, (ST6), 1137-1153 (1979).

209) Z.P.Bazant "Physical Model for Steel Corrosion in Concrete Sea Structures - Application". ASCE J.,Structural Division, Proc. 105,(ST6), 1155-1166 (1979).

210) P.Schiessl "Corrosion of Reinforcement". Proc. CEB-Rilem Int. Workshop Durability of Concrete Structures, Copenhagen, May 1983, S.Rostam Ed.,73-93 (1984).

211) K.C.Clear "Solving Rebar Corrosion Problems in Concrete Research Update : Methods and Materials". Proc. Sem. on "Solving Rebar Corrosion Problems in Concrete", Chicago, Sept.1982, Paper no. 4, NACE, Houston TX.

212) D.Whiting "Corrosion Control-Concrete Design and Construction Practices". Proc. Sem. on "Solving Rebar Corrosion Problems in Concrete", Chicago Sept 1982, NACE, Houston TX.

213) J.H.Fitzgerald III "Design Considerations and Construction Practices". Proc. Sem. on "Solving Rebar Corrosion Problems in Concrete", Chicago Sept 1982, NACE, Houston TX.

214) R.F.Stratfull "Solving Rebar Corrosion Problems in Concrete-Past,Present and Future". Proc. Sem. on Solving Rebar Corrosion Problems in Concrete", Chicago, Sept. 1982, Paper no. 16, NACE, Houston TX.

215) M. Schupak "Design of Permanent Seawater Structures to Prevent Deterioration". Concrete Int., (3),19-27 (1982).

216) W.P.Kilareski "Corrosion Induced Deterioration of Reinforced Concrete - An Overview". Mat. Performance, 19,(3), 48-50 (1980).

217) K. Katawaki, M. Ota, T. Yanagida, and K.Kokubu "Corrosion and Protection Technologies for Concrete Structures in Marine Atmosphere". Proc. 4th Asian-Pacific Corrosion Control Conf., Tokyo, May 1985,531-538.

218) H.Roper "State of the Art of Practical Prevention and Control of Corrosion in Concrete Structures". Proc. 4th Asian-Pacific Corrosion Control Conf., Tokyo, May 1985,716-722.

219) R.D.Browne "Protection and Repair of Concrete Structures". Proc. Sem. on "Corrosion and Degradation of Building Materials and System Building", London, Oct.1985, Oyez.

220) P.Bertrandy,and A.Vincens "Comportement de Structures en Beton Arme et Precontraint Exposees a la Mer", Proc. Int. Symp. on "Behaviour of Offshore Concrete Structures", III-3, C.N.E.X.O. (1980).

221) M.Makita,Y.Mori,and K.Katawaki "Performance of Typical Protection Methods for Reinforced Concrete in Marine Environment". ACI SP-65, American Concrete Institute, Chicago MI, 453-471 (1980).

222) C.M.Preece,F.O.Gronvold,and T.Frolund "The Influence of Cement Type on the Electrochemical Behaviour of Steel in Concrete", in A.P.Crane "Corrosion of Reinforcement in Concrete Construction", Ellis Horwood, Chichester, 393-405 (1983).

223) O.E.Gjorv "Durability of Concrete Containing Condensed Silica Fume ". ACI SP-79 Fly Ash, Silica Fume, Slag and Other Mineral By-Products in Concrete, American Concrete Institute, Detroit MI, 695-708 (1983).

224) O.Vennesland,and O.E. Gjorv "Silica Concrete - Protection Against Corrosion of Embedded Steel".ACI SP-79,Fly Ash,Silica Fume,Slag and Other Mineral By-Products in Concrete, American Concrete Institute, Detroit MI, 719-729 (1983).

225) C.M.Preece,H.Arup,and T.Frolund "Electrochemical Behaviour of Steel in Dense Silica-Cement Mortar". ACI SP79, Fly Ash, Silica Fume, Slag and Other Mineral By-Products in Concrete, American Concrete Institute, Detroit MI, 785-796 (1983).

226) K.P.Fischer,O.Bryhn,and P.Aagaard "Corrosion of Steel in Concrete:Some Fundamental Aspects of Concrete with Added Silica". Corrosion 83, Anaheim, Paper no. 175, NACE (1985).

227) K.P.Fischer,O.Bryhn,and P. Aagaard "Corrosion of Steel in Concrete:Some Fundamental Aspects of Concrete with Added Silica". Corrosion, 40,(7), 358-365 (1984).

228) J.B.Newman, P.J.E.Sullivan, and A.M.Bell "In - Service Performance of Reinforced Concrete Structures Containing Fuel Ash". Concrete,(12), 9-12 (1983).

229) R.L.Yuan,and W.F.Chen "Behaviour of Sulfur - Infiltrated Concrete in Sodium Chloride Solution". ACI SP-65, American Concrete Institute, Chicago MI, 291-307 (1980).

230) D.W.Pfeifer,and M.J.Scali "Concrete Sealers for Protection of Bridge Structures". NCHRP Report 244, Transportation Research Board, Washington DC (1981).

231) D.W. Pfeifer, and W.F. Perenchio "Coatings, Penetrants and Specialty Concrete Overlays for Concrete Surfaces". Proc. Sem. on "Solving Rebar Corrosion Problems in Concrete". Paper no. 12. Chicago Sept 1982, NACE, Houston TX.

232) J.D.Scantlebury "The Prevention of Corrosion in Reinforced Concrete Structures by Coatings". Proc. 2nd. Eur. Sem. on "Failure and Repair of Corroded Reinforced Concrete Structures", London, Oct.1984, Oyez.

233) R.I.Frascoia "Vermont's Experience with Bridge Deck Protective Systems". ASTM STP 629,D.E.Tonini and S.W.Dean Eds.,69-81 (1977).

234) L.E.Kuckaka "The Use of Concrete Polymer Materials for Bridge Deck Applications". ASTM STP 629, D.E.Tonini and S.W.Dean Eds, 100-109 (1977).

235) K.H.Wong,R.E.Weyers,and P.D.Cady "The Retardation of Reinforcing Steel Corrosion by Alkyl-Alkoxy Silane". Cem. Concr. Res.,13, 778-788 (1983).

236) W.P.Kilareski "Epoxy Coatings for Corrosion Protection of Reinforcing Steel". ASTM STP 629, D.E. Tonini and S.W.Dean Eds, 82-88 (1977).

237) H.J.Schmidt,Jr " Variations in Epoxy Coated Rebar Specifications". Proc. Sem. on "Solving Rebar Corrosion Problems in Concrete", Chicago Sept.1982, Paper no. 9, NACE, Houston TX.

238) B.J.McFadden "Application and Fabrication of Epoxy Coated Reinforcing Steel". Proc. Sem. on "Solving Rebar Corrosion Problems in Concrete",

Chicago Sept.1982, Paper no .8, NACE, Houston TX.

239) F.Ellyin,and R.A.Matta "Bonding and Corrosion Protection Properties of Two Coatings for Prestressing Steels". ACI J.,79, 366-371 (1982).

240) Korrosioncentralen ATV "Galvanized Steel in Concrete, a Necessary Warning". Steel in Concrete Newsletter, no.1, 1-2 (1978).

241) A.Hofsoy,and I.Gukild "Bond Studies on Hot Dip Galvanized Reinforcement in Concrete". ACI J., 66,(3), 174-184 (1969).

242) W.K. Boyd, and A.B. Triple, Jr. "Corrosion of Reinforcing Steel Bars in Concrete". Mat. Prot., 7,(10), 40-47 (1968).

243) G.Sergi,N.R.Short,and C.L.Page "Corrosion of Galvanized and Galvannealed Steel in Solutions of pH 9-14". Corrosion 85, Boston, Paper no. 272, NACE (1985).

244) C.Andrade,A.Macias,A.Molina,and J.A.Gonzales "Advances in the Study of the Corrosion of Galvanized Reinforcements Embedded in Concrete". Corrosion 85, Boston,Paper no. 270, NACE (1985).

245) J.A. Gonzales, A.J. Vasquez, G. Jauregui, and C. Andrade "Effect of Four Coating Structures on Corrosion Kinetics of Galvanized Reinforcement in Concrete". Mat. Constr.,17,(102), 409-414 (1984).

246) M.T.Blanco,C.Andrade,and A.Macias "SEM Study of the Corrosion Products of Galvanized Reinforcements Immersed in Solutions in the pH Range 12.6 to 13.6". Br. Corrosion J.,19,(1), 41-48 (1984).

247) J.A. Gonzales, and C. Andrade "Effect of Carbonation, Chlorides and Relative Ambient Humidity on the Corrosion of Galvanized Rebars Embedded in Concrete". Br. Corrosion J. ,17,(1), 21-28 (1982).

248) H.Okamura,and Y.Hisamatsu "Effect of Use of Galvanized Steel on the Durability of Reinforced Concrete". Mat. Prot.,15,(7), 43-47 (1976).

249) T.J.Kinstler "An Update on Galvanized Reinforcing Steel". Proc. Sem. on "Solving Rebar Corrosion Problems in Concrete", Chicago Sept.1982, Paper n.10, NACE, Houston TX.

250) ASTM A767-79 "Standard Specification for Zinc-Coated (Galvanized) Steel Bars for Concrete Reinforcement" (1979).

251) W.H. Hartt, and A.M.Rosenberg "Influence of $Ca(NO_2)_2$ on Sea Water Corrosion of Reinforcing Steel in Concrete". ACI SP 65, American Concrete Institute, Chicago MI, 609 (1980).

252) A.L.Walitt "Calcium Nitrite Offers Long-Term Corrosion Prevention in Concrete Constructions". Concrete Constructions, Apr.1985, 355 (1985).

253) Y.P.Virmani,K.C.Clear,and T.J.Pasko Jr. "Time to Corrosion of Reinforcing Steel in Concrete Slabs, vol.5 : Calcium Nitrite Admixture or Epoxy-Coated Reinforcing Bars as Corrosion Protection Systems", FHWA/RD 83/012 (1983).

254) W.H.Hartt,B.Voshardt,and A.M.Rosenberg "Influence of $Ca(NO_2)_2$ on Sea Water Corrosion of Reinforcing Steel in Concrete-Part II". Corrosion 81, Toronto, Paper no. 52, 609-622 (1981).

255) N.S.Berke "The Effects of Calcium Nitrite and Mix Design on the Corrosion Resistance of Steel in Concrete (Part I)". Corrosion 85, Boston, Paper no. 273 (1985).

256) J.E. Slater, D.R. Lankard, and P.J. Moreland "Electrochemical Removal of Chlorides from Concrete Bridge Decks". Mat. Performance,15,(11),21-26 (1976).

257) J.B.Vrable "Cathodic Protection for Reinforcing Steel in Concrete". ASTM STP 629, American Society for Testing and Materials, Philadelphia, 124-149 (1977).

258) P.M.Ward "Cathodic Protection : A User's Perspective". ASTM STP 629, American Society for Testing and Materials, Philadelphia, 150 (1977).

259) M.Arpaia "Conduites en beton Precontraint et Phenomenes de Corrosion". Tribune du Cebedeau, n.250-251, 1-11 (1965).

260) D.A.Hausmann "Criteria for Cathodic Protection of Steel in Concrete Structures", Mat. Protection 8,(10), 23-25 (1969).

261) J.B.Vrable,and B.E.Wilde "Electrical-Potential Requirements for Cathodic Protection of Steel in Simulated Concrete Environments". Corrosion, 36,(1), 18-23 (1980).

262) W.R.Schutt "Steel in Concrete Cathodic Protection-Results of a 10 years Experience". Corrosion 85, Boston, Paper no. 267, NACE (1985).

263) R.Cigna,and O.Fumei " Sulla protezione catodica dei ferri del calcestruzzo armato". Ind. Ital. Cemento, 41,(9), 595-600 (1981).

264) F.Carassiti, R.Cigna, B.Di Miceli, and O.Fumei "Protezione catodica dell'armatura del calcestruzzo in presenza di cloruri". Ind. Ital. Cemento, 42,(11), 855-860 (1982).

265) R.F.Stratfull " Criteria for the Cathodic Protection of Bridge Decks", in A.P.Crane "Corrosion

of Reinforcement in Concrete Construction" Ellis Horwood, Chichester, 287-331 (1984).

266) O.E.Gjorv,and O.Vennesland " Cathodic Protection of Steel in Offshore Concrete Platforms". Mat. Performance, 19,(5), 49-52 (1980).

267) H.C.Schell,and D.G.Manning " Evaluating the Performance of Cathodic Protection Systems on Reinforced Concrete Bridge Substructures". Mat. Performance, 24,(7), 18-25 (1985).

268) R.E.Weyers, and P.D.Cady "Cathodic Protection of Concrete Bridge Decks". ACI J.,81,618-622 (1984).

269) R.P.Brown,and R.G.Powers " Update on the Use of Conductive Materials for Cathodic Protection of Steel in Concrete". Corrosion 85, Boston, Paper no. 264, NACE (1985).

270) R.P.Brown,and R.J.Kessler " A New Concept in Cathodic Protection of Steel in Concrete.The Use of Conductive Materials". Corrosion 83, Anaheim, Paper no. 179, NACE (1983).

271) D.Noran " Solar Energy for Production Applications". Oil Gas J., March 6, 80-90 (1978).

272) L.E.Bell,and T.L.Canfield " Solar Energy: A Reality for Cathodic Protection". Pipeline Industry, April, 67-74 (1977).

273) W.Von Baeckmann,D.Funk,H.Hildebrand,and W.Shwenk "Polarisierbarkeit von Sandboeden bei Anwendung des Kathodischen Korrosionsshutzes". Werkstoffe u. Korrosion, 28,(11), 757 (1977).

274) R.F.Stratfull "Experimental Cathodic Protection of Bridge Deck". TRB 500, 1 (1974).

275) H.J.Fromm,and G.P.Wilson " Cathodic Protection of Bridge Decks:Study of 3 Ontario Bridges". TRB 604, 38 (1976).

276) B.Heuze "Cathodic Protection on Concrete Offshore Platforms".Mat.Performance,19,(5),24-33 (1980).

277) O.T.de Rincon,and C.E.Locke " Experiences with Sacrificial Anodes for Protection of the Pilings of the General Rafael Urdaneta Bridge over Lake Maracaibo". Corrosion 85, Boston, Paper no. 260, NACE (1985).

278) W.Perenchio " Condition Survey:Test Methods and Equipment". Proc. Sem. on " Solving Rebar Corrosion Problems in Concrete", Chicago Sept.1982, Paper no. 3, NACE, Houston TX.

279) J.L.Dawson " Corrosion Monitoring of Steel in Concrete", in A.P.Crane "Corrosion of Reinforcement in Concrete Construction, Ellis Horwood, Chichester, 175-191 (1983).

280) UMIST " CAPCIS Corrosion Monitoring MUSYC Box". Bainsbridge House Laboratories, Manchester (1983).

281) H.Naifeng,W.Donglin,and H.Ming " Electrochemical Method for Comprehensive Evaluation of Steel Corrosion in Concrete". Proc. 4th Asian-Pacific Corrosion Control Conf, Tokyo, May 1985, 757-764.

282) H.J.Fromm " Measurement of Polarized Potentials in Concrete Bridge Decks". Transportation Research Record, no.692, 23-28 (1978).

283) A.M.Rosenberg,and J.M.Gaidis " Methods of Determining Corrosion Susceptibility of Steel in Concrete". Transportation Research Record no.692, 28-34 (1978).

284) R.F.Stratfull " Corrosion Autopsy of a Structurally Unsound Bridge Deck". Highway Res. Record no. 433, 1-11 (1973).

285) R.F.Stratfull " Corrosion Testing of Bridge Decks". TRB Record 539, 50-59 (1975).

286) P.R.Vassie " Non-Destructive Evaluation of the Corrosion of Concrete Reinforcement by Chlorides". Proc. Symp. on "Corrosion of Steel Reinforcements in Concrete Construction", London, SCI, 57-78 (1978).

287) J.R.Van Daveer " Techniques for Evaluating Reinforced Concrete Bridge Decks". ACI J.72,, 697-704 (1975).

288) ASTM C 876-80 " Standard Test Method for Half Cell Potentials of Reinforcing Steel in Concrete" (1980).

289) H.ARUP " Copper/Copper Sulfate Half Cells Should Not be Used on Concrete". Mat. Performance, 20,(6), 26 (1981).

290) C. L. Page, and J. Havdahl "Electrochemical Monitoring of Corrosion of Steel in Microsilica Cement Pastes". Mater. Constr. (Paris),18,(103), 41-47 (1985).

291) P.G.Cavalier,and P.R.Vassie " Investigation and Repair of Reinforcement Corrosion in a Bridge Deck". Proc. Instn. Civ. Engrs., Part 1, 70, 461-480 (1981).

292) D.G.John,J.Lomas,J.Dawson,and P.Searson " Electrochemical Techniques for the Investigation and Monitoring of the Corrosion of Reinforcing Steel in Concrete". Proc. 1st Arabian Conf. on Corrosion, Kuwait Feb.1984, 755-772.

293) K.Hladky,and J.L.Dawson " The Measurement of Corrosion using Electrochemical 1/f Noise". Corrosion Sci., 22, 231-237 (1982).

294) D.F.Griffin " Corrosion of Reinforced Concrete in Marine Environments". Mat. Protection, 4,(11), 8-11 (1965).

295) M.Stern,and A.L.Geary "Electrochemical Polarization I. A Theoretical Analysis of the Shape of Polarization Curves". J. Electrochem. Soc., 104, 56-63 (1957).

296) C. Andrade, and J.A. Gonzales " Quantitative Measurements of Corrosion Rate of Reinforcing Steels Embedded in Concrete Using Polarization Resistance Measurements". Werkstoffe u. Korrosion, 29, 515-519 (1978).

297) C.E.Locke,and A.Siman " Measurement of Steel Corrosion Rates in Salt Contaminated Concrete". Proc. 7th Int. Congr. on Metallic Corrosion. Rio de Janeiro Oct.1978, 1399-1417.

298) H.C.Schell,and D.G.Manning " Evaluating the Performance of Cathodic Protection Systems on Reinforced Concrete Bridge Substructures". Corrosion 85, Boston, Paper no. 263, NACE (1985).

299) E.Locke,and A.Siman " Electrochemistry of Reinforcing Steel in Salt-Contaminated Concrete". ASTM STP 713, D.E.Tonini and J.M.Gaidis Eds, American Society for Testing and Materials, 3-16 (1980).

300) M.Arpaia " Corrosione delle armature in acciaio dei manufatti in calcestruzzo". Proc.BBM 75, 8th Int. Congr. on the Precast Concrete Industry, Stresa, May 1975.

301) D.G.John,P.C.Searson,and J.L.Dawson " Use of AC Impedance Technique in Studies on Steel in Concrete in Immersed Conditions". Br. Corrosion J., 16,(2), 102-106 (1981).

302) C.Andrade,and V.Castello " Practical Measurement of the AC Impedance of Steel Bars Embedded in Concrete by Means of Spectrum Analyser (Fast Fourier Transform)". Br. Corrosion J., 19,(2), 98-100 (1984).

303) K.Hladky,L.M.Callow,and J.L.Dawson " Corrosion Rates from Impedance Measurements:An Introduction". Br. Corrosion J., 15,(1), 20-25 (1980).

304) F.Wenger,J.Galland,and L.Lemoine " Methode de Controle de la Corrosion des Armatures de Beton en Milieu Marin". Proc. Int. Symp. on " Behaviour of Offshore Concrete Structures", Brest Oct. 1980, C.N.E.X.O.III-8.

305)J.A.Gonzales,A.Molina,M.Escudero,and M.C.Andrade "A Comprehension of Linear Polarization and A.C. Impedance in the Determination of Corrosion Rates of Reinforcements Embedded in Concrete". Corrosion 85, Boston, Paper no.257, NACE (1985).

306) J.A.Gonzales,A.Molina,M.L.Escudero,and C.Andrade "Errors in the Electrochemical Evaluation of Very Small Corrosion Rates-II-Other Electrochemical Techniques Applied to Corrosion of Steel in Concrete". Corrosion Sci., 25,(7), 519-530 (1985).

307) D.G.Manning,and F.B.Holt "Detecting Delamination in Concrete Bridge Decks". Concrete Int., Nov.1980, 34-41 (1980).

308) M.S.Weng, S.E.Dunn, W.H.Hartt, and R.P.Brown "Application of Acoustic Emission to Detection of Reinforcing Steel Corrosion in Concrete". Corrosion, 38,(1), 9-14 (1982).

309) S.E.Dunn, J.D.Young, W.H.Hartt, and R.P.Brown "Characterization of Corrosion Induced Damage of Reinforced Concrete Using Acoustic Emission". Corrosion 83, Anaheim, Paper no.171, NACE (1983).



8.º Congresso Internacional de Química do Cimento

8th International Congress on the Chemistry of Cement

8e Congrès International de la Chimie des Ciments

Communications
THEME 1
Volume II

22-27 de setembro de 1986
Rio de Janeiro — Brasil

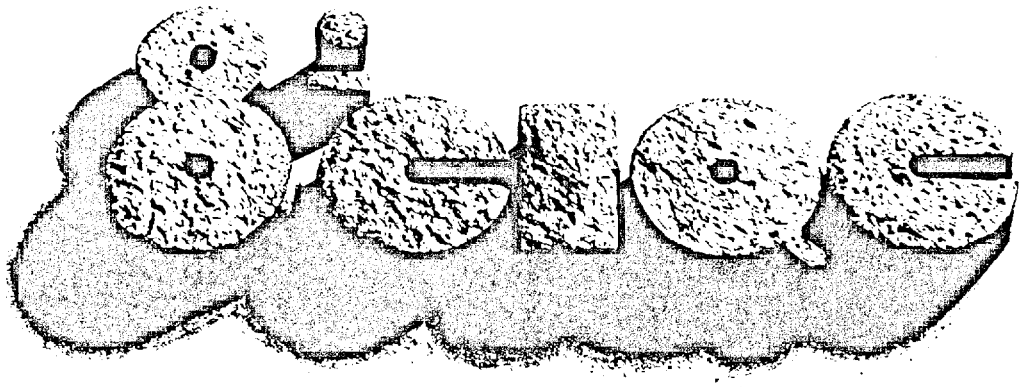

8.º Congresso Internacional de Química do Cimento

8th International Congress on the Chemistry of Cement

8e Congrès International de la Chimie des Ciments

Communications
THEME 1
Volume II

22-27 de setembro de 1986
Rio de Janeiro — Brasil

Não é permitida a reprodução dos Anais sem prévia autorização da Comissão Organizadora do Congresso.

The Proceedings are not to be reprinted without a previous permission of the Organizing Commission of the Congress.

La reproduction des Annales est interdite sans, au-devant, l'autorisation de la Commission d'Organisation du Congrès.

• • •

A substância e a forma de apresentação dos trabalhos que compõem os Anais do Congresso são de exclusiva responsabilidade de seus autores.

The substance and the form of presentation of the papers that compound the Proceedings of the Congress are exclusive responsability of their authors.

Le fond et la forme de publier les travaux qui composent les Annales du Congrès sont d'exclusive responsabilité de leur auteurs.

Secretaria Geral do 8º CIQC:
Rua da Assembléia, 10 - 40º and. - Gr. 4001
Tel.: 221-6562 – Telex: (021) 33191
20011 Rio de Janeiro – RJ – Brasil

Apoio financeiro da

finep FINANCIADORA DE ESTUDOS E PROJETOS

ORGANIZING COMMISION:

PRESIDENT:	JOSÉ ERMÍRIO DE MORAES FILHO	BRASIL
EXECUTIVE VICE-PRESIDENT:	PAULO MÁRIO FREIRE	BRASIL
TECHNICAL DIRECTOR:	FRANCISCO DE ASSIS BASÍLIO	BRASIL
ADMINISTRATIVE DIRECTOR:	JOÃO BATISTA MENESCAL FIUZA	BRASIL
DIRECTORS:	ALBERTO LUIZ GONÇALVES SOARES	BRASIL
	ENRIQUE GUNTHER DREWES	BRASIL
	EPAMINONDAS MELO DO AMARAL FILHO	BRASIL
	MARCÍLIO DE BRITO	BRASIL
	NEWTON GOULART	BRASIL

SCIENTIFIC COMMITTEES:

- SOUTH AMERICA:
  - PRESIDENT:

FRANCISCO DE ASSIS BASÍLIO	BRASIL
ALVARO AUGUSTO ALVES PINTO	BRASIL
DANTE E.J. VERONELLI	ARGENTINA
FLEMING OEST	BRASIL
HANS BUCHER	BRASIL
JOÃO GASPAR DJANIKIAN	BRASIL
LUIZ ROBERTO MARTINS DE MIRANDA	BRASIL
MARIA DAS GRAÇAS JAQUÁ	BRASIL
MARIA LUIZA MOREIRA DE MORAES	BRASIL
NEY JOSÉ DE SOUZA E SILVA	BRASIL
PABLO KITTL D.	CHILE
PAULO RODRIGUES	BRASIL
ROBERTO R. COELHO	BRASIL
YASUKO TESUKA	BRASIL
YUSHIRO KIHARA	BRASIL

- NORTH AND CENTRAL AMERICA, AND FAR EAST:
  - PRESIDENT:
  - MEMBERS:

JAN P. SKALNY	U.S.A.
DELLA M. ROY	U.S.A.
GEOFFREY FROHNSDORFF	U.S.A.
GERARD G. LITVAN	CANADA
HIROSHI UCHIKAWA	JAPAN
J. FRANCIS YOUNG	U.S.A
JORGE MARIO VILLASENOR	MEXICO
R.E. OBERHOLSTER	SOUTH AFRICA
SIDNEY DIAMOND	U.S.A.
S.W. TRESOUTHICK	U.S.A.
WU ZHONG-WEI	CHINA

- EUROPE, ASIA AND AFRICA:
  - PRESIDENT:
  - MEMBERS:

JEAN PAUL MERIC	FRANCE
C. CHARRETON	FRANCE
FRANCO MASSAZZA	ITALY
FRANÇOIS LE BEL	FRANCE
FRIEDRICH W. LOCHER	WEST GERMANY
F. YAGIZ	TURKEY
H.W.W. POLLITT	ENGLAND, U.K.
JOSE CALLEJA	SPAIN
J. TALLABER	HUNGARY
LABO KADA ABOUBACAR	NIGERIA
O.P. MTCHEDLOV-PETROSSIAN	U.S.S.R.
P. DUTRON	FRANCE
RENATO BUCCHI	ITALY
S.K. CHOPRA	INDIA
T.V. KOUZNETSOVA	U.S.S.R.
WIESLAW KURDOWSKI	POLAND

INDEX

AUTHORS'NAMES/NOMS DES AUTEURS	SUB-THEMES/SOUS-THÈMES
A	
ABDUL-MAULA, S.	1.2
AGARWAL, R.K.	1.1 – 1.3
AHLUWALIA, S.C.	1.1 – 1.2
AL'BATS, B.S.	1.2
AMICARELLI, V.	1.2
ANGELOVA, T.	1.2
ASAKURA, E.	1.2
B	
BEDÓ, M.	1.2
BESSMERTNYKH, A.V.	1.1
BHASKARA RAO, P.	1.1 – 1.2
BIKBAOU, M.Y.	1.3
BOIKOVA, A.I.	1.2 (2)
BOLIN, WU	1.2
BRAUN, H.	1.1
BRYTOV, I.A.	1.1
BÜRGER, D.	1.3
BÜRKI, P.	1.1
C	
CARIN, V.	1.2
CASTANET, R.	1.1
CHATTERJEE, A.K.	1.1 – 1.2 (2) – 1.3
CHOUBINE, V.	1.2
CHUAN-YUAN, YIN	1.2
CONG-YUN, HUANG	1.2
CONJEAUD, M.	1.1
COSTA, U.	1.2
COTTIN, B.	1.1
D	
DESHMUKH, V.V.	1.2
DE-XUN, SHEN	1.2
DRAGICEVIC, LJ.M.	1.1
E	
F	
FAYOS, J.	1.2
FENG, QIHUANG	1.1
FILLIPPOVA, L.S.	1.2
FIODOROV, N.F.	1.1
FOMITCHEVA, O.I.	1.2 (2)
FRIGIONE, G.	1.2
FUNDAL, E.	1.2
G	
GADAEV, A.I.	1.3
GAVRILOV, A.P.	1.1
GHOSH, D.	1.1 – 1.2
GROSH, S.N.	1.3
GILIOLI, C.	1.2
GOUDA, G.R.	1.2
H	
HANDOO, K.	1.1 – 1.2
HARGAVE, R.V.	1.2
HEPHER, N.M.	1.3

I	
IENTCH, Y.G.	1.3
IVANOV, B.SH.	1.1
IVANOV, N.I.	1.1
J	
JAVORONKOV, N.M.	1.3
JOST, K.	1.3
JUN'AN, DENG	1.3
K	
KAWABATA, H.	1.2
KHADILKHAR, S.A.	1.1
KHALINA, O.M.	1.1
KHLOUSOV, V.B.	1.3
KHNYKINE, Y.	1.2
KHOKHLOV, V.K.	1.1
KIHARA, Y.	1.2
KISELYEVA, I.I.	1.1
KOGAN, N.P.	1.3
KOUGIA, M.V.	1.3
KOUZNETSOVA, T.V.	1.1 – 1.2
KOZYREVA, N.A.	1.1
KRIVOBORODOV, Y.	1.2
L	
LEBEDEVA, E.L.	1.2
LEMPERLE, M.	1.1
LEWANDOWSKA-KANAS, A.	1.2
LIN, ZONGSHOU	1.2
LUDWIG, U.	1.3 (2)
M	
MASSAZZA, F.	1.2 (3)
MATHUR, V.K.	1.1 – 1.2 – 1.3
MATKOVIC, B.	1.2
MINGFEN, FENG	1.2
MIN-KANG, TENG	1.2
MOIR, G.K.	1.3
MTCHEDLOV-PETROSSIAN, O.P.	1.3
MUDHBHATKAL, G.A.	1.1
MÜLLER, A.	1.3
MUNTEAN, M.	1.2
MUZHEN, S.U.	1.3
N	
NAGASHIMA, M.	1.2
NANRU, YANG	1.3
NIKIFOROV, U.V.	1.3
NOUDELMAN, B.I.	1.3
O	
ODLER, I.	1.2
OSEN, E.	1.1
OSSOKIN, A.	1.1
OVCHARENKO, G.I.	1.3
P	
PAGE, C.H.	1.2
PARALKAR, S.V.	1.3
PARASHAR, A.K.	1.3
PÉREZ-MÉNDEZ, M.	1.2
PETERSEN, I.F.	1.1
PEZZUOLI, M.	1.2 (2)
PÖHLMANN, R.	1.3
POTAPOVA, E.	1.1
PUERTAS, F.	1.2
Q	
QING-JUN, DING	1.2

R	
RAINA, S.J.	1.1
ROUANET, A.	1.1 (2)
RUILIN, YE	1.2
S	
SAMUEL, G.	1.1 – 1.2
SARASWAT, I.P.	1.2
SAUMAN, Z.	1.2
SCHEUBEL, B.	1.2
SERSALE, R.	1.2
SEYDEL, R.	1.3
SHELUDKO, V.V.	1.1
SHI-ZHONG, LONG	1.2
SLOTA, R.J.	1.2
SOKOLOVA, N.A.	1.3
SORRENTINO, F.P.	1.1
SOUDAKAS, L.G.	1.3
STARK, J.	1.3
SUDRIGEAN, T.	1.2
SUMNER, M.S.	1.3
T	
TEOREANU, I.	1.2
TONG, DAMAO	1.2
TRIVIÑO, F.	1.2
TSUKERMAN, E.A.	1.1
U	
UBBRIACO, P.	1.2
UDA, S.	1.2
V	
VENKATESWARAN, D.	1.2
VERNET, C.	1.2 – 1.3
VERDIAN, M.A.	1.2
W	
WEI, SHEN	1.2
WEISWEILER, W.	1.1
WERYNSKA, A.	1.2
WERYNSKI, B.	1.2
WOLTER, A.	1.1
X	
XINRONG, WANG	1.2
XIU-JI, FENG	1.2 – 1.3
Y	
YANMOU. WANG	1.3
YIEWEI, ZHENG	1.3
YOUNG, J.F.	1.2
YU, SHANGREN	1.1
YUFENG, ZHU	1.3
Z	
ZDOROV, A.I.	1.3
ZOUBEKHIN, A.P.	1.2

CONTENTS/TABLE DE MATIÈRES

THEME/THÈME 1
CLINKER FORMATION AND PROPERTIES/FORMATION ET PROPRIETÉS DU CLINKER
Chairman/Président: C.D. POMEROY (England, U.K.) – Secretary/Secrétaire: M.S. MARINHO (Brasil)

SUB-THEME/SOUS-THÈME 1.1
Kinetic of Clinker Formation/Cinétique de la Formation du Clinker
Chairman/Président: O.P. MTCHEDLOV-PETROSSIAN, (U.S.S.R.)
Principal Reporter/Rapporteur Principal: F.P. GLASSER (Scotland, U.K.)

Pages	Authors (Countries)/Auteurs (Pays)	Titles of Papers/Titres des travaux
15	Qihuang Feng, Shangren Yu (China)	A study on the kinetics of the burning of portland cement clinker in different processes.
21	I.F. Petersen (Denmark)	The ability of clinker nodule formation.
25	A. Rouanet (France)	Réactions en phase solide entre la chaux et l'alumine.
31	B. Cottin, A. Rouanet, M. Conjeaud (France)	Transformations minéralogiques des crus chaux-silice-alumine a 830°C.
36	R. Castanet, F.P. Sorrentino (France)	Study of clinkering reactions by hight temperature isothermal calorimetry.
40	S.C. Ahluwalia, V.K. Mathur (India)	Thermal studies on the effect of some transition metal oxides on the kinetics of formation and stabilization of -dicalcium silicate.
46	S.J. Raina, P. Bhaskara Rao, S.K. Handoo, G. Samuel (India)	A new approach for estimation of heat requirement for clinkerization.
50	D. Ghosh, S.A. Khadilkar, R.K. Agarwal, A.K. Chatterjee (India)	Specific surface as a parameter for raw mix burnability and its relation with volume change of fired raw mix pellets.
56	P. Bürki, H. Braun (Switzerland)	Investigations on influence of raw mix reactivity and rate of upheating upon clinker formation.
62	N.F. Fiodorov, A.P. Gavrilov, N.I. Ivanov, O.M. Khalina (U.S.S.R.)	Cinétique de la synthèse des aluminates de calcium par le traitement thermique dans le milieu des caloporteurs métalliques fondus.
67	A.V. Bessmertnykh, V.K. Khokhlov, V.V. Sheludko (U.S.S.R.)	Thermodynamic study of decarbonation kinetics.
72	A. Ossokin, E. Potapova (U.S.S.R.)	Formation de minéraux dans les bains fondus.
77	T.V. Kouznetsova, I.A. Brytov, N.A. Kozyreva, B.Sh. Ivanov, I.I. Kiselyeva, E.A. Tsukerman (U.S.S.R.)	Auger electron spectroscopic study of calcium silicates and aluminates.
83	W. Weisweiler, E. Osen, M. Lemperle (West Germany)	Effect of Fe_2O_3 and Al_2O_3 admixtures on the reaction kinetics between CaO – and SiO_2 – powder compacts.
89	A. Wolter (West Germany)	Phase composition of calcined raw meal.
95	Lj.M. Dragicevic (Yugoslavia)	Prognosis of the physical-mechanical characteristics of portland cement.

SUB-THEME/SOUS-THÈME 1.2

Relationship of Processing Parameters to Clinker Properties; Influence of Minor Components.
Rapport entre les Paramètres du Processus et les Proprietès du Clinker; Influence des Éléments Mineurs

Chairwoman/Président: A.I. BOIKOVA (U.S.S.R.)
Principal Reporter/Rappoteur Principal: I. MAKI (Japan)

Pages	Authors (Countries)/Auteurs (Pays)	Titles of Papers/Titres des travaux
105	Y. Kihara (Brasil)	Influence of high ash content mineral coal in portland cement clinker characteristics.
111	Shen Wei, Feng Mingfen (China)	A study of the effects of CaF_2 on clinker doped with compound mineralizer.
117	Damao Tong, Zongshou Lin (China)	The role of CaF_2 and $CaSO_4$ in cement clinkering.
122	Ye Ruilun, Wu Bolin, Wang Xinrong (China)	The synthesis and crystal structure of a new compound $Ca_8Mg(Sio_4)_4Cl_2$.
128	Feng Xiu-ji, Long Shi-zong, Ding qing-jun, Huang Cong-yun, Shen De-Xun, Teng min-kang, Yin Chuan-yuan (China)	Investigation of dopped β -C_2S with positron annihilation.
134	Z. Sauman (Czechoslovakia)	Influence of fluorides and silicofluorides on the hydration of cement.
139	E. Fundal (Denmark)	The description of a new potassium-alumina phase in OPC.
146	C. Vernet (France)	Quissons réductrices – Conséquences relatives à la stabilité des phases du clinker.
152	C.H. Page, D. Ghosh, A.K. Chatterjee (India)	Influence of mineralizers on the constitution and properties of industrial clinkers.
158	P. Bhaskara Rao, S.K. Handoo, G. Samuel (India)	Radio tracer technique: a diagnostic method for evaluation of raw meal and clinker movement, in a cement rotary kiln.
162	I.P. Saraswat, V.K. Mathur, S.C. Ahluwalia (India)	Thermal decomposition and phase transformation studies of $CaCO_3$-SiO_2 (2:1) system in presence of sodium and potassium carbonate.
167	R.V. Hargave, D. Venkateswaran, V.V. Deshmukh, A.K. Chatterjee (India)	Quantification of clinker microstructure – An approach for prediction of cement strength.
173	C. Gilioli, F. Massazza, M. Pezzuoli (Italy)	Solid state relationships in the lime-richest part of the CaO-Al_2O_3-Na_2O-Fe_2O_3 system.
180	F. Massazza, M. Pezzuoli (Italy)	Interactions between alkaline vapours and coal ashes.
187	U. Costa, F. Massazza (Italy)	Influence of the burning degree on the rheological and strength properties of clinkers.
194	R. Sersale, V. Amicarelli, G. Frigione, P. Ubbriaco (Italy)	A study on the utilization of an italian steel slag.
199	M. Nagasnima, E. Asakura, S. Uda, H. Kawabata (Japan)	Characteristics of alite in portland cement clinker and C_3S solid solution.
205	R.J. Slota, A. Lewandowska-Kanas (Poland)	Modification of clinker phase composition and strength properties of a high-alkali cement clinker by gypsum addition.
211	B. Werynski, A. Werinska (Poland)	Influence of the isomorphic components on the clinkerization process.
217	I. Teoreanu, M. Muntean, M. Bedó, T. Sudrigean (Romania)	Belitic portland cements with various content of MgO and SO_3.
223	M. Pérez-Méndez, J. Fayos (Spain)	A very modified apatite-type structure: $Ca_2K_3(SO_4)_3F$.
228	F. Puertas, F. Triviño (Spain)	Modifications clinker phase and mechanical strength in relation to type of Quenching.
234	G.R. Gouda (U.S.A)	Microstructure and properties of high-alkali clinker.

240	Y. Krivoborodov, O.I. Fomitcheva, A.I. Boikova (U.S.S.R.)	Composition des phases des clinkers contenant des sulfoaluminates et sulfoferrites.
243	A.I. Boikova, O.I. Fomitcheva, A.P. Zoubekhin (U.S.S.R.)	Chemical composition of phases relations in unbleached and bleached clinkers.
249	T.V. Kouznetsova (U.S.S.R)	Influence des facteurs différents sur la composition de phase et les proprietés du clinker.
253	V. Chouvine, Y. Khnykine (U.S.S.R.)	Modification des clinkers de belite.
258	B.S. AL'Bats, M.A. Verdian, L.S. Fillippova, E.L. Lebedeva (U.S.S.R.)	Durée de cuisson du clinker et ses proprietés.
265	I. Odler, S. Abdul-Maula (West Germany), T. Angelova (Bulgaria)	Effect of burning conditions on clinker structure and properties of resultant cements.
270	B. Scheubel (West Germany)	Investigations on the influence of the kiln system on clinker quality.
276	B. Matkovic, V. Carin (Yugoslavia), J.F. Young (U.S.A.)	Dicalcium silicates doped with phosphates.

SUB-THEME/SOUS-THÈME 1.3
Low Energy Clinker Formation/Formation D'Un Clinker Consommant Peu D'Énergie

Chairman/Président: J.P. MERIC (France)

Principal Reporter/Rapporteur Principal: F.W. Locher (West Germany)

Pages	Authors (Countries)/Auteurs (Pays)	Titles Papers/Titres des travaux
285	Feng Xiu-ji, Zhu Yufeng (China)	Research on an early strength cement containing high content of iron.
293	Zheng Yiewei, Yang Nanru (China)	Mossbauer study of $C_2A_xF_{(1-x)}$ solid solution.
300	Wang Yanmou, Deng Jun'an, Su Muzhen (China)	An investigation into cement $CaO-SiO_2-Al_2O_3-Fe_2O_3-SO_3$ system.
306	J. Stark, A. Müller, R. Seydel, K. Jost (East Germany)	Conditions of the existence of hydraulically active belite cement.
310	M.S. Sumner, N.M. Hepher, G.K. Moir (England, U.K.)	The influence of a narrow cement particle size distribution on cement paste and concrete water demand.
316	C. Vernet (France)	Cuissons de belite à basse température – reactivité.
322	S.N. Ghosh, V.K. Mathur, A.K. Parashar (India)	Microstructure et solutions solides dans les clinkers elaborés à basse température.
327	R.K. Agarwal, S.V. Paralkar, A.K. Chatterjee (India)	Chloride salts as reaction medium for low temperature clinkerization – a probe into alinite technology.
334	N.M. Javoronkov, O.P. Mtchedlov-Petrossian, N.P. Kogan, A.I. Zdorov, Y.G. Ientch (U.S.S.R.)	Clinkerisation à basse consommation d'énergie lors de la cuisson des mélanges contenant d laitier non broyé.
338	L.G. Soudakas, U.V. Nikiforov, M.V. Kougia, N.A. Sokolova (U.S.S.R.)	Étude des clinkers à basse basicité.
343	V.B. Khlousov (U.S.S.R.)	Clinker alitosulfoalumineux: réalisation et proprietés.
347	B.I. Noudelman, A.I. Gadaev (U.S.S.R.)	Aspects phisico-chimiques de la cristallisation des chlorsilicates lors de la clinkerisation à basse température dans le bain fondu de sel.
352	M.Y. Bikbaou (U.S.S.R.)	Formation, crystal chemistry and properties of alinite and jasmundite.
358	G.I. Ovcharenko (U.S.S.R.)	Technological aspects of structure replication in silicates.
363	U. Ludwig, R. Pöhlmann (West Germany)	Investigations on the production of low lime portland cements.
372	D. Bürger, U. Ludwig (West Germany)	Synthesis of calcium silicates at low temperatures and influence on their reactivity.

THEME/THÈME 1

Clinker formation and properties. Formation et proprietés du clinker.

Chairman/Président
C.D. Pomeroy
Cement & Concrete Association
England, U.K.

Secretary / Secrétaire
M.S. Marinho
ICI — Brasil S/A
São Paulo, Brasil

SUB-THEME/SOUS-THÈME 1.1

Kinetic of clinker formation.
Cinétique de la formation du clinker.

Chairman/Président
O.P. Mtchedlov-Petrossian
Cement Research Institute
Kharkov, U.S.S.R.

Principal Reporter/Rapporteur Principal
F.P. Glasser
University of Aberdeen
Scotland, U.K.

Qihuang Feng, Shangren Yu

A study on the kinetics of the burning of portland cement clinker in different processes 1.1

Une recherche sur la dynamique de la fussion du clinker de ciment portland dan les procédés différent

A STUDY ON THE KINETICS OF THE BURNING OF PORTLAND CEMENT CLINKER IN DIFFERENT PROCESSES

ABSTRACT

To find a saving energy method of clinker formation, the authors suggested a rapid burning process and compared it with the ordinary method used in rotary kiln using the kinetic point of view in laboratory. Ginstling-Brounshtein diffusion equation and Arrhenius equation were used to detect and calculate the velocity constant Kt and diffusion activation energy Ea of the process of clinker formation. As a result, these two methods gave very different kinetic at the same temperature range 1280-1320°C. The velocity constants Kt of slowly burning method were much smaller than that of the rapid burning and the activation energy Ea of the slowly burning was much greater than that of the rapid burning. It may be explained as follows. As the mixtures burnt at burning temperature directly, a series of chemical reactions including dehydration and decomposition of clay and carbonates, solid phase reactions such as formation of calcium aluminate, calcium alumino-ferrite, dicalcium silicate and tricalcium silicate formation are all overlaped. The reactants are in the nascent state and are highly active, so that this method can give higher velocity constants Kt and a lowe activation energy Ea. On the other hand, as the raw mixtures were heated slowly, the solid phase reactions are prolonged, leading to the passivation of decomposition products of clay, carbonates, etc. Thus reduce reactivity of the reactants, leading to lowering Kt and increasing activation energy Ea. By the kinetic point of view, therefore, the rapid burning method is much better than the ordinary method. It is a significant process of lowering burning temperature and saving energy.

SUMÁRIO

Para descobrir um método de economizar a energia para a formação de clínquer, os autores sugerem um processo de queima rápida e comprovam-no com o método usual empregado em forno rotatório usando o ponto de vista cinético em laboratório. A equação de difusão de Ginstling-Brounshtein e a equação de Arrhenius foram usadas para determinar e calcular a constante de velocidade Kt e a energia de ativação de difusão Ea do processo de formação do clínquer. Como resultado, esses dois métodos forneceram constantes cinéticas muito diferentes na faixa de temperaturas de 1280-1320°C. As constantes de velocidade Kt com o método de queima lenta foram muito menores que as de queima rápida e a energia de ativação Ea da queima lenta foi muito maior do que a de queima rápida. Pode-se explicar da seguinte forma. A medida que a mistura queima numa temperatura de queima diretamente, uma série de reações químicas incluindo a desidratação e decomposição da argila e carbonatos, reações de estado sólido como a formação de aluminato de cálcio, ferro-aluminato de cálcio, silicato bicálcico e silicato tricálcico são sobrepostas. Os reagentes estão em uma forma nascente e são altamente ativos, portanto este método pode fornecer maiores constantes de velocidade Kt e uma menor energia de ativação Ea. Por outro lado, à medida que a mistura crua é aquecida vagarosamente, as reações de estado sólido são prolongadas, levando à uma passivação dos produtos de decomposição da argila, carbonatos, etc. Portanto, reduzindo a reatividade dos reagentes, ocasionando um abaixamento de Kt e aumentando a energia de ativação Ea. Pelo ponto de vista cinético, portanto, a queima rápida é muito melhor que o método usual. É um método significativo de abaixamento da temperatura de queima e de economia de energia.

Qihuang Feng, Shangren Yu

A study on the kinetics of the burning of portland cement clinker in different processes 1.1

Une recherche sur la dynamique de la fussion du clinker de ciment portland dan les procédés différent

A STUDY ON THE KINETICS OF THE BURNING OF PORTLAND CEMENT CLINKER IN DIFFERENT PROCESSES

1. Introduction

For finding a process of burning portland cement clinker at lower temperature without using any mineralizer, the authors compared the different burning methods in laboratory. One was a rapid burning method that the raw materials were exposed to the burning temperature directly; and the other one was a ordinary method, then the raw materials were heated with a heating rate about 350°C/hr to burning temperature as in rotary kiln. The rate constants Kr and activation energies Ea of these two methods have been detected and calculated, and then compared them with the kinetic point of view. Therefore, a better method for burning of clinker at lower temperature could be found, in order to suggest the engineers designing a process similar to it in industry.

2. Principle

The burning of portland cement clinker is a solid state reactions. It contains some simple physical and chemical processes eg. the phase boundary reaction, chemical reaction, diffusion, crystallization etc. The rate of the reaction is controlled by the slowest step. At burning temperature about 1300°C, many chemical reactions such as the formation of C_2S, C_3A, C_4AF and C_3S take place almost simultaneously, however, the slowest step of the whole process is the diffusion of calcium ion Ca^{2+}. So the authors adopted the Ginstling- Brounshtein diffusion equation to calculate the rate constant Kr. Ginstling-Brounshtein equation is:

$$f(\alpha)= 1-\frac{2}{3}\alpha-(1-\alpha)^{2/3}=Krt \qquad (1)$$

where α----- degree of conversion

Kr---- rate constant

t----- time

The activation energy may be calculated with the Arrhenius equation.

$$Kr=C_0 EXP(-Ea/RT) \qquad (2)$$

where C_0 ---- constant

T----- absolute temperature

Ea---- activation energy

R----- gas constant

Taking the logarithm gives:

$$lnKr=lnC_0-Ea/RT \qquad (3)$$

3. Experiment

The authors adopted three industrial materials—— limestone, clay and pyrite cinder to make the raw meal, of which the composition is given in table 1.

Table1 Composition of the raw meal (%)

SiO_2	Fe_2O_3	Al_2O_3	CaO	MgO	Loss
14.01	2.01	3.14	41.14	1.13	35.97

The raw meal was burnt with the rapid method and the ordinary method respectively.

a. Rapid burning method

The raw meal was pressed at 2000kg/cm^2 to form tablets with an area of 1cm^2, height of 5mm and cut into 4 pieces. The burning conditions were in the range of 1280°C to 1320°C with 5 levels at 10°C intervals and each for 3, 5, 10, 15 and 20 minutes[1]. The burning was done in a carborundum electric furnace with a precise automatic temperature controller. The furnace temperature fluctuation

was controlled within a range of ±0.5 C. f_{CaO} and loss of the burning products were determind. The analytical results are shown in table 2.

b. Ordinary method

The tablets were made as before and placed in the electric furnace, but with a speed of temperature rise about 350°C/hr. As the temperature rase to 1280°C, the tablets were all taken out and burnt in the range of 1280 to 1320°C with 5 levels at 10°C intervals for 5, 10, 15, 20 and 30 minutes. Then f_{CaO} and loss of the burning products were determind. The analytical results of the burning products are given in table 3.

4. Results and discussion

a. Rapid burning

The rate constants Kr might be calculated using Ginstling equation. First of all, it was how to get α which was expressed by the conversion of CaO in the reaction. Since the reactions were not completed in these experiments, different amounts of limestone were left not to be decomposed and could be calculated with the data of ignition loss. The calcium oxide combined in unchanged limestone togather with the free lime were not taken part in the formation of clinker minerals in these experiments. So the formular for calculating degree of conversion is:

$$\alpha = \frac{CaO-(f_{CaO}+\frac{56}{44}\times L)\times\frac{100}{100-L}}{CaO} \qquad (4)$$

where CaO----total content of CaO in clinker

L------loss of burning product

f_{CaO}---free lime in burning product

56, 44---molecular weights of CaO and CO_2, respectively.

Then, reaction rate constants Kr and Ca^{2+} ion diffusion energy Ea in the formation of clinker were obtained by calculating α for different durations of burning at variable temperature using formula (4). The processing results are shown in table 2. Plotting $f(\alpha)$ against t according to equation (1) are shown in figure 1.

In figure 1 the graph for $f(\alpha)$ against t was some sharp bent lines, of which each consisted of two straight lines. The turning points were around 5 minutes of burning. The graphs before turning points were one set of straight lines, while after that were another set. The former were resulted predominantly from the bourndary reactions such as the formation of calcium aluminate, calcium aluminoferrite, dicalcium silicate and some tricalcium silicate was also formed, hence the reactions were more complecated; the latter straight lines were derived from the calcium ion diffusion and the main reactions were the tricalcium silicate formation and a small amount of dicalcium silicate formed. It can be seen from the X-ray diffraction patterns[2]. The X-ray diffraction patters for different durations of burning at 1300°C are shown in figure 2. The deviation of the last point of 1320°C in figure 1 might be caused by the equilibrium of the reaction at 1320°C. In case of equilibrium, it did not fit Ginstling equation. From the kinetic point of view the process of clinker formation is identical with that of alite formation. The rate of which is the controlling factor[3].

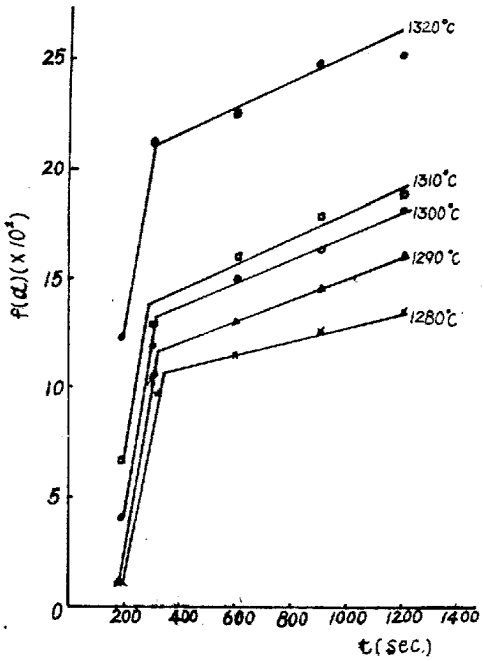

Fig.1 $f(\alpha)$ vs t for rapid burning

Table 2. Data and results for rapid burning

T(°C)	t(sec)	f_{CaO}%	L%	α %	f(α)	Kr	lnKr	1/T	Ea(kj/mol)
1280	180	40.66	2.56	0.298	0.0115				
	300	15.21	1.17	0.737	0.0982				
	600	12.83	0.79	0.782	0.116				
	900	11.43	0.75	0.806	0.127	3.32×10^{-5}	-10.31	6.44×10^{-4}	
	1200	10.31	0.74	0.824	0.136				
1290	180	39.01	3.66	0.294	0.0112				
	300	14.27	1.02	0.755	0.105				
	600	10.07	1.28	0.816	0.133				
	900	8.43	1.37	0.839	0.145	4.85×10^{-5}	-9.93	6.40×10^{-4}	
	1200	7.67	0.65	0.867	0.161				
1300	180	28.71	1.18	0.524	0.0411				
	300	12.47	0.77	0.789	0.120				
	600	8.96	0.49	0.850	0.151				
	900	7.65	0.44	0.872	0.164	5.29×10^{-5}	-9.85	6.36×10^{-4}	303
	1200	6.02	0.41	0.898	0.183				
1310	180	21.47	1.28	0.636	0.0661				
	300	11.30	0.58	0.812	0.130				
	600	7.89	0.42	0.868	0.162				
	900	6.37	0.40	0.892	0.179	6.27×10^{-5}	-9.68	6.32×10^{-4}	
	1200	5.47	0.54	0.904	0.187				
1320	180	12.28	0.56	0.797	0.123				
	300	3.66	0.48	0.933	0.213				
	600	2.82	0.55	0.945	0.225				
	900	1.62	0.48	0.965	0.250	6.10×10^{-5}	-9.71	6.28×10^{-4}	
	1200	1.50	0.47	0.967	0.253				

Table 3. Data and results for ordinary burning

T(°C)	t(sec)	f_{CaO}%	L%	α %	f(α)	Kr	lnKr	1/T	Ea(kj/mol)
1280	300	13.46	0.70	0.775	0.113				
	600	12.87	0.70	0.784	0.117				
	900	12.10	0.56	0.799	0.124				
	1200	12.05	0.45	0.803	0.125	4.62×10^{-6}	-12.29	6.44×10^{-4}	
	1800	11.46	0.62	0.808	0.129				
1290	300	13.06	0.52	0.785	0.118				
	600	12.22	0.40	0.801	0.125				
	900	11.44	0.41	0.813	0.131				
	1200	11.00	0.36	0.821	0.135	7.50×10^{-6}	-11.80	6.40×10^{-4}	
	1800	10.68	0.32	0.827	0.138				
1300	300	11.94	0.34	0.807	0.128				
	600	11.34	0.62	0.810	0.130				
	900	10.25	0.59	0.828	0.139				
	1200	9.99	0.22	0.840	0.145	1.24×10^{-5}	-11.30	6.36×10^{-4}	981
	1800	9.40	0.23	0.849	0.150				
1310	300	12.42	0.44	0.797	0.123				
	600	9.42	0.40	0.845	0.148				
	900	8.48	0.40	0.860	0.157				
	1200	7.73	0.27	0.874	0.166	2.43×10^{-5}	-10.62	6.32×10^{-4}	
	1800	6.28	0.46	0.893	0.179				
1320	300	12.24	0.52	0.798	0.124				
	600	9.25	0.38	0.848	0.150				
	900	7.45	0.37	0.876	0.168				
	1200	6.48	0.34	0.892	0.179	2.78×10^{-5}	-10.49	6.28×10^{-4}	
	1800	5.19	0.41	0.911	0.193				

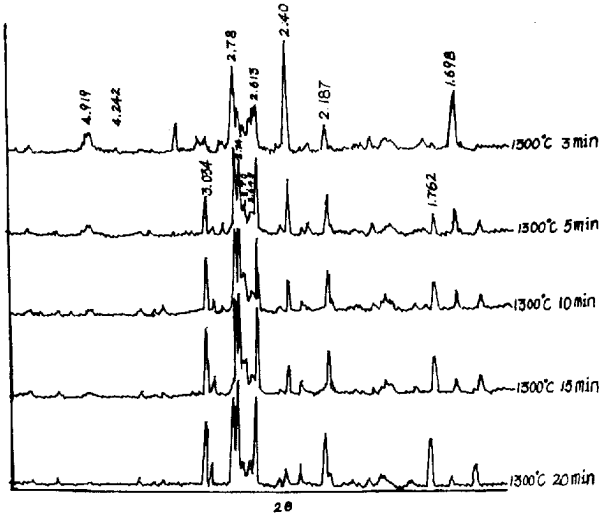

Fig.2 X-ray diffraction patterens

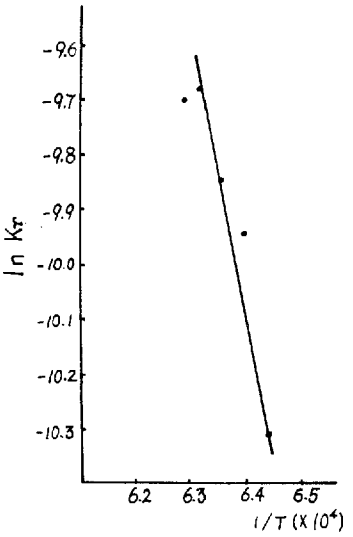

Fig.3 lnkr vs 1/T for rapid burning

Owing to the later straight lines representing mainly the Ca^{2+} diffusion and tricalcium silicate formation reactions, the authors adopted them to calculate Kr and Ea with equation (1) and (3)[4] by the least square method-regression analysis using an electric computer. The processing results are shown in table 2 and figure 3. The correlation coefficients of the liner equation relating $f(\alpha)$ to t were above 0.97, which proved the rapid burning process of raw meal in the temperature range of 1280-1320°C within 20 minutes conformed to Ginstling-Brounshtrin equation. The activation energy calculated by us for the formation of tricalcium silicate as the main reaction was 303 kj/mol, closs to the value of 205-361 kj/mol obtained by Von St. Chromy.

b. Ordinary method

The reaction rate constants Kr and Ca^{2+} ion diffusion activation energy Ea in the formation of clinker were obtained as described in a. The results are shown in table 3 and figure 4-5.

The activation energy was 981 kj/mol, much more greater than the rapid burning method's and the rate constant at every temperature was smaller than that of the rapid burning

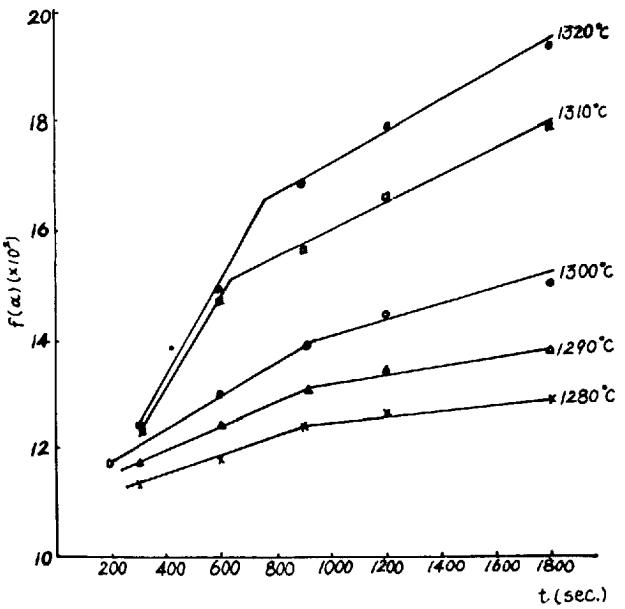

Fig.4 $f(\alpha)$ vs t for ordinary burning

method. It may be explained as follows: As the raw meal burnt at burning temperature directly, a series of chemical reactions including dehydration and decomposition of clay and carbonates, solid state reactions such as formation of calcium aluminate, calcium alumino-ferrite, dicalcium silicate and tricalcium silicate formation are all over-

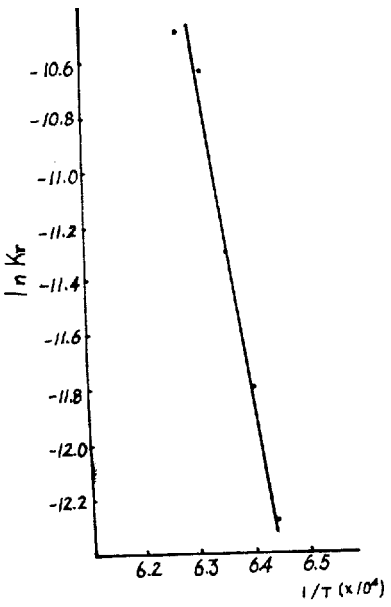

Fig.5 lnKr vs 1/T for ordinary burning

laped. The reactants are in the nacent state and are highly reactive, so the method can give higher rate constants Kr and a lower activation energy Ea. On the other hand, as the raw meal heated gradually, the solid phase reactions are prolonged, leading to the passivation of decomposition products of clay, carbonates etc. Thus the reactivity of reactants is reduced resulting in a lower Kr and a higher activation energy Ea. By the kinetic point of view, therefore, the rapid burning method is much better than the ordinary method. So the authors propose the engineers to design a process similar to the rapid burning and then it should be a significant process of lowering burning temperature and hence saving energy.

The authors are indebted to Mr. Xian-Lin Guan, Miss Jian Quan and the others for their assistance in carrying out the experiments.

References

1. Renichi Kondo, reaction velocity in portland clinker formation, chemistry of cement Proc. 4th Int. Symp. Washington, 1960 Vol.1 pp107-112.
2. F. M. Lea, The chemistry of cement and concrete, third edition , London 1970 pp.858-866 (in chinese).
3. Von St. Chromy, process of portland cement clinker formation, part Ⅱ: Kinetics of clinker formation, Zement-Kalk- Gips, Vol.35 No.7. 1982, pp.368-373.
4. K.J.D. Mackenziet and N. Hadipour, formation kinetics of portland cement clinker phases Ⅲ. β-dicalcium silicate and tricalcium silicate, Transactions and Journal of the British Ceramic Society. Vol.77. No.6, 1978, pp.168-172.

Ib Finn Petersen, Chemical Engineer, M.Sc.
F.L. Smidth & Co. A/S, R&D Dept.
Copenhagen, Denmark.

The Ability of Clinker Nodule Formation.

1.1

Aptitude à la formation des nodules de clinker.

SUMMARY: Little attention has been devoted to the physical processes accomplishing the burning of raw meal into clinker. These processes are responsible for the agglomeration of the clinkering material into clinker nodules during the burning in an industrial rotary kiln. This agglomeration process consists fundamentally in a reduction in the specific surface area of the clinkering material. Clinker melt formation at the beginning of the burning zone rearranges the crystals into clinker nuclei followed by nodule growth by coalescence of these nuclei and layering of clinker nuclei onto the surfaces of the formed nodules. This agglomeration process is difficult to imitate in the laboratory. However, it is possible to elucidate physical characteristics of the clinkering material by isothermal burning of a number of raw meal compacts for different times in the laboratory, followed by investigations of the pore structure in the resulting samples. From earlier research concerning such sintering experiments it has been concluded that the clinkering material obtains strength due to capillary action of the melt phase and that the clinkering material in rheological sense resembles a liquid with very high viscosity. In addition, methods for estimation of the capillary pressure and the ratio between specific surface energy and viscosity have been established. In the present paper such data are used for the evaluation of the ability of clinker nodule formation. This involves an estimation of the binding force that can develop between two clinker nodules in contact during one kiln revolution in comparison to the force of gravity.

SUMÁRIO

Pouca atenção tem sido devotada aos processos físicos acontecidos na queima da mistura crua para formação do clínquer. Esses processos são responsáveis pela aglomeração do material de clinquerização em nódulos de clínquer durante a queima num forno industrial rotativo. Esse processo de aglomeração consiste fundamentalmente numa redução da superfície específica do material de clinquerização. A formação do clínquer fundido no início da zona de queima, rearruma os cristais no núcleo do clínquer, seguido do crescimento do nódulo por coalescencia desses núcleos e da formação de camadas nos núcleos do clínquer em direção às superfícies dos nódulos formados. Esse processo de aglomeração é difícil de ser imitado em laboratório. Entretanto, é possível elucidar as características físicas do material em clinquerização pela queima isotérmica de certo número de misturas cruas compactas em diferentes tempos no laboratório, seguido de investigações da estrutura de poros nas amostras resultantes. Pelas pesquisas iniciais, relativas a estas experimentações de sinterização, concluiu-se que o material em clinquerização obtém resistência devido a ação capilar da fase fundida e que o material de clinquerização, em sentido reológico, assemelha-se a um líquido com muito alta viscosidade. Além disso, foram estabelecidos métodos para avaliação da pressão capilar e a relação entre a energia específica da superfície e a viscosidade. No presente trabalho esses dados são usados para uma avaliação da habilidade da formação de nódulos do clínquer. Isso envolve uma estimação das forças de aderência que podem se desenvolver entre dois nódulos de clínquer em contato durante uma rotação do forno, em comparação com a força da gravidade.

INTRODUCTION

The size distribution of rotary kiln cement clinker is a result of the agglomeration process in the burning zone of the kiln. It has been concluded that the main mechanisms of this agglomeration are coalescence of clinker nodules together with layering of particulate material onto the surface of the clinker nodules [1].

Investigations concerning the sintering properties of Portland cement raw meals have revealed the following physical characteristics [2]. At burning temperatures the clinkering material obtains strength due to the capillary action of the melt in the interstices between the crystals. The condensed material (crystals + melt) resembles in clinker at high temperature a liquid with high viscosity. In addition, methods have been derived for estimation of the capillary pressure relative to the specific surface energy and the viscosity of the condensed material, also relative to the specific surface energy from isothermal sintering experiments.

Knowing these physical properties of the clinkering material it is obviously of interest to consider how these characteristics are interrelated with the agglomeration process in the burning zone of the kiln.

STRESSES WITHIN THE CHARGE OF THE KILN

The cascading movement of the charge in a rotary kiln is shown in fig. 1. At the lower part of the charge surface material incorporates in the part of the charge following the kiln rotation as a fixed bed.

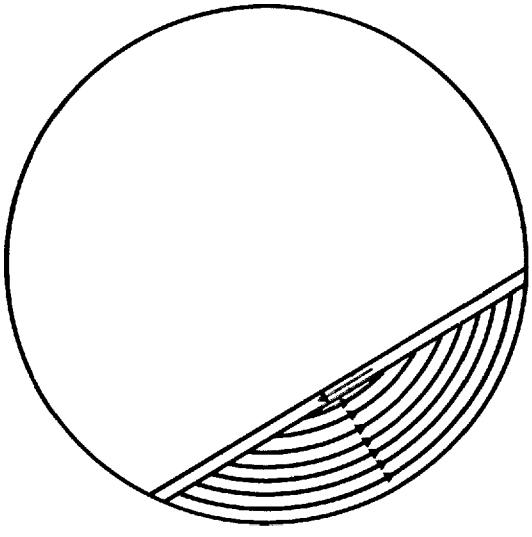

When the charge surface is reached, again gravitation outbalances the effect of material friction and cohesion, and a layer of material rolls and slides down the surface.

The moderate rotational speed - approx. 10% of the critical speed - of a rotary kiln indicates that the centrifugal force can be neglected. The stress distribution within a bulk material can always be described by means of three perpendicular, principal compressive stresses $\sigma 1 \geq \sigma 2 \geq \sigma 3$. The major principal stress $\sigma 1$ within the kiln charge is equal to the gravitational load of overlaying charge and is directed vertically downwards. Neglecting the modest inclination of the kiln axis, the medium and minor principal compressions $\sigma 2$ and $\sigma 3$ can to a first approximation be assumed to be equal to zero.

The greatest magnitude of the major principal stress will be at the periphery of the charge. At this location it can be calculated [3] according to:

$$\sigma 1 = 0.5 \cdot \rho \cdot g \cdot D \, (\cos(\theta - \phi) - \cos v)/\cos\phi \quad (1)$$

where ρ denotes charge bulk density, g the acceleration of gravity, and the rest of the symbols are described in fig. 2.

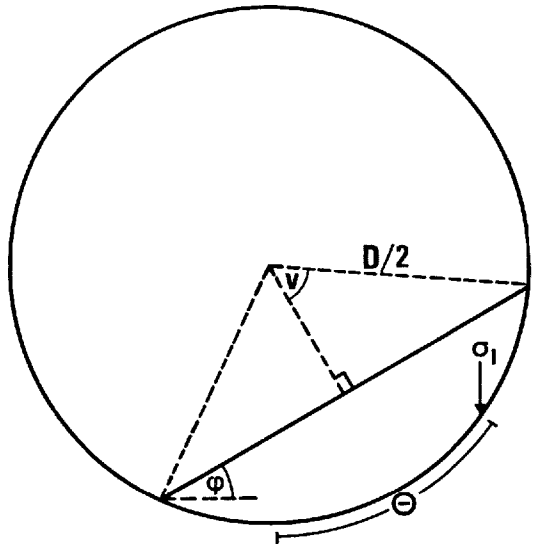

Fig. 2

When the magnitudes and directions of the principal compressive stresses are known, it is possible to calculate normal and shear stresses transmitted in a plane of any direction in the charge. The normal stress $\sigma(\psi)$ and the shear stress $\tau(\psi)$ transmitted in a plane, whose normal is orientated at an angle ψ against the direction of the major principal stress $\sigma 1$, can be calculated as [4]:

$$\sigma(\psi) = 0.5 \cdot \sigma 1 \cdot (1 + \cos 2\psi) \quad (2)$$

$$\tau(\psi) = 0.5 \cdot \sigma 1 \cdot \sin 2\psi \quad (3)$$

GRANULATION SUBJECT TO THE STRESS DISTRIBUTION

The stresses in the charge will affect the granulation process. These stresses have to be transmitted as normal forces $N(\psi)$ and shear forces $T(\psi)$ among contacting nodules or nuclei of nodules. Taking advantage of the theoretical work of Molerus [4], these forces between nodules of diameter d in a charge with a void fraction ε are related to the corresponding stresses:

$$\sigma(\psi) = \frac{1-\varepsilon}{\varepsilon} \cdot \frac{N(\psi)}{d^2} \quad (4)$$

$$\tau(\psi) = \frac{1-\varepsilon}{\varepsilon} \cdot \frac{T(\psi)}{d^2} \quad (5)$$

The normal force $N(\psi)$ transmitted between two contacting nodules will tend to consolidate this contact by forming a neck with a contact area growing in time. This is a consequence of the viscous behaviour of clinkering material at high temperature. Expression (6) for the development of such a neck between two viscous spheres, when the contact is subject to an external force F, has been derived by Rumpf et al [5] from a solution of the general Navier-Stoke equation

$$(\frac{b}{d})^2 = (\frac{4}{5} \cdot \frac{\gamma}{d} + \frac{2}{5\pi} \cdot \frac{F}{d^2}) \cdot t/\eta \quad (6)$$

b: neck radius

d: diameter of spheres

γ: specific surface energy

η: viscosity

t: time

F: external normal force over the contact

However, the shear force $T(\psi)$ transmitted by a contact will tend to break the contact by shearing the nodules apart. As a matter of fact, the normal force $N(\psi)$ and the shear force $T(\psi)$ are transmitted by the neck area πb^2. The neck will be sheared apart if the shear stress $T(\psi)/\pi b^2$ in the neck is greater than the internal friction of the neck. The internal friction of the neck is related to the total compressive stress over the neck by the coefficient of the internal friction μ. The total compressive stress over the neck contains two contributions. The material cohesion gives rise to an internal contribution equal to the capillary pressure in the material ΔPc.

The load of the charge gives rise to an external contribution of the magnitude $N(\psi)/\pi b^2$. Consequently the neck will be sheared apart in cases where:

$$|T(\psi)/\pi b^2| > \mu \cdot (\Delta Pc + N(\psi)/\pi b^2) \quad (7)$$

WORST CASE MODEL

A computer programme has been established on the basis of the above principles. This programme calculates whether a contact established between two clinker nodules at the foot of the charge will be consolidated into a permanent contact or sheared apart, as it follows the kiln rotation subject to the stresses at the periphery. Because the stresses at the periphery are of greater magnitude, this calculation is to be considered as a worst case. The charge follows the kiln rotation as a fixed bed apart from the surface layer. Consequently the orientation of a contact between two nodules will remain fixed, relative to the kiln rotation. The direction of the principal compressive stress is always vertical. Accordingly the angle ψ will change, as the contact follows the kiln rotation. Consequently the magnitudes of the normal and shear forces transmitted by the contact will change during this passage. When the kiln dimension, rotational speed, degree of filling, and angle of repose are specified, the time elapsed from the contact entered the rotating part of the charge until it has reached a given position can be calculated. This time is necessary in order to evaluate the neck development. Actually a contact between two nodules may have any orientation when it enters the rotating part of the charge. Therefore the programme considers all possible orientations and calculates the fraction surviving.

Such results from calculations corresponding to six different cases are presented in fig. 3. All cases concern a kiln having a 4.2 m internal diameter exclusive of lining and coating, making one revolution in 30 sec., having 15% filling with 1300 kg/m^3 bulk density, and a 35 deg. angle of repose. For the clinkering material, physical properties covering the range observed in experiments at 1400-1450 deg. C have been used [2].

From a generalized yield locus for clinkering material [2] the angle of internal friction is estimated at 40 deg., corresponding to a coefficient of internal friction $\mu = \tan 40 = 0.84$. No estimate for the specific surface energy exists. However, the good wetting properties of the clinker melt towards the crystals indicate that this quantity is of the same order of magnitude as the surface tension of the melt, approx. $\gamma = 0.5$ N/m. The capillary pressure ΔPc and the viscosity η have been varied among the cases as listed below:

Case No.	ΔPc kPa	η MPa s
1	125	5
2	60	5
3	25	5
4	125	20
5	60	20
6	25	20

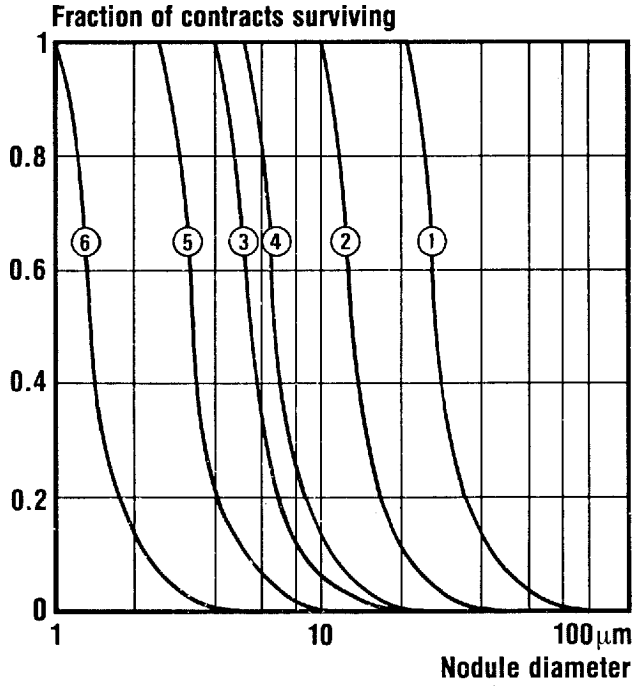

Fig. 3 Fraction of contacts surviving versus nodule diameter

DISCUSSION

Qualitatively the model responds reasonably upon changes in the physical properties of the clinkering material. When the capillary pressure decreases, the cohesion of the material decreases, and the size of the nodules that can form contacts that are able to survive the treatment in the charge decreases. The capillary pressure is in particular influenced by the raw meal mineralogy and micro level homogeneity. Especially the content of coarse-grained silica in the raw meal has a decreasing influence on the capillary pressure [2] and accordingly upon the agglomeration. An increase in the viscosity of the clinkering material has a similar effect. When the viscosity increases, the neck development between contacting nodules slows down. The viscosity of the clinkering material increases when the amount of melt is reduced [2].

Quantitatively the order of magnitude of the size of nodules that can form permanent contacts appears to be too small and corresponds rather to clinker crystals than to clinker nodules. The reason for this could be that the viscosities used in these calculations correspond to condensed material (crystals + melt) and do not take into account that the nodules also contain pores. It is to be expected that this porosity will lower the apparent viscosity of the clinker nodules and speed up the neck development. However, an adequate treatment of the viscosity of polyphase systems, which could quantify this effect, is presently lacking.

CONCLUSIONS

A worst case computational model has been established, relating the physical properties of clinkering material observed in sintering experiments with the agglomeration process in a rotary kiln based upon the mechanics of bulk solids. The model responds qualitatively reasonably upon changes in the physical properties of the clinkering material, whereas the model appears to be too critical regarding the size of nodules that can form permanent contacts surviving the charge load. The model considers the situation at the charge periphery and is therefore also considered relevant concerning formation of coating.

BIBLIOGRAPHY

1. I.F. PETERSEN (1980), "A Model for the Size Distribution of Rotary Kiln Cement Clinker", World Cement Technology 11, pp. 435-439, 467-470.

2. I.F. PETERSEN (1983), "Isothermal Sintering of Portland Cement Raw Mixes", World Cement Technology 14, pp. 188-196, 220-228.

3. M. CROSS (1979), "The Transverse Motion of Solids Moving Through Rotary Kilns", Powder Technology 22, pp. 187-190.

4. O. MOLERUS (1975), "Theory of Yield of Cohesive Powders", Powder Technology 12, pp. 259-275.

5. H. RUMPF, K. SOMMER & K. STEIER (1976), "Mechanismen der Haftkraftverstärkung der Partikelhaftung durch plastisches Verformen, Sintern und viskoelastisches Fliessen", Chem.-Ing.-Tech. 48, pp. 300-307.

A. ROUANET 1
Chargé de recherche au CNRS, en détachement à LAFARGE COPPÉE RECHERCHE, actuellement au Laboratoire des Ultra-Réfractaires, CNRS-Odeillo, France.

REACTIONS EN PHASE SOLIDE ENTRE LA CHAUX ET L'ALUMINE 1.1
Solid-state reactions between lime and alumina

RESUME.

Il s'agit d'une contribution à la connaissance des systèmes réactionnels établis entre la chaux et l'alumine et à l'approche de la cinétique des réactions. Une première étude macroscopique est effectuée sur des mélanges d'oxydes d'aluminium et de calcium de granulométrie contrôlée dont les proportions correspondent aux cinq composés connus du diagramme C-A, et traités dans l'air à diverses températures ($900 < T < 1500^{o}C$). Le taux de combinaison de la chaux, la nature des aluminates et les vitesses d'avancement de la réaction globale vers l'équilibre thermodynamique sont appréhendés par diffraction X à la température ordinaire ou "in situ" selon des isothermes ou des montées linéaires de la température. Les mécanismes réactionnels sont interprétés à la lumière des résultats d'une étude microscopique complémentaire réalisée sur des échantillons plans et massifs d'alumine pure placés au contact de chaux pulvérulente. Les analyses sont effectuées par microscopie électronique à balayage et microsonde électronique. Le schéma réactionnel suit le modèle topochimique du grain d'alumine à coeur rétrécissant. La formation de l'aluminate tricalcique semble au contraire procéder d'une diffusion de l'alumine dans la chaux et indiquer la présence d'une double diffusion à contre courant. On a établi par ailleurs une corrélation entre les grandeurs cinétiques obtenues par les deux méthodes d'analyse.

SUMÁRIO.

Trata-se de uma contribuição ao conhecimento dos sistemas reacionais estabelecidos entre a cal e a alumina e a uma aproximação da cinética das reações. Um primeiro estudo macroscópico é efetuado em misturas de óxidos de alumínio e cálcio de granulometria controlada cujas proporções correspondem aos cinco compostos conhecidos do diagrama C-A, e tratados ao ar em diversas temperaturas ($900 < T < 1500^{o}C$). A taxa de combinação da cal, a natureza dos aluminatos e as velocidades de avançamento da reação global em direção ao equilíbrio termodinâmico são determinados por difração de R.X à temperatura ordinária ou "in situ" de acordo com as isotermas ou das subidas lineares da temperatura. Os mecanismos reacionais são interpretados à luz dos resultados de um estudo microscópico complementar realizado sobre amostras planas e massas de alumina pura colocadas em contato com a cal pulverulenta. As análises são efetuadas por microscopia eletrônica de varredura e microsonda eletrônica. O esquema reacional segue o modelo topoquímico do grão de alumina com interior em retração. A formação do aluminato tricálcico parece ao contrário provir de uma difusão de alumina na cal e indicar a presença de uma dupla difusão em contra corrente. Estabeleceu-se, por outro lado, uma correlação entre as grandezas cinéticas obtidas pelos dois métodos de análise.

1. INTRODUCTION.

Nombreuses sont les études qui relèvent de la compréhension des mécanismes de formation des aluminates de calcium par réaction à l'état solide entre la chaux et l'alumine. On distingue chronologiquement une première période au cours de laquelle les travaux ont porté pour l'essentiel sur des analyses qualitatives (caractérisation des aluminates formés) et pseudo-quantitative à partir des mélanges d'oxydes ou de carbonates et oxydes (approche des lois de vitesses de formation). Les méthodes utilisées (diffraction X) ne permettent qu'une observation globale des phénomènes à l'exclusion de celle des séquences élémentaires de la formation des phases d'équilibre. Les résultats présentés par les différents auteurs (1 à 9) ne sont pas toujours en bon accord car ils dépendent étroitement des conditions expérimentales dans lesquelles les réactions ont été opérées. Plus récemment une série de travaux ont été effectués (10 et 11) au moyen de techniques microscopiques permettant l'analyse plus fine des mécanismes sur le grain isolé de matière. Dans le travail présenté ici on a recherché une meilleure définition des réactions de formation des aluminates par l'analyse des phénomènes de diffusion unidirectionnelle dans un système matériel constitué d'un bloc monolithique d'alumine noyé dans la chaux pulvérulente. De plus, on a tenté d'expliciter les phénomènes observés sur des mélanges de poudres d'oxydes à la lumière des résultats précédemment acquis.

2. ETUDE DES REACTIONS CHAUX-ALUMINE A PARTIR D'UNE INTERFACE PLANE DEFINIE.

2. 1 - Conditions expérimentales.

L'alumine de haute pureté est fondue au foyer d'un concentrateur d'énergie solaire (T > 2200°C) dans l'air sous forme de globule pseudo-sphérique de 8 mm de diamètre environ. L'échantillon refroidi à vitesse lente est ensuite poli selon une surface plane mise au contact de la poudre de carbonate de calcium. Une charge mécanique permet d'assurer un meilleur contact au moment de la cuisson. Les températures de traitement varient de 980°C à 1370°C et les périodes de quelques heures à quelques dizaines d'heures selon la température choisie. La température limite T = 1370°C est légèrement inférieure à la température du premier eutectique C_3A + $C_{12}A_7$ annoncé sur le diagramme d'équilibre ($T_{eut.}$ ~ 1390°C). On a pu constater en effet, sur des échantillons portés à 1400°C qu'un film de liquide se forme à la surface du bloc d'alumine modifiant brutalement le comportement du matériau par diffusion des espèces dans la phase liquide. Les matériaux traités sont taillés selon un plan perpendiculaire au front de diffusion et examinés par microscopie optique ou électronique. Après attaque sélective des phases soit dans une solution de soude à 2 % soit d'acide fluorhydrique à 20 %, on définit l'épaisseur moyenne des couches successives des différents aluminates formés -moyenne évaluée à partir de plusieurs mesures effectuées en différents sites de l'échantillon (on a, pour ce faire, choisi les zones de diffusion les plus homogènes où le front réactionnel est sensiblement parallèle à l'interface initiale). Parallèlement des mesures locales du rapport C/A sont effectuées par EDX en différents points de la couche de produit. Les profils de concentration sont définis par la méthode de l'analyse en ligne.

2. 2 - Résultats.

L'examen morphologique du matériau après traitement révèle la présence d'une couche de produit nouvellement formée dans le bloc d'alumine compacte. Cette couche est elle-même constituée de plusieurs couches élémentaires (Fig. 1) dont le nombre et l'épaisseur relative sont fonction de la température. Cette couche de produit est compacte et l'on ne note pas de fissure entre chacune des phases la constituant. L'analyse par diffraction X de la surface de la couche compacte révèle dans tous les cas l'existence de la phase $C_{12}A_7$. Au fur et à mesure que l'on pénètre à l'intérieur du produit apparaissent successivement les phases CA, CA_2 CA_6 conformément à la décroissance du potentiel chimique en calcium. Le domaine de chacune de ces phases est bien défini, tel qu'il apparaît (Figs. 2 et 3) sur les profils de concentration en calcium et aluminium. Toutefois, la phase CA_6 n'apparaît significativement qu'aux températures les plus élevées.

Les gradients de concentration en calcium et aluminium sont très prononcés aux voisinages des zones de changement de phases. Ces mêmes zones sont séparées par des domaines où les concentrations, seniblement monotones, traduisent l'existence de phases stoechiométriquement bien définies. D'un autre côté, l'examen par diffraction X de la zone de produit pulvérulent au voisinage de l'interface poudre-monolithe révèle l'existence de la seule phase C_3A. L'ensemble de ces phénomènes s'expliquent bien par une diffusion unidirectionnelle du calcium dans l'alumine compacte et d'une diffusion à contre-courant de l'ion aluminium dans la chaux. Ces résultats sont en bon accord avec ceux de WEISWEILLER et coll. (11) qui observèrent, à l'inverse de nos expériences, la formation d'aluminates (C_3A et $C_{12}A_7$) dans un monolithe de calcite noyé dans la poudre d'alumine.

Sur le plan de la thermodynamique, l'existence des cinq types d'aluminates C_xA_y est possible dans la gamme des températures choisie. Toutefois, leur ob-



Fig. 1 - Micrographie (x 380) d'une section de produit formé sans l'alumine (traitement à 1310°C - 16 heures). Les trois zones correspondent -de bas en haut- aux alumine-aluminates (CA, CA_2) et aluminate $C_{12}A_7$.

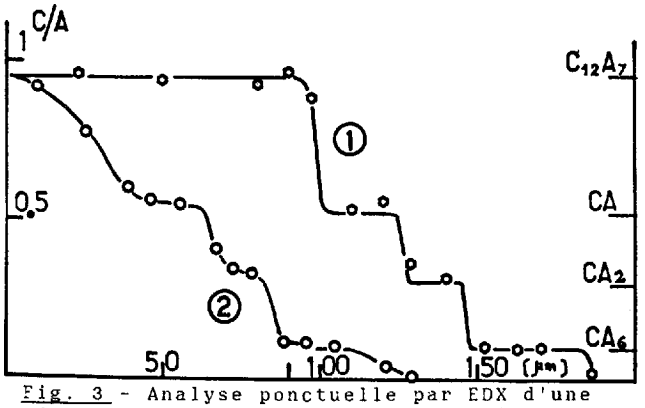

Fig. 3 - Analyse ponctuelle par EDX d'une série de microdomaines localisés le long d'une ligne perpendiculaire au front de réaction. -1-Alumine traitée à 1370°C sous potentiel chimique de calcium maintenu constant à l'extérieur du bloc monolithique. -2- Alumine traitée à 1370°C par attaque à la chaux - puis ultérieurement en l'absence de chaux. On note alors une régression de la zone $C_{12}A_7$ qui devient ainsi la source en calcium.

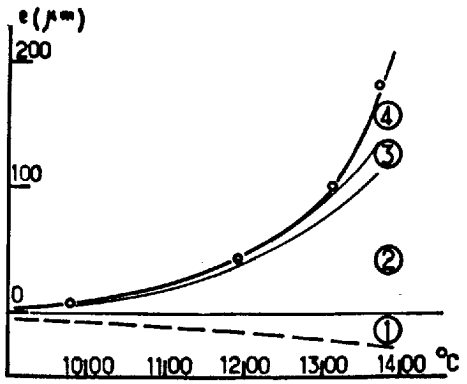

Fig. 4 - Profondeur de pénétration du calcium dans le monolithe d'alumine à différentes températures et à échéance constante (t = 30 heures). Les zones 2 - 3 et 4 représentent les épaisseurs estimées pour $C_{12}A_7$, (CA + CA_2) et CA_6. La zone 1 représentative de l'épaisseur estimée de la phase C_3A est située en dehors du bloc monolithique.

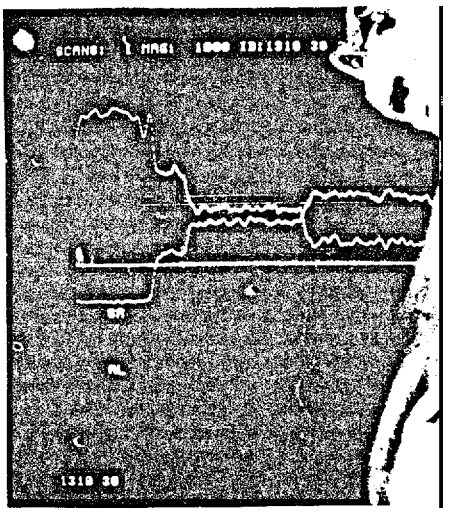

Fig. 2 - Analyse en ligne des concentrations en calcium et aluminium au travers de la couche de produit formé. Les concentrations en calcium sont croissantes de gauche à droite. Les quatre paliers correspondent aux zones suivantes : alumine - aluminates CA_2, CA et $C_{12}A_7$ (x 3000).

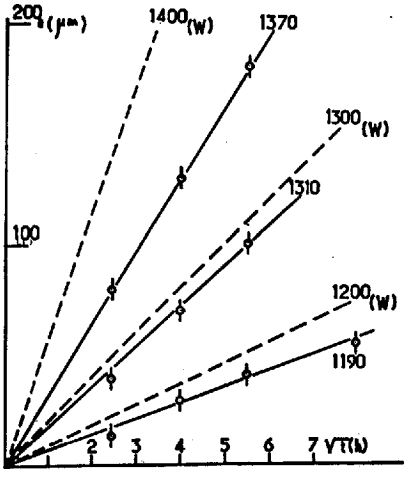

Fig. 5 - Evolution dans le temps de l'épaisseur totale de la couche de produit formé dans le monolithe d'alumine à différentes températures. Représentation quasi-linéaire de la fonction $e = k't^{.5}$. Les fonctions linéaires tracées en tiretés représentent les valeurs observées par WEISWEILLER (11).

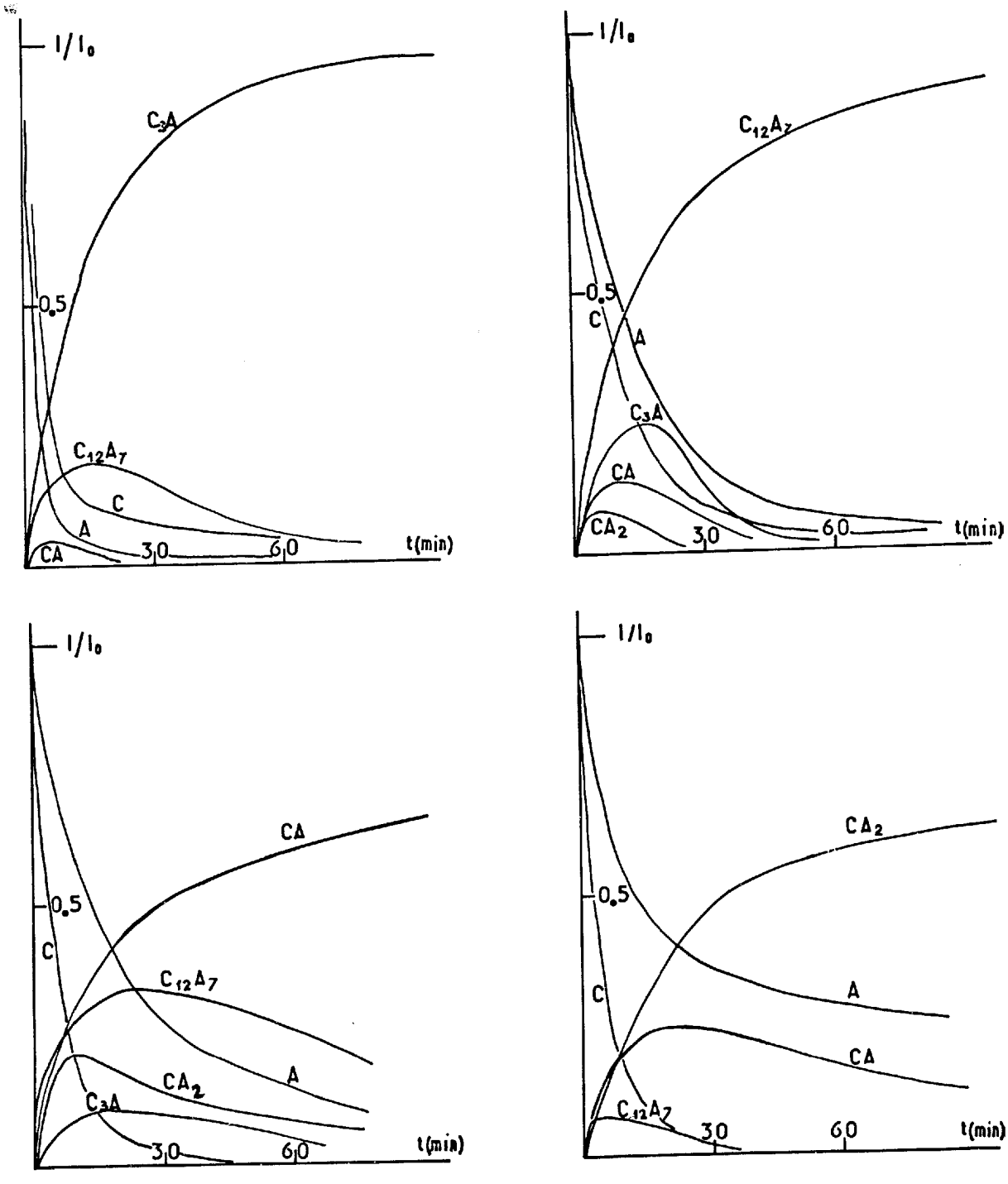

Fig. 6 à 9 - Evolution en fonction du temps du système des phases apparaissant lors des réactions devant donner lieu aux aluminates (phases d'équilibre) C_3A, $C_{12}A_7$, CA et CA_2.

servation dépend de l'étendue de leurs domaines respectifs. Dans les conditions expérimentales où nous nous sommes placés (diffusion unidirectionnelle en milieux semi-infinis) l'état du système même aux échéances les plus longues est très éloigné de l'état d'équilibre. De l'évolution de ce système en régime transitoire on a retenu quelques aspects d'ordre cinétique.

Ainsi, dans l'hypothèse où le potentiel chimique en calcium est maintenu constant à la source on observe (Fig. 4) :

- la prépondérance du domaine de la phase $C_{12}A_7$ pour 980°C < T < 1370°C sur les autres domaines ainsi que sa croissance rapide en fonction de la température ;
- une faible évolution du domaine CA + CA_2 en fonction de la température;
- un rapport CA/CA_2 ~ 5 dans tous les cas expérimentaux observés
- un domaine de phase CA_6 identifiable seulement à T = 1370°C.

En ce qui concerne la phase C_3A, identifiée dans le produit pulvérulent, il n'a pas été possible d'estimer la profondeur de son domaine d'existence avec une bonne précision. Il semblerait cependant que sa croissance en fonction de la température et du temps soit nettement moins prononcée que celle de la phase $C_{12}A_7$.

L'évolution de l'épaisseur totale de la couche de produit dans l'alumine compacte [$\sum C_xA_y$ sauf C_3A] est définie en fonction du temps pour T = 1190, 1310 et 1370°C (Fig. 5). Cette évolution se traduit de façon satisfaisante par la loi parabolique : $e^2 = kt$, où e est l'épaisseur de la couche et k le coefficient de croissance dont les valeurs sont les suivantes :

$k(1190°C) = 0,126\ 10^{-9}$ $(cm^2.s^{-1})$
$k(1310°C) = 0,912\ 10^{-9}$
$k(1370°C) = 2,84\ 10^{-9}$

L'énergie d'activation calculée à partir de ces valeurs est E ≃ 330 $kJ.mole^{-1}$.

3. ETUDE DES REACTIONS CHAUX-ALUMINE A PARTIR DES MELANGES D'OXYDES.

Selon une méthode utilisée par de nombreux auteurs, nous avons étudié l'avancement et les modes de transformation de cinq mélanges de chaux et d'alumine dont les compositions initiales $xC + yA \rightarrow C_xA_y$ correspondent aux cinq aluminates connus. Les produits de départ sont la calcite de haute pureté et l'alumine électrofondue broyée finement (granulométrie centrée sur 3 µm). Les barbotines séchées sont pressées sous une charge de 5 t/cm^2 sous forme de pastilles de 6 mm d'épaisseur. Aprés traitement thermique aux températures de 980, 1190, 1310 et 1370°C les produits sont analysés par diffraction X. Seule la phase C_xA_y qui tend vers son état d'équilibre est quantitativement définie en mesurant le rapport de l'intensité de la raie X la plus intensse aux instants t = t quelconque et t = τ (état d'équilibre atteint). Les autres phases sont définies d'une façon pseudo-quantitative. Les résultats concernant la formation des phases C_3A, $C_{12}A_7$, CA et CA_2 à la même température T = 1370°C sont consignés sur les figures 6 à 9. De ces résultats on tire les observations suivantes :

a) la vitesse de l'épuisement de la chaux autour des grains est d'autant plus rapide que la concentration relative de cet oxyde est plus faible. On distingue donc statistiquement deux périodes dans l'évolution du matériau ; la première où le système présente les interfaces chaux-aluminates et aluminates-alumine [$C/\sum C_xA_y/A$], la deuxième où l'interface chaux-aluminates a disparu [$\sum C_xA_y/A$]. On note entre ces deux zones une variation sensible de la loi d'avancement de la réaction globale. Ce phénomène n'est toutefois pas très significatif dans le cas du système $3C + A \rightarrow C_3A$ pour lequel l'épuisement en alumine paraît plus rapide que celui de la chaux, ce qui induit que l'ultime réaction avant l'établissement de l'équilibre serait du type :

$$1/7\ C_{12}A_7 + 9/7\ C \rightarrow C_3A.$$

b) si l'on se réfère au modèle cinétique de l'interface plane (cf. loi de vitesse de pénétration du front réactionnel) il apparaît (bien que le modèle du grain sphérique serait ici en meilleure conformité) que le temps moyen nécessaire à l'ion calcium pour atteindre le coeur du grain d'alumine serait de l'ordre de quelques minutes seulement à T = 1370°C. Dès lors on peut distinguer deux périodes distinctes :

- la première au cours de laquelle les domaines respectifs de tous les aluminates sont en expansion alors que le coeur du grain d'alumine n'a toujours pas réagi (régime transitoire court) ;
- la seconde (régime transitoire long) au cours de laquelle les phases sous saturées en calcium par rapport à la phase d'équilibre régressent grâce à l'apport continu de calcium ainsi que les phases sursaturées qui, elles, s'épuisent en calcium.

La transition entre les deux périodes s'effectue, pour chacune des phases transitoires, à l'instant $t^*_{[C_xA_y]}$.

A cette valeur t^* du temps la courbe $(I/I_0) = f(t)$ passe par un maximum (Figs. 6 ~ 9). Pour chacun des systèmes réactionnels $xC + yA \rightarrow (C_xA_y)_{eq.}$ on observe une augmentation des valeurs t^* de chaque phase sous-saturée dans le sens des valeurs croissantes du potentiel chimique du calcium. A l'inverse la progression de t^* de chaque phase sursaturée s'effectue dans le sens des valeurs décroissantes du potentiel chimique du calcium. A titre d'exem-

ple pour la réaction C - A → CA, on aura le schéma suivant :

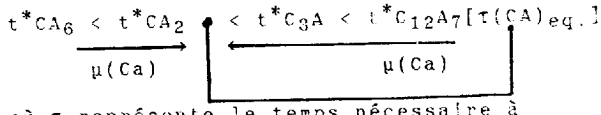

où τ représente le temps nécessaire à l'obtention de l'équilibre et μ le potentiel chimique croissant selon le sens de la flèche.

Notons enfin que l'évolution vers l'équilibre du système C - 6A → CA_6 à T = 1370°C est très lente. La phase CA_6 n'apparaît qu'au delà de 2 heures de traitement et procède de la seule réaction élémentaire :

$$CA_2 + 4\ A \rightarrow CA_6$$

Selon le schéma proposé ci-dessus on aurait donc pour cette réaction :

$$t^*_{C_3A} < t^*_{C_{12}A_7} < t^*_{CA} < t^*_{CA_2}[\tau(CA_6)]_{eq}$$

Les valeurs de t^* pour C_3A, $C_{12}A_7$, CA sont suffisamment faibles pour que la présence de ces phases n'ait pas été observée expérimentalement. On peut considérer que la période initiale où existe l'interface $C/\Sigma C_xA_y$ est de très courte durée.

BIBLIOGRAPHIE

1. J. WILLIAMSON et F.P. GLASSER, J.Appl.Chem., Vol. 12, 535 (1962).
2. K.I. REPENKO, Sb.Nauch.Tr.Ukr.Nauchn.-Issl.Inst.Ogneuporov,318 (1963).
3. M. DELIGNE, P. FIERENS, P. PICQUET et J. VOTQUENNE, Silicates Indust., 6, 261 (1977).
4. K.J.D. MACKENZIE et R.K. BANERJEE, Trans.J.of the British Ceram.Soc., 77, 88 (1978).
5. V.K. SINGH et M.M. ALI, Trans.J.of the British Ceram.Soc., 79, 112 (1980).
6. K.S. CHOU et G. BURNET, Cement and Concrete Research, 11, 57 (1981).
7. K.S. CHOU et G. BURNET, Cement and Concrete Research, 11, 167 (1981).
8. V.K. SINGH et U.K. MANDAL, Trans.J.of the British Ceram.Soc., 81, 112 (1982).
9. T.D. ROBSON, Symp.Chemistry of Cements, Tokyo (1968).
10. I. KOHATSU et G.W. BRINDLEY, Z.Phys.Chem., 60, 79 (1968).
11. W. WEISWEILLER et S.J. AHMED, Zement, Kalk, Gips, 2, 84 (1980).

B.COTTIN*, A.ROUANET**, M.CONJEAUD*
* LAFARGE COPPEE RECHERCHE, FRANCE
** LABORATOIRE des ULTRA-REFRACTAIRES, CNRS, ODEILLO

1.1

TRANSFORMATIONS MINERALOGIQUES des CRUS CHAUX-SILICE-ALUMINE à 830°C
MINERALOGICAL CHANGES of LIME-SILICA RAW MATERIALS at 830°C

L'étude vise à simuler les traitements de quatre crus modèles et à examiner l'évolution minéralogique du système pendant la décarbonatation et au cours du début de clinkérisation. Ces crus sont constitués de matières naturelles dont la composition globale se situe, dans le diagramme C.S.A., approximativement sur le pseudo-binaire C_2S-$C_{12}A_7$. Chacun d'eux présente différentes caractéristiques morphologiques (compactage, cobroyage). La température unique de traitement est de 830°C. On a examiné l'influence du milieu gazeux sur la nature des phases et sur les vitesses de transformation. L'étude a permis de mettre en évidence le rôle prépondérant du cobroyage (en raison, probablement, d'une plus grande finesse) et de la pression de vapeur d'eau sur la cinétique de décarbonatation et de clinkérisation.

Esse estudo visa simular os tratamentos de quatro crus modelos e a examinar a evolução mineralógica do sistema durante a decarbonatação e durante o início da clinquerização. Esses crus são constituídos de materiais naturais cuja composição se situa, no diagrama C-S-A, aproximadamente sobre o pseudo-binário C_2S-$C_{12}A_7$. Cada um deles apresenta diferentes características morfológicas (compactação, co-moagem). A temperatura única de tratamento é de 830°C. Examinou-se a influência do meio gasoso sobre a natureza das fases e sobre as velocidades de transformação. O estudo permitiu colocar em evidência o papel preponderante do co-moagem (em virtude, provavelmente, de uma maior finura) e da pressão do vapor d'água sobre a cinética da descarbonatação e de clinquerização.

B. COTTIN, A. ROUANET, M. CONJEAUD

INTRODUCTION

Divers prélèvements effectués à différents niveaux des cyclones ont déjà montré que les taux de combinaison de la chaux naissante pouvaient atteindre des grandeurs élevées pour des crus portés à des températures de l'ordre de 800°C. L'étude ci-dessous consiste à examiner pour des matières traitées dans des conditions simulées en laboratoire les taux respectifs de décarbonatation et de combinaison de la chaux ainsi que la nature des phases obtenues.

PROTOCOLE EXPERIMENTAL

L'étude porte sur quatre crus différents obtenus à partir des mélanges de calcaire très pur et de matières silico-alumineuses dont les compositions respectives ont été calculées pour correspondre à une composition globale située, dans le diagramme ternaire C-S-A, sur le pseudobinaire $C_{12}A_7 - C_2S$. On a éliminé les compositions surdosées en calcium qui, au-delà de cette ligne $C_{12}A_7$-C_2S, conduiraient théoriquement à la formation du C_3S. Dans le domaine de température envisagé ce composé ne peut en effet se former et l'on serait alors en présence de taux très élevés de chaux libre. Les échantillons sont les suivants :

N°1 - calcaire + sable kaolinique.
[C = 63,6 % - S = 31 % - A = 4,8 %]

N°2 - calcaire + kaolin
[C = 61,7 % - S = 27,8 % - A = 10,5 %]

N°3 - calcaire + bauxite
[C = 55,3 % - S = 14,3 % - A = 30,4 %]

Pour cette dernière composition on n'a pas tenu compte des 27 % d'oxyde de fer que contient la bauxite du VAR, pour le calcul du dosage en calcaire. On a donc préparé un quatrième cru (N°4) de mélange calcaire-bauxite, surdosé en chaux de telle sorte que tout l'oxyde de fer puisse s'y combiner.

Les matières sont préparées par mélange des poudres -(3 000 Blaine pour les produits et 10 000 pour le kaolin)- ou par compactage de ces mélanges -(pastillage de cylindres de 1,7 mm d'épaisseur sous une charge de 1,6 tonne)- ou encore par cobroyage à l'Aurec (durée de 1 minute sur 15 grammes de poudres). La température unique de traitement est de 830°C. Les traitements s'effectuent dans un four tubulaire sous courant d'argon sec ou humidifié par passage préalable dans un bouilleur (étude de l'influence catalytique de la vapeur d'eau). Les durées de traitement sont respectivement de 20 et 40 minutes. Ces ordres de grandeurs ont été choisis afin de permettre des taux de décarbonatation d'échantillons compacts suffisamment élevés pour que les taux de combinaison soient eux mêmes significatifs. En effet les phénomènes de décarbonatation sont assujetis aux deux facteurs limitants que sont :

- les transferts thermiques au sein du solide,
- les transferts de masse gazeuse, soit au travers du milieu poreux en cours de formation, soit au travers de la couche limite de diffusion extra-granulaire.

Compte tenu des taille et morphologie des échantillons, il s'imposait de traiter la matière aussi longuement afin de ne pas être limité par ces transferts.

Des essais préliminaires de décarbonatation de calcaire pur ont préalablement permis de justifier de telles durées de traitement.

Les produits traités sont analysés par voie chimique (dosage du CO_2 résiduel, de la chaux totale et de la chaux libre) et par diffraction X (analyse quantitative des phases de chaque système).

RESULTATS

a) Influence des paramètres opératoires sur la décarbonatation (Tableaux 1 et 2)

Les taux de décarbonatation de tous les échantillons sont élevés à l'échéance de 20 minutes. On remarque cependant, pour les produits cobroyés à l'Aurec, un effet notable de la taille des grains sur la vitesse relative de décarbonatation. Par contre, la compacité du milieu solide apparaît comme un facteur secondaire. Il semble donc que la résistance au transfert de CO_2 soit plus élevée dans la couche de produit décarbonaté de chaque grain de calcaire que dans le milieu poreux intergranulaire, même lorsqu'il s'agit d'échantillons compactés sous charge. En ce qui concerne le rôle de la pression partielle de vapeur d'eau (estimé à partir des valeurs du coefficient γ), il apparaît que ce dernier s'exerce significativement sur les produits non cobroyés ($1 < \gamma < 1,6$). L'effet "catalytique" de la vapeur d'eau sur la décarbonatation a été par ailleurs décrit (1) comme une fonction inverse de la température. A 830°C la pression d'équilibre de CO_2 est déjà très élevée et l'on comprend que sur un plan strictement thermodynamique, l'effet catalytique tend à s'annuler lorsque $p(CO_2) \longrightarrow 1$ atm. En revanche, l'effet "vapeur d'eau" présentera un intérêt accru lorsque la matière non décarbonatée transitera dans des zones où la température sera inférieure à 800°C. Cet effet "catalytique" de la vapeur d'eau peut s'expliquer par une amélioration des transferts de chaleur dans la couche de produit décarbonaté formée autour du grain de calcaire (modification de la conductivité thermique du gaz) et des transferts de masse (accélération de la diffusivité de CO_2 dans la vapeur d'eau). Enfin et probablement à un degré plus élevé, la catalyse de la décarbonatation stricto sensu pourrait s'expliquer par un phénomène d'adsorption dissociative de la vapeur d'eau à l'interface réactionnelle (2 et 3). Celui-ci suppose l'existence probable d'ions OH^- sur la surface du carbonate.

B.COTTIN, A.ROUANET, M.CONJEAUD

1.1

TABLEAU I

		Sous argon sec						Sous argon - vapeur d'eau					
		t = 20 min.			t = 40 min.			t = 20 min.			t = 40 min.		
	Ech.	X	Y	Z	X	Y	Z	X	Y	Z	X	Y	Z
1	A	53,8	30,4	10,1	59,8	44.8	0,4	60,5	33,8	0,7	59,2	30.4	0,7
	B	55,5	32,4	6,9	59,5	36.0	0.6						
	C	59,5	23,0	1.0	59.2	21,3	1.0	60,7	10,8	0,5	61,5	7.0	0,4
2	A	43,9	24,6	14,2	50,6	41,0	0,9	57,8	32,9	2.4	59,2	28,0	0.3
	B	43,6	19,4	15.6	50,7	40,8	1,0						
	C	50,9	7,3	1,25	50,6	6,5	1.3	58,5	1,35	0,4	58.9	0.6	0.4
3	A	44,5	28,2	4,9	46,2	33,7	0,8	46,7	23.2	0.3	46.6	18.5	0,4
	B	43,1	25,5	8.5	46,4	34,5	0,6						
	C	46,0	4,1	1,4	46,1	4,3	0,7	46,5	0,2	0,4	46,9	0.2	0,4
4	A	51,0	33,2	3,9	53,8	39,2	0,3	60,5	33,8	0,7	59,2	30,4	0,7
	B	51,9	38,9	0,6	52,6	40,3	0,5						
	C	52,4	8,5	0,7	52,8	7,4	0,7	60,8	10,3	0,5	61,5	7.0	0,4

Légende - A : mélangeage ; B : pastillage ; C : broyage Aurec ;
X : CaO % ; Y : CaO libre % ; Z : CO_2 %.

TABLEAU II

		Cuisson sous argon sec				Cuisson sous argon - vapeur d'eau			
Ech.		t = 20 min.		t = 40 min.		t = 20 min.		t = 40 min.	
		X	Y	X	Y	X	Y	X	Y
1	A	76,0	19,6	99.1	24,2	98,5 (γ=1.3)	42.6 (γ=2.18)	97,5 (γ=1)	47.1 (γ=1,95)
	B	84,3	26.5	98,7	38,2				
	C	97,9	59,2	97.7	61,8	99,0 (γ=1,01)	81.1 (γ=1,37)	99.2 (γ=1,02)	88.5 (γ=1,43)
2	A	58.8	2,8	97,8	16,5	94,7 (γ=1,6)	37,7 (γ=13,5)	99,4 (γ=1,02)	52.1 (γ=3,15)
	B	54.3	9,9	97,5	16,9				
	C	96,8	82,30	96,7	83,9	99,2 (γ= 1)	96.8 (γ=1,18)	99,2 (γ=1,02)	98,0 (γ=1,18)
3	A	85,8	22,6	97,8	24,9	99,2 (γ=1,16)	49,5 (γ=2,2)	99 (γ=1,01)	59,1 (γ=2.37)
	B	74,5	15,7	98,3	23,8				
	C	97,8	87,4	98,1	89,0	99,2 (γ=1,01)	98.6 (γ=1,13)	99 (γ=1,01)	98,4 (γ=1,11)
4	A	90.3	25,1	99,3	26,4	99,1 (=1,1)	49,9 (= 2)	99,1 (=1)	55.3 (=2.1)
	B	98,5	23,6	98,7	22,3				
	C	98,3	82,2	98,3	84,2	99,1 (γ=1,01)	97,4 (γ=1,18)	99,3 (γ=1,01)	98,6 (γ=1,17)

Légende - A : mélange ; B : pastillage ; C : cobroyage Aurec ; X : taux de décarbonation ; Y : taux de combinaison de la chaux.
γ : facteur multiplicatif ; rapport de X (ou Y) sous atmosphère humide sur X (ou Y) sous argon sec.

TABLEAU III et IV

CRU N°1 — CRU N°2

			phases d'équilibre C_2S	$C_{12}A_7$	CS	C_3A	C_2AS	C	phases d'équilibre C_2S	$C_{12}A_7$	CS	C_3A	C_2AS	C
A	1	a			f			FF	ff	ff	f		ff	FF
		b	ff	ff	f	ff		FF	ff	ff	f		ff	FF
	2	a	m			m		FF	F			ff	m	F
		b	F	f	m	f	m	FF	FF				F	F
B		a			m			FF	ff	ff	f	f	f	F
		b	f	ff	m	ff		FF	ff	ff	f	f		F
C	1	a	F	f	f	m		F	F	F	ff			f
		b	F	m	f	F		F	F	F	ff			f
	2	a	F	f	m	m	ff	m	F	F		f	m	F
		b	F	m	f	F		f	FF	FF				

CRU N°3 — CRU N°4

			phases d'équilibre C_2S	$C_{12}A_7$	(AF)	CS	C_3A	C_2AS	CA	C	phases d'équilibre C_2S	$C_{12}A_7$	(AF)	CS	C_3A	C_2AS	C
A	1	a		ff		f	ff			F				f			F
		b		ff		f	ff			F		ff		f	ff	ff	F
	2	a	m		m		m	m		m	m		f		m	f	m
		b	F		F		m	F	f	f	F		m		m	f	m
B		a				f		ff		F				f		f	F
		b				f		ff		F				f		f	F
C	1	a	f	F	F	f		f		ff			FF	f		f	f
		b	F	F	F	f		f		ff			FF	F		f	f
	2	a	F	F	F			ff	f		FF	FF	FF				
		b	F	F	F			ff	f		FF	FF	FF				

Légende - A : mélange ; B : pastillage ; C : broyage Aurec
1 : traitement sous argon
2 : traitement en présence de vapeur d'eau - a : 20 minutes : b : 40 minutes.
F : forte intensité des pics de diffraction ; FF : très forte ; m : médium ;
f : faible ; ff : très faible.

TABLEAU V

	Résistance à 1 jour (MPa)	Eau liée %	Phases observées
Echantillon N°2 (40 min./vapeur d'eau)	2	20,5	C_4AH_{13} C_2ASH_8 $-C_2S$
Echantillon N°3 (20 min./argon)	5	41,6	C_2AH_8 C_2ASH_8 (AF) $-C_2S$
Echantillon N°3 (20 min./vapeur d'eau)	non mesurable	43,0	C_3AH_6 C_2ASH_8 C_2AH_8 $-C_2S$
Echantillon N°4 (20 min./vapeur d'eau)	non mesurable	32,4	C_3AH_6 $-C_2S$

b) Influence des paramètres opératoires sur la combinaison (Tableau 2)

Quelle que soit la nature du cru, le taux de combinaison est fondamentalement relié à celui de la décarbonatation. Toutefois, les vitesses d'avancement des réactions sont dans les deux cas (décarbonatation et combinaison) nettement différenciées suivant les crus. Plus spécifiquement ici, ce sont les produits cobroyés (non compactés) qui présentent les taux de combinaison les plus élevés en raison de la grande finesse des grains et par conséquent de la grande surface spécifique des grains de composés "acides" au travers desquels diffuse la chaux. A l'inverse, le compactage ne modifie pas significativement le taux de combinaison de la matière en ne jouant que très peu sur les surfaces de contact entre grains "acides" et grains "basiques". Quant au rôle de la vapeur d'eau sur la combinaison, il apparaît considérable [$2 < \gamma < 3$] sur des produits non cobroyés (le gain sur les produits cobroyés est moins sensible avec un coefficient $\gamma < 1,5$). On ne sait pas à quel stade des des mécanismes réactionnels s'exerce l'influence de la molécule d'eau pour les réactions à l'état solide, mais on peut penser qu'il s'agit d'une modification des propriétés de surface des grains où diffuse la chaux.

c) Nature des phases des différents systèmes (Tableaux 3 et 4)

Les phases identifiées par diffraction X sont :

- d'une part les phases d'équilibre du système : C_2S et $C_{12}A_7$ pour les matières ne contenant pas ou peu d'oxyde de fer et C_2S, $C_{12}A_7$, ainsi que des aluminoferrites (AF) pour les matières contenant à l'origine de la bauxite. Les phases AF sont très probablement C_4AF et C_6A_2F.

- d'autre part des phases "hors d'équilibre". Il s'agit du silicate CS, des aluminates C_3A et CA (ce dernier n'apparaît significativement que dans l'échantillon N° 3) et du silico-aluminate C_2AS. Les résultats de l'étude minéralogique sont en bon accord avec ceux de l'analyse chimique, à savoir que, seules les matières cobroyées pour lesquelles les taux de combinaison sont proches de la valeur maximum conduisent après traitement à la formation des phases d'équilibre.

On a calculé pour deux cas types (calcaire + kaolin N° 2 et calcaire + bauxite N° 4) les compositions minéralogiques des produits traités en prenant en compte pour les alumino-ferrites, soit la composition C_4AF, soit C_6A_2F.

Produits cobroyés traités sous vapeur d'eau	C_2S	$C_{12}A_7$	C_4AF	C_6A_2F
Calcaire + kaolin Echantillon N° 2	80 %	20 %		
Calcaire + bauxite Echantillon N° 4	37 % 37 %	27 % 14 %	36 %	49 %

En ce qui concerne la formation des phases en régime transitoire on note que le composé CS est le premier à apparaître, précédant les silico-aluminates et aluminates et en conformité avec la grande affinité de la chaux pour l'oxyde le plus acide du système.

d) Tests de réactivité

On a procédé à des tests de réactivité de quatre matières traitées après gâchage (E/C = 1) en mesurant les résistances mécaniques en compression et l'eau liée. Les nouvelles phases formées ont été définies. Les résultats sont reportés sur le tableau 5.

BIBLIOGRAPHIE

1. A.CASALONGA - "Etude de la décomposition de la dolomie en présence de vapeur d'eau" - Thèse, Université de PERPIGNAN, 1983.

2. R.BARDEL - "Influence de l'atmosphère gazeuse sur la cinétique de décomposition d'un solide - Application au carbonate d'argent" - Thèse, Université de GRENOBLE, 1973.

3. T.L.SLAGER et Coll., J.Phys. Chem. (1972), 76 (6), p. 940/3.

R. CASTANET (C.N.R.S. MARSEILLE France)
F.P. SORRENTINO (LAFARGE COPPEE RECHERCHE France)

STUDY of CLINKERING REACTIONS by HIGH TEMPERATURE ISOTHERMAL CALORIMETRY

ETUDE des REACTIONS de CLINKERISATIONS par MICROCALORIMETRIE ISOTHERME HAUTE TEMPERATURE

SUMMARY : The evolution of the enthalpy during the firing of industrial cements has been measured by isothermal calorimetry and calculated from published data.

The calculations account the final total enthalpy at 1450°C, necessary to obtain the clinker and found experimentaly (1000 kcal/kg of clinker). They explain the shape of curve giving the enthalpy as function of the temperature.

As opposite the experimental results show an important endothermal effect up to 1100° and an important exothermal effect from 1100° to 1250°. These phenomena cannot be explained quantitatively by the known theory.

SUMÁRIO: A evolução da entalpia durante o cozimento de cimentos industriais foi medida por calorimetria isotérmica e calculada a partir de dados publicados.

Os cálculos fornecem a entalpia final total de 1450°C necessária para obter o clínquer e a determinada experimentalmente (1000 kcal/kg de clínquer). Eles explicam a forma da curva fornecendo a entalpia como função da temperatura.

Contrariamente, os resultados experimentais demonstram um importante efeito endotérmico até 1100° e um importante efeito exotérmico de 1100 a 1250°. Estes fenômenos não podem ser explicadas quantitativamente pela teoria conhecida.

INTRODUCTION:

In order to determine the yield of an industrial process, it is necessary to know the quantity of heat consummed during the transformations, i.e., from the initial stage (raw material) to the final stage (clinker). In order to improve a process ,it is necessary to know the optimum conditions to supply this energy i.e. the change of enthalpy as function of temperature.
These variations are dependent on the variations of enthalpy of each of the constituents and on the change due to their combinations.It is,thus necessary to know the sequence of clinkering reactions : this has been largely studied during the past and reviewed exhaustively (1)
From these data,from the knowledge of specific heat and the enthalpy of formation of the compound,it is possible to calculate the enthalpy of clinkerisation at a fixed temperature .(2).The sum at 1450°is a basic calculation for the thermal balance of the process.This sum can be predicted,with a good agreement by a formula given by ZURSTRASSEN (3)
To obtain these informations ,there is an experimental approach by D.T.A (4).The results of these studies allow the determination of the temperature at which a reaction occurs and the quality of the thermal effect (exo or endothermal),but do not give quantitative results concerning the change of enthalpy. On the other hand it is a non-isothermal method and thus difficult to compare with data obtained from an isothermal method. This is the reason why we have undertaken experiments by means of isothermal high temperature microcalorimetry.

EXPERIMENTAL:

Up to 1051°, the experiments have been carried out with a high temperature CALVET calorimeter.The thermal effect is measured by thermocouple Pt/Pt,Rh (0,13%). Above this temperature,a very high temperature calorimeter SETARAM (CALVET type) is used; the thermo couples are Pt/Pt,Rh (6,30%).The containers holding the samples are from alumina;the atmosphere is argon.The standardisation of the calorimeters are controlled by the thermal effect of a known,standart materials,provided by the N.B.S. laboratory. It must be mentioned here that both calorimeters are checked to give the same measurement in an overlapping range of temperatures. During the experiments,the calorimeter is set at the desired temperature, the sample being at room temperature.The experiment starts when the sample is dropped into the furnace of the calorimeter. The quantity of heat necessary for the sample to reach the fixed temperature is measured. After the run,the sample is cooled, and analysed by X ray diffraction: the free lime content is determined by the classical ethylene-glycol method.
A D.T.A measurement has been carried out in order to get a complete set of results.

RESULTS and DISCUSSION

The chemical composition of the industrial raw material is given table 1

SiO2	AL2O3	Fe2O3	CaO	MgO	K2O	Na2O	L.O.I.	Total
14.2	3.30	1.00	43.6	0.65	0.47	0.23	36.2	99.65

TABLE 1
Chemical composition of the raw material

Table 2, (2^{d} column),and the figure 1 show the evolution of the enthapy as function of the temperature.The figures are given for one gram of raw material.The curve 2 figure 1 shows the free lime

Temperature °C	H cal/g measured	H cal /g calculated
401	104	98
498	130	123
501	128	124
597	167	199
699	222	225
850	313	265
874	477	587
894	520	592
925	564	601
996	628	620
1028	680	629
1051	691	635
1102	780	648
1126	530	579
1153	530	583
1201	558	590
1305	573	607
1451	641	649

TABLE 2
Comparison of measured and calculated enthalpy for one gram of raw material

Table 3 gives the results of the phases analysis by X rays diffraction.

Temperature	°C Phases identified By X rays diffraction
850°	$CaCO_3$ /C_2S /CaO / quartz
1100	C2S / C3A / CaO / Quartz
1200	C2S / C3A / C4AF / CaO
1300	C3S / C2S / C4AF / C3A /CaO
1450°	C3S / C2S / C4AF / C3A / CaO

TABLE 3

Phases identified by X rays diffraction analysis

The phases found and the sequence of the reactions which can be deduced are consistent with the previously published results (1).For the sake of calculations ,we have fixed a defined temperature to a defined reaction, for exemple,850° for the decarbonation,1100° for the C_3A and C_2S formation,1200° for the C_4AF ,1300° for the C_3S and liquid phase formation ,keeping in mind that ,(depending on the degree of freedom),the heat involved in the reaction should be ,or not spread over a range of temperature.(for example the decarbonation starts at 650°C and is still going on at 1050°.....)

The mineralogical composition of the final clinker ,according the Bogue calculations is C_4AF 4.77%.....C_3A 11.07%.....C_2S 21.28%....C_3S 55.7 %...and 4% of free lime .

We have used the following enthalpy of formation (kcal/kg of final product,and referenced to the initial oxides)

$CaO + CO_2$------$CaCO_3$ +405.3 at 900° (5)

3 C + A ,-------C_3A -19.1 at 1100° (5)

2 C + S--------C_2S -177.6 at 1100° (5)

4C +A + F ----C_4AF -37.6 at 1200° (5)

C + C_2S -------C_3S +10.8 at 1300° (5)

The figure used as specific heat are given in the reference 2

We did not taken into account the heat consummed for the liquid phase formation because of the lack of reliable data for this transformation.

The result of the calculation are given in column 3 table 2 and are plotted with a cross on the figure 1

The agreement is good for the temperature below 800° and for the final figure which correspond to the generaly admitted theoretical heat of clinkering (448 Kcal/Kg of clinker)

Some discrepencies are created artificialy by the method of calculation, as has been explained above.This is the case for the point a at 600° which accumulates the heat of dehydration of kaolinite.The point b does not include the heat of decarbonation....and we know by DTA that the decarbonation has started at 650°...thus we understand why the point b is situed lower than the measured point. On the other hand we have reported the

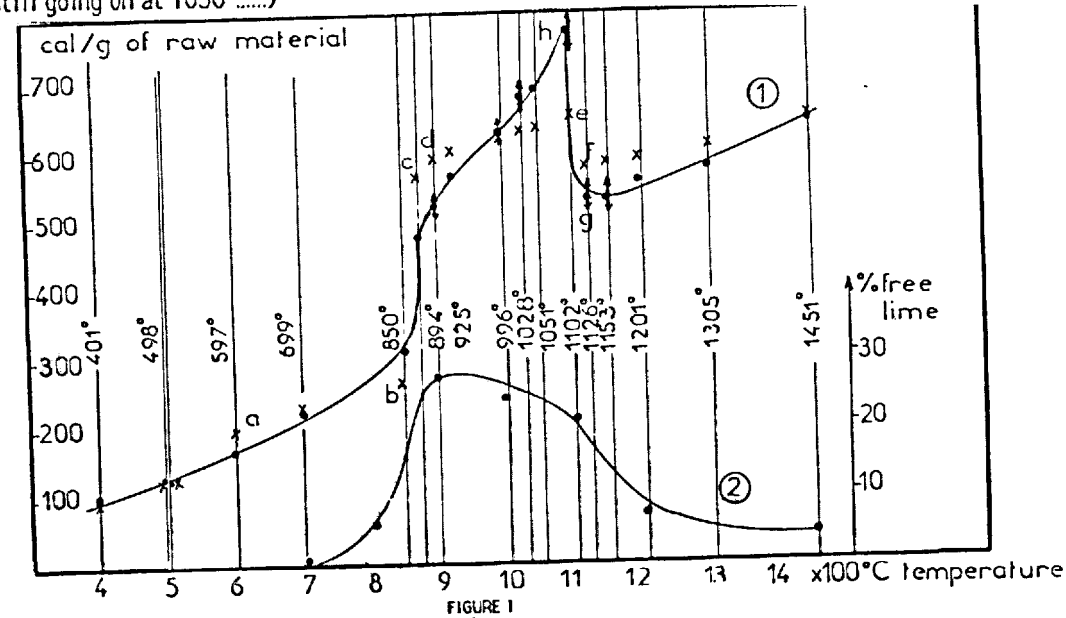

FIGURE 1

VARIATIONS OF ENTHALPY AS FUNCTION OF TEMPERATURE
Curve 1:Experimental measurement of enthalpy
Cross : Calculated values
Curve 2 Free lime

total heat of decarbonation on the points c,d,e, which are plotted too high. By considering these remarks the calculated points a,b,c,d will join the experimental curve. The break at 1100°C is qualitatively explained by the exothermicity of the the C2S formation but the published figures will lead to point f and not to point g. Neither is explained the endothermal effect situated between points e and h.

The differences e---h ,e----f,e---g, are respectively 132,69,118 cal/g of raw material,and are very far from the standart deviation admitted for the measurements (arrows on the points of the figure 1. The differences represent an endothermal effect of 207 Kcal/Kg of clinker (45% of the theoretical heat) and a release of heat (between h and g)of 392 Kcal/Kg of clinker.This will correspond to an important phenomena which cannot be explained by the occurence of new phases (we have detected only classical phases by X rays).

By involving the activation energy of C2S (8) the endothermal effect could be explained 108 cal/g against 132 +/- 40 cal/g. If we admit that this energy is restituted during the reaction it will lead to point f and not g., thus 77 cal/g of clinker remains unexplained.

CONCLUSIONS

The use of high temperature isothermal microcalorimetry allows an accurate measurementof the change of enthalpy during the clinkering process.

The comparison between calculations and measurements highlights thermal effect occuring in the range of temperature 1050°/1150

In order to find explanations to these phenomena further studies are now underway to study the influences of differents parameters such as the impurities, the fineness of the raw material and so on ...

REFERENCES

1 CHATTERJEE T.K. et al
World cem. techno. vol 4,5 p 81 (1980)
vol 9 p 171 (1980)
Cement technology Pergamon press
Edt GHOSH (1981)

2 ZURSTRASSEN H.
Zement Kalk Gips 10 , 1 (1957)

3 ANSELM W.
Radex rundschau 1, (1950)

4 DEHEUL et al
Zement Kalk Gips 8, p 390 (1979)

5 RIBOUD P.V. et al
Techniques de l'ingénieur M 1726 (1980)

6 BABUSHKIN V.I. et al
Thermodynamics of silicates Spring. Verlag(1985)
Inter. symp. on chem.of cements Moscou (1976)

7 JONS E.S.
Cem. and Conc. res vol10 p103 (1980)

8 MACKENZIE et al
Trans. J. Brit. ceram. soc.77,168,(1978)

S.C. AHLUWALIA and V.K. MATHUR,
National Council for Cement and Building Materials,
M-10, South Extension - II, New Delhi - 110 049, INDIA.

Thermal studies on the effect of some transition metal oxides on the kinetics of formation and stabilization of β-dicalcium silicate

ETUDE THERMIQUE DES EFFETS DE QUELQUES METAUX DE TRANSITION SUR LA CINETIQUE DE FORMATION ET DE STABILISATION DU SILICATE BICALCIQUE.

SUMMARY : The energy consumption in the formation of silicate phases during clinkerization can be considerably improved by bringing about the reaction at a lower temperature and accelerating the rate of reaction. With a view to understanding the factors which affect the reaction kinetics of the formation of dicalcium silicate, mixtures of calcium carbonate and silica in a 2:1 molar ratio were subjected to thermal analysis. Transition metal oxides such as chromium oxide, Titanium dioxide and manganese dioxide in varying concentrations upto 5.0 percent by weight of dicalcium silicate were added to study the effect of these dopants on the activation energy, enthalpy of decomposition and the formation of dicalcium silicate. These studies have also been used to determine the order of reaction.

It was observed that the application of first order kinetic equation provides an adequate description of the DTA curve and activation energy values calculated from the thermal data. The investigations also provide valuable information on the stabilization of various polymorphs such as α', β and γ-C_2S.

SUMÁRIO

O consumo de energia na formação das fases de silicato durante a clinquerização pode ser consideravelmente melhorado pela reação em mais baixa temperatura e acelerando o andamento da reação. Com o objetivo de entender os fatores que afetam a cinética da reação da formação do silicato dicálcico, misturas de carbonato de cálcio e silica com razão molar de 2:1 foram submetidas a análises térmicas. Óxidos metálicos de transição como óxido de cromo, dióxido de titânio e dióxido de manganês, em várias concentrações, até 5,0% em peso do silicato dicálcio, foram adicionados para o estudo do efeito desses dopantes na energia de ativação, entalpia da decomposição e a formação do silicato dicálcio. Esses estudos foram também usados para determinar a seqüência da reação.

Foi observado que a aplicação da equação cinética de primeira ordem fornece uma descrição adequada da curva de DTA e os valores da energia de ativação calculada com os dados térmicos. A investigação também forneceu informações valiosas sobre a estabilização de vários compostos polimórficos como os α', β e γ-C_2S.

INTRODUCTION

The effect of minor constitutents on the kinetics of clinker formation and the structural properties of portland cement clinker have been the subject of interest in the past many years. Chromium, Titanium and manganese are generally present in small amounts in cement raw materials and have been reported to affect both these properties significantly.

Pashehenko Etal (1) studied the x-ray petrography and I.R. spectral studies of C_2S obtained from CaO and SiO_2 at 1400°C with the addition of 1-2.75 percent Cr_2O_3. Chromium has also been reported to act as an stabilizer of β - C_2S phase when present in concentration range of 0.5 - 3.0 percent in the raw mix (2).

Titanium oxide (TiO_2) occurs in clinker to a small extent (0.2 - 0.5 percent) being derived from clay, shale or corrective materials like bauxite, red mud etc. The burning of cement raw materials is favourably affected by TiO_2 and it gets incorporated in different amounts in the four principal phases of clinker (3).

Manganese oxide (MnO_2) is found in clinkers generally derived from manganese bearing limestone. MnO_2 is derived from slag, where it is used as a raw material. The presence of manganese oxide gives different colours to clinker and substitutes iron in the liquid phase and does not significantly affect the hydraulic properties of cement. A compound 4 CaO, Al_2O_3, Mn_2O_3 analogous to 4 CaO. Al_2O_3, Fe_2O_3 exists and the two form a continuous series of solid solution (4).

No systematic study on the effects of the presence of these cations on the decomposition of $CaCO_3$ in $CaCO_3$-SiO_2 (2:1) mixture leading to the formation of dicalcium silicate phase has been reported. A series of investigations have been carried out at National Council for Cement and Building Materials on these systems using dopants (5, 6). These investigations relate to the study of the effects of cationic dopants, Cr_2O_3, TiO_2 and MnO_2 on the kinetics and energetics of decomposition in a $CaCO_3$-SiO_2 (2:1) system and formation of various polymorphs of C_2S phase.

EXPERIMENTAL

(a) Materials and Sample preparation :

Varying amounts of reagent grade Cr_2O_3, TiO_2 and MnO_2 (0.1 - 5.0 percent) were added to the 2:1 molar mixture of reagent grade $CaCO_3$ and quartz powder (purity > 99.5 percent). The resulting mixtures after thorough mixing, grinding and passing through 100 μm sives, were shaped in the form of nodules with small amount of distilled water. The samples after drying at 100 ± 5°C for 2 h were tested to ensure complete homogenisation. These dried samples were stored for the experimental Work.

(b) Thermal analysis

The measurements were made on Mettler Thermal Analyser (TA-1) which simultaneously records the DTA, DTG and TG curves. The samples (60 mg) were heated to 1450°C at a rate of 8°C min^{-1} in a platinum crucible of the thermal analyser. α-Al_2O_3 (previously burnt to 1500°C for 30 minutes) was used as the reference material. The activation energy (Ea) of $CaCO_3$ decomposition was calculated from DTG curve (7). The enthalpy (Δ H) and the order of reactions were determined from the DTA curve (8, 9).

(c) X-ray diffraction studies

The samples for analysis were powdered to pass through 45 μm sieve and pressed into a sample holder. The instrument used was Phiips model PW 1120 having Cu target and Ni filter.

(d) Examination of the Intermediate Phases

The samples in the form of nodules were heated in a quench furnace at the rate of 8°C min in a platinum bucket to the termination temperature of the DTA peak, retained for 30 minutes at that temperature and immediately quenched in liquid nitrogen.

(e) Estimation of Free Lime

The free lime in the final products (obtained after heating to the final DTA peak temperature for 2 h) was estimated by titrating the ethylene glycol extract against standard Hcl (10).

RESULTS AND DISCUSSION

Thermal curves of $CaCO_3$ - SiO_2 (2:1) system using Cr_2O_3, TiO_2 and MnO_2 dopants (0.1 - 5.0 percent) have been given in Figs. 1-3. Kinetic parameters for the decomposition reaction such as Ea, Δ H and n have been calculated as per the standard methods (7-9) and are presented in Tables 1-3.

Effect of Cr_2O_3 on the decomposition of $CaCO_3$ and formation of C_2S Phase

Thermal analysis of samples doped with 0.1, 0.5, 1.0 and 5.0 percent Cr_2O_3 by weight of C_2S have been given in Fig. 1. The threshold (Ti), peak (Td) and termination (Tf) temperature of decomposition of $CaCO_3$ in the $CaCO_3$-SiO_2 (2:1) system as determined from the curves have been presented in Table 1.

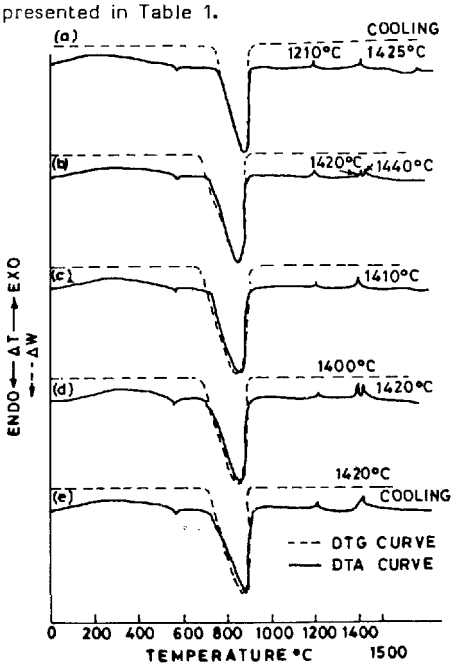

FIG 1 THERMAL CURVES OF (a) $2CaCO_3$:SiO_2;(b) $2CaCO_3$:SiO_2+0.1% Cr_2O_3 (c) $2CaCO_3$:SiO_2+0.5% Cr_2O_3 (d) $2CaCO_3$:SiO_2+1% Cr_2O_3 (e) $2CaCO_3$:SiO_2+5% Cr_2O_3

TABLE - 1 : Thermal analysis and XRD data of Cr_2O_3 doped $CaCO_3$-SiO_2 (2:1) System

Concentration of Cr_2O_3 (% wt) in $CaCO_3$-SiO_2 (2:1) System	Temperature of decomposition of $CaCO_3$ and other kinetic parameters							Exothermic Peaks observed by DTA after decomposition of $CaCO_3$ ^oC	Constituents formed as discernible by XRD of liquid nitrogen quenched Sample
	Threshold T_i ^oC	Peak T_d ^oC	Termination T_i ^oC	Activation energy (Ea) from DTG kJ mol^{-1}	Enthalpy (ΔH) from DTA $kJ\ mol^{-1}$	Shape Index (S)	Order of reaction (n)		
0.0	740	855	910	247	160	0.143	0.48	1210 1425 1420	β-C_2S, γ-C_2S, Cristobalite, Free Lime (High) β-C_2S γ-C_2S Free lime (Low) β - C_2S, γ-C_2S Free lime (1-2%)
0.1	685	860	885	225	146	0.250	0.63	1440	($\gamma > \beta$) β - C_2S, γ-C_2S ($\gamma > \beta$)
0.5	680	860	900	216	142	0.307	0.70	1410 1400	β - C_2S, γ-C_2S ($\beta > \gamma$) Free lime (0.60%) β -C_2S, γ-C_2S (little)
1.0	680	860	890	202	139	0.360	0.76	1420	Free lime (0.50%) β -C_2S (Most predominant) $CaCrO_4$ Free lime (0.50%)
5.0	700	870	890	210	156	0.419	0.82	1420	β- C_2S (Most predominant) α'-C_2S (Small Qty) Ca CrO_4 (little) Cr_2SiO_4 (little) Free Lime (0.30%)

TABLE - 2 : Thermal analysis and XRD data of TiO_2 doped $CaCO_3$-SiO_2 (2:1) System

0.0	740	885	910	247	160	0.143	0.48	1210 1425	As above
0.1	670	870	900	181	158	0.270	0.65	1420	β -C_2S, γ-C_2S Free lime (1.60%)
0.5	660	865	900	172	160	0.300	0.69	1420	β -C_2S, Free Lime (0.64%)
1.0	650	860	890	161	163	0.340	0.73	1410	β -C_2S, Free lime (0.31%) $CaTiSiO_5$ (little)
5.0	660	875	890	184	166	0.360	0.76	1375	β -C_2S, $CaTiSiO_5$ $CaTiO_3$ (little) Free lime (nil)

TABLE - 3 : Thermal analysis and XRD data of MnO_2 doped $CaCO_3$-SiO_2 (2:1) System

0.0	740	885	910	247	160	0.143	0.48	1210 1425	As above
0.1	675	870	900	217	152	0.210	0.58	1425	β -C_2S
0.5	670	870	890	200	150	0.288	0.68	1410	β -C_2S
1.0	670	860	855	183	147	0.316	0.71	1400	β -C_2S
5.0	670	870	895	232	154	0.332	0.73	1390	β -C_2S $CaMn_3O_7$ (Small Qty) $MnSiO_3$ (Small Qty)

Activation energy (Ea) and enthalpy (Δ H) of $CaCO_3$ decomposition progressively decreased with increase in concentration of Cr_2O_3 from 0.1 - 1.0 percent and the Ea attained the minimum value at 1.0 percent concentration (202 kJ mol^{-1}) after which there was an increase in the activation energy with increase in concentration of the dopant (210 kJ mol^{-1} with 5.0 percent Cr_2O_3 dopant). The enthalpy of decomposition of $CaCO_3$ (Δ H) also decreased from 160 kJ mol^{-1} without dopant to 139 kJ mol^{-1} with 1.0 percent dopant. The value of enthalpy showed an increase to 156 kJ mol^{-1} with 5.0 percent Cr_2O_3. The shape indices showed an increasing trend with increasing concentration of the dopant and so also the order of reaction. The thermal curves give two exothermic peaks at 1420°C and 1440°C at 0.1 percent of the dopant. 0.5 percent doped sample gave one exotherm at 1410°C, 1.0 percent doped sample gave two exotherms at 1400°C and 1420°C and only one exotherm at 1420°C was observed with 5.0 percent dopant. The exotherm could be attributed to the formation of dicalcium silicate phase.

The liquid nitrogen quenched sample at 1430°C (the exotherm was observed at 1420°C) using 0.1 percent Cr_2O_3 gave a mixture of β and γ-C_2S phase and free lime determined by XRD. The peaks at d (A°) 2.77, 2.40, 1.70 and 1.45 confirmed the presence of free lime. The sample was subjected to free lime estimation by extraction method (10) and was found to have 1.2 percent free lime indicating in complete reactions. The same mix on heating to 1450°C with 1/2 hr retention and quenching in liquid nitrogen gave mostly γ-C_2S and a small quantity of β-C_2S phase. The free lime as determined chemically was 0.8 percent. The sample with 0.5 percent Cr_2O_3 on heating to 1420°C and quenching in liquid nitrogen gave a mixture of β and γ-C_2S phase. However, an increase in β-C_2S was noticed. 1.0 percent doped sample gave two exotherms at 1400 and 1420°C in the DTA curve. The starting material heated to 1420°C for ½ h and quenched in liquid nitrogen gave predominantly β-C_2S phase along with small amount of γ-C_2S phase. A few week lines corresponding to $CaCrO_4$ (d values (A°) 3.62, 2.88, 2.68, 2.38) also appeared in the XRD pattern. Free lime as determined chemically was found to be 0.5%

5.0 percent Cr_2O_3 doped sample gave a DTA exotherm at 1420°C, XRD pattern of the liquid nitrogen quenched sample heated to 1430°C for 1/2 h. indicated the presence of predominently β-C_2S phase alongwith a small quantity of α'-C_2S phase (d values (A°) 2.73, 2.66, 2.26 and 1.92). However γ-C_2S was found to be completely absent. The final products formed have been given in Table - 1.

Effect of TiO_2 on the decomposition of $CaCO_3$ and formation of C_2S phase

Thermal data of TiO_2 doped smaples (Fig. 2) having 0.1, 0.5, 1.0 and 5.0 percent TiO_2 by weight of C_2S have been given in Table 2. The caclulated value of Ea, Δ H and n have also been given in Tables The value of Ea decreased from 247 kJ mol^{-1} to 161 kJ mol^{-1} (1.0 percent TiO_2 dopant) through 181 kJ mol^{-1} (0.1 percent dopant). However, the enthalpy of the reaction remained nearly same. The shape indices of the decomposition curve showed an increasing trend with increasing concentration of the dopant and so also the order of reaction.

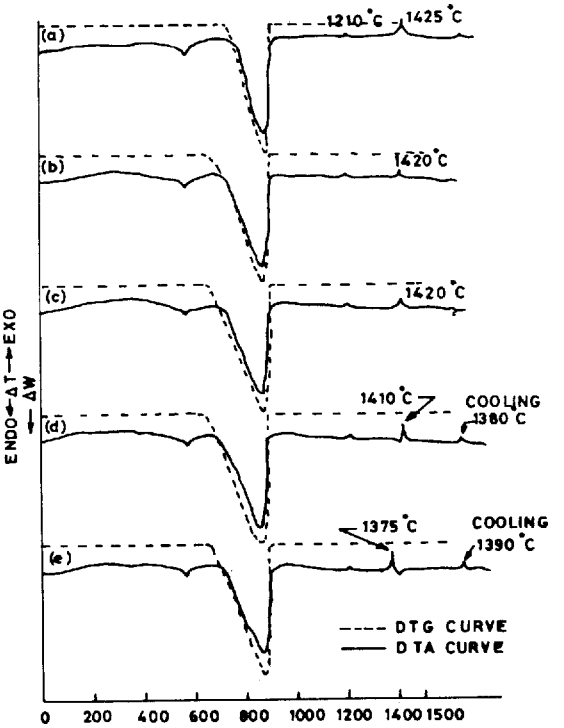

FIG 2 THERMAL CURVES OF (a) $2CaCO_3 : SiO_2$ (b) $2CaCO_3 : SiO_2$ + 0.1% TiO_2 (c) $2CaCO_3 : SiO_2$ + 0.5% TiO_2 (d) $2CaCO_3 : SiO_2$ + 1% TiO_2 (e) $2CaCO_3 : SiO_2$ + 5% TiO_2

TiO_2 (0.1 percent) dopant showed an exotherm at 1420°C in the DTA curve. The reacting mixture heated to 1430°C for 1/2 h and quenched in liquid nitrogen indicated the presence of both β and γ-C_2S phases, along with free lime. Free lime determined chemically was found to be 1.60 percent. TiO_2 (0.5 percent) gave an exotherm at 1420°C and the sample heated to 1430°C and quenched in liquid nitrogen gave peaks corresponding to β-C_2S phase in the XRD. Free lime determined by extraction method was found to be 0.64 percent. The sample having TiO_2 (1.0 percent) gave an exothermic peak at 1410°C and the sample heated to 1420°C showed peaks corresponding to β-C_2S and free lime. Free lime determined chemically was found to be 0.31 percent. Traces of calcium-titanium silicate (Ca Ti SiO_5 d values (A°) 3.25, 3.00, 2.61) were also observed in the XRD pattern. Free lime determined chemically was found to be 0.31 percent. The sample having 5.0 percent TiO_2 dopant gave an exotherm at 1375°C. The starting material (2 $CaCO_3$-SiO_2 + 5 percent TiO_2) heated to 1385°C and quenched in liquid nitrogen showed Ca Ti SiO_5 and Ca TiO_3 (d values (A°) 2.70, 1.91, 1.57). No free lime could be detected by XRD or by extraction method.

Effect of MnO_2 on the decomposition of $CaCO_3$ and formation of C_2S Phase.

the thermal curves of MnO_2 doped $CaCO_3$-SiO_2 system have been given in Fig. 3. The Ti, Td and Tf of the DTG peaks for the decomposition of $CaCO_3$ have been recorded in Table 3 along with the calculated values of activation energy (Ea), enthalpy (ΔH), shape Index and the order of reaction (n) Fig. 4. All the thermal curves (0.1 - 5.0 percent MnO_2) gave a short exothermic peaks at 1210°C due to partial formation of β -C_2S along with the transformation of quartz to cristobalite (11). Exotherms have been obtained at 1425°C, 1410°C, 1400°C and 1390°C with 0.1, 0.5, 1.0 and 5.0 percent respectively of the dopant. The products formed at the above temperatures have been identified by heating the samples to the temperature where the peaks terminate, retained for 1/2 h and quenched in liquid nitrogen. The quenched products have been identified by XRD.

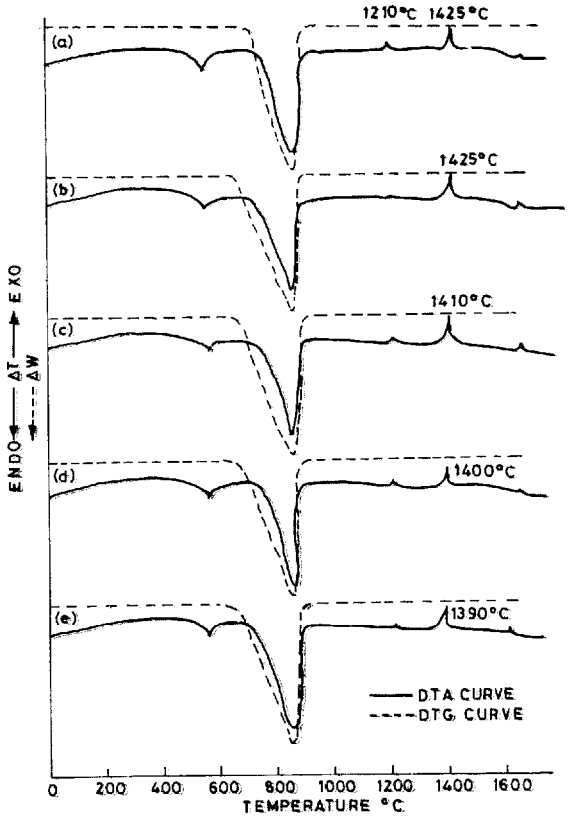

FIG 3 THERMAL CURVES OF (a) $2CaCO_3$:SiO_2 (b) $2CaCO_3$:SiO_2 +0.1% MnO_2 (c) $2CaCO_3$:SiO_2 + 0.5% MnO_2 (d) $2CaCO_3$:SiO_2 + 1% MnO_2 (e) $2CaCO_3$:SiO_2 +5% MnO_2

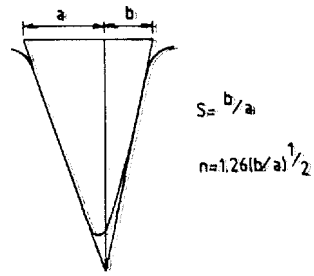

FIG. 4 SHAPE INDEX FROM DTA DECOMPOSITION PEAK

The sample having 0.1 percent dopant showed an exothermic peak at 1425°C and the sample heated to 1435°C and quenched in liquid nitrogen gave pre-dominantly β -C_2S phase with no free lime and free quartz indicating that 0.1 percent dopant was sufficient to complete the reaction. The sample having MnO_2 (0.5 - 5 percent) gave mainly β -C_2S along with $CaMn_3O_7$ (d values (A°) 2.67, 2.41, 1.79) these peaks also appeared with 1.0 and 5.0 percent dopant. No free lime peaks were observed indicating that manganese does not substitute calcium but Si^{4+}. This is also observed by knoefel etal (12) on the incorporation of manganese in tricalcium silicate phase.

CONCLUSION

1. Cr_2O_3, TiO_2 and MnO_2, which occur as minor constituents in cement raw materials lower the decomposition temperature of $CaCO_3$ and formation of C_2S phase with increase in concentration of dopants from 0.1 - 1.0 percent. The Ea and ΔH also show a decreasing trend upto 1.0 percent concentration of the dopants.

2. Formation temperature of β - dicalcium silicate phase is not significantly affected upto a concentration of 1.0 percent of the dopants. TiO_2 and MnO_2 at 5.0 percent concentration significantly lowef the temperature of formation of β -C_2S.

3. Significant amount of free lime have been detected with Cr_2O_3 and TiO_2 showing a decreasing trend with increase in concentration of the dopants, probably due to the formation of new compounds where these dopants get fixed as anions.

ACKNOWLEDGEMENT

This paper is based on the experimental work relating to Doctoral Thesis of one of the authors (VKM) carried out at the National Council for Cement and Building Materials. The authors are grateful to Dr. H.C. Visvesvaraya, Chairman and Director General of the Council for his encouragement and permission to carry out the studies. This paper is communicated with his permission.

REFERENCES

1.- A.A. PASHEHENKO, E.A. STARCHEVSKAYA and L.I. KUSHCH (1978), "Effects of chromium oxide on the synthesis and properties of dicalcium silicate" (In ukrain) Dopov, Akad, Nauk, UKr, RSR, Ser B Geol, Khim Biol, Wanki, 42.

2.- P. FIERENS and J. TIRLOIQ, "Nature and Concentration effect of stabilizing element of β -Dicalcium silicate on its hydration rate", cem. and concr. Res. - 13, 21, 26.

3.- D. KNOEFEL (1977). "Modifying some properties of portland cement by TiO_2" Zem. Kalk. Gips 30, 4, 191.

4.- T.W. PARKAR (1952). "Discussion on ferrite phase", Proc. 3rd Inter. Symp. chemistry of Cement. London, 143.

5.- I.P. SARASWAT, V.K. MATHUR and S.C. AHLUWALIA (1985). "Effect of alkaline earth metal dopants on the thermal decomposition of the $CaCO_3$-SiO_2 system, Part I, Thermochim. Acta 87, 37.

6.- I.P. SARASWAT, V.K. MATHUR and S.C. AHLUWALIA (1985). "Thermal studies of $CaCO_3$ -SiO_2 (2:1) system containing Lithium as dopant, Thermo-Chem Acta (In press).

7.- A.W. COATS and J.P. RED FERN (1964). "Kinetics Parameters from thermogravimetric data, Nature 201, 68.

8.- D.M. SPEROS and R.L. WOOD house (1968). "Realization of quantative differential thermal analysis II" J. Phys Chem. 72, 2346.

9.- K.E. KISSINGER (1957). "Reaction Kinetics by DTA" Anal, Chem, 29, 1702.

10.- M.P. JAVELLANA and I. JAWED (1982). "Extraction of free lime in Portland Cement and Clinker by ethylene glycol, Cem. and Concr. Res. 12, 399.

11.- I.P. SARASWAT, V.K. MATHUR and S.C. AHLUWALIA, (1985). "Effect of alkaline earth metal dopants on the thermal docomposition of $CaCO_3$-SiO_2 system Part - II - Formation of dicalcium silicate. Thermo-Chim. Acta., 95, 201.

12.- D. KNOEFEL, J. STRUNGE and H.U. BAMBAUER (1983). "Effect of Manganese on the properties of portland cement clinker and portland cement, Zem. Kalk. GIPS 36, 7, 407.

S.J. RAINA, P. BHASKARA RAO, S.K. HANDOO and GEORGE SAMUEL
National Council for Cement and Building Materials,
M-10, N.D.S.E. Part - II, New Delhi - 110 049, INDIA.

A new approach for estimation of heat requirement for clinkerization.

SUMMARY : Zur Straussen's poineering work towards the determination of theoretical heat requirement for clinkerization of conventional raw mixes is well known. While the conventional raw mixes containing simple minerals like calcite, kaolinite etc can be dealt with very easily using his method, its application becomes difficult for nonconventional raw mixes. Such mixes necessarily require quantitative estimation of their mineral constituents which is quite complex. hence an experimental approach based on differential thermal analysis has been developed for estimation of heat required for clinkerization, which does not require the estimation of mineral composition.

The heat required (HR) is expressed as

$$HR = A - B - C$$

Where A is the amount of heat received by the raw mix from ambient upto clinkerization temperature, B is the heat recoverable from gaseous products such as H_2O and CO_2. A is obtained by superimposing the DTA curves of the raw mix and that of α-Al_2O_3, recorded under similar experimental conditions, thus obtaining a heat equivalent of the area generated in the thermodynamic sense. The values of B and C are calculated by using the experimental data along with data available in literature.

É bem conhecido o trabalho pioneiro de Zur Straussen visando a determinação da quantidade teórica de calor requerida para a clinquerização de misturas cruas convencionais. Se bem que as misturas cruas convencionais contendo minerais simples como calcita, kaolinita,etc... podem ser tratadas facilmente usando este método, sua aplicação torna-se difícil para misturas cruas não convencionais. Essas misturas requerem necessariamente uma estimativa quantitativa dos seus minerais constituintes o que é bastante complexo. Então foi desenvolvida uma aproximação experimental, baseada na análise termo-diferencial, para estimar o calor requerido para a clinquerização, que não necessita a avaliação da composição mineral.

O calor requerido (HR) é expresso assim:

$$HR = A - B - C,$$

onde A é a quantidade de calor recebido pela mistura crua do ambiente até à temperatura de clinquerização. B é o calor recuperável dos produtos gasosos como H_2O e CO_2. A é obtido superpondo as curvas DTA da mistura crua e as do α-Al_2O_3, registradas sob condições experimentais similares, obtendo assim o calor equivalente da área gerada em sentido termodinâmico. Os valores de B e C são calculados usando os dados experimentais juntamente com os dados disponíveis na literatura.

INTRODUCTION

In the calculations of heat balance of any pyroprocessing system used for the production of cement, the theoretical heat requirement of clinker formation happens to be one of the most important items. This subject was dealt earlier by Zur Strassen (1) who had summarised all the other approaches adopted till then and also gave simplified equations for the calculation of theoretical heat requirement in terms of oxide composition of clinker. These equations have been widely used subsequently and are also presented in a number of books (2, 3) on the subject. A closer examination of the original paper of Zur Strassen (1) shows that these equations based on oxide composition are valid only for certain types of raw meals made up of limestone rich in calcite, and clay made up of equal contributions from the principal clay minerals - kaolinite, montmorillonite and illite. This limitation is explicitly made clear by Zur Strassen (1). On the other hand if the cement raw meal has a widely different mineralogical composition, the approach to be adopted for the derivation of the relevant equations has also been given by Zur Strassen (1). However since this approach needs vital data on the quantitative mineralogical composition of the raw meal and the heats of formation of the minerals concerned (which is not easy to obtain for low grade and complex raw materials), it is not generally adopted. In practice the readymade equations given by Zur Strassen (1) and subsequently adopted in the handbooks (2,3) are used irrespective of the complexity of the mineralogical compositon of the cement raw meal.

Cement industry, in India, is using low grade limestones with considerable free silica content, alongwith complex types of corrective materials including industrial wastes like red mud from aluminium industry in some cases. The coal available to the Cement Industry is generally rich in ash with ash contents reaching upto 40% in some cases. Under these conditions, it was felt necessary that the calculations of theoretical heat requirement be reexamined and a need was felt for a simple method of determination without requiring any data on the mineralogical composition of raw meal or the heats of formation of the complex minerals. In the present work an attempt is made to present an independent experimental method based on differential thermal analysis for the determination of theoretical heat requirement.

EXPERIMENTAL

Five clinker compositions were designed using different raw materials and the analysis of raw materials are listed in Table I.

The proportions of raw materials in each clinker alongwith the oxide and the computed(with simple Bogue's formulae) mineral compositions are listed in Table II.

TABLE - I

CHEMICAL ANALYSES OF RAW MATERIALS

Raw Material	LOI	SiO_2	Fe_2O_3	Al_2O_3	CaO	MgO	Na_2O	K_2O
Limestone (LS-1)	38.42	11.62	0.74	1.52	46.35	1.32	0.08	0.18
Limestone (LS-2)	42.60	2.20	0.40	0.40	54.10	0.48	Traces	Traces
Limestone (LS-3)	37.00	12.46	1.15	2.01	45.45	1.39	0.12	0.29
Kaolinite (K)	15.80	42.62	1.28	32.03	3.14	1.37	1.62	0.44
Clay (Cl)	10.14	54.30	9.61	16.87	2.70	1.94	1.90	2.31
Bauxite (B)	15.15	10.00	2.44	70.15	0.15	0.91	Traces	Traces
Iron Ore (IO)	3.30	8.65	77.55	8.62	1.75	Traces	0.33	Traces
Coal Ash (CA)	0.23	58.86	8.23	29.42	1.59	0.16	1.19	0.91
Ferric Oxide (FO)	AnalaR Chemical Reagent							

TABLE - II

PROPORTIONS OF RAW MATERIALS AND COMPOSITION OF CLINKER

Raw Mix No.	Proportions of Materials %	Composition of Clinker								
		SiO_2	Fe_2O_3	Al_2O_3	CaO	MgO	C_3S	C_2S	C_3A	C_4AF
1.	LS-2 - 75.00 K - 7.93 CI - 15.07 FO - 2.00	20.24	5.90	8.25	63.17	1.17	39.4	28.5	11.9	17.9
2	LS-2 - 77.00 K - 7.59 CI - 14.41 FO - 1.00	19.76	4.32	8.01	65.52	1.17	56.5	14.4	13.9	13.2
3	LS-2 - 76.00 K - 7.93 CI - 15.07 FO - 1.00	20.41	4.40	8.31	64.42	1.18	45.0	24.8	14.6	13.4
4	LS-1 - 91.71 B - 1.90 IO - 1.62 CA - 4.77	21.65	3.71	6.78	65.73	1.91	52.1	23.1	11.7	11.3
5	LS-3 - 93.16 B - 1.14 IO - 0.86 CA - 4.84	22.65	3.34	6.53	64.55	2.00	41.9	33.6	11.7	10.2

The selection of raw materials for clinkers 1, 2 & 3 was made such that their mineral composition is as close as possible to the assumptions made by Zur Strassen (1), discussed already in the introduction i.e. the contribution of Al_2O_3 from each of the argillaceous raw materials was kept the same. Clinkers 4 and 5 were made with relatively impure raw materials and the coal ash absorption was also accounted for. For example in this case the limestone had about 9 - 10% free silica and the coal ash absorption assumed was about 7.4% on clinker which is a typical figure in India.

As a step towards the determination of theoretical heat requirements, the total heat received by each of the above raw meals for heating from 25°C to 1450°C (A) was determined using the DTA method already published elsewhere (4) and the equipment used was a Mettler TA - 1 thermal analyser. The heat recoverable from the cooling of clinker from 1450° to 25°C (B) was computed based on the equations of specific heats of minerals (5) and the computed mineral composition of each clinker. Here a simplification had to be done and the clinkers were assumed to be made up of only the four conventional major phases. The contents of these phases were proportionately corrected as to add up to 100%.

The heat recoverable from the gaseous products (C) was also calculated using the standard equations on specific heats of water vapour and carbon dioxide (6). No other gaseous product was considered in the laboratory study. For the determination of C the DTA and TG curves were used and the temperature range in which a gaseous product was evolved, was divided into convenient narrow zones. The mass of any gaseous product in a particular zone was assumed to be evolved at the average temperature of the zone and the heat recoverable from this mass was calculated with reference to cooling from this average temperature to 25°C. The water vapour, in particular, was assumed to be lost in vapour state only, at 25°C. The experimentally computed theoretical heat requirement was obtained by subtracting the sum of B and C from A. Secondly, the comparative figures on theoretical heat requirement (Q) based on oxide composition (ignoring alkalies) were also calculated using the readymade equation given by Zur Strassen (1). All these results are presented in Table III.

TABLE - III

COMPARATIVE RESULTS ON THEORETICAL HEAT REQUIREMENT

Raw Mix/ Clinker No.	Heat Values Kcal/kg Clinker			Theoretical Heat Requirement Clinker Kcal/kg	
	A	B	C	Present Work	Ref. 1
1	875	347	117	411	417
2	917	348	126	443	438
3	889	349	121	419	427
4	876	350	125	401	430
5	863	351	122	390	416

RESULTS AND DISCUSSION

It is seen that the agreement between the values of theoretical heat requirement obtained by the present method and Zur Strassen's method (1) is reasonably close in the case of clinkers 1, 2 and 3, owing to the selection of pure raw materials closer to the assumptions made by Zur Strassen (1). On the other hand the agreement is not so good in the case of clinkers 4 and 5 in which the mineral composition of raw materials and the influence of coal ash indicate a considerable deviation from the assumptions made by Zur Strassen (1). Such deviations in the case of clinkers made with commercial raw materials may be significant to the designers and machinery manufacturers, particularly in view of the lower specific heat consumption of the order of 700-800 kcal/kg presently obtained with the modern dry process as compared to the figure of 1400 kcal/kg prevalent earlier for the conventional wet process.

CONCLUSION

The new method of experimental determination of theoretical heat requirement is simple and independent of the complexity of raw materials. The method requires a high precision thermal analyser and experience remains to be gained with different types of thermal analysers commercially available.

ACKNOWLEDGEMENTS

The work described here was carried out as a part of the R & D programme of the National Council for Cement and Building Materials and the authors are grateful to Dr H C Visvesvaraya, Chairman and Director General of the Council for his permission to communicate this work.

REFERENCES

1.- H. ZUR STRASSEN (1957), "Der theoretische Warmebedarf des Zement brandes", Zement Kalk Gips. 10(1), 1-12.

2.- O.LABAHN (1971), "Cement Engineers Handbook". 3rd English edition, Bauverlag GmbH, Wiesbaden and Berlin.pp 234-36.

3.- W. H. DUDA (1977), "Cement-data book", 2nd edition, Bauverlag GmbH, Wiesbaden and Berlin, pp 88.

4.- P. BHASKARA RAO, V.N. VISWANATHAN, S.J. RAINA, V.K. ARORA and A.K. CHATTERJEE (1977), "Estimation of heat requirement for burning cement raw mixes-A Practical approach" Cement (Bombay). 11(4), 5-9.

5.- C.P.M. PETROSIAN and V.I. BABUSHKIN (1974), "Thermodynamics and thermochemistry of cement", Principal paper, VI International Congress on Chemistry of Cement, Moscow.

6.- S. GLASSTONE (1964), "Thermodynamics for Chemists", Van Nostrand, Affiliated East West Press. Student Edition, pp 503.

Specific Surface as A Parameter for Raw Mix Burnability and its Relation with Volume Change of Fired Raw Mix Pellets. 1.1

D. GHOSH, S.A. KHADILKAR, R.K. AGARWAL, G.A. MUDHBHATKAL AND A.K. CHATTERJEE,
The Associated Cement Companies Ltd.,
Central Research Station, Thane 400 604, INDIA.

Abstract :

The quantification of burnability of a raw mix is often attempted through the application of either Jander's or Ginstling's equations to the data obtained on combined lime of the fired raw mix. It is well known that the above equations are derived on the basic concept of diffusion of monodisperse spherical particles. The application of the above technique to industrial raw mixes turn out to be problematic because of polydisperse nature of industrial raw mixes. In view of this limitation an attempt has been made to modify the above equation by considering the specific surface of raw mixes as a parameter modifying its burnability characteristics.

Raw mixes of a specific composition but varying specific surfaces have been subjected to firing at different temperatures and different soaking time. 1) The relationship between residual free lime, temperature, soaking time and specific surface has been established 2) Based on these relationship an empirical equation has been arrived at to quantify the burnability of a raw mix.

The theoretical burnability thus obtained is of appreciable help in predicting the burnability of a given raw mix with change in its specific surface. The extent of correlation attained between the theoretical prediction and experimental determination of burnability for a few raw mixes have been reported.

Another new approach of assessing the lime combinability reaction through determination of volume change of raw mix pellets fired at different temperatures has also been in practice in the laboratory of the authors. A qualitative correlation between the trend of volume change of fired pellets with the burnability of raw mixes of varying specific surface as determined through the modified empirical equation has also been reported.

A quantificação da aptidão de queima de uma mistura crua freqüentemente é tentada pela aplicação das equações de Jander ou de Ginstling para dados obtidos na cal combinada de mistura crua queimada. Sabe-se bem que as equações acima são derivadas sobre o conceito básico de difusão de partículas esféricas monodispersas. A aplicação da técnica acima a misturas cruas industriais pode ser problemática por causa da natureza polidispersa das misturas cruas industriais.Tendo em vista esta limitação, fez-se uma tentativa para modificar a equação acima, levando em consideração a superfície específica dos crus como um parâmetro que modifica suas características de aptidão de queima.

Misturas cruas com uma composição específica, mas com superfícies específicas variáveis, foram submetidas à queima à diversas temperaturas e por diferentes períodos de embebimento. 1) Foi estabelecida a relação entre cal livre residual, temperatura, tempo de embebimento e superfície específica. 2) Com base nestas relações, chegou-se a uma equação empírica para quantificar a aptidão de queima de uma mistura crua.

A aptidão teórica de queima obtida desta forma é uma ajuda considerável para a predição da aptidão de queima de uma dada mistura crua com mudança de sua superfície específica. Informa-se a correlação existente entre a predição teórica e a determinação experimental da aptidão de queima de uns poucos crus.

Outra nova aproximação para avaliação da reação de capacidade de combinação da cal, por determinação da mudança de volume de pelotas de cru queimadas a diferentes temperaturas, também foi praticada em laboratório pelos autores. Também se consigna uma correlação qualitativa entre a tendência de mudança de volume das pelotas queimadas e a aptidão de queima dos crus com superfície específica variável, conforme determinada pela equação empírica modificada.

I. INTRODUCTION

The prediction of burnability of a raw mix is quite difficult as it not only depends on the raw material characteristics, chemical composition, fineness but also on the fuel characteristics, system design and operating controls. The basic approach towards determination of burnability are either theoretical or experimental. All these experimental approaches are based on the determination of residual free lime after a given burning period or the time of burning required to attain a given value of residual free lime. These are mostly evaluated qualitatively. Quantitative approaches are also available and for quite sometime, the equation by Jander's (1) and Ginstling's (2) were used in the author's Laboratory.

The equation of Jander's and Ginstling's are associated with the diffusion mechanism of monodisperse spherical particles and considers the reduction of the reaction interface with time. The application of these equations to industrial raw mixes pose limitations because of the polydisperse nature of the raw mixes. In view of this, an attempt has been made to consider the specific surface as a parameter and develop an equation for predicting burnability of industrial raw mixes.

An approach practiced in the Laboratory of the authors is the assessment of lime combinability through determination of volume change of raw mixes on firing. This method gives an overall behavioral change of raw mixes with rise in temperature. Here a qualitative correlation has also been made of the two approaches.

II. EXPERIMENTAL

The burning experiments were performed in an electric furnace at temperatures from 1100°C to 1500°C at intervals of 100°C and with retention time ranging from 5 to 25 min. The raw mixes were pelletised (25.4 x 15 cms) at 500 kg/Sq. cm. pressure. The residual free lime and total lime were determined after burning as well as the volume change noted due to burning.

III. BURNABILITY EQUATION

A raw mix (RM-1) of the composition shown in Table 1 was prepared and ground to different surface areas (1700 to 5300 Sq. cm/gm). This was subjected to heating at different temperatures and retention time. The lime combinability $(CaO_{total} - CaO_{free}/CaO_{total})$ was determined for each temperature and retention time.

Following emerges from the plot of lime combinability against temperature for each surface areas (Fig 1 a to d)

- Irrespective of surface area and temperature the lime combinability increases with increase in retention time. However, at higher surface area ($>$ 4000 sq.cm/gm) and higher temperatures ($>$1400°C), the lime combinability is almost the same for all retention time from 5 to 25 min.

- At lower surface areas ($<$4000 sq.cm/gm) the relationship between lime combinability and temperature appears to be curvilinear which tends to become linear at higher surface areas ($>$4000 sq.cm/gm).

It is apparent from above that surface area, temperature, and retention time have considerable influence on the lime combinability. The other factors which would also influence the lime combinability are the mineralogy of the raw mix and its chemical composition. Ten industrial raw mixes of varying chemical composition (Table 1) and mineralogy were subjected to the same schedule of experiments.

Multiple regression technique was used to fit a curve on these data points and the equation for best fit was found out. The multiple correlation coefficient was found to be 0.87 with 110 data points.

The lime combinability (α) in the equation is a ratio of the total lime combined to the total lime in the raw mix hence this ratio cannot exceed the value 1.0. The equation derived is applicable within a temperature range of 1200°C to 1500°C and for all retention time, surface area and total lime on the mix provided the α value remains within the limit 1.0. Any of these parameters responsible for the increase of α value above 1.0 is unreal for the raw mix under study.

The equation is useful in the

- prediction of lime combinability or free lime expected at a given temperature and retention time, knowing the surface area of the raw mix and expected total lime (designed value) after firing.

- the retention time or temperature required for achieving a certain lime combinability for a given raw mix with known surface area.

- Since theoritically the maximum lime combinability can be achieved is 1.0, the limits of the equation for a given raw mix in terms of surface area or temperature or retention time can be determined. This limit would serve as the maximum value of the parameter for the given raw mix. For eg. in case of a raw mix with 66.0 total lime, the lime comibnability is maximum at 1450°C with 20 migutes retention time when the surface area is 5400 cm^2/gm. Further, grinding or increasing fineness of the same raw mix is unwanted.

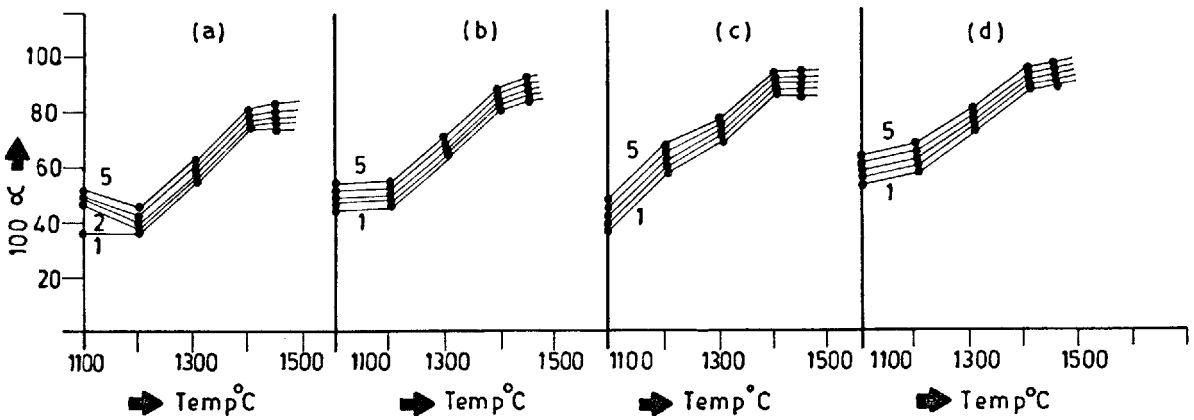

FIG-1 RELATION OF LIME COMBINABILITY WITH TEMPERATURE FOR SURFACE AREA (a)1700 (b)3600(c)4100 AND (d)5300. CURVES 1 TO 5 DENOTES THE DIFFERENT RETENTION TIME 5,10,15,20 AND 25 MINUTES.

The regression equation for Burnability is :

$$\mathcal{L} = 0.7396 + 2.158 \times 10^{-3}\rho_1 + 6.2094 \times 10^{-4}\rho_2 + 3.6046 \times 10^{-5}\rho_3 - 0.0133\rho_4$$

where

$\mathcal{L}$ - Lime Combinability ratio

ρ_1 - Retention time in minutes

ρ_2 - Temperature in °C

ρ_3 - Surface area cm^2/gm

ρ_4 - Percent total CaO in raw mix after burning.

IV. APPLICATION TO INDUSTRIAL RAW MIXES

Three industrial raw mixes were collected for investigating the burnability with the help of the equation derived earlier. The Plant-A with precalcination technology uses limestone of sedimentary origin and the Plant B & C are wet process plants using fine grained crystalline limestone. The chemical composition of the raw mixes along with Coal Ash component from fuel due to absorption is given in Table 2.

The calculated lime combinability of these three raw mixes at three different surface areas at temperatures 1350°C, 1400°C, 1450°C with retention time 20 minutes was determined. Similar data on the same raw mixes with the same parameters was also determined experimentally.

The calculated value of lime combinability in all cases is lower (.005 - .08) than the experimental value. The influence of minor elements which often acts as a mineraliser has not been considered in the equation might explain the higher experimental lime combinability value than the calculated value. Figure 2 shows the close relation between the lime combinability values calculated and experimental.

V. EXPANSION/SHRINKAGE STUDIES

The volume change inthe fired raw mix pellets of the three industrial raw mixes was determined (Fig.3 a to c). The firing expansion/shrinkage patterns of raw mix pellets are characteristic of each of them and no two patterns are alike. These patterns provide qualitative information about the lime combinability, solid state reactions forming intermediate phases, appearance & quantity of liquid and finally the compressive strength of the pellet

TABLE 1

CHEMICAL COMPOSITION OF RAW - MIXES USED IN THE DERIVATION OF THE EQUATION OF BURNABILITY.

	SiO_2	Al_2O_3	Fe_2O_3	CaO	MgO	LOI	M_S	M_A	LSF
RAW-MIX-1	12.53	3.18	1.66	42.9	1.4	36.26	2.58	1.91	1.07
RAW-MIX-2	15.1	4.1	2.6	43.0	0.2	33.9	2.25	1.57	0.88
RAW-MIX-3	13.8	2.1	2.6	44.0	1.0	35.7	2.94	0.81	1.02
RAW-MIX-4	13.3	3.2	2.5	43.7	1.0	35.2	2.33	1.28	1.00
RAW-MIX-5	13.5	3.4	1.8	41.1	1.7	36.9	2.60	1.89	0.93
RAW-MIX-6	13.0	3.9	1.8	42.6	1.6	35.2	2.28	2.17	0.98
RAW-MIX-7	13.1	2.3	1.2	44.3	3.2	34.7	3.70	1.92	1.08
RAW-MIX-8	14.4	2.7	1.1	43.8	0.9	35.8	3.79	2.45	0.97
RAW-MIX-9	14.8	2.5	2.6	42.3	1.3	35.3	2.91	0.96	0.91
RAW-MIX-10	13.2	3.7	2.4	43.0	0.6	36.0	2.16	1.54	0.98
RAW-MIX-11	12.3	2.3	3.1	45.2	0.6	36.0	2.72	0.74	1.15

at 1400°C throws light on the expected granulometry of the clinker in the industrial situation. The details of the method & interpretation has been described elsewhere (3).

Following conclusions can be drawn from the expansion/shrinkage pattern (Fig. 3 a to c) of the three plant raw mixes ground to three different surface areas.

i) In case of Plant - A & B (Fig. 3 a & b), an expansion maxima occurs at 1200°C indicating the formation of high lime aluminates (C_3A) and high lime silicates(C_2S). The liquid formation initiates at around 1250°C - 1300°C. The rate of reaction, either solid state or liquid-solid, is higher for the higher surface area than the lower surface area as exemplified by higher value of expansion at 1200°C and shrinkage at 1450°C for the same raw mix. The difference inthe two raw mixes (Plant A and Plant B) is shown by the value of maximum expansion and shrinkage signifying the rate of lime combinability and quantity of liquid being different for the two raw mixes.

ii) The raw mix from Plant-C shows an expansion at 1200°C followed by shrinkage and then another expansion maxima at 1350°C. The above characteristic is indicative of the formation of intermediate phases and incipient liquid formation between the two stages of silicate and aluminate formation. However, this rate of reaction is higher for the higher surface area in the raw mix. Based on the firing shrinkage/expansion studies, the three plants can be rated in order of their lime combinability and reactivity as Plant - A (Max. shrinkage : 16.4%) followed by Plant - B

TABLE 2

CHEMICAL COMPOSITION OF THREE INDUSTRIAL RAW MIXES

	SiO_2	Al_2O_3	Fe_2O_3	CaO	MgO	LOI	LSF	M_S	M_A
Plant A	13.8	3.8	2.4	43.5	1.0	34.6	0.97	2.2	1.58
Plant B	15.0	3.2	2.4	44.6	0.8	34.0	0.94	2.7	1.33
Plant C	15.5	3.0	1.9	43.2	0.6	34.1	0.89	3.2	1.58

(Max. shrinkage 14.43%) and, then Plant-C (Max. shrinkage 5.89). The same rating can be maintained from the lime combinability values obtained from the equation viz., the lime combinability at 1400°C for Plant A, B and C are 0.968, 0.925 and 0.920 respectively.

VI. CONCLUSION

The equation derived is successful in predicting the lime combinability/free lime of a raw mix with known surface area for a given temperature and retention time of burning. It can also be used for decisions on the fineness of a raw mix under a given burning condition. However, the behavioral aspects of a raw mix due to heating like the course of reaction, appearance of melt and quantity of melt cannot be derived from the equation but such information is available from the firing shrinkage/expansion studies. The mineralogical and minor elements influence on burning and reactivity of raw mixes cannot be brought out selectively from the use of the equation alone but the experimental determination of lime combinability ($\mathcal{L}$) together with the shrinkage/expansion characteristics would help in deciphering them.

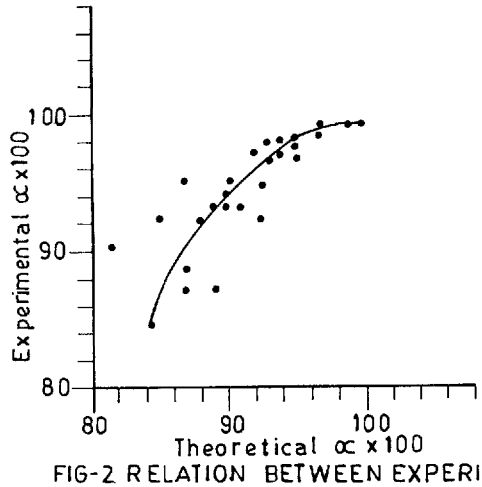

FIG-2 RELATION BETWEEN EXPERIMENTAL AND-THEORETICAL BURNABILITY

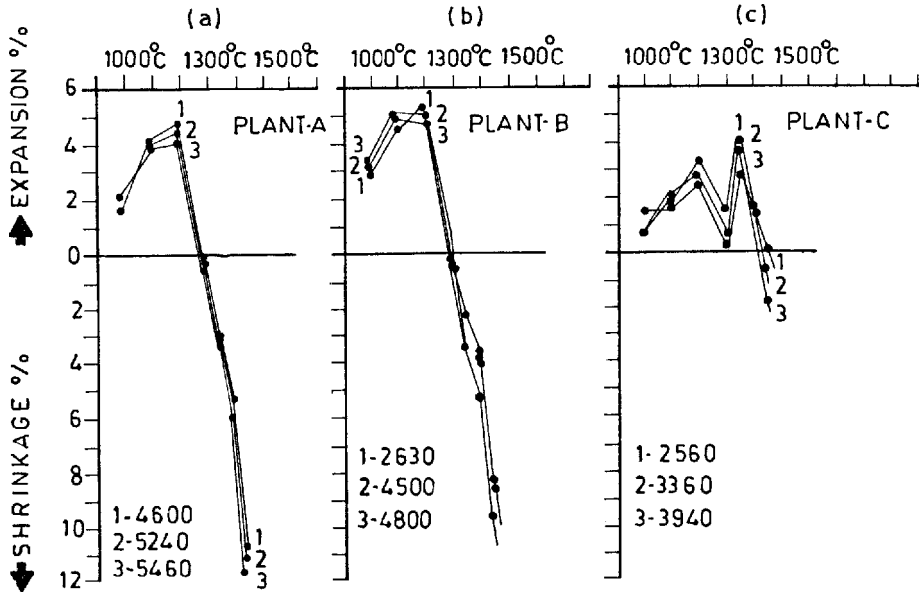

FIG-3 EXPANSION/SHRINKAGE OF THREE RAW MIXES WITH DIFFERENT SURFACE AREA

REFERENCES

1. W. Jander (1931) "Die Grundlagen der Reaktionen in Festernb Zustande and ihre Bedeutung fur die Erzeugung des Zements". Zement 20, 936-39, 951-53.

2. A.M. Ginstling and B.I. Braunstein, (1950) "Diffusion Kinetics of Reactions of Spherical Particles". J. Applied Chemistry (USSR), 23, No.12.

3. A.K. Chatterjee, C.H. Page & D. Ghosh(1985) Industrial Experience of using mineralisers, Paper submitted at the Int. Seminar on Energy Conservation, Beijing.

P. Bürki and H. Braun, "Holderbank" Management and Consulting Ltd., Switzerland

Investigations on Influence of Raw Mix Reactivity and Rate of Upheating upon Clinker Formation

Investigations de l'influence de la Réactivité du Cru et du Taux de Chauffage sur la Formation du Clinker

SUMMARY

Clinker formation kinetics remain a topic of great practical relevance. This is again apparent in latest kiln technologies designed for rapid throughput of the kiln charge through the calcining and transition zones to maintain high reactivity of intermediate products up to the sinter-zone.

In this context, the question arises as to what extent the reactions between calcination and formation of melt phase (i.e. 1000 - 1250°C) influence the final clinker formation not only concerning the reaction rate but also clinker granulation and microstructure. Given the great petrological variety of raw materials, it seems worthwhile to clarify whether this reaction interval is equally important for all raw mixes, and - ultimately - whether the new technologies are applicable regardless of the raw material nature.

With the above objective, the reaction kinetics of numerous industrial raw meals in the temperature range 900 - 1500°C was examined by means of a laboratory test ("reactivity test"): cylinders of different raw meals are burnt simultaneously in a programmable furnace at distinct rates of upheating and withdrawn after preselected temperature or time intervals. The reaction process is expressed on basis of the residual free lime content.

Measuring the dimensional changes of the cylinders provided information on the sintering behaviour. For selected meals the sequence of mineral formation and the development of clinker structure were studied using appropriate techniques.

The "reactivity test" revealed considerable differences between raw meals regarding the amount of residual free lime and its rate of combination within the temperature range 1000 - 1250°C. They arise from different degrees of raw meal microhomogeneity, an inherent property of the raw components.

Also significantly dependent on the microhomogeneity is the development of the clinker microstructure.

The effects of rapid heating upon selected raw mixes are studied. They would seem to be most advantageous for mixes of pronounced microhomogeneity, where the well-advanced CaO-combination after calcination leads to an apparently inactive transition period until alite formation commences.

SUMÁRIO

A cinética de formação do clínquer permanece um tópico de grande relevância prática. Isto é aparente nas mais recentes tecnologias de forno projetadas, para o rápido despacho da carga do forno através das zonas de calcinação e transição para manter a alta reatividade dos produtos intermediários até a zona de sinterização.

Neste contexto, a pergunta que surge é até que extensão as reações entre calcinação e formação de fase líquida (i.e. 1000 - 1250°C) influenciam a formação final do clínquer não apenas relacionado à velocidade de reação mas também à granulometria e microestrutura do clínquer. Dada a grande variedade petrográfica das misturas cruas, é significativo clasificar se este intervalo de reação é igualmente importante para todas as misturas cruas e - ultimamente - se novas tecnologias são aplicáveis, independentemente da natureza da mistura crua.

Com este objetivo, a cinética da reação para várias misturas cruas industriais na faixa de temperatura de 900 - 1500°C foi examinado por meio de testes laboratoriais ("teste de reatividade"): cilindros de misturas cruas diferentes foram cozidas simultaneamente em uma fornalha programável para diferentes velocidades de aquecimento e resfriamento após temperatura pré-selecionada ou intervalos de tempo. O processo da reação é expresso em base do conteúdo de cal livre.

A medição das mudanças dimensionais dos cilindros forneceu informação no comportamento da sinterização. Para crús selecionados, a sequência de formação mineral e o desenvolvimento da estrutura do clínquer foram estudadas usando técnicas apropriadas.

O "teste de reatividade" revelou consideráveis diferenças entre misturas cruas considerando a quantidade de cal livre residual e sua velocidade de combinação dentro da faixa de temperatura de 1000-1250°C. Elas surgem devido a diferentes graus de micro-homogeneidade da mistura crua, uma propriedade inerente das misturas cruas.

O desenvolvimento da microestrutura do clínquer é também significativamente dependente da micro-homogeneidade.

Os efeitos de aquecimento rápido em misturas cruas selecionadas foram estudadas. Eles parecem ser mais vantajosos para misturas de pronunciada micro-homogeneidade, onde a bem avançada combinação do CaO após a calcinação leva a um aparente período de transição inativo até que a formação da alita começe.

P. Bürki and H. Braun, "Holderbank" Management and Consulting Ltd., Switzerland

1. INTRODUCTION

Determination of the rate of clinker formation is an important step in assessing the in-kiln behaviour of industrial cement raw meals. In most cases, a comparative assessment is made, based - for reasons of simplicity - on isothermal burning tests, supplemented by chemical and mineralogical data, which permit an optimization of raw meal composition and fineness.

For a more comprehensive understanding of the burning process - as is increasingly required for the efficient operation of modern kilns - it is necessary to include additional aspects, such as clinker granulation [1], dust development, coating formation and others, i.e. not simply the burnability but the overall burning behaviour must be considered. Furthermore, in view of the subsequent grinding process and cement properties, the development of the clinker microstructure is also of interest.

The above mentioned aspects are determined by the ongoing chemical reactions, occurring over the entire temperature range in the rotary kiln. Thus, it seems appropriate to investigate the progress of reaction over an extended temperature range, in order to characterize the influences of raw meal characteristics and of heating rate upon the various stages of clinker formation [2].

Rapid upheating of the kiln charge, as achieved in precalciner kilns with short rotary sections, is said to be advantageous not only with respect to sinter-zone temperature, but also to clinker granulation and microstructure [3].

2. OBJECTIVES

In the "Holderbank" laboratories a non-isothermal reactivity test is employed to characterize the burning behaviour of raw meals over a wide temperature range. The test was designed to combine practical relevance with experimental simplicity and so make it attractive for both routine and special investigations. The test serves two purposes, namely:

- to permit a comparative characterization of raw meals, as performed under constant test conditions (standard reactivity test)
- to assess the effect of distinct, individual process conditions, such as maximum burning temperature or upheating rate on clinker formation (modified reactivity test).

These tests may be supplemented by further experimental investigations (microscopy, X-ray diffraction, thermoanalysis).

3. TEST DETAILS

Materials preparation: Raw meal cylinders, 15 mm in diameter and height, are formed by pressing a moist paste into holes of the above dimensions, drilled in a steelplate, followed by drying at 100°C.

Reactivity test: A programmable, electrically heated 1600°C "Naber" muffle furnace is used. It can accommodate 32 raw meal cylinders (normally 8 cylinders each from 4 different raw meals), distributed on 8 ceramic sample holders (see photo 1). The loaded sample holders are all entered at 700°C and individually withdrawn at selected temperatures (or times); the burnt cylinders are allowed to cool in air, after which their diameter, height and free lime are measured, the latter according to the Schläpfer-Bukowski method using ethylene-glycol extraction.

Further investigations: X-ray diffraction diagrams were recorded using CuK -radiation on a Philips APD 10 diffractometer. The microstructure was examined by reflected light microscopy on polished and etched test cylinders after burning to various temperatures and times respectively.

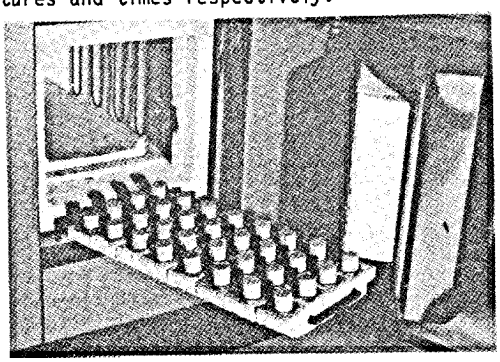

Photo 1: Test furnace

4. RESULTS

4.1 Raw Mix Characterization by Standard Reactivity Test

Test procedure: upheating rate of 8°C/min from 700 to 1400°C. Samples are withdrawn in 100°C intervals starting at 900°C, and after 15 and 30 minutes retention time at 1400°C.

Out of the numerous raw meals, four spread over the range encountered are selected for presentation. Their chemical moduli, mineralogical composition and fineness are shown in Table 1. The raw component characteristics are as follows:

Meal A: A complex mixture of marly to high grade limestone and slate containing quartz and highly crystalline silicates, such as micas and chlorite.

Meal B: A microcrystalline, marly, chalky limestone of cementstone composition containing poorly crystalline montmorillonite as major argillaceous mineral.

Meal C: A hard, high-grade limestone and an alluvial, quartz-rich river deposit (sand to gravel) as siliceous component.

Meal D: A mixture of high and low grade, rather inhomogeneous limestones. Very high calculated clinker liquid phase (approx. 30%).

P. Bürki and H. Braun, "Holderbank" Management and Consulting Ltd., Switzerland

TABLE 1: RAW MEAL PROPERTIES

Raw meal	A	B	C	D
Chemical moduli				
Lime saturation	90.2	100.1	97.2	93.2
Silica ratio	3.08	3.14	3.74	2.13
Alumina ratio	1.72	3.00	1.71	2.05
LPh 1338°C	19.7	13.0	16.5	22.9
LPh 1400°C	23.0	21.5	19.0	29.7
Mineralogical composition				
Calcite	75.5	76.5	74.5	73.5
Dolomite	0.5	-	4.0	-
Quartz	12.0	4.0	8.0	7.5
Feldspars	2.5	-	3.0	4.0
Kaolinite	-	-	4.0	-
Micas	4.0	3.0	1.5	4.0
Chlorite	4.0	-	-	6.0
Montmorillonite	-	6.0	-	-
Fineness				
Sieve residue: 200 µm	1.0	1.3	1.8	2.2
90 µm	14.8	13.6	22.6	24.0

The free lime development for the four raw meals in the standard reactivity test is shown in Figure 1.

The residual free lime content at 1400°C characterizes the burnability, i.e. the ease of alite formation in the reacting meals. In the cases of meals A, C and D, the distinct burnabilities can be satisfactorily explained by models expressing the burnability as a function of lime saturation, silica modulus, and the amount of coarse quartz and calcite ("Holderbank" physico-chemical burnability model; [4],[5]). Meal B, however, lies outwith the scope of this model: the free lime content is unexpectedly low for its high lime saturation and silica ratio; the excellent reactivity has to be explained by the exceptional raw meal microhomogeneity.

Very different reactivities of the raw meals during and after calcination are revealed by the different free lime contents in the temperature range 1000 - 1200°C. Assuming that at 1000°C all clinker minerals can be formed except alite, a relative degree of lime combination can be calculated (100% means that all remaining CaO is exclusively available for the conversion of belite into alite). The figures for the four meals are:

Relative degree of lime combination at 1000°C (%)

A	B	C	D
37.7	89.4	59.3	46.4

Since the chemical transformations at around 1000°C are solid state reactions, the degree of lime combination depends mainly on the contact area of the reacting components and is, thus, a measure of the microhomogeneity of the meal. It appears that the microhomogeneity is not so much a matter of the grinding fineness in the typical range for raw meals but rather of the inherent petrographic texture of the raw components. This is evidenced both by the reactive meal B based on a cementstone-like, microcrystalline raw material and by the low reactive meal A made from rather heterogeneous, well crystalline rocks (see photos 2 and 5).

Depending on the degree of lime combination achieved at 1000°C, either an appreciable reaction rate is still observed in the upheating period up to melt formation (meals A, C, D), or the meal passes through an apparently inactive period of almost no net transformation (meal B) in which, however, crystal growth or recrystallization reactions take place. For the industrial process a rapid transit through the temperature range from 1000 to 1250°C (corresponding approx. to the transition-zone) seems to be desirable for type B meals, whereas for types A, C and D the advantages are not immediately obvious and require some clarification. This will be further discussed in section 4.2.

In Figure 2, the changing volume of the burnt raw meal cylinders (referred to the original volume) is shown. The shrinkage behaviour at sintering temperature, which primarily depends on the liquid phase content, provides an indication of the granulation and coating behaviour of the meal. A more profound interpretation, however, requires an examination of the microstructure and a more detailed consideration of melt phase properties [6].

4.2 Influence of Upheating Rate on Burnability and Microstructure

As pointed out by Wolter [3], the most significant differences in the temperature profile of modern kiln systems occur in the transition-zone, which, to take extremes, is either long, as in a precalciner kiln with a length to diameter ratio of approx.14:1, or of a rather limited length, as in a short precalciner kiln (10 : 1).

This situation was simulated by the upheating sequence in the modified reactivity tests:

slow upheating: 50°C/min from 700 to 1000°C and from 1300 to 1500°C; 2.5°C/min from 1000 to 1300°C

rapid upheating: 50°C/min from 700 to 1500°C

sampling: at 100°C intervals, starting at 1000°C, and after 10 and 20 minutes retention time at 1500°C

(During calcination the temperature within the relatively large raw meal cylinders was certainly not uniform. Although the free lime curve was thus falsified in this range, the final conclusions remain unchanged).

Included in the investigations were the low reactive meal A and the very reactive meal B.

P. Bürki and H. Braun, "Holderbank" Management and Consulting Ltd., Switzerland

Fig. 1 DEVELOPMENT OF FREE LIME

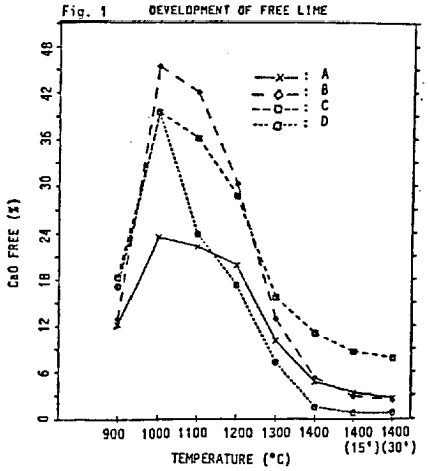

Fig. 3 DEVELOPMENT OF FREE LIME

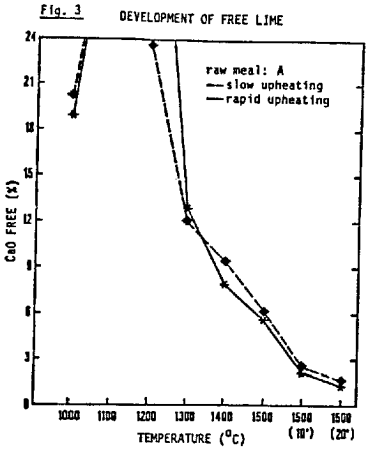

Fig. 4 DEVELOPMENT OF FREE LIME

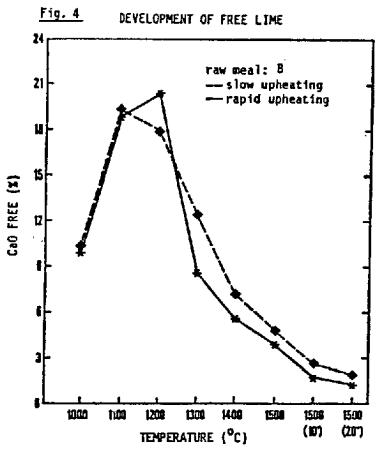

Fig. 2 DEVELOPMENT OF PERCENTAGE VOLUME CHANGE

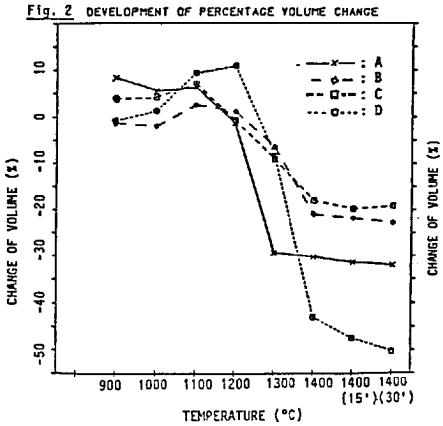

Fig. 5 DEVELOPMENT OF PERCENTAGE VOLUME CHANGE

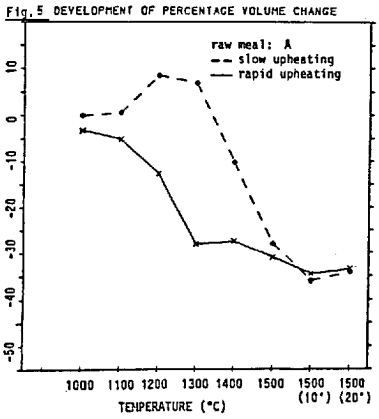

Fig. 6 DEVELOPMENT OF PERCENTAGE VOLUME CHANGE

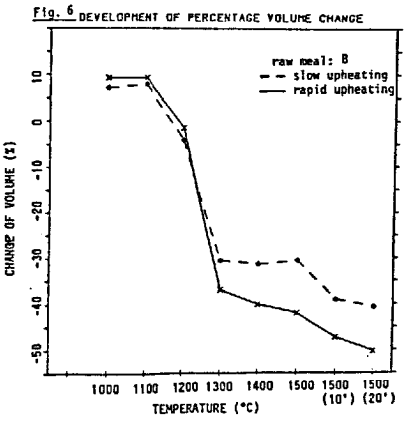

Influence on burnability

Figs. 3 and 4 display the free lime development of the two meals under slow and rapid upheating conditions. In both cases, the residual free lime content at and above 1400°C is lower in the case of rapid upheating than after a prolonged tempering period between 1000 and 1300°C. For the reactive meal B, a much further advanced degree of reaction of the rapidly burnt sample is already observed at 1300°C.

It has been suggested that the gain in reactivity is due to the preservation of small and disordered intermediate minerals up to the stage of alite formation [2],[3]. This should be reflected in the X-ray diffraction peak width, in particular of free lime and belite. At 1300°C no differences were observed in the diffraction peaks of free lime, while a noticeable increase in peak width and a decrease in peak resolution were observed for belite in the rapidly heated samples, as shown in Fig. 7.

Fig. 7

BELITE PEAK WIDTH IN FUNCTION OF HEATING RATE (1300°C)

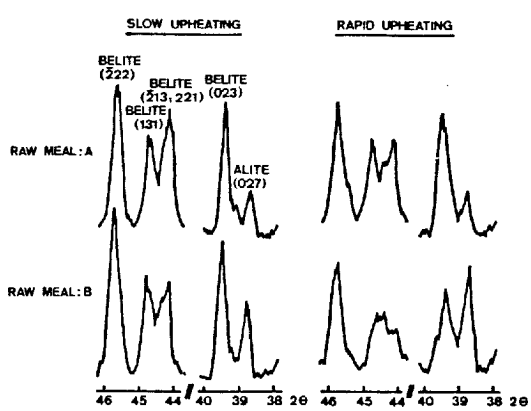

P. Bürki and H. Braun, "Holderbank" Management and Consulting Ltd., Switzerland

Influence on microstructure

A definite influence of the upheating rate upon microstructure development is apparent from the observed volume changes of the burnt raw meal cylinders as shown in Figs. 5 and 6: for meal A, the shrinkage at the final sintering temperature is about the same for both the slowly and rapidly heated samples; however, at lower temperatures, a lower upheating rate leads to a temporary volume increase, while upon rapid upheating an immediate shrinkage is observed. In the case of meal B, the differences rather occur at sintering temperature, where a markedly increased shrinkage results from rapid upheating.

The development of clinker microstructure was studied in detail by optical microscopy. Only the granulated raw meal and the final clinker after 20 minutes retention time at 1500°C are depicted (photos 2 - 7).

It is evident that the characteristics of the clinker structure are principally determined by the raw meal properties and only to a lesser extent influenced by the upheating program.

The main features distinguishing the clinkers produced from mixes A and B, as a result of their intrinsic properties, are:

Mix A: This meal consists of rather coarse, monomineral particles, the size of which is strongly affected by the grinding process (photo 2). The resulting clinker is coarsely structured, consisting of extended regions of dense sintered material and large pores. The clinker minerals are heterogeneously distributed and have a large crystal size (photos 3 and 4).

Mix B: This meal is extremely fine grained and homogeneous (photo 5), a feature inherent to the components and not produced by grinding. The resulting clinker is fairly dense, the remaining porosity almost exclusively consisting of fine pores. The clinker minerals are very homogeneously distributed and are small in size.

The influence of the different upheating conditions is readily visible in the case of mix B: from the start of sintering to the final stage, a denser structure, intersected by larger pores, is formed in the case of rapid upheating.

A similar trend to a coarser structure upon rapid heating is also found in the final clinker of mix A, though far less pronounced than in mix B. The rather striking difference in volume shrinkage at 1300°C (Fig. 5) is also apparent in the microstructure (not shown here): after rapid heating, the sintering process has progressed much further than after prolonged tempering.

A significant difference in crystal size in the final clinker after slow and rapid upheating cannot be detected in either of the two clinkers.

5. CONCLUSIONS

By means of the standard reactivity test, the burning behaviour of cement raw meals can efficiently be determined over the temperature range from 1000 to 1400°C.

The residual free lime content at 1400°C - used to characterize the burnability of a meal - can in most, but not all cases, be explained by statistical models. Highly reactive meals, for which these models are not valid, are distinguished by an exceptional microhomogeneity, which is inherent to the raw components and is not significantly affected at the grinding fineness typical for industrial raw mills.

The microhomogeneity can be determined by various methods:

- indirectly after calcination by the free lime content, or the degree of lime combination, as determined by the reactivity test;
- by means of a microscopical assessment of the (nodulized) raw meal;
- by microprobe analysis of small areas (30 x 30 um) as recently proposed by Grigel et al. [7].

The observed effects of rapid upheating - as compared to prolonged tempering between 1000 and 1300°C - on clinker formation are twofold:

- The alite formation rate is definitely increased within the investigated cases, the acceleration being more effective in the homogeneous meal, which is in agreement with [2].
- The development of the clinker structure is influenced in such a way that larger pores are formed. This is considered to be rather unfavourable regarding clinker grindability. On the other hand, no influence on the final size of alite and belite is observed. Thus, our results from laboratory experiments differ to some extent from those that Wolter reports [3] on the basis of industrial trials.

The remaining uncertainties on the influence of process conditions on the clinker microstructure certainly require - in view of their significant impact on grindability and cement properties - further clarification.

LITERATURE

[1] F. MacGregor Miller, Rock Products (1980), 152
[2] H. Bomas, U. Ludwig, A. Wolter, Tonind. Ztg. 105 (1981), 144
[3] A. Wolter, Zement-Kalk-Gips, 38 (1985), 612
[4] E. Fundal, World Cement Technology 10 (1979), 195
[5] U. Ludwig, Zement-Kalk-Gips, 34 (1981), 175
[6] I.F. Petersen, World Cement (1983), 188 and 220
[7] W. Grigel, G. Oberheuser, A. Wolter, Zement-Kalk-Gips, 38 (1985), 589

P. Bürki and H. Braun, "Holderbank" Management and Consulting Ltd., Switzerland

MICROGRAPHS

MEAL A

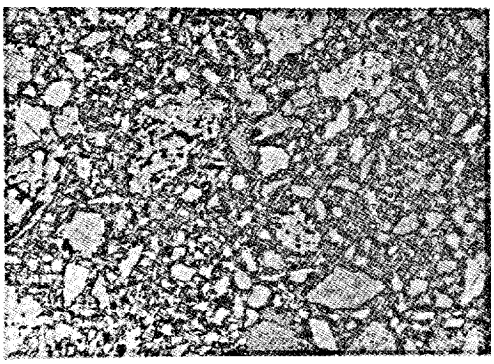

Photo 2 128 x
Raw meal

MEAL B

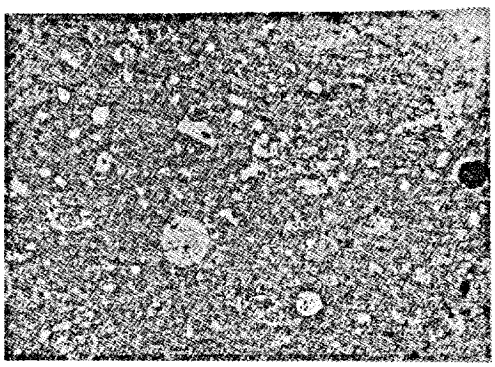

Photo 5 128 x
Raw meal



Photo 3 128 x
1500°C, 20 minutes,
slow upheating

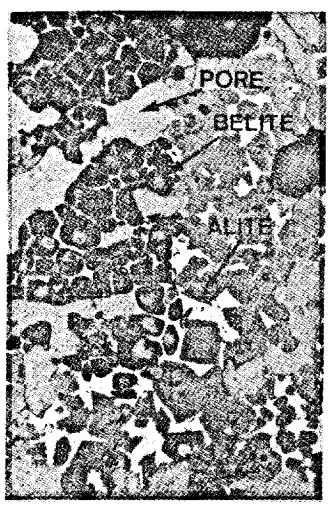

Photo 4 128 x
1500°C, 20 minutes
rapid upheating



Photo 6 128 x
1500°C, 20 minutes
slow upheating

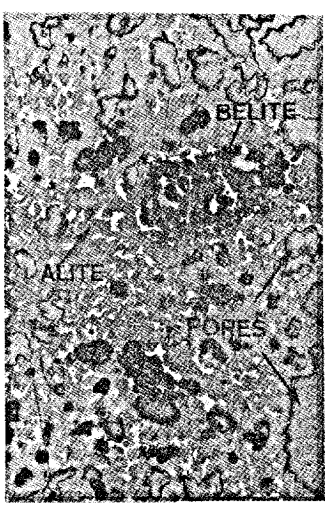

Photo 7 128 x
1500°C, 20 minutes
rapid upheating

N.F. FIODOROV,
A.P. GAVRILOV,
N.I. IVANOV,
O.M. KHALINA, Institut technologique Lensovet de Leningrad, U.R.S.S.

1

CINETIQUE DE LA SYNTHESE DES ALUMINATES DE CALCIUM PAR LE TRAITEMENT THERMIQUE DANS LE MILIEU DES CALOPORTEURS METALLIQUES FONDUS

1.1

Les auteurs ont étudié la cinétique de la synthèse en phase solide des $3CaO \cdot Al_2O_3$, $12CaO \cdot 7Al_2O_3$, $CaO \cdot 2Al_2O_3$ qui sont les constituants principaux des ciments alumineux et siliceux. Les tablettes cylindriques ont été pressées à partir de la charge crue composée de $CaCO_3$ et Al_2O_3. Les tablettes ont subi le traitement thermique au moyen de l'immersion dans le bain fondu de fonte. La durée de traitement thermique était de 30 à 2000 s. Le degré d'achèvement de la synthèse a été contrôlé par les méthodes chimiques, pétrographiques et aux rayons X.

Les auteurs ont constaté que, indépendamment de la composition du cru initial, à l'exception de celui pour l'obtention de $CaO \cdot 2Al_2O_3$, se sont des $CaO \cdot Al_2O_3$ et $12CaO \cdot 7Al_2O_3$ qui se forment aux étapes initiales de l'interaction. Dans tous les cas, la durée de la synthèse diminue brusquement par rapport aux conditions traditionnelles de sa réalisation et constitue 300-2000 s. Dans les conditions normales, la synthèse de ces aluminates exige le traitement thermique de plusieurs heures.

Le traitement cinétique des données expérimentales montre que la synthèse de $CaO \cdot Al_2O_3$ et $12CaO \cdot 7Al_2O_3$, pour tous les degrés de transformation, est décrite par l'équation de Guinstling-Brooutstein, tandis que la synthèse de $3CaO \cdot Al_2O_3$ - par l'équation de Karter-Valensi.

Les valeurs de la préexponentielle et de l'énergie d'activation sont obtenues.

Os autores estudaram a cinética da síntese, em fase sólida, dos C_3A, $C_{12}A_7$, CA_2 que são os constituintes principais dos cimentos aluminosos e silicosos. Os corpos de prova cilíndricos foram comprimidos a partir da carga crua composta de $CaCO_3$ e AL_2O_3. As lâminas sofreram o tratamento térmico por meio de imersão em um banho de ferro fundido. A duração do tratamento térmico era de 30 a 2000 s. O grau de terminação da síntese foi controlado por métodos químicos, petrográficos e de Raios X.

Os autores constataram que, independentemente da composição do cru inicial, com exceção daquele para a obtenção do CA_2, são o C.A e $C_{12}A_7$ que se formam nas etapas iniciais da interação. Em todos os casos, a duração da síntese diminui bruscamente em relação às condições tradicionais de sua realização e constitui 300-2000 s. Em condições normais, a síntese desses aluminatos exige o tratamento térmico de várias horas.

O tratamento cinético dos dados experimentais mostra que a síntese do CA e $C_{12}A_7$, para todos os graus de transformação, é descrita pela equação de Guinstling-Brooutstein, enquanto que a síntese do C_3A, pela equação de Karter-Valensi.

Os valores da prê exponencial e da energia de ativação foram obtidas.

I.F. FIODOROV,
A.P. GAVRILOV,
V.I. IVANOV,
O.M. KHALINA

1.1

Les aluminates de calcium: $CaO \cdot Al_2O_3$, $CaO \cdot 2Al_2O_3$, $I2CaO \cdot 7Al_2O_3$ présentent les constituants principaux des ciments alumineux et des ciments alumineux à teneur d'alumine élevée qui, grâce à la combinaison d'une haute résistance absolue et d'une vitesse de son accroissement, trouvent l'utilisation toujours croissante en qualité des matériaux réfractaires /I/. La production industrielle de ces ciments est basée sur deux méthodes de fabrication: fusion et cuisson à voie du ciment Portland normal. En réalisant la derniere méthode de fabrication, on rencontre des grandes difficultés liées avec un petit intervalle de cuisson des crus aluminates et avec la formation d'anneaux dans le four rotatif. Les températures assez élevées de fusion des aluminates de calcium rendent également assez difficile du point de vue technologique la fabrication des ciments alumineux suivant la première méthode.

A l'occasion de ci-dessus, à notre avis, il apparaît assez perspectif le traitement thermique des crus en milieu ou sur la surface des fluides caloporteurs métalliques en vue de fabriquer les ciments alumineux et les ciments alumineux à teneur d'alumine élevée. Nous avons montré les avantages principales de cette méthode de traitement thermique dans le travail portant sur la synthèse des minéraux du clinker de ciment Portland qui a été présenté au Congrès précédent. Ces avantages sont les suivantes: I) accroissement multiple de vitesse des réactions de synthèse de phase solide; 2) absence de pollution de la matière à traiter par les produits de combustion; 3) possibilité de traiter la matière première minérale avec récupération des produits gazeux; 4) élimination complète d'entrainement de poussière de l'unité de cuisson; 5) simplicité de contrôle précis de la température permettant d'éliminer complètement le surchauffage de la matière, ce qui est important pour le traitement thermique des crus du ciment alumineux.

La présente recherche est effectué dans le but d'obtenir les données sur la cinétique de la synthèse des phases solides des aluminates de calcium et de leurs mélanges qui correspondent aux compositions des ciments alumineux et des ciments alumineux à teneur d'alumine élevée et dans le but d'avoir les données concernant les propriétés liantes des produits de cuisson obtenus dans les conditions tellement extraordinaires. Les données sur la première et la seconde question sont nécessaires pour apprécier l'utilité de la production des ciments alumineux par la méthode de synthèse fondue thermique.

En qualité des matériaux de départ on a utilisé: carbonate de calcium, type "CP"; β - alumine, type "CP"; oxyde d'aluminium technique; γ - alumine, type "P"; mélange cru à base du calcaire naturel et de l'alumine technique (pour la composition, voir le Tableau n°I).

En qualité du caloporteur on a utilisé le métal fondu (fonte grise de mauvaise qualité, type C4-00). On juge de la cinétique d'interaction dans les charges comptées sur l'obtention des C_3A, $C_{12}A_7$ et CA selon le degré de fixation de l'oxyde de calcium et dans les charges comptées sur l'obtention du CA_2 et des ciments alumineux à haute teneur d'alumine - selon le degré de fixation de l'oxyde d'aluminium. Les données concernant la cinétique d'assimilation des constituants de base sont présentées dans les Tableaux n°2 et n°3.

L'analyse de ces données montre le suivant. La vitesse de synthèse de toutes les substances étudiées est beaucoup plus grande que la vitesse de synthèse en conditions de chauffage traditionelles avec l'utilisation des caloporteurs gazeux, lorsqu'il est nécessaire, pour achever la synthèse, quelques heures à la température 1673 K.

La température et le degré de broyage des agents de départ exercent la plus grande influence sur la cinétique de synthèse. La nature des constituants de base est aussi d'une grande importance.

La composition de phase des produits

Tableau n°I

Al_2O_3	Fe_2O_3	CaO	MgO	K_2O	Na_2O	TiO_2	SiO_2	Perte au feu
67,75	0,31	17,34	0,74	0,1	0,44	0,14	1,44	11,83

Tableau n°2

Teneur en CaO libre dans les produits de cuisson

Minéral	Surface spécifique, m^2g	Température de cuisson, °K	Durée d'exposition, s.					
			60	180	300	600	1200	2400
$3CaO \cdot Al_2O_3$	0,16	1573	56,0	49,1	48,5	46,7	45,4	43,1
	0,45	1573	53,1	45,9	42,9	39,4	33,2	20,8
	supérieure à 0,5	1573	37,0	7,5	6,5	2,2	1,0	0
	0,16	1663	53,2	21,1	12,9	11,9	10,7	0,5
	0,45	1663	45,3	18,8	10,8	9,9	0	0
	supérieure à 0,5	1663	11,6	4,4	2,5	0	0	0
$12CaO \cdot 7Al_2O_3$	0,35	1573	48,5	46,0	45,0	36,5	31,4	23,3
	0,35	1623	46,0	40,2	36,6	26,8	18,9	9,5
	0,35	1663	47,1	35,1	24,4	19,2	9,7	0,9
$CaO \cdot Al_2O_3$	0,31	1573	35,4	27,5	26,3	22,4	18,3	1,5
	0,31	1623	33,4	25,0	23,1	16,9	11,0	0,8
	0,31	1663	30,2	9,0	0	0	0	0

d'interaction obtenue par les analyses pétrographiques, radioscopiques et spectroscopiques infrarouges montre que ce sont $CaO \cdot Al_2O_3$ et $12CaO \cdot 7Al_2O_3$ qui se forment aux étapes initiales de la synthèse. l'interaction ultérieure mène à la fixation complète de l'oxyde de calcium et à la formation du produit correspondant à la stoechiométrie de la charge de départ. L'exception est faite pour le processus dans les charges comptées sur l'obtention du dialuminate de calcium. Pendant le traitement thermique de ces charges, aux étapes initiales, le monoaluminate de calcium et le dialuminate de calcium synthétisent simultanément.

Le rapport de ces phases dépend de la température et de l'activité de la charge initiale. L'augmentation de température du fluide caloporteur mène à l'accroissement de rendement du dialuminate de calcium. Il faut souligner que l'utilisation des formes actives de l'alumine pour la synthèse du dialuminate de calcium, contrairement aux attentes, ne donne pas un effet positif. Le rendement du dialuminate est plus grand dans les charges composées avec l'utilisation de l'alumine technique ou du corindon.

L'augmentation de dispersité de la charge initiale dans tous les cas mène à l'accélération de la formation des minéraux.

Le traitement des données obtenues avec l'utilisation de l'analyse cinétique formelle montre que les équations suivantes

N.F. FIODOROV,
A.P. GAVRILOV,
N.I. IVANOV,
O.M. KHALINA

Tableau n°3

Bilan des matériaux des produits de cuisson des charges comptées sur l'obtention du dialuminate de calcium

T K	Temps, s	CA_2 r.x	Al_2O_3 en poids	CaO libre glycér.	CA calc.	Al_2O_3 calc.	CaO calc.	Débalance
		Pourcentage de masse						
		Charge sur la base de Al_2O_3						
	120	20	40,0	5,13	34,87	78,61	21,39	0,45
1573	240	24	33,0	0	43,0	80,09	19,91	-1,0
	480	28	24,2	0	47,8	77,59	22,41	1,5
	960	29	24,2	0	46,8	77,73	22,27	1,34
	120	25	37,0	0	38,0	81,61	18,39	-2,5
1673	240	34	28,0	0	38,0	79,73	20,27	-0,66
	480	46	17,5	0	36,5	77,74	22,26	1,36
	960	48	16,3	0	35,7	77,60	22,40	1,47
	120	32	22,3	0	45,7	77,48	22,52	1,59
1773	240	43	16,2	0	40,8	76,88	23,12	2,19
	480	58	13,3	0	28,7	77,93	22,07	1,14
	960	59	13,3	0	27,7	78,06	21,94	1,01
		Charge sur la base de Al_2O_3 technique						
	120	12	46,3	18,17	23,53	71,16	28,84	7,92
1573	240	23	41,0	14,63	21,37	73,16	26,84	5,91
	480	33	29,0	8,7	29,3	74,25	25,75	4,82
	960	34	28,0	2,16	35,84	78,31	21,68	0,75
	120	24	42,0	11,16	22,39	75,62	22,48	3,45
1673	240	37	27,1	10,8	25,10	72,77	27,23	6,3
	480	55	19,5	2,5	23,00	78,02	21,98	1,04
	960	55	18,5	1,55	24,95	78,3	21,70	0,77
	120	45	32,2	0	22,8	82,89	17,31	-3,6
1773	240	57	21,2	0	21,8	80,52	19,48	-1,45
	480	74	12,5	0	13,5	79,84	20,16	-0,77
	960	75	12,5	0	12,5	79,79	20,21	-0,9

décrivent les données expérimentales avec la plus grande confiance:

$CaO \cdot Al_2O_3$; $I - \frac{2}{3}\alpha - (I-\alpha)^{\frac{2}{3}} =$

$= 4,4 \cdot 10^{20} \exp\left(\frac{762000}{RT}\right)(\tau - 51,6)$

$12CaO \cdot 7Al_2O_3$; $I - \frac{2}{3}\alpha - (I-\alpha)^{\frac{2}{3}} =$

$= 3,8 \cdot 10^{8} \exp\left(\frac{-401000}{RT}\right)(\tau - 49,8)$

$3CaO \cdot Al_2O_3$; $\frac{3}{2} - (I-\alpha)^{\frac{1}{3}} - \frac{1}{2}(I+2\alpha)^{\frac{2}{3}} =$

$= 1,4 \cdot 10^{10} \exp\left(\frac{-370000}{RT}\right) \ln(\tau - 58,2)$

Pour évaluer les propriétés techniques, nous avons synthétisé les clinkers comptés

Tableau n° 4

n° du ciment	Teneur calculée		Résistance à la compression (MPa) à l'âge de			
	$CaO \cdot Al_2O_3$ % de masse	$CaO \cdot 2Al_2O_3$ % de masse	1 jour	3 jours	7 jours	28 jours
1	50	50	18*/42**	108/54	102/69	121/96
2	40	60	18/-	114/-	132/-	162/-
3	30	70	18/45	86/63	112/85	124/101

* - numérateur (données des auteurs),
** - dénominateur (données de la référence bibliographique /3/).

sur l'obtention des ciments alumineux à teneur d'alumine élevée ayant un rapport différent du CA et du CA_2. La synthèse a été effectuée par le traitement thermique du mélange cru formé en bande continue à la surface de la fonte en fusion. La bande du mélange cru a été formée par laminage à la pression spécifique de 0,5 MPa et avait l'épaisseur de 5 mm et la largeur de 35 mm. Les particularités constructives de l'installation sont décrites dans le travail (voir référence bibliographique /4/). Ces particularités constructives permettent d'utiliser, outre le clinker, le gaz carbonique qui se forme lors de la dissociation de calcite.

La cuisson a été effectuée à la température de la fonte en fusion de 1723 K et à la conservation à la surface pendant 120 s, ce qui correspond au rendement spécifique du produit de 500 kg par mètre carré de surface de la fonte en fusion.

Le clinker obtenu a été broyé jusqu'à la surface spécifique de 0,5 m^2/g.

Les résultats des essais du clinker par la méthode de petits échantillons en comparaison avec les données /3/ sont présentés sur le Tableau n°4.

L'analyse de ces données montre d'une façon claire que les ciments obtenus par le traitement thermique en milieu des bains fondus de la fonte ne cèdent pas aux ciments habituels alumineux à teneur d'alumine élevée obtenus par les méthodes traditionnels et, dans certains cas, dépassent même un peu ces derniers.

Le clinker calculé pour la teneur de 40% en CA et de 60% en CA_2 a la plus haute résistance à la synthèse fondue thermique.

Il en résulte que le traitement thermique en milieu des métaux fondus peut être utilisé avec succès en vue d'obtenir des ciments alumineux et des ciments alumineux à teneur d'alumine élevée dont la production peut être combinée avec l'obtention simultanée du gaz carbonique qui sera nécessaire en grandes quantités pour augmenter le rendement des forage à pétrole.

Références

1. Бутт Ю.М., Тимашев В.В., Сычев М.М. "Технология вяжущих веществ". Из-во "Высшая школа". М. 1980 г.
2. Федоров Н.Ф., Гаврилов А.П., Кузяк В.А. В книге "Химия и технология вяжущих веществ, силикатных и неорганических материалов". Из-во ЛТИ им. Ленсовета, Л. 1977 г., с. 33-42.
3. Применение жаростойких бетонов и конструкций из них. Обзор по материалам международного симпозиума под редакцией К.Д. Некрасова. М. 1973 г.
4. Гаврилов А.П., Федоров Н.Ф., Иванов Н.И., Уполовникова Л.К. "Технологические принципы расплавотермического обжига клинкера". Цемент № II. 1984 г., с. 20-21.

A.V. BESSMERTNYKH,
V.K. KHOKHLOV,
V.V. SHELUDKO, Cement Research Institute, Moscow, USSR

THERMODYNAMIC STUDY OF DECARBONATION KINETICS

ETUDE THERMODYNAMIQUE DE LA CINETIQUE DE DECARBONATATION.

On a consistent ground of the thermodynamics of irreversible processes, the present study approaches a complicated process of decarbonation of carbonaceous components floating in a supported (buoyant) state and accompanied by the processes of heat and mass transfer.

There have been derived a dissipative function of the system "supporting medium - solid decarbonated particles" and a set of linear kinetic Onsager equations based on the principle of mutually penetrating continua.

The rate of a decarbonation reaction is given as a function of quantities which can be determined experimentally.

Em fundamentos consistentes da termodinâmica de processos irreversíveis, o presente estudo analisa um complicado processo de descarbonatação de componentes carbonosos flutuantes em um estado suporte e acompanhado por processo de transferência de calor e de massa.

Foram derivadas funções dissipativas do sistema "meio suporte-partículas sólidas descarbonatadas" e um conjunto de equações cinéticas lineares de Onsager baseadas no princípio de contínuos mutualmente penetráveis.

A velocidade da reação de descarbonatação é dada como função das quantidades que podem ser determinadas experimentalmente.

A.V. BESSMERTNYKH,
V.K. KHOKHLOV,
V.V. SHELUDKO

In out report to the 7th Congress on the Chemistry of Cement we referred to the methods of non-equilibrium thermodynamics in order to perform the kinetic analysis of formation of alite. Non-equilibrium, or irreversible, thermodynamics which has evolved as an independent discipline of macroscopic physics within the recent decades is accumulating major applications and brings about profoundly new results primarily in the studies of transfer processes associated with chemical and/or phase transformations. This is due to the fact that all actual processes are irreversible and their temporal behaviour (kinetics) cannot be studied within the conceptual framework of classical thermodynamics (actually thermostatics) which fails to explicitly involve the concept of time. Apart from that, the phenomena in most processes of actual life are interrelated and influence each other's behaviour. The only theory capable of studying this relation quantitatively seems to be NET.

Two ways are possible in approaching a thermodynamic description of decarbonation in the heterogeneous system of the gas-solid particles type. The first treats the system as being continuous, that is having no discontinuities in its thermodynamic functions. This approach assumes that the system has no clear cut interfaces between the phases. The transfer processes such as heat transfer and diffusion are governed by vector thermodynamic motive forces, namely, temperature gradients and concentration gradients since in each point of such a system there exists a finite gradient of the respective scalar quantity.

With such a continuous description, it would be natural to conclude that there exist no effect of the motive forces of heat and mass transfer that are vectors on the kinetics of the chemical reaction whose motive force, affinity, as a scalar quantity (Curie's symmetry principle).

This approach seems to be inaccurate for systems exhibiting clear cut interphases. In this case each phase may be deamed homogeneous, and the thermodynamic functions suffer finite discontinuities on the interphases. This standpoint appears to be fruitful in considering the phenomena occurring in the decarbonation of carbonaceous components, constituing cement raw mixes, being in suspension.

Consider the irreversible (in the thermodynamics sense) processes of decarbonation of $CaCO_3$, and interphase heat and mass transfer in a heterogeneous system whose homogeneous phases are separated from each other by a natural interface. We assume that the system as a whole is a closed one, while each of its subsystems (phases) is open. The phases are deamed to be isotropic. For a thermodynamic description of this system we draw up the balances of mass, energy and entropy. The subscript 1 relates to the gaseous phase, the subscript 2 to the solid phase. The interface is assumed to be penetrable for CO_2 species.

Mass balance

Introduce a chemical variable ξ for the solid phase, where the reaction of decarbonization takes place, as follows:

$$d\xi = -dn_{CaCO_3} = dn_{CaO} = dn_{CO_2}$$

where n is the mole number.

Then for each phase i (i = 1, 2),

$$dn_{1,CO_2} = d_e n_{CO_2} \qquad (1a)$$

$$dn_{2,CO_2} = d\xi - d_e n_{CO_2} \qquad (1b)$$

where $d_e n_{CO_2}$ is the number of moles of CO_2 escaping through the interface.

Energy balance

The first-law equations for each of the system phases are as follows

$$dQ_1 = dU_1 + p_1 dV_1 + h_{1,CO_2} d_e n_{CO_2} \qquad (2a)$$

$$dQ_2 = dU_2 + p_2 dV_2 - h_{2,CO_2} d_e n_{CO_2} \qquad (2b)$$

where h_{i,CO_2} is the molar enthalpy of CO_2 in phase i.

A.V. BESSMERTNYKH,
V.K. KHOKHLOV,
V.V. SHELUDKO

Entropy balance

We draw up the balances of entropy for each of the phases on the basis of the Gibbs fundamental equation whose validity with respect to irreversible processes is substantiated by Prigozhin's principle of local equilibrium

$$TdS = dU + pdV - \sum_i \mu_i dn_i \qquad (3)$$

where μ_i is the chemical potential of component i, and S the entropy of the system.

In view of (1a) and (2a) equation (3) may be written for phase 1 as

$$T_1 dS_1 = dQ_1 - h_{1,CO_2} d_e n_{CO_2} - \mu_{1,CO_2} d_e n_{CO_2} \qquad (4a)$$

The same for the solid phase

$$T_2 dS_2 = dQ_2 + h_{2,CO_2} d_e n_{CO_2} + A d\xi + \mu_{2,CO_2} d_e n_{CO_2} \qquad (4b)$$

where $A = -\mu_{CaCO_3} + \mu_{CaO} + \mu_{CO_2}$ is de Donder's affinity of the decarbonation reaction.

Differentiating (4a) and (4b) with respect to time and observing the property of additivity of entropy and the fact that $dQ_2 = -dQ_1 = dQ$ we arrive at the expression describing the production of entropy in the entire system (called the dissipative function):

$$\frac{d_i S}{d\tau} = \frac{dQ}{d\tau}\left(\frac{1}{T_2} - \frac{1}{T_1}\right) + \frac{d_e n_{CO_2}}{d\tau}\left(\frac{h_{1,CO_2}}{T_1} - \frac{h_{2,CO_2}}{T_2}\right) + \left(\frac{\mu_{2,CO_2}}{T_2} - \frac{\mu_{1,CO_2}}{T_1}\right) + \frac{d\xi}{d\tau} A \qquad (5)$$

The term within the brackets is the motive force of interphase mass transfer, which consists of the enthalpic motive force, in the first parentheses, and the Planck potential difference, in the second parentheses.

Assuming the gaseous phase being the mix of perfect gases, it may be demonstrated (we will not do this for the lack of space) that the motive force of the interphase mass transfer, X, can be presented in the form

$$X_{CO_2} = C_{p,CO_2} \ln \frac{T_1}{T_2} + 2R \ln \frac{p_{2,CO_2}}{p_{1,CO_2}} \qquad (6)$$

where C_{p,CO_2} is the CO_2 specific heat capacity on a mole basis in the temperature range between T_1 and T_2.

To simplify the expression of dissipative function we note that it has been derived under rather general assumptions and is valid for both dependent and independent flows and forces. In our case, with the mass transfer being the direct consequence of the chemical reaction, it may be maintained that the molar diffusion flow never exceeds the reaction rate, i.e.,

$$d_e n_{CO_2}/d\tau \leq d\xi/d\tau$$

Moreover, from the general physical considerations it may be concluded that the system tends to assume a state where

$$d_e n_{CO_2}/d\tau = d\xi/d\tau = dn/d\tau \qquad (7)$$

where $dn/d\tau$ is the decarbonation reaction rate.

In view of (7) and the affinity of the decarbonation reaction $A = RT \ln(p_{2,CO_2}/p_{1,CO_2})$, the dissipative function (5) rewrites as

$$\frac{d_i S}{d\tau} = \frac{dQ}{d}\left(\frac{1}{T_2} - \frac{1}{T_1}\right) + \frac{dn}{d}\left(3\frac{A_2}{T_2} + C_{p,CO_2} \ln \frac{T_1}{T_2}\right) \qquad (8)$$

It is worth noting an important feature of (8), namely, the right-hand side is the sum of products of scalar quantities, that is, all the flows and generalized forces are

tensors of the same, zero rank.

Thus we have demonstrated that for a gaseous suspension whose solid phase comprises a mechanical mix of neutral compounds and calcium carbonate being decarbonated through one reaction, the dissipative function has a bilinear form in which $dQ/d\tau$ and dn/τ are the generalized flows (heat flux, reaction rate), and $X_T = (1/T_2 - 1/T_1)$ and $X_A = \left[3A_2/T_2 + C_{p,CO_2} \ln(T_1/T_2)\right]$ are the generalized thermodynamic forces.

For the dissipative function (8), the linear kinetic relationships that the linear NET asserts to exist between the generalized flows and forces can be written in the form

$$\frac{dQ}{d\tau} = L_{11}\left(\frac{1}{T_2} - \frac{1}{T_1}\right) + L_{12}\left(3\frac{A_2}{T_2} + C_{p,CO_2}\ln\frac{T_1}{T_2}\right) \quad (9)$$

$$\frac{dn}{d\tau} = L_{21}\left(\frac{1}{T_2} - \frac{1}{T_1}\right) + L'_{22}\left(3\frac{A_2}{T_2} + C_{p,CO_2}\ln\frac{T_1}{T_2}\right)$$

where L_{ij} are the phenomenological coefficients connected by Onsager's reciprocity relation, $L_{12} = L_{21}$.

The set of equation (9) provides a complete phenomenological description for the transfer processes and chemical kinetics in a gaseous suspension with a decarbonation reaction in the solid phase. The first equation in (9) may be used to derive the cross-coefficient $L_{21} = L_{12}$ on the base of experimental data. Before we embark on this determination we would like to clarify the physical meaning of the direct coefficient L_{11}.

In the absence of chemical reactions

$$dQ/d\tau = L_{11}(1/T_2 - 1/T_1) \quad (10a)$$

On the other hand, the heat flux can be expressed via the heat transfer coefficient

$$dQ/d\tau = \alpha_F\, a(Mn_0/K)(T_1 - T_2) \quad (10b)$$

where α_F is the heat emission coefficient, a the specific surface of solid phase particles containing one mole of $CaCO_3$, K the initial mass concentration of $CaCO_3$ in the solid phase, n_0 the initial content of $CaCO_3$ on a mole basis, and M the molecular weight of $CaCO_3$.

Comparing (10a) and (10b) yields

$$L_{11} = \alpha_F a(n_0/K)T_2T_1 \quad (11)$$

The heat transferred from the gaseous phase is expended on the endoeffect of the reaction and on the heating of the solid phase from the initial temperature to the temperature of the onset of the reaction, T_{eq}, and then from T_{eq} to T_1:

$$Q = H_T n + \frac{Mn_0}{K} C\,(T_{eq} - T_0) + \left(\frac{Mn_0}{K} - 0.44Mn\right)(c(T_1 - T_{eq})$$

whence

$$\frac{dQ}{d\tau} = \frac{dn}{d\tau}\left[\Delta H_T - 0.44MC(T_1 - T_{eq})\right]$$

The difference $T_1 - T_{eq}$ is normally small so that the second term in the brackets may be safely neglected and, returning to the first equation in (9), we get

$$L_{12} = L_{21} = \frac{H_T}{X_A}\frac{dn}{d\tau} - \frac{\alpha_F a n_0 (T - T_2)}{K X_A} \quad (12)$$

With experimental data on hand this equation can be used to determine the cross coefficients.

The coefficient L'_{22} can be derived from the second equation in (9). It should be taken into account that no matter what the in-

terphase heat transfer, the rate of the reaction is proportional to the number of nonreacted moles of $CaCO_3$. Introducing a modified L_{22} coefficient as $L'_{22} = L_{22}(n_0-n)$ carries the second equation of the set to

$$dn/d = L_{21}X_T + L_{22}(n_0 - n)X_A \qquad (13)$$

Solving this linear differential equation under the initial conditions $\tau = 0$ and $n = 0$ we get for the degree of decarbonation φ

$$\varphi = \frac{n}{n_0} = \left(\frac{1}{n_0}\,\frac{L_{12}}{L_{22}}\,\frac{X_T}{X_A} + 1\right)(1 - e^{-L_{22}X_A}) \qquad (14)$$

This equation describes the kinetics of decarbonation. It is based on the linear thermodynamics of irreversible processes and takes into account mutual influence of the processes of heat and mass transfer and the decarbonation reaction proper. The validity region for this equation is where the process of interphase heat transfer in a gaseous suspension is governed by the interphase heat transmission resistance rather than by the internal heat-transfer resistance of the solid particles. This domain is rather well investigated and treated in many courses on heat transfer theory.

A. OSSOKIN,
E. POTAPOVA, Institut de génie chimique Mendéléev de Moscou, URSS

1

FORMATION DE MINERAUX DANS LES BAINS FONDUS

1.1

Les auteurs analysent la corrélation entre la structure, les propriétés de la matière fondue et la cinétique de la formation de minéraux. Suivant la nature et la concentration des modifiants, il y a formation, au sein du grain de clinker, d'une matière en fusion constituée d'oxydes ou d'oxydes et de sels, dont les propriétés sont déterminées par les rapports quantitatifs des éléments dans le volume local du granule de clinker en formation. L'apparition d'un constituant salin est due aux phénomènes de lamellation. La tendance à la ségrégation s'accentue avec l'accroissement de l'acidité des éléments p et de la basicité des éléments s. Suivant la concentration d'ions, il se produit une microlamellation ou une macrolamellation, on observe dans les phases coexistantes une solubilité mutuelle des constituants. Dans les sels fondus à haute mobilité, il se produit une dissolution intense des oxydes du clinker fondu et une synthèse de silicates de calcium. On a établi qu'il y a variation de la cinétique et du mécanisme de formation de minéraux en fonction de la composition des matières fondues lamellées. La régulation de la composition et des propriétés de la matière en fusion et du rapport entre les phases lamellées permet d'intensifier la formation de minéraux tout en optimisant la microstructure des clinkers.

Os autores analisam a correlação entre a estrutura, as propriedades da matéria fundida e a cinética da formação de minerais. Segundo a natureza e a concentração dos modificantes, há formação, no interior do grão de clínquer, de uma matéria em fusão constituída de óxidos ou óxidos e sais, cujas propriedades são determinadas pelas relações quantitativas dos elementos no volume local do grão de clínquer em formação. O aparecimento de um constituinte salino é devido aos fenômenos de lamelação. A tendência à segregação se acentua com o aumento da acidez dos elementos p e da basicidade dos elementos s. Segundo a concentração de íons, produz-se uma microlaminação ou uma macrolaminação, observa-se nas fases coexistentes uma solubilidade mútua dos constituintes. Nos sais fundidos de alta mobilidade, produz-se uma dissolução intensa dos óxidos do clínquer fundido e uma síntese de silicato de cálcio. Mostrou-se que há variação da cinética e do mecanismo de formação de minerais em função da composição das matérias fundidas lamelares. A regulação da composição e das propriedades da matéria em fusão e da relação entre as fases lamelares permite intensificar a formação de minerais e ao mesmo tempo otimisando a microestrutura dos clínqueres.

A. OSSOKIN,
E. POTAPOVA

Le processus de formation de minéraux représente un ensemble d'interactions acide-base se déroulant dans des bains fondus de composition différente. En fonction de la nature et de la concentration des modificateurs (F, Cl, S, Mg et autres) dans le grain de clinker se forment des bains fondus d'oxyde ou d'oxyde-sel dont les propriétés sont déterminées par le rapport des éléments contenus dans le volume local de la granule de clinker en formation. Une régulation de la micro- et de la macrostructure du bain fondu de clinker grâce à une introduction de modificateurs permet de modifier sensiblement ses paramètres (viscosité, tension superficielle, densité et mobilité d'ions) [1, 2] ce qui influence la cinétique des processus de formation de minéraux.

Lorsque la teneur en R_2SO_4 (où R^+ est K^+ ou Na^+) dépasse 1 % en masse, il se produit une microlamellation du bain fondu de clinker. Les dimensions des zones de lamellation augmentent de $(0,6\text{-}1,3)\cdot10^3$ Å (1 % en masse de K_2SO_4) à $(1\text{-}3)\cdot10^3$ Å (1 % en masse de Na_2SO_4) (fig. 1, a) à mesure que l'électronégativité des cations (des s-éléments) diminue. Quand la concentration de R_2SO_4 dépasse 3 % en masse, la microlamellation passe en macrolamellation: la phase saline se sépare de celle d'oxyde. En additionnant au bain fondu en lamellation à un cation fort un composant où le cation est plus faible, on le voit se répartir entre les phases correspondantes ce qui conduit à une augmentation de l'énergie superficielle du bain fondu et à une modification de ses propriétés. Pour cette raison, à l'introduction de l'oxyde de magnésium dans un bain fondu de sulfate-alcali en lamellation, la solubilité des sulfates alcalins augmente dans la composante d'oxyde tandis que les phénomènes de lamellation faiblissent. Ainsi, en présence du complexe R_2O+ MgO+SO_3 (le rapport entre les éléments étant: R_2O:MgO:SO_3 = 1:11:8) dans un bain fondu, on ne constate pas de macrolamellation dans ce dernier. Une modification du rapport indiqué entre les éléments conduit à une formation de nouveaux complexes qui provoque un changement des propriétés du bain fondu aboutissant à sa ségrégation (fig. 1, b).

Les phénomènes de lamellation sont observés dans les bains fondus halogénés à des concentrations d'anions plus basses que dans les bains fondus sulfatés et même en présence de cations alcalino-terreux seulement. Les bains fondus fluorés se lamelle à des concentrations de F^- égales à 1 % en masse (la dimension des gouttes étant de $(2\text{-}3)\cdot10^3$ Å) et les bains fondus chlorés à une plus grande concentration d'ions (3 % en masse). La loi analogue est propre également aux bains fondus additionnés d'eutectiques salines. Les domaines de lamellation propres aux verres fluorés ont un aspect de gouttes dont les dimensions diminuent de $(6\text{-}12)\cdot10^3$ Å (pour 1 % en masse de CaF_2+ $CaSO_4$) (fig. 1, c) à $(0,5\text{-}1,0)\cdot10^3$ Å (pour 1 % en masse de CaF_2+$CaCl_2$). Les bains fondus composés d'oxydes et de sels formés par suite de la lamellation sur la base des systèmes R_2O+$CaSO_4$+MgO, $CaCl_2$+$CaSO_4$, CaF_2+$CaSO_4$ et d'autres sont caractérisés par une viscosité inférieure d'un ou de deux ordres et par une tension superficielle deux ou quatre fois inférieure à celles des bains fondus d'oxydes formés dans le système C-A-F-S. Aussi, leur présence contribue-t-elle à intensifier les processus de dissolution et de cristallisation des minéraux.

Au sein des bains fondus a lieu un processus de dissolution mutuelle des composants du bain fondu d'oxyde et de celui de sel. Cependant, contrairement aux données de Glasser (3), dans les bains fondus salins ayant pour base R_2SO_4 il se produit la dissolution de 5,90 à 5,95 % en masse de CaO et de 1,3 à 1,4 % de SiO_2 tandis que les oxydes de Al et de Fe sont pratiquement insolubles. La concentration de CaO dans les bains fondus à la base des complexes R_2SO_4+ $MgSO_4$; $Na_2SO_4\cdot3MgSO_4$; $K_2SO_4\cdot2MgSO_4$ constitue de 13,49 à 13,78 %. D'autre part, on y constate une augmentation de la teneur en SiO_2 de 1,93 à 2,31 % et la dissolution de

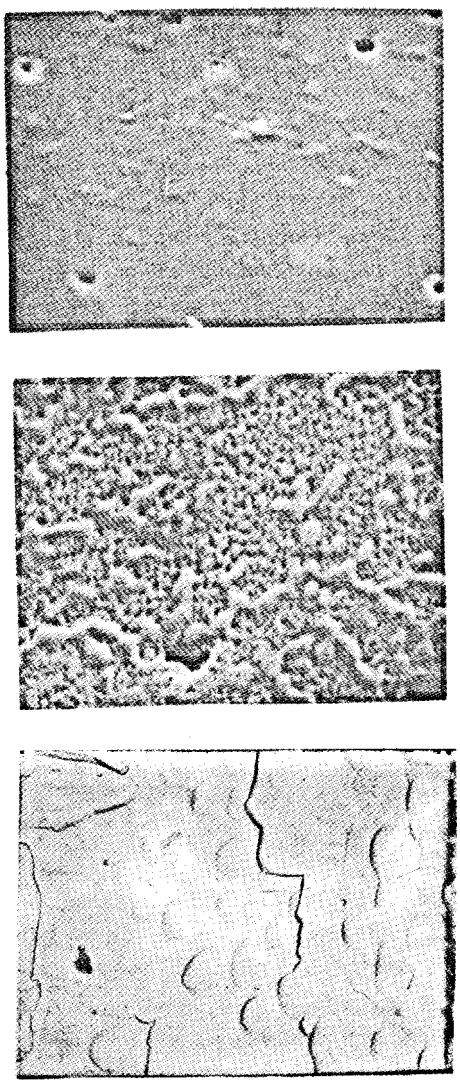

Fig. 1. Microstructure des verres de clinker obtenus par un brusque refroidissement des bains fondus contenant (% en masse): a - $2Na_2SO_4$; b - $K_2SO_4 \cdot 2MgSO_4$; c - $1CaF_2+CaSO_4$

Al_2O_3 et Fe_2O_3 en quantités de 0,19 à 1,09 %. La solubilité du CaO entrant dans les bains fondus composés de CaF_2+CaSO_4, $CaCl_2+CaSO_4$, CaF_2+CaCl_2 varie de 8,21 à 15,38 % avec un accroissement de la température dans une gamme de 1223 à 1500 K. La solubilité maximale du CaO (12-150) à 1373-1573 K est observée dans le bain fondu salin basé sur $CaCl_2+CaSO_4$. Ses valeurs diminuent à un remplacement successif des anions dans la série $Cl^- - F^- - SO_4^{2-}$. Dans des bains fondus salins à haute mobilité le CaO se dissout plus intensivement grâce à quoi ils remplissent la fonction d'un milieu de transport pour les cations de calcium qui se diffusent dans des domaines locaux enrichis de composants siliciés où se produit la formation et la cristallisation d'alite. Ainsi, par suite de la cristallisation des bains fondus de sulfate-alcali, il se forme de 5 à 10 % de silicates de calcium lesquels constituent des composants de cristallisation lors de la synthèse des C_2S et C_3S dans un bain fondu d'oxyde.

Le processus de formation d'alite est contrôlé par la vitesse de diffusion d'ions de calcium dans le bain fondu (1, 2, 4, 5). Une étude de la vitesse de diffusion de Ca^{2+} dans des systèmes multiples a montré que la valeur du coefficient de diffusion efficace (D_{Ca}) varie de $1,12 \cdot 10^{-9}$ à $2,82 \cdot 10^{-9}$ m^2/s en fonction de la composition des systèmes en diffusion mutuelle, de la température et du temps de frittage isothermique. La modification du bain fondu de clinker aboutit à une augmentation de la vitesse de diffusion de Ca^{2+}. Ainsi, à une introduction dans le bain fondu de 3 % en masse de CaF_2+CaSO_4 et $R_2O+MgO+SO_3$, les valeurs de D_{Ca} augmentent de $2,50 \cdot 10^{-9}$ à $21,3 \cdot 10^{-9}$ et à $4,1 \cdot 10^{-9}$ m^2/s respectivement en se soumettant à la loi de Stokes-Einstein.

La nature de l'influence des éléments sur les processus de formation de minéraux concorde avec leur action sur les propriétés structurales et sensibles du bain fondu de clinker et est conditionnée tant par la variation de la viscosité de la composante d'oxyde que par l'apparition de zones de lamellation de la composition saline (fig.2,3). En présence de Mg^{2+} le degré de fixation accroît intensivement à mesure de l'augmentation de la teneur en MgO proportionnellement à la réduction de la viscosité du bain fondu par suite d'une augmentation de la vitesse de dissolution de CaO et C_2S et de la diffusion des ions Ca^{2+} et SiO_4^{4-} (6). Mais lorsqu'on introduit des sulfates alcalins le processus de formation d'alite croît d'inten-

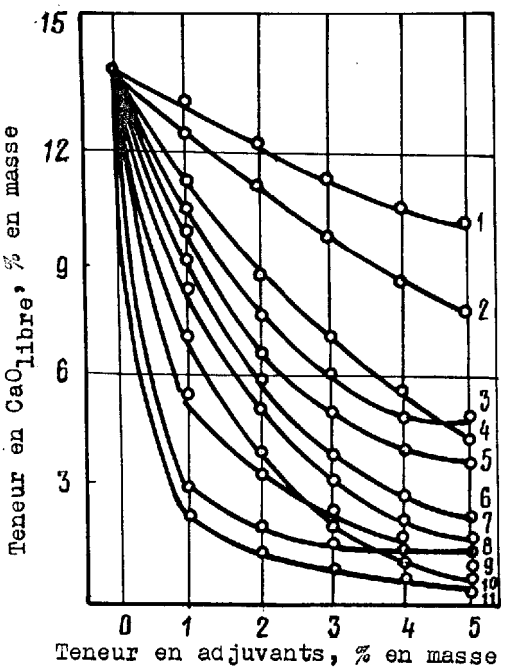

Fig. 2. Influence de la teneur en adjuvants sur la fixation du CaO libre en présence de: 1 - Na_2SO_4; 2 - $K_2SO_4 \cdot 2MgSO_4$; 3 - $R_2SO_4+MgSO_4$; 4 - MgO; 5 - Na_2SO_4; 6 - $R_2O+MgO+SO_3$; 7 - Cl; 8 - $CaCl_2+CaSO_4$; 9 - CaF_2+CaSO_4; 10 - CaF_2+CaCl_2; 11 - F (T=1573 K; τ= 20 min)

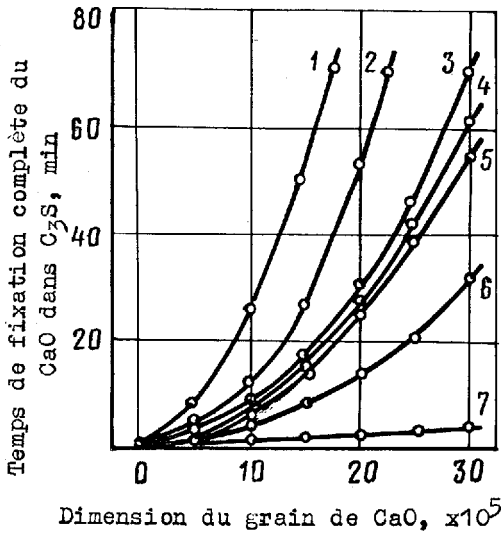

Fig. 3. Influence de la dimension moyenne du domaine de l'oxyde de calcium sur la durée de la formation d'alite dans des bains fondus contenant de divers éléments: 1 - R_2O; 2 - bain fondu de départ; 3 - MgO; 4 - SO_3; 5 - $R_2O+MgO+SO_3$; 6 - F; 7 - CaF_2+CaSO_4

sité, essentiellement, grâce à une accélération sensible des réaction de dissolution de C_2S à la suite d'un changement de son mécanisme en présence de R^+ (1). A une réduction de la viscosité du bain fondu le degré de transformation du CaO augmente mais cette loi est perturbée avec l'apparition de bains fondus salins. Dès que le bain fondu commence à augmenter sa tendence à la ségrégation dans la série $R_2O+MgO+SO_3$ - $Na_2SO_4 \cdot 3MgSO_4$ - $R_2SO_4+MgSO_4$ - $K_2SO_4 \cdot 2MgSO_4$ - Na_2SO_4 on observe un ralentissement du processus de fixation de l'oxyde de calcium (fig. 2) ce qui concorde avec l'influence des cations sur la liquation de Mg - Na - K. Cette loi est déterminée par une solubilité réduite de Ca et la vitesse de dissolution de CaO dans les bains fondus sulfates-alcalis. La suppression de la macrolamellation contribue à une activisation du processus. Etant donné que pour le système $R_2O+MgO+SO_3$ la macrolamellation est observée à une teneur en oxydes (plus de 3 % en masse) plus grande que pour d'autres compositions sulfate-alcali, cette propriété s'exprime par sa capacité catalytique maximale. A noter qu'avant l'apparition de la lamellation le processus se déroule intensivement tandis qu'à l'apparition de bains fondus salins (la concentration du complexe étant supérieure à 3 % en masse) le processus ralentit.

Dans les bains fondus halogénés les phénomènes de lamellation catalysent le processus de formation d'alite et le degré de fixation de l'oxyde de calcium (fig. 2) accroît par suite d'un remplacement des ions dans la série $SO_4^{2-} \rightarrow Cl^- \rightarrow F^-$ qui concorde avec la série typique pour l'amplification de la capacité de lamellation du bain fondu de clinker. A des concentrations absolues égales, l'efficacité maximale revient au F, mais les compositions des systèmes eutecti-

ques salins dépassent considérablement, au point de vue de l'intensité, son influence individuelle (fig. 2). Ainsi, à une introduction de F^- dans un bain fondu, le temps de l'assimilation complète du grain de l'oxyde de calcium de 40 mm de dimension diminue de 52 à 14 min (fig. 3). Dans le bain fondu d'oxyde-sel $CaF_2 + CaSO_4$ la durée de frittage diminue pratiquement 5 fois (τ = 3 min).

Une analyse et un traitement mathématique des relations cinétiques obtenues ont permis de proposer une équation à l'aide de laquelle il est possible d'apprécier la durée de frittage requise du clinker de ciment Portland pour une assimilation du grain (du domaine) de l'oxyde de calcium de dimension requise en fonction des propriétés des phases de réaction. Dans l'ensemble, l'équation se présente sous l'aspect suivant: $\tau = K_1 \cdot K_2 \cdot \eta^2 \cdot r_o^2$, où K_1 est la constante déterminée par les propriétés des phases solides; K_2 est la constante qui dépend de la quantité de bain fondu; η est la viscosité; r_o est la dimension des grains de CaO.

La nature de l'influence de la composition et des propriétés des bains fondus d'oxydes-sels sur la microstructure des clinkers concorde avec la variation de la vitesse de dissolution et de cristallisation des minéraux. En présence d'un bain fondu d'oxyde à haute mobilité ou de domaines halogénés on constate que $I_{CaO} > I_{C_2S}$ et la vitesse de réaction est déterminée par la dissolution du silicate bicalcique tandis que l'alite à cristallinité moyenne se forme dans les domaines enrichis de C_2S. A une apparition de bains fondus de sulfates-alcalis $I_{C_2S} > I_{CaO}$ et la réaction est limitée par la vitesse de dissolution de l'oxyde de calcium tandis que le clinker formé est caractérisé par une structure à gros cristaux. Une suppression de la lamellation de sulfates-alcalis et une régulation du rapport entre les vitesses de dissolution de CaO et C_2S permettent d'intensifier le processus de formation d'alite et contribuent à une formation de la structure à cristaux moyens des clinkers.

De cette façon, les phénomènes de liquation catalysent le processus de formation de minéraux dans les bains fondus halogénés. L'effet catalyseur maximal s'obtient en présence de bains fondus salins complexes ce qui permet de les utiliser en qualité de milieu réactif pour la formation de la phase d'alite. La régulation de la composition et des particularités du bain fondu et du rapport entre les phases en lamellation permet d'intensifier le processus de formation de minéraux en combinaison avec l'optimisation de la microstructure des clinkers. La synthèse des clinkers dans les bains fondus en lamellation constitue une méthode efficace de réduction de la consommation d'énergie et d'augmentation de la qualité du ciment Portland.

REFERENCES

1. Тимашев В.В., Осокин А.П. Химия высокоосновных алюмоферросиликатных расплавов. Обзорная информация. – М.: ВНИИЭСМ, 1980. – 64 с.
2. Тимашев В.В., Осокин А.П. Физико-химические основы формирования структуры и свойств клинкера. – Цемент, 1982, № 9, с. 4-6.
3. Glasser F.P., Marr I. Sulfates in cement clinkering immishribility between sulfates and oxyde melts: at 1350°C. – Cem. and Concr. Res., 1980, v. 10, – No. 6, p. 753-758.
4. Timashev V.V. The kinetik of clinker formation. The structure and composition of clinker and its phases. – 7 Internat. Congress of the Chemistry of Cement. – Paris, 1980, v. 1, p. 3/1-28.
5. Johansen V. Model for Reactions Between CaO Particles and Portland Cement Clinker. – J. Amer. Ceram. Soc., 1973, v. 56, No. 9, p. 450-454.
6. Timashev V.V., Osokin A.P., Potapowa E.N. Mechanism and kinetik of crystall in the mikrovolumes of clinker grains. – 7 Internat. Congress of the Chemistry of Cement. – Paris, 1980, v. 2, p. 1/241-246.

T.V. KUZNETSOVA, 1
I.A. BRYTOV,
N.A. KOZYREVA,
B.SH. IVANOV,
I.I. KISELYEVA,
E.A. TSUKERMAN, Mendeleyev Institute of Chemical Technology, Moscow, USSR 1.1
Burevyestnik Research and Production Agglomerate, Leningrad

AUGER ELECTRON SPECTROSCOPIC STUDY OF CALCIUM SILICATES AND ALUMINATES

To date Auger spectroscopy has not been applied to analysis of calcium silicates and aluminates. The use of the indium matrix procedure and electron beams with energies below 3 keV enable us to obtain stable surface charging for a number of minerals of interest: C_3S, γ-C_2S, β-C_2S, C_3A, CA, and CA_2. The reference lines has been those of C, Ar, and In. Different spectra and amount of charging for the studied minerals have been identified and a number of additional bands and satellite lines in the fine structure of the spectra have been assigned. Comparison of the spectra of the same elements in silicates and aluminates has revealed relative shift of the peaks with respect to the position of the pure element line.

These studies lead us to conclude that the structure of minerals affects their Auger spectra, specifically, that the coordination sphere of the elements influences the shape, half-width and position of lines, and that the fine structure of the spectrum may be connected with the electron density distribution in a valence band within the surface layer of 15-20 Å.

Até hoje a spectroscopia Auger não foi aplicada à análise dos silicatos de cálcio e aluminatos. O uso do procedimento da matrix de indium e feixes de electron com energia abaixo de 3 keV permite-nos a obtenção de uma superfície de carga estável para certo número de minerais de interesse: C_3S, γ-C_2S, β-C_2S, C_3A, CA e CA_2. As linhas de referência são ao do C, Ar e In. Diferentes espectros e quantidades de carga para os minerais estudados foram identificados e um certo número de faixas adicionais e linhas satélites na estrutura fina dos espectros foram assinaladas. A comparação dos espectros dos mesmos elementos nos silicatos e aluminatos revelou deslocamentos relativos dos picos em relação a posição da linha do elemento puro.

Esses estudos levam à conclusão que a estrutura do mineral afeta seu espectro Auger, especificamente, que a esfera de coordenação dos elementos influencia a forma, a meia-largura e a posição das linhas, e que a estrutura fina do espectro pode ser relacionada com a distribuição da densidade dos electrons numa faixa de valência na camada superficial de 15-20 Å.

T.V. KUZNETSOVA,
I.A. BRYTOV,
N.A. KOZYREVA,
B.SH. IVANOV,
I.I. KISELYEVA,
E.A. TSUKERMAN

Prior to this study we have not been able to trace in the literature any report concerning Auger electron spectroscopy (AES) applied to calcium silicates and aluminates, the basic mineral components of cementitius materials. We undertook the AES investigation of these minerals to evaluate the feasibility of using AES for analysis of a broader class of such minerals and to resolve the basic methodological problems on the way to such an expansion.

The compound composition of the studied polycrystalline specimens was as follows: Ca_3SiO_5 (C_3S), ß-, γ-Ca_2SiO_4 (C_2S), $Ca_3Al_2O_6$ (C_3A), $CaAl_2O_4$ (CA), and $CaAl_4O_7$ (CA_2). The reference specimens were pure poly- and monocrystalline silicon, α-quartz, calcium hydroxide, graphite, and Al, Al_2O_3, $Al(OH)_3$ and hydrocarbon films.

Integral spectra were recorded over the range from 0 to 1650 eV for silicates and from 0 to 1500 eV for aluminates; in both cases E_p = 2 keV, I_p = 80 nA, and sweep speed = 50 eV/s. Fine structure fragment spectra were recorded at a sweep rate of 5-10 eV/s with an energy resolution of 0.27%, in the following bands: 0-60 eV for Al, 0-90 eV for Si, 200-350 eV for Ca, and 450-550 eV for O. The electron probe was 2-5 µm diameter.

The crucial problem in AES investigation of dielectrics, to which the studied compounds belong, concerns the removal, compensation or account of the electrostatic charge /12/ that occurs on the sample being irradiated by an electron beam. The gradually accumulating charge causes the Auger lines to shift by a few electronvolts thus hampering the chemical shift evaluation.

After a number of attempts to prepare specimens for the study - securing large pieces in a holder, fixing finely chipped platelets of minerals, etc. - we recognized the most suitable preparation technique being the indentation of fine chips or powder (prepared by slowly grinding these minerals in agate mortar) of the minerals to be studied into an indium matrix. This procedure stabilized surface charging so that the reference lines of C, Ar, and In, appearing in different spectral bands, occurred shifted by the same value relative to their no-charge counterparts.

It may be recalled that a layer of carbon or hydrocarbons on the surface of specimen holders and the dielectric specimen is in electrical equilibrium until electron bombardment occurs. An electron bombardment upsets this equilibrium, and the true amount of charge may be inferred from the difference of carbon KLL-lines from the hydrocarbon layers on the specimen and on the holder electrically connected with the spectrometer frame. Even most accurately performed, this method, however, is not free from errors which may be incurred by the carbon being oxidated when affected by the electron beam. This results in a shift of both KLL-lines, from the specimen and the holder, with respect to the line of pure carbon.

To eliminate this error we made use of the Ar LMM-line at 215 eV which is recorded in ionically purified specimens. Argon is inert, so the position of its line is fairly reliable and not subject to any inflicted chemical chifts. We also employed for this purpose the MNN-line of indium at 405 eV, recorded both in a point near the holder and in a point of the specimen's contact with the indium matrix. This triple reliability check provided a basis for accurate measurements of the shifts due to specimen charging.

The spectra of certain elements from cement clinker minerals consist of single peaks appearing very close to each other on the energy scale; for example, the B transition is at 179 eV, and that for Cl at 181 eV. To assign such peaks we took account of the different lineshapes in the respective pure-element spectra. For instance, a large negative swing is typical of the boron lineshape whereas the clorine Auger peak is practically symmetrical about the background level.

The Auger line analysis in the spectra

T.V. KUZNETSOVA,
I.A. BRYTOV,
N.A. KOZYREVA,
B.SH. IVANOV,
I.I. KISELYEVA,
E.A. TSUKERMAN

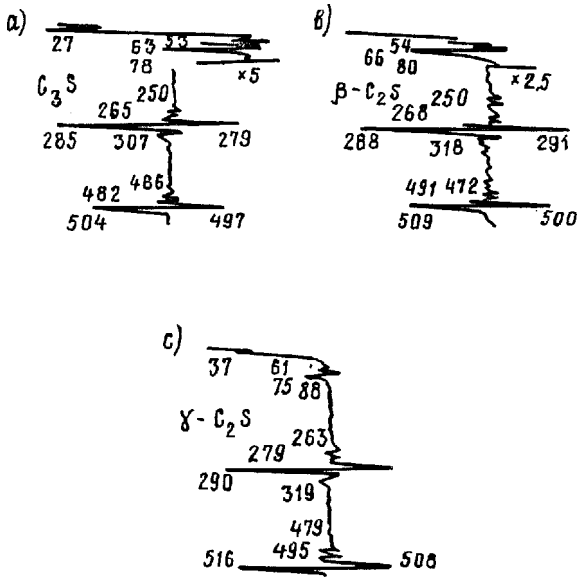

Fig. 1. Spectra Auger of calcium silicates a) C_3S; b) β-C_2S; c) γ-C_2S

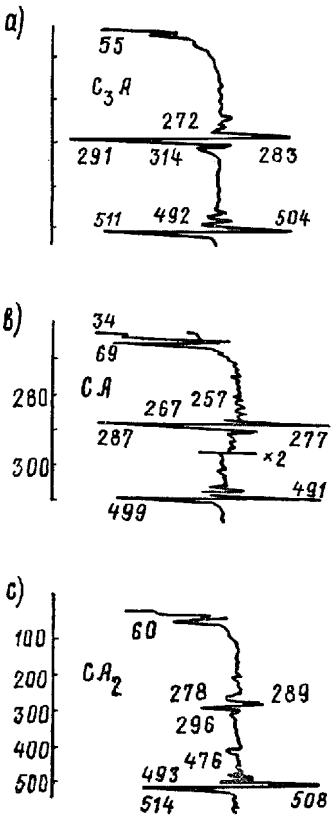

Fig. 2. Spectra Auger of calcium aluminates a) C_3A; b) CA; c) CA_2

of the minerals took account of the fact that the available reference data for the positions of pure element lines are prone to significant errors. The spectrum albums /1-4/ and some other references quote the line positions of the same elements differing by up to 5 eV. This discrepancy may be attributed to the fact that the researchers might have used substances of various purity, or containing different admixtures, or reported line positions from various compounds without due account of the chemical chifts, or used different, and probably inadequate, methods of accounting for specimen charging. To avoid these misfortunes, we employed a comparative analysis in which the spectra of investigated coumpounds were compared with the spectra of the respective reference materials. The reference materials were the parent materials for the clinker minerals being investigated. The spectra of the studied minerals and reference compounds were run simultaneously and in the same experimental conditions. The Auger spectra of calcium silicates exhibited different values of charging for different compounds: 9 eV for Ca_3SiO_5, -7 eV for β-Ca_2SiO_4, and -5 eV for α'-Ca_2SiO_4; given identical recording conditions, the value of a charging was reproduced accurate to within ± 1 eV. This experimental finding, never noted before, may be an indicative of the charging being an individual characteristic of the electronic structure of these minerals.

Figures 1-6 show the Auger spectra of calcium silicates and aluminates. Figs. 7-10 plot fragments of these spectra to reveal the fine structure.

In the calcium silicate spectra we tracked the following lines: $M_{2,3}VV$ and $L_{2,3}M_{2,3}M_{2,3}$ for calcium; $L_1M_1M_1$, L_3M_1V and $L_{2,3}VV$ for silicon; and KL_1L_1, KL_1V and KVV lines for oxygen. The same oxygen lines were traced in the aluminate spectra, but the $M_{2,3}VV$ line of calcium was not traced becau-

T.V. KUZNETSOVA,
I.A. BRYTOV,
N.A. KOZYREVA,
B.SH. IVANOV,
I.I. KISELYEVA,
E.A. TSUKERMAN

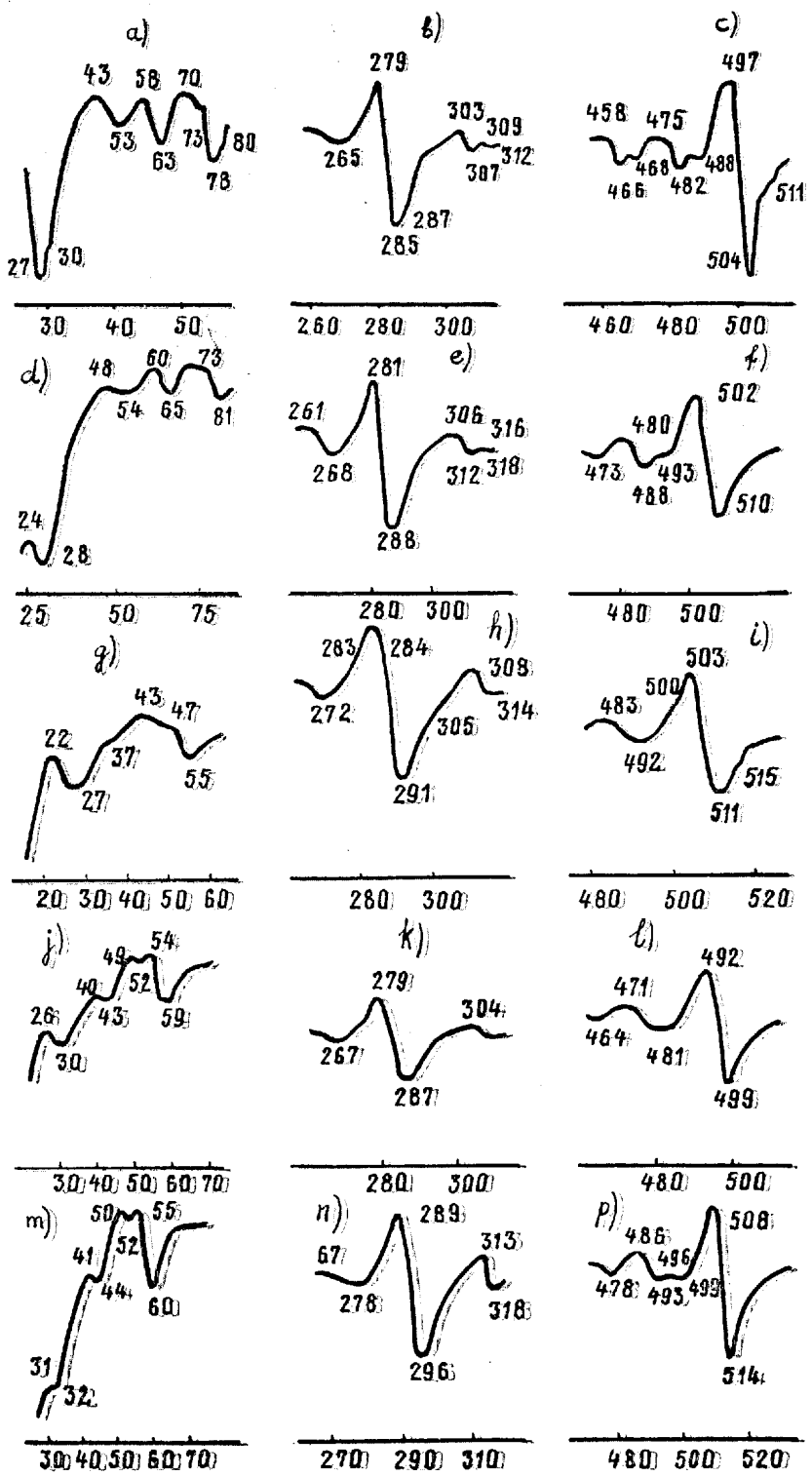

Fig. 3. Fragments of spectra Auger of fine structure
a, b, c – C_3S; d, e, f – βC_2S; g, h, i – C_3A; j, k, l – CA; m, n, p – CA_2

se of intense background. Aluminium lines were recorded in the following positions: $L_{2,3}M_1M_1$, $L_1L_{2,3}M_1$, $L_3M_1M_1$, and $L_1M_1M_1$. Also observed in the spectra of aluminates and silicates were satellite lines /8/ and a number of additional peaks, revealed after a fine structure analysis of the fragment spectra, which cannot be traced to the effect of plasmon losses /9/.

Comparison of the silicate and aluminate spectra reveals changes in lineshape and various relative shifts of the same lines relative to the lines of the pure elements. The pure calcium line $L_{2,3}M_{2,3}M_{2,3}$ is observed as the dublet of $L_3M_{2,3}M_{2,3}$ and $L_2M_{2,3}M_{2,3}$ at 291 and 294 eV. No dublet splitting was observed in the silicate and aluminate spectra, the $L_{2,3}M_{2,3}M_{2,3}$ line being recorded at 285 eV for C_3S, at 288 eV for ß-C_2S, and at 298 eV for γ-C_2S. A similar shift was found for the $KL_{2,3}L_{2,3}$ oxygen line which for the respective minerals was found at 504, 509, and 516 eV. The same phenomenon was observed for silicon peaks (identified in the figures). The uncertainty of ±1 eV fails to include the experimentally observed shifts of the Auger lines studied. To illustrate, the calcium lines $L_{2,3}M_{2,3}M_{2,3}$ and $M_{2,3}N_{1,2}N_{1,2}$ of C_3S and γ-C_2S appear at 258 eV and 261 eV, respectively. The spacing between oxygen lines also changed from one compound to another. It was only the position of the silicon lines that remained practically unchanged.

The ratio of intensities of calcium and silicon lines varies insignificantly for silicates; the pattern of relative intensities of calcium and oxygen lines is similar for C_3S and ß-C_2S, whereas for γ-C_2S the relative intensity of oxygen line increases almost 1.5 times.

The purity of the aluminate series studied, C_3A, CA, and CA_2, was tested by x-ray analysis. An x-ray phase analysis revealed that the CA sample contained some CA_2 and vice versa. The C_3A sample was found to be x-ray pure. Comparison of Auger spectra within the series C_3A, CA, and CA_2 indicates the presence of chemical shifts for most lines: the KVV oxygen line was recorded respectively at 511, 499, and 514 eV; the $L_{2,3}M_{2,3}M_{2,3}$ calcium line, at 291, 287, and 296 eV; the $L_3M_1M_1$ aluminium line, at 55, 59, and 60 eV. For comparison, the literature positions /1/ of these lines for pure Al and Ca are 68 eV and 292 eV, respectively; no reference can be quoted for oxygen, as in the literature its lines are documented for different compounds.

To exclude the possibility of error due to charging of the specimens, we took for analysis the energy intervals between the lines of oxygen and calcium, and oxygen and silicon, in the same way as we did for silicates. In the series C_3A, CA, and CA_2, these differences amounted respectively to 220, 212, 218 eV, and 456, 440, and 454 eV. Differences between the aluminate spectra are quite obvious, the relative shifts for the respective lines in the CA and CA_2 spectra being smaller compared to the C_3A spectrum.

The performance and resolution of modern AES spectrometers are such that in addition to line positions, one can compare linewidth, lineshape and some subtle spectral features, say additional lines due to plasmon losses /8-12/. Comparison of the lineshapes in the aluminate spectra indicates that CA and CA_2 have more in common that either of them with C_3A. Note also that the inflexion maxima in the low energy part of CA, CA_2, and C_3A spectra are more clear cut than in the high energy portion of C_3A spectrum and in the ß-C_2S spectrum. These spectral features and the unambiguous distinction of line positions in the ß- and γ-C_2S spectra lead us to speculate on the bearing of the structure of minerals on their Auger spectra, specifically, to conclude that the coordination sphere of elements influences the lineshape, linewidth and position of their Auger lines. It is not unlikely also that there exist a correlation between the distribution of electron density over the material structure and the

T.V. KUZNETSOVA,
I.A. BRYTOV,
N.A. KOZYREVA,
B.SH. IVANOV,
I.I. KISELYEVA,
E.A. TSUKERMAN

features of the Auger spectrum.

The elucidated experimental findings suggests that AES is an efficient and fruitful method for analyzing cement minerals and similar compounds. They demonstrate a higher potential of Auger spectroscopy for the investigation of materials with low electric conductivity than has been recognized by most researchers in the field until recently.

REFERENCES

1. P.W. Palmerg, C.E. Riach, P.E. Weber, N.C. McDonald: Handbook of Auger Electron Spectroscopy (PHI Inc., Minn. 1972).
2. L.E. Dairs, N.C. McDonald, P.W. Palmberg, C.E. Riach, R.E. Weber: Handbook of Auger Electron Spectroscopy (PHI Inc., Minn. 1976).
3. G.E. Mc Guire: Auger Electron Spectroscopy References Manual (Plenum Press, New York, 1979).
4. T. Sekine, Y. Nagasawa, M. Kudoch, Y. Sakai, A.S. Parkes, J.D. Geller, A. Mogami: Handbook of Auger Electron Spectroscopy (JEOL, 1982).
5. T.A. Carlson: Photoelectron and Auger Spectroscopy (Plenum Press, New York 1975).
6. C.C. Chang, in: D.F. Kanc (ed.) Characterization of Solid Surfaces (Plenum Press, New York 1974).
7. C. Dipankar: The Theory of Auger Transitions (Academic Press 1976).
8. C.J. Powell: Appl. Phys. Lett. 20, 335 (1972).
9. R.A. Pollak, L. Ley, F.R. Mc Feely, S.P. Kowalczyk, and D.A. Shirley: J. Electron Spectr. 3, 381 (1974).
10. M.F. Chang and L.H. Jenkins: Surf. Sci. 28, 649 (1971).
11. M. Salmeron: Surf. Sci. 41, 584 (1974). J.J. Melles, L.F. Davis, and L.L. Levinston: Phys. Rev. B9, 4618 (1974).
12. B. Goldstein and D.E. Carlson: J. Am. Ceram. Soc. 55, 51 (1972) see also B. Carriere, J-P Devill and S. Goldstaub: C.R. Acad. Sci. Paris 274B (1966).

W. Weisweiler, E. Osen, M. Lemperle

Effect of Fe_2O_3 and Al_2O_3 admixtures on the reaction kinetics between CaO- and SiO_2-powder compacts

Effet des additions de Fe_2O_3 et Al_2O_3 sur la cinétique des réactions entre comprimés de poudre de CaO et SiO_2

Summary

The phase formation between CaO- and SiO_2-powder compacts containing 0.3, 3, 5 and 10 % by weight of Fe_2O_3 or Al_2O_3 has been studied at temperatures between 1100 and 1450 °C using electron microprobe analysis. This method is essential for quantitative, non-destructive determination of the local distribution of elements in the micron range of solids.

For diffusion couple experiments, hot-pressed specimens were held in contact by a screw loaded sample holder and fired for periods up to five days in dry argon atmosphere.

The kinetics of phase formation depend on the amount of sesquioxide added to CaO or SiO_2. Small additions generally decrease overall phase formation compared to the system without any addition whereas further addition continuously increases overall phase growth. In all cases, C_2S is found to be the major phase developed in a temperature range below 1400 °C while the CS phase dominates between 1400 and 1450 °C. Along with CS, a glassy phase with an approximate composition of "CS_2" is formed in each system. C_3S and C_3S_2 are also formed but only in minute amounts.

The growth of all product layers is shown to obey a parabolic rate law for diffusion-controlled solid state reactions . Reaction rate constants and activation energies are presented and discussed.

Sumário

A formação de fase entre pó compacto de CaO e SiO_2 contendo 0,3, 3.5 e 10% em peso de Fe_2O_3 ou Al_2O_3 foi estudada a temperaturas entre 1100 e 1450°C usando-se análise com microsonda. Este método é essencial para a determinação quantitativa, e não destrutiva da distribuição local de elemento em sólidos da ordem de micros.

Para ensaios de difusão, corpos de provas prensados a quente foram mantidos em contacto por uma carga mantida no suporte da amostra e aquecidos por períodos de até cinco dias em uma atmosfera de argônio seca.

A cinética da formação de fase depende da quantidade de sesqui-óxidos acrescentados ao CaO ou SiO_2. Pequenas adições geralmente decrescem a formação da fase geral comparada ao sistema sem qualquer adição, ao passo que maiores adições aumenta constantemente o crescimento geral da fase. Em todos os casos, o C_2S é a principal fase desenvolvida numa faixa de temperatura abaixo de 1400°C, enquanto a fase do CS domina entre 1400 e 1450°C. Juntamente com o CS, uma fase vitrex com uma composição aproximada de "CS_2" é formada em cada sistema. C_3S e C_3S_2 são também formados mas em quantidades mínimas.

O crescimento de todas as camadas do produto obedece uma lei de velocidade parabólica para as reações de estado sólido controladas por difusão. As constantes da velocidade de reação e energia de ativação são apresentadas e discutidas.

Introduction

The solid state reactions between CaO and SiO_2 are of great interest in cement clinker manufacturing. Though extensive work is reported in literature, the system is not well understood in all details. Nowadays research is mainly concerned with reaction kinetics and mechanisms. There is a need for a fundamental understanding of the process, of its rate determining parameters and of the types of rate effects observed. Kinetic studies in the CaO-SiO_2 system were carried out by various workers using either powder mixtures /1-5/ or diffusion couple techniques with polycrystalline bulk materials or single crystals respectively /6-9/. The orthosilicate was found to be the favourite product in the initial state of the reaction. C_3S_2, CS and the C_3S phases occurred later on at the phase boundaries depending on reaction time and temperature as well as on the experimental conditions.

In order to investigate the reactions between planar CaO-SiO_2 interfaces we used hot-press technique, contacting heat-treatment and analytical investigation with electron probe microanalysis /10/. No reaction product was found below 1000 °C in spite of long annealing periods. In the first step of reaction only the C_2S phase was formed between 1000-1250 °C. Above this temperature, CS and a glassphase with a composition of about 65-68 % SiO_2 and 35-32 % CaO (="CS_2") occurred in small amounts (1300-1350 °C). Up to 1400°C the C_2S phase dominated though CS and "CS_2" grew very fast. Also the C_3S_2 phase occurred and crystal growth CS in the glassphase was observed. The reaction of the powder compacts was completed by the formation of CS according to the initial CaO:SiO_2 molar ratio of 1:1. In the observed temperature range (1000-1450 °C) no kinetic data were available for the formation of the C_3S and C_3S_2 phases within the multiphase layers. As reported by Wolter /11/, C_3S can already be formed around 1260 °C using highly activated starting materials. Non activated oxide mixtures markedly react at higher temperatures (>1450 °C) depending on the grain sizes and the contact between the particles. The reaction will be accelerated by a melt consisting of CaO, SiO_2, Al_2O_3 and Fe_2O_3. That is why technical raw material blendings for cement clinker burning are adjusted compositionally to these four oxides by clinker modules calculations.

The present paper describes the influence of Fe_2O_3 or Al_2O_3 admixtures on the kinetics of solid state reactions between compact powder specimens of CaO and SiO_2 in a diffusion couple arrangement at high temperatures. Electron probe microanalysis (EPMA) and optical microscopy have been applied to study the phase formation at the interface.

Experimental

The specimens were prepared from analytical grade $CaCO_3$, Fe_2O_3 and Al_2O_3, amorphous SiO_2-powder and dense silica glass. First, two series of samples were produced with Fe_2O_3 admixed to CaO (calcinated from $CaCO_3$) or to SiO_2 respectively in amounts of 3, 5 and 10 % by weight. In the following series Al_2O_3 was introduced to either CaO- or SiO_2-powder (0.3, 3, 5 and 10 % by weight.
After thorough mixing the powder mixtures were densified to compact bulk materials ("compacts") using a high-frequency hot-press. The specimens were cut after cooling, polished on one side, cleaned and finally brought into a graphite boat with a straining screw to reach the necessary contact (for detailed informations see /10/). The diffusion couples were annealed in an electric furnace between 1100-1450 °C for periods from 15 min up to several days.
The air-quenched specimens were embedded in mounting resin, sectioned, ground, polished and cleaned. After being studied by optical microscopy the surfaces were carbon-coated for the electron microprobe examination.

The microanalyses were performed by a scanning microscope JEOL JXA 50 A, equipped with two crystal spectrometers. The sample was moved across the reaction zone at a constant speed rate of 10 µm/min while recording the CaKα-, SiKα-, FeKα- or AlKα-X-ray impulses (mechanical line-scanning). The conversion of the determined relative X-ray intensities I_{rel} = I (element in specimen) / I_o (element in standard) into concentrations was achieved by use of a calibration curve /10/.

Results and Discussion

The kinetics of solid state reactions were determined by evaluation of the X-ray intensity / path diagrams or line-scans. Along with the layer thickness, the local and temporal sequence of the product phases could be detected directly from the line-scans. Total and individual layer thicknesses were measured and the maximum values of a number of measurements on the specimen were used. These maximum values most closely satisfy the condition of ideal contact between the reactants.

The influence of 3, 5 and 10 % by weight of Fe_2O_3, added to CaO, on the total reaction layer thickness is illustrated in Fig.1.

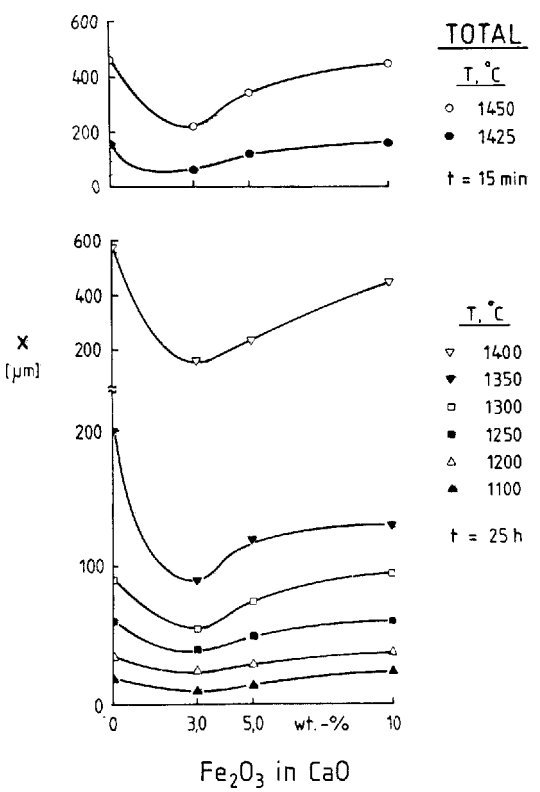

FIG.1

Total layer thickness x vs amount of Fe_2O_3, added to CaO.

Here pure silica glass served as diffusion partner. Additionally the x-values of the undoped $CaO-SiO_2$ system are applied /10/.
Addition of 3 % Fe_2O_3 generally decreases the overall reaction rate. In the temperature range between 1100-1300 °C this decrease is not as distinct as at higher temperatures (1350-1450 °C). Further addition again increases the thickness of total reaction zone giving values which are similar to those of the undoped series.

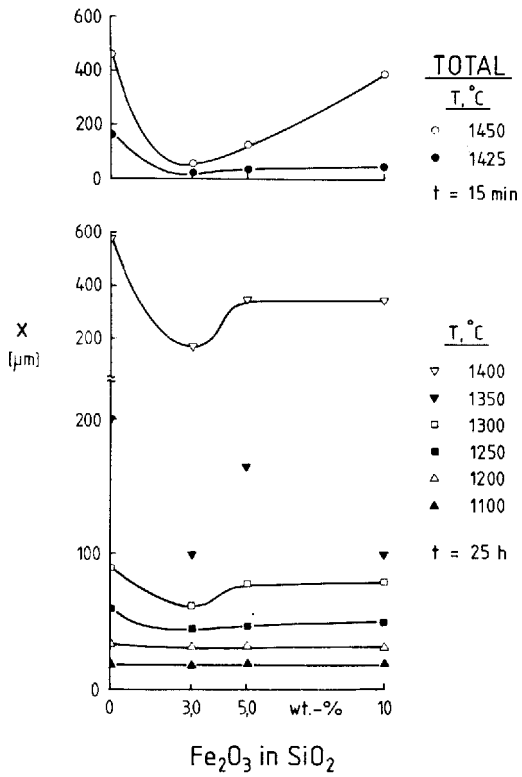

FIG.2

Dependence of total layer thickness x on the amount of Fe_2O_3, added to SiO_2.

The effect of Fe_2O_3 admixtures to silica on the growth of the total reaction zone is shown in Fig.2. Again a considerable decrease can be observed by adding 3 % iron oxide. Compared to Fig.1 the reactions seem to be much more hindered, especially at 1425 and 1450 °C. Furthermore there is no steady increase with higher addition and the x-values do not much differ going from 5 to 10 %, with exception at T = 1450 °C, where higher additions cause an increase in total layer thickness. Varying results are obtained for the diffusion couples fired at 1350 °C. Here, the samples with 5 and 10 % Fe_2O_3 addition show inhomogeneous Ca-Diffusion zones in the SiO_2 compact which do not contribute to the total reaction zone. The temperature range below 1250 °C is not much influenced by the addition of Fe_2O_3.

The total reaction zone is formed additively by the different clinker phases like C_2S, CS and a glassphase with an approximate composition of "CS_2". In some samples the C_3S_2 phase is formed but only at 1450 °C. C_3S as the most important clinker phase could not be clearly detected presumably caused by the dusting of C_2S which made microanalytical investigation more difficult.
Both total and individual layer thicknesses follow a parabolic rate law for diffusion-controlled solid state reactions. Adopting the parabolic equation $dx / dt = k \cdot 1 / x$ or $k = x^2 / 2 \cdot t$, reaction rate constants k can be calculated for each phase (Table 1 a,b).

TABLE 1

Reaction rate constants k ($cm^2.s^{-1}.10^{-11}$) in the system $CaO-SiO_2$, added with Fe_2O_3 (Table 1a - Fe_2O_3 in CaO ; Table 1b - Fe_2O_3 in SiO_2). The values for the undoped system are taken from /10/.

a)

T (°C)		1100	1200	1250	1300	1350	1400	1425	1450
0%	C_2S	1.7	7.8	20	31.3	86.8	245	680	1390
	CS	-	-	-	2.2	18.1	218	2347	18000
	"CS_2"	-	-	-	0.55	6.8	170	1390	6720
3%	C_2S	0.4	3.5	8.9	11.2	35.5	86.8	347	-
	CS	-	-	-	0.5	2.2	5.0	125	1390
	"CS_2"	-	-	-	-	-	0.55	170	8680
5%	C_2S	1.3	5.0	7.1	19.6	35.6	125	1563	11681
	CS	-	-	1.1	2.7	8.9	13.9	347	3125
	"CS_2"	-	-	-	-	-	7.8	1125	12500
10 %	C_2S	3.5	10.3	20	27	49	222	1681	8681
	CS	-	-	0.9	2.2	5.4	87	2722	22781
	"CS_2"	-	-	-	-	-	43	694	6722

b)

T (°C)		1100	1200	1250	1300	1350	1400	1425	1450
3%	C_2S	0.9	2.4	5.2	11.9	21.7	85	174	890
	CS	0.2	0.4	1.3	2.0	7.8	28	63	222
	"CS_2"	-	-	-	-	-	-	-	-
5%	C_2S	1.4	2.4	7.1	20	76	174	390	6250
	CS	0.2	0.4	1.3	3.5	14	31	56	250
	"CS_2"	-	-	-	-	-	-	-	-
10 %	C_2S	2.0	2.7	7.1	13.9	21.7	170	444	11110
	CS	0.2	0.5	1.3	3.5	7.8	32	63	11110
	"CS_2"	-	-	-	-	-	-	-	-

In the presence of Fe_2O_3 the C_2S phase dominates in the temperature range between 1100-1400 °C like in the undoped $CaO-SiO_2$ system. Above 1400 °C either CS or glassphase "CS_2" are predominant. The formation of the CS phase is shifted to lower temperatures (1250 °C, 1100 °C) by addition of Fe_2O_3 to CaO or SiO_2 respectively. In the SiO_2-doped series the CS phase is

1.1

following directly to the SiO_2 compact. No continuous layer of "CS_2" is formed but some inclusions of glass-phase are observed in the above mentioned Ca-diffusion zone.

From microanalytical investigations it is seen that Fe_2O_3 is spread in minute amounts all over the reaction zone, accumulated at grain and phase boundaries. The Fe_2O_3-content in homogeneous C_2S grains or layers varies from 0.3 - 0.9 %, in CS from 0.2 - 0.7 % and in the "CS_2" phase from 0.1 up to 1.7 %, no matter whether in CaO- or SiO_2-doped systems. Higher Fe_2O_3 addition does not markedly influence its content in the calciumsilicate phases but considerably increases the amount of Fe_2O_3 at grain and phase boundaries, up to 8 %.

Results concerning Al_2O_3 admixtures to CaO / SiO_2 diffusion couples will be presented below. Here, another series with 0.3 % by weight of Al_2O_3, added to CaO or SiO_2 respectively, was carried out to determine the influence of minute admixtures on the reaction rates. Fig.3 shows the dependence of total layer thickness x on the amount of alumina added to calciumoxide. At all temperatures a sharp decrease of total layer thickness x can be noticed from 0 to 0.3 % which is more distinct than drawn in the Fe_2O_3 added systems where no runs with 0.3 % were made however.

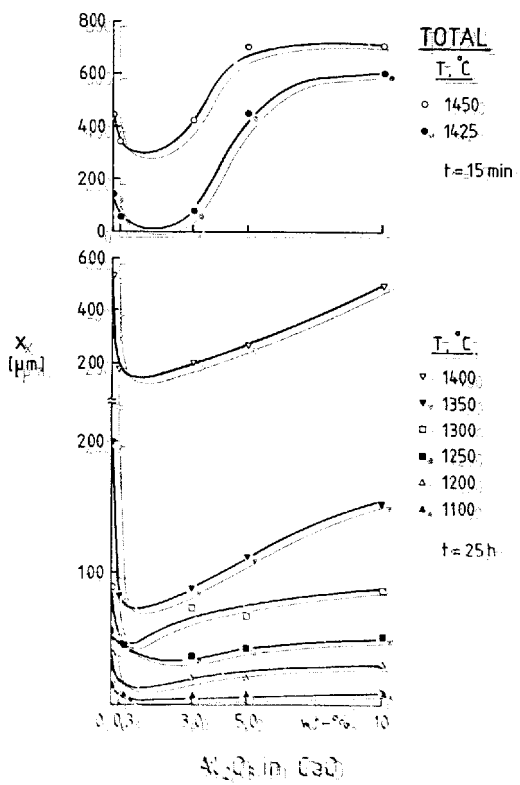

FIG.3

Total layer thickness x vs the amount of alumina added to calciumoxide.

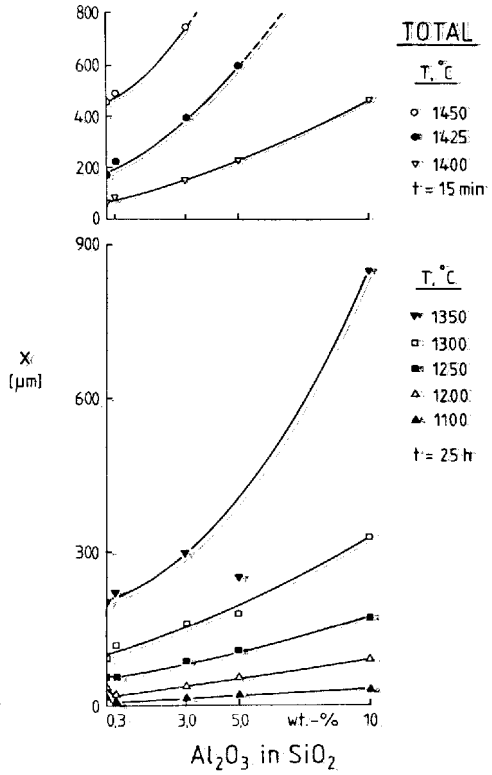

FIG.4

Total layer thickness x vs the amount of alumina added to silicondioxide.

Different findings are obtained by adding 0.3, 3, 5 and 10 % by weight of Al_2O_3 to SiO_2 as shown in Fig.4. Apart from T = 1100 and 1200 °C a continuous increase in total layer thickness is observed at all temperatures. In samples added with 5 or 10 % by weight of alumina and fired for some minutes at 1425 and 1450 °C a complete reaction of the diffusion couple had taken place leaving mainly CS and "CS_2" phases.

The partial composition of the total reaction zones and the corresponding reaction rate constants can be taken from Table 2a and 2b. Again the C_2S phase dominates between 1100-1400 °C in the $CaO (Al_2O_3) / SiO_2$ or 1100-1350 °C in the $CaO / SiO_2 (Al_2O_3)$ system respectively. Above those temperatures the CS phase or CS together with "CS_2" are predominant.
Spherical separations of C_3S_2 in the CS phase are already observed at 1400 °C (5 % and 10 % Al_2O_3 in CaO) or 1200 °C (10 % Al_2O_3 in SiO_2) respectively, which get more and more frequent towards the C_2S phase.

Contrary to the results described before, some grains of tricalciumsilicate, C_3S, are detected at 1350 °C (10 % Al_2O_3 in CaO) or 1300 °C (10 % Al_2O_3 in SiO_2) respectively. It was not possible, however, to evaluate kinetic data for the C_3S- and C_3S_2-phase formation because its growth was found to be irregular at different temperatures and reaction times.

TABLE 2

Reaction rate constants k ($cm^2 . s^{-1} . 10^{-11}$) ; Table 2a - Al_2O_3 in CaO ; Table 2b - Al_2O_3 in SiO_2

a)

T (°C)		1100	1200	1250	1300	1350	1400	1425	1450
0.3 %	C_2S	0.94	2.9	5.3	10.7	21.4	121	760	6968
	CS	-	-	-	0.2	0.7	29.6	142	12500
	"CS_2"	-	-	-	-	0.13	6.8	939	2275
3 %	C_2S	0.36	2.2	5.3	17.4	32.1	128	1680	3208
	CS	-	-	-	0.7	0.9	13.9	125	45760
	"CS_2"	-	-	-	-	0.2	1.4	200	2568
5 %	C_2S	0.27	2.7	7.6	18.1	37.4	252	5555	10275
	CS	-	-	-	1.1	2.7	20.7	54080	54080
	"CS_2"	-	-	-	-	1.4	3.5	5555	12500
10 %	C_2S	0.36	5.0	11.1	31.3	61.3	781	5555	12500
	CS	-	-	-	1.4	5.0	55.6	54080	54080
	"CS_2"	-	-	-	-	0.4	3.5	5555	15308

b)

T (°C)		1100	1200	1250	1300	1350	1400	1425	1450
0.3 %	C_2S	0.55	2.2	10.2	27.2	86.8	1380	1390	5555
	CS	-	0.14	1.13	6.8	20.0	86.8	5555	34722
	"CS_2"	-	-	0.07	1.6	8.89	420	2722	12500
3 %	C_2S	1.25	3.47	15.6	40.1	101	3125	5555	12500
	CS	-	0.55	2.2	11.3	55.5	2347	22220	68055
	"CS_2"	-	0.14	1.6	5.0	23.5	681	5555	34720
5 %	C_2S	2.2	6.8	20.0	55.5	80.0	888	5555	-
	CS	-	1.25	8.88	31.3	93.9	7347	50000	-
	"CS_2"	-	-	-	-	-	5014	22220	-
10 %	C_2S	5.0	6.8	27.2	67.2	222	1388	-	-
	CS	-	2.2	5.0	27.2	500	34722	-	-
	"CS_2"	-	8.9	35.0	125	680	16055	-	-

Homogeneous C_3S, C_2S and CS regions only contain small amounts of Al_2O_3 (< 0.3 %) whereas the glassphase "CS_2" shows values of 4-5 %. Comparable high amounts of Al_2O_3 are found in the spherical C_3S_2-separations which may stabilize this phase at lower temperatures. The same holds for the glassphase "CS_2" already occurring at 1200 °C in CaO / SiO_2 (Al_2O_3) diffusion couples. In those systems additions of Al_2O_3 produce accelerated diffusion rates.

The experimental findings of the CaO / Fe_2O_3 and CaO / Al_2O_3 systems shown in Figure 1 and 3 may be interpreted on the basis of the disorder in CaO.

TABLE 3

Activation energies E_A (kJ/mol) for the formation of the calciumsilicate phases ; Table 3a - addition of Fe_2O_3 , Table 3b - addition of Al_2O_3.

a)

Addition of		Fe_2O_3 in CaO		Fe_2O_3 in SiO_2	
wt.-%	Phase	E_A *)	E_A +)	E_A *)	E_A +)
0 %	C_2S	230	-	230	-
	CS	845	-	845	-
	"CS_2"	1085	-	1085	-
3 %	C_2S	325	-	240	1210
	CS	480	2685	255	1000
	"CS_2"	-	4610	-	-
5 %	C_2S	245	2170	470	-
	CS	370	2590	450	-
	"CS_2"	-	3540	-	-
10 %	C_2S	195	1750	190	2000
	CS	370	2665	270	2810
	"CS_2"	-	2420	-	-

b)

Addition of		Al_2O_3 in CaO		Al_2O_3 in SiO_2	
wt.-%	Phase	E_A *)	E_A +)	E_A *)	E_A +)
0.3 %	C_2S	490	505	380	660
	CS	730	4610	650	2865
	"CS_2"	-	2590	1060	1700
3 %	C_2S	390	1200	335	660
	CS	1070	3830	615	1695
	"CS_2"	-	3040	660	1700
5 %	C_2S	360	1370	335	1265
	CS	630	4035	565	1925
	"CS_2"	-	3720	-	-
10 %	C_2S	380	1915	450	-
	CS	825	4790	708	-
	"CS_2"	-	3720	567	-

*) low temperature range (1100-1400 °C)
+) high temperature range (1400-1450 °C)

According to Hauffe and Tränckler /12/ CaO is a p-type semiconductor for $p_{O_2} > 10^{-2}$ mbar. Vacancies in the cation sublattice are regarded to be the most important defects as to the mobility of calcium ions. The concentration of the cation vacancies, however, can be markedly altered by introducing trivalent ions into the calcium sublattice. Small additions of sesquioxides may result in filling up the cation vacan-

cies according to the reaction

$$Me_2O_3 + 6\ h^{\cdot} + 2\ V''_{Ca} = 2\ Me^{\cdot}_{Ca} + {}^3/_2\ O_2\ ,$$

where $h^{\cdot}$ denotes the positively charged electron hole, V''_{Ca} the negatively charged calcium vacancy and Me_{Ca} the positively charged metal ion occupying a calcium site. According to the Kröger symbolism /13/ all charges are given relative to the ideal crystal. This mechanism would account for the decrease in reaction rate at small Fe_2O_3- or Al_2O_3-concentrations. At higher admissions the number of electron holes will be reduced to such an extent that the following competitive reaction will become dominating:

$$Me_2O_3 + 3\ Ca^x_{Ca} = 3\ CaO + 2\ Me_{Ca} + V''_{Ca}$$

i.e. new cation vacancies are created if divalent calcium ions are substituted by trivalent iron or aluminum ions.
It should be noted that higher admixtures of Al_2O_3 lead to the formation of calciumaluminate phases ($C_{12}A_7$, C_3A) throughout the CaO compact, which in addition may cause an enhanced diffusion of the Ca-species.
In the upper temperature range (>1400 °C) the high solubility of Al_2O_3 in "CS_2" accelerates its phase formation followed by the enormous increase of the now dominating CS phase.

Arrhenius plots of the reaction rate constants lead to the corresponding activation energies listed in the Tables 3a and 3b. It is known from literature that activation energies for the formation of calciumsilicate phases strongly depend on the experimental conditions. For instance, the activation energy for the C_2S formation is found to range from 210-420 kJ / mol /8,14,15/. Our E_A-values obtained for the formation of the C_2S phase fit quite well into above mentioned data. The extremely high activation energies ascertained for the formation of the C_2S, CS and "CS_2" phases at temperatures higher than 1400 °C indicate that another reaction mechanism is involved. At low temperatures, however, we again find activation energies for the CS formation which show an acceptable accordance to literature data.

References

/1/ J.W. Cobb, J.Soc.Chem.Ind., 29, 69 (1910).

/2/ W. Dyckerhoff, Zement, 14, 3 (1925).

/3/ K. Hild, G. Trömel, Z.Anorg.Allg.Chemie, 215, 211 (1933).

/4/ W. Jander, E. Hoffmann, Z.Anorg.Allg.Chemie, 218, 211 (1934).

/5/ W.L. de Keyser, Bull.Soc.Belg., 62, 235 (1953).

/6/ J. Gebauer, E. Fitzer, ZKG, 22, 402 (1969).

/7/ J. Gebauer, W. Weisweiler, High temp.-High Press, 1, 277 (1969).

/8/ A.S. Burte, P.S. Nicholson, J.Am.Ceram.Soc., 55, 469 (1972).

/9/ P.V. Kichas, D.I. Stul'pinas, Dokl.Akad.Nauk SSSR, 270, 360 (1983).

/10/ W. Weisweiler, E. Osen, J. Eck, H. Höfer, Cem.Concr.Res., 16, 283 (1986).

/11/ A. Wolter, Die untere Bildungstemperatur und Stabilität von C_3S, Diss., TH Aachen, 1979.

/12/ K. Hauffe, G. Tränckler, Z.Phys., 136, 166 (1953).

/13/ F.A. Kröger, The Chemistry of Imperfect Crystals, 2. ed., North-Holland Publ. Comp., Amsterdam, 1974.

/14/ K. Segawa, J.Jap.Ceram.Assoc., 56, 99 (1948).

/15/ M.R. Montierth, R.S. Gordon, I.B. Cutler, Mater.Sci.Res., 4, 522 (1969).

DNR. 100315 E.29.09.17 BG

A. Wolter
KHD Humboldt-Wedag AG, Cologne, West Germany

PHASE COMPOSITION OF CALCINED RAW MEAL

1.1

COMPOSITION DE PHASE DES FARINES CRUES CALCINÉES

SUMMARY

The more precalcining techniques become common practice in cement plants the more data about intermediate phase formation during calcination of industrial raw meals become available. Investigations on this subject have been by way of X-ray diffraction, chemical and SEM analyses.

The composition of calcined meals extracted from operating plants varies over a wide range depending on the degree of calcination, heterogeneity of the raw meal and recirculation of kiln dust and of condensed volatiles. Calcium aluminate and -ferrite are easily formed during calcining. The range of silica reaction to C_2S or spurrites varied from 10 to 60 % . Correspondingly, the free lime content was found to vary between less than 5 % by weight and more than 40 % by weight. This percentage tends to be less upon spurrite formation.

As a general rule it can be said that the degree of lime combination is significantly higher during practical operation than ascertained in the laboratory. Additional information is given with respect to splitting of exothermic heat in calciner and kiln, as well as on the use of calcined meal for nearly any type of cement.

SUMÁRIO

A medida que as técnicas de pré-calcinação tornam-se uma prática comum nas fábricas de cimento, aumenta-se a informação sobre a formação da fase intermediária durante a calcinação de matérias-primas industriais. Investigações sobre este assunto foram realizadas utilizando-se difração de raios X, análises químicas e de SEM.

A composição da alimentação calcinada extraída de fábricas em operação variam em uma grande faixa, dependendo do grau de calcinação, heterogeneidade da alimentação bruta e da recirculação do pó do forno e de voláteis condensados.

Aluminatos e ferritos de cálcio são facilmente formados durante a calcinação. A faixa da reação de sílica para C_2S ou espurritas variam de 10 a 60%. Correspondentemente, a quantidade de cal livre variou entre menos de 5% em peso a mais de 40% em peso. A percentagem tende a ser menor dependendo da formação da espurrita.

Como regra geral, pode ser dito que o grau de combinação da cal é significativamente maior durante operação prática do que a realizada em laboratório. Informação adicional é dada com relação à divisão do calor exotérmico no calcinador e forno, assim como no uso de alimentação calcinada para quase qualquer tipo de cimento.

1. INTRODUCTION

The formation of phases during calcining of cement raw meals and during heating up to sintering temperature has from the very beginning of cement research been of particular interest /1,2,3,4,5/. However, current knowledge on this complex topic is based almost exclusively on experimental work. Due to the introduction of the precalcining technology on plant scale industrially produced cement raw meals, calcined up to 98% can be sampled and examined today.

Calcined meal can be withdrawn as portion of the continuous production run. It is a new type of hydraulic binder, i.e. either in anhydrous or hydrated form /6/. For instance, substituting clinker in cement by calcined meal results in a proportionate saving of grinding energy and permits at the same time controlled modification of the cement properties. Withdrawing meal portions means that rotary kiln and preheater are relieved from circulating volatiles without accumulating a waste product difficult to handle - as it is typical of a conventional kiln gas bypass.

The composition of clinker as main product has to meet clearly defined requirements and, consequently, the composition of calcined meal is allowed but little variation. Calcined meals are characterized by the 'Lime Saturation Factor' LSF, the 'Silica Ratio' SR and the 'Alumina Ratio' AR, as well as by

* the 'Degree of Calcination' DCAL,
* the 'Degree of Lime Combination' K' or the 'relative Degree of CaO Reaction" DCR resp. and
* the 'Degree of Belite Formation" DC_2S.

(For details of calculation see formulae attached)

2. PROCEDURE

Samples of kiln inlet meal have been taken in about 20 rotary kiln systems fitted with cyclone preheater. These samples have been examined in the laboraties of KHD by identical methods. The majority of the investigated kilns was equipped with precalciners. The principal components of the meal samples have been ascertained with the aid of X-ray fluorescence analysis and the minor components by wet chemical processing. X-ray diffraction analyzing has been carried out whenever high concentrations of volatiles were noticed. Some of the samples have subsequently been treated with salicylic acid /7/ and the residue subjected once again to X-ray diffraction analysis. For verifying purposes, the eluate has in a few cases been subjected to wet analysing. Similarly, investigations have been carried out with the X-ray scanning micro analyser.

For kiln systems operated with a bypass also the bypass dust has been examined. These dusts are characterized by a higher concentration of volatile compounds than meal samples taken at the kiln inlet which means that they are particularly suitable for the X-ray diffraction phase analysis. XRD analyses of bypass dusts have been included in table 1 but not those obtained by analyzing coatings from the cyclone preheater.

3. RESULTS

Table 1 is a summary of the crystallized phases that have definitely been evidenced to exist in kiln inlet meals and in bypass dusts. Some phases display very poor crystallinity. It is even assumed that amorphous portions exist which are not detectable by XRD. Similarly, they could not be determined by the methods of chemical analyzing applied so far.

Table 1: Phases identified in calcined meals

	soluble in salicylic acid?
Group 1: not reacted raw meal phases	
$CaCO_3$ calcite	no
SiO_2 quartz	no
mica	no
feldspars	no
Group 2: new formed phases	
CaO free lime	yes
MgO periclase	no
β-C_2S belite	yes
$2C_2S \cdot CaCO_3$ spurrite	yes
$C_{12}A_7$	no
$C_2(A,F)$ ferrite	no
Group 3: condensed volatiles	
KCl sylvine	yes
NaCl halite	yes
K_2SO_4 arcanite	no
$K_3Na(SO_4)_2$ aphtitalite	no
$CaSO_4$ anhydrite	no
Group 4: clinker dust and coal ash	
C_3S alite	yes
Group 5: phases formed after hydration	
$Ca(OH)_2$ portlandite *)	yes
$CaSO_4 \cdot 0.5\ H_2O$ hemihydrate **)	no

*) from free lime
**) from anhydrite during salicylic acid treatement

The specific stages of clinker burning enable differentiating between five categories of phases:

* the first category includes the raw meal phases that have undergone either no reaction at all or only partial reaction during calcination. These phases being in particular calcite and quartz, will predominate the XRD pattern especially upon a low degree of calcination. It is a general rule that dolomite and pyrite can never be located in meal samples taken at the kiln inlet. Similarly, there can be detected no more than weak traces of the basic peaks of clay minerals.

* The phases that have formed new during calcination originate from liberated CaO. There is a particularly pronounced reactivity of CaO with the thermally activated decomposition products of the clay minerals. Their aluminate ferrite portion is responsible for the formation of $C_2(A,F)$. Reasonable excess of Alumina will normally entail the additional formation of $C_{12}A_7$. Phases of lower lime content, such as CA and CA_2, have not been evidenced. C_2AS(gehlenite) could neither be definitely identified nor its nonexistance be evidenced beyond any doubt. Even if gehlenite would have formed, it could be of very small quantity only compared with the belite that has formed evidently. Poorly crystallized belite (β-C_2S) and frequently spurrite are formed from the portion of SiO_2 included in the clay minerals and - to a certain extent - from quartz. The "sulfate spurrite" described by GUTT and SMITH /8/ has not been noticed. In spite of occasionally significant chloride contents (see further below), no alinites /9/have been located. Similarly, no silicate phases have formed that featured a lower lime content than C_2S.In case of incomplete calcining and extremely heterogeneous raw material, the free lime content can raise to more than 40 % by weight. MgO always predominantly exists as periclase.

* The third important category are the salts some of which may occur at high concentrations in the evaporation/condensation circuit between rotary kiln and waste gas utilizing section of lower temperature (preheater - raw mill - dryer - filter). The concentration of chlorine in the form of KCl is particularly striking. The KCl concentration may reach levels of more than 10 % by weight. KCl contents ranging between 0.5 and 2 % by weight are frequently found in operating plants without bypass. NaCl is, on the contrary, located in exceptional cases only. Apparently, potassium displays much stronger affinity for chlorine at high temperatures than sodium. It is a well-known fact that sodium is preferably incorporated in calcium aluminates. Normally, the alkali content of the raw meal at the kiln inlet is ample for stoichiometrically compensating chlorine. For the few cases where excess chloride had been ascertained by calculation, no additional chloride phase could be detected. It is presumed that - similar to fluoride - this Cl is incorporated in $C_{12}A_7$ or in spurrite as solid solution.
The kiln inlet meals and bypass dusts often include alkali sulfates with K_2SO_4 (arcanite) occuring frequently, $K_3Na(SO_4)_2$ (aphtitalite) seldom, and Na_2SO_4 (thenardite) occuring not at all. The double salt $K_2Ca_2(SO_4)_3$ has been located only in in coatings originating from the top cyclone stages but not in meal taken from the kiln inlet. Alkali carbonates, such as K_2CO_3 or $K_2Ca(CO_3)_2$ cannot be evidenced, even not at sulfurization degrees of less than 50 %. It has been impossible to furnish unambigous proof as to wether the alkalies are incorporated in these cases into other phases as foreign ions or wether they form separate amorphous phases that are unable to be detected by XRD.
In case of significant excess sulfate, i.e. at a sulfurization degree of far beyond 100 %, $CaSO_4$ is formed as anhydrite II . However, the anhydrite peaks are in all cases smaller than expected on the basis of the calculated portion. It should be noticed that neither $2C_2S{\cdot}CaSO_4$ nor $3CA{\cdot}CaSO_4$ are formed which are known from coatings. In general, sulfates are not affected by treatement with salicylic acid.

* Coal of high ash content and clinker tending to develop dust will entail considerable portions of these substances being included in the kiln inlet meal. They are difficult to identify although alite can be reliably evidenced from a clinker dust portion of about 10 % by weight onward. Ash particles originating from the kiln firing system can occasionally be identified in a SEM by their spherical shape - a configuration well-known from fly ash discharged from power plants.

* To the fifth category all phases belong which are formed secondary during sample storaging or treatement, like $Ca(OH)_2$ from CaO or hemihydrate from anhydrite.

4. FURTHER EVALUATION OF EXPERIMENTAL AND OPERATIONAL WORK

In the course of the tests made attention has been focused on the interrelation between the formation of new phases and the degree of calcination. It is impossible to take samples covering the complete range from 0 to 100 % calcining in only one running plant with operating conditions being comparable for all samples taken. Hence, for carrying out pertinent tests,

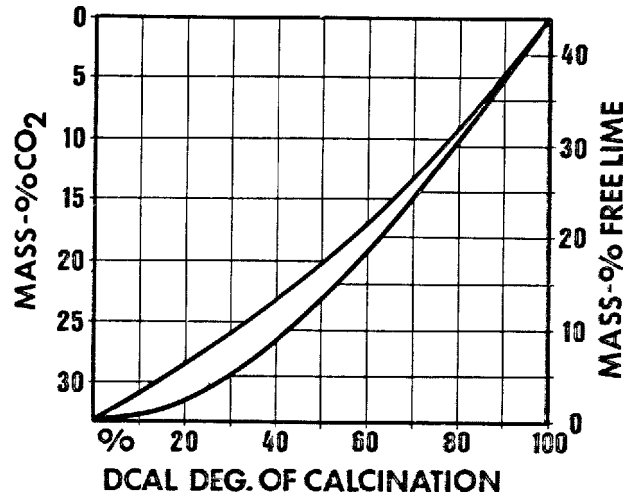

Fig. 1: CO_2 and free lime content during calcination

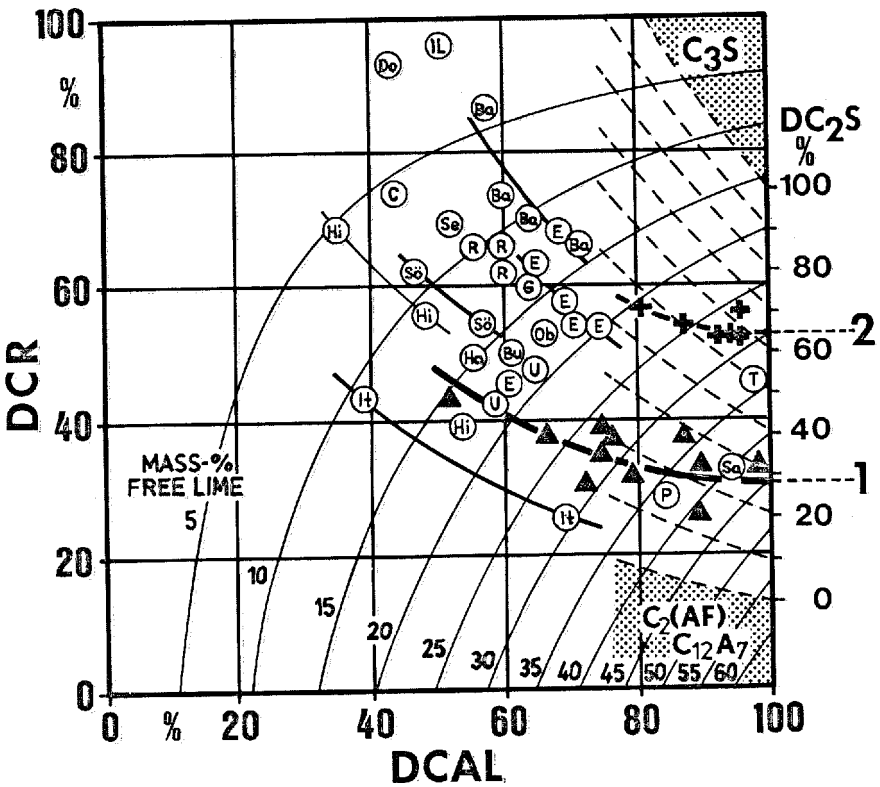

Fig. 2: Relative degree of CaO reaction DCR vs. degree of calcination DCAL DC_2S significates the degree of belite formation (DC_2S and isolines of free lime calculated on basis of KSt = 95 %, SR = 2.5, AR = 1.8, C+S+A+F = 95 % by weight)

a laboratory scale fluidized bed reactor has been fed with industrially produced raw meals which were calcined under isothermal conditions. The typical pattern of CO_2 and free lime content is given in figure 1 vs. the degree of calcination. The ranges of CO_2 and free lime have been correlated such for the example shown that the starting and terminating points of the plotted curves coincide. Assuming the portion of decarbonized lime that combines with hydraulic factors direct - such portion being identical with the relative degree of CaO reaction DCR - remaining constant over the complete range of calcination, the two curves should be congruent. However, free lime is formed only reluctantly upon starting calcination. This means that at the beginning of calcination the DCR is significantly higher than at a calcination degree above 80 % at which the curves are extensively adapted to each other. At this level an approximately constant DCR value is achieved. With calcining having reached that high level, the formation of aluminate and ferrite has been terminated to such an extent that additional CaO reaction can be calculated on the basis of C_2S. This belite portion will continuously increase until complete calcination has been attained.

Figure 2 is a graphic survey of DCR vs. DCAL of all kiln inlet meals analyzed. Two plants from which a particularly large number of samples has been taken are identified by separate symbols. The remaining values have been entered with a circle including an index characterizing each plant.

For plant 1, the free lime content equals approx. 45 % by weight at complete calcination. This value corresponds to a DCR of more than 30 %, and hence, to a DC_2S amounting 25 - 30 %.

Plant 2, also characterized by extensive precalcining, reaches a DCR of more than 50 %, and, consequently, a DC_2S value of 60 %. These differences can be attributed to the heterogeneity of the raw meals examined.

The majority of kiln inlet meals featured degrees of calcination between 40 and 70 % approx. which are correlated to DCR's ranging from 30 to 75 %, in rare cases even above 90 %. The free lime content of meals taken from plants without precalciner amounts between 5 and 10 %.

In general, the DCR decreases with increasing degree of calcination so that the free lime content raises exponentially. Upon complete calcining the DC_2S value can be extrapolated to become on average 40 - 50 %. this, in turn, is identical to a belite portion of 25 - 30 % by weight, subject to average LSF and SR.

Partially calcined raw meal may be characterized by marked portions of spurrite having formed instead of belite. These two phases can be easily differentiated upon XRD. It seems probable that the existance of spurrite impairs the flow properties of the hot meal.

5. CONCLUDING REMARKS

The reaction between free lime and 'hydraulic factors', especially with SiO_2, liberates significant amounts of exothermal heat which reduces the amount of heat required for calcining within the particles involved. Hence, it is obvious that at the beginning of calcination such particles or aggregates are preferably decarbonized in which $CaCO_3$ and hydraulic factors are intimately intergrown. These early stages of calcination are associated with only little formation of free lime. Correspondingly, the specific amount of heat required for the final calcining is much higher, thereby most of liberated lime remaining uncombined and less belite being formed. Upon the increasing temperature, however, the belite formation is accelerated again towards final calcination.

The degree of belite formation DC_2S has a direct effect on the design of calcining and firing systems as it is directly proportional to the amount of exothermic heat already released. That degree indicates the splitting of exothermal heat between calciner and rotary kiln which is required to be known for establishing separate thermal balances for rotary kiln and calciner/preheater respectively. It is a well-known fact that but negligible amounts of heat are liberated due to the formation of calcium aluminate and ferrite phases /10/.

Figure 3 shows two examples for the interrelation between heat released as a result of belite formation and

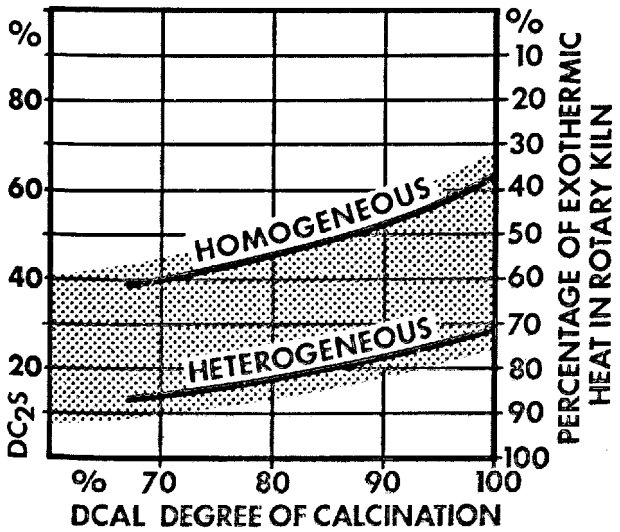

Fig. 3: Portion of the exothermic heat in the kiln as a function of the degree of calcination and the heterogeneity of the raw meal

the degree of calcination. Subject to complete calcining, the range of exothermic heat liberated in the rotary kiln varies between a minimum of 30 % (for very homogeneous meal) and a maximum of 80 % (for extremely heterogeneous meal).

As to plants not equipped with precalciners it can be assumed that in absolute figures more than 70 to 90 % of exothermic heat will be released in the rotary kiln.

With respect to the calculation of DCAL, DCR and DC_2S recirculation of volatile salts and of clinker dust are of importance. The presence of clinker dust not only results in an apparently higher degree of calcination but also falsifies the DCR level towards higher values. Meal whirled up from the inlet chamber increases DCAL and DCR to a comparable extent, hence it does not falsify the DCR level in relation to DCAL. Sulfate circuits stimulate CaO combination and increase the DCR level. For these reasons, it is not surprising that the DCR ascertained during practical operation often exceeds the laboratory figures of the same raw meal samples approx. 20 % in abs. fig. Differences of that extent have been determined in spite of retention times of no more than a few seconds in industrial-size calciners.

Calcined meal offers itself for most versatile applications. For instance, it can substitute clinker in fly ash- and slag cements, act as main component of hydraulically active binders, for solidifying waste material, as filler and drying agent as well as in hydrated form as substitute of $Ca(OH)_2$, for example in the dry waste gas desulfurization. For the majority of the above applications, the contents of free lime and/or of belite are decisive quality aspects. Hence, not only the thermal but also the mineralogic value of the meal increases by an exponential function with the degree of calcination. There are applications where the specific surface and full availability of $Ca(OH)_2$ during the concrete preparation are of particular importance. This is the case, for instance, for little ground Portland cements where these properties are to increase the water requirement for avoiding "bleeding".

$C_{12}A_7$ may involve problems since it enhances "false setting" and complicates control of setting. Similarly, an occasionally occuring concentration of alkali salts may restrict applicability of calcined meal.

However, expansion caused by free lime or magnesia can

be excluded because both phases exist finely grained and chemically active thereby guaranteeing very quick hydration.

APPENDIX OF FORMULAE

The degree of calcination has been defined as the ratio between CaO not bonded to CO_2 and total CaO content of a sample. In terms of interpretation it should be added that from a point of view of process engineering this is the 'apparent' degree of calcination while it is the 'actual' degree with respect to the meal and its intended use. This value is normally calculated from the ratio between CO_2 content in the raw meal (G) and CO_2 content in the calcined meal (g) /11/:

$$PHI = \frac{100\ (G - g)}{G\ (100 - g)} \times 100\,\% \qquad [\ 1\ ]$$

During practical operation , the CO_2 values are mostly substituted by the losses of ignition of raw meal and of calcined meal respectively. Apart from this inaccuracy PHI is additionally falsified by salt concentrations (diluting and volatilizing effects), ash entry and circulating dust, if the LSF of the latter differs from that of the raw meal.

It is more reliable to calculate the degree of calcination exclusively from the CaO and the CO_2 content of the calcined meal (values in % by weight):

$$DCAL = \left(1 - \frac{CO_2 \times 1.274}{CaO}\right) \times 100\,\% \qquad [\ 2\ ]$$

The decarbonized lime partially exists as free lime, partially as combined in newly formed phases. The term 'degree of lime combination' has been introduced for identifying the ratio between lime combined in oxides and total lime /12/:

$$K' = \frac{CaO - CO_2 \times 1.274 - CaO_{free}}{CaO} \qquad [\ 3\ ]$$

The above ratio correlates with a simple graphic presentation plotted by HASTRUP /13/ (accord. fig. 4).

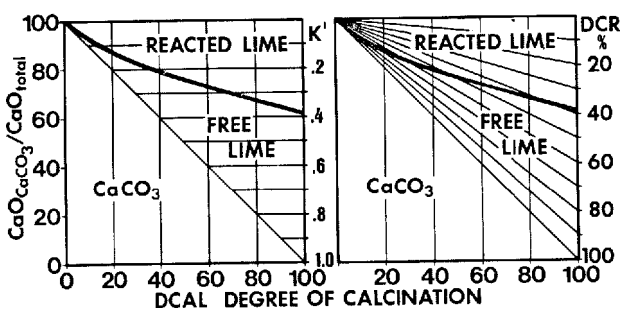

Fig. 4: Ratio between $CaCO_3$, free lime and combined lime correlated with K' (left) and DCR (right)

Since K' is related to total CaO, that ratio always has to be related to the degree of calcination. Such 'detour' will not be necessary when taking the 'relative degree of lime reaction' as a basis:

$$DCR = \frac{CaO - CO_2 \times 1.274 - CaO_{free}}{CaO - CO_2 \times 1.274} \qquad [\ 4.1\ ]$$

$$\triangleq \left(1 - \frac{CaO_{free}}{CaO - CO_2 \times 1.274}\right) \times 100\,\% \qquad [\ 4.2\ ]$$

Figure 1 indicates that DCR yields a better approximation to the typical curve of lime combination than K' does.

In case of high-grade calcining, the reactions of Al_2O_3 and Fe_2O_3 with CaO to become $C_2(A,F)$ and $C_{12}A_7$ have been essentially completed so that the remaining free lime permits calculating the 'degree of belite formation':

$$DC_2S = \frac{CaO - .94\,A - .70\,F - 1.274\,CO_2 - C_{fr.}}{1.87\,S} \times 100\,\% \qquad [\ 5\ ]$$

The belite content given in % by weight will then equal by calculation:

$$C_2S = 2.87\,S \times \frac{DC_2S}{100} \qquad [\ 6\ ]$$

In the event that spurrite exists instead of belite, its content will be calculated analogously, although the restriction attributable to the residual portion of CO_2 will have to be duly considered:

$$2C_2S{\cdot}CaCO_3 = 3.70\,S \times \frac{DC_2S}{100} \qquad [\ 7.1\ ]$$

$$\leq 9.71 \times CO_2 \qquad [\ 7.2\ ]$$

Moreover, it is recommended to calculate the sulfurization degree 'SG' of the alkalies and the CaO portion in case of excess sulfur free of $CaSO_4$:

$$SG = \frac{SO_3}{.85\,K_2O + 1.29\,Na_2O - 1.13\,Cl} \times 100\,\% \qquad [\ 8\ ]$$

$$CaO_{CaSO_4\text{-free}} = \left(CaO - .70\,SO_3 \times \frac{SG - 100}{SG}\right) \times 100\,\%. \qquad [\ 9\ ]$$

REFERENCES

/ 1/ LUDWIG, U.: ZKG 34 (1981) 4, 175 - 186 (p. 178)

/ 2/ KEIL, F.: Zement, Springer 1971, p. 67

/ 3/ KUPPER, D.: Dissert. Clausthal 1984, p. 154

/ 4/ MOIR, G.K.: World Cem. 13 (1982) 374 - 382 (p. 378)

/ 5/ WOLTER, A.: Forschungsberichte des Landes Nordrhein-Westfalen, No. 3092, Opladen 1982

/ 6/ HENKEL, F.: VDZ-Congress '85, Techn. Sess. 5

/ 7/ LOCHER, F.W. et al.: ZKG 29 (1976) 10, 435 - 442

/ 8/ GUTT, W. and SMITH, M.A.: Trans. Brit. Ceram. Soc., 67 (1968) 487 - 509

/ 9/ ILUKHINE, V. et al.: Nature 269 (1977) 5627, 397 - 398

/10/ ANSELM, W.: Radex-Rundschau (1950) 3 ff. in: SCHWIETE, H.E. u. ZIEGLER, G.: ZKG 9 (1956) 6, 3 - 8

/11/ KEIL, F.: Zement, Springer 1971, p. 319

/12/ KIESER, J. et al: ZKG 32 (1979) 9, 442 - 447

/13/ HASTRUP, N.E.: ZKG 29 (1976) 5, 202 - 206

Lj. M. Dragićević - The Highway Institute, Belgrade

1

PROGNOSIS OF THE PHYSICAL-MECHANICAL CHARACTERISTICS OF PORTLAND CEMENT

1.1

SUMMARY: In the Work we made a prognosis of flexural and compressive strengths of portland cement after 3 and 28 days, and pointed out importance of application of determined mathematical methods, which can be used for forming mathematical models. Using of D-optimal plans and plans including "pseudo components" realized original mathematical models, which make possible, for diferent composition of four-component C-S-A-F system, to determine strength values of portland cement, after 3 and 28 days.

For forming corresponding mathematical models for realization qualitative prognosis, used polynomial of fourth order. Calculation polynomial coeficients and determination of analytically form made on calculator PDP 11/40.

Adequateness of obtained mathematical models has examined by Student's t-test, and in all cases calculated values of t-test are less then tabulated at $\alpha = 0.05$. That means, that by obtained mathematical models can be established exact functional dependence between composition of portland cement clinker and characteristics of portland cement.

SUMÁRIO: Neste trabalho, foi feito um prognóstico das resistências à flexão e compressão do cimento portland depois de 3 e 28 dias e foi indicada a importância da aplicação de determinados métodos matemáticos que podem ser usados para a formulação de modelos matemáticos.

Usando planos de D-ótimo e planos incluindo "pseudo componentes" foram realizados modelos matemáticos originais, que tornaram possível para diferentes composições do sistema quaternário C-S-A-F, a determinação dos valores do cimento portland, depois de 3 e 28 dias.

Para a criação de modelos matemáticos que realizem prognósticos qualitativos foram utilizados polinômios de quarta ordem. O cálculo dos coeficientes dos polinômios e determinação da forma analítica foi feita num computador PDP 11/40.

A adequação dos modelos matemáticos obtidos foi examinada por um teste t de Student, e em todos os casos os valores calculados do teste-t foram menores do que os tabelados para $\alpha = 0,05$. Isto significa que ao obterem-se modelos matemáticos pode-se estabelecer uma dependência funcional exata entre a composição do clínquer de cimento portland e as características do cimento portland.

Lj. M. Dragičević - The Highway Institute, Belgrade

PROGNOSIS OF THE PHYSICAL-MECHANICAL CHARACTERISTICS OF PORTLAND CEMENT

Everyday's demands of contemporary technique for new inorganic materials caused an intensive work on problems of prognosis of composition, physical and chemical features. Problems that have be solved in contemporary research of materials are exceptionally complex, more complicated then problems relatied to physics and chemistry of solid state.

Contemporary technique, in widest range, from civil engineering to electrical engineering, sets in first plan development of new silicate materials and prediction of features and optimization of production procedures.

In this work we have made prognosis of compressive strengths for portland cement and pointed out importance of application of determinated mathematical methods for prognosis of characteristics of polycomponent materials. We obtained original mathematical models, which make possible, for different composition of four-component C-S-A-F system, to determine compressive strength values of portland cement, after 3 and 28 days.

1. EXPERIMENTAL WORK

Prognosis of physical-mechanical characteristics of portland cement is subject of interest of numerous investigations [1-3]. First attempts for prediction of portland cement strengths, on the base of chemical composition of portland cement clinker, attained a limited importance, because in most cases obtained mathematical models are not adequate for determination dependence between mechanical characteristics and chemical composition of portland cement clinker. In frame of experimental work we investigated concentracion C-S-A-F area, which is interesting for sphere of portland cement clinker. In order to define concentracion area [4], we have used four kind of portland cement clinker, which are different with regard to chemical composition, modular characteristics,saturation degree and contents of particular minerals:

- portland cement clinker, designed as z_1,
- portland cement clinker, designed as z_2,
- portland cement clinker, designed as z_3,
- portland cement clinker, designed as z_4,

Lj. M. Dragićević - The Highway Institute, Belgrade

PROGNOSIS OF THE PHYSICAL-MECHANICAL CHARACTERISTICS OF PORTLAND CEMENT

1.1

To portland cement clinkers we have added 3% of gypsym dyhidrat, and then clinker is separately milled in laboratory ball mill of 10 lit. volume, until obtained specific surface 3 200 $\pm$ 50 cm^2/g.

We have made chemical and mineralogical investigations of portland cement clinkers, and then on the base of chemical compositions and Boque equation, calculated potential mineral composition. Table I. shows potential mineral composition of portland cement clinkers, calculated for the base 100.

Table I. Potential mineral composition calculated for the base 100

	Clinker designations			
	z_1	z_2	z_3	z_4
x_1-C_3S	73.04	40.95	73.73	53.34
x_2-C_2S	6.89	41.05	7.43	21.04
x_3-C_3A	10.05	4.82	5.89	13.59
x_4-C_4AF	10.02	13.18	12.95	12.03

On this way unknowns x_i (i=1,2,3,4) satisfy conditions which regulate D-optimal plans |5-14| and there is also determinated concentracion area in which exist corresponding mathematical models:

$$\begin{aligned} 40.95 \leq x_1 \leq 73.73 \\ 6.89 \leq x_2 \leq 41.05 \\ 4.82 \leq x_3 \leq 13.59 \\ 10.02 \leq x_4 \leq 13.18 \end{aligned} \qquad (1)$$

Fig. 1 shows concentration area defined by assembley (1) in concentration triangle C_2S-C_3A-C_4AF, and obtained from table I, by eliminatic 1 phase C_3S (x_1=0), and remaining three phases are re- lculated with base 100, and obtained values for C_2S, C_3A and C_4AF projected in concentration triangle C_2S-C_3A-C_4AF.

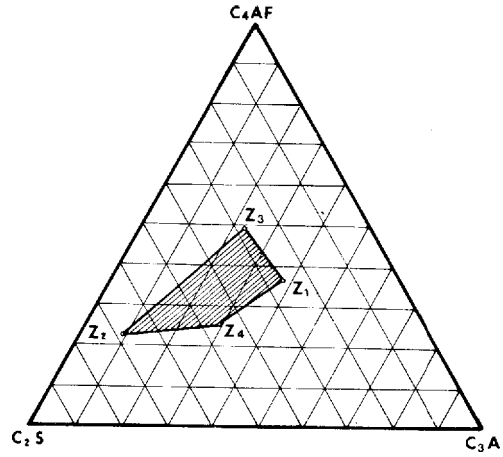

Fig. 1. Concentration area of investigated portland cement clinkers.

Area is bordered with coordinates of "pseudocomponents" (z_1-z_2-z_3-z_4) of an irregular shape, i.e. not corresponding to regular simplex for girder {4.4}.

1.1. Working matrix of experiment

For forming working matrix of experiment we have used a plan, including pseudocomponents, and experimental points are shown in coordinates of pseudocomponents *) z_i (i=1,2,3,4) Pseudocomponents represent portland cement clinker and theirs relations, which used for experimental determination compressive strengths after 3 and 28 days. The plan of experiment is compiled in accordance with requirements of D-optimal plans, and number of experimental points for pseucocomponental system and polynomial of fourth order is determined by relation:

$$N = C^{n}_{n+q-1} = C^{4}_{4+4-1} = \frac{7!}{4!} = 35 \qquad (2)$$

On the right of working matrix are values of compressive strength, obtained by wxperiment realization. Table II shows working matrix and results of experiment.

*) On the base of data from table I. and pseudocomponent in determined point of plan, it is possible to recalculate mineralogical compositions of portland cement clinders, for each point of plan.

Table II. Working matrix and results of experiment

N	Pseudocomponents				Response function	
					Pressure, MPa	
	z_1	z_2	z_3	z_4	3	28
1	1	0	0	0	17.5	47.5
2	0	1	0	0	19.8	38.4
3	0	0	1	0	24.3	46.4
4	0	0	0	1	18.2	36.6
5	0.5	0.5	0	0	17.2	45.8
6	0.5	0	0.5	0	20.6	50.3
7	0.5	0	0	0.5	19.0	45.0
8	0	0.5	0.5	0	21.6	43.2
9	0	0.5	0	0.5	18.9	39.0
10	0	0	0.5	0.5	23.1	43.9
11	0.8273	0.1727	0	0	18.0	48.7
12	0.1727	0.8273	0	0	19.2	41.3
13	0.8273	0	0.1727	0	17.3	51.4
14	0.1727	0	0.8273	0	21.3	48.1
15	0.8273	0	0	0.1727	18.1	45.2
16	0.1727	0	0	0.9273	19.6	38.4
17	0	0.8273	0.1727	0	19.8	40.6
18	0	0.1727	0.8273	0	22.5	44.7
19	0	0.9273	0	0.1727	19.2	40.0
20	0	0.1727	0	0.8273	19.3	40.1
21	0	0	0.8273	0.1727	21.4	46.8
22	0	0	0.1727	0.2773	20.8	36.3
23	0.5670	0.2165	0.2165	0	23.0	52.5
24	0.5670	0.2165	0	0.2165	20.2	46.2
25	0.5670	0	0.2165	0.2165	22.2	48.2
26	0.2165	0.5670	0.2165	0	22.4	43.9
27	0.2165	0.5670	0	0.2165	21.9	43.4
28	0	0.5670	0.2165	0.2165	23.9	39.4
29	0.2165	0	0.5670	0.2165	24.8	43.5
30	0	0.2165	0.5670	0.2165	25.8	42.3
31	0.2165	0.2165	0.5670	0	25.5	43.0
32	0.2165	0.2165	0	0.5670	21.8	37.5
33	0.2165	0	0.2165	0.5670	22.7	43.0
34	0	0.2165	0.2165	0.5670	23.0	41.0
35	0.25	0.25	0.25	0.25	24.8	46.8

1.2. Forming of mathematical models

Calculation procedure of mathematical models is following: Select polynomial for corresponding polycomponent system, with we wish to describe investigated feature system. Polynomial selection depends of accuracy we wish achieve by prognosis a certain feature. In our case polynomial of fourth order is selected. Then, by using corresponding mathematical relations [5-14] and data from table II, calculate polynomial coefficients. Calculation of polynomial coefficients and determination of analytically form was made on calculator PDP 11/40. On that way we have obrained following expressions for prognosis investigated feature of portland cement:

a - mathematical model for prognosis of compressive strength after 3 days has a following form:

$$\begin{aligned}\zeta_3 = {} & 17.5z_1+19.8z_2+24.3z_3+18.2z_4-5.8z_1z_2-1.2z_1z_3+ \\ & + 4.6z_1z_4-1.8z_2z_3-0.4z_2z_4+7.4z_3z_4+1.63z_1z_2(z_1-z_2) \\ & - 0.26z_1z_3(z_1-z_3)-5.57z_1z_4(z_1-z_4)+1.31z_2z_3(z_2-z_3) \\ & - 6.13z_2z_4(z_2-z_4)-18.14z_3z_4(z_3-z_4)+12.72z_1z_2 \\ & (z_1-z_2)^2-19.25z_1z_3(z_1-z_3)^2+5.60z_1z_4(z_1-z_4)^2- \\ & - 10.50z_2z_3(z_2-z_3)^2+5.02z_2z_4(z_2-z_4)^2-19.72z_3z_4 \\ & (z_3-z_4)^2+196.45z_1^2z_2z_3+36.64z_1^2z_2z_4+121.65z_1^2z_3z_4+ \\ & + 44.08z_1z_2^2z_3+192.02z_1z_2^2z_4+179.36z_2^2z_3z_4+218.85 \\ & z_1z_3^2z_4+193.75z_2z_3^2z_4+225.30z_1z_2z_3^2+ 78.34z_1z_2z_4^2- \\ & - 56.70\ z_1z_3z_4^2-40.73z_2z_3z_4^2-189.10z_1z_2z_3z_4. \end{aligned} \quad (3)$$

b - mathematical model for prognosis of compressive strength after 28 days has a following form:

$$\begin{aligned}\zeta_{28} = {} & 47.5z_1+38.4z_2+46.6z_3+36.6z_4+11.4z_1z_2+13.4z_1z_3+ \\ & + 11.8z_1z_4+3.2z_2z_3+6.0z_2z_4+9.6z_3z_4+7.71z_1z_2 \\ & (z_1-z_2)+13.79z_1z_3(z_1-z_3)-1.79z_1z_4(z_1-z_4)+6.08 \\ & z_2z_3(z_2-z_3)-6.83z_2z_4(z_2-z_4)+21.84z_3z_4(z_3-z_4) + \\ & + 6.88z_1z_2(z_1-z_2)^2+14.47z_1z_3(z_1-z_3)^2-31.62z_1z_4 \\ & (z_1z_4)^2-3.38z_2z_3(z_2-z_3)^2+27.65z_2z_4(z_2-z_4)^2- \\ & - 21.58z_3z_4(z_3-z_4)^2+334.93\ z_1^2z_2z_3+95.65z_1^2z_2z_4+ \\ & + 57.75z_1^2z_3z_4-27.31z_1z_2^2z_3+183.19z_1z_2^2z_4-142.77 \\ & z_2^2z_3z_4-385.55z_1z_3^2z_4-158.21z_2z_3^2z_4-369.19z_1z_2z_3^2- \\ & - 430.56z_1z_2z_4^2+146.67z_1z_3z_4^2+139.83z_2z_3z_4^2+847.45 \\ & z_1z_2z_3z_4. \end{aligned} \quad (4)$$

Obtained mathematical models (3) and (4) are presented in form not much convenient for calculations. On the other hand, presentation mathematical models in more convenient form, in form of intial coordinates x_i, in which are represented minerals of portland cement clinker (C_3S, C_2S, C_3A, C_4AF), is difficult also, because of big dimensions of mathematical model. For to solve these two opposite requirements, program is conceived, that is possible on the base of contents C, S, A and F in portland cement clinker and by Boque formula, calculate contents of C_3S, C_2S, C_3A and C_4AF (coordinates x_i). Dependence transformation between system coordinates x_i and z_i ($i = 1,2,3,4$) is assigned by means of matrix equation $Z = A^{-1}X$.

On the base of data from table I, we form matrix A in form:

$$A = \begin{vmatrix} 0.7304 & 0.4095 & 0.7373 & 0.5334 \\ 0.0689 & 0.4105 & 0.0743 & 0.2104 \\ 0.1005 & 0.0482 & 0.0589 & 0.1359 \\ 0.1002 & 0.1318 & 0.1295 & 0.1203 \end{vmatrix} \quad (5)$$

Since $Z = A^{-1}X$, it is:

$$\begin{vmatrix} z_1 \\ z_2 \\ z_3 \\ z_4 \end{vmatrix} = \begin{vmatrix} 0.7304 & 0.4095 & 0.7373 & 0.5334 \\ 0.0689 & 0.4105 & 0.743 & 0.2104 \\ 0.1005 & 0.0482 & 0.0589 & 0.1359 \\ 0.1002 & 0.1318 & 0.1295 & 0.1203 \end{vmatrix}^{-1} \times \begin{vmatrix} x_1 \\ x_2 \\ x_3 \\ x_4 \end{vmatrix} \quad (6)$$

Solwing above matrix:

$$\begin{vmatrix} z_1 \\ z_2 \\ z_3 \\ z_4 \end{vmatrix} = \begin{vmatrix} 5.517 & 5.600 & 0.484 & -34.660 \\ 1.300 & 4.051 & -4.627 & -7.623 \\ -2.295 & 5.481 & -5.811 & 26.324 \\ -3.523 & -3.203 & 10.921 & 16.926 \end{vmatrix} \times \begin{vmatrix} x_1 \\ x_2 \\ x_3 \\ x_4 \end{vmatrix} \quad (7)$$

From matrix (7):

$$\begin{aligned} z_1 &= 5.517\,x_1 + 5.600\,x_2 + 0.484\,x_3 - 34{,}660\,x_4 \\ z_2 &= 1.300\,x_1 + 4.051\,x_2 - 4.627\,x_3 - 7{,}603\,x_4 \\ z_3 &= -2.295\,x_1 - 5.481\,x_2 - 5.811\,x_3 + 26.324\,x_4 \\ z_4 &= -3.523\,x_1 - 3.203\,x_2 - 10.291\,x_3 + 16.926\,x_4 \end{aligned} \quad (8)$$

For each value x_i ($i = 1,2,3,4$) by means of (8), calculate values for z_i ($I = 1,2,3,4$), which then change in mathematical models (3) and (4), after that, on exit from calculating system will be printed values of prognostic quality characteristics, in our case compressive strength after 3 and 28 days.

2. DISCUSSION OF OBTAINED RESULTS

During forming mathematical models (3) and (4), 70 experiments were realized in total (35 for each model); experimental data are then used for calculation polynomial coefficients. During polynomial selection, which will describe feature dependance on chemical composition, was selected polynomial of fourth order, since it makes possible in selected concentration area, obtain high prognosis accuracy (deviations between prognostic and experimental values are minimal).

An adequateness of obtained mathematical models is examined by Student t-test, and in all casses calculated values of t-test are less then tabulated at = 0.05. In addition, that verification was made also in points of plan, and obtained results are presented in table III. As shown in table III, differences between prognostic (R) and experimental (E) results are insignificant, so prognostic values deviations are 0.4-0.6% (for compressive strength after 28 days). As shown, a good coincidence is obtained between experimental and prognostic compressive strength after 3 and 28 days.

Comparing our results, obtained by means of models (3) and (4), with results of L.Aldriges [1], we can see that is possible, by means of our mathematical models, obtain a reliable prognosis of investigated features. Models proposed by L. Aldriges are unreliable and in most cases, have not described causal-consequent connection between composition and features of cement.

As shown in table III, there is a good coincidence between prognostic and experimental results. However, that still not means that mathematical models can be used successfully for strength prognosis in cement factories. Theirs accuracy and application will depend, before all, on accuracy of chemical and physical-mechanical investigations, which take place in cement factories and which sometimes can be considered only for orientation. With exact input data for particular minerals of portland cement clinker will be provided exact values for obtaining coordinates of "pseudocomponents" z_i, i.e. compressive strength after 3 and 28 days.

As on compressive strengths after 3 and 28 days, besides mineralogical composition, conditions of age and investigations have a certain influence, it is necessary to coordinate these conditions with prescribed conditions of corresponding standard, during practical application our models, as obtained models can be used for accurate prognosis of compressive strengths after 3 and 28 days.

As on compressive strength after 3 and 28 days, besides mineralogical composition, conditions of age and investigations have a certain influence, it is necessary to coordinate these conditions with prescribed conditions of corresponding standard, during practical application our models, as obtained models can be used for accurate prognosis of compressive strengths after 3 and 28 days.

Table III. Results of experimental (E) and prognostic (R) values of strength after 3 and 28 days

N	Pseudocomponents				Response function Pressure, MPa			
	z	z						
	z_1	z_2	z_3	z_4	E	R	E	R
1	1	0	0	0	17.5	17.5	47.5	47.5
2	0	1	0	0	19.8	18.9	38.4	38.4
3	0	0	1	0	24.3	24.3	46.4	46.4
4	0	0	0	1	18.2	18.2	36.6	36.6
5	0.5	0	0	0	17.2	17.2	45.8	45.8
6	0.5	0	0.5	0	20.6	20.6	50.3	50.3
7	0.5	0	0	0.5	19.0	19.0	45.0	45.0
8	0	0.5	0.5	0	21.6	21.6	43.2	43.2
9	0	0.5	0	0.5	18.9	18.9	39.0	39.0
10	0	0	0.5	0.5	23.1	23.1	43.9	43.9
11	0.8273	0.1727	0	0	18.0	18.1	48.7	48.6
12	0.1727	0.8273	0	0	19.2	19.1	41.3	41.2
13	0.8273	0	0.1727	0	17.3	17.4	51.4	51.3
14	0.1727	0	0.8273	0	21.8	21.8	48.1	48.1
15	0.8273	0	0	0.1727	18.1	18.0	45.2	45.2
16	0.1727	0	0	0.8273	19.6	19.6	38.4	38.3
17	0	0.8273	0.1727	0	19.8	19.7	40.6	40.6
18	0	0.1727	0.8273	0	22.5	22.5	44.7	44.7
19	0	0.8273	0	0.1727	19.1	19.1	40.0	40.0
20	0	0.1727	0	0.8273	19.3	19.3	40.1	40.1
21	0	0	0.8273	0.1727	21.4	21.4	46.8	46.7
22	0	0	0.1727	0.8273	20.8	20.9	36.3	36.2
23	0.5670	0.2165	0.2165	0	23.0	23.1	52.5	52.4
24	0.5670	0.2165	0	0.2165	20.2	20.1	46.2	46.1
25	0.5670	0	0.2165	0.2165	22.2	22.2	48.2	48.2
26	0.2165	0.5670	0.2165	0	22.4	22.4	43.9	43.9
27	0.2165	0.5670	0	0.2165	21.9	21.9	43.4	43.4
28	0	0.5670	0.2165	0.2165	23.8	23.8	39.4	39.4
29	0.2165	0	0.5670	0.2165	24.8	24.7	43.5	43.5
30	0	0.2165	0.5670	0.2165	25.1	25.2	42.3	42.3
31	0.2165	0.2165	0.5670	0	25.5	25.5	43.0	43.0
32	0.2165	0.2165	0	0.5670	21.8	21.7	37.5	37.5
33	0.2165	0	0.2165	0.5670	22.7	22.7	43.0	43.0
34	0	0.2165	0.2165	0.5670	23.0	23.0	41.0	41.0
35	0.25	0.25	0.25	0.25	24.8	24.7	46.8	46.7

C O N C L U S I O N

For prognosis of portland cement features and establishement of dependance between chemical composition of portland cement clinker and mechanical strengths of portland cement, we have used D-optimal plans and plans with included pseudocomponents.With the help of these methods we have obtained mathematical models, which make possible qualitative prognosis with minimal deviations between prognostic and experimental values. Adequateness of obtained athematical models is examined by means of Student t-test, and in all cases calculated values of t-test are less then tabulated at $\alpha = 0.05$. Calculating programs are developed, what makes possible wide use of calculators, as for calculation of polynomial coefficients so for testing of corresponding mathematical models.

R E F E R E N C E S

|1| L. Aldrige, Composition of Portland Cement, Proc. 7th Inter.Cong. of the Chem. of Cem. III, VI-83, Paris, (1983)

|2| S. Popovics, Composition of Portland Cement, Proc 7th Inter. Conf. of the Chem. of Cem. III, VI-47, Paris, (1983)

|3| V. Šein, O. Mčedlov - Petrosjan, Cement, 9, 15 (1973)

|4| Lj. Dragićević, Prognosis of materials properties of multicomponent composition by example of silicate system, Doctoral thesis, CMS (88-103), Beograd 1984

|5| R. Fisher, A. Mackenzie, J. Agricultural Sci. 13, 311 (1933)

|6| G. Box, K. Wilson, J. Roy, Statist. Soc 13, 1 (1951)

|7| J. Kiefer, Roy, Statist. Soc 21, 272 (1959)

|8| I. Zedginidze, matematičeskoe planirovanie eksperimenta dla isledovania mnogokomponentnih sistem, Nauka, Moskva, 1976

|9| J. Gorman, J. Hinman, Simplex Tablice Desings Tok multicomponent sistems, Tehnometries 4, 463 (1962)

|10| H. Scheffe, J. Roy. Statist. Soc. 20, 344 (1958)

|11| O. Kasatkin, Primenie matematičeskih metodov dla isledovenia mnogokomponentnih sistem, Metalurgia, Moskva, 1974.

|12| I.Zedginidze, Matematičeskoe planirovanie eksperimenta dla isledovania i optimizacii svojstv cmesej, Mecniereba, Tbilisi, 1971.

|13| J. Kiefer, Optimum Designs of Regresion Problems, II Ann. Matt.stat. I, 398 (1962)

|14| T.Kemleva, Primenenie matematičeskih metodov dla isledovania mnogokomponentnih sistem, Metalurgia, Moskva, 1974.

SUB-THEME/SOUS-THÈME 1.2

Relationship of processing parameters to clinker properties; influence of minor components.

Rapport entre les paramètres du processus et les proprietés du clinker, influence des éléments mineurs.

Chairman/Président:

A.I. Boikova
Academy of Sciences of the U.S.S.R.
Leningrad, U.S.S.R.

Principal Reporter/Rapporteur Principal:

I. Maki
Nagoya Institute of Technology
Nagoya, Japan

YUSHIRO KIHARA, Research Mineralogist, Department of Physicochemistry, Associação Brasileira de Cimento Portland and Assistant Professor, Department of Mineralogy and Petrology, University of São Paulo, Brazil. 1

INFLUENCE OF HIGH ASH CONTENT MINERAL COAL IN PORTLAND CEMENT CLINKER CHARACTERISTICS L'INFLUENCE DU CHARBON MINÉRAL À HAUTE TENEUR EN CENDRES DANS LES CARACTÉRISTIQUES DU CLINKER DE CIMENT PORTLAND 1.2

ABSTRACT: The necessity of reducing the fuel oil consume and its consequent replacement by coal in cement industry, had a strong influence over the behavior of rotary kiln running as well as over clinker composition and quality.

Besides the ash content and composition, inadequate conditions of coal preparation and firing, influence greatly the production process and sintering reactions, which are responsible for formation or instability of coating, low durability of refractory bricks, changes in burnability, inhomogeneity and modifications in clinker composition.

High ash content (35 - 54%) of Brazilian mineral coals used in cement industry not only determines their low calorific value (5200 - 3300 kcal/kg), but also causes modifications in clinker composition and microstructure. Such modifications are basically due to the addition of SiO_2 and $A\ell_2O_3$ originated from the ash. The changes in the microstructure are those related to the corrosion of the C_3S, to the appearance of irregular zones of C_2S, to changes in the dimension and morphology of cristals, etc.

Industrial clinkers obtained under coal substitution rates and differentes firing systems, were studied by optical microscopy and submitted to chemical analyses in order to characterize the influence this substitution has in clinker structure and quality.

In addition, comments are made on the influences clinker microstructural changes may have over its potential quality.

Sumário A necessidade de reduzir o consumo de óleo e, em consequência, sua substituição por carvão, tem uma forte influência sobre o comportamento na marcha do forno relativo e também sobre a composição e qualidade do clinquer.

Além do conteúdo de cinzas a composição, condições inadequadas no preparo do carvão e queima, influencia grandemente o processo de produção e reações de sinterização, as quais são responsáveis pela formação ou instabilidade da crosta, baixa durabilidade dos tijolos refratários, alterações de queima, falta de homogeneidade e modificações na composição do clinquer.

Alto conteúdo (35 - 54%) dos carvões minerais brasileiros usados na indústria do cimento não só determina o seu baixo poder calorífico (5.200 - 3.300 kcal/kg) mas causa também modificações na composição e na microestrutura do clinquer. Tais modificações são basicamente devidas à adição de SiO_2 e $A\ell_2O_3$ originadas da cinza. As modificações na microestrutura são as relacionadas da corrosão do C_3S, do aparecimento de zonas irregulares de C_2S, a mudança na dimensão e morfologia de cristais, etc.

Clinqueres industriais obtidos com diferentes quantidades de substituição de carvão e diferentes sistemas de queima, foram estudados por microscopia ótica e submetidos à análises químicas de modo a caracterizar a influência que essas substituições tem na estrutura e qualidade do clinquer.

Além disso, são feitos comentários sobre a influência que as mudanças na microestrutura do clinquer pode ter sobre a sua qualidade potencial.

INTRODUCTION

The energy crisis of the seventies made it economically impracticable for the Brazilian Cement Industry to maintain the same degree of dependance on fuel oil, mostly imported. In search for alternative solutions, mineral coal turned out to be the best substitute, among other alternatives like vegetal coal, siderugical, petrochemical and industrial wastes, rice husk, etc.

The increasing use of mineral coal in the cement industry influenced not only the kiln production, but also the composition and the quality of the clinker. The aim of this paper is to establish the correlation between clinquer quality and its microstructural features as influenced by burning conditions of high ash content mineral coal with different degrees of technological improvement.

CHARACTERISTICS OF MINERAL COAL USED AS FUEL

When compared to coals used in other countries, brazilian mineral coals are characterized by high ash contents and low calorific values. Distinct regional characteristics are due to differences in origin and mineralogical composition. As seen from Table 1, which exhibits analysis of some coals used by the cement industry, coals from Rio Grande do Sul (RS) are characterized, in a general way, by higher volatile and moisture contents, lower fixed carbon and sulfur contents and lower coalification degrees (sub-bituminous).

Mineralogically, the inorganic portion of coals is made up of quartz (SiO_2) and clay minerals (hydrated silico-aluminates, some with alkalies). Feldspar (alkali-aluminosilicate), calcite ($CaCO_3$), pyrite (FeS_2) and gypsum ($CaSO_4.2H_2O$) can occur secondarily among others. An x-ray diffraction pattern of a brazilian mineral coal sample is shown in Figure 1.

The coal ashes have a silico-aluminous composition, with lesser quantities of iron, calcium, magnesium and alkalies. Elements like titanium, phosphorus, manganese, strontium, vanadium, chlorine and rare earth elements occur in trace quantities. Average chemical compositions of various coal ashes are shown in Table 2. It is important to observe that the values in this Table represent the mean composition of various ashes, as these can exhibit great compositional variability. These variations are caused by differences in the sedimentary country rock characteristics.

Considering that part of the ashes is added to the clinker, chemical composition control of major and minor elements constitutes an important parameter to evaluate clinker quality, the durability of refractories and kiln stability.

Knowledge of the characteristics of coal used as fuel is an important factor for the clinker fabrication process and for the quality of the clinker so produced.

INTERACTION MECHANISMS OF MINERAL COAL ASHES IN THE PORTLAND CEMENT CLINKER

During coal burning, the mineralogy of inorganic compounds is modified by the downbreak of clay minerals and by the decomposition of carbonates,

TABLE 1 - Analysis of some mineral coals used by brazilian cement industries

Sample	1	2	3	4	5	6
Origin	RS	RS	RS	RS	RS	SC
Residual moisture (%)	10,86	6,84	8,68	5,59	15,20	3,17
Hygroscopic moisture (%)	11,30	9,68	9,20	9,74		1,56
Volatile matter (%)	44,98	38,26	41,98	39,71	22,30	24,99
Ash content (%)	18,80	33,15	33,58	34,59	52,00	32,46
Fixed carbon (%)	36,21	28,59	24,44	25,70	2 7,60	42,55
Carbon (%)	58,10	52,20	51,50	47,50	–	54,20
Hidrogen (%)	3,80	3,60	3,60	3,20	–	3,60
Sulfur (%)	0,60	0,80	0,80	1,00	1,90	3,30
Calorific values (kcal/kg)	5994 5803	5158 4967	4800 4608	4633 4466	3200 –	5254 5062

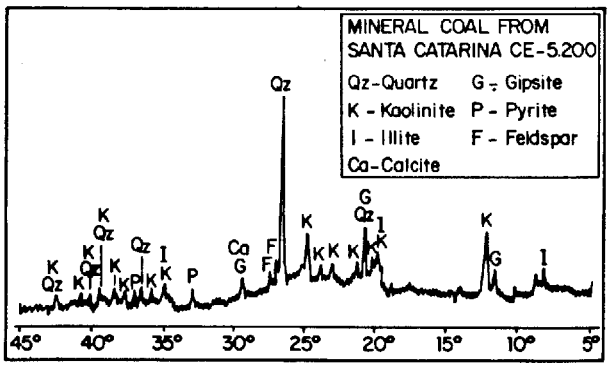

FIGURE 1 - X-ray diffraction pattern of brazilian mineral coal sample

TABLE 2 - Coal ash chemical analysis

Oxide \ Origin	Candiota (RS)	Charqueadas (RS)	Leão (RS)	Tubarão (SC)
SiO_2	71,7	65,1	58,2	56,7
Al_2O_3	18,2	23,0	26,8	26,3
CaO	1,0	3,1	1,4	2,2
MgO	0,6	0,6	0,4	0,9
Fe_2O_3	4,9	2,9	5,4	7,6
TiO_2	0,9	1,2	1,2	2,5
MnO_2	0,1	0,1	<0,1	0,2
K_2O	1,3	1,5	1,1	2,4
Na_2O	0,6	1,1	1,4	0,2
P_2O_5	0,1	0,1	0,08	0,1
SO_3	0,2	0,3	0,2	0,7
SiO_2 / Al_2O_3	3,93	2,83	2,17	2,15
Al_2O_3 / Fe_2O_3 (MA)	3,71	7,93	4,96	3,46
$\frac{SiO_2}{Al_2O_3 + Fe_2O_3}$ (MS)	3,10	2,51	1,81	1,67

sulphates and sulphides, with later formation of a silico-aluminous principal phase. The chemical composition and the reactivity of the ashes is controlled by the varying proportions of minerals that occur associated in the coal.

Mineralogical studies in ashes obtained by calcinating coal at 1400°C (Figure 2) demonstrated that they are made up of a vitreous silico-aluminous phase, residual quartz and secondarily crystallized mullite ($Si_2O_{13}Al_6$), cristobalite (SiO_2), magnetite and hematite.

Interaction of coal ashes with the clinker during fabrication process produces an eutetic with a lower softening point than in coal ashes and in the clinker separately[1]. A liquid phase is developed at lower temperatures, at the clinker-ash interface, and favours the assimilation reactions of the ashes by the clinker. High SiO_2 and Al_2O_3 content ashes, in contact with the clinker develope a reaction border characterized by the appearance of secondary C_2S. The higher ionic mobility of silicium when compared to calcium facilitates the attack and penetration of the ashes to the interior of the clinker, provoking the reconversion of C_3S crystals into C_2S and free secondary lime. At the same time, all free lime available in the area under ash influence participates in the formation of new C_2S crystals. The C_2S crystals formed at the beginning of the reaction tend to be elongated and oriented, following ash penetration directions, and with further development of the reaction they become more developed and ameboid (digitated), loosing the oriented aspect.

Kihara and Zampieri[2] undertook an experimental study on the influence of coal ashes from Santa Catarina (SC) and Rio Grande do Sul (RS) on portland cement clinker and, through microscope analysis, recognized three very distinct domains (Figure 3) in the experimental clinkers, similar to the zones observed by Heilmann[3]

The Z_1 (outer) domain corresponds to the initial ash zone. In this domain, ameboid or dendritic, commonly twinned C_2S crystals, as well as secondary, prismatic crystals identified as gehlenite ($Ca_2Al_2SiO_7$) by x-ray diffraction pattern can be observed, embedded in an abundant fused silico-aluminous phase (Figure 4).

The Z_2 (intermediate) domain is made up exclusively of twinned and rather densely distributed C_2S crystals with a relatively small quantity of interstitial phase. It corresponds to the original clinker zone modified by the ashes, and with a complete transformation of the previous C_3S in C_2S. Many times the C_2S crystals produced by these transformation are oriented, showing the ash action directions (Figure 5). The composition of the modified clinker is characterized essentially by the C_2S and by the increase in C_3A content.

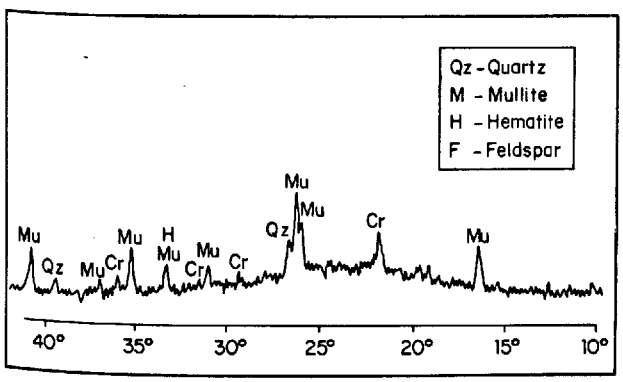

FIGURE 2 - X-ray diffraction pattern of a mineral coal calcinated at 1.400 °C

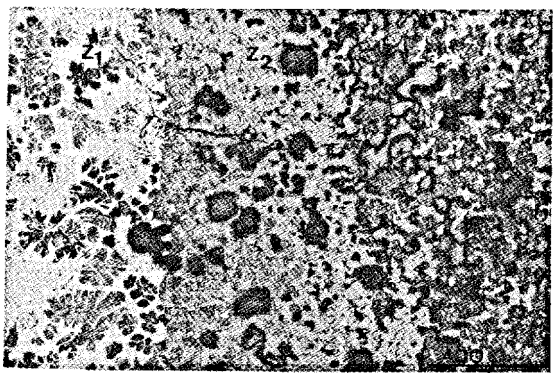

Figure 3: Ash reaction border, showing the three domains: Z_1 (outer), Z_2 (intermediate) and Z_3 (inner).

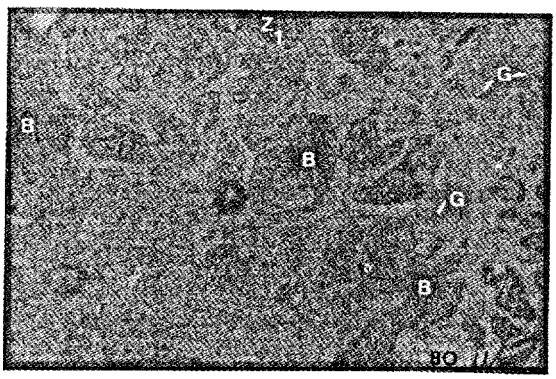

Figure 4: Twinned and ameboidal C_2S (B) and prismatic gehlenite (G) crystals in the Z_1 domain.

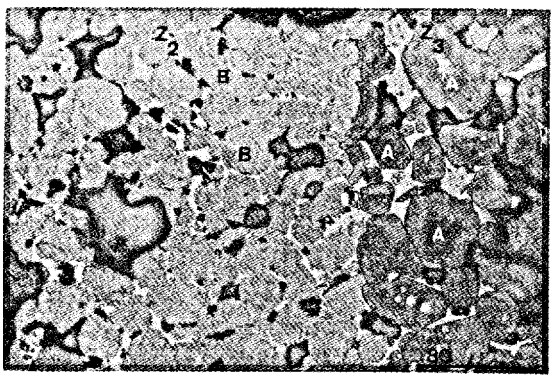

Figure 5: C_2S (B) region in the Z_2 domain, some crystals elongated following the direction of ash attack and practically unaltered C_3S (A) crystals of the Z_3 domain.

The Z_3 (inner) domain represents the almost unaltered clinker, where occasionally only part of the free CaO has been subtracted, mainly in the region close to the C_2S domain. The Z_3 domain is characterized by unaltered C_3S crystals in its mineralogy (Figure 3 e 5).

The boundaries between these three domains are well defined and change with ash and clinker characteristics as well with the reaction time length. There is an effective tendency between the ashes (characteristically acid) and the portland cement clinker (basic) towards a physico-chemical equilibrium.

Features similar to those observed under experimental conditions were recognized in localized regions in the interior of some industrial clinkers. Whenever this regions occur, they were observed to be associated to coarse coal fragments. The intensity of the assimilation reaction of the ashes by the clinker depends on grain size and burning conditions, being more favorable the thinner the coal grain size.

INFLUENCE OF MINERAL COAL ON CLINKER COMPOSITION AND MICROSTRUCTURE

Mineral coals with high ash contents modify original raw mix composition. The moduli values that control the raw mix should be adjusted to the ash content and ash composition of the coals being used. Ignoring these parameters could affect the raw mix burnability and the obtention of a suitable composition.

Table 3 shows some chemical analysis of brazilian industrial raw mixes and clinkers from dry process kiln ran with fuel oil and mineral coals from Rio Grande do Sul and Santa Catarina which allow the recognition of chemical and mineralogical composition variations due to the influence of ashes in the clinker. The following conclusions can be reached by analysing this table:

- The increasing modification of raw mix by coal ashes is revealed by a decrease of the lime saturation factor (LSF) and the silica ratio (SR) and by an increase of the alumina ratio (AR). The higher the ash content and the substitution degree of fuel oil by coal, the higher will be LSF variation. Among the chemical moduli, the LSF is the one which displays the most significative changes, thus influencing composition and clinker quality;

- The increasing use of high ash content coals, like those from Candiota (3200 kcal/kg) with 50% ash content implies in the use of high LSF raw mix. The Candiota coal is being used as an approximately 30% weight percentage mixture with coal from Santa Catarina (5200 kcal/kg) and LSF 1.2 to 1.3; and,

- Mineralogically there is a decrease in the C_3S/C_2S ratio, and an increase in the interstitial phase, specially of C_3A, as well as a decrease in silicate content.

TABLE 3 - Brazilian industrial raw mix and clinker chemical analysis

	PLANT A*		PLANT B**		PLANT C***		PLANT D****	
	Raw mix	Clinker	Raw mix	Clinker	Raw mix	Clinker	Raw mix	Clinker
L.I.	35,00	0,40	35,35	0,17	35,53	0,14	37,91	0,04
SiO_2	14,19	21,57	13,67	21,92	12,31	21,90	10,76	20,03
Al_2O_3	3,99	5,93	3,00	5,41	2,85	5,38	2,52	5,65
Fe_2O_3	2,10	3,02	2,04	3,45	1,84	3,22	2,34	4,17
CaO	42,45	65,44	44,01	65,26	44,64	65,70	43,91	64,03
MgO	0,35	0,38	0,97	1,60	0,99	1,43	2,41	4,11
SO_3	0,25	0,93	-	1,43	-	-	0,30	1,30
Na_2O	0,53	0,73	0,09	0,06	0,36	0,47	-	-
K_2O	0,08	0,05	0,28	0,52	0,78	1,01	-	-
LSF	0,93	0,95	1,02	0,92	1,15	0,94	1,27	0,98
SR	2,33	2,41	2,71	2,47	2,63	2,55	2,21	2,04
AR	1,90	1,96	1,47	1,57	1,55	1,67	1,08	1,35

* burned with fuel oil

** burned with 50% mineral coal from Rio Grande do Sul (CE-4700)

*** burned with 100% mineral coal from Santa Catarina (CE-5200)

**** burned with 100% mineral coal in 3:1 proportion from Santa Catarina (CE-5200) and Rio Grande do Sul (CE-3200), respectivaly

In the dry kilns, when coal ashes are carried beyond the clinkerization zone, a good diffusion with the raw mix will take place, without prejudice to clinker microstructure (Figure 6), apart from changes in its composition (4, 5, 6). On the other hand, unfavorable effects occur when the ashes are deposited on clinker grains (7) or when the coal has an improper grain size that would not permit a complete absorption and diffusion of the ashes (Figure 7 and 8). As a result, segregated silicatic zones will be formed, apart from the corrosion and decomposition of the previously formed C_3S (Figure 4 and 5).

Heterogeneous microscopic features which evidence improper ash absorption and burning conditions can be observed more frequently in clinkers where the burning system consists in granulated coal injection in air-suspention pre-heater or in coarse coal injection through the primary air tube. Coal grain size heterogenity, inadequate coal grain size, moisture, feeding and combustion gases are sensible factors in these burning systems and affect kiln production and, as a consequence, ash absorption and the development of characteristic microstructural features. The chief microscopic features which characterize clinkers inadequately burnt with high ash content coals are the following:

1 - varied and irregular porosity due to ash action on grain surfaces originating a more porous crust; or an increase in clinker porosity in a way similar to grinding deficiency or insatisfactory clinkerization conditions.

2 - brownish colours in some regions of the clinker, possibly due to locally more reducing conditions[9]. This feature has been frequently observed in national industrial clinkers, particularly after the more widespread use of coal.

3 - coal nodules, partially calcinated, mainly in clinkers in which part of the burning system is by granulated coal injection (with diameter sometimes as large as 1,5 inches) in the pre-heater.

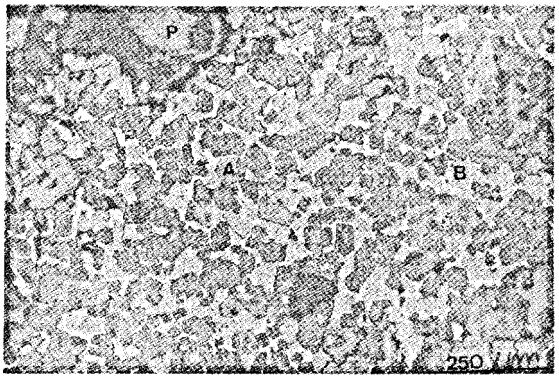

Figure 6: Clinker calcinated with 100% micropulverized coal showing an appropriate ash absorption as seen from the homogeneous distribution of the C_3S (A) and C_2S (B) crystals (P = pores).

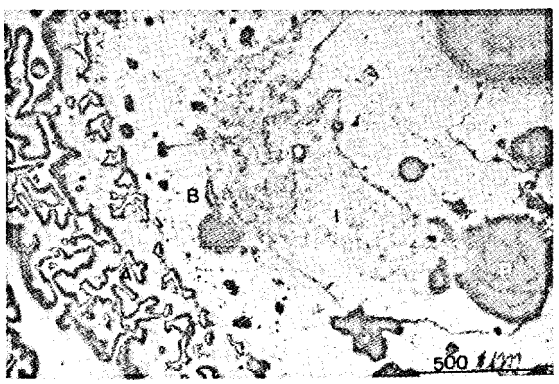

Figure 7: Heterogeneous aspect due to improper absorption of granulated coal ashes.
I: central silico-aluminous zone
B: calcic zone, mainly C_2S
C: external zone, unattacked clinker

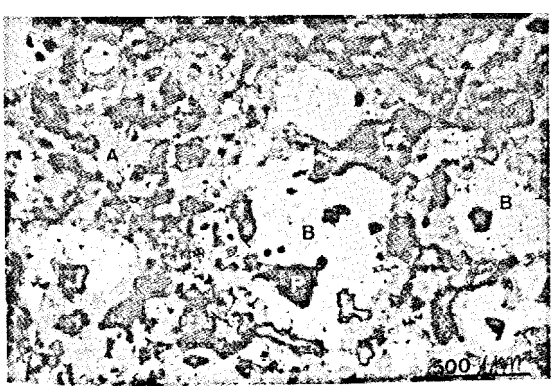

Figure 8: C_2S (B) zones due to the burning of high ash content granulated coal.

Inadequate grain-size and moisture are the factors responsible for incomplete combustion and the later incorporation of the granules by the clinker. Indiscriminated siliceous zones, decomposed C_3S crystals, spherical metallic inclusions, calcium shulphides (oldhamite) and brownish colors are commonly associated to the nodules;

4 - irregular C_2S zones (Figure 7 and 8), originated from coarse-grained coals with high ash contents or by the incorporation of fused ash particles through precipitation over grain surfaces and penetration in the voids and fissures of the clinker. The C_2S are generally digitated and occur associated to a more widespread interstitial phase. Exceptionally, C_2S γ crystals are observed in more acid regions with low local LSF. Regular C_2S zones (Figure 8), similar to those produced when inefficient grinding of quartz in the raw material takes place, can be originated by the ashes, due to a higher concentration of quartz grains, specially in coals from Rio Grande do Sul;

5 - decomposed C_3S crystals led to the formation of C_2S (Figure 5), due to their reaction with the more acid ashes. Coal ashes cause a reconvertion of the C_3S, with the formation of C_2S and transference of CaO to the ashes. Some times the C_2S crystals remind the original C_3S crystal shapes;

6 - excessive growth of the C_3S and C_2S crystals caused by longer burning conditions thus indicating characteristics of a longer flame;

7 - C_3S crystals with exsolutions, indicating reducing conditions[9]. These features are more common in clinkers calcinated with coal than in those calcinated with fuel oil; and,

8 - metallic inclusions, associated to an intersticial phase rich in C_3A, suggesting local reducing conditions, due to improper burning of granulated coal.

THE INFLUENCE OF COAL IN CLINKER QUALITY

A good quality portland cement clinker is obtained from adequatily selected and dosed raw materials, so that the formation of hidraulic minerals (C_3S, C_2S, C_3A and C_4AF) is guaranteed during the clinkerization reactions, maintaining the projected characteristics without the formation of microstructural features typical of improper grinding or homogenization of the raw materials. The burning and cooling conditions should guarantee the stability and reactivity of the formed minerals.

The quality of a clinker can be prejudiced when improperly prepared and burned high ash content mineral coal is used. Underisable microstructural

features are thus produced, affecting the reactivity and stability of the formed crystals.

C_2S zones produced by the incorporation of the coal ashes, sometimes joined by C_2S γ can influence the grindability and reactivity of the clinkers.

C_3S crystals developed with corrosion and/or exsolution microstructural features, accompanied by low reactivity C_2S forms, influence the development of low mechanical resistence in the cement, specially at later ages.

The increase in C_3S contents, due to the arrival of Al_2O_3 from the ashes and/or to reducing conditions, influences the setting time, the heat of hydration, the optimal gypsum content and the evolution of mechanical strength at early ages.

Modifications in silicate content and decrease in the C_3S/C_2S ratios can influence cement behaviour at longer ages.

CONCLUSIONS

The use of high ash content mineral coal modifies clinker characteristics, changing their composition and reactivity. When inadequately prepared and burnt, it forms the development of crystalline forms and microstructural features underisable for the reactivity and stability of the formed crystals, which can in extreme situations undermine the quality of the cement so produced.

Irregularities in the coal burning and in the assimilation of the ashes by the clinker are shown by the segregated distribution of the C_2S crystals, corrosion and excessive growth of the C_3S crystals, digitation of the C_2S crystals, formation of C_2S γ crystals and exsolution in the C_3S crystals, appearance of reduced phases, and variation in the C_3S, C_2S and C_3A contents.

The petrographic study of clinker, based on the microscopic observation of mineralogical and microstructural features of the crystals represents a great help for the control and improvement of coal burning as well as evaluates the quality of the cement so obtained.

References

1 ALEGRE, R. *Formation et suppression des anneaux de cendres dans les fours rotatifs à ciment.* Paris, CERILH, 1958. (Pub. tecn. n. 95)

2 KIHARA, Y. & ZAMPIERI, V. A. *Aspectos microscópicos da interação das cinzas do carvão mineral com o clínquer de cimento portland.* "Cerâmica", São Paulo, 31(185):99-104, junho 1985.

3 HEILMANN, T. *Reactions of coal ash with portland cement clinker during the burning process.* In: INTERNATIONAL Symposium on the Chemistry of Cement, 4th, Washington, D.C., 1960. v.1, p.87-98.

4 CHATTERJEE, A.K. *Phase composition, microstructure, quality and burning of portland cement clinkers; a review of phenomenological interrelations.* World Cement Technology, London, 10(4): 127-35, May; (5):165-73, Jun. 1979.

5 HAWTHORNE, F. & RICHEY, F. & DEMOULIAN, E. *Influence of the fuel and burning process on the microscopic structures and characteristics of the clinker.* In: GOUDA, G.R., ed. Proceedings of the third International Conference on Cement Microscopy, Houston, Texas, March 16-19, 1981. Duncanville, International Cement microscopy Association, 1981. p.121-6.

6 DOBROWSKY, F. *Le charbon pulverisé et les combustibles de remplacement pour l'industrie cimentière.* Ciments, Bétons, Plâtres, Chaux, Paris, (729):93-101, jan/fév. 1981.

7 L'HOPITALLIER, P. & JAMES, L.M. *Le clinker de ciment artificel vu au microscope en lumière réfléchie.* Revue des Matériaux de Constructions et de Travaux Publics, Paris, (416):17-28, oct. 1950.

8 KIHARA, Y. *A influência do carvão mineral nas características do clínquer de cimento portland.* "Cerâmica", São Paulo, 31(189):201-206, out. 1985.

9 LONG, G.R. *The effect of burning environment of the microscopic characteristics of portland cement clinker.* In: GOUDA, G.R., ed. Proceedings of the fourth International Conference on Cement Microscopy, Las Vegas, Nevada, March 28-April 1, 1982. Duncanville, International Cement Microscopy Association, 1982. p.128-40.

SHEN WEI, Asso. Prof., Dept. of Material Science and Engineering, Tongji University, Shanghai, China. 1
FENG MINGFEN, Asso. Prof., Dept. of Material Science and Engineering, Tongji University, Shanghai, China.

A STUDY OF THE EFFECTS OF CaF_2 ON CLINKER DOPED WITH COMPOUND MINERALIZER

1.2

ABSTRACT: The purposes of present paper are to study the distribution of fluorine in the main phase of clinker, separate the silicate phase from the clinker and study the effects of fluorine on the hydration performance of Alite and its relation to the petrographic morphology.

Four clinkers with considerable differences in the amount of CaF_2 were prepared for chemical extraction, QXRD, EPMA, image analysis and measuring the hydration heat evolution, strength test, etc.

Experiments show that as the CaF_2 content is increased, the content of Alite increases, the amount of $\bar{F}$ solvated in this phase is increased also, and its morphology changes gradually from incomplete to complete appearence, the crystal size becomes smaller. It was found that the increment of hydration heat evoluted within 1 hr was almost proportional to the increment of Alite content. Thus, we propose that apart from the change of Alite morphology which favoured the strength development, the $\bar{F}$ solvated in Alite phase does not alter the hydraulic activity of Alite obviously in the early age.

As finalidades do presente trabalho são o estudo da distribuição de fluorite nas fases principais do clínquer, a separação da fase do silicato do clínquer e o estudo do efeito da fluorite no mecanismo de hidratação da alita e sua relação com a morfologia petrográfica.

Quatro clínqueres com diferenças consideráveis na quantidade de CaF_2 foram preparados para a extração química, QXRD, EPMA, análise de imagem e medição da evolução do calor de hidratação, testes de resistência, etc.

Experiências demonstram que à medida que o conteúdo de CaF_2 aumenta, a quantidade de alita aumenta, a qualidade de $\bar{F}$ solvato nesta fase aumenta também, e sua morfologia muda gradualmente de aparência incompleta para completa, o tamanho dos cristais torna-se menor. Foi também descoberto que o aumento da evolução do calor de hidratação em 1 hr foi quase proporcional ao incremento do teor de alita. Portanto, não propomos que a parte da mudança da morfologia da alita que favorece o aumento de resistência, o $\bar{F}$ solvato na fase da alita não altera a atividade hidráulica da alita sensivelmente nas primeiras idades.

SHEN WEI
FENG MINGFEN

1.2

INTRODUCTION

In recent years, the use of gypsum-flourite as compound mineralizer for lowering the clinkering temperature, increasing the klin production and energy saving has significant progress in China. The mechanism of compound mineralizer, i.e. the effects of fluorine in the presence of sulphate is consistently a subject of common interest. Some authors have reported, after containing the fluorine, the hydraulic activity of the Alite decreases, but the results are not all the same [1,2,3]. Moreover, the Alite phase in clinker has some differences from those in most of the studies using pure synthetic minerals. As for the relations among the solid solubility of fluorine, petrographic morphology and the properties of Alite, especially the difference from the clinker doped with fluorite only, few report can be found.

The purposes of the present paper are to study the distribution of fluorine in the main phase of clinker, separate the silicate phase from the clinker and study the effects of fluorine on the hydration performance of the Alite and its relation to the petrographic morphology. Four clinkers with considerable difference in the amount of fluorine were prepared in laboratory burnt at 1350°C. The chemical composition of the clinkers are given in Table 1.

Table 1. Chemical Composition of the Clinkers (%)

Sample	CaO	SiO_2	Al_2O_3	Fe_2O_3	MgO	SO_3	F	f-CaO
F_0	62.76	20.27	7.77	4.08	1.17	2.01	0.013	0.62
F_1	62.93	20.09	7.81	4.43	1.18	1.96	0.20	0.38
F_2	63.66	19.19	7.42	4.66	1.47	2.22	0.55	0.41
F_3	64.55	18.24	7.03	4.43	1.50	2.22	0.91	0.47

1. THE DISTRIBUTION OF FLUORINE IN CLINKER MINERALS

The distribution of fluorine in clinker minerals was measured by chemical extraction analysis and EPMA.

1.1 Chemical Extraction Analysis

The sample was ground into powder all passed through a No. 0080 sieve. The silicate phase was dissolved into liquid by using salicylic acid-methanol (SM) solution. The XRD patterns of the residue (Fig. 1) indicate that the silicate phase has been separated completely. By determining the fluorine content in the original clinker and the residue respectively by an ion-specific electrode, the fluorine contents distributed in the silicate phase and interstitial phase were obtained. The measured results are given in Table 2.

Table 2. Fluorine Distribution in Clinkers (%)

Sample	Content in clinkers	Interstitial phase		Silicate phase		
		content	fraction of total $\bar{F}$	content	fraction of total $\bar{F}$	solid solubility
F_0	0.013	0.0034	26.15	0.0096	73.85	0.0134
F_1	0.20	0.037	18.48	0.163	81.52	0.229
F_2	0.55	0.108	19.64	0.442	80.36	0.611
F_3	0.91	0.178	19.57	0.732	80.43	0.986

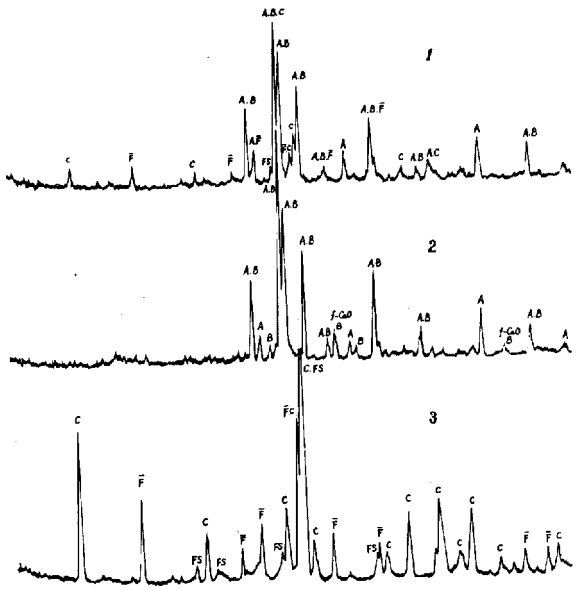

Fig. 1 XRD patterns before and after the chemical extraction

A - Alite; B - Belite;
C - C_4AF; $\bar{F}$ - $C_{11}A_7 \cdot CaF_2$;
FS - $3(C_2S \cdot C\bar{S}) \cdot CaF_2$

1 - F_3, original;
2 - after treatment using potassium-sucrose (KOSH) solution;
3 - after SM treatment.

1.2 Electron Probe Microanalysis

An electron-probe microanalyzer of Shimadzu EPM-810 was used. The $\bar{F}$ distribution measurement was conducted under the condition of 20 KV accelerating voltage and 10 nA probe current. The point analysis results are obtained by accumulating the counts in the period of 5 sec. in order to meet the condition that the energy of secondary radiation of fluorine is very low. The results obtained in F_2 clinker ($\bar{F}$ = 0.55%) at the points of Alite (Fig. 2,A), Belite (Fig.2,B) and interstitial phase (Fig. 2,C) are given in Table 3.

These results indicate that $\bar{F}$ concentration is highest in Alite phase, lower in Belite phase, lowest in interstitial phase. It can be seen from the data in Table 2: for the four clinkers studied in this paper, the $\bar{F}$ distributed at interstitial phase is only 18.48 ~ 26.15% of its total amount, most of the $\bar{F}$(73.85 ~ 81.52%) are distributed at silicate phase and its solid solution concentration is 0.0134~0.986%. It should be noted that as the $\bar{F}$ content in clinker is increased. It was found that the solid solubility of $\bar{F}$ in silicate phase varies nearly in proportion to the $\bar{F}$ content in the clinker.

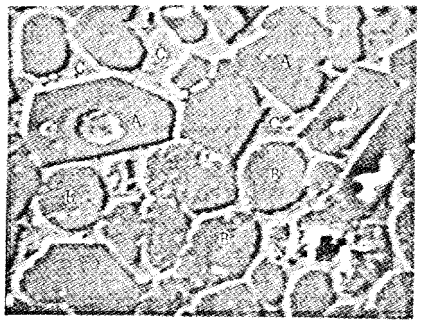

Fig. 2 Electron back scatter photograph of $\overline{F}_2$ clinker (× 1000)

Table 3. $\overline{F}$ element analysis at given points of F_2 clinker

Locations	A (Alite)	B (Belite)	C (Interstitial phase)
Counts*	251.6	201.5	103.7
	283.8	200.8	93.3
	264.4	208.5	101.6

* Average of 10 measurements

2. THE CORRELATION BETWEEN $\overline{F}$ CONTENT AND PETROGRAPHIC MORPHOLOGY

The polished surface of clinker was etched with 1% nitric acid in alcohol solution. The petrographic morphology of each clinker are given in Fig. 3. In the sample F_0, the size of Alite crystal is relatively large (50 ~ 60 μm), its amount is about 25% only and usually with incomplete appearence, some of them are in harbour shape. The white enclosures always existed in the Alite phase are large in size. The Belite phase appears as rounded grains with regular shape, about 15 μm in size. It can be seen that as the $\overline{F}$ content was increased, the Alite phase changed gradually from incomplete to complete appearence with more flattened periphery, and its amount was increased correspondingly. Furthermore, its crystal size became smaller, but with larger aspect ratio. As for the Belite phase, its amount was decreased with the increase of $\overline{F}$ content in the clinker, and transferred from round to brain, finger or leaf-like shape, turned more and more irregular. For example, in sample F_3 which contained more fluorine, the amount of Alite phase increased to a significant proportion, generally exceeded 70%. Most of the crystal was rather small (10 ~ 15 μm) and appeared as tabular or prismatic configuration with relatively sharp outline. The crystal shape was long and thin, with aspect ratio greater than 2. The Belite phase appeared to be leaf-like shape, its amount decreased obviously.

The amount of Alite phase in these four clinkers was estimated by Opton Photo-III Scanning Microscope Photometer with IBAS Interactive Image Analysis System and by Point Counter method under reflecting microscope respectively. The data obtained are given in Table 4.

Table 4. The Estimation of Alite Content in clinkers (%)

Sample	By IBAS Image Analysis System	By Point Count Method
F_0	29.27	27
F_1	42.91	38
F_2	58.62	59
F_3	71.93	73

The positive effects of CaF_2, $CaSO_4$ on the clinkering process have been extensively investigated by various researchers. They have found that the effect of these mineralizer is related to lowering the temperature at which liquid phase is formed and thus reduces the clinkering temperature. The temperature of initial liquid phase formation is reduced by several hundred degree and the clinkering temperature by 50 - 100°C by the addition of 3% CaF_2[2]. According to Y.M. Butt[4], as the content of CaF_2 in the melt is less than 1.0%, its viscosity and surface tension can be reduced more significantly, thus the average size of precipitated crystals correspondingly decreased[5]. In addition to the aforementioned changes in the liquid phase, the formation of transitional phases is an important factor for forming more Alite phase by decomposing itself at lower temperature. Moreover, in the presence of CaF_2, the formation of C_3A is hindered and replaced by $C_{11}A_7 \cdot CaF_2$, some additional lime is available for formation of Alite. The data obtained in present paper further demonstrates that in the presence of SO_3, the amount of Alite estimated by the two methods adapted increases with the increase of $\overline{F}$ content in clinker. These estimated values are approximately coincident with the change of peak height in the XRD patterns (Fig. 4). And the estimated values by these two methods (Table 4) are obviously comparable.

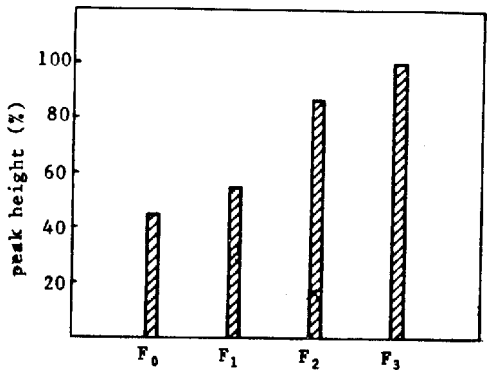

Fig. 4 The peak heights in XRD pattern of F_0 ~ F_3 clinker

3. EFFECTS OF FLUORINE ON THE HYDRATION PERFORMANCE OF ALITE

Relevant studies indicate that the $\overline{F}$ solvated in Alite leads to some variation of its hydration performance, but the descriptions are different. In the present study, the solution of pottasium hydroxide and sucrose (KOSH) was used to separate silicate phase from the clinker. Then, by using the method of reheating to

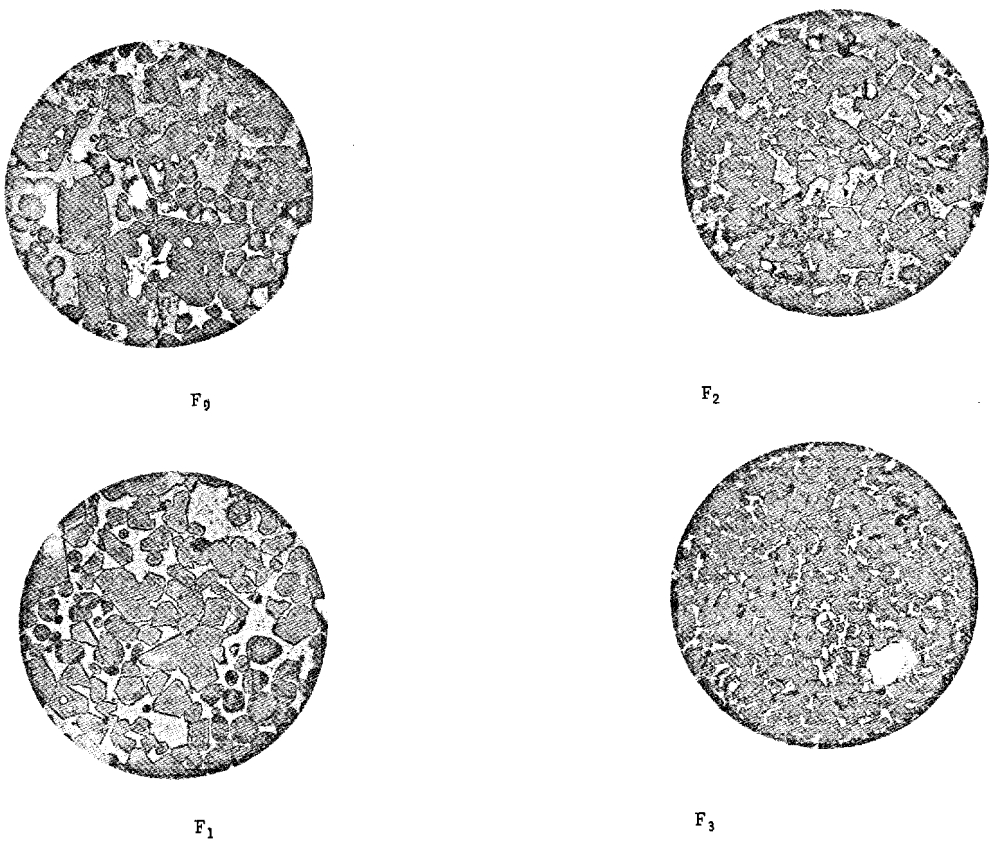

Fig. 3 The petrographic morphology characteristics of F_0 - F_3 clinker reflected light (256 ×)

950°C and then cooling down slowly, let the Belite phase transform to Y-C_2S. After such "passivation" treatment, the initial hydration performance of Alite may be measured under the condition that the Belite interference would be negligible. The hydration heat evolution rate was measured with a conductive microcalorimeter of RD-1 type, its calorimeter constant $K = 6.4577 \times 10^{-3}$ J/mm^2. The results obtained are given in Fig. 5. Ground the clinker with 3% gypsum (SO_3 = 1.32%) to a specific fineness, then 2 × 2 × 2 cm paste specimens were prepared with w/c = 0.3, fog cured for various times. The compressive strength results measured at 1d, 3d, 7d and 28d are listed in Table 5.

Table 5. Compressive Strength of Cements Made From F_0 ~ F_3 Clinker (MPa)*

Sample	1d	3d	7d	28d
F_0	24.5	42.7	51.0	64.0
F_1	35.2	56.5	72.5	93.8
F_2	42.4	71.6	90.8	104.4
F_3	40.4	87.6	130.0	140.4

* 2 × 2 × 2 specimen, w/c = 0.3

The study of A.F. Krapliya[6] indicates that close correlation exists between the completeness of the clinker mineral crystallization and its hydration dynamics. Actually, the heat evolution of one day for the clinker with coarse and complete crystals is 50% less than that for the clinker with incomplete ones. It was always considered that the reactivity of Alite crystal with the size of 15 μm is higher than that with the size of 40 μm, and the larger the aspect ratio, the greater its reactivity in general. On the other hand, I. Odler has reported that $\overline{F}$ retarded the rate of hydration, and the intrinsic properties of the hydration products were altered, resulting in decreased compressive strength[1]. From Fig. 5, it can be seen that the first peak of heat evolution (181.7 J/g·h) for Alite phase separated from F_0 clinker is the lowest one. As the $\overline{F}$ content in Alite phase was increased, the peak height also increased though the peak occuring durations in the measurements were all within 5 ~ 8 min. The heat evolution peak of F_3 sample is 281.4 J/g·h, which makes significant difference from that of F_0 sample. By comparing the amount of hydration heat evoluted within 1 hr, it can be found that the heat evolution is increased with the increase of $\overline{F}$ content in clinker (Table 6). Plotting the value of heat evolution within 1 hr as the function of Alite % in KOSH residue, it can be seen that the increase of heat evolution is approximately proportional to the increase of Alite %. But it should be noted that, when the Alite % exceeds 60%, the values of heat evolution gradually deviate from the straight line (Fig.6). This means, as the $\overline{F}$ content in the clinker increases, not only the content of

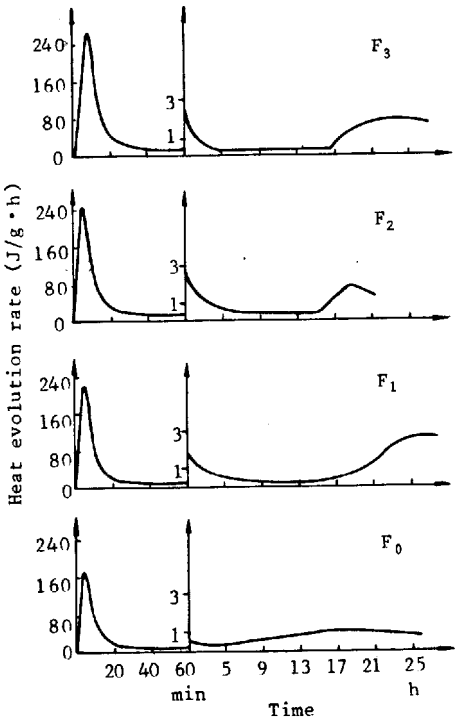

Fig. 5 Hydration heat evolution curves of Alite separated from F_0 ~ F_3 clinker

Alite is increased, but also the hydraulic activity of Alite has been somewhat improved. This may be explained by the smaller crystal size of the Alite present in the clinker with higher $\overline{F}$ content. Meanwhile, the results of our strength measurement also show such a general regularity.

Table 6. The heat evolution and its peak height of Alite separated from F_0 ~ F_3 clinker

Sample	Alite in residue (%)	Heat evolution (1h, J/g)	1st Peak height (J/g·h)
F_0	41.43	25.16	181.7
F_1	60.22	30.23	231.1
F_2	81.40	38.25	258.3
F_3	97.05	46.01	281.4

Hence, we propose that with the increase of $\overline{F}$ content, the increase of heat evolution is mainly due to the increase of Alite content, however, the hydraulic activity is somewhat improved. That is, the solid solution of $\overline{F}$ do not alter the hydraulic activity of Alite substantially, it seems to be not a significant factor in strength development. After having studied the $CaO-SiO_2-CaF_2$ system, M. Tanaka et al[7] pointed out that the low hydraulic activity of Alite containing $\overline{F}$ in solid solution is due to the effect of $Ca_{12}Si_4O_{19}F_2$, which is formed in the slow cooling process in particular. This intermediate phase shows only little hydraulic activity and usually presents

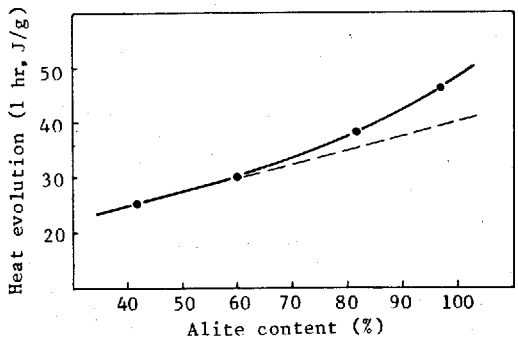

Fig. 6 Heat evolution as the function of Alite % in residue

together with Alite phase in the surrounding of it. However, in a more recent work[8] it was concluded that if $CaSO_4$ is added to this system and its amount exceeds 1.35%, the formation of $Ca_{12}Si_4O_{19}F_2$ is wholly obstructed. That is, in the case of compound mineralizer, the situation is quite different. For the four clinkers studied in this paper, the SO_3 content is 1.96 ~ 2.22%, we have not observed any peritectic structure of this intermediate phase by petrographic examination, and also not found in XRD analysis. Hence, we propose that when doping with compound mineralizer, in the presence of appropriate amount of SO_3, the cause of decline in hydraulic activity of $\overline{F}$-containing Alite phase has been eliminated. Moreover, because of the small size of Alite crystals containing more $\overline{F}$, the hydraulic activity is somewhat increased.

CONCLUSIONS

1. In the four clinkers studied, most of $\overline{F}$ (73.85 ~ 81.52%) are distributed in silicate phase, and its concentration is relatively higher in Alite phase. More $\overline{F}$ content in the clinker is in correspondence with more $\overline{F}$ solvated in the silicate.

2. As the $\overline{F}$ solubility is increased, the appearence of Alite phase under a microscope changes from incomplete crystallization to complete, and the crystal size gradually becomes smaller.

3. The heat evolution within 1 hr is closely related with the Alite contents. There existed an approximate linear correlation between them, especially when the $\overline{F}$ content is lower.

4. In the case of doping with gypsum-fluorite as compound mineralizer, the beneficial effect of $\overline{F}$ is mainly due to increase of Alite contents in clinker burnt in lower temperature, but the smaller crystal size may enhance the hydraulic activity somewhat.

REFERENCES

(1) I. Odler et al, "Structure and Properties of Portland Cement Clinker Doped with CaF_2", J. Amer. Ceram. Soc. 63, 11-12, pp. 654-659.

(2) F.M. Lea, "The Chemistry of Cement and Concrete", 3rd. ed., 1970, pp. 156.

(3) W.A. Kleen and I. Jawed, "Mineralizer and Fluxes in the Clinkering Process", Proc. 7th Int.

Congr. Chem. Cement, I, pp.152.

(4) Y.M. Butt, "The Mechanism of Clinker Formation Processes and the Modification of its Structure", Proc. 6th Int. Congr. Chem. Cement, 1974, I, pp. 132.

(5) V.V. Timashev, "The Kinetics of Clinker Formation, The Structure and Composition of Clinker and its Phases", Proc. 7th Int. Congr. Chem. Cement, I. pp. 3.

(6) A.F. Krapliya, "The effect of Clinker Phase Composition and Microstructure on Cement Hydration Kinetics", Cement 1982. 7. pp. 5 (in Russian).

(7) M. Tanaka et al, "New Compound $Ca_{12}Si_4O_{19}F_2$ in the System $CaO-SiO_2-CaF_2$ and the Role of CaF_2 in the Burning of Cement Clinker", Proc. 5th Int. Congr. Chem. Cement I, pp. 122.

(8) Ren Xiangtai, "The Study of Mechanism of Silicate Formation in $CaO-C_2S-CaF_2-CaSO_4$ System", Symp. Cement Committee of Chinese Silicate Soc. 1980-1981, pp. 209 (in Chinese).

Damao Tong & Zongshou Lin
Wuhan Institute of Building Materials
Wuhan, China

1

THE ROLE OF CaF_2 AND $CaSO_4$ IN CEMENT CLINKERING

1.2

SUMMARY: $2C_2S \cdot CaF_2$ can't be detected in the mix with $F/SO_3 > 0.158$ burned at 1,000 or 1,080 °C. $3C_3S \cdot CaF_2$ can hardly form at 1,140 °C even in the mix according to its stoichiometric composition, and can't form in the presence of SO_3. $2C_2S \cdot CaSO_4$ occurs only in the mix with $F/SO_3 < 0.158$ burned at 1,140 °C. $3C_2S \cdot 3CaSO_4 \cdot CaF_2$ forms easily at 940 °C owing to the melting of eutectic mix at 910 °C. It begins to melt at 1,225 °C and the corresponding endothermic peak is at 1,260 °C. Its melting point may be reduced to 1,180 - 1,248 or 1,160-1,248 °C when $Al_2O_3+Fe_2O_3$ or $Al_2O_3+Fe_2O_3+MgO$ is added.

Both CaF_2 and $CaSO_4$ can depress the melting point of eutectic mix T_2. The melting point of mix may be reduced to 850-900 °C when large quantities of CaF_2+CaSO_4 are added. It seems probable that a small quantity of melt may be produced at some points in the raw meal with CaF_2+CaSO_4 before 900 °C, it promotes $3C_2S \cdot 3CaSO_4 \cdot CaF_2$ forming. Both CaF_2 and $CaSO_4$ also increase the fluidity (or reduce the viscosity) of eutectic melt.

Both CaF_2 and CaF_2+CaSO_4 can promote the clinker formation at lower temperature. The clinkering temperature of cement with CaF_2+CaSO_4 could be reduced to 1,300 - 1,350 °C. The mix near the inner side of refractory in clinkering zone of shaft kiln could be well burned, and the industrial wastes such as coal gangue might be used when mineralizer is added.

Não se pode detectar $2C_2S.CaF_2$ na mistura com $F/SO_3 > 0,158$ queimado a 1.000 ou 1.080°C. $3C_3S.CaF_2$ dificilmente pode se formar a 1.140°C mesmo na mistura de acordo com sua composição estequiométrica, e não pode formar-se na presença de SO_3. $2C_2S.CaSO_4$ acontece somente na mistura $F/SO_3 < 0,158$ a 1.140°C. $3C_2S.3CaSO_4.CaF_2$ se forma facilmente a 940°C devido à fusão de mistura eutética a 910°C. Ele começa a fundir a 1.225°C e o pico endotérmico correspondente se dá a 1.260°C. Seu ponto de fusão pode ser reduzido para 1.180 - 1.248 ou 1.160 - 1248°C quando há adição de $Al_2O_3+Fe_2O_3$ ou $Al_2O_3+Fe_2O_3+MgO$.

CaF_2 e $CaSO_4$ podem baixar o ponto de fusão de mistura eutética T_2. O ponto de fusão da mistura pode ser reduzido para 850-900° quando são adicionadas grandes quantidades de CaF_2+CaSO_4. Parece provável que uma quantidade pequena de fusão pode ser produzida em alguns pontos no cru com CaF_2+CaSO_4 antes de 900°C, promovendo a formação de $3C_2S.3CaSO_4.CaF_2$. Os dois, CaF_2 e $CaSO_4$, também aumentam a fluidez (ou diminuem a viscosidade) da fusão eutética.

Os dois, CaF_2 e $CaSO_4$, podem promover a formação de clinquer a temperatura mais baixa. A temperatura de clinquerização do cimento com CaF_2+CaSO_4 poderia ser reduzida para 1.300 - 1.350°C. A mistura próxima do lado interno do refratário, na zona de clinquerização do forno, poderia ser bem queimada e os rejeitos industriais, como ganga de carvão, poderiam ser usados quando se adicionasse mineralizador.

1. INTRODUCTION

Utilizing mineralizer to lower the clinkering temperature of portland cement is among the important measures to save energy. Up to now, it is still worth while to study what causes the cement with mineralizer clinkering at lower temperature. In this article, we make a study of the formation of intermediate phase, the fluxing effect of mineralizer and the cement with mineralizer clinkering at lower temperature.

2. FORMATION OF INTERMEDIATE PHASE

The sulphur introduced by coal affects the formation of intermediate phase. According to C. Gilioli[1], $2C_2S{\cdot}CaF_2$ may form in the mix with $F/SO_3 > 0.158$ in the system $CaO\text{-}C_2S\text{-}CaF_2\text{-}CaSO_4$. In our experiment, two batches of the mix with SiO_2 30.52%, CaO 15.08%, CaF_2 19.83%, $CaSO_4$ 34.57%, F/SO_3=0.471 were burned at 1000 and 1,080 °C, cooled and examined by XRD respectively, and a mix with SiO_2 19.62%, Al_2O_3 5.40%, Fe_2O_3 5.48%, CaO 64.40%, MgO 1.40%, CaF_2 1.20%, SO_3 2.50%, F/SO_3=0.234 was studied by high temperature XRD, the results show that no $2C_2S{\cdot}CaF_2$ but $3C_2S{\cdot}3CaSO_4{\cdot}CaF_2$ is detected.

9 mixes proportioned according to table 1 were burned at 1,140 °C for 1 hr and examined by XRD in order to study the formation of $3C_3S{\cdot}CaF_2$ and $2C_2S{\cdot}CaSO_4$. The results showed in table 2 show that $3C_3S{\cdot}CaF_2$ and $2C_2S{\cdot}CaSO_4$ occur only in mix H_0 and H_8 respectively, but $3C_2S{\cdot}3CaSO_4{\cdot}CaF_2$ in all mixes with SO_3.

Table 1 Compositions of mixes H

No	Composition %				F/SO3	3C3S·CaF2 : CaSO4 molal ratio by calculation
	SiO2	CaO	CaF2	CaSO4		
H0	23.63	66.14	10.23			1 : 0
H1	22.81	63.86	9.80	3.45	2.370	1 : 0.2
H2	22.05	61.74	9.55	6.66	1.187	1 : 0.4
H3	21.34	59.75	9.24	9.67	0.791	1 : 0.6
H4	20.67	57.88	8.95	12.47	0.593	1 : 0.8
H5	20.05	56.13	8.68	15.14	0.474	1 : 1
H6	17.41	48.75	7.54	26.30	0.237	1 : 2
H7	15.39	43.08	6.66	34.86	0.159	1 : 3
H8	13.78	38.60	5.97	41.65	0.119	1 : 4

Table 2 Results of XRD of mixes H

No	Mineral detected
H0	CaO, SiO_2, CaF_2, C_2S, $3C_3S{\cdot}CaF_2$(little)
H1-H7	CaO, CaF_2, C_2S, $3C_2S{\cdot}3CaSO_4{\cdot}CaF_2$
H8	CaO, C_2S, $3C_2S{\cdot}3CaSO_4{\cdot}CaF_2$, $2C_2S{\cdot}CaSO_4$

3 mixes were made up according to table 3. Mixes G_1 and G_2 were added $Al_2O_3{+}Fe_2O_3$ and $Al_2O_3{+}Fe_2O_3{+}MgO$ respectively.

Table 3 Compositions of mixes G

No	SiO2	Al2O3	Fe2O3	CaO	MgO	CaF2	CaSO4
G0	17.97			33.54		7.78	40.71
G1	17.62	0.98	0.98	32.88		7.63	39.91
G2	17.53	0.98	0.98	32.72	0.49	7.59	39.72

2 pieces of sample about 0.3 mm thick were made from mix Go in a model under a pressure. One was directly burned at 1,000°C for 5 sec, the other was heated to 1,000 °C from room temperature at the rate of 10°C/min, and both samples were taken out and cooled in air.

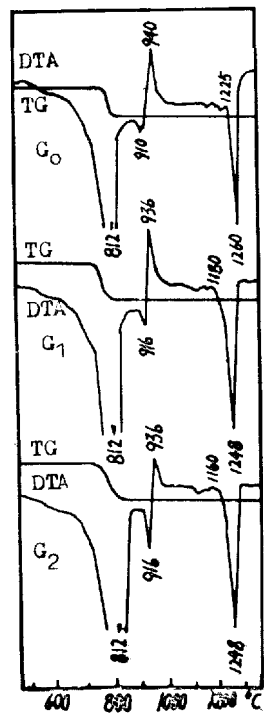

Fig. 1 DTA curves of mixes G

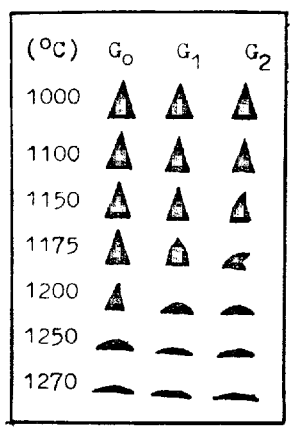

Fig. 2 Melting point of mixes G

The results of XRD of these two samples also confirm that the intermediate phase is only $3C_2S \cdot 3CaSO_4 \cdot CaF_2$.

The results of DTA and melting point of mixes G_o, G_1, and G_2 are shown in Fig. 1 and 2. From it, we might get that the exothermic peak of formation of $3C_2S \cdot 3CaSO_4 \cdot CaF_2$ at 940 °C is behind the endothermic peak of the melting of eutectic mix at 910 °C. $3C_2S \cdot 3CaSO_4 \cdot CaF_2$ begings to melt at 1,225 °C and the corresponding endothermic peak is at 1,260 °C. $3C_2S \cdot 3CaSO_4 \cdot CaF_2$ with $Al_2O_3 + Fe_2O_3$ and with $Al_2O_3 + Fe_2O_3 + MgO$ begin to melt at 1,180 °C and 1,160 °C respectivily and the corresponding endothermic peaks are both at 1,248 °C.

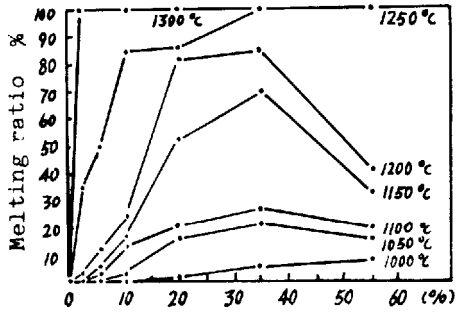

Fig. 3 Effect of CaF_2 on mix melting

Mix E_o (SiO_2 4.0%, Al_2O_3 3.0%, Fe_2O_3 5.0%, CaO 3.0%, CaF_2 35.0%, $CaSO_4$ 50.0%) and mix E_1 (SiO_2 3.85%, Al_2O_3 2.88%, Fe_2O_3 4.81%, CaO 2.88%, CaF_2 33.65%, $CaSO_4$ 48.08%, MgO 1.92%, K_2SO_4 0.96%, Na_2SO_4 0.96%) were proportioned with a great quantities of $CaF_2 + CaSO_4$ in order to study what temperature the melting point of mix may be reduced to. The results are shown in Fig. 5 and 6. Mix E_o begins to melt at 936—950 °C, the corresponding endothermic peak is at 960 °C. The melting point of mix E_1 with $MgO + K_2SO_4 + Na_2SO_4$ in comparison with that of Mix E_o is more reduced. Its relative values are 850-900 and 936 °C.

From the results above mentioned, we could deduce that a small quantity of melt may be produced at some points in the raw meal with CaF_2 and $CaSO_4$ before 900 °C, it promotes the formation of $3C_2S \cdot 3CaSO_4 \cdot CaF_2$.

3. FLUXING EFFECT OF MINERALIZER

3.1 Melting of mix

After adding various quantities of CaF_2 or $CaSO_4$ into the eutectic mix of the system $C_2S - C_3S - C_3A - C_4AF$ separately, every mix was molded into seger cones, and burned at various temperatures for 10 min for melting test. The initial height a before burning and final height b after burning were measured, and the melting ratio MR was calculated according to equation $MR=(a-b)/a \times 100\%$. The results showed in Fig. 3 and 4 show that the mix added CaF_2 is more meltable than that added $CaSO_4$.

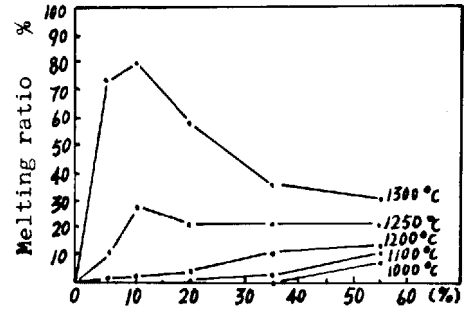

Fig. 4 Effect of $CaSO_4$ on mix melting

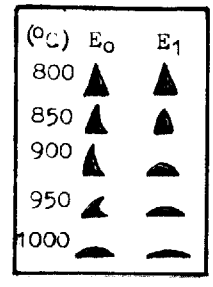

Fig. 5 Melting of mixes E

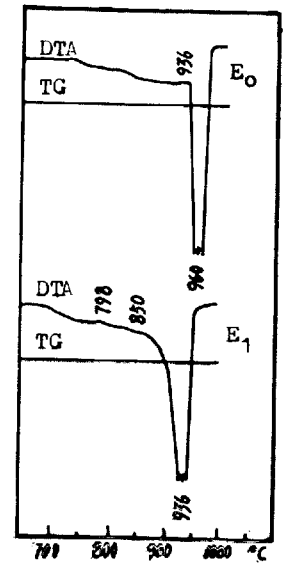

Fig.6 DTA curves of mixes E

3.2 Fluidity of melt

The fluidity of the eutectic melt of the system C_3S-C_2S-C_3A-C_4AF with 0%, 1%, 2% and 3% CaF_2 or $CaSO_4$ was studied. A predesigned quantity of mix (every batch of mix tested was calculated in same quantity of melt) was placed in a cylindrical platinum crucible, burned melting completely at 1,340 °C, then turned the mouth of crucible down at -15° angle with horizontal so that the melt flowed down slowly. The more quantity of mineralizer is added, the longer distance melt flows. The flowing distances of another group of melts proportioned according to table 4 were measured at 1,340 °C, The influence of temperature on the flowing distance of melt N_3 was studied. The results are shown in Fig. 8 and 9. At 1,340 °C, the flowing distances of melts N_1 and N_3 are longer than that of melts T_2 and N_2. The flowing distance of melt N_3 at 1,250 °C is equal to that of melt T_2 at 1,340 °C.

Table 4 Chemical compositions of melts N

No	SiO_2	Al_2O_3	Fe_2O_3	CaO	CaF_2	SO_3	MgO	Na_2O
T_2	6.00	22.70	16.50	54.80				
N_1	5.84	22.08	16.05	53.31	0.78	1.94		
N_2	5.85	22.15	16.10	53.46			1.46	0.98
N_3	5.70	21.56	15.67	52.04	0.76	1.90	1.42	0.95

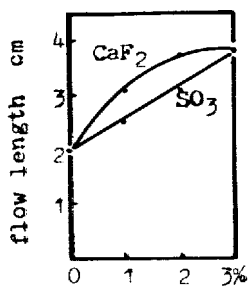

Fig. 7 Flowing distance of melt

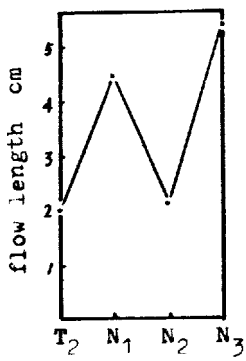

Fig. 8 Flowing distances of melts N

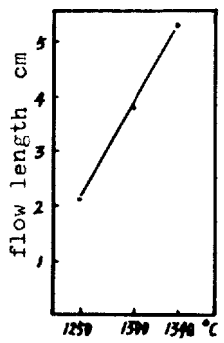

Fig. 9 Influence of temperature on flowing distance of melt N_3

4. CEMENT CLIKERING AT LOWER TEMPERATURE

The mixes having composition SiO_2 21.62 %, Al_2O_3 6.82 %, Fe_2O_3 5.13 %, CaO 66.43 % with 3 % different kind of mineralizer were burned at 1,300 °C for 1 hr respectively. The free lime of mix burned with CaF_2 is less than 2%, and that of mix burned with CaF_2 + $CaSO_4$ is much less than 2 %.

On the basis of this result, 3 batches of mix with composition SiO_2 20.03 %, Al_2O_3 5.62 %, Fe_2O_3 5.57 %, CaO 64.41 %, MgO 1.41 %, CaF_2 0.79 %, SO_3 2.37 % were burned at 1,270, 1,300 and 1,330 °C for 1 hr and cooled in air

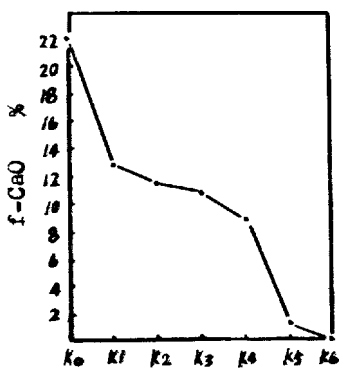

Note: The mineralizer added to K_0 is:
K_1, $CaSO_4$;
K_2, Na_2SO_4;
K_3, K_2SO_4 ;
K_4, MgO ;
K_5, CaF_2 ;
K_6, CaF_2+$CaSO_4$.

Fig. 10 Free limes of mixes with different kind of mineralizer

Table 5 Physical properties of cement C

No	temp °C	f-CaO %	Fineness cm^2/g	Normal consistency	Time of setting		Soundness	strength
					Int	Fnl		
C_1	1,270	6.74	3,700	28.87	1:40	3:04	cracked	see Fig. 11
C_2	1,300	0.92	3,730	27.74	2:36	4:43	fine	
C_3	1,330	0.29	3,710	28.64	4:20	7:51	fine	

respectively. Free limes in clinkers C_2,C_3 are less than 1 % except C_1. Clinkers were ground with 3.64 % gypsum to examine their physical properties. The results showed in table 5 and Fig. 11 show that the clinkering temperature of cemenet with CaF_2+SO_3 must not be lower than 1,300 - 1,330 °C.

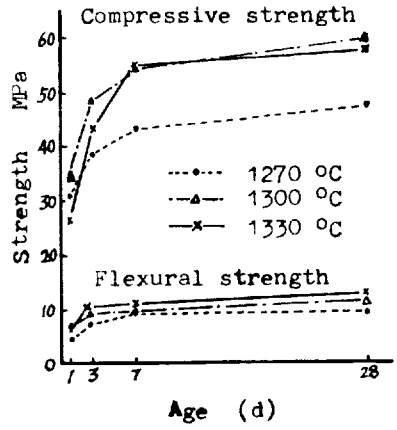

Fig. 11 Strength of cement C

The temperature near the inner side of refractory in clinkering zone of shaft kiln is often lower than 1,400 - 1,450 °C, it gives under-burned clinker. The Clinker shall be well burned even at 1,300-1,350 °C when mineralizer is added(2). A technical experiment of clinkering cement at lower temperature using coal gangue as argillaceous material with mineralizer was also made on a shaft kiln, the good result was obtained although the clinker contained 4.75-5.25 % Al_2O_3, 2.79 -3.21 % Fe_2O_3 rather less than the normal(3).

5. CONCLUSION

From above results, we might draw conclusions as follows:

1) $2C_2S{\cdot}CaF_2$ and $3C_3S{\cdot}CaF_2$ can hardly form in the presence of SO_3, and $2C_2S{\cdot}CaSO_4$ occurs only in the mix with $F/SO_3 < 0.158$.

2) $3C_2S{\cdot}3CaSO_4{\cdot}CaF_2$ forms easily owing to the melting of eutectic mix. It forms at about 940 °C, and melts at the interval of 1,225 - 1,260 °C. Its melting point could be reduced to 1,180-1,248 or 1,160-1,248 °C when Al_2O_3+Fe_2O_3 or Al_2O_3+Fe_2O_3+MgO is added.

3) Both CaF_2 and $CaSO_4$ can depress the melting point of eutectic mix T_2 and increase the fluidity (or reduce the viscosity) of eutectic melt.

4) Both CaF_2 and CaF_2 + $CaSO_4$ can promote the clinker formation at lower temperature.

5) The clinkering temperature of cement with CaF_2 + $CaSO_4$ could be reduced to 1,300-1,350 °C. Therefore, the mix near the inner side of refractory in clinkering zone of shaft kiln could be well burned, and the industrial wastes such as coal gangue might be used when mineralizer is added.

REFERENCES

1. Gilioli C., Massazza F., Pezzuoli, Cem. and Conc. Res., 1979, Vol. 9, No. 3, PP. 295-301

2. Tong Damao, Lin Zongshou, A study on Mineralizer, 1985

3. Tong Damao, Yang Wenyan, Li Jianxi, Yong Hong, Utilization of coal Gangue as Argillaceous Material and Active Addition in Producing Cement, 1985

Ye Ruilun, Wu Bolin and Wang Xinrong, Wuhan Institute of Building Materials, China.

THE SYNTHESIS AND CRYSTAL STRUCTURE OF A NEW COMPOUND $Ca_8Mg(SiO_4)_4Cl_2$

SUMMARY: The function of MgO in cement clinker and cement technique has been considerably studied, and the formation of the intermediate compounds containing magnesium has been discussed, but so far no consistent recognition has been obtained. The formation of the intermediate compounds containing magnesium has therefore received much attention.

A new compound that is chlorine calcium silicate containing magnesium $Ca_8Mg(SiO_4)_4Cl_2$ in $CaO-MgO-SiO_2-CaCl_2$ system was synthesized in the laboratory. The raw materials used were A.R.. When the batches prepared in certain proportions are heated up to 760°C in air, this new compound begins to form and it decomposes at 1265°C in air, the decomposition product is mainly $\alpha'-Ca_2SiO_4$.

The crystal of $Ca_8Mg(SiO_4)_4Cl_2$ belongs to cubic system and the crystal pattern is a regular octahedron, it is colourless and transparent with the density $D_m = 3.08$ g/cm^3, refractive index n=1.691, unit cell parameter a=15.065Å, space group is Fd3m, Z=8. In this paper we analysed the compound by using chemical analysis, differential thermal analysis, infrared absorption spectrum, high temperature X-ray diffractometer and determined mainly the crystal structure. The crystal structure was solved by direct method SHELXTL. Refinement of atomic coordinates and thermal parameter were acheived by tetrainture block matrix least-squares method to a final value of R=0.073.

In $Ca_8Mg(SiO_4)_4Cl_2$ crystal structure, the anion frame is constructed by oxygen and chlorine atoms, and chlorine atoms in $\bar{3}m(000)$ positions. Calcium atoms are in the positions of two sets of equivalent dots, and Ca(1) with 0 atoms form hexa-coordination octahedrons, one Ca(2) with two Cl and six O atoms form octa-coordination polyhedrons. Si-O tetrahedrons are isolated from each other, Si-O bond averaged length is 1.626Å, and O-Si-O averaged bond angle is 109.25°. Mg atoms stand in high-symmetric $\bar{4}3m(1/8,1/8,1/8)$ positions, and form tetra-coordination regular tetrahedron together with the neighbouring four O atoms belonging to individually the apexes of four silicon-oxygen tetrahedrons. Mg-O bond length is 1.860Å and bond angle is 109.5°. Mg atom combined with four O atoms to form strong covalent intermediate chemical bond in SP^3 hydrid orbits. Magnesium atoms existed in the form of (MgO_4) tetrahedrons in the crystal structure. It is unusual that the Mg-O tetra-coordination exists in the crystal structure of silicate minerals.

A função do MgO na técnica do clinquer-de-cimento e do cimento tem sido amplamente estudada e se tem discutido a formação de compostos intermediários contendo magnésio, mas até agora não se obteve conhecimento consistente. Por isso, a formação dos compostos intermediários contendo magnésio tem sido objeto de muita atenção.

Um novo composto que é silicato de cálcio clorado contendo magnésio $Ca_8Mg(SiO_4)_4Cl_2$, no sistema $CaO-MgO-SiO_2-CaCl_2$ foi sintetizado em laboratório. As matérias-primas usadas foram A. R.. Quando as bateladas preparadas em proporções definidas são aquecidas a até 760°C em ar, este novo composto começa a se formar e se decompõe a 1.265°C em ar, sendo principalmente $\alpha'-Ca_2SiO_4$ o produto de decomposição.

O cristal de $Ca_8Mg(SiO_4)_4Cl_2$ pertence ao sistema cúbico e a matriz do cristal é um octaedro regular; é incolor e transparente com densidade de $D_m = 3,08$ g/cm^3, índice refrativo n = 1,691, parâmetro de célula unitária a = 15,065Å, grupo espacial Fd3m, Z = 8. Neste trabalho analisamos o composto usando análise química, análise termodiferencial, espectro de absorção infra-vermelha, difratômetro de raios X de alta temperatura, e determinamos principalmente a estrutura do cristal. A estrutura do cristal foi solvida pelo método direto SHELXTL. Conseguiu-se o refinamento de coordenadas atômicas e parâmetro térmico pelo método de quadrados-mínimos de matriz de bloco "tetrainture" para um valor final de R = 0,073.

Na estrutura do cristal $Ca_8Mg(SiO_4)_4Cl_2$ a armação aniônica é construída por átomos de oxigênio e cloro, e átomos de cloro em posições $\bar{3}m(000)$. Os átomos de cálcio estão nas posições de dois conjuntos de pontos equivalentes, e Ca(1) com átomos de O formam octaedros de hexa-coordenação, um Ca(2) com dois Cl, e seis átomos de O formam poledros de octo-coordenação. Tetraedros Si-O estão isolados uns dos outros, sendo o comprimento médio de ligação de Si-O de 1,626Å, e o ângulo médio de ligação O-Si-O de 109,25°. Átomos de Mg ficam em posições alto-simétricas $\bar{4}3m$ (1/8, 1/8, 1/8), e formam tetraedro regular de tetra-coordenação juntamente com os 4 átomos de O próximos, pertencendo individualmente aos quatro ápices de quatro tetraedros silício-oxigênio. O comprimento de ligação Mg-O é de 1,860Å e o ângulo de ligação é de 109,5°. O átomo de Mg combinou com quatro átomos de O para formar forte ligação química intermediária covalente em órbitas de hidreto SP^3. Existiam átomos de magnésio em forma de tetraedros (MgO_4) na estrutura do cristal. Não é usual que a tetra-coordenação de Mg-O exista na estrutura do cristal de minerais silicatos.

Ye Ruilun, Wu Bolin and Wang Xinrong, Wuhan Institute of Building Materials,China.

THE SYNTHESIS AND CRYSTAL STRUCTURE OF A NEW COMPOUND $Ca_8Mg(SiO_4)_4Cl_2$

1. Introduction

The function of magnesium oxide in cement clinker and cement technique has been considerably studied, and the formation of the intermediate compounds containing magnesium has been discussed. But so far a consistent recognition has not been reached. The formation of the intermediate compounds containing magnesium has therefore received much attention. Alinite cement is a new kind of saving energy cement which has drown many interests for its many outstanding properties.

A new compound, i.e., chlorine calcium silicate containing magnesium $Ca_8Mg(SiO_4)_4Cl_2$ in $CaO-SiO_2-MgO-CaCl_2$ system was synthesized in the laboratory/1/. The monocrystal up to 0.3 ×0.3×0.3 mm^3 in size was obtained. We analysed the crystal of the compound by using the methods of electron probe and chemical analysis and determined the molecular formula to be $Ca_8Mg(SiO_4)_4Cl_2$.

2. Research on the Compound

2.1. Crystal description

The crystallinity of chlorine calcium silicate containing magnesium $Ca_8Mg(SiO_4)_4Cl_2$ is grained and is octahedral in symmetry. Fig.1 shows the shape of the ideal crystal. The crystal belongs to cubic crystal system with space group $m3m(O_h)$ and growes along (111) plane. The crystal is clear and transparent with the outerfaces unbroken. The crystal is extinctive under orthogonal polarizing microscope and has not interference figure under conical lens. Its refractive index is $1.691\pm 0.003(20^{\circ}C)$ under natural rays.

We measured the crystal density by using density bottle method. The sample was dried an hour at 105°C. The measuring was performed in vacuum and the medium was alcohol 99.5% with density 0.7886(20°). The average value of the crystal density is $D_m=3.08\ g\cdot cm^{-3}$.

2.2. DTA Experiment

Fig. 2 shows the DTA curves of $Ca_8Mg(SiO_4)_4Cl_2$. The curve shows that the reaction of mixture sample starts at 760°C and followed is the gradual formation of chlorine calcium silicate containing magnesium. A sharp endothermic peak at 810°C shows the formation of the compound in large quantity. An endothermic peak at 1265°C correspounds to the loss of about 5.85% in weight shown in thermogratimetric curve, which indicates the incongruent decomposition of the compound at the temperature with endothermic effect. From the analysis for the high temperature X-ray diffraction and petrography, we know that the following reaction of the compound with water vapour exists:

$$Ca_8Mg(SiO_4)_4Cl_2 + H_2O(g) \xrightarrow[1265^{\circ}C]{\Delta} 4\alpha'\text{-}Ca_2SiO_4 + MgO + 2HCl$$

2.3. Analysis to the Infrared Absorption

The KBr technique was used for the experiment of infrared absorption. The infrared spectrum (Fig.3) was obtained from the spectrophometer (FT-IR SX-170).

From the infrared spectroscopic analysis we know that the peaks at about 953,935,910,875 and 851 cm^{-1} are attributed to the stretching vibrations of (SiO_4) groups, and 565 and 524 cm^{-1} to the bending vibrations of (SiO_4) groups/2/. The double peak bending vibration V_4(Fig.3) appearing at 524°C indicates that (SiO_4) group are isolated in the structure. Therefore the structure formula of the crystal may be written as $Ca_8Mg(SiO_4)_4Cl_2$.

2.4. Powder X-ray diffraction analysis

Walking rundown method was used in the X-ray diffraction of powder crystal $Ca_8Mg(SiO_4)_4Cl_2$. Fig.4 shows the diffraction spectrum. The data are listed in Table 1.

By observing the systematic extinctions in the X-ray diffraction of cubic crystal system the crystal lattice is determined as the cubic lattice(cubic F). The calculated unit cell parameter a=15.064Å. And we could inferinitially its space group Fd3m.

3. Crystal Structure Determination

3.1. The collection of Intensity Data and the Analysis of the Crystal Structure

The diffraction intensity data were collected in Sintex-P3/R3 four circle diffractometer with θ:2θ scanning, $2\theta_{max}=60°$, $hkl_{max}=22,22,22$. The scanning speed could be changed from 4°—29.3°/min. The ratio of background to scanning time was 0.2. The number of independent intensity data collected was 1386 with those $I=1.96\ (I)$ 74.24% of the total. From the intensity data collected, we found that the systematic extinctions appeared in hkl type when h,k,l, mixtured in odd and even, in hkl type when h+l=2n+1, in 0kl type when k+l≠4n, and in 00l type when l≠4n. Thus the space group of the crystal can be determined uniquely to be $Fd3m(O_h^7)$ which has confirmed the inference from the result of the powder X-ray diffraction analysis. The unit cell parameter refined from the least square method a=15.065 (4)Å. Table 2 shows the related crystallographic data. The intensity data were refined by emperical absorption correction of ψ scanning, the PL refinement and then were reduced by using Wilson statistical method. The calculated scale factor K=1.51 and total temperature factor $B=0.018\ Å^2$.

The crystal structure was solved by direct method of SHELXTL program. Atomic coordinates and enantiomorphic thermal factors were refined by using block matrix least square method to a final discrepence R=0.073.

$$\left(R = \frac{\sum \left||F_o| - |F_c|\right|}{\sum |F_o|}\right).$$

Table 3 shows the atomic coordinates and thermal factors.

3.2. Structure Description

There are 8 $Ca_8Mg(SiO_4)_4Cl_2$ molecules and 248 atoms in a cell of the crystal structure in which the anion frame is constructed by the O and Cl atoms, the latter are in the $\bar{3}m(000)$ positions. In Table 4 listed are the data of bond lengthes and angles calculated from the atomic coordinates. Fig. 5 shows the stero-

Ye Ruilun, Wu Bolin and Wang Xinrong, Wuhan Institute of Building Materials,China.

1.2

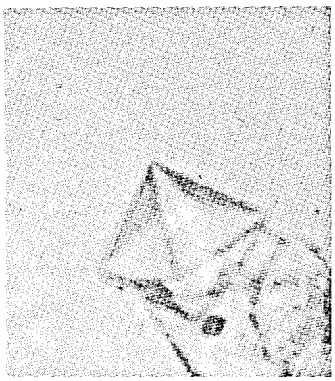

Fig.1 The ideal crystal shape of the new compound

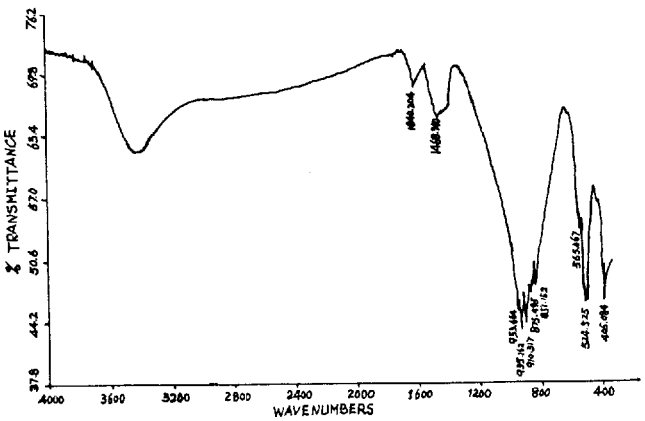

Fig.3 The infrared spectrum of the new compound

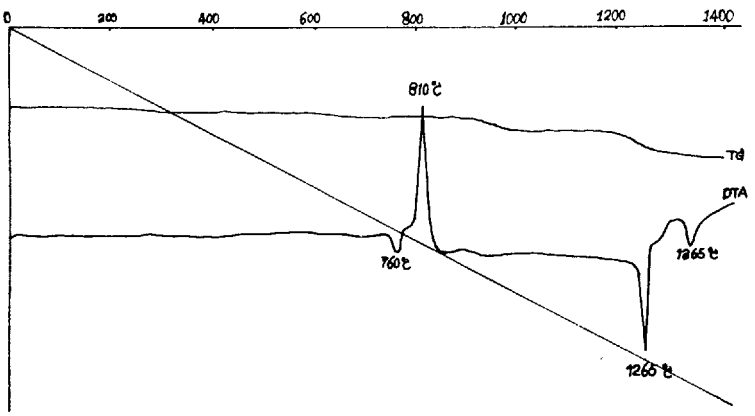

Fig.2 The DTA curve of the starting material

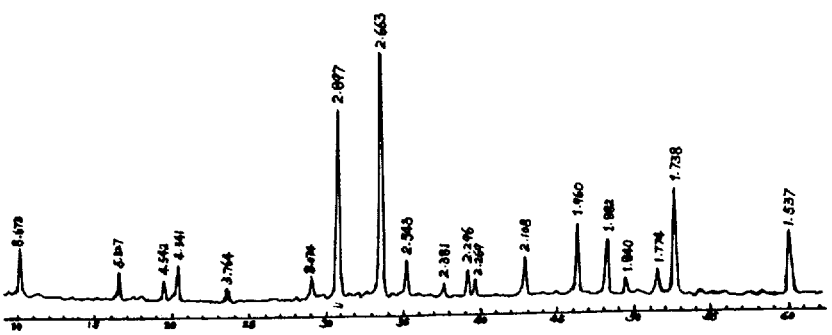

Fig.4 The X-ray diffraction spectrum of the new compound

Ye Ruilun, Wu Bolin and Wang Xinrong, Wuhan Institute of Building Materials, China.

Table 1. X-ray diffraction data and calculated results

No.	d(Å)	2θ(degree)	I/I_1	$3\times(\sin^2\theta/\sin^2\theta_1)$	hkl
1	8.673	10.198	30	3.0	111
2	5.327	16.640	30	8.0	220
3	4.542	19.545	20	11.0	311
4	4.341	20.459	30	12.0	222
5	3.764	23.638	10	16.0	400
6	3.074	29.047	20	24.0	422
7	2.897	30.867	80	27.0	511,333
8	2.663	33.654	100	32.0	440
9	2.543	35.294	30	35.1	531
10	2.381	37.783	10	40.0	620
11	2.296	39.237	20	43.0	533
12	2.269	39.723	10	44.1	622
13	2.108	42.900	30	51.1	711, 551
14	1.960	46.322	40	59.1	731, 553
15	1.882	48.362	30	64.1	800
16	1.840	49.538	10	67.0	733
17	1.774	51.514	20	72.1	822
18	1.738	52.662	50	75.1	751
19	1.537	60.206	40	96.1	844
20	1.456	63.938	30	107.0	773
21	1.332	70.726	10	127.9	880
22	1.256	75.726	10	143.9	884
23	1.191	80.672	10	160.0	12,40
24	1.152	84.008	20	171.0	993

Table 2. the crystallographic data of the crystal

chemical formula: $Ca_8Mg(SiO_4)_4Cl_2$, M=784.17
crystal system: cubic
space group: Fd3m
lattice constant: a=15.065(4) Å
unit cell volume: V=3419.17 $Å^3$
mole number of a cell: Z=8
density: D_m=3.08 g/cm^3, D_c=3.05 g/cm^3
total number of electrons in a cell: F(000)=3120(e)
linear absorption coefficient: μ=30.38 cm^{-1}(Mo)

Table 3. atomic coordinates($\times10^4$) and thermal factors($\times10^4$)

atom	X	Y	Z	B_{11}	B_{22}	B_{33}	B_{12}	B_{13}	B_{23}	K
Mg	1250	1250	1250	144	144	144	0	0	0	0.0417
Ca_1	5000	2500	2500	159	159	159	35	-35	-35	0.0833
Ca_2	9092	1250	1250	174	162	162	0	0	0	0.2500
Si	7408	7408	7408	133	133	133	0	0	0	0.1667
Cl	2500	2500	2500	196	196	196	-36	-36	-36	0.0833
O_1	1963	1963	1963	156	156	156	0	0	0	0.1667
O_2	5194	2958	1011	161	145	144	0	0	0	0.5

$T=\exp(-\frac{1}{4}(B_{11}h^2a^{*2}+B_{22}k^2b^{*2}+B_{33}l^2c^{*2}+2B_{12}hka^*b^*+2B_{13}hla^*c^*+2B_{23}klb^*c^*))$

structure of the crystal in an unsymmetrical unit and the coordination states of canions Ca_1, Ca_2, Si and Mg and their connections with anions. Fig.6 illustrates the sterostructure of 1/8 cell ($0\leq x,y,z,\leq 1/2$). Other part ofthe cell can be determined by symmetrical translations of Fd3m. Ca_1 and O_2 atoms form the octahedron with hexa-coordination, Ca_2, two Cl, four O_2 and two O_1 atoms form the polyhedra with octa-coordination. Si and O_1 and three O_2 atoms form (SiO_4) tetrahedron, Mg and four O_1 atoms form (MgO_4) tetrahedron whose apexes are connected with those of (SiO_4) tetrahedron. All angles of Mg-O-Si are 180°, From bond lengthes and angles, we know that the (SiO_4) tetrahedron, characterized by somewhat longer Si-O_1 bond (1.641Å) sharing apex with (MgO_4) tetrahedrons than other three Si-O_2 bond (1.621Å), is a little distorted. The (SiO_4) tetrahedron is a regular one with O-Mg-O angle 109.5°, and Mg-O distance 1.680Å which is 9.3% shorter than the ionic bond distance 2.05Å of Mg-O with hexa-coordination. The tetra-coordination of Mg-O is very rare in the crystal structures of silicates minerals.

4. Dicussion

4.1. Crystal chemistry analysis to the tetra-coordination of Mg-O in the structure

In $Ca_8Mg(SiO_4)_4Cl_2$ crystal structure, Mg

atoms and O atoms form regular tetrahedrons with Mg tetra-coordinated, and Mg atoms stand in the center of the neighbouring and secondary neighbouring tetrahedrons(Fig.6). Mg^{2+} ions are polarized by the secondary neighbouring four Cl atoms while polarized by the neighbouring four O atoms. The polarization effect so produced on Mg atoms makes the electron densities between Mg and O atoms largely increased, which means the pure Mg-O ionic bond has changed into the bond with covalent characters, and the forming-bond orbits of Mg atoms with O atoms are heavely confused by the ionic polarization effect of Cl^- ions. Thus Mg and O atoms form SP^3 hybrid obital with all four hybrids equevalent and therefore they constructe a regular tetrahedron. The bond length 1.860Å of Mg-O with strong covalent character just coincides with the calculated value from the following formula in tetra-coordination with covalent bonds/3/:

$$d_{A-B}=r_A+r_B-0.09(x_A-x_B)$$

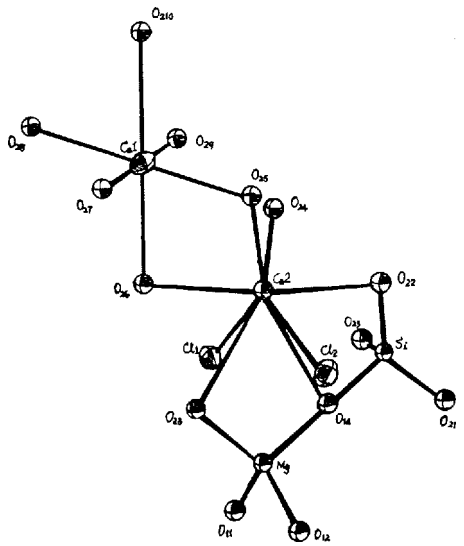

Fig.5 sterostructure of the crystal in an unsymmetrical unit

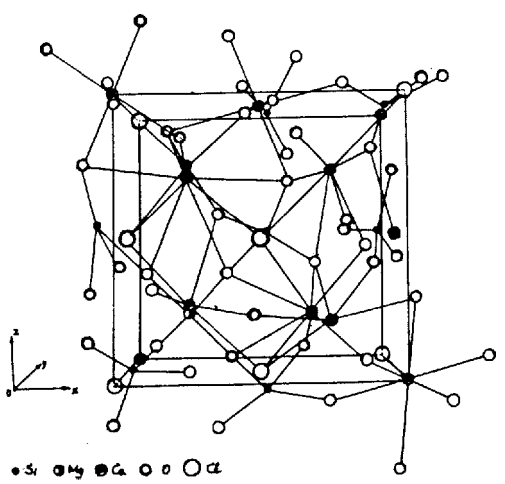

Fig.6 sterostructure of 1/8 cell ($0 \leq x,y,z \leq 1/2$)

Where r_A and r_B are covalent radius, x_A and x_B are electronegativity.

4.2. The Disordered Arrangement of Part O Atoms in the Crystal Structure

From the determination of the crystal structure, we know that there are 128 O atoms in a cell in the crystal of $Ca_8Mg(SiO_4)_4Cl_2$, among them 96 O atoms,i.e., O_2 in Table 3, stand in general symmetric positions with site occupation factor 0.5, which indicates that there are three O atoms in every one (SiO_4) tetrahedron being distributed disorderly in the structure. This will causes the orientational disorder of (SiO_4) tetrahedron. This is because on one base plane of the (SiO_4) tetrahedron there are six symmetric positions which have the same crystallographic surrundings, and the three O atoms on this plane will random distribute in the positions. So that the possibility of their occupations is 0.5.

Because of the orientation disorder of (SiO_4) groups, the crystal structure possesses higher symmetry.

4.3. The Relation of Crystal Structure to the Stability of the Compound

So far as we know, the new compound $Ca_8Mg(SiO_4)_4Cl_2$ has no polymorphism. The compound begins to form at 760°C and decompose at 1265°C. The property of decomposition at high temperature is because the chemical bonds in the structure are mainly covalent bond to which Mg-O connections contribute, and this increases the chemical stability of the compound at high temperature. Therefore we could infer that the compound will not have strong hydrition effect. It is well known that the calcination temperature of alinite cement clinker is about 1100°C. When higher Mg content exists in the raw materials of alinite cement clinkers, the chlorine calcium silicate containing magnesium will tend to form in the product and the following two effect will appear: firstly the formation of the compound is easy at lower temperature and the decomposition begins a above the calcination temperature. This will consume some useful components including $CaCl_2$ and SiO_2. Secondly because of the formation of the compound during the calcinating process,MgO will be stablized in the compound so that the sintered product will contain less free-MgO, thus soundness of cement is incresed. The other physical and chemical properties of the new compound will be further researched.

Table 4. bond lengthes (Å) and angles (°) between atoms

Si-O tetrahedron

O_{21}-Si-				1.621
O_{22}-Si-	113.8			1.621
O_{23}-Si-	113.8	113.8		1.621
O_{24}-Si-	104.7	104.7	104.7	1.641
	O_{21}	O_{22}	O_{23}	

MgO- tetrahedron

O_{11}-Mg-				1.860
O_{12}-Mg-	109.5			1.860
O_{13}-Mg-	109.5	109.5		1.860
O_{14}-Mg-	109.5	109.5	109.5	1.860
	O_{11}	O_{12}	O_{13}	

Ca-O octahedron

O_{25}-Ca_1-						2.365
O_{26}-Ca_1-	78.7					2.365
O_{27}-Ca_1-	78.7	101.3				2.365
O_{28}-Ca_1-	180.0	101.3	101.3			2.365
O_{29}-Ca_1-	101.3	78.7	180.0	78.7		2.365
O_{210}-Ca_1-	101.3	180.0	78.7	78.7	101.3	2.365
	O_{25}	O_{26}	O_{27}	O_{28}	O_{29}	

Ca-O (or Cl) polyhedron

Cl_1-Ca_2-								2.994
Cl_2-Ca_2-	125.6							2.994
O_{13}-Ca_2-	68.0	68.0						2.655
O_{14}-Ca_2-	68.0	68.0	69.8					2.655
O_{22}-Ca_2-	106.1	77.3	126.8	60.2				2.486
O_{24}-Ca_2-	79.1	148.2	143.5	112.5	76.4			2.362
O_{25}-Ca_2-	148.2	79.1	112.5	143.5	98.3	87.4		2.362
O_{26}-Ca_2-	77.3	106.1	60.2	126.8	172.8	98.3	76.4	2.486
	Cl_1	Cl_2	O_{13}	O_{14}	O_{22}	O_{24}	O_{25}	

References

/1/ Ye Ruilun and Wang Xinrong,JOURNAL OF THE CHINESE SILICATE SOCIETY,13(2) 250-51 (1985).

/2/ V.C.Farmer; Infrared Spectra of Minersis, London, 1980.

/3/ Erwin Parthe: Crystal Chemistry of Tetrahedral Structure, 1960.

Dr-Ing. Feng Xiu-ji, M.S.Long Shi-zong, Ding qing-jun and Huang Cong-yun: 1
Wuhan Institute of Building Materials, China; Shen De-Xun: Nanjing University, China. Teng min-kang, Yin Chuan-yuan: Nanjing University, China.

INVESTIGATION ON DOPED β-C_2S WITH POSITRON ANNIHILATION 1.2

ETUDE SUR β-C_2S DOPÉ EN UTILISANT L' ANNIHILATION DE POSITRON

ABSTRACT The lifetime spectrum of positron in β-C_2S of added Na_2O and P_2O_5 is studied with positron annihilation teehnique. According to the theory of the capture of positron, we discuss the relationship between lifetime spectrum parameters obtained through experiment and the microstructure of β-C_2S. The results show that the long living component τ_2 (about 500 ps) represents the capture of positrum in the defects of Ca^{2+} vacancies; the intensity I_2 of τ_2 decreases with the increasing of Na^+ and increases with the increasing of P^{5+}. The results also verify that Na^+ replaces Ca^{2+} and creates anion vacancies; but P^{5+} replaces Si^{4+} and creates cation vacancies; Vacancy concentration increases with the increasing of Na^+ and P^{5+}. Our work shows that the positron annihilation technique is a useful tool for studying the change of microstructure defects in doped β-C_2S.

This article also studies and discusses the relationship between heat treatment and hydration activity of doped β-C_2S and its impurities.

Estuda-se o espectro de duração de positron em β-C_2S de Na_2O e P_2O_5 adicionados, empregando-se técnica de aniquilação de positron. De acordo com a teoria de captura de positron, discutimos a relação entre parâmetros de espectro de duração, obtidos através de experiência, e a microestrutura de β-C_2S. Os resultados mostram que o componente τ_2 de duração mais longa (cerca de 500 ps) representa a captura de positron nos defeitos de carências de Ca^{2+}; a intensidade I_2 de τ_2 diminui com o aumento de Na^+ e aumenta com o aumento de P^5 Os resultados constatam também que Na^+ substitui Ca^{2+} e cria carências de aníon; mas P^{5+} substitui Si^{4+} e cria carências de catíon; a concentração de carência aumenta com o aumento de Na^+ e P^{5+}. Nosso trabalho mostra que a técnica de aniquilação de positron é um instrumento útil para estudo da mudança de defeitos de microestrutura em β-C_2S dopado.

O artigo também estuda e discute a relação entre tratamento térmico e atividade de hidratação de β-C_2S dopado e suas impurezas.

Dr-Ing. Feng Xiu-ji, M.S.Long Shi-zong, Ding qing-jun and Huang Cong-yun: Wuhan Institute of Building Materials, China; Shen De-Xun: Nanjing University, China. Teng min-kang, Yin Chuan-yuan: Nanjing University, China.

INVESTIGATION ON DOPED β-C_2S WITH POSITRON ANNIHILATION

ETUDE SUR β-C_2S DOPÉ EN UTILISANT L' ANNIHILATION DE POSITRON

1. INTRODUCTION

Adding Impurities to C_2S can affect its microstructure, polycrystalline change, rate of firing reaction and hydraulic properties. Foregoing the microstructure defects of doped β-C_2S were usually studied with electron microscope and so on (1,2,3,4). But we haven't seen published reports about the studies of defects in doped β-C_2S with positron annihilation so far.

Positron annihilation is a experimental medium developed rapidly in recent years(5). Positrons are very sensitive to vacancy-type defects in solid substance, in ionic compound, for example, the cation vacancy of halides of alkaline metals and the defects of F cantre are able to capture the positrons and increase the intensity of long living component of lifetime spectrum.(6).

Let us imagine that the Ca^{2+} vacancies in C_2S crystal possess equivalent negative charges which are able to capture positron due to coulomb attraction between positive and negative charges. The anion vacancies in C_2S crystal possess equivalent positive charges which repel positrons and hinder Ca^{2+} vacancies from capturing positrons. In this article, the microstrueture defects in doped β-C_2S are studied with positron annihilation.

2. PREPARATION OF SAMPLES

The samples for measurement of positron annihilation are made of chemicals of AR degree according to molar ratio $CaCO_3$:SiO_2=2:1 Added Na_2O and P_2O_5 come from $Na_2C_2O_4$ and $NH_4H_2PO_4$ respectively. The quantities of impurities of various samples are given in table 1. Raw materials are mixed uniformly and pressed into pieces, then burned at 1450°C for 5 hours in electric oven and then quenched in air. Pure C_2S is burned at 1450°C trebly and amounts to 18 hours. XRD spectra of samples show that the samples are β-C_2S with little free lime. After grinding, the samples are sieved, a portion between 140 and 180 mesh is for the measurement of positron annihilation.

Table 1 Samples of doped β-C_2S

No.	1	2	3	4	5	6	7
impurities	-	Na_2O	Na_2O	Na_2O	P_2O_5	P_2O_5	P_2O_5
wt%	0	1.0	1.5	2.0	0.5	1.0	1.5

3. METHODS AND RESULTS OF EXPERIMENT

^{22}Na is used for radioactive source. The source and samples are placed as a sandwich structure. The circumstance temperature is 23±1°C when measurement is performed. Lifetime spectra are filed with standard positron fit program.[7] The results of free fit lifetime spectra are given in table 2. In this table, τ_1, τ_2 and τ_3 represent the lifetime of three living components and I_1. I_2 and I_3 are corresponding intensities of those components respectively. Because I_1=1-I_2-I_3, therefore intensities of I_1 are omitted in table 2.

In order to compare better intensities of long living component τ_2 and get more satisfactory fit, a controlled fit of three living components is made in the condition of constraining τ_1, τ_2 and τ_3 to be constant. The results are given in table 3. Based on average values in table 2, we force that τ_1=225 ps, τ_2=470 ps and τ_3=2050 ps. A constant forced τ_2 means that it represents the lifetime of certain positron state, it is able to help us easily to discuss the corresponding relationship between defect concentration and positron parameters.

Table 2. The character of Positron Annihilation of doped C_2S (free fit)

No.	τ_1(ps)	τ_2 (ps)	τ_3 (ps)	I_2 (%)	I_3(%)
1	249	493	2188	13.76	2.31
2	209	429	2120	15.38	3.83
3	216	452	1969	9.17	2.94
4	214	463	2013	9.45	2.23
5	244	478	2196	16.09	2.13
6	240	492	1683	34.05	2.70
7	258	498	2091	18.85	2.14

4. ANALYSIS AND DISCUSSION

We adopt curve fit of three living com-

Dr-Ing. Feng Xiu-ji, M.S.Long Shi-zong, Ding qing-jun and Huang Cong-yun: Wuhan Institute of Building Materials, China; Shen De-Xun: Nanjing University, China. Teng Min-kang, Yin Chuan-yuan: Nanjing University, China.

INVESTIGATION ON DOPED β-C_2S WITH POSITRON ANNIHILATION
ETUDE SUR β-C_2S DOPÉ EN UTILISANT L' ANNIHILATION DE POSITRON

Table 3. The Character of Positron Annihilation of doped C_2S (controlled fit)

No.	τ_1 (ps)	τ_2(ps)	τ_3(ps)	I_2(%)	I_3(%)
1	225	470	2050	17.08	1.91
2	225	470	2050	7.95	3.71
3	225	470	2050	5.94	2.71
4	225	470	2050	5.84	2.13
5	225	470	2050	17.35	1.79
6	225	470	2050	22.48	1.34
7	225	470	2050	23.71	1.62

ponents. Both free and controlled fit can only get two significant components τ_1 and τ_2 (refering table 2 and 3). The intensity of longest living component τ_3 is very small. It may be due to positron annihilation in the radioactive source and on sample surface. τ_1 separated from spectra does not represent any positron state directly. According to the capture model[8,9] it represents the annihilation of free positron. The long living component τ_2 is important parameter in our work. It may be produced in three conditions. One of them is that positrons are captured on the surface of C_2S granulae, forming a bound state on the intersurface. Another is that if positrons form positronium, "pick-off" annihilation process represents long lifetime.[10] Third, positrons are captured in cation vacancies. Based on the analysis of experiment results, former two possibilities can be eliminated.

According to W.Brandt's formula about[11] the surface contribution of positron annihilation, the intensity of surface annihilation is:

$$I_s = 1-\exp\left[-\frac{3.3}{R}\left(\frac{0.1D_+}{\lambda_f-\lambda_s+n}\right)^{\frac{1}{2}}\cdot\left(1-\frac{\lambda_s}{\lambda_f}\right)\right]$$

Our prepared C_2S samples are similar in the way of raw material granula and firing regulation, So we believe that R, D_+, λ_f and λ_s of every sample are approximately identical, so is I_s. Therefore we can consider that the regular change of the intensity I_2 of τ_2, owing to different quantities of added impurities, is not caused by the surface capture.

Positronium is a bound state of a couple of positron and electron, it will be formed when positron capture electron around in substance. Its basic state a single one 1^1S_0 (paro-positronium, abbr to P-P_s) and a triple one 1^3S_1 (ortho-positronium, abbr to O-P_s). The lifelime of P-P_s which is selfannihilated into two photons is 125 ps. The lifetime of O-Ps which decays with discharging three photons is 142 ns. In the medium, O-Ps has another "pick-off" annihilation, which competes against 3γ annihilation. In the process of "pick-off", the positron of O-Ps crashes into an "outcomer" electron, which possesses opposite spin and causes 2γ annihilation. Thus the lifetime of O-Ps in solid substance decreases to a few ns. In our experiment, there is no any reason to say that the regular change of intensity of τ_2 with the quantitative change of added impurities is caused by "pick-off" annihilation of positronium. (If so, we can obtain useful information of defects with positronium also)

Therefore, we consider that the component τ_2 in the lifetime spectra does not come from boundary of granulae and "pick-off" annihilation of positronium, it mainly comes from cation vacancies. In C_2S, Na^+ replaces Ca^{2+}. It is able to create anion vacancies, (oxygen vacancies) in order to keep electric neutral. Oxygen vacancies possess equivalent positive charges which may bind Ca^{2+}vacancies and form a complex of vacancy couple of cation and anion. This weakens the effect of Ca^{2+} vacancies' capturing positron. Thus, as added Na^+ increases, the vacancy concentration increases, and I_2 inclines to decrease (see table 3, #1 and #5-#7). When P^{5+} replace Si^{4+}, it is able to create Ca^{2+} vacancies. Ca^{2+} vacancies possess equivalent negative charges which may capture positron. Therefore when added P^{5+} increases, the Ca^{2+} vacancy concentration increases, the effect of capturing positron increases. Thus, I_2 inclines to increase. (see table 3, 1- 4).

In order to verify the above experiment, we have studied thermodynamics of doped C_2S. It is well-known that, at high temperature,

the combination of CaO with SiO_2 produces C_2S through the following process: Ca^{2+} diffuses toward the surfuce of C_2S granulae. First of all, a layer of C_2S is produced on the surface, the reaction goes on continuously, Ca^{2+} spread from outside to inside of granulae through the layer of surface product. The rate of C_2S formation is determined by the rate of diffusion of Ca^{2+} from outside to inside. When the activation energy of vacancy diffusion of ion in crystal is smallest, vacancy has biggest diffusion coefficient. If the previous produced dicalcium silicate has bigger concentration of vacancy defects, the diffusion of Ca^{2+} from outside to inside and the rate of Ca_2SiO_4 formation will be rapid at all, on the contrary, the above relationship is also correct.

We consider that the rate of reaction in pure C_2S goes on more slowly, because its concentration of vacancy defects is smaller. But the rate of formation of C_2S of added Na^+ or P^{5+} is rapide due to producing more Ca^{2+} or O^{2-} vacancies. The more quantites of added Na^+ or P^{5+} are, the higher the concentration of vacancies is, the rapider the rate of reaction is, too.

Table 4 and 5 give the formation rate (α) of doped Na^+ or P^{5+} dicalcium silicate burned at 1300 °C and different time. The definition of α is

$$\alpha = 1 - \frac{f}{c}$$

in which: f= weight percent of free lime.
c=CaO content in C_2S.

It's noticed from 4 and 5 that the rate of formation of C_2S added Na^+ or P^{5+} is both much rapider than that of pure C_2S. As long as quantities of added Na^+ or P^{5+} are raised, the rate of formation of C_2S becomes rapider. This told us clearly that the above assumption is correct. We have carried out the similar experiments at 1100 °C and 1200 °C. Their results are completely the same as that at 1300°C. There is no liquid phase to appear in the samples. The above facts show that the increase of the rate of C_2S formation mainly results from the organization of vacancy diffusion.

Table 4. The rate of doped Na_2O C_2S formation (at 1300°C)

Firing time (min) / Na_2O %	20	40	60	90
0	16.9	20.1	26.1	33.6
1.0	21.5	46.7	50.5	57.8
1.5	49.2	57.0	60.7	65.4
2.0	65.4	75.4	80.8	86.0

Table 5. The rate of doped P_2O_5 C_2S formation (at 1300°C)

Firing time (min) / Wt%	20	40	60	90
0.5	21.7	27.6	34.6	38.2
1.0	26.6	30.3	37.9	43.8
1.5	30.0	34.9	40.4	46.2

Calcium carbonate and silicate dioxide used in these experiments are all AR pure chemical agents. Magnitude of raw material granulae, preparation and firing condition are strictly controlled in the same condition. The temperature in the electric oven rises to due firing one in advance. Then, raw material is placed in the oven. As soon as due time is reached, samples are removed out. Free lime is tested with the method of glycerol and ethgl aleohol. After testing, it is recongnized that there is no free lime residue in different samples.

5. HYDRATION OF DOPED β-C_2S

After impurities is added to β-C_2S, how is the behaviour of its hydration? Many scholars have ever studied about that, (12, 13, 14) their conclusions at last are inconsistent. By means of testing chemical combined water, we deal with the rate of hydration of C_2S added Na^+. The results are given in table 6. The experimental results show that the hydration activity of β-C_2S decreases with the increasing of added Na^+, this is consistent with I.M. Pritts' result. As mentioned earlier, after Na^+ is added to β-C_2S,

Dr-Ing. Feng Xiu-ji, M.S.Long Shi-zong, Sing qing-jun and Huang Cong-yun: Wuhan Institute of Building Materials, China; Shen De-Xun: Nanjing University, China. Teng Min-kang, Yin Chuan-yuan: Nanjing University, China.

INVESTIGATION ON DOPED β-C_2S WITH POSITRON ANNIHILATION

ETUDE SUR β-C_2S DOPÉ EN UTILISANT L' ANNIHILATION DE POSITRON

anionic vacancies are produced. Moreover, vacancy concentration increases with the increasing of added Na^+, because the defects in crystal increase, the result should have higher activity. But the is just contrary, how to explain this phenomenon?

Table 6.The combined H_2O of β-C_2S added Na_2O

H_2O % / Na_2O % / time of hydration (d)	1.0	1.5	2.0
3	2.00	1.94	1.90
7	2.88	2.77	2.69
15	3.20	3.14	2.76
25	3.61	3.69	2.99
35	4.87	4.16	3.78

We consider that vacancy defects in crystal is the type of point defect that occurs in the crystal granula. The main factor determining the hydration activity of mineral should be crystal boundary of C_2S granulae, its surface structure and its component. The authors ever explored the mechanism of stability of doped β-C_2S. We consider that part of added ions as Na^+ and P^{5+} that are able to stabilize β-C_2S is distributed in crystal according to statistics regulation, another is enriched in the crystal dislocation crystal boundary and its surface, this is verified by ESCA.(15)

Because Na^+ is enriched in crystal boundary of β-C_2S crystal and on its surface. It makes structure dislocation and reduces free energy of crystal boundary and its surface. Therefore hydration activity lower. The more quantities of added Na^+ are, the larger the area of crystal boundary at which Na^+ is enriched, the more the reduction of free energy of the whole surface and the lower the hydration activity.

6. CONCLUSION

1). That the vacancy defects of Ca^{2+} in β-C_2S the capture positron has been verified with positron annihilation technique. The lifetime of positron annihilation is about 470 ps in Ca^{2+} vacancies in β-C_2S.

2). Adding Na^+ to β-C_2S can create anionic vacancies (oxygen vacancies). Oxygen vacancy concentration increases with added Na^+; oxygen and Ca^{2+} vacancies can form a couple of cation and anion vacancies. It weaken the ability of Ca^{2+} vacancies' capturing positron.

3). Adding $P^{5+}$to β-C_2S can create Ca^{2+} vacancies. Ca^{2+} vacancy concentration and the ability of capturing positron increase with doped P^{5+}.

4). The vacancy concentration and the rate of C_2S formation increase with doped Na^+ and P^{5+}.

5). That Na^+ is enriched on the surface of β-C_2S granulae will reduce free energy of crystal boundary and its hydration activity.

REFERENCES

(1) Boikova A.I., Dehen M.G., Parmoncra V.A., 6th-ISCC, Vol 1, Moscow.

(2) MAYCOCK, J.N. et MC CARTHY, M.Jr. (1973) "Crystal lattice deffect in dicalcium silicate", Proc. 11 th Conf. Silicate Ind. Budapest P 1, 389

(3) G.W.GROVES, Portland cement clinker viewed by transmission electron microscory « Journal of materials science », Vol 16, 4, 1981.

(4) J.N.Maycaky, Cement and Concret Research 4, p835-847, (1974).

(5) R.N.West, Adv. Phys., 22 [3] 263 (1973).

(6) W.Brandt, in A.T.Stewart and L.O.Roellig Eds. « Positron Annihilation », Academic Press, New York, London, 179 (1967).

(7) P.Kirkegaard and M.Eldrup, Computer Phys. Commun., 7 [7] 401 (1974).

(8) M.Bertolaccini, A.Bisi, G.Gambarini, et al., J.Phys. C, Solid state phys., 4,734 (1971).

(9) K.Hinode, S.Tanigawa, H.Kumakura, et al.,

J.Phys. Soc, Japan, 45 [6] 1858 (1978).

(10) A.Dupasquier, in P.Hautojarv; Ed. « Positrans in Solids », Springer-Verlag, Berlin Heidelberg, New York, Chap. 5, 197 (1979).

(11) W.Brandt, Appl. Phys., 5 [1] 1 (1974).

(12) I.M.Pritts and K.E. Daugherty, Cement and Concrete res. 6, (6) 783-795 (1976).

(13) H.Funk, Z. anorg. U. allgem. Chem. 291 276 (1957).

(14) L.E.Capeland and D.L.Kantro, Proceedings of the Fifth International Symposium on the chemistry of cement, Part Z, Session 5, P.12, 7 Tokyo (1968).

(15) Feng Xiuji and Long Shizong, Journal of the chinese Silicate Society, Vol.13, No. 4, 423, (1985).

Z. ŠAUMAN, Technical University Brno, Czechoslovakia

INFLUENCE OF FLUORIDES AND SILICOFLUORIDES ON THE HYDRATION OF CEMENT

SUMMARY : Through the use of industrial gypsum as a cement setting regulator and considerably reduced the initial strengths of cement paste or mortar.

The retardation of the growths of strengths is in agreement with the low liberated portlandite contents; after more than 7 days storage the $Ca(OH)_2$ contents as well as the attained strengths approach the values for cement without the presence of silicofluorides.

It was shown that to this phenomenon contributes already a small quantity of silicofluorides, contained in the gypsum, mainly Na_2SiF_6, whereas CaF_2 does almost not influence the initial strengths.

It was found that Na_2SiF_6 accelerates considerably the formation of ettringite and reduces the degree of alite hydration in the initial pe_ ods of the reaction.

SUMÁRIO: Pelo uso de gesso industrial como regulador de pega do cimento são consideravelmente reduzidas as resistências iniciais de pasta e argamassa de cimento.

O retardamento do crescimento das resistências está de acordo com o baixo conteúdo de portlandita liberada; após mais de 7 dias o conteúdo de $Ca(OH)_2$, assim como as resistências, atingem os valores para cimento sem a presença de silicofluoretos.

Foi mostrado que para esse fenômeno já contribui uma pequena quantidade de silicofluoretos, contido no gesso, principalmente Na_2SiF_6, ao passo que CaF_2 quase não influi nas resistências iniciais.

Descobriu-se que Na_2SiF_6 acelera consideravelmente a formação de etringita e reduz o grau de hidratação da alita no período inicial da reação.

Z. ŠAUMAN, Technical University Brno, Czechoslovakia

INTRODUCTION

In the production of cement is generally employed a suitable quantity of natural gypsum as a setting regulator. In connection with a deficiency of natural resources of this raw material on one hand and the ever increasing volume of waste products from the chemical industry which contain $CaSO_4.2H_2O$ on the other hand, it appeared desirable to use for those purposes industrial gypsum. The replacement of natural gypsum by industrial gypsum has caused, however, a considerable retardation in the growth of strengths of the standard cement mortar during the initial period of time. After 3 and especially 7 days storage the strengths, however, already correspond to values for cement with natural gypsum. With regard to the fact that industrial gypsum contains a certain fraction of X-ray amorphous $Fe(OH)_3$, the effect of this component onto the growth of cement paste strengths was studied and it was found that its effect is negligeable. It was shown, however, that the main cause may lie in fluorine compounds which are contained in the waste gypsum. These include mainly CaF_2, Na_2SiF_6 and K_2SiF_6, respectively.

For this reason the experimental studies were aimed at the clarification of the influence of fluorides and silicofluorides onto the attained strengths, especially in the initial hydration period. At the same time it was desirable to study the influence of selected fluorine compounds on simpler systems. Even though the kinetics of ettringite formation was studied relatively thoroughly (1-5), the influence of fluorides and silicofluorides, respectively onto the setting of cement was investigated sporadically. Schwiete at al. (6) have shown that the action of $MgSiF_6$ and $ZnSiF_6$ manifests itself in a prolongation of the setting period which in mixed cements is markedly increased.

Ludwig et al. (7) have investigated the influence of inorganic and organic materials added to the cement as decelerators of the setting process with the result that the $MgSiF_6$ additive exhibits a pronounced effect.

EXPERIMENTAL

For the actual work was used portland cement clinker M with usual chemical composition.

The clinker was first of all ground in a laboratory ball mill onto the specific surface 310 $m^2.kg^{-1}$ and then were added 7% natural gypsum and a graded quantity (0-5%) of fluorides - CaF_2, NaF and silicofluorides - Na_2SiF_6, K_2SiF_6. From the homogenized mixtures were preparted in the form of paste (w=0,32) micro-beams with the dimensions 20x20x100 mm which were stored in a 100% relative humidity environment for 12 and 24 h at 20°C; after this period the compressive strengths were determined. The prepared mixtures and the obtained compressive strengths are shown in Table 1.

It follows from the compressive strength values after a 12 hour hydration of the cement paste that the CaF_2 additive exerts practically no influence onto the cohesions in this period. The situation is the same also after 24 hours of storage; in both cases is observed a slight increase of strengths with a growing CaF_2 content; quite different are the results when using NaF, since its 1% addition (related to gypsum contents) decreases significantly the strengths with a growth of the NaF contents the strength no longer changes more substantially, on the contrary in the case of 5% NaF can be seen a mild increase of the latter.

Table 1

Composition of mixtures and compressive strength values

Quantity of fluorides in gypsum (wt. %)		Storage period and compressive strengths 12h (MPa)	24h (MPa)
-	-	3,90	17,80
1	CaF_2	3,97	17,90
3	CaF_2	4,04	18,10
5	CaF_2	4,07	18,15
1	NaF	2,62	17,60
3	NaF	2,33	17,10
5	NaF	2,94	17,72

After 24 hours of hydration the compressive strength values are comparable with a cement paste without fluoride.

In the same manner was carried out the determination of the effect of silicofluorides (Na_2SiF_6, K_2SiF_6) onto the attained cohesions of the cement mortar (Table 2).

It follows from the compressive strength values that in both components there occurs a considerable retardation of the growth of strength in the course of a 12 hour storage, a higher effect is exhibited by Na_2SiF_6. With a growth of the contents of silicofluorides is considerably reduced the strengths of the paste, so that at 5% contents of the two components the strengths after 12 hours can no longer be measured. A pronounced reduction of strengths was proven also after 24 hours of hydration, especially in the case of Na_2SiF_6.

Table 2

Composition of mixtures and compressive strength values

Quantity of silicofluorides in gypsum (wt. %)		Storage period and compressive strengths 12 h (MPa)	24 h (MPa)
-	-	3,90	17,80
1	Na_2SiF_6	0,49	10,58
3	Na_2SiF_6	0,14	3,08
5	Na_2SiF_6	not meas.	0,67
1	K_2SiF_6	1,17	13,96
3	K_2SiF_6	0,37	11,43
5	K_2SiF_6	not meas.	9,13

Analogical experiments were carried out with both $CaSiF_6$ and $MgSiF_6$ and there was also confirmed their negative influence on the growth of strengths in the initial hydration period of the cement paste.

To the degree of strength reduction corresponds essentially the liberated $Ca(OH)_2$ content, so that in the case of 5% silicofluoride contents can be identified only a slight quantity of the formed portlandite.

For the clarification of the above mentioned phenomenon it was desirable to carry out experiments, by which it would be possible to delimitate the influence, if any, of CaF_2 and Na_2SiF_6 onto the formation of ettringite and other components, respectively.

RESULTS AND DISCUSSION

Study of the system C_3A - $CaSO_4$ - CaF_2 or Na_2SiF_6 - H_2O

For the investigation of the considered system were prepared mixtures of C_3A and $C\bar{S}H_2$ (in a molar ratio 1:3) with the addition of a graded quantity of CaF_2 and Na_2SiF_6 (0, 1, 3 and 5%), converted onto $C\bar{S}H_2$ contents.

The mixtures in the form of a paste (relation of solid phase: H_2O = 1:2) were exposed to an environment with 100% relative humidity for a period of 1, 24 and 72 h and 28 days. After dewatering with absolute ethanol and acetone they were subjected to further studies.

Apart from DTA was investigated by X-ray diffraction analysis the relative quantity of gypsum, ettringite and monosulphate on the basis of their typical diffractions. The results are presented in Table 3.

Table 3

R e s u l t s of semi-quantitative X-ray determination

Composition of mixes and determined phases			Hydration period and X-ray data 1 h count	24 h count	72 h count	7 d count	28 d count
C_3A + 3 $C\bar{S}H_2$ (without additive)	$C\bar{S}H_2$	(7,56 Å)	8622	5210	1288	800	83
	$C_6A\bar{S}_3H_{32}$	(9,73 Å)	60	190	800	1076	1629
	$C_4A\bar{S}H_{12}$	(8,92 Å)	-	-	101	182	202
C_3A + 3 $C\bar{S}H_2$ (5% CaF_2)	$C\bar{S}H_2$	(7,56 Å)	5530	3779	1357	906	484
	$C_6A\bar{S}_3H_{32}$	(9,73 Å)	-	214	543	779	1461
	$C_4A\bar{S}H_{12}$	(8,92 Å)	-	-	85	90	166
C_3A + 3 $C\bar{S}H_2$ (5% Na_2SiF_6)	$C\bar{S}H_2$	(7,56 Å)	2650	158	-	-	-
	$C_6A\bar{S}_3H_{32}$	(9,73 Å)	336	1347	1921	1971	2031
	$C_4A\bar{S}H_{12}$	(8,92 Å)	-	120	125	138	184

As can readily be seen, in the case of a mixture containing Na_2SiF_6 is formed after a 1 hour reaction a significantly higher ettringite quantity in comparison with the two other systems. Its quantity increases considerably with time; the ettringite contents after 24 h of hydration is several times higher than in the systems with CaF_2 and without an additive. Only towards the end of the investigated period (28 days) there occurs a partial balancing of its contents. This fact is in good agreement with the relative gypsum quantity, since after 72 h in the system with Na_2SiF_6 it is no longer possible to identify $C\bar{S}H_2$.

Also to a greater extent - with regard to the two systems - is formed monosulphate up to a period of approx. 72 h. With regard to the fact that in a system with Na_2SiF_6 is formed within a very short period of time a pronounced quantity of ettringite, mixtures with an identical composition were stored for a very short period of time, beginning with 60 s, in an environment with 100% relative humidity.

The mixture without an additive is characterized by particles of gypsum and C_3A, the surface of which is not disturbed (Fig. 1).



Fig. 1 Mixture C_3A : 3 $C\bar{S}H_2$ (without additive) 60 s/20°C

An analogical character exhibits the mixture with CaF_2 (Fig. 2).

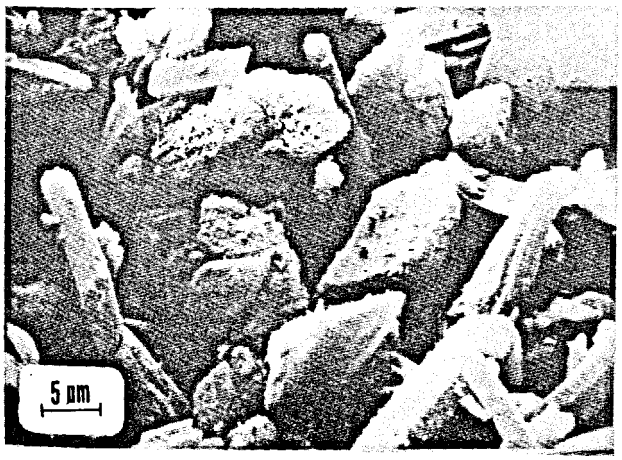

Fig. 2 Mixture C_3A : 3 $C\bar{S}H_2$ (5% CaF_2) 60 s/20°C

In both cases can be observed only sporadically appearing ettringite micro - needles. Substantially different is the situation in the sample with Na_2SiF_6 (Fig. 3).

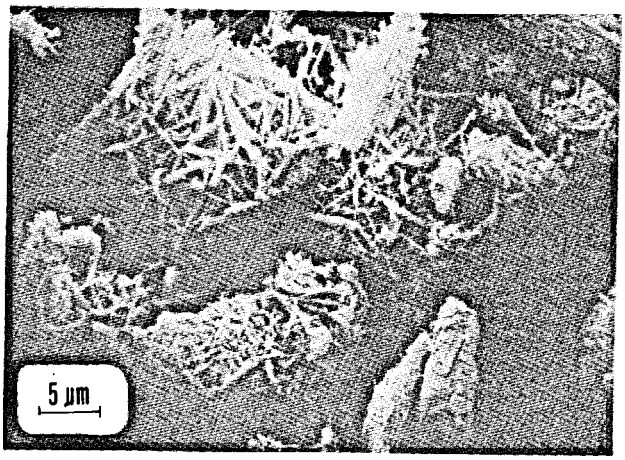

Fig. 3 Mixture C_3A : 3 $C\bar{S}H_2$ (5% Na_2SiF_6) 60 s/20°C

There can readily be seen a considerable quantity of needle- and bar-shaped, respectively ettringite particles of considerably larger dimensions in comparison with the two previous mixtures. Only after a long-period hydration is formed in the mixtures without silicofluoride a pronounced fraction of this phase, but the dimension of its crystals is substantially smaller.

Delimitation of the influence of CaF_2, NaF and Na_2SiF_6 onto the hydration of 3 $CaO.SiO_2$

It was proven experimentally that both Na_2SiF_6 and NaF increase the solubility of gypsum, whereas in the case of CaF_2 this phenomenon was not proven. This fact is connected with the formation of a pronounced quantity of ettringite in the first time period of the reaction.

In order to explain the effect of the above compounds including gypsum onto the degree of C_3S hydration were prepared mixtures containing 97% C_3S, 7% $C\bar{S}H_2$ and 1, 2, 3 and 5% CaF_2, NaF and Na_2SiF_6 (converted to gypsum contents).

Samples in paste form were stored in an environment with 100% relative humidity for a period of 4, 8, 12, 24, 72 h and 28 days. It was shown that already in the case of 1% Na_2SiF_6 is considerably suppressed the hydration of C_3S.

A lower retardation effect exhibits NaF and finally CaF_2. From Fig. 4 can readily be seen the effect of 5% of the above components onto the hydration of C_3S. In the case of the mixture with Na_2SiF_6 it is no longer possible after 12 hours of hydration to identify thermogravimetrically liberated portlandite (contents of $Ca(OH)_2$ and second. formed $CaCO_3$, converted to CaO).

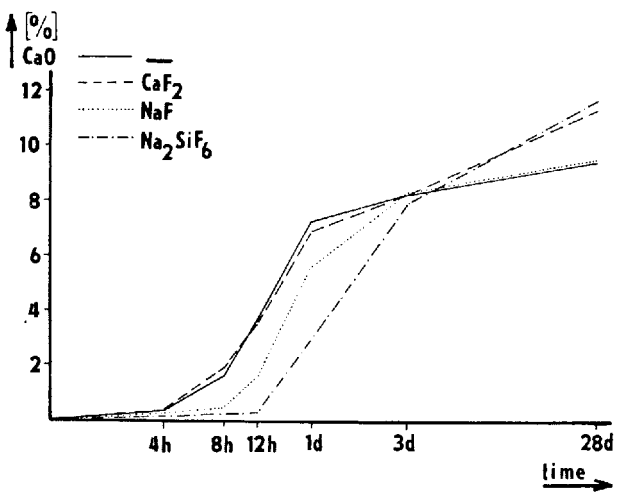

Fig. 4 Influence of fluorides and silicofluride onto the hydration of C_3S

After 28 days of hydration the CaO quantity in the mixture with CaF_2 and Na_2SiF_6 is somewhat higher in comparison with a specimen without additive.

CONCLUSIONS

Upon using industrial gypsum - waste from the chemical industry - as setting regulator for cements, has been proven a pronounced retardation of the growth of the initial strengths of the standard mortar.

It was found that an influence onto the slow growth of strengths during the initial hydration period exert the silicofluorides contained in the gypsum, mainly Na_2SiF_6. By a significantly lower effect is characterized NaF, whereas CaF_2 does almost not influence the development of initial strengths.

The above phenomenon was determined through the addition of those compounds to the system clinker - $C\bar{S}H_2$ - H_2O. It was shown at the same time that in the presence of Na_2SiF_6 on one hand there is formed a substantially higher quantity of ettringite which is characterized by considerably larger crystals which do not, however, exhibit binding effect, on the other hand the alite hydration is substantially slower.

REFERENCES

1. F.E. JONES, J.Phys.Chem. 48, 311 (1944)
2. H.E. SCHWIETE, U.LUDWIG, Proc. Fifth Int.Symp.Chem. Cem. II,37 (Tokyo 1968)
3. J. BENSTED, Cem. Concr. Res. 12, 341 (1982)
4. M. ISH-SHALOM, A. BENTUR, Cem. Concr. Res. 4, 519 (1974)
5. P.J.M. MONEIRO, P.K. MEHTA, Cem. Concr. Res. 15, 378 (1985)
6. H.E. SCHWIETE, U.LUDWIG and K. SEILER, Zement - Kalk - Gips 23, 354 (1970)
7. U. LUDWIG, H.E. SCHWIETE and K. SEILER, Proc. X. Conf. Silic. Ind., 409 (Budapest 1970)

Erling Fundal, Ph. D.
F.L. Smidth & Co. A/S, R&D Dept., Copenhagen, Denmark.

1

1.2

The Description of a New Potassium-alumina Phase in Ordinary Portland Cement.

Le description d'une nouvelle phase d'aluminate de potassium dans le ciment portland ordinaire.

SUMMARY: Raw mixes with differing amounts of K_2O in excess of sulphur have been examined with the purpose of proving the existence of free K_2O in cement clinker. The suspicion of the existence of such a phase originated from scanty observations of a strongly hygroscopic phase in some clinker. The hygroscopic reaction originates from the existence of both K_2O and $K_2O \cdot Al_2O_3$ as proven by observation of the aeration products and different extraction methods. The free K_2O in clinker has a strong influence on the determination of free CaO by the glycol titration method. The presence of both K_2O and Na_2O promotes the formation of the so-called alkali aluminate which is proven not to crystallize by prolonged burning time at normal sintering temperature. This is shown by micrographs and microscopical point counting on clinker samples with increasing duration of burning at 1450°C. The existence of a water soluble alkali not being a sulphate has also been suspected by some researchers from examination of cement properties. The presence of free alkali in clinker with its hygroscopic properties is expected to exceed a perceptible influence on cement strength as well on storage properties.

Foram examinadas misturas cruas com diferentes quantidades de K_2O em excesso de enxofre, com a finalidade de provar a existência de K_2O livre no clinquer de cimento. A suspeita da existência de tal fase derivou de observações insuficientes de uma fase fortemente higroscópica em alguns clínqueres. A reação higroscópica tem origem na existência de K_2O e $K_2O.Al_2O_3$, conforme provado por observação de produtos de aeração e métodos diferentes de extração. O K_2O livre no clinquer tem forte influência sobre a determinação do CaO livre pelo método de titulação de glicol. A presença de K_2O e Na_2O proporciona a formação do chamado aluminato alcalino, que ja se provou que não se cristaliza por queima em período prolongado sob temperatura normal de sinterização. Isto é mostrado por microfotografias e contagem microscópica de ponto em amostras de clinquer com aumento da duração de queima a 1.450°C. A partir do exame das propriedades do cimento, há também a suspeita de alguns pesquisadores quanto à existência de um álcali solúvel em água, que não é um sulfato. Espera-se que a presença de álcali livre em clinquer com suas propriedades higroscópicas vá além de uma influência perceptível sobre a resistência do cimento bem como sobre as propriedades de armazenagem.

INTRODUCTION

When concerned with microscopy of cement clinker from time to time one may experience bad etching of polished sections, especially when HF-vapor is applied.

Early we thought in our laboratory the phenomena to originate from bad cleaning of the surface. The etching fault is very often observed as more or less circular areas not receiving the etch. Also when a section was not etched immediately after polishing we experienced that some clinker despite storage in exsiccator very soon became so bad that a repolish was needed.

Using alkali-rich raw materials in burning a series of clinker a strongly hygroscopic phase was found.

A similar hygroscopic phase was found by sintering lime and nepheline syenite (an alkaline rock type) forming belite and alkali aluminate.

Besides this scanty observations we were recently faced with a potential cement raw mix with very high potassium content originating from mica (muscovite) where again we observed a hygroscopic phase.

In the literature concerned with clinker microscopy according to our knowledge these phenomena has not been described hitherto, although hints of a soluble phase of alkali not being a sulphate may be found in papers concerned with cement properties.

As a consequence of this we have tried to identify the phase and it follows from the experiments described below that free K_2O in clinker must be expected to be rather common. Thus we have found that the so-called alkali aluminate forming in alkali-rich clinker by cooling is sensitive to the duration of burning gradually being substituted by the crystallization of ferrite and aluminate.

Observations in the Microscope:

A raw mix with the chemical modules shown in Table 1 as R_1 was burned in a 300 g batch from 1 to 2 hours in a closed platinum crucible at 1500°C and examined in polished section.

It is noticed from Table 1 that the sodium content is nearly zero and that only about 10% of the alkali has evaporated.

It was observed that immediately after cleaning droplets started to migrate over the clinker surface when exposed to the atmosphere. This is seen in fig. 1 representing 30 sec. exposure. Besides droplets also initial reaction products are seen as a positive relief, especially in the center of the micrograph.

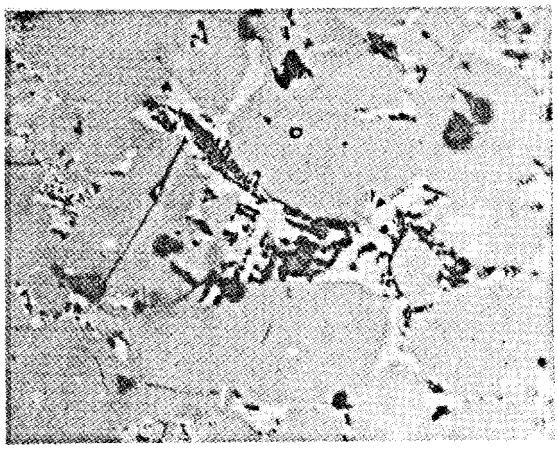

Fig. 1. Clinker R_1 from Table 1, unetched but exposed to the atmosphere for 30 sec. Besides droplets also reaction products are observed situated in the white ferrite. Reflected light x 800.

When treated with a saturated solution of K_2SO_4 the general melt phase structure is better observed. A cross-hatched texture of the ferrite is characteristic and it is seen that some interstitial matter between the ferrite laths has been removed. Typical C_3A is not observed and is hardly present as also confirmed by XRD.

The high solubility of the phase can be used for quantitative determination of its composition, as will be described below.

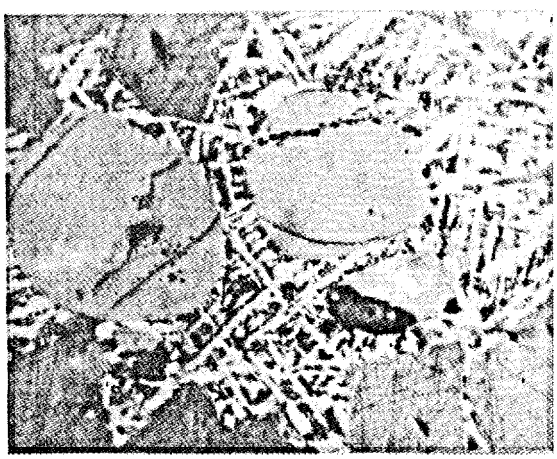

Fig. 2. Clinker R_1 from Table 1 etched with saturated solution of K_2SO_4 for 10 sec. The hygroscopic phase has been dissolved and the characteristic cross-hatched structure of the ferrite is distinctly seen. Belite light grey, alite medium grey with scratches from the polish. Reflected light x 800.

Another method for identification of the phase follows from the fact that any soluble K_2O in the polished surface may be precipitated as K_2CO_3 during a treatment with humid air and CO_2. If $K_2O \cdot Al_2O_3$ is present in the surface also gibbsite should precipitate.

An example of the surface reaction products is seen in fig. 3. The whole polished surface of the clinker is now covered with reaction products. The most pronounced reaction product is the large prismatic mineral easily identified by EDAX or in polarizing microscope as the expected K_2CO_3.

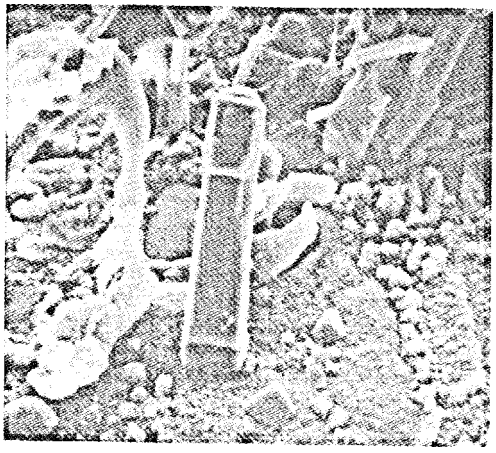

Fig. 3. Clinker R_1 from Table 1 exposed to humid air with CO_2. Original polished section. Sample dried at 60°C for 1 hour. Silicates are covered with reaction products. Large crystals are K_2CO_3. SEM x 1000.

As mentioned above also gibbsite is expected and by examining the EDAX spectra of different features in the surface spherical products as shown in fig. 4 were found to consist of K and Al making a mixture of K_2CO_3 and $Al(OH)_3$ likely. Not all products of the aeration have been identified, but there are indications of double carbonates of K and Ca.

When K_2SO_4 is present in a clinker the aeration has comparatively less influence and the aeration products are not similar (fig. 5), but syngenite and $Ca(OH)_2$ then seem to be among the initial reaction products.

Thus, there are strong indications that both K_2O and $K_2O \cdot Al_2O_3$ are present in this clinker, and both of these are expected to be hygroscopic.

Both do not occur in regions larger than a few micron.

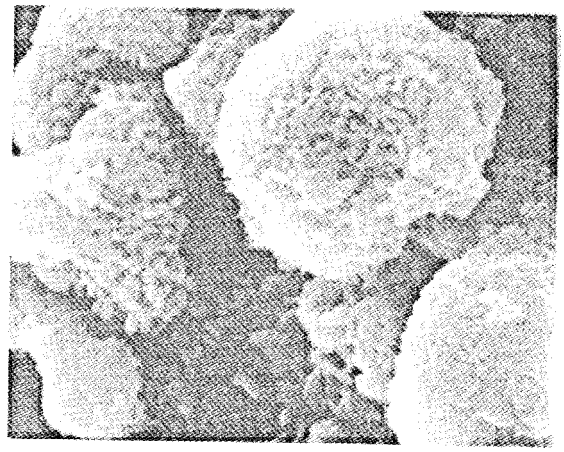

Fig. 4. Clinker R_1 from Table 1 exposed to humid air with CO_2. Original polished section. Sperical reaction product, probably a mixture of K_2CO_3 and $Al(OH)_3$. SEM x 6000.

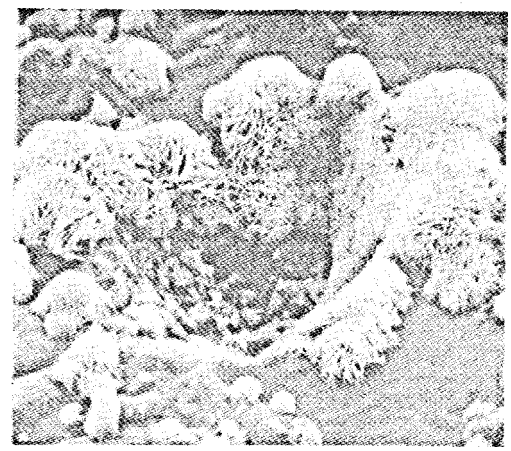

Fig. 5. Clinker R_1 from Table 1, with 0.6% K_2SO_4 added to the raw mix. Polished surface exposed to humid air with CO_2. Reaction product not identified. SEM x 1000.

Chemical Extraction of Clinker:

As soluble potassium compounds have been proven a quantitative extraction is a natural continuation.

100 g of the R_1 from Table 1 were sintered in a closed platinum crucible at 1500°C for 1 hour.

a) 25 g of the freshly ground clinker were treated with 100 ml of destilled water for 15 min. at 70°C and in addition washed with 100 ml of the same temperature.

b) 25 g of the freshly ground clinker were treated with 100 ml solution of 34.2 g Na_2CO_3 and 6.45 g per liter for 15 min. at 70°C, and in addition washed with 100 ml water of the same temperature.

400 g of R_1 were sintered in a closed platinum crucible at 1500°C for 2 hours.

c) 3 g of the clinker sample were treated with 50 ml dry ethylene glycol for 30 min. at 110°C.

All the filtrates were analysed by atomic absorption and the results are presented in Table 2.

It follows from test a) and b) that approximately 1.4% K_2O is soluble in distilled water constituting 70% of the total alkali in clinker, and that the mole ratio K_2O: Al_2O_3 in the basic extraction is larger than 1, indicating that both K_2O and $K_2O \cdot Al_2O_3$ are present in amounts calculated to be 0.6 and 1.7% of clinker, respectively. It is trivial to conclude that K_2O contributes to free CaO as determined by titration of ethylene glycol.

This statement leads to the conclusion that a determination of free K_2O is needed in clinker with alkalies in excess of sulphur, when correct free CaO is analysed for.

Clinker Burning with Increasing K_2O-Content.

We have examined a series of raw mixes with increasing content of K_2O. The mixes R_{11} to R_{15} and R_{21} to R_{25} from Table 1 were prepared from Muscovite (with 10.4% K_2O), pyrite ash, coral limestone, bauxite, clay A (1.4% K_2O) and clay B, hematite, Al_2O_3 and $CaCO_3$, the three last mentioned of analytical grade. The chemical modules of the mixes are shown in Table 1. A gradual increment in the K_2O-content has been obtained with nearly constant modules. Only for R_{23}, R_{24} and R_{25} the M_a is somewhat off.

A few grammes of each mix was burned in a closed platinum crucible at 1450°C for 30 min. after a calcination at 1000°C for 1 hour. The same heating and cooling rate was established for all burnings (cooling 500°/min. down to 1000°C) in an atmosphere consisting of 2% O_2, 30% CO_2 and 68% N_2.

During this procedure approximately half of the K_2O was lost due to evaporation (Table 1) compared to only 10% of R_1. This is probably due to the difference in the batch size.

The free CaO was determined by the ethylene glycol method and the filtrate was analysed with atomic absorption. In addition the free CaO and the melt phase compounds were determined by point counting in polished sections of the clinker.

The results are shown in Table 2. The content of free K_2O increases with the amount of K_2O in the clinker. In the filtrate sodium and alumina are fairly constant.

There is a distinct difference between the chemical and microscopic determination of free CaO, and the difference increases with the increasing amount of free K_2O. The relation is approximately $\Delta CaO = 3.7\ K_2O_{free}$. A relation of the same order of magnitude has been found by other investigations in our laboratory.

As a conclusion it follows that for some clinker a determination of free K_2O is needed, thus comprising the sum of K_2O and K_2O from the phase $K_2O \cdot Al_2O_3$, if correct free CaO values are to be determined.

The existence of free alkali has been discussed by Politt and Brown (1), Osbaeck (2) and Costa and Massazza (5) in connection with cement properties, probably mostly found as K_2CO_3 because of the high reactivity of the K_2O.

Melt Phase Structure:

It is natural to devote the melt phase structure some interest. By microscopy it appeared that the whole series of clinker described above possessed the melt phase structure depicted in fig. 6. This phase is normally called an alkali aluminate and is lamelliform often with a poikilitic growth. When comparing R_{21} with $M_a = 2.0$ with R_1 with $M_a = 1.4$ there is a large dissimilarity (fig. 2 and 6).

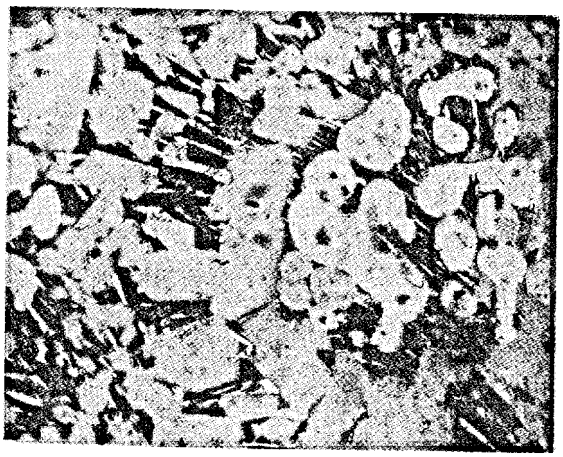

Fig. 6. R_{21} from Table 1. Polished section etched with 10% NaOH solution. Alkali aluminate and free lime. Reflected light x 800.

The texture of fig. 2, also sometimes seen in industrial clinker, is by some attributed to fast cooling as stated for instance by Woermann (3), but the same structure may be produced by increasing the burning time with origin in the structure of fig. 6, as will be proven here.

R_{21} was sintered at the same circumstances as described above, only increasing the burning time in steps to 3 hours. The loss in K_2O has not been analysed, but the change in the melt phase texture is drastic. Fig. 7 and 8 show the structure after 1 and 2 hours and practically no change is observed from 2 to 3 hours.

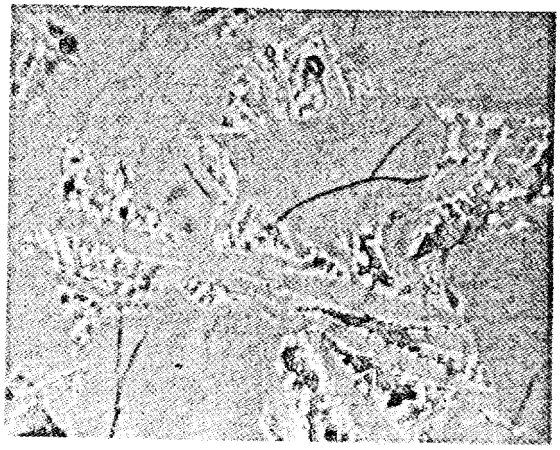

Fig. 7. R_{21} from Table 1 burned at 1450°C for 1 hour. Polished section etched with a K_2SO_4 solution. Reflected light x 800. Ferrite, aluminate and alkali aluminate.

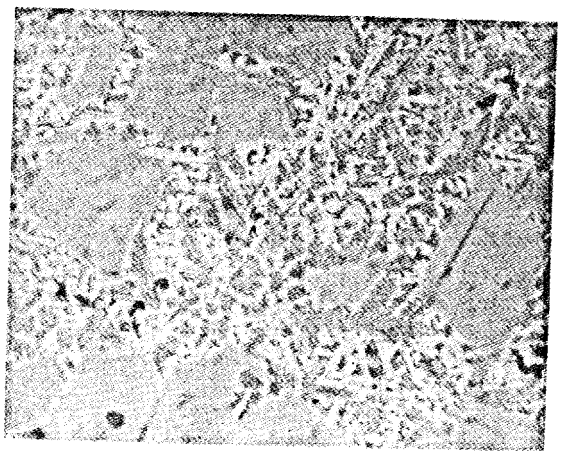

Fig. 8. Same as for fig. 7 but 2 hours. Ferrite and aluminate.

The alkali aluminate disappears and the cross-hatched ferrite develops. An intermediate texture is shown in fig. 9 leading most of all the thoughts towards liquid phase immiscibility.

On the other hand, the cross-hatched ferrite indicates an octahedral symmetry, i.e. two principal sections with 90° and 120° between lamellas.

This indicates a formation of a cubic phase which subsequently exsolves ferrite and aluminate during cooling.

Anyhow, the duration of burning has a strong effect on the relative distribution of ferrite and aluminate as appears in Table 3. A strong reduction of the amount of the alkali aluminate happens between 1/2 and 1 hour's duration of burning and vice versa for the ferrite.

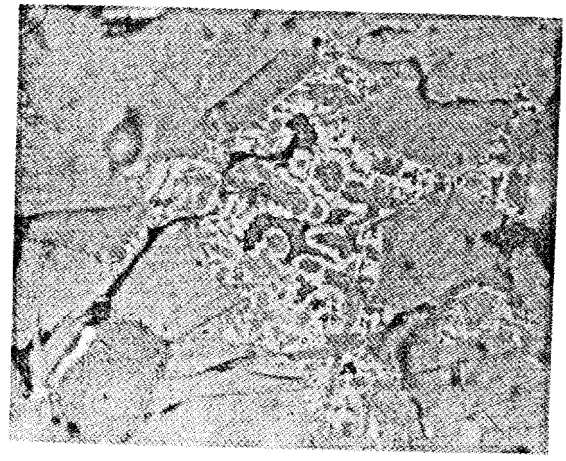

Fig. 9. As for fig. 8.
Intermediate structure.

The conclusion must be that the alkali aluminate also contains rather much Fe. That true ferrite appears after prolonged burning is confirmed by the observation of the characteristic peak around $2\theta=34^{\circ}$ in XRD.

Fe in rhombic aluminate has also been reported by Cromý and Gregor (7) and Regourd and Mortureux (6).

As virtually no Na_2O is present in the clinker it must be concluded that the K_2O stabilizes rhombic alkali aluminate, in contrary to the statement by Shin and Glasser (4). On the other hand, Locher et al (5) and Regourd and Mortureux (6) state that K_2O may equally well be incorporated in the aluminate.

Cement Properties:

Because of the strong hygroscopic properties of both K_2 and $K_2O{\cdot}Al_2O_3$ local humid and strongly basic environment prevails.

The same will apply for Na_2O and $Na_2O{\cdot}Al_2O_3$ to be expected in raw mixes using basic rocks (andesite or equal) as adjusting materials. The liquor formed easily dissolves true aluminate and from saturated solutions new minerals may crystallize leading to lump formation. But also changes of setting properties and early strength may be expected. With respect to the last mentioned Osbaeck (9) and Costa and Massazza (8) have discussed that alkalies in surplus with respect to formation of sulphate exceed a negative influence on the cement strength at all ages.

Variations in the melt phase structure has mostly been attributed to changes in the chemistry and the cooling conditions, for instance as discussed by Locher et al (5), but as shown above also the duration of burning is very important. By redistribution of the melt phase compounds also a change of the reactivity of these is expected and consequently setting behaviour and strength properties.

References:

1. H.W.W. Politt and A.W. Brown. The Distribution of Alkalies in Portland Cement Clinker. Proc. of the Fifth Int. Symp. on the Chemistry of Cement. Tokyo 1968 I-126, 322-333.

2. B. Osbaeck. Calculation of Content of Water-soluble Alkalies in Portland Cement Clinker. Zement-Kalk-Gips. Heft 9/1984. 486-493.

3. E. Woermann. Die mikroskopische Untersuchung von Klinker und Zementproben. Schriftenreihe der Zementindustrie. Heft 29/1962. 79-97.

4. G.Y. Shin and F.P. Glasser. Interdependence of Sodium and Potassium Substitution in Tricalcium Aluminate. Cem. Concr. Res., Vol. 13, No 1 1983. 135-141.

5. F.W. Locher, W. Richartz, S. Sprung und H.-M. Sylla. Erstarren von Zement, Teil III. Einfluss der Klinkerherstellung. Zement-Kalk-Gips No 12/1982, 669-676.

6. M. Regourd and B. Mortureux. Tricalcium Aluminate in Synthetic Solid Solutions and in Cements. Presented at the seminar. "Reaction of Aluminate during the Setting of Cement", Eindhoven. April 1977.

7. S. Chromý and M. Gregor. Zur sogenannten "Primatische Phase" in Portland Klinker. Zement-Kalk-Gips. 11/1968, 451-456.

8. Umberto Costa, Franco Massazza. Interstitial Mass Composition and Setting Irregularities of Portland Cements. Il Cemento 4/1975, 181-191.

9. B. Osbaeck. Der Einfluss von Alkalien auf de Festigheitseigenschaften von Portland Zement. Zement-Kalk-Gips. Heft 2/1979, 72-77.

TABLE 1 - RAW MIXES

(All raw mixes burned at 1450°C for 30 min. - except R_1 at 1500°C for 2 hours)

	R_{11}	R_{12}	R_{13}	R_{14}	R_{15}	R_{21}	R_{22}	R_{23}	R_{24}	R_{25}	R_1
Ms	2.5	2.4	2.5	2.4	2.4	2.2	2.2	2.2	2.2	2.2	2.3
Ma	2.1	2.2	2.3	2.3	2.7	2.0	2.3	2.7	3.1	3.8	1.4
LSF	92.0	92.0	92.0	92.0	95.0	95.0	95.0	95.0	95.0	95.0	92.5
% K_2O Clinker	0.41	0.68	0.67	1.07	1.15	1.11	1.00	1.23	1.54	1.35	2.05
% Na_2O "	0.19	0.20	0.23	0.25	0.21	0.25	0.24	0.26	0.26	0.26	-
% S_{tot} "	0.006	0.018	0.010	0.005	0.013	0.006	0.013	0.021	0.005	0.002	0.15
% K_2O expected	0.48	0.96	1.36	1.90	2.0	1.90	2.00	2.09	2.22	2.27	2.25
% Na_2O "	0.17	0.17	0.21	0.20	0.20	0.21	0.21	0.21	0.23	0.23	0.03
% K_2O evapor.	15	29	5	44	42	41	50	41	31	40	9

TABLE 2 - EXTRACTION OF R_1 (1500°C for 2 hours) AA

	a	b	c
	Destil. H_2O	Basic extract	Glycol extract 110°
% K_2O	1.35	1.49	1.72
% Al_2O_3	0.01	0.91	0.86
% CaO	0.31	0	2.24
% MgO	0	0	

TABLE 3 - MELT PHASE COMPOSITION AND FREE CAO

	% CaO_{1450} titr.	% CaO_{1450} LM	"C_3A" LM	C_4AF LM	% K_2O extract	% Na_2O extract	% Al_2O_3 extract
R_{11}	4.6	4.2	10	3	0.010	0.011	0.100
R_{12}	3.4	2.6	9	2	0.034	0.020	0.080
R_{13}	3.2	2.3	8	1	0.022	0.010	0.086
R_{14}	3.7	3.0	11	2	0.090	0.016	0.086
R_{15}	4.8	3.3	8	2	0.100	0.016	0.058
R_{21}	5.1	3.9	15	2	0.110	0.022	0.078
R_{22}	4.8	3.4	16	2	0.080	0.050	0.052
R_{23}	4.8	3.6	15	2	0.120	0.020	0.093
R_{24}	4.4	2.9	15	2	0.160	0.020	0.180
R_{25}	4.8	3.4	16	1	0.250	0.020	0.110

NB: Extraction in 60°C glycol.

TABLE 4 - MELT PHASE COMPOSITION AND DURATION OF BURNING

	T°C	hours	% C_3A Calc.	% C_4AF Calc.	% "C_3A" LM	% C_4AF LM	% CaO LM
R_1	1500	2	4.7	7.9	2.6	9.0	1.8
R_{21}	1450	0.5	7.7	7.0	15.0	2.0	3.9
R_{21}	1450	1.0	7.7	7.0	5.7	8.1	1.9
R_{21}	1450	2.0	7.7	7.0	3.7	9.7	0.3
R_{21}	1450	3.0	7.7	7.0	5.8	10.2	-

C. VERNET, Société des CIMENTS FRANÇAIS - C.E.R.E.G. (FRANCE)

CUISSONS REDUCTRICES - CONSEQUENCES RELATIVES A LA STABILITE DES PHASES DU CLINKER
REDUCING CONDITIONS IN KILNS - STABILITY AND HYDRAULICITY OF PHASES

RESUME

L'utilisation de certains combustibles solides peut conduire à la création accidentelle de conditions de cuisson réductrice. Nous avons observé des clinkers industriels et des produits de synthèse alitiques, obtenus en faisant varier la nature du réducteur, la vitesse de refroidissement et la température de trempe. Nous avons étudié les modifications de la minéralogie (par D.R.X), de la morphologie (microscopie optique, MEB), de la composition chimique (microsonde de Castaing) et de l'hydraulicité des phases.
Dans le cas des produits de synthèse, nous avons remarqué:
- La réduction de CaO par le carbone, qui commence dès 1280°C et s'accélère dans le liquide. Dans ce cas, il y a enrichissement en bélite, sans formation de CaO libre secondaire.
- L'absence de réduction de l'alite par le carbone à 1500°C.
L'instabilité des silicates serait plutôt liée à la décomposition thermique. Les transformations reconstructives de la bélite semblent facilitées, d'où une forte incidence de la vitesse de refroidissement. L'analyse à la microsonde des domaines de morphologie myrmékitique donne un rapport CaO/SiO_2 voisin de 2.
Les réactions REDOX affectent principalement la composition du liquide.
Dans le cas des clinkers industriels observés ici, l'analyse des cristaux à la microsonde n'a pas permis de mettre en évicence l'action spécifique de réductions localisées (charbon mal broyé). Ce phénomène est sans doute masqué par le processus d'assimilation des cendres des gros grains de combustible, produisant d'importants gradients de teneur en éléments mineurs dans des domaines enrichis en bélite. Pour mieux utiliser les combustibles solides, il semble judicieux de les brûler dans les systèmes de précalcination, ce que laisse plus de temps aux cendres pour se combiner complètement. L'analyse à la microsonde montre alors une plus grande régularité de composition des cristaux.
La cinétique d'hydratation des clinkers réduits est affectée par les modifications de la minéralogie. La réduction entraine l'augmentation de C_3A et la diminution de C_3S, ce qui aboutit à des variations anarchiques de temps de prise, observées surtout lorsque le gypsage n'a pas été modifié en conséquence.

SUMÁRIO

A utilização de certos combustíveis sólidos pode conduzir à criação acidental de condições cozimento redutoras. Nós observamos clínqueres industriais e produtos de síntese alíticos, obtidos fazendo variar a natureza do redutor, a velocidade de resfriamento e a temperatura de têmpera. Estudamos as modificações da mineralogia (por D.R.X.), da morfologia (microscópio ótico, MEV), da composição química (microssonda Castaing) e da hidraulicidade das fases.
No caso de produtos de síntese, nós notamos:
- A redução do CaO pelo carbono, que começa desde 1280°C e se acelera no líquido. Neste caso, há um enriquecimento em belita, sem formação de CaO livre secundária.
- Ausência de redução de alita pelo carbono a 1500°C.
A instabilidade dos silicatos seria ligada à decomposição térmica. As transformações reconstrutivas da belita parecem facilitadas, donde uma forte incidência da velocidade de resfriamento. A análise por microssondas dos domínios de morfologia mismekitica dá uma relação CaO/SiO_2 próxima de 2.
As equações REDOX afetam principalmente a composição do líquido.
No caso de clínqueres industriais observados aqui, a análise dos cristais na microssonda não permitiu por em evidência a ação específica de redução localizada (carvão mal moído). Este fenômeno é sem dúvida mascarado pelo processo de assimilação das cinzas dos grãos grandes do combustível, produzindo importantes gradientes de teores em elementos menores nos domínios enriquecidos em belita. Para melhor utilizar os combustíveis sólidos, parece judicioso de queimá-los em sistemas de precalcinação, o que deixa mais tempo às cinzas para se combinar completamente. A análise na microssonda mostra então maior regularidade de composição dos cristais.
A cinética da hidratação dos clínqueres reduzidos é afetada pelas modificações da mineralogia. A redução acarreta o aumento de C_3A e a diminuição de C_3S, o que conduz à variações anárquicas no tempo de pega, observadas sobretudo quando o teor de gesso não foi modificado em consequência.

1 - INTRODUCTION

Les processus de réduction qui se manifestent au cours de la cuisson du clinker sont habituellement interprétés dans les trois cas suivants :

1/ Réduction superficielle, liée à la présence d'une atmosphère réductrice. La réoxydation en aval de la zone de cuisson, où les gaz sont plus riches en oxygène, amène à la présence de couches successives dans l'écorce des granules. La masse de clinker affectée par le phénomène est relativement faible, dépendant de la granulométrie du clinker.

2/ Réduction localisée, par des particules carbonées provenant du combustible. Les zones réduites montrent alors diverses figures de décomposition des phases du clinker. Leur localisation dans les granules est variable, selon la partie du four où se produit le contact entre les particules et la matière. Ceci met en jeu la forme de la flamme, la vitesse des gaz et la masse des particules projetées par la tuyère. Il semblerait que dans la majorité des cas, le contact se produise en amont de la zone de cuisson.

3/ Réduction localisée par ajout de combustible à la matière crue. Le cas typique est celui de la cuisson en four vertical. Ce cas est plus rarement observé dans les fours rotatifs, où les ajouts combustibles ont en général le temps de brûler complètement, avant d'arriver en zone de cuisson. La formation d'une "peau" d'eutectiques alcalins sur les granules de cru, en voies semi-sèche, peut empêcher le contact avec l'oxygène ou ralentir sa diffusion, lorsque les granules ne sont pas brisés en aval de la grille. La réduction peut alors affecter le coeur des granules, même lors d'une cuisson oxydante.

Dans chacun de ces trois cas de réduction, des modifications de la morphologie des phases, de la composition et des propriétés hydrauliques du clinker ont été observées /1//2//4//6//7//10//11//14/.

- Les auteurs constatent de façon unanime la décomposition de l'aluminoferrite, dont le mécanisme mettrait en jeu la réduction des ions ferriques dans le liquide du clinker. Il se formerait d'abord des solutions solides de plus en plus riches en alumine, le long de la ligne C_4AF-C_6AF_2 /10/, puis du C_3A secondaire et de la chaux libre secondaire. Le fer ferreux serait substitué au calcium et réparti dans les phases en fonction de sa solubilité dans chacune d'elles. Des modifications de la morphologie et de la composition du clinker sont également constatées, en fonction de la vitesse de refroidissement et de la vitesse de trempe /14/. La tendance à l'effusement par formation de gamma-C_2S est souvent remarquée.
- Les points de désaccord concernent l'interprétation du mécanisme de changement de couleur, la solubilité du fer ferreux dans les phases et surtout le processus de transformation des silicates. L'hypothèse faite par certains auteurs /1/ /14/, de la décomposition de l'alite en bélite et chaux libre secondaires, par réduction, est remise en question par un certain nombre de faits expérimentaux. En effet, la chaux libre secondaire, autre que celle provenant de la décomposition du ferrite, n'a jamais pu être détectée, ni par les méthodes chimiques, ni par diffraction X. Par ailleurs, diverses études menées dans des conditions réductrices extrêmes n'ont pas montré de décomposition de l'alite. Celle-ci n'a été observée, ni en atmosphère d'hydrogène /9/, ni dans un clinker obtenu par fusion à 1900°C, en milieu très réducteur, produisant la transformation totale de Fe_2O_3 en fer métallique /15/.

Dans cette étude nous tentons de préciser les mécanismes de réduction et leurs conséquences, en observant, d'une part, des mélanges simples, cuits au laboratoire, puis des clinkers industriels.

2 - CUISSONS DE LABORATOIRE - PLAN D'EXPERIENCES

2.1 - COMPOSITIONS CHIMIQUES

Nous avons étudié plusieurs séries de cuissons de produits alitiques, préparées à l'aide d'un four électrique programmable. La composition chimique des mélanges de départ figure au *Tableau 1*.

TABLEAU 1 COMPOSITION CHIMIQUE DES CRUS ALITIQUES

COMPOSITION TYPE	A I	A II	A III	A IV	A V	A VI
% CaO	71,261	70,964	70,667	70,370	70,075	69,780
% SiO2	26,022	26,004	25,986	25,968	25,950	25,935
% Al2O3	0,902	0,901	0,900	0,900	0,899	0,892
% MgO	1,782	1,781	1,779	1,778	1,777	1,776
% Li2O	0,033	0,033	0,033	0,033	0,033	0,033
% FeO	0,000	0,317	0,635	0,951	1,267	1,583

2.2 - MODE DE PREPARATION

Nous avons fait varier la nature du réducteur (fer ferreux sous forme sulfate, oxalate, carbone), le programme de cuisson et de refroidissement, et le mode de trempe.

3 - RESULTATS

3.1 - ASPECT GENERAL

Les produits de synthèse sont constitués de cristaux d'alite jointifs, d'une dimension de 10 à 20 microns, accompagnés d'une proportion variable de très gros cristaux de bélite et d'une faible proportion de phase interstitielle, constituant les joints de grains. La morphologie des cristaux de bélite évolue en fonction du mode de refroidissement et de trempe, suite aux transitions allotropiques bien connues alpha → alpha prime → béta, qui s accompagne d'une suite de striations caractéristiques révélées par le réactif d'attaque (acide nitrique à 0,1 % dans éthanol anhydre) [*Photo 1*].

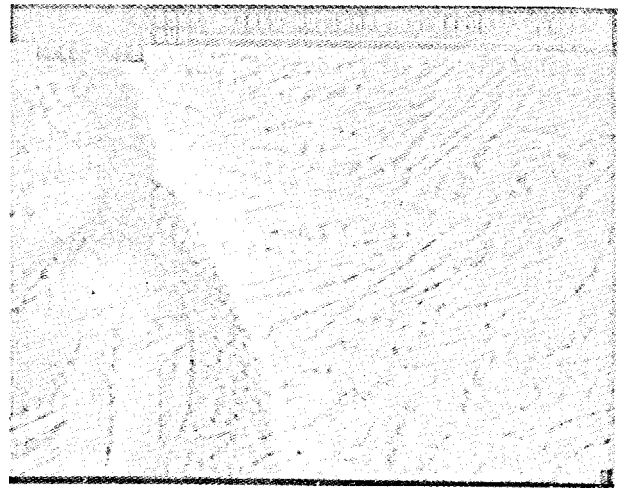

PHOTO 1

TRANSITIONS DE LA BELITE - MILIEU OXYDANT

Cristaux de bélite ayant subi la suite de transformations alpha → alpha prime → beta. Détail des lamelles de beta, formées dans les inclusions initiales de alpha prime. On distingue des exsolutions, sous forme de microcristaux ne dépassant pas 0,1 micromètre.

1.2

Dans le cas des échantillons refroidis lentement, ces striations sont remplacées par des ponctuations très rapprochées, donnant au cristaux une apparence "myrmékitique", terminologie employée par WOERMANN /1/ (*Photo 2*).
Comme le montre l'observation au M.E.B. (*Photo 3*), cette apparence est liée à la présence de nombreuses inclusions ponctuelles, d'une dimension inférieure au micromètre, dont l'attaque par le réactif est plus lente, et qui apparaissent donc en relief, après attaque de la surface polie initiale.
Ces échantillons présentent également des exsolutions de périclase. Aucun produit ne présente d'amas de chaux libre, dont le dosage chimique par dissolution dans le glycol donne des valeurs comprises entre 0,3 et 0,8 %. Les raies de CaO ne sont visibles en D.R.X dans aucun échantillon.

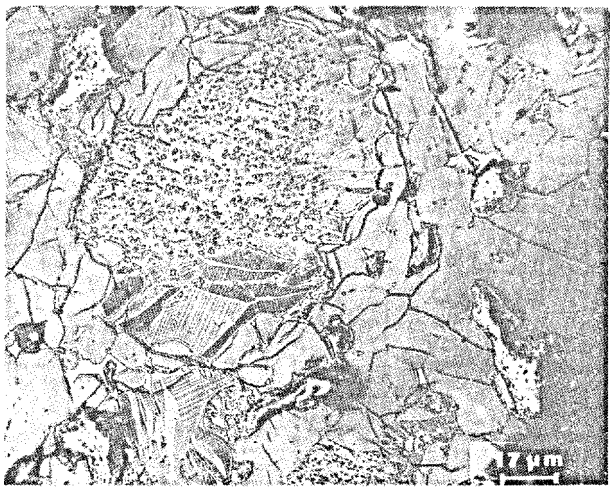

PHOTO 2
TRANSITIONS DE LA BELITE EN MILIEU REDUCTEUR
ALITE TYPE A5 (oxalate ferreux)
Apparition du maclage polysynthétique (trempe à 1150°C). Une partie du cristal commence à prendre une allure "myrmékitique" caractristique du milieu réducteur.
Le rapport C/S, mesuré à la microsonde, est ici = 2.

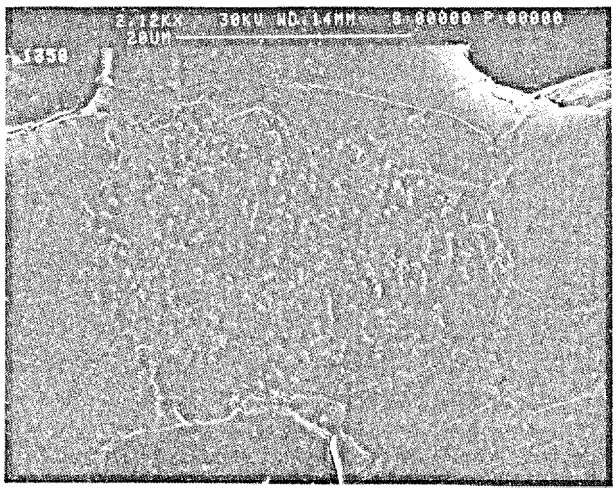

PHOTO 3 (x2120)
Inclusions apparaissant en relief après l'attaque chimique d'une section polie (cristal du type de la photo 2).

3.2 - COMPOSITION CHIMIQUE

L'analyse chimique effectuée sur les produits décarbonatés à 1000°C, puis en fin de cuisson, montre des écarts par rapport à la composition théorique qui augmentent avec la teneur en carbone. Ces écarts ne sont pas significatifs pour les produits cuits en atmosphère oxydante, ni pour ceux qui ont été préparés avec du fer métallique ou du sulfate ferreux. Par contre, les synthèses avec oxalate ferreux ont un rapport C/S un peu plus faible que le cru et cette tendance s'accentue pour les synthèses avec ajout de carbone, ou faites en creusets de carbone. On pourrait penser que ceci est dû à la réduction de l'alite par le carbone. Nous avons testé cette hypothèse en recuisant avec du carbone une alite préparée auparavant en milieu oxydant. Le produit ne présente aucune variation significative de composition, après une heure de cuisson. Ce résultat est en accord avec ceux de HRABE /9/ et de MAKI /15/.Il faut donc en conclure que la réduction se produit par d'autres mécanismes.

3.3 - ORIGINE DES ECARTS DE COMPOSITION. REDUCTION DE CaO PAR LE CARBONE

Nous avons mesuré la vitesse de la réduction de CaO par le carbone, par thermogravimétrie. La réaction commence vers 700°C et s'accélère au cours de la montée en température. A 1450°C, le taux de réaction atteint 10,7 %. Au cours d'un palier à 1450°C, la réaction se poursuit, pour atteindre un taux de 41,3 % au bout de 26 h. La vitesse de réduction de la chaux par le carbone est donc suffisante pour expliquer les variations de composition chimique que nous avons observées plus haut.

3.4 - COMPOSITION MINERALOGIQUE

Tableau 2 - Evolution de la composition minéralogique des synthèses

REF.	Methode ! CaO.Lib!	C3S	C2S	C3A	C4AF	MgO
CRU A1	Comp.Pot. 0,0	86,2	9,6	2,4	0,0	1,8
A1 OX.1500°C	Comp.Pot 0,0	86,5	9,0	2,2	0,0	1,9
	D.R.X....	97,4				
	Dissol...		2,0	1,4 (C3A + MgO)		
A1 Atm.N2	Comp.Pot.	74,6	21,1	2,4		1,9
1500°C	D.R.X.	89,3	15,4			
Creuset carbone	Dis.Selec 0,8			0,9 à 2,8 (C3A + MgO)		
	Microscop	91,7	8,3			
A1 + carbone	Comp.Pot.	47,5	48,3	1,8		1,6
1500°C	D.R.X.	59,2	35,4			
Creuset carbone	Dis.Selec 0,3			2,1 (C3A + MgO)		
	Microscop	46,6	53,4			
Cru A5	Comp.Pot.	79,9	14,1	0,0	4,3	1,8
Cuisson A5	Comp.Pot.	70,2	22,6	0,0	4,4	1,9
1500°C	D.R.X.	82,5	13,9		1,7	
Creuset Platine	Dis.Selec 0,3				3,0	C4AF+MgO
	Microscop	85,9	12,1		2,8	

La minéralogie des produits de syynthèse est affectée par la variation de la composition chimique. L'augmentation de la teneur en bélite est très significative dans les échantillons cuits avec carbone. Les résultats du *Tableau 2* sont cohérents, compte tenu de l'incertitude des dosages et de la proportion d'impuretés en solution solide dans les phases, produisant l'écart habituel entre composition potentielle et composition réelle. La teneur en alite passe de 97,4 % (A1 cuisson oxydante) à environ 50 % (A1 avec carbone), en milieu très réducteur, ce qui montre l'intensité des processus de réduction, lorsque la quantité de carbone (provenant ici de l'ajout au cru et du creuset) est importante.

3.5 - COMPOSITION DES CRISTAUX
DOSAGE A LA MICROSONDE DE CASTAING

Les dosages ont porté au total sur 12 échantillons, soit environ 300 cristaux. Le *Tableau 3* montre que la composition des cristaux d'alite est relativement indépendante de l'atmosphère de cuisson. On remarquera cependant, pour l'alite cuite avec carbone, l'augmentation de la teneur en Al_2O_3, qui s'accompagne de la diminution de la teneur en MgO. Dans ce cas, les teneurs en impuretés montrent une distribution statistique bimodale, ce qui peut être relié à la présence de deux formes cristallines, M_{Ia} et M_{Ib}, identifiées par D.R.X. Il est possible que cette diminution de MgO soit due à une réaction avec le carbone et permette l'entrée en solution solide d'une plus grande quantité d'alumine.

- Tableau 3 - COMPOSITION CHIMIQUE MOYENNE DES CRISTAUX -

Ref. Ech.	CaO	SiO2	Fe2O3	Al2O3	MgO	Total
- Cristaux d'alite -						
A1 OX.....	71,71	26,03	0,02	0,48	1,76	100,00
A1 Azote.....	71,42	26,26	0,02	0,48	1,79	99,97
A1 + carbone.....	72,77	25,60	0,00	0,84	0,80	100,01
A5 (oxalate Fe)..	70,72	26,65	0,94	0,59	1,10	100,00
- Cristaux de bélite -						
A1 OX.....	65,25	33,02	0,02	1,01	0,69	99,99
A1 Azote.....	64,77	33,60	0,00	0,89	0,72	99,98
A1 + Carbone.....	65,21	33,52	0,00	0,91	0,36	100,00
A5 (Oxalate Fe)..	63,66	33,37	1,52	1,05	0,40	100,00
- Cristaux de ferrite -						
A5 (oxalate Fe)..	51,91	7,11	22,12	14,87	3,99	100,00

Dans les cristaux de bélite, les différences de composition sont beaucoup plus marquées que dans les cristaux d'alite. L'incidence de la température de trempe sur la teneur en magnésium des cristaux est significative et plus grande que celle de l'atmosphère ou de la teneur en réducteur. La distribution des concentrations est monomodale dans le cas des trempes à 1500°C, où la bélite est principalement sous la forme alpha. La distribution s'élargit ou devient bimodale pour la trempe à 1350°C, ce qui correspond à l'apparition de la forme alpha prime, qui est alors caractérisée en microscopie par la présence de stries larges en "lame de couteau" (*Photo 4*).

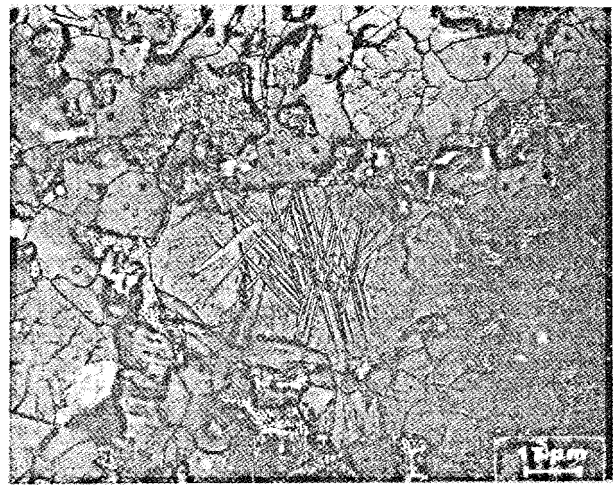

PHOTO 4
ALITE TYPE A 5 (OXALATE FERREUX). TREMPE 1350°C
TRANSITIONS DE LA BELITE.
Inclusions de la forme alpha prime dans un cristal de alpha C_2S.

La distribution est trimodale dès les températures inférieures à 1150°C. Ceci s'accompagne du maclage polysynthétique, montré précédemment par les *photos 1 et 2*. Bien que le pouvoir de résolution spatial de la sonde ne permette pas de faire une analyse quantitative distincte des lamelles et des exsolutions qui les séparent, on peut observer dans celles-ci l'abondance de l'aluminium.
Le ferrite montre une teneur en MgO décroissant fortement avec la température de trempe, dont l'abaissement produit la cristallisation de périclase. Sous réserve des interférences de voisinage, nous avons trouvé dans les produits cuits en milieu réducteur, des cristaux de composition proche de C_6A_2F.

3.6 - TENEUR EN Fe^{2+} DES CRISTAUX

Ce problème est difficile à résoudre, en l'absence de méthode directe de microanalyse spécifique de l'ion ferreux. Les méthodes chimiques donnent une indication globale et il suffit d'une très faible quantité de ferrite dans un produit de synthèse pour fausser l'estimation de la teneur en fer dans la phase étudiée. Nous avons utilisé ici, d'une part, une approche chimique, en mesurant la teneur moyenne en fer ferreux des synthèses et, d'autre part, une approche structurale, en essayant d'évaluer les déplacements du fer des sites tétraédriques vers les sites octaédriques.

Approche chimique

Les dosages ont été effectués par titrage potentiométrique à courant nul, en suivant l'oxydation du fer ferreux par un sel cérique. Pour éviter l'oxydation lors de la préparation de l'échantillon (broyage, mise en solution), les pastilles après trempe ont été dissoutes directement dans une solution concentrée d'acide citrique chaude, sous atmosphère d'azote.

Une partie du fer ferreux introduit dans le cru s'est oxydée durant les opérations de broyage associées au cycle de cuisson. Une partie du fer ferrique ainsi produit a formé la phase interstitielle, l'autre est entrée en solution solide dans les silicates. Nous avons calculé la quantité de fer correspondante à partir des dosages à la microsonde de la phase interstitielle et de l'insoluble salicylique (*Fig. 1*). Le bilan du fer montre que la majeure partie du fer ferreux se trouve dans les silicates, où sa teneur atteint rapidement un palier vers 0,4 % (FeO), pour une teneur en fer ferrique variant de 0 à 0,6 % (Fe_2O_3) [*Fig. 2*].

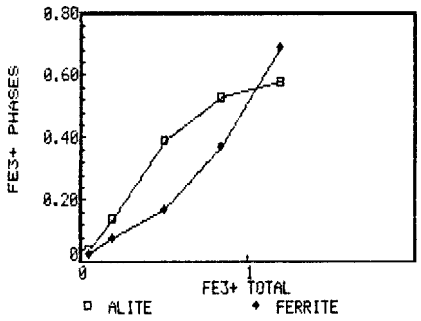

FIG. 1 - ECH. A5

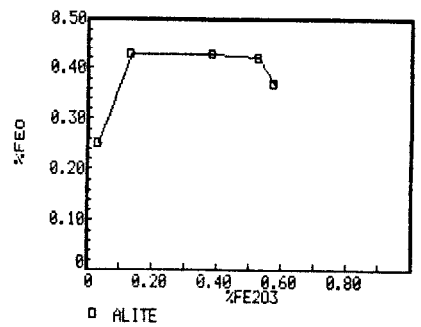

Fig. 2 - ECH. A5 REPARTITION DU FER

Les teneurs en fer mesurées à la microsonde pour nos synthèses sont supérieures au valeurs habituelles mesurées sur les clinkers industriels, la différence étant de l'ordre de grandeur du % FeO dosé ci-dessus. Les résultats sont en bon accord avec ceux de SYLLA /14/ pour des clinkers cuits en atmosphère de CO. Il faut donc en conclure que, même en atmosphère fortement réductrice, la limite de solubilité de FeO dans l'alite, qui serait de l'ordre de 1 à 2,6 % /1//6//10bis/, n'est pas atteinte dans la majorité des cas de figure.

Approche cristallographique

Le mode de substitution de Fe et Al dans le réseau de l'alite peut être étudié à partir des résultats des dosages à la microsonde, en reportant les points figuratifs des échantillons dans un diagramme constitué des courbes théoriques correspondant à différents modes de substitution. Pour établir ce diagramme, on utilise les variables suivantes (en mMol/100g) :

$A = C_{eq}/S_{eq}$, $a = (Al_2O_3 + Fe_2O_3)/S_{eq}$, $b = Fe_2O_3/S_{eq}$

où $C_{eq} = CaO + MgO + K_2O + Na_2O + BaO$

et $S_{eq} = SiO_2 + SO_3 + TiO_2 + P_2O_5$

A titre d'exemple, l'hypothèse correspondant à un mode de substitution de (Fe+Al), réparti pour moitié en sites tétraèdriques et pour moitié en sites octaèdriques, conduit à la courbe théorique d'équation : A = (3-a/2)/(1-a/2) [C'est en général autour de cette courbe que se distribuent les points représentatifs des alites des clinkers].

Le report des points figuratifs des alites de synthèse dans le diagramme montre l'accentuation de l'occupation des sites octaèdriques avec le degré de réduction, pour les échantillons contenant du fer. Le fer contenu dans l'alite A5 serait à 100 % en sites octaèdriques.

4 - ETUDE DE QUELQUES CLINKERS INDUSTRIELS

Nous avons observé à la microsonde de Castaing, 4 clinkers susceptibles de présenter des phénomènes de réduction. Le premier était fabriqué avec un ajout de matière combustible dans le cru. Le second était fabriqué avec injection de 20 % de déchets combustibles à la tuyère, le combustible habituel étant le gaz. Le troisième et le quatrième proviennent de la même usine, comportant deux fours voie sèche alimentés par le même cru. Ces deux fours se distinguaient par le réglage du broyeur à charbon, (charbon grossier, Réf. GF3) et par l'existence d'un système de précalcination (Réf. GF4).

Les zones présentant en microscopie optique l'apparence de cristaux d'alite décomposés ont un rapport C/S égal à 2, ce qui exclut la présence de chaux libre secondaire. Nous n'avons pas trouvé de corrélation systématique entre la présence de ce type de cristaux et l'existence de processus de réduction, qui se traduiraient par un passage du fer en sites octaèdriques (point figuratif dans le diagramme A = f(b). Par contre, il semblerait que ces décompositions soient liées à l'homogénéité de la matière au moment de la clinkérisation. Ceci est le cas avec l'injection à la tuyère de combustibles solides riches en cendres minérales, et comportant des grains grossiers. En effet, nous avons observé dans ces zones, l'existence de gradients de teneurs en éléments mineurs, sur des distances de l'ordre d'une centaine de micromètres. Il s'agirait donc de configurations apparentées aux classiques "rosaces bélitiques", mais avec un degré d'assimilation plus élevé des cendres. Un meilleur broyage du combustible et l'utilisation de la précalcination suppriment ces phénomènes. La distribution statistique des impuretés devient alors beaucoup plus étroite.

5 - COMPORTEMENT HYDRAULIQUE DE SPRODUITS CUITS EN MILIEU REDUCTEUR

Les tests d'hydraulicité comprenaient des mesures cinétiques en réacteur agité, sur des suspensions concentrées de rapport eau/solide voisin de 4, des essais mécaniques et des observations au M.E.B. sur des micromortiers compactés. Les résultats de ces mesures sont plus significatives de l'interaction alite-bélite que des propriétés intrinsèques des alites étudiées. La durée de la période dormante augmente avec la teneur en bélite. La quantité de portlandite libérée au cours de l'hydratation diminue quand la teneur en bélite augmente, mais moins que par un simple effet de dilution de l'alite.

Les hauteurs des pics de flux thermique, pendant la période de prise étant très voisines, ceci nous amène à penser que la réactivité de l'alite varie peu, en comparaison de la réactivité des bélites, ce qui concorde avec l'évolution de leur microstructure et de leur composition.

Les échantillons cuits en milieu réducteur montrent des résistances initiales plus faibles et des temps de prise plus longs que les témoins cuits en milieu neutre ou oxydant. Vers 2 jours, les performances deviennent équivalentes, puis les échantillons cuits en milieu réducteur deviennent plus résistants que les témoins. L'observation au M.E.B. montre alors une pâte constituée de CSH plus compact et moins riche en portlandite, pour les échantillons réduits. Nous avons également étudié le comportement cinétique d'un clinker industriel, recuit au laboratoire avec des teneurs croissantes en carbone (0,1 ; 1 ; 10 %). Ceci produit des anomalies que nous attribuons à la présence d'une plus grande quantité de C_3A, de haute réactivité, provenant de la réduction du ferrite, dans les échantillons réduits.
On peut prévoir, pour des clinkers ainsi traités, des défauts de rhéologie, liés à une réaction trop rapide des aluminates, si le gypsage n'est pas augmenté suffisamment. Dans le cas des pâtes et mortiers, l'augmentation de la durée de la période dormante due à l'augmentation de la teneur en bélite serait alors compensée de façon anarchique par la formation plus ou moins abondante d'ettringite. Il en résulte des variations importantes des temps de prise, ainsi qu'une grande sensibilité à l'éventement et une diminution des performances initiales, sans préjudice pour les peformances à long terme.

6 - CONCLUSIONS

Notre étude avait pour objectif de préciser les mécanismes par lesquels certains processus de réduction aboutissent à des perturbations de la minéralogie des clinkers, et d'en évaluer les conséquences vis-à-vis des caractéristiques dynamiques et des performances des ciments. Nos conclusions porteront, d'une part, sur la nature de ces mécanismes, et d'autre part, sur l'aspect industriel du problème.
Nos synthèses au laboratoire ont permis de mettre en évidence une réaction qui avait jusqu'ici échappé aux investigations : la réduction de CaO par le carbone permet d'expliquer l'apparition de bélite, bien que l'alite soit stable en milieu réducteur, ce que nous avons confirmé. En utilisant différentes méthodes d'observation complémentaires, cette étude nous amène à conclure que le milieu réducteur affecte assez peu la structure, la composition chimique et la réactivité des cristaux d'alite. Au contraire, les cristaux de bélite voient leurs transformations allotropiques s'accélérer avec des modifications importantes de leur composition et de leur réactivité.
L'étude parallèle d'échantillons industriels a montré que dans les fours rotatifs, certaines causes de décomposition de l'alite, associées à des défauts localisés d'assimilation des cendres de charbons siliceux, se superposent au processus de réduction. Dans ce cas, il est évidemment difficile de distinguer la part respective des deux mécanismes, les mêmes grains grossiers de combustible, porteurs à la fois de carbone et de cendres minérales, étant à l'origine de chacun d'eaux, avec des conséquences très semblables. Les dosages à la microsonde ont montré également que, même lorsqu'ils sont fabriqués dans des conditions difficiles, certains clinkers peuvent atteindre un degré d'homogénéité remarquable sur le plan de la distribution des impuretés en solution solide dans les phases, ce qui constitue sans doute la principale cause de leurs meilleures performances. Les problèmes techniques associés à l'utilisation de combustibles particuliers peuvent donc être maitrisés, conciliant ainsi les nécessités d'économie d'énergie et de maintien de la qualité des produits.

BIBLIOGRAPHIE

/1/ WOERMANN E. "Decomposition of alite in technical Portland cement clinekr" - 4th ISCC, Washington, 1960, Vol.1, Paper II-S8, pp 119-128.
/2/ SUZUKAWA Y. ; SASAKI T. "Influence of reducing atmosphere on the constitution of clinker". Ibid., Paper II-S3, pp 83-85.
/3/ LONGUET P. "Note on the behaviour of tetracalcium aluminoferrite in an atmosphere of hydrogen". Ibid., Paper II-S9, pp 131-133.
/4/ TERRIER P. ; HORNAIN H. "Sur l'application des méthodes minéralogiques à l'industrie des liants hydrauliques". Publication technique CERILH N° 180, pp 1-59.
/5/ LEA F.M. "The chemistry of cement and concrete". Ed. E. Arnold, 3rd Ed., 1970, pp 58-59 "The system $CaO-SiO_2-FeO$".
/6/ AKATSU K. ; HIGUCHI K. "On the strength and color of the Portalnd cement clinker burned under reducing atmosphere". CAJ Rev. of the 24th. Meet., Tokyo, 1970, pp 23-25.
/7/ LUGININA I.G. et Coll. "L'atmosphère réductrice des fours et ses conséquences". Cement, Mai 1971, N°5, 15-6.
/8/ MANDER J.E. ; SKALNY J.P. "Calcium alkali sulfates in clinker". Ceramic Bulletin, Vol. 56, n° 11, 1977, pp 987-990.
/9/ HRABE Z. ; JESENAK V. "The influence of furnace atmosphere on the reaction rate between Ca_2SiO_4 and CaO". CCR, Vol. 10, 1978, pp 195-202.
/10/ TOLOCHKOVA M.G. et Coll. "L'oxyde ferreux dans le clinker" 7th ISCC, Paris, 1980, Vol. II, Thème I, I-47.
/10bis/ PONOMAREV I.F. et Coll. "Particularités cristallochimiques et propriétés des phases du clinker de ciment portland en fonction des conditions de cuisson et de refroidissement". Ibid., pp I/166 - I/169.
/11/ DEMOULIAN E. et Coll. "Anomalies de cuisson, structure microscopique, propriétés des clinkers et ciments". Ibid., pp I/212-I/215.
/12/ ONO M. et Coll. "Effect of Na_2O on the stability of calcium aluminoferrite under reducing atmosphere. Ibid., Vol. 2, pp I/124-I/127.
/13/ MOISSET J. et Coll. "La bélite dans les ciments portland obtenus par fusion". Ibid., Vol. II, pp I/218-I/222.
/14/ SYLLA H.M. "Einffluss reduzierenden Brennens auf die Eigenschaften des Zementklinkers". Zement Kalk Gips, Dtsch, N° 12, 1981, pp 618-630.
/15/ MAKI I. et Coll. "Characterisation of fluorine-bearing alite in rapid-hardening high strength cement clinker manufactured by fusion". Il Cemento, N° 1, 1984, pp 3-11.
/16/ SAMUEL G. et Coll. "Influence of the burning process on the morphology and microstructure of Indian cement plants". 6th ISCC, Microscopy, Albuquerque, 1984, pp 20-36.

Influence of Mineralisers on the Constitution and Properties of Industrial Clinkers

C.H. PAGE, D. GHOSH AND A.K. CHATTERJEE
The Associated Cement Companies Ltd.,
Central Research Station, Thane 400604, INDIA.

ABSTRACT

As a part of the comprehensive programme for productivity optimisation, energy conservation and trouble shooting, The Associated Cement Companies Ltd. (ACC) an organization with 17 factories, 48 kilns and about 9 million tonnes of installed capacity have been taking advantage of plant scale use of mineralisers under diverse process conditions. This approach has led to extensive use of fluorite, fluorosilicate and sulphate compounds as the mineralisers in wet and semi-dry kiln systems of 300-600 tpd range.

In order to reveal the thermo-chemical effect of different mineraliser on industrial raw mixes a new technique based on firing shrinkage of kiln feed pellets have been developed. The application of this technique for predicting the change in the course of lime combinability reaction with and without use of mineralisers has been reported in the present article.

The changes obtained in the quality of clinker with the use of Fluorspar as mineraliser under actual plant conditions have been studied. Attempts have been made to find out the retention and distribution pattern of mineralising ions in various phases of the industrial clinkers. An endeavour has been made to correlate the change in clinker quality with distribution pattern of mineralising ions in clinker phases as well as with the course of lime combinability reactions established through the technique of firing shrinkage of raw mix pellets.

SUMÁRIO

Como uma parte de um programa abrangente de optimização da produtividade, de conservação da energia e de resolução dos problemas, a Associated Cement Companies Ltd. (ACC), uma organização com 17 fábricas, 48 fornos e com uma capacidade instalada de cerca e 9 milhões de toneladas, tem tirado vantagens do uso de mineralizadores em escala industrial sob diversas condições de operação. Este enfoque levou ao uso extensivo de fluoreto, fluorisilicato e compostos de sulfato como mineralizadores em sistemas úmidos e semi-únidos em fornos na faixa de 300-600 tpd.

Com a finalidade de analisar os efeitos termo-químicos dos diferentes mineralizadores nas misturas cruas industriais, uma nova técnica baseada na retração dos "pellets" no forno foi desenvolvida. A aplicação desta técnica para a predição de mudanças durante as reações da cal com ou sem o uso de mineralizadores é relatada no presente artigo.

As mudanças obtidas na qualidade do clínquer com o uso de espatofluor como mineralizador sob condições reais de fábrica foram analisadas. Tentativas foram feitas para descobrir padrões de retenção e distribuição dos ions mineralizantes nas várias fases do clínquer industrial. Um esforço foi feito para correlacionar a mudança na qualidade do clínquer com os padrões de distribuição dos ions mineralizantes nas fases do clínquer; assim como durante as reações da cal, estabelecida através da técnica de retração dos "pellets" da mistura crua.

I. INTRODUCTION

The use of mineraliser in clinker burning is well established due to its multifarious benefits. The Associated Cement Cos. Ltd. (ACC), India, have been taking advantage of plant scale use of mineraliser for quite sometime. The energy saving in industrial application and the technique for selection of mineralisers has been highlighted in earlier communications (1,2). The present paper discusses the improvement in quality of clinker with use of mineralisers in four plants and its correlation with distribution of mineralising constituents in clinker phases.

II. MINERALISER SELECTION

The technique of firing shrinkage/expansion of raw mixes was used for the selection of mineraliser. This technique provides considerable advantage over conventional methods already highlighted (2).

In brief, the method provides information on the rate of lime combinability, formation of phase assemblage and appearance of liquid. Based on the above approach the mineralisers were selected for the four plants (J,L,M & S) chosen for reporting in this paper, of which in three situations the mineraliser was used for improvement in clinker quality and/or reduction in the high grade limestone consumption. In Plant J, a Lepol kiln (600 tpd) with grate coolers, Plant M wet process (300 tpd) with planetary coolers and Plant L wet process (400 tpd) with planetary coolers, the mineraliser selected was Fluorspar. Whereas in the case of Plant S a wet process kiln (300 tpd) with planetary coolers, the mineralising constituents (F, SO_3,P_2O_5) are available from an industrial waste which normally constitutes 30-40% of the raw mix.

The shrinkage/expansion patterns with and without mineraliser for the three plant raw mixes (Fig. 1) was used to decipher the changes in the course of reactions due to addition of mineraliser. The expansion phenomenon is normally due to the appearance of high lime silicates (C_2S) and aluminates (C_3A). The addition of mineraliser in plant J & L (Fig. 1 a&b) enhanced the expansion characteristics from that without mineraliser indicating reactions favourable for the formation of C_2S & C_3A. The shrinkage indicating the appearance of liquid starts at a temperature around 1250°C has not changed due to the addition of mineraliser but the quantity of liquid exemplified by the value of shrinkage (Fig.1) has increased considerably due to the addition of mineraliser. The rate of shrinkage with temperature as shown by the slope of the shrinkage curve (Fig.1) for plant L indicates improvement in C_3S formation whereas in the case of plant J the liquid was enormous in quantity and because of grate coolers the most of the liquid solidified as glass without promoting C_3S formation. The above is confirmed from microscopic studies by the determination of actual phase composition and phase microstructure described later.

In the case of plant M, a shrinkage was found before the maximum expansion which attributes to the formation of intermediate phases and poor development of C_2S. The addition of mineraliser to some extent improved the situation by arresting the formation of intermediate phases and promoting C_2S formation and consequently improving C_3S development. This fact also receives confirmation through microscopic studies.

III. EXPERIMENTAL

The distribution of mineralising constituents in clinker phase was studied after separating the clinker phases by selective solvent dissolution technique (3) with slight modifications to suit clinker under evaluation. The F, in separated phases were estimated by Specific Ion Analyser and SO_3 & P_2O_5 by conventional classical methods.

The quantification of actual phases and their morphology in clinker was carried out by Optical Microscope corroborated by Scanning Election Microscope studies. The data of chemical composition, potential and actual phase composition, compressive strength of the four plant clinkers with and without mineraliser are given in Table 1. The distribution of mineralising ions in the different phases of the mineralised clinker is given in Table 2. The values in Table 2 are the percentage of the total mineralising constituent present in the clinker.

IV. RESULTS AND DISCUSSION

The compressive strength of cement mortar cubes prepared from the clinkers with and without mineraliser (Table 1) indicate that even though the chemical composition of the clinkers in both situations remaining same, the quality of cement in the case of plant L & M are significantly better with mineraliser, whereas no such improvement is evident from the cliners of plant J. Between plant - L & M clinkers with mineraliser the improvement in compressive strength was higher for plant - L (400 Kg/Cm^2 at 3 days) than plant - M (330 Kg/Cm^2).

An attempt has been made in the following paragraphs to explain the improvement in quality with mineraliser in case of plant - L & M and no improvement in the case of plant - J with the help of data on phase composition, microstructure and distribution of mineralising constituents in clinker phases.

The addition of mineraliser increases the actual C_3S content (determined by microscope) by about 10% in plant - L and 15% in plant - M from that of without mineralised clinker. The level of strength increase with mineraliser addition in plant - L is much higher than that of plant - M, though the C_3S content is within a close range and F concentration in C_3S is of the same order. The C_3S crystals are well developed in case of plant - L(Fig.2). In plant - M clinker, the C_2S development was poor in both the cases with (Fig. 3a) and

Table 1 - CHEMICAL COMPOSITION, PHASE COMPOSITION AND COMPRESSIVE STRENGTH OF CLINKER AND CEMENT.

Plant		Chemical Composition %								Actual Phase Composition %				Compressive Strength kg/Cm^2		
		SiO_2	Al_2O_3	Fe_2O_3	CaO	MgO	F	SO_3	P_2O_5	C_3S	C_2S	C_4AF	C_3A	3 days	7 days	28 days
J	Normal	21.6	6.8	3.8	63.5	2.5	-	-	-	38.0 (43.0)	47.0 (30.0)	2.0 (11.7)	13.0 (11.6)	340	400	450
	With Mineraliser	22.5	6.2	3.5	63.9	2.4	0.3	-	-	41.0 (42.4)	46.0 (32.6)	2.0 (10.6)	11.0 (10.5)	350	390	455
L	Normal	23.2	6.3	4.0	64.6	1.2	-	-	-	40.0 (38.5)	46.0 (37.5)	10.0 (12.2)	4.0 (10.0)	260	320	450
	With Mineraliser	23.4	6.0	4.2	64.7	1.0	0.33	-	-	49.0 (39.2)	36.0 (37.6)	12.0 (12.8)	3.0 (8.8)	400	550	640
M	Normal	24.0	4.6	3.2	66.1	1.1	-	-	-	32.0 (51.1)	58.0 (30.3)	8.0 (9.7)	2.0 (6.8)	250	330	480
	With Mineraliser	24.3	4.8	3.3	65.8	1.0	0.30	-	-	46.0 (46.1)	44.0 (35.0)	8.0 (10.0)	2.0 (7.1)	330	410	590
S	With Mineraliser	23.4	3.0	1.6	66.7	2.0	0.6	2.1	1.3	55.0 (65.2)	35.0 (18.0)	5.0 (4.8)	5.0 (5.2)	320	440	600

Figures in bracket are the potential phase composition.

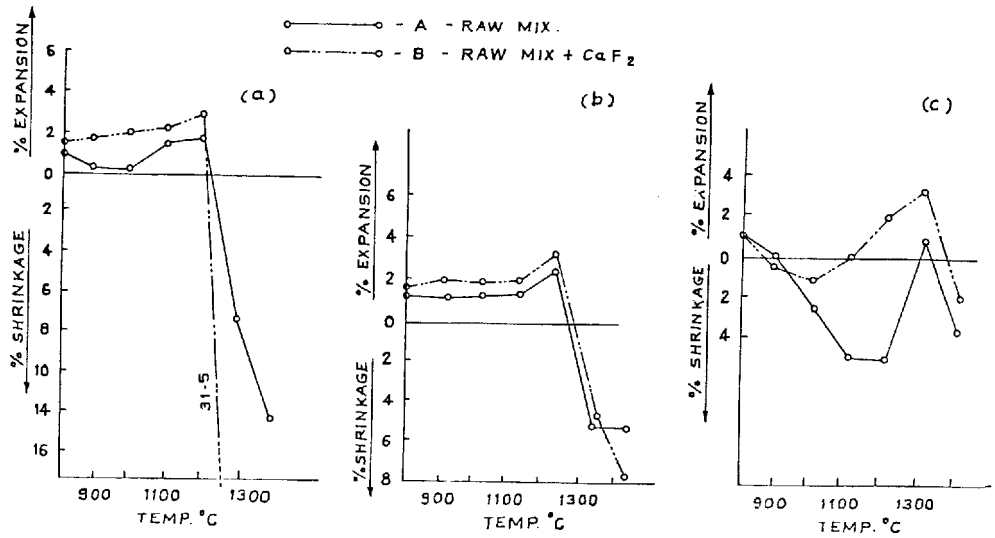

Fig. 1 : EXPANSION / SHRINKAGE (%) WITH TEMPERATURE (°C)
a - PLANT J, b - PLANT, c - PLANT M.

without (Fig. 3b) mineraliser compared to plant - L. This feature was also brought out by the expansion/shrinkage studies as explained earlier. However, some improvement of C_3S was noticed (Fig.3a). Further correlation of potential phase composition and actual phase composition of plant - M clinkers indicate that without mineraliser the potential C_3S which was 51%, the actual C_3S obtained in the clinker is only 32%. Where as the potential C_3S with mineraliser is 46% and the actual obtained is also 46%. Hence the addition of mineraliser did favoured the formation of C_3S but the full potential (51%) is not achieved. However, in case of plant - L the C_3S content in the mineralised clinker is higher by 10% from the potential.

In the case of plant - J where no improvement in cement strength was noticed. The addition of mineraliser did not lead to increase in C_3S content from that without mineraliser (Table 1), even though the concentration of F in C_3S was almost comparable with the other two plants. The F mineralising ion accentuated the formation of liquid as evidenced by the expansion/shrinkage studies (Fig. 1a). The actual C_4AF was found to be 2% when the potential C_4AF was 11% indicating that a substantial amount of the liquid might have formed a glassy phase. The mineralising ions have concentrated preferentially within C_3S and C_3A+C_4AF. The well developed aluminates were also observed (Fig. 4)

- The comparison of the distribution of F in all the clinkers of the plants (J, L & M) indicates their concentration in C_3S at almost the same level.

- The improvement incement quality for the plant - L & M can be explained as due to the quantity and better crystallisation of C_3S because of addition of mineraliser. The higher level of strength in plant - L mineralised clinker in comparison to plant - M mineralised clinker is due to better development of the phases. In case of plant - J clinker with mineraliser no improvement in compressive strength, may be attributed to the poor formation of phases, no improvement in C_3S content and substantial amount of liquid phase leading to the formation of glass. This also shows that the incorporation of 'F' in C_3S or other clinker phases, by itself, cannot ensure better hydraulic potential

Table 2 - DISTRIBUTION OF MINERALISING CONSTITUENTS

Plant	Mineralising Constituents(M.C.)	% M.C. Total	% M.C. of total in		
			C_3S	C_2S	C_3A+C_4AF
J	F	0.30	50.0	4.0	46.0
L	F	0.33	61.0	18.0	21.0
M	F	0.30	51.0	26.0	23.0
S	F	0.60	40.0	47.0	13.0
	SO_3	2.10	9.0	59.0	32.0
	P_2O_5	1.30	44.0	16.0	40.0

of a clinker.

In case of plant S where the C_3S content is the highest (55%) among the four plants under study, the strength development is almost comparable to plant - M (C_3S-46%) and much less compared to plant - L (C_3S-49%). The actual F concentration is also maximum (Table 2) in C_3S. The low order of strength development particularly in early ages is possibly due to the concentration of P_2O_5 in C_3S and C_3A+C_4AF. The sulphate has mostly deposited as Calcium Sulphate on the clinker phase (Fig. 5)

From the limited data on mineralising ion distribution (Table 2) in clinker phases, it can be observed that a minimum of 50% of the total mineralising ion gets absorbed in C_3S phase, for systems where only one type of mineraliser is present.



FIG-2 Well developed C_3S in plant-L
(SEM-photograph x4000)

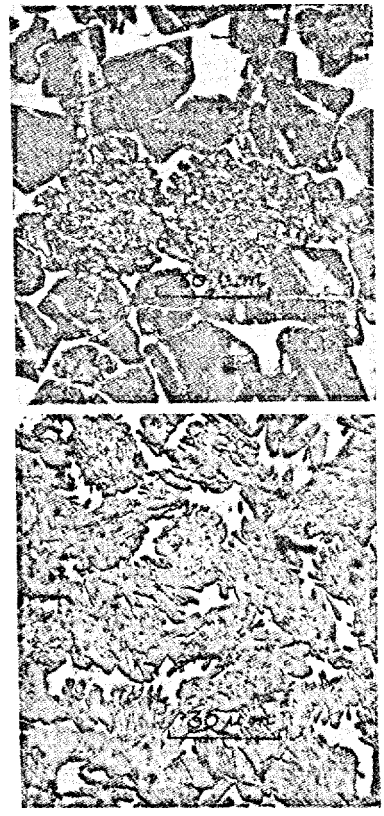

(a) With mineraliser
(b) Without mineraliser

FIG-3 POOR DEVELOPMENT OF C_2S (Optical microscope)



FIG-4 Aluminates in plant-J with mineraliser (SEM- photograph x12000)

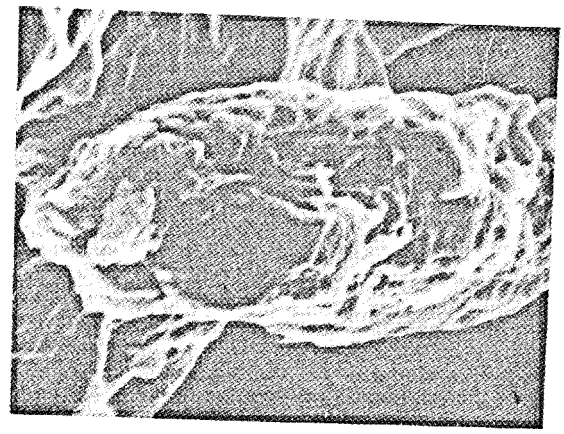

FIG-5 Sulphate deposits on clinker phases (SEM - photograph x6000)

V. CONCLUSIONS

The increase in compressive strength of cement mortar cubes from mineralised clinkers of plant L & M were higher than that without mineraliser and between L & M the development is better in plant - L. There was no improvement in cement compressive strength for plant - J. The improvement in the quality is related to the addition of mineraliser which favoured the formation of C_3S in clinkers of plant - L & M and the phase development, microstructure in plant - L appears to be better than plant - M. But in plant - J the liquid formation was increased due to mineraliser addition without resulting in improvement of C_3S formation. The distribution of the mineralising ions in the clinkers of plant - L, M & J were of the same order in C_3S phase. In view of this, the formation and development of C_3S phase due to mineraliser addition can be primarily attributed to the higher strength development in the resultant cement than the incorporation of mineralising ions in the structure of phases.

In the case of plant S where the mineralising ions are three, inspite of higher C_3S formation compared to plant M & J the strength level was not commensurately higher. This is due to the complex reactions involved for the three mineralisers (F,SO_3 & P_2O_5) and also the incorporation of P_2O_5 in the structure of C_3S thereby retarding its hydraulicity.

ACKNOWLEDGEMENT

The authors thank the help rendered by Mrs. V.S. Bapat, Mr. P.G. Lele and Mr. V.M.Sequeira at various stages of the study.

REFERENCES

1. A.K. Chatterjee & C.H. Page (1984) "Industrial application of Mineralisers for improved Clinker Burning - Illustrative case studies". Seminar on Cement & Allied Building Materials, Cem. Res. Inst. India, Vol. III pp 192-209.

2. A.K. Chatterjee, C.H. Page & D. Ghosh (1985) "Industrial experience of using Mineralisers", International Seminar on Energy Conservation, Beijing.

3. W.A. Gutteridge (1979). "On the dissolution of the Interstitial Phases in Portland Cement" Cem. & Conc. Res. Vol. 9, pp. 319-324.

P. BHASKARA RAO, S.K. HANDOO and GEORGE SAMUEL
National Council for Cement and Building Materials,

Radio tracer technique : a diagnostic method for evaluâtion of raw meal and clinker movement, in a cement rotary kiln. 1.2

TECHNIQUES DES TRAVAUX RADIO ACTIFS : METHODE DE DIAGNOSTIC POUR LE SUIVI DES CRUS ET DES CLINKERS DANS LE FOUR ROTATIF.

SUMMARY : Radiotracer technique has been used for monitoring the movement of material in a wet process cement rotary kiln for the first time in India. These studies were required for obtaining the time - temperature schedule to which the raw meal is subjected, under normal condition of operation of a commercial cement kiln.

An isotope of La^{140} with γ - activity was added in solution form, from the feed end of a wet process kiln. Movement of the radiotracer was monitored at various predetermined locations along the length of the kiln with the help of detectors placed outside the kiln shell.

The studies have shown that the assumptions made in the existing equations defining the material movement phenomenon in rotary kilns are valid only over a very limited length within which the material is in the form of a dry flowing powder without any appreciable physico-chemical change. This zone in a wet proces kiln is limited to the conventional preheating zone. The present study revealed that the material movement in transition and burning zone was much faster than the fine powdery material which is explained by the fact that nodulization takes place in this zone.

It is concluded that such studies are essential for each type of kiln to arrive at realistic figure regarding material movement. Subsequently this data can be used for improving the burnability of raw mixes and out put of existing kilns.

SUMÁRIO: A técnica de radiotraço foi utilizada para medir o movimento do material em um processo de via úmida em um forno rotatório de cimento pela primeira vez na Índia. Estes estudos foram requeridos para a obtenção da programação tempo-temperatura à qual a mistura crua está sujeita sob condições de operação normal de um forno comercial de cimento.

Um isotopo do LA^{140} com atividade L foi usado em forma de solução desde a entrada de alimentação de um forno de via úmida. O movimento do radiotraço foi medida em várias localizações pré-determinadas ao longo do comprimento do forno com o auxílio de detetores localizados fora do casco do forno.

Os estudos mostraram que as hipóteses, feitas nas equações existentes para a definição do fenômeno de movimentação do material em forno rotatório, são válidas apenas em um comprimento muito limitado dentro do qual o material está na forma de um pó seco em corrente, sem qualquer apreciável mudança físico-química. Esta zona em um forno de via úmida é limitada para a zona convencional de pré-aquecimento. O presente estudo revelou que o movimento do material na zona de transição e queimas foi muito mais rápido que material fino em pó, que é explicado pelo fato de que uma modulação ocorre nesta zona.

Foi incluído que tais estudos são essenciais para cada tipo de forno para chegar a figuras realísticas com relação ao movimento do material. Subsequentemente, estes dados podem ser utilizados para melhorar a queima de misturas cruas e os resultados dos fornos existentes.

INTRODUCTION

It is well known that the reactivity of intermediate phases formed in a cement rotary kiln is affected by soaking at a temperature lower than that required for the relevant reaction in which the intermediate phases are to take part. Secondly the heating schedule of the material in terms of variation of temperature with time, varies very considerably with the type of process adopted - wet, semidry, dry process with suspension preheating only, dry process with precalcinator, etc. Even for the same process, there can be minor variations in this heating schedule depending on the minor differences in the design and operation of the pyroprocessing systems.

Therefore in order to undertake burnability studies on a cement raw mix specific to the system in which the raw mix is processed under commercial conditions, a knowledge of the actual heating schedule, to which the raw meal is subjected was required.

Working with a commercial 600 tpd wet process rotary kiln, 165 m in length, the heating schedule was sought to be evaluated by (i) knowing the lengths traversed by the material in the direction of the axis of the kiln in various intervals of time, with the help of radiotracer studies (ii) attempting to evaluate the material temperature in the kiln at any location with a knowledge of (a) the surface temperature of the kiln (b) the thermal conductivities of refractories used at various locations and (c) the dimensional details of the kiln design, and using conventional equations of steady state heat transfers, besides making certain essential approximations.

The results obtained above were converted into a length vs time curve and a length vs temperature curve respectively. By eliminating the length as a common variable, a time temperature schedule experienced by the material was obtained (1). The present paper reports only the studies carried out using radiotracer techniques to obtain the length vs time curve valid for the specific conditions of normal operation of the kiln.

EXPERIMENTAL

A suitable dose of Lanthanum 140 isotope was selected for the study after considering (i) the dilution factor (ii) minimum radiation level detectable from outside the kiln depending on the absorption of radiation by the refractory lining and kiln shell (iii) the half life of the isotope and (iv) safety requirements.

A solution of La^{140} isotope with β & γ- activity was introduced into the slurry at the delivery trough, at the head of the kiln at zero time on the time scale. At predetermined locations along the length of the kiln the γ-activity was monitored from outside the kiln shell with the help of radiation detectors duly protected from the heat radiation of the kiln shell with the help of water cooled jackets.

RESULTS AND DISCUSSION

The location of radioactivity detectors along the kiln length and the calculated times of arrival are shown in Table I.

TABLE - I

MATERIAL MOVEMENT INSIDE KILN AS A FUNCTION OF TIME

Location No.	Distance from Feed End, Metres	Cumulative time of Arrival, Minutes from Feed End			
		As per Radioactive Tracer Studies	Calculated values as per the formulae from		
			Ref. 2	Ref. 3	Ref. 4
1	8.7	4.0	14.0	13.3	13.6
2	19.9	28.0	32.6	30.9	31.7
3	34.8	34.5	58.1	55.0	56.4
4	50.0	51.0	84.8	80.3	82.3
5	63.2	69.5	109.8	104.0	106.6
6	75.3	90.0	133.1	126.1	129.2
7	87.6	98.5	156.8	148.5	152.2
8	106.0	121.0	192.3	182.1	186.6
9	112.5	131.0	205.8	194.0	198.8
10	125.0	142.0	229.0	215.9	221.2
11	136.4	171.0	249.1	234.8	240.7
12	145.0	169.0	264.4	249.3	255.5
13.	155.6	208.0	283.3	267.2	273.8
14	163.5	204.0	297.4	280.5	287.5

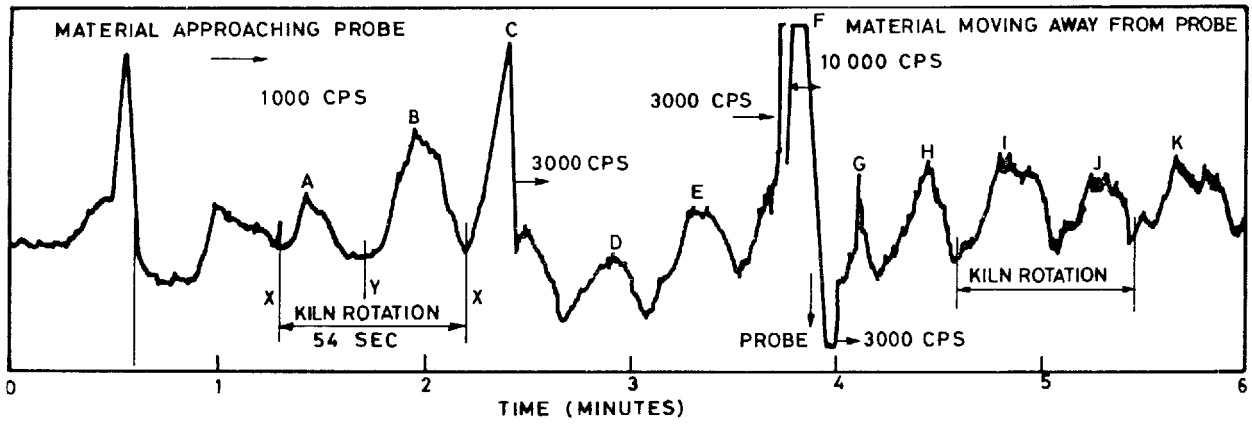

Fig. 1 : Radioisotope record of material movement in kiln. Survey at 9 m from feed end (A,B,C,D, are points of closest approach to probe.)

At any given location along kiln length the variation of γ-radioactivity as a function of time passed through a maximum and decayed slowly as the material containing the radiotracer passed across the location. At the first point of measurement situated at 9 m from feed end, the dilution of the tracer in the slurry was minimum and the peak of radioactivity was very sharp as can be seen on the radio-isotope record of material movement inside the kiln, given in Fig. 1.

Owing to the high concentration of tracer at this location, many other detials can be seen in this curve. In addition to the principal sharp peak, several secondary maxima could also be seen corresponding to the motion of the mateiral in the direction perpendicular to the kiln axis, caused by the rotation of the kiln. It is observed that there is a set of two maxima and two minima corresponding to every cycle of kiln rotation (kiln speed 54 sec/cycle). The appearance of secondary maxima is atributed to the positions A and B taken by the radiotracer (See Fig. 2) and the secondary minima correspond to the positions X and Y taken by the tracer in one cycle of kiln rotation. Further more, owing to the bulk of material between points A and B, the tracer at position A is screened by the material and therefore it may be expected that one of the secondary maxima in any set is slightly higher than the other secondary maximum of the same set. However no evidence of such finer details is seen in the radio-tracer curves. The heights of these secondary maxima are also influenced by the distance of the radio-tracer from the detector, in a direction parallel to the kiln length. Therefore the heights of secondary maxima decreased gradually with distance from the detector on either side of it.

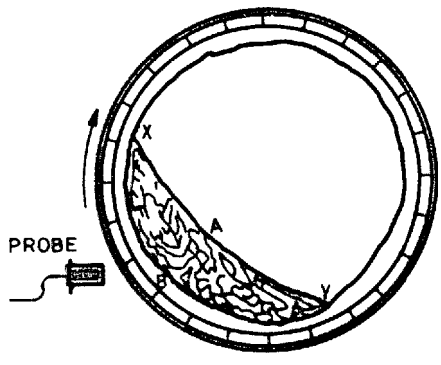

Fig. 2 : Position of the feed inside kiln relative to the probe.

The time of arrival of the radioactive tracer at each location of the kiln length is shown in Fig. 3. A closer examination of the trends in Fig. 3 shows that the free-flowing slurry entering the kiln moves quite rapidly up to the start of the chain zone. In the chain zone the movement is somewhat slowed down owing to the chains and also the thickening of the slurry. Towards the end of the chain zone and through the zone of crosses, the moisture content is sufficiently reduced and a nodulisation of the raw meal takes place. These nodules move down the kiln by rotation and traverse faster. Towards the end of the drying zone the nodules break up into powder owing to further loss of moisture and the movement is once again slowed down. This rate of movement continues up to the end of the calcining zone (125 m). Beyond 125 m of kiln length, i.e. in the transition and burning zones, it is seen that the spread of observations in Fig. 3 has become so wide that the times of arrival of tracer at locations 12 and 14 (see Table 1) are marginally earlier than those at 11 and 13. The spread may be attributed to the size enlargement of the material into a wide range of sizes from say 5 cm to 100 µm. While the coarser nodules tend to move faster by rolling, the finer grains follow as a tail by sliding only. Since the volume of material containing the activity at location 10 (i.e. 125 m) gets distributed statistically into all particle sizes moving at different speeds, the total length of the radioactivity front became very much elongated. It is possible that coarse nodules containing the activity had reached detector position 12 before the tail of finer grains reached even position 11.

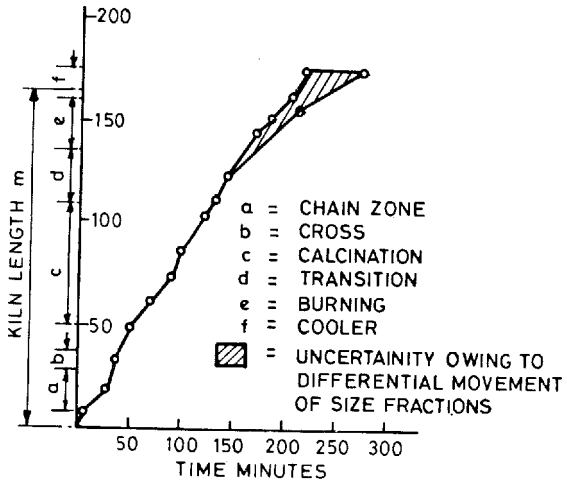

Fig. 3 : Material movement profile as indicated by Radio-tracer.

This being the first experiment of its kind to be conducted in the country, the length of this elongated front could not be anticipated before hand to station the limited number of available detectors, over a longer range. The degree of uncertainity caused by this phenomenon is depicted by the shaded area in Fig. 3.

A number of formulae describing the transport of material inside the kiln by Otto Labahn (2) Duda (3) and Peray and Waddell (4) are already available in the literature. A comparison of the results obtained by the use of these various formulae and the results obtained in the present study are presented in Table 1. It is seen from this Table that the results obtained by the use of all these existing formulae are almost closely in agreement with one another but are at variance with this experimental study, except in a narrow zone of the kiln prior to calcination where the material is a free flowing dry powder not influenced by any parameters such as (a) moisture content (b) gas evolution within the bulk through calcination resulting in a partial fluidization, however low the degree of fluidization may be, and (c) size enlargement, be it due to nodule formation at the appropriate moisture content towards the end of the drying zone, or due to sintering and clinkerization in the transition and burning zones. This variance is easily understandable because the parameters described above, do influence the state of aggregation and the effective angle of repose, whereas all these existing equations are based on simple models assuming that the material can be approximated to a free flowing powder with a constant angle of repose.

CONCLUSION

The movement of material in a cement rotary kiln cannot be described accurately with the help of any of the existing formulae in the literature which are based on simplified models. In a wet process kiln the progressive change in the state of aggregation of material through the stages of free flowing slurry, wet sticky lumps, nodules, free flowing powder, partly fluidized powder and sintered material changes the flow properties through these various stages inspite of the angle of inclination and the speed of rotation of the kiln remaining constant. Secondly incorporations in any particular kiln such as chains, crosses, lifters, and tapering sections, depending on the design, also influence the material movement. Therefore it is necessary to evaluate the material movement experimentally whenever the design features are different.

ACKNOWLEDGEMENTS

The authors have freely drawn upon completed R & D work of NCB. They are thnakful to M/s. India Cements Ltd., for all the cooperation received in the study at their plant. It is also desired to place on record the valuable technical help received from the Bhabha Atomic Research Centre, Bombay, in the selection and handling of the radioactive tracer and in the monitoring of the activity. The authors are grateful to Dr. H.C. Visvesvaraya Chairman and Director General, NCB for permitting to present this paper.

REFERENCES

1.- CEMENT RESEARCH INSTITUTE OF INDIA (1983), "Burnability Based on Process Parameters for Better Clinker production", - Research Bulletin R B - 25 - 83.

2.- O. LABAHN (1971), "Cement Engineers' Hand Book". 3rd English edition, Bauverlag GmbH, Wiesbaden and Berlin, 1971, pp 234-36.

3.- W.H. DUDA, "Cement-data book," 2nd ed. Bauverlag GmbH, Wiesbaden and Berlin, 1977, pp 88.

4.- K.E. PERAY and J.J. WADDELL, "The rotary cement kiln," Chemical Publishing Company Inc, New York, 1972, pp 86.

I.P.Saraswat,Ph.D,Scientist emeritus,University of Roorkee,Roorkee(U.P) India.
V.K.Mathur,M.Sc. and S.C.Ahluwalia, Ph.D, National Council for Cement & Building Materials, M-10 N.D.S.E - II New Delhi - 110 049.

THERMAL DECOMPOSITION AND PHASE TRANSFORMATION STUDIES OF $CaCO_3$-SiO_2 (2:1) SYSTEM IN PRESENCE OF SODIUM AND POTASSIUM CARBONATE.

ETUDES DES DECOMPOSITIONS THERMIQUES ET DES TRANSFORMATIONS DE PHASE DU SYSTEM $CaCO_3$-SiO_2 EN PRESENCE DE CARBONATES DE SODIUM ET DE POTASSIUM.

SUMMARY: Mixtures of $CaCO_3$ - SiO_2 (2:1) molar ratio were subjected separately to thermal analysis with varying concentrations of Na_2CO_3 and K_2CO_3 as dopants (calculated as % Na_2O/K_2O). The activation energy (E_a), Enthalpy (ΔH) of $CaCO_3$ decomposition shows a decreasing trend with 0.1-1.0% dopant but increases with 5% dopant. 0.1-0.5% alkali dopants lead to the formation of a mixture of β-and γ-C_2S phases, while 1% dopants assist in the formation of more desired β-C_2S phase alongwith some C_3S phase. 5% dopants give a mixture of β-and α'-C_2S phases alongwith some C_3S and alkali silicate phases at a much lower temperature.

SUMÁRIO: Misturas de $CaCo_3$ - SiO_2 de 2:1 de relação molar foram submetidas separadamente à análise térmica com concentrações variáveis de Na_2CO_3 e K_2CO_3 como dopantes(calculado como % Na_2O/K_2O). A energia de ativação (E_a), entalpia (ΔH) da decomposição do $CaCO_3$ mostra uma tendência decrescente com 0,1 - 1,0% de dopante, mas aumenta com 5% de dopante. 0,1 - 0,5% do dopante conduz à formação de uma mistura de fases β e γ C_2S, enquanto que 1% de dopante apóia na formação mais desejada da fase β C_2S juntamente com algum C_3S. 5% de dopante dá uma mistura das fases β e α' C_2S e fase de silicato alcalino em muito menor temperatura.

I.P.Saraswat
V.K. Mathur
S.C.Ahluwalia

INTRODUCTION

An important step in the formation of various calcium silicate phases from the mixtures of calcium carbonate and silica is the decomposition of the former. The process is highly energy intensive and efforts are being made to bring about the reaction at a lower temperature and with relative ease. Studies on the kinetics of the decomposition of pure $CaCO_3$ and effects of various dopants on it have been reported (1-4). A good deal of work has also been done on the thermal dissociation of naturally occuring limestone containing impurities (5-7). From the literature survey, it was found that a systematic study of sodium and potassium carbonate dopants on the thermal transformations leading to the formation of dicalcium silicate phases from 2:1 molar $CaCO_3$ and SiO_2 mixture has virtually received no attention.

Since alkali metal salts are found in naturally occuring clays and limestones used for cement manufacture and are fixed as solid solutions in clinker, this study was called for to see the effects of smaller amount of it on the thermal behaviour of 2:1 molar $CaCO_3$ and SiO_2 mixture.

EXPERIMENTAL

Reagent grade $CaCO_3$ and quartz powder (purity > 99.5% in 2:1 molar ratio were mixed with the varying amounts of Na_2CO_3/K_2CO_3 (calculated as 0.1-5.0% oxides). The resulting mixtures after through mixing, grinding and passing through 100 micron sieve, were shaped in the form of nodules of 10 mm dia with small amounts of distilled water. The complete homogenisation of the sample was tested by quantitative estimation of $CaCO_3$ after drying at 100 ± 5°C (2h). These dried samples (I) were stored for the experimental work.

Thermal measurements were made on Mettler thermal analyser (TA-1), which simultaneously records the DTA, DTG and TG curve. The rate of heating of the sample was maintained at 8°C min^{-1} in the platinum crucible of the thermal analyser from room temperature to 1450°C with $-Al_2O_3$ as the reference material. The activation energy (Ea), the enthalphy of $CaCO_3$ decomposition (ΔH) were determined from the DTG and DTA curves respectively (8,9). The intermediate peaks as observed by DTA curve were examined by XRD as follows:

The starting materials (I) were heated in a platinum bucket in a quench furnace (8°C min^{-1}) to the temperature where the peak ends, retained for 1/2 h and immediately quenched to liquid nitrogen temperature (LNT). The products so obtained and the final products, as observed by the final DTA peaks, were examined by Philips X-ray diffractometer PW 1120 using Cu target and Nickal filter.

Free lime in the final products (obtained after heating to final DTA peak temperature for 1 h) was estimated by enthylene glycol method (10).

RESULTS AND DISCUSSION

An endothermic DTA peak at 160°C was observed with 1.0 & 5.0% K_2CO_3 due to its phase transformation. The α-β quartz transformation at 575°C was not disturbed by the presence or concentration of the dopant studied.

The threshold (T_i), decomposition temperature (T_d) and termination temperature (Tf) of $CaCO_3$ in a doped $CaCO_3$-SiO_2 (2:1) mixture have been given in Table 1 and 2. The shape index of the DTA peaks alongwith other kinetic parameters have also been given in Tables. Following things are observed from Table 1 and 2.

Ti value are no doubt reduced by dopants more so by Na_2CO_3 dopant, but the change of concentration has no effect on Ti value. The Tf is practically unaffected by either of the dopants. The Td is not affected by K_2CO_3 dopant but Na_2CO_3 dopant brings it down. Activation energy (Ea) is decreased by both the dopants in the concentration range 0.1-1.0%. However,, for 5% concentration, Ea shot up remarkably to 218 KJ mol^{-1} for K_2CO_3 dopant and to 209 KJ Mol^{-1} for Na_2CO_3 dopant. This trend was also observed in the enthalpy of $CaCO_3$ decomposition (ΔH), through the magnitude was less. The shape index (S) values (Fig. 3) no doubt increased with the concentration of the dopant but the increase was sharper for K_2CO_3 dopant. The various exotherms observed in the DTA plots after the decomposition of $CaCO_3$ with various concentrations of the dopants and the products identified by XRD have been given below:

A sharp exotherm appeared at 1210°C for the pure system $2CaCO_3$: SiO_2. The sample quenched to LNT from this temperature showed the formation of some β-and γ-C_2S phases along with excess of free lime. Sharp d lines of cristobalite also appeared. This exotherm appeared for both the dopants in the concentration range 0.1 - 5%.

Na_2CO_3 (0.1%) dopant gave two exotherms at 1410°C and 1440°C (Fig. 1. Table 1) after the decomposition of $CaCO_3$. The reacting mixture (I) heated to 1410°C and quenched in liquid nitrogen gave a mixture of β - and small amount of γ-C_2S phases alongwith some free lime as observed in XRD. The liquid nitrogen quenched sample at 1440°C showed only β-C_2S phase and not the γ-C_2S phase in the XRD. Free lime was found to be in traces (< 0.1%). Na_2CO_3 (0,5%) dopant gave two exotherms at 1410°C and 1425°C.

TABLE-I THERMAL ANALYSIS AND XRD DATA OF $2CaCO_3 : SiO_2$ MIXTURE IN PRESENCE OF Na_2CO_3

Concentration of Na_2CO_3 (Calculated as % Na_2O by wt) in 2:1 molar $CaCO_3:SiO_2$ system.	Temperature of $CaCO_3$ decomposition and other kinetic Parameters						Exotherm obtained after the decomposition of $CaCO_3$ °C	Constituents formed as discerned by XRD of liquid nitrogen quenched samples.
	Threshold (Ti)	Peak (Td)	Termination (Tf)	Activation Energy (Ea) KJ Mol^{-1}	Enthalphy $(\Delta H)_1$ KJ mol^{-1}	Shape Index from DTA Peak (s)		
0.0	740	885	910	247	160	0.143	1210	β-C_2S, Cristobalite, γ-C_2S, Free lime (High)
							1425	β-C_2S, Free lime (Low) γ-C_2S.
0.1	660	855	910	234	155	0.145	1410	β-C_2S, γ-C_2S, Free Lime (High)
							1440	β-C_2S, Free Lime (< 0.1%)
							1410	β-C_2S, γ-C_2S (Traces)
0.5	660	850	910	216	150	0.150	1425	β-C_2S, C_3S (Small qty) Free lime (< 0.1%)
1.0	660	840	890	200	148	0.152	1410	β-C_2S, C_3S (Small qty) Free lime (0.32%)
5.0							1290	α'-C_2S, β-C_2S, Na_2CaSiO_4 Free lime (Small qty)
	670	840	880	209	152	0.171	1440	β-C_2S, Na_2CaSiO_4 (Small qty) Free lime (0,36%) C_3S (Small qty)

TABLE-II THERMAL ANALYSIS AND XRD DATA OF 2 $CaCO_3:SiO_2$ SYSTEM IN PRESENCE OF K_2CO_3

0.0	740	885	910	247	160	0.143	1210	β-C_2S, Cristobalite γ-C_2S, Free lime (High)
							1425	β-C_2S, γ-C_2S Free lime (Low)
0.1							1410	β-C_2S, γ-C_2S Free lime (High)
	690	880	900	216	159	0.158	1435	β-C_2S, γ-C_2S (Small qty) Free lime (0.40%)
0.5	690	875	905	210	148	0.212	1435	β-C_2S, γ-C_2S (Small qty) Free lime (0.40%)
1.0	690	875	900	195	140	0.290	1390	β-C_2S, γ-C_2S (Small qty) Free lime (0.30%)
							1420	β-C_2S, C_3S, K_2CaSiO_4 $K_2Si_2O_5$
5.0	700	880	900	218	145	0.385	1380	β-C_2S, γ'-C_2S, Free lime (0.20%) K_2CaSiO_4, $K_2Si_2O_5$

I.P.Saraswat
V.K.Mathur
S.C.Ahluwalia

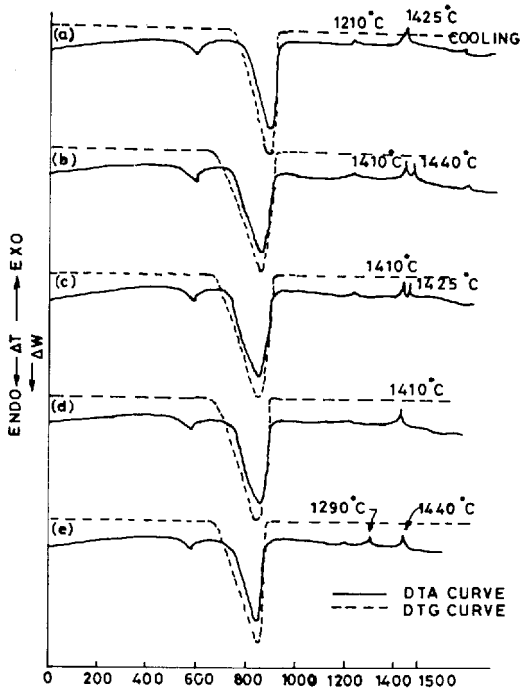

FIG 1 THERMAL CURVES OF (a) $2CaCO_3:SiO_2$ (b) $2CaCO_3:SiO_2$ + 0.1% Na_2CO_3 (c) $CaCO_3:SiO_2$ + 0.5% Na_2CO_3 (d) $2CaCO_3:SiO_2$ + 1% Na_2CO_3 (e) $2CaCO_3:SiO_2$ + 5% Na_2CO_3

The quenched sample showed the formation of β-C_2S and small amounts of γ-C_2S at 1410°C and only β-C_2S alongwith some weak lines of C_3S (d values) (A^o), 3,02, 2.76, 2.73) at 1425°C. This also confirms the views of Koneev and Bygalina (11) that γ-C_2S gets transformed to β-C_2S on heat treatment. Free lime was found to be in traces (< 0.1%). Na_2CO_3 /1.0%) dopant gave only one exothermic peak at 1410°C and the products identified were β-C_2S alongwith little C_3S in the quenched sample by XRD. Free lime was found to be 0.32%. Na_2CO_3 (5%) dopant gave one exothermic peak at 1290°C and the products formed were found to be β-C_2S, α'-C_2S (d values (A^o) 2.73, 2.66, 2.26, 1.92) and small amount of Na_2CaSiO_4 (d values (A^o) 4.33,2.65, 1.88, 1.53) in the liquid nitrogen quenched sample. Another exotherm appeared at 1440°C which showed the presence of most predominant β-C_2S phase alongwith appreciable amounts of Na_2CaSiO_4 and small quantity of C_3S. Probably the α'-C_2S phase got transformed to β-C_2S phase as no lines for this phase appeared in the XRD pattern. The sample (I) heated to 1450°C (1 h) confirmed the above phases formed at the final DTA peak temperature. Free lime in the sample heated to 1450°C was found to be 0.38%.

K_2CO_3 (0.1%) dopant gave two exotherms at 1410°C and 1435°C (Fig. 2, Table 2). The XRD of the liquid nitrogen quenched sample at 1410°C gave a mixture of β and γ-C_2S phases alongwith high free lime. At 1435°C, a major transformation of γ-C_2S to β-C_2S took place leaving only a small quantity of γ-C_2S as detected by the weak lines in the XRD pattern. Free lime determined chemically was found to be 0.40%. One exotherm at 1435°C was observed with 0.5% K_2CO_3 dopant and the XRD of the liquid nitrogen quenched sample confirmed only β-C_2S alongwith a little γ-C_2S phase. Free lime was found to be 0.46%. Few weaklines of $K_2Si_2O_5$ (d values (A^o) 3.82, 2.96, 2.43) also appeared in the XRD.

K_2CO_3 (1.0%) dopant gave two exothermic peaks at 1390° and 1420°C in the DTA curve. The liquid nitrogen quenched sample at 1390°C showed only β-C_2S alongwith very little γ-C_2S phase as discerned in XRD. Free lime determined chemically was found to be 0.30%. The XRD of the sample (I) heated to 1420°C and quenched in liquid nitrogen, showed only β-C_2S. γ-C_2S phase was found to be absent. Free lime values also went down to 0.20%. Few weak lines of C_3S alongwith K_2CaSiO_4 and $K_2Si_2O_5$ appeared in the XRD. K_2CO_3 (5.0%) gave only one exotherm at 1380°C and the reacting mixture heated to 1390°C and quenched indicated the most predominant β-C_2S alongwith α'-C_2S, K_2CaSiO_4 and $K_2Si_2O_5$ in the XRD pattern.

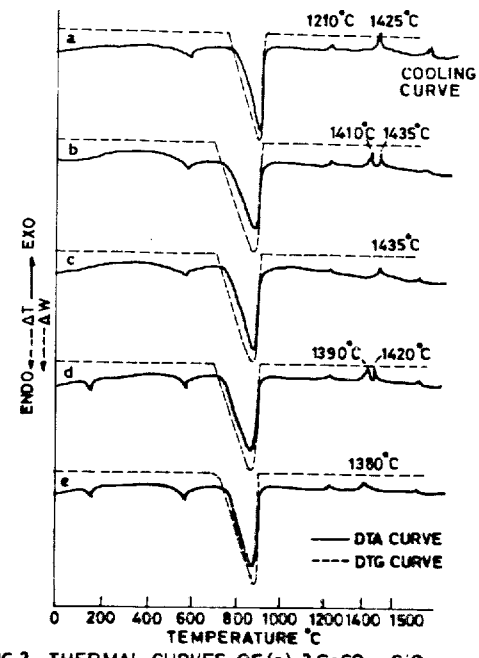

FIG 2 THERMAL CURVES OF (a) $2CaCO_3, SiO_2$ (b) $2CaCO_3, SiO_2$ + 0.1% K_2CO_3 (c) $2CaCO_3$ SiO_2 + 0.5% K_2CO_3 (d) $2CaCO_3, SiO_2$ + 1% K_2CO_3 (e) $2CaCO_3, SiO_2$ + 5% K_2CO_3

Free lime determined chemically was found to be 0.20%. A phase previously considered to be definite compound of composition K_2O 23 CaO. 12 SiO_2 was shown by Suzukawa (12) to be a solid solution of K_2O in the form of $\alpha'C_2S$. However, at higher temperature this phase transforms to β-C_2S as also observed by Welch and Gutt (13).

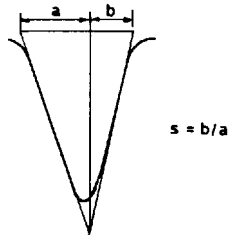

FIG 3 SHAPE INDEX FROM DTA DECOMPOSITION PEAK

CONCLUSION

The activation energy and enthalpy of $CaCO_3$ decomposition is minimum with 1.0% dopant in $CaCO_3$-SiO_2 (2:1) system. The magnitude of β-C_2S phase increases with increasing percentage of dopant (0.1-1.0%). 5.0% dopant give most predominant β-C_2S phase alongwith a little α'-C_2S, C_3S and alkali silicates. Na_2CO_3 (5.0%) is found to be most effective in bringing down the temperature of formation of most desired α' - and β-phases of C_2S than K_2CO_3, resulting in reduced fuel consumption.

ACKNOWLEDGEMENT

The authors are thankful to Dr. H.C.Visvesvaraya, Chairman and Director General, National Council for Cement and Building Materials, for providing research facilities in pursuing Ph.D Studies to one of the authors(VKM).

REFERENCES

1. G.V.SUBBA RAO, M.NATRAJAN, C.N.R.RAO (1968) J.Am. Ceram SOC, 51, 3, 179.

2. B.D.CHATTARAJ, S.N.DUTTA, M.S.IYER (1973) J.Thermal Analysis 5, 43.

3. C.R.M.RAO & P.N.MEHROTRA (1977) Ind J. Chem 15A, 1016.

4. P.K.GALLAGHER & D.W.JHONSON (1976) Thermochim Acta 14, 3, 255.

5. I.MASOOD, N.G.DAVE, R.S.GUPTA (1982) Ind Ceram, Ceram, 25, 4, 83.

6. A.K.GUPTA, MOHAN RAI (1977) Chemical Age of India 28, 3, 199.

7. G.E.KIND & M.V.KONGIYA (1976) Tr GOS V ses Nauchne-Issled Instt. Tsem. Prom Sti 37, 11.

8. N.G.DAVE & S.K.CHOPRA (1966) Z Phys. Chem. Neuefolge 48, 5/6 257.

9. D.M.SPEROS & R.L.WOOD HOUSE (1968) J. Phys. Chem. 72, 2846.

10. M.P.JAVELLANA & I.JAWED (1982) Cem.and Concr. Res. 12, 399.

11. V.I.KORNEEV & E.B.BYGALINA, (1968)Proc. of the fifth Inter. Symp. on the Chemistry of Cement, Tokyo 285.

12. Y.SUZUKAWA, (1956) Zem. Kalk. GIPS 9, 390.

13. J.H.WELCH & W.GUTT (1960) Proc. of the fourth Inter. Symp. on Chemistry of Cement, Washington Vol. I, 59.

Quantification of OPC Clinker Microstructure - An Approach for Prediction of Cement Strength

1.2

R.V. HARGAVE, D.VENKATESWARAN, V.V. DESHMUKH, AND A.K. CHATTERJEE,
The Associated Cement Cos. Ltd.,
Central Research Station, Thane 400604, INDIA .

SUMMARY :

The influence of clinker microstructure on its quality and cement strength is extensively reported in the literature, but its effective application has been limited due to the absence of proper quantification of various microstructural parameters.

The problems in quantifying clinker microstructure have been the difficulty in drawing representative samples from plants, involvement of a large number of parameters of varying significance, absence of universally acceptable techniques for quantifying parameters; other than chemical and phase composition, break up of each parameters into sub-parameters and difficulty of comparing certain parameters that are quantified in range intervals.

Keeping in view the above shortcomings of available technique, the quantification approach adopted by the authors have the following features :

- Rationalised sampling procedure.
- Quantitative estimation of phases based on chayes' IC number and corresponding measurement area with distributed point counts.
- Conversion of phase analysis into a single ratio.
- Quantification of morphology of alite phase through a graphical technique.
- Quantification of belite morphology on the basis of their roundness.
- Graphical integration of silicate crystal size distribution.
- Quantification of clustering, twinning etc.

Based on the above quantified approach as extended to a large number of industrially produced clinkers, a multiple linear regression analysis has been performed to obtain an empirical equation correlating the clinker microstructural parameters with 28 days cement strength. The equation thus obtained has been applied to unknown samples to compare the match between the theoretical prediction and experimentally determined strength values. The method has also been compared with ONO's technique for prediction of cement strength. The potential of the new quantification approach has been highlighted.

A literatura aborda amplamente a influência da microestrutura do clinquer sobre sua qualidade e a resistência do cimento, mas sua aplicação efetiva tem sido limitada devido à falta de quantificação de vários parâmetros microestruturais.

Os problemas para quantificação da microestrutura do clinquer têm sido a dificuldade de obtenção de amostras representativas das fábricas, envolvimento de grande número de parâmetros de significação variável, falta de técnicas aceitas universalmente para parâmetros de quantificação; além de composição química e de fase, divisão de parâmetros em sub-parâmetros e dificuldade de comparação de certos parâmetros que são quantificados em intervalos de escala.

Tendo em mente as deficiências acima de técnica disponível, a aproximação de quantificação adotada pelos autores tem as seguintes características:

- processo racionalizado de amostragem;
- estimativa quantitativa de fases com base no número IC de "chayes" e correspondente área de medição com contagens distribuídas de ponto;
- conversão da análise de fase numa relação única;
- quantificação da morfologia da fase de alita por meio de uma técnica gráfica;
- quantificação da morfologia da belita com base em sua redondeza;
- integração gráfica da distribuição de tamanho do cristal de silicato;
- quantificação de grupamento, geminação, etc...

Com base na aproximação quantificada acima, estendida para um grande número de clínqueres produzidos industrialmente, foi feita uma análise de regressão linear múltipla para se obter uma equação empírica correlacionando os parâmetros microestruturais do clinquer com a resistência do cimento aos 28 dias. A equação obtida desta forma foi aplicada a amostras desconhecidas para se comparar a semelhança entre os valores de predição teórica e os da resistência determinada experimentalmente. O método foi também comparado com a técnica de ONO para predição da resistência do cimento. Ficou evidenciado o potencial da nova aproximação de quantificação.

1. INTRODUCTION

In the past a few serious attempts have been made to use the clinker microstructure to predict cement strength. But the total impact of microstructural characterisation of clinker for quality control and prediction of cement strength by and large remained qualitative due to absence of quantification of important microstructural parameters.

Ono(1,2) is probably first to use quantified microstructural parameters determined by transmitted light microscopy for predicting 28D cement compressive strength. Sometime back the present authors took up a comprehensive investigation and proposed a systematic approach of quantification of significant microstructural parameters under reflected light microscopy with a view to integrate the quantitative 'indices' into an empirical relation to predict 28-D cement strength (3,4,5)

2. QUANTIFICATION APPROACH.

In the present day practice the microstructural characteristics of OPC clinker is essentially based on the following parameters.

a) Relative proportion of various clinker phases.
b) Crystal size of silicates.
c) Crystal morphology.
d) Various polymorphic modifications of major phase.
e) clustering of silicate phases.

The problems in quantifying the above parameters have been

- Drawing the representative samples from bulk.
- Involvement of a number of parameters of varying significance.
- Absence of universally acceptable techniques for quantifying parameters; other than chemical and phase composition.
- Breakup of each parameters into sub-parameters.
- Difficulty in comparing certain parameters that are quantified in range intervals.

Keeping in view the above shortcomings a rationalised sampling procedure was devised and more significant microstructural parameters were quantified as seven 'indices' on the basis of techniques developed by authors (3,4). They are

- Phase index (PHI)
- Crystal size index of alite (CSI-A)
- Crystal size index of belite (CSI-B)
- Morphology index of alite (MOI-A)
- Morphology index of belite (MOI-B)
- Twinning Index (TWI)
- Cluster Index (CLI).

3. EXTENSION OF THE APPROACH TO INDUSTRIAL CLINKER.

Following the approach of quantification of microstructural parameters (3,4) various 'indices' of a large number of industrially produced clinkers from 18 cement plants, covering wide range of raw materials and processes were determined and correlated with 28D compressive strength of coresponding laboratory ground OPC cement. Attempts were made to keep the Blaines and sulphate content in all the samples as close as possible but occasional marginal fluctuations could not be avoided. However, an assessment of 28D cement strength with cement specific surface area and SO_3 content did not show any systematic correlation. (Fig. 1 & 2)

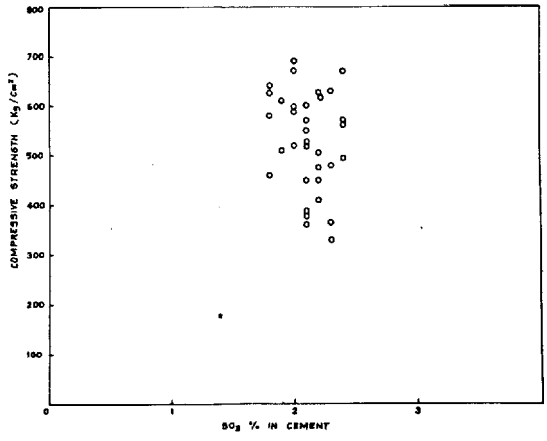

Fig. 1 Correlation of 28D Compressive strength of Laboratory ground cement with SO_3 content.

Chemical composition and other physical data on clinker samples are available with the authors but to paucity of space it is not being presented here.

4. SIGNIFICANCE OF INDIVIDUAL MICROSTRUCTURAL PARAMETERS ON CEMENT STRENGTH.

Based on our study (4) Correlation coefficient (r) value of some more significant microstructural parameters were identified in relation with compressive strength of cement. They are -

- Crystal size index of alite (CSI-A)
- Crystal size index of belite (CSI-B)
- Phase index (PHI)
- Cluster index (CLI)

However, it was concluded that for any effective quantification of either individual or composite effect of microstructural 'indices' on cement strength, a multiple linear regression analysis has to be considered (4).

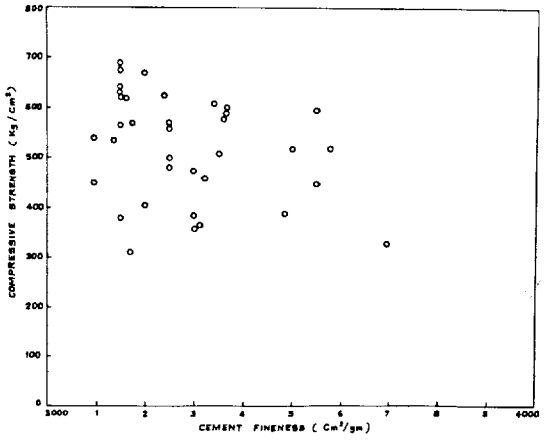

Fig. 2 Correlation of 28D compressive strength of cement samples with their specific surface area.

5. APPLICATION OF MULTIPLE LINEAR REGRESSION ANALYSIS AND FORMULATION OF AN EQUATION.

The multiple linear regression analysis was done on a large number of data (Table-1, Fig. 3) on DCM Spectrum 3 computer to assign proper weightage to various microstructural 'indices'. The tentative equation arrived at is as follows :

28D strength = 0.028 + 98.598 (PHI) + 90.571 (CSI-A) + 1.539 (CSI-B) + 61.437 (MOI-A) + 2.943 (MOI-B) + 85.049 (TWI) - 84.308 (CLI)

The co-efficient of multiple correlation (r) is 0.836 and the standard error of estimate is 52.794. the F-test (ratio of variances) and t-test (ratio of standard deviation) were also computed and the significance of total equation and significance of individual parameters were established :-

F test value - 9.610

T test value - CSI-A (3.154)
MOI-A (2.752)
PHI (1.871)
CLI (1.292)
TWI (0.472)
CSI-B (0.057)
MOI-B (0.054)

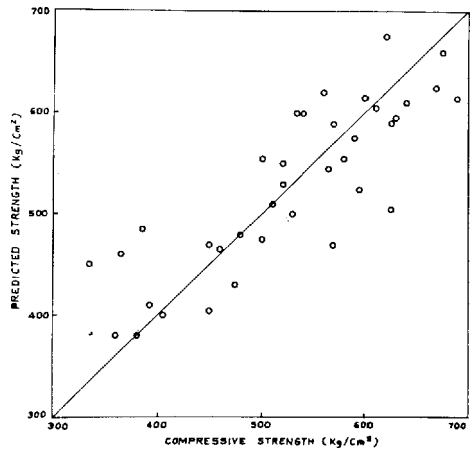

Fig. 3 Correlation between 28D cement compressive strength with predicted strength by CRS Technique.

6. PREDICTION OF 28D COMPRESSIVE STRENGTH OF UNKNOWN CEMENT SAMPLE.

Ten unknown OPC clinker from various sources were evaluated for their microstructural 'indices' and they were processed with the equation. The compressive strength obtained by the equation were compared with the actual strength determined as per I.S. specification (Table 2).

Following observations were made

- All the predicted values of strength are in close agreement with actual values (variation ± $<10\%$).
- The difference of the predicted values varied between + 19 and - 42 Kg/cm^2.
- Except in one case the predicted strength values are within $\lesssim 7\%$ range.
- Inspite of having wide variation in true strength value (360 - 612 Kg/cm^2), the equation is able to predict 28D strength quite accurately.

7. COMPARISON OF CRS TECHNIQUE WITH THAT OF ONO AND ITS POTENTIAL.

Same ten OPC clinker which has been evaluated by CRS technique for prediction of 28D strength were tested by Ono's technique (2) and the respective values were compared (Table 3).
Following are comments

(a) Both the techniques uses optical light microscope as the basic tool and quantify the selected microstructural parameters of clinker.
(b) In Ono's technique the required parameters are determined on clinker powder/section in trans-

TABLE - 1

Microstructural Indices of clinker by CRS Technique and Actual and Predicted Strength of Corresponding Cement

S. No.	CRS MICROSTRUCTURAL INDICES							CEMENT STRENGTH (Kg/Cm^2)		
	PHI	CSI-A	CSI-B	MOI-A	MOI-B	TWI	CLI	Compressive Strength	Predicted Strength	Difference
1	0.670	1.585	1.860	3.057	0.320	0.90	0.346	331	448.635	-117.635
2	0.970	2.810	1.835	2.985	0.760	0.74	0.148	624	589.082	34.917
3	0.750	2.170	2.095	2.670	0.390	0.90	0.195	532	499.029	32.971
4	0.430	2.555	2.765	2.020	0.270	0.90	0.257	364	457.865	-93.864
5	0.740	1.950	2.255	2.775	0.400	0.85	0.229	482	477.725	4.274
6	0.820	2.593	1.715	2.816	0.540	0.93	0.200	496	555.199	-59.198
7	0.560	1.849	1.394	2.018	0.170	0.92	0.280	405	403.973	1.026
8	0.960	2.358	1.527	2.879	0.460	0.92	0.280	564	543.469	20.531
9	0.740	1.851	1.397	2.667	0.170	0.93	0.215	572	468.110	103.89
10	0.780	1.630	1.270	3.360	0.600	0.81	0.225	384	484.635	-100.634
11	1.000	1.540	1.270	2.740	0.550	0.97	0.205	503	475.231	27.769
12	0.900	1.115	1.145	2.930	0.410	0.96	0.300	476	429.087	46.913
13	0.703	2.815	2.715	2.710	0.420	0.71	1.107	460	463.265	- 3.264
14	0.614	3.490	2.135	2.895	0.410	0.87	0.254	642	611.592	30.408
15	0.540	2.420	2.300	2.867	0.620	0.89	0.226	509	510.598	- 1.597
16	0.680	3.406	2.780	2.605	0.890	0.92	0.187	608	604.981	3.019
17	0.695	2.550	2.600	2.320	0.830	0.85	0.192	625	504.593	120.407
18	1.069	2.365	2.005	3.150	0.780	0.85	0.219	588	572.366	15.633
19	0.697	1.850	1.840	3.007	0.340	0.78	0.261	452	469.215	-17.215
20	0.639	1.540	1.480	2.560	0.290	0.79	0.211	387	412.322	-25.321
21	0.784	2.150	2.160	3.200	0.260	0.91	0.271	520	527.293	- 7.292
22	0.599	1.975	2.620	3.625	0.420	0.93	0.249	595	524.048	70.952
23	0.792	2.060	2.240	3.665	0.300	0.88	0.256	518	547.452	-29.452
24	1.160	2.785	2.785	2.680	0.050	0.90	0.220	631	593.724	37.276
25	0.820	3.190	3.685	3.025	0.060	0.88	0.274	689	613.239	75.761
26	1.200	3.070	2.880	2.600	0.400	0.95	0.204	671	625.343	45.657
27	1.030	3.550	3.220	2.980	0.700	0.87	0.317	675	660.477	14.522
28	1.170	2.925	2.622	2.955	0.660	0.96	0.426	599	613.565	- 14.564
29	1.090	3.047	3.158	2.708	0.690	0.99	0.231	566	621.457	-65.456
30	0.470	2.573	2.617	1.216	0.209	0.080	0.571	378	378.658	- 0.657
31	0.737	1.836	1.816	1.866	0.320	0.85	0.560	360	382.441	-22.44
32	0.508	2.196	1.895	1.929	0.428	0.94	0.551	451	405.191	45.809
33	1.507	3.157	2.870	2.755	0.534	0.99	0.231	621	674.519	-53.519
34	1.084	2.810	2.893	1.950	0.600	0.98	0.182	578	555.438	22.562
35	0.826	3.353	2.662	2.183	0.487	0.94	0.173	570	590.163	-20.162
36	0.866	3.090	3.089	2.610	0.329	0.93	0.107	542	601.427	-59.426
37	0.875	3.327	2.833	2.175	0.420	0.92	0.101	534	596.583	-62.583

Multiple Correlation Coefficient(r) = 0.8359. Std. Error of Estimate = 52.794.

TABLE - 2

Prediction of 28 D Compressive Strength of Unknown Cement Sample by CRS Technique

S. No.	CRS MICROSTRUCTURAL INDICES							CEMENT STRENGTH (Kg/Cm^2)		
	PHI	CSI-A	CSI-B	MOI-A	MOI-B	TWI	CLI	Compressive Strength	Predicted Strength	Difference
1	0.932	2.704	1.314	2.409	0.89	0.835	0.221	505	541.83	- 36.83
2	1.556	2.31	3.323	2.54	0.82	0.99	0.193	612	594.156	17.843
3	1.036	2.85	2.63	2.608	0.876	0.92	0.258	542	583.628	- 41.628
4	0.9	2.104	2.127	2.363	0.5	0.875	0.507	419	460.908	- 41.908
5	1.39	2.131	1.555	2.9	0.74	0.883	0.259	548	566.074	- 18.074
6	0.795	1.13	2.087	2.122	0.577	0.982	0.276	396	376.283	19.716
7	0.692	1.24	2.393	2.736	0.485	0.983	0.283	418	413.508	4.491
8	0.805	1.912	2.01	2.021	0.502	0.992	0.282	425	441.887	- 16.887
9	0.559	1.357	2.308	2.194	0.396	0.989	0.313	402	375.278	26.721
10	0.740	1.836	1.816	1.866	0.320	0.850	0.560	360	382.000	-22.000

mitted light, while CRS technique is based on the measurement of microstructural parameters on clinker polished section.

(c) Ono (2) has considered only size of silicate crystals, birefringence of alite and colour of belite, whereas CRS technique is more comprehensive and considers silicate size and morphology, distribution and proportion of phases, polymorphic forms apart from rationalised sampling of clinker which represents the bulk. However, both the techniques use multiple linear regression analysis to assign proper weightage to the various parameters and formulation of equation.

(d) Tentatively we have observed that predicted result is more accurate with CRS technique, probably because of various considerations described in (c) (Table 2, Fig.4).

(e) Eventhough Ono seems to be faster than CRS technique, the element of personal judgement present in the Ono technique is a negative factor.

(f) Moreover, some practical difficulties were encountered by the authors while using Ono 's technique for 28D strength prediction, such as coatings of ferrites on silicates which curtailed the visibility of grains and often accurate measurement become difficult. Further, in some Indian clinker due to high manganese the belite crystals gave a colour which does not fit in the Ono 's suggested range.

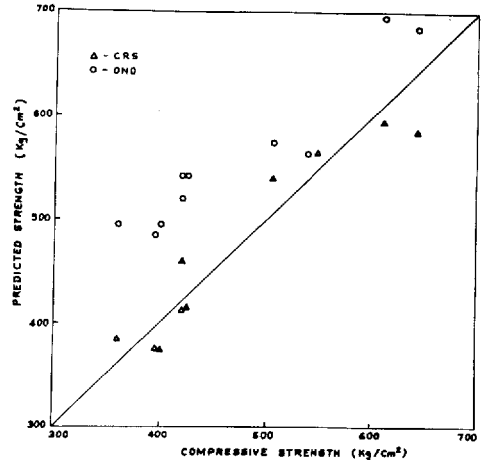

Fig. 4 Comparison of strength prediction of unknown cement samples by CRS and Ono 's technique.

TABLE - 3

COMPARISON OF STRENGTH PREDICTION OF UNKNOWN CEMENT SAMPLES BY CRS AND ONO'S TECHNIQUE

S. No.	ONO'S PARAMETERS				Compressive Strength Kg/Cm^2	ONO'S PREDICTION Kg/Cm^2		CRS PREDICTION Kg/Cm^2	
	A.S.	A.B.	B.S.	B.C.		Strength	Difference	Strength	Difference
1	24	0.0027	27	FY	505	573	-68	542	-37
2	39	0.0026	34	FY-C	612	706	-94	594	18
3	39	0.0041	31	FY	542	685	-143	584	-42
4	24	0.0023	22	Y	419	543	-124	461	-42
5	30	0.0020	18	Y	548	566	-18	566	-18
6	20	0.0029	17	Y-A	396	483	-87	376	20
7	23	0.0026	20	Y-A	418	519	-101	414	4
8	25	0.0030	23	Y	425	542	-117	415	17
9	20	0.0028	18	Y	402	496	-94	375	27
10	22	0.0017	17	A	360	489	-129	382	-22

(g) CRS technique has potential to replace the normal physical method of 28D strength determination of OPC cement. And possibly with computer programming of the measurement techniques, the prediction may become faster.

8. REFERENCES

1. Ono Y, Kawamura S, and Soda Y (1968) "Microscopic observation of alite and belite and hydraulic strength of cement." Proceeding of 5th International Symposium of Chemistry of cement, Tokyo 1, 275-284.

2. Ono Y (1981) "Microscopical observation of clinker, for the estimation of burning condition, grindability and hydraulic activity." Proc. of the 3rd International conference on Cement Microscopy, Houston, USA, 198-210.

3. Hargave R.V., Venkateswaran D, Chatterjee A.K. and Rangnekar B.S.(1982) "Prospect of Quantifications in Portland cement Clinker Microscopy". Microscope, 30, 291-313.

4. Hargave R.V., Venkateswaran D, Chatterjee A.K. and Rangnekar B.S.(1983) "Assessment of process effects on clinker microstructure through its quantification" Proc. of the 5th International Conference on Cement Microscopy, Nashville, U.S.A. 99-120.

5. Hargave R.V., Venkateswaran D, Deshmukh V.V. and Chatterjee A.K. (1985) "Quantification on varying effects of a set of clinker microstructural parameters on cement strength at various ages." Proc. of 7th International Conference on Cement Microscopy, Fort Worth, USA.

C. GILIOLI, Dr. of Chemistry, Italcementi, Laboratorio Chimico Centrale, Bergamo, Italy
F. MASSAZZA, Professor of Applied Chemistry, Italcementi, Laboratorio Chimico Centrale, Bergamo, Italy
M. PEZZUOLI, Dr. of Chemistry, Italcementi, Laboratorio Chimico Centrale, Bergamo, Italy

1

SOLID STATE RELATIONSHIPS IN THE LIME-RICHEST PART OF THE $CaO-Al_2O_3-Na_2O-Fe_2O_3$ SYSTEM

1.2

RELATIONS A L' ETAT SOLIDE DANS LA PARTIE LA PLUS RICHE EN CHAUX DU SYSTEME $CaO-Al_2O_3-Na_2O-Fe_2O_3$

SUMMARY

The solid state relationships existing at 1200°C in the most basic part of the system $CaO-Al_2O_3-Fe_2O_3-Na_2O$ were studied.

The results led to ascertain that in the examined system there is no formation of quaternary compounds and sodium preferentially dissolves in calcium aluminates.

This solubility extends calcium aluminate stability inside the quaternary system.

In fact, cubic C_3A containing up to 1.88 wt % Na_2O is in equilibrium with the terms of the solution $C_4AF-C_6A_2F$ but, owing to the Na_2O values between 3.60 wt % and 5.59 wt % its stability field extends up to C_6AF_2.

$C_{12}A_7$ can dissolve up to about 2.2 wt % Na_2O in its lattice. This limit solid solution is compatible with C_5AF_2 whereas, without sodium, it can only be in equilibrium with C_6A_2F.

SUMÁRIO

As relações de estado sólido existente a 1200°C na maior parte básico do sistema CaO, $Al_2O_3-Fe_2O_3-Na_2O$ foram estudadas.

Os resultados levaram a verificar que no sistema examinado não existe a formação de compostos quaternários e que o sódio preferencialmente dissolve em aluminato de cálcio.

Esta solubilidade estende a estabilidade do aluminato de cálcio dentro do sistema quaternário.

De fato, o C_3A cúbico contendo até 1.88% de Na_2O em peso está em equilíbrio com os termos da solução $C_4AF-C_2A_2F$ mas, devido aos valores de Na_2O entre 3,60% e 5.590% em peso o seu campo de estabilidade estende até C_2AF_2.

$C_{12}A_7$ pode dissolver até 2.2% Na_2O em sua rede. Este limite de solução sólida é compatível com C_2AF_2 desde que, sem sódio, pode estar apenas em equilíbrio com C_2A_2F.

SOLID STATE RELATIONSHIPS IN THE LIME-RICHEST PART OF THE $CaO-Al_2O_3-Na_2O-Fe_2O_3$ SYSTEM 1.2

1. INTRODUCTION

1.1. This work gives a contribution to the knowledge of the equilibrium relationships among the phases concerning portland cement clinker.

The purpose of this study is mainly to ascertain in what extent the presence of Na_2O can change the solid-state equilibrium relationships between C_3A, $C_{12}A_7$* and the solid solution of calcium aluminoferrites.

1.2. The literature reports a great deal of works about the $CaO-Al_2O_3-Fe_2O_3$ ternary system. The knowledge on this system can be considered good since the results obtained in the latest studies (1) (2) (3) (4) are in excellent agreement. According to all the Authors the C_2F - "C_2A" solid solution extends to a final term having a composition very similar to $C_2A_{0.7}F_{0.3}$, whereas the intermediate member compatible with C_3A and CaO, has a composition like that of brownmillerite ($C_2A_{0.5}F_{0.5}$). A limited Al^{3+}-Fe^{3+} substitution also occurs in C_3A and $C_{12}A_7$.

1.3. The $CaO-Al_2O_3-Na_2O$ ternary system was first studied by Brownmiller and Bogue (5) who drew the relative phase diagram. This work pointed out the presence of the NC_8A_3 ternary compound, compatible with C_3A in the solid state.

The existence of this compound was doubted by Suzukawa (6) who declared that its stability is conditioned by the presence of small amounts of SiO_2 in its crystalline structure.

Moore (7) in her studies on clinker phases ascertain the presence of a non-cubic tricalcium aluminate,but in some clinkers the amount of sodium attributed to this phase did not correspond to that contained in NC_8A_3.

Conwicke and Day (8), Fletcher, Midgley, Moore (9) and Maki, Nishi and Sugimura (10), through their studies about the equilibrium relationships along the join C_3A-NC_8A_3, revealed the existence of a series of mixed crystals in this subsystem. Chromy and Gregor (11) established by high temperature microscopy that this solid solution can exist in 3 polymorphic forms.

Maki (12) found that the prismatic phase in portland cement clinker coincides with the terms of the C_3A-NC_8A_3 series and proved that C_3A can dissolve in its lattice up to 6.2 wt.% Na_2O. Beyond this value C_3A decomposes partially into CaO and $NaAlO_2$. Moreover, for Na_2O contents above 4.6 wt.%, C_3A has a monoclinic symmetry.

Regourd et al. (13)(14) studied again the C_3A+Na_2O solid solutions completely and established the existence of four crystalline phases of C_3A. Furthermore they ascertained that Na_2O solubility in tricalcium aluminate extends up to a peak value of 5.7 wt.%. Since over this value the cell parameters vary no longer, they inferred that the solubility limit had been reached.

According to these Authors, a cubic phase of C_3A with a Pa3 spatial group is stable up to 1.9 wt.% Na_2O, the orthorombic phase I with Pbca spatial group is stable from 3.7 to 4.6% and the orthorombic phase II with Pba2 or Pbam spatial group is from 4.6 to 5.7%.

For Na_2O contents above 3.7 wt.%, at temperatures exceeding 450°C, a fourth tetragonal phase with probable P4/mbm spatial group is stable. This variety, obtained by quenching, is unstable at room temperature.

Takeuchi, Nishi, Maki (15) essentially agree with Regourd et al.'s(13)(14) results and showed by a crystallographic study that the orthorombic phase II was actually monoclinic with $P2_1/a$ spatial group and the tetragonal phase was actually orthorombic.

Tavasci, Massazza and Costa (16) studied in their turn the relationships between orthorombic and monoclinic phases and found that there is a narrow two-phase area between them. This area has a common point at 550°C corresponding to the NC_8A_3 compound, which surely exists.

Lee, Banda and Glasser (17), determined the combined role of Na^+ and Fe^{+++} replaced in C_3A and proved that the orthorombic phase II is stabilized by high sodium and iron contents.

The same Authors essentially accept the existence of the NC_8A_3 phase: "since the orthorombic solid solutions extend up to the NC_8A_3 composition, we accept that C_3A and NC_8A_3 are two distinctly different phases". Moreover, in agreement with Takeuchi et al. (15), they maintain that the tetragonal phase is actually orthorombic.

1.4. It is known that the exact compostion and stability of $C_{12}A_7$ were and still are the subject of disagreement and dispute. However, it is ascertained that only traces of oxygen or humidity are enough to stabilize a phase of this type, containing hydroxyl ions or peroxidic oxygen in its own lattice (18). Therefore, to the purpose of this study, this aluminate was considered as a stable phase in the $CaO-Al_2O_3$ system.

2. EXPERIMENTAL RESULTS

2.1. Working modes

The work was carried out on samples obtained by firing mixes of r.g. $CaCO_3$, Al_2O_3, Na_2CO_3. The mixes were made by homogenizing the components under cyclohexane in an agathe jar mill. After the cyclohexane evaporation, the mixes were dried and calcined at 950°C for one hour, pelletized and fired twice, with

* The standard nomenclature of the chemistry of cement is used: C = CaO, A = Al_2O_3, F = Fe_2O_3, N = Na_2O

an intermediate grinding, for 24 hours at 1200°C. To avoid losses caused by the sodium volatility, it was necessary to introduce the pellets into small platinum cylinders that were then welded at atmospheric pressure.

After firing, the sodium content was checked by atomic absorption spectrophotometry.

The phases in the fired samples were determined by X-ray diffractometry and optical microscopy.

2.2. Results

The presence of many solid solutions and singular points in the same made the study of the equilibrium relations inside this system rather complicated.

The mineralogical examination of the numerous samples allowed the phase diagram of the CaO-C_2F-$C_{12}A_7$-$N_2C_3A_5$-NA subsystem to be drawn.

The relationships between the different phases and the singular points of the solid solutions, defined at 1200°C, are shown in the phase diagram of figure 1.

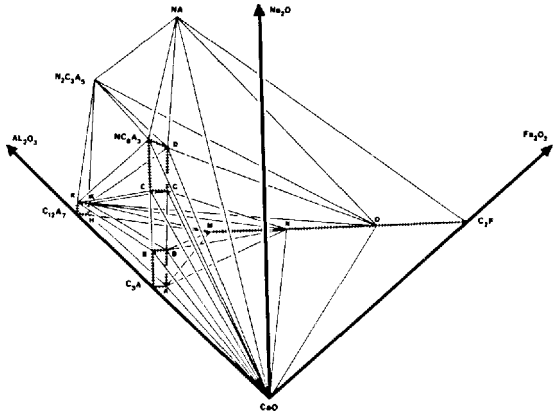

Fig. 1

The compositions of the solid solutions and the singular points here illustrated are summarized in table I. The composition of points A, H, B', C', M, N, and NC_8A_3 was derived from previous works (4) (5) (13)(19). From figures 1-2 it results that the phase diagram can be subdivided into the volumes briefly described later on.

1) CaO-A-B-B'-C_3A
2) CaO-B-B'-C'-C
3) CaO-C-C'-NC_8A_3-D
4) CaO-NC_8A_3-D-NA
5) C_3A-A-B-B'-K'-K-H-$C_{12}A_7$
6) B'-B-C-C'-K'-K
7) C'-C-D-NC_8A_3-K'-K
8) NC_8A_3-D-K-K'-$N_2C_3A_5$
9) NC_8A_3-D-$N_2C_3A_5$-NA
10) CaO-A-B-N
11) CaO-B-C-N
12) CaO-C-D-O-N
13) CaO-D-NA-O
14) CaO-C_2F-O-NA
15) A-B-M-N
16) A-B-K-H-M
17) B-N-K-M
18) B-N-K-C
19) C-D-O-N-K
20) K-O-$N_2C_3A_5$-D
21) $N_2C_3A_5$-D-NA-O

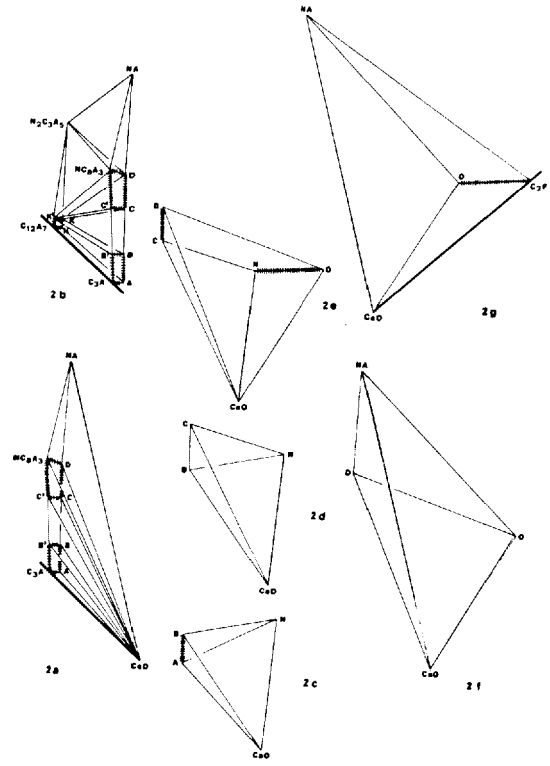

Fig. 2

2.2.1. CaO-C_3A-NC_8A_3-NA-D-A- volume

This subsystem (fig. 2a) includes four volumes characterized by the constant presence of CaO in equilibrium with tricalcium aluminate containing varying amounts of Na_2O and Fe_2O_3 in solid solution (C_3A_{ss}).

To define the compositions of the B,C,D solid solution limits suitable mixes were prepared in the C_3A-"N_3A"-"F_3A" plane. The results are given in table 1.

C_3A_{ss} with composition lying inside the C_3A-A-B-B' plane always shows a cubic symmetry, whereas that lying on the C'-C straight line has an orthorombic sym-

metry.

However, as the Na_2O content increases, the lines 400 and 040 of the orthorombic lattice tend to approach each other and they cannot be distinguished when the C_3A_{ss} composition corresponds to that of point D. This fact is visible in the X-ray diffraction patterns of fig. 3 obtained by using a Guinier de Wolff camera.

Therefore C_3A_{ss} with the composition of point D shows an X-ray diffraction pattern like that given by Regourd et al. (13) for the tetragonal phase.

The mixes having a higher sodium content than that of point D are no longer single-phase but, depending on the composition, they contain $N_2C_3A_5$, NA and another calcium aluminoferrite of varying composition as equilibrium phases.

2.2.2. C_3A-NC_8A_3-$N_2C_3A_5$-$C_{12}A_7$-H-A-D-NA volume

It was ascertained by electron microprobe that $C_{12}A_7$ can dissolve small amounts of Fe_2O_3 and Na_2O in its crystalline lattice. The composition of the K and K' singular points is given in table 1.

The subsystem shown in fig. 2b is made up of five volumes.

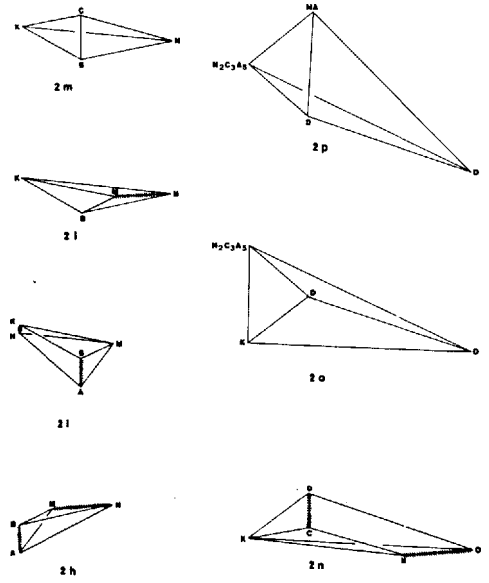

Fig. 2 bis

The C_3A-A-B-B'-K'-K-H-$C_{12}A_7$ volume is two-phase, since cubic C_3A_{ss} and $C_{12}A_{7ss}$ coexist.

On the contrary the B'-B-C-C'-K'-K volume is three-phase since, besides cubic C_3A_{ss} and $C_{12}A_{7ss}$, C_3A_{ss} with orthorombic I simmetry appears as an equilibrium phase.

The K'-K-C-C'-NC_8A_3-D is again two-phase since now, besides $C_{12}A_{7ss}$, only a C_3A_{ss} with a non-cubic symmetry is present.

In the two remaining volumes having a higher Na_2O content the non-cubic C_3A_{ss} is now in equilibrium with $C_{12}A_{7ss}$ and $N_2C_3A_5$ or with $N_2C_3A_5$ and NA.

2.2.3. CaO-A-B-N/CaO-B-C-N/CaO-C-D-O-N volumes

CaO is always present in these three subsystems as an equilibrium phase.

In the first three-phase tetrahedron (fig. 2c) the cubic C_3A_{ss} cohexists with CaO and C_4AF (point N). This can be seen in fig. 4 which shows the presence of three phases having a clearly different refractive index. In the second four-phase volume (fig. 2d), besides CaO, there are the solid solution limit of cubic C_3A (point B), the first non-cubic term of the same solid solution (point C) and C_4AF (point N).

In the third three-phase volume (fig. 2e) cubic C_3A is absent and the terms of the C-D and O-N solid solutions, together with CaO, are present (fig. 5)

From the above it results that non-cubic C_3A_{ss} can only cohexist with the terms included between C_3A_{ss} N and O of the aluminoferrite solid solution.

2.2.4. CaO-D-NA-O/CaO-NA-C_2F-O volumes

In the former of these subsystems (fig. 2f) C_3A_{ss} (point D) is in equilibrium with a calcium aluminoferrite having a composition which corresponds roughly to C_6AF_2 (point O). The other present phases are CaO and NA (fig. 6).

In the latter subsystem (fig. 2g) C_3A is no longer stable and the stable phases in its inside are CaO, NA and a calcium aluminoferrite with a varying composition included between C_6AF_2 and C_2F (fig. 7).

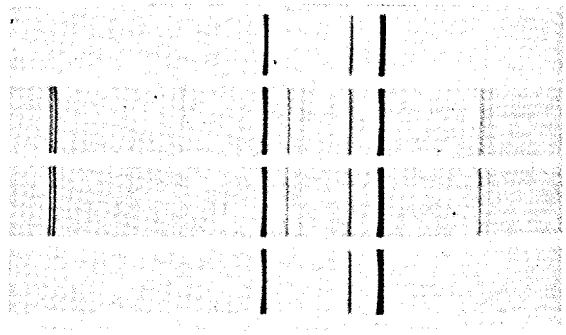

Fig. 3 - a. C_3A_{ss} with composition corresponding to point C
b. C_3A_{ss} with composition corresponding to point D

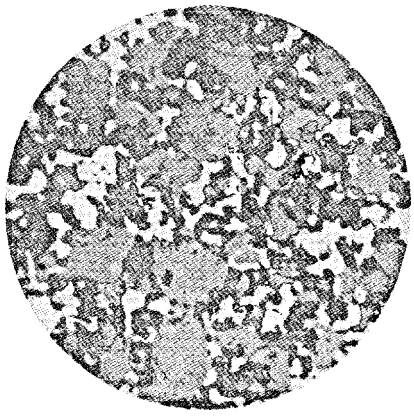

550X

Fig. 4 - CaO-A-B-N subsystem etched with alc. HNO_3. Ferrite: light - CaO: grey with dark boundary - C_3A_{ss}: grey

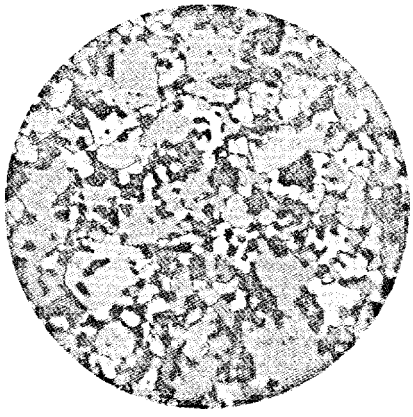

550X

Fig. 5 - CaO-C-D-O-N subsystem, etched with alc.HNO_3. Ferrite: light - CaO: grey with dark boundary - C_3A_{ss}: grey

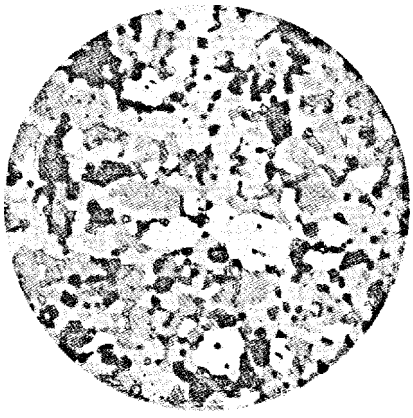

400X

Fig. 6 - CaO-D-NA-O subsystem, etched with alc. HNO_3. CaO: black-ferrite: light - C_3A_{ss}: light grey -NA: dark grey

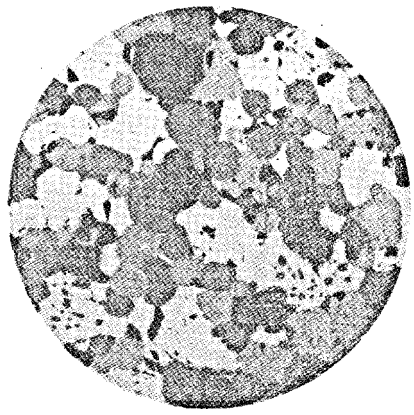

300X

Fig. 7 - CaO-C_2F-O-NA subsystem, unetched. Ferrite: light - CaO: light grey - NA: dark grey - pores: black

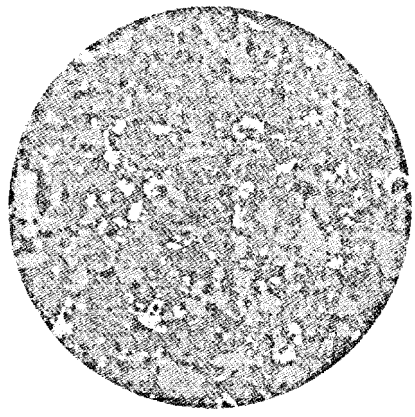

350X

Fig. 8 - A-B-K-H-M subsystem, etched with H_2O. Ferrite: light - C_3A_{ss}: dark grey - $C_{12}A_{7ss}$: grey

2.2.5. A-B-N-M/A-B-H-K-M volumes

In the former of these small volumes (fig. 2h) the terms included between A and B of the C_3A_{ss} cubic solid solution are in equilibrium with the terms of the aluminoferrite solid solution included between M and N. Therefore cubic C_3A is not stable in the presence of calcium aluminoferrites having a lower Al_2O_3 content than C_4AF.

The latter volume is three-phase (fig. 2i) since the last term of the C_2F - "C_2A" solid solution (point M) is in equilibrium with C_3A_{ss} (join A-B) and $C_{12}A_{7ss}$ (join H-K) (fig. 8).

2.2.6. B-N-K-M/B-C-K-N volumes

These two tetrahedra are adjacent through the B-K-N plane: the former (fig. 2l) is three-phase since the K and B solid solution limit are stable in the pre-

sence of calcium aluminoferrites having a composition included between M and N (fig. 9).

On the contrary the second volume (fig. 2m) is four-phase, the K,N,B and C solid solutions being present together.

2.2.7. C-D-O-N-K/K-D-O-$N_2C_3A_5$/NA-$N_2C_3A_5$-O-D volumes

The two first volumes were adjacent through the K-O-D plane (fig. 2n-2o). The first is three-phase and in its inside $C_{12}A_{7ss}$ (point K) is in equilibrium with the terms of the N-O-D-C two-phase surface (fig. 10).

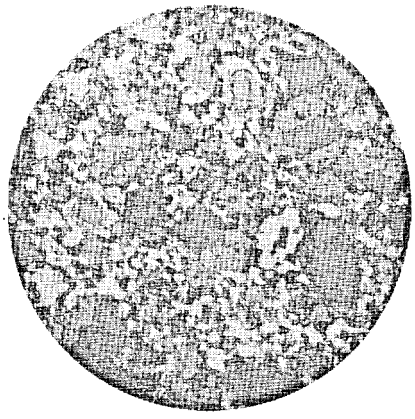

500X

Fig. 9 - B-N-K-M subsystem, etched with Nital. Ferrite: light - C_3A_{ss}:light grey with dark boundary - $C_{12}A_{7ss}$: dark grey

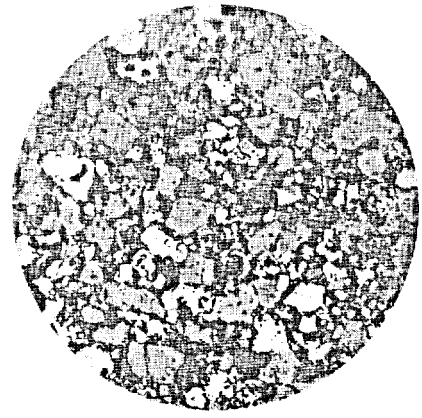

350X

Fig. 10 - C-D-O-N-K subsystem, unetched. Ferrite: light- C_3A_{ss} :grey - $C_{12}A_{7ss}$: dark grey

Table n° 1 - Composition of some phases present in the CaO-Al_2O_3-Fe_2O_3-Na_2O system

STOICHIOMETRIC FORMULAS	SYMBOLS	CHEMICAL COMPOSITION				REMARKS
		CaO	Al_2O_3	Fe_2O_3	Na_2O	
$C_3A_{0.94}F_{0.06}$	A (19)	61.48	35.02	3.50	-	Solid solution limit of "C_3F" in C_3A
$C_{2.917}N_{0.083}A_{0.94}F_{0.06}$	B	59.67	34.96	3.49	1.88	Cubic solid solution limit of Na^+ and Fe^{3+} in C_3A
$C_{2.917}N_{0.083}A$	B' (13)	60.43	37.67	-	1.90	Cubic solid solution limit of "N_3A" in C_3A
$C_{2.84}N_{0.16}A_{0.92}F_{0.08}$	C	57.75	34.02	4.63	3.60	Non-cubic solid solution of Na^+ and Fe^{3+} in C_3A
$C_{2.84}N_{0.16}A$	C' (13)	58.74	37.60	-	3.66	Non-cubic solid solution of "N_3A" in C_3A
$C_{2.75}N_{0.25}A_{0.90}F_{0.10}$	D	55.58	33.07	5.76	5.59	Solid solution limit of Na^+ and Fe^{3+} in C_3A
$C_{2.67}N_{0.33}A$	NC_8A_3 (5)	54.95	37.46	-	7.59	Solid solution limit of "N_3A" in C_3A
$C_{12}A_{6.8}F_{0.2}$	H (19)	48.13	49.59	2.28	-	Solid solution limit of "$C_{12}F_7$" in $C_{12}A_7$
$C_{11.5}N_{0.5}A_{6.8}F_{0.2}$	K *	46.03	49.48	2.28	2.21	Solid solution limit of Fe^{3+} and Na^+ in $C_{12}A_7$
$C_{11.5}N_{0.5}A_7$	K' *	46.41	51.36	-	2.23	Solid solution limit of "$N_{12}A_7$" in $C_{12}A_7$
$C_2A_{0.67}F_{0.33}$	M (4)	48.10	29.30	22.60	-	Solid solution limit of "C_2A" in C_2F
$C_2A_{0.5}F_{0.5}$	N (4)	46.16	20.98	32.86	-	Singular point of the solid solution C_2F-"C_2A"
$C_2A_{0.33}F_{0.67}$	O	44.37	13.31	47.37	-	Singular point of the solid solution C_2F-"C_2A"

* Composition determined by electron microprobe analysis

On the contrary, the second volume is four-phase since in its inside the D and K solid solution limits and the singular point O of the $C_2(A,F)$ solid solution are in equilibrium with $N_2C_3A_5$.

In the third volume (fig. 2p) the solid solution limit in C_3A (point D) is in equilibrium with the $N_2C_3A_5$, ^3NA compounds and with the singular point O. Therefore $C_{12}A_7$ containing Na_2O and Fe_2O_3 in solid solution extends its compatibility as far as this term, poor in Al_2O_3, of the aluminoferrite solid solution.

2.3. CONCLUSIONS

The results allow some conclusions to be drawn. The addition of Na_2O to mixes of CaO, Al_2O_3 and Fe_2O_3 does not essentially modify the equilibrium relationships between cubic tricalcium aluminate and calcium aluminoferrites.

In fact, the cubic C_3A_{ss} is only in equilibrium with the terms of the C_2F-"C_2A" solid solution included between C_4AF and C_6A_2F (M-N), as happens in the absence of sodium.

In fact the non-cubic solutions of C_3A are only compatibles with calcium aluminoferrites relatively poor in Al_2O_3, with composition included between N and O.

As regards $C_{12}A_7$, small percentages of Na_2O dissolved in its lattice extend its compatibility as fas as about C_6AF_2 (point O), whereas in the absence of sosium it is only stable with C_6A_2F (point M).

Neither $C_{12}A_{7ss}$ nor C_3A_{ss} are stable any longer beyond the CaO-O-NA-plane.

REFERENCES

1) T.F. NEWKIRK, R.D. THWAITE, J. Res. N.B.S., 1958, 61 (4), 1

2) A.J. MAJUMDAR, Trans. Brit. Ceram. Soc., 1965, 64 (2), 105

3) R.R. DAYAL, F.P. GLASSER, Proc. 3rd Conf. "Science of Ceramics", Vol. 3 (Bristol, July 1965), 191

4) D.H. LISTER, F.P. GLASSER, Trans. Brit. Ceram. Soc. 1967, 66 (7), 293

5) L.T. BROWNMILLER, R.H. BOGUE, Amer. J. Sci.,1932, 23 (138), 501

6) Y. SUZUKAWA, Zement Kalk Gips, 1956 (8), 345

7) A.E. MOORE, Nature, 1963, 199 (4892), 480

8) J.A. CONWICKE, D.E. DAY, J. Am. Ceram. Soc.,1964, 47 (2), 654

9) K.E. FLETCHER, H.G. MIDGLEY, A.E. MOORE, Mag. Concr. Res., 1965, 17 (53), 171

10) I. MAKI, M. NISHI, T. SUGIMURA, J. Ceram. Soc.Japan 1971, 79 (911), 241

11) S. CHROMY, M. GREGOR, Zement Kalk Gips, 1968 (11), 451

12) I. MAKI, Cem. Concr. Res., 1973, 3 (3), 295

13) M. REGOURD, S. CHROMY, L. HJORTH, B. MORTUREUX,A. GUINIER, J. Appl. Cryst., 1973, 6, 355

14) M. REGOURD, S. CHROMY, L. HJORTH, H. HORNAIN, B. MORTUREUX, Rev. Mat. Constr., 1973 (682), 7

15) Y. TAKEUCHI, F. NISHI, I. MAKI, Zeitschrift für Kristallographie, 1980, 152 (3/4), 259

16) B. TAVASCI, F. MASSAZZA, U. COSTA, 7th Int. Congr. Chem. Cem., Vol. IV (Paris, June-July 1980), 432

17) F.C. LEE, H.M. BANDA, F.P. GLASSER, Cem. Concr. Res., 1982, 12 (2), 237

18) C. BRISI, M. LUCCO BORLERA, Il Cemento, 1983 (3), 155

19) F. MASSAZZA, M. PEZZUOLI, C. GILIOLI, Rev. Mat. Constr., 1970 (663), 357

F. MASSAZZA, Professor of Applied Chemistry, Italcementi, Laboratorio Chimico Centrale, Bergamo, Italy
M. PEZZUOLI, Dr. of Chemistry, Italcementi, Laboratorio Chimico Centrale, Bergamo, Italy

1

INTERACTIONS BETWEEN ALKALINE VAPOURS AND COAL ASHES
INTERACTIONS ENTRE VAPEURS ALCALINES ET CENDRES DE CHARBON

1.2

SUMMARY

The consumption of coals in cement kilns is constantly increasing. Generally they have a considerable content in ashes (5-20 wt.%) which are obviously involved in the reactions occurring in the clinker burning.

Coal ashes brought to high temperature are capable of fixing high amounts of K_2O from atmospheres containing potassium carbonate or sulphate vapours.

The combined potash amount depends on the nature of the used salt, the temperature, the duration of the thermal treatment and, in particular, the preparation modes of the ash sample. These conditions mainly affect the absorption from a K_2SO_4 atmosphere. In fact in this case, to obtain consistent and reproducible results, it is necessary to standardize the porosity of these samples through a strong compaction under pressure (350 N/mm^2).

By working under these conditions, the amount of K_2O fixed by ashes was clearly higher at all the examined temperatures (between 1250 and 1450°C), in the presence of vapours from K_2CO_3.

After 60 minutes' treatment at 1450°C in the presence of K_2CO_3, K_2O absorption was higher than 32 wt.% with a lignite ash and tham 19 wt.% with a coal one. In the presence of K_2SO_4 the corresponding values were about 8 wt. % and 5 wt.% respectively. These values lower as the temperature and the duration of the thermal treatment decrease.

SUMÁRIO

O consumo de cargão nos fornos de cimento está constantemente aumentando. Geralmente eles possuem um considerável conteúdo de cinzas (5 – 20% em peso) que irão obviamente envolver-se nas realizações que ocorrem na queima do clínquer.

As cinzas do carvão levadas à altas temperaturas são capazes de fixar altas quantidades de K_2O de atmosferas contendo carbonato de potássio ou vapores de sulfato.

A quantidade combinada de potássio depende da natureza do sal utilizado, da temperatura, da duração do tratamento térmico e em particular da preparação da amostra de cinza. As condições principalmente afetam a absorção de uma atmosfera de K_2, SO_4. De fato neste caso, para obter resultados consistentes e reproduzíveis, é necessário estandardizar a pôrosidade destas amostras através de uma forte comparação sob pressão (350 N/mm^2).

Ao trabalho sob essas condições, a quantidade de K_2O fixado pelas cinzas foi claramente maior em todas as temperaturas examinadas (entre 1250 e 1450°C), na presença de vapores de K_2CO_3.

Após tratamento de 60 minutos a 1450°C na presença de K_2CO_3, a absorção de K_2O foi maior que 32% em peso com um cinza de linhito e que 19% com uma de carvão. Na presença de K_2SO_4 os valorês correspondentes foram de aproximadamente de 8% e 5% em peso respectivamente.

Estes valores diminuiram à medida que a duração do tratamento térmico diminui.

INTERACTIONS BETWEEN ALKALINE VAPOURS AND COAL ASHES

1. INTRODUCTION

The literature (1)(2) and a previous work (3) pointed out that the coal ash coatings forming in cement rotary kilns have high alkali contents, especially K_2O. High potash contents correspond to the presence of phases rich in potassium (kaliophilite, leucite, feldspar).

A recent work (4) showed that the enrichment in potash could be attributed to an interaction, in the burning zone, between fuel ashes and alkaline vapours present in the kiln atmosphere. In fact, the tests performed to confirm this assumption showed that the alkaline vapours from the potassium sulphate or carbonate vaporization react with the coal ashes, however in different ways.

As a matter of fact, in the presence of K_2CO_3 vapours, all the examined ashes absorbed regularly increasing amounts of K_2O as a function of the process temperature (from 1250°C to 1450°C). Nevertheless, with K_2SO_4, the K_2O absorption increased from 1250 to 1350°C but it varied irregularly between 1350 and 1450°C.

The phenomenon of the potash absorption by ashes is examined again in this work which shows the results of the research performed to explain the anomalies found in the absorption of K_2O from K_2SO_4.

2. EXPERIMENTAL

2.1. Materials

The tests were performed on the ashes of two solid coals of different origin, a lignite from Sulcis coal field (Sardinia, Italy) (S) and a lithanthrax from South Africa (M). Ashes were obtained by burning the coals at 815°C, according to the procedure provided by ISO Standards (5). Their chemical composition is given in table 1.

The two ashes had a BET specific surface of 2.94 and 3.01 $m^2.g^{-1}$ respectively and a porosity, determined by N_2 adsorption, prevailingly formed of pores having radius less than 3-4 nm.

Reagent grade potassium sulphate and carbonate were used as a source of potassium vapours.

2.2. Thermal treatments

The two ashes were exposed to alkaline vapours, for different times, at temperatures of 1250, 1300, 1350, 1400 and 1450°C, by following the working modes that will be explained later on.

2.3. Testing methods

The chemical analysis of the two ashes was carried out by X-ray fluorescence. The alkali contents of the thermally treated samples were determined by Atomic Absorption Spectrophotometry and the SO_3 ones did by semi-automatic pyrolytic analyzer.

The mineralogical analysis was based on X-ray diffraction but, in some cases, also microscopic examinations on powder under the mineralogical microscope were made.

3.RESULTS

3.1. Preliminary thermal treatments

The tests performed in a previous work (4) were repeated by defining the working modes better. 0.5 g of ash were put in a Pt container, laid on an upside-down Pt crucible, contained in its turn in another crucible of the same metal (see figure 1A).

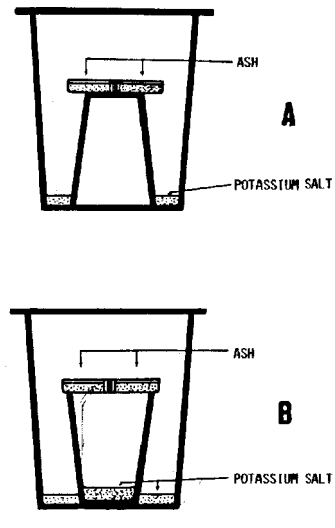

3 g of the potassium salt were put on the bottom of the latter. The crucible was covered with a Pt lid and the whole was introduced into the furnace at the prefixed temperature where it was left for 10-30-60 minutes.

Fig. 1 - Device for the ash heating in an environment containing potassium salt

3.2. Change in the chemical composition

After heating, the ash samples were analyzed to determine the K_2O, Na_2O and SO_3 content.
The results are given in tables 2 and 3 and, as regards K_2O, in figures 2 and 3.
These show that in both cases the absorption of K_2O from K_2CO_3 is an increasing function of both temperature and the treatment duration. The increase in K_2O content is accompanied by a quick decrease in the sulphur trioxide one.
The phenomenon is remarkable in the case of ash "S" that has a very high initial SO_3 content (18,23%).
Heating in an environment containing K_2SO_4 vapours generally causes a K_2O enrichment for the ashes, but the values cannot be related to a regular scheme. In any case the obtained results are similar to the previous ones (4).
At 1250°C and for burning times of 10 and 30 minutes, the sulphate vapours seem to be able to slow down the sulphur trioxide evaporation (ash "S") and even to cause a sligh SO_3 enrichment, in the case of ash "M".

	ASH "S"	ASH "M"
L.o.i.	1.68	0.51
SiO_2	24.89	50.03
Al_2O_3	12.21	34.14
Fe_2O_3	24.88	3.79
CaO	12.58	4.21
MgO	3.51	0.40
SO_3	18.23	1.75
Na_2O	0.51	0.10
K_2O	0.87	0.60
SrO	0.12	0.32
Mn_2O_3	0.04	0.02
P_2O_5	0.15	1.34
TiO_2	0.55	1.77
Acid moles / Basic moles	2.81	12.96
Soften. temp.	°C 1250	°C 1320
Fluid temp.	°C 1290	°C 1550

Table 1 - Composition of the coal ashes

3.3. Thermal treatments by different working modes

The results of figures 2A and 3A confirm that, in the presence of sulphate vapours, the K_2O absorption by ashes occurs with an irregular and quite unexpectable trend. Since, also at the end of the longer tests, a certain amount of salt was still present on the bottom of the crucible, it can be excluded that the observed anomalies are justified by an atmosphere not satured with potassium vapours.

By assuming that the working modes could affect the potassium vapour absorption, the inner arrangement of the support and the amount of potassium salt were changed and the following testing configurations were used:

a) inner upside-down support (see figure 1A) and 3 g of potassium salt introduced into the interspace between the two crucibles,

b) arrangement as above, but with 20 g of salt,

c) upright inner support (see figure 1B) and 3 g of potassium salt introduced into the interspace and the inner crucible,

d) arrangement as above, but with 20 g of salt.

	As receiv.	1250°C 10'	1250°C 30'	1250°C 60'	1300°C 10'	1300°C 30'	1300°C 60'	1350°C 10'	1350°C 30'	1350°C 60'	1400°C 10'	1400°C 30'	1400°C 60'	1450°C 10'	1450°C 30'	1450°C 60'
		IN THE PRESENCE OF K_2CO_3														
SO_3 %	18.23	0.58	0.52	0.42	0.22	0.32	0.20	0.12	0.05	0.03	0.05	0.06	0.05	0.02	0.03	0.02
Na_2O %	0.5	0.59	0.60	0.57	0.57	0.53	0.49	0.52	0.54	0.60	0.63	0.64	0.48	0.68	0.56	0.44
K_2O %	0.87	1.17	2.85	5.01	2.08	3.80	7.79	2.04	5.35	11.55	3.09	7.47	14.04	3.50	11.17	23.26
		IN THE PRESENCE OF K_2SO_4														
SO_3 %	18.23	13.83	10.75	7.64	4.80	0.87	2.50	0.87	0.79	0.52	2.05	0.50	0.01	0.37	0.03	0.01
Na_2O %	0.51	0.46	0.43	0.48	0.45	0.48	0.38	0.44	0.47	0.51	0.48	0.38	0.49	0.45	0.67	0.53
K_2O %	0.87	13.75	14.74	13.94	8.46	9.58	14.14	8.50	13.93	9.69	9.33	12.10	16.24	12.67	6.47	5.49

Table 2 - SO_3, Na_2O and K_2O contents of ash "S" as received and heated for increasing times in an atmosphere containing potassium salts

	As receiv.	1250°C 10'	1250°C 30'	1250°C 60'	1300°C 10	1300°C 30'	1300°C 60'	1350°C 10'	1350°C 30'	1350°C 60'	1400°C 10'	1400°C 30'	1400°C 60'	1450°C 10'	1450°C 30'	1450°C 60'
		IN THE PRESENCE OF K_2CO_3														
SO_3 %	1.75	0.03	0.04	0.06	0.03	0.05	0.04	0.03	0.02	0.05	0.04	0.01	0.06	0.01	0.01	0.02
Na_2O %	0.10	0.20	0.16	0.14	0.16	0.16	0.23	0.31	0.26	0.19	0.20	0.37	0.19	0.19	0.23	0.18
K_2O %	0.60	0.83	2.32	6.35	1.54	3.21	6.33	2.36	5.58	10.03	2.54	7.17	12.68	3.49	9.79	16.97
		IN THE PRESENCE OF K_2SO_4														
SO_3 %	1.75	3.99	4.80	0.90	1.25	0.63	0.87	1.27	1.23	0.20	0.12	0.01	0.12	0.58	0.01	0.01
Na_2O %	0.10	0.18	0.17	0.14	0.16	0.20	0.16	0.19	0.18	0.17	0.24	0.23	0.19	0.48	0.24	0.23
K_2O %	0.60	13.75	18.40	12.60	9.61	11.24	13.71	13.10	17.90	12.48	8.93	11.36	13.28	8.38	4.90	4.94

Table 3 - SO_3, Na_2O and K_2O contents of ash "M" as received and heated for increasing times in an atmosphere containing potassium salts

Ash	Determination	Testing modes a	b	c	d	Testing modes a	b	c	d
		in the presence of K_2SO_4				in the presence of K_2CO_3			
M	SO_3 %	0.01	tr.	tr.	tr.	0.02	-	-	tr.
	Na_2O %	0.16	0.16	0.16	0.16	0.18	-	-	0.12
	K_2O %	5.56	7.34	8.38	11.06	16.97	-	-	21.37
S	SO_3 %	0.02	0.03	0.03	tr.	0.02	-	-	tr.
	Na_2O %	0.57	0.56	0.58	0.59	0.44	-	-	0.26
	K_2O %	5.67	5.87	7.46	8.40	23.26	-	-	26.41

Table 4 - Alkali and SO_3 contents of tests performed at 1450°C for 1 h with different testing configurations

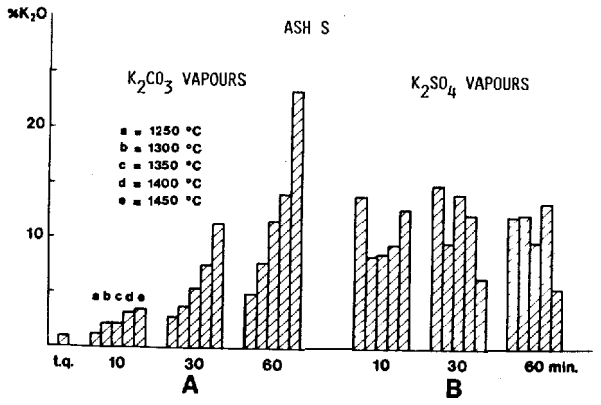

Fig. 2 - K_2O content of ash "S" as received and heated for increasing times in an atmosphere containing potassium salts

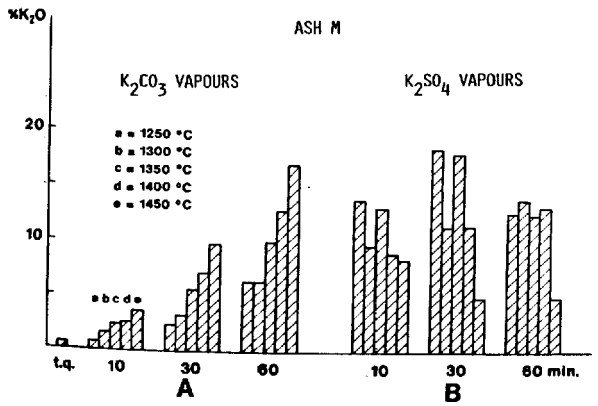

Fig. 3 - K_2O content of ash "M" as received and heated for incresing times in an atmosphere containing potassium salts

The obtained results, given in table 4 show that the testing modes have a strong influence on the absorption of K_2O from sulphate vapours, whereas they cause minor differences in the presence of K_2CO_3 vapours. It is pointless to remind that the tests were performed without aiming at reaching the equilibrium conditions.

4. DISCUSSION

4.1. At high temperature, K_2CO_3 evaporates and decomposes completely (6)(7)(8)(9)(10)(11)(12).

Some Authors (11) have found K^+ ions among the thermal decomposition products of K_2CO_3 and think that the carbonate decomposition occurs according to the reaction

$$K_2CO_3(l) \longrightarrow 2\,K(g) + CO_2(g) + \tfrac{1}{2}O_2(g) \qquad 1)$$

However, it is generally thought that decomposition occurs according to the following reaction:

$$K_2CO_3(l) \longrightarrow K_2O(g) + CO_2(g) \qquad 2)$$

This would be the primary reaction, whereas others, such as

$$K_2O(g) \longrightarrow 2K(g) + \tfrac{1}{2}O_2(g) \qquad 3)$$

would take place later on (10). This sequence is in agreement with the analytical data obtained by a mass spectrometer that allowed the presence of CO^+, K^+, CO_2^+ and K_2O^+ to be detected.

Without going into these complex thermodynamic problems, to the purposes of this study it is sufficient to observe that, at the temperatures reached in the present study, potassium carbonate has appreciable vapour and decomposition tensions (see table 5).

4.2. At the same temperatures, potassium sulphate has a lower vapour pressure and the vaporized fraction, contrarily to carbonate, decomposes only partially. According to some Authors, the evaporation would occur only in the completely indissociated form (12),

$$K_2SO_4(l) \longrightarrow K_2SO_4(g) \qquad 4)$$

However, it is a largely shared opinion that volatilization is accompanied by a partial decomposition with formation of metallic potassium vapours (13)(14)(15)(16), according to the equation

$$K_2SO_4(g) \rightleftharpoons 2K(g) + SO_2(g) + O_2(g) \qquad 5)$$

or with the intermediate formation of K_2O (10)

$$K_2SO_4(g) \rightleftharpoons K_2O(g) + SO_2(g) + \tfrac{1}{2}O_2(g) \qquad 6)$$

Also in this case the formation of K would constitute a following evolution of the system and reaction 6) would be primary (10).

As the temperature rises, both the partial pressure of undissociated K_2SO_4 and that of its dissociation products (see table 5) increase. At the temperatures attained during this work, the undissociated sulphate prevails clearly in the vapour phase (15).

Table 5 also shows that the saturated vapour pressure of K_2SO_4 is lower by about one order of magnitude than that of K_2CO_3.

Temperature • C	K_2CO_3			K_2SO_4					
				P_i	P_d			P_i	P_d
1250	11.7	11.2	63.8	0.3	0.2	1.7	0.8	0.8	0.2
1300	15.1	20.9	109.9	0.6	1.0	3.2	1.5	1.4	0.4
1350	19.6	37.2	183.7	1.0	4.5	5.8	2.7	2.5	0.7
1400	35.6	-	297.2	1.7	18.0	-	4.6	4.3	1.5
Ref.	(8)	(12)	(10)	(10)		(12)	(15)	(16)	

P_i = vapour pressure of the undissociated salt
P_d = vapour pressure of the dissociation products

Table 5 - Vapour pressure P_i and dissociation pressure P_d of potassium carbonate and sulphate - mm_{Hg}

4.3. The K_2SO_4 vaporization at the molecular state can explain the irregularities found in the potash absorption (see figures 2B and 3B) and the higher combined amount with respect to when K_2CO_3 is present (see figure 2A and 3A), although the vapour pressure of sulphate is much lower than that of carbonate.

As known, the vapour tension of a liquid is affected by the bending of its surface and, in particular, the vapour pressure of a liquid contained in a capillary pore (p) is lower than that of a plane surface (p_o). Their ratio can be calculated by the equation:

$$\ln \frac{p}{p_o} = - \frac{2\gamma}{r\varrho} \frac{M}{RT}$$

where:
M is the molecular weight of vapour
r is the pore diameter
ϱ is the density of liquid
γ is the surface tension of liquid.

The ash particles have pores having sizes below 3-4 nm, that is they can favour the condensation in their inside of the undissociated potassium sulphate vapours present in the atmosphere.
Once condensed, K_2SO_4 reacts much more efficaciously and quickly than the vapours, diluted by air.

The ashes were put in the crucible without considering their higher or lower degree of agglomeration and this favoured, differently from sample to sample, the penetration and condensation of potassium sulphate.

Finally, if it is considered that the thermal treatments of ashes were not performed as far as the attainment of the chemical equilibrium, but for constant and limited times, the irregular absorption of potash from sulphate vapours becomes understandable.

The K_2SO_4 condensation on ashes was proved by the mineralogical examination since the samples heated at the lower temperatures in a sulphate environment often contained arcanite (K_2SO_4). In the case of ash S, rich in anhydrite, calcium langbeinite ($2CaSO_4.K_2SO_4$) is also present. Both arcanite and calcium langbeinite, that crystallizes from a liquid containing K_2SO_4 and $CaSO_4$ (17), are absent in the samples treated at temperatures above 1300°C. However, this does not exclude that also in these cases condensation phenomena inside the thinnest pores had occurred. These remarks lead to conclude that, to have consistent and reproducible results when potassium sulphate is present, it is necessary to check the sample porosity as much as possible.

4.4. To comply with this condition, 0.4 g of ash were pelletized under a pressure of about 3500 kg/cm^2 and disks about 1.5 mm high and with a diameter of about 14 mm were obtained. By using these disks the tests shown in figures 2 and 3 were repeated. The K_2O amounts measured in the so treated ashes are given in figures 4 and 5 and, together with those of Na_2O and SO_3, in tables 6 and 7.

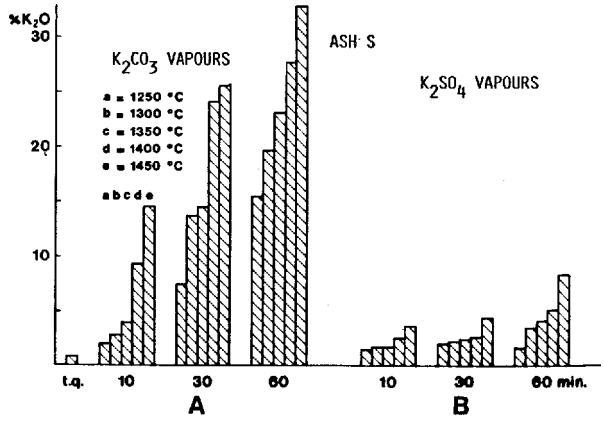

Fig. 4 - K_2O content of ash "S" as received and heated after pelletization for increasing times in an atmosphere containing potassium salts

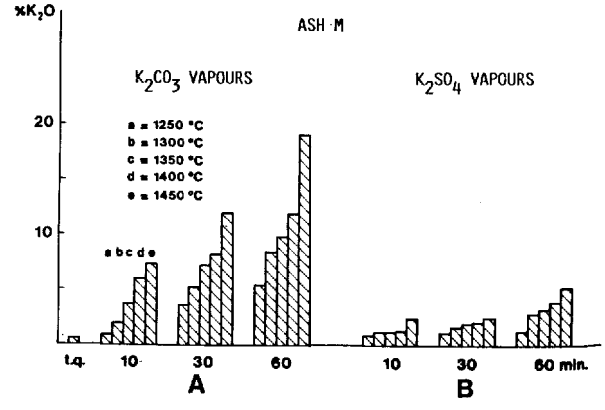

Fig. 5 - K_2O content in ash "M" as received and heated after pelletization for increasing times in an atmosphere containing potassium salts

As regards the potash absorbed from carbonate vapours, the trends observed in the previous tests are confirmed, whereas that absorbed from the sulphate vapours

shows a quite regular behaviour.

	As receiv.	IN THE PRESENCE OF K_2CO_3														
		1250°C			1300°C			1350°C			1400°C			1450°C		
		10'	30'	60'	10'	30'	60'	10'	30'	60'	10'	30'	60'	10'	30'	60'
SO_3 %	18.23	0.92	1.06	0.36	0.44	0.32	0.56	0.13	0.08	0.02	0.12	0.04	0.08	0.09	0.02	0.01
Na_2O %	0.51	n.d.	n.d.	n.d.	n.d.	n.d.	n.d.	n.d.	n.d.	n.d.	n.d.	n.d.	n.d.	n.d.	n.d.	n.d.
K_2O %	0.87	2.06	7.43	15.38	2.81	13.72	19.55	3.90	14.44	22.98	9.32	24.01	27.62	14.44	25.32	32.70
		IN THE PRESENCE OF K_2SO_4														
SO_3 %	18.23	1.42	0.95	0.96	0.54	0.46	0.29	0.47	0.16	0.16	0.49	0.03	0.01	0.02	0.02	0.01
Na_2O %	0.51	n.d.	n.d.	n.d.	n.d.	n.d.	n.d.	n.d.	n.d.	n.d.	n.d.	n.d.	n.d.	n.d.	n.d.	n.d.
K_2O %	0.87	1.37	1.78	1.66	1.66	2.19	3.35	1.65	2.32	4.10	2.49	2.65	5.21	3.55	4.36	8.18

Table 6 - SO_3, Na_2O and K_2O contents of ash "S" compacted under 3500 kg/cm^2 and heated for increasing times in an environment containing potassium salts

	As receiv.	IN THE PRESENCE OF K_2CO_3														
		1250°C			1300°C			1350°C			1400°C			1450°C		
		10'	30'	60'	10'	30'	60'	10'	30'	60'	10'	30'	60'	10'	30'	60'
SO_3 %	1.75	0.02	0.04	0.03	0.03	0.02	0.05	0.05	0.06	0.03	0.04	0.05	0.06	0.19	0.02	0.01
Na_2O %	0.10	n.d.	n.d.	n.d.	n.d.	n.d.	n.d.	n.d.	n.d.	n.d.	n.d.	n.d.	n.d.	n.d.	n.d.	n.d.
K_2O %	0.60	1.00	3.61	5.52	2.07	5.28	8.48	3.69	7.26	9.91	6.03	8.23	11.94	7.28	11.99	19.20
		IN THE PRESENCE OF K_2SO_4														
SO_3 %	1.75	0.02	0.02	0.01	0.01	0.01	0.01	0.02	0.01	0.01	0.02	0.01	0.01	0.08	0.01	0.01
Na_2O %	0.10	n.d.	n.d.	n.d.	n.d.	n.d.	n.d.	n.d.	n.d.	n.d.	n.d.	n.d.	n.d.	n.d.	n.d.	n.d.
K_2O %	0.60	0.90	1.19	1.40	1.24	1.76	2.98	1.19	2.05	3.40	1.37	2.21	3.94	2.48	2.61	5.32

Table 7 - SO_3, Na_2O and K_2O contents of ash "M" compacted under 3500 kg/cm^2 and heated for increasing times in an environment containing potassium salts

The K_2O amount fixed under these conditions in a sulphate environment is lower than that found in a carbonate environment but, above all, much lower than that fixed by the loose ashes (see figures 2 and 3). These two facts can be interpreted by the same mechanism.

The condensation of the potassium sulphate vapours in the ash pores is hindered by the compactness of the pellet and the phenomenon remains limited to the surface pores which are therefore quickly obstructed.

By using pellets, only the interaction between potassium vapours and ashes can occur. Since the K_2CO_3 volatility is higher than that of K_2SO_4, the ashes will absorb more K_2O from the atmosphere containing K_2CO_3 vapours. The pelletized ashes, heated in the presence of potassium carbonate vapours, almost always fix a higher amount of K_2O than the loose ones. This phenomenon was not studied in this work.

5. CONCLUSIONS

The tests confirmed the strong tendency of coal ashes to combine the potash from the evaporation of K_2CO_3 and K_2SO_4.

By standardizing the external surface of ashes through a vigorous compaction under pressure, the irregularities in the potash absorption found when the ash heating occurs in an environment containing potassium sulphate have disappeared.

Under these conditions the K_2O absorption is lower than that observed with loose ashes and that ascertained when the environment contains potassium carbonate, consistently with the higher vapour pressure of this salt with respect to K_2SO_4. This difference is attributed to the more limited condensation of the K_2SO_4 vapours in the smallest pores of the ash.

This result is in agreement with what found in the practice, that is an equilibrated ratio between alkalis and SO_3 prevents efficaciously deposits and coatings from forming in the cement kilns (18)(19).

The alkali absorption in the coal ashes and in the coatings present in cement kilns is a complex process which depends not only on the concentration of the alkaline element but also on the composition of the atmosphere and the materials present in the kiln, the structure of the solid phases, a.s.o.

REFERENCES

1) ALEGRE, R., Rev. Mat. Constr. (509), 1958, 33-44

2) FOREST, J., Rev. Mat. Constr. (607), (608), 1966, 137-150, 195-201

3) MASSAZZA, F., PEZZUOLI, M., GILIOLI, C., I Materiali per l'Ingegneria, Atti del 1° Convegno Nazionale ASMI (Milano, 1983), 485-496

4) MASSAZZA, F., PEZZUOLI, M., AITEC 25°: Il Cemento e il Calcestruzzo negli Anni '80 (Parma, 17-18 ottobre 1985), 59-68

5) ISO 1171, Combustibles minéraux solides - Détermination des Cendres, 1985

6) LEBEAU, P., Ann. Chim. Phys., 6, 1905, 426

7) JACKSON, D.D., MORGAN, J.J., Ind. & Eng. Chem., 13 (2), 1921, 110-118

8) HOWARTH, J.T., TURNER, W.E.S., J. Soc. Glass Technol. 15, 1931, 360-364

9) KROGER, C., STRATMAN, J., Glastechn. Ber., 34, 1961, 311-320

10) KOSUGI, T., Bull. Chem. Soc. Jap., 45 (1), 1972, 15-19

11) GOROKHOV, L.N., Proc. 3rd Int. Symp. on High Temp. Technology, Butterworths, London, 1967

12) DUBOIS, J., MILLET, J., Compte Rendus des Séances de l'Académie des Sciences, vol. 256, Serie C, 1968, 852-855

13) FICALORA, P.J., UY, O.M., MEUNOW, D.W., MARGRAVE, J.L., J. Am. Ceram. Soc., 51 (10), 1968, 574-577

14) HALSTEAD, W.D., Transactions of the Faraday Society, 66 (572), 1970, 1966-1973

15) ELIEZER, I., HOWALD, R.A., The J. Chem. Phys., 65, (8), 1976, 3053-3062

16) LAU, K.H., CUBICCIOTTI, D., HILDENBRAND, D.L., J. Electrochem. Soc., 126 (1), 1979, 490-495

17) ROWE, J.J., MOREY, G.W., HANSEN, I.D., J. Inorg. Nucl. Chem., 27 (1), 1965, 53-58

18) GARRETT, H.M., Mining Engineering, 32 (2), 1980, 188-198

19) BUCCHI, R., World Cement Technology, 12 (5) (6), 1981, 210-231, 258-273

U. COSTA, *Dr. of Chemistry - Italcementi, Laboratorio Chimico Centrale, Bergamo, Italy*
F. MASSAZZA, *Professor of Applied Chemistry - Italcementi, Laboratorio Chimico Centrale, Bergamo, Italy*

1

INFLUENCE OF THE BURNING DEGREE ON THE RHEOLOGICAL AND STRENGTH PROPERTIES OF CLINKERS

1.2

Influence du degré de cuisson sur les propriétés rhéologiques et de résistance de clinkers

SUMMARY

Clinker obtained by burning 8 industrial raw meals and a mixture of r.g. SiO_2, Al_2O_3, Fe_2O_3 and $CaCO_3$ were prepared in the laboratory.

By changing the heating time, three clinker samples characterized by a different burning degree were made from each raw mix. As this parameter increased, variations of the chemical composition and morphology were observed in the main constituents of clinker. The loss of the most volatile elements and the increase in the sizes of alite and belite crystals were the most evident phenomena.

In some cases the reactivity of the aluminate phases reduced as the burning degree increased, in others it remained unaltered, whereas the alite reactivity showed a general reduction. The reactivity variations corresponded to changes in the rheology and mechanical strengths of the cement pastes.

When the burning degree increase caused a reactivity reduction of the aluminate phases, rheology improved.

The reduction in the alite reactivity involved in its turn the decrease in early strengths.

Foram preparados em laboratório clínqueres obtidos por queima de 8 farinhas industriais e uma mistura de r. g. SiO_2, Al_2O_3, Fe_2O_3 e $CaCO_3$.

De cada mistura crua, mudando o tempo de aquecimento, foram feitas três amostras de clinquer caracterizadas por diferente grau de queima. Na medida em que este parâmetro aumentou, foram observadas variações da composição química e da morfologia nos constituintes principais do clinquer. Os fenômenos mais evidentes foram a perda de grande parte dos elementos voláteis e o aumento nos tamanhos dos cristais de alita e belita.

Em alguns casos a reatividade das fases de aluminato se reduziram, na medida em que cresceu o grau de queima; em outros ela permaneceu inalterada, enquanto a reatividade da alita apresentou uma redução geral. As variações da reatividade correspondem a mudanças na reologia e nas resistências mecânicas das pastas de cimento.

Quando o grau de queima aumentou, causou uma redução da reatividade das fases de aluminato, a reologia melhorou.

A redução da reatividade da alita implicou por sua vez na diminuição das resistências iniciais.

1. INTRODUCTION

Important properties of mortars and concretes such as workability and early mechanical strengths, depend on the initial stages of the cement hydration process.
This process is affected by the chemical composition and reactivity of clinker (1)(2), the nature of set retarders (3) and hydraulic active or inert additions (4)(5).

Among the factors determining the clinker reactivity an important role was attributed to the joint effect of the burning temperature and duration. In fact these parameters affect composition, structure and morphology of the clinker phase crystals (6).
If burning is prolonged, the larger alite and belite crystals grow to the detriment of the small ones. The growth process is accompanied by an appreciable decrease in the foreign ions present in the lattices of the two constituents and, sometimes, by changes in the crystal simmetry (7). The growth kinetics is conditioned by the amount and viscosity of the liquid phase (8).
As regards the rheological and mechanical performances of the oil well cements, an important role was ascribed to some features of the crystals, such as shape regularity and size (9)(10).

This paper gives the preliminary results of a study undertaken to emphasize the consequences of different burning degrees of clinker on the rheological and mechanical properties of pastes.

2. EXPERIMENTAL

2.1 Materials

Clinkers were prepared by using 8 industrial raw meals from different plants having C_3A content (according to Newkirck) ranging between 6 and 13%.
A clinker, n° 9, prepared with r.g. $CaCO_3$, SiO_2, Al_2O_3 and Fe_2O_3 was utilized as a control sample.
As all the plants used coal for burning clinkers, the lime saturation factors of the industrial raw meals generally exceeded the value of 0.95 to balance the contribution of coal ashes. For this reason the saturation factors were corrected in the laboratory, by adding a fly ash, to the standard value of 0.90.
The raw meal finenesses gave the following oversizes on the average: 40μ-35%; 63μ-23%; 90μ-12%; 200μ-1%.
Before burning the mixes were pelletized under a pressure of 100 N/mm^2 in pellets having a 2 cm diameter and a 10 g mass.

The clinker burning (150 g) was made in an electric laboratory furnace according to a heat cycle including a decarbonation isothermal treatment at 950°C for 1 hour; a heating stage from 950° to 1450°C for 1.5 hours; a final treatment at the temperature of 1450°C for duration of 1, 3 or 6 hours. At the end of the treatment the material was air-quenched by pouring it on a wire net hit by an air jet.

The clinkerization rate increases exponentially with the difference between the burning (T_{max}) and the critical alite formation temperatures ($T_o \simeq 1250$°C) and proportionally with the burning time (t).

Therefore the burning degree can be expressed by the relation

$$F = a \cdot t \exp\left(b(T_{max} - T_o)\right)$$

where **a** and **b** are constants (11).
As a consequence it can be thought that since T_{max} (1450°C) and T_o (1250°C) were fixed, the burning degree is proportional to t.

The clinkers were crushed to a maximum size of 2 mm, and then they were ground with the optimum amounts of gypsum, varying from 3 to 6%. Grinding was performed in a laboratory agatha jar mill to a fineness of about 3000 cm^2/g (Blaine).

2.2 Characterization of clinkers and cements

The samples were submitted to chemical analysis, microscopic observations by reflected light and X-ray diffraction analysis to point out the differences in composition, morphology and crystalline structure due to the thermal treatment.

The BET specific surface measurement was carried out since it gives information on the sintering degree of clinker and affects the rheology and the initial reactivity of cements.

The initial reactivity of cements was determined by measuring the heat evolved during the first 24 hours' hydration. The used conduction calorimeter allowed the measurement of the heat evolved starting from the contact between cement and water (12).

Strength was determined on cubic paste specimens having the side of 1.73 mm. The paste was made at a w/c ratio = 0.4 by using a small blade mixer. The cement (60 g) was added to the water (24 g) kept in slow shaking, in the space of 1 min. After a minute of stop, mixing was resumed with a speed of 600 rev/min for 1 min. Afterwards the paste was transferred into a suitable mould and compacted by vibration.
The specimens were demoulded after 24 hours and water-cured. The compressive strength was determined immediately after demoulding and after 28 days. Each value represents the average of at least 2 measurements.

A portion of the paste prepared for the mechanical tests was used also to determine the flow curves by the rotational viscometer HAAKE RV2 equipped with SVIIP measurement system. The rheological measurements started 6 min after the mixing had begun. The decreasing step procedure was adopted in the tests (13).

The maximum speed of the rotor was changed from 512 to 8 rev/min in 6 steps. The rotation speed was manually reduced by half when the shear stress took a constant value.

3. RESULTS

3.1 Characteristics of clinkers

Tables 1-9 give the chemical composition of clinkers. As regards the composition ratios, it can be observed that the clinkers reveal very slight differences in

L.S.F. and, therefore, in the hydraulic modulus. On the contrary, the silica modulus varies from 2.4 to 3 and the iron modulus from 0.75 to 2.70.
The burning time prolongation causes a general reduction in the more volatile elements (Na, K, S and Pb). The potassium concentration reduces by about 50% when the thermal treatment time passes from 1 to 6 hours, whereas the sodium volatilization is more limited and, in some cases, zero. The alkali loss corresponds to a SO_3 loss, above all in clinkers where this element is present in a higher concentration.

X-ray diffraction analysis did not point out any structural difference in the silicate phases of clinkers as a function of either the type of raw materials or the burning degree. In all cases alite appeared in the monoclinic crystalline form. Nevertheless, a systematic increase in the X-ray diffraction peaks of silicate was observed as the burning time lengthened. This was attributed to the improvement of the crystal lattice order.

The X-ray diffraction patterns carried out on the salicylic residues **(14)** showed that the tricalcium aluminate of clinkers 1,3,4,6 and 7 is prevailingly present in the anisotropic forms, in agreement with the low sulphate modulus **(15)** of these clinkers.

The microscopic observations showed that the alite and belite crystals are generally formed better and have sharper boundaries than those in industrial clinkers. Also in the interstitial phase a rather clear distinction was observed between ferrite and aluminate phases. This morphology is attributed to the quicker cooling of these clinkers than that of the industrial ones **(16)**. The crystal sizes was in any case similar to those observed in the industrial clinkers.
In some clinkers the sizes of the alite crystals exceed those of belite, in others the opposite occurs. Anyway the grading of the two phases varies in a rather large range, as can be observed in table 10 which gives the minimum and maximum sizes of crystals as a function of clinker type and burning time.
The table also shows the more frequent size. It is generally noticed that the crystal size tends to increase as the burning time prolongs. By extending heating from 1 to 6 hours, the average size of the cristals increases by 10-20 micronsfor alite, and by 10-30 micronsfor belite.

TABLE 10: Sizes of alite and belite crystals determined under the optical microscope

Clinker	Burning time (h)	Max size (μm)		Min. size (μm)		More frequent size (μm)	
		Alite	Belite	Alite	Belite	Alite	Belite
Clinker n° 1	1	65	50	<5	10	15-35	30
	3	80	65	5	15-20	20-25	40
	6	70	70	5-10	10	20-35	45-50
Clinker n° 2	1	75	40	5	5	25-30	20
	3	80	80	5-10	5-10	30-35	35-40
	6	120	80	10	15-20	45	50
Clinker n° 3	1	45	50	5	5	20	30
	3	45	60	5	5-10	25-30	35-40
	6	60	100	5	5-10	30	40
Clinker n° 4	1	50	60	<5	5-10	20-30	40
	3	50	60	5	10	20-25	40
	6	55	80	5	10	30	45-50
Clinker n° 5	1	60	70	<5	5	10-15	20
	3	80	90	5	5-10	20-30	35-40
	6	80	80	5	15-20	20	30
Clinker n° 6	1	40	50	<5	5	15-20	25
	3	60	55	5	5-10	20-25	30-35
	6	120	80	5	10	30	45
Clinker n° 7	1	50	55	<5	5-10	25	25
	3	60	75	5	10	20-25	30
	6	60	60	5-10	15-20	25-35	35-40
Clinker n° 8	1	80	60	5	5-10	20-30	35
	3	70	80	5	10	20-40	40
	6	80	80	5	10	25-45	45
Clinker n° 9	1	50	50	<5	5-10	20	30-35
	3	100	160	5	10	20-25	30
	6	120	120	5	10	30	50

3.2 Properties of cements

The composition and specific surface (BET and Blaine) of the cements are shown in table 11.
It can be seen that there is no correlation between the Blaine and BET specific surface values. In fact, the Blaine values range between 0.28-0.30 m^2/g whereas the BET specific surface values varies between 0.35 -0.80 m^2/g.

Obviously, not only the size of grains but also their porosity play an important role on this parameter. In fact, it is noted that a prolonged clinker burning causes a more or less marked reduction in the BET specific surface, since the clinker porosity decreases as a result of sintering. This porosity reduction was confirmed microscopically.

TABLE 11: Composition, specific surface and heat of hydration of cements

Composition	Spec.surf. BET (m^2/g)	Spec.surf. Blaine (m^2/g)	Hydr. heat after 1 h (J/g)	End induct. period (h)	Hydr.heat between 1 - 24 h (J/g)
Clinker 1(1h)+5% gypsum	0.63	0.2920	13.93	3.3	107
" (3h)+" "	0.63	0.2823	9.87	3.5	119
" (6h)+" "	0.63	0.2747	9.20	3.5	111
Clinker 2(1h)+4% gypsum	0.45	0.2877	13.43	1.8	149
" (3h)+" "	0.42	0.2831	10.37	1.7	149
" (6h)+" "	0.43	0.2906	8.58	2.1	143
Clinker 3(1h)+4% gypsum	0.61	0.3026	11.51	1.9	114
" (3h)+" "	0.37	0.2836	8.37	2.5	98
" (6h)+" "	0.37	0.2943	7.32	2.5	97
Clinker 4(1h)+5% gypsum	0.54	0.2876	9.46	1.7	98
" (3h)+" "	0.70	0.2952	9.87	2.8	99
" (6h)+" "	0.68	0.2944	9.56	4.4	90
Clinker 5(1h)+3% gypsum	0.54	0.3016	7.95	3	131
" (3h)+" "	0.53	0.2880	7.53	3.2	110
" (6h)+" "	0.50	0.2992	7.74	3.9	107
Clinker 6(1h)+4% gypsum	0.58	0.3185	12.66	2.1	120
" (3h)+" "	0.56	0.3129	15.06	1.9	126
" (6h)+" "	0.55	0.2993	15.10	2.1	119
Clinker 7(1h)+6% gypsum	0.76	0.3063	10.44	1.6	120
" (3h)+" "	0.64	0.3083	10.58	2.7	115
" (6h)+" "	0.78	0.3080	9.12	3.0	114
Clinker 8(1h)+4% gypsum	0.51	0.3167	10.06	4.5	104
" (3h)+" "	0.60	0.3202	7.03	5.0	98
" (6h)+" "	0.54	0.3220	5.56	5.5	86
Clinker 9(1h)+5% gypsum	0.70	0.3094	10.41	2.5	113
" (3h)+" "	0.63	0.3076	8.53	2.1	105
" (6h)+" "	0.64	0.2953	9.20	2.2	110

3.2.1 Initial reactivity

The heat evolved during the initial hydration of cement is shown in table 11. Figure 1 gives an example

of the heat flow curves relevant to cements made with clinker 5.

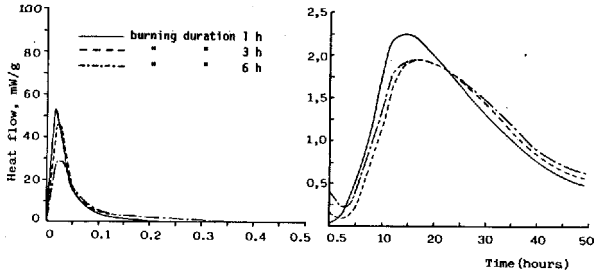

FIG. 1: Heat evolution rate curves relevant to the cements made with clinker n° 5

The heat evolved during the first hour of hydration is chiefly attributable to the reaction of the aluminate phases and the hydration of free lime. The heat released after the induction period mainly depends on the alite hydration. The values of table 11 show that the heat of hydration after 1 hour varies considerably as a function of both the clinker nature and the thermal treatment.

This heat evolution cannot be correlated with the BET specific surface values, as evidenced by clinker 1 and 2 that have different surfaces but develop the same heat of hydration.
Moreover cements from clinker 1, that have unchanging surface values as the burning time lengthens, display, an appreciable reduction in the evolved heat.

Cements from clinker 5 and 8 develop a lower amount of heat after 1 hour's hydration. This fact can be ascribed to their limited tricalcium aluminate and/or free lime contents. These samples, similarly to 4, 6 and 7, do not show changes in the evolved heat as the burning degree increases. In the remaining cements, the lowering of the evolved heat as a function of the burning degree is sometimes appreciable.

Since cements 7 have free lime contents similar to those of sample 1, it can be assumed that the differences found in the calorimetric data as a function of the burning degree are mainly attributable to chemical-physical changes. These concern the aluminate phase rather than a reduction in the free lime content.
The influence of the heat treatment on the alite reactivity is shown from both the induction period duration and the heat evolved between 1 and 24 hours. The induction period lengthening, caused by extention of the burning time, is very marked in the case of cements from clinker 4 (+ 2.7 h), whereas it is low in cements from clinker 1 (+ 0.2 h).

The heat evolved at 24 hours generally tends to reduce as the burning time prolongs.

3.2.2 Mechanical strength

The mechanical strength values of the cement pastes are given in table 12. The 24 hour-strength undergoes a generalized reduction by 17 to 50% as the burning time lengthens.

TABLE 12: Compressive strengths (N/mm^2)

Cements made with:	1 day			Δ(1h-6h) %	28 days			Δ(1h-6h) %
	t=1 h	t=3 h	t=6 h		t=1 h	t=3 h	t=6 h	
Clinker 1	10.8	10.0	7.6	-29.6	71.5	76.0	69.6	- 2.7
Clinker 2	16.8	16.5	13.9	-17.3	76.5	78.0	65.4	-14.5
Clinker 3	11.1	6.7	8.0	-27.9	85.6	74.0	81.4	- 4.9
Clinker 4	10.7	7.4	5.5	-48.6	86.5	83.1	78.1	- 9.7
Clinker 5	15.0	11.8	10.1	-32.7	88.0	87.1	79.8	- 9.3
Clinker 6	9.5	6.0	5.1	-46.3	85.6	92.0	95.7	+11.8
Clinker 7	10.5	8.9	6.6	-37.1	101.3	98.4	101.9	+ 0.6
Clinker 8	8.3	5.2	4.1	-50.6	71.4	71.6	65.6	- 8.1
Clinker 9	10.2	6.1	5.4	-47	79.8	73.6	75.7	- 5.1

t = burning time

The long-term strengths, even though they are less affected than those at 24 hours, reveal in any case a reduction ranging between 3 and 15%.
By comparing the strengths of the different cements, there appear substantial differences that increase as the burning time prolongs. Cements from clinkers 2 and 5 show clearly better early strengths than the others in agreement with the higher reactivity of alite detected calorimetrically. These two samples have some peculiarities as regards the chemical composition: in fact the former has high SrO and SO_3 contents, the latter a relatively high SO_3 content.

The remaining cements, except for number 8, show strength ranging in a very limited values. From this point of view also the cement made with pure reagents does not deviate from the others.

3.2.3 Rheology of pastes

Table 13 gives the yield stress (τ_0) and the initial viscosity (η_{in}) deduced from the flow curves relevant to the different cement pastes. The experimental values of "shear stress" (τ) and "shear rate" (D) were interpolated according to the parabolic equation:

$$D = \alpha\tau^2 + \beta\tau + \delta$$

The parameters α, β and δ allowed τ_0 and η_{in} to be calculated (17).
The fitting of the experimental points to this model is generally very good, as results qualitatively from the flow curves, shown in figure 2 as an example. The correlation coefficients were never below 0.9986.
The τ_0 values are more affected than the initial viscosity (η_{in}) by the burning time. When the heat treatment passes from 1 to 6 hours, some cements display a decrease in the "yield stress" and others have a constant rheological behaviour.

Most cements, even if they were made with different raw materials, show similar rheological parameters, at least after 1 hour's burning. Only cements from clinkers 1

TABLE 13: Rheological parameters of pastes

Cements made with:	t = 1 h		t = 3 h		t = 6 h	
	τ_o Pa	η_{in} Pa·s	τ_o Pa	η_{in} Pa·s	τ_o Pa	η_{in} Pa·s
Clinker 1	21.7	0.21	16.6	0.22	18.6	0.21
Clinker 2	18.6	0.22	17.5	0.22	16.9	0.14
Clinker 3	24.0	0.30	22.0	0.28	22.3	0.23
Clinker 4	18.8	0.24	21.7	0.25	18.4	0.24
Clinker 5	18.2	0.21	20.9	0.20	20.7	0.23
Clinker 6	18.9	0.24	21.3	0.28	16.4	0.30
Clinker 7	18.9	0.24	18.9	0.19	21.6	0.22
Clinker 8	18.1	0.23	19.2	0.18	19.1	0.19
Clinker 9	20.4	0.25	17.6	0.22	17.0	0.23

t = burning time
τ_o = yield stress
η_{in} = initial viscosity (shear rate D = 0)

and 3 have higher τ_o and η_{in} and therefore they give pastes with poorer rheological properties than the others. This could depend on the joint effect of a high tricalcium aluminate content and a high BET specific surface (18).

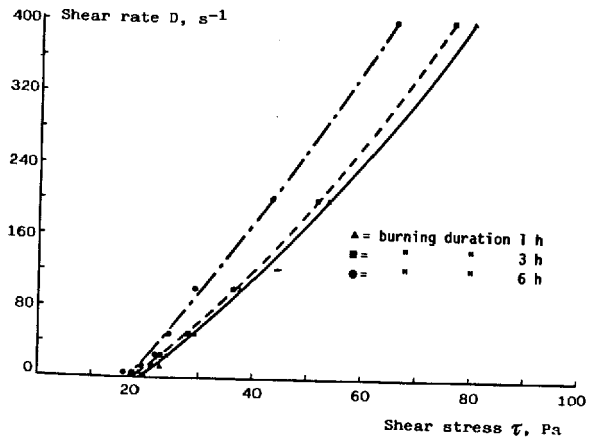

FIG. 2: Flow curves relevant to the cements made with clinker n° 2

4. CONCLUSIONS

The increase in the burning degree causes changes in the composition and structure of clinker and, therefore, in the properties of the resulting cements. The chemical composition changes on a macroscopic scale are observed mainly as regards alkalis, whose content decreases as the heating duration lengthens.
Volatilization not only involves the alkalis combined as sulphates but also those present in solid solution in the clinker phases. The alkali loss can affect the tricalcium aluminate and bicalcium silicate structures since these elements stabilize the anisotropic forms of the former (19) the monoclinic ones, α and α', of the latter (20).
Changes in the crystalline structure of alite are not noticed as the burning degree increases. The intensification of the X-ray peaks and the growth of the C_3S and C_2S crystals are signs of an increase in the crystalline lattice order, as heating time prolongs.

The reactivity variations of the aluminate phase are correlatable with the rheology modifications of pastes. Significant decreases in the rheological parameters are observed as the burning time lengthens and the reactivity lowers.
A burning degree increase causes in all cements an extension of the induction period and a slowing down of the hydration rate of alite. The changes undergone by C_3S have a slight influence on the paste rheology. In all cases a reduction in the strengths at early ages is observed. Owing to the slowness of C_2S hydration, it was not possible to correlate its chemical and structural variations with reactivity.
The lowering of reactivity could be partly due to the increase in the crystal sizes and/or the reduction in the clinker porosity. Nevertheless the reasons of these reactivity changes are likely to be searched in the crystal defects of crystallografic or chemical type (21). The former include lattice dislocations and atom removal that leave vacancies in the crystalline structure. The latter involve the substitution of an atom for a different one and the incorporation of an atom in an interstitial position in the lattice. It was proved that both categories of defects play an important role in determining the hydraulicity of the clinker phases (22).

It also resulted from thermoluminescence studies that the number and the physical characteristics of these defects considerably depend on the thermal history undergone by the specimen (23)(24).
It is difficult to establish whether the crystallographic or the chemical defects have a preminent role in the reactivity. If the results obtained with the control clinker containing the four main oxides are considered, it should be concluded that the defects of chemical origin have a poor influence. Nevertheless it must be remembered that each of the four main elements is present in the clinker phases and, therefore, the latter are different from the pure compounds.

In any case the work point out that the relationships existing between composition and structure of clinker and rheological and mechanical properties of cements are very complex. For this reason it seems that only an investigation technique cannot correlate the composition and structure of clinker with the cement properties.

REFERENCES

(1) **J. SKALNY, J.F. YOUNG,** *7th Int. Congr. on the Chem. of Cement (Paris, June 1980), vol. I, II-1/3*

(2) **U. UCHIKAWA, K. OGAWA, S. UCHIDA,** *Cem. Concr. Res, 1985, 15 (4), 561-572*

(3) F.W. LOCHER, W. RICHARTZ, S. SPRUNG, *Zement Kalk Gips 1976, (10), 435; 1980 (6),271; 1982 (12),669*

(4) K. TAKEMOTO, U. UCHIKAWA, *7th Int. Congr. on the Chem. of Cement, (Paris,June 1980),vol.I,IV-2/1*

(5) J. BENSTED, *World Cement Technology 1980, 11 (8), 395; 1983, 14 (10), 383*

(6) H. UCHIKAWA, S. UCHIDA, K. OGAWA, S. HANEHARA, *Cem. Concr. Res. 1984, 14 (5), 645*

(7) I. MAKI, H. HABA, S. TAKAHASHI, *Cem. Concr.Res. 1983, 13 (5), 689*

(8) G.B. EGOROV, M.M. SYCHEV, CH. A NOORMETZ, G.F. ERMAKOV, R.M. KAPRALOVA, *Tsement 1981, (7), 11*

(9) W.J. CAVENY, W. WEIGAND, D.E. BAILEY, *Oil and Gas Journal, Sept. 1983*

(10) W.J. CAVENY, W. WEIGAND, *World Oil 1985, 201 (5), 79*

(11) Y. ONO, *7th Int. Congr. on the Chem. of Cement (Paris, June 1980), vol. II, I-206*

(12) F. MASSAZZA, M.T. FRANCARDI, U. COSTA, *Colloque CEMBUREAU - Manifestation Thermiques de l'Hydratation au Cours de la Prise du Ciment (Paris, 1969), pp. 15*

(13) R. LAPASIN, A. PAPO, S. RAJGELJ, *Cem. Concr.Res. 1983, 13 (3), 349*

(14) S. TAKASHIMA, F. AMANO, *Sement Gijutsu Nenpo 1959, 13, 50*

(15) H.W.W. POLLITT, A. W. BROWN, *V Int. Symp. on the Chem. of Cement (Tokyo, 1968), 322*

(16) H.F.W. TAYLOR, *The Chemistry of Cements 1964, vol. I, Academic Press, London, p. 103*

(17) C. ATZENI, L. MASSIDDA, U. SANNA, *Il Cemento 1983, (3), 141*

(18) J.P. BOMBLED, *Proc. 7th Int. Congr. on the Chem. of Cement (Paris, June 1980), vol. III, VI-164*

(19) B. TAVASCI, F. MASSAZZA, U. COSTA, *7th Int.Congr. on the Chem. of Cement (Paris, June 1980),vol.IV, 432*

(20) W. GUTT, G.J. OSBORNE, *Cem.Technol.1970,1(4),121*

(21) J.H. SCHULMAN, W. DALE COMPTON, *Int.Series on Monogr. on Solid State Physics - vol. 2: Color Centers in Solids, Pergamon Press, 1962, 1*

(22) J.N. MAYCOCK, J. SKALNY, R. KALYONCU, *Cem.Concr. Res. 1974, 4 (5), 835*

(23) P. FIERENS, J.P. VERHAEGEN, *Cem. Concr..Res.1975, 5 (6), 587*

(24) P. FIERENS, A. VERHAEGEN, J.P. VERHAEGEN, *Cem. Concr. Res. 1974, 4 (3), 381*

TABLE 1: Chemical composition of clinker 1

	t = 1 h	t = 3 h	t = 6 h
L.o.I.	0.38 %	0.43 %	0.26 %
SiO_2	22.41	22.54	22.66
Al_2O_3	5.94	5.94	6
Fe_2O_3	2.47	2.45	2.47
CaO	64.93	65.23	65.25
MgO	2.23	2.24	2.22
SO_3	0.04	0.01	0.01
Na_2O	0.62	0.47	0.40
K_2O	0.55	0.38	0.26
SrO	0.02	0.02	0.02
Free lime	0.70	0.14	0.06
OLIGOELEMENTS			
Mn	417 ppm	487 ppm	417 ppm
P	393	349	349
Ti	1738	1738	1738
Cu	260	256	286
Zn	96	113	123
Pb	14	8	9
Ni	44	37	33
As	31	29	36
Cr	29	37	36
NEWKIRCK POTENTIAL COMPOSITION			
C_3S	58.30 %	59.98 %	58.46 %
C_2S	12.32	14.59	18.47
$KC_{23}S_{12}$	11.50	8.27	5.84
C_3A	3.47	5.31	6.34
NC_8A_3	8.03	6.23	5.29
C_4AF	7.50	7.46	7.52
Na_2SO_4	0.02	0.01	0.01
K_2SO_4	0.06	-	-
Lime saturation factor	0.91	0.91	0.90
Hydraulic modulus	2.11	2.11	2.10
Silica modulus	2.67	2.68	2.68
Iron modulus	2.41	2.42	2.42

TABLE 2: Chemical composition of clinker 2

	t = 1 h	t = 3 h	t = 6 h
L.o.I.	0.37 %	0.47 %	0.55 %
SiO_2	20.87	20.83	20.89
Al_2O_3	5.79	5.84	5.78
Fe_2O_3	3.03	3.05	3.04
CaO	61.81	62.14	62.15
MgO	1.93	1.98	1.96
SO_3	2.06	1.80	1.61
Na_2O	0.39	0.34	0.49
K_2O	0.90	0.77	0.71
SrO	2.24	2.27	2.25
Free lime	2.04	0.45	0.25
OLIGOELEMENTS			
Mn	974 ppm	1043 ppm	974 ppm
P	742	742	742
Ti	1618	1618	1618
Cu	185	187	225
Zn	221	217	228
Pb	16	11	11
Ni	39	33	40
As	25	23	25
Cr	30	30	31
NEWKIRCK POTENTIAL COMPOSITION			
C_3S	45.09 %	53.25 %	54.93 %
C_2S	28.98	22.71	21.63
C_3A	10.21	10.32	10.17
C_4AF	9.21	9.27	9.23
$CaSO_4$	1.33	1.20	0.63
Na_2SO_4	0.90	0.77	1.12
K_2SO_4	1.67	1.42	1.31
Lime saturation factor	0.90	0.90	0.91
Hydraulic modulus	2.08	2.09	2.09
Silica modulus	2.37	2.34	2.37
Iron modulus	1.91	1.91	1.90

TABLE 3: Chemical composition of clinker 3

	t = 1 h	t = 3 h	t = 6 h
L.o.I.	0.45 %	0.22 %	0.20 %
SiO_2	22.90	22.84	22.89
Al_2O_3	5.95	5.89	5.98
Fe_2O_3	2.21	2.23	2.21
CaO	65.45	65.73	65.94
MgO	1.34	1.38	1.43
SO_3	0.10	0.11	0.11
Na_2O	0.04	0.12	0.01
K_2O	0.72	0.55	0.38
SrO	0.12	0.12	0.10
Free lime	0.64	0.08	0.08
OLIGOELEMENTS			
Mn	765 ppm	765 ppm	765 ppm
P	655	698	655
Ti	1558	1558	1558
Cu	204	180	208
Zn	97	92	82
Pb	10	8	5
Ni	22	27	29
As	25	29	39
Cr	32	31	33
NEWKIRCK POTENTIAL COMPOSITION			
C_3S	51.57 %	55.85 %	55.14 %
C_2S	15.94	16.48	20.90
$KC_{23}S_{12}$	14.12	10.12	6.32
C_3A	11.76	10.55	12.26
NC_8A_3	0.27	1.30	-
C_4AF	6.73	6.79	6.73
Na_2SO_4	0.04	0.05	0.05
K_2SO_4	0.16	0.18	0.18
Lime saturation factor	0.90	0.90	0.90
Hydraulic modulus	2.11	2.12	2.12
Silica modulus	2.80	2.81	2.79
Iron modulus	2.69	2.64	2.71

TABLE 4: Chemical composition of clinker 4

	t = 1 h	t = 3 h	t = 6 h
L.o.I.	0.40 %	0.26 %	0.26 %
SiO_2	22.05	22.24	22.27
Al_2O_3	5.99	6.05	6.05
Fe_2O_3	2.54	2.52	2.55
CaO	64.58	64.93	65.15
MgO	1.88	1.91	1.92
SO_3	0.22	0.15	0.12
Na_2O	0.37	0.33	0.14
K_2O	0.73	0.47	0.38
SrO	0.09	0.08	0.08
Free lime	0.22	0.03	0.06
OLIGOELEMENTS			
Mn	348 ppm	278 ppm	348 ppm
P	2139	2139	2139
Ti	1679	1738	1679
Cu	266	306	283
Zn	153	157	160
Pb	15	9	9
Ni	32	27	35
As	13	14	11
Cr	33	30	31
NEWKIRCK POTENTIAL COMPOSITION			
C_3S	59.07 %	58.59 %	58.31 %
C_2S	10.12	15.38	17.08
$KC_{23}S_{12}$	11.97	7.54	6.13
C_3A	7.30	7.84	10.19
NC_8A_3	4.31	3.96	1.54
C_4AF	7.73	7.67	7.76
Na_2SO_4	0.10	0.07	0.05
K_2SO_4	0.36	0.24	0.20
Lime saturation factor	0.91	0.91	0.91
Hydraulic modulus	2.11	2.11	2.11
Silica modulus	2.58	2.58	2.59
Iron modulus	2.35	2.36	2.37

TABLE 5: Chemical composition of clinker 5

	t = 1 h	t = 3 h	t = 6 h
L.o.I.	0.40 %	0.27 %	0.25 %
SiO_2	23.03	22.93	23.13
Al_2O_3	4.59	4.70	4.62
Fe_2O_3	2.89	2.89	2.89
CaO	63.83	64.41	64.55
MgO	2.79	2.80	2.78
SO_3	0.68	0.56	0.43
Na_2O	0.48	0.33	0.35
K_2O	0.83	0.51	0.37
SrO	0.13	0.13	0.13
Free lime	0.17	0.08	0.05
OLIGOELEMENTS			
Mn	349 ppm	417 ppm	348 ppm
P	436	436	480
Ti	1139	1139	1139
Cu	321	320	310
Zn	192	186	191
Pb	45	20	8
Ni	19	24	22
As	91	81	95
Cr	16	16	16
NEWKIRCK POTENTIAL COMPOSITION			
C_3S	60.42 %	62.24 %	62.07 %
C_2S	19.06	21.96	22.98
$KC_{23}S_{12}$	4.98	0.34	-
C_3A	2.70	4.54	3.79
NC_8A_3	4.52	2.94	3.50
C_4AF	8.79	8.80	8.78
Na_2SO_4	0.30	0.25	0.20
K_2SO_4	1.12	0.92	0.69
Lime saturation factor	0.88	0.89	0.89
Hydraulic modulus	2.09	2.11	2.11
Silica modulus	3.08	3.02	3.08
Iron modulus	1.59	1.62	1.60

TABLE 6: Chemical composition of clinker 6

	t = 1 h	t = 3 h	t = 6 h
L.o.I.	0.38 %	0.43 %	0.53 %
SiO_2	22.27	22.32	22.20
Al_2O_3	6.44	6.42	6.41
Fe_2O_3	2.38	2.34	2.36
CaO	65.18	65.68	65.86
MgO	1.28	1.28	1.31
SO_3	0.16	0.12	0.16
Na_2O	0.40	0.32	0.29
K_2O	0.79	0.56	0.41
SrO	0.07	0.07	0.11
Free lime	0.64	0.14	0.11
OLIGOELEMENTS			
Mn	557 ppm	557 ppm	557 ppm
P	524	524	524
Ti	1858	1858	1858
Cu	148	136	128
Zn	87	82	82
Pb	9	5	3
Ni	38	39	38
As	37	34	37
Cr	31	32	31
NEWKIRCK POTENTIAL COMPOSITION			
C_3S	52.80 %	55.88 %	57.30 %
C_2S	12.76	14.97	17.62
$KC_{23}S_{12}$	14.54	10.09	5.95
C_3A	8.08	9.04	9.49
NC_8A_3	4.86	3.92	3.40
C_4AF	7.24	7.12	7.17
Na_2SO_4	0.07	0.05	0.07
K_2SO_4	0.27	0.20	0.26
Lime saturation factor	0.91	0.91	0.92
Hydraulic modulus	2.10	2.11	2.13
Silica modulus	2.53	2.55	2.53
Iron modulus	2.70	2.74	2.72

TABLE 7: Chemical composition of clinker 7

	t = 1 h	t = 3 h	t = 6 h
L.o.I.	0.68 %	0.30 %	0.35 %
SiO_2	21.7	21.76	22.04
Al_2O_3	5.92	5.81	5.99
Fe_2O_3	3.13	3.12	3.18
CaO	65.45	65.99	65.70
MgO	1.31	1.34	1.38
SO_3	0.39	0.28	0.29
Na_2O	0.25	0.33	0.24
K_2O	0.74	0.54	0.41
SrO	0.07	0.05	0.04
Free lime	0.92	0.25	0.08
OLIGOELEMENTS			
Mn	278 ppm	278 ppm	278 ppm
P	305	305	349
Ti	1678	1618	1678
Cu	173	172	160
Pb	109	111	117
Ni	5	3	2
As	30	29	33
Cr	34	32	30
NEWKIRCK POTENTIAL COMPOSITION	35	30	27
C_3S	58.18 %	63.71 %	59.39 %
C_2S	12.63	10.99	18.08
$KC_{23}S_{12}$	8.95	6.50	3.43
C_3A	8.00	6.46	7.99
NC_8A_3	2.30	3.58	2.41
C_4AF	9.51	9.48	9.66
Na_2SO_4	0.17	0.12	0.13
K_2SO_4	0.64	0.45	0.47
Lime saturation factor	0.93	0.94	0.92
Hydraulic modulus	2.13	2.15	2.11
Silica modulus	2.40	2.44	2.40
Iron modulus	1.89	1.86	1.88

TABLE 8: Chemical composition of clinker 8

	t = 1 h	t = 3 h	t = 6 h
L.o.I.	0.11 %	0.08 %	0.07 %
SiO_2	22.51	22.50	22.43
Al_2O_3	3.60	3.56	3.55
Fe_2O_3	4.78	4.79	4.78
CaO	64.26	64.57	64.67
MgO	2.55	2.50	2.56
SO_3	0.17	0.11	0.07
Na_2O	0.53	0.44	0.51
K_2O	0.17	0.13	0.08
SrO	0.07	0.07	0.07
Free lime	0.24	0.10	0.09
OLIGOELEMENTS			
Mn	348 ppm	348 ppm	348 ppm
P	829	829	829
Ti	4196	4196	4196
Cu	536	549	460
Zn	114	108	110
Pb	5	3	2
Ni	27	27	27
As	82	73	82
Cr	42	44	42
NEWKIRCK POTENTIAL COMPOSITION			
C_3S	68.83 %	70.50 %	72.11 %
C_2S	15.58	14.07	13.01
$KC_{23}S_{12}$	0.46	0.69	0.35
NC_8A_3	6.49	6.45	6.58
C_4AF	14.54	14.57	14.62
Na_2SO_4	0.08	0.06	0.03
K_2SO_4	0.28	0.19	0.12
Lime saturation factor	0.91	0.92	0.92
Hydraulic modulus	2.08	2.09	2.10
Silica modulus	2.68	2.69	2.69
Iron modulus	0.76	0.74	0.74

TABLE 9: Chemical composition of clinker 9

	t = 1 h	t = 3 h	t = 6 h
L.o.I.	0.38 %	0.32 %	0.39 %
SiO_2	23.27	23.13	23.26
Al_2O_3	6.43	6.43	6.39
Fe_2O_3	2.58	2.57	2.57
CaO	67.57	67.65	67.64
MgO	≤0.01	0.02	0.04
SO_3	≤0.01	≤0.01	0.01
Na_2O	≤0.01	≤0.01	≤0.01
K_2O	0.03	0.04	0.03
SrO	0.01	≤0.01	≤0.01
Free lime	1.71	0.62	0.31
OLIGOELEMENTS			
Mn	70 ppm	70 ppm	70 ppm
P	44	44	44
Ti	60	60	60
Cu	61	67	76
Zn	58	63	64
Pb	7	7	10
Ni	10	10	10
As	59	57	62
Cr	2	2	2
NEWKIRCK POTENTIAL COMPOSITION			
C_3S	42.07 %	47.98 %	48.54 %
C_2S	37.15	32.07	32.25
$KC_{23}S_{12}$	0.47	0.70	0.47
C_3A	12.57	12.59	12.48
NC_8A_3	0.11	0.11	0.11
C_4AF	7.86	7.82	7.81
K_2SO_4	0.02	0.02	0.02
Lime saturation factor	0.91	0.91	0.91
Hydraulic modulus	2.09	2.11	2.10
Silica modulus	2.58	2.57	2.60
Iron modulus	2.49	2.50	2.49

R. SERSALE, Department of Materials and Production Engineering, University of Naples, Italy.
V. AMICARELLI, Institute of Applied Chemistry, Faculty Engineering, University of Bari, Italy.
G. FRIGIONE, Department of Chemistry, Faculty Engineering, University of Calabria, Cosenza, Italy.
P. UBBRIACO, Institute of Applied Chemistry, Faculty Engineering, University of Bari, Italy.

A STUDY ON THE UTILIZATION OF AN ITALIAN STEEL SLAG.

SUMMARY: The Authors deal with the subject of the industrial utilization of a sample of steel slag, reasonably typical of the major Italian production, in order to select appropriate technical applications.

The effects of a partial substitution of the limestone in the raw meal for Portland clinker manufacture, burnt in an industrial kiln, have been investigated and it has been demonstrated that such a substitution, at a rate of 10% of steel slag, appears to be effectual, without detriment of the technical behaviour of the resultant cements and with energy saving for the clinkering process.

It has been pointed out, too, that the steel slag under examination can be used also as aggregate for concretes with high compressive strength and abrasion resistance, but without fire endurance.

SUMÁRIO: Os autores tratam da questão da utilização industrial da amostra de escória de aço, razoavalmente típica da maioria da produção italiana, de modo a selecionar apropriadas aplicações técnicas.

O efeito de parcial substituição do calcário na mistura crua para fabricação de clínquer portland, queimado num forno industrial, foi investigado e foi demonstrado que essa substituição, na proporção de 10% de escória de aço, parece ser efetiva, sem prejuizo do comportamento do cimento resultante e com economia de energia no processo de clinquerização.

Foi também assinalado que a escória de aço em exame pode também ser usada como agregado para concreto com alta resistência à compressão e à abrasão, mas sem suportar fogo.

R. SERSALE
V. AMICARELLI
G. FRIGIONE
P. UBBRIACO

INTRODUCTION.

In the frame of the experimental researches devoted to turn wastes discharged from factories efficiently to account (1), in a previous paper (2) a sample of steel slag, reasonably typical of major Italian production, was fully characterized. The chemical composition (Tab.I) and the X-ray diffraction pattern (Fig.1) which gave evidence of the main lines of β--dicalcium silicate, dicalcium and monocalcium ferrite, were performed. Two phases were identified by means of optical microscopy and electron probe microanalysis : the first one, compact, containing iron as predominant element and magnesium and manganese as accessory constituents and appearing to be the ground phase: the second one, incoherent, more or less dispersed, containing calcium and silicon as predominant elements, with negligible iron and manganese content.

Table I - Chemical Composition of the Products Used (per cent).

	Limestone	Clay	Pyrite Ash	LD Slag
l.o.i.	42.8	19.4	0.4	1.3
SiO_2	1.0	44.3	4.3	12.0
Al_2O_3	0.4	10.0	2.2	1.4
Fe_2O_3	0.6	3.8	87.4	29.9
CaO	53.7	10.7	1.8	41.9
MgO	0.7	2.1	-	4.3
Na_2O	0.2	0.8	0.1	0.6
K_2O	0.2	1.9	0.1	0.1
CaO free				16.0
MnO				6.0
P_2O_5				1.4
TiO_2				0.8

The tests on the aptitude for combining with lime, in view of a possible utilization for blended cement manufacture, pointed out that the sample, previously ground to 420 m^2/kg Blaine surface area, shaken with constantly saturated lime solution, virtually did not combine with lime, either in the presence or in the absence of calcium sulphate. It was also noticed that the same sample, in contact with previously boiled distilled water, allowed 18.4 mmols/l of CaO and 39 mmols/l OH^- to enter into solution, after 28 days at room temperature. The low reactivity towards lime was also confirmed by means of transmission electron microscopy investigation on the deposits of slag/lime and slag/lime+calcium sulphate suspensions.

Compressive strength tests on ISO-RILEM mortars (3) manufactured with blended cements obtained by adding steel slag, brought to 420 m^2/kg Blaine surface area, to an industrial clinker at a rate of 15,30 and 50% respectively, gave evidence of a remarkable lowering of the values that, all conditions being equal, could be reached substituting steel slag for blast furnace slag, in the same ratio. Steam curing of the specimens manufactured by adding, to the clinker, 30% steel slag and precured two hours at 20°C ± 2 and successively six hours at 80°C, showed moreover an improvement of the compressive strength at short ages but a worsening at long ones, according to the ordinary behaviour of Portland cement.

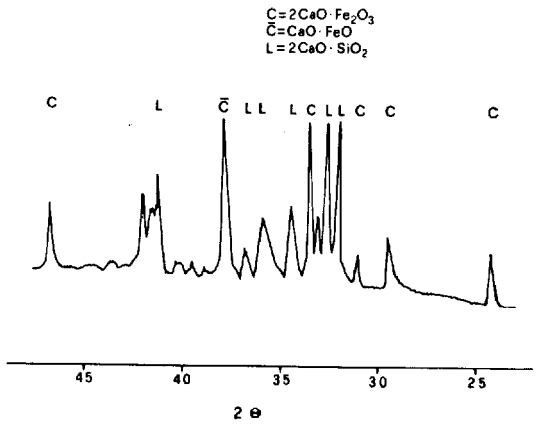

Fig. 1 - Diffractogram of steel slag sample.

Finally, as regards grindability, an energy consumption was pointed out higher than that required for granulated blast furnace slag, owing to the presence of small amounts of iron enclosed in the minute masses which escaped magnetic separation.

The results of the whole investigation (2) led to the disregarding of the of use of this slag as active addition to the clinker, suggesting, at the same time, its utilization as partial substitute of granulated blast furnace slag in slag cements, at a rate of about 10%. Such a substitution resulted in fact in a slight reduction of the water amount for mixtures with standard consistency, in a slight acceleration of the initial set and delay of the final, in a decrease in the whiteness of the end product - a real advantage for countries of the Mediterranean area - and in a slight lowering of the compressive strength, quite acceptable at long ages.

As a continuation and completion of the previous research (2), we deemed it interesting to investigate further possible industrial applications of the same steel slag and we have therefore examined its utilization either for clinker manufacture, as partial substitute of limestone, or as aggregate for concrete endowed with high compressive strength and high durability in terms of abrasion resistance.

An account of the overall results of the tests carried out and of the conclusion reached is give hereafter.

EXPERIMENTAL.

It's well known that more than 80% of the heat consumption for Portland cement manufacture is spent for the clinkering process and that the higher fraction of this consumption involves limestone dissociation (4). Reasonable energy savings can therefore be made through partial substitution of the raw materials entering in the raw meals for industrial by--products with energy content stored in previous technological cycles. Steel slag owing to its high calcium oxide content, represents a possible partial substitute of limestone, sharing in the reduction of heat consumption for clinker formation (5). Further advantages appear to be: the lowering of the volume of exhausted gases, owing to the lower carbon dioxide evolution, resulting at the same time in an abatement of the speed of volatile components, as well of the entrained dusts and calorie losses. As regards transportation, the product does not undergo successive weight losses because of gas evolution.

The above mentioned short considerations induced us to start an experimental investigation, carried out by means of an industrial plant, for evaluating, first of all, the possible differences arising in the technical behaviour of the end products in consequence of a partial substitution of limestone for steel slag, or secondarily, of clay, in the raw meal for Portland clinker manufacture. Table I shows the average values of the composition of the product used, including the steel slag sample.

Two kind of raw meals have therefore been prepared, the first one pertaining to the normal production of the factory and being the term of reference, of the following chemical composition: Limestone 71%, Clay 27.5%, Pyrite ash 1.5%; the second one, concerning this investigation: Limestone 66%, Clay 26.7%, Steel Slag 7.3%.

The burning process of the two series of mixes carried out in a rotary kiln having a diameter 3.6 m an 130 m length and a couple of cyclones for preheating the raw mix, supplied clinkers of the following composition during the whole investigation period:

- Lime standard 95 ± 1%
- Hydraulic modulus 2.10 ± 0.06
- Silica modulus 2.17 ± 0.18
- Alumina modulus 1 ± 0.15

Average value of the specific heat consumption for clinkering in the case of a raw mix containing steel slag was found to be 985 Kcal/kg, in comparison to 1050 Kcal/kg, which represents the average heat consumption for the burning of an ordinary raw mix.

RESULTS.

Both the types of raw meals supplied clinkers with chemical, physical and mechanical properties corresponding to the normal industrial production.

At his point, using the clinker obtained by burning raw mix containing steel slag in the mentioned ratio, we have prepared:

- a rapid hardening Portland cement
- a rapid hardening blast furnace slag cement
- a slag cement

whose characteristics are summarized in Tab.2. It's to be noticed that all the parameters fit very well with the Specification values and that a lengthening of the initial and final set, increasing with the steel slag content, is to be seen.

Another possible utilization of the same slag concerns the manufacture of concretes endowed with particular abrasion resistance.

It's well known that one of the manifold aspects of the concrete durability is represented by the abrasion resistance (6) which is also affected, all conditions being equal, by the lowering of the water/cement ratio, as well by the increase of compressive strength and hardness of aggregate (7).

We have therefore prepared a series of concrete specimens, whose characteristics are summarized in Tab. 3. Steel slag has been used as aggregate, terms of reference being in turn either the basalt or the calcareous aggregate (7). The abrasion resistance has been tested according to Italian Specification for road surface materials (8), estimating the abrasion resistance on the basis of weight loss in standard conditions. Average values obtained by testing four specimens manufactured with each type of aggregate (Tab.3) show, all conditions being equal, that abrasion resistance is twice as much for the concrete with steel slag, in comparison to those manufactured with basalt or calcareous aggregate.

Comparative tests showed moreover that thermal treatment (9) at 200°C for 24 hours considerably lowers compressive strength of concrete specimens with steel slag as aggregate, cured 28 days in wet environment.

Specimens appear significantly cracked, probably owing to the free lime content, so that the production of concretes with fire endurance must therefore be disregarded.

CONCLUSIONS

The whole of the experimental results allows us to select the following effectual utilization of the steel slag examined:

- as partial substitute of blast furnace slag, at a rate of 10%, for the manufacture of slag cements (2), without perceptible influence on the strength progress and with lowering of the whiteness of the end product, a requisite particularly demanded in

Table II - Characteristics of the Cements as a Function of Raw Mix Composition.

	Raw mix	Blaine Value m^2/kg	Set (hours-min.)		Compressive Strength (MPa)			
			Initial	Final	1 day	3 days	7 days	28 days
Rapid hardening Portland Cement	A	382	2.10	3.20	16.8	29.2	36.2	45.9
	B	374	2.20	3.35	14.8	29.4	36.6	45.0
Rapid hardening Portland Blast Furnace Slag Cement	A	400	2.10	3.10	13.5	27.5	37.2	48.0
	B	400	2.30	3.35	13.3	27.8	38.5	49.8
Ordinary Portland Blast Furnace Slag Cement	A	324	3.35	5.10	-	11.8	24.8	44.3
	B	325	4.15	5.45	-	11.7	22.8	44.1

A = Raw mix with Ordinary Components.
B = Raw mix Containing also LD Slag.

Table III - Characteristic of the Concretes as a Function of the Type of Aggregate.

	Basalt	Limestone	LD Slag
Fraction 25/15 (kg/m^3)	480	390	468
" 12/ 7 "	357	487	573
" 5/ 3 "	336	292	343
" 3/ 1 "	336	292	343
Siliceous Sand "	476	487	573
Cement "	350	350	350
Slump (cm)	6.0	6.2	6.0
Compressive Strength :			
1 day (MPa)	16.1	15.6	16.3
3 days "	36.7	36.5	37.5
7 days "	44.7	42.6	50.0
28 days "	54.4	53.0	58.5
After 24 h thermal treatment at 200 °C (MPa)	67.0	64.4	30.0
Wear (loss on weight, g)	1.2	1.4	0.6

the Mediterranean countries;
- as partial substitute of limestone in the raw mix of Portland clinker, likewise at a rate of 10%, without affecting the technical behaviour of the resultant cements and with lowering of the heat consumption for the clinker burning;
- as aggregate for the manufacture of concretes endowed with high compressive strength and abrasion resistance.

REFERENCES.

1. Idemitsu T., Takayama S.I., Watanabe A. (1981), "Utilization of Converter Slag as a Constituent of Slag Cement". Transactions of the Japan Concrete Institute, Vol.3, pp.33-38.

2. Sersale R., Amicarelli V., Frigione G., Ubbriaco P. (1986), "Characterization and Potential Uses of Steel Slag". Silicates Industriels (in press).

3. ISO Recommendation (1968), R.679, March 1968.

4. Frigione G. (1984), "Utilizzazione di loppe d'altoforno per la produzione di Clinker Portland" Rend.Acc.Sc.Fis. e Mat., Napoli, Serie IV, Vol. 51/1, pp 49-60.

5. Baoxun W., Yonghao F. (1985), "Investigation on the Formation Process of Cement Clinker from Raw Meal Using Steel-Slag as Raw Materials". 1985 Bejing International Symposium on Cement and Concrete. China Academic Publishers. p 37.

6. Alexander M.G. (1985), "Towards Standard Tests for Abrasion Resistance of Concrete. Report on a Limited Number of Tests Studied, with a Critical Evaluation". Matériaux et Constructions, Vol.18, n. 106, pp 297-307.

7. Liu T.C. (1981), "Abrasion Resistance of Concrete",

ACI Journal, Vol.78, n.5, pp 341-350.

8. Norme per l'accettazione dei materiali per pavimentazioni. (1940), Suppl. Ordinario Gazzetta Ufficiale Italiana n.92, 18/4/1940. pp 42-45.

9. Abrams M.S. (1981), "Compressive Stength of Concrete at Temperatures to 1600 F". Temperature and Concrete. ACI Publication SP 25-2, pp 33-58.

M. NAGASHIMA, E. ASAKURA, S. UDA and H. KAWABATA, Research and Development Laboratory, Mitsubishi Mining and Cement Co., Ltd. JAPAN

1.2 Characteristics of Alite in Portland Cement Clinker and C_3S Solid Solution

SUMMARY : Alites in portland cement clinkers and C_3S solid solutions have been examined, especially in their modifications, birefringence and hydration properties.

Alite in clinker occurs in two forms, M_1 and M_3. M_1 is always observed when burnt for short time. It converts into M_3 with longer burning time. However if the clinker burnt slowly, M_1 is hard to convert into M_3. Birefringence of M_1 is constantly 0.003, while that of M_3 varies from 0.004 to 0.007 with the burning time and shows the maximum value after some time. It is suggested that the change of birefringence in M_3 might be due to the displacive transition. MgO content of alite after 5 minute burning is really high up to 1.8 % and decreases as the holding time becomes longer.

C_3S solid solutions were prepared from chemical reagents. C_3S solid solutions containing a certain amount of Al_2O_3 and Fe_2O_3 are M_1 with low MgO content and M_3 with high MgO content. The lattice constants of M_3 change corresponding to the MgO content, while birefringence is nearly constant in the range of 0.0044 to 0.0054. Any M_3 burnt for different time does not show significant change of birefringence although M_3 in clinker does.

The hydration properties of the rapid hardening portland cement containing alites with different birefringence have been studied. M_3 reacts more slowly than M_1 at early stage, but the hardened cement with M_3 is denser and has greater strength after 3 days. There seems to be a little difference of strength among samples containing M_3 with different birefringence.

Foram examinadas alitas em clínqueres de cimento portland e em soluções sólidas de C_3S, especialmente em suas modificações, birrefringência e propriedades de hidratação.

A alita acontece no clínquer sob duas formas: M_1 e M_3. Sempre se observa M_1 quando a queima é de curta duração. Ela se converte em M_3 quando a queima é por tempo mais longo. Contudo, se o clínquer é queimado lentamente, é mais fácil a conversão de M_1 em M_3. A birrefringência de M_1 é constantemente 0,003, enquanto a de M_3 varia de 0,004 a 0,007 com o tempo de queima e apresenta o valor máximo após algum tempo. Sugere-se que a mudança de birrefringência de M_3 possa ser devida à transição deslocadora. O teor de MgO da alita depois de 5 minutos de queima, de até 1,8%, é realmente alto e diminui na medida em que o tempo de retenção se torna maior.

A partir de reagentes químicos foram preparadas soluções sólidas de C_3S. As soluções sólidas contendo uma certa quantidade de Al_2O_3 e Fe_2O_3 são M_1 com baixo teor de MgO, e M_3 com alto teor de MgO. As constantes de rede de M_3 se alteram, correspondendo ao teor de MgO, enquanto a birrefringência é quase constante na faixa de 0,0044 a 0,0054. Qualquer queima de M_3 por tempo diferente não apresenta alteração significativa da birrefringência, embora o M_3 no clínquer apresente.

Foram estudadas as propriedades de hidratação do cimento portland de endurecimento rápido, contendo alitas com birrefringência diferente. M_3 reage mais lentamente do que M_1 no estágio inicial, mas o cimento endurecido com M_3 é mais denso e tem resistência maior aos 3 dias. Parece que há uma pequena diferença de resistência entre amostras contendo M_3 com birrefringência diferente.

M. NAGASHIMA, E. ASAKURA, S. UDA and H. KAWABATA, Research and Development Laboratory,
Mitsubishi Mining and Cement Co., Ltd. JAPAN

INTRODUCTION

Alite in portland cement clinker is C_3S solid solution corresponding to the modification M_1 or M_3 of C_3S(1-4). M_3 was recently found and was proved to correspond to M_{Ib} of C_3S solid solution by Maki et al.(1,4). However, M_3 was called M_{IIb} in some works (5,6). There may exist some discrepancies as to the phase identification of alite.

In this study, the character of both alite in clinker and C_3Sss (C_3S solid solution prepared by solid state reaction) was investigated at ambient temperature, with special reference to birefringence, to elucidate the characteristics of alite in clinker as compared with C_3Sss. Further, the hydration property of alite with different character was studied.

C_3Sss PREPARED BY SOLID STATE REACTION

C_3Sss which are almost the same as those of Woermann et al.(7) were prepared and studied on the lattice constant, birefringence and the amount of impurities of them. C_3Sss were obtained by burning at 1550 °C for 8 hours, adding impurities such as Al_2O_3, Fe_2O_3 and MgO. The chemical compositions are shown in the modification diagram originally drawn by Woermann et al. (Fig.1). The chemical composition of C_3Sss was analysed with EPMA. As shown in Fig.2, the amount of impurities in C_3Sss was almost the same as those added to specimens.

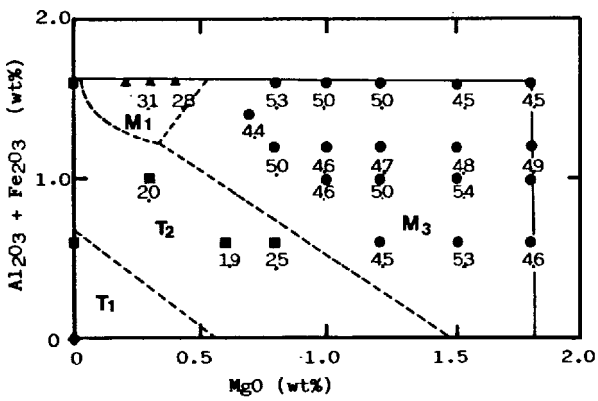

Fig.1 Birefringence and modification of C_3Sss.

◆:T_1 ■:T_2 ▲:M_1 ●:M_3

The broken line indicates the boundary of modification. Al_2O_3/Fe_2O_3=1. Birefringence :$x10^{-3}$.

XRD data of specimens employed in this study were in agreement with those obtained by Woermann et al. Lattice constants of C_3Sss were calculated using d-spacings of (402), (009), (620) and (040). The lattice constants of C_3Sss vary with the amount of impurities(Fig.3 and 4). All the constants decrease as the amount of MgO increases, while they increase as the amount of Al_2O_3+Fe_2O_3 increases.

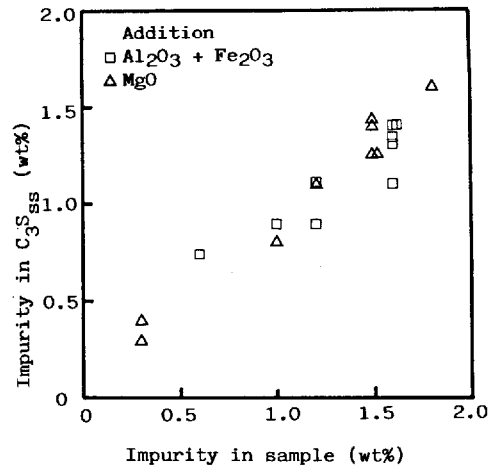

Fig.2 Impurity contents in C_3S_{ss} and samples.

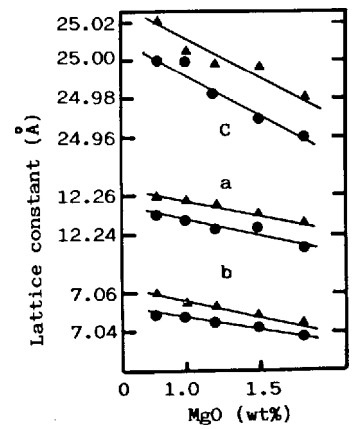

Fig.3 Change in lattice constant of C_3Sss with the addition of MgO.

●:Fe_2O_3 0.6wt% , Al_2O_3 0.6wt%

▲:Fe_2O_3 0.8wt% , Al_2O_3 0.8wt%

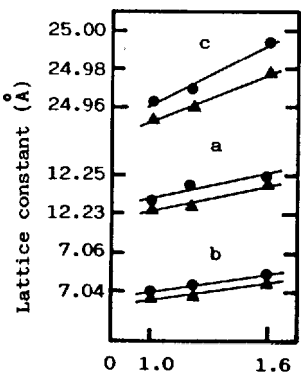

Fig.4 Change in lattice constant of C_3Sss with the addition of (Fe_2O_3 + Al_2O_3).

●: MgO 1.5wt% ▲: MgO 1.8wt%
Al_2O_3 / Fe_2O_3 =1.

Birefringences of C_3Sss were measured in thin sections including quartz prism as reference whose Y axis was normal to the section and were shown in Fig.1. From these data it follows that M_{Ia} identified by Woermann et al.is equivalent to M_1 and M_{Ib} is to M_3. As shown in Fig.1, birefringence of M_1 and T_2 is about 0.003 and about 0.002 respectively. Birefringence of M_3 is ranging from 0.0045 to 0.0055 and seems to be scarcely influenced by the amount of impurities.

The results described above can be summarized as follows. Modification and lattice constant are determined by the amount of impurities. Birefringence of M_3 is less than 0.0055, and is independent of the amount of impurities.

ALITE IN CLINKER

The raw mixes for rapid hardening portland cement (HM 2.3, SM 2.8, IM 1.8) were prepared using industrial materials or chemical reagents and were burnt under various conditions. The amount of MgO was changed from 1 to 3 wt% on clinker base and Blaine fineness was from 500 to 970 m^2/kg. The burning conditions were varied in the heating rate, the maximum temperature and the holding time. Alites in the run products were observed with an optical microscope to determine their birefringence and modification.

The modification of alite is influenced by the burning condition and the MgO content in clinker. The results are shown in Table 1. M_1 is always observed at the attainment of the maximum temperature in any burning condition and converts into M_3 with longer holding time. However, when the clinker is burnt slowly, alite is difficult to convert into M_3 even if the holding time is long.

The increase of MgO content in the clinker is of advantage to the occurence of M_3 (Table 1). This might suggest that the amount of impurities determines the modification of alite in a similar manner as C_3Sss. In certain cases, however, M_1 with high MgO content is found in clinker. The cases are shown as follows.

Fig.5 shows the amount of impurities (MgO, Al_2O_3, Fe_2O_3) and birefringence of alites in the clinkers burnt at different maximum temperatures. It indicates that the amount of impurities decreases with increasing maximum temperature. Burnt at 1400°C, the amount of impurities in alite is the largest and birefringence of alite corresponds to M_1. Burnt at 1500 and 1600°C, however, alite shows higher birefringence corresponding to M_3 despite the less amount of impurities.

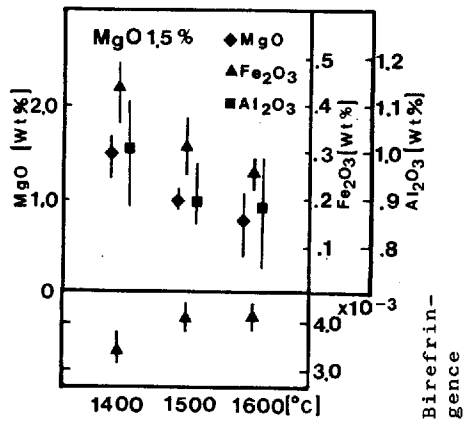

Fig.5 Impurity contents and birefringence of alites in clinkers burnt for 30 minutes(500 m^2/kg, industrial materials, rapid burning).

The amount of impurities in alite of the clinker burnt at 1500°C for different holding time is shown in Fig.6. MgO content is really high reaching up to 1.8 wt% at 5 minute holding time and decreases as the holding time becomes longer. This suggests that drastic incorporation of Mg ions into alite takes place at the beginning of the crystal precipitation from the melt. On the contrary, the amount of Al_2O_3+Fe_2O_3 is neary constant in the range of 1.0 to 1.5 wt% for any clinker. As M_1 occurs at first under any burning condition, M_1 contains large amount of MgO in this case as well.

Table 1 Modification and birefringence of alites in clinkers burnt under different conditions.

burning condition			birefringence ($X10^{-3}$) and alite phase	
burning rate	temp.(°C)	holding time	MgO 1%	MgO 3%
rapid	1500	2 min	2.3-2.7 (2.5) , M1	2.5-3.5 (3.0) , M1
slow	〃	〃	1.5-3.5 (2.7) , M1	1.9-3.7 (2.5) , M1
rapid	〃	1 hr	2.4-6.1 (3.5) , M1<M3	2.1-4.9 (4.0) ,M1<M3
rapid	〃	2 hr	2.5-6.3 (4.0) , M3	3.4-7.1 (4.8) , M3
slow	〃	〃	2.3-3.8 (2.8) , M1	2.9-4.7 (3.5) ,M1<M3
rapid	1400	〃	2.6-3.9 (3.5) , M1.M3	3.2-4.8 (3.9) ,M1<M3

( ): mean value

M. NAGASHIMA, E. ASAKURA, S. UDA and H. KAWABATA, Research and Development Laboratory, Mitsubishi Mining and Cement Co., Ltd. JAPAN

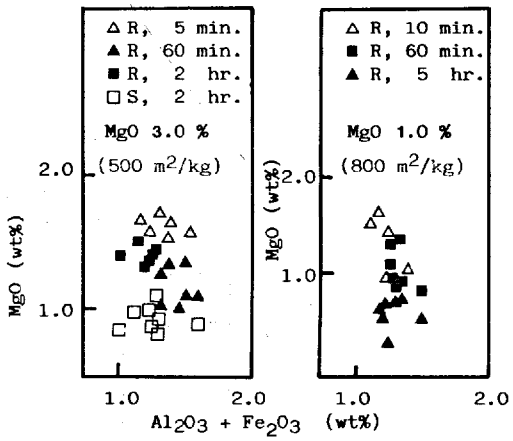

Fig.6 Impurity contents of alites in clinkers burnt at 1550°C (industrial materials). R=rapid burning, S=slow burning.

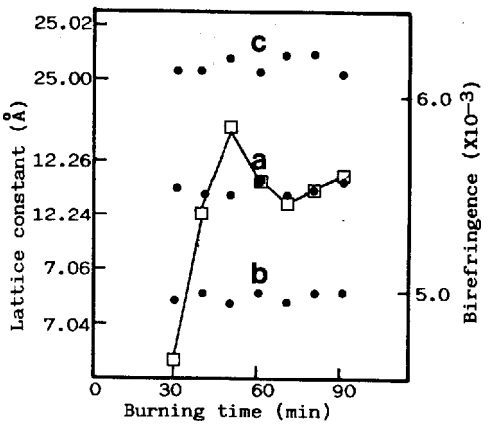

Fig.8 Change of lattice constant and birefringence with burning time.
•:lattice constant □:birefringence

Birefringence of M_1 in clinker is constantly 0.003, while that of M_3 varies from 0.004 to 0.007 corresponding to the burning condition or the character of raw mix. Birefringence of M_3 alite changes with the holding time and shows the maximum value after a certain holding time (Fig.7). The maximum point appears at shorter time when the burning temperature is higher and the raw mix is finer. Fig.8 shows lattice constants and birefringence of alite in clinker burnt at different holding time. Lattice constants of alites scarcely vary with the burning time in spite of the change of their birefringence. Alite coexisting with melt at high temperature is considered to be R type. Monoclinic modification, that is M_1 and M_3, may probably depend on the structure of these R alites. Seeing the XRD peak profiles of alites in clinker, the XRD peak of (009) varies little in its position and intensity, while those of (040) and (620) do remarkably. Single peak of (220) splits into doublet of (040) and (620) when the form of alite changes from R to M. Therefore, the structural variance of M_3 alite could be detected by the change of (220) of R alite. R alite was obtainable when the clinker was quenched by being dropped into oil. The raw mixes prepared from chemical reagents were burnt at 1500 to 1700°C, varying holding time from 3 to 130 minutes. XRD was carried out to determine the FWHM (full width at half maximum intensity) of (009) and (220) peak. The FWHM of (009) peak is almost constant at any burning condition, while that of (220) peak varies. THe ratio of the FWHM of (002) peak to (009) peak varies with holding time and shows the maximum value as the birefringence does (Fig.9). The relation between the burning temperature and the appearance time of the maximum value has

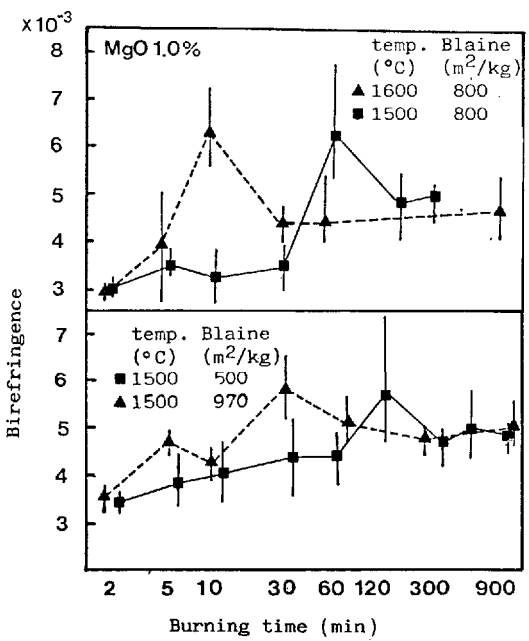

Fig.7 Change in birefringence of alites in clinkers burnt rapidly using industrial materials (500, 800 m^2/kg) and chemical reagents (970 m^2/kg).

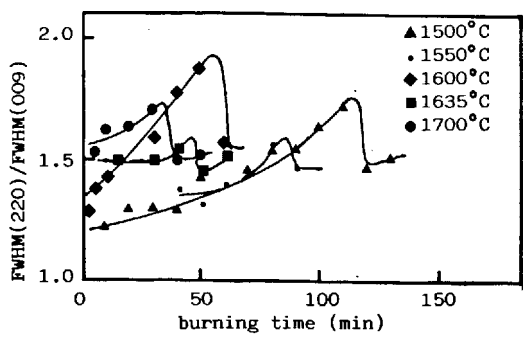

Fig.9 Change in the ratio of FWHM(220) and FWHM(009) with burning time.

M. NAGASHIMA, E. ASAKURA, S. UDA and H. KAWABATA, Research and Development Laboratory, Mitsubishi Mining and Cement Co., Ltd. JAPAN

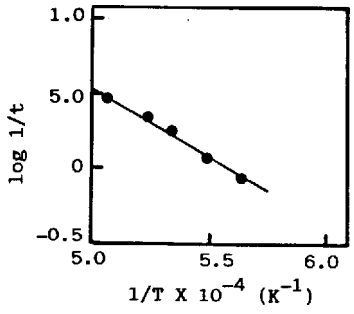

Fig.10 Arrenius plot.

been well implied by the Arrenius plot (Fig. 10). The activation energy obtained from the plot is about 171 kJ/mol which is very small compared to the dissociation energy of Ca-O and O-Si-O bond. It suggests that the displacive transition might occur in M_3 when being kept at high temperature.

Alite in clinker is different from C_3Sss in two aspects; the form of alite does not necessarily depend on the amount of impurities and M_3 sometimes shows very high birefringence over 0.006. As mentioned above, the forms of alite in laboratory clinkers occur as M_1 with low birefringence, M_3 with high birefringence (0.004-0.006) and M_3 with very high birefringence (>0.006). In addition, zoned alite, in which M_3 usually overgrows M_1, occurs in industrial clinkers. From the study of alites in laboratory clinker, it is thought that each type of alite in industrial clinkers reflects the burning conditions. M_3 with very high birefringence may be formed by rapid burning and its grain is fine, prismatic, euhedral and clear with little entraped inclusions. On the other hand M_1 is usually coarse grain and may be formed when burnt slowly or burnt under lower temperature. With prolonged holding time at high temperature, M_1 may change to M_3 with high birefringence. Such M_3 sometimes contains numerous fine inclusions which appear dusty. Zoned alite may be formed when the marked change of the burning condition happens.

HYDRATION PROPERTY OF ALITE

The hydration properties of alite M_1 and alite M_3 with different birefringence were studied. The raw mixes for rapid hardening portland cement (HM 2.3, SM 2.9, IM 1.6) were prepared using industrial materials and were burnt under various conditions to change birefringence of alite in clinker. Table 2 shows burning conditions and the results of cement tests. Alite formed under low burning rate was M_1 (birefringence $\leq$ 0.0037) and M_3 (birefringence $\geq$ 0.0041) under high burning rate. The maximum birefringence was obtained in clinker (F) burnt for 34 minutes.

Heat evolution curves of cement pastes indicates that alite with higher birefringence ($\geq$0.0045) tends to have longer dormant period than alite with lower birefringence ($\leq$0.0041). Each cement used in the study differs more or less in f.CaO content. Adding f.CaO on 0.7 wt% to cement F, the dormant period became 20 minute shorter, but was far longer than cement A-B containing M_1 alite.

Fig.11 shows the SEM photographs of hardened pastes. At 1 day, type I particle of C-S-H and needlelike crystal of ettringite are formed much more in the samples containing M_1 alite (A and B) compared with those containing M_3 alite (C-I). At 3 days, in the case of M_3 alite, cement particles agglomerate each other, resulting in forming blocks and large open spaces among them. On the other hand, in the case of M_3 alite, cement particles are homogeneously distributed and fill open spaces. The former is more porous than the latter.

Fig.12 shows pore volume of hardened mortars after strength test. At 3 days, in the case of M_3 alite, the pore volume is large. At other ages, clear difference is not recognized in any sample.

Fig.13 shows the compressive strength of cements at the age of 1,3,7 and 28 days. At 1 day, the strength of cement containing M_1 alite is higher than that of cement containing M_3, although after 3 days the former is

Table 2 Burning Condition and Result of Cement Test.

Sample	Burning condition: Burning rate	Temp. (°C)	Holding time(min)	Alite: Biref. (X10^{-3})	Phase	Time of the 2nd peak of heat evol. (hr-min)	Blaine (m^2/kg)	f.CaO (wt %)
A	slow *	1550	0	3.6	M1	9-25	418	0.89
B	slow *	1500	10	3.7	M1	9-05	424	1.01
C	rapid	1550	14	4.1	M3	9-20	420	0.91
D	rapid	1550	20	5.1	M3	10-30	427	0.54
E	rapid	1550	28	4.7	M3	10-50	423	0.31
F	rapid	1550	34	6.0	M3	11-10	417	0.31
G	rapid	1550	36	4.5	M3	11-00	417	0.39
H	rapid	1550	40	5.1	M3	11-10	419	0.25
I	rapid	1550	60	4.8	M3	10-40	417	0.19

* : 5 °C/min

M. NAGASHIMA, E. ASAKURA, S. UDA and H. KAWABATA, Research and Development Laboratory,
Mitsubishi Mining and Cement Co., Ltd. JAPAN

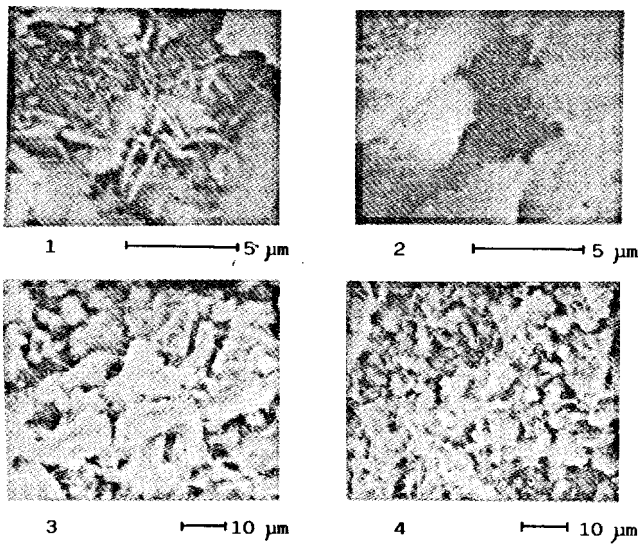

Fig.11 SEM micrograph of fracture surface of hardened cement paste (W/C=50%).
1:sample A, 1 day 2:sample F, 1 day
3:sample A, 3 days 4:sample C, 3 days

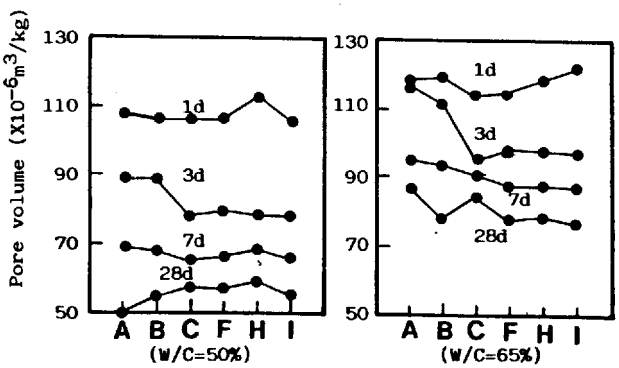

Fig.12 Pore volume of mortar.

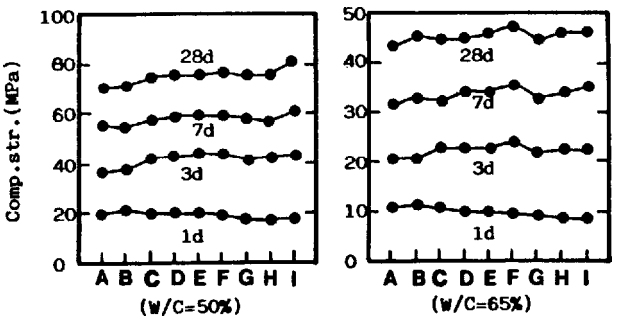

Fig.13 Compressive strength of mortar.

lower than the latter. The strength of cement containing M_3 alite with different birefringence seems not to vary too greatly. Similar result was ascertained for industrial clinker.

CONCLUSIONS

(1) Modification and lattice constant of C_3Sss are determined by the amount of impurities. Birefringence is ranging from 0.0045 to 0.0055 for M_3, about 0.003 for M_1 and about 0.002 for T_2. Birefringence of M_3 is independent of the amount of impurities.

(2) M_1 alite in clinker is always observed when clinker is burnt for short time or by slow burning. It converts into M_3 with prolonged burning at high temperature. High MgO content favors the conversion from M_1 to M_3. Impurity content in M_3, however, is not necessarily higher than in M_1.

(3) Birefringence of M_1 is constantly 0.003, while that of M_3 varies from 0.004 to 0.007 with the burning time and after certain time shows the maximum value that is not detected in C_3Sss. The appearance of the maximum value suggests that the displacive transition might occur in M_3.

(4) M_3 alite hydrates more slowly than M_1 alite at early stage. After 3 days, the hardened cement containing M_3 is denser than that containing M_1 and the former shows greater strength than the latter. However, there seems to be little difference of strength in M_3 with different birefringence.

REFERENCES

1) I.Maki and S.Chromý (1978), "Characterization of the alite phase in portland cement clinker by microscopy", Cemento, 75, 247.

2) I.Maki (1979), "Phase constitution of the alite in portland cement clinker from modern manufacturing process", Cemento, 76, 167.

3) I.Maki, T.Ogiwara and S.Chromý (1981), "Differential thermal analysis of portland cement clinker and phase constitution of alite", Cemento, 78, 53.

4) I.Maki and K.Kato (1982), "Phase identification of alite in portland cement clinker", Cement Concrete Res., 12, 93.

5) M.Regourd (1979) "Physique cristalline — polymorphisme du silicate tricalcique, nouvelles données de la diffraction des rayons X", C.R.Acad.Sci.Paris, série B, 17.

6) M.Regourd (1979) "Fundamentals of cement production: the crystal chemistry of portland cement minerals. New data", Cement Production and Use, Engineering Foundation N.Y., 41.

7) E.Woermann, W.Eysel and Th.Hahn (1969), "Chemische und strukturell untersuchungen der mischkristallbildung von tricalciumsilikat", Zement-Kalk-Gips, 22, 414.

Rudolf J. Słota , Institute for the Industry of Building Bond Materials , Opole , Poland ;
Anna Lewandowska-Kanas , Institute for the Industry of Building Bond Materials , Opole , Poland .

1.2

Modification of Clinker Phase Composition and Strength Properties of a High - Alkali Cement Clinker by Gypsum Addition

Modification de la composition du clinker et des résistances d'un clinker à haute teneur en alcalis par addition de gypse.

SUMMARY: Studies were undertaken to determine whether the properties of a high-alkali clinker can be improved by gypsum addition to the raw mix. As the principal component of the raw meal,an unconventional raw material was used,namely a by-product obtained in the process of alumina manufacturing according to the Grzymek method (1 , 2) .

X-ray diffractometry and optical microscopy data of investigated clinkers are presented.

Strength properties of cements made from Na_2O containing raw materials are discussed with regard to the modified by gypsum addition structure of clinker.

The optimum value of gypsum requirement has been determined.

SUMÁRIO: Estudos foram feitos para determinar se as propriedades de clínquer com alto teor de álcalis podem ser melhorados com adição de gesso na matéria-prima. Como princi pal componente da matéria-prima, um material não convencional foi usado, um subproduto obtido no processo de manufatura da alumina de acordo com o método Grzymek (1,2).

São apresentados dados de difratometria de raios X e de microscopia ótica.

Propriedades de resistência de cimentos feitos com matéria-prima contendo Na_2O são discutidas em face da modificação de estrutura do clínquer pela adição de gesso.

O valor ótico do gesso requerido foi determinado.

INTRODUCTION

The effect of alkalies on phase composition and properties of cement clinker have been widely discussed in the literature. A review by Jawed and Skalny (3,4) summarizes the knowledge in this subject up to 1978.

Many authors have reported that the deleterious effect of alkalies on the mechanical properties of cement may be considerably reduced by addition of gypsum to the raw meal(5,6,7,8).

Other researchers,in turn,have indicated the negative effect of higher SO_3 content in the clinker on the hydraulic reactivity of the cement.Due to the reaction of β-C_2S and the sulfate compound the reactivity of belite is decreased and less alite is formed in the clinker.Also,the hydraulic reactivity of β-C_2S itself can be lowered (9,10,11,12) .

Recant studies performed by Stunge et al. (13,14) provided a large set of new data. They have found that a higher SO_3 content in the clinker lowers the strength of the cement made from it.However,the strength reductions can be compensated by raising the silica modulus.

It has to be emphasized that the reactivity of a gypsum-doped raw meal is strongly related to the nature of raw materials used.The form in which the alkalies occur in the raw materials may play a significant role in the burning of clinker.

It is reported in the literature that for every cement an optimum SO_3 level can be determined with regard to setting behaviour and strength developement.

In our experiments an unconventional raw material was used in the preparation of clinker.It is known as a so-called post-extraction slime,a by-product in the alumina manufacturing according to the Grzymek method (2) . Due to its origin it may contain large quantities of Na_2O, predominantly as Na_2CO_3. This fact determines the reactivity of the raw meal as well as the properties of clinker manufactured from it.

Thus,we have felt it worthwile to study if the clinker produced from this particular raw material could gain a more reactive mineral structure by increasing the SO_3 content in the raw mix.

EXPERIMENTAL

Four different in Na_2O content raw mixes were prepared of approximately 80 % post-extraction slime and 20 % lime stone. Prior to blending both ingredients were dried and grinded to pass the 200μm sieve. The composition of mixes was calculated according to (15) by assuming the LSF = 0.98 .The silica module was 4.15 . Na_2O content in the raw mixes was gradually raised by Na_2CO_3 admixtures.Thus,resultant blends contained 0.7 (no admixture of Na_2CO_3) , 1.2 , 1.7 and 2.2 % of Na_2O.

The amounts of gypsum added to the raw mixes were 0 , 1 , 2 , 3 , 4 and 5 % by mass.

Components of the mix were thoroughly blended and afterwards pelletized. Firing was performed in a laboratory oven in the temperature 1450 °C .

Structural studies of clinkers were performed by X-ray diffractometry (XRD) and optical microscopy methods.

The chemical composition of clinkers was determined by routine analytical methods. Strength properties were evaluated according to the Polish Specifications (16). Specific surface area for all tested cements was approximately 3000 cm^2/g (Blaine) .

RESULTS AND DISCUSSION

Clinkers obtained in our experiments contained 0.9 , 1.4 , 1.8 and 2.3 % of Na_2O.

The SO_3 content in the prepared clinkers varied from 0.3 to 3.0 per cent by mass. In Fig. 1 X-ray diffraction pattern of post-extraction slime is presented.

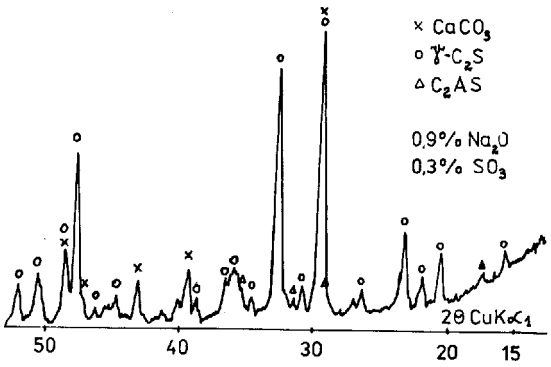

FIG. 1
Post-extraction slime (raw)

Effect of gypsum addition on the mineralogy of clinkers having different Na_2O content is shown in Fig. 2 .
XRD examinations revealed significant changes in the structure of clinkers caused by sodium and sulphates which are present in the studied systems.

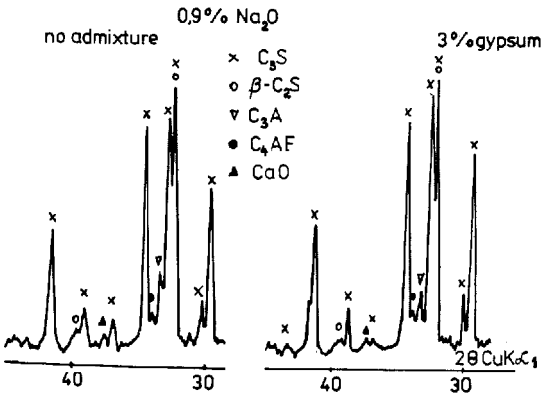

FIG. 2
Effect of gypsum addition on the phase composition of clinkers containing Na_2O

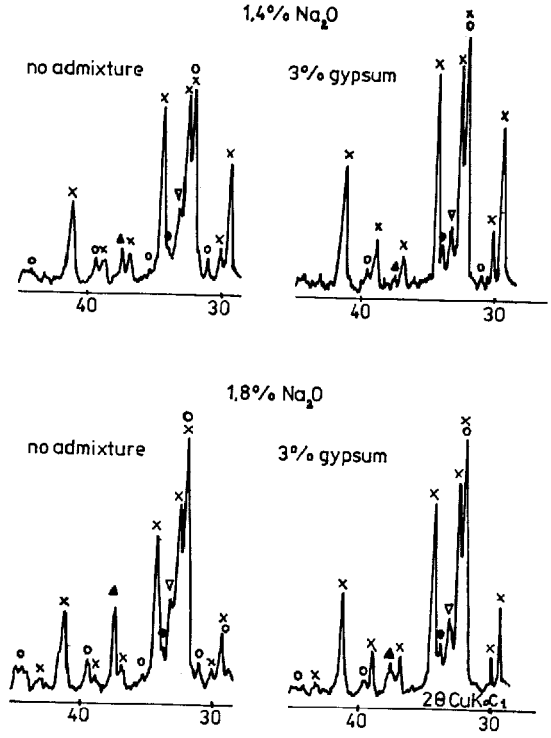

Cont. of FIG. 2

It can be noticed that by increasing the Na_2O content in clinker less quantities of alite are formed, while more free lime occurs as a separate phase. Also, the β-C_2S phase is encountered in the clinker in larger quantities if more Na_2O is present in the system.
Alterations can be seen in the appearance of the C_3A peak in the range of 2θ = 33 - 33.5 . After Regourd et al. (17) this phenomenon may be assigned to phase transformation of cubic C_3A into the "prismatic" aluminate phase in the clinker due to the raise of sodium content.
Similar effect can be observed in the case of aluminoferrite phase.
Microscopy analysis confirmed the XRD da-

ta. Micrographs presented in Fig. 3 show the average structure of chosen clinkers. In particular, the corrosion of alite crystals due to the action of sodium and phase transformation of C_3A can be distinguished.

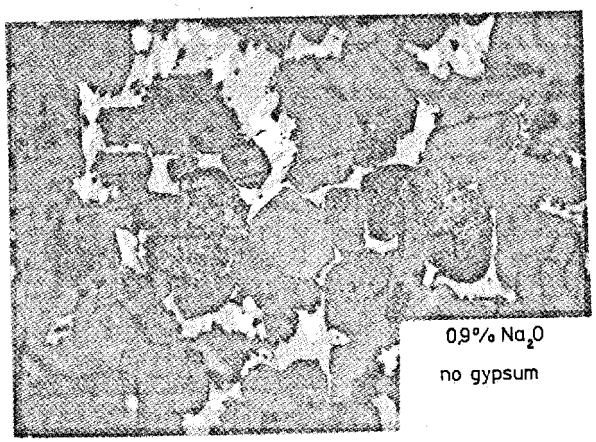

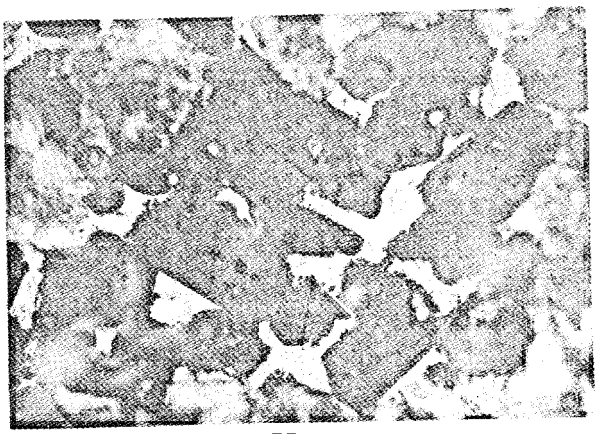

FIG. 3
Effect of gypsum addition on the microstructure of clinkers containing Na_2O (800 x)

Introduction of gypsum to the raw meal has led to a modification of the clinker structure. It has been proved that an increase in SO_3 content is followed by a formation of more alite. Also, the clinker contains both β-C_2S and free lime in less quantities.
The effect of gypsum admixture on the reactivity of the raw meal, characterized by

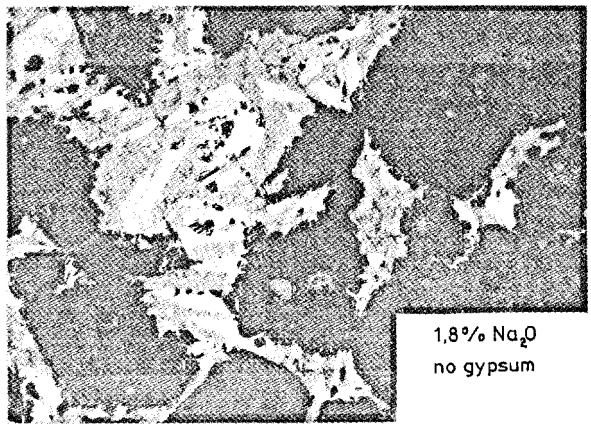

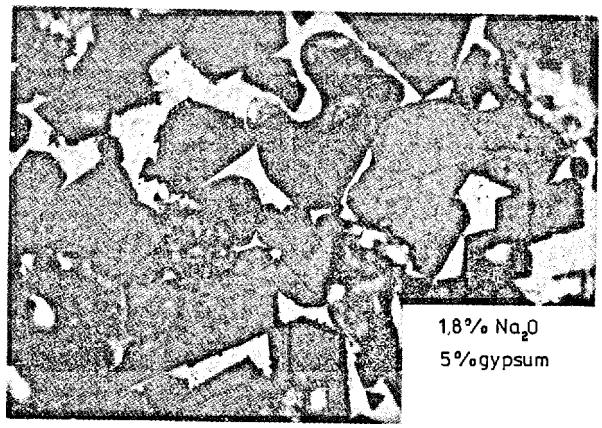

cont. of FIG. 3

free lime content in the clinker, is presented in Fig. 4 .
Besides, an increase of SO_3 content in the clinker leads to a raise in the quantity of cubic C_3A considered as the most reactive form of this compound. It has appeared that in clinkers containing 0.9 or 1.4 % Na_2O the C_3A phase occurs predominantly in the cubic form when respectively 3 or 5 % of gypsum was added to the raw meal. In contrary, when no gypsum was added the "prismatic" aluminate phase was found all over the clinker structure.
Results on compressive strength of cements made from clinkers containing different quantities of Na_2O and SO_3 are

shown in Fig. 5 .

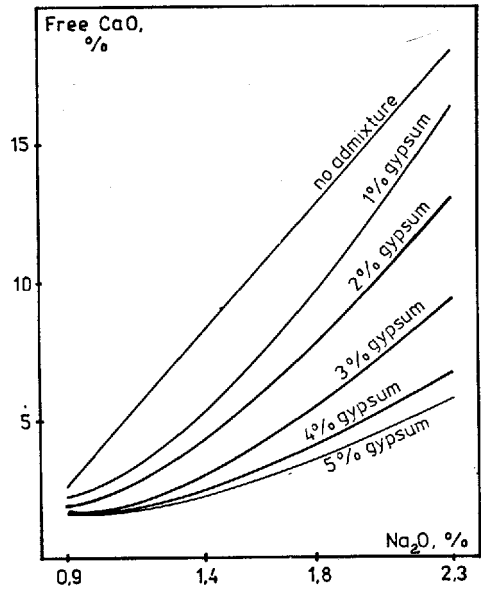

FIG. 4

Effect of gypsum addition to the raw meal on free lime content in the clinker

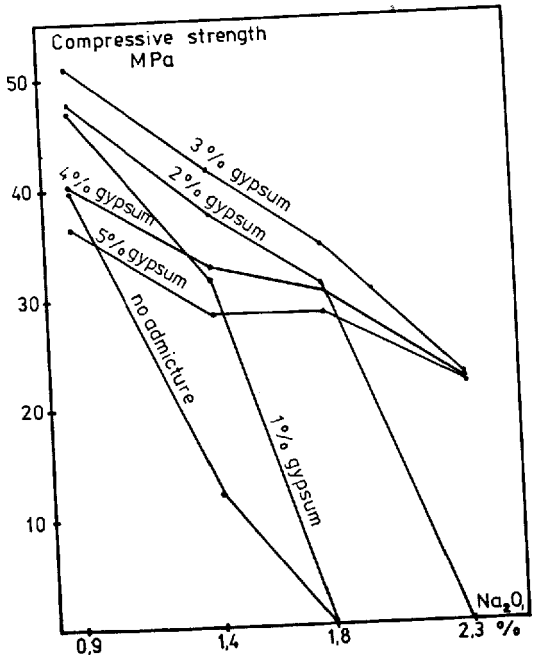

FIG. 5

28-day compressive strengths vs. Na_2O content in clinker and % of gypsum in the raw meal

It has been proved that strength of an alkali containing cement can be considerably improved by introducing gypsum to the raw meal. The best strengths exhibited cements when 3 % gypsum was added to the raw mix. This corresponds to the optimum value of SO_3 content in the clinker, widely discussed in the literature (3 , 4 , 6 , 7 , 8 , 13 , 14) .

However, when 4 or 5 % of gypsum was introduced to the raw meal, resulting cements have manifested a decrease in compressive strength. In this point, neither qualitative nor quantitative changes in the clinkers have been revealed by XRD examination; the X-ray patterns did not differ from XRD traces for clinkers produced from raw meals containing 3 % of gypsum. Also, no increase in free lime has occured in clinkers as it can be seen in Fig. 4 .

It is believed that Na_2O is preferentially combined with SO_3 to form Na_2SO_4. However, some SO_3 may be incorporated into the belite phase thus lowering the hydraulic reactivity of clinkers.

This is, what we believe, the reason of strength reduction of cements made from raw meals containing more than 3 % of gypsum.

No evidence for the formation of silicosulphate phases (e.g. $2C_2S \cdot CaSO_4$) has been found by XRD examination both in our study and that reported by Stunge et al. (13) . However it has been proved (13) that belite contains much more sulphur than other clinker phases.

Our report relates to a specific set of raw materials. It should be emphasized that the behaviour of different alkali containing raw materials is strongly dependent on their physicochemical nature.

Thus, in any particular case, the "optimum" gypsum requirement must be determined experimentally.

CONCLUSIONS

1. Addition of gypsum to Na_2O containing raw meals leads to the modification of the clinker structure towards the better developed alite and belite crystals. Reactivity of the raw mix is increased so that more C_3S can be formed and the C_3A phase tends to crystalize in the cubic form. Thus, the compressive strength of cement is increased.
2. In the present study the optimum gypsum addition is to be 3 %, however, different raw materials may require a different admixture of gypsum.
3. When 4 or 5 % of gypsum was introduced to the raw meal, the compressive strength of resultant cements decreased. It is believed that this is caused due to reduction of the hydraulic reactivity of β-C_2S.

REFERENCES

(1) Grzymek J. et al.: Cement Wapno Gips, 8-9 (1980), 210
(2) Patent PRL nr 43444
(3) Jawed I., Skalny J.: Cem. Conc. Res., Vol.7 (1977), 719
(4) Jawed I., Skalny J.: Cem. Conc. Res., Vol.8 (1978), 37
(5) Sudakas A.G. et al.: Tsement, 12 (1978) 11
(6) Butt J.M. et al.: Tsement, 4 (1971), 14
(7) Luginina J.G., Luginin A.N.: Tsement, 11 (1974), 13
(8) Jelenic J., Panovic A.: Cem. Conc. Res. Vol.10 (1980), 463
(9) Gutt W.: Build. Res. Station, V Int. Symp. Tokyo, 1968
(10) Knorel D., Spohn E.: Zement Kalk Gips, 22 (1969), 471
(11) Gutt W., Smith M.A.: Nature, 210 (1966) 408
(12) Pliego-Cuervo Y.B., Glasser F.P.: Cem. Conc. Res., Vol.8 (1978), 455
(13) Strunge J. et al.: Zement Kalk Gips, 3 (1985), 150
(14) Strunge J. et al.: Zement Kalk Gips, 8 (1985), 441
(15) Duda W.H.: Cement Data-Book, 2 Ed., 1977, Bauverlag GMbH, Wiesbaden and Berlin
(16) PN-80/B-04300.
(17) Regourd M. et al.: J. Appl. Cryst., 6 (1973), 355

Prof. B. WERYNSKI, D. Eng., Building and Bonding Materials Industry Research Institute, Opole, Poland.

A. WERYNSKA, D. Eng., Building and Bonding Materials Industry Research Institute, Opole, Poland.

1.2

INFLUENCE OF THE ISOMORPHIC COMPONENTS ON THE CLINKERISATION PROCESS

SUMMARY: Main minerals of portland clinker have higher hydraulic activity in case of deformation of their crystallic structure. One of the factors introducing such a deformation is the penetration of other minerals or oxides into the structure of main minerals and forming solid solutions. Special ability to form solid solutions have isomorphic components of natural raw materials such as MgO, K_2O, Na_2O, $\overline{S}$, A and F. In the clinkerisation process these components play a role of mineralizers increasing the amount of the liquid phase, i.e. changing the crystallisation conditions, which leads in turn to differentiation of crystallic microstructures and crystal dimensions thus increasing the hydraulic activity of the minerals. Main importance of the isomorphic components is their influence on modification of clinker phases connected with forming new phases and significant change of their hydraulic activity.

Investigation of the hydraulic activity of clinkers with different concentrations of MgO, Na_2O, K_2O, A and F based on early and late strenght measurements is presented in this paper. Moreover the clinker microstructure was investigated observing the influence of the liquid phase on crystal forms. The results are shown on photographs. The influence of the isomorphic components on clinker hydraulic activity is explained by investigation of their distribution in clinker phases, using the microprobe. The results are shown on photographs. From microscopic studies occurs, that somewhat higher amount of the liquid phase improves the clinkering conditions. Main alite phase crystallizes in form of polyhedrons and pseudo-hexagonal shallows with visible belite inserts. The samples show high hydraulic activity measured as 28 days strength. The clinkers with lower amount of the liquid phase are more porous, the alite crystals are of dendrite form and the belite appears in form of grown together rings.

Analysis of the characteristic X-ray radiation distribution over particular clinker phases shows, that Mg^{2+} is evently distributed in all phases, but its concentration is higher in alite and highest in filling substances consisting mainly of tricalcium aluminate and tetra calcium alumino-ferrite. The microprobe analysis results confirm the literature data i.e. the fact, that Mg^{2+} replaces Ca^{2+} ions in the crystallic net of the tricalcium silicate forming the solid solution. Na^+ and K^+ ions are built in the alite and belite crystallic structure forming solid solutions. The presence of the isomorphic components modifies the microstructure and texture of the clinker phases increasing their hydraulic activity.

Os principais minerais de clínquer portland têm atividade hidráulica mais alta em caso de deformação de sua estrutura cristalina. Um dos fatos que ensejam uma deformação é a penetração de outros minerais ou óxidos na estrutura dos minerais principais e formação de soluções sólidas. Têm especial aptidão para formar soluções sólidas os componentes isomórficos das matérias primas naturais, tais como MgO, K_2O, Na_2O, S, A e F. No processo de clinquerização estes componentes exercem um papel de mineralizadores, aumentando a quantidade da fase líquida, isto é, mudando as condições de cristalização, o que leva por sua vez à diferenciação de microestruturas cristalinas e dimensões de cristal, aumentando assim a atividade hidráulica dos materiais. A principal importância dos componentes isomórficos é sua influência sobre a modificação das fases do clínquer, interligada com a formação de novas fases e mudança sigmificativa de sua atividade hidráulica.

Neste trabalho é apresentada investigação sobre a atividade hidráulica de clínqueres com concentrações diferentes de MgO, Na_2O, K_2O, A e F, com base nas medições da resistência inicial e final. Adicionalmente foi investigada a microestrutura do clínquer, observando-se a influência da fase líquida sobre as formas cristalinas. Os resultados são apresentados em fotografias. A influência dos componentes isomórficos é explicada pela investigação de sua distribuição nas fases do clínquer, usando microsonda. Os resultados são mostrados por fotografias. Verifica-se a partir dos estudos microscópicos que de certa maneira a maior quantidade de fase líquida melhora as condições de clinquerização. A fase principal de alita se cristaliza em forma de poliedros e bancos pseudo-hexagonais com visíveis inserções de belita. As amostras apresentam atividade hidráulica elevada, medida como resistência aos 28 dias. Os clínqueres com menor quantidade de fase líquida são mais porosos, os cristais de alita têm a forma de dendrita e a belita aparece em forma desenvolvida juntamente com anéis.

Análise da distribuição característica de radiação de raios-X em fases específicas do clínquer mostra que Mg^{2+} se distribui uniformemente em todas as fases, mas sua concentração é mais alta na alita e máxima nas substâncias de enchimento, que consistem principalmente de aluminato tricálcico e ferroaluminato tetracálcico. Os resultados de análise de microsonda confirmam os dados de literatura, isto é, o fato de que Mg^{2+} substitui íons Ca^{2+} na rede cristalina do silicato tricálcico formando a solução sólida. Íons Na^+ e K^+ são criados na estrutura cristalina da alita e belita formando soluções sólidas. A presença de componentes isomórficos modifica a estrutura e a textura das fases do clínquer, aumentando sua atividade hidráulica.

INTRODUCTION

Main components for the production of clinker are: limestone, chalk, marl and clay. In case, when the chemical composition of a raw mix does not meet the technological requirements the correcting materials are added, such as slags, sands, ashes, iron - containing components etc.

The origin of raw materials - natural or artificial - their mineralogical composition and physical and chemical properties have indubitable influence on the clinkerisation process. The mineralogical form of main raw mix components, i.e. C, S ,A, F has an influence on the kinetics of formation of calcium aluminates and silicates.

The share of the main oxides in the subsequent stages of forming main clinker minerals is shown on Fig. 1.

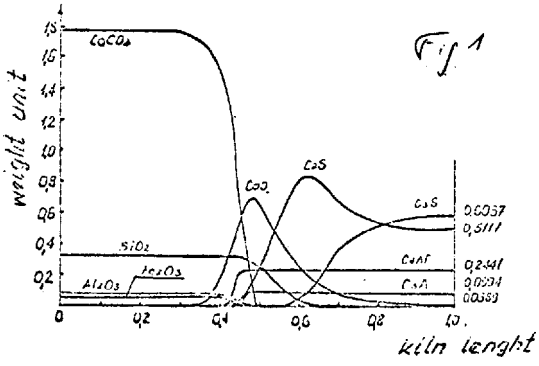

Figure 1. Course of the reactions between different oxides in the clinkerisation process.

Considerable influance on the clinkerization process have different isomorphic additions, directly built in the crystallic structure of minerals. Most common isomorphic inclusions in the calcite are the Mn, Cr, Fe, Li, B, Ba and Ni oxides. The presence of these inclusions lowers the synthesis temperature of the minerals with lower lime saturation degree.

During the burning of the cement clinkier in high temperature the reactions between silicates take place partly in the solid phase and partly in liquid one. In the buring zone of the kiln reactions take place in the solid phase. The speed of these reactions depends first of all on the speed of diffusion, which in this phase is directly proportional to the temperature and inversely proportional to the tightness of the reagent's structure. The silicates structure is rather loose because of tetrahedronal ions coordination Si^{+4}.

In the clinkerisation process the isomorphic components play a role of mineralisators. Presence of A, F, MgO, Na_2O, K_2O lowers the temperature of the formation of entectics, which are important for initiating the reactions and decreases the vislosity of alloys, which in turn fascilites the ions movement and thus the reactions course.

As it is known silicate alloys have high viscosity resulting from considerable part of atomic bond Si-O in the SiO_4^{4-} anion. Substituting the oxygen by one-valence ions in this anion or introducing kations modyfying the properties of the silicate alloy causes the decrease of its viscosity.

The isomorphic components of the raw mix have also a crystallic influence on the clinkerisation process/ for example Fe in $CaCO_3$ and illites/.

Most important factor for accelleration and fascility of reactions in the solid state is the irregularity of adjacent crystals. The higher the irregularity is, the less energy is required to initialize the reactions.

The knowledge of isomorphic components influence on physical and chemical properties of the liquid phase allows to modify the process of the formation of clinker minerals thus changing their hydraulic activity.

Many research works on the mechanism of clinker phases formation show, that solid solutions of main minerals with isomorphic components are formed from the polymineral liquid phase containing these components.

Presented research study is the contribution for an explanation the role of isomorphic components of the raw mix in the process of forming the clinker minerals.

Explanation of this mechanism is possible by testing the distribution of isomorphic components in indyvidual clinker phases and investigating the texture of the crystals. Such possibility is given by an electron microscope equipped with microprobe.

THE EXPERIMENTAL PART

The influence of isomorphic components on the formation of clinker minerals was investigated basing on clinkers produced from natural raw materials containing small amounts of Na_2O, K_2O, MgO and traces of ZnO, CuO, V_2O_5, MnO_2, Cr_2O_3, PbO and NiO.

The concentration of the trace elements was established using the atomic absorption spectrometry technique.

The sintering test of raw materials were carried out using the high temperature microscope. The results show, that the sintering temperature of raw materials lies between 1150 and 1250°C.

In laboratory conditions the clinkers of different chemical and mineralogical compositon were produced using the limestone consisting mainly of calcite and small amounts of kaolinite and clay / haolinite, illite, chlorite/.

Investigation of mineral composition of clinkers was done using the microscope.

Structural investigation of clinker minerals was carried out using electron scanning microscope with microprobe. The microstructure of clinkers was observed by means of the signal of secondary electrons emitted from the surface and representing the sample topography. The distribution character of Mg, K, Na, Fe and Al and alterations of their concentration along chosen lines was investigated in some microregions of alite and belite, measuring the intensity alterations of their x-ray characteristic radiation.

The results of the observations of clinkers on the electron scanning microscope are shown on Figures 2, 3 and 4.

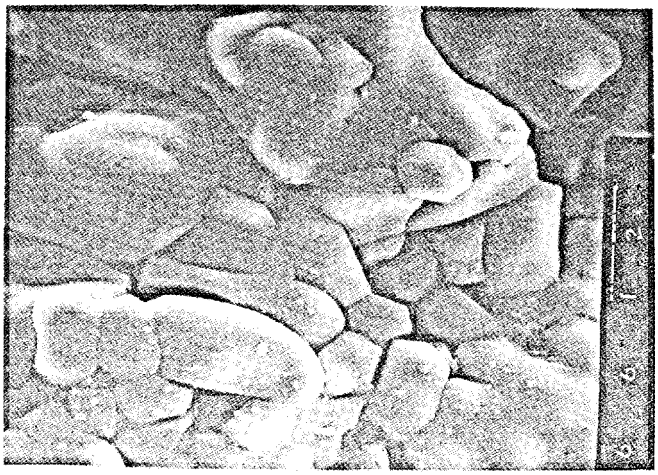

Figure 2. Microstructure of clinker with LSF = 0,92. Magnification 1000 x.

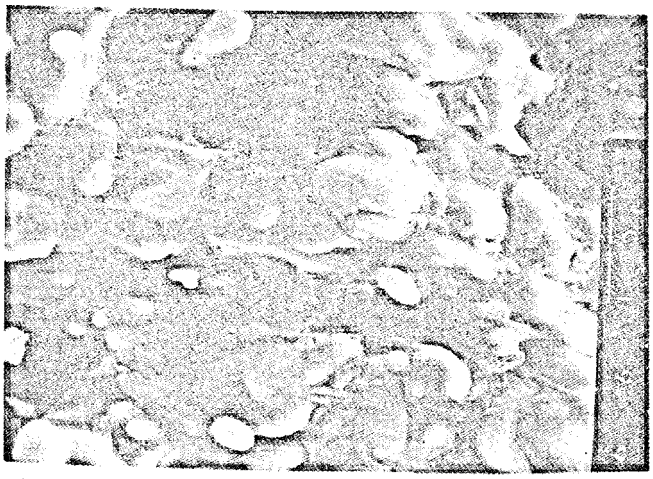

Figure 3. Microstructure of clinker with LSF = 0,93. Magnification 1000 x.

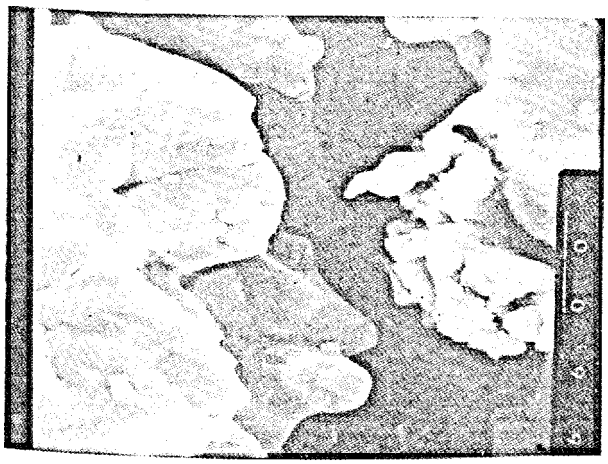

Figure 4. Microstructure of clinker with LSF = 0,94. Magnification 1000 x.

The photographs show clinker fractures with visible well shaped grains of calciferous silicates. The main alite phase is present as pseudohexagonal plates and polieders. On the alite surface the belite inserts are visible / Figure 2 /. Minerals of the clinker with LSF = 0,93 are sunk in glass phase filling the area between the grains / Figure 3 /. The alite phase of that clinker appears in form of polieders and hexagonal plates. Comparing with others this clinker has the highest concentration of MgO, K_2O and Na_2O / 1,4%/, the presence of which created profitable condi tions for cristallisation and forming the alite with higher symmetry and higher hydraulic activity.

The clinker with LSF = 0,94 is of the lowest concentration of isomorphic components. The microstructure of the fracture shows very rich porous structure with different grain sizes.

The pores are free spaces between the grains or have a character of micro-cracks. Numerous dendrite belite coalescences are visible as well as plate-shaped alite rings / Figure 4/. This type of clinker has the highest hydraulic activity measured as 1-day strenght, because the high porosity fascilites the pe netration of water particles during hydration pro- cess. The clinker had lower concentration of isomorphic components /1,205%/ as well as lower concentration of aluminium and iron oxides /A + F = 8,1%/. The concentration of the liquid phase estimated according to Murray was 23,6% comparing with 25,5% of the clinker with LSF = 0,93. Small difference in the chemical composition of the two clinkers and the same burning conditions for the clinkers with different a- mount of the liquid phase resulted in two products with different hydraulic activity.

To explain the influence of isomorphic components on the hydraulic activity their distribution in particular clinker phases was investigated.

Observing the polished and pickled microsections in reflected electron beam one could to investigate the crystallic structures and to carry out the quality microanalyses of clinkers. The x-ray microprobe allo wed to investigate the distribution character of Mg, Al, Fe, Na and K and the change of elements concentra tion along choosen lines, measuring the change of in- tensity of their characteristic x-ray radiation.

The results of the clinker tests are shown on photographs 5, 6, 7, 8, 9, 10, 11 and 12.

The analysis of characteristic radiation intensity changes shows that Mg is evently distributed along the alite and belite area. Comparison of Figure 5 and 9 shows distinctly that there is much more Mg^{2+} ions in alite crystals than in those of belite, but most of them are present in the filling substance con sisting of calcium aluminates and tetracalcium alumi- noferrite. Microanalysis results confirm the literature data according to which ion Mg forms the solid solution with three - calcium silicate replacing Ca^{2+} ions in its crystal latice.

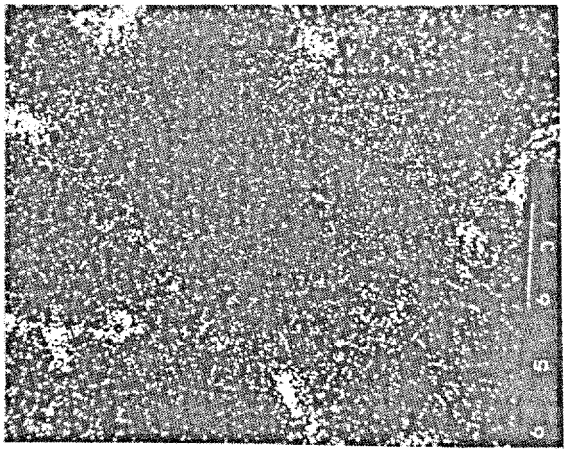

Figure 5. Distribution of Mg in the alite microarea.

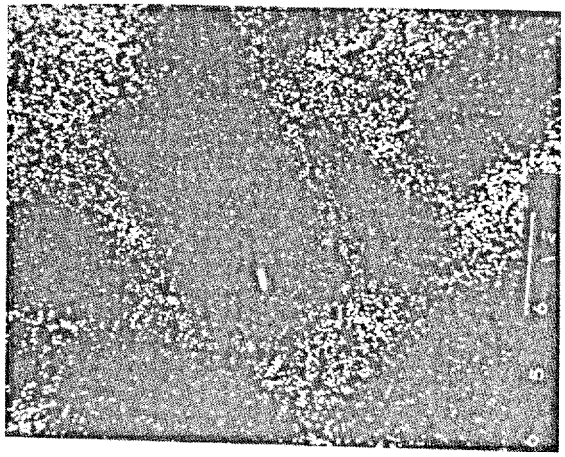

Figure 6. Distribution of Fe in the alite microarea.



Figure 7. Distribution of Al in the alite microarea.

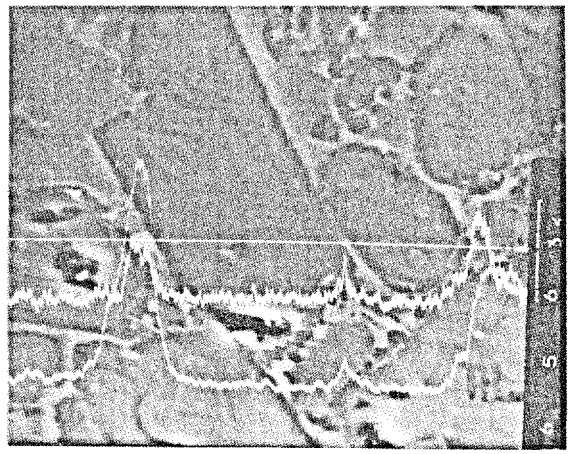

Figure 8. Changes of concentration Mg and Al along chosen line in the alite microarea.

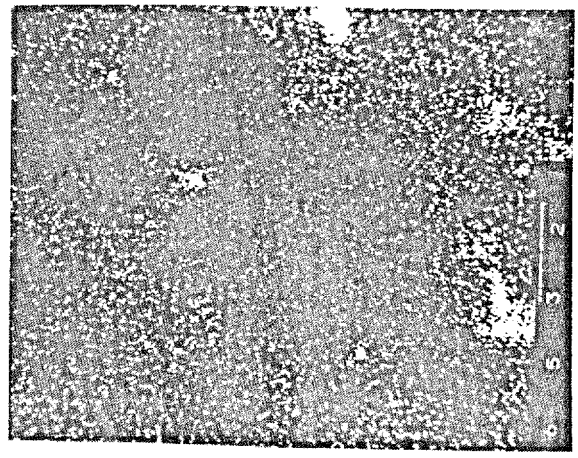

Figure 9. Distribution of Mg in the belite microarea.

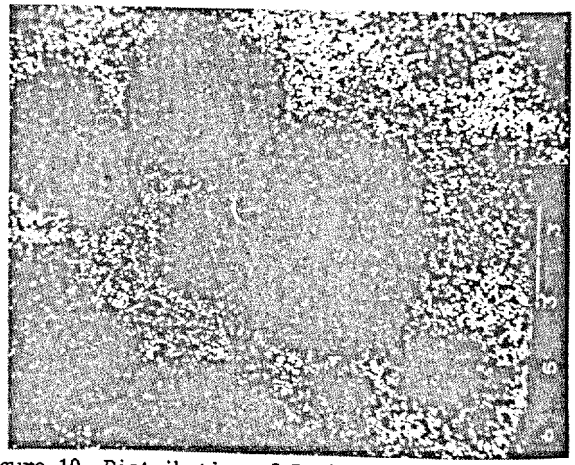

Figure 10. Distribution of Fe in the belite microarea.

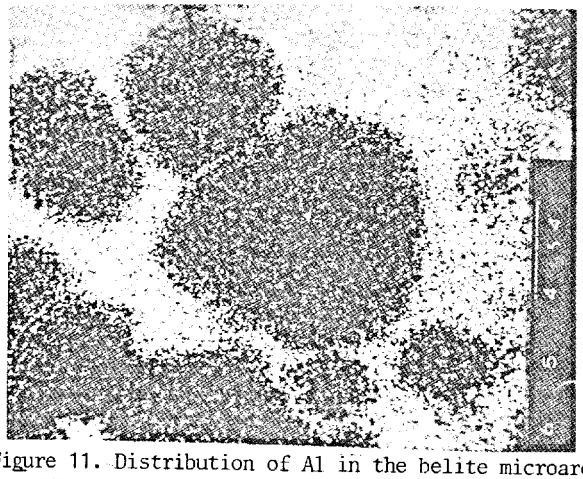

Figure 11. Distribution of Al in the belite microarea

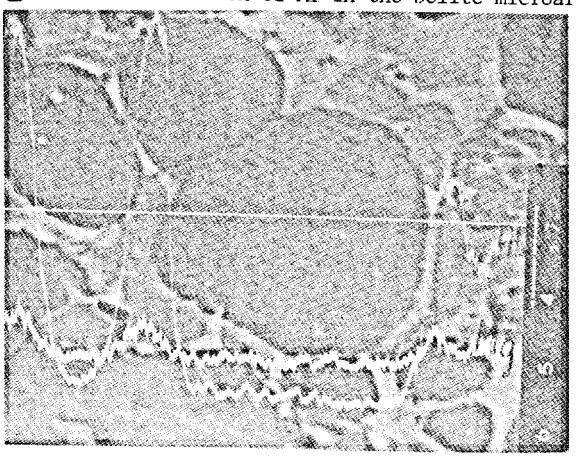

Figure 12. Changes of concentration Mg and Al along chosen line in the belite microarea.

Iron ions are also entering the alite crystal latice but in very small amount. More iron ions are observed in the belite /Figure 6 and 10/.

Aluminium is built into alite lattice in much highier degree then iron, also highier into belite, but evenly in the whole crystal area, which is visible on photographa 7 and 11.

K and Na distribution was investigated in the same microregions as Mg, Fe and Al. Presented photographs /Figures 13 - 16/,show equal K^+ distribution in alite, belite and filling substance. The same applies to Na^+ ions, but in much smaller amounts. Due to very small concentrations of Na^+ and K^+ ions the photographa of their noice were taken to confirm their presence.

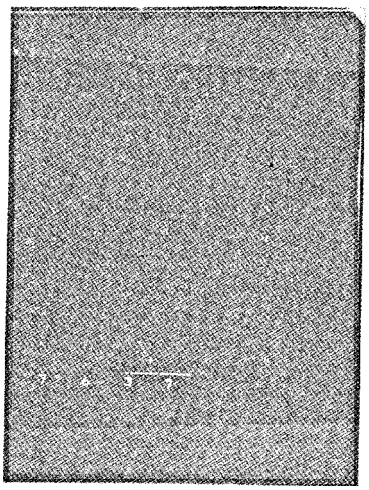

Figure 13. Distribution of Na in the alite microarea.

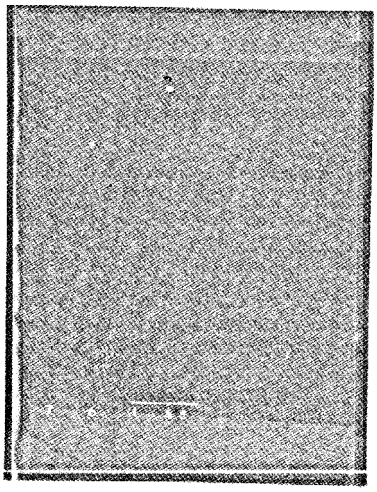

Figure 14. Distribution of Na in the belite microarea.

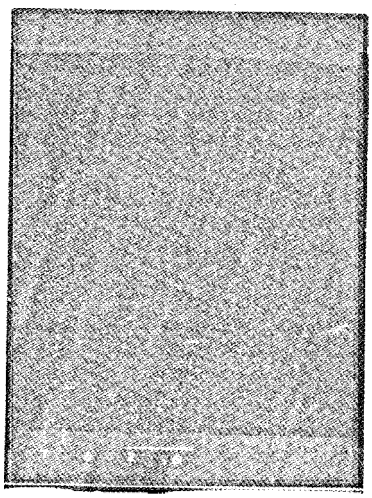

Figure 15. Distribution of K in the alite microarea.

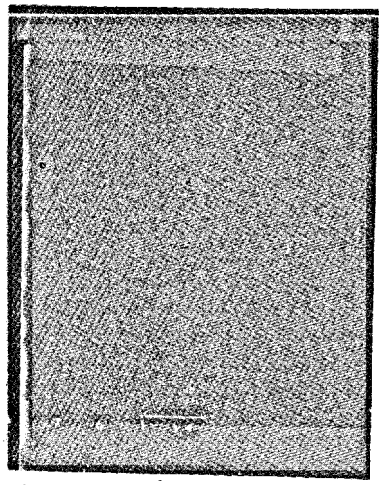

Figure 16. Distribution of K in the belite microarea.

The microprobe analyses confirmed the fact, that calcium aluminates, calcium silicates and tetracalcium aluminoferrietes are not pure minerals, but solid solutions of the minerals with Mg, Fe, Al, Na and K ions built inirregulary into the crystal lattice or replacing Ca and Si ions.

The isomorphic components mentionned above play a role of mineralizers in the sintering process lowering the surface tension of the liquid phase and improving the conditions for silicate and aluminate crystallization. The main significance of the isomorphic components is their modification of hydraulic activity.

Isomorphic components from the liquid phase enter the crystal lattice of minerals forming solid solutions. They also play a role of stabilizers of polimorphic modifications. The presence of the oxides of elements of potassium group in the solutions results in ophaining higher symmetry and increased hydraulic activity of three-calciferous aluminates.

Increasing the MgO concentration to about 4% gives the increase of the hydraulic activity of the three-calciferous silicate. The fact is confirmed by strength tests of cement with highest MgO and potassium group oxides concentration. The presence of those components caused the modification of the mineral composition of clinker and creating new phases by destroing their structure during the process of forming of solid solutions.

Simultaneously the hydraulic activity of a phase depends on the irregularity of its crystallic structure caused by the presence of "foreign" ions in the lattice, which gives energetic potencial of minerals deciding about their chemical reactivity.

The investigation on influence of isomorphic components on the clinker hydraulic activity shows that certain concentrations of these components give optimal increase of activity.

Overfulfilling the saturation limits of isomorphic components gives, however, even destructive efects, callsing desintegration of clinker phases to lower orders with secreting of free C.

BIBLIOGRAPHY

1 - P.P. BUDNIKOV, E.B. EUTIN, A.P. BIELOV /1967/, "O viazkosti jidkoi fazy portland-cementnogo klinkiera", DAN SSSR, № 3.

2 - I.M. BUTT, V.V. TIMASHEW /1965/, "Portland clinkers of a reguired crystal structure and cements of a high quality obtained on their phase", Jurnal of the Mendelejev National Chemical Association in Moscow, № 5.

3 - M. Reguard, A. Guiner /1976/ "The Crystal Chemistry and Crystalochemistry of Cement Minerals", VI I.C.C.C., Moscow, Vol. I.

4 - D. Knofel /1979/, "Tonindustrie Zeitung", № 12.

5 - Sk. Takagi Yamaguchi, "Present - Day Methods of Investigation of the Clinker Formation Mechanism and Clinker Phase Compositions", Japan.

Ion Teoreanu, Marcela Muntean, Institutul Politehnic Bucureşti,
Maria Bedő, Traian Sudrigean, Institutul Cercetări Proiectări Industria
Lianţilor şi Azbocimentului, Bucureşti, Romania.

Belitic Portland Cements with various content of MgO and SO_3

Des ciments Portland bélitiques avec contenu variable de MgO et SO_3

SUMARY: The obtaining of low firing temperature binding masses, without lowering physical-mechanical properties of the resulting cements is a very important problem for the binder industry. In the present paper, belitic Portland cements with various contents of MgO (to lo %) and SO_3 (5 %), were synthetized, in the conditions in which the raw materials Fe_2O_3 content is low, at the following temperatures: 1,25o°, 1,3oo°, 1,35o° and 1,38o°C/3o min. In these conditions a sulphate aluminate compound is formed, which determines changes in the mineralogical composition of the Portland cement clinker. The burning ability of the synthetised masses was followed using DTA and the free lime content analyses. The compositional modifications and the physical-mechanical properties of the samples were determined using X-ray analysis and mechanical strengths determinations. The above mentioned clinkers may be synthetised from raw materials with a higher MgO content.

SUMÁRIO: A obtenção de massas aglomeradas de baixa temperatura de queima, sem redução das propriedades físicas e mecânicas dos cimentos resultantes é um problema muito importante para a indústria de aglomerantes. No presente trabalho, cimento portland belítico com vários conteúdos de MgO (até 10%) e SO_3 (5%) foram sintetisados, em condições nas quais o conteúdo de Fe_2O_3, na mistura crua, é baixo, às seguintes temperaturas: 1250°, 1300° e 1380°C em 30 minutos. Nessas condições o composto sulfoaluminato se forma, o que determina alterações na composição mineralógica no clínquer do cimento portland. A facilidade de queima das massas sintetisadas foram seguidas com o uso de DTA e análise do conteúdo de cal livre. As modificações de composição e as propriedades físico-mecânicas das amostras foram determinadas usando análise de raio-X e por determinações de resistências mecânicas. Os clínqueres acima mencionados podem ser sintetisados com matéria-prima com alto conteúdo de MgO.

INTRODUCTION

The obtaining of binding masses at lower firing temperatures, in comparison with ordinary Portland clinkers, without lowering theirs physical-mechanical properties is a interesting problem for the binder industry. The possibility to produce some belitic clinkers with physical-mechanical properties comparable with those of the ordinary Portland clinkers, at relative low firing temperatures (1,3oo - 1,37o°C) from various raw materials was tested by numerous researchers / 1-14 /.

In the present paper were studied white belitic clinkers, synthesized from usual raw materials, with various content of MgO (introduced as $MgCO_3$) and a constant content of SO_3 (introduced as gypsum). The modifications induced by $MgCO_3$ and $CaSO_4 \cdot 2H_2O$ admixtures, both upon the burning behaviour of the raw materials, as well as, upon the binding properties of the resulted cements were examined.

EXPERIMENTAL

A series of laboratory clinkers have been prepared from usual raw materials, characterized by reduced Fe_2O_3 content (adequate to manufacture some white clinkers) and which have the chemical composition presented in Table 1.

The clinkers have lime saturation factors of 75, 8o and 85 and the same modular chracteristics: silica modulus about 5.1o and alumina modulus approximately 27; in this case, the alumina modulus loses its significance, because the Fe_2O_3 content of the clinkers is under o.5 %.

Table 1.

Chemical composition of raw materials.

Oxide	Chemical composition, wt.%		
	Limestone	Kaolinite clay	Bentonite
CaO	55,1o	1.51	7.55
SiO_2	o.32	75.9o	51.5o
Al_2O_3	o.16	14.o1	18.2o
Fe_2O_3	o.o4	o.4o	o.7o
MgO	o.71	o.25	2.1o
Na_2O	o.24	2.o8	2.o6
K_2O	o.o6	2.8o	2.13
SO_3	o.o7	o.o5	o.22
L.I.	43.3o	3.oo	15.54

The raw materials mixtures have been finely ground (under 63 /um), pelletized at about 5 MPa and fired for 3o minutes in an electric furnace at 1,25o°, 1,3oo°, 1,35o° and 138o°C. The resulted clinkers were quenched in air and ground without gypsum to a Blaine specific surface area of 38o m^2/kg.

The burning behaviour and the mineralogical composition of the synthesized masses have been followed by chemical analysis of the free lime content, XRD (performed on TUR-M.75, diffractometer using CuK_α radiation) and DTA (Erdely-Pauling, 1o°/min.).

The physical-mechanical properties of all cements have been determined by standard testing methods.

RESULTS.

The determinations of the free lime (CaO_f) content evidence, for all examined samples, a good clinkerization degree at 1,35o°C. The masses with lime saturation factors equal to 75 and 8o have the recommended content of free lime (CaO_f = 2 %), even when these mixtures were fired at lower temperatures for example, at 1,3oo° and 1,25o° (see Table 2).

Table 2

Free CaO, wt.% on the masses

Samples	MgO %	Firing temp.°C/3o min.			
		125o	13oo	135o	138o
A	1.6	2.45	1.43	o.85	o
A_1	7.o	1.36	o.9o	o.22	o
A_2	1o.o	2.33	1.36	o.79	o.56
B	1.2	3.38	1.97	1.2o	o.91
B_1	7.o	1.8o	1.15	o.57	o.3o
B_2	1o.o	3.21	1.9o	1.o2	o.79
C	o.9	3.87	2.8o	1.34	1.o2
C_1	7.o	2.3o	1.92	o.88	o.6o
C_2	1o.o	4.1o	2.31	1.31	o.98

A,B,C (reference clinkers) S_K = 75, 8o, 85
MgO = wt.%, in clinkers

In all cases a positive influence is remarked when the clinkers contain 7% MgO and 5% SO_3 (constant value for all clinkers). The corresponding CaO_f values suggest in this case an acceleration of the clinkerization processes. When biger proportions of the MgO, were added, as to have up to 1o % MgO in the clinkers, for a constant proportion of SO_3 (5%), no semnificative modifications of the CaO_f was observed in comparison with the reference clinkers.

The obtained free lime value are in concordance with XRD analysis, fig.1-3. As expected, the increase of the synthesis temperature determines the increase in the content of the well crystallized silicate compounds (C_2S+C_3S - 2.78 Å; C_3S - 1.76 Å) lowering, in the same time, the CaO_f content of the clinkers. Simultaneously, the XRD data show

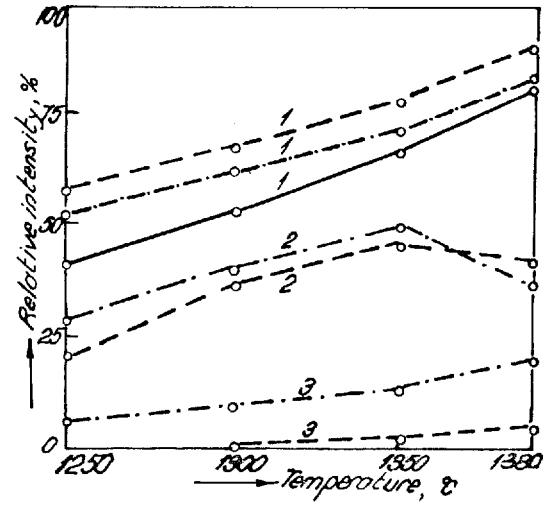

Fig.1. Relative intensity vs. temperature: (1)-C_2S+C_3S; (2)-$(C,M)_4A_3\bar{S}$; (3)-MgO. ——(A); -.- -(A_1) and -•-•- (A_2).

a maximum line at 3.72 - 3.74 Å which was attributed to the formation of a sulphate aluminate compound resulted as a consequence of the SO_3 presence in the samples. The fact that the maximum is not at 3.76 Å (the line foe pure $C_4A_3\bar{S}$) may be explained by the probable presence of a variable quantity of the MgO in the crystalline latice of the latter compound, with the result of the formation of a sulphate aluminate of $(C,M)_4A_3\bar{S}$ type /15/. The $(C,M)_4A_3\bar{S}$ content

of the clinkers increases with the increase of the MgO content of the samples; this is

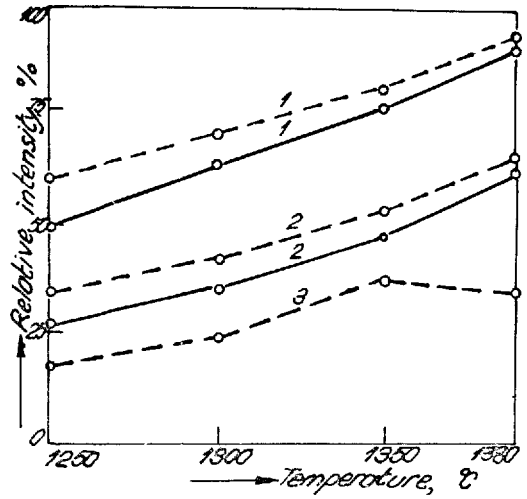

Fig.2. Relative intensity vs.temperature: (1)-C_2S+C_3S; (2)-C_3S; (3)-$(CM)_4A_3\bar{S}$; ——(B); - - -(B_1).

not the case for the masses fired at temperature greater than 1,38o°, when a partial decomposition of the $(C,M)_4A_3\bar{S}$ may take place, resulting periclase (2.1o Å) and a higher proportion of free lime.

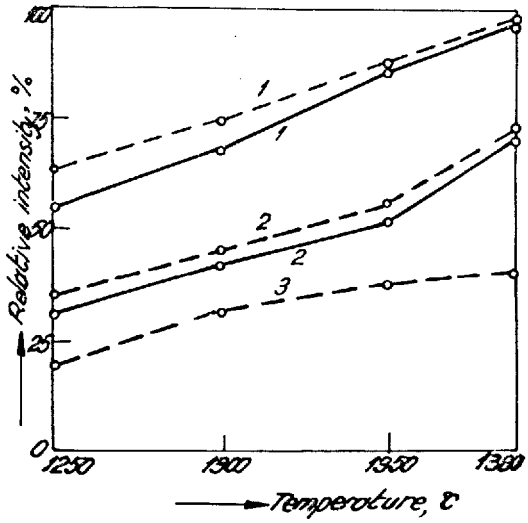

Fig.3.Relative intensity vs temperature (1)-C_2S+C_3S; (2)-C_3S; (3)-$(C,M)_4A_3\bar{S}$; ——(C); - - - (C_1)

The formation of the above mentioned sulphate aluminate compound in clinker with 7 and lo % MgO and a constant content of SO_3 (5%) is also evidenced by the DTA analysis, which show an exothermic peak at 1265°/16/, fig.4. The DTA curves also, show that the increase of the MgO content in the samples, determines a shift of some thermic effects: for example these for decarbonation and for clinkerization.

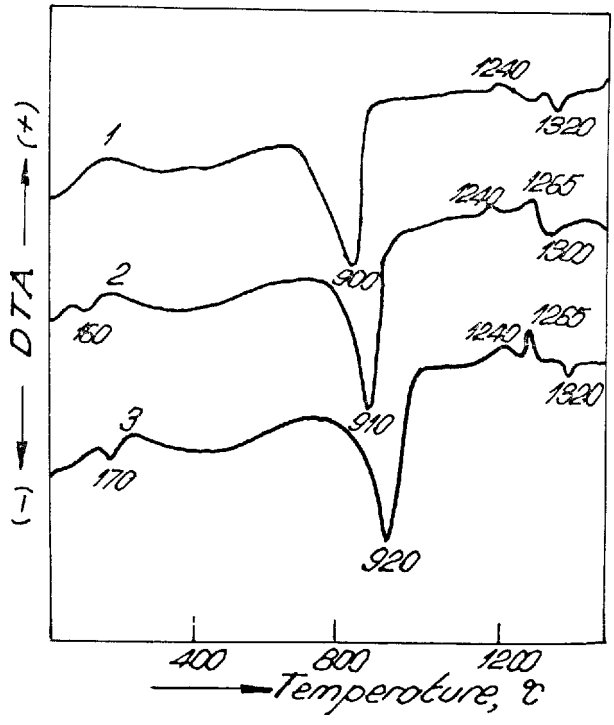

Fig.4. DTA curves.
(1)-A; (2)-A_1; (3)-A_2.

The mechanical properties of the binding masses, especially for the samples with 7% MgO and 5% SO_3, burnt at 125o° are relatively good and they are very good when these samples were burnt at 13oo° and 135o°C, see fig.5-6. For normal hardening conditions, these cements are characterized by a good volume constancy.

This behaviour of the cements may be attributed to the formation of the $(C,M)_4A_3\bar{S}$. In the early stage of the interaction with water the $(C,M)_4A_3\bar{S}$ compound may be an accelerating agent of the hydration-hydrolysis processes.

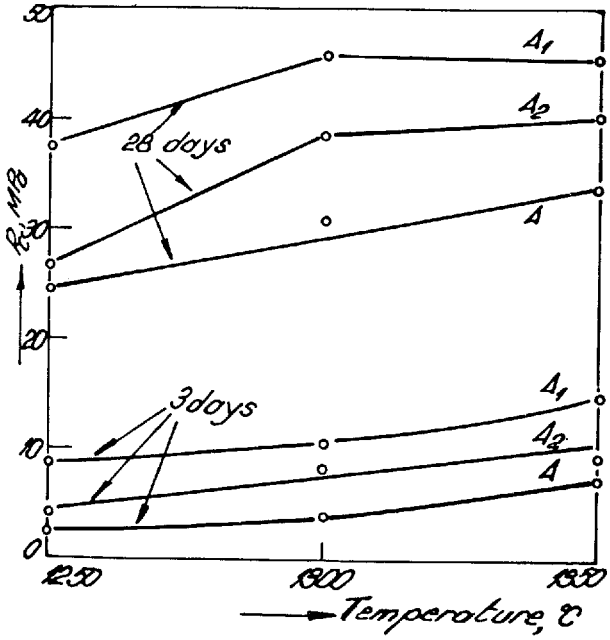

Fig.5. Compressive strength vs temperature.

The normal consistency water values is in the usual limits: 27 - 3o %, and the setting time begins after 1^h35^{min} - 2^h15^{min} and ends after 7 - 9 hours. For the reference cements the setting time and the $H_2O_{n.c.}$ have the upper limit values of the above given domains.

These binding masses can be utilized as white cements. It must be noted that a very good whiteness (an increase with 7-9% in comparison with reference clinkers) is observed for the samples with 7-1o % MgO and 5 % SO_3. These cemants showed also, a good mechanical strengths, above 33-35 MPa, after 28 days of normal hardening, /17-18/.

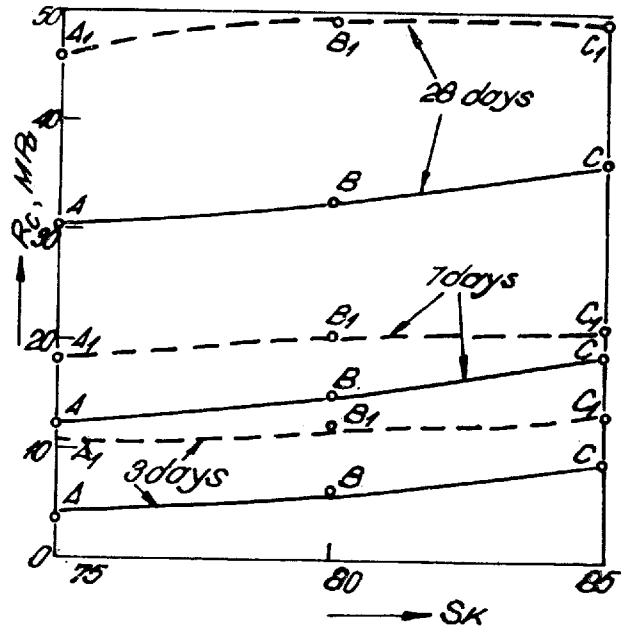

Fig.6. Compressive strength vs lime saturation factor.

CONCLUSIONS

The present investigations have led us to the following conclusions:

- belitic clinkers can be prepared from usual cheap raw materials have a reduced content of Fe_2O_3, even at 125o° - 13oo°C in the presence of the MgO and SO_3 admixtures;

- these clinkers may be utilized as white cements;

- in the presence of MgO and SO_3 both, the whiteness of the clinkers and the mechanical strengths of the resulted cements are good, even when the firing temperatures are with approximatevely 2oo°C lower;

- the MgO proportion introduced in the samples must be correlated with the SO_3 proportion of the clinker, because in this way is possible to incorporate all MgO in the crystalline latice of the sulphate aluminate compound of $(C,M)_4A_3\overline{S}$ type.

REFERENCES

1. Ghosh, S.N., Mathur, V.K., Chopra, S.K., CCR, 14, 437 (1984).

2. Müller, A., Stark, J., Mielke, J., Silikattechnik, 35, 276 (1984).

3. Mehta, K., USPatent 4,o36,657-Co48, 7/82 (1977).

4. Mielke, I., Müller, A., Stark, J., 9 Intern.Baustoff Silikattagung, Weimar, 17-21 Juni, S.l.,82(1985).

5. Skomorowski, E., Cement Wapno Gips, 33, 334 (198o).

6. Stark, J., Müller, A., Rümpler, K., ZKG., 34, 476 (1981).

7. Viswanathan, V.N., Raina, S.J., Chatterjee, A.K., World Cement Technology, 9, lo9, (1978).

8. Stark, J., Müller, A., Schrader, R., Rümpler, R., Dahm, B., Silikattechnik, 3o, 357 (1979).

9. Mielke, I., Müller, A., Stark, J., Mat. Construcţii, 15, 138 (1985).

lo. Seydel, R., Jost, K.H., Lampe, F.V., Stark, J., Müller, A., Materiale de Construcţii, 15, 142 (1985).

11. Kuś L.I., 9 Intern.Baustoff Silikattagung, Weimar, 17-21 Juni, S.l, 98(1985).

12. Radeikova-Ianev, W.E., Ianev, I.L., Siliconf, Budapesta, 228 (1984).

13. Teoreanu, I., Muntean, Marcela., CCR, 13, 711 (1983).

14. Ziemer, B., Altrichter, B., Jesenak, V., CCR., 14, 686 (1984).

15. Teoreanu, I., Muntean, Marcela., Dragnea, I., Type $3CA.M_x.\overline{S}_y$ compounds and compatibility relations in CaO-$CaO.Al_2O_3$-$M_x(SO_4)_y$ systems, Il Cemento, (under press, 1986).

16. Budnikov, P.P., Kuznethova, I., Saveliev, G.V., Silikattechnik, 16, 414 (1965).

17. Teoreanu, I., Muntean, Marcela., Revue Roumaine Chimie, 19, 1483 (1974).

18. Protocol Institutul Politehnic Bucureşti - Inst.Cercetări Proiectări pt. Industria Lianţilor Azbocimentului, Braşov (1984-1985).

M. Pérez-Méndez* and J. Fayos+, Chemical Crystallography Laboratory, 9 Parks Road, University of Oxford, United Kingdom.

1

A Very Modified Apatite-Type Structure: $K_3Ca_2(SO_4)_3F$.
Une structure Apatite-Type trés déformée.

1.2

SUMMARY: $K_3Ca_2(SO_4)_3F$, compound identified in coatings of heat recovery cyclones in portland cement kilns, crystallizes in space group $Pn2_1a$ -pseudo Pnma - with: a=13.415(7), b=10.493(8), c=9.127(5) A. The structure was refined to R=0.105 based on 1102 observed reflections. It is a very distorted analog of apatite $M_5(YO_4)_3X$. Both $K_3Ca_2(SO_4)_3F$ and apatite can be described as parallel columns of central F's along the pseudo-screw a-axis, and the 6_3 c-axis respectively surounded by levels of three M-polyhedra enclosing SO_4 groups. The main difference being that whilst in apatite the Ca_3 triangular cation-coordination of F imposes a ternary symmetry for the three surrounding Ca_9 cages, in $K_3Ca_2(SO_4)_3F$, the Ca_2K_2 tetrahedral cation-coordination of F, leaves a pseudomirror symmetry for the surrounding M_8 and $2M_9$ cages. Different F columns are related by parallel screw-axes or inversion centres as in apatite.

$K_3Ca_2(SO_4)_3F$, composto identificado em colagens de ciclone de recuperação de calor em fornos de cimento portland, se cristaliza no grupo espacial $Pn2_1a$ - pseudo Pnma - com: a = = 13,415(7), b = 10,493(8); c = 9,127(5) A. A estrutura foi refinada para R = 0,105 com base nas reflexões observadas de 1102. Ele é um análogo muito deformado de apatita $M_5(YO_4)_3X$. Ambos $K_3Ca_2(SO_4)_3F$ e apatita podem ser descritos como colunas paralelas de F's central ao longo do eixo "a" de um pseudo-parafuso, e o eixo "c" 6_3 respectivamente rodeados por níveis de três poliedros M fechando grupos de SO_4. A diferença é que enquanto na apatita a coordenação catiônica triangular Ca_3 de F impõe uma simetria ternária às três gaiolas Ca_9 circundantes, no $K_3Ca_2(SO_4)_3F$ a coordenação catiônica tetraédrica Ca_2K_2 de F deixa uma simetria de pseudo-espelho para as gaiolas circundantes M_8 e $2M_9$. Diferentes colunas F são relacionadas por eixos de parafuso ou centros de inversão como na apatita.

* On leave from Instituto Eduardo Torroja, Madrid, Spain
+ On leave from Instituto Rocasolano, Madrid, Spain

M. Pérez-Méndez and J. Fayos, Chemical Crystallography Laboratory, 9 Parks Road, University of Oxford, United Kingdom

INTRODUCTION

Recently, $K_3Ca_2(SO_4)_3F$ has been identified by Trivino-Vazquez (1985) in coatings of heat recovery cyclones in the portland cement manufacture process.

Kreidler and Hummel (1970) had previously reported it in a study of structure fields of fluor- and chlorapatites. Compounds of general formula $M_5(YO_4)_3X$, where M = Ca, Sr, Ba, Pb; Y = P, As, V and X = F, Cl, were reported for all combinations as hexagonal apatite types. When Y = S, metal-mixed fluorapatites such as: $Na_3Ca_2(SO_4)_3F$ and $Na_3Pb_2(SO_4)_3F$ were also described as apatite structures; but metal-mixed fluorapatites including potasium of the form $K_3M_2(SO_4)_3F$ were reported as non-apatite type for M = Ca, Cd, Sr, Pb, Ba. The title compound is one of them. In addition, the same authors report some apatite-distorted structure as $Ca_5(CrO_4)_3F$ and $Na_3Pb_2(SO_4)_3Cl$ which are considered as slight deformations of the apatite one.

In the present paper, the crystal structure of $K_3Ca_2(SO_4)_3F$ is studied from a synthetic single crystal and it is compared with the hexagonal apatite structure.

EXPERIMENTAL

Single crystals were obtained by firing stoichiometric mixtures of $CaSO_4$, K_2SO_4 and CaF_2, together with 3% excess CaF_2 and K_2SO_4, at 960°C for 17 hours, afterwards quenching in water. Substantial yields of phase $K_3Ca_2(SO_4)_3F$ were obtained, but the preparations were never phase-pure. Single crystals were handpicked under the petrographic microscope. All of them gave broad diffraction peaks but were considered suitable for X-ray analysis.

Precession photos showed observed reflections allowed in space groups Pnma or $Pn2_1a$.

A cell of a=13.415(7), b=10.493(8), c=9.127(5) Å with Z=4 was confirmed by least squares refinement of 25 convenient reflections. Intensity data for 2988 independent reflections were obtained out to $2\theta=70°$, from a crystal flake, on an automated single crystal diffractometer. Monochromatic MoK_α radiation was used. The CRYSTALS package by Watkin et al. (1985) was used for all calculations except for Direct Methods.

Statistical tests based on N(Z) and $|E|^2$ distributions and the Patterson function analysis, indicated the structure to be acentric.

The structure could be better refined in the space group $Pn2_1a$. After an isotropic refinement, potasium and calcium were distinguished by geometrical considerations. This model was then refined (anisotropic for potasium and calcium atoms and isotropic for the rest).

Afterwards eight oxygen atoms around S2 (sulphur in the pseudomirror plane) were found by (2Fo-Fc) Fourier difference. These were interpreted as two statistically desordered tetrahedra $S2(O2)_4$ and $S21(O21)_4$ pseudo m-related with atomic population 0.5.

A final refinement including these oxygens (isotropic) was done, the final R factor was 0.105 for 1102 reflections with $I > 5\sigma(I)$. Table 1 shows the fractional coordinates and thermal parameters for all atoms after the last refinement.

Table 1. Fractional atomic coordinates and thermal parameters (with their l.s.s.d. in parenthesis) of $K_3Ca_2(SO_4)_3F$. Coordinates of K and Ca atoms are multiplied by 10^4. Coordinates for the rest of the atoms are multiplied by 10^3. U[ISO] being in $Å^2 \times 10^3$. U[ISO] of * atoms are calculated as UEQUIV= $1/3 \sum_i \sum_j Uij\ a^*_i a^*_j \bar{a}_i . \bar{a}_j$.

Atom	pp	U[ISO]	x	y	z
K 1	1.0	23(5)*	5735(8)	5415(12)	6939(11)
K 2	1.0	29(4)*	7128(4)	2500(19)	3481(8)
K 3	1.0	33(4)*	7755(4)	2472(19)	8055(9)
CA 1	1.0	25(4)*	5763(7)	-475(10)	6897(13)
CA 2	1.0	21(3)*	9873(3)	2500	5128(6)
F 1	1.0	21(3)	903(1)	272(2)	302(2)
S 2	0.5	8(3)	1027(1)	237(1)	901(2)
O 12	0.5	19(9)	994(3)	282(3)	755(3)
O 22	0.5	99(32)	1114(3)	153(4)	883(6)
O 32	0.5	49(16)	947(3)	168(4)	979(5)
O 42	0.5	26(10)	1053(3)	353(3)	988(4)
S 21	0.5	27(5)	1025(1)	268(2)	924(2)
O121	0.5	48(16)	991(4)	210(4)	784(4)
O221	0.5	23(9)	1126(2)	317(4)	899(4)
O321	0.5	120(41)	958(4)	371(4)	971(6)
O421	0.5	42(13)	1028(3)	166(3)	1036(4)
S 1	1.0	25(2)	841(1)	535(1)	546(1)
O 11	1.0	35(6)	861(2)	398(3)	591(3)
O 21	1.0	59(9)	913(3)	613(3)	632(4)
O 31	1.0	27(5)	744(2)	579(2)	589(3)
O 41	1.0	74(12)	857(3)	571(4)	407(5)
S 11	1.0	16(1)	853(1)	-32(1)	579(1)
O111	1.0	37(7)	854(2)	102(3)	540(3)
O211	1.0	58(9)	932(3)	-81(3)	680(4)
O311	1.0	44(7)	755(2)	-61(3)	652(3)
O411	1.0	58(9)	877(3)	-103(3)	436(4)
.S 1					

The refinement in Pnma space group proved to have some difficulties for the thermal parameters giving a R=0.235 was obtained for 1102 reflections, with $I > 5\sigma(I)$.

We can then summarize that the structure is very close to centrosymmetric with deviations large enough to give a better fit in the non-centrosymmetric $Pn2_1a$ space group. Some significant interatomic distances are given in Table 2.

M. Pérez-Méndez and J. Fayos, Chemical Crystallography Laboratory, 9 Parks Road, University of Oxford, United Kingdom.

RESULTS

Geometrical considerations

The greater radius for K than Ca is evident in Table 2 for K2, K3 and Ca2, so there is no doubt about its actual nomination. That difference is not so clear between K1 and Ca1, although the given nomination seems to be more probable if more weight is assigned to the distances to F and to the not-restrained oxygens. However, the distance K1-O31 is very short and it could be explained by some Ca/K substitutions in this possition. Unfortunatelly, the thermal parameters did not help for that discrimination. On the other hand, the possible Ca/K substitution had to be accompanied by O/F substitution. Nevertheless, the Ca-F distances of $\sim$ 2.20 Å, shown in Table 2 are closer to those expected for Ca-F = 2.33 Å than to the Ca-O = 2.40 Å for a similar atomic arrangement (Fayos et al.,1985). Hence there is no crystallographic evidence for O/F substitution.

Description of the structure

The crystal structure can be described by the packing of the cation-polyhedra cages enclosing the SO_4 and F anions. Fig.1 shows the arrangements of these polyhedra.

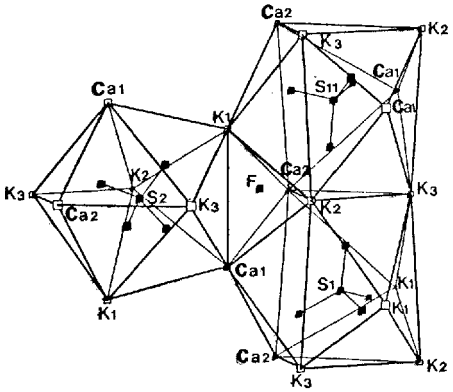

Fig. 1 The cation-polyhedra arrangement surounding the anions SO_4 and F (both in full squares) in $K_3Ca_2(SO_4)_3F$ structure. Only one half populated $S2O_4$ tetrahedron has been represented.

The F atoms are placed at the centre of Ca_2K_2 tetrahedra forming columns along the pseudo-screw axis parallel to a (existing in the Pnma pseudo-symmetry). Around each column, one CaK edge of the tetrahedron is shared with a Ca_3K_5 polyhedron enclosing a statistically desordered SO_4 group (only one represented). The two tetrahedral faces Ca_2K_1 and Ca_1K_2 not containing that edge are shared by two Ca_4K_5 and Ca_3K_6 polyhedra enclosing two SO_4 groups respectively. These two K_9 polyhedra are trigonal-tricaped prisms which are pseudo-mirror related sharing a face.

The whole group of the three polyhedra repeates every 6.74 Å by the pseudo-screw axis parallel to a. The columns are related by parallel screw axes.

The distances between S and K or Ca atom in a cage range from 3,14(2) to 4,09(2) Å, with an average value of 3,6 ± 0,2 Å.

The distances between cations in the same polyhedra range from 3,82(1) to 5,29(1)Å, with average 4,4 ± 0,5 Å. The averaged cation-cation distance on the tetrahedron surounding F has a smaller value of 3,9 ± 0,2 Å.

Its relationship with the hexagonal apatite structure

The orthorhombic unit cell of $K_3Ca_2(SO_4)_3F$ has a volume almost double that of the hexagonal apatite, with similar formula, $Na_3Ca_2(SO_4)_3F$ with a = 9.39, c = 6.89 Å, and space group $P6_3/m$ (Kreidler and Hummel, 1970). In addition, both cells can be related through an intermediate cell defined as: $\bar{a}_{IM} = \bar{b}_o$, $\bar{b}_{IM} = -1/2\ \bar{b}_o - \bar{c}_o$ and $\bar{c}_{IM} = 1/2\ \bar{a}_o$, which would be a typical apatite cell: $a_{IM} = 10.52$, $b_{IM} = 10.57$, $c_{IM} = 6.74$ Å and $\gamma = 120.3^o$.

Hence, a parallel relationship between the crystal structure of $K_3Ca_2(SO_4)_3F$ and hexagonal apatite is expected. A previous crystallographic study on apatite $Ca_5(PO_4)_3X$ structures for X = F, Cl, OH (Wickoff, 1965, p. 228), shows that F atoms are in the centre of Ca_3 triangles perpendicular to the ternary c-axis, whilst Cl or OH are above and below that triangle $\sim$ 0.5 Å.

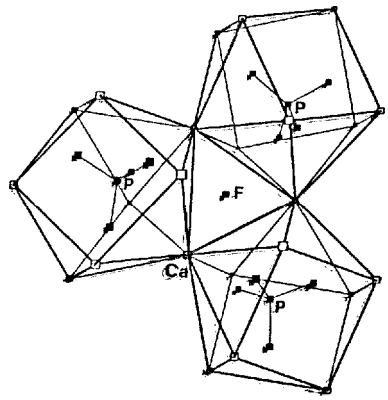

Fig. 2 The cation-polyhedra arrangement surounding the anions PO_4 and F (both in full squares) in apatite $Ca_5(PO_4)_3F$ structure.

According to the analysis based on the cation-polyhedra sublattice, the apatite structure, represented in Fig.2, can be described as columns of parallel Ca_3 triangles with F atoms in the centre, along the 6_3 c-axis, which corresponds to the $K_3Ca_2(SO_4)_3F$ a-axis.

M. Pérez-Méndez and J. Fayos, Chemical Crystallography Laboratory, 9 Parks Road, University of Oxford, United Kingdom.

Surounding each column, and sharing the edges of the triangles Ca_3, there are three equivalent Ca_9 polyhedra cages enclosing SO_4 groups. The whole group repeats here, by the screw-axis every 3.5 Å (a half that in $K_3Ca_2(SO_4)_3F$) for the trigonal packing around the FCa_3 allows closer packing between F's than in the title compound. Columns in the apatite structure are related by inversion centres. Figs. 3 and 4 show de packing of both crystal structures in similar orientation.

Accordingly, both structures can be described as parallel columns of central F's surounded by the three M-polyhedra enclosing SO_4 groups. The Ca_3 trigonal cation-coordination of F in apatite, imposes a ternary symmetry for the three Ca_9 cages, whilst the Ca_2K_2 tetrahedral cation-coordination around F in $K_3Ca_2(SO_4)_3F$, causes a pseudomirror symmetry for the M_8 and $2M_9$ cages.

The differences between apatite and $K_3Ca_2(SO_4)_3F$ structures are, however, not enough to identify the later as apatite-related by inspection its the X-ray powder diffraction patern. A synthetic pattern calculated from its atomic coordinates in Table 1 confirms that fact.

ACKNOWLEDGEMENTS

The authors thank Dr. G. W. Groves of the Department of Metallurgy and Sciences of Materials, Oxford University, for all the facilities in the laboratory during the synthesis.

Table 2. Interatomic distances in A, less than 3.57 Å for K and Ca to O and F atoms, the average 1.s.s.d. is 0.03 Å. Average distances to oxygens are in the last column with their σ_{n-1} standard deviations, $([n\Sigma x^2-(\Sigma x)^2]/n(n-1))^{1/2}$. Distances to the eigh restrained Oi2 and Oi21 are averaged, their σ_{n-1} standard deviations being in parenthesis. Bond distances for S1 and S11 to O atoms are shown with an averaged 1.s.s.d. of 0.03 Å.

Atom	F	⟨Oi2,Oi21⟩	O11	O21	O31	O41	O111	O211	O311	O411	⟨O⟩
K 2	2.59	2.9(1)	3.36	2.96	3.03	--	3.01	3.05	2.71	--	3.0(2)
K 3	--	3.0(1)	2.77	--	3.14	2.72	3.05	--	3.55	2.84	3.0(3)
K 1	2.63	2.6(3)	--	2.78	2.50	--	3.36	--	--	2.76	2.9(4)
Ca1	2.17	2.9(5)	--	--	--	2.52	--	2.30	2.44	--	2.4(1)
Ca2	2.24	2.4(2)	2.41	2.36	--	2.91	2.38	2.73	--	2.43	2.5(2)
S 1	--		1.51	1.50	1.44	1.33					
S11							1.45	1.49	1.50	1.54	

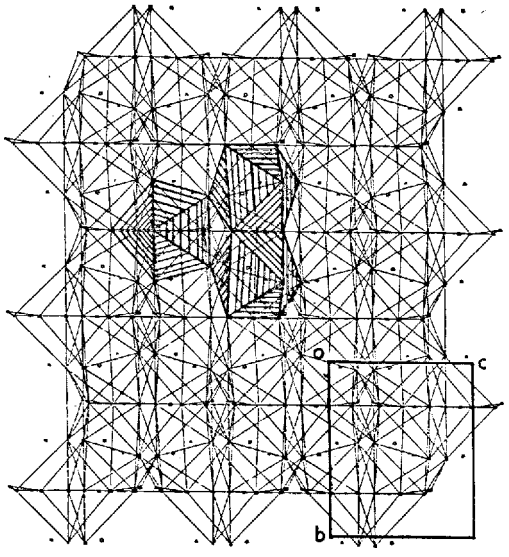

Fig. 3 Packing of $K_3Ca_2(SO_4)_3F$, viewed along the a axis. The unit cell is indicated in the right lower corner.

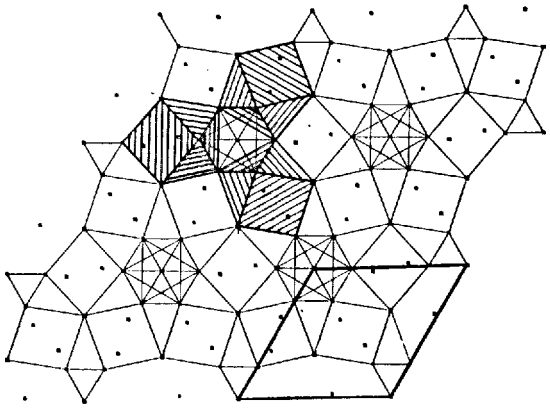

Fig. 4 Packing of apatite $Ca_5(PO_4)_3F$ viewed along the c axis. The unit cell is indicated in the right lower corner.

REFERENCES

Fayos, J., Glasser, F. P., Howie, R. A., Lachowski, E., Perez-Mendez, M. (1985) Structure of dodecacalcium potassium fluoride tetrasilicate bis(sulphate), $KF.2[Ca_6(SO_4)(SiO_4)_2C]$: a fluoride-containing phase encountered in cement clinker production process. Acta Crystallographica, C41, 814-816.

Gilmore, C. J. (1983) MITHRIL, a computer program for the automatic solution of crystal structures from x-ray data. Department of Chemistry, University of Glasgow, U. K.

Kreidler, E. R. and Hummel, F. A. (1970) The crystal chemistry of apatite: structure fields of fluor and chlorapatite. American Mineralogist, 55, 170-184.

Trivino-Vazquez, F. (1985) A new compound: $K_3Ca_2(SO_4)_3F$, identified in coatings of heat recover cyclones. Cement and Concrete Research, 15 [4], 581-584.

Watkin, D. J., Carruthers, J. R. and Betteridge, P. W. (1985) CRYSTALS User Guide. Chemical Crystallography Laboratory, University of Oxford, U. K.

Wickoff, R. W. G. (1965) Crystal structures, Vol. 3, p. 228-229. Second Ed. Wiley-Interscience, New York.

F.PUERTAS, Lic. Chem.Sd.
F. TRIVIÑO, Dr. Chem.Sci. CSIC. Inst. Eduardo Torroja (Madrid) ESPAÑA

MODIFICATIONS CLINKER PHASE AND MECHANICAL STRENGTH IN RELATION TO TYPE OF QUENCHING

MODIFICATIONS DE PHASE CLINKER ET LEURS RESISTENCES MECANIQUES EN RELATION AVEC LA MANIERE DE TREMPE

RESUME: Les effects de la trempé dans la estabilité des phases de differents clinkers et aussi les résistences mecaniques à flexion et compression à 7 et 28 jours sont etudiés.

Les clinkers sont rechauffés a 1576°C pendant 30 minutes et sont trempés de deux façons differentes:

A l'air la temperature ambiente et par immersion sous l'eau.

Les échantillons ont été étudiés à travers les suivantes méthodes: D.R.X., microscope optique et analyse dispersive de rayon X.

Le clinker trempé sous l'eau contient alite de structure trigonale avec Al et Mg dans solution solide. Le clinker trepé à l'air contient alite monoclinique.

Les résistences mecaniques à 7 et 28 jours des clinkers tremprés à l'air, qui étaient superiers et plus hauts suivant que la temperature de trempé augmentait.

L'alite trigonale s'hydrate plus doucement que l'alite monoclinique.

SUMÁRIO: Os efeitos da têmpera na estabilidade das fases de diferentes clínqueres e também as resistências mecânicas à flexão e à compressão de 7 e 28 dias são estudadas.

Os clínqueres são reaquecidos a 1576°C durante 10 minutos e são temperados de duas maneiras diferentes:

Ao ar à temperatura ambiente e por imersão em água.

As amostras foram estudadas pelos seguintes métodos: D.R.X., microscópio ótico e análise dispersiva de raios X.

O clínquer temperado debaixo d'água contém alita de estrutura trigonal com Al e Mg em solução sólida. O clínquer temperado ao ar contém alita moniclínica.

As resistências mecânicas a 7 e 28 dias dos clínqueres temperados ao ar, são superiores, e mais elevadas de acordo com o aumento da temperatura de têmpera.

A alita trigonal se hidrata mais lentamente que a alita monoclínica.

1. INTRODUCTION

The main reasons for the rational cooling of clinker are:

- Clinker just out of the kiln is not transportable.
- Hot clinker is difficult to mill. Its friction with mill materials would draw the temper out of the steel and the gypsum would dehydrate explosively.
- To take advantage of the hot clinker's thermal content which is about 200 Kcal/kg of clinker. This would lower the costs of production.
- An improvement in clinker properties and thereby a quality improvement in the cement.

Clinker leaves the clinkerization zone of the kiln at a temperature of about 1350ºC - 1500ºC. As of this moment the cooling progresses more or less rapidly on which type of cooler is used (1). The clinker leaves the cooler at a temperature that fluctuates between 50ºC - 300ºC.

The clinker cooling rate influences the relationship between the crystalline and vitreous phases (2). If the cooling is slow the clinker's phases continue their evolution reacting among themselves until they reach the point of complete crystallization. If the cooling is very fast crystal formation is slowed down and a large part of the liquid phase solidifies into a vitreous state.

Under normal production conditions the cooling is neither too fast to freeze the vitreous phase nor too slow for total crystallization. In rotary-kiln clinker the percentage or liquid phase is about 20 - 25%. A relatively fast cooling down from clinkerization temperatures is necessary if one wants to avoid the tendency of tricalcic silicate to decompose (3). K. Mohan and F.P. Glasser (4) say that decomposition of C_3S begins at temperatures between 1210ºC - 1025ºC with slow cooling.

Portland cement clinker phases are seen to be affected according to the type of cooling method used:

Alite: With slow cooling C_3S decomposes above 1025ºC in accordance with the reaction:

$$C_3S \longrightarrow C_2S + C$$

This lime s called secondary lime. The large alite crystals a e slow to hydrate thereby diminishing the initial and final mechanical strenght.

Belite: If the large belite crystals do not have enough stabilizers and their size is greater than 10m they tend to favour polimorphic transformation $\beta \rightarrow \gamma$ with which the clinker would desintegrate and the mechanical strengt diminish considerably.

Tricalcium Aluminate: The large C_3A crystals have a slower hydration rate in the presence of gypsum thereby slowing down the beginning and final stages of the setting. In a fast cooling the C_3A remains in a vitreous state and isn't very susceptible to magnesium and sodium sulphate solution attacks.

Ferritic Phase: The large C_4AF crystals are less reactive in the presence of water and gypsum.

Periclase: The hydration of large periclase crystals is accompanied by an increase in volume. It flows more slowly than in the other clinker phases and this alters the volume stability of the cement during its hardening. period. Rapid cooling of the clinker permits a large MgO content.

In the present work we have studied the influence of different types of quenching (air and water) on various clinkers with respect to its phase formations and mechanical strength: flexotraction and compression.

2. EXPERIMENTAL WORK

Two Portland cement clinkers were used, 1 and 3. Their compositions in percentages by weight are in Table 1. A laboratory clinker was also prepared with the same chemical composition as nº 1 which has been called nº 2.

TABLE 1

Clinkers	SiO_2	Al_2O_3	Fe_2O_3	CaO	MgO	SO_3	Na_2O	K_2O	Free Lime
1	22.07	5.04	2.93	66.34	2.20	0.50	0.23	0.53	0.38
2	22.07	5.04	2.93	66.72	2.20	0.50	-	0.50	-
3	20.44	6.14	3.89	66.87	1.42	1.30	-	-	0.76

From Bogue's calculations the potencial compositions of these clinkers is as follows:

	1	2	3
C_3S	61.24%	64.33%	63.19%
C_2S	17.16%	14.83%	11.01%
C_3A	8.4%	8.4%	9.69%
C_4AF	8.9%	8.9%	11.82%

Clinker nº 1 was heated in an electric kiln at the following temperatures: 1100ºC, 1206ºC, 1320ºC, 1460ºC and 1576ºC for a period of thirty minutes. For each temperature the clinkers were quenched in two different ways.

A.- Outside at air temperature of A.Q.S. (air quenching clinker).

B.- Water submersion at ambient temperature or W.Q.C. (water quenching clinker).

Clinkers nº 2 and nº 3 were only heated at 1576ºC and the two previously described quenching methods were employed:

A Philips P.W. 1700 difractometer and a Kevex System 7000 for the dispersive X-Ray analysis were used.

Some samples were treated with salicylic-methanol solution in order to disolve the silicate phases and detect the composition of the clinker's vitreous phase which remains insoluble (5 and 6).

It was prepared a prismatic mortar samples of 1 x 1 x 6 cm with a sand/cement ratio of 3:1 and a water/cement ratio of 0.66 for all the treated samples of clinkers nº 1, nº 2 and nº 3.

3. RESULTS

3.1.- X-Ray Diffraction

3.1.1.- Anhydrous samples

The X-Ray diffraction patterns of all the A.Q.C. (figure nº 1) had similar characteristics: its alite crystallizes in the monoclinic system, possibly the $M_3 + M_1$ type, identified by a peak of 51.70º. Its ferritic phase has a composition between C_4AF and C_6A_2F. This means a ferritic phase with a high alumina con-

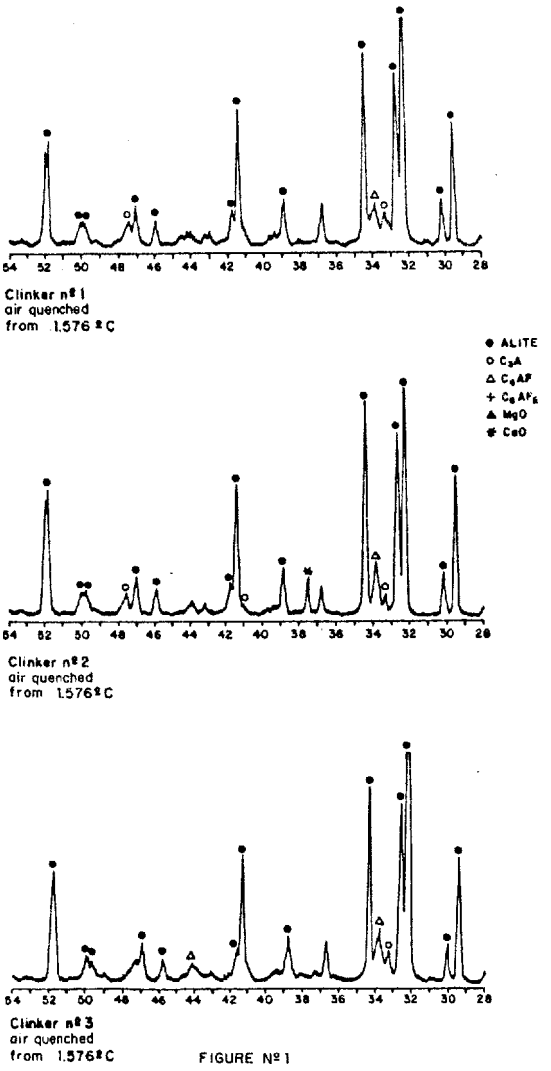

FIGURE Nº1

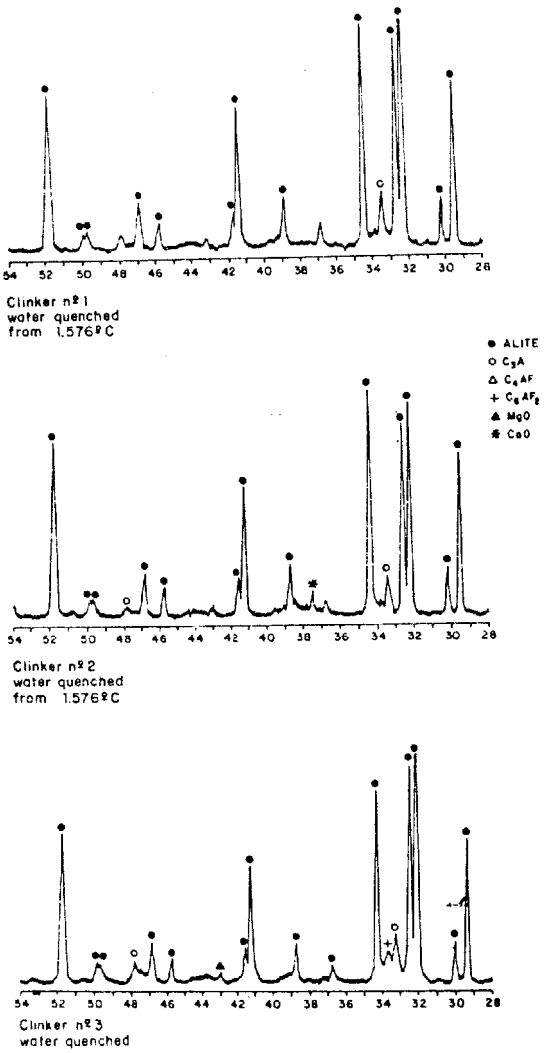

FIGURE Nº2

tent. In those A.Q.C. very little tricalcium aluminate is seen.

The X-Ray diffraction patterns of the W.Q.C (figure nº 2) have the following characteristics in common: Their alites crystallize in the trigonal system and they have very little crystallized ferritic phase. This being so it is very poor in aluminate with a composition close to C_6AF_2. On the other hand it has a large tricalcium aluminate content, possibly with iron in solution, which distorts the lattice.

In the figure nº 3 are the X.R.D. patterns of the samples were treated by salicylic-methanol solution of clinker nº 1 heated at 1576ºC and quenched by the two methods described (air and water).

3.1.2.- Hydrated samples

The X.R.D. patterns of the hydrated paste of A.Q.C. and W.Q.C. nº 1, appear in figure 4. In the X.R.D. patterns of the A.Q.C. nº 1 hydrated product the alite cannot be detected. However, in the rest of the hydrated products of the other clinkers that have been quenched by different methode, a certain amount of alite is always detected. This amount is conside-

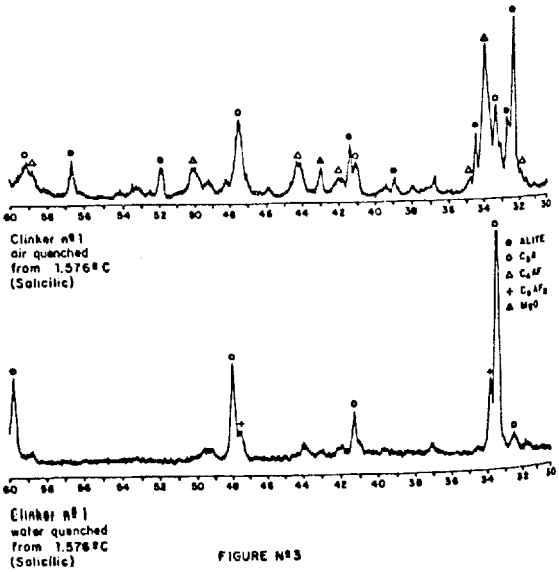

FIGURE Nº3

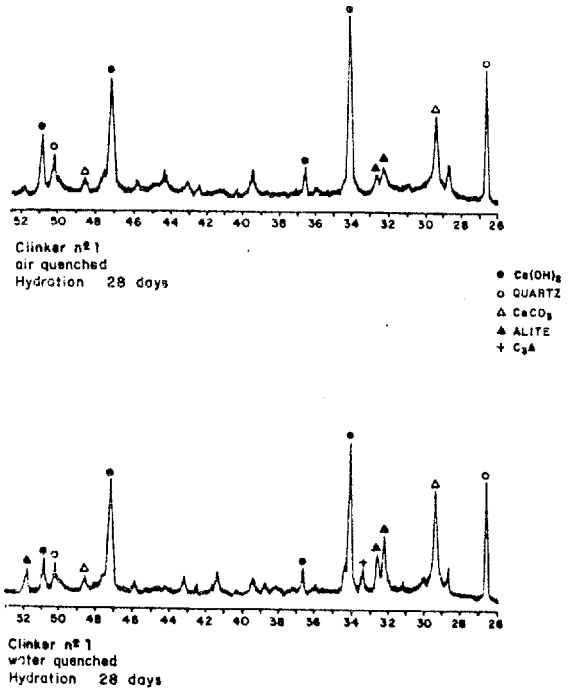

FIGURE Nº 4

rably higher in the W.Q.C. In the hydrated paste of all the W.Q.C. there is always tricalcium aluminate which is not detected in those quenched by air.

3.2.- Optic Microscopy

Clinker nº 1 treated at 1100ºC and 1576ºC, A.Q.C.and W.Q.C. nº 2 and nº 3 treated at 1576ºC, also A.Q.C. and W.Q.C. were studied under a petrographic microscope. The samples, pressed in resin, were polished and treated with Nital to differentiate the phases.

The figure nº 5.1 corresponds to clinker nº1 without reheating. The same A.Q.C. heated at 1576ºC is presented in figure 5.2; figure nº 5.3 shows the same W.Q.C. It is seen that the alite and belite crystals are larger in the W.Q.C. than in the A.Q.C. and the clinker without reheating. Likewise W.Q.C. nº1 seems to have less interstitial phase quantity than the A. Q.C. one.

In the figure nº 6.1 correspond to A.Q.C nº1 heated at 1100ºC, and figure nº 6.2 and W.Q.C. It is seen that the edges of the alite grains are clearer and straighter in the W.Q.C. ones than in the A.Q.C.ones

3.3.- Dispersive X-Ray Analysis

a) A.Q.C. nº 1 from 1576ºC

- The elements present in the interstitial phase are:

Ca, Si, Al, Ti and Fe

- The elements detected in the alite crystals are:

Ca, Si, Ti and K

- In the belite crystals appear:

Ca, Si, K, Ti and Fe

b) W.Q.C. nº 1 from 1576ºC

- The elements present in the interstitial phase are:

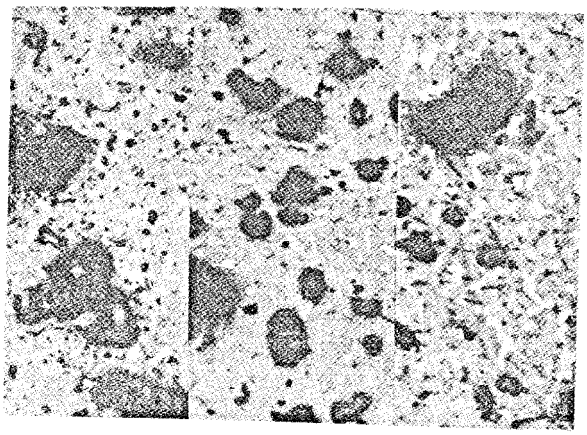

Clinker nº 1

without reheating W.Q.C. 1576ºC A.Q.C. 157ºC

FIG. 5-1 FIG. 5-2 FIG. 5-3

Ca, Si, Al, Ti and Fe, Mg, K

- The elements detected in the alite cristals are:

Ca, Si, Al and Mg, Fe

- The elements detected in the belite cristals are:

Ca, Si and K

3.4.- Mechanical strength

For clinker nº 1 with a 7 day curing period the greatest flexotraction and compression resistances were obtained by the clinker without reheating followed by the A.Q.C. as can be seen in figures nº 7 and nº 8. The mechanical resistances of the W.Q.C. nº 1 remained practically constant for all temperatures.

For the 28 day cured ones (figures nº 7 and nº 8) there is little difference in the mechanical strength between the clinker without reheating and the A.Q.C. one from 1576ºC. The W.Q.C. had strenght of the same order or inferior to those of the other two at all temperatures studied except at 1100ºC.

The W.Q.C. had strength of the same order or inferior to those of the other two at all temperatures studied except at 1100ºC.

Figure nº 9 represent the mechanical strength by flexotraction and compression breakage of clinkers nº 2

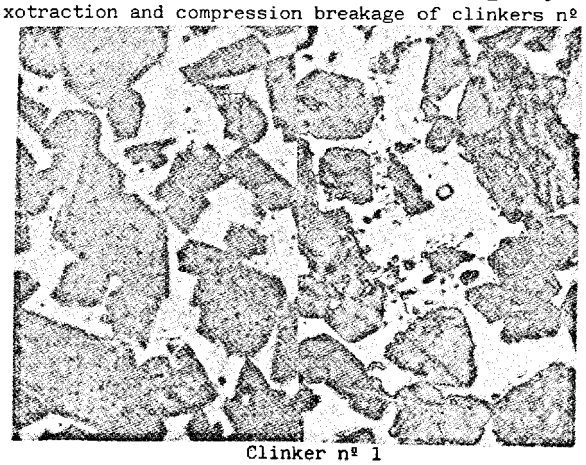

Clinker nº 1

W.Q.C 1100ºC A.Q.C. 1100ºC

FIG. 6 FIG. 6-2

1.2

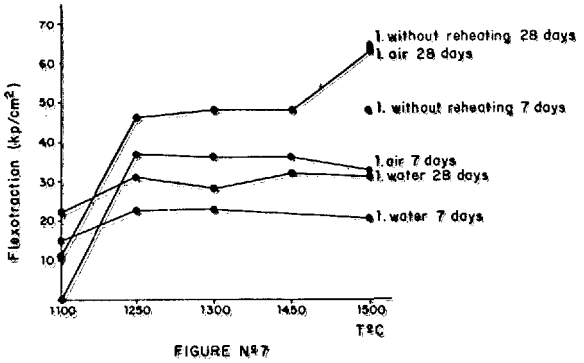

FIGURE Nº 7

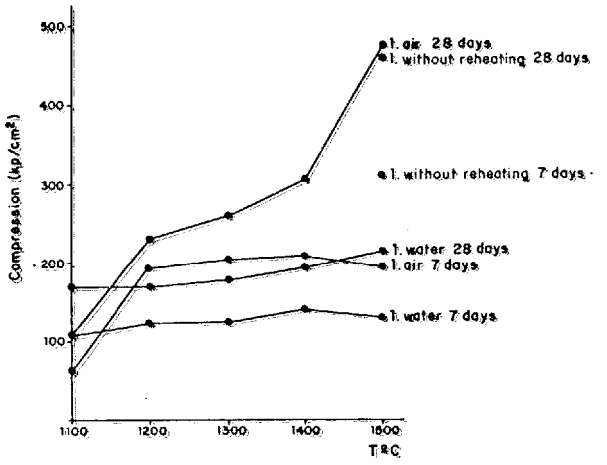

FIGURE Nº 8

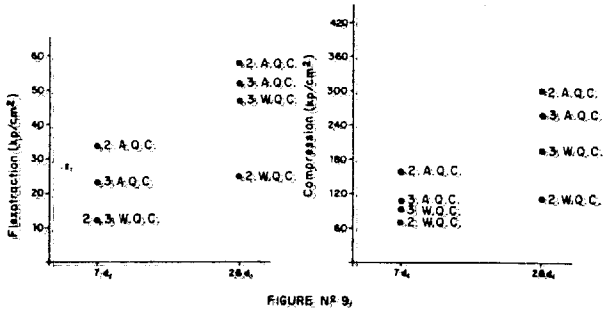

FIGURE Nº 9

and nº 3, A.Q.C. and W.Q.S. treated at 1576ºC, and cured in deionized water for a period of 7 and 28 days. In all casses it is appreciated that the A.Q.C. have greater strength than the W.Q.C. ones.

3.5.- Granulometry

Figure nº 10 represent the percentage of retained material before a meshed-screen light of clinker nº 1 A.Q.C. and W.Q.C. from 1576ºC, and clinker without reheating.

Figure 11 represents the granulometry of the clinker before milling. We can appreciate that the grain sizes of the clinker without reheating are superior to the A.Q.C. and W.Q.C. ones. After milling it is been that the finest grains belong to the clinker without reheating, the largest size belongin to the W.Q.C.

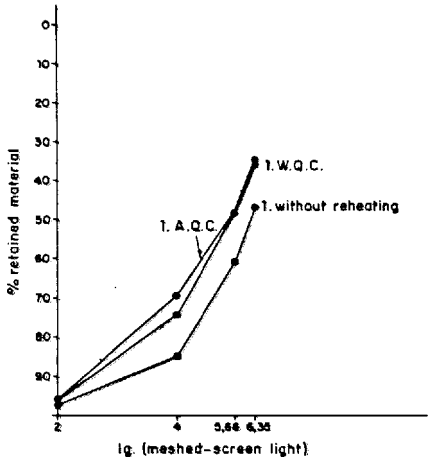

FIGURE Nº 10

3.6.- Clinker colouration

There is a marked difference in the clinkers colouring depending on the type quenching used and these can be seen with the naked eye. W.Q.C. from high temperatures (1576ºC) is yellow, not only experimentally but also internally as well. This yellow colour is lost as the treatment diminishes. At 1460ºC the yellow colour is still there although it is darker. At 1320ºC the clinker granules are normal greycolour.

4. DISCUSSION

The experimental results we obtained do not seem to be in accordance with bibliographic data with respect to the influences of quenching in clinker phase crystallization and its mechanical resistance.

It must be taken into account that in our case the treatment temperatures were very high (1576ºC) and the A.Q.C. and W.Q.C. was much rougher than commercial clinker treatment.

From microscopy it has been established that the alite in Portland cement clinker appears in the following forms: M_1 and M_3 (7) (8) (9). By X-Ray diffraction the two identified forms are: R (trigonal) and M_1 (of the M_{1b} type) (10). The M_{1b} form had an X-Ray diffractogram very similar to M_3 (11).

We have identified, through the X-Ray diffraction patterns, a trigonal structured alite in the W.Q.C. wich is the highest temperature polimorphic form. The A.Q.C. had an alite of the monoclinic type, possibly a mix of the M_1 and M_3 forms.

A possible justification for the low mechanical strength obtained from the W.Q.C. could be the establishment of this trigonal alite which has its Ca and Al substituded by Mg and Al respectively (observed by dispersive X-Ray analysis). These substitution make room for the formation of relatively large sized crystals with very marked and straight profiles, therefore having less reactivity in the presence of water thereby justifying the low flexotraction and compression strength of the water quenched clinkers. On the other hand, it is known that the decrease of distance of the Ca-O bond by metalic substitution diminishes reactivity.

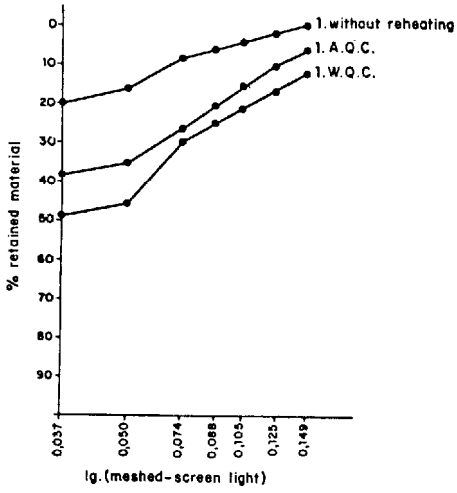

FIGURE Nº11

The air quenched clinkers have a monoclinic alite and the ionic substitutions observed are quite a bit smaller than in the trigonal alite, This monoclinic alite is comparable to that of a commercial clinker in so far as its reactivity with the water is proportional to the quenching temperature, within wide limits, and with high treatment temperatures has high mechanical strength.

The ferritic phase of the W.Q.C. has an aproximate composition of C_6AF_2 which means it is rich in iron oxide and poor in alumina. The ferritic phase of the A.Q.C. has a composition between C_4AF-C_2A_6F, that is to say, it is much more richer in alumina. This last data obtained by us agrees with the conclusions of authors T. Vázquez, M.T. Blanco-Varela and A. Palomo (12).

5. CONCLUSIONS

- In all the W.Q.C. from 1100ºC a trigonal structured alite was obtained. If the quenching was done in the air from the same temperatures monoclinic type alite, possibly a mixture of the M_1 + M_3 forms, was obtained.
- The trigonal structured alite has Mg and Al in solid solution and hydrates with much more difficulty than the monoclinic structured alite which does not contain the mentioned clinkers.
- The mechanical resistances: flexotraction and compression of clinkers nº 1, nº 2 and nº 3, W.Q.C. are always inferior to those of the A.Q.C.
- The mechanical resistances of W.Q.C. nº 1 are independent of the treatment temperature while the mechanical resistances of the A.Q.C. are greater with higher treatment temperatures between 1100ºC and 1576ºC.

6. BIBLIOGRAPHY

1.- W.H. Duda. Manual Tecnológico del cemento, 265-281 (1977)

2.- F. Soria. Estudio de Materiales, 127-132 (1976)

3.- S. Sprung, VII Congres International de la Chimie des Cements, 1-2 1-17 (1980)

4.- K. Mohan and F.P. Glasser, Cem. and Concr, Res. 7 (1977)

5.- Takashima, S. Semento Gijutzu Nempo XII, 12-13 (1958)

6.- F. Triviño, Materiales de Construcción, nº 143-21-25 (1971)

7.- I. Maki and S. Chromy. Il Cemento 75, 247 (1978)

8.- I. Maki. Il Cemento 76, 167 (1979)

9.- V.V. Timashev, A.T. Suleimenov. A. Yu. Sychkareva and A.I. Tleubertenova. Cement nº 5, 8 (1979)

10.- M. Regourd and A. Guinier, Principal paper presented at 6 Th.Int. Symp. Chem. Cement, Moscow (1974)

11.- E. Woerman, W. Eysel and Th. Hahn, Zement-Kalk -Gips 22, 414 (1969)

12.- T. Vázquez, M.T. Blanco-Varela and A. Palomo Proceeding nº 35 British Ceramic Society, edited by F.P. Glasser (1984)

George R. Gouda, Consultant
Allentown, Pennsylvania, U.S.A.

1

Microstructure and Properties of High-Alkali Clinker

Microstructure et Proprietés du clinkera Haute Teneur Alcaline

1.2

Summary: The alkali contents of portland clinker alter significantly the clinker microstructure, affect the behaviour of the cement and accordingly properties of concrete during the process of its placing and while it develops strength. Two different clinker samples, (with low and high percentages of alkalies bearing compounds, from the same plant at different conditions) were examined by SEM and EDX.

The microstructure of the low-alkali clinker showed that most of Na, K and S are incorporated with the crystalline lattice of the clinker as well as, the interstitial material. The morphology of the calcium silicates is defined and clear. Higher amounts of Na, K and S alter the structure of the clinker as the alkali sulfates are crystallized and precipitated over the calcuim silicate grains as small crystallites and fine polysynthetical stripes. Belite crystals showed higher concentration of K and it seems that the structure of C_2S changed to $KC_{23}S_{12}$, which contributes to lower strength at late ages.

In this paper, influence of alkalies on the setting time, slump loss, workability and strength development are discussed and related to observations of the microstructure.

SUMÁRIO: O conteúdo de álcalis no clínquer portland altera significativamente a microestrutura do clínquer, afeta o comportamento do cimento e, em conseqüência, as propriedades do concreto durante o processo de sua colocação e enquanto desenvolve resistência. Duas amostras diferentes de clínquer (com alta e baixa porcentagem de compostos possuindo álcalis, na mesma fábrica e em diferentes condições) foram examinadas pelo SEM e EDX.

A microestrutura do clínquer de baixo álcalis mostrou que muito do Na, K e S são incorporados na rede cristalina do clínquer, bem como no material intersticial. A morfologia dos silicatos de cálcio é definida e clara. Mais altos teores de Na, K e S alteram a estrutura do clínquer à medida que os sulfatos alcalinos cristalisam-se e precipitam sobre os grãos de silicato de cálcio como pequenos cristalitos e estreitas bandas polisintéticas. Cristais de belita apresentam mais altas concentrações de K e parece que a estrutura do C_2S muda para $KC_{23}S_{12}$, que contribui para diminuir a resistência a longo prazo.

Neste trabalho, a influência dos álcalis no tempo de pega, na perda de consistência, trabalhabilidade e desenvolvimento de resistência são discutidas e comparadas com observações da microestrutura.

INTRODUCTION

Raw materials for cement are generally natural deposits such as limestone, chalk, clay, shale, and marl. All these materials contain variable amounts of alkalies and sulfates. The alkalies are in the form of finely dispersed aluminosilicate minerals such as mica, feldspar, and illite, and sulfur compounds are in the form of sulfide minerals such as pyrite, sulfate, and marcasite.

Using coal as a fuel contributes to the alkalies and sulfates, and any variation in S content and coal composition poses difficulties in an Sp-type kiln, as well as in clinker quality, even if other types of kilns are used. Coal ash is deposited and mixed, to some extent, with the raw mix during the burning process; it is brought forward to the burning zone, where it becomes part of the clinker.

Most coal S compounds are absorbed by the kiln feed in the preheater tower or in the calcining zone of the rotary kiln. In an Sp system, the contact between the gas and the solids is more intensive than in other kiln systems, so more SO_2 is absorbed. When the exhaust gas from the Sp system is used to dry the raw mix, the SO_2 is almost completely absorbed by the mix (1).

Alkalies are found in clinkers partly as soluble sulfates and partly as constituents of the clinker minerals. Previous work (2,3,4) showed that when different percentages of alkalies are incorporated in the structure of the clinker minerals, their crystalinity and crystal lattice change. This can change the hydraulic properties of the clinker and affect its strength. Several studies on alkalies in clinkers have been comprehensively reviewed. (5,6).

SCOPE OF THIS STUDY

The scope of this study is to diagnose and analyse the microstructure of two clinker samples produced from the same cement plant using the same process, (Sp system) raw materials and fuel (coal). For several years, the clinker produced at this plant and, accordingly, the cement and concrete were more or less homogenous. Then, suddenly the quality of the concrete greatly changed; it was found to be because the clinker had changed. The clinkers were examined by SEM and by EDX, and the properties of the concrete were taken into account in the diagnosis. It was discovered later that the quality of the coal was greatly changed; to poor quality.

CLINKER SAMPLES

A normal clinker (the first sample) had a low alkali content (maximum total alkali calculated as Na_2O = 0.60%). The second clinker sample had a total alkali content of 1.76%. The major and minor oxides and the constituents of each clinker are given in Table I.

TABLE 1

Chemical Analysis and Composition of Clinker Samples

	Low-Alkali Clinker	High-Alkali Clinker
SiO_2	21.81	21.34
Al_2O_3	5.63	5.49
Fe_2O_3	2.76	2.51
CaO	64.63	63.09
MgO	2.85	2.55
Na_2O	0.30	0.86
K_2O	0.42	1.58
SO_3	1.32	2.02
L.O.I.	0.35	0.54
Total	100.07	99.98
Free lime	0.75	1.25
C_3S	55.57	54.18
C_2S	20.61	20.31
C_3A	10.25	8.25
C_4AF	8.40	7.64
S.M.	2.60	2.54
A.M.	2.04	2.19
H.M.	2.14	2.15
L.S.F.	0.93	0.93
CaO/SiO_2	2.96	2.96
Equiv.Na_2O	0.58	1.76
K_2O/Na_2O	1.40	1.84
$SO_3/Na0+K_2O$	1.83	0.83
K_{tot}	0.88	2.83
M_{SO_3}	1.77	0.83

The chemical analysis shows less CaO and more Na_2O, K_2O, SO_3, and free lime in the high-alkali clinker sample. Although the Bogue formula shows approximately the same minerals in both clinkers, their behaviour is completely different. The second clinker sample shows higher equivalent Na_2O and its K_2O/Na_2O ratio is higher. The SO_3 to Na_2O+K_2O ratio in the high-alkali clinker sample is approximately half that in the low-alkali clinker. Total alkali content, expressed as K_2O equivalent ($K_{tot}=K_2O+1.52 \times Na_2O$), is higher in the high-alkali clinker. The molar ratio of sulfur to alkali ($M_{SO_3}=SO_3/0.85xK_{tot}$) is 1.77 in the low-alkali clinker and 0.83 in the high-alkali clinker.

PROPERTIES OF CEMENT AND CONCRETE

Table II shows the main properties of the cement and concrete prepared from the same two clinker samples.

TABLE II

Properties of Cement and Concrete

	Clinker	
	Low-Alkali	High-Alkali
Cement:		
Specific Surface	:3450	3570 cm^2/g
Setting Time (I)	: 155	85 min
(F)	: 3 h 18 min	1 h 55 min
Autoclave Expansion	:0.08%	0.27%
Concrete:		
Slump Test	: -32mm	-8mm
Comprehensive Strength:		
1 day	106	123 kg/cm^2
3 days	156	184 kg/cm^2
7 days	245	237 kg/cm^2
28 days	305	242 kg/cm^2

The cement produced from the high-alkali clinker is characterized by:

1. More free lime.
2. Faster setting time (initial and final).
3. Higher autoclave expansion.
4. Early stiffening because of slump loss and low workability.
5. Slightly more compressive strength initially, but less after 7 and 28 days.

SEM STUDIES

The regular clinker (low-alkali content) shows a normal microstructure (Figure 1) in which C_3S and C_2S crystals can be seen. The C_3S crystals are more abundant and larger than the C_2S crystals. Twinning of the C_2S crystals is observed (Figure 1b). The interstitial material and the porosity are clearly shown. Alkali sulfates are precipitated on the outside surface of the silicate crystals, with different morphology and thickness. Alkalies were also detected by EDX in the silicate crystals and in the interstitial materials. K, Na, and S are the main constituents of these depositions, and their intensities are higher than those of the solid solution of the silicate crystals and interstitial material.

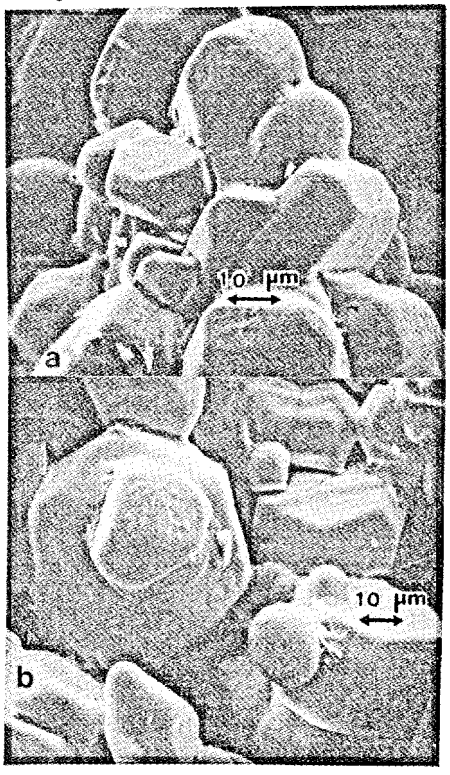

Figure 1: Microstructure of low-alkali clinker.

The microstructure of the high-alkali clinker is different from that of the regular clinker (Figures 2,3,4,5). The Ca-silicate crystals are completely coated by small crystallites, forming a thin skin. The alkali sulfates encircled the crystals and covered them. EDX analysis showed precipitation of K, Na, and S and, in some cases, Ca. In some spots, monosulphates were identified with either Na or K and S (Figure 2). Figure 2a shows that these netted precipitates are cracked, which may have been caused by moisture absorption during sample preparation.

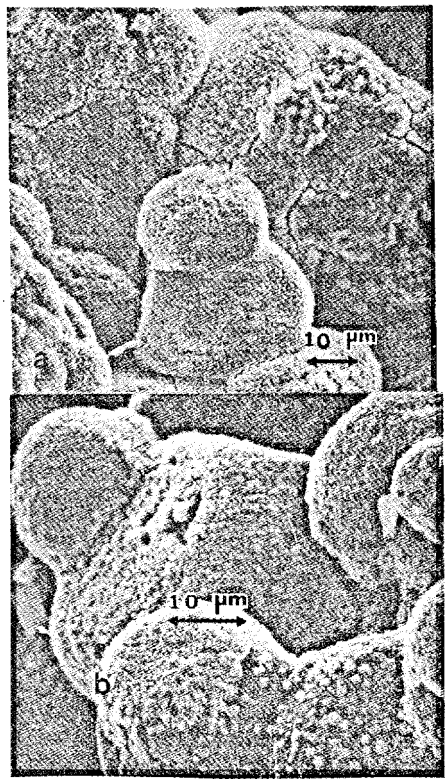

Figure 2: Microstructure of high-alkali clinker.

The structure of C_3S-silicates is composed of well developed compact prismatic alite crystals consisting of Ca and Si (major) and of Mg, Al, Fe, Na, K, and S (minor) (Figure 3a). The skin of the alite crystal is formed from K, Na, S & Ca. The distribution of these elements, in both the internal structure and the skin of the alite, is not consistent in the spots checked by EDX since the intensity differs greatly. Figure 3b shows two kinds of precipitation over the Ca-silicate grains. The skin of the big crystal (top right) is thin and netted; the other crystals have a thin crust of alkali sulfates. The netted layer has more Na than the crust layer. K and S are present in both layers. Rectangular crystals of periclase (MgO) are seen between the two crystals on the right side of Figure 3b and in the top left of Figure 2a. The cracks in the C_3S crystal (Figure 3a)may have been caused by poor cleavage or sample preparation, or may be an effect of stress released during cooling.

Another clinker sample with a high alkali content was analyzed. Its microstructure had Ca-silicate crystals that were more or less rounded; these were in addition to the crystals described in Figures 2 and 3. Some of these crystals have a "cover" or "lid" on the top whereas others have a cavity (Figure 4a). These crystals , which are probably an altered C_2S, are covered by thin lathe-like layers in different directions (Figure 4b). Examination by EDX shows that the crystals are composed of C, Si, Al, Fe, Na, K, Mg, and S. The amount of K is much greater than that in Figure 2. The lathes consist mainly of K, Ca, and S,

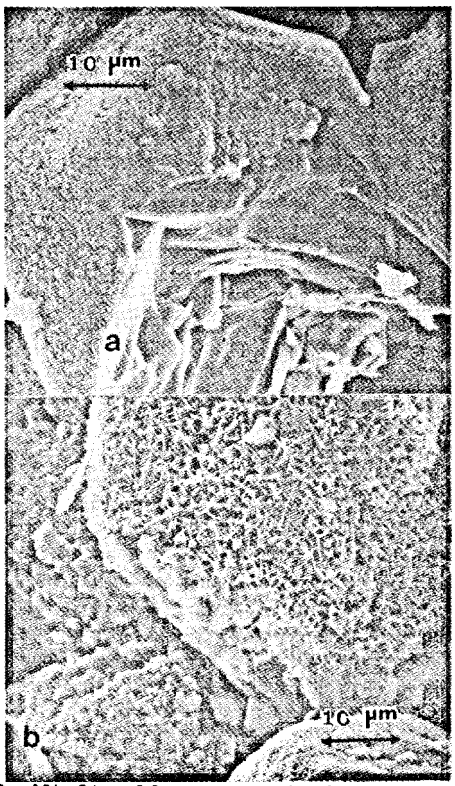

Figure 3: Alkali sulfates coat the Ca-silicate crystals.

and, in some spots, Na. This suggests that the crystals are $KC_{23}S_{12}$, whereas the needle-like precepitates are single and/or double sulfates.

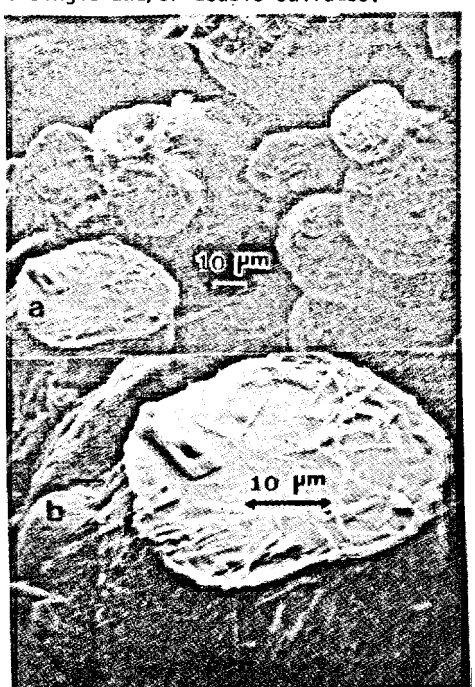

Figure 4: Ca-silicate crystals of high-alkali clinker, most probably $KC_{23}S_{12}$.

Figure 5 shows a single round crystal of Ca-silicate with a "lid"; the needles have different orientations. X-ray diffraction showed the presence of $KC_{23}S_{12}$ and single/double alkali sulfates.

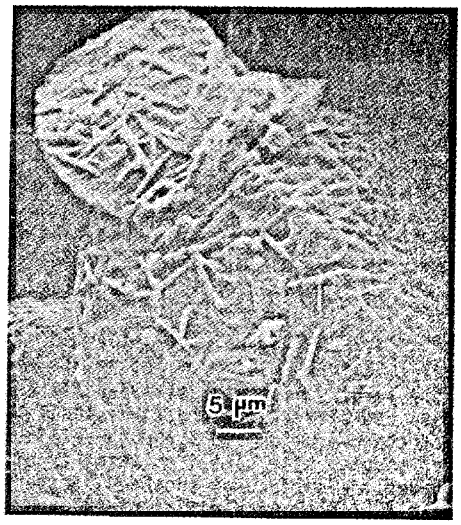

Figure 5: A Ca-silicate crystal, ($KC_{23}S_{12}$); of high-alkali clinker.

DISCUSSION

Cement plants that burn coal, particularly high-sulfur coal, increase the S content in the clinker. If alkalies are available, the sulfur combines with them. In kilns with suspension preheaters (which may or may not have a precalciner), the sulfur and the alkalies are almost fully absorbed. An alkali by-pass can help reduce the amount of alkali sulfate absorbed by the raw mix, but this depends on the size of the by-pass.

The presence of alkali sulfates greatly affect the morphology and structure of the clinker, the reaction kinetics of clinker formation, and the equilibrium and composition of the phases (7). In an oxidizing medium, sulfur compounds are considered to be "transfer agents" of alkalies into clinker (8).

Alkali sulfates found in the clinker are usually single or double (Table III).

Table III: Alkali Sulfates in Portland Cement Clinker

	Na	K	Ca
Single Sulfate	Na_2SO_4 (thenardite)	K_2SO_4 (arcanite)	$CaSO_4$ (anhydrite)
Double Sulfate	$Na_2SO_4.3K_2SO_4$ (aphthitalite)	$2CaSO_4.K_2SO_4$ (calcium langbeinite)	

They are partly soluble sulfates and partly incorporated with the solid solutions of the clinker minerals (C_3S, C_2S, and the liquid phase). In clinkers,

potassium sulfate is likely to occur either alone or in one of the two double sulfate forms. This depends on the availability of the second sulfate (9). Sodium sulfate most probably occurs as double alkali sulfate whereas calcium sulfate occurs either as single or double salt, subject to prior information of double alkali sulfates (9).

Alkalies usually combine with available sulfates during the burning process to form an alkali phase that contains both K_2O and Na_2O, with K_2O predominating, until either alkali or sulfate is satisfied (5). Excess alkalies and sulfates then combine and are incorporated in each phase of the clinker. Na combines with the aluminate phase forming NC_8A_3 and free lime, and K combines with the silicate (preferably C_2S), forming $KC_{23}C_{12}$ (10), which is K stabilized in the form of β-C_2S. The high-alkali clinker contains a high percentage of K_2O, which greatly modifies the C_2S crystal (Figures 3,4, 5). The belite absorbs distinctly larger amounts of alkali-sulfate than alite does and alters its structure significantly, which affects hydration and strength development in the later stages. The alkali sulfates crystallize, deposit over the surface of the Ca-silicate grains, and almost coat them with different thicknesses and morphology, depending on their concentrations and constituents, the clinker temperature, the cooling process, etc.

The C_2S crystals in the high-alkali clinker are more or less ellipsoidal with a relative degree of dismemberment that develops into a "flat cover"; they have excessive amounts of alkalies and sulfates in their lattices. They are without normal multidirectional lamellae. This alteration will result in different forms of new phases of alkali belite containing foreign inclusions. Since the belite is responsible for late hydration, it is expected that the strength will be changed due to the alteration of the original crystal. The foreign inclusions (Na, K, S) in the alkali-belite are considered to be higher than in the regular belite. The impurities have no hydraulic or strength properties so lower strength is expected due to low Ca and Si constituents.

In their studies, Strunge et al. (11) showed that, with increasing SO_3 content in the clinker, the alite content increases and the belite content decreases correspondingly, which may be responsible for the strength decrease at 28 days. In this study, the high-alkali clinker sample has high K_2O, and the belite structure is completely altered. The alite crystals are covered with a "net" of alkali sulfates different from the belite crystals, which have needle-like precipitation on their surfaces.

A substantial fraction of the total alkalies passes into the cement solution within a few minutes, when water is mixing with it, producing an alkali-rich solution. The setting time is accelerated by the K_2SO_4, which results in the formation of syngenite ($CaSO_4.K_2SO_4.H_2O$). The setting time decreases significantly when alkali sulfate is present in the cement; K_2SO_4 is more effective than Na_2SO_4 (12). Early stiffening and low workability can be attributed to the presence of K_2SO_4 and syngenite formed by the reaction of gypsum and K_2SO_4 in the aqueous phase (13). The soluble alkali sulfates increase the pH value and lower the $Ca(OH)_2$ concentration in the solution. This will result in changing the rate of nucleation and crystalization of the hydration products and in increasing the hydration velocity of C_3A. Accordingly, rapid setting caused by the formation of aluminate hydrate and alkali ions depresses the solubility of the solubility of the Ca^{2+} ions (14).

Alkalies can affect strength development as they enhance strength in the early stages (1-3 days), but decrease it at later stages (7-28 days). This is attributed to changes in the hydraulic properties of the clinker minerals (caused by incorporating alkalies in their lattice) and to changes in the composition of the liquid phase (caused mainly by the alkali sulfates) (15). The specific area of hydrated Ca-silicate decreases at all stages in the presence of alkalies; the morphology and microstructure also change.

Alkali sulfates and double sulfates in high-alkali cement are rapidly dissolved in the aqueous phase when the cement hydrates; alkalies in the silicate, aluminate, and ferrite phases are released more slowly. Solid products of hydration incorporate alkalies in their structure, changing the morphology and composition of fresh and hardened concrete (16). It was found in this study that alkalies changed the clinker microstructure, particularly the belite, which was characterized by fine polysynthetical strips on its outside surface.

CONCLUSION

Variations in raw materials and coal can add alkali sulfate to the clinker. Coal contributes a varying percentage of SO_3 and ash, which greatly affects the process and, accordingly, the cement quality. Introducing SO_3 cycles will lead to desposition of either $CaSO_4$ or alkali sulfate, depending on the amount of SO_3. Alkali sulfates are incorporated in the crystal lattice of clinker minerals; they are also deposited on the surface of the Ca-silicate grains and coat the grains with small thin crystallites. They are frequently found as incrustation on the surface of the silicate grains. In the case of higher percentage of alkalies, belite is stabilized to $KC_{23}S_{12}$. The presence of alkali sulfates changes the morphology of the crystals, which results in changed hydration properties, early setting and stiffening, slump loss, early increase and late decrease in strength. The most important parameters influencing strength are the soluble potassium oxide and the alteration of the Ca-silicate grains, especially C_2S, which is responsible for strength during the later stages.

Limits of sulfur and ash in the coal to be used as fuel should be specified. Then clinker quality should be analysed by microscope to monitor any changes in the microstructure.

REFERENCES

1. Reports on VDZ congress, "Reactions of Kiln Gases and Ring Formation", Cement Technology, Vol. 3, No. 3, May/June 1972, P. 94.

2. M. Regourd and B. Mortureux, "Tricalcium Aluminate in Synthetic Solid Solutions and in Cement", Summaries of Contributions to a Seminar at the University of Technology, Eindoven, Netherlands, April 13 - 14, 1977.

3. A. Boikova, et al. "The Influence of Na_2O on the Structure and Properties of 3 CaO. Al_2O_3", Cement and Concrete Research Vol. 7, No. 5, 1977, PP 243-252.

4. Y. Ono, et al., "On the Influence of Na_2O, K_2O and MgO on the development of Strength of Portland Cement Mortar", The Cement Association of Japan, 1969, PP. 61 - 69.

5. I. Jawad and J. Skalny, "Alkalies in Cement: A Review, I. Forms of Alkalies and Their Effect on Clinker Formation", Cement and Concrete Research, Vol. 7, No. 6, 1977, PP. 719 - 730.

6. I. Jawad and J. Skalny, "Alkalies in Cement: A Review, II. Effects of Alkalies on Hydration and Performance of Portland Cement", Cement and Concrete Research, Vol. 8, No. 1, 1978, PP. 37 - 52.

7. R. Bucchi, "Features on the Role of Minor Compounds in Cement Clinker", Part I, World Cement Technology, June 1981, P. 21.

8. R. Bucchi, "Features on the Role of Minor Compounds in Cement Clinker", Part II, July 1981, P. 67.

9. H.W. Pollitt and A. Brown, Proc. 5th International Symposium on Chemistry of Cement, Tokyo, Vol. I, 1968, P. 322.

10. F. Hogan, "The Effect of Alkalies on the Properties of Portland Cement", Task Group Report to ASTM C.01.32 on Alkalies, Nov. 1978.

11. J. Strunge and al, "Influence of Alkalies and Sulfur on the Properties of Cement, Part I: Effect of SO_3 Content on the Cement Properties" Zement-Kalk - Gips, Vol. 38, No. 3, 1985, pp. 150 - 158.

12. I. Older and R. Wonneman, "Alkalies Present in Form of Sulfates", Part II, Cement and Concrete Research, Vol. 15, 1983, PP. 771 - 777.

13. S. Sprung, "Effects of Mill Atmosphere on the Setting and Strength of Cement", Zement - Kalk - Gips, Vol. 26, 1973, P. 67.

14. H. Vivian, Proceedings Symposium Effect of Alkalies on Properties of Concrete, September 1976, Cement and Concrete Association, London, 1977, P. 9.

15. B. Osbeack and E. Jons, "The Influence of the Content and Distribution of Alkalies on the Hydration Properties of Portland Cement", Proceeding of 7th International Congress on Chemistry of Cement, Paris, Vol. I, 1980, PP II 135 - 140

16. J. Skalny and W. Klemm, "Alkalies in Clinker: Origin, Chemistry, Effects", Proceedings of the Fifth International Congress on Alkali-Aggregate Reaction in Concrete, Capetown, South Africa, S252/1, 1981, PP. 1 - 7.

Y. KRIVOBORODOV,
O. FOMITCHEVA,
A. BOÏKOVA, NIICIMENT, Institut de la chimie des silicates, Moscou, Léningrad, URSS

COMPOSITION DES PHASES DES CLINKERS CONTENANT DES SULFOALUMINATES ET SULFOFERRITES

1.2.

Les recherches avaient pour objet d'étudier les phases des clinkers, leur composition chimique, les particularités de l'isomorphisme dans les phases contenant un certain nombre d'impuretés dans le réseau des minéraux.

Les auteurs ont établi par analyse radiographique, microscopique et microradiospectrale que le sulfoaluminate et la bélite constituent les principales phases d'un clinker à base de sulfoaluminate, obtenu dans les conditions industrielles. Les taux de $12CaO \cdot 7Al_2O_3$ et de $4CaO \cdot Al_2O_3 \cdot Fe_2O_3$ sont faibles. La composition de ceux-ci est compliquée par la présence d'impuretés isomorphes: MgO, SiO_2, Fe_2O_3, Na_2O, K_2O, TiO_2.

Les clinkers industriels à base de sulfoferrites contiennent, suivant la composition du cru initial, des solutions solides de sulfoferrites de calcium et de Bélite, dans lesquelles sont présents, à titre d'impuretés isomorphes, Na_2O, MgO, MnO, Al_2O_3, TiO_2.

Le rapport entre les phases et la nature des impuretés incorporées dans le réseau des minéraux précités prédéterminent l'activité d'hydratation et les propriétés des ciments obtenus.

As pesquisas tiveram por objetivo estudar as fases dos clínqueres, sua composição química, as particularidades do isomorfismo nas fases contendo um certo número de impurezas na rede dos minerais.

Os autores constataram pela análise radiográfica, microscópica e microradioespectral que o sulfoaluminato e a belita constituem as principais fases de um clínquer com base de sulfoaluminato, obtido em condições industriais. As porcentagens de $C_{12}A_7$ e de C_4AF são fracas. A sua composição é complicada pela presença de impurezas isomórficas: MgO, SiO_2, Fe_2O_3, Na_2O, K_2O, TiO_2.

Os clínqueres industriais de base de sulfoferritos contêm, de acordo com a composição do cru inicial, soluções sólidas de sulfoferritos de cálcio e de belita, nas quais estão presentes, como impurezas isomorfas: Na_2O, MgO, MnO, Al_2O_3, TiO_2.

A relação entre as fases e a natureza das impurezas incorporadas na rede dos minerais precitados predeterminam a atividade de hidratação e as propriedades dos cimentos obtidos.

Y. KRIVOBORODOV
O. FOMITCHEVA,
A. BOIKOVA

Introduction. Une des tendances perspectives dans la chimie du ciment consiste dans l'obtention des composés se formant sur la base de l'orthosilicate, monoaluminate et monoferrite de calcium contenant le fluor, chlore et le soufre: $2(2CaOSiO_2)\cdot CaSO_4$, $2(CaOSiO_2)\cdot CaF_2$, $2CaOSiO_2\cdot CaCl_2$, $3CaO\cdot 3Al_2O_3\cdot CaSO_4$, $3CaO\cdot 3Al_2O_3\cdot CaF_2$, $3CaO\cdot 3Al_2O_3\cdot CaCl_2$, $3CaO\cdot 3Fe_2O_3\cdot CaSO_4$, etc.

Une haute volatilité du fluor, du chlore et du soufre conditionne une inconstance de composition de ces combinaisons, ce qui exige une précision de leur structure et de leurs propriétés. Le but de ce travail est d'étudier la composition de phase des clinkers, la composition chimique des phases de clinker réelles, les particularités de l'isomorphisme dans les phases contenant un complexe d'additifs isomorphes dans le réseau des minéraux.

Objets et méthodes de recherche. Dans le travail, on a utilisé les substances chimiquement pures et les matières premières naturelles en vue d'obtenir les minéraux dans les conditions de laboratoires, semi-industrielles et industrielles. Les recherches ont été effectuées à l'aide des méthodes d'analyse différentes: méthode radiographique, microspectrale aux rayons X, microscopie électronique et méthode d'analyse chimique. En outre, on a utilisé la microscopie optique, la spectroscopie infrarouge et l'analyse thermique différentielle.

Résultats. Dans le système $CaO-Al_2O_3-SiO_2-CaSO_4$, les premiers produits de cuisson sont $CaO\cdot Al_2O_3$ et C_2S dont la formation s'effectue simultanément. Ensuite, sur la base de ces produits, $3CaO\cdot 3Al_2O_3\cdot CaSO_4$ et $2(2CaOSiO_2)\cdot CaSO_4$ cristallisent. Les données obtenues sont conformes à celles du travail /1, 2/.

A l'aide des analyses aux rayons X, microscopiques et microspectrales aux rayons X, on constate que les phases principales du clinker sulfoaluminate obtenu dans les conditions industrielles sont présentées par le sulfoaluminate et la bélite. $12CaO\cdot 7Al_2O_3$ et $4CaO\cdot Al_2O_3\cdot Fe_2O_3$ sont présents en faibles quantités (Fig. 1). La composition de chaque phase se complique à cause de leur teneur en additifs isomorphes: MgO, SiO_2, Fe_2O_3, Na_2O, K_2O, TiO_2. Par exemple, $3CaO\cdot 3Al_2O_3\cdot CaSO_4$ peut contenir MgO de 0,2 à 1,0 % en poids; SiO_2 - de 1,0 à 2,0 % en poids; Fe_2O_3 - de 1,3 à 3,5 % en poids; Na_2O - de 0,1 à 0,5 % en poids; K_2O - de 0,3 à 1,0 % en poids; TiO_2 - de 0 à 0,2 % en poids. La bélite (C_2S) peut contenir: Na_2O - de 0,0 à 0,1 % en poids; K_2O - de 0,1 à 0,7 % en poids; MgO - de 0,1 à 0,3 % en poids; MnO - de 0,1 à 0,0 % en poids; Al_2O_3 - de 0,1 à 0,7 % en poids; Fe_2O_3 - de 0,1 à 0,7 % en poids; TiO_2 - de 0,0 à 0,1 % en poids; SO_3 de 0,1 à 1,1 % en poids.

L'aluminate de calcium $C_{12}A_7$: Na_2O - - 0,1-0,4; K_2O - 0,2-1,0; MgO - 0,3-1,5; Fe_2O_3 - 0,3-3,0; SiO_2 - 0,5-3,0; TiO_2 - - 0,1; SO_3 - 0,5-5,0.

Le sulfosilicate de calcium a une composition très hétérogène par suite de la cuisson du clinker qui s'effectue à la température proche à celle de décomposition de cette combinaison en C_2S et $CaSO_4$ (1350 °C). A la microscopie, les cristaux de ce composé sont fortement corrodés. Les quantités moyennes approximatives des additifs dans le sulfosilicate de calcium (en % de masse): Na_2O - 0,0-0,1; K_2O - 0,1-1,0; MgO - - 0,0-0,1; MnO - 0,1-4,0; Al_2O_3 - 0,2-6,1; Fe_2O_3 - 0,1-1,0; TiO_2 - 0,1-0,3.

Dans le système $CaO - Fe_2O_3-CaSO_4$, $CaO\cdot Fe_2O_3$, $2CaO\cdot Fe_2O_3$ et ses solutions solides avec le sulfate de calcium se forment en fonction du rapport CaO/Fe_2O_3. L'intercalation du sulfate-ion dans les ferrites de calcium modifie les paramètres de leur réseau cristallin et affaiblit l'énergie de liaison Ca - O (Tableau 1).

Dans les clinkers sulfoferrites, en fonction de la composition du mélange cru initial, les solutions solides des sulfoferrites de calcium et la bélite sont présentes contenant Na_2O, MgO, MnO, Al_2O_3 en qualité des additifs isomorphes.

Le rapport de phase et le type des additifs intercalés dans le réseau des minéraux

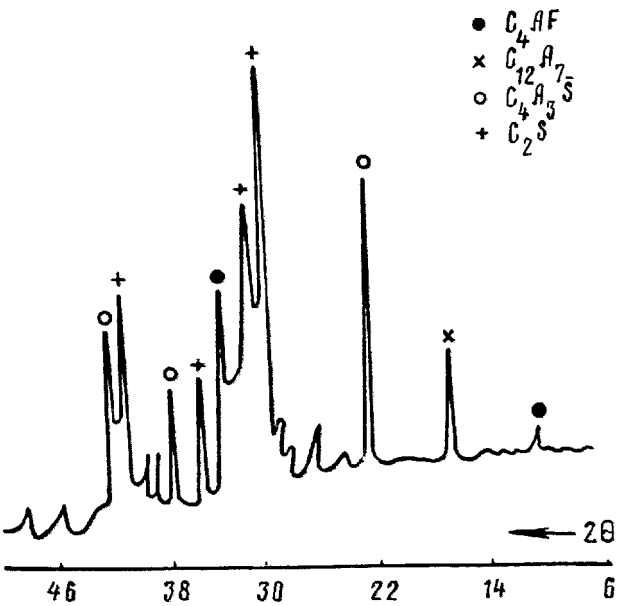

Fig. 1. Diagramme radiographique du clinker sulfoaluminate

Tableau 1

Paramètres de la cellule cristallographique et énergie de liaison des minéraux

Minéral	Paramètres Å			Energie de liaison Ca-O, kJ/mole
	a	b	c	
$CaO \cdot Fe_2O_3$	9,323	10,740	3,015	1148,9
$CF \cdot 0,3C$	9,349	10,678	3,023	1141,0
$2CaO \cdot Fe_2O_3$	5,579	14,758	5,428	1091,0
$C_2F \cdot C$	5,355	15,028	5,420	1084,4

Pour les additifs Na_2O, MgO, MnO, Al_2O_3, TiO_2, voir Tableau 2.

mentionnés prédéterminent l'activité d'hydratation et les propriétés des ciments (Fig. 2).

Conclusions. La modification des phases du clinker sulfoaluminate et sulfoferrite à l'aide des additifs et du régime thermique permet de régler les propriétés des phases isolées et les propriétés des ciments contenant ces phases.

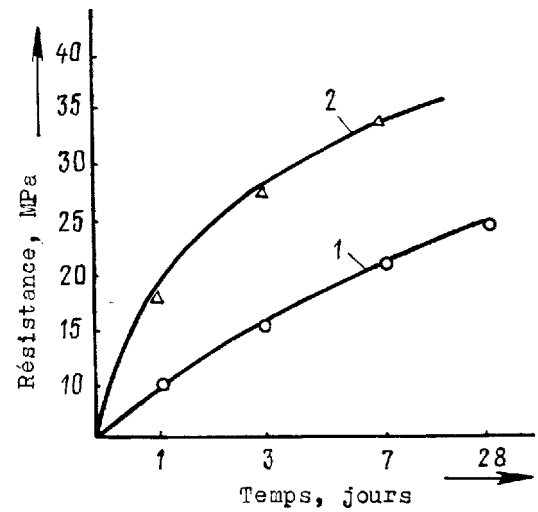

Fig. 2. Résistance de la pierre de ciment lors du durcissement dans les conditions normales
1 - ciment ferrite
2 - ciment sulfoferrite

Tableau 2

Additifs isomorphes dans les phases du clinker sulfoferrite

Oxyde	Quantité dans les phases, % de masse			
	C_2F	C_2S	$2(C_2S) \cdot CS$	$C_2F \cdot CS$
Na_2O	0,1	0,1	0,1	0,1
K_2O	0,1	0,1-0,3	0,1-0,3	0,1-0,4
MnO	0,2-2,0	0,2	0,2	0,1-0,3
Al_2O_3	0,5-3,5	0,1-0,5	0,1-0,3	0,1-0,3
Fe_2O_3	-	0,9-1,0	1-2,5	-
SiO_2	0,5-2,5	-	-	0,2-0,6

BIBLIOGRAPHIE

1. Кузнецова Т.В., Безрукова С.Г. Изучение сульфоалюминатного клинкера на основе различных сырьевых материалов. - Труды НИИЦЕМЕНТА, 1977, № 45, с. 40-44.
2. Кузнецова Т.В. Химия и технология расширяющихся и напрягающих цементов. - Обзорная информация ВНИИЭСМ, 1980 - с. 59.

A.I. BOIKOVA, Dr. Chem. Sc., Senior Research Scientist, 1
O.I. FOMICHEVA, Junior Research Scientist, Institute of Silicate Chemistry of the USSR Acad. Sci., Leningrad,
and A.P. ZUBEKHIN, Dr. Tech. Sc., Novocherkassk Polytechnical Institute, Novocherkassk.

Chemical composition of phases and phase relations in unbleached and bleached clinkers. 1.2

SUMMARY: Bleached and unbleached industrial clinkers of similar composition have been studied using EPMA, X-ray, microscopic and chemical methods to the purpose of elucidating the factors responsible for the whiteness. The Fe_2O_3 contents in the clinkers were 0.4-1.1 wt%.

The quantitative phase composition of the clinkers, the chemical composition of the phases, the coefficients (K_{Fe}) which represent the ratio of the mean Fe_2O_3 quantity in the phases to its total content in the clinker, the coefficients of whiteness (K_w) are given. Calcium aluminoferrite has been found in none of the clinkers. This implies that Fe^{3+} is distributed between the alite, belite, aluminate and glassy phases.

Special attention has been paid to the experimental control of Fe^{3+} distribution among the clinker phases and to the comparison of the quantitative phase relations in bleached and unbleached clinkers. The increase of the quantity of alite in bleached clinkers is due to the reaction between C_2S and CaO liberated by incongruent melting of C_3A. The C_3A content in bleached clinkers decreases significantly.

The value of the coefficients K_{Fe} for the silicate phases is less than unity which evidences for the distribution in these phases of only an insignificant part of the total Fe^{3+} content in clinkers. The majority of Fe^{3+} is concentrated in the aluminate and glassy phases, the latter being also enriched with silicon and aluminium. Two types of belite have been found which differ in crystallinity and impurity content.

An important conclusion is drawn from the study of impurities distribution among the phases. It is shown that the Fe^{3+} content in alite and belite of bleached and unbleached clinkers does not practically change. This desagreees with the existing point of view not confirmed experimentally.

Usando-se EPMA, raios-X, métodos químicos e microscópicos, foram estudados clínqueres industriais branqueados e não branqueados de composição semelhante, com o fim de esclarecer os fatores responsáveis pela brancura. Os teores de Fe_2O_3 nos clínqueres eram de 0,4 - 0,1% em peso.

São dadas a composição quantitativa de fase dos clínqueres, a composição química das fases, os coeficientes (K_{Fe}) que representam a relação de quantidade média de Fe_2O_3 das fases com o seu teor total no clinquer, os coeficientes de brancura (K_w). Em nenhum dos clínqueres se constatou o ferroaluminato de cálcio. Isto implica na distribuição do Fe^{3+} entre as fases de alita, belita, aluminato e vítrea.

Foi dedicada atenção especial ao controle experimental da distribuição de Fe^{3+} entre as fases do clinquer e à comparação das relações quantitativas de fase nos clínqueres branqueados e não branqueados. O aumento da quantidade de alita nos clínqueres branqueados se deve à reação entre C_2S e CaO liberado pela fusão incongruente do C_3A. O teor de C_3A nos clínqueres branqueados diminui significativamente.

O valor dos coeficientes K_{Fe} para as fases de silicato é menor que a unidade, o que evidencia a distribuição nestas fases de apenas uma parte insignificante do teor total de Fe^{3+} nos clínqueres. A maior parte do Fe^{3+} está concentrada nas fases de aluminato e vítrea, sendo a última também enriquecida com silício e alumínio. Foram encontrados dois tipos de belita, que diferem em teor de cristalinidade e impureza.

Tira-se uma conclusão importante do estudo da distribuição das impurezas entre as fases. Ficou demonstrado que o teor de Fe^{3+} praticamente não se altera na alita e belita dos clínqueres branqueados e não branqueados. Isto discorda do ponto de vista existente, não confirmado experimentalmente.

A.I. BOIKOVA
O.I. FOMICHEVA
A.P. ZUBEKHIN

INTRODUCTION

The most important characteristic of the quality of white cement is its whiteness which depends on several factors /1-4/. Among these factors are the content of iron oxides, the burning and cooling schedules, the methods of cooling. Usually the following factors are considered: the relation of phases (silicate, aluminate, aluminoferrite, glassy phases) in unbleached and bleached clinkers, the Fe^{3+} and Fe^{2+} contents in the phases and their distribution among them, the grain size of the phases and the uniformity of their mutual arrangement.

At present, however, we are lacking experimental data on the chemical composition of the real phases of unbleached and bleached clinkers, the distribution of iron among the phases during their formation in clinkers, the change in phase relations during bleaching. All these factors can be indicative of the physico-chemical peculiarities of the bleaching process and they are the main topics of the present work.

EXPERIMENT, RESULTS AND DISCUSSION

Five pairs of clinkers were investigated (I-unb, I-b; II-unb, II-b; III-unb, III-b; IV-unb, IV-b; V-unb, V-b). Each pair contained one unbleached (unb) and one bleached (b) clinker. Table 1 gives the contents of Fe_2O_3 and FeO in the samples determined by chemical analysis. Table 2 represents the results of determination of the quantitative phase composition of clinkers, conditions of their formation and coefficients of whiteness (K_w).
Figure 1 shows the X-ray diffraction patterns of bleached and unbleached clinkers V-b and V-unb. All bleached and unbleached clinkers contain the monoclinic alite, the β-modification of belite, the C_3A-based aluminate phase; the quenched (bleached) clinkers contain the glassy phase.

It is noteworthy that the quantitative phase relations in unbleached and bleached clinkers can be evidence of the physico-chemical processes occurring on bleaching. It was observed that in bleached clinkers the quantity of alite increases, whereas that of belite and aluminate decreases (Table 2). The decrease of the aluminate content in bleached clinkers is clearly seen in the X-ray diffraction pattern as the change of the maximum intensity at 33-34° 2θ (Fig. 1, notation □).

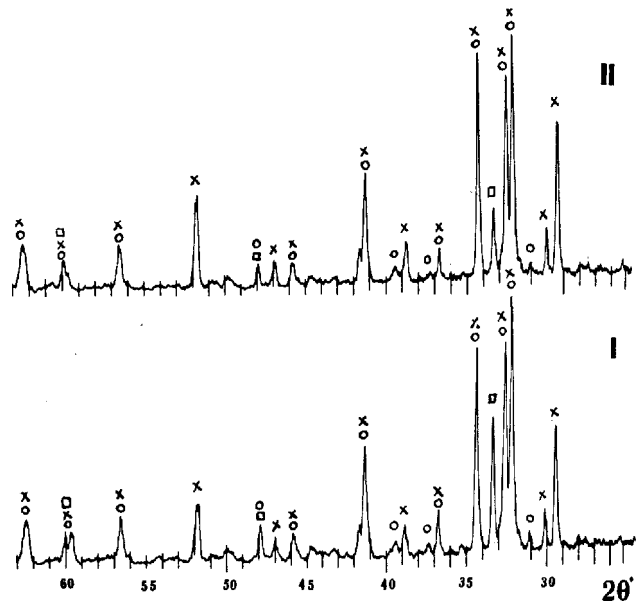

Fig. 1 - X-ray diffraction patterns of bleached V-b (curve 1) and unbleached V-unb (curve 2) clinkers; x - alite, o - belite, □ - aluminate phase.

As is known, C_3A melts incongruently yielding the formation of CaO and a liquid of the C_5A_3 composition /5/. The liberated CaO entering into reaction with C_2S is the reason of increasing alite content. It is this state that is "frozen" by bleaching (quenching).

Hence it can be concluded: the higher the burning temperature and the quicker the cooling, the greater amount of the liquid phase is formed and the greater amount of alite and the smaller amount of belite and aluminate will be present in the bleached clinker; the amount of glassy phase increases in this case.

As a result, the coefficient of whiteness increases as the glassy phase possesses a better degree of whiteness than the aluminate /1/. The influence of atmosphere and burning temperature on the increase of K_w can be proved by the fact that clinker

TABLE 1

Clinker	I		II		III		IV		V	
Oxide (wt%)	unb	b	unb	b	unb	b	unb	b	unb	b
Fe_2O_3	0.5	0.5	0.7	0.7	0.2	0.2	1.1	1.1	0.4	0.4
FeO	0.1	0.1	0.1	0.1	0.3	0.3	-	-	-	-

III-unb fired in a reducing atmosphere and at higher temperature contains 6% and 3% larger amounts of alite and belite, respectively, than clinker III-b obtained from the same initial material, and shows a higher degree of whiteness (Table 2).

It is worth noting that neither the X-ray nor microscopic methods permitted to find calcium aluminoferrite in any of the clinkers studied. This indicates that all iron enters as an isomorphous impurity into the silicate, aluminate and glassy phases of clinkers.

The microscopic investigation of the clinkers shows that clinker V-b is characterized by the most uniform distribution of the phases and is more finely crystallized. This clinker differs from other bleached clinkers with a higher coefficient of whiteness. Figure 2 is the back-scattered electron image of a grain section of clinker V-b with the concentration profile of iron along the indicated scanning line. It is seen that the largest iron quantity is concentrated in the interstitial phase (glassy and aluminate phases).

To study the composition of real clinker phases and the distribution of iron among them, the EPMA was made. Figure 3 shows the back-scattered electron image of the surface part of a grain of white clinker III-b (a) and the characteristic X-ray image of Al (b), Si (c), Ca (d), Fe (e). One can clearly see the grains of alite "immersed" in the interstitial phase (aluminate and glassy phases). The X-ray images are qualitative pictures of Al, Si, Ca and Fe distributions at the chosen surface part. The microscopic study of clinker III-b showed the non-uniform distribution of the phases. The major part of the grain section of clinker III-b is occupied by closely distributed alite and belite crystals. Such a part of the grain section with the clearly observable glassy phase is specially separated in the figure.

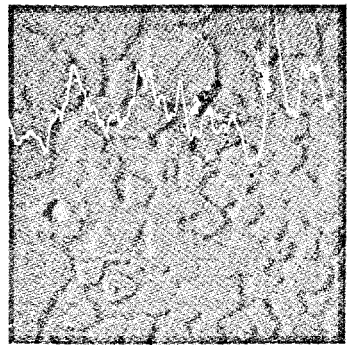

Fig. 2 - Back-scattered electron image of the grain section of clinker V-b and concentration profile of iron. Magnification x 800.

The chemical composition of the clinker phases was determined by the methods reported in /6-8/. Table 3 represents the mean chemical composition of the phases of the clinkers studied.

An important result of the determination of the composition of phases is that the Fe_2O_3 content in alites of bleached and unbleached clinkers does not change practically and is within the limits of 0.2-0.3 wt%.

TABLE 2

Clinker		Phase composition (wt%)				Regime		K_w
		alite	belite	aluminate	glassy phase	burning condition	cooling condition	
I	unb	49.0	32.0	19.0		1450 °C, air	air	53
	b	56.0	28.0	11.0	5.0	1450 °C, air	water quenching	70
II	unb	55.0	32.0	12.0		1450 °C, air	air	62
	b	65.0	20.0	5.0	10.0	1450 °C, air	water quenching	80
III	unb	62.0	20.0	18.0		1500 °C, reduc.atm.	reducing atm.	76
	b	56.0	17.0	19.0	8.0	1450 °C, air	water quenching	72
IV	unb	60.0	32.0	8.0		1450 °C, air	air	54
	b	63.0	26.0	6.0	5.0	1450 °C, air	water quenching	74
V	unb	71.0	13.0	16.0		1450 °C, air	air	75
	b	76.0	7.5	9.0	7.5	1450 °C, air	water quenching	85

In all clinkers under study two types of belite have been found which differ in the crystal shape and total impurity content. Belite of the first type forms in the solid phase and under the microscope it represents crystals of indefinite form; it contains a minor amount of impurities (1.6-1.7 wt%). The second type of belite is crystallized from the melt and contains a greater (3.5-5.2 wt%) amount of impurities; under the microscope it looks as grains of the rounded form. The total content of impurities in alite and belite of white clinkers when calculated for the same amount of oxides does not exceed 3.5 and 3.7 wt%, respectively.

The aluminate of bleached clinkers was found to contain a greater amount of impurities (8-15 wt%) compared to that of unbleached clinkers (7-11 wt%).

A large body of experimental data obtained permitted us to calculate the coefficients K_{Fe} which represent the ratio of the mean Fe_2O_3 content for each phase to the total content of this oxide in the clinker (Table 4). As seen from this table, the coefficients K_{Fe} of the silicate phases of white clinkers are less than unity which indicates that only an insignificant part of the total amount of iron is contained in them. The major amount of iron enters the interstitial substance - the aluminate and glassy phases.

CONCLUSION

The increase of the coefficient of whiteness can be attained by burning at the highest possible temperature, by sharp quenching and by decreasing time of burning which promotes the fine crystallization of the phases.

The increase of whiteness at water bleaching of the clinkers studied can be attained by changing the clinker phase composition: by the increase of the amount of alite, by the decrease of the amounts of aluminate and belite with high impurity contents, by the formation of the glassy phase and by the

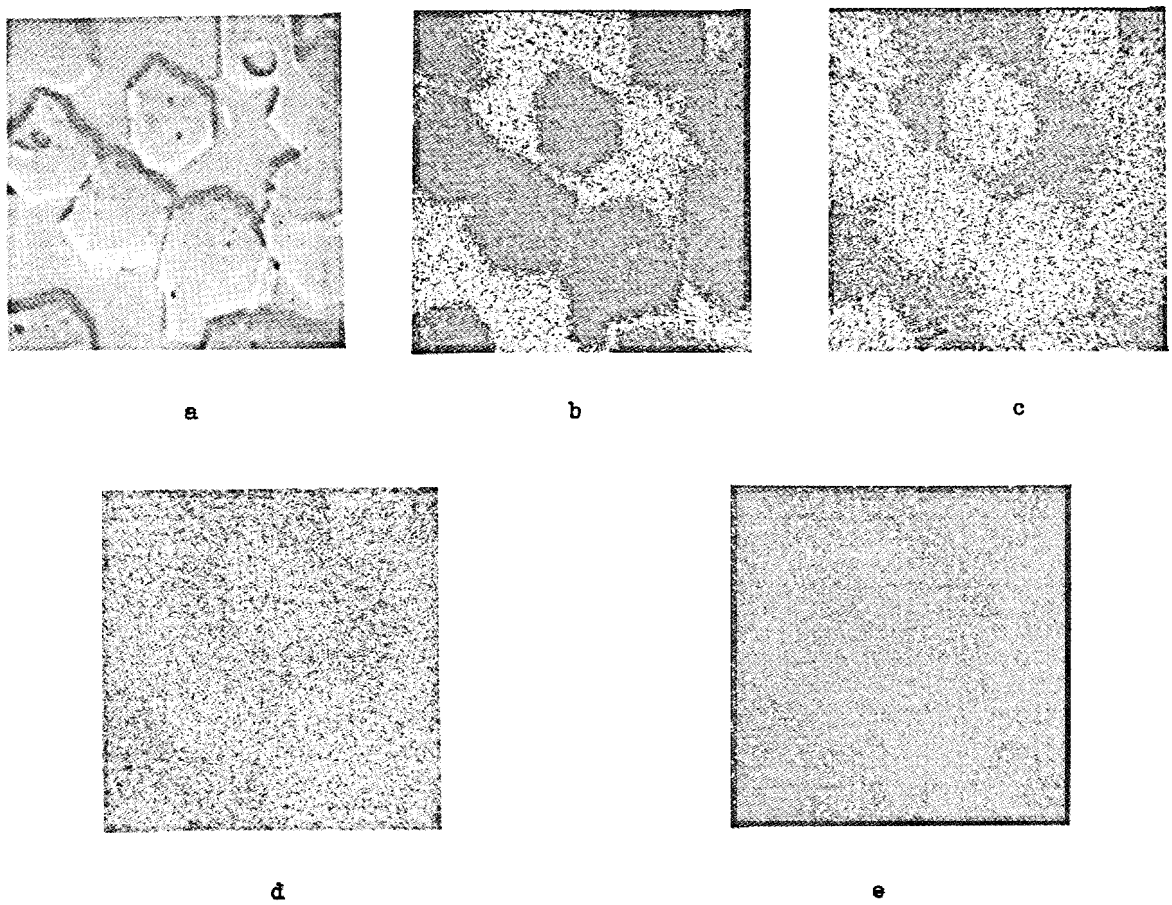

Fig. 3 - Back-scattered electron image (a) and characteristic X-ray images of Al (b), Si (c), Ca (d), Fe (e) on the grain section of clinker III-b

TABLE 3

Clinker	Phase	Chemical composition of phases of white clinkers (mean values, wt%)							
		CaO	SiO_2	Al_2O_3	Na_2O	K_2O	MgO	Fe_2O_3	TiO_2
I-unb	alite	73.3	24.4	0.8	0.0	0.1	1.0	0.2	0.1
	belite	64.9	32.2	1.4	0.1	0.4	0.5	0.2	0.1
	aluminate	59.3	4.0	32.9	0.2	0.4	0.3	2.0	0.6
I-b	alite	73.7	23.5	1.0	0.0	0.2	1.1	0.3	0.2
	belite	65.2	31.2	2.1	0.1	0.3	0.7	0.2	0.2
	aluminate	52.8	7.0	33.0	0.2	0.7	2.0	3.3	0.5
	glass	53.8	18.6	22.7	0.2	0.3	1.9	2.0	0.4
II-unb	alite	72.5	23.9	1.3	0.0	0.1	1.8	0.2	0.2
	belite	63.8	32.7	1.8	0.1	0.5	0.8	0.3	0.1
	aluminate	56.7	6.0	32.7	0.2	0.3	0.9	3.0	0.2
II-b	alite	73.7	23.4	1.0	0.0	0.2	1.3	0.3	0.1
	belite	63.9	32.9	1.8	0.1	0.2	0.6	0.3	0.2
	aluminate	56.4	6.4	28.9	0.2	0.8	2.0	4.6	0.5
	glass	51.9	15.2	24.1	0.2	0.6	4.0	3.7	0.6
III-unb	alite	74.0	23.7	0.9	0.1	0.1	0.7	0.2	0.2
	belite	66.3	31.6	1.0	0.1	0.3	0.3	0.2	0.2
	aluminate	53.0	5.5	37.5	0.2	0.3	1.5	1.3	0.2
III-b	alite	73.4	23.6	1.1	0.0	0.1	0.8	0.2	0.3
	belite	64.9	32.3	1.6	0.1	0.3	0.3	0.1	0.2
	aluminate	54.6	5.3	37.5	0.2	0.4	0.9	0.9	0.2
	glass	52.9	12.1	32.2	0.1	0.2	1.0	0.9	0.3
IV-unb	alite	73.3	23.6	1.6	0.0	0.2	0.7	0.3	0.3
	belite	64.9	31.0	1.9	0.0	0.5	0.2	0.5	0.2
	aluminate	53.5	5.4	35.2	0.1	0.6	1.9	2.6	0.4
IV-b	alite	74.1	23.4	1.2	0.0	0.1	0.6	0.3	0.2
	belite	64.2	31.8	2.1	0.0	0.5	0.2	0.6	0.3
	aluminate	48.8	6.2	34.8	0.1	0.6	1.0	6.5	0.6
	glass	56.0	15.9	19.7	0.1	0.2	1.2	2.5	0.7
V-unb	alite	74.0	23.9	1.1	0.1	0.1	0.7	0.2	0.1
	belite	66.8	30.2	2.3	0.1	0.1	0.3	0.2	0.2
	aluminate	60.6	4.7	32.8	0.2	0.2	0.7	1.4	0.2
V-b	alite	73.5	24.3	1.1	0.1	0.1	0.7	0.2	0.1
	belite	64.6	32.3	2.2	0.1	0.1	0.3	0.2	0.2
	aluminate	58.4	6.2	33.1	0.2	0.1	0.7	1.8	0.5
	glass	52.0	8.2	32.8	0.2	0.1	2.2	0.9	0.5

TABLE 4

Phase \ Clinker	I-unb	I-b	II-unb	II-b	III-unb	III-b	IV-unb	IV-b	V-unb	V-b
alite	0.33	0.40	0.25	0.38	0.40	0.40	0.27	0.27	0.50	0.50
belite	0.33	0.33	0.38	0.38	0.40	0.20	0.45	0.50	0.50	0.50
aluminate	3.30	5.50	3.75	5.75	2.60	1.80	2.36	5.90	3.50	4.50
glass		3.33		4.62		1.80		2.27		2.25

change of the crystallization features of the minerals.

The best coefficient of whiteness is observed in such a bleached clinker (V-b in our case) in which R^{3+} is mainly concentrated in the glassy phase and is characterized by fine crystallinity and uniform distribution of the phases among each other.

The Fe_2O_3 content in alite and belite of low-iron clinkers does not change practically on bleaching and shows a considerably lower value compared to the limiting one. The major part of Fe_2O_3 of white clinkers goes to the aluminate and glassy phases.

Two types of belite are crystallized in low-iron clinkers. Not all the amount of belite formed in the solid phase goes to the liquid phase, part of belite is retained in the solid phase and present in the final product. The total amount of impurities in such a belite is lower than in the one crystallized from the melt.

REFERENCES

1.- A.P. ZUBEKHIN (1979), "Effective methods of burning and bleaching the clinkers during preparation of decorative cements.", Review Information, VNIIESM, Moscow, 59 p.

2.- M. TEOREANU (1976), "Chemistry of white cements.", Proc. 6th Intern. Congr. on the Chem. of Cement, v.3, 255-267, Stroiizdat, Moscow.

3.- K. DOLEZHAI (1976), "Influence of colored metal oxides and the degree of cooling on the whiteness of white Portland cement clinker", Proc. 6th Intern. Congr. on the Chem. of Cement, v. 3, 278-282, Stroiizdat, Moscow.

4.- G. FRIGIONE and F. ZENONE (1985), "Influences on the whiteness of cements", Il Cemento 82, 2, 95-106.

5.- N.A. TOROPOV (1956), "Chemistry of Cement", Stroiizdat, Moscow, 271 p.

6.- A.I. BOIKOVA, A.K. ESAYAN and V.B. LAZUKHIN (1980), "Distribution of impurities among the minerals of industrial clinkers", Tsement N 1, 10-12.

7.- A.I. BOIKOVA, O.I. FOMICHEVA, T.V. KUZNETSOVA and N.I. KOMAROVA (1982), "On the composition of phases of white clinkers", Short Abstracts of Papers Presented at the 6th All-Union Conf. on the Chem. and Technol. of cement, Moscow, VNIIESM, 27-31.

8.- O.I. FOMICHEVA, A.I. BOIKOVA and A.P. ZUBEKHIN (1984), "Physico-chemical features of the whitening process of low-iron clinkers", Tsement N 6, 12-15.

T.V.Kouznetsova, Institut de chimique Mendéléev, Moscou, U.R.S.S.

1

INFLUENCE DES FACTEURS DIFFERENTS SUR LA COMPOSITION DE PHASE ET LES PROPRIETES DU CLINKER

1.2

Beaucoup de chercheurs étudiaient l'interliaison entre la composition-structure et les propriétés du clinker. Cependant, ce problème reste important jusqu'à présent. Le but du travail est d'étudier la composition de phase et la microstructure des clinkers industriels et de déterminer leur influence sur la qualité du ciment. Le rôle des microadditions dans la stabilisation des différentes modifications d'alite, de bélite et des compositions des aluminoferrites de calcium est défini. On présente les données concernant l'influence des paramètres d'obtention du clinker sur sa microstructure, caractère de cristallisation des minéraux, defectuosité des cristaux des phases principales et sur leur activité d'hydratation. On montre que, en fonction des conditions de cuisson, l'alite des clinkers industriels est présentée par la modification triclinique et monoclinique, la belite - sous forme des modifications γ, β, α, α' tandis que la composition des aluminoferrites de calcium varie de C_6AF_2 à C_6A_2F. Ces variations se reflètent avec évidence sur la microstructure du clinker. La combinaison de la microscopie optique avec la méthode d'analyse microradiospectrale peut être utilisée pour résoudre les problèmes d'amélioration de la qualité du ciment.

Muitos pesquizadores estudavam a interligação entre a composição-estrutura e as propriedades do clínquer. Entretanto, este problema continua importante até agora. O objetivo deste trabalho é estudar a composição de fase e a microestrutura dos clínqueres industriais e de determinar sua influência sobre a qualidade do cimento. O papel das microadições na estabilização das diferentes modificações da alita, da belita e das composições dos aluminoferritos do cálcio é definido. Apresentam-se os dados relativos à influência dos parâmetros de obtenção do clínquer sobre sua microestrutura, caráter de cristalização dos minerais, defeitos dos cristais das fases principais e sobre a sua atividade de hidratação. Mostra-se que, em função das condições de queima , a alita dos clínqueres industriais é caracterizada pela modificação triclínica em monoclínica, a belita sob a forma das modificações γ, β, α e α' enquanto que a composição dos aluminoferritos de cálcio varia de C_6AF_2 a C_6A_2F. Essas variações se refletem com evidência sobre a microestrutura do clínquer. A combinação da microscopia ótica com o método de análise microradioespectral pode ser utilizada para resolver os problemas de melhoria da qualidade do clínquer.

Introduction. L'interaction entre l'activité d'hydratation du ciment et la microstructure du clinker et sa composition chimico-minéralogique a bénéficié d'une étude suffisanment approfondie. A l'heure actuelle, on attache l'attention principale à la defectuosité des cristaux des phases du clinker (1), à l'influence des composunts mineurs sur leurs transformations polymorphiques (2). Un nombre d'ouvrages donne une analyse du rapport entre les dimensions des cristaux d'alite, la structure de cette derniere et sa composition chimique (3,4), la forme des cristaux d'alite et de bélite et l'activité du clinker (5). Cependant, une étude systématique sous les aspects du problème avec application de méthodes d'analyse modernes n'a pas été encore faite. Le présent ouvrage a pour but d'étudier l'influence de divers facteurs sur les propriétés, les modifications polymorphiques, la forme des cristaux des principales phases du clinker et l'activité du ciment.

Objets d'étude. Sur la base des matériaux chimiquement purs SiO_2, $CaCO_3$, Fe_2O_3, Al_2O_3 on a fabriqué une pâte brute qui a servi pour obtenir en laboratoire un clinker à FS=0,9 (fact. de sat. en chaux); MS=2,1 (mod. sil.); MA=1,3 (mod. alum.). Pour régler la quantité d'impuretés dans la pâte brute, cette dernière a été additionnée aussi de matériaux chimiquement purs $MgCO_3$, Na_2CO_3, $CaSO_4$. On a étudié, en outre la constitution de phase, la modification et la forme des cristaux des principaux minéraux utilisés à 30 cimenteries.

Résultats des expériments. Il a été établi à l'aide de la méthode d'analyse des phases aux rayons X, des méthodes microradiospectrale et chimique et de la microscopie optique que la constitution et la proportion des constituants du clinker dépendent de la quantité d'impuretés, de la température et du milieu gazeux de la cuisson.

En cas de cuisson du clinker dans un milieu neutre, une teneur en MgO de 3% et plus provoque une altération sensible de la structure microcristalline: les cristaux d'alite et de bélite revêtent une forme indéterminée. Pendant la cuisson du clinker dans un milieu réducteur, l'altération de sa microstructure n'a été observée qu'en présence de 5 % de MgO et plus en comparaison avec le clinker-témoin exempt de MgO. Les cristaux d'alite et de bélite des clinkers contenant de 2 à 3 % de MgO avaient, par contre, une forme plus régulière et les faces de l'alite possédaient un moindre degré de corrosion.

La constitution de phase des clinkers varie tout comme leur structure microcristalline sous l'influence du MgO en fonction des conditions de cuisson. Ainsi, les méthodes de recherche radiographique, rationnelle chimique et d'autres ont permis d'établir qu'avec une augmentation de la quantité de MgO dans les clinkers de cuisson neutre, le rapport des phases d'aluminate et d'aluminoferrite subit un décalage vers une réduction de la fraction du C_3A et une augmentation de celle du $C_2A_xF_{1-x}$ (fig. 1). Ce changement n'a pas un caractère monotone mais se porte au maximum lorsque la teneur en MgO est d'environ 3 %. A mesure que la teneur en MgO augmente, celle en

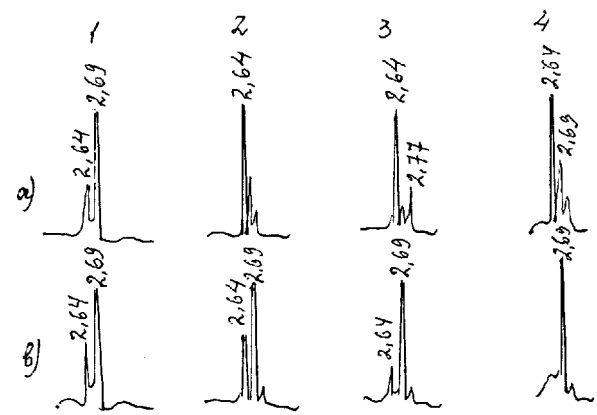

Fig.1. Secteurs des diagrammes radiographiques des phases d'aluminate et d'aluminoferrite de clinkers inductriels cuits dans un milieu neutre (a) et réducteur (b): 1 - 0,2 % de MgO; 2 - 2 % de MgO; 3 - 3 % de MgO; 4 - 4,9 % de MgO

C_3A commence de nouveau à s'élever. Appliqéée aux clinkers de cuisson réductrice, cette loi change quelque peu sa nature: la valeur maximale de décalage est observée la teneur en MgO est d'environ 2 % et la valeur relative ée déphasage diminue.

Il est établi également que dans le domaine des clinkers à magnésium il se produit non seulement un décalage de phases mais les propriétés deces dernières changent elles aussi. Les plus grands changements subit la phase d'aluminoferrite C_4AF (tabl. 1) qui s'enrichit d'Al_2O_3 en présence de MgO. Dans la phase d'aluminoferrite des clinkers soumis à la cuisson dans un milieu neutre, le rapport Al_2O_3/Fe_2O_3 augmente avec l'augmentation de la teneur en MgO. Elle atteint une valeur de 0,8 en présence de 4,90 % de MgO dans le clinker. Pour ce qui est des clinkers cuits un milin réducteur, ce rapport change peu et reste proche de 0,64.

Tableau 1

Milieu de cuisson du clinker	Teneur en, %		Constitution minéralogique, %				Al_2O_3/Fe_2O_3 dans la phase d'aluminoferrite
	MgO	FeO	C_3S	C_2S	C_3A	Phase d'aluminoferrite	
Neutre	0,20	0,11	68,3	8,4	10,0	12,7	0,65
	2,16	0,09	69,2	8,2	6,1	15,3	0,72
	3,16	0,05	67,6	8,0	6,1	16,4	0,74
	4,90	0,05	64,3	9,7	6,9	18,2	0,80
Réducteur	0,24	0,93	59,6	15,7	10,2	10,5	0,56
	2,16	0,52	58,6	16,2	9,5	13,0	0,63
	3,40	0,44	57,0	15,9	10,0	13,4	0,66
	5,27	0,44	57,1	15,6	10,9	13,2	0,65

Ces résultats donnent lieu à supposer qu'en cas de cuisson dans un milieu réducteur, la phase d'aluminoferrite des clinkers à magnésium subit des changements moindres que ceux propres aux clinkers exempts de MgO. La conclusion donnée est bien soutenue par les données relatives à la teneur en FeO des clinkers de cuisson réductrice: en de MgO la quantité de FeO diminue sensiblement.

A une augmentation de la quantité de FeO dans le clinker, les cristaux de bélite changent de forme: des grains compacts arrondis qu'ils étaient en l'absence de FeO revêtent une forme de grains à bords rugueux et de plaques distinctes (fig. 2).

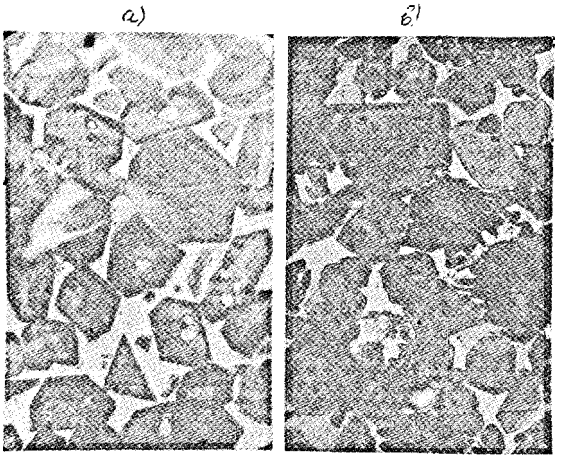

Fig. 2. Microstructure du clinker cuit dans un milieu neutre (a) et réducteur (b)

En présence de Na_2O la constitution de la phase d'aluminoferrite change aussi (fig. 3), la valeur du rapport Al_2O_3/Fe_2O_3 diminuant dans les aluminoferrites de calcium. La présence de plus de 2 % de Na_2O dans le clinker s'accompagne même de la formation de $2CaO.Fe_2O_3$.

Une addition de $CaSO_4$ dans la pâte brute change radicalement la nature de la microstructure du clinker: l'alite se cristallise sous la forme de prismes allongés bien réguliers et les cristaux de bélite prennent une surface striée.

Une intercalation d'ions de Mg^{2+}, Na^+ et S^{6+} entraîne l'augmentation de dislocations dans la structure des mineraux et des changements de modification (tabl. 2). L'intercalation d'ions d'addition le réseau cristallin des minéraux jusqu'à une certai-

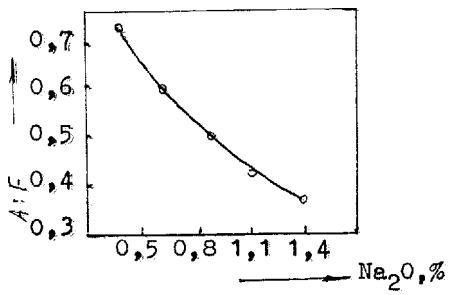

Fig. 3. Rapport Al_2O_3:Fe_2O_3 dans les aluminoferrites de calcium en fonction de la quantité de Na_2O dans le clinker

Tableau 2

Caractéristique des solutions d'alite solides des clinkers industriels

Type d'adjuvants	Modification of C_3S	Densité des dislocations, m^{-2}
MgO + $CaSO_4$	M_1. P	$7,8.10^3$
MgO	T_1. M_1	$3,1.10^{12}$
Na_2O	T_1	$3,2.10^{12}$

ne limite accroît l'activité du clinker. Ces limites sont les suivantes: 2 % pour MgO, 0,5 % SO_3 et 1 % pour Na_2O. Le dépassement de ces valeurs aboutit à un changement du rapport de phase dans le clinker et même une formation de phases indépendantes à magnésium, sulfate et alcali ce qui provoque une altération de la qualité du ciment.

Ainsi, une nette interaction est établie entre la constitution de phases, leur modification polymorphique, les forme des cristaux et l'activité du ciment ce qui permet d'appliquer la méthode de microscopie optique à l'appréciation correcte de la qualité du clinker.

Bibliographie

1. Timaschev V.V., Akimov V.G. Influence des defonts ponstuels sur l'activite d'hydration des constitutions de clinker. - 7 Intern. Congress de la Chemie des cements, Paris, 1980, p.11-27
2. Counlend L.E., Kantro D.A. International Congress of Chemie of Cement, Tokijo, 1968
3. Судакас Л.Г. и др. Гидравлическая активность промышленных клинкеров с различными формами алита. -Цемент, 1982, № 9, с.13-14
4. Maki i., Goto K. Factors influencing the phase constitution of alite in portland cement clinker. - Cement and Concrete Research, 1982, v.12, p.301-308
5. Кривобородов Р.Т., Кузнецова Т.В. Влияние структуры клинкера на прочность тампонажного цемента. - Цемент, 1963, № 3, с. 11-14

V. CHOUBINE,
Y. KHNYKINE NIIciment, Moscou, URSS

MODIFICATION DES CLINKERS DE BELITE

Les auteurs ont étudié la relation entre la composition, l'aptitude à la cuisson, les traitements thermiques subis et la structure des bélites, ainsi que l'influence qu'exercent ces facteurs sur leur activité et leur résistance mécanique. Les auteurs ont examinés les analogues structuraux β, α'-C_2S.

Les auteurs ont montré que les clinkers à base de bélites peuvent être obtenus à des températures de 250 à 300°C inférieures à celles prévues pour les clinkers classiques du ciment Portland; grâce à certains artifices technologiques, on peut accroître l'activité d'hydratation des clinkers à base de bélites.

Les auteurs analysent la nécessité et la suffisance de certains facteurs chimiques et technologiques pour une stabilisation fiable des variétés de bélite nécessitant de hautes températures, pour modifier la défectuosité de sa structure, pour faire varier dans le sens voulu les caractéristiques de la bélite et des ciments à sa base.

Sur le plan pratique, les résultats de ces recherches peuvent être utilisés pour réduire la consommation de chaleur et d'énergie et pour valoriser des ressources secondaires (déchets provenant d'autres productions).

Os autores estudaram a relação entre a composição, a aptidão à queima, os tratamentos térmicos sofridos e a estrutura das belitas, bem como a influência que esses fatores exercem sobre a atividade e sua resistência mecânica. Os autores examinaram os análogos estruturais β, α'-C_2S.

Os autores mostraram que os clínqueres com base em belitas podem ser obtidos em temperaturas de 250 a 300°C inferiores às previstas para os clínqueres clássicos do cimento Portland; graças a alguns artifícios tecnológicos, pode-se aumentar a atividade de hidratação dos clínqueres com base em belitas.

Os autores analisam a necessidade e a suficiência de certos fatores químicos e tecnológicos para uma estabilização confiável das variedades da belita necessitando altas temperaturas para modificar os defeitos de sua estrutura, para fazer variar no sentido desejado, as características da belita e os cimentos com base nelas.

No plano prático, os resultados dessa pesquisa podem ser utilizados para reduzir o consumo de calor e de energia e para valorizar recursos secundários (resíduos provenientes de outras produções).

Introduction. On sait que les liants à base de bellites présentent un certain nombre d'avantages. Leur principal inconvénient réside dans leur activité d'hydratation peu élevée. Un bon nombre de facteurs qui influent sur l'activité d'hydratation de la bellite et les caractéristiques mécaniques des liants à base de bellites compliquent la recherche d'un procédé d'obtention d'une bellite très active.

Le présent ouvrage est consacré à la recherche d'une relation entre la composition chimique, la structure et la morphologie de certaines bellites, d'une part, et leur activité d'hydratation, la morphologie et la composition des néo-formations hydratées, ainsi que les caractéristiques mécaniques des échantillons de bellites hydratées et de liants à base de bellites, d'autre part.

Produits de départ, appareils, modes opératoires. On a examiné des bellites synthétisées par cuisson de γ-C_2S en présence d'ions modifiants Na^+, B^{3+}, P^{5+}, Cr^{6+} et d'ions Al^{3+} et Fe^{3+} présents à titre d'impuretés, ainsi que des clinkers à base de bellites. La synthèse des bellites et des clinkers à leur base a été opérée dans un four électrique de laboratoire, en milieu d'air et avec un refroidissement effectué à une vitesse de 500 degrés par minute. On broyait les agglomérats jusqu'à une surface spécifique de 310±10 m^2/kg, on gâchait les poudres en leur donnant la forme de cubes d'une longueur de l'arête de 14,1 mm qu'on conservait en milieu d'air humide.

La composition par phases des agglomérats, la composition des cristallohydrates et le taux d'hydratation des matériaux étudiés ont été déterminés par des méthodes d'analyse radiographique et thermique différentielle. La morphologie des cristaux des agglomérats et des échantillons hydratés a été étudiée à l'aide d'un microscope électronique.

La réactivité (l'aptitude à la cuisson) des mélanges bruts a été estimée d'après le taux maximal d'oxyde de calcium libre contenu dans les agglomérats (A) et d'après la surface comprise entre la courbe représentative de la CaO libre = f (T) pour une cuisson pendant 1 heure et l'abscisse (T).

Résultats des expériences. Les données relatives à la réactivité d'un certain nombre de mélanges bruts sont résumées au tableau 1. Les compositions, les modifications, les taux d'hydratation, les caractéristiques mécaniques de plusieurs bellites, ainsi que des caractéristiques des produits de leur hydratation sont présentés au tableau 2. Les résultats des recherches sur l'activité d'hydratation des bellites figurent dans le dessin.

Caractéristiques des compositions et aptitude à la cuisson des mélanges bruts

Tableau 1

n°n° d'ordre	Constituants du mélange	KH	p	r	Valeur de A*	B**	C***, °C
1	Matériaux naturels qui	0,91	2,1	0,9	48	16	200 1 400
2	Marnes	0,92	2,0	1,1	31	11	300 1 350
3	Réactifs $CaCO_3$, SiO_2, Al_2O_3, Fe_2O_3	0,93	2,0	1,2	43	14	500 1 400
4	Réactifs $CaCO_3$, Al_2O_3, SiO_2, Fe_2O_3	0,67	1,7	1,2	28	4	100 1 250
5	Calcaire, constituant alumino-fère, gypse	0,74	0,6	7,2	10	1	300 1 000

* A, valeur maximale du taux de CaO libre dans les agglomérats (% en masse).

** B, valeur intégrale du taux de CaO libre dans les agglomérats (% en masse)

*** C, température de synthèse des clinkers conditionnés pour une cuisson durant une heure

Discussion des résultats. Une des vertus des liants à base de bellites est une moindre consommation de combustibles lors de la fabrication de ces liants par rapport aux ciments Portland ordinaires à base d'alites. La différence des températures de synthèse des clinkers des liants en question peut atteindre 400°C. La réactivité du mélange brut à base de bellites, qui n'a pas dans sa composition d'impuretés minéralisantes, est nettement supérieure en valeur de B, à celle d'un mélange ordinaire analogue d'un ciment Portland classique (tableau 1, mélanges 3 et 4).

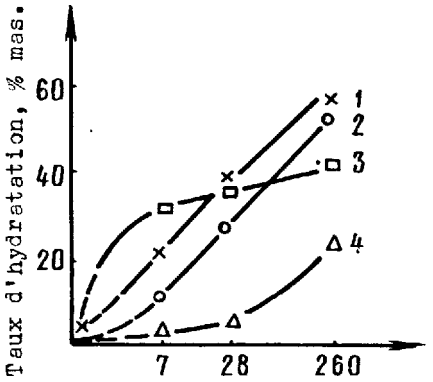

Fig. Vitesse d'hydratation des bellites
1. '-C_2S phosphoré d'une composition non stoechiométrique;
2. β-C_2S
3. '-C_2S contenant le sodium;
4. β-C_2S d'un ciment à base de bellite et d'alumine en abscisse: durée d'hydratation, jours (lg τ) en ordonnée: taux d'hydratation, % en masse

La formation des solutions solides de bellites à forte teneur en impuretés est accompagnée d'une stabilisation sous refroidissement de leurs modifications exigeant de hautes températures et ayant des structures plus défectueuses. Les potentialités de l'activité d'hydratation des bellites sont probablement d'autant plus élevées que leur modification est de plus haute température.

Il existe une interdépendance déterminée entre la composition chimique, le caractère de cristallisation et l'activité d'hydratation des bellites. Des différences relativement peu importantes entre les compositions chimiques des analogues structuraux de β et surtout de α'-C_2S peuvent conduire à des différences notables des caractères de leur cristallisation, de l'activité d'hydratation et de la résistance mécanique. Les bellites ayant un motif structural commun β-C_2S sont caractérisées par une activité d'hydratation peu élevée dans les premières phases de durcissement et une vitesse d'hydratation régulière, obéissant à la relation TH (taux d'hydratation) = $K_\beta \lg \tau$ au bout de 5 à 7 jours de durcissement (à l'issue de la période d'accélération). Une moindre vitesse d'hydratation correspond à une cristallisation plus nette de β-C_2S. Quand le β-C_2S contient des quantités appréciables d'impuretés, surtout d'impuretés alcalines, on observe des phénomènes de recristallisation et un certain accroissement de l'activité d'hydratation, mais la résistance n'en change pratiquement pas.

Une activité d'hydratation relativement basse des échantillons correspond à une cristallisation très prononcée de α'-C_2S. Ce sont les solutions solides de C_2S et de C_3P isostructuraux qui présentent l'activité d'hydratation la moins élevée. Ainsi, le taux d'hydratation de $C_{2,15}P_{0,05}S$, refroidi à une vitesse de 500°C par minute, constitue, au bout de 28 jours, 10% environ, alors que si la vitesse est de 100°C par minute, il est pratiquement égal à zéro.

Les α'-C_2S contenant des alcalis et se distinguant par une structure défectueuse à petits cristaux ont l'activité d'hydratation la plus grande dans les premières

V. CHOUBINE,
Y. KHNYKINE

Tableau 2

Compositions, températures de synthèse de la modification et résistance mécanique des bellites, taux d'hydratation (TH), taux d'eau combinée (EC) et de CaO libre, compositions des hydrosilicates de calcium (HSC) dans des bellites hydratées pendant 260 jours

nos d'ordre	Compositions des bellites	Températures de la synthèse, °C	Modification	Résistance à la compression, MPa au bout de tant de jours				TH, % en masse	Teneur en		Compositions des HSC
				3	7	28	260		EC, % en masse	CaO libre, % en masse	
1.	$C_{2,00}{}^{B}O_{0,01}{}^{S}$	1500		9	16	46	81	46	17,1	4,17	$C_{1,85}H_{1,82}$
2.	$C_{2,00}{}^{B}O_{0,01}{}^{S}$	1400		7	15	59	76	61	15,8	4,91	$C_{1,81}H_{1,81}$
3.	$C_{2,00}\ 0,05{}^{F}O_{0,03}{}^{S}$	1500		-	9	17	78	53	18,8	4,10	$C_{1,84}H_{2,06}$
4.	$C_{2,00}\ 0,13{}^{F}O_{0,04}{}^{S}$	1500		11	14	31	51	52	19,9	3,87	$C_{1,88}H_{2,23}$
5.	$C_{2,00}\ 0,21{}^{F}O_{0,03}{}^{A}O_{0,04}{}^{S}$	1500		20	34	46	65	44	22,1	3,08	$C_{1,88}H_{2,59}$
6.	$C_{2,00}{}^{P}O_{0,05}{}^{S}$	1470		9	23	56	87	54	18,4	4,20	$C_{1,84}H_{2,00}$
7.	$C_{2,06}{}^{P}O_{0,05}{}^{S}$	1500		8	21	64	100	55	16,9	3,68	$C_{1,86}H_{1,80}$
8.	$C_{2,15}{}^{P}O_{0,05}{}^{S}$	1500		-	10	25	54	35	15,9	3,56	$C_{1,87}H_{1,68}$
9.	$C_{2,00}{}^{B}O_{0,10}{}^{S}$	1370		8	14	38	45	30	16,1	2,87	$C_{1,83}H_{1,80}$

étapes de durcissement. La résistance des α'-C_2S contenant des alcalis est, elle aussi, la plus grande dans les premiers 7 jours en comparaison des autres bellites. Plus tard, la résistance et l'activité d'hydratation des α'-C_2S contenant des alcalis deviennent inférieures à celles des autres bellites, la croissance de la resistance se ralentissant le plus.

Les auteurs ont établi que la grandeur du rapport CaO/SiO_2 dans les hydrosilicates de calcium (HSC) résultant de l'hydratation de β-C_2S pendant 260 jours est de 1,81 à 1,85, alors que pour l'hydratation de α'-C_2S, elle est de 1,83 à 1,88. La teneur des HSC en eau d'hydratation varie, suivant les compositions des bellites de départ, dans des limites relativement étendues; une moindre résistance des échantillons hydratés correspond à une valeur plus grande du rapport $H_2O/C_{1,83\pm0,03}$. Il paraît que les HSC plus hydratés forment des agrégats de cristaux relativement moins solides.

Des écarts à la stoechiométrie de la forme α' de bellite favorisent la formation d'une structure cristalline plus défectueuse de celle-ci, l'accroissement de l'activité d'hydratation et de la résistance mécanique des échantillons hydratés. Selon toute probabilité, il existe un domaine des compositions de bellites, à l'intérieur duquel des écarts à la stoechiométrie de α'-C_2S entraînent un accroissement maximal de leur activité d'hydratation. Parmi les bellites phosphorées, ce sont les solutions solides ayant des compositions proches de $C_{2+1,5p}\ P_pS$ où le taux d'anhydride phosphorique P_p est de 3 à 7% en masse qui présentent la résistance mécanique et l'activité d'hydratation les plus élevées.

Quand il s'agit des liants à base de bellites, la tâche principale est d'obtenir avec eux une bonne résistance mécanique dès les premières étapes de durcissement. Cet objectif peut être atteint par synthèse d'un liant d'une composition déterminée par pha-

ses, notamment un ciment à base de bellite et de sulfoaluminate ou d'autres compositions. On peut obtenir des ciments de ce genre avec une consommation modérée de combustibles pour leur cuisson, ils ont une bonne résistance mécanique dès les premières étapes de durcissement (de 6 heures à 7 jours), mais le taux d'hydratation de β-C_2S au sein de ces ciments pendant 28 jours ne s'élève qu'à 5 à 15% par rapport à la masse de la bellite et la résistance mécanique ne croît pas suffisamment rapidement à l'âge de 3 à 28 jours.

A part les autres moyens d'accroissement de la résistance mécanique des liants à base de bellite, on peut le faire par une synthèse orientée des bellites stabilisées sous forme α', dont les compositions présentent des écarts à la stoechiométrie. Dans ce cas, une vitesse élevée de refroidissement du clinker, qui favorise la stabilisation de la modification de haute température de la bellite pour des concentrations relativement peu élevées d'ions modifiants dans le clinker, peut avoir son utilité.

B.S. AL'BATS,
M.A. VERDIAN,
L.S. FILLIPPOVA,
E.L. LEBEDEVA, NiiCement, Moscou, URSS

1

DUREE DE CUISSON DU CLINKER ET SES PROPRIETES

1.2

Les auteurs ont effectué les études du rapport des paramètres du processus de cuisson, de la variation de composition, de la structure et des propriétés des clinkers à obtenir pour les différents crus industriels.

Les régimes actuels de cuisson et de refroidissement ne sont pas optima car ils assurent un temps prolongé de rétention de la matière dans la zone des hautes températures. Cela mène à l'inhibition du processus de formation de l'alite dans le clinker et à la diminution de son activité.

Les expériments industriels avec utilisation de la méthode des indicateurs radioactifs ont confirmé les résultats des essais laboratoires.

La dépendance quantitative entre la température et le temps du maintien isotherme est calculée pour les crus de cimenterie.

Os autores efetuaram os estudos da relação dos parâmetros do processo de queima, da variação de composição, da estrutura e das propriedades dos clínqueres a serem obtidos para os diferentes crus industriais.

Os regimes atuais de queima e de resfriamento não são ótimos pois asseguram um tempo prolongado de retenção na zona de altas temperaturas. Isso conduz à inibição do processo de formação de alita no clínquer e à diminuição de sua atividade.

As experiências industriais com a utilização do método dos indicadores radioativos confirmaram os resultados dos ensaios em laboratório.

A dependência quantitativa entre a temperatura e o tempo mantido isotérmico foi calculado para crus de fabricação.

B.S. AL'BATS,
M.A. VERDIAN,
L.S. FILLIPPOVA,
E.L. LEBEDEVA

On a étudié le comportement des mélanges crus industriels au cours du traitement thermique, y compris les conditions de la cuisson industrielle, la composition et les propriétés des bains fondus, la cinétique de formation de l'alite comme un minéral principal du clinker, les propriétés du clinker et le rôle du facteur "température-temps" lors de la cuisson.

Pour les essais, on a choisi les mélanges crus se distinguant d'après les compositions minéralogiques et chimiques (tableau I). Pour rapprocher au maximum l'identité de la dispersité des particules, tous les mélanges ont été tamisés à travers le tamis 02 (mailles 20 μ).

La cuisson des échantillons-tablettes de 0,01 m de diamètre pressés sous la pression de 5 MPa a été effectuée dans le four de silite dans un intervalle de température 1593-1698°K, tous les 15° avec les maintiens à chaque température de 120, 300, 600, 1200, et 1800 s. La vitesse de montée de la température a été 0,083 degrés/s. Pour les mélanges crus 2 et 4 on a effectué un cycle d'essai analogue avec une grande vitesse de chauffage. Dans ce cas, les maintiens ont été les mêmes qu'en cas du chauffage lent.

Tableau I

Composition minéralogique et chimique des mélanges crus

Composition chimique % de masse	Composition minéralogique					
	marne, craie	loess calcaire	kaolinc, argile, craie	schlamm de néphéline, calcaire	marne, marne	limon de montmorillonite, calcaire
Perte au feu	34,34	34,00	34,12	21,86	34,06	33,83
SiO_2	15,12	14,08	13,93	18,31	14,66	15,22
Al_2O_3	2,65	3,17	2,70	2,80	2,25	3,52
Fe_2O_3	1,93	2,66	3,04	3,24	3,25	2,34
CaO	43,97	43,60	44,32	50,71	42,86	41,88
MgO	0,82	1,03	0,61	1,84	0,80	1,49
MnO	0,01	0,06	0,04	0,10	0,08	0,06
SO_3	0,33	0,44	0,36	0,20	0,41	0,33
TiO_2	0,14	0,17	0,22	0,23	0,15	0,32
Cr_2O_3	traces	traces	traces	traces	traces	traces
Na_2O	0,30	0,47	0,29	0,48	0,18	0,40
K_2O	0,58	0,49	0,49	0,37	0,44	0,70
P_2O_5	0,12	0,12	0,09	0,04	0,04	0,06

Composition et propriétés des bains fondus

Dans les bains fondus des mélanges I et 6, on a observé les zones de lamellation dont les compositions sont enrichies en oxydes de soufre et d'alcalis. Le bain fondu du mélange 5 se distingue par une teneur élevée totale en oxydes de manganèse, de soufre et de titane (3,18%) à une teneur totale relativement faible en oxydes de magnésium et d'alcalis (7,04). Apparemment, ce fait explique la viscosité diminuée des matières fondues des mélanges mentionnés (à la température de 1673°K - 0,09; 0,07 et 0,095 Pa·s conformément).

Les matières fondues des mélanges 2, 3, 4 ont une viscosité de 0,135; 0,165 et 0,11 Pa·s à la température de 1673°K. Cela peut-être expliqué par une influence dominante des oxydes de magnésium et d'alcalis dont la teneur totale est de 9,95; 8,15 et 10,08% de masse.

La dépendance "viscosité-température", en cas des matières fondues des mélanges 3 et 6, porte un caractère nettement exponentiel, pour la matière fondue du mélange 4, cette dépendance s'approche de la fonction exponentielle, pour la matière fondue du mélange 2, elle prend un caractère linéaire, tandis qu'en cas des matières fondues des mélanges I et 5, elle est complexe (l'exponentielle a des zones isolées linéaires à des basses températures).

La tension superficielle des matières fondues, à l'exception des mélanges 1, 3 et 6, varie d'une façon non linéaire. En cas des mélanges 4 et 5, la tension superficielle diminue principalement dans un intervalle de 1673-1723°K et en cas du mélange 2 - dans un

intervalle de 1623-1673°K.

Cinétique de formation de l'alite et propriétés du clinker

On voit sur la figure I que lors du chauffement lent, toutes les courbes possèdent paratiquement les zones représentant un retardement de l'assimilation de CaO.

Les données de l'analyse de phases à rayons X (figure I) témoignent de périodicité de la formation de l'alite. Dans ce cas, les zones de températures de l'inhibition de formation de l'alite sont proches des zones du retardement de l'assimilation de CaO.

L'énergie d'activation du processus de formation de l'alite pour les mélanges 1-6 est conformément: 53, 27; 79,96; 82,81; 89,75; 45,08 et 53,13 kJ/mole. Selon les valeurs indiquées de l'énergie d'activation, les mélanges I, 5, 6 peuvent être rapportés aux mélange à cuisson facile, tandis que les autres - aux mélanges à cuisson difficile qui exigent des dépenses de chaleur élevées. Cette classification conventionnelle correspond aux données sur la viscosité des matières fondues des mélanges en question.

La périodicité de formation de l'alite est liée, probablement, au caractère de cristallisation de ce minéral. Le cristal de bélite se dissout dans la matière fondue avec la formation des ions $[Si_nO_m]^{-k}$ relativement peu mobiles et des ions plus mobiles Ca^{2+}. Il se forme une zone de germination de l'alite où migrent les ions Ca^{2+} formés par suite de la dissolution des cristaux CaO dans la matière fondue. Selon les données de V. Timachev et autres auteurs, les valeurs de l'énergie d'activation pour dissoudre C_2S sont de 419 kJ/mole et celles pour dissoudre CaO sont de 264 kJ/mole. Pour cette raison, il est bien probable qu'il y a une germination des cristaux d'alite autour des cristaux de bélite dissolvants, leur croissance suivante, la recristallisation et la fusion avec les autres cristaux croissants jusqu'à la formation d'une couche continue d'alite autour du cristal de bélite initial.

Le volume de la matière fondue entre les cristaux de bélite et la couche d'alite formée est sursaturé rapidement par les ions Ca^{2+} et $[Si_nO_m]^{-k}$, et l'équilibre se déplace dans le sens de la substance initiale (bélite). Simultanément, l'accès des ions Ca^{2+} dans la zone de la matière fondue fermée cesse. L'équilibre acido-basique entre les volumes de la matière fondue des deux côtés du cristal d'alite croissant est perturbée. La cristallisation ultérieure de l'alite a un caractère déséquilibré. Des conditions se forment pour un écart de la stoechiométrie dans la composition des zones périphériques et internes des cristaux d'alite.

Dans la structure du cristal d'alite, des contraintes supplémentaires se forment représentant une source de déformations du cristal qui mènent à sa destruction (figure I). Dans ce cas, une diminution de quantité des défauts des cristaux d'alite est inévitable car la destruction s'effectue dans les endroits de leur concentration maximum. Les ondes des contraintes provenant des cristaux croissants d'alite détruisent tout l'échantillon qui, malgré la présence de la phase liquide, subit des déformations empêchant le retrait et menant parfois à l'expansion de l'échantillon (figure I). En pratique, cela peut aboutir à la destruction des grains du clinker et à la formation de la poussière.

La coincidence des effets d'inhibition dans la formation de l'alite, de décomposition des grains du clinker et de diminution de l'activité d'hydratation de ce dernier est observée en cas des clinkers industriels quand la matière se trouve relativement longtemps en zone de cuisson (figure 2).

L'analyse des paramètres de base caractérisant la structure hydrodynamique du flux de la matière dans le four rotatif industriel montre que si le temps de séjour de la matière dans la zone de cuisson (déter-

B.S. AL'BATS,
M.A. VERDIAN,
L.S. FILLIPPOVA,
E.L. LEBEDEVA

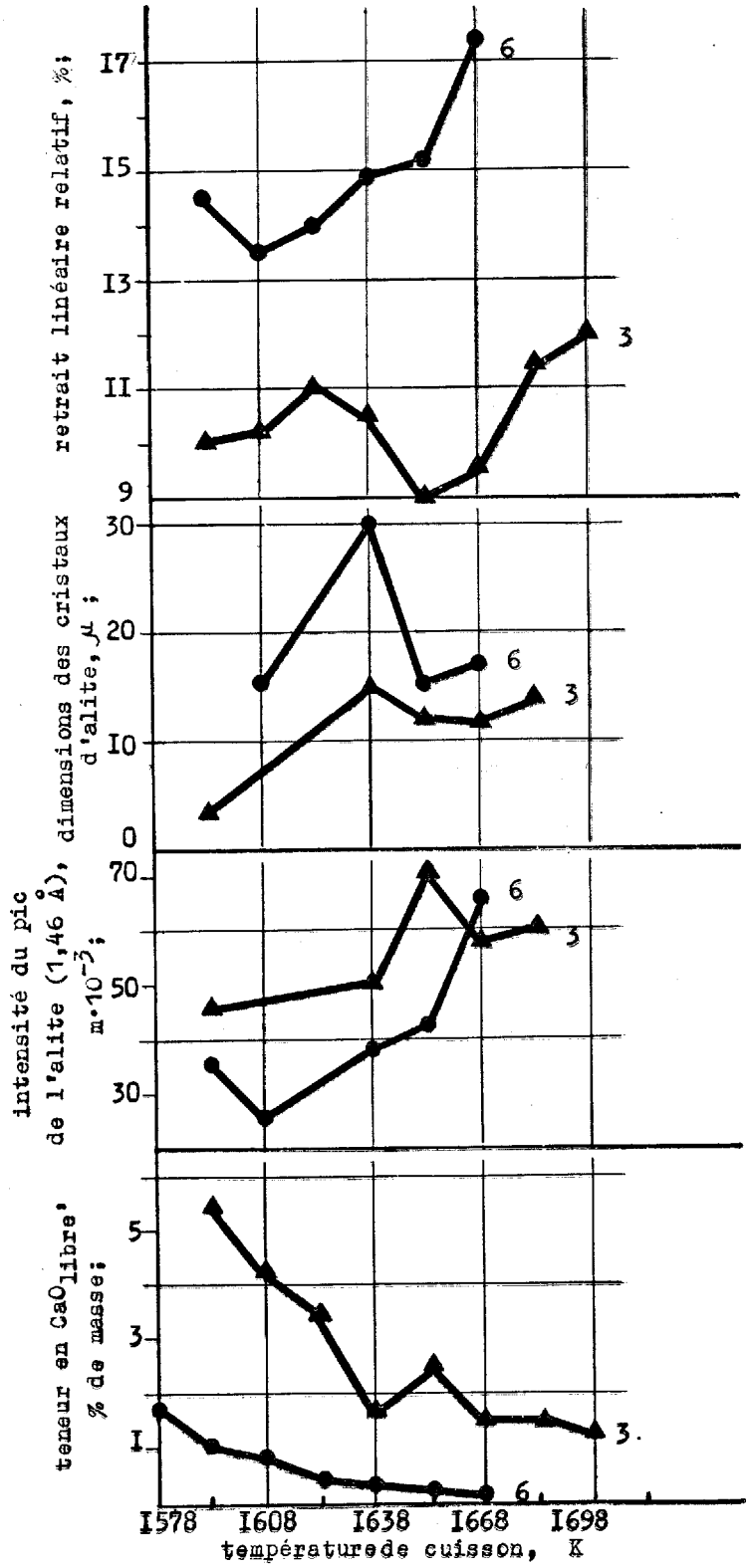

Fig. 1. Teneur en CaO_{libre}, quantité et dimensions des cristaux d'alite et retrait relatif linéaire en fonction de la température de cuisson (en cas de la cuisson pendent 600 s);
3 - mélange n°3; 6 - mélange n°6

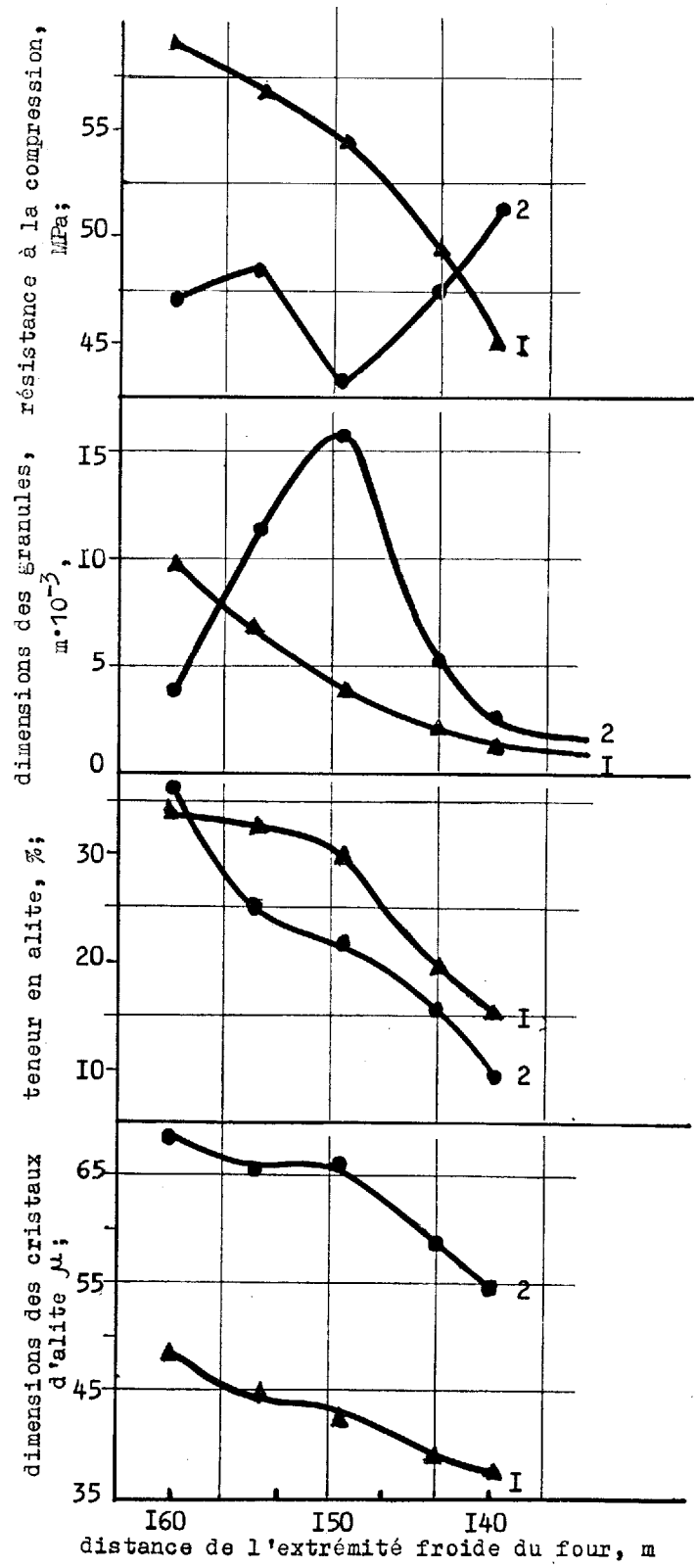

2. Caractère de la formation des minéraux, des cristaux et des grains et l'activité du clinker par la longueur de la zone de cuisson du four rotatif 4,5 x 170 m (I - zone de cuisson courte, 2 - zone de cuisson longue)

Tableau 2

Durée du traitement thermique et degré de cuisson de la matière dans le four rotatif industriel

Zone du four	Temps moyen de séjour, s	Vitesse de passage de la matière, m/s	Teneur en CaO_{libre} (%/masse) de la matière par la longueur de la zone de cuisson (m. de l'extrémité froide du four 4,5 x 170)					
			135	140	145	150	155	160
Zone de séchage	2230	0,025						
Zone de chauffement	930	0,049						
Zone de décarbonisation	557	0,057						
Zone de cuisson et de refroidissement	5080	0,010	10,1	9,0	4,0	0,4	4,4	0,3

miné par la méthode des indicateurs radioactifs) dépasse considérablement le temps nécessaire à l'achèvement de la réaction de formation de l'alite, la teneur en ce dernier diminue. Parfois, à l'aide de la méthode chimique, on fixe une augmentation de teneur en CaO_{libre} (tableau 2).

Au cours de l'analyse des échantillons cuits selon un régime de grande vitesse, on n'a pas observée l'inhibition dans le processus de formation de l'alite.

Lors de la cuisson brusque, les conditions pour la recristallisation de la bélite et de l'oxyde de calcium ne se forment pas, la dissolution de ces minéraux dans la matière fondue s'effectue au moment de leur formation et avec une grande vitesse. Il en résulte, comme règle, une structure à cristallisation fine sans inclusions des cristaux de bélite n'ayant pas eu assez de temps pour se dissoudre dans les cristaux d'alite.

Interdépendance entre la température et la durée de cuisson

En se basant sur un grand nombre de données expérimentales, on a construit des dépendances entre la température et la durée de cuisson correspondant à une même teneur en CaO_{libre} des échantillons dans des limites de 0,58-0,87% pour des mélanges différents.

Les dépendances obtenues sont décrites d'une façon satisfaisante à l'aide de l'équation suivante:

$$T = T_0 \cdot e^{-k \ln \frac{\tau}{\tau_0}},$$

où T est la température de cuisson en degrés: τ est la durée de cuisson en s; T_0 est la température conventionnelle à laquelle on obtient une valeur prédéterminée pour la teneur en CaO_{libre} pendant la cuisson égale à τ_0; K est la constante caractérisant la vitesse de chauffement de l'échantillon, I/degré.

Pour les valeurs T_0 et K des mélanges analysés, voir tableau 3.

Tableau 3

Valeurs T_0 est et K pour les mélanges analysés

Constante	Numéro du mélange					
	I	2	3	4	5	6
T_0, K	1656	1709	1813	1815	1695	1631
$K \cdot 10^{-2}$, 1/deg.	1,64	1,15	1,61	1,44	1,93	0,78

Comme on le voit des données présentées, la gamme de températures conventionnelles des mélanges crus industriels est extrêmement large et varie de 1631 à 1815 K. Cela est conditionné par la nature du cru ainsi que par sa composition chimique.

Donc, pour produire le clinker de ciment Portland avec une haute activité hydraulique conditionnée par la teneur en alite optimum et par la défectuosité maximum de ses cristaux, il est nécessaire de maintenir un certain rapport entre la température et la durée de cuisson conformément à un mélange cru concret.

I. Odler, S. Abdul-Maula. Technical University Clausthal, D-3392 Clausthal-Zellerfeld, Federal Republic of Germany and T. Angelova. Cement Research Institut, Sofia, Bulgaria.

1

The effect of burning conditions on the structure of portland clinker and the reactivity of the resultant cement.

1.2

L'effet des conditions de cuisson sur la structure du clinker Portland et la réactivité du ciment résultant.

SUMMARY: From a single raw meal clinkers were burned using variable heating rates, burning temperatures, burning times and rates of cooling. The alite crystal size distribution was mainly affected by variations of burning temperature and burning time. Different burning conditions affected the progress of hydration of cements made from these clinkers only within the first hours of hydration. Here, the rate of alite hydration and ettringite formation were accelerated with increasing burning rate and with decreasing burning temperature. The strength development of the cements was only unsignificantly affected by the burning conditions employed.

Empregando índices de aquecimento, temperaturas de queima, tempos de queima e índices de resfriamento variáveis, foram preparados clínqueres de uma única farinha. A distribuição de tamanho de cristal de alita foi afetada principalmente por variações de temperatura e do tempo de queima. Condições diferentes de queima afetaram o desenvolvimento da hidratação dos cimentos feitos com estes clínqueres apenas durante as primeiras horas de hidratação. No caso, a velocidade de hidratação da alita e a formação de etringita foram aceleradas com o índice de aumento da queima e com a diminuição da temperatura de queima. O desenvolvimento da resistência dos cimentos foi afetado apenas insignificantemente pelas condições de queima empregadas.

I. Odler, S. Abdul-Maula. Technical University Clausthal, D-3392 Clausthal-Zellerfeld, Federal Republic of Germany and T. Angelova. Cement Research Institut, Sofia, Bulgaria.

Within this paper the effect of burning conditions i.e. of the heating rate, the maximum temperature, the duration of burning and the cooling rate on the structure of portland clinker and the reactivity of the resultant portland cement was studied. The main aim of this study has been to determine whether a relationship between the size of the formed alite crystals and cement reactivity exists and whether and to what an extent both parameters can be controlled by burning conditions.

EXPERIMENTAL

For preparations of the clinkers a raw meal made out of pure $CaCO_3$, SiO_2 (quartz), Al_2O_3 and Fe_2O_3 was used. Its potential phase composition (as calculated by Bogue) was 70 per cent of C_3S and 10 per cent of each C_2S, C_3A and C_4AF. Compressed pelets made from the blend (total amount about 200 g) were placed into Pt-dishes and burned in an electric furnace under variable conditions. The different burning programmes employed are shown graphically in Fig. 1.

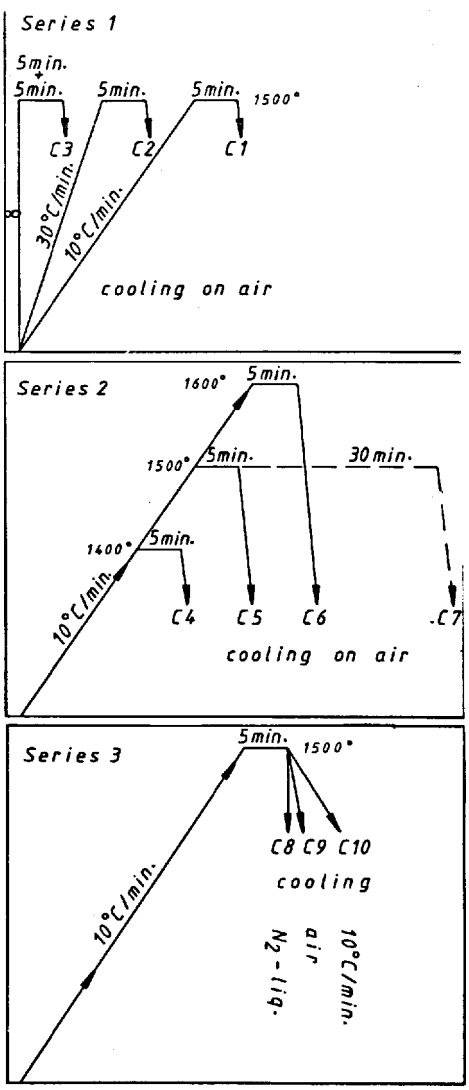

FIG. 1: Graphic representation of the burning programmes employed

Series 1 - Effect of heating rate

The raw meal was heated up to 1500 °C with rates of 10 and 30 °/min and by inserting the Pt-dish with the raw meal directly into a furnace preheated to the above temperature. After 5 min of burning the samples were cooled on air. In the sample placed into the furnace directly, additional 5 min of burning were allowed to obtain a thermal equilibrium.

Series 2 - Effect of burning temperature and duration of burning

The raw meal was heated up to temperatures of 1400, 1500 and 1600 °C at a constant rate of 10 °C/min, held at the maximum temperature for 5 min and subsequently cooled on air. A separate sample was held at 1500 °C for 30 rather than for 5 min.

Series 3 - Effect of cooling

Samples that were burned at 1500 °C for 5 min were cooled a) with a rate of 10 °C/min, b) by quenching on air and c) by trowing the material into liquid N_2.

In the obtained clinkers the alite crystal size distribution and the length/width ratio of the crystals was determined by optical microscopy. The determination was made on polished clinker surfaces etched with an ammonium citrate solution.

Experimental cements were prepared from the clinkers by grinding them with amounts of gypsum equal to 3.0 per cent SO_3 to a specific surface area of 3000 cm^2/g (Blaine).

The strength development of the experimental cements was studied on specimens 15 x 15 x 60 mm made out as ISO-mortars with a water-solid ratio of 0.5 (room temperature, curing under water).

The progress of hydration was studied on cement pastes (w/s = 0.27) that were allowed to hydrate for different periods of time. The hydration process was stopped and the non reacted water was removed by grinding the paste with an excesss of acetone, filtering the obtained suspension, washing the residue on the filter with additional acetone and ethyl ether and drying it at 40 °C.

The bound water content was determined as the ignition loss of the obtained hydrated material and the fraction of non reacted tricalcium silicate by quantitative X-ray-diffraction. The progress of gypsum consumption and ettringite and calcium hydroxide formation as well as the ettringite to monosulphate conversion were studied by DTA.

In separate studies the development of hydration heat was studied by adiabatic conduction calorimetry. Here, for technical reasons, a higher water-cement

ratio i.e. 0.7 had to be employed.

RESULTS

1. Effect on clinker structure

The size distribution of the alite crystals is shown in Fig. 2. It appears that the average size of the formed alite crystals increased distinctly with extended burning time. Which increasing burning temperature the alite size distribution curve became wider while the average size of alite crystals was little affected. Variations of the heating rate and the rate of cooling had little effect on the alite crystal size. The distribution of the length/width ratio of the alite crystals exhibited a maximum at l/d~1.5 regardless on the conditions of burning.

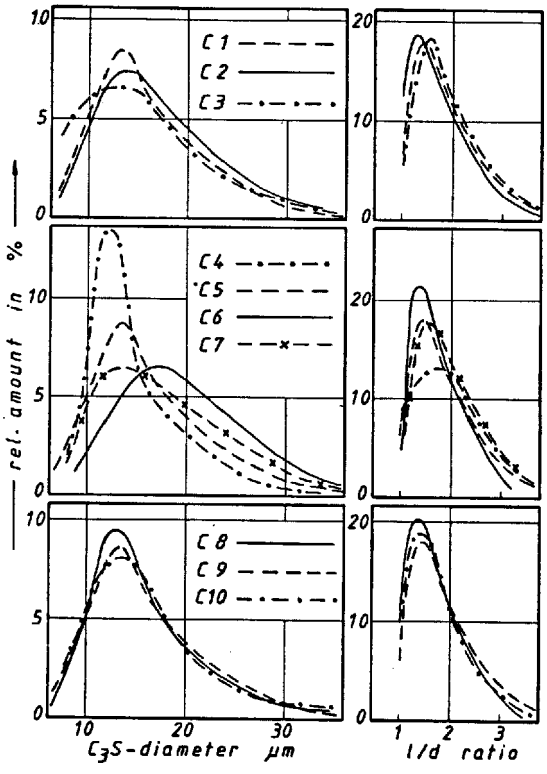

FIG. 2: Effect of burning conditions on alite crystal size and length/width ratio distribution

2. Effect on the progress of hydration

The hydration heat evolution of the obtained cements is shown in Fig. 3. The obtained data indicate a significant effect of the burning conditions on the intensity of the "first" peak that indicates the amount of heat liberated in the first minutes of the hydration process. It appears, that this peak, which is due to a simultaneous hydration of tricalcium silicate and tricalium aluminate, increased with an increasing heating rate, with decreasing burning temperature and with an increasing cooling rate. The intensity of the main peak, that is due mainly to the hydration of tricalcium silicate, was little affected by burning conditions. Its development became moderately retarded with a decreasing heating rate and accelerated at lower burning temperatures. The "third" peak, thats due to the ettringite to monosulfate conversion, was most affected by cooling conditions. It almost disapeared in the slowly cooled clinker and became significantly more intensive and even split into two peaks upon cooling with liquid N_2.

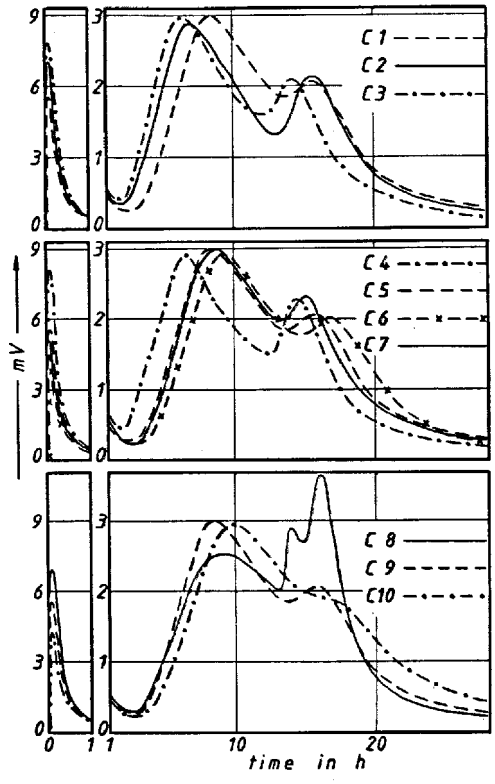

FIG. 3: Effect of burning conditions on the hydration heat evolution of the resultant cements

In Tab. I data on the degree of C_3S hydration and the combined water content are summarized. It appears that both values were affected by the burning procedure only after short hydration times, if at all. The amount of C_3S that hydrated within 8 hours declined with decreasing heating rate, with increasing burning temperature, and with extended burning time and was little dependent on the cooling rate. The bound water values generally followed those of the degree of C_3S hydration.

Fig. 4 shows the DTA curves of cement pastes after different hydration times. With increasing heating rate the intensity of the peak belonging to ettringite increased and that of gypsum declined, indicating an increased C_3A reactivity under these conditions. With increasing burning temperature the intensity of the peak belonging to ettringite declined while that belonging to gypsum increased, indicating a declining C_3A-reactivity. Finally, an extended burning time and different cooling rates had little effect on the intensity of the two peaks and thus

I. Odler, S. Abdul-Maula. Technical University Clausthal, D-3392 Clausthal-Zellerfeld, Federal Republic of Germany and T. Angelova. Cement Research Institut, Sofia, Bulgaria.

Tab. I: Effect of burning conditions on the degree of C_3S hydration and combined water content in hydrated cement pastes

Series	cement	α C_3S in %			H_2O comb. in g/100 g			
		8 h	1 d	28 d	4 h	8 h	1 d	28 d
1	C 1	12	49	86	3.4	6.7	16.8	28.4
	C 2	16	49	86	4.5	7.9	16.7	28.6
	C 3	19	52	85	5.2	9.2	17.2	29.5
2	C 4	16	49	88	5.2	8.5	16.9	29.5
	C 5	13	49	86	3.4	6.7	16.8	28.4
	C 6	11	51	85	3.1	5.5	17.0	28.4
	C 7	8	49	85	3.0	5.0	16.3	28.1
3	C 8	10	47	85	3.4	6.7	16.9	28.4
	C 9	13	49	86	3.4	6.7	16.8	28.4
	C10	12	44	84	3.3	6.1	17.3	28.3

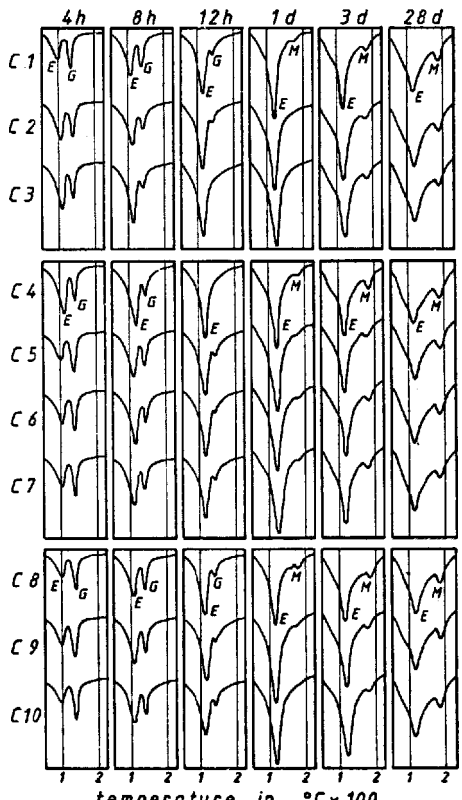

FIG. 4: DTA curves of cements made out of clinkers burned under different conditions

C_3A reactivity. Unlike the DTA curves of pastes with short hydration times, those found after longer hydration times, were not affected by the conditions of burning.

3. Effect on compressive strength

Tab. II shows the compressive strength development of the experimental cements studied. It appears that the strength obtained were affected by the conditions of burning only unsignificantly. Only in the cement made out of a clinker cooled with liquid N_2 the one day strength was distinctly lower than those in other cements.

Tab. II: Effect of burning conditions on compressive strength development

Series	cement	N/mm²				
		1 d	3 d	7 d	28 d	90 d
1	C 1	18	39	60	79	84
	C 2	19	37	61	84	89
	C 3	21	41	63	84	88
2	C 4	18	41	65	82	85
	C 5	18	39	60	79	84
	C 6	16	38	60	77	79
	C 7	16	37	60	77	82
3	C 8	12	34	55	76	85
	C 9	18	39	60	79	84
	C10	17	40	58	73	80

DISCUSSION

The obtained data revealed distinct, though not very great variations in the alite size distribution brought about by the employed conditions of burning. The observed increase of the alite crystall size due to increased burning temperatures and burning times is in line with previous observations (1,2,3,4,5). On the other hand a reduction of the alite crystall size due to a rapid temperature increase as reported by (6), could not be confirmed.

Another parameter that could be studied by optical microscopy was the porosity of the clinkers prepared. It has been found in our experiments, that the porosity of the produced clinkers increased significantly with decreasing burning temperature, apparently due to a smaller amount and higher viscosity of the liquid phase formed under these conditions.

Of practical importance is the existing effect of burning conditions on setting time and strength of the resultant cement. In our own experiments we found that even very substantial variations of burning conditions affected only the initial reactivity of the resultant cement. The progress of hydration has been altered distinctly only within the first hours after mixing with water. On the other hand the later course of hydration has been affected only unsignificantly by the conditions of burning. The finding of only relatively small differences in reactivity may be due to the fact, that the burning conditions employed allowed in all instances the formation of sufficiently well burned clinkers, with well developed crystal textures and low free lime contents, from the raw meal used in our series of experiments. The setting behaviour of the obtained cements was not studied extensively within this study. It was noted, however, that the setting time was distinctly shorter in those cements that exhibited increased initial reactivity

as determined by chemical method. On the other hand variations of the burning condition exhibited only little effect on strength development of the cements studied. In related studies a positive effect of fast heating rates on strength was reported by (6) and (7) while similar data reported by (8) were inconclusive. According to (5) the heating rate is of little significance for cement strength. Data on the effect of burning temperature on cement strength are not uniform either. Ludwig und Rückensteiner (8) found an increase of cement strength with decreasing temperature of burning. In studies on clinkers burned at excessively high temperatures both favorable (2,9,10) anddetrimental effects (11) were reported. As to the effect of burning time a favorable effect of extended burning on strength was reported by (3,4,6). Also data on the optimum cooling rate are not uniform as both rapid and slow cooling were reported to be favorable for high cement strengths (5,6,7,12,13,14,15,16).

CONCLUSIONS

1. Variations in heating rate, burning temperature, duration of burning at maximum temperature and cooling rate brought about only small, though distinct variations in the size of alite crystals formed. The average alite crystal size increased distinctly with increasing burning temperature. Variations of other factors such as of heating rate, duration of burning and of cooling rate had little effect on alite crystal size.

2. The initial cement hydration was accelerated with increasing heating rate and retarded with increasing burning temperature and burning time.

3. The progress of hydration after about one day and more, just as the strength development, were only little affected by the conditions of clinker burning.

REFERENCES

1. J.M. Butt, V.V. Timashev and J. Stark: Phase composition and crystal size of rapidly burned portland cement clinker (in German). Silikattechnik 24, 10-12 (1973).
2. Y. Suzukawa and K. Fukunaga: High temperature burning of portland cement clinker. Cem. Assoc. Japan, Rev. 18. Cem. Meeting, Tokyo 1964, pp. 96-99.
3. B.V. Volconsky, L.G. Sudakas: A.F. Kraplia and L.G. Bernstein: Control of microstructure and activity of clinker (in French). Proc. 7th Internat. Congr. Chem. Cem. Paris 1980, Vol. 2, pp. I-17 to 20.
4. A.F. Kraplia, L.G. Sudakas and M.V. Kougia: Interrelation between commercial clinker micro-structure and hydraulic activity and hydration heat (in Russian) Proc. 13th Conf. Silicate Industry, Budapest 1981, Vol. 3, pp. 111-118.
5. F.W. Locher: Effect of clinker manufacture on the properties of cement (in German). Zement-Kalk-Gips 28, 265-272 (1975).
6. Y. Ono: Microscopical examination of burning conditions and quality of clinker. Proc. 7th Internat. Congr. Chem. Cem. Paris 1980, Vol. 2, pp. I-206 to 211.
7. P. Frühauf, S.E. Ibrahim and U. Ludwig: Effect of heating-up rate and cooling on the formation and properties of clinker (in German). TIZ-Fachberichte 103, 594-602 (1979).
8. U. Ludwig and G. Rückensteiner: Effects on raw meal burning and clinker quality (in German). Tonindustrie-Zt. 97, 313-315 (1973).
9. J.M. Butt, V.V. Timashev and D.A. Vysockij ref. (1).
10. K. Watanabe et.al. Jap. pat. 38-70091 (1963).
11. J.M. Butt and V.V. Timashev: Dependence of hardening properties of clinker minerals on burning temperature and crystal structure (in Russian). Tsement (russ.) 7, 17-22 (1961).
12. F. Keil and A. Narjes: On the effect of steam curing on cement clinkers of different composition (in German). Zement-Kalk-Gips 12, 129-136 (1959).
13. K. Tomita et.al.: The effect of cooling rate of cement clinker on the strength of cement. Cem. Assoc. Japan, Rev. 23 Gen. Meeting, Tokyo 1969, pp. 81-86.
14. H.M. Sylla: Effect of clinker cooling on the setting and strength of cement (in German). Zement-Kalk-Gips 28, 357-362 (1975).
15. F.W. Locher: Influence of burning conditions on clinker characteristics. World Cement Technol. 67-73 (1980).
16. T.K. Chatterjee and S.N. Ghosh: The effect of cooling rate on cement properties - a review. World Cem. Technol., 252-257 (1980).

B. Scheubel, KRUPP POLYSIUS, Research Center, Beckum, Germany 1

Investigation on the Influence of the Kiln System on Clinker Quality
Recherches de l'influence du système de four sur la qualité du clinker 1.2

SUMMARY: The quality of portland cement clinker is decisively influenced by the chemical and mineralogical composition of the raw mix on the one hand and by the treatment of the kiln feed material as a function of temperature and time on the other hand. The temperature profile of the material is influenced by burnability and kiln system.

The thermodynamically active intermediate phases generated by the dehydration and calcination of clay and carbonate minerals can loose their activity through the healing up of lattice defects by a flat material-temperature profile. A long calcination zone accelerates the recrystallisation of CaO and the formation of large belite crystals, which on their part obstruct the alite formation. This results in a flat distribution curve of alite crystal sizes together with a large mean diameter and a more difficult clinker grindability.

In short rotary kiln system even without precalcining the raw meal is heated up to about 800°C within seconds. The calcining and heating zones in the kiln are passed faster, which especially leads to smaller primary belite crystals. These support the granulization and promote rapid alite formation because of their large reactive surface. A steep frequency distribution of the alite particle sizes and a small mean phase diameter improve the grindability.

If a precalcined is added to the system, only a very small part of the calcining zone remains in the rotary kiln. On the other hand, the heating zone becomes longer whereas the retention time is shortened. Nevertheless, the flat temperature profile in the kiln itself may cause a flat frequency distribution of the alite particle sizes. This applies especially to non-ideal raw materials with a more difficult burnability.

If the raw material conditions are ideal (natural cement), all modern kiln systems, even those with a very low L/D ratio, can produce clinker of good quality. That means small silicate crystals, uniform granulometry and easy grindability.

A qualidade do clinquer de cimento portland é decisivamente influenciada, de um lado pela composição química e mineralógica da mistura crua, e de outro lado pelo tratamento do material alimentado ao forno, em função da temperatura e do tempo. O perfil da temperatura do material é influenciado pela aptidão para queima e pelo sistema do forno.

As fases intermediárias termodinamicamente ativas, geradas pela desidratação e calcinação da argila e dos minerais carbonatados, podem perder sua atividade através de correção de defeitos de entrelaçamento por um perfil plano de material-temperatura. Uma zona longa de calcinação acelera a recristalização do CaO e a formação de grandes cristais de belita, que por seu lado dificultam a formação de alita. Isto dá como resultado uma curva plana de distribuição dos tamanhos de cristal de alita juntamente com um diâmetro médio grande e moabilidade mais difícil do clinquer.

No sistema de forno rotativo curto, mesmo sem precalcinação, a farinha é aquecida até cerca de 800°C em questão de segundos. As zonas de calcinação e aquecimento no forno são percorridas mais depressa, o que especialmente leva a cristais menores de belita primária. Estes suportam a granulação e promovem a formação rápida de alita por causa da sua grande superfície reativa. Uma distribuição de alta freqüência de tamanhos de partícula de alita e um pequeno diâmetro médio de fase melhoram a aptidão de moagem.

Se ao sistema for acrescentado um precalcinador, apenas uma parte muito pequena da zona de calcinação fica no forno rotativo. Por outro lado, a zona de aquecimento torna-se mais longa enquanto o tempo de permanência é encurtado. Todavia, o perfil plano de temperatura no forno propriamente dito pode causar uma distribuição plana de freqüência de tamanhos de partícula de alita. Isto se aplica especialmente às matérias-primas não ideais com uma maior dificuldade para serem queimadas.

Se as condições da matéria são ideais (cimento natural), todos os fornos modernos, mesmo aqueles com uma relação comprimento/diâmetro muito baixa, podem produzir clinquer de boa qualidade. Isto significa cristais pequenos de silicato, granulometria uniforme e moabilidade fácil.

CLASSIFICATION OF THE PYROPROCESSING

For the quality of the end product, the thermal treatment of the material with a given chemical composition is of decisive significance. During the pyroprocessing, the clay minerals and carbonates are dehydrated and calcined. If this is brought about by a steep heatup slope, thermodynamically reactive phases are generated which are characterized by their defective lattice structures and the presence of a large number of molecular faults (1). The excessive enthalpy and entropy as well as the high surface area caused by the dissociation reactions permits the first solids reactions to occur already in the temperature range below 900 °C.

For the further observation of the pyroprocessing, the temperature range up to approximately 1280 °C, often termed the transition zone, is particularly critical. Up to that temperature, reactions generally only occur between solids. A decisive new phase generation, however, is the reaction between CaO and SiO_2 to form belite (C_2S). If the SiO_2 is also present in its active form, for example from the dissociation of clay minerals, a rapid temperature increment leads to the generation of small belite crystals. A steep temperature profile not only enhances the formation of smaller defective crystals but also preserves most of the CaO activity since the existing lattice defects cannot be healed quickly enough. Also the solubility of foreign ions increases as the temperature rises (2). Once the material temperature rises above 1250 - 1280 °C, the liquid phase begins to form. No later than this temperature level, the main reaction becomes the generation of alite from belite and free lime. Since the reaction is primarily diffusion controlled, it is enhanced by small defective belite and free lime crystals since they dissolve more readily in the liquid phase. A steep temperature increment to the maximum burning temperature reinforces this behaviour due to the exponential relationship between temperature and viscosity, diffusion coefficients and speed of dissolution (2). The increased reaction turnover per time period leads to the formation of numerous small alite crystals.

Figure 1 schematically shows the relationship between the material temperature profile and the frequency distribution of alite crystal sizes. For simplicity, a linear heatup rate was utilized for the temperature range shown. Range 1 up to approximately 1200 °C is primarily characterized by the generation of belite and the recrystalization of CaO. Given a flat temperature increment (A), fewer but consequently larger belite crystals are formed. The CaO increasingly loses its activity. Conversely, given a steep temperature profile (B), smaller crystals are generated and the phase activity is largely preserved.

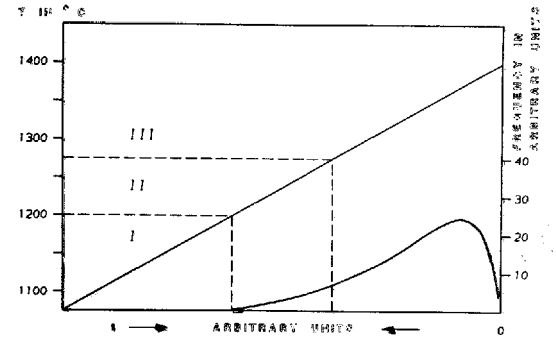

Fig. 1 A : Expected Distribution of Alite Crystal Sizes Given a Flat Temperature Profile (Schematic)

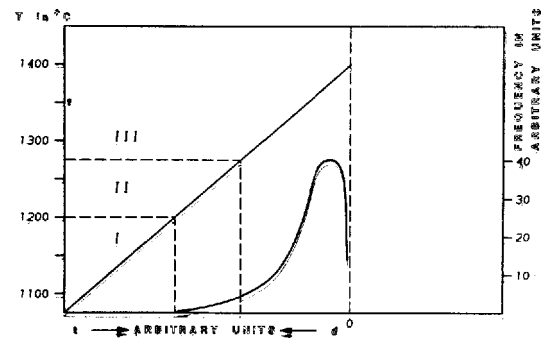

Fig. 1 B : Expected Distribution of Alite Crystal Sizes Given Steep Temperature Profile (Schematic)

After rising above approximately 1200 °C (Area 2), the first alite structures are generated as a solids reaction between belite and free lime (3). Though the reaction turnover rate is still secondary, the few crystals can grow well given a longer retention time in this temperature range with only a slight temperature increment. Since, even after attaining the temperature of the eutectic liquid phase (Area 3), the nucleation with a flat temperature profile proceeds more slowly than if this temperature range is more rapidly spanned, the already existing alites can continue to grow quite well.

In this temperature range, the material also begins to granulate. This granulation is impeded by the size of the already existing crystals which could lead to the formation of fine particulate clinker, that is, with high gas velocities the kiln tends to have a dusty atmosphere. The increase in temperature promotes the formation of further alite crystals. The increase in the distribution curve of the alite crystal sizes is, however, in this case flatter (A) as is the case with a steep temperature profile (B) since the solubility of CaO and belite in the liquid phase is lower due to their lesser activity and larger crystal size. A flat temperature profile thus leads to a self-induced reduction in the burnability. A rapid temperature increase leads to the formation of smaller crystals due to an increased mass turnover rate per time interval.

TESTING PROCEDURES

Based on Figure 1, it follows that a simple test procedure to depict the material temperature profile in a rotary kiln system would be microscopic clinker analysis, taking into account the parameters describing the structure, such as the average phase diameter and frequency distribution. The structural analysis, here linear analysis (5, 10), refers to the measured chord lengths wherein the average chord length (d_H) is not identical to the average phase diameter. Given a high statistical reliability, that is with a large number of measured chord lengths, the average chord length does, however, provide a measure for the average crystal diameter. Analogously, the same applies to the relationship between the frequency distribution of chord lengths and crystal diameters.

As per Figure 1, a tight frequency distribution of alite chord lengths is to be expected for a steep temperature profile. Accordingly, the average chord length d_H range should fall in the range up to approximately 20 micron. In case of a flat temperature increment, the chord length distribution should be broader and d_H should shift to higher micron values.

RESULTS

For the following tests, clinker samples from 62 different plants were subjected to microscopic linear analysis.

In the following evaluation the samples are not generally evaluated individually, but rather summarized within each kiln system. For each kiln system this minimizes the effect of the different raw material burnability values and the influence of the subsidiary constituents, which affect the alite formation by changing the viscosity and surface tension of the liquid phase. Having the same raw material prepared in the same way but subjected to differing firing systems is an exception. Where that is, however, the case, the individual kiln lines will be compared. The same applies for systems in which the raw material was deliberately modified.

THE LONG ROTARY KILN

In long rotary kiln systems (dry and wet systems are here summarized together) with a length to diameter ratio of approximately 35/1, about 2/3 of a kiln length is required for the preheating, dehydration and calcining of the material. Assuming 25 - 30 minutes of retention time for the transition and firing zone in each case, then for the temperature range of 900 - 1300 °C (transition zone) there is a linear heatup rate of approximately 15°/min. and of approximately 6°/min. for the firing zone of 1300 - 1450 °C. This flat temperature profile leads to thermodynamically non-active intermediate phases where fewer crystal nuclei are generated. This produces a flat frequency distribution of the alite crystal sizes characterized primarily by overly large crystals and a large average phase diameter.

Figure 2 shows the frequency distribution of the measured alite chord lengths with a chord length class interval width of 10 micron. The curve depicts the average value drawn from 11 long kiln clinkers. The maximum attains 20 - 25 % relative frequency. The average chord length is approximately 35 micron, though extreme individual values can easily exceed 120 micron (chord lengths!).

In order to demonstrate the effect of raw material on the temperature profile and thus upon the frequency distribution of the alite crystal sizes, Figure 3 plots the frequency distributions of the measured alite chord lengths in a kiln for different raw material parameters. Both curves are also incorporated in Figure 2.

By improving the burnability (finer silica-bearing components, reduction of the silica ratio, increase of the liquid phase component), the temperature profile also became steeper. The frequency distribution clearly shows the higher portion of smaller crystals. The average chord length has dropped from 48 to 36 micron whereby the grindability according to the Zeisel test referred to 3200 cm^2/g (Blaine) improved by more than 10 kWh/t (6, 10).

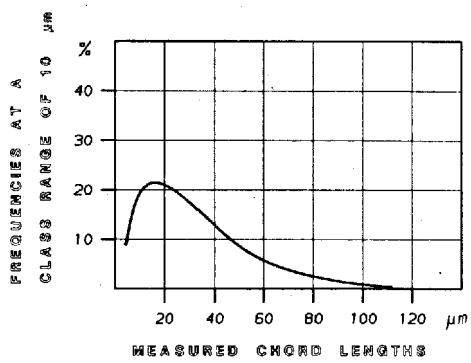

Figure 2 : Frequency Distribution of Alite Chord Lengths form 11 Long Kiln Clinkers

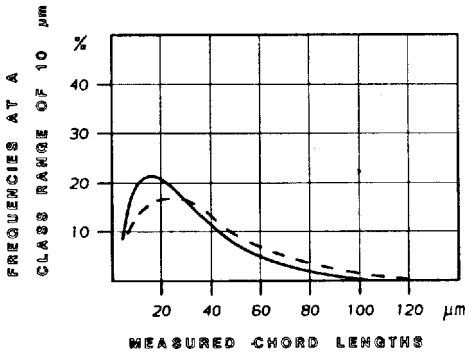

Figure 3 : Affect of Burnability on the Alite Frequency Distribution

THE SHORT ROTARY KILN

THE SHORT ROTARY KILN WITH GRATE PREHEATER

In these kiln systems, the pelletized raw material is preheated on a travelling grate but reaches the short rotary kiln only partially calcined to approximately 20 %. The short rotary kiln has a length to diameter ratio of 12 - 14. Approximately half the kiln is required to calcine the pellets. The remaining approximately 25 minutes of retention time are divided into approximately 10 minutes for the transition zone and 15 minutes for the firing zone. Thereby, the heatup rates are approximately 40-60 °/minute for the transition zone. Due to its steep temperature slopes the short transition zone produces many small alite crystals which can only grow very slightly in the firing zone. The frequency distribution of the alite crystal sizes should thus correspond to the case in figure 1 - B. Figure 4 plots the frequency distribution of the alite chord lengths from 6 travelling grate kiln systems. The average chord length is approximately 15 micron.

These clinkers are generally porous and easily ground, which reflects the small crystal size. Since for pellet strength, a certain component of clay minerals must be present in the raw material, the raw mixes are generally not hard to burn. Burnability and temperature profile in the kiln have a positive impact on the quality (7).

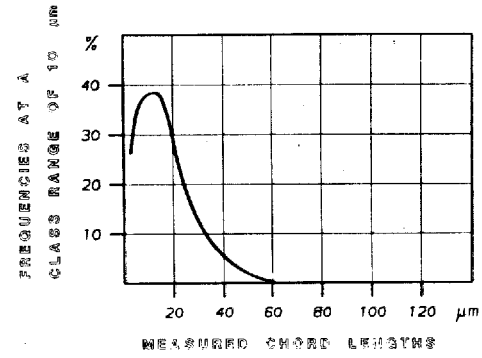

Figure 4 : Frequency Distribution of Measured Alite Chord Lengths of 6 Clinkers from Kilns with Grate Preheaters

THE SHORT ROTARY KILN WITH SUSPENSION PREHEATER

In this kiln system the feed material is preheated in several cyclone stages within a few seconds to approximately 800 °C and then burned in a kiln with an L/D ratio of 12 - 17. This means that the degree of calcination at the kiln inlet is only approximately 20 - 30 % and the remaining calcining requires approximately 2/3 of retention time in the kiln. Since in this context the temperature of the feed material hardly exceeds 900 °C, the heatup slope is 40 - 80 °/min. for the temperature range up to approximately 1300 °C, given a retention time of 5 - 10 minutes. This rate then drops again in the firing zone to 10 - 15 °/min. One should therefore expect a steep frequency distribution of the alite crystal sizes. The evaluation of 19 clinkers from suspension preheater kilns in Figure 5 confirms the steep curve of the material temperature in this system. In contrast with clinkers from travelling grate kilns, only slight differences can be found due often to the somewhat harder burnability of suspension preheater feed material. Harder burnability requires sharper burning, thereby changing the material temperature profile in the kilm.

An extended firing zone enhances the growth of crystals or permits recrystalization on the alites. Both lead to a flatter frequency distribution of the crystal sizes (Figure 6). Given the same preconditions, both systems provide clinker of the same quality (8).

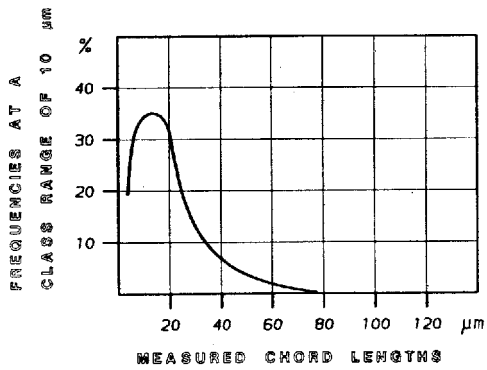

Figure 5 : Frequency Distribution of Measured Alite Chord Lengths of 19 Clinkers from Suspension Preheater Kilns

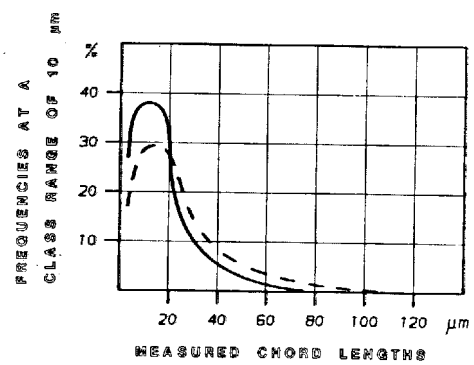

Figure 6 : Effect of Burnability on Frequency Distribution of Alite Crystals for Clinkers from Suspension Preheater Kilns

a) Good Burnability
b) Poor Burnability

KILN SYSTEMS WITH PRECALCINING

In these kiln systems, the raw meal is calcined to approximately 90 - 95 % before entering the actual kiln. This is attained by supplying energy through calcining burners in the upstream calciner. The required combustion air is either drawn through the kiln or else conducted through a separate tertiary air duct to the secondary firing area after being drawn off at the cooler or kiln hood. This two part process permits, on the one hand, the use of so-called substitute fuels in the calciner and, on the other hand, an increase in capacity since only a very small amount of material still has to be calcined in the kiln itself. Thereby, the kiln itself has an extended transition zone, since the burning zone is restricted to the flame radiation area. In this case too, a shorter retention time due to more rapid kiln rotation guarantees a steep temperature increment of 25 - 30 °/min. Apart from cost savings due to the at least partial use of cheaper substitute fuels and the increased system flexibility in modifying the material temperature profile, this approach is particularly suitable for use with problematic raw material conditions. For raw material which naturally has the desired composition, moreover with fine homogenous distribution of the mineral components (natural cement), the rotary kiln can operate effectively even with lower length to diameter ratios (9, 11). This is, for example, also the case with travelling grate kiln thanks to their easily burnable raw material. Figure 7 shows the average frequency distribution of alite chord lengths of 25 clinkers from precalcining kiln systems, while Figure 8 plots the effect of the burnability on the alite crystal size distribution in precalcining systems.

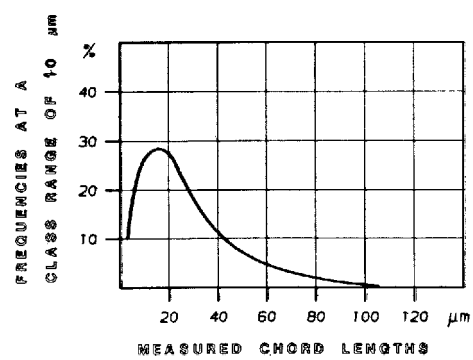

Figure 7 : Frequency Distribution of Measured Alite Chord Lengths of 25 Clinkers from Precalcining Systems

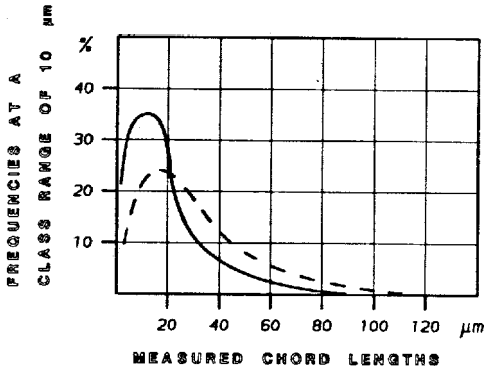

Figure 8 : Frequency Distribution of Alite Sizes with Easier and Harder Burnability in Kiln Systems with a Precalciner and Separate Tertiary Air Ducting

CONCLUSION

As the structural analytic evaluations of 62 Portland Cement clinkers show, microscopic methods can be used to obtain information regarding the thermal history of the clinker. The statistical evaluation of the alite crystal diameters or chord lengths permits simple representation of the material temperature profile in the kiln. Given knowledge of the kiln system and certain raw material parameters, the measured data can be used as the basis for suggestions for improving the clinker quality and optimizing the burning process.

Since the use of grate preheater systems requires plastic raw materials, which as a rule are easily burnable, the burning process is simple and the clinker produced is of good quality.

Non-homogenous raw materials, such as those containing coarse quartz, cannot be so easily burned. From the perspective of the burning process, the kiln system has to be more flexible, that is capable of adjusting to extrem conditions.

These requirements can best be met by the use of precalcining systems which are adequately sized to assure reserve burning capacities.

LITERATURE

1. TORKAR, K.: Zur Thermodynamik fester Stoffe, "Reactivity of Solids", S. 400-408, ELSEVIER PUBLISHING COMPANY 1961
2. SEIDEL, G., HUCKAUF, H., STARU, J.: Technologie der Bindemittelbaustoffe Bd. 3 Brennprozeß und Brennanlagen VEB Verlag für Bauwesen 1978
3. WOLTER, A.: (1982) Zur Bildung und Stabilität von Trikalziumsilikat und Aliten Forschungsbericht des Landes Nordrhein-Westfalen Nr. 3092
4. MACGREGOR MILLER, F. (1980):Dusty Clinker and Grindability Problems, Rock Products, H. 4, S. 151 - 157
5. SCHEUBEL, B. (1984): Exact Characterisation of Portland Cement Clinker Using Visual Linear Analysis, Proc. 6th International Conf. Cem. Microscopy, S. 427-437
6. SCHEUBEL, B. (1985): Microscopically Determinable Parameters and their Relationship to Kiln System and Clinker Grindability, Proc. 7th Intern. Conf. Cem. Microscopy, S. 131-153
7. WEBER, P. (1960): Der Wärmeübergang im Drehofen unter Berücksichtigung der Kreislaufvorgänge und Phasenneubildungen, Zement-Kalk-Gips, Sonderausgabe Nr. 9
8. WEBER, P. (1963): Über die Entwicklung der Zementdrehöfen und die Wahl des zweckmäßigsten Brennverfahrens, Polysius teilt mit - Heft 3
9. HERCHENBACH, H. und WOLTER, A. (1982): Auswahlkriterien für den Einsatz des kurzen Zementdrehofens Zement-Kalk-Gips 35, Nr. 9, S. 450-455
10. SCHEUBEL, B. und BALZER, H.-J. (1983): Mikroskopische Untersuchungen an Zementklinkern mit Hilfe der Linearanalyse zur Bestimmung der Klinkermahlbarkeit Zement-Kalk-Gips 36, Nr. 11, S. 624-627
11. WOLTER, A. (1985): Einfluß des Ofensystems auf die Klinkereigenschaften Zement-Kalk-Gips 38, Nr. 10, S. 612-614

B. Matkovic, "Rudjer Boskovic" Institute, 41001 Zagreb, Yugoslavia; V. Carin, R. Halle, "JUCEMA" - The Association of the Yugoslav Cement and Asbestos Cement Producers, 41001 Zagreb, Yugoslavia
J. F. Young, The University of Illinois, Urbana, IL 61801, USA

Dicalcium Silicates Doped with Phosphates
Reactivité du Silicate Dicalcique Stabilisé avec Phosphate

SUMMARY: Results are presented on the stabilization of β- and α'-modifications, quantitative elemental composition, reaction products and strength development of C_2S solid solutions stabilized by phosphates. Variations in microanalyses are discussed in terms of doped belite microstructure. Estimates of hydration products obtained by thermal methods and strength testing correlate well and show that α-modification develops C-S-H gel and strength faster than β, and samples made from chemical reagents react faster than those from natural materials. The level of dopant and other minor elements in dicalcium silicate solid solution influence strength development much more than do the preparatory conditions.

SUMÁRIO: São apresentados resultados sobre a estabilização do β e α' modificações, composição quantitativa elementar, produtos de reação e desenvolvimento de resistência de soluções sólidas de C_2S estabilizadas com fosfatos. Variações na microanálise são discutidas em termos de microestrutura da belita dopada. Estimativas de produtos de hidratação obtidos por métodos térmicos e ensaios de resistência apresentaram boa correlação e mostraram que a modificação α desenvolve gel de C-S-H e resistência mais rápida que β, e amostras feitas com reagentes químicos reagem mais rápido que aqueles com materiais naturais. O nível de dopantes e de outros elementos menores na solução sólida de silicato dicálcio influencia o desenvolvimento de resistência muito mais do que nas condições preparatórias.

INTRODUCTION

As a part of a study concerning belite cements (1-9), solid solutions of C_2S doped by $Ca_5(PO_4)_3OH$ have been investigated (2-4,7). Previous studies gave much information about the bulk chemical compositions of belites doped by various stabilizers, the phases present and their polymorphic forms, the morphology and the microstructure, their reactivity with water and the reaction products formed, as well as strength development. It has been observed (5,7-9) that the stabilizing element tends to be concentrated in a glassy grain boundary phase, or in microscopic inclusions, and that the level of stabilizer in the C_2S crystals is much less than indicated by bulk analyses. In this paper we present results of microanalyses for phosphorous-doped samples not previously reported as well as additional information concerning hydration and strength development.

EXPERIMENTAL DATA

Reagent-grade chemicals,[1] or natural raw materials[2] were used for the preparation of doped C_2S, which included samples (1, P1-P4) from a previous study (4). Specimens for compressive strength measurements and hydration studies were prepared using procedures previously described (4) and testing were done on samples after first, second, and fourth firings (the samples were not ground before the third and fourth firing). Specimens for electron probe microanalysis (EPMA) were mounted in epoxy and polished to 0.25 μm using standard metallographic techniques. The chemical compositions of raw materials and fired samples were determined by standard wet analytical methods. Free CaO or $Ca(OH)_2$ were estimated by the glycerol-ethanol method (10). Phases and their modifications present in a clinker were determined by x-ray diffraction[3] (6) and by optical microscopy (OM)[4] in reflected light on polished samples (2,4). EPMA were made in a microprobe[5] equipped with an energy dispersive spectrometer[6] (9). Instrumental parameters were accelerating voltage 20 kv, beam current 2-4 x 10^{-9} Amps, tilt angle 35°. Quantitative analyses were made with the help of an in-house computer program[7] including ZAF corrections and compensation for drift in the beam current. Calibrations were made using mineral standards. The hydration products were estimated using differential thermal analysis (DTA), thermogravimetry (TG) and derivative thermogravimetry (DTG)[8].

RESULTS AND DISCUSSION

1. Chemical and Phase Bulk Composition

Chemical and phase bulk compositions are presented in Table I. The polymorphism is in agreement with earlier studies except for the

[1] $CaCO_3$, SiO_2, and $Ca_5(PO_4)_3OH$

[2] High purity natural limestone (SiO_2; Fe_2O_3, 0.07; CaO, 55.90; Loss of ignition (LOI), 43.88 wt. %) and quartz and (SiO_2, 97.20; Al_2O_3, 0.97; Fe_2O_3; CaO, 0.63; LOI, 0.43 wt. %.

[3] X-ray diffractionmeter, Phillips Gloeilampenfubricken, N.V., Eindhoven, the Netherlands.

[4] Optical Microscope, Leitz, Wetzlar, BRD (West Germany)

[5] JXA-50A Electron Probe Microanalyzer, JEOL, Ltd., Tokyo, Japan.

[6] TN-2000 X-ray analyzer, Tracon Northern Co., Middleton, Wisconsin, USA.

[7] Devleoped by D. E. Anderson, Department of Geology, University of Illinois.

[8] Mettler Thermobalance, Mettler Inc., Zurich Switzerland.

persistence of the β form in sample T-40 and P4, which were synthesized from natural raw materials.

2. Quantitative EPMA Analyses

Table II presents mean values and ranges in 247 EPMA quantitative analyses from 10 samples identified as C_2S grains. Apart from added phosphorus, the other minor elements are impurities from the raw materials. Other possible minor elements (e.g., Na, Ti, Cr, Mn) were not analyzed. The majority of data for all 10 samples are similar; the C/S ratio was close to 2.0 and the mean phosphorus content close to the bulk analysis in β, but lower in α' C_2S samples. However, within each sample the composition varies significantly from one point to another. Related electron-optical studies (5,7-9,11) have shown the presence of significant quantities of glassy grain boundary phases (forming agglomerates of grains), and exsolutions or precipitates within the grain, all of which are rich in the dopant and other minor elements. Thus, it is likely that individual point analyses can contain a contribution from these second phases, in a random manner, since the size of individual crystals is probably between 1 and 0.2 μm, and therefore less than the size of the excited area. TEM micrographs of phosphorous-doped belites showed that lamellae (single or twin crystals) are narrow, less than 0.5 μm (11). Crystals of α'-modification are, probably, somewhat larger. The minimum sampling area using the SEM probes at 20 kV has a diameter of about 1.5 μm around the point of electron beam impact on a specimen surface (12). Thus the true level of minor elements in the crystals would be somewhat less than the observed values. Unfortunately the imaging capabilities of the instrument were not sufficient to allow the presence of second phases to be unequivocally established. However, they have been reported (11) in C_2S preparations doped with phosphorous. Some randomness in the analyses would be expected anyway since solid state substitution would be essentially a random process. The broadening of the α'->α phase transformation peak seen by DTA (2) is evidence for an inherent variation of this kind.

Results presented in Table III represent 44 EMPA quantitative analyses within the grains that do not correspond to C_2S solid solution. Areas having a C/S molar ratio slightly above 1 have significantly lower levels of P (dependent upon the amount of dopant in the raw mix) and a higher level of Al, Fe and Mg than the other parts of sample whose composition corresponded to the C_2S solid solution. Since x-ray analyses did not reveal any other phase except C_2S, the phase which corresponded to wollastonite composition was a glass (interstitial melt) as was confirmed by electron diffraction studies (11). TEM studies of belites doped with other elements also show an amorphous phase at grain boundary and between agglomerates of grains (7-9).

Glassy areas large enough to be analyzed by EPMA were detected only in samples which were prepared from natural raw materials and fired once. Samples which were refired, or were made from the pure laboratory reagents did not show such areas. Areas rich in phosphorous were detected in samples T-40 and P4, which had been fired once (see Table III). Areas corresponding to C_3S were found only in sample P4 (Table III); they contained less phosphorus.

Some effects of repeated firing could be drawn from the data listed in Table II. The C_2S solid

solution had somewhat different chemical composition, becoming richer on phosphorous in refired samples but variations in compositions were still large. This could be due to a more even distribution of the glassy phase over grain boundaries.

3. Hydration Products Determined by Thermal Analyses

Combined water associated with C-S-H gel and $Ca(OH)_2$ were determined on paste samples at different hydration times by simultaneous TG and DTG analyses. Any calcium carbonate present was assumed to be formed from the carbonation of $Ca(OH)_2$; both were expressed as CaO total and were considered as $Ca(OH)_2$. The loss of water at temperatures between 100 and 350°C was used to estimate the amount of C-S-H. The results are plotted in Figure 1. Three distinct groups of curves, which begin to converge only after 6 months of hydration can be seen. The samples containing the α'-modification (T-38), formed more C-S-H than those containing the β-form (T-37 and T-39). T-37 develops significantly more C-S-H than does T-39.

Present results are in an agreement with previous work (4) (i.e., β-C_2S samples from laboratory reagents fired twice developed higher contents of C-S-H than β-C_2S samples from natural raw materials fired once). In contrast, C-S-H from α'-C_2S is not affected by the number of firings. The effect of the polymorphic form or of the incorporation of other minor elements into β-C_2S solid solution (use of laboratory reagents v. natural materials) on C-S-H formation is more pronounced than the effect caused by the preparation conditions. From Figure 1 it is obvious that α'-C_2S has the most rapid C-S-H formation between 7 and 28 days of hydration time when the difference between α' and β modifications is most marked. β-C_2S made from laboratory reagents develops gel most rapidly between 28 and 50 days and, up to the age of 3 months, faster than the β-modification which is formed from natural materials. The latter approaches the other samples in the quantity of gel formed only after 1 year hydration. The formation of $Ca(OH)_2$ shows similar, but more variable, trends to those observed from measurements of C-S-H.

4. Compressive Strength Development

Strength curves, determined for mortars, are shown in Fig. 2. Curves of P2 and P3 (a mixture of β and α'-C_2S, with β-C_2S being a major phase) lie between the curves of T39 and P1 and (β-C_2S) and P4 and T-40 (almost pure α'-C_2S). Since a higher level of phosphate in the raw mix causes an increase of α'-modification in a fired sample, the higher strength in P2 and P3 (compared to T39 and P1) are attributed to the presence of α'-form. Strength development in P4 is in agreement with the strength curve for T-40; both samples have α'-modification as the major phase. These observations are in general agreement with previous conclusions regarding the reactivity of α' and β forms (1-5,7,13).

CONCLUSIONS

1. Quantitative EPMA analyses of C_2S grains show a stoichiometric composition. Variations in analyses are attributed to some contributions from the adjacent grain boundary phase.
2. When the interstitial phase has a composition approximating to a C/S ratio of 1.0, it contains much less phosphorous than do the C_2S grains but concentrates other impurity elements. In contrast, the interstitial phase, which was rich

in phosphorous contains only small amounts of other impurities and has a C/S ratio >2.

3. Refirings of samples cause a reaction between C_2S solid solution and interstitial phase, and result in the formation of C_2S solid solution with a slightly modified chemical composition.
4. Solid solutions of α'-form develop strength much faster than those in β-modification, due to faster hydration.
5. The change of crystal modification and impurity types, levels, or distributions changes only the rate of hydration.

ACKNOWLEDGMENTS

This work was supported by: the U.S. Department of Transportation; the Selfmanaging Community of Interest for Scientific Research of the S. R. Croatia; and the National Science Foundation, Grant CEE83-00268. The EPMA analyses were carried out at the Center of Microanalysis, University of Illinois, Urbana, Illinois, USA. We thank Professor D. E. Anderson for supplying the computer program and general assistance with the analyses.

REFERENCES

1. B. Matković (1982), "Doped dicalcium silicates," Proc. Yugoslav Center Crystallography, 17, 67-88.
2. B. Matkovic et al. (1981), "Development of strength in cements," pp. 26-34; 42-46; 49-56; 66; Report No. FHWA/RD-80/128, Federal Highway Adminstration, Washington, DC. (Available from the National Technical Information Service, Springfield, Virginia 22161.)
3. B. Matković et al. (1984), "Development of strength in cements," pp. 3-21; Report No. FHWA/RD-83-049, Federal Highway Adminstration, Turner-Fairbank Highway Research Center, McLean, Virginia 22101 (see Ref. 2).
4. B. Matković, V. Carin, T. Gacesa and R. Halle (1980), "Reactivity of belite stabilized by $Ca_5(PO_4)OH$, " pp. I/189-I/194, Proc. 7th Int. Congress Chem. Cement, Vol. II. Ed. Septima, Paris, France.
5. B. Matković, V. Carin, T. Gacesa, R. Halle, I. Jelenić and J. F. Young (1981), "Influence of $BaSO_4$ on the formation and hydration properties of calcium silicates: I. Doped dicalcium silicates," Am. Ceram. Soc. Bull. 60(8), 825-829.
6. B. Bobesić, R. Halle, M. Mikoc, B. Matković, and J. F. Young (1981), "Influence of $BaSO_4$ on the formation and hydration properties of calcium silicates: II. Laboratory Belite-rich clinkers," Am. Ceram. Soc. Bull. 60(11), 1164-1167.
7. S. Chopra, A. Ghose and J. F. Young (1983), "Electron-optical studies of stabilized α'- and β-dicalcium silicate," Proc. 5th Int. Conf. Cement Microscopy. pp. 11-22, Int. Cement Microsc. Assoc., Duncanville, Texas 75137, USA.
8. A. Ghose, S. Chopra and J. F. Young (1983), "Microstructural characterization of doped dicalcium silicates," J. Mater. Sci. 18, (10) 2905-2914.
9. A. Ghose, C.-T.Y. Chan, W. Kriven and J. F. Young (1985), "Microstructure of non-stoichiometric dicalcium silicate containing potassium or aluminum oxide," Proc. Int. Symp. Cem. Concr. Beijing, China, May, 1984, in press.
10. Yugoslav Standard JUS B.C8.020 (1975), "Methods of chemical analysis of cements produced by portland clinker," p. 5, Beograd.
11. S. Chopra (1983), "Electron-optical studies of stabilized α'- and β-dicalcium silicates," M. S. Thesis, Univ. Illinois, Urbana, Illinois, 61801, USA.
12. S. Diamon, J. F. Young and F. V. Lawrence, Jr. (1974), "Scanning electron microscopy - energy dispersive x-ray analysis of cement constituents - some cautions," Cem. Concr. Res., 4(6), 899-914.
13. I. Jelenić and A. Bezjak (1981), "On the hydration kinetics of α'- and β-modifications of dicalcium silcate," Cem. Concr. Res. 11(3), 467-471.

TABLE I. The Chemical and Phase Bulk Composition of C_2S Samples

Sample	Raw Mix	$Ca_3(PO_4)_2OH$ in Raw Mix	Bulk Chemical Composition in wt.%[a] CaO[b]	SiO_2	P_2O_5	Fe_2O_3	Al_2O_3	Free CaO	Modification
T-37	LR	1.18	64.80	34.62	0.44	nd	nd	-	β, γ(<5%)
T-38	LR	11.0 5	64.22	31.01	4.85	nd	nd	0.08	α'
T-39	NRM	1.18	63.65	34.39	0.47	0.24	0.47	0.42	β
T-40	NRM	11.05	63.23	31.48	4.52	0.14	0.45	0.58	α', β[c]
1	LR	1.18	65.03	34.47	0.50	nd	nd	-	β
P1	NRM	2.40	64.04	33.24	0.78	0.14	0.64	nd	β
P2	NRM	3.45	63.02	33.21	1.42	0.20	0.64	nd	β, α'(trace)
P3	NRM	5.70	63.80	32.88	2.27	0.31	0.27	nd	β, α'[c]
P4	NRM	11.00	64.05	31.24	4.02	0.10	0.46	nd	α', β[c]

LR Laboratory reagents
NRM Natural raw materials
nd Not determined

[a] Determined after first firing.
[b] Free CaO included
[c] Small amounts

Table II. Composition of C_2S Crystals in Doped Belites.

Sample: (No. of Firings)	Percentages by weight* CaO	SiO_2	SO_3	P_2O_5	Al_2O_3	Fe_2O_3	K_2O	MgO	C/S Molar Ratio	No. of Determinations
T-37	63.64	35.65	0.10	0.80	0.09	0.01	0.01	0.01	1.91	
(1x)	62.34	34.53	-	0.09	-	-	-	-		34
	64.57	36.55	0.23	0.91	0.09	0.08	0.08			
T-37	64.97	34.32	0.11	0.44	0.01	0.02	0.01	0.03	2.03	
(4x)	63.84	33.59	-	-	-	-	-	-		18
	65.63	35.66	0.66	0.98	0.10	0.11	0.06	0.15		
1	65.15	34.06	0.06	0.61	<0.005	0.01	0.05	0.01	2.05	
(2x)	63.60	33.38	-	0.25	-	-	-	-		31
	65.98	35.79	0.18	1.18	0.09	0.11	0.12	0.11		
P1	64.46	34.60	0.10	0.46	0.06	0.04	0.04	0.21	2.00	
(1x)	62.96	34.21	-	0.10	-	-	-	-		34
	65.01	35.30	0.29	0.79	0.32	0.19	0.10	1.66		
T-39	64.74	34.46	0.09	0.34	0.16	0.03	<0.005	0.10	2.01	
(1x)	63.20	34.00	-	0.22	-	-	-	-		16
	65.67	35.62	0.29	0.47	0.34	0.15	0.06	0.27		
T-39	63.18	35.64	0.14	0.39	0.15	0.17	0.04	0.26	1.90	
(2x)	61.90	34.92	-	0.15	-	-	-	-		21
	64.15	36.32	0.25	0.55	0.82	1.48	0.12	2.13		
T-39	64.78	33.77	0.12	0.54	0.20	0.14	0.02	0.24	2.05	
(4x)	62.56	32.77	-	0.33	-	-	-	-		38
	65.63	34.85	0.27	0.77	0.56	0.51	0.08	1.29		
P1	64.44	33.09	0.08	2.25	0.04	0.02	0.02	0.03	2.09	
(1x)	60.31	31.66	-	-	-	-	-	-		38
	67.85	35.70	0.23	3.64	0.29	0.12	0.09	0.23		
T-40	64.11	33.11	0.06	2.43	0.05	0.04	0.03	0.15	2.07	
(1x)	63.52	32.57	-	1.25	-	-	-	-		11
	64.49	33.97	0.22	3.47	0.17	0.16	0.10	0.45		
T-40	63.65	32.00	0.08	3.55	0.20	0.07	0.01	0.19	2.13	
(2x)	62.98	31.73	-	2.24	0.12	-	-	0.12		6
	64.63	32.38	0.24	4.32	0.33	0.20	0.08	0.26		

*The three values denote the mean, the smaller and the largest value, respectively. The composition corresponds to the C_2S solid solution.

Table III. Composition of Other Phases in Doped Belites (Samples Fried only Once)

Sample	Percentages by weight* CaO	SiO_2	SO_3	P_2O_5	Al_2O_3	Fe_2O_3	K_2O	MgO	C/S Molar Ratio	No. of Determinations
T-39	47.99	47.66	0.14	0.03	1.75	0.96	0.01	0.95	1.08	
	47.33	47.17	-	-	1.62	0.31	-	0.29		16
	48.57	48.15	0.27	0.20	1.89	0.55	0.04	1.01		
P1	48.66	48.09	0.10	0.06	1.67	0.43	0.05	0.88	1.08	
	48.26	46.20	-	-	1.58	0.32	-	0.71		9
	50.66	48.50	0.16	0.16	1.75	0.52	0.11	0.96		
T-40	49.87	46.05	0.15	0.81	1.81	0.50	0.03	0.76	1.15	
	49.69	45.70	-	0.65	1.74	0.46	-	0.02		5
	50.26	46.32	0.30	1.02	1.93	0.55	0.06	1.06		
T-40	62.27	29.75	0.17	7.31	0.05	0.06	0.04	0.31	2.24	
	59.84	26.19	-	6.45	-	-	-	-		4
	63.22	29.92	0.28	12.52	0.13	0.15	0.08	0.93		
P4	63.26	31.33	0.05	5.13	0.05	0.01	0.02	0.10	2.16	
	62.10	30.39	-	4.11	-	-	-	-		7
	63.80	33.38	0.19	7.30	0.16	0.05	0.04	0.21		
P4	72.32	26.51	0.16	0.67	0.06	0.02	0.04	0.22	2.93	
	72.25	25.44	0.10	-	-	-	-	0.10		3
	72.46	27.41	0.22	1.42	0.10	0.06	0.07	0.37		

*The three values denote the mean, the smallest and the largest value. The composition is different from C_2S solid solution.

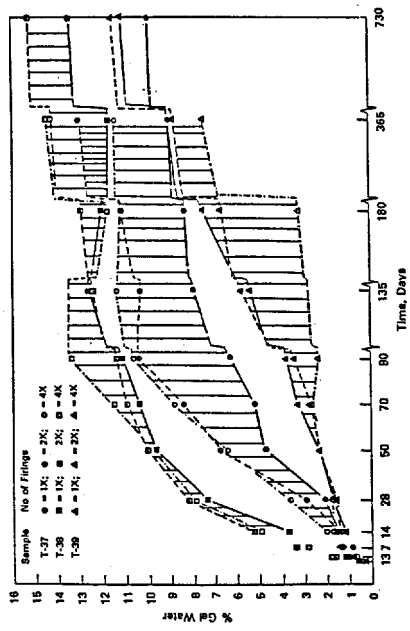

Fig. 1: Development of C-S-H gel during hydration of different C_2S preparations doped with phosphates.

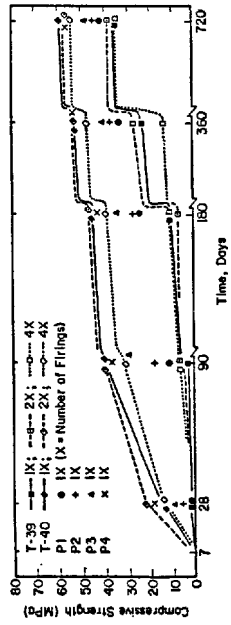

Fig. 2: Compressive strength development for C_2S preparations doped with phosphates.

SUB-THEME/SOUS-THÈME 1.3

Low energy clinker formation.
Formation d'un clinker consommant peu d'énergie.

Chairman/Président
J.P. Meric
Societé des Ciments Français
Paris, France

Principal Reporter/Rapporteur Principal
F.W. Locher
Forschungsinstitut der Zementindustrie
Dusseldorf, West Germany

Dr.-Ing Feng Xiuji M.S. Zhu Yufeng: Wuhan Institute of Building Materials China 1

RESEARCH ON AN EARLY STRENGTH CEMENT CONTAINING HIGH CONTENT OF IRON
UNE RECHERCHE SUR LE CIMENT DE L'INTENSITE' INITIALE CONTENANT UNE FORTE PROPORTION DE FER.

1.3

ABSTRACT

Formation and hydraulic characteristics of C_4AF are studied in the paper, showing that C_4AF is a cement mineral having good hydraulic properties; and some metallic ions of the 4th group of periodic system such as V^{5+}, Ti^{4+} and Mn^{4+}, can improve the hydraulic characteristics of iron phase obviously. For these phenomena, some discussions and explanations are made on bases of some concepts of solid physics and structural chemistry. A new type of cement with high early strength has been prepared. Content of iron phase in the clinker of this cement is moderately high, which plays an important role on the development of the strength of cement. Special properties of this type of cement are: low clinkering temperature, high early strength when curing in water or air, and still very high strength of this clinker after dusting. Meanwhile, formation mechanism of clinker of this cement has been studied and the relation between the physical properties of the cement and the clinker composition has also been discussed.

Sumário

São estudados neste trabalho, a formação e as características do C_4AF, mostrando que o C_4AF é um mineral do cimento tendo boas propriedades hidráulicas; e alguns íons metálicos do 4º grupo do sistema periódico como V^{5+}, Ti^{4+} e Mn^{4+}, podem melhorar obviamente as características hidráulicas da fase ferro. Para esses fenômenos, algumas discussões e explanações são feitas com base em conceitos da física dos sólidos e química estrutural. Um novo tipo de cimento de alta resistência inicial foi preparado. O conteúdo da fase ferro no clínquer desse cimento é moderadamente alto, e apresenta um importante papel no desenvolvimento da resistência do cimento. Propriedades especiais desse cimento são: baixa temperatura de clinquerização, alta resistência inicial, quando curado ao ar ou com água e ainda muito alta resistência do seu clínquer mesmo contendo pó. Além disso, o mecanismo de formação do clínquer desse cimento foi estudado e a relação entre as propriedades físicas do cimento e a composição do clínquer foram também discutidas.

Dr.-Ing Feng Xiuji M.S. Zhu Yufeng : Wuhan Institute of Building Materials China.

RESEARCH ON AN EARLY STRENGTH CEMENT CONTAINING HIGH CONTENT OF IRON
UNE RECHERCHE SUR LE CIMENT DE L' INTENSITE' INITIALE CONTENANT UNE FORTE PROPORTION DE FER 1.3

1. GENERAL DESCRIPTION

C_4AF is a well-known cement compound but how much hydraulicity does C_4AF possess has still remained a problem up to now. Many scholars believed that C_4AF is poor in cementing ability while some people do not think so. Indeed the evidences provided by individual scientists are variant wildly.

Table 1 Compressive strength of C_4AF paste(kg/cm^2)

Author	3 d	7 d	28 d	90 d	180 d	360 d
С.Д.Окноков	117	124	147	185	279	-
Ю.М.Бутт	-	300	384	-	493	595

Comparing the hydraulicity of C_4AF with other Portland cement compounds, there are different conclusions. R.H.Bogue and H.F.W. Taylor thought that C_4AF is a poorest one of the four Portland cement compounds. However the experimental data from Ю.М.Бутт greatly depart from those of them. The compressive strength of C_4AF obtained by Ю.М.Бутт is much higher than ever before.

Table 2 Compressive strength of mineral paste given by Ю.М.Бутт (kg/cm)

Mineral	7 d	28 d	180 d	360 d
C_3S	322	466	512	584
β-C_2S	24	42	193	325
C_3A	118	124	0	0
C_4AF	300	384	493	595

1:1 mortar, 2x2x2cm prism

The reason why there are so big differences among these experimental data are seemingly relating to structural complexity of C_4AF that changes bitterly with different conditions under which C_4AF forms. C_4AF, forming under different conditions, i.e. different temperature, various chemical environment and miscellaneous firing system, possesses certainly some differences in chemical composition and crystal structure. These

Dr.-Ing Feng Xiuji M.S. Zhu Yufeng: Wuhan Institute of Building Materials China.

RESEARCH ON AN EARLY STRENGTH CEMENT CONTAINING HIGH CONTENT OF IRON
UNE RECHERCHE SUR LE CIMENT DE L' INTENSITE' INITIALE CONTENANT UNE FORTE PROPORTION DE FER 1.3

differences of C_4AF in chemical composition and crystal structure probably cause the strength differences of C_4AF paste.

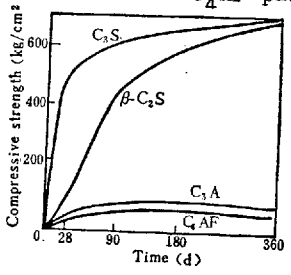

Fig.1 Compressive strength of minerals at different ages [2]

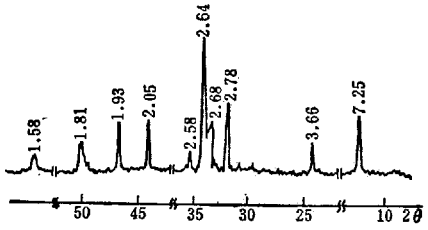

Fig.2 XRD diagram of C_4AF

Authors of this paper have synthesized C_4AF with chemical agents (molar ratio, C:A:F =4:1:1) by melting in an electric oven in 1360±10 °C. The f-CaO of melt products is zero. XRD diagram shows (Fig.2) that there is nothing but C_4AF. The clinker of C_4AF, added with 3% gypsum, is ground into specific surface area of about 3000 cm^2/g. Its compressive strength is given on table 3. For confirming the reliability the experiment mentioned above was repeated three times.

Table 3 Compressive strength of C_4AF 1:1 mortar 2x2x2 cm w/c 0.3

Sample No	Time of test	Compressive strength (kg/cm²)		
		3 d	7 d	28 d
f_1	1st	309	432	559
	2nd	422	479	554
	3rd	445	564	672

It is clear that C_4AF has indeed rather active hydraulicity according to experimental results listed on table 3. Thus developing the strength of C_4AF is not only necessary but also possible.

In 1980 P.K.Mehta discovered that C_4AF forming at rather lower temperature has rather higher hydraulicity than that acquired at higher temperature. He present a so-called energy-saving cement with high C_4AF content. Principle compounds of the clinker are C_4AF, $C_4A_3\bar{S}$, β-C_2S, and an amount of anhydrate. Further research work on C_4AF was not reported in Mahta's paper.

Authors of this paper presented a new type of early strength cement. The clinker of this cement contains $C_4A_3\bar{S}$, $C_{11}A_7CaF_2$, βC_2S, C_4AF. It should be noticed that the iron content can be very high and C_4AF is one of the principle minerals which contribute the early strength of cement. Besides this the lower clinkering temperature and high early strength are also its outstanding characteristics.

Table 4 Mineral composition and physical properties of high early strength cement prepared by authors

Item		a_{32}	F_{10}	F_1	F_9	F_{12}	F_{15}
Mineral composition (%)	C_4AF	30	35	40	50	60	75
	C_2S	23	20	18	12	8	0
	$C_4A_3\bar{S}$	34	33	32	27	23	17
	$C_{11}A_7 \cdot CaF_2$	12	12	10	11	9	8
Blaine (cm^2/g)		3656	2738	3770	3395	4220	—
Setting time	water added (W/C)	0.267	0.267	0.267	0.267	0.267	—
	initial set (h:min)	0:20	0:10	0:12	0:47	0:40	—
	final set (h:min)	0:25	0:19	0:26	1:33	1:00	—
Compressive strength (kg/cm^2)	1d	454	484	421	320	351	254
	3d	623	520	491	548	689	535
	7d	652	685	637	623	662	592
	28d	824	790	789	656	769	571

1:2 mortar, 2×2×2cm, cured in air (temp.20°C, R.H.76%).

2. CLINKER-BURNING PROCESS

In order to know proper conditions under which clinker forms and to determine the optimum temperature range of burning, some research work has been carried out. The raw materials are prepared as that listed on the table 5 and burnt in an electric oven: temperature-raising rate is 10°C/min. After being kept at every fixed temperature for 15 minutes, the burned sample is taken out and quenched in the air. Measure the free-lime of clinker by glycerin-alcohol method and identify the phase composition by XRD. Meanwhile differential thermal analysis has been car-

ried out. The experimental results are given as follows:

Table 5

Item	Potential mineral composition (%)			
	C_2S	C_4AF	$C_4A_3\bar{S}$	$C_{11}A_7 \cdot CaF_2$
F_3	18	40	24	18

Table 6 Amount of f-CaO of raw mix burnt under different temperatures

Temp.(°C)	1000	1050	1150	1200	1230	1250	1280
fCaO(%)	20.70	15.73	12.66	-	4.83	4.21	0

From the DTA curve we can see that decomposition temperature of calcium carbonate is about 750-850 °C that is lower than that at normal condition due to existance of CaF_2. The endothermic peak at 980 °C shows that liquid phase appears. From 1020 to 1100 °C there are successively three minor exothermic peaks that hint the formation of C_2S, C_2F, $C_4A_3\bar{S}$, $C_{11}A_7CaF_2$ and so on. The endothermic at 1189°C has something to do with an amount of liquid phase formation. An amount of liquid phase helps the aluminium ions moving into crystal lattice of C_2F and speeds up the formation of C_4AF. Thus following exothermic peak can be considered to be caused by formation of C_4AF.

The XRD diagram (Fig. 4) illustrates more clearly the process of formation and transformation of individul components existing at each given temperature. At beginning (1000 °C) appear the specific lines of CA(2.50, 2.95), C_2F(2.67, 2.71) and $3C_2S.3C\bar{S}.CaF_2$(2.82). Along with disappearance of CA, $C_4A_3\bar{S}$(3.76) comes into being first at 1050 °C. This is due to following chemical reaction take place:

$$3\ CA + CaSO_4 = C_4A_3\bar{S}$$

Specific lines of $C_{11}A_7CaF_2$(4.87) appears somewhat latter, but the intensity of XRD lines of two early strength compounds reach their peak value at 1200 °C. Afterwards the intensity of XRD lines of $C_4A_3\bar{S}$ starts dropping a bit. The XRD diagram also reflects the formation of ferrite phase. The strongest (141) line of ferrite phase occuring from 2.68 to 2.63 can be seen clearly. It shows that the crystal structure of ferrite phase changes progressively from space group, Pnma, to Imma that has more symmetrical elements and that the chemical composition changes from C_2F to C_4AF. The clinkering process ends with formation of C_4AF.

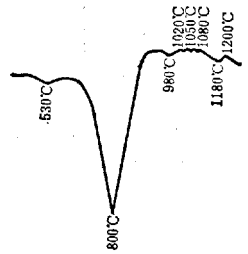

Fig.3 DTA curve of raw mix

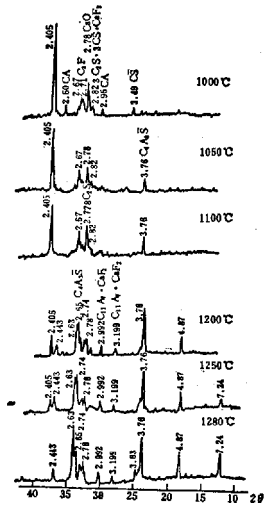

Fig. 4 XRD diagram of raw mix burnt under different temperatures

3. MINERAL COMPOSITION AND PHYSICAL PROPERTIES

(A). Mineral composition and physical properties of clinker.

It is noticed that there exist two early strength compounds $C_4A_3\bar{S}$ and $C_{11}A_7CaF_2$ simulteneously in the clinker. They have different hydration characteristics. Being cellular structure, $C_{11}A_7CaF_2$ absorbs water intensely and hydrates very quickly so that the increase in strength can be measured even every other hour. Unfortunately its later strength is not very high, even regress

Dr.-Ing Feng Xiuji M.S. Zhu Yufeng : Wuhan Institute of Building Materials China.

RESEARCH ON AN EARLY STRENGTH CEMENT CONTAINING HIGH CONTENT OF IRON
UNE RECHERCHE SUR LE CIMENT DE L' INTENSITE' INITIALE CONTENANT UNE FORTE PROPORTION DE FER 1.3

sometimes. $C_4A_3\overline{S}$ has both early and later strength. Although its early strength is a bit lower than $C_{11}A_7CaF_2$. Thus proper proportion of these two early strength compounds has a significant influence both on the clinker-burning process and on the cementing properties.

Table 7 shows a group of sample with different $C_4A_3\overline{S}$:$C_{11}A_7\cdot CaF_2$. Being mixed carefully and shaped into a pie of 30x10 mm, the raw materials are burnt in electric oven. Keep a constant temperature of 1250 C for one hour to escape the temperature gradient in the pie, then quench them in the air, the f-CaO is found to be zero.

Table 7

Item	Potential mineral composition (%)			
	C_2S	C_4AF	$C_4A_3\overline{S}+C_{11}A_7\cdot CaF_2$	$C_4A_3\overline{S}:C_{11}A_7\cdot CaF_2$
a_{11}	23	30	46	100:0
a_{32}	23	30	46	74:26
a_2	23	30	46	57:43
a_{41}	23	30	46	47:53
d_3	23	30	46	30:70

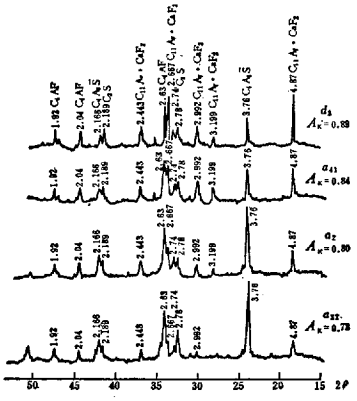

Fig.5 XRD diagram of clinkers with different amount of $C_{11}A_7\cdot CaF_2$

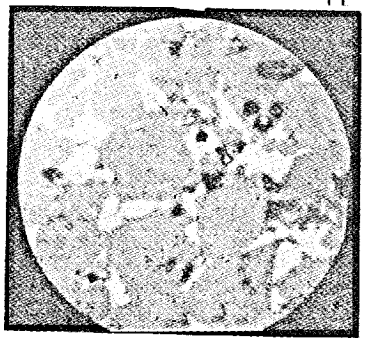

Fig.6 Micrograph of clinker d_3 Reflected light 500x

Fig. 5 is XRD diagram of clinkers listed on table 7. It can be clearly seen that the intensity of XRD line of $C_{11}A_7CaF_2$(4.87) increases steadily along with the increase in $C_{11}A_7\cdot CaF_2$. At the sametime the intensity of XRD line of $C_4A_3\overline{S}$(3.76) drops accordingly.

Petrographic analysis gives the configuration and quantity of these minerals more directly. By microscope examination of polished section of clinker without etching, two phases can be seen distinctly: the one is white phase composed mainly of ferrite phase which has stronger light-reflecting ability, the other is gray phase composed mainly of two early strength compounds $C_4A_3\overline{S}$ and $C_{11}A_7CaF_2$ have different appearances that makes it easy to distiguish them. $C_{11}A_7CaF_2$ takes mostly square-like form with smooth surfaces and size order of 15-30 μm(Fig.6). $C_4A_3\overline{S}$ looks like a gathering of countness roundy or drop-like particles with size order of 2-6 μm (Fig.7). Both $C_4A_3\overline{S}$ and $C_{11}A_7CaF_2$ belong to cubic system, refractory index of former is 1.601-1.605, of later is 1.568.

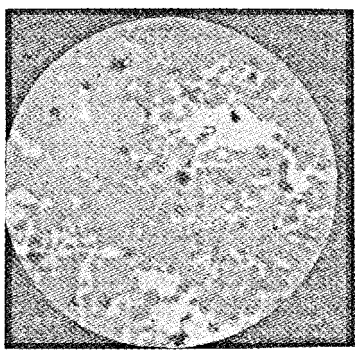

Fig.7 Micrograph of clinker a_{32} Reflected light 500x

(B). Mineral composition and physical properties of clinkers with different iron modulus ($f=SiO_2:Fe_2O_3$).

One of most outstanding characteristics of this cement is its high ferrite phase content which plays important role in both early and later strength development. This is the difference from other cements ever made before. Up to now the ferrite phase has been regarded

Dr.-Ing Feng Xiuji M.S. Zhu Yufeng : Wuhan Institute of Building Materials China.

RESEARCH ON AN EARLY STRENGTH CEMENT CONTAINING HIGH CONTENT OF IRON
UNE RECHERCHE SUR LE CIMENT DE L' INTENSITE' INITIALE CONTENANT UNE FORTE PROPORTION DE FER1.3

as a fusion-assistant mineral in Portlant cement. The contribution of ferrite phase to strength development remains uncertain. As an opinion of ours, the hydraulicity of ferrite phase should be taken into consideration in following two aspects:

(1) How much hydraulicity does the ferrite phase possess by itself?

(2) Under what conditions the strength of ferrite phase can be developed fully?

It is known that C_2F is a hydrability-lacking mineral. But once some iron ions in C_2F crystal lattice are replaced by aluminum ions and C_4AF forms, the hydrability increases markedly. One reason is the structure changes of ferrite phase. Aluminium ions, with smaller ion radius, manage to take the tetrahedron coordinate positions where the iron ions originally stay. In this way the Fe-O bond becomes weakened, the stability of lattice is lowered, and the hydraulicity of ferrite phase get hightened. Another reason is perhaps relevant to hydration reaction and its hydration products. Anhydrous C_2F reacts with water very slowly and does not offer strength. However the hydration rate of C_4AF is much greater than C_2F. This is possibly because there is somewhat solid solution formation among ferrite, aluminate and their compound salts, which is beneficial to the strength development of C_4AF.

We know that the hydration products of $C_4A_3\bar{S}$ and $C_{11}A_7CaF_2$ and form a series of solid solution with the hydration products of C_4AF. Further more owing to absence of calcium hydroxide in hydration products, and added by control of gypsum amount as additive, an adequate circumstance for the hydration of C_4AF can be acquired[4,5]. All of these will facilitate the strength development of C_4AF.

Fig.8 is XRD diagram of clinkers with different iron modulus (f). It can be seen that while the iron modulus increases XRD line of C_4AF(2.63) become stronger and the XRD lines of $C_4A_3\bar{S}$(3.76) and of $C_{11}A_7CaF_2$ (4.87) get weaker.

Tab. 4 lists the compressive strength that supports a fact that with the increase in C_4AF content and the decrease in total amount

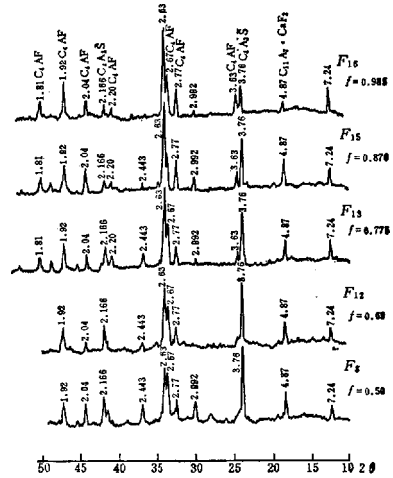

Fig. 8 XRD diageam of clinkers with different iron modulus

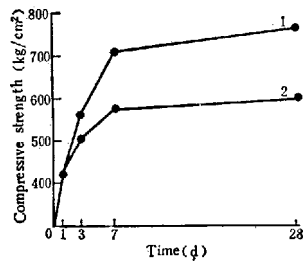

Fig.9 Compressive strength of raw mix F_1 cured in different conditions
1. Cured in air 2. Cured in water

of early strength compounds, the compressive strength of these clinkers at 3 day or 7 day ages can increases quickly and becomes nearly close each other, although there is some difference in one-day sthength. That indicates that in cooperation with $C_4A_3\bar{S}$ and $C_{11}A_7CaF_2$, the hydraulicity of C_4AF can be developed in full and C_4AF exhibits some early strength characteristics in this case.

It is interestingly observed that there is rather big difference in compressive strength between those test cubes both cured in water and in air. Although the test cubes are made of identical cement and shaped under same conditions, the strength of cubes cured in air is greater than cured in water. (see Fig. 9) It is probably because the reaction of carbon dioxide in air to hexagonal plate hydration products resists the transformation to cubic calcium aluminate through formation

Dr.-Ing Feng Xiuji M.S. Zhu Yufeng : Wuhan Institute of Building Materials China.

RESEARCH ON AN EARLY STRENGTH CEMENT CONTAINING HIGH CONTENT OF IRON
UNE RECHERCHE SUR LE CIMENT DE L' INTENSITE' INITIALE CONTENANT UNE FORTE PROPORTION DE FER 1.3

of C_3ACaCO_3 aq. which still possesses hexagonal plate crystal structure. It is no doubt useful for simplying the curing system of cement products.

(C) The influences of silica modulus (S= $SiO_2:Fe_2O_3$) on mineral composition and physical properties of clinkers.

The silicate compounds existing in this clinker take form of dicalcium silicate. Fig. 10 shows that β-C_2S distributing in the clinker is roundy striped particle with size order of 2-8μ.

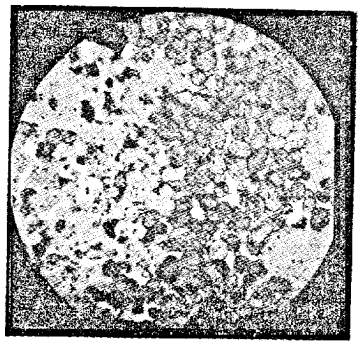

Fig.10 Micrograph of clinker C_2 with 10% NH_4Cl etching 10s
Reflected light 500x

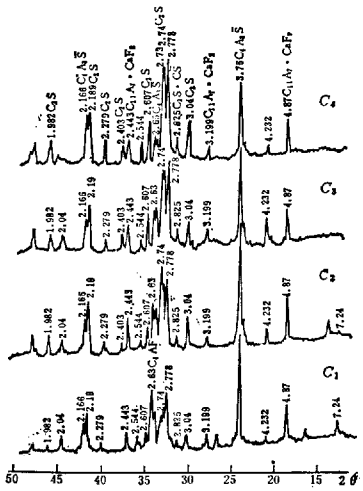

Fig.11 XRD diagram of clinker with different silica modulus

The silicate-containing phases in clinker have some effects on promoting formation of clinker at lower temperature. The formation of transient phases such as $2C_2S{\cdot}CaSO_4$, $3C_2S{\cdot}3CaSO_4{\cdot}CaF_2$, lowers the liquid-formation temperature and facilitates the formation of other minerials.

What is the contribution of dicalcium silicate to strength of cement? Tab.8 lists a group of raw mix with rather high silica modulus. Fig.11 is XRD diagram of C group clinkers. The relative intensity of XRD lines of main minerals, $C_4A_3\overline{S}$(3.76), $C_{11}A_7CaF_2$(4.87), C_4AF(2.63), β-C_2S(2.778 2.74), shows that the mineral composition acquired corresponds with the composition designed before. The compressive strength of C group clinkers here given on Tab.9. For purpose of comparison Tab.9 also lists the mineral composition and compressive strength of F group clinkers.

Table 8

No \ Item	Index of raw mix	Potential mineral composition (%)			
	s	C_2S	C_4AF	$C_4A_3\overline{S}$	$C_{11}A_7{\cdot}CaF_2$
C_1	2.36	40	18	24	18
C_2	4.42	50	12	22	16
C_3	5.65	60	8	18	14
C_4		70	0	17	13

Table 9 Influence of silica modulus on compressive strength of clinkers

No	Item	Mineral composition (%)			Compressive strength (kg/cm^2)			
		C_2S	C_4AF	$C_4A_3\overline{S}+C_{11}A_7{\cdot}CaF_2$	1 d	3 d	7 d	28 d
1	C_1	40	18	42	199	317	316	312
	F_1	18	40		419	510	578	580
2	C_2	50	12	38	161	322	391	341
	F_9	12	50		326	469	579	592
3	C_3	60	8	32	107	280	343	329
	F_{12}	8	60		351	634	605	623
	C_4	70	0	32	110	224	237	265
	F_{14}	0	70		358	576	563	570

1:2 mortar, 2x2x2cm; standard curing in water.

It is obvious that although the same amount of early strength compounds do both C and F group clinkers have, there is big difference in compressive strength between both groups: the compressive strength of F group (with lower S) is much higher than of C group (with higher S). By comparison C_4AF has more hydration activities than β-C_2S in such a circumstance.

In experiment there is a interesting discover that during the cooling process dusting

Dr.-Ing Feng Xiuji M.S. Zhu Yufeng : Wuhan Institute of Building Materials China.

RESEARCH ON AN EARLY STRENGTH CEMENT CONTAINING HIGH CONTENT OF IRON
UNE RECHERCHE SUR LE CIMENT DE L' INTENSITE' INITIALE CONTENANT UNE FORTE PROPORTION DE FER 1.3

of clinker often occurs due to transformation from β-C_2S to γ-C_2S, however the dusting clinker still possesses a good hydraulicity.

Table 10 Compressive strength of dusting clinkers

Dusting clinker	Mineral composition (%)					Compressive strength (kg/cm^2)			
	C_2S	C_4AF	$C_4A_3\bar{S}$	$C_{11}A_7CaF_2$	fCaO	1 d	3 d	7 d	28 d
a_{32}	23	30	34	12	0	464	712	698	796
F_1^{2m}	18	40	32	10	0	330	589	722	749

XRD diagram of dusting clinkers (Fig.12) shows that original mineral composition still remains unchangeable except that XRD lines of γ-C_2S (3.002) 2.728 1.928) replace those of β-C_2S. It can be seen clearly that without β-C_2S in clinker, C_4AF and two early strength compounds can still contribute to paste a high strength. It is a further proof that C_4AF plays an important role in establishing both early and ultimate strength of paste.

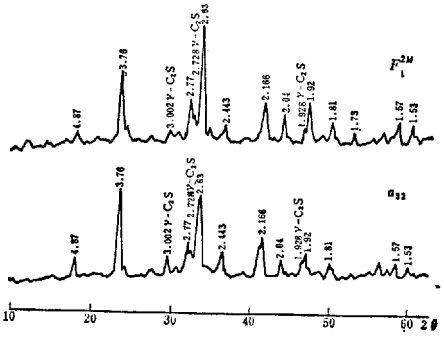

Fig.12 XRD diagram of dusting clinker

4. SUMMARY

From experiment at this stage following conclusions can be made:

(A) Under certain conditions C_4AF can develope fine hydraulicity and become a valuble cementing material. It is necessary to have a right assessment of the effect of ferrite phase in various cements and to research into some effective measures for making a full use of its hydrability.

(B) C_4AF combining with $C_4A_3\bar{S}$ and $C_{11}A_7CaF$ can give rise to high strength paste. On basis of this a new type of cement with high iron content, high early strength and low burning temperature, has been presented.

REFERECENCES

1 F.M. Lea, « Chemistry of cement & concrete » 3rd Ed, (1970)

2 H.F.W. Taylor, « Chemistry of cement » (1964)

3 P.K. Mehta, World Cement Techn. 11 [4] 166 (1980)

4 I.Jawed, S.Goto, & K.Koudo. Cement & Concrete Res. 6 [3] 441 (1976)

5 R. Sanzhaasuren, E.P.Andreeva & N.Slukalova, 7-th Intern. Cogr. On chem. of Cement. Paris, Vol I , 176 (1980)

Zheng Yiewei, Yang Nanru
Nanjing Institute of Chemical Technology, Nanjing, China

Mössbauer Study of $C_2A_xF_{1-x}$ Solid Solution

SUMMARY: It is well known that in the investigations of structure and hydration behavior of the iron-bearing phase in cement, many advantages have been revealed by using ^{57}Fe-Mössbauer spectroscopy.
In the present paper, the general distribution behavior of Al^{+3} and Fe^{+3} ions in the solid solution $C_2A_xF_{1-x}$ ($x=0\sim0.7$) on the crystal lattice sites was investigated by Mössbauer spectroscopy, IR and magnetic susceptibility measurement. The solid solution was prepared from analytical grade reagents $CaCO_3$, Al_2O_3 and Fe_2O_3. The mixtures were fired at temperature 1553 K and in oxidizing atmosphere in order to prevent the reduction of Fe^{+3} ions. The Mössbauer spectra of all the samples were taken at room temperature 295 K. But for the samples with x=0.3 and 0.5, in addition to 295 K, the spectra at 315, 335 and 365 K were also recorded.
Through analysing the Mössbauer spectra of $C_2A_xF_{1-x}$ and comparing them with that of ferromagnetic microcrystal materials, it was found that the diamagnetic Al^{+3} ions not only occupy the tetrahedral sites in preference, but their distribution in the sublattices is not at random. With the increase of Al^{+3} ions in the structure , the Al^{+3} and Fe^{+3} ions tend to segregate. The authors suggest that very small Al^{+3}-rich and Fe^{+3}-rich regions, or called clusters, may appear in the structure. This idea was also supported by the IR spectra and magnetism of $C_2A_xF_{1-x}$.
By applying the Hesse's method for continuous hyperfine field H_{hf} distribution to computer analysis of the Mössbauer spectra, the Hhf distribution and paramagnetic percentage of some solid solution members were obtained. And at the same time, the size distribution of Fe^{+3}-clusters in $C_2A_{0.3}F_{0.7}$ was derived according to the collective magnetic excitation theory proposed by Mörup et al.. If the magnetic anisotropy constant K_1 is assumed to be 10^3 J/m^3, the most probable size of Fe^{+3}-clusters is about 350 Å.

SUMÁRIO: É bem conhecido que, na investigação da estrutura e no comportamento da hidratação da fase possuindo ferro no cimento, tem-se revelado vârias vantagens no uso da espetroscopia ^{57}Fe-Mössbauer.

No presente trabalho, o comportamento da distribuição dos íons Al^{+3} e Fe^{+3} na solução sólida $C_2A_xF_{i-x}$ ($x = 0,0 \sim 0,7$) em pontos da rede do cristal foi investigado por espetroscopia Mössbauer, IR e medidas de susceptibilidade magnética. A solução sólida foi preparada com reagentes $CaCO_3$, Al_2O_3 e Fe_2O_3, de grau analítico. As misturas foram queimadas à temperatura de 1553 K e em atmosfera oxidante de módo a evitar a redução dos íons Fe^{+3}. Os espectros Mössbauer de todas as amostras foram tomados à temperatura ambiente de 295 K. Mas, para as amostras com x = 0,3 e 0,5, além dos 295 K, os espectros à 315, 335 4 365 também foram anotados.

Pela análise dos espectros Mössbauer do $C_2A_xF_{1-x}$ e comparando-os com os de materiais de microcristais ferromagnéticos, verificou-se que os íons diamagnéticos Al^{+3} não somente ocupam de preferência pontos no tetraedro, mas que sua distribuição nas subredes não é aleatória. Com o aumento de íons Al^{+3} na estrutura os íons Al^{+3} e Fe^{+3} tendem a segregar. Os autores sugerem que pequenas regiões ricas em Al^{+3} e ricas em Fe^{+3}, chamados grupamentos, podem aparecer na estrutura. Essa idéia foi também apoiada pelo espectro IR e magnetismo do $C_2A_xFe_{1-x}$.

Aplicando o método de Hesse para distribuição de campos contínuos hiperfinos H_{hf} na análise de computador dos espectros Mössbauer, a distribuição H_{hf} e a porcentagem para magnética de alguns casos de soluções sólidas, foram obtidos. E, ao mesmo tempo, o tamanho da distribuição dos grupamentos Fe^{+3} no $C_2A_{0.3}Fe_{0.7}$ foi deduzido de acordo com a teoria proposta por Morup et al sobre a excitação magnética coletiva. Se a constante K_1 de anisotropia magnética é admitida de ser 10^3 J/m^3, o mais provável tamanho do grupamento Fe^{+3} é de cerca de 350 Å.

1. INTRODUCTION

It is well known that the so-called ferrite phase in cement clinker is a series of solid solution $C_2A_xF_{1-x}$ where x=0.0~0.7. But regarding its cementitious property, researchers have not obtained an unambiguous understanding as yet.

As early as 1950s, Butt et al.(1) indicated that the ferrite phase was a good cementitious mineral owing to its relatively high compressive strength. But the majority of researchers(2,3) still maintained that the cementitious property of ferrite phase was the worst in Portland cement clinkers. In recent years, some researchers (4,5) have found the way to produce high iron-bearing phase cement with steel slags or blast furnace slags so as to reduce the fuel consumption and fully use industrial wastes. P.K.Mehta (6) and many researchers(7,8,9) in China, for example, have made an energy-saving cement containing β-C_2S, C_4AF and $C_4A_3\bar{S}$ as major minerals, in which the amount of ferrite phase is much larger than that of ordinary Portland cement. It has been established that the cement with high content of ferrite phase hydrates rapidly and exhibits expected properties.

However, it is still very hard to make a pertinent evaluation of cementitious property of the ferrite phase, because we know only a little about it. In the past, much less attention was paid to the ferrite phase than other cement clinker minerals, the ferrite phase being often simply regarded as C_4AF leaving the fact out of consideration that its properties may vary with its composition and structure. Consequently, it is of interest to investigate the correlation between the chemical composition, structure and properties of the solid solution $C_2A_xF_{1-x}$ as to better understand the function of the ferrite phase in high iron-bearing phase cement and to develop its cementing potential.

In the present paper, it was only concerned to investigate the general distribution behaviour of the Al^{+3} and Fe^{+3} ions in the crystal lattice sites of the solid solution $C_2A_xF_{1-x}$(x=0.0~0.7) by Mössbauer spectroscopy, IR and magnetic susceptibility measurements. Some studies on the inherent connection between the composition and properties of $C_2A_xF_{1-x}$ on the base of this structural level will be published elsewhere. Mössbauer spectroscopy(10), as a new technique, is ideally suited to the characterization of the iron-bearing phase in cement clinkers. Recently, this technique has been applied to cement science and many advantages have been revealed(11~16).

2. EXPERIMENTAL

2.1 Preparation of Samples

The analytical grade reagents $CaCO_3$, Al_2O_3 and Fe_2O_3 were accurately weighed, and blended for 12 hours to obtain the homogeneous mixtures of desired chemical composition as shown in Table 1. The small pellets (ϕ1.5X0.6 cm) made from the mixtures at pressure 200 Kg/cm^2 were fired at temperature 1553 K and in oxidizing atmosphere to prevent the reduction of Fe^{+3} ions The content of f-CaO was determined to be less than 0.1 % for all samples. XRD patterns, measured at Rikagu-D/max-12Kw XRD, indicated that all the samples were in excellent crystal state and the solid phase reactions were rather complete. The typical XRD pattern was shown in Fig.1.

The bulk samples were ground in agate mortar to the fineness so that the powder entirely passed through the 170-mesh standard sieve.

2.2 Measuring Instruments and Methods

A contant acceleration type Mössbauer spectrometer (MF-1) coupled with a 512 channels pulse analyser (FH-451) was employed to record the spectra. The absorbers used for measurement were prepared by pressing the powder into discs containing 7.5 mg/cm^2 of natural iron.The Mössbauer sourse, 50mc-$^{57}Co/Rh$, was used and kept at room temperature (295 K). The velocity scale was calibrated by using high pure metallic iron foil.

The infrared spectra of the samples were determined by Nicolet-175sx type FFT-Infrared Spectrophotometer and the magnetic-balance method was adopted to measure the magnetic susceptibility of the samples.

Table 1 The Conditions of Preparing Samples

Symbol	FR-1-0~7	FR-2-3~7	FR-3-3~7
Component (x)	0,0.1,0.2, ...,0.7	0.3,0.5,0.7	0.3,0.5,0.7
Firing-temperature	1553 K	1553 K	1553 K
Cooling model	*	**	***

* Cooled with furnace to room temperature.
** Cooled with furnace to 1273 K, and maintained at 1273 K for 10hrs, then cooled to room temperature in 5 mins.
***Cooled with furnace to 1273 K and maintained at 1273 K for 30hrs, then cooled to room temperature in 5 mins.

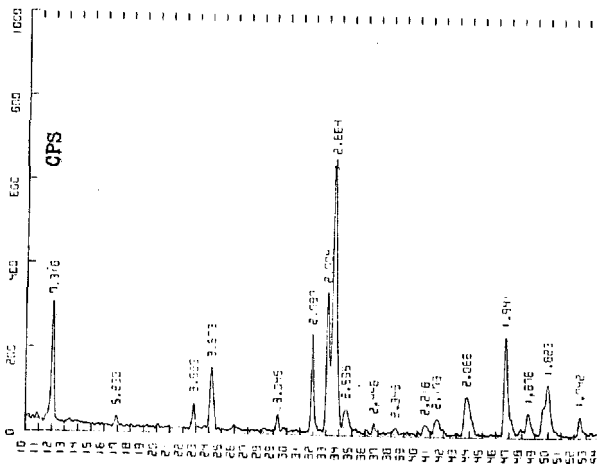

Fig.1 The typical XRD pattern for $C_2A_xF_{1-x}$

3. RESULTS AND DISCUSSION

3.1 Mössbauer Spectra and Their Characteristics

Fig.2 shows the Mössbauer spectra for $C_2A_xF_{1-x}$ (x = 0.0~0.7). It can be easily found that the spectral lines clearly vary with the change of chemical composition. The spectrum of C_2F (i.e. x=0) manifests two sets of six-line subspectra that arises from the Fe^{+3} in the tetrahedral and octahedral sublattices, respectively. With increasing Al^{+3} ions,the six-line subspectra are gradually transformed into two-line ones. This phenomenon reveals that Al^{+3} ions' entering C_2F crystal structure will cause the crystal to change from magnetically ordered state to paramagnetic state. The features for the variation of the

spectra with the compositions may be summerized as follows:

i) When Al^{+3} ions enter the crystal lattices of C_2F, for instance x=0.1, the outer lines in the spectra of it will shift inwards in comparison with that of C_2F. A slight asymmetry of the absorption peaks appears and the intensity of the subspectrum resulting from Fe^{+3} ions in the tetrahedral sites obviously decreases with increasing Al^{+3} ions. This is in accordance with the results obtained by D.K.Smith(17) and J. C. Grenier et. al.(18).

ii) With x increasing from 0.1 to 0.5, besides the tendency mentioned above, the asymmetry of the absorption peaks is getting clearer and clearer and a considerable overlap of the two subspectra is observed. The paramagnetic absorption peaks appear at the center of the spectra when x=0.3, and gradually replace the ferromagnetic ones as x increasing. When x= 0.5, the spectra is mainly composed of paramagnetic absorption lines and the whole spectra pattern exhibits a continuous undulation.

iii) When x>0.5, the intensity of magnetic absorption lines quickly decreases with increasing x. Finally, at x=0.7, the magnetic absorption lines completely vanish.

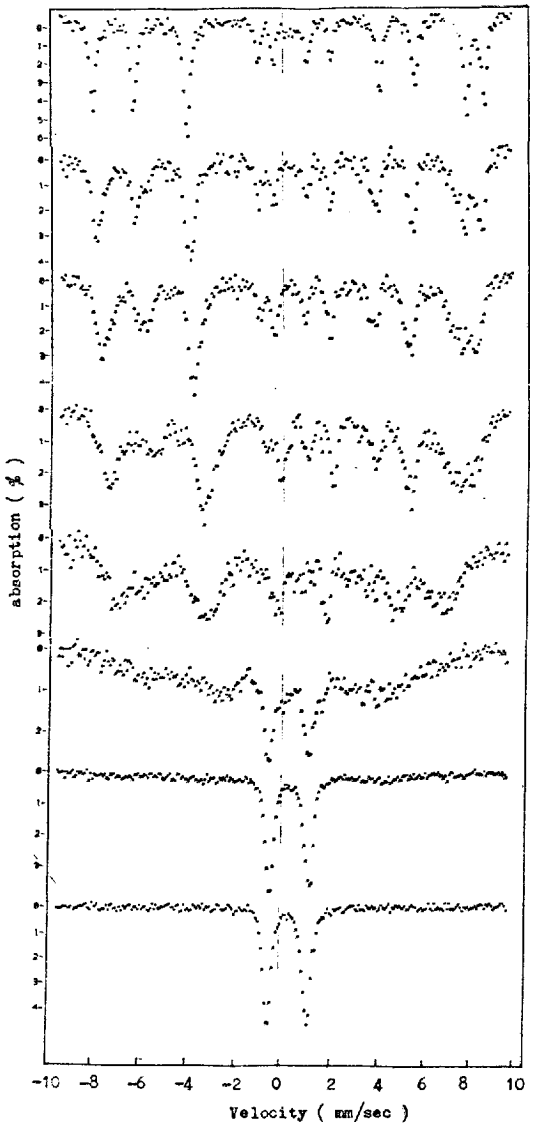

Fig.2 The Mössbauer spectra of $C_2A_xF_{1-x}$ (x=0~0.7) at room temperature 295 K

The Mössbauer spectra at temperatures over 295 K for the solid solution $C_2A_xF_{1-x}$ were also measured. As is shown in Fig.3, taking example by sample FR-3-3, the effect of temperature on the Mössbauer spectra of solid solution $C_2A_xF_{1-x}$ is similar to that of chemical composition. And it is more important, as given in experiments, that this effect is almost the same as that of the temperature far below Nèel point on the spectra of ferromagnetic superfine microcrystals.

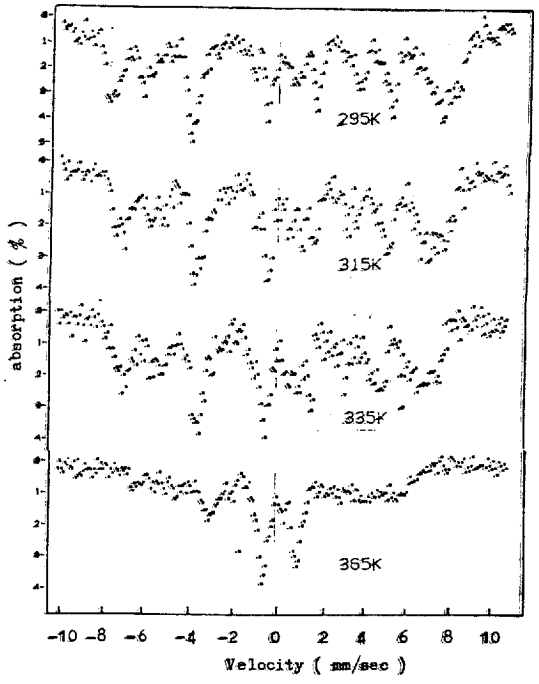

Fig.3 The Mössbauer spectra for FR-3-3 at various temperatures.

The room-temperature Mössbauer spectra for the sample groups FR-2 and FR-3 are shown in Fig.4. It can be found that the preparing conditions will influence the Mössbauer spectra of samples, too.

3.2 Ferromagnetic Microcrystals and its Mössbauer Spectra

The system of ferromagnetic microcrystallines is composed of a large quantity of fine enough magnetically ordered crystal particles so that thermal energy kT at room temperature may become comparable to the magnetic anisotropy energy of a single particle. In such fine particles, the magnetization vector is no longer fixed in an easy direction, but fluctuates in a random way.

A six-lines Mössbauer spectrum undoubtedly results

from the Zeeman interaction of the nuclear magnetic moment with the magnetic hyperfine field H_{hf}. When the magnetization fluctuates, the time-average H_{hf} will decrease in proportion to the fluctuation relaxation time t. And when this time t is short compared with the Larmor precession time t_L of the nuclear magnatic moment, the H_{hf} will nearly equal zero, and so the Mössbauer spectrum with six lines will be not obtained, but one with two peaks. Consequently, the Mössbauer spectrum of magnetic microcrystals depends on the relative magnitude of the Larmor precession time t_L (approximately equal to $1.2X10^{-7}$ sec. for ^{57}Fe) and the time scale of the fluctuation relaxation which is determined by the temperature and the sizes of magnetic microcrystals as well as their anisotropy energy constant. Some theoretical Mössbauer spectra at various relaxation times that have been caculated by Wickman(19) are shown in Fig.5.

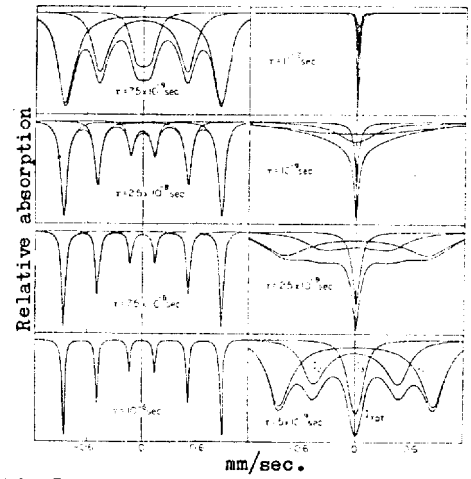

Fig.5 Theoretical Mössbauer spectra for various relaxation times, H_{hf}=550KG

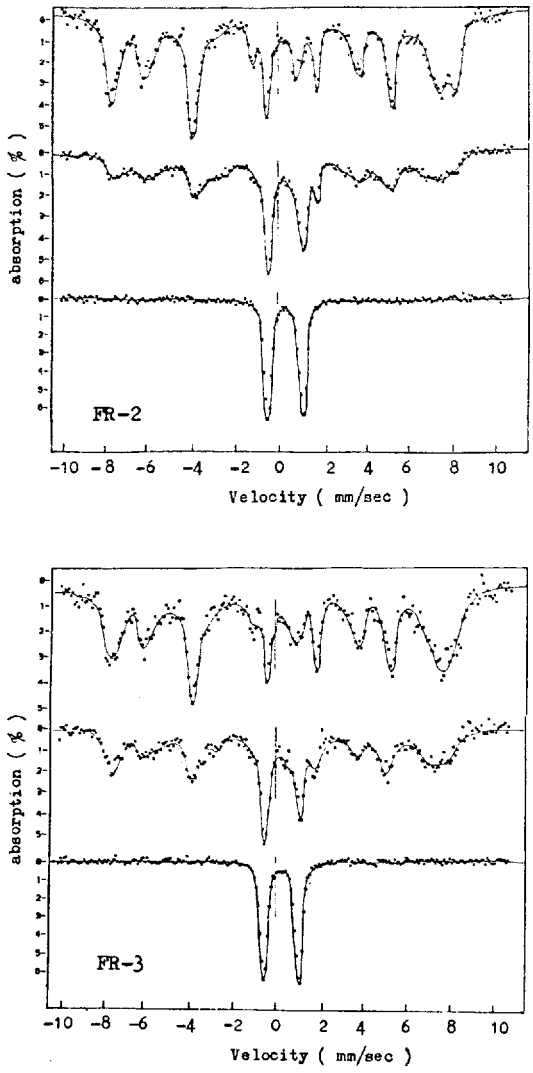

Fig.4 The Mössbauer spectra the sample groups FR-2 and FR-3, at 295 K

3.3 Fe^{+3}-cluster Structure in the C_2AxF_{1-x}

The solid solution C_2AxF_{1-x} exhibits similar Mössbauer spectra to that of magnetic microcrystals, but their physical nature are quite different from each other. It is proposed by the easults that the Mössbauer spectra of C_2AxF_{1-x} are determined by the distribution behavior of Fe^{+3} and Al^{+3} ions on the crystal lattice sites. And following physical picture may be thought to be possible: with increasing the Al^{+3} in the structure, the heterogeneous distribution of Al^{+3} ions on the lattice sites will appear so that a large quantity of small Al^{+3}-rich and Fe^{+3}-rich regions, or called clusters, are formed in the structure, but the Fe^{+3}-spins in the Fe^{+3}-clusters may arrange still in order. Therefore, such an aggregation of all the Fe^{+3}-clusters, which are separated by the diamagnetic Al^{+3} ions, will be equivalent to the system of magnetically ordered microcrystals, so far as Mössbauer effect is concerned.

Obviously, it is reasonable to assume that the size of the Fe^{+3}-clusters dispersed in the structure will be different from each other. At certain temperature, thermal energy kT will cause the magnetization vector of each Fe^{+3}-cluster to fluctuate, and each cluster has a definite relaxation time depending on its size. If some Fe^{+3}-clusters are smaller than some critical volume, the fluctuation relaxation time t will be so short that the H_{hf} nearly equals zero. Hence, the size distribution of Fe^{+3}-clusters may be reflected by the distribution of relaxation time t or magnetic hyperfine field H_{hf} by means of Mössbauer effect.

3.4 The Other Facts of Existence of Fe^{+3}-clusters

The infrared spectra of C_2AxF_{1-x} is shown in Fig.6 . It is noteworthy that, in addition to the frequency shift of spectral bands, some new absorption bands turn up with increasing x.

It is well known that infrared spectroscopy is sensitive to short-range order in crystal structure. The substitution of some foreign ions for host ions may change or not change the space group symmetry of a crystalline. According to the factor group analysis , if the cations are orderly distributed among nonequivalent sites, the rotational symmetry will not alter, the number of normal modes as well as their selection rules for the substituted crystal being exactly the same as for the parent structure. So no new

bands will appear in infrared spectrum. And if the cations are ordered in sublattice sites, however, the rotational symmetry will partially lose in proportion to the order degree. Thus, some new spectral bands will appear.

Consequently, the IR spectra seem to suggest that not only the Al^{+3} ions replace the Fe^{+3} ions in two non-equivalent sites, but the cations which occupy these sites are ordered in the crystal structure of $C_2A_xF_{1-x}$.

Another proof of existence of Fe+3-clusters is the fact that the magnetic susceptibility of the solid solution $C_2A_xF_{1-x}$ varies regularly with its chemical composition x. The curve of room-temperature specific magnetization σ(emu./mole Fe+3) versus x at the field 12.35 Koe is plotted in Fig.7 for samples FR-1. It can be seen from the figure that when $x < 0.3$, the mole magnetic susceptibility of $C_2A_xF_{1-x}$ decreases with increasing x; but it increases in proportion to x when $x > 0.3$. This behavior is explainable in terms of the Fe^{+3}-cluster hypothesis.

When x is small, the amount of weakly Fe^{+3}-bound on the boundaries of Fe^{+3}-clusters is small and the large mole magnetic susceptibility arises mainly from the incomplete counteraction of the spin magnetic moments of Fe^{+3} ions in the two sublattices. This explaination can be supported by the magnetization curves in Fig.8. As the Al^{+3} in the structure increases and the Fe^{+3}-clusters develop in quantities, however, the weakly Fe^{+3}-bound content will quickly increases, which leads to an augment in the magnetic susceptibility of $C_2A_xF_{1-x}$. In fact, the curve in Fig.7 may be regarded as the superposition of the two parts, one of which is attributed to the incomplete counteraction of the Fe+3-spins and another to the paramagnetism produced by the weakly Fe^{+3}-bound on the boundaries of the clusters.

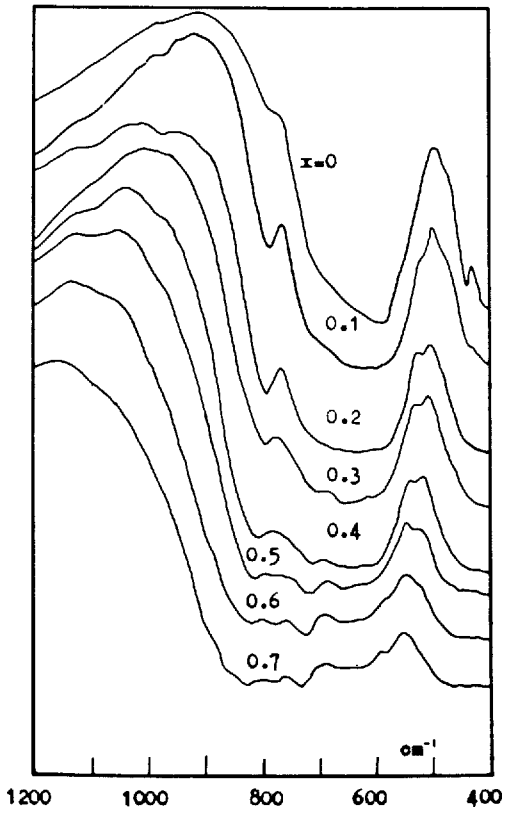

Fig.6 The Infrared Spectra of $C_2A_xF_{1-x}$ at 297 K

3.5 The Computer Analysis of The Mössbauer Spectra

In order to make a quantitative discription about the cluster structure in $C_2A_xF_{1-x}$, Hesse's method for continuous hyperfine field H_{hf} distribution and stripping spectrum technique have been applied to the computer analysis of some Mössbauer spectra containing both ferromagnetic and paramagnetic absorption. The Mössbauer spectra of C_2F and $C_2A_{0.7}F_{0.3}$, however, remained to be simply fitted to Lorentzian line shape under some restrictive conditions. Some analysis results have been illustrated in Table2, Fig.9 and 10.

Table 2 Mössbauer Parameters for the Samples C_2F and $C_2A_{0.7}F_{0.3}$,at 295 K

	C_2F		$C_2A_{0.7}F_{0.3}$	
	(Tet.)	(Oct.)	(Tet.)	(Oct.)
H_{hf}(Koe)	473	513	-	-
QS(mm/sec)	1.55	1.20	1.62	1.60
IS(mm/sec)	0.05	0.43	0.32	0.21

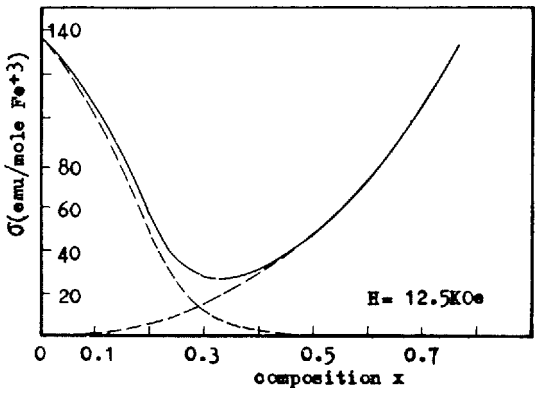

Fig.7 The Relation Between the Specific Magnetization σ and Chemical Composition x for $C_2A_xF_{1-x}$, at 12.5 KOe and 295 K

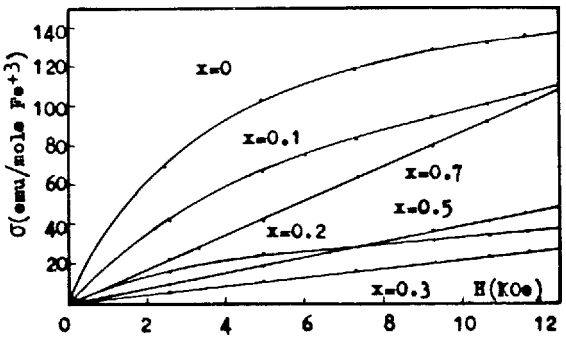

Fig.8 The Magnetization Curves for the Samples FR-1, at Temperature 295K

Fig.9a shows the probability distribution of the magnetic hyperfine field H_{hf}, P(H), for the samples FR-2-3 and FR-3-3. Each curve can be approximately divided into two separated parts, one of which, located at the high field range, may be attributed to the octahedral sublattice of $C_{2A}xF_{1-x}$ and another at low field range, to the tetrahedral one. The non-single-value distribution of H_{hf} proves the existence of the Fe^{+3}-clusters of various sizes in the structure.

An intergral of the probability distribution P(H) with respect to H_{hf} shows that the ratio of the area at low field range to the total area is 0.376 and 0.382 for the samples FR-2-3 and FR-3-3, respectively. And if we suppose that the recoil-free fractions did not differ significantely for the Fe^{+3} ions in two sublattices in $C_{2A}xF_{1-x}$, the amount of Al^{+3} ions in the tetrahedral sites are 79.0 % and 77.6 %, respectively. This result shows that Al^{+3} ions prefer to occupy the tetrahedral sites.

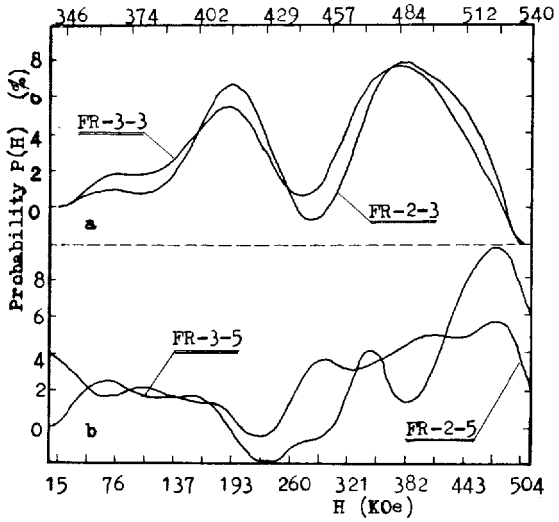

Fig.9 The distribution probability of H_{hf}, P(H), for samples FR-2-3,5 and FR-3-3,5

The relation between the paramagnetic component, the ratio of the paramagnetic absorption area to the total absorption area of Mössbauer spectra, and chemical composition x of $C_{2A}xF_{1-x}$ has been shown in Fig.10. It can be seen that the paramagnetic component increases almost exponentially with x. It appears that this phenominon is closely related to the developing of the Fe^{+3}-clusters of small sizes. Moreover, it should be noted that the paramagnetic component of the samples FR-3 is more than that of FR-2, which indicates that the paramagnetic component of the samples which were maintained at an appropriate temperature for a longer time may be more than those for a shorter time. Thermodynamically, this phenomenon can be ascribed to the diffusion of Al^{+3} and Fe^{+3} ions from small clusters towards larger ones, which gives rise to increase in the average sizes of the clusters. The probability distribution of H_{hf} for the samples FR-2-5 and FR-3-5, as shown in Fig.9b, can give the same conclusion as above.

According to the collective magnetic excitation theory proposed by Mörup et al(20):

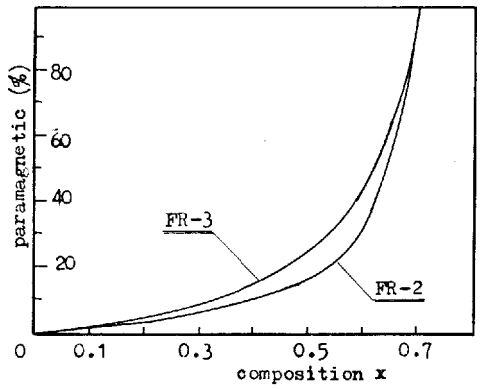

Fig.10 The paramagnetic (%) ~ X

$$H(V,T) = H(\infty,T)\langle\cos\theta\rangle_T$$

$$\langle\cos\theta\rangle_T = \int_0^{\pi/2} \exp\left[-\frac{W(\theta)}{kT}\right]\sin\theta\cos\theta d\theta \Big/ \int_0^{\pi/2} \exp\left[-\frac{W(\theta)}{kT}\right]\sin\theta d\theta$$

$$W(\theta) = K_1 V \sin^2\theta$$

where H(V.T) is the average value of hyperfine field in the Fe^{+3}-clusters of volume V; $H(\infty,T)$ the hyperfine field in a large crystal at the same temperature; and K_1 the magnetic anisotropy constant, the probability distribution P(H) can be transformed into the size distribution P(d). In the present paper, the magnetic anisotropy constant K_1 was estimated at 10^3 (J/m3) and every cluster supposed to be spherical (e.g. $V=4\pi d^3/3$). So the size distribution of the Fe^{+3}-clusters in FR-2-3 and FR-3-3 were obtained and shown in Fig.11.

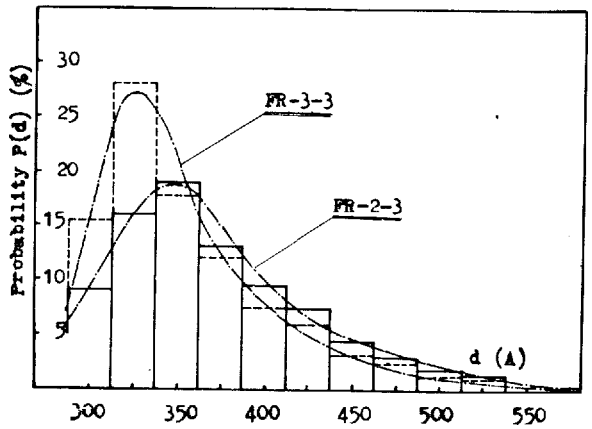

Fig.11 The distribution of the size of Fe^{+3}-clusters for FR-2, 3-3

From Fig.11, it is to be noted that the most probable sizes of the Fe^{+3}-clusters are about 350 Å and 325 Å for the samples FR-2-3 and FR-3-3, respectively; but that the clusters less than 350 Å in FR-3-3 were more than ones in FR-2-3. Obviously, this phenomenon is caused by the difference in heat treatment conditions of samples.

4. CONCLUSION

i) The diamagnetic Al^{+3} ions not only occupy the tetrahedral sites preferentially, but their distribution on the sublattices is not at random. With the increase of Al^{+3} ions in the structure of $C_{2A}xF_{1-x}$, the Al^{+3} and Fe^{+3} ions tend to gather individually to form the cluster structure.

ii) The size of the cluster in the structure varies with the average chemical composition of the solid solution. While the amount of Al^{+3} ions in $C_2AxF1-x$ increases, the size of Al^{+3}-cluster gradually becomes larger and the size of Fe^{+3}-cluster smaller. For the sample with x=0.3, the size of Fe^{+3}-cluster mainly ranges from 250 to 500 Å.

iii) The size of the cluster may also vary with the conditions under which the samples were treated. At an appropriate temperature, to prolong the time period, in which the samples are maintained a desired temperature, is helpful to the growth of the clusters.

REFERENCES:

1. Yu.M.Butt, V.M.Koffbasov et al., " The Chemistry of Cement and Concrect", 3rd Ed.,(Translated in Chinese), P103, China Building Press (1970)
2. H.F.W. Taylor, " The Chemistry of Cements " vol.1, P6, Academic Press, London and New York (1964)
3. F.M.Lee, "The Chemistry of Cement and Concrete", 3rd Ed., P200, Edward Arnold Ltd, London(1970)
4. R.Kondo, S.Diamond,et al., Proceedings of The 5th Mineral Waste Utilization Symposium, Chicago, P329(1976)
5. M.Matousek, Proc. of V Mine. Waste Utili. Sym., Chicago,P257(1976)
6. P.K. Mehta, World Cement Techn., 11(4)166(1980)
7. Deng Junan, Su Muzhen et al., Cements (in Chinese), (8)3(1982)
8. Zhu Yufeng, Dissertation for Master, Wuhan Institute of Building Materials, Wuhan in China (1982)
9. Yue Meixi, Tan Minsu, J. of Nanjing Institute of Chemical Technology, Special Volumn for Silicates, (2)71(1982)
10. V.G. Bhide, "Mössbauer Effect and its Applications", Tata, McGraw-Hill publishing Co., New Delhi (1973)
11. F.Pobell,F.Wittmann, Phys. Letters,19,175(1976)
12. F.Wittmann, F.Pobell et al., Z. Angew. Phys.19, 281(1965)
13. F.D. Tamas, A. Vertes, Cem. Concr. Res., 7, 399 (1977)
14. D.E. Rogess, L.P. Aldridge, Cem. Concr. Res.,7, 399(1977)
15. K.J.D. Mackenzie, L.P. Aldridge, Trans. J. Briti. Ceram. Sci., 79(2)29(1979)
16. K.J.D. Mackenzie, J. Mater. Sci., 17,1834(1982)
17. D.K. Smith, Acta. Crysta., 15, 1146(1962)
18. J.C. Grenier, M. pouchard et al., J. Sol. State Chem., 13,93(1975)
19. I.J.Gruverman, "Mössbauer Effect Methodology", Vol.2, P39, Plenum Press, New York(1966)
20. S. Morup, H. Topose et al., J. Physique, 37, C6-287(1976); Appli. Phys., 11,63(1976)

Wang Yanmou, Senior Engineer, Vice Minister, China State Administration of Building Materials Industry.

Deng Jun'an, Enginner. Su Muzhen, Engineer. Cement Research Institute, Research Institute of Building Materials, Guanzhuang, Beijing, China

AN INVESTIGATION INTO CEMENT $CaO-SiO_2-Al_2O_3-Fe_2O_3-SO_3$ SYSTEM

A series of energy saving sulfoaluminate cements of superior property and multiple uses in C.S.A.F.$\bar{S}$ quinary system has been established using natural bauxite with high content of ferric oxide or silica. It is found that clinkers with appropriate proportion of C_2S, C_4AF and C_4A_3S can be burnt under 1300±50°C. Different types of cements with the properties of high early strength, micro-expansion, expansion and self-stressing can be produced from these clinkers.

Production on an industrial scale shows: the raw meal of these cements contains less limestone than that of Portland cement. The burning temperature of the clinkers is low and their grindability is high. The energy consumption for the production of these cements is only two thirds of that of Portland cement.

The compressive strength/bending strength of the sulfoaluminate cement with high iron content produced industrially attains 19.7/30.7 and 101.8/12.4 MPa in 1 day and 3 days, respectively. The strengths of high silica content cement with up to 55% C_2S reach 46.9/7.6, 65.6/7.7 and 75.5/8.1 MPa in 1,3 and 28 days, respectively.

The authors explored the process of formation of $C_4A_3\bar{S}$, C_4AF and C_2S in the system C-A-S-F-$\bar{S}$. Studies have been made of the formation and decomposition of the intermediate phases $2C_2S.CaSO_4$, C_2AS and f-CaO and also the external form, morphology and the situation of solid-solution and substitution of the main clinker phases.

Hydration kinetics and strength development of the cements as well as the physical and chemical factors that influence the strength development have been studied. Measures have been proposed to improve the strength development of the cements.

The cements of this cement series are being produced in some cement plants in China and have been used satisfactorily in house building, harbour construction and permeable resisting constructions. They also find application in winter construction, shotcreting and making self-stressing pressure pipes.

Preparou-se uma série de cimentos de sulfoaluminato economizadores de energia de propriedades superior e usos múltiplos no sistema quinário C.S.A.F.$\bar{S}$, usando-se bauxita natural com alto teor de óxido de ferro ou sílica. Constatou-se que clínqueres com proporção apropriada de C_2S, C_4AF e C_4A_3S podem ser queimados a temperaturas inferiores a 1.300 ± 50°C. Diferentes tipos de cimentos com propriedades de alta resistência inicial, micro-expansão, expansão e auto-estressamento podem ser produzidos com estes clínqueres.

A produção em escala industrial mostra: a matéria crua destes cimentos contém menos calcário que o cimento portland. A temperatura de queima dos clínqueres é baixa e sua aptidão de moagem é alta. O consumo de energia para produção destes cimentos é de apenas 2 terços do consumo do cimento portland.

A resistência à compressão/resistência à tensão do cimento de sulfoaluminato com alto teor de ferro, produzido industrialmente, atinge 19,7/30,7 e 101,8/12,4 MPa em 1 e 3 dias, respectivamente. As resistências do cimento com alto teor de sílica com até 55% de C_2S atinge 46,9/7,6 65,6/7,7 e 75,5/8,1 MPa em 1, 3 e 28 dias respectivamente.
Os autores exploraram o processo de formação de $C_4A_3\bar{S}$, C_4AF e C_2S no sistema C-A-S-F-$\bar{S}$. Estudou-se a formação e decomposição das fases intermediárias $2C_2S.CaSO_4$, C_2AS e f-CaO e também a forma externa, morfologia e situação da solução sólida e substituição das fases principais do clínquer.

Foram estudadas as cinéticas de hidratação e desenvolvimento da resistência dos cimentos, bem como os fatores físicos e químicos que influenciam o desenvolvimento da resistência. Foram propostas medidas para melhorar o desenvolvimento da resistência dos cimentos.

Os cimentos desta série de cimento estão sendo produzidos em algumas fábricas na China e têm sido usados satisfatoriamente na construção civil, construção portuária e construção resistente permeável. Encontram também aplicação em construção de inverno, concreto projetado e tubos de pressão auto-estressante.

Deng Jun'an, Su Muzhen, Engineers; Wang Yanmou, Senior Engineer
Cement Research Institute, Research Institute of Building Materials, Guanzhuang, Beijing, China

INTRODUCTION

Cement Researchers have begun to attach importance to C_4AF in these years out of their concern for energy saving. Professor P.K. Mehta[1][2][3] is among the most important ones. Some research workers[4][5] have been engaged in the study of the hydration of C_4AF.

The authors[6] developed in 1973 the sulfoaluminate clinker in the C-A-S-$\bar{S}$ system with $C_4A_3\bar{S}$ and C_2S as its main component. By adding different amounts of gypsum, high early strength cement, expansive cement and self-stressing cement can be produced. Low temperature concrete and sub-zero concrete used in the Chinese "Great Wall" Investigation Station in the Antarctic were made from the high early strength cement.

We have since 1978 engaged in the study of C-A-S-F-$\bar{S}$ system[7], noticing that in the production of clinker with $C_4A_3\bar{S}$, C_2S and C_4AF as their main components, ferruginous bauxite or Al, Si, Fe and sulphide containing industrial wastes can be used as the raw material. The cement with high ferrite content is referred to as ferroaluminate cement and that with high silicate content as silicosulfoaluminate cement[8].

This paper deals mainly with the matching of $C_4A_3\bar{S}$, C_4AF and C_2S, the clinker formation and the hydration characteristics of these cements.

It should be pointed out that C_4AF is a component in the C_2F-C_6AF_2 solid solution system. In different burning conditions and in different raw material proportioning, this compound may exist in the form of C_6A_2F or C_6AF_2. For the sake of convenience they are referred to here as C_4AF.

The mineral composition of ferroaluminate cement clinker lies in the following range: C_4AF 15-45%, $C_4A_3\bar{S}$ 35-60%, C_2S 15-30%. The burning temperature is 1250°C. This cement is produced on an industrial scale and is used in harbour constructions, ordinary construction projects, water impermeable works, winter constructions, shotcreting, sealing and anticorrosion projects. It is also used to make cement products and self-stressing pressure pipes and good results have been achieved. This is an energy saving cement and is superior in various properties.

STUDY ON FERROALUMINATE CEMENT CLINKER

1. Study on the formation of some minerals in the C-A-F-$\bar{S}$ system

Different amounts of $CaSO_4$ (0, 2, 5, 9.4, 30%) are added to C_4AF raw meal which is burnt at 1100-1400°C. Results show $CaSO_4$ may take up Al_2O_3 and form $C_4A_3\bar{S}$. With gypsum in excess, calcium sulfate exists in the form of γ-$CaSO_4$. The ferrite phase may turn to C_6AF_2 when Al_2O_3 in C_4AF is taken up by $CaSO_4$ in the greatest amount. When gypsum is added in the amount of 5%, the formation temperature of C_4AF will be decreased to 1300°C. C_4AF crystals are small in the initial stage but become larger with the rise in burning temperature. From XRD and OM analyses $C_4A_3\bar{S}$ is observed in addition to C_4AF (Fig.1).



Fig.1 Optical micrograph showing C_4AF and $C_4A_3\bar{S}$ (300 X)

Table 1 The composition of raw meals (calculated as the ratio of three potential minerals)

Number	$C_4A_3\bar{S}$	C_4AF	$CaSO_4$
A - 1	50	50	0
A - 2	40	40	20
A - 3	40	20	40
A - 4	20	40	40

When Fe_2O_3 is added into $C_4A_3\bar{S}$ raw meal in the amount of 2, 5, 10 and 15% the temperature of formation of $C_4A_3\bar{S}$ is lowered. At 1150-1200°C $C_4A_3\bar{S}$ is formed in large amounts and coexist with CF and C_2F. As the temperature rises to 1300°C, the coexisting phases are $C_4A_3\bar{S}$ and C_4AF or C_6A_2F.

*Participants of the investigation are: Zhou Haihong, Diao Jiangjing, Liu Xiaoxin, Han Guihua.

Deng Jun'an, Su Muzhen, Engineers; Wang Yanmou, Senior Engineer
Cement Research Institute, Research Institute of Building Materials, Guanzhuang, Beijing, China

Raw meals were prepared with chemical reagents according to the proportion of $C_4A_3\bar{S}$:C_4AF:$CaSO_4$ given in Table 1. They were burnt at 1300 and 1350°C for two hours. XRD shows $C_4A_3\bar{S}$, C_4AF and $CaSO_4$ exist together (Fig.2).

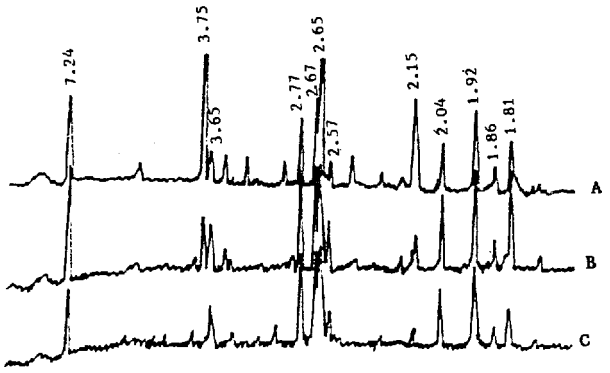

Fig.2 XRD diageam of sintered samples in C-A-F-$\bar{S}$ system

A - C_4AF raw mix

B - C_4AF raw mix + 15% $CaSO_4$

C - $C_4A_3\bar{S}$ raw mix + 10% Fe_2O_3

C_4AF : 2.74, 2.77, 2.67, 2.63, 1.92 Å

$CaSO_4$: 3.50, 2.85 Å

$C_4A_3\bar{S}$: 3.76, 2.65, 2.16 Å

2. Study on the formation of some minerals in C-A-S-$\bar{S}$ system

At burning temperature of 1200°C three minerals, i.e., C_2AS, $2C_2S{\cdot}CaSO_4$, and $C_4A_3\bar{S}$, may coexist in the C-A-S-$\bar{S}$ system. C_2AS is formed at 900°C and dissolves at 1200°C. At 1200-1250°C C_2S, $2C_2S{\cdot}CaSO_4$ and $C_4A_3\bar{S}$ coexist in the system. At 1280°C $2C_2S{\cdot}CaSO_4$ is resolved into C_2S and $CaSO_4$. The test result shows that C_3A may be appearing in small amounts when $CaSO_4$ is insufficient. C_3S and $C_4A_3\bar{S}$ do not coexist when $CaSO_4$ is greater than 5%.

3. Study on the formation of some minerals in the C-S-A-F-$\bar{S}$ system

Raw meals with different composition were prepared and burnt in a furnace for one hour. The course of the reaction can be represented as follows:

830°C	Decomposition of $CaCO_3$
1000°C	Formation of C_2AS and $C_4A_3\bar{S}$
1150°C	Formation of C_2S
1200°C	Decomposition of C_2AS
1250°C	End of lime absorbing, f-CaO=0
1300°C	The final clinker minerals $C_4A_3\bar{S}$, C_4AF, C_2S and $CaSO_4$ are formed

Beginning from 1100°C the ferrite containing phase transforms in the following order : CF — C_2F — C_4AF (C_6A_2F).

4. Study on the burning of ferroaluminate clinker with natural raw materials

Raw meals of the ferroaluminate clinker were prepared with limestone, gypsum and ferruginous bauxite. The latter may be replaced by Al, Si, Fe and sulphide containing industrial wastes.

The burnability of ferroaluminate clinker and the process of clinker formation are studied in the light of two typical raw meals (LF-17 and LF-30) from the 33 combinations.

Chemical compositions and mineral compositions of LF 17 and LF 30 are listed in Table 2 and Table 3. From Table 3 one can see that the amount of $CaCO_3$ in the ferroaluminate raw meal is much lower than that in portland cement. This is favorable to energy saving.

Table 2 Chemical composition of L-17 and L-30

Number	Ignition loss	SiO_2	Al_2O_3	Fe_2O_3	TiO_2	CaO	MgO	SO_3
Raw meal LF-17	28.69	6.42	18.20	6.09	0.65	31.82	1.07	7.05
Raw meal LF-30	27.84	3.38	18.75	9.63	0.84	31.07	0.73	7.14
Clinker LF-17		9.83	25.39	8.62	0.92	43.88	1.49	9.88
Clinker LF-30		5.66	26.07	13.34	1.14	42.27	1.01	9.69

Table 3 Mineral compositions of LF-17 and LF-30

Number	$C_4A_3\bar{S}$	C_4AF	C_2S	others
LF-17	40	26	28	6
LF-30	35	41	16	8

XRD, DTA, high temperature XRD and SEM-EDAX have been employed to analyze the various clinkers burnt at different temperatures. The results show that the order

Deng Jun'an, Su Muzhen, Engineers; Wang Yanmou, Senior Engineer
Cement Research Insitute, Research Institute of Building Materials, Guanzhuang, Beijing, China

of formation of the clinker minerals burnt from raw meals prepared with chemical reagents. However, the reaction temperature of the formation of various minerals are greatly lowered. Fig.3 shows the XRD diagrams of the raw meal burnt at different temperatures.

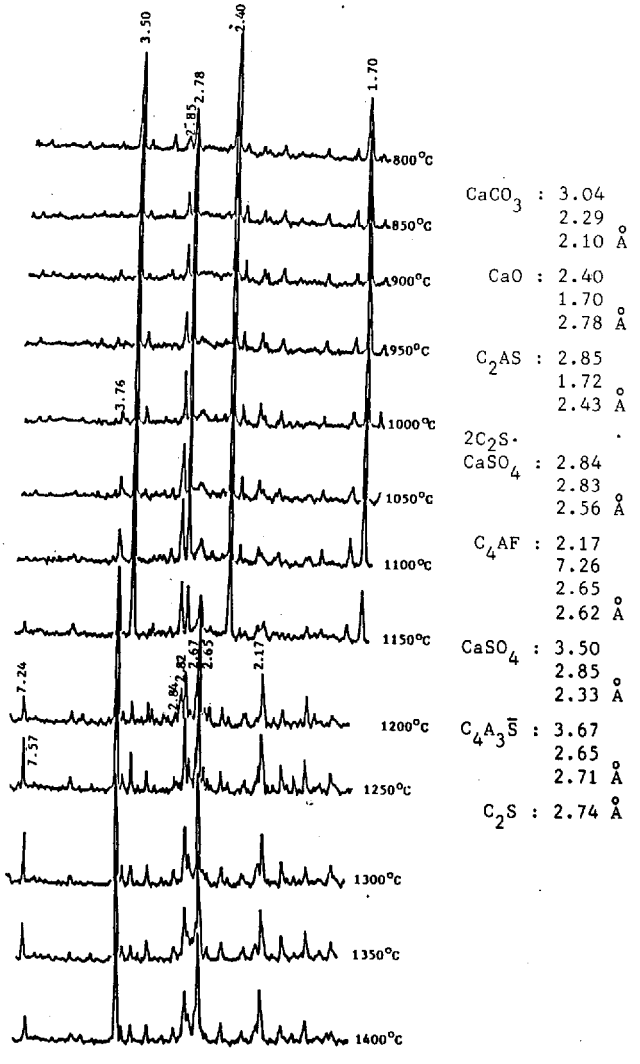

Fig.3 XRD curves of clinkers burnt at different temperatures

a. $CaCO_3$ Decomposition begins at 800°C and ends at 850°C

b. γ-$CaSO_4$ Its peaks are the highest at 800°C and lowest at 1200°C. It goes up again at 1250°C, indicating the decomposition of $2C_2S \cdot CaSO_4$

c. C_2AS begins to form at 800°C and dissolves at 1200°C.

d. $2C_2S \cdot CaSO_4$ is formed in large amounts at 1200°C and decomposes at 1250°C.

e. $C_4A_3\bar{S}$ is formed at 1000°C. Its amount is the greatest at 1250°C. It disappears at 1400°C.

f. Ferrite phase appears in the form of CF (2.66 Å) at 1000°C. At 1200°C it exists in the form of C_4AF (7.24, 2.63 Å). With the rise of temperature, crystals grow larger and the composition turns gradually to C_6AF_2 (7.17, 2.62 Å).

SEM-EDAX analysis is made of the ferroaluminate clinker. The average chemical composition comes out of 5-10 points and is listed in Table 4. Fig.4 and Fig.5 are the SEM micrographs of $C_4A_3\bar{S}$ and ferrite phase. According to the data of Table 4, large amounts of $\bar{S}$, S and Ti are taken up as solid solution in ferrite phase, and Fe is taken up to as much as 4.9% in $C_4A_3\bar{S}$. The minerals formed at lower temperature are ill-crystallized and contain large amounts of impurities. They are more active than pure minerals where the rate of hydration is concerned. Moreover, the minerals complement and accelerate each other in hydration. That is why this clinker is much superior to the mixture of several pure minerals.

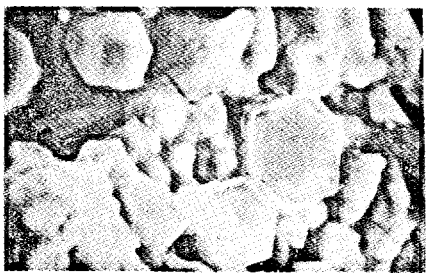

Fig.4 SEM micrograph of $C_4A_3\bar{S}$ in ferroaluminate clinker (1500 X)



Fig.5 SEM micrograph of C_4AF in ferroaluminate clinker (1500 X)

Deng Jun'an, Su Muzhen, Engineers; Wang Yanmou, Senior Engineer
Cement Research Institute, Research Institute of Building Materials, Guanzhuang, Beijing, China

Table 5 Weight percentage of elements in the minerals (by EDAX analysis)

Minerals*	Al	Si	S	Ca	Ti	F	O
C_4AF	10.10	2.86	2.73	26.65	2.34	18.74	36.58
C_6A_2F	20.77	3.23	4.27	25.86	0.47	7.93	38.47
$C_4A_3\bar{S}$	22.51	1.82	5.62	23.20	-	4.95	41.90
C_2S	1.43	15.71	2.31	40.79	0.31	1.88	37.52
C_6AF_2	4.62	3.41	0.28	25.59	3.41	19.56	43.39

*All the minerals are incorporated with other elements as solid solution

Table 6 Performance of high early strength ferroaluminate cement

Cement code	Compressive strength (MPa)					Bending strength (MPa)				
	12hr	1d	3d	28d	730d	12hr	1d	3d	7d	730d
FA-0	-	19.7	101.8	102.6	-	-	3.7	12.4	12.7	-
F-2	45.8	51.3	54.8	65.0	95.1	7.3	8.1	8.1	8.6	8.5
LFC-1-15	-	59.1	79.2	87.1	-	-	8.2	9.2	9.9	-
LFC-1-20	-	59.0	74.4	83.2	-	-	7.7	8.5	9.2	-

HYDRATION OF FERROALUMINATE CEMENT AND ITS PROPERTIES

C_4AF, $C_4A_3\bar{S}$, C_2S and $CaSO_4$ are the principle minerals of ferroaluminate cement. Part of the gypsum and limestone are added into the cement in grinding to adjust the hydration and hardening. The replacement of limestone for gypsum has the advantage of eliminating the retrogression of bending strength of the cement in certain age. The has been reported in another paper[9].

As the hydrated phases of ferroaluminate cement consist of AFt, AFm, AH_3, FH_3, C-S-H and small amounts of $Ca(OH)_2$, the incorporation of limestone will result in the formation of $C_4A\bar{C}\cdot 11H_2O$ and C_2ASH_8. The properties of this cement come from its hydration products. Table 6 shows the properties of high early strength cement produced in several plants. Table 7 shows the properties of self-stressing cement.

The pH value of the cement is 12-12.5 which lies between that of porltand cement and sulfoaluminate cement. It coutains sulfoaluminate and ferroaluminate minerals. This cement has the properties of high early strength, stable increase of strength in late age, high resistance to chemical sttack (Table 8, Fig.6 and Fig.7) and frost resistance. It is also characterized by its excellent resistance to permeation brought about by the large amount of FH_3 it contains.

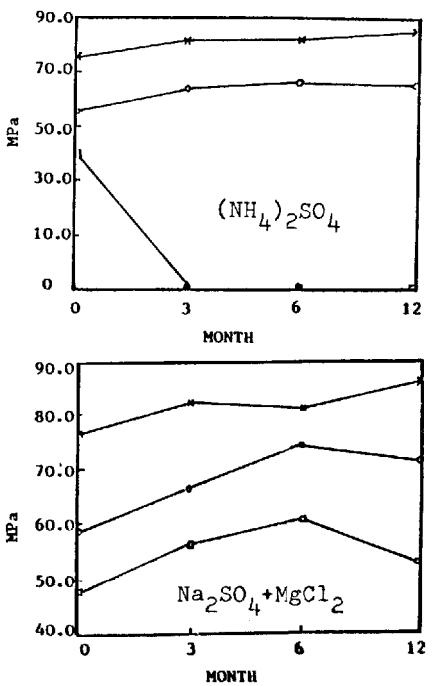

Fig.6 Compressive strength of the concrete immersed in $(NH_4)_2SO_4$ and Na_2SO_4 + $MgCl_2$
■ - 525# portland cement
x, o - Ferroaluminate clinker with admixtures

Deng Jun'an, Su Muzhen, Engineers; Wang Yanmou, Senior Engineer
Cement Research Institute, Research Insitute of Building Materials, Guanzhuang, Beijing, China

Table 7 Performance of self-stressing ferroaluminate cement

No	Curing system	Cement : sand	Free expansion % / Self-stressing value (MPa) 1d	3d	7d	14d	28d	*	Compressive strength (MPa) 1d	3d	7d	14d	28d
F-40	45 C x 50 min	1:2	0.11 / 3.08	0.18 / 4.08	0.20 / 4.95	0.21 / 5.08	0.21 / 5.20	143	270	260	360	430	470
F-4	"	"	0.05 / 1.83	0.14 / 3.77	0.27 / 5.60	0.91 / 6.70	0.93 / 6.80	120	323	458	491	-	664
F-6	"	"	0.09 / 1.37	0.23 / 2.51	0.29 / 3.43	0.29 / 4.71	0.31 / 4.94	146	-	455	403	543	611
F-35	"	"	0.31 / 2.40	0.69 / 4.50	1.46 / 6.60	1.84 / 7.50	1.85 / 7.60	251	-	-	296	565	655

*Immediately after demoulding

Table 8 Ratio of bending strength after and before immersion ($K_{6\ month}$)

Type of cement	3% $NaSO_4$	10% NaCl
Ferroaluminate cement	1.05	1.0
Aluminate cement	0.86	0.91
Sulfate-resisting cement	0.99	0.81
Sulfoaluminate cement	0.98	0.89

CONDLUSIONS

1. Ferruginous bauxite, limestone and gypsum are used to produce ferroaluminate cement clinker in the C-S-A-F-$\bar{S}$ quinary system. The mineral composition of this clinker is $C_4A_3\bar{S}$ 35-60%, C_4AF 15-45% and C_2S 15-30%. By adjusting the amount of admixing limestone and gypsum high early strength cement, expansive cement and self-stressing cement can be manufactured.

2. The burning temperature of the ferroaluminate cement clinker is low (1250°C), the grindability of which is high. The limestone in its raw meal is much lower than that in the raw meal of PC. Thus, this cement is an energy saving cement.

3. As the pH value of the ferroaluminate cement is low (pH=12-12.5), $Ca(OH)_2$ exists only in small amounts in its hydration products. Thus, it is non-dusting, frost resistant and permeation resistant. It is also superior in chemical resistance owing to the large amount of FH_3. The expansive cement and self-stressing cement are characterized by their high self-stressing value, low free expansion, high strength and short interval to attain stability.

REFERENCES

1. P.K. Mehta, United States Patent 4, 036, 657, 1977.7.19

2. P.K. Mehta "World Cement Technology" No.4 1980

3. P.K. Mehta "World Cement Technology" No.4 1978

4. M. Fuicuhaka, So Croto, K. Asaga "Cement and Concrete Research" 1981, No.3

5. Akita Arujazami, Proc 5th Internat Symp. Chem. Cement. Vol.2, p134-141 p36-67, 1969

6. Deng Jun'an, Ge Wenmin, Su Muzhen, Proceedings of the 7th International Symposium on the Chem. of Cement, Vol.4, p381-386, 1980

7. Wang Yanmou, Su Muzhen, Deng Jun'an, Journal of the Chinese Silicate Society, Vol.10, No.4, 369-376

8. Wang Yanmou, Su Muzhen, Deng Jun'an, International Symposium on Cement and Concrete, Beijing, 1985

9. Wang Yanmou, Deng Jun'an, Su Muzhen, International Symposium on Cement and Concrete, Beijing, 1985

Dr.-Ing. J. Stark
Dr.-Ing. A. Müller
Dipl-Phys. R. Seydel
Dr. sc. K. Jost

VEB Zementanlagenbau Dessau
Institut Weimar - DDR
Akademie der Wissenschaften
Berlin - DDR

Conditions of the existence of hydraulically active belite cement

Active belite cement (ABC) is a cement which belite as the main clinker mineral takes the place of alite. By thermal and chemical activation the belite is influenced in a way that it corresponds in its strength and its other structural properties to a Portland cement of OPC-type.
The experiments show that the cooling schedule is the most important factor for the hydraulic activity. Under the conditions.
. rapid cooling by about 1000 K/min
. temperature intervall for rapid cooling from 1300 to 900 ^{o}C
an active belite clinker can be produced with a sufficent erly strength and a very good strength after 28 days.
The tests in a pilot plant with an output of 20 t/d have shown, that the rapid cooling with about 1000 K/min is feasible on a technological scall. ABC allows the production of Ordenary Portlan cement with a 420 kj/kg cl. lower specific heat consumption and the use of limestone or limemarl with a lower $CaCO_3$-contet than is necassaru to the manufacture of Portland cement.

Sumário

Cimento de Belita Ativa (ABC) é um cimento no qual a belita como o principal mineral do clinquer toma o lugar da alita. Por ativação térmica e química a belita influência de tal modo que corresponde por sua resistência e outras propriedades estruturais ao cimento portland do tipo CPC.

As experiências mostram que o esquema de resfriamento é o fator mais importante para a atividade hidráulica. Sob as condições de

- rápido resfriamento de cerca de 1000 K/min.
- intervalo de temperatura para resfriamento rápido de 1300°C 900°C.

Um clinquer de belita ativa pode ser produzido com suficiente resistência inicial a uma nuito bôa resistência após 28 dias.

Os ensaios numa usina piloto com uma produção de 20 t/d mostrou que o resfriamento rápido de cerca de 1000K/min é factivel numa escala tecnológica. ABC permite a produção do cimento portland comum com menos 420 KJ/Kg cl. de consumo específico de calor e o uso de calcáreo ou morna com menor teor $C_a\ C^3_o$ que o necessário à produção de cimento portland.

Dr.-Ing. J. Stark
Dr.-Ing. A. Müller
Dipl.-Phys. R. Seydel
Dr. sc. K. Jost

VEB Zementanlagenbau Dessau
Institut Weimar - GDR
Akademie der Wissenschaften
Berlin - GDR

1.3

Conditions of the existence of hydraulically active belite cement

Active belite cement (ABZ) is a cement in which belite as the main clinker mineral takes the place of alite. By thermal and chemical activation the belite is influenced in a way that it corresponds in its strength and its other structural properties to a Portland cement of OPC-type /1/ /2/ /3/.
The production of an active belite clinker with a lime standard according to KÜHL KSt I = 80 ... 82 allows the reduction of energy consumption to about 10 ... 14 % and the decrease of the burning temperature by at least 100 K. Besides the manufacture of ABC allows the use of limestone or limemarl with a lower $CaCO_3$-content than is necessary to the production of Portland cement production as they do not allow the burning of an alite rich clinker, are suitable for the production of belite cement.

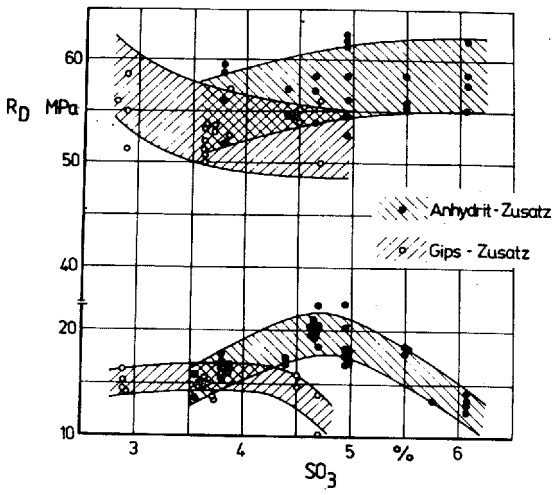

Fig. 1: Compressive strength after 3 and 28 days versus SO_3-content for clinker with 12 % C_3A (BOGUE)

- Results of laboratory experiments

The laboratory experiments /1/ /2/ have shown that the cooling schedule is the most important factor for the hydraulic activity. Under the conditions

- rapid cooling by about 1000 K/min
- temperature intervall for rapid cooling from 1300 to 900 °C

an active belite cement can be produced with a sufficient early strength and a very good strength after 28 days.
At grinding of active belite clinker natural anhydrite is added which is more suitable to control the setting behaviour than gypsum (Fig. 1).
The optimum content of SO_3 for active belite clinker with a lower C_3A-content ($\leq$ 10 %) amounts 3 ... 3,5 %. The use of limestone as a mineral admixture ($\leq$ 5 %) gives a better grindability of clinker, a higher early strength and a better workability of ABC.

- Phase composition and active state

Active belite clinker differ in phase composition and in the minor oxid content of the clinker minerals from an inactive clinker burnt from same raw mix and cooled slowly. X-ray phase analysis of clinkers (Fig. 2 and 3) burnt in a laboratory furnace and in a pilot plant have shown, that the active clinkers (cooling rate $\Delta\vartheta/\Delta\tau_K \geq$ 1000 K/min) contain more alite and α'-belite and less ß-belite, C_3A and $C_2(A,F)$ than inactive ones (cooling rate $\leq$ 100 K/min) /5/.

Dr.-Ing. J. Stark
Dr.-Ing. A. Müller
Dipl.-Phys. R. Seydel
Dr.sc. K. Jost

VEB Zementanlagenbau Dessau
Institut Weimar - GDR
Akademie der Wissenschaften
Berlin - GDR

Conditions of the existence of hydraulically active belite cement

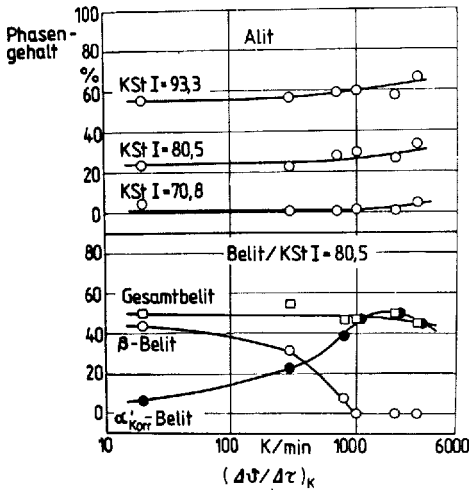

Fig. 2: Alite and α'-belite content as a function of the cooling rate (α'_{korr}-belite means the whole content of α'-belite according to /5/)

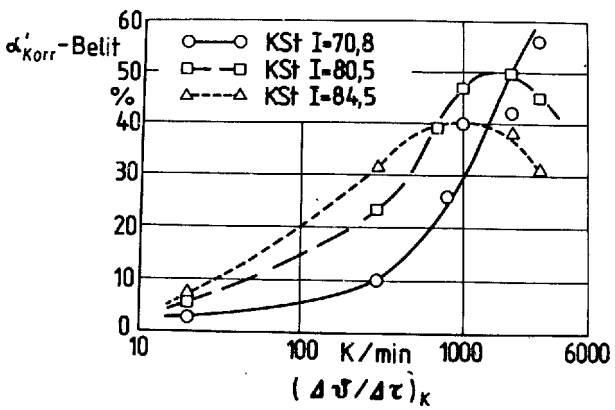

Fig. 3: α'-belite content as a function of the cooling rate at various lime standards

The differences in phase composition of active and inactive belite clinker are shown in Table 1 by example of a typical belite clinker with lime standard KSt I = 80.

Table 1: Phase composition of a clinker (%) with lime standard KSt I = 80,5; SM = 2,4; TM = 2,4; CaO_{frei} < 1,0 %

cooling rate K/min	1000	20
alite	30	24
α'-belite	48	7
ß-belite	0	44
C_3A	10	15
C_2 (A,F)	9	6
MgO	3	4
amorphous interstitial phase	0	0

- Pilot plant investigations

By means of pilot plant investigations - output 20 t/d - it has been shown that rapid cooling with temperature gradients of around 1000 K/min is technically feasible. The clinkers produced in this way attain after grinding on a laboratory ball mill (3200 cm^2/g) cement compressive strengths of 16 - 22 MPa at 3 days and 50 - 60 MPa at 28 days. Grinding of larger quantities of clinker in a classifier mill showed, that by variation of particle size distribution a strength after 3 days >30 MPa is also possible.
Under pilot plant conditions the effect of the cooling rate on the strength of cement is manifested in the strength decreasing in the following order:

- quenching in water
- fluidized bed cooler
- high speed rotary cooler
- planetary cooler.

The cooling temperature gradient decreases in the same order. The rapid cooling of clinker requires a fine-grained clinker (grain size up to 12 mm). For more coarse clinker (12 ... 50 mm) therefore an impact crusher is incorporated into the cooling process.

The impact crushing of hot belite clinker is a practicable way, because the crushing strength of clinker by temperatures from 1300 to 1350 °C is nearly zero. The abrasion of the crushing segments during testperiods in the pilot plant was minimum.

Literature

/1/ Stark, J.; Müller, A.; Schrader, R.; Rümpler, K. u. a.: Silikattechn. 30 (1979)12, S. 357-362; Silikattechn. 31 (1980) 2, S. 50- 52; Silikattechn. 31 (1980) 6, S. 168-171

/2/ Stark, J.; Müller, A.; Schrader, R.; Rümpler, K.: Zement-Kalk-Gips 34 (1981) 9, S. 476-481

/3/ Stark, J.: betontechn. 1982, 3, S. 72-80

/4/ Müller, A.; Stark, J.: Silikattechn.35 (1984) 9, S. 276-278

/5/ Jost, K.; Seydel, R.; v.Lampe, F.; Müller, A.; Stark, J.; Mielke, I.: Silikattechn. 36(1985) 12, S.

M. S. Sumner, N. M. Hepher and G. K. Moir
Blue Circle Industries PLC, Research Division, Greenhithe, Kent.

THE INFLUENCE OF A NARROW CEMENT PARTICLE SIZE DISTRIBUTION ON CEMENT PASTE AND CONCRETE WATER DEMAND

L'INFLUENCE D'UNE GRANULOMETRIE ETROITE DU CIMENT SUR LES EXIGENCES EN EAU DES PATES DU CIMENT ET DES BETONS

The production of narrow particle size distribution cements, using either vertical spindle mills or closed-circuit ball mills with high efficiency separators, offers substantial savings in grinding cost. However, these narrow particle size distribution cements can have significantly different properties from those of conventional cements. In particular, cement paste and concrete water demands can be increases to such a level that the potential energy savings are reduced or even negated when the cements are tested for strength in concrete gauged to a constant level of slump.

This paper identifies the important influences of a narrow particle size distribution on cement properties.

Investigations, using inert material, into the effect of physical properties on cement paste and concrete water demands for wide and narrow particle size distributions are described. Results for cements produced from separately ground clinker, with wide and narrow particle size distribuition, blended with varying gypsum/ /hemihydrate additions are also discussed.

Finally, resulting from this work, methods that enable the production of narrow particle size distribution cements with satisfactory water requirements, whilst maintaining the associated economic benefits, are outlined.

SUMÁRIO

A produção de cimentos com uma distribuição estreita do tamanho de partículas, usando tanto moinhos verticais de fuso ou moinhos de bolas de circuito fechado com separadores de alta eficiência, oferece uma grande economia nos custos de moagem. Entretanto, esses cimentos com uma distribuição estreita no tamanho de partículas possuem propriedades significativamente diferentes dos cimentos convencionais. Particularmente, a demanda de água da pasta de cimento e do concreto podem ser aumentados a um tal nível que as economias potenciais de energia são reduzidas ou são mesmo negativas quando os cimentos testados à resistência, em concretos com slump constante.

Este artigo identifica as influências importantes de uma distribuição estreita do tamanho de partículas nas propriedades do cimento.

Investigações, usando material inerte, no efeito das propriedades físicas da demanda de água na pasta de cimento e no concreto para uma distribuição larga e estreita do tamanho das partículas são descritas. Resultados para cimentos produzidos a partir de clínquer moído separadamente, com uma distribuição larga e estreita do tamanho de partículas, misturados com adições variáveis de gesso/hemidrato são também discutidos.

Finalmente, como resultado deste trabalho apresentam-se métodos que permitem a produção de cimentos com uma distribuição estreita do tamanho de partículas com requerimentos de água satisfatórios, e ao mesmo tempo mantendo o efeito econômico benéficos.

M. S. Sumner, N. M. Hepher and G. K. Moir
Blue Circle Industries PLC

1. INTRODUCTION

Portland cement is normally produced by grinding clinker and gypsum in ball mills operated in either open or closed-circuit. These mills produce cement with characteristic particle size distributions.

A suitable method of presenting particle size distributions is by using the Rosin-Rammler distribution function which generally yields a linear relationship for ground brittle materials.[1]

$$\ln \ln \frac{100}{R} = n (\ln x - \ln x_o)$$

The distribution can be described by the slope, n, and x_o. Decreasing values for x_o, with constant n, indicate an overall finer cement and increasing values for n indicate a narrow range of particle sizes. Typical particle size distributions for cements ground in conventional open and closed-circuit mills are shown in Table 1.

% Finer	Open-Circuit		Closed-Circuit	
	Typical	Range	Typical	Range
90 μm	98	96 - 100	99	97 - 100
63	95	90 - 98	95	91 - 97
45	88	81 - 93	88	82 - 92
30	75	69 - 81	74	67 - 80
20	60	53 - 65	59	55 - 64
15	48	44 - 52	47	44 - 52
10	36	32 - 39	35	32 - 38
5	21	18 - 23	19	18 - 21
2	8	7 - 9	7	7 - 8
SSA (m^2/kg)	363	341 - 394	352	329 - 376
x_o (μm)	22.1	26.4 - 18.5	22.2	23.0 - 19.9
Slope, n	1.03	0.99 - 1.07	1.06	1.02 - 1.10

Table 1 - Cement Particle Size Distributions

Slope can be influenced by a number of mill design and operating parameters. For example, operation in closed-circuit should narrow the range of particle sizes as a consequence of a reduction in the degree of overgrinding and elimination of coarse particles. However, due to the inherent poor efficiency of conventional separator types, closed-circuit mills yield a product with only a marginally narrower particle size distribution compared to that produced by efficient open-circuit grinding.

Recently interest has arisen in the development of high efficiency separators for ball mills[2,3], and of vertical spindle milling for cement grinding.[4,5] These both allow cement production at a reduced power consumption, as much as 30% lower, and also produce cements with narrower particle size distributions. In fact, from our own studies, (see Figure 1), it would appear that increases in milling efficiency (reduced kWh/tonne) coincide with the production of narrower cement particle size distributions.

2. INFLUENCE OF A NARROW PARTICLE SIZE DISTRIBUTION ON CEMENT PROPERTIES

2.1 Operating Data

Table 2 shows data for cement production on a 300 kW mill fitted with a high efficiency separator.

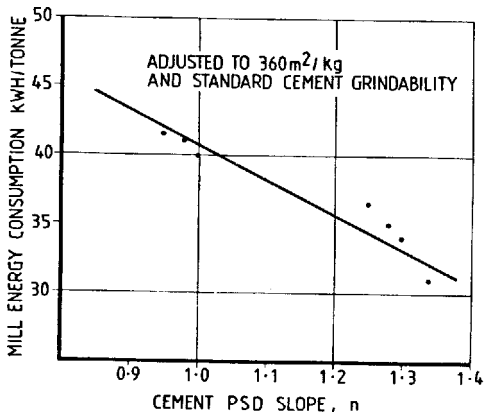

Figure 1 - Relationship Between Cement Granulometry and Mill kWh/tonne

Cement	IA	IB	IC	ID	Clinker I	
Mill Operation	O/C	C/C	C/C	C/C	C_3S	52.3
Mill Output	1.00	1.20	1.38	1.05	C_2S	15.6
SSA (m^2/kg)	346	346	310	375	C_3A	11.8
Residue, 45μm (%)	9.0	2.0	5.0	1.2	C_4AF	8.9
PSD Slope, n	1.07	1.25	1.28	1.23	LSF	96.2
x_o (μm)	21.0	17.0	19.0	15.8	SR	2.1
Paste Water Demand (%)(1)	25.5	29.0	29.0	29.2	FL	1.0
Initial Set (mins)	240	210	230	200	K_2O	0.71
Final Set (mins)	300	290	305	285	Na_2O	0.12
Concrete w/c	0.60	0.60 0.65	0.60	0.63	SO_3	0.86
Concrete Slump (mm)(2)	40	15 40	10	40		
Concrete Strength(3) 1d	10.3	11.1 8.1	9.5	10.1		
MPa 28d	46.2	48.7 42.7	46.2	46.3		
Milling Temp (°C)	110	75	70	78	(1) BS 4550	
Cement SO_3 (%)	2.7	2.8	2.8	2.7		
SO_3 ex Nat. $CaSO_4$ (%)	0.2	0.2	0.2	0.2	(2) BS 1881	
$CaSO_4.2H_2O$ (%)	0.6	1.4	1.5	1.3		
$CaSO_4.\frac{1}{2}H_2O/CaSO_4$ (%)	1.0	0.3	0.2	0.3	(3) BS 4550	

Table 2 - Operating Data for a 300 kW Mill

Cement IA represents that typically produced in open-circuit and IB and IC represent cements, produced by closed-circuit, at the same SSA and same 28 day concrete strength respectively.

Closed-circuit operation has resulted in the production of cements with a narrow granulometric composition (n = 1.23 - 1.28 compared to 1.07) and, in agreement with our general observations, have been produced with a lower kWh/tonne.

The production of narrow particle size distribution cements, either by vertical spindle milling or high efficiency separation is achieved at lower temperatures.[2,7] From Table 2 it can be seen that, consistent with the lower milling temperature, the level of dehydrated gypsum in the closed-circuit milled cements (0.2 - 0.3%) was lower than that in the open-circuit milled cement (1.0%).

Cement IB gave higher strengths than cement IA when tested at a fixed water/cement ratio of 0.60. If the target quality parameter is a constant 28 day concrete strength then cements with a narrow granulometry have a lower SSA, as for cement IC.

To explain the variation in concrete strength obtained using cements of similar SSA but varying granulometry one can postulate relationships between particle size distribution, SSA and degree of hydration.

2.2 Relationship Between Particle Size Distribution and SSA

Defining SSA by:

$$SSA = \sum_{i=1}^{i=m} \frac{6}{d_i \rho} \cdot \frac{W_i . F}{100} \quad m^2/kg$$

From this relationship it is deduced that for ordinary Portland cement (OPC) approximately 40% of the total SSA is contributed by the finest size fraction (-2μm) which is only 7 - 9% by weight of the cement. Conversely less than 2% of the total SSA is due to the coarsest size fraction (+45μm) which can be some 10 - 20% by weight.

2.3 Relationship Between Particle Size Distribution and Degree of Hydration

Hydration can be considered to be a diffusion reaction which propagates on a uniform front on the cement particle surface towards the centre.[6] The actual depth of hydration at any time will depend on the clinker chemistry and mineralogy. However to examine the influence of only granulometry a simple model can be used to determine the extent of hydration at any time:

$$\% \text{ Hydration} = \sum_{i=1}^{i=m} \frac{d_i^{\,3} - (d_i - 2h)^3}{d_i^{\,3}} W_i$$

If $2h > d_i$ then $(d_i - 2h) = 0$

Using this approach it is apparent that it is the presence of coarser particles which have the greatest influence in reducing the degree of hydration and hence strength, thus emphasising the practical importance of cement residue levels.

2.4 Effect on Water Demand

Comparing cements IC and IA it is apparent that the production of narrow particle size distribution cement offers substantial savings in grinding costs. However, it is also noted that the cement paste water demand is increased, from 25.5% to 29.0% and that the concrete slump is lower, 10mm compared to 40mm. In practice this latter effect results in an increased concrete water content when the cement is tested for strength in concrete gauged to a constant level of slump.

The influence of this higher concrete water demand is demonstrated in Table 2 for cement IB and ID gauged to give a slump of 40mm. For constant SSA the concrete strengths are lower than those obtained for cement IA. When a narrow particle size distribution cement is produced to a target of constant concrete strength and slump (cement ID) an increase in mill output compared to the production of cement IA of only 5% is recorded. Hence the increase in concrete water demand, apparently brought about by the narrowing of the particle size distribution of the cement, is so significant as to virtually negate the energy benefits achieved during grinding.

For the large proportion of cement applications the higher concrete water demand is important and a route for slump improvement is vital if the potential energy savings associated with the production of narrow particle size distribution cements are to be fully realised.

Possible explanations for the higher water demand are:

i) The physical influence of the narrower granulometry and SSA.
ii) The influence of the narrow granulometry on the cement's chemical behaviour and early reactivity.
iii) The effect of less gypsum dehydration as a result of lower milling temperatures.

3. THE PHYSICAL INFLUENCES OF NARROW PARTICLE SIZE DISTRIBUTION ON WATER DEMAND

3.1 Introduction

In practice changes in physical and chemical parameters which influence the water demand due to changes in the cement particle size distribution and SSA are inter-related. For instance, it has been shown that the early setting behaviour is influenced by the amount of C_3A reacting before the rest period.[8] This reactivity is influenced by a number of parameters such as overall C_3A level, potassium level, etc.[9] and also the cement SSA and granulometry.[10] Therefore, in order to isolate the purely physical influence, granulated blastfurnace slag was ground to 'normal' and narrow particle size distributions and tested for rheological properties in both 'paste' and 'concrete' (Table 3). Granulated blastfurnace slag behaves similarly to clinker during grinding and is essentially inert to water during the period of the rheological tests performed.

Sample		S1	S2	S3	S4
SSA (m^2/kg)		364	268	349	306
Residue, 45μm (%)		14	24	1	1
PSD slope, n		1.02	1.08	1.37	1.40
x_o (μm)		23.2	32.3	17.3	18.9
Bulk Density (kg/m^3)		1450	1570	1330	1410
Voidage (%)		49.7	45.3	53.7	51.0
'Paste' Water Demand (%)		28.5	27.5	35.5	35.0
'Concrete' Slump	0.55 w/c	15	2	8	0
mm	0.60 w/c	35	22	30	18
	0.65 w/c	140	70	100	65

Table 3 - Properties of Ground Slags

3.2 'Paste' Water Demand

The small differences in water demand observed for Portland cements are usually attributed to small fluctuations in properties such as C_3A, alkalies and SSA. However, the significantly higher water demands observed for narrow granulometry cements cannot be accounted for by existing relationships.

If a chemical mechanism was mainly responsible a generally lower level of water demand for ground slags compared to cements would be expected, together with little sensitivity to changes in the slag particle size distribution.

From Table 3 it is noted that the general level of

water demand for a slag paste is marginally higher than for cements. Furthermore, the slags with a narrow granulometry have a higher water demand than the slags with a normal granulometry as has been observed for cement pastes.

Water demand is determined for constant material weight not material volume. If the results are adjusted to a basis of water demand per volume, as carried out elsewhere,[11] then the water demands for the slags are found to be similar or slightly lower to that found for cement.

Materials with a narrow range of particle sizes pack less well than materials with a wider range of particle sizes and hence have a higher voidage. This is seen for the slags in Table 3 and Figure 2 shows the relationship between particle size distribution and voidage found for 12 cements. The voidage is also influenced by the SSA and this is indicated in Figure 2 by the average SSA for the cements above and below the line.

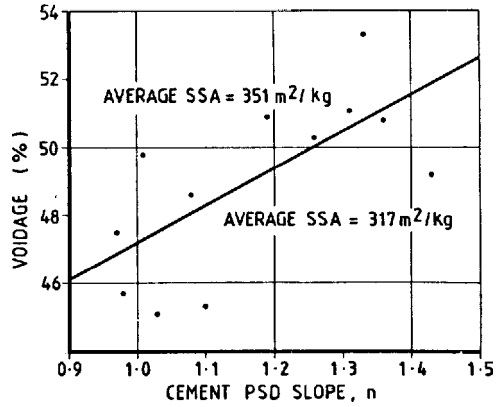

Figure 2 - Relationship between Granulometry and Voidage

The higher voidage results in more water being required to fill spaces before acting to 'lubricate' the particles. Therefore cements with a higher voidage tend to exhibit a higher paste water demand as shown in Figure 3.

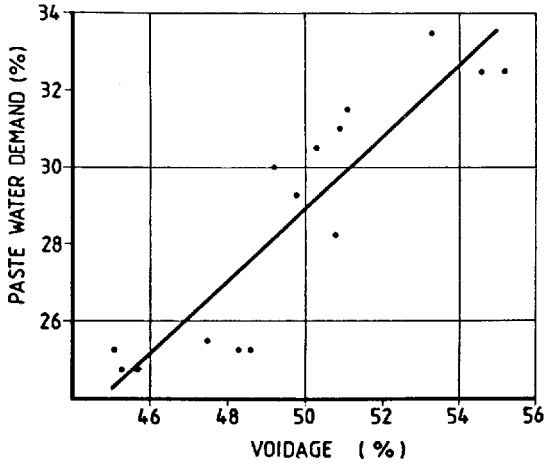

Figure 3 - Relationship between Voidage and Water Demand

3.3 'Concrete' Water Demand

The influences of SSA and granulometry on 'concrete' water demand are shown in Figure 4 using results taken from Table 3. As discussed in Section 2, the increased concrete water demand with cement attributed to the narrow granulometry resulted in an increase in water/cement ratio of 0.05. However, the increase in water demand attributed to the physical influences of the narrower particle size distribution only is found, from Figure 4, to be an increase of approximately 0.005 - 0.01 in the water/cement ratio. This small increase in the 'concrete' water demand is considered to be as a result of the increased voidage, although the influence is naturally diluted for a 'concrete' mix compared to that for the 'paste' mix due to the presence of aggregate.

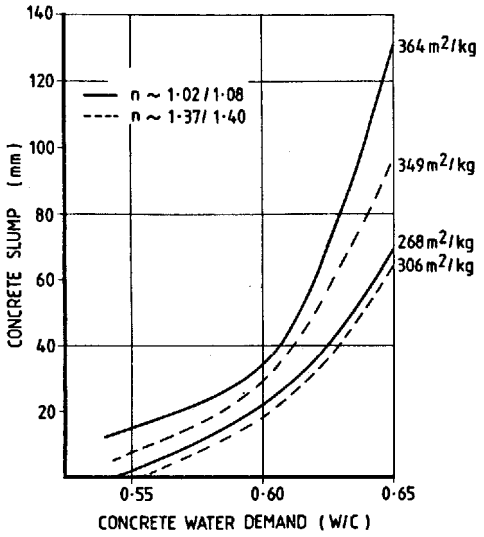

Figure 4 - Effect of Granulometry and SSA on 'Concrete' Water Demand for Slag

It is also noted from Figure 4 that increased SSA decreases the water demand for 'concrete' as expected. This is considered to be as a result of increased SSA improving water retention properties of the powder thus enhancing lubrication of aggregate particles. Overall the influence of the SSA was found to be approximately a 0.01 reduction in water/cement ratio for an increase of 50 m^2/kg in the SSA.

Therefore it is concluded that for the production of narrow particle size distribution cements at lower SSA's the increased concrete water demand due to physical effects alone would only result in an increase in the water cement ratio in a typical concrete of approximately 0.01 to 0.015.

4. CHEMICAL PROPERTIES OF A NARROW PARTICLE SIZE DISTRIBUTION INFLUENCING WATER DEMAND

4.1 Introduction

It has been reported that the granulometry may also influence the chemical behaviour, e.g. C_3A reactivity.[10] Also, during the milling process, because of lower temperatures, less gypsum

dehydration occurs (see Table 2). In production these two parameters are inter-related, and were therefore investigated separately by blending clinker, ground to wide and narrow granulometric composition, with various proportions of gypsum and hemihydrate.

In order to simulate a realistic cement the SO_3 additive needs to be very fine.[12] The gypsum/hemihydrate used was therefore prepared to a fineness of 1000 - 1200 m^2/kg.

Cements were produced from two clinkers with both 'normal' and narrow particle size distributions (see Table 4) for a range of gypsum/hemihydrate levels and tested for water demand. The influence of gypsum/hemihydrate, expressed as the percentage SO_3 arising from dehydrated gypsum ($D.SO_3$) on concrete water demand is shown in Figure 5.

	CLINKER II		CLINKER III	
	N	W	N	W
SSA (m^2/kg)	295	304	295	294
Residue, 45μm (%)	1	18	1	18
PSD slope, n	1.36	1.03	1.33	1.01
x_0 (μm)	17.9	25.8	16.4	26.0
Bulk Density (kg/m^3)	1560	1760	1470	1580
Voidage (%)	50.8	45.1	53.3	49.8
Paste Water Demand (%)	28.3	25.3	33.5	29.3
C_3S	63.5		60.6	
C_2S	11.2		13.0	
C_3A	8.0		14.0	
C_4AF	10.9		7.3	
LSF	98.6		98.3	
SR	2.3		2.2	
LOI	0.69		0.75	
FL	1.3		0.7	
Clinker SO_3	1.0		0.7	
Cement SO_3	2.5		2.5	
K_2O	0.71		0.56	
Na_2O	0.08		0.29	

Table 4 - Properties of Cements Produced from Clinkers II and III

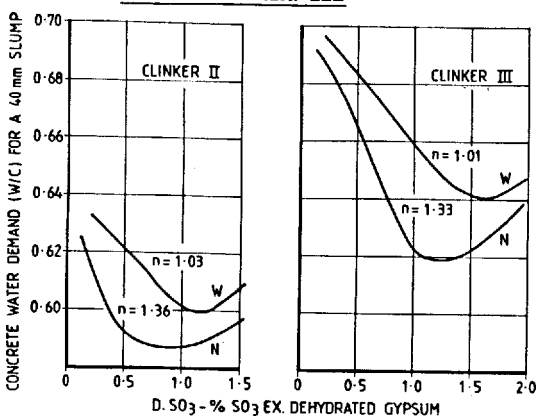

Figure 5 - Effect of Dehydrated Gypsum on Concrete Water Demand for Clinkers II and III

4.2 Paste Water Demand

As expected the paste water demand is higher for the cements (N) with a narrow granulometry compared to the cements (W) with a 'normal' granulometry as a result of the increased voidage. Furthermore, the paste water demands are higher for clinker III. Initially this could be attributed to the higher C_3A level, however the cements have a higher voidage, possibly due to particle surface properties, which largely account for the higher paste water demand.

4.3 Concrete Water Demand

For the initial rheological properties of concrete, optimisation of available soluble SO_3 in relation to the level and reactivity of C_3A is important.[8] Insufficient supply of SO_3 can lead to uncontrolled hydration of C_3A and thus cause stiffening and increased water demand for constant slump. Conversely excessive supply of SO_3 can cause stiffening and increased water demand due to crystallisation of gypsum (so-called false set). Therefore there is an optimum level of $D.SO_3$ for each cement as shown in Figure 5. For each clinker the level of $D.SO_3$ to achieve minimum water demand is lower for the narrow granulometry cement than for the wider granulometry cement. Furthermore the general level of concrete water demand is higher for the wider granulometry cements, i.e. opposite to that found for cement pastes. It is therefore postulated that the narrower particle size distribution has rendered the clinker less reactive. This is in agreement with work reported from the examination of roller milled cements.[7]

This does not help to understand the higher concrete water demands observed for narrow granulometry cements. However, as already stated, due to lower milling temperatures, the level of $D.SO_3$ can be very low, 0.2 - 0.3% for narrow granulometry cements compared to $\sim$ 1.0% for cements with a normal granulometric composition. From Figure 5 this would increase water demands from water/cement ratios of approximately 0.60 to 0.62 for clinker II and from 0.64 to 0.69 for clinker III. Hence it would appear that the lower level of available soluble SO_3, as indicated by a lower level of $D.SO_3$, results in an increase in water demand from stiffening due to a certain degree of uncontrolled C_3A hydration. Also, the level of increase in water demand appears to depend on the early reactivity of the clinker in question (in this case due to C_3A level).

Examination of clinker I for the influence of $D.SO_3$ on concrete water demand is shown in Figure 6. From this it is apparent that a reduction in $D.SO_3$ from approximately 1.0% to 0.2/0.3% leads to an increase in water demand of about 0.04 in the water/cement ratio. Therefore the higher concrete water demand observed for cement IC is explained partially by the physical influence of the narrower granulometry ($\sim$0.01) but mainly by the lower level of gypsum dehydration ($\sim$ 0.04).

It is therefore postulated that a reduction in the concrete water demand for narrow particle size distribution cements can be achieved by the optimisation of the amount of gypsum dehydration during milling by revised operating targets for mill cooling in the case of closed-circuit ball milling and by the use of process gases to raise milling temperatures or gypsum heat treatment in the case of vertical spindle milling.

As a final test, cement sample IC was heat treated for various times and re-tested for $D.SO_3$ and

concrete water demand. The results are shown in Table 5 and are in general agreement with those shown in Figure 6 when the lower SSA is taken into consideration.

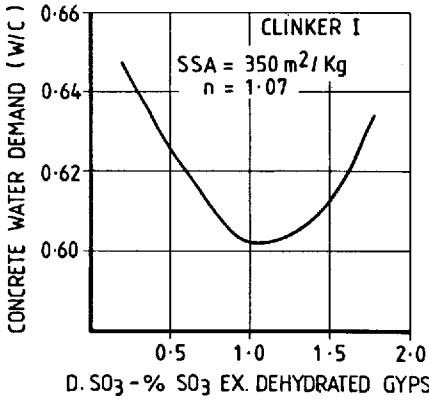

Figure 6 - Effect of Dehydrated Gypsum on Concrete Water Demand for Clinker I

D. SO_3 (%)	0.20	0.35	1.40	1.80
Concrete Water Demand (w/c) for 40mm Slump	0.661	0.643	0.619	0.637

Table 5 - Heat Treatment of Sample IC

5. CONCLUSIONS

1) The higher paste water demand for standard consistency associated with a narrow particle size distribution is attributed to a higher voidage.

2) The higher concrete water demand seen for narrow particle size distribution cements is partly attributed to the physical influence of the particle size distribution and lower SSA, but mainly to the lower level of gypsum dehydration which results in insufficient supply of available soluble SO_3.

3) The concrete water demand penalty associated with narrow particle size distribution cements can be reduced or even eliminated by ensuring an adequate level of dehydrated gypsum in the final cement.

6. ACKNOWLEDGEMENTS

The authors wish to thank Mr. R. S. Ogden and Mr. C. Plumb for their assistance in the practical work and Blue Circle Industries PLC for permission to publish.

NOMENCLATURE

d_i	Mean size for particle size fraction i (m)
D.SO_3	Percentage SO_3 arising from dehydrated gypsum ($CaSO_4.\frac{1}{2}H_2O$ - $CaSO_4$)
F	Surface shape factor (found to be 1.10 - 1.15 for cement when using a psd determined by x-ray sedigraph)
h	Depth of hydration (m)
m	Number of size fractions
n	Rosin-Rammler particle size distribution slope
PSD	Particle size distribution, granulometry
R	Percentage retained on size x
SSA	Specific surface area (m^2/kg)
w_i	Weight percentage of size fraction i
w/c	Water/cement ratio
x	Particle size (μm)
x_o	Particle size where R = 1/e = 36.79% (μm)
ρ	Apparent particle density (kg/m^3)

REFERENCES

1. Beke, B. : Principles of Comminution. Akadémaai Kiado, Budapest, 1964, pp 27
2. Onuma, E., and Furukawa, T. : O-Sepa - A New High Performance Air Classifier. World Cement 15 (1984), No. 1, pp 13-24.
3. Klumpar, I.V., and Zoubov, N.N. : New Sturtevant High Efficiency SD Classifier at Keystone Cement. World Cement 16 (1985), No. 8, pp 302 - 307.
4. Lukas, K.P. : MPS Roller Mills - Modern Grinding Plants for the Cement Industry. World Cement 14 (1983), No. 7, pp 266 - 270.
5. Beke, B. : Importance of Roller Milling in Cement Production. World Cement Technology (1982), pp 76 - 81.
6. Locher, F. W., Sprung, S., and Korf, P. : The Effect of Particle Size Distribution on the Strength of Portland Cement. Zement-Kalk-Gips, 26 (1973), No. 8, pp 349 - 355.
7. Wessel, H. F. : Quality Characteristics of Cements Ground in a Roller Mill. Zement-Kalk-Gips, 35 (1982), No. 8, pp 425 - 431.
8. Locher, F. W., Richartz, W., and Sprung, S. : Setting of Cement Part II : Effect of Adding Calcium Sulphate. Zement-Kalk-Gips, 33 (1980), No. 6, pp 271-277.
9. Locher, F. W., Richartz, W., Sprung, S., and Sylla, H. M. : Setting of Cement Part III : Influence of Clinker Manufacture. Zement-Kalk-Gips, 35 (1982), No. 12, pp 669 - 676.
10. Kuhlmann, K., Ellerbrock, H.G., and Sprung, S. : Particle Size Distribution and Properties of Cement Part I : Strength of Portland Cement. Zement-Kalk-Gips 38 (1985), No. 4, pp 169 - 178.
11. Sprung, S., Kuhlmann, K., and Ellerbrock, H.G. : Particle Size Distribution and Properties of Cement Part II : Water Demand of Portland Cement. Zement-Kalk-Gips 38 (1985), No. 9, pp 528 - 534.
12. Helmuth, R.A. : Phase I. Energy Conservation Potential of Portland Cement, Particle Size Distribution Control. Final Report, March 1979 Construction Technology Laboratories, Portland Cement Association, Stokie, Illinois, USA.

C. VERNET, Société des CIMENTS FRANCAIS - C.E.R.E.G. (FRANCE)

CUISSONS DE BELITE A BASSE TEMPERATURE - REACTIVITE

LOW TEMPERATURE SYNTHESIS OF BELITE - REACTIVITY

RESUME

Contrairement à l'alite, dont l'enthalpie libre de formation à partir de C_2S et CaO devient positive au-dessous de 1250°C, C_2S peut se former à basse température. Il faut alors trouver des conditions opératoires donnant une vitesse de réaction et une réactivité suffisantes. L'aspect cinétique du problème peut être abordé en recherchant la formation d'un liquide à basse température. Diverses méthodes permettent d'obtenir ce résultat au-dessous de 1000°C, mais la plupart ne permettent pas de produire des distorsions au réseau, et une bonne réactivité. Nous étudions ici les mécanismes pouvant conduire à ces distorsions à basse température. Il est possible par exemple d'obtenir des bélites réactives au-dessous de 800°C, dans un liquide constitué de $Ca(NO_3)_2$ fondu. La réaction commence dès 560°C et devient rapide dès 700°C. Le produit obtenu montre des raies D.R.X. larges, indiquant la désorganisation du réseau. Recuit entre 800°C et 1200°C, il se transforme en βC_2S, moins réactif avec des raies D.R.X. très fines. Il faut recuire au-dessus de 1200°C pour observer un nouvel élargissement des raies. Le même phénomène est observé lorsqu'on prépare βC_2S en milieu $CaCl_2$ fondu, ou à partir du chlorosilicate de LE CHATELIER $C_2S,CaCl_2$, et qu'on le recuit à température croissante. En considérant les processus de diffusion des impuretés et de relaxation des défauts de réseau, ceci nous amène à discuter les possibilités d'obtention de réseaux distordus, donnant des produits réactifs, dans trois gammes de température : 500-800°C, 800-1200°C, 1200-1500°C.

SUMÁRIO

Ao contrário da alita, cuja entalpia livre de formação a partir do C_2S e CaO torna-se positiva acima de 1250°C, C_2S pode formar-se em baixa temperatura.

É preciso então encontrar condições operatórias dando uma velocidade de reação e uma reatividade suficiente. O aspecto cinético do problema pode ser abordado procurando a formação de um líquido em baixa temperatura. Diversos métodos permitem obter esse resultado abaixo de 1000°C, mas a maior parte não permite produzir as distorções na rede, e uma boa reatividade. Nós estudamos aqui os mecanismos que possam conduzir a essas distorções em baixa temperatura. É possível, por exemplo, obter belitas reativas abaixo de 900°C, em um líquido constituído de $Ca(NO_3)_2$ fundido. A reação começa desde 560°C e torna-se rápida desde 700°C. O produto obtido mostra raias de DRX largas, indicando a desorganização da rede. Recozido entre 800°C e 1200°C, ela se transforma em βC_2S, menos reativo com raias de DRX muito finas. É preciso recozer acima de 1200°C para observar um novo alargamento das raias. O mesmo fenômeno é observado quando se prepara βC_2S em meio de $CaCl_2$, fundido, ou a partir do clorossilicato de Le Chatelier C_2S, $CaCl_2$ e que seja recozido em temperaturas crescentes. Considerando os processos de difusão das impurezas e da relaxação dos defeitos da rede, isso nos conduz à discutir as possibilidades de obtenção de redes distorcidas, dando produtos reativos, em três gamas de temperatura: 500-800°C; 800-1200°C e 1200-1500°C.

1 - INTRODUCTION

Il est peu probable que l'on parvienne un jour à fabriquer de l'alite, constituant le plus hydraulique du clinker portland, au-dessous de 1250°C. En effet, l'enthalpie libre de la réaction $C_2S + C \rightarrow C_3S$ est de l'ordre de +2,7 kcal.mol^{-1} à 25°C, et ne devient négative qu'au-dessus de 1200-1250°C /1/ /2/. Néanmoins, il existe un grand nombre d'applications pour lesquelles l'utilisateur peut se contenter d'une croissance plus lente des résistances mécaniques. Ceci est obtenu avec des liants bélitiques, fabriqués actuellement vers 1300-1350°C dans divers pays. Les études concernant ce type de liants ont montré que leur réactivité varie dans de larges proportions selon la trempe et la température de cuisson /3/ à /6/, ainsi que la teneur en impuretés /7/ à /12/, et la nature des matériaux de départ /13/ /14/.

Mais la fabrication de liants bélitiques pourrait être beaucoup plus économique : en effet, il est thermodynamiquement possible d'opérer à plus basse température, l'enthalpie libre de la réaction $2\ C + S \rightarrow C_2S$ étant très négative, même à température ordinaire (-43 kcal.mol^{-1} à 25°C). Cependant les conditions cinétiques pour exploiter les potentialités de cette réaction ne sont pas toujours satisfaites, et si C_2S est bien l'un des premiers produits formés dans les fours à ciment /15/, le taux de réaction reste faible s'il ne se forme pas de liquide favorisant la décarbonatation de la calcite et la dissociation de la silice. Dans de bonnes conditions, C_2S peut être obtenu dès 450°C /15bis/, mais il semble maintenant bien établi que la réactivité des bélites augmente avec la distorsion du réseau /16//17/, or ceci est habituellement obtenu avec des formes haute température /11/, /18/. Il n'est donc pas évident qu'il existe à basse température des conditions opératoires donnant une vitesse de réaction et une réactivité du produit suffisantes. Quelques tentatives ont été faites dans ce sens. D.BRETON /17/ a montré en 1978 que ceci peut être obtenu dès 750°C, en utilisant une silice fossile particulière (spongolithe), en ajoutant au cru une forte proportion de nitrate d'ammonium, ce qui accélère la décarbonatation de la calcite, et environ 5 % de sulfate de calcium. Bien que ce procédé ne soit pas industriellement rentable, compte tenu de la dépense d'énergie nécessaire pour recycler les vapeurs nitreuses, il nous a paru intéressant de reprendre l'une de ces variantes, pour étudier les mécanismes permettant d'obtenir des distorsions de réseau à basse température. En effet, dans l'intervalle 500-800°C, la vitesse de diffusion et l'agitation thermique sont beaucoup plus faibles que vers 1300-1400°C, ce qui devrait conduire au contraire à des réseaux moins distordus.

Nous avons donc porté une attention particulière à l'évolution du réseau en fonction de la température et cherché à élargir le champ expérimental. Pour cela, nous avons fait varier le rapport chaux/silice, qui d'après PANCRASI /15bis/ modifie la cristallinité du réseau, et comparé le comportement des bélites préparées par "voie nitrique" à celui du C_2S préparé au-dessous de 1000°C, soit en milieu $CaCl_2$ fondu, soit par hydrolyse du chlorosilicate C_2S, $CaCl_2$, réaction étudiée par LE CHATELIER, dès 1904 /19/ ("voie chlorhydrique").

2 - PARTIE EXPERIMENTALE

2.1 - SYNTHESE PAR VOIE NITRIQUE. METHODOLOGIE

L'utilisation de nitrate d'ammonium conduisant à une formation intermédiaire de nitrate de calcium /17/ nous avons choisi de partir directement de ce dernier. Ceci a l'avantage de supprimer l'étape de décarbonatation et d'augmenter la quantité de liquide présent à 560°C, ce qui facilite l'assimilation de la silice, et permet d'obtenir des bélites à très basse température.

Nous avons opéré, d'une part, avec des produits purs, les mélanges ayant des rapports C/S variant de 1 à 3, et d'autre part, en traitant à l'acide nitrique des crus de cimenterie dont le facteur de saturation était ajusté pour obtenir de la bélite comme seul silicate. Les essais ont été réalisés dans un four spécialement aménagé pour permettre la circulation des vapeurs corrosives contenant des oxydes d'azote. Lors de chaque cuisson, des prélèvements ont été effectués à différentes températures et des analyses cristallographiques ont été faites par diffraction X.

2.2 - RESULTATS

2.2.1 - Produits purs, 1ère série d'essais

Nous avons utilisé une silice hydratée très fine et du nitrate de calcium P.A., en ajoutant 5 % de gypse au mélange, pour obtenir un réseau déformé. Le mélange homogène a été introduit dans le four à 400°C, puis a subi une montée en température à la vitesse de 10°C.mn^{-1}

Le degré de distorsion du réseau de la bélite semble indépendant du rapport C/S. Il évolue essentiellement en fonction de la température (fig.1).

A 500°C, la silice a déjà subi des transformations, et donne un produit non identifié. Le nitrate et le sulfate de calcium sont présents.

A 600°C, le nitrate de calcium, qui commence à se dissocier vers 560°C a complètement disparu, en donnant un composé intermédiaire. Nous n'observons pas la formation de CaO libre lorsque le rapport C/S est inférieur ou égal à 2. Le sulfate de calcium est présent.

A 700°C, à la suite d'une réaction très rapide (quelques minutes), le produit intermédiaire précédent s'est transformé en bélite, montrant des raies diffuses. Le sulfate de calcium est présent.

A 800°C, les constituants majeurs restent les mêmes, mais l'allure du spectre X évolue alors avec le temps de cuisson. Les raies de la bélite s'affinent, en se rapprochant de celles de βC_2S. Les raies du sulfate de calcium s'amenuisent. Dans les mélanges avec C/S = 3, la spurrite sulfatique commence à apparaître. Dans les mélanges avec C/S = 1, il se forme de la wollastonite β, puis la variété α. Dans les mélanges avec C/S = 3, la spurrite sulfatique disparait vers 1100°C. Au-dessus de 1200°C, on observe un nouvel élargissement des raies de la bélite, coïncidant avec la transition $\alpha' \rightarrow \alpha C_2S$, et l'apparition de l'alite.

2.2.2 - 2ème série d'essais - Crus bélitiques

Les mélanges préparés à partir de crus de cimenterie montrent une évolution similaire, à laquelle s'ajoute la séquence de formation des aluminates et aluminoferrites, comportant la formation intermédiaire de $C_{12}A_7$ et de sulfoaluminate $(CA)_3CaSO_4$. Les crus contenant des gros grains de quartz réagissent plus difficilement que ceux qui contiennent uniquement des argiles.

Fig. 1 - SYNTHESE DE C_2S PAR VOIE NITRIQUE - EVOLUTION DE LA CRISTALLINITE EN FONCTION DE LA TEMPERATURE

Diagrammes DRX entre 2,5 Å ET 3 Å

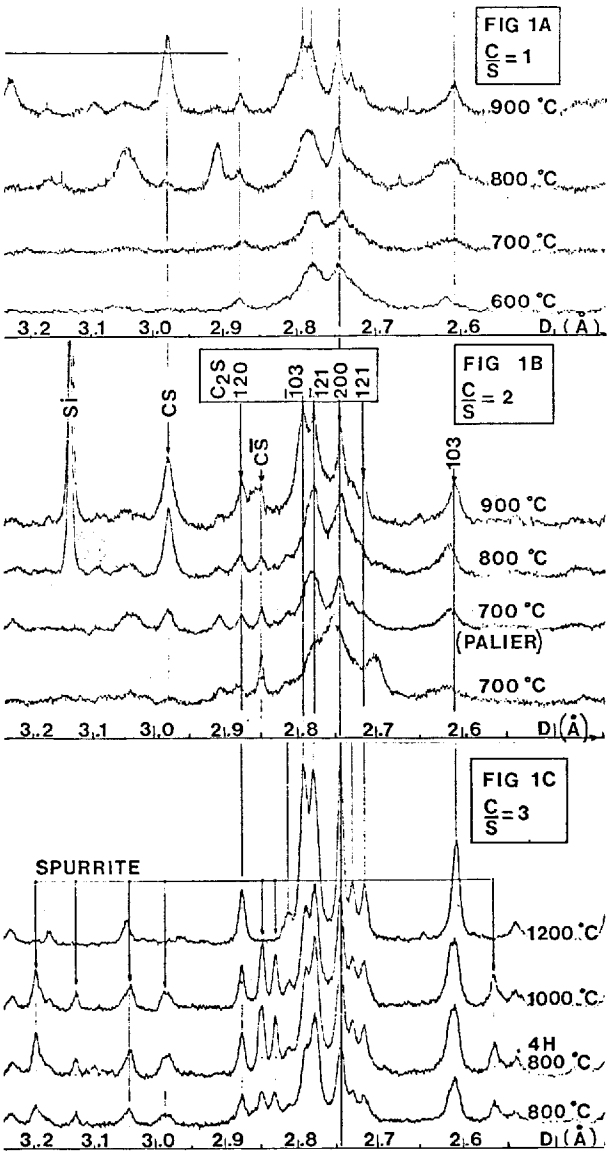

2.3 - SYNTHESE PAR VOIE CHLORHYDRIQUE

La combinaison de la silice est réalisée ici par formation intermédiaire de chlorosilicate $C_2S,CaCl_2$, dans un liquide à base de $CaCl_2$, dont le point de fusion est voisin de 700°C. Diverses réactions permettent d'obtenir facilement ce composé :

(1) $SiO_2 + 3\ CaCl_2 + 2\ H_2O \rightarrow C_2S,CaCl_2 + 4\ HCl$ (hydrolyse à 720°C)

(2) $SiO_2 + 2\ CaCL_2 + CaCO_3 \rightarrow C_2S,CaCl_2 + CO_2$ (à 720°C)

(3) $SiO_2 + CaCl_2 + 2\ CaCO_3 \rightarrow C_2S,CaCl_2 + 2\ CO_2$ (à 720°C)

Les 3 réactions ci-dessus peuvent être produites avec un excès de silice. Il se forme alors intermédiairement un peu de wollastonite. L'hydrolyse obéirait par exemple à une réaction du type :

(4) $2SiO_2 + 4CaCl_2 + 3H_2O \rightarrow C_2S,CaCl_2 + CS + 6HCl$

Les produits obtenus, recuits entre 940 et 1000°C donnent un βC_2S très bien cristallisé, avec une tendance à la transformation en gamma, qui peut être empêchée par ajout de sulfate de calcium (*Fig. 2*). L'hydrolyse permet d'obtenir des produits exempts de chlorure :

(5) $C_2S,CaCl_2 + CS + H_2O \rightarrow 2\ C_2S + 2\ HCl$

Comme dans le cas des synthèses nitriques, l'élargissement des raies n'est observé qu'au-dessus de 1250°C.

2.4 - SYNTHESE EN MILIEU $CaCl_2$ FONDU

Cette méthode présente l'inconvénient de donner un produit contenant du chlorure de calcium résiduel. Le silicate bicalcique se forme vers 700°C. La réaction est rapide au-dessus de 800°C et donne à 900°C un produit présentant des raies très fines, qui ne s'élargissent qu'au-dessus de 1250°C, avec formation d'alite (*Fig. 2*).

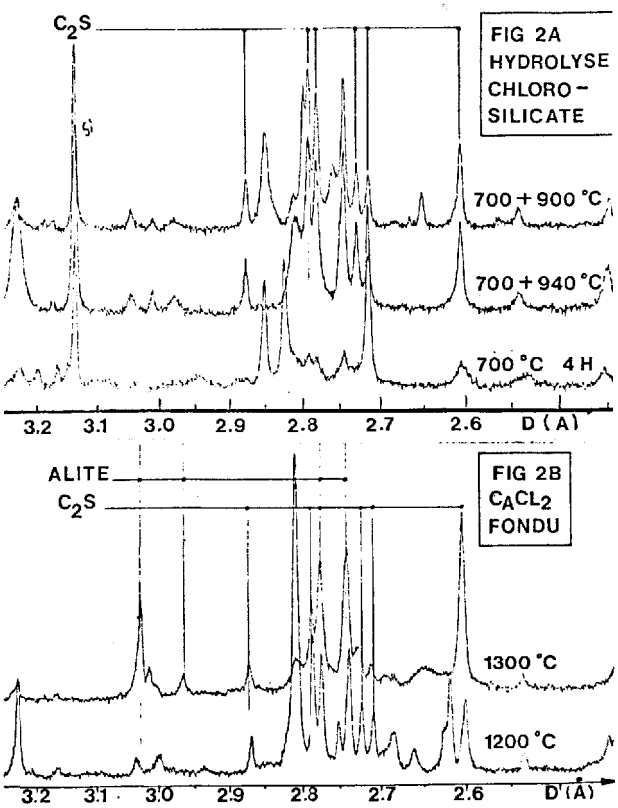

2.5 PROPRIETES HYDRAULIQUES DES PRODUITS OBTENUS

Nous avons effectué quelques tests d'hydraulicité sur les diverses bélites obtenues par les 3 méthodes de synthèse. En effet, s'il est admis que la désorganisation du réseau est une condition nécessaire à l'obtention d'une bonne réactivité, le travail de BRETON /17/ semble indiquer que cette condition n'est pas suffisante, et que la nature des produits de départ joue un rôle important. Nos mesures confirment ce point de vue. Parmi les produits précédents, ce sont les synthèses nitriques effectuées à partir de crus bélitiques (§ 2.2.2) qui montrent la meilleure réactivité, tant sur le plan cinétique que sur le plan des résistances. Ces échantillons ont un comportement intermédiaire entre celui du C_2S et celui des ciments portland (*Fig.3*). Les hydratés formés sont des produits habituels : CSH, portlandite, sulfoaluminates (*Photos 1 et 2*).

FIG 3 RESISTANCE EN COMPRESSION

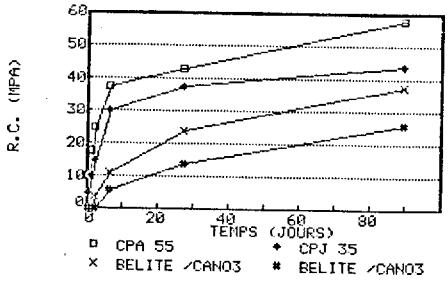

x Produits impurs

Photo.1 - Bélite nitrique hydratée 7 jours
E/C = 0,35. Morphologie du CSH

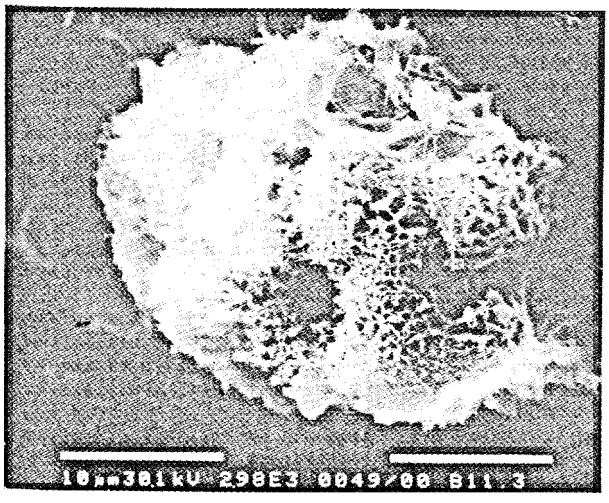

Photo. 2 - Même échantillon
Aspect des hydrates dans un pore



3 - INTERPRETATION. DISCUSSION

Les résultats précédents montrent que l'obtention de réseaux distordus et réactifs n'est possible que dans des conditions très précises. Ces conditions sont liées, d'une part, aux interactions avec le liquide générateur, qui s'inscrivent dans le cadre général des réactions sans les sels fondus /24/, et d'autre part, aux transformations des phases solides en fonction de la température, et à leurs conséquences sur la réactivité /25/.

Sous le premier aspect, deux faits expérimentaux nous paraissent essentiels :

- La très grande vitesse de réaction dans le nitrate de calcium fondu, ce qui semble indiquer l'intervention d'un mécanisme de dissolution/cristallisation;
- L'influence de la nature des produits de départ, et en particulier de la source de silice, ce qui n'est pas sans rappeler le problème des "précurseurs", produits intermédiaires de la fabrication des catalyseurs.

Ces deux faits sont apparemment contradictoires, car si l'on admet que les produits de départ sont dissociés au cours de la dissolution, il ne peut plus de produire d'effet de substrat, ce dernier ayant été détruit.

Pour lever cette contradiction, on est amené, soit à abandonner l'idée du mécanisme de dissolution/précipitation, soit à envisager une dissociation incomplète de la source de silice. Dans le premier cas, le mécanisme pourrait être du type "topotactique" et mettre en jeu la propagation interne de liaisons épitaxiques. Les impuretés présentes dans le réseau de départ se retrouveraient alors, avec une répartition sensiblement identique, dans le produit final. Dans le second cas, la silice étant répartie sous différentes formes dans les sels fondus, on peut penser que certains sels fondus, comme le nitrate de calcium, ne sont pas suffisamment dissociants pour briser des groupements du type Si-O-Al, par exemple. Ces groupements participeraient alors à la construction du nouveau réseau, au cours de la précipitation. Ce dernier mécanisme expliquerait bien la tendance à la cristallisation des produits synthétisés en présence de chlorures, qui sont des solvants très dissociants /24/.

Le deuxième aspect, à savoir l'évolution thermique du réseau, se résume alors aux phénomènes bien connus d'évolution des phases métastables. De nombreux exemples /25/ montrent que des phases métastables, souvent amorphes, sont obtenues dans un premier stade, lors des combinaisons d'oxydes à température relativement basse. Le recuit à température plus élevée, en permettant la relaxation des dislocations et la diffusion des impuretés vers les joints de grains, donne des phases mieux cristallisées. Ce n'est que par chauffage à température beaucoup plus élevée que l'on obtient ensuite des solutions solides, qui montrent à nouveau des réseaux désorganisés. Sur le plan énergétique, ceci correspond à la faible énergie d'activation de diffusion des dislocations (moins de 1 eV) par rapport à l'énergie d'activation de diffusion des impuretés (1 à 2 eV) et celle, encore plus élevée, de la création des défauts de réseau (4 à 5 eV). Ce comportement se traduit par l'existence de processus mécanochimiques induits par broyage, et par des changements de pente des droites représentant la loi d'Arrhénius, pour les coefficients de diffusion ou les conductivités électriques.

4 - CONCLUSIONS

La multiplicité des sels fondus ouvre un champ d'investigation très prometteur pour la synthèse à basse température de liants hydrauliques.
Dans le cas particulier de la bélite, notre étude permet de délimiter 3 domaines de température, dans lesquels la cristallinité et la réactivité des produits seront différentes :

T < 800°C. Dans ce domaine, la création de bélite mal cristallisée est possible si l'on choisit bien les conditions de synthèse, et en particulier le pouvoir dissociant du liquide. L'utilisation de produits initiaux très purs donne des bélites de réactivité moyenne, probablement à la suite de la ralaxation de certains défauts de réseau au cours du broyage, ou à des différences relatives à la nature des défauts. L'utilisation de produits initiaux impurs donne des bélites très réactives (les impuretés pouvant bloquer la relaxation des dislocations, et produire des défauts plus actifs, sur le plan énergétique).

800 <T< 1200°C. Ce domaine est peu favorable à l'obention d'une réactivité élevée, car la température est insuffisante pour activer la diffusion des impuretés extérieures au réseau, mais peut rendre la relaxation très rapide. Cependant, il n'est pas impossible que l'on puisse y obtenir des réseaux déformés. Il faudrait pour cela utiliser un sel fondu peu dissociant où la réaction soit très rapide, des produits de départ très impurs, et une trempe assez violente pour empêcher la relaxation des défauts.
T > 1200°C. Dans ce domaine, déjà utilisé, c'est la forme alpha qui est la plus réactive et les méthodes pour la stabiliser à température ordinaire sont bien connues.

BIBLIOGRAPHIE

/1/ LUDWIG U. ; WOLTERR A. "Formation and stability of C_3S and alites" - VIIth ISCC Paris, 1980, vol.2, thème 1, pp 1/99 à 1/103
/2/ JONS E.S. "Thermodynamic driving force for formation of tricalciumsilicate" - C.C.R., 1980, vol. 10, pp 103/106.
/3/ STARK J. "Uber aktiven belit-zement" Silikattechnik, 31, 1980, Heft 6, pp 168-171.
/4/ STARK J. et coll. "Existenzbedingungen von hydraulisch aktiven Belit-Zement". Zement-Kalk-Gips, Sept. 1981, n°9, pp 476-481.
/5/ FIERENS P. ; TIRLOCQ J. "Effect of synthesistemperature and cooling conditions of beta-dicalcium silicate on its hydration rate". C.C.R., 1983, vol.13, pp 41-48.
/6/ GHOSH S.N. et coll. "Low temperature OPC-type cement containing superhydraulic C_2S phase". C.C.R., 1984, vol 14, pp 437-438.
/7/ WELCH J.H. ; GUTT W."The effect of minor components on the hydraulic activity of the calcium silicates" Proc.4th ISCC, Washington, 1960, vol.1, pp 59-68.
/8/ YAMAGUCHI G. "Strength of mortars made from the modifications of Ca_2SiO_4". CAJ Rev. of the 17th Gen.Meet., Tokyo, 1963, pp 39-43
/9/ BIKBAU M.Y. "On hydration activity of silicates" VIth ISCC, Moscou, 1974, suppl.paper, section 2, 1-6, II-1, pp 1-13.
/10/ MATKOVIC B. et coll. "Reactivity of belite stabilized by $Ca_5(PO_4)_3OH$", VIIth ISCC, Paris, 1980, I-189 à I-194.
/11/ SUZUKI K. "Hydration of α, α', and β-dicalcium silicates stabilized with Na-Al, K-Al, Na-Fe, and K-Fe". VIIth ISCC, Paris, 1980, II-47 à II-51.
/12/ ABO-EL-ENEIN S.A. et coll. "Hydration and microstructural characteristics of β-dicalcium silicate". 7th I.C.C. of Microscopy, Fort-Worth, 1985, pp 255-266.
/13/ HEDVALL J.A. "Influence of solid state prócesses at relatively low temperatures in the production of cement and silicate products in general". VIth ISCC, Moscou, 1974, suppl.paper, section 1.
/14/ PASHCHENKO A.A. "Research in belite synthetized in the low temperature area". (ibid.), suppl.paper, section 1, 1-4.
/15/ CHATTERJEE T.K. et coll.. "Clinkerisation reactions in Portland Cement manufacture. A review of sequence and kinetics". Silicates Industriels, 1980, 4-5, pp 81-87.

/15bis/ PANCRASI et coll. "Increase of the reactivity of solids in the system CaO, Al_2O_3, SiO_2 by the sol gel technique". 10th ISRS, Dijon, 1984, pp 19-20.

/16/ STRUILLOU R. "Etude des possibilités de fabrication de liants hydrauliques entre 600 et 900°C". Rapport de recherche Ecole des Mines, Centre de Géologie de l'Ingénieur, Paris, Déc. 1975, pp 1-15.

/17/ BRETON D. "Contribution à l'étude d'un silicate dicalcique β très réactif synthétisé à 750°C". Thèse 3e cycle Univ. Paris VI, 29 Nov. 1978, pp 1-121.

/18/ REGOURD M. ; GUINIER A. "Cristallochimie des constituants du clinker de ciment portland". VIth ISCC, Moscou, 1974, Rev. des Mat. Constr., n° 695, 1975, pp 201-215.

/19/ LE CHATELIER H. "Recherches expérimentales sur la constitution des mortiers hydrauliques", Paris, 1904, Ed.Dunod.

/20/ KURDOWSKI W. "Formation des silicates bi et tricalciques jusqu'à température de 1300°C". Silicates Industriels, 1965, 30, pp 500-506.

/21/ Von R. CZAYA "Darstellung und kristallographische daten von $Ca_2SiO_4.CaCl_2$". Zeitschrift fur anorganische und allgemeine Chemie. Band 375, 1970, pp 124-127.

/22/ NUDELMAN B.I. "Clinker formation in calcium chloride melt". VIth ISCC, Moscou, 1974, suppl.paper, section I, I-4, pp 1-15.

/23/ PACKTER A. ; ZAIDI S.A. "The heterogeneous reactions of silica powders with calcium oxide solutions in calcium chloride melts to form βdicalcium silicate : kinetics and mechanisms". Silicates Industriels, 1981, N°9, pp 173-177.

/24/ CHARLOT G. ; TREMILLON B. "Les réactions chimiques dans les solvants et les sels fondus". Gauthier-Villars Ed., 1963.

/25/ Extended abstracts of the 10th International Symposium of the Reactivity of Solids, Dijon University, 1984.

S.N. Ghosh, V.K. Mathur, A.K. Parashar
National Council for Cement and Building Materials,
M-10, N.D.S.E. Part - II, New Delhi - 110 049. India.

Sub-Theme 1.3 - Microstructures and solid solutions of Low Temperature clinkers.

MICROSTRUCTURE ET SOLUTIONS SOLIDES DANS LES CLINKERS ELABORES A BASSE TEMPERATURE.

SUMMARY: Electron Microscopy with EDXA of cement clinker made in our laboratory furnace and pilot plant kilns using marginal grade plant raw materials at 1360°C revealed interesting microstructural features and solid solubility behaviour of silicate phases. High early strength cement was also obtained in some cases. Crystals of alites and belites were of irregular shapes. An apparent correlation of structural features with solid solubility of elements in the silicate phases appears to exist.

SUMÁRIO: Microscopia eletrônica com EDXA de clínquer de cimento feito em fornalha e em forno piloto em nosso laboratório, usando matéria-prima de graduação marginal da fábrica, a 1360°C revelou interessantes características microestruturais e o comportamento de solubilidade dos sólidos da fase silicato. Cimento de alta resistência inicial também foi obtido em certos casos. Cristais de alita e belita eram de formas irregulares. Uma correlação aparente entre as características estruturais e a solubilidade sólida dos elementos das fases silicatos parece existir.

INTRODUCTION

The synthesis of a reactive belite phase using low grade cement plant raw materials has been the main thrust in our research for quite sometime. Preliminary studies in this area were published (1,2). The present paper is an extension of these earlier studies besides the incorporation of pilot plant investigations. The clinkers obtained were primarily belitic in the bench scale pilot plant studies similar to our laboratory studies while a dry process pilot plant of 2.5 TPD capacity produced clinkers of both belitic and alitic composition.

EXPERIMENTAL

Cement grade limestone having low CaO content (~ 43%) from an Indian Cement Plant was used in conjuction with clay, which was not being used in the plant and has been dumped as a quarry waste. Proper raw mixes were prepared as per following moduli values :

Lime Saturation Factor	Silica Modulus	Alumina Modulus
LSF	Ms	Ma
0.76	2.33	1.23

The chemical composition of raw materials and raw mix is given in Table - 1.

Raw mix composition made out of these two component system passing 90 μm seive (~ 10 percent residue) were thoroughly mixed in a ball mill. Nodules of sizes 8 - 10 mm were obtained adding appropriate quantity of water in a pan nodulizer. The nodules were dried in an over at 100 ± 5°C for 2 hrs before being introduced in the laboratory furnace or bench scale pilot plant furnace - rotary furnace fired by oxy-acetylene gas (Cap. 2 kg/hr). Dry mixes as such were used in our experiments on oil fired pilot plant (Cap. 2.5 TPD) having four stage suspension preheaters and rotary grate coolers. Normal air quenching of clinkers was practised and very little dusting observed in laboratory or pilot plant clinker.

X-ray diffraction studies of the clinkers were conducted using Phillips X-ray diffractometer (PW-1120) having Cu-target and Ni filter for identification of phases. Electron microscopic studies (Phillips S (T) EM 301 G) with EDXA (707 B) were carried out on Au-coated clinker samples.

TABLE - 1

Raw Materials	Percent Chemical Composition							
	LOI	SiO_2	Al_2O_3	Fe_2O_3	CaO	MgO	Na_2O	K_2O
Limestone (1)	36.98	12.03	3.39	1.60	43.22	3.00	0.03	0.02
Limestone (2)	36.80	12.59	1.59	1.35	43.69	3.08	0.09	0.24
Clay (1)	9.89	52.57	18.99	10.32	4.38	1.55	0.55	2.17
Clay (2)	11.79	46.64	17.34	15.73	4.86	0.06	0.44	2.00
Clay (3)	14.48	40.84	12.69	15.38	10.83	1.90	0.84	1.58
Raw mix (Average)	34.00	16.00	3.80	3.07	39.00	2.70	ND	ND

RESULTS AND DISCUSSION

The chemical analysis of clinkers produced in the laboratory indicated the C_2S content 60% and C_3S content 12% as per Bogue calculation. The C_3S content in the pilot plant clinker was however higher (27%) and C_2S correspondingly lower (47%). This could possible be due to inadvertent lime-enrichment of the raw mix during preheating by slight loss of fine clay fraction. The oxide composition of laboratory, bench scale pilot plant, and dry process pilot plant is presented in Table - II.

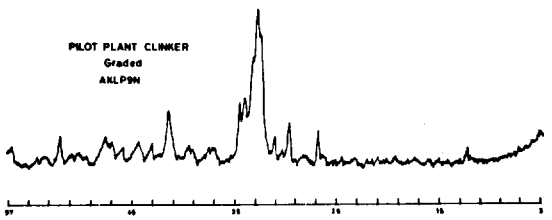

Fig. 1 : X-ray diffraction (2θ) trace of belite clinker

TABLE - II

Nature of Clinker	Percent Chemical Compositon							
	LOI	SiO_2	Al_2O_3	Fe_2O_3	CaO	MgO	Na_2O	K_2O
Lab. Clinker (1350°C)	1.00	24.12	5.78	4.63	59.08	4.10	0.20	0.60
Bench Scale Pilot Plant Clinker (1325-1350°C)	1.16	24.02	6.02	4.28	59.16	4.16	0.21	0.64
Pilot Plant (Dry Process) (1325-1365°C)	1.12	23.36	5.36	4.10	60.66	4.20	0.18	0.52

The X-ray diffractogram of the belite clinker is shown in Fig . 1. It will be seen that the intensity of the alite phase at 29.5 (2θ) and 51.8 (2θ) is very weak suggesting high belitic composition of the clinker.

The compressive strength data of belite cement from lab clinkers (IS: 269-1976) are as follows:

	1 Day	3 Days	7 Days	28 Days
kg/cm^2	144	320	460	548

W/C=0.385; Fineness (Baline's) = 3138 cm^2/g

Thus, the strength data point to the existence of reactive type of belite phase in the system. On examining the electron micrographs (Fig. 2) of the belite clinkers the above conclusion appears to be confirming. Elongated, tapered, Fig. 2 (a) and deformed (egg shaped, etc) morphology Fig. 2 (b) and 2 (c) of the belite crystals can be observed. The presence of α'-C_2S phase can be inferred from electron micrographs and also from X-ray diffraction trace (33° (2θ) peak).

The alitic clinker obtained from dry process pilot plant presented some interesting features. For example, the morphology of crystals as observed under electron microscope, Figs. 3 (a), (b) and (c) is different from that of normal alites. The compressive strength of cement obtained from pilot plant clinker are as follows:

	1 Day	3 Days	7 Days	28 Days
kg/cm^2	194	365	467	645
	(W/C = 0.38; fineness = 2934 cm^2/g			
	290	516	535	690
	(W/C = 0.39; fineness = 4009 cm^2/g			

The morphology and solid solution behaviour of the clinkers under study are given in Table 3.

TABLE - 3

Microstructure	Solid Solution Species	Fig.
Belitic compsotion		
Elongated Crystals	K, Fe	2 (a)
Egg -shaped crystals	K, Al, Fe	2 (b), (c)
Alitic Composition		
Rectangular crystals	Fe	3 (a)
Rod-like crystals	Fe, Cr, Al, Mg	3 (c)
Multifaced crystals (chopped off)	Al, Fe, Cr	3 (b)

Fe was found to be present in all silicate crystals as detected by EDXA. An apparent correlation between the morphology of the crystal and solid solution characteristics appears to exist. Dumb-bell shaped belite crystals contained Al, Cr, Fe in solid solution, rectangular shaped alites/belites contained only Fe in solid solution while elongated tubular belite crystals contained Al, Fe and Mg or K, Al and Fe in solid solution.

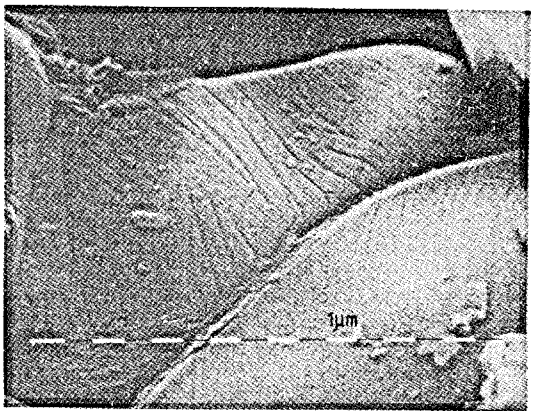

(a)

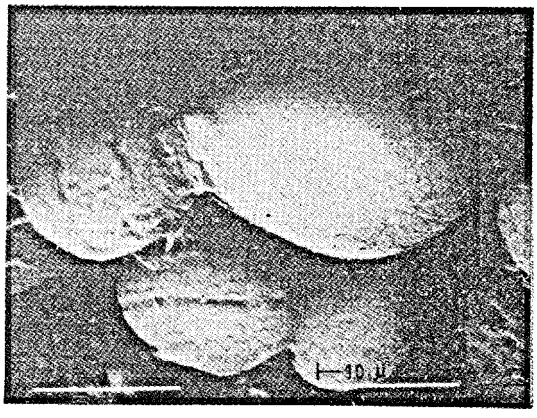

(b)

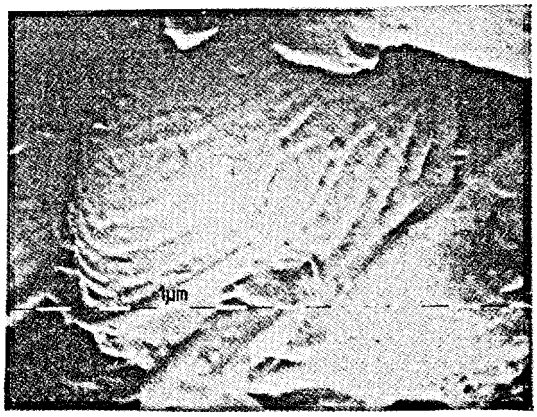

(c)

Fig. 2. Scanning electron micrographs of belite clinker

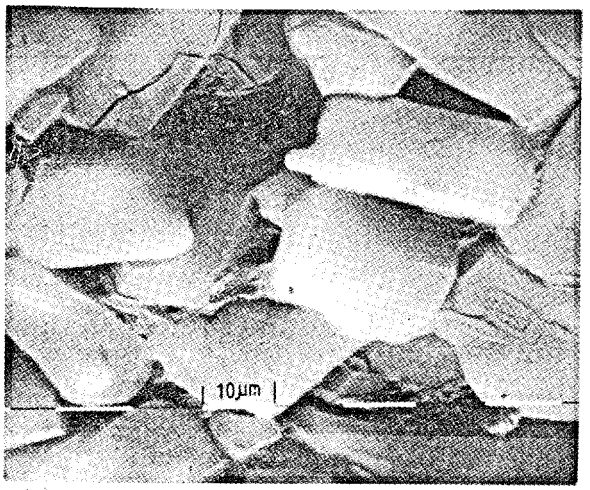

(a)

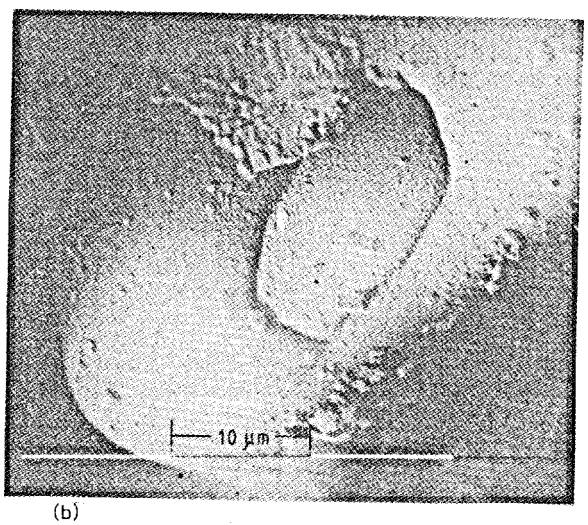

(b)

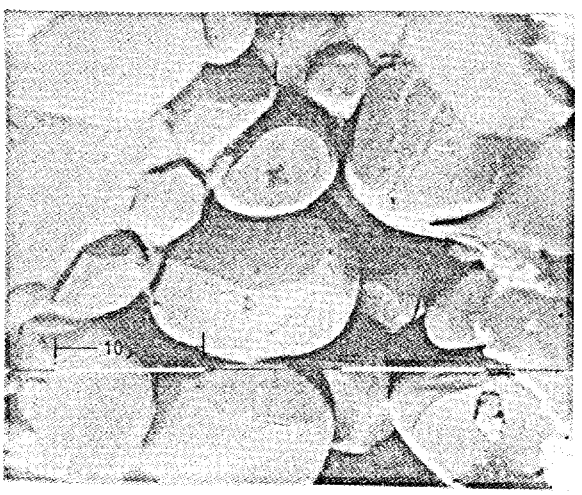

(c)

Fig. 3 : Scanning electron micrographs of low temperature (~1360°C) relatively alitic clinker.

CONCLUSION

Reactive belite cement and low temperature alitic cement prepared in the laboratory and in the pilot plants have irregular morphology leading to early development of strength.

ACKNOWLEDGEMENT

The authors have freely drawn upon completed R&D work/ status reports of NCB and some of the unpublished work of NCB. This paper is being published with the permission of the chairman and Director-General, NCB.

REFERENCES

1.- S.N. GHOSH, V.K. MATHUR, S.K. CHOPRA (1984). "Low temperature OPC type cement containing super hydraulic cement". Cement and Concrete Research, 14, 47.

2.- S.N. GHOSH (1985). "Hydration of Polymorphs of dicalcium silicate". Il Cemento, 82 (3), 139-146.

1.3

CHLORIDE SALTS AS REACTION MEDIUM FOR LOW TEMPERATURE CLINKERISATION - A PROBE INTO ALINITE TECHNOLOGY

R.K. AGARWAL, S.V. PARALKAR AND A.K. CHATTERJEE
The Associated Cement Companies Ltd.,
Central Research Station, Thane 400604, INDIA.

Abstract :

Although "chlorides" were recognised as "mineralisers" in clinker formation since the classical work of Le Chatelier, the practical application was inhibited on two accounts: less effectiveness of Cl in mineralising action compared to SiF_6^{2-}, F^- and SO_4^{2-} and apprehension regarding the corrosion effect of residual chlorides in clinker on concrete reinforcement. Lately the interest in the chloride salts as a reaction medium in clinkerisation has been revived with the development of Alinite technology in the USSR.

Samples of Alinite clinker and cement obtained from the USSR have been evaluated by the authors at the Central Research Station of The Associated Cement Companies Ltd. in India and the salient results of evaluation have been processed in the article.

In order to understand the fundamentals of clinker formation with chlorides as the reaction medium the following experiments have been conducted with the help of differential thermal analysis technique :

- Effect of increasing addition of $CaCl_2$ in the range of 0.8 - 11.7% on the reaction sequence of a given raw mix.
- Thermochemical changes of different raw mixes fired with the optimum dosage of $CaCl_2$.
- Combined effect of magnesium salts (in the form of carbonate, chloride or dolomite) along with $CaCl_2$ on the firing behaviour of a raw mix.
- Effect of non-calcium chloride salts and other combinations on the reaction sequence.

From the above experimental studies, an endeavour has been made to establish the fundamental course of reactions in lime combinability and formation of intermediate phases in the process and their breakdown. The extent of lowering of calcining and burning temperatures has been tentatively estimated. The problems and prospects of attaining the clinker/cement quality achieved through Alinite technology in the USSR have been highlighted.

SUMÁRIO

Embora os "cloretos" sejam reconhecidos como "mineralizadores" na formação do clínquer desde o trbalho clássico de La Chatelier, a aplicação prática era inibida por dois fatores: menor eficácia do Cl na ação mineralizante comparada com o SiF_6^{2-}, F^- e So_4^{2-} e a preocupação em relação ao efeito residual dos cloretos no clínquer sobre a corrosão no concreto armado. Posteriormente o interesse nos sais de cloreto como um meio de reação de clinquerização foi reavivada com o desenvolvimento da tecnologia da Alinita na USSR.
Amostras de clínquer de Alinita e de cimento obtidos na USSR foram avaliadas pelos Autores na "Central Research Station of The Associated Cement Companies Ltd" na India e os interessantes resultados de avaliação são apresentados neste trabalho.
Com o objetivo de compreender os fundamentos da formação do clínquer com cloretos como o meio de reação os seguintes experimentos foram realizados com auxílio da técnica da DTA:
- Efeito do aumento da adição de $Ca\ Cl_2$ nos limites de 0,80 a 11,7% na seqüência da reação de uma certa mistura crua.
- Alterações termoquímicas de diferentes misturas cruas queimadas com a dosagem ótima de $Ca\ Cl_2$.
- Efeito combinado dos sais de magnésio (na forma de carbonatos, cloretos, ou dolomita) com $Ca\ Cl_2$ no comportamento de queima da mistura crua.
- Efeito de sais não cloreto de cálcio e outras combinações na seqüência das reações.

Como resultado dos estudos experimentais acima, um esforço foi feito para estabelecer a seqüência fundamental das reações de combinação de cal e formação de fases intermediárias no processo de sua decomposição. A extensão da redução das temperaturas de queima e calcinação foi estimada aproximadamente. Os problemas e objetivos de atingir a qualidade do cimento e do clínquer obtida através da tecnologia da USSR, foram esclarecidos.

INTRODUCTION

In the context of the new development of the Soviet LTS or Alinite technology[1,2] an investigation was conducted by the R & D Division of the Associated Cement Cos. Ltd., the largest manufacturer of cement in India, on various fundamental aspects of clinkerisation in the Chloride Salt medium. Some of the salient features of this investigation are presented in this paper.

BROAD EVALUATION OF INDUSTRIAL ALINITE CLINKER

The Alinite clinker samples from the operating experimental commercial plant at Akhangaran in the USSR having a wet process kiln of 2.75 x 75 m size as well as from the dry process pilot plant at Tashkent, having a capacity of 24 TPD, were evaluated in the authors' laboratory with respect to compositional characteristics and phase stability. The chemical composition of the clinker samples lies in the following ranges :

S 22.7-23.3	A 4.4-4.6	F 3.6-4.8
C 62.5-63.9	M 2.0-2.2	LOI 0.7-1.0
Cl(total)1.0-2.9	Cl(free)0.04-0.12	
CaO(free) $\angle$ 0.5		

Unlike Portland clinkers, these samples were characterised by(i) Low C/S (2.74-2.75) and A/F(0.96-1.22) ratios, (ii)high levels of fixed chloride (iii) very low levels of free chloride. From subsequent detailed chemico-mineralogical examinations it was revealed that even when the total chloride content is one percent, the Alinite formation is quite appreciable and further the fluctuations in the free chloride levels in clinker has no relation with the total Cl content; in other words, at high levels of total Cl (say 2.9%) the free Cl was 0.04%. The X-ray diffractograms of these clinkers confirmed the presence of chloroaluminate and chlororthosilicate phases in addition to the primary Alinite phase.

The morphological and microstructural features of alinite clinkers do have strong resemblance with those of Portland clinker (see Plate 1), although certain features like zoning in Alinite crystals and simple twining with elongated crystal habit for chlororthosilicate phase are quite distinctive.

In order to ascertain the stability of alinite and other phases in LTS clinkers, a sample was subjected to reheating in electric static furnace which resulted in the following changes:

	Before Heating	1200°C	1400°C
% CaO(free)	0.5	3.0	0.80
% Cl^- (total	1.0	0.83	0.55
% Cl^- (free)	0.04	0.01	0.04
Intensity of Alinite X-ray reflection	100	85	Nil

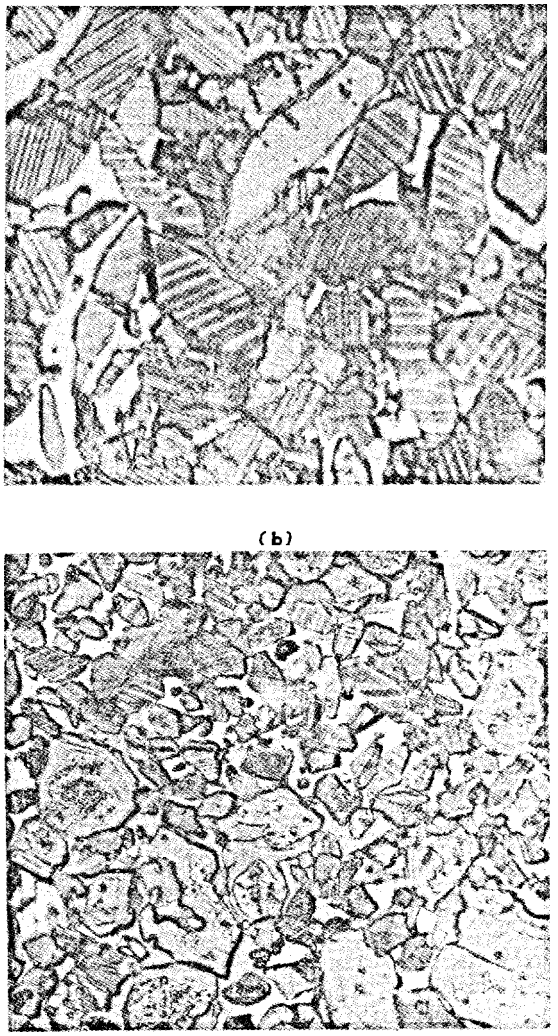

(b)

Plate 1 (a) Elongated chlororthosilicate with simple twining. Nital etch x 625

(b) Alinite crystals showing zoning and elongated chlororthosilicate with simple twining. Nital etch x 400

The experiment demonstrated (i) the instability of Alinite phase at temperatures between 1100-1200°C (ii) complete conversion of alinite to alite with loss of chloride at temperatures below 1400°C, (iii) rigid bond of chloride even in non-alinitic phases not permitting its loss even at 1400°C.

The reheat studies of alinitic clinkers by DTA/TG analysis (Fig.1) and Hot stage microscopy (Fig.2) also confirm the above observations and in addition indicate that alinitic clinkers on overheating may

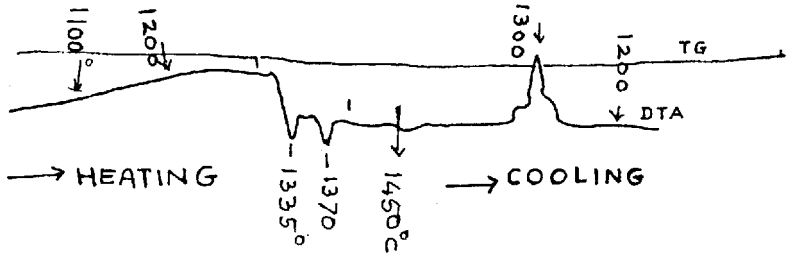

FIG. 1 DTA / TG : REHEAT STUDIES OF ALINITE CLINKER.

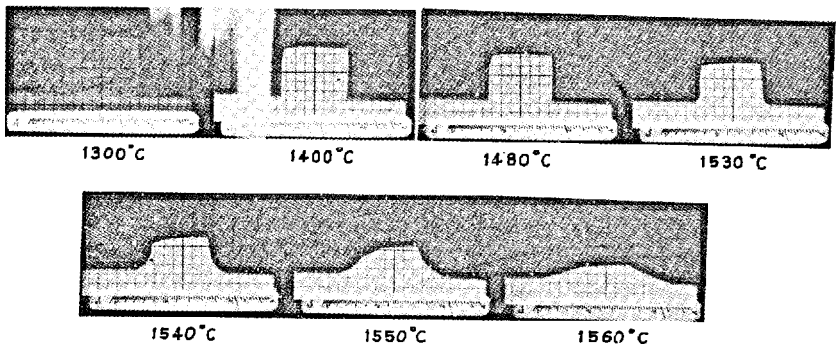

Fig. 2 : Reheat studies of Alinite clinkers by Hot stage Microscopy.

show the formation of oxidic melt phase around 1300°C and the thermophysical behaviour of alinitic clinker is no different from normal Portland variety.

REACTION SEQUENCE IN $CaCl_2$ MELT

The DTA studies (Fig.3) of a raw mix (RM1 in Table I) prepared with the addition of $CaCl_2$ in the range of 0.8 to 11.7% unfolded the following reaction concept :

- The addition of 6.6% $Cacl_2$ leads to the maximum reduction in the decarbonation peak area from 54.8Cm^2 in control sample to 36.4 Cm^2, the corresponding reduction in decarbonation temperature maximum being 35°C (Fig. 4).
- The DTA traces remain identical with all dosages of $Cacl_2$; the patterns vary only in magnitude.
- Apparently, the reaction sequence proceeds with
  - i) Loss of water of crystallisation from $Cacl_2$ at temperatures below 150°C.
  - ii) Formation and decomposition of $CaCO_3$. $CaCl_2$ at temperatures close to 570°C.
  - iii) Decomposition of $CaCO_3$ around 780°C.

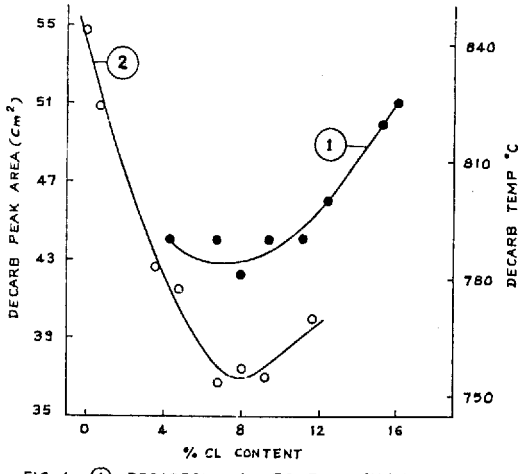

FIG. 4 (1)- DECARBONATION TEMP. Vs (%) Cl CONTENT
(2)- DECARBONATION PEAK AREA Vs (%) Cl CONTENT

- iv) Formation and decomposition of spurrite phase around 810°C.

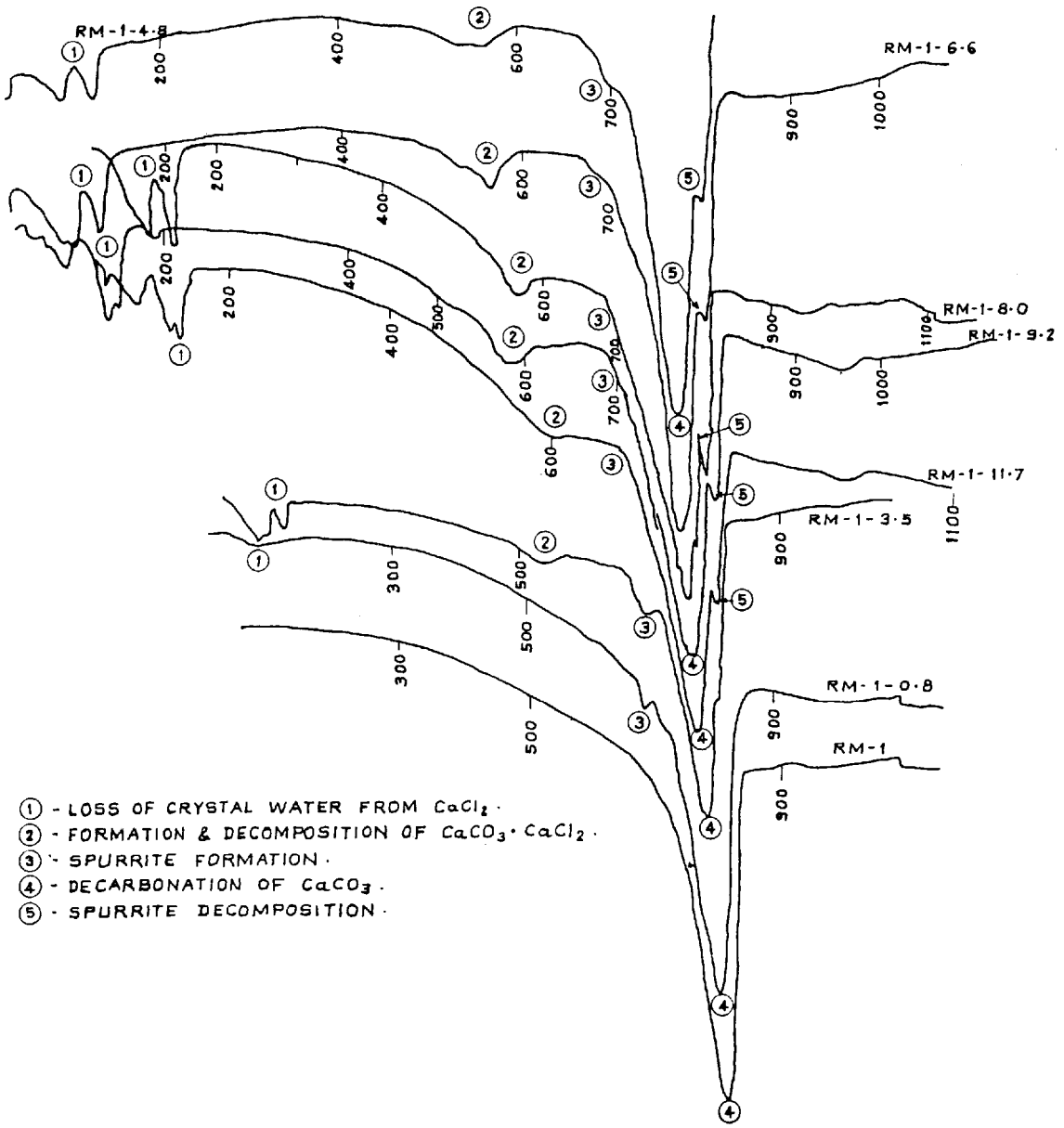

FIG. 3 THERMOGRAMS OF RM-1 WITH ADDITION OF $CaCl_2$

The above patterns of DTA traces were also observed to hold good when different raw mixes (Table I) were subjected to thermal analysis with optimum dosage of $CaCl_2$(6.0-6.6%)(Fig.5). In other words no changes in the basic reaction sequence was observed with changing composition of raw mixes.

Table-I : Composition of Raw Mixes

Sample No.	S	A	F	C	M	LOI
RM 1	12.4	4.0	2.6	42.8	1.2	35.2
RM 2	15.4	2.7	2.2	42.8	0.7	34.3
RM 3	15.3	4.0	0.35	42.2	1.0	35.6

As the DTA studies did not reveal a clear picture about the clinker phase formation, the products of firing of RM 3 with 6.5% $CaCl_2$ addition were subjected to X-ray Diffractometry(Fig.6). From Fig.6 it is evident that at 700°C the intensive diffraction reflections of raw mix minerals like calcite and Quartz are discernible, which gradually give way to spurrite formation at 755°C. Around 780°C, the new formation of calcium chloroaluminate ($C_{11}A_7CaCl_2$) is detected. Around 900°C the decomposition of spurrite and formation of chlororthosilicate and alinite become evident. With rise in temperature from 900 to 1400°C, the characteristic intensity of alinite reflection (d=2.81A°) gradually reduces and disappears at 1400°C, when the normal clinker phases are detected.

The above observations were also confirmed by repeating this experiment with firing of RM 2,

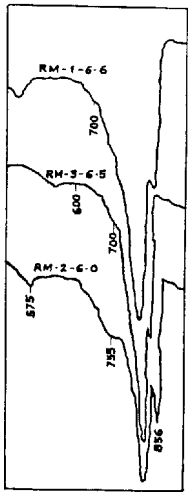

FIG·5. THERMOGRAMS OF DIFFERENT RAW MIXES

the results of which are not reproduced here for brevity.

The typical free lime combinability curves for such instances are shown in Fig.7, which shows that the lime combinability reactions in alinite clinker phase formation is sluggish under normal circumstances and should call for special measures. Needless to mention that with high temperature firing and conversion of alinite phase to normal alites, the lime combinability drastically improves.

EFFECT OF Mg SALTS, NON-$CaCl_2$ SALTS AND OTHER COMBINATIONS

In the preceding section, we have seen that the fired samples had high residual lime content. In order to improve upon lime assimilation process,

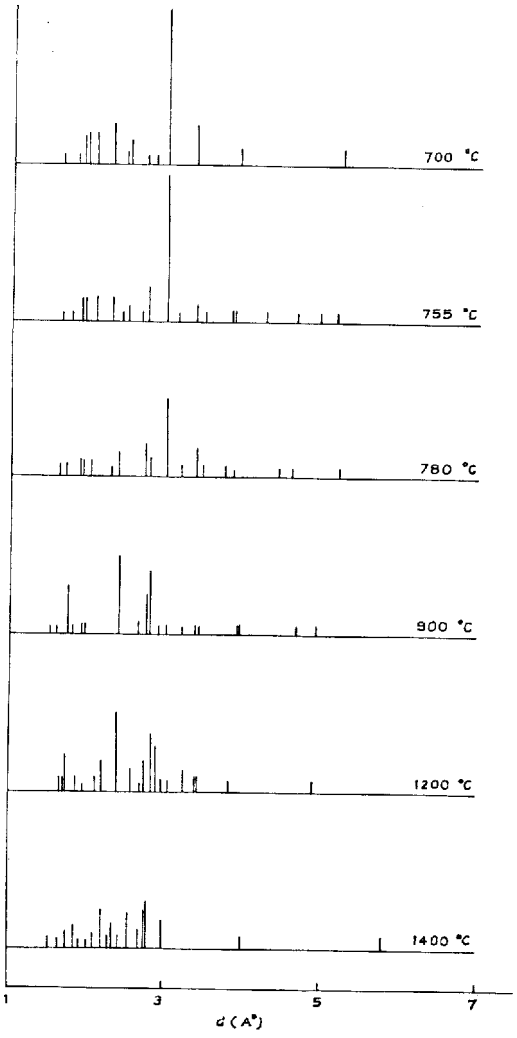

FIG·6 X-RAY POWDER PATTERNS FOR ALINITE ASLINE DIAGRAMS.

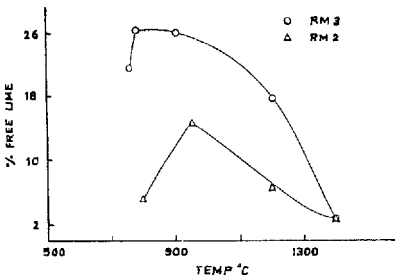

FIG. 7 CHANGE IN THE CONTENTS OF FREE LIME VS. TEMPERATURE

without losing sight of our main objective of energy savings, we tried additions of Mg salts and also non-calcium chloride salts in combination with $CaCl_2$ to RM 2, (Fig. 8) expecting an improvement in the melt properties.

It is seen that magnesium salts, irrespective of their form, when mixed with $CaCl_2$ are more effective as a mineraliser than $CaCl_2$ alone. The data given below, also shows that $MgCO_3$ and $MgCl_2$, both are equally effective in lowering the decarbonation temperature even though the total chloride is much lower than that of raw mix containing $CaCl_2$ alone.

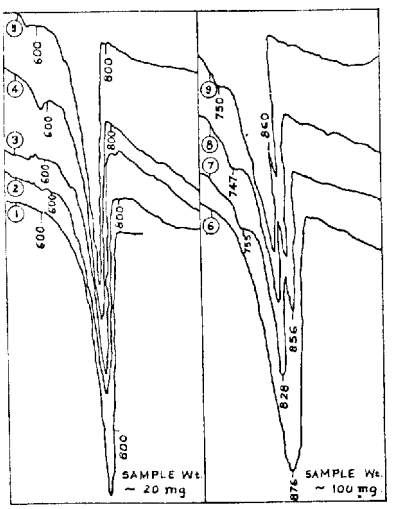

FIG 8 : THERMOGRAMS OF RM-2

①- RM-2 , ②- RM-2 - $CaCl_2$ - Na_2SO_4
③- RM-2 - $CaCl_2$ - K_2SO_4 , ④- RM-2 - $CaCl_2$
⑤- RM-2 - $CaCl_2$ - $BaCl_2$, ⑥- RM-2 , ⑦- RM-2 - $CaCl_2$
⑧- RM-2 - $CaCl_2$ - $MgCO_3$, ⑨- RM-2 - $CaCl_2$ - $MgCl_2$

It is also observed, on comparison of endo-peak area which is related to heat requirement for the calcination step that $CaCl_2$ alone and Mix $CaCl_2$-$BaCl_2$ has more or less same effect on the energy requirement. The decarbonation temperature is brought down to 775° from 815° for control sample. The raw mix containing alkali suphates along with $CaCl_2$ as additive has higher peak area indicating their less effectiveness to bring down the heat requirement.

Sample	Decarb. Temp. Max. °C	Decarb. Peak Area, Sq.Cm.	Additive %
RM 2	876	20.0	
RM 2 + $CaCl_2$	828	13.5	3.8 Cl
RM 2 + $CaCl_2$ + $MgCO_3$	828	7.0	2.2 Cl 2.2 MgO
RM 2 + $CaCl_2$ + $MgCl_2$	836	7.1	2.1 Cl 1.4 MgO
Control RM 2	815	13.9	
RM 2+$CaCl_2$	775	2.2	3.7 Cl
RM 2+$CaCl_2$ + $BaCl_2$	775	8.2	2.9 Cl
RM 2+$CaCl_2$ + K_2SO_4	775	9.33	3.7 Cl 1.8 SO_3
RM 2+$CaCl_2$ + Na_2SO_4	775	10.07	4.4 Cl 2.1 SO_3

CONCLUSION

From the fundamental lab-scale studies it appears that clinkerisation is possible at temperatures much below 1200°C with chloride salt as the reaction medium. However, in this process the lime combinability reaction appears to be sluggish under normal circumstances. Magnesium salt appear to improve the lime combination. In practical situations the residence time and judicious design of raw mix composition may become critical needs.

The optimum concentration of $CaCl_2$ when used as the reaction medium seems to be 6-7%. However, this concentration is what is needed inside a reactor and should be distinguished from the make-up dosage under practical conditions, depending on the internal or external recycles phenomena.

The formation temperature of alinite phase appears to be around 900°C under optimum conditions and the phase may be stable upto 1150°C. The formation and decomposition of alinite is not detectable in DTA curves, as probably these reactions get masked by other concurrent endothermic reactions. Regorous maintenance of firing temperature in a practical situation is essential for the stability of alinite.

The alinite clinkers are distinctly characterised by the presence of chloride in fixed and free forms. The presence of fixed chloride is not only in the

alinite phase but also in other silicate and aluminate phases. Very low levels of free chloride ($\angle$ 0.05%) are possible to achieve even when the total chloride in clinker is above 2.5%. With optimum dosages the fixation of chloride has little relation with the total chloride available in the system and hence is likely to be highly dependent on stability of operation of a kiln system. The fixation of chloride through proper burning is critical in achieving the optimum proportion of alinite in a clinker. In industrial clinkers the fixed chloride of 2.0-2.5% as generally maintain, would ensure 50-60% alinite formation.

The clinker reheat experiments revealed that the chloride fixation in non-alinitic phases is apparently structurally even more rigid as total removal of chloride could not be achieved even on reheating at 1400°C, when alinite phase had totally disappeared. All these are indirect evidences of lattice bond of fixed chloride which may presumably reduce the danger of their easy release on hydration.

ACKNOWLEDGEMENT

Participation in this study by Mr. V. Mohan and Mr. S.A. Khalidkar is greatfully acknowledged.

REFERENCES

1. B. Nudelman (1976) VI International Congress on the Chemistry of cement. "Clinkerisation dans la fusion de sel de la Chlorure de calcium" tome I, pp.217 - 221 (Russe)

2. M. Bikbaou (1980) IV, 7th International Congress on the Chemistry of cement "Mineral formation process and phase composition of alinite clinker", theme V, pp.285 - 290 (French)

N.M. JAVORONKOV,
O.P. MTCHEDLOV-PETROSSIAN,
N.P. KOGAN,
A.I. ZDOROV,
Y.G. IENTCH, Académie des sciences de l'URSS, Youjguiprociment, Kharkov, URSS

1

CLINKERISATION A BASSE CONSOMMATION D'ENERGIE LORS DE LA CUISSON DES MELANGES CONTENANT DU LAITIER NON BROYE

1.3

L'analyse de l'évolution de l'équipement pour la cuisson du clinker montre que le four rotatif restera la principale unité de fabrication du clinker. Afin de pouvoir déterminer la consommation totale de chaleur par ces unités aux différents stades et pour la cuisson du clinker, il faut savoir les effets thermiques correspondant à ces stades et à l'ensemble du processus. Le calcul de la consommation théorique de chaleur peut fournir une estimation fiable de l'efficacité de l'utilisation de divers déchets pour la fabrication du clinker. A cet effet, en se basant sur la formule de Zur-Strassen et une analyse méticuleuse des divers laitiers métallurgiques on a établi des coefficients nouveaux à l'aide desquels on peut donner une estimation énergétique concernant l'utilisation éventuelle de toute une série de scories métallurgiques. Les calculs montrent qu'en cas de remplacement du constituant argileux par une scorie, la consommation théorique de chaleur pour la formation du clinker se chiffre à 1 061 kJ/kg·kl., d'ou l'on conclut sur l'utilité de la mise en oeuvre de ces déchets pour la fabrication du ciment.

A análise da evolução do equipamento de cozimento do clínquer mostra que o forno rotativo continuará a principal unidade de fabricação do clínquer. A fim de poder determinar o consumo total de calor por essas unidades em diferentes estágios e para o cozimento do clínquer, é preciso saber os efeitos térmicos correspondentes a esses estágios e ao conjunto do processo. O cálculo do consumo teórico de calor pode fornecer uma estimativa confiável da eficácia da utilização de diversos resíduos para a fabricação do clínquer. Com esse objetivo, baseando-se na fórmula de Inz-Strassen e uma análise meticulosa de várias escórias metalúrgicas estabeleceu-se novos coeficientes com auxílio dos quais pode-se dar uma estimativa energética em relação à utilização eventual de uma série de escórias metalúrgicas. Os cálculos mostram que, em caso de substituição do constituinte argiloso por uma escória, o consumo teórico de calor para a formação do clínquer será de 1061 kJ/kg.kL, donde se conclui pela utilidade de por em uso esses resíduos para a fabricação do cimento.

N.M. JAVORONKOV,
O.P. MTCHEDLOV-PETROSSIAN,
N.P. KOGAN,
A.I. ZDOROV,
Y.G. IENTCH

L'analyse du développement de la technique de cuisson dans l'industrie du ciment permet de conclure que le four rotatif restera l'appareil principal de fabrication du clinker à l'avenir.

Une particularité du travail calorifique d'un four rotatif consiste dans le fait que la zone de combustion d'où se dégage la totalité ou la plus grande partie de l'énergie chimique du combustible coincide avec la zone de frittage de la matière où se déroulent des réactions exothermiques et il y a un important excès de chaleur. Grâce à cela la vitesse d'amenée de la chaleur à la surface de la matière est tellement grande qu'elle ne limite pas la vitesse de cuisson totale qui est aussi fonction de la vitesse du flux de chaleur à l'intérieur d'une particule de la matière en cuisson et de la vitesse d'interaction chimique. Cette fonction peut être présentée sous son aspect général à l'aide de l'équation ci-après:

$$K = \frac{1}{c\gamma/a_t + d/a + \delta/s + 1/K^r} \qquad (1)$$

où: K est la vitesse linéaire de la cuisson, m/s; c est la capacité calorifique de la matière, kJ/kg K; γ est la densité de la matière, kg/m^3; a_t est le coefficient de transmission de chaleur à la surface d'une particule, W/m^{2}K; d est la dimension d'une particule, m; a $-\lambda/c\gamma$ est la conductibilité de la température de la matière, m^2/s; δ est la dimension moyenne des grains du mélange, m; S est le coefficient de diffusion réduit, m^2/s; K^r est la vitesse réduite de l'interaction chimique, m/s.

Il résulte de la présente équation que l'utilisation dans la composition du mélange brut de sous-produits industriels et, en premier lieu, de laitiers sidérurgiques dont les indices thermophysiques sont supérieurs à ceux des minérais de ciment naturels conduira à une accélération de la vitesse de cuisson. L'introduction du laitier non broyé dans le four, même au stade de préparation de la matière contribue à une intensification de l'échange calorifique grâce à une baisse de la vitesse de mouvement de la matière et à une amélioration de la composition granulométrique dans la couche.

Le laitier non broyé représentant un système physicochimique indépendant dans la composition du mélange de ciment brut se fond à une température réduite et forme un bain fondu à faible viscosité (1). Il peut être considéré comme agent de transfert de chaleur et de masse efficace au stade de frittage du clinker. Ces propriétés du laitier ainsi que la présence dans les mélanges de laitiers bruts d'une quantité importante d'oxyde de calcium qui est déjà lié dans des composés silicieux, expliquent le fait que l'assimilation de la chaux dans l'intervalle de températures de 1523 à 1623 K y est plus complète que dans les mélanges dépourvus du laitier.

Pour déterminer la consommation de chaleur totale nécessaire à des stades distincts du processus et au processus de cuisson du clinker en entier on doit connaitre les effets thermiques correspondants propres à ces stades et au processus en entier. Le calcul de la consommation de chaleur théorique qui est l'article principal du bilan calorifique de tout processus thermochimique offre des difficultés dues à la détermination de la composition de phase et des températures de formation des composés faisant partie du laitier. Cela étant, on est amené normalement à admettre un nombre de suppositions de simplification. On considère, par exemple, l'argile comme du kaolin à inclusions de silice ou comme un mélange de minérais d'argile: kaolin, montmorillonite et illite et en ce qui concerne le laitier, on utilise sa composition de phase réduite à la moyenne (2).

Dans la composition des scories métallurgiques de remblai entrent, outre les oxydes de calcium, de silicium, d'aluminium et de magnésium, des oxydes de fer, de manganèse et leurs inclusions métalliques qui sont capables de s'oxyder dans l'atmosphère du four et, par conséquent, de dégager de

la chaleur. On doit en tenir compte lorsqu'on établit des équations des réactions chimiques de clinkérisation et lorsqu'on déduit des formules pour déterminer la chaleur théorique du processus. La formule connue de Zur-Strassen servant à déterminer la chaleur de clinkérisation théorique

$$Q_{cl}=17,21\ A_{cl}+32,01\ C_{cl}-21,42\ S_{cl}-2,466\ F_{cl} \qquad (2)$$

est applicable pour des mélanges de ciment bruts traditionnels à chaux-argile et la formule

$$Q_{cl}=17,21(A_{cl}-A_{lg})+32,01(C_{cl}-C_{lg})+3,71\ C_{lg}-3,6A_{lg}-14,14\ S_{lg}-21,42(S_{cl}-S_{lg})-2,466\ F_{cl} \qquad (3)$$

(lg est le laitier granulé)
pour des mélanges contenant du laitier granulé de haut fourneau constitué par C_2S, C_2AS, CS. Les calculs faits d'après la formule (3) ont montré qu'à une introduction de 18% de laitier granulé dans le mélange, on obtient une réduction de la chaleur de clinkérisation théorique égale à 347,5 kJ/kg cl. La précision de cette formule en tenant compte de la phase d'okermanite montre qu'on obtient dans ce cas une faible augmentation de la chaleur de clinkérisation de 17 kJ/kg cl. Cependant, une plus large utilisation de résidus métallurgiques en qualité de composants bruts du mélange de ciment qui contiennent des phases autres que le laitier granulé exige une introduction de nouveaux coefficients de calcul. Des études (3) réalisées ont établi qu'un nombre de scories métallurgiques de remblai sont représentées essentiellement par des mélanges cristallins tels que

C_2S, $CaO{\cdot}FeO{\cdot}SiO_2$(CfS),
$CaO{\cdot}MnO{\cdot}SiO_2$(CmS), C_2AS et FeO

Pour déterminer l'enthalpie d'une telle scorie, procédons de façon analogue (2) en décomposant les phases cristallines en oxydes isolés ce qui nécessite respectivement des chaleurs:

$C_2S=2CaO+SiO_2+736,33$ kJ/kg,

$CfS=CaO+FeO+SiO_2+565,64$ kJ/kg,

$CmS=CaO+MnO+SiO_2+438,78$ kJ/kg,

$C_2As=2CaO+Al_2O_3+SiO_2+475,22$ kJ/kg.

En décomposant la combinaison de phase donnée d'après la formule de Bogue (4) en oxydes isolés, obtenons:

$C_2S=1,536C-1,20f'-1,21m'-1,688A$

$CfS=2,62f'$

$CmS=2,63m'$

$C_2AS=2,688A$

où: f' est le FeO fixé dans $CaO{\cdot}FeO{\cdot}SiO_2$,
m' est le MnO fixé dans $CaO{\cdot}MnO{\cdot}SiO_2$.

En multipliant par chaleurs respectives de la décomposition et faisant la somme $Q_{C_2S} + Q_{CfS} + Q_{CmS} + Q_{C_2AS}$ obtenons:

$$1131C + 598,38f' + 263m' + 34,41A \qquad (4)$$

A la différence du laitier granulé, dans la scorie de remblai les combinaisons existent sous une forme cristalline ce qui permet de négliger la chaleur de dévitrification. En revanche, on doit tenir compte de la chaleur qui se dégage par suite de la suroxydation des oxydes ferreux et manganeux

$2FeO+0,5O_2-1816$ kJ/kg$=Fe_2O_3$

$2MnO+0,5O_2-1274$ kJ/kg$=Mn_2O_3$.

Dans ce cas, l'équation (4) prend la forme ci-dessous:

$$1131C+598,38f'+263m'+34,41A-1816f_\Sigma'-1274m_\Sigma \qquad (5)$$

où: f_Σ est la teneur totale du laitier en FeO;
m_Σ est la teneur totale du laitier en MnO.

En amenant les coefficients en conformité de l'équation (2), obtenons

$$11,31C+5,98f'+2,63m'+0,344A-18,16f_\Sigma-12,74m_\Sigma \qquad (6)$$

Alors:

$$17,21(A_{cl}-A_{sr})-0,866A_{sr}+$$
$$+32,01(C_{cl}-C_{sr})+11,787C_{sr}+$$
$$+5,98f'+2,63m'-18,16f_{\Sigma}-12,74m_{\Sigma}-$$
$$-21,42S_{cl}-2,466F_{cl}. \qquad (7)$$

(sr est la scorie de remblai).

L'introduction d'un laitier à composition chimique: SiO_2 = 30,33 %; Al_2O_3 = = 2,43 %; MnO = 15,148 %; FeO = 11,87 %; CaO = 33,73 %; MgO = 6,51 % en quantité de 3, 6, 12, 18 et 36 % permet de réduire la consommation théorique de chaleur pour la clinkérisation (tabl. 1).

Comme le montrent les données du tableau, le remplacement du composant argileux par le laitier donne une consommation théorique de chaleur de clinkérisation de 1061 kJ/kg cl. Ainsi, lorsqu'on se sert de la formule de Zur-Strassen pour déterminer la consommation théorique de chaleur de clinkérisation, on doit y introdure de nouveaux coefficients qui sont en fonction de la composition de phase concrète du laitier à utiliser. Les calculs montrent qu'au point de vue de la réduction d'énergie nécessaire à la fabrication du clinker, l'introduction du laitier métallurgique dans la composition du mélange brut de ciment Portland nous paraît bien justifiée. En même temps, la résolution de ce problème est impossible sans une étude détaillée de l'influence que le laitier exerce en tant que constituant sur tous les stades du processus technologique de cuisson du clinker et des processus physicochimiques de clinkérisation.

Tableau 1

Consommation théorique de chaleur de clinkérisation en fonction de la quantité de laitier à introduire

Fraction en masse du laitier, % en masse	Consommation théorique de chaleur de clinkérisation	
	kcal/kg cl	kJ/kg cl
0	416	1742
3	402	1683
6	382	1599
12	340	1422
18	317	1326
36	253	1061

REFERENCES

1. Интенсификация процесса получения цементного клинкера за счет обжига шихты, состоящей из независимых исходных физико-химических систем (Н.П. Коган), О.П. Мчедлов-Петросян, А.И. Здоров и др. - ДАН СССР, 1978, № 2, 238 (en russe).
2. Zur-Strassen, H. Der theoretische Wärmebedarf des Zementbrandes. - Zement-Kalk-Gips, Nr. 1, S. 1-12, 1957.
3. Енч Ю.Г., Коган Н.П., Мчедлов-Петросян О.П. - возможности использования отвальных доменных шлаков. - Цемент, 1983, № II (en russe).
4. Bogue, H.R. The Chemistry of Portland Cement -- New York, 1955.

L.G. SOUDAKAS,
U.V. NIKIFOROV,
M.V. KOUGIA,
N.A. SOKOLOVA, Guiprocement, Léningrad, URSS

1

1.3

ETUDE DES CLINKERS A BASSE BASICITE

Dans la communication, les auteurs analysent les résultats des recherches de laboratoire, semi-industrielles et expérimentales des clinkers peu basiques (KS est inférieur à 0,84).

On présente les caractéristiques thermodynamiques et cinétiques d'obtention des clinkers ayant une large gamme de compositions, on évalue la chaleur théoriquement nécessaire à leur cuisson.

On considère les particularités des caractéristiques physico-mécaniques des clinkers en fonction des conditions d'obtention et de l'état des minéraux dans le clinker.

La diminution de basicité des clinkers est une direction parmi les plus importantes pour résoudre les questions d'abaissement de la consommation de combustible pendant la production du ciment.

Sumário

Na comunicação, os autores analisam os resultados das pesquisas em laboratório, semi-industriais e experimentais de clínqueres pouco básicos (KS é inferior a 0,84).

Apresentam-se as características termodinâmicas e cinéticas de obtenção de clínqueres tendo uma larga faixa de composições, e avaliou-se o calor teoricamente necessário ao seu cozimento.

Foram consideradas as particularidades das características físico-mecânicas dos clínqueres em função das condições de obtenção e do estado dos minerais no clínquer.

A diminuição da basicidade dos clínqueres é uma direção, entre as mais importantes, para resolver as questões sobre o abaixamento do consumo de combustível durante a produção do cimento.

L.G. SOUDAKAS,
U.V. NIKIFOROV,
M.V. KOUGIA,
N.A. SOKOLOVA

Introduction. Au cours des dernières années, du fait de l'accroissement de l'importance du problème des ressources naturelles, on note l'augmentation de l'intérêt pour l'élaboration des technologies peu consommantes en combustible et énergie dans l'industrie cimentière. L'une des voies pour la réalisation de l'objet désigné réside dans la modification de la composition de phase traditionnelle de clinker de ciment.

Certes, la perspective de l'obtention et d'utilisation des clinkers à basse basicité est conditionnée par des facteurs tels que le gain énergétique possible et l'obtention de l'activité hydraulique assez haute du ciment durci. Pour répondre aux questions posées, l'institut Giprotzement réalise une étude systématique des clinkers à basse basicité, dont une partie des résultats est entrée dans la présente communication.

Caractéristiques thermodynamiques et cinétiques. Pour apprécier les avantages des clinkers à basse basicité vis-à-vis des dépenses énergétiques les chaleurs de clinkérisation ont été calculées selon l'équation suivante:

$$q_{cl.}=7,70+5,13(A-S)-0,59F+92,9 \text{ kJ/kg.cl.}$$

où C, A, F et S - teneur en oxyde du clinker en mass %.

Les calculs ont été faits pour une large gamme des compositions ayant le coefficient de saturation KS de 0,90 jusqu'à 0,76, MS = 1,8÷3,0, MA = 1,0÷2,0. La figure 1 montre que l'abaissement de la basicité des clinkers et l'optimisation de leur composition selon le module silicique MS et alumoferrique MA font possible la diminution de la chaleur de clinkérisation de 8 à 12%.

Pour le contrôle expérimental des résultats obtenus il a été déterminé la chaleur de dissolution des échantillons réels des clinkers à basse basicité et à base de celle-là les valeurs de la chaleur de formation des minéraux ont été établies. Les études réalisées ont confirmé les tendances établies par calcul, et elles ont montré que du point de vue thermodynamique les compositions qui se caractérisent par KS = = 0,76÷0,80 et par MS avoisinant à 3 et MA égal à 1,0÷2,0 sont les plus avantageuses.

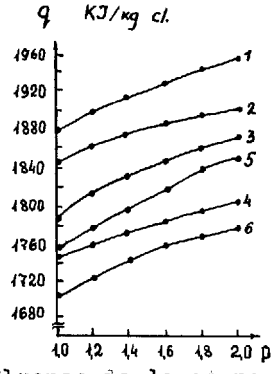

Fig. 1. Influence de la composition chimique sur la chaleur de clinkérisation
1 - KS = 0,90, MS = 1,8;
2 - KS = 0,90, MS = 3,0;
3 - KS - 0,80, MS = 1,8;
4 - KS = 0,80, MS = 3,0;
5 - KS = 0,76, MS = 1,8;
6 - KS = 0,76, MS = 3,0.

La cinétique de la consommation de la chaux lors de la cuisson du clinker à basse basicité en comparaison de la composition traditionnelle est présentée sur la figure 2. Les résultats cités montrent qu'à l'abaissement du coefficient de saturation KS de 0,90 jusqu'à 0,76, les modules silicique et alumoferrique étant invariables, la clinkérisation s'est achevée aux plus basses températures (jusqu'à 100°); pour les compositions dont KS était inférieur à 0,90 on a noté une combinaison plus rapide de la chaux.

Production du clinker et son activité hydraulique. 39 compositions ont été synthétisées dans les limites des variations des caractéristiques chimiques cités ci-dessus. Les cuissons ont été effectuées dans le four à silite à la vitesse de la montée en température de 5K par minute (à partir de 873K), les échantillons étant conservés pendant 30 minutes à la température limite désirée. Chaque composition a été refroidie selon 2 régimes: rapide (vi-

L.G. SOUDAKAS,
U.V. NIKIFOROV,
M.V. KOUGIA,
N.A. SOKOLOVA

Tableau

Caractéristiques physico-mécaniques des clinkers semi-industriels
(mélange avec 5% du gypse)

N° de série	N° d'ordre	Caractéristique du clinker				Epaisseur normale	E/C	Affaissement du cône	Résistance à la compression (MPa)			
		KS	n	p	CaO_{libre}				1 jours	3	7	28
I	1	0,90	2,2	1,2	2,4	25,00	0,40	114	14,7	29,3	37,9	52,4
	2	0,81	2,2	1,1	0,40	23,50	0,40	113	8,8	18,4	24,4	42,7
	3	0,80	3,1	1,0	0,90	22,25	0,38	113	9,3	14,3	21,7	49,9
II	4	0,90	2,3	1,1	0,60	24,00	0,40	114	-	32,1	40,9	58,0
	5	0,76	2,1	1,0	0,20	24,25	0,40	115	-	13,5	19,3	48,7
	6	0,76	3,0	1,2	0,20	24,50	0,40	114	-	15,7	21,2	49,6
	7	0,82	3,1	1,2	1,20	23,50	0,40	114	-	23,3	29,2	51,2
III	8	0,80	3,01	1,37	1,8	22,25	0,40	113	-	13,1	16,3	31,8
	9	0,80	2,56	1,21	0,50	22,00	0,40	115	-	17,2	21,8	37,9

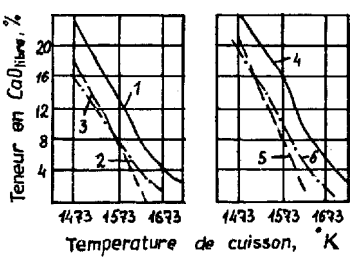

Fig. 2. Influence de la composition chimique sur la cinétique de consommation de l'oxyde de calcium
1 - KS = 0,90, MS = 1,8, MA = 1,0;
2 - - KS = 0,80, MS = 1,8, MA = 1,0;
3 - KS = 0,80, MS = 3,0, MA = 1,0;
4 - KS = 0,90, MS = 3,0, MA = 2,0;
5 - KS = 0,80, MS = 1,8, MA = 2,0;
6 - KS = 0,80, MS = 3,0, MA = 2,0.

tesse de montée - 400÷600 K/min) et lent (V ≈ 5 K/min). La figure 3 montre qu'à partir de clinkers rapidement refroidis on obtient des ciments de plus haute qualité.

Après 28 jours du durcissement la résistance des ciments obtenus à partir des clinkers qui, du point de vue thermodynamique, étaient les plus avantageux, n'a pas été inférieure à 42 MPa.

Par cuisson dans un four rotatif (pas grand) des parties des clinkers ont été produites à la vitesse de refroidissement identique à celle adoptée dans les expériments de laboratoire. Présentés dans le tableau, les résultats des essais physico-mécaniques des ciments à base de ces clinkers confirment les conclusions faites par les études de laboratoire sur la possibilité de l'obtention stable des valeurs A_{28} n'étant pas inférieures à 42 MPa. Pourtant certains échantillons n'avaient pas eu des caractéristiques satisfaisantes. Pour l'étude de la nature des variations de la propriété fondamentale les analyses microscopiques et de phase aux rayons X des échantillons ont été effectuées et la cinétique du dégagement de chaleur lors d'hydratation a été déterminée.

Etat des phases minérales. La formation du bélite de forme α' [1], hydrauliquement active, à haute température est estimée comme le facteur principal qui conditione les caractéristiques de résistance satisfaisantes des ciments obtenus à partir des clinkers à basse basicité. Parmi les méthodes possibles pour la stabilisation des modifications à haute température du silicate bicalcique celle qui a été reliée au refroidissement intense du clinker pour l'obtention

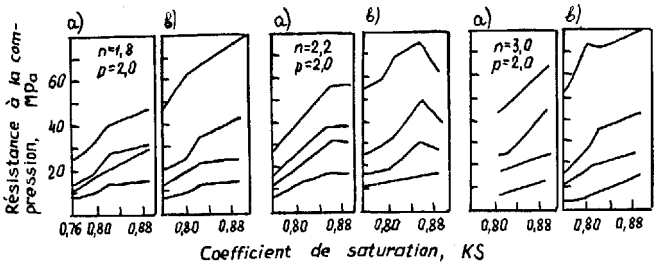

Fig. 3. Activité hydraulique des clinkers lentement (a) et rapidement (b) refroidis à la composition chimique variable

du α'-C_2S a fait l'objet du présent travail. En effet, l'analyse par fluorescence X des clinkers de laboratoire a montré que la partie bélite dans les échantillons rapidement refroidis est représentée par la forme α'. β-C_2S, étant une seule variété polymorphe du silicate bicalcique, a été révélé dans certains échantillons lentement refroidis.

Dans les clinkers de synthèse semi-industrielle, malgré le refroidissement aux grandes vitesses, α'-C_2S n'a pas été identifié dans de nombreux échantillons bien qu'ils aient atteint une assez haute activité hydraulique.

L'étude microscopique détaillée des sections polies des clinkers de laboratoire et semi-industriels, compte tenu de leurs propriétés physico-mécaniques, a permis d'établir qu'il y a des facteurs supplémentaires et, en premier lieu, se sont la morphologie des phases et la microstructure du clinker.

Auparavant, sur des compositions traditionnelles a été montré que ces caractéristiques sont étroitement liées aux conditions de cuisson [2]. Le même phénomène a été marqué pour des clinkers à basse basicité. Ainsi, dans les échantillons de la cuisson en laboratoire lors du refroidissement lent, tous les autres indices étant égaux, la présence du bélite friable, crénelé, souvent finement écailleux et de l'alite mal formée,

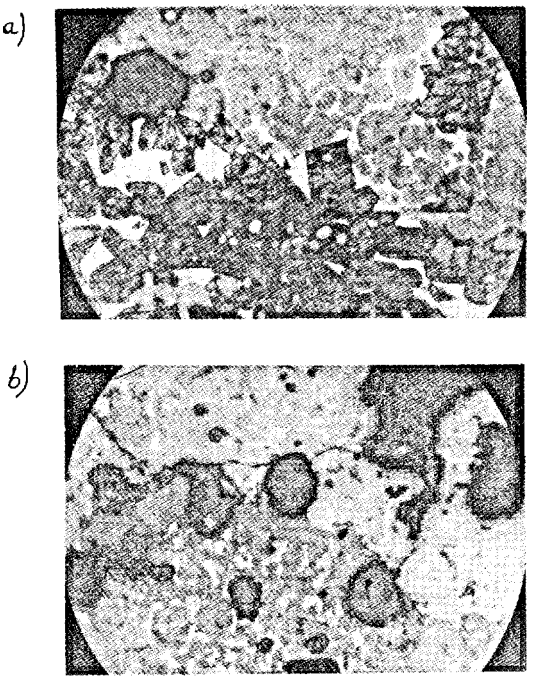

Fig. 4. Microphotographies des clinkers à basse basicité

donnant en général une microstructure peu nette, a été notée. Lors du refroidissement rapide se sont formés: le bélite rond, aux bords denses et l'alite bien différenciée, la cristallisation étant nette.

Obtenus par les expériments semi-industriels, identiques par leurs compositions de phase calculées et réelles, mais se diffèrent par leur microstructure (fig. 4) les clinkers se distinguaient par leur activité chimique lors de l'interaction avec de l'eau, ce qui a fait apparaître la différence des valeurs de A_{28} jusqu'à 10-15 MPa.

Ainsi, il a été déterminé que l'activité hydraulique assez haute des clinkers à basse basicité peut être assurée aussi, sauf la stabilisation haute température de C_2S en α'-modification, par la microcomposition favorable des grains et la morphologie des minéraux du clinker.

BIBLIOGRAPHIE

1. Stark J., Müller A., Schrader R., Rumpler K., Dahm B. "Über aktiven Belit-Zement", Silikattechnik, 1980, H. 2, 50-52.

2. Volkonski B.V., Soudakas L.G., Kraplia A.F., Bernstein L.G. "Contrôle de la microstructure et de l'activité des clinkers", 7 Congrès International de la Chimie des Ciments", 1980, V. II, 1-17.

V.B. KHLOUSOV, NIICement, Moscou, URSS

CLINKER ALITOSULFOALUMINEUX: REALISATION ET PROPRIETES

1

1.3

Il est connu que des températures de la formation de sulfoaluminate de calcium et de l'alite se diffèrent beaucoup.

Dans le présent travail l'auteur analyse des conditions de l'obtention simultanée de l'alite et de sulfoaluminate.

Des résultats sur la cinétique de la formation des minéraux, ainsi qu' une courbe du durassement du ciment à base des clinkers industriels cuits dans le four rotatif 4,5x170 m sout presentés.

É sabido que as temperaturas de formação do sulfoaluminato de cálcio e da alita são muito diferentes.

No presente trabalho o autor analisa as condições de obtenção simultânea da alita e dos sulfoaluminatos.

Os resultados sobre a cinética da formação dos minerais, bem como uma curva do endurecimento do cimento de clínqueres industriais cosidos em forno rotativo de 4,5 x 170 m, são apresentados.

1.3

L'industrie cimentière soviétique se propose comme buts, de l'un côté la réduction de la consommation énergétique, de l'autre côté - l'amélioration de la qualité du ciment.

Ces deux problèmes peuvent être résolus, à un certain degré, par l'organisation de la production des ciments alitosulfoalumineux qui ont la basse température de cuisson du clinker et des propriétés de construction améliorées.

Il est connu (1) que la présence de sulfoaluminate de calcium dans le ciment assure l'accélération considérable du durcissement, en particulier, dans les premiers heures et jours. Le durcissement de tels ciments se produit sans retrait et expansion à densité élevée de la pierre de ciment, et la présence de l'alite crée des conditions pour la croissance active de la résistance dans des délais ultérieurs et pour la formation de $Ca(OH)_2$ lors du processus d'hydratation activant la formation de l'ettringite.

Pourtant, l'obtention simultanée de l'alite et de $C_4A_3\bar{S}$ est compliquée parce que $C_4A_3\bar{S}$ se forme activement à 1200-1250°C et se décompose à 1300°C, tandis que la formation de l'alite à partir des crus ordinaires commence à 1400-1450°C.

Le but de ce travail consistait en création des conditions nécessaires pour la formation précoce de la phase liquide à haute réactivité assurant la formation de l'alite à températures moins élevées. En même temps la composition du cru doit assurer la formation de $C_4A_3\bar{S}$, c'est-à-dire une teneur en Al_2O_3 et $CaSO_4$ doit être suffisante. C'est pourquoi les crus destinés à obtenir les clinkers alitosulfoalumineux étaient préparés partiellement à partir des matières premières naturelles et partiellement à partir des déchets industriels riches en oxyde d'aluminium et contenant de certains fondants.

Il est connu (2) que le taux de l'achevement des processus de la formation d'alite est une fonction de la vitesse de dissolution de CaO et du C_2S dans le bain fondu de clinker, parce que la vitesse de la cristallisation de C_3S se produit assez vite et ne limite pas le processus. A son tour, le processus de dissolution est limité par la mobilité des ions Ca^{2+} et SiO_4^{4-} qui s'augmente avec la diminution de la viscosité du bain fondu, dont la composition comprend des ions Ca^{2+}, des radicaux SiO_4^{4-} et des Al et Fe amphotères faisant partie de groupes MeO_4^{5-} ou MeO_6^{9-}. L'anion acide de S fait déplacer un équilibre acide-basique du bain fondu et contribue à l'augmentation de la teneur en MeO_6^{9-}, ce qui mène à la diminution de la viscosité du bain fondu et à l'accélération du processus de dissolution de CaO et de C_2S (2).

L'étude des procédés se déroulant lors du chauffage des crus (tabl.) a montré que la première apparition de la phase liquide avait lieu déjà à 780°C; à 1100°C la formation de $C_4A_3\bar{S}$ se produit activement et arrive à son maximum à 1200°C. A cette température on a fixé la quantité maximale de la phase liquide et le commencement de la formation de l'alite. Si la température augmente, le sulfoaluminate se décompose et la quantité de l'alite s'élève (fig. 1). Ultérieurement, on a obtenu dans les conditions industrielles (four rotatif 4,5x170 m) les clinkers alitosulfoalumineux à teneur en alite 35 à 60% et en sulfoaluminate 5 à 15%.

Tableau

Composition des crus

n° des crus	Teneur en oxydes, %					
	SiO_2	Al_2O_3	Fe_2O_3	CaO	MgO	SO_3
1	18,13	10,55	4,36	63,06	1,05	2,70
2	20,00	11,80	4,60	60,60	1,17	2,07

Sur la fig. 2 on présente des radiogrammes des clinkers obtenus dans le four 4,5x170 m à teneur variable en alite.

Des analyses de la composition minéralo-

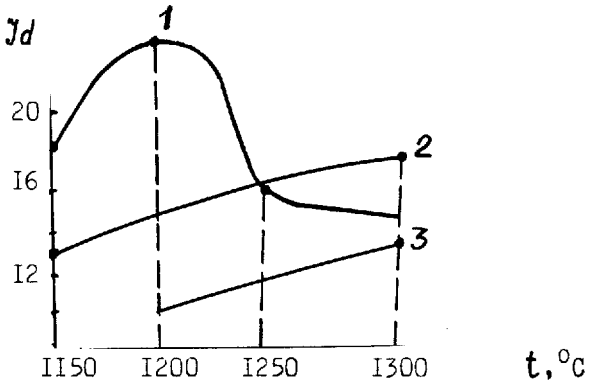

Fig. 1. Variation de l'intensité des lignes de diffraction des minéraux lors de la cuisson du clinker alitosulfoalumineux: 1 - $C_4A_3\bar{S}$; 2 - C_3S; 3 - C_3A

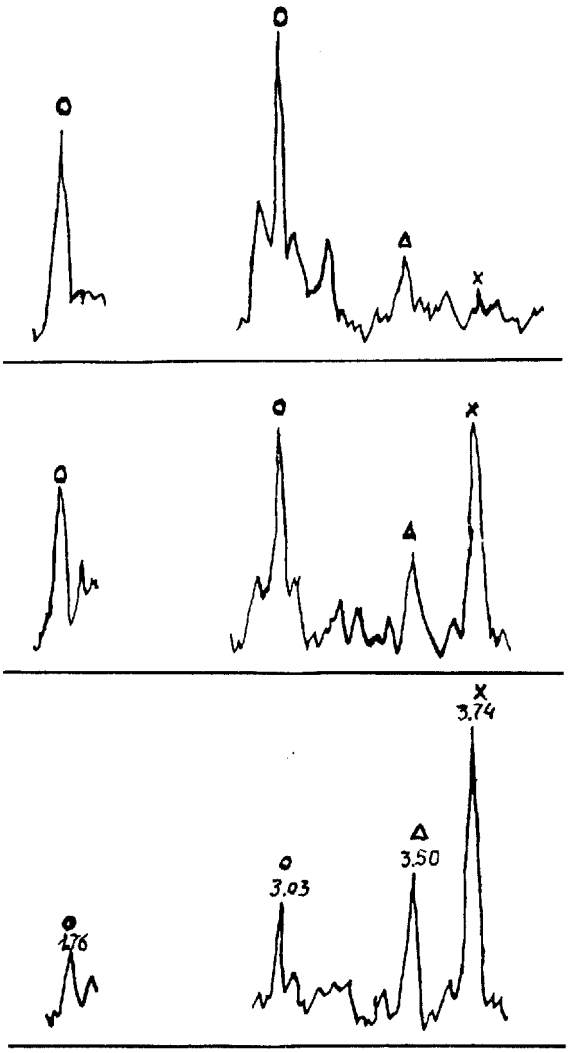

Fig. 2. Radiogrammes des clinkers alitosulfoalumineux
a. KS = 0,95; C_3S - 61%; $C_4A_3\bar{S}$-5,6%;
b. KS=0,90; C_3S-43%; $C_4A_3\bar{S}$-8,3%;
c. KS=0,87; C_3S-36_; $C_4A_3\bar{S}$-11,7%;
o - C_3S; x - C_3A_3S; Δ -$CaSO_4$

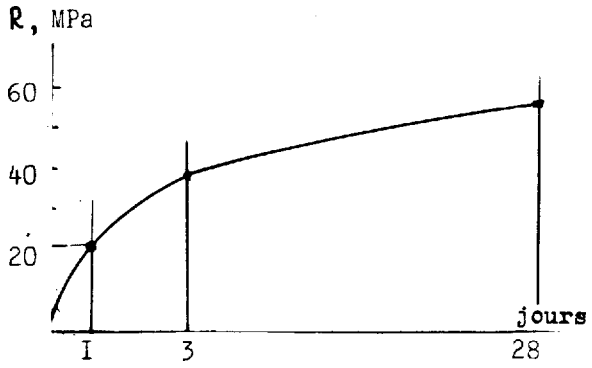

Fig. 3. Dépendance de la résistance du ciment alitosulfoalumineux du temps

gique réelle du clinker alitosulfoalumineux ont manifesté qu'en présence de l'excédent de sulfate de calcium il ne se produit pas la combinaison complète de l'oxyde d'aluminium en sulfoaluminate de calcium. Dans le clinker sont présentés: alite (C_3S), bélite (ß-C_2S), sulfoaluminate de calcium ($C_4A_3\bar{S}$), aluminates de calcium dont la composition dépend d'une basicité du cru ($C_{12}A_7$, C_3A), alumoferrite (C_4AF), sulfate de calcium ($C\bar{S}$), gehlenite (C_2AS).

L'intensification du processus de clinkérisation permet d'abaisser la température de cuisson jusqu'à 1250-1300°C, réduire la consommation énergétique à 18% et augmenter la capacité horaire du four à 27%.

Une courbe caractéristique de la résistance du ciment à base des clinkers alitosulfoalumineux industriels est représentée sur la fig. 3.

Cette courbe veut dire que des ciments alitosulfoalumineux sont ceux à durcissement rapide et à résistance élevée.

1.3

Bibliographie

I. Ямадзаки, Т.Мондзи, К.Сугиура. Поведе-
Поведение расширяющихся растворов и бетонов в начальные сроки твердения с использованием добавок системы $CaO-CaSO_4-4CaO\cdot 3Al_2O_3\cdot SO_3$ - В кн.: Труды УI Международного конгресса по химии цемента. - М., Стройиздат, I976, т.Ш,с.I92-I96.
2. Осокин А.П. Автореферат докторской диссертации. Химия и технология клинкерообразования в оксидно-солевых расплавах. Киев, I985, с. 5-I3.

B.I. NOUDELMAN,
A.I. GADAEV, NIIstromproykt, Tachkent, URSS

ASPECTS PHYSICO-CHIMIQUES DE LA CRISTALLISATION DES CHLORSILICATES LORS DE LA CLINKERISATION A BASSE TEMPERATURE DANS LE BAIN FONDU DE SEL

On a étudié le processus de formation des mineraux principaux et intermédiaires dans la technologie de la production du clinker d'alinite.

On établit que dans le processus de formation des germes de minéraux, se sont les interphases "gaz-liquide-solide" qui jouent le premier rôle.

Les auteurs soulignent deux mécanismes de la cristallisation des chlorsilicates. Le premier est lié avec des propriétés des interphases, le deuxieme avec des propriétés volumetriques de la phase liquide.

On a mis en évidence la concentration superficielle des atomes d'oxygène, ce qui peut indiquer à la concentration superflue des oxydes de Ca, Si, Fe dans la couche superficielle, assurant ainsi la formation de germes.

On a établi l'existence de deux mode de la phase liquide: oxyde et oxyde-sel formant des interphases "liquide-liquide" qui ont les propriétés analogue à celles "liquide-gaz", et "liquide-solide".

On a montre qu'en présence de germes dans les interphases, la surface maximale de ces dernières était désirée pour l'augmentation de la cinétique de la formation des minéraux.

Estudou-se o processo de formação dos minérios principais e intermediários na tecnologia da produção do clínquer de alinita.

Verificou-se que, no processo de formação de germens dos minerais, são as interfases "gás -líquido-sólido" que representam a principal parte.

Os autores assinalam dois mecanismos da cristalização dos clorossilicatos. O primeiro está ligado às propriedades das interfases; o segundo com as propriedades volumétricas da fase líquida.

Pôs-se em evidência a concentraçao superficial dos átomos de oxigênio, o que pode indicar a concentração supérflua dos óxidos de Ca, Si, Fe na camada superficial, assegurando assim a formação de germens.

Verificou-se a existência de dois modos da fase líquida: óxido e óxido-sal formando as interfases "líquido-líquido" que têm propriedades análogas às do "líquido-gás" e "líquido-sólido".

Mostra-se que, em presença de germens nas interfases, a superfície máxima dessas últimas era desejada para aumento da cinética da formação dos minerais.

La nouvelle technique de fabrication du ciment Portland à basse consommation d'énergie se distingue grâce à l'utilisation, en qualité de principal minéral pour obtenir le clinker, de l'alinite - silicate de calcium à haute basicité contenant du chlore ($21CaO \cdot 6SiO_2 \cdot Al_2O_3 \cdot CaCl_2$). Les phases minérales intermédiaires à chlore sont le chlororthosilicate ($4CaO \cdot 2SiO_2 \cdot CaCl_2$), le chloraluminate ($11CaO \cdot 7Al_2O_3 \cdot CaCl_2$) et le chloraluminoferrite de calcium ($4CaO \cdot Al_2O_3 \cdot Fe_2O_3 \cdot CaCl_2$) dont il ne reste vers le moment de formation de l'alinite que le chloraluminate. Le chloraluminoferrite se décompose en ferrite et en chloraluminate de calcium tandis que le chlororthosilicate se décompose en C_2S et $CaCl_2$. Les produits de décomposition des minéraux indiqués et le chloraluminate servent de base pour la germination de cristaux d'alinite.

Une analyse de la formation de l'alinite et du chlororthosilicate de calcium en fonction de la teneur du système en $CaCl_2$ à une température déterminée (fig. 1) permet de concevoir l'existence, en principe, de deux mécanismes de cristallisation des phases minérales dans la production du clinker. Le premier mécanisme est lié à la nécessité d'assurer les conditions de germination des cristaux aux interphases liquide (L) - gaz (G) et liquide (L) - solide (S) et des zones adjacentes (concentration d'impuretés, propriétés physico-chimiques). Il existe, apparemment, un rapport optimal déterminé entre les surfaces des interphases L-G et L-S permettant la cristallisation de tel ou tel minéral. Ainsi, pour l'alinite, ce rapport optimal est assuré en présence dans le système de 8 à 14 % de $CaCl_2$ (v. fig. 1). Une variation de la quantité de la phase liquide saline dans un ou dans l'autre sens aboutit à un changement du rapport et, finalement, à une perturbation des conditions de germination et de cristallisation de l'alinite.

Pour le chlororthosilicate, le paramètre déterminant au stade de germination est l'interphase L-G. De ce fait, dans les limites des concentrations de $CaCl_2$ soumises à l'essai, la cristallisation du chlororthosilicate est proportionnelle à sa teneur dans le système (v. fig. 1).

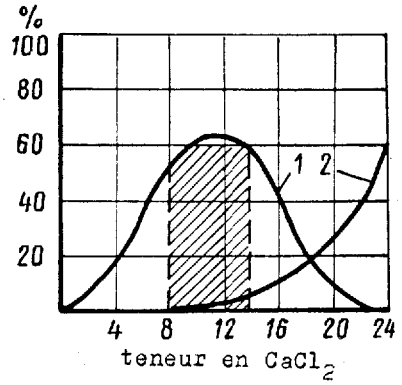

Fig. 1. Formation de minéraux en fonction de la quantité de $CaCl_2$ à 1100 °C: 1 - alinite; 2 - chlororthosilicate

La nécessité de limiter la quantité de la phase liquide (dans le cas de l'alinite) peut être justifiée par le fait que l'énergie superficielle de L-S est plusieurs fois supérieure dans le bain fondu salin par rapport à celle de L-G (1) (500 à $600 \cdot 10^{-3}$ N/m^2 pour le système L-S et 100 à $150 \cdot 10^{-3}$ N/m^2 pour le système L-G). Aussi, les conditions de cristallisation à l'interphase L-S ou à proximité d'elle sont-elles prépondérantes. Le bain fondu de la chlorure de calcium y joue un rôle de solvant et d'agent de transport servant à approvisionner le front de cristallisation en composants nécessaires (CaO, SiO_2, Fe_2O_3, $Al_2O_3 \cdot MgO$, etc.). A mesure que la cristallisation se développe, son front progresse en profondeur en gagnant ainsi tout le volume du bain fondu salin et en passant du domaine de L-G à celui de L-S.

Le fait que les conditions ci-dessus s'établissent dans la couche superficielle du bain fondu est confirmé par les résultats d'étude de la couche superficielle du bain fondu de $CaCl_2$ saturé d'oxydes de Ca, Si, Al, Fe, Mg. Les études ont été réalisées d'après la méthode de spectrométrie Auger (fig. 2). Elles ont montré que les premières couches moléculaires contiennent

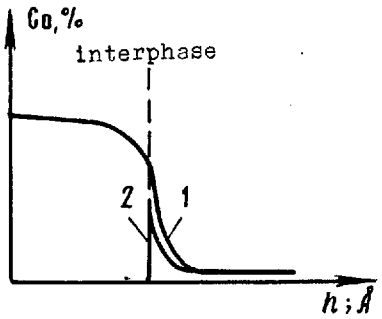

Fig. 2. Concentration des atomes d'oxygène à l'interphase:
1 - $CaCl_2$ - air; 2 - $CaCl_2$ - platine

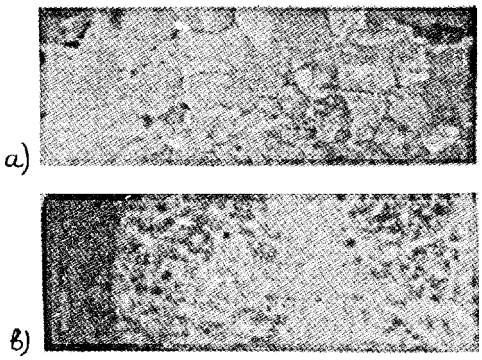

Fig. 3. Cristallisation des chlorosilicates à la surface du bain fondu:
a) chlorsilicate, b) alinite

beaucoup plus d'atomes d'oxygène et, par conséquent, d'oxydes que les couches suivantes. Cela concerne aussi bien l'interphase L-G que l'interphase L-S. Il est évident que la nature des phènomènes est la même pour les deux interphases. Les données de la spectrométrie Auger témoignent en même temps de l'importance du rôle de l'oxygène au cours de la germination des chlorsilicates.

Une des conditions qui influencent la crostallisation des chlorsilicates est la concentration de molécules ou d'ions dans la solution, leurs coefficients de diffusion. Les valeurs de ces derniers déterminent les valeurs des collisions "productives" des unités structurales de la solution lesquelles aboutissent en fin de compte à la formation d'un motif structural déterminé (fig. 3). La comparaison des conditions de cristallisation des minéraux à l'aide des procédés classique et à basse température montre que la principale distinction outre celle de température est la composition des phases liquides du clinker (tabl. 1).

Une plus basse concentration des oxydes dans la phase liquide saline peut être compensée dans une certaine mesure par de hates valeurs des coefficients de diffusion (tabl. 2). La cristallisation des chlorosilicates montre que cette condition peut être suffisante pour le premier mécanisme de cristallisation.

Tableau 1

Concentrations d'équilibre des oxydes dans le bain fondu de $CaCl_2$ et dans le bain fondu d'oxyde-silicate, %

Composants	Température, °C						
	Bain fondu salin de $CaCl_2$					Bain fondu d'oxyde eutectique (2)	
	1000	1100	1200	1300	1400	1340	1475
CaO	7,7	9,1	12,9	18,3	22,2	54,8	56,3
SiO_2	0,95	1,38	2,77	3,15	3,54	6,0	6,7
Al_2O_3	0,15	0,27	0,56	0,82	1,08	22,7	18,5
Fe_2O_3	0,10	0,22	0,37	0,98	1,48	16,7	18,5

Tableau 2

Coefficients de diffusion des oxydes dans le bain fondu de $CaCl_2$ et dans le bain fondu d'oxyde-silicate (cm^2/s)

Composants à étudier	Température, °C					
	Bain salin					Bain d'oxyde
	1000	1100	1200	1300	1400	1450
CaO	10^{-5}	10^{-4}	10^{-3}	10^{-2}	10^{-1}	$1,2 \cdot 10^{-6}$
SiO_2	10^{-6}	10^{-6}	10^{-3}	10^{-3}	10^{-2}	$1,1 \cdot 10^{-7}$
Al_2O_3	10^{-6}	10^{-5}	10^{-3}	10^{-3}	10^{-2}	$4,0 \cdot 10^{-7}$
Fe_2O_3	10^{-6}	10^{-4}	10^{-3}	10^{-2}	10^{-1}	$3,5 \cdot 10^{-6}$

Pour réunir ensemble tous ces faits, on se sert d'un modèle statistique de germina-

tion dans la solution qui est basé sur la théorie des phénomènes rares. Dans notre cas, c'est la probabilité de collisions productives aboutissant à la formation du motif structural du minéral. La probabilité de collisions productives est déterminée d'après la formule de Poisson transformée de façon à être appliquée au processus de diffusion (3):

$$P = \frac{V_1 n}{V \cdot m^2 (m-1)} \cdot e^{-\frac{V_1 n}{V}},$$

où P est la probabilité de collisions productives, V_1 est le volume de la cellule cristallographique, V est la volume du bain fondu, m est le nombre des éléments composant la cellule, n est la concentration des composants dissous.

Etant donné que le nombre des éléments qui constituent la cellule cristallographique d'alinite est supérieur à celui de chlororthosilicate (tabl. 3), la "P" au au cours de la cristallisation de l'alinite est beaucoup plus basse du fait qu'à des mêmes concentrations la valeur de "P" au cours de la bain fondu elle est déterminée, de règle, par la valeur de "m". Une augmentation de la valeur de "P" est possible grâce à un accroissement de la concentration des réactifs, c'est à-dire, des oxydes dans le bain fondu que l'on obtient soit en augmentant la température ce qui augmente en même temps le coefficient de diffusion, soit en créant un autre bain fondu, celui d'oxyde-sel où les concentrations des oxydes s'approchent de celles des bains fondus silicieux.

La formation de la phase liquide oxyde-sel (4) modifie les conditions de germination et de cristallisation des chlorsilicates. En présence d'un bain fondu homogène d'oxyde-sel la cristallisation des chlorosilicates s'y déroule dans tout le volume du bain fondu par suite d'un appauvrissement progressif de l'agent de chlore. Dans ce cas, le deuxième mécanisme de cristallisation des chlorosilicates commence à se manifester qui est lié aux conditions de sursaturation ou de sous-refroidissement de la solution et à la formation de centres de cristallisation dans tout le volume. Dans le cas contraire, la phase liquide se lamelle en deux liquides de compositions différentes (oxyde-sel et sel). La formation de la phase liquide oxyde-sel conduit à un accroissement considérable de la concentration des oxydes en le faisant s'approcher des valeurs du bain fondu silicieux. Les phénomènes de lamellation (5) se produisant dans le bain fondu de $CaCl_2$ créent plusieurs domaines de compositions différentes (fig. 4). L'apparition de phases liquides oxyde-sel et sel aboutit à une création d'une importante interphase favorisant l'initiation de la germination dans le volume du bain fondu. Dans ces conditions, les lois citées pour les systèmes L-G et L-S sont aussi valables pour le système L-L (premier mécanisme de cristallisation).

Avec une augmentation de la température, le bain fondu lamellé se transforme en un bain fondu homogène d'oxydesel où la cris-

Tableau 3

Caractéristiques des éléments structuraux de l'alinite et du chlorosilicate

Minérai	Paramètres de la structure des minérais			
	Type de la structure	Nombre d'atomes dans la cellule élémentaire	Volume de la cellule élémentaire	Nombre des éléments composant la cellule élémentaire
Alinite	$D_5^{12}=I\bar{4}2m$	91	943,8	6
Chlorortho-silicate	C_2^5 h=p $\frac{2_1}{c}$	68	725,3	4

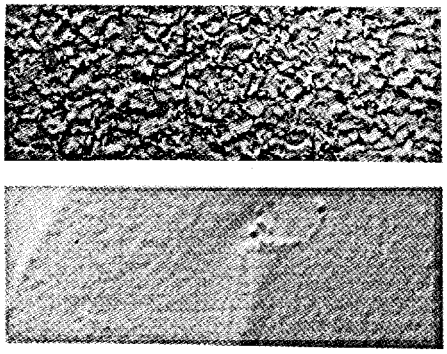

Fig. 4. Bain fondu d'oxyde-sel à:
a - 1200 °C, b - 1350 °C.
x 15000

tallisation s'amorce par suite de la sublimation d'un des composants (chlorure de calcium) et de l'obtention grâce à cela du point de passage liquide-solide pour une température déterminée.

Ainsi, les aspects physicochimiques cités de la cristallisation des minéraux chlorés formateurs du clinker permettent de conclure qu'une partie active de formation de minéraux est la mince couche superficielle. Ceci révèle la nécessité de création d'une interphase très développée pour obtenir de hauts paramètres cinétiques des processus de formation de minéraux pour la fabrication du clinker de ciment.

REFERENCES

I. Гадаев А.Н., Нудельман Б.И., Ишкова С.А., Бикбау М.Я. "Некоторые особенности взаимодействия жидкой солевой фазы с силикатами кальция". В кн. "Теоретические основы и технология получения цементов низкотемпературного синтеза". М., 1984, с. 22-29.
2. Бутт Ю.М., Тимашев В.В. "Портландцементный клинкер". М., "Стройиздат", 1967.
3. Нудельман Б.И. "Клинкерообразование в солевом расплаве и основы низкотемпературной технологии производства цемента" - Дисс. докт. т.н., - Ташкент, 1973.
4. Гадаев А.Я. "Состав и свойства жидкой фазы клинкера низкотемпературной технологии производства цемента". Материалы УІ Всесоюзного научно-технического совещания по химии и технологии цемента. М., 1983, с. 191-196.
5. V. Timachev. "Cinétique de la clinkérisation, structure et composition du clinker et ses phases", VII Cong. int. de la chimie des ciments, Paris, 1980.

M.Y. BIKBAOU, Cement Research Institute, Moscow

FORMATION, CRYSTAL CHEMISTRY AND PROPERTIES OF ALINITE AND JASMUNDITE

FORMATION, PROPRIETES ET CRISTALLOCHIMIE DE L'ALINITE ET DE LA JASMUNDITE.

1.3

The kinetic parameters of the formation of high-basicity calcium silicates with mixed anions are reported, and the activation energy of the process being about 83 kJ/mol for a temperature interval of 1370-1370 K.

A mechanism is suggested for the formation of a new high-basicity structural motif in calcium silicates, which is basically the formation of calcium-oxygen clusters which are being centered on chlorine or sulfur atoms in oxide-saline melts at the stage of mineral crystallization. The central atoms take on an unusual for them part of complex agent in oxide-saline clinker melts.

The data are presented on the structural features, morphology, and properties of alinite and jasmundite. The partial substitution of the oxygen portion of cement silicates reduces the power expenditure for the synthesis of minerals and clinkers on their base, and opens up possibilities for control of cement properties.

São reportados os parâmetros da cinética de formação de silicatos de cálcio de alta basicidade com mistrua de aníons, sendo a energia de ativação do processo de aproximadamente ' 83 kJ/mol para um intervalo de temperatura de 1.370 - 1370 K.

Sugere-se um mecanismo para a formação de um novo motivo estrutural de alta basicidade em silicatos de cálcio, que é basicamente a formação de grupos de cálcio-oxigênio que têm como centro átomos de cloro ou enxofre em fusões óxido-salinas no estágio de cristalização mineral. Os átomos centrais assumem um papel, não usual para eles, de agente complexo nas fusões óxido-salinas de clínquer.

São apresentados dados de características estruturais, morfologia, e propriedades da alinita e jasmundita. A substituição parcial de porção de oxigênio dos silicatos reduz o gasto de energia para a síntese de minerais e clínqueres em sua base, e abre possibilidades para controle de propriedades do cimento.

Based on the data on the formation and properties of alinite and alinite clinker /1, 2/, this paper reports our study into the general mechanisms of mineral formation in chloride and sulfide clinker systems. To be more specific, we investigated the formation of new high-basicity calcium silicates in the systems

$$CaCO_3(CaO) - SiO_2 - Al_2O_3 - MgO - Fe_2O_3 - CaCl_2$$

and

$$CaCO_3(CaO) - SiO_2 - Al_2O_3 - FeS_2(CaSO_4)$$

Finely ground and homogenized mixes were burned as tablets and in melts: the chloride-containing systems were treated in oxidizing conditions, whereas the sulfur-containing systems in reducing and normal conditions. As a result, both systems exhibited polycrystalline and monocrystalline structures of the new minerals

alinite, $Ca_{21}Mg\left[(Si_{0.75}Al_{0.25})O_4\right]_8O_4Cl_2$,

and

jasmundite, $Ca_{22}\left[SiO_4\right]_8O_4S_2$

The yield of alinite and jasmundite as a function of calcination time at 1373 K, 1423 K, and 1473 K was revealed by a quantitative x-ray analysis of the calcination products (analytical reflections at 3.24 Å and 1.85 Å; external reference, α-quartz). The formation kinetics for these systems, shown in Fig. 1, indicates that the crystallization rate for alinite and jasmundite exceeds that of C_3S /3/ by 7-8 times, in spite of lower by 300-400 K temperatures of the synthesis.

The kinetic curves for the formation of alinite and jasmundite were fit with the Kolmogorov-Erofeyev equation

$$\alpha = 1 - \exp(B\tau^A)$$

where α is the advancement of reaction, τ time of conditioning, in minutes, and A and B equation constants.

The rate of the reaction was estimated as a function of temperature in the temperature range 1373-1473 K with the Arrhenius equation. The activation energies of formation were found to be 83 kJ/mol for alinite and 114 kJ/mol for jasmundite, these being considerably lower than the activation energy of C_3S formation which is known /3/ to be 203 kJ/mol in the temperature interval 1670-1770 K.

The composition of interim compounds has been reported to alter in the process of formation of alinite clinker /2/. The process of formation of jasmundite exhibits oldgamite, belite, and calcium sulfide-aluminate, $C_{11}A_7CaS$. In the oxidazing environment of calcination, jasmundite decomposes yielding C_2S and $CaSO_4$, and at temperatures above 1600-1650 K loses S^{2-} and converts into tricalcium silicate.

Single crystals of alinite exhibit a variety of ditetragonal-dipyramidal habitus. In the absence of impurities, their ordinary and extraordinary refractive indices are $n_o = 1.704$ and $n_e = 1.696$. These are colorless, monoaxial crystals of negative optic sign and a density of 3074 kg/m^3.

Single crystals of jasmundite, containing iron impurities, exhibit a pyramidal habitus and a prismatic habitus, yellow-pink color, and a weak pleochroism with $n_o = 1.731$ and $n_e = 1.723$. These synthetic studies into new calcium silicates have evolved a crystallization mechanism for minerals with mixed anions. According to this mechanism for minerals with mixed anions. According to this mechanism, alinite crystallizes not in a saline melt of calcium chloride, as has been assumed earlier /4/, but rather in a silicate melt containing some dissolved chlorine. Jasmundite also crystallizes in a silicate melt containing sulfur as S^{2-}. The solubility of chlorine and S^{2-} in silicate-saline melts at 1500-1600 K amounts to 4-5 wt %. As the

proportion of chlorine and sulfur dissolved in a simicate-saline melt increases, micro-liquation phenomena take place with the evolution of chlorine-silicate liquid phase. This phase evolves crystals of calcium chlor-meta- and ortosilicates. Overheating of such melts above 1350-1450 K causes their segregation into saline and saline-silicate melts.

Analysis of F, Cl, and S effects on the properties of silicate melts /5/ suggests that there exist general regularities expressable as a marked decrease in the formation temperature of the melt, its viscosity and surface tension, an acceleration of the ion exchenge processes in the melts, and a more intense solidification of minerals.

A most important implication of the silicate-saline melt's ability to solidify is an unusual role of the anions Cl^-, S^{2-}, and F^- which, after Weil and Marboe /6/, form in such melts complexes with least charged cations. At the early stage of alinite clinker formation, the composition of the clinker liquid phase is consistent with the chlor-silicate mechanism, and the relative content varies as follows:

	CaO	SiO_2	Al_2O_3	Fe_2O_3	MgO	$CaCl_2$
wt %	35-45	18-23	3-5	2-5	1-2	20-35

The melting temperature of such compositions varies in accord with the proportion of calcium chloride, from 1270 to 1170 K. The experimentally found melting points for these compositions were verified by the specific features in the curves of electric conductivity, differential gravimetry, and shrinkage in heating the respective mixes.

As the clinker melt receives more oxides of raw mix components and the active anions of chlorine volatile (or migrate into solid particles of the mix), the chlorine-silicate melt experiences liquation and stratifies giving rise to zones of silicate-saline melt. It is exactly in these zones, where the chlorine content is under 4-5 wt %, that Cl^- anions take on the role of complexing agents. They group in their coordination sphere the largest possible number of calcium atoms, i.e., form a new high-basicity structural motif, or cluster /5/. Considerable concentration of movable calcium atoms in the silicate-saline melt aids a rapid impregnation of the melt with such complexes. These being connected with each other produce a spatial pseudo-crystalline structure first in this silicate-saline melt and then evident in the solidified alinite.

This mechanism was verified by a successful synthesis of jasmundite in a silicate melt saturated with S^{2-}. It is also in good agreement with an established negative effect on alinite and jasmundite crystallization of low charged cations of alkali metals which screen the complex agents Cl^- and S^{2-} from Ca^{2+} and hamper the formation of a new structural motif (Fig. 2).

The chemical analyses of the synthetized single crystals of alinite and jasmundite are close to that given by the chemical formulas, except a reduced proportion of Al_2O_3 (about 4 wt %) as compared to the theoretical. The crystallographic structure of this alinite has been treated by Ilyukhin et al. /7/ and in the work of Dent-Glasser and Lee /8/ on a sample of a natural mineral of jasmundite there was shown its authenticity to alinite. The synthetic single crystals of jasmundite (symmetry group 14m2) exhibit the following parameters of a tetragonel cell a = 10.452 (1) Å and c = 8.6977(9) Å.

It was a rather surprising experience to find out that jasmundite fails to react with water. Polycrystalline alinite, jasmundite and C_2S ground to a specific surface of about 450 m^2/kg were mixed with water at a W/C ratio of 0.35 to determine the compression strength and cementitious properties in setting under normal conditions. The jasmundite paste failed to set and therefore no hardening could be reported for this material. Table summarizes the findings of quantitative x-ray analysis of hydration degree and the strength tests after conditioning in humid air.

For alinite, hydration heat evolution be-

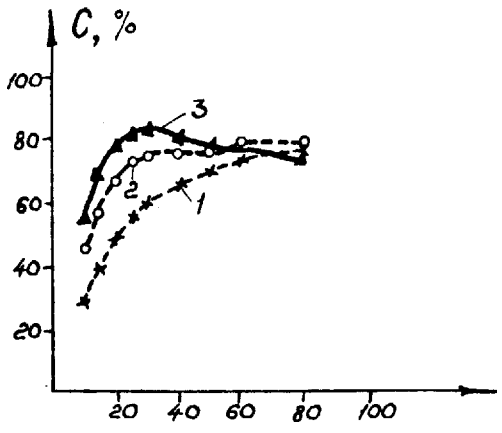

Fig. 1. Alinite formation kinetics at three temperatures: 1373 K (1), 1423 K (2), and 1374 K (3), derived by a quantitative x-ray analysis of calcination products from the Akhangarinsk cement plant

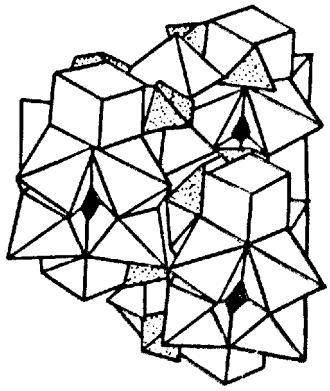

Fig. 2. A model of crystallographic structure of alinite and jasmundite. Si(Al) - tetrahedrons are outlined with a dot-line. In the cluster joints of Ca-polyhedrons the atoms of Cl and S are blackened

Table

X-Ray Analysis of Mineral Degree of Hydration and Compressive Strength Tests

Compound	Degree of hydration, % (numerator), and compressive strength, MPa (denominator) at 0.35 W/C ratio, 293 K, and age (days) indicated							
	1 hr	3 hr	6 hr	1	3	7	28	90
alinite	15	33	39	62 / 22	74 / 32	79 / 45	96 / 57	100 / 64
C_3S	5	10	15	30 / 12	39 / 21	45 / 41	53 / 54	59 / 58
jasmundite	0	0	0	0 / 0	0 / 0	4 / 0	8 / -	24 / -

gins immediately after mixing at a level of 9 J/kg s, but already in the first 15 minutes drops to 2 J/kg s, and after 5 hours settles at a gradually, but constantly falling pattern of 0.4 J/kg s. Analysis of the heat evolution curves for alinite also suggests a higher hydration reactivity than that of C_3S and alite.

The x-ray quantitative analysis of hardening paste indicated considerable difference in the hydration rates of polycrystalline alinite, jasmundite, alite, and C_3S. At all setting ages, the rate of alinite reaction with water is, on the average, twice as high as that of alite hydration. The higher hydration rate of alinite as compared with that of alite and C_3S is due to the incorporation of chlorine atoms in the crystal lattice of alinite.

In the sequence alinite-alite-C_3S-jasmundite, the minerals are rather close in their compound composition (specifically in their Ca content - the principal element of cementitious materials, in the proportion of basic and acid oxides, and in some other features), and the crystalline structure of alinite and jasmundite is the same. It was rather surprising therefore to find out that the hydration rates of these compounds differ significantly within this sequence. This difference fails to obtain a reasonable explanation within the framework of the approach

to hydration reactivity adopted by many researchers, saying that mineral's reactivity toward water is higher, the higher the mineral basicity.

To substantiate the point, the Ca content of inert jasmundite is 50.49, of alite 52.66, and of the most reactive phase, alinite, 48.50 wt %. Similarly, the basicity of alinite, 2.87, is close to that of C_2S, 2.80, but alinite reacts with water 1.5-2.5 times as actively as C_3S.

An explanation of the different hydration rates found for isostructural alinite and jasmundite, obtained one from another by isostructural substitution of Cl^- for S^{2-}, may be given by relating their ability to interact with water to the ionicity or covalency of atomic bonds in silicates. Indeed, the presence of chlorine atoms in the key positions of chlorsilicate structure provides active species at the surface and in the bulk of the crystals. In alinite, a chlorine atom plays a role of a bridge element (a lock that opens in hydration) for eight calcium atoms each of which is coordinated by five oxygen atoms which together with chlorine atoms form a distorted octahedron around the calcium atoms.

In actual mineral structure, the cations from with Cl unequal bonds, some with higher ionicity as a partial replacement of oxygen with Cl, F, or OH in oxygen-containing compounds is known to increase the ionicity of bonds in fragments of the type O-Ca-O.

The markedly lower ionicity of sulfur atom bonds with calcium is due to a larger donation of the S^{2-} charge, as compared with that of Cl^-, into the binding orbitals of coordinating Ca atoms. Sulfur differs from chlorine and, in a larger degree, from oxygen and fluorine by the lower ionization potentials. Owing to the lower ionization energies of valent states, s-, p-, and d-orbitals of sulfur mix heavily with the orbitals of coordinating Ca atoms. In jasmundite, there forms a stabilizing state of structural motif pattern: the sulfur atom assumes an electronic configuration of the "transargon" sulfur, and the coordinating Ca atoms assume the electronic configuration of argon.

The bonds of sulfide sulfur atoms, being more covalent, bind a considerable proportion of the positive charge of coordinating Ca atoms, thereby causing a radical reduction in the hydration rate of the new high-basicity calcium silicate. Although jasmundite contains only about 3.7 wt % sulfur, these atoms prove to be enough in number to considerably alter the properties of the mineral. Chemically this occurs because in an elementary cell, each of two sulfur atoms binds eight Ca atoms, that is only six in twenty two Ca atoms have no bonds with sulfur.

Thus, with one and the same structural motif pattern in two identically built and closely compounded minerals, the nature of anions, in which the minerals differ, caused in one (chlorine in alinite) active interaction with water, while in the other (sulfur in jasmundite) caused a radical retardation of hydration.

REFERENCES

1. Бикбау М.Я., Нудельман Б.И. Минералогия алинитового клинкера- в кн.:Краткие тезисы докладов на УI Всесоюзном совещании по химии и технологии цемента.- М., ВНИИЭСМ,1982, с.48-55.
2. Bikbaou M. Prosessus de formation de mineraul et la composition des phases du clinker alinitique - In 7. Congr. inter. de la chimie des ciments. v. 4. - Paris, 1981, pp. 285-290.
3. Бутт Ю.М., Тимашев В.В. Портландцементный клинкер. - М., Стройиздат,1967
4. Нудельман Б.И. Клинкерообразование в расплаве хлористого кальция.- В кн.: Шестой Международный конгресс по химии цемента,т.I.- М.,Стройиздат,1976, с.217-222.
5. Бикбау М.Я. Открытие 210.Новое научное направление в химии и технологии цемента Цемент,.Каз.НТИ,1988- 114с

6. Weil W.A., Marboe E.C. Conditions of glassformation a simple compounds - Glass. Ind., 1960, v. 41, No. 8-12, 1961, v. 42, No. 1.
7. Ilyukhin V.V., Nevsky N.N., Bikbaou M.Y., Howie R.A. Crystal structure of alinite - Nature, 1977, v. 269, No. 5627, pp. 397-398.
8. Dent-Glasser L.S., Lee C.K. The structure of Jasmundite, Ca_{22} SiO_4 $_8O_4S_2$ - Acta Cryst., 1981, v. 37, pp. 803-808.

G.I.Ovcharenko, assistant professor of the Altay Polytechnical institute, candidate of technical science, Barnaul, USSR.

Technological Aspects of Structure Replication in Silicates

Aspects technologiques de la replique de la structure dans les silicates

SUMMARY: Based on the idea of structure replication in silicate reactions, attempts have been made to explain technological peculiarities of binding material production.

Structure replication of γ-Ca_2SiO_4 in topotactic reactions of dehydration of highly based calcium hydrosilicates has been shown by X-ray diffraction. This structure replication can be modified by stabilization of belit by lime.

A crystal chemical model and mechanism for belit stabilization by lime are also given.

Structure replication of lime in belite-containing melted or sintered cements is shown by X-ray microanalysis. Undesirable alumina-silica interection in melted or sintered cements are avoided binding alumina into another compounds or by changing technological conditions.

Transformation of ortosilicate structure in the process of hydration into the structure of tilleite-cuspidine or zeolite similar type is shown by X-ray and TMS-analyses.

Com base na idéia de réplica da estrutura em reações do silicato, foram feitas tentativas para explicar as peculiaridades tecnológicas da produção do material ligante.

Por difração de raiox-X se mostrou a réplica de estrutura de γ-Ca_2SiO_4 em reações topotáticas de desidratação de hidrossilicatos de cálcio altamente baseados. Esta réplica de estrutura pode ser modificada por estabilização da belita por cal.

Também são dados um modelo químico de cristal e o mecanismo para estabilização da belita por cal.

A réplica de estrutura de cal em cimentos fundidos ou sintetizados contendo belita é mostrada por microanálise de raios-X. A interação indesejável alumina-sílica nos cimentos fundidos ou sintetizados é evitada ligando alumina com outros compostos ou mudando as condições tecnológicas.

Mostrou-se por análises de raio-X e TMS a transformação da estrutura de ortossilicato no processo de hidratação para a estrutura de tuleíta-cuspidina ou tipo similar ao zeólito.

Replication of the silicon-oxygen framework in transforming minerals from one kind into another was convincingly shown by academician Belov, using a larg number of silicates as an exampl, if in its structure cation has a subordinate function (silicates with fine cations). And vice versa. The structure replication of oxide motive of the large cation and subordinate of the silicon-oxygen tetrahedron structure (1).

His collegues showed replication of the lime structure in ortosilicate, which decreases in the series α -, α' -, β -modification and is hardly followed in γ -C_2S. worth considering crystalchemical model and stabilization mechanizm of polymorphic modifications C_2S offered by the author.

Crystalchemical Model

The conformity of the main structural ortosilicates constituets is taken as a principle of the offered crystalchemical model: the lengthes of the rib Si-tetrahedrone and rib's lengthes of cation polyhedrone. Moreover the basic rib's size Si-tetrahedrone is chosen as it's length in fayalite. The least was equal to rib's length of octahedron $[FeO_6]$. This chice is explained by the fsct, that fayalite is crystalized

Table 1

The size discrepancy of the cation polyhedrons and tetrahedron $[SiO_4]$ ribs in fayalite

Admixtural ion	The difference in tetrahedron and cation polyhedron rib lengthes at different coordinative number (CN) by oxygen (10^{-10}m)				Allowable (CN) of the admixtural ion
	CN=4	CN=6	CN=8	CN=12	
Al^{3+}	+0,192	-0,240			4-6
Mn^{3+}	+0,273	-0,170			6
Cr^{3+}	+0,306	-0,141			6
Fe^{3+}	+0,335	-0,099			6
Mg^{2+}		-0,057			6
Fe^{2+}		0			6
Cr^{2+}		+0,069			6
Mn^{2+}		+0,113	-0,462		6
Ca^{2+}		+0,374	-0,256		6-8
Sr^{2+}		+0,608	-0,058		8
Ba^{2+}		+ ,891	+0,174	-0,112	8-12
Na^{+}		+0,340	-0,277		6-8
K^{+}		+0,778	+0,080	-0,197	8-12

(-) -the rib length deficiency of cation polyhedron in relation to the Si-tetrahedron's rib in fayalite;

(+) -the rib length excess of cation polyhedron over tetrahedron's rib length in fayal.

Nikiforov (2) thoroughly described the fragments preservation of the kaolin ring type in different reactions with alùmosilicates participation.

In the present paper an attemp is made to explain technological peculiarities of getting binding materials on the base of common idea of replication. The binding systems considered are mainly based on calcium ortosilicate. Therefore it is preliminary in strictly hexagonal symmetry, as Belov noted (1) and it points out good structural conformity of its polyhedron.

Basic quantitative ratios of the given model are given in table 1. Taking into account that coordination of large cation (which may substitute calcium in the structure C_2S) by oxigen equals: 6 -for γ-C_2S; 6-7 -for β-C_2S; 8 -for α'-C_2S; 8-12 -for α -C_2S may be explained by corresponding

cations. In particular, cation Ca^{2+} may stabilize β-C_2S, so if it is in octahedron, there will be excessive rib discrepancy of polyhedrons ($+0{,}374 \cdot 10^{-10}$m). But Ca^{2+} cannot stabilize α'-C_2S, because in this case the size discripancy will be observed to - wards opposite diretion. Thus, it is theoretically possible to stabilize β-C_2S by lime.

Dehydration of the high based calcium hydrosilicates

Belov showed (1), that the structure of high based calcium hydrosilicates is presented by olivine part (γ-C_2S) using different com inations with portlandit. H.F.W. Taylor (4) showed, that dehydration of the Ca hydrosilicates is carrisd aut by topotaxic mechanizm and by Bukle data leads to the obtain of γ-C_2S and CaO. And accoding to Heyker and Zalkind data - to the mixture β-C_2S and CaO.

Table 2

The composition of dehydration products

Hydrosilicate	Dehydration temperature, °C	Pressure of dehydration, Pa	Crystalline products
TSH	670	Atmospheric 0,1 - 1,0	CaO, TSH, C_5S_2H β-C_2S, CaO, C_5S_2H
	900	Atmospheric 0,1 - 1,0	γ-C_2S, CaO β-C_2S, CaO, C_3S
C_5S_2H	700	Atmospheric 0,1 - 1,0	γ-C_2S, CaO β-C_2S, CaO, C_3S
hydrates C_2S	600 - 900	1300	β + γ-C_2S, CaO

Stabilization mechanizm

While sintering lime and silica to get C_2S with the lime excess it is impossible to stabilize β-C_2S. But at a relatively low temperature sintering (800-1100°C) of γ-C_2S and CaO one can succeed in stabilysing β-C_2S. Similar phenomena have been found in metal systems by Arharov (3) and are called intercrystalline internal adsorbtion (IIA). The essence of this phenomena is in the fact that som admixture atoms can not be kep by crystal matrix lattice and they are forced out into intercrystalline sections during the process of cooling (gorofilic ions). However, it is possible to direct such gorofilic ions into crystalline matrix and keep them there after cooling by means of repeated low temperature kilning. This phenomenon has thermodynamic base. It may be concluded, that Ca ion is a gorofilic ion for C_2S, and under certain conditions (IIA-mechanizm) lime may stabilize β-C_2S.

On the base of crystalchemical model data and mechanism IIA, it can be assumed that during the process of dehydration of the high based calcium hydrosilicates, it is possible to direct CaO into γ-C_2S, to stabilize β-modification and thus to modify the negative replication of the structure in this case. Competitive reaction - sintering of CaO into larger crystals - it is possible to remove by dehydration in vacuum.

Binding meterials obtained by dehydration

The high based calcium hydrosilicates (TSH, Ca-chondrodite (C_5S_2H) and α-, α'-, β - dicalcium silicate hydrates) were subjected to dehydration in the temperature interval 500 - 900°C under the atmospheric pressure and in the vacuum. The conditions of the dehydration and the phase composition

of the products are given in table 2. The hydraulic activity of the binding materials obtained by means of dehydration in vacuum formed 25-40 MPa.

Binding materials obtained by melting and sintering

As it was already noted, Ca_2SiO_4 replicates the lime structure and it can be well seen from our belit X-ray microanalyses data, obtained in the result of tempering of the silicate meltings (table 3).

alumina and silica as in the solid phase reaction and under melting process as well.

In this case we are faced with the negative replication of alumina-silica interaction. If to examine the reactions of clinkering, it may be noted, that alongside with the positive replication process of the lime structure, the negative process takes place - replication of the alumosilicates structure. To get rid of the latter, the technologists are obliged to add much CaO

Table 3

Molecular composition of ortosilicates

Kind of melting	Factor of saturation	The composition of Ca-ortosilicates		
		By quantity Ca and Si	By quantity Ca, Si and admixtures: Fe, Al, Mg	In comparison with theoretical content CaO in C_2S
High alumina Al_2O_3 15-20%	0,33	2,744	2,412	2,093
	0,80	2,664	2,453	2,107
High iron Fe_2O_3 15-20%	0,33	2,423	2,245	2,059
	0,50	2,179	2,094	1,927
	0,80	2,181	1,956	1,867

Table 4

Diorthogroup content in autoclaved belit with additions

	Mixture composition, %			Content
$-C_2S$	SiO_2	$CaCO_3$	CaF_2	Si_2O_7, %
100	not hydrated			13,46
100	-	-	-	20,71
86,1	14,9	-	-	15,21
90	-	10	-	25,21
78,3	13,6	9,1	-	23,17
90	-	-	10	53,58
78,3	13,6	-	9,1	45,22

At the time when silica may not be enough in the C_2S structure by a number of reasouns, the presence of lime is always near the standard. But even under such active C_2S with the abundance of lime, the hydrolic activity of the melting cements remains low (0-10 MPa) in the high alumina melts.

According to our data, the reason of it is constant interaction of

to the system and it leads to the large expenditure of energy (1500°C).

It is possible to remove alumina - silica interaction at less energy expenditure by binding alumina into sulpo-, fluorine-, chlorine aluminates and othe compounds as well as by low temperature raw mixture sintering containing neithe alumina nor silica

in one component, but containing the abundance of iron oxides. Sintering of such mix ture under the 1150°C made it possible to get cement activity 100 MPa (in paste) in twenty four hours.

The questions of hydration and structu ra formation of new phases take an important place in the studied problem.

Binding materials and industrial waste products, cotaining a large quantity of cal cium orthosilicate, may be effectivly used in autoclave technology. It is considered, that the system with mole ratio $CaO:SiO_2=1$ provide the best property.

However, we assumed and showed experimentally, that calcium ortosilicate structure is easy to transform into the structure of tilleit ($Ca_4 Si_2O_7 .CO_3$) and cuspidine ($Ca_4 Si_2O_7 .(F,OH)_2$) type. It is explained by the fact, that diorthogroup Si_2O_7 is well commensurable with calcium octahedrone rib.

Chemically pure belite (stabilizing agent 0,5% B_2O_3) was hydrated in autoclave at 1 MPa during 6 hours with $CaCO_3$ and CaF_2 presence. The amount of diorthogroup Si_2O_7 in stone was determined by method of derivatization by trimethylsilyl (TMS) groups. Hydration of β-C_2S is essentially increased in the presence of $CaCO_3$ and CaF_2 and transformation degree of SiO_4 in Si_2O_7 may exceed 50% (in the case of CaF_2 addition - see table 4).

Such systems, where belit structure transforms into zeolite similar phases in the presence of other components in hydration process are likely to be considered another trend of the effective use of ortosilicate and cements on it's base.

It may be provided by hydration of such systems in alkali conditions. Our investigations with F.D.Tamás, using trimethylsilyl derivatives, showed, that belit hydration degree is compared with alit hydration degree in lignosulfonate-alkali mixed cements (table 5).

Thus, considerations of such binding systems on the base of the Ca-ortosilicate with low energy consuming, allow to suggest more effective ways of their use, taking in to account peculiarities of the replication structures and structural conformity.

Table 5

Diorthogroup content in cement stone after 28 days hydration

Cement composition, %			Content Si_2O_7, %
Clinker	Kind of clinker	Granulated slag	
100	Belit	-	27,8
100	Alit	-	37,7
50	Belit	50	36,0
50	Alit	50	36,7

BIBLIOGRAPHY

I.- Белов Н.В. (1976), Очерки структурной минералогии, Москва, Недра.

2.- Никифоров К.А. (1977), Кристаллохимические основы топотаксических реакций в твердых телах, Новосибирск, Наука.

3.- Архаров В.И. (1976), Физико-химическая механика материалов, т.12, № 3, с.21.

4.- Тейлор Х.Ф.У.(1969), Химия цемента, Москва, Стройиздат.

5.- Хейкер Д.М., Залкинд А.И.(1961), Сб. трудов НИИ Асбестоцемент, № 11, с.34.

U. Ludwig and R. Pöhlmann, Institut fur Gesteinshüttenkunde, RWTH Aachen, West-Germany

Investigations on the Production of Low Lime Portland Cements

Summary: The manufacturing of low-lime Portland cements was investigated in order to come to further optimization within the process of clinker and cement production. The laboratory examinations based on natural marl revealed the pros and cons of the production of Portland cements with lime standards between 100 and 75%.

There are two ways to produce low-lime Portland cements with sufficient hydraulic reactivity:

1) reduce the lime standard of ordinary Portland cements to 85 - 80% approximately;
2) mix and mill alite-free with alite-rich clinkers.

The advantages of the reduction of the carbonate content on the one hand are as follows:

1) exploitation of raw material deposits of lower lime content;
2) less energy demand and better homogenity in the raw meal preparation;
3) reduced energy requirement in the burning process due to the decreasing necessary heat consumption and a temperature reduced by more than 100 K or
4) higher furnace output under normal conditions;
5) less strain to the refractory linings;
6) reduces NO_x formation in the flue gas due to the lower temperature in the sintering zone;
7) improved grindability;
8) less heat of hydration.

Sumário: A fabricação de cimento portland de baixo conteúdo de cal foi investigada de chegar-se a avançar na otimização dentro do processo de produção de clínquere de cimento. Os exames de laboratório baseados em marga natural revelaram os pros e contras da produção de cimento com o padrão de cal entre 100 e 75%.

Há dois modos de produzir cimento portland de baixo cal com suficiente reatividade hidráulica:

1 - reduzir o padrão de cal de cimento portland comum a 85-80% aproximadamente;
2 - misturar e moer clínqueres sem alita com clínqueres riscos em alita.

As vantagens da redução do conteúdo de carbonatos de um lado são as seguintes:

1 - exploração de depósitos de matérias-primas com baixo teor de cal;
2 - menos demanda de energia e melhor homogeneidade na preparação de mistura crua;
3 - reduzida energia requerida no processo de queima devido ou decréscimo do calor consumido necessário e as temperatura reduzida em mais de 100 k ou
4 - maior produção do forno em condições normais;
5 - menor deformação da camada de refratários;
6 - reduz a formação de NO_x na corrente de gás devido à menor temperatura da zona de sinterização;
7 - melhoria da moagem;
8 - menor calor de hidratação.

Por outro lado, o uso de adições de pozolanas em clínqueres de baixa cal, seria limitado.

U. Ludwig and R. Pöhlmann, Institut für Gesteinshüttenkunde, RWTH Aachen, West-Germany

INTRODUCTION

In recent years the specific energy consumption for the burning of Portland cement clinker could be reduced by almost 50 % due to a systematic improvement of the technical production process. Especially the development of the drying process replacing the wet process as well as the optimization of the whole burning process were of significant importance. Presently, the main aim of research is the reduction of the specific energy consumption in the production process of Portland cement clinker, which is strived for in the following ways:

1. Addition of sintering agents, such as mineralizers and fluxes, for the acceleration of the lime combination or the decrease of the burning temperature (1-8).

2. Reduction of the lime content in the raw mix for the production of belite-rich Portland cement clinker with suitable hydraulic reactivity (9-11).

3. Modification of the normal composition of Portland clinker in order to receive higher C_3S-* and C_4AF-content or to stabilize the sulphate-containing calcium aluminates (e.g. C_3A_3Cs) (12-14).

4. Reduction of the clinker content in the production of mixed cements, because the clinker compound is more energy-specific than that of the puzzolanic or latent hydraulic admixtures (12,13).

Concerning the further optimization of the burning process the production of Portland cements with low or very low lime content is very important in many respects. On the one hand, it leads to a decrease of the theoretical energy consumption of about 1850 to 1550 kJ/kg clinker (i.e. by about 15 %)** by the reduction of the carbonat content in the raw mix, i.e. by the production of alite-free instead of alite-rich clinkers (LSt III = 75 - 100 %). On the other hand, it leads to the expected effective improvements in the burnability, i.e. to lower sintering temperatures (17-21).

Moreover, the advantages in the treatment of low-lime marls are to be stressed, so that finally the admixing of a limestone can be avoided, which impairs the favourable burnability of natural marl due to the worse comminution properties (19-22). In addition, the possible decrease of the burning temperature, which leads to a lower thermal stress on the sintering zone, can reduce various technical problems in the burning process, as there are: the kiln lining wear, the formation of circulations, and the exit gases stress. It also implies an improvement in the clinker grindability. Under these aspects a further reduction of the whole energy consumption in the Portland cement production can be reached, if the occuring impairment of the strength development at early stages can be balanced.

The investigations described in the following present a review on the burning behaviour of natural raw mixes with or without sintering admixtures - e.g. MgO, SO_3, ZnO, CaF_2, or to a certain degree their combinations - depending on the lime standard. The results are discussed concerning the reachable temperatures at complete burning and clinker properties, as there are porosity and grinding behaviour, as well as the behaviour of technical mortars of the so produced cements.

EXPERIMENTAL

raw mix / index (i)	$K\,75_i$	$K\,80_i$	$K\,84_i$	$K\,89_i$	$K\,94_i$	$K\,100_i$
without admixture	SM = 2.40 - 2.52					
	TM = 2.10 - 2.31					
	HG * = 0.14 - 0.17					
	C_3S = 0 - 71 (wt.-%)					
	C_2S = 71 - 0 (wt.-%)					
	$C_3A + C_4AF$ = 23 - 20 (wt.-%)					
2 M	MgO-admixture up to 2.0 wt.-% MgO as $Mg(OH)_2$					
3 M	MgO-admixture up to 3.0 wt.-% MgO as $Mg(OH)_2$					
SO_3	sulfating of alkalis (c. 0.9 wt.-% SO_3) as H_2SO_4					
ZnO	admixture of 1.0 wt.-% ZnO (0.8 wt.-% Zn^{++}) as ZnO					
CaF_2	admixture of 1.0 wt.-% CaF_2 (0.4 wt.-% F^-) as CaF_2					
.5CaF_2+.5ZnO	admixture of 0.5 wt.-% CaF_2 and 0.5 wt.-% ZnO					
CaF_2 + ZnO	admixture of 1.0 wt.-% CaF_2 and 1.0 wt.-% ZnO					
.5 CaF_2 + SO_3	admixture of 0.5 wt.-% CaF_2 and sulfating of alkalis					
CaF_2 + SO_3	admixture of 1.0 wt.-% CaF_2 and sulfating of alkalis					
.5 ZnO + SO_3	admixture of 0.5 wt.-% ZnO and sulfatinf of alkalis					
ZnO + SO_3	admixture of 1.0 wt.-% ZnO and sulfating of alkalis					

* corresp. to (20)

Table 1 Data of the investigated Portland cement raw materials with and without admixtures

As raw materials natural marls with different carbonate contents were used, which were adapted to the values of the lime standard III of 100 to 75%, with

* The following abbreviations are used: C=CaO, S=SiO_2, A=Al_2O_3, F=Fe_2O_3, s=SO_3, etc.

** calculated according to (15),(16)

or without admixtures (sintering agents). Table 1 informs about the chemical and mineralogical data and the different sintering agents.

For the measuring of the burnability as well as the clinker properties the raw mixes were pressed in testing cylinders (11 mm ø, 11 mm h) and burned stationarily in a gradient kiln. This kiln system allows an exact temperature-time control, so that the parameters: heating (50 K/min) - holding (20 min) - cooling (about 800 K/min) can be kept at an optimal degree (23).

Afterwards, an electrically heated laboratory rotary kiln* served for the homogeneous burning of raw mixes pellets in the kg-field for hydration investigations, where heating gradients of ≥ 100 K/min, cooling gradients of about 800 K/min and again a burning time of 20 min were applied. Then the clinkers were fine-grained together with different calcium sulphates.

The results described in the following are presented as a summary of works on the possibilities of Portland cement production which are characterized by a significant decrease in the lime standard.

INVESTIGATIONS ON THE BURNABILITY

Figures 1 and 2 show the complete burning temperatures**, which based on the lime binding processes of the isochronic pilot burnings, as well as the bulk densities of the clinkers with various sintering agents as parameters depending on the lime standard.

It is obvious that a reduction of the lime standard leads to a markedly improved burnability especially of the very lime-rich raw mixes (figure 1). This corresponds with a reduction of the burning temperature for natural mixes ("without admixtures") in the high lime standard range of about 12 K and with a lime standard of < 94 % of about 2.5 - 3 K per percent of lime standard. The reduction of the burning temperature by about 130 K occuring when the lime standard is decreased from 100 to 75 % stands in accordance with investigations made in model as well as technical raw mixes (9,17,18). From present investigations, however, it can be taken that a lime content, which is being decreased in the raw mix, does not automatically imply a linearly decreasing burning temperature. Alite-rich clinkers generally show a sufficiant lime binding at a 20minute burning time only when a melting phase is present (> 1250°C).
The increase of the relatively low MgO content from about 1 to 2 - 3 wt.-% MgO ("2M, 3M") only leads to a quicker lime binding at high complete burning temperatures when a liquid phase is present. Thus, the clinker formation in this range is accelerated, which is directly connected with the favourable influence of the clinker melt with the help of MgO, as well as with the reduction of the formation temperature and the viscosity of the liquid phase.

The same is true for the influence of a sulphatisation of alkalies ("SO_3"), which only is effective to the complete burning temperature in the high lime standard range. From the separate in-

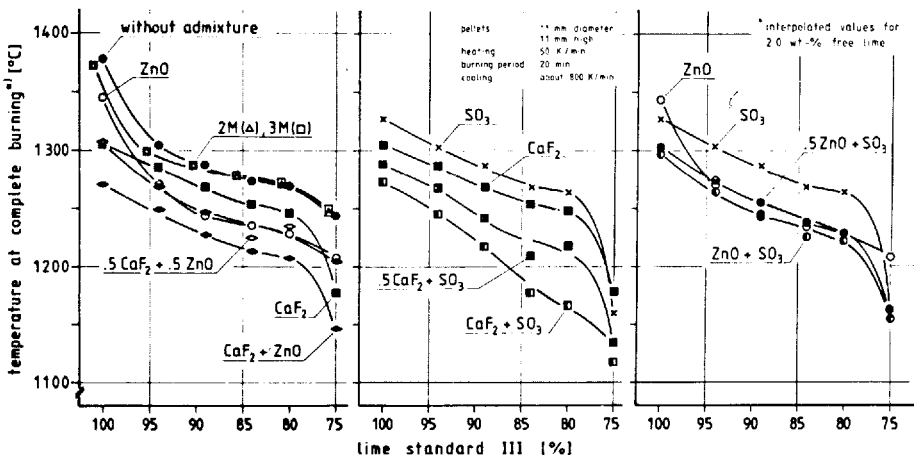

Figure 1
Burning temperatures of Portland cement raw mixes in the complete burning range as a function of lime standard and sintering agents

* as described in (20)
** defined for CaO_{free} = 2.0 wt.-%

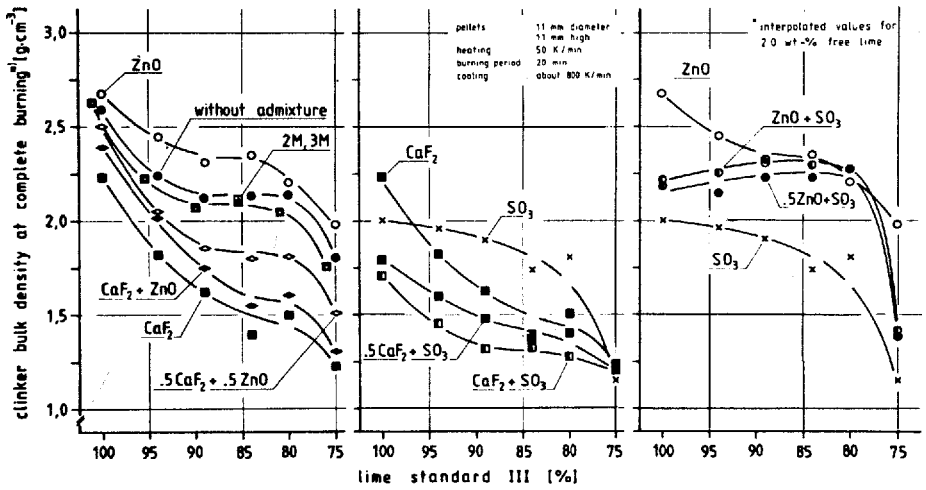

Figure 2
Clinker bulk densities of Portland cement raw mixes in the complete burning range as a function of lime standard and sintering agents

vestigations it can be seen that the quicker lime binding is especially due to a quicker transformation in the final phase of the clinker formation, i.e. a quicker alite formation. Two phenomena described in literature are involved: a reduction of viscosity of the liquid phase (24,25) and a alkali stabilization of belite (8,26,27) which takes place partly or not at all in the presence of sulphate or by the formation of alkali sulphates. The quicker lime formation of the alite-free clinker, however, is due to a favoured formation of C_3A instead of the $C_{12}A_7$, which normally is present in this low-lime range.

The accelerating reaction effect of fluor and zinc additions, which is also described in literature (2,5,7,8) resp. (2,6), is confirmed in the present results, too. CaF_2 and ZnO are favourable to the clinker formation when used individually ("CaF_2", "ZnO") as well as when used in combination (".5CaF_2+.5ZnO", "CaF_2+ZnO") in the whole lime standard range. However, it is interesting to note that the mineralizing effect of CaF_2 is very strong especially at very high and very low lime standards, whereas ZnO additions only show better effects when the complete burning of the raw mixes takes place at the same time as the evidently earlier forming of the clinker melt (≥ 1225°C).

Compared to the effect of the individual components the combined addition of fluor and sulphate (".5CaF_2+SO_3", "CaF_2+SO_3") clearly leads to the quickest lime binding (35). Especially in extreme low-lime sectors complete burning temperatures of less than 1200°C could be measured. The increase of the CaF_2 content from 0.5 to 1.0 wt.-% also brings about an increase in the reactivity.

Compared to the raw mixes with zinc or sulphate additions the presence of the combined "ZnO+SO_3" shows a purely additive effect independently from the zinc content (36). This means that especially for clinkers with high and low alite contents a more favourable lime binding behaviour is to be expected. On the other hand, in the range of the melting phase formation, which starts at lower temperatures, the effectivity of ZnO is dominant and is not impaired by the presence of sulphate.

According to figure 2 the course of the clinker bulk density, i.e. of the measured structure densification, is almost parallel to that of the complete burning temperatures. The porcsity of the addition-free clinker increases from about 20 to more than 40 vol.-% with a reduction of the lime standard fom 100 to 75 %. To use clinkers produced at such low temperatures gives a markedly improved grinding behaviour, which will be described later. Similarly, clinkers, which contain fluor and sulphate, show a clear reduction of the bulk density at the same lime binding rate in the whole lime standard range. The porosities rise to values of up to 60 vol.-%. The formation of fine-grained and porous clinkers is caused by a lessened surface tension of the clinker melt or by its increasing specific volume in the presence of fluor and sulphate (25,27,28). The strong flux-like effect of ZnO, however, causes a structure densification of the clinker.

Occasionally, the improvement of the clinker grinding by highly porous clinkers can bring about an increased dust development in the technical processing and thus reduce the positive effect. With the help of exact employment of structure-densifying or -loosing sintering agents there is the possibility of a direct influence on the formation of the clinker structure. The clinker properties change additively in the direction of higher densification in the presence of zinc.

Figure 3 informs about the behaviour of the different sintering agents in the burning process, i.e. the affinity to the gaseous phase resp. the clinker in the kiln.

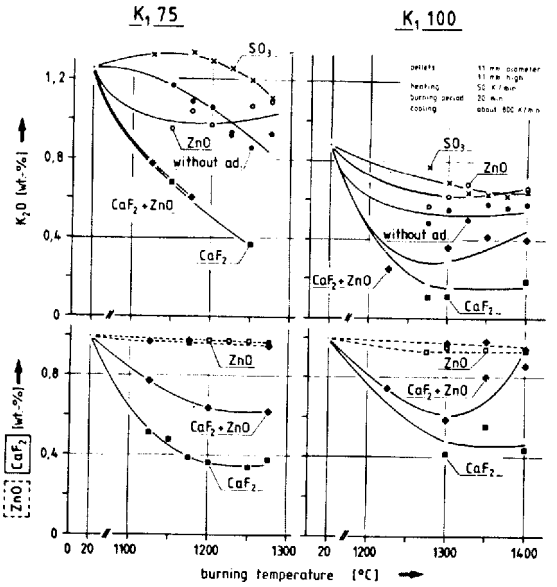

Figure 3
Binding of alkali (K_2O), zinc (ZnO), and fluor (CaF_2) as a function of the different raw mixes ("without admixture", "SO_3", "CaF_2", "ZnO", "CaF_2+ ZnO") and of the burning temperature

Besides an altogether higher alkali binding of the belite-rich clinker (LSt III = 75%), a sulphatisation of the alkalies ("SO_3") leads to an alkali binding which is higher than that of the basic raw mix ("without admixture") and connected with the formation of more stable alkali sulphates. The binding degree of zinc always reaches values of > 90 wt.-%. In contrast, fluor is strongly volatile during the open laboratory burning. Already at 900°C slight fluor losses were measured which averaged values of up to 60 wt.-% of the added CaF_2 contents in the range of the complete burning.

The different densifications of the doted clinker influence the vaporization behaviour of the very volatile components such as alkali and fluor. For example, significantly higher fluor contents are measured in the clinker (up to 90 wt.-% CaF_2) even at high burning temperatures when zinc is present ("CaF_2+ZnO") and the densification degree is correspondingly high. At this, fluor is increasingly enclosed into the calcium silicate clinker phases. Similar interrelations were observed for the volatility of alkalies or the binding of zinc.

INVESTIGATION ON THE REACTIVITY

The changes in the phase compositons and the properties of laboratory rotary kiln clinkers with varied lime standards are shown as an example in Figure 4.

sample	$K75_{1230°C}$	$K75_{1244°C}$	$K75_{1265°C}$	$K75_{1285°C}$	$K80_{1285°C}$	$K85_{1285°C}$	$K90_{1295°C}$	$K95_{1328°C}$
phase composition [wt.-%]		β-C_2S		C_3A		C_3S		
burning temp. [°C]	1230	1244	1265	1285	1285	1285	1295	1328
burning period [min]	30	20	20	20	20	20	20	20
density [g/cm³]	3,18	3,20	3,22	3,24	3,21	3,21	3,19	3,18
porosity [vol.-%]	44,7	45,0	37,3	29,9	33,0	33,3	35,4	32,1
grindability [cm²/g s]	81	85	50	41	43	38	37	33
BET / Blaine	n.d.	3,0	2,5	2,3	2,3	2,2	2,1	2,0

Figure 4
Clinker phase composition and properties of Portland cement clinkers in relation to the lime standard

A reduction of the lime standard leads automatically to an increasing belite- and a decreasing alite-content, so that with a lime standard III of 75% a alite-free cement is burned. With lime values below LSt III = 75%, $C_{12}A_7$ is formed instead of the lime-richer C_3A.

Apart from a reduction of the burning temperature special attention should be paid to the changed clinker properties. With decreasing lime standard, generally, the following properties can be stated: an increased porosity of the clinker pellets, an improved clinker grindability (grindability index) and an increased relation between the specific surface to BLAINE and BET, i.e. an increased surface reactivity. The growing clinker density is due to the augmenting β -C_2S portion. There are two reasons

U. Ludwig and R. Pöhlmann, Institut für Gesteinshüttenkunde, RWTH Aachen, West-Germany

for the decreasing density, when alit-free clinker (K 75) is burned in decreasing temperatures: firstly, the formation of $C_{12}A_7$, secondly, the progressing destabilization of belite, i.e. a γ-C_2S formation.

The results from grinding tests on the grinding behaviour are shown in figure 5. The grindability index is defined as surface increase per time unit.

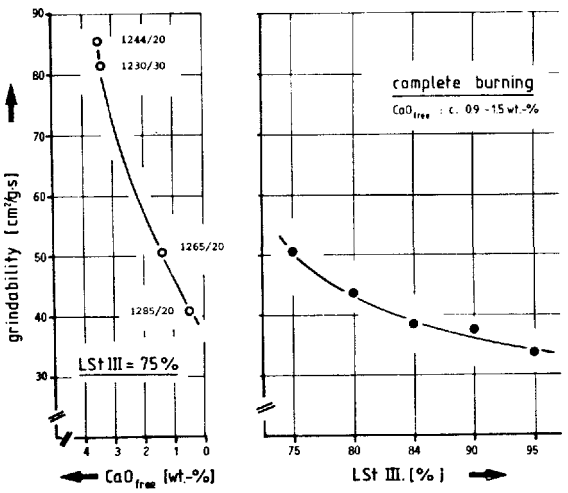

Figure 5
Grindability index of clinkers with a lime standard from 95 to 75% as a function of the burning degree (free lime) and the lime standard

With the same contents of residual free limes, i.e. with the same burning degrees, and falling lime standards, an obvious improvement in the grindability can be stated. Another significant effect is the influence of the burning degree with a chemically similar raw mix.

What can be taken from the results is that for the assessment of the grindability of Portland cement clinkers the adjustment of a previously defined burning degree (free lime content) is absolutely necessary. Rising burning temperatures for the same clinkers, together with growing portions of melting phase as well as low free lime values or clinker porosities, lead to a deteriorisation of the grinding behaviour. The negative influence of the grindability with an decreasing C_3S/C_2S ratio, which was often mentioned in literature (30-32), could not be confirmed. Using a standardized burning degree, i.e. a burning temperature adjusted to the raw mix, there are again obvious improvements in the grindability up to the finest range of more than 7000 cm^2/g for the clinkers with decreasing C_3S/C_2S ratio.

To what extend favourable influences from the reduction of lime standard in the production process can be applied for the production of hydraulic sufficiantly active Portland cements, is shown in figures 6 and 7.

First investigations in the whole lime standard range from 99 to 75% showed that the production of Portland cements is possible especially for lime standards of 89 resp. 85%, the strength developments of which are sufficiant even in the early period of hydration (28 days) (figure 6).

Differences in the early strength developments (up to 7 days) could be balanced with the help of finer grinding. Yet the use of even lower lime standards leads to an increasingly worse workability, a higher water demand with the same sulphate portion as well as to a quick setting with insufficiant strengths.

We tried to accelerate the reaction of belite-rich clinkers by applying higher cement fineness and more calcium sulphate, by optimizing the sulphate bearer and the burning conditions with the result that for an alite portion of only about 28 wt.-% (K 85) there were favourable early and final strengths (figure 7). The retardation and workability of low-lime Portland cements give hardly any problems when applied under appropriate conditions (kind and dosing of calcium sulphate). For mortar compressive strengths of up to 15 N/mm^2 after 2, 37 N/mm^2 after 7 and above 50 N/mm^2 after 28 days, the highest reachable strength classes according to DIN 1164 are Z35F resp. Z45L. A further reduction of the alite content to a rest content of about 15 wt.-% with a lime standard of 80% results in a marked drop in reactivity, which up to now could not be balanced. The DIN class Z25 is not reachable due to reduced early strengths ($\beta_{D,2d} < 10$ N/mm^2). According to the present investigations the cooling rates of up to 3000 K/min, which are demanded as the most important criterion for the production of hydraulic active belite cements (9), are not in any case necessary. The optimized belite-rich cements of clinkers with lime standards of 85 to 80% show comparable strengths.

The alite-free cements with lime standards of 75% react even more slowly. The clinker with the highest burning degree (1285°C) shows the comparably most favourable strength development.

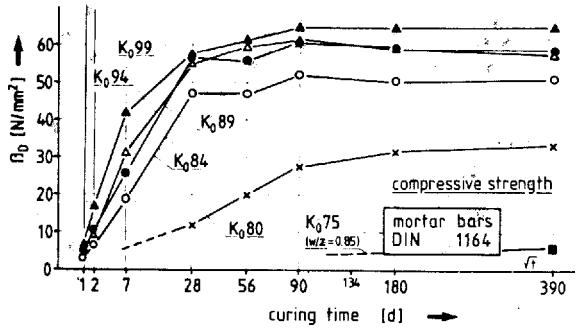

Figure 6
Strength development of Portland cements on passing from lime standard III of 99% to 75% (spec. surface about 3000 cm^2/g; 2.5 wt.-% SO_3, DH:A II = 1:1)

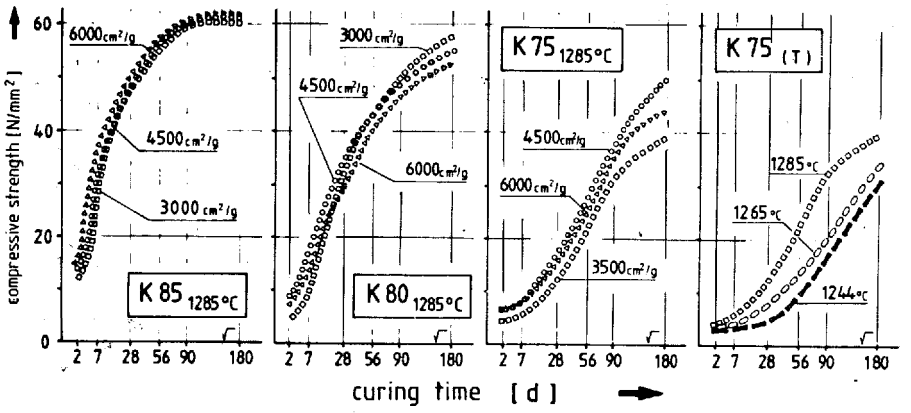

Figure 7
Compressive strength development of Portland cements with LSt III = 85% as a function of fine-grinding and burning conditions (2.5-4.0 wt.-% SO_3 as DH, HH, and A II; measurements on small mortar specimens in compliance with DIN 1164)

To reduce the burning temperature from 1265 to 1244°C does not entail a gain in reactivity. The determination of the reactivity of pure belite clinkers (LSt III = 75%) showed that all belite cements can be stimulated by the addition of alite to the same degree, which has already been stated for pure clinker phases, too (33,34). It was found out that the hydration reactivity is independent from the burning degree. The favourable hydraulic properties of belite-rich clinkers are thus directly dependent on the presence of a necessary residue of alite.

Figure 8 informs on the results of initial investigations on cement mortars from alite-rich (LSt III = 90%) resp. belite-rich clinkers (LSt III = 80%), which were burned with the additives mentioned above (37).

The setting behaviour of all cements is in general without problems. Yet there is the exception of the fluor-modified clinker that tends to set very quickly due to the stabilization of $C_{12}A_7 \cdot CaF_2$, which, however, probably can be parried by an increase of the calcium hydroxide concentration. In the same way, all mortars with an extension of 17 to 20 cm (flow test) show a good workability, which is true not only for the addition-addition-free but also for the mineralised cements.

On the whole, these results show that cements where alite content were reduced from about 40 to 12 wt.-% have a reduced strength on all curing periods. Comparing the hydraulic reactivity of cements without additions to those mineralised with clinkers, which were produced in the complete burning range ("c.b."), especially for the period of 28 days the negative influences can clearly be observed. Only when the alkalies are sulphatized, the alite-rich clinker shows unchanged properties. In general, the unfavourable influence on hydration evoked by the mentioned sintering agents is stronger for the belite-rich cements. According to X-ray phase analyses the hydration of the calcium silicates is blocated so that a clear hardening could be stated at a later curing period (up to 180 days), which is probable to entail a strength balance.

Varying the burning degrees of the addition-free raw mixes with different lime standards lead to an interesting and astonishing effect. For example, the increase of the 28-day compressive strength; at first, the strength increase can be attributed to the complete

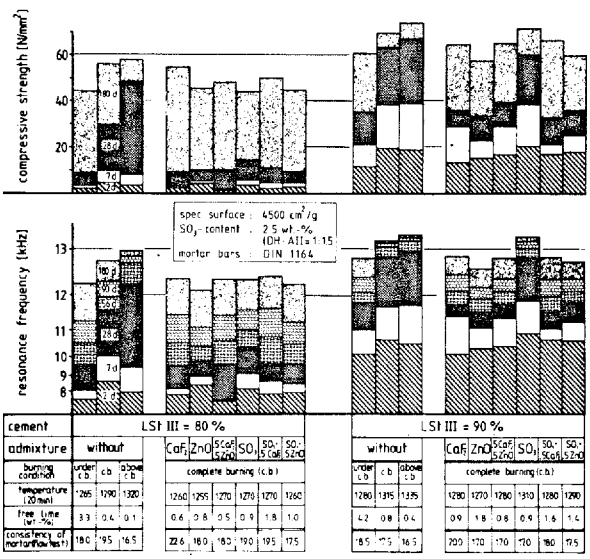

Figure 8
Compressive strength and resonance frequency of Portland cement mortars made of clinkers with different lime standards as a function of the burning degree and of a "mineralization"

lime binding, which is normal for the higher burning temperatures and finally results in a higher alite content (about 12 wt.-% C_3S). Yet, for a further strength increase, which is clearly observed especially for the low-lime cements, the explanation of an alite content increase is no longer valid, as the free lime and accordingly the C_3S content hardly show any changes at all due to an increase of the burning temperature.

CONCLUSION

According to the present investigations the production of low-lime Portland cements is possible up to lime standards of ≥ 80% with keeping favourable properties similar to the nowadays usual Portland cements. The decisive fact for a favourable reactivity behaviour is the minimum residue of alite which also can be added in mixing or grinding to an alite-free clinker. In that case, the special importance lays in the reduction of the theoretical energy consumption, the use of a significantly lower burning temperature as well as the positive influencing of the clinker grindability.

For values of LSt III ≤ 90%, an additional "mineralization" leads to an only minimal improvement in the burnability and does not imply an improvement in the hydraulic reactivity. According to the results reached up to now the application of such materials will be confined to alite-rich clinkers; what remains to be examined is the significant influence of the burning temperature on the hydration properties.

ACKNOWLEDGEMENT

This work was financially supported by the Deutsche Forschungsgemeinschaft in Bonn, to which we want to express our thanks.

LITERATURE

(1) Tsuboi,T., Ito,T., Hokinoue,Y., Matsuzaki,Y.: Die Einflüsse von MgO, SO_3 und ZnO auf die Sinterung von Portlandklinker. Zement-Kalk-Gips (1972) 426-431

(2) Odler,I., Abdul-Maula,S.: Einfluss von Mineralisatoren auf das Brennen des Portlandzementklinkers. Teil I: Kinetik des Brennprozesses. Zement-Kalk-Gips 33 (1980), 132-136 Teil II: Wirkungsweise von Mineralisatioren. Zement-Kalk-Gips 33 (1980) 278-282

(3) Odler,I.: Abdul-Maula,S.: Effect of oxid composition on Portland cement raw meal burnability. World Cement Technology (1980) 330-336

(4) Klemm,W.A., Jawed,I.: Burnability of synthetic and industrial raw mixes. VII. Int. Cong. Cem. Chem., Paris (1980), Vol. II, I/150-155

(5) Klemm,W.A., Jawed,I., Holub,K.J.: Effects of calciumfluoride mineralization on silicates and melt formation in Portland cement clinker. Cement & Concrete Research 9 (1979) 489-496

(6) Knöfel,D.: Beeinflussung einiger Eigenschaften des Portlandzementklinkers und des Portlandzementes durch ZnO und ZnS. Zement-Kalk-Gips 31 (1978) 157-161

(7) Christensen,N.H., Johansen,V.: Mineralizers and fluxes in the clinkering process. II. Kinetic effects on alite formation. VII. Int. Cong. Cem. Chem., Paris (1980), Vol. II, I/1-5

(8) Ludwig,U., Wolter,A.: Zur Bildung und Stabilität von Tricalciumsilikat und Aliten. Forschungsbericht des Landes NRW, Nr. 3092, Westdeutscher Verlag Opladen (1982) und Zement-Kalk-Gips (1979) 455-459

(9) Stark,J., Müller,A., Schrader,R., Rümpler,K.-H.: Existenzbedingungen von hydraulisch aktivem Belit-Zement. Zement-Kalk-Gips 34 (1981) 476-481

(10) Gosh,S.N., Mathur,V.K.,Chapra,S.K.: Low temperature OPC-type cement containing superhydraulic C_2S phase. Cement & Concrete Research 14 (1984) 437-438

(11) Rangnekar,B.S., Srinivasam,V.R.G., Paj,V.N.: An early hardening C2S-phase made by rapid heating technique. VI. Int. Cong. Cem. Chem., Moskau (1974), Suppl. Paper 1-4

(12) Metha,P.K.: Energy, resources and the environment - a review of the US cement industry. World Cement Technology 9 (1978) 144-160

(13) Metha,P.K.: Investigations on energy-saving cements. World Cement Technology 11 (1980) 166-177

(14) Sudho,G., Ohta,T., Harada,H.: High strength cement in the CaO-Al_2O_3-SiO_3-SO_3 system and its application VII. Int. Cong. Cem. Chem., Paris (1980), Vol. III/V-152

(15) Schwiete,H.E., Ziegler,G.: Beitrag zur Thermochemie von Zementrohstoffen. Zement-Kalk-Gips 9 (1956) 257-262

(16) Strassen,H.z.: Der theoretische Wärmebedarf des Zementbrandes. Zement-Kalk-Gipsö 10 (1957) 1-12

(17) Mussgnug,G.: Sinterfähigkeit von Rohmehl. Zement-Kalk-Gips 6 (1953) 46-53

(18) Heilmann,T.: The influence of the fineness of cement raw mixes on the burnability. III. Int. Cong. Cem. Chem., London (1952) 711-749

(19) Ludwig,U.: Einflüsse auf das Sinterverhalten von Zementrohmehlen. Zement-Kalk-Gips 34 (1981) 175-186

(20) Ludwig,U., Ibrahim,S.E.: Burnability of Portland cement raw mixes. VII. Int. Cong. Cem. Chem., Paris (1980), Vol.II, I/114-118

(21) Ludwig,U., Ruckensteiner,G.: Einflüsse auf die Brennbarkeit von Zementrohmehlen. Forschungsbericht des Landes NRW, Nr. 2372, Westdt. Verlag Opladen (1973) und Cement & Concrete Research 4 (1974) 239-246

(22) Ibrahim,S.E.: Zur Optimierung des Brennens von Zementrohmehlen. Diss. RWTH Aachen (1979)

(23) Billmeier,W., Ludwig,U., Pöhlmann,R.: Automatisierung von Brennprozessen mit exakt definierten Temperatur-Zeit-Programmen im Labor. Ceramic Forum International 62 (1985) 445-449

(24) Butt,Y.M., Timashev,V.V.: The mechanism of clinker formation processes and ways of modification of clinker structure. VI. Int. Cong. Chem., Moscov (1974), Princ. Paper

(25) Timashev,V.V.: The kinetics of clinker foramtion - the structure and composition of clinker and its phases. VII. Int. Cong. Cem. Chem., Paris (1980), Princ. Paper, Vol. I-3/1-20

(26) Newkirk,T.F.: The alkali phases in Portland cement clinker. III. Int. Cong. Cem. Chem., London (1952) 151-168

(27) Jawed,I., Skalny,J.: Alkalies in cement: a review - I. Forms of alkalies and their effect on clinker formation. Cement & Concrete Research 7 (1977) 719-730

(28) Glasser,F.P., Marr,J.: Sulfates in cement clinkering: Imsicibility between sulfate and oxide melts at 1350°C. Cement & Concrete Research 10 (1980) 753-758

(29) Sprung,S.: Technologische Probleme beim Brennen des Zementklinkers, Ursache und Lösung. Habilitationsschrift RWTH Aachen (1982)

(30) Mussgnug,G.: Beitrag zur Frage der Mahlbarkeit von Hochofenschlacken (Zementschlacken) und Klinkern. Zement 31 (1942) 183-193

(31) Schmid,A.: Abhängigkeit der Mahlbarkeit von Zementklinker und Kalkstein von den Stoffeigenschaften. Schriftenreihe der Zementindustrie (1953), Heft 14

(32) Beke,B.: Einiges über Mahlbarkeitsbestimmungen. Zement-Kalk-Gips 28 (1975) 325-330

(33) Odler,I., Schüppstuhl,J.: Combined hydration of tricalciumsilicate and β-dicalciumsilicate. Cement & Concrete Research 12 (1982) 13-20

(34) Kawada,N., Nemoto,A.: Calciumsilikate im frühen Verlauf der Hydratation. Zement-Kalk-Gips 20 (1967) 65-71

(35) Hatzigianelis,I.: Zum Einfluss von CaF_2 und Sulfat auf den Portlandzementklinkerbrand bei unterschiedlichem Kalkstandard. Studienarbeit, Institut für Gesteinshüttenkunde, RWTH Aachen (1984), unpublished

(36) Aran,Y.: Zum Einfluss von ZnO und Sulfat auf den Portlandzementklinkerbrand bei unterschiedlichem Kalkstandard. Studienarbeit, Institut für Gesteinshüttenkunde, RWTH Aachen (1984), unpublished

(37) Bei,R.: Untersuchungen zur Reaktivität von Portlandzementen in Abhängigkeit vom Kalkstandard, Brenngrad und Sinterhilfsmitteln beim Klinkerbrand. Diplomarbeit, Institut für Gesteinshüttenkunde, RWTH Aachen (1985), unpublished

D. Bürger and U. Ludwig, Institut fur Gesteinshüttenkunde, RWTH Aachen, West-Germany

Synthesis of Calcium Silicates at Low Temperatures and Influences on their Reactivity

Summary: The main component of Portland cement is tricalcium silicate, i.e. the solid solution, alite. In this paper, we present some results obtained from C_3S, alite and alinite produced at lower temperatures (1050 - 1350°C) and measurements of hydration processes of these synthetics.

Beside the possibility to save burning energy the purpose of the investigations was to obtain knowledge about the correlation between burning reactivity, development of microstructure dependent on burning conditions and the hydraulic reactivity of the tricalcium silicates.

As the most effectful sintering agents we used zinc oxide, calcium fluoride and manganese fluoride. Zinc oxide caused a high sintering of the granules by means of an increased molten phase formation (above 1200°C). The ZnO-alite was burned completely (free lime 1 wt.-%) at 1250°C/20 min in a laboratory rotary kiln.

Calcium fluoride accelerated the solid state diffusion reactions over the entire temperature range above 1100°C, the stability temperature of fluorine-alite[1]). A complete burning of CaF_2-alite was performed at 1150°C/20 min already.

Using manganese fluoride and the usual oxides A. F, M as mineralizers the attempt to synthezise a doped mineral called alinite has been successful at 1050°C/30 min (fluorine-alinite is stable from 950 to 1100°C and crystallizes in the tetragonal crystal lattice). Further the application of these mineralizers led to the formation of C_3S mixed crystals with triclinic, monoclinic and rhombohedral modifications.

Regarding the results of the hydration measurements one can summarize that ZnO accelerated whereas fluorine-ions retarded the alite-water-reactions considerably. This was particularly true for MnF_3-doped alinite.

Because of the high specific surface areas corresponding with fine-grained crystallites in a loosened homogeneous microstructure, the triclinic materials - especially C_3S burned at low temperatures - had a remarkably improved hydraulic reactivity.

O componente principal do cimento portland é o silicato tricálcico, isto é, a solução sólida, alita. Neste trabalho, apresentamos alguns resultados obtidos com C_3S, alita e alinita produzidos a temperaturas mais baixas (1.050 - 1.350°C) e medições dos processos de hidratação destes produtos sintéticos.

Além da possibilidade de economia de energia, o objetivo das investigações foi adquirir conhecimento a respeito da correlação entre reatividade de queima, desenvolvimento de microestrutura em função da queima e condições da queima, e reatividade hidráulica dos silicatos tricálcicos.

Como agentes mais eficientes de sinterização utilizamos óxido de zinco, fluoreto de cálcio e fluoreto de manganês. O óxido de zinco causou uma alta sinterização dos grânulos por meio de um aumento da fase líquida (acima de 1.200°C). O ZnO-alita queimou-se completamente (cal livre < 1% em peso) a 1.250°C, por 20 minutos em forno de laboratório.

O fluoreto de cálcio acelerou as reações de difusão do estado sólido em toda a faixa de temperatura acima de 1.100°C, temperatura de estabilidade de fluor-alita. Uma queima completa de CaF_2-alita se consumou a 1.150°C, por 20 minutos.

Usando fluoreto de manganês e os óxidos usuais A, F, M como mineralizadores, a tentativa para sintetizar um mineral dopado chamado alinita obteve sucesso a 1.050°C, por 30 minutos (fluor-alinita é estável de 950 a 1.100°C e se cristaliza em rede de cristais tetragonais).

Posteriormente a aplicação destes mineralizadores ocasionou a formação de cristais de C_3S misturados com modificações triclínicas, monoclínicas e romboédricas.

Com relação aos resultados das medições da hidratação, podemos resumir que o ZnO acelerou, enquanto íons fluor retardaram consideravelmente as reações alita-água. Isto foi particularmente verdadeiro para alinita dopada com MnF_3.

Devido às áreas de superfície específica altas correspondentes aos cristais finamente granulados em microestrutura homogênea frouxa, os materiais triclínicos - especialmente C_3S queimado a baixas temperaturas - tiveram uma reatividade hidráulica notavelmente melhorada.

D. Bürger and U. Ludwig, Institut für Gesteinshüttenkunde, RWTH Aachen, West-Germany

INTRODUCTION

The Technical Portland cement, which is generally produced in the temperature range from 1400 to 1500°C, consists of a phase composition of various clinker minerals.
The main components are the tricalcium silicate (C_3S) and dicalcium silicate (C_2S), that is their respective solid solutions, alite and belite. In this paper, we will present some results obtained from C_3S- and alite production at lower temperatures(1150-1350°C) and measurements of hydration processes of these synthetics. The purpose of the investigations is to get knowledge about the correlation between crystal symmetry, burning reactivity, development of microstructure dependant on burning conditions, and the hydraulic reactivity of the tricalcium silicates with and without additional agents.
A decrease of the sintering temperature of Portland cement clinker by chemical activation of the alite formation may lead to possibilities of energy saving, by some lower milling energy or diminished heat consumption.

EXPERIMENTAL

The first step in the experimental plan was the preparation of reactive alites and C_3S raw mixtures using very pure fine-grained crystalline or amorphous starting materials such as amorphous silica and precipitated hydroxides or oxides with high specific surface areas. Additionally, a spray drying technique and wet milling in a laboratory ball mill have been applied as homogenizing methods.
The second step was the examination of the burnability by determining the free lime content of the sintered products (with Franke's method) which is a measure for the burning performance:

C_3S-Formation

$$(1)\quad C_2S + C \xrightarrow{\geq\ 1264°C} C_3S \qquad 1)$$

$$(2)\quad C_3S\ (wt.-\%) = 100 - (4{,}072 \times C_{free})$$

The characterization of the sintered products was realized with SEM for the microstructure and morphology, BET and Blaine for specific surface area determinations and laser granulometer for grain size distributions of the grinding stock.

The hydraulic reactivity measurements have been carried out by means of conduction calorimeter traces (heat liberation) and quantitative x-ray analysis to determine the unreacted C_3S residue in the hydrated patterns and from that the degree of hydration.
Measurements of the rheological and setting properties of the alite pastes were realized using a rotational viscosimeter with specially made measuring cells.
The development of compressive strength of the hydrated samples and partly studies of the hydrated phases (morphology, C/S and H/S) permits us to describe the technological properties of the tricalcium silicates.
All applied methods are specified elsewhere[2].

REACTION MIXES AND THEIR PROPERTIES (C_3S, Alites, Alinite)

A survey on the produced lime-rich calcium silicates is given in Table 1. The pure tricalcium silicates were burned as pellets in the electrically fired chamber kiln, the alites and alinite as granules in the rotary kiln.

Synthetic Calcium Silicates

Electrical oven furnace (C_3S)

C_3S	: 1500°C, 14 h , C_{free} < 1,0 wt.-%	triclinic T_I, T_{II}
C_3S	: 1350°C, 24 h , C_{free} < 1,0 wt.-%	
C_3S	: 1375°C, 12 h , C_{free} < 1,0 wt.-%	

Electrical rotary kiln (alites)

C_3S (F,M)*)	: 1274°C, 20 min, C_{free} = 6,3 wt.-%	
C_3S (F,M)	: 1330°C, 20 min, C_{free} < 1,0 wt.-%	triclinic T_{III}
C_3S (F,M)	: 1350°C, 20 min, C_{free} < 1,0 wt.-%	
C_3S (A,F)	: 1284°C, 60 min, C_{free} = 2,4 wt.-%	
C_3S (A,F)	: 1307°C, 60 min, C_{free} < 1,0 wt.-%	monoclinic M_{Ia}
C_3S (A,F)	: 1350°C, 60 min, C_{free} < 1,0 wt.-%	
C_3S (A,F,M)	: 1274°C, 20 min, C_{free} = 3,7 wt.-%	inverse
C_3S (A,F,M)	: 1310°C, 20 min, C_{free} < 1,0 wt.-%	monoclinic M_{Ia}
C_3S (A,F,M)	: 1350°C, 20 min, C_{free} < 1.0 wt.-%	
C_3S (A,F,M) +2 wt.-% ZnO	: 1250°C, 20 min, C_{free} < 1.0 wt.-%	$M_{Ia} \longrightarrow$ Rh
C_3S (A,F,M) +2 wt.-% CaF_2	: 1150°C, 20 min, C_{free} < 1.0 wt.-%	rhombohedral Rh

Electrical rotary kiln (fluorine-alinite)

C_3S (A,F,M, 1 wt.-% MnO_2, 4,4 wt.-% CaF_2) 1050°C, 30 min, C_{free} = 5,8 wt.-%	Symmetry : tetragonal

*) F=Fe_2O_3 1 wt.-% A=Al_2O_3 1 wt.-% M=MgO (1-2 wt.-%)

Table 1 Synthetic Polycalcium Silicates

It is obvious that the synthesis of the higher symmetrical forms is possible by using the mineralizing oxides A, F, M (inverse monoclinic) and the additional sintering agents zinc oxide and calcium fluoride (rhombohedral modification).

The classification of the alite modifications was carried out according to [1), 3), 4)].
Fluorine alinite takes a special position within the group of lime-rich calcium silicates which according to literature[1),5)] consists of 3 mol C_3S and 1 mol CaF_2 (stoichiometric composition: $C_{11}S_4 \cdot 2CaF_2$[1)]) and occurs as a stable compound between 950 and 1100°C in the tetragonal crystal class, if the components A, F, and M as well as manganese oxide are applied as mineralizers.
Correlating with the increase in symmetry properties the burning temperatures, which are necessary for the complete burning, decrease, which is especially true for ZnO (2 wt.-%) and CaF_2 (2 wt.-%)-alites produced at very low temperatures and short burning periods (20 min). They could already be transformed completely at 1250 resp. 1150°C.
The relatively high lime content of the fluor alinite at burning conditions of 1050°C and 30 min is partly due to a too high lime content of the raw mixture[2)].

BURNING REACTIVITY OF THE ALITES

Pilot burnings were produced under defined burning conditions using calcium fluoride and zinc oxide respectively the A, F, M-oxides as alite forming admixtures. The furnace used was an electrical kiln permitting defined heating and cooling conditions and getting accurate sintering temperature and burning periods.
The results of these pilot tests are drawn up in the next graphs of figure 2 and 3. Further measurements may be found in literature[1),2)].

The results of the burning tests are here summarized:
Calcium fluoride and zinc oxide accelerated the alite formation in the represented temperature range between 1200 and 1400°C considerably, which agrees with other results[1)]. This is especially valid for CaF_2. Zinc oxide caused a high sintering of the pellets by means of an increased melting phase formation (iron-rich melting) above 1200°C corresponding with a small sintering intervall between 1200 and 1250°C.
Calcium fluoride accelerated the solid state diffusion reaction over the entire temperature range (increase of the free formation energy).
In the temperature range defined by free lime content < 2 wt.-% when a complete burning performance is practicable, the influence of a longer period is relatively slight, so that a short time of sintering applies to be the most economic way of manufacturing.

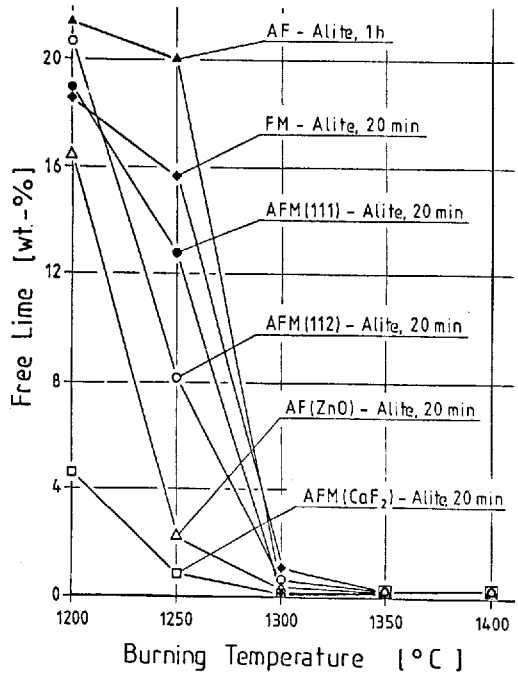

Figure 1
Burnability of alites with and without admixtures ((heating rate 100°C/min, rapid air cooling)

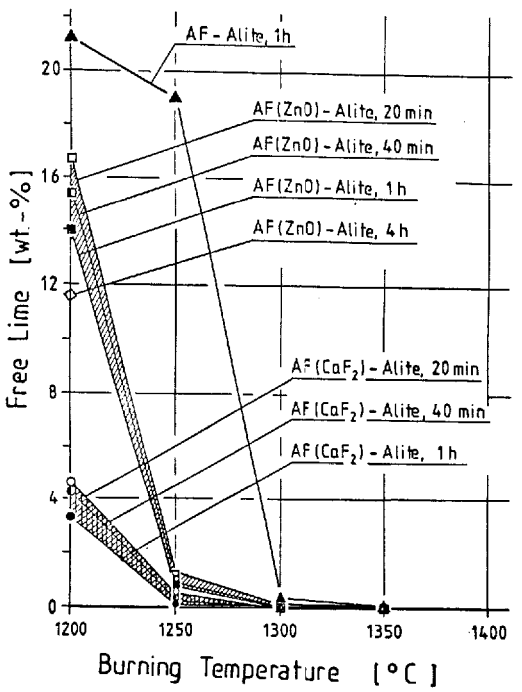

Figure 2
Free lime vs. burning temperature and burning period of the ZnO- and CaF_2-alites

D. Bürger and U. Ludwig, Institut für Gesteinshüttenkunde, RWTH Aachen, West-Germany

STRUCTURE DEVELOPMENT IN THE TRICALCIUM SILICATES

Instead of single results, a summarizing description of the results of structure investigations should be tried (table 2).

As an example for structure development serves figure 3 where the surfaces of C_3S and some alite sintering products are demonstrated.

Alltogether we can make the following statements:
All added mineralizing oxides (A,F,M) and especially the additives calcium fluoride and zinc oxide caused a greater sintering of the burned products at low temperatures. With this one can associate a partly strong grain growth, increased micropore share and low pore volume.

Corresponding to this the physical properties of the burning products changed. The granules were harder and more difficult to mill to a comparable fineness (favourable Blaine-value 4000 cm^2/g). An similar influence on the microstructure was affected by an increase of the burning temperature or lengthening of the burning time, as can be taken from figure 3 for pure C_3S.

Microstructure of the Tricalcium Silicates

(1)
reticulate homogenous structure
(cristallites 0,5-4 µm)
specific surface area (BET) in the burning products
4000-8000 cm^2/g
C_3S → FM-Alite → AF-Alite
(1375°C,14 h) (1330°C,20 min) (1307°C,60 min)
triclinic T_I triclinic T_{III} monoclinic M_{Ia}
(2)
homogenous structure, advanced up to strong recrystallization
(cristallites 4-16 µm)
porosity 10-25 Vol.-% ,
specific surface area 1000cm^2/g, strongly sintered products <200m^2/g
C_3S → FM-Alites → AF-Alites overburnt ≥ 1350°C → **→AFM-Alites** (1310°C,20 min)
inverse monoclinic M_{Ib}
(3)
Influence of special agents
CaF_2 in AFM-Alites (1150°C,20 min):
raising degree of sintering
ZnO in AFM-Alites (1250°C,20 min):
formation of melting phase, highly sintered

Table 2
Characterization of the microstructure of alites and C_3S (SEM, high pressure mercury porosimeter, BET)

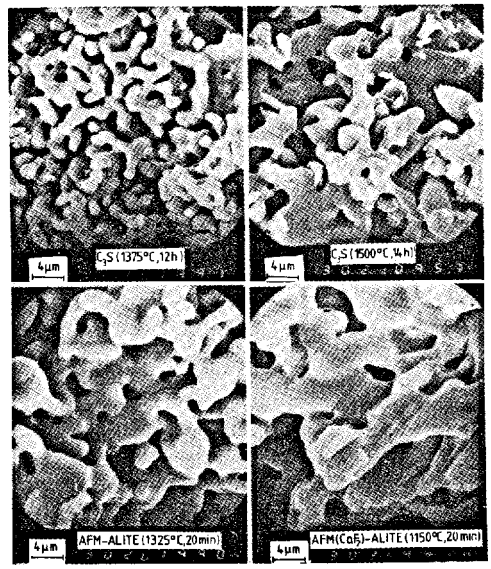

Figure 3
SEM photographs of C_3S, alite, and fluorine alite

The reaction mixes which were softly burnt at low temperatures - that is C_3S and FM-alites particularly - must be milled to a fineness more than 4000 cm^2/g to obtain similar grain size distribution determinated with laser granulometer[2]. Nevertheless, the milling energy needed was very low. In this field there are possibilities to save energy at the one hand, and to produce high-reactivity calcium silicates on the other hand.

HYDRAULIC REACTIVITY OF THE CALCIUM SILICATES

Figure 4 illustrates the reaction traces of various (low temperature) alites and C_3S with free lime contents < 1 wt.-% hydrated for 3 days in a microcalorimeter at 30°C with a water/solid ratio of one.

The influence of the burning temperature on the heat liberation determinated with this conduction calorimeter is shown in figure 5-7.

Measurements of the rheological properties (shear stress vs. shear rate) and setting (shear stress vs. time of hydration) are represented in figures 8 and 9. Table 3 and 4 exhibits the values of compressive strength and the degree of hydration as a function of curing time (pastes w/s = 0.5) for C_3S, alite, and alinite reaction mixes.

RESULTS

Discussing the results upon hydraulicity of calcium silicates the influence of the degree of burning, lime binding and microstructure features must be taken into account. The results of the experiments carried out can be summarized as follows:

1. Influence of the burning temperature

Reactive free lime as well as a favourable microstructure (high specific surface, size of the crystallites 1-4 µm) in the alites and in C_3S burned at very low temperatures caused partly substantial reaction accelerations in the hardening and setting processes (Table 4, Figures 10-11, AFM- and FM-alites at 1274°C). Both materials showed comparably high compressive strengths over the whole observation period of hydration. A swelling effect could not be stated.

The overburning of the reaction mixes (1350°C for FM-, AF-, and AFM-alites; 1500°C for C_3S) always led to a diminished reactivity.

There was less energy needed when the low-temperature alites were grinded, which showed fine-grained crystallites and a loosened microstructure, than for the samples burnt at high temperatures. The reactivity can be controlled by the burning temperature and the fineness (e.g. AFM (1274°C), FM-alites, C_3S (1375°C)).

The paste viscosity is appreciably increased with the help of an absorbent microstructure for the same W/S value. The regulation of the hardening process is possible for the higher sintered samples by the variation of the W/S value (e.g. ZnO-alite, Figure 8).

2. Influence of the chemical-mineralogical composition

The complete burning of the low-symmetrical forms of the tricalcium silicates needs more burning energy (e.g. C_3S (1375°C) and FM-alites). The resulting products were characterized by a higher porosity and relatively temperature-stable structure. Under the preposition that the grain size distribution is the same, the higher specific surfaces lead to an accelerated setting and hardening and to a higher heat evolution up to 3 days in the calorimeter (e.g. C_3S, FM-, and AF-alites, Figure 4).

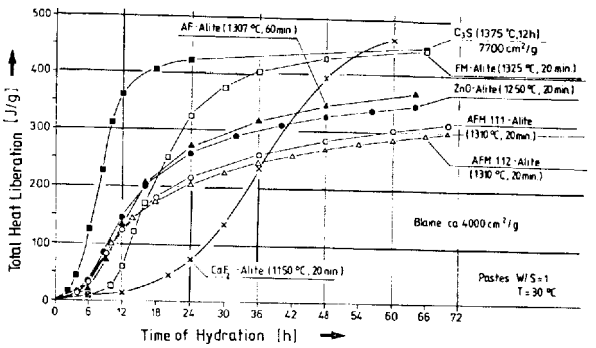

Figure 4
Heat evolution of hydrating alites and C_3S produced at low temperatures (free lime < 1wt.-%)

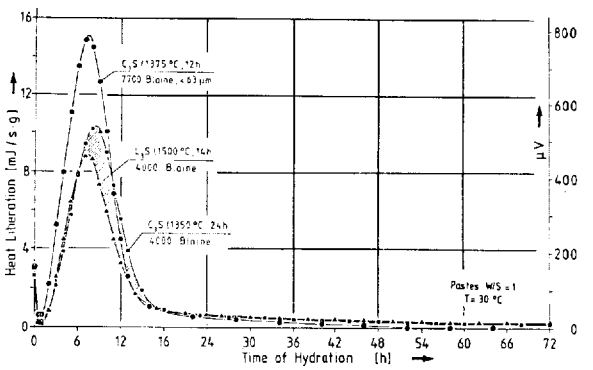

Figure 5
Influence of burning temperature on the rate of heat evolution of triclinic C_3S

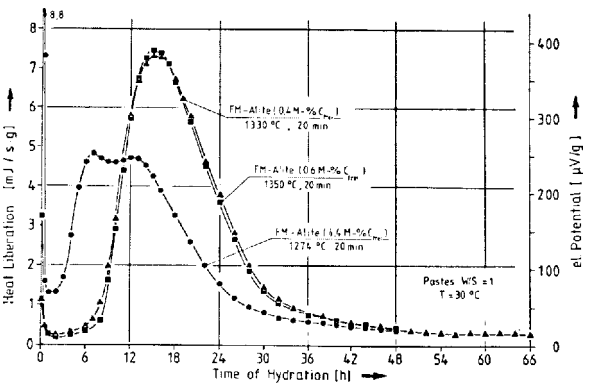

Figure 6
Influence of the degree of burning and burning temperature on the rate of heat evolution of triclinic FM-alite

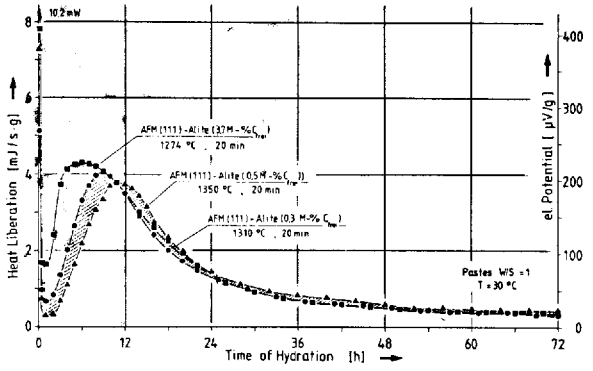

Figure 7
Effect of the degree of burning and the temperature on the rate of heat evolution of inverse monoclinic AFM-alites

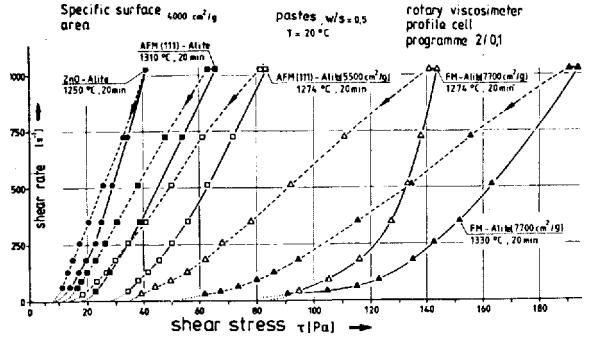

Figure 8
Rheological properties of alites: shear stress as a function of the shear rate (rheometer)

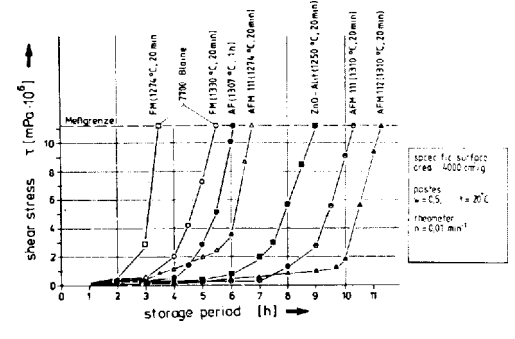

Figure 9
Setting properties of alites: Shear stress as a function of duration of the hydration (rheometer, n = constant)

Homogenizing Method : Spray-Drying-Technique								
Material	Burning Condition			Fineness (Blaine)	Degree of Hydration (%) Compressive Strength (N/mm²)			
	°C	h	min	cm²/g	1 (2)	3 (14)	28	90
C_3S	1500	14	-	4010	36,6 5,5	61,0 13,2	87,3 45,8	93,7 66,3
C_3S	1375	12	-	7700	79,5 25,8	87,6 40,3	96,6 58,4	97,7 77,2
Alite (A=1, F=1 M=2)	1325	-	20	4020	31,6 2,2	65,7 13,4	93,1 48,6	97,3 49,3
CaF_2-Alite	1150	-	20	4050	(24,8) (-)	50,5 7,1	92,0 40,3	95,5 45,3
Fluorine-Alinite	1050	-	20	4100	- -	(37,9) (4,1)	77,8 19,1	97,2 35,3

Table 3
Degree of hydration and compressive strength vs. duration of storage of triclinic C_3S, inverse monoclinic AFM-alite, rhombohedral CaF_2-alite and tetragonal fluorine alinite (pastes, W/S = 0.5, curing under water)

Homogenizing Method : Grinding in a Ball Mill							
Alite + 3 wt.-% Gypsum	Burning Condition		Fineness (Blaine)	Degree of Hydration (%) Compressive Strength (N/mm²)			
	°C	min	cm²/g	1	3	28	90
AFM (111) -Alite	1274	20	5500	51,4 9,5	65,7 20,4	82,6 47,1	88,8 56,6
	1310	20	3970	35,6 5,1	57,7 18,8	80,7 45,7	88,6 58,5
(M_{Ib})	1350	20	4140	36,5 6,5	63,6 16,0	84,2 46,5	89,8 50,6
AFM (112)	1310	20	4140	38,9 5,4	51,1 16,2	80,8 47,1	87,6 55,7
FM-Alite	1274	20	7700	54,6 8,3	71,7 17,8	91,6 56,4	96,3 59,5
(T_{III})	1330	20	7700	48,3 9,2	79,7 28,6	88,4 51,4	93,1 55,3
ZnO-Alite (M_{Ib}→Rh)	1250	20	4140	44,9 9,6	59,9 17,2	78,0 38,1	85,1 49,9

Table 4
Degree of hydration and compressive strength of various alites dependent on burning temperature and storage period (pastes, W/S = 0.5, curing under water)

3. Influence of special mineralizers

The ZnO-doped alite, which was completely burnt at 1250°C with comparable granulometric datas, had shorter setting times and higher early strengths than "normal alites", so that this alite could be ranged as reactive for the burning as well as for the behaviour of setting and hardening (Figure 9, Table 4). The glassy surfaces, which were caused by the melting phase, brought about a clear reduction of the paste viscosity. Doting with CaF_2 the lattice symmetry changed (rh) and brought about retarded hydraulic reactions of the alite (Table 3). With adding appropriate additives (e.g. gypsum) it became possible to activate this low-temperature alite (1150°C) and adapt its behaviour to that of normal alites[2].
The fluorine alinite had hydraulic reactivity, too, but in comparison to the fluorine alite showed more retardation in reaction in the chosen composition (table 3).

CONCLUSION

One of the essential findings of our research work is that it became possible to reduce partly to a markable degree the burning temperature for the synthesis of the calcium silicates in homogeneous raw mixtures and, at the same time, to save grinding energy and keep the hydraulic activity or even to increase it. It is to be expected that even under technical conditions the burning temperatures will be reduceable without any diminution in reactivity of the calcium silicates. The reactivity was especially high for the triclinic tricalcium silicates and alites, which were produced at low temperatures and hardly sintered. Their microstructure allowed a quick grinding to high fineness and accordingly a accelerated setting and hardening.
The use of the sintering agents CaF_2 and ZnO permitted the synthesis of alites at 1150 resp. 1250°C and led to a retarded (calcium fluoride) resp. a slightly accelerated reaction (zinc oxide) compared to "normal" alite.

ACKNOWLEDGEMENT

We are grateful to the LAND NORDRHEIN-WESTFALEN for the financial support.

LITERATURE

(1) Wolter A.: Zur Bildung und Stabilität von Tricalciumsilikat und Aliten Forschungsbericht des Landes NRW, Nr. 3092, Westdt. Verlag, Opladen, 1982
Ludwig U., Wolter A., ZKG 32 (1979) p. 455-459

(2) Bürger D.: Beitrag zur Synthese und Reaktivität von Calciumsilikaten, Dissertation RWTH Aachen 1985

(3) Woermann E., Hahn Th., Eysel W.: Chemische und strukturelle Untersuchungen der Mischkristalle von Tricalciumsilikat, 1.-4. Bericht, ZKG 16 (1963), p. 370-375, ZKG 20 (1967) p. 385-390, ZKG 21 (1968), p.241-251 ZKG 22 (1968), p. 235-241

(4) Guinier A., Regourd M., Principal Paper: Structure of Portland Cement Minerals V. Int. Congr. Chem. Cem. Tokyo (1968), Vol. I, 1-14

(5) Gutt W., Osborne G.J.: The System $CaO-2CaO\cdot SiO_2-CaF_2$, Trans. Brit. Cer. Soc. (1970), 125-129

Abla Gráfica e Editora Ltda.
Rua Júlia Lopes de Almeida, 15 e 15-A
Telefones: 253-6054, 253-6296, 253-6325
Rio de Janeiro – RJ

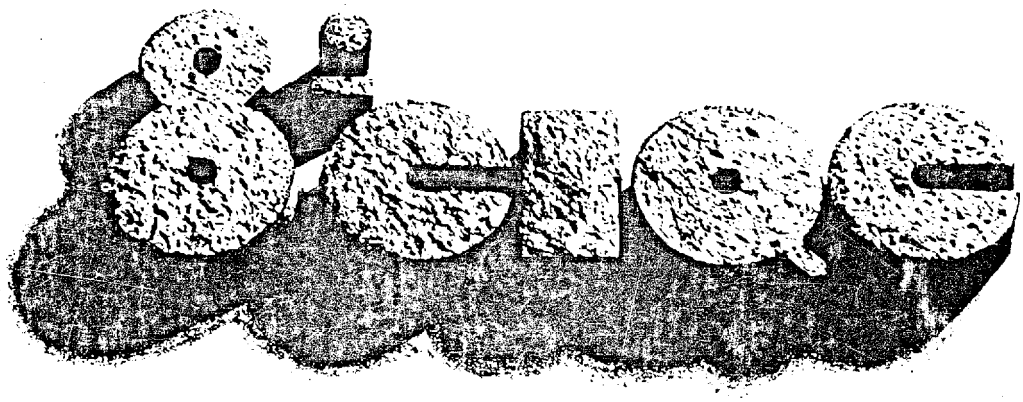

8.º Congresso Internacional de Química do Cimento

8th International Congress on the Chemistry of Cement

8e Congrès International de la Chimie des Ciments

Communications
THEME 2
Volume III

22-27 de setembro de 1986
Rio de Janeiro — Brasil



8.º Congresso Internacional de Química do Cimento

8th International Congress on the Chemistry of Cement

8e Congrès International de la Chimie des Ciments

Communications
THEME 2
Volume III

22-27 de setembro de 1986
Rio de Janeiro — Brasil

Não é permitida a reprodução dos Anais sem prévia autorização da Comissão Organizadora do Congresso.

The Proceedings are not to be reprinted without a previous permission of the Organizing Commission of the Congress.

La reproduction des Annales est interdite sans, au-devant, l'autorisation de la Commission d'Organisation du Congrès.

• • •

A substância e a forma de apresentação dos trabalhos que compõem os Anais do Congresso são de exclusiva responsabilidade de seus autores.

The substance and the form of presentation of the papers that compound the Proceedings of the Congress are exclusive responsability of their authors.

Le fond et la forme de publier les travaux qui composent les Annales du Congrès sont d'exclusive responsabilité de leur auteurs.

Secretaria Geral do 8º CIQC:
Rua da Assembléia, 10 - 40º and. - Gr. 4001
Tel.: 221-6562 – Telex: (021) 33191
20011 Rio de Janeiro – RJ – Brasil

Apoio financeiro da

finep FINANCIADORA DE ESTUDOS E PROJETOS

ORGANIZING COMMISION:

PRESIDENT:	JOSÉ ERMÍRIO DE MORAES FILHO	BRASIL
EXECUTIVE VICE-PRESIDENT:	PAULO MÁRIO FREIRE	BRASIL
TECHNICAL DIRECTOR:	FRANCISCO DE ASSIS BASÍLIO	BRASIL
ADMINISTRATIVE DIRECTOR:	JOÃO BATISTA MENESCAL FIUZA	BRASIL
DIRECTORS:	ALBERTO LUIZ GONÇALVES SOARES	BRASIL
	ENRIQUE GUNTHER DREWES	BRASIL
	EPAMINONDAS MELO DO AMARAL FILHO	BRASIL
	MARCÍLIO DE BRITO	BRASIL
	NEWTON GOULART	BRASIL

SCIENTIFIC COMMITTEES:

– SOUTH AMERICA:		
• PRESIDENT:	FRANCISCO DE ASSIS BASÍLIO	BRASIL
	ALVARO AUGUSTO ALVES PINTO	BRASIL
	DANTE E.J. VERONELLI	ARGENTINA
	FLEMING OEST	BRASIL
	HANS BUCHER	BRASIL
	JOÃO GASPAR DJANIKIAN	BRASIL
	LUIZ ROBERTO MARTINS DE MIRANDA	BRASIL
	MARIA DAS GRAÇAS JAQUÁ	BRASIL
	MARIA LUIZA MOREIRA DE MORAES	BRASIL
	NEY JOSÉ DE SOUZA E SILVA	BRASIL
	PABLO KITTL D.	CHILE
	PAULO RODRIGUES	BRASIL
	ROBERTO R. COELHO	BRASIL
	YASUKO TESUKA	BRASIL
	YUSHIRO KIHARA	BRASIL
– NORTH AND CENTRAL AMERICA, AND FAR EAST:		
• PRESIDENT:	JAN P. SKALNY	U.S.A.
MEMBERS:	DELLA M. ROY	U.S.A.
	GEOFFREY FROHNSDORFF	U.S.A.
	GERARD G. LITVAN	CANADA
	HIROSHI UCHIKAWA	JAPAN
	J. FRANCIS YOUNG	U.S.A
	JORGE MARIO VILLASENOR	MEXICO
	R.E. OBERHOLSTER	SOUTH AFRICA
	SIDNEY DIAMOND	U.S.A.
	S.W. TRESOUTHICK	U.S.A.
	WU ZHONG-WEI	CHINA
– EUROPE, ASIA AND AFRICA:		
• PRESIDENT:	JEAN PAUL MERIC	FRANCE
MEMBERS:	C. CHARRETON	FRANCE
	FRANCO MASSAZZA	ITALY
	FRANÇOIS LE BEL	FRANCE
	FRIEDRICH W. LOCHER	WEST GERMANY
	F. YAGIZ	TURKEY
	H.W.W. POLLITT	ENGLAND, U.K.
	JOSE CALLEJA	SPAIN
	J. TALLABER	HUNGARY
	LABO KADA ABOUBACAR	NIGERIA
	O.P. MTCHEDLOV-PETROSSIAN	U.S.S.R.
	P. DUTRON	FRANCE
	RENATO BUCCHI	ITALY
	S.K. CHOPRA	INDIA
	T.V. KOUZNETSOVA	U.S.S.R.
	WIESLAW KURDOWSKI	POLAND

INDEX

AUTHORS' NAMES/NOMS DES AUTEURS	SUB-THEMES/SOUS-THÈMES
A	
ABBIATI, G.	2.1
AFSHAR, A.B.	2.1 (2)
AKIMOV, G.V.	2.1 (3)
AMELINA, E.A.	2.1
ANDREEVA, E.P.	2.1
ARLIGUIE, G.	2.3
ASAGA, K.	2.1
B	
BACHIORRINI, A.	2.2
BAIQIAN, ZHONG	2.1
BAILEY, J.E.	2.2 (2)
BAILLEUL, P.	2.1
BALEK, V.	2.1
BAOYUAN, LIU	2.3
BARAGAÑO, J.R.	2.1
BARON, J.	2.2
BARRET, P.	2.1 (2)
BARTOS, P	2.3
BEAUDOIN, J.J.	2.2
BERTRANDIE, D.	2.1
BLUMENFEL'D, A.L.	2.1
BOIKOVA, A.I.	2.1
BROWN, P.W.	2.1
BUCK, A.D.	2.2
C	
CAMPOS, G.	2.1
CEBECI, O.Z.	2.2
CHENGJU, GUO	2.1
CHOI, S.H.	2.1
CHOUKIN, E.D.	2.1
CHPYNOVA, L.	2.2
CLAYDEN, N.J.	2.1
CLIFTON, J.R.	2.1
COLLEPARDI, M.	2.1 (4)
CONJEAUD, M.	2.2
COURTAULT, B.	2.1
CRAIEVICH, A.F.	2.2
CUSSINO, L.	2.1 (2)
D	
DAIMON, M.	2.1
DIAZ, G.	2.3
DJANIKIAN, J.G.	2.2
DMITRIEV, A.M.	2.1
DOBSON, C.M.	2.1
DOHNÁLEK, J.	2.1
DOMANSKY, A.I.	2.1
E	
EDEN, N.B.	2.2
F	
FEDIN, E.I.	2.1
FELDMAN, R.F.	2.2
FIERENS, P.	2.1
FRIGIONE, G.	2.3
FROHNSDORFF, G.	2.1
FUKAYA, Y.	2.1
FUSHII, Y.	2.1

G	
GARTNER, E.	2.1
GAWLICKI, M.	2.1
GEORGESCU, M.	2.1
GRANDET, J.	2.3
GRISHCHENKO, L.V.	2.1
GROVES, G.W.	2.1
GRUTZECK, M.W.	2.1
H	
HAN, K.S.	2.1
HANNAWAYYA, F.	2.1
HARA, N.	2.1
HASEGAWA, T.	2.1
HENDERSON, E.	2.2
HENRY, F.	2.1
I	
ILIOUKHINE, V.	2.2
INOUE, N.	2.1
ISOZAKI, K.	2.2
J	
JAMBOR, J	2.2
JENNINGS, H.M.	2.1
JIA, WANG	2.3
JONGSHAN, XIE	2.3
K	
KABUEMA, Y.	2.1
KAMEGAI, N.	2.1
KATO, K.	2.1
KAWANO, Y.	2.1
KILLOH, D.C.	2.1
KISHI, K	2.1
KITTL, P.	2.3
KNUDSEN, T.	2.2
KOBAYAKAWA, S.	2.1
KOCHMAI, A.	2.1
KONTOROVITSH, S.I.	2.1
KOUDRIAVTSEV, A.B	2.1 (2)
KOUZNETSOVA, T.V.	2.1 (4)
KRÍZ, J	2.1
KURDOWSKI, W.	2.1 – 2.2
KUZEL, H.–J.	2.1
L	
LACH, V.	2.2
LETELLIER, M.	2.1
M	
MARCHESE, B.	2.3
MCCARTER, W.J.	2.1 (2)
MEHTA, P.K.	2.3
MELNIK, S.	2.2
MINGSHU, TANG	2.3
MINO, I.	2.1
MISKIEWICZ, K.	2.1 – 2.2
MITSUDA, T.	2.1
MLAKAR, V.	2.1
MONOSI, S.	2.1 (4)
MONTANARO, L.	2.1 – 2.2
MONTEIRO, P.J.M.	2.3
MOON, J.Y.	2.1
MORICONI, G.	2.1 (3)
MORTUREUX, B.	2.1
MTCHEDLOV-PETROSSIAN, O.P.	2.1 (2)
N	
NAKAGAWA, K.	2.2
NANRU, YANG	2.1
NEGRO, A.	2.1 (2) – 2.2
NEKHOROCHEV, A.V.	2.1
NOCÚN-WCZELIK, W.	2.1 (2)
NOMA, H.	2.1

O	
ORSZÁGH, J.	2.1
OUCHEROV-MARCHAK, A.V.	2.1
P	
PANCRAZI, F.	2.1
PANIOUCHKINE, V.	2.1
PARROTT, L.J.	2.1
PATEL, R.G.	2.1
PAURI, M.	2.1 (3)
PHALIPPOU, J.	2.1
PING, LU	2.2
POLAK, A.	2.1
PÖLLMANN, H.	2.1
PONOMAREV, I.D.	2.1
PRATT, P.L.	2.3
PURI, A.	2.1
Q	
QINGHAN, BIAN	2.3
R	
RAMACHANDRAN, A.R.	2.1
REGOURD, M.	2.1
RODGER, S.A.	2.1
S	
SAKAI, E.	2.1
SANITSKI, M.	2.2
SCRIVENER, K.L.	2.2 – 2.3
SEBÖK, T.	2.1
SERSALE, R.	2.3
SHRESTHA, P.R.	2.1
SIBATA, S.	2.1
SINGH, A.K.	2.1
SINGH, N.B.	2.1
SINGH,S.P.	2.1
SKALNY, J.P.	2.1
SKVÁRA, F.	2.2
SONGSHAN, XIE	2.3
SOROTSHKIN, M.A.	2.1
SORRENTINO, F.P.	2.1
SUFEN, HAN	2.3
SYCHEV, M.M.	2.1
SZUBA, J.	2.1
T	
TALEB, H.	2.1
TENOUTASSE, N.	2.1
TEOREANU, I.	2.1
TESUKA, Y.	2.2
TIRLOCQ, J.	2.1
TORAYA, H.	2.1
U	
UCHIDA, S	2.2
UCHIKAWA, H.	2.2
USHIYAMA, H.	2.1
V	
VAN DAMME, H.	2.1
VERNET, C.	2.1 (2)
VOLLET, D.R.	2.2
W	
WENDA, R.	2.1
X	
XIO-ZHONG, ZHANG	2.3 (2)
XUEQUAN, WU	2.3

Y	
YANO, K	2.1
YIUN-YUAN, HUANG	2.2
YUDOVITCH, B.E.	2.1
Z	
ZAPOLSKY, A.K.	2.1
ZARZYCKI, J.	2.1
ZHANWEN, WANG	2.1
ZHI-YUAN, CHEN	2.3 (2)
ZHONGWEI, WU	2.3

CONTENTS/TABLE DE MATIÈRES

THEME/THÈME 2
HYDRATION OF CLINKER COMPONENTS INDIVIDUALLY AND IN CEMENTS/HYDRATATION DES COMPOSANTS DU CLINKER ET DES CIMENTS

Chairman/Président: G. FRONHSDORFF (U.S.A.) – Secretary/Secrétaire: P.J.M. MONTEIRO (Brasil)

SUB-THEME/SOUS-THÈME 2.1
Physical Chemistry of Hydration Process; Influence of Minor Components and Admixtures. Physico-Chimie du Processus D'Hydratation; Influence des Éléments Mineurs et des Matières D'Additions

Chairman/Président: A.M. DMITRIEV (U.S.S.R.)

Principal Reporter/Rapporteur Principal: H.F.W. TAYLOR (Scotland, U.K.)

Pages	Authors (Countries)/Auteurs (Pays)	Titles of Papers/Titres des travaux
17	P. Fierens, Y. Kabuema, J. Országh, N. Tenoutasse, J. Tirlocq (Belgium)	Mécanisme réactionnel et cinétique de l'hydratation du silicate tricalcique en présence de chlorure de calcium.
22	Yang Nanru, Zhong Baiqian, Wang Zhanwen (China)	An active β -dicalcium silicate preparation and hydration.
28	Guo Chengiu (China)	Accelerating effect of chloride salts on the hydration of portland cement.
34	T. Sebök (Czechoslovakia)	Effects the molar parameters of sulphonated melamine and formaldehyde polycondensates on mortar properties.
40	V. Balek, J. Kríz, J. Dohnálek (Czechoslovakia)	Influence of temperature and admixtures on the C_3S and cement hydration investigated by radiometric emanation method.
46	L.J. Parrott, D.C. Killoh, R.G. Patel (England, U.K.)	Cement hydration under partially saturated curing conditions.
51	N.J. Clayden, C.M. Dobson, G.W. Groves, S.A. Rodger (England, U.K.)	The application of solid state nuclear magnetic resonance spectroscopy techniques to the study of the hydration of tricalcium silicate.
57	F. Henry, P. Bailleul, B. Courtault (France)	Hydration des phases pures du ciment et de mélanges synthétiques par relaxation en microondes.
64	C. Vernet (France)	Flux thermique et cinétique d'hydratation – Tentative d'approche thermodynamique et analytique du comportement interactif des ciments.
70	C. Vernet (France)	Séquence et cinétique des réactions d'hydratation de l'aluminate tricalcique en présence de gypse, de chaux et de fillers calcaires.
75	F. Pancrazi, J. Phalippou, J. Zarzycki, F.P. Sorrentino (France)	Synthesis of "C-S-H" gel.
79	D. Bertrandie, P. Barret (France)	Étapes élémentaires interfaciales de l'hydratation des aluminates de calcium, constituants des ciments.
86	P. Barret (France)	Mécanisme d' hydratation des silicates de calcium (C_3S, C_2S) constituants du ciment, vu à travers les concepts généraux de la réactivité des solides.

93	M. Letellier, H. Van Damme, B. Mortureux, M. Regourd (France)	Mécanisme d'action des fluidifiants etudié par RMN du proton.
101	N.B. Singh, A.K. Singh, S.P. Singh (India)	Retardation of portland cement hydration by citric acid.
109	A. Negro, G. Abbiati, L. Cussino (Italy)	Sur l'emploi du calcaire comme régulateur de prise du ciment.
114	L. Cussino, L. Montanaro, A. Negro (Italy)	Action de l'anhydride vanadique sur l'hydratation du ciment.
120	S. Monosi, M. Collepardi (Italy)	Effect of silica fume on the hydration products of C_3A-CSH_2 system.
125	M. Pauri, S. Monosi, G. Moriconi, M. Colepardi (Italy)	Effect of triethanolamine on the tricalcium silicate hydration.
130	S. Monosi, G. Moriconi, M. Pauri, M. Colepardi (Italy)	Effect of retarding admixtures on the portland cement hydration.
136	G. Moriconi, S. Monosi, M. Pauri, M. Colepardi (Italy)	Effect of alkali content in the clinker on the cement hydration with and without sodium gluconate.
142	Y. Fukaya, K. Kato (Japan)	Adsorption of superplasticizers on CSH(I) and ettringite.
148	K. Asaga, M. Daimon, S. Sibata, K. Kishi, K. Yano, P.R. Shrestha (Japan)	Effects of thermal history and additives on the hydration of β -Ca_2SiO_4.
154	H. Ushiyama, Y. Kawano, N. Kamegai (Japan)	Effect of carbonates on early stage of hydration of alite.
160	N. Hara, N. Inoue, H. Noma, T. Hasegawa (Japan)	Formation and characterization of jennite.
167	I. Mino, Y. Fushii, E. Sakai (Japan)	Early hydration of alite at low water to powder ratio.
173	T. Mitsuda, S. Kobayakawa, H. Toraya (Japan)	Characterization of hydrothermally formed C-S-H.
179	W. Kurdowski, W. Nocun-Wczelik, K. Miskiewicz, J. Szuba (Poland)	Induction period in calcium silicate hydration in light of some new experimental results.
183	M. Gawlicki, W. Nocun-Wczelik (Poland)	-Ca_3SiO_4 hydration in the presence of electrolytes.
187	I. Teoreanu, A. Puri, M. Georgescu (Romania)	Hardening processes in some C_4AF – additives – water system.
193	A.B. Afshar, W.J. McCarter (Scotland, U.K.)	Monitoring the influence of admixtures and composition on the early hydration characteristics of cement paste using AC electrical response techniques.
198	W.J. McCarter, A.B. Afshar (Scotland, U.K.)	Monitoring chemio-physical changes and microestructure development in OPC during early hydration.
204	J.Y. Moon, K.S. Han, S.H. Choi (South Korea)	Effect of calcium lignosulfonate on the early hydration process of portland cement.
211	J.R. Barragaño, G. Campos (Spain)	Extension of setting time by means of mineralized clinkers.
217	F. Hannawayya (Sweden)	The properties of C_4AF hydrated for 8 years.
225	A.R. Ramachandran, M.W. Grutzeck (U.S.A.)	Hydration of tricalcium silicate at fixed pH.
231	P.W. Brown (U.S.A.)	The implications of phase equilibria on hydration in the tricalcium silicate-water and the tricalcium aluminate-gypsum-water systems.
239	H.M. Jennings, H. Taleb, G. Frohnsdorff, J.R. Clifton (U.S.A.)	Interpretation of the effects of retarding admixtures on pastes of C_3S, C_3A plus gypsum, and portland cement.
244	E. Gartner, J.P. Skalny (U.S.A.)	Computation of solubility relationships for hydrating cement systems.
251	T.V. Kouznetsova, G.V. Akimov (U.S.S.R.)	Bicalcium slicate and calcium aluminates.
256	A.M. Dmitriev, A.K. Zapolsky, T.V. Kouznetsova, B.E. Yudovitch, I.D. Ponomarev (U.S.S.R.)	Alliage d'hydrolicité des ciments.

260	G.V. Akimov, T.V. Kouznetsova, A.B. Koudriavtsev, V. Paniouchkine (U.S.S.R.)	Défectuosités de structure et activité d'hydratation des minéraux entrant dans le clinker du ciment portland.
266	E.I. Fedin, T.V. Kouznetsova, A.V. Nekhorochev, M.A. Sorotshkin, A.L. Blumenfel'd, A.B. Koudriavtsev, G.V. Akimov (U.S.S.R.)	Étude de la cinétique de l'hydratation du ciment portland par la serie de méthodes nucleaires.
271	A.I. Boikova, L.V. Grishchenko, A.I. Domansky (U.S.S.R.)	Hydration activity of chlorine-containing phases.
277	M.M. Sychev (U.S.S.R.)	Cement hydration control.
281	A. Polak (U.S.S.R.)	Certaines nouvelles conceptions sur le mécanisme d'hydratation des liants.
285	O.P. Mtchedlov-Petrossian, A.V. Oucherov-Marchark (U.S.S.R.)	Classification des processus de durcissement des liants.
290	A. Kochmai, O.P. Mtchedlov-Petrossian (U.S.S.R.)	Phénomènes électrochimiques intervenant aux premiers stades d'hydratation et de formation de la structure des pâtes de ciment.
295	E.D. Choukin, E.P. Andreeva, S.I. Kontorovitsh, E.A. Almelina (U.S.S.R.)	Rôle des processus de la polycondensation au cours du durcissement d'hydratation des liants siliceux.
300	H. Pöllmann (West Germany)	Solid solution of complex calcium aluminate hydrates containing Cl^-, OH^- and CO_3^{2-} - anions.
307	R. Wenda, H.-J. Kuzel (West Germany)	B^{3+} in calcium aluminate hydrates.
314	V. Mlakar (Yugoslavia)	The role of kinetic parameters on the properties of hydrating cement paste.

SUB-THEME/SOUS-THÈME 2.2

Microstructure of Hardened Cement Paste and its Effects on its Behaviour
Microstructure de la Pâte de Ciment Hydraté et ses Effets dans son Comportement

Chairman/Président: P.K. MEHTA (U.S.A)

Principal Reporter/Rapporteur Principal: S. DIAMOND (U.S.A.)

Pages	Authors (Countries)/Auteurs (Pays)	Titles of Papers/Titres des travaux
323	Y. Tezuka, J.G. Djanikian (Brasil) H. Uchikawa, S. Uchida (Japan)	Hydration characteristics and properties of mixtures of cement and high content of calcium sulfate.
330	D.R. Vollet, A.F. Craievich (Brasil)	Structure and kinetics of formation of the gel phase in hydrated tricalcium silicate.
337	J.J. Beaudoin, R.F. Feldman (Canada), J. Baron, M. Conjeaud (France)	Dependence of degree of silica polymerization and intrinsic mechanical properties of C-S-H on C/S ratio.
343	Lu Ping, Huang Yiun-yuan (China)	A study of the intrinsic properties of hardened cement pastes (HCP).
349	V. Lach (Czechoslovakia)	The formation of $C_2SH(A)$ and C_3SH at the hydration of portland cement.
356	F. Skvára (Czechoslovakia)	Microstructure of hardened pastes of gypsum-free portland and slag cements.
363	J. Jambor (Czechoslovakia)	Pore structure and strengths of hardened cement pastes.
369	T. Knudsen (Denmark)	The dispersion model for hydration of portland cement.
375	E. Henderson, J.E. Bailey (England, U.K.)	Structure and morphological aspects of calcium silicate hydrates.

382	N.B. Eden, J.E. Bailey (England, U.K.)	Crack tip processes and fracture mechanism in hardened hydraulic cements.
389	K.L. Scrivener (England, U.K.)	A study of the microstructure of two old cement pastes.
394	A. Negro, L. Montanaro, A. Bachiorrini (Italy)	Sur l'hydratation de la phase ferrite en présence de chaux et gypse.
401	K. Isozaki, K. Nakagawa (Japan)	Behaviour of ettringite in high strength hardened cement paste.
407	W. Kurdowski, K. Miskiewicz (Poland)	$Ca_3SiO_4Cl_2$ hydration under hydrothermal conditions.
412	O.Z. Cebeci (Saudi Arabia)	Hydration and porosity of cement paste cured in warm and dry environment.
417	A.D. Buck (U.S.A.)	Relationships between ettringite and chloroaluminate, strength, and expansion in paste mixtures.
425	L. Chpynova, V. Ilioukhine, M. Sanitski, S. Melnik (U.S.S.R.)	Phénomènes cristallochimiques intervenant dans l'hydratation des minéraux du ciment.

SUB-THEME/SOUS-THÈME 2.3
Bond: Paste-Aggregate, Paste-Reinforcement and Paste-Fibres.
Adhérence: Pâte-Granulat, Pâte-Armature et Pâte-Fibres.

Chairman/Président: J.P. SKALNY (U.S.A.)

Principal Reporter/Rapporteur Principal: F. MASSAZZA (Italy)

Pages	Authors (Countries)/Auteurs (Pays)	Titles of Papers/Titres des travaux
433	P.J.M. Monteiro (Brasil), P.K. Mehta (U.S.A.)	Improvement of the aggregate-cement paste transition zone by grain refinement of hydration products.
438	P. Kittl, G. Diaz (Chile)	Compatibility of copper fibre with compacted cement and low thermal-skock fatigue thereof.
444	Chen Zhi-yuan, Zhang Xio-Zhong (China)	Investigations on the zinc/hydrated-cement-paste interfacial zone.
449	Chen Zhi-yuan, Zhang Xio-Zhong (China)	Distribution of $Ca(OH)_2$ and of the CSH phase in the oolithic marble/hydrated cement paste.
454	Wu Xuequan, Han Sufen, Bian Qinghan, Tang Mingshu (China)	Effect of pretreatment of aggregate surface on the properties of concrete.
460	Wang Jia, Liu Baoyuan, Xie Songshan, Wu Zhongwei (China)	Improvement of paste-aggregate interface by adding silica fume.
466	K.L. Scrivener, P.L. Pratt (England, U.K.)	A preliminary study of the microstructure of the cement/sand bond in mortars.
472	G. Arleguie, J. Grandet (France)	Durabilité de la liason acier galvanisé-patê de ciment portland.
478	G. Frigione, B. Marchese, R. Sersale (Italy)	Microcrackings propagation in flexural loaded portland and high slag cement concretes.
485	P. Bartos (Scotland, U.K.)	Bond in cements reinforced with bundles of fibres.

THEME/THÈME 2

Hydration of clinker components individually and in cements.

Hydratation des composants du clinker et des ciments.

Chairman/Président:

G. Fronhsdorff
National Bureau of Standards
Gaithersburg, MD, U. S. A.

Secretary/Secrétaire:

P. J. M. Monteiro
Companhia de Cimento Portland
Paraiso
Rio de Janeiro, Brasil

SUB-THEME/SOUS-THÈME 2.1

Physical chemistry of hydration process, influence of minor components and admixtures.

Physico-chimie du processus d'hydratation; influence des éléments mineurs et des matières d'additions.

Chairman/Président:

A. M. Dmitriev
Institute Niicement
Moscow, U.S.S.R.

Principal Reporter/Rapporteur Principal:

H.F.W. Taylor
Department of Chemistry University of Aberdeen
Scotland, U. K.

P. FIERENS, KABUEMA Y., J. ORSZÁGH, N. TENOUTASSE et J. TIRLOCQ
- Université de Mons et Université Libre de Bruxelles (Belgique) -

1

Mécanisme réactionnel et cinétique de l'hydratation du silicate tricalcique en présence de chlorure de calcium.
Reaction Mechanism and Kinetic of Tricalcium Silicate Hydration in the presence of Calcium Chloride.

2.1

RESUME

L'influence du chlorure de calcium sur la cinétique d'hydratation du silicate tricalcique a été mesurée par microcalorimétrie isotherme à conduction. Le dégagement de chaleur dû à la réaction d'hydratation est précédé d'une période d'induction dont la longueur augmente avec la concentration en $CaCl_2$.

La constante de la relation d'Avrami qui décrit l'étape d'accélération de l'hydratation augmente linéairement en fonction de la concentration du $CaCl_2$. L'influence de cet adjuvant sur l'étape de décélération, décrite par l'équation de Jander, ne semble être qu'un simple effet de relaxation calorifique. La variation de la longueur de la période d'induction est expliquée à l'aide d'un schéma réactionnel faisant intervenir deux réactions consécutives où l'adjuvant influence les grandeurs d'activation. On admet que, pendant la période d'induction, des germes potentiels se forment et donnent naissance à des centres réactionnels actifs dont le nombre doit atteindre une valeur limite pour que la phase de croissance puisse démarrer.

SUMÁRIO

A influência do cloreto de cálcio sobre a cinética da hidratação do silicato tricálcio foi medida por microcalorimetria isotérmica por condução. O desprendimento de calor devido à reação de hidratação é precedido de um período de indução cuja extensão aumenta com a concentração do $Ca\ Cl_2$.

A constante da relação de Avrami, que descreve a etapa de aceleração da hidratação, aumenta linearmente em função da concentração do $Ca\ Cl_2$. A influência desse aditivo sobre a etapa de desaceleração, descrita pela equação de Jander, não parece ser senão um simples efeito de relaxação calorífica. A variação da extensão do período de indução é explicado com o auxílio de um eschema reacional com a intervenção de duas reações consecutivas onde o aditivo influencia as grandezas de ativação. Admite-se que, durante o período de indução, germes potenciais se formam e dão nascimento a centros reacionais ativos cujo número deve atingir um valor limite para que a fase de crescimento possa começar.

Mécanisme réactionnel et cinétique de l'hydratation du silicate tricalcique en présence de chlorure de calcium. 2.1
Reaction Mechanism and Kinetic of Tricalcium Silicate Hydration in the presence of Calcium Chloride.

1. Introduction

Le chlorure de calcium est utilisé depuis longtemps pour accélérer la prise et le durcissement du ciment de Portland.

Son mode d'action est imputable, entre autres, à l'un des phénomènes suivants (1,2): formation des oxychlorures de formule générale x CaO.y $CaCl_2$.z H_2O, adsorption physicochimique, diminution du pH de la solution interstitielle ou action catalytique.

TENOUTASSE et DE DONDER (3) ont observé que la cinétique de l'hydratation du silicate tricalcique est décrite par le modèle cinétique d'Avrami et que celui-ci n'est pas modifié par la présence du $CaCl_2$. Par ailleurs, le même modèle reste valable en présence d'autres adjuvants (4).

Dans le présent travail, nous avons montré que la partie descendante de la courbe calorimétrique, qui correspond à un processus diffusionnel (5), est bien décrite par le formalisme mathématique proposé par JANDER (6).

La cinétique d'hydratation du silicate tricalcique a été suivie par microcolorimétrie isotherme à conduction. L'étude a porté sur l'influence de la concentration en $CaCl_2$ sur la durée de la période d'induction et sur la valeur des constantes cinétiques des équations d'Avrami et de Jander.

2. Résultats expérimentaux

Les expériences d'hydratation ont été réalisées à l'aide de solutions contenant de 0,05 à 1,00 mole/litre de $CaCl_2$, avec un rapport massique solution/solide égal à 1.

La figure 1 représente la vitesse de dégagement de chaleur dQ/dt pendant l'hydratation en fonction du temps et en fonction de la concentration en $CaCl_2$. L'effet accélérateur du $CaCl_2$ se traduit par une réduction de période d'induction t_i et par une augmentation de la vitesse réactionnelle. La vitesse maximum de dégagement de chaleur (Figure 2) augmente avec la concentration en $CaCl_2$. Par contre, la quantité totale de chaleur dégagée (Figure 3) passe par un maximum.

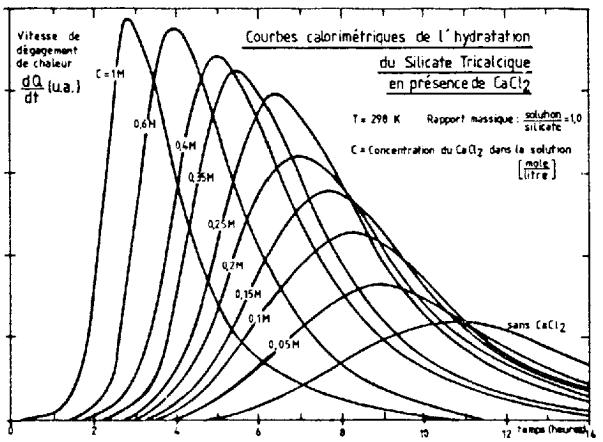

Figure 1

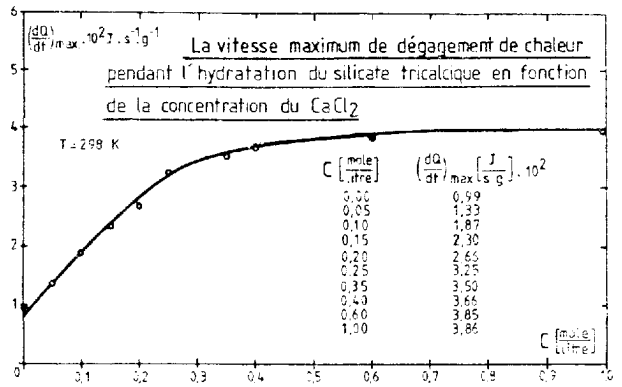

Figure 2

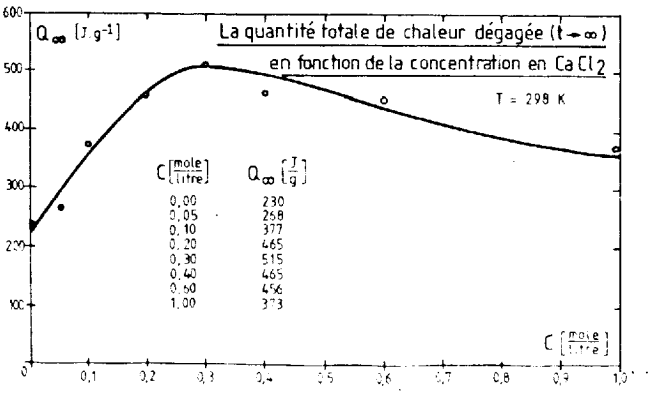

Figure 3

3. Interprétation des résultats

3.1. Etape d'initiation

La variation de la période d'induction t_i peut être représentée par la relation empirique :

$$\ln t_i = \ln t_i^\circ - bC \qquad [1]$$

où t_i° est la période d'induction sans $CaCl_2$, b = 1,2531 litre/mole est une constante ajustable et C est la concentration en $CaCl_2$.

Le Tableau I reprend les valeurs de t_i mesurées en fonction de C.

Tableau I

C $\left[\frac{\text{mole}}{\text{litre}}\right]$	10^{-3} t_i [S]
0,00	15,00
0,05	12,00
0,10	11,88
0,15	11,34
0,20	10,38
0,25	9,96
0,35	8,64
0,40	8,04
0,60	6,24
1,00	4,08

Cette relation peut être justifiée par un calcul qui découle d'un modèle réactionnel simple de deux réactions consécutives. Nous admettons que les germes de la réaction d'hydratation se forment à une vitesse constante au cours de la période d'induction qui précède la phase d'accélération de la courbe calorimétrique.

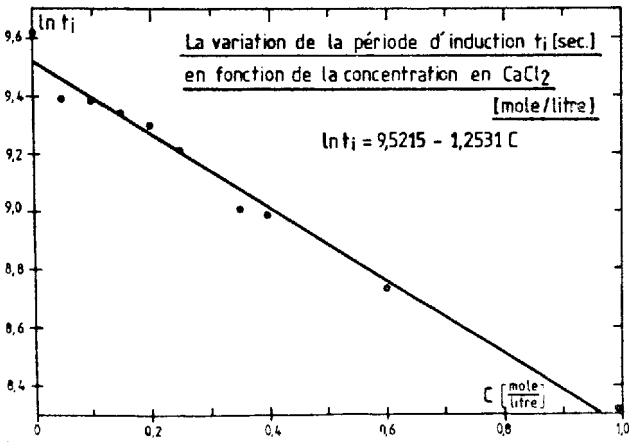

Figure 4

Le début de l'étape de croissance des hydrates ne peut avoir lieu qu'après la formation d'un certain nombre de germes. La vitesse de formation de ceux-ci est inversément proportionnelle à t_i. La grandeur $\frac{1}{t_i}$ peut être assimilée à la constante de vitesse d'un phénomène activé où le $CaCl_2$ influence l'enthalpie d'activation. Par ailleurs, FIERENS (7) a montré que $\frac{1}{t_i}$ obéit à la relation d'Arrhénius. On obtient ainsi, par un raisonnement classique, une relation d'énergie libre. En effet, l'enthalpie d'activation de la formation des germes $\Delta H^{\neq}$ est une fonction linéaire de la concentration C en $CaCl_2$:

$$\Delta H^{\neq} = \Delta H_o^{\neq} + \kappa C \qquad [2]$$

où κ est un coefficient de couplage exprimé en joule.litre.mole^{-1}, dont le signe est déterminé par le caractère accélérateur ou retardateur de l'adjuvant. Introduisons la relation [2] dans l'expression générale de $\frac{1}{t_i}$ suivant la théorie des vitesses absolues :

$$\frac{1}{t_i} = \frac{kT}{h} \exp \frac{\Delta S_o^{\neq}}{R} \cdot \exp \left(-\frac{\Delta H^{\neq}}{RT}\right) \qquad [3]$$

pour obtenir :

$$\ln t_i = \left(\frac{\Delta G_o^{\neq}}{RT} - \ln \frac{kT}{h}\right) + \kappa \frac{C}{RT} \qquad [4]$$

sachant que l'énergie libre d'activation de la germination sans adjuvant est :

$$\Delta G_o^{\neq} = \Delta H_o^{\neq} - T\Delta S_o^{\neq} .$$

On voit immédiatement que les relations [1] et [4] ont la même forme mathématique et à l'aide des valeurs du Tableau I, on obtient : $\Delta G_o^{\neq}$ = 86,48 k Joule.mole^{-1} et κ = -3,14 kJoule.litre.mole^{-2}. Le signe négatif de κ exprime l'effet accélérateur du $CaCl_2$. La valeur de $\Delta G_o^{\neq}$ est du même ordre de grandeur que celles qu'on observe pour l'énergie libre de la formation des lacunes dans les solides cristallins (8).

3.2. Etape d'accélération lors de la formation des hydrates

La constante de vitesse k de l'équation d'Avrami :

$$\left(\ln \frac{1}{1-\alpha}\right)^{1/3} = kt \qquad [5]$$

(α est le degré d'avancement de la réaction d'hydratation) varie d'une façon linéaire en fonction de la concentration C en chlorure de calcium (Figure 5). Cette variation est bien décrite par la relation empirique :

$$k - k_o = b.C \qquad [6]$$

où $k_o = 3,7.10^{-5} S^{-1}$ est la constante cinétique mesurée sans adjonction de CaCl, tandis que b est une constante ajustable dont la valeur numérique est $1,261.10^{-4}$ litre.mole^{-1} S^{-1}.

Toutefois, pour des concentrations

C>0,6 mole.litre^{-1}, l'équation [6] cesse d'être valable. (Cfr. Figure 6).

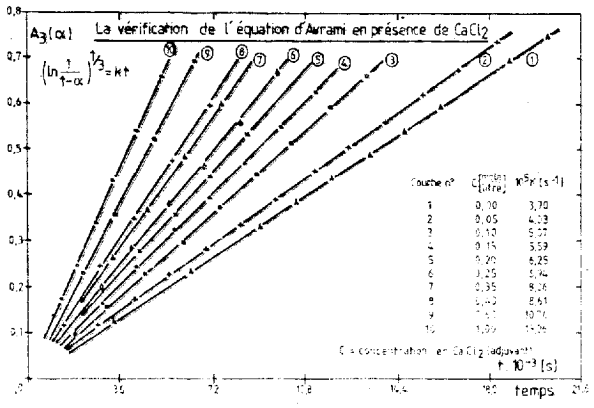

Figure 5

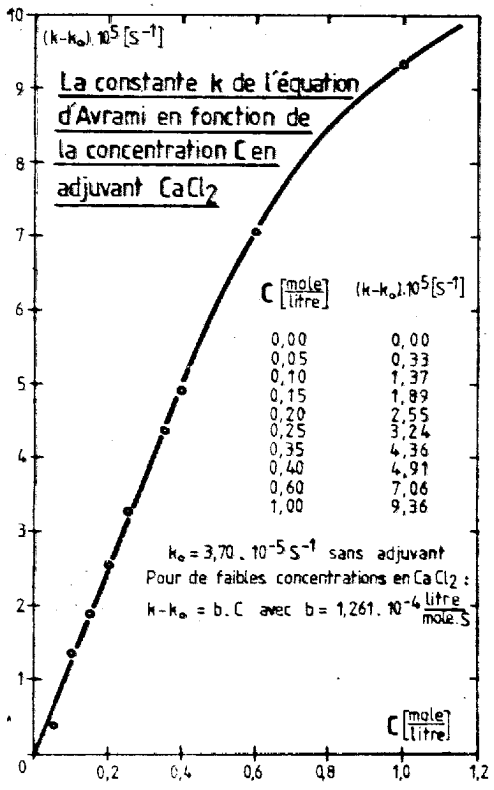

Figure 6

3.3. Etape de décélération

L'influence de la concentration en $CaCl_2$ sur la constante cinétique k_d de l'équation de Jander :

$$[1-(1-\alpha)^{1/3}]^2 = k_d t \qquad [7]$$

ne peut pas être décrite par une corrélation simple comme le montre le Tableau II.

Tableau II

C [mole/litre]	$10^5 k_d$ [S^{-1}]
0,00	0,133
0,05	0,209
0,10	0,534
0,20	1,293
0,30	2,439
0,40	1,333
0,60	1,328
1,00	0,686

Toutefois, on peut constater que, pour une concentration de 0,3 mole.litre^{-1}, l'effet accélérateur est le plus marqué. Par ailleurs, c'est à la même concentration que la quantité totale Q_∞ de chaleur dégagée (Figure 3) est la plus élevée. Vu la similitude des deux phénomènes, à savoir :

- la quantité totale de chaleur dégagée (position de l'équilibre),
- la vitesse de décroissance de l'hydratation en fin de réaction,

on peut se demander s'il ne s'agit tout simplement pas d'un effet de relaxation calorifique dû à l'évacuation de la chaleur réactionnelle.

4. Conclusions

La cinétique d'hydratation du silicate tricalcique C_3S, responsable des propriétés mécaniques du ciment de Portland présente encore de nombreux points à éclaircir. Les travaux effectués, ces dernières années en Belgique, ont montré que celle-ci obéit à la loi d'Avrami et à celle de Jander, même en présence de chlorure de calcium.

L'effet accélérateur de cet adjuvant se manifeste à la fois par le raccourcissement de la période d'induction et par l'augmentation de la vitesse de dégagement calorifique pendant la prise. L'effet catalytique du $CaCl_2$ sur la formation des germes d'hydratation peut être décrit à l'aide d'une relation d'énergie libre.

On a également pu mettre en évidence un déplacement d'équilibre de l'hydratation dû à la présence du $CaCl_2$ par une augmentation de l'ordre de 200 à 500 Joules/g de la quantité totale de chaleur dégagée.

5. Bibliographie

(1) - J. SKALNY, J.N. MAYCOCK
Journal of Testing and Evaluation
3 (4) 303 (1975).

(2) - V.S. RAMACHANDRAN
Mater. Constr. 4 (19) 3 (1971).

(3) - N. TENOUTASSE et A. DE DONDER
Silicates Ind. 35, 301 (1970).

(4) - P. FIERENS, KABUEMA Y.
Silicates Ind. Tome XLII, 313 (1977).

(5) - J.F. YOUNG
Colloque International sur les
adjuvants du ciment et du béton,
Mons, Novembre 1977.

(6) - KABUEMA Y.
Thèse de Doctorat ès Sciences -
Université de Mons (1979).

(7) - P. FIERENS
Il Cemento, 75, 195 (1978).

(8) - J.N. MAYCOCK, M. McCARTY
Cem. and Concr. Res., 3 (6) 701 (1973).

(9) - M.H. ROBERTS
Int. Admixtures for Mortar and Concrete, Brussels, August 30th -
September 1st (1967).

Yang Nanru, Zhong Baiqian and Wang Zhanwen
Nanjing Institute of Chemical Technology, Nanjing, China

1

An Active β-Dicalcium Silicate Preparation and Hydration

2.1

SUMMARY: A kind of active β-C_2S was synthesized by using a new technique in 1982. A mixture of CaO and SiO_2 (aerosil or silica gel) with stoichiometic composition of C_2S was subjected to hydrothermal treatment at about 373K for several hours, and then ignited at temperature 1123-1223K without stabiliser. The product obtained was examined by X-ray, IR. It was confirmed to be in pure β-form. The silicate polymerization distribution in hydrothermal treated mixture was determined by TMS technique (modified Tamas method) followed by GLC and GPC . It was evident that the polymer of silicate preferably forms during hydrothermal process, but is eliminated in subsequent ignition. The formation of active β-C_2S is attributed to dehydration of C_2SH_x formed in hydrothermal condition and reaction of polymer silicate with free CaO remained. The characteristic of active β-C_2S is mainly exhibited at early stage hydration. The heat evolution of the hydration of active β-C_2S within 1 hour is much higher than that of controlled β-C_2S (burned at 1613K). The heat evolution of active β-C_2S in 10 and 30 mins are even higher than C_3S. The strength development of active β-C_2S is extremely different from that of controlled one. The active paste not only gives a significant strength at 3 days, but also shows a greater increment of compressive strength between 7 and 28 days, e.g. 9.3 Kg/cm^2 per day against to 0.91 Kg/cm^2 for controlled species. The rate of hydration determined by the amount of combined H_2O gives the similar results. The morphology of hydration products at early stage and long term hydration was observed by SEM. The formation mechanism of active β-C_2S was studied in this paper as well.

Em 1982, usando-se uma técnica nova, foi sintetizado um tipo de β-C_2S ativo. Uma mistura de CaO e SiO_2 (aerosil ou gel de sílica), com composição estequiométrica de C_2S, foi submetida a tratamento hidrotérmico a cerca de 373K durante várias horas, e então queimada a temperatura de 1.123 a 1.223 K sem estabilizador. O produto obtido foi examinado por Raio X, IR (infra-vermelho). Confirmou-se ser forma pura de β. A distribuição da polimerização do silicato na mistura tratada hidrotermicamente foi determinada por técnica de TMS (método modificado de Tamas), seguido por GLC e GPC. Ficou evidente que o polímero de silicato se forma preferencialmente durante o processo hidrotérmico, mas é eliminado na combustão subseqüente. A formação de β-C_2S ativo é atribuída à desidratação de C_2SH_x formado em condição hidrotérmica e reação de silicato de polímeto com CaO livre remanescente. A característica do β-C_2S ativo se manifesta principalmente no estágio inicial de hidratação. A evolução de calor da hidratação de β-C_2S ativos no período de 1 hora é muito mais alta que a do β-C_2S controlado (queimado a 1.613K). A evolução de calor de β-C_2S ativo em 10 e 30 minutos é até mesmo mais alta que a do C_3S. O desenvolvimento da resistência de β-C_2S ativo é muitíssimo diferente do desenvolvimento da resistência do β-C_2S controlado. A pasta ativa não só dá uma resistência significativa aos 3 dias, mas também apresenta um aumento maior da resistência à compressão entre 7 e 28 dias, por exemplo, 9,3 kg/cm^2 por dia contra 0,91 kg/cm^2 dos espécimes controlados. A velocidade de hidratação determinada pela quantidade de H_2O combinada dá resultados semelhantes. A morfologia dos produtos de hidratação foi observada por microscópio eletrônico de varredura (SEM) no estágio inicial de hidratação e a longo prazo. Neste artigo se estuda também o mecanismo de formação do β-C_2S ativo.

1. INTRODUCTION

Dicalcium silicate, existing in meta-stable form i.e. β-form at room temperature, is commonly found in Portland cement as one of the major four constituents, which gives promissing hydraulicity,especially at the latter stage of hydration. The hydration products of β-C_2S are quite similar to those of C_3S (1). It is well known that β-C_2S is characterized by high ultimate strength, even higher than that of C_3S after hydrating for one year(2). However, the regretable fact is that the early hydration rate of C_2S is too low, which gives so slow a strength development. For this reason, no sufficient attention has been paid to it before in both research and practice.But many years ago, Nurse(3) has suggested already that the acquirement of the early strength development of C_2S is not impossible. The lower hydralic activity of C_2S in Portland cement may be attributed(impute) to the high burning temperature, at which β-C_2S crystallized in relatively perfect form and forms crystals in larger size. If the formation temperature of β-C_2S(or cement) can be decreased, the reactivity of C_2S with water may be increased to a certain extent, especially for the first days of hydration. Thus β-C_2S might be an alternative hydraulic mineral in Portland cement to minimize, if not eliminate, the content of C_3S. Accordingly, investigators in many countries in past years were diverted from their interest in C_3S to C_2S Some of them attempted to make a cement in which C_2S is a predominant mineral, such as Porsal cement(4), belite aluminate cement (5-7), energy-saving cement, (8-9), active belite cement (10-13) etc. In addition, the pure active β-C_2S has been also prepared by different ways, namely: 1) evaporation spray drying technique by D.M.Roy and S.O.Oyefesobi(14); 2) melting and decomposing $Ca(NO_3)_2$, then reacting with SiO_2 at 1023 K(15); 3) by addition of activators, such as K^+ Na^+, Sr^{+2} , and Ba^{+2} salts(16-17); 4) by addition of stablizer to form α'-C_2S(18-19); 5) with different thermal treatment, for instance by means of thermal shock(20-21), etc. The authors of present paper have synthesized β-C_2S, which possesses high early hydration rate, from aerosil, trass, silica gel and CaO (CaO/SiO_2=2) under hydrothermal treatment followed by ignition at 1223K (22). This technique was also used to produce a sort of belite cement-special low lime fly ash cement consisting of β-C_2S and $C_{12}A_7$ as predominant minerals(23).

2. EXPERIMENTAL

2.1 Preparation of β-C_2S

Materials used SiO_2: aerosil, ignition loss is about 7-8 %.
CaO : analytical grade.

Procedure of preparation A CaO/SiO_2=2 mixtures with a small amount of water was moulded into cylinders or cubes, then put into a steel vessel and subjected to hydrothermal treatment at 368-373K. The vessel was sealed with a small hole on the top of the lid for the purpose to prevent the contamination of CO_2 in the air. The treatment was prolonged for several hrs. The sample was then taken out and ground in an agte mortar in order to peel off the hydration products conering over the SiO_2 grains, and then treated under hydrothermal condition again. The procedure was repeated untill the content of f-CaO in the mixture is less than 10 %. After then the mixture was heated at 1223K without any stabilizer. While the product was cooled, no dusting phenomenon was observed. The XRD and IR spectra for the product showed that there was noly pure β-C_2S present in it (Fig.1). For comparison the controlled β-C_2S was also synthesized at high temperature, namely 1623K with B_2O_3 as stablizer.

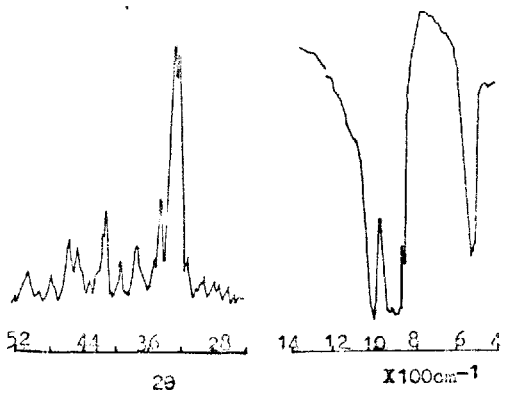

Fig.1 The XRD and IR of synthesized β-C_2S

2.2 Methods for the Determination of Hydration

2.2.1 IR-75 Spectrometer, made in DDR, with wave lengths 400-4000 cm^{-1} was used for IR spectrum in the present work. KBr disc method was employed for the preparation of samples.

2.2.2 XRD: Y-2 X-Ray diffractometer, made in China , was adopted.

2.2.3 SEM observation: on DX-3A SEM, made in China.

2.2.4 Heat of hydration: conductive calorimeter was used in the measurement.

2.2.5 Trimetyl silylation (TMS) technique combined with GLC and GPC to determine the degree of polymerization of C-S-H gel.

Hydrated C_2S indifferent ages derivatized by TMS technique according to the procedure of Tamas et al. (24) and the present authors(25). N-C_{14} was used as internal standard. The TMS derivatives were then followed by GLC or GPC analysis.

SC-7 gas chromatograph(made in China), used in this study, was equipped with H_2 ionic detector and SCOT OV-101 capillary column in ϕ0.2mmX20m. Waters 200 ALC Gel permeation Chromatograph was used with two 500 u-styrogel columns in series. The elution agent was toluene and the rate of elution 1.0 ml/min. RI (ϕX) refractometer was adopted as detector.

2.2.6 Physical properties of β-C_2S pastes were tested by standard specifications.

3. RESULTS AND DISCUSSION

3.1 Physical properties of β-C_2S

	active C_2S	controlled C_2S
specific gravity, g/cm^3	3.20	3.252
specific area, m^2/g	8.72	0.74
consistency, %	55	42

It can be seen that the specific gravity of two type of C_2S is very close, but the specific surface of area and consequently the consistency of active C_2S is much higher than the controlled one.

The compressive strength development of pastes within 3 days to 90 days after hydration was measured. For the purpose of comparison early strength of C_3S was

also taken. The results were illustrated in Table 1 .

Table 1 Compressive strength of pastes (MPa)

Hydration time (days)	3	7	14	28	90
active C_2S	0.5	1.15	7.34	20.67	40.81
controlled C_2S	-	0.57	0.73	2.46	26.69
C_3S	-	5.72	12.87	17.23	46.16

Table 1 shows: 1) In spite of higher consistency, there is a measurable strength at early stage hydration (3 days) for active C_2S. On the contrary there is no detectable strength for ordinary C_2S. The strength development of active C_2Sincreased rapidly between 7-28 days. This is distinctly different from ordinary C_2S, the strength development of which is appreciably enhanced only after 28-days of hydration. The 7-days and 14-days strength of active C_2S is 2 and 10 times that of the controlled C_2S respectively. 2) The strength of active C_2S is comparable to that of C_3S after 28-days. It is well known that the strength of C_2S gets close to C_3S normally only after one year of hydration.

3.2 Hydration rate determination

The hydration of the pastes was stopped with acetone in desired ages. The samples were then dried at 333 K and put into sealed tubes for the following measurements.

3.2.1 The content of combined H_2O and $Ca(OH)_2$ formed

The content of combined H_2O was determined by ignition of the samples at 1223 K. The amount of $Ca(OH)_2$ formed during the hydration was measured by glycerine ethyl alcohol method. The results are shown in Table2.

Table 2 Content of combined H_2O and $Ca(OH)_2$ (%)

Hydration time (days)	3	7	14	28	90
		combined H_2O			
active C_2S	2.3	4.38	5.91	11.95	25.11
controlled C_2S	-	1.34	1.49	2.54	11.18
		$Ca(OH)_2$ formed			
active C_2S	-	0.56	2.05	3.70	4.23
controlled C_2S	-	0.07	0.14	0.59	4.26

3.2.2 The amount of unhydrated C_2S determined by TMS-GLC analysis

Von H. Stade and W.Wieker have identified (26) that the primary product of hydration of C_3S is monosilicate, but it condenses at 275K forming disilicate. At higher temperature a C-S-H phase is formed, consisting of di- and poly-silicates. Therefore, it may be assumed that no monosilicate hydrate will be present during the hydration of C_3S and C_2S at room temperature. So it might be possible to determine the quantity of unhydrated C_2S and C_3S with the help of gas chromatogram of TMS derivatives, i.e. from the area of monomer's peak. In this study, samples of both type C_2S, hydrated for 3,7,185 days and 4 years, were examined. The gas chromatogram of the TMS derivatives are shown in Fig.2. The calibration curve of C_2S (mg) versus area ratio of monomer/I.S. was used to evaluate the quantity of unhydrated C_2S remaining in the hydrated samples. The results are indicated in Tab.3.

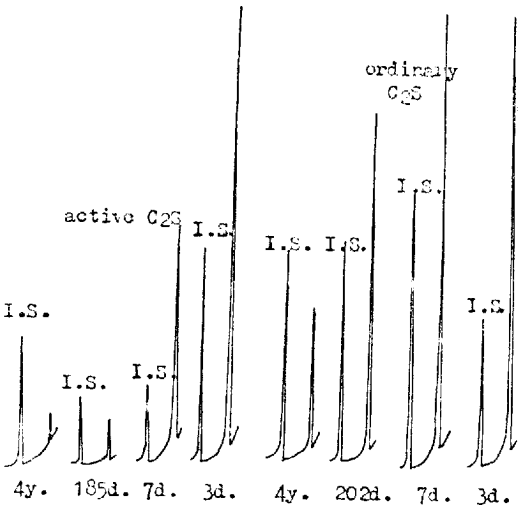

Fig.2 Gas chromatograms of C_2S (only monomer has been shown)

Table 3 Area ratio of monomer/I.S. and quantity of C_2S unhydrated(mg)

Hydration time(days)		3	7	185	4y.
active C_2S	area ratio	3.533	2.643	0.639	0.233
	unhydrated(mg)	76.80	57.46	13.89	5.07
controlled C_2S	area ratio	4.204	3.520	1.898 (202d)	0.654
	unhydrated(mg)	91.39	76.52	41.26 (202d)	14.22

It is clear from Fig.2 and Tab.3 that the active C_2S hydrated far more rapidly than controlled one.

3.2.3 The long term hydration characteristics

The 4-years hydration pastes were subjected to XRD and IR examinations. The results are shown in Fig.3 and Fig.4. For active C_2S, as is shown in Fig.3, there is only a little amount of unhydrated C_2S, most of it having been hydrated already. However, there is still an appreciable amount of C_2S unhydrated in controlled C_2S sample. The IR spectra showed the same results. As can be seen in Fig.4, the characteristic absorption band of C_2S disappears, instead a high absorption frequency, denoted at 1180 cm^{-1} shows up due to the polymerization of SiO_4^{-4} and the occurence of anions of Si-O-Si bond for the case of active C_2S. On the contrary, the absorption band of controlled C_2S hydrates show only a shoulder at 1160 cm^{-1}. The characteristic band of C_2S remains apparently. These results fairly agree with those described above.

3.3 Heat of hydration

The present investigation on the heat of hydration of both kinds of C_2S and C_3S was carried out by utilizing a conductive calorimeter, with W/S=0.7.The period of measurement was lasted up to 32 hrs. The rate of heat evolution during hydration was calculated and is shown in Fig.5 . The main points from the results may

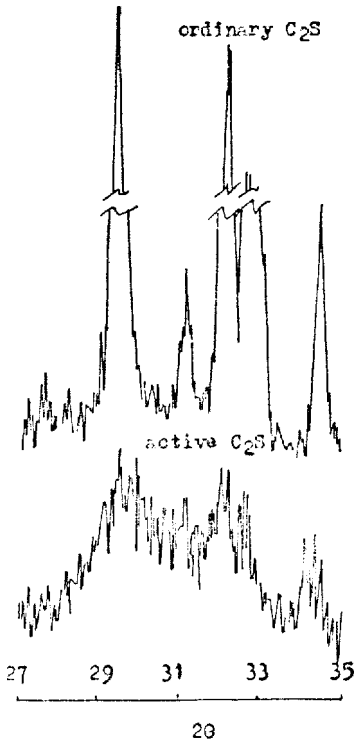

Fig.3 The XRD of both type of C_2S hydrated pastes for four years

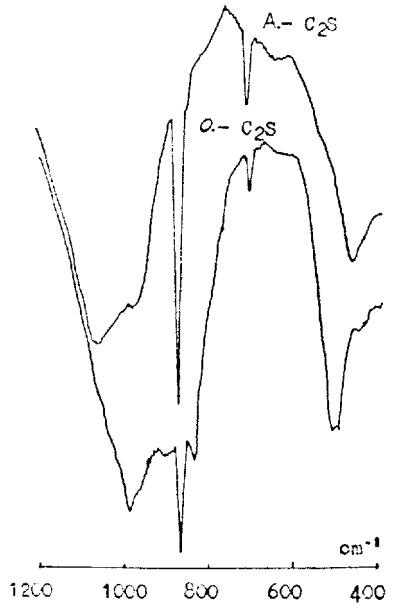

Fig.4 The IR of both type of C_2S hydrated pastes for four years

be summarized as follows: 1) The reactivity of active C_2S with water is far higher than controlled C_2S during the first peak of heat evolution, but it drops sharply after the first hour of hydration. The heat of hydration of active C_2S in the first hour is even higher than C_3S. 2) There is no second peak of hydration at all for both kinds C_2S samples. 3) The total quantity of heat evolution of active C_2S is much less than that of C_3S. The total amount of heat, evoluted during hydration of C_3S within 32 hrs., was 29.56 cal g^{-1} under the experimental conditions, at the meanwhile, it was only 4.93 cal$\cdot g^{-1}$ for active C_2S, and 0.724 for controlled one.

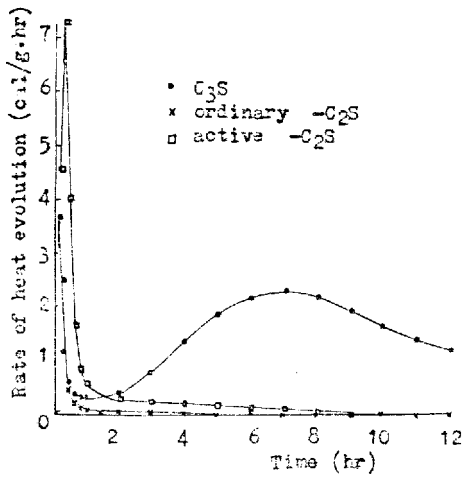

Fig.5 The heat evolution rate of C_2S and C_3S at the early stage of hydration

3.4 SEM observation

Photos 1-4 show the SEM of both type C_2S hydrated for 7 days and 4 years. It is clear that active C_2S has hydrated to a significant extent for 7 days, the hydration product C-S-H can be seen in photo 1. As for ordinary C_2S, the profile of C_2S grains are obviously visible. It is noted that the sight field is fully covered by type-IV C-S-H for active C_2S hydrating up to 4 years, but the situation is not the same in the case of ordinary C_2S.

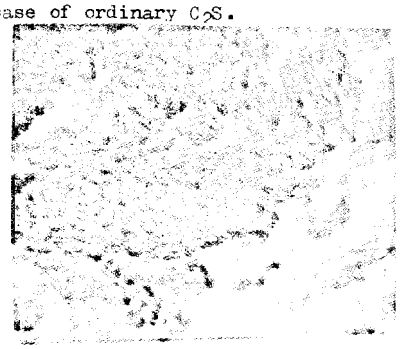

Photo 1. SEM of active C_2S hydrated for 7 days (3300X)

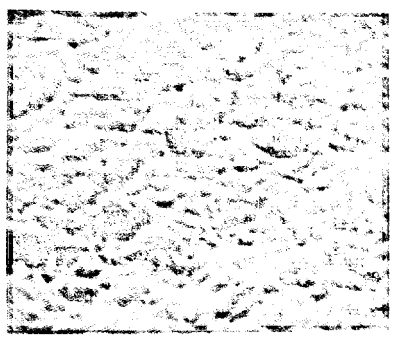

Photo 2. SEM of active C_2S hydrated for 4 years (4500X)

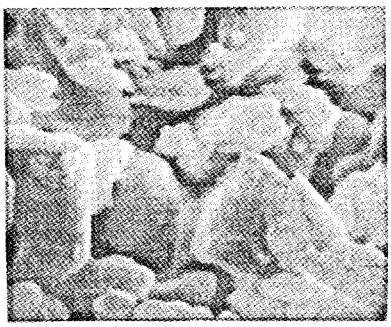

Photo 3.
SEM of ordinary C_2S hydrated for 7 days (4500X)

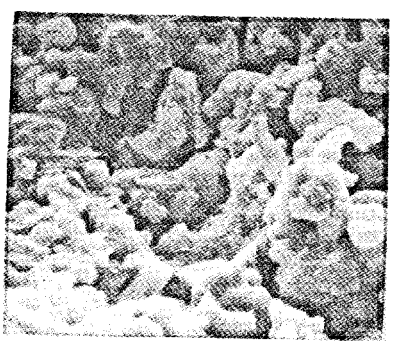

Photo 4.
SEM of ordinary C_2S hydrated for 4 years (4500X)

3.5 Some aspects of active C_2S

3.5.1 The formation of active C_2S

Since the active C_2S is synthesized under hydrothermal treatment and followed by a lower temperature ignition, it is conceivable that C_2S is formed in two ways: one is from the decomposition of C_2SH_x, produced during hydrothermal treatment. The another is by the reaction of CaO with SiO_2 in solid states, the resulting C_2S being designated as " secondary formed" C_2S.

3.5.2 The formation mechanism of active C_2S

It is well acknoledged that in CaO-SiO_2 system the first product of reaction is always C_2S, regardless of the initial ratio of CaO to SiO_2 used. O.P.Mchedlov-Petrosyn(24) has suggested that in CaO-SiO_2-H_2O system some trimer or tetramer silicate hydrates may be obtained under autoclaving condition. This is also found true for the present case. To explore the formation mechanism of the active C_2S, TMS derivatives of CaO-SiO_2 mixtures, treated under hydrothermal condition for different time(0.5, 2, 4 and 8 hrs.), were analysed by GPC. The gel permeation chromatogram of the samples are illustrated in Fig.6. In the figure only di- and polymer distribution are indicated. It is shown clearly from the figure that rather complex polysilicate hydrates are formed, the amount of which increases with the time treatment. In addition, there are small peaks lying around the molecular weight,890 and 1040, the intensities of which are augmented with treatment time. These peaks belonged to cyclic and linear tetramer, which have molecular weight 888 and 1050 respectively. The largest molecular weight of the polymer is about 10000. So it can be concluded that CaO/SiO_2 mixtures, treated under hydrothermal condition, contain very complex silicate hydrates apart from C_2SH_x.

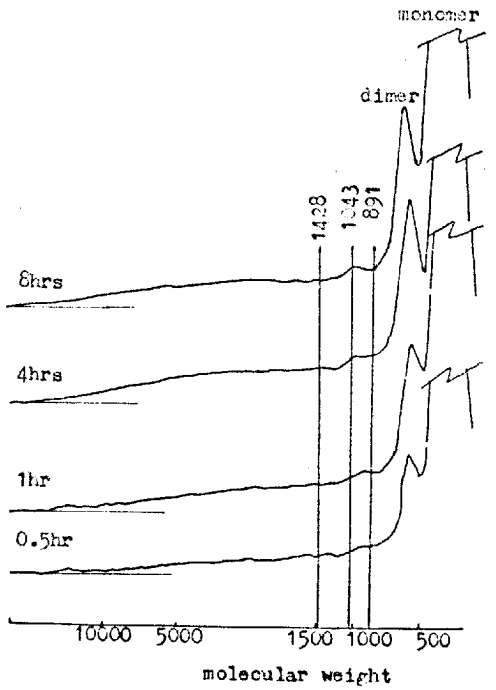

Fig.6 GPC of hydrothermal CaO/SiO_2 mixture, treated under different time

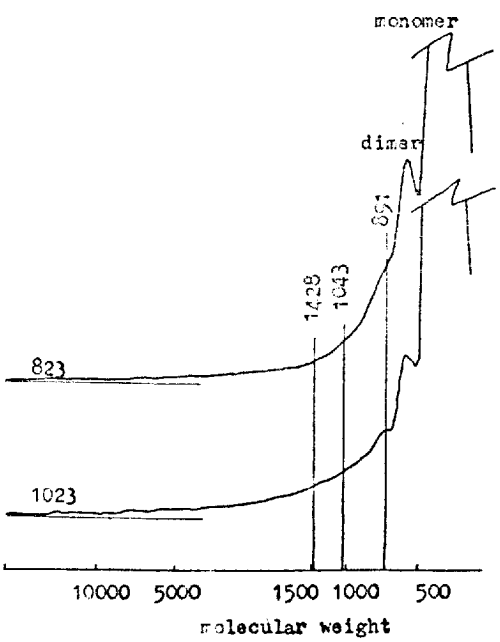

Fig.7 GPC of samples, ignited at 823,1023K

The change of the polymerization degree of the mixtures, treated for 8 hrs hydrothermally, followed by 823 and 1023 K ignition for 2 hrs is illustrated in Fig.7. The results show that the derivatives of higher molecular weight(3000) disappear, and simultaneously the amount of the derivatives of molecular weight 891 and 760 increases apparently, especially for

those samples ignited at 1023K. These facts demonstrated that active C_2S may be formed through the intermediate products, namely tetramer and trimern in addition to C_2SH_x.

The higher early hydration reactivity of active C_2S may be atributed to 1) the higher specific surface of area and 2) the lower preparation temperature.

4. CONCLUSION

1). It is possible to obtain β-C_2S by a new technique. A mixture of CaO/SiO_2=2 was subjected under hydrothermal treatment for several hours, then followed by a ignition at lower temperature, a pure C_2S was produced.

2). The early hydraulic reactivity of this active C_2S is much higher than ordinary C_2S, synthesized at 1273 and 1623K. The early strength of active C_2S is close to that of C_3S(28 days). The strength development of active C_2S is most apparent between 7-28 days.

3). The formation mechanism of active C_2S is in somewhat different from the mechanism of formation of C_2S in solid state reaction.

REFERENCES:

1. H.F.W.Taylor, "The Chemistry of Cements" Vol.1, (1964)
2. W.C.Hansen, Proc. of IV Int. Sym. on Chem. of Cem.,Vol.II, P1000, Washington, (1960)
3. B.S.Rangnakar, V.R.G.Srinivasan and V.N. Pai, Proc. of VI Int. Sym. on Chem. of Cem., Vol.I, P179, Moscow, (1974) (in Russian)
4. V.N. Viswannathan, World Cement Technology, 9 (4), 109(1978)
5. L.A. Zaxalov, see ref.3 Vol.3,P153(in Russian)
6. L.A. Zaxalov, Proc. of 9th Confer. on the Sili. Indust. P303, Budabest (1968)
7. L.A. Zaxalov, "Belite-Aluminate Cement", in Russian (1969)
8. P.K. Mehta, World Cement Technology, 11 (4) 166 (1980)
9. Deng Junan, Su Muzhen et al., Cements (in Chinese) (8)3 (1982)
10. J.Stark, A.Muller, R.Schrader et al., Silikattechnik 30 (12) 351 (1979)
11. J.Stark, A.Muller, R.Schrader et al., ibid, 31 (6) 168 (1980)
12. F.Hannawayya, Materal Science and Engineering, 17-18, 81-115 (1975)
13. Murry et al., United States Patent No. 4042408 (1977)
14. S.O.Oyefesobi, D.M.Roy, Cem. Concr. Res. 7,(1) 95 (1977)
15. R.Struillou, M.Arnuuld, Proc. of VII Int. Sym. on Chem. of Cem., Vol.III, V-75 Paris, (1980)
16. J.F.Young, Sym. of Int. Confer. on Cem. and Concr., Vol.1, P11, Beijing (1985)
17. B.Ziemer and G.Oliew, Silikattechnik, 33(6), 176 (1982)
18. A.A.Pashenko, E.A.Starchevskaya and P.P.Serbin, see ref.3, P200, Vol.2
19. W.Gutt and G.J.Osborne, Cement Technology, 7/8, 121 (1970)
20. S.N.Ghosh, A.K.Paul and A.K.Thakur, J. of mater. Science, 13 (7) 1602 (1978)
21. W.A.Klemm, R.L.Berger, J. of American Ceramic Society,55, 485 (1972)
22. Yang Nanru and Zhong Baiqian, J. of Silicate Society(in Chinese) 10 (2)161 (1982)
23. Min Panrong, Yang Nanru, Zhong Baiqian et al., see ref.16, Vol.1 P444
24. F.D. Tamas, A.K.Sarkar and D.M.Roy, Proc. of Confer. on Hydraulic Cement Pastes, Sheffield, P55 (1976)
25. Yang Nanru, Wang Zhanwen and Zhang Chengjun et al., J. of Silicate Society, 11(1), 112 (1983) (in Chinese)
26. Von H. Stade, W.Wieker and G.Garzo, Z. Anorg. Allg. Chem., 500, 123 (1983)
27. O.P.Mchedlov-Petrosyn " Thermodynamic of Silicate", Translated in Chinese,(1983)

Guo Chengju, Research Professor, China Academy of Railway Sciences
Beijing, China

Accelerating Effect of Chloride Salts on the Hydration of Portland Cement

L'Effet Accéléré du Sels Chlorures sur L'Hydratation du Ciment Portland

Summary: Calcium hydroxide, though a moderately soluble substance, behaves very sluggishly in water. It dissolves, diffuses and crystallizes all at low speeds. Removal of $Ca(OH)_2$ generated during the hydrolysis of the silicate components of portland cement away from the reaction site is a prerequisite for the reaction to go on, and thus determines the rate of the process.

The dissolution, diffusion and crystallization of calcium hydroxide are markedly intensified when calcium chloride is present along with it in a solution, presumably on account of the formation of a basic salt, i. e., the calcium oxychloride. Owing to the lowering of concentration of discrete $Ca(OH)_2$ molecules in the liquid at the surfaces of cement grains, in addition to the enhanced lime transporting capability of oxychloride molecules, excretion of $Ca(OH)_2$ is facilitated and the hydration of cement accelerated. The role of $CaCl_2$ is nothing other than that of a catalyzer with the oxychloride acting as the intermediate product.

Similar accelerating effect may be borne of other chloride salts due to the calcium chloride produced when chloride ions are caught by calcium ions.

O hidróxido de cálcio, apesar de ser uma substância moderadamente solúvel, comporta-se muito lentamente em água. Ele se dissolve, se difunde e se cristaliza a velocidades baixas. O afastamento do $Ca(OH)_2$, gerado durante a hidrólise dos componentes de silicato do cimento portland, para fora do sítio da reação é um pré-requisito para que a reação prossiga, e assim determina a velocidade do processo.

A dissolução, difusão e cristalização do hidróxido de cálcio são marcadamente intensificadas quando há presença de cloreto de cálcio juntamente com aquele numa solução, presumivelmente em decorrência da formação de um sal básico, isto é, o oxicloreto de cálcio. Devido à diminuição de concentração de moléculas separadas de $Ca(OH)_2$ no líquido nas superfícies dos grãos de cimento, acrescida ao aumento da capacidade de transporte de cal das moléculas de oxicloreto, fica facilitada a excreção do $Ca(OH)_2$ e se acelera a hidratação do cimento. O papel do $CaCl_2$ não é outro senão o de catalizador, atuando o oxicloreto como o produto intermediário.

Outros sais de cloreto podem proporcionar efeito acelerador semelhante, em decorrência do cloreto de cálcio produzido quando íons de cloreto são colhidos por íons de cálcio.

2.1

INTRODUCTION

It has been well recognized that the rapid hardening of portland cement pastes and concretes containing calcium chloride admixtures is due to the accelerating effect of the salt on the hydration of cement. Attempts have been made to detect the presence of any chlorine-containing compound in the hardened cement pastes so as to be able to speculate about the possible reactions between the chloride and the cement minerals. Yet there is no evidence for the existence of such reaction products except the calcium chloroaluminates, which may be found in a dried paste by means of X-ray analysis. Inasmuch as the accelerating effect of calcium chloride is also pronounced for the hydration of low alumina portland cements or even C_3S, as well as for the slaking of quicklime, it is unlikely that such effect is a result of its reaction with aluminates. More reasonably, account should be taken of a series of phenomena on the part of calcium hydroxide, including its formation, dissolution, migration and crystallization, rather than the overall reactions of cement being altered.

BACKGROUND

Calcium hydroxide, being the base of an alkali earth metal, can combine with acids at various proportions forming several types of salt, namely, the normal salt and the basic salts. In the case of hydrochloric acid, the final product may be $CaCl_2$, $CaCl_2 \cdot 2H_2O$, $CaCl_2 \cdot 6H_2O$, $CaO \cdot CaCl_2 \cdot 2H_2O$ or $3CaO \cdot CaCl_2 \cdot 15H_2O$, depending on the relative amounts of HCl, CaO and H_2O available for the reaction. While the true composition of the dissolved substances in a solution containing CaO and $CaCl_2$ is practically indeterminate, however, the change of solubility of $Ca(OH)_2$ due to the addition of $CaCl_2$, as pointed out by Zahorsky and other investigators, infers the presence of basic salts in such solutions /1/.

Early at the beginning of this century, Shreinemaker worked out a trinary equilibrium diagram for the $CaO-CaCl_2-H_2O$ system, which is shown in Fig. 1 /1/. From the diagram, it is seen that in case there is a surplus of CaO but the ratio of $CaCl_2$ to H_2O is below 0.15, the solid phase in coexistence with the liquid is limited to the slightly soluble calcium hydroxide. As the concentration of $CaCl_2$ increases up to a $CaCl_2:H_2O$ ratio of 0.30, the solid phase changes to the more soluble oxychloride ($3CaO\ CaCl_2 \cdot 15H_2O$), and at a ratio higher than 0.30, the still more soluble solid $CaO \cdot CaCl_2 \cdot 2H_2O$ stands instead. Thus, calcium oxychloride is merely a metastable substance which can by no means exist in case water is either abundant or in deficiency.

The writer was able to collect the crystalline substances excreted from cement pastes cured in water as well as in $CaCl_2$ solutions, and studied some of their properties. The needle like crystals up to 5 cm long found in curing liquids having a $CaCl_2$ concentration higher than 15% were identified as the oxychloride of calcium, while the hexagonal ones found in dilute $CaCl_2$ solutions or pure water were nothing other than portlandite/2/.

While the equilibria of the three phases have been clarified, the processes of reaching these equilibria are generally ignored when problems like hydration of cement are dealt with.

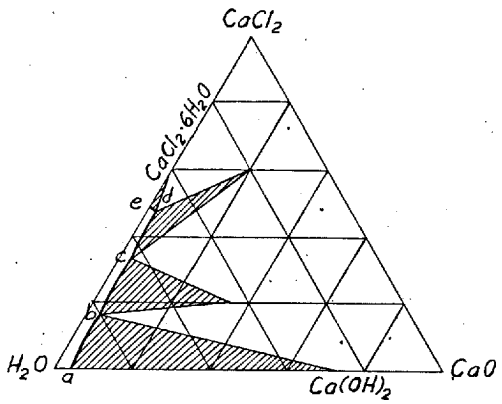

Fig. 1 Equilibrium Diagram of $CaO-CaCl_2-H_2O$ System

Solubility curve:

ab -- the solid phase being $Ca(OH)_2$
bc -- " " " " $3CaO \cdot CaCl_2 \cdot 15H_2O$
cd -- " " " " $CaO \cdot CaCl_2 \cdot 2H_2O$
de -- " " " " $CaCl_2 \cdot 6H_2O$

SOLUBILITY OF CALCIUM HYDROXIDE

The equilibrium concentration of aqueous solution of calcium hydroxide is a variable not only dependent upon the temperature, but also different for different types and grain sizes of the solid /3/. Values from various sources are quite diverse one from another. As a result of careful determinations made on crystalline calcium hydroxide (portlandite), which had been extracted from portland cement paste during its hydration, the writer found the concentration of the solution in equilibrium with crystals 0.3 mm in diameter at 25°C to be 1.13 g CaO/L. The figures given in many handbooks are somewhat higher, which probably are pertaining to slaked lime instead of crystalline $Ca(OH)_2$.

The solubility of portlandite in aqueous solutions of $CaCl_2$ varies with the concentrations of the salt. Fig. 2 represents the amount of $Ca(OH)_2$ entering $CaCl_2$ solutions of various concentrations at 25 C. It should be noticed that the solubility of $Ca(OH)_2$ is lowered in dilute $CaCl_2$ solutions as compared with that in pure water, being 0.88 g CaO/L in a solution containing 1.0 g $CaCl_2$ per liter. Thenceforth, it in-

creases straight forward almost in direct proportion with the concentration of $CaCl_2$, and exceeds the normal solubility at a $CaCl_2$ concentration of 8%. These seem to indicate that only a scanty portion of $Ca(OH)_2$ entering the solution stands as discrete molecules, while another portion in the form of complex salts.

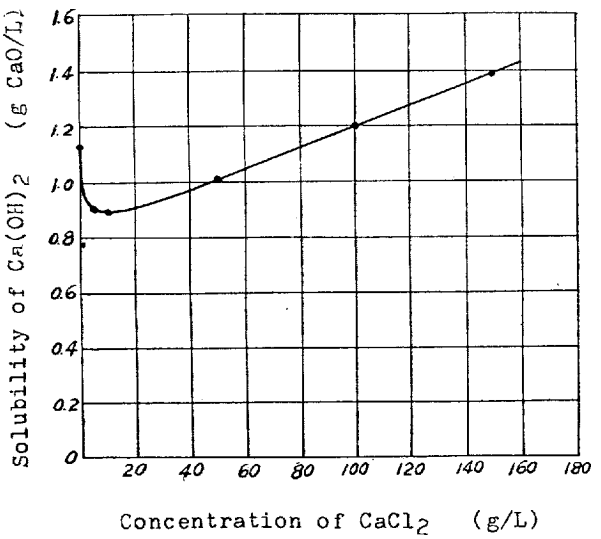

Fig. 2 Solubility of $Ca(OH)_2$ in $CaCl_2$ Solutions

RATE OF DISSOLUTION OF $Ca(OH)_2$

Calcium hydroxide, although moderately soluble in water, behaves very sluggishly when dissolved. It may take years for the solution to be saturated when $Ca(OH)_2$ crystals coexists with water without disturbance. the process of dissolution may be greatly accelerated by the aid of $CaCl_2$. The change of rate of dissolution was demonstrated by a simple experiment.

To a glass flask containing 500 mL of water or $CaCl_2$ solutions having various concentrations, 1.5 g of crystalline $Ca(OH)_2$ 0.3-0.5 mm in size were added in. The flask was stoppered and shaked at intervals (10 min for the first hour, 1 hr for the remainder of the first day and 8 hr up to the end of the test). At each time scheduled, 10 mL of clear liquid were taken out (filtration not permitted) and titrated against 0.05 N HCl solution with methyl orange as indicator. The concentrations of $Ca(OH)_2$ were calculated and plotted against time as shown in Fig. 3.

From the isotherm (25°C) obtained, it is seen that the dissolution of crystalline $Ca(OH)_2$ in water is a time-taking process, the rate of which decreases with the elapsed or in other words, with the rise of the concentration of the solution. By the aid of mixing according to the schedule adopted, equilibrium was reached not earlier than

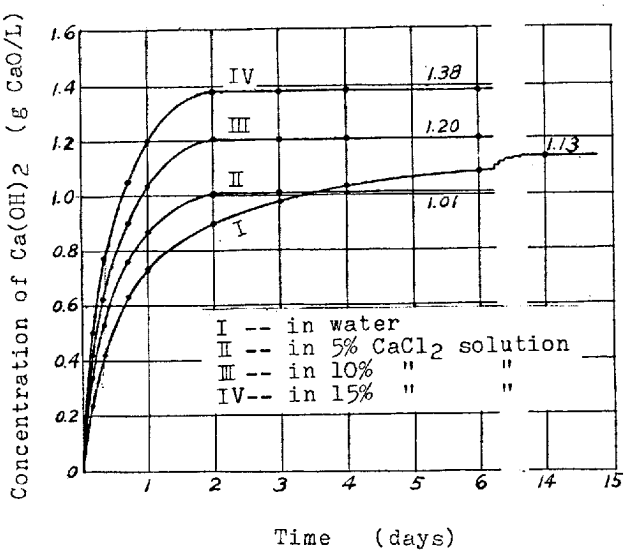

Fig. 3 Isotherm of Dissolution of $Ca(OH)_2$

14 days after the first mixing for the case for the case of pure water, but moved up to 2 days when $CaCl_2$ was present in the solution. The reason for the acceleration appears to be due to the formation of oxychloride molecules, which have higher affinity for water and are more diffusive than $Ca(OH)_2$ molecules.

RISE AND FALL OF $Ca(OH)_2$ CONCENTRATION OF THE LIQUID PHASE OF CEMENT PASTE

It is known that when portland cement (or quicklime) is mixed with water, the latter will soon become saturated or even supersaturated with $Ca(OH)_2$. The supersaturation may last for a few days and then fades away as hydration proceeds. Detailed investigations have been made into the $Ca(OH)_2$ concentration of the liquid phase of cement pastes, yet the results usually lead to diverse interpretations. In order to avoid painstaking procedures for the extraction of pore liquids from hardened cement pastes, the writer had found a reasonable approach to the settlement of the problem, and arrived at due conclusions.

Prismatic bars 1 x 1 x 6 cm in size were molded from cement paste made of a low alkali content cement at a water cement ratio equal to 0.40. After being stored in moist air for 24 hr, they were demolded and stripped of any dust on the surfaces. Six of them were placed in a 200 mL beaker with their longest edges standing vertical and kept clear one from another by the aid of spacers. 150 mL of water or 5% $CaCl_2$ solution were added in so that the prisms were completely immersed. The beaker was then sealed with membranes and stored at 25°C. An appropriate number of samples thus composed were prepared both for pure water and for

$CaCl_2$ solution. Each sample contained 50.0 g of cement and 170 g of water, and the water cement ratio of the system was 3.40.

At each time as scheduled, a sample was unsealed, and 10 mL of clear liquid were taken out and titrated against 0.05 N HCl solution for OH^- concentration. Meanwhile, Na^+ and K^+ concentrations were determined on another portion of the liquid by means of atomic absorption spectrophotometry. The difference between the molar concentration of OH^- and the sum of those of the two alkalis were taken as the equivalent concentration of $Ca(OH)_2$, which, after being reduced to g CaO/L, were plotted against the time elapsed since the prisms were first immersed, as shown in Fig. 4.

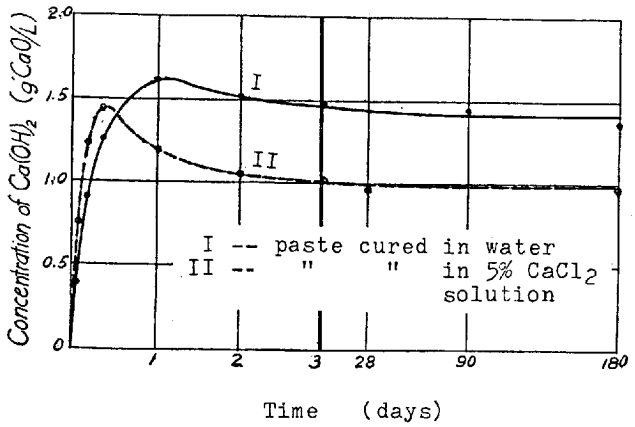

Fig. 4 Concentration of $Ca(OH)_2$ in curing liquids

From the figure, it is seen:(i) although the water cement ratio of the system was as high as 3:1 and the prisms were treated with water or $CaCl_2$ solution one day after they were fabricated, the $Ca(OH)_2$ concentrations of the liquids in all samples tested from the very beginning up to 28 days were above the saturation level, whether or not there was $CaCl_2$ present in the liquid. In view of the continuous accumulation of solid $Ca(OH)_2$ (portlandite) in the liquid (we shall see it later), it seems to be natural that the pore liquid within a cement should likewise be supersaturated with $Ca(OH)_2$ as long as the hydration of cement takes place, unless the cement contains pozzolana or other lime taking minerals.

(ii) In the case cement paste prisms were treated with pure water, rise of $Ca(OH)_2$ concentration took place during the first 24 hr until a summit value of 1.8 g CaO/L or so was reached. The process was significantly hastened by $CaCl_2$. It took only 8 hr for the $Ca(OH)_2$ concentration to get to the summit value, which was only about 1.5 g CaO/L, however. These situations suggest that the nascent $Ca(OH)_2$ set free during the hydration of cement dissolves much more rapidly than portlandite crystals and the rate of dissolution is still higher when $CaCl_2$ is present.

In order to have a keener insight into the descension of $Ca(OH)_2$ concentration after the summit was over, the liquids from the above mentioned samples were analyzed at times with the prisms removed. 300 mL of clear liquid were collected by decanting from a few samples prepared with water or 5% $CaCl_2$ solution at the moment when the $Ca(OH)_2$ concentration came to the respective summit value. The liquid was then sealed in in a flask. At each time scheduled, 10 mL were taken out and titrated against 0.05 N HCl solution for OH^- concentration (mol/L). From the values obtained, the molar concentration of the alkalis determined as before was deducted, and the differences divided by two were taken as the molar concentrations of $Ca(OH)_2$. The latter, after being reduced to g CaO/L, were plotted against the time elapsed since the collection of the liquid, as shown in Fig. 5.

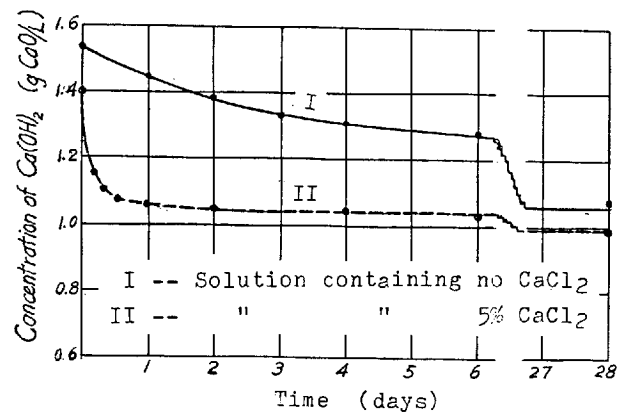

Fig. 5 Fading away of Supersaturation of $Ca(OH)_2$ Solution

Fig. 5 indicates that the lowering of $Ca(OH)_2$ concentration of the supersaturated solutions was by itself a gradual and time taking process. It took many weeks for the supersaturation to fade away completely, but there was no evidence for the concentrations to drop below the saturation levels. Inspection revealed that the liquid remained clear and transparent all along up to the end of the experiment. Thus, the lowering of concentration must be a result of growth of portlandite crystals instead of being a process of rapid precipitation. As shown in the figure, this process of crystallization was greatly accelerated when $CaCl_2$ was present in the liquid.

RATE OF EXCRETION OF $Ca(OH)_2$ FROM CEMENT PASTE

In view of the fact that both dissolution and crystallization of $Ca(OH)_2$ are markedly accelerated by $CaCl_2$, it is expected that more $Ca(OH)_2$ will be excreted during the hydration of cement and transferred to some lime-short spots in a given space of time by the aid of $CaCl_2$. This was confirmed by the following experiment.

Samples composed of cement paste prisms and water or 5% $CaCl_2$ solution were prepared as described before. At each time scheduled, one of them was unsealed and the 6 prisms taken out. With the aid of a penknife and a wash bottle, the crystals adhered on the surfaces of the prisms were carefully stripped off and returned to the beaker. The clear liquid was decanted into another beaker, and the residues were dissolved by dropping in from a burette sufficient amount of 0.5 N HCl solution to change the color of methyl orange indicator. The two solutions were combined, and an additional amount of the acid was dropped in until the liquid turned red again. From the total amount of acid consumed, the amount of $Ca(OH)_2$ excreted from the 6 prisms or 50 g of cement was calculated. The amount of excretion represented as mg CaO/g of cement were plotted against the time elapsed since the beginning of immersion of the prisms, as shown in Fig. 6.

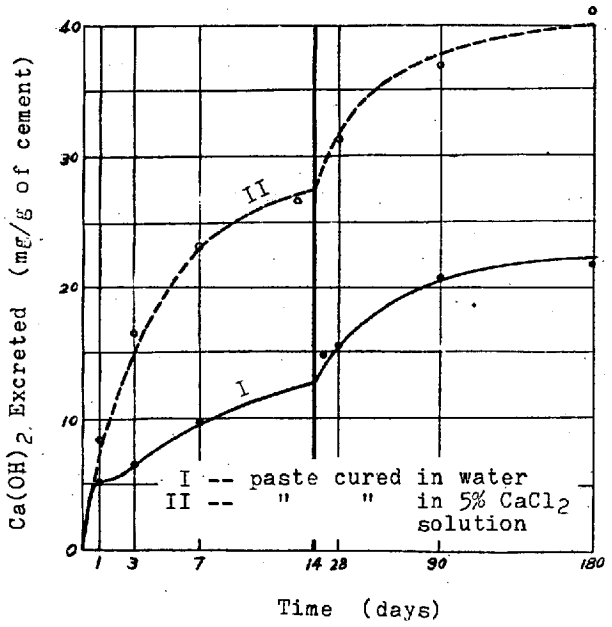

Fig. 6 Isotherm of Excretion of $Ca(OH)_2$

As can be seen from Fig. 6, $Ca(OH)_2$ was continuously excreted from cement as the hydration was carried on up to an age of 180 days. However, the process of excretion was more impetuous when cement paste was cured in $CaCl_2$ solution than in water. In the first case, the amount of $Ca(OH)_2$ excreted within the first 7 days even exceeded the cumulative amount accrued in water within half a year. These situations were in accordance with what we have known about the processes of hydration of cement.

MECHANISM OF THE ACCELERATING EFFECT

The hydration of portland cement comprises mainly the hydrolysis of lime rich silicates of calcium at the surface of cement grains, forming hydrosilicates of lower basicity on the one part and calcium hydroxide on the other. Such reactions may be roughly represented by the following equations:

$$2(3CaO\cdot SiO_2) + 6H_2O = 3CaO\cdot 2SiO_2\cdot 3H_2O + 3Ca(OH)_2$$

$$2(2CaO\cdot SiO_2) + 4H_2O = 3CaO\cdot 2SiO_2\cdot 3H_2O + Ca(OH)_2$$

Being heterogeneous reactions which take place only at the contact surface between the unreacted cement minerals and the surrounding water, the hydration as a rule retards itself as it proceeds. The retardation is generally ascribed to the deposition of the non-soluble hydrosilicates, which obstructs the access of water to the reaction site. Little attention has been arrested on the $Ca(OH)_2$ set free in company with the hydrosilicates.

As we have pointed out before, calcium hydroxide is a moderately soluble substance, but behaves very sluggishly in water. It dissolves, diffuses and crystallizes all at low speeds. Supersaturated solutions are formed when $Ca(OH)_2$ in its nascent state is delivered into water during the hydration of a cementing material like quicklime, portland cement, etc.

According to LeChatelier's principle, which is unive-rsally true for all physical and chemical processes, the rete-ntion of $Ca(OH)_2$ at the reaction site as supersaturated solutions must throw impediments in the way of the hydrolysis of cement along with the deposition of hydrosilicates. Therefore, the removal of $Ca(OH)_2$ away from the reaction site should be a prerequisite for the hydrolysis to go on. That a cement hydrates in a self-retarding manner is at least partly due to the reluctant diffusion and crystallization of the dissolved $Ca(OH)_2$ in water. Hydration will be accelerated whenever condition changes in favor of the $Ca(OH)_2$ to be excreted. As an example may be mentioned the rapid hardening of concrete at elevated temperatures, in which case so much $Ca(OH)_2$ are excreted as to give concrete the bright colors.

Then, the mechanism of the accelerating effect of $CaCl_2$ is very clear. When cement grains come into contact with $CaCl_2$ solution, the $Ca(OH)_2$ generated dissolves more rapidly than in the case of pure water, forming a kind of complex solution, which contains less discrete $Ca(OH)_2$ molecules in a given volume than an ordinary saturated or supersaturated $Ca(OH)_2$ solution. The dissolved lime bearing substance, probably a basic chloride of calcium, then diffuses from the reaction site to some remote places and crystallizes there, both at intensified rates. The solid resulted in may be either portlandite or calcium oxychloride, depending upon the $CaCl_2$ concentration of the pore liquid where crystallization takes place.

As we have stated before, calcium oxychloride is a metastable phase, which can stand in equilibrium with a solution containing

15-30 parts of $CaCl_2$ in every 100 parts of water. In a liquid having a higher or lower $CaCl_2$ concentration, it decomposes. The probable reactions are:

$$3CaO\cdot CaCl_2\cdot 15H_2O \rightarrow 3Ca(OH)_2 + CaCl_2\cdot 6H_2O + 6H_2O \quad (\text{when } CaCl_2:H_2O < 0.15)$$

$$3CaO\cdot CaCl_2\cdot 15H_2O \rightarrow CaO\cdot CaCl_2\cdot 2H_2O + 2Ca(OH)_2 + 11H_2O \quad (\text{when } CaCl_2:H_2O > 0.30)$$

When a cement paste containing $CaCl_2$ is either treated with an ample amount of water or dried up in low humidity environments, no oxychloride will be included in its composition.

It can then be concluded that the role of $CaCl_2$ in accelerating the hydration of portland cement is that of a catalyzer, with the basic salts produced acting as the intermediate products.

Similar accelerating effect may be borne of some other chloride salts, such as NaCl, $MgCl_2$, $AlCl_3$, etc., on account that $CaCl_2$ will be formed when chloride ions are caught by calcium ions, which are always in abundance in the pore liquid of cement pastes.

$$2NaCl + Ca(OH)_2 \rightarrow 2NaOH + CaCl_2$$

$$MgCl_2 + Ca(OH)_2 \rightarrow Mg(OH)_2 + CaCl_2$$

$$2AlCl_3 + 3Ca(OH)_2 \rightarrow 2Al(OH)_3 + 3Ca(OH)_2$$

Of course, such effect may be different in magnitude with different salts, owing to the possible interference of the various bases produced with the hydration of cement.

REFERENCE

1. J.W. Mellor, A comprehensive treatise on inorganic and theoretical chemistry, volume II, 1941.
2. Guo Chengju, Some properties of calcium hydroxide liberated during the hydration of portland cement. (unpublished)
3. F.M. Lea, The chemistry of cement and concrete. 3rd edition. London, 1970.

T. SEBÖK, Building Research Institute Prague, Laboratory of Building Constructions, 764 32 Gottwaldov, Czechoslovakia

EFFECTS THE MOLAR PARAMETERS OF SULPHONATED MELAMINE AND FORMALDEHYDE POLYCONDENSATES ON MORTAR PROPERTIES

Les parametres molaires des condensats de mêlamine et de formaldéhyde et leur influence sur les propriétés des mortiers

SUMMARY: The effects of chemical additives on the properties of mortar mixtures and mortar specimens after 28 days of hardening depend significantly on their chemical structure and other properties.

The efficiency of sulphonated melamine and formaldehyde polycondensates on the rheological properties of mortars with cement bond as well as on the strength after 28 days depends on their molar parameters mainly on the molar weight (Mw) and polydispersity (Rp).

From the values of correlation parameters obtained it can be judged that besides the chosen molar parameters, included in the analysis, further variables take part in the change of the strength and plasticity of the specimens of mortars with additives; their effects can be expressed by the approximate value of 30 up to 40 per cent.

From the results of the ridge analysis it was found that with approximately the same values of Mw and Rp of the specimens of additives the change in the investigated properties of the mortars with additives will also be effected by parameters of the synthesis.

Additives based on sulphonated melamine and formaldehyde polycondensates consist of fractions of molecules with different distribution of molar weight. The sorption of molecules on the surface of cement in cement bond suspension after 20 minutes of hydration is not selective.

All fractions are sorbed in the same range. These results prove that the electro kinetc effects that have been studied by a lot of authors so far are taken part in by all fractions sorbed on the cement surface.

Os efeitos de aditivos químicos sobre as propriedades de misturas de argamassa e corpos de prova de argamassa, depois de 28 dias de endurecimento, dependem significativamente de sua estrutura química e de outras propriedades.

A eficiência da melamina sulfonada e dos policondensados de formaldeído sobre as propriedades reológicas de argamassas com liga de cimento, bem como sobre a resistência depois de 28 dias, depende de seus parâmetros molares, principalmente do peso molar (Mw) e da polidispersividade (Rp).

A partir de valores de parâmetros de correlação obtidos, pode-se avaliar que, além dos parâmetros molares escolhidos, incluídos na análise, outras variáveis participam da mudança da resistência e da plasticidade de espécimes de argamassas com aditivos; seus efeitos podem ser expressos pelo valor aproximado de 30 a 40%.

A partir dos resultados da análise se constatou que, com aproximadamente os mesmos valores de Mw e Rp dos espécimes de aditivos, a mudança nas propriedades investigadas das argamassas com aditivos serão também afetadas pelos parâmetros da síntese.

Aditivos baseados em melamina sulfonada e policondensados de formaldeído consistem de frações de moléculas com distribuição diferente de peso molar. A sorção de moléculas sobre a superfície de cimento na suspensão de liga de cimento depois de 20 minutos de hidratação não é seletiva. Todas as frações são sorvidas na mesma escala. Estes resultados provam que os efeitos eletrocinéticos que foram estudados por inúmeros autores participam amplamente por todas as frações sorvidas na superfície de cimento.

INTRODUCTION

The principle of action of sulphonated melamine and formaldehyde polycondensates (MFP) is a subject of the intensive study.
At present there is a general opinion that the workability of suspensions with cement bond is improved by MFP in the way that as a result of the sorption of their molecules on the surface of cement particles the negative potential ζ increases. The change in the potential ζ up to a certain limit causes a change in the rheological properties of mortars.
In the study of the effect of MFP on the formation of the solid structure and on the kinetics of hydration it has been found that they slow down hydration C_3A in a significant way. Their influence on the kinetics of C_3S and β- C_2S hydration is smaller.
The decisive part of the existing knowledge of the effects of MFP on the properties of specimens with cement bond has been gained using commercial types of polycondensates. So far there has been very little publication of the results of work aimed at the study of the effect of the chemical structure and molar parameters of MF polycondensates on the properties of specimens with cement bond. Therefore in this paper the attention is concentrated just on clearing up the above mentioned connections.

EXPERIMENTAL

Components used

Cement: For the tests the cement was used the comcosition of which is given in Table I

Table I - Chemical analysis of industrial cement used /%/

SiO_2	Al_2O_3	Fe_2O_3	TiO_2	CaO	MgO	K_2O
24.25	5.58	2.31	0.30	54,71	3,96	0.78
Na_2O	SO_3	MnO	Ignition loss		Non soluble rest	
0.51	3.46	0.29	1.15		2.55	

Additives: In the experiments, specimens of polycondensates were prepared with a significant difference in the conditions of synthesis and also in their properties. Basic data of the specimens are given in TablesII and III.

Aggregates: For the preparation of mortars standard sands were used i. e. those specified for test of cement strength according to ČSN 72 2117.

Water: Distilled water was used for the tests.

Testing method

According to ČSN 72 2117 specimens of mortars were prepared without additions and with an additive of 0.5 per cent of the dry substance of MF polycondensates from the cement mass. The plasticity of the mortars was also found using the procedure according to the standards ČSN 72 2440 and ČSN 72 2441; photographic paper was put under the glass plate of the shaking table. After five taps the specimen was exposed. In this way an accurate recording of the change in the area of the cake was obtained (an example of the recording is in Fig. 1).

Table II - Properties of synthetized additives with various time of sulphonation

No. of additive	Properties of additive			Molar parameters	
	Solid %	CH_2O %	pH	$Mw.10^{-3}$	Rp
8	19.78	0.99	8.08	931	3.97
9	19.85	1.00	8.87	1 548	6.50
10	19.25	0.84	10.42	2 849	5.81
11	20.46	1.08	8.96	1 712	5.23
12	19.31	1.04	9.68	1 032	4.22
13	20.23	0.91	8.17	2 080	5.53
14	19.88	1.08	9.02	2 441	5.83
15	20.29	0.86	8.47	2 803	6.16
16	19.65	0.82	8.10	543	3.89
17	19.49	0.56	8.25	1 591	5.70
18	19.95	0.59	8.20	731	4.72
19	19.80	0.62	8.15	284	2.96
20	19.77	0.36	9.11	650	4.46
21	19.34	0.52	8.18	272	2.97
22	19.41	1.17	8.76	540	3.09
25	19.50	1.06	9.75	864	3.66
28	19.75	1.20	8.59	-	-
29	19.84	1.12	9.21	693	3.58

Table III - Properties of synthetized additives with constant time of sulphonation

No. of additive	Properties of additive			Molar parameters	
	Solid %	CH_2O %	pH	$Mw.10^{-3}$	Rp
45	20.28	0.76	8.55	3 415	17.72
46	19.95	0.64	8.05	2 662	15.56
47	19.75	0.85	9.03	4 305	17.56
48	20.00	0.68	9.27	2 862	13.91
49	19.68	0.73	9.26	3 984	15.74
50	20.05	0.70	9.22	3 594	16.54
51	20.62	0.67	9.35	3 506	15.54
52	19.53	0.55	9.54	2 865	14.68
53	19.86	0.74	8.51	2 622	15.60
54	19.95	0.65	9.48	1 838	14.05

As a criterion of the plasticity the surface of the cake, found by planimeter after 15 taps, was chosen. The results are given in TablesIV and V.
Using the same specimens small beams 4 by 4 by 16 cm were made and cured as well as tested according to ČSN 72 2117. The strength values found are given in Tables IV and V.
MF polycondensates were analysed on a liquid chromatograph SP 8000 by SPECTRA PHYSICS company (USA). In the analysis a differential refractometer (model R 401 of WATERS ASSOCIATION USA) was also used. As an eluent distilled water with sodium

azoimide (0.02 per cent) was used. The chromatographic column was 6 mm in the inner diameter and 250 mm long. As chromatographic packing gel Sepharon Hema 1000 was used; it is characterized by particle size of 7 - 16 m and by the separation range of molar weight of 10^3 to $5 . 10^5$ g/mol. GPC system was calibrated to dextrans made by Fine chemicals Uppsala. Therefore the molar parameters found and given in TablesII and III are only valid for the calibration conditions used. The total chromatograms were evaluated using the computer according to programme 7 described in the literature (1).
In GPC analysis there were the following parameters: passage 20 ml per hour pressure 3.5 MPa. The following values were obtained by the analysis: Mw - molar weight (g/mol); Rp - polydispersity (-). The values are given in TablesII and III.
On the basis of the GPC method research has been done on the sorption of all components of MF polycondensates and on the change of differential mass distribution of molar masses of additives after 20 minutes of interaction of components in modified cement suspension (w_c = 1.0).
Tested cement and a solution of additive (1 % concentration) were mixed. After 20 minutes of hydration the vaccuum filtration of the suspension through a nitrocellulose filter of the pore size 6000 ± 1000 Å was carried out. To make full comparison possible a GPC analysis of the solution before sorption and that of the filtrate after sorption was always made. An example of the results is in Fig. 2.

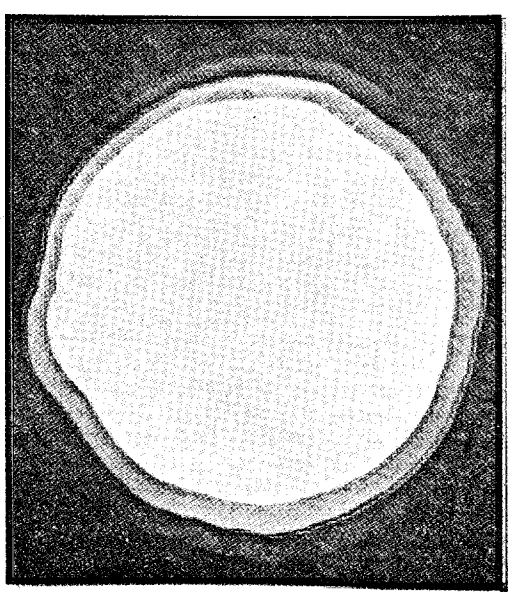

Figure 1. An example of the recording of plasticity of mortar.

2.1

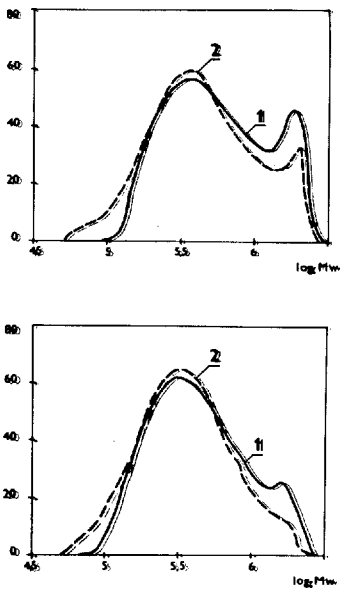

Figure 2. An example of the change in distribution functions of tested MF polycondensates before (1) and after sorption (2).

EVALUTION OF THE RESULTS

The approximation of functional dependences between Mw (X_1), Rp (X_2) and the properties of modified mortar specimens (Y) was determined by a computer using the programme for a multifactor regression analysis.
By the analysis it was found that the following mathematical model proves suitable to express the dependence.

$$Y = B_0 + \sum_{i=1}^{n} B_i . X_i \qquad / 1 /$$

B_0 , B_i - regression coefficients
X_i - independant variable
Y - dependant variable

The concrete mathematical model was further analysed using the programme for a ridge analysis. Its results are given in Figs. 3, 4, 5, 6. The figures illustrate the course of changes of variable Y depending on the change in the value of mediating factor R, which is a radius of n - dimensional ball, the magnitude of which can be expressed by relation.

$$R^2 = \sum_{i=1}^{n} X_i^2 \qquad / 2 /$$

Using the data from Tables II and IV the approximate dependence between Mw, Rp and the plasticity of mortar was analyzed.

Table IV - Properties of mortar samples with additives (Table II)

No. of additive used	Plasticity /cm^2/	Strength /MPa/	
		1 day	28 days
8	185	17.0	57.6
9	181	13.0	55.2
10	186	13.9	58.4
11	163	6.0	52.0
12	189	10.0	58.4
13	193	13.0	62.4
14	190	12.0	63.4
15	185	12.7	61.6
16	259	14.5	64.8
17	188	12.9	61.6
18	250	12.8	69.6
19	224	14.1	70.4
20	178	12.1	61.6
21	249	16.3	69.6
22	187	13.2	59.2
25	193	11.2	64.0
28	175	10.9	58.4
29	192	11.0	62.4
Control	172	12.1	50.8

Table V - Properties of mortar samples with additives (Table III)

No. od additive used	Plasticity /cm^2/	Strength /MPa/	
		1 day	28 days
45	240	14.0	66.4
46	197	10.5	66.4
47	190	11.0	64.0
48	198	12.9	64.5
49	184	14.5	58.4
50	207	9.7	64.0
51	185	12.6	63.3
52	193	13.6	62.4
53	204	13.6	60.8
54	252	14.5	63.4
Control	172	12.1	50.8

The regression analysis made it possible to obtain coefficients of multiple correlation R_k = 0.7492 and those of multiple determination R_d = 66.12 per cent on the level of 5 per cent. It means that variables Mw and Rp included in the analysis influence the change of plasticity by about 66 per cent. Further effects not included in the analysis influence the change of plasticity by about 34 per cent.
Taking the range given in the literature as the criterion for the assessement of the significance of correlation features for multiple regressions we can then state that there is a very good correlation between the variables analyzed. The results of the ridge analysis in Fig. 3 can be evaluated as follows:

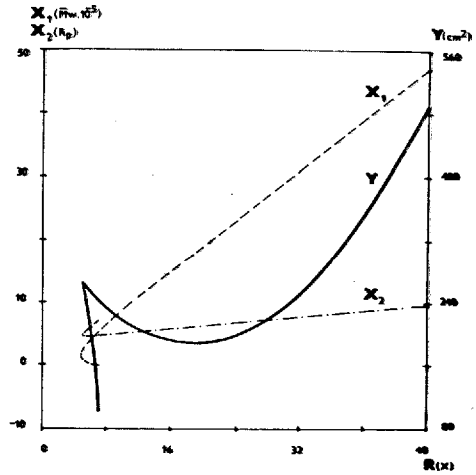

Figure 3. The results of ridge analysis using values of Mw, Rp and plasticity from Tables II and IV.

In the interval of the values Mw (0 - 200) g/mol.10^3 and Rp (4.8 - 7.2) the plasticity (Y) grows with increasing value Mw and decreasing value Rp. Further considerable increase of value Mw and a moderate increase of Rp results in the decrease of functional dependence Y = f (Rx) to the value of the local minimum. Further increase in the values of both molar parameters already causes a considerable increase of the plasticity.
In the same way an analysis was made of the approximate dependence between Mw, Rp and the compression strength after 28 days of hardening using the data from Tables II and IV. By the regression analysis the following coefficients have been obtained: R_k = 0.7629 and R_d = 58.2 per cent on the level of 5 per cent.
It follows from the characteristics mentioned above that the chosen variables Mw, Rp have decisive effects on the compression strength of the specimens and thus also on the other processes connected with and deciding on the kinetics in the formulation of the solid structure.
The results of the ridge analysis have shown that the values analyzed are positive for the mean ridge. From Fig. 4 it can be concluded that the compressive strength of the modified specimens grows with increasing value Mw and decreasing value Rp in the interval of the experimentally found values of variables in Tables II and IV. From the further course of dependences we can make conclusions as to a probable change of variables X_i and Y in the interval of changes determined by the calculation only besides the value interval found experimentally.
The results achieved have also been confirmed using other cements.

2.1

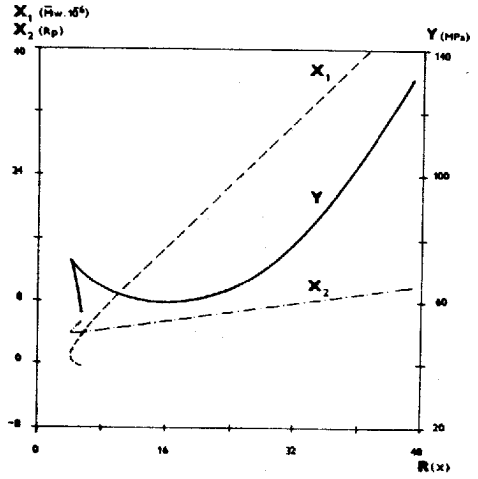

Figure 4. The results of ridge analysis using values of Mw, Rp and strength after 28 days from Tables II and IV.

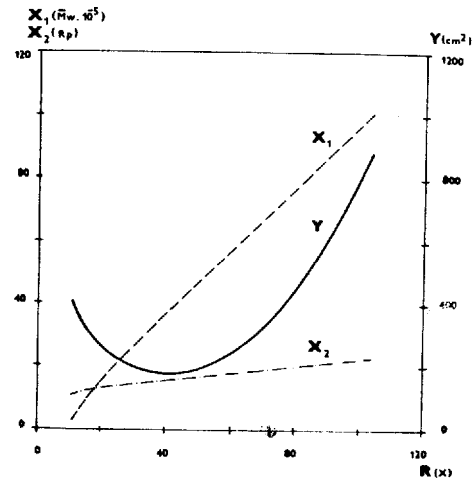

Figure 5. The results of ridge analysis using values of Mw, Rp and plasticity from Tables III and V.

Using the same method the approximate determination of functional dependences between the variables was carried out in Tables III and V. These specimens of additive were made from the same raw materials and with the change of the same parameters of synthesis in mutual combinations except the time of sulphonation, which was constant with all specimens. With specimens in Table II even the time of sulphonation was variable to a large extent.

By multifactor regression analysis it was found that between Mw, Rp and the plasticity there is a very good correlation dependence. This can be concluded from values R_k = 0.8748 and R_d = 76.52 per cent. From the results of the ridge analysis in Fig. 5 it follows that in this case the plasticity in the value interval in Table V decreases with increasing values Mw and Rp to the value of local minimum of Y.

By regression analysis it was also found that with specimens in Table III there is a very good correlation between Mw, Rp and the compression strength of the specimens. This is proved by coefficients R_k = 0.7744, R_d = 59.96 per cent. The results of the ridge analysis are in Fig. 6

In this case is evident that there is a very good correlation between the variables analyzed.

From the value of coefficient of multiple determination we can to derive that variables Mw and Rp included in the analysis influence the change of strength by about 60 per cent. Further effects not included in the analysis influence the change of plasticity by about 40 per cent.

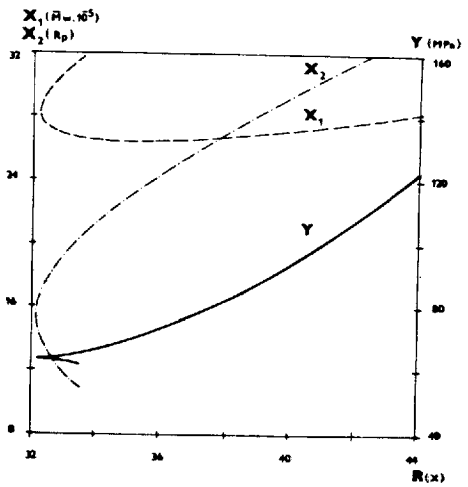

Figure 6. The results of ridge analysis using values of Mw, Rp and strength from Tables III and V.

CONCLUSION

There is a significant dependence between the changes in values Mw and Rp of MF polycondensates as well as in their effects on the change in rheological properties and the strength of mortar specimens with cement bond. Therefore the basic key to explain the principle of the efficiency of the additives should be searched for in clearing up further dependences between the characteristics of polycondensate molecules and their effects on the properties of the specimens with cement bond.

These dependences have been studied in a complex research programme and some of them also defined. They will be published successively.
From the change of differential distribution functions of molar masses after sorption on the surface of cement it is evident that the sorption of all fractions of molecules is equal.

Acknowledgement

The autor wishes to thank Dipl. Ing. František Čermák for synthesis of specimens of additives.

BIBLIOGRAPHY

1. Spectra Physics Instruction Manual Part No. A 0098-01, 3/78

2. Casassa, E. F., J. Polym. Sci.,B5,773 (1967)

3. Moore, J. C., J. Polymer Sci., A2, 835 (1964)

4. Mayerhoff, G., Makromol. Chemistry, 134, 129, (1970)

5. Vinklárek, Z., Stráněl, O., GPC of Melamine - Formaldehyde polycondensates, Report of Technical University Brno (1982)

6. Šauman, Z., Thesis, Brno, (1973)

7. Jambor, J., Stavebnický časopis, 33, No. 9, (1985)

8. Collepardi, M., et al., Cement and Concrete Research, 10, 455 (1980)

9. Daimon, M., Roy, D. M., Cement and Concrete Research, 8, 753, (1978)

10. Daimon, M., Roy, D. M., Cement and Concrete Research, 9, 103, (1979)

11. Helmuth, R. A., 7th Int. Congress on the Chemistry of Cement, Paris, (1980)

12. Sebök, T., Cement and Concrete Research (to be published)

13. Proc. International Symp. Superplasticizers in Concrete, Ottawa, (1978)

14. Petrie, E. M., Ind. Eng. Chemistry, 15, 242, (1976)

15. Stein, H. N., J. Coll, Sci, 28, 203, (1968)

16. Somasundaran, P., and Kulkalrni, R. D., J. Coll., Interface, Sci., 45, 591

17. Vosnesenskij, V. A., Statistica, 62, Moskow, (1974)

18. Ratimov, V., et al. Proc. of the Int. Symp. Pore structure and properties of materials, Vol III., 205, (1973)

19. Stein, H. N., J. Coll., Sci., 15, 578, (1960)

20. Hattori, T. M., Proc. Int. Symp. Superplasticizers in Concrete, Ottawa, (1978)

V. Balek, Nuclear Research Institute, Řež, Czechoslovakia
J. Kříž, Paint Research Institute, Prague, Czechoslovakia
J. Dohnálek, Building Research Institute, Technical University Prague, Czechoslovakia

1

Influence of Temperature and Admixtures on the C_3S and Cement Hydration Investigated by Radiometric Emanation Method

2.1

Influence de la température et des adjuvants sur l'hydratation du C_3S et des ciments, étudiée par la méthode des émanations radioactives.

SUMMARY: The possibilities of the radiometric emanation method (REM) in the study of C_3S and cement hydration in various conditions are shown. For the REM measurements the surface of the samples to be studied is impregnated by a non-aqueous solution containing trace amounts of the radioisotopes Th-228 and Ra-224 which give rise to Rn-220 in the sample. The REM curves, representing time dependences of the radon release rate from the samples, indicate the changes of the surface and microstructure during the sample hydration.

The changes in the kinetics of C_3S hydration caused by the C_3S activation on heating and rapid cooling, by the presence of 0.1 % of xylose and elevated temperatures were estimated by means of REM. This method has been applied to the investigation of the influence of elevated temperatures (to 85 °C) and the presence of sulphate ions on the kinetics of the changes in the microstructure of Portland cement paste in the early hydration.

Mathematical model of the radon release curves during the C_3S hydration, taking into account the effects of temperature and admixtures, is suggested. A good agreement between the theoretical REM curves derived by computer simulation and the experimental REM results was found.

SUMÁRIO: São mostradas as possibilidades do método de emanação radiométrica (REM) para o estudo da hidratação do C_3S e do cimento em várias condições. Para as medições pelo REM a superfície das amostras a serem estudadas é impregnada com uma solução não-aquosa, contendo quantidades de traço dos radioisótopos Th-228 e Ra-224, que dão origem a Rn-220 na amostra. As curvas REM, representando as dependências do tempo na velocidade de liberação de radon das amostras, indica as mudanças da superfície e da microestrutura durante a hidratação da amostra.

As mudanças na cinética de hidratação do C_3S pela ativação do C_3S sob aquecimento e resfriamento rápido, pela presença de 0,1% de xilose e temperaturas altas, foram estimadas por meio do REM. Este método foi aplicado na investigação da influência de temperaturas altas (até 85°C) e da presença de íons de sulfato sobre a cinética das mudanças na microestrutura da pasta de cimento Portland na hidratação inicial.

Sugere-se modelo matemático das curvas de liberação de radon durante a hidratação do C_3S, levando em consideração os efeitos da temperatura e dos aditivos. Encontrou-se uma boa concordância entre as curvas teóricas REM obtidas por simulação de computador e os resultados experimentais REM.

V.Balek
J Kříž
J.Dohnálek

INTRODUCTION

Numerous attempts have been made to explain the complex processes of the C_3S hydration and the influence of various factors on its kinetics. Various methods have been used for the study of the hydration of cement and clinker minerals. In the recent years these methods have been supplemented by the radiometric emanation method /1,2/ enabling us to receive a new insight into the hydration processes, especially those taking place during the early hydration stage.

PRINCIPLES OF THE METHOD AND EXPERIMENTAL PROCEDURES

The radiometric emanation method (REM) is based on the measurement of the radon release from the samples, previously labelled by its parent isotopes (i.e. Th-228 and Ra-224). The radon Rn-220 atoms formed in the sample by the radioactive decay, do not react with the labelled sample, the rate of their release depends on the surface area and diffusion properties of the labelled sample.

The rate of the radon release from the hydrating cement grain reflects the structural and chemical changes taking place as the results of the hydration in the surface layers and the bulk of the sample. An interaction of the labelled sample with the surrounding medium or a change occuring within the solid sample causes a sudden release of Rn-atoms trapped in the structure.

Sample labelling. In the sample labelling the C_3S and cement were impregnated with an acetone solution containing Th-228 and Ra-224 atoms in the concentration of the order 10^5 Bq cm^{-3}. The radionuclides were adsorbed on the surfaces of the cement grains and the aceton was evaporated. The specific radioactivity of the labelled samples was 10^4 Bq g^{-1}. Due to the recoil effect the atoms of Ra-224 and Rn-220 are incorporated into the surface layers of the grains to maximum depth of 120 nm.

Characteristics of the samples
C_3S, supplied by the Institute of Inorganic Chemistry, Academy of Sciences of the GDR, Berlin, has the surface area of 0.4 m^3 g^{-1}; Portland cement supplied by Cement Plant Lochkov, ČSSR, exibited the surface area of 0.35 m^2 g^{-1}. The phase composition of the ground portland cement clinker was: C_3S - 71.9 %, C_2S - 13 %, C_3A + C_4AF - 11.6 %, Free CaO - 3.5 %; the amount of 30 % of slag was present in the slag cement.

The samples of the water suspensions of C_3S or cement were prepared by the addition of water to solid labelled samples, the ratio water:solid being 0.4 in the case of C_3S or 0.3 in the case of cement. The labelled samples were stored before the hydration in a closed container in dessicator.

REM measuring procedure. The suspensions in the amount of about 1 – 3 g were homogenized by mixing in a PVC vessel and inserted into the measuring device described elsewhere /2/. This device is commercially produced by Messrs. NETZSCH-Ltd., Selb, F.R.G. /3/.

In the measuring device the sample is held at the required temperature and overflowed by air of controlled humidity at constant flow-rate. Radon atoms released from the sample are carried into the radioactivity measuring chamber by the air saturated with water vapour at the temperature of hydration. For the detection of alpha-radiation of radon a scintillation detector with a photomultiplier was used /2/. The REM results are presented as time dependences of the relative radon release rate E calculated from the experimental data as $E = A_{gas}/A_{solid}$, where A_{gas} is the radioactivity of radon released from the sample, and A_{solid} is the total radioactivity of the sample, being proportional to the rate of radon formation in the sample.

RESULTS AND DISCUSSION

Fig. 1 shows the time dependences of the radon release rate during C_3S hydration at 25 °C, where the reactivity of C_3S has been affected.

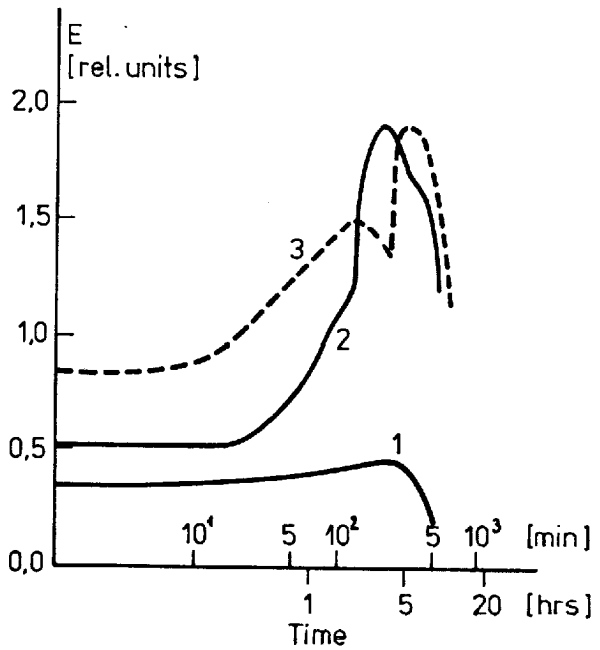

Fig. 1: REM curves measured during the hydration of C_3S in the mixture with water w/c = 0.4 at 25 °C using (a) C_3S 6 months stored - curve 1, (b) thermally activated C_3S - curve 2, (c) thermally activated C_3S and 0.1 % xylose solution for the paste preparation - curve 3.

As it follows from Fig. 1 the activation of C_3S enhanced the rate of C_3S hydration. The difference in the hydration rates of activated and non-activated samples is indicated since the very beginning of the hydration. The REM results confirm the concept of the lattice defect influence on the initial hydration stage of C_3S /4,5/.

It should be pointed out that no sudden decrease of the E value at the beginning of the C_3S hydration took place, as it could be expected if a layer of hydration products impermeable for water molecules was formed. As the diameter of radon atoms is comparable to that of water molecules the REM results confirm the hypotheses of the mechanism of early hydration by Fierens and Verhaegen /5,6/, Tadros /7/, Taylor /8/ and other authors reviewed by Skalny and Young /9/.

In the post-induction period, the increase of radon release rate reflects the enormous increase of the surface area of the sample. It was shown by Tretin and Wieker /10/ that the surface area of geleous C-S-H hydration products formed in this hydration stage attain the value above 100 $m^2 g^{-1}$.

In the subsequent time-interval, the changes of E reflect the changes of the microstructure of hydrated products; the radionuclides Th-228 and Ra-224 initially introduced into the C_3S are incorporated into the hydration products formed from the C_3S.

The decelerating effect of sugars on the C_3S hydration is well known /11/ and it was of interest for us to ascertain how this effect is reflected by the REM. The curve 3 in Fig. 1 represents difference in the kinetics of early hydration C_3S in the suspension containing of 0.1 % of xylose in comparison to that in the pure water suspension. The presence of xylose causes the slowing down of the hydration rate in the post-induction period which is expressed by the separation of the effects in curve 3, as compared with the curve 2 in Fig. 1.

The influence of temperature on C_3S hydration can be investigated by the REM very easily. The curves in Fig. 2 demonstrate the effect of the temperature increase in the kinetics of C_3S early hydration: at 35 °C (curve 2) the induction period is considerably shortened and the hydration rate in the post-induction period is enhanced, when compared to the behaviour of the system at 25 °C (curve 1). This is in a perfect agreement with the results of other methods reviewed by Skalny and Young /9/.

We have already shown /2/ that the radiometric emanation method enabled us to distinguish individual stages of the cement hydration, i.e. the induction, post-induction and diffusion periods /9/. The changes of the emanation rate related to the hydration processes of cement were discussed and compared with the measurements of surface area, porosity, calorimetry, penetration resistance and compressive strength /2/.

The changes of emanation rate of the cement paste during hydration at 25 °C and the effect of the temperature shock from 25 to 55 °C lasting 20 minutes are shown in Fig. 3. The temperature shock in the post-induction period of cement hydration caused a sharp increase of the emanation rate (see curve 2, Fig. 3). As it follows from Fig. 3, after the end of this shock the emanation rate does not reach the level shown in the curve 1, immediately. The curves 1 and 2 in Fig. 3 proximate after 10 – 15 hours of the hydration only. Consequently, the temperature dependence of the development of the microstructure of the cement paste can be indicated by the REM measurements.

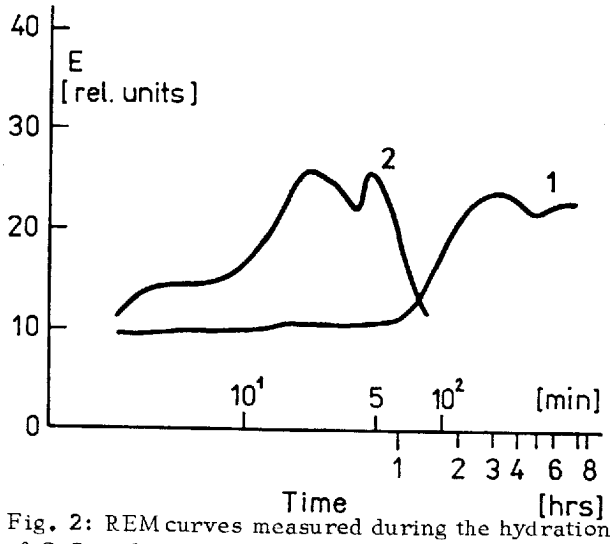

Fig. 2: REM curves measured during the hydration of C_3S in the mixture with water w/c = 0.4 at the temperature of 25 °C (curve 1) and 35 °C (curve 2).

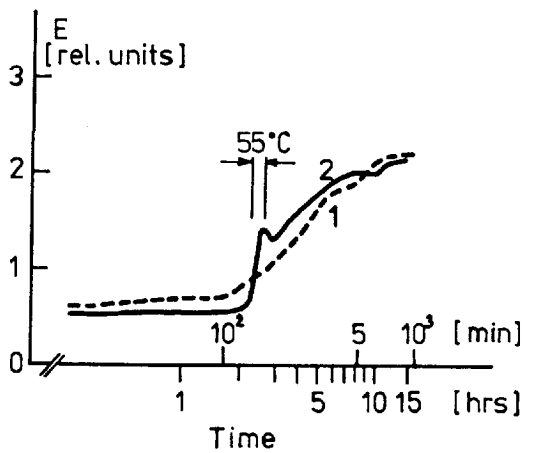

Fig. 3: REM curves measured during the Portland cement hydration w/c = 0.3 at the temperature of 25 °C (curve 1); curve 2 corresponds to the experimental conditions when a thermal shock from 25 to 55 °C lasting 20 minutes was applied.

The dependences of the emanation rate and penetration resistance measured during hydration of Portland cement at temperatures of 35, 45, and 85 °C are demonstrated in Fig. 4. The REM curves in Fig. 4 confirmed that the hydration of Portland cement performed from the very beginning at elevated temperatures is characterized by a shorten induction period and an enhanced velocity of the hydration in the post-induction period. We suppose that the subsequent slowing down of the emanation rate (curves 1 – 3, Fig. 4) is caused by the compactization of the

microstructure of the hydration products and corresponds to the time intervals where the penetration resistance of the cement paste starts to increase (cf. curves 1′ – 3′, Fig. 4). The shift of the REM curves and the corresponding penetration resistance curves of the samples hydrated at 45 and 85 °C is due to the interruption of the sample curing at elevated temperatures caused by the penetration resistance measurements, which were performed at room temperature.

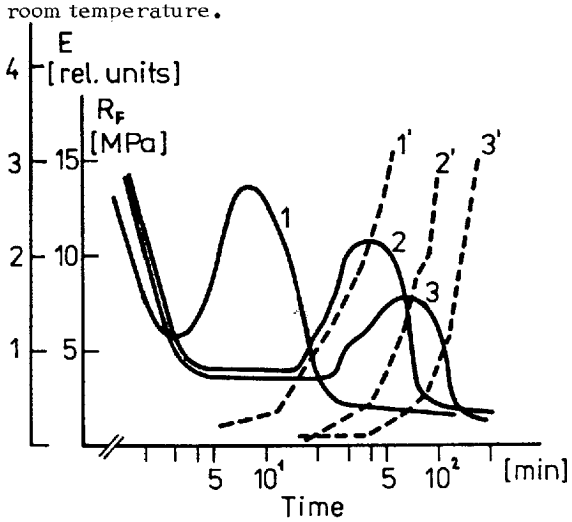

Fig. 4: REM curves and penetration resistance curves measured during the Portland cement hydration, w/c = 0.3, at the temperatures of 85 °C - curves 1, 1′; 45 °C - curves 2, 2′; and 35 °C - curves 3, 3′, respectively.

We have found with all samples hydrated at 35, 45, and 85 °C that at the time interval corresponding to the boottom of the respective REM curves after the emanation rate decrease, the degree of hydration attained 15 ±1 %. We suppose that at these time intervals the hydration of the radioactively labelled surface layers of the thickness of appr. 120 nm is terminated.

Consequently the REM can be used for a rapid estimation of the hydration process in the surface layers and of the temperature influence on the cement hydration.

The decelerating effect of sulphate on the cement hydration was widely investigated /9,13/. In Fig.5 the effect of the presence of Na_2SO_4 in the concentration of 3380 mg/1 liter on the Portland cement hydration at 45 °C is shown. The differences in the kinetics of the early stage of hydration of Portland cement caused by the presence of sulphate ions can be investigated at required temperature by means of REM.

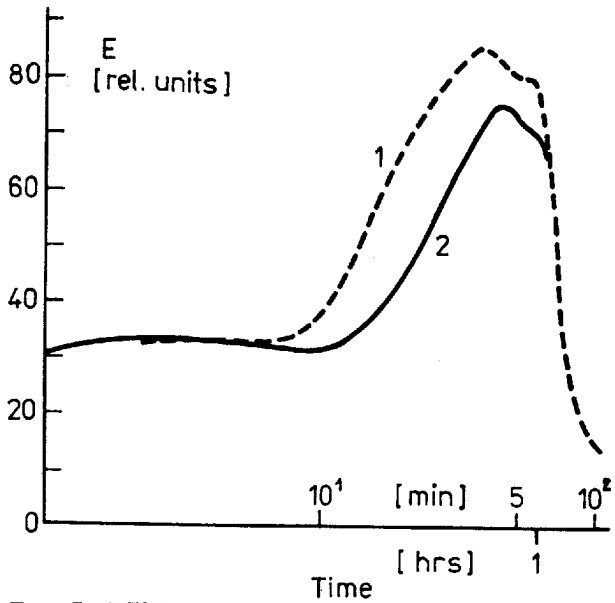

Fig. 5: REM curves measured during the Portland cement hydration, w/c = 0.3, at the temperature of 45 °C in presence of 3380 mg Na_2SO_4 per 1 liter water (curve 1), and in absence of any admixtures (curve 2).

MATHEMATICAL MODELLING OF THE REM CURVES

In the mathematical model, the quasi-continuum-domain (QCD) approximation of the system has been used /14,15/. It is assumed that the inert gas is released by recoil from the spherical domains of C_3S into the porous space and is transported by diffusion to the surface of the sample. Under such conditions, its concentration c follows the equation (1)

$$\frac{\partial c}{\partial t} = D \frac{\partial^2 c}{\partial x^2} - \lambda c + \zeta \qquad (1)$$

where λ is the decay constant of radon, D is the diffusion coefficient of radon and ζ is the source function. Both D and ζ are dependent on the degree of hydration α according to the equations (2) and (3)

$$D_t = D_o \exp(-\delta_1 \alpha) + D_\infty \qquad (2)$$

and

$$\zeta = \left\{\zeta_o + (\zeta_m - \zeta_o)\exp\left[1 - \frac{\alpha_c}{\alpha}\right]\right\}\exp(-\delta_2 \alpha) \qquad (3)$$

Here, D_o corresponds to the initial Knudsen diffusion /15/, i.e. $D_o = 0.5\, r_g\, (8RT/3\pi M)^{0.5}$, r_g - being the initial grain radius. ζ_o and ζ_m in Eq. (3) are the initial and maximum recoil functions, respectively, i.e. /15,16/

$$\zeta_o = \frac{\pi \Lambda_T c_T}{2\varrho_R \varrho_r}\left\{(2r_g - \varrho_R)\varrho_r \varrho_R - (r_g^2 - \varrho_r^2)\varrho_R + 1/3\left[r_g^3 - (r_g - \varrho_R)^3\right]\right\} \qquad (4a)$$

and

$$\zeta_m = 4\pi\Lambda_T c_T r_g^2 \qquad (4b)$$

Equation (2) reflects the experimentally verified dependence of the gas diffusion coefficient on the degree of hydration α. Equations (3) and (4) express the approach that the atoms of the intermediate nuclide Ra-224 released by the parent decay into the grain are brought to the surface of the grain by the hydration products.
The filling of the porous space by the hydration products, however, leads to a more effective trapping of the released gas atoms and to the corresponding sinking of the source function for higher values of α.

In the QCD approximation, the approximation, the emanation rate E_R is then expressed as follows

$$E_R = \frac{r_g^2\sqrt{\beta}}{4} D \left.\frac{\partial c}{\partial x}\right|_{x=0} \qquad (5)$$

where the first derivative $\partial c/\partial x$ follows from the solution of Eq. (1) /16/.

In the computer simulations, the dependence of E_R on time has been obtained from the model suggested by Pommersheim and Clifton /17/ with the following values of the parameters: water/solid = 0.4, a = 1, γ = 3.2, ν = 2.2, $D_i(0) = 1.35 \cdot 10^{-5}$, $E_i = 4 \cdot 10^4$ J/mole, $D_x(0) = 8.2 \cdot 10^{-6}$, $E_x = 4.5 \cdot 10^4$ J/mole, $D_o(0) = 2.23 \cdot 10^{-5}$, $E_o = 3 \cdot 10^4$ J/mole, $x_o = 3.5 \cdot 10^{-8}$ m, n = 3, $\beta_o = 6 \cdot 10^{-6}$, $E_\beta = 4 \cdot 10^4$ J/mole, $K_o = 8.1$, $E_K = 4 \cdot 10^4$ J/mole, $r_g = 3.4 \cdot 10^{-6}$ m. Additionally, the parameters of our model were: $\alpha_c = 0.15$, $\delta_1 = 3$, $\delta_2 = 6.5$.

Using this model, the theoretical REM curves for C_3S hydration in the conditions of various temperatures were obtained by computer simulations. The results of this simulations for c_o = 0.1 mole/liter are shown in Fig. 6. In accordance with the experimental results, the model REM curves show a maximum which is shifted to a higher reaction time by the lower temperature.

In Fig. 7 the model REM curves are shown for C_3S at the temperature of 20 °C, supposing the change of the concentration c_o (corresponding to the Ca^{2+} concentration). The maximum in the REM curves is shifted to a higher reaction time by lowering the values of c_o.

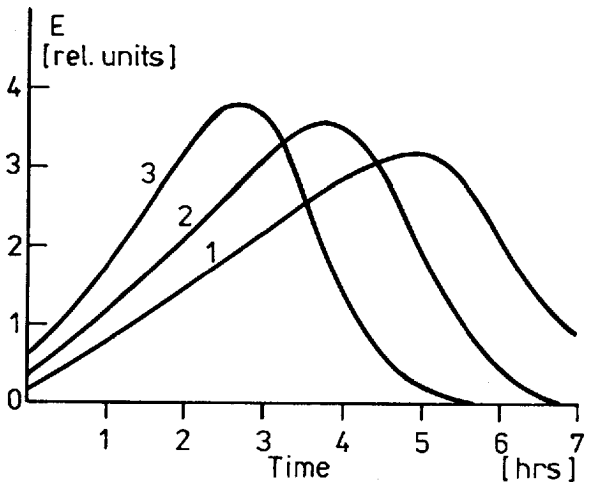

Fig. 6: Theoretical REM curves obtained by computer simulation of C_3S hydration at various temperatures: 20 °C (curve 1), 40 °C (curve 2) and 60 °C (curve 3).

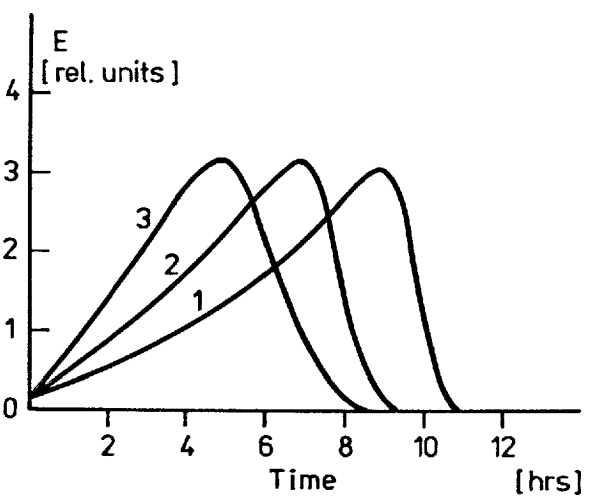

Fig. 7: Theoretical REM curves obtained by computer simulation of C_3S hydration at 20 °C in the presence of admixtures causing the decrease of Ca^{2+} concentration in the solution. Curves 1 – 3 correspond to the concentrations c_o = 0.1, 0.05 and 0.025 mole of Ca^{2+} per liter, respectively.

CONCLUSION

The experimental results proved the suitability of the radiometric emanation method for the investigation of the kinetics of early hydration of C_3S and cement as influenced by temperatures and various admixtures. The experimental results of REM agree fairly well with the theoretical curves obtained by computer simulation on the basis of the theoretical model formulated. This model enables us to describe mathematically the release rate of radon during the C_3S hydration under various experimental conditions.

REFERENCES

1. V. Balek, V. Šatava, J. Dohnálek, Proc. 7th Int. Congress on the Chemistry of Cement, Paris 1980, II/6-72
2. V. Balek, J. Dohnálek, Cement and Concr. Res. 13 (1983) 1
3. V. Balek, W. D. Emmerich, High Temp.-High Pressures 5 (1973) 67
4. J. M. Maycock, J. Skalny, R. Kalyoncu, Cem. and Concr. Res. 4 (1979) 835
5. P. Fierens, J. Verhaegen, Silic. Ind. 39 (1974) 125
6. P. Fierens, J. Verhaegen, Cement and Concr. Res. 6 (1976) 287 and 337
7. M. E. Tadros, J. Skalny, R. S. Kalyoncu, J. Amer. Ceram Soc. 59 (1976) 344
8. H.F.W. Taylor, Cement Production and Use, Proc. Eng. Found Conf. 1979
9. J. Skalny, J. F. Young, Proc. 7th Congress on the Chemistry of Cement, Paris 1980, II-1/3
10. R. Trettin, R. Wieker, ibid, III/6-163
11. I. Odler, J. Schüppstuhl, Cement and Concr. Res.11 (1981) 765
12. J. F. Young, Cement and Concr. Res. 2 (1972) 415
13. C. R. Wilding, A. Walter, D. D. Double, Cement and Concr. Res. 14 (1984) 185
14. J. Kříž, V. Balek, Thermochim. Acta 71 (1983) 175
15. J. Kříž, V. Balek, ibid 78 (1984) 377
16. V. Balek, J. Kříž, Cement and Concr. Res., to be published
17. J. M. Pommersheim, J. R. Clifton, Cement and Concr. Res. 12 (1982) 765

ACKNOWLEDGEMENTS

The authors wish to thank Dr. R. Trettin, Institute of Inorganic Chemistry, Berlin, G.D.R., for the C_3S samples and fruitfull discussions, and Mrs. F. Hrdličková for carefull typewritting of this manuscript.

L J Parrott, D C Killoh and R G Patel

CEMENT HYDRATION UNDER PARTIALLY SATURATED CURING CONDITIONS

SUMMARY: Curing of concrete under field conditions will be impaired by exposure of surfaces to a dry atmosphere at early ages. The surface layer is expected to protect reinforcing steel but, if prematurely dried, cement hydration is curtailed and the pore structure will be coarsened. Thus the surface layer will be of lower quality than the interior concrete and the difference will depend upon the duration of moist curing, the relative humidity of the environment and the reactivity of the binder. Modelling of these hydration and microstructural gradients is hindered by lack of published data on the effects of microstructural development under partially saturated conditions. The present investigation reports data on OPC and OPC + pfa pastes mixed with a water/binder ratio of 0.59 and exposed, after limited initial curing, at selected relative humidities. After specific exposure periods, changes in hydration and pore structure were measured using thermogravimetric analysis, quantitative x-ray diffraction and methanol adsorption. The various methods of measurement all showed that even moderate drying greatly reduced the rates of OPC and pfa reaction. There were no indications that the reactions changed under partially saturated conditions. The relative volume of pores smaller than 4 nm wide reduced markedly when there was a drop in relative humidity during curing due to their dependence upon hydration and their partial collapse when the pastes were dried. The measured degrees of hydration were consistent with predictions of a mathematical model of cement hydration in which curing relative humidity was a variable.

A cura do concreto sob condições de trabalho será prejudicada pela exposição de superfícies a uma atmosfera seca nas idades iniciais. Espera-se que a camada de superfície proteja o aço da armadura mas, se secada prematuramente, a hidratação do cimento é encurtada e a estrutura de poro ficará grossa. Assim a camada de superfície terá qualidade inferior à do concreto interno, e a diferença dependerá da duração da cura úmida, da umidade relativa do ar e da reatividade do ligante. A modelação desta hidratação e dos gradientes microestruturais' é prejudicada pela falta de dados publicados sobre os efeitos do desenvolvimento microestrutural sob condições parcialmente saturadas.

A presente investigação relata dados de pastas de cimento portland comum e de cimento portland comum + pfa, (cinza volante) preparadas com relação água/ligante de 0,59 e expostos, após cura inicial limitada, a umidades relativas escolhidas. Após períodos específicos de exposição, foram medidas as mudanças na hidratação e na estrutura de poro, usando-se análise termogravimétrica, difração quantitativa de raio X e adsorção de metanol. Todos os diversos métodos de medição mostraram que, mesmo sob secagem moderada, reduziram-se grandemente as velocidades de reação do cimento portland comum e de pfa. Não houve indicações de alteração das reações sob condições parcialmente saturadas. O volume relativo de poros com abertura menor que 4 nm reduziu-se acentuadamente quando houve uma queda na umidade relativa no período de cura, devido à sua dependência da hidratação e de seu colapso parcial quando as pastas secaram. Os graus de hidratação medidos foram consistentes com predições de um modelo matemático de hidratação do cimento em que a umidade relativa de cura foi variável.

INTRODUCTION

Site curing of concrete typically involves an initial period where moisture loss is virtually prevented by formwork and curing procedures. When the formwork is stripped the concrete will normally start to dry and near to the drying surface, the cement will react with the residual pore water at a reduced rate. If the relative humidity of the surrounding air is low enough the cement reactions will stop, first at the exposed surface and subsequently at increasing depths. Thus drying can cause gradients of cement hydration that are deeper and more severe the sooner drying starts, the lower the exposure humidity, the faster the rate of drying and slower the cement reacts. This investigation examines the effects of curing relative humidity upon OPC and OPC + pfa reactions and microstructure under experimental conditions that are relevant to a) practical curing of concrete and b) mathematical modelling of reaction rates in terms of relative humidity. The reactions and microstructural changes are monitored by x-ray diffraction, thermogravimetry and methanol adsorption.

EXPERIMENTAL DETAILS

Two slabs of paste, each with a water binder ratio of 0.59 by weight were cast in sealed moulds. The moulds were slowly rotated during setting to avoid sedimentation of the binder. The binders used were an OPC and a 70/30 blend by weight of OPC and pfa. Details of OPC and pfa are given in Table 1. Slices 3 mm thick were sawn from the saturated slabs at 2 days for the OPC paste and at 7 days for the OPC + pfa paste. The slices were then conditioned in vacuum desiccators where the relative humidities were controlled by saturated salt solutions. The OPC + pfa paste was conditioned at the later age of 7 days to help isolate the effects of curing relative humidity upon the pozzolanic reaction. At ages of 14 days and 90 days, OPC samples were tested by thermogravimetry (1), methanol adsorption (1), loss on ignition (1) and quantitative x-ray diffraction (2). OPC + pfa samples were tested at ages of 28 days and 90 days by thermogravimetry and methanol adsorption.

RESULTS AND DISCUSSION

OPC hydration versus curing relative humidity.

The effect of relative humidity during curing upon OPC hydration at 14 days can be observed in Figure 1; there is a marked drop in hydration between curing at relative humidities of 97% and 70%, while below 70% there is little evidence of hydration. The 90 day results in Figure 2 are similar to the 14 day results apart from the slight long-term hydration observed below 70% curing relative humidity. The three different indicators of hydration, i.e. quantitative x-ray diffraction (QXRD), loss on ignition 105 to 900°C (LOI) and thermogravimetric loss 100 to 750°C (TG), all exhibit similar patterns. The degree of hydration by x-ray diffraction is a weighted mean value for the four main cement compounds. Figures 1 and 2 are broadly consistent with the small amount of existing data reviewed in reference 3 and suggest that the rate of OPC hydration is related to the amounts of water in the larger capillaries rather than the amounts of water in the porous hydrate coatings that surround residual, unhydrated cement

Table 1 Properties of cement and pfa

Oxide (wt %)	Cement	Pfa
SiO_2	20.32	47.74
Fe_2O_3	2.36	9.10
Al_2O_3	5.47	25.96
CaO	64.00	1.67
MgO	2.30	1.33
SO_3	2.80	0.84
Others	1.59	6.33
Loss on ignition	1.06	5.84
Density (kg/m^3)	3160	2395
Specific surface (m^2/kg)	320	375

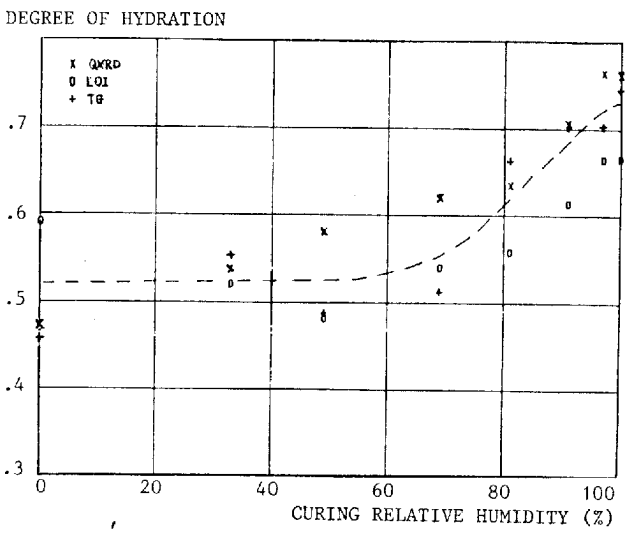

FIG. 1 HYDRATION VERSUS CURING RELATIVE HUMIDITY AT 14 DAYS

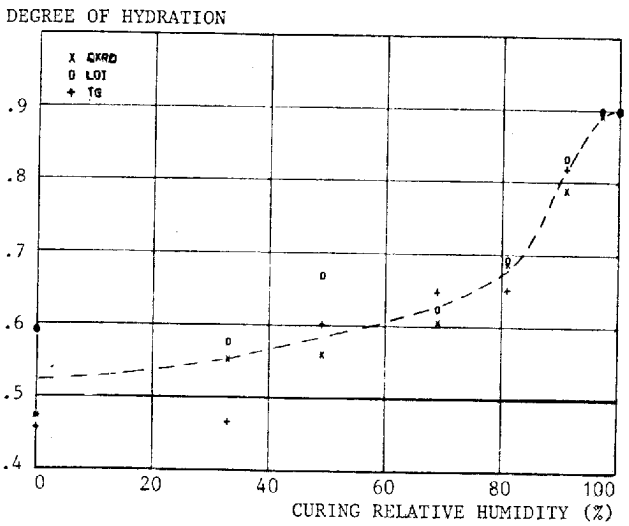

FIG. 2 90 DAY HYDRATION VERSUS CURING RELATIVE HUMIDITY

grains. Possibly this indicates that drying causes a reduction of the concentration gradient of some outward diffusing species across the hydrate coating. However, it is also feasible that any diffusion associated with hydration is hindered by the partial collapse of small diameter pores that accompanies drying (4,5).

Pfa reactions versus curing relative humidity.

The pozzolanic reaction between pfa and the calcium hydroxide produced by the OPC reaction is affected by the curing relative humidity as illustrated in Figure 3; at 28 days the calcium hydroxide in OPC + pfa pastes is dominated by the OPC reactions and an increase is observed at high relative humidities. At 91 days the effect of the pozzolanic reaction is evident and there is a consumption of calcium hydroxide at high curing relative humidities. The effect of curing relative humidity upon the pozzolanic reaction is best represented by the difference between the 28 and 91 day curves. There is little evidence of much pozzolanic reaction at curing relative humidities below 80%, although the OPC again shows signs of slight reactivity at lower humidities.

Bound water distribution.

Thermogravimetric data were examined for evidence that reactions under partially saturated conditions alter the bound water distribution in the reaction products. The single linear relationship in Figure 4 suggests that the broad distribution of water bound in products other than calcium hydroxide is not significantly affected by either curing relative humidity or by the presence of pfa. Figure 5 illustrates that calcium hydroxide is produced by OPC reactions and is consumed by the pozzolanic reaction but there was no obvious effect of curing relative humidity upon the distribution of bound water between calcium hydroxide and other products with a given binder system.

Amount and physical nature of gel products.

Assuming that calcium hydroxide formations are relatively large and have a low specific surface area, the amount of gel product can be viewed in terms of a thermogravimetric loss that excludes calcium hydroxide e.g. from 100 to 425°C. Figure 6 indicates that for OPC pastes the amount of gel formed is consistent with the hydration results shown in Figures 1 and 2 and again suggests that slow, long-term hydration is possible at curing relative humidities below 70%. Parallel data for OPC + pfa pastes, Figure 7, show no clear sign of pozzolanic reaction except under near-saturated conditions. Comparison of Figures 6 and 7 indicates that there is more gel in the OPC paste than in the OPC + pfa paste after 90 days at curing relative humidities above 40%, even though the OPC pastes were moist cured for a shorter time.

The gel pores detected by methanol adsorption increase with the amount of gel but are reduced by drying (1,4,5). The relative volume of pores less than 4 nm wide are plotted against curing relative humidity for OPC paste in Figure 8 and for OPC + pfa paste in Figure 9. Figure 8 shows that at high humidities the volume of gel pores is higher at 90 days than at 14 days as would be expected from

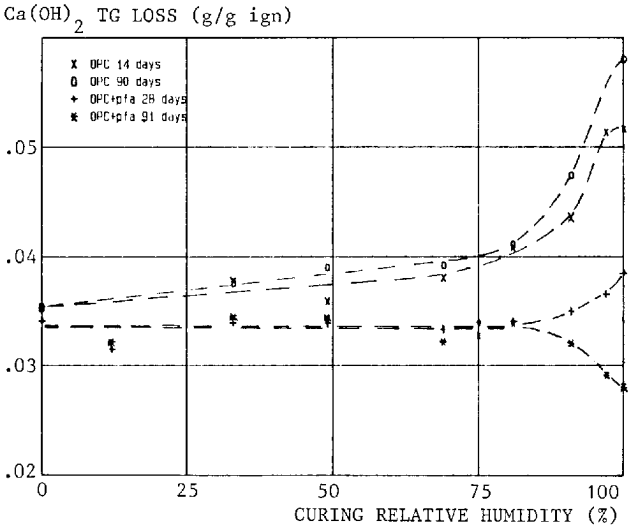

FIG. 3 CALCIUM HYDROXIDE TG LOSS VERSUS CURING RELATIVE HUMIDITY

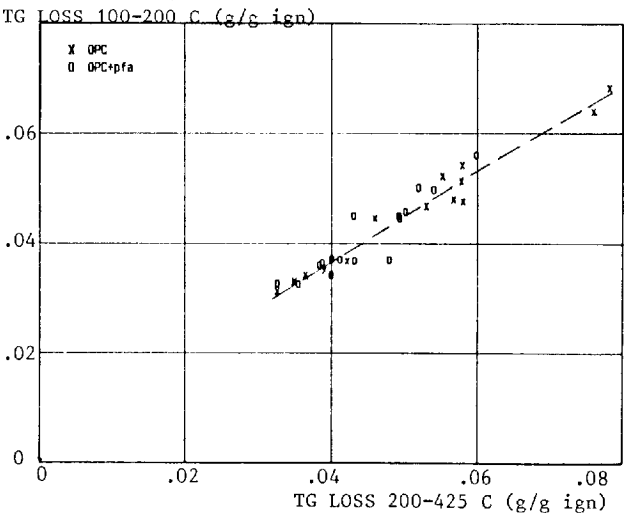

FIG. 4 TG LOSSES 100-200 VERSUS 200-425 C

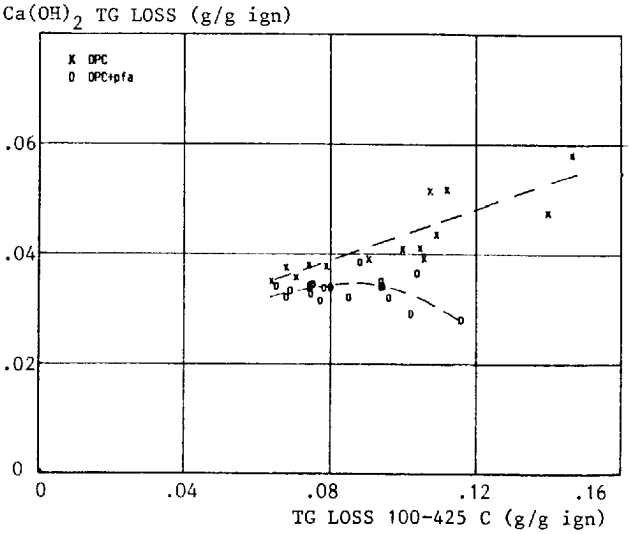

FIG. 5 CALCIUM HYDROXIDE TG LOSS VERSUS TG LOSS 100-425 C

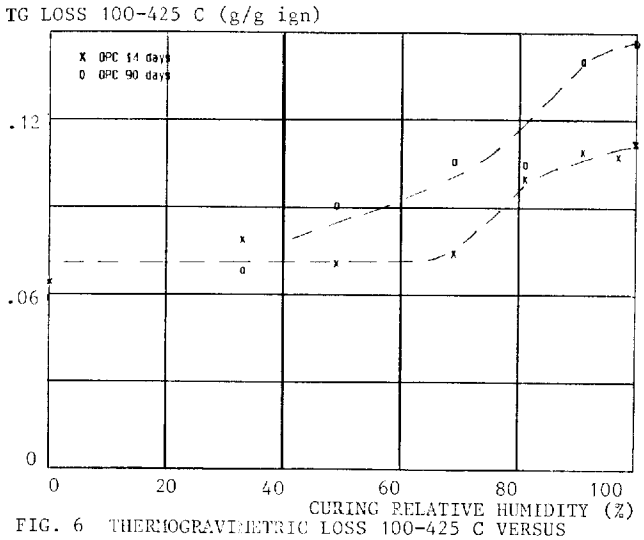

FIG. 6 THERMOGRAVIMETRIC LOSS 100-425 C VERSUS CURING RELATIVE HUMIDITY

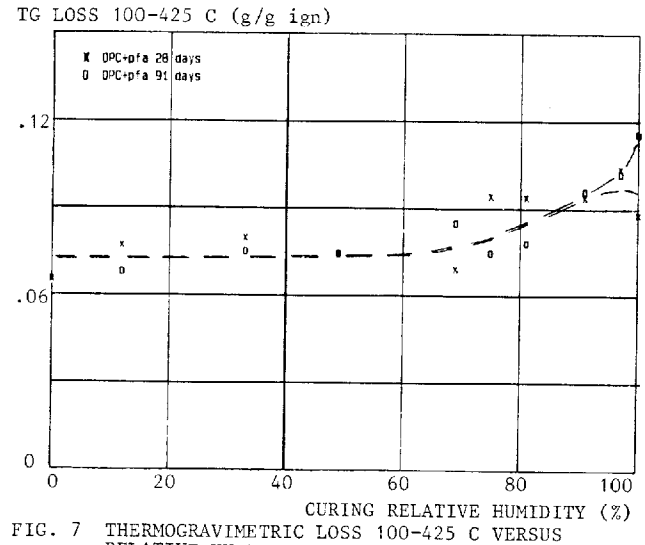

FIG. 7 THERMOGRAVIMETRIC LOSS 100-425 C VERSUS RELATIVE HUMIDITY

Figure 6; below 95% curing relative humidity it is believed that partial collapse of the gel pores induced by drying dominates and the trend is reversed. The bulk of this gel pore collapse might reasonably be attributed to the calcium silicate hydrates, since similar behaviour was observed with hydrated alite paste (5). The gel pores in OPC + pfa paste are formed partly by OPC reactions and partly by the pozzolanic reaction. However, Figure 9 shows that they are affected by drying in a similar way to the gel pores in OPC paste.

Comparison of Figures 8 and 9 indicates that there is generally a greater volume of pores smaller than 4 nm wide in the OPC paste than in the OPC + pfa paste for a given curing relative humidity or age. However, the pozzolanic reaction increases the volume of gel pores above that expected solely from the OPC.

Mathematical description.

The effect of relative humidity, H, upon the rate of cement hydration relative to that at saturation, R, has been described previously (3) by the relationship $R = ((H - .55)/.45)^4$ for $H > .55$; $R = 0$ for $H < .55$. The equation was based upon a limited amount of published data and it was one intention of the present study to check its validity. The equation can not be derived directly from the experimental results because the rate of hydration depends upon the average degree of hydration during a time increment and in the present study this varied with relative humidity. Instead, a relationship was assumed and was used in a recently developed model of cement hydration (6) to estimate hydration under the relative humidity histories appropriate to the test conditions. Table 2 shows that the relationship above yielded good results for the OPC data. The standard error of the predicted degree of hydration was 0.035 and variations with relative humidity were well represented.

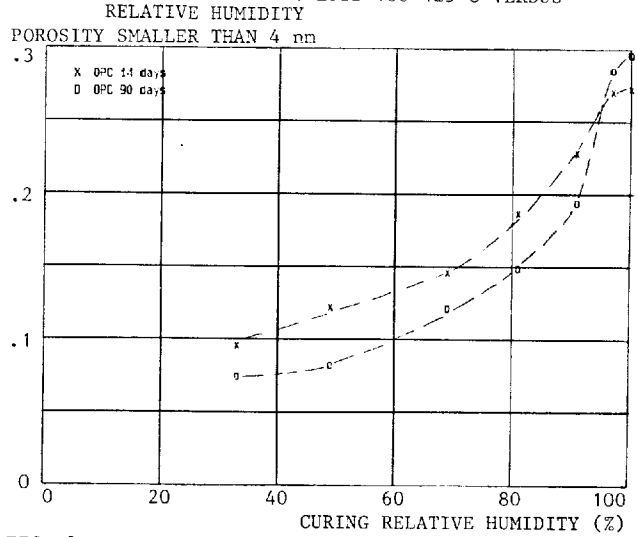

FIG. 8 PORES SMALLER THAN 4 nm VERSUS CURING RELATIVE HUMIDITY

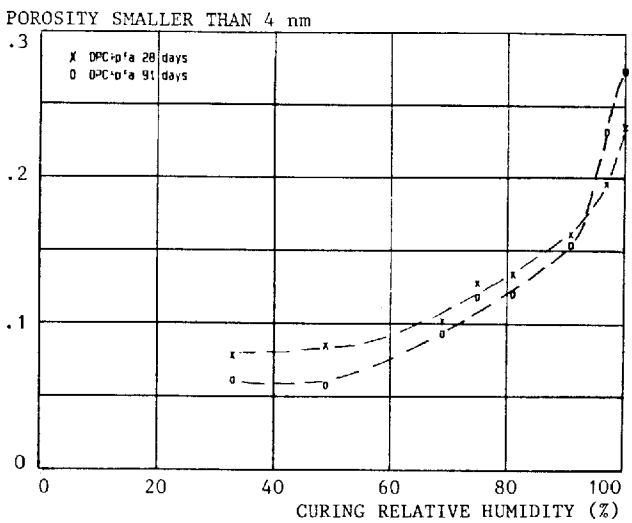

FIG. 9 PORES SMALLER THAN 4 nm VERSUS CURING RELATIVE HUMIDITY

Table 2 Comparison of predicted* and measured** degrees of OPC hydration

Curing relative humidity %	33	49	69	81	91	97	100
14 day hydration measured	.538	.517	.558	.619	.674	.711	.724
predicted	.544	.544	.583	.625	.694	.735	.755
90 day hydration measured	.532	.610	.625	.677	.813	.896	.899
predicted	.544	.544	.610	.741	.824	.846	.854

* Hydration rate factor = $((H - .55)/.45)^4$ for $H > .55$
= 0 for $H \leq .55$

** Mean of x-ray, ignition loss and thermogravimetry data.

CONCLUDING REMARKS

Three independent measures of hydration showed that a drop in relative humidity below saturation during curing reduced the rates of OPC hydration and pfa reaction, particularly in the range 100 to 70%; below 70% relative humidity there was little evidence of pfa reaction and any OPC hydration was slow. The results suggested that the rate of cement hydration was related to the amounts of water in the larger capillaries rather than the amounts of water in the porous hydrate coatings that surround residual, unhydrated cement grains. There were no indications from an examination of bound water distribution that the nature of the reactions changed under partially saturated conditions. The relative volume of pores smaller than 4 nm wide reduced markedly with a drop in relative humidity during curing due to their dependence upon hydration and their partial collapse when dried. The reduction in the relative volume of small pores due to drying was accompanied by an increase in the relative volume of larger pores. This behaviour and its practical implications will be considered at greater length in a subsequent paper.

The effects of relative humidity observed in this study are consistent with reported gradients of microstructure in drying, hydrated cement paste (1). Thus it may be concluded that the surface of prematurely dried concrete will have a low degree of reaction, a higher proportion of large diameter pores and will offer less protection to underlying concrete and any steel reinforcement. The results of the present study enable this variation of concrete quality to be modelled with greater confidence.

ACKNOWLEDGEMENT

The authors are indebted to Mr W A Gutteridge for undertaking the x-ray measurements and to Mr J A Martin for his assistance with the other measurements.

REFERENCES

1. Patel, R., Parrott, L., Martin, J. and Killoh, D. Cement and Concrete Research, 1985,, V. 15, N. 2, pp 343-356.

2. Gutteridge, W. Proc. British Ceramic Soc. Sept 1984, N. 35, pp 11-23.

3. Parrott, L. and Killoh, D. Proc. British Ceramic Soc. Sept. 1984, N. 35, pp 41-53.

4. Sellevold, E. and Bager, D. Technical University of Denmark, 1980. Technical Report No. 86/80.

5. Parrott, L. Cement and Concrete Research, 1981, V 11, pp 651-658.

6. Parrott, L. 'Modelling the development of microstructure'. To be published in Proceedings of Engineering Foundation Conference on Cement Manufacture and use, New Hampshire, July 1985.

N.J. Clayden and C.M. Dobson. Inorganic Chemistry Laboratory, Oxford University, England.
G.W. Groves and S.A. Rodger. Dept. of Metallurgy and Material Science, Oxford University, England.

The Application of Solid State Nuclear Magnetic Resonance Spectroscopy Techniques to the Study of the Hydration of Tricalcium Silicate. 2.1
L'Application des Methodes Spectroscopique de la Resonance Magnetique Nucleaire dans l'Etat Solide pour l'Etude de l'Hydration du Silicate Tricalcique.

SUMMARY: A detailed study of the products formed during the hydration of tricalcium silicate has been carried out using solid state ^{29}Si nuclear magnetic resonance spectroscopy and cross polarisation techniques. It has been found that the initial product contains hydrated monomeric silicate units and that this product persists throughout the hydration process. At the end of the induction period material containing dimeric silicate units is formed and at later stages in the reaction a more highly polymerised silicate unit appears. The nature of the CSH products formed during the post induction period can be followed using ^{29}Si nmr in conjunction with other techniques. In particular the hydration process has been studied with and without admixtures present using solid state ^{29}Si nmr, scanning electron microscopy and thermogravimatric analysis. It has been found that considerable changes in the morphology of the CSH gel are accompanied by only small variations in the degree of polymerisation of the silicate units involved.

SUMÁRIO: Realizou-se um estudo pormenorizado dos produtos formados durante a hidratação do silicato tricálcico, utilizando-se técnicas de espectroscopia de ressonância magnética nuclear de estado sólido de ^{29}Si e técnicas de polarização transversal. Constatou-se que o produto inicial contém unidades de silicato monomérico hidratado, e que este produto persiste durante o processo de hidratação. Ao final do período de indução forma-se material contendo unidades de silicato dimérico, e nos últimos estágios da reação aparece unidade de silicato mais altamente polimerizado. Pode-se acompanhar a natureza dos produtos CSH formados durante o período de pós-indução usando-se ^{29}Si nmr conjuntamente com outras técnicas. O processo de hidratação com ou sem aditivos foi estudado de forma particular, empregando-se ^{29}Si nmr de estado sólido, microscopia eletrônica de varredura e análise termogravimétrica. Verificou-se que mudanças consideráveis na morfologia do gel de CSH são acompanhadas apenas por pequenas variações no grau de polimerização das unidades de silicato envolvidas.

N.J. Clayden and C.M. Dobson. Inorganic Chemistry Laboratory, Oxford University, England.
G.W. Groves and S.A. Rodger. Dept. of Metallurgy and Material Science, Oxford University, England.

INTRODUCTION

Tricalcium silicate is the major constituent of ordinary portland cements. Its hydration reaction, responsible for the development of much of the strength of cement, has been studied in detail for many years. Two aspects of the reaction are of particular interest. One is the induction period. This is the stage of the reaction following the first exotherm caused by the addition of water to C_3S . It may easily be characterised as the period of low heat evolution from the paste before the material begins to harden (see figure 1). The induction period is extremely important because during this time the paste remains workable, thus facilitating mixing with aggregate and placing of the cement. However the reasons for its existence remain a source of controversy. The second area of interest is the action of accelerators and retarders. These are chemical compounds which when added to the hydrating water of C_3S have dramatic effects on the hydration reaction. Again this can be clearly seen using isothermal calorimetry (see figure 1). An accelerator such as calcium chloride will shorten the induction period and raise the maximum of the second exotherm whilst a retarder such as malic acid will lengthen the induction period and reduce the height of the second heat peak. The way in which these admixtures act is not clearly understood.

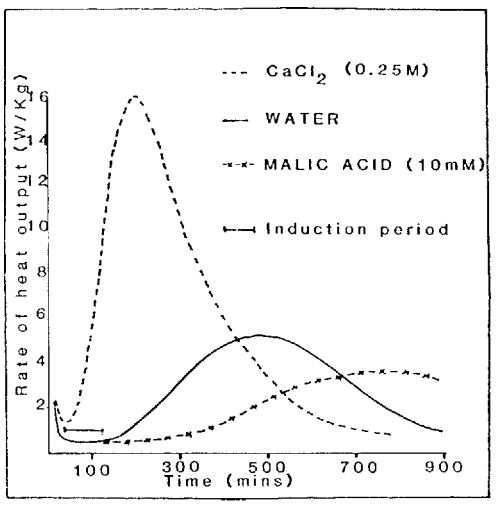

Figure 1. Heat evolution curves obtained from hydrating C_3S with various solutions (T = 25°C, w/s = 0.5).

Over the past few years it has been shown that high resolution solid state ^{29}Si nuclear magnetic resonance spectroscopy can be used successfully to follow the hydration of C_3S (1,2,3). The frequency of the resonance obtained from any ^{29}Si nucleus depends on its local environment. Thus information may be obtained about ^{29}Si nuclei in both the amorphous CSH as well as in the crystalline anhydrous C_3S. Distinct resonances may be obtained from ^{29}Si nuclei in different silicate units. The connectivity of an SiO_4 unit in a silicate material can be given a symbol Q^n where n = 0 - 4. Thus Q_0 corresponds to isolated silicate tetrahedra, Q^1 to chain end units and Q_2 to middle units in silicate chains. In a previous paper (2) we have shown that the anhydrous C_3S shows five well resolved resonances in the range -69.1 to -74.5 ppm. The first new signal that can be observed in the conventional "onepulse" spectrum of hydrating C_3S appears at the beginning of the acceleratory period and corresponds to end units in silicate chains, at -79 ppm. In the absence of any signal from middle units this must indicate the presence of dimeric silicate units in the hydrate. As hydration proceeds a resonance corresponding to middle units in silicate chains, at -83 ppm, appears thus indicating the presence of more highly polymerised silicate units in the CSH gel. We have not observed any Q_3 , chain branching units, or Q_4 , units in a three dimensional network , in the hydrating C_3S system using solid state nmr.

One great advantage of the use of solid state nmr is that no chemical manipulation of the sample is neccessary before information can be obtained. Hence no spurious side reactions can occur. If the spectra are acquired with a long recycle time to prevent saturating the Si resonance the areas beneath the peaks give quantitative values for the percentage of each silicate unit present.

In this paper we shall present the results of a study of the products of the hydration of C_3S in the presence of admixtures using solid state nmr, thermogravimetric analysis and scanning electron microscopy. We shall also present some of the preliminary results of a series of experiments using solid state nmr techniques to examine the reaction products during the induction period.

RESULTS AND DISCUSSION

A. Admixtures.

Samples of C_3S were hydrated for various time intervals up to the end of the second exotherm in the presence of a selection of admixtures (w/c = 0.5, T = 25° C). The hydration reaction was quenched by the addition of propan-2-ol followed by vacuum outgassing. The admixture solutions used were 0.5M cadmium chloride, 0.5M lead nitrate and 5mM malic acid. The first is a good accelerator whilst the other two are retarders. The Si solid state nmr spectrum was obtained from each sample and the areas beneath each resonance measured. The results are shown in figure 2. where the percentage of each type of silicate unit present is plotted against the time of hydration. Also included is a line corresponding to the % hydration of the sample. The control shows the typical pattern of the development of the silicate structure of the CSH. First solely Q_1 , and so dimer, units appear and then the Q_2 resonance begins to grow. The same pattern is repeated when admixtures are used be they accelerating or retarding. The difference between the control and when admixtures are present is simply in the rate of growth of the hydrate product. The Q_1/Q_2 ratio at any particular degree of hydration remains much the same. Any variation in the ratio is small and the is no systematic difference between that in the presence of accelerators or retarders.

This is an interesting result particularly when considered in the light of the thermogravimetric analysis (TGA) results. Here portions of the same specimens which had been examined in the solid state nmr work were used. TGA was used to find the calcium hydroxide content of the sample and thus the C/S ratio of the CSH gel material produced.

N.J. Clayden and C.M. Dobson. Inorganic Chemistry Laboratory, Oxford University, England.
G.W. Groves and S.A. Rodger. Dept. of Metallurgy and Material Science, Oxford University, England.

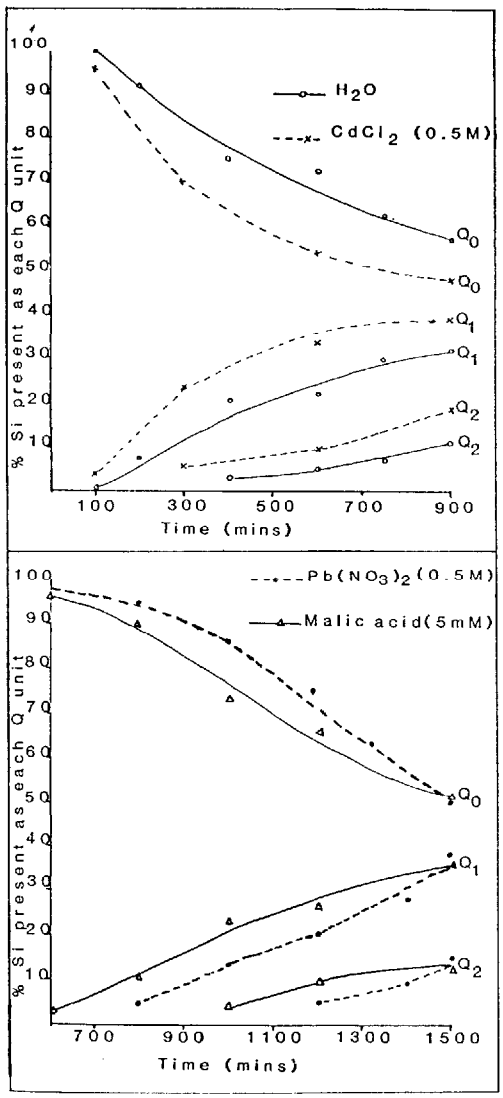

Figure 2. The distribution of silicate units in C_3S hydrated with water and various admixtures for short time intervals.

The results are shown in table 1. There is only a small variation in the C/S ratio of the gel materials, all the values lying around 1.7.

Table 1. Average C/S ratios of the CSH gel produced when C_3S is hydrated with various admixtures determined by TGA.

Admixture	C/S
water	1.8 + 0.1
cadmium chloride (0.5M)	1.75 + 0.1
lead nitrate (0.5M)	1.8 + 0.1
malic acid (5mM)	1.7 + 0.1

This result shows that the admixtures do not have any significant effect on the chemical composition or the silicate structure of the CSH produced during the hydration reaction. The sole effect appears to be on the kinetics of the reaction.

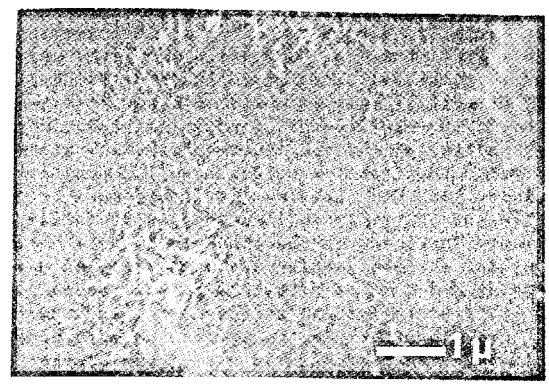

Plate 1. C_3S hydrated with water.

However if scanning electron microscopy is used to examine the fracture surfaces of the specimens it is clear that the addition of accelerating and retarding admixtures may produce quite dramatic changes in the morphology of the CSH. Plate 1 shows the typical morphology of the CSH produced when C_3S is hydrated with water. This morphology has been found by many authors (4,5). The surface of the grain is covered with CSH material which has been described as fibrils or crumpled foils.The fibrils are often triangular in profile and taper to a point. They are very thin, being almost electron transparent in places and some appear striated along the long axis although this may be a result of thickness profiles.

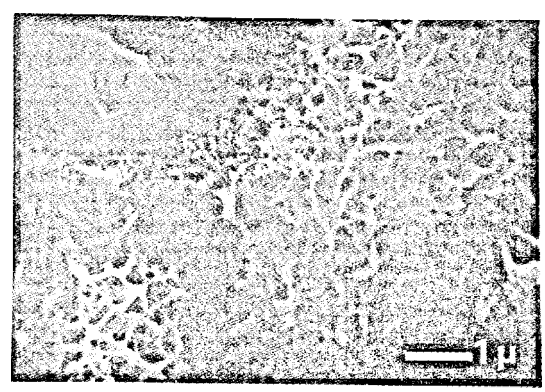

Plate 2. C_3S hydrated with cadmium chloride solution.

Plate 2 shows the morphology of the CSH formed when cadmium chloride is used as an accelerator. The C_3S sample is hydrated to almost exactly the same degree as the C_3S sample in plate 1. The CSH is now much less fibrillar . It has a much more open honeycombed outer product. Similar changes in morphology have been found by other workers when calcium chloride solutions have been used to accelerate the hydration of C_3S (6).Changes in the morphology of the gel to a greater or lesser extent have been found when lead nitrate or malic acid are used as admixtures. Thus

N.J. Clayden and C.M. Dobson, Inorganic Chemistry Laboratory, Oxford University, England.
G.W. Groves and S.A. Rodger, Dept. of Metallurgy and Material Science, Oxford University, England.

although the composition and silicate structure of the CSH is unaffected by the addition of admixtures the rate of formation of the gel and the morphology may be greatly altered. It is not clear from these results if the rate of formation of the gel is changed by the altered morphology or vice versa. However Ottewill (7) and Double (8) have suggested that the CSH may be treated as a typical colloid that will be affected by the ionic species in solution. They propose that ions in solution will coagulate or flocculate the CSH causing it to be more or less permeable and thus it will hinder or facilitate hydration. This cannot be the only factor involved because, for example, while calcium nitrate is a good accelerator and cadmium nitrate a poorer accelerator lead nitrate is in fact a retarder. Another important factor must be the the nature of the precipitates other than CSH that are formed when admixtures are used. Cadmium compounds appear to result in crystalline precipitates whilst lead ones produce a voluminous amorphous precipitate which may block further hydration.

Solid state nmr has also been used to follow the much longer term hydration of C_3S with water and in the presence of 0.25M calcium chloride solution.

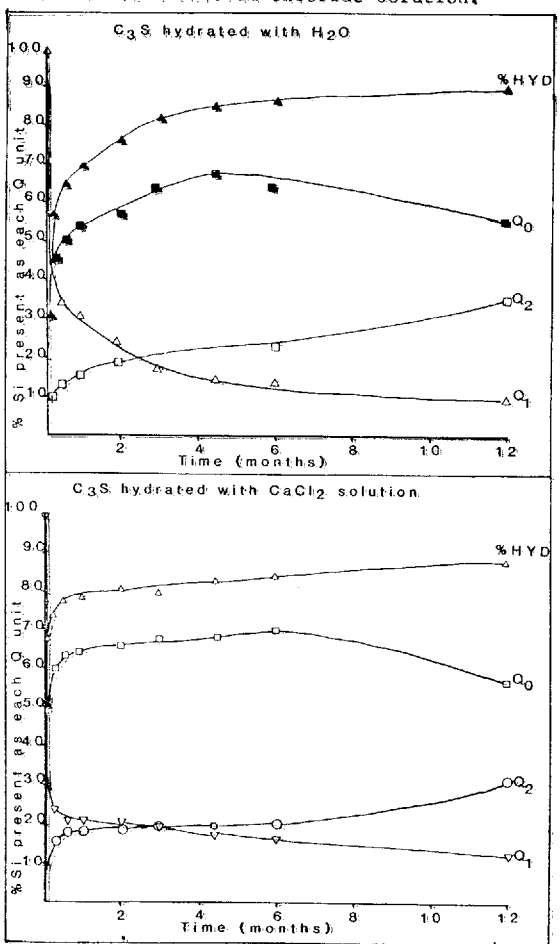

Figure 3. The degree of hydration of C_3S as a function of time. The percentage of each type of silicate unit present are also shown.

Again there are few differences between the average chain lengths of the silicate structures in the two cases although the rates of the reactions involved are different. Figure 3 shows the changing Q_0,Q_1 and Q_2 percentages over a 12 month period of hydration. In both cases after about four to six months there is a marked decrease in Q_1 units and an increase in Q_2 units with a small decrease in Q_0 content. No Q_3 units have yet been observed. It has been suggested that CSH formed after the end of the induction period can be considered as disilicate units deposited onto short calcium hydroxide like sheets (9) shown schematically in figure 4. Up to about 10 - 15% hydration only dimeric units are present . Further polymerisation may take place by a single monomer unit linking two dimer units forming a pentamer. Later pentamer and dimer may be linked to form octamer. Trimethylsilylation studies suggest that pentamer and octamer are the predominant higher polymeric species present (10,11). The nmr results could be used to support these findings. For the C_3S/water samples from six months to one year the Q_1 units decrease by about 4% , the Q_1 decrease by 10% whilst the Q_2 units increase by 14% . This would suggest that a polymerisation reaction involving dimer units as described is the dominant reaction at this stage of hydration. However at earlier stages both a dimerisation reaction and the production of higher polymers must be taking place as both Q_1 and Q_2 units increase at the expense of the Q_0.

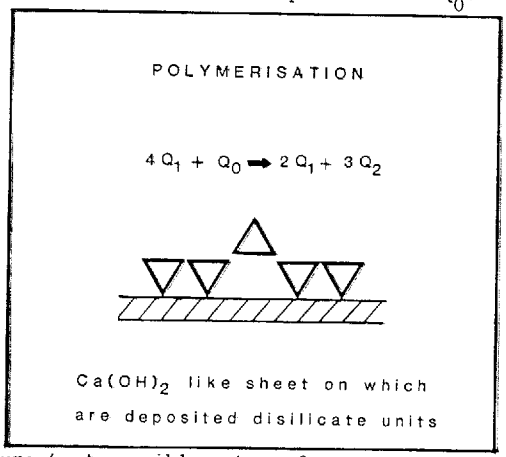

Figure 4. A possible scheme for the polymerisation of the silicate units in CSH (adapted from ref.9).

B THE INDUCTION PERIOD.

We have shown how basic solid state ^{29}Si nmr can follow the hydration reaction of C_3S giving a degree of hydration and an idea of the structure of the silicate units involved in the CSH. However the results so far have shown that the first hydrate material to be detected contains dimeric units and appears at the beginning of the acceleratory stage. This cannot be used as evidence to rule out the formation of a small quantity of hydrated monomeric silicate containing material since the resonance of the latter would be swamped by those of the anhydrous monomeric silicate in the C_3S. It has been shown that cross polarisation (CP) techniques can be used to observe selectively the signal from silicon nuclei close to protons (12). We have used this technique to initiate studies of the reactions occurring within the induction period of C_3S hydration.

A number of experimental problems must be overcome if an attempt is to be made to follow the development and composition of the CSH formed during the

N.J. Clayden and C.M. Dobson. Inorganic Chemistry Laboratory, Oxford University, England.
G.W. Groves and S.A. Rodger. Dept. of Metallurgy and Material Science, Oxford University, England.

induction period. Firstly there is a problem of sensitivity. Although CP will enhance the signal of silicons close to protons , as there is only a very small amount of material present in the sample it takes a very long time to acquire a spectrum with an adequate signal to noise ratio. To avoid this we found it necessary to use a sample of C_3S which had been enriched in ^{29}Si to a level of 30%[3] (natural abundance 4.7%). Secondly it was necessary to add an internal standard in order to be able to compare quantitatively the spectra obtained after different hydration times . A silicon - naphthol complex containing octahedral silicon was used to give a ^{29}Si resonance well away from those of hydrating C_3S . This complex responded well to CP.

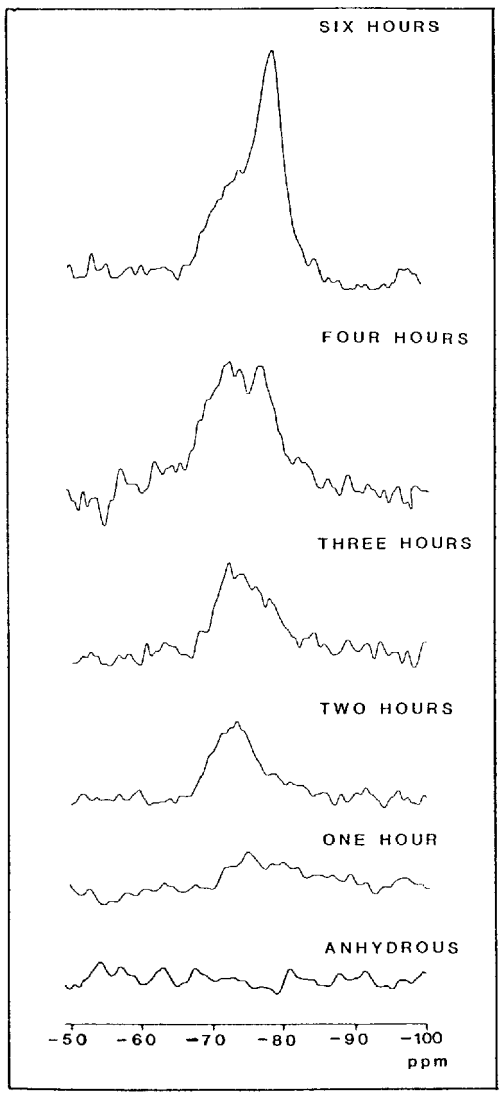

Figure 5. CP ^{29}Si nmr spectra from C_3S samples hydrated for various short time intervals.

A series of spectra obtained from these experiments using C_3S hydrated for time intervals up to six hours are shown in figure 5.Full experimental details will be given elsewhere (13). A CP spectrum from anhydrous C_3S shows no resonances. Even with CP and enrichment the technique would not be sensitive enough to pick up signals from a single surface layer of hydrated silicate units. After one hour a small peak has appeared with a chemical shift corresponding to a hydrated monomeric silicate. After two hours this has grown and at three hours a new resonance has appeared at the Q_1 position. At four hours this has grown further and at six hours it is beginning to dominate the spectrum.

A further CP spectrum was obtained after three days of hydration when substantial hydration had taken place. This spectrum also shows a small shoulder in the monomer position and it is of approximately the same magnitude as that at the end of the induction period.

This set of results has some interesting implications. It is clear from chemical analyses of the solution phase in contact with C_3S pastes that some hydrated silicate species must be formed during the induction period since the solution C/S ratio is >>3 (14). Similarly ESCA and HVEM studies have detected some hydration products on the surface of the grains at these very early times (4,15,16). However this study has shown that, firstly, CSH is formed steadily throughout the induction period and contains largely a hydrated monomeric silicate species and, secondly, that approximately the same amount of hydrated monomeric silicate units remain at three days hydration as are present at the end of the induction period.

These results can be rationalised in terms of both a nucleation theory and a barrier layer theory. If we consider a nucleation theory, the results suggest that it is the calcium hydroxide that has to overcome the nucleation barrier since a hydrated silicate species is formed during the induction period. However the fact that CSH containing dimeric silicate units only appears after the end of the induction period suggests that calcium hydroxide may be an essential precursor for its formation. The results have more far reaching implications for a barrier layer theory. Firstly,as the CSH containing monomeric silicate units increases steadily in quantity through the induction period it is clear that any barrier layer cannot be formed solely during the first few minutes of hydration. Secondly as the material persists at a similar quantity through later hydration the results favour a theory in which the barrier layer is physically disrupted or undergoes a phase change to become more permeable. If the initial hydrated monomeric silicate units dimerise at the end of the induction period they must be continually produced to the same level during subsequent hydration. In terms of a layer around the anhydrous material this would imply that a continually thickening layer of CSH containing monomeric silicate units must be formed as the C_3S core shrinks.
Further experiments are planned to determine the effect of the admixtures on hydrate formation during the induction period.

CONCLUSION

The solid state nmr technique has been shown to be a powerful investigative tool for following C_3S hydration. At its simplest it is an effective means of determining the degree of hydration and the average silicate chain lengths in the CSH. To

N.J. Clayden and C.M. Dobson. Inorganic Chemistry Laboratory, Oxford University, England.
G.W. Groves and S.A. Rodger. Dept. of Metallurgy and Material Science, Oxford University, England.

investigate specific problems such as the induction period the experiments must be carefully considered and designed. It can then provide plentiful new information.

This work has been supported by the SERC. NJC and SAR thank Shell, Thornton Research Centre, for financial support and we acknowledge the advice and support of Dr. A.D.H. Clague.

REFERENCES

1. E. Lippmaa, M. Magi, M. Tarmak, W. Wieker and A-R. Grimmer. Cem. Conc. Res. 12, 597, (1982).
2. N.J. Clayden, C.M. Dobson, C.J. Hayes and S.A. Rodger. J. Chem. Soc. Chem. Commun. 1396 (1984).
3. N.J. Clayden, C.M. Dobson, G.W. Groves, C.J. Hayes and S.A. Rodger. Proc. Brit. Ceram. Soc.35, 55, (1984)
4. H.M. Jennings, B.J. Dalgleish and P.L. Pratt. J. Am. Ceram. Soc.64 (10),587, (1981).
5. J.E. Bailey and H.R. Stewart. Proc. Brit. Ceram. Soc. 35, 193, (1984).
6. P.J. LeSueur, D.D. Double and G.W. Groves. Proc. Brit. Ceram. Soc. 35, 177,(1984)
7. R.H. Ottewill. Phil. Trans. R. Soc. Lond A. 310, 67, (1983).
8. D.D. Double. Phil. Trans. R. Soc. Lond A. 310,56, (1983).
9. J.D. Birchall and N.L.Thomas. Proc. Brit. Ceram. Soc. 35, 305, (1984).
10. L.S.Dent Glasser, E.E. Lachowschi, M.Y. Qureshi, H.P. Calhoun, D.J. Embree, W.D. Jamieson and C.R. Masson. Cem. Conc. Res. 11, 775, (1981).
11. J. Hirljac, Z.-Q. Wu and J.F. Young. Cem. Conc. Res. 13, 877, (1983).
12. D.W. Sindorf and G.E. Maciel. J. Phys. Chem. 86, 5208, (1982).
13. N.J. Clayden, C.M. Dobson, G.W. Groves and S.A. Rodger. To be published
14. P.W. Brown, E. Franz, G. Frohnsdorff and H.F.W. Taylor. Cem. Conc. Res. 14, 259, (1984).
15. D. Ménétrier, I. Jawed, T.S. Sun and J. Skalny. Cem. Conc. Res. 9, 473, (1979).
16. M. Regourd, J.H. Thomassin, P. Baliff and J.C. Touray. Cem. Conc. Res. 10, 223, (1980).

F. HENRY - C.N.R.S. - Thiais France
P. BAILLEUL, B. COURTAULT - C.E.R.I.L.H. - Paris France

Hydratation des phases pures du ciment et de mélanges synthétiques par relaxation diélectrique en microondes
Hydration study of pure phases of cement and synthetic mixtures by microwave dielectric relaxation

Une nouvelle méthode de mesure par hyperfréquences des paramètres diélectriques d'un matériau est présentée. Elle est basée sur la mesure de la perturbation de la fréquence complexe d'une cavité résonnante, contenant le matériau et travaillant en transmission. Cette méthode est appliquée à l'étude de l'hydratation du C_3S, du C_3A et de mélanges synthétiques. Des mesures d'eau liée par thermogravimétrie, dans le cas du C_3S , permettent de corréler la permittivité à la quantité d'eau libre restant dans le matériau.

Apresenta-se um método novo de medição por meio de hiperfreqüência dos parâmetros dielétricos de um material. O método se baseia na medição da freqüência complexa de uma cavidade ressonante, contendo o material e trabalhando em transmissão. Este método se aplica ao estudo da hidratação do C_3S, do C_3A e de misturas sintéticas. Medições, por termogravimetria, da água ligada permitem fazer-se a correlação da permitividade com a quantidade de água livre remanescente no material.

INTRODUCTION

Les méthodes diélectriques centrées sur la relaxation de l'eau ont déjà été utilisées pour suivre les processus liés à la prise des ciments /1-7/. Cependant la mise en oeuvre relativement lourde de telles techniques n'ont pas permis de suivre en dynamique l'hydratation d'un ciment et notamment dès les premiers instants.

Dans la région du gigahertz, maximum de l'absorption dipolaire de l'eau libre, HENRY et BERTEAUD ont développé /8,9/ une méthode à fréquence fixe permettant de suivre en dynamique et simultanément les variations des paramètres diélectriques (ϵ' et ϵ'') obtenues par la théorie des petites perturbations et des pertes pondérales (microbalance de CAHN) de tout matériau inséré dans une cavité résonnante travaillant en transmission.

Cette nouvelle technique de mesures diélectriques par hyperfréquences a été appliquée à l'étude des processus d'hydratation des constituants de base du ciment, C_3A et C_3S et de mélanges synthétiques avec ou sans gypse. Le C_3S a été plus particulièrement étudié. Parallèlement, des mesures d'eau liée par thermogravimétrie ont été effectuées ainsi qu'une détection de flux de chaleur par microcalorimétrie isotherme.

1. METHODOLOGIE

1.1 PARAMETRES DIELECTRIQUES

L'action d'un champ électrique sur un milieu possédant un moment dipolaire se traduit par une orientation de celui-ci dans le champ. Cela représente le phénomène de relaxation souvent caractérisé par la décroissance temporelle de la polarisation $\vec{P}$ du diélectrique après suppression du champ excitateur $\vec{E_o}$ appliqué. On définit alors le vecteur déplacement électrique:

$\vec{D} = \vec{P} + \epsilon_o \vec{E_o}$ où ϵ_o est la permittivité du vide. Comme la polarisation du matériau est proportionnelle au champ excitateur:

$\vec{D} = \epsilon_o \ \epsilon \vec{E_o}$ avec $\vec{P} = \epsilon_o \ (\epsilon - 1) \ \vec{E_o}$

Dans le cas où $\vec{E_o}$ est un champ électrique statique, ϵ, permittivité du matériau testé, est alors un scalaire. Cependant dès que la fréquence du champ excitateur augmente, on observe en général que $\vec{P}$ n'est plus instantanément en phase avec le champ appliqué $\vec{E_o}$. La fréquence à laquelle les molécules ne peuvent plus s'orienter dans le champ est la fréquence de relaxation. Pour formaliser d'une part le déphasage (dispersion) et d'autre part les pertes énergétiques par rotation gênée ou par frottement on définit une constante diélectrique complexe:

$$\epsilon^* = \epsilon' - j \ \epsilon'' \quad (1) \quad \text{et} \quad \vec{D} = \epsilon_o \ \epsilon^* \ \vec{E_o}$$

Dans cette formule, ϵ' est la permittivité. Elle traduit physiquement la dispersion de l'onde dans le matériau. Cette grandeur est très liée à la mobilité ou à la fluidité moléculaire.

ϵ'' représente les pertes diélectriques. En effet on peut montrer que l'énergie dissipée dans un matériau est proportionnelle à:

$W = f \ E_o^2 \ \epsilon'' v$ où v est le volume du matériau.

Dans le cas des matériaux ioniques, il convient d'ajouter aux pertes par relaxation diélectrique les pertes par conduction. La constante diélectrique complexe généralisée s'écrit alors:

$\epsilon^* = \epsilon' - j \ (\epsilon'' + \sigma / 2\pi \ f \ \epsilon_o)$ (2) où σ est la conductivité du matériau.

1.2 PROPRIETES DIELECTRIQUES DE L'EAU

La courbe d'HASTED /10/ présentée ici (fig.1) montre que l'eau possède plusieurs domaines de relaxation. Plus l'eau est liée (adsorbée, solide) plus sa fréquence est basse.

L'intérêt de la région microondes réside dans son action pratiquement sélective vis-à-vis de l'eau libre. A plus basse fréquence le chevauchement des différents domaines ne permet pas une aussi bonne discrimination.

Au cours de l'hydratation d'une pâte de ciment, parmi les nombreuses réactions simultanées, les plus importantes vis-à-vis d'un champ microondes sont:

- le passage de l'eau libre à l'eau liée (adsorbée),
- l'évolution de la concentration en ions dans la solution aqueuse,
- l'effet thermique de l'hydratation provoquant un déplacement des processus de relaxation (fig. 2).

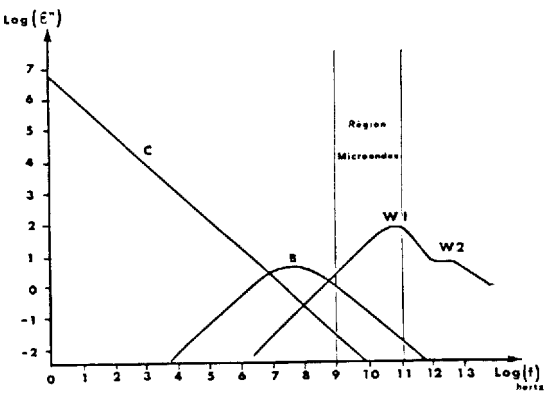

Fig.1 - Représentation des différentes contributions aux pertes diélectriques en fonction de la fréquence d'après /10/.
C: conductivité ionique
B: relaxation de l'eau liée
W_1: relaxation principale de l'eau libre
W_2: seconde relaxation de l'eau libre

1.3 PRINCIPE DE MESURE

Il est basé sur la mesure de la perturbation de la fréquence complexe d'une cavité résonnante contenant le matériau à pertes diélectriques:

$$\frac{\Delta w^*}{w^*} = \frac{\Delta f}{f_o} + \frac{1}{2} \ j \ \Delta (1/Q) = \frac{\epsilon_o (\epsilon^* - 1) \iiint E_i^* \ E_o \, dv}{4 \ W}$$

$\Delta f = f - f_o$: fréquences de la cavité perturbée et non perturbée

$1/Q$, $1/Q_o$: facteurs de surtension en charge et à vide

ϵ^* : permittivité complexe du matériau

E_i^* : champ électrique dans le volume perturbant v

E_o : champ électrique dans la cavité de volume V

W : énergie totale emmagasinée.

Pour un champ appliqué E_o constant, pour une forme de matériau constante, l'intégration sur le volume perturbant conduit aux relations linéaires suivantes:

$$\frac{\Delta f}{f_o} = \beta \frac{v}{V} (\epsilon' - 1) \qquad (3)$$

$$1/2\,\Delta(1/Q) = \beta \frac{v}{V} \epsilon'' \qquad (4)$$

Ces formules ne sont linéaires que pour une perturbation v faible dans le volume V de la cavité/8/.

β est appelé habituellement facteur de forme ou de dépolarisation. Il traduit suivant la forme géométrique le rapport du champ électrique au niveau du matériau au champ électrique excitateur circulant dans la cavité.

Pour un volume V de cavité donné (fig. 3) les évolutions de fréquence et de surtension traduisent les variations de volume, de forme et de constantes diélectriques.

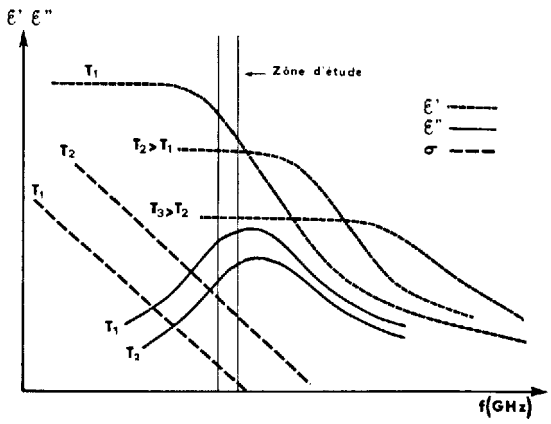

Fig. 2 - Variations de la permittivité (ϵ'), des pertes diélectriques (ϵ'') et de la conductivité (σ) en fonction de la température.

1.4 APPAREILLAGE DE MESURE

Il est représenté à la figure 4. Il convient de signaler que la séparation des constantes ϵ' et ϵ'' n'est rendue possible que grâce à l'asservissement de fréquence de l'oscillateur (Klystron) sur celle de la cavité chargée. D'autre part les iris de couplage à l'entrée et à la sortie maintiennent un train d'ondes stationnaires permettant d'amplifier l'énergie emmagasinée dans la cavité (surtension). Comme dans un circuit oscillant classique, on définit une cavité résonnante par son coefficient de surtension Q.

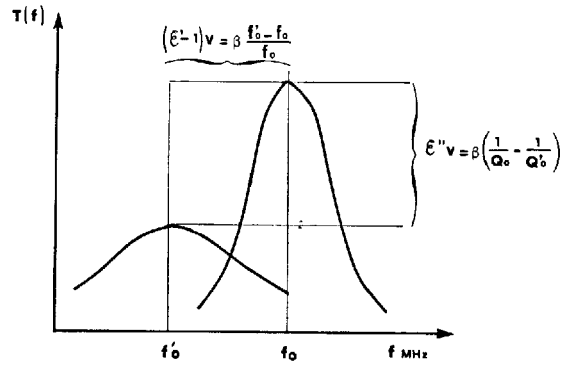

Fig. 3 - Variation de la transmission d'une cavité résonnante due à une perturbation de volume v.

Pour l'étude des matériaux polaires, nous avons confectionné une cavité résonnante, stabilisée thermiquement, dans un mode particulier TE 1, 3 , 13 qui empêche la cavité de trop rayonner par l'orifice nécessaire à l'introduction de l'échantillon. Le volume important de la cavité permet de minimiser la perturbation.

Les variations de fréquences sont obtenues à partir d'un fréquencemètre de précision "Systron Donner".

Les variations de surtension sont atteintes par le coefficient de transmission de la cavité ($\tau = kQ^2$) calculé à l'aide d'une détection quadratique bas niveau, linéaire en puissance.

Les conversions analogiques digitales sur douze bits et parallèles (PIO) de ces mesures permettent un enregistrement simultané sur microordinateur.

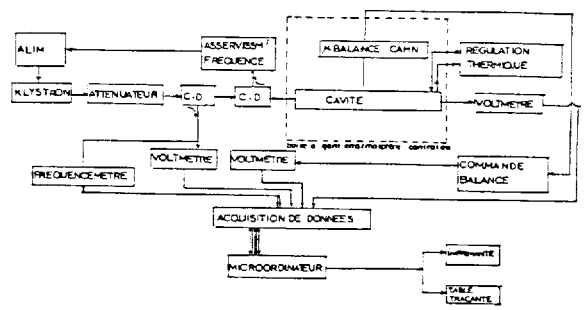

Fig.4 - Schéma de l'appareillage

1.5 FORMULATION DIELECTRIQUE

La complexité d'une pâte de ciment où à tout instant l'eau se partage en eau liée non évaporable et en eau libre évaporable réparties dans une structure évolutive nous incite à utiliser une loi de mélange diélectrique additive et linéaire telle que la formule de WIENER:

$\epsilon^*_m = \rho_1 \epsilon^*_1 + \rho_2 \epsilon^*_2 + \rho_3 \epsilon^*_3$ (5) avec $\rho_1 + \rho_2 + \rho_3 = 1$

ρ_1, ρ_2, ρ_3 sont, respectivement, les fractions volumiques de l'eau libre, de l'eau liée et du matériau; ϵ^*_1, ϵ^*_2, ϵ^*_3 les constantes diélectriques complexes correspondantes. Aux fréquences microondes, le matériau ne relaxant pas et l'eau liée ayant des constantes diélectriques beaucoup plus faibles que celles de l'eau libre ($\epsilon''_{libre} / \epsilon''_{liée} = 250$ à 9 GHz - fig.1) la relation (5) peut encore s'écrire:

$\epsilon^*_m = \epsilon^*_e \rho_e + \epsilon^*_c \rho_c$ (6) avec $\rho_e + \rho_c = 1$ d'où $\rho_c = 1 - \rho_e$

ρ_e, ϵ^*_e : fraction volumique et constante diélectrique complexe de la solution aqueuse.

ρ_c, ϵ^*_c : fraction volumique et constante diélectrique complexe du matériau en cours d'hydratation.

Pour tenir compte du facteur de forme β de l'eau dans le matériau selon l'approche de POLDER et VAN SAUTEN, la formule précédente devient alors:

$$\epsilon^*_m = \epsilon^*_c + \rho_e \beta (\epsilon^*_e - \epsilon^*_c) \quad (7)$$

D'après les formules (3) et (4) et si l'on néglige ϵ^*_e devant ϵ^*_c, les paramètres observés sont proportionnels à:

$$\frac{\Delta f}{f} \alpha \beta V_e (\epsilon'_e - \epsilon'_c) \quad (8)$$

$$\Delta(1/q) \alpha \beta \frac{V_e}{2} (\epsilon''_e - \epsilon''_c) \quad (9), \text{ sachant que:}$$

$$\rho_e = v_e / v_m$$

Ainsi exprimés, ils montrent de manière simplifiée l'influence de:

- la solution aqueuse par ϵ^*_e et V_e volume de cette solution.

- du matériau par ϵ^*_c évoluant selon son état de surface.

- du facteur de dépolarisation par β.

D'autre part, selon les résultats de ZELWER /11/ et l'équation (2), la contribution maximale de la conductivité ionique aux pertes diélectriques est de 10 %.

2. APPLICATION AU CIMENT

2.1 CONDITIONS EXPERIMENTALES

La quantité de matière anhydre étudiée est de l'ordre de cent milligrammes. Le rapport E/C est de 1 pour les phases pures et de 0,7 pour les mélanges synthétiques. Les surfaces spécifiques sont pour le C_3S de 3400 cm^2/g et pour le C_3A de 3450 cm^2/g. Le C_3A gypsé contient 5 % de gypse. Un mélange comprenant 90 % de C_3S et 10 % de C_3A a été testé. Le gâchage est effectué sous un vide primaire (10^{-2} Torr). Le premier point de mesure a lieu trois minutes après le début du gâchage.

La fréquence de résonnance de la cavité est 9150 MHz. La fréquence et la surtension de la cavité à vide, stabilisée à 25°C, sont celles obtenues lorsqu'elle ne contient que le porte échantillon. Les atténuateurs d'ondes sont réglés de façon à obtenir la même valeur de surtension à vide q pour chaque expérience. Les unités des variables ϵ'/m et ϵ''/m sont arbitraires; m étant la masse totale du matériau.

2.2 INTERPRETATION DES RESULTATS

2.2.1 *Phases pures*

Il convient de rappeler le rôle complémentaire de ϵ' et de ϵ''. La permittivité ϵ' appelée aussi dispersion est une grandeur traduisant la mobilité de l'eau dans le matériau tandis que les pertes diélectriques ϵ'' rendent compte des interactions solution aqueuse-substrat.

Le tableau I résume les variations de ϵ'/m et de ϵ''/m au cours de l'hydratation des phases pures.

Tableau I

Variations de ϵ'/m et ϵ''/m au cours de l'hydratation du C_3S et du C_3A

	C_3S		C_3A	
Temps en min	ϵ'/m	ϵ''/m	ϵ'/m	ϵ''/m
3	16,0	10,8	23,9	13,2
30	15,2	9,7	20,9	10,7
90	14,7	9	19,3	10,2
300	14,0	7,3	17,8	9,7
550	13,0	6,0	17,5	9,3

2.2.1.1 *C_3S (fig.5)*

Au contact de l'eau, un premier hydrate se forme immédiatement, C_3SHn, qui se tranforme ensuite en C-S-H 1 ce qui se traduit pour la réponse diélectrique par une décroissance rapide de ϵ' et ϵ'' dans le premier quart d'heure, celle de ϵ'' étant plus prononcée que celle de ϵ' malgré l'augmentation de la conductivité de la solution aqueuse. L'effet thermique initial (adsorption d'eau et premier hydrate) provoque un déplacement des processus de relaxation vers les hautes fréquences. Entre 25°C et 30°C, $d\epsilon''/d\theta = -0,6°C^{-1}$ et $d\epsilon'/d\theta = -0,2°C^{-1}$.

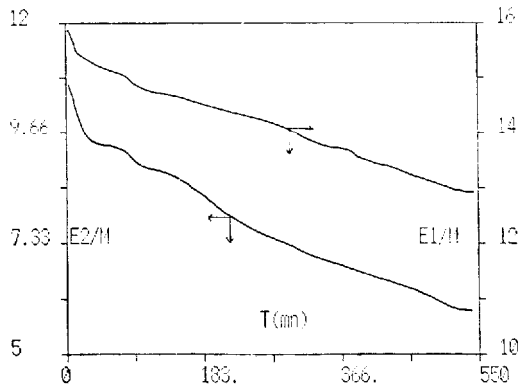

Fig. 5 - Variations de la permittivité E1/M et des pertes diélectriques E2/M au cours de l'hydratation d'une pâte de C_3S

2.1

Durant la période dormante, au-delà de quinze minutes, les variations de ϵ' et ϵ'' observées sont faibles et en accord avec les mesures microcalorimétriques d'hydratation (fig. 6) dont le flux de chaleur est minimum à vingt minutes ainsi qu'avec les variations du rapport C/S des couches superficielles du C_3S mesurées par la technique ESCA/12/. Ce rapport décroît jusqu'à 15 minutes de 2,75 à 2,1 pour atteindre 1,9 à 4 heures.

Le début de la période d'accélération marquée par la précipitation de la portlandite qui entraîne une reprise de la dissolution du C_3S provoque une décroissance rapide mais de faible amplitude de la permittivité et des pertes diélectriques, après 100 minutes.

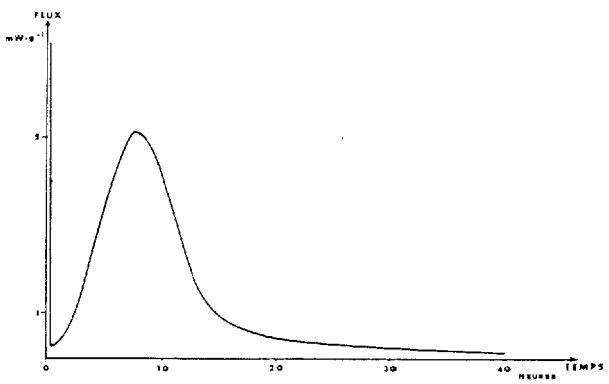

Fig. 6 - Microcalorimétrie de l'hydratation de C_3S

La permittivité est en relation avec la teneur en eau libre dans le matériau. Les mesures d'eau liée, réalisées par thermogravimétrie, conduisent, par différence, à la teneur en eau libre exprimée dans le tableau II par rapport à la quantité d'eau totale dans le matériau. L'expression de la droite de régression linéaire liant la permittivité et la teneur en eau libre, représentée à la figure 7, est de la forme:

$$\epsilon'/m = 0{,}32 \text{ \% eau libre} - 16{,}9 \quad r^2 = 0{,}89.$$

La corrélation des pertes diélectriques en fonction du pourcentage d'eau libre est moins satisfaisante: ϵ''/m étant plus fortement influencé par la température.

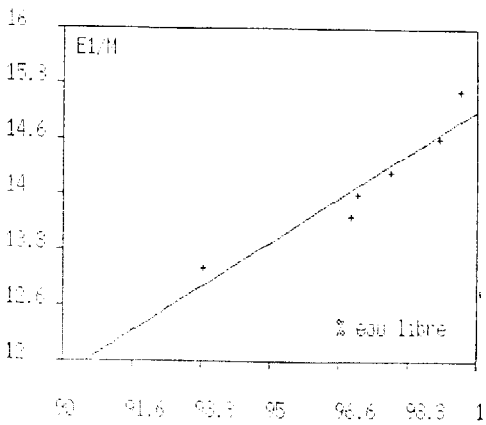

Fig. 7 - Droite de régression (ϵ'/m) = f(% eau libre)

Tableau II

Pourcentage d'eau libre dans la pâte de C_3S et évolution de la permittivité

temps en heures	ϵ'/m	% eau libre
0,5	15,2	99,6
2	14,8	99,1
4	14,2	97,9
5	14	97,1
6	13,7	96,9
8	13,1	93,4

2.2.1.2 *C_3A (fig. 8 et 9)*

L'aluminate tricalcique réagit très rapidement avec l'eau en donnant les hydrates C_2AH_8 et C_4AH_{13} puis C_3AH_6. La forte décroissance de ϵ'/m et ϵ''/m dans les trente premières minutes reflète à la fois la liaison de l'eau et l'effet thermique dû à l'hydratation immédiate du C_3A. Elle est nettement plus importante que celle mesurée par le C_3S (tableau I).

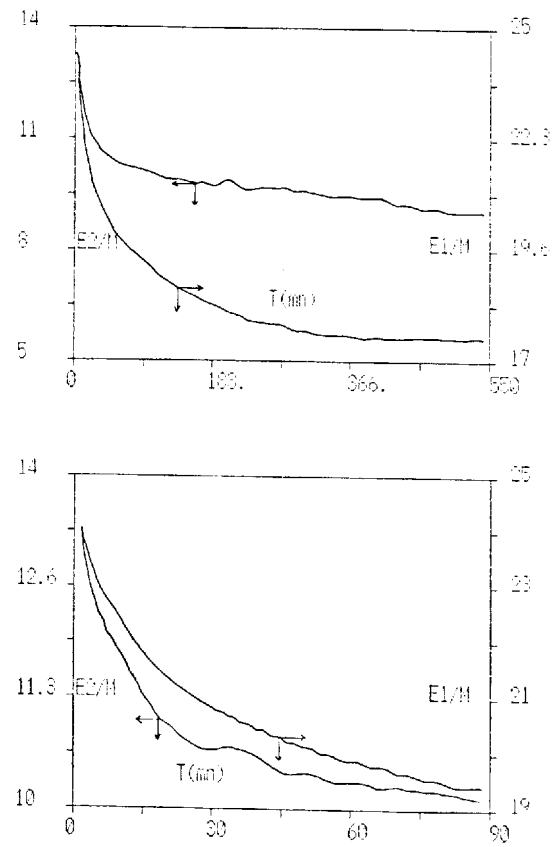

Fig. 8 et 9 - Variations de la permittivité E1/M et des pertes diélectriques E2/M au cours de l'hydratation d'une pâte de C_3A.

Globalement, la permittivité et les pertes diélectriques diminuent par fluctuations successives marquant la compétition entre les formations des différents hydrates notamment celle de C_3AH_6 qui s'accompagne d'une libération d'eau. Interprétation renforcée par l'absence de similitude entre les deux courbes. Les modifications de texture au sein du matériau influent essentiellement sur ϵ', tandis que ϵ'' est plus sensible aux réactions chimiques.

Les mesures sont en concordance avec les résultats obtenus en diffraction X par CABRERA et PLOWMAN /13/ et représentés à la figure 10. Ainsi, la décroissance rapide initiale est attribuée à la formation de C_2AH_8 et C_4AH_{13} et la faible évolution de ϵ''/m entre 25 et 45 minutes correspond à la fin de l'effet thermique concomitant de la transformation des hydrates hexagonaux en hydrates cubiques. Il y a compensation entre l'eau se liant dans le C_3AH_6 formé à partir du C_3A et celle libérée au cours de la cristallisation du C_3AH_6 à partir du C_2AH_8. De même, la disparition du C_2AH_8 après 4h 30 mn se traduit par un palier de ϵ'/m d'une dizaine de minutes et un changement de pente de la courbe.

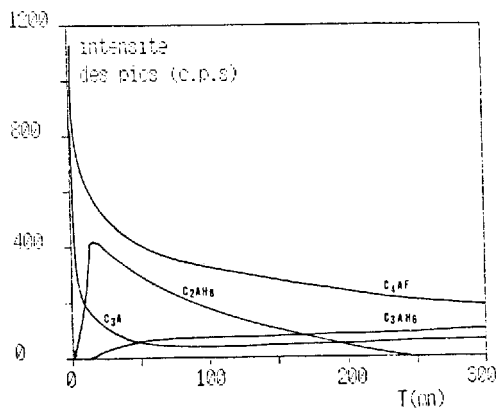

Fig. 10 - Intensité des pics de diffraction X des produits d'hydratation de C_3A + C_4AF en fonction du temps selon/13/.

2.2.2 *Mélanges synthétiques*

2.2.2.1 *C_3A gypsé (fig. 11)*

Le tableau III indique les variations de la permittivité et des pertes diélectriques au cours de l'hydratation du mélange.

La présence de gypse amène la formation d'ettringite dès les premiers instants après le gâchage et a également pour effet de réduire l'effet thermique initial comparativement à celui observé pour le C_3A seul. Cependant après un quart d'heure d'hydratation, la quantité d'eau non évaporable est comparable à celle du C_3A malgré une hydratation moindre. L'ettringite contient en effet plus d'eau que les aluminates de calcium hydratés.

La mesure de la constante diélectrique complexe indique **trois** phases distinctes de la cinétique d'hydratation tant pour ϵ'/m que pour ϵ''/m: jusqu'à 30 minutes, de 30 à 60 minutes et au-delà. La première

Tableau III

Temps en min	ϵ'/m	ϵ''/m
3	31,5	34,4
30	25,3	17,6
60	23,1	14,1
270	21,2	10,1

Variations de ϵ'/m et ϵ''/m au cours de l'hydratation du mélange C_3A + gypse

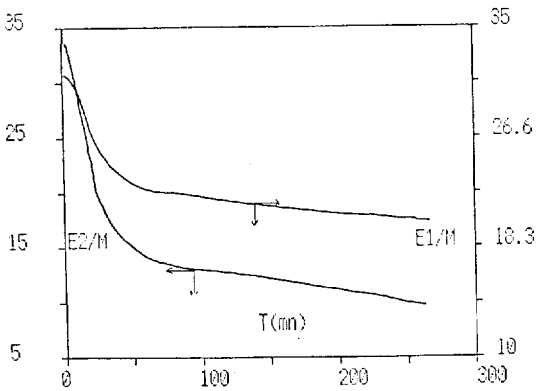

Fig. 11 - Variations de la permittivité E1/M et des pertes diélectriques E2/M au cours de l'hydratation d'une pâte de C_3A gypsé.

phase correspond à l'adsorption de l'eau sur la surface du matériau et à la formation de l'ettringite ou du monosulfoaluminate de calcium $C_3A\,\overline{CS}H_{12}$. STEIN a observé un dédoublement du premier pic calorifique pour de faibles pourcentages de gypse qu'il attribue à la formation d'alumine amorphe /14/. CORTANJE et collaborateurs considèrent la précipitation de $Al(OH)_3$ comme la cause du retard du C_3A gypsé quand la concentration en sulfate devient trop faible pour la formation de $C_3A\,\overline{CS}H_{12}$ /15/. Dans le cas présent, en raison de la teneur limitée en gypse du mélange, c'est à la précipitation d'alumine qu'est attribuée la seconde phase de la cinétique d'hydratation, entre 30 et 60 minutes.

2.2.2.2 *90 % C_3S + 10 % C_3A (fig. 12)*

Le tableau IV indique les variations de la permittivité et des pertes diélectriques au cours de l'hydratation du mélange.

En présence de la chaux libérée par l'hydrolyse du C_3S , l'hydratation du C_3A conduit à C_4AH_{13}. Les courbes de réponse en ϵ'/m et ϵ''/m donnent une information sur le début de durcissement de la pâte situé à 8h 30. Par addition de 5 % de gypse au mélange, il a lieu à 6 heures environ. Ces courbes sont du même type que celles observées dans le cas des ciments industriels. Bien que leurs allures générales soient comparables d'une expérience à l'autre, une disparité entre les niveaux initiaux de ϵ' et ϵ'' peut être observée qui est liée à la mise en place du matériau dans la cellule de mesure et au volume occupé par celui-ci.

Tableau IV

temps en min.	ϵ'/m	ϵ''/m
5	34,2	33,5
45	33,7	33,0
120	33,3	32,1
470	32,4	32
510	32	31,5
870	30,7	27,3

Variations de ϵ'/m et de ϵ''/m au cours de l'hydratation du mélange $C_3A + C_3S$

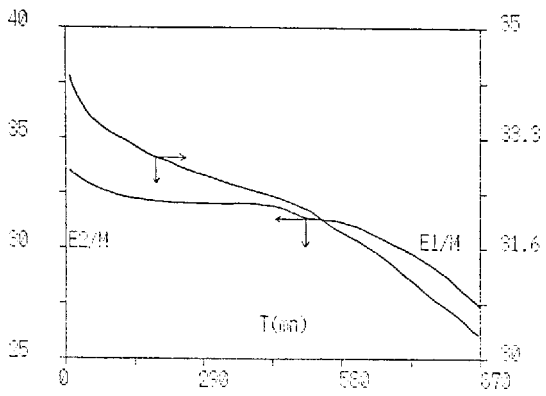

Fig. 12 - Variation de la permittivité E1/M et des pentes diélectriques E2/M au cours de l'hydratation du mélange $C_3S + C_3A$.

CONCLUSION

Une nouvelle méthode de mesure des paramètres diélectriques par hyperfréquences, continue et non destructive, a été appliquée à l'étude de l'hydratation, dès les premiers instants, des phases pures du ciment et de mélanges synthétiques. La mesure de la permittivité permet d'accéder à la teneur en eau libre présente dans le matériau, il est ainsi possible de suivre de manière continue l'avancement de l'hydratation des ciments.

BIBLIOGRAPHIE

1 TOBIO J.M.
Journées Internationales d'Etudes des Liants (1957)

2 DE LOOR G.P.
Appl. Sci. Res. B, 9,297 (1961)
Appl. Sci. Res. B, 11, 330 (1961)

3 LE BOT J.J.
Journal de Physique et le Radium (1957), 18,638

4 LE BOT C.R.
C.R. Acad. Sciences (1962), 255, 2247

5 WITTMANN F.H.
Cement and Concrete Research (1975), vol 5,63

6 REBOUL J.P.
Journal of Microwave Power (1981), 16 (1)

7 GORUR K, SMIT M.K., WITMANN F.H.
Cement and Concrete Research (1982), vol 12,447

8 HENRY F, BERTEAUD A.J.
Journal of Microwave Power (1980) 15 54)

9 HENRY F.
Thèse de doctorat d'état, paris VI (1982)

10 HASTED
"Aqueous Dielectrics" Chapman et Hall (1973)

11 ZELWER A.
Publication CERILH n° 227 (1973)

12 THOMASSIN J.H., REGOURD M., BAILLIF P.,TOURAY J.C.
C.R. Acad. Sciences (1978), 288,93

13 CABRERA J.G., PLOWMAN C.
Congrès Aluminates de Calcium, Turin (1982), 182

14 STEIN H.N.
J. Appl. Chem. July (1965), 15

15 CORSTANJE W.A., STEIN H.N., STEVELS J.M.
Cement and Concrete Research (1973), vol 3, 791
Cement and Concrete Research (1974), vol 4, 193 et 417

C. VERNET, Société des CIMENT FRANCAIS - C.E.R.E.G. (FRANCE)

FLUX THERMIQUE ET CINETIQUE D'HYDRATATION - TENTATIVE D'APPROCHE THERMODYNAMIQUE ET ANALYTIQUE DU COMPORTEMENT INTERACTFIC DES CIMENTS.

2.1

CONDUCTION CALORIMETRY AND HYDRATION KINETICS - A THERMODYNAMICAL AND ANALYTICAL APPROACH OF THE INTERACTIVE BEHAVIOUR OF CEMENTS.

RESUME

Pour estimer la réactivité des contituants, la calorimétrie à conduction est souvent utilisée. Or l'interprétation des pics de flux thermique est délicate, car ils sont produits par plusieurs réactions. Dans ce cas, il faut effectuer des mesures simultanées des taux de réaction, du flux thermique et de la composition de la phase liquide, pour évaluer la contribution de l'une des phases au dégagement de chaleur. En abordant le problème de cette manière, nous avons constaté que la réactivité d'un constituant dépend parfois autant des variables liées au système, que de ses propriétés intrinsèques : c'est le cas du C_3A, selon les conditions du milieu. Nous donnons d'autres exemples, qui montrent que les interactions dans le système affectent à la fois les vitesses et les compositions, et qu'elles ne se limitent pas à quelques réactions couplées. Elles agissent de façon générale, ce que nous traduisons par le concept de milieu dynamique interactif. Elles peuvent être de nature chimique (réactions couplées) ou thermique. Il apparait que leur intensité augmente avec la finesse de broyage et avec la température, ce qui permet, en première approximation, de définir une énergie d'activation globale, dans chacune des périodes de la séquence des réactions.

L'intensité des interactions diminue lorsqu'on augmente le rapport eau/ciment. Cependant, elles ne s'annulent jamais complètement: elles sont donc liées à des processus irréversibles localisés à l'interface entre les grains anhydres polyphasés et l'eau. Il faut considérer les gradients et non pas uniquement les concentrations loin de l'interface. La composition de la phase liquide à elle seule ne permet pas d'accéder directement à la réactivité des constituants.

Au cours de son déplacement dans le diagramme d'équilibre, le point figuratif d'un système chimique parcourt le "chemin des compositions". Celui-ci est stable dans le TEMPS. Par contre, dans un système dynamique, vu sous l'angle de la thermodynamique des processus irréversibles, le TEMPS est une variable fondamentale: divers trajets énergétiques, correspondant à des vitesses différentes de crâtion d'entropie interne peuvent être suivis selon les relations existant entre les flux (de matière, d'énergie) et les forces qui les produisent (gradients de température et de concentrations, potentiels chimiques).

Freqüentemente se utiliza a calorimetria por condução para avaliação da reatividade dos constituintes. Mas a interpretação dos picos de fluxo térmico é delicada, porque eles são produzidos por inúmeras reações. Neste caso se faz necessário realizar medições simultâneas das taxas de reação, do fluxo térmico e da composição da fase líquida, para avaliar a contribuição de uma das fases à liberação de calor. Abordando o problema sob este ângulo, constatamos que a reatividade de um constituinte às vezes depende tanto de variáveis ligadas ao sistema , como de suas propriedades intrínsecas: é o caso do C_3A, conforme as condições do meio. Damos outros exemplos, que mostram que as interações no sistema afetam às vezes as velocidades e as composições, e que elas não se limitam a algumas reações emparelhadas. Elas atuam de forma geral, o que traduzimos pelo conceito de meio dinâmico interativo. Elas podem ser de natureza química (reações emparelhadas) ou térmica. Parece que sua intensidade aumenta com a finura da moagem e com a temperatura, o que permite, numa primeira aproximação, definir-se uma energia de ativação global, em cada um dos períodos da seqüência das reações.

A intensidade das interações diminui na medida em que aumenta a relação água/cimento. Todavia, elas nunca se anulam completamente: portanto, estão ligadas a processos irreversíveis localizados na interface entre os grãos anidros polifásicos e a água. Faz-se necessário considerar os gradientes, e não apenas as concentrações afastadas da interface. A composição da fase líquida por si só não permite ter-se acesso diretamente à reatividade dos constituintes.

No curso de seu deslocamento no diagrama de equilíbrio, o ponto figurativo de um sistema químico percorre o "caminho das composições". Este é estável no TEMPO. Ao contrário, num sistema dinâmico, visto sob o ângulo da termodinâmica dos processos irreversíveis, o TEMPO é uma variável fundamental: diversos trajetos energéticos, correspondentes a velocidades diferentes de criação de entropia interna, podem ser acompanhados de acordo com as relações existentes entre os fluxos (de matéria, de energia) e as forças que os produzem (gradientes de temperatura e de concentrações, potenciais químicos).

INTRODUCTION

La réactivité des ciments a été longtemps définie par rapport à l'évolution de la résistance mécanique. Or celle-ci est la résultante d'un très grand nombre de paramètres, dont certains sont purement physiques. Ceci empêche l'interprétation rationnelle des variations de réactivité en fonction de la nature et de la composition des phases. Depuis les travaux de TIAN et CALVET /1/, l'utilisation de la calorimétrie à conduction a ensuite permis de grands progrès dans l'étude cinétique des réactions chimiques. Pour une réaction chimique unique et déterminée, la grandeur mesurée, à savoir le flux thermique dQ/dt, est le produit de l'enthalpie et de la vitesse de réaction. Connaissant l'enthalpie, on peut donc obtenir la vitesse, avec l'avantage de disposer d'un signal enregistré en continu et ne laissant échapper aucun évènement. Le taux d'avancement de réaction peut être obtenu par simple intégration de dQ/dt, puis en calculant le rapport $Q(t)/Q_r$, où Q_r est la chaleur de réaction, correspondant à un temps infini. Diverses informations à caractère cinétique peuvent en être tirées, en comparant les résultats ainsi obtenus à des modèles ou des courbes de référence. L'étude de la même réaction a différentes températures permet de faire varier la constante de vitesse et de déterminer l'énergie d'activation de la réaction. Peut-on appliquer cette démarche à un processus aussi complexe que l'hydratation du ciment portland, mélange de phases dont chacune d'elles fait intervenir plusieurs réactions chimiques ? Quelle est la validité des résultats obtenus et quelles informations peut-on en espérer, vis-à-vis de la réactivité de chaque constituant ? Nous tentons dans cette étude d'apporter quelques éléments de réponse à ces questions fondamentales, et, dans une première approche, nous aborderons l'étude d'une phase prise isolément.

1 - CAS DU SILICATE TRICALCIQUE

La réaction globale d'hydratation de C_3S peut s'écrire /2/ :

(1) $2Ca_3SiO_5 + 7H_2O \rightarrow Ca_{2x}(OH)_{(4x-2)}H_4Si_2O_7 + (6-2x)Ca(OH)_2$

avec $0,8 < x < 1,8$, la valeur de x variant en fonction de la teneur en chaux de la solution /2//3/. La réaction s'effectue en plusieurs périodes, au cours desquelles le dégagement de chaleur subit des variations importantes (*Fig.1*).

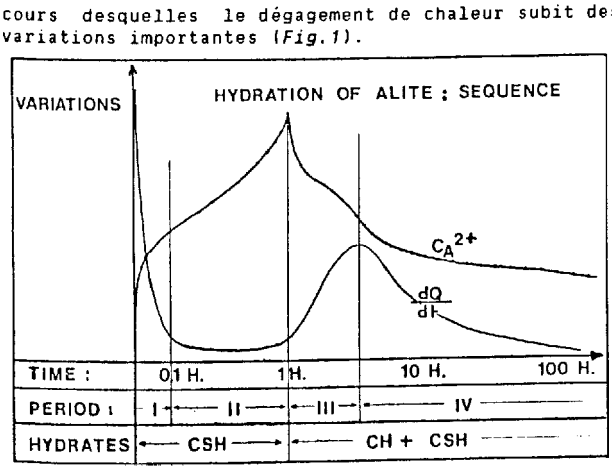

I - *Période initiale*, avec réaction rapide et flux thermique élevé.

II - *Période "dormante"*, avec flux très faible, réaction très lente, au cours de laquelle la solution se sursature en chaux.

III - *Période de prise*, débutant avec la précipitation de la portlandite,

(2) $Ca^{2+} + 2\ OH^- \rightarrow Ca(OH)_2$,

avec accélération de la réaction *(1)* et apparition d'un second pic de flux thermique.

IV - *Période de ralentissement*, liée à la consommation de C_3S et à l'épaississement de la couche d'hydrates.

L'interprétation rigoureuse des mesures thermiques pose ici les problèmes suivants :

1/ L'enthalpie de la réaction *(1)* n'est définie que si l'on connait l'évolution de la variable x jusqu'à un taux de réaction de 100 %. Or, cette variable dépend des conditions dans lesquelles s'est déroulée la réaction, par exemple le rapport eau/solide, la température.

2/ Il est probable que la réaction *(1)* comporte plusieurs étapes, par exemple la chimisorption d'eau sur le C_3S avec rupture des liaisons chimiques du réseau, la solvatation des ions, leur diffusion en solution et la précipitation des CSH /2/. La définition de la réactivité devient alors difficile, la vitesse du processus global étant limitée par le mécanisme intermédiaire le plus lent. Si l'on recherche par exemple à établir un lien entre la réactivité et la structure cristalline ou la teneur en impuretés de l'alite, on s'intéressera plus particulièrement à l'étape de dissolution, regroupant la chimisorption, la rupture des liaisons, et la solvatation. Il sera alors préférable d'opérer dans un milieu qui empêche la précipitation des CSH, par exemple un réacteur en circuit ouvert ou une solution formant un complexe avec les ions calcium et suffisamment basique pour éviter la formation de gel de silice.

3/ Dès la fin de la période dormante, à la réaction globale *(1)* se superpose la réaction supplémentaire *(2)*, dont l'enthalpie vient s'ajouter algébriquement à celle de *(1)*. Il devient alors indispensable de savoir si les deux réactions sont liées ou indépendantes. Si elles sont liées, il est encore possible de définir une réaction et une vitesse globales, à condition d'établir la relation liant les vitesses ou les taux de réaction. Faute de cette relation, comme dans le cas de réactions indépendantes, il faut mesurer l'une des deux vitesses de réaction, par une autre méthode et procéder par différence. La nécessité de mesurer la teneur en silicate tricalcique ou en $Ca(OH)_2$ en fonction du temps complique l'approche expérimentale du problème, en particulier au niveau de la simultanéité des mesures thermiques et de l'analyse quantitative de phases.

Nous voyons donc qu'un cas apparemment simple comme celui du système C_3S-H_2O doit être abordé avec précaution. Le cas des ciments portland est beaucoup plus complexe et exige par conséquent la mesure simultanée d'un plus grand nombre de paramètres (Fig. 1b). Bien évidemment, ces mesures ne sont plus possibles dans un simple calorimètre à flux, ni de façon continue. C'est pourquoi nous avons développé depuis une dizaine d'années un appareillage spécialement adapté /4/.

2.1

Lorsque l'on décompose une réaction solide-liquide en étapes élémentaires, il apparait aussitôt des phénomènes qui font intervenir, d'une part les propriétés intrinsèques du solide et d'autre part, les conditions de milieu. Pour cette raison, nous avons cherché à approfondir le concept de réactivité en prenant en compte les interactions. Dans le cas du silicate tricalcique, si l'on se réfère aux points 1/, 2/ et 3/ ci-dessus, les conditions de milieu peuvent modifier la stoechiométrie du CSH ou la proportion de portlandite, par exemple par la présence d'un constituant supplémentaire consommant de la chaux, ou donnant lieu à une réaction exothermique. Elles peuvent intervenir dès la première étape de la dissolution et également dans l'étape de précipitation de CSH, en présence d'adjuvants subissant une chimisorption. Les réactions du C_3A nous donnent un autre exemple, caractéristique des interactions dans le système ciment-eau.

2 - REACTIVITE DE C_3A. INTERACTIONS

L'étude de la réactivité de l'aluminate tricalcique a fait l'objet de très nombreuses études, où le calorimètre à conduction a souvent été utilisé. L'influence de certaines impuretés, en particulier le sodium, permettant d'obtenir la forme orthorhombique, a donné lieu à des interprétations contradictoires. Nous pensons que la variété des comportements observés a pour origine la variété des conditions opératoires et des systèmes étudiés. L'interprétation de ces comportements ne devient cohérente que si l'on prend en compte les interactions dans chaque système. L'utilisation du réacteur-filtre-calorimétrique, mis au point au CEREG à partir de 1978, nous a permis de mesurer simultanément de nombreux paramètres au cours de l'hydratation de C_3A dans différents milieux. Ces mesures ont montré que l'on ne peut généraliser au cas des ciments, les observations faites sur des systèmes simples, pour les raisons suivantes :

1/ Dans les clinkers portland, les propriétés intrinsèques du C_3A sont liées aussi bien à la présence du potassium en solution solide, qu'à la forme cristalline, cubique ou orthorhombique. En France, l'abondance du potassium par rapport au sodium dans les produits de carrière lui donne naturellement un rôle plus important. L'ion K^+, en déformant le réseau de C_3A par son rayon ionique élevé (1,33 A) joue un rôle inverse de celui du sodium et augmente la réactivité de l'aluminate /4/ /5/.

2/ La vitesse de réaction de C_3A dans les ciments dépend autant des variables liées au système que de ses propriétés intrinsèques /4/ /6/. La nature et les quantités des différents sulfates, gypse, hémihydrate, anahydrite, K_2SO_4, la finesse de broyage, les proportions d'alite et d'aluminate, la consommation de chaux, d'ions aluminate ou sulfate par les ajouts, sont des variables qu'il faut prendre en compte.

3/ Les interactions de C_3A avec le système ne sont pas de simples déplacements d'équilibre et ne mettent pas seulement en jeu la consommation d'un certain nombre de réactifs pour donner des produits de réaction. Elles font intervenir, non seulement des quantités, mais aussi des flux de matière. Ces derniers ne peuvent exister que par la situation hors d'équilibre du système. Les forces ainsi développées jusqu'à ce que l'enthalpie libre de la réaction atteigne une valeur nulle peuvent être de plusieurs natures : forces électriques de surface, variations de potentiel thermique, chimique ou thermodynamique, variations de tension superficielle.

Nous avons montré par exemple que la vitesse de réaction de C_3A avec le gypse est liée au gradient de concentration en ions SO_4^{2-} à l'interface /6/. Des gradients différents sont obtenus lorsque la source d'ions sulfate possède une solubilité ou une surface plus élevée, ce qui explique la différence bien connue des comportements en présence d'une quantité identique de gypse et de semi-hydrate. De même, la vitesse de réaction de C_3A avec des calcaires de différentes réactivités est modifiée selon la valeur du gradient d'ions carbonates /6/.

4/ Contrairement aux mélanges de produits de synthèse préparés au laboratoire, le ciment est principalement constitué de grains polyphasés, où le C_3A se trouve en contact étroit avec les autres phases du clinker. Cette situation favorise des interactions de caractère thermique et chimique, en particulier avec l'alite. Celle-ci bénéficie plus ou moins de l'activation thermique par l'importante chaleur de réaction du C_3A, selon la valeur des paramètres cités en 2/.

La calorimétrie à conduction nous apporte ici une aide précieuse, pour mesurer l'intensité de ces "couplages" entre phases. Nous nous proposons de montrer que ceux-ci apparaissent comme le cas général dans le système ciment-eau.

LE SYSTEME CIMENT-EAU, "MILIEU DYNAMIQUE INTERACTIF"

Dans la séquence des réactions d'hydratation des ciments portland (*Fig. 2*), nous pouvons définir 4 périodes principales, liées au constituant le plus abondant, l'alite, et marquées par des changements du flux thermique, suite aux réactions décrites au §1.

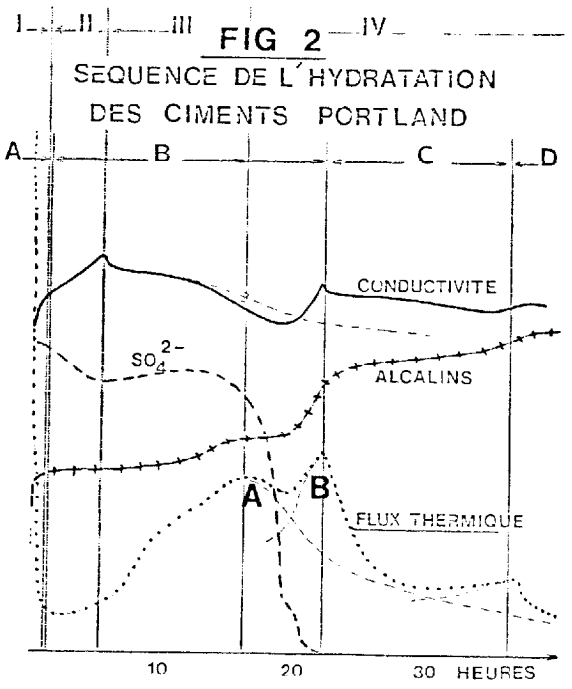

FIG 2
SEQUENCE DE L'HYDRATATION DES CIMENTS PORTLAND

A ces variations dominantes se superposent des variations supplémentaires dues aux réactions des autres phases, parmi lesquelles le C_3A présente l'enthalpie d'hydratation la plus élevée : le pic thermique initial est beaucoup plus intense et lorsque la teneur en C_3A est suffisante, un pic supplémentaire B apparait pendant la période de prise

Grace aux possibilités d'analyse simultanée offertes par le réacteur-filtre-isotherme, nous voyons que ce pic se produit aussitôt après l'épuisement du sulfate, lorsque l'ettringite commence à réagir avec l'excédent de C_3A, pour donner du monosulfoaluminate. Il est donc naturel que sa position et son intensité varient en fonction du gypsage et des paramètres agissant sur la vitesse de réaction du C_3A, cités précédemment.

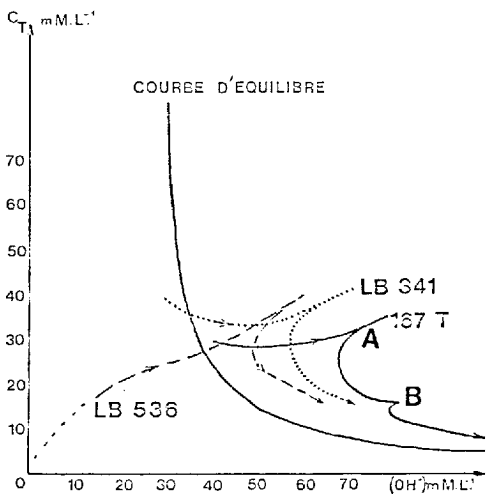

Fig. 3 - EQUILIBRE DE SOLUBILITE DE LA PORTLANDITE TRAJET DU POINT FIGURATIF DE LA SOLUTION

Mais la possibilité de mesurer les taux de réaction des autres phases nous a amené à des observations beaucoup plus intéressante /4/. Il apparait que, pendant cette période, toutes les vitesses de réaction sont augmentées, en particulier la vitesse de dissolution de l'alite. Le taux de sursaturation en chaux augmente, ce qui indique que l'énergie ainsi libérée contribue à éloigner le système de l'équilibre *(Fig. 3)*.

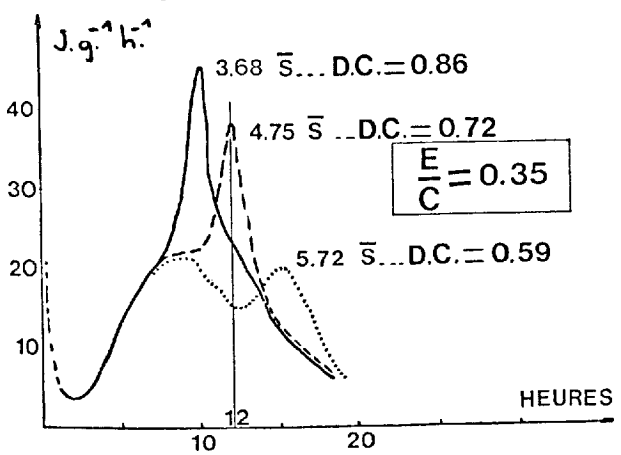

Fig. 4 - OPTIMUM DE GYPSE ET DEGRE DE COUPLAGE

Réciproquement, l'augmentation de l'une des vitesses de réaction au cours des périodes précédentes accélère la consommation du gypse et le pic se produit plus tôt. Les interactions que nous avions évoquées à propos du C_3A se manifestent ici de façon générale .

Dans chaque période de l'hydratation, l'une des phases est l'objet d'une réaction principale, qui est la plus rapide dans le système. Mais les autres réactions ne poursuivent pas leur déroulement initial de façon indépendante. Elles subissent une activation et leur vitesse augmente avec celle de la réaction principale. Ceci constitue un caractère essentiel de l'hydratation du ciment portland et justifie pour ce matériau l'appellation de "milieu dynamique interactif" Le comportement cinétique du ciment est conditionné principalement par l'interaction entre ses deux constituants majeurs, l'alite et le C_3A. On peut dire qu'il existe entre ces deux phases un véritable "couplage" ce terme étant pris au sens large, comme dans le cas de deux circuits électroniques couplés et prenant en compte les interactions entre deux familles de réactions et de phénomènes d'interface. Cette définition élargie doit intégrer par exemple les interactions qui ont été observées entre alite et bélite /7/, ainsi qu'entre C_3A et C_4AF /4/. Il est possible de quantifier le "degré de couplage" alite-C_3A, par exemple en utilisant la variable $D_c = \exp(-\Delta t)$, où Δt est le rapport $ABS[(t_1 - t_2)/t_m^c]$, où t_1 et t_2 désignent les temps correspondant aux maxima des pics thermiques, et t_m la moyenne de ces temps. La première conséquence pratique de l'augmentation de tous les taux de réaction avec le degré de couplage est l'existence d'un optimum de gypse vis-à-vis des résistances initiales, correspondant à un degré de couplage voisin de 1 *(Fig. 4)*. Il en résulte également que chaque ciment possède une "personnalité", due à l'association des proportions et des propriétés de tous ces constituants. Ce comportement interactif permet aussi d'expliquer l'échec des nombreuses tentatives qui ont été faites pour relier la chaleur d'hydratation ou les résistances mécaniques des ciments à leur composition minéralogique, en utilisant des calculs de régression multiple : cette méthode ne peut s'appliquer lorsque les variables ne sont pas indépendantes.

MECANISMES DES INTERACTIONS

En se référant aux exemples précédents concernant l'alite et le C_3A, il apparait que le degré de couplage varie en fonction, d'une part, de paramètres de composition et d'autre part, en fonction des paramètres agissant sur les flux ioniques.

• L'intervention des compostions est évidente : prenons l'exemple de la réaction d'un excès de C_3A avec le gypse dans un ciment portland. L'évolution du système aboutit à une solution solide de C_4AH_{13}, en passant par la formation d'hydrates intermédiaires (ettringite, monosulfoaluminate). Ce sont les proportions initiales des constituants qui conditionnent les quantités formées à chaque instant, calculables en fonction de l'avancement de la réaction. On peut donc prévoir le "chemin des compositions", indépendant du temps, suivi par le système. Mais aucun calcul de ce type ne pemet de prévoir le temps nécessaire à l'épuisement du gypse. On sait qu'il faudra un temps plus long pour consommer une plus grande quantité de gypse, mais il faut connaitre l'évolution de la vitesse pour déterminer ce temps, que l'on peut considérer comme le rapport de la quantité de gypse et du flux de dissolution moyen.

♦ Les paramètres agissant sur les flux peuvent être mis en évidence en analysant les mécanismes de l'hydratation et également en étudiant les effets cinétiques de la température, du rapport eau/solide, du régime d'agitation, de la finesse de broyage, et des adjuvants.
On pourrait penser, par exemple, que l'interaction due à l'activation thermique serait supprimée en opérant en milieu parfaitement isotherme. Nous avons constaté le contraire : dans un système agité, régulé à moins de 1/100 de degré près, ce type d'interaction diminue, mais ne s'annule jamais complètement. Il en est de même lorsqu'on augmente le rapport eau/solide (*Fig. 4b*). Ce comportement ne peut s'expliquer que par l'intervention d'un phénomène de surface, produisant une distribution hétérogène de la chaleur. Nous sommes ainsi amenés à envisager l'intervention de gradients thermiques, localisés à l'interface des grains polyphasés. L'activation thermique n'est pas seulement un phénomène d'échauffement de masse, cependant, il peut s'en rapprocher lorsque la proximité des grains devient suffisante et que les transferts de chaleur sont facilités. Dans le cas des pâtes pures, il serait donc possible de définir une énergie d'activation globale, pour chacune des périodes de l'hydratation où l'on a affaire au même système chimique. Dans ce cas, l'augmentation du degré de couplage permettrait de considérer l'hydratation comme une réaction unique, en première approximation. Des mesures calorimétriques /8/ confirment ce point de vue, en montrant que les courbes de chaleur d'hydratation obtenues à différentes températures en régime isotherme obéissent à une loi d'affinité.

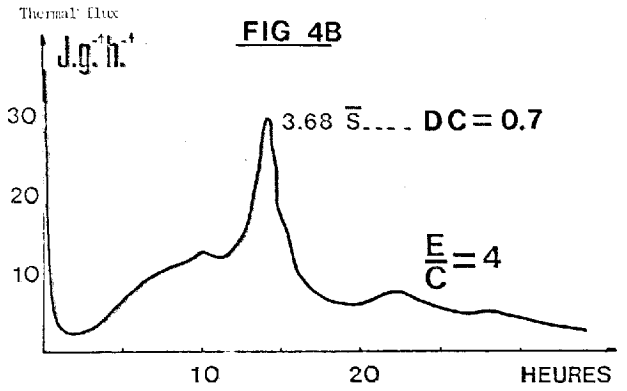

Fig. 4b - COUPLAGE AVEC E/C ELEVE

La finesse de broyage est le paramètre prépondérant pour l'augmentation du degré de couplage. Elle favorise à la fois les transferts thermiques et les transferts ioniques. L'hydratation étant une réaction de surface, les débits ioniques de dissolution des phases sont augmenter avec la finesse, ce qui se traduira par des taux de réaction plus élevés et des réactions plus rapides. Cet effet est particulièrement visible au niveau de la vitesse de consommation du régulateur de prise (*Fig. 5*) et de la vitesse de sursaturation en chaux pendant la période dormante (*Fig. 3*).

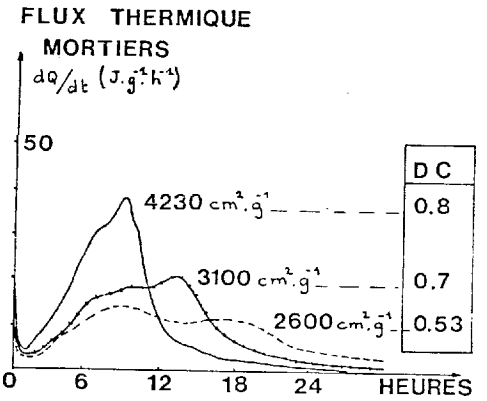

Fig. 5 - EVOLUTION DU DEGRE DE COUPLAGE AVEC LA FINESSE DE BROYAGE

L'ensemble des données expérimentales nous amène à considérer que le mécanisme des interactions est lié à l'irréversibilité de l'hydratation. A ce titre, la thermodynamique des processus irréversibles (T.P.I.) nous apporte un éclairage intéressant /9/. Un système dynamique ou structure dissipative chimique peut sous cet angle, parcourir divers trajets énergétiques, correspondant à des vitesses différentes de création d'entropie interne. Ces trajets sont conditionnés par les relations entre les flux (ioniques, thermiques, électriques) et les forces qui les produisent. Pendant l'hydratation des ciments, lorsque le trajet des points figuratifs de la solution dans chacun des diagrammes d'équilibre des hydrates ne s'éloigne pas trop de la courbe d'équilibre, on se trouve dans le cas où les flux restent proportionnels aux forces (équations phénoménologiques linéaires).
Le système évolue alors vers un état stationnaire obéissant à la règle du minimum de création d'entropie interne /9/ /10/ /11/ /12/. Lorsque le taux de sursaturation est élevé, le système se trouve plus loin de l'équilibre, dans le domaine non-linéaire. Il peut alors montrer différents comportements, selon la nature des étapes élémentaires du mécanisme réactionnel :
- Soit il continue à se comporter comme au voisinage de l'équilibre,
- Soit il donne lieu à l'apparition d'une instabilité, source de la création de nouvelles structures. Ce cas se produit lorsque l'une des étapes réactionnelles est auto-catalytique, ou donne lieu à un processus de catalyse croisée. C'est ainsi par exemple que le processus de dissolution est accéléré par le processus de précipitation et réciproquement.
Dans ce cadre, des couplages peuvent lier, non seulement les réactions chimiques, mais aussi des réactions chimiques et des phénomènes physiques, ou des phénomènes physiques entre eux. Le couplage d'un gradient thermique et d'un gradient ionique donne lieu par exemple au phénomène de thermodiffusion, dont l'effet s'ajoute au simple effet de la température sur les constantes cinétiques. A une autre échelle, celle de la double couche électrochimique, des couplages peuvent également se manifester entre des gradients électriques et des gradients ioniques, d'où une interaction possible entre la charge de surface et la vitesse de transfert interfacial.

Sur la plan chimique, le mécanisme de dissolution-précipitation, met en jeu le couplage entre un ou plusieurs gradients ioniques et une ou plusieurs réactions de précipitation, en interaction avec les phénomènes précédents.

CONCLUSIONS

A travers le thème de la calorimétrie des ciments, nous avons fait apparaitre toute la complexité des phénomènes de l'hydratation, bien que dans certains cas, ces phénomènes se simplifient par le jeu des interactions, en se ramenant à l'équivalent d'une réaction unique. Il faut essayer de mieux analyser l'intimité des mécanismes, si l'on veut maitriser le comportement dynamique des ciments. La recherche appliquée se voit donc amenée à faire appel de plus en plus à des approches qui sont celles de la recherche fondamentale. En essayant, d'une part, d'approfondir le concept de réactivité, en mettant l'accent, d'autre part, sur le comportement interactif du ciment et sur son origine dans l'irréversibilité de l'hydratation, nous avons tenté d'apporter une contribution à l'étude pratique des liants hydrauliques. L'optimisation des ciments en fonction des caractéristiques particulières demandées par l'utilisateur, qu'il s'agisse du temps de prise, de l'évolution du dégagement de chaleur, de la vitesse d'augmentation des résistances, des propriétés rhéologiques, fait appel à des plans d'expérience. il nous parait important, pour mieux les élaborer et pour mieux en interpréter les résultats, de savoir qu'en faisant varier un paramètre ou en ajoutant un constituant nouveau, ou encore un adjuvant, il en résulte systématiquement des conséquences indirectes. La grandeur ou la propriété que l'on cherchait à faire varier dans le plan d'expérience n'est donc jamais la seule à varier et l'analyse de ses causes de variation exige la mesure d'un nombre suffisant de paramètres. A ce titre, la mesure du flux thermique, même avec des moyens simplifiées comme la bouteille isolante, peut donner des indications précieuses sur la réponse dynamique de l'ensemble du système, mais cette grandeur étant une résultante, son interprétation doit faire appel à des techniques d'investigation complémentaires.

BIBLIOGRAPHIE

/1/ CALVET E., PRAT H. "Récents progrès en microcalorimétrie". Monographie. Ed. Dunod, Paris, 1958.

/2/ BARRET P. "Modélisation et réactivité des matériaux". Rev. Ciments, Bétons, Plâtres, Chaux, N° 755, 4/1985, pp 237-244

/3/ MICHAUX, O. MENETRIER D., BARRET P. C.R. Ac.Sciences, Paris, II, 219, 1983.

/4/ VERNET C. "Etude de la cinétique des réactions d'hydratation des ciments industriels, méthodologie et applications". Thèse CNAM Ing. Phys., Paris, OCt 1982.

/5/ REGOURD M. "Solutions soldes de C_3A avec K_2O+SiO_2, $Na_2O + SiO_2$ et leur hydratation. CERILH. Rapport d'activités 1976, pp 12-15.

/6/ VERNET C. "Séquence et cinétique des réactions d'hydratation de l'aluminate tricalcique en présence de gypse, de chaux et de fillers calcaires". 8th ISCC Rio, à paraitre.

/7/ SCHUPPSTUHL J. "Investigations dans le système $C_3S-C_2S-H_2O$". Thèse présentée à l'Institut des Matériaux non métalliques, Université Technique de Clausthal, résumée dans Tonindustr. Ztg., Dtsch, Fev. 1985, Vol. 109, N°2, pp 77-78.

/8/ REGOURD M., GAUTHIER E. "Comportement des ciments soumis au durcissement accéléré". Ciments, Bétons, Plâtres et chaux, N° 725, 4/80, pp 240-249.

/9/ PRIGOGINE I. "Physique temps et devenir" Ed. Masson, Paris, 1982.

/10/ CHARTIER P., GROSS M., SPIEGLER K.S."Applications de la thermodynamique du non-équilibre" Ed. Hermann.

FIG 1B

CINETIQUE DE L'HYDRATATION

CPA 987

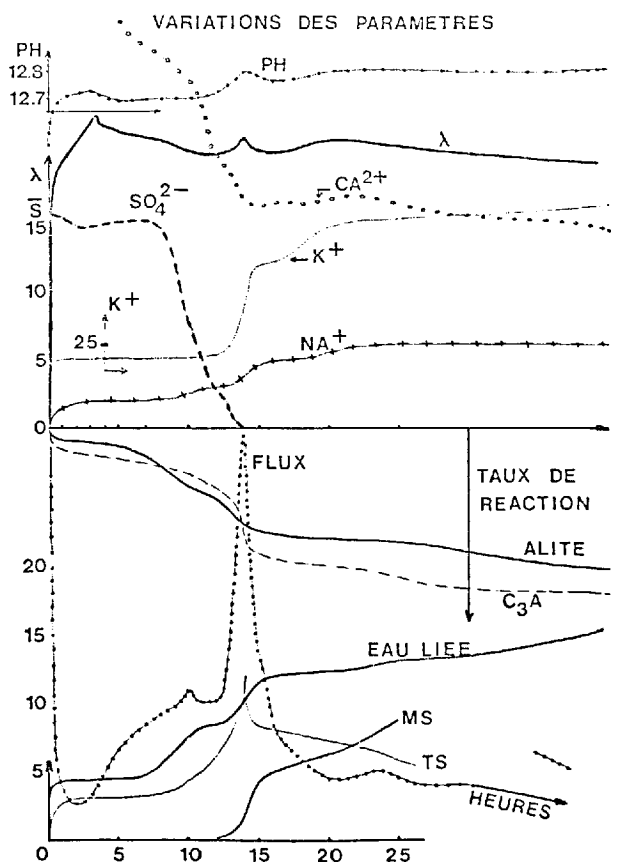

Fig. 1 b

C. VERNET, Société des CIMENTS FRANCAIS - C.E.R.E.G. (FRANCE)

SEQUENCE ET CINETIQUE DES REACTIONS D'HYDRATATION DE L'ALUMINATE TRICALCIQUE EN PRESENCE DE GYPSE, DE CHAUX ET DE FILLERS CALCAIRES

SEQUENCE AND KINETICS OF HYDRATION REACTIONS OF C_3A WITH GYPSUM, LIME AND CALCAREOUS FILLERS.

RESUME

En présence de fillers calcaires, la séquence des réactions de formation des sulfoaluminates est modifiée de la manière suivante :

- Dans une première période, définie par la présence de gypse, il se forme principalement de l'ettringite. Les réactions sont pratiquement les mêmes qu'en l'absence de calcaire.
- Au contraire, dès que le gypse est épuisé, ce sont les réactions du calcaire qui dominent. En aucun cas, nous n'avons observé la formation de monosulfoaluminate. La formation du monocarboaluminate comporte une réaction intermédiaire, avec formation d'une solution solide de C_4AH_{13} contenant des ions sulfate et carbonate.
- En cas d'épuisement du C_3A, les composés stables à l'équilibre sont l'ettringite et le carboaluminate.

D'une façon générale, la vitesse de réaction calcaire-C_3A est beaucoup plus faible en présence de gypse. Ceci montre qu'il faut intégrer les conditions de milieu dans le concept de réactivité. Par ailleurs, il apparait que l'on peut modifier le taux de réaction des fillers calcaires en ajustant le gypsage des ciments.

Em presença de "fillers" calcários, a seqüência das reações de formação dos sulfoaluminatos é modificada da seguinte forma:

- num primeiro período, definido pela presença de gesso, forma-se principalmente etringita. As reações são praticamente as mesmas que na ausência de calcário.
- ao contrário, assim que o gesso é consumido, são as reações do calcário que predominam. Em nenhum caso chegamos a observar a formação de monosulfoaluminato. A formação de monocarboaluminato inclui uma reação intermediária, com formação de uma solução sólida de C_4AH_{13} contendo íons de sulfato e carbonato.
- em caso de desaparecimento do C_3A, os compostos estáveis para o equilíbrio são a etringita e o carboaluminato.

De um modo geral, a velocidade de reação calcário-C_3A é muito mais fraca em presença de gesso. Isto mostra que é preciso integrar as condições do meio no conceito de reatividade. Por outro lado, parece que se pode modificar a taxa de reação dos "fillers" calcários, ajustando-se o teor de gesso dos cimentos.

INTRODUCTION

Les ajouts calcaires ne peuvent être considérés comme des inertes lors de l'hydratation des ciments /1/ /2/ /3/ /6/ /7/ /8/ /11/. De nombreux auteurs ont attribué cette réactivité des calcaires à la formation de carboaluminate : en effet, le gachage du mélange C_3A + $CaCO_3$ produit une réaction rapide et exothermique /1//3/ /11/. Or, il semble que dans la pâte de ciment avec filler calcaire, le monocarboaluminate ne se forme que très lentement, après 3 jours /2/ /5/ /6/ /7/. Supposant que cette différence de comportement du calcaire était liée à la présence, ou l'absence de gypse dans le système, nous avons étudié de façon détaillée la cinétique des réactions chimiques dans le système [C_3A, $C\bar{C}$, $C\bar{S}H_2$, CH, H] en nous plaçant dans des conditions proches de celle de la prise des ciments (saturation en chaux, rapports molaires $\bar{C}/A$ et $\bar{S}/A$ identiques à ceux d'un ciment fillérisé).

MESURES - RESULTATS

La méthodologie a été la suivante :
- Mise en suspension des constituants dans un réacteur-filtre calorimétrique, avec un rapport eau/solide voisin de 4.
- Mesure en continu du flux thermique de la conductivité électrique et du pH.
- Dosage séquentiel des ions OH^- et SO_4^{2-}.
- Dosage des phases solides par DRX et ATG.

Notre étude a comporté 3 étapes :

1/ - ESSAI TEMOIN SANS $CaCO_3$

Cet essai a permis de tester la réactivité des produits de synthèse (C_3A cubique, gypse, chaux) pris dans les conditions standards du plan d'expériences. La *figure 1 a* montre la séquence bien connue des transformations des sulfoaluminates, lors de chaque modification du système par épuisement d'un constituant.

2/ - VARIATION DU RAPPORT $CaCO_3$/GYPSE AVEC CALCITE DE SYNTHESE

Nous avons étudié les réactions entre C_3A, $CaCO_3$ et gypse, pour 7 teneurs en gypse s'échelonnant entre 5 et 50 g, pour 100 g de C_3A et 100 g de calcite. Il apparait (*Fig. 1b*) que la séquence des réactions est modifiée par rapport à l'essai témoin.

- *Dans la première période*, c'est-à-dire avant que le gypse soit épuisé, la formation d'ettringite est prépondérante. La formation de carboaluminate qui aurait été très rapide en l'absence de gypse /11/, est ici stoppée dès les premières secondes. La hauteur du premier pic thermique diminue avec la teneur en gypse (*Fig. 2*). Le temps d'épuisement du gypse augmente avec la teneur en gypse (*Fig.3*), selon une loi de la forme :

$$t_e = \frac{k_g . s_g (m_g - m_{og})}{k_c . s_c (3.m_c - r.m_g)}$$

où les indices g et c désignent les phases gypse et C_3A, k la constante de vitesse de dissolution, s la surface spécifique, m la masse de gypse consommée pendant la réaction initiale. L'application de ce modèle montre que le rapport k_g/k_c est proportionnel à m_g. Nous en déduisons que durant la croissance des cristaux d'ettringite, le flux d'ions sulfates, proportionnel à la masse de gypse, conditionne la valeur des gradients ioniques à l'interface C_3A-solution. La relation ci-dessus permet d'expliciter, de façon quantitative, le rôle joué par la proportion et la solubilité du régulateur de prise.

FIG 1A CINETIQUE à E/C = 4 25°C

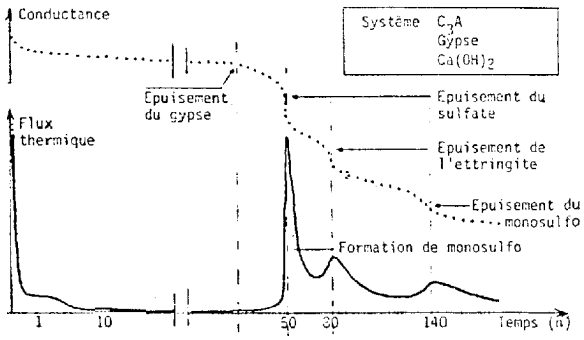

FIG 1 B

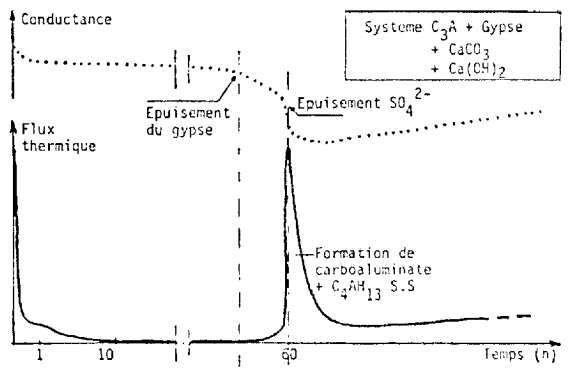

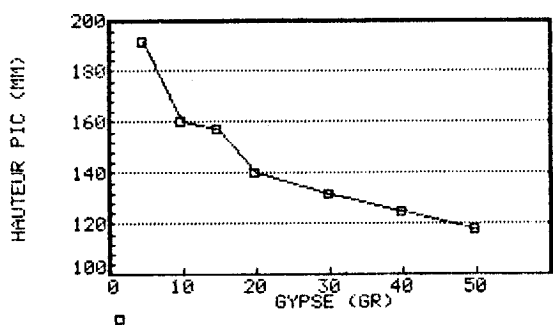

Fig. 2 - 1er PIC THERMIQUE

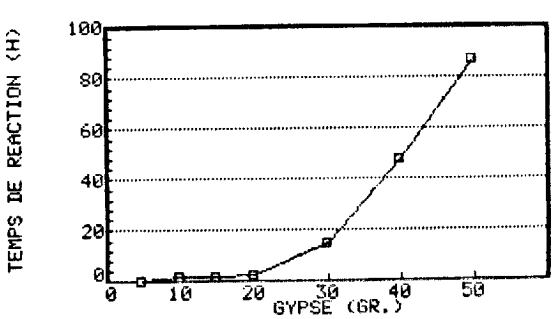

Fig. 3 - EPUISEMENT DU GYPSE

2.1

- *Dans la deuxième période* située après l'épuisement du gypse, nous observons la formation de carboaluminate et d'une solution solide de C_4AH_{13}, au lieu de la formation habituelle de monosulfoaluminate.
La hauteur du second pic de flux thermique varie presque linéairement ave cla teneur en gypse (*Fig.4*). L'ettringite, seul composé sulfaté présent à cet instant est donc l'un des réactifs donnant lieu aux réactions exothermiques mises en jeu ici, ce qui indique que la solution solide contient des sulfates.

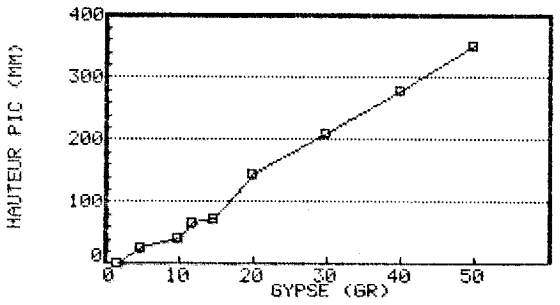

Fig. 4 - 2nd PIC THERMIQUE

Lorsqu'on augmente la quantité de gypse, la proportion de solution solide passe par un maximum, correspondant à un rapport gypse/C_3A compris entre 1/2 et 2/3. L'ettringite n'étant qu'en partie consommée lors de la formation de la solution solide, cette dernière présente donc probablement un rapport $\bar{S}/A$ inférieur à 1/2.
La solution solide est un produit intermédiaire. Elle réagit lentement avec la calcite, au cours de la période suivante, pour donner un carboaluminate et de l'ettringite secondaire. Les mesures par DRX montrent alors que le rapport carboaluminate/ettringite varie très peu et de façon quasi-proportionnelle au temps de réaction.

3/ - COMPARAISON DE DIFFERENTS FILLERS CALCAIRES
Les proportions standard reproduisent celles d'un ciment avec 10 % de filler, soit 100 g C_3A + 100 g filler + 40 g gypse, la suspension, de rapport eau/solide voisin de 4, est tamponnée par 2 g de CaO. Nous avons comparé 7 calcaires, dont la calcite de synthèse précédente et 6 fillers provenant de diverses carrières et contenant les impuretés habituelles : quartz, argiles, feldspaths. Dans ces échantillons, la calcite présente un état de cristallisation variable (largeur des raies DRX).

On constate que la hauteur du premier pic de flux thermique et le temps d'épuisement du gypse varient dans une fourchette très étroite. Ceci est logique, puisque nous avons ici une proportion constante C_3A/gypse et que dans la première période, les réactions du filler jouent un rôle mineur.
Au contraire, la hauteur du 2e pic thermique varie dans de très larges proportions. Les mesures par DRX montrent que ces différences de flux thermique correspondent principalement à la formation de la solution solide du type C_4AH_{13} (*Fig. 5*). Cette dernière contient donc des ions carbonate.

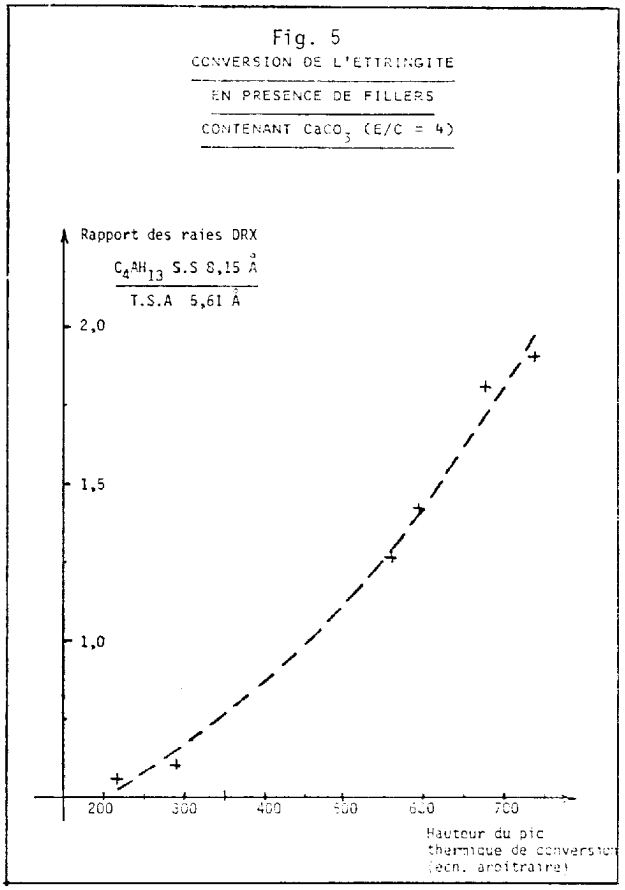

INTERPRETATION

1 - Séquence des réactions chimiques

Sur la base des observations précédentes, nous pouvons maintenant écrire la succession des équations des réactions les plus probables à l'interface C_3A - solution :

1/ Période initiale

$C_3A + CH + (x-1)H \rightarrow C_4AH_x$ *(1)*

$C_3A + 1/2\,CH + 1/2\,C\bar{C} + yH \rightarrow [C_3A, 1/2\,CH, 1/2\,C\bar{C}, Hy]$ *(2)*

$C_3A + C\bar{C} + 11\,H \rightarrow [C_3A, C\bar{C}, H_{11}]$ *(3)*

$C_3A + 3\,C\bar{S}H_2 + 25\,H \rightarrow [C_3A, 3C\bar{S}H_2, H_{31}]$ (ettringite) *(4)*

Cette réaction *(4)* étant inibitrice des précédentes.

2/ Période dormante
La consommation de gypse continue lentement par la réaction *(4)*.

3/ Période accélérée (2e pic de flux thermique).
Lors de l'épuisement du gypse, une quantité aliquote de l'ettringite est consommée pour donner la solution solide :

$C_3A + x(C_3A, 3C\bar{S}H_2, H_{31}) + yC\bar{C} + wCH + zH \rightarrow$

$(1+x)[C_3A, y/1+x\,C\bar{C}, 3x/1+x\,C\bar{S}, w/1+x\,CH, Hz)$ *(5)*

Les coefficients stoechiométriques étant liés par la relation :
$2x + y + w = 1$ avec $3x/x+1 < 1/2$, soit $x < 1/5$

le deuxième pic thermique est constitué principalement de la chaleur fournie par la relation ci-dessus.

Simultanément, du carboaluminate peut de former selon la réaction *(3)*, et la réaction suivante :

$$[C_3A,y/1+x\ C\bar{C},3x/1+x\ C\bar{S},w/1+x\ CH,H_z]+(1-y/1+x)C\bar{C}+vH \rightarrow x/1+x[C_3A,3C\bar{S}H_2,H_{31}]+1/1+x[C_3A,C\bar{C},H_{11}]+w/1+x\ CH \quad (6)$$

4/ Lorsque le C_3A est épuisé, seule la réaction *(6)* continue, les produits finaux étant l'ettringite et le carboaluminate.
La séquence ci-dessus est en accord avec toutes les observations des pâtes de ciment fillérisés, ou des auréoles de transition pâte-granulat dans les bétons, figurant dans la bibliographie /5/ /6/ /7/ /8/. Les mesures en réacteur agité à E/C = 4, comme nous l'avons déjà montré /12/, reproduisent bien les conditions chimiques des bétons.

2 - Rôle des gradients

Nos propres observations au M.E.B. de bétons avec fillers calcaires *(Fig.6)* montrent que la formation de carboaluminate a lieu essentiellement au voisinage des grains de C_3A, plutôt que sur les grains de calcite. Ceci confirme le rôle important joué par la diffusion des ions d'un grain vers un autre, à travers la solution. Les ions aluminate sont apparemment piégés par les réactions de précipitation, dans un gradient de concentration très élevé à l'interface C_3A - solution. Par contre, rien ne s'oppose à la diffusion des ions carbonate depuis la calcite, ce qui permet le déplacement de l'équilibre de solubilité de la calcite. Ce mécanisme expliquerait bien, d'une part, l'analogie des comportements des bétons et des suspensions concentrées, la microstructure et la distance de diffusion des ions sulfate et carbonate jouant alors un rôle mineur, et d'autre part, la coexistance de réactions transitoires simultanées, hors de l'équilibre. La séquence des réactions serait donc, non seulement temporelle, mais également spatiale : nous retrouverons ici un comportement classique, sous l'angle de la thermodynamique des systèmes irréversibles.

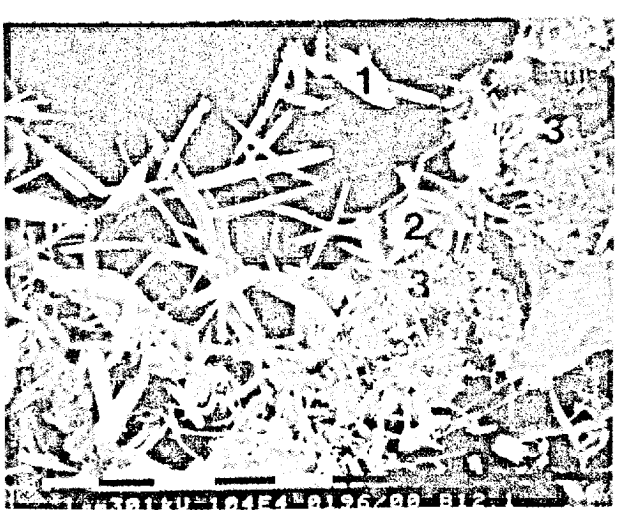

Fig. 6 - OBSERVATION AU M.E.B. :
BETON DE CIMENT FILLERISE
1 Ettringite 2 Carboaluminate
3 Grain de clinker

La différence de réactivité des fillers va se traduire par des valeurs différentes du gradient d'ions carbonate autour des grains de C_3A.
Ce gradient sera fonction de la solubilité du calcaire dans le système considéré, en régime dynamique. Les mesures par DRX montrent en effet que les calcaires les plus réactifs vis à vis du C_3A forment plus rapidement du carboaluminate, ce qui consomme beaucoup d'ions carbonates. Au contraire, les calcaires moins réactifs produisent beaucoup de solution solide et peu de carboaluminate.

CONSEQUENCES

1/ Comment définir la réactivité d'un filler calcaire ?

La réactivité est souvent définie par rapport à l'évolution de la résistance mécanique. Celle-ci est malheureusement la résultante d'un trop grand nombre de paramètres, pour que l'on puisse en dégager la contribution des propriétés d'un constituant, et encore moins évaluer quantitativement cette contribution. Les résultats précédents montrent à l'évidence que l'évaluation de la réactivité d'un calcaire incorporé dans un ciment n'est pas un problème simple et que les conditions de milieu (ici, la proportion de gypse) jouent un rôle aussi important que les propriétés intrinsèques. D'autres interactions peuvent se produire. Certains éléments mineurs du clinker, comme les alcalins, peuvent modifier la réactivité du calcaire avec C_3A. En effet, l'écriture des produits de solubilité du carboaluminate et de C_4AH_{13} montre que l'activité des ions OH^- y apparait à la puissance 4, pour le premier, et à la puissance 6, pour le deuxième. On peut donc prévoir que l'augmentation du pH produite par l'accumulation des alcalins dans la solution, va favoriser la précipitation de C_4AH_{13}, ce qui pourrait diminuer le taux de réaction du calcaire.

La formation de complexes comme $CaOH^+$ peut modifier la solubilité de la calcite, lorsque la concentration en OH^- augmente. Par ailleurs, on ne peut négliger l'incidence de la pression partielle de CO_2 sur les équilibres des phases carbonatées /13/ 714/, qui dans les bétons sera liée à la porosité.

2/ Réactivité et solubilité

Nous pouvons tenter de concilier l'exigence d'une définition rigoureuse de la réactivité et la complexité des interactions, en remarquant que, quel que soit le nombre des réactions mises en jeu par ces dernières, chacune d'entre elles utilise les potentialités du calcaire, résultant de ses propriétés intrinsèques. A ce titre, la solubilité en régime dynamique nous parait essentielle. Il faut essayer de la mesurer en séparant les variables, c'est-à-dire dans un système chimique débarassé des interactions. Pour cela, il est indispensable de s'entourer de quelques précautions (respect de l'identité du mécanisme, élimination des espèces solubles, normalisation de la surface).

3/ Réactivité et structure cristalline

Il est bien établi maintenant que la dissolution des cristaux de calcite est plus rapide selon certaines faces cristallines /8/ /9/, ou sous l'action d'une contrainte mécanique /15/. Diverses impuretés peuvent modifier sa solubilité /16/.

C'est en approfondissant le concept de réactivité et en continuant à dégager les rôles respectifs des propriétés intrinsèques et du milieu, que l'on ouvrira de nouvelles perspectives, autant dans le domaine de l'activation des fillers par broyage, que dans celui de leur sélection.

CONCLUSIONS

Nous sommes maintenant en mesure de prévoir quelques aspects du comportement d'un ciment contenant un filler calcaire, en fonction du gypsage. Tout d'abord, il apparait qu'en présence de calcaire, les réactions du C_3A peuvent être fortement ralenties, avec un gypsage très faible. La calcite peut donc jouer un rôle de régulateur de prise. Cependant, le mécanisme réactionnel est alors différent et comme le montre la *Figure 4*, une diminution excessive du sulfate ferait perdre le bénéfice de taux de réaction apporté par le 2e pic thermique. or la chaleur libérée durant ce pic contribue à l'augmentation de l'ensemble des vitesses de réaction, ce qui permet, en optimisant le gypsage, d'obtenir les meilleures résistances initiales /12/. Si l'on recherche cet optimum, il parait donc souhaitable de gypser à une teneur légèrement inférieure à celle du ciment portland pour tenir compte de la formation initiale de carboaluminate.
Inversement, un gypsage très faible devrait conduire à un ciment de plus faible chaleur d'hydratation, avec une progression régulière des performances. Ceci donne au fabricant une nouvelle possibilité de moduler les caractéristiques dynamiques du ciment, selon les besoins de l'utilisateur, mais ne doit pas être obtenu au prix d'une moins bonne durabilité : s'il est admis que la formation de carboaluminate contribue à l'augmentation des performances mécaniques /2/, il faut prendre garde, dans quelques applications particulières, au risque de décomposition de cet hydrate au contact de solutions salines concentrées (chlorures, sulfates), ce que les données thermodynamiques permettent de prévoir.

BIBLIOGRAPHIE

/1/ T. MANABE ; N. KAWADA ; M. NISHIYAMA "Studies on $3CaO.Al_2O_3.CaCO_3.nH_2O$ (Calcium Monocarboaluminate Hydrate" - C.A.J. Rév. 1961, pp 48-55.

/2/ E. SPOHN ; W. LIEBER "Reactionen zwischen calciumcarbonat und portlandzement" - Zement Kalk Gips N°9, 1965, pp 483-485.

/3/ M.H.ROBERTS "Calium aluminate hydrates and related basic salt solid solutions"- 5e ISCC Tokyo, 1968, Suppl.paper (Abstract) Part II, pp.21-25.

/4/ S.J.AHMED ; L.S.DENT GLASSER ; H.F.W.TAYLOR "Crystal structures and reactions of C_4AH_{12} and derives basic salts" - Ibid. pp.26-30.

/5/ J.GRANDET ; JP. OLLIVIER "Etude de la formation du monocarboaluminate de calcium hydraté au contact d'un granulat calcaire dans une pâte de ciment portland"- CCR, vol.10, 1980, pp 759-770.

/6/ B.MORTUREUX ; H.HORNAIN ; M.REGOURD "Liaison pâte de ciment-filler dans les ciments composés". RILEM Colloque International "Liaison pâte de ciment-matériaux associés", Toulouse, 1982, A.64.

/7/ A.CARLES-GIBERGUES ; J.GRANDET ; JP.OLLIVIER "Evolution dans le temps de la pâte de ciment portland contenant des ajouts", Ibid. B.11.

/8/ JP.OLLIVIER ; J.GRANDET ; B.THENOZ "Influence de la température sur la raction marbre-pâte de ciment portland". Bull.Minral.(1982), 105, pp 267-272.

/9/ A.NEGRO ; A.BACCHIORINI ; L.CUSSINO "Interazione carbonato di calcio - Aluminati. Seminario Internationale Totino (Italia), 1982, pp 219-229.

/10/ R. FICHER ; H.J.KUZEL "Réinvestigation of the system $C_4A.nH_2O$ - $C_4A.CO_2.nH_2O$ - CCR Vol.12, 1982, pp 517-526.

/11/ P.LONGUET "Réactivité des fillers calcaires"- Ciments Bétons Plâtres et Chaux, n° 742, 3/83, pp 176-179.

/12/ C.VERNET "Etude de la cinétique des réactions d'hydratation des ciments industriels - Méthodologie et applications" - Thèse CNAM, Ing.phys., Oct. 1982.

/13/ P.BARRET ; D.BERTRANDIE ; D.BEAU "Calcium hydrocarboaluminate, carbonate, alumina gel, and hydrated aluminates solubility diagram calculated in equilibrium with CO_{2g} and with Na^+_{aq} ions". CCR, Vol. 13, 1983, pp 789-800.

/14/ M.SOUSTELLE ; B.GUILHOT ; AA. FOURNIER ; M.MURAT A.NEGRO "Stabilité thermodynamique des phases dans le système $CaO-Al_2O_3-CO_2-H_2O$ - CCR, Vol.15, 1985, pp 421-430.

/15/ A.GIROU et coll. "Dissolution expérimentale d'un rhomboèdre de calcite soumis à une contrainte" - Bull.Minéral. (1982), 105, pp 301-306.

/16/ F.LIPPMANN "Stable and metadtable solubility diagrams for the system $CaCO_3-MgCO_3-H_2O$ at ordinary temperature". Bull. Mineral. (1982), 105, pp 273-279.

F. PANCRAZI, J. PHALIPPOU, J. ZARZYCKI (C.N.R.S. MONTPELLIER France)
F.P. SORRENTINO (LAFARGE COPPEE RECHERCHE France)

1

SYNTHESIS of "C-S-H" GEL
SYNTHESE des GELS de C-S-H

2.1

SUMMARY : "C-S-H" gels, of high C/S ratios have been prepared either by sol gel process, either by hydrolisis and polycondensation of metal alkoxydes. These methods of preparation by solubilisation of the species and gelation seem closer of the way of formation of the "C-S-H" formed during C_3S hydration, than the usual method of preparation by coprecipitation of salts.

Foram preparados géis de C-S-H com relações altas de C/S, seja pelo processo de gel sol, seja por hidrólise e policondensação de óxidos alcalino-metálicos. Estes métodos de preparação por solubilização de espécies e gelação parece mais próximo do modo de formação do "C-S-H" formado durante a hidratação do C_3S, do que o método usual de preparação por co-precipitação de sais.

F. PANCRAZI, J. PHALIPPOU, J. ZARZYCKI (C.N.R.S. MONTPELLIER France)
F.P. SORRENTINO (LAFARGE COPPEE RECHERCHE France)

INTRODUCTION

The microscopic examination of hardened C_3S paste shows an amorphous phase in which it is possible to recognize anhydrous C_3S and hexagonal plates of $Ca(OH)_2$, (1). This amorphous compound, called "C-S-H" is responsible of the setting and hardening of C_3S or Portland Cement. It fills up the space between grains of cement or C_3S, bridging them and giving the rigidity of the paste. The continuous formation of "C-S-H" keep filling the capillary pores, leading to a decrease of the total porosity of the paste and to an increase of the strengths (2).

The real nature of the atomic ordering of "C-S-H" which provides the strength of the paste is still today an open question. Several models have been proposed (POWERS 1958, (3), KANTRO 1962, (4), ISHAI 1962 (5), FELDMAN and SEREDA 1968 (6), SIERRA 1973 (7)...). It is generaly accepted that the elementary particle of "C-S-H" is a foil, composed from 2 or 3 layers, each layer being formed with calcium octaedron sandwitched by 2 layers of silica tetraedra. The discrepencies concern mainly the distribution of water in the "C-S-H". It is possible to distingish :

- hydroxyl water in which OH is bound to Si or Ca atoms in the structur ; they are located on the internal and external surfaces of the foil,
- interlayer water, fixed between the layer by hydrogen bound,
- interfoil water, less fixed.

The rigidity of the paste can be attached to the cohesive strength (VAN der WAALS, Hydrogen) dues to the structuration of interfoil or interlayer water and to interparticles chemical bound. Whatever the precise nature of the bound which still remains at the stage of hypothesis, the rigidity of the paste is caused by the presence of the amorphous compound "C-S-H" whose the colloidal nature may have its origin in the colloidal nature of silica itself, (8). We try to understand in our last chapter how it is possible to go from the silica gel structure to the "C-S-H" layers.

A colloidal solution of silica is formed by polymerised silicic acid particles. The silica atoms occupy tetraedric sites and are bound to hydroxyl groups, which allow to make up their coordinance at the surface. In a recent work (9), the silica particles could be formed by a linear, weakly polymerised condensate branched together with hydrogen bound. The stability of colloidal silica is insured by the formation of electric layer between hydroxyl ions absorbed at the surface of the particles and the cations present in the water. By reducing the potential energy of interaction between the electric double layer of particles in equilibrium, the colloidal solution will destabilize, few type of phenomena will occur : coagulation, floculation coacervation, gelation. Although most of these phenomena involve the formation of a tridimensional network of colloidal particles, a fundamental difference exists between gelation and the other types of aggregations.

When the gelation occurs, the colloidal solution becomes viscous, and develops a rigidity. When a floculation or a coagulation occurs, a pricipitat forms and separate from the aquous media. The difference is easy to see when the solution is diluted but difficult when the solution is concentrated.

The figure 1 shows the differences :

figure 1

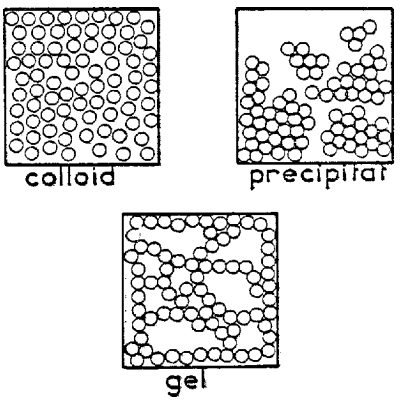

The gel formation by colloidal solution destabilization is used industrialy as hardener or binder of mineral fiber. By setting, the gel can link particles and by driyng the gel will change in insoluble silica ; these properties are typical to these type of aggregation.

It is possible to produce gels by an other way such as hydrolysis of tetraethoxysilane (TEOS). This method is used to bound refractory mortar (10) ; the setting of the gel allows a strength of the particles at low temperature ; these bound will change as ceramics bound at higher temperature.

In the case of silica, both process lead to a tridimensional network of silica tetraedron, but in the case of mixed gel, the colloidal silica destabilisation process will lead to a gel in which the minimal size of silica particles will be the size of the starting silica particles, while the hydrolisis of "TEOS" may lead to a particle os filica acid.

The synthetis of "C-S-H" has been studied and reviewed by many authors and we mention here only the more narrowly defined category of gels as opposed to precipitated : these studies (11 to 19) have shown that the synthesis of "C-S-H".

Gels in alimited range of C/S or pH was possible, but the recent works concern mainly the phenomenon of colloidal solution destabilisation. ALLEN and MATIJEVIC (16), FROLOV and MILOVICH (18), DEPASSE and WATILLON (19), determine the parameters leading to the precipitation of silica in presence of electrolyte, but none systematic studies have been done concerning the gelation in the system CaO, SiO_2.

In this study, we have tried to produce "C-S-H" of ratio as near as those found during C_3S or Portland cement hydration and to define the conditions of their formation.

EXPERIMENTAL RESULTS

A colloidal silica solution (Ludox as 40 Dupont de Nemours) formed from particle of 20 nm diameter, is mixed with a calcium nitrate solution ; the proportion being calculated to reach a given C/S ratio. When the products are mixed, the solution must be clear ; the presence of a precipitat cancels the experiment. The pH is then setted up and the sample is

kept out CO_2 until the setting occurs.

The curves of the figure 2 show the field of gelation and precipitation of "C-S-H". For a calcium concentration more than 2.10 mole. L-1, the pH boundary is constant and equal to 8.5. When the calcium concentration is less than 2.10-1 mole. L-1, the curve will change of slope to higher pH, which show clearly the possibility of gelation in the field of pH 10 for a calcium concentration less than 10-3 moles L-1, this is confirmed by the work of ALLEN and MATIJEVIC (curve 2, figure 2...(16)). The differences between curve 1 and 2 come from the differences of concentration of the starting colloidal silica.

figure 2

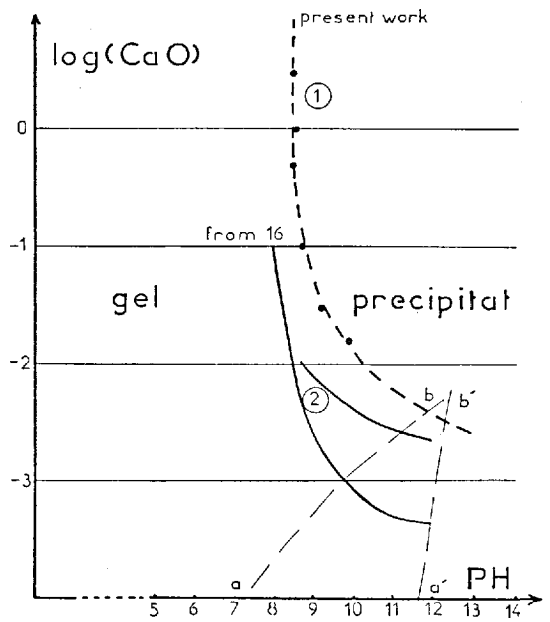

In order to change the ratio C/S we have used a solution of calcium nitrate of 3 mole.L-1 and changed the quantity of silica solution, the pH being 8.5, in this conditions we have obtained gels of ratio C/S in the range 0.01,3. In all cases, the evolution of the process of gelation is the same ; the solution becomes whiter and whiter to reach an opaque gel.

The figure 3 shows the variation of setting time as function of the ratio C/S. It is clear that calcium ions accelerate the setting time of the gel.

In a previous study (15), we have seen that the gels of "C-S-H" can be obtained from metal alkoxydes. The required amount of "TEOS", is mixed with the appropriate amount of ethanol, depending on the composition of the gel to be prepared ; the batch was allowed to reflux at 70 degre for two hours under vigorous stirring ; the solution was cooled to room temperature and calcium nitrate, dissolved in a minimum quantity of ethanol was added. No precipitate occurs at this stage and stirring was maintained for 1/2 hrs. The solution was hydrolysed by a mixture of water and ethanol ; by this method, it has been possible to obtain "C-S-H" gel of C/S=4.

figure 3

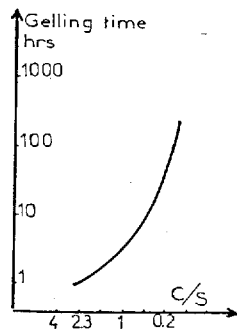

The gels of "C-S-H" obtained by these techniques are solid, but soft and contain a large amount of water with NO_{3-} and NH_{4+} ions in solution. Stored in air, the gels of ratio greater than 1.6 show cristallization of calcium nitrate. When the ratio is less than 1.6 the cristallization does not occur and the gel hardens.

The infra red spectrum shows the caracteristics bands of NO_3 (810 and 1030 cm-1), a band of polymerized silica (1100 cm-1) a band of dimeric silica at 970 cm-1.

DISCUSSION

The usual method of preparing "C-S-H" consist in reacting a solution of calcium with colloidal silica, solution of silica, organic silica (TEOS) or alcali silicate. When we mix the solution, "C-S-H" precipitate and we never obtain calcium and silica in solution together without solid "C-S-H". The pH of the solution and the ions concentration are high, so we are in the right part of the figure 2, i.e in the precipitation area of "C-S-H". These methods of preparation do not represent what is going on during the hydration of C_3S, for which there are calcium and silica in solution during a certain time. In the case of the technique described in this work, we really have calcium and silica in the solution before any coagulation effect so we are close to the formation of the outer product (i.e the "C-S-H" deposited in the space initialy occupied by water) during the C_3S hydration. The mechanism of formation of the inner product may be different (20).

The "C-S-H" formed during C_3S contains polymeric silica. From the trimethylsilylation technique, evidence is that for $C/S \geqslant 0,8$ there is combinations of anions with 2,5 % Si atoms, the distribution shifting upwards as Ca/Si decreases (21). In the sol gel process, silica is already highly polymerised and the calcium ions are located at the surface of the particles of silica (200 A°) : there is no evidence why the addition of calcium would reduce the degre of polymerisation inside the particles : in this case we are not similar to the layer structure of "C-S-H". During the organic "TEOS" process the starting silica in monomeric and an evolution to highly degre of polymerisation is possible : this later process could give a "C-S-H" closer to the compound obtained during the C_3S hydration.

The studies of C_3S hydration show a congruent dissolution of C_3S followed by a coagulation of "C-S-H" of ratio C/S = 1 ; this ratio increases during the induction period up to 1.5/1.7 (22) ; starting from a ratio water/solid = 100, for example, C_3S dissolves and the solution contains calcium and silica with a ratio equal to 2.96, 3.18 (23). The quantity of calcium is 3.8 10-3 mole. L-1 and the pH = 11,7. The figure 2 shows that, there is a precipitation and not a gel formation.

Nevertheless, when C_3S is introduced in solution, the pH is 7, and the evolution of the dissolution of the dissolution of C_3S can be represented by the line a...b (figure 2, we are in the gelling field. If we keep the pH artificialy equal to 7 or if we maintain the calcium concentration less than 4 10-4 mole. L-1 we should be in the gelation condition I.E. the formation of gel of C/S = 3. We have seen experimentaly that the gel of high C/S ratio (higher than 1.6) are not stable and decompose in "C-S-H" of lower ratio and calcium salt. At the end of this first step the pH is definitly fixed at 11.5,12, the route of the evolution of the hydration is then a'...b' (figure 2) i.e., we cross the field of gelation for low local calcium concentration to reach the precipitation field of "C-S-H" ; the step of gelation is transitory and allows a structuration of water and silica which are found in the "C-S-H" precipitat as hydroxyl water, the hypothesis being that the layer structure of "C-S-H" is created by the alternative process gelation-precipitation.

CONCLUSIONS

It has been possible to prepare, either by sol gel process, either by hydrolisis and polycondensation of metal alkoxides "C-S-H" gels of high C/S ratio. These method of preparation by solubilisation of the species and gelation seems closer of the way of formation of the "C-S-H" formed during C_3S hydration, than the usual method of preparation by coprecipitation of salts and could allow to find explanation in the setting and hardening of Portland cement, at least in the early stages (first day) : however it is important to remember that cement paste is a composite material in which those are not only "C-S-H", but also calcium sulfoaluminate, unreacted product, $Ca(OH)_2$ etc ... and in general a very complex heterogeneous structure.

ACKNOWLEDGMENT

The authors want to express their thanks to Professor H.F.W.TAYLOR for his helps in questions of structure of "C-S-H" and for his general comments on this work.

REFERENCES

1 - DIAMOND S.-Proc. of the conference of sheffield on the hydraulic cement pastes. Cement and concrete assoc. 8,9 April (1976).

2 - SOROKA I.-Portland cement paste and concrete. The Mac MILLAN Press LTD (1979)

3 - POWERS T.C.-J. Amer. Ceram. Soc. 41.1.1,6. (1958)

4 - KANTRO D.L. et al.-J. Phys. Chem. 66. 1804,9 (1962)

5 - ISHAI O.-Proc. Conf. the structure of concrete and its behavior under load. cement and concrete assoc. LONDON (1965)

6 - FELDMAN R.F. et al.-Eng. J. 53.819. 53,9. (1970)

7 - SIERRA R.-Rapport de recherche n° 39, Laboratoire des Ponts et Chaussées. Sept. (1974)

8 - OTTERWILL R.H.-Phil. Trans. R. Soc. LONDON A.310 67,78. (1983)

9 - ACKER E.G.-J. Colloid int. SCI.32 (1). 41,54 (1970)

10 - EMBLEN H.G. - Silicate industriel 12.231 (1980)

11 - ROY R.-J. Amer . Ceram. SOC. 52.344 (1969)

12 - MC CARTHY et al-J. Amer. Ceram Soc. 54.344 (1969)

13 - DISLICH H.-Angewante chem. int. ed. 10.363 (1971)

14 - ROY D.M. J.-Amer. Ceram. Soc. 60.178.80. (1977)

15 - PANCRAZI F. et al.-Journal of non cristalline solid 63.1.1. Fev. (1984)
Journal de physique .C9. Supplement n° 12,43 DEC (1984)

16 - ALLEN H. et al.-Journal colloid and int. Sci. 33.420 (1970) - 35.66 (1971)

17 - HAYASHI T. et al-Journal of Mat. SCI. 15.1971,77. (1980)

18 - FROLOB Y.G. et al-Kolloid J. of URSS 431,6. (1970)

19 - DEPASSE J. et al.-J. Colloid and SCI.33.430 (1970)

20 - TAYLOR HFW-10th intern. Symp.. reactivity, of solids (DIJON 1984)

21 - TAYLOR HFW-Private communication

22 - TAYLOR HFW - Rilem Committee 68. MMH. Task group 3.457,68 (1984)

23 - MENETRIER D.-Thesis DIJON - France (1977)

D. BERTRANDIE et P. BARRET

Hydration elementary interfacial steps of calcium aluminates as cement compounds

2-1

Etapes élémentaires interfaciales de l'hydratation des aluminates de calcium, constituants des ciments.

La dissolution des aluminates de calcium anhydres présente un caractère d'irréversibilité et il est bien connu que le calcul du produit de solubilité de ces phases à partir des ΔG^{o} de formation des partenaires de la réaction conduit à des produits de solubilité aberrants parce que beaucoup trop élevés.

Notre interprétation suppose qu'une telle différence est la conséquence d'une réaction interfaciale directe irréversible entre la surface du solide anhydre et l'eau, aboutissant à l'hydroxylation, sur leurs propres sites cristallographiques, des anions anhydres superficiels tels que AlO_2^- et O^{2-}. Cette hydroxylation les transforme en ions $[Al(OH)_4]^-$ et OH^- et un équilibre est alors susceptible de s'établir entre ces ions (qui occupent les sites superficiels du solide à la manière d'impuretés de substitution) et les ions de même nature en solution. L'hydroxylation superficielle, dans le cas de $CaAl_2O_4$, ne concerne que des ions AlO_2^- dont la transformation en $[Al(OH)_4]^-$ est le résultat d'une réaction d'addition ne nécessitant pas la coupure des molécules d'eau.

En revanche, dans le cas des aluminates de calcium, de rapport C/A > 1 comme $C_{12}A_7$ ou C_3A, l'hydroxylation superficielle nécessite la coupure d'une partie des molécules d'eau pour assurer la protonation des ions O^{2-}, ce qui crée simultanément des ions OH^- sur les sites superficiels correspondants du solide et des ions OH^- excédentaires dans la solution. La fréquence du transfert en solution des anions déjà hydroxylés accompagnés des cations Ca^{2+} correspondants règlerait donc la vitesse d'ensemble et imposerait la congruence de la dissolution.

D'un point de vue macroscopique, le tracé sur le diagramme chaux-alumine-eau des courbes de solubilité des aluminates de calcium superficiellement hydroxylés et la position, par rapport à ces courbes, des courbes de supersolubilité des hydrates qui délimitent les domaines de composition au-delà desquels leur nucléation devient immédiate permettent de comprendre pourquoi la précipitation de certains hydrates peut être provoquée, à une température donnée, par un simple changement de composition tandis que celle d'autres hydrates ne peut pas l'être. De nombreux comportements des ciments alumineux peuvent alors être expliqués ou prévus.

A dissolução dos aluminatos anidros de cálcio apresenta um caráter de irreversibilidade, e se sabe bem que o cálculo do produto de solubilidade destas fases, a partir de ΔG^{o} de formação dos associados da reação, leva a produtos anômalos de solubilidade porque muito elevados.

Nossa interpretação supõe que tal diferença é conseqüência de uma reação interfacial direta irreversível entre a superfície do sólido anidro e a água, confinando à hidroxilação, em seus próprios locais, os aníons anidros superficiais como o AlO_2^- e O^{2-}. Esta hidroxilação os transforma em íons $(Al(OH)_4)^-$ e OH^-, e então é suscetível a ocorrência de um equilíbrio entre estes íons (que ocupam os sítios superficiais do sólido à maneira de impurezas de substituição) e os íons de mesma natureza em solução. A hidroxilação superficial, no caso de $CaAl_2O_4$, refere-se apenas aos íons AlO_2^-, cuja transformação em $(Al(OH)_4)^-$ é o resultado duma reação de adição, não precisando da dissociação das moléculas de água.

Ao contrário, no caso dos aluminatos de cálcio, com relação C/A > 1 com $C_{12}A_7$ ou C_3A, a hidroxilação superficial precisa da dissociação de uma parte das moléculas de água para garantir a protonação dos íons O^{2-}, o que cria simultaneamente íons OH^- sobre os sítios superficiais correspondentes do sólido e íons OH^- excedentes na solução. A freqüência da transferência em solução de aníons já hidroxilados, acompanhados de catíons Ca^{2+} correspondentes, regulará, portanto, a velocidade de conjunto e imporá a congruência da dissolução.

Sob um ponto de vista macroscópico, o traçado no gráfico cal-alumina-água das curvas dos aluminatos de cálcio superficialmente hidroxilados e a posição, em relação a estas curvas, das curvas de supersolubilidade dos hidratos que delimitam os domínios de composição, além dos quais sua nucleação torna-se imediata, permitem que se compreenda por que a precipitação de certos hidratos pode ser provocada, a uma dada temperatura, por uma simples mudança de composição, enquanto a de outros hidratos não pode ser provocada. Assim se pode prever e explicar inúmeros comportamentos dos cimentos aluminosos.

1) INTRODUCTION :

Dans le problème de l'hydratation des constituants des liants hydrauliques, le processus d'hydratation par l'intermédiaire de la solution, suivant l'hypothèse de Le Chatelier (1), semble généralement admis lorsqu'il s'agit des aluminates de calcium alors qu'il est beaucoup plus controversé dans le cas des silicates de calcium.

Plusieurs raisons peuvent être invoquées pour expliquer cette différence d'attitude :

a) *Le C-S-H se sépare très difficilement des grains de C_3S ou de βC_2S* autour desquels il s'est formé. Récemment Hassan (2) et Longuet (3) ont pu réussir une telle séparation grâce à une forte abrasion produite par le malaxage sous l'effet de deux pistons d'une pâte de ciment blanc ou de C_3S en cours d'hydratation dans une vessie souple.

En revanche, après agitation pendant 48 heures en suspension aqueuse de rapport pondéral liquide/solide = 10, nous avons pu séparer par simple décantation les grains résiduels de Fondu (broyé en gros grains et tamisé) des hydrates (CAH_{10}, C_2AH_8 et AH_3) qui s'étaient formés (4). La couleur noire du premier et blanche des seconds facilitait le contrôle de l'opération (Fig. 1).

En outre, les grains de Fondu prélevés dans la suspension aqueuse et observés au microscope optique et au microscope électronique à balayage n'étaient pas recouverts d'une couche d'hydrates et ne portaient que de rares germes dans les anfractuosités. Des hydrates ne se rencontraient sur et entre les grains qu'en milieu stagnant (Fig. 2).

En collant quelques grains de Fondu sur de fines lamelles en matériau plastique et en les introduisant dans la suspension agitée, on pouvait observer, au bout de 3 heures environ, des germes d'hydrates adhérents à la lamelle et entourant la base des grains (Fig. 3). Cette expérience montre (4) qu'une faible protection contre les courants dans la suspension agitée permettait aux germes d'hydrates de se déposer autour et au voisinage immédiat des grains

b) *La nucléation des aluminates de calcium hydratés présente un caractère de nucléation homogène :*

Des nombreuses expériences que nous avons faites sur la cinétique d'évolution de suspensions aqueuses agitées de CA et comparativement de filtrats prélevés au maximum de concentration (5), il résulte que la présence des grains et donc d'interfaces ne modifie pratiquement pas la longueur de la période d'induction précédant la précipitation massive des hydrates. Le caractère homogène de leur nucléation est ainsi mis en évidence.

c) *Aux concentrations élevées en chaux, la concentration des ions aluminates reste toujours relativement importante* et facilement mesurable par rapport à la concentration des ions silicates. La première est de l'ordre de la millimole alors que la seconde est de l'ordre de la micromole par kilogramme.

Or, à de si faibles concentrations en ions silicates, le processus d'hydratation par l'intermédiaire de la solution ne correspond plus à une hypothèse satisfaisante pour l'esprit.

d) *L'imperméabilité des produits d'hydratation qui se développent dans une pâte de ciment alumineux est moins invoquée* que celle des produits d'hydratation dans une pâte de ciment Portland, voire même dans une pâte de C_3S pur.

Pour ces diverses raisons, *l'hypothèse d'un*

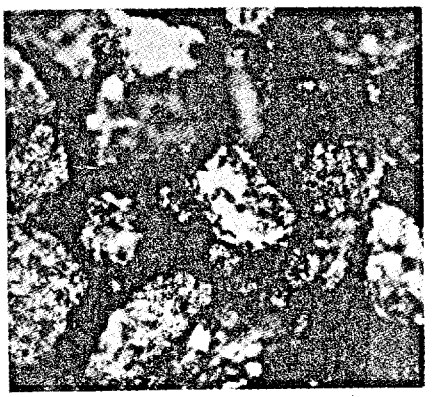

Fig. 1 : Grains résiduels de Fondu (x 150) séparés par décantation d'une suspension aqueuse après 48 heures.



Fig. 2 : Grains de Fondu (x 150) hydratés en milieu stagnant : hydrates au contact des grains et entre eux.



Fig. 3 : Grains de Fondu (x 50) collés sur une lamelle et hydratés en suspension aqueuse.

processus d'hydratation "topochimique" n'a pas connu la même faveur dans les ciments alumineux que dans les ciments Portland.

Cependant, en dépit des cas d'espèces, nous croyons à l'existence de concepts généraux s'appliquant au mécanisme de la formation des hydrates à partir des phases anhydres, que celles-ci soient des aluminates ou des silicates de calcium. Pour faire apparaître les similitudes et aussi certaines différences, nous nous proposons de développer ici, parallèlement à la synthèse que nous avons faite dans le cas des silicates C_3S et C_2S (6) un exposé sur nos hypothèses, nos idées et leur support expérimental et théorique en ce qui concerne les étapes élémentaires de l'hydratation des principaux aluminates de calcium utilisés dans les ciments.

Nous espérons ainsi contribuer à l'élaboration d'un modèle conceptuel général de l'hydratation des constituants des ciments.

2) SOLUBILITE THEORIQUE DES PHASES SOLIDES ANHYDRES :

La dissolution des phases solides anhydres du type oxysel, qu'il s'agisse des aluminates aussi bien que des silicates de calcium, *présente un caractère d'irréversibilité* et il est bien connu que le calcul du produit de solubilité de ces phases à partir des ΔG^o de formation des partenaires de la réaction conduit à des valeurs aberrantes parce que beaucoup trop élevées.

Cependant, dans les exemples traités par H.N. Stein (7), ceux de C_3S et de C_3A, on ne dispose pas de valeurs expérimentales fiables auxquelles comparer les valeurs calculées, car la précipitation des hydrates vient masquer l'existence d'un éventuel équilibre de solubilité.

Un tel inconvénient n'existe pas avec l'aluminate monocalcique CA. Dans une suspension agitée de cet aluminate, il est bien connu qu'à 25°C par exemple, les concentrations exprimées en CaO et Al_2O_3 plafonnent toujours aux mêmes valeurs limites telles que $[CaO] = 21{,}3.10^{-3}$ mol.kg^{-1}, $[Al_2O_3] = 19{,}9.10^{-3}$ mol.kg^{-1} et qu'elles s'y maintiennent approximativement pendant une vingtaine d'heures avant que les hydrates ne se mettent à précipiter massivement.

En utilisant les données bibliographiques rassemblées par H.N. Stein (7) et reportées dans le tableau I, nous avons calculé (8) la solubilité théorique de $CaAl_2O_4$ d'après l'équation :

$$(1)\quad CaAl_2O_4 + 4H_2O_\ell \rightleftarrows 2[Al(OH)_4]^-_{aq} + Ca^{2+}_{aq}$$

Tableau I

	$[Al(OH)_4]^-_{aq}$	Ca^{2+}_{aq}	OH^-	H_2O_ℓ
$\Delta_f G^o_{298}$ kJ.mol^{-1}	-1293,25	-522,51	-157,14	-236,96
	$CaAl_2O_4$	C_3A	$C_{12}A_7$	
	-2206,62	-3405	18392,84 (18)	

Pour cela, on calcule d'abord l'enthalpie libre normale de cette réaction soit $\Delta_r G^o_{298} = 15{,}45$ kJ.mol^{-1}, puis on en tire la valeur de la constante d'équilibre : $K_{(1)} = 1{,}96.10^{-3}$.

Les concentrations des ions Ca^{2+}_{aq}, $[Al(OH)_4]^-$ exprimées en molalités, sont désignées respectivement par x, y et ψ. Ces concentrations doivent satisfaire à la relation d'électroneutralité :

$$(2)\quad 2x = y + \psi$$

Si l'on admet que les ions en solution sont dans le même rapport stœchiométrique que dans le composé anhydre, on aura $y = 2x$.

Etant donné la valeur relativement élevée de la concentration x à calculer, on n'utilise pas, pour exprimer les coefficients d'activité γ_i des ions, la formule de Debye et Hückel simplifiée, mais on fait appel à l'extension de Davies :

$$(3)\quad \log \gamma_i = -0{,}507\, Z_i^2 \frac{\sqrt{I}}{1+\sqrt{I}} - 0{,}2\, I$$

Z_i est la charge électrique de l'ion et I la force ionique donnée par la relation :

$I = \frac{1}{2} \sum_i m_i Z_i^2$ où m_i est la molalité.

Ici $I = 3x$. L'équation à résoudre est alors :

$$(4)\quad 4x^3.10^{-3},042 \frac{\sqrt{3x}}{1+\sqrt{3x}} - 0{,}6x. = 1{,}96.10^{-3}$$

La valeur x = 0,164 mol.kg^{-1} satisfait à cette équation. Les résultats exprimés en $[CaO]$ et $[Al_2O_3]$ seraient donc : $[CaO] = [Al_2O_3] = 0{,}164$ mol.kg^{-1}.

Ce n'est qu'un ordre de grandeur en raison de l'approximation faite sur le calcul des γ_i en utilisant l'extension de Davies, mais comparées aux valeurs limites observées, on voit que les concentrations calculées sont près de huit fois plus élevées. Il convient de remarquer en outre que le rapport stœchiométrique n'est pas exactement conservé dans les valeurs limites expérimentales pour lesquelles le rapport C/A est toujours supérieur à 1. Ici, C/A = 1,07.

3) INTERPRETATION PROPOSEE DE L'ECART ENTRE SOLUBILITE THEORIQUE ET VALEURS LIMITES OBSERVEES :

Bien que les valeurs des solubilités calculées pour C_3S et C_3A anhydres lui soient apparues comme anormalement élevées, H.N. Stein avait admis qu'elles pouvaient être atteintes au voisinage immédiat de l'interface, où devait alors régner un très fort gradient de concentration.

Notre position diffère essentiellement de celle de H.N. Stein par le fait que *nous postulons l'existence d'une étape irréversible d'hydroxylation superficielle s'accompagnant d'un abaissement d'enthalpie libre susceptible d'expliquer la différence entre la solubilité théorique calculée et les valeurs limites des concentrations observées.*

D'ailleurs une réaction telle que (1) est une réaction globale qui ne traduit pas uniquement une dissolution, puisque son premier membre exprime une combinaison entre l'aluminate anhydre et l'eau.

Il manque donc une étape intermédiaire, celle qui donnerait le produit solide susceptible de véritablement se dissoudre et de prendre part à un équilibre de solubilité avec les ions en solution.

Mais nous ne considérons pas que ce solide intermédiaire doit être un produit d'hydratation dans lequel le solide anhydre se serait d'abord intégralement transformé. Notre hypothèse consiste à admettre qu'un simple état hydroxylé, *produit par interaction interfaciale directe (certains diraient : "par un processus topochimique") entre les molécules d'eau et les ions oxygénés appartenant à la surface du solide anhydre,* permet l'établissement d'une situation d'équilibre entre les ions en solution et les ions identiques créés de cette manière à la surface du solide.

La dissolution du solide se produit alors *grâce à une séquence répétitive d'étapes exigeant que les sites superficiels hydroxylés se découvrent par dé-*

part de leurs occupants pour permettre l'hydroxylation des sites sous-jacents. Formation de l'état superficiellement hydroxylé et dissolution sont conçues en quelque sorte comme des réactions simultanées.

La formulation de ces étapes utilise la représentation des défauts ponctuels ou des impuretés de substitution dans un cristal en faisant appel conjointement au système des unités de construction et à celui des éléments de structure (9).

Une unité de construction est représentée par la formule chimique du composé solide placée entre parenthèses avec un indice précisant sa localisation, par exemple *s* pour "surface". Un élément de structure est représenté par son symbole ou sa formule chimique avec, en indice, un symbole ou une formule qui désigne la nature du site cristallographique qu'occupe cet élément. S'il existe une différence de charge électrique entre la particule qui occupe réellement un site et la particule qui devrait normalement l'occuper, il en résulte une charge effective q_e qui est la différence $q_r - q_n$ entre la charge q_r occupant réellement le site et la charge q_n qui devrait normalement l'occuper. Pour simplifier, les charges ioniques ne sont pas écrites, étant supposées connues par le contexte. Ainsi un ion Ca^{2+} occupant un site normal s'écrira : Ca_{Ca}, tandis qu'un ion OH^- occupant un site d'ion O^{2-} s'écrira $OH_O^{\cdot}$. Pour les différencier des charges ioniques, les charges effectives positives sont représentées par des points et les charges effectives négatives, par des virgules. Par exemple une lacune d'ion Ca^{2+} s'écrira V''_{Ca} (V pour vacancy).

L'étape d'hydroxylation superficielle portant sur une unité de construction de $CaAl_2O_4$ peut alors s'écrire :

$$(5) \quad (Ca[AlO_2]_2)_s + 4H_2O_\ell \rightarrow (Ca[Al(OH)_4]_2)_s$$

Traduite en éléments de structure, cette équation devient :

$$(6) \quad (Ca_{Ca} + 2AlO_2^{\cdot}{}_{AlO_2})_s + 4H_2O_\ell \rightarrow (Ca_{Ca} + 2[Al(OH)_4]^{\cdot}_{AlO_2})_s$$

ce qui manifeste que l'ion hydroxylé $[(Al(OH)_4]^-$ se comporte comme une impureté de substitution en occupant un site cristallographique du réseau appartenant à un ion AlO_2^-. *L'état hydroxylé est donc constitué d'une telle monocouche qui ne forme pas une phase distincte du solide anhydre*. Il convient de remarquer ici *qu'un anion hydroxylé est le produit d'une réaction d'addition de deux molécules entières d'eau sur un ion AlO_2^-* et que la *charge de l'ion n'est pas changée* ; la charge effective q_e est donc nulle.

En partant de l'hypothèse que les valeurs limites des concentrations observées par agitation dans l'eau de $CaAl_2O_4$ correspondent à l'équilibre de solubilité de l'état superficiellement hydroxylé, noté CA_{sh}, on peut calculer le produit de solubilité relatif à l'équation suivante (7) dont la forme est vraiment celle d'une dissolution :

$$(7) \quad (Ca[Al(OH)_4]_2)_s \rightleftarrows Ca^{2+}_{aq} + 2[Al(OH)_4]^-_{aq}$$

Mais si la dissolution est congruente, les ions en solution doivent se trouver dans le rapport stoechiométrique $2x/y = 1$, comme dans l'état hydroxylé.

Le fait que le rapport $2x/y = C/A$ observé n'est pas 1, mais 1,07 environ, peut s'expliquer autrement que par la non-congruence de la dissolution. Nous avons déjà fait remarquer (10, 11) que, quand le rapport $C/A \rightarrow 1$, le degré de sursaturation β_o du gel d'alumine en milieu basique (pH > 10) augmente très rapidement et même β_o tendrait vers l'infini si la molalité ψ des ions OH^-_{aq} tendait vers zéro (ce qui est exclu car il ne serait plus possible de raisonner exclusivement avec des ions $[Al(OH)_4]^-_{aq}$ si le pH descendait notablement au-dessous de 10).

La réaction de précipitation du gel d'alumine s'écrit :

$$(8) \quad [Al(OH)_4]^-_{aq} \rightleftarrows OH^-_{aq} + Al(OH)_3 \downarrow$$

En désignant par $K_o = 1,60$, la constante d'équilibre de la réaction inverse, β_o est défini par le rapport :

$$(9) \quad \beta_o = \frac{\uparrow}{K_o} \frac{y}{\psi} \frac{\gamma[Al(OH)_4]^-}{\gamma OH^-}$$

Les γ_i exprimés ici à l'aide de la formule de Debye et Hückel simplifiée :

$$(10) \quad \log \gamma_i = -0,507 Z_i^2 \sqrt{I}$$ sont égaux, de sorte que $\beta_o = \frac{\uparrow}{K_o} \frac{y}{\psi}$.

En vertu de la relation d'électroneutralité (2) $\psi = 2x - y = y(C/A - 1)$ et l'on a :

$$\beta_o = \frac{\uparrow}{K_o(C/A - 1)} \quad (\beta_o \rightarrow \infty \text{ quand } C/A \rightarrow 1)$$

En fait, pour pH = 10, $\psi = 10^{-4}$ et $y \simeq 20.10^{-3}$ mol.kg^{-1} ; par suite, $C/A = 1,005$ et $\beta_o = 125$.

Le degré de sursaturation β_o varie très rapidement et pour $C/A = 1,07$, il n'est plus que de 8,9, c'est-à-dire qu'il est 14 fois plus faible qu'à pH = 10.

Ainsi, notre interprétation est que la dissolution est bien congruente, mais qu'elle est accompagnée d'une légère précipitation de gel d'alumine dont la cinétique, bien mise en évidence et interprétée par l'un de nous (9, 10) est étonnante puisque la précipitation cesse aux faibles valeurs de β_o, quoiqu'encore nettement supérieures à 1 (équilibre). Elle semble se stabiliser lorsque la composition de la solution est celle qui correspond, sur le diagramme chaux-alumine-eau à une courbe (m) (Fig. 4) thermodynamiquement définie (10) comme *la courbe d'instabilité minimale dans le domaine des solutions simultanément sursaturées par rapport au gel d'alumine et à C_2AH_8*.

C'est pourquoi pour calculer le produit de solubilité $K_{(7)}$ de la réaction (7), il convient de prendre la valeur de $x = 21,3.10^{-3}$ mol.kg^{-1} avec $y = 2x$.

En utilisant la formule simplifiée de Debye et Hückel (10) on obtient : $K_{(7)} = xy^2 10^{-5,269\sqrt{x}}$ soit $K_{(7)} = 6,58.10^{-6}$ (à comparer avec $K_{(1)} = 1,96.10^{-3}$).

L'enthalpie libre normale de la réaction (7) est alors $\Delta_r G^o_{298} = 29,562$ kJ.mol^{-1} et à l'aide des données du tableau I, on peut calculer l'enthalpie libre normale de formation rapportée à une mole de l'état superficiellement hydroxylé, soit : $\Delta_f G^o_{298} = -3168,57$ kJ.mol^{-1}.

Enfin, ayant déterminé à partir de la courbe de solubilité expérimentalement établie de CAH_{10}, l'enthalpie libre normale de la réaction :

$$(11) \quad 2[Al(OH)_4]^-_{aq} + Ca^{2+}_{aq} + 6H_2O_\ell \rightleftarrows Ca[Al(OH)_4]_2,6H_2O \quad \text{soit } \Delta_r G^o_{298} = -43,01 \text{ kJ.mol}^{-1}$$

on en déduit l'enthalpie libre normale de formation de CAH_{10} : $\Delta_f G^o_{298} = -4603,78$ kJ.mol^{-1}.

Dans le tableau II, sont rassemblées les valeurs des enthalpies libres normales de formation de

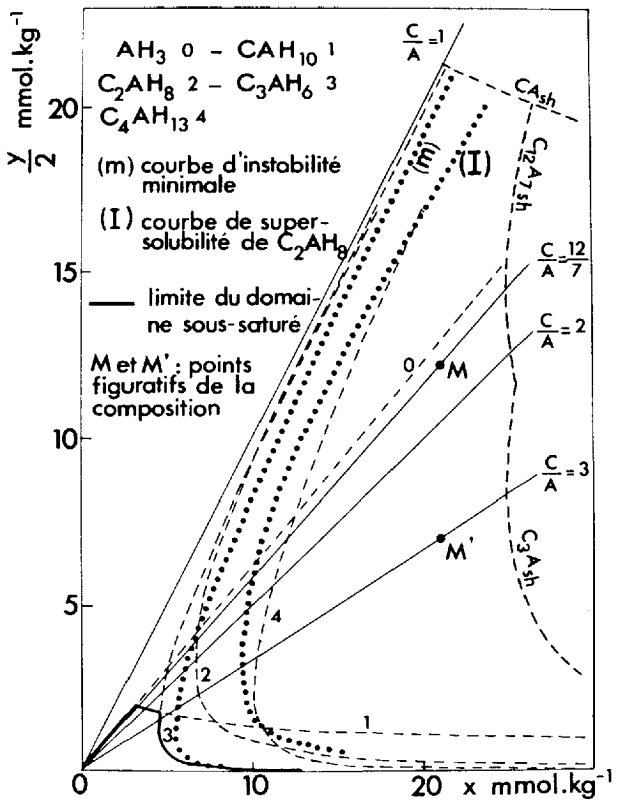

Fig. 4 : Courbe de solubilité de CA_{sh} et courbes de solubilité hypothétiques de $C_{12}A_{7\,sh}$ et de C_3A_{sh} reportées sur le diagramme chaux-alumine-eau.

CA anhydre, de CA_{sh} et de CAH_{10}. Les écarts entre ces valeurs illustrent bien le rôle d'intermédiaire que joue l'état superficiellement hydroxylé entre l'aluminate monocalcique anhydre et l'hydrate de même rapport C/A :

Tableau II

	$CaAl_2O_4$	$(Ca[Al(OH)_4]_2)_s$	CAH_{10}
$\Delta_f G^o_{298}$ kJ.mol^{-1}	-2206,62	- 3168,57	- 4603,78
Ecart kJ.mol^{-1}	-961,95		-1435,21

Il est assez remarquable de constater que l'abaissement d'enthalpie libre est de l'ordre de -240,5 kJ par mole d'eau fixée au cours de l'hydroxylation superficielle et que, lors du passage de l'état superficiellement hydroxylé à l'hydrate CAH_{10}, au cours duquel 6 moles d'eau supplémentaires sont fixées, l'abaissement d'enthalpie libre est encore proche de 240 kJ par mole d'eau. Il est exactement de 239,20 kJ.

D'autre part, l'expression d'équilibre de la réaction (7) :

(12) $xy^2.10^{-5,269\sqrt{x}} = 6,58.10^{-6}$

permet de tracer sur le diagramme chaux-alumine-eau la courbe de solubilité de CA_{sh}, conformément à nos hypothèses (Fig. 4).

4) EXTENSION A D'AUTRES ALUMINATES DE CALCIUM :

a) Cas de $C_{12}A_7$. $C_{12}A_7$ est un aluminate de calcium basique dont l'unité de construction peut être représentée par la formule $([Ca(AlO_2)_2]_7, [CaO]_5)$.

L'hydroxylation d'une unité de construction superficielle exprimée en éléments de structure s'écrira :

(13) $(12Ca_{Ca} + 14\underset{AlO_2}{\overset{AlO_2}{}} + 5O_O)_s + 33H_2O_\ell \rightarrow$

$(12Ca_{Ca} + 14\underset{AlO_2}{\overset{Al(OH)_4}{}} + 5OH_O^{\cdot})_s + 5OH^-_{ad}$

Il convient de remarquer que l'hydroxylation superficielle résulte ici de deux réactions différentes : une réaction d'addition de 28 molécules d'eau sur les sites AlO_2^- et une réaction de protonation de 5 sites O^{2-} nécessitant la coupure de 5 molécules d'eau dont les OH^- résiduels, dans la solution, neutralisent les 5 charges effectives positives apparues sur les sites O^{2-} protonés. L'interaction entre ces charges de signes opposés doit conduire à une adsorption des ions OH^- et favoriser le passage en solution de deux ions Ca^{2+} neutralisés par 4 de ces ions OH^- sur 5.

En se basant sur les observations faites par ESCA au cours de la période initiale de l'hydratation de C_3S (12, 13) et de C_2S (14) et sur les interprétations de la forme des courbes Ca/Si en fonction du temps que nous avons données (15), les prévisions suivantes peuvent être avancées :

- Dans le cas de $CaAl_2O_4$ dont l'hydroxylation superficielle résulte d'une simple addition des molécules d'eau, la dissolution devrait être congruente dès le premier contact avec l'eau et la courbe ESCA du rapport Ca/Al en fonction du temps ne devrait pas présenter de minimum initial.
- Dans le cas de $C_{12}A_7$, une libération privilégiée dans la solution de 2 ions Ca^{2+} sur 12 rejoignant 4 sur 5 des ions OH^- résiduels pourrait donner lieu à un léger écart initial à la congruence de la dissolution susceptible de se traduire par un faible minimum de la courbe du rapport Ca/Si en fonction du temps.

b) Cas de C_3A. Il s'agit également d'un aluminate basique dont l'unité de construction peut être représentée par la formule $(Ca[AlO_2]_2, [CaO]_2)$.

L'hydroxylation d'une unité de construction superficielle exprimée en éléments de structure donnera :

(14) $(3Ca_{Ca} + 2\underset{AlO_2}{\overset{AlO_2}{}} + 2O_O)_s + 6H_2O_\ell \rightarrow$

$(3Ca_{Ca} + 2\underset{AlO_2}{\overset{Al(OH)_4}{}} + 2OH_O^{\cdot})_s + 2OH^-_{ad}$

L'hydroxylation superficielle résulte donc aussi d'une réaction d'addition de 4 molécules d'eau et d'une réaction de protonation exigeant la coupure de 2 molécules d'eau. C'est donc ici 1 ion Ca^{2+} sur 3 dont, au premier contact avec l'eau, le passage en solution serait favorisé par l'existence de 2 ions OH^-_{ad}, au lieu de 2 ions Ca^{2+} sur 12 dans le cas de $C_{12}A_7$.

Si comme dans le cas de C_3S et de C_2S, cela se traduit par un écart initial à la dissolution congruente, il est possible que la courbe ESCA du rapport Ca/Al passe, dans les toutes premières secondes du contact avec l'eau, par un minimum beaucoup plus net que dans le cas de $C_{12}A_7$. Par la suite, la

necessité qu'un site sous-jacent O^{2-} soit découvert pour subir à son tour l'hydroxylation peut permettre de prévoir, comme pour C_3S et C_2S (6,15) un retour progressif à la dissolution congruente. A notre connaissance, de tels essais comparatifs n'ont pas été effectués systématiquement dans des conditions rigoureuses. Leurs résultats permettraient d'infirmer ou de confirmer nos considérations théoriques et si le minimum initial existe dans le cas de $C_{12}A_7$ et de C_3A, de se rendre compte, par la profondeur de pic, si seuls les ions calcium susceptibles de neutraliser les OH^-_{ad} passent préférentiellement en solution, ou si les ions calcium accompagnés des hydroxyles formés par protonation des sites O^{2-} du solide le font aussi. Pour $C_{12}A_7$, cela ferait passer de 2 à 5 sur 12 et pour C_3A de 1 à 2 sur 3, le nombre d'ions Ca^{2+} concernés. Des essais ont bien été effectués par ESCA sur C_3A par M.E. Tadros, W.Y. Jackson et J. Skalny (16). Mais ces essais ont été faits, non pas sur des plaquettes frittées comme ultérieurement sur C_3S et βC_2S (12, 13, 14), mais sur une suspension aqueuse agitée dont la composition était déterminée après filtration au bout d'une minute tandis que le résidu solide était examiné par ESCA et spectroscopie Auger. Dans le filtrat, un rapport $x/y \simeq 1{,}9$ était observé (avec $x \simeq 1{,}05.10^{-2}$ mol.kg^{-1}) tandis qu'à la surface du solide, le rapport Ca/Al était égal à l'unité. Ce dernier résultat semblerait suggérer, en considérant la réaction (14), qu'initialement, un seul ion Ca^{2+} sur 3 rejoindrait en solution les $2OH^-_{ad}$, ce qui donnerait, à la surface du solide, un rapport Ca/Al = 1. Mais alors, on ne devrait pratiquement pas trouver d'ions $[Al(OH)_4]^-$ en solution et le temps d'observation devrait être de l'ordre de la seconde et non de la minute. Les auteurs déclarent que la dissolution est incongruente. Il faudrait alors que, par unité de construction, en régime dynamique, 1 ion $[Al(OH)_4]^-$ sur 2 passe en solution accompagné par deux ions Ca^{2+} dont l'un serait neutralisé par les $2OH^-_{ad}$ ainsi que par l'un des deux OH^- produits par protonation et qu'il reste comme résidu solide superficiel :

$$(2V''_{Ca} + Ca_{Ca} + V^{\cdot}_{AlO_2} + Al(OH)_4{}_{AlO_2} + V^{\cdot\cdot}_{O} + OH^{\cdot}_{O})_s$$

c'est-à-dire $(Ca\ Al(OH)_4\ OH)_s$. Il convient de remarquer que de telles unités de construction résiduelles seraient électriquement neutres et devraient se réorganiser en un noyau insoluble d'un hydroaluminate monocalcique basique. Une telle transformation paraît hautement improbable. Dans les travaux que nous avons faits ultérieurement (17), nous avons été amenés à conclure à une dissolution congruente en régime établi, mais nous n'avons pas fait d'analyses complémentaires sur le solide.

5) PASSAGE EN SOLUTION DES UNITES DE CONSTRUCTION SUPERFICIELLES HYDROXYLEES DE $C_{12}A_7$ ET C_3A ET EQUILIBRE HYPOTHETIQUE DE SOLUBILITE :

Dans le cas de l'aluminate monocalcique, le passage en solution, conduisant à un équilibre de solubilité de l'état superficiellement hydroxylé (équation 7) ne pose pas de problème.

Il est facile de voir que l'abaissement de la solubilité calculée de CA_{sh} (équation 7) par rapport à la solubilité théorique de CA anhydre (équation 1), provient de ce que l'enthalpie libre normale est de $-240{,}5$ kJ.mol^{-1} par mole d'eau fixée dans CA_{sh}, tandis que, dans l'équation 1, n'intervient que l'enthalpie libre normale de formation de l'eau liquide libre $\Delta_f G^o_{298} = -236{,}96$ kJ.mol^{-1}. La différence : $-3{,}5$ kJ qui représente l'enthalpie libre normale moyenne de liaison de l'eau dans CA_{sh} est petite, mais elle suffit pour faire passer la solubilité calculée de 0,164 mol.kg^{-1} à $21{,}3.10^{-3}$ mol.kg^{-1}.

Avec $C_{12}A_7$ et C_3A apparaît une difficulté que l'on retrouve encore aggravée dans le cas de C_3S et de C_2S (6). Cette difficulté est due à l'hydroxylation partielle par protonation (avec C_3S et C_2S elle est totale) qui produit une charge électrique positive à la surface du solide équilibrant la charge des OH^- provenant de la coupure des molécules d'eau. De l'attraction électrostatique, doit résulter une association entre ces ions OH^- et les charges superficielles du solide, mais, en l'absence de données sur la force de la liaison ainsi établie, nous sommes conscients qu'il est quelque peu aventureux de considérer $C_{12}A_{7sh}$ et C_3A_{sh} comme des entités superficielles aussi bien définies que CA_{sh}. En particulier, comme dans le cas de C_3S et de C_2S, nous avons postulé au paragraphe 4 le passage privilégié en solution d'une partie des ions Ca^{2+} compensant ces OH^-_{ad} lors du premier contact avec la phase liquide et par la suite, la régulation de la dissolution congruente par la fréquence du transfert en solution des ions hydroxylés et des cations qui les accompagnent. Cette fréquence impose celle de l'hydroxylation des sites sous-jacents découverts. Dans ces conditions, peut-il s'instaurer un équilibre de solubilité de $C_{12}A_{7sh}$ et de C_3A_{sh} d'après les équations suivantes exprimées en éléments de structure ?

Pour $C_{12}A_7$ (voir équation 13) :

$$(15)\quad (12Ca_{Ca} + 14Al(OH)_4{}_{AlO_2} + 5\ OH^{\cdot}_{O})_s + 5\ OH^-_{ad} \rightleftarrows 12Ca^{2+}_{aq} + 14[Al(OH)_4]^-_{aq} + 10\ OH^-_{aq} + (12V''_{Ca} + 14V^{\cdot}_{AlO_2} + 5V^{\cdot\cdot}_{O})_s$$

Pour C_3A : (voir équation 14) :

$$(16)\quad (3Ca_{Ca} + 2Al(OH)_4{}_{AlO_2} + 2\ OH^{\cdot}_{O})_s + 2\ OH^-_{ad} \rightleftarrows 3Ca^{2+}_{aq} + 2[Al(OH)_4]^-_{aq} + 4\ OH^-_{aq} + (3V''_{Ca} + 2V^{\cdot}_{AlO_2} + 2V^{\cdot\cdot}_{O})_s$$

On a fait figurer au second membre de ces équations l'unité de construction vide, électriquement neutre, pour rappeler que c'est le dégagement des unités de construction superficielles qui permet l'hydroxylation des sites oxygénés sous-jacents.

Il convient d'abord de remarquer, dans l'hypothèse d'une dissolution congruente dans l'eau pure que les seconds membres de ces équations équivalent :
pour $C_{12}A_7$: à la dissolution simultanée de 7 CA_{sh} et de 5 $Ca(OH)_2$
pour C_3A : à la dissolution simultanée de 1 CA_{sh} et de 2 $Ca(OH)_2$.
C'est-à-dire que le point M figuratif de la composition sur le diagramme chaux-alumine-eau se déplaçant sur une droite de rapport C/A = 12/7 pour $C_{12}A_7$ et sur une droite de rapport C/A = 3 pour C_3A, pénétrerait rapidement dans des domaines sursaturés par rapport à différents hydrates (Fig. 4) et rencontrerait notamment la courbe de supersolubilité de C_2AH_8 (10, 11). Il en résulterait la précipitation immédiate de cet hydrate et à terme, en l'absence de carbonatation, celle des hydrates les plus insolubles : CAH_{10} ou le mélange CAH_{10} et C_3AH_6 dans le cas de $C_{12}A_7$; C_3AH_6 dans le cas de C_3A. Dans ce dernier cas, la pénétration plus profonde du point figuratif sur la droite C/A = 3 permettrait de prévoir également la précipitation de C_4AH_{13}.

Cela explique l'absence de période d'induction lors de l'hydratation de $C_{12}A_7$ et de C_3A et justifie l'impossibilité de déterminer la solubilité de leurs états superficiellement hydroxylés.

Une telle solubilité ne peut donc être qu'hypothétique et en l'absence de données, nous allons nous contenter de calculer quel serait l'abaissement moyen d'enthalpie libre normale par mole d'eau fixée nécessaire pour amener la solubilité de l'état superficiellement hydroxylé à une valeur arbitrairement choisie, par exemple, $x = 25.10^{-3}$ mol.kg^{-1} dans les conditions de congruence de la dissolution. Celles-ci correspondent à $y = 7/6$ de x avec $C_{12}A_{7sh}$ et $y = 2x/3$ avec C_3A_{sh}.

En utilisant l'extension de Davies de la formule de Debye et compte tenu de la relation d'électroneutralité (2), les constantes d'équilibre hypothétiques auraient comme valeurs :

$$(19)\quad K_{C_{12}A_{7sh}} = x^{12}y^{14}(2x-y)^{10}10^{-36,50\left(\frac{\sqrt{3x}}{1+\sqrt{3x}} - 0,6x\right)} = 1,488.10^{-65}$$

$$(20)\quad K_{C_3A_{sh}} = x^3y^2(2x-y)^4 10^{-9,126\left(\frac{\sqrt{3x}}{1+\sqrt{3x}} - 0,6x\right)} = 8,012.10^{-17}$$

A partir des données du tableau I, on peut calculer les $\Delta_rG^o_{298}$ des équations (15) et (16) qui sont respectivement : $\Delta_rG^o_{298}(15) = 369,85$ kJ et $\Delta_rG^o_{298}(16) = 91,83$ kJ. On en déduit les $\Delta_fG^o_{298}$ des états superficiellement hydroxylés, soit : $\Delta_fG^o_{298}(C_{12}A_7)_{sh} = -26676,87$ kJ.mol^{-1} et $\Delta_fG^o_{298}(C_3A)_{sh} = -4964,42$ kJ.mol^{-1}.

Comparées à l'enthalpie libre normale de formation (tableau I) de C_3A (- 3405 kJ.mol^{-1}) tirée d'une publication de H.N. Stein (7) et à celle de $C_{12}A_7$ (- 18393,84 kJ.mol^{-1}) tirée d'une publication de O.P. Mchedlov-Petrosyan (18) , les abaissements observés correspondent à une enthalpie libre normale moyenne par mole d'eau liée de - 251,03 kJ dans le cas de $C_{12}A_{7sh}$ et de - 259,90 kJ dans le cas de C_3A.

Il ne faut pas oublier que les valeurs des solubilités ont été arbitrairement choisies afin d'être d'un ordre de grandeur comparable à la solubilité de CA_{sh}. Ainsi, les enthalpies libres moyennes normales de liaison par rapport à l'eau libre ($\Delta_fG^o_{298} = -236,96$ kJ.mol^{-1}) prendraient respectivement les valeurs suivantes : - 14 kJ par mole d'eau dans le cas de $C_{12}A_{7sh}$ et de - 23 kJ dans le cas de C_3A_{sh}. Ce sont des valeurs nettement supérieures à celles calculées pour CA_{sh} : - 3,5 kJ par mole d'eau fixée par simple addition sur les ions AlO_2^- superficiels.

En même temps que la courbe de solubilité de CA_{sh} tracée à partir de l'équation :

$$(17)\quad xy^2.10^{-3,042\left(\frac{\sqrt{3x}}{1+\sqrt{3x}} - 0,6x\right)} = 1,029.10^{-5}$$

dont la constante correspond à une solubilité congruente de $x = 21,3.10^{-3}$ mol.kg^{-1}, on a porté sur le diagramme de la Fig. 4 les courbes de solubilité hypothétiques de $C_{12}A_{7sh}$ et de C_3A_{sh}.

6) CONCLUSION :

La réalité du processus d'hydroxylation superficielle est particulièrement bien établie, par la possibilité exceptionnelle qu'offre l'aluminate monocalcique CA d'avoir accès à des données expérimentales sur la solubilité de son état hydroxylé CA_{sh}. L'existence de cet équilibre de solubilité est confirmée par le calcul, car l'obtention d'une enthalpie libre normale par mole d'eau liée supérieure de quelques kilojoules à l'enthalpie libre normale molaire de formation de l'eau ne peut être fortuite. La longue durée de vie de la solution obtenue, due, dans notre hypothèse au fait que la courbe de solubilité de CA_{sh} (Fig. 4) n'a pas, à la température considérée, de courbes de supersolubilité d'hydrates située au-dessous d'elle, (sauf à son tout début, celle du gel d'alumine), la différencie des courbes de solubilité des autres aluminates $C_{12}A_{7sh}$ et C_3A_{sh} qui, bien qu'hypothétiques sont, selon toute vraisemblance, situées au-delà de la courbe de supersolubilité de C_2AH_8. La précipitation immédiate de cet hydrate qui en résulte, voire celle de C_4AH_{13} dans le cas de C_3A et à terme celle des hydrates les plus insolubles, CAH_{10} et C_3AH_6, en l'absence de carbonatation, empêche irrémédiablement l'accès à des mesures sur la solubilité des états hydroxylés de ces aluminates basiques.

REFERENCES :

(1) H. le Chatelier, Recherches expérimentales sur la constitution des mortiers hydrauliques. Thèse, Paris (1887).
(2) M. Hassan, Effet d'une action dispersive continue au cours de l'hydratation des pâtes de ciment. Thèse Doctorat d'Etat (1983), Paris VI.
(3) G. Bellina, M. Hassan, P. Longuet, Ciments, Bétons, Plâtres, Chaux, n° 755, 4 (1985) pp. 245-249.
(4) P. Barret, Etude du mécanisme de la prise des ciments alumineux (t I et II). Rapport privé Sté Lafarge.
(5) P. Barret, D. Ménétrier et D. Bertrandie, Cem. and Concr. Res., 4 (1974) pp. 545-556.
(6) P. Barret, Hydration mechanism of calcium silicates (C_3S, C_2S) cement compounds, through the general concepts of the reactivity of solids. 8th International Congress on the Chemistry of Cement. Rio-de-Janeiro, Brésil (1986).
(7) H.N. Stein, Cem. and Concr. Res., 2 (1972) pp. 167-177.
(8) P. Barret et Ph. Dufour, C.R. Acad. Sc. Paris, 286 (1978) série C, pp. 569-571.
(9) R.A. Kröger, The Chemistry of imperfect crystals, North-Holland Publishing Company (1964) p. 208.
(10) D. Bertrandie, Contribution à l'étude cinétique de la formation des hydrates dans les solutions aqueuses obtenues à partir des ciments alumineux. Thèse de l'Université de Dijon (1977).
(11) P. Barret, D. Bertrandie, Minimum instability curve in a metastable solution of CA, Proceedings of the 7th International Congress on the Chemistry of Cement, Paris (1980) V-175.
(12) D. Ménétrier, I. Jawed, T.S. Sun, J. Skalny, Cem. and Concr. Res., 9 (1979) pp. 473-482.
(13) J.H. Thomassin, M. Regourd, P. Baillif, C.R. Acad. Sc. Paris, série C, 288 (1979) p. 93 et 290 (1980) p. 1.
(14) D. Ménétrier, I. Jawed, T.S. Sun and J. Skalny, Cem. and Concr. Res., 10 (1980) pp. 425-432.
(15) P. Barret, D. Ménétrier and D. Bertrandie, Cem. and Concr. Res., 13 (1983) pp. 728-738.
(16) M.E. Tadros, W.Y. Jackson and J. Skalny, Study of the dissolution and electrokinetic behavior of tricalcium aluminate, Proc. Coll. Interf. Sci. Conf. Puerto Rico, June 1976, vol 4, Acad. Press. N.Y. (1976) pp. 211-223.
(17) P. Barret et D. Bertrandie, Hydration of C_3A in lime water. Proceedings of the 7th International Symposium on Cement Chemistry, Paris (1980).
(18) O.P. Mchedlov-Petrosyan, Thermodynamics and Thermochemistry of Cement. Proceedings of the VIth International Congress on the Chemistry of Cement, Moscou (1974).

P. BARRET

Hydration mechanism of calcium silicates (C_3S, C_2S) cement compounds, through the general concepts of the reactivity of solids.

2.1

Mecanisme d'hydratation des silicates de calcium (C_3S, C_2S) constituants du ciment, vu à travers les concepts généraux de la réactivité des solides.

Dans une récente publication (9), H.F.W. Taylor, tout en admettant la validité des concepts généraux que nous avons formulés (1, 2) sur le mécanisme d'hydratation de C_3S et de C_2S, suggère que la formation de C-S-H à partir des ions libérés dans la phase liquide par ces solides superficiellement hydroxylés (passage par la solution) ne s'applique qu'à la période initiale de l'hydratation : celle qui donne naissance au "C-S-H extérieur". Il suppose qu'en pâte, après les 12 premières heures, alors que la cinétique est contrôlée par la diffusion, c'est un mécanisme topochimique qui donne naissance au "C-S-H intérieur". Ce mécanisme prend toujours en compte la protonation des ions O^{2-} et SiO_4^{4-}, comme nous l'avons suggéré, mais il revient à supposer la constitution d'une couche protectrice, formée de C-S-H et de C-H qui empêche un contact direct entre l'eau moléculaire et le silicate non encore hydraté.

Nous avons toujours postulé que les mécanismes d'hydratation par l'intermédiaire de la solution et topochimiques ne s'excluaient pas mutuellement, mais qu'ils étaient à considérer comme mettant en jeu des réactions concurrentes (20), la prédominance de l'une ou de l'autre dépendant des conditions et des contraintes du milieu.

Nous nous proposons de montrer que les étapes élémentaires interfaciales de l'hydratation que nous avons formulées à partir de concepts généraux de la réactivité des solides, se conservent dans les différentes variantes de mécanismes soit par l'intermédiaire de la solution, soit topochimiques et que, non seulement elles s'adaptent au cas limite d'une couche totalement protectrice envisagé par H.F.W. Taylor, mais qu'en outre, elles permettent de prévoir un cas de mécanisme topochimique intermédiaire, sans couche protectrice.

Ces étapes sont écrites sous forme d'équations quasichimiques mettant en jeu les ions et les éléments de structure de la surface du silicate de calcium représentés dans la notation de Kröger et Vink (16). Elles sont illustrées par des schémas et justifiées à partir de faits expérimentaux et au moyen d'arguments théoriques.

Ces réflexions peuvent ainsi servir de base à un modèle conceptuel reflétant les différents stades du mécanisme d'hydratation des silicates de calcium constituants des ciments et rendant compte d'un grand nombre d'observations expérimentales.

Em publicação recente (9), H. F. W. Taylor admite a validade dos conceitos gerais que formulamos (1, 2) sobre o mecanismo de hidratação do C_3S e do C_3A, mas sugere que a formação de C-S-H a partir dos íons liberados na fase líquida por estes sólidos parcialmente hidroxilados (passagem pela solução) aplica-se apenas ao período inicial da hidratação: aquele que dá origem ao "C-S-H externo". Ele supõe que na pasta, depois das 12 primeiras horas, assim que a cinética é controlada pela difusão, é um mecanismo topoquímico que dá origem ao "C-S-H interno". Este mecanismo leva sempre em consideração a protonação dos íons O^{2-} e SiO_4^{4-}, como havíamos sugerido, mas ele volta a supor a constituição de uma camada protetora, formada de C-S-H e de C-H, que impede um contato direto entre a água molecular e o silicato ainda não hidratado.

Sempre postulamos que os mecanismos de hidratação, quer pela intermediação da solução, quer os topoquímicos, não se excluem mutuamente, mas que eles deviam ser considerados como colocando em jogo reações concorrentes (20), dependendo das condições e das limitações do meio a predominância de uma sobre a outra.

Propomo-nos mostrar que as etapas elementares interfaciais da hidratação, que formulamos a partir de conceitos gerais sobre a reatividade dos sólidos, se mantêm nas diferentes variantes de mecanismos, seja pela intermediária da solução, sejam topoquímicas, e que elas não só se adaptam ao caso limite de uma camada totalmente protetora admitida por H. F. W. Taylor, mas além disso elas permitem prever-se um caso de mecanismo topoquímico intermediário, sem camada protetora.

Estas etapas são apresentadas sob a forma de equações quasequímicas, colocando em jogo os íons e os elementos de estrutura da superfície do silicato de cálcio, representadas na notação de Kröger e Vink (16). Elas são ilustradas por esquemas e justificadas a partir de fatos experimentais e por meio de argumentos teóricos.

Assim, estas reflexões podem servir de base para um modelo conceitual, refletindo os diferentes estágios da hidratação dos silicatos de cálcio que constituem os cimentos e prestando conta de grande número de observações experimentais.

1) INTRODUCTION :

Dès 1977, nous avons publié (1) les bases fondamentales du mécanisme d'hydroxylation superficielle que nous avons proposé comme étape essentielle de l'hydratation du silicate tricalcique C_3S et que nous avons étendu par la suite à l'hydratation du silicate dicalcique βC_2S (2). Nous avions souligné que cette étape devait être impliquée aussi bien dans un mécanisme d'hydratation par l'intermédiaire de la solution que dans un mécanisme d'hydratation topochimique.

Par la suite nous avons approfondi notre modèle de mécanisme pour montrer comment il était capable de rendre compte d'un processus transitoire de dissolution non congruente (2) lors du contact initial avec l'eau de C_3S ou de C_2S et de l'établissement progressif de la dissolution congruente dans la période suivante.

Nous avons pu ainsi expliquer quantitativement (2) le passage par un minimum du rapport Ca/Si déterminé par ESCA en fonction du temps dans la période initiale de l'hydratation de C_3S et de βC_2S (3, 4, 5, 6, 7) et sa remontée progressive correspondant à l'établissement de la dissolution congruente.

Dans une récente étude collective du Comité 68-MMH de la RILEM, H.F.W. Taylor (8) a donné une représentation schématique (Fig. 1) de notre mécanisme de dissolution de C_3S, basé sur une séquence répétitive de 3 étapes A, B, C.

Ultérieurement, H.F.W. Taylor (9), se basant sur l'existence d'un C-S-H extérieur et d'un C-S-H intérieur, a formulé une hypothèse suivant laquelle le produit extérieur se formerait partiellement ou totalement par dissolution et précipitation, tandis que la formation du produit intérieur serait topochimique.

Mais, d'après cet auteur, la très basse concentration en ions silicates dans la solution laisserait cependant supposer que la migration du silicium a lieu partiellement et même principalement, par le processus dit de "filled-empty tetrahedron migration" à travers le C-S-H extérieur. Ce processus illustré par la Fig. 2, consisterait en le saut d'un atome de silicium du centre d'un tétraèdre dans une lacune de silicium existant au centre du tétraèdre voisin, les deux tétraèdres étant accolés par une face qui serait traversée par l'atome de silicium migrant. Ce processus a été originellement proposé par Dent Glasser (10).

D'après H.F.W. Taylor, la cinétique d'hydratation du ciment, après les deuze premières heures, est généralement contrôlée par la diffusion. La migration du Si pourrait bien être l'étape limitant la vitesse. Cet auteur suggère (Fig. 3) que les molécules d'eau fournissent des protons qui migrent d'oxygène en oxygène à travers la couche de C-S-H intérieur jusqu'à ce qu'ils atteignent le C_3S inattaqué. Ils se fixent sur les ions O^{2-} et SiO_4^{4-} de C_3S qui laisse alors échapper une partie de son calcium et de son silicium. H.F.W. Taylor suppose que cette étape du processus se produit conformément au mécanisme que nous avons décrit (2), mais que la totalité des Ca, des Si et probablement des O n'est pas relâchée. Il considère que, dans la zone interfaciale, d'ailleurs non détectée expérimentalement et d'épaisseur inconnue, interviennent de substantiels mouvements locaux d'atomes, contribuant à la formation de C-S-H. D'après son hypothèse, les atomes de Ca et de Si migrent vers l'extérieur à travers le produit intérieur, car, le C-S-H possèdant une structure en couches, les ions Ca^{2+} peuvent facilement emprunter les espaces entre les couches. Les atomes de Si peuvent se mouvoir par le processus de "filled-empty tetrahedron migration" décrit ci-dessus. Mais l'auteur insiste sur le fait que le mécanisme qu'il suggère ne concerne pas la période initiale de la réaction. Dans le ciment, l'existence, durant les premiers jours, d'un intervalle entre les grains anhydres et le C-S-H conformément aux observations de Pratt et Ghose (11) et de Scrivener et Pratt (12), laisse supposer qu'au cours de cette période, la réaction procède par dissolution et précipitation. De tels intervalles n'ont pas été observés avec C_3S pur et il semblerait que dans ce cas, le mécanisme décrit ci-dessus puisse intervenir plus tôt. En revanche, dans le cas d'un plus grand rapport eau/solide, par exemple dans les suspensions agitées, l'auteur écrit que les résultats de Barret et al. (2) indiquent que, au moins dans le cas des silicates de calcium purs, le mécanisme par l'intermédiaire de la solution est prédominant, probablement à tous les stades.

Nous nous proposons de montrer que *les étapes*

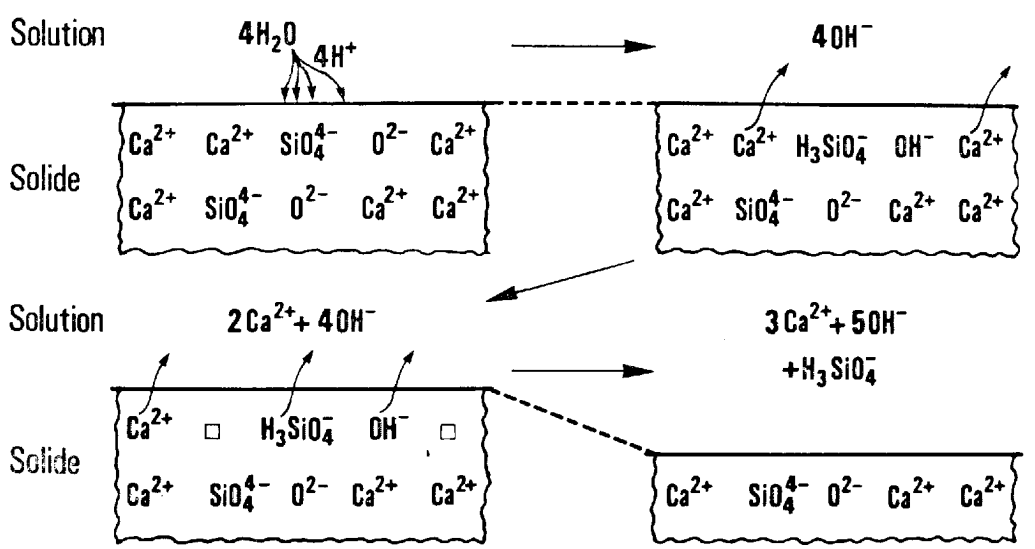

Fig. 1 : Mécanisme de dissolution de C_3S basé sur une séquence répétitive de trois étapes A, B et C : représentation schématique par H.F.W. Taylor (8) du modèle de P. Barret et al. (1, 2).

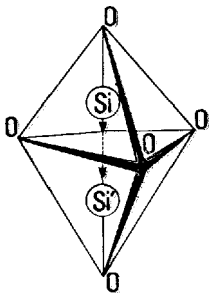

Fig. 2 : Migration d'un atome de Si de tétraèdre en tétraèdres.

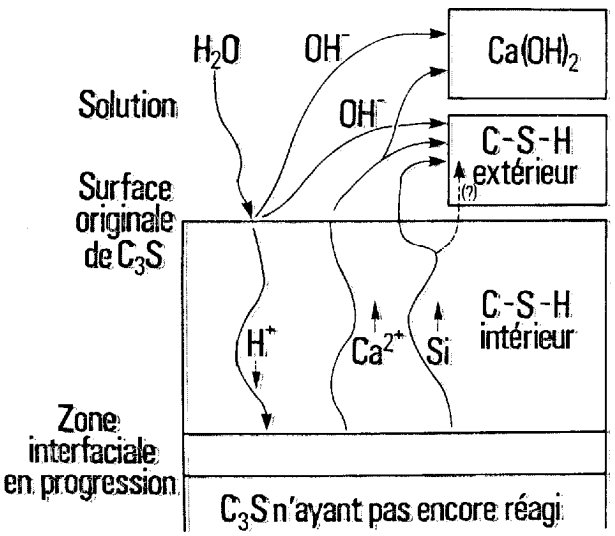

Fig. 3 : Représentation schématique suggérée par H.F.W. Taylor (9) pour la réaction du silicate tricalcique avec l'eau dans une pâte de ciment.

élémentaires interfaciales de l'hydratation, que nous avons formulées à partir des concepts généraux de la réactivité des solides se conservent dans les différentes variantes de mécanismes envisageables, soit par l'intermédiaire de la solution, soit topochimiques. Nous ferons valoir en outre que ces étapes élémentaires sont non seulement susceptibles de s'adapter au *cas limite d'une couche totalement protectrice* qui est en fin de compte celui envisagé par H.F.W. Taylor, mais qu'en outre, elles permettent de *prévoir un cas de mécanisme topochimique* aboutissant à la croissance de *germes individuels*. L'existence d'une couche non protectrice formée de germes individuels en cours de croissance peut être observée dans de nombreuses réactions de l'état solide. Une telle couche constitue parfois un stade intermédiaire (13) aboutissant à une couche protectrice par recouvrement latéral des germes.

2) PREMIER CONTACT AVEC L'EAU ET POURSUITE DE L'HYDRATATION.

2.1. Départ d'une partie des ions Ca^{2+} :

Avec C_3S et C_2S, l'hydroxylation superficielle résulte non pas d'une simple addition des molécules d'eau sur les sites superficiels oxygénés, comme dans le cas de $CaAl_2O_4$ (14, 15), *mais d'une protonation qui laisse dans la phase liquide des ions OH^- provenant de la coupure des molécules d'eau.*

Exprimée dans le système des unités de construction (16) les réactions s'écrivent :

- Avec C_3S :

$$(Ca_3SiO_5)_s + 4H_2O_\ell \rightarrow (Ca_3OH\ H_3SiO_4)_s^{\cdot\cdot\cdot\cdot} + 4OH^-_{aq}$$

- Avec C_2S :

$$(Ca_2SiO_4)_s + 3H_2O_\ell \rightarrow (Ca_2H_3SiO_4)_s^{\cdot\cdot\cdot} + 3OH^-_{aq}$$

La traduction de ces réactions en éléments de structure donne : [pour les symboles, voir notre 2ème papier (15)]

- Avec C_3S :

$$(3Ca_{Ca} + O_O + SiO_4^{SiO_4})_s + 3H_2O_\ell \rightarrow (3Ca_{Ca} + OH_O^{\cdot} + H_3SiO_4^{SiO_4})_s + 4OH^-_{aq}$$

- Et avec C_2S :

$$(2Ca_{Ca} + SiO_4^{SiO_4})_s + 3H_2O_\ell \rightarrow (2Ca_{Ca} + H_3SiO_4^{\cdot\cdot}{}^{SiO_4})_s + 3OH^-_{aq}$$

La représentation schématique de notre mécanisme (Fig. 1), donnée par H.F.W. Taylor comme une séquence répétitive de trois étapes A, B, C n'est en fait valable que pour le premier contact de C_3S ou de C_2S avec l'eau.

En effet, tous les sites oxygénés superficiels ont pu s'hydroxyler à ce premier contact, à moins qu'une partie d'entre eux ne l'ait déjà été au contact de l'air humide ambiant. En raison de la forte interaction électrostatique devant exister entre les charges effectives superficielles du solide et les ions OH^-_{aq} libérés dans l'eau par la protonation des sites oxygénés, on peut écrire OH^-_{ad} (adsorbé) au lieu de OH^-_{aq}, et lors du premier contact avec l'eau, *nous admettrons un passage massif en solution* des entités superficielles constituées par $[2(Ca_{Ca})_s + 4OH^-_{ad}]$ dans le cas de C_3S ou $[(Ca_{Ca})_s + 2OH^-_{ad}]$ dans le cas de C_2S suivant la réaction :

$$(Ca_{Ca})_s + 2OH^-_{ad} \rightleftarrows (V''_{Ca})_s + Ca^{2+}_{aq} + 2OH^-_{aq}$$

C'est ce passage massif initial d'hydroxyde de calcium dans la solution qui dans notre interprétation (2) permet d'expliquer la brusque chute du rapport Ca/Si superficiel observé par ESCA dans les toutes premières secondes du contact avec l'eau aussi bien avec C_3S qu'avec C_2S (4, 5, 6) et qui laisse des unités de construction partiellement lacunaires et électriquement neutres telles que :

$(2V''_{Ca} + Ca_{Ca} + OH_O^{\cdot} + H_3SiO_4^{\cdot\cdot}{}^{SiO_4})_s$ dans le cas de C_3S

et $(V''_{Ca} + Ca_{Ca} + H_3SiO_4^{\cdot\cdot}{}^{SiO_4})_s + OH^-_{ad}$ dans le cas de C_2S

Mais par la suite, un tel processus massif ne peut pas se reproduire car il n'existe plus d'ions OH^-_{aq} excédentaires dans la solution au voisinage immédiat de l'interface. *Le renouvellement des ions*

OH^-_{aq} se fera alors individuellement à la fréquence avec laquelle de nouveaux sites oxygénés seront découverts grâce au départ des anions précédemment hydroxylés, par la mise en œuvre de l'un des quatre types de transfert que nous allons examiner.

La protonation des sites découverts est supposée instantanée *tant qu'il existe un contact direct avec l'eau*. Le dégagement des sites hydroxylés sera donc l'étape déterminant la vitesse.

2.2. Transformation intermédiaire des unités de construction partiellement lacunaires :

Aux valeurs du pH comprises entre 12,6 et 12,9 où les ions $H_2SiO^{2-}_{4aq}$ deviennent majoritaires par rapport aux ions $H_3SiO^-_{4aq}$, on peut imaginer une organisation interne de chaque unité de construction superficielle suivant les réactions :

$$(2V''_{Ca} + Ca_{Ca} + OH^\cdot_O + H_3SiO^{\cdot\cdot}_{4\ SiO_4})_s \rightleftarrows (2V''_{Ca} + Ca_{Ca} + V^{\cdot\cdot}_O + H_2SiO^{\cdot}_{4\ SiO_4})_s + H_2O_\ell$$

dans le cas de C_3S et :

$$(V''_{Ca} + Ca_{Ca} + H_3SiO^{\cdot\cdot\cdot}_{4\ SiO_4})_s + OH^-_{ad} \rightleftarrows (V''_{Ca} + Ca_{Ca} + H_2SiO^{\cdot}_{4\ SiO_4}) + H_2O_\ell$$

dans le cas de C_2S.

Mais, alors que dans C_3S et C_2S les ions silicates sont sous forme monomère, il a été établi que dans C-S-H, même aux valeurs du rapport Ca/Si proches de 1, les ions silicates étaient dimères à 96 % (22, 23). On peut donc se demander si ces ions dimères ne se forment que lors de la nucléation et la croissance du C-S-H où s'ils préexistent en totalité ou en partie. Leur préexistence peut être expliquée par la transformation intermédiaire de deux unités de construction voisines suivant les schémas réactionnels :

Pour C_3S :

$$2(2V''_{Ca} + Ca_{Ca} + OH^\cdot_O + H_3SiO^{\cdot\cdot}_{4\ SiO_4})_s \rightleftarrows H_2O_\ell + (2V''_{Ca} + Ca_{Ca} + OH^\cdot_O + V^{\cdot\cdot\cdot\cdot}_{SiO_4})_s + (2V''_{Ca} + Ca_{Ca} + OH^\cdot_O + H_4Si_2O^{\cdot\cdot}_{7\ SiO_4})_s$$

Pour C_2S :

$$2(V''_{Ca} + Ca_{Ca} + H_3SiO^{\cdot\cdot\cdot}_{4\ SiO_4})_s + 2OH^-_{ad} \rightleftarrows H_2O_\ell + (V''_{Ca} + Ca_{Ca} + V^{\cdot\cdot\cdot\cdot}_{SiO_4}) + 2OH^-_{ad} + (V''_{Ca} + Ca_{Ca} + H_4Si_2O^{\cdot\cdot}_{7\ SiO_4})$$

3) CONSERVATION DES ETAPES ELEMENTAIRES INTERFACIALES DE L'HYDRATATION DANS LES DIFFERENTES VARIANTES DE MECANISMES :

3.1. Dégagement des sites superficiels hydroxylés par transfert en solution :

C'est l'étape C de la figure 1 grâce à laquelle les unités de construction superficielles qui ont déjà perdu une partie de leurs ions Ca^{2+} (équation 2) achèvent de se vider et découvrent les unités de construction non encore hydroxylées de la couche sous-jacente. Suivant le processus général décrit dans le paragraphe précédent, elles le font, non pas simultanément, mais à des dates échelonnées au hasard dans le temps. En conséquence, les sites sous-jacents sont réhydroxylés successivement et non plus simultanément ce qui entraîne l'installation progressive de la dissolution congruente se manifestant sur les courbes ESCA par la remontée vers la valeur du rapport Ca/Si = 3, après le minimum initial (4, 5, 6).

Il existe d'abord une période de dissolution pure qui se manifeste dans les suspensions aqueuses agitées de C_3S de rapport liquide/solide, ℓ/s = 5, 10, 20 ... La limite de cette période est marquée (Fig. 4) par le maximum de la courbe de la silice et simultanément par le début du palier que présente la courbe de la chaux (21). Ce palier est dû à un état

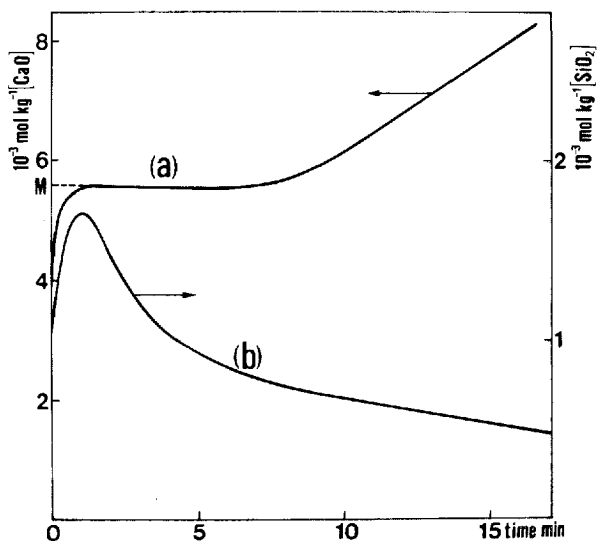

Fig. 4 : Période de dissolution pure et palier intermédiaire de la courbe de concentration des ions calcium entraînés dans un précipité de C-S-H avec les ions silicates accumulés en solution sursaturée de concentration maximale. a) Ca^{2+}, b) $H_3SiO^-_4$.

stationnaire correspondant à la précipitation sous forme de C-S-H des ions silicates qui se sont accumulés dans la solution en même temps que les ions calcium avec lesquels ils ont constitué une solution sursaturée par rapport au C-S-H.

Le domaine de sursaturation est délimité supérieurement, non par la courbe de solubilité de C_3S_{sh} (comme ce serait le cas avec CA_{sh}), mais dans notre interprétation (19, 20) par *la courbe de supersolubilité de C-S-H en fonction de la composition de la solution à température constante.*

Lorsque, par accroissement des concentrations en ions silicates et en ions calcium, cette courbe est atteinte, la précipitation de C-S-H a lieu sans délai et la solution est le siège de deux réactions consécutives:

La dissolution de C_3S_{sh} suivant l'équation :

1) $$2(Ca_3OHH_3SiO_4)^{\cdot\cdot\cdot\cdot}_s + 8OH^-_{ad} \rightleftarrows 6Ca^{2+}_{aq} + 10\ OH^-_{aq} + 2H_3SiO^-_{4aq}$$

Et la précipitation de C-S-H (supposé ici de rapport C/S = 1) suivant l'équation :

2) $$2Ca^{2+} + 2OH^- + 2H_3SiO^-_4 \rightleftarrows Ca_2(OH)_2H_4Si_2O_7 + H_2O_\ell$$

En désignant par ξ_1 et ξ_2 les degrés d'avancement de ces réactions et par $n(Ca^{2+})$ le nombre molaire d'ions Ca^{2+}, les vitesses de variation du nombre d'ions Ca^{2+} du fait de chacune de ces réactions serait :

$$\frac{d_1 n(Ca^{2+})}{dt} = 6\,\frac{d\xi_1}{dt} \quad \text{et} \quad \frac{d_2 n(Ca^{2+})}{dt} = -2\,\frac{d\xi_2}{dt}$$

La vitesse de variation globale serait alors :

$$\frac{dn(Ca^{2+})}{dt} = \frac{d_1 n(Ca^{2+})}{dt} + \frac{d_2 n(Ca^{2+})}{dt} = 6v_1 - 2v_2$$

$v_1 = \frac{d\xi_1}{dt}$ et $v_2 = \frac{d\xi_2}{dt}$ sont respectivement les vitesses des réactions 1) et 2). Le palier dans la courbe de la chaux correspond à la chute de concentration de la silice après le maximum, dont la vitesse est telle que, fortuitement $\frac{dn(Ca^{2+})}{dt} \simeq 0$, c'est-à-dire $v_2 \simeq 3v_1$, pendant cette courte période (dépendant du rapport liquide/solide). Puis, par la suite, c'est la concentration des ions silicates qui varie peu, restant dans un état quasi stationnaire. Par un calcul semblable au précédent, on tire de $\frac{dn(H_3SiO_4^-)}{dt} \sim 0$ $\quad v_1 \sim v_2$.

Après le palier, la concentration en chaux va donc de nouveau augmenter jusqu'à un maximum ($\sim 36.10^{-3}$ mol.kg^{-1}) correspondant, dans notre interprétation (2!) au point de supersolubilité de l'hydroxyde de calcium (portlandite) à la température considérée. Lorsque ce point est atteint, une troisième réaction simultanée, consécutive à la réaction 1, parallèle à la réaction 2, débute :

3) $\quad Ca^{2+}_{aq} + 2OH^-_{aq} \rightarrow Ca(OH)_2$

Il est utile d'insister sur la simulitude des concepts (courbe ou point de supersolubilité) qui permettent d'interpréter ici le déclenchement, d'abord de la précipitation du C-S-H, ensuite, de celle de l'hydroxyde de calcium.

Remarquons également, que dans notre conception, il convient de faire *la distinction entre le processus d'hydratation de C_3S ou de C_2S et le processus de formation du C-S-H et de l'hydroxyde de calcium*. En effet, le processus d'hydratation est le résultat de *l'étape d'hydroxylation superficielle* qui apporte, par séquences répétitives, tous les H^+ et les OH^- aux phases anhydres en interaction directe avec les molécules d'eau (certains diraient "par un processus topochimique").

La formation du C-S-H et celle de l'hydroxyde de calcium *correspondent à des stades ultérieurs qui ne changent pratiquement pas, ou assez peu, le nombre des molécules d'eau d'hydratation*, car ils résultent de la combinaison des ions déjà hydroxylés (par protonation, plus le reliquat d'ions OH^-_{aq}).

Dans un processus dit "par l'intermédiaire de la solution" le transfert des ions superficiels hydroxylés et des cations qui les accompagnent a lieu dans la phase liquide au voisinage immédiat de l'interface et la formation du C-S-H, ainsi que celle de l'hydroxyde de calcium résultent de processus de précipitation.

3.2. Dégagement des sites superficiels hydroxylés par transfert interfacial direct dans une phase hydratée :

Hormis le cas de *l'interface solide-solution* ci-dessus envisagé, les exemples que l'on rencontre habituellement en réactivité des solides conduisent à considérer *deux types d'interfaces solide-solide* que nous appelerons *"interface ouverte"* et *"interface fermée"*. Ces cas sont illustrés par les schémas a) et b) des figures 5 et 6. Ces figures se rapportent respectivement à la formation d'un C-S-H de rapport Ca/Si = 1 et à celle d'un C-S-H de rapport Ca/Si = 2.

Cas a : Le cas a) est celui de la croissance individuelle d'un germe de C-S-H en relation d'épitaxie avec le substrat. *L'interface est dite ouverte* parce que la famille des plans cristallographiques qui délimitent l'interface C_3S/C-S-H vient couper la surface du cristallite. Dans cette hypothèse, les espèces chimiques peuvent alors être échangées directement

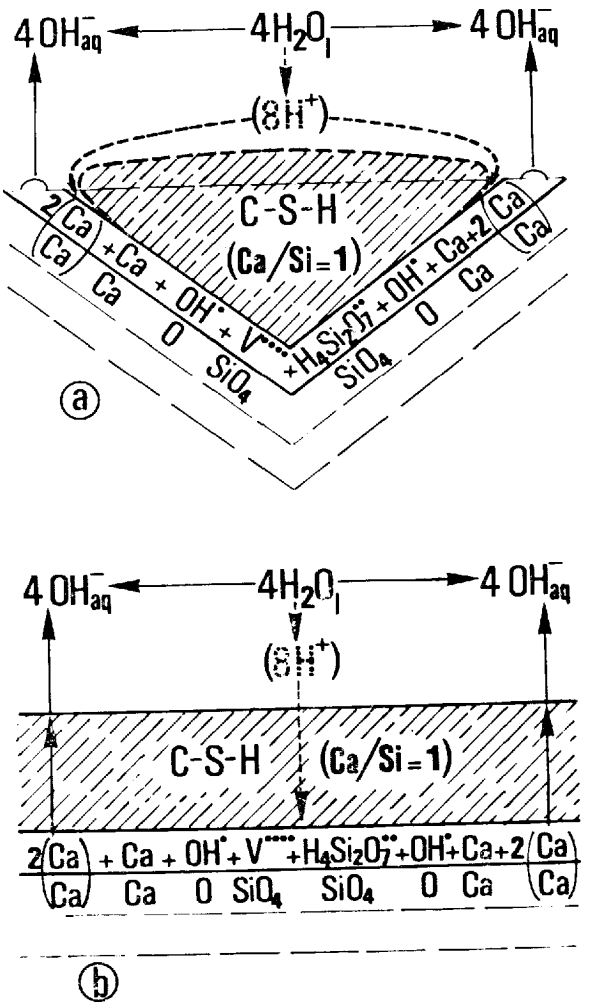

Fig. 5 : Représentation schématique d'un mécanisme de croissance de C-S-H de rapport Ca/Si = 1 : a) dans le cas d'une interface ouverte (germe individuel), b) dans le cas d'une interface fermée supposant une couche protectrice de C-S-H siège de la diffusion des ions H^+ et Ca^{2+}.

entre l'extérieur et l'interface dans laquelle elles sont susceptibles de diffuser. Ce peut être le cas pour les ions H^+ de l'eau dont la diffusion dans l'interface permettra de réaliser la protonation des ions oxygénés. En outre, quatre ions Ca^{2+} sur six, ou deux sur six, selon que le rapport Ca/Si du C-S-H est 1 (Fig. 5) ou 2 (Fig. 6) devront diffuser le long de l'interface pour rejoindre les ions OH^- dans la solution. Dans le second cas, les quatre OH^- excédentaires en solution devront également diffuser le long de l'interface en sens opposé, afin de compléter les deux unités de construction représentées. On a supposé que celles-ci avaient subi la transformation des ions hydrogénosilicates monomères en ions dimères.

Mais l'acte essentiel qui confèrerait à ce type de transformation *le caractère topochimique* serait *le transfert direct, à travers l'interface, des unités de construction ainsi préparées par ces étapes préliminaires et leur agrégation au germe de C-S-H.*

On voit que la distinction entre processus purement topochimique et processus par l'intermédiaire de la solution est assez délicate à établir expérimentalement et repose essentiellement dans notre modèle, sur la largeur de l'interface et la possibilité offerte ou non aux molécules d'eau d'y pénétrer et d'y jouer leur rôle de solvant.

Cas b : Le cas b) est celui de l'augmentation d'épaisseur d'une couche protectrice de C-S-H interdisant le contact direct des molécules d'eau et du C_3S ou du C_2S restant. *L'interface interne entre C_3S (ou C_2S) et C-S-H est dite fermée* parce que les échanges ioniques avec la phase aqueuse ne peuvent se faire que par diffusion volumique à travers la couche de C-S-H protectrice. Ce cas correspond exactement à l'hypothèse formulée par H.F.W. Taylor (9) (Fig. 3). Mais nous ne ferons pas la distinction, qui ne semble pas encore très bien fondée expérimentalement (24) entre C-S-H intérieur et C-S-H extérieur. On voit (Fig. 5) que pour obtenir un C-S-H de rapport Ca/Si = 1 à partir de C_3S, il faudrait, d'une part que les protons de l'eau diffusent à travers la couche de C-S-H pour provoquer la protonation des sites superficiels oxygénés du C_3S restant et que, d'autre part quatre ions Ca^{2+} sur six appartenant à deux unités de construction interfaciales diffusent en sens opposé à travers la couche de C-S-H pour rejoindre les ions OH^- résultant de la dissociation des quatre molécules d'eau qui ont fourni les protons.

Pour obtenir un C-S-H de rapport Ca/Si = 2 (Fig. 6) ce serait seulement deux ions Ca^{2+} sur six qui devraient diffuser à travers la couche de C-S-H tandis que les quatre OH^- escédentaires devraient diffuser en sens opposé pour venir compléter les deux unités de construction qui sont représentées, comme dans le cas a), en supposant la formation intermédiaire d'un ion dimère $H_4Si_2O_7^{2-}$.

Comme précédemment, l'acte essentiel à caractère topochimique serait le dégagement par transfert interfacial direct des sites hydroxylés grâce à ces étapes diffusionnelles préliminaires et leur agrégation à la base de la couche de C-S-H protectrice dont l'épaisseur irait ainsi en croissant.

Sans exclure la possibilité d'une diffusion du silicium envisagée par H.E.W. Taylor dans son modèle, nous constatons qu'une telle diffusion, sans devoir être exclue, n'apparaît pas comme indispensable pour expliquer, par ces mécanismes topochimiques à l'interface ouverte et à interface fermée, la croissance de germes individuels ou d'une couche protectrice de C-S-H. Dans la croissance de couches d'oxydes protecteurs sur les métaux, selon le type de défauts ponctuels prédominant, ce sont soit les cations, soit les anions qui diffusent, parfois les deux simultanément.

Les cas où la composition du C-S-H serait intermédiaire entre 1 et 2 peuvent être prévus de la même façon. Du C-S-H de rapport Ca/Si = 1,5 par exemple pourrait être obtenu par diffusion vers la phase liquide, à travers la couche protectrice de C-S-H, de trois ions Ca^{2+} sur six et la diffusion en sens opposé vers l'interface, de seulement deux ions OH^- provenant de la dissociation des quatre molécules d'eau.

3.3. Dégagement des sites superficiels hydroxylés par diffusion volumique vers l'intérieur de la phase anhydre :

On peut supposer l'existence d'une diffusion des protons fixés sur les sites oxygénés superficiels vers l'intérieur du solide anhydre. Des sites inter-

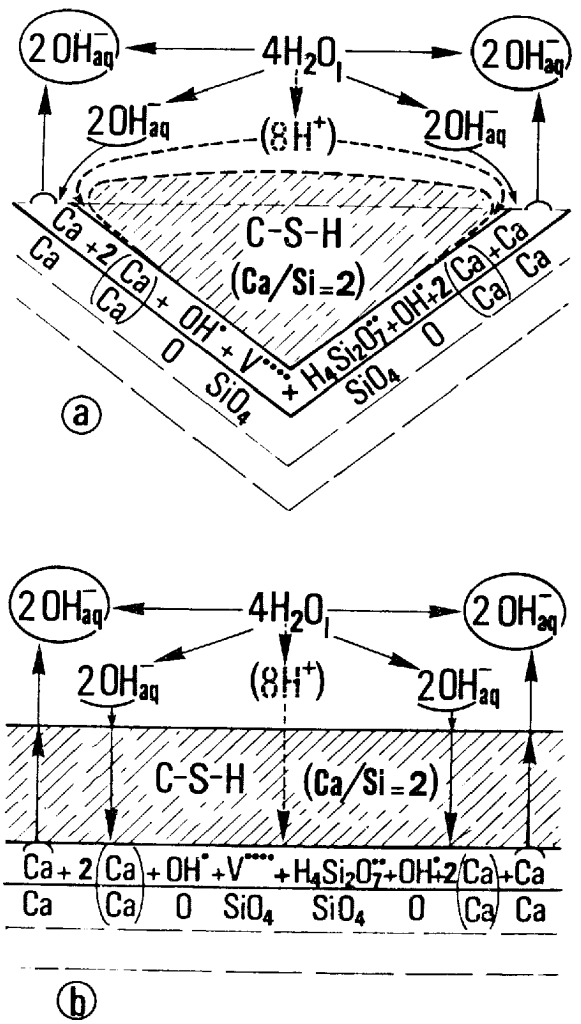

Fig. 6 : Représentation schématique d'un mécanisme de croissance de C-S-H de rapport Ca/Si = 2 : a) cas d'une interface ouverte (germe individuel), b) cas d'une interface fermée supposant une couche protectrice de C-S-H siège de la diffusion des ions H^+ Ca^{2+} et OH^-.

nes se trouveraient ainsi hydroxylés tandis que des sites superficiels seraient déshydroxylés sans pour autant découvrir les sites sous-jacents. Ces sites superficiels pourraient donc être de nouveaux hydroxylés et un état de régime serait ainsi censé s'établir. Il faut toutefois penser que le renouvellement des protonations superficielles conduirait à une accumulation des ions OH^-_{ad} formés dans la solution au voisinage immédiat de l'interface. Or une telle accumulation n'est pas possible. Des ions Ca^{2+} devraient donc quitter la surface du solide et passer avec ces ions OH^-_{ad} dans la solution suivant le mécanisme précédemment envisagé. Les lacunes d'ions Ca^{2+} ainsi créées pourraient favoriser un processus de diffusion des ions Ca^{2+} de l'intérieur du solide anhydre vers l'interface afin de perpétuer leur passage en solution pour y neutraliser les ions OH^-_{ad} nouvellement créés. Cependant, les unités de construction partiellement lacunaires, telles que :

$(2V''_{Ca} + Ca_{Ca} + OH^{\cdot}_{O} + H_3SiO_4^{\cdot\cdot})$ qui apparaîtraient
$\quad\quad\quad

M. LETELLIER*, H. VAN DAMME*, B. MORTUREUX** et M. REGOURD**
*CRSCCI - Orléans (France), ** CERILH - Paris (France)

Mechanism of the action of superplasticizers studied by the proton NMR.
Mécanisme d'action des fluidifiants étudié par RMN du proton.

RESUME L'hydratation de différents constituants du ciment Portland C_3S, C_3A, C_3A + gypse, de mélanges C_3S + C_3A avec et sans gypse et de ciment blanc a été suivie par Résonance Magnétique Nucléaire à impulsions, en présence de fluidifiants et dans des pâtes témoins sans adjuvants.

Les paramètres étudiés sont le rapport eau/solide, la nature du fluidifiant (base naphtalène sulfonate, lignosulfonate ou mélamine formaldéhyde) et son dosage, la finesse de broyage et la proportion de C_3A dans les mélanges et dans le ciment.

Les mesures de temps de relaxation Spin-réseau T_1 sont faites dès les premières minutes après le gachâge et jusqu'à 28 jours pour certains échantillons. Elles montrent la progression de l'aire interfaciale solide-eau développée dans la pâte de ciment en cours d'hydratation, l'importance relative des constituants dans le mélange et l'action très différenciée des fluidifiants sur les silicates et les aluminates de calcium.

A hidratação de diferentes componentes do cimento Portland - C_3S, C_3A, C_3A + gesso, misturas de C_3S + C_3A com e sem gesso e cimento branco foi acompanhada por Ressonância Magnética Nuclear de impulsos, em presença de fluidificantes e em pastas testemunho sem aditivos.

Os parâmetros estudados são a relação água/sólido, a natureza do fluidificante (base sulfonato de naftaleno, lignossulfonato ou melamina formaldeída) e sua dosagem, a finura de moagem e a proporção de C_3A nas misturas e no cimento.

As medidas de tempo de relaxação Spin-rede T_1 são feitas desde os primeiros minutos após o amassamento e até aos 28 dias para algumas amostras. As medidas mostram a progressão do ar interfacial sólido-água desenvolvido na pasta de cimento no decorrer da hidratação, a importância relativa dos constituintes na mistura, e a ação muito diferenciada dos fluidificantes sobre os silicatos e os aluminatos de cálcio.

INTRODUCTION

Les essais décrits dans cette étude utilisent la Résonance Magnétique Nucléaire (RMN) et la mesure des temps de relaxation du proton.

Des études ont déjà été réalisées en RMN sur du silicate tricalcique ou du ciment dont LAHAJNAR et al (1) ont suivi l'hydratation, distinguant, à partir des mesures de relaxation du proton (T_1 spin-réseau ou T_2 spin-spin) l'eau d'adsorption de l'eau de cristallisation. Les mêmes auteurs ont également utilisé la RMN du solide sur ^{27}Al. D'après BLINC et al (2), les molécules d'eau sont hautement mobiles dans la couche adsorbée et s'échangent rapidement avec l'eau des pores à leur contact. MACTAVISH et al (3) ont pu décomposer les signaux RMN en différents groupes de spins correspondant aux hydrates formés et aux catégories d'eau liée. DIMIC et DROLJC (4) KOCUVAN et URSIC (5) ont présenté des courbes de variation de T_1 en absence et en présence d'adjuvants dans des pâtes de ciment Portland.

Nous avons appliqué la RMN du proton aux constituants du ciment Portland, C_3S et C_3A, étudiés séparément puis en mélanges avec le gypse ceci afin de mieux décomposer les cinétiques d'hydratation et de mettre en évidence l'action des fluidifiants et l'influence du rapport Eau/Solide.

I TECHNIQUE

Rappelons que certains noyaux atomiques possèdent un moment angulaire de spin p auquel est associé un moment magnétique $\mu = \gamma p$, γ étant le rapport gyromagnétique caractéristique de chaque noyau. La composante de ce moment magnétique sur une direction donnée Z est, d'après la Mécanique Quantique $\mu z = \gamma m h/2\pi$, h étant la constante de Planck; m ne peut prendre que des valeurs discrètes, $\pm \frac{1}{2}$ dans le cas le plus simple du proton.

Si un champ magnétique extérieur B_o est appliqué le long de l'axe Z, il apparaît un terme d'énergie d'interaction entre le champ et le moment magnétique nucléaire de la forme $E = -\mu_z B_o = -\gamma \hbar m B_o$ ($\hbar = h/2\pi$).

Il en résulte que les niveaux d'énergie du noyau sont clivés avec un écart $\Delta E = \gamma \hbar B_o$, la résonance entre ces deux niveaux d'énergie peut être excitée à une fréquence appropriée ν_o telle que $\Delta E = h\nu_o$ soit $\nu_o = \gamma B_o/2\pi$.

Nous avons utilisé la spectroscopie RMN par impulsions. L'impulsion de fréquence appropriée ν_o a pour effet de modifier la répartition des populations de spins entre les deux états $+\frac{1}{2}$ et $-\frac{1}{2}$ et donne un état de magnétisation excité M_z. Si l'irradiation est stoppée, la composante M_z se relaxe suivant $M_t = M_z\ (1-e^{-t/T1})$, T_1 étant le temps de relaxation longitudinal ou spin-réseau, l'échange d'énergie ayant lieu entre les spins et le réseau cristallin dans le cas des solides, l'ensemble des molécules en mouvement dans un liquide.

La valeur de T_1 proton est donc étroitement reliée à la mobilité des molécules d'eau ou à la structure des hydrates d'où son intérêt pour l'étude de l'hydratation des ciments.

Un deuxième temps de relaxation T_2 est défini ; il concerne la composante de M perpendiculaire au champ (temps de relaxation spin-spin), les deux valeurs T_1 et T_2 n'étant pas égales dans le cas d'une structure non liquide.

L'appareil utilisé est un spectromètre BRUKER SXP à impulsions et transformée de Fourier, fréquence de résonance du proton 90 MHz. Le temps de relaxation T_1 est mesuré grâce à une séquence d'impulsions $\pi\tau\pi/2$, τ variable. Quelques mesures de T_2 ont été faites par la méthode de l'écho de spin ou séquence $\pi/2\ \tau\ \pi$ et ultérieurement par la méthode CARR PURCELL (impulsion $\pi/2$ suivie d'un série d'impulsions π).

II ESSAIS SUR C_3S AVEC ET SANS FLUIDIFIANT

II.1 Expérimentation :

Le C_3S préparé au CERILH, de surface spécifique Blaine 2040 cm^2/g a été gâché avec de l'eau distillée au rapport E/S = 0,40 ou 0,28. Les mesures de T_1 sont faites dès cinq minutes d'hydratation et jusqu'à 24 ou 48 heures. La décroissance de T_1 en fonction du temps apparaît sur la figure 1.

Quelques mesures de T_2 ont été faites sur l'échantillon n°2 à E/S 0,40, la valeur observée par spin-écho après 12 minutes d'hydratation est de 9 à 10 ms. Cette valeur ainsi que celles de T_1 semblent en accord avec des résultats antérieurs (1-2) et nous en donnons ci-après une interprétation originale.

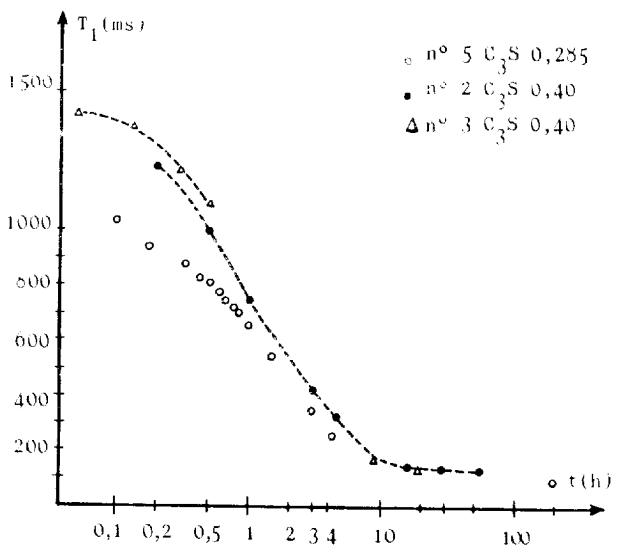

Fig.1 - Variation du temps de relaxation T_1 en fonction du temps.

Un fluidifiant commercial à base de polynaphtalène sulfonate de sodium (NSS) est ajouté à l'eau de gâchage à raison de 0,9 % en poids du ciment. Ce produit a un effet extrêmement important sur l'hydratation de C_3S: sur l'échantillon E/S = 0,40 T_1 reste constant de 5 minutes jusqu'à 4 heures (1,55 s). Cette valeur est proche de celle observée initialement sur les témoins E/S = 0,40.

II.2 Interprétation des résultats :

Des résultats intéressants peuvent être déduits de la représentation de $1/T_1$ en fonction du temps. Cette variation apparaît linéaire au moins jusqu'à 9 heures d'hydratation (figure 2). Elle se prête à l'application d'un modèle à deux phases "a" et "b"

de temps de relaxation respectifs T_{1a} et T_{1b}, proches de l'eau libre pour a et d'eau fortement perturbée par la surface des hydrates sur quelques couches (phase b). Des études antérieures sur des suspensions d'argile ont montré que seules les molécules d'eau situées à moins de 10 Å de la surface solide avaient leurs temps de relaxation perturbé (6-7). Connaissant la quantité d'eau ayant une relaxation perturbée, il est possible d'en déduire la surface de la phase solide.

Les deux phases a et b étant supposées en échange rapide le temps de relaxation moyen T_1 est $T_1^{-1} = a\ T_{1a}^{-1} + b\ T_{1b}^{-1}$, a et b étant les fractions molaires des deux phases ($a + b = 1$). La valeur initiale de T_1 n'est plus égale à celle de l'eau libre (2,85 s), il existe donc dès le début de l'hydratation, une fraction b_o d'eau liée, d'où l'hypothèse $b = b_o + \beta t$, le volume de phase b augmentant avec le temps comme la surface développée des grains hydratés. Ce modèle semble bien vérifié jusqu'à une dizaine d'heures environ, après quoi, la variation de T_1^{-1} s'infléchit et tend vers un palier correspondant à la disparition de la phase a.

Si K est la pente de $T_1^{-1} = f(t)$, sensiblement égale à E/S = 0,40 ou 0,28, K = 160 x 10^{-6} s^{-2}, alors $\beta = K/(1/T_{1b} - 1/T_{1a})$, la valeur $1/T_{1a}$ correspondant à l'eau libre, $1/T_{1b}$ est pris égal à la valeur correspondant au palier (T_{1b} = 145 ms) lorsqu'a

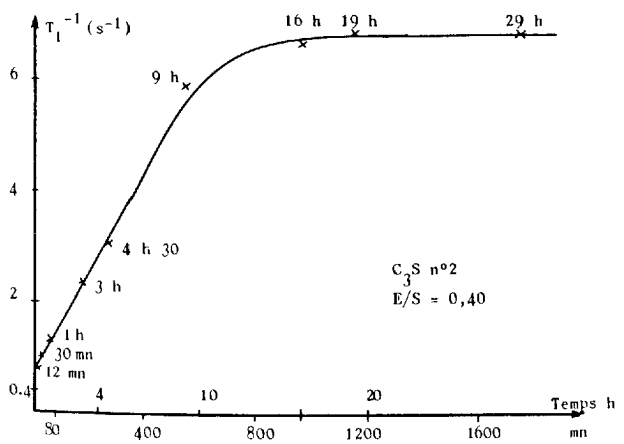

Fig.2 : C_3S . Variation de $1/T_1$ en fonction du temps

disparu la phase a, β = 24,4 x 10^{-6} s^{-1}

La valeur initiale de la proportion d'eau liée b_o dépend du rapport E/S: l'application de la relation $(1/T_1)_o = 1/T_{1a} + b_o\ (1/T_{1b} - 1/T_{1a})$ donne pour E/S = 0,40 b_o = 4,5 % et pour E/S = 0,28, b_o = 8,7 %. Ces valeurs relativement faibles et les surfaces spécifiques que l'on peut en déduire, semblent confirmer le fait qu'une très faible partie du C_3S soit intéressée au tout début de l'hydratation (8). D'autre part, l'effet du fluidifiant sur C_3S semble figer cet état initial de l'eau dans le système au moins jusqu'à 20 h, le développement des produits d'hydratation reprenant ensuite suivant une cinétique qui reste à préciser.

II.3 Mesures de T_1 à longue échéance:

Certains échantillons conservés dans les tubes RMN bouchés ont fait l'objet de mesures de T_1 à plus longue échéance. Nous donnons ci-après les résultats des mesures après une semaine.

Au bout de 28 jours, nous ne trouvons plus en général une seule valeur de T_1. Un calcul graphique simple permet de connaître les proportions M_1/M_o et M_2/M_o des deux groupes de spins et les valeurs des temps T_1 long et T_1 court.

Echantillon	Echéance	T_1 ms
1 E/S = 0,4	11 jours	140
2 E/S = 0,4	10 jours	140
3 E/S = 0,4	10 jours	140
5 E/S = 0,28	8 jours	95
6 E/S = 0,28 + 1 % NSS	8 jours	145

C_3S E/S = 0,40 30 jours T_{1l} = 100 ms (80 %), T_{1c} = 8,7 ms (20%)

C_3S E/S = 0,28 28 jours T_{1l} = 60 ms (60 %), T_{1c} = 11 ms (40 %)

Ces valeurs et les pourcentages des contributions indiquées sont approximatifs, ils montrent en tous cas que l'approximation de l'échange rapide n'est plus valable et qu'il y a compartimentage entre différentes catégories d'eau liée (3).

III ESSAIS SUR C_3A

Le C_3A présentait une surface spécifique BLAINE de 2150 cm^2/g. Deux rapports E/S ont été utilisés 0,40 et 0,60, un troisième échantillon étant gâché à E/S = 0,40 mais avec fluidifiant NSS dans l'eau de gâchage dosé à 0,75 %.

III.1 C_3A seul (non gypsé)

. *C_3A E/S = 0,40* : dans ce cas nous trouvons deux valeurs de T_1. Si les valeurs des deux T_1 varient relativement peu (600 ms et 150 à 200 ms), les proportions évoluent rapidement avec le temps d'hydratation (figure 3). Des mesures ont été faites jusqu'à 46 h : la proportion de constituant à temps long est alors très fortement réduite, T_1 = 400 ms pour 10% environ, le T_1 court étant de 83 ms. Si nous ne tenons compte que de T_{1c} majoritaire dès 20 minutes d'hydratation, la courbe de variation $T_1 = f(t)$ est voisine de celle obtenue par d'autres auteurs (4) et indiquerait une forte augmentation de la proportion d'eau liée dès les premiers instants (figure 4).

. *C_3A E/S = 0,60* : le comportement de cet échantillon est très différent du précédent: un seul T_1 est observé et sa valeur augmente avec le temps (330 ms à 10min et 700 ms à 2 h).

. *C_3A avec fluidifiant E/S = 0,40* : le fluidifiant est le même qu'avec C_3S , à base NSS et dosé à 0,75 % en poids de C_3A. Il semble avoir peu d'effet sur C_3A: le comportement de cet échantillon a été assez proche de celui du témoin jusqu'à 40 minutes (deux valeurs de T_1 en proportions variables) puis à partir de 1 heure n'apparaît plus qu'un seul T_1 (165 ms) qui

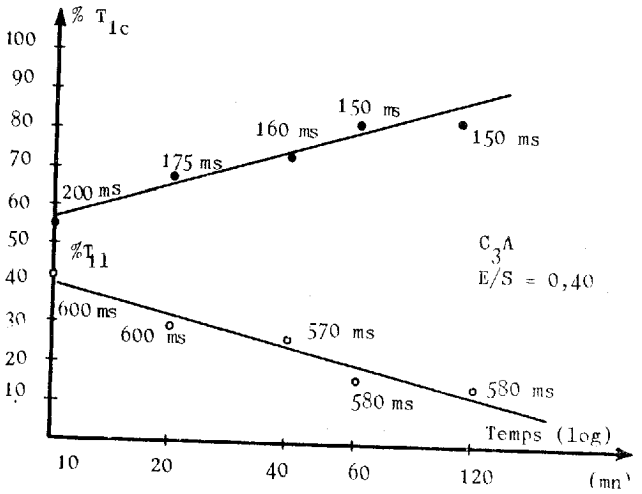

Fig. 3: C_3A, E/S = 0,40 . Mesures de T_1

tend à augmenter par la suite. Comme dans le cas du témoin E/S = 0,60, cette augmentation pourrait avoir pour cause la cristallisation lente de C_3AH_6 en cristaux de plus en plus gros ayant pour effet de diminuer la surface développée ou le rapport S/V des hydrates (diminution de la phase b) en même temps que de libérer une certaine quantité d'eau faiblement liée (9-11). D'après la Diffraction des Rayons X, la composition en hydrates et anhydres des trois échantillons diffère très nettement :

. *C_3A E/S = 0,6* : l'hydrate bien défini et bien cristallisé est C_3AH_6. Il reste très peu de C_3A anhydre

. *C_3A E/S = 0,4* : il y a trois à quatre fois moins de C_3AH_6 que dans l'échantillon précédent, la présence d'aluminates hydratés hexagonaux mal cristallisés est certaine et il reste beaucoup plus de C_3A anhydre.

C_3A E/S = 0,4 + 0,75 % NSS : l'effet du fluidifiant à cette échéance (140 h) est très net et étonnant: à même E/S, cet échantillon est beaucoup plus hydraté que le témoin essentiellement à l'état de C_3AH_6, le diagramme est pratiquement identique à celui de l'échantillon E/S = 0,6, le fluidifiant modifie donc la nature des phases présentes et le taux d'hydratation.

Ces observations peuvent être reliées aux comportements différents à l'échelle moléculaire en RMN: si l'hydratation conduit à du C_3AH_6 (cas E/S = 0,6 ou E/S = 0,4 avec fluidifiant) le temps de relaxation moyen du proton a tendance à augmenter. Sur le témoin subsiste une forte population de protons à T_1 court alors qu'il s'est formé en abondance des aluminates hexagonaux plus ou moins mal cristallisés. Ceux-ci peuvent soit présenter une grande surface spécifique, soit intervenir par leurs OH de structure dans un groupe de spins: dans leur structure se trouvent des couches d'aluminium octaédrique faites de Al^{3+} et Ca^{2+} régulièrement disposés ainsi que les OH^-. Dans la structure de C_3AH_6 d'après (10) les OH sont très faiblement liés entre eux, une perturbation des spins se relaxe mal et le temps T_1 est long (1,4 s d'après nos mesures).

III.2 C_3A + Gypse :

Les mesures de T_1 ont été faites sur un mélange C_3A 80 % Gypse $CaSO_4\ 2H_2O$ pur 20 %, le rapport E/S étant de 0,50 avec et sans fluidifiant.

. *C_3A + gypse témoin* : la pâte obtenue est très maniable. T_1 égal à 1s après 10 minutes se maintient autour de 800 ms jusqu'à 2 h. Les mesures n'ont pu être faites au-delà de 2 h mais reprises après 18 h de contact eau-C_3A + gypse (figure 4).

. *C_3A + gypse + fluidifiant* : avec le même fluidifiant à base NSS dosé à 1 % en poids du solide, les valeurs de T_1 relevées jusqu'à 7 h sont très voisines de celles du témoin et généralement plus courtes. Les valeurs finales trouvées (autour de 120 ms après 72 h) sont du même ordre avec et sans fluidifiant et aussi avec C_3A (fig. 4).

Le fluidifiant utilisé semble donc avoir peu d'effet sur la première hydratation de C_3A en présence de gypse telle qu'on peut l'observer par RMN du proton. Il n'est pas certain pour autant

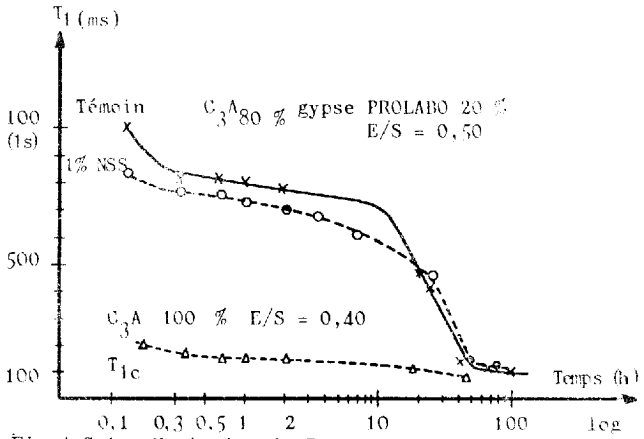

Fig.4 C_3A : Variation de T_1

que ce produit n'agisse pas sur les propriétés rhéologiques et le malaxage de cet échantillon a paru plus facile que sur le témoin. Le comportement rhéologique d'un tel système dans la période dormante dépend pour une large part de la cristallisation ou morphologie de l'ettringite primaire formée plutôt que de sa quantité totale. Cette cristallisation peut être influencée par de nombreux paramètres comme la proportion relative C_3A/Gypse, la solubilité de ce gypse et précisément les adjuvants (12-13).

IV MELANGES C_3S - C_3A AVEC ET SANS GYPSE

Les composés C_3S et C_3A précédemment étudiés ont été mélangés en proportions 80/20 (finesse BLAINE moy. 2200 cm^2/g) et hydratés avec ou sans addition de gypse à E/S = 0,40 ou 0,285. Nous avons également étudié le fluidifiant à base NSS sur ces mélanges ainsi que sur un mélange à 10 % de C_3A.

. *Mélange C_3S_{80} - C_3A_{20} sans gypse:*

E/S = 0,40 le temps de relaxation T_1 évolue suivant la courbe 1 de la figure 5. Une seule valeur est observée et évolue progressivement jusqu'à 6h 30. Les T_1 sont beaucoup plus courts qu'avec C_3S au même rapport E/S: la première mesure entre 4 et 7 minutes d'hydratation indique 450 ms (influence de C_3A).

T_1^{-1} varie linéairement au moins jusqu'à 6h 30 avec une pente K = 44 x 10^{-6} s^{-2} plus faible qu'avec C_3S seul, puis sa variation s'accélère ensuite, T_1 passant de 280 ms à 100 ms entre 6h 30 et 16h. Cette période d'accélération est apparue plus nette encore avec les mélanges gypsés.

Avec fluidifiant (0,75 %), les valeurs de T_1 sont pratiquement identiques durant les premières heures et au-delà: T_1 ± 90 ms à 24 h comme sur le témoin. L'effet du fluidifiant paraît donc peu important sur le mélange C_3S + C_3A sans gypse qui donne par ailleurs dès le gâchage des temps de relaxation moyens plutôt courts.

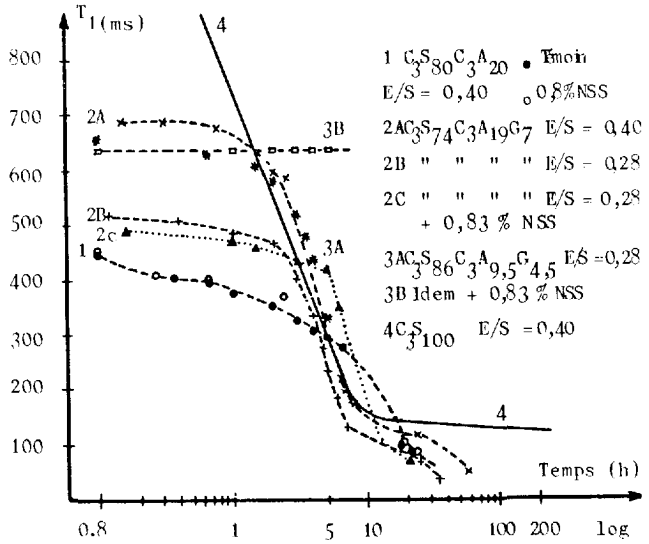

Fig. 5: Mélanges C_3S + C_3A, variation de T_1

. *Mélange C_3S_{80} C_3A_{20} gypsé:*

Le mélange précédent est additionnée de 7 % de gypse naturel ($CaSO_4 2H_2O$ + $CaCO_3$). Les valeurs de T_1 obtenues dès 10 minutes sont indiquées sur la figure 5.

. Influence du rapport E/S: à E/S =0,40 la valeur initiale T_1 = 680 ms se maintient pendant 1 h environ. Elle est nettement plus faible qu'avec C_3S seul mais aussi plus longue qu'avec le mélange C_3S C_3A non gypsé, ce qui confirme l'influence de C_3A et du gypse dans les premiers temps de l'hydratation: même si la quantité de C_3A mise en jeu dans les premiers instants est faible et du même ordre de grandeur avec et sans gypse (12) la nature différente des aluminates formés implique une mobilité différente de l'eau révélée par les valeurs de T_1.

Après le palier de 1 h (période dormante), la valeur moyenne de T_1 chute jusque vers 8 h. Sur la même figure sont rappelées les valeurs obtenues au même rapport E/S sur C_3S seul. Dans la période correspondant à une forte augmentation de la proportion d'eau liée et de croissance des interfaces, l'hydratation de C_3S paraît être le phénomène principal.

A E/S = 0,285, il y a par rapport à E/S = 0,40 diminution de la valeur initiale de T_1 (500 ms) due à une augmentation du volume relatif de phase b, puis une avance de la période de variation rapide de T_1. Des valeurs courtes sont atteintes dès 7 h (135 ms). L'écart entre les deux courbes E/S = 0,40 et 0,285 est de 1 h environ (figure 5). C'est sur un mélange gypsé E/S = 0,285 qui se rapproche sensiblement des conditions du ciment qu'a été testée l'influence du fluidifiant.

. Influence du fluidifiant (0,8 %): la valeur initiale T_1 = 480 ms proche du témoin est constante pendant 1 h et diminue peu jusqu'à 5 h d'hydratation (figure 5). Il y a allongement du palier initial, la décroissance rapide de T_1 n'intervient qu'au delà de 5 h. L'écart entre les deux courbes avec et sans fluidifiant à même E/S 0,285 est de 3 heures environ.

. *Influence de la teneur en C_3A*

Un dernier essai a été fait sur un mélange gypsé à plus faible taux de C_3A (10 %) au rapport E/S 0.285 en présence de fluidifiant au dosage de 0,8 %. Toutes les mesures effectuées depuis 7 minutes après le gâchage jusqu'à 6 h ont donné la même valeur de T_1 = 640 ms. Le palier initial est donc très allongé et le fluidifiant semble donner sa pleine efficacité au moins jusqu'à 6 heures. Le même mélange sans fluidifiant a été suivi jusqu'à 5 h d'hydratation (courbes 3 A et B de la figure 5).

V COMPARAISON DE L'EFFET DE DIFFERENTS FLUIDIFIANTS

Une deuxième série d'essais a porté sur des mélanges C_3S + C_3A + Gypse à 20 % de C_3A et 5 % de sulfate $CaSO_4 2H_2O$ en présence de trois fluidifiants commerciaux à base Naphtalène Sulfonate de Sodium (NSS) déjà utilisé, Lignosulfonate de Sodium (LSS) et Mélamine sulfonée condensée par le Formaldéhyde (MSF). Ces trois produits étaient ajoutés à l'eau de gâchage au dosage de 1 % en poids des solides, E/S = 0,40.

Les variations de T_1 et de T_2 CARR PURCELL sont indiquées sur les figures 6 et 7.

Témoin sans fluidifiant: les valeurs de T_1 sont légèrement différentes de celles obtenues en IV, le gypse n'étant pas le même. T_1 est constant jusqu'à 1h 30 environ, a encore très peu varié à 2 h (750 ms) puis décroît très rapidement ensuite jusque vers 6 - 7 h d'hydratation où commence une troisième période de ralentissement. Les variations de T_2 semblent plus sensibles que celles de T_1 en début d'hydratation: T_2 décroît dès 40 minutes sur le témoin.

Avec NSS 1 % l'effet observé précédemment est confirmé: valeurs initiales de T_1 identiques avec et sans fluidifiant, mais variant plus progressivement en début de prise (jusqu'à 4 h) et retard de 1h 30 à 2 h de la période d'accélération.

Les valeurs de T_2 sont plus élevées avec ce fluidifiant et surtout restent plus longtemps à des niveaux proches de la valeur initiale: à 3h 20 T_2 = 20 ms contre 13 ms sur le témoin. Cet effet d'évolution ralentie du T_2 semble commun aux fluidifiants utilisés (5).

Avec MSF 1 % (figure 7): en T_1 l'effet retardateur est important, de l'ordre de 6 à 7 h: la valeur initiale de T_1 légèrement inférieure à celle du témoin (740 ms contre 800 ms) diminue peu jusqu'à 7 h 45 (700 ms) alors que le témoin semble avoir terminé sa prise avec un temps T_1 de 225 ms.

En T_2 la valeur initiale est inférieure à celle du témoin (19 ms au lieu de 24) mais, comme T_1, évolue peu jusqu'à 8 h.

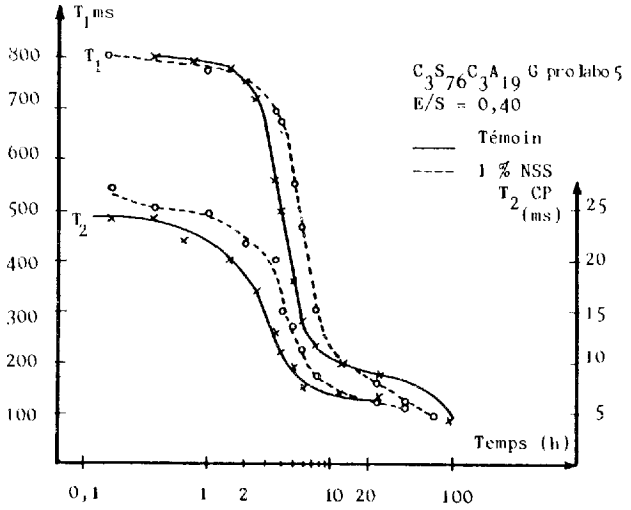

Fig. 6 : Mélange $C_3S + C_3A$ sans et avec 1 % NSS

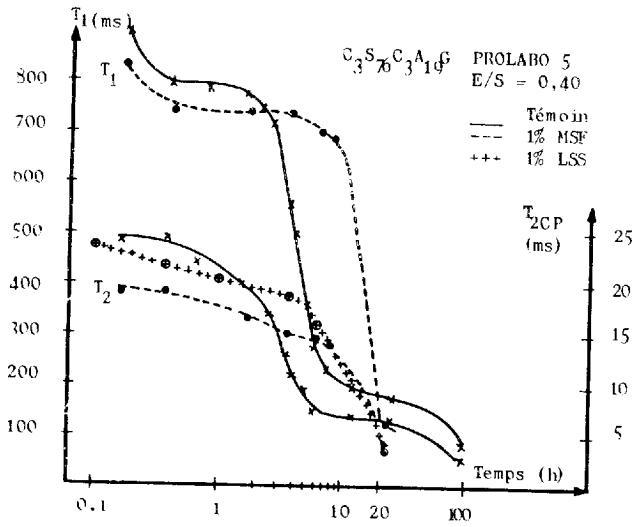

Fig. 7: Mélange $C_3S + C_3A$ sans et avec 1 % LSS ou MSF

La période active de l'hydratation semble ensuite accélérée puisqu'à 23 h les valeurs de T_1 et T_2 sont sensiblement plus courtes que sur le témoin: 120 et 3,5 ms contre 175 et 6,8 ms respectivement.

Avec LSS 1 %: il est apparu que ce produit modifiait la relaxation de l'eau en l'absence de ciment probablement en raison d'impuretés entraînant des valeurs courtes de T_1. Seules les variations de T_2 sont indiquées sur la figure 7. La valeur initiale de 24 ms proche de celle du témoin diminue très peu jusqu'à 4 h.

Conclusion des essais avec fluidifiants:

Sur les mélanges $C_3S_{76}C_3A_{19}G_5$ quelques caractéristiques générales concernant l'effet des fluidifiants peuvent être dégagées: les valeurs initiales des temps de relaxation T_1 et T_2 sont généralement proches de celles du témoin, parfois un peu inférieures mais elle se maintiennent plus longtemps. Nous ne connaissons pas actuellement les valeurs de T_1 et T_2 correspondant à des seuils des propriétés rhéologiques mais si nous prenons par exemple le T_2 dont la variation est très sensible en début d'hydratation, T_2 reste supérieur à 12 ms pendant 3h 30 (témoin) 10h (MSF) 5h (NSS) et 9h (LSS). Lorsque cet effet des fluidifiants cesse, la réaction d'hydratation du mélange semble reprendre normalement mais avec une vitesse plus élevée que sur le témoin. Sur la figure 8 sont rassemblées les courbes de variations de $1/T_1$ en fonction du temps. On y voit outre l'influence des fluidifiants, l'évolution comparée de C_3S seul

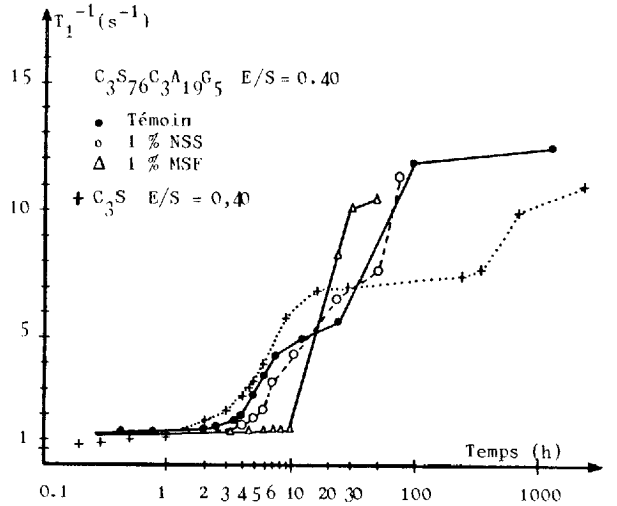

Fig. 8: Mélanges $C_3S + C_3A$. Variation de $1/T_1$

(au même rapport E/S=0,40) et des mélanges C_3S-C_3A-Gypse: C_3S semble commander la variation de T_1^{-1} dans le mélange au cours des premières heures, la courbe expérimentale $T_1^{-1} = f(t)$ du mélange témoin est proche d'une combinaison linéaire de $(C_3A + \text{Gypse})1/4$ et de C_3S 3/4, le gypse ayant pour effet, rappelons le, de ramener le T_1 de C_3A hydraté aux environs de 800 ms.

Le fluidifiant inhibe le développement des interfaces pendant un temps variable au-delà duquel celui-ci reprend avec une cinétique qui sera précisée par de nouvelles mesures: la pente obtenue lors de cette reprise est-elle la même qu'en l'absence de fluidifiant et une nouvelle addition de produit peut-elle à nouveau interrompre le développement des interfaces?

VI MESURES SUR CIMENT

Les mesures ont porté uniquement sur un ciment blanc afin d'éviter la relaxation sur les centres paramagnétiques électroniques que constituent les atomes de fer dans le CPA normal.

Le développement des interfaces semble plus rapide que pour C_3S mais suit toujours un modèle linéaire, un palier semble atteint vers 7h d'hydratation (figure 9).

VII QUANTIFICATION DES INTERFACES MESURES EN D_2O

Un essai d'hydratation de C_3S pur par l'eau lourde à E/S = 0,40 a permis de confirmer le modèle utilisé.

La résonance de ^2H est suivie à la fréquence de 13,85 MHz, les temps de relaxation T_1 et T_2 mesurés

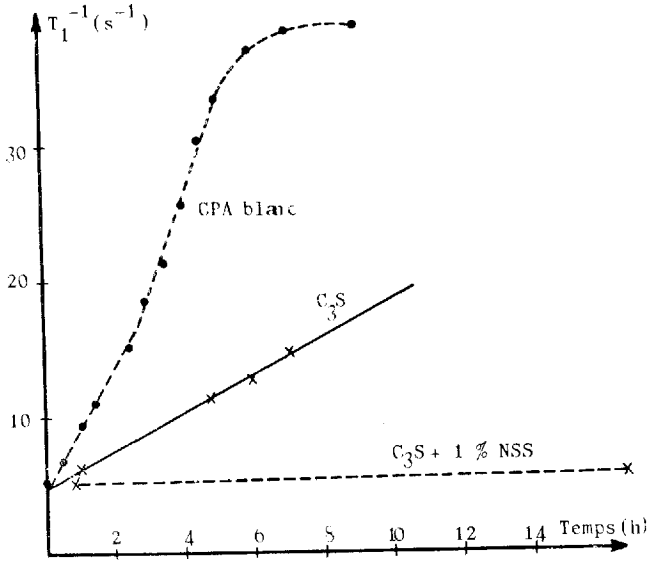

Fig. 9: Ciment blanc. Variation de $1/T_1$

comme pour le proton en adaptant la durée des impulsions du champ de radiofréquence (séquence $\pi, \tau, \pi/2$ etCARR PURCELL). Les variations de T_1 et T_2 sont indiquées dans le tableau I. Si nous considérons comme pour le proton la vitesse de relaxation T_1^{-1} en fonction du temps d'hydratation, vitesse liée aux proportions des phases a et b, ses variations sont relativement peu sensibles en début de réaction comme cela avait déjà été montré sur des suspensions d'argile à faible concentration (7). Une régression linéaire sur cinq points de mesure entre 0 et 10h est indiquée sur la figure 10.

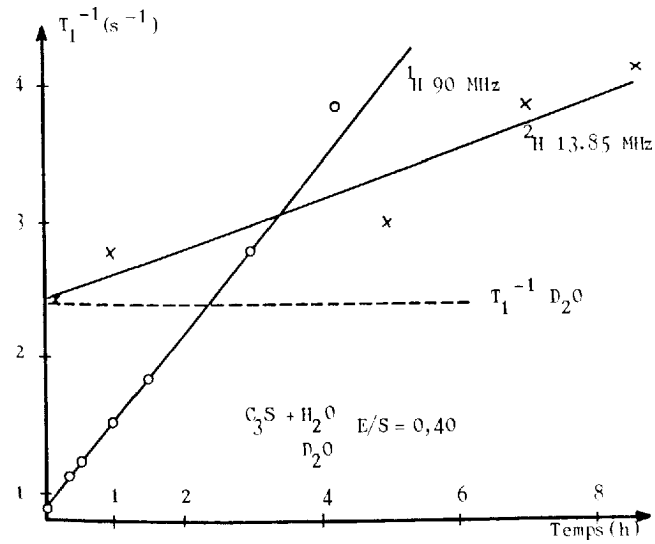

Fig. 10: C_3S hydraté avec H_2O et D_2O. Variation de $1/T_1$

L'intérêt des mesures en D_2O est que la relaxation de ^2H est beaucoup moins sensible aux impuretés paramagnétiques éventuellement présentes dans les produits étudiés (6-7).

Tableau I: $C_3S + D_2O$. Variation de T_1 et T_2

t^h_{min}	10	17	30	1h	3h	4h	7h	9h	24h
T_{1ms}	410	360	-	360	330	360	260	240	75
T_{2ms}	-	-	80	70	-	29	21	17.5	6.5

Essai de quantification des interfaces:

Compte tenu des valeurs mesurées de T_{1a} (eau libre) et de T_{1b} un premier calcul sur C_3S a donné la valeur initiale de la fraction b_o d'eau liée : $b_o = 0,046$ (E/S = 0,40) et $b_o = 0,087$ (E/S = 0,285). Cette fraction d'eau liée exprimée comme un rapport des volumes des phases b et a est:

$$b = S_b Z^* C \quad \text{où } Z^* \text{ est}$$

l'épaisseur de la couche d'eau perturbée estimée à 10 Å (6), S_b la surface des grains accessibles à l'eau et C le rapport masse de solide/masse totale d'eau. Le calcul étant fait sur 1g de solide, S_b est la surface développée en cm^2/g et C est l'inverse du rapport E/S,

d'où $b_o = 0,046 = (Sb \times 10\text{-}7)/ 0,40$
(cas E/S = 0,40) $Sb = 18\ m^2/g$

ou $b_o = 0,087 = (Sb \times 10^{-7})/0,28$
et $Sb = 24\ m^2/g$ (E/S = 0,28)

La surface initialement accessible à l'eau serait de l'ordre de 20 m^2/g. Cette valeur semble en bon accord avec des mesures de surface B.E.T. aux premiers âges citées par POWERS. Si nous cherchons de même à chiffrer l'accroissement de cet interface pour une variation observée de T_1^{-1}, par exemple de une unité soit entre 0 et 100 minutes d'hydratation à E/S = 0,285. nous trouvons $b_{100\ mn} = 0,24$ soit $\Delta b = 0,15$ et $\Delta S = 43 m^2/g$.

Le même calcul en fin d'expérience, lorsqu'il ne reste plus de phase a et que la proportion de phase b tend vers 1, donnerait des valeurs de surfaces spécifiques de l'ordre de 200 m^2/g. Des valeurs de B.E.T. H_2O de cet ordre sont effectivement citées dans la littérature (14).

VIII CONCLUSION

. La RMN du proton est une technique appropriée pour suivre en continu la prise dès les premières minutes.

. Dans le cas simple de C_3S la variation de T_1^{-1} est linéaire jusqu'à 10 heures environ et permet de suivre le développement de la surface des hydrates. Ce modèle linéaire semble compatible avec la formation de C-S-H en fines aiguilles autour des grains comme observé au Microscope Electronique à Balayage.

. Les résultats sur C_3A seul paraissent plus difficiles à interpréter [3] et dépendent beaucoup du rapport Eau/Solide.

. Dans les mélanges C_3S-C_3A, le temps de relaxation moyen du proton est sous la dépendance essentielle de C_3A. Nous avons suivi l'influence du gypse et de teneurs en C_3A différentes.

. A E/S égal, l'ajout de différents fluidifiants aux mélanges C_3S - C_3A - Gypse ne modifie pas le temps de relaxation moyen du proton mais allonge le palier en début de réaction d'autant plus que la teneur en C_3A est faible. Le fluidifiant inhibe le développement des surfaces pendant un temps variable au-delà duquel celui-ci reprend avec une cinétique qui fera l'objet de recherches ultérieures.

. Les essais sur ciment blanc montrent la même loi de développement de l'interface dans les premières heures d'hydratation.

. Le changement de rapport E/C affecte la valeur initiale de T_1 et la cinétique d'hydratation.

La RMN du proton fera l'objet d'autres applications en vue de préciser la microstructure poreuse des ciments hydratés en particulier par la technique du gradient de champ permettant d'atteindre le libre parcours moyen des molécules d'eau soit en cours de prise, soit dans des pâtes durcies.

BIBLIOGRAPHIE

1. G. LAHAJNAR, R. BLINC, V. RUTAR On the use Pulse NMR Technique for the Study of Cement Hydration Cem. Conc. Res Vol 17, pp 385-394, (1977)

2. R. BLINC, M. BURGAR, G. LAHAJNAR, M. ROZMARIN and V. RUTAR NMR Relaxation Study of Adsorbed Water in Cement and C_3S Paste J.A.C.S. Vol 61, n° 1-2, pp. 35-37, Janv. 1978.

3. J.C. MACTAVISH, L. MILJKOVIC, M. PINTAR Hydration of White Cement by Spin Grouping NMR. Cem. Concr. Res. Vol 15, pp. 367-377, (1985)

4. D. DIMIC, S. DROLJC The Influence of Sulfonated Melamine Formaldehyde Condensate on the Hydration of C3S and C3A Measured by NMR Method. RILEM Symposium Technology of Concrete when Pozzolanas, Slags and Chemical Admixtures are used Monterrey (MEXICO) march 1985.

5. I.KOCUVAN, J.URSIC, G. LAHAJNAR, R.BLINC, M.ROZMARIN. Evaluation of Various Cement Additives by Pulse NMR. Silic. Ind. n° 10, pp. 223-228, (1978).

6. J. FRIPIAT, M. LETELLIER, P. LEVITZ Interaction of Water with Clay Surfaces Phil. Trans. R. Soc. London A311, pp. 287-299 (1984).

7. J. FRIPIAT et al Thermodynamic and Microdynamic Behavior of Water in Clay Suspensions and Gels. Journal of Colloid Interf. Sc. Vol 89 n°2 pp. 378-400, Oct. 82.

8. M. REGOURD Microanalytical Studies (XPS) of Surface Hydration Reactions of Cement Compounds. Phil. Trans. R. Soc. London A 310, pp. 85-92 , (1983).

9. E. BREVAL Gas-phase and Liquid Phase Hydration of C_3A. Cem. Concr. Res. Vol 17 pp. 297-304 (1977).

10. R. KIRIYAMA, H. KIRIYAMA, M. TAKAGAWA Proton Magnetic Resonance Studies of C_3AH_6. Supplementary paper II-27 Vth Symp. Chem. Cements TOKYO 1968.

11. J. SKALNY, I. JAWED, H.F.W. TAYLOR Studies on Hydration of Cement Recent Developments World Cement Technology Sept 78.

12. M. REGOURD Microstructure et Propriétés des Ciments Mortiers et Bétons Rev. Ciments Bétons Plâtres Chaux n° 734, pp. 41-48, Janv. 82.

13. FW LOCHER, W. RICHARTZ, S. SPRUNG Setting of Cement. Part II Effect of Adding Calcium Sulphate Zement Kalk Gips n° 10 (1976).

14. G.C. LITVAN Cem. Concr. Research. 6,139 (1976)

N.B. Singh, A.K. Singh and (Mrs.) S. Prabha Singh
Chemistry Department, Gorakhpur University, Gorakhpur (U.P.), India

2.1

Retardation of Portland Cement Hydration by Citric Acid.

Abstract : Citric acid is found to be a strong retarder for portland cement hydration. Calorimetric measurements show that in presence of citric acid the sequence of the hydration of aluminate and silicate phase is changed. X-ray diffraction analysis shows that before the renewed hydration of the aluminate phase gypsum is consumed and ettringite starts decomposing into monosulphate. Differential thermal analysis indicates that the amount of $Ca(OH)_2$ increases with hydration time but it was always lower in the presence of citric acid. Electrical conductivity measurements of the paste indicate that in presence of citric acid, the concentration and mobilities of the charge carriers are decreased. Compressive and tensile strengths are changed considerably in presence of citric acid. Zeta potential measurements give a definite proof regarding the adsorption of citric acid on the portland cement surfaces and in its presence the values become negative.

Constatou-se que o ácido cítrico é um poderoso retardador da hidratação do cimento portland. Medições calorimétricas mostram que a sequência da fase de hidratação do aluminato e do silicato se altera em presença de ácido cítrico. Análise por difração de raio X mostra que antes de renovada a hidratação da fase de aluminato, o gesso é consumido e a etringita começa a se decompor em monosulfato. Análise termo-diferencial indica que a quantidade de $Ca(OH)_2$ aumenta com o tempo de hidratação, mas é sempre menor em presença de ácido cítrico. Medições de condutividade elétrica da pasta indicam que, em presença do ácido cítrico, diminuem a concentração e a mobilidade dos condutores de carga. Em presença do ácido cítrico, as resistências à compressão e à tração mudam consideravelmente. Medições de potencial Zeta proporcionam uma prova definitiva da absorção do ácido cítrico nas superfícies do cimento portland e em sua presença os valores se tornam negativos.

N.B. Singh, A.K. Singh and (Smt.) S.Prabha Singh
Chemistry Department, Gorakhpur University, Gorakhpur (U.P.), India

Introduction

Setting and hardening of portland cement envolves chemical reaction with water. These processes can be influenced by addition of certain admixtures. Both accelerating and retarding admixtures are well known. Amongst the retarders sugars and the sugar acids have been studied extensively[1-7]. The important factor for an acid to be a strong retarder is that it must contain α and β hydroxy carboxylic group.[8,9] Recently Double[10] studied the effect of series of aliphatic acids on the hydration of portland cement and found that citric acid is one of the most powerful retarder. However, the mechanism of its action is not fully understood.

The present paper describes the mechanism of action of citric acid on the hydration of portland cement.

Experimental

Materials: Portland cement of following composition was used for the hydration studies:

Oxides	Composition (%)
CaO	60.1
SiO_2	23.0
Al_2O_3	5.94
Fe_2O_3	2.72
TiO_2	0.41
MgO	3.81
SO_3	2.38
K_2O	1.15

The mineralogical composition is as follows:

C_3S	C_2S	C_3A	C_4AF
26.0%	46.3%	11.1%	8.3%

The blain surface area was 4420 cm^2/g.

Citric acid (M. Sarabhai) was used as an admixture. In this paper portland cement is referred as PC and citric acid as CA and the concentration of the citric acid is always represented as weight percent.

Method:

1. Preparation of hydrated samples: Known amounts of PC were taken in polythene bags and mixed with water, 0.1, 0.2, 0.3 and 0.4 wt % CA solutions in such a way that the water-solid ratio was equal to one. The samples were allowed to hydrate at room temperature ($30 \pm 2^{\circ}C$). The hydration at different intervals of time was stopped with isopropyl alcohol and ether and dried at $105^{\circ}C$. The dried samples were stored in sealed polythene bags in a desiccator.

2. Determination of setting time: The initial and final setting times in the presence and absence of CA were determined with vicat needle. The water solid ratio was kept 0.2.

3. Non-evaporable water content: Non-evaporable water contents for hydrated samples were determined by heating nearly one gram of its sample first at $105^{\circ}C$ for one hour and then at $1000^{\circ}C$ for one hour. From the loss in weight, the non-evaporable water contents were determined.

4. X-ray diffraction studies: X-ray diffraction pattern of the samples were taken with a X-ray diffractograph using $CuK\alpha$ radiation. Following lines were used for analysis:

	d(A°)
Calcium hydroxide (CH)	4.9
Gypsum ($C\bar{S}H_2$)	7.56
Ettringite	9.73
Tetra calcium aluminate monosulphate 12-hydrate	8.92

5. Thermal analysis: DTA curves of hydrated samples were obtained by thermal analyser (Paulik-Paulik Erdeymom derivatograph, Hungary). The rate of heating was maintained at $10^{\circ}C$/min. from ambient temperature to $1000^{\circ}C$ in atmospheric air. The weight of each sample was ≈ 500 mg.

6. Compressive strength: Compressive strength of the PC in the form of cubes ($7.06 \times 7.06 \times 7.06$ cm^3) was determined in the presence of different concentrations of CA solutions at 3, 7, 15 and 28 days with water-cement ratio equal to 0.35.

N.B. Singh, A.K. Singh and (Smt.) S.Prabha Singh
Chemistry Department,Gorakhpur University, Gorakhpur, (U.P.),India

The experiments were made at room temperature. The cubes were kept in mould for 24 hours (72 hours in case of 0.3 and 0.4 wt % CA), the moulds were removed and submerged in clean fresh water until taken out just prior to breaking. The testings were done by an universal testing machine, manufactured by AIMIL, New Delhi.

7. Tensile strength: Tensile strengths of PC in the form of briquettes (7.6 cm length and 2.5 cm thick) were determined in the presence of different concentrations of CA solutions at 3, 7, 15 and 28 days with water-cement ratio equal to 0.35. The experiments were made at room temperature. The briquettes were kept in the mould for some hours and after which the moulds were removed and kept in clean fresh water until taken out just prior to breaking. The testings were done by an universal tensile testing machine, manufactured by AIMIL, New Delhi.

8. Electrical conductivity measurements: Electrical conductivities of the cement pastes in the presence of 0, 0.1 and 0.4% CA were measured with the help of a digital conductivity meter 304 (systronics) at 30°C with a water-cement ratio of one.

9. Liquid-phase analysis: 50 grams of PC were taken in different polythene bags and mixed with 50 CC of water or CA solutions. The cement was thoroughly mixed with steel spatula for nearly 30 seconds and then sealed. The bags were then kept in a thermostat maintained at 35°C. At different intervals of time, the solutions were quickly filtered in a carbon dioxide free atmosphere. The OH^- ions were determined by titrating against 0.1 NHCl, Ca^{++}, Na^+ and K^+ ion concentrations were determined with the help of a flame photometer.

10. Zeta potential measurements : For measurements of zeta potential, 0.02 gm of PC was dispersed in 100 ml water or CA solutions ultrasonically for 5 minutes and the suspension was placed in the electrophoretic cell of the zeta meter and the zeta potentials were determined by measuring electrophoretic mobilities.

11. Heat of Hydration : Heat of hydration was measured by a conduction calorimeter at 30°C in the presence and absence of 0.1% CA. The rate of heat liberation was recorded with a recorder. The actual rate of heat liberation and total heat evolved was calculated with a programable calculator.

Results and Discussion

The variation of initial and final setting times are given in fig. 1. Both the initial and final setting times are reduced

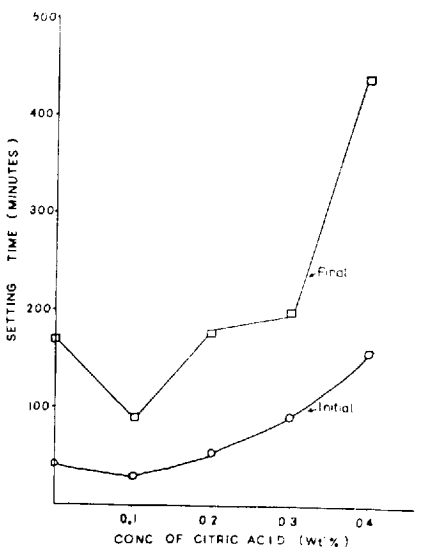

Fig.1. Effect of citric acid on the initial and final setting time.

in presence of 0.1% CA, whereas in presence of other concentrations of CA they are increased considerably. The increase in setting times increases with the increase in CA concentrations. From these results one can say that either 0.1% CA accelerates the hydration or it changes the nature of hydration products which reduced the setting times. Further it is quite clear that 0.2, 0.3 and 0.4% CA retards the hydration.

The variation of non-evaporable water content (W_n) very clearly indicate that

N.B. Singh, A.K. Singh and (Smt.) S.Prabha Singh
Chemistry Department, Gorakhpur University, Gorakhpur (U.P.), India

the values of W_n are constant during the induction period and after that increases. The induction period increases with the increase of CA concentrations. Also the values of W_n are always lower in the presence of CA than in its absence. This confirms that CA retards the hydration of PC and the retarding power increases with the increase in CA concentration.

The variation of concentrations of calcium hydroxide formed during the hydration as determined by x-ray diffraction shows that upto 3 days of hydration, the concentration of CH in the hydrated cement is maximum in the absence of CA and minimum in the presence of 0.3% CA. There is no indication of the formation of CH upto 3 days in presence of 0.4% CA indicating complete retardation of hydration. The results further confirms that upto 3 days of hydration, the retarding power increases with the increase of CA concentration. However, at 28 days of hydration, there is no sequence and the values are very close to each other.

Differential thermal analysis of hydrated cement shows an endothermic peak at around 570°C. This peak is due to the decomposition of $Ca(OH)_2$ formed during hydration. The variation of peak area in the presence and absence of CA are given in fig. 2. From the curves it is quite clear that in the absence of CA, the area

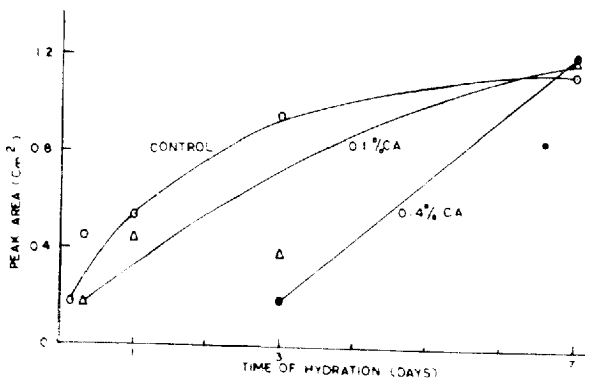

Fig. 2. Variation of DTA peak area for $Ca(OH)_2$ in hydrating portland cement.

increases with hydration time, indicating the increased formation of $Ca(OH)_2$. In the presence of CA also the area increases with hydration time but it is always lower than without CA except at 7 days of hydration, where, there is no definite sequence. It appears that at 7 days of hydration, the amount of $Ca(OH)_2$ formed in the presence and absence of CA, is nearly the same. In the presence of 0.4% CA, $Ca(OH)_2$ was detected only at 3 days of hydration. The results thus indicate that the amount of $Ca(OH)_2$ increases with hydration time and decreases with CA concentration. This means that PC hydration is retarded in presence of CA and the retarding power increases with the increase in CA concentration. It is also observed that the peak temperature decreases with the increase of CA concentration. This may be due to the following reasons :

(i) The amount of $Ca(OH)_2$ formed in presence of CA is lower as compared to that in its absence,

(ii) the crystallinity and compactness of $Ca(OH)_2$ crystals in presence of CA may be lower,

(iii) there may be morphological changes in $Ca(OH)_2$ crystals.

In presence of 0.1% CA the value of compressive strength is higher upto 15 days and remains nearly the same at 28 days than that of without CA. In presence of 0.2, 0.3 and 0.4% CA the values are always lower upto 15 days and the lowering increases with increase of CA concentrations. However, at 28 days, there is no regular sequence. In the presence of 0.4% CA the strength could be measured only at 15 and 28 days because upto 7 days, there was practically no strength. The higher values of compressive strength may be attributed due to changed nature of hydration products giving more strength.

The tensile strength continuously decreases with the increase of CA

N.B. Singh, A.K. Singh and (Smt.) S.Prabha Singh
Chemistry Department, Gorakhpur University, Gorakhpur (U.P.),India.

concentration.

Variation of electrical conductivities of the cement paste with hydration time in presence of 0.0, 0.1 and 0.4% CA are given in fig. 3. In the absence of CA, the electrical conductivity increases rapidly and

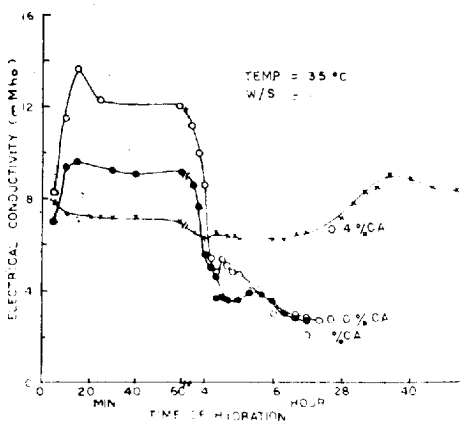

Fig. 3. Effect of citric acid on the electrical conductivities of cement paste.

reaches a maximum value at 15 minutes of hydration and then decreases till 5 hours. Again after 5 hours, there is an increase and the value is maximum at 7 hours and then the conductivity decreases. If the temperature and the system is constant, the conductivity will depend mainly on (1) concentration of charge carriers and (2) ionic mobility. In the present case as soon as cement comes in contact to water, dissolution and hydrolysis of cement start and the liquid phase rapidly becomes saturated or even supersaturated with respect to $Ca(OH)_2$. The first peak in the conductance curve may be due to this factor. After the saturation or supersaturation of the liquid phase, the process of crystallization of hydration products, adsorption of ions by the hydrated products and the association of ions start. These reduce the concentration of charge carriers and the ionic mobility of the ions and hence the conductivity decreases. Further after the induction period, acceleration of hydration starts and generally it reaches to its maximum within 7-8 hours. The second peak at 7 hours may correspond to this effect. In the presence of 0.1% CA, the conductivity is decreased but the first maximum is at the same hydration time. The second maximum is shifted towards higher hydration time. In the presence of 0.4% CA, the conductivity is further decreased and the first maxima disappeared and the second maxima shifted further towards higher hydration time (38 hours). This indicates that in presence of CA, the dissolution and hydrolysis of cement decrease and hence the concentration of charge carriers and may be ionic mobility also decreased. CA might be getting adsorbed at the cement particles causing reduction in dissolution or citric acid forms calcium citrate and being feebly soluble gets precipitated. This may cause lowering in Ca^{++} ion concentration in solution.

Variation of OH^- and Ca^{++} ions concentration in the liquid phase in presence and absence of CA are given in Fig. 4. In the absence of CA, OH^- ion concentration increase considerably upto 1 hour and then becomes practically constant upto 5 hours and again increases with a maximum at 7 hours of hydration. It indicates that as soon as cement comes in contact to water, hydrolysis starts and the alkalies of the cement also go into solution and the solution becomes saturated or even supersaturated within a hour and during the induction period it remains constant. After the induction period is over, it again starts

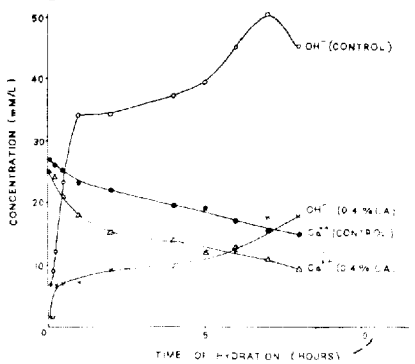

Fig.4. Variation of concentration of Ca^{++} and OH^- ions in liquid phase extracted from the hydrating paste, w/s = 1.

N.B. Singh, A.K. Singh and (Smt.) S. Prabha Singh
Chemistry Department, Gorakhpur University, Gorakhpur (U.P.), India

increasing and when the hydration becomes diffusion controlled, it decreases slowly.

In the absence of CA, the Ca^{++} ion concentration (Fig. 4) is maximum at 5 minutes of hydration (before this time measure-ments could not be made) and then continuously decreases upto 4 hours and then it becomes practically constant. This indicates that soon after mixing water, the solution becomes saturated or even supersaturated with respect to Ca^{++} ion and when the ionic product increases the solubility product, $Ca(OH)_2$ starts precipitating and as a result of this Ca^{++} ion concentration starts decreasing. Since OH^- ions come also from alkalies, it does not decrease. However, in presence of CA, the concentration of Ca^{++} ions is much lower and remains practically constant (Fig. 4) indicating that the hydrolysis of cement is decreased. OH^- ion concentrations are also much lower in presence of 0.4% CA and remain practically constant. These results indicate that as soon as cement comes in contact to CA solution, its surface is covered with CA molecules, which causes reduction of hydrolysis and hydration.

The variation of Na^+ and K^+ concentrations have also been studied. In the absence of CA, concentration of both the ions increases slowly whereas in presence of CA, they are much lower and remain practically constant. This can again be explained as a result of CA adsorption at the cement surface.

The variation of zeta potential in presence of different concentration of CA is given in fig. 5. In the absence of CA, the zeta potential is positive, whereas in presence of CA it becomes negative and the minimum value is at 0.2% CA. The negative sign of zeta potential very clearly indicates that citrate ions with negative charge are adsorbed at cement grains at the stern layer. Beyond this concentration, the zeta potential has increasing tendency indicating that desorption of ions may start. Because of the adsorbed

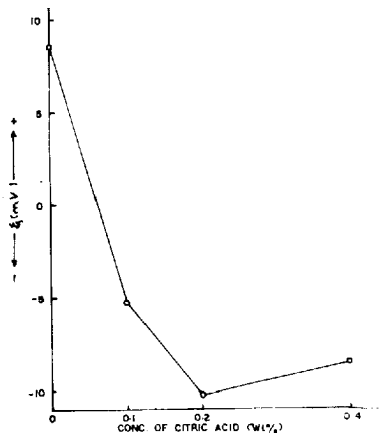

Fig. 5. Effect of citric acid on zeta potential.

citrate ions, which are bigger in size, the approach of water molecules to the cement grains are hindered and the hydration is retarded considerably in presence of CA.

In order to confirm whether the citric acid is adsorbed at the portland cement surfaces or on the surfaces of the hydrated products, the setting times were determined in two ways. Firstly the setting times were determined in a normal way as reported earlier. Secondly water was mixed with the cement to have a paste and after 10 minutes of hydration appropriate amount of citric acid was added in the paste which did not affect the setting times. This shows that the citric acid is adsorbed at the anhydrous portland cement and not the hydrated product.

The rate of heat evolution and the total heat evolved during the hydration of PC in presence and absence of 0.1% CA are given in figure 6 and 7. In the absence of CA, there are three peaks in the heat liberation curves. As soon as PC comes in contact to water, rapid heat evolution starts and sharp peak is obtained at 10 minutes of hydration. This peak is due to cement wetting, solution of alkalies and gypsum,

N.B. Singh, A.K. Singh and (Smt.) S. Prabha Singh
Chemistry Department, Gorakhpur University, Gorakhpur (U.P.), India.

hydration of free lime and the formation of ettringite. After the first peak, decrease

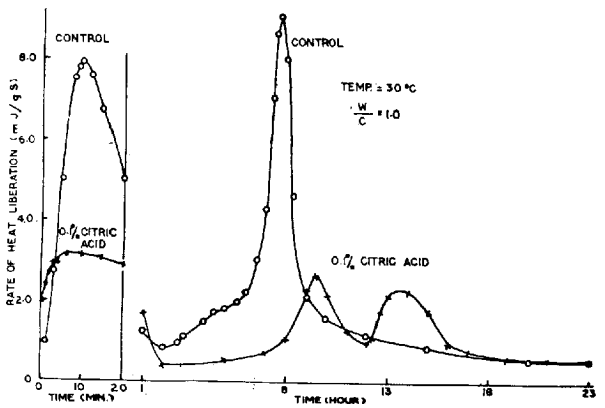

Fig. 6. Effect of citric acid on rate of heat liberation during the hydration of portland cement.

in heat evolution occurs and the reaction becomes very slow upto 2 hours. This period

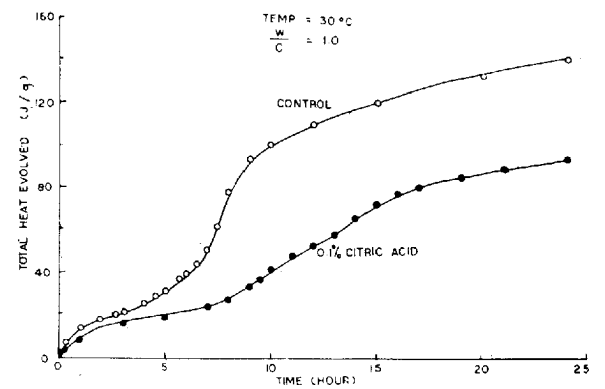

Fig. 7. Effect of citric acid on total heat evolved during the hydration of portland cement.

is known as the induction period. After the induction period is over, an acceleration of hydration starts, and the rate of heat liberation increases and reaches to a maximum value at arround 6 hours. This is mainly due to the hydration of alite. Before deceleratory period of alite hydration starts the rate of heat liberation increases considerably and reaches to a maximum value at 7.7 hours of hydration. This peak corresponds to renewed hydration of the aluminate phase. X-ray diffraction studies indicate that at 6 hours of hydration, there is no detectable gypsum and ettringite starts decomposing into monosulphate. Thus the third peak of the calorimetric curve is the renewed hydration of C_3A and during this period ettringite is converted into monosulphate.

In the presence of 0.1% CA, the rate of heat evolution and the total heat evolved are decreased considerably. Again there are three peaks in the calorimetric curve but with the change in the sequence of hydration. The first peak comes at arround 10 minutes of hydration. The induction period is increased and continues upto 5 hours. Now here renewed hydration of aluminate phase and the conversion of ettringite to monosulphate occurs before the alite hydration and a peak at 7.5 hours of hydration corresponds to this effect. This has been confirmed by X-ray diffraction also. The third peak at 14 hours of hydration correspond to alite hydration. Thus the hydration of both C_3A and alite is retarded in the presence of 0.1% CA. However the retardation of the alitephase is much more as compared to the aluminate phase. It appears that CA molecules are adsorbed at alite and aluminate surface, causing retardation of hydration. However, there may be preferential adsorption i.e. CA is adsorbed more at alite surface whereas it is adsorbed less at the aluminate surface. This preferential adsorption may be one of the reasons for renewed hydration of aluminate phase before the alite hydration in presence of CA.

Conclusion

The results indicate that the citric acid retard the hydration of portland cement at all concentrations. The hydration of both aluminate and alite phase is retarded. In the presence of citric acid the sequence of hydration is changed and the renewed hydration of C_3A and conversion of ettringite into monosulphate occurs before the hydration of

N.B. Singh, A.K. Singh and (Smt.) S.Prabha Singh
Chemistry Department, Gorakhpur University, Gorakhpur (U.P.), India

alite. Thermal analysis show that the amount of $Ca(OH)_2$ formed and its crystallinity and compactness in presence of citric acid is lower as compared to that in its absence. Zeta potential measurements clearly indicate the adsorption of citrate ions at the alite surface. This is one of the cause for retardation.

References

1. N.B. Singh, Cem. Concr. Res., 5, 545 (1975).
2. N.B. Singh and P.N. Ojha, J. Material Science, 16, 2675 (1981).
3. G.M. Breuer, Nature, 212, 502 (1966).
4. J.H. Taplin, Proc. 4th Int. Symp. Chem Cem. Washington, NBS Monogr. 43, Vol. II, 927 (1960).
5. R.W. Previt, Cement Concr. Research, 1, 301 (1971).
6. N.B. Milestone, J. Amer. Ceram. Soc., 62, 321 (1979).
7. N.L. Thomas and J.D. Birchall, Cement Concr. Research, 13, 830 (1983).
8. Gaidzhorov, Chem. Abst. 95, 208415 (1981).
9. S.A. Rodger and D.D. Double, Cem. Concr. Res., 14, 73 (1984).
10. D.D. Double, "Technology in 1990s Developments in hydraulic cements", The Royal Society, London, 53 (1983)

A. Negro, G. Abbiati - Dipartimento di Scienza dei Materiali e Ingegneria Chimica, Politecnico di Torino, Italia
L. Cussino - Ricerca e Sviluppo UNICEM SpA, Casale Monferrato, Italia.

SUR L'EMPLOI DU CALCAIRE COMME REGULATEUR DE PRISE DU CIMENT
ON THE USE OF LIMESTONE TO CONTROL CEMENT SETTING

Resumé

L'emploi de combustibles ayant des teneurs en soufre plus importantes que dans le passé, limite, quelques fois, l'ajout de gypse pendant le broyage du clinker. Le calcaire peut être substitué au gypse comme régulateur de prise.
Le but de la recherche est l'étude des caractéristiques d'un ciment dans lequel le gypse est remplacé par du calcaire.
Avec un clinker, dont la teneur en SO_3 était du 1,45%, ont été preparés cinq ciments additionnés de 6; 4,5; 3; 1,5; et 0% de $CaSO_4.2H_2O$ et respectivement de 0; 1,5; 3; 4,5; et 6% de $CaCO_3$.
On a constaté que le remplacement progressif du gypse par le calcaire influence la surface specifique Blaine et les temps de prise du ciment, en particulier quand le $CaSO_4.2H_2O$ est remplacé complètement par le carbonate.
Le comportement rhéologique des pâtes est également modifié: un remplacement partiel du gypse par le calcaire entraîne une diminution de la viscosité et de la seuil de cisaillement.
En ce qui concerne le comportement mécanique, l'effet de la substitution est significatif.
Si on remplace le 25% du gypse par le calcaire on a un accroissement de la résistence à la compression; des substitutions plus importantes donnent, au contraire, une diminution des résistences mécaniques.
Le retrait est influencé par le remplacement de 75% du $CaSO_4.2H_2O$ par du carbonate.
D'aprés ces résultats, on à constaté qu'il est possible de remplacer 50% de gypse par le calcaire sans porter prejudice au comportement des ciments et que, pendant l'hydratation, le carbonate, en reagissant pour donner du carboalluminate hydrate, joue le rôle d'un composant actif du ciment.
Des essais complémentaires sur des clinkers, dont la teneur en SO_3 dépasse les 2%, ont démontré que le calcaire joue un rôle encore plus important comme régulateur de prise.

SUMÁRIO

O emprego de combustíveis contendo teores de enxofre maiores do que no passado, limita, algumas vêzes, a adição de gesso durante a moagem do clínquer. O calcáreo pode substituir o gesso como regulador da pega.
O objetivo da pesquisa é o estudo das caracteristicas de um cimento no qual o gesso foi substituído por calcáreo.
Com um clínquer, cujo teor de SO_3 era de 1,45%, foram preparados cinco cimentos com adição de 6; 4,5; 3; 1,5 e 0% de $CaSO_4.2H_2O$ e respectivamente 0; 1,5; 3; 4,5 e 6% de $CaCO_3$.

Constatou-se que a substituição progressiva do gesso pelo calcáreo influencia a superfície específica Blaine e os tempos de pega do cimento, em particular quando o $CaSO_4.2H_2O$ é substituído completamente pelo carbonato.

O comportamento reológico das pastas é igualmente modificado: uma substituição parcial do gesso pelo calcáreo acarreta uma diminuição da viscosidade e do patamar de cisalhamento.
Quanto ao comportamento mecânico, o efeito da substituição é significativo. Se se substitui 25% do gesso por calcáreo obtém-se um aumento da resistência à compressão; substituições maiores dão, ao contrário, uma diminuição das resistências mecânicas.
A retração é influenciada pela substituição de 75% do $CaSO_4.2H_2O$ pelo carbonato.

De acordo com esses resultados, constatou-se que é possível substituir 50% do gesso pelo calcáreo sem causar prejuizo ao comportamento dos cimentos e que, durante a hidratação, o carbonato, reagindo para dar origem ao carboaluminato hidratado, torna-se um componente ativo do cimento.
Ensaios complementares em clínqueres, cujo teor em SO_3 ultrapassa 2%, demonstraram que o calcáreo tem um papel ainda mais importante do que regulador de pega.

Introduction

Le recours à des combustibles présentant des teneurs en soufre plus élevées que dans le passé, impose parfois une limitation à l'addition de gypse comme régulateur de prise.

Etant donné que le soufre reste lié au clinker, l'ajout de gypse doit être réduit afin que le pourcentage de SO_3 dans le ciment rentre dans les limites de la norme.

Ce problème s'est révélé d'une telle importance qu'il a été considéré comme prioritaire tant par l'U.S. Energy Research and Development Administrarion (E.R.D.A.) que par l'International Energy Agency (I.E.A.), qui ont proposé la mise à jour de la réglementation concernant la teneur en SO_3 dans le ciment et des recherches de substituants du gypse afin de stimuler l'utilisation de carbones à haute teneur en soufre, économiquement plus valables sur le plan du coût énergétique.

Babrowshi (1) et Bensted (2,3) ont suggéré récemment de remplacer le gypse par le calcaire; l'Agence Internationale de l'Energie semble orientée elle aussi vers ce type de solution.

Une étude préliminaire sur l'hydratation du C_3A (4) nous a confirmé que la substitution partielle de $CaSO_4.2H_2O$ par $CaCO_3$ determine des temps de prise et des expansions acceptables.

Les présent travail entend vérifier les caractéristiques physico-mécaniques de ciments dans lesquels le gypse a été remplacé par du carbonate de calcium.

Matériaux et méthodes

Avec un clinker dont la teneur en SO_3, est moyennement elevée (Tableau 1) nous avons réalisé des ciments à différentes teneurs en $CaSO_4.2H_2O$ et $CaCO_3$. De même nous avons préparé un ciment dans lequel une partie du gypse a été remplacée par de la silice.
Le clinker a été broyé en maintenant constant le temps de travail pour contrôler l'influence du remplacement du gypse par le carbonate de calcium sur la surface spécifique Blaine (ssB).
Le Tableau 2 indique la composition des ciments et leurs caractéristiques physiques.

La quantité d'eau pour réaliser la pâte normale et les temps de prise ont été déterminés conformément aux normes italiennes.

La cinétique d'hydratation a été suivie à l'aide de l'analyse calorimétrique différentielle (DSC), de la diffraction des rayons X, de la microscopie électronique à balayage (4).

Le comportement rhéologique des pâtes a été déterminé à 24°C en utilisant un rapport e/c = 0,45 (5,6).

Les Figures 1-3 présentent les résultats obtenus.

Sur les mortiers normals nous avons déterminé la consistance, le retrait après traitement des échantillons pendant 27 jours dans l'eau, la résistance à la compression selon les normes italiennes (Figures 4,5).

Résultats et discussion

La substitution progressive du gypse par du calcaire comporte une diminution de la surface spécifique; à la différence du calcaire et de la silice, le gypse agit comme adjuvant de broyage, comme l'a déjà signalé Hobbs (7).

La quantité d'eau de malaxage pour réaliser la pâte normale semble ne pas différer fondamentalement d'un ciment à l'autre.

Les temps de prise se révèlent acceptables, même lorsque 75% de $CaSO_4.2H_2O$ sont remplacés par $CaCO_3$ (ciment D); on a toutefois l'impression que le rôle de retardateur joué par le calcaire est négligeable: il suffit pour cela de comparer les temps de prise des ciments C et F.

L'analyse DSC, indique la formation initiale d'ettringite pour les ciments A-D,F et de carboaluminate pour le ciment E. Dans le ciment A, la présence de gypse est encore

Tableau 1 - Composition du clinker

ppc%	SiO_2%	Al_2O_3%	Fe_2O_3%	CaO%	MgO%	K_2O%	Na_2O%	SO_3%	N.D.%	CaO lib.%
0,64	21,90	4,89	2,63	63,78	2,65	0,92	0,42	1,45	0,72	1,34

C_3S%= 51,02; C_2S% = 24,31; C_3A% = 8,49% C_4AF% = 8,00

importante même après 6 heures d'hydratation.

L'analyse aux rayons X confirme les résultats de l'analyse thermique (DSC).

La viscosité des pâtes décroît en substituant 25% de gypse avec du calcaire, et prend des valeurs à peu près égales à celle du ciment témoin lorsque la substitution atteint 50%, pour augmenter nettement en cas de substitutions plus importantes (Figure 1).

leurs basses jusqu'à ce que 75% de gypse aient été remplacés par le calcaire (Figure 2).

Les valeurs des aires hystérésis (Figure 3) sont affectées de façon marquée par les substitutions du gypse dépassant 50%, surtout pour des temps supérieurs à l'heure.

La substitution d'une partie du gypse avec de la silice, améliore elle aussi le comportement rhéologique du ciment (Figures 1-3).

Le comportement rhéologique des ciments peut

Tableau 2 - Composition des ciments et caracteristiques physiques

Ciment	Composition %					ssB cm2/g	Pâte normale H_2O%	Temps de prise	
	Clinker	Gypse	Calcaire	Silice	SO_3% totale			D	F
A	94	6	-	-	3,93	3598	23,4	$2^h45'$	$5^h40'$
B	94	4,5	1,5	-	3,29	3540	22,8	$2^h35'$	$4^h55'$
C	94	3	3	-	2,64	3376	22,6	$2^h50'$	5^h
D	94	1,5	4,5	-	2,00	3365	22,2	$2^h55'$	$4^h45'$
E	94	-	6	-	1,36	3111	22,8	$0^h20'$	$1^h50'$
F	94	3	-	3	2,64	3281	23	$2^h45'$	$4^h40'$

De même, le seuil de cisaillement décroît en remplaçant le gypse par du carbonate de calcium; cette grandeur se maintient à des va-

trouver une explication dans l'étude de Locher et coll. (8). Ces derniers ont mis en évidence que l'apport des sulfates au début

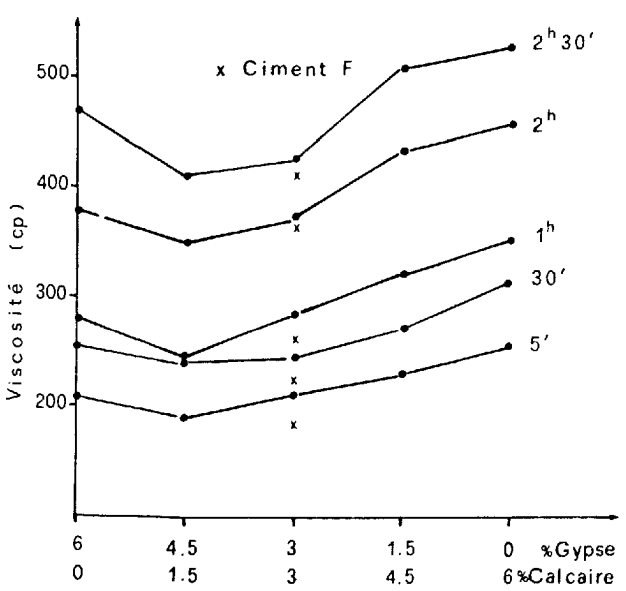

Fig. 1 - Valeurs de la viscosité des pâtes en fonction de la teneur en gypse et en calcaire.

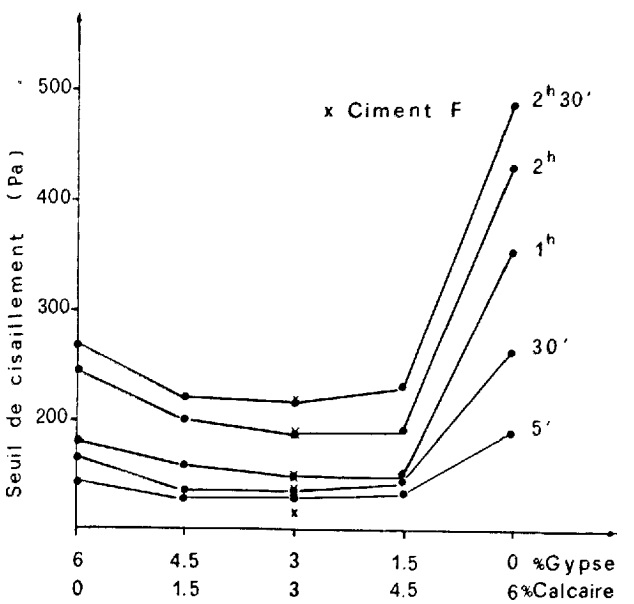

Fig. 2 - Valeurs de seuil de cisaillement des pâtes en fonction de la teneur en gypse et en calcaire.

de l'hydratation doit être tel que tout le C_3A se transforme en ettringite: en cas d'excédent de sulfates, du gypse secondaire se forme; en cas de défaut, en plus de l'ettringite se forment des aluminates de calcium hydrates ou du monosulfoaluminate.

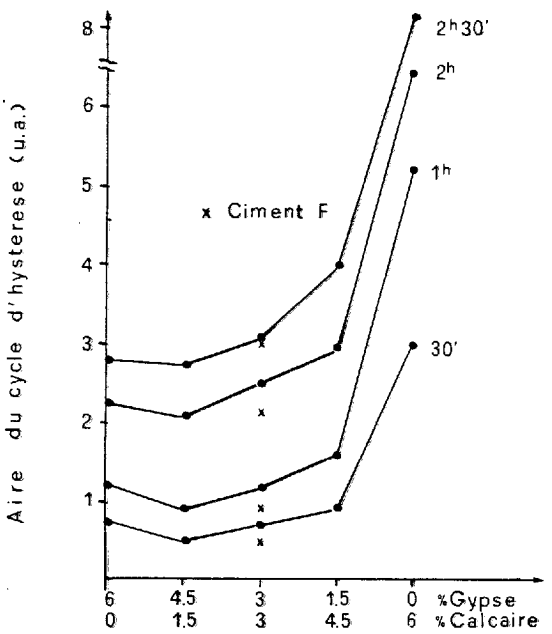

Fig. 3 - Aires d'hystérésis des pâtes en fonction de la teneur en gypse et en calcaire.

Les cristaux aciculaires de gypse secondaire ou bien les cristaux tabulaires d'aluminate ou de monosulfoaluminate hydraté constituent une structure rigide qui provoque un épaississement de la pâte de ciment.

Dans le cas examiné, le ciment A contient un excédent de gypse; les ciments D-E pauvres en gypse s'hydratent en formant, en plus de l'ettringite, des aluminates de calcium hydrates et du carboaluminate. Dans les deux cas se crée une structure plus rigide qui détermine un écoulement réduit de la pâte.

Par contre, les ciments B, C et F ont une teneur en gypse telle qu'au début de l'hydratation au moins, de l'ettringite seulement se forme sur la surface des grains de ciment. Puisque aucun pont ne s'établit entre ces grains, la pâte ne devient pas rigide.

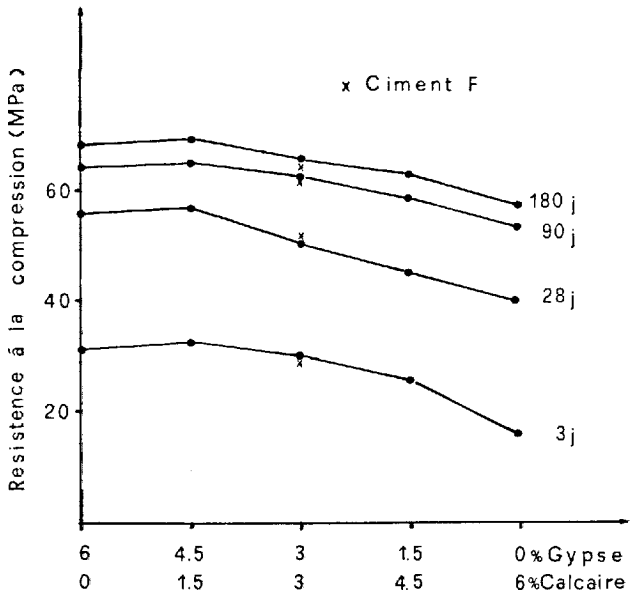

Fig. 4 - Résistance en compression des mortiers en fonction de la teneur en gypse et en calcaire.

Ce que nous venons d'exposer est confirmé en observant que l'ampleur des aires d'hystérésis (qui dépendent de la rupture du système thixotropique (9), c'est-à-dire des liaisons qui se sont établies entre les particules de ciment (6)) augmente avec la teneur en $CaCO_3$ (Figure 3).

De même, la résistance mécanique des mortiers est influencés par la substitution du gypse par du calcaire (Figure 4), comme il en ressort aussi de recherches précédentes (1-3).

De plus, il est confirmé qu'il existe une quantité optimale de gypse déterminant le maximum de résistance à la compression (10).

Le comportement mécanique des ciments peut s'expliquer aussi bien à la lumière des théories qui interprètent l'action du contenu optimal en gypse (11), qu'en admettant que le $CaCO_3$, en plus de former du carboaluminate hydraté, modifie la réactivité de l'alite et/ou la structure du CSH. Nos études en cours semblént confirmer cette hypothése.

En tout cas, il faut souligner que le pourcentage de calcaire qui peut remplacer le gypse, en fournissant les performances mécaniques les plus élevées, est variable, et

dépend probablement tant de la teneur en C_3A qu'en SO_3 soluble contenu dans le ciment.

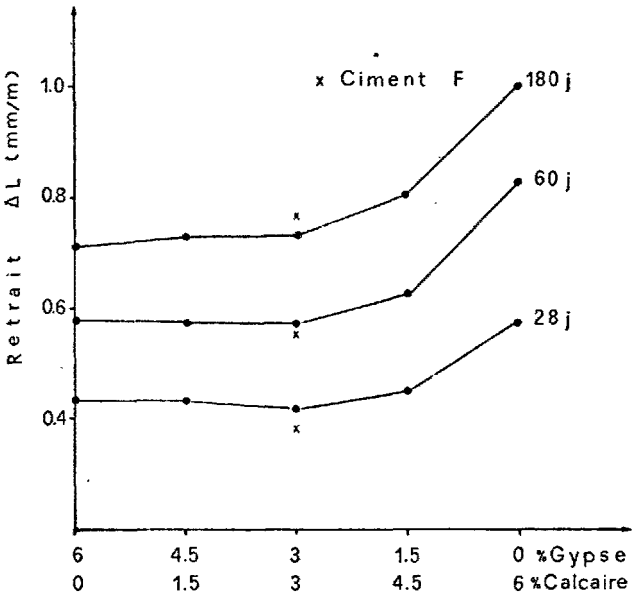

Fig. 5 - Retrait des mortiers en fonction de la teneur en gypse et en calcaire.

Par exemple, d'après de expériences récentes, dans un clinker ayant des teneurs de 6,98% de C_3A et de 2,35% de SO_3, il nous a été possible de remplacer totalement le gypse par le calcaire, en conservant des temps de prise et des résistances mécaniques absolument valables.

En dernier lieu, on peut faire remarquer que seules des substitutions dépassant 50% de $CaSO_4.2H_2O$ avec $CaCO_3$ influencent le retrait (Figure 5).

Cela est probablement en rapport avec la quantité d'ettringite qui s'est formée aux premiers stades d'hydratation et/ou à l'action du SO_3 sur la composition et la morphologie du CSH (11).

Conclusions

Les résultats obtenus permettent de tirer les conclusions suivantes:

- Il est possible de substituer 50% de gypse avec du calcaire sans compromettre le comportement des ciments.
- En accord avec les données de la littérature, il existe un rapport optimal gypse/calcaire qui détermine les meilleures performances du ciment.
- Le carbonate, tout en jouant parfois un rôle limité en tant que régulateur de prise, interagit en tout cas pour donner du carboaluminate, et se comporte donc comme un composant actif du ciment.

Bibliographie

1) G.S. Bobrowski, J.L. Wilson, K.E. Daugherty, (1977), Rock Products 80, 64.
2) J. Bensted, (1980), World Cement Tech. 11, 395.
3) J. Bensted, (1983), World Cement Tech. 14, 383.
4) A. Negro, L. Cussino, G. Abbiati, sous presse.
5) M. Collepardi, (1971), Il Cemento 3, 99.
6) P.F.G. Banfill, D.C. Sanders, (1981), Cem.Concr. Res. 11, 363.
7) D.W. Hobbs, (1977), World Cement Tech. 8, 75.
8) F.W. Locher, W. Richartz, S. Sprung, (1980), Zement Kalk Gips 10, 435 (1976) et 6, 271.
9) M.I. Shalon, S.A. Greenberg, (1960), Proc. IV ISSC vol. II, 731 Washington.
10) B. Cottin, (1977), Rev. Int. Hautes Temp. et Réfract. 14, 123.
11) J. Jawes, J. Skanly et J.F. Young (1983) en Structure and Performance of Cement, P. Barnes ed., App.Sci.Publisher, pp. 298, London.

Nous remercions Md.me A.A. Fournier de l'E.N.S.M. de St. Etienne pour la révision du texte.

Ce travail a été accompli avec la contribution du C.N.R. cont. n. 84.02663.59.

L. Cussino - Ricerca e Sviluppo UNICEM SpA, Casale Monferrato, Italia
L. Montanaro, A. Negro - Dipartimento di Scienza dei Materiali e Ingegneria Chimica, Politecnico di Torino, Italia.

ACTION DE L'ANHYDRIDE VANADIQUE SUR L'HYDRATATION DU CIMENT
VANADIUM PENTOXIDE EFFECT ON CEMENT HYDRATION

Resumé

On a étudié l'influence de l'anhydride vanadique sur les caractéristiques du ciment, ayant constaté que les bétons additionés de cendres volantes, provenantes de la combustion mixte de feul lourd et de houille et contenant ce composé, presentaient des retards au durcissement très importants.

Notre étude a été réalisé sur neuf ciments: deux de référence; deux ayants en solution solide dans lé clinker respectivement 0,20 et 0,45% de V_2O_5; quatre additionnés de 0,10; 0,25; 0,40; 0,60% de V_2O_5; un ciment de cendres volantes qui contenaient 0,45% de V_2O_5.

On a verifié que l'anhydride vanadique dissoute dans le clinker, surtout dans la bélite, ne perturbe pas ni la prise ni le durcissment contrairement à ce qui se passe si elle est simplement ajoutée au ciment. Dans ce cas les temps de prise sont d'autant plus longs que la teneur en V_2O_5 est plus grande. Pour des teneurs superieures à 0,25%, les temps de prise, mesurés par la methode de Vicat, diminuent; ceci est du à un épaississement de la pâte sans avoir une progression dans l'hydratation comme le mettent en evidence les courbes calorimétriques.

Le retard de prise est, probablement, du à la formation d'un vanadate de calcium amorphe qui, enrobant les grains de ciment, limite l'hydratation.

Les retards de prise et de durcissement influencent à court terme les résistences mécaniques des ciments, mais après vingthuit jours on retrouve des valeurs presque normales des résistences.

Le retrait est egalement influencé par l'anhydride vanadique.

Il semble donc que les cendres volantes qui contiennent V_2O_5 peuvent être employées, aprés controle, pour la production des ciments pouzzolaniques.

Au contraire l'utilisation imprudente de ces cendres dans la réalisation du béton peut être à l'origine de certains problèmes.

Foi estudada a influência do anidrido vanádico sobre as características do cimento, tendo-se constatado que os concretos com adição de cinzas volantes, provenientes da combustão mista de combustível pesado e de óleo e contendo este composto, apresentavam demoras muito relevantes no endurecimento.

Nosso estudo foi feito com nove cimentos: dois de referência; dois tendo respectivamente 0,20 e 0,45% de V_2O_5 em solução sólida no clínquer; quatro adicionandos respectivamente com 0,10, 0,25, 0,40, 0,60 de V_2O_5; um cimento de cinzas volantes contendo 0,45% de V_2O_5.

Verificou-se que o anidrido vanádico dissolvido no clínquer, sobretudo na belita, não prejudica nem a pega nem o endurecimento, contrariamente ao que acontece se ele simplesmente é adicionado ao cimento. Neste caso os tempos de pega são tão mais longos quanto maior o teor de V_2O_5. Para teores maiores que 0,25%, os tempos de pega, medidos pelo método de Vicat, diminuem; isto se deve a um espessamento da pasta sem uma progressão na hidratação, como se evidencia pelas curvas calorimétricas. O atraso da pega é devido, provavelmente, à formação de um vanadato de cálcio amorfo que, envolvendo os grãos de cimento, limita a hidratação.

Os atrasos de pega e de endurecimento influenciam a curto prazo as resistências mecânicas dos cimentos, mas depois de 28 dias encontram-se valores quase normais das resistências.

A retração é igualmente influenciada pelo anidrido vanádico.

Parece, portanto, que as cinzas volantes contendo V_2O_5 podem ser empregadas, após controle, para produção de cimentos pozolânicos.

Ao contrário, a utilização imprudente destas cinzas na preparação de concreto pode dar origem a certos problemas.

Introduction

Ayant constaté dans l'application pratique que l'ajout, dans le béton, de quantites importantes de cendres volantes, contenant du V_2O_5, se traduit par un retard du durcissement, les auteurs ont étudié l'enfluence du V_2O_5 sur les caracteristiques du ciment.

Rappelons que les cendres volantes, dérivées de la combustion mixte de fuel lourd dense et de houille, peuvent contenir des teneurs élevées en V_2O_5.

Une recherche précédente (1) avait établi que l'anhydride vanadique retarde considérablement l'hydratation du C_3S et la conversion de l'ettringite en monosulfoaluminate. Après avoir mis en évidence la formation d'un vanadate de calcium amorphe, nous avons formulé une hypothèse fondée sur la théorie de Kondo (2); le vanadate forme une enveloppe étanche autour des grains du solide qui sont ainsi isolés de la solution.

Partie expérimentale

Pour déterminer l'influence du V_2O_5 sur les performances du ciment quatre clinkers marqués A, B, C, D ont été utilisés.

Le premier a été synthétisé au laboratoire à partir d'une farine industrielle.

Le deuxième et le troisième ont été préparés dans les mêmes conditions en utilisant la même farine additionnée de façon à obtenir dans le clinker des teneurs en V_2O_5 de 0,20 et 0,45% respectivement.

Le quatrième était un clinker industriel obtenu à partir de la même farine utilisée pour la synthèse des trois précédents.

L'ajout de gypse dans les clinkers A, B, C a permis l'obtention des ciments A1, B1, C1; le clinker D a été broyé avec du gypse avec des quantités variable de V_2O_5 pour produire les ciments D1 - D5.

En vue de déterminer le comportement effectif du vanadium présent dans une cendre volante, nous avons de plus préparé le ciment D6 contenant 33% de cendres volantes.

L'analyse des clinkers et de la cendre a été exposée au cours d'un travail précédent (1); le Tableau 1 présente la composition des ciments.

Résultats et discussion

Il a été établi dans un premier temps, grâce à l'analyse par microsonde, que le vanadium dans les clinkers B et C se répartit de préférence dans la bélite (Figure 1); cela concorde avec les observations de Hornain (3).

Tableau 1 - Composition des ciments

Ciment	Gypse%	V_2O_5%	Cendre%
A1	5	-	-
B1	5	0,20^{+}	-
C1	5	0,45^{+}	-
D1	5	-	-
D2	5	0,10	-
D3	5	0,25	-
D4	5	0,40	-
D5	5	0,60	-
D6	5	0,13^{++}	33

+ V_2O_5 contenu dans le clinker

++ V_2O_5 apporté par la cendre

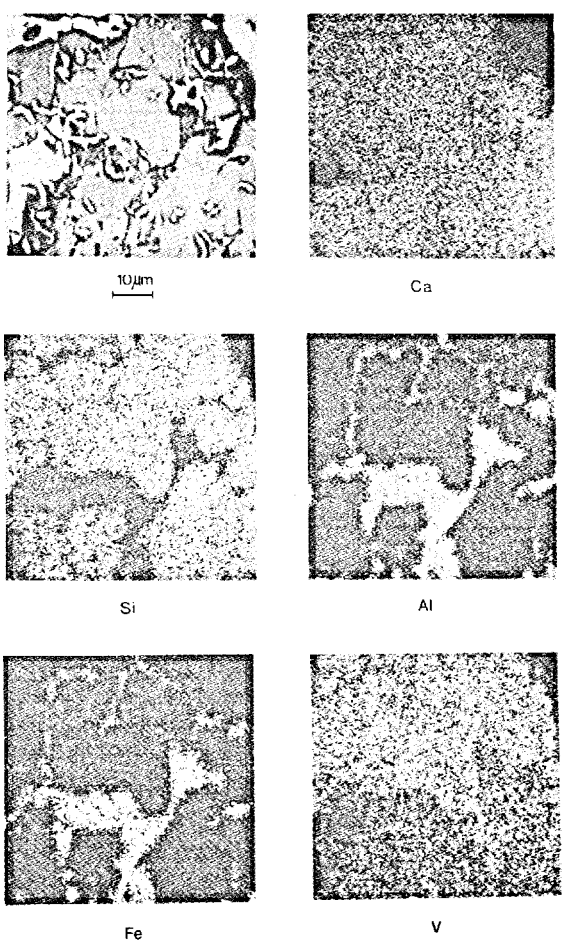

Fig. 1 - Image en électrons absorbés et analyse à la microsonde du clinker C.

Le pourcentage d'eau nécessaire pour réaliser la pâte normale s'élève à 23% environ pour tous les ciments, à l'exception du ciment aux cendres volantes (28%); ceci s'explique par sa plus grande surface spécifique Blaine (ssB) et par la nature de l'ajout.

Les valeurs du "flow" sont très similaires entre elles: 110 mm environ.

Le V_2O_5 présent dans le clinker modifie peu les temps de prise; par contre, nous constatons des retards très prononcés, quand il est ajouté au ciment dans des quantités allant jusqu'à 0,25% aussi bien comme composé pur que comme élément de la cendre volante.

A des teneurs dépassant 0,25% se produit un épaississement de la pâte sans toutefois déterminer la prise (Tableau 2).

Tableau 2 - Caractéristiques physiques des ciments.

Ciment	ssB cm^2/g	H_2O pour pâte normale %	Temps de prise	
			Début	Fin
A1	3710	23,2	2h05'	3h35'
B1	3705	22,8	1h55'	3h15'
C1	3715	23,0	1h35'	2h50'
D1	3638	23,0	2h20'	4h05'
D2	3696	22,8	6h	10h
D3	3710	22,6	6h30'	17h30'
D4	3724	22,6	2h15'	14h30'
D5	3750	22,8	1h15'	8h30'
D6	4492	28,4	5h10'	8h45'

Les courbes calorimétriques confirment les résultats précédents: l'effet exothermique, associé à l'hydratation apparaît après la même période pour les ciments A1 - C1 (Figure 2), alors qu'il se manifeste à des temps toujours plus longs pour les autres ciments en raison de la quantité de V_2O_5 additionnée (Figure 3).

En raison du peu de matériau disponible, la résistance en compression des ciments A1-C1 a été déterminée sur des échantillons de mortier cubiques de 2 cm. de côté (Figure 4); celle des ciments D1 - D6, conformément à la réglementation italienne.

Les échantillons on été conservés soit dans l'eau à 20°C durant 90 jours soit à l'air à

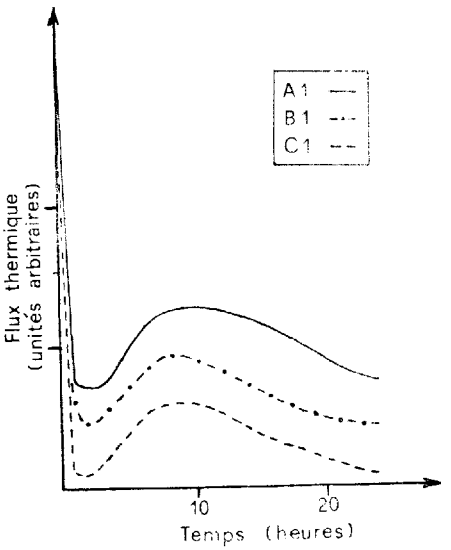

Fig. 2 - Courbes calorimétriques des ciments A1-C1.

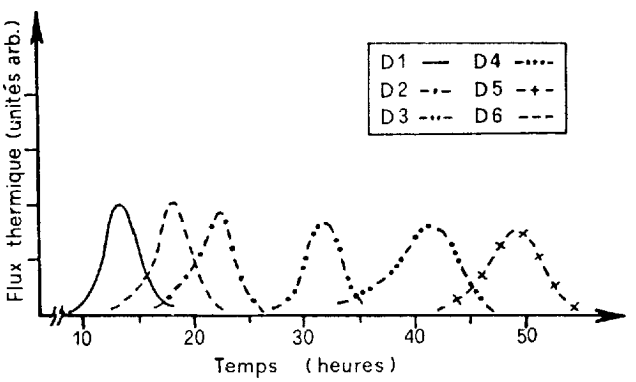

Fig. 3 - Courbes calorimétriques des ciments D1-D6.

20°C et à 50% H.R., durant 365 jours.

L'examen de la Figure 4 et du Tableau 3 fait ressortir nettement que, si l'anhydride vanadique se trouve dans le clinker, il n'influence pas la progression des résistances mécaniques, excepte une légère modification de la valeur absolue lorsque le V_2O_5 s'y trouve dans un pourcentage de 0,45; par contre, s'il est ajouté au ciment, il exerce une action prononcée sur la résistance en compression. Aux courtes échéances, les résistances mécaniques sont d'autant plus réduites que la teneur en V_2O_5 est plus élevée, cela est à mettre en relation avec le retard de prise mis en évidence par les courbes calorimétriques.

La résistance en compression du ciment D5 est caractérisée par un retard de durcissement moins prononcé. Le comportement de ce ciment

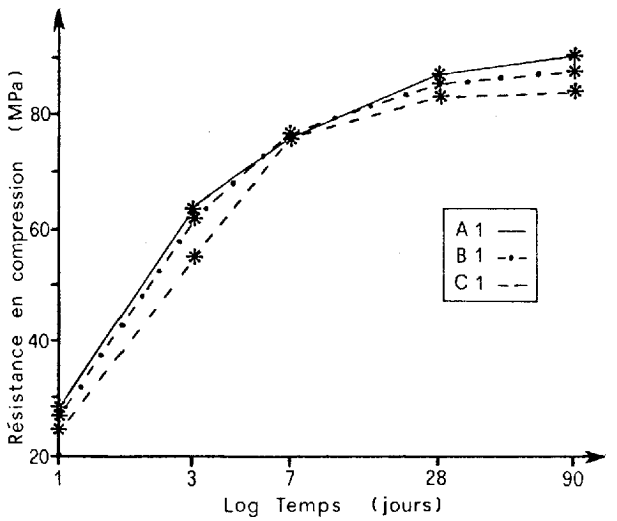

Fig. 4 - Evolution de la résistance à la compression sur micro-éprouvettes des ciments A1 - C1 en fonction du temps.

Tableau 3 - Résistance en compression (MPa) des ciments D1 - D6.

Temps de traitement (jours)	Ciments					
	D1	D2	D3	D4	D5	D6
1	11	-	-	-	-	4
2	25	19	2	1.5	8	-
3	33	29	14	14	19	19
7	46	41	34	35	40	32
28	60	59	58	58	62	48
90	66	63	60	62	70	65
365 à l'air, H.R. 50%, t = 20°C	69	69	94	66	60	65

peut s'expliquer en admettant d'une part que le vanadate de calcium amorphe, formé à la suite de la réaction entre V_2O_5 et $Ca(OH)_2$ (1), ralentit le processus d'hydratation, et que d'autre part il exerce une faible action liante, diminue la porosité du mortier, réduit le rapport eau/ciment en liant de l'eau.

A partir du 28ème jour, nous assistons pour tous les ciments contenant de l'anhydride vanadique à une augmentation notable des résistances.

Il est donc évident que la présence de V_2O_5 influence uniquement les premières phases de la prise et du durcissement, mais n'altère pas le comportement mécanique du ciment au cours des phases plus avancées d'hydratation; au contraire, à 90 jours, certains ciments contenant de l'anhydride vanadique offrent des performances supérieures à celles du ciment témoin, à condition que le traitement se fasse dans l'eau.

Un traitement de 28 jours dans l'eau et d'une année à l'air, pour le ciment à 0,6% de V_2O_5, se traduit par une diminution des résistances entre 90 et 365 jours.

Pour le ciment D6 il n'y pas de changement de resistance entre 90 et 365 jours.

Ce dernier résultat a besoin de confirmations ultérieures, étant donné que la résistance pourrait être influencée par le milieu de traitement excessivement sec et donc non adapté à un ciment contenant des cendres volantes.

En dernier lieu, l'action provoquée par le V_2O_5 dans l'application pratique a été vérifiée à l'aide d'essais sur des bétons.

La composition des bétons préparés avec les ciments D1, D3, D4, D6 et les valeurs de résistance mécanique sont indiquées au Tableau 4 et sur la Figure 5.

Le béton Cz6 a été préparé avec du ciment D6 et une partie du sable a été remplacée par la cendre volante.

Comme dans les mortiers, le V_2O_5 provoque dans les bétons des retards de prise sensibles, au point de ne pas permettre le démoulage des échantillons après 24 heures; ces retards sont proportionnels à la teneur en V_2O_5 et l'effet sur le béton est plus marqué quand on réalise des consistances fluides. Si le béton n'est pas perturbé pendant la période dormante, la reprise des résistances est assurée graduellement et, dans le cas du béton avec cendre, elle est même plus élevee à 28 jours.

Enfin, les essais de retrait ont été effectués sur des échantillons de mortier normal conservés dans l'eau pendant 28 jours et, ensuite, dans un milieu à 20°C et 50% H.R. (figure 6).

Pendant le traitement dans l'eau, la présence de V_2O_5 détermine une plus grande expansion et, pendant le séchage, un plus fort retrait.

Nous pouvons donc admettre que le V_2O_5, qui

Tableau 4 - Composition et caractéristiques des bétons

Béton	Cz1	Cz3	Cz4	Cz6
Dosage du ciment kg/m3	250	250	250	250
Cendre volante kg/m3	-	-	-	100
Pourcentage de V_2O_5 dans le ciment	-	0,25	0,40	0,13+
Rapport E/C	0,85	0,87	0,88	0,84
Slump	15	15	15	15
+ Pourcentage de V_2O_5 provenant de la cendre volante				

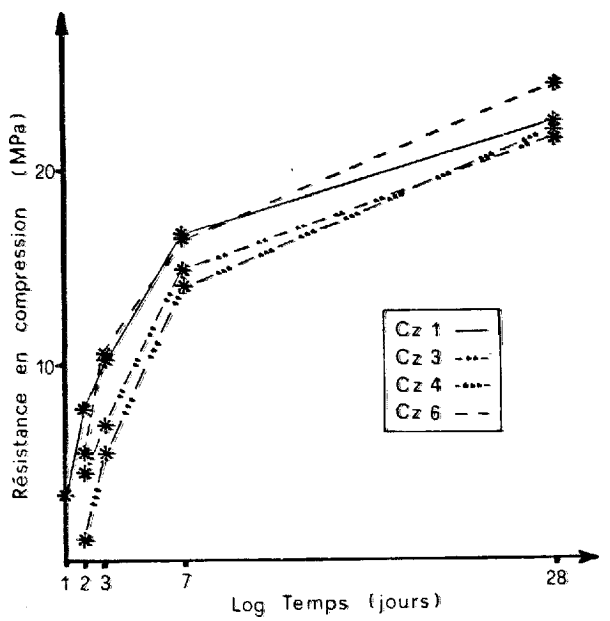

Fig. 5 - Evolution de la résistence en compression des bétons Cz1, Cz3, Cz4, Cz6 en fonction du temps.

s'est transformé en vanadate de calcium amorphe, donne lieu au début à une expansion; par la suite, le vanadate cristallise en provoquant une contraction de volume.

Cette diversité de comportement du ciment D2, dont l'expansion dans l'eau est moindre que celle du ciment D1, peut s'expliquer en admettant que le retrait provoqué par le V_2O_5 sur l'hydratation et donc sur l'expansion de la pâte, n'est pas compensé par l'expansion du gel de vanadate de calcium, car ce dernier s'y trouve en petite quantité.

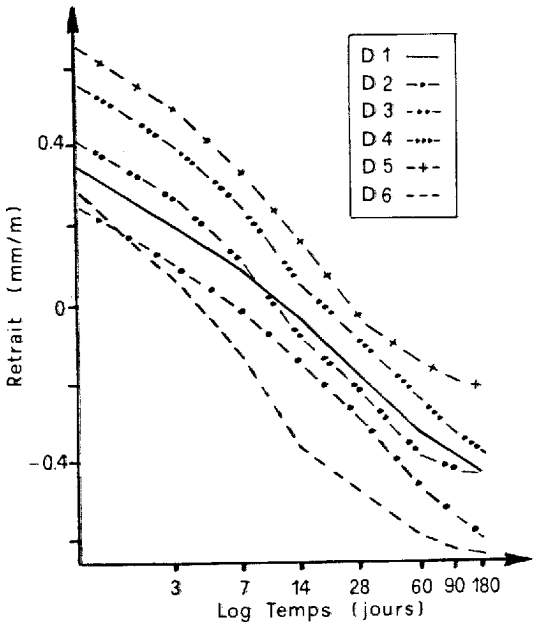

Fig. 6 - Evolution du retrait des ciments D1 - D6 en fonction du temps.

Conclusions

D'après les résultats obtenus il est possible de tirer les conclusions suivantes:

- L'anhydride vanadique en solution solide dans le clinker, particulièrement dans la bélite, ne perturbe ni la prise ni le durcissement;
- Au contraire, le V_2O_5 additionné au ciment provoque un retard des temps de prise et de durcissement en fonction de la quantité ajoutée;
- Le retard des temps de prise et de durcissement est à imputer probablement à la formation d'un vanadate de calcium amorphe qui, enrobant les grains de ciment, en ralentit l'hydratation;
- Le ralentissement du processus d'hydratation se répercute évidemment de façon marquée sur les résistances mécaniques à court terme, même si après 28 jours de traitement, nous ne constatons plus que de très faibles differences;
- L'anhydride vanadique, en ralentissant la vitesse d'hydratation, permet aux longues échéances l'obtention de résistances mécaniques élevées des échantillons conservés dans l'eau;
- Les échantillons préparés avec des ciments additionnés de 0,6% de V_2O_5, après 28 jours de conservation dans l'eau et une année de traitement à l'air, presentent une diminution des résistances mécaniques;

- D'après ce qui précède, il semble possible de préparer des farines en utilisant des cendres volantes contenant de l'anhydride vanadique dans certaines limites, sans que cela se répercute de façon significative sur les caractéristiques physico-mécaniques du ciment;
- L'utilisation de cendres volantes contenant du V_2O_5 en cimenterie pour la production de ciments pouzzolaniques peut être contrôlée en faisant appel aux essais ordinaires de conformité aux normes et en intervenant là où cela est nécessaire. Par contre, l'emploi indiscriminé ou imprudent des cendres dans la préparation du béton peut créer des problèmes qui ne permettent ni interventions ni remèdes, à part une attente prolongée pour les décoffrages.

Bibliographie

1) A. Negro, L. Montanaro et L. Cussino (1985), "Vanadium pentoxide effect on hydratation of C_3S and C_3A in the presence of gypsum and lime". Il Cemento 82 (1), 41-8.
2) R. Kondo, M. Daimon, E. Sakoi et H. Ushiyama (1977) "Influence of inorganic salts on the hydration of tricalcium silicate", J. Appl. Biotechnol. 27, 191-197.
3) H. Hornain (1971) "Sur la répartition des éléments de transition et leur influence sur quelques propriétés du clinker et du ciment", Rev.Mat.Constr. 671/672, 203-219.

Nous remercions Md.me Regourd du C.E.R.I.L.H. de Paris pour les analyses par microsonde et Md.me A.A. Fournier de l'E.N.S.M. de St. Etienne pour la revision du texte.

S. Monosi, M. Collepardi, University of Ancona, Ancona, Italy 1

EFFECT OF SILICA FUME ON THE HYDRATION PRODUCTS OF C_3A-$C\bar{S}H_2$ SYSTEM

2.1

EFFET DE FUMEE DE SILICE SUR LES PRODUITS D'HYDRATATION DU SYSTEMA C_3A-$C\bar{S}H_2$

SUMMARY: The hydration of C_3A-$C\bar{S}H_2$ systems at 20°C has been studied in the presence of quartz (considered to be inert) or silica fume. Moreover, since silica fume is generally used in cement mixes in combination with superplasticizers, the effect of polymer based on naphthalene sulfonated has been also examined.

The hydration products have been identified by thermal analysis (DTG). In some cases XRD analysis has been also carried out.

In the presence of quartz the usual hydration products of the C_3A-$C\bar{S}H_2$ system have been observed: ettringite is initially produced and then it is transformed into monosulfate.

When silica fume replaces quartz the conversion the ettringite into monosulfate is accelerated. Moreover, in the presence of silica fume, beside the monosulfate after some days a new product is formed with a DTG peak at about 370°C and a group of XRD lines at 5.06, 3.32, 3.11, 2.79, 2.27, 2.02 Å.

On the basis of these data the new product has been identified as a hydrogarnet of chemical composition $C_3AS_xH_{6-2x}$.

With a combined additon of silica fume and naphthalene sulfonated polymer to the C_3A-$C\bar{S}H_2$ system the hydrogarnet production is retarded or completely inhibited (at least up to 28 days) depending on the polymer dosage (0.4 or 2% by weight respectively). Moreover, at the higher dosage of polymer the formation of ettringite and its conversion into monosulfate are both retarded.

Sumário :

A hidratação dos sistemas C_3A-$C\bar{S}H_2$ à 20°C foi estudada em presença de quartzo (considerado inerte) ou microsílica. E mais, como a microsílica é geralmente usada nos concretos em combinação com superplastificante, também foi examinado o efeito de polímeros com base em naftalenos sulfonados.

Os produtos de hidratação foram identificados por análise termo-gravimétrica (DTG). Em alguns casos também foram feitas análises por difração de raios X (XRD).

Em presença do quartzo os produtos usuais de hidratação do sistema C_3A-$C\bar{S}H_2$ foram observados: etringita é inicialmente formada e depois é transformada em monosulfato.

Quando a microsílica substitui o quartzo, a conversão da etringita em monosulfato é acelerada. E mais, em presença da microsílica, além do monosulfato após alguns dias um novo forma-se com um pico DTG a cerca de 370°C e um grupo de linhas XRD com 5,06, 3,32, 3,11, 2,79, 2,27 e 2,02 Å.

Com base nesses dados, o novo produto foi identificado como sendo uma hidrogranada de composição química $C_3AS_xH_{6-2x}$.

Com uma combinação na adição de microsílica e polímero naftaleno sulfonado ao sistema C_3A-$C\bar{S}H_2$, a formação da hidrogranada é retardada ou completamente inibida (ao menos até 28 dias) dependendo da dosagem do polímero (0,4 a 2% em peso respectivamente). Além disso, com dosagens mais elevadas do polímero a formação de etringita e sua conversão em monosulfato são ambas retardadas.

Introduction

Since the last few years, it is well known that the need for conserving energy through the lower percentage of clinker in cements has revived the interest in materials having chemical composition and surface properties similar to those of pozzolans.

In recent times research works have been directed towards investigations of silica fume, a by-product resulting from the manufacture of silicon steel. Silica fume appears to possess rather interesting characteristics.

A number of authors (1) have found that, when used as partial substitution of cement, silica fume shows a good pozzolanic activity, because of its high content in amorphous silica and its high fineness (20 m^2/g). This extraordinary fineness also results in high demand for mix water to obtain concrete with good workability; yet, the addition of a superplasticizing admixture can conduce to relatively low water/solid ratios again. Moreover, added water being equal, a content of silica fume up to 30% seems to impart improved mechanical properties to concrete.

In the present paper, the influence of silica fume on the C_3A-gypsum system in the presence or absence of superplasticizer is investigated in order to assess the variation both in the kinetics of hydration and in the nature of the hydrated products.

Materials

Four mixes were prepared whose composition is shown in Table 1.

Table 1 Composition of anhydrous mixes (Q=quartz, SF=silica fume, NS=dry polymer of calcium naphthalene sulfonate)

C_3A	Q	SF	$C\bar{S}H_2$	NS
50	40	--	10	--
50	--	40	10	--
50	--	40	10	0.4
50	--	40	10	2

Tricalcium aluminate was the same material already used in other works (2,3). Silica fume, with the fineness of 20.70 m^2/g was the same which was used in a previous work (4). Finely ground quartz (passing the 37-mm sieve) was used as an inert material in order to obtain the same amount of C_3A in the mixes without silica fume.

Tricalcium aluminate and silica fume (or quartz) were dry mixed with gypsum and naphthalene sulfonate polymer in powder form, obtained by drying out a proprietary admixture made of a 40% aqueous solution of polymer.

Specimens were hydrated with a given quantity of water in order to obtain a water/solid ratio of 0.5 and then they were maintained at 20°C. At given times, from 6 hours to 28 days, the reaction was blocked by grinding the specimens in methyl alcohol; filtered specimens were tested by thermogravimetric analysis and, in some cases, also by X-ray diffraction.

Results and Discussion

Figure 1 indicates the DTG curves of the C_3A-quartz-gypsum mix. At about 150°C the anhydrous mix shows the peak attributed to bihydrated gypsum. After a 6 hours hydration, one peak at 120°C, due to the thermal decomposition of ettringite, and two peaks (at 200 and 280°C) of monosulfate, are present. At 1 day, the peaks of monosulfate are considerably higher and only traces of ettringite are present. At later ages, monosulfate is the only product of the reaction left, as it had already been found and discussed in a previous work (5).

Figure 2 shows the DTG curves of the reaction products of the C_3A-silica fume-gypsum mix. The substitution of quartz with silica fume, which is more reactive, determines interesting variations of both the hydration kinetics, and, above all, the type of products obtained. At 6 hours the conversion of ettringite into monosulfate is almost completed. Moreover, the XRD analysis indicates that the percentage of hydrated C_3A appears to be higher in the presence of silica fume than in the presence of quartz. An analogous behaviour has been pointed out in other publications in connection with the hydration of C_3A, pozzolan and gypsum mixes (6,7). The conversion of ettringite into monosulfate is completed after 1 day. At 3 days, a new peak at about 370°C appears, in

2.1

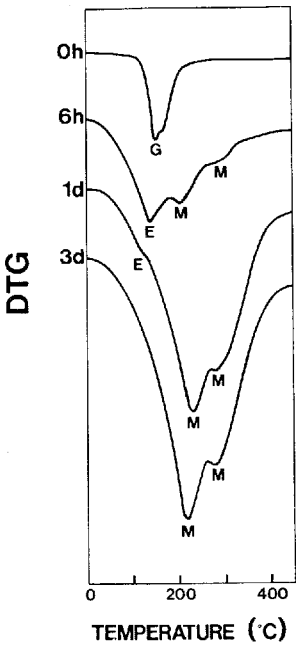

Fig.1 DTG curves of the hydration products of the C_3A-quartz-gypsum mix. G=gypsum; M=monosulfate; E=ettringite.

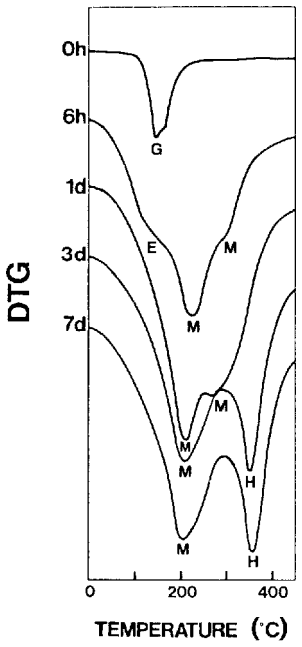

Fig. 2 DTG curves of the hydration products of the C_3A-silica fume-gypsum mix. H=hydrogarnet.

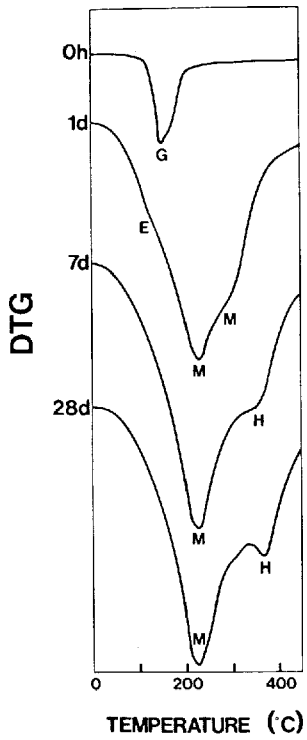

Fig.3 DTG curves of the hydration products of the C_3A-silica fume-gypsum mix in the presence of 0.4% superplasticizer.

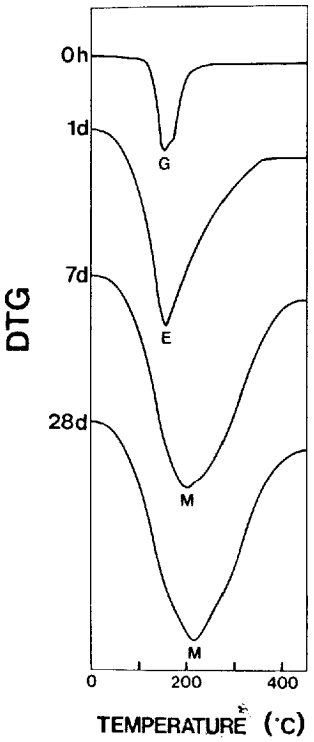

Fig.4 DTG curves of the hydration products of the C_3A-silica fume-gypsum mix in the presence of 2% superplasticizer.

2.1

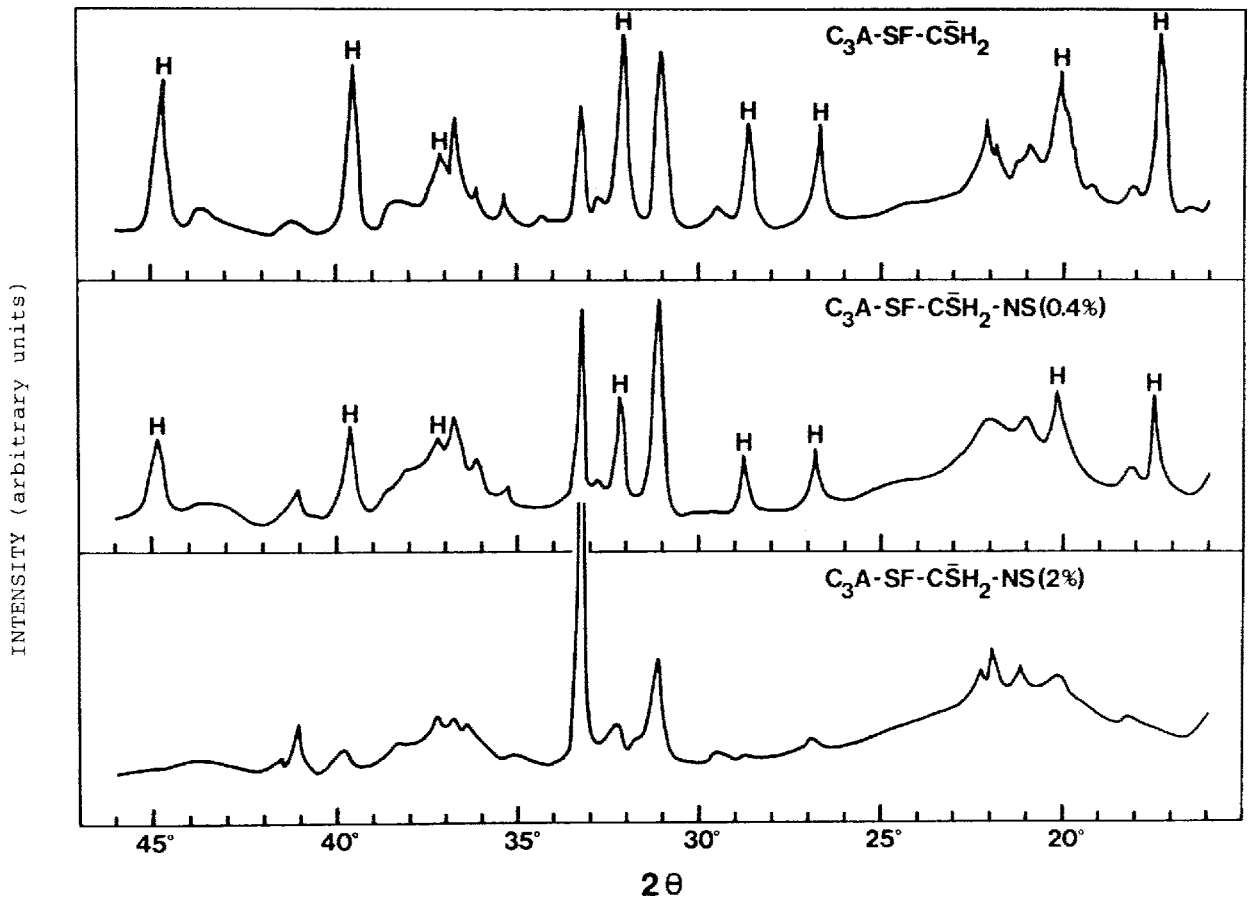

Fig. 5 XRD patterns of the hydration products of the C_3A-silica fume-gypsum mix. H = hydrogarnet

addition to the peak already mentioned. Comparing the XRD patterns obtained with the existing data in the literature (8) allowed to identify this new peak as hydrogarnet ($C_3AS_xH_{6-2x}$).

Figure 3 shows the DTG peaks of the C_3A-silica fume-gypsum mix, hydrated at 0, 1, 7, 28 days in the presence of 0.4% of superplasticizer by weight of cement. At 1 day, the peaks of monosulfate and a shoulder attributed to residual ettringite are observed. Comparing these results with the one obtained at 1 day without admixture (Fig. 2), it can be concluded that the superplasticizer slightly retards the conversion of ettringite into monosulfate. Only at 7 days, the peak attributed to the hydrogarnet appears at about 370°C; the presence of the admixture retards its appearance and strongly retards its rising. It does not reach the amount it had in the mix without admixture at 3 days, not even at 28 days.

The increase in the dosage of superplasticizing admixture (2%) retards the conversion of ettringite into monosulfate strongly (Fig. 4). For example, at 1 day the DTG peak of ettringite at 120°C is predominant.

Figure 5 indicates the X-ray diffraction patterns of the C_3A-silica fume-$C\bar{S}H_2$ system hydrated at 7 days with and without superplasticizing admixture. The XRD analysis confirms the presence of hydrogarnet in the sample without superplasticizer and in the sample with a lower dosage (0.4%) of admixture. In the last case, the intensity of XRD peaks is weaker. Even the XRD analysis does not indicate the presence of hydrogarnet in the specimen with a higher dosage of superplasticizer (2%).

Conclusion

The addition of silica fume to the C_3A-$C\bar{S}H_2$ system accelerates the production of ettringite and its conversion into monosulfate. Moreover, it causes the formation of hydrogarnet ($C_3AS_xH_{6-2x}$) which is strongly evident after 3 days of hydration.

Naphthalene sulfonate based superplasticizer, added at the dosage rate of 0.4% to the C_3A-silica fume-$C\bar{S}H_2$ system, slows down both the conversion of ettringite into monosulfate and the formation of hydrogarnet. The strong effect obtained with the dosage of 2% hinders the production of hydrogarnet at least up to 28 days.

References

(1) G.G. Carette and V. M. Malhotra, "Silica Fume in Concrete - Preliminary Investigation", CANMET Report 82-1E, Canada, February 1982.

(2) S. Monosi, G. Moriconi, M. Pauri, M. Collepardi, "Influence of Gluconate, Lignosulfonate or Glucose on the C_3A Hydration", Cem. Concr. Res., 13, 568-574, 1983.

(3) M. Collepardi, S. Monosi, G. Moriconi and M. Pauri, "Influence of Gluconate, Lignosulfonate or Glucose on the C_3A Hydration in the Presence of Gympsum With or Without Lime", Cem. Concr. Res., 14, 105-112, 1984.

4) S. Chatterji, M. Collepardi and G. Moriconi, "Pozzolanic Property of Material ans Synthetic Pozzolans: a Comparative Study", First International Conference on the Use of Fly Ash, Silica Fume, Slag and other Mineral By-products in Concrete, Montebello, Canada, July 31-August 5, 1983, Vol. 1, pp 221-232.

5) M. Collepardi, G. Baldini and M. Pauri, "Tricalcium Aluminate Hydration in the Presence of Lime, Gypsum or Sodium Sulfate", Cem. Concr. Res., 8; 571-580, 1978.

6) M. Collepardi, G. Baldini and M. Pauri, "The Effect of Pozzolans on the Tricalcium Aluminate Hydration", Cem. Concr. Res., 8, 741-752, 1978.

(7) H. Uchikawa and S. Uchida, "Influence of Pozzolana on the Hydration of C_3A", 7th International Congress on the Chemistry of Cement, Paris 1980, Vol. III, Theme IV 24-29.

(8) H.F.W. Taylor, "The Chemistry of Cements", Vol. I, pg 344, Academic press, London, (1964).

M. Pauri, S. Monosi, G. Moriconi and M. Collepardi, University of Ancona, Ancona, Italy 1

EFFECT OF TRIETHANOLAMINE ON THE TRICALCIUM SILICATE HYDRATION 2.1

EFFET DE LA TRIETHANOLAMINE SUR L'HYDRATATION DU SILICATE TRICALCIQUE

SUMMARY: The effect of triethanolamine (TEA) on the C_3S hydration at 20°C with and without (or $N_{0.25}C_{2.75}A$) and gypsum was studied.

Addition of TEA (0.1%) to a pure C_3S paste (water/solid ratio = 0.50) slightly retarded the early hydration process particularly during the first 6 hours. After 1 day no substantial change in C_3S hydration process was caused by TEA addition.

This retarding effect was almost completely eliminated when C_3S hydrated in the presence of C_3A (or $N_{0.25}C_{2.75}A$) and gypsum. On the other hand, TEA accelerated the early ettringite production and its transformation into monosulfate particularly in the C_3S-$N_{0.25}C_{2.75}A$-$C\bar{S}H_2$ system. It would seem that the adsorption of TEA molecules on ettringite could remove the admixture from the aqueous phase and consequently decrease or eliminate the slight retarding effect on the C_3S hydration.

SUMÁRIO: Estudou-se o efeito da trietanolamina (TEA) sobre a hidratação do C_3S a 20°C, com e sem C_3A (ou $N_{0,25}C_{2,75}A$) e gesso.

A adição de TEA (0,1%) a uma pasta de C_3S puro (relação de água/sólido = 0,50) retardou ligeiramente o processo inicial de hidratação, particularmente durante as primeiras 6 horas. Depois de 1 dia, a adição de TEA não causou mudança substancial no processo de hidratação do C_3S.

Este efeito retardador foi quase completamente eliminado quando o C_3S se hidratou em presença de C_3A (ou $N_{0,25}C_{2,75}A$) e gesso. Por outro lado, a TEA acelerou a produção inicial de etringita e sua transformação em monossulfato, particularmente no sistema C_3S-$N_{0,25}C_{2,75}A$-$C\bar{S}H_2$. Poderia parecer que a absorção de moléculas de TEA na etringita poderia remover aditivo da fase aquosa e, conseqüentemente, diminuir ou eliminar o ligeiro efeito retardador sobre a hidratação do C_3S.

Introduction

Triethanolamine (TEA) is usally used as raw material in many concrete admixtures. Use of pure water reducing agents often prolongs setting time and extends induction period so that hydration of cement is significantly delayed. Addition of TEA achieves intent to limit retarding effect on these admixtures on cement hydration (1).

Triethanolamine alone has been found to act as a retarding on C_3S hydration (2) but an accelerator of ettringite formation (3).

In the present paper the effect of TEA on the hydration of C_3S-C_3A (or NC_3A) system in the presence of gypsum has been studied.

Experimental

a) Hydration

Tricalcium aluminate (C_3A) and C_3A-Na_2O solid solution (NC_3A) were prepared according to a methodology employied in previous works (4) (5). Blaine specific surface area of C_3A and C_3A-Na_2O solid solution were 3100 and 3050 cm^2/g respectively.

Tricalcium silicate was also prepared from reagent grade $CaCO_3$ and SiO_2 according to the method described in a previous paper (6). The Blaine specific surface area of C_3S was about 3250 cm^2/g.

Gypsum, calcium hydroxide, TEA reagent grade were also used.

Tricalcium silicate alone and mixes of C_3S (75%)-C_3A (20%)-$C\bar{S}H_2$ (5%) or of C_3S (75%)-NC_3A (20%)-$C\bar{S}H_2$ (5%) hydrated with water or a 2000 mg/l TEA aqueous solution. With water/solid ratio of 0.50, such as that used for the hydration, the TEA percentage by weight of solid was 0.1%.

The hydration at 20°C was blocked after a certain period of time (from 0.5 hours to 7 days) by grinding the hydrated samples under methyl alcohol and then vacuum-drying them at about 2 mmHg.

Differential thermal analysis (DTA) and differential thermogravimetry (DTG) were simultaneously carried out by a Netzsch thermoanalyzer to identify the hydration products. Only DTG curves are reported in the present paper. In same cases X-ray diffraction (XRD) analysis was also carried out to confirm the presence of certain phases.

b) Triethanolamine adsorption

One liter of TEA (2000 mg/l) aqueous solution was mixed with 25 g of ettringite prepared according to the method described by Mehta (7). After a certain period of time (from 0.5 hours to 1 day) the filtered aqueous solution was analyzed by UV method to determine the amount of TEA adsorbed on ettringite.

Results

From DTG curves the area corresponding to the peak of $Ca(OH)_2$ produced by C_3S hydration was determined by taking into account also the $Ca(OH)_2$ transformed into $CaCO_3$. The amount of $Ca(OH)_2$ in arbitrary units is shown as a function of time in Fig. 1. The two curves are representative of the C_3S hydration kinetics with and without TEA. The addition of TEA blocks the $Ca(OH)_2$ production at 0.5 hours and retards the C_3S hydration until 6 hours, whereas no substantial change is recorded after 1 day of hydration.

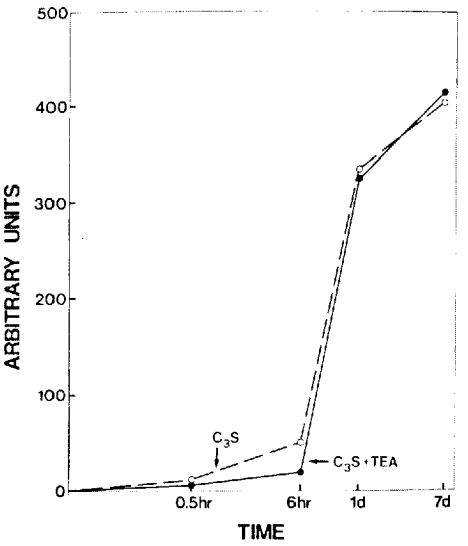

Fig.1 Amount of $Ca(OH)_2$ produced by C_3S hydration as a function of time for the C_3S and C_3S+TEA systems.

The DTG curves for the C_3S-C_3A-$C\bar{S}H_2$ system with and without TEA at different hydration times are shown in Fig. 2. In the the presence of TEA the ettringite production appears to be accelerated confirming the results obtained by Ramachandran (3). For example at 6 hours the DTG gypsum peak is present only in the absence of TEA. The XRD analysis confirmed that in the presence of TEA gypsum was absent after 6 hours of hydration.

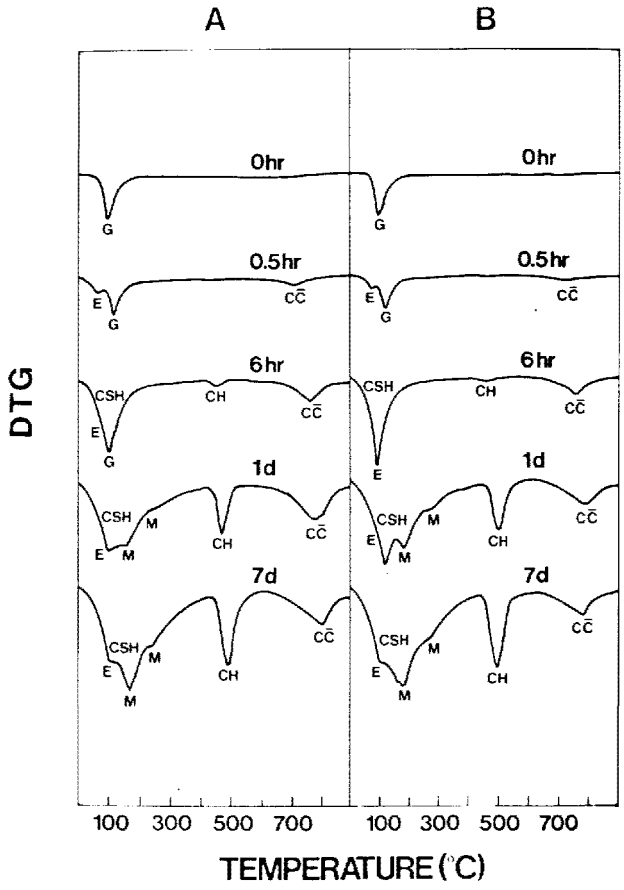

Fig. 2 DTG curves mixes of C_3S-C_3A-$C\bar{S}H_2$ (A) and C_3S-C_3A-$C\bar{S}H_2$ + TEA (B) hydrated from 0.5 hours to 7 days. The top curve refers to the anhydrous mix. G = gypsum; E = ettringite; M = monosulfate; CH = calcium hydroxide; $C\bar{C}$ = calcium carbonate; CSH = calcium silicate hydrate.

In Fig. 3 the effect of TEA on the $Ca(OH)_2$ production for the C_3S-C_3A-$C\bar{S}H_2$ system is shown. The TEA addition retards the C_3S hydration less than it does when C_3S hydrates alone (Fig. 1).

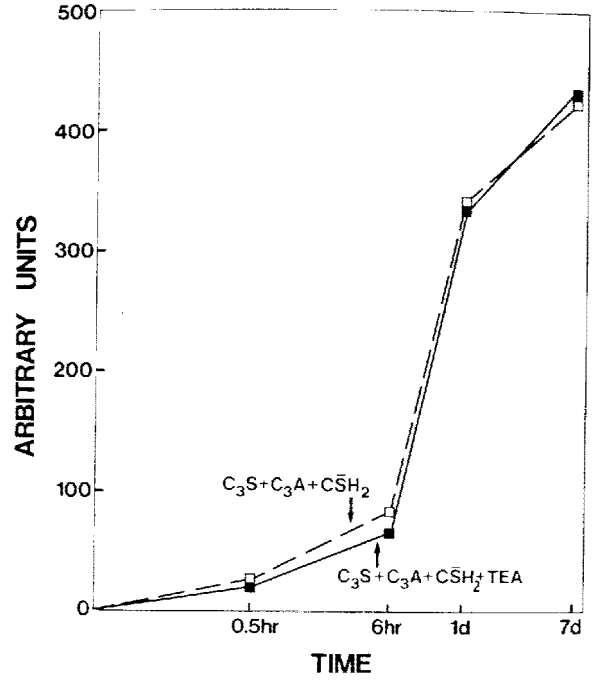

Fig. 3 Amount of $Ca(OH)_2$ produced by C_3S hydration as a function of time for the C_3S-C_3A-$C\bar{S}H_2$ and C_3S-C_3A-$C\bar{S}H_2$ + TEA systems.

In Fig. 4 the DTG curves for C_3S-NC_3A-$C\bar{S}H_2$ mixes hydrated with and without 0.1% TEA are shown. During the first 6 hours ettringite production and its transformation into monosulfate appears to be accelerated by TEA addition. At subsequent times the effect of TEA on C_3A hydration seems to be negligible. The $Ca(OH)_2$ production for the C_3S-NC_3A-$C\bar{S}H_2$ system with and without TEA is shown in Fig. 5. The C_3S hydration rate is slightly retarded in the presence of TEA. However the retarding effect, particularly during the first 6 hours, is much smaller than that found for the hydration of C_3S alone (Fig. 1).

2.1

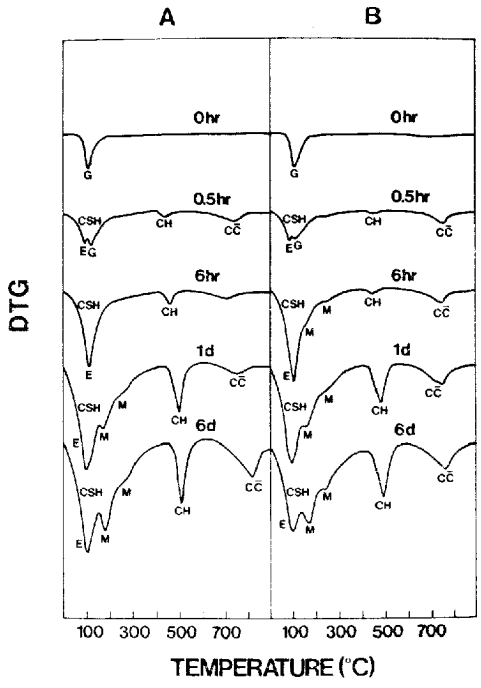

Fig. 4 DTG curves of mixes of C_3S-NC_3A-$C\bar{S}H_2$ (A) and C_3S-NC_3A- $C\bar{S}H_2$ + TEA (B) hydrated from 0.5 hours to 7 days. The top curve refers to the anhydrous mix. G = gypsum; E = ettringite; M = monosulfate; CH = calcium hydroxide; $C\bar{C}$ = calcium carbonate; CSH = calcium silicate hydrate.

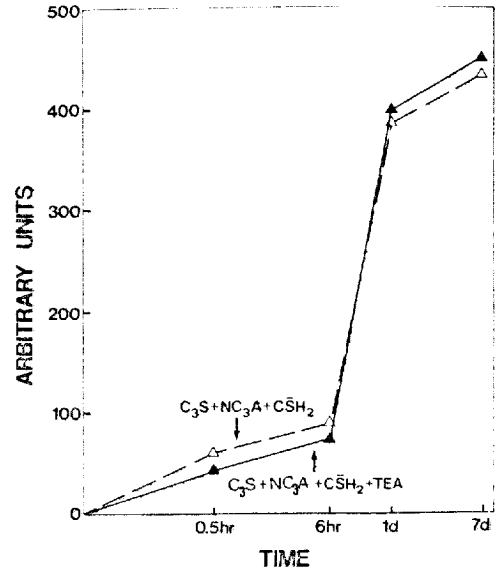

Fig. 5 Amount of $Ca(OH)_2$, produced by C_3S hydration as a function of time for the C_3S-NC_3A-$C\bar{S}H_2$ and C_3S-NC_3A-$C\bar{S}H_2$ + TEA systems.

All these results demonstrate that in the presence of C_3A or NC_3A the retarding effect of TEA on C_3S hydration decrases (8). This could be ascribed to the adsorption of TEA molecules on the hydration product of C_3A (ettringite) so that the concentration of TEA in mixing water is reduced and consequently the retarding effect on the C_3S hydration also decreases.

In order to verify this hypothesis a sample of 25 g of ettringite was left in contact with 1 liter of aqueous solution containing 2000 mg of TEA per liter of water. The amount of TEA which remained in solution after different times is reported in Fig. 6. Triethanolamine is gradually removed from the aqueous solution, and during the first 6 hours, the ettringite adsorbs about 50% of TEA molecules originally present. This experiment seems to confirm that ettringite is responsible for the reduction in the retarding effect of TEA on C_3S hydration. On the other hand TEA accelerates the ettringite production. Therefore the retarding effect of TEA on the C_3S hydration in Portland cement could strongly depend on the C_3A content in Portland cement. The higher the C_3A content, the weaker the retarding effect on the C_3S hydration. It does not seem that the alcali content in C_3A affects the influence of TEA on the C_3S hydration.

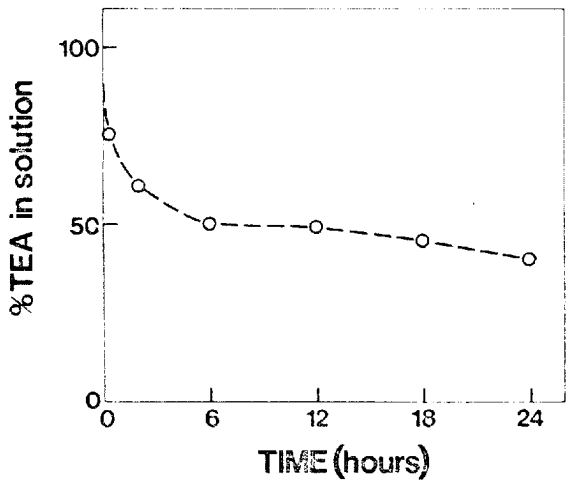

Fig.6 Amount of TEA remained in solution after different times of contact with ettringite.

Conclusion

Addition of TEA (0.1%) to a C_3S paste slightly retards the early hydration process during the first 6 hours.

This retarding effect is almost eliminated when C_3S hydrates in the presence of C_3A (or NC_3A) and $C\bar{S}H_2$. Addition of TEA accelerates the early production of ettringite and its conversion into monosulfate. It seems that adsorption of TEA molecules on ettringite can remove the admixture from the aqueous phase and reduce the retarding effect on the C_3S hydration.

References

(1) V.S. Ramachandran, "Hydration of Cement. Role of Triethanolamine", Cem. Concr. Res., 6, 623-632, (1976).

(2) V.S. Ramachandran, "Influence of Triethanolamine on the Hydration Characteristics of Tricalcium Silicate". J. App. Chem. Biotechnol., 22,1125-1138, (1972).

(3) V.S. Ramachandran, "Action of Triethanolamine on the Hydration of Tricalcium Aluminate", Cem. Concr. Res., 3, 41-54, (1973).

(4) S. Monosi, G. Moriconi, M. Pauri, M. Collepardi, "Influence of Lignonsulfonate, Glucose and Gluconate on the C_3A Hydration", Cem. Concr. Res., 13, 568-574, (1983).

(5) M. Pauri, G. Ferrari, M. Collepardi, "Combined Effect of Lignosulfonate and Carbonate on Pure Portland Clinker Compounds Hydration. IV. Hydration of Tricalcium Aluminate-Sodium Oxide Solid Solution". Cem. Concr. Res., 13, 61- 68, (1983).

(6) S. Monosi, G. Moriconi, M. Collepardi, "Combined Effect of Lignosolfonate and Carbonate on Pure Portland Clinker Compound Hydration. III. Hydration of Tricalcium Silicate Alone and in the Presence of Tricalcium Aluminate", Cem. Concr. Res., 12, 425-435, (1982).

(7) P.K. Mehta, "Mechanism of Expansion Associated with Ettringite Formation", Cem. Concr. Res., 3, 1-6, (1973).

(8) T.D. Ciach, E.G. Swenson, "Morphology and Microstructure of Hydrating Portland Cement and its Costituents. IV. Changes in Hydration of a C_3S, C_2S, C_3A, C_4AF and Gypsum Paste with and without the Admixtures Triethanolamine and Calcium Lignosulphonate". Cem. Concr. Res., 1, 367-383, (1971).

S. Monosi, G. Moriconi, M. Pauri and M. Collepardi, University of Ancona, Ancona, Italy

EFFECT OF RETARDING ADMIXTURES ON THE PORTLAND CEMENT HYDRATION 2.1

EFFECT DES ADJUVANTS RETARDANTS SUR L'HYDRATATION DES CIMENTS PORTLAND

SUMMARY: Type I and V Portland cements have been hydrated (water/cement ratio = 0.50) at 20°C with and without glucose, sodium gluconate and sodium lignosulfonate (0.3% by weight of cement).

Minislump tests have been carried out to determine the fluidifying effect of the admixtures on cement pastes. The cement hydration rate has been studied by thermal analysis (DTG).

Sodium gluconate, which appeared to be the most effective in fluidifying the cement pastes, retard both the ettringite production and the calcium silicates hydration. The retarding effect was much more remarkable on type V Portland cement with null C_3A content.

Sodium lignosulfonate did not significantly retard after ettringite production or calcium silicates hydration.

Glucose accelerated the ettringite production for type I and type V Portland cements, and this seems to be related with the reduction of fluidity caused by the addition of this admixture. On the other hand, glucose strongly retard the calcium silicates hydration particularly when type V Portland cement was used.

SUMÁRIO: Cimentos Portland Tipos I e V foram hidratados (relação de água/cimento = 0,50) a 20°C, com e sem glicose, gliconato de sódio e lignossulfonato de sódio (0,3% em peso de cimento).

Foram realizados testes de mini-trabalhabilidade para determinar o efeito fluidificante do aditivo sobre as pastas de cimento. Por análise térmica (DTG) se estudou a velocidade de hidratação do cimento.

O gliconato de sódio, que parece ser o mais eficiente em termos de fluidificação das pastas de cimento, retarda tanto a produção de etringita como a hidratação dos silicatos de cálcio. O efeito retardador foi muito mais marcante no cimento Portland tipo V com teor nulo de C_3A.

O lignossulfonato de sódio não retardou significativamente depois da produção de etringita ou da hidratação dos silicatos de cálcio.

A glicose acelerou a produção de etringita nos cimentos Portland tipos I e tipo V, e isto parece estar relacionado com a redução de fluidez causada pela adição deste aditivo. Por outro lado, a glicose retardou fortemente a hidratação dos silicatos de cálcio, em particular quando se usou o cimento Portland tipo V.

Introduction

In previous works (1-5) the influence of some water reducers/retarders on the hydration of pure components of Portland cement has been examined. In particular, the effect of glucose, gluconate and sodium lignosulfonate on the hydration of C_3A and C_4AF with and without lime and gypsum, and on the hydration of the C_3S-C_3A-gypsum and C_3S-C_4AF-gypsum systems was investigated.

In the present work the research program extends to the study of the hydration of Portland cement, choosing two samples of cement, having a significantly different content in C_3A and C_4AF.

Experimental

Two Portland cements were used: a white Portland cement type I and a ferric Portland cement type V substantially without C_4AF and C_3A respectively.

Table 1 Chemical analysis (%) of Portland cements used.

	WHITE CEMENT	FERRIC CEMENT
CaO	65.39	63.13
SiO_2	22.16	19.97
Al_2O_3	3.54	4.01
Fe_2O_3	0.29	5.71
Na_2O	0.66	0.14
K_2O	0.20	0.81
MgO	1.51	1.74
SO_3	2.75	2.97
Free CaO	0.77	0.77
C_3S	65.0	61.3
C_2S	13.5	9.9
C_3A	8.9	1.0
C_4AF	0.9	17.4

Glucose (G), gluconate (NG) and sodium lignosulfonate (LGS), are the same materials as those used in other works (1-5).

Hydration occurred at 20°C with a water/cement ratio (w/c) of 0.50 in the absence or in the presence of the admixtures (0.3% by weight of cement). The reaction was blocked at given times by grinding and vacuum drying some portions of paste in methyl alcohol.

To evaluate the influence of the admixtures on the hydration of silicates and aluminates, DTG analysis was carried out by the methods already described in a previous paper (1).

Minislump tests were also carried out, to determine the fluidity of cement pastes (7).

Results and Discussion

Figures 1 to 4 show the DTG curves for white cement.

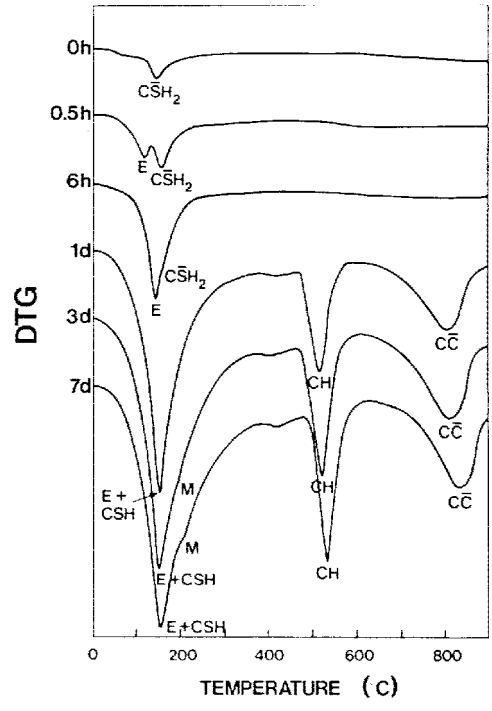

Fig.1 DTG curves of white cement hydrated up 7 days. E=ettringite; M=monosulfate.

In the absence of admixtures (Fig. 1), the peak at about 150°C in the anhydrous specimen is attributed to the dehydration of gypsum. At 0.5 hour and at 6 hours the presence of a new peak at about 120°C is observed. This due to the thermal decomposition of ettringite which begins to form. At 1 day the peak is significantly higher also because at about the same

temperature (130-140°C) C-S-H, produced by the hydration of silicates, decomposes. The formation of C-S-H is confirmed by the appearance of the CH peak at about 500°C and by that of $C\bar{C}$ at 800°C approximately. At 3 days, in addition to a higher degree of hydration of silicates, the conversion of ettringite into monosulfate starts, as shown by the shoulder in the thermogram at about 200°C.

Figure 2 shows the termograms of the same cement hydrated in the presence of lignosulfonate. This admixture has negligible effects on the kinetics of hydration of the various components: the peak of ettringite at 0.5 h is lower, while, at 1 day, a slight lowering of the C-S-H and CH peaks is observed.

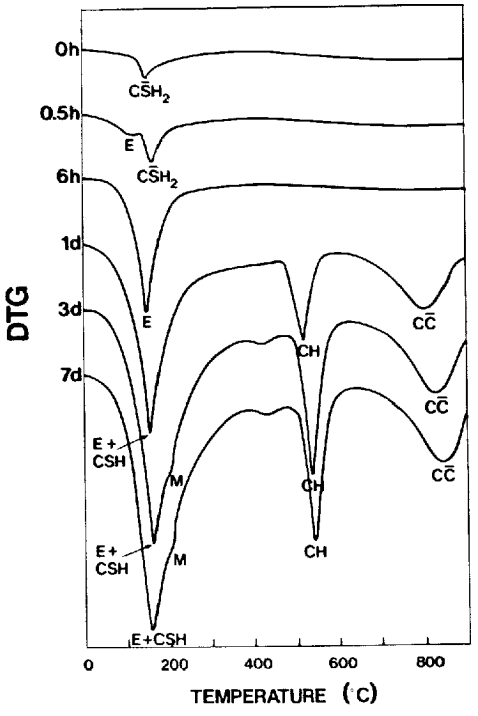

Fig.2 DTG curves of white cement hydrated in the presence of sodium lignosulfonate up to 7 days.

Figure 3 indicates the thermograms of the cement hydrated in the presence of gluconate. The retarding action of the admixture occurs quite clearly both on aluminates and on silicates. Only after 1 day of hydration an amount of ettringite comparable to that produced without admixture at 0.5 h is formed. Moreover, 7 days are required to obtain, in the presence of gluconate, the same CH as that obtained without admixture at 1 day.

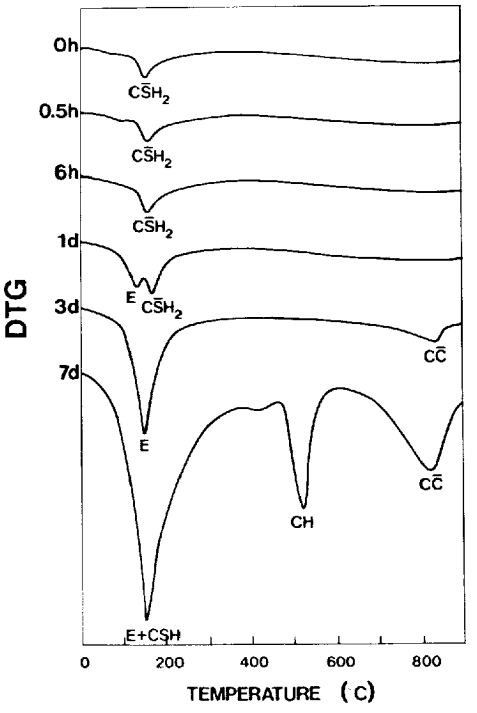

Fig.3 DTG curves of white cement hydrated in the presence of sodium gluconate up to 7 days.

Figure 4 indicates the accelerating effect of glucose on the ettringite production: after 6 hours only, the peak of gypsum is no longer evident and only the presence of ettringite is recorded. However, even at 7 days there is no tendency of ettringite to converse into monosulfate. Even this admixture, as well as gluconate, shows a strong retarding effect on the hydration of silicates. A significant increase of the peaks of C-S-H, CH and $C\bar{C}$ is observed only after 7 days.

Figures 5 to 8 show the thermograms of the hydration products of cement type V without C_3A. Fig. 5 concerns the DTG curves of the cement without admixtures.The effects of the three admixtures (Fig. 6-8) are comparable to the one found out in white

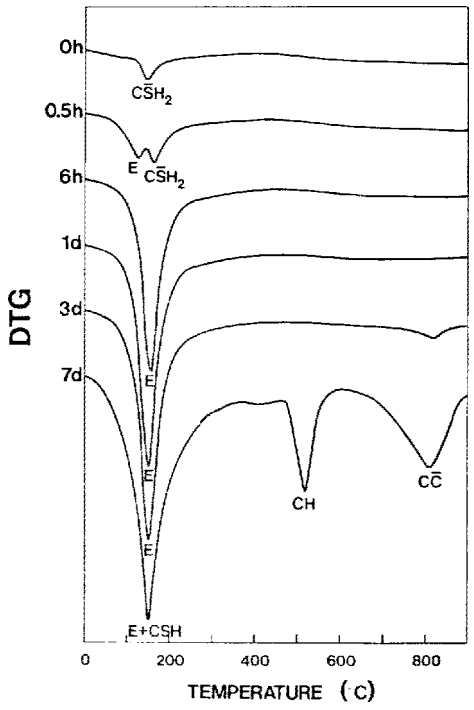

Fig.4 DTG curves of white cement hydrated in presence of glucose up to 7 days.

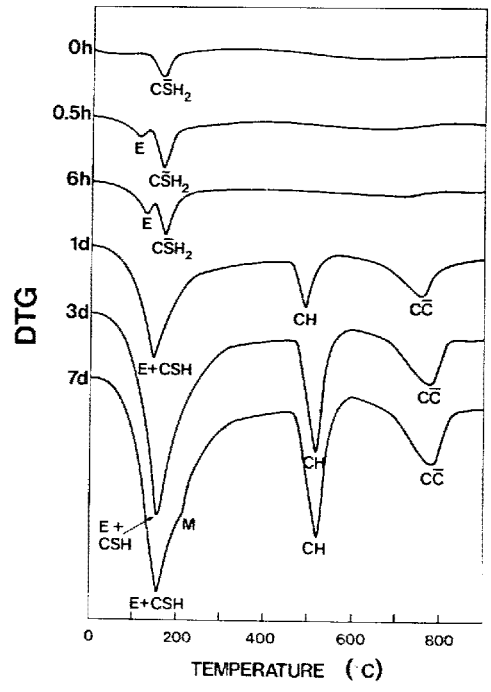

Fig.5 DTG curves of ferric cement hydrated up to 7 days.

cement type I. The differences which can be noticed are certainly due to the kinetics of hydration of C_4AF that is slower than that of C_3A.

Lignosulfonate shows negligible effects on the hydration of both C_4AF and silicates (Fig. 6).

Gluconate (Fig. 7) is confirmed as the most efficient retarder: even at 14 days, in addition to the peak of ettringite, the peak of gypsum is present, while the hydration of silicates is still blocked.

Glucose (Fig. 8) accelerates the production of ettringite and strongly retards the hydration of silicates: a moderate peak of CH is present only at 14 days.

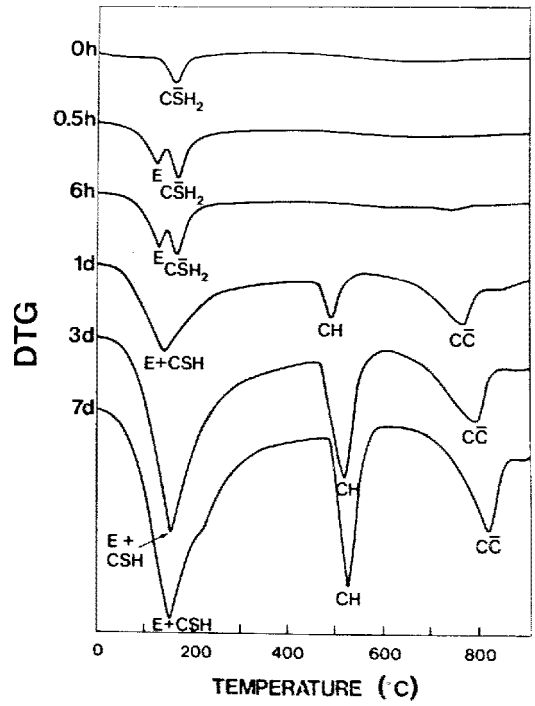

Fig.6 DTG curves of ferric cement hydrated in presence of sodium lignosulfonate up to 7 days.

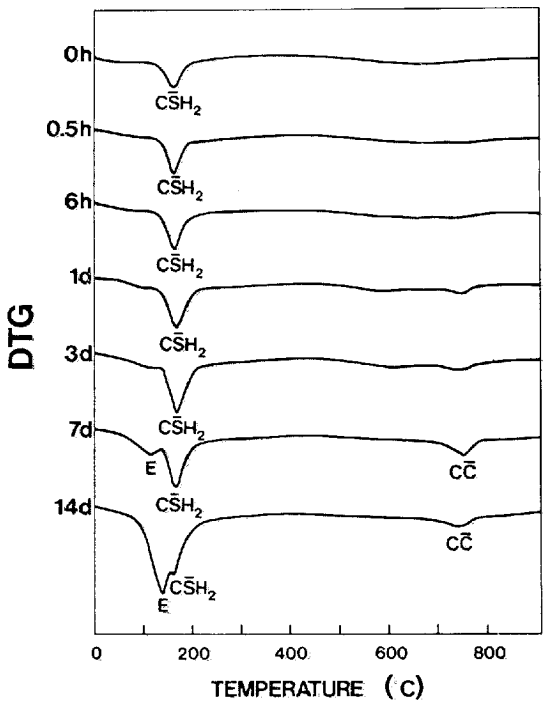

Fig. 7 DTG curves of ferric cement hydrated in presence of sodium gluconate up to 7 days.

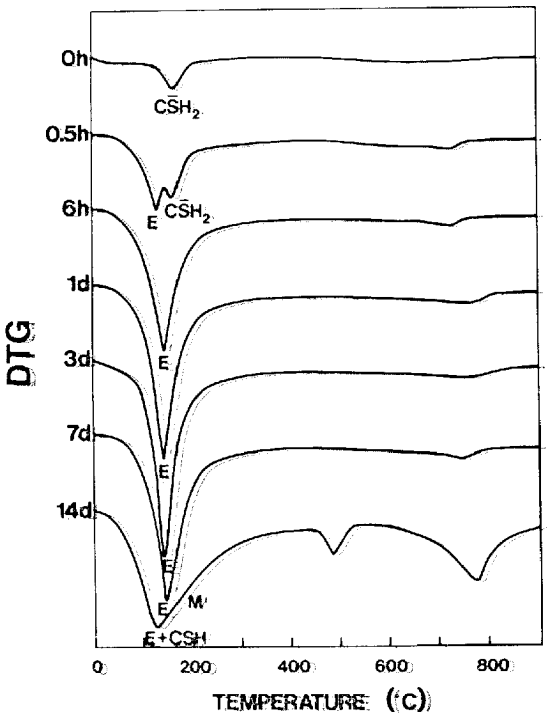

Fig. 8 DTG curves of ferric cement hydrated in presence of glucose up to 7 days.

Figure 9 shows the minislump of the pastes manufactured with the two cements in the presence and in the absence of admixtures. Among the admixtures tested, gluconate is markedly the most plasticizing one; in cement type V, the effect is more noticeable and extends for a longer period of time this being in accordance with the higher retardation in the production of ettringite. Also lignosulfonate plasticizes the paste manufactured with the low C_3A cement more than it does with the white cement rich in C_3A. Conversely, glucose reduces the fluidity of the cement pastes and this behaviour has to be correlated with the accelerating effect on the initial production of ettringite.

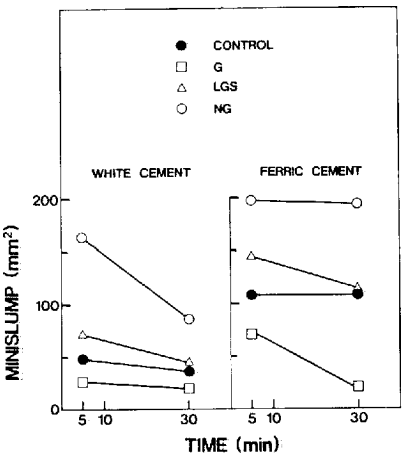

Fig.9 Minislump of cement pastes with and without admixtures (G = glucose; LGS = lignosulfonate; NG = gluconate).

Conclusion

The effects of three chemical products used as raw materials for admixtures in concrete were tested on two cements, one without C_4AF, the other without C_3A.

Gluconate, which proves to be the most effective plasticizer of cement pastes, retards both the production of ettringite and the hydration of silicates: the effects are more marked on cement without C_3A and rich in C_4AF.

Lignosulfonate does not retard the hydration of cement significantly, even if it shows an initial fluidifying effect.

Glucose has no fluidifying effect. This has to be correlated with the accelerating effet on the production of ettringite. Glucose retards the hydration of C_3S only.

References

(1) S. Monosi, G. Moriconi, M. Pauri and M. Collepardi, "Influence of Lignosulfonate, Glucose and Gluconate on the C_3A Hydration", Cem. COncr. Res., 13, 568-574, (1983).

(2) M. Collepardi, S. Monosi, G. Moriconi and M. Pauri, "Influence of Gluconate, Lignosulfonate or glucose on the C_3A hydration Hydration in the presence of gypsum with or without Lime", Cem. Concr. Res., 14, 105-112, (1984).

(3) S. Monosi, G. Moriconi, M. Pauri and M. Collepardi, "Influence of Lignosulfonate, Gluconate or Glucose on the hydration of C_3A or $N_{0.25}C_{2.75}$ Solid Solution in the Presence of Lime and Gypsum", Proceeding of the 1th National Meeting ASMI, Engineering Materials, 437-444, Milano, Italy, October 26-27, 1983.

(4) M. Collepardi, S. Monosi, G. Moriconi and M. Pauri, "Influence of Gluconate, Lignosulfonate and Glucose on the Tricalcium Aluminoferrite Hydration in the Presence of Gypsum with or without Lime", J. Am. Cer. Soc., 68, C 126-128, (1985).

(5) S. Monosi, G. Moriconi, M. Pauri and M. Collepardi, "The Influence of Glucose, Lignosulfonate and Gluconate on the Hydration of C_3S-C_4AF-$CaSO_4 2H_2O$ System, Il Cemento, 82, 147-152, (1985).

(6) M. Collepardi, "Water Reducers/Retarders" in Concrete Admixtures handbook, Ed. by V.S. Ramachandran, pg 116-210, Noyes Publications, Park Ridge, (1984).

(7) W.F. Perenchio, D.A. Whiting and D.L. Kantro, "Water Reduction, Slump Loss, and Entrained Air-Void Systems oa Influenced by Superplasticizers", Superplasticizers in Concrete, American Concrete Institute, Special SP-62, 137-156, (1979).

G. Moriconi, S. Monosi, M. Pauri and M. Collepardi, University of Ancona, Ancona, Italy

EFFECT OF ALKALI CONTENT IN THE CLINKER ON THE CEMENT HYDRATION WITH AND WITHOUT SODIUM GLUCONATE

EFFECT DU CONTENU D'ALCALI DANS LE CLINKER SUR L'HYDRATATION DU CIMENT AVEC ET SANS GLUCONATE DE SODIUM

SUMMARY: An industrial clinker (with Na_2O=0.22% and K_2O=0.54%) was heated in a laboratory kiln at 1350°C in the presence of Na_2CO_3, so that its Na_2O content became 0.56%. In order to obtain comparative results, the clinker as received and that heated in the kiln without Na_2CO_3 were also studied.

In a laboratory mill the three clinkers were ground with 5% of gypsum to a Blaine fineness of about 4500 cm^2/g.

With these three cements, pastes were prepared (water/cement ratio = 0.40) with and without pure sodium gluconate (0.2% by weight of cement). The cements were hydrated at 25°C, and the hydration products were determined by thermal analysis (DTG). Minislump tests of fresh cement pastes were also carried out in order to evaluate the plasticizing effect of the admixture.

The thermal treatment of the clinker in the absence of Na_2CO_3 made the corresponding cement much more rapid in the production of ettringite and its transformation into monosulfate. No substantial change in the calcium silicates hydration was observed.

The cement prepared with the clinker heated in the presence of Na_2CO_3 became significantly slower, in the production of ettringite and its conversion into monosulfate, with respect to the cement prepared with the clinker thermally tratec without Na_2CO_3. On the other hand, the retarding effect, due to the alkali increase in the clinker, was negligible for the calcium silicates hydration.

The addition of sodium gluconate significantly retarded both the ettringite production and the calcium silicates hydration for all the three cements. The retarding action was particularly effective for the cement of the admixture.

Em um forno de laboratório se aqueceu um clínquer industrial (com Na_2O = 0,22% e K_2O = 0.54%) a 1350°C em presença de Na_2CO_3, de modo que o seu teor de Na_2O passou para 0,56%. Com a finalidade de obter resultados comparativos, estudou-se também o clínquer conforme fora recebido e aquele aquecido no forno sem Na_2CO_3.

Os três clínqueres foram moídos em moinho de laboratório, com 5% de gesso, a uma finura Blaine de cerca de 4.500 cm^2/g.

Com estes três cimentos foram preparadas pastas (relação de água/cimento = 0,40) com e sem gliconato de sódio puro (0,2% em peso de cimento). Os cimentos foram hidratados a 25°C, e os produtos de hidratação foram determinados por análise térmica (DTG). Testes de mini-trabalhabilidade de pastas frescas de cimento foram feitos a fim de se avaliar o efeito plastificante da mistura.

O tratamento térmico do clínquer sem a presença de Na_2CO_3 fez o cimento correspondente muito mais rápido na produção de etringita e em sua transformação em monossulfato. Não se observou mudança significativa na hidratação dos silicatos de cálcio.

O cimento preparado com o clínquer aquecido em presença de Na_2CO_3 tornou-se significativamente mais lento na produção de etringita e em sua transformação em monossulfato, em comparação com o cimento preparado com o clínquer tratado termicamente sem Na_2CO_3. Por outro lado o efeito retardador, devido ao aumento de álcali no clínquer, foi desprezível para a hidratação dos silicatos de cálcio.

A adição de gliconato de sódio retardou significativamente tanto a produção de etringita como a hidratação dos silicatos de cálcio nos três cimentos. A ação retardante foi particularmente efetiva no cimento com teor mais alto de álcali, cuja pasta de cimento tornou-se muito mais fluida na presença do aditivo.

Introduction

Sodium gluconate is one of the most widely used raw materials in the production of water-reducing admixtures for concrete (1). Generally these admixtures cause, as a secondary effect, a retard in the Portland cement early hydration particularly during the setting time, though anomalous phenomena of quick set caused by these admixtures were also observed (1-4).

The influence of pure water-reducing admixtures such as sodium gluconate and lignosulfonate on the hydration of pure Portland clinker compounds was examined in previous papers (5-10).

On the other hand, the study of the hydration of Portland cements having different tricalcium aluminate contents with or without those plasticizing admixtures was carried out in other works (11,12).

The results of these works, as far as the sodium gluconate effects are concerned, are summarized in Table 1 in terms of changes in the rate of ettringite production, ettringite conversion into monosulfate and silicates hydration.

These results indicate that sodium gluconate acts actually as a retarder for the hydration of both the aluminate phase and silicates when it is used as admixture for portland cements. On the other hand, when gluconate is added to pure Portland cement compounds or their mixes it acts always as a retarder only for C_3S hydration, whereas not definite results are obtained for the C_3A and C_4AF hydration. Therefore it seems that the effect of gluconate on the ettringite production and its transormation into monosulfate, such as to be studied on systems containing pure C_3A or C_4AF, cannot be extended to the C_3A or C_4AF hydration in Portland cements. Thus the influence of the alkali content in a clinker Portland cement on the effect of a plasticizer such as gluconate on Portland cement hydration does not seem to be evaluable by examining the hydration of pure C_3A and Na_2O-C_3A solid solution (Table 1).

In order to study this influence, clinkers having the same matrix and a different alkali content were used to produce Portland cements which hydrated with and without sodium gluconate.

Table 1 Effect of pure sodium gluconate on ettringite production, its conversion into monosulfate, and silicates hydration.

SYSTEM	ETTRINGITE PRODUCTION	ETTRINGITE CONVERSION INTO MONOSULFATE	SILICATES HYDRATION	REF.
C_3A+gypsum	Weakly accelerated	Weakly retarded	—	8
C_3A+gypsum + calcium hydroxide	No effect	Retarded	—	7,8
N-C_3A+gypsum + calcium hydroxide	No effect	No effect	—	7
C_4AF+gypsum	Retarded	Retarded	—	10
C_4AF+gypsum + calcium hydroxide	Accelerated	No effect	—	10
C_3S	—	—	Very strongly retarded	6,9
C_3S+C_3A + gypsum	No effect	Retarded	Retarded	6
C_3S+C_4AF + gypsum	Retarded	No effect	Strongly retarded	9
Ordinary Portland cement (type I)	Retarded	—	Retarded	12
White Portland cement (type I)	Retarded	—	Retarded	11
Ferric Portland cement (type V)	Strongly retarded	—	Strongly retarded	11

Experimental

An industrial clinker, with Na_2O and K_2O contents of 0.22% and 0.54% rispectively, was heated in a laboratory kiln for 3 hours at 1350°C in the presence of 1% Na_2CO_3 (13, 14), so that its Na_2O

content became 0.56%. The same industrial clinker was thermally trated for 3 hours at 1350°C in the absence of Na_2CO_3. The chemical analysis of the clinker as received is shown in Table 2. No change was found in the chemical analysis of the annealed clinker, whereas only negligible changes were found in the alcali-modified clinker due to the increase in the Na_2O content from 0.22 to 0.56%.

Table 2 Chemical analysis of the clinker as received.

	%
SiO_2	21,61
Al_2O_3	5,38
Fe_2O_3	3,06
CaO	64,77
MgO	1,71
SO3	0,78
Na_2O	0,22
K_2O	0,54
Insoluble residue	0,07
Free CaO	1,31

The three clinkers were subjected to the extraction of the silicate phases by using a solution of salicylic acid in methanol, in order to isolate the aluminate phases (14). These aluminate phases were analyzed by XRD which showed that the aluminate obtained from the clinker thermally treated with Na_2CO_3 was a monoclinic form (13, 17, 18) displaying the characteristic splitting of each major diffraction peak of the cubic C_3A into doublets or triplets. The aluminates extracted from the clinker as received and the annealed clinker were mainly in a cubic form. These results agree with the Na_2O content in the clinkers (18,19): 5% by weight of C_3A in the alkali modified clinker and 2% for the other two clinkers.

The three clinkers were ground in a laboratory mill, with 5% of $C\bar{S}H_2$, to a Blaine fineness of about 4500 cm^2/g.

The three cements so obtained hydrated with and without 0.2% of sodium gluconate at 25°C with a water/cement ratio of 0.40.

The hydration products were determined by differential thermogravimetric (DTG) as described in a previous paper (6).

Minislump tets (19) on fresh cement pastes were also carried out after 2 minutes mixing in order to evaluate the plasticizing effect of the admixture.

Results and discussion

Figures 1 and 2 show the DTG curves of the hydration products of the three cements, as a function of the hydration time, in the absence and in the presence of sodium gluconate respectively.

The DTG peak at about 150°C with a shoulder on the right side is assigned to a stepwise thermal decomposition of $C\bar{S}H_2$ into $C\bar{S}H_{0.5}$ and $C\bar{S}$. The peak at about 120°C is attributed to the thermal dehydration of ettringite, whereas the peaks at about 200°C and 280°C are attributed to the thermal dehydration of monosulfate. Generally after 1 day hydration a peak at about 140°C due to the C-S-H thermal decomposition appears, which overlaps the gypsum and the aluminates hudration products peaks in the temperature range 100-200°C. At the same time a peak at about 500°C, caused by the thermal decomposition of CH, appears. Finally, two different peaks may appear for the decomposition of carbonated products (6, 8). The former at about 780°C is due to the thermal decomposition of calcium carbonate ($C\bar{C}$), the latter at about 800°C is attributed to the thermal loss of CO_2 in the monocarboaluminate obtained by carbonation of the monosulfate.

Figure 1 shows the DTG curves of cements hydrated in the absence of sodium gluconate. The thermal tratment of the clinker in the absence of Na_2CO_3 caused in the corresponding cement (Fig. 1B) an acceleration in the ettringite production and its conversion into monosulfate with respect to the control cement produced with the clinker as received (Fig. 1A). After 0.5 hour of hydration, for instance, only monosulfate was observed in the cement with the annealed clinker (Fig. 1B), whereas gypsum with traces of ettringite was present in the control cement (Fig. 1A). No substantial change in the hydration of silicates was caused by the treatment in the

2.1

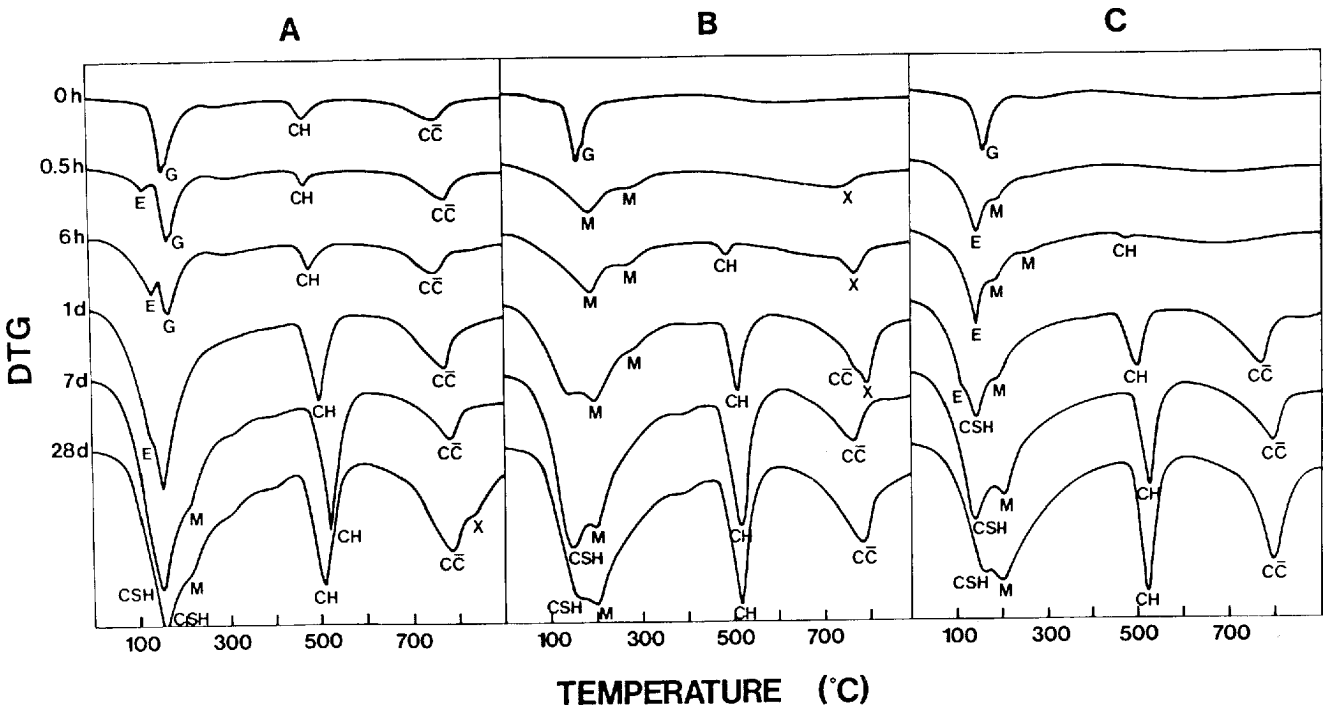

Fig. 1 DTG curves of the cements prepared with the as received clinker (A), the annealed clinker (B), the alkali modified clinker (C), in the absence of sodium gluconate. G = gypsum; E = ettringite; M = monosulfate; X = monocarboaluminate.

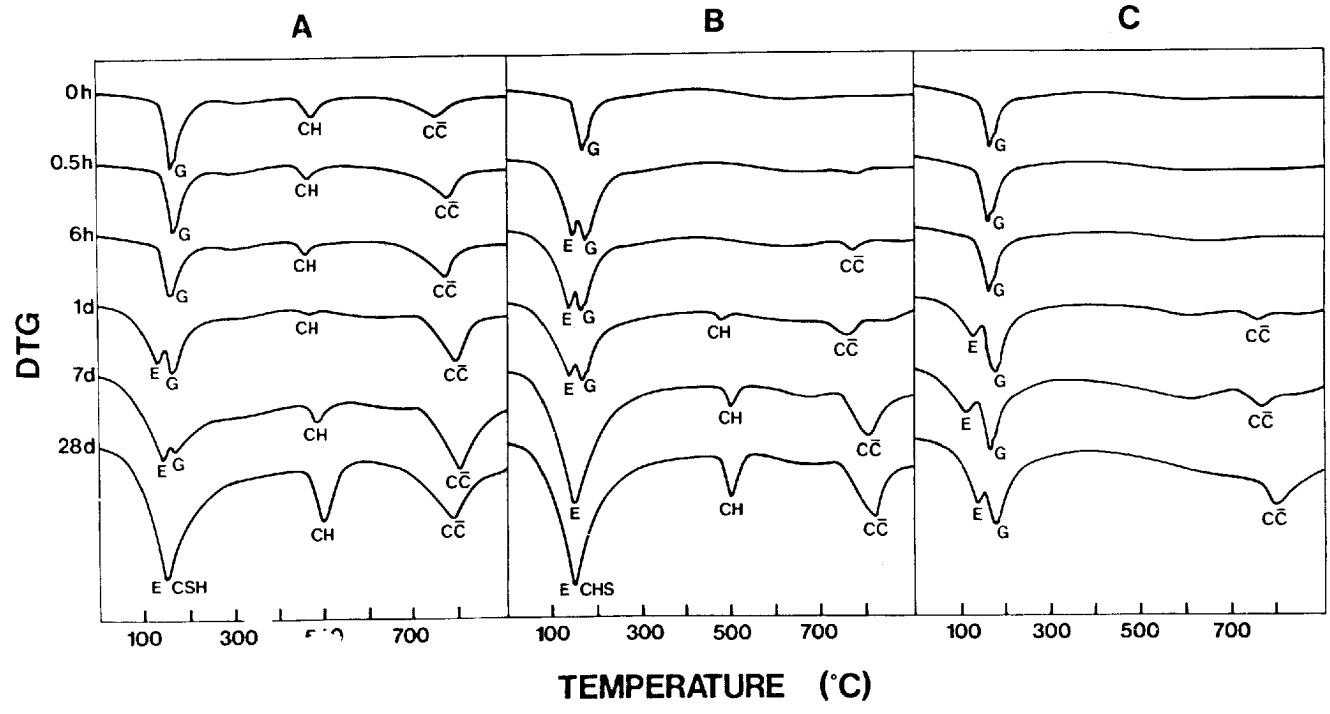

Fig. 2 DTG curves of the cements as thus shown in Fig. 1 in the presence of sodium gluconate.

absence of Na_2CO_3, as it can be found through the CH peaks at different hydration times (Fig. 1A and B).

The hydration rate of the aluminate phase for the cement produced with the alkali modified clinker (Fig. 1C) was between that of the control cement (Fig. 1A) and that of the cement manufactured with the annealed clinker (Fig. 1B). After 0.5 hour of hydration, for instance, both ettringite and monosulfate were present in the cement with the alkali modified clinker. Therefore, the increase in Na_2O content in the cement manufactured with the thermally treated clinkers caused a retardation in ettringite production and its transformation into monosulfate. On the other hand, no change in the silicates hydration was recorded as a a result of the increase in the alkali content (Fig. 1B and C).

The addition of sodium gluconate (Fig. 2) significantly retarded both the ettringite production and the calcium silicates hydration for all the three cements. This retarding action was particularly effective for the cement with the higher alkali content (Fig. 2C), so that after 28 days of hydration gypsum is still present and no hydration product from C_3S and C_2S did yet appear.

The influence of sodium gluconate on the fluidity of cement pastes is shown in Table 3. The plasticizing effect of the admixture is higher in the cement with the annealed clinker than in the control cement. Still higher is the the fluidifying effect on the cement with the clinker thermally treated in the presence of Na_2CO_3.

Table 3 Influence of sodium gluconate on the minislump test of cement pastes.

TYPE OF CEMENT	MINISLUMP (cm^2)	
	WITHOUT NG*	WITH NG*
Control cement	45	55
Cement with annealed clinker	25	53
Cement with annealed clinker in the presence of Na_2CO_3	32	80

* NG = Sodium gluconate

Conclusions

The increase in the alkali content in cements manufactured with clinkers subjected to the same thermal treatment makes the gluconate addition more effective both as plasticizer and as retarder on the hydration of the aluminate phase and silicates.

References

(1) M. Collepardi, "Water Reducers/ Retardes" in Concrete Admixtures Handbook, Ed. V.S. Ramachandran, pg. 116-210, Noyes Publications, Park Ridge, (1984).

(2) L.H. Thuthill, R.F. Adams and J.H. Hemmie Jr., ASTM Special Publication No. 266, 97-117, (1960).

(3) K.T. Greene, Transportation Research Record, No. 564, 21-26, (1976).

(4) P. Seligmann and N.R. Greening, Highway Research Record, Highway Research Board No. 62, 80-105, (1976).

(5) S. Monosi, G. Moriconi, M. Pauri and M. Collepardi, Cement and Concrete Research, 13, 568-574, (1983).

(6) M. Collepardi, S. Monosi, G. Moriconi and M. Pauri, "Influence of Pure Water Reducers and High-Range Water Reducers on the Hydration of C_3S and C_3A in the Presence of Gypsum", Symposium on Chemical and Mineral Admixtures for concrete, St. Lous, Missouri, USA, April 6-13, 1984.

(7) S. Monosi, G. Moriconi, M. Pauri and M. Collepardi, Preceedings of the 1st National Meeting ASMI, Milan, Italy, October 26-27, (1983).

(8) M. Collepardi, S. Monosi, G. Moriconi and M. Pauri, Cement and Concrete Research, 14, 105-112, (1984).

(9) S. Monosi, G. Moriconi, M. Pauri and M. Collepardi, Il Cemento, 82 (3), 147-152, (1985).

(10) M. Collepardi, S. Monosi, G. Moriconi and M. Pauri, Journal of American Ceramic Society, 68 (5), C126-C128, (1985).

(11) S. Monosi, G. Moriconi, M. Pauri and M. Collepardi, "Effect of retarding Admixtures on the Portland Cement Hydration", paper presented at the VIII International Congress on the Chemistry of Cement, Rio the Janeiro, Brasil, September 22-27, (1986).

(12) S. Monosi and M. Collepardi, Proceedings of the Symposium "Il Cemento ed il Calcestruzzo negli Anni 80", pg 71-77, Parma, Italy, October (1985).

(13) I. Maki, Cement and Concrete Research, 3, 295-313, (1973).

(14) J.E. Mender, L.D. Adams and E.E. Larkin, Cement and Concrete Research, 4, 533-544, (1974).

(15) A.A. Tabikh and R.J. Weht, Cement and Concrete Research, 1, 317-328, (1971).

(16) W.A. Gutteridge, Cement and Concrete Research, 9, 319-324, (1979).

(17) A.I. Boikova, A.I. Romansky, V.A. Paramonova, G.P. Stavitskaja and V.M. Nikushchenko, Cement and Concrete Research, 7, 483-492, (1977).

(18) M. Regourd, Il Cemento, 75 (3), 323-336, (1978).

(19) W.F. Perenchio, D.A. Whiting and D.L. Kantro, "Superplasticizers in Concrete", American Concrete Institute, SP-62, 137-156, (1979).

YASUBUMI FUKAYA, Chief Chemist, Research Department,
KAZUMI KATO, Senior Research Chemist, Chichibu Cement Co., Ltd., JAPAN

Adsorption of Superplasticizers on CSH(I) and Ettringite

SUMMARY: A research was made about the adsorption mechanism of β-naphthalene sulfonate formaldehyde condensates (NSF) and lignosulfonate (LS) on ettringite and CSH(I) synthesized from pure reagents.
The surface basicity of the hydrates used was reduced with the adsorption of an admixture. From the relationship between this basicity and the amount of adsorption, it was found that NSF is adsorbed on the surface of the hydrate in flat form. Also, it was made clear that NSF is adsorbed on CSH(I) in monolayer while ettringite forms multilayers in its adsorption thereon. The adsorption of LS on hydrates, on the other hand, could not be clarified for the complexity of the molecular structure of LS.
This fact, together with the experiments on the amount of adsorbed NSF and the surface basicity of inorganic compounds with low solubility other than hydrates shows that the basic site may function as an adsorption site for adsorption of the first layer.
As a result of studying the effect of various ions coexisting with an admixture in liquid phase, it was found that Na^+ or K^+ ion does not adsorb on ettringite but on CSH(I). The adsorption of these cations did not affect the amount of adsorption of the admixture. On the other hand, it was found that Ca^{2+} ions adsorb on either CSH(I) or ettringite, while at the same time increasing the amount of adsorbed admixture, indicating that Ca^{2+} ions have a direct effect on the adsorption mechanism of an admixture.

Foi feita uma pesquisa a respeito do mecanismo de absorção de condensados de formaldeído de sulfonato de β-nafatalina (NSF) e lignosulfonado (LS) na etringita e CSH (I) sintetizados a partir de reagentes puros.

A basicidade de superfície dos hidratos usados foi reduzida com a adsorção de uma mistura. A partir da relação entre esta basicidade e a quantidade de adsorção, constatou-se que NSF é adsorvido na superfície do hidrato em uma forma plana. Também, ficou claro que NSF é adsorbido no CSH(I) em monocamada, enquanto a etringita forma multicamadas em sua adsorção. A adsorção de LS em hidratos, por outro lado, não pôde ser esclarecida devido à complexidade da estrutura molecular do LS.

Este fato, juntamente com as experiências sobre a quantidade de NSF adsorvido e a basicidade da superfície de compostos inorgâncios com baixa solubilidade, além de hidratos, mostra que o sítio básico pode funcionar como um sítio de adsorção para adsorver a primeira camada.

Como resultado do estudo do efeito de íons diversos coexistindo com uma mistura em fase líquida, verificou-se que íon de Na^+ ou K^+ não adsorve em etringita mas em CSH(I). A adsorção destes cátions não afeta a quantidade de adsorção da mistura. Por outro lado, verificou-se que íons de Ca^{2+} adsorvem seja em CSH(I), seja em etringita, enquanto ao mesmo tempo aumenta a quantidade de mistura adsorvida, indicando que íons de Ca^{2+} têm um efeito direto sobre o mecanismo de adsorção de uma mistura.

YASUBUMI FUKAYA, Chief Chemist, Research Department,
KAZUMI KATO, Senior Research Chemist, Chichibu Cement Co., Ltd., JAPAN

INTRODUCTION

The adsorption of an organic admixture is important for the interaction between the organic admixture and cement hydrate. The amount and manner of adsorption of an admixture is generally dependent on the type of a hydrate involved. The adsorption of an admixture, therefore, is considered to have deep relationship with the crystalline structure or surface characteristics of the hydrate as well as the molecular structure of the admixture. In the adsorption of lignosulfonate on hexagonal phase (C_2AH_n-C_4AH_n), for example, it has been reported that the admixture penetrates between the layers of the hydrate crystals and form an interlayer complex (1). There are, however, few researches conducted on the adsorption from the viewpoint of the crystalline structure or surface characteristics of a hydrate (2). This research deals with the adsorption behaviour studied by use of the acidity or basicity of the solid surface as an index of the surface characteristics of hydrates including CSH(I) and ettringite. Further, study was made about the relationship between the liquid phase composition and the adsorption.

EXPERIMENTAL

Materials

CSH(I) was obtained in such a manner that the solution of ethanol of ethyl silicate was adjusted to Ca/Si ratio of 1.0 against the 0.01 mol/dm^3 solution of calcium hydroxide in the N_2 gas environment, and after being stirred for three days at room temperature, the product was separated by filtering. The obtained product was dried in vacuum. To obtain ettringite (Ett), $Al_2(SO_4)_3$ solution was dropped into the saturated solution containing the equivalent of CaO and $CaSO_4 \cdot 2H_2O$, and after being left to stand for three days at room temperature, the material deposited was filtered. The product was dried in a 70% H_2SO_4 desiccator. The synthesized CSH(I) and Ett were checked by X-ray and DTA. The composition and specific surface area measured by BET method are shown in Table I. The admixtures used are available on the market.

TABLE I

HYDRATE	CHEMICAL COMPOSITION (%)					MOLAR RATIO		BET specific surface area (m^2/g)
	CaO	SiO_2	Al_2O_3	SO_3	H_2O	C/S	H/S	
CSH(I)	35.9	45.0	—	—	19.1	0.85	1.42	78.7
Ett	27.3	—	8.3	19.7	44.7	—	—	7.4

β-naphthalene sulfonate formaldehyde condensates (NaNSF) contained 32.5% sulfonic group, while calcium lignosulfonate (CaLS) contained 18.5% sulfonic group, 8.6% methoxyl group, 3.5% carboxyl group, 1.8% phenolic hydroxyl group and 5.5% reducing sugar. Using those two admixtures as a base, the salts converted by cation exchange resin column, that is, potassium salt (KNSF) of NaNSF, and sodium salt (NaLS) and potassium salt (KLS) of CaLS were prepared. By use of the ultrafilter, the products of high molecular weight (H) and low molecular weight (L) were separated. They were abbreviated as H-CaLS and L-CaLS for CaLS, and H-NaNSF and L-NaNSF for NaNSF respectively. The ultrafilter used was for dividing the molecular weight of protein of 50000 and 10000. The GPC analysis showed that the admixtures were divided in level.

Measurement of adsorption and desorption

1.0g of hydrate or inorganic compound were dispersed in 80 cm^3 of pure water, and subjected to preliminary agitation for 30 minutes. After that, 20 cm^3 of admixture solution was added and stirred at 20±0.1°C for an hour. The adsorbed amount of admixture was determined by measuring the concentration of the solutions before and after adsorption, performed by UV absorption spectroscopy. In a desorption test, a certain amount of the liquid phase used for the adsorption test was collected, and mixed with the same amount of water for reducing the equilibrium concentration, and then the amount of desorption was measured.

Influence of liquid phase composition on adsorption

The reagents including $CaCl_2$, $CaSO_4 \cdot 2H_2O$ and KCl were all of reagent grade, and were added with different concentrations in the stage of preliminary agitation in the adsorption test. For analysis of the liquid phase, the atomic absorption spectrometry was used for sodium and potassium, the EDTA titration method for calcium and the mercury (II) thiocyanate method for chlorine.

Measurement of basicity

A 0.5g sample was taken in a flask, and with 20 cm^3 benzene and 1 cm^3 indicator (0.5g phenolphthalene dissolved in 100 cm^3 benzene), was sealed together. The sample in this solution becomes red when it has a basicity. After being left to stand for 24 hours, the mixture was titrated with the benzene solution of benzoic acid at intervals of four hours, and the basicity was measured by the amount of the benzoic acid consumed.

Analysis of infrared spectra

In order to obtain the infrared spectrum of the sample surface, the sample of adsorption test was dried and investigated by the diffuse reflection method with Fourier transform infrared spectroscopy. By reducing the spectrum of the sample not adsorbed, the spectrum of the admixtures adsorbed was detected.

YASUBUMI FUKAYA, Chief Chemist, Research Department,
KAZUMI KATO, Senior Research Chemist, Chichibu Cement Co., Ltd., JAPAN

RESULTS AND DISCUSSION

Adsorption isotherm

The adsorption isotherms of NaNSF and CaLS adsorbed on CSH(I) and Ett are shown in Fig. 1. More CSH was adsorbed the larger the molecular weight of the admixtures. The undivided admixture exhibited the characteristic intermediate the adsorption isotherms of the admixtures low molecular weight (L) and high molecular weight (H). This results coincided with the report (3) that polymer NaNSF was adsorbed more than monomer NaNSF in cement paste. The adsorption isotherms of Ett, on the other hand, were different from that of CSH. In the adsorption of NaNSF, H-NaNSF reached the saturated adsorption with the equilibrium concentration of about 0.1 μg/cm^3, and beyond this concentration, the adsorption of L-NaNSF exceeds that of H-NaNSF. In the case of CaLS, the amount of adsorption of L-CaLS approaches that of H-CaLS with the increase in the equilibrium concentration, though not so extremely as NaNSF. For both the admixtures, the amount of adsorption of the undivided one exceeded that of the divided one. This difference between CSH and Ett in the adsorption isotherm, as described later, is considered due to the fact that the adsorption on CSH is in monolayer while that to Ett is in multilayer. By the way, a calculation using Langmuir's equation of monolayer adsorption from the data of adsorption isotherm shows a considerable coincidence for CSH but not for Ett. As a result of the desorption measurement conducted from several points on the NaNSF adsorption isotherm of CSH and Ett, it was made clear that NaNSF was not desorbed at all, indicating an irreversible adsorption. By type of the adsorption isotherm of the admixtures, different reports were obtained among the cement (or cement minerals) type (4), admixture type (5) and solvent type (5, 6).

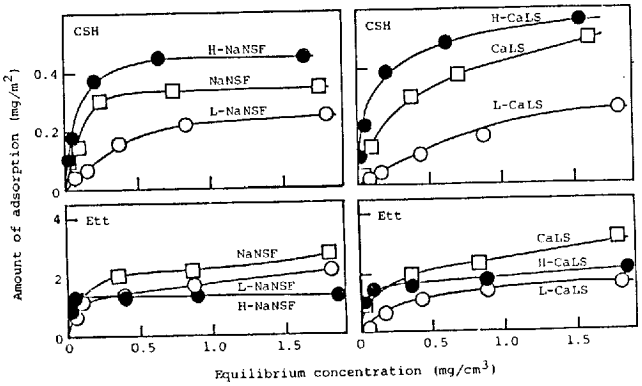

Fig. 1 Adsorption isotherm of admixture on CSH and Ett.

Relationship between Ca^{2+} ion concentration and amount of adsorption

For the purpose of determining the influence of Ca^{2+} ion concentration in the liquid phase, the amount of adsorption of NaNSF in the $CaSO_4 \cdot 2H_2O$ or $CaCl_2$ aqueous solution of different concentrations was measured. The result is shown in Fig. 2. The amount of adsorption increases with the Ca^{2+} concentration. The amount of Ca^{2+} (Ceq) in the equilibrium liquid phase is smaller than the total amount (Cto) of Ca derived from the added reagent and NaNSF and Ca released from CSH into pure water. Fig. 3 shows the relationship between the amount (Cto - Ceq) and the amount of adsorption of NaNSF on CSH. This relationship is considered to show that Ca^{2+} ions are adsorbed with the adsorption of the admixtures.

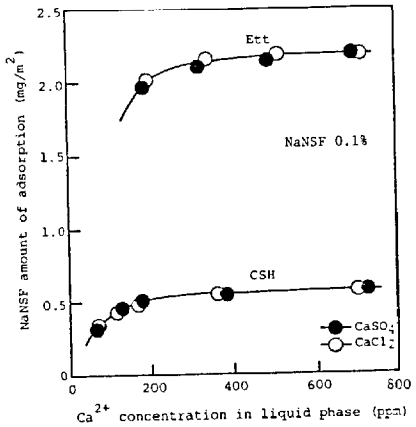

Fig. 2 Relationship between Ca^{2+} concentration and amount of adsorption in adsorption equilibrium liquid phase

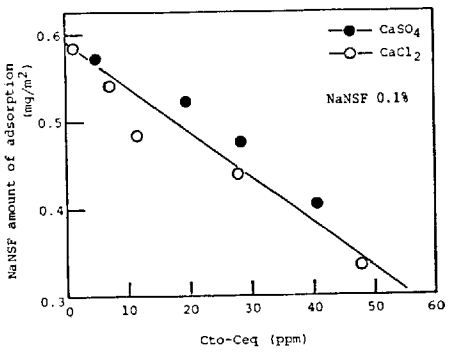

Fig. 3 Relationship between Cto-Ceq and amount of adsorption

Adsorption of cations of admixture molecules

In order to determine the behaviour of the admixture molecular cations, CSH or Ett in three-level weights was added to the 0.1% solution of the admixtures of NaNSF, KNSF and KLS respectively. The relationship involved between the residual concentration of survival rate of the admixtures and of the R^+ (R = Na, K) in the equilibrium liquidphase is shown in Fig. 4. In the case of Ett, Na^+ or K^+ ions are not substantially adsorbed but remain in the liquid phase. For CSH, on the other hand, Na^+ and K^+ ions

YASUBUMI FUKAYA, Chief Chemist, Research Department,
KAZUMI KATO, Senior Research Chemist, Chichibu Cement Co., Ltd., JAPAN

decrease with the residual admixtures. Although the cations of the admixtures are not substantially adsorbed on Ett, therefore, but on CSH. The above results seem to suggest that these cations enter the interlayers of CSH.

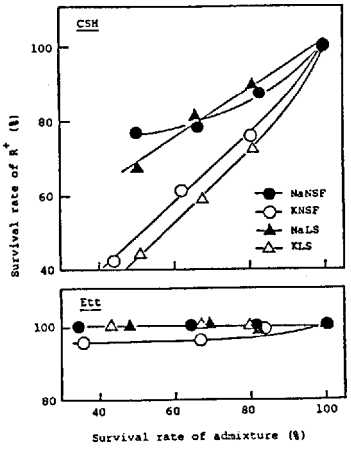

Fig. 4 Behaviour of cations of admixture molecules

$$\text{Survival rate (\%)} = \frac{\text{equilibrium concentration (mg/cm}^3\text{)}}{\text{initial concentration (mg/cm}^3\text{)}} \times 100$$

Adsorption of NaNSF in KCl aqueous solution

The relationship between the concentration of KCl added and the amount of NaNSF adsorbed is shown in Fig. 5. The amount of adsorption of NaNSF on CSH remained constant regardless of the concentration of KCl added. Also, Cl^- ions were not adsorbed at all, while K^+ ions were adsorbed in increasing amounts with the concentration. It appears, however, that with the increase in NaNSF concentration and hence the amount of adsorption, the maximum amount of adsorption

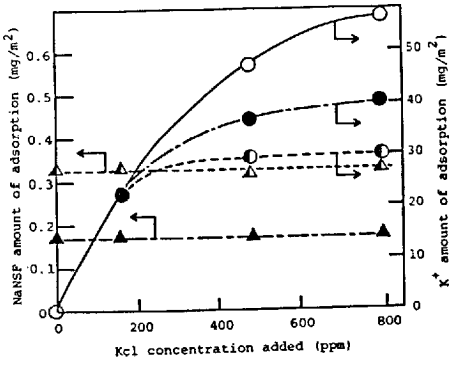

Fig. 5 Relationship between NaNSF adsorption on CSH and KCl concentration.

—○— NaNSF 0%, —●— —▲— NaNSF 0.02%, —◐— —◭— NaNSF 0.1%

of K^+ ions decreases. This is considered not the result of the competitive adsorption on the same site, but may have been caused by the fact that the steric hindrance formed by the adsorption of NaNSF prevents the adsorption of K^+ ions.

Surface basicity of hydrate and adsorption of admixtures

As a result of a preliminary experiment on the surface acidity, CSH did not any substantial acidity while Ett exhibited a small acidity (methyl red indicator, pKa = +4.8), but it did not have any great relations with the adsorption of the admixtures. On the other hand, basicity as strong as to redden the phenolphthalene (pKa = +9.3) was observed, and this basicity was utilized as a surface character of the hydrate surface. The relationship between the surface basicity of CSH and Ett on which NaNSF is adsorbed and the amount of adsorption thereof is shown in Fig. 6. Before the admixtures were adsorbed, the basicity was 3.00 μmol/m^2 for CSH and 2.96 μmol/m^2 for Ett. The decrease in the basicity was found to be proportional to the increase in the adsorption. CSH and Ett are positioned on the same straight line (Fig. 6). A calculation of the increase in adsorption with the reduction by 1 mole of the basicity from the gradient of this straight line shows the result of 240 g/mol. Since the molecular weight equivalent to monomeric unit of NaNSF is 242 (212 excluding Na atoms of sulfonic group), it follows that the admixtures are adsorbed in such a relationship that one basic site corresponds to a monomeric unit of NaNSF molecule. This indicates NaNSF molecules are adsorbed in flat form to the surface of CSH or Ett particles. For Ett, however, the form of the straight line changes at the point representing the adsorption of about 0.6 mg/m^2, the gradient of the straight line being smaller beyond this adsorption amount. The lack of a measuring point of CSH in this region is due to the fact that the color presented by the phenolphthalene was to obscure to measure. Since other many data indicate that the maximum amount of CSH adsorption is thought to be 0.7 to 0.8 mg/m^2, the relationship between basicity and amount of adsorption of CSH may be obtained by extending the initial linear relationship downward. As compared with CSH, Ett is apparently has a greater amount of adsorption per unit area, and data is obtained reaching as much as 3.0 mg/m^2 beyond the amount of adsorption (about 1.4 mg/m^2) as the point associated with the basicity zero as determined from Fig. 6. Taking into consideration the fact that in the case of CSH, adsorption does not occur beyond the amount associated with the basicity zero even if $CaCl_2$ is added, the adsorption of NaNSF on CSH may remain only in monolayer. In view of the fact that the amount of monolayer adsorption on CSH is about 0.7 mg/m^2 and that the Ett amount of adsorption of about 1.4 mg/m^2 associated with the basicity zero is twice the amount

YASUBUMI FUKAYA, Chief Chemist, Research Department,
KAZUMI KATO, Senior Research Chemist, Chichibu Cement Co., Ltd., JAPAN

of monomolecular adsorption of CSH, therefore, the process of adsorption in the amount of 0.7 to 1.4 mg/m^2 on Ett (that is, the second linear relationship) is understandable as the process of formation of two molecular layers. The NaNSF molecules adsorbed in the first layer are in flat form on the surface of particles, and therefore have a rough surface coverage, so that basic sites are considered to appear from gaps of adsorbed molecules. These residual basic sites are completely covered by the second layer adsorption. The reason why CSH permits adsorption of only monolayer is probably that most of the admixture molecules enter the interlayers of CSH, thus making it difficult to form the second layer.

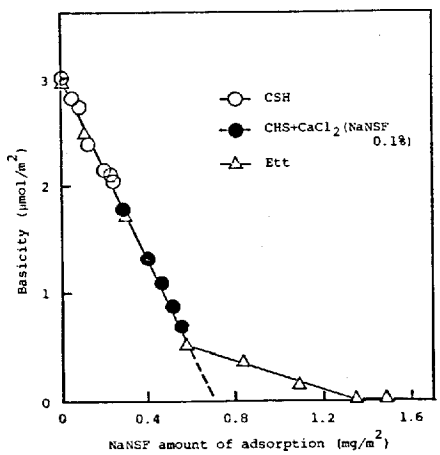

Fig. 6 Relationship between surface basicity of hydrate and amount of admixture adsorbed.

Role of basic site as adsorption site

It is possible that the relationship described above between the basicity of the hydrate surface and the amount of NaNSF adsorption may be the apparent one. In other words, an admixture is adsorbed on the surface of a hydrate regardless of basic sites, with the result that the basic sites are concealed to reduce the basic sites. To confirm this, the relationhip between the basicity before adsorption and the amount of NaNSF adsorption was studied about inorganic compounds other than hydrates which are hard to solve in water. Each of the compounds was used after being dried for three hours at 100°C. The adsorption was carried out from two types of liquid, pure water and 0.2% $CaCl_2$ solution. The concentration of the admixtures was set to 0.1% for both. The result of the study is shown in Fig. 7. In the case of adsorption in pure water, the correlationship was obtained that the amount of adsorption increases with basicity. Assuming that one basic site corresponds to a monomeric unit of NaNSF, the relationship between basicity and the amount of adsorption is shown by the straight line ① in Fig. 7. In the case of adsorption in pure water, each compound is located almost along this line. The maximum amount of adsorption of CSH (in 0.2% $CaCl_2$ solution) also exists on this line. As Ett is comparatively large in the amount of dissolution, the adsorption of it is shown by the same symbol as that of the 0.2% $CaCl_2$ aqueous solution. As explained above, the relationship shown by the straight line ① concerns the completion of the monomolecular layer adsorption. In similar manner, the relationship associated with the completion of the two or three-molecular layers are given by straight line ② or ③, respectively. In each case, the adsorbed molecules are assumed to be flat. The adsorption in the 0.2% $CaCl_2$ solution, therefore, is presumed to be 1.5 to 3 molecular layer one. These results appear to show also that Ca^{2+} ions are involved in the adsorption of multilayers. Also, the fact that the change in basicity per unit area increases the amount of adsorption per unit area substantially proportionately in the adsorption in pure water may indicate that the basic sites are related to the adsorption sites directly but not apparently.

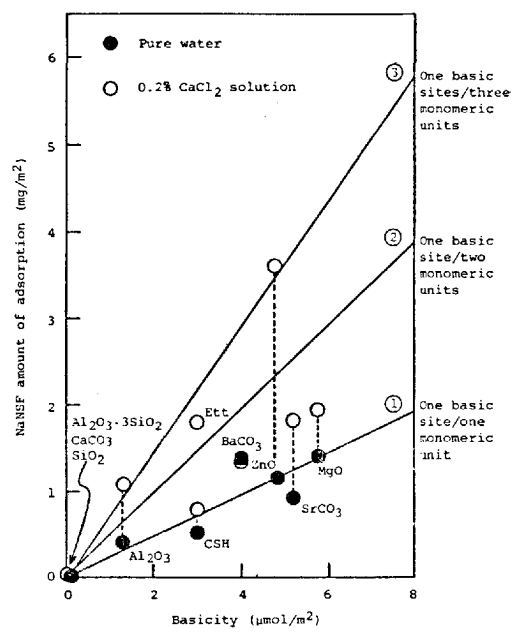

Fig. 7 Relationship between surface basicity of inorganic compound and amount of NaNSF adsorbed.

The basic sites of the solid are known as a electron-pair donor. The researchs on the surface basic sites of a cement-related compounds are still few (8, 9), and the structure thereof have not yet made clear. According to Krylov, et al (10), O^{2-}, OH^-, OH^- adjacent to the O^{2-} may be the basic sites of MgO. Tanabe (11) maintains that as shown in the example of CaO of Fig. 8, the strong basic sites of the oxides of alkali earth metal are made up of O^{2-} atoms on the surface. A similar result is given by Niiyama et al (7). In CSH and Ett also,

therefore, the surface O^{2-} and OH^- may be the main basic sites. Hansen and Steiner, on the other hand, points out that the carboxyl group and hydroxyl group of organic admixture molecules having a set retarding action are coupled to Ca^{2+} and adjacent O^{2-} respectively on the surface of cement particles and that the important mechanism of adsorption is probably provided by chelation of these atoms on the surface (12). Since the structure of the basic sites are not yet clear, it is still impossible to specify the manner in which the admixture molecules are coupled to the surface basic sites. The differential spectrum by FT-IR of MgO that has adsorbed NaNSF is shown in Fig. 9. The main absorption bands (8.3, 8.9, 9.6 μm) of NaNSF adsorbed on MgO are observed. The absorption band at 8.3 μm SO_3^- group shows no chemical shift but its split is clearly seen. This suggests that the sulfonic group is concerned with the adsorption. Though not shown in the drawing, the absorption band at 2.7 μm (free-OH group) remained unchanged with the adsorption of NaNSF. Therefore, it follows that there is no interaction between the hydroxyl group and NaNSF on the MgO surface. As regards CSH and Ett, a clear differential spectrum could not obtained due to the absorption bands of the admixtures and hydrates superimposed one on the other.

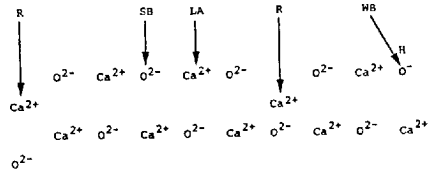

Fig. 8 Surface model of CaO.R: reducing site, SB: strong basic site, LA: Lewis acid site, WB: weak basic site. (11)

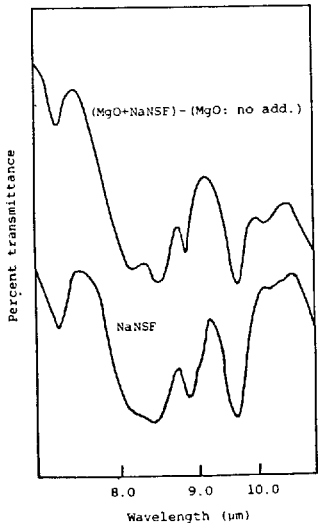

Fig. 9 FT-IR spectrum of NaNSF adsorbed on MgO surface

ACKNOWLEDGEMENTS

The authors wish to express their thanks to the top management and Mr. O. Suzuki, Manager of Research Department, and Mr. M. Tanaka, Chief Chemist of Chichibu Cement Co., Ltd., for invaluable advices and allowing us to publish this paper.

REFERENCES

1.- V.S. RAMACHANDRAN (1983), "Adsorption and hydration behavior of tricalcium aluminate-water and tricalcium aluminate-gypsum-water system in the presence of superplasticizers," A.C.I. Journal, May-June, 235-241.

2.- E.D. SHUKIN, E.A. AMERINA, E.P. ANDREEVA and S.I. KONTOROVICH (1980), "Agglutination (bridging) of particles during hydration hardening and the effect of surface active additives," 7th Int. Sym. Chem. Cem., Vol. II, (Paris), II167-171.

3.- M. COLLEPARDI, M. CORRADI, G. BALDINI and M. PAULI (1980), "Influence of sulfonated naphthalene on the fluidity of cement paste," 7th Int. Sym. Chem. Cem., Vol. III, Paris, VI20-25.

4.- B. BLANK, D.R. ROSSINGTON and L.A. WEINLAND (1963), "Adsorption of admixtures on Portland cement" Journal of the American Ceramic Society, Vol. 46, No.8, 395-399.

5.- U. COSTA, F. MASSAZZA and A. BARRILA (1982), "Adsorption of superplasticizers on C_3S: Changes in zeta potential and rheology of pastes," Il Cemento, (4), 323-336.

6.- U. COSTA, F. MASSAZZA (1984), "Adsorption of superplasticizers on $-C_2S$ - Changes in zeta potential of particles and the rheology of pastes," Il Cemento, (3), 127-139.

7.- H. NIIYAMA and E. ECHIGOYA (1971), Journal of the Chemical Society of Japan (Kogyo Kagaku Zasshi) Vol. 74, No.4, 560-563.

8.- G. SUDOH, T. AKIBA, T. IWASAKI (1976), "Some studies on calcium sulfoaluminate hydrates," CAJ Review of the 30th General Meeting - Technical Session -, 42-44.

9.- G. SUDOH, T. AKIBA, K. ARAI, S. NAWATA (1973), "The correlation between surface activity and hydraulic quality in C_3S," CAJ Review of the 27th General Meeting -Technical Session -, 32-35.

10.- O.V. KRYLOV, et al., (1965), Kinetics and Catalysis, (USSR), Vol. 6, 128.

11.- K. TANABE, (1981), Catalyst-Science and Technology, Springer, Chapt. 5.

12.- J.F. YOUNG (1972), "A review of the mechanisms of set-retardation in Portland cement pastes containing organic admixtures," Cement and Concrete, Research, Vol. 2, 415-433.

Kiyoshi ASAGA, Masaki DAIMON, Sumio SIBATA,
Kazuhiro KISHI, Koumei YANO and P.R.SHRESTHA
(Dpartment of Inorganic Materials,
Tokyo Institute of Technology, Japan)

2.1

Effects of Thermal History and Additives on the Hydration of β-Ca_2SiO_4
Les Effects de L'histoire Thremique et des Additifs sur la Hydration de β-Ca_2SiO_4

SUMMARY ; β-C_2S without or with additives such as Fe_2O_3, Fe_2O_3+K_2O and B_2O_3 were prepared under various thermal treatments. β-C_2S without additives was formed as a single phase, when γ-C_2S was heated at about 1000 ℃ and then rapidly quenched (β-phase quenched from α' phase), or when quenched from the temperature higher than the α' - α transformation temperature (β-phase quenched from α phase). And these treatments were also favorable to produce β-C_2S with additives.

Effects of thermal history and additives on the hydration kinetics and composition of hydrate were studied.

Thermal history largely affected hydration kinetics of β-C_2S. There was large difference in the rate of hydration between the β-C_2S from α' phase and α phase. The hydration of β-C_2S from α phase proceeded actively at early stage , and became very slow in later stage. In the case of β-C_2S from α' phase, it hydrated slowly in the beginning, but rapidly in later stage. In the hydration in later stage, the additives retarded the hydration, and B_2O_3 was the strongest retarder.

The additives have significant effects upon the composition of hydration products. $Ca(OH)_2$ was hardly formed from β-C_2S prepared without additibes. However, $Ca(OH)_2$ appeared formed at early stage, and continuously increased during the hydration of β-C_2S prepared with additives. The amount of $Ca(OH)_2$ formation varied with the kind of additives. Composition of produced C-S-H changed with the curing time, and became almost constant after 2 mounths. The final composition of C-S-H was about $C_2SH_{2.4}$ from pure sample, $C_{1.8}SH_{2.5}$ from Fe_2O_3+K_2O bearing sample, and $C_{1.6}SH_{2.3}$ from the sample with B_2O_3. Composition of produced C-S-H was not remarkably affected by the thermal history to prepare of the starting β-C_2S and the curing temperature.

Sob vários tratamentos térmicos se preparou β-C_2S com ou sem aditivos, tais como Fe_2O_3, Fe_2O_3+K_2O e B_2O_3. β-C_2S sem aditivos se formou como uma fase única, quando se aqueceu γ-C_2S a cerca de 1000°C e se resfriou rápidamente a seguir (fase β resfriada a partir de fase α'), ou quando resfriada a partir de temperatura mais alta que a temperatura de transformação α' - α (fase β resfriada a partir de fase α). E este tratamento foi também favorável para a produção de β-C_2S com aditivos.

Foram estudados os efeitos da história térmica e dos aditivos sobre a cinética de hidratação e a composição do hidrato.

A história térmica afeta grandemente a cinética de hidratação de β-C_2S. Há grande diferença na velocidade de hidratação de β-C_2S proveniente da fase α' e da fase α. A hidratação de β-C_2S oriundo da fase α se processou ativamente no estágio inicial, e se tornou muito lenta no estágio final. No caso de β-C_2S proveniente da fase α', sua hidratação foi lenta no começo, mas rápida no estágio final. Na hidratação em estágio final, os aditivos retardaram-na, e B_2O_3 foi o mais forte retardator.

Os aditivos tem efeitos significativos sobre a composição dos produtos de hidratação. Com β-C_2S sem aditivos a formação de $Ca(OH)_2$ foi pouca. Contudo, durante a hidratação de β-C_2S preparado com aditivos, houve a formação de $Ca(OH)_2$ no estágio inicial, e seu crescimento foi contínuo durante a hidratação. A quantidade de formação de $Ca(OH)_2$ variou conforme o tipo de aditivos. A composição do C-S-H produzido se alterou com o tempo de cura, e tornou-se quase constante depois de 2 meses. A composição final do C-S-H de amostra pura foi de cerca de $C_2SH_{2.4}$, $C_{1.8}SH_{2.5}$ de amostra com Fe_2O_3+K_2O e $C_{1.6}SH_{2.3}$ de amostra com B_2O_3. A composição do C-S-H produzido não foi marcantemente afetada pela história térmica na preparação de β-C_2S inicial e na temperatura de cura.

1 INTRODUCTION

In order to discuss the hydration process of β-C_2S, it is necessary to clarify the kinetics and the stoichiometry of hydration. Many investigation have been performed to study the hydration of β-C_2S, by using the β-C_2S with various additives as stabilizer (1-5). Kinetics of hydration of β-C_2S varies with the kind and quantity of additives (2,6,7), and the hydration mechanism is thought to be affected by additives. The hydration process of β-C_2S without additives must be studied in order to discuss the mechanism of hydration of β-C_2S and effect of additives. There is less studies to discuss the hydration of β-C_2S without additives because of the difficulty of the synthesis (6,8).

The authers found out the preparation methods of pure β-C_2S, and showed that the hydration process was largely affected by the thermal history when it was prepared (8).

There have been reported several studies on the effect of thermal history on hydration of β-C_2S (7,9), but there have been no report on the effect of thermal history and additives togather at instance. In this study, β-C_2S without or with additives were prepared under various thermal treatment, and the effect of thermal history and additives on the kinetics and the stoichiometry of the hydration were discussed.

2 EXPERIMENTAL PROCEDURES

2-1 Preparation of β-C_2S

$CaCO_3$, SiO_2, Fe_2O_3, KOH and B_2O_3 were mixed in the ratio listed in the Table 1. The mixtures were heated in platinum crucible in an electric furnace at 1500°C for 1-1.5 hours and cooled in the air. γ-C_2S was the only polymorph in when no additive was introduced, and the mixtures of γ-C_2S and β-C_2S were obtained in the case with additives. The β-C_2S was synthesized by firing these C_2S as the starting materials. The starting materials were heated in platinum crucible in an electric furnace at verious temperatures from 1000°C to 1500°C for 10 minuites -48 hours and were quenched in the water. The products were imediately washed with aceton to prevent hydration. The products were identified by XRD, and the ratios of γ-C_2S/total C_2S were determined.

2-2 Hydration

The starting materials mentioned above were heated at verious temperatures from 1000°C to 1500°C for 1 hour, as shown in Table 2, in order to study the hydration of β-C_2S. The samples were grounded to the Blain fineness about 0.4-0.5 m^2/g. The specific surface area was determined by BET method using Kr as adsobate.

The rate of heat liberation for 48 hours were carried out by conduction calorimeter, at W/C ratio of 1 at 20°C. The experiments of paste hydration were carried out at W/C ratio of 0.6 at 20°C and 70°C. The hydrated pastes were dried under the water vapor pressure of 3×10^{-2} mmHg. The degree of hydration of β-C_2S was measured by quantitative XRD using CaF_2 as internal standard. Loss on ignition was determined by heating at 1000 C and the amount of $Ca(OH)_2$ was determined by DSC.

Table 1 Chemical composition of the starting materials (mol %)

	CaO	SiO_2	B_2O_3	Fe_2O_3	K_2O
without	2	1			
Fe_2O_3	2	0.97		0.015	
Fe_2O_3+K_2O	1.97	0.97		0.015	0.015
B_2O_3	2	0.97	0.015		

Table 2 Characters of the β-C_2S for hydration

	reheated temp.(C)	Blain surface area (m^2/g)	Kr surface area (m^2/g)
without	1000	0.58	2.3
	1500	0.46	
Fe_2O_3	1000	0.51	0.88
	1500	0.50	
Fe_2O_3+K_2O	1000	0.424	1.02
	1500	0.436	0.98
B_2O_3	1000	0.442	1.23
	1500	0.406	1.13

3 RESULTS AND DISCUSSIONS

3-1 Preperation of β-C_2S

Fig.1 shows the changes in the γ-phase/total C_2S ratio with soaking time of the samples without additives and with Fe_2O_3 heated at 1000-1500°C. In the case without additives, the amounts of γ-C_2S were less in the samples heated at 1000°C and 1500°C, and showed little change with time, whereas they were larger in the samples heated at 1200-1400°C, and changed with time. Fe_2O_3 addition restrain-ed β- γ transformation at any temperatures, especially when the soaking time was short. γ-C_2S was not exsisted in the samples heated at 1000°C and 1500°C independently on soaking time, and it was increased with soaking time when the starting material was heated at 1200-1400°C.

In the case of the other additives, β-C_2S was also formed as a single phase, when the samples were heated at 1000°C and then rapidly quenched, or when quenched from 1500°C, which was higher than the α'-α transformation temperature.

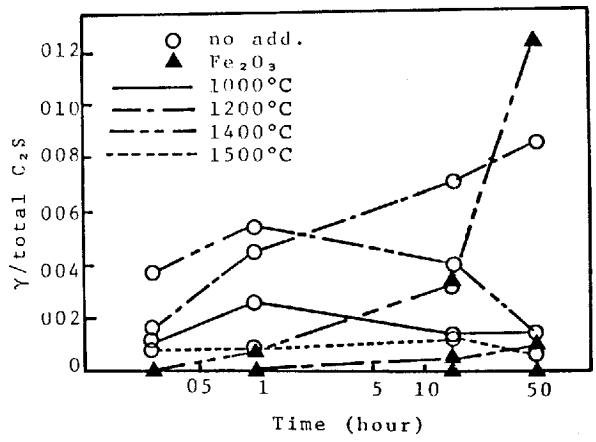

Fig.1 - Canges in the γ-phase/total C_2S ratio with soking time of the samples without and with Fe_2O_3.

It was found that the transformation of C_2S was complicatedly influensed by the thermal history and the impurities. The authors discussed on this issu in detail, in the previous reports concerning pure C_2S (10) and Fe_2O_3 bearing C_2S (11).

3-2 Hydration during the eary stage.

The rate of heat liberation for the β-C_2S without additives and with Fe_2O_3 prepared at verious temperatures are plotted against time in Figs.2 and 3. It was observed in the both cases that the rate of heat liberation for the samples heated at 1500°C was different from those of 1000-1400°C. Total calorific value for 24 hours of the samples heated at 1500°C was 40J/g and 35J/g respectively, whereas those of 1000-1400°C were 5-10J/g and 3-5J/g. The heat liberation curve for the sample without additives heated at 1500°C showed the broad peak at 6 hours after mixing with water. Those with Fe_2O_3 showed the peak at 20 hours. The hydration during the early stage was retarded by the Fe_2O_3 addition. The heat liberation curves for the samples heated at 1000-1400°C shows the small peaks at 1-2 hours and very small heat liberation after 10 hours.

The rate of hydration during the early stage was affected by the thermal history of the samples than by the additives. The samples quenched from α-C_2S hydrated much faster than those quenched from α'-C_2S. The similar results were obtained for the samples containing the other additives.

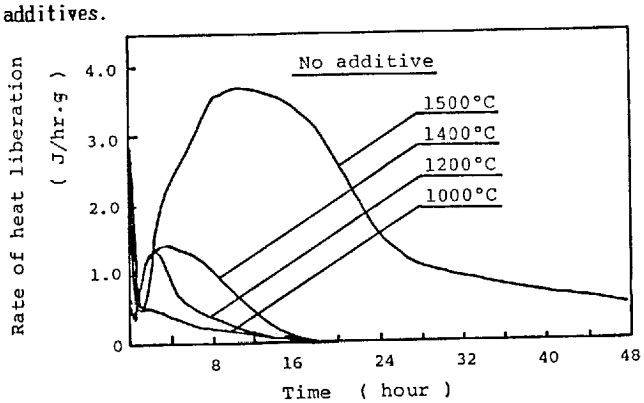

Fig.2 - Effect of the preparation temperatures on the rate of heat liberation curve; without additives.

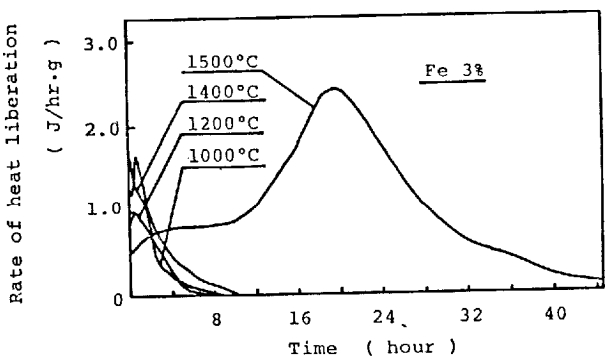

Fig.3 - Effect of the preparation teppera-tures on the rate of heat liberation curve; with Fe_2O_3.

3-3 Hydration of pastes at 20°C

All values of the results were shown on the ignited basis.

Fig.4 shows the percentage of hydration in the paste with W/C ratio of 0.6, cured at 20°C. The sample without additives heated at 1000°C hydrated at an extremely slow rate in the early stage, it was not possible to detect the hydration within 7 days. But it hydrated rapidly after two weeks, and over 80% of the sample had consumed within 50 days, and hydrated completly before 120 days. The sample without additives heated at 1500°C hydrated faster than that of 1000°C in the early curing time. It hydrated gradually, and about 70% hydrated at 60 days. The rate of hydration became slow after 60 days. The rate of hydration of the sample with B_2O_3 heated at 1500°C was not markedly differnt from that without additives heated at 1500°C in the early stage, but it became slower in the later stage. The the rate of hydration of the sample with Fe_2O_3+K_2O heated at 1500°C was intermediate between those of two.

Fig.5 shows the amount of loss on ignition of the hydrated samples at different curing times. The curves of the loss on ignition were almost same as the curves of the percentage of the hydration, except that the sample with B_2O_3 showed larger values than others at the early stage of hydration.

The formation of $Ca(OH)_2$ during the β-C_2S hydration is plotted against the curing time in Fig.6. In the hydrated pastes of both the samples without additives heated at 1000°C and 1500°C, the amount of $Ca(OH)_2$ was very small and was not markedly increased with curing time. The value up to 150 days was below about 1.5%. The large amounts of $Ca(OH)_2$ was liberated in the hydrated pastes of the samples with additives. The formation of $Ca(OH)_2$ in B_2O_3 containing system was greater than the others from the very beginning, and it continuously increased in the later stages. In the case with Fe_2O_3+K_2O the amount of $Ca(OH)_2$ increased up to 50 days hydration, and became almost constant there after.

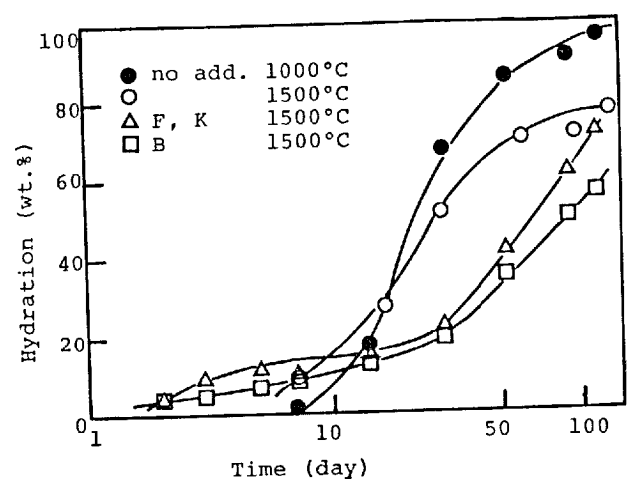

Fig.4 - Canges of the percentage of hydration with curing time at 20°C.

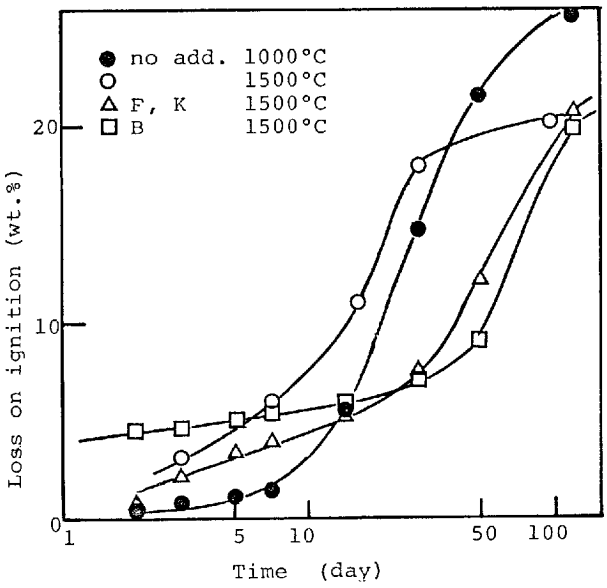

Fig.5 - Changes of the loss on ignition with curing time at 20°C.

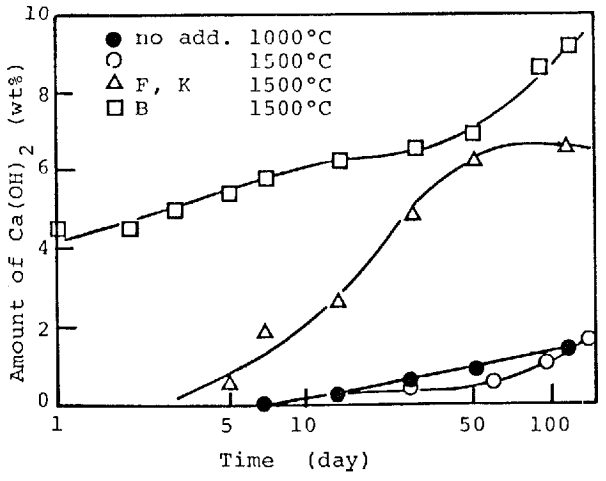

Fig.6 - Changes of the amount of $Ca(OH)_2$ with curing time at 20°C.

The molar ratio of CaO and SiO_2, H_2O and SiO_2 of the produced C-S-H calculated from the ratio of hydration, loss on ignition and amount of $Ca(OH)_2$ are plotted against curing time in Figs.7 and 8. C/S ratio of the C-S-H produced from the samples without additives was almost constant at about 2 throughout the hydration. On the other hand, it changed with curing time in the case with additives. In the case with B_2O_3, C/S ratio was very low in the early stage and increased untill 50 days, and became constant at the value of about 1.6. It was high as about 2 in the beginning, and decreased up to 50 days, and became almost constant at the value of about 1.8 for the C-S-H produced from the sample with $Fe_2O_3+K_2O$.

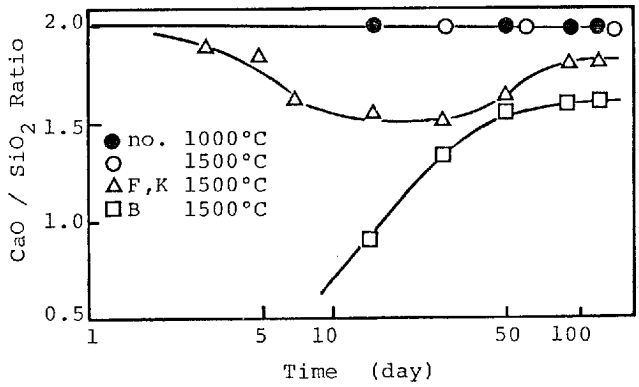

Fig.7 - Changes of molar ratio of CaO and SiO_2 of the produced C-S-H, with curing time at 20°C.

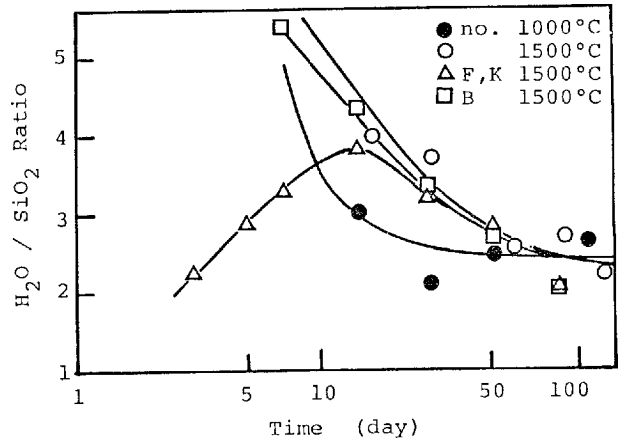

Fig.8 - Changes of the molar ratio of H_2O and SiO_2 of the produced C-S-H with curing time at 20°C.

Although the data of H/S ratio of the C-S-H were slightly scattered, It had a tendency of decreasing with hydration and became almost constant at the value about 2.3-2.5. It did not markedly change with the additives except the early hydration of the sample with $Fe_2O_3+K_2O$.

The composition of formed C-S-H varied with the starting β-C_2S. It also changed with curing time, and it did not changed after 2 mounths for each sample. The final composition of C-S-H was about $C_2SH_{2.4}$ from pure sample, $C_{1.8}SH_{2.5}$ from $Fe_2O_3+K_2O$ bearing sample, and $C_{1.6}SH_{2.3}$ from the sample with B_2O_3.

The results with B_2O_3 is agreed with Kantro and Weise (5). But B_2O_3 bearing β-C_2S hydrates in a very different way from β-C_2S with the other additives. It is suggested that B_2O_3 is not sutable as stabilizer in order to study the hydration mechanism of β-C_2S.

Recently, the composition of C-S-H is directly measured by analytical electron microscope. The results show that average composition of C-S-H produced β-C_2S is 1.4 (12). These values are smaller than that of results of

this work and the other studies. One of the reasons is thought to be that analytical electron microscope may measure outer C-S-H. The values calculated from the amount of $Ca(OH)_2$ are average values of the outer and inner C-S-H The more precise study must be carried out.

3-4 Hydration of pastes at 70°C

Fig.9 shows the percentage of β-C_2S hydration in pastes, cured at 70°C. The rate of hydration was very fast compared with the results of 20°C. But the rate of hydration of the samples with B_2O_3 became slow in the later stage, and the amount of hydration was smaller than that at 20°C. This agreed with the result of Kantro et al (2). The sample without additives heated at 1000°C hydrated in very slow rate within 16 hours, products could not be detected. But it hydrated rapidly after 1 day, and hydrated almost completely after 168 hours (7 days). It was observed, in the samples with additives, that the rate of early hydration of the samples heated at 1500°C was faster than those of 1000°C, and that the rate of hydration after 24 hours was slower. The amount of hydration of the B_2O_3 bearing β-C_2S, in later stage, was as small as 20°C hydration.

The results of loss on ignition are in Fig.10, which show very similler tendencies to Fig.9. But in the case with Fe_2O_3+K_2O, the loss on ignition of the samples heated at 1500°C was more than that of 1000°C even at the same degree of hydration.

The amount of $Ca(OH)_2$ liberated during the hydration is plotted against the curing time in Fig.11. In the samples without additives, the amount of $Ca(OH)_2$ was as small as in the paste curing at 20°C. B_2O_3 sample liberated larger amount of $Ca(OH)_2$ than other samples, too. But $Ca(OH)_2$ liberations were smaller, in all samples, than that of 20°C at the same degree of hydration. The effect of thermal treatment was not observed in the samples with B_2O_3, but in the case with Fe_2O_3+K_2O, larger amount of $Ca(OH)_2$ was formed from the samples heated at 1500°C.

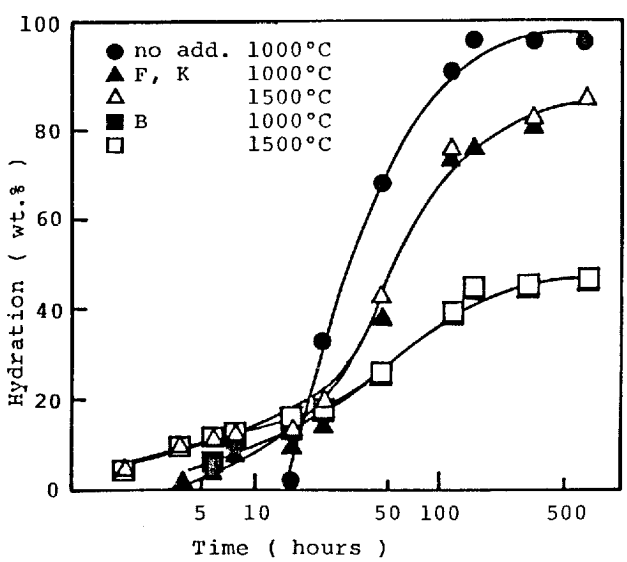

Fig.9 - Changes of the percentage of hydration with curing time at 70°C.

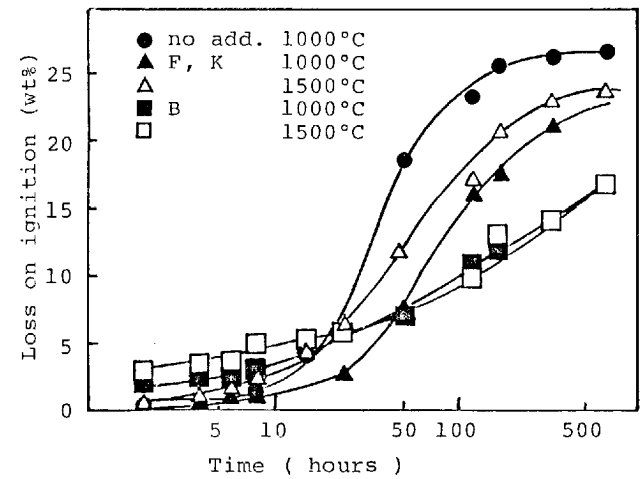

Fig.10 - Changes of the loss on ignition with curing time at 70°C.

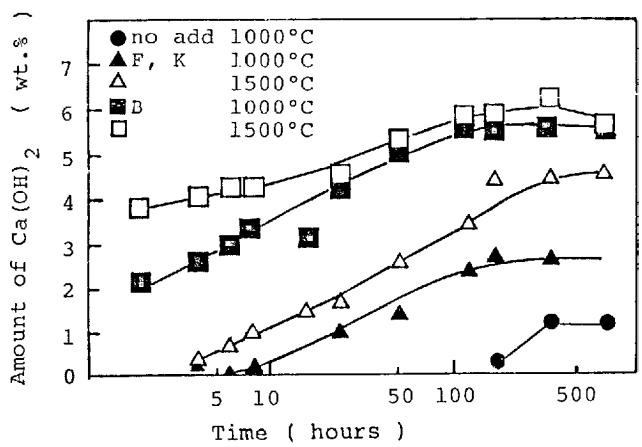

Fig.11 - Changes of the amount of $Ca(OH)_2$ with curing time at 70°C.

The changes in the molar ratio of CaO and SiO_2, H_2O and SiO_2 of the produced C-S-H are shown in Figs 12 and 13 The C/S ratio changed similarlly to 20°C, although the values were slightly larger than those of 20°C. The effect of thermal treatment was not observed in the samples with B_2O_3, and the value was about 1.7 in the late stage. In the case with Fe_2O_3+K_2O, C/S ratio was higher for 1000°C sample than for 1500°C, and the value was 1.8 and 1.9 respectively.

The results of H/S ratio were very similler to the results of 20°C hydration.

The compositions of the C-S-H produced from hydration at 70°C were almost identical with 20°C.

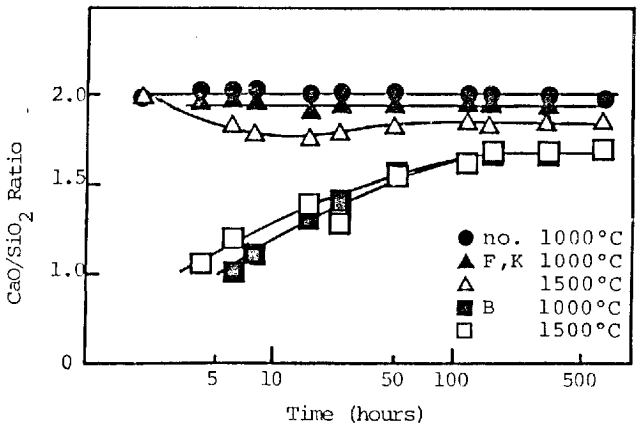

Fig.12 - Changes of the molar ratio of CaO and SiO_2 of the produced C-S-H with curing time at 70°C.

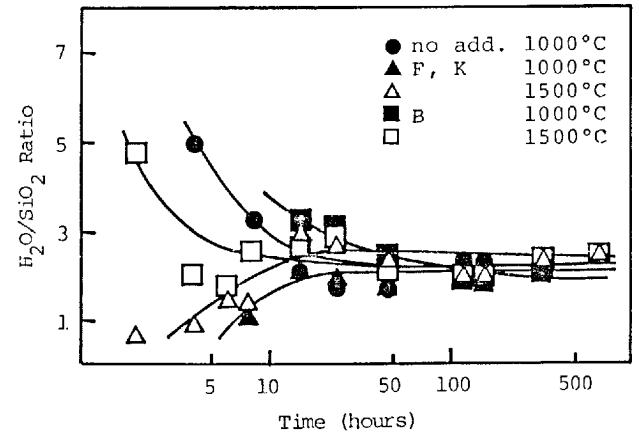

Fig.13 - Changes of the molar ratio of H_2O and SiO_2 of the produced C-S-H with curing time at 70°C.

5 CONCLUSIONS

β-C_2S without or with additives such as Fe_2O_3, Fe_2O_3+K_2O and B_2O_3 were prepared at various thermal treatment. And the effects of thermal history and additives on the hydration kinetics and stoichometry were studied. The results were summerised as follows.

1) β-C_2S without additives was formed as a single phase, when γ-C_2S was heated at about 1000°C and then rapidly quenched, or when quenched from the temperature higher than the α'-α transformation temperature. And these treatments were also favorable to make β-C_2S in the case with additives.

2) There is large difference in the rate of hydration between the β-C_2S from α' phase and α phase. The hydration of β-C_2S from α phase proceeded activly at early stage, and became very slow in later stage. In the case of β-C_2S from α Phase, it hydrated slowly in the beginning , but rapidly in later stage.

3) In the hydration in later stage, the additives retarded the hydration, and B_2O_3 was the strongest retarder.

4) The additives have important effects upon the composition of formed C-S-H. $Ca(OH)_2$ was hardly formed from the hydration of β-C_2S prepared without additibes. However, $Ca(OH)_2$ appeared at early stage, in the hydration of β-C_2S prepared with additives, and continuously increased during hydration prosess. The amount of $Ca(OH)_2$ changed with the kind of additives.

5) Composition of produced C-S-H changed with the curing time, and became almost constant after 2 mounths. The final composition of C-S-H was about $C_2SH_{2.4}$ from pure sample, $C_{1.8}SH_{2.5}$ from Fe_2O_3+K_2O bearing sample, and $C_{1.6}SH_{2.3}$ from the sample with B_2O_3.

6) Composition of produced C-S-H was not significantly affected by the thermal tretment of the starting β-C_2S and the curing temperature.

7) B_2O_3 is not sutable as stabilizer in order to study the hydration mechanisms of β-C_2S.

REFERENCES

1.- S.Brunauer and S.A.Greenberg, "The hydration of tricalcium silicate and β-dicalcium silicate at room temperature", Proc. 4th Intl. Symp. Chem. Cement, Washington 1960 Vol.1, 135-153 (1962).

2.- D.L.Kantro, S.Brunauer and C.H.Weise, "Development of surface in the hydration of calcium silicates. 2 Extension of investigations to earlier and later stage of hydration", J. Phys. Chem., 66, 1804-1809 (1962).

3.- K.Fujii and W.Kondo, "Rate of mechanism of hydration of β-dicalcium silicate", J. Am. Ceram. Soc., 62, 161-167 (1979).

4.- F.M.Lea, "The chemistry of cement and concrete", Edward Arnold, London, 1970, pp 176-183.

5.- D.L.Kantro and C.H.Weise, "Hydration of various beta-dicalcium silicate preparations", J. Am. Ceram. Soc., 62, 621-626 (1979).

6.- I.M.Pritts and K.E.Daugherty, "The effect of stabilizing agents on the hydration rate of β-C_2S", Cem. Concr. Res., 6, 783-796 (1976).

7.- P.Fierens and J.Tirlocq, "Nature and concentration effect of stabilizing elements of beta-dicalsium silicate on its hydration rate", Cem. Concr. Res., 13 , 267-276 (1976).

8.- S.Shibata, K.Kishi, K.Asaga, M.Daimon and P.R.Shrestha, "Preparation and hydration of β-C_2S without stabilizer", Cem. Concr. Res., 14, 323-328 (1976).

9.- A.A.Pashohenko, E.A.Starchevskaya and V.P.Serbin, "Research in belite synthesized in the low temperature area", Proc. 6th Intl. Cong. Chem. Cement Suppl. Paper Section 1, Moscow (1974).

10.- S.Shibata, K.Kishi, K.Asaga and M.Daimon, "Effect of thermal history on β -γ transformation of pure β-C_2S" (in Japanese), Yogyo Kyokai-Shi, 91, 497-502 (1983).

11.- S.Shibata, K.Kishi, K.Asaga and M.Daimon, "Effect of thermal history on β -γ transformation of β-C_2S in presence of F_2O_3" (in Japanese), Yogyo Kyokai-Shi, 92, 71-76 (1984).

12.- K.Mohan and H.F.W.Taylor, "Analytical electoron microscopy of cement pastes; 4 β-dicalcium silicate ", J. Am. Cerm. Soc., 64, 717-719 (1981).

Hirotaka Ushiyama,Yutaka Kawano and Nobuo Kamegai Tokuyama Soda Co., Ltd Japan

Effect of Carbonates on Early Stage of Hydration of Alite

2.1

Effect du carbonate sur l'hydration initial de l'alite

ABSTRACT

It is well known that carbonates affect the rate of cement hydration in the early stage. So carbonate is used as one agent of cement additives.
In this paper,influence of various carbonates including bicarbonates on the early stage of hydration of Alite which is the main component of portland cement was studied.
Alite was synthesized in the structure of $105CaO \cdot 2MgO \cdot Al_2O_3 \cdot 35SiO_2$, and ground to a specific surface area of $2920 cm^2/g$.
As carbonates and bicarbonates,Na_2CO_3,K_2CO_3,Li_2CO_3,Cs_2CO_3,$NaHCO_3$,$KHCO_3$,and $LiHCO_3$ were used.
It is shown that by addition of small amount of carbonates or bicarbonates the early hydration of Alite is retarded and by addition of large amount of them it is accelerated.

Sabe-se bem que os carbonatos afetam a velocidade de hidratação do cimento no estágio inicial. Assim, o carbonato é usado como um agente de aditivos de cimento.

Neste trabalho se estuda a influência de vários carbonatos, incluindo bicarbonatos, sobre o estágio inicial de hidratação da alita, que é o componente principal do cimento portland. A alita foi sintetizada na estrutura de $105CaO.2MgO.Al_2O_3.35SiO_2$, e moída até uma área de superfície específica de $2.920 cm^2/g$.

Foram usados Na_2CO_3,K_2CO_3, Li_2CO_3, Cs_2CO_3, $NaHCO_3$, $KHCO_3$ e $LiHCO_3$, como carbonatos e bicarbonatos.

Ficou demonstrado que, com adição de pequena quantidade de carbonatos e bicarbonatos, a hidratação inicial da alita é retardada, e com adição de grande quantidade deles, ela é acelerada.

Hirotaka Ushiyama,Yutaka Kawano and Nobuo Kamegai Tokuyama Soda Co., Ltd Japan

INTRODUCTION

As soluble carbonates have a distinct inflence on the early stage hydration of portland cement, they are able to be utilized as an accelerator(1) or one of water-reducer's agents(2).
It has been reported by some researchers that the hydration of tricalcium silicate is accelerated by the addition of the carbonates.(3,4,5,6)
However, there has been little work about the hydration of Alite which contains a small amount of MgO and Al_2O_3.
In this study,the influence of vorious cabonates including bicarbonates on the early stage of the hydration was studied by using mainly a Alite synthesized in laboratory. Conduction calorimetry, paste hydration and suspension were measured.
In addition, the effect of carbonates on the hydration of the commercial portland cements is studyed by calorimetry in order to compare that of Alite.

EXPERIMENTAL

(1) Materials
Alite was synthesized from a mixture of $CaCO_3$,MgO , Al_2O_3 and SiO_2,proportioned to give $105CaO \cdot 2MgO \cdot Al_2O_3 \cdot 3SiO_2$. The mixture was sintered two times at 1520 ℃ for 6 hours with intermediate grinding, and finally ground to a Blaine finess of 2920cm^2/g.
The Alite obtained had a free lime content of 0.08 percent, and the X-ray diffraction pattern(in Fig.1) showed the polymorphic modification to be monoclinic. Table 1 gives the chemical analysis of two commercial portland cements used in this study.

Carbonates and bicarbonates used were Na_2CO_3 ,$NaHCO_3$, K_2CO_3 ,$KHCO_3$,Cs_2CO_3 ,Li_2CO_3 ,and $LiHCO_3$, of which the former two were mainly used.
$LiHCO_3$ was prepared by blowing CO_2 gas into Li_2CO_3 solution, and the solution obtained was a mixture of 97mol% $LiHCO_3$ and 3mol% Li_2CO_3.
Amounts of carbonate or bicarbonate added were 2,4,8, 16 milli-mol per 100g solid(8 m-mol Na_2CO_3 per 100g so lid corresponds to 0.85 wight percent).
And beforehand dissolved in water, carbonates or bicarbonates were used.

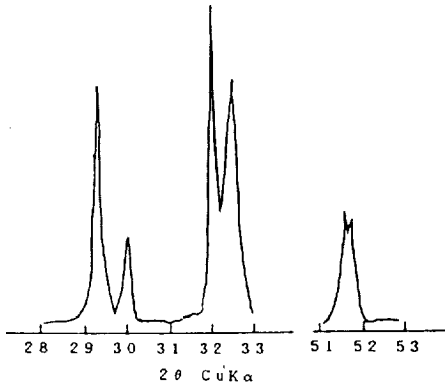

Fig.1 Fragment of X-ray diffraction pattern of Alite

(2) Hydration condition

Hydration temperature was 20℃ in all experiments.
Water to solid ratio was 0.65 in case of paste hydration and conduction calorimetry, and 5.0 in case of suspention hydration.
Suspension hydration was performed using a shaker, which vibrated horizontally in the amplitude of 40mm and 100 reciplocations a minute.

RESULTS AND DISCUSSION

(1) Rate of heat liberation
Fig.2 and 3 give the rate of heat liberation in the hydration of Alite without additive and with carbonate or bicarbonate.
As shown in these figures there is no significant difference in the effect of carbonates on the hydration of Alite among the cations contained in them.

No	amount of carbonate added per 100g Alite (m-mol)
1	No addition
2	Na_2CO_3 2.0
3	〃 4.0
4	〃 8.0
5	〃 16.0
6	$NaHCO_3$ 8.0

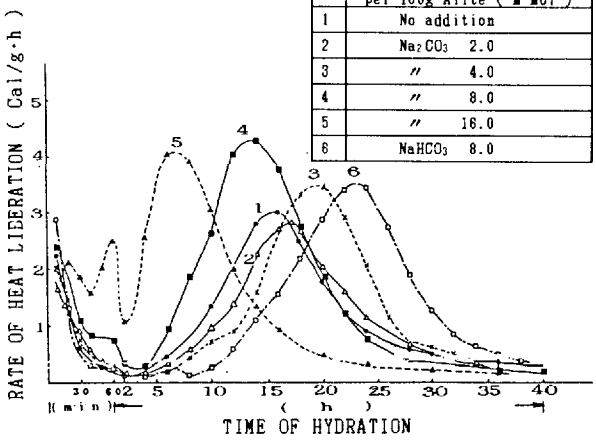

Fig.2 Variation of heat liberation of Alite with amount of carbonate or bicarbonate added

No	amount of carbonate addeed per 100g Alite (m-mol)
1	No addition
2	Li_2CO_3 8.0
3	K_2CO_3 8.0
4	Cs_2CO_3 8.0
5	$LiHCO_3$ 8.0
6	$KHCO_3$ 8.0
7	Li_2CO_3 4.0

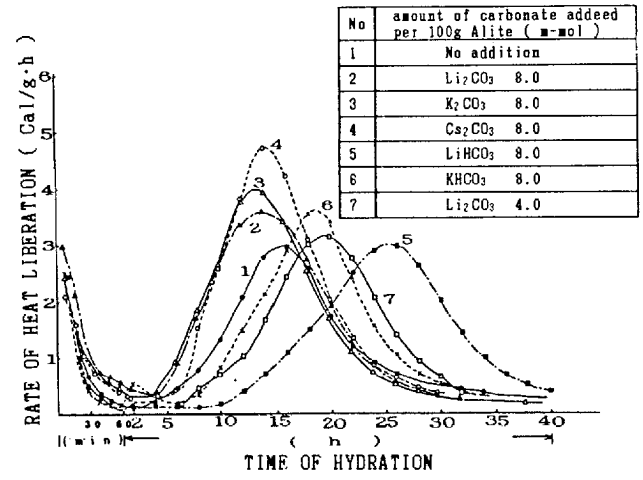

Fig.3 Variation of heat liberation of Alit with amount of carbonate or bicarbonate added

Table 1 Chemical analysis of portland cement

Sample	Ig.loss	In.sol	SiO_2	Al_2O_3	Fe_2O_3	CaO	MgO	SO_3
A	0.6	0.1	22.7	5.5	2.9	62.9	1.6	2.1
B	1.0	0.1	22.3	5.0	2.9	63.5	1.7	2.0

Hirotaka Ushiyama,Yutaka Kawano and Nobuo Kamegai Tokuyama Soda Co., Ltd Japan

The hydration was retarded below 8 m-mol of Na_2CO_3. On the contrary, with Na_2CO_3 more than 8 m-mol the hydration was accelerated and the dormant period was shortened.
It is so-called accelerating period in which the rate of heat liberation is rising up to the final peak in Fig.2 and 3.
In case that the amount of carbonates added is 8 m-mol, with any carbonate the final peak appeared rather promptly and has larger value than without addition. On the other hand, in case the amount of bicarbonate added in 8 m-mol, with any bicarbonate the final peak appeared in delay.
As shown in Fig.4 and 5, the hydration of two portland cements with $NaHCO_3$ (amount of 8 m-mol) is retarded.
So, it seems that the hydration of portland cement is affected in the same manner as that of Alite by the addition of carbonates or bicarbonates.
Fig.6 shows the relation between the amount of Na_2CO_3 or $NaHCO_3$ added and the time of appearence of final peak in rate of heat liberation of Alite. In case of small amount addition, $NaHCO_3$ has a larger effect on the delay of hydration rate of Alite than Na_2CO_3 has. However, it is noticiable that with increasing the amount of addition of $NaHCO_3$, the hydration rate is changed from retarding to accelerating, as well as Na_2CO_3.

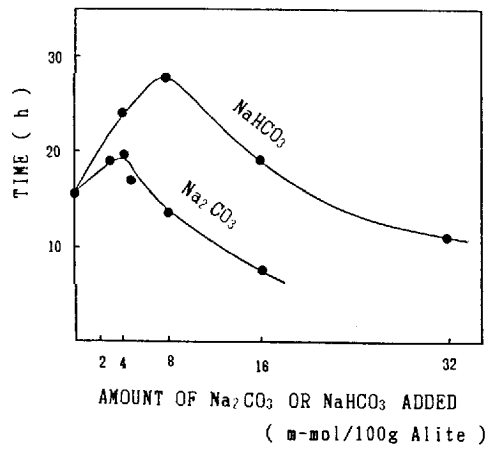

Fig.6 Relation between amount of Na_2CO_3 or $NaHCO_3$ and time of appearence of final peak in rate of heat liberation of Alite

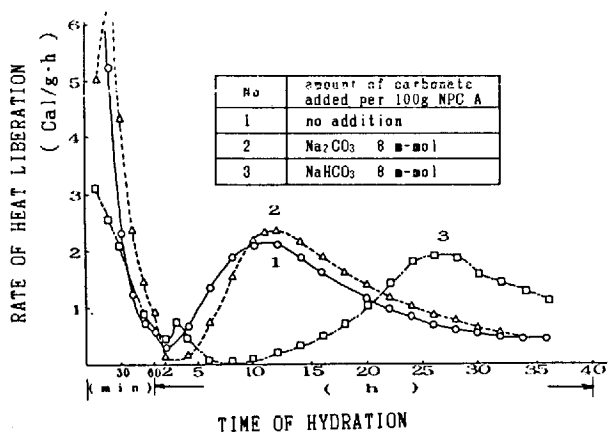

Fig.4 Variation of heat liberation of portland cement A

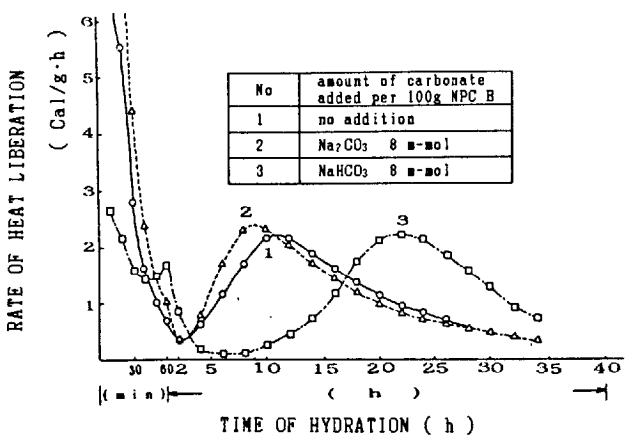

Fig.5 Variation of heat liberation of portland cement B

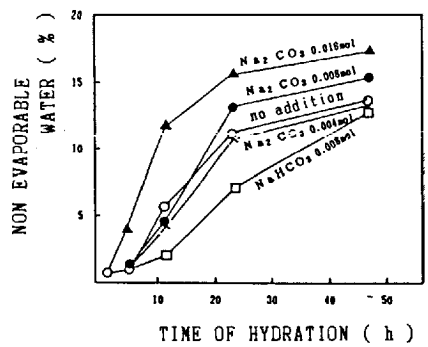

Fig.7 Variation of non evaporable water content in hydrated Alite with amount of Na_2CO_3 or $NaHCO_3$ added per Alite 100g

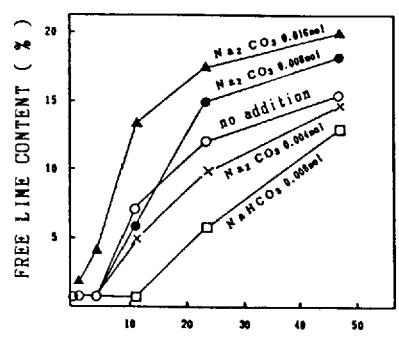

Fig.8 Variation of free-lime content in hydrated Alite with amount of Na_2CO_3 or $NaHCO_3$ added per Alite 100g

(2) Non-evaporable water and free-lime contents in paste hydration

In order to determine non-evaporable water and free-lime contents of hydrated Alite, the samples which were hydrated for different intervals of time at 20 C, were stopped with aceton and dried for 24 hours by means of D-dry method.
The determined data are shown in Fig.7 and 8.
It is considered that the non-evaporable water and free lime contents are not exactly but approximately in proportion to the degree of hydration. So, as can be seen from Fig.7,and 8, the degree of hydration for ages up to 48 hours is in the order of

$NaHCO_3$(0.008mol) < Na_2CO_3(0.004mol) < no-addition < Na_2CO_3(0.008mol) < Na_2CO_3(0.016mol).

This order agrees well with the curves of rate of heat liberation shown in Fig.2 and 3.

(3) Scanning electron microscope examination

Fig.9 and 10 show the morphology of the surface of anhydrous and hydrated Alite without additive and with 8 m-mol $NaHCO_3$ or with 16 m mol Na_2CO_3 respectively.
At ten minutes, the surface of Alite without additive is already coated with dense hydrate , while with $NaHCO_3$ the surface remains still nearly anhydrous.
With Na_2CO_3 the surface is covered with needle-like hydrates which are not observed in case of no-addition or addition of $NaHCO_3$.
Moreover, it is observed that the disintegration of coating around the particle of hydrated Alite with NaHCO3 takes place in delay in comparison with no-addtion or addition of 16 m mol Na_2CO_3.
This means that the diffusion rate of H_2O molecule or ions through the coating by addition of $NaHCO_3$ is smaller than that by no-addition.

With Na_2CO_3 the hydrate morphology changes from needle-like to ciger-shaped(at 1 hour) and to more dense ciger-shaped(at 5 hour), which means that a violent reaction occurs in this early stage.
This violency is consistent with the figure of the curve of heat liberation rate by addition of 16 m-mol Na_2CO_3(Fig.2).

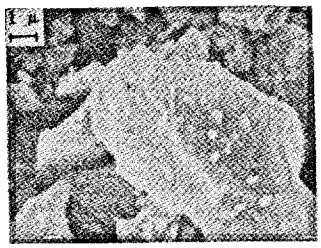

Fig.9 SEM of surface of anhydrous Alite

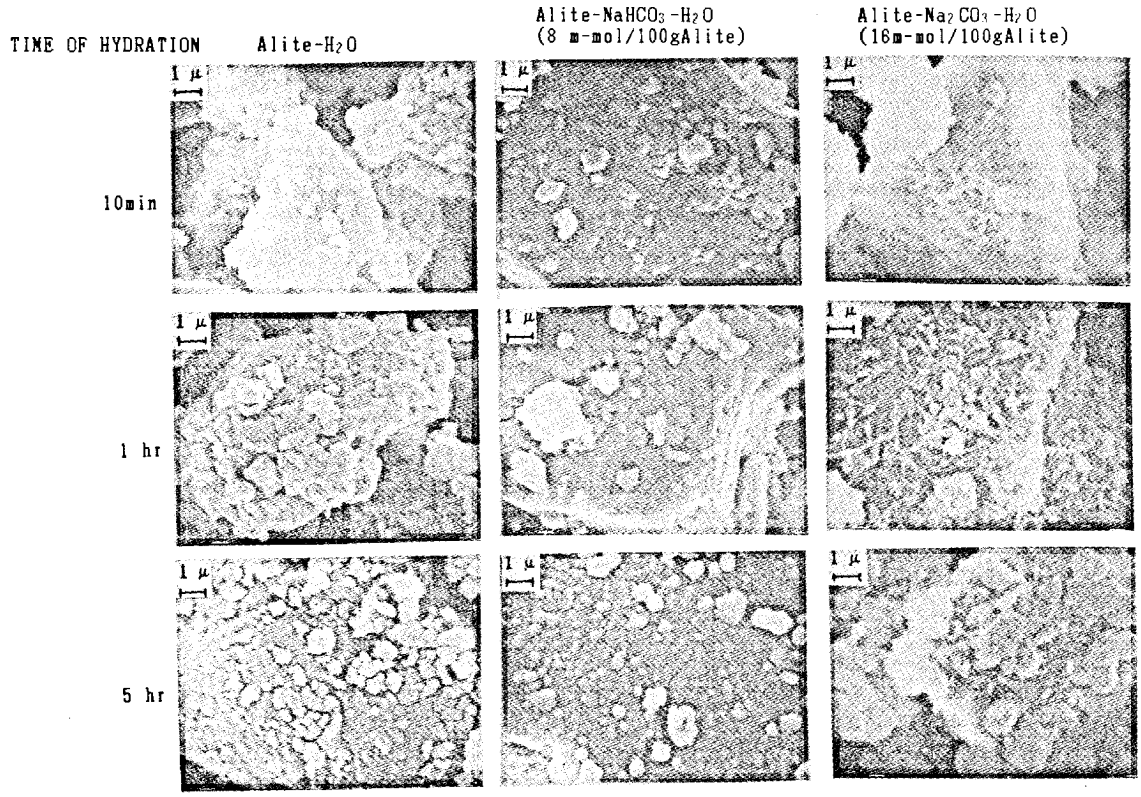

Fig.10 SEM of surface of hydrated Alite

Hirotaka Ushiyama,Yutaka Kawano and Nobuo Kamegai Tokuyama Soda Co., Ltd Japan

(4) Ion concentrations of liquid phase in suspension hydration

Hydroxide ion was determined by acid-base titration with 1/20N-HCl solution (used phenolphthalein as an indicator), Ca ion determined by cheletometric titration with 1/100M-EDTA and SiO_2 determined by colormetric method with ammonium molibdate.
It is considered that acceleration period in the hydration of Alite starts when the concentration of Ca^{++} ion of liquid phase reaches a peak(3).
Without additive or with 8 m-mol Na_2CO_3 this peak appears after 7 hours, and with 8 m-mol $NaHCO_3$ it appears after 8 hours. This fact explains that with 8 m-mol $NaHCO_3$ the hydration is retarded.
The appearance time at which acceleration period starts in curve of rate of heat liberation (Fig.2) differs from that in suspension hydration (Fig.11). This difference is attributed to the difference of the ratios of water/solid: in measurement of rate of heat liberation the ratio is 0.65 and in suspension hydration 5.0.

Without additive the concentration of Ca ion of liquid phase increases until 7 hour, and that of SiO_2 is rather low and constant within 1 hour.
While with Na_2CO_3 or $NaHCO_3$ the concentration of Ca ion is rather low and constant within 30 min and that of SiO_2 decreases rapidly with time. This phenomena imply that with Na_2CO_3 and $NaHCO_3$ Ca ion which dissolves from solid to liquid phase reacts with SiO_2 which remains in liquid, and calcium silicate hydrate formed is precipitated onto solid phase.
At very early stage (30minutes), with Na_2CO_3 or $NaHCO_3$ the concentration of SiO_2 in liquid phase is higher than that without additive. This phenomena may be explained as follows; with Na_2CO_3 or $NaHCO_3$ the concentration of Na and OH are rather high, thereby SiO_2 is easily drawn from solid to liquid phase from the moment of contact of Alite with the solution.

Furthermore, at very early stage by 10 minutes, with $NaHCO_3$ the concentration of SiO_2 in the solution is higher than that with Na_2CO_3. This may be explained as follows; with $NaHCO_3$ the hydrate layer formed around Alite grain at the moment of contact of Alite with the solution has a smaller diffusibility of ions than that with Na_2CO_3, thereby the dissolution of Ca ion into the $NaHCO_3$ solution is surpressed and the decrease in the concentration of SiO_2 by formation of CSH-gel occurs in delay.
However, with $NaHCO_3$ the concentration of SiO_2 of the solution decreases rather repidly. This may be explained as follows; the concentration of OH^- in $NaHCO_3$ solution is lower than in Na_2CO_3 solution, thereby in $NaHCO_3$ solution CSH-gel is more easily formed and SiO_2 ion remains more difficult than in Na_2CO_3.
And also this difference of the change in concentration of SiO_2 with time between in $NaHCO_3$ solution and in Na_2CO_3 solution was observed in the experiment of suspension hydration of portland cement.

(5)From above mentioned, it may be concluded that with small amount of carbonate the early hydration of Alite is retarded, and with large amount of carbonate it is accelerated.
The process of early hydration of cement is one of complicated reactions in the interface between solid and liquid. Nevertheless, the mechanism of early hydration of Alite with carbonate or bicarbonate may be given as an outline by following; with small amount of carbonate, immediatly after contact of Alite with solution, a formation of very small $CaCO_3$ particles occurs, which make the hydrate layer formed around the Alite grain to be more dense, and to be more impermeable in ion passing through, and the subsequent hydration is retarded.
On the other hand, with a large amount of carbonate the hydrate layer formed around Alite grain immediatly after contact of Alite with solution is disintegrated by an excess amount of CO_3 , thereby the rate of diffusion of ion or water through the layer is made higher, the dormant period is shortened and the subsequent hydration is accelerated.

(6)Furthermore discussions comparing with the reports described previously
Young, Tong and Berger(5) examined the hydration of C_3S(monoclinic) in the presence of admixturs, and analyzed the liquid phase in paste hydration.
Comparing the effect of NaF with that of Na_2CO_3 on the hydration, they stated that with the former the hydration is retarded, while with the latter it is accelerated. And they stated that it is not clear why there is this difference between the two additives, but possibly the answer lies in their effects on the soluble silicate species. However, in their experiment

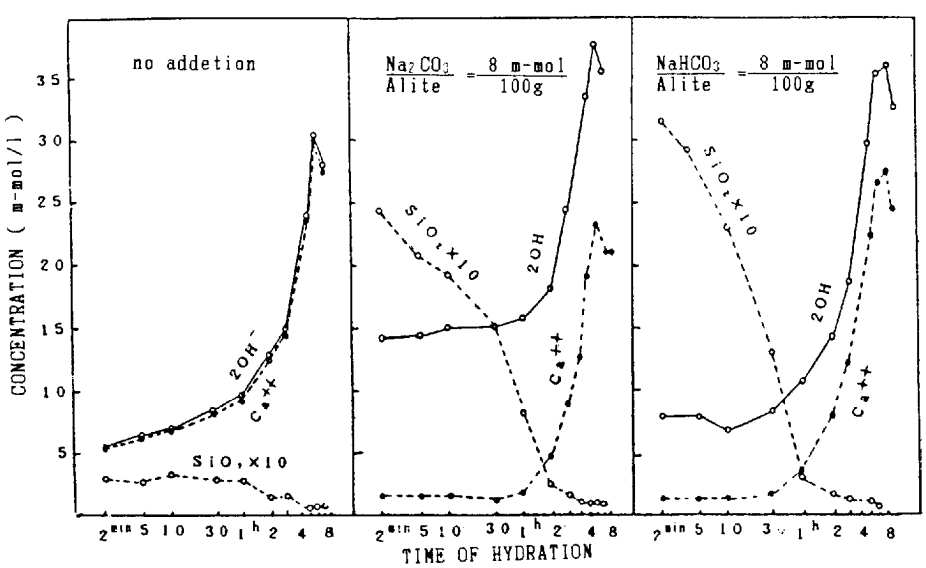

Fig.11 Variation with time of the ion concentrations of liquid phase in suspension hydration of Alite without additive or with Na_2CO_3 or $NaHCO_3$

the amount of Na_2CO_3 added is 9 m-mol per 100g C_3S and this amount of 9 m-mol may be thought to be one which accelerates the hydration, as obtained in our experiment.

Mori et al.(3) examined the hydration of nearly pure C_2S(triclinic) in the presence of Na_2CO_3 more than 0.23% by weight to C_3S.
They stated that a small amount of 0.23% already retards the hydration of C_3S.
It is considered that as to the way how the hydration in the presence of carbonate is affected, there is no big difference between C_3S(triclinic) and Alite(monoclinic) and if the amount of Na_2CO_3 is below 0.23% by weight to C_3S the hydration may be retarded.

Niël(7) examined the physical and chemical properites of hydrating paste of laboratory synthesized portland cement "M" in the presence of K_2CO_3. This cement contains C_2S,C_3A and C_4AF besides C_3S. And it is stated that by measuring setting time, consistency and change in temperature inside the paste with time the hydration is retarded with K_2CO_3 below 0.25% by weight to cement and accelerated with K_2CO_3 above 2.5%

CONCLUSION
The following points were clarified and discussed as a result of this study.
(1) A small amount of carbonates or bicarbonates delays but a large amount accelerates the hydration
(2) The difference of cation in carbonates or bicarbonates little causes the change of hydration rate.
(3) The degree of delay-effect addition of bicarbonates on hydration is larger than that of carbonates.

(4) A mechanism of the above phenomena of (1) was discussed by the results of electron microscopy, changes in ionic concentration such as SiO_2,OH^- and Ca^{++} with hydration time in suspension hydration.

BIBLIOGRAPHIE

1. A.YA.ARDEEV,E.L.DESHKO and V.A.OTRASHKEVICH "Setting Accelerator for Concrete Mixture"U.S.S.R.503,831,Feb 25 1976;Chem.Abstr.,84 154749(1976)
2. K.NATSUUME,Japan Kokai 77-137436 Nov 16 1977.
3. H.MORI,K.MINEGISHI,T.OHTA and T.AKIBA,Cemento Gijutsu Nenpo 24 48 (1970)
4. J.N.MAYCOCK and J.SKALNY,"Hydration of Ca_3SiO_5-K_2CO_3 System",Thermochimica Acta,8 167-176 (1974)
5. J.F.YOUNG,H.S.TONG and R.L.BERGER,"Composition of Solution in Contact with Hydrating C_3S Pastes", J.Am.Ceram.Soc.,60 [5-6],193-198 (1977)
6. N.B.SINGH,"Study of Ca_3SiO_5-$TlCO_3$-H_2O System", Cem. Concr. Res.5 [4],377-380 (1975)
7. EGIDE M.M.G.NIËL,"The Influence of Alkali-Carbonate of the Hydration of Cement", Vth Int. Symp. Chem. Cem. Tokyo 2,472-488,1968)

N. Hara, N. Inoue and H. Noma, Government Industrial Research Institute, Kyushu, Japan
T. Hasegawa, Aso Cement Co., Ltd., Japan

Formation and Characterization of Jennite

SUMMARY : In the series of hydrothermal reactions of fumed silica with lime in a suspension state at temperatures ranging from 60 to 120°C for duration up to 300 days, the optimum synthetic condition of well crystalline jennite and the effect of addition of Al-ions to the reaction mixtures were investigated.
Besides, the formation of jennite was tried by hydrothermal reaction at 80°C of β-C_2S and C_3S with and without addition of fumed silica, and of pulverized rice husk ash.

The results obtained are as follows :

1. The optimum temperature for the hydrothermal formation of jennite is 80°C. Siliceous materials with high amorphosity and high surface area, such as fumed silica and rice husk ash, are recommended to be used for its synthesis.
2. Jennite tends to be replaced by the formation of tobermorites on prolonging the reaction time, i.e. 14Å tobermorite in absence of Al-ions and 11Å tobermorite in presence of them.
3. The infrared absorption spectra of heated jennite suggest that a remarkable change occurs in its structure during conversion to meta-jennite. The existence of Si-Al substitution in jennite was confirmed by the displacement of Si-O stretching band toward lower frequencies, which was observed in the spectra of Al-bearing jennite.
4. Hydration of β-C_2S and C_3S at 80°C did not give the formation of jennite. However, addition of fumed silica to β-C_2S enabled to obtain jennite. It is suggested that the existence of a certain amount of silicate ions is favourable for the formation of jennite not only in these mixes but also in portland cement pastes.

Na série de reações hidrotérmicas de sílica fumaçada com cal num estado de suspensão, com temperaturas na faixa de 60 a 120°C, por período de até 300 dias, investigou-se a condição sintética ótima da jenita bem cristalizada e o efeito da adição de íons de Al às misturas de reação.

Além disso foi tentada a formação de jenita por reação hidrotérmica de β-C_2S e C_3S a 80°C, com e sem adição de sílica fumaça, e de cinza de casca de arroz pulverizada.

Os resultados obtidos são os seguintes:

1. A temperatura ótima para a formação de jenita é 80°C. Materiais silicosos com alta amorfia e alta área de superfície, como sílica enfumaçada e cinza de casca de arroz, são recomendados para uso nesta síntese.
2. A jenita tende a ser substituída pela formação de tobermoritas com o prolongamento do tempo de reação, isto é, tobermorita 14Å na ausência de íons Al, e tobermorita 11Å na presença deles.
3. O espectro de absorção infra-vermelho da jenita aquecida sugere a ocorrência de uma mudança marcante em sua estrutura durante a conversão para meta-jenita. A existência de substituição Si-Al na jenita foi confirmada pelo deslocamento da banda dispersante Si-O no sentido de frequências mais baixas, o que foi observado no espectro de jenita portadora de Al.
4. A hidratação de β-C_2S e de C_3S a 80°C não levou à formação de jenita. Entretanto, a adição de sílica fumaçada a β-C_2S possibilitou a obtenção de jenita. Sugere-se que a existência de determinada quantidade de íons de silicato é favorável para a formação de jenita não só nestas misturas, mas também em pastas de cimento portland.

N. Hara, N. Inoue and H. Noma, Government Industrial Research Institute, Kyushu, Japan
T. Hasegawa, Aso Cement Co., Ltd., Japan

Formation and Characterization of Jennite

INTRODUCTION

The occurrence of jennite was firstly reported by Carpenter et al (1), which was found in Crestmore, California, and secondly by Gross (2) in the Hatrurim formation, Israel. Taylor (3) once suggested the possibility of structural resemblance of jennite to C-S-H formed during hydration of portland cement. Gard and Taylor (4) offered a hypothesis in which jennite, C-S-H(II) and the fibrous constituents of C-S-H of cement pastes may form a sequence of decreasing crystallinity of the same material. Taylor and Roy (5), however, introduced a doubt on assumptions of this kind such as correlating certain crystalline calcium silicate hydrates with C-S-H in cement pastes.
It seems, therefore, important to establish a synthesis of jennite and to investigate characteristics of the synthetic ones in order to clarify relationships among these hydrates.

The formation of jennite was first accomplished by the present authors and has already been reported together with some characteristics of the synthetic ones (6, 7).

Subsequently, additional experiments were performed in order to clarify the optimum synthetic condition of well crystalline jennite, effect of Si-Al substitution, characteristics etc.
Furthermore, the formation of jennite was tried by hydrothermal reaction at 80 °C of β-C_2S and C_3S with and without addition of fumed silica.

Results obtained in these experiments are summarized in this paper. Moreover, the relationship of jennite to hydrated calcium silicate phases of portland cement was discussed on the basis of these results.

METHODS

Starting materials used in the present preparations are listed in Table 1 with some properties. CaO was prepared by calcining reagent $CaCO_3$ (precipitated) at 1100°C for 4 hours.

TABLE I

Fumed silica SiO_2 99.8% ; 200+25 m^2/g(BET)
* Produced by oxidizing $SiCl_4$.

	Ig loss	CaO	SiO_2	Al_2O_3+Fe_2O_3	C/S
β-C_2S	0.14	63.81	34.84	1.24	1.96
C_3S	0	73.06	26.44	0.34	2.96

* Ground to pass through a 44μ m sieve.

Rice husk ash: Ig loss 5.04, SiO_2 91.26, Al_2O_3 0.58, Fe_2O_3 0.60, TiO_2 0.09, CaO 0.54, MgO 0.32, Na_2O tr., K_2O 1.04, P_2O_5 0.45 ; Total 99.92%
* Amorphous ; Coarsely ground.

Starting materials.

All the preparations were performed in a suspension state with the water/total solid weight ratio of 20. The suspensions of mixes were sealed in a polyethylene bottle and placed in a water bath regulated at 80°C for required periods of reaction time. For preparations at 60, 100 and 120°C, pressure vessels of stainless steel with Teflon liner were used instead, and placed in a drying oven regulated at each temperature.

Fumed silica was mixed with CaO at starting C/S ratios of 1.1, 1.15 and 1.2.
γ-Al_2O_3 (<0.05μm) was added to some of the preparations at 0.5-8.8% to the total of fumed silica and CaO by weight.
Rice husk ash used here was amorphous judging from its X-ray powder diffraction pattern. The ash, coarsely pulverized, was reacted with CaO at 80 °C for up to 150 days. β-C_2S and C_3S were hydrated with and without addition of fumed silica at 80°C for up to 13 weeks. In the case of addition of fumed silica, the starting C/S mole ratio of the mixes was set at 1.5.

At required intervals a portion of each preparation was pipetted from the reaction vessel, filtered and dried in a vacuum desiccator at room temperature. Filtrates from the mixes containing β-C_2S and C_3S were rinsed first by ethanol and then by ethyl ether to prevent from further hydration during filtration and drying.

All the preparations were examined by X-ray powder diffractometry (XRD) and DTA-TG, and some of them by transmission and scanning electron microscopy (TEM, SEM), and selected area electron diffraction (SED).
For some preparations, infrared absorption (IR) spectra were measured on KBr disks containing 0.3% of each sample with a KBr disk in the reference beam by Hitachi EPI-G3 double-beam grating spectrophotometer.

RESULTS

1. Synthesis of Jennite

In order to find out the optimum temperature for the formation of jennite, the suspensions of fumed silica and CaO were heated at different temperatures ranging from 60 to 120 C for up to 70 days. Reaction products thus obtained are summarized in Table 2, which were identified by XRD, DTA-TG and EM. The starting C/S mole ratios ranging from 1.1 to 1.2 were chosen for these preparations based on the previous experiment (7), where well crystalline form of jennite was obtained within short periods of reaction time compared with the other mixing ratios when fumed silica was used.

Reaction products from rice husk ash are listed in Table 3, along with those from fumed silica with and without addition of γ-Al_2O_3. For the preparations from fumed silica, the reaction time was prolonged up to 300 days to evaluate the stability of synthetic jennite. Jennite showed a tendency

N. Hara, N. Inoue and H. Noma, Government Industrial Research Institute, Kyushu, Japan
T. Hasegawa, Aso Cement Co., Ltd., Japan

Formation and Characterization of Jennite

to be replaced by the formation of 14Å tobermorite in absence of Al-ions. To the contrary, 11Å tobermorite was formed in presence of Al-ions.

Typical morphology of synthetic jennite was observed as blade-shaped or lath-like crystals as shown in Fig. 1 (Stereomicrograph). A high resolution electron micrograph of synthetic jennite lying on (001) is given in Fig. 2, which was taken by a JEM-200CX electron microscope incorporated with minimum dose system at 200kV accelerating voltage. The lattice planes of 10Å, 3.6Å and 2.9Å apart were resolved, which correspond to 200, 020 and 420 planes, respectively. The SED pattern of synthetic jennite was given elsewhere (6, 7).

2. Infrared Absorption Spectra of Jennite

The IR absorption was measured on two kinds of specimens, viz. jennite and Al-bearing jennite. Both specimens were synthesized by reactions at 80°C for 100 days using fumed silica and CaO. The starting C/S mole ratios were 1.4 and 1.2, respectively. For the preparation of Al-bearing jennite, γ-Al_2O_3 was added by 8.8% to the mix of fumed silica and CaO by weight. Their syntheses and characteristics have been detailed elsewhere (6, 7).
The IR absorption spectra of jennite, heated jennite and Al-bearing jennite are illustrated in Fig. 3. The same heating temperatures as used by Carpenter et al (1) were applied for the synthetic jennite in two ways, i.e. i) the sample, heated separately

TABLE II

Reaction temp., °C	Starting C/S	Reaction time, d 20	40	70
60	1.1	11.9bC	12.0bC	10.5 J
	1.15	11.4bC	11.9bC	10.5 J
	1.2	11.9bC	11.8bC	10.5 J
80	1.1	12.3bC	10.5 J	10.5 J
	1.15	10.5 J	10.5 J	10.4 J
	1.2	10.5 J	10.4 J	10.4 J
100	1.1	11.6bC	10.5 J	10.5 J
	1.15	11.8bC	10.5 J	10.5 J
	1.2	11.6bC	10.5 J	10.5 J
120	1.1	12.3bC	12.3bC 10.7sJ	11.9sT
	1.15	11.9bC	11.7bC	11.7bC
	1.2	11.6bC	11.6bC	11.4bC

Reaction products from fumed silica with basal spacings (Å).

C : C-S-H, poorly crystalline.
J : Jennite. T : Tobermorite.
b : Broad diffraction.
s : Small diffraction peak.
* C-S-H was formed along with jennite or tobermorite, however, not listed here.

TABLE III

1) Rice husk ash

Starting C/S	Reaction time, d 7	28	91	150
0.8	C-S-H	10.5 J	14.0 T 11.6sT	14.0 T 11.5sT

2) Fumed silica (Starting C/S = 1.15)

γ-Al_2O_3	Reaction time, d 40	100	180	300
0	10.5 J	10.4 J	10.5 J	10.5 J 14.0sT
2	10.5 J	10.4 J 11.7 T	10.5 J 11.6 T	10.5 J 11.6 T
5	12.4 T	12.1 T	12.0 T 10.5 J	11.7 T 10.5 J

Reaction products from rice husk ash and fumed silica with basal spacings (Å).

* Symbols are the same as shown in Table 2.



Fig. 1. - SEM stereomicrograph of jennite.

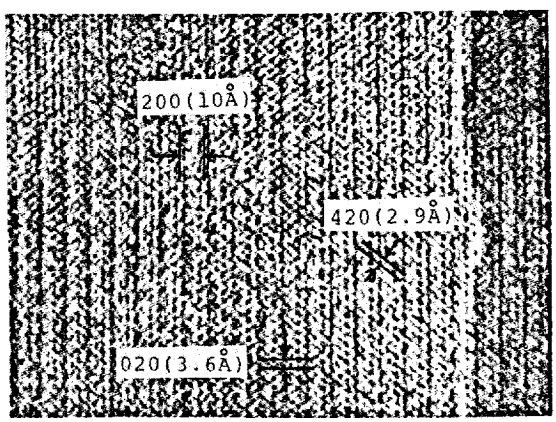

Fig. 2. - High resolution electron micrograph of jennite.

N. Hara, N. Inoue and H. Noma, Government Industrial Research Institute, Kyushu, Japan
T. Hasegawa, Aso Cement Co., Ltd., Japan

Formation and Characterization of Jennite

2.1

at a required temperature, was moulded to a KBr disk respectively, and ii) the sample was first moulded to a KBr disk and then heated at successively higher temperatures in the KBr disk. Since very similar spectra were observed in both ways, those obtained from the former method are summarized in

3. Hydration of ß-C_2S and C_3S at 80°C with and without Addition of Fumed Silica

Reaction products are listed in Table 4, where C-S-H(I) and C-S-H(II) were identified morphologically with help of TEM and SEM.

The formation of fibrous C-S-H, which was observed as fibre bundles well oriented and elongated parallel to b by EM, was detected in all the preparations. Jennite was only formed in the preparation from the mix of ß-C_2S and fumed silica. Jennite thus obtained gave blade-shaped or lath-like crystals as shown in Fig. 4. Since fibrous C-S-H gave a SED pattern similar to C-S-H(II), this phase was identified as C-S-H(II).
On prolonging the reaction time, fibrous C-S-H showed a tendency to increase its crystal width parallel to a, and this tendency was accelerated by addition of fumed silica.

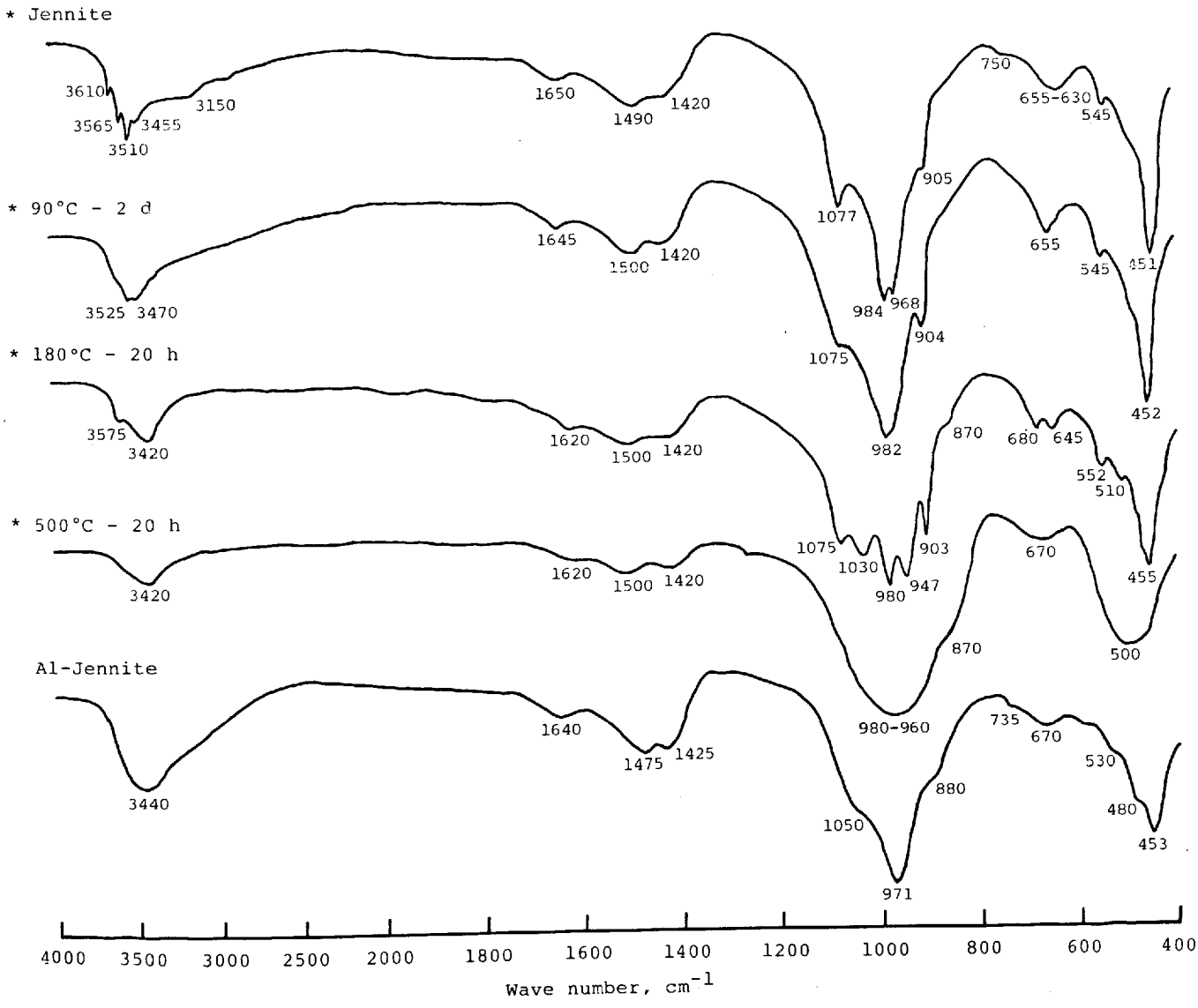

Fig. 3. - Infrared absorption spectra of jennite, mata-jennite and Al-bearing jennite.

N. Hara, N. Inoue and H. Noma, Government Industrial Research Institute, Kyushu, Japan
T. Hasegawa, Aso Cement Co., Ltd., Japan

TABLE IV

Starting material	Reaction time, d 7	28	91
β-C_2S	C-S-H CH, β-C_2S	C-S-H(II) CH, β-C_2S	C-S-H(II) CH
β-C_2S+FS*	C-S-H β-C_2S	C-S-H(I) β-C_2S	Jennite β-C_2S
C_3S	C-S-H(II) CH	C-S-H(II) CH	C-S-H(II) Afw, CH
C_3S + FS*	C-S-H	C-S-H(II)	C-S-H(II)

Reaction products from β-C_2S and C_3S with and without addition of fumed silica.

FS : Fumed silica. CH : $Ca(OH)_2$.
Afw : Afwillite, $C_3S_2H_3$.
* Starting C/S mole ratio of mix = 1.15 .

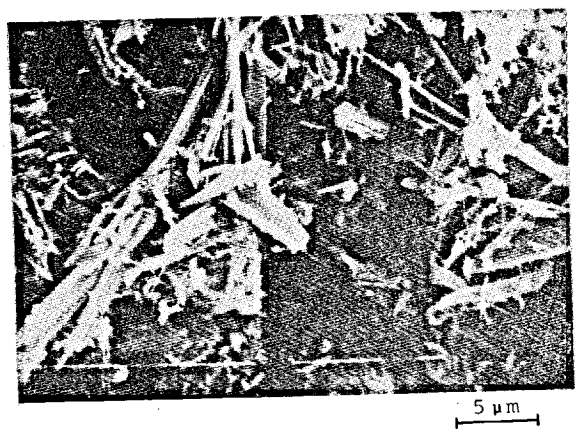

Fig. 4. - SEM micrograph of jennite formed from β-C_2S with addition of fumed silica.

DISCUSSION

1. Synthesis of Jennite

The formation of jennite was possible over a wide temperature range from 60 to 120 C as shown in Table 2. However, in terms of the reaction time required for its formation and its crystallinity thus obtained, it could be concluded that the optimum temperature is 80°C. Jennite formed at temperatures except 80°C was poorly crystalline, and at 120°C the formation of tobermorite tended to replace that of jennite. This is compatible with the fact that jennite remains stable up to 70°C (1). On heating in the air at 70-90 °C, it loses a part of molecular water to give meta-jennite. This relationship is quite similar to that observed between hydrothermal synthesis of 14Å tobermorite and its convertion to 11Å tobermorite by partial dehydration. Namely, the optimum temperature for the synthesis of 14Å tobermorite is 80°C, however, it loses a part of molecular water at 60°C on heating in the air to give 11Å tobermorite (8).

In terms of the reactivity at temperatures around 80°C, it is advisable to use amorphous silica with high surface area, since this kind of formation takes place by through solution reaction mechanism. Fumed silica is, in this sense, the most suitable for the formation of jennite.

Rice husk ash is an interesting siliceous material characteristic in its SiO_2 content, amorphosity, porosity and surface area. All of these are quite high. On heating at high temperatures for long duration, it crystallizes into tridymite and cristobalite. Even in these crystalline forms, rice husk ash is more reactive than quartz-based siliceous materials at temperatures below 100°C.
Jennite was obtainable in the reaction at 80 °C using amorphous rice husk ash as shown in Table 3. On prolonging the reaction time, jennite was replaced by the formation of 14Å and 11Å tobermorites. Among them, 14Å tobermorite was dominant in quantity compared with 11Å tobermorite. This tendency is contrary to Al-bearing jennite formed under similar reaction conditions by using either silica glass with addition of γ-Al_2O_3 or volcanic glass containing Al_2O_3 as a constituent, where Al-bearing jennite was replaced by the formation of 11Å tobermorite with the passage of reaction time(7, 8). 'Al-bearing jennite' was first reported as '10Å tobermorite' (8), however, it was corrected later to the present name(7).

Jennite prepared from fumed silica showed a tendency similar to the abovementioned as shown in Table 3. In spite that the starting C/S mole ratio of 1.15 and the reaction time of 80°C were the optimum to synthesize well crystalline jennite, jennite itself was not stable under these conditions. On prolonging the reaction time up to 300 days, degeneration of jennite was observed along with the formation of 14Å tobermorite in absence of Al-ions, and contrarily the formation of 11Å tobermorite in presence of Al-ions.
These results suggest that tobermorite is more stable than jennite over a wide range of reaction conditions, and that the presence of Al-ions accelerates this replacement.

2. Infrared Absorption Spectra of Jennite

The IR spectra of synthetic jennite were substantially similar to those reported by Carpenter et al (1). However, in detail there were observed several differences. Regarding the bands between 3700-3400 cm^{-1} attributable to the stretching vibration of weakly hydrogen bonded OH, the synthetic jennite when unheated gave 4 peaks, among which 3610 and 3455 cm^{-1} were not resolved by Carpenter et al (1). The sharp band at 3610 cm^{-1} can be attributed to OH groups coordinated to Ca ions (9). On heating in the air, these peaks and the band at 1620 cm^{-1} attri-

butable to molecular water deteriorated to less definite and smaller bands due to dehydration.
The bands at 1500 and 1420 cm^{-1} may be due to CO_3 ions, since TG curve of this sample gave 1.1% of the weight loss at about 800°C. The broad group of bands between 1080 and 900 cm^{-1} are due to Si-O stretching. The spectra of this region showed a remarkable change during conversion to meta-jennite, i.e. meta-jennite formed at 180°C gave well separated 5 peaks in this region. It may be useful to point out in this connection that the basal spacings of meta-jennite formed at 90°C and 200°C were 8.73Å and 8.56Å respectively (7). A certain definite change seems to occur during this transition.
Besides, the decrease of crystallinity on heating resulted in the diffuseness of the bands in this region.
Stubican and Roy (10) clarified that the Al for Si substitution in the tetrahedral sites results in the displacement of the Si-O stretching band in the region from 1100 to 900 cm^{-1} toward lower frequencies as the result of the average increase of (Si, Al)-O distance and of the ionic character of the bond. This tendency was clearly observed in the spectra of jennite and Al-bearing jennite. The present authors (7) suggested the possibility of Si-Al substitution for jennite based on the Al Kα line shift of Al-bearing jennite determined by X-ray fluorescence analyser. The IR data shown in Fig. 3 have assured the reliability of this suggestion. The diffuseness in this region of Al-bearing jennite may be due to the irregularity of Si-Al substitution. This is compatible with the diffuseness of the exothermic peaks at about 850°C detected by DTA of Al-bearing jennite, which are attributed to conversion to β-CS, β-C_2S and C_2AS (7).

3. Hydration of β-C_2S and C_3S at 80°C with and without Addition of Fumed Silica

The formation of jennite was possible only from the mix of β-C_2S and fumed silica by 91 day hydration. The XRD pattern of this jennite was rather similar to meta-jennite with the basal spacing of 8.8Å. This decrease of the basal spacing may be caused not only by its low crystallinity but also by the drying condition where ethanol and ethyl ether were used for rinsing before vacuum pumping.

The C/S mole ratios of β-C_2S and C_3S seem to be too high to form jennite. Addition of fumed silica functions to decrease the C/S mole ratios of products, and resulted in an increase of the crystal width of C-S-H(II) parallel to a. Similar morphological difference was also observed between C-S-H(II) formed from β-C_2S and that from C_3S, i.e. the former were more platey compared with the latter in detail. Since this morphological change of C-S-H(II) seems to be closely related to its potentiality to crystallize into jennite, the possible formation of jennite should be searched on this extension.

Hagiwara and Harada (11) reported the formation of jennite in the press-moulded compact of ordinary portland cement and quartz with the starting C/S mole ratio of 1 after cured at 80°C for 180 days. Jennite was observed by SEM as lath-like crystals projecting out from fibrous C-S-H formed on the surface of quartz particles.

This result supports the aforementioned suggestion that the existence of a certain amount of silicate ions is favourable for the formation of jennite even in cement pastes. However, an excess of silicate ions may favour the formation of tobermorites instead, viz. 14Å tobermorite in absence of Al-ions and 11Å tobermorite in presence of them.

CONCLUSIONS

1. The optimum temperature for the hydrothermal formation of jennite is 80°C. Siliceous materials with high amorphosity and high surface area, such as fumed silica and rice husk ash, are recommended to be used for its synthesis.
2. Jennite tends to be replaced by the formation of tobermorites on prolonging the reaction time, i.e. 14Å tobermorite in absence of Al-ions and 11Å tobermorite in presence of them.
3. The IR absorption spectra of heated jennite suggest that a remarkable change occurs in its structure during conversion to meta-jennite.
The existence of Si-Al substitution in jennite was confirmed by the displacement of Si-O stretching band toward lower frequencies, which was observed in the spectra of Al-bearing jennite.
4. Hydration of β-C_2S and C_3S at 80°C did not give the formation of jennite. However, addition of fumed silica to β-C_2S enabled to obtain jennite. It is suggested that the existence of a certain amount of silicate ions is favourable for the formation of jennite not only in these suspensions but also in portland cement pastes.

REFERENCES

1.- A.B. CARPENTER, R.A. CHALMERS, J.A. GARD, K. SPEAKMAN and H.F.W. TAYLOR (1966), "Jennite, a new mineral", Am. Mineral. 51, 56-74.

2.- S. GROSS (1977), "The mineralogy of the Hatrurim formation, Israel", Geological Survey of Israel Bulletin No.70.

3.- H.F.W. TAYLOR (1969), "The calcium silicate hydrates", Proc. 5th Int. Symp. Chem. Cement, Tokyo 1968, Vol.2, 1-26.

4.- J.A. GARD and H.F.W. TAYLOR (1976), "Calcium silicate hydrate (II) ("C-S-H(II)")", Cem. Concr. Res. 6, 667-678.

5.- H.F.W. TAYLOR and D.M. Roy (1980), "Structure and composition of hyd-

rates", Proc. 7th Cong. Chem. Cement, Paris 1980, Vol.1, II-2/1-13.

6.- N. HARA and N. INOUE (1980), "Formation of jennite from fumed silica", Cem. Concr. Res. **10**, 677-682.

7.- N. HARA and N. INOUE (1982), "Formation of jennite and its thermal behaviour", Proc. 1st Int. Symp. Hydrothermal Reactions, Yokohama 1982, 849-858.

8.- N. HARA and N. INOUE (1980), "Formation of 10Å and 14Å tobermorite from pozzolanic glassy silica", Proc. 7th Int. Cong. Chem. Cement, Paris 1980, Vol.3, IV-13-18.

9.- J.A. GARD, T. MITSUDA and H.F.W. TAYLOR (1975), "Some observations on Assarsson 's Z-phase and its structural relations to gyrolite, truscottite and reyerite", Mineral. Mag. **40**, 325-333.

10.- V. STUBICAN and R. Roy (1961), "Infrared spectra of layer-structure silicates", J. Am. Ceram. Soc. **44**, 625-627.

11.- G. HAGIHARA and M. HARADA (1983), "Surface reaction of aggregates and strength development of cement mortars cured at 80°C", Semento Gijutsu Nempo **37**, 124-127 (in Japanese).

I. MINO, Y. FUSHII and E. SAKAI
Central Reseach Laboratory, DENKI KAGAKU KOGYO K.K.

Early hydration of alite at low water to powder ratio.
L'hydratation initiale de l'alite à un faible rapport eau poudre

SUMMARY: Recently, ultra-high strength cement has been developed as a new material. This material consists of cement, ultra-fine particles such as silica fume and superplasticizer. The water to powder ratio is less than 20% and therefore it can be assumed that the cement particles are densely packed. These are called DSP materials meaning "Densified systems containing homogeneously arranged particles". The hydration of cement and synthesized alite at low water to powder ratio (in DSP materials) has been investigated compared with the hydration of cement and alite at ordinary water to powder ratio.

By the twin transient state cylindrical probe method, the thermal conductivity of fresh cement paste is measured at early hydration stage. The very early hydrated morphology and packing state of cement is observed by wet-SEM. The thermal conductivity of fresh cement paste is dependent on the packing state of cement particles: the higher the packing fraction of cement, the grater the thermal conductivity of fresh cement paste. When the same dosage of superplasticizer was used, the hydration was related to the packing state of cement particles. At low water to powder ratio(in DSP), the ratio of cement hydration was lower than the case of ordinary water to powder ratio. But, the porosity of hardened cement was decreased by the densely packing of powders and the cement hydration at an early stage. At a late stage, the porosity of hardened DSP was decreased by the pozzolanic reaction of ultrafine particles.

Recentemente foi desenvolvido como um novo material um cimento de resistência ultra-alta. Este material consiste de cimento,partículas ultra-finas como microsílica e superplastificante. A relação de água para pó é inferior a 20% e, por isso, pode-se admitir que as partículas de cimento são densamente aglomeradas. Chama-se a isso de materiais DSP, que significa "sistemas densificados contendo partículas dispostas homogeneamente". A hidratação do cimento e da alita sintetizada com baixa relação de água/pó (em materiais DSP) foi investigada, em comparação com a hidratação de cimento e alita com relação normal de água/pó.

Pelo método de corpo de prova cilíndrico gêmeo de estado transiente mediu-se a condutividade térmica da pasta fresca de cimento no estágio inicial de hidratação. Foi observada a morfologia hidratada imediata e o estado de adensamento do cimento por meio de microscopia eletrônica de varredura (SEM) a úmido. A condutividade térmica da pasta fresca de cimento depende do estado de adensamento das partículas de cimento: quanto maior a porção adensada de cimento, maior a condutividade térmica da pasta fresca de cimento. Quando se usou a mesma dosagem de superplasticidade, a hidratação foi relacionada com o estado de adensamento das partículas de cimento. Com uma baixa relação de água/pó (em DSP), a relação de hidratação do cimento foi mais baixa do que no caso da relação habitual de água/cimento. Mas a porosidade do cimento endurecido foi diminuída pelos pós densamente aglomerados, bem como a hidratação no estágio inicial. Num estágio tardio, a porosidade do DSP endurecido foi diminuída pela reação pozolânica das partículas ultra-finas.

INTRODUCTION

Ultra high strength cement has been studied by many investigators among whom Bache's study(1) is especially important for practical use. Bache's ultra high strength cement based materials are called DSP materials meaning "densified systems containing homogeneneously arranged particles". In Japan, the demands that DSP materials are exploited not only as building materials also as industrial castable ceramics are recently increasing (2). This promising field of application has just begun. More detailed basic investigation for DSP materials is required.

DSP is a combination of cement particles, ultrafine particles such as silica fume and superplasticizer. DSP can be mixed with a minimum amount of water because a large quantity of superplasticizer is mixed with ultrafine particles one or two order of magnitude smaller than portland cement and dispersis these particles. The water to solid ratio is less than 20wt% and therefore it can be assumed that the cement particles are densely packed. Because of the densely packing of particles, DSP has minimal space between the cement particles in the fresh paste, and that space is filled by the ultrafine particles. In addition to the densely packed particles, ultrafine particles such as silica fume react with $Ca(OH)_2$ and only very small capillary pore exist (3). Thus, DSP has an ultra high strength and also has a good fluidity for casting due to the effect of dispersed ultrafine particles.

Many investigators have studied DSP materials and high strength cement containing silica fume (5,6). However, there are few systematic and detailed studies on the influence of packing state of particles on the hydration of cement and alite and the pozzolanic reaction of silica fume.

In order to understand the relation between the hydration of cement and the packing state of particles, the hydration of cement and silica fume reaction with $Ca(OH)_2$ have been investigated at various low water to solid ratios. Also, the packing state of particles have been studied by means of thermal conductivity and the wet-SEM observation method. Thermal conductivity of fresh paste is also very important in connection with the thermal stress analysis of mass concrete.

EXPERMENTAL

Chemical composition and specific surface areas (BET) of the used alite, portland cement and silica fume are shown in Table 1. Alite was synthesized from reduced LD-slag which was provided by NIPPON KOKAN K. K. (6). Silica fume contained 2.8% carbon and about 3% quartz and a small amount of magnesioferrite. X-ray diffraction analysis (X-RD) shows the main component of silica fume to be amorphous phase. By TEM, the diameters of silica fume are less than 0.2 μm.

An experiment was carried out at 20°C and 50°C. The water to solid ratios were respectively 0.16, 0.20, 0.25, 0.3 and 0.4. When the water to solid ratio (W/S) was less than 0.25, the solid consisted of portland cement or alite and silica fume and the dosage of superplasticizer (sodium salts of β-alkyl napthalene sulfonate formaldehyde condensate) was 2 wt% by weight of solid. The ratio of cement or alite and silica fume was 80:20.

When the water to solid ratio was 0.3, the dosage of superplasticizer was 0.5 wt% by weight of portland cement or alite. In the case of W/S=0.3 and 0.4, silica fume was not added.

Heat liberation of early hydration was measured by conduction calorimeter. Further, after curing for 1, 3, 7, 14 and 28 days respectively, the hydration was stopped by acetone and the samples were dreid at 105°C. Loss on ignition, amounts of $Ca(OH)_2$, unreacted alite, pore size distribution and total pore distribution and total pore volume of samples were measured. Amounts of $Ca(OH)_2$ were measured by DSC and unreacted alite was detected by means of X-RD. The pore size distribution was determined by Hg-porosimetry and the total pore volume was measured by the method of weighing in water.

In connection with the packing state of solid, thermal conductivity of fresh paste was measured by twin transient-state cylindrical probe method (7), and the packing state of fresh paste was observed by wet-SEM (K. K. Akashi Seisakusho).

A block diagram of the apparatus of the transient state cylindrical probe method is shown in Figure 1.

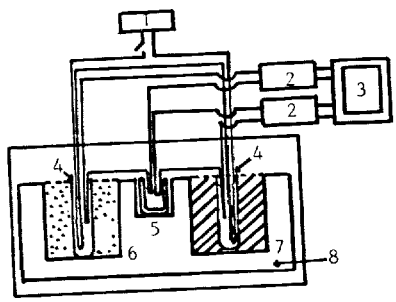

1. Constant voltage
2. Amplifier
3. X-Y recorder
4. Probe
5. Zero point
6. Standard
7. Sample
8. Thermostat

Figure 1 Twin type of non-stationary probe method.

Probes are made of stainless steel pipes with a 0.10 cm outer diameter, 0.05 cm inner diameter and 5.00 cm length. Heating wire made of enameled constantan wire 0.01 cm in diameter and thermocouple which, in turn, was of enameled copper and constantan wire of the same diameter were placed the pipe, and the residual space was filled with paraffin wax. Temperature of the thermostat was set at 20°C. One probe was introduced into the center of the standard materials and the other into the sample being

Table 1 Chemical composition and specific surface area

	$S_{BET}(m^2/g)$	Ig. loss	SiO_2	Al_2O_3	Fe_2O_3	CaO	MgO	SO_3	R_2O	Total
Cement	1.21	0.8	21.7	4.9	3.0	64.9	0.9	3.0	0.5	99.7
Alite	1.54	—	25.2	1.3	—	72.6	0.8	—	—	99.9
Silica fume	22.60	3.8	90.7	0.3	3.0	0.3	0.3	0.4	1.0	99.8

(%)

measured. Although, the standard material was water, its low viscosity caused the convection current of heat. To remove the influence of this convection current, aqueous polyacrylic acid solution was used instead of water. An electric current was passed through the heating wires for about 30 sec. and the ratio of the increases and decreases in temperature were detected by an X-Y recorder. If the thermal conductivity of sample and the standard material were the same value, the tangent of the locus in X-Y recoder was 45°. Based on standard material, the thermal conductivity was calculated by the tangent of the locus.

The initial contact of fresh paste with water was observed by wet-SEM. The wet-SEM (AKASHI WS-250) is equipped with a unique low-vacuum viewing function which allows direct observation of moist specimens previously regarded as very difficult to observe. The low-vacuum environment is always free from "charge up", thus removing the necessity of deposition or coating on specimens.

RESULTS AND DISCUSSION

Packing state of particles and thermal conductivity

Thermal conductivity of fresh paste with various water to solid ratios measured by the twin type of non-stationary probe method is shown in Figure 2. A correlation was observed between the thermal conductivity of fresh paste at early stage of hydration and the water to solid ratio. The lower the water to solid ratio, the greater the thermal conductivity of fresh paste. But, at a late stage of hydration, about the same values of thermal conductivities of cement pastes with various water to powder ratios are obtained.

Figure 3 shows "wet-SEM" photographs of fresh paste with water after 15 and 25 min.. These photographs clear show that the powder particles are packed more densely in DSP materials. At water to solid ratio of 16 wt%, a crack is observed in the matrix. This is caused by the drying of water in a vacuum condition of wet-SEM (about 10^{-1} mmHg). In soil mechanics, it has been reported that the thermal conductivity is dependent on the ratio of soil phase, and thermal conductivity of the solid solid particles is larger than that of water(8). In DSP materials, solid particles may be in contact with each other. These results are consistent with the observation results of wet-SEM.

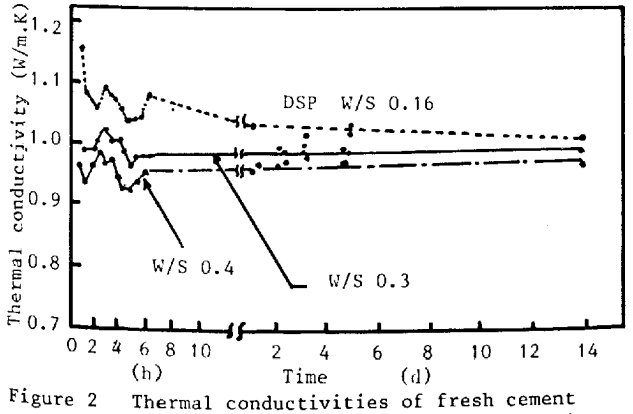

Figure 2 Thermal conductivities of fresh cement paste with various water to solid ratios.

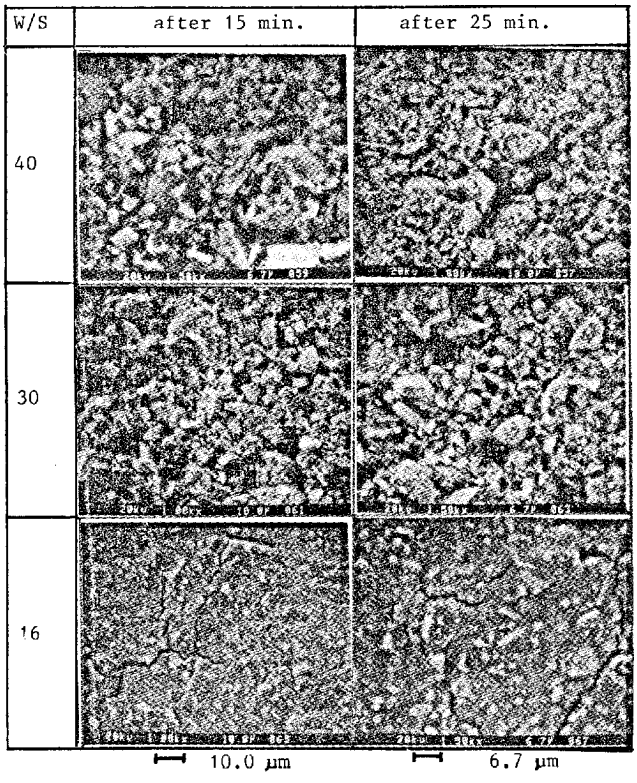

Figure 3 Wet-SEM photographs of fresh cement paste with various water to solid ratios.

However, the thermal conductivity of hardened paste with various water to powder ratios shows values comparable to the progress of cement hydration. This may be due to the formation of hydrated morphology and the thermal conductivity of hydrated products may have the same value.

Hydration and packing state of particles

The heat liberation curves owing to cement hydration at various water to solid ratios are shown in Figure 4. In DSP materials, the early hydration of cement was retarded and the ratio of cement hydration was reduced compared with the conventional cement paste. Retardation of cement hydration in DSP materials may be caused by the large amount of superplasticizer and the densely packing of solid particles. The ratio of cement hydration was related to the packing state of particles. The hydration ratio of cement was gradually decreased by the augmentation of packing fraction.

Figure 5 shows the relation between the loss on ignition and the water to solid ratio. In DSP materials, the values of loss on ignition are smaller than that of materials with normal water to solid ratio. The values of loss on ignition are reduced with the decrease of the water to solid ratio. This tendency becomes more and more obvious with curing time.

Figure 6 shows the changes in loss on ignition of portland cement at 50°C with curing time. These results are consistent with the results at 20°C.

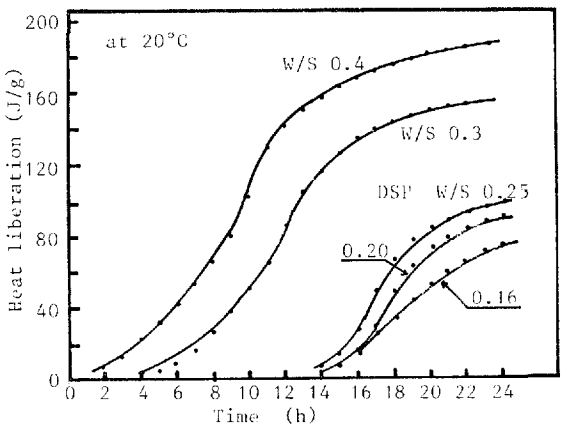

Figure 4 Heat liberation of cement.

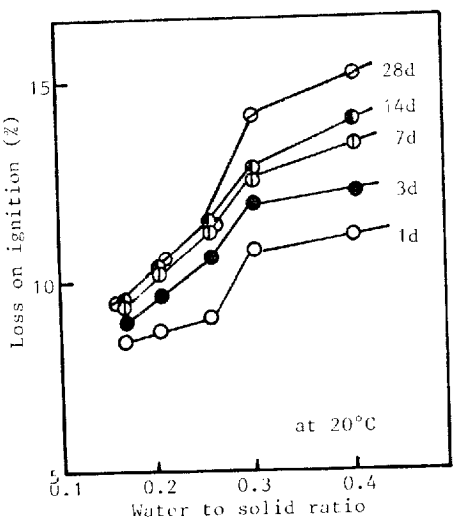

Figure 5 Relation between the loss on ignition and the water to solid ratio.

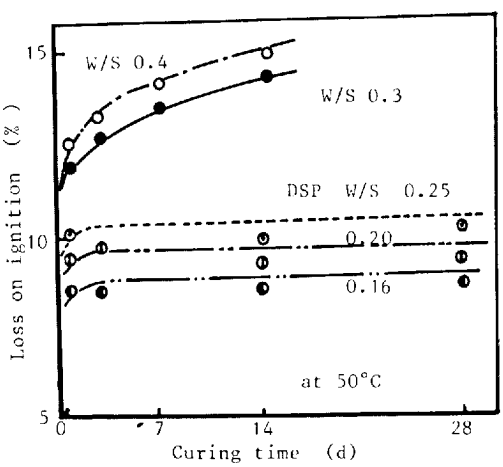

Figure 6 Changes in loss on ignition of portland cement with curing time.

In the case of normal water to cement ratio, the values of loss on ignition are gradually increased with curing time. But in DSP materials, the values of loss on ignition do not increase and the about same values are indicated after 3 days.

The loss on ignition with alite has the same tendency as with portland cement as shown in Figure 7. The values of loss on ignition when alite is used are slightly larger than when portland cement is used. Thus, it may be sufficient to investigate the hydration of the alite in portland cement without considering the hydration of aluminate phase.

Figure 8 shows the changes of unreacted alite in portland cement with curing time as measured by X-RD. The relative X-RD peak values (I/I_0) of unreacted alite in portland cement are related to the water to solid ratios; the greater these ratios, the smaller the relative X-RD peak values of unreacted alite. In other words, the lower the water to solid ratios, the smaller the hydration ratio of alite. Therefore, a large amount of unreacted cement particles remain in DSP materials. And it may be adequate that the residual cement grain cores act as strong internal filler or microaggregate as mentioned by S. Diamond (9). In addition, cement acts as a source of $Ca(OH)_2$ supply.

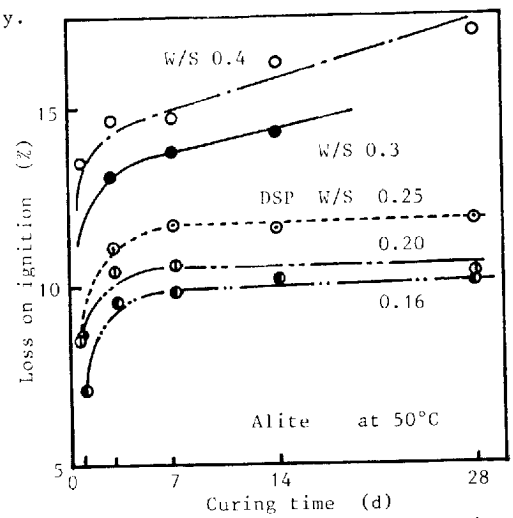

Figure 7 Changes in loss on ignition of alite.

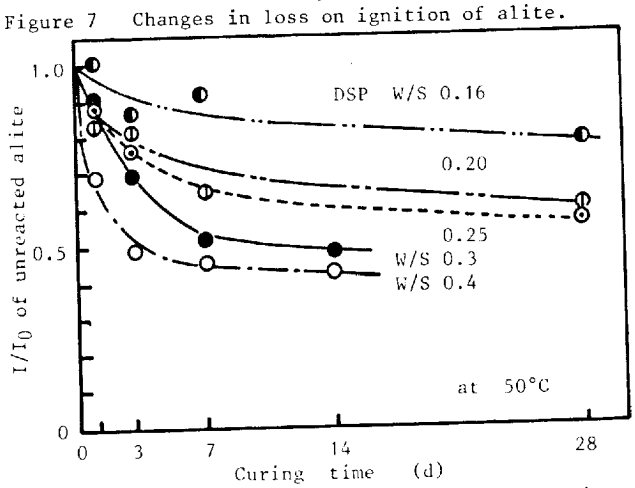

Figure 8 Changes of unreacted alite in portland cement with curing time.

Figure 9 shows the amount of $Ca(OH)_2$ with curing time at various water to solid ratios. DSP materials contain silica fume. Without silica fume, $Ca(OH)_2$ is produced rapidly with in a day and the amounts of $Ca(OH)_2$ are smaller than that of the samples with higher water solid ratio. In DSP materials, the amounts are scarcely detected, because of the reaction of silica fume and $Ca(OH)_2$ (3). As shown in Figure 8, the smaller the water to solid ratio, the lower the rate of cement hydration.

The hydration ratio was decreased by the augmentation of packing fraction. Thus, the amounts of $Ca(OH)_2$ are insufficient to obtain the complete reaction of silica fume. Considering the reaction of silica fume, it may be the optimum ratio of silica fume and cement is determined by the water to solid ratio (packing fraction).

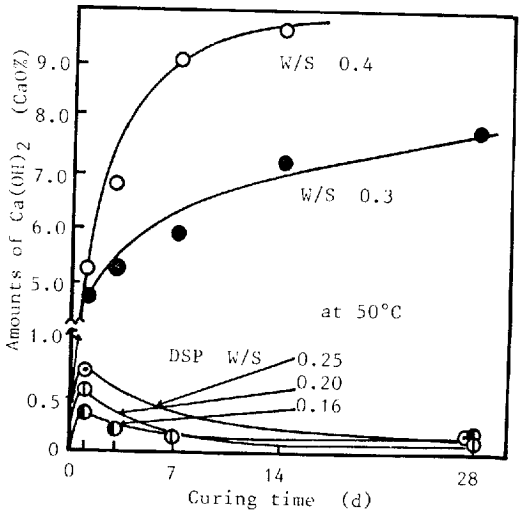

Figure 9 Amounts of $Ca(OH)_2$ in hardened paste.

Porosity of hardened pastes

Figure 10 shows the relation between the total pore volume and the water to solid ratio.

Calculated values of total pore volume in DSP materials start to decrease rapidly with the augmentation of packing fraction of particles compared with the case of normal water to solid ratio. At an early stage of hydration, the same tendency is found, but, after a long curing time, an approximately linear relationship exists between the total pore volume of materials and the water to solid ratio. Decrease rates of total pore volume of DSP materials are lower than that of the case of normal water to solid ratio. This is caused by the hydration ratio of cement, which is reduced by the increase of packing fraction as previously decribed.

However, the pore sizes of DSP materials become smaller than those of samples with higher water to solid ratio as shown in Figure 11. The pore volume as measured by Hg-porosimeter is decreased with the augmentation of packing fraction .

This is based on the pozzolanic reaction of silica fume and cement and the adjustment of packing fraction are very important.

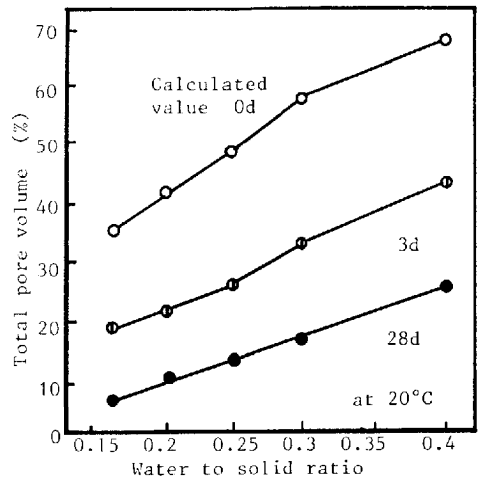

Figure 10 Relation between the total pore volume of hardened paste and the water to solid ratio.

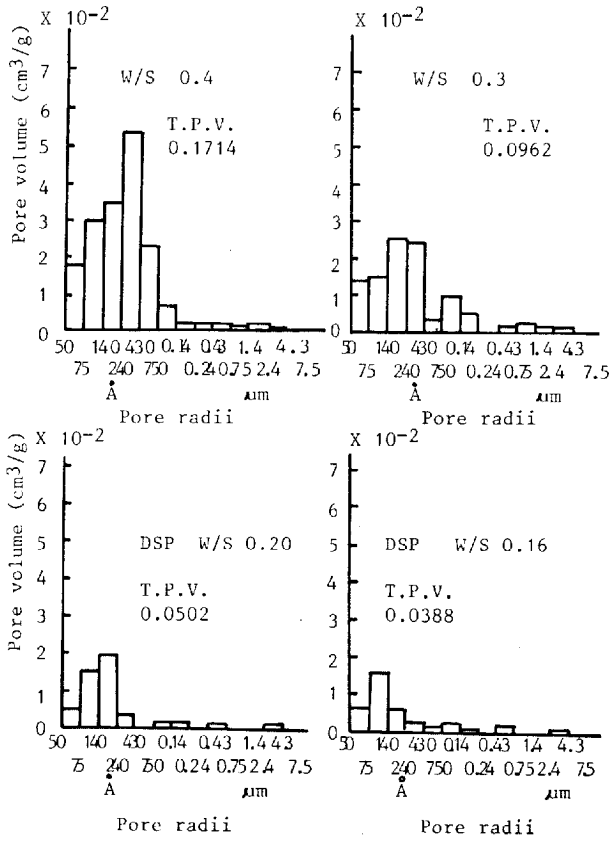

Figure 11 Pore size distribution of hardened paste (at 20°C, 7days).

CONCLUSIONS

Relation between the packing fraction of particles and the hydration of cement and alite is discussed by the measurement of thermal conductivity, wet-SEM, heat liberation, loss on ignition, unreacted alite, the amounts of $Ca(OH)_2$ and the porosity of DSP and conventional cement paste.

The packing state of particles was observed by wet-SEM. The thermal conductivity of fresh paste was dependent on the packing state of particles: the higher the packing fraction the larger the thermal conductivity of fresh paste.

The hydration ratio of cement was gradually decreased by the augmentation of packing fraction of particles. In DSP materials, cement particles act as a strong internal filler and the source of $Ca(OH)_2$ supply. The total pore volumes of DSP are small and the pore sizes of DSP materials become small compared with conventional cement paste with the increase of packing fraction and the pozzolanic reaction of silica fume. Considering the reaction of cement and silica fume, the control of relation between the packing fraction and the hydration of hydraulic materials appears to be very important in DSP materials.

ACKNOWLEDGEMENTS

We are grateful to Prof. M. Daimon and Dr. K. Asaga, Tokyo Institute of Tchnology, for their helpful advice. We wuold like to thank Dr. T. Kasubuchi, National Institute of Agro-Enviromental Science, for his help in the measurment of thermal conductivity.

REFERENCES

1.- H. H. BACHE (1982), "Densified cement/ultra-fine particle-based materials", Presented at Proc. 2nd Int'l Conf. on Superplasticizer in Concrete, Ottwa, Canada.
2.- Denki Kagaku Kogyo Technical Information.
3.- K. ONO, K. ASAGA and M. DAIMON (1985), "Hydration in the system of cement and silica fume", Semento Gijutsu Taikai,28.
4.- Proc. of the CANMET/ACI First Int'l Conf. on the Use of FLY ASH, SILICA FUME, SLAG and Other MINERAL BY-PRODUCTS in Concrete,1983, Montebello, Canada, edited by V. M. Malhotra, ACI SP-79 (1983)
5.- Materials Research Society Symp. Proc. vol 42 1984, edited by J. F. Young, "Very high strength Cement-Based Materials" (1985).
6.- S. KUBODERA, T. KOYAMA, R. ANDO and R. KONDO," An approach to the full utilization of LD-slag", The Iron and Steel Institute of Japan Meeting, 1978, at University of Tokyo.
7.- T.KASUBUCHI (1977), " Twin transient-state cylindrical-probe method for the determination of the thermal conductivity of soil", Soil Science,124, 255.
8.- T.KASUBUCHI (1984), "Heat conduction model of saturated soil and estimation of thermal conductivity of soil solid phase", Soil Science,138,240.
9.- S. DIAMOND, ibid ref 5 ,p 233,"very high strength cement-based materials- a prospective".

T. Mitsuda, S. Kobayakawa and H. Toraya
Ceramics Research Laboratory, Nagoya Institute of Technology, Japan.

1

CHARACTERIZATION OF HYDROTHERMALLY FORMED C-S-H

2.1

SUMMARY

Hydrothermal treatment of lime-silica mixtures under saturated steam pressures below 250°C usually gives C-S-H as an initial product, which reacts further to give crystalline calcium silicate hydrates. In the present paper, C-S-H was prepared using CaO and silicic acid at Ca/Si ratios of 0.4 to 3.0 and 120°to 210°C. The C-S-H was characterized by X-ray and electron diffraction, thermal analysis, infra-red spectroscopy, and surface area determination.

The C-S-H showed variable Ca/Si ratios; the mean upper limit was 1.67 and the lower limit was about 0.5. For all specimens except those with 0.8 ratio, irrespective of temperature of treatment, the C-S-H formed initially consisted of crumpled foils, and the same morphology was retained until crystallization took place for the 0.5-0.6 preparations. For the preparations higher than 1.0 ratio, initially formed C-S-H having crumpled foils reacted further to give mixtures of crumpled foils and fibre aggregates before crystallization occurred. In the case of 0.8 ratio, the mixtures were initially formed at even 120°C-2h treatment and crystallized further to 11 Å tobermorite.

X-ray diffractometry of all the C-S-H showed bands at 3.0 (v strong), 2.8 (weak), 1.83 (medium), 1.66 (weak) with very weak bands at 5.4, 2.1-2.0, 1.53 and 1.40 Å. The 0.8 ratio preparations gave an additional weak band at 11 Å. These X-ray results agree well with those of originally named C-S-H (I) by Taylor.

Electron diffractometry for the preparations higher than 1.0 ratio showed that the fibre aggregates consist of different units of structure in the fibre direction: mixtures of tobermorite and xonotlite and/or foshagite. In the present preparations, C-S-H (II) was not detected by SED in all runs. The values for the specific surface area were 180-380 m^2/g (50-24 Å thick) for typical crumpled foils. On heating the C-S-H gave a gradual water loss up to 900°C with a strong exotherm at 820-900°C, and then decomposed to wollastonite for the specimens less than 1.0 ratio and wollastonite with β-C_2S for the specimens higher than 1.3.

O tratamento hidrotérmico de misturas de cal-sílica sob pressões de vapor saturado a baixo de 250°C usualmente dá C-S-H como produto inicial, o qual reage posteriormente para dar hidratos cristalinos de cálcio. Neste artigo o C-S-H foi preparado usando-se CaO e ácido sílico em relações Ca/Si de 0,4 a 3,0 e temperaturas de 120 a 210°C. O C-S-H foi caracterizado por meio de difração por raio X e eletrônica, análise térmica, espectroscopia infra-vermelha, e determinação da área de superfície.

O C-S-H apresentou relações variáveis de Ca/Si: o limite médio superior foi de 1,67 e o limite inferior de cerca de 0,5. Com todos os espécimes, exceto os com relação de 0,8, independentemente de temperatura de tratamento, o C-S-H formado inicialmente consistia de folhas rugosas, e se mantinha a mesma morfologia até que ocorresse a cristalização nas amostras com 0,5 - 0,6. Nas com relação superior a 1,0, formou-se inicialmente C-S-H tendo folhas rugosas, que a seguir reagiram para dar misturas de folhas rugosas e agregados de fibra antes de ocorrer a cristalização. No caso da relação 0,8, as misturas se formaram inicialmente até mesmo a 120°C com duas horas de tratamento e se cristalizaram posteriormente em tobermorita 11Å.

A difratometria de raio X de todos os C-S-H apresentou bandas em 3,0 (muito forte), 2,8 (fraca), 1,83 (média), 1.66 (fraca), com bandas muito fracas em 5,4, 2,1 - 2,0, 1,53 e 1,40 Å. As preparações de relação 0,8 deram uma banda adicional fraca em 11Å. Estes resultados de raio X coincidem bem com aqueles chamados originalmente de C-S-H(I) por Taylor.

A difratometria eletrônica dos espécimes com relação superior a 1,0 mostraram que os agregados de fibra consistem de unidades diferentes de estrutura na direção da fibra: misturas de tobermorita e xonotlita e/ou foshagita. Nestas preparações não foi detectado C-S-H(II) por SED em todas as provas. Os valores de área de superfície específica foram de 180 - 380 m^2/g (espessura de 50 - 24Å) para as folhas rugosas típicas. O aquecimento do C-S-H teve como resultado uma perda gradual de água até 900°C com forte exotermia a 820 - 900°C, e então se decompôs em wolastonita nos espécimes com relação menor que 1,0 e wolostonita com β-C_2S nos espécimes com mais que 1,3.

T. Mitsuda, S. Kobayakawa and H. Toraya
Ceramics Research Laboratory, Nagoya Institute of Technology, Japan.

2.1

CHARACTERIZATION OF HYDROTHERMALLY FORMED C-S-H

Introduction

In hydrothermal preparations for calcium silicate hydrates, calcium silicates such as C_3S, β-C_2S, or γ-C_2S used as starting materials with or without silica, react to give initially crystalline calcium silicate hydrates; α-dicalcium silicate hydrate, tricalcium silicate hydrate or kilchoanite. However, hydrothermal treatment of lime-silica mixtures under saturated steam pressures below 250°C usually gives ill-crystallized calcium silicate hydrate (C-S-H) as an initial product, which reacts further to give crystalline calcium silicate hydrates; tobermorite, xonotlite, foshagite or gyrolite. Some of those are important because of their relevance to cements and autoclaved building or insulating materials.

In this work, the formation of C-S-H from mixtures of silicic acid and lime above 120° C was investigated, and some data on chemical composition, morphology, structure, and thermal behaviour of the C-S-H are also presented.

Results and Discussion

Preparations

All reactions were done using CaO and silicic acid at saturated steam pressures. CaO was made by heating analytical grade $CaCO_3$ at 1050° C for 3h. Silicic acid was of reagent grade with 12.0% loss. Those in stirred suspensions at 150 rpm were carried out at various Ca/Si ratios of crystalline materials such as 0.4 (K-phase) to 3.0 (tricalcium silicate hydrate) and 120° to 210°C for 2h to 7d using a water/solids weight raito of 30. Stirring was stopped after the first 4h. The preparations were continued until a crystalline phase was detected in the products by X-ray diffraction. The products were filtered and dried in a vacuum at 80°C.

Initial Formation of C-S-H and Reaction Sequences

Table 1 gives the phases detected in the products by X-ray and electron diffraction. The C-S-H was always formed as an initial product of crystalline phase. The present results can be explained if the following sequence of reactions occures in the runs at 120 - 210°C.

Runs with Ca/Si = 0.5 - 0.6:
C-S-H (crumpled foils) ⟶ Assarsson's Z-Phase ⟶ gyrolite
Runs with 0.8:
C-S-H (mixtures of crumpled foils and fibre aggregates) ⟶ 11 Å tobermorite
Runs with 1.0 - 1.5:
C-S-H (cumpled foils) ⟶ C-S-H (mixtures of crumpled foils and fibre aggregates) ⟶ xonotlite at 1.0 ratio, xonotlite or foshagite at 1.3, α-C_2S hydrate or foshagite at 1.5
Runs with 2.0 - 3.0:
C-S-H (crumpled foils) + $Ca(OH)_2$ ⟶ C-S-H (mixtures of crumpled foils and fibre aggregates) + $Ca(OH)_2$ ⟶ α-C_2S hydrate or hillebrandite.

These results for crystalline phases formed after C-S-H agreed with those reported by many workers. For the preparations ranging from 2.0 to 3.0 ratios, C-S-H always contained unreacted lime.

TABLE 1
Hydrothermal Results

Mixture Ca/Si	Temperature (°C)	Time 2h	4h	16h	36h	1w
3.0 - 2.0	210	XXXXXXX	Hil			
	180	XXXXXXXXXXXXXXXXXXXX	Hil			
	150	XXXXXXXXXXXXX	α-C_2SH			
	120	XXXXXXXXXXXXXXXXXXXXXXXXXXXXXX				
1.5	210	xxxxxxxxxxxxxx	Fos			
	180	xxxxxxxxxxxxxxxxxxxx	Fos			
	150	xxxxxxxxxxxxx	α-C_2SH			
	120	xxxxxxxxxxxxxxxxxxxxxxxxxxxxxxxx				
1.3	210	xxx	Fos			
	180	xxxxxxxxxxxxxxxxxxxx	Fos			
	150	xxxxxxxxxxxxxxxxxxxxxxxxxxx	Xo			
	120	xxxxxxxxxxxxxxxxxxxxxxxxxxxxxxx				
1.0	210	xxx	Xo			
	180	xxxxxxxx	Xo			
	150	xxxxxxxxxxxxxxxxxxxx	Xo			
	120	xxxxxxxxxxxxxxxxxxxxxxxxxxxxxxx				
0.8	210	xxx	To			
	180	xxx	To			
	150	xxxxxxxxxxxxxx	To			
	120	xxxxxxxxxxxxxx	To			
0.6 - 0.4	210	xxxxxxx	Z-p			
	180	xxxxxxxxxxxxxx	Z-p			
	150	xxxxxxxxxxxxxxxxxxxxxxxxxxx	Z-p			
	120	xxxxxxxxxxxxxxxxxxxxxxxxxxxxxx				

XXX = pure C-S-H with unreacted $Ca(OH)_2$; xxxx = pure C-S-H; Hil = hillebrandite, α-C_2SH = α-dicalcium silicate hydrate; Fos = foshagite; Xo = xonotlite; To = tobermorite; Z-p = Assarsson's Z-phase.

Ca/Si Ratio

The C-S-H showed variable Ca/Si ratios; the mean, upper limit was 1.67 and the lower limit was about 0.5. Table 2 shows the upper limit of Ca/Si ratios, which are obtained by difference using determination of unreacted lime by a TG method for the preparations of 2.0 - 3.0 ratios. The lower limit is less certain, because unreacted silicic acid in the products was examined by TEM. In all runs unreacted lime or silica were finely dispersed in C-S-H aggregates, so it is difficult to correctly determine the upper or lower limit of Ca/Si ratios for C-S-H using a ATEM method.

TABLE 2
Upper Limit of Ca/Si Ratios for C-S-H

Mixture Ca/Si	Temperature (°C)	No. of analyses	Range of Ca/Si
3.0	210	1	1.70
	180	3	1.65 - 1.75
	150	2	1.68 - 1.75
	120	5	1.71 - 1.74
2.5	210	1	1.59
	180	3	1.61 - 1.68
	150	2	1.60 - 1.67
	120	5	1.65 - 1.73
2.0	210	1	1.65
	180	3	1.63 - 1.66
	150	2	1.61 - 1.66
	120	5	1.59 - 1.66

No. of analyses, 33; Mean Ca/Si = 1.67; Range of Ca/Si = 1.59 - 1.75; std. deviation, 0.05.

T. Mitsuda, S. Kobayakawa and H. Toraya
Ceramics Research Laboratory, Nagoya Institute of Technology, Japan.

CHARACTERIZATION OF HYDROTHERMALLY FORMED C-S-H

Specific Surface Area

Table 3 gave specific surface area results for all runs contained C-S-H only by nitrogen adsorption using the BET method. Typical values for the specimens having crumpled foils are 180 - 230 m^2/g (Ca/Si = 1.0 - 1.5) and 260 - 380 m^2/g (0.5 - 0.6). Layer thicknesses were also calculated by assuming the density to be 2.2 g/cm^3 for C-S-H and by neglecting edge effects. Results gave a mean foil thickness of 24 - 50 Å, i.e. between 2 and 5 elementary layers, assuming the structure of 11 Å tobermorite. This agreed well with the evidence of X-ray examination.

TABLE 3
Specific Surface Area for C-S-H

Mixture Ca/Si	Temperature (°C)	No. of analyses	m^2/g Mean	Range
	180	2	180	175 - 185
1.5	150	1		192
	120	3	201	194 - 214
	180	2	215	202 - 228
1.3	150	3	212	195 - 232
	120	3	233	226 - 241
1.0	150	2	221	214 - 228
	120	3	230	206 - 247
0.8	150	1		129
	120	1		114
	180	2	363	348 - 377
0.6	150	4	377	366 - 381
	120	3	356	350 - 361
	180	2	264	262 - 265
0.5	150	2	285	260 - 309
	120	3	318	297 - 331

X-ray Examination

All specimens were examined in a nitrogen gas flow by using a diffractometer with monochromatized CuKα radiation (40kV- 40mA) and a step scan technique: step width = 0.02°(2Θ), fixed time = 2s and 2Θ range = 3°to 75°. High purity Si powder was used as an external standard. Fig. 1 gives a typical X-ray powder patterns for the C-S-H prepared hydrothermally and dried in a vacuum at 80°C. The D-dried specimens also gave the same results. The specimens give crumpled foils except the preparations at 0.8 ratio, which are mixtures of crumpled foils and fibre aggregates even at treatment of 120° C for 2 h. In spite of various Ca/Si ratios for the preparations, all specimens gave substantially the same X-ray powder patterns: characteristic peaks at 5.4, 3.0, 2.8, 1.83, 1.66 and 1.40 Å. For the preparations at 0.8 and 0.5 - 0.6 ratios, additional weak peaks were obtained at 11 Å as a basal spacing and 3.6 Å respectively.

Table 4 gives results. X-ray powder data for the C-S-H prepared hydrothermally agree well with those of orginally named C-S-H (I) by Taylor (1), and natural plombierite reported by McConnell (2). The peaks at 1.66 and 1.40 Å are particularly useful for distinguishing C-S-H (I) from other forms of C-S-H. Assuming that the C-S-H is a structurally imperfect tobermorite and give largely 2-dimensional diffraction effects, all the reflections except 5.4 Å, 3.6 Å, and 1.9 - 2.1 Å band are indexable as hk0 peaks from a body-centred orthorhombic lattice with a=5.6, b=3.6 and c=11 Å (3). These X-ray results also agree with evidence of surface area determination, giving only a few elementary layers thick of 11 Å tobermorite.

TABLE 4
X-Ray Powder Data

C-S-H (I) by Taylor (4,5) d	I	hkℓ	Plombierite (2) d	I	The Present Work d	I
12.5	vs	001			11.7	vvw/d*
5.3	vvw	(?)	5.48	wb	5.4	vvw
					3.6	vvw/d**
3.07	vs	220	3.17 3.01	msb	3.0	vs
2.80	s	400	2.81	ms	2.8	w
2.4	w/d	(?)				
2.1	w/d	(?)	2.07	w	2.0 2.1	vvw/d
1.83	s	040	1.83	ms	1.83	m
1.67	mw	620	1.67	w	1.66	w
1.53	vw	440			1.53	vvw/d
1.40	w	800	1.403	vw	1.40	vw

Observed for the preparations at Ca/Si =0.8* and at 0.5 - 0.6**.

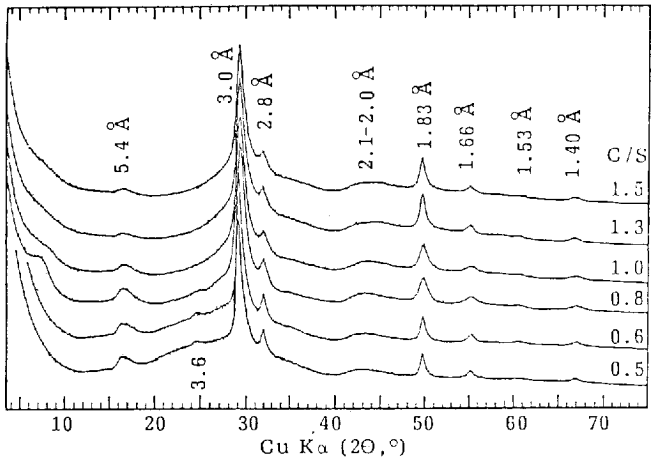

FIG. 1

X-ray powder patterns of C-S-H

Electron Microscopy and Diffraction

The C-S-H specimens were examined by a transmission electron microscope operating at 200 kV. Micrographs for the C-S-H were classified for convenience into two types described as A and B (Fig. 2). The A type showed a typical form of crumpled foils and gave a ring pattern, reflections at 3.1, 2.8 and 1.8 Å which agreed with those observed by X-ray diffraction. The B type was mixtures of the crumpled foils (A type) and fibre aggregates oriented along the fibre axis. Most of fibre aggregates gave spots by selected-area electron diffraction. By X-ray powder diffraction the C-S-H gave no difference between the type A and B.

T. Mitsuda, S. Kobayakawa and H. Toraya
Ceramics Research Laboratory, Nagoya Institute of Technology, Japan.

CHARACTERIZATION OF HYDROTHERMALLY FORMED C-S-H

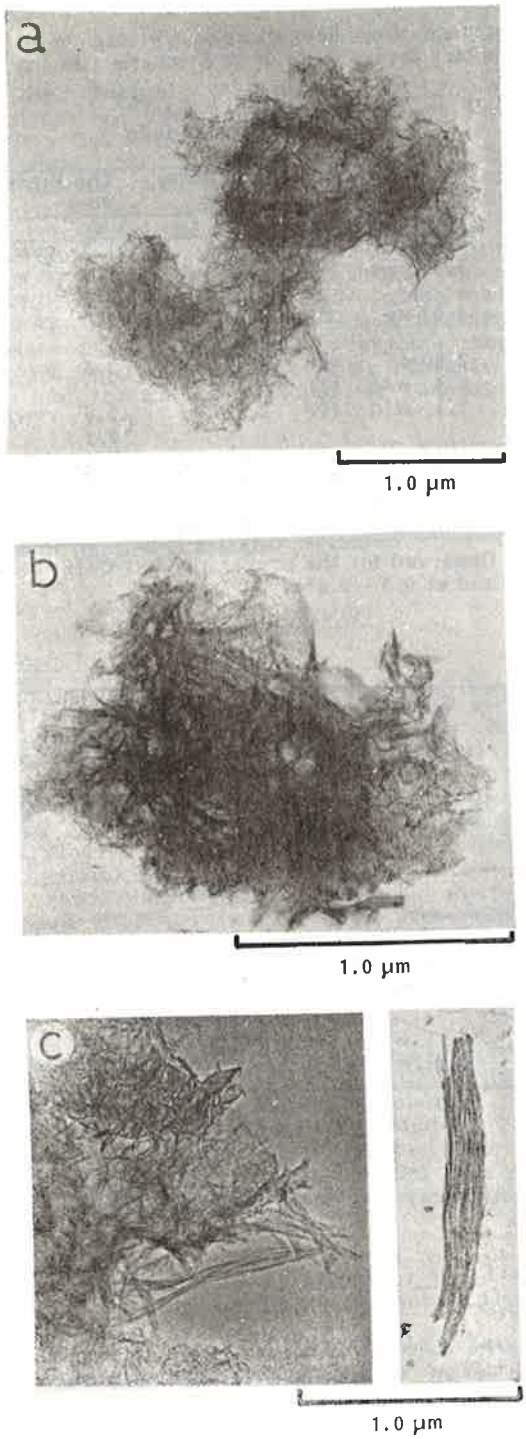

FIG. 2

TEM micrographs of C-S-H showing crumpled foils (A type) in the preparations (a) at 0.6 ratio and (b) at 1.3 ratio. (c) shows mixtures of crumpled foils and fibre aggregates (B type) in the preparations higher than 0.8 ratios.

For all specimens at 0.5 - 0.6 ratios, irrespective of temperature of treatment, the C-S-H formed initially consistent of A type and retained the same morphology until crystallization to Assarsson's Z-phase took place. However, all specimens prepared with higher than 1.0 ratio gave initially A type C-S-H and reacted further to give B type, increasing fibre aggregates before crystalline calcium silicate hydrates were formed. The 0.8 preparations gave B type C-S-H as an initial product even at 120° C - 2h treatment and further reacted to give 11 Å tobermorite.

For the fibre aggregates in the B type C-S-H, SED patterns were well-defined layer lines corresponding to a repeat distance of 7.3 - 7.4 Å in the fibre direction, which will be called b, and gave strong and diffused reflections. The layer lines for the odd number of indicies were very weak, and could not be observed for some specimens. The fibre aggregates gave strong reflections of approximate spacings 1.84 Å with k=4, 2.82 Å with k=0 and 3.08 Å with k=2, which coincided in their positions and intensities with those of 040, 400 and 220 of tobermorite respectively. In addition to these strong spots for the fibre aggregates, weak reflections showed some differences in positions and intensities according to the Ca/Si ratios for the preparations. The identifications of diffraction patterns were incomplete due to the missing of the most of spots to be observed for an assumed crystal. However, they were generally interpreted as the composite of hk0 and 0kℓ reciprocal patterns of tobermorite for the 0.8 ratio preparations, and were also identified by adding further a pattern with hk0 reciprocal plane of xonotlite for the 1.0 ratio preparations. Finally in the case of 1.3 and 1.5 ratios, they were interpreted by assuming the composite of the hk0 plane of xonotlite and/or hk0 plane of foshagite superposed on the hk0 and 0kℓ planes of tobermorite. These results suggest that the fibre aggregates in the B type C-S-H are structurally based on dreier ketten in the fibre direction and a tobermorite like phase, and some fibres in Ca-rich C-S-H higher than 1.0 ratio consist of adding different units: partly similar to xonotltie or foshagite.

In the present preparations, we could not find any reflections at 3.09 Å with k=0 and 2.8 - 2.9 Å with k=2, which are characteristic reflections for C-S-H (II) reported by Gard and Taylor (6).

Thermal Behaviour

DTA and TG curves were obtained at 20°C/min for specimens with various Ca/Si ratios of A type C-S-H and with the 0.8 ratio of B type one. Fig. 3 gave TG curves, expressed as the H_2O/SiO_2 molar ratio. The water loss was gradual and increased with rise in the Ca/Si ratios. This could be directly related to the C-S-H structure. For some specimens, a step loss was observed at about 800°C, which could be due to decarboxylation for partly carbonated C-S-H.

DTA results (Fig. 4) gave a strong exotherm at 800 - 900°C for all specimens and another weak one at 800°C for Ca-rich C-S-H higher than 1.3 ratio. Those are due to conversion into wollastonite for the former and β-C_2S for the later. The Ca/Si

T. Mitsuda, S. Kobayakawa and H. Toraya
Ceramics Research Laboratory, Nagoya Institute of Technology, Japan.

ratios for C-S-H gave effect on the exothermic temperature for the decomposition into wollastonite (Fig. 5); apart from the 0.8 - 1.0 ratios the exotherm shifted to higher temperatures. Kalousek (7) first reported DTA results for C-S-H prepared at 25°C that exothermic temperature was minimal at 830°C for 0.8 and 1.0 ratios, and increased with rise of Ca/Si ratios up to 900°C for 1.33 ratio.

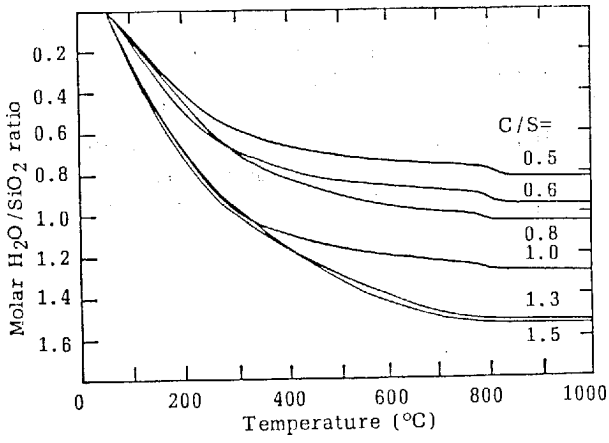

FIG. 3

TG curves of C-S-H

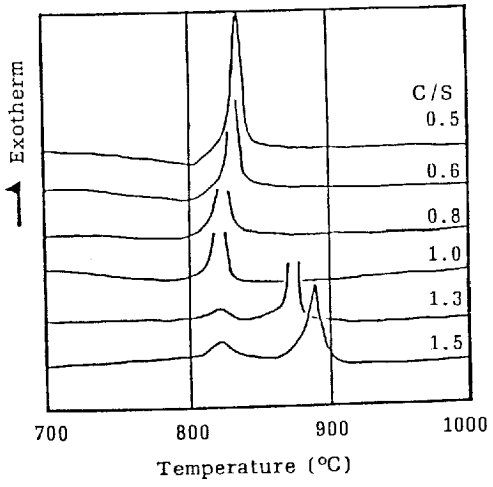

FIG. 4

DTA curves of C-S-H

Table 5 gave X-ray results for specimens, obtained in air by step heating for 1 h at 50°C intervals. In the preparations, it is significant that, Si-rich C-S-H such as 0.5 - 0.6 ratios, which crystallized to Assarsson's Z-phase and reacted further to give gyrolite, converted into wollastonite on heating at 800°C. If the Si-rich C-S-H has a layer structure like Assarsson's Z-phase or gyrolite group minerals, they could decompose into pseudowollastonite on heating at 700-800°C (8).

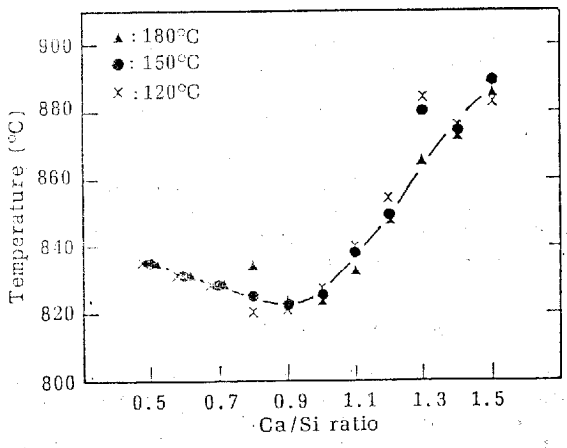

FIG. 5

Effect of Ca/Si ratio of C-S-H on exotherm of DTA. Specimens were prepared at 120 - 180 °C.

TABLE 5
Thermal Decomposition for C-S-H

Ca/Si ratio of C-S-H	Crystalline phase(s) formed on decomposition
1.5	β-C_2S at 750°C β-C_2S + wollastonite at 800°C
1.3	wollastonite + β-C_2S at 800°C
1.0	wollastonite at 800°C
0.8	wollastonite at 750°C
0.6, 0.5	wollastonite at 800°C

Infrared Absorption Spectra

Fig. 6 gave spectra obtained using the KBr disk method and Nujol mulls for unheated C-S-H specimens with various Ca/Si ratios. Spectra were also recorded for the samples after heating for 1 h at 300° and 500° C and then quickly immersing in

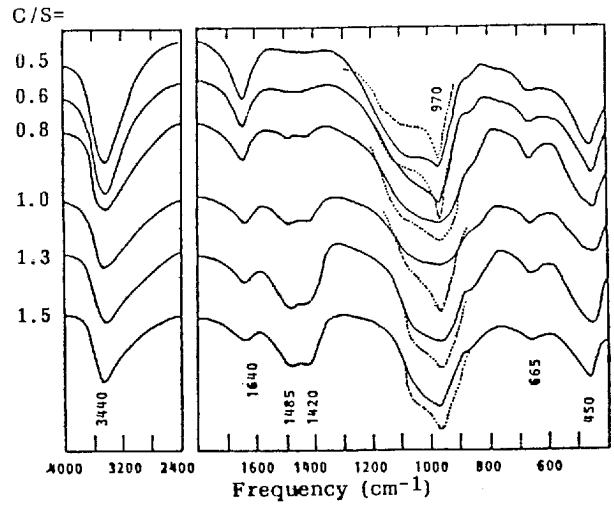

FIG. 6

Infrared absorption spetra of C-S-H.
(The dotted lines were obtained by Nujol mulls)

T. Mitsuda, S. Kobayakawa and H. Toraya
Ceramics Research Laboratory, Nagoya Institute of Technology, Japan.

CHARACTERIZATION OF HYDROTHERMALLY FORMED C-S-H

Nujol. The bands at 3440 and 1640 cm^{-1} given by the unheated samples show the presence of molecular water and SiOH. These bands were also markedly weaker in the heated samples. The remaining bands are attributable to carbonate (1420 - 1485 cm^{-1}) and silicate ions. The Ca/Si ratio for C-S-H caused little change in the pattern of Si-O stretching absorption at 970 - 1100 cm^{-1}; the shoulder extended to higher frequency with decrease of the Ca/Si ratios.

Acknowledgements

We thank Professor H.F.W. Taylor, University of Aberdeen for his helpful comments on C-S-H structure. We also thank the Asahi Glass Foundation for Industrial Technology, and the Japanese Government for a grant-in aid for scientific research to T. Mitsuda and H. Toraya.

References

1. H.F.W. Taylor, J. Chem. Soc. (London), 3682 (1950).
2. J.D.C. McConnell, Miner. Mag., 30, 293 (1954).
3. T. Mitsuda and H.F.W. Taylor, Miner. Mag., 42, 229 (1978).
4. L. Heller and H.F.W. Taylor, In: Crystallographic Data for the Calcium Silicates, HMSO, London (1956), p.42.
5. H.F.W. Taylor, In:The Chemistry of Cements, H.F.W. Taylor (ed), Academic Press, London (1964), vol.2, p.372.
6. J.A. Gard and H.F.W. Taylor, Cem. Concr. Res., 6, 667 (1976).
7. G.L. Kalousek, Proc. 3rd Int. Congr. Chem. Cement, London, 1952, 296 (1954).
8. J.A. Gard, T. Mitsuda and H.F.W. Taylor, Miner. Mag., 40, 325 (1975).

W.KURDOWSKI, W.NOCUŃ-WCZELIK, K.MIŚKIEWICZ, J.SZUBA, University of Mining and Metallurgy, 30-059 Kraków, Al.Mickiewicza 30, Poland

Induction period in Calcium Silicate Hydration in Light of Some New Experimental Results.
La periode d'induction au cours de l'hydratation des silicates de calcium en vue des nouvelles donnees experimentales.

2.1

ABSTRACT: The early stages of the tricalcium ortosilicate C_3S and calcium chlorosilicate C_2S $CaCl_2$ hydration process has been studied with the aim to establish the main factors responsible for retardation of the process in so-called induction or dormant period.
Microcalorimetry, analysis of liquid phase coexisting with the hydrating material and solid phase composition analysis by QXRD and DTA were used as the basic investigation methods. The results obtained indicate that the liquid phase supersaturation plays a decisive role as a rate controlling factor in the hydration process acting either directly or indirectly. The importance of the processes occuring in the liquid phase has been confirmed also during examination of the chain - -wollastonite hydration under hydrothermal conditions.

Foram estudados os estágios iniciais do processo de hidratação do ortossilicato tricálcico C_3S e do clorossilicato de cálcio C_2SCaCl_2, com o objetivo de se estabelecerem os fatores principais, responsáveis pela retardação do processo no chamado período de indução ou de dormência.

Foram utilizadas análises de microcalorimetria, de fase líquida coexistente com o material hidratante, e análise de composição de fase sólida por QXRD e DTA como métodos básicos de investigação. Os resultados obtidos indicam que a supersaturação da fase líquida exerce um papel decisivo como um fator controlador de velocidade no processo de hidratação, atuando tanto direta como indiretamente. A importância dos processos que ocorrem na fase líquida foi confirmada também durante o exame da hidratação da cadeia de wolostonita sob condições hidrotérmicas.

W.KURDOWSKI, W.NOCUŃ-WCZELIK, K.MIŚKIEWICZ, J.SZUBA, University of Mining and Metallurgy, 30-059 Krakow, Al.Mickiewicz 30, Poland

The calcium silicates hydration mechanism has not yet been completely explained (1,2). The silicates of high hydraulic activity, e.g. tricalcium silicate $Ca_3(SiO_4)O$, calcium chlorosilicate $Ca_2SiO_4CaCl_2$ and even the alinite phase reveal on the heat evolution curve socalled induction or dormant period which is the matter of numerous investigations (3-10). In order to elucidate, which of the following phenomena:

- calcium silicate hydrate nucleation,
- calcium hydroxide or basic calcium chloride nucleation,
- liquid phase supersaturation with Ca^{2+} or other ions in relation to hydration products, is the main factor hindering the initial hydration of C_3S and $C_2S.CaCl_2$ the following series of experiments have been carried out;
- the tricalcium silicate and calcium chlorosilicate hydration with some admixtures acting as Ca^{2+} binding agents,
- the hydrothermal reaction of chain-wollastonite either in water or in water vapour alone, has been examined additionally to supplement the previous investigations.

The thermal effects of the C_3S and $C_2S.CaCl_2$ hydration process were measured using the microcalorimetry.

The chemical composition of the liquid phase was analysed and the phase composition of solids was investigated by XRD and DTA. C_3S and $C_2S.CaCl_2$ hydration was carried out at w/s=10.

The experiments with wollastonite were carried out in autoclave under following conditions:

- the dry samples were exposed to the saturated steam action or,
- the pastes made of wollastonite mixed with water were introduced into autoclave.

The hydration heat evolution curves for all C_3S and $C_2S.CaCl_2$ samples with admixtures are shown in Figs 1 - 6.

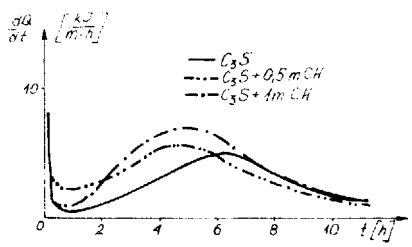

Fig. 1 - Heat evolution curves of C_3S hydrated with CH additon.

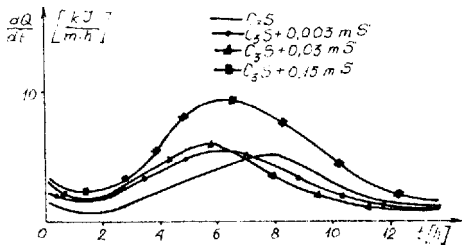

Fig. 2 - Heat evolution curves of C_3S hydrated with silica addition (0,003 - 0,15 mole S for 1 mole C_3S)

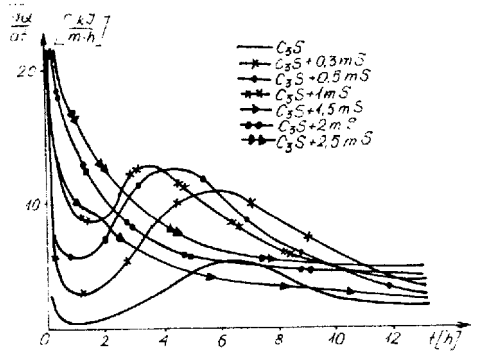

Fig. 3 - Heat evolution curves of C_3S hydrated with silica additon (0,3 - 2,5 mole S for 1 mole C_3S)

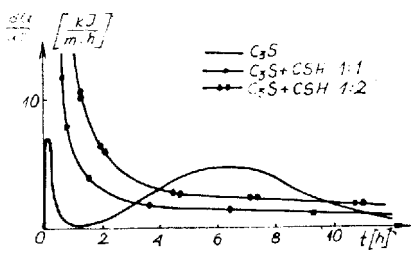

Fig. 4 - Heat evolution curves os C_3S hydrated with CSH addition.

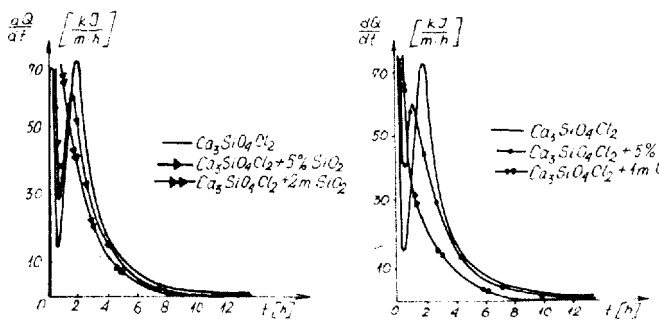

Fig. 5- Heat evolution curves of $Ca_3SiO_4Cl_2$ hydrated with SiO_2 additon

Fig. 6- Heat evolution curves of $Ca_3SiO_4Cl_2$ hydrated with CSH addition

It can seen that both the C_3S hydration and the $C_2S.CaCl_2$ hydration proceed in four sta-

W.KURDOWSKI, W.NOCUŃ-WCZELIK, K.MIŚKIEWICZ, J.SZUBA, University of Mining and Metallurgy, 30-059 Krakow, Al.Mickiewicza 30, Poland

ges with the induction period between the two thermal peaks, but the heat evolution is much more intensive for the chlorosilicate. In the presence of all admixtures applied i.e. SiO_2, CSH and CH a shortening of the induction period takes place, until its complete disappearance as the SiO_2 or CSH additives increase. The influence of CH addition on C_3S hydration is less pronounced (compare Fig. 1 with 2 and 3).

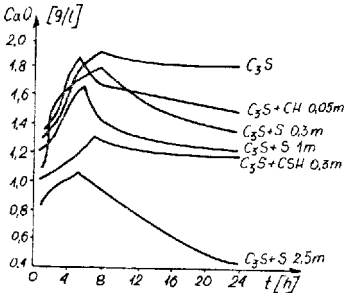

Fig.7- CaO concentration in the liquid phase during C_3S hydration with different additives

As can be seen from the liquid phase analysis during the C_3S hydration, active silica, calcium hydroxide or CSH generally bring about a Ca^{2+} concentration decrease with the increasing additive content though at first, relatively high Ca^{2+} concentrations are measured in C_3S water suspension containing small amounts of these additives. The Ca^{2+} concentration lowering is clearly visible when the 1 mole or higher quantities of CSH or silica are added. The silica concentration during the C_3S hydration is substantially lower than (Ca^{2+}) and does not exceed the ppm level. On the other hand calcium chlorosilicate when hydrating with water only releases Ca^{2+}, Cl^- and silicate anions into the solution in such proportion that we may say about its congruent dissolution. This process proceeds generally with greater rate than the C_3S hydrolysis. As it was stated in a previous work (4), a high silica concentration is retained for a long time (Fig. 8).

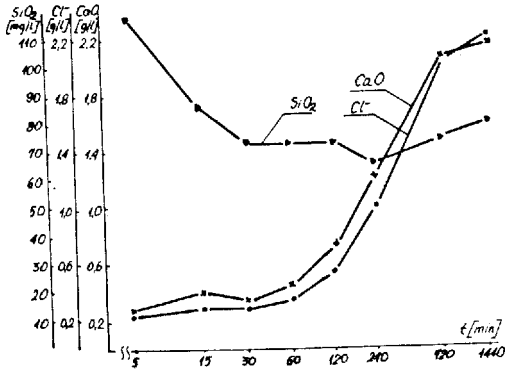

Fig. 8 - CaO. SiO_2 and chloride ions concentration during $Ca_3SiO_4Cl_2$ hydration

The SiO_2 or CSH phase addition reduces the silica concentration to a very low value, comparable with that for C_3S - H_2O suspension. Simultaneously the Ca^{2+} and Cl^- contents attain the values 10 times exceeding the concentration for $C_2S.CaCl_2$ hydration without any admixtures (Fig. 9 and 10).

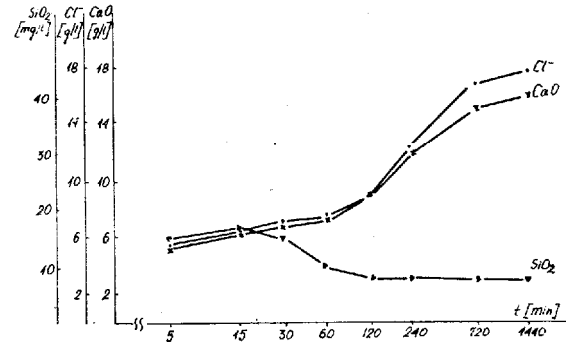

Fig. 9 - CaO, SiO_2 and chloride ions concentration during $Ca_3SiO_4Cl_2$ hydration with 5% SiO_2 addition

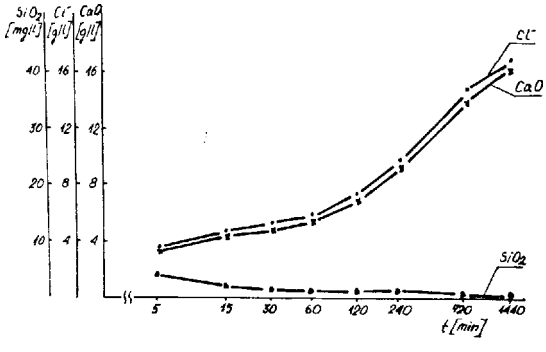

Fig. 10 - CaO, SiO_2 and chloride ions concentration during $Ca_3SiO_4Cl_2$ hydration with 5% CSH phase addition.

The action of admixtures described above have been confirmed by XRD and DTA examination. The pure phases react relatively slowly with water as it results from the unreacted phases determination. The hydration degree versus time increases with increasing admixture content (Fig. 11).

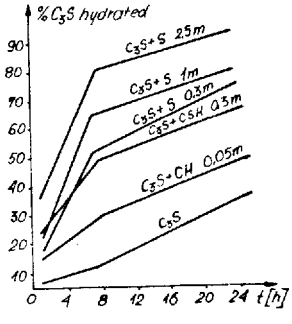

Fig.11 - The influence of additives on C_3S hydration degree according to XRD data.

The accelerating action of SiO_2 and CSH admixtures involves a rapid formation of hydration products, especially of CSH phase, which appears in substantial amount during the first hour of reaction. The CSH phase forming when the active silica is added, is of low C/S ratio (11). In the case of silica

to C_3S molar ratio higher than 1, the CSH phase is the only C_3S hydration product (12). The CH addition increases in some extent the hydration degree and the rate of hydration products formation - this last statement relates particularly to the calcium hydroxide crystallisation - but its effect is smaller than that of SiO_2 or CSH. The results of β-wollastonite reaction with water are listed in table 1.

Table 1.
Phase composition of β-wollastonite samples after thermal treatment.

Sample preparation	Temp. (°C)	Time (h)	Sample components (XRD and DTA measurement)
Water vapour	200	168	CS, no detective products,
Dry sample	220	168	CS, xonotlite appears.
Paste with W/C=0.5	200	48	CS, xonotlite
	220	24	CS, xonotlite
		48	Xonotlite, CS
		96	Xonotlite, CS-traces
		336	Xonotlite

The results indicate, that in the hydration process the liquid phase plays a decisive role as a rate controlling factor acting either directly or indirectly. The small quantities of CSH, SiO_2 and $Ca(OH)_2$, i.e. "nuclei" accelerate the process of the C_3S hydration and diminish the induction period, but their influence rises proportionally to the additive content as concerning the CSH and SiO_2 phases.
It means that the nucleation process is not the decisive factor hindering the reaction in this stage. The additivies mentioned above can act obviously as a nucleation barrier eliminating agent but mainly they modify the reaction in the liquid phase. When a high amount of SiO_2 or CSH phase is introduced into the hydrating C_3S - H_2O mixture the complete disappearence of the induction period is observed the active silica is the best acceleration as it ensures relatively fast Ca^{2+} ions combination and considerable Ca^{2+} ions supersaturation decrease with a simultaneous CSH phase formation.
The situation is analogous when the calcium chlorosilicate hydration is studied. This phase reacts with water much more quickly than C_3S but after initial rapid congruent dissolution it also reveals an induction period with a high saturation of the liquid phase with Ca^{2+}, Cl^- and silicate anions. CSH or SiO_2 accelerates the CHS phase formation and brings about a considerable silica concentration decrease. It results from these data that the liquid phase supersaturation with lime or silica plays a decisive role in Ca_3SiO_5 or $Ca_3SiO_4Cl_2$ hydration. The formation of an impermeable layer of the primary product cannot be excluded, but when the liquid phase is not supersaturated in respect to the hydration products, this layer does not cause the induction period, probably because of its composition.
The results concerning β-wollastonite hydration under hydrothermal conditions confirm the above conclusions relating generally to the decisive role of the liquid phase. The wollastonite phase, of relatively low reactivity, under hydrothermal conditions, in contact with saturated water vapour gives X-ray decetable xonotlite only after 168 h treatment at 220° while after the same time at 200°C the sample contains no detectable hydration products. The same wollastonite in contact with liquid phase at 200°C gives the xonotlite phase as early as after 48 h and at 220°C after 24 h of hydration. This results indicate an important role of the liquid phase also under hydrothermal conditions.
Summarising, the authors should underline the decisive significance of the liquid phase and of its composition for the hydration process of different calcium silica phases.

REFERENCES:

1. H.F.W.Taylor - Cement Production and Use, Proc. of the Conf. New Hampshire, USA, 1979.
2. Proc. of the 7th Int. Congress on the Chemistry of Cements, Paris, 1980.
3. R.Kondo, M.Daimon - Amer. Ceram. Soc., 52, 503, 1967.
4. W.Kurdowski, K.Miśkiewicz - Cem. Concr. Res., 15, 785, 1985.
5. W.Wieker - Round Table Conference on Calcium Chlorosilicates in the Chemistry of Cements, Cracov, Poland, 1985.
6. J.G.M. de Jong, H.N.Stein, J.M.Stevels - Appl. Chem., 17, 246, 1967.
7. D.D.Double, N.W.Thomas, D.A. Jameson - 7th Int. Congress on the Chemistry of Cements, II/256, Paris, 1980.
8. J.I.Young, H.S.Tong, R.W.Berger - J.Amer. Ceram. Soc., 60, 193, 1977.
9. P.Barret, D.Menetrier, D.Bertrandie, M. Regourd - 7th Int. Congress on the Chemistry of Cements, II/279, Paris, 1980.
10. C.Vernet, E.Damoulian, P.Gourdin, F.Hawthorn - 7th Int. Congress on the Chemistry of Cements, II/267, Paris, 1980.
11. W.Kurdowski, W.Nocuń-Wczelik - Proc. of the XIV Conf. on Silicate Industry and Silicate Science, 120-127, Budapest, 1985.
12. W.Kurdowski, W.Nocuń-Wczelik - Cem-Concr. Res. 13, 341, 1985.

M. GAWLICKI and W. NOCUŃ-WCZELIK, University of Mining and Metallurgy, Kracow, Poland 1

-Ca_3SiO_4 Hydration in the Presence of Electrolytes.
Hydration du -Ca_2SiO_4 en presénce des eléctrolytes.

2.1

SUMMARY: ß-C_2S hydration with K_2SO_4, Na_2SO_4, K_2CO_3 and Na_2CO_3 addition has been studied. The degree of hydration of ß-C_2S phase as well as the liquid phase composition in the suspensions of W/S = 50 have been determined. It has been found that all the additives used accelerated ß-C_2S hydration at early stages owing to the faster leaching and consumption of Ca^{2+} ions from the liquid phase as a result of hydration products formation.

SUMÁRIO: A hidratação de ß-C_2S com adições de K_2SO_4, Na_2SO_4, K_2CO_3 e Na_2CO_3 foi estudada. Foi determinado o grau de hidratação da fase de ß-C_2S em função do tempo, bem como a composição da fase líquida nas suspensões de A/S = 50. Constatou-se que os aditivos utilizados aceleravam a hidratação de ß-C_2S nas idades iniciais graças ao aumento da lixiviação e consumo dos íons de Ca^{2+} da fase líquida como resultado da formação dos produtos de hidratação.

M. GAWLICKI and W. NOCUŃ-WCZELIK, University of Mining and Metallurgy, Cracow, Poland

The role of chemical admixtures in β-C_2S hydration is not completely well explained till now. The most of works refers to the kinetics of the process or to the strength development and structure formation in the presence of some additives either accelerating or deccelerating the course of reaction /1-5/. The investigation of the liquid phase separated from the C_2S - H_2O - admixture suspension can give very useful informations concerning the admixture action /6,7/.
The β-C_2S hydration with K_2SO_4, Na_2SO_4, K_2CO_3 and Na_2CO_3 addition has been studied.
The sulphates and carbonates used as additives are known as components of mixed concrete admixtures and their effect is not widely examined.
C_2S was synthesized by heating the calcined $CaCO_3$ and silica mixture at 1500°C for 3h. P_2O_5 with equivalent $CaCO_3$ addition was used as a β-C_2S stabilizer. The X-ray investigation did not reveal any other phases than β-C_2S. The sintered material was ground to the specific surface of 3400 cm^2/g or 4500 cm^2/g.
The hydration was carried out at room temperature, in water and in 2% Na_2SO_4, K_2SO_4, Na_2CO_3 and K_2CO_3 water solutions.
The suspensions of water or solution to solid ratio equal to 50 were subjected to mechanical shaking. After a proper time the suspensions were filtered through the vacuum miliporous filter. The solid residue was rinced with acetone and ether and dried at 105°C.
CaO concentration in the liquid phase thus separated was analysed using EDTA solution. SiO_2 content was determined colorimetrically as a yellow molybdate complex. Solid components were examined by QXRD method.

The results of the liquid phase analyses were plotted in Fig. 1-4.

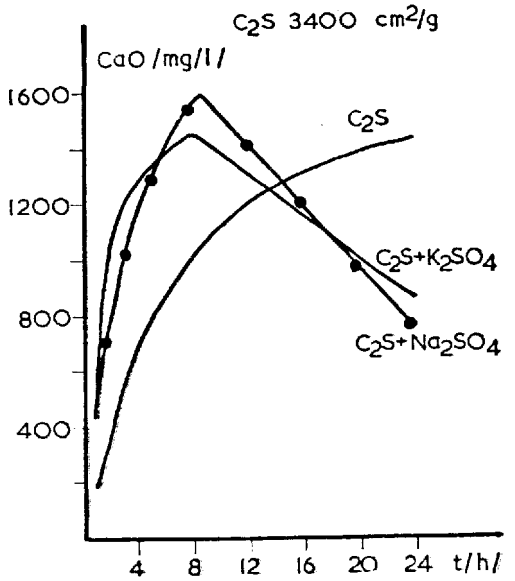

Fig. 2 - CaO content in the liquid phase. β-C_2S hydrated in water, 2% Na_2SO_4, 2% K_2SO_4 solutions. W/S = 50.

As it can be noticed in Fig. 1 and Fig. 2, the β-C_2S specific surface augmentation from 3400 cm^2/g to 4500 cm^2/g gives no considerable difference in Ca^{2+} leaching into the liquid phase. The Ca^{2+} concentration increases slowly during the first hour of

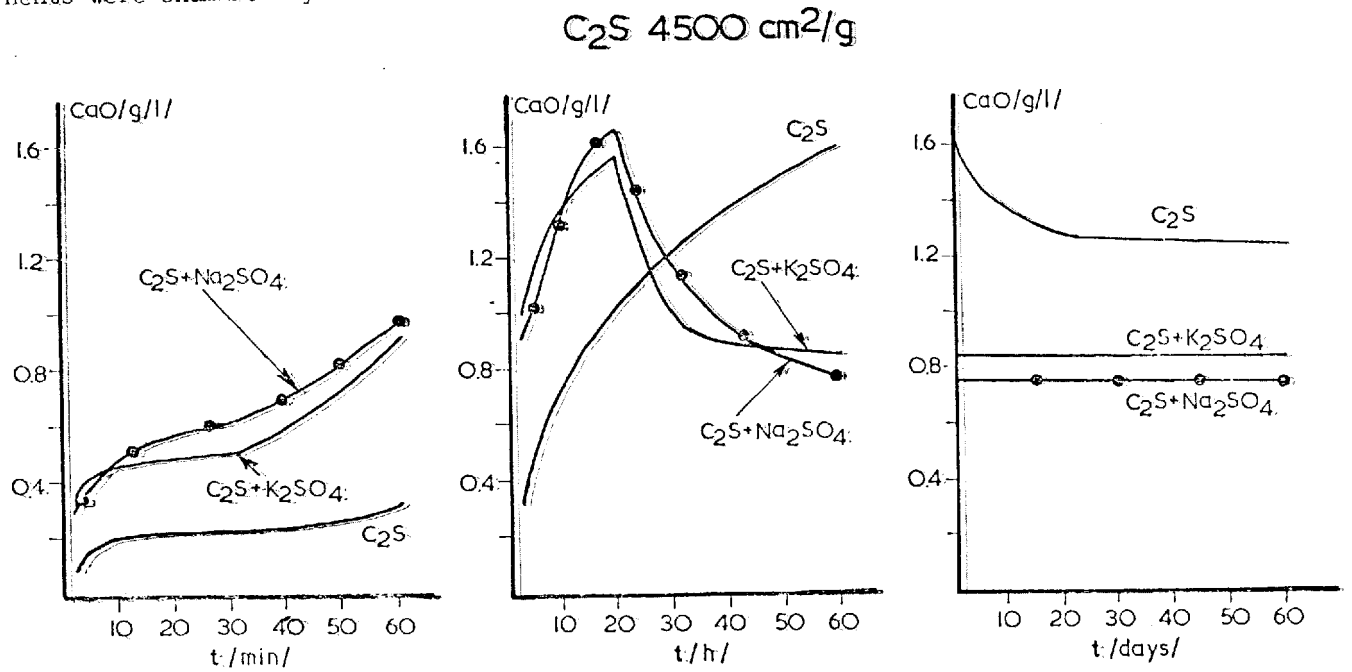

Fig. 1 - CaO content in the liquid phase. β-C_2S hydrated in water, 2% Na_2SO_4, 2% K_2SO_4 solutions. W/S = 50

reaction and then it rises faster up to 24h, pass the $Ca(OH)_2$ saturation value, attain the maximum equal to 1.6g/l and falls down to the constant level of 1.3g/l as it is shown in the Fig. 1.

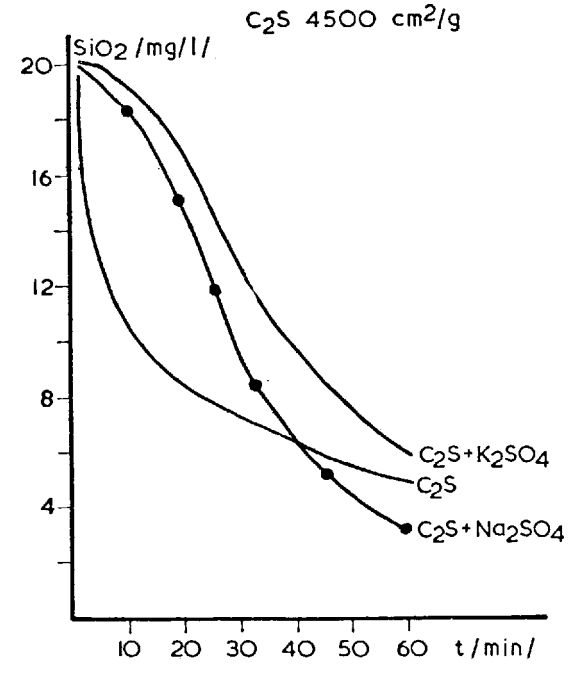

Fig. 3 - SiO_2 content in the liquid phase. β-C_2S hydrated in water, 2% Na_2SO_4 and 2% K_2SO_4 solutions. W/S = 50.

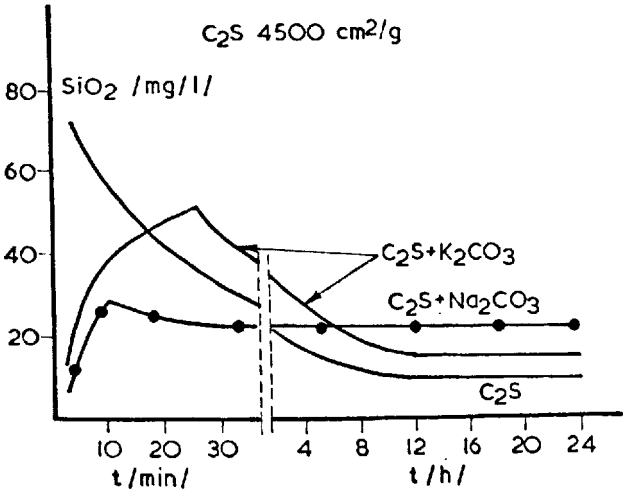

Fig. 4 - SiO_2 content in the liquid phase. β-C_2S hydrated in water, 2% K_2CO_3 and 2% Na_2CO_3 solutions. W/S = 50.

When the K_2SO_4 or Na_2SO_4 solutions are used, Ca^{2+} leaching proceeds faster. Ca^{2+} ions concentration maxima are attained by 8-12h and then the Ca^{2+} considerably diminishes and stabilizes on the level of 0.8g/l. The silica concentrations in the very early stages by 3-5min. are relatively high and then they rapidly fall down. K_2SO_4 or Na_2SO_4 addition supports a little higher silica concentration during the first 20-30min. but after 24h in all samples the silica content is about 1mg/l.

When the K_2CO_3 or Na_2CO_3 solutions are used the situation is quite different. Ca^{2+} ions concentration is very low and constant owing to $CaCO_3$ precipitation. The slow silica concentration increase to the value of about 30-50mg/l canbe seen in Fig. 4 and later it slowly lowers.

The QXRD measurements proved that the additives used accelerate the β-C_2S hydration during the first 24h /Fig. 5 and 6/.

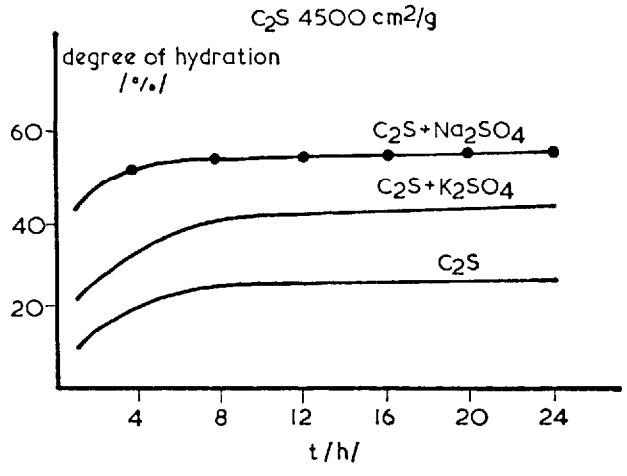

Fig. 5 - Degree of hydration of β-C_2S in water, 2% Na_2SO_4 and 2% K_2SO_4 solutions. W/S = 50.

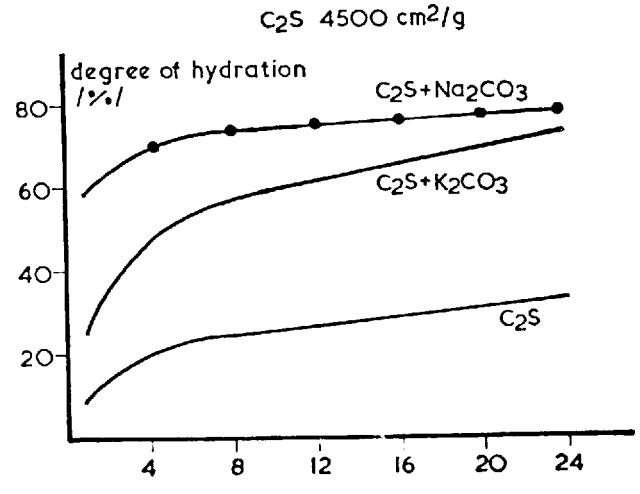

Fig. 6 - Degree of hydration of β-C_2S in water, 2% K_2CO_3 and 2% Na_2CO_3 solutions. W/S = 50.

Sodium salts act stronger than potassium

salts, specially at the beginning of reaction. Carbonates are better β-C_2S hydration accelerators than sulphates. Thus the most active admixture used is Na_2CO_3. 2% Na_2CO_3 addition rises the degree of β-C_2S hydration from about 40% to 80% after 24h. It should be mentioned that after 3days all the samples reveal similar degree of hydration exceeding 80%.

Summarizing the above data the authors would state that the compounds used, i.e. Na_2SO_4, K_2SO_4, Na_2CO_3 and K_2CO_3 accelerate β-C_2S hydration in early stages as it results from the degree of hydration determination by QXRD. The liquid phase data prove that K_2SO_4 and Na_2SO_4 addition facilitate calcium and silica leaching into the solution. Therefore the liquid phase supersaturation occurs earlier than in a suspension without any admixture and as a consequence, the precipitation of solid products takes place. When the Na_2CO_3 and K_2CO_3 additives are introduced, the carbonate anions combine the calcium kations forming $CaCO_3$. $CaCO_3$ precipitation favourizes further β-C_2S hydrolysis and CSH phase formation and results in relatively very fast unhydrated β-C_2S decrease. The authors succeeded in obtaining the two exact thermal effects on the microcalorimetric curves of β-C_2S paste with carbonate solutions as it can be seen in Fig. 7 illustrating the heat evolution curves of β-C_2S reaction with water /only one peak attributed to initial wetting/ and with carbonate solutions /two peaks/.

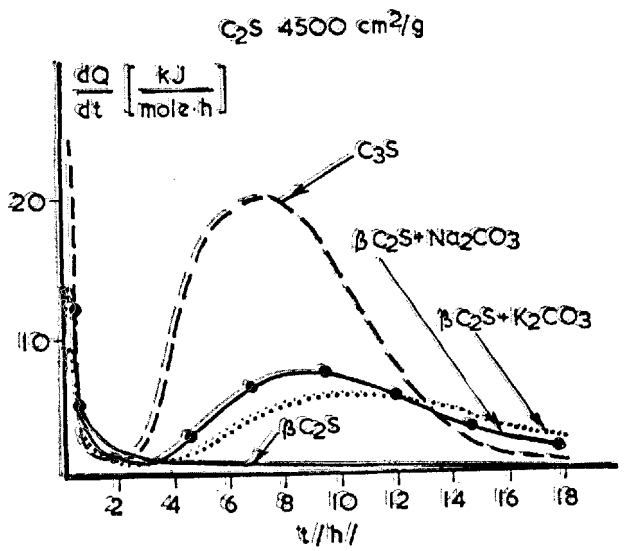

Fig. 7 - Microcalorimetric curves for C_3S, β-C_2S + 2% Na_2CO_3 and 2% K_2CO_3 pastes. W/S = 0.5.

It should be underlined that the accelerating influence of admixtures mentioned above relates to the early stages of β-C_2S hydration, i.e. to 1-3 days.

REFERENCES

1.- J.F. YOUNG and H.S. TONG /1977/, "Microstructure and strength development of beta-dicalcium silicate pastes with and without admixtures", Cem. Concr. Res., 7, 627-636.

2.- M. RADENKOWA-YANEVA, J. YANEV, R. PAUNOW, I. NIKOLOV and E. MILETOVA /1982/, "Hydration and structure formation in beta-dicalcium silicate pastes in the presence of chemical additives", Tekh. Misul. 19, 67-73. Chem. Abstr. /1983/, 98, 165966.

3.- G.L. VALENTI, D. RINALDI and V. SABATELLI /1984/, "Effect of some accelerating admixtures on the hardening of beta-dicalcium silicate", 3, 821-824. Jour. Mat. Sci.

4.- M. COLLEPARDI, S. MONOSI, G. MORICONI and M. PAURI /1984/, "Combined effect of lignosulfonate and carbonate on pure Portland Cement Clinker compounds hydration. Hydration of dicalcium silicate alone and in the presence of tricalcium aluminate", Cem. Concr. Res., 14, 275-284.

5.- E.P. ANDREEVA and I. EVTUKOVA /1982/, "Mechanism of effect of calcium chloride on procesess of disperse structure formation and chemical interaction in the hydration of beta-dicalcium and tricalcium silicates", Kolloid. Zh., 44, 633-639.

6.- H.S. TONG and J.F. YOUNG /1977/, "Composition of solutions in contact with hydrating beta-dicalcium silicate", J. Am. Ceram. Soc., 60, 321-325.

7.- N.L. THOMAS, D.D. DOUBLE /1983/, "The hydration of Portland Cement, C_3S and C_2S in the presence of calcium complexing admixture /EDTA/", Cem. Concr. Res., 13, 391-400.

8.- V.S. RAMACHANDRAN /1983/, "Admixtures", Cement Research Progress, Chapter 6, 110-128.

9.- P.A. ROSSKOPF, F. KINNEY, D.A. LUPYAN and A. McFARLAND /1984/, "Admixtures", Cement Research Progress, Chapter 6, 109-126.

Ion Teoreanu, Annemarie Puri and Maria Georgescu, Polytechnical Institute Bucharest, Romania.

Hardening processes in some C_4AF - additives - water systems

Processus de durcissement de quelques systèmes C_4AF - additifs - eau

SUMMARY: The object of this paper was to obtain informations about the processes that occur in the interaction with water and in the hardening of some C_4AF-additives-water systems, in comparision with the C_4AF-water system.

The results concerning the obtaining of workable compositions with relatively lower water/binder ratios wich evolves high resistant hardening structures, by association of C_4AF with gypsum (5%) and an industrial product (0.2%) containing mostly dimethylterephtalate (DMTP), are to be remarked. In this case, over the more retarding effect of gypsum (on the hydrocompounds conversion, especially), overlaps the lower retarding effect of DMTP, wich favour the development of a microcrystalline hardening structure.

O objetivo deste artigo foi obter informações a respeito dos processos que ocorrem na interação com água e no endurecimento do alguns sistemas C_4AF-aditivos-água, em comparação com o sistema C_4AF-água.

Devem ser observados os resultados relativos à obtenção de composições trabalháveis com relações relativamente baixas de água/ligante, que desenvolvem estruturas de endurecimento de alta resistência, por associação de C_4AF com gesso (5%) e um produto industrial (0,2%) contendo principalmente dimetiltereftalato (DMTP). Neste caso, sobre o efeito mais retardante do gesso (principalmente na conversão dos hidrocompostos), sobrepõe-se o efeito menos retardante do DMTP, que favorece o desenvolvimento de uma estrutura microcristalina de endurecimento.

Ion Teoreanu, Annemarie Puri, Maria Georgescu

1. Introduction

The iron containing phases of portland cement clinker are less reactive than the calcium aluminates. Their interaction with water becomes less intense as the amount of iron(III) oxide increases /1-6/. According to Tsumura /7/, in the early stages the hydration rate of C_4AF (1,65 /um/h) is about 3 times lower than of C_3A (4,6 /um/h).

Flint /8/ has shown that in C_4AF-water pastes are present metastable solid solutions of hexagonal hydroaluminates and hydroferites ($C_4(A,F)H_n$) as well as cubic solid solutions $C_3(A,F)H_6$. The X-ray diffraction and Moessbauer spectroscopy have also detected hydroferrite aluminate solid solutions richer in Al_2O_3 and $Fe(OH)_3$ /9-12/.

Calorimetric data published by Tenoutasse /13/ deal with the effect of variable additions of $CaSO_4.2H_2O$ (10-30%) on the hydration of C_4AF. These data show that the second exothermal effect due to hydration heat shifts towards longer durations of the process as the amount of gypsum increases, wich proves the retarding effect of the latter. This effect is still obvious, but less intense, at small gypsum concentrations /14/.

There are relatively few published data on the formation of hardening structures in C_4AF-additives-water systems. The factors wich controll this process are: its kinetics, ratio of hexagonal vs. cubic compounds, their stability, temperature conditions, amount of ferric hydroxide formed and its change in time /9,11,12,14/.

2. Experimental

The aim of this work is to present informations on the processes occuring upon the interaction with water and hardening of some C_4AF-additive-water systems. As a reference, the C_4AF-water system has been used.

C_4AF was prepared by a thermal treatment of a stoichiometric mixture of $CaCO_3$, Al_2O_3 and Fe_2O_3 at 1330°C. The mixture was kept 2 hours at this temperature, then cooled and the product was ground to 3000 cm^2/g (Blaine surface area).

The additions used were $CaSO_4.2H_2O$ and an industrial product containing dimethylterephtalate (DMTP). The main part of this investigation was a study of DMTP influence on hardening of C_4AF.

The hydration-hydrolysis processes and the formation of the hardening structure has been investigated by chemical analysis (Ca^{2+} released by hydrolysis and chemically bound water), thermal analysis, X-ray diffraction and measurements of mechanical strength.

3. Discussion

The results of chemical, thermal and X-ray diffraction analyses provided the informations regarding the modifications determined by the above mentioned additions in the formation mechanism, the kinetics and the chemical and morphological composition of the new compounds resulted from the hydration of C_4AF. The results are presented in figures 1 to 5 and in table 1.

The additions exert a retarding effect on C_4AF-water interaction, as well as on the conversion of hexagonal hydroferrite aluminates into cubic ones. The composition of the liquid phase in equilibrium with the hydrated phases is affected by modifications in the kinetics of chemical processes involved. A quantitative evaluation is provided by the time variation of Ca^{2+} concentration in suspensions of binder (Fig.1), as well as by the composition and relative amounts of solid phases present in hardening systems.

The use of DMTP is of relatively little consequence on the hydration degree (mainly for longer interactions) and of no practical importance with respect to the conversion of hydrated compounds, regardless of the duration of the binder-water interaction.

Ion Teoreanu, Annemarie Puri, Maria Georgescu

Table 1

Composition (%)			Blaine surface area (cm^2/g)	Chemical bound water (%), after:			
C_4AF	Gypsum	DMTP		1 day	3 days	7 days	28 days
100	-	-	3034	15,22	17,41	19,38	19,4o
95	5	-	2978	15,54	15,72	16,5o	18,91
90	10	-	2933	3,o8	4,97	-	17,32
99,8	-	0,2	3023	14,86	16,93	19,97	2o,46
94,8	5	0,2	3020	15,5o	-	19,3o	18,76
89,8	10	0,2	3122	3,22	6,44	-	2o,o7

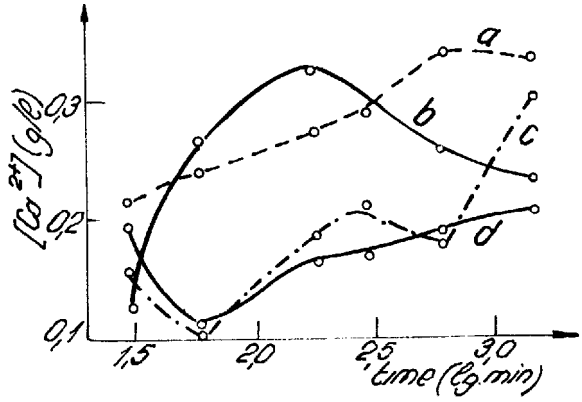

Figure 1 Time variation of Ca^{2+} concentration in binder-water suspensions:
a - C_4AF; b - C_4AF + 0,2% DMTP; c - C_4AF + 5% $CaSO_4.2H_2O$; d - C_4AF + 5% $CaSO_4.2H_2O$ + 0,2% DMTP.

Calcium sulphate dihydrate exerts its expected retarding effect both on hydration kinetic and conversion of hydrated compounds. In the masses with 10 wt% gypsum the chemical bound water is less important with respect to the reference system and the other systems, even after 3 to 7 days. In the early days of the hardening process differences between systems with and without $CaSO_4.2H_2O$ additions are visible in the amounts of hydrated hexagonal phases (see in Figures 2-3 the following reflexions: 8.20-8.30 Å, 2.88-2.90 Å and on the DTA curves in Figures 4-5 the effects at 110-135° and 180-195°C) and cubic phases (see in Figures 2-3 the following reflexions: 5.08-5.14 Å, 4.40-4.45 Å, 3.31-3.36 Å, 3.12-3.14 Å, 2.80-2.82 Å, 2.26-2.30 Å, 2.02-2.04 Å and on the DTA curves in Figures 4-5 the effects at 290-320° and 440-475°C), both in systems with gypsum additions. Hydrosulphates are also formed in the hydration of systems with $CaSO_4.2H_2O$. This is more obvious in systems with higher amounts of additive. Thus, ettringite is present even after the first day of hydration in the sample with 10 wt% gypsum; its X-ray interferences recorded by us were at 9.55 Å, 5.53 Å, 2.76 Å and 2.54 Å. The thermal effects assigned to hydrosulphate aluminates overlap those assigned to calcium hydroferrite aluminates and ferric hydroxides.

The addition of DMTP together with gypsum does not affect essentially the kinetics of the hydration and conversion processes and the relative amounts of phases formed. Its presence determines a finer grain size of resulted hydrated compounds, seen on the TEM micrographs. The microcrystalline structures evolved from such compounds are more compact.

The formation of hardening structures is a consequence of chemical processes wich occur in binder systems and their kinetics, of chemical and morphological nature of resulted hydrated compounds and of their aptitude to generate compact structures. Mechanical strength measurements were done on investigated masses on microprisms (15x15x40 mm) made of plastic mortars. The results are given in table 2 and are in good agreement with our observations and interpretations regarding the alterations induced by the used additions on the C_4AF-water interaction, in the conversion of resulted hydrocompounds and in their

chemical and morphological nature.

The moderate retarding effect of some additives wich signifiantly affect the conversion processes only, but do not affect to such a degree the hydration processes, is associated to the formation of a compact microcrystalline hardening structure wich determines the development of high mechanical strengths, wich steadily increase in time, without exhibiting any undesirable discontinuities. Such results are noted when $CaSO_4 \cdot 2H_2O$ (5%) is associated to DMTP (0.2%). This is a consequence of the formation of hydrated compounds with smallgrain sizes and of the possibility to prepare workable (plastic) mortars with lower water/binder ratios than for the reference system.

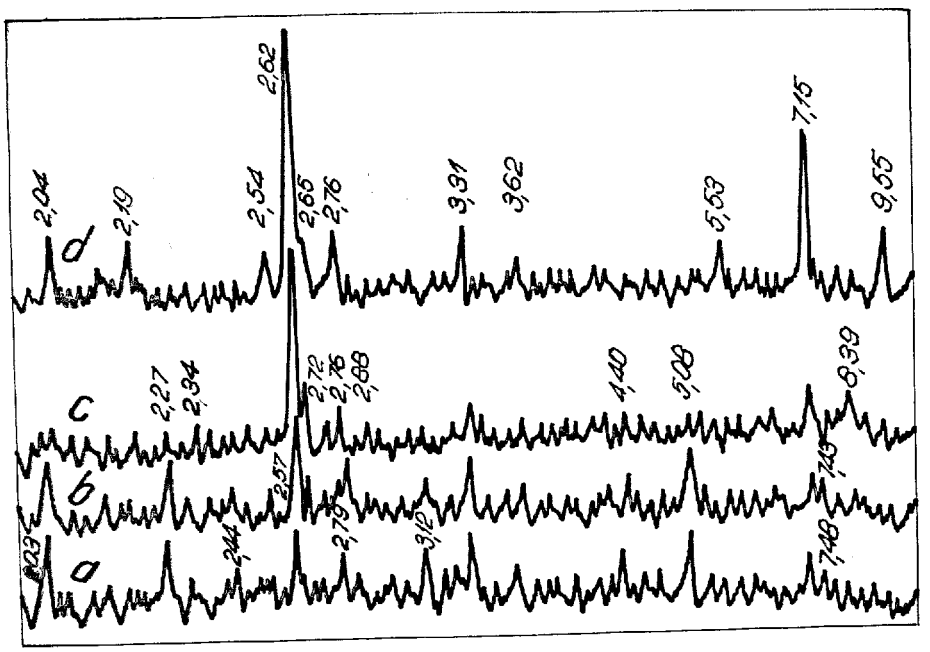

Figure 2 X-ray diffraction patterns of 1 day hydrated binders:
a - C_4AF;
b - C_4AF + 0.2% DMTP;
c - C_4AF + 5% $CaSO_4 \cdot 2H_2O$;
d - C_4AF + 10% $CaSO_4 \cdot 2H_2O$.

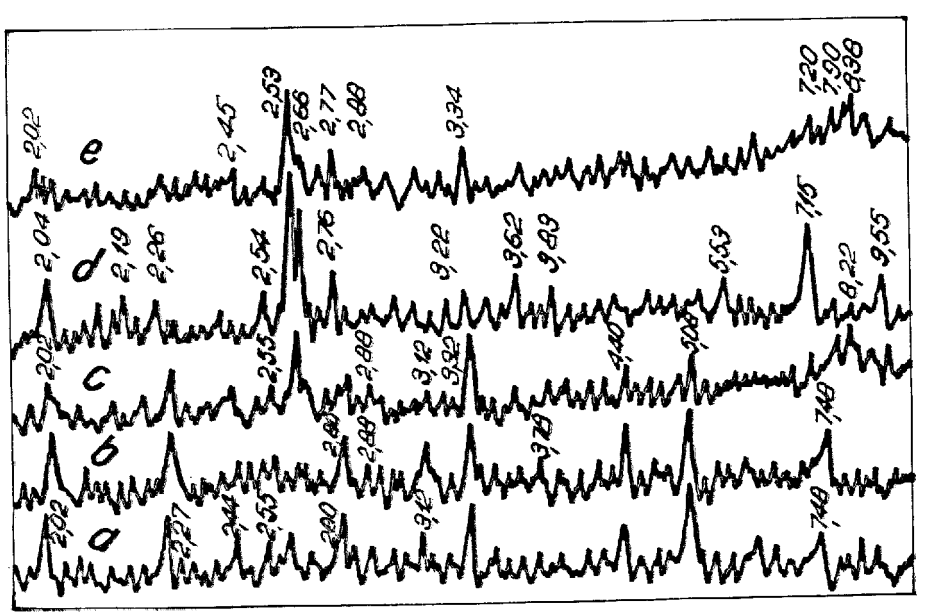

Figure 3 X-ray diffraction patterns of 28 days hydrated binders:
a - C_4AF;
b - C_4AF + 0.2% DMTP;
c - C_4AF + 5% $CaSO_4 \cdot 2H_2O$;
d - C_4AF + 10% $CaSO_4 \cdot 2H_2O$;
e - C_4AF + 5% $CaSO_4 \cdot 2H_2O$ + 0.2% DMTP.

Ion Teoreanu, Annemarie Puri, Maria Georgescu

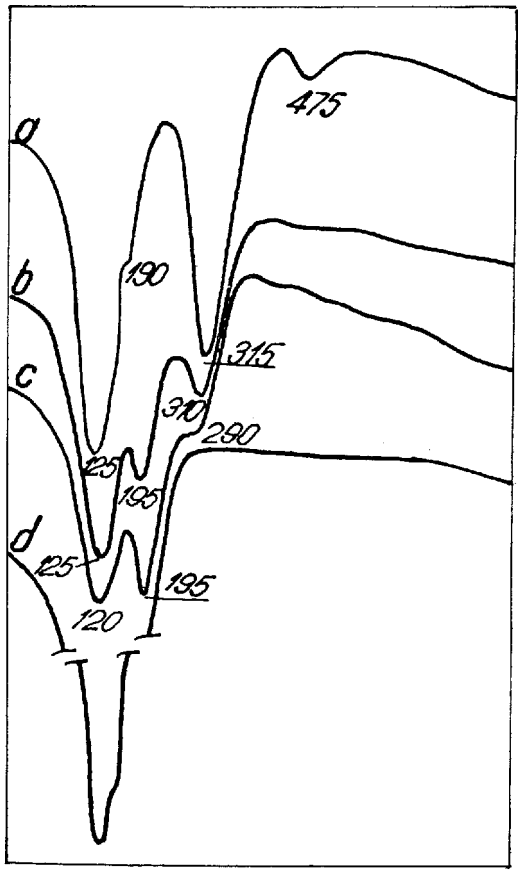

Figures 4 DTA curves of 1 day hydrated binders:
a - C_4AF; b - C_4AF + 5% $CaSO_4 \cdot 2H_2O$;
c - C_4AF + 5% $CaSO_4 \cdot 2H_2O$ + 0,2% DMTP;
d - C_4AF + 10% $CaSO_4 \cdot 2H_2O$.

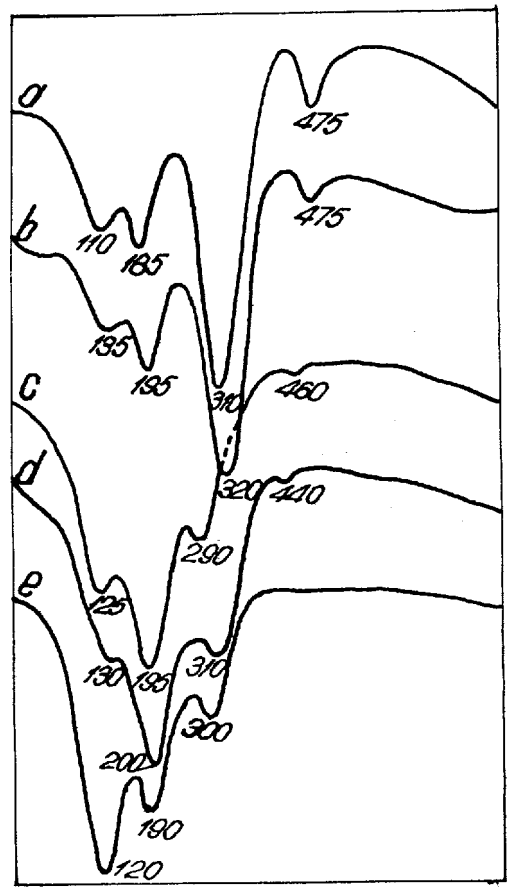

Figures 5 DTA curves of 28 days hydrated binders:
a - C_4AF; b - C_4AF + 0.2% DMTP; c - C_4AF + 5% $CaSO_4 \cdot 2H_2O$; d - C_4AF + 5% $CaSO_4 \cdot 2H_2O$ + 0.2% DMTP; e - C_4AF + 10% $CaSO_4 \cdot 2H_2O$.

Table 2

Composition (%)			Blaine surface area (cm^2/g)	water/binder ratio	Compressive strength (daN/cm^2) after:				
C_4AF	Gypsum	DMTP			1 day	3 days	7 days	28 days	60 days
100	-	-	3024	0,6	33.0	16.0	28.6	41.0	37.0
99,8	-	0.2	3023	0.6	37.0	20.6	24.5	27.6	38.2
95	5	-	2980	0.5	103.0	88.7	81.6	137.7	115.9
90	10	-	2933	0.5	0	0	0	23.7	24.7
94.8	5	0.2	3020	0.5	90.5	167.0	159.0	336.0	328.0
89.8	10	0.2	3122	0.5	0	0	4.4	7.6	5.0

4. Conclusions

The kinetics of hydration and conversion of hydrated compounds resulted in the hardening process of aluminate binders, and their chemical-morphological nature exert an essential influence on the characteristics of the hardening structure. The control of these processes in association with the preparation of workable masses characterized by relatively low water/binder ratios, may lead to high strength structures. Such a result is obtained for C_4AF by the joint use of a relatively low amount of gypsum (5%) and an industrial by-product - DMTP (0.2%). In this case, the more important retarding effect of gypsum, wich is exerted mainly on the conversion processes, and the similar but less important effect of DMTP, wich leads to microcrystalline hardening structures, are overlapped.

References

1. I.Teoreanu a.o. - Bazele fizico-chimice ale întăririi lianţilor anorganici, EDP Bucureşti 1972
2. I.Teoreanu - Bazele tehnologiei lianţilor, ET Bucureşti 1975
3. H.E.Schwiete, T.Iwai - Zement-Kalk-Gips 17,(2),53,1964
4. L.V.Smirnova, A.I.Boikova - Tement, nr.9, 1977
5. S.I.Ivaşcenko, M.T.Vlasova - Tement nr.11, p.13, 1982
6. A.M.Dmitriev, M.T.Vlasova a.o. - Siliconf XIII, vol.3, p.11, 1981
7. S.Tsumura - Zement-Kalk-Gips 19,(11), 511, 1966
8. E.P.Flint a.o. - J.Res.Nat.Bur.Stand. 26,13,1941
9. C.Hriţcu - Dissertation, IPB Bucureşti 1979
10. I.Teoreanu, G.Filoti a.o. - Il Cemento 76,(1),19,1979
11. V.Moldovan - Mat.de Constr. 2,(1),16, 1972
12. V.Moldovan, N.Butucescu - Mat. de Construcţii 6,(2),65,1976
13. N.Tenoutasse - Rev. des Mat. de Constr. nr.614, p.452, 1966.
14. I.Teoreanu, M.Muntean - Rev. des Mat. de Constr. nr.697, p.317, 1975

A B Afshar and W J McCarter
Department of Civil Engineering
Heriot-Watt University, Edinburgh, Scotland, UK.

MONITORING THE INFLUENCE OF ADMIXTURES AND COMPOSITION ON THE EARLY HYDRATION CHARACTERISTICS OF CEMENT PASTE USING AC ELECTRICAL RESPONSE TECHNIQUES

Summary: The authors have developed a method for monitoring hydration processes in cement paste and entails measuring the changes in electrical response during the initial 24 hours after gauging with water. This method is used in this paper to show that AC electrical response methods can be used as a diagnostic for the determination of cement hydration characteristics and assessing the effect of admixtures, cement composition and environmental conditions on the hydration characteristics of cement.

Os autores desenvolveram um método de monitoração dos processos de hidratação da pasta de cimento, com medição das mudanças na resposta elétrica, no decorrer das primeiras 24 horas após a mistura com água. Neste artigo, o método é usado para mostrar que métodos de resposta elétrica AC podem ser empregados como um diagnóstico para determinação das características de hidratação do cimento e para avaliação do efeito de aditivos, da composição do cimento e das condições ambientais sobre as características de hidratação do cimento.

INTRODUCTION

The increasing use of admixtures by the construction industry, as a substitute to using special cements, warrants the need for a thorough investigation into the effects of admixtures on the physical characteristics and chemical processes occurring during cement hydration. The effect of admixtures on the physical characteristics of cement based materials cannot be generalised, for example, some salts accelerate setting while others retard; certain groups of salts retard the setting process when used in small percentages and accelerate setting when used in larger percentages (1). Moreover, similar admixtures have different effects on, for example, cements of different chemical composition; similar cements manufactured at different plants or even cement stored under different environmental conditions.

The most important physical characteristic of cement paste is setting. Setting is the physical consequence of the chemical reactions which take place when water is added to cement. Setting time has been measured using the Vicat Needle apparatus to various standards, and attempts have been made (1,2) to correlate the results of setting times with pull-out and heat of hydration methods.

The Vicat Needle and pull-out methods relate to the physical state of the paste, however, it is known that setting is the direct consequence of chemical reactions and crystal formation occurring during hydration. Monitoring the chemical reactions would give better indicators as to setting and hardening. Moreover, although the heat of hydration method relates hydration to setting by measuring the amount of heat evolved, the small sample size, together with high water/cement ratios used in the test, does not represent typical mixes used in practice. Furthermore, "....since the heat evolution curve represents a dynamic balance between the heat evolved by the hydrating C_3S and the heat lost by the calorimeter to its surroundings, the exact shape and position of the peaks depend on the particular instrument used" (2). There is thus a need for a precise chemio-physical test to,

(a) ensure correct setting of cement, and,
(b) assess and quantify the influence of admixtures on the hydration process.

THE ELECTRICAL METHOD AND THE PARAMETERS MEASURED

Previous papers by the authors (3-5) contain full details of a technique for monitoring the hydrolysis and the hydration processes in cement paste during the initial 24-hours after gauging with water. In essence, the technique entails accurately monitoring the variation in electrical resistivity and dielectric constant of the paste. A typical electrical response curve is given in Fig 1, with the frequency of the applied electrical field at 1kHz. The change in the internal temperature of the paste is also given and resembles, in shape, that of the heat evolution curve produced by various investigators (2,6).

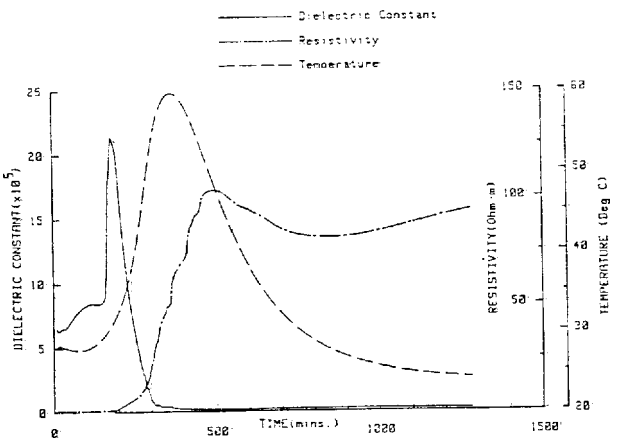

Fig 1 Variation of dielectric constant, restivity and internal temperature of cement paste during initial 24-hours after gauging

Hydration occurs in a number of stages and it has been proposed by the authors that this sequence can be followed by the dielectric constant and resistivity curves, similar to that using heat evolution curves. The authors postulate that the dielectric constant and resistivity curves are better indicators as to the physical and chemical state of the paste during early hydration and the rate of change of these parameters are indicative of the rate at which reactions are progressing. The dielectric constant and resistivity are sensitive to physical and chemical changes taking place as hydration proceeds; whereas in conduction calorimetry there may be a lag between the time chemical reactions take place and the time the exothermic effects are recorded.

Referring to Fig 1, the initial stages of hydration are characterised by a relatively high dielectric constant value and a low resistivity value, caused by high ionic concentrations, particularly Ca^{2+} and OH^- ions, leached from the cement grains. There is a small drop in dielectric value over the initial 30 minutes as first hydration products are formed before the induction period commences (30-180 minutes). This is characterised by a gradual increase in dielectric constant and constant resistivity. The induction period is terminated by a rapid rise in dielectric value and the authors (7) believe this to be the result of the rupture of the protective membrane, caused by osmotic pressure (8,9) build-up within the protective membrane. The sudden drop in dielectric value coincides with the rise in resistivity value and a general increase in rigidity of the mix due to the formation of CH and more stable C-S-H hydrates. The authors have, for the purposes of this paper, redefined the initial set as the peak in dielectric constant following the induction period which coincides with the initial rise in resistivity (≈180 minutes), while the final set is taken as the peak in resistivity curve (≈500 minutes), as reaction rates by this time are considerably reduced. Thus, the period 180-500 minutes, as inferred from the electrical response curves, is one of rapid

chemical activity. The gradual drop in resistivity and rise in dielectric constant over the period 500-1000 minutes is associated with large scale formation of ettringite and monosulpho-aluminate.

EXPERIMENTAL

A full account of the experimental procedure is given in reference 3. The in-phase (resistance) and quadrature (capacitance) components of the impedance were measured over a range of frequencies using an impedance analyser. In addition, the internal temperature changes within the specimens were monitored. The instruments were controlled and the data logged and analysed using a microcomputer controlled data acquisition system.

Tests were carried out using Ordinary Portland Cement (OPC); High Alumina Cement (HAC); Rapid Hardening Portland Cement (RHPC); and Sulphate Resisting Portland Cement (SRPC). The water/cement ratio was kept constant at 0.27 by weight. Two common admixtures, sugar and calcium chloride, were used which, respectively, retard and accelerate the setting of cement paste.

The specimens for electrical measurements were made from single batches of cement to minimise the effects of variability in materials. Tap water was used for all experiments. The cement was mixed using a Hobart planetary motion rotary mixer and, to facilitate electrical measurements, the specimens were compacted into a calibrated dielectric cell.

DISCUSSION OF RESULTS

Representative results from the tests are given in Figs 2, 3 and 5 for an applied frequency of 1kHz.

Fig 1 shows the change in the measured parameters over the 24-hour test period for OPC paste without any admixture (taken as the datum mix). Assuming initial set occurs at the first peak in dielectric constant following the induction period, then by comparing Fig 1 with Fig 2, it is evident that the addition of sugar to the mix has the effect of delaying this peak. Fig 2(a) and 2(b) shows variation in measured parameters when 0.02% and 0.1% sugar is added to the mix respectively; 0.02% sugar delays setting by 220 minutes and 0.1% sugar delays setting by 620 minutes. The retarding agent has the effect of delaying the reaction of the C_3S phase (associated with the peak in dielectric constant) and increasing the induction period; the peak in dielectric constant curve is progressively delayed as the proportion of retarder is increased. The delay in setting is

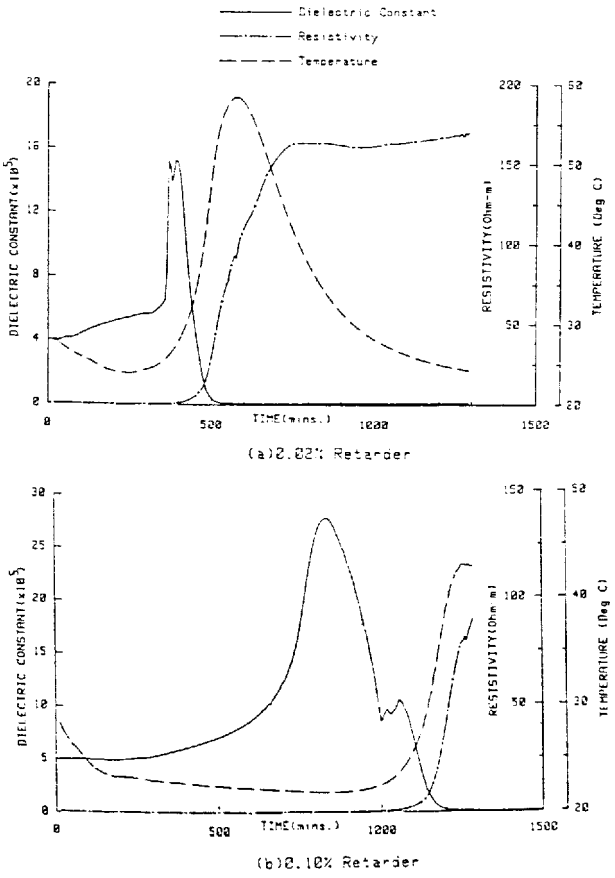

Fig 2 The effect of retarder (sugar) on measured parameters

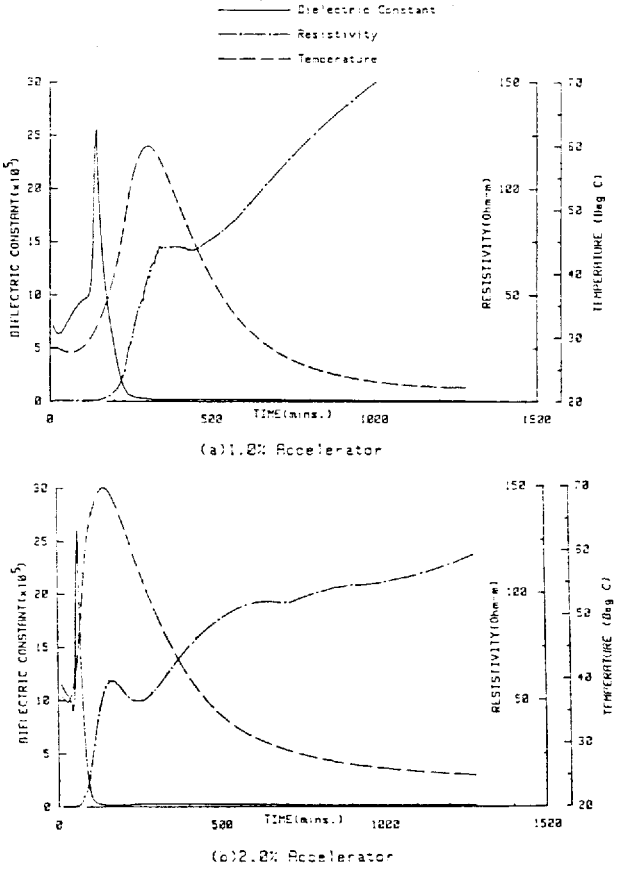

Fig 3 The effect of accelerator (calcium chloride) on measured parameters

directly proportional to the quantity of sugar added, although it is possible to kill setting by the addition of more than 0.2% sugar.

The addition of calcium chloride accelerates the setting process; Fig 3(a) and 3(b) show the variation in measured parameters when 1% and 2% of calcium chloride is added to the mix respectively; 1% calcium chloride accelerates the setting by 50 minutes and 2% calcium chloride accelerates setting by 120 minutes. The induction period is reduced and reaction rates considerably increased. The curves are compressed compared to that of the standard mix.

Fig 4 displays the results of a series of tests obtained by adding various percentages of retarder (sugar) and accelerator (calcium chloride) to the standard paste. In this figure, P_r is defined as the time at which the peak in dielectric constant occurs in the paste with admixture added; P_n is the time at which the peak in dielectric constant occurs in the datum mix; and the ratio P_r/P_n is used to quantify the effect of the admixture on the setting of the paste. P_a is percentage, by weight, of admixture added.

Although in this instance, only the graph for sugar and calcium chloride is presented, similar graphs could be produced for other commonly used admixtures. These graphs can be used to assess the percentage of admixture that is required to be added to the standard mix to achieve a specified setting time. It is evident from this figure that small percentages of calcium chloride (less than 0.2%) retard setting, and is in agreement with other investigators (1,2).

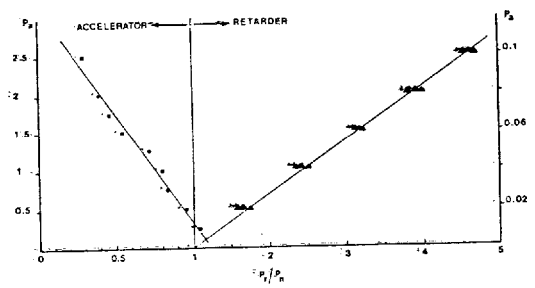

Fig 4 The relationship between setting time and the percentage of admixture added

When cements of differing chemical composition were tested, similarities in the response graphs to those of OPC were noted; Figs 5(a), 5(b) and 5(c) display the variation in measured parameters for HAC, RHPC and SRPC respectively.

Considering Fig 5(a), the absolute values of dielectric constant and resistivity are, respectively, lower and higher than those for OPC in Fig 1, and would indicate an overall reduction in ionic concentrations. Three peaks are observed on the dielectric constant curve; the first peak

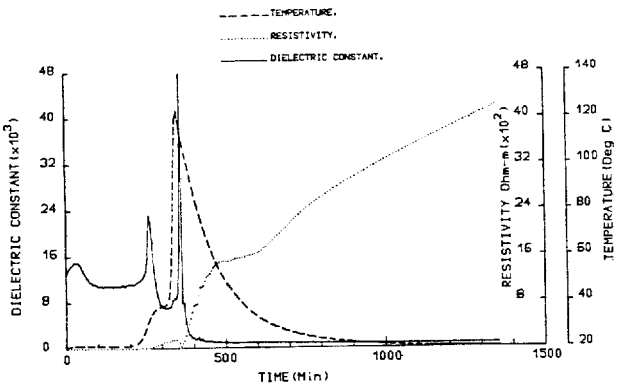

(a) HAC

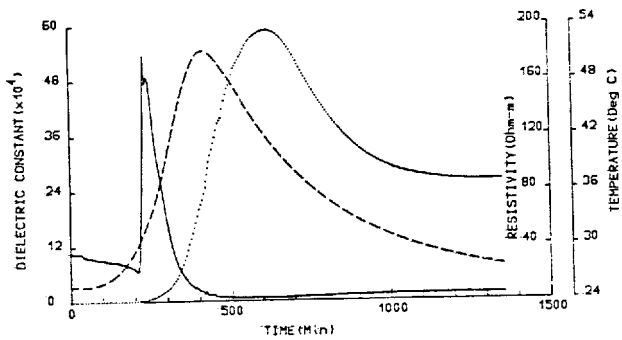

(b) RHPC

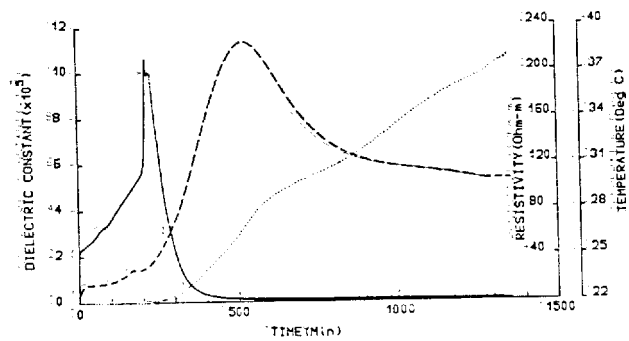

(c) SRPC

Fig 5 Influence of cement composition on measured parameters

is associated with the gradual leaching of ions from the grains and formation of a weak aluminous hydrate gel on the grain surface; following a dormant period peak 2 is the result of renewed activity on the CA phase forming CAH_{10} and C_2AH_8 and leads to an increase in rigidity of the mix. At temperatures > 25°C these hydrates undergo conversion to C_3AH_6. The authors attribute the third peak in dielectric constant (and drop in resistivity) to a combination of C_3AH_6 formation and the considerable rise in temperature.

Fig 5(b) displays the change in measured parameters for RHPC and, comparing this Figure with Fig 1, it is evident that the peak in dielectric constant occurs at approximately the same time (i.e. setting occurs at the same time). However, certain differences should be noted,

a) the absolute values for resistivity and dielectric constant are higher and lower respectively. Indeed, after the peak in dielectric constant at ≈200 minutes, the resistivity rises considerably indicating a rapid gain in strength as the cement grains segment and capillary pores become blocked.

b) the drop in resistivity and rise in dielectric constant after 500 minutes is more considerable than that for OPC, indicating an increase in activity on the C_3A phase.

Fig 5(c) displays the results for SRPC (lower C_3S and C_3A content, and higher C_2S content than OPC). The peak in dielectric constant at 200 minutes is still evident, however, the rate at which the resistivity increases (after this peak) is reduced, possibly due to the reduction in C_3S content of the cement. What is also noticeable is the absence of the peak in resistivity at 500 minutes, which the authors have attributed to the reduction in the C_3A content of this cement.

CONCLUSIONS

The following conclusions can be drawn from the present study:

a) The method developed offers a technique for monitoring hydration characteristics and physical changes taking place during the early hydration of cements of various chemical compositions.

b) The influence of admixtures on the hydrolysis and hydration processes can be quantified. As this method is measuring the chemical processes within the paste, the arbitrary terms "initial" and "final" set could have more meaning if redefined in terms of these electrical parameters.

c) A relationship has been established and graphs given to enable the required percentage of additive to be calculated for a given setting time. However, it is essential to carry out a datum mix test for the cement type being used to establish a P_n value before the graph could be used.

ACKNOWLEDGEMENTS

The authors wish to thank Professor A Bolton, Head of the Department of Civil Engineering, Heriot-Watt University for placing the facilities of his Department at their disposal. The receipt of a research grant from the Science and Engineering Research Council is gratefully acknowledged (GR/D/38200).

REFERENCES

1. LEA F M
"The chemistry of cement and concrete"
Edward Arnold Publishers Ltd, 1970

2. JAWED I, SKALNY J and YOUNG J F
"Structure and performance of cements"
(P Barnes & A Chose, Eds), Applied Science Publishers, London, 1983, pp 236-260

3. McCARTER W J and AFSHAR A B
"A study of the early hydration of Portland Cement"
Proc Instn of Civil Engrs, part 2, 1985, 79, Sept, pp 585-6-4

4. McCARTER W J and AFSHAR A B
"Further studies in the early hydration of Portland Cement paste"
Jnl of Material Science Letters 4 (1985), pp 405-408

5. AFSHAR A B and McCARTER W J
"Early hydration characteristics of Aluminous Cement"
Jnl of Material Science Letters 4(1985), pp 851-854

6. DOUBLE D D
"Technology in the 1990's. Developments in hydraulic cements"
Proc of a Royal Society Discussion Meeting, Feb 1983, pp 43-103

7. McCARTER W J and AFSHAR A B
"Some aspects of the electrical properties of coment paste"
Jnl of Material Science Letters 3(1984) pp 1083-1086

8. DOUBLE D D, HELLAWELL A and PERRY S
"The hydration of Portland Cement"
Proc Royal Soc, London, A359, 1978, pp 435-451

9. BIRCHALL J D, HOWARD A J and BAILLY J E
"On hydration of Portland Cement"
Proc Royal Soc, London, A 360, 1978, pp 445-453.

W J McCARTER and A B Afshar
Department of Civil Engineering
Heriot-Watt University, Edinburgh, Scotland, UK

MONITORING CHEMIO-PHYSICAL CHANGES AND MICROSTRUCTURE DEVELOPMENT IN OPC DURING EARLY HYDRATION

SUMMARY: Scanning electron microscopy techniques have been extensively used to examine micro-structure development of cement paste during hydration. Differences between early, middle and late products of hydration have been identified and these differences have been related to the stages of hydration using isothermal calorimetry. In this paper, the authors present an AC electrical response technique for monitoring chemical and structural building processes within cement paste, with particular attention being given to the initial 24 hours, as it is during this period that the paste changes from a fluid to rigid state. From SEM micrographs; heat evolution and strength development curves, undertaken in conjunction with electrical tests, it is shown that electrical response techniques could be used to identify regions of crystal growth and formation and throw light on the mechanisms of hydration.

SUMÁRIO: Técnicas de microscopia eletrônica de varredura foram usadas largamente para exame do desenvolvimento da micro-estrutura da pasta de cimento durante a hidratação. Foram identificadas diferenças entre produtos imediatos, mediatos e retardados de hidratação, e estas diferenças foram correlacionadas com as etapas de hidratação usando-se calorimetria isotérmica. Neste trabalho, os autores apresentam uma técnica de resposta elétrica AC para monitoração dos processos de construção química e estrutural dentro da pasta de cimento; foi dada atenção especial às 24 primeiras horas, uma vez que é durante este período que a pasta passa de um estudo fluído para rígido. A partir de micrografias SEM, curvas de evolução de calor e de desenvolvimento da resistência, realizadas conjuntamente com testes elétricos, demonstra-se que técnicas de resposta elétrica podem ser empregadas para identificar regiões de crescimento e formação de cristal e esclarecer os mecanismos de hidratação.

INTRODUCTION

The reaction between cement clinker and water is an exothermic reaction and calorimetric techniques have been widely used in monitoring the hydration characteristics of cement, particularly over the initial period of setting and hardening. Attempts have been made in relating the heat evolution/time curve with the stages of hydration and the early, middle and late products of hydration. Considering the initial 24-hours, the stages of hydration are shown on the calorimetric curve in Fig 1(1). Stage 1 is a period of rapid chemical activity; stage 2 is the induction period; stage 3 is the period of renewed chemical activity, and stage 4 is the beginning of the period of hardening.

According to investigators(1-4), peak A is the result of the initial hydration products forming around the grain surfaces - primarily CSH and CAH; peak B is due to secondary hydration of C_3S forming more crystalline hydrates, and precipitation of CH; the shoulder in the curve at C is associated with C_3A reaction and large-scale formation of ettringite and monosulpho-aluminate, and that occurring at D (≈30 hours) is the result of C_4AF hydration.

In contrast to calorimetric observation, the authors have monitored the changes in electrical response of OPC over the initial 24-hours of the hydration process(5-7). In this paper we focus on a detailed investigation of the electrical properties of cement paste and attempt to relate mechanisms of hydration and crystal growth and formation to variations in electrical response of cement paste.

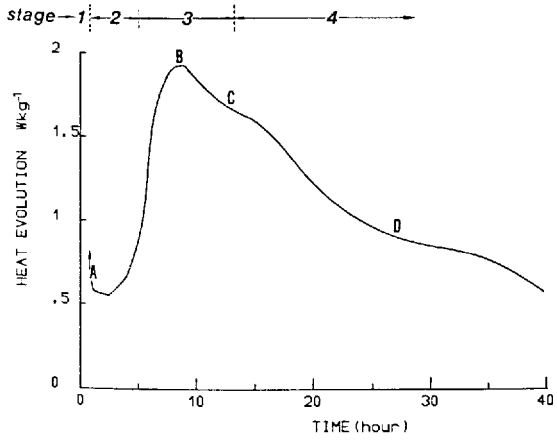

Fig 1: A conduction calorimetric curve for OPC

ELECTRICAL RESPONSE MEASUREMENT

Much work has been undertaken on measuring the change in conductivity (reciprocal of resistivity) of cement paste throughout the setting and hardening processes(8-10), and attempts have been made to relate changes in the physical state of the paste with changes in conductivity. Little attempt has been made to relate changes in conductivity with mechanisms of hydration; the rate at which reactions are progressing or changes in crystal morphology; furthermore, lack of standardisation of specimen size, electrode configuration and measuring techniques, together with a general lack of data points over the initial 24-hours make results vary within wide limits.

When an AC electrical field is applied to cement paste, some ions are free to drift through the material and discharge at the electrodes producing a conduction effect. Other charges, e.g. charges electrostatically held to grain surfaces, whilst not available for conduction are able to oscillate under the action of the electrical field. Oscillation of charges (without conduction) produces a polarization which can be measured in terms of a polarization current and is quantitatively expressed in the capacitance, and hence the dielectric constant of the medium.

The frequency of applied electrical field has a significant influence on dielectric constant with certain polarization mechanisms only operative over a particular frequency band. In cement paste, possible polarization mechanisms are double -layer [Fig 2 (a)] and interfacial [Fig 2(b)] effects, the latter mechanism being an accumulation or build-up of charges of crystal boundary or particle interfaces.

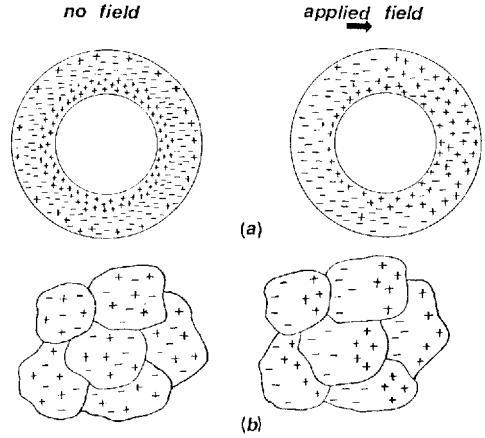

Fig 2: Polarisation mechanisms within cement paste (a) double layer, and (b) interfacial

EXPERIMENTAL

The experimental programme was developed on two fronts - the electrical response of the paste was monitored over the initial 24-hours after gauging and, in parallel, SEM observations on fracture surfaces were undertaken.

OPC (ASTM Type 1) was used in all tests and had a Bogue calculated composition of C_3S - 54.8%; C_2S - 13.7%; C_3A - 9.3% and C_4AF - 10.3%. A water/cement ratio (w/c) of 0.27 was used, this producing a paste of standard consistency (11). Samples were contained in a dielectric cell which had been calibrated to eliminate errors due to field fringing effects.

The in-phase (resistance) and quadrature

(capacitance) components of impedance were measured at 28 spot frequencies over the range 20Hz - 300kHz; in addition, the internal temperature changes within the specimens were monitored. The instruments were controlled and the data were logged and analysed using a micro-computer controlled data acquisition system, details of which can be found elsewhere(6,7). Experiments were run over a 24-hour period with a reading cycle being initiated every 300 seconds.

DISCUSSION OF RESULTS

Typical electrical response curves have been given in Fig 3. Superimposed on these graphs is the variation of internal temperature within the paste. Fig 4 shows the results of a series of strength tests carried out on cement paste cubes, and Fig 5 displays a sequence of micro-graphs taken over the 24-hour test period.

Figure 3(a)-(e)

This figure displays the electrical response curves for OPC at five spot frequencies taken over four decades of frequency (i.e. 20 Hz - 200kHz).

A general feature of the dielectric constant curve is the considerable variation over the 24-hour period, decreasing by almost two orders of magnitude at all frequencies. This, in broad terms, can be attributed to an irrotational binding of charges and crystallization of the various hydrates as the paste changes from a fluid to a solid state. It is also evident that as the frequency of the electrical field is increased from 20Hz to 200kHz the 'shape' of the dielectric constant curve changes quite markedly and values reduce; indeed, at any particular point in time the high frequency value of dielectric constant (200kHz) is almost three orders of magnitude lower than the low frequency (20Hz) value.

Considering this latter point, at low frequencies, several polarisation mechanisms contribute to the dielectric constant - primarily double layer and interfacial effects - as the frequency increases the contribution from double layer polarisation will diminish as charges find it difficult to follow the alternations of the electric field, and interfacial effects will tend to predominate.

Over the initial 50 minutes, the rate of change of dielectric constant is rapid and leads into a period of rate reduction (up to ≈170 minutes). Although obscured by scale, the resistivity over the initial 50 minutes reduces indicating electrolytic saturation of the bulk aqueous phase, thereafter, and up to ≈170 minutes, the resistivity remains relatively constant. The authors have ascribed the initial change in electical parameters (0 - 50 minutes) as the initial period of chemical activity (stage 1). At intermediate frequencies (200Hz - 2kHz) the gradual increase in dielectric constant up to 170 minutes would indicate an increase in charges adjacent to grain surfaces, possibly due to dissolution of the grain by imbibition of water through the gelatinous C-S-H coating formed on initial hydration.

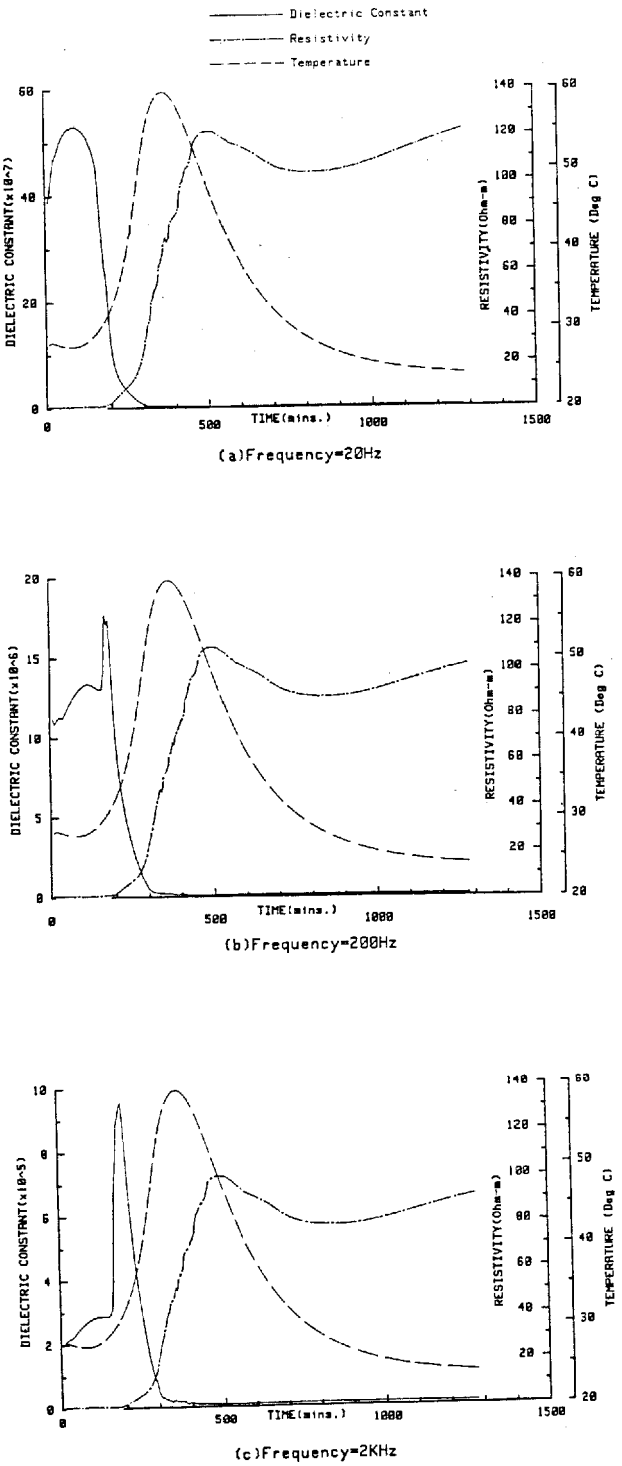

Fig 3: Variation of measured parameters during initial 24 hours after gauging for the frequency range 20Hz - 200kHz

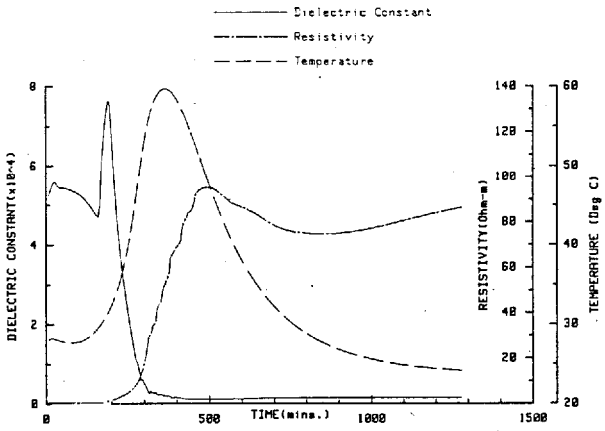

(d)Frequency=20KHz

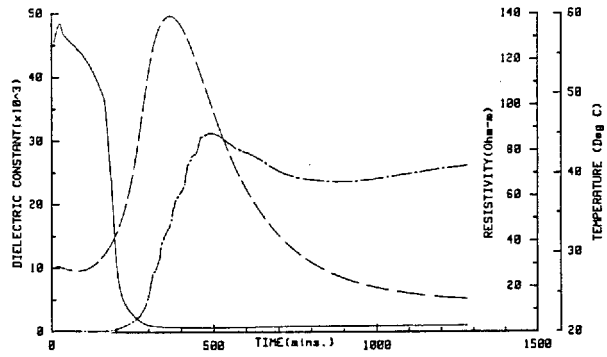

(e)Frequency=200KHz

Fig 3 (continued)

At ≈170 minutes there is an increase in dielectric constant and is more marked over the frequency range 200Hz - 20kHz. The authors have attributed the peak in dielectric constant at ≈200 minutes to renewed chemical activity on the C_3S phase which leads to a rapid gain in rigidity of the paste; the renewed activity being associated with the grain surface and not the bulk aqueous phase. If the renewed activity resulted in a release of charges in the continuous capillary pores then a reduction in resistivity should be detected and from the work presented this is not the case. The temporary increase in polarizability of the paste (hence dielectric constant) could be the result of charges being squeezed through the ruptured semi-permeable silicate hydrate coating. These charges (primarily hydrosilicate) quickly recombine with the Ca^{2+} ions to precipitate C-S-H. It is noticeable that after the peak there is a considerable drop in dielectric constant observed at all frequencies and the resistivity (and temperature) begins to increase signifying that the renewed chemical activity has resulted in segmentation of grains, a reduction in ionic concentrations due to crystallization, and blocking of capillary pores.

Over the period 200 - 500 minutes the resistivity rises sharply as the rigidity of the paste increases. The period 170 - 500 minutes could be visualised as stage 3 of the hydration process. After 500 minutes the resistivity of the paste reduces and, coinciding with this, there is a gradual rise in dielectric constant which is more noticeable at higher frequencies. This must signify further chemical activity within the paste, although reaction rates, as inferred from the rate of change of electrical parameters, are much reduced. This activity could be that associated with C_3A hydration (c.f. shoulder, C, on Fig 1) and formation of ettringite and monosulpho-aluminate.

The authors ascribe the period from 500 minutes onwards as stage 4 of the hydration process.

The effect of frequency on resistivity is not as marked as its effect on dielectric constant. In general, the resistivity decreases with increasing frequency, although it becomes more evident after 200 minutes (rise in resistivity) when the cement paste is gaining rigidity. By comparing the resistivity curve in Fig 1(a) with that in 1(e), the difference becomes quite apparent as hydration progresses. If ρdc is the resistivity at 20Hz and ρac is the resistivity at 200kHz then the frequency effect ratio (FER) $(\rho dc - \rho ac)/\rho dc$, increases as the cement grains segment. This ratio can be related to the blocking of conduction paths (i.e. capillary pores) through the paste - the greater the ratio the more numerous the blocked conduction paths. From work conducted to date, on cement pastes of varying consistency, as the water/cement ratio increases, not only do the absolute values of resistivity decrease but also the FER (at corresponding times) is also reduced. The FER could thus give a measure of the permeability and rigidity of the paste, with a small FER indicative of a more 'open' porous structure.

Figure 4

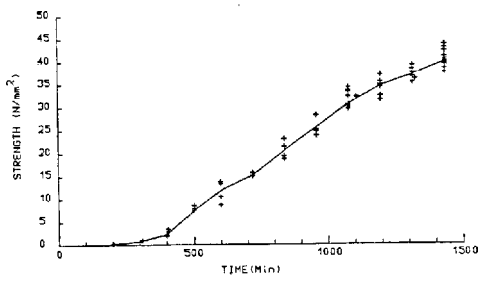

Fig 4: Strength development of paste over initial 24-hours

One of the first physical consequences of hydration is the transformation of the plastic paste into a rigid material, with the C_3S phase

being responsible for normal setting and strength development(12). It has been proposed that the renewed activity on the C_3S phase (stage 3), which leads to an increase in rigidity of the paste, can be identified by changes in electrical response. A series of strength tests were carried out on cement paste prisms (w/c = 0.27) to investigate the strength development of the paste over the initial 24-hours and the results have been given in Fig 4. By 200 minutes (peak in dielectric constant) the paste has gained sufficient strength to be demoulded and at 300 minutes the failure pattern of the prisms is that of a 'wedge' failure, similar to one observed in mature cement specimens. This would indicate that the paste is taking on the behaviour of the solid material. The strength increases rapidly from 300-1000 minutes, indeed, by the end of this period it has achieved approximately 30% of its 28-day strength (90 N/mm^2).

Figure 5(a)-(e)

A series of SEM micrographs was taken over the 24-hour period to investigate if changes in electrical response can be linked to changes in crystal growth and morphology. Fig 5(a) was taken at ≈200 minutes (peak in dielectric constant and of rise in resistivity). A reticulated crystal structure is evident (CSH(II)) with interaction and bridging between grains.

Fig 5(b) was taken at ≈300 minutes (rapid rise in resistivity and plateauing in dielectric constant). This micrograph displays stubby, needle-like acicular crystals associated with CSH(I). It is apparent that a change in morphology has occurred over the peak in dielectric constant, with the unstable primary product CSH(II) converting to CSH(I). The paste is rapidly gaining rigidity and Fig 5(c) shows the formation of CH crystals (taken at 500 minutes). Fig 5(d) is taken at 700 minutes and shows the presence of ettringnite and foils of monosulpho-aluminate. Fig 5(e) is taken at the end of the test period showing overall crystal structure in set cement paste - ettringite and CSH(I) is present. Evidence of a Hadley grain can also be seen in this micrograph (top centre left).

CONCLUSIONS AND CONCLUDING REMARKS

The following conclusions can be drawn from the present study:

a) the work presented offers a method for continuous monitoring of hydration processes in cement paste.

b) changes in electrical response can be related to physical and chemical changes within OPC paste and the rate of change of the measured electrical parameters are indicative of the rate at which hydration is progressing.

c) from the SEM work undertaken, tentative predictions as to hydrate morphology have been linked to electrical response.

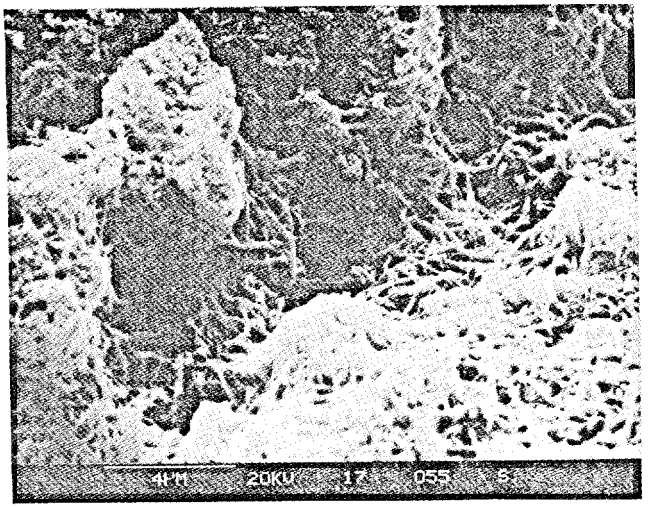

(a) 200 mins.

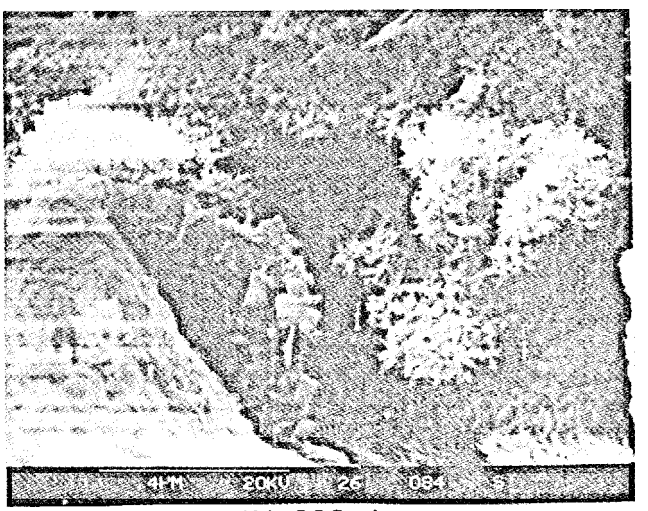

(b) 300 mins.



(c) 500 mins.

Fig 5: A series of micrographs taken over test period showing crystal growth

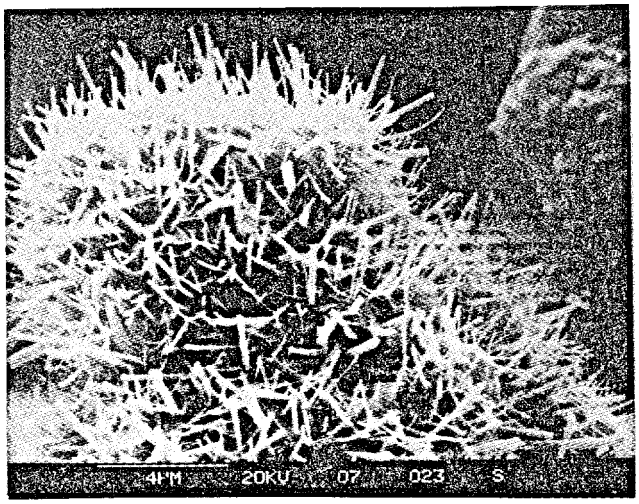

(d) 700 mins.



(e) 1200 mins.

Fig 5 (continued)

Further development of electrical response methods could offer an additional technique for monitoring the structure building processes and micro-structure development in cement paste. Electrical response curves could be used as a 'fingerprint' to ensure correct setting and hardening of the cement.

ACKNOWLEDGEMENTS

The authors wish to thank Professor A Bolton, Head of Department of Civil Engineering, Heriot-Watt University, for placing the facilities of his Department at their disposal. The receipt of a research grant (GR/D/38200) from the Science and Engineering Research Council is gratefully acknowledged.

REFERENCES

1. P L PRATT, A GHOSE
Phil Trans Royal Soc (London), A310, 1983, pp 93-103

2. D D DOUBLE, A HELLAWELL, S PERRY
Proc Royal Soc (London), A359, 1978, pp 435-451

3. I D BIRCHALL, A J HOWARD, J E BAILLY
Proc Royal Soc (London), A360, 1978, pp 445-453

4. B J DALGLEISH, P L PRATT, E TOULSON
Jnl Matl Sci, 17, 1982, pp 2199-2207

5. W J McCARTER, P N CURRAN
Mag of Conc Res, Vol 36, No 126, Mar 1984 pp 42-49

6. W J McCARTER, A B AFSHAR
Jnl Matl Sci Lett, 3, 1984, pp 1083-1086

7. W J McCARTER, A B AFSHAR
Proc Instn Civil Engrs, Pt 2, 1985, 79, Sept, pp 585-604

8. J CALLEJA
Jnl Amer Conc Inst, Vol 23, 1952, pp 525-536

9. R SRIRAVINDRARAJAH, R N SWAMY
Cement, Concrete and Aggregates (ASTM), Vol 4, 2 (Winter), 1983, pp 73-80

10. J WILSON, H W WHITTINGTON, M C FORDE
NDT International, Vol 18, Pt 2, 1985, pp 79-84

11. BRITISH STANDARDS INSTITUTION
BSI, London, 1978, BS4550, Pt 3, Section 3.5.

12. I JAWED, J SKALNY, J F YOUNG
in, Structure and performance of Cement and Concrete. Editor: P Barnes and A Ghose. Applied Science Publishers, London, 1983, pp 292.

J.Y. Moon, Director, Ssang Yong Cement Industrial Co., Ltd. Seoul,
K.S. Han, Professor, Inha University, Inchon,
S.H. Choi, Professor, Hanyang University, Seoul, Korea

1

Effect of Calcium Lignosulfonate on the Early Hydration Process of Portland Cement
Effet de lignosulfate de calcium dans le procédé a l'hydratation de ciment portland

2.1

RESUME: Les Caractéres d'hydratation de clinker, le mécanisme de retard à fixer et le contenu optimum de gypse dans le ciment sont été étudié en ajoutant lignosulfate de calcium (CLS) dans les plusieurs sortes de ciment.

Quant on a ajouté 0.5% de CLS dans C_3S l'hydrátation étais en petit peu retardé, mais la reaction à retarder étais retrouvé en melangant avec C_3A par resultat de l'adsorption de CLS sur C_3A. Par contre, la reaction d'hydratation étais extrement retardé en ajoutant C_4AF à C_3S.

En presence d'excés de CLS et gypse insuffisante, l'hydratation de C_3S-C_3A-C_4AF étais retardé par la reaction de C_3A et gypse pour produire ettringite fit l'adsorption de CLS abaisser.

En conséquence le contenu optimum de gypse pour arrêter ce phénoméne de retard étais 2.0% (basé sur SO_3) quand 0.25% de CLS étais ajouté et 2.5% de SO_3 quand 0.5% de CLS etais ajouté.

Os caracteres de hidratação do clinquer, o mecanismo de retardo a ser fixado e o teor ótimo de gesso no cimento foram estudados, com adição de lignosulfato de cálcio (CLS) nos diversos tipos de cimento.

Com a adição de 0,5% de CLS ao C_3S a hidratação foi bem pouco retardada, mas a reação de retardação foi retomada com a mistura com C_3A, como resultado da adsorção de CLS sobre o C_3A. Ao contrário, a reação de hidratação foi extremamente retardada com adição de C_4AF ao C_3S.

Em presença de excesso de CLS e insuficiência de gesso, a hidratação de C_3S-C_3A-C_4AF foi retardada pela reação do C_3A e gesso para produzir etringita, baixando a adsorção de CLS.

Em consequência, o teor ótimo de gesso para sustar o fenômeno de retardo foi de 2,0% (com base no SO_3) quando a adição de CLS era de 0,25% e 2,5% de SO_3 quando a adição de CLS era de 0,5%.

J.Y. Moon, Director, Ssang Yong Cement Industrial Co., Ltd. Seoul,
K.S. Han, Professor, Inha University, Inchon,
S.H. Choi, Professor, Hanyang University, Seoul, Korea

INTRODUCTION

A lignosulfonate salt is a commercial admixture for concrete which is used primarily as water-reducing agent. But even small amount of lignosulfonate salt can change considerably the physical-mechanical properties of concrete(1) and make hardening of concrete abnormally(2) sometimes.

To improve these undesirable phenomena, there have been attempted many investigations to study the behaviour of the admixture in cement (3-10), but their hydration mechanisms have not been proposed satisfactorily with the observed effects.

In present investigation, the early hydration characteristics for each clinker minerals such as tricalcium silicate (C_3S), tricalcium aluminate(C_3A), tetracalcium aluminoferrite (C_4AF) and the mixture of these minerals, the effect of gypsum added to the clinker minerals, and the set-retarding phenomena are studied when calcium lignosulfonate (CLS) is added.

EXPERIMENTAL

The clinker minerals used in the experiments synthesized not to detect other phases by X-ray diffraction analysis. CLS in the form of powder was supplied by Carl Roth GmbH Co.

Each samples were prepared by blending of the clinker minerals and gypsum with mixing ratio given in Table 1.

CLS was dissolved in CO_2-free distilled water and the concentration of the solutions were 0, 0.25, and 0.5% CLS by weight. A series of pastes was prepared with these solutions (water/solid=0.5) at 20°C and hydration was carried out in a curing cabinet at 20±1°C. At selected intervals (3hrs, 1day, 3days), the hydration was stopped by the addition of acetone and dried in vacuum.

The hydrates were analysed by XRD, DT-TGA, and microstructure of hydrates were observed by SEM. The multicell conduction calorimeter was used to study the heat evolution of hydration for the sample with water to solid ratio of 0.5 at 20°C.

Table 1. Mixing ratio of Samples with clinker minerals.

(wt, %)

Sample No.	C_3S	C_3A	C_4AF	Gypsum (SO_3 %)
A-0	100	-	-	-
B-0	-	100	-	-
B-20	-	100	-	20
C-0	-	-	100	-
C-20	-	-	100	20
D-0	90	10	-	-
D-2	90	10	-	2
E-0	90	-	10	-
E-2	90	-	10	2
F-0	80	10	10	-
F-1	80	10	10	1
F-2	80	10	10	2
G-0	80	7	13	-
G-1	80	7	13	1
G-2	80	7	13	2
H-0	80	3	17	-
H-1	80	3	17	1
H-2	80	3	17	2

To analyse the liquid phase composition of the each hydrating samples, the paste with a water to solid ratio of 10 and CLS solutions of 0, 0.25 and 0.5% concentration were respectively prepared.
After different periods of hydration at 20±1°C, the liquid phase was removed from the solids by centrifugation and analysed for Fe^{3+}, SO_4^{2-} and lignosulfonate. The concentration of lignosulfonate was determined by absorbance measurements at a wavelength of 280 nm on a UV-Visible spectrometer.

RESULTS

Hydration of clinker minerals

The cumulative heat liberation profiles (Fig. 1) and XRD data (Table 2) of each samples in the presence of CLS showed the different types of hydration process. In the hydration of A-0 (C_3S only), the rate of heat evolution and the amount of $Ca(OH)_2$ produced were affected slightly by adding 0.25% of CLS, but 0.5% of CLS reacted considerably.
The hydration of B-0 (C_3A only) and C-0 (C_4AF Only) without CLS in this period produced mainly C_3AH_6 hydrate of cubic phase. As the hydration progresses, the amounts of the cubic phase were increased continuously by the conversion.

J.Y. Moon, Director, Ssang Yong Cement Industrial Co., Ltd. Seoul,
K.S. Han, Professor, Inha University, Inchon,
S.H. Choi, Professor, Hanyang University, Seoul, Korea

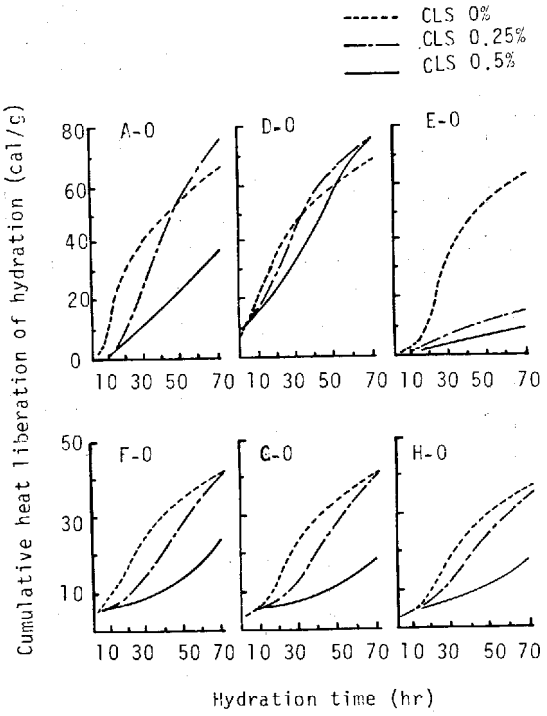

Fig. 1 The curves of cumulative heat liberation for various samples with CLS.

of the hexagonal phase of $C_4A(F)H_{13}$ formed. By adding CLS, the hydration of B-0 and C-0 produced mainly $C_2AH_8(C_2AFH_8)$ and $C_4AH_{13}(C_4AFH_{13})$ hydrates of hexagonal phase. It is suggested that CLS impeded the conversion of hexagonal to cubic phase.

In the hydration of D-0(C_3S-C_3A system), the rate of heat liberation and the amount of $Ca(OH)_2$ produced by adding of CLS were nearly the same with no addition of CLS, but that of E-0 (C_3S-C_4AF system) with 0.25% of CLS retarded extremely the C_3S hydration reaction. It is also observed by SEM(Fig.2). There were many hydrates on C_3S particles in D-0 with 0.5% of CLS, but only a few hydrates in E-0 with 0.25% of CLS. The hydration of F-0, G-0, H-0 (C_3S-C_3A-C_4AF system) with 0.5% of CLS were impeded, and the hydration of F-0 with more C_3A content was a little superior than that of G-0 and H-0 with less C_3A content.

Table 2. The result of XRD analysis for hydrates of various samples with CLS.

Sample No.	Added CLS (%)	Hydration period	C_2AFH_8	C_4AFH_{13}	$C_3A(F)H_6$	Portlandite
A-0	0	3 hrs 1 day 3 days				+ +++++ ++++++++++
	0.25	3 hrs 1 day 3 days				++++ +++++++++
	0.5	3 hrs 1 day 3 days				+ ++
B-0	0	3 hrs 1 day 3 days		+ + +	++++ +++++ ++++++++	
	0.25	3 hrs 1 day 3 days	+ ++ ++	++ +++ +++	++ ++ ++	
	0.5	3 hrs 1 day 3 days	+ ++ ++	++ +++ +++		
C-0	0	3 hrs 1 day 3 days		+ +	++ +++ +++++	
	0.25	3 hrs 1 day 3 days	+ + +	+ ++ ++	+ +	
	0.5	3 hrs 1 day 3 days	+ + ++	+ + ++		
D-0	0	3 hrs 1 day 3 days			+ + +	++ ++++++ ++++++++++
	0.25	3 hrs 1 day 3 days		+ +		++ ++++++ ++++++++++
	0.5	3 hrs 1 day 3 days		+		++ ++++++ +++++++++
E-0	0	3 hrs 1 day 3 days			+ +	+ ++++ +++++
	0.25	3 hrs 1 day 3 days		+		+ ++ ++++
	0.5	3 hrs 1 day 3 days				+ +++
F-0	0	3 hrs 1 day 3 days		+ + +		+ ++++++ +++++++++
	0.25	3 hrs 1 day 3 days		+ + +		+ ++ +++++++++
	0.5	3 hrs 1 day 3 days		+ + +		+ + ++++
G-0	0	3 hrs 1 day 3 days		+ + +		+ ++++++ ++++++++++
	0.25	3 hrs 1 day 3 days		+ + +		+ ++ ++++++++
	0.5	3 hrs 1 day 3 days		+ +		+ + +++
H-0	0	3 hrs 1 day 3 days		+		+ +++++ ++++++++++
	0.25	3 hrs 1 day 3 days		+		++ +++++++
	0.5	3 hrs 1 day 3 days		+ +		+ +++

Remarks: + very little, ++ little, +++ - ++++ medium
+++++ much, ++++++ - ++++++++++ very much

J.Y. Moon, Director, Ssang Yong Cement Industrial Co., Ltd. Seoul,
K.S. Han, Professor, Inha University, Inchon,
S. H. Choi, Professor, Hanyang University, Seoul, Korea

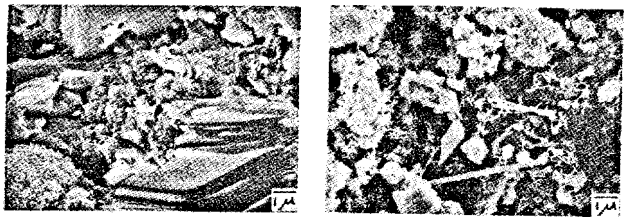

D-2, with CLS 0.5% E-2, with CLS 0.25%

Fig. 2 SEM micrographs for hydrates of sample D-0 and E-0 with CLS for 3 days.

Hydration of clinker minerals with gypsum

Fig. 3 and Table 3. showed the curves of cumulative heat liberation and XRD analysis of hydrates for hydration of clinker minerals with gypsum.

The hydration of B-20 produced ettringite considerably in early stage and then ettringite was converted to monosulfate. By adding CLS, conversion reaction of ettringite to monosulfate delayed.
These situation was the same for C-20 hydration.
But the reaction between C_4AF and gypsum was slower than the reaction between C_3A and gypsum.

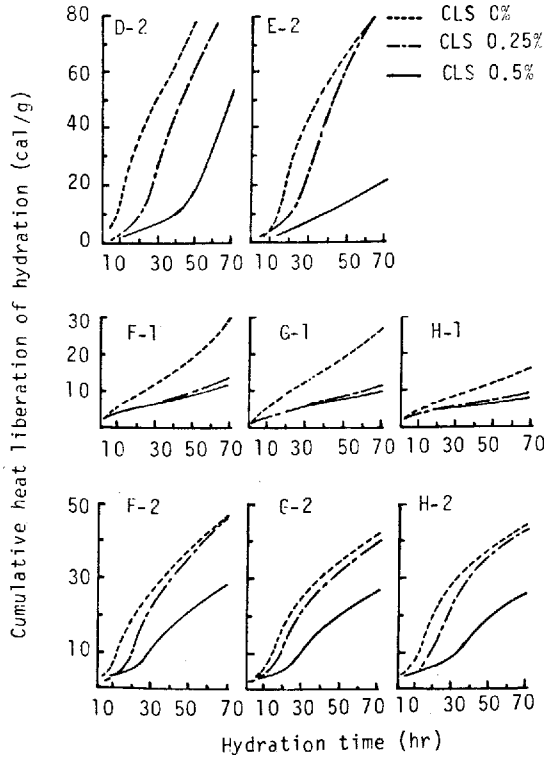

Fig. 3 The curves of cumulative heat liberation for various samples with CLS.

Table 3. The result of XRD analysis for hydrates of various samples with CLS and gypsum.

Sample No.	Added CLS (%)	Hydration period	C_4AH_{13}	Ettringite	Monosulfate	Portlandite
B-20	0	3 hrs 1 day 3 days		++++ +++ ++	+ ++++ ++++++	
	0.25	3 hrs 1 day 3 days		+++++ ++++ +++	+ +++ +++++	
	0.5	3 hrs 1 day 3 days		++++++ +++++ ++++	+ +++	
C-20	0	3 hrs 1 day 3 days		+ ++ +++	 ++++	
	0.25	3 hrs 1 day 3 days		+ +++ +++++	 +	
	0.5	3 hrs 1 day 3 days		 +++ +++++	 +	
D-2	0	3 hrs 1 day 3 days		++ ++	 +++	+++++ +++++++++
	0.25	3 hrs 1 day 3 days		+ ++ +	 +	++ +++++++
	0.5	3 hrs 1 day 3 days		+ ++ ++	 	 ++++
E-2	0	3 hrs 1 day 3 days		+ ++	 +	+++++ ++++++++
	0.25	3 hrs 1 day 3 days		+ ++ ++	 	 ++ ++++++
	0.5	3 hrs 1 day 3 days		+ ++ ++	 	 ++++
F-1	0	3 hrs 1 day 3 days	 ++ ++	+	 ++ ++	+ ++ ++++++
	0.25	3 hrs 1 day 3 days	+ ++ ++	+ +	 + ++	 + ++
	0.5	3 hrs 1 day 3 days	+ ++ ++	+ + +	 + +	 + +
H-1	0	3 hrs 1 day 3 days	 + +	+ + +	 + +	 ++ ++++++
	0.25	3 hrs 1 day 3 days	 ++ ++	+ ++ ++	 	 + +
	0.5	3 hrs 1 day 3 days	 ++ ++	+ ++ ++	 	 + +
F-2	0	3 hrs 1 day 3 days		+ + +	 + +	+ ++++ +++++++++
	0.25	3 hrs 1 day 3 days		+ ++ ++	 + 	 +++ +++++++++
	0.5	3 hrs 1 day 3 days	 +	++ ++ +	 +	 + +++
H-2	0	3 hrs 1 day 3 days		+ + +	 	 +++++ +++++++++
	0.25	3 hrs 1 day 3 days		++ ++ ++	 	 +++ +++++++++
	0.5	3 hrs 1 day 3 days	 +	+++ ++ ++	 +	 +

Remarks: + very little, ++ little, +++ - ++++ medium
+++++ much, ++++++ - ++++++++++ very much

J.Y. Moon, Director, Ssang Yong Cement Industrial Co., Ltd. Seoul,
K.S. Han, Professor, Inha University, Inchon,
S.H. Choi, Professor, Hanyang University, Seoul, Korea

The hydration of D-2 were retarded a little more than that of D-0. On the other hand, the hydration of E-2 with CLS was recovered rather than that of E-0. These facts are also observed by SEM (Fig. 4).
The effect of gypsum addition to C_3S-C_3A and C_3S-C_4AF system showed reversely each other.

The hyuration of C_3S-C_3A-C_4AF system (F-, G-, H-series) with CLS were proceeded according to gypsum content, When 0.25% of CLS is added, the hydration of F-1, G-1 and H-1 were greatly retarded. But the hydration of F-2, G-2, H-2 were normally progressed. From these results, we coula see the facts that there would be a certain optimum gypsum content to prevent such retarding phenomena.
Fig. 5 showed the curves of $Ca(OH)_2$ content calculated by DT-TGA with various samples hydrated. When SO_3 content were 0 and 0.5%, $Ca(OH)_2$ content were nearly the same. But when SO_3 content was from 1 to 2, the $Ca(OH)_2$ content was quite low. When SO_3 content was 2.5 and 3.0%, the $Ca(OH)_2$ content was almost the same in the case without gypsum.

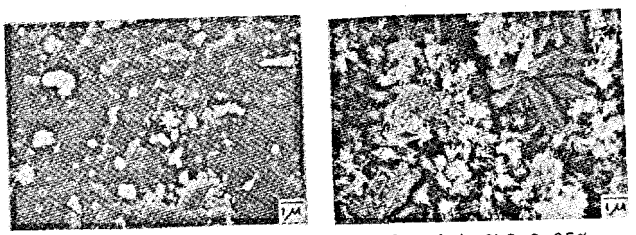

D-2, with CLS 0.5% E-2, with CLS 0.25%

Fig. 4 SEM micrographs of hydrates of various samples with CLS for 3 days.

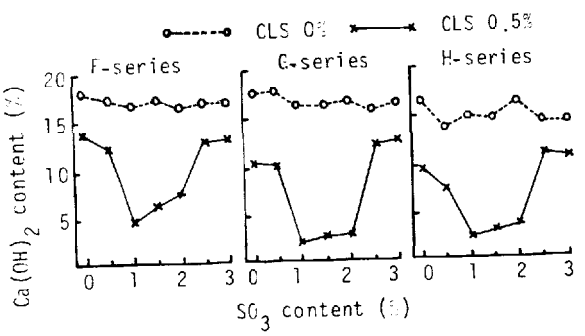

Fig. 5 Amount of $Ca(OH)_2$ produced on the hydration of various samples with CLS 0.5% for 3 days.

Accordingly, when 0.5% of CLS added to portland cement, 2.5% or more SO_3 content had to be added.

Liquid phase composition

Fig. 6 showed the CLS concentration in liquid removed from the solution of various samples with CLS.

The CLS concentration in the solution of A-0 was higher than those of B-0 and C-0. The CLS concentration in the solution of B-20 including gypsum was lower than that of C-20.

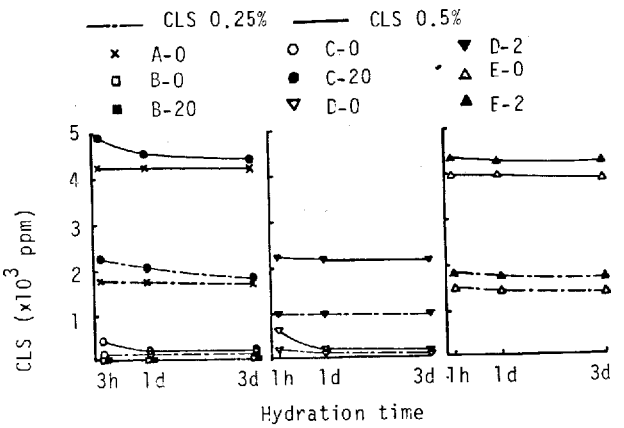

Fig. 6 Concentration of CLS in liquid phase removed from the solution of hydrated samples with CLS 0.25%, 0.5% for various time.

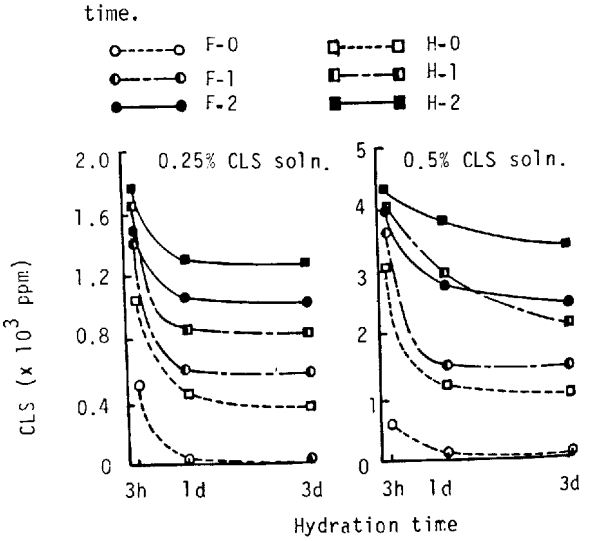

Fig. 7 Concentration of CLS in liquid phase removed from hydrated samples with CLS 0.25%, 0.5% solution for various time.

J.Y. Moon, Director, Ssang Yong Cement Industrial Co., Ltd. Seoul,
K.S. Han, Professor, Inha University, Inchon,
S.H. Choi, Professor, Hanyang University, Seoul, Korea

Also the CLS concentration in the solution of D-0 and D-2 were lower than those of E-0 and E-2. In general, the CLS concentrations in the solution of samples with more C_3A and less gypsum were lower than others (Fig. 7). Accordingly, the adsorbability of CLS was in the order of $C_3A > C_4AF >> C_3S$.

When CLS was added, the SO_4^{2-} concentration in the solution of various samples is lower than that when CLS was not added. On the contrary, the Fe^{3+} concentration in the solution of C-0 with CLS was higher than that of C-0 only but the Fe^{3+} concentration in the solution of C-20 was lower than that of C-0 (Fig. 8,9)

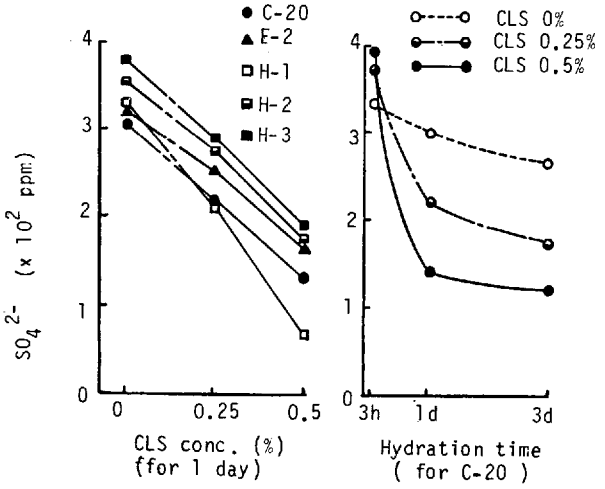

Fig. 8 Concentration of SO_4^{2-} in liquid phase removed from hydrated samples with CLS.

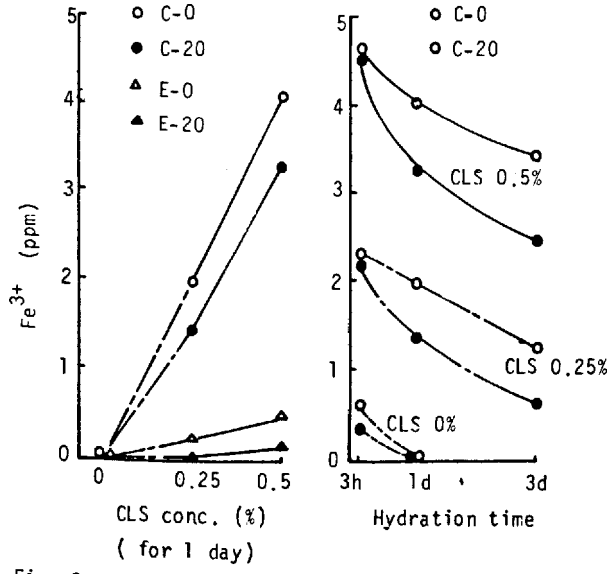

Fig. 9 Concentration of Fe^{3+} in liquid phase removed from hydrated samples with CLS

DISCUSSION AND CONCLUSIONS

The retardation of C_3S hydration when CLS is added seems to be related to the amount of C_3A, C_4AF and gypsum. By adding 0.5% of CLS to C_3S, the hydration of C_3S is slightly retarded, but the retarding reaction is recovered by mixing of C_3A as a result of CLS adsorption. On the contrary, the hydration reaction is extremely retarded through addition of C_4AF to C_3S.

In the hydration of C_3S-C_3A-C_4AF system with 0.25% of CLS, the retardation did not occur but the hydration reaction is interrupted by adding 0.5% of CLS in the system.

Under the presence of CLS and gypsum, the hydration of C_3S-C_3A system is retarded, since the reaction of C_3A and gypsum to form ettringite lower the adsorption of CLS. Noticeable decrease of the CLS concentration in the liquid phase of C_3S-C_3A system, in the first hour after mixing, means the adsorption of CLS and the hydration of C_3S is not retarded. On the contrary, though the CLS concentration in the liquid phase of C_3S-C_4AF system with 0.25% of CLS is lower than that of C_3S-C_4AF-gypsum system, the former hydration is rather retarded. It is supposed that the hydration of C_3S is not affected with only the adsorption of CLS by hydrate.

In the hydration of samples, when the amount of CLS is increased, SO_4^{2-} concentration is decreased and Fe^{3+} concentration is increased gradually (Fig.8,9). When the gypsum is added to the samples, Fe^{3+} concentration is lower than that of samples without gypsum (Fig. 9).

Consequently, it is suggested that the retardation in the hydration of clinker minerals is related largely to the amount of C_4AF and gypsum. And also, it is believed that the hydration phenomena of C_3S in C_3S-C_3A-C_4AF system is varied considerably in accordance with the content of gypsum and CLS.

The optimum content of gypsum is considered as follows; when 0.25% of CLS is added to portland cement, the amount of SO_3 needed is 2.0% while addition of 0.5% of CLS requires 2.5% of SO_3.

REFERENCES

1. V.S. Ramachandran, "Interaction of Calcium Lignosulfonate with Tricalcium Silicate, Hydrated Tricalcium Silicate, and Calcium Hydroxide", Cem. Concr. Res., Vol. 2(2), pp. 179-194(1972)

2. L.H. Tuthill, R.F. Adams, "A Case of Abnormally Slow Hardening Concrete for Tunnel Lining." J. Am. Concr. Inst., Vol. 32(3), pp. 1091-1109 (1961)

3. W.C. Hansen, "Symposium of Effect of Water-Reducing Admixtures and Set-Retarding Admixtures on Properties of Concrete," Am. Soc. Test. Mater., STP No. 265, pp. 3 (1959)

4. J.H. Taplin, "Some Chemical Additions and Admixtures in Cement Paste and Concrete," Proc. 4th, Inter, Symp. Chem. Cem., Washington, Vol. II, pp. 909-925 (1960)

5. K.E. Doughtery, M.F. Kowalewski, "Effect of Organic Compounds on the Hydration Reactions of C_3A, "Proc. 5th Inter. Symp. Chem., Tokyo, Vol. IV. pp. 42-52 (1968)

6. J.F. Young, "Reaction Mechanism of Organic Admixtures with Hydrating Cement Compounds." Transp. Res. Record, No. 564, pp. 1-9 (1976)

7. I. Jawed, W.A. Klemm, J. Skalny, "Hydration of Cement-Lignosulfonate-Alkali Carbonate System," J. Am. Ceram. Soc., Vol. 62(9-10), pp. 461-464 (1979)

8. I. Odler, U. Duckstein, Th. Becker, "On the Combined Effect of Water Solubles Lignosulfonates and Carbonates on Portland Cement and Clinker Pastes" Cem. Concr. Res. Vol. 8(4), pp. 469-480 (1978)
I. Odler, R. Schoenfeld. H. Doerr, Cem. Concr. Res. Vol. 8(5), pp. 525-538 (1978)

9. V.S. Ramachandran, "Elucidation of the Role of Calcium Lignosulfonate in the Hydration of C_3A." Proc. 7th Inter. Cong. Chem. Cem. Paris, Vol. IV. pp. 535-540 (1980)

10. M. Collepardi, S. Monosi, G. Moriconi, "Combined Effect of Lignosulfonate and Carbonate on Pure Portland Clinker Compound Hydration." Cem. Concr. Res. Vol. 10(4), pp. 445-462 (1980)
M. Pauri, G. Baldini, M. Colleparidi, Cem. Concr. Res. Vol. 12(2), pp. 271-277 (1982)

J.R. BARAGAÑO. Dr. Chem. Sc. ASLAND SA - VILLALUENGA DE LA SAGRA (TOLEDO) SPAIN
G. CAMPOS. Chemist. ASLAND SA. NIEBLA (HUELVA) SPAIN

EXTENSION OF SETTING TIME BY MEANS OF MINERALIZED CLINKERS

SUMMARY

The obtaining of clinkers that produce cements with different setting times, using natural gypsum as regulator, may be achieved by adding certain minor elements (P and F) as components of raw meals.

Other elements such as Cu-Zn have not produced the expected results.

However, in the case of P, the amount of natural fluorapatite may be found high (5%) if an initial setting of 3 hours is required, while the same results may be obtained with only 0,8% of natural fluorite.

In this case, the setting time is related to the percentage used. It has been observed that there is a minimum below which its effect is not felt. Above that figure, there is a clear relation between the percentage of F^- and the different crystallization of C_3A (cubic or tetragonal) and the possible formation of a new $C_{11}A_7CaF_2$ aluminate.

It was also verified that the F^- acts as a fluxing agent and mineralizer, with which it was possible to calcinate high SK raw meals, which not only offset any possible decreases of strength in the early days, but on the contrary increased strenght, in particular after three days had elapsed, having reached 600 kp/cm^2 in 28 days in ISO/RILEM prismatic specimens, a strength difficult to obtain without increasing the thermal load of the kiln and shortening the life of refractories.

In all case, industrial tests of 1000 mT/day each were conducted in two Lepol kilns, where a minimum of 10.000 mT with Cu-Zn was obtained, reaching a maximum of 200.000 mT with F^- after five months' operation.

SUMÁRIO

Pela adição de certos elementos menores (P e F) como componentes da farinha, pode-se conseguir a obtenção de clínqueres que produzem cimentos com diferentes tempos de pega, empregando-se gesso natural como regulador.

Outros elementos como Cu - Zn não produziram os resultados esperados.

Todavia, no caso de P, a quantidade de fluor-apatita natural (5%) pode ser considerada alta se for exigida uma pega inicial de 3 horas, enquanto se pode obter os mesmos resultados com apenas 0,8% de fluorina natural.

Neste caso, o tempo de pega está relacionado com a porcentagem usada. Observou-se que há um mínimo abaixo do qual seu efeito não é sentido. Acima deste valor, existe uma relação clara entre a porcentagem de F^- e a cristalização diferente do C_3A (cúbica ou tetragonal) e a possível formação de um novo aluminato $C_{11}A_7CaF_2$.

Verificou-se também que F^- atua como um agente fundente e mineralizador, com o qual foi possível calcinar farinhas com SK alto o que não apenas contrabalançou qualquer possível queda de resistência nos primeiros dias mas, ao contrário, aumentou a resistência, particularmente depois de 3 dias, tendo atingido 600 kp/cm^2 aos 28 dias com corpos de prova prismáticos ISO/RILEM, resistência difícil de ser obtida sem aumento da carga térmica do forno e diminuição da vida dos refratérios.

Em todo caso, foram realizados testes em escala industrial de 1.000 tm/dia cada em dois fornos Lepol, em que foram obtidas 10.000 tm com Cu - Zn, atingindo-se um máximo de 200.000 tm com F^- após 5 meses de operação.

J.R. BARAGAÑO. Dr. Chem. Sc. ASLAND SA - VILLALUENGA DE LA SAGRA (TOLEDO) SPAIN
G. CAMPOS. Chemist. ASLAND SA - NIEBLA (HUELVA) SPAIN

2.1

EXTENSION OF SETTING TIME BY MEANS OF MINERALIZED CLINKERS

1. INTRODUCTION

A clinker low in alkalis, of moderate C_3A content, is normally obtained in one of our plants which, when ground at 350 m^2/kg Blaine with an amount of high purity natural gypsum, has a Vicat setting considered normal (Initial Setting 1h58', Final Setting 2h35') as compared with other clinkers of the Company and similar to the majority of Spanish cements.

Because of its qualities, it was selected for export but due to the climatic conditions of the country, the client required the cement to have a setting time considerably longer than normal; this had to be achieved with the least amount of retarder possible, since the client had to import gypsum at high cost.

Another limitation of a chemical nature was to maintain the C_3A between 6 and 9.

Various tests were therefore urgently undertaken, both in the Laboratory and on an industrial scale, to verify the actions produced on the raw meals by small percentages of different components containing elements such as Cu, Zn, P and F, which were selected for this purpose after a detailed study of the wide, though contradictory, bibliography on the subject.

The purpose of this paper is to describe the results obtained both in the Laboratory and on an industrial scale in two Lepol kilns with a production capacity of 1000 mT/day, where 10.000 mT of clinker was obtained with Cu and Zn, 20.000 mT with P and over 200.000 mT with F.

II. STANDARD CLINKER

The standard characteristics of the clinker were as follows: SK-93; SM-2,4; AM-1,7; Free CaO-1,8; Na_2O-equivalent 0,48; C_3S-52; C_2S-24; C_3A-9; C_4AF-11; Vicat setting (Initial, 1h58"; Final 2h35"); S.S. Blaine 350 m^2/kg; mechanical strengths according to ISO-RILEM (kp/cm^2): 1 day 36/146 - 3 days 57/293 - 7 days 71/394 - 28 days 87/534.

III. CLINKER WITH COPPER AND ZINC (Cu-Zn)

III.1. Industrial test

A vitreous slag from copper metallurgy was used for this purpose, composed principally of fayalite (Fe_2SiO_4) in which the CuO content was 1,5% and the ZnO content 4,0%.

In addition, an effort was made to reduce the C_3A to values approaching 6%, since the ASTM-V type clinkers usually had slightly longer setting times.

However, on average only an extension of some 10 minutes was obtained. The results obtained were: SK-96 SM-2,3; AM - 1,3; Free CaO-2,1; Na_2O equivalent 0,56; CuO-0,06; ZnO-0,18; C_3S-55; C_2S-20; C_3A-7; C_4AF-12; Vicat setting (Initial 2h05"; Final 2h45"); S.S. Blaine 350 m^2/kg; mechanical strengths (ISO-RILEM) (kp/cm^2): 1 day 33/148 - 3 days 66/333 - 7 days 70/411 - 28 days 86/536.

The operation of the kiln was a little more irregular than with normal raw meal, production remaining constant.

IV. CLINKER WITH PHOSPHORUS (P)

IV.1. Laboratory tests

Firstly an industrial raw meal and chemically pure $Ca_3(PO_4)_2$ in percentages of 0,25; 0,50 and 1,0%, expressed as P_2O_5, was used and after calcination in an electric furnace at 1420ºC for 45' and rapid air cooling, the clinker was milled with natural gypsum at 350 m^2/kg, maintaining the SO_3 constant at 2,5%.

Setting increased in proportion to the $\%P_2O_5$ added, reaching a maximum of 22' at the Initial and 27' at the Final settings. This encouraged us to continue the tests, but using natural phosphorite.

IV.1.1. Natural phosphorite and raw meal (SK-99 and SM-2,2

The phosphorite consisted of: SiO_2-4,9; Al_2O_3-0,64; Fe_2O_3-0,34; CaO-49,8; MgO-0,51; SO_3-1,6; K_2O-0,11; Na_2O-0,67; P_2O_5-28,8; Cl^--0,03; F^--2,5; LOI-9,8.

By X-ray diffraction (Philips PW 1700/00 with copper anticathode) it was verified that it consisted mainly of fluor-apatite $3Ca_3(PO_4)_2CaF_2$.

The raw meal (9,6% over 90μ and 18,6% over 64μ; SK-99 and SM-2,2) was calcinated, under the same conditions as before, with four additions of P_2O_5. Setting times increased on the basis of the P_2O_5 content.

	Raw Meal I (R.M-I)	R.M-I 0,4%P_2O_5	R.M-I 0,6%P_2O_5	R.M-I 0,8%P_2O_5	R.M-I 1%P_2O_5
SK	99	99	99	100	100
Free CaO	2,9	2,8	2,7	2,5	2,2
Initial set	1h30'	1h40"	2h05"	2h10"	2h15"
Final set	1h48"	1h56"	2h20"	2h25"	2h50"

With a NETZSCH (STA 429) apparatus capable of performing the DTA and the GTA simultaneously, it was observed that the area of the fusion peak (1310ºC) increases with the addition of P_2O_5, no significant variation being observed by X-ray diffraction in the C_3S, C_2S and C_3A content, the latter being in cubic form.

IV.1.2. Natural phosphorite and raw meal (SK-101 and SM-2,3)

The test was repeated using a raw meal more difficult to combine (13% over 90μ, 21,6% over 64μ, SK-101 and SM-2,3) and also increasing the range of the phosphorite added.

	Raw Meal-II (R.M-II)	R.M-II 0,4%P_2O_5	R.M-II 1%P_2O_5	R.M-II 1,5%P_2O_5	R.M-II 2%P_2O_5
SK	101	101	102	103	104
Free CaO	3,6	3,0	3,2	3,7	4,0
Initial set	1h47"	2h33"	2h45"	2h45"	3h30"
Final set	2h10"	2h45"	3h15"	3h20"	3h55"

Free lime decreases with additions of up to 1% of P_2O_5 but increases above that percentage in accordance with the greater SK obtained by the addition of phosphorite.

Setting times become longer with percentages from 0,4% of P_2O_5 and increase accordingly on that basis.

J.R. BARAGAÑO. Dr. Chem. Sc.ASLAND SA - VILLALUENGA DE LA SAGRA (TOLEDO) SPAIN
G. CAMPOS. Chemist. ASLAND SA. NIEBLA (HUELVA) SPAIN

When raw meal with 1% P_2O_5 is calcinated at higher temperatures, the free lime content decreases, setting times being maintained without any remarkable variation.

Mechanical strengths with 0,4% of P_2O_5 increase after 3 days and are 70 kp/cm^2 greater at 28 days, while with 1% P_2O_5 strengths are lower up to 7 days, although at 28 days they exceed those of the initial clinker, by 50 kp/cm^2.

After these results were obtained, it was considered desirable to make an industrial test, establishing the appropriate value at between 0,4 and 1% of P_2O_5.

IV.2. Industrial tests

The dosage of the phosphorite, of a size similar to that of sand (<4 mm) and moisture of 1% was made at the mill inlet in percentages of 1,1; 1,6 and 2,2%, or in other words, the raw meals contained P_2O_5 between 0,53 and 0,90%.

Setting performance was variable; even lower values than usual with low additions of phosphorite were detected. In the most favourable case, they increased by about 25'.

	Standard clinker	Clinker 0,5%P_2O_5	Clinker 0,7%P_2O_5	Clinker 0,9%P_2O_5
SK	93	95	96	97
Free CaO	1,8	1,9	2,4	2,3
Initial set	1h58'	1h35'	2h00'	2h25'
Final set	2h35'	2h15'	2h30'	2h55'

The SK was increased to counter the effect of the reduction of initial strength, but the free lime content increases with no substantial improvement in setting, up to relatively high P_2O_5 (0,9%) contents, equivalent to 2,2% of mineral, which represented quite a considerable cost.

In a balance made, it was observed that all P comes out practically with the clinker. The kiln operation was regular and performance increased by approximately 2%.

The average characteristics of this test (20.000 mT) were: SK-96; SM-2,6; AM-1,8; Free CaO-2,2; NaO equivalent 0,60; C_3S-64; C_2S-14; C_3A-9; C_4AF-9; mechanical strengths (ISO-RILEM) (kp/cm^2): 1 day 34/147 - 3 days 62/333 - 7 days 73/418 - 28 days 90/545.

By X-ray diffraction, observed under normal conditions and after selective attacks with salicylic acid and methanol to dissolve the silicates, it showed great similarity to the clinker obtained in the laboratory. The C_3A appears in cubic form.

V. CLINKER WITH FLUOR (F)

V.1. Laboratory tests

V.1.1. Natural fluorites (60 and 85% in CaF_2 and raw meal (SK-99 and SM-2,2)

In this case, the raw meal difficult to combine used in IV.1.2. was again taken (13% over 90µ, 21,6% over 64µ, SK-101 and SM-2,3) for mixing with two natural fluorites of varying purity (60% CaF_2+19% $CaCO_3$+12% SiO_2-(+ 4%$BaSO_4$) and (85% CaF_2+12% SiO_2-µ).

Calcination carried out at 1420ºC for 45' consisted of mixtures with each of the fluorites, with values expressed as F^- ranging from 0,12% to 0,62%, so that the addition of mineral in both cases varied according to its purity.

The free lime decreases according to the greater F^- content, at the same time as the setting lengthen (4h0'/4h36', with 0,62% F^-).

Mechanical strengths (ISO-RILEM) at one day remain constant or decrease slightly, and they increase from 3 days on, exceeding 50 kp/cm^2 at 28 days for percentages of F^- around 0,4% in raw meal.

To enable the interpretation of these data they were compared with those obtained under identical conditions with phosphorite, in which the figures achieved industrially were already known.

As shown in the following table, for an initial set of 2h45' about 4% of phosphorite (1,5% P_2O_5) was needed, and 0,7% or 0,9% of fluorite (0,41% F^-); when the required set was 3h30', the difference between the percentages of each component were more marked (6% for phosphorite and 1% for fluorite 85%).

PHOSPHORITE

	Raw Meal-II (R.M-II)	R.M-II 0,4%P_2O_5	R.M-II 1%P_2O_5	R.M-II 1,5%P_2O_5	R.M-II 2%P_2O_5
SK	101	101	102	103	104
Free CaO	3,6	3,0	3,2	3,7	4,0
Initial set	1h47'	2h33'	2h45'	2h48'	3h30'
Final set	2h10'	2h45'	3h15'	3h20'	3h55'

FLUORITE (85%)

	Raw Meal-II (R.M-II)	R.M-II 0,12%F^-	R.M-II 0,21%F^-	R.M-II 0,27%F^-	R.M-II 0,41%F^-
SK	101	101	100	100	100
Free CaO	3,6	2,8	2,0	1,8	1,4
Initial set	1h47'	2h00'	2h30'	2h50'	3h38'
Final set	2h10'	2h30'	2h47'	3h10'	4h07'

FLUORITE (60%)

	Raw Meal-II (R.M-II)	R.M-II 0,15%F^-	R.M-II 0,20%F^-	R.M-II 0,27%F^-	R.M-II 0,41%F^-
SK	101	100	100	100	99
Free CaO	3,6	3,0	2,5	2,0	1,2
Initial set	1h47'	2h10'	2h30'	2h45'	3h27'
Final set	2h10'	3h00'	3h10'	3h11'	3h56'

Since the price of fluorite was almost half that of phosphorite, a deeper study was required, using various analytical techniques.

The original raw meal R.M-II, that of 0,15%F^- (0,5% CaF_2(60%)), that of 0,41% F^-(1,4%CaF_2(60%) and 1% CaF_2(80%)) were selected as the values between which the future industrial raw meals should be located.

V.1.2. Studies by DTA-GTA

There is an endothermal peak at 1150ºC for the formation of a liquid originating from the fluorite in raw

J.R. BARAGAÑO. Dr. Chem. Sc. ASLAND SA - VILLALUENGA DE LA SAGRA (TOLEDO) SPAIN
G. CAMPOS. Chemist. ASLAND SA - NIEBLA (HUELVA) SPAIN

EXTENSION OF SETTING TIME BY MEANS OF MINERALIZED CLINKERS

meals with 0,4% of F^-, while this is not detected in raw meals with 0,15% of F^- and R.M-II.

The area of the peak of the formation of the liquid phase which appears at 1320ºC increased with the addition of F^-, and the same occurs in the cooling with the cristalization peak of that phase, which would explain the increase of reaction speeds.

RAW MEAL	Peak area Melting (mm^2)	Peak area Cristalization (mm^2)
RM-II	29	59
RM-II+0,15% F^-	39	63
RM-II+0,41% F^-	46	70
RM-II+0,41% F^-	69	73

V.1.3. Study by X-ray diffraction

The former raw meals calcinated at 1420ºC, were directly observed in order to verify the form of the silicates and after a selective attack on the latter, the composition of the aluminates is studied.

For this purpose two criteria were followed, one comparing with pure cristaline forms synthetically prepared and the other following the work of Burkes and Buck (1) which permit the differentiation between cubic and non-cubic forms and a mixture of the two.

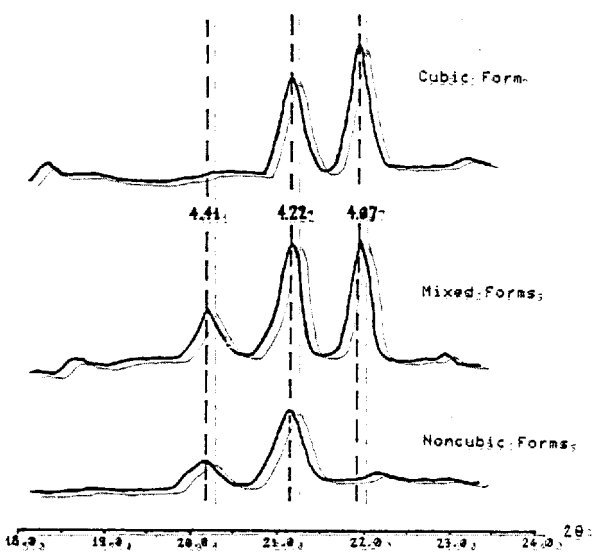

Criteria for identification of C_3A type by x-ray diffraction (Burkes and Buck)

It was detected that while in the clinker without F^-, the C_3A is in cubic form, in the others it decreases, the tetragonal form increasing according to the $\%F^-$, and the possible presence of $C_{11}A_7CaF_2$ also being detected, which would explain the lengthening of the setting time.

V.1.4. Study by Microscopy

An universal camera microscope REICHERT (MeF) using the reflected light technique was used.

After selective attacks with Nital and Nital+KOH, a planimetric counting was conducted, with the following results:

CLINKER	%Alite	%Belite	%Interstitial phase	%Free Lime
RM-II	59	20	16	4,4
RM-II+0,15% F^-	67	12	18	2,8
RM-II+0,41% F^-	77	9	12	1,3
RM-II+0,41% F^-	78	9	12	1,5

There is a clear increase of alite with the reduction of belite and free lime on increasing the addition of CaF_2.

VI. INDUSTRIAL TEST

VI.1. Fluorite with 60% CaF_2

Fluorite of this kind is obtained by flotation and for this reason its great fineness and residual moisture give rise to handling problems.

Its behaviour in the kiln does not show any anomalies although in principle, in spite of having a high SK, its greater burning facility caused fused clinker to be obtained.

After adjusting the parametres of the process to the variables caused by the introduction of the fluorite in the raw meal, it was not only possible to stabilize the operation of the kilns, but also production increased, without affecting the life of the refractories or the possible atmospheric pollution by fluorides.

VI.1.1. Distribution of the F^-

Independently from the theoretical calculations according to the F^- of the daily raw meal at the kiln inlet and of the clinker obtained, a study was conducted for five days weighing and analysing the dust collected in the cyclones and that from the electrofilter, deducing that 93% of the F^- leaves with the clinker.

	$\%F^-$	$\%F^-$ (kg/day)	%
Raw meal kiln inlet	0,10	1498	100
Clinker	0,15	1387,5	93
Filter dust	0,52	23,4	1
Grate dust	0,72	88,1	6

VI.1.2. Relation between $\%F^-$ in clinker and setting times

Logically the addition of fluorite was modified according to the setting times required.

In the attached graph, it is observed that when F^- increases, not only the initial set is lenghtened, but also the interval between the initial and the final time increases.

Furthermore, figures below a certain minimum have no measurable effect on it, this minimum being approximately 0,12% F^-.

This was verified by reducing the F^- to figures between 0,08 and 0,10% for several days, maintaining

J.R. BARAGAÑO. Dr. Chem. Sc. ASLAND SA - VILLALUENGA DE LA SAGRA (TOLEDO) SPAIN
G. CAMPOS. Chemist. ASLAND SA - NIEBLA (HUELVA) SPAIN

EXTENSION OF SETTING TIME BY MEANS OF MINERALIZED CLINKERS

the high SK (98).

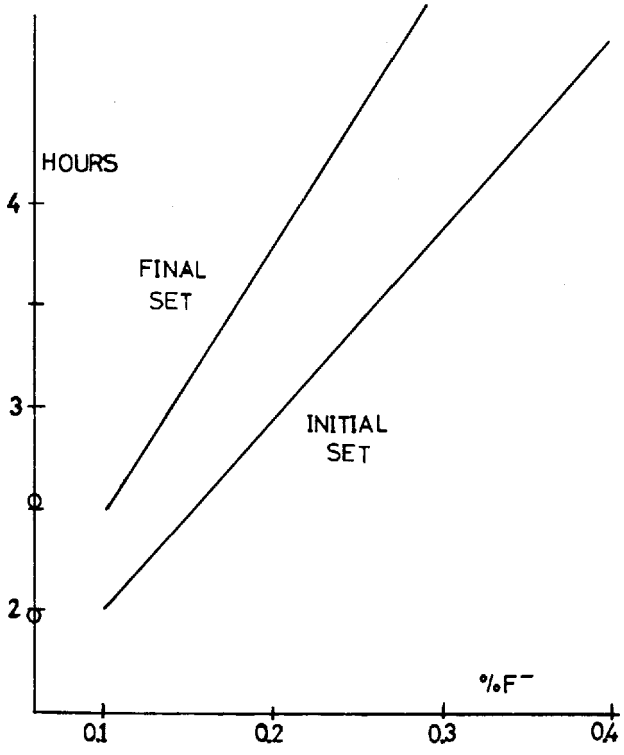

Not only did setting times reduce to the normal levels, but also the free lime was abnormally high (3 and 4%). A further increase of the F^- gave rise to the reduction of free lime and the lengthening of setting times.

VI.1.3. Quality of clinker obtained

The clinker, with an SK of 96; SM-2,4; AM-1,7; free lime-1,6; Na_2O equivalent 0,52; F^- 0,16% and C_3S-65; C_2S-8; C_3A-8; C_4AF-10, does not cause expansion to the autoclave and ground at 350 m^2/kg, improves mechanical strengths at all stages, in particular from 3 days on (1 day 38/156 - 3 days 62/340 - 7 days 73/437 and 28 days 88/558 kp/cm^2).

The greater ease of calcination make it possible to obtain clinkers with more SC_3, which produces greater strength, even during the first days. For SC_3 contents similar to those of standard clinker, strengths at 1 day are rather lower, remaining higher at 28 days.

VI.2. Fluorite with 85% CaF_2

In this case, the fluorite has a granular aspect (< 3 mm) and less moisture, so that its addition causes no problems.

Due to its greater concentration of F^-, the average contents in raw meal is 0,45% instead of 0,71% previously used to maintain an approximate figure of 0,16% F^-.

The ease with which these raw meals may be combined continues to be as good as in the preceding case, and no problem of wear of the refractories or of coating was observed.

The clinker obtained continues to have setting times closely linked with the % of F^-, with no measurable effect for values of 0,10% or below.

In general kiln production was 3% higher when using fluorite.

VI.2.1. Quality of the clinker obtained

The ease of burning caused by the addition of fluorite means that even high SK clinkers (97) have low free lime, and cause high strength at all places, completely in accordance with the high SC_3 contents.

Compared with the strengths of the standard clinker, it is observed that the increase caused at 1 day (28 kp/cm^2) is less than the strengths existing from 3 days on (59 to 73 kp/cm^2), and thus if the same SK are maintained as in the clinkers without F^-, the initial strengths are lower.

CLINKER	SK	Free lime	C_3S	ISO-RILEM (kp/cm^2) 1 day	3 days	7 days	28 days
Standard	93	1,8	56	36/146	57/293	71/394	87/534
Cu-Zn	96	2,0	64	33/148	66/333	70/411	86/536
P	96	2,2	63	34/147	62/333	73/418	90/545
F(60%)	96	1,6	63	38/156	62/340	73/437	88/558
F(85%)	97	1,6	65	41/174	64/352	76/467	89/602

VII. SUPPLEMENTARY TESTING

VII.1. Grindability tests

The Work Index (WI) of the first clinker obtained was determined using the Bond method (2) since the performance of the industrial mills had diminished; a rate of 17,3 kw.h/mT was obtained, which was of some concern as it was harder than the standard clinker (14.6 kw.h/mT). However it is possible to attribute this rate to the fact that due to the ease of burning the clinker was at first partly fused.

Subsequently, under normal operation, the WI varied between 14.1 and 15.4 kw.h/mT, similar to the clinker without fluorite.

VII.2. Analysis by X-ray Diffraction

Following the same premises as those used in the laboratory clinker studies, we wished to verify whether the same occurred in industrial clinkers.

For this purpose, one standard clinker, two clinkers with different F^- content, made with 60% fluorite, and another made with 85% fluorite were employed.

The main question was to verify the state of cristalization of the C_3A, based on samples from which the silicates had been eliminated by selective dissolution.

It can be observed in the attached graph that to the extent the % of F^- increases, independently from the type of fluorite, the characteristic peak of the cubic state decreases and even vanishes, and another

J.R. BARAGAÑO. Dr. Chem. Sc. ASLAND SA - VILLALUENGA DE LA SAGRA (TOLEDO) SPAIN
G. CAMPOS. Chemist. ASLAND SA. NIEBLA (HUELVA) SPAIN

2.1

EXTENSION OF SETTING TIME BY MEANS OF MINE[illegible]FD CLINKERS

one appears corresponding to the tetragonal s:

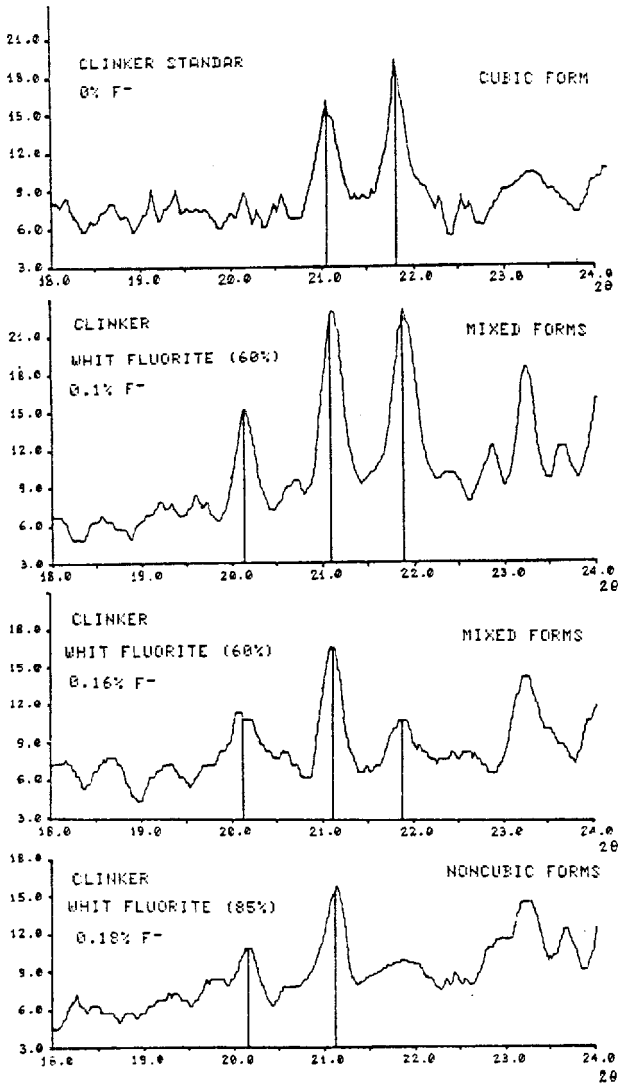

It also seems that the presence of $C_{11}A_7.CaF_2$ can be observed, but in this case it is more doubtful.

Furthermore, the C_3S also increases in clinkers with fluorite; these have a higher SK with less free lime than clinkers considered standard.

VII.3. Optical microscopic test

We took clinkers with very high SK (99-100 and 101), with F^- of 0,17; 0,18 and 0,25% respectively which due to their good calcination had had low figures of free lime.

	SK-99 SM 2,3 F^- 0,17%	SK-100 SM-2,2 F^- 0,18%	SK-101 SM 2,4 F^- 0,25%
%Alite	75	75	65
%Belite	13	9	13
%Interstitial	11	16	20
%Free CaO	0,8	0,5	1,6

The large amount of alites formed may be explained by the satisfactory behaviour of the fluorite, both as a fluxing agent facilittating the burning of high SK raw meals, and as a mineralizer, sppeding up the formation of alite.

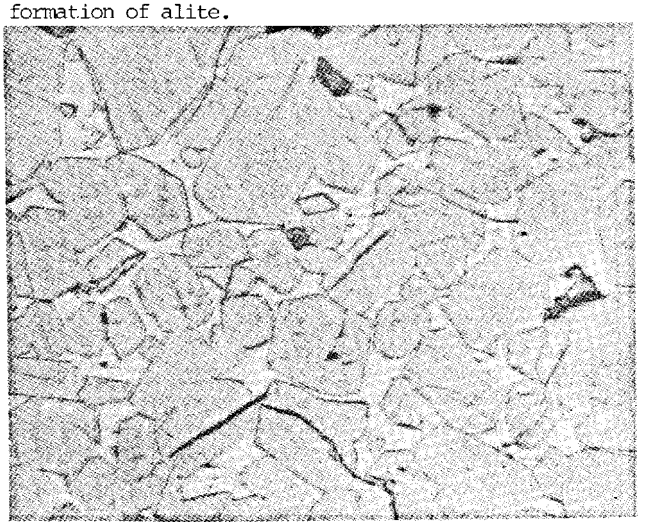

Clinker (SK-99, SM-2,3, F^- 0,17%) 370x. Attack: H_2O+ +Nital+alcohol. Field of alites with well-defined edges.

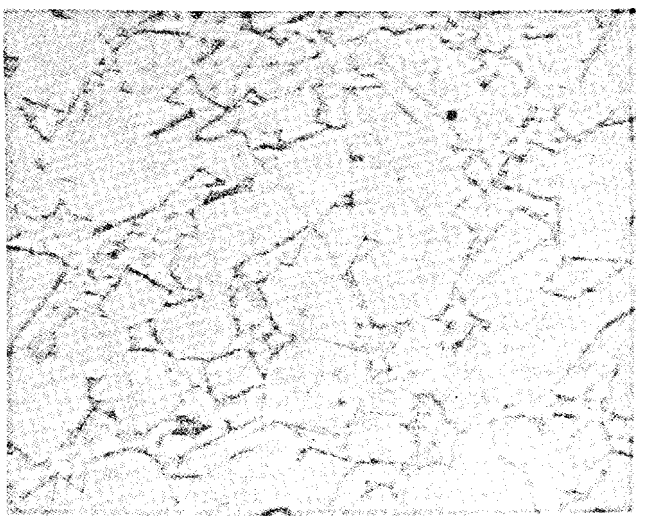

Clinker (SK-100, SM 2,2; F^- 0,18%).370x.Attack: H_2O+ +Nital+alcohol. Well developed alite crystals with relatively high interstitial matter.

REFERENCES

1. Use of selective dissolution and X-ray diffraction to determine form of trical ium aluminate in Portland cement.
Burkes and Buck.
Proccedings of the 5 th International Conference on Cement Microscopy, pp 247-251.USA March 1983.
2. Crushing & grinding calculations.
Fred C. Bond. British Chemical Engineering. June 1961. Vol. 6 Nº 6. August 1961. Vol 6. Nº 8.

FRANCISA HANNAWAYYA
DOCTOR OF CHEMICAL TECHNOLOGY:NATIONAL SWEDISH BOARD FOR TECHNICAL DEVELOPMENT,STOCKHOLM SWEDEN

THE PROPERTIES OF C_4 AF HYDRATED FOR 8 YEARS

2.1

SUMMARY:
The system $CaO-Al_2O_3-Fe_2O_3$ wich occurs in Portland cement and High Alumina Cement is of particular interest. The Tetracalcium Aluminoferrite (C_4AF) phase also resembles the other major constituents of Clinker cement.
The mineral C_4AF was synthetic, the procees of which the preparation should be as closely similar as possible to the practical Clinker burning process with the degree of purity between 96-98 percent.
Hydrated C_4AF past has been examined by SEM and X-ray diffraction after 1 day, 7 days, 28 days and one year and also after 8 years, especially, to clarify its microstructural kinetics and crystal formation. The main hydration products are: $C_4(A,F)H_n$ (hexagonal plates) and $C_3(A,F)H_6$ (isometric), and there is also a solid solution series between the two. After a period of time all hexagonal hydrate is coverted to isometric hydrate, the stable end phase of hydration . C_4AF reacted with gypsum forming mixtures of Monosulfate ($C_4A\bar{S}H_{12}$,$C4A\bar{S}H_{18}$) and Trisulfate (Ettringite). The rate of the reaction decreased as the Fe_2O_3/Al_2O_3 ratios of the hydrate increased. The purpose of this study is : (1) to relate certain identifying characteristics of C_4AF paste hydration to its composition, and (2) to find out if its hydration products have significant strength as they effect the behaviour of cement.

SUMÁRIO:
O sistema $CaO-Al_2O_3-Fe_2O_3$ que ocorre no cimento Portland e no cimento aluminoso é de particular interesse. A fase Ferro-aluminato tetracálcico (C_4AF) também se assemelha a outros dos maiores constituintes do clinquer de cimento.
O mineral C_4AF era sintético, com um processo de preparação o mais similar possível do clinquer industrial queimado, com um grau de pureza entre 96-98 por cento.
Pastas hidratadas de C_4AF foram examinadas por SEM e difração de raios-X após 1 dia, 7 dias,28 dias e um ano e também após 8 anos, especialmente para esclarecer sua cinética microestrutural e formação do cristal. Os principais produtos de hidratação são : $C_4(A,F)H_n$ (em placas hexagonais) e $C_3(A,F)H_6$ (isométrico),e também há uma série de soluções sólidas entre os dois.
Após um período de tempo,todo o hidrato hexagonal é convertido em hidrato isométrico, a fase final estável de hidratação.
C_4AF reagiu com gesso formando misturas de Monosulfato ($C_4A\bar{S}H_{12}$, $C_4A\bar{S}H_{15}$) e trisulfato (etringite).
A rapidez da reação decresce quando a relação Fe_2O_3/Al_2O_3 do hidrato aumenta.
A finalidade desse estudo é : (1) - relacionar algumas características identificadoras de hidratação das pastas de C_4AF com a sua composição, e (2) verificar se os seus produtos de hidratação têm resistência significativa e como afetam o comportamento do cimento.

FRANCISA HANNAWAYYA

2.1

INTRODUCTION:

In the manufacture of clinker-cement, Iron is always present in the raw materials entering into a ternary composition with Calcium Oxide and Alumina to form a reddish brown crystalline Tetracalcium Aluminoferrite ($4CaO.Al_2O_3.Fe_2O_3$ or C_4AF). The compound C_4AF was first reported in 1928 by Hansen, Brownmiller, and Bogue /1/, later on by Solacolu/2/, a single crystal investigation has been made by Büssen /3/ The unit cell was analyzed by rotary diagrams: a = 5.34Å; b=14.44Å; c=5.52Å. The unit cell is th therefore pseudo-tetragonal with the ac-plane as basic plane. The unit cell contains 2 molecules $4CaO.Al_2O_3.Fe_2O_3$. Numerous investigations, using X-ray, magnetic, thermal and chemical methods, have found the existence of a series of solid solutions between C_2F and a hypothetical C_2A, terminating in a limiting solid solution usually given as $6CaO.2Al_2O_3.Fe_2O_3$ /4, 5 and 6/. The existence of a solid solution series between the known C_2F and hypothetical C_2A, extending as far as C_6A_2F, has been shown by previous investigators /7/. A review of research in this field up to 1964 has been given by Welch /8/. In a more recent paper, Majumdar /9/ places the limit at 70 mol-percent C_2A. Research of the system $CaO-Al_2O_3-Fe_2O_3$ has shown that the solid solution series extending from $2CaO.Fe_2O_3$ to $4CaO.Al_2O_3.Fe_2O_3$ (C_2F to C_4AF) is beyond C_4AF. The investigations in this field were summarized by Nurse /10/ for the fourth International Symposium on the Chemistry of cement (1960). More recently, the crystal structure has been investigated by Smith/11/, who gives the generalized formula for the series as $Ca_8(Fe_{1-p}Al_p)_8O_{20}$.

The present author Hannawayya emphasizes that the ternary solid solution is important because of its presence in Portland cement clinker. The $Al_2O_3:Fe_2O_3$ ratio in clinker varies with that in the raw mix, but it has been shown that the relationship is not simple. For many clinkers the composition approximates C_4AF, although, the C_4AF composition is not a distinct compound. The solid solution often is referred to as the Ferrite phase. The present paper describes research which deals with reactions of the C_4AF at hydration in paste form. The purpose of this study is: (1) to relate certain identifying characteristics of C_4AF paste hydration to its composition, and (2) to find out if its hydration products have significant strength as they effect the behaviour of cement.

MATERIALS AND PROCEDURE:

The mineral C_4AF was synthetic, the process of which the preparation shoud be as closely similar as possible to the practical clinker burning process with the degree of purity between 96-98 percent as follows:

Calcium Carbonate (guarantee 99%) is slightly burned in a large platinum crucible in a muffer furnace for at least, two hours at 1050°C to get CaO. It is important that the temperature is checked, it must not be considerably higher, for it means, if so be the case, that the Calcium gets burned crisp and that thereby the possible continued reaction will be considerably reduced.

The materials, reagent weight according to the stoichiometric of C_4AF, Calcium Oxide, Aluminum Hydroxide (Gibbsite) and Ferric Oxide, were mixed dry, passed through a No. 48 sieve, and again mixed dry for two hours in bottles on a rotaring wheel. The mixture was then heated in open platinum dish in an electric furnace at 1320°C for two to three hours, cooled, ground, and reheated in the same manner. the preparation was ground to pass a No. 200 sieve. The specification of the compound C_4AF is given in table 1.

Table 1.

Compound	Detected by X-ray	CaO	Al_2O_3	Fe_2O_3	Free CaO	Specific surface area Cm²/gm (Blaine)
C_4AF	C_4AF (C_6AF_2, C_6A_2F)	45.2%	20.9%	31.95	0.04%	1210

The relation between the products of hydration and the Oxide composition of the C_4AF compound in system $CaO.Al_2O_3.Fe_2O_3$ is studied. The C_4AF component was mixed at a water/solid ratio of 0.5. A series of specimens with and without gypsum was prepared and stored inside the desiccator containing cold water for the proper period of test at a constant room temperature of 22-25°C. After one day, some of the stored specimens were removed and placed in water; after 7 days, they were removed from the water and stored again inside the desiccator up to 8 years. The X-ray apparatus was a North American Philips Geiger counter diffractometer, with CuK_α radiation. The specimens were scanned at a rate of 1° 2θ/min. Hannawayya /12/ presents a scheme of qualitative measurements by X-ray diffraction in all systems which reads as follows: 5000 CPS (Count Per Secont) represent maximum. The morphology of the specimen were identified by Scanning Electron Microscopy.

RESULTS AND DISCUSSIONS:

The ternary compound of the composition $4CaO.Al_2O_3.Fe_2O_3$ hydrated rapidly so that at the end of 28-day-hydration, the anhydrous phase had disappeared. The C_4AF/H_2O mixture with water/solid ratio of 0.5 forms a mud. There was no abnormal rise of temperature during mixing. The colour of the mixture was deep brick red and did not change during hydration.

The compound absorbed in fixed combination about 25 percent of water in one day; this increased slightly, reaching 29 percent after one year /13/.

The $4CaO.Al_2O_3.Fe_2O_3$ phase resembles the other major constituents of clinker-cement in that it reacts with water to form crystalline hydrated compounds and thereby sets to a hard polycrystalline mass. The hydrated products of C_4AF consisted as follows:

1- Crystalline phases:
   (a) $C_4(A,F)H_n$ (hexagonal plates)
   (b) $C_3(A,F)H_6$ (isometric)
   (c) A solid solution series between (a) and (b)
2- An amorphous phase Iron, or Aluminum Hydroxide $(A,F)H_3$.
3- Lime (Calcium Hydroxide or CH).

The reaction of C_4AF with water as follows:

$$2C_4AF + 17H \longrightarrow 2C_3(A,F)H_6 + (A,F)H_3 + 2CH$$

The Aluminum and Iron Hydroxide combines with Hydroxide of lime from the supersaturated solution forming as follows:

$$(A,F)H_3 + 3CH \longrightarrow C_3(A,F)H_6$$

If the hydration reaction would result in a product richer in Alumina than the parent material, part of the Fe_2O_3 would have to appear in some other form.

(i) X-RAY DIFFRACTION DIAGRAMS:

(a) 100 vol.parts $C_4AF + H_2O$, W/C = 0.5. after 4 hours at a temperature of 18-20°C, X-ray diffraction revealed that α-$C_2(A,F)H_8$ was the major hydration product at 18.26° (or 10.7Å). It was sharp in outline and strongly visible, probably reflecting superior crystallinity of the hydrate.

The α_1-$C_4(A,F)H_{13}$ of weak intensity was detected as well as a trace of $C_3(A,F)H_6$ with strong intensity of unreacted C_4AF.

The high-iron-alumina members give the di-tetra-calcium compound, presumably a solid solution containing both Ferric Oxide and Alumina. The free $Ca(OH)_2$ is formed during paste hydration of C_4AF. The Iron or Alumina separates as Ferric or Alumina Hydroxide during the hydration of C_4AF, but cannot be detected by X-ray.

The present author Hannawayya can explain that tnese components occur because the Iron Oxide of C_4AF became amorphous Iron Hydroxide (the same is true for Alumina). In this case the C:A molar ratio would have been 4 and the presence of $C_2(A,F)H_8$ means that $Ca(OH)_2$ had to be released in an amorphous form.

$C_4(A,F)H_{13}$ is the stable form in the presence of free lime, because the amorphous lime is very reactive.

After 1 day, metastable hydrates phases (α-$C_2(A,F)H_8$, α_1-$C_4(A,F)H_{13}$) transfomed to

$C_3(A,F)H_6$ phase, which is stable at room temperature. Monocarbonate ($C_4(A,F)\bar{C}H_{11}$) of weak intensityr was detected. This detection is compatible with the explanation that the α-hydrate was formed progressively by action of atmospheric CO_2 on the moist C_4AF paste. After 7 days, the product was rich in $C_3(A,F)H_6$ phase, but C_4AF had decreased to medium weak intensity, $C_4(A,F)\bar{C}H_{11}$ also appeared. The present author, Hannawayya, can explain the occurrence of these compounds by stating that the Iron Oxide transforms into amorphous Iron Hydroxide (the same is valid for Alumina). In this case the C:A molar ratio would have been 4 and the presence of $C_2(A,F)H_8$ means that $Ca(OH)_2$ had to be released in an amorphous forms. $C_4(A,F)H_{13}$ is the stable form in the presence of free lime, because the amorphous lime is very reactive.

After 28 days, X-ray diffraction revealed that anhydrate phase C_4AF had reached depletion. The hydration product was richer in $C_3(A,F)H_6$ phase. $C_4(A,F)\bar{C}H_{11}$ was also detected. After 1 year, X-ray diffraction revealed the same products as after 28 days. Table 1, Fig. 1. After 8 years, X-ray diffraction revealed that the mixture gets a certain concentration of CH amorphous phase (cannot be detected by X-ray), of which follows that $C_3(A,F)H_6$ phase with very strong intensity is stable in the presence of CH amorphous phase at room temperature, $C_4(A,F)\bar{C}H_{11}$ increased somewhat to medium intensity. Table 1.

Hannawayya emphasizes that from the kinetic data results of X-ray diffraction presented in table 1 of the present paper, it would appear that the Ferrite phase in Portland cement hydrates will show no significant change in the A/F ratio of the remaining unhydrated material. Hence, one might assume that the product of hydration can be a solid solution of Ferrite and Aluminate such that the A/F ratio of solid solution is the same as it was in the original Ferrite phase. Thus, if the original Ferrite phase had an A/F ratio of unity, then the hydration product in question would be an equipolar solid solution of Ferrite phase with an Aluminate as a necessary component. The crystalline hydration products of $C_4AF + H_2O$ are:

(1): $4CaO.(Al_2O_3,Fe_2O_3).13H_2O$ and α-$2CaO.(Al_2O_3,Fe_2O_3).8H_2O$,

(2): $3CaO.(Al_2O_3,Fe_2O_3).6H_2O$.

The first phases were stable below 18°C, the second above 25°C. This difference may partly depend on differences in the nature on the rate of reaction, which in turn is controlled by the Fe_2O_3/Al_2O_3 ratio of the Aluminoferrite phase and the hydration products.

Hannawayya /4/ has investigated the hydration product of C_4AF in the presence of Silicates (C_3S, β-C_2S) and found that addition of C_3S retards the hydration of C_4AF somewhat, a deduction based on the absence of crystal phase $C_3(A,F)H_6$ and also that the unhydrated phase C_4AF still appears after one year. It should be emphasized that the observations on the reactions of Tetracalcium Aluminoferrite on paste hydration as reported in the present report do not necessarily indicate that these materials would behave in the same way in the hydration of cement, in the presence of Silica, Calcium Sulfate, excess Calcium Hydroxide, and other substances. It is, therefore, interesting to study the interaction between Calcium Sulfate (Gypsum, $C\bar{S}$) and the hydration products obtained during hydration of C_4AF.

(b) 67 vol.parts C_4AF + 33 vol.parts $C\bar{S}$ + H_2O, W/C = 0.5.

Initially, Gypsum ($C\bar{S}$) retarded the setting of C_4AF. C_4AF, Gypsum and water is a more fluid mixture than C_4AF and water. The temperature of the paste was normal. The paste hardened somewhat between 1 and 7 days. The colour of the paste was deep brick red and did not change over time.

After 4 hours at 18-22°C, X-ray diffraction revealed that C_4AF and $C\bar{S}H_2$ were the main hydration products. No other crystalline phase was visible and CH phase in amorphous state could not be detected by X-ray. Addition of Gypsum to C_4A retards its hydration products.

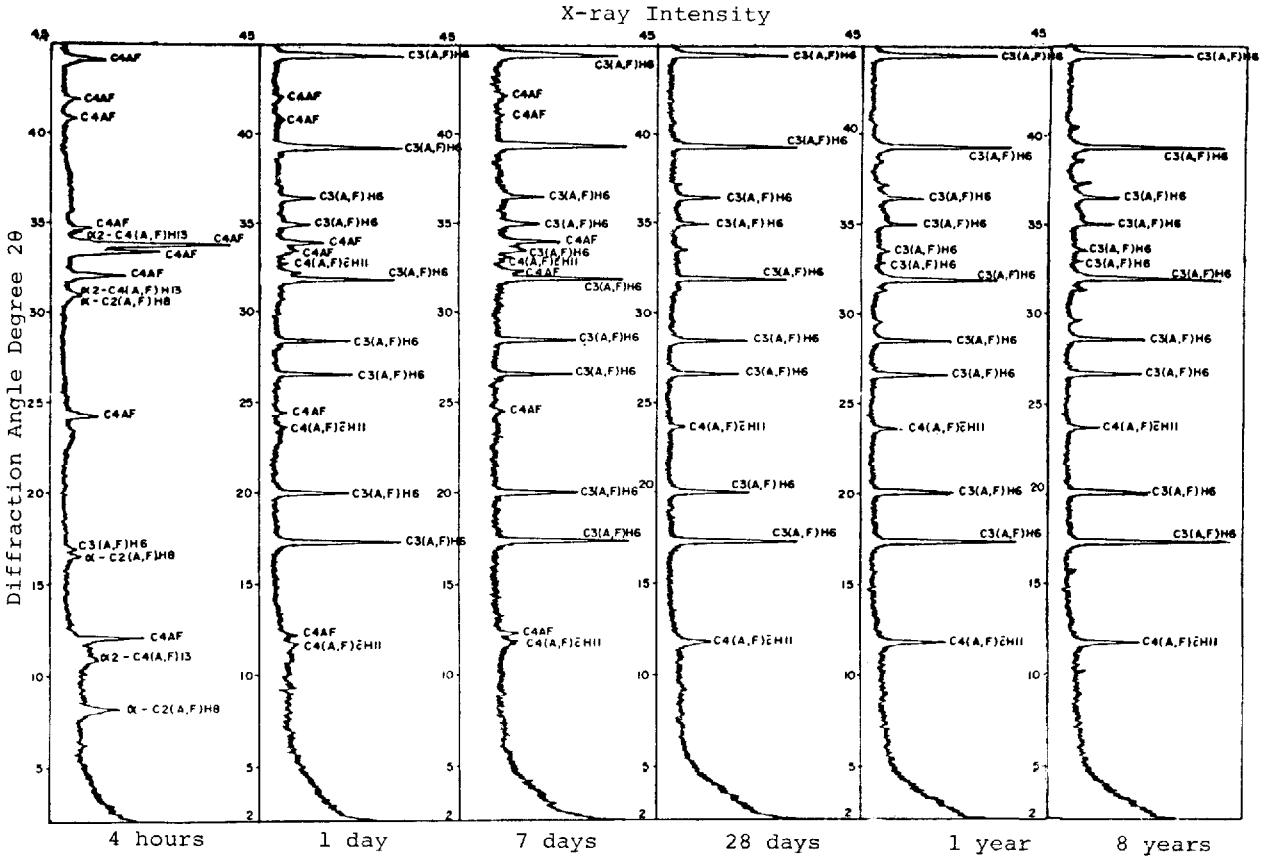

Fig. 1. X-ray diffraction Diagrams of 100 vol.parts $C_4AF + H_2O$

Table 1. Data of X-ray diffraction of the reaction: 100 vol.parts $C_4AF + H_2O$, W/C = 0.5.

$C_4AF + H_2O$	4h	1d.	7d.	28d.	1y.	8y.
C_4AF	s	m	mw	-	-	-
$C_3(A,F)H_6$	tr.	ms	s	s	ms	vs
α-$C_2(A,F)H_8$	mw	-	-	-	-	-
α_1-$C_4(A,F)H_{13}$	w	-	-	-	-	-
$C_4(A,F)\bar{C}H_{11}$	-	w	w	mw	m	ms

vvs = very very strong
vs = very strong
s = strong
ms = medium strong
m = medium
mw = medium weak
w = weak
tr = trace

Table 2. Data of X-ray diffraction of the reaction: 67 vol.parts C_4AF + 33 vol. parts $C\bar{S} + H_2O$, W/C = 0.5.

$C_4AF+C\bar{S}+H_2O$	4h	1d.	7d.	28d.	1y.	8y.
C_4AF	vs	vs	s	w	-	-
$C\bar{S}H_2$	vvs	vs	s	-	-	-
$C_6(A,F)\bar{S}_3H_{32}$	-	w	mw	mw	-	-
$C_4(A,F)\bar{S}H_{18}$	-	-	-	mw	ms	s
$C_4(A,F)\bar{S}H_{12}$	-	-	-	vvs	vs	s

After 1 and 7 days, X-ray diffraction revealed mainly unreacted C_4AF, Gypsum of very strong intensity, Ettringite of medium weak intensity CH was detected in an amorphous phase. The reaction leading to a product, type Ettringite, may be formulated as follows:

$$4CaO.(Al_2O_3,Fe_2O_3).13H_2O + 3CaSO_4 + aq. \xrightarrow{20\ H_2O} 3CaO.(Al_2O_3,Fe_2O_3).3CaSO_4.32H_2O + Ca(OH)_2.$$

$$3CaO.(Al_2O_3,Fe_2O_3).6H_2O + 3CaSO_4 + aq. \xrightarrow{26\ H_2O} 3CaO.(Al_2O_3,Fe_2O_3).3CaSO_4.32H_2O.$$

After 28 days, Ettringite of medium intensity was visible. Gypsum had reacted completely and C_4AF had decreased to weak intensity. Monosulfate Hydrates ($C_4(A,F)\bar{S}H_{18}$, $C_4(A,F)\bar{S}H_{12}$) appeared with medium weak and very very strong intensity, respectively.

After 1 year, both Ettringite and unreacted C_4AF had reacted completey, converting into

Monosulfate Hydrate, $C_4(A,F)\bar{S}H_{18}$, thus increased over time to medium strong intensity It appears that after this length of time, the reaction between Ettringite and C_4AF to form low Sulfoaluminate progresses at a faster rate than the reaction between C_4AF and Gypsum to form Ettringite. Therefore, the main hydration products were Monosulfate Hydrate $C_4(A,F)\bar{S}H_{12}$ of very strong and $C_4(A,F)\bar{S}H_{12}$ of medium strong intensity.

After hydration for 8 years, X-ray diffraction revealed that Monosulfate Hydrate $C_4(A,F)\bar{S}H_{18}$ had increased to strong intensity, while Monosulfate Hydrate, $C_4(A,F)\bar{S}H_{12}$, had decreased to strong intensity. Table 2.

The present author explains the existence of both Monosulfates as the final products after hydration for 8 years from the fact that the solid solution is continuous between the end members. The formation of both Monosulfates Hydrates indicates that either the solid solution was not continuous or that it took a longer time to reach equilibrium in the case of paste hydration, and that the mobility of the SO_4^{-2} ions must have been considerably restricted.

Hannawayya /15/ studied the interaction between Calcium Sulfate (from Gypsum and $C_4A_3\bar{S}$) and the hydration products, obtained during hydration of C_4AF (or system $C_4AF + C_4A_3\bar{S} + C\bar{S} + H_2O$).

(ii) SCANNING ELECTRON MICROSCOPY RESULTS

SEM was used to show the morphological structure and the location of the various products of hydration. It can be seen how the character of the products of hydration changes with time and enviroment.

(a) MORPHOLOGY OF HYDRATION IN AIR

Already after hydration for 24 hours, a certain tendency is noticed towards development of crystal surfaces. The mass of gel splits once in a while into thin flakes, this possibly in connection with the continuous binding with the water.

SEM, observed after hydration for 3 days (Fig. 2), revealed some flat, irregular, hexagonal-shaped crystal discs getting more and more numerous, with a mass of gel arround the particles.

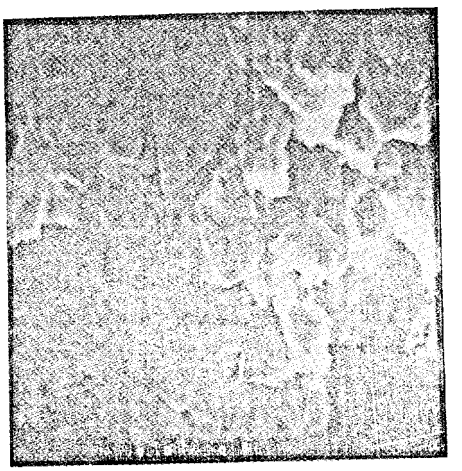

Magnified X 3000

Fig. 2. Paste of 100 vol.parts $C_4AF + H_2O$, hydrated for 3 days.

SEM, observed after hydration for 28 days, revealed that the main part is an amorphous gel, which fills out all the spaces between the grains and gives to the structure a certain stability and tenacity. When drying, the gel shrinks and gives rise to several internal microcracks, which shows that the adhesion to the grains is stronger than the very tenacity or cohesion of the gel. The gel component does not resemble the grain product given by AH_3. It is completely without structure except for the fact that it easily splits into thin flakes, which is an indication that it has been formed in several thin layers. It is possible to guess by this lack of structure and by the reddish-brown colour of the experimental prisms that the gel is mainly made out of FH_3. Thus, the hydration reaction might take place in the following way:

$2C_4AF + aq. \longrightarrow C_3AH_6 + FH_3 + CH$ (dissolved)

C_3AH_6 (amorphous) $\longrightarrow C_3AH_6$ (crystals).

C_3AH_6 is first deposited in the form of an amorphous layer, which then slowly crystallizes into a concentration of regular cubic crystal grains. See Fig. 3, which represents the area of the hydration product, discussed above, of course, most of cubic C_3AH_6 crystal are also observed.

In the one-year-hydration, the crystals were thicker and larger, but their nature remained the same.



Figure 3. Magnification X 3000



Figure 4. Magnification X 1000



Figure 5. Magnification X 1000

(b) MORPHOLOGY OF HYDRATION IN WATER + HYDRATION IN AIR

(1) 1-day hydration in air + 3-day hydration in water: SEM shows crystals resembling many irregular shapes of crystals, but some very thin, small cubic (C_3AH_6) crystals were visible, Fig. 4.

(2) 1-day hydration in air + 7-day hydration in water + up to 28-day hydration in air: SEM revealed that the structure change is considerable. The structure holds together rather well, but the porosity increases with the degree of crystallization which is without strength. Fig. 5.

(C) MORPHOLOGY OF HYDRATION FOR 8 YEARS IN AIR

(1) The C_4AF/H_2O mixture with water/solid ratio 0.5: SEM revealed that the main structure is isometric crystalline phase C_3AH_6 in which cubically shaped crystals seem to be frequent after hydration for 8 years together with thin, irregular edges of crystals. This structure is completely without adhesion and porous, lowering the tenacity. Fig. 6.

(2) The $C_4AF + C\bar{S}/H_2O$ mixture with wter/solid ratio 0.5: SEM revealed that the addition of Gypsum ($C\bar{S}$) to system $C_4AF + H_2O$ led to bigger change in the hydration products. After hydration for 8 years, t appears clearly by the micropictures (Fig. 7) that hexagonal, prismatic crystals (Monosulfates) have increased in number as a final hydration product. The observations were confirmed by X-ray diffraction. The presence of Gypsum in $C_4AF + H_2O$ appeared to hinder the formation of Calcium Carbonate, $C_4(A,F)CH_{11}$, hydrate.

CONCLUSIONS:

The ternary compound of composition $4CaO.Al_2O_3.Fe_2O_3$ resembles the other major constituents of clinker-cement in that it reacts with water to form hydration products as follows: (1): A crystalline phase, (2): A solid series, (3): An amorphous phase. The crystalline hydration products of $C_4AF + H_2O$ are: (1): $4CaO.(Al_2O_3,Fe_2O_3).13H_2O$ and α-$2CaO.(Al_2O_3,Fe_2O_3).8H_2O$ (hexagonal crystals), (2): $3CaO.(Al_2O_3,Fe_2O_3).6H_2O$ (isometric), which is the final product after hydration for 8 years.



MAGNIFICATION X 6000

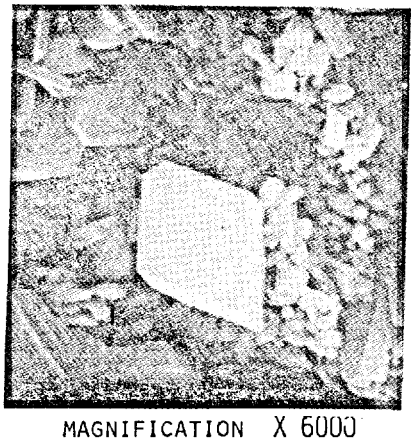

MAGNIFICATION X 6000

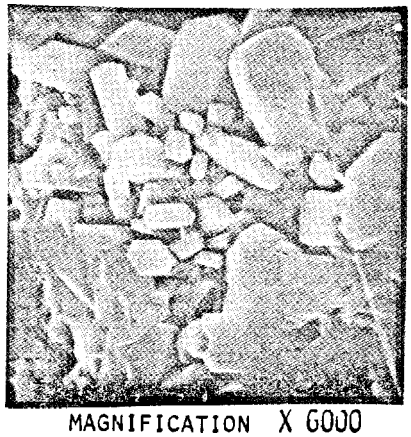

MAGNIFICATION X 6000

Fig. 6. 100 vol.parts $C_4AF + H_2O$, Hydration for 8 years in air.

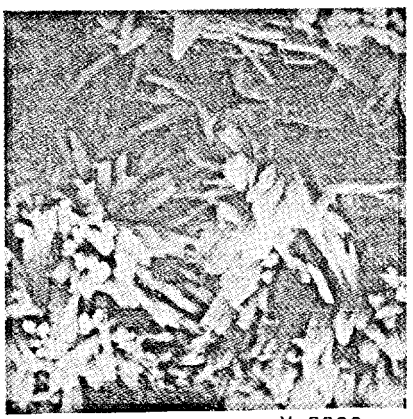

MAGNIFICATION X 6000

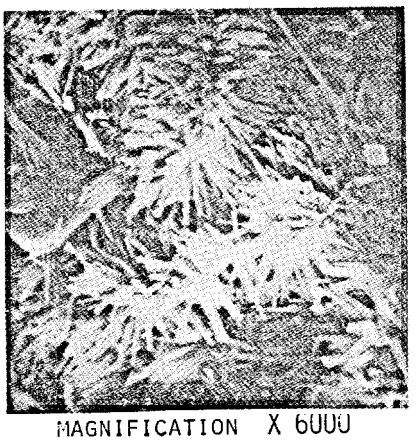

MAGNIFICATION X 6000

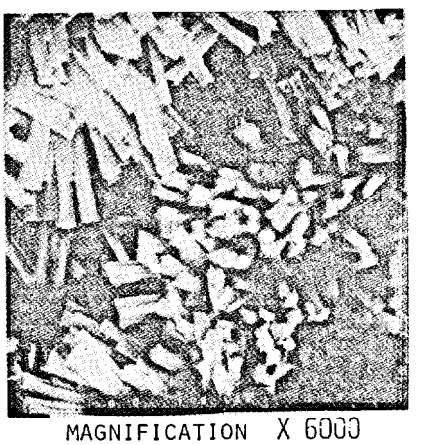

MAGNIFICATION X 6000

Fig. 7. 67 vol.parts C_4AF + 33 vol.parts $C\bar{S}$ + H_2O. Hydration for 8 years in air.

The first phase was stable below 18°C, the second above 25°C. From the kinetic data results of X-ray diffraction presented in table it would appear that the Ferrite phase in Portland cement hydrates will show no significant change in the A/F ratio of the remaining unhydrated material. Hence, one might assume that the product of hydration can be solid solution of Ferrite and Aluminate. The logical conclusion to be drawn from this discussions is that paste C_4AF + H_2O does not behave in the same way in the hydration of cement, in the presence of Silica, Calcium Sulfate, excess Calcium Hydroxide, and other substances. Therefore, the hydration of C_4AF + Gypsum($C\bar{S}$) leads to a product, type Ettringite which over time converts into Monosulfate hydrates.
The present author explains the existence of both Monosulfates as the final products after hydration for 8 years from the fact that either the solid solution was not continuous or that it took a longer time to reach equilibrium in the case of paste hydration, and that the mobility of the SO_4^{-2} ions must have been considerably restricted. The present report certainly contains interesting results, and SEM micrographs and other documentation supplied in it, are contributed for further research in Cement Chemistry.

ACKNOWLEDGEMENTS:

The author is deeply indebted to Chief Engineer Paul Forsgren, Head of the Industrial P2 and to Director Carl-Otto Frykfors of the National Swedish Board for Technical Development (Styrelsen för Teknisk Utveckling, STU) for all help recived in supporting grant for this research.

REFERENCES:

/1/ W.C. Hansen, L.T. Broownmiller, and R.H. Boque, "Studies on the system Calcium Oxide Alumina-ferric Oxide, J. Am. Chem. Society 50, 396-406 (1928).

/2/ S. Solvacolu, Zement, 1932, 21, 301.

/3/ W. Büssen, Fortschn. Mineral, Krist Petrog, 1937, 22, XXXI.

/4/ T. Yamauchi, J. Japan Ceramic Assoc. 45, 433, 6-4, 880 (1937).

/5/ M.A. Swayze, Am. J. Sci. 244, 1 (1946).

/6/ G.L. Malquori and V. Cirilli, Symposium London 1952, 120.

/7/ F.M. Lea and C.H. Desch. The Chemistry of cement and concrete, 2nd ed., Edward Arnold, Ltd., London Ch. IV, 1956.

/8/ H.F.W. Taylor, The Chemistry of Cements, Academic Press, New York Vol. 1, Ch. 2, by J.H. Welch, 1964.

/9/ A.J. Majumdar, The Ferrite phase in cement Trans. brit. Ceram. Soc. 64, 105-119,1965.

/10/ R.W. Nurse, Phase equilibria & Constitution of Portland cement clinker, Proc. 4th International Symposium on the Chem. of Cement, NBS Mono. 43, 9-37, 1962.

/11/ D.K. Smith, Crystallographic changes with the substitution of Aluminum for Iron in Dicalcium Ferrite, Acta Cryst. 15, 1962, 1146-1152.

/12/ F. Hannawayya, Studies of Hydration Reaction of Cement Components & Sulfoaluminate ($C_4A_3\bar{S}$) Swedish Cement & Concrete Institute, Forskning 2:75, 1975, p. 32.

/13/ R. H. Bogue & William Lerch, Hydration of Portland cement compounds, Industrial and Engin. Chem. vol. 26,No. 8, 837, (1934).

/14/ F. Hannawayya (Thesis) "X-ray Diffraction Studies of Hydration Reaction of Cement Components & Sulfoaluminate ($C_4A_3\bar{S}$), Part IA. Silicates Mixed With Different Components. The Royal Institute of Technology, S-100 44 Stockholm, Sweden)1975).

/15/ F. Hannawayya, "X-ray Diffraction Studies of Hydration Reaction of Cement Components Part IB. Aluminates Mixed With Different Components", Material Science and Engineering, 17, 1975, pp. 247-281, Printed in the Netherland, Elsevier Sequois Lausanne.

A.R. Ramachandran and M.W. Grutzeck, Materials Research Laboratory,
The Pennsylvania State University, University Park, PA 16802 USA

Hydration of Tricalcium Silicate at Fixed pH

ABSTRACT

The hydration of tricalcium silicate (alite) has been studied as a function of pH (8-12) and temperature (10°-40°C) for up to two days. The samples were bottle hydrated at a water/solid ratio of 500/1. The solutions, sampled at different time intervals, were analyzed for calcium and silica concentrations and the morphology of the gels formed on the surfaces of the tricalcium silicate particles were examined using the scanning electron microscope (SEM).

Kinetic data obtained from fixed pH solution analyses are presented which can be interpreted in terms of congruent dissolution followed by nucleation and growth of a silica gel and/or a C-S-H gel from a solution containing calcium, silicate and hydroxide ions. The data suggest that the activity of the hydroxide ion may play a determinant role in governing observed solution and solid compositions which in turn affect the morphology of the gels formed. The data have been used to model the hydration of tricalcium silicate, invoking the concept of invariancy as defined by Gibbs' phase rule, to explain the induction period.

Estudou-se a hidratação do silicato de cálcio (alita) em função do pH (8 - 12) e da temperatura (10 - 40°C) no decurso de até dois dias. As amostras foram hidratadas em garrafa com uma relação de água/sólido de 500/1. As soluções, amostradas a intervalos diferentes de tempo, foram analisadas em termos de concentrações de cálcio e sílica, e se examinou a morfologia dos géis formados sobre as superfícies das partículas de silicato tricálcio, usando-se microscópio eletrônico de varredura (SEM).

Os dados cinéticos apresentados, obtidos de análises de solução com pH fixo, podem ser interpretados em termos de dissolução congruente, seguida por nucleação e crescimento de um gel de sílica e/ou um gel de C-S-H proveniente de uma solução contendo cálcio, silicato e íons de hidróxido. Os dados sugerem que a atividade do íon de hidróxido pode exercer um papel determinante no governo da solução observada e das composições sólidas que, por sua vez, afetam a morfologia dos géis formados. Os dados foram usados como modelo da hidratação do silicato tricálcio, invocando o conceito de invariância conforme definido pela regra de fase de Gibbs, para explicar o período de indução.

INTRODUCTION

Different hypotheses have been advanced to explain the early hydration behavior of tricalcium silicate [1] (C_3S) and the phenomenon of the "induction period." With the exception of the osmotic membrane theory, all theories propose the formation of an initial precipitate which converts to a more stable phase with time. The types of precipitates referred to in these theories could be formed under different pH conditions prevailing in the solution phase at different times during the course of hydration. Most published studies concerning the suspension hydration of C_3S have concentrated on calcium and silica concentrations in solution and have failed to isolate the effects of the hydroxide ion concentration upon observed results.

Recently there have been a few isolated studies [2-5] which report the hydration behavior of C_3S under controlled pH conditions. McCurdy and Stein [4] have shown the existence of a "plateau" in their Ca^{2+} and OH^- ion concentrations which coincides with a maximum in their silica concentration for the same pH. They have also shown [5] that the formation of an initial C-S-H with a higher silica content leads to a longer plateau whereas the formation of one with a higher calcium content leads to a shorter plateau. The plateau was most pronounced when the pH was fixed at 11.5. They suggest that the plateau represents a state of equilibrium between the early protective coating of C-S-H and solution, which converts to a second type of less protective C-S-H at the end of the plateau.

Our objective was to further study the effect of pH upon the suspension hydration of tricalcium silicate at three temperatures. In addition to conventional solution analyses we also studied the morphology and chemical composition of the coexisting solid phases in order to delineate pH regimes in which different precipitates were present. Experiments were carried out at pH 10, 11 and 12 at three temperatures (10°, 25°, 40°C) and at pH 8 and 11.5 at 25°C. A silica gel containing a small amount of calcium was found to be stable at pH 8. The amount of calcium incorporated in the precipitate increased with pH and Type II C-S-H was observed above a hydroxide ion activity of $10^{-2.5}$ (pH 11.5 at 25°C).

EXPERIMENTAL METHODS

The tricalcium silicate (alite)* used in the experiments was synthesized by reacting a well mixed stoichiometric blend of reagent grade calcium carbonate and colloidal silica (Cab-O-Sil) at 1550°C. The sintered powder was ground in an agate mortar and then pressed into pellets which were fired again at 1600°C for approximately 5 hours. The alite sample used in the dissolution experiments was obtained by crushing the fired pellets and sieving the resulting coarse powder. The 300μm to 425μm (ASTM -40 to +50 mesh) size fraction was used throughout (see Figure 1). The chemical analysis of the alite is given in Table 1. Powder x-ray diffraction analysis showed the polymorph to be T_{II}. The specific surface area of the alite was found to be 0.07 m^2/g by nitrogen BET measurement.

All experiments were carried out in one liter, high density polyethylene bottles. A very high liquid to solid ratio (500/1) as well as a coarse particle size was selected with the hope of obtaining slower rates of dissolution. Freshly boiled deionized (DI) water was used to reduce the effects of carbonation. Carbon dioxide-free nitrogen gas was bubbled through the DI water for 15 minutes prior to and passed over the solution surface during the course of the experiments. Temperature control was achieved by using a Haake refrigerated water bath (Model A82) and was maintained within ±0.1°C of the set point. The solutions were stirred magnetically using water-driven magnetic stirrers and Teflon-coated stirring bars. The lids of the bottles (wide mouth) were modified to accept a nitrogen gas supply tube, acid-containing pipet or dropper, a Ross pH electrode (Orion Model 810300) and an adjustable pipetter (MLA) for periodic sampling.

Table 1. Chemical Analysis of Alite Used in Dissolution Experiments.

Oxide	wt. %
CaO	72.07
SiO_2	25.72
Al_2O_3	1.78
Free CaO	<0.01
TOTAL	99.57

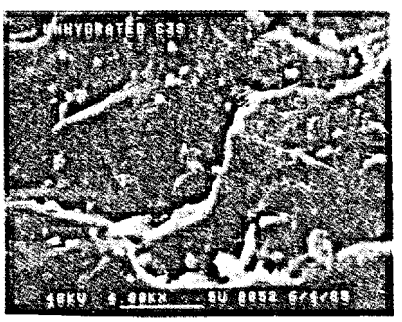

Figure 1. Unhydrated alite showing a dense pore-free surface and fine particles. The effect of the latter upon dissolution is assumed to be negligible.

The pH of the solution was controlled to within ±0.1 pH unit by means of a pH stat (Horizon Model 5651) and syringe pump (Sage Model 355) equipped with 60 cc syringes filled with dilute HCl solutions. The pH meter (Orion Model 611) was calibrated with respect to both pH and temperature.

Although the pH stat proved quite reliable for maintaining required pH, at earliest times, at low pH (8, 10), early pH control was achieved by manual additions of more concentrated HCl solutions. For this reason, some of the data begin as late as two

*Approximately 0.5 wt. Al_2O_3 was added to the mixture before milling with alumina balls. Alumina was added in order to stabilize C_3S and thus we are calling our substituted material alite.

hours rather than at two minutes, which was more common. Initial pH was adjusted using KOH.

Once the system had reached thermal equilibrium, two grams of alite was introduced into the bottle. The stirring dispersed the alite grains, carried them upward forming a halo approximately one inch below the surface of the solution. This prevented grinding of the grains by the stirring bar and allowed us to easily remove both liquid and solid samples at regular intervals. Fifteen mL of solution and a few (20-30) alite grains were withdrawn with a pipet equipped with disposable plastic tips. The grains of alite which settled in the pipet tip were dropped into a vial containing acetone, rinsed with fresh acetone, allowed to air dry for approximately five minutes and then stored in a CO_2-free desiccator until viewed with a SEM (ISI DS-130) equipped with EDX (KEVEX) capabilities. Solutions were filtered through a 0.2μm filter into a polyethylene vial which was closed and further sealed with Parafilm. The solutions were analyzed for Ca, Si, Al and K using a DC plasma emission spectrometer (Spectrametrics SpectraSpan IIIB). The chloride analysis was carried out using a Dionex Anion Chromatograph (Model 2010i). The effects of K, Al and Cl concentrations are assumed to be of minor importance and therefore are not reported here. Data are available from the authors upon request.

RESULTS

Fixed pH

The variation in calcium and silica concentration as a function of time and pH is shown in Figure 2. The marked effect that pH has on the hydration phenomenon is demonstrated by the final silica concentrations attained at the end of the experiments. At pH 8, the silica concentration suggests saturation of the solution with respect to amorphous silica. The silica concentrations at pH 11.5 and 12 agree with similar published data such as those of Brown et al. [6]. Accompanying SEM photomicrographs depicting the typical microstructural features of the developing precipitates on the alite particles at pH 8, 10 and 12 are given in Figure 3. It should be noted that the photomicrographs represent typical features. We have selected the most representative pictures and as such a one-to-one comparison between Figures 2 and 3 is not our intention. The precipitate at pH 8 was found to be silica rich (see EDX plots given in Figure 4) whereas at pH 10 and 12 the precipitate was found to be richer in calcium. At pH 12, one observes a progressive development of the precipitate's morphology which is more suggestive of that found during the conventional hydration of cement. Figure 3I shows a denser Type III C-S-H gel evolving from Type II C-S-H at earlier ages (Fig. 3H) without experiencing a significant change in solution chemistry. Thus, at high and low pH, we can conclude that C-S-H and an amorphous silica gel containing a small amount of calcium are the respective stable phases. The results at pH 10 and 11 are more difficult to interpret and as such will be discussed later in the paper.

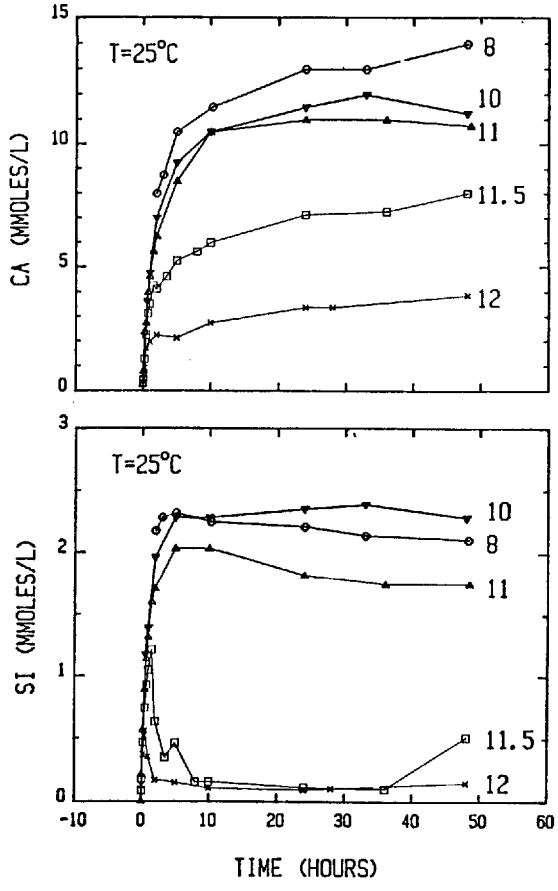

Figure 2. Calcium and silica concentrations as a function of pH. Temeprature was fixed at 25°C.

The calcium versus silica data have also been plotted in Figure 5 in order to establish whether the dissolution is congruent or incongruent. As far as we can see, the data suggest (as did McCurdy and Stein's [4]) that dissolution is congruent. The deviation is attributed to formation of a hydrated phase. The data points fall reasonably close to the 0.333 slope (Si/Ca) for alite.

Temperature Effect

The effect of temperature on the hydration of alite is demonstrated in Figure 6. It can be seen that both the calcium and silica concentrations shift to lower values with increasing temperature. The experiments were performed under conditions where pH was kept constant over a range of temperatures. However, the dissociation constant of water (K_w) is a function of temperature; ranging from $10^{-14.5}$ at 10°C to $10^{-13.5}$ at 40°C. Therefore the a_{OH^-} is not what it first appears to be, the a_{OH^-} varies with temperature. For example, at pH 11 and 40°C (Fig. 6D) silica is severely depressed due to calcium-rich C-S-H formation, yet this effect is absent at 10° and 25°C. Discounting the possibility of equilibrium conditions not being achieved in the runs due to the limited length of hydration (48

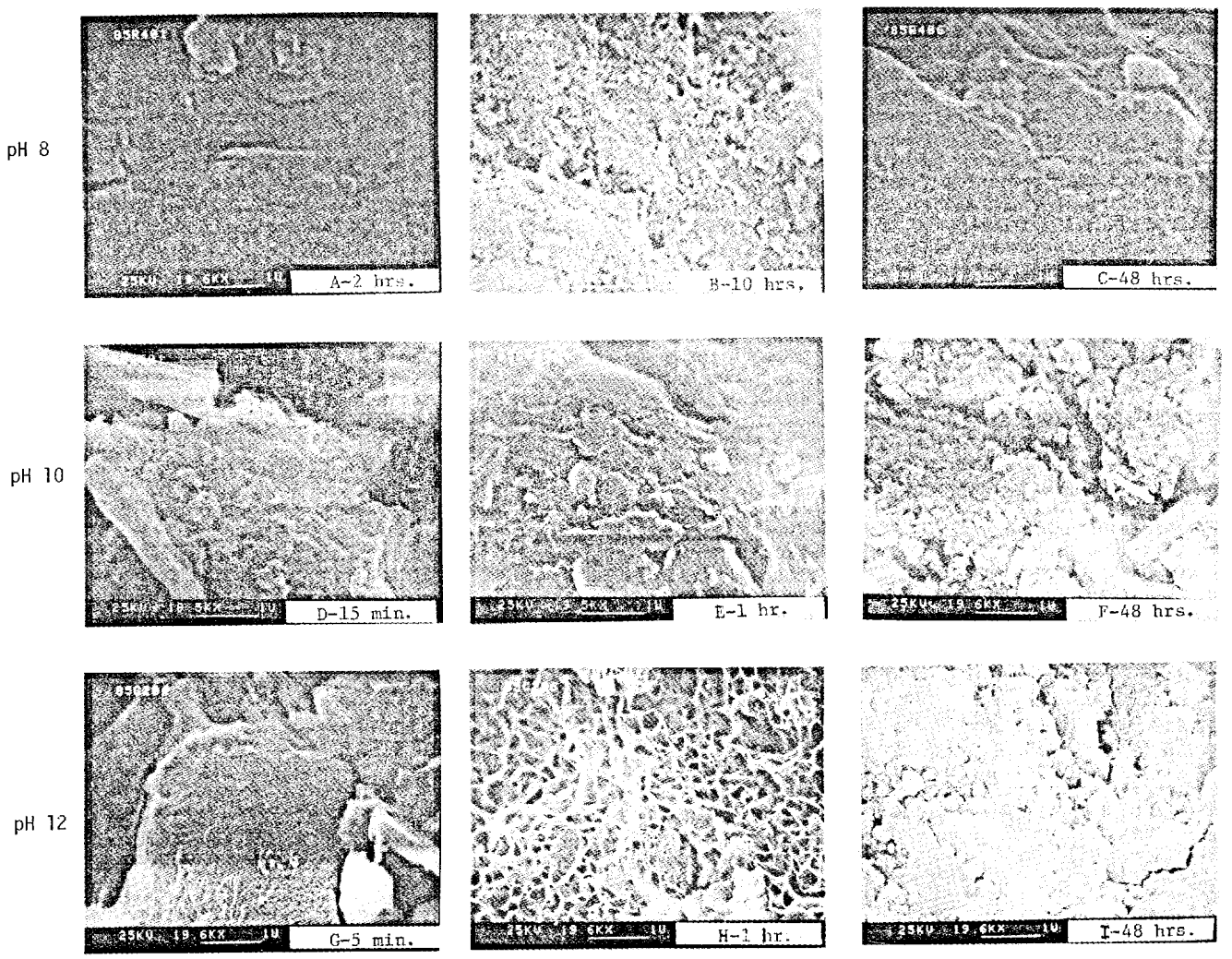

Figure 3. Representative SEM photomicrographs of alite particles hydrated at pH 8, 10 and 12. Photos A-C are taken from pH 8 25°C solutions; photos D-F are from pH 10 40°C solutions; and photos G-I are from pH 12 40°C solutions. The three images for each pH represent a progression of time ranging from early (0-2 hr) through intermediate (1-10 hr) to long-term hydration (48 hr). The horizontal bar at the bottom of each photograph is 1μm long.

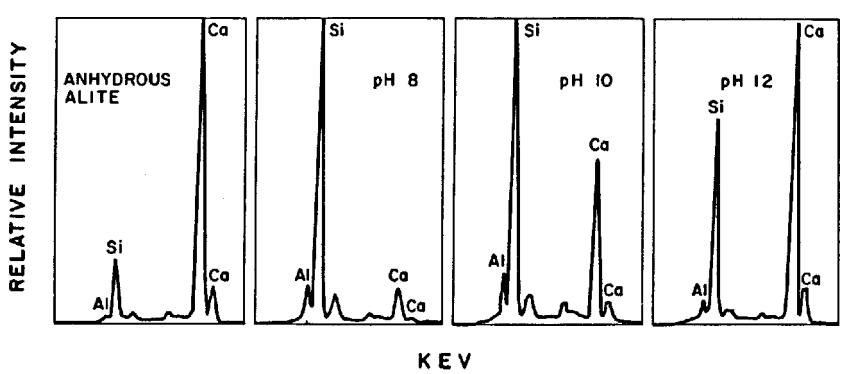

Figure 4. EDX traces of anhydrous alite and alite grains hydrated at pH 8, 10 and 12 for 2 days at 25°C. The precipitate becomes increasingly rich in calcium with pH.

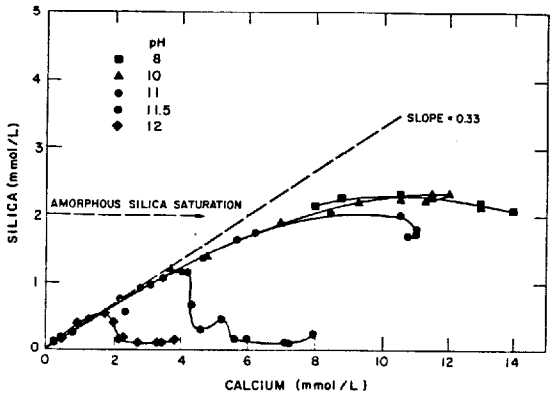

Figure 5. Calcium versus silica in solution as a function of pH at 25°C. Initial dissolution appears to be congruent. At pH 8 the solution rapidly equilibrates with precipitating amorphous silica. At pH 11.5 and 12 reticulated C-S-H precipitates. At pH 10 and 11, a lower c/s ratio C-S-H is precipitating.

hrs.), a more likely explanation would be to attribute the observed difference in behavior to OH^- ion activity. At 40°C and pH 11, the OH^- ion concentration is $10^{-2.5}$. At 10°C and pH 12 the OH^- ion concentration is also $10^{-2.5}$. If the OH^- concentration does effect the concentration of ions in solution the calcium and silica plots should be very close under these conditions--which, in fact, they are (see Figure 6C-F). Small deviations may be due to kinetic effects directly attributable to temperature.

DISCUSSION

Data

For ease of discussion we have plotted our 24-48 hour silica data (which we assume is nearly at equilibrium) on a concentration versus pH plot also including the solubility of amorphous silica (Figure 7). In the absence of calcium, the solubility of amorphous silica increases beyond pH 9. Our data do not (Fig. 5), which suggests another hydrate regulating the concentration of silica in solution. It was this observation which originally suggested the presence of two gel phases, the stability of

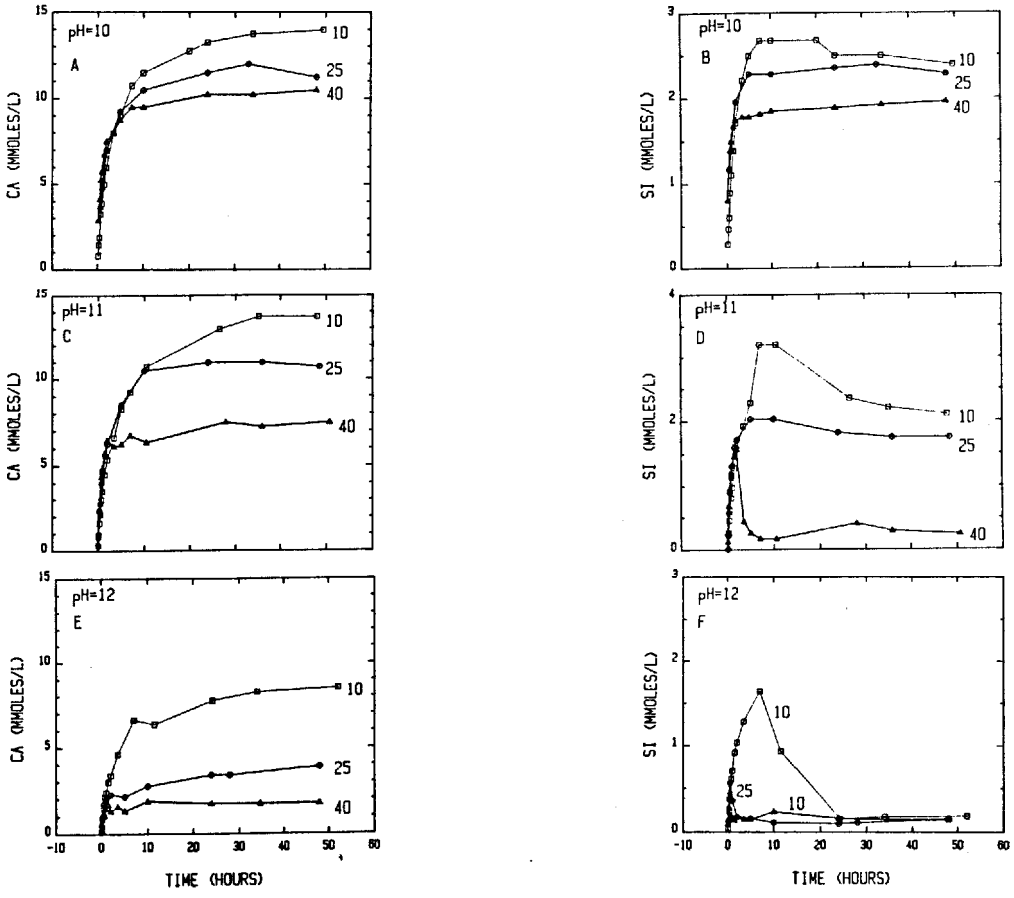

Figure 6. The effect of temperature on the dissolution of alite at pH 10 (AB), 11 (CD) and 12 (EF). Both calcium and silica decrease with increasing temperature.

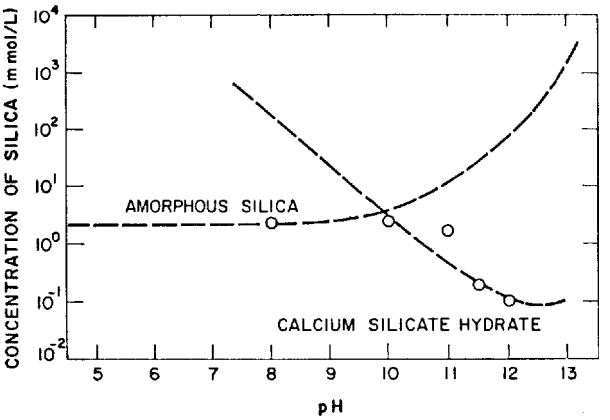

Figure 7. Concentration of silica in solution versus pH for amorphous silica at 25°C (adapted from Stumm and Morgan [6]) and our present 24-48 hour, 25°C silica data. The solubility of silica in solution is determined by the least soluble precipitate. It appears as if the crossover between amorphous silica and C-S-H gel is at about pH 10.

which were dependent upon the activity of the hydroxide ions.

The activity of the hydroxide ion determines, to a large extent, the concentration of ions in solution and the nature of the precipitate formed. Although a crossover point of pH 10 ($a_{OH^-}^{25°C} = 10^{-4}$M) is suggested as a boundary between silica gel (containing a few percent calcium) and C-S-H gel (Fig. 7), the typical Type II reticulated structure for C-S-H gel is not apparent until one approaches or exceeds an activity of hydroxyl ion equal to $10^{-2.5}$. In our experiments, the reticulated structure developed only at pH 11 (40°C), pH 11.5 (25°C) and pH 12 (10°, 25°, 40°C) all of which had an a_{OH^-} equal to or greater than $10^{-2.5}$M. From our EDX data, we conclude that the C-S-H which forms becomes progressively richer in calcium with increasing pH. Therefore, we suggest the following: At pH 10 the sheet-like structure of C-S-H can accommodate calcium ions between the layers. However at a pH equivalent to an a_{OH^-} equal to or greater than $10^{-2.5}$ (11.5 at 25°C) all of the calcium no longer can fit between the layers and therefore the sheets begin to roll up causing a reticulated structure to form.

McCurdy and Stein's [4,5] observation of a pronounced plateau at pH 11.5 in their calcium and hydroxide plots coincides with our finding that a reticulated C-S-H begins to form at this same pH at 25°C. Perhaps their plateau is associated with the process of reticulation. Unfortunately, due to differences in experimental procedures, it is difficult to directly compare results.

Model

The proposed model is consistent with previous theories in that it suggests the conversion of one gel phase to another. However, in addition it also provides a much needed raison d'etre for the induction period based upon Gibbs' phase rule.

At equilibrium, the pH 10 crossover point depicted in Figure 7 represents an invariant point in the system $CaO-SiO_2-H_2O$. At this point, two gels can coexist with a solution having a fixed composition (Ca^{2+}, silicate and OH^-). As one moves either to higher or lower pHs, the composition of the solution will remain fixed until one of the phases dissolves and converts to the other (reconstructive transformation). It is suggested that the induction period observed during the paste or solution hydration of tricalcium silicate may be a reflection of the time it takes to convert a silica gel formed at initially low pHs to a C-S-H gel stable at higher pHs. Conceivably, such a gel might form in the vicinity of the grains due to differences in rates of diffusion of Ca^{2+} (fast) versus silicate ion (slow) as well as pH considerations. Once the silica gel coats the hydrating grains and isolates the anhydrous cores of alite, allowing only slow diffusion of calcium through the layer, the observed induction period may actually be a period of near invariancy during which the system is constrained (zero degrees of freedom) and cannot react until the silica gel (containing a few percent calcium) has been converted into a calcium-poor C-S-H gel.

REFERENCES

1. H.F.W. Taylor et al., RILEM Committee 68-MMH, Task Group 3, "The Hydration of Tricalcium Silicate," Materiaux Constructions 17, pp. 457-468 (1984).
2. K.G. McKurdy and B.P. Erno, "Influence of pH on the Kinetics of Hydration of Tricalcium Silicate," Canadian J. Chem. 47, pp. 833-836 (1971).
3. K.G. McKurdy and B.P. Erno, "Influence of Surface Area Variation on the Kinetics of Hydration of Tricalcium Silicate," Canadian J. Chem. 50, pp. 701-706 (1972).
4. K.G. McCurdy and H.N. Stein, "Suspension Hydration of C_3S at Constant pH. I. Variation of Particle Size and C_3S Content," Cem. Concr. Res. 3, pp. 247-262 (1973).
5. K.G. McCurdy and H.N. Stein, "Suspension Hydration of C_3S at Constant pH. II. Effect of Previously Formed Hydrates and of Additives," Cem. Concr. Res. 3, pp. 509-520 (1973).
6. P.W. Brown, E. Franz, G. Frohnsdorff and H.F.W. Taylor, "Analyses of the Aqueous Phase During Early C_3S Hydration," Cem. Concr. Res. 14, pp. 257-262 (1984).
7. W. Stumm and J.J. Morgan, Aquatic Chemistry 2nd ed., John Wiley and Sons, New York (1981).

ACKNOWLEDGEMENTS

The support of NSF Grant No. CEE-8304076 is gratefully acknowledged. We are also deeply grateful to W. Bathgate who typed the final manuscript.

P.W. Brown, Center for Building Technology, National Bureau of Standards, Gaithersburg, MD 20899, USA.

The Implications of Phase Equilibria on Hydration in the Tricalcium Silicate-Water and the Tricalcium Aluminate-Gypsum-Water Systems

SUMMARY: The mechanisms and kinetics of hydration in the C_3S-H_2O and C_3A-gypsum-H_2O systems are discussed within the context of the relevant phase equilibria. The development of a layer of C-S-H of variable composition results in the onset of the induction period. The composition gradient in this layer causes a morphological transformation leading to the onset of the acceleratory period. The first-formed aluminate-containing phase in the C_3A-gypsum-H_2O system may be AH_3 or ettringite, depending on the initial solution composition. The rate of early C_3A hydration is lowest when ettringite is the first-formed phase. This suggests that initial AH_3 formation does not have a major influence on retardation.

No contexto dos importantes equilíbrios de fase são discutidos os mecanismos e cinéticas de hidratação nos sistemas C_3S-H_2O e C_3A-gesso-H_2O. O desenvolvimento de uma camada de C-S-H de composição variável tem como resultado o início do período de indução. O gradiente de composição nesta camada causa uma transformação morfológica que leva ao início do período de aceleração. A primeira fase formada, contendo aluminato, no sistema C_3A-gesso-H_2O pode ser AH_3 ou etringita, dependendo da composição da solução inicial. A velocidade de formação inicial de AH_3 não tem influência maior sobre a retardação.

Introduction

The mechanisms and kinetics of hydration of C_3S and of C_3A in the presence of gypsum remain incompletely understood. Both the kinetics of the hydration processes in these systems and the mechanisms of hydration are controlled by the morphologies and compositions of the product phases which form. These, in turn, depend on the thermodynamics of the hydration processes involved. It is the objective of this paper to discuss the phase relationships which influence the mechanisms and kinetics of hydration of C_3S and C_3A with gypsum in terms of the relevant stable and metastable phase equilibria in the systems: $CaO-SiO_2-H_2O$ and $CaO-Al_2O_3-CaSO_4-H_2O$.

TRICALCIUM SILICATE

Various authors [1-3] have recently considered the hydration of C_3S in the context of the relevant phase equilibria in the system $CaO-SiO_2-H_2O$. However, considerations of this type extend back to the investigations of Flint and Wells [4], Bessey [5], and Roller and Ervin [6]. Steinour [7] has reviewed the early investigations of phase equilibria in this system and Jennings [8] has reviewed more recent investigations. Each of these studies has attempted to further elucidate the relevant solubility curves and invariant points in this system.

Figure 1 schematically represents the water-rich portion of the $CaO-SiO_2-H_2O$ system at 25°C. The solution region is bounded by the curve O-A-I-J. O-A is the solubility curve for SiO_2·aq. A-I is the solubility curve for C-S-H and extends from the invariant point A: SiO_2·aq-(C-S-H)-solution, (ca. 1 mmol/l SiO_2 and 1 mmol/l CaO) to the invariant point I: (C-S-H)-CH-solution, (ca. 1 µmol/l SiO_2 and 22.5 mmol/l CaO) [3]. The curve I-J is the solubility curve for CH and extends from the ternary invariant point I to the binary invariant point J on the CaO axis (22.3 mmol/l CaO [9]).

The line of congruent C_3S dissolution intersects the C-S-H solubility curve at B. Following Barret et al. [10], C_3S dissolves congruently until the composition of the solution intersects the C-S-H solubility curve at point B. Subsequent congruent dissolution results in a solution supersaturated with respect to C-S-H. Supersaturation is relieved by the precipitation of C-S-H at compositions parallel to the tie lines indicated in figure 1. Continued dissolution and precipitation enrich the solution with respect to CaO and the composition of the solution moves along the curve B-I.

The two-phase region, (C-S-H + solution), is bounded by the solubility curves A-I, A-C, C-M, and M-I. Various investigations have shown that the C/S ratio of the C-S-H

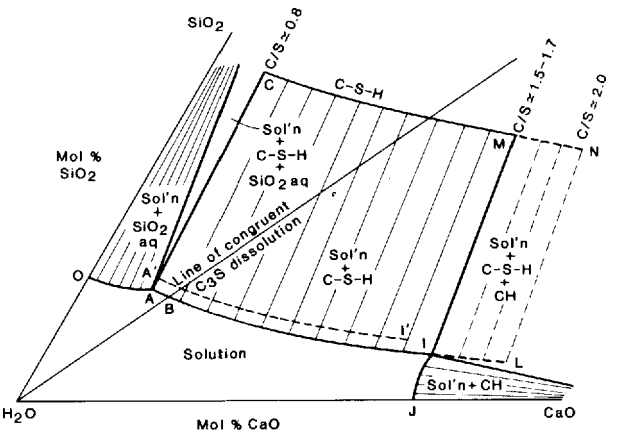

Figure 1. A schematic representation of the water-rich portion of the system $CaO-SiO_2-H_2O$. Not drawn to scale.

increases as calcium ion concentration in solution increases [c.f. 11]. The tie lines connecting curves A-I and C-M schematically represent this increase. The C/S ratio of the first formed C-S-H is near 0.8, while that of the C-S-H forming as the solution composition reaches the invariant point at I is in the range of 1.5 to 1.7. Under equilibrium conditions, C_3S hydration should then result in the formation of CH, C-S-H of composition M, and a saturated solution of composition I. However, it is well known that CH does not immediately precipitate at its saturation concentration. Rather, the C-S-H solubility curve, A-I extends metastably to point L (ca. 0.5 µmol/l SiO_2 and 30 mmol/l CaO [3]). The metastable extensions I-L of the solubility curve A-I and M-N of curve C-M representing the C-S-H composition are shown in figure 1. As a result of these metastable extensions, the formation of C-S-H having C/S ratios in excess of 1.7 would be expected and observations of C-S-H having ratios approaching 2.0 have been cited by Taylor and Newbury [12]. However, after several hours of hydration, CH precipitation initiates and the composition of the solution moves to the left along I-L, reaching the invariant point, I, within about 24 hours.

Taylor has proposed the existence of two modifications of C-S-H: tobermorite-like and jennite-like [13,14]. Jennings [8], based on a review of published solubility data, has suggested the existence of a second solubility curve, curve A'-I' in figure 1. Specifically, the solubility curve A-I was suggested to be associated with tobermorite-like C-S-H while curve A'-I' with a jennite-like modification. However, the specific conditions under which each modification

preferentially forms and whether the two solubility curves converge as the invariant point, I, is approached are yet to be determined.

Discussion

Thomas and Double [1] pointed out that an equilibrium relationship between calcium and silica will also exist in the presence of other species in solution. The concentrations of calcium ions and soluble silicate species in cement pore solutions, along with the composition of the C-S-H, will be affected by a variety of species including alkali, hydroxyl, sulfate, aluminate, and chloride ions and mineral admixtures. As a consequence, variability in the C/S ratio of C-S-H formed in cements should be anticipitated.

From the standpoint of kinetics, the rate controlling steps in C_3S hydration remain a matter of debate. Figure 1 indicates the existence of local equilibria between the composition of the C-S-H and the solution from which it precipitates. However, this data does not directly provide kinetic information. Clearly, the C/S ratio of C-S-H progressively increases throughout its precipitation. It is not clear, however, whether the previously-formed C-S-H adjusts its composition to maintain equilibrium with the solution or whether its composition departs from equilibrium. SEM observations on hydrating C_3S single crystals suggest the latter [15]. It was observed that a featureless layer of hydration product developed on the C_3S single crystal during the initial period of rapid heat evolution. The induction period initiated once this layer had formed and ended when this layer underwent a morphological transformation. The observation of a layer surrounding a C_3S crystal is consistent with the view that a diffusion barrier controls the rate of C_3S hydration at early ages. The rapid transformation of this layer to an acicular morphology appeared to result in the onset of the acceleratory period. Since the acicular product is far less effective in shielding the anhydrous C_3S from the solution, the hydration rate is unlikely to depend on a diffusional process. Rather, a rate of hydration which depends on the C_3S-solution interfacial area would be likely. The occurrence of this phase transformation in the surface layer would indicate thermodynamic instability, the source of which may be a compositional gradient in the C/S ratios of the C-S-H forming as the system moves along the solubility curve A-I-L in figure 1 or a similar curve.

TRICALCIUM ALUMINATE AND GYPSUM

The hydration of C_3A can be considered in the context of the ternary system: $CaO-Al_2O_3-H_2O$. However, the phase equilibria relevant to the hydration of C_3A in the presence of gypsum require analyses of the quaternary system: $CaO-Al_2O_3-CaSO_4-H_2O$. Our understanding of the stable and metastable phase equilibria in these systems is principally due to the investigations of Wells et al. [16], Jones [17-19] and D'Ans and Eick [20,21].

The system $CaO-Al_2O_3-H_2O$ may be plotted on an ordinary ternary phase diagram; however, it is typical to plot the relevant solubility curves on orthogonalized axes. The quaternary system is more difficult to represent. The projection techniques used by Jones [18,19] are awkward. D'Ans and Eick [21] and Eitel [22] reduced this difficulty by plotting the logarithms of the concentrations of CaO, Al_2O_3, and $CaSO_4$ on orthogonal axes with water at the origin. Unfortunately, this construct is also somewhat awkward since molar ratios, such as C/A ratios, plot as parallel lines that do not emanate from the origin. However, this problem has been eliminated by using the convention of plotting the 10th root of the molar concentrations rather than their logarithms. When plotted in this way, molar concentrations scale from 0 (H_2O) at the origin to unity at 1 mol/l. Figure 2 is a representation of the stable quaternary system plotted in this way. The crystallization surfaces for the various phases in this stable system are labeled. The quaternary invariant points determined by D'Ans and Eick at 20°C [21] and those determined by Jones at 25°C [18] are shown. The points determined by Jones are labeled "(J)". The phases in the stable quaternary system are: gypsum, lime, ettringite, hydrargillite, and C_3AH_6. The data from which this and subsequent figures were drawn are presented in table 1.

In discussing the phase equilibria that affect the early hydration of C_3A, it is more relevant to consider the metastable ternary and quaternary systems than the stable systems. In the metastable systems, alumina gel exists in place of hydrargillite and AFm phases exist in place of C_3AH_6. Figure 3 represents the metastable ternary system and figure 4 the metastable quaternary system. Figure 3 also represents the x-y plane of figure 4 and the CaO and Al_2O_3 axes are drawn with the same orientation.

In the subsequent discussion, consideration will be given to the hydration of C_3A under the following circumstances:

1. a mechanical mixture of C_3A and gypsum particles in water,

2. a mechanical mixture of C_3A and gypsum particles in a saturated gypsum solution,

3. a mechanical mixture of C_3A and gypsum particles in a solution saturated with respect to both gypsum and $Ca(OH)_2$.

Table 1

Invariant Points in the Stable and Metastable $CaO-Al_2O_3-H_2O$ and $CaO-Al_2O_3-CaSO_4-H_2O$ Systems. Points F(J), E_2(J), G(J), and H_2(J) were obtained at 25°C [18]. The remaining points were obtained at 20°C [20,21]. g=gypsum, E=ettringite, M=monosulfate.

Point	Solid Phases	Concentration, mmol/l		
		CaO	Al_2O_3	$CaSO_4$
w	CH	20.7		
b	g			15.2
a_2	Y-AH_3		~0.009	
o	AH_3 (gel)		~0.01	
c	CH, g	19.7		12.4
j_2	Y-AH_3, g		0.0079	15.2
j	AH_3, g		~0.01	15.2
s_2	Y-AH_3, C_3AH_6	5.63	0.248	
t	CH, C_3AH_6	20.9	0.0322	
p	AH_3, C_3AH_6	5.79	6.74	
y	C_2AH_8, C_4AH_{19}	10.9	0.94	
v	C_4AH_{19}, CH	21.5	0.0329	
F(J)	CH, E, g	19.2	0.0606	12.4
F	CH, E, g	20.6	0.0272	12.2
E_2(J)	g, Y-AH_3, E	0.675	0.0252	15.0
E_2	g, Y-AH_3, E	0.316	0.0914	14.8
G(J)	CH, E, C_3AH_6	19.0	0.0101	0.181
G	CH, E, C_3AH_6	21.4	0.0259	0.107
H_2(J)	Y-AH_3, E, C_3AH_6	3.12	0.911	0.375
H_2	Y-AH_3, E, C_3AH_6	2.84	0.16	0.263
n	AH_3, E, M	5.98	1.55	5.88
d	CH, E, M	21.1	0.022	0.0294
e	AH_3, E, g	15.2	0.103	0.151
q	AH_3 solubility curve (after [23]).	0.761	0.223	
		1.17	0.341	
		1.83	0.610	
r		2.91	0.957	

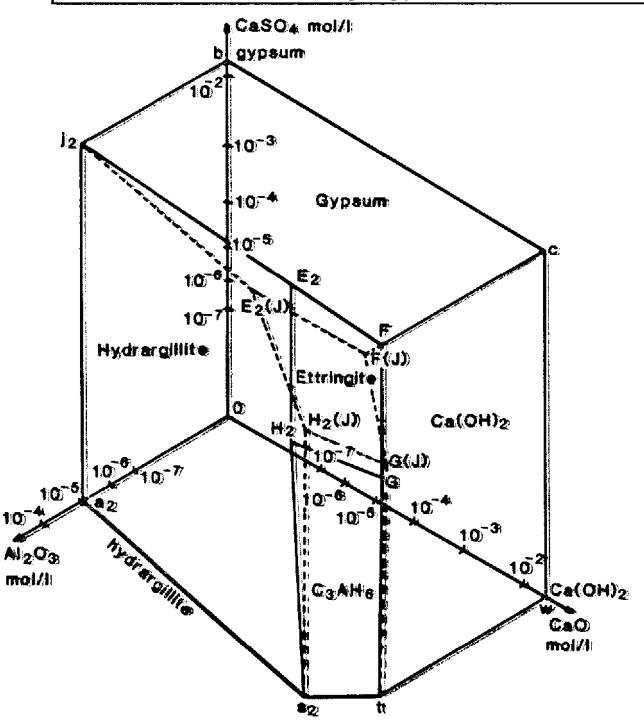

Figure 2. The stable system $CaO-Al_2O_3-CaSO_4-H_2O$ showing the quaternary invariant points determined by Jones (J) at 25°C and D'Ans and Eick at 20°C. Data are plotted as the 10th root of their molar concentrations.

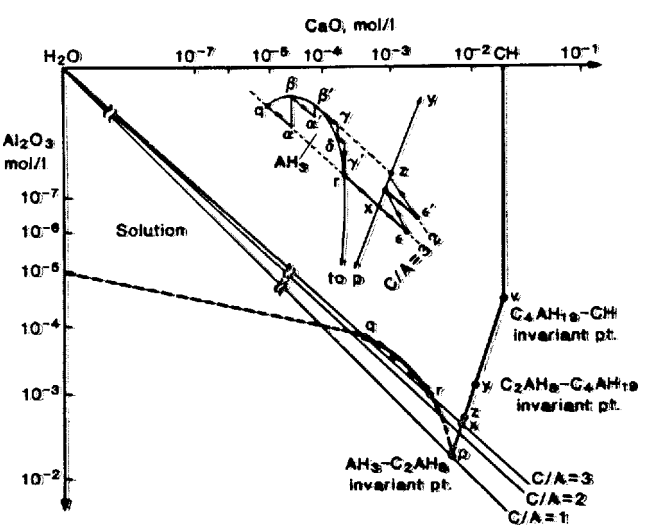

Figure 3. The metastable system $CaO-Al_2O_3-CaSO_4$ determined by D'Ans and Eick. Data are plotted as the 10th root of their molar concentrations.

4. a mechanical mixture of C_3A and gypsum particles in a saturated $Ca(OH)_2$ solution.

C_3A and Gypsum Particles in Water

In this case, two alternatives may occur depending on the rate at which calcium sulfate, entering solution as a result of the dissolution of gypsum, approaches the vicinity of the hydrating C_3A particle. If, in the first instance, it is assumed that the calcium sulfate concentration in solution near the hydrating C_3A particle remains negligible during the initial dissolution process, figure 3 may be used to illustrate the initial phase relationships. As this figure shows, C_3A dissolution proceeds congruently at a C/A ratio of 3 until reaching point q. The curve q-r was obtained from the data of Glasser and Marinho [23] and their data points are indicated on the figure. Continued congruent dissolution to point α, shown in the insert in this figure, results in a solution supersaturated with respect to AH_3. Supersaturation is relieved by AH_3 precipitation along the line α-β until the point β on the AH_3 solubility curve is reached. Continued C_3A dissolution, driving the solution composition towards supersaturation at α', and precipitation of AH_3 causes the solution to reach point β'. Further C_3A dissolution drives the solution composition towards point Y. This point is undersaturated with respect to AH_3 and, under the conditions of metastable equilibrium, AH_3 dissolution should occur along the line Y-δ. Continued C_3A dissolution brings the system to point Y', which is also undersaturated with respect to AH_3. AH_3 dissolution then brings the system to point r. Finally, further C_3A dissolution brings the solution composition to point x on the C_2AH_8 solubility curve. However, should a departure from equilibrium occur as a result of incomplete AH_3 dissolution, continued C_3A dissolution causes the solution composition to intersect the C_2AH_8 solubility curve somewhere between points x and z. This latter possibility is in accord with the findings of Glasser and Marinho [23] who calculated that an AH_3 layer between 1 and 5 μm in thickness formed during the early hydration of C_3A.

After the composition of the solution reaches the C_2AH_8 solubility curve, further C_3A dissolution supersaturates the system with respect to C_2AH_8 bringing the solution composition to point ε. C_2AH_8 precipitation at a C/A ratio of 2 returns the solution composition to the C_2AH_8 solubility curve. Continuing dissolution and precipitation occurs along the line x-z-y until the C_2AH_8-C_4AH_{19} invariant point is reached.

If it is assumed that calcium sulfate, entering solution as a result of gypsum dissolution, reaches the vicinity of the C_3A particle when the system is at the invariant point y, the composition of the solution moves towards the line n-d along a plane on the AFm crystallization surface defined by the lines y-n and y-m. The precise position on this plane depends on the rates at which C_2AH_8 and C_4AH_{19} are converted to a sulfate-bearing phase. In moving along the plane n-m-y, an AFm solid solution precipitates, with the monosulfate phase, $C_3A{\cdot}Cs{\cdot}H_{12}$, forming as the terminal member of this solid solution series. Continuing C_3A dissolution then results in the formation of ettringite as the ettringite crystallization surface is intersected, and the solution composition moves towards the invariant point n.

However, calcium sulfate may reach the vicinity of the hydrating C_3A particle before the composition of the solution reaches the line x-y in figure 4. If calcium sulfate enters the system when the solution composition is at some arbitrary point between q and r, the solution composition moves along a line parallel to the calcium sulfate axis. This is represented in figure 4 as occuring at point q in which case the composition of the solution moves along the line q-k. Continuing C_3A dissolution supersaturates the system with respect to AH_3 as the AH_3 crystallization surface is intersected and sequential AH_3 precipitation and C_3A dissolution results in the system moving along the line k-e towards the quaternary invariant point e, as schematically represented.

C_3A and Gypsum Particles in a Saturated Gypsum Solution

In this case the initial solution composition lies on point b in figure 4. C_3A dissolution causes the solution composition to move along the line b-u on the gypsum crystallization surface. As the solution composition intersects the AH_3 crystallization surface, AH_3 precipitation causes the composition of the solution to move towards the quaternary invariant point e, as shown schematically.

C_3A and Gypsum Particles in a Solution Saturated with Gypsum and Lime

If C_3A particles are placed in a solution saturated with respect to both $Ca(OH)_2$ and gypsum, the initial solution composition lies on point c in figure 4. In this instance, C_3A dissolution causes the composition of the solution to move along the line c-F. c-F defines the boundary between the $Ca(OH)_2$ and gypsum crystallization surfaces and the C/A ratio along this line is 3. As a consequence, C_3A dissolution simply causes the system to approach the invariant point F without precipitating any other phases.

2.1

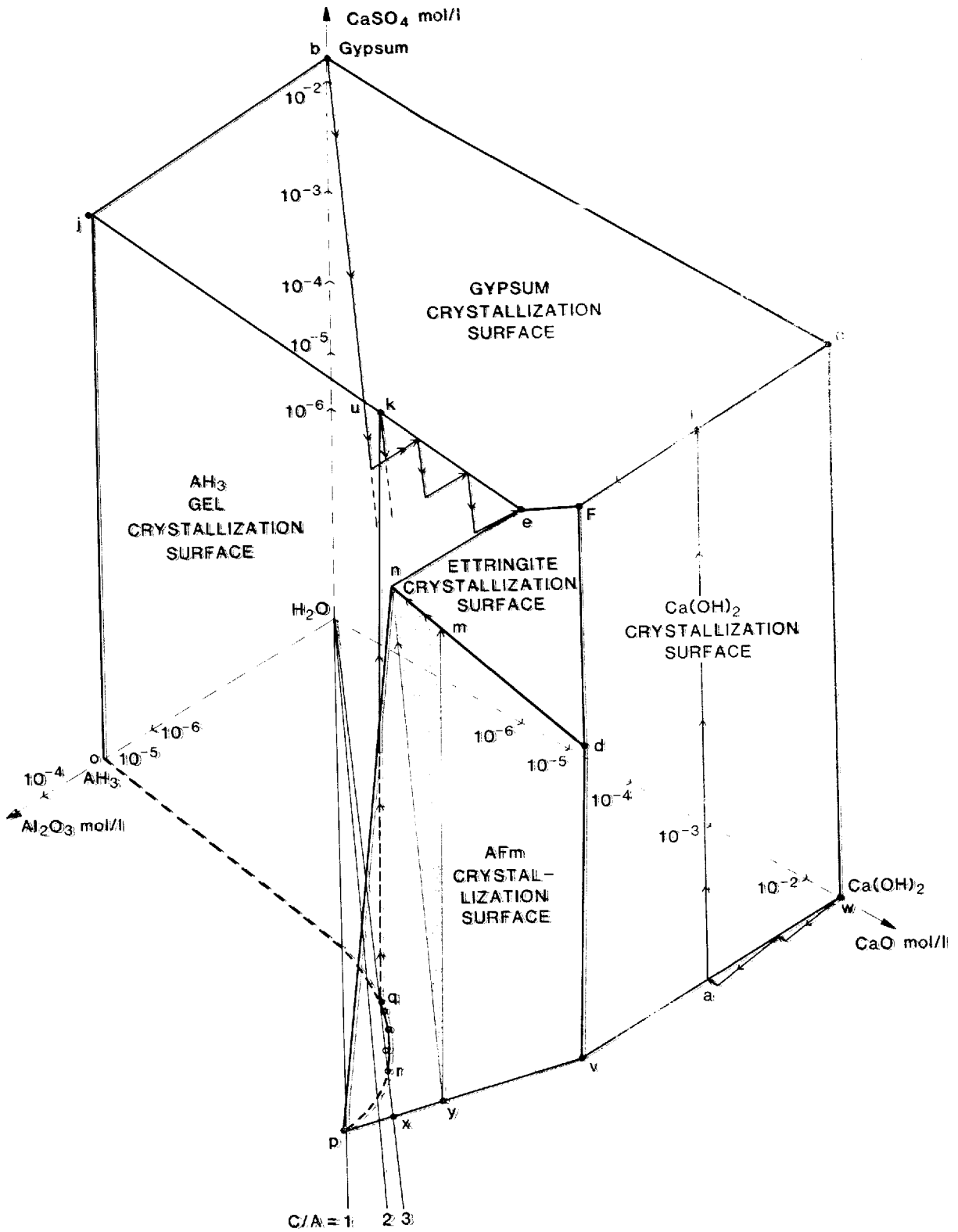

Figure 4. The metastable system $CaO-Al_2O_3-H_2O$ plotted on orthogonal axes. Data are plotted as the 10th root of their molar concentrations.

C_3A and Gypsum Particles in a Lime-Saturated Solution

In this instance the initial composition lies on point w in figure 4. C_3A dissolution and $Ca(OH)_2$ precipitation move the composition of the solution along the line w-v, as shown schematically. If calcium sulfate, from the dissolution ofgypsum, approaches the reacting C_3A particle at some arbitrary point a on the line w-v, the solution composition moves along the $Ca(OH)_2$ crystallization surface on the line a-1 until the line c-F is intersected. Subsequent C_3A dissolution moves the composition of the solution towards the invariant point F.

Discussion

The relevant phase equilibria indicate the dissolution of C_3A to be congruent, regardless of the presence of gypsum. However, the AH_3 solubility curve appears to intersect the line of congruent C_3A dissolution leading to the precipitation of AH_3. Thus, AH_3 is the first-formed hydrate in the metastable quaternary system when C_3A and gypsum are hydrated in water or in a saturated gypsum solution.

It has been suggested by Stein and coworkers [24-7] that C_3A hydration in the presence of gypsum is retarded by the formation of an alumina gel layer. The phase relationships previously discussed suggest that alumina gel formation occurs when C_3A and gypsum are hydrated in water or in a solution initially saturated with respect to gypsum. On the other hand, calorimetric data obtained by Collepardi et al. [28] indicate the rate of C_3A hydration to be more strongly retarded in the presence of lime and gypsum than in the presence of gypsum alone. Initial formation of alumina gel would not be expected when the solution is saturated with respect to lime or saturated with respect to both lime and gypsum. Rather, ettringite is the first-formed aluminate-containing phase under these conditions. This suggests that the presence of AH_3 does not initially have a significant retarding effect on the rate of hydration of C_3A.

As with the C_3S-water system, the above analysis only considers the phase relationships involving the bulk solution. For example, hydration in a lime-gypsum solution predicts ettringite to be the first-formed phase. However, the subsequent phase relationships in the interfacial zone between the ettringite and the C_3A will depend on the relative rates at which water, and calcium and sulfate ions enter this region. For instance, should water reach the interfacial zone relatively rapidly and calcium and sulfate ions relatively slowly, the ettringite will tend to decompose to AFm phases, and AH_3 formation may also occur. In this case the phases that exist within the interfacial region will be:

C_3A--AH_3--AFm--ettringite--solution (saturated with respect to lime and gypsum). Macroscopically, this is a departure from equilibrium; however, locally, conditions will be close to those of equilibrium.

ACKNOWLEDGEMENT:

The author wishes to thank Prof. H.F. W.-Taylor and Dr. Karen Scrivener for many stimulating discussions which contributed significantly to this paper.

REFERENCES

1. N. L. Thomas and D. D. Double, "The Hydration of Portland Cement, C_3S and C_2S in the Presence of a Calcium Complexing Admixture (EDTA)," Cem. Concr. Res. 13, 391 (1983).

2. F. P. Glasser, M. J. Angus, C. E. McCulloch, D. MacPhee, and A. A. Rahman, "The Chemical Environment in Cements," Matls. Res. Soc. Proc. 44, 849, C. M. Jansen, J. A., Stone, and R. C. Ewing, Eds., Matls. Res. Soc., Pittsburgh (1985).

3. P. W. Brown, E. Franz, G. Frohnsdorff, and H. F. W. Taylor, "Analyses of the Aqueous Phase During Early C_3S Hydration," Cem. Concr. Res. 14, 257 (1984).

4. E. P. Flint and L. S. Wells, Study of the System $CaO-SiO_2-H_2O$ at 30°C and of the Reactions of Water on the Anhydrous Calcium Silicates," J. Res. N. B. S. 12, 751 (1934).

5. G. E. Bessey, "The Calcium Aluminate and Silicate Hydrates," Symp. Chem. Cem., 178, Ingeniorsvetenskapsakademien, Stockholm (1939).

6. P. S. Roller and G. Ervin, Jr., "The System Calcium Oxide-Silica-Water at 30°," J. Am. Chem. Soc. 62, 461 (1940).

7. H. Steinour, "The System $CaO-SiO_2-H_2O$ and the Hydration of the Calcium Silicates," chem. Revs. 40, 391 (1947).

8. H. M. Jennings, "Equilibria Between Aqueous Phase and Two Types of Calcium Silicate Hydrate," J. Am Ceram. Soc., accepted.

9. R. Hedin, Sven. Forskn. Cem. Betong. K. Tek. Hoegsk. Stockholm, No. 33 (1962).

10. P. Barret, D. Bertrandie, and D. Menetrier, "Comparative Study of C-S-H Formation from Supersaturated Solutions and C_3S Solution Mixtures," Proc. 7th Intl. Cong. Chem. Cem. II, II-261, Editions Septima, Paris (1980).

11. H. F. W. Taylor, "Hydrated Calcium Silicates. Part I, Compound Formation at Ordinary Temperatures," J. Chem. Soc. 3682 (1950).

12. H. F. W. Taylor and D. E. Newbury, "Calcium Hydroxide Distribution and Calcium Silicate Hydrate Composition in Tricalcium Silicate and β-Dicalcium Silicate Pastes," Cem Concr. Res. 14, 93 (1984).

13. H. F. W. Taylor, "The Calcium Silicate Hydrates," Proc. 5th Intl. Sym. Chem. Cem. 2, 1, Cement Assoc. of Japan. Tokyo (1968).

14. H. F. W. Taylor, "Jennite, 1.4 nm Tobermorite, and C-S-H Gel," J. Am. Ceram. Soc., submitted for publication.

15. J. B. Ings, P. W. Brown, and G. Frohnsdorff, "Early Hydration of Large Single Crystals of Tricalcium Silicate," Cem. Concr. Res. 13, 843 (1983).

16. L. S. Wells, W. F. Clark, and H. F. McMurdie, "Study of the System $CaO-Al_2O_3-H_2O$ at 21°C and 90°C," J. Res. N.B.S. 30, 367 (1943).

17. F. E. Jones, "The Quaternary System $CaO-Al_2O_3-CaSO_4-H_2O$ at 25°C," Trans. Faraday Soc. 35, 1484 (1939).

18. F. E. Jones, "The Quaternary System $CaO-Al_2O_3-CaSO_4-H_2O$ at 25°C; Equilibria with Crystalline $Al_2O_3 \cdot 3H_2O$, Alumina Gel, and Solid Solutions," J. Phys. Chem. 48, 311 (1944).

19. F. E. Jones and M. H. Roberts, "The System $CaO-Al_2O_3-H_2O$ at 25°C," DSIR Bldg. Res. Stat. Note E 965. HMSO, London (1962).

20. J. D'Ans and H. Eick, "Das System $CaO-Al_2O_3-H_2O$ bei 20°C und das Erharten der Tonerdezemente," Zem. Kalk Gips 6, 197 (1953).

21. J. D'Ans and H. Eick, "Das System $CaO-Al_2O_3-CaSO_4-H_2O$ bei 20°C," Zem. Kalk Gips 6, 302 (1953).

22. W. Eitel, "Recent Investigations of the System Lime-Alumina-Calcium Sulfate-Water and its Importance in Building Research Problems," J. Am. Concr. Inst. 28, 679 (1957).

23. F. P. Glasser and M. B. Marinho, "Early Stages of the Hydration of Tricalcium Aluminate and its Sodium-Containing Solid Solutions," Brit. Ceram. Soc. Proc. 35, 221 (1984).

24. W. A. Corstanje, H. N. Stein, and J. M. Stevels, "Hydration Reactions in Pastes $C_3S+C_3A+CaSO_4 \cdot 2aq+H_2O$ at 25°C," Part I, Cem. Concr. Res. 3, 791 (1973); Part II, Cem. Concr. Res. 4, 193 (1974); Part III, Cem. Concr. Res. 4, 417 (1974).

25. W. A. Corstanje, H.N. Stein, and J. M. Stevels, "Hydration Reactions in Suspensions of $C_3A+C_3S+CaSO_4 \cdot 2aq$ in Water," Cem. Concr. Res. 4, 581 (1974).

26. C. L. M. Holton and H. N. Stein, "Influence of Quartz Surfaces on the Reaction $C_3A+CaSO_4 \cdot 2H_2O+Water$," Cem. Concr. Res. 7, 291 (1977).

27. H. N. Stein, "The Colloid Chemistry of Calcium Aluminate Hydrates," Proc. 7th Intl. Cong. Chem. Cem. IV, 449, Septima Editions, Paris (1980).

28. M Collepardi, G. Baldini, M. Pauri, and M. Corradi, "Tricalcium Aluminate Hydration in the Presence of Lime, Gypsum, or Sodium Sulfate," Cem. Concr. Res. 8, 571 (1978).

H. M. Jennings, H. Taleb, G. Frohnsdorff and J. R. Clifton, Building Materials Division, Center for Building Technology, Gaithersburg, MD 20899, U.S.A. 1

Interpretation of the Effects of Retarding Admixtures on Pastes of C_3S, C_3A plus Gypsum, and Portland Cement 2.1

SUMMARY: From studies of the effects of a range of organic retarders on pastes of C_3S and of C_3A-gypsum, it may be concluded that the two systems have different, possibly independent, influences on the concentrations of retarders in the aqueous phase of a portland cement paste. In the case of C_3S, some of the retarder is incorporated into the layer of product which forms around the grains during the early stages of reaction. It appears that a process which controls the induction period occurs within this C-S-H layer and that the incorporation of a retarder in it somehow slows the process. It may be that a phase change, or other reaction which ends the induction period by making the layer more permeable, is poisoned by the retarder which is incorporated into the layer. The C_3A-gypsum-water system removes a large amount of retarder from the aqueous phase during the early stages of hydration, with the rate of removal falling with time. Delaying retarder addition, therefore, decreases the amount of retarder which can be incorporated into a C-S-H layer. Thus these systems affect, in separate ways, a retarder's ability to extend the induction period of a portland cement. There is a delay time after initial mixing, when it is most efficient to add a retarder. It seems probable that, at least for some organic retarders, the effects on the portland cement reaction may be considered to be a combination of separate processes occuringin the C_3S-water and C_3A-gypsum-water subsystems.

Através de estudos dos efeitos de uma série de retardadores orgânicos sobre pastas de C_3S e de C_3A-gesso, pode-se concluir que os dois sistemas têm influências diferentes, possivelmente independentes, sobre a concentração de retardadores na fase aquosa de uma pasta de cimento portland. No caso do C_3S, parte do retardador se incorpora na camada de produto que se forma ao redor dos grãos durante os estágios iniciais da reação. Parece que um processo, que controla o período de indução, ocorre dentro desta camada de C-S-H e que a incorporação de um retardador nela desacelera o processo de algum modo. Pode ser que uma mudança de fase, ou outra reação que encerre o período de indução fazendo a camada mais permeável, seja envenenada pelo retardador que é incorporado na camada. O sistema C_3A-gesso-água retira da fase aquosa uma grande quantidade de retardador, durante os estágios iniciais de hidratação, com a velocidade de retirada diminuindo com o tempo. Portanto, o atraso na adição do retardador diminui a quantidade deste que pode ser incorporado na camada de C-S-H. Assim este sistema afeta, de formas diferentes, a aptidão de um retardador para ampliar o período de indução de um cimento portland. Há um tempo de atraso depois da mistura inicial, quando é mais eficaz adicionar-se um retardador. Parece provável que, pelo menos para alguns retardadores orgânicos, os efeitos sobre a reação do cimento portland pode ser considerada como sendo uma combinação de processos separados que acontecem nos sub-sistemas C_3S-água e C_3A-gesso-água.

INTRODUCTION

The influence of retarding admixtures on the hydration of portland cement has been extensively studied. There remains, however, an incomplete understanding of the mechanisms by which retarders control the rate of cement hydration and the time of set. The problem is complex because portland cement is a mixture of several minerals, each of which may interact individually with a retarder.

Several different stages are observed in the hydration of a typical portland cement. A short initial period of rapid reaction is followed by a period of slow reaction, known as the induction period. During these first two stages, the paste is plastic. After the induction period, the reaction accelerates and the paste begins to stiffen or "set." The lengths of the induction periods for both portland cement and pure C_3S are similar (1) which suggests that the main contributor to the reactions which end the induction period is the same in both cases. If this is so, it must be the C_3S reaction which ends the induction period. The length of the induction period can be increased by the addition of retarders, sometimes extending it from the normal few hours to many days. Portland cement has a characteristic "time of set" which occurs early in the period of accelerating reaction, and is influenced by retarders in the same way as the length of the induction period.

The reactions between cement and water which end the induction period could occur in any of three types of sites (3): 1) on the surface of the anhydrous material (or of the hydration product), 2) in the aqueous phase, and 3) in the hydration product. Although retarders are normally added to the aqueous phase, they could influence reactions in the other two types of sites by adsorption on to a surface or incorporation into a product. This paper discusses how retarders might influence the reaction mechanism in the different sites in each of two subsystems in portland cement: 1) C_3S-water, and 2) C_3A-gypsum-water. There are other subsystems such as C_2S-water and C_4AF-water in portland cement pastes but, they generally make much smaller contributions to the early reactions because they either react slowly, and/or make up only a small percentage of a portland cement; they appear not to have an obvious effect on the length of the induction period and they will not be discussed here.

Experimental results to be discussed in the present paper are drawn from a recent investigation of the influence of retarding admixtures on the hydration of C_3S (3-5) and from the literature data on the C_3A-gypsum-water system (6,7). The effects discussed in this paper are illustrated primarily with sucrose as a retarder, but similar phenomena have been observed with a variety of retarders (3-5).

INTERPRETATION OF CONCENTRATIONS OF LIME AND SILICA IN THE AQUEOUS PHASE IN THE C_3S SYSTEM

It is believed (8) that C_3S grains in a C_3S paste are surrounded by a layer of calcium silicate hydrate (C-S-H). A solubility curve for the C-S-H which surrounds C_3S during the induction period has been defined recently; because the data points fall on a smooth curve, AB in Fig. 1., it has been suggested (8) that the outer surface of the layer is near to equilibrium with the aqueous phase. Fig. 1 summarizes these data (solid line AB) along with other data points obtained with and without retarders in the original mixing water (3-5). The presence of retarders does not move the data points from the line and therefore does not alter the state of near-equilibrium established without retarders.

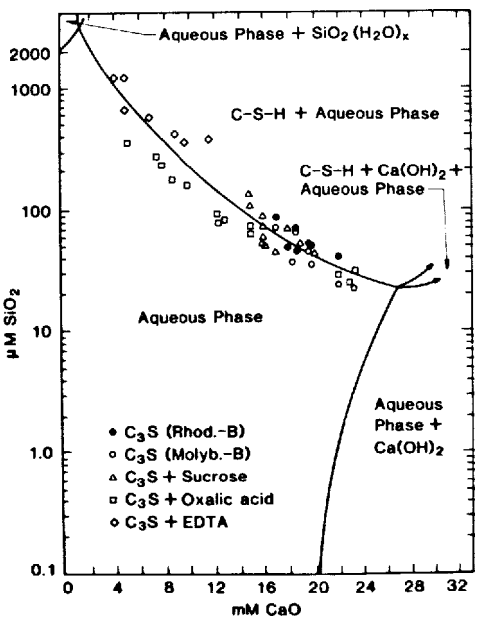

Figure. 1 Concentrations of CaO and SiO_2 in aqueous solution which have been mixed with C_3S. The points associated with EDTA and oxalic acid are values for free calcium ion and do not include calcium which has been chelated or precipitated. Silica concentrations were determained using the molybdenum blue and rhodamine B methods (4,6). In all cases w/c=2 and T=20°C.

Some aspects of the chemistry of the surface layer on the C_3S grains can be deduced from the solubility curve. As time passes after mixing, the data points always move along the curve, AB, from A at the upper left towards B at the lower right. The data

points in Fig. 1 were taken between one and sixty minutes after mixing. The temperature and the initial water:C_3S ratio were kept constant at 20°C and 2.0, respectively. The course of the C_3S-water reaction appears to be as follows. Upon mixing C_3S with water, the solid dissolves congruently and the concentrations of the components in the aqueous phase rise until the solubility curve (AB) is reached. Congruent dissolution implies that the curve is approached at concentrations of about CaO = 4mM and SiO_2 = 1.3 mM. When the solution is saturated (i.e. when AB is reached), a layer of C-S-H hydration product soon forms (8) on the surface of the C_3S grains and near-equilibrium is established between its external surface and the aqueous phase. As the C_3S continues to dissolve, the C-S-H continues to form and the layer on the C_3S grains thickens. The C-S-H has a Ca:Si ratio of about 1.7 (9) which is much smaller than the ratio of 3 for C_3S; as a result, the Ca concentration in the aqueous phase continues to rise. In order to maintain the observed near-equilibrium concentration of Fig.1, some SiO_2 must be removed from solution by precipitation of additional quantities of C-S-H product. This causes the data points to continue to move along the solubility curve towards B.

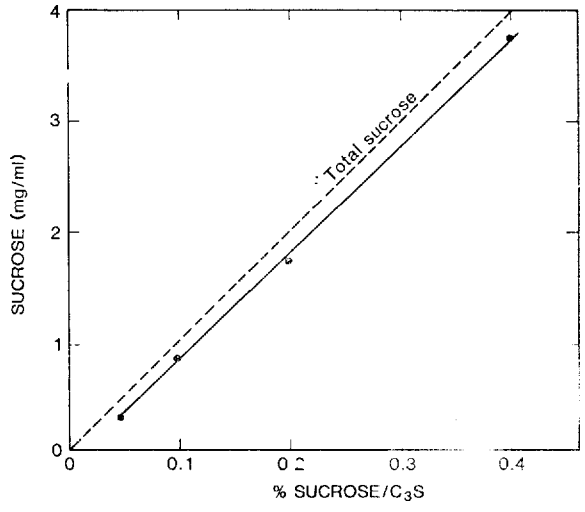

Figure 2. Concentrations of sucrose in the aqueous phase 15 minutes after mixing C_3S with aqueous sucrose solutions of various concentrations (4,6); w/c=2, T=20°C.

EFFECTS OF SUCROSE, EDTA AND OXALIC ACID ON THE LENGTH OF THE INDUCTION PERIOD OF C-S-H PASTES

Sucrose is a strong retarder for the setting of C_3S and portland cement. The 2% solution by mass associated with data points of Fig.1 extends the induction period from the normal few hours to about seven days. When used at the same concentration by mass, EDTA is less effective a retarder than sucrose, and oxalic acid shows a small acceleration effect. Fig. 1 shows that data for mixtures incorporating EDTA and oxalic acid are close to one another and are separated from data for mixtures incorporating sucrose and no admixture which are also close to one another. Thus, there is apparently no correlation between the length of the induction period and the positions of the data points on the solubility curve. The equilibrium between the aqueous phase and the surface of the C-S-H is not altered significantly by the presence of retarders. It is concluded, therefore, that the concentrations in solution of the components associated with C-S-H (CaO and SiO_2) are not directly responsible for changing the length of the induction period.

INTERPRETATION OF THE EFFECTS OF RETARDER IN THE AQUEOUS PHASE OF THE C_3S-WATER SYSTEM

Fig. 2 shows, as a function its concentration in the initial mixture, the concentration of sucrose in the aqueous phase of a C_3S paste 15 minutes after mixing. The vertical distance between the two lines in Fig. 2 represents the amount ofsucrose removed from solution in the 15 minutes; it is a measure of the amount of sucrose adsorbed on, or incorporated within, the product layer on the C_3S grains. Clearly, most of the retarder remains in solution. The concentration of a retarder in the mixing water has a strong influence on the retardation (3-6) with greater concentrations causing longer induction periods. Further, it has been observed recently (3-5) that, for C_3S pastes, the retarder is most effective when it is added to the water prior to being mixed with C_3S. Fig. 3 provides data which shows that, for a given quantity of sucrose, delayed addition reduces the effect on the induction period (compared to the induction period if sucrose is added first to the water). A 5 minute delay reduces the retardation by one half, and longer delay reduces the retardation still more. These observations suggest (3-6) that the reaction which brings the induction period to an end takes place somewhere within the product layer which surrounds the C_3S grains. They suggest, further, that retarder present in the aqueous phase during the early stages is incorporated into the layer thereby delaying the termination of the induction period (3-5). If, as we believe, the end of the induction period is associated with a phase change in the product layer, then the retarders may retard the phase change by hindering the first-formed product from converting into a second product which causes the layer to become more permeable. This conversion may be a nucleation and growth process.

2.1

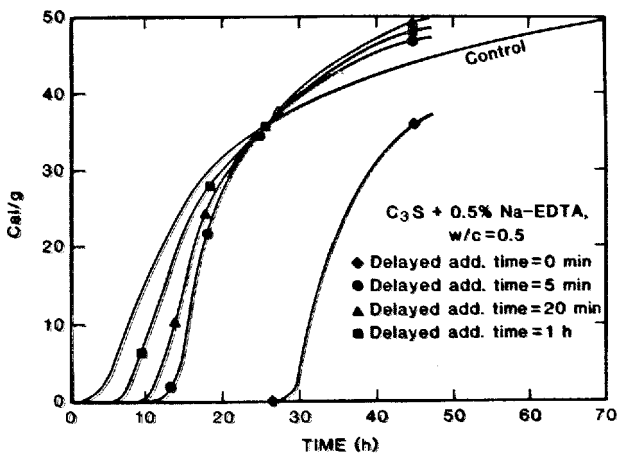

Figure 3. Plot of heat required to decompose $Ca(OH)_2$ in C_3S pastes (mixed at w/c = 2, T = 20°C) as a function of time after mixing. Sucrose was added to the pastes at the times indicated. The greater the heat the more the $Ca(OH)_2$. The formation of $Ca(OH)_2$ begins at the end of the induction period. Delayed addition of sucrose shortens the induction period as compared to addition with the original mixing water (4,6).

CONCENTRATION OF RETARDER IN THE AQUEOUS PHASE IN THE C_3A-GYPSUM-WATER SYSTEM

The C_3A-gypsum-water system consumes a substantial amount of retarder during the early stages of hydration (6,7), significantly reducing its concentration in the aqueous phase. Further, the amount of retarder removed from solution is less if the retarder addition is delayed (7). These observations suggest that retarder is incorporated in the hydration product which forms during the early stages of reaction.

THE EFFECT OF DELAYED ADDITION OF RETARDERS ON THE TIME OF SET OF PORTLAND CEMENT

The C_3S-water and C_3A-gypsum-water systems influence the concentration of retarder in the aqueous phase of portland cement pastes in different ways. With the C_3A-gypsum-water system, the earlier the retarder is added, the more is removed from the aqueous phase. In contrast, the C_3S-water system removes only a small amount of retarder from the aqueous phase. It seems likely that, in portland cements, the two systems will make separate and different contributions to the quantity of retarder which is incorporated within the C-S-H layer during the early stages of reaction.

Since the time of set in portland cement is correlated with the length of the induction period of the C_3S-water system, then it may be proposed that the effects of the two systems, C_3S-water and C_3A-gypsum-water, can be combined as illustrated in Fig. 4. The ability of a retarder to lengthen of the induction period tends to increase with delay time because the C_3A-gypsum-water system will then remove less retarder from the solution and leave more in the aqueous phase to retard the C_3S hydration. On the other hand, if the addition is delayed too long, the retarder will have less effect on the hydration of C_3S. A plot of experimental results is shown in Fig. 5. The length of the induction period has been scaled by an arbitrary factor so that it can be more easily compared with the time of set. As can be seen, there is an optimum time after mixing portland cement and water at which a retarder should be added if the greatest retardation is desired. This time may vary with cement composition and other factors, such as water:cement ratio and temperature of hydration, because the contributions from the different sub-systems will vary. More data are needed to establish whether or not the effects of the different systems on the set time are independent. Also, the interaction between retarders and the other subsystems including C_2S and C_4AF must be considered to establish whether the effects are always as small as has been assumed in this paper.

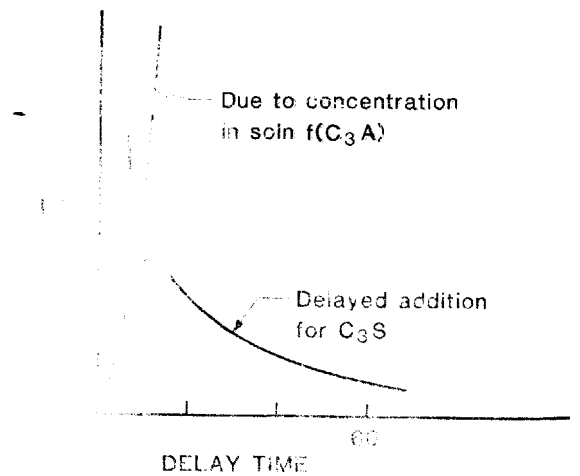

Fig. 4. Variation of induction period with delay in adding retarder to portland cement. Schematic representing a superposition of the separate effects of 1) the C_3S-water system and, 2) the C_3A-gypsum-water system, on the delayed addition of a fixed amount of retarder to a portland cement. At early delay times C_3A-gypsum controls the I.P. At late delay times C_3S controls the I.P.

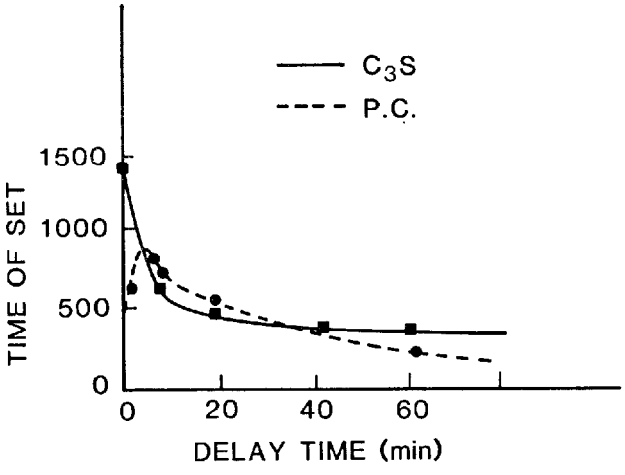

Figure 5. Influence of delay time on time of set. Dotted line is for portland cement pastes. Solid line is for C_3S pastes. The influence of delay time on portland cement pastes can be largely attributed to the C_3S-water subsystem.

CONCLUSIONS

From studies of the effects of a range of organic retarders on pastes of C_3S and of C_3A-gypsum, it may be concluded that the two systems have different, possibly independent, influences on the concentrations of retarders in the aqueous phase of a portland cement paste. In the case of C_3S, some of the retarder is incorporated into the layer of product which forms around the grains during the early stages of reaction. It appears that a process which controls the induction period occurs within this C-S-H layer and that the incorporation of a retarder in it somehow slows the process. It may be that a phase change, or other reaction which ends the induction period by making the layer more permeable, is poisoned by the retarder which is incorporated into the layer. The C_3A-gypsum-water system removes a large amount of retarder from the aqueous phase during the early stages of hydration, with the rate of removal falling with time. Delaying retarder addition, therefore, decreases the amount of retarder which can be incorporated into a C-S-H layer. Thus these systems affect, in separate ways, a retarder's ability to extend the induction period of a portland cement. There is a delay time after initial mixing, when it is most efficient to add a retarder. It seems probable that, at least for some organic retarders, the effects on the portland cement reaction may be considered to be a combination of separate processes occuringin the C_3S-water and C_3A-gypsum-water subsystems.

ACKNOWLEDGEMENTS

The authors wish to thank J. Skalny and L. Struble for helpful discussions.

REFERENCES

1. I. Jawed, J. Skalny and J.F. Young, "Hydration of Portland Cement," Structure and Performance of Cements, ed. P. Barnes, Applied Science Publishers, New York-London (1983) 237.

2. H.M. Jennings, "The Developing Microstructure in Portland Cement," Advances in Cement Technology, ed, S.N. Ghosh, Pergamon Press, Oxford (1983) 349.

3. H. Taleb, Analytical and Mechanistic Aspects of the Action of Selected Retarders on the Hydration of Tricalcium Silicate, the Major Component of Portland Cement, PhD Thesis, Georgetown University, Washington D.C. (1985).

4. H.M. Jennings and H. Taleb, "The Influence of Selected Retarders on the Hydration of Tricalcium Silicate," Proceedings of the Engineering Foundation Conference on Cement Production and Use, Henniker, New Hampshire, (1985) in press.

5. H. Taleb and H.M. Jennings, to be published.

6. V.S. Ramachandran, Concrete Admixtures Handbook, Noyes Publications, New Jersey (1984).

7. V.S. Ramachandran, "Admixture Interactions in the Cement Water System," Paper presented at Engineering Foundation Conference on Cement Production and Use, Henniker, New Hampshire (1985).

8. H.M. Jennings, "Aqueous Solubility Relationships for Two Types of Calcium Silicate Hydrate,"J. Amer. Ceram. Soc., in press.

9. H.F.W. Taylor et al. "The Hydration of Tricalcium Silicate," Committee Report, Materials and Structures RILEM, 17, [102] (1984) 457.

Ellis Gartner and Jan Skalny, W. R. Grace & Co., Research Division, Columbia, Maryland, U.S.A.[1]

COMPUTATION OF SOLUBILITY RELATIONSHIPS FOR HYDRATING CEMENT SYSTEMS 2.1
CALCUL DES RELATIONS DE SOLUBILITÉ POUR DES CIMENTS HYDRATANTS

SUMMARY: The use of liquid phase analysis to assess the state of hydrated cement systems is discussed. Assumptions regarding the form of the relationship between ionic strength and the activities of each thermodynamic component of the cement system are made. Using published solubility data and ionic association constants where available, it is shown that the liquid phase chemical potentials of calcium hydroxide silica and calcium sulfate decrease with age during hydration of portland cement. This is interpreted as being due to formation of stable hydrates from metastable hydrates formed at earlier ages. The lack of comprehensive phase equilibrium data for the cement water system is noted, and further work in this area is recommended.

Discute-se a utilização da análise da fase líquida para avaliar o estado de sistemas de cimentos hidratados. São feitas suposições relativas à forma de relação entre resistência iônica e as atividades de cada componente termodinâmico do sistema de cimento. Usando dados de solubilidade publicados e constantes de associação iônica quando disponíveis, mostra-se que os potenciais químicos da fase líquida de hidróxido de cálcio - sílica e sulfato de cálcio diminuem com o tempo de duração da hidratação do cimento portland. Admite-se ' que este fato seja devido à formação de hidratos estáveis, a partir de hidratos metastáveis' formados nas idades iniciais. É observada a falta de dados completos do equilíbrio de fase para o sistema de água cimento, pelo que se recomenda trabalho adicional nesta área.

Introduction

Substantial progress has been made toward understanding hydration mechanisms and microstructure development, and their relationship to the mechanical properties of hardened concrete. This progress, together with advancements in computer technologies, have recently led to attempts to develop comprehensive, state-of-the-art models of cement hydration and microstructural development(1). Generally, these developments have been slow due to several factors, among which is the lack of some fundamental data needed for further advancement of the field. An example of the latter problem is an inadequate data base in phase relationships such as the dynamic (time-dependent) and equilibrium solid-liquid interactions during cement hydration.

In this paper, we outline some of the essential aspects of a standardized approach to the interpretation of liquid-solid phase equilibria in the cement/water system. A considerable amount of aqueous phase compositional data has been generated by various workers, using such methods as filtering, centrifuging, and pressing of cement pastes (e.g., refs. 2, 3, 4, 5). At times beyond set, pressing is the only technique available. Comparison of the concentrations of the ions found in the extracted solutions should, in principle, allow prediction of the solid phases which may be forming from or in equilibrium with the solutions. However, estimation of saturation with respect to many of the phases of interest is difficult and subject to serious limitations in analytical and in computational techniques.

Because of limited experimental data, the approach taken in this paper deals only with a few selected aspects of the problem. We welcome suggestions by others as to how to extend this approach and improve it.

Notation

In order to develop any such standardized approach, a clear and readily interpretable notation seems desirable. We intend to follow notation used by Gartner, et al,(3) with some minor changes. In this notation, square brackets indicate the concentration of the enclosed solvated species and curved brackets indicate activity*; the two are related by the activity coefficient, γ:

$$\gamma_i [i] = (i) \qquad (1)$$

where i may be any ionic or neutral dissolved species.

Following Debye-Huckel theory for dilute aqueous solutions, γ_i is a function only of the ionic strength, I, and the charge, Z_i on the species i at constant temperature. Ionic strength is defined below:

$$I = 0.5 \sum_i [i] Z_i^2 \qquad (2)$$

Ionic species behave essentially independently in dilute aqueous solution, but clearly cannot be isolated in a solid phase without an equal number of opposite charges. Thus, to define the thermodynamic components of any part of the cement-water system, the neutral elements or their oxides or other compounds are generally used. Any independent set of components may be chosen, but clarity is enhanced if the components chosen are those which represent the normal limits of the hydrated cement system. Thus, instead of the oxides H_2O, CaO, SiO_2, Al_2O_3, Fe_2O_3, SO_3, Na_2O, K_2O, CO_2, etc. (shorthand notation H, C, S, A, F, $\bar{S}$, N, K, $\bar{C}$), we prefer to use CH, S, AH_3, FH_3, $C\bar{S}$, NH, KH, and $C\bar{C}$. Non-oxide anionic groups, such as chloride, can be represented conveniently in oxide notation by symbols such as C' (representing $2Cl^- - O^{2-}$); however, we prefer to use $CaCl_2$ as the independent component, which we may also write as CC'. The choice of the calcium salts of anions and the hydroxide salts of cations in the above basis set reduces the number of steps in solubility calculations.

Theory

The chemical potential, μ_i, of each species, i, in the aqueous phase is conventionally related to its activity by equation (3) (which constitutes the definition of activity):

$$\mu_i = \mu^\circ_i + RT \ln (i) \qquad (3)$$

where μ°_i represents the chemical potential of solvated species i in the state of unit activity. The chemical potential of any of the above-listed components in solution is related to the activities of any combination of species which uniquely defines that component, and we can choose whichever combination gives the greatest ease of computation. Thus, for example:

$$\mu_{CH} = \mu^\circ_{CH} + RT \ln \{(Ca^{2+})(OH^-)^2\} \qquad (4)$$

$$\mu_S = \mu^\circ_S + RT \ln \{(H_4SiO_4^\circ)\} \qquad (5)$$

*[Note: Ionic concentrations, activities, etc., are conventionally in units of molality unless otherwise specified. For the dilute solutions typical of cement/water, molarity is approximately equal to molality and they are often used interchangeably without serious error. The shorthand M is used to represent units of molarity (g-mols/litre solution).]

$$\mu_{AH_3} = \mu^\circ_{AH_3} + 2RT \ln\{(Al(OH)_4^-)/(OH^-)\} \quad (6)$$

$$\mu_{C\bar{S}} = \mu^\circ_{C\bar{S}} + RT \ln\{(Ca^{2+})(SO_4^{2-})\} \quad (7)$$

$$\mu_{NH} = \mu^\circ_{NH} + 2RT \ln\{(Na^+)(OH^-)\} \quad (8)$$

Note that we have made the tacit assumption that the chemical potential of water is always zero relative to the reference state of pure liquid water. Over the range of concentrations of interest (submolar) this is a reasonable and convenient approximation. All that remains is to determine the reference state for each component. The simplest and safest assumption is to set μ°_i equal to zero and thereby use unit activity as the reference state. Then, for the components which are relatively insoluble, values of μ_i at saturation are readily computed from the solubility of the pure component. For example:

$$\mu^{sat}_{CH} = + \left| RT\{\ln(Ca^{2+})(OH^-)^2\} \right| \text{at saturation} \quad (9)$$

The conventional equilibrium solubility product, Kp, for portlandite is also defined by equation (9). Thus, we may also write equation (4) as:

$$\mu_{CH} - \mu^{sat}_{CH} = RT(\ln Pp - \ln Kp) = RT \ln Sp \quad (10)$$

In this case, Pp is the actual ionic activity product and Sp is the "saturation factor" of the solution with respect to portlandite(3). Values of Sp greater than unity represent supersaturation of the solution and, hence, an increased chemical potential of the component CH relative to the reference state, portlandite. Similar relationships will apply for any chosen solid phase of interest.

Computational Method

Since the various formulae which may be used to estimate the activity coefficients, γ_i, are all non-linear, we must generally resort to iterative methods for solving the equations relating concentration to chemical potential. Bailey and Hampson(6) showed in outline a simple first order iterative method, and we have continued to use such methods ourselves. (However, with increasing numbers of species, higher order convergence techniques may become desirable to minimize computing time.) Use of Davies' equation(7) (equation 11) simplifies the calculation of activity coefficients since there is no need to estimate solvated ionic radii:*

$$\log_{10} \gamma_i = AZ^2_i \left[0.3I - \sqrt{I}/(1+\sqrt{I})\right] \quad (11)$$

* (NOTE: The variation in A with temperatures is approximated by the equation $A = 0.490 + 8.87 \times 10^{-4}(T,°C)$ over the range 20-30°C.)

However, since all equations of this type are only approximations, it is necessary also to assume the existence of discrete "associated ions" in many cases, even when such species may in reality be only very loose associations. Thus, we assume the existence of the species $CaOH^+$, $CaSO_4^\circ$, $NaSO_4^-$, KSO_4^-, as in ref.(6). We must also consider a wide variety of possible silicate species: $H_4SiO_4^\circ$, $H_3SiO_4^-$, $H_2SiO_4^{2-}$, $HSiO_4^{3-}$, and possibly also complexes between these species and calcium and alkali ions. At this time, we do not have reliable estimates of the formation constants of associated calcium and alkali silicate species; thus we are forced either to neglect them in our calculations or to assume values based on those observed for other species. Likewise, we have little reliable information on the interactions of the aluminate anion with other species, although we believe that direct association between aluminate and silicate anionic species is insignificant at the low concentrations found in hydrating cement systems. Values of ionic association constants used in this work are listed in Table 1.

Table 1

Compound Ions and Their Assumed Activity Products

Compound Ion, (i)	Association Activity Product (Pi)	Value Assumed for Pi	Reference
$CaOH^+$	$\frac{(CaOH^+)}{(Ca^{2+})(OH^-)}$	24 M^{-1}	(8)
$CaSO_4^\circ$	$\frac{(CaSO_4^\circ)}{(Ca^{2+})(SO_4^{2-})}$	204 M^{-1}	(6)
KSO_4^-	$\frac{(KSO_4^-)}{(K^+)(SO_4^{2-})}$	5 M^{-1}	(6)
$NaSO_4^-$	$\frac{(NaSO_4^-)}{(Na^+)(SO_4^{2-})}$	10 M^{-1}	(6)
$H_3SiO_4^-$	$\frac{(H_4SiO_4^\circ)(OH^-)}{(H_3SiO_4^-)}$	6.3×10^{-5}M	(9)
$H_2SiO_4^{2-}$	$\frac{(H_3SiO_4^-)(OH^-)}{(H_2SiO_4^{2-})}$	6.3×10^{-3}M	(9)
$HSiO_4^{3-}$	$\frac{(H_2SiO_4^{2-})(OH^-)}{(HSiO_4^{3-})}$	1OM	(9)

Establishment of Equilibrium Solubility Products for Selected Phases

(a) Portlandite and Gypsum

In order to establish the value of μ_i^{sat} for a solid phase, it is preferable to compute values of μ_i (=RT ln P_i) for various solutions known to be in equilibrium with the given solid phase, and determine how effectively our ionic association assumptions work to minimize variation in μ_i^{sat} with changing solution conditions. This was done in ref.(3) for portlandite and gypsum, using Hansen and Pressler's equilibrium solubility data(10), but applying different relationships between ionic strength and activity coefficient than those used here, and following P_i^{sat} rather than μ_i^{sat}. It has now been repeated, using equation (11), together with the ionic association constants listed in Table 1. It was also assumed that all uncharged species were at unit activity throughout, as opposed to the more complex relationship suggested in ref.(6) and used in ref.(3).

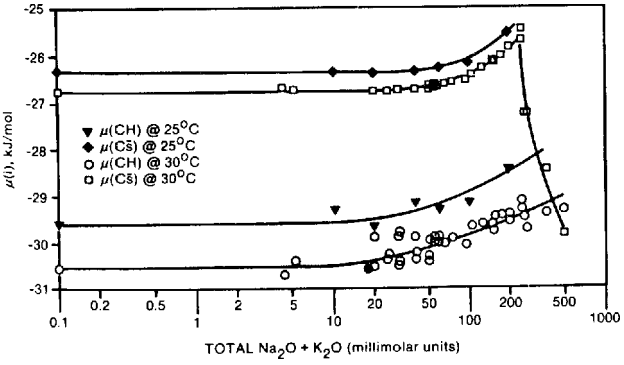

Figure 1: Computed chemical potentials for CH and CS̄ for solutions saturated with respect to portlandite and gypsum from (data in ref. 10).

Figure 1 shows the computed values of μ_{CH}^{sat} for portlandite and $\mu_{C\bar{S}}^{sat}$ for gypsum on the ordinate vs. the total molar alkali concentration as the abscissa, on a logarithmic scale. There is clearly an upward curvature of both μ^{sat} curves at 25°C and 30°C, which becomes severe above about 100mM alkali oxide (R_2O). This must be due to the limited accuracy of our assumptions regarding ionic strength and ionic association effects. Nonetheless, the simple formulae used in this work do not appear to be significantly less accurate than the more complex formulae used in ref. (3), following ref.(6); therefore, we have determined to adhere to the simpler formulae used herein. Averaging all data points for alkali concentrations below 100 mM as R_2O, we obtain the equilibrium constants listed in Table 2. In order to make reasonable estimations of saturation factors for

Table 2

Equilibrium Solubility Data Computed for Gypsum and Portlandite

Phase:	Gypsum		Portlandite	
Temperature:	25°C	30°C	25°C	30°C
μ^{sat} ([R_2O]<100 mM)				
mean (kJ/mol):	-26.34	-26.69	-29.42	-30.17
Std. deviation:	0.04	0.06	0.23	0.27
Number of points:	5	24	5	24
μ^{sat} ([R_2O]>100 mM)				
Intercept at [R_2O] = 0 (kJ/mol):	-26.45	-26.89	-29.58	-30.36
95% confidence limits (kJ/mol):	0.46	0.19	0.61	0.21
Slope (kJ/mol/mM):	+0.0042	+0.0051	+0.0054	+0.0049
Number of points included:	7	34	7	34
Coefficient of determination:	0.88	0.96	0.84	0.74

R_2O>100mM, we instead plot μ_{CH}^{sat} or $\mu_{C\bar{S}}^{sat}$ vs. [R_2O], as shown in Figure 2, and in this case a linear regression vs. [R_2O] is quite good, giving the regression parameters as also listed in Table 2. These can be used in computations of saturation factors for gypsum or portlandite at alkali concentrations up to at least 500mM as R_2O, and possibly beyond. However, it must be noted that gypsum may not be the most stable form of calcium sulfate at 30°C and high ionic strengths (i.e., the divergence of such points from the curve in Figure 1 may be due to formation of another phase, which we presume to be anhydrite).

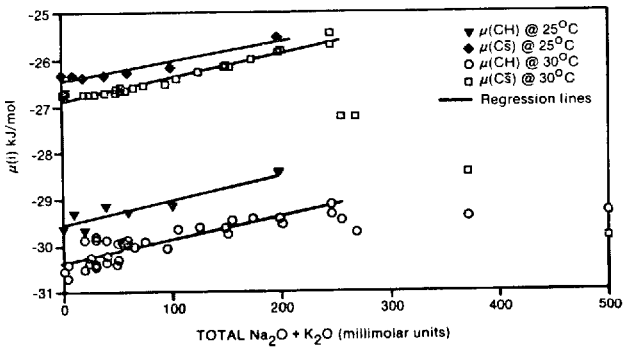

Figure 2: As for Figure 1 but showing linear regression vs. alkali concentration.

(b) Calcium Silicate Hydrates

The development of equilibrium activity products for the calcium silicate hydrate phase found in hydrated cement systems is more complicated. The difficulty in measuring the low concentrations of silica in equilibrium with the hydrates has frequently led to large experimental errors. Published solubility data for calcium silicate hydrates have recently been summarized by Jennings(11), and a further analysis by Gartner and Jennings(12) indicates that C-S-H behaves as a hydrate of fixed C/S

ratio for total calcium hydroxide concentrations in the range 7 to 28 mM, i.e., covering the subsaturation to supersaturation range usually encountered in hydrating cement systems. There are apparently two distinct C-S-H solubility curves, one representing a stable product, (C-S-H(s)), obtained by precipitation methods, and one apparently representing a metastable product, (C-S-H(m)), formed at early ages during the hydration of C_3S. The values of μ_{C-S-H}^{sat} are different for each of these products, and the analysis(12) indicated that different lime-silica ratios must be assumed for each product. Unfortunately the computed lime silica ratio in the solid phase depends on the degree of association assumed between Ca^{2+} and $H_2SiO_4^{2-}$ ions in solution, and the "true" association constants are not known. Therefore, we will use the simplest assumption, of no association, which leads to the following equations, for the free energy of solution of these phases at about 25°C:

$$\Delta\mu^{soln.}_{(C\text{-}S\text{-}H(s))} = 0$$
$$= 1.54\ \mu_{CH} + \mu_S + 101.9\ \text{kJ/mol} \qquad (14)$$

$$\Delta\mu^{soln.}_{(C\text{-}S\text{-}H(m))} = 0$$
$$= 1.77\ \mu_{CH} + \mu_S + 102.6\ \text{kJ/mol} \qquad (15)$$

These two equations relate the chemical potentials of CH and S if the two components are present in equilibrium with either form of C-S-H. It is of considerable interest to determine whether these relationships can be extended into the more complex system typical of portland cements. The only equilibrium study of the C-S-H system with added alkali of which we are aware is Kalousek's study of the N-C-S-H system at 25°C(13). Solution concentrations reported for N-C-S-H gels in the presence of excess portlandite (Table I of ref.13) were analyzed by the methods outlined above, for data obtained at submolar alkali levels (the approximations are not valid at higher concentrations). As is shown in Figure 3, μ_{CH} remained approximately independent of alkali concentration, as would be expected, if the three clearly divergent data points at 600mM Na_2O are discounted.

Taking the data for only the ten points with [NH]<400mM, we obtain the following mean values for solutions reportedly in equilibrium with portlandite and C-S-H:

$$\mu_{CH} = -30.86 \pm 0.49 \quad \text{kJ/mol} \qquad (17)$$

$$\mu_S = -58.4 \pm 2.2 \quad \text{kJ/mol} \qquad (18)$$

The scatter in these data are clearly much greater than in Hansen and Pressler's data, and the values for μ_{CH} at 25°C do not agree. It is difficult, therefore, to draw any strong conclusions regarding the effect of alkali on the chemical potential of C-S-H in the N-C-S-H system; but, nevertheless, it is of interest that μ_S appears to decline with increasing alkali concentrations, as opposed to the behavior of μ_{CH} and μ_{CS}. This suggests that Na_2O is actually incorporated into the C-S-H phase, as indicated by Kalousek's analytical data.

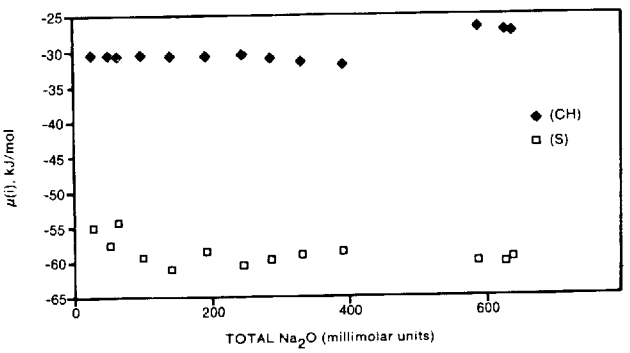

Figure 3: Computed chemical potentials for CH and S versus sodium hydroxide concentration, for C-S-H gels in equilibrium with portlandite at 25°C (from data in Table I of ref. 13).

A regression of μ_S vs. [NH] for the thirteen data points included in Figure 3 gives the following relationship:

$$\mu_S = -57.27 - 0.0052\ [\text{NH, mM}] \qquad (19)$$

Combining the extrapolated value of μ_S at zero alkali from eqn.(19) with the mean value of μ_{CH} from (17) and substituting in eqn.(14) gives $\Delta\mu^{soln.}_{C\text{-}S\text{-}H(s)} = -2.9$ kJ/mol, implying that Kalousek's concentration measurements are lower than the literature averages used to obtain eqn.(14). If, however, we use the more accurate value for μ_{CH} obtained for portlandite at 25°C in Table 2 (-29.42 kJ/mol), the computed value of $\Delta\mu_{C\text{-}S\text{-}H(s)}$ is only -0.7 kJ/mol, indicating that it may have been an error in measuring calcium concentrations which led to the apparently low saturation concentrations in Kalousek's data.

Application to Portland Cements

To test the relationships derived for pure component systems on portland cements, it is necessary to measure the concentrations of all of the principal components in solutions extracted from cement pastes. Unfortunately, this is rarely done due to experimental difficulties. We have analyzed one set of data, including SiO_2 concentrations presented in a recent paper by Xue, et al,(14). Chemical potential values computed from these data are shown in Table 3 for portland cement pastes, with and without two different glass "aggregates", at ages from 5 hours to 180

days. Apart from the alkali hydroxides, chemical potentials of all components tend to decrease with age. This is particularly apparent for sulfate. At 5 hours, the values for $\mu_{C\bar{S}}$ in Table 3 correspond very closely with the expected value of -26.0 for gypsum saturation at 20°C extrapolated from data in Table 2. SO_3 levels in solution were usually below the limit of detection beyond the first few days, due to exhaustion of gypsum, and formation of stable calcium aluminate hydrates as discussed in ref. 3.

Table 3

Chemical Potential for Species in Cement Paste Pore Fluid
(computed from data of Xue, et al., ref. 14)

Component:		Chemical Potential at 20°C, kJ/Mol			Total Alkali
		CH	S	$C\bar{S}$	$[R_2O]$,mM
Age, Days	Paste				
0.2	PC	-26.57	-52.52	-26.08	37
	PC + AG	-26.56	-54.05	-25.90	44
	PC + ARG	-26.44	-53.41	-25.82	44
	mean	-26.52	-53.33	-25.93	42
	S.dev.	.07	.77	.13	4
1	PC	-27.20	-56.99	-36.77	73
	PC + AG	-27.01	-56.23	---	70
	PC + ARG	-26.97	-56.29	---	71
	mean	-27.06	-56.50	-36.77	71
	S.dev.	.12	.42		2
3	PC	-27.53	-57.23	-40.22	88
	PC + AG	-27.16	-57.64	---	95
	PC + ARG	-26.59	-56.98	---	101
	mean	-27.09	-57.28	-40.22	95
	S.dev.	.47	.33		7
7	PC	-27.55	-55.07	---	101
	PC + AG	-27.36	-58.07	---	116
	PC + ARG	-27.62	-58.07	---	136
	mean	-27.51	-57.07		118
	S.dev.	.13	1.73		18
28	PC	-27.32	-57.36	-39.33	128
	PC + AG	-27.16	-58.26	-41.97	160
	PC + ARG	-27.36	-56.77	-39.08	145
	mean	-27.28	-57.46	-40.1	144
	S.dev.	.11	.75	1.6	16
90	PC	-27.89	-57.32	---	146
	PC + AG	-27.35	-58.05	---	175
	PC + ARG	-27.65	-57.35	---	158
	mean	-27.63	-57.57		160
	S.dev.	.27	.41		15
180	PC	-28.06	-57.39	---	160
	PC + AG	-27.84	-57.27	---	196
	PC + ARG	-28.00	-56.42	---	170
	mean	-27.97	-57.02		175
	S.dev.	.11	.53		19

*NOTE: PC = portland cement; AG = alkali glass; ARG = alkali resistant glass

Calcium hydroxide saturation also decreases with time, approaching a limit which should correspond to a value of μ_{CH}^{sat} of about -28.8 kJ/mol, at zero alkali content based on a linear extrapolation of the data in Table 2 to 20°C. However, the increasing alkali concentration of the pore solution influences the saturation value, so that for the final value of close to 175 mM K_2O, μ_{CH}^{sat} is estimated (again extrapolating the data in Table 2) to be about -27.9 kJ/mol. This is equal to the average values observed for the 180 day old pastes.

The upward trends in alkali concentration, which are also reflected in upward trends in μ_{NH} and μ_{KH}, are more strongly and consistently influenced by the presence of glass, especially alkali glass at later ages. This is because the glass is a source of alkali, and alkali is relatively weakly bound in the hydrated phases.

In contrast, the downward trends in the chemical potentials of CH, S, and $C\bar{S}$ with age are about the same for all three cement pastes included in Table 3, regardless of the presense or absence of glass. This suggests that similar hydrates form in all three cases. Thus, in order to examine these overall trends more closely, it is convenient to examine the mean values, so as to minimize the discrepancies apparently caused by random experimental errors in some of the measurements. This has been done for μ_{CH} vs. μ_S in Figure 4, the ellipses representing one standard deviation for μ_{CH} and μ_S at each of the ages studied, based on data from all three pastes. There is a clear decreasing trend in both μ_{CH} and μ_S with increasing paste age. The lines for C-S-H solubility from equations (14) and (15) are included for reference in this figure, and all points except the one at 5 hours fall between the stable and metastable curves, suggesting a slow formation of the stable C-S-H phase from the initial metastable phase found at early ages. The exact positions of the C-S-H solubility curves at 20°C may be somewhat different from those shown, because they are based on an average of data over a range of temperatures (about 20-30°C), although the temperature coefficient is believed to be small(12).

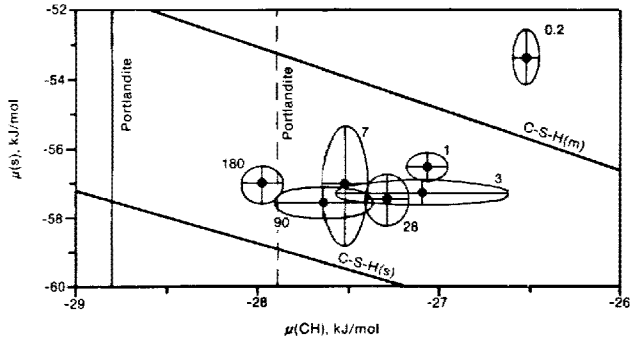

Figure 4: Computed chemical potentials for S vs. CH for averaged data from three sets of portland cement pastes at ages from 0.2 to 180 days (from data in ref. 14). Ellipses indicate one standard deviation from mean. Numbers indicate paste age in days. Solid lines approximately indicate saturation with respect to solid phases indicated, as computed for zero alkali content. Broken line computed for portlandite saturation at 175mM alkali oxide.

Saturation factors can be computed for CH and C-S-H based on distances from the equilibrium curves in Figure 4, using equation (10). For CH, however, the effect of alkali concentration on the equilibrium curve is quite large, as shown by the dashed line in the figure. Thus alkali concentration must be considered in computing saturation by this method. It is not yet clear whether the apparent decrease in the saturation factor of C-S-H with respect to the stable phase is influenced so severely by alkalis, or by the aluminates or sulfates present in the system. However, it must be remembered that all of these components are known to dissolve to some extent in C-S-H, (15) and would therefore be expected to lower its chemical potential in much the same way as was observed for Na_2O alone in Kalousek's data. In the absence of reliable equilibrium studies on the C-S-H system with such impurities present, we can draw no stronger conclusions at this time regarding the proximity to equilibrium of the C-S-H in the hydrating cement system.

Concluding Remarks

It is our belief that return to in-depth fundamental studies of chemical and physical phenomena, together with engineering application of the generated data (taking into account the real-world environment of concrete use), will lead to novel and cost-effective advancements in the concrete construction industry. Better understanding of the phase relationships, as has been achieved in the fields of metallurgy and ceramics, is one of the conditions for such advancement. Specifically, understanding and control of the solid-liquid interactions, of composition and stability fields of cementitious hydrated formed during hydration, could, when intelligently applied, lead to extended durability of concrete products, improved quality assurance procedures, and technology-based standards.

We would like to propose that, in the coming years, a concentrated worldwide emphasis be put on phase equilibrium studies, and that the results of such studies be handled in a special session of the 9th International Symposium on the Chemistry of Cements.

References:

(1) L. J. Parrott, "Critical Questions in Modeling the Development of Microstructure", Engineering Foundation Conference on "Cement Manufacture and Use", Henniker, New Hampshire, 1985 (to be published).

(2) C. D. Lawrence; pp 378-91 in Symposium on the Structures of Cement Pastes and Concretes, Highway Research Board Special Report No. 90, 1966.

(3) E. M. Gartner, F. J. Tang and S. J. Weiss, "Saturation Factors for Calcium Hydroxide and Calcium Sulfates in Fresh Portland Cement Pastes", J. Am. Ceram. Soc., 68 (12) pp 667-673 (1985)

(4) P. Longuet, L. Burglen and A. Zelwer "La Phase Liquid du Ciment Hydraté", Revue des Materiaux de Construction, 676 pp 35-41, (1973).

(5) R. S. Barneyback, Jr., and S. Diamond, Cem. Concr. Res., 11, pp 279-286 (1981).

(6) J. E. Bailey and C. J. Hampson "The Chemistry of the Aqueous Phase of Portland Cement", Cem. Conc. Res., 12, (2) pp 227-236 (1982).

(7) C. W. Davies, "Ion Association" pp 34-53, Butterworths, London (1962).

(8) F. G. R. Gimblett and C. B. Monk, Trans. Farad. Soc., 50, 965, (1954).

(9) D. Darby, T. Griffiths, A. R. Jacques and D. Pawson, p 338 in "The Modern Inorganic Chemicals Industry", Special Publication No. 31, Royal Society of Chemistry, London (1977).

(10) W. C. Hansen and E. E. Pressler, "Solubility of $Ca(OH)_2$ and $CaSO_4 \cdot 2H_2O$ in Dulute Alkali Solutions", Ind. Eng. Chem., 39, (10) pp 1280-1282 (1947).

(11) H. M. Jennings, "Equilibria Between Aqueous Phase and Two Types of Calcium Silicate Hydrate", (in press).

(12) E. M. Gartner and H. M. Jennings, "Solution Thermodynamics of Calcium Silicate Hydrates", to be presented at the annual meeting of the American Ceramic Society, Chicago, 1986.

(13) G. L. Kalousek, "Studies of Portions of the Quaternary System Soda-Lime-Silica-Water at 25°C", J. Research N.B.S., 32, pp 285-302, (1944).

(14) Xue Jun-gan, Xu Wen-xia and Ye Ming-xun, J. Chinese Silicate Society, 11, (3), pp 277-287, (1983).

(15) L. E. Copeland, E. Bodor, T. N. Chang and C. H. Weise, "Reactions of Tobermorite Gels with Aluminates, Ferrites and Sulfates", J. PCA Res. Devel. Labs, 9 (1) pp 61-74 (1967).

T. KUZNETSOVA,
V. AKIMOV, Mendelejev Institute of Chemical Technology, Moscow, USSR

1

BICALCIUM SILICATE AND CALCIUM ALUMINATES

2.1

The implanting of different elements into the crystalline lattice of minerals leads to the formation of the additional amount of dislocations, vacancies, paramagnetic centres, free charge carriers, the total concentration of which changes in a wide range of values. More effectively (in 10-10^4 times) the concentration of free charge carriers goes up that considerably exceeds the number of forming dislocations and vacancies of atoms of calcium, silicon and oxygen. The dependence of the rate and kinetics of hydration of minerals upon defectivity of their structure has been established. The results obtained could be used for prediction of hydration activity of minerals and clinkers.

A implantação de elementos diferentes dentro da rede cristalina de minerais leva à formação de quantidade adicional de deslocamentos, centros paramagnéticos, transportadores de carga livre, cuja concentração total se altera numa faixa ampla de valores. Mais efetivamente (em 10 - 10^4 vezes) a concentração de transportadores de carga livre cresce a ponto de exceder consideravelmente o número de deslocações que se formam e os vazios de átomos de cálcio, sílica e oxigênio. Foi estabelecida a dependência da velocidade e cinética de hidratação em relação à deficiência de sua estrutura. Os resultados obtidos poderão ser usados para predição da atividade de hidratação de minerais e clínqueres.

T. KUZNETSOVA,
V. AKIMOV

Introduction. The analysis of bicalcium silicate and calcium aluminates structural features has indicated the substantial dependence of the minerals hydration activity upon the un stoichiometry of their composition and point defects concentration in the structure of basic phases of portland cement clinker. It is established that an increase in concentration of free charge carriers leds to stepping up C_2S and C_3A reactivity. Adding (injection) of impurity elements to the mineral composition, their direct distribution in the cristals volume for extra defects provides more active solid-liquid interaction.

Experiments. Bicalcium silicate solid solutions K_2O, B_2O, Al_2O_3, Fe_2O_3 Mn_2O_3, Cr_2O_3 and so on were formed by means of repeated calcination of starting mixture and by grinding of subsidiary products to particles of 40-60 . The curing time at 1450°C is two hours in all stages of calcination. The synthesis of calcium aluminates was carried out at 1380°C and at the cure of 3 hours. The study of calcination products was made by methods of chemical, differential thermal, X-ray, X-ray microanalysis, electron microscopic analyses. The concentration of free charge carriers was determined from change in parameters of Hall effect at room temperatures. Minerals reactivity at water-solid ratio of 0,5 (for C_2S) and of 0,7 (for C_3A) was determined by microcalorimetric methods, by X-ray phase analysis and by nuclear magnetic resonance (spic echo).

Results. In crystal of belite as well as alite the basic and impure ions are distributed irregularly, the central part of mineral's grains gaining calcium. Analyses of the structure of bicalcium silicate solid solutions with K_2O, B_2O_3, Al_2O_3, Fe_2O_3, Mn_2O_3, Cr_2O_3 and so on have shown that change of concentration of free charge carriers in the mineral is occurred as a result of restoichiometry of its composition and as a result of replacement of ions Ca^{2+}, Si^{4+} by microelements which can penetrate into the structure cavities. Formation of free charge carriers p-type of C_2S was established; their concentration is changed in the interval $3{,}0\cdot10^{18}$ up to $8{,}0\cdot10^{18}$ m^{-3}. Electron conduction is characteristic feature of solid solutions of C_2S and iron, cobalt and nickel. Dislocation density and concentration of paramagnetic centres, formed by irradiation of samples at the temperature of liquid nitrogen, is changed in more narrow interval $3{,}0\cdot10^{11}$ - $9{,}0\cdot10^{11}$ m^{-2} and $4{,}2\cdot10^{21}$ - $8{,}1\cdot10^{21}$ kg^{-1} respectively. Thus mineral reactivity is considerably affected first of all by concentration of free charge carriers (tabl. 1). It is necessary to mention that the results of the analyses carried out by methods of nuclear magnetic resonance (spin echo), microcalorimetric methods and X-ray phase analysis is agreed with each other and is indicative of the efficient phases of the proceeding process at interaction of a monomineral binder and water. The reduction of time of spin-lattice relaxation of protons is observed in the initial stage of hydration. It is bound up not only with the transition of H_2O molecules from adsorbed state into gellike layer, but also with passing of Ca^{2+} ions and mixtures into solution. The period of time is 60-120 minutes for β-C_2S with different mixtures additions, and 15-90 minutes for C_3S, thus the higher presence of defects, the less the duration. The second period of hydration goes on for tens of hour and is characterized by practically constant time of spin-lattice relaxation of protons.

Degree of hydration of minerals even in later periods depends on presence of defects of their structure (fig. 1, 2, table 1), thus by T_1 in the early stages estimating degree of hydration of bicalcium silicate 2 weeks old from the moment of addition of water to a material. Such regularity appears to be useful for reactivity prediction and binding properties of a mineral. However, the presence of substantial amount of paramagnetic ions in crystal lattice of main portland cement phases leds to consi-

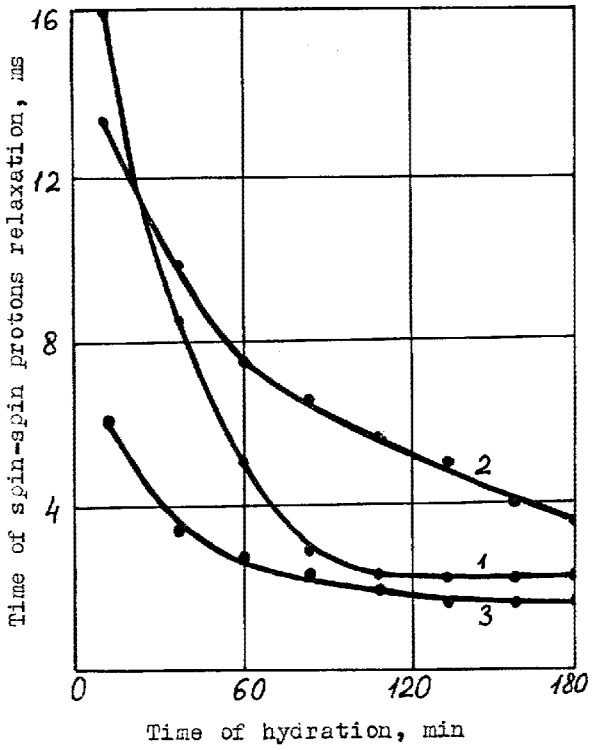

Fig. 1. Variation of time of spin-spin protons relaxation during the minerals hydration:
1 - $Ca_{1,87}K_{0,01}B_{0,03}Si_{1,04}O_4$;
2 - $Ca_{1,87}Al_{0,01}B_{0,03}Si_{1,04}O_4$;
3 - $Ca_{1,87}Fe_{0,02}B_{0,03}Si_{1,04}O_4$;

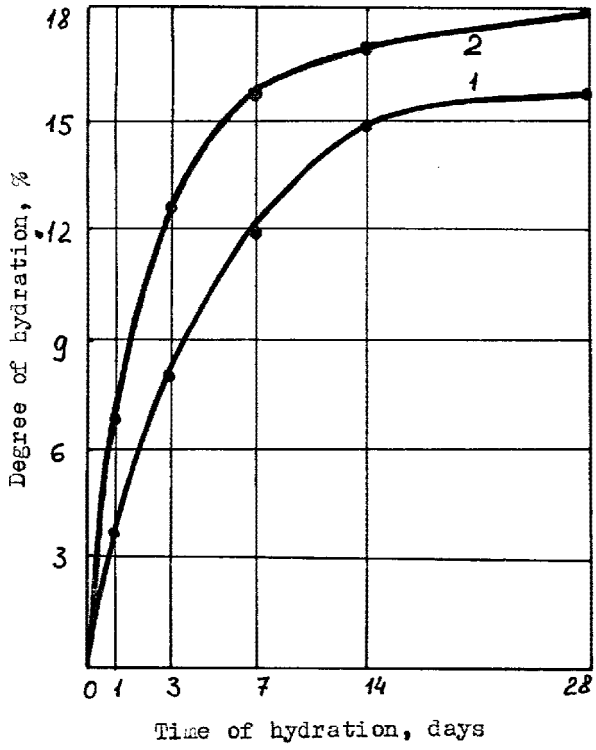

Fig. 2. Degree of minerals hydration:
1 - $Ca_{1,87}Al_{0,01}B_{0,03}Si_{1,04}O_4$;
2 - $Ca_{1,87}Fe_{0,02}B_{0,03}Si_{1,04}O_4$

derable errors while analysing the processes going on at the solid-water interaction. Estimation of H_2O molecules mobility at hydration of C_2S solid solutions with Cr (up to 2 mass. % C_2O_3) confirms the conclusion.

It is determined 1-3 that at the initial moment of addition of water to the samples an decrease of T_1 and T_2 (for pure water T_1 T_2 3s), caused by decrease of H_2O molecules mobility at their adsorption onto the active centres of the surface of a solid is observed (fig. 3). So long as a dependence of T_1 on the time of correlation $_c$ is in the form of V, for the simple interpretation of a change of T_1 as a result of deceleration or speed acceleration up of the molecular motion, it is determined that the studies have been made on the right branch of a curve $T_1 = f(\ _c)$. Therefore, the decrease of T_1 observed in the initial stage of hydration is connected with the transition of H_2O molecules from adsorbed state into gellike layer. The sharp decrease of T_1 and T_2 at an increase of concentration of Cr_2O_3 in a starting mixture from 0,25 up to 1,5 mass. % is induced by formation of extra amount of paramagnetic centres in the C_2S structure. Though, in spite of the fact that the concentration of paramagnetic centres in the mineral structure proceeds increasing at the content of Cr_2O_3 of 1,5-2,0 mass. %, T_1 and T_2 are not decreased, but are increased on the contrary. It is bound up with the amplification (gain) of hydration activity of a mineral as a result of 5-6 times more increase in concentration of free charge carriers while for-

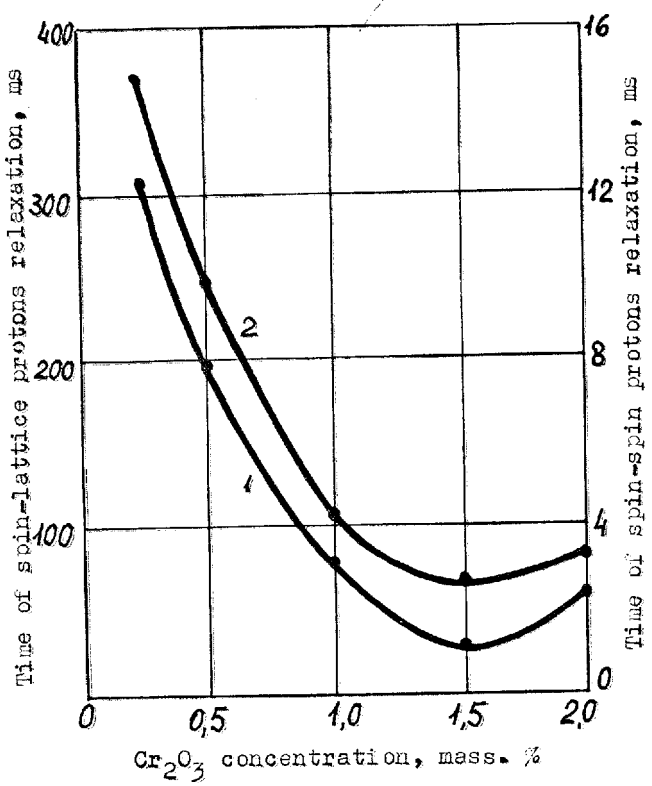

Fig. 3. Dependence of spin-lattice (1) and spin-spin (2) protons relaxation upon chrome concentration in C_2S (30 min of hydration)

ming $-C_2S$ solid solutions with chromium. Thus, the presence of considerable amount of paramagnetic elements in minerals impedes determination of their reactivity by nuclear magnetic resonance (spin echo). It is necessary to note that T_2 is more sensitive to the presence of paramagnetic ions in the structure then T_1.

Studies of calcium aluminates of nestoichiometry content have also indicated the dependence of the hydration activity of the mineral on the concentration of free chage carriers of p-type (table 2, fig. 4, 5). A decrease of hydration degree and time of spin-lattice relaxation of protons at hydration of the calcium aluminate, if the range of C/A ratio is 3,0-2,6, has been caused by decrease in content of holes by an order of magnitude grater. Injection of paramagnetic mixtures leds to fall in magnitudes of time of relaxation of protons (as well

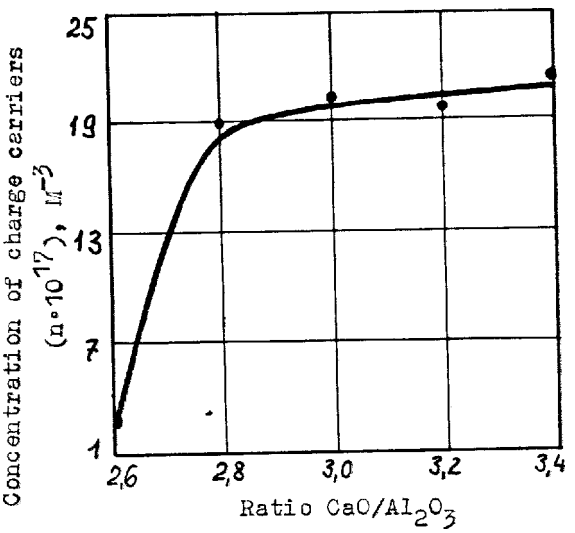

Fig. 4. Dependence of free charge carriers concentration upon composition of calcium aluminates

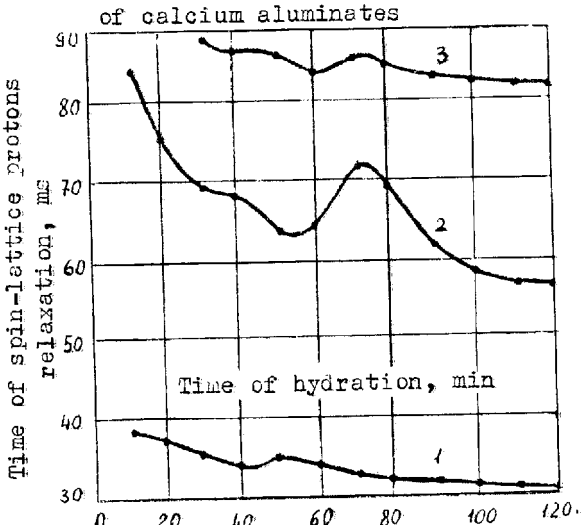

Fig. 5. Variation of time of spin-lattice protons relaxation during minerals hydration

as at hydration of calcium silicates) though a mineral reactivity may be precisely estimated by T_1. The analogous regularity holds true for $C_{12}A_7$ hydration.

Conclusion. The studies of structural peculiarities of minerals of industrial clinkers and synthesized phases and their hydration activity have indicated the dependence of hydration degree and kinetics of calcium silicates hydration on the presence of defects of their structure. In this connection

Table 1

Hydration Activity of Bicalcium Silicate Solid Solutions in Different Periods of Hydration

Mineral	Concentration of charge carriers, m^{-3}	Time of spin-lattice protons relaxation, ms			
		2 min	36 min	60 min	84 min
$Ca_{1,87}\ K_{0,01}\ B_{0,03}\ Si_{1,04}\ O_4$	$5,7 \cdot 10^{18}$	92	50	27	18
$Ca_{1,87}\ Al_{0,01}\ B_{0,03}\ Si_{1,04}\ O_4$	$2,0 \cdot 10^{16}$	100	62	50	45
$Ca_{1,87}\ Fe_{0,02}\ B_{0,03}\ Si_{1,04}\ O_4$	$1,5 \cdot 10^{16}$	98	78	74	73

Table 2

Degree of Hydration of Tricalcium Aluminate, %

Mineral	Time of hydration, days			
	1	3	7	28
$C_{2,6}A$	57	63	74	82
$C_{2,8}A$	71	81	80	87
$C_{3,0}A$	73	87	89	92
$C_{3,2}A$	72	86	90	94
$C_{3,4}A$	72	84	91	94

it seems to be advisable the direct adjustment of microelements distribution in the volume of crystals aimed at an increase in concentration of the point defects and the crystal dislocation and as a result of it an increase of reactivity of minerals at their interaction with water.

REFERENCES

1. Timashev V.V., Akimov V.G. 7th International Congress on the Chemistry of Cement, Paris, 1980, v. 4, p. 203-207.
2. Тимашев В.В., Акимов В.Г., Кудрявцев А.Б., Панюшкин В.Н. Тр. МХТИ им. Д.И. Менделеева, 1980, вып. 116, с. 106-109.
3. Акимов В.Г. Тезисы докл. IУ Всес. совещания по гидратации и твердению вяжущих, Львов, 1981, с. 61.

A.M. DMITRIEV,
A.K. ZAPOLSKY,
T.V. KOUZNETZOVA,
B.E. YUDOVITCH,
I.D. PONOMAREV, Moscou, Kiev, Kharkov, URSS

2.1

ALLIAGE D'HYDROLICITE DES CIMENTS

On a étudié les nouveaux types d'adjuvants à introduire dans la composition du ciment lors de la mouture: (1) composants cristallisants (crentes) contenant sulfates d'Aluminium, de Fer, Silice actif, Méta-kaolin et d'autres; (2) ligno-sulfonates techniques modifiés contenant les atomes actifs d'Azote dans les chaînes latérales des molécules de ligno-sulfonates. Les adjuvants peuvent augmenter l'activité hydraulique des ciments de 12-25 (1) et de 10-15 (2) MPa.

Les principes physico-chimiques d'action des adjuvants sont liés à l'influence: (1) à la germination, au nombre d'hydrates, au degré de polimérisation des hydro-silicates de groupes oxygéno-siliceux; on a noté de l'accélération de liage des films de silicegélé avec de la chaux dans la périphérie des particules alites, ainsi que le phénomène d'alliage d'hydratation de nouvelles formations; (2) à la composition granulométrique des ciments grâce à l'accroissement de la sortie de la fraction moyenne (5-30 μ) et (3) au rapport "eau-ciment" dans les béton se réduisant de 0,07-0,12 sans ralentissement de la vitesse de la hydratation.

Foram estudados os novos tipos de adjuvantes a serem introduzidos na composição do cimento quando da moagem: (1) componentes cristalizantes, contendo sulfatos de alumínio, ferro, sílica ativa, metacaolim e outros; (2) lignossulfonatos técnicos modificados, contendo os átomos ativos de azoto nas cadeias laterais de moléculas de lignossulfonatos. Os adjuvantes podem aumentar a atividade hidráulica dos cimentos de 12 - 25 (1) e de 10 - 15 (2) MPa.

Os princípios físico-químicos de ação dos adjuvantes estão ligados à influência de: (1) germinação, número de hidratos, grau de polimerização dos hidrossilicatos de grupos oxigeno-silicosos; notou-se aceleração de ligação das películas de silica-gel com a cal na periferia das partículas de alita, bem como o fenômeno de combinação de hidratação de novas formações; (2) composição granulométrica dos cimentos, graças ao crescimento da porção da fração média (5 - 30μ); e (3) relação água/cimento no concreto reduzindo-se de 0,07 - 0,12 sem diminuição da velocidade de hidratação.

A.M. DMITRIEV,
A.K. ZAPOLSKY,
T.V. KOUZNETZOVA,
B.E. YUDOVITCH,
I.D. PONOMAREV

L'utilisation des amorces de cristallisation composées des propres produits d'hydratation des liants hydrauliques, pour accélérer leur hydratation, est connue depuis longtemps, mais elle n'a pas été efficace que dans les condition hydrothermales /I-3/. Les dernières années, les auteurs de la présente étude ont élaboré des "KRENT" (abréviation des mots russes "кристаллизационные компоненты" "constituants de cristallisation" adoptée dans l'industrie). Ces constituants de cristallisation sont des adjuvants synthétiques chimico-minéraux destinés pour le ciment et introduits dans celui-ci lors du broyage réagissant avec les constituants du ciment pour former les produits hydratés qui allient le ciment et jouent le rôle des amorces, également efficaces à des températures normales du milieu.

Dans le présent travail, les auteurs considèrent les bases physico-chimiques de l'influence des "KRENT" sur la cinétique et la composition de phase des produits d'hydratation du ciment et sur les propriétés de construction techniques des ciments.

Pour déterminer le critère d'efficacité de l'influence des "KRENT" sur la cinétique de l'hydratation des ciments, utilisons, l'équation de Ratinov-Lavout /4/ reliant les constantes de vitesse de dissolution du liant initial K_I et celles d'hydratation des formations nouvelles K_2 avec la masse du liant m_I et la masse de la phase nouvelle m_2 (calculées pour la substance anhydre) à l'instant et à l'instant τ_c /$m_{1,0}$ et $m_{2,0}$/. Désignons également par D le coefficient de diffusion et par $C_{1,2}$, $\gamma_{1,2}$, $N_{1,2}$, $l_{1,2}$ et $\rho_{1,2}$ conformément: solubilité, coefficient de forme, nombre, dimension caractéristique et densité des particules du liant et des formations nouvelles. Dans ce cas, selon /4/, pour le premier stade du processus on a:

$$K_1^{-1}(m_1^{1/3}-m_{1,0}^{1/3})-K_2^{-1}(m_2^{1/3}-m_{2,0}^{1/3})= \\ = -D^{2/3}(C_1-C_2)\tau \qquad (1)$$

où

$$m_{1,2}=\gamma_{1,2} N_{1,2} \rho_{1,2} \quad \text{et} \\ K_{1,2}=A_{1,2}\rho_{1,2}^{-2/3}\gamma_{1,2}^{1/3} N_{1,2}^{1/3} \qquad /2/$$

A l'absence des amorces de cristallisation, en cas où $\tau = \tau_o$, $m_{2,0}=0$ $m_2 \longrightarrow 0$, le deuxième membre dans la partie droite de l'équation /I/ disparaît. Si on admet $-D^{2/3}(C_I - C_2)$ = const, K_I est minimum pour tout instant.

Introduisons maintenant l'adjuvant de cristallisation ($m_{2,0} \geqslant 0$). L'analyse de l'équation /I/ montre que dans ce cas K_I augmente, et le degré de cette augmentation est d'autant plus, d'autant est plus lente la cristallisation des formations nouvelles ($A_o \longrightarrow$ min). Donc, les amorces doivent agir plus efficacement sur les liants dont l'hydratation et le durcissement sont lents. Puisque la diminution des différences des solubilités du liant et des formations nouvelles dans l'équation /I/ mène (à condition des autres paramètres fixés) à l'augmentation du K_2, le besoin de l'amorce dans ce cas est minimum. L'affirmation opposée étant également valable, les amorces les plus efficaces doivent être présentées par les amorces de cristallisation des formations nouvelles peu solubles dans l'eau. En cas des valeurs élevées du coefficient de diffusion dans le système (fortes dilutions ou température élevée du milieu), il est nécessaire d'augmenter le dosage de l'amorce pour conserver son effet d'action. Enfin, il résulte de l'équation /I/ une conclusion triviale concernant la possibilité de diminuer le dosage de l'amorce ($m_{2,0}$) en gardant une haute efficacité de celle-ci.

Les conditions /2/ exigent les limitations supplémentaires suivantes: l'amorce doit comprendre un nombre maximum des particules ($N_{2,0} \longrightarrow$ max). Cela, en cas de la masse fixée $m_{2,0}$, ne s'obtient qu'à la dimension minimum des particules ($l_{2,0} \longrightarrow$ min). Une telle amorce, grâce à l'augmentation simultanée du $m_{2,0}$ et du K_2, doit être la plus efficace.

Cela est en contradiction avec une notion intuitive sur l'utilité d'avoir dans l'amorce de gros cristaux bien facettés, mais, comme on le montre ci-dessous, ce fait est en concordance avec les données expérimentales. Il devient plus claire l'inefficacité des tentatives faites en vue d'utiliser en qualité des amorces les produits d'hydratation du ciment préparés préalablement qui, dans l'air, tendent à vieillir et à recristalliser ($l_{2,0} \rightarrow$ min, $N_{2,0} \rightarrow$ max). Evidemment, il faut obtenir les amorces directement avant l'utilisation et encore mieux - au moment de l'utilisation, quand elles "in statu nascendi" sont les plus efficaces. Sur ce fait est basés l'idée d'utilisation en qualité des "KRENT" des agents de départ en vue de synthétiser les formations nouvelles hydratées du liant donné. Cependant, pour satisfaire à la condition $m_{2,0} \gg 0$, il est nécessaire que la constante de vitesse de la synthèse de ces formations nouvelles hydratées à partir de la substance des "KRENT" ou avec l'utilisation des "KRENT" (K) soit beaucoup plus grande que la constante K_2.

Les résultats des essais effectués avec l'utilisation d'une série des "KRENT" semi-industriels d'une nature différente montrent que les "KRENT" accélèrent considérablement les processus de formation de l'hydrosulfoaluminate de calcium du type tricalcique /TTCAK / et des hydrosilicates de calcium /TCK /, ce qui mène, en fin de compte, à l'intensification du processus d'hydratation, à l'augmentation du degré d'hydratation en améliorant l'utilisation de l'énergie chimique de la partie clinker du ciment. Tous ces facteurs, pris ensemble, favorisent l'accroissement de résistance du ciment.

La microstructure de la pierre de ciment (qui a été méticuleusement étudiée en présence des "KRENT" au cours des recherches à "NIICement" et à "Ujgiprocement") se perfectionne: la teneur moyenne en TTCAK sur les clivages aux premiers âges de durcissement augmente, la longueur des fibres diminue un peu et l'épaisseur s'accroît. Cela est caractéristique pour la cristallisation de masse en présence des amorces.

Le rôle des "KRENT", cependant, ne se ramène pas à la fonction unique des amorces. Les données obtenues montrent que les "KRENT" préviennent le passage du TTCAK en forme monosulfate de l'hydrosulfoaluminate de calcium (HTCAK) et accélèrent la conversion des C_4AH_{13} en C_3AH_6. Cela favorise de plus l'augmentation de résistance du ciment avec les "KRENT" car le passage du TTCAK en MTCAK diminue le nombre de contacts de cristallisation dans la pierre de ciment libérant, en outre, de l'eau avec un grand pouvoir dissolvant et des impuretés, type H_2SiO_3, qui initient, après le dégagement, les transformations de phase dans les TCK. A son tour, l'accélération de la conversion des C_4AH_{13} en C_3AH_6 mène à la création dans la structure, pas encore formée, des C_3AH_6 stables n'empêchant pas l'augmentation ultérieure de résistance du ciment et prévient l'évolution de ce phénomène plus tard, quand il est capable de diminuer les paramètres de résistance du ciment.

Les causes de la stabilisation des TTCAK et de la destabilisation des C_4AH_{13} en présence des "KRENT" révèlent un grand intérêt. Les données obtenues donne une base pour supposer que la phase siliceuse entrant dans la composition des "KRENT" et comprenant les polyanions (SiO_4^{4-}) interagit avec les impuretés siliceuses dans les phases hydratées. Cela aboutit à la diminution de la teneur en ces impuretés dans les phases hydratées, à la stabilisation des TTCAK et à la destabilisation des C_4AH_{13} par suite de la substitution, en premier cas, du SiO_3^{2-} par un anion d'un acide plus fort SO_4^{2-} et en deuxième cas, par un anion d'un acide plus fable AlO_3^{3-}. Evidemment, les "KRENT" exercent également une influence sur le rapport Al/Fe dans les phases hydratées et sur la teneur en SO_3 dans ces dernières en variant dans l'ensemble la basicité et le degré de polymérisation des anions. Donc,

A.M. DMITRIEV,
A.K. ZAPOLSKY,
T.V. KOUZNETZOVA,
B.E. YUDOVITCH,
I.D. PONOMAREV

Tableau 1

Conservation des ciments d'alliage
t = 15°C, φ = 60 - 70%

Ciment, type	Durée de conservation, jours	Rapport eau/ciment	Résistance à la compression, MPa/%			
			I jour	3 jours	7 jours	28 jours
ciment témoin	I	0,38	191 / 100	326 / 100	458 / 100	640 / 100
	360	0,37	21 / 11	124 / 38	272 / 59	46,9 / 73
ciment avec 5% de "KRENT	I	0,35	20,2 / 100	37,4 / 100	57,7 / 100	73,0 / 100
	360	0,36	4,2 / 21	22,8 / 61	47,9 / 83	65,0 / 89

Tableau 2

Résistance aux sulfates des ciments d'alliage /K_c - coefficient de la résistance aux sulfates/

Composition du ciment, %			Procédé de fabrication du "KRENT"	Rapport eau/ciment	K_c en solution de Na_2SO_4(5%)	
Clinker	Gypse	"KRENT"			3 mois	6 mois
94	6	-	-	0,37	1,37	0,73
89	6	5	sec	0,37	1,47	1,0
89	6	5	humide	0,37	1,44	1,1

les "KRENT" peuvent exercer une action d'alliage sur les produits d'hydratation du ciment.

En tenant compte des bases physico-chimiques mentionnées concernant l'effet des "KRENT", on propose l'alliage d'hydratation des ciments comme une voie de l'augmentation de qualité et de la production des ciments spéciaux.

A l'aide des "KRENT" en combinaison avec les clinkers d'alite ayant une microstructure optimum et à une granulométrie du ciment choisie rationnellement, l'activité du ciment Portland peut être portée à 80,0 MPa. Dans les conditions industrielles, on a fabriqué avec les "KRENT" les lots d'essais industriels du ciment ayant une haute résistance et une activité de 65,0 MPa.

Les produits de leur hydratation tendent moins à la corrosion par carbonates. Pour cette raison, les pertes de l'activité des ciments avec "KRENT" (y compris les ciments finement broyés), en cas de leur conservation d'une longue durée, sont beaucoup plus petites par rapport aux ciments à haute résistance sans "KRENT" (tableau I).

Les ciments avec "KRENT" ont une imperméabilité et une résistance au gel élevées de 30-50% par rapport aux ciments témoins, en cas des conditions comparables des essais. Ce fait s'explique par l'hydratation accélérée de leurs parties de clinker et par la densitée élevée de la submicrostructure de la pierre de ciment.

L'utilisation des "KRENT" en combinaison avec le clinker type alite permet d'augmenter considérablement la résistance aux sulfates du ciment jusqu'à un niveau caractérisant les variétés des ciments à résistance aux sulfates.

Donc, l'alliage d'hydratation de la pierre de ciment permet d'obtenir les ciments à objectifs différents.

REFERENCES

I. Бутт Ю.М., Рашкович Л.Н. Твердение гидравлических вяжущих веществ при повышенных температурах. М., Стройиздат, I96I.
2. Маедер А.А. Труды УШ Менделеевского съезда по общ. и прикл. химии. Секц. силикатов, I958, I2-I5.
3. Тимашев В.В., Сычева Л.И. Труды Московск. хим.-технол. ин-та им. Д.И. Менделеева, I979, № 92.
4. Ратинов В.Б., Лавут А.П. Доклады АН СССР, I962, т. I46, № I, I48.

V. AKIMOV,
T. KOUZNETSOVA,
A. KOUDRIAVTSEV,
V. PANIOUCHKINE, Institut de génie chimique Mendéléev de Moscou, URSS

1

DEFECTUOSITES DE STRUCTURE ET ACTIVITE D'HYDRATATION DES MINERAUX ENTRANT DANS LE CLINKER DU CIMENT PORTLAND

2.1

Les auteurs ont étudié les particularités de la structure des solutions solides de silicates de calcium ainsi que l'alite et de la bélite des clinkers industriels. La répartition des ions des micro-additifs dans les cristaux des minéraux, pour des conditions différentes de la cuisson du mélange de matières premières, a été mise en évidence par la méthode d'analyse radiospectrale locale. On a établi que l'incorporation de divers éléments dans le réseau cristallin des silicates de calcium conduit à la formation d'une quantité supplémentaire de dislocations, de vacances, de centres paramagnétiques, de libres porteurs de charge, dont la concentration totale varie dans de larges limites, ce qui permet de réguler l'aptitude réactionnelle des phase tant au début qu'à la fin de l'hydratation. Des recherches diversifiées des phénomènes intervenant lors de l'interaction du corps solide et de l'eau, recherches effectuées par des méthodes d'analyse radioscopique des phases, de microcalorimétrie et de résonance magnétique nucléaire (spin-écho), ont montré la dépendance du taux et de la cinétique de l'hydratatuin des minéraux vis-à-vis des défauts de leur structure. Les résultats obtenus peuvent être utilisés pour établir des prévisions de l'activité d'hydratation du ciment.

Os autores estudaram as particularidades da estrutura das soluções sólidas de silicatos de cálcio, bem como a alita e belita dos clínqueres industriais. Pelo método de análise radioespectral local foi posta em evidência a repartição dos íons de microaditivos nos cristais dos minerais, de conformidade com condições diferentes de cocção da mistura de matérias-primas. Estabeleceu-se que a incorporação de diversos elementos na rede cristalina dos silicatos de cálcio leva à formação de uma quantidade suplementar de deslocamentos, vazios, centros paramagnéticos, portadores livres de carga, cuja concentração total varia em limites amplos, o que permite regular-se a aptidão de reação de fases tanto no início como no fim da hidratação. Pesquisas diversificadas dos fenômenos que intervêm quando da interação do corpo sólido e água, pesquisas feitas pelos métodos de análise radioscópica de fases, microcalimetria e ressonância magnética nuclear (spin-écho) mostraram a dependência do teor e da cinética da hidratação dos minerais, face aos defeitos de sua estrutura. Os resultados obtidos podem ser utilizados para se fazerem previsões da atividade de hidratação do cimento.

V. AKIMOV,
T. KOUZNETSOVA,
A. KOUDRIAVTSEV,
V. PANIOUCHKINE

La défectuosité de la structure cristalline des minéraux du clinker est un facteur qui influe sur l'activité d'hydratation du ciment Portland. L'absence de données exhaustives sur la concentration des divers types de défauts dans les silicates, les aluminates et les alumoferrites de calcium empêche de faire une analyse objective des phénomènes intervenant lors de l'interaction du corps solide et de l'eau. La mise en oeuvre d'une microscopie électronique à haut pouvoir résolvant a confirmé l'hypothèse énonçant que l'hydratation n'intéresse pas toute la surface des cristaux mais essentiellement les centres actifs et que la dissolution intervient dans des régions déterminées du solide, en premier lieu aux endroits d'émergence de dislocations à sa surface (1-4). Les défauts superficiels résultant d'un traitement mécanique ou thermique des cristaux influent directement sur la durée de la période d'induction lors de l'hydratation du silicate tricalcique, principal minéral du clinker du ciment Portland (5), alors que les électrons captés par les centres actifs prennent part à l'établissement des liaisons avec les molécules d'eau, les ions H^+ et OH^- (6,7). Aussi les recherches sur la défectuosité structurale des principaux minéraux du clinker sont-elles d'actualité.

La modification de la structure des minéraux du clinker, en premier lieu de l'alite, par des micro-additifs, et cela aux régimes divers de la cuisson, est un procédé des plus efficaces pour induire des défauts. En déterminant, par une méthode d'analyse radio-spectrale locale, les taux des principaux éléments étrangers dans divers points des cristaux d'alite de certains clinkers industriels, on a établi que les valeurs moyennes des concentrations de Al_2O_3, Fe_2O_3, MgO, TiO_2, K_2O, Na_2O varient respectivement dans les limites de 0,90 à 1,30; 1,18 à 1,48; 0,53 à 0,82; 0 à 0,3; 0,15 à 0,23; 0 à 0,2 % en masse. La répartition des ions Mg^{2+} et leur quantité exercent une influence sur celle des autres éléments étrangers, principalement l'aluminium et le fer, dans le volume des cristaux d'alite. La concentration des ions Mg^{2+} dans les cristaux des minéraux dépend sensiblement du rapport C/S. A noter que pour $C/S < 3$ les zones périphériques des grains de C_3S sont enrichies en magnésium. Etant donné que les ions Mg^{2+} remplacent les ions Ca^{2+} dans les noeuds du réseau cristallin, il faut s'attendre à ses déformations les plus importantes à la limite des grains du minéral par suite de l'accroissement de la quantité des ions aluminium et fer tétraédriquement coordonnés et de l'incorporation d'une partie de ceux-ci dans les interstices. Le potassium et le titane enrichissent également les zones périphériques des grains du minéral, mais le titane est réparti plus uniformément.

En portant la durée de la cuisson du clinker du ciment Portland de laboratoire de 15 à 25 mn, à une température de 1 673°K, on provoque un accroissement de la quantité de Al, de Fe, de Mg simultanément au centre et dans les zones périphériques des grains d'alite, et en cas d'un maintien plus long, on voit s'accroître sensiblement la part des ions localisés dans les régions centrales. En portant la durée de la cuisson du clinker de 15 à 25 mn, à une température de 1 743°K, on obtient une baisse de la quantité de Al, de Fe et de Ti dans la partie centrale des cristaux du minéral. On a mis en évidence la relation qui existe entre la répartition des ions aluminium et celle des ions fer dans le volume des cristaux du minéral: dans les régions à haute teneur en aluminium, le fer est présent en quantités moindres, et vice versa, ce qui est une conséquence de la répartition des ions étrangers dans des positions identiques du réseau cristallin de C_3S.

L'incorporation des divers éléments dans le réseau cristalline de C_3S conduit à une quantité supplémentaire de dislocations dans la structure du mineral. La densità des dislocations varie de $3,0 \times 10^{12}$ à $4,1 \times 10^{14}$

V. AKIMOV,
T. KOUZNETSOVA,
A. KOUDRIAVTSEV,
V. PANIOUCHKINE

m^{-2}, suivant la concentration et la nature chimique de l'élément incorporé. On observe également un accroissement de la concentration des centres paramagnétiques électroniques sur les vacances oxygèniques, qui passe de $1,3x10^{21}$ à $1,0x10^{22}$ kg^{-1}. La concentration des centres à trou sur les vacances des atomes de calcium passe de $1,6x10^{21}$ à $2,1x10^{22}$ kg^{-1} en cas de remplacement des ions Si^{4+} par S^{6+}, Ti^{4+}, Al^{3+}. On a établi par voie expérimentale qu'il y a formation de libres porteurs de charge dans les cristaux du minéral, la conduction par trous se muant en conduction électronique en cas d'incorporation d'ions fer, cobalt et nickel dans la structure des cristaux de C_3S pur (tableau 1). L'incorporation des ions Na^+, Mg^{2+}, Ba^{2+}, Al^{3+}, S^{6+}, Zn^{2+}, Cd^{2+}, Cu^{2+}, Cr^{5+}, Mn^{2+}, Ti^{4+} dans le réseau cristallin de C_3S conduit à une multiplication de trous par 10 à 10^4 fois, chiffres nettement supérieurs au nombre des vacances en cours de formation chez les atomes de calcium, de silicium et d'oxygène.

Des recherches diversifiées sur la réactivité des solutions solides de C_3S et d'un alite de composition complexe (le rapport eau: solide étant de 0,5) ont permis d'établir que la durée des premiers stades d'hydratation du minéral diminue de 5 à 80% si le rapport entre la concentration des libres porteurs de charge et la densité des dislocations à sa surface dépasse 10^3 m^{-1}. Ce phénomène est plus caractéristique d'un alite contenant au plus 2,5 miles % d'ions étrangers. Le taux d'hydratation est également fonction de la concentration des libres porteurs de charge, dont la formation est due à l'incorporation des ions des micro-additifs dans la structure de C_3S (fig. 1).

Les ions principaux et les ions étrangers sont répartis dans les cristaux de bélite d'une manière aussi irrégulière que dans ceux d'alite, la partie centrale des grains du minéral étant enrichie en calcium. On voit ainsi apparaitre la possibi-

Tableau 1

Propriétés galvanomagnétiques des solutions solides de C_3S

n°	Additif	Concentration de l'additif, moles %	Concentration des porteurs de charge, m^{-3}	Mobilité des porteurs de charge, m^2/vs	Type de porteur de charge
1	-	-	$2,6 \cdot 10^{15}$	$1,0 \cdot 10^{-7}$	n
2	Fe_2O_3	0,8	$8,0 \cdot 10^{16}$	$3,0 \cdot 10^{-7}$	p
3	-"-	1,2	$9,2 \cdot 10^{16}$	$3,4 \cdot 10^{-7}$	p
4	CoO	0,8	$2,0 \cdot 10^{17}$	$2,7 \cdot 10^{-6}$	p
5	-"-	1,6	$4,3 \cdot 10^{17}$	$3,0 \cdot 10^{-6}$	p
6	-"-	3,2	$5,7 \cdot 10^{17}$	$3,2 \cdot 10^{-6}$	p
7	NiO	1,2	$7,2 \cdot 10^{17}$	$5,8 \cdot 10^{-6}$	p
8	-"-	1,8	$9,8 \cdot 10^{17}$	$7,4 \cdot 10^{-6}$	p
9	-"-	2,4	$2,0 \cdot 10^{18}$	$8,6 \cdot 10^{-6}$	p
10	BaO	0,4	$2,1 \cdot 10^{18}$	$1,1 \cdot 10^{-6}$	p
11	-"-	0,8	$9,5 \cdot 10^{18}$	$7,2 \cdot 10^{-6}$	n
12	-"-	1,6	$8,5 \cdot 10^{17}$	$3,5 \cdot 10^{-7}$	n
13	MgO	1,4	$3,5 \cdot 10^{15}$	$7,0 \cdot 10^{-7}$	n
14	-"-	2,8	$4,6 \cdot 10^{15}$	$4,6 \cdot 10^{-7}$	n
15	-"-	5,6	$2,7 \cdot 10^{19}$	$9,5 \cdot 10^{-6}$	n
16	TiO_2	0,7	$5,1 \cdot 10^{17}$	$1,2 \cdot 10^{-7}$	n
17	-"-	1,4	$8,2 \cdot 10^{16}$	$2,5 \cdot 10^{-7}$	n
18	-"-	2,8	$2,1 \cdot 10^{16}$	$6,8 \cdot 10^{-7}$	n

lité de contrôler la structure et les propriétés du minéral, aux différentes étapes d'hydratation, en induisant dans sa structure de différents types de défauts (tableau 2).

La variation de la concentration de libres porteurs de charge dans le silicate dicalcique est due aux écarts à la stoechiométrie de la composition du minéral, du remplacement des ions Ca^{2+} par K^+, Al^{3+}, Fe^{3+}, et Si^{4+} par Al^{3+}, B^{3+}, ainsi que de l'incorporation des ions étrangers dans son réseau cristallin. L'introduction des ions Fe^{3+} dans la composition de la solution solide conduit à la formation de libres porteurs de charge du type p, la réactivité du minéral variant sensiblement aux premiers stades d'hydratation (fig. 2,3). La cinétique de l'hydratation des solutions solides de silicate dicalcique (le rapport

Tableau 2

Défectuosité de structure des solutions solides de silicate dicalcique

66

n°	Minéral	Concentration des défauts		
		dislocations, m^{-2}	centres paramagnétiques, kg^{-1}	porteurs de charge, m^{-3}
1	$Ca_{1,87}\ K_{0,01}\ B_{0,03}\ Si_{1,04}\ O_4$	$9 \cdot 10^{11}$	$6,8 \cdot 10^{21}$	$5,7 \cdot 10^{18}$
2	$Ca_{1,98}\ K_{0,01}\ B_{0,03}\ Si_{0,99}\ O_4$	$6 \cdot 10^{11}$	$5,8 \cdot 10^{21}$	$7,2 \cdot 10^{15}$
3	$Ca_{2,07}\ K_{0,01}\ B_{0,03}\ Si_{0,94}\ O_4$	$5 \cdot 10^{11}$	$5,9 \cdot 10^{21}$	$6,0 \cdot 10^{15}$
4	$Ca_{1,87}\ Al_{0,01}\ B_{0,03}\ Si_{1,04}\ O_4$	$4 \cdot 10^{11}$	$6,5 \cdot 10^{21}$	$2,0 \cdot 10^{16}$
5	$Ca_{1,98}\ Al_{0,01}\ B_{0,03}\ Si_{0,99}\ O_4$	$8 \cdot 10^{11}$	$6,5 \cdot 10^{21}$	$1,0 \cdot 10^{18}$
6	$Ca_{2,07}\ Al_{0,01}\ B_{0,03}\ Si_{0,94}\ O_4$	$4 \cdot 10^{11}$	$5,9 \cdot 10^{21}$	$3,7 \cdot 10^{15}$
7	$Ca_{1,87}\ Fe_{0,02}\ B_{0,03}\ Si_{1,04}\ O_4$	$5 \cdot 10^{11}$	non déterminée	$1,5 \cdot 10^{16}$
8	$Ca_{1,98}\ Fe_{0,02}\ B_{0,03}\ Si_{0,99}\ O_4$	$8 \cdot 10^{11}$	non déterminée	$8,0 \cdot 10^{18}$
9	$Ca_{2,07}\ Fe_{0,02}\ B_{0,03}\ Si_{0,94}\ O_4$	$6 \cdot 10^{11}$	non déterminée	$6,0 \cdot 10^{17}$

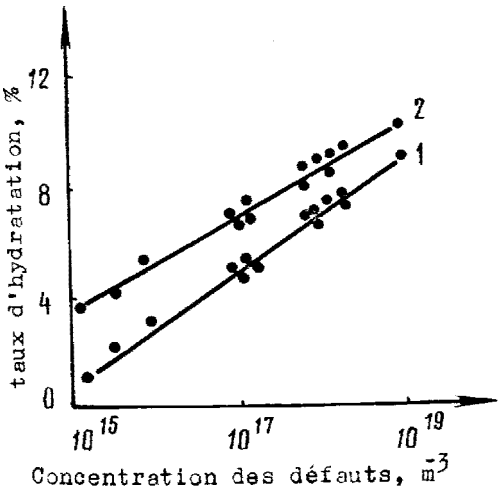

Fig. 1. Influence de la concentration de libres porteurs de charge sur le taux d'hydratation de C_3S (1 - 12 mn, 2 - 24 mn)

eau: solide étant de 0,5) a été étudiée par la méthode de résonance magnétique nucléaire. Les courbes de la relaxation des protons spin-milieu (T_1) et spin-spin (T_2) s'accordent, comme pour l'hydratation de C_3S [7], avec les données relatives au dégagement de chaleur et au taux d'hydratation des minéraux, en attestant la pluralité des stades des processus en cours lors de l'interaction d'un liant monominéral avec l'eau. Le décroissement de la valeur de T_1 observé au début de l'hydratation est dû au passage des molécules de H_2O de l'état adsorbé dans une couche géliforme, ainsi qu'au passage d'ions étrangers et d'ions Ca^{2+} dans la solution. Il est à noter que pour β-C_2S doté de différents additifs, cette période dure 60 à 120 mn, et pour C_3S, 15 à 90 mn, sa durée étant fonction de la défectuosité de structure du minéral. La seconde phase d'hydratation, caractérisée pratiquement par une constance de T_1, peut durer plusieurs dizaines d'heures. Le taux d'hydratation des minéraux, même plus tard, dépend de la défectuosité de leur structure. On peut juger, d'après la valeur de T_1 aux premiers stades, du taux d'hydratation du silicate dicalcique qu'on aura plusieurs jours après le gâchage du matériau avec de l'eau. Ce sont les aluminates de calcium qui s'hydratent le plus activement à la première étape (fig. 4).

Les recherches sur les particularités de la structure des minéraux des clinkers industriels et des phases synthétisées, ainsi que sur leur activité d'hydratation ont

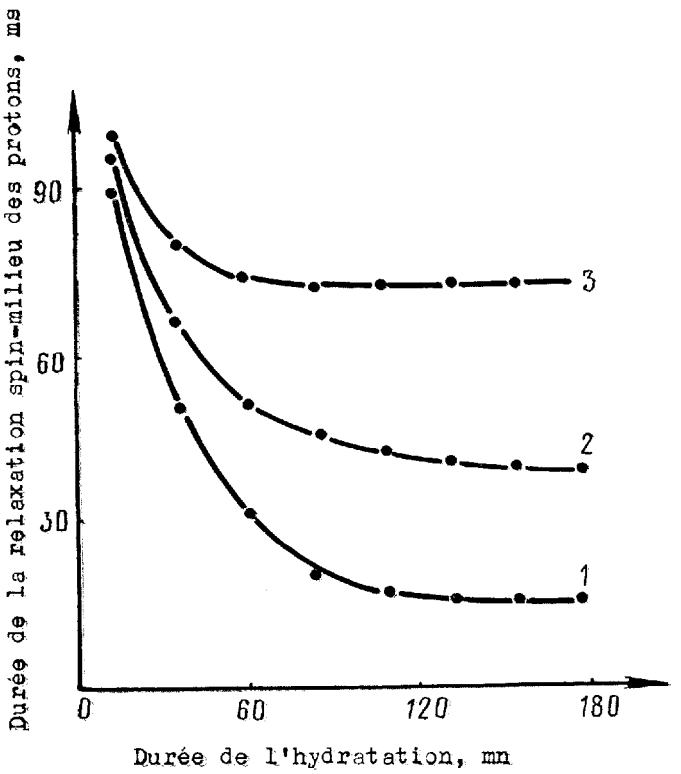

Fig. 2. Variation de la durée de la relaxation spin-milieu des protons lors de l'hydratation des minéraux:
1 - $Ca_{1,87}\ K_{0,01}\ B_{0,03}\ Si_{1,04}\ O_4$
2 - $Ca_{1,87}\ Al_{0,01}\ B_{0,03}\ Si_{1,04}\ O_4$
3 - $Ca_{1,87}\ Fe_{0,02}\ B_{0,03}\ Si_{1,04}\ O_4$

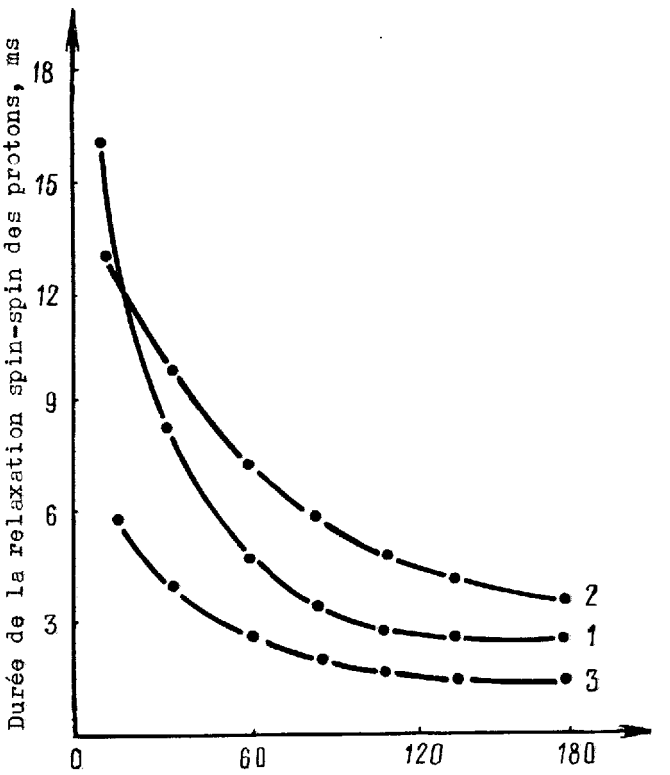

Fig. 3. Variation de la durée de la relaxation spin-spin des protons lors de l'hydratation des minéraux:
1 - $Ca_{1,87}\ K_{0,01}\ B_{0,03}\ Si_{1,04}\ O_4$
2 - $Ca_{1,87}\ Al_{0,01}\ B_{0,03}\ Si_{1,04}\ O_4$
3 - $Ca_{1,87}\ Fe_{0,02}\ B_{0,03}\ Si_{1,04}\ O_4$

donc montré qu'on a intérêt à réguler la répartition des éléments-traces dans le volume des cristaux en vue d'augmenter la défectuosité structurale et, partant, la réactivité lors de l'interaction avec l'eau.

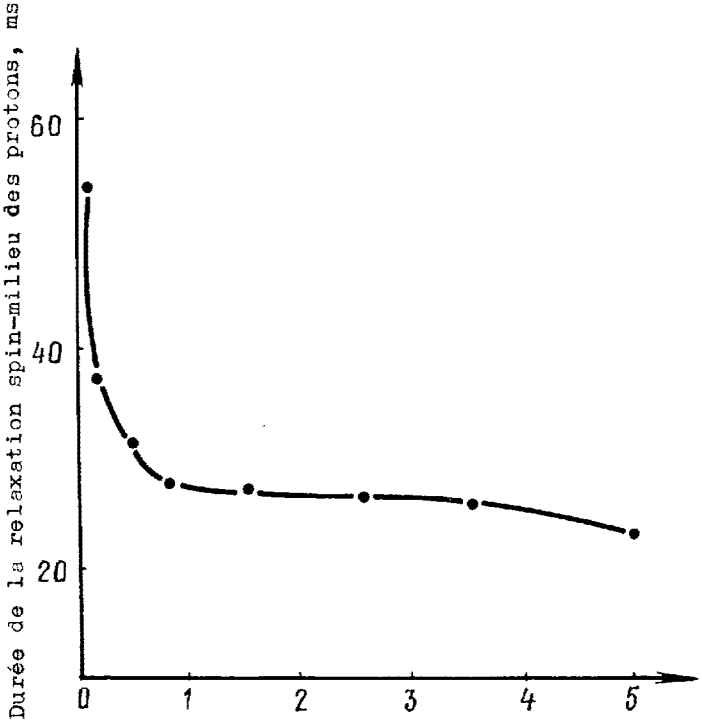

Fig. 4. Variation de la durée de la relaxation spin-réseau des protons lors de l'hydratation de C_3A.

REFERENCES

1. Regourd M., Thomassin J.H., Baillif P., Touray J.C. 7-th International Congress on the Chemistry of Cement, 1980, V. 11, p.p. 123-128.
2. Timachev V. Ciment Portland. Stroizdat, 1974, 328 p. (en russe).
3. Timachev V. - 7-th International Congress on the Chemistry of Cement, 1980.
4. Toropov N.A., Degen M.G., Baikova A.J. Silikattechnik, 1971, V. 22, n° 12, p.p. 400-402.
5. Maycock J.N., Skalny J., Kaluoncu R. Cem. Concr. Res., 1974, V. 4, n° 5, p.p. 835-847.
6. Сычев М. Цемент, 1984, № 4, стр. 10-13.
7. Timachev V., Akimov V. 7-th International Congress on the Chemistry of Cement, 1980, V. IV, p.p. 203-207.

E.I. FEDIN,
T.V. KOUZNETSOVA,
A.V. NEKHOROCHEV,
M.A. SOROTSHKIN,
A.L. BLUMENFEL'D,
A.B. KOUDRIAVTSEV,
G.V. AKIMOV, Institut de génie chimique D.I. Mendéléev de Moscou, U.R.S.S.

2.1

ETUDE DE LA CINETIQUE DE L'HYDRATATION DU CIMENT PORTLAND PAR LA SERIE DE METHODES NUCLEAIRES

Les méthodes d'analyse des phases aux rayons X, de résonance magnétique nucléaire et celles d'analyse à γ-résonance nucléaire sont utilisées pour l'étude des processus ayant lieu au cours du durcissement des pâtes (eau/ciment = 0,16; 0,2; 0,33; 0,5) sur la base des ciments et du silicate tricalcique. L'évaluation de qualité du gel tobermorite est donnée pour tous les délais de durcissement. L'épaisseur des films hydratés et la viscosité dans les couches minces sont calculées.

L'utilisation de la série des méthodes nucléaires (résonance magnétique nucléaire, analyse à γ-résonance nucléaire) pour l'étude de la cinétique d'hydratation du ciment et C_3S a permis d'expliquer l'allure anomale des processus aux étapes initiales, de démontrer la cristallisation initiale des phases polyaqueuses et la présence de l'eau de phase solide et des processus de recristallisation au cours du durcissement.

Foram utilizados métodos de análise de fases por raios X, ressonância magnética nuclear e ressonância nuclear γ para estudo dos processos que ocorrem durante o endurecimento de pastas (água/cimento = 0,16; 0,2; 0,33; 0,5) com base de cimentos e de silicato tricálcico. A avaliação da qualidade gel tobermorita é feita em todos os atrasos de endurecimento. São calculadas a espessura das películas hidratadas e a viscosidade nas camadas finas.

A utilização da série de métodos nucleares (ressonância magnética nuclear, análise por ressonância nuclear γ) para o estudo da cinética de hidratação do cimento e do C_3S permitiu explicar a evolução anormal dos processos nas etapas iniciais, e demonstrar a cristalização inicial das fases poliaquosas e a presença de água da fase sólida, e os processos de recristalização no decorrer do endurecimento.

E.I. FEDIN,
T.V. KOUZNETSOVA,
A.V. NEKHOROCHEV,
M.A. SOROTSHKIN,
A.L. BLUMENFEL'D,
A.B. KOUDRIAVTSEV,
G.V. AKIMOV

Les questions de la formation de structure à son stade initial et les processus de polymérisation-recristallisation se déroulant dans des délais plus avancés de durcissement, constituent des aspects des plus importants de la théorie de l'hydratation des liants minéraux. Le présent ouvrage étudie l'allure des processus de durcissement des pâtes fabriquées sur la base des ciments et du C_3S, à l'aide des méthodes APX (analyse de phase aux rayons X), RMN (résonance magnétique nucléaire) et γ-RN (γ-résonance nucléaire).

On a retenu pour le paramètre caractérisant la qualité du gel de tobermorite à tous les délais de durcissement, le rapport entre la résistance à la compression et le degré d'hydratation (R/γ). En présence de rapports bas eau/solide le paramètre $\frac{R}{\gamma}$ (fig. 1) qui caractérise la qualité du gel, est à sa valeur maximale. Ceci peut être dû tant à la formation de phases polyhydratées des hydrocilicates au stade initial de l'hydratation (1) qu'aux processus de polymérisation-recristallisation se déroulant intensivement dans des délais plus avancés (2).

Au stade initial de l'hydratation, on a étudié la variation du temps de relaxation spin-réseau T_1 selon la méthode du "point zéro" à l'aide d'une série d'impulsions $\frac{\pi}{2} - \tau - \frac{\pi}{2}$ (fig. 2). En présence d'un haut rapport eau/solide durant une période de 36 à 72 mn, il n'y a pas de baisse monotone de T_1 (fig. 2). Mais c'est durant cette période justement que l'on observe une brusque chute d'intensité du dégagement de chaleur (3), une modification des propriétés des pâtes de ciment (4) et une réduction du volume d'eau libre (effet d'"aspiration hydraulique") (5).

En présence d'un bas rapport eau/solide, l'eau structuralisée ne doit pas être considérée comme un liquide à faible viscosité (6) et comme le veut la théorie générale de la RMN (7) à $\omega_0 r \approx 1$

$$\frac{1}{T_1} = 0{,}52\,\frac{\gamma_1^4\, h^2 I(I+1)\tau_c}{r^6} \qquad (1)$$

où: I est le spin;

ω_0 est la fréquence de résonance de Larmor;

γ_1 est le rapport hydromagnétique;

h est la constante de Planck;

$\tau_s = \frac{4\,a^3\,n}{3K}$ est le temps de corrélation;

η est la viscosité de l'eau.

Ainsi, on peut caractériser les données expérimentales de variation du temps de relaxation spin-réseau T_1 comme variation de viscosité des minces couches d'eau ($h < 0{,}15\ \mu$). D'après la fonction connue (8) où la viscosité (η) dépend de l'épaisseur h de la couche d'eau et de la voscosité de l'eau libre $\eta_0 \simeq \frac{1}{(T_1)_0}$

$$\eta\,(h) \approx \eta_0\left(1 + \frac{K}{h}\right) \qquad (2)$$

En se basant sur les données de la figure 2 on a déterminé les épaisseurs h des films hydratés (formule 3) et les surfaces spécifiques S_0 au stade initial de l'hydratation (4):

$$h = \frac{K}{\frac{(T_1)_0}{T_1} - 1},$$

$$S_0 = \frac{(E/C)\left(\frac{(T_1)_0}{T_1} - 1\right)}{K},$$

où: $K = (3{,}76 \pm 0{,}18)\cdot 10^{-7}$ m;

$(T_1)_0 = 3000$ ms.

Au cours de l'hydratation à E/C = 0,2 durant une période de 3 heures l'épaisseur des films hydratés a diminué de $1{,}07\cdot 10^{-7}$ à $0{,}4\cdot 10^{-7}$ m, la viscosité a accru dans les minces couches de $4{,}5\,\eta_0$ à $10{,}3\,\eta_0$ et la surface spécifique S_0 a augmenté de 2 à 5 m^2/g (fig. 3).

Une variation non monotone de T_1 (courbe 4 de la figure 2) et des variations anoma-

E.I. FEDIN,
T.V. KOUZNETSOVA,
A.V. NEKHOROCHEV,
M.A. SOROTSHKIN,
A.L. BLUMENFEL'D,
A.B. KOUDRIAVTSEV,
G.V. AKIMOV

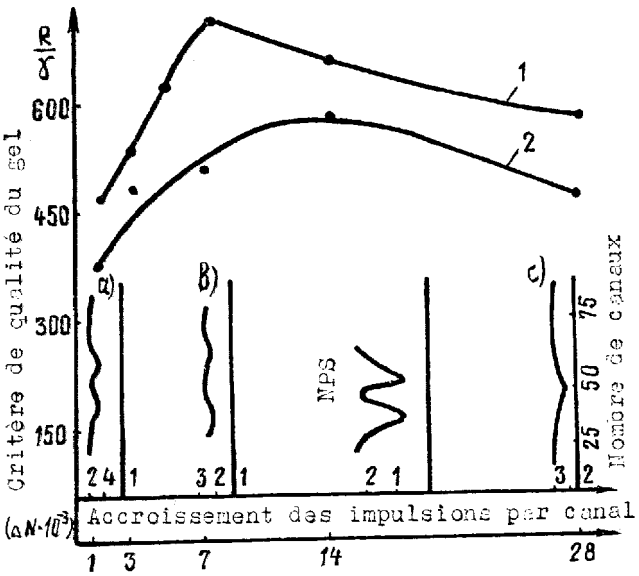

Fig. 1. Variation du critère de la qualité du gel de tobermorite $\frac{R}{\gamma}$ au cours du durcissement (1, 2) et γ-RN-spectres du ciment Portland de base (a) et du ciment durci au bout de 7 jours (b) et de 28 jours (c). NPS - diagramme d'étalonnage du nitroprussiate de sodium

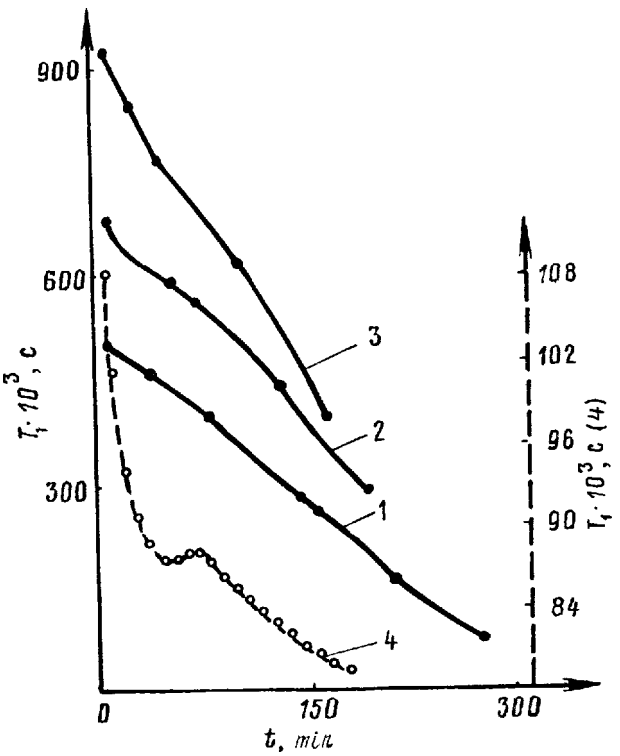

Fig. 2. Variation temporelle T_1 de la relaxation spin-réseau en fonction du temps de l'hydratation du C_3S pour de différents rapports eau/solide: 0,16 (1); 0,2 (2); 0,33 (3); 0,5 (4)

les des autres paramètres dans les délais de 30 à 70 mn du début de l'hydratation (3, 4, 5) sont liées aux processus d'immobilisation de l'eau libre, de coagulation de nouvelles formations dispersées, à leur précipitation à la surface, à une augmentation de l'épaisseur h de la couche d'eau et à un accroissement régulier du temps de relaxation spin-réseau T_1. Le fait que le critère de la qualité du gel ($\frac{R}{\gamma}$) se porte à l'extrême au cours de l'hydratation (courbes 1, 2 de la figure 1) est dû à la cristallisation initiale des phases polyhydratées (1) et au déroulement des processus de polymérisation-recristallisation dans des délais plus avancés. Les hydrosilicates polyhydratés primaires ne contiennent pas d'eau en phase solide que l'on déterminait à l'aide de la méthode RMN selon la décroissance d'induction libre. Après la $-\frac{\pi}{2}$ impulsion l'aimantation décroît suivant la fonction exponentielle (7)

$$M(t) = M_0\left(e^{-\frac{t_1}{T_2'}} + e^{-\frac{t_1}{T_2''}}\right),$$

où T_2' et T_2'' sont les valeurs temporelles de la relaxation spin-spin. Etant donné que l'eau libre et l'eau contenue dans les hydrosilicates ont des valeurs temporelles de relaxation différentes T_2' et T_2'', il est possible de définir d'après les aimantations M_l et M_s (fig. 4) la tenue de la phase solide en eau (7). Au bout de 24 heures, lorsque la qualité du gel est encore basse (fig. 1), on n'a décelé que des traces de la présence d'eau en phase solide mais vers le quatrième jour la présence d'eau en phase solide indépendamment des rapports eau/solide atteint déjà 6,5 à 8 % en poids du liant et subit

E.I. FEDIN,
T.V. KOUZNETSOVA,
A.V. NEKHOROCHEV,
M.A. SOROTSHKIN,
A.L. BLUMENFEL'D,
A.B. KOUDRIAVTSEV,
G.V. AKIMOV

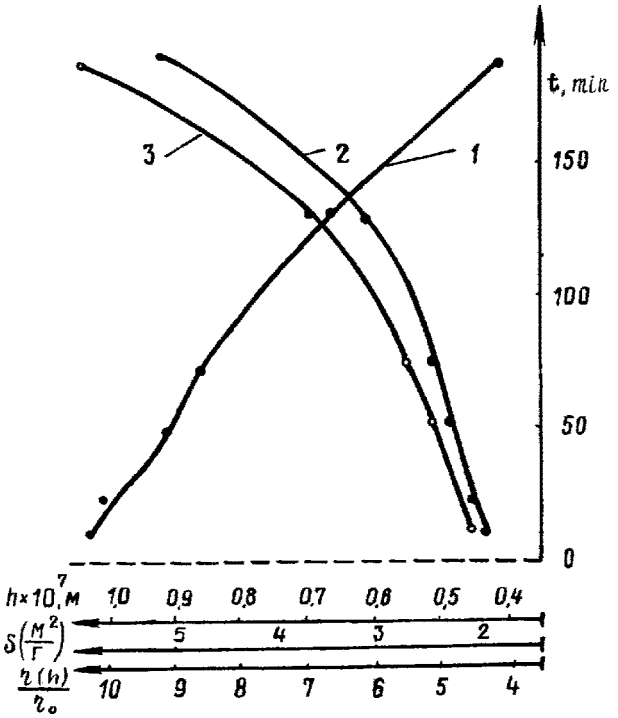

Fig. 3. Variation de l'épaisseur h (1) des couches hydratées en phase solide, de la surface spécifique S_g (2) et de la viscosité d'eau $\frac{\eta(h)}{\eta_0}$ dans de minces couches en fonction du temps de l'hydratation initiale à un bas rapport eau/solide (0,2)

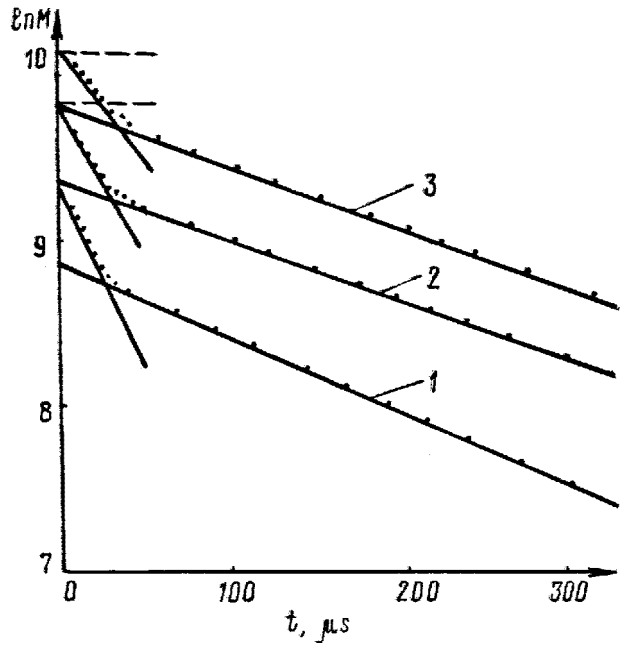

Fig. 4. Variation de l'aimantation (ln M) de la décroissance d'induction libre en fonction du temps de relaxation (t) pour les pâtes de C_3S en durcissement 56 jours à partir du moment de gâchage.
(1) - E/C = 0,16; (2) - E/C = 0,2;
(3) - E/C = 0,33

de faibles variations vers le 28-e jour (8 à 9 %). Au fur et à mesure que l'hydratation se poursuive, au bout de plus de 24 heures, dans des conditions encore plus "restreintes" commencent à se produire des phénomènes du type "synérèse" conduisant à une compression des couches hydratées, à un déplacement de l'eau en excès et à une limitation de la mobilité des molécules de H_2O restées dans les hydrosilicates. Les molécules pareilles sont enregistrées à l'aide de la méthode RMN comme celles appartenant à la phase solide.

Une altération de la qualité du gel de tobermorite dans les délais de 7 à 28 jours de durcissement est due aux processus de polymérisation-recristallisation (2) liés à la variation des formes de liaison d'ions de fer dans le réseau cristallin. Dans le ciment de départ et dans celui en hydratation il se produit au bout de 1, 3, 7 jours une décomposition quadripolaire des lignes des γ-RN-spectres où $\delta E_Q \approx 9{,}374 \cdot 10^{-8}$ eV (fig. 1 a, b) et au bout de 7 à 28 jours des processus de polymérisation-recristallisation ce qui aboutit à une brusque variation des formes de liaison d'ions de fer. Au bout de 28 jours la décomposition quadripolaire (fig. 1, c) cède la place à un déplacement chimique ($\delta E_I = 0{,}9468 \cdot 10^{-8}$ eV). Ainsi, une altération du critère de la qualité du gel observée expérimentalement en présence de bas rapports eau/solide dans les délais de 7 à 28 jours de durcissement s'explique par des processus de recristallisation intenses.

L'utilisation d'un ensemble de méthodes nucléaires (RMN et γ-RN) à l'étude de la

cinétique de l'hydratation du ciment et du C_3S a permis d'expliquer le déroulement anomal du processus à un stade précaire, de prouver expérimentalement la cristallisation initiale des phases polyhydratées, la présence d'eau en phase solide et des processus de recristallisation au cours du durcissement.

REFERENCES

1. Сычев М.М., ЖПХ, 1981, № 9, с. 2036.
2. Jawed J., Menetrier D., Skalny J., Lachowski E., Mohan K., Taylor H.F.W., World Cem. Technol., 1981, v. 12, No. 3, p. 124-126, 128-132, 134-135, 137-138.
3. Timachev V.V., Akimov V.G. 7th Int. Congr. on the Chemistry of Cement, Paris, 1980, No. 4, p. 203-207.
4. Гранковский И.Г., Чистяков В.В., ЖПХ, 1981, 54, № 1, с. 15-20.
5. Сорочкин М.А., Шуров А.Ф., Журина Л.П., Зайченко Ю.П. Тезисы Всесоюзной конференции "Повышение эффективности и качества бетона и железобетона", Горький, 1977, с. 82.
6. Сычев М.М. Цемент, 1981, № 1, с. 7-9.
7. Лундин А.Г., Федин Э.И. Ядерный магнитный резонанс, Наука, Новосибирск, 1980, с. 192.
8. Бондаренко Н.Ф., Железный Б.В. Сб. "Связанная вода в дисперсных системах". изд-во МГУ, 1980, вып.5, с.34.

A.I. BOIKOVA, Dr. Chem. Sc., Senior Research Scientist,
L.V. GRISHCHENKO, Junior Research Scientist
et A.I. DOMANSKY, Junior Research Scientist, Institute of Silicate Chemistry of the USSR Acad. Sci., Leningrad.

1

Hydration activity of chlorine-containing phases.

2.1

SUMMARY: The hydration activity of chlorine-containing phases of clinkers obtained by special technology was studied by X-ray diffraction method. Although the use of such clinkers is limited, the search for the ways of their application in combination with other components can be effective. The main phase of these clinkers - alinite - contains up to 4% Cl_2. According to the atomic structure data, the chemical composition of alinite corresponds to the formula $Ca_{11}(Si_{0.75}Al_{0.25})O_{18}Cl$. However, recent investigations by Italian and German workers showed that Mg is necessarily contained in alinite.

The alinite used in our work contained ~ 4 wt% MgO, ~ 3.5 % Cl_2 and a small amount of Fe (0.14 wt% Fe_2O_3). The hydration activity of alinite in clinker was also studied. The other chlorine-containing phase studied was calcium aluminate $C_{11}A_7 \cdot CaCl_2$, both without and with impurities in the lattice. For comparison, the hydration activity of $C_{12}A_7$ was studied. The curves for the degree of hydration of C_3S and alites of complex composition are given.

The hydration kinetic curves of alinites show that alinite without impurities in the lattice is more active in the early and later hydration stages than alinite in clinker. The simultaneous hydration of other phases of alinite-based clinkers and the hydration products formed not only decrease significantly the activity of alinite in clinker in the early stage but promote a more "smooth" reaction with water in the later stage.

Among the calcium chloroaluminates studied, the aluminate $C_{11}A_7 \cdot CaCl_2$ is most active in the early stage. Impurity-containing chloroaluminate phases of the real composition are less active in the early stage than "pure" $C_{11}A_7 \cdot CaCl_2$. However, in the early stage their reaction with water is more intense. The analysis of the hydration kinetic curves permit us to conclude that the higher the hydration activity of calcium chloroaluminate in the early stage, the sooner the retardation of the reaction in the later stage.

Utilizando o método de difração por raio X, estudou-se a atividade de hidratação de fases de clínqueres contendo cloro, obtidos através de tecnologia especial. Embora a utilização destes clínqueres seja limitada, pode ser útil a pesquisa das formas para sua aplicação em combinação com outros componentes. A fase principal destes clínqueres - alinita- contem até 4% de Cl_2. De acordo com os dados de estrutura atômica, a composição química da alinita corresponde à fórmula $Ca_{11}(Si_{0,75}Al_{0,25})O_{18}Cl$. Todavia investigações recentes desenvolvidas por cientistas italianos e alemães modstraram que a alinita necessariamente contém Mg.

A alinita utilizada em nossa pesquisa continha, em peso, ~4% de MgO, ~3,5% de Cl_2, e uma pequena quantidade de Fe (0,14% em peso de Fe_2O_3). Também foi estudada a atividade de hidratação da alinita no clínquer. A outra fase contendo cloro, que foi estudada, foi aluminato de cálcio $C_{11}A_{17} \cdot CaCl_2$, com ou sem impurezas na rede. Para comparação se estudou a atividade de hidratação de $C_{12}A_7$. São fornecidas as curvas do grau de hidração de C_3S e de alitas de composição complexa.

As curvas da cinética de hidratação das alinitas mostram que alinita sem impurezas na rede, nos estágios inicial e final de hidração é mais ativa do que a alinita em clínquer. A hidratação simultânea de outras fases de clínquer baseado em alinita e os produtos de hidratação formados não só diminui significativamente a atividade da alinita no clínquer no estágio inicial, mas proporciona uma reação mais "suave" com água no estágio final.

Entre os cloroaluminatos de cálcio estudados, o aluminato $C_{11}A_7 \cdot CaCl_2$ é o mais ativo na etapa inicial. Fases do cloroaluminato contendo impureza na composição real são menos ativas no estágio inicial do que $C_{11}A_7 \cdot CaCl_2$ "puro". Entretanto, no estágio inicial, sua reação com água é mais intensa. A análise das curvas de cinética de hidratação nos permite concluir que quanto maior for a atividade de hidratação do cloroaluminato de cálcio no estágio inicial, mais rápida e a retardação da reação no estágio final.

A.I. BOIKOVA
L.V. GRISHCHENKO
A.I. DOMANSKY

INTRODUCTION

The study of the interaction between water and chlorine-containing phases - high-basic calcium chlorosilicate (alinite) and calcium chloroaluminate $Ca_{11}Al_{14}O_{32}\cdot CaCl_2$ ($11CaO\cdot 7Al_2O_3\cdot CaCl_2$) is of interest as these phases are constituents of clinkers rich in chlorine. These phases contain in their lattice a considerable amount of chlorine. The alinite content in clinkers is 55-65 wt%; the amount of the chloroaluminate phase can reach 5-10 wt% /1/.

Although the application of alinite clinkers is limited at present, the search for the ways of their use can be rather effective. One way is the use of alinite clinkers in mixtures with other components /2/. Another way is such a change of the clinker phase composition which leads to the formation of some amount of alite along with alinite. This can be realized by increase of clinkering temperature.

The main phase of chlorine-containing clinkers - alinite - contains ~ 3.5 wt% Cl_2 in the lattice. Based on the data of structural analysis of alinite /3/, the formula of this new mineral can be written as $Ca_{11}(Si_{0.75}Al_{0.25})_4O_{18}Cl$.

However, recent investigations /4,5/ showed that alinite free of magnesium in the lattice cannot be obtained. It should be supposed that in the alinite lattice Mg occupies positions analogous to those of calcium. According to /4/ the refined composition of alinite is as follows: $3(CaO_{0.875}\cdot MgO_{0.070}CaCl_{2}_{0.055})(SiO_{2}_{0.885}Al_2O_{3}_{0.115})$; and according to /5/: $Ca_{9.9}Mg_{0.8}\square_{0.3}[(SiO_4)_{3.4}(AlO_4)_{0.6}O_{1.9}Cl_{1.0}]$.

Under real conditions of industrial production the composition of alinite becomes more complex due to the presence in the lattice of impurities which substitute isomorphously the main structural elements. Thus the EPMA study of the alinite contained in industrial clinkers permitted to reveal that along with the main structural elements - Ca, Mg, Al, Si, Cl (oxygen is also implied) it also contains impurities Na, K, Fe, Ti, P /6/. The amounts of Na, K, Ti and P are small and do not exceed 0.3, 0.3, 0.6, 0.2 wt%, respectively when calculated for the same amount of oxides. As to iron, its content as an isomorphous impurity is somewhat greater in the real crystals and varies from 0.5 to 2.5 wt%. It is worth noting that manganese has been found only in the aluminoferrite phase whose amount in the clinker is rather low. The given values of impurities contents in alinite are not final because of insufficiency of the experimental data.

EXPERIMENT AND RESULTS

The composition of alinite studied in our work was as follows (wt%): SiO_2 - 23.14; Al_2O_3 - 4.06, Fe_2O_3 - 0.14, CaO - 63.51, MgO - 3.86, Cl - 3.20, the loss on ignition being 2.25 wt%. The hydration activity was studied by X-ray method taking into account the change of integral intensity of the definite diffraction maxima.

The hydration activity of alinite in alinite clinkers was also studied. The experiment was unusual in that the alinite phase was not separated from the clinker and the process of its interaction with water was observed directly in clinker in the presence of all other phases.

In the X-ray diffraction patterns we selected such maxima which were overlapped neither by the maxima of other phases (belite, chloroaluminate and aluminoferrite phases) nor by the ones of the hydration products formed. These were the maxima at 27.55° and 49.20° $2\theta, CuK_\alpha$, hkl 031 and 440, respectively (see Fig. 1). Samples were prepared in the paste form with a w/c ratio of 0.4, the experimental temperature was ~ 20°C.

Figure 1 shows X-ray diffraction patterns of alinite and alinite clinker. It is clearly seen that the main phase of clinker is alinite.

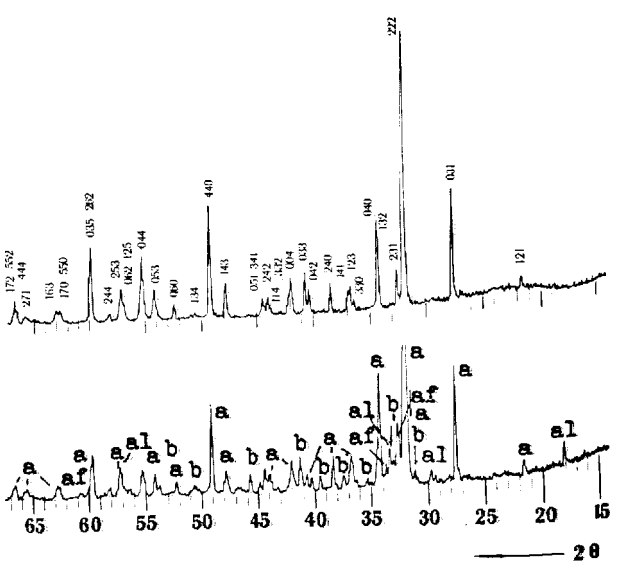

Fig. 1 - X-ray diffraction patterns of alinite (top) and alinite clinker.
a - alinite, b - belite, al - chloroaluminate phase, af - aluminoferrite phase.

A.I. BOIKOVA
L.V. GRISHCHENKO
A.I. DOMANSKY

The X-ray diffraction pattern of clinker also exhibits reflections characteristic of other phases - belite, chloroaluminate and aluminoferrite.

Figure 2 represents hydration kinetic curves for alinite (I), alinite in clinkers (II,IV,V) and alinite in cement (III). The curves of the degree of hydration for C_3S and alites of complex composition analogous to alites of commercial clinkers (Fig. 3) are given for comparison of the hydration processes of alinite and alite.

The kinetic curves permit us to reveal the main features of the hydration of a new high-basic mineral - alinite. Firstly, it is a much higher activity of the mineral in the early and later stages compared to C_3S and alites of complex composition containing several varieties of impurities in the lattice. This is well demonstrated by the curves. Thus after 1 h of the reaction with water the degree of hydration is ~22% for alinite and ~ 10% for C_3S; after 12 h it amounts up to ~ 70% for alinite and ~ 20% for C_3S. After 1 day the degree of hydration is ~ 80% and ~25% for alinite and C_3S, respectively.

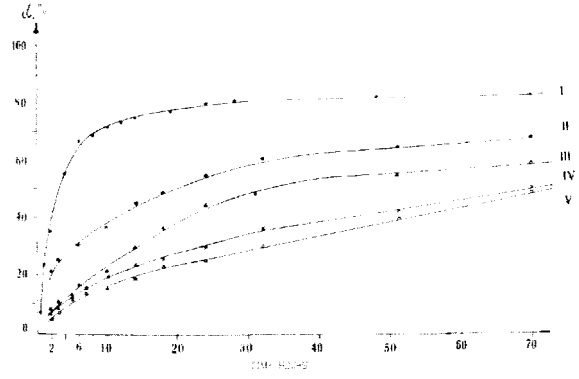

Fig. 2 - Hydration kinetic curves for alinite (curve I) and alinite in clinkers (curves II,IV,V) and in cement (curve III)

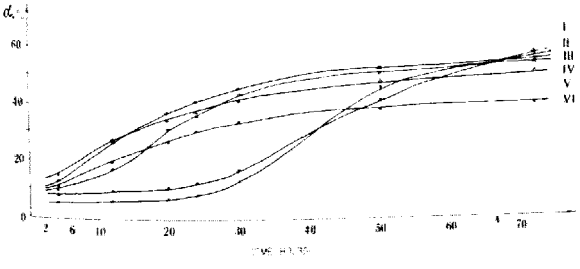

Fig. 3 - Hydration kinetic curves for C_3S (curve VI) and alites of complex composition (curves I-V).

Attention is drawn to the fact that the form of the curve for alinite hydration is similar to those for C_3A, its solid solutions with Na_2O and aluminate phases of complex composition /7,8,9/. However, the time of intense reaction of the aluminate with water is measured in minutes and that of alinite - in hours. Nevertheless three stages of hydration have been observed for the alinite studied by us. The first stage is characterized by active reaction of alinite with water and is due to the peculiarities of the chemical composition and atomic structure of the mineral itself. At the second stage the reaction slows down due to the formation of a layer of hydration products on the surface of crystals. This retards the diffusion of the liquid phase to the unreacted substance. The third hydration stage is a delayed reaction with water. After 28 days the reaction of alinite with water (the degree of hydration ~ 97%) has been completed.

The hydration kinetic curves for alinite show that pure alinite is much more reactive in the early and later stages than alinite contained in clinker. It is obvious that the simultaneous hydration of other phases in alinite clinkers, mainly of the belite and chloroaluminate, as well as the hydration products formed not only retard the hydration of clinker alinite in the early stage but promote a more smooth reaction in the later stage.

At the same time the different activity of alinite in clinkers has been observed. Thus after 1 day the degree of hydration of alinite in clinker II is ~ 50%, in cement (curve III) ~ 40%, in clinker IV ~ 30% and in clinker V ~ 25%. When analyzing the values of the degree of hydration attention should be paid to the fact that the degree of hydration of alinite in clinker II is twice as much as that of alinite in clinker V. One of the sure reasons of this difference in hydration rates of alinites is the presence of impurities in the lattice. Chemical analysis showed that all the four materials under study contain SiO_2, Al_2O_3, Fe_2O_3, CaO, MgO, Cl as well as TiO_2, P_2O_5 (except for clinker V), SO_3 (except for clinker IV) and small amounts of Na_2O (except for clinker IV), K_2O (except for clinker IV), MnO.

Alinites of the clinkers studied contain in their lattices different amounts of impurities Na, K, Fe, Ti, P and S. At present it is difficult to estimate the influence of each of the impurities mentioned on the hydration of alinite. However, there are grounds to assume that Fe decreases the activity of alinite. Alinite in clinker contains about 2.0 wt% Fe_2O_3 in the lattice, whereas pure alinite (Sample 1, Fig. 2) contains ~ 0.14 wt% Fe_2O_3 and its degree of hydration is much higher than that of alinite in clinker.

It should be mentioned once more that the hydration activity of alinite in clinker depends not only on the chemical composition of the real clinker but also on some other factors.

The same preliminary conclusion can also be drawn about the influence of Ti and P. The total contents of TiO_2 and P_2O_5 in clinker II and cement III are about 0.85 and 0.60 wt%, respectively, whereas in clinkers IV and V they amount to 0.45 and 0.20 wt%. The hydration activity of alinite in materials II and III is higher than in IV and V (Fig. 2). After 28 days the degree of hydration of alinite in samples II, III, IV, V was 82, 83, 77 and 76 %, respectively. It should be noted in conclusion that many tests will be needed to reveal the influence of different impurities on the hydration of alinite.

Another chlorine-containing phase under study was the aluminate $C_{11}A_7 \cdot CaCl_2$ (~ 5.0 wt% Cl_2), both without and with impurities in the lattice.
Under industrial conditions the chloroaluminate phase of alinite clinkers is formed also with impurities in the lattice. The main impurities in the aluminate determined by EPMA are iron and silicon. The amount of the former when calculated for the same amount of Fe_2O_3 can reach 6 wt% and that of the latter 4.5-5 wt%. Much less amount of Na, Mg and Ti can be present in the aluminate.

To study the hydration activity we synthesized samples of $C_{11}A_7 \cdot CaCl_2$ at different temperatures (1200 and 1400 °C, burning for 1 h). Aluminate phases with impurities in the lattice have also been obtained on the basis of this compound. One of these phases (phase I) is analogous in composition to the chloroaluminate phase of industrial alinite clinker, another phase (II) is similar to the chloroaluminate phase of white industrial clinker. The chloroaluminate phases were synthesized at 1300 °C for 3 h. Samples in the form of tablets were fired in sealed platinum crucibles.
Tables 1 gives the results of chemical analysis of two synthesized chloroaluminate phases of complex composition.

The compositions of the phases differ first of all in contents of iron, silicon and magnesium oxides. As was to be expected, the amount of Fe_2O_3 in the chloroaluminate phase of white clinker (II) is much less than in phase I of the usual alinite clinker. The total amount of impurities (in the oxides) is ~ 8.0 wt% in phase I and ~ 6.0 wt% in phase II.

Figure 4 shows X-ray patterns of the chloroaluminate phase I of complex composition and the compound $C_{11}A_7 \cdot CaCl_2$ (curve II) synthesized at 1400 °C for 1 h. As seen from the figure, the chloroaluminate phase (X-ray pattern I) retains completely the $C_{11}A_7 \cdot CaCl_2$ matrix; only a small shift of the maxima to the region of small angles is observed. An analogous X-ray pattern is shown by the chloroaluminate phase II.

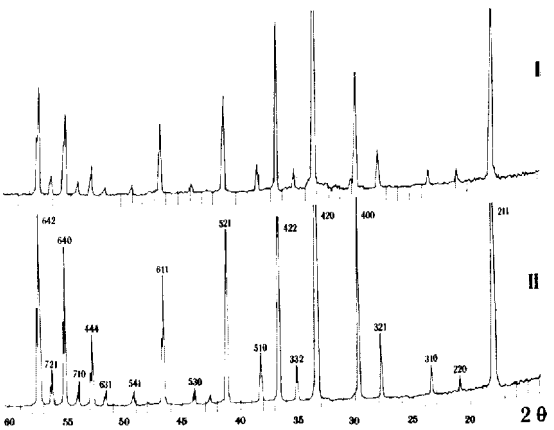

Fig. 4 - X-ray diffraction patterns of the impurity-containing chloroaluminate phase (curve I) and $C_{11}A_7 \cdot CaCl_2$ (curve II).

The calculated unit cell parameter a is as follows:
1) for $C_{12}A_7$ - 11.982 ± 0.003 Å,
2) for $C_{11}A_7 \cdot CaCl_2$ - 12.010 ± 0.003 Å,
3) for the chloroaluminate phase I $(11CaO \cdot 0.08MgO \cdot 0.02Na_2O) \cdot (5.80Al_2O_3 \cdot 0.48Fe_2O_3 \cdot 0.48SiO_2 \cdot 0.03TiO_2) \cdot 0.77CaCl_2$ - 12.018 ± 0.005 Å
4) for the chloroaluminate phase II $(11CaO \cdot 0.28MgO \cdot 0.01MnO \cdot 0.03Na_2O) \cdot (5.72Al_2O_3$

TABLE 1

Oxides / Phases	SiO_2	TiO_2	Al_2O_3	Fe_2O_3	CaO	MgO	MnO	Na_2O	Cl	L.O.I. 1000°C	Σ	Oequiv. to Cl	Σ
PHASE I	2.09	0.17	42.34	5.55	47.40	0.22	-	0.10	3.90	0.15	101.65	0.88	100.77
PHASE II	3.97	-	42.74	0.98	48.41	0.80	0.09	0.10	3.60	0.10	100.69	0.81	99.88

TABLE 2

Phases	$C_{12}A_7$	$C_{11}A_7 \cdot CaCl_2$	Chloroaluminate phase I	Chloroaluminate phase II
Refraction indices	1.61	1.634	1.648 - 1.652	1.635 - 1.638

$\cdot 0.08Fe_2O_3 \cdot 0.89SiO_2) \cdot 0.69CaCl_2$ - 12.020 ± 0.005 Å.

The given formulae of the chloroaluminates of complex composition with cationic and anionic groups should be considered approximate because such elements as Na, Mg, Mn can also be present in the $CaCl_2$ lattice.

By means of X-ray and microscopical methods, the samples of calcium chloroaluminates of complex composition are shown to contain a small amount of aluminate $CaO \cdot Al_2O_3$ (the maximum at the angle of reflection 2θ of 30°) and calcium aluminoferrites (the maximum near 2θ of 34°). The indices of refraction for the aluminates have been measured (Table 2); the aluminates are isotropic.
A considerable increase of the index of refraction of phase I is due to the presence in the lattice of significant amount of iron.

To study the hydration activity, five samples of the aluminates have been taken: $C_{12}A_7$, $C_{11}A_7 \cdot CaCl_2$ (synthesis at 1200 °C and 1400 °C, for 1 h), chloroaluminate phase I (analogous in composition to the chloroaluminate phase of the usual alinite clinker) and chloroaluminate phase II (analogous in composition to the chloroaluminate phase of white alinite clinker). Samples were prepared in the paste form with a w/c ratio of 0.6; the experimental temperature was ~ 20 °C. For X-ray measurements of the degree of hydration of the aluminates we selected the maxima with 2θ of 33.3° and 41.1°; for $C_{12}A_7$ - with 2θ of 33.4° and 41.15°. Preliminary hydration tests showed that these maxima are not overlapped by the maxima of hydration products.

Figure 5 shows the hydration kinetic curves for the aluminates. The reaction with water of the aluminate $C_{12}A_7$ as the matrix of all the aluminate phases studied was also investigated. Analysis of the hydration curves showed that in the early stage $C_{12}A_7$ is most active (curve IV). After 10 minutes the degree of hydration of $C_{12}A_7$ is ~ 35%. The intense reaction in the early stage leads to the formation of a considerable amount of hydration products on the surface of $C_{12}A_7$ crystals which sharply hinders the further course of the process. Already after 1-2 h of hydration a sharp bend appears in the curve (Fig. 5, curve IV). From this time the hydration exibits a smooth delayed behaviour.

Among the chloroaluminates, the phase $C_{11}A_7 \cdot CaCl_2$ free of impurities is most active in the early stage. The degree of its hydration after 10 minutes is ~ 22% for the synthesis conditions 1200 °C, 1 h (Fig. 5, curve V) and ~ 15% for 1400 °C, 1 h (Fig.5, curve III). It is worth noting that chloroaluminate phases with impurities in the lattice are less reactive in the early stage but in the later stage their reaction with water is more intense.

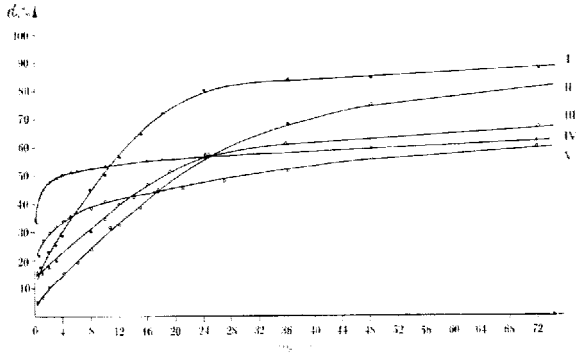

Fig. 5 - Hydration kinetic curves for the chloroaluminate phases with impurities in the lattice (curves I and II), $C_{11}A_7 \cdot CaCl_2$ synthesized at 1400 °C for 1 h (curve III), $C_{12}A_7$ (curve IV), $C_{11}A_7 \cdot CaCl_2$, synthesis at 1200 °C (curve V).

After 1 day the degree of hydration of phase I corresponding in composition to the chloroaluminate phase of alinite clinker reaches 80% (Fig. 5, curve I) and from this time the slowing down of the process is observed.

A comparison of the degree of hydration of phase I and $C_{11}A_7 \cdot CaCl_2$ (sample V) shows that after 1 day the degree of hydration of the latter is twice as low as that of the former. After 3 days the highest degree of hydration is shown by the chloroaluminate phases with impurities in the lattice.

The hydration kinetic curves permit us to reveal the general fact: the higher the hydration activity of the aluminate in the early stage, the sooner the retardation of the process in the later stage. This retardation is due to the layer of hydration

products formed on the surface of crystals. The higher the hydration rate in the early stage, the greater amount of hydrates is formed and the less amount of the liquid phase diffuses to the surface of the unreacted substance, and on the contrary. The samples which hydrate rather slowly in the early stage can reach a higher degree of hydration in the later stage than the ones which are active in the early stage. As a result, the hydration kinetic curves will intersect after a certain period of time different for each sample. Thus after 28 days the degree of hydration of the aluminate was as follows: sample I - 96%, II - 88%, III - 100%, IV - 70%, V - 79%.

In the later stage (weeks, months, years) the hydration behaviour is determined not only by the structural peculiarities and chemical composition but also by other factors such as the kind of the layer of hydration products, the growth of crystal hydrates, their recrystallization etc.

DISCUSSION AND CONCLUSION

Two chlorine-containing phases active with respect to water are present in clinkers obtained in the presence of considerable amount of $CaCl_2$:

1. High-basic calcium chlorosilicate - alinite $Ca_{9.9}Mg_{0.8}\square_{0.3}[(SiO_4)_{3.4}(AlO_4)_{0.6}O_{1.9}Cl_{1.0}]/57$ containing 3.5% Cl_2 in the lattice is much more active in the early stage than alite. The degree of hydration of alinite after 1 day is more than twice as much as that of C_3S and alites with impurities in the lattice. The form of the kinetic curve shows that the hydration process of alinite is similar to that of C_3A and aluminate phases of any composition (solid solution of C_3A with Na_2O, aluminate phases of complex composition). Alinite of commercial clinkers hydrated in the presence of other clinker phases (belite, chloroaluminate, aluminoferrite) is much more inactive with respect to water than pure alinite, and its degree of hydration can be 2-4 times as low as that of the pure sample.

One of the reasons of slower hydration of real alinites is the presence of isomorphous impurities in the lattice. Another reason is the simultaneous hydration of other phases.

2. Hydration activity of $C_{11}A_7 \cdot CaCl_2$-based chlorine-containing phases in the early stage is promoted (along with the peculiarities of the atomic structure and composition) by isomorphous impurities present in the lattice (the real phases) and by the degree of crystallization (the quality of crystals).

The hydraulic activity of these phases in the early stage is rather high like that of alinite. Thus after 1 day the degree of hydration of alinite and chlorine-containing phase with isomorphous impurities in the lattice is $\sim$ 80% (see Figs. 2, 5).

3. As the hydration activity of each of the studied phases is different in the early stage due to the different reasons, the thickness of the layer of hydration products formed on the crystal surface will also be different. Consequently the rate of reaction of the unreacted substance with water after the completion of the early stage will be much more dependent on the hydration products formed.

An important practical problem of hydration is to elucidate the presence of chlorine in the liquid phase and in the composition of hydration products. Preliminary tests show that chlorine enters both the liquid phase and the hydrates formed.

REFERENCES

1.- B. NOUDELMAN, M. BIKBAOU, V. ILYUKHIN and A. SVENTSITSKI (1980), "Structure and properties of alinite and alinite cements", 7th Intern. Congr. Chem. Cem., v.3, V-169-174.
2.- B.I. NOUDELMAN (1981), "Low-temperature technology of cement production", Tsement N 6, 12-13.
3.- V.V. ILYUKHIN, N.N. NEVSKY, R.A. HOWIE, M.Ya. BIKBAOU and N.V. BELOV (1977), "Crystal structure of alinite", Dokl. AN SSSR 237, 4, 834-836.
4.- F. MASSAZZA and C. GILIOLI (1983), "Contribution to the alinite knowledge", Il Cemento 80, 2, 101-106.
5.- F.V. LAMPE, W. HILMER, K.-H. JOST, G. RECK and A.I. BOIKOVA (1986), "Synthesis and thermal decomposition of alinite", Cem. Concr. Res. (in press).
6.- A.I. BOIKOVA, A. K. ESAYAN, R.A. SOKOLOVA, A.I. DOMANSKY and M.M. PIRYUTKO (1981), "Physical-chemical investigation of alinite clinkers", Tsement N 6, 13-15.
7.- A.I. BOIKOVA, A.I. DOMANSKY, V.A. PARAMONOVA, G.P. STAVITSKAYA and V.M. NIKUSHCHENKO (1977), "The influence of Na_2O on the structure and properties of $3CaO \cdot Al_2O_3$", Cem. Concr. Res. 7, 5, 483-492.
8.- M. REGOURD and B. MORTUREAUX (1977), "Tricalcium aluminate in synthetic solid solutions and in cements", Summaries of Contributions to a Seminar at the University of Technology, Eindhoven, The Netherlands, April 13-14, 1977.
9.- A.I. BOIKOVA, L.V. GRISHCHENKO and A.I. DOMANSKY (1980), "Hydration of C_3A and solid solutions of various composition", 7th Intern. Congr. Chem. Cem., v. 4, 460-464.

M.M. SYCHEV, Lensoviet Technological Institute, Leningrad, USSR

1

CEMENT HYDRATION CONTROL

SUIVI DE L'HYDRATATION.

2.1

It is demonstrated that the cementitious phases emerging in hydration possess surface active centres where dissociative adsorption of water molecules and the occurrence of its active groups takes place, thus facilitating the autocatalythic character of hydration in the surface area when the induction period expires. Because the specific surface of cementitious phases exceeds that of the cement powder by an order of magnitude, the process assumes a chain mode: branching over the material - branching over the surface.

Key subjects. The nature and properties of active centres on the surface of silicate phases. The role of free charge carriers in the formation of properties of active centres. Donor, acceptor, and protodonor centres. Dissociative chemosorption of water molecules supplying H^+ and OH^- ions for local reaction areas. The surface mechanism of bond rupture leading to Ca^{2+} leaching (bond protonation), an increase in the coordination number of certain surface silicon atoms up to 5-6 at the expence of free d-orbitals and the rupture of Si-O-Si bonds. A decreasing value of the dielectric constant in the interfacing layers of water as a cause of hydrate phase evolution on the surface of cement minerals. Activation of hydration from the standpoint of the zone model. Activation of hydration by ionosorption, UV radiation, and electric fields.

Demonstra-se que as fases cimentosas emergentes na hidratação possuem centros de superfície ativa, em que acontecem absorção dissociativa de moléculas de água e ocorrência de seus grupos ativos, facilitando então o caráter autocatalítico de hidratação na área de superfície quando termina o período de indução. Pelo fato de que a superfície específica das fases cimentosas é superior à do pó de cimento por uma ordem de grandeza, o processo assume um modo decorrente: ramificação sobre o material - ramificação sobre a superfície.

Pontos-chave: A natureza e prioridades dos centros ativos na superfície das fases de silicato. O papel de carreadores livres de carga na formação de propriedades de centros ativos. Centros doadores, receptores e protodoadores. Quimissorção dissociativa de moléculas de água fornecedoras de íons H^+ e OH^- para áreas de reação local. O mecanismo de superfície de ruptura da ligação levando à lixívia de Ca^{2+} (protonotação de ligação), um aumento no número de coordenação de determinados átomos de silício da superfície até 5 - 6 à custa de d-orbitais livres e da ruptura das ligações Si-O-Si. Uma diminuição do valor da constante dielétrica nas camadas interfaciais de água, como causa da evolução da fase de hidrato na superfície dos minerais do cimento. Ativação da hidratação a partir de um ponto de vista de modelo de zona. Ativação da hidratação por ionossorção, radiação UV e campos elétricos.

2.1

Earlier it has been demonstrated /1-3/ that there are electron donors and acceptors and proton donors at the surface of clinker minerals. Acceptor species are where dissociative adsorption of water molecules takes place to initiate hydration. The rupture of the bonds -Ca-O-Si- is due to the protonation of oxygen atoms [Brunauer, Danilov; 7th Congress on the Chemistry of Cement] and brings about leaching Ca^{++} ions and increasing pH, the necessary factors for the stability of hydrate phases - cement dispersions, self-organized systems. Therefore, hydration can be activated by increasing the concentration of acceptor species /3, 4/.

The rupture of ≡Si-O-Ca- bonds in cement minerals proceeds through the formation of complexes of the surface silicon atoms involving d-orbitals and increasing the coordination number of these atoms to 5 or 6 /5, 1/. This rupture initiates the polymerization of anion species leading to the formation of hydrosilicates /6/. Electrochemical methods and vacuum IR spectroscopy have given an insight into how hydration is related to the processes of electron-hole recombination and to the concentration of free charge carriers /7, 3/.

Dissociative adsorption involved the following recombination processes

$$OH^- + p^+ \longrightarrow OH_{ad}$$

$$H_2O + e^- \longrightarrow H_{ad} + OH^-$$

$$H_{ad} + OH_{ad} \rightleftharpoons H_2O_{ad}$$

The latter is involved in the rupture of -Ca-O-Si≡ bonds, surface hydration of Ca^{++} ions, and release of these ions into solution. Thus, the factors that increase the concentration of surface traps and free charge carriers will activate the process of cement setting. This statement is substantiated by the correlation of free carrier concentration and the length of induction period /8/.

The concentration of active species can be improved and their properties controlled by introducing admixtures and doping components into the clinker minerals, and electrolites into the mixing water. Electrolites introduced in the mixing water take part in the chemosorption (ionosorption and ion exchange both with the surface atoms of cement minerals and with filler, specifically with hydroxylated atoms of quartz sand: $=Si=(OH)_2 + Ca^{++} \longrightarrow =Si=O_2=Ca + 2H^+$. Evidence on the adsorption of the components of the Fe(III)/Fe(II) redox system from the water of mixing indicates that this leads to the formation of new active recombination species which have a large capture cross-section for both electrons and holes, thus accelerating the hydration process.

Electrolites can activate not only the surface of cement minerals, thus increasing the concentration of acceptor species, as for example in chromate ion absorption, but also the adhesive interactions of cementitious phases with the structural materials. The boundary layers of water are influenced by nonsaturated fields of water, specifically by the electrostatic field which polarizes water and affects its structure. This structural effect is of sensible magnitude at a distance of up to 1000 Å, i.e., penetrates dozens of monolayers of water. As the result of such structural ordering, the permittivity of water, that is, its dissolving power, diminishes and causes the formation of hydrate phases in these boundary layers of water, and affects the diffusive removal of Ca^{++} and OH^- from the zone of rupture of the bonds -Ca-O-Si≡. Consequently, the chemical potential of boundary water layers and diffusion in the reaction zone can be controlled by an appropriate choice of electrolites whose ions produce a disordering or ordering effect on the structure of water (positive or negative hydration after Samoilov).

Recently Grankovsky /9/ and Svatovskaya et al. /10/ have demonstrated the possibility of influencing the structure of water by small amounts of solid, highly dispersive phase. This possibility may be used to

control the reaction of hydration and the rheology of cement dispersive systems. Electrolites introduced in the mixing water cause changes in the morphology of the hydrate phases, which occur due to the surface activating effect of ion adsorption on the growing surphases of hydrate phases and due to the ion activators being included in the structure of hydrates (Al^{+++}, K^{+}, Na^{+}, SO_4^{--}, etc.). Nuclear gamma resonance studies of the behavior of oxidizing and reducing species added into the water of mixing /10/ indicated that the surface of cement minerals contains acceptor species. Comparison of this behavior within the sequence Sn-Mn-Cr has revealed that the acceptors have enough oxidizing power to change the valency of tin or manganese, but it is insufficient to convert Cr^{+6} to Cr^{+3}. Hence, the activating effect of chromium ions is due to ionosorption, whereas that of manganese or tin compounds is due to their oxidation-reduction properties.

Ionosorption alters the energy characteristics of active species (capture cross-section of electrons and holes) behaving as the traps for electrons and holes, so it can be used to activate the hydration process (by predominantly affecting the acceptor species) or retard it (by affecting the recombination processes or donor species). Oxidizers added in the mix increase the concentration of acceptor species by way of depleting the traps of electrons being consimed to convert Sn^{+4} to Sn^{+2} or Mn^{+4} to Mn^{+2} so that there increases the concentration of acceptors which play an important part in the mechanism of elementary acts of hydration /3/.

Bronsted's acid centres (≡Si-OH) on the surface of clinker minerals, hydrate phases and structural materials provide the gradient of pH required for the matched development of a number of processes in setting (hydrolisis of clinker minerals, polymerisation processes, stabilization of hydrate phases). For a portland cement added by a solid, finely ground activator having acidic species on the surface (themoactivated or modified agrillaceous minerals, ceolites, disperse silica), there exists a correlation between the Bronsted acidity of the activator and the compressive strength of the portland cement. Acid species of alumosilicate activator dissociate in the alkali medium by the acid type and thereby locally rise the concentration of protons and facilitate the hydrolisis of clinker minerals. Hand in hand with this process, the silicon rich pseudophase intensely develops, in the presence of active protons, a polymerization of silicon-oxygen ions, the process being limited in the alkali medium by the transfer of neutral molecules of silicic acid. Thus, the presence of a solid, finely ground, acidic activator facilitates the appearance of nuclei of high-polymeric hydrosilicate phase - fibrous calcium silicate hydrates of morphological form which positively affects the kinetics of hydration and setting /11/.

The possibility of activating clinker minerals by admixtures has been demonstrated by a number of authors /12-14/ and later a physico-chemical analysis of this activation has been given /15-18/. The heterovalent and isomorphic substitution or non-stoichiometry /17/ lead to uncompensated charges, vacancies, local changes in electron density, and capture phenomena, all being reflected in the concentration and properties of active species and affecting the intensity of hydration. Recently we have demonstrated the possibility of integrating the doping, ion exchange and ion sorption processes by intergrinding solid activators /19, 20/. This way is attractive as it enables using the wastes of chemical and mining industries as such activators. We have also demonstrated /18/ that ions activating clinker (Ba, Cr, Mn, Fe) when introduced in the raw mix may achieve the same effect if interground in a mill where they can be introduced in the form of oxides and salts.

In order to find ways of accelerating hydration it is important to understand the

autocatalitic nature of hydration after the induction period /1/ (the acceleration period by Kondo). The phenomenon is based on the chain, nonstationary hydration process that occurs due to an avalanche-like increase of the solid-liquid interface by emerging disperse hydrates whose surface contains active species supplying active groups (H^+ and OH^-) into the reaction zone /3/.

In the presence of ions with "surface properties" adsorption intensifies the process in the acceleration period as a result of a growth of the specific surface of hydrate phases. More intense polarisation of the boundary layers of water, by lowering the permittivity, and diminishing as a result the dissolving property of the water, leads to a higher dispersive state of hydrates. The structure of the boundary layers may be changed still more by doping the clinker with admixtures of Cr, Ln, and P /4/.

REFERENCES

1. Сычев М.М. Некоторые вопросы механизма гидратации цемента. Цемент, 1981, № 1, стр. 8-10.
2. Тимашов В.В., Акимова А.А., Туспонов М.Б., Якуб Ю.Н. Труды МХТИ им. Менделеева, 1979, вып. 108.
3. Сычев М.М. Роль электронных явлений при твердении цементов. Цемент, 1984, № 8, стр. 10-12.
4. Сычев М.М. Способы повышения активности клинкера и цемента. Цемент, 1985, № 3, стр. 19-21; № 7, стр. 14-16.
5. Стелко В.В. Теоретическая и экспериментальная химия, 1974, 10, № 13.
6. Taylor H.F.W., Roy D.M., 7-th International Congress on the Chemistry of Cement. Paris, 1980, vol. II.
7. Стрижов Е.Ф., Сычев М.М., Гермаш Н.Ю. Цемент, 1985, № 3.
8. Ferens P., Verchagen V.P. Cement and Concr. Res., 1975, No. 5, No. 7.
9. Гранковский И.Г. Структурообразование в минеральных вяжущих системах. Наукова думка, Киев, 1984.
10. Сватовская Л.Б., Сычев М.М., Досмагамбетова Т.С. Цемент, 1980, № 10.
11. Сычев М.М., Казанская Е.Н., Петухов А.А. ЖПХ, 1982, т. 55, № 7, стр. 1684-1686; № 11, стр. 2553-2555.
12. Сычев М.М., Корнеев В.И., Зозуля П.В. Цемент, 1984, № 9.
13. Бутт Ю.М., Тимашов В.В. Портландцемент. Стройиздат, 1974.
14. Бойкова А.И. Цемент, 1976, № 8.
15. Сычев М.М. Цемент, 1977, № 12.
16. Туркина Л.И., Сычев М.М., Судакас Л.Г. ЖПХ, 1981, № 6, стр. 1315-1319.
17. Акимов В.И. В сб.: Структура технических силикатов. М., 1976.
18. Сычев М.М. Цемент, 1985, № 3, стр. 19-21, стр. 14-16.
19. Сычев М.М., Сватовская Л.Б., Сватовская М.Б. Цемент, 1980, № 11, стр. 6-8.
20. Сычев М.М., Минкина В.Н., Тандилова К.Б., Папушвили С.Н. Цемент, 1983, № 3, стр. 18-20.

A. POLAK, Institut de pétrole, Oufa, URSS 1

CERTAINES NOUVELLES CONCEPTIONS SUR LE MECANISME D'HYDRATATION DES LIANTS

2.1

En se basant sur les données fournies par une analyse radiographique des phases et un examen au microscope électronique, l'auteur estime que l'hydratation de la phase initiale (X) fournit d'abord une phase intermédiaire - l'hydrate primaire (Y) -, et et ensuite une phase stable: l'hydrate secondaire (Z).

L'ordre de succession de l'apparition des phases ($X \longrightarrow Y \longrightarrow Z$) nécessite, selon Ostwald, une relation déterminée entre les potentiels chimiques ($M_x \longrightarrow M_y \longrightarrow M_z$) et les solubilités ($C_x \longrightarrow C_y \longrightarrow C_z$) de ces phases. En outre, l'auteur invoque la règle de Folmer, selon laquelle les germes des phases Y et Z doivent se former sur des supports constitués de phases X et Y respectivement.

Vu ce qui vient d'être dit, l'auteur dégage le principe déterminant l'allure de l'hydratation. Elle se déroule par un mécanisme qui régit le processus dans une solution de part en part, mais elle peut aussi adopter un mécanisme topochimique. L'auteur cite les conditions d'apparition et d'achèvement de la période d'induction et celles de passage d'un mécanisme à l'autre.

Com base em dados fornecidos por uma análise radiográfica de fases e um exame com microscópio eletrônico, o autor estima que a hidratação da fase inicial (X) proporciona de imediato uma fase intermediária - o hidrato primário (Y) -, e em seguida uma fase estável: o hidrato secundário (Z).

A ordem de sucessão do aparecimento das fases ($X \rightarrow Y \rightarrow Z$) precisa, segundo Ostwald, de uma relação determinada entre os potenciais químicos ($M_x \rightarrow M_y \rightarrow M_z$) e as solubilidades ($C_x \rightarrow C_y \rightarrow C_z$)' destas fases. Por outro lado, o autor invoca a regra de Folmer, segundo a qual os germes das fases Y e Z devem ser formados sobre suportes constituídos de fases X e Y, respectivamente.

Face ao exposto, o autor emite o princípio determinante do processo da hidratação. Ele se desenvolve por um mecanismo que rege o processo de uma solução, mas ele pode também adotar um mecanismo topoquímico. O autor cita as condições de aparecimento e de conclusão do período de indução e as condições de passagem dum mecanismo para o outro.

2.1

Des études faites ces dernières années par plusieurs auteurs à l'aide de la microscopie électronique et de l'analyse des phases aux rayons X ont montré de façon évidente (1-2) que par suite de l'hydratation de la phase initiale des liants (PI) - x se forment d'abord une phase intermédiaire - hydrate primaire (HP) - y et puis une phase stable - hydrate secondaire (HS) - z. Une telle suite de déroulement du processus de formation $x \rightarrow y \rightarrow z$ exige que soient établis des rapports concrets des potentiels chimiques d'après Ostwald ($\mu_x > \mu_y > \mu_z$) et, respectivement, des solubilités de ces phases ($C_{x\infty} > C_{y\infty} > C_{z\infty}$).

Il serait intéressant de noter que les circonstances ci-dessus sont tout à fait suffisantes pour décrire la cinétique de ces processus (3). On peut le faire sur la base des travaux de Folmer (4) et de leur développement (5,6) qui tient compte de l'énergie interphase localisée aux points de siège des nouvelles formations. D'après Folmer, la probabilité d'apparition de phases nouvelles s'exprime par la loi exponentielle (1):

$$W_i = W_0 \exp^{-A_i/CT} \qquad (1)$$

où A_i est le travail de germination, C est la constante de Bolzman, T est la température absolue. Etant donné que le travail de germination A_g dans le volume de la solution est plus important que celui de germination A_{gc} à la surface de la phase PI, alors la probabilité de germination $W_{gc} > W_g$. Il n'est pas impossible que les germes formés s'arrachent à la surface ce qui nécessite l'exécution du travail $A_{ar} = A_g - A_{gc}$, où

$$A_{gc} = A_g\, 0{,}5\chi \quad A_{ar} = A_g(1 - 0{,}5\chi) \qquad (2)$$

ici χ est le facteur d'inhomogénéité physique et chimique en fonction de la valeur de l'énergie interphase. Pour la lyophobisation limite entre le substrat et la nouvelle formation $\chi = 2$, pour la lyophilisation limite $\chi = 0$ et dans les autres cas $0 < \chi < 2$ (5-7).

Si $\chi = 2$ et il n'y a pas d'affinité physique et chimique entre le substrat et la nouvelle formation, alors $A_i = A_g$, $W_i = W_g$ et les germes ne se forment que dans le volume de la solution. A la surface de la phase PI les dépôts hydratés (DH) n'apparaissent pas et le coefficient β qui exprime la fraction des nouvelles formations qui reste à la surface du substrat constitue $\beta = 0$.

Si $1 < \chi < 2$, l'affinité est encore peu importante mais les germes commencent déjà à se former sur le substrat. Mais du fait qu'en même temps $W_{ar} > W_{gc} > W_g$, la plupart des germes s'arrachent de nouveau à la surface et passent dans le volume de la solution. Dans ce cas il est admis que $\beta = 0$.

Si $\chi_c < \chi < 1$, l'affinité physique et chimique entre le substrat et la nouvelle formation est déjà sensible: $W_i = W_{gc} > W_{ar}$, l'arrachement des germes à la surface devient difficile et des DH commencent à se former. Néanmoins, l'arrachement a lieu et par conséquent $0 < \beta < 1$.

Si $\chi < \chi_c$ (où $\chi_c = 0{,}25$) l'affinité est très proche de la valeur maximale ($\chi = 0$). Dans ces conditions commencent à se former des germes de croissance qui sont incapables de s'arracher à la surface et par conséquent $\beta = 1$.

Sur la base de l'exposé, l'interprétation linéaire donne en qualité de première approximation pour le coefficient de précipitation di dépôt à la surface de la PI

$$\beta_i = (1 - \chi_c)/(1 - \chi_c) \qquad (3)$$

Il résulte du texte ci-dessus que les surfaces de la PI - S_x et de l'HP - S_y se couvrent partiellement de dépôts des phases y et z si $\chi_{(i/j)} < 1$ tout en laissant découverte la superficie des surfaces F_x et F_y respectivement où

$$F_x = S_x - \beta_1 S_y \quad F_y = S_y - \beta_2 S_2 \qquad (4)$$

De cette manière, si la concentration de la solution $C_{x\infty} > C > C_{y\infty}$ la phase x se dissout mais la phase y qui vient de paraître, croît. Par conséquent, un moment peut arriver où $\beta_1 S_y = S_y$ et $F_x = 0$. Dans ce cas, le processus de dissolution cesse. Ce moment

2.1

arrive très vite, au début du processus d'hydratation et peut être identifié comme le début de la période d'induction. Par suite du passage de la substance dissoute de la solution aux phases y et z, la concentration de la solution diminue et se matérialisent enfin les conditions $C_{y\infty} > C > C_{z\infty}$. A ce stade, l'hydrate primaire (y) se redissout, la surface de la phase initiale (x) se dénude et le processus de dissolution se renouvelle. Cela marque la fin formelle de la période d'induction et le début de la principale étape du processus d'hydratation. Dans ces conditions, la vitesse du processus augmente d'abord étant donné que la croissance de l'HS fait diminuer la concentration de la solution. Mais comme suite de la croissance de l'HS, la phase initiale x se couvre du composant de la phase z et, il est évident, qu'un moment peut arriver où simultanément $F_x = 0$ et $F_y = 0$. Dans ces conditions, tout le système est recouvert de molécules de la phase z ce qui aboutit à un équilibre chimique et le processus d'hydratation à travers la solution (PTS) cesse (3).

Notons qu'en ce moment les densités des composants pris à part atteignent les valeurs $\xi_c = X_c/X_o$, $h_c = Y_c/Y_1 \sim 0$, $\zeta_c = Z_c/Z_1$. Mais les particules de la PI - x se trouvent dans le système sous une couche de molécules de la phase y ce qui ne les empêche pas d'entrer en réaction avec le milieu liquide dont les molécules diffusent à travers les formations friables des HS à la surface de l'HP en direction de la PI. Un tel processus doit être qualifié (7) comme un processus d'hydratation topochimique (PTC). On trouve le critère de ce processus TO_1 désignant la quantité de la PI qui peut être hydratée par le procédé topochimique, en divisant la masse relative de la phase non hydratée ξ_c par la masse relative de la nouvelle formation ζ_c compe tenu du fait que $F_x = 0$ et $F_y = 0$ en même temps.

$$TO_1 = \xi_c / \zeta_c = (\beta_1 \cdot \beta_2 \; C_2)^{3/2} \qquad (5)$$

où $\xi_{c2} = \dfrac{(\beta_1 \beta_2 C_2)^{3/2}}{1+(\beta_1 \beta_2 C_2)^{3/2}}$;

$$\zeta_c = \frac{1}{1+(\beta_1 \beta_2 C_2)^{3/2}} ;$$

$$C_2 = S_{zc}/S_{xo} \qquad (6)$$

Pour illustrer les résultats obtenus, calculons les valeurs des coefficients χ et les critères des processus topochimiques TO_1 suivant les formules (7) découlant des formules (3), (5) et (6) et portons les résultats reçus au tableau 1.

$$1 - \chi = \left(\frac{c}{1 - \xi_c}\right)^{1/3} \qquad \frac{0.75}{\sqrt{C_2}} ;$$

$$TO_1 = 2{,}37 \; (1 - \chi)^3 \; C_2^{3/2} \qquad (7)$$

Comme le montrent les données du tableau 1, la fraction de la phase qui ne s'est pas encore dissoute $x - \xi_c$ comme celle de la phase nouvellement formée $z - \zeta_c$ peuvent varier considérablement par suite de la variation de C_2 ce qui amène à un brusque changement du paramètre TO_1.

Pour déterminer la vitesse de ce processus, divisons la vitesse du processus topochimique V(PHT) par celle des processus se déroulant à travers les solutions V(PTS) et calculons les paramètres TO_2 d'après la formule (8)

$$TO_2 = V(PHT)/V(PTS) \qquad (8)$$

L'analyse (8) montre que $TO_2 > 1$ si le coefficient de diffusion de l'eau à travers les dépôts friables de l'HP est supérieur à $D \gtrsim 10^{-13}$ cm^2 c^{-1} ce qui apparemment a lieu compte tenu de la friabilité des dépôts de l'HP.

Ainsi, la prise en compte du processus hétérogène de germination et du facteur d'inhomogénéité physique et chimique permet d'un côté d'expliquer le stade initial du processus d'hydratation et de l'aut-

2.1

Tableau 1

N° d'ordre	C_2	ξ_c	ζ_c	χ	TO_1	Type du monominéral
1	1600	0,85 à 0,65	0,15 à 0,35	0,97 à 0,98	4,10 à 1,21	$\sim C_3A$
2	10	0,10 à 0,05	0,40 à 0,95	0,89 à 0,91	0,11 à 0,05	

Tableau 2

Variété du processus	χ		Mécanisme d'hydratation	Type du liant monominéral
	$\chi(y/x)$	$\chi(z/y)$		
A	$\geqslant 1$	$\geqslant 1$	PTS	$CaSO_4 \cdot 0,5H_2$
B	< 1	$\geqslant 1$	PTS	
C	< 1	< 1	PTS + PHT	C_3A, C_4AF, C_3S, C_2S

re, de montrer qu'en fonction des valeurs des coefficients $\chi(y/x)$ et $\chi(z/y)$ il y a lieu de distinguer trois variétés du processus d'hydratation réunies au tableau 2.

A la variété A du processus il faut porter par exemple, le gypse, à la variété C les silicates et les aluminates de calcium. Ayant obtenu l'appréciation des coefficients des inhomogénéités physique et chimique χ ainsi que les constantes de la vitesse de dissolution de la PI, de formation des HP et HS on peut calculer la cinétique du processus d'hydratation (3).

REFERENCES

1. Шпинова Л.Г. и др. VI Международный конгресс по химии цемента, Стройиздат, 1976, т. 2.
2. Людвиг У. Там же.
3. Полак А.Ф. ДАН СССР, 1984, т. 274, № 3.
4. Volmer M. Kinetik d. Phasenbildung. Dresden-Leipzig, 1938.
5. Mtschedlow-Petrosian O.P., Polak A.F., Silikattechnik, 22, 1971, H. 2.
6. Полак А.Ф. В сб. Физико-химическая механика. М., Наука, 1966.
7. Третьяков Ю.Д. Твердофазные реакции. М., Химия, 1978.

O.P. MTSHEDLOW-PETROSIAN,
A.V. OUCHEROV-MARCHAK, Kharhov, U.R.S.S.

CLASSIFICATION DES PROCESSUS DE DURCISSEMENT DES LIANTS

2.1

L'analyse des études théoriques et expérimentales est effectuée. Elle concerne les régularités de manifestation des propriétés liantes et de systématisation des liants inorganiques. Les problèmes de connaissance de la nature des réactions d'hydratation sont considérés des positions de la méthodologie chimique moderne, notamment, des positions de la chimie des réactions hétérogènes. On montre l'utilité de la détermination des régularités communes et caractéristiques et de la création de la classification des processus de durcissement à la base desquelles se trouvent les critères de vitesse et de plénitude des réactions.

On présente les moments principaux concernant l'analyse thermocinétiques des processus en question des liants inorganiques permettant d'évaleur quantitativement le changement des indices de vitesse et de plénitude des réactions d'hydratation suivant les données de la microcalorimétrie différentielle. On communique l'information sur l'appareil de traitement élaboré et l'interprétation des résultats des mesures avec utilisation des ensembles de calcul automatisés.

En se basant sur l'étude thermocinétique de l'hydratation des oxydes de calcium et de magnésium, du semi-hydrate de sulfate de calcium, des minéraux de clinker, des ciments traditionnels et spéciaux durcissant aux températures normales et élevées, on propose de classifier les processus de durcissement en trois types.

Le premier type comprend les processus de durcissment rapides des liants les plus réactifs: CaO, C_3A, C_4AF. Ces processus sont accompagnés par les grands indices du dégagement de chaleur. La période d'induction de l'hydratation manque. Le maximum de vitesse du processus correspond au début de transformation ($\alpha \simeq 0,05$–$0,1$).

Le deuxième type est caractéristique pour le durcissement de la plupart des liants. Les périodes d'induction, accélérées et ralenties sont fixées au cours de l'hydratation. La durée des changements fixables des indices du dégagement de chaleur ne dépasse pas un jour. La valeur maximale de vitesse de l'hydratation correspond à $\alpha \simeq 0,3$–$0,5$.

La vitesse extrêmement basse de la réaction à l'étendue considérable (jusqu'à quelques mois) est caractéristique pour les liants tels que les laitiers, verres, cendres dont la réactivité ne se manifeste pas pratiquement dans les conditions normales. Le maximum de vitesse et du degré de transformation coincident à $\alpha \simeq 0,6$–$0,8$.

L'application des actions réglant la vitesse et la plénitude des réactions d'hydratation (température, additions) peut conditionner les passages des régularités établies de l'un type à un autre type ce qui confirme la validité de la constatation sur la dualité de la réactivité.

La classification des processus de durcissement proposée apparaît assez efficace à la prédiction des propriétés liantes dea matériaux traditionnels et perspectifs.

Faz-se a análise dos estudos teóricos e experimentais. Ela se refere às regularidades de manifestação das propriedades ligantes e de sistematização dos ligantes inorgânicos. Os problemas de conhecimento da natureza das reações de hidratação são considerados, a partir das posições da moderna metodologia química, notadamente das posições da química das reações heterogêneas. Mostra-se a utilidade da determinação das regularidades comuns e características, e da criação da classificação dos processos de endurecimento, com base nos quais se encontrem os critérios de velocidade e de plenitude das reações.

São apresentados os momentos principais relativos à análise termocinética dos processos em questão dos ligantes inorgânicos, que permitem a avaliação quantitativa da mudança dos índices de velocidade e de plenitude das reações de hidratação, de acordo com os dados da microcalorimetria diferencial. Comunica-se a informação sobre o aparelho de tratamento elaborado e a interpretação dos resultados das medidas, com utilização de conjuntos automatizados de cálculo.

Com base no estudo termocinético da hidratação dos óxidos de cálcio e de magnésio, do hemi-hidrato de sulfato de cálcio, dos minerais de clínquer, dos cimentos tradicionais e especiais com endurecimento a temperaturas normais e elevadas, propõe-se classificar os processos de endurecimento em três tipos.

O primeiro tipo compreende os processos rápidos de endurecimento dos ligantes mais reativos: CaO, C_3A, C_4AF. Estes processos são acompanhados pelos grandes índices de liberação de calor. O período de indução da hidratação é insuficiente. O máximo de velocidade do processo corresponde ao início de transformação ($\alpha \simeq 0,05 - 0,1$).

O segundo tipo é característico para o endurecimento da maior parte dos ligantes. Os períodos de indução, acelerados e retardados, são fixados no decurso da hidratação. A duração das mudanças determináveis dos índices de liberação de calor não passa de um dia. O valor máximo de velocidade da hidratação corresponde $\alpha \simeq 0,3$–$0,5$.

A velocidade extremamente baixa da reação com duração considerável (de até alguns meses) é característica de ligantes como as escórias, vidros, cinzas, cuja reatividade praticamente não se manifesta nas condições normais. O máximo de velocidade e do grau de transformação corresponde a $\alpha \simeq 0,6 - 0,8$.

A aplicação de ações reguladoras da velocidade e da plenitude das reações de hidratação (temperatura, adições) pode condicionar as passagens das regularidades estabelecidas de um tipo para outro tipo, o que confirma a validade da constatação sobre a dualidade da reatividade.

A proposta classificação dos processos de endurecimento parece bastante eficaz para a predição das propriedades ligantes dos materiais tradicionais e .os em perspectiva.

O.P. MTSHEDLOV-PETROSIAN,
A.V. OUCHEROV-MARCHAK

Le problème de la systématisation des liants, y compris des ciments ordinaires et spéciaux, devient de plus en plus actuel ce qui s'explique par deux raisons. La première consiste dans un accroissement des volumes de la production et un élargissement de la nomenclature des ciments, la composition de ces derniers devenant en même temps de plus en plus complexe grâce à l'utilisation de résidus industriels et de produits spécialement synthétisés sous la forme d'adjuvants et de germes. La deuxième est due à la tendance à intensifier autant que possible la production de matériaux et d'articles sur la base des ciments tout en réduisant la consommation de matériaux et d'énergie et en accroissant la stabilité et la durabilité.

Une étude sous tous les aspects des problèmes de la chimie et de la technique du ciment et du béton nous a permis de formuler aux années 60 le principe de correspondance fondamental dont l'essence consiste à tenir compte des caractéristiques physico-chimiques des processus de durcissement des ciments (réactivité, vitesse d'hydratation et de formation de la structure) en choisissant et en déterminant les paramètres des facteurs (thermiques, chimiques, mécaniques et combinés) qui influent le durcissement. La justesse du principe de correspondance a trouvé sa confirmation théorique et expérimentale grâce au recours à l'appareil de la thermochimie et de la thermodynamique, de la cinétique des réactions hétérogènes, de l'électrochimie et d'autres domaines de la connaissance. La réalisation des thèses de ce principe en pratique a permis d'obtenir quelques variétés de ciments expansifs à autocontrainte et de ciments composés avec l'utilisation de laitiers sidérurgiques et de mâchefers ainsi que d'augmenter l'efficacité de leur utilisation dans la technique du béton grâce à l'addition d'adjuvants chimiques individuels et combinés, de réduire la durée des régimes de traitement à la chaleur humide, etc. (1).

La manifestation des propriétés liantes est en rapport, comme on le sait, avec leurs tendances thermodynamique et cinétique ainsi qu'avec les possibilités de réalisation de transformations durant le durcissement. Cela étant, des indices très importants qui permettent d'évaluer quantitativement et de classifier les processus de durcissement et les propriétés liantes sont la vitesse et la totalité des réactions liées aux facteurs d'ordre extérieur.

On voit s'accroître le rôle et l'importance de l'unité des aspects technologiques et méthodologiques de la chimie du ciment. La résolution des problèmes de la génèse des propriétés et de la réactivité doit être basée sur le système méthodologique "composition-structure-processus-propriété" (2).

Le fait que les processus sont de nature compliquée, comportent plusieurs stades et ne sont pas stoechiométriques ainsi qu'ils peuvent se dérouler selon des mécanismes différents avec la réalisation simultanée de divers types de transformations propres aux systèmes hétérogènes (3) impliquent l'utilité des lois générales à établir pour les processus de durcissement.

A notre point de vue, aux thèses qui viennent d'être examinées correspond la méthodologie de l'étude thermocinétique d'un des principaux phénomènes qui accompagnent l'hydratation - le dégagement de chaleur. Une particularité caractéristique de l'analyse thermocinétique est l'appréciation des indices de la vitesse et de la totalité des processus, la distinction de trois périodes: celle d'induction, accélérée et ralentie selon trois types de relations: $\alpha Q/d\tau = f(\tau)$, $Q = f(\tau)$ et $\alpha Q/d\tau = f(Q)$.

Le problème essentiel de la thermocinétique vu sous le jour de son application à la chimie du ciment consiste à établir des lois générales et particulières des processus de durcissement, à distinguer des stades et périodes d'hydratation, à régler sur cette base les indices de la vitesse et de la totalité des réactions en déroulement

grâce à l'application de facteurs extérieurs avec le respect du principe de correspondance.

La résolution des problèmes de la thermocinétique se réalisait grâce à la méthode de microcalorimétrie différentielle a l'aide d'ensembles de mesure et de calcul automatiques et de l'appareil d'interprétation des données d'analyse (4).

La systématisation des études thermocinétiques de l'hydratation d'une large gamme de liants mono- et polyminéraux, y compris des ciments spéciaux et de leurs minérais (4), a démontré (fig. 1) que les lois des processus de durcissement se divisaient selon les indices de leur vitesse et de leur totalité en trois types (5).

Le premier type de lois réunit les processus à durcissement rapide des liants les plus réactifs tels que CaO, $3CaO \cdot Al_2O_3$ et $4CaO \cdot Al_2O_3 \cdot Fe_2O_3$. Ces processus sont caractérisés par des indices d'intensité et de dégagement de chaleur total élevés. En ce qui concerne les relations thermocinétiques, on n'y peut distinguer que les périodes d'hydratation accélérée et ralentie. La période accélérée dure des minutes tandis que la période ralentie, de 1 à 2 heures. Le maximum de la vitesse du processus correspond, au début de la transformation des liants, à α de l'ordre de 0,05 à 0,1.

Le deuxième type de liants est propre au durcissement de la majeure partie des liants: $CaSO_4 \cdot 0,5H_2O$, $3CaO \cdot SiO_2$, aux minérais du ciment alumineux $CaO \cdot Al_2O_3$ et $CaO \cdot 2Al_2O_3$, aux ciments ordinaires. On y voit se manifester deux effets exothermiques séparés par un intervalle où le dégagement de chaleur se produit à une vitesse constante. L'hydratation s'effectue en trois périodes nettement distinctes, y compris celle d'induction. La durée des modifications enregistrées des indices de dégagement de chaleur varie de quelques heures à une période de 24 à 72 heures. La vitesse maximale du processus correspond à α d'une valeur de 0,3 à 0,5.

Une vitesse extrêmement basse des réactions étalées considérablement dans le temps (de quelques jours à quelques mois) est typique pour les liants dont la réactivité ne se manifeste presque pas dans les conditions normales de l'interaction liant-eau. Les lois d'hydratation de ce type de liants ($2CaO \cdot SiO_2$), de laitiers et de cendres peuvent être groupées dans le type III. La coincidence de valeurs maximales de la vitesse et du degré de transformation à α de l'ordre de 0,6 à 0,8 est naturelle pour les processus pareils.

L'établissement des lois générales des processus de durcissement reflète la possibilité de leur réalisation avec l'acquisition des caractéristiques techniques exigées: solidité, durée de prise, contraintes, déformations dues à la dilatation, concentration, indices de maniabilité et de durabilité des mélanges, etc. Les hydrates des liants qui se durcissent suivant le type I ne forment pas de structures solides. En cas d'utilisation des liants dont les processus de durcissement se rapportent au type III, il convient de les soumettre aux effets d'activation thermiques ou chimiques, à la compression, à l'extrusion, etc.

La connaissance des paramètres de la thermocinétique de l'hydratation facilite le pronostic quant aux liants et aux régimes de durcissement dans de différentes conditions. Une double nature de la réactivité fait que l'application des effets régulateurs peut donner lieu au passage de la loi établie d'un type à un autre. Cette circonstance confirme une fois de plus la justesse du principe de correspondance et la nécessité de le respecter dans la technique des liants et des bétons étant donné que la variation de la vitesse de transformation sous l'action d'effets, surtout thermiques, entraîne inévitablement un écart des établies ce qui, à son tour, conduit à des changements de la composition de phase, de la structure et des propriétés du produit obtenu.

La classification citée établit les lois générales des processus de durcissement

des liants dans des conditions normales. Il est naturel que des variantes intermédiaires, des mélanges et des déviations de fluctuation sont possibles tant pour la forme des relations thermocinétiques que pour les valeurs absolues de leurs paramètres. On peut citer comme exemple l'hydratation de $12CaO \cdot 7Al_2O_3$ lorsque dans les relations $dQ/d\tau = f(\tau)$ on ne constate pas la présence de la période d'induction mais les valeurs absolues des effets exothermiques (dont un est principal et les autres, secondaires) qui se manifestent à la recristallisation des hydrates ne sont pas à mesurer avec les paramètres des lois du type I.

Il convient de signaler surtout les manifestations des changements plus compliqués de la vitesse de dégagement de chaleur que nous avons établies pour la première fois, par exemple, à l'étude des modèles expansifs et à auto-contrainte du type "aluminate-gypse-chaux-eau". De tels phénomenes sont propres au caractère auto-oscillatoire des changements de concentration des vitesses des réactions type Béloussov-Jabotinski (6) ce qui est dû à une formation spontanée de structures à auto-organisation dans des systèmes métastables désordonnés (7).

L'établissement des lois thermocinétiques de manifestation des propriétés liantes et la classification des liants eux-mêmes sur la base quantitative d'après les indices de la vitesse et de la totalité d'hydratation nous paraissent un pas en avant sur le chemin de la résolution des problèmes théoriques, expérimentaux et appliqués de la chimie du ciment.

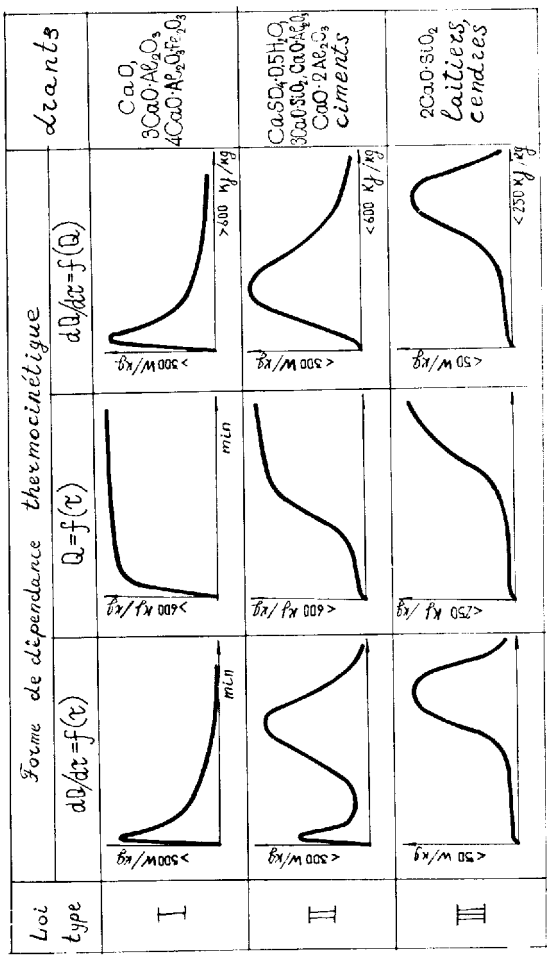

REFERENCES

I. Мчедлов-Петросян О.П. Химия неорганических строительных материалов. - М.: Стройиздат, 1970, с.

2. Кузнецов В.И. Диалектика развития химии. - М.: Наука, 1973, с. 327.

3. Дельмон Б. Кинетика гетерогенных реакций. - М.: Мир, 1972, с. 554.

4. Мчедлов-Петросян О.П., Ушеров-Маршак А. В., Урженко А.М. Тепловыделение при твердении вяжущих веществ и бетонов. - М.: Стройиздат, 1984, с. 224.

5. Ушеров-Маршак А.В. Общие закономерности процессов твердения неорганических вяжущих веществ. Доклады АН СССР, 1984, т. 276, № 2, с. 417-420.

6. Жаботинский А.М. Концентрационные автоколебания. - М.: Наука, 1974. - 179 с.
7. Хакен Г. Синергетика. - М.: Мир, 1980. - 404 с.

A. KOCHMAI,
O. MTCHEDLOV-PETROSSIAN, Youjguiprociment, Kharkov, URSS

1

PHENOMENES ELECTROCHIMIQUES INTERVENANT AUX PREMIERS STADES D'HYDRATATION ET DE FORMATION DE LA STRUCTURE DES PATES DE CIMENT

2.1

Les auteurs ont étudié les phénomènes électrochimiques intervenant dans les systèmes en durcissement "liant-eau" et dus au développement d'un réseau dynamique de microcapillaires et de pores dont le rayon est commensurable avec l'épaisseur de la double couche électrique à l'interface du solide et du liquide.

Les auteurs ont montré que l'interaction des phases faisait apparaitre des potentiels transmembraneux, de membrane, de concentration et du type de celui de Donnan.

Les recherches sur les phénomènes électrochimiques sont à la base de l'interprétation et des méthodes pratiques de contrôle de l'hydratation et de la formation de la structure aux premiers stades de durcissement des pâtes de ciment, notamment au cours de la période d'induction et des périodes de prise normale et anomale.

Les auteurs ont mis en évidence l'interdépendance de l'hydratation, de la formation de la structure et des phénomènes électrochimiques et dégagé les principes qui permettent de la mettre à contribution pour orienter et réguler le durcissement des pâtes de ciment.

Os autores estudaram os fenômenos eletro-químicos que intervêm nos sistemas "ligante-água" em endurecimento, e devidos ao desenvolvimento de uma rede dinâmica de microcapilares e de poros, cujo raio é compatível com a espessura da dupla camada elétrica na interface do sólido e do líquido.

Os autores mostraram que a interação das fases fazia aparecerem potenciais transmembranosos, de membrana, de concentração e de tipo igual ao de Donnan.

As pesquisas sobre os fenômenos eletro-químicos se realizam com base na interpretação e nos métodos práticos de controle da hidratação e da formação da estrutura nas primeiras etapas de endurecimento das pastas de cimento, principalmente no decorrer do período de indução e dos períodos de pega normal e anormal.

Os autores colocaram em evidência a interdependência da hidratação, da formação da estrutura e dos fenômenos eletro-químicos, e estabeleceram os princípios que permitem utilizá-la para orientar e regular o endurecimento das pastas de cimento.

Le durcissement des pâtes de ciment s'accompagne du développement d'un réseau dynamique de capillaires et de pores dont une grande partie possède un rayon (r) commensurable avec l'épaisseur (h) de la zone de diffusion de la double couche bipolaire (DCB) à l'interphase solide et liquide. Le modèle de Grème décrit la DCB des systèmes examinés (1,2), c'est-à-dire:

$$E = \pm\sqrt{\frac{2RT}{\xi}\sum m_i\left[\exp\left(-\frac{Z_iF\chi_1}{RT}\right) - 1\right]} \quad (1)$$

$$\sigma = -\sigma_2 = E\xi, \quad (2)$$

où: E est l'intensité du champ dans la zone de diffusion de la DCB;
R est la constante de gaz;
T est la température thermodynamique;
ξ est la perméabilité diélectrique de la phase liquide;
m_i est la molalité des i-ions;
Z_i est la charge et le signe d'un i-ion;
F est la constante de Faraday;
χ_1 est le potentiel de la phase liquide dans le plan d'approche maximale des ions de la surface de la phase solide;
σ et σ_2 est la densité des charges superficielles des phases solide et liquide dans le champ de la DCB.

Il apparaît entre les volumes de la phase liquide dans le champ de la DCB et en dehors de ses limites une répartition irrégulière d'ions qui fait apparaître des potentiels de concentration (ψ_c) et ceux du type Donnan (ψ_D) et se développer la pression osmotique résultante. Cela découle de la transformation de l'équation 1:

$$\frac{\xi}{2}(E)^2 = RT\sum m_i\exp\left(-\frac{Z_iF\chi_1}{RT}\right) - RT\sum m_i, \quad (3)$$

où: $\frac{\xi}{2}(E)^2 \equiv P_{él}$ est la composante électrique de la pression de Maxwell de la force pondéromotrice dans le champ de la DCB (tension de contraintes de Maxwell);

$RT\sum m_i\exp\left(-\frac{Z_iF\chi_1}{RT}\right) \equiv \tilde{\rho}_{osm}$ est la pression osmotique dans le champ de la DCB;

$RT\sum m_i \equiv \rho_{osm}$ est la pression osmotique dans le volume libre de la phase liquide.

Le champ de la DCB modifie la mobilité des ions (u_i) jusqu'à certaines valeurs $\tilde{u}_i$. Il est évident que $\tilde{u}_i \longrightarrow u_i$ à $\rho_{osm} \to \tilde{\rho}_{osm}$. Alors

$$\tilde{u}_i \approx u_i\,\frac{\rho_{osm}}{\tilde{\rho}_{osm}} = \frac{\sum m_i}{\sum m_i\exp\left(-\frac{Z_iF\chi_1}{RT}\right)} \quad (4)$$

Cela étant, les nombres de transfert de t_i changent du fait que $t_i = u_iZ_im_i/\Sigma u_iZ_im_i$. Par conséquent, des potentiels de membrane ψ_m (type de diffusion) apparaissent entre les volumes de la phase liquide dans le champ de la DCB et en dehors de ses limites.

Le durcissement s'accompagne de changement de la surface des particules de départ, de la morphologie des nouvelles formations, de la quantité relative de capillaires et de pores à $r \approx h$, $r > h$, $r \gg h$, de la composition ionique de la phase liquide.

Les particules hydratées ont des valeurs variables de signes opposés σ ($\sigma_{CSH} < 0$, $\sigma_{AFt} > 0$, $\sigma_{AFm} > 0$, $\sigma_{C\bar{S}H_2} > 0$, $\sigma_{CH} > 0$), la charge totale de la phase solide étant négative ($\Sigma\sigma < 0$) (1,2). Une superposition compliquée des champs de la DCB apparaît aux interphases ce qui fait changer les grandeurs ψ_c, ψ_D, $\rho_{él}$, U_i, t_i, ψ_m.

L'interaction des processus d'hydratation et de cristallisation d'un côté et les phénomènes électrochimiques de l'autre est analysée dans la chaine

Ag, AgCl, $KClm_1$ /Pâte de ciment/ $KClm_2$, AgCl, Ag,

où m_1 et m_2 sont des concentrations des solutions de KCl.

Dans les systèmes à diffusion difficile

$$V = \varphi_2 + \varphi_{trm} - \varphi_1 = \\ = \varphi_2 + \varphi_{1(2)} \pm \varphi_m - \varphi_{1(1)} - \varphi_1, \quad (5)$$

où: V est la tension électrique de la chaîne;
φ_1 et φ_2 sont les potentiels d'électrodes;
φ_{trm} est le potentiel transmembrane;
$\varphi_{1(1)}$ et $\varphi_{1(2)}$ sont les potentiels pour les solutions de KCl.

Pendant la mesure de V à compensation du champ intramembrane ($\varphi_m = 0$), les équations 1, 2, 5 donnent (1)

$$\varphi^c_{trm} = \frac{2RT}{Z_i F} \left(\operatorname{Arsh} \frac{\sigma}{\sqrt{8\varepsilon m_2 RT}} - \right. \\ \left. - \operatorname{Arsh} \frac{\sigma}{\sqrt{8\varepsilon m_1 RT}} \right), \quad (6)$$

où $\varphi^c_{trm} = \varphi_{trm}$ si $\varphi_m = 0$.

En mesurant V et en déterminant φ_{trm} (φ^c_{trm}) on peut calculer les valeurs de σ, χ_1, $\tilde{\rho}_{osm}$, $\rho_{él}$, U_i, φ_m à l'aide des équations 1 à 6. Une analyse de ces dernières révèle l'analogie qualitative qui caractérise la variation des grandeurs σ, χ_1 et $\rho_{él}$ ainsi que des grandeurs φ_{trm} et φ_m.

On voit sur les figures 1 et 2 les caractéristiques des processus de durcissement exprimées par les termes des grandeurs φ_{trm} et $\rho_{él}$.

Lorsque le durcissement des ciments Portland se déroule de façon normale (courbes 1 à 3 des figures 1 et 2) on peut identifier cinq périodes:

1. Période de réactions rapides liée à l'hydratation des C_3A et C_3S et à une formation prépondérante des AFt-phases. Du fait que $\sigma_{AFt} > 0$, les valeurs négatives totales des grandeurs σ et χ_1 diminuent selon le module /$|\Sigma\sigma|$ /:/$|\Sigma\sigma|$/ en provoquant la chute des $\tilde{\rho}_{osm}$ et $\rho_{él}$. Il en résulte que les grandeurs u_i et t_i accroissent (l'équation 4) et entraînent un accroissement de φ_m. Cela détermine un accroissement monotone de la grandeur φ_{trm}.

2. Période d'induction liée au développement des processus de formation des CSH-phases. Etant donné que $\sigma_{CSH} < 0$, alors $|\Sigma\sigma|$ et $|\Sigma\chi_1|$ augmentent et la grandeur $\rho_{él}$ commence à accroître au lieu de diminuer. Cependant, l'accroissement de φ_m continue ce qui est dû au développement d'un réseau de capillaires et de pores ($r \approx h$) formés par les CSH-phases et, respectivement, à l'accroissement de t_i. Il s'en suit que la grandeur φ_{trm} accroît de façon monotone.

3. Période de prise liée au croissement des cristaux d'ettringite allongés et au remplissage de l'espace entre eux par du gel hydrosilicieux. Pendant ce processus il se produit une augmentation rapide du nombre de microcapillaires et de pores. Cela provoque un accroissement brusque des valeurs de σ, χ_1, $\rho_{él}$, φ_m et φ_{trm}. A la fin de la prise commence la cristallisation de portlandite. Etant donné que $\sigma_{CH} > 0$, l'accroissement des $\Sigma\sigma$ et $\Sigma\chi_1$ ralentit. En même temps commence à ralentir l'accroissement des φ_m et φ_{trm} par suite de la diminution de $|\Sigma\sigma|$ sur les surfaces internes des microcapillaires et des pores grâce à la germination de cristaux d'éttringite et de portlandite dans le gel hydrosilicieux. Le contrôle du début et de la fin de l'accroissement brusque de la grandeur φ_{trm} peut servir à l'identification pratique de la période de prise des pâtes de ciment Portland (1).

4. Période de durcissement liée au développement des processus propres à la fin de la période de prise. On y constate qu'un accroissement ralenti de φ_{trm} continue tandis que la valeur de $\rho_{él}$ diminue et augmente périodiquement grâce aux processus de formation du gel hydrosilicieux et de germination de cristaux d'éttringite et de portlandite dans le gel.

5. Période de formation de la structure du ciment durci liée à une formation ultérieure des CSH-phases et au début des processus de leur polycondensation. Ce dernier facteur provoque une réduction de σ_{CSH}. Dans

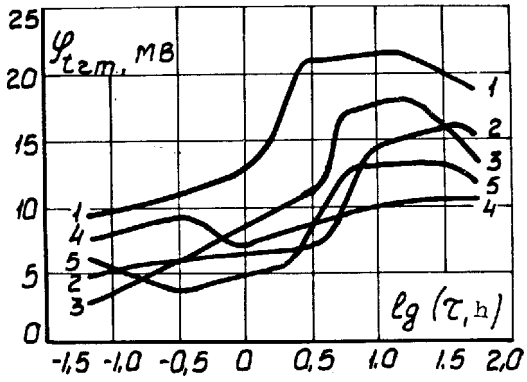

Fig. 1. Variation de la grandeur φ_{trm} au cours du durcissement des pâtes de ciment Portland: 1, 2, 3 - durcissement normal; 4 - prise rapide; 5 - fausse prise

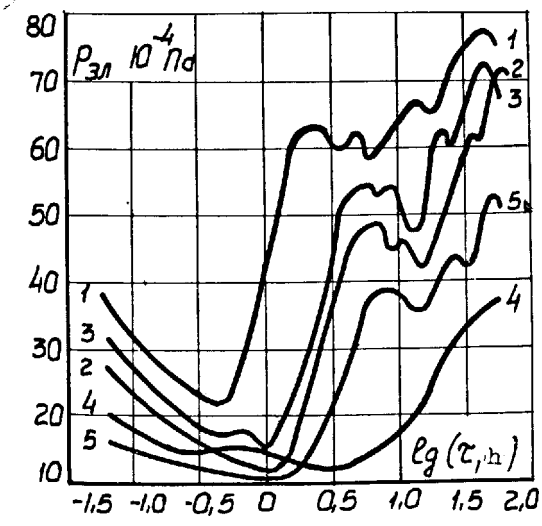

Fig. 2. Variation de la grandeur $\rho_{él} = \tilde{\rho}_{osm} - \rho_{osm}$ au cours du durcissement des pâtes de ciment Portland: 1, 2, 3 - durcissement normal; 4 - prise rapide; 5 - fausse prise

ce cas, commence la chute de la grandeur $\rho_{él}$ au lieu de son accroissement ainsi qu'une réduction de φ_{trm}.

Une prise rapide est liée aux structures non thyxotropes formées par les AFt-phases. Etant donné que $\sigma_{AFt} > 0$, il se produit une baisse durable de $\rho_{él}$ et la grandeur φ_{trm} qui était au début de sa croissance commence à diminuer (courbes 4 des fig. 1, 2).

Une fausse prise est liée aux structures thyxotropes formées par les AFt-phases ($\sigma_{AFt} > 0$) ou aux structures rhéopexiques des grilles tridimensionnelles du gypse dihydraté ($\sigma_{\overline{CSH}_2} > 0$). Dans ce cas, durant un certain temps à partir du moment de gâchage du ciment il se produit une baisse des $\rho_{él}$ et φ_{trm} (courbes 5 des fig. 1, 2). Ainsi, la nature de variation de la grandeur φ_{trm} peut être utilisée au contrôle pratique des processus de prise anomale (1).

Une analyse des phénomènes électrochimiques montre que la prise propre au durcissement normal commence après un accroissement brosque des grandeurs $\rho_{él}$ et $\Sigma\sigma$.

Dans ces conditions, le rapport $\rho_{osm}/\tilde{\rho}_{osm}$ est de valeur minimale. En modifiant les valeurs de $\Sigma\sigma$, $\rho_{él}$ et en changeant le moment où le rapport $\rho_{osm}/\tilde{\rho}_{osm}$ devient minimal, on peut influer sur la période de prise grâce à un choix de la minéralogie du clinker ou à une addition d'adjuvants chimiques. Une baisse de $\Sigma\sigma$, le rapport $\rho_{osm}/\tilde{\rho}_{osm}$ étant de valeur maximale, pendant la période de durcissement réduit l'excès de cations de Ca^{2+} et le manque d'anions de OH^- dans le champ de la DCB. Il en résulte que la formation de portlandite faiblit et celle des CSH-phases devient plus intense ce qui permet d'obtenir une structure plus homogène, plus dense et plus solide du ciment durci (2). Par conséquent, il existe une liaison réciproque entre les processus d'hydratation et de cristallisation d'un côté et les phénomènes électrochimiques de l'autre. L'utilisation de cette liaison peut ouvrir de nouvelles possibilités dans le domaine de la régulation dirigée des processus de durcissement.

REFERENCES

1. А.С. Кошмай и О.П. Мчедлов-Петросян "Электрохимические и структурно-механические свойства цементных паст" - В сб. "Реология бетонных смесей и ее технологические задачи". - Тезисы докладов IУ Всесоюзного симпозиума. ч. П. Юрмала, 1982, с. 194-197.
2. А.С. Кошмай, И.Ф. Пономарев и А.Г. Хо-

лодный. "Взаимосвязь между электрохимическими процессами и действием добавок при твердении цемента" - Цемент, 1933, №5, с. 14-16.

E.D. CHOUKIN,
E.P. ANDREEVA,
S.I. KONTOROVITSH,
E.A. AMELINA, Université de Moscou, URSS

1

ROLE DES PROCESSUS DE LA POLYCONDENSATION AU COURS DU DURCISSEMENT D'HYDRATATION DES LIANTS SILICEUX

2.1

Les auteurs ont étudié les processus de formation des structures dans les pates ß-$2CaOSiO_2$ et $3CaOSiO_2$ (en mélange avec corps de remplissage). L'accroissement de résistance au cours de l'hydratation de ces minéraux dans l'eau et dans les mortiers du chlorure de calcium se produit irrégulièrement. On observe une disproportion brusque entre le degré d'hydratation des silicates de calcium et l'accroissement de résistance. Pendant toute la période de l'hydratation des silicates de calcium dans l'eau et dans les mortiers du chlorure de calcium, il se produit une polycondensation des anions siliceux dans les hydrosilicates de calcium. L'accroissement intensif de résistance commence en cas d'obtention d'une certaine proportion de la fraction à haute polymérisation des hydrosilicates de calcium, quand les produits ayant une haute valeur de polycondensation se forment et sont susceptibles de la cyclisation et, pour cette raison, de former les bandes condensées entre elles s'approchant par leur structure des éléments du tobermorite.

Le role de la polycondensation dans la formation des contacts lors de la création des structures de durcissement des liants siliceux se fait sentir également en cas des études portant sur la jonction des particules de silice. Le principe des expériences est basé sur les mesures des forces de cohésion dans le contact entre les cylindres de quartz (diamètre 2-1 cm) couverts des particules de l'acide silicique précipitées des milieux sursaturé. On montre que la jonction de ces particules peut être considérée comme le résultat du dégagement d'une nouvelle phase condensée à partir de la solution sursaturée. Cette jonction est déterminée par la cinétique de la réaction de polycondensation de l'acide silicique.

Os autores estudaram os processos de formação de estruturas nas pastas ß-$2CaOSiO_2$ e $3CaOSiO_2$ (em mistura com materiais de enchimento). O aumento de resistência no decorrer da hidratação destes minerais com água e nas argamassas de cloreto de cálcio, ocorre irregularmente. Observa-se uma desproporção brusca entre o grau de hidratação dos silicatos e cálcio e o crescimento da resistência. Durante todo o período da hidratação dos silicatos de cálcio na água e nas argamassas de cloreto de cálcio, produziu-se uma policondensação dos aníons silicosos nos hidrossilicatos de cálcio. O crescimento intensivo da resistência começa no caso de obtenção de certa proporção da fração de alta polimerização dos hidrossilicatos de cálcio, quando se formam produtos possuidores de um valor alto de policondensação e são susceptíveis à formação de ciclos e, por esta razão, à formação de faixas condensadas entre si, aproximando-se por sua estrutura dos elementos da tobermorita.

O papel da policondensação na formação de contatos fora da criação das estruturas de endurecimento dos ligantes silicosos se faz sentir igualmente no caso de estudos sobre a junção das partículas de sílica. O princípio das experiências se baseia na medição das forças de coesão no contato entre os cilindros de quartzo (diâmetro de 2 - 1 cm) cobertos de partículas de ácido silícico precipitadas de meios super-saturados. Mostra-se que a junção destas partículas pode ser considerada como o resultado do isolamento de uma nova fase condensada a partir da solução super-saturada. Esta junção é determinada pela cinética da reação de policondensação do ácido silícico.

E.D. CHTCHOUKINE,
E.P. ANDREEVA,
S.I. KONTOROVITCH,
E.A. AMELINA

Le processus de formation des structures dispersées sur la base des $\beta 2CaO\ SiO_2$ et $3CaO\ SiO_2$ en hydratation qui sont responsables de la solidité définitive du ciment Portland, reste jusqu'à présent, malgré des études entreprises, peu connu. Un intérêt particulier éveille l'interaction qui relie les propriétés résistantes de la pierre artificielle obtenue à la base de ces minéraux au degré de polycondensation des silicat-anions dans les hydrosilicates de calcium se dégageant durant leur hydratation.

L'accroissement de la résistance au cours de l'hydratation des silicates de calcium s'effectue d'une façon irrégulière, en plusieurs étapes (fig. 1). Le fait qui attire l'attention est une brusque disproportionnalité entre le nombre d'hydrosilicates de calcium en formation (le degré d'hydratation des silicates de calcium anhydres) et l'accroissement de la résistance (fig. 2). Durant la formation d'hydrosilicates de calcium métastables l'accroissement de la résistance est faible et se produit dans les conditions où le rapport CaO/SiO_2 (C/S) s'approche de la stabilité dans les hydrosilicates de calcium à la période de l'hydratation de 20 à 30 % des silicates de calcium anhydres.

Durant toute la période de l'hydratation des silicates dans l'eau et dans les solutions de la chlorure de calcium, on voit se produire des processus de polycondensation d'ions silicieux. Ces processus se produisent de façon que d'abord sont extraits les hydrosilicates de calcium à bas degré de polycondensation ("n") correspondant à n = 1 à 4. Pendant le processus de l'hydratation on observe une augmentation de la valeur moyenne de "n" et de la fraction à haute polymérisation où le degré de polycondensation est égal et supérieur à 6,5 ($Q\ \%_n \geqslant 6,5$) avec une diminution simultanée de la fraction à faible polymérisation (fig. 3). La composition des milieux liquides exerce une influence sensible sur les processus de polycondensation: les va-

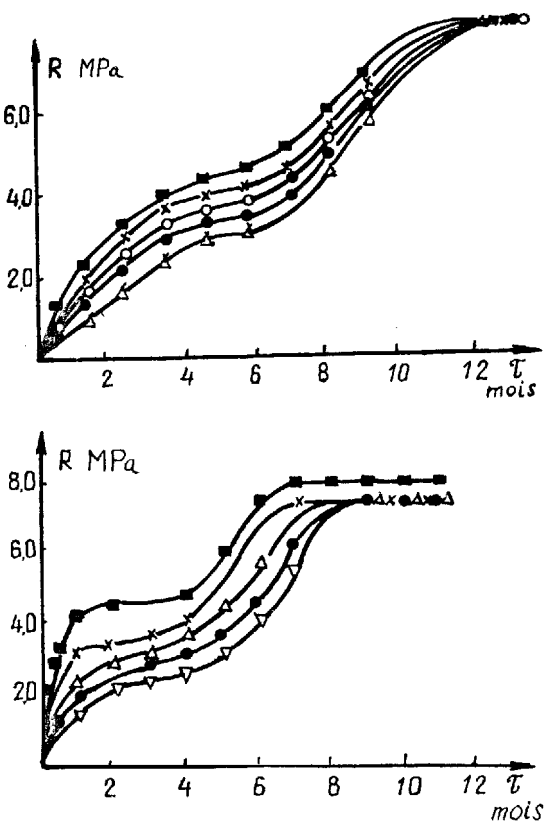

Fig. 1. Processus de formation de structure au cours de l'hydratation de $3CaO \cdot SiO_2$ et $\beta 2CaO \cdot SiO_2$ dans l'eau et dans les solutions de $CaCl_2$. Courbes: 1 - H_2O; 2 - solution de $CaCl_2$ à 0,01N; 3 - ibid. 0,1N; 4 - ibid. 0,5N; 5 - ibid. 1,0N; 6 - ibid. 3N. Composition des pâtes: 10 % $C_3S(\beta C_2S)$ + 90 % $CaCO_3$ + 25 ml H_2O ou de la solution de $CaCl_2$ pour 100 g de mélange sec (le temps est en mois)

leurs les plus probables du degré de polycondensation des silicat-anions et des hydrosilicates de calcium, "n", sont plus hautes dans les solutions de $CaCl_2$ que dans l'eau non seulement pour le même temps de l'hydratation mais aussi pour le degré de l'hydratation. La chlorure de calcium fait diminuer la valeur de pH de la solution et provoque un déplacement de la composition ionique dans le sens de l'augmentation de la fraction d'anions à faible charge et de

E.D. CHTCHOUKINE,
E.P. ANDRIEVA,
S.I. KONTOROVITCH,
E.A. AMELINA

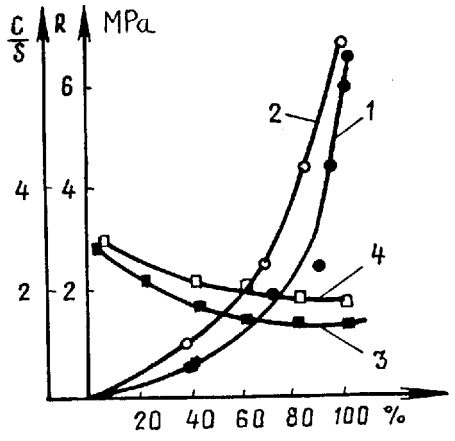

Fig. 2. Variation de R (courbes 1, 2) et de CaO/SiO_2 (3, 4) dans la composition des hydrosilicates de calcium en fonction du degré d'hydratation de $3CaO \cdot SiO_2$ dans l'eau (1, 3) et dans la solution de $CaCl_2$ à 1N (2, 4). Composition des pâtes: 10 % $3CaO \cdot SiO_2$ + 90 % $CaCO_3$ + 25 ml H_2O où de la solution de $CaCl_2$ pour 100 g de mélange sec.

l'acide silicique lesquels sont les plus adaptés à la réaction de polycondensation (v. tableau).

Dans les chaînes linéaires des hydrosilicates de calcium oligomériques le rapport C/S = 1 à 1/n. L'accroissement du degré de polycondensation des anions silicieux dans ces chaînes correspond à une réduction du rapport C/S. Pour les polymères cycliques, selon leur formule générale $K^{+(2x+y)}(Si_nO_{3n})^{-2n}$, où K = x + y, X est le nombre d'ions de calcium, y est le nombre d'ions d'hydrogène, la valeur de K à y = 0 ne dépend pas de celle de "n". Le fait que le rapport C/S est devenu stable durant l'hydratation, peut signifier que dans les hydrosilicates qui se dégagent les anions forment des cycles.

La comparaison des caractéristiques de polycondensation des hydrosilicates de calcium avec les processus de formation de la structure montre (fig. 4) qu'un accroissement intense de la résistance est observé

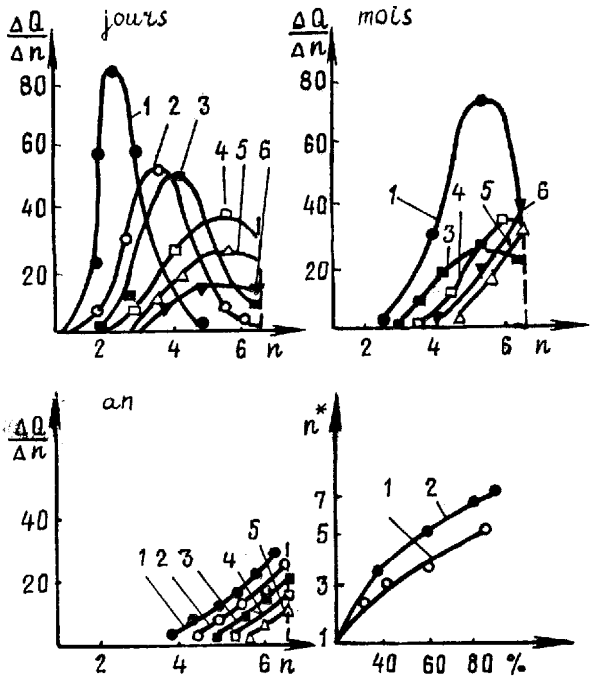

Fig. 3. Courbes de répartition différentielles de la teneur en poids des oligomères hydrosilicieux selon le degré de polycondensation moyen (n) au cours de l'hydratation de $3CaO \cdot SiO_2$ dans l'eau et dans les solutions de $CaCl_2$. Courbes: 1 - H_2O; 2 - solution de $CaCl_2$ à 0,01N; 3 - ibid. 0,1N; 4 - ibid. 0,5N; 5 - ibid. 1N; 6 - ibid. 3N. Variation de la valeur la plus probable du degré de polycondensation moyen (n*) en fonction du degré d'hydratation de $3CaO \cdot SiO_2$ dans l'eau (1) et dans la solution de $CaCl_2$ à 1N (2). Composition des pâtes: 10 % C_3S + 90% $CaCO_3$ + 25 ml H_2O ou de la solution de $CaCl_2$ pour 100 g de mélange sec

lorsque la fraction à haute polymérisation atteint une certaine valeur ($Q\,\%_n \geqslant 6{,}5$) quand les hydrosilicates de calcium à haute valeur de "n" peuvent se former. Ces hydrosilicates sont capables de former des bandes condensées entre elles, proches d'après leur

Tableau

Teneur en $CaCl_2$, gramme-équivalent par litre	Temps d'hydratation	Type d'anions				
		SiO_4^{4-}	$HSiO_4^{3-}$	$H_2SiO_4^{2-}$	$H_3SiO_4^{1-}$	H_4SiO_4
0	15 mn	0,773	4,34	24,4	68,6	1,76
	1 h	1,33	5,86	27,4	64,1	1,36
	6 h	3,31	10,5	33,1	52,4	0,75
1	15 mn	$3,6 \times 10^{-3}$	0,130	4,68	82,0	13,2
	1 h	$6,9 \times 10^{-3}$	0,201	5,76	83,1	10,9
	6 h	$1,41 \times 10^{-3}$	6,30	6,30	62,8	1,28

La teneur en ions silicieux et en H_4SiO_4 est exprimée au tableau en %% de la teneur générale en SiO_2. La composition de la suspension est de 0,25 g de βC_2S dans 100 ml de solution.

structure des éléments de tobermorite.

Le rôle des processus de polycondensation dans la création des contacts au cours de la formation des structures de durcissement des liants silicieux se fait voir à l'étude de la jonction des particules du silicium. La réalisation de l'expériment au cours de telles recherches est décrite en détail dans les ouvrages publiés auparavant. Le principe de l'expérimentation est basé sur la mesure des forces de cohésion entre des cylindres de quartz (de 1 à 2 mm de diamètre) en contact entre eux. Les cylindres sont recouverts de particules de SiO_2 précipitées à partir des sols instables de l'acide silicique dans des milieux sursaturés. Il est montré que la jonction de ces particules peut être considérée comme résultat de séparation d'une nouvelle phase condensée de la solution sursaturée et est déterminée par la cinétique de la réaction de polycondensation de l'acide silicique.

On sait que la cinétique de la polycondensation est tres sensible aux variations de la valeur de pH. Sur la figure 5 sont représentées, en fonction de la valeur de pH, et comparées entre elles (a) les probabilités de jonction (W, %) des particules de l'acide polysilicique et (b) de concentration de la fraction bas-moléculaire (C, % moléculaire) de l'acide silicique obtenue vers un même instant et caractérisée par la vitesse de polycondensation. On voit que le maximum de la jonction est observé lorsque les valeurs de pH sont de 6 à 8. Dans ce cas, la valeur de C est minimale, c'est-à-dire, la vitesse de polycondensation est maximale. L'influence de pH sur la vitesse de polycondensation peut être liée à un changement du rapport entre les fractions ionisées et bas-moléculaires de la silice dans les solutions. La vitesse de jonction maximale est assurée par leur rapport optimal obtenu à pH = 6 à 8. Etant donné qu'en fonction de la valeur de pH les courbes de sursaturation de la solution et de concentration de la silice dissoute sont analogues, une haute probabilité de jonction à pH = 6 à 8 correspond à la sursaturation minimale et non pas maximale. Cela signifie que la probabilité de jonction est déterminée non seulement par la valeur de la sursaturation mais aussi par la vitesse de la réaction de polycondensation. Par conséquent, la jonction des particules nécessite une fluctuation de la concentration d'associations de molécules contenant des formes telles que H_4SiO_4 qui sont capables, au moment où elles apparaissent entre les particules en contact, de former des liaisons de siloxane.

E.D. CHTCHOUKINE,
E.P. ANDREIEVA,
S.I. KONTOROVITCH,
E.A. AMELINA

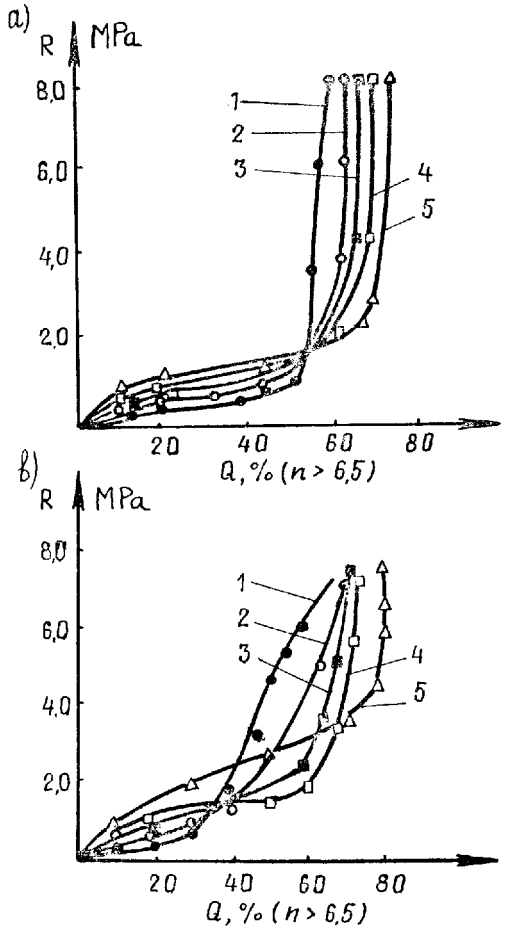

Fig. 4. Variation de R en fonction de la teneur en fraction à haute polymérisation $Q\,\%_{n \geqslant 6,5}$ au cours de l'hydratation de $\beta 2CaO \cdot SiO_2$ (a) et $3CaO \cdot SiO_2$ (b) dans l'eau et dans les solutions de $CaCl_2$. Courbes: 1 - H_2O; 2 - solution de $CaCl_2$ à 0,01N; 3 - ibid. 0,1N; 4 - ibid. 0,5N; 5 - ibid. 3N. Composition des pâtes: 10 % C_3S + 90 % $CaCO_3$ + 25 ml H_2O ou de la solution de $CaCl_2$ pour 100 g de mélange sec

Le fait que la polycondensation joue un rôle important est témoigné aussi par l'influence qu'elle exerce sur la jonction des particules des additifs d'électrolyte, par exemple, de NaCl dans un milieu dispersé sursaturé. En faisant varier la concentration de $7 \cdot 10^{-3}$ à 3.0 M, la probabilité de la jonction augmente de 7 à 28 %. L'effet

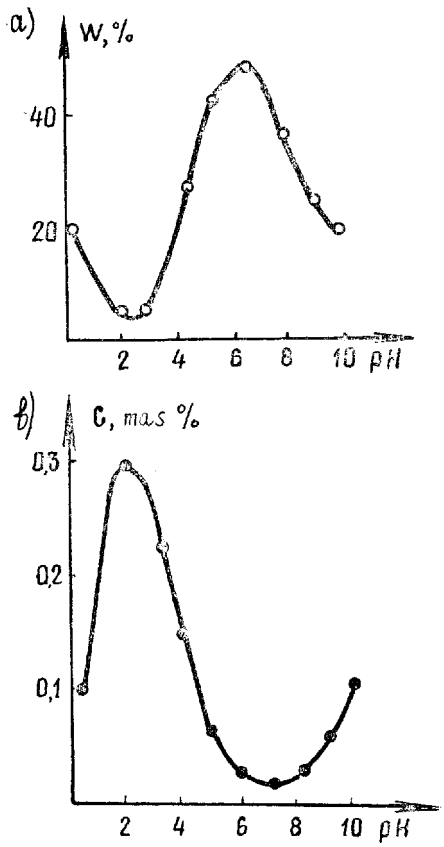

Fig. 5. Probabilités de jonction des particules de l'acide polysilicique (a) et de concentration de l'acide silicique bas-moléculaire (b) en fonction de pH du milieu

indiqué est observé dans un milieu acide (à pH = 3) où la vitesse de polycondensation est faible et représente un stade limitant le processus de jonction. La croissance de la concentration de NaCl conduit à une augmentation de la vitesse de polycondensation et, comme suite, à une augmentation de la probabilité de jonction des particules.

Pöllmann Herbert

2.1

Solid solution of complex calcium aluminate hydrates containing Cl^-, OH^- and CO_3^{2-} - anions

SUMMARY:

Replacement of hydroxyl-anions in the crystal structure of lamellar calcium aluminate hydrates by chloride and carbonate was examined. Solid solution occurs in the boundary systems and over an extended range of composition in the system $C_3A.Ca(OH)_2.aq$ - $C_3A.CaCO_3.aq$ - $C_3A.CaCl_2.aq$. It can be described as follows:

$$Ca_4\left[Al_2(OH)_{12}\right]^{2+}\quad\left[(x)\ Cl_2.(y)\ CO_3.(z)\ (OH)_2.aq\right]^{2-}$$

$$0 \leqslant x \leqslant 1$$
$$0 \leqslant y \leqslant 0.83\ x + y + z = 1$$
$$0 \leqslant z \leqslant 0.66$$

Complete solid solution along the join $C_3A.CaCl_2.aq$ - $C_3A.1/2Ca(OH)_2.1/2CaCO_3.aq$ was observed. Two miscibility gaps occur in the system:

The compound $C_3A.CaCO_3.aq$ coexists with

$$Ca_4\left[Al_2(OH)_{12}\right]^{2+}\quad\left[(5/6-2/6x)CO_3.(1/6-1/6x)\ Cl_2.(3/6x)\ (OH)_2.aq\right]^{2-}$$

$$0 \leqslant x \leqslant 1$$

and the compound $C_3A.Ca(OH)_2.aq$ coexists with

$$Ca_4\left[Al_2(OH)_{12}\right]^{2+}\quad\left[(4/6-1/6x)\ (OH)_2.(2/6-2/6x)Cl_2.(3/6x)CO_3.aq\right]^{2-}$$

$$0 \leqslant x \leqslant 1$$

Crystallographic, chemical and thermoanalytical data of the solid solution serie are given. Thermal stability of solid solution series increases with increasing chloride content.

SUMÁRIO:

Foi estudada a substituição de anions de hidroxila na estrutura do cristal de hidratos lamelares de aluminato de cálcio por cloreto e carbonato. A solução sólida ocorre nos sistemas limítrofes e numa faixa ampla de composições no sistema $C_3A.Ca(OH)_2.aq$ - $C_3A.CaCO_3.aq$ $C_3A.CaCL_2.aq$. Pode ser descrito conforme abaixo:

$$Ca_4\left[Al_2(OH)_{12}\right]^{2+}\quad(x)Cl_2.(y)\ CO_3.(z)\ (OH)_2.aq\Big]^{2-}$$

$$0 \leqslant x \leqslant 1$$
$$0 \leqslant y \leqslant 0{,}83\ x + y + z = 1$$
$$0 \leqslant z \leqslant 0{,}66$$

Observou-se solução sólida completa ao longo da junção $C_3A.CaCl_2.aq$ - $C_3A.1/2Ca(OH)_2.CaCO_3.aq$.

Ocorrem duas falhas de miscibilidade no sistema:

O composto $C_3A.CaCO_3.aq$ coexiste com

$$Ca_4\left[Al_2(OH)_{12}\right]^{2+}\quad\left[(5/6-2/6x)CO_3.(1/6-1/6x)\ Cl_2.(3/6x)\ (OH)_2.aq\right]^{2-}$$

$$0 \leqslant x \leqslant 1$$

e o composto $C_3A.Ca(OH)_2.aq$ coexiste com

$$Ca_4\left[Al_2(OH)_{12}\right]^{2+}\quad\left[(4/6-1/6x)\ (OH)_2.(2/6-2/6x)Cl_2.(3/6x)CO_3.aq\right]^{2-}$$

$$0 \leqslant x \leqslant 1$$

Dados cristalográficos, químicos e termoanalíticos da série de solução sólida são fornecidos. A estabilidade térmica da série de solução sólida aumenta com o aumento do teor de cloreto.

Pöllmann Herbert

Introduction

Some of the lamellar calcium aluminate hydrates play an important role in the chemistry of cement hydration and in deterioration of already hardened cement stone. Besides the well-known accelerating effect of Cl^--ions the influence of deicing salts, seawater etc. on hardened cement stone is of great interest in relation to the corrosion behaviour of embedded steel-reinforcement. The aggressiveness of $CaCl_2$-containing solutions to concrete may be caused by the crystallisation of complex salts with $CaCl_2$, $Ca(OH)_2$ and/or $CaCO_3$ (Chatterji,(7)).

Complex calcium aluminate hydrates conform to the general formula $C_3A \cdot CaX_2 \cdot nH_2O$ or $C_3A \cdot CaY \cdot nH_2O$ ($X = Cl^-, OH^-, ..$ / $Y = CO_3^{2-}, .$) Crystal structure determinations are based on a main layer $Ca_2\left[Al(OH)_6\right]^+$ and an interlayer $\left[X \cdot nH_2O\right]^-$ (Ahmed & Taylor (2), Allmann(3), Terzis, Fillipakis, Kuzel & Burzlaff (33)).

The purpose of the present investigation is to examine the possible crystallisation of solid solution series and to determine formation conditions and crystallographic properties.

Experimental Procedure

Synthesis of all solid solution series were made by mixing calcium salts ($CaCO_3$, $CaCl_2 \cdot 2H_2O$ p.a.) , calcined CaO and monocalciumaluminate with a definite amount of freshly distilled water. The reaction mixtures were placed in sealed polyethylene bottles and shaken continously. After 12 month the crystalline phases were filtrated in a glove box and then investigated by X-ray analysis, infrared spectroscopy, thermal analysis, chemical analysis and electron microscopy. To avoid contamination by atmospheric CO_2 all the specimen were treated under an inert gas atmosphere.

X-ray powder diffraction data were collected from moist (100 % r.h.) and dried (35% r.h.) samples using Si (99.999%, a_o=5.4308 Å) as internal standard. The lattice parameters were refined by least squares methods. Differential thermal analysis, dynamic weight loss curves and chemical analysis were made of specimen dried to constant weight at room temperature over 35% r.h. The chloride content of solutions and crystalline phases has been measured using argentometric methods.

Results

1. Unit cells and space groups of compounds in the ternary system $C_3A \cdot CaCl_2 \cdot aq$ - $C_3A \cdot CaCO_3 \cdot aq$ - $C_3A \cdot Ca(OH)_2 \cdot aq$

The compounds in this system had been characterized in detail by Fischer & Kuzel(14), Kuzel(21), Pöllmann(27), Roberts (31) and Wenda(37). A summary of crystallographic data is given in table 1.

Composition	lattice parameters(pm)						space group
	a_o	b_o	c_o	α	ß	γ	
α-$C_3A \cdot CaCl_2 \cdot 10H_2O$(40°C)	997	574	1630	-	104.5	-	C2/c , Cc
ß-$C_3A \cdot CaCl_2 \cdot 10H_2O$(40°C)	574	-	4688	-	-	-	R3c , $R\bar{3}c$
$C_3A \cdot CaCO_3 \cdot 11H_2O$	578	574	786	92.6	101.96	120.04	P 1 , $P\bar{1}$
$C_3A \cdot Ca(OH)_2 \cdot 12H_2O$	573	-	9530	-	-	-	R3c , $R\bar{3}c$
$C_3A \cdot 1/2Ca(OH)_2 \cdot 1/2CaCO_3 \cdot 11.5H_2O$	577	-	4920	-	-	-	R3c , $R\bar{3}c$

Tab.1 : Unit cells and space groups of compounds

2.Solid solution in boundary systems

$C_4A \cdot aq - C_3A \cdot CaCl_2 \cdot aq$ / $C_3A \cdot CaCO_3 \cdot aq -$
$C_3A \cdot CaCl_2 \cdot aq$ / $C_3A \cdot CaCO_3 \cdot aq - C_4A \cdot aq$

Phase relations in the boundary systems are shown by variation of short layer distance c´in fig.1.

System $C_4A \cdot aq - C_3A \cdot CaCO_3 \cdot aq$
intermediate compound with following composition(Fischer(15)) :

$3CaO \cdot Al_2O_3 \cdot 1/2Ca(OH)_2 \cdot 1/2CaCO_3 \cdot 11.5H_2O$

System $C_4A \cdot aq - C_3A \cdot CaCl_2 \cdot aq$
limited solid solution (Pöllmann & Kuzel (26)) :

$3CaO \cdot Al_2O_3 \cdot (1-x)CaCl_2 \cdot (x)Ca(OH)_2 \cdot aq$

$0 \leqslant x \leqslant 0.67$

System $C_3A \cdot CaCO_3 \cdot aq - C_3A \cdot CaCl_2 \cdot aq$
limited solid solution (Pöllmann(25)) :

$3CaO \cdot Al_2O_3 \cdot (1-x)CaCl_2 \cdot (x)CaCO_3 \cdot aq$

$0 \leqslant x \leqslant 0.83$

3.Solid solution along the join

$C_3A \cdot 1/2CaCO_3 \cdot 1/2Ca(OH)_2 \cdot 11.5H_2O -$
$C_3A \cdot CaCl_2 \cdot 10H_2O$

The results obtained with different reaction mixtures proved complete solid solution. X-ray powder diffraction data were indexed on the basis of hexagonal pseudocells. The linearity of lattice parameter c_o in solid solution series is interrupted significantly at a molar ratio of $CaCl_2/Al_2O_3$ 0.33. (fig.2). With further decreasing chloride content of the crystalline phases c_o increases linear to c_o of $C_3A \cdot 1/2Ca(OH)_2 \cdot 1/2CaCO_3 \cdot 11.5H_2O$. (fig.2).
The variation of the interlayer can be described as follows :

$$\left[(Cl)_2 \cdot 4H_2O\right]^{2-} \longleftrightarrow \left[(OH) \cdot 1/2CO_3 \cdot 5.5H_2O\right]^{2-}$$

Refined lattice parameters of solid solution series are tabulated in table 2.
The water content of solid solution series increases with decreasing Cl^--content.

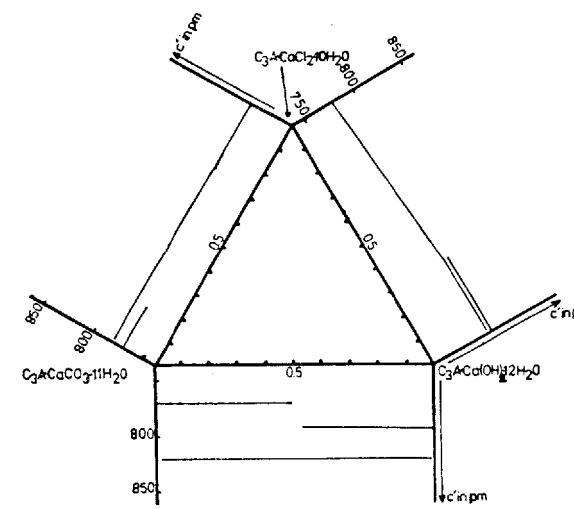

Fig.1:Phase relations in boundary systems

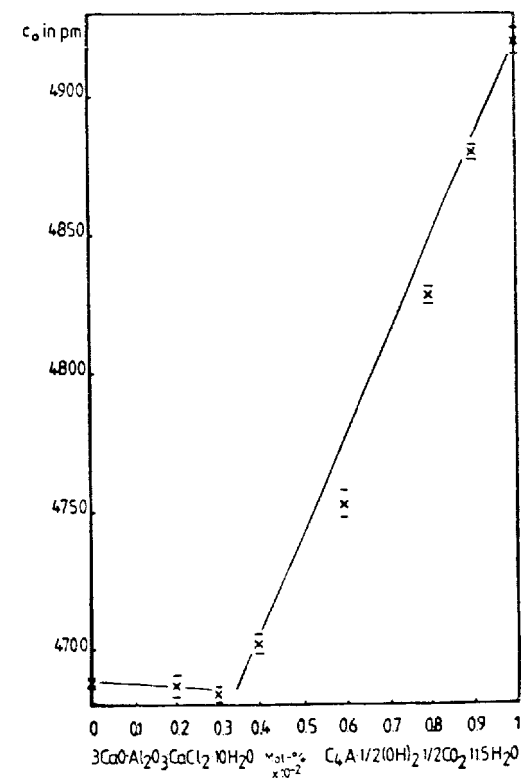

Fig.2:Variation of lattice parameter c_o of solid solution series in the system $C_3A \cdot CaCl_2 \cdot 10H_2O - C_3A \cdot 1/2Ca(OH)_2 \cdot 1/2CaCO_3 \cdot 11.5H_2O$ at 35 % r.h.

Composition $CaCl_2/Al_2O_3$	Lattice parameter (pm) a_o	c_o
1.0(40°C)	573.8 ± 1	4688.4 ± 3
0.9	574.2 ± 1	4688.0 ± 3
0.8	574.7 ± 1	4686.9 ± 4
0.7	575.0 ± 1	4682.5 ± 6
0.6	575.3 ± 1	4702.0 ± 4
0.5	575.5 ± 1	4724.9 ± 4
0.4	575.8 ± 1	4751.1 ± 6
0.3	575.9 ± 1	4791.2 ± 5
0.2	575.9 ± 1	4828.0 ± 5
0.1	576.4 ± 1	4880.0 ± 4
0	577.0 ± 1	4919.9 ± 5

Tab.2: Lattice parameters of solid solution series in the system $C_3A \cdot CaCl_2 \cdot 10H_2O$ - $C_3A \cdot 1/2Ca(OH)_2 \cdot 1/2CaCO_3 \cdot 11.5H_2O$

4. Thermal investigations

With increasing temperature molecular water is reversibly removed from the interlayer and some different lower hydrates are formed. The results of thermal dynamic loss curves and high temperature x-ray diffraction show the decreasing thermal stability of solid solution series with decreasing chloride content.

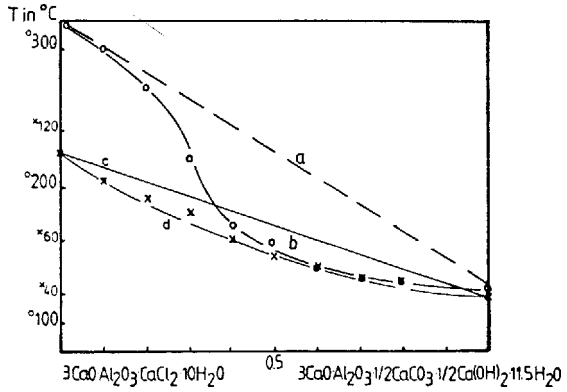

Fig. 3 : Thermal stability of solid solution series
a) Deterioration of main layer(linear equation)
b) Detericration of main layer(measured)
c) First loss of water from the interlayer(linear equation)
d) First loss of water from the interlayer (measured)

5. Solid solution of lamellar calcium aluminate hydrates in the ternary system $C_3A \cdot CaCl_2 \cdot aq$ - $C_3A \cdot CaCO_3 \cdot aq$ - $C_3A \cdot Ca(OH)_2 \cdot aq$

a) Miscibility gaps :

The compound $C_3A \cdot Ca(OH)_2 \cdot 12H_2O$ coexists with solid solution series of the following composition :

$$Ca_4\left[Al_2(OH)_{12}\right]^{2+}\left[(4/6-1/6x)(OH)_2 \cdot (2/6-2/6x)Cl_2 \cdot (3/6x)CO_3 \cdot aq\right]^{2-} \quad 0 \leq x \leq 1$$

The compound $C_3A \cdot CaCO_3 \cdot 11H_2O$ coexists with solid solution series of the following composition :

$$Ca_4\left[Al_2(OH)_{12}\right]^{2+}\left[(5/6-2/6x)CO_3 \cdot (1/6-1/6x)Cl_2 \cdot (3/6x)(OH)_2 \cdot aq\right]^{2-} \quad 0 \leq x \leq 1$$

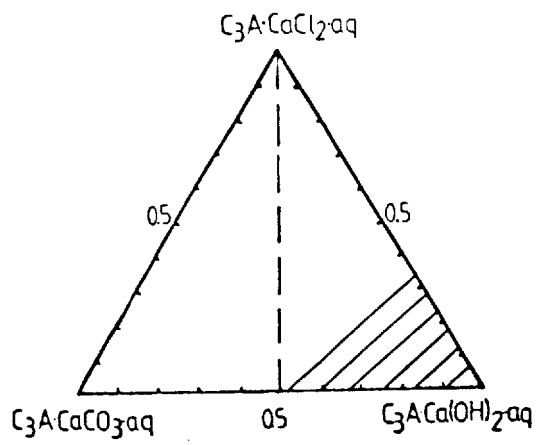

Fig.4 : Stability field of $C_3A \cdot Ca(OH)_2 \cdot aq$

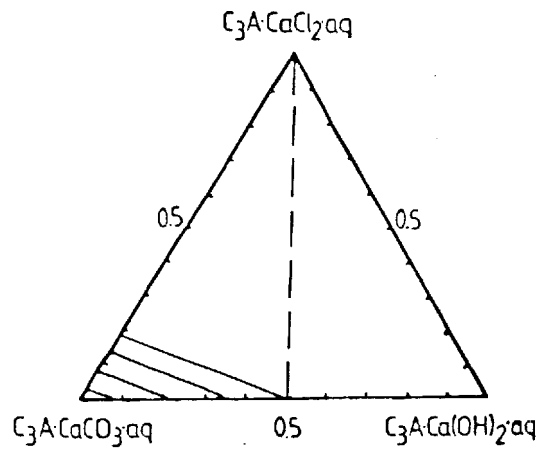

Fig.5 : Stability field of $C_3A \cdot CaCO_3 \cdot aq$

b)Solid solution series

X-ray diffraction measurements on about 100 reaction mixtures proved complete solid solution over an extended area of compositions. All ternary cristalline phases could be indexed on the basis of hexagonal pseudocells. The significant fracture in the course of c_o which had been described along the join $C_3A \cdot CaCl_2 \cdot aq$ - $C_3A \cdot 1/2Ca(OH)_2 \cdot 1/2CaCO_3 \cdot aq$ pursues in the whole system. For better presentation the system is divided up along this compatibility join. The variation of lattice parameter c_o is shown in fig.6 and fig.7. Some selected examples of lattice parameters are tabulated in table 3.

With decreasing Cl^--content of the ternary solid solution series the thermal stability decreases very rapidly.

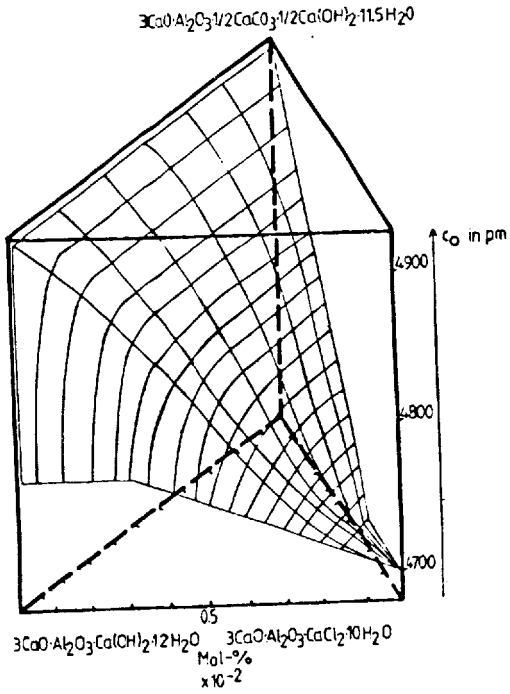

Fig.6:Variation of lattice parameter c_o(schematically)in the system $C_3A \cdot Ca(OH)_2 \cdot aq$-$C_3A \cdot 1/2Ca(OH)_2 \cdot 1/2CaCO_3 \cdot aq$ - $C_3A \cdot CaCl_2 \cdot aq$ at 35% r.h.

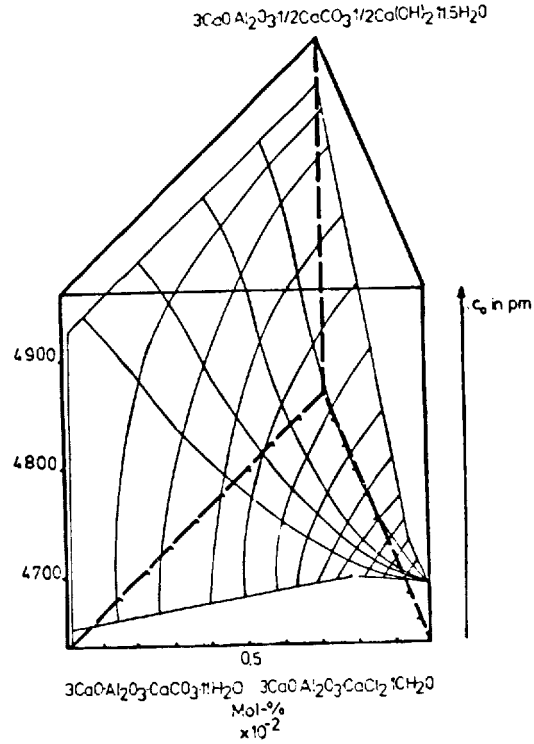

Fig.7:Variation of lattice parameter c_o(schematically) in the system $C_3A \cdot CaCl_2 \cdot aq$-$C_3A \cdot CaCO_3 \cdot aq$ - $C_3A \cdot 1/2CaCO_3 \cdot 1/2Ca(OH)_2 \cdot aq$ at 35% r.h.

Composition			Lattice parameter(pm)	
$CaCl_2/Al_2O_3$	$Ca(OH)_2/Al_2O_3$	$CaCO_3/Al_2O_3$	a_o	c_o
0.7	0.2	0.1	574.8 ± 1	4698.1 ± 3
0.7	0.1	0.2	575.2 ± 1	4692.9 ± 2
0.5	0.4	0.1	575.7 ± 2	4796.2 ± 4
0.5	0.2	0.3	575.4 ± 1	4701.7 ± 5
0.4	0.4	0.2	576.1 ± 2	4815.1 ± 4
0.3	0.6	0.1	575.6 ± 1	4854.2 ± 6
0.3	0.1	0.6	577.1 ± 2	4747.5 ± 4
0.2	0.5	0.3	576.7 ± 2	4863.1 ± 8
0.2	0.2	0.6	577.4 ± 1	4810.4 ± 5
0.1	0.8	0.1	576.6 ± 2	4882.0 ± 4
0.1	0.1	0.8	577.7 ± 1	4795.3 ± 5

Tab.3:Lattice parameters of solid solution series $C_3A \cdot CaCl_2 \cdot aq$ - $C_3A \cdot Ca(OH)_2 \cdot aq$ - $C_3A \cdot CaCO_3 \cdot aq$ (selected examples)

Thus solid solution in the ternary system can be described as follows :

$$Ca_4\left[Al_2(OH)_{12}\right]^{2+}\left[x(Cl)_2 \cdot y(CO_3) \cdot z(OH)_2 \cdot 4x \cdot 5y \cdot 6z\ H_2O\right]^{2-}$$

$$0 \leq x \leq 1$$
$$0 \leq y \leq 0.83 \qquad x + y + z = 1$$
$$0 \leq z \leq 0.66$$

Conclusions

The now available data, obtained on complex calcium aluminate hydrates containing Cl^-, OH^- and CO_3^{2-}, give a substantial clarification of the existing uncertanties with regard to solid solution, water content and composition. Misinterpretation of available data for precise identification may be caused by the following factors :

1. Carbonation effects(caused by contamination of CO_2 from air)
2. Water content(precise control of different hydration stages is needed)
3. Stacking faults of layer structures
4. Order-disorder problems of anions in the interlayer

Acknowledgements

The author wishes to thank Prof.Dr.H-J.Kuzel for high interest in this work and constant support. Furthermore he wishes to thank Dr. R.Wenda for helpful discussions and the "Deutsche Forschungsgemeinschaft" for financial support.

References

1. Ahmed,S.J.,Dent Glasser,L.S. & Taylor,H. F.W.,"Crystal structures and reactions of C_4AH_{12} and derived basic salts", Proc. V. Int. Symp. on the chemistry of Cement,Tokyo,Suppl.-Paper II-77,118-127,(1968)
2. Ahmed,S.J. & Taylor,H.F.W.,"Crystal structures of the lamellar calcium aluminate hydrates", Nature 215,622-623,(1967)
3. Allmann,R,"Refinement of the hybrid layer structure $Ca_2\left[Al(OH)_6\right]^+\left[1/2SO_4 \cdot 3H_2O\right]^-$" N.Jb.Min.Mh.7,136-143,(1977)
4. Ben-Yair,M.,"Studies on the stability of calcium-chloroaluminate",Is.J.Ch.9,529-536,(1971)
5. Berntsson,L. & Chandra,S.,"Damage of concrete sleepers by calcium chloride", Cem. Concr.Res.12,87-92,(1982)
6. Blenkinsop,J.C.,"The effect on normal 3/8 reinforcement of adding calcium chloride to dense and porous concrete",Mag.Concr. Res.15,33-38,(1963)
7. Chatterji,S.,"Mechanism of the $CaCl_2$-attack on Portland Cement concrete",Cem. Concr.Res.8,461-468,(1978)
8. Chatterji,S. & Damgaard,A.,"Studies of the mechanism of calcium chloride attack on Portland Cement",Nordisk Betong, 5-6, (1975)
9. Clemmer,H.F. & Burggraf,F.,"An investigation in the use of calcium chloride as a curing agent and accelerator of concrete" Proc.Am.Soc.Test.Mat.23,Part II,(1923)
10. Collepardi,M.,Marcialis,A. & Turriziani, R.,"Penetration of chloride ions into cement pastes and concrete",J.Am.Ceram. Soc.55,534-535,(1972)
11. Cottinger,P. & Kendall,H.-G.,"The use of calcium chloride as protection against freezing of concrete",Concrete 22, 150-155,(1923)
12. Dosch,W. & Keller,H.,"On the crystal chemistry of tetracalcium aluminate hydrate",Proc. VI.Int. Symp. on the chemistry of Cement, Moscow,Suppl.-Paper,Section II -4
13. Darr,G.M. & Ludwig,U.,"The incorporation of chloride in calcium aluminate hydrates" Ind.Chim.Belg.39,687-692,(1974)

14.Fischer,R. & Kuzel,H.-J.," Reinvestigation of the system $C_4A \cdot nH_2O$ - $C_4A \cdot CO_2 \cdot nH_2O$",Cem.Concr.Res.12,517-526,(1982)

15.Fischer,R.," About the incorporation of CO_3^{2-} in laminar earth-alkalimetal aluminate hydrates",(in german),Thesis Univ. Erlangen-Nürnberg,(1977)

16.Fischer,R.,Kuzel,H.-J. & Schellhorn,H., "Hydrocalumit:Solid solution between Friedels Salt"$3CaO \cdot Al_2O_3 \cdot CaCl_2 \cdot 10H_2O$" and Tetracalciumaluminatehydrate?",(in german),N.Jb.Min.Mh.7,322-334,(1980)

17.Friedel,P.M.,"Sur un chloro-aluminate de calcium hydrate se maclant par compression",Bull.Soc.Fran.Min.Crist.20,122-136, (1897)

18.Gjorv,O.E. & Vennesland,O.,"Diffusion of chloride ions from seawater into concrete Cem.Concr.Res.9,229-238,(1979)

19.Keller,H.,"Inorganic exchange reactions of $Ca_2 Al(OH)_6 \cdot OH \cdot aq$ and derived solid solution",(in german), Thesis,Univ. Mainz (1971)

20.Kuzel,H.-J.,"X-ray investigation in the system $3CaO \cdot Al_2O_3 \cdot CaSO_4 \cdot nH_2O$ - $3CaO \cdot Al_2O_3 CaCl_2 \cdot nH_2O$",(in german),N.Jb.Min.Mh.7, 193-200,(1966)

21.Kuzel,H.-J.,"X-ray investigations of some complex calcium aluminate hydrates and related compounds",Proc.V.Int. Symp. on the chemistry of Cement,Tokyo,Suppl.-Paper II-19,92-97,(1968)

22.Lea,F.M.,"The chemistry of Cement and Concrete,London,(1970)

23.Lieber,W. & Bleher,K.,"Calciumchloride aggressive to steel?",(in german),Beton 9,207-209,(1959)

24.Newman,A.J.,"Effects of the addition of calciumchloride to the Portland Cement Concrete",Concr. and Constr. Eng.38,159-167,(1943)

25.Pöllmann,H.,"Solid solution in systems $C_3A \cdot CaCl_2 \cdot aq$ - $C_3A \cdot CaCO_3 \cdot aq$ and $C_3A \cdot CaCl_2 \cdot aq$ - $C_3A \cdot Ca(OH)_2 \cdot aq$",(in german),Univ. Erlangen-Nürnberg,M.Sc.(1981)

26.Pöllmann.H. & Kuzel,H.-J.,"Chloridecontaining Calcium aluminate hydrates",(in german),Fortschr.Min.60,165-166,(1982)

27.Pöllmann,H.,"Crystal chemistry of new compounds formed under the influence of destructive agents to Cement",(in german) Thesis,Univ.Erlangen-Nürnberg,(1984)

28.Pöllmann,H. & Wenda,R.,"Quaternary calcium aluminate hydrates - formed by hardening of cement",(in german),Fortschr. Min.63,187,(1985)

29.Richartz,W.,"Bonding of chloride among cement hardening",(in german),ZKG 10,447-456,(1969)

30.Roberts,M.H.,"Effect of calcium chloride on the durabilility of pre-tensioned wire in prestressed concrete", Mag.Concr.Res. 14,143-154,(1962)

31.Roberts,M.H.,""Calcium aluminate hydrates and related basic salts solid solutions", Proc.V.Int. Symp. on the chemistry of Cement,Tokyo,Suppl.-Paper II-29, 104-117 (1968)

32.Schwiete,H.E. & Ludwig,U.,"Bonding of Calciumchloride and Calciumsulphate among hydration of aluminatic and ferritic components",(in german),ZKG 5,225-234,(1969)

33.Serb-Serbina,Y.A.,Savina,V. & Zhurina,V., "The formation of hydrated calcium chloro aluminates and their effect on the structure of cement pastes",Dokl.Akad.Nauk. SSSR 3,659-662,(1956)

34.Terzis,A.,Fillipakis,S.,Kuzel,H.-J. & Burzlaff,H.,"The crystal structure of $Ca_2Al(OH)_6 \cdot Cl \cdot 2H_2O$,Z.Krist.(in press) (1986)

35.Traetteberg,A. & Grattan-Bellew,P.E., "Hydration of $3CaO \cdot Al_2O_3$ and $3CaO \cdot Al_2O_3$ + Gypsum with and without $CaCl_2$",J.Am.Ceram Soc.58,221-227,(1975)

36.Turriziani,R. & Schippa,G.," Contribution to the knowledge of hydrated calcium chloroaluminates",(in italian),Ric.Scient 25,3102-3106,(1955)

37.Wenda,R.,"Investigations among crystal chemistry of hydration products from borate containing cements",(in german), Thesis,Univ. Erlangen-Nürnberg,(1984)

R. Wenda, Keimfarben GmbH Neusäß and H.-J. Kuzel, Mineralogisches Institut der Universität Erlangen-Nürnberg, Germany

B^{3+} in Calcium Aluminate Hydrates

SUMMARY: In the course of experiments with borate containing high alumina cements the incorporation of B^{3+} in calcium aluminate hydrates has been investigated. At low concentrations of B^{3+} a new compound of composition $C_4A \cdot 1/2B_2O_3 \cdot 12H_2O$ is formed. The crystal structure is closely related to that of monosulfate $C_3A \cdot CaSO_4 \cdot 12H_2O$. The phase is stable in pastes up to 60°C. Its formation is most probably responsible for the reported "stabilisation" of aluminous cements by borates. With increasing concentration of B^{3+} in the pastes and at temperatures below 40°C ettringite-like phases of composition $6CaO \cdot Al_2O_3 \cdot 2B_2O_3 \cdot 39H_2O$ and $6CaO \cdot Al_2O_3 \cdot B_2O_3 \cdot 42H_2O$ have been observed. By precipitation from lime-sucrose solutions the hydroxyl-ettringite $C_3A \cdot 3Ca(OH)_2 \cdot 33H_2O$ has been prepared. The infrared spectra of the new phases are discussed and their crystallographic data are given.

No decorrer de experiências com cimentos alto-aluminosos contendo borato, foi investigada a incorporação de B^{3+} nos hidratos de aluminato de cálcio. Com baixas concentrações de B^{3+} ocorre a formação de um novo composto cuja composição é $C_4A.1/2B_2O_3.12H_2O$. A estrutura do cristal está estreitamente relacionada com a de monosulfato $C_3A.CaSO_4.12H_2O$. A fase é estável em pastas até 60°C. Muito provavelmente sua formação é responsável pela relatada "estabilização" de cimentos aluminosos por boratos. Com o aumento da concentração de B^{3+} nas pastas e sob temperaturas abaixo de 40°C foram observadas fases semelhantes à etringita com composição $6CaO.Al_2O_3.2B_2O_3.39H_2O$ e $6CaO.Al_2O_3.B_2O_3.42H_2O$. Preparou-se hidroxil-etringita $C_3A.3Ca(OH)_2.33H_2O$ a partir de precipitações de soluções de cal-sacarose. São discutidos os espectros infravermelhos das novas fases e informados seus dados cristalográficos.

R. Wenda, Keimfarben GmbH Neusäß and H.-J. Kuzel, Mineralogisches Institut der Universität Erlangen-Nürnberg, Germany

INTRODUCTION

It has been reported in the literature (1,2,3,4) that boric acid and borates affect the setting and strength development of portland cement depending on their concentration in the pastes. Lieber and Richartz (5) have shown that additions of 0,1 to 1,0 weight percent of boric acid retards the sulfate binding and the formation of ettringite. They observed that the setting of the pastes was slightly accelerated whereas the hardening of the cement was retarded.

A patent of 1974 claims a method for retarding the hydration reactions of rapid hardening cements containing $C_{12}A_7$ and C_4AF by small amounts of boric acid, sodium or potassium borates (6). The addition of 2 to 5 weight percent of calcium borates to high alumina cements is reported in another patent of 1972 (7) to prevent the conversion of the hydrates CAH_{10} and C_2AH_8 into stable C_3AH_6 up to 60°C.

In the course of experiments with borate containing rapid-hardening cements and "stabilized" high alumina cements X-ray reflections of new crystalline phases have been observed.

The purpose of this work is to clear the chemical compositions, formation conditions and crystallographic properties of the apparently B^{3+}-containing new compounds.

EXPERIMENTAL

The composition and formation conditions of the new compounds were studied by hydration of pastes prepared with CA, calculated amounts of freshly calcined CaO, solutions with different concentrations of H_3BO_3 or suspensions of finely ground natural colemanite $Ca[B_3O_4(OH)_3] \cdot H_2O$. The mixtures were placed in sealed polyethylene bottles and shaken for several weeks at different temperatures between 5°C and 60°C in large containers filled partly with soda lime to avoid contamination by atmospheric CO_2.

Monocalcium aluminate was prepared in a laboratory furnace from reagent grade $CaCO_3$ and Al_2O_3 and ground to a Blaine fineness of about 2500cm^2/g. In some cases Secar 250 or "Ciment Fondu" containing appreciable quantities of Fe-oxide were used.

After filtration in a glove box under CO_2-free conditions the solutions and the crystalline phases were analyzed for Ca^{2+} and Al^{3+} using flame photometry and AAS. B^{3+} was determined colourimetrically. The solids were then examined by X-ray diffraction methods, infrared spectroscopy, optical and scanning electron microscopy, dynamic weight-loss curves and differential thermal analysis.

At every stage of preparation and examination of the samples rigorous precautions were taken against uncontrolled contamination by CO_2.

RESULTS AND DISCUSSION

Three new quaternary calcium aluminate hydrates have been detected in the pastes.

$C_4A \cdot 1/2B_2O_3 \cdot 12H_2O$. At low concentration of B^{3+} in the pastes a compound with the composition $C_4A \cdot 1/2B_2O_3 \cdot 12H_2O$ is formed. It crystalizes as thin biaxial negative plates with pseudohexagonal morphology and perfect (0001) cleavage (Fig. 1). Penetration twins are common. Crystals up to 0,3mm diameter were collected from samples of appropriate composition which had been

shaken for 12 months at 40°C. Single crystal photographs and X-ray powder diffraction diagrams showed that the hydrate had mono-

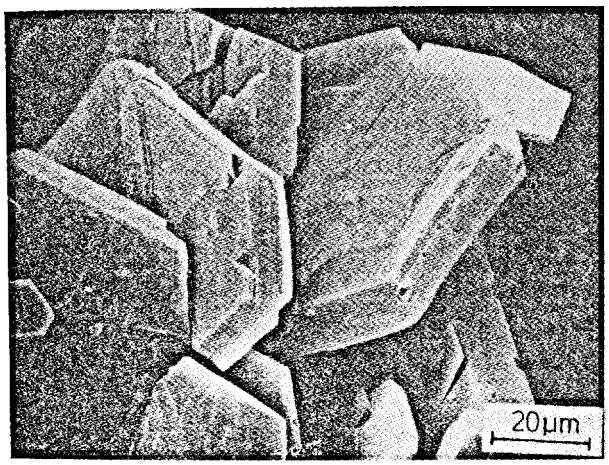

Fig. 1. SEM micrograph of $C_4A \cdot 1/2B_2O_3 \cdot 12H_2O$

clinic symmetry with the lattice constants a_o=10,005 ± 0,002Å, b_o=5,765 ± 0,001Å, c_o=16,840 ± 0,003Å and ß=101,3 ± 0,1°. The space group is probably Cc or C2/c.
At T= 60°C the compound transforms without loss of molecular water to a phase with probable space group R3c or $R\bar{3}c$ and the unit cell a_o=5,776±0,001Å, C_o=49,511±0,007Å. The observed data support the assumption that $C_4A \cdot 1/2B_2O_3 \cdot 12H_2O$ has a layer structure which is closely related to that of monosulfate $C_3A \cdot CaSO_4 \cdot 12H_2O$ (9,10,11). The infrared absorption spectra of the monoclinic and the hexagonal polymorph are shown in Fig. 2. The patterns are very similar to those of other calcium aluminate hydrates which have been discussed in detail by Houtepen and Stein (12), Volant (13) and Fischer and Kuzel (14). Of special interest are the absorption bands due to B-OH-vibrations at 1180 and 1150cm^{-1} in both polymorphs.
As a consequence of the lower symmetry at 20°C the ν_3 band of the BO_3^{3-}-group is split into two components at 1420 and 1475 cm^{-1}. Thus the formula of the new compound may be written as

$$\{Ca_4[Al(OH)_6]_2\} \cdot \{HBO_3 \cdot 5,5H_2O\}.$$

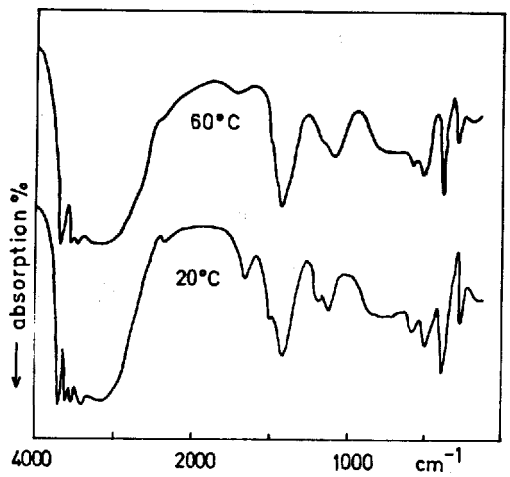

Fig. 2. IR diagrams of monoclinic (20°C) and hexagonal (60°C) $C_3A \cdot CaHBO_3 \cdot 11,5H_2O$

The results of high temperature X-ray diffraction, DTA and dynamic weight-loss curves are given in Fig. 3. In the temperature range up to 200°C the molecular water is reversibly removed step by step and lower hydrates of interlayer composition $[HBO_3 \cdot 4,5H_2O]^{2-}$ (c'=7,85Å), $[HBO_3 \cdot 3,5H_2O]^{2-}$ (c'=7,50Å), $[HBO_3 \cdot 1\text{-}2H_2O]^{2-}$ (c'=6,70Å) and $[HBO_3]^{2-}$ (c'=6,50Å) are formed.
At 20°C solid solution between the end members $C_4A \cdot 1/2B_2O_3 \cdot 12H_2O$ and the quaternary carbonate hydrate $C_4A \cdot 1/2CO_2 \cdot 12H_2O$ exists. With increasing molar ratio CO_2/Al_2O_3 the largest basal spacing c'=8,252Å of $C_4A \cdot 1/2B_2O_3 \cdot 12H_2O$ is continuously lowered to the layer thickness c'=8,202Å of the carbonate hydrate (Fig. 4). At the composition $C_3A \cdot 0,7CaHBO_3 \cdot 0,15CaCO_3 \cdot 0,15Ca(OH)_2 \cdot$

$11,5H_2O$ the transformation of the monoclinic 2-layer structure of the borate hydrate to the hexagonal 6-layer structure of the carbonate hydrate occurs.

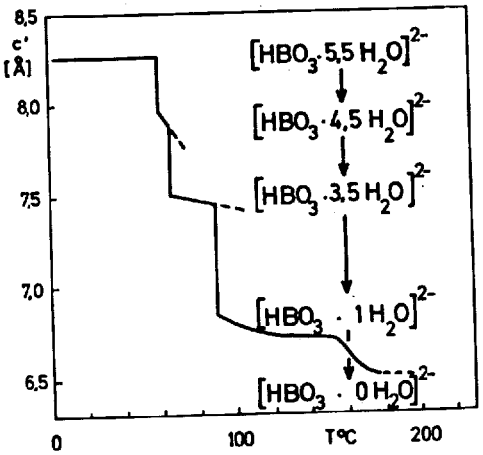

Fig. 3. Dehydration of $[Ca_4Al_2(OH)_{12}] \cdot [HBO_3 \cdot 5,5H_2O]$

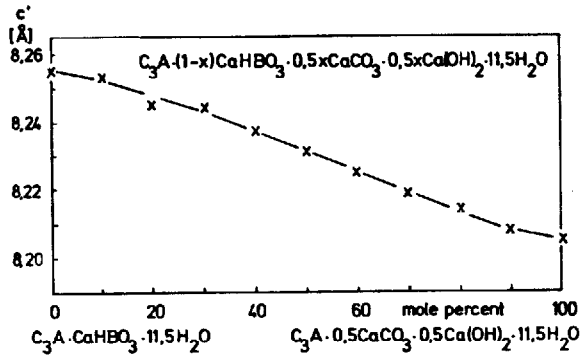

Fig. 4. c'-values of the solids in the system $C_3A \cdot CaHBO_3 \cdot 11,5H_2O$ - $C_3A \cdot 1/2CaCO_3 \cdot 1/2Ca(OH)_2 \cdot 11,5H_2O$ at 22°C and 35% relative humidity

Al^{3+} of $C_4A \cdot 1/2B_2O_3 \cdot 12H_2O$ can be completely replaced by Fe^{3+} if the pastes are prepared with C_2F instead of CA. The hydrate $C_4F \cdot 1/2B_2O_3 \cdot 12H_2O$ has hexagonal symmetry with $a_o = 5,904 \pm 0,001$Å and $c_o = 48,731 \pm 0,006$Å. The space group is probably R3c or $R\bar{3}c$.

Ettringite phases. If the molar ratio H_3BO_3/CA exceeds 0,25 in the pastes at $T < 40^\circ$ another new compound with the composition $6CaO \cdot Al_2O_3 \cdot 2B_2O_3 \cdot 39H_2O$ crystallizes as very small hexagonal prisms. The size of the crystals did not exceed 1 µm and no material suitable for single crystal X-ray work could be obtained. In its qualitative composition, morphology and X-ray powder diffraction diagram the compound resembles ettringite $6CaO \cdot Al_2O_3 \cdot 3SO_3 \cdot 32H_2O$.

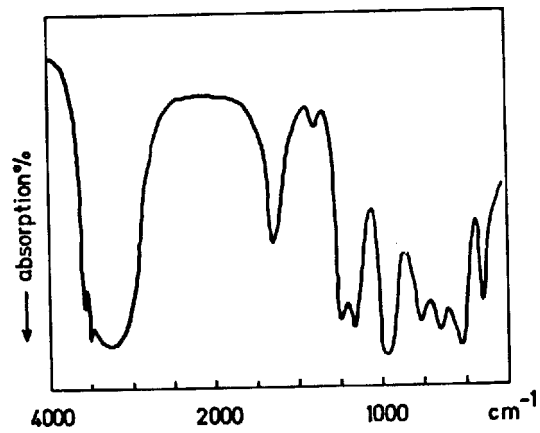

Fig. 5. IR-diagram of $6CaO \cdot Al_2O_3 \cdot 2B_2O_3 \cdot 39H_2O$

The infrared absorption spectrum shows B-OH bands at 1185 and 1240cm^{-1} and a strong ν_3-vibration of $B(OH)_4$ at 975cm^{-1}. It is therefore assumed that the structure channels contain $B(OH)_4$-tetrahedra and the constitution of the compound is tentatively written as

$$\{Ca_6[Al(OH)_6]_2 \cdot 24H_2O\} \cdot \{4B(OH)_4 \cdot 2OH\}.$$

The weak band at 1420cm^{-1} is ascribed to the asymmetric stretching mode of the CO_3^{2-} -group due to contamination of the sample by CO_2. The X-ray powder diffraction

pattern has been indexed by aid of an ettringite-like hexagonal unit cell. The lattice constants are given in table 1. On heating at 65°C the borate complex looses all of its molecular water.
After shaking the pastes in the temperature range 5°C to 20°C for 12 months some additional unknown X-ray reflections of low intensity have always been observed. This led to another B^{3+} containing ettringite-like phase which crystallizes in characteristically short hexagonal prisms (Fig.6).

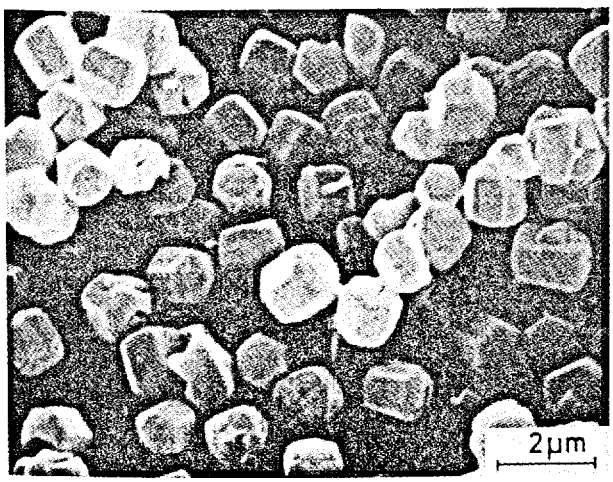

Fig. 6. SEM micrograph of $6CaO \cdot Al_2O_3 \cdot B_2O_3 \cdot 42H_2O$

Attempts to prepare the borate complex in a pure state were only successful if the compound was precipitated from aquous lime-sucrose solutions by adding calculated amounts of $NaAl(OH)_4$ and H_3BO_3. A similar method was used by Carlson and Berman (15) in the preparation of the carbonate ettringite $C_3A \cdot 3CaCO_3 \cdot 32H_2O$.
Its composition was determined to be $6CaO \cdot Al_2O_3 \cdot B_2O_3 \cdot 42H_2O$ at 35 per cent relative humidity. In its main features the IR-pattern shown in Fig. 7 is similar to that of $6CaO \cdot Al_2O_3 \cdot 2B_2O_3 \cdot 39H_2O$ indicating the presence of $B(OH)_4$-tetrahedra in the channels of the crystal structure. The constitution of this phase is possibly given by the formula

$$\{Ca_6[Al(OH)_6]_2 \cdot 24H_2O\} \cdot \{2B(OH)_4 \cdot 4OH \cdot 6H_2O\}.$$

The compound is hexagonal too. The lattice constants are given in table 1.

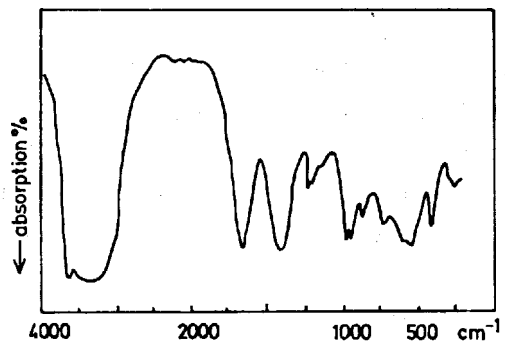

Fig. 7. IR-diagram of $6CaO \cdot Al_2O_3 \cdot B_2O_3 \cdot 42H_2O$

The hydroxyl-ettringite described by Flint and Wells (16) has been prepared by the same method at 20°C. Although this phase is extremely sensitive against attack of carbon dioxide it could be synthesized nearly CO_2-free. Chemical analysis of the material after drying at 35 per cent relative humidity, infrared and X-ray data have shown the composition and constitution to be $C_3A \cdot 3Ca(OH)_2 \cdot 33H_2O$ or

$$\{Ca_6[Al(OH)_6]_2 \cdot 24H_2O\} \cdot \{6OH \cdot 3H_2O\}.$$

Like all other minerals of the ettringite group the phase has a hexagonal unit cell. The crystallographic data are tabulated in table 1.

R. Wenda, Keimfarben GmbH Neusäß and H.-J. Kuzel, Mineralogisches Institut der Universität Erlangen-Nürnberg, Germany

Table 1. Crystallographic data of the hydrates

Composition	Lattice constants (Å)				Space group
	a_o	b_o	c_o	ß	
$C_4A\cdot 1/2B_2O_3\cdot 12H_2O$	10,005±2	5,765±1	16,840±3	101,3±3	Cc,C2/c
$C_4A\cdot 1/2B_2O_3\cdot 12H_2O$	5,776±1	-	49,511±4	-	R3c,R$\bar{3}$c
$C_4F\cdot 1/2B_2O_3\cdot 12H_2O$	5,904±1	-	48,731±6	-	R3c,R$\bar{3}$c
$C_6A\cdot 2B_2O_3\cdot 39H_2O$	11,022±1	-	21,388±4	-	-
$C_6A\cdot B_2O_3\cdot 42H_2O$	11,015±1	-	21,232±3	-	-
$C_6A\cdot 36H_2O$	10,900±1	-	21,274±4	-	-

The lamellar hydrate $C_4A\cdot 1/2B_2O_3\cdot 12H_2O$ is stable in pastes up to 60°C. At T > 60°C decomposition to $2CaO\cdot B_2O_3\cdot H_2O$ occurs. The formation of this compound is responsible for the reported stabilisation of aluminous cements by borates. With the addition of approximately 5 per cent of colemanite only 50 per cent of the hydrates CAH_{10} and C_2AH_8 are converted to $C_4A\cdot 1/2B_2O_3\cdot 12H_2O$ and the trasformation of this fraction to stable C_3AH_6 is blocked. On addition of more than 5 per cent of calcium borates to the pastes the setting and hardening of the cement is vigorously retarded.

Table 2. X-ray powder diffraction data

$C_3A\cdot CaHBO_3\cdot 11,5H_2O$ (monoclinic)

d(Å)	I/I_o	hkl	d(Å)	I/I_o	hkl	d(Å)	I/I_o	hkl
8,253	100	002	2,728	<5	311	2,317	<5	404,222
4,635	<5	$\bar{2}02$	2,722	<5	022	2,234	<5	402
4,126	30	004	2,631	<5	$\bar{2}06$,115	2,222	5	206
3,894	5	202	2,558	5	312	2,218	<5	$\bar{1}17$
3,883	5	$\bar{1}13$	2,554	5	023	2,175	<5	314
2,891	5	$\bar{2}04$	2,453	5	400	2,172	<5	025,$\bar{3}16$
2,887	10	$\bar{3}11$,$\bar{1}15$	2,448	5	$\bar{2}22$	2,064	<5	008
2,881	5	020	2,366	<5	313	2,054	<5	117
2,838	<5	021	2,362	<5	024,$\bar{3}15$			

$C_3A\cdot CaHBO_3\cdot 11,5H_2O$ (hexagonal)

d(Å)	I/I_o	hkl	d(Å)	I/I_o	hkl	d(Å)	I/I_o	hkl
8,251	100	006	2,631	<5	1016	2,063	<5	0024
4,638	<5	104	2,555	5	119	2,052	<5	1022
4,125	30	0012	2,452	5	204	2,041	<5	2014
3,893	5	108	2,365	<5	1112	1,992	<5	1118
3,519	<5	1010	2,319	<5	208	1,780	<5	1026
2,888	5	110	2,233	5	2010	1,759	5	2020
2,845	<5	113	2,220	5	1020	1,667	5	300
2,726	5	116	2,172	5	1115			

$C_3A\cdot 2Ca[B(OH)_4]_2\cdot Ca(OH)_2\cdot 30H_2O$ (hexagonal)

d(Å)	I/I_o	hkl	d(Å)	I/I_o	hkl	d(Å)	I/I_o	hkl
9,55	100	100	3,182	5	300	2,373	5	314
5,511	50	110	2,993	20	116	2,180	30	226
5,347	<5	004	2,756	10	220	2,145	<5	322
4,899	10	112	2,734	20	304	2,125	10	316
4,665	30	104	2,668	5	222	2,045	5	412
3,838	30	114	2,647	<5	310	2,026	5	324
3,608	5	210	2,570	10	312	1,941	5	414
3,563	10	204	2,536	50	216	1,840	5	2110
3,418	30	212	2,449	<5	224	1,780	10	408

$C_3A\cdot Ca[B(OH)_4]_2\cdot 2Ca(OH)_2\cdot 36H_2O$ (hexagonal)

d(Å)	I/I_o	hkl	d(Å)	I/I_o	hkl	d(Å)	I/I_o	hkl
9,53	100	100	2,979	10	116	2,173	30	226
5,500	30	110	2,753	10	220	2,143	10	323
4,886	10	112	2,726	20	304	2,119	20	316
4,766	5	200	2,567	20	312	2,082	<5	410
4,635	20	104	2,525	50	216	2,024	10	324
3,812	40	114	2,443	5	224	1,938	10	414
3,548	10	204	2,366	5	314	1,908	10	500
3,411	30	212	2,313	<5	208	1,874	<5	318
3,178	10	300	2,189	<5	320	1,830	<5	2110

$C_3A\cdot 3Ca(OH)_2\cdot 33H_2O$ (hexagonal)

d(Å)	I/I_o	hkl	d(Å)	I/I_o	hkl	d(Å)	I/I_o	hkl
9,45	100	100	2,972	5	116	2,317	<5	208
5,453	20	110	2,724	10	220	2,161	20	226
4,852	10	112	2,708	20	304	2,122	5	322
4,633	10	104	2,620	<5	310	2,106	10	316
3,806	20	114	2,542	10	312	2,006	<5	324
3,531	10	204	2,515	40	216	1,887	5	500
3,386	20	212	2,425	<5	224	1,827	5	2110
3,144	<5	300	2,349	<5	314			

The authors are indebted to Dr. K. Damm and Dr. J. Bartsch, ARDEX-Chemie, for many helpful discussions and for material support. We would also gratefully acknowledge the financial support of the Deutsche Forschungsgemeinschaft.

REFERENCES

(1) Venuat,M. (1972): Zusammensetzung und Wirkungsweise von Betonzusatzmitteln.- Betonwerk und Fertigteiltechnik 38, 571-580.

(2) Lieber,W. (1973): Wirkung anorganischer Zusätze auf das Erstarren und Erhärten von Zementen.- Zement-Kalk-Gips,75-79.

(3) Uchikawa,H. and Uchida,S. (1977): Influence of boric acid on hydration of ultra rapid hardening cement.- J.Res. Onoda Cem.Comp. Tokyo, 29, 43-51.

(4) Joisel,A. (1967): Activite chimique des adjuvants: accelerateurs et retardeurs.- Int.Symp. on Admixtures for Mortar and Concrete, Topic II, Bruxelles.

(5) Lieber,W. and Richartz,W. (1972): Einfluß von Triäthanolamin, Zucker und Borsäure auf das Erstarren und Erhärten von Zementen.- Zement-Kalk-Gips, 403-409.

(6) Auslegeschrift 2408412, Deutsches Patentamt 1977.

(7) Offenlegungsschrift 1771911, Deutsches Patenamt 1972.

(8) Kuzel,H.-J and Kiehne,H. (1969): Ein einfacher Heizaufsatz für Pulverdiffraktometer bis 800°C.- N.Jb.Miner. Mh., 235-239.

(9) Taylor,H.F.W. (1973): Crystal structures of some double hydroxide minerals.- Min.Mag. 39, 377-389.

(10) Allmann,R. (1977): Refinement of the hybrid layer structure $[Ca_2Al(OH)_6]^+ \cdot [1/2SO_4 \cdot 3H_2O]^-$.- N.Jb.Miner.Mh., 136-143.

(11) Kuzel,H.-J. (1968): X-ray investigation of some complex calcium aluminate hydrates and related compounds.- Proc.V. Int.Symp.Chem.Cem., Tokyo,II-19,92-97.

(12) Houtepen,C.J.M. and Stein,H.N. (1976): An IR investigation on some calcium aluminate hydrates, $CA_2Al(OH)_6^+X^- \cdot yH_2O$ ($=3CaO \cdot Al_2O_3 \cdot CaX_2 \cdot nH_2O$, X^-=univalent anion).- Spectrochim.Acta 32A,1409-1414.

(13) Volant,H. (1968): Etude par spectrometrie infrarouge d'aluminates de calcium hydrates.- Rev.Mater.Constr. 623-634, 191-197,257-272,313-322,432-450.

(14) Fischer,R. and Kuzel,H.-J. (1982): Reinvestigation of the system $C_4A \cdot nH_2O$-$C_4A \cdot CO_2 \cdot nH_2O$.- Cement and Concrete Res. 12, 517-526.

(15) Carlson,E.T. and Berman,H.A. (1060): Some observations on the calcium aluminate carbonate hydrates.- J.Res.NBS 64A, 333-341.

(16) Flint,E.P. and Wells,L.S. (1944): Analogy of hydrated calcium silicoaluminates and hexacalcium aluminate to hydrated calcium sulphoaluminate.- J.Res. NBS 33, 471-478.

V. MLAKAR Cementarna Trbovlje, Yugoslavia

THE ROLE OF KINETIC PARAMETERS ON THE PROPERTIES OF HYDRATING CEMENT PASTE

SUMMARY : Calculated were the rate constants for the characteristic processes of hydration: nucleation and growth of hydration products, phase-boundary,interaction, and diffusion through growing hydration layer on a group of commercial cements and synthetic cement by adding alkali sulfates. The constants were obtained on the basis of kinetic study of alite hydration of these samples, using the method of kinetic parameter determination taking into account the α-t dependence and polydispersity of the examined systems.
Distribution of the characteristic processes, depending on percentage of particles, which at determined stage of alite hydration react after one of these processes is in correlation with the kinetic constant values and with mechanical properties, especially with the cement paste compressive strength.

It is supposed that for normal strenght development with time, the rate constants for each reaction must be within very close optimal limits.

Foram calculadas as constantes de velocidade para os processos característicos de hidratação: nucleação e crescimento de produtos de hidratação, interação, fase-contorno e difusão através da camada crescente de hidratação, num grupo de cimentos comerciais e de cimento sintético, por adição de sulfatos alcalinos. As constantes foram obtidas com base em estudo da cinética de hidratação da alita destas amostras, usando o método de determinação do parâmetro cinético, levando-se em conta a dependência α-t e a polidispersividade dos sistemas examinados.

A distribuição dos processos característicos, dependente da procentagem de partículas, que em determinado estágio de hidratação da alita reagem após um destes processos, está correlacionada com valores de constante cinética e com propriedades mecânicas, especialmente com a resistência à compressão da pasta de cimento.

Supõe-se que para desenvolvimento normal da resistência com o tempo, as constantes de velocidade para cada reação devem ficar dentro de limites ótimos muito estreitos.

V. MLAKAR, Cementarna Trbovlje, Yugoslavia

INTRODUCTION

The kinetic hydration study, i.e. calculated kinetic constants for the characteristic processes: nucleation and growth of hydration products,phase-boundary interaction and diffusion through the growing hydration layer, is very important for examining the development of mechanical properties of hydrated cement paste. A big problem are the so-called inverse correlations of compressive strenghts which were found on a great number of daily production cement samples. Correlation between parameters acting on the development of cement compressive strenghts (chemical,phase, and granulometric compositions) and the tested compressive strenghts often do not exist,which causes certain dilemmas regarding the technical process control.

EXPERIMENTAL DATA

The mean phase and chemical chemical characteristics of the examined cements (marked T-I...T-6) are given in Table I. T-4 cement was a synthetic one, prepared by adding 1% K_3NS_4($3K_2SO_4$. Na_2SO_4) to T-3 cement. Phase composition was determined by X-ray diffraction. Content of total and soluble alkalies and sulfates in clinkers, is illustrated in Table II. Particle size distribution for the samples T-1,T-2,T-3 determined with Sartorius sedimental weight is given in Fig.1 and for the T-5 and T-6 specimens, by the Coulter-Counter method, in Fig.2. In Table III shows the specific surface and the mechanical strenghts of cement samples.

All cement specimens were paste-hydrated at 0,5 water-to-solid ratio at 20°C. After different ages the specimens were ground, washed with acetone, dried in vacuum for 1 hour and hermetically closed in plastic bags. To determine the degree of alite hydration the method of internal standard was used. The degree of hydration in time "t" was determined from the ratio of analitical diffraction's, the maximum intensity of alite hydrated cement, and the original unhydrated specimen (d_A= 1,76 Å).

RESULTS AND DISCUSSION

Table IV shows the degrees of alite hydration for different ages of examined cement samples. Rate constants of alite hydration of the specimens were calculated by the method developed by A. Bezjak and I.Jelenić presented at the 7th International Congress on the Chemistry of Cement (Paris,1980). The results are given in Table V for all time intervals (marked I,II,III) together with the compressive strenghts of cements tested.

The calculated rate constants for a group of cements, differing in the contents of alite,C_3A, readily soluble alkalies,sulfates,particle size distribution vary from sample to sample an the differences in the decrease of diffusion constants vary from interval to interval. The specimen of T-2 cement which has the highest degree of hydration (69%) after 24 hours, has the highest kinetic constants in all three processes and in all three time intervals. Likewise, the T-3 specimen which after 24 hours has the lowest degree of alite hydration (37%) shows the lowest kinetic constants for the phase-boundary interaction and diffusion processes. Diffusion constants are the lowest of all time intervals.Among all tested cements T-3 specimen has the lowest content of C_3A, of total and readily soluble alkalies and sulfates, and the lowest particle size fraction under 5 μm. In contrast the T-2 specimen has the highest content of total and readily soluble sulfates and a very high C_3A/C_3S ratio. The value of kinetic constants influences the distribution of

V.MLAKAR, Cementarna Trbovlje, Yugoslavia

kinetic processes in dependence on the amount of hydrated particles. This can easily be seen from Fig.3, showing the Q - α dependence of kinetic processes in specimens with low (T-3) and high (T-2) kinetic constants.

The early beginning of slow diffusion causes formation of good quality gel and good final strength , but early strength are low. The development of compressive strength of the T-3 specimen is in agreement with this conclusion.

Later beginning and slower development of diffusion i.e. longer phase-boundary interaction and nucleation and growth processes for a certain percentage of particles result in higher early strength , while the 28 day strength are at the low required limit; this is reflected in compressive strength development of the T-2 specimen.

In normal strength development the nucleation and growth process couldn't exist at a higher degree of hydration of a certain percentage of particles. As can be seen from Fig.4 in case of T-5 specimen, there remain 25 % of particles after the nucleation and growth process at 80% hydration, whereas diffusion occurs at a higher degree of hydration and develops slowlier. The reason is the low rate constant of the nucleation and growth process, the high rate constant of the diffusion process in the first time interval and the great difference (the greatest in all the examined specimens) between diffusion rate constants in the first and the second time interval. Because of such distribution of processes the final strength are low, and the early strength higher.

Fig.4 shows that the difference in distribution of processes between the specimens T-3 and T-5 is really a drastic one, this being in correlation with the compressive strenght development of these cements.

While the T-3 cement has the highest 28-day compressive strenght of all specimens examined, the 28-day compressive strenght of the T-5 cement is under the required value. At the lowest value of readily soluble alkalies and sulfates and C_3A content the T-3 cement has the lowest content of the finest fraction (6% of particles are under 5 μm). In contrast, the content of readily soluble alkalies and C_3A are much higher in the T-5 specimen, which contains three times as many finest particles (under 5μm) as the T-3 specimen.

Consequently it is easy to understand that in the T-3 specimen diffusion occurs at low degree of hydration. The particles of this cement are coarser (the average particle diameter is 27μm) and in case of high percentage of the finest particles of the T-5 specimen (the average particle diameter is 18μm) the nucleation and growth mechanism lasted too long for a certain percentage of cement particles, so the final strenghts cannot be good enough. It is obvious that also in the particle size distribution there is a certain optimum to achieve a desired compressive strenght development.

It can be assumed that the distribution of processe for the Q- α dependence is in correlation with the development of mechanical properties.

Fig.5 shows the distribution of kinetic processes of T-3 and T-6 cements, which have low early and good final strenghts. The similarity of curves is obvious.

An interesting thing is that the cements with similar strenght development and distribution of kinetic processes have similar constant ratios for each kinetic process and vice versa. This can be seen from Table VI, which shows two examples of cement pairs T-3— T-6 and T-3—T-5. The compressive strength of the compared specimens are also shown. One-day compressive strengths cannot be predicted on the basis of the values of rate constants of the nucleation and growth and phase-boun-

dary interaction. By examining the diffusion constants at all time intervals the correlation with 28-day compressive strenghts was obtained.

Fig.6 presenting the rate constants of diffusion depending on hydration time at different time intervals, shows the lines of different coefficients of tendency.A lower 28-days compressive strength is accompanied by greater change in the coefficient of tendency.

It is obvious that changes in kinetic parameters for each process in C_3S hydration are in correlation with mechanical properties of cement pastes.

Table I

Phase and Chemical Characteristies Cement Samples

	T-1	T-2	T-3	T-4	T-5	T-6
% C_3S	66	47	62	62	47	68
% C_3A	5	5	2	2	7	6
C_3A/C_3S	0,075	0,106	0,032	0,032	0,148	0,088
% SO_3	2,050	3,091	1,056	2,050	3,028	3,030
SO_3/C_3S	0,037	0,083	0,025	0,040	0,070	0,049
% Na_2O	0,042	0,037	0,034	0,037	0,032	0,028
% K_2O	0,065	0,062	0,039	0,074	0,056	0,048

Table II

Total and Readily Soluble Alkalies and Sulfates (%) of Clinker Samples

Sample	SO_3	Na_2O	K_2O
T_K - 1	1,44	0,45	0,76
	0,80x	0,30x	0,60x
T_K - 2	1,93	0,39	0,56
	0,86x	0,22x	0,42x
T_K - 3	0,75	0,34	0,33
	0,48x	0,14x	0,25x
T_K - 5	1,05	0,30	0,70
	0,69x	0,14x	0,58x
T_K - 6	1,06	0,34	0,57
	0,71x	0,14x	0,52x

x readily soluble

Table III

Specific Surface and Mechanical Strengths of Cements

	T-1	T-2	T-3	T-5	T-6
Spec.surf. (cm^2/g)	4717	4443	4298	4374	4468
Strength (MPa)					
tensile/compressive					
1 day	6,32/31,4	5,35/26,3	2,83/12,2	4,23/19,4	3,47/17,4
3 days	6,78/43,5	6,68/43,8	5,60/29,2	5,53/32,7	6,32/38,2
28 days	7,93/50,5	8,49/51,6	8,30/65,1	7,58/48,4	7,54/53,2

REFERENCES

1. A Bezjak, I. Jelenić, Cem.Concr.Res.10,553 (1980)
2. I.Jelenić-Bezjak Kinetics of Hydration of Cement Phases, Advances in Cement Technology, S.N.Ghosh, ed. (Pergamon Press, 1983)
3. A. Bezjak,Cem.Concr.Res.13,305 (1983)
4. J.H.Taplin, 5th ICCC, Tokyo, II,249(1969)
5. J.H.Taplin, 5th ICCC,Tokyo, II,337(1969)
6. T.Knudsen, 7th ICCC,Paris,II-I,170(1980)
7. J.Alexander,Cem.Concr.Res.,2,663 (1972)
8. S.Popovics, ibid 6,343 (1976)
9. J.Jambor, Proceedings of a Conference held at University of Sheffield (1976)
10. I.Jelenić,A.Panović,A.Bezjak, Cem.Concr. Res.10,463 (1980)
11. A.Bezjak,I.Jelenić,V.Mlakar,A.Panović, 7th ICCC, Paris, II-I,III (1980).

Table IV

Degree of Alite Hydration

Time (h)	Sample T-1	T-2	T-3	T-4	T-5	T-6
4	12	10		10	6	6
5	13	13				
6	14	18	4	13	8	10
7	16	24				
8	18	31	7	16	12,5	17,0
9	21	37				
10	24	42	12	20	17,5	25,0
11	28	47				
12	33	51	19	24	22,5	31,5
13	36	54				
14	39	57	24	29	28,5	37,0
15	42	59				
16	44	62	28	33	35,0	40,5
17	47	64				
18	49	65	32	38	41,5	46,0
19	51	66				
20	52	67	35	44	47,0	48,5
22	55	68				
24	57	69	37	53	54,0	54,0
32	64	72	42	56	60,5	60,5
40	69	74	45	59	65,5	65,0
48	73	77	49	61	69,5	68,0
56	75	79	52	62	73,0	71,0
64	77	81	54	63	76,0	73,5
72	78	82	55	65	77,5	75,5

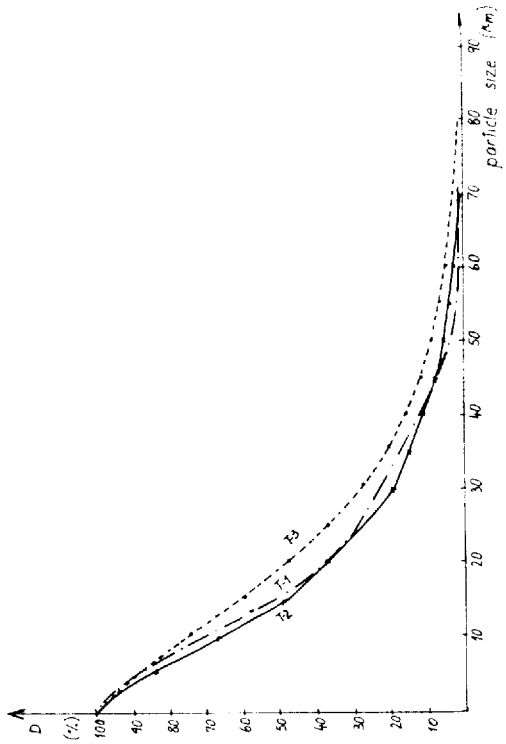

Fig. 1
Particle Size Distribution in the Samples of Cement T-2, T-3, T-4

Table V

Rate Constants for Alite Hydration in Cement Pastes

Interval		T-1	T-2	T-3	T-4	T-5	T-6
I	$k_1(h^{-1})$	0,051	0,070	0,055	0,023	0,037	0,060
	$k_2(umh^{-1})$	0,110	0,128	0,067	0,114	0,091	0,110
	$k_3(um^2h^{-1})$	0,200	0,345	0,083	0,364	0,327	0,180
II	k_3	0,143	0,207	0,059	0,179	0,130	0,106
III	k_3	0,039	0,073	0,040	0,054	0,008	-
1	(MPa)	41,4	26,3	12,2		19,4	19,4
28		50,5	51,6	65,1		48,4	53,2

Table VI

Ratios of Rate Constants for Pairs of Cement Samples

$$\frac{K_{11}^{T-3}}{K_{11}^{T-6}} = 0,91 \qquad \frac{K_{11}^{T-3}}{K_{11}^{T-5}} = 1,48$$

$$\frac{K_{21}^{T-3}}{K_{21}^{T-6}} = 0,61 \qquad \frac{K_{21}^{T-3}}{K_{21}^{T-5}} = 0,74$$

$$\frac{K_{31}^{T-3}}{K_{31}^{T-6}} = 0,46 \qquad \frac{K_{31}^{T-3}}{K_{31}^{T-5}} = 0,25$$

$$\frac{K_{32}^{T-3}}{K_{32}^{T-6}} = 0,56 \qquad \frac{K_{32}^{T-3}}{K_{32}^{T-5}} = 0,45$$

$$\frac{K_{33}^{T-3}}{K_{33}^{T-5}} = 0,41$$

T-6	T-3	T-5
σ'_1=17,4	σ'_1=12,2	σ'_1=19,4(MPa)
σ'_{28}=53,2	σ'_{28}=65,1	σ'_{28}=48,4(MPa)

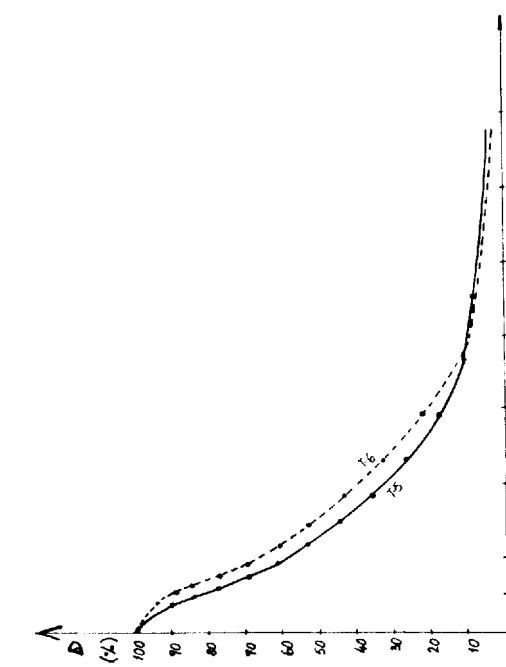

Fig. 2
Particle Size Distribution in the Samples of Cement T-5, T-6

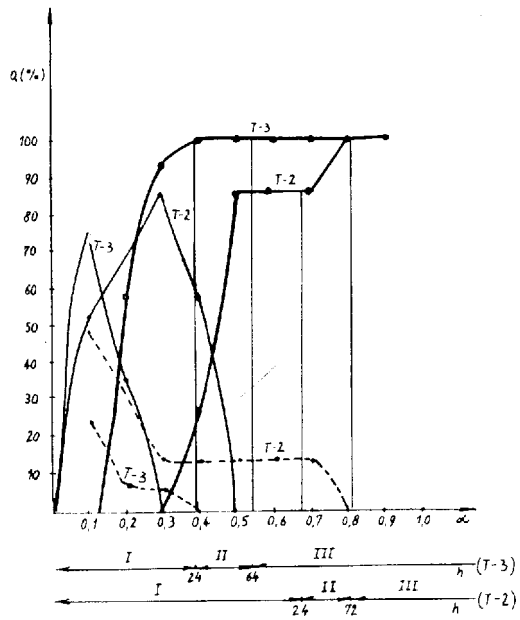

Fig. 3

Percentages of particles (Q) samples T-3, T-2 that react according to the nucleation and growth process (dotted line) phase-boundary interaction process (thin line) and diffusion process (full line) at various α.

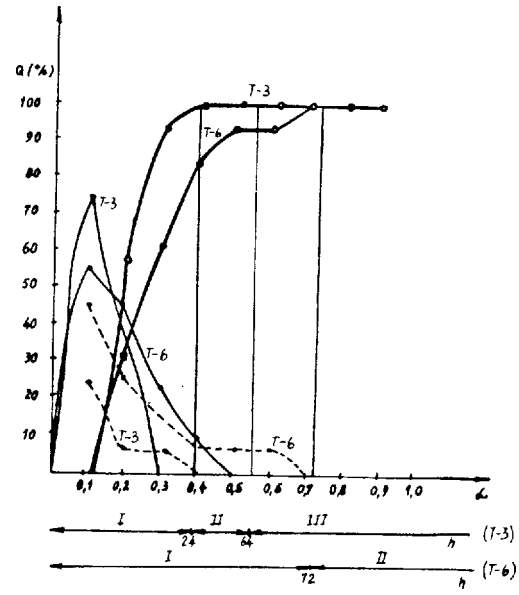

Fig. 5

Percentages of particles (Q) samples T-3, T-6 that react according to the nucleation and gorwth process (dotted line) phase-boundary interaction process (thin line) and diffusion process (full line) at various α.

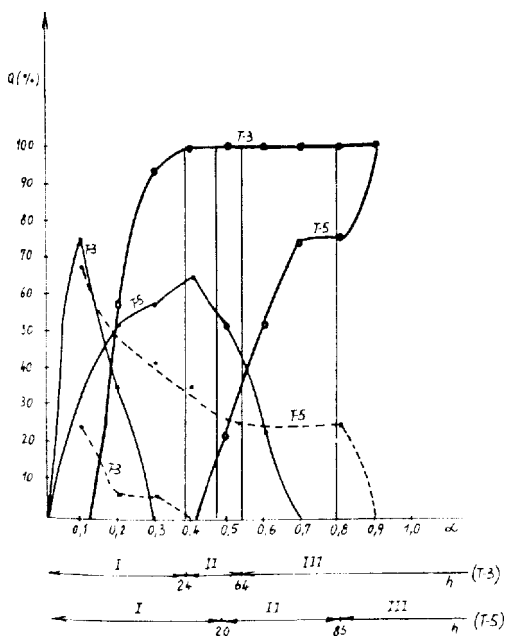

Fig. 4

Percentages of particles (Q) samples T-5, T-3 that react according to the nucleation and growth process (dotted line) phase-boundary interaction process (thin line) and diffusion process (full line) at various α.

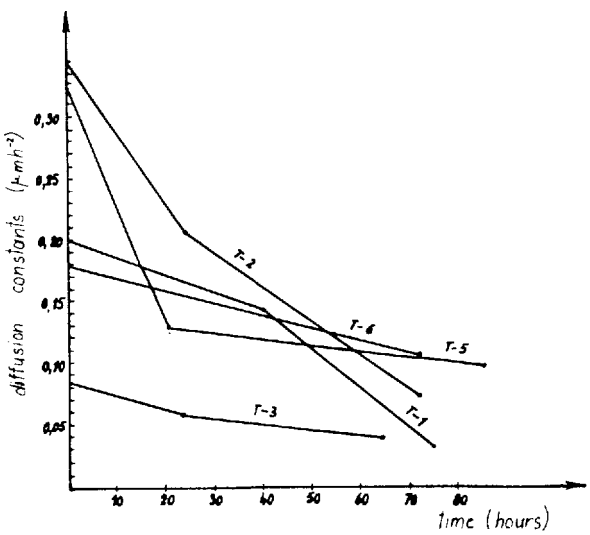

Fig. 6

Diffusion constants depending on transition time of the hydration rate

SUB-THEME/SOUS-THÈME 2.2

Microstructure of hardened cement paste and its effects on its behaviour.

Microstructure de la pâte de ciment hydraté et ses effets dans son comportement.

Chairman/Président:

P. K. Mehta
Civil Engineering Department
University of California, Berkeley
Berkeley, CA, U.S.A.

Principal Reporter/Rapporteur Principal:

S. Diamond
School of Civil Engineering
Purdue University
West Lafayette, IN, U.S.A.

Y.TEZUKA, Inst. Pesquisas Tecnológicas S. Paulo, Brasil; J.G. DJANIKIAN, Serrana S.A. de Mineração, Brasil; H. UCHIKAWA, Onoda Cement Co, Ltd, Japan and S.UCHIDA, Onoda Cement Co, Ltd, Japan.

1

Hydration Characteristics and Properties of Mixtres of Cement and High Content of Calcium Sulfate

2.2

Caractéristique de l'Hydratation et Proprieté du Mélange de Ciment avec Haut Teneur de Sulfate de Calcium

SUMMARY: Mixtures of calcium sulfate and cement are used as a low-cost building material such as for walls and panels. However, when various kinds of calcium sulfates and admixtures were used, troublès often occur in such properties as setting time, development of expansion.

To take effective action for these unfavourable problems, it is the most important occurately to grasp the basic hydration characteristics of these mixtures.

In this paper, influence of kind of cement and calcium sulfate on hydration of the mixtures with and without various admixtures was studied by measuring heat evolution rate, amount of combined water and hydrates formed and cappilary space, and by observing the texture in hardened paste, and then relationship between the results obtained and the properties was discussed.

Sumário

Misturas de sulfato de cálcio e cimento são usadas como materiais de construção de baixo custo para paredes e painéis. Entretanto, vários tipos de sulfato de cálcio e adições são usados, às vezes ocorrem problemas em algumas propriedades como tempo de pega e ocorrência de expansão.

Para tomar medidas efetivas para esses problemas desfavoráveis, é da maior importância conhecer com precisão as características básicas da hidratação dessas misturas.

Neste trabalho, a influência da espécie do cimento e do sulfato de cálcio na hidratação das misturas com ou sem várias adições foi estudada pela medida variação do calor desprendido, quantidade de água combinada e hidratos formados e espaço capilar, e pela observação da testura da pasta hidratada, e então as relações entre os resultados obtidos e as propriedades foram discutidas.

Y.TEZUKA, Inst. Pesquisas Tecnológicas S.Paulo, Brasil; J.G.DJANIKIAN, Serrana S.A. de Mineração, Brasil; H.UCHIKAWA, Onoda Cement Co, Ltd, Japan and S.UCHIDA, Onoda Cement Co, Ltd, Japan.

Hydration Characteristics and Properties of Mixtures of Cement and High Content of Calcium Sulfate

Caractéristique de l'Hydratation et Proprieté du Mélange de Ciment avec Haut Teneur de Sulfate de Calcium

1. Sample and Experimental Procedure

The chemical composition of ordinary portland cement (OPC) and pozzolanic cement (POZ), natural gypsum (GYP) α-hemihydrate (aH), β-hemihydrate (bH) of calcium sulfate and anhydrite (AN), their specific gravity, blaine and BET specific surface area are showed on Table 1. The mineralogical composition of OPC calculated as C_3S, C_2S, C_3A and C_4AF is 56%, 13%, 9% and 11%, respectively while POZ contains 20% pozzolan.

Table 1-Chemical Composition, Specific Surface Area and Specific Gravity of Samples Used

sample	ig.loss	insol	SiO_2	Al_2O_3	Fe_2O_3	CaO	MgO	SO_3	Na_2O	K_2O	P_2O_5	Total	Blaine (cm^2/g)	BET(m^2/g)	Specific gravity
OPC	1.7	0.4	19.6	5.3	3.8	59.0	4.3	3.5	0.2	0.6	1.0	99.4	3450	1.08	3.14
POZ	3.9	20.6	13.5	3.7	3.8	45.7	4.0	2.7	0.1	0.6	0.8	99.4	4260	1.41	2.97
GYP	20.9		0.8			32.3		46.0				100.0	2500	0.91	2.34
aH	6.6		0			37.8		55.5				99.9	1330	0.32	2.74
bH	3.4		1.0			39.3		55.9				99.6	7960	6.47	2.54
AN	0.5		6.5			47.8		41.3				96.1	5900	1.36	3.00

OPC- ordinary portland cement GYP- natural gypsum bH-β hemihydrate
POZ- pozzolanic cement aH -α hemihydrate AN- anhydrite

Hydrated samples were prepared by the mixing ratio showed in Table 2.
Each sample was mixed with water solid ratio of 0.50 at 20ºC, and after being cured for 1, 3, 28, 91 days, its hydration was stopped by immersion in acetone.Part of the hydrated samples were dried under the condition of 11% relative humidity and used for measurement of the amount of $Ca(OH)_2$ and ettringite by DSC, the other samples were used for other purposes after D-drying.

Table 2-Samples Mixing Proportion

	proportion (weight %)		
cement (OPC, POZ)	30	50	70
calcium sulfate (GYP, aH, bH, AN)	70	50	30

The retarder (tartaric acid), accelerator(K_2SO_4) and additive A (expansion regulator - solution having PVA) was added 0.05% for hemihydrate content in the mixture, 1.5% for AN mixture and 37.5% for calcium sulfate content, respectively.
Heat evolution rate was measured by conduction calorimeter. The amount of combined water was calculated from the ignition loss at 800ºC of the unhydrate sample and that of each hydrated sampe D- dried.
Identification and quantitative analysis of hydrates produced were measured by powder X-ray difraction.
The amount of ettringite and $Ca(OH)_2$ produced were determined by DSC.
The cappilary space of which diameter is 30 Å or more and its pore size distribution were measured by mercury penetration porosimeter. The texture and Morphology of hydrate in the hardened paste was observed under SEM (JECL, JSM-T300).The setting time and compressive strenght were measured by French method AFNORNF B12-401, and the change in length according to ASTM C 452.

2. Heat Evolution Rate

The Fig. 1 shows the heat evolution curve of OPC, POZ and various calcium sulfate-cement mixtures. The first peak immediately after mixed with water is caused, by formation of ettringite by hydration of the interstitial phase such as C_3A and C_4AF and the second by vivid hydration of alite.

From these results, it seems that the calcium sulfate hemihydrate is hydrated actively immediately after mixed with water, bH being higher than aH in hydration rate. With the addition of 0,05% of retarder, the active hydration is retarded by about 5 to 10 minutes for bH and about an hour for aH. These are considered to depend upon to the difference in their specific surface area and polymorphism. In the case of AN, its hydration is promoted by addition of K_2SO_4, and the active hydration thereof coincides in timing with vivid hydration of alite in cement.
When each kind of calcium sulfate was added, in particular, the induction period of the alite in the cement is shortened. The effect was larger on the sequence of bH, aH, GYP and AN. Uchikawa, Uchida,Ogawa and Hanehara (1) reported that the earlier the maximum of peak of $Ca(OH)_2$ saturation ratio in the liquid phase of paste appeared, the more the induction period of hydration of alite was shortened. The above mentioned difference in the effect of promoting hydration among different kinds of calcium sulfate is considered to be caused by the dissolution rate of calcium sulfate, so that the higher the dissolution rate, the earlier the $Ca(OH)_2$ saturation ratio in the liquid phase of paste attains maxium value, shortening the induction period of alite. Uchikawa, Uchida and Okamura (2) studied on the influence of characters of blending component on the hydration of ordinary portland cement and showed that the active hydration of alite corresponding to the second

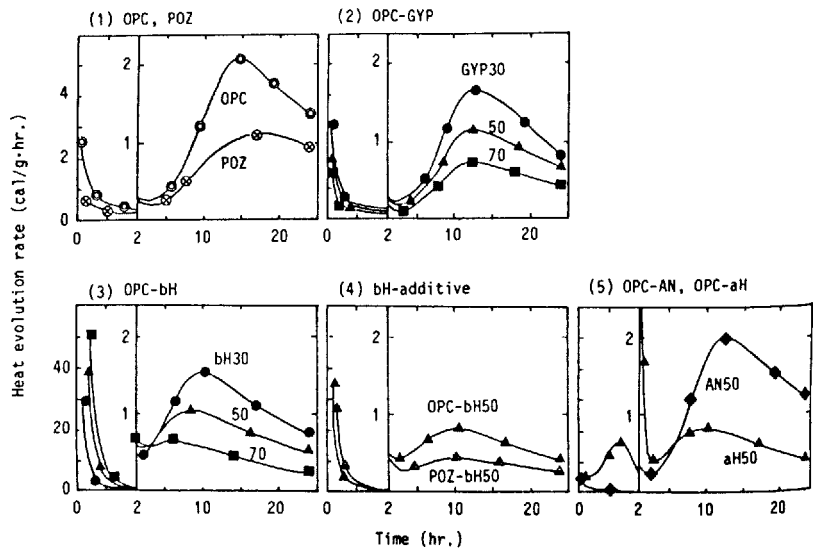

FIG. 1 Heat evolution curve of calcium sulfate and cement mixture

Y.TEZUKA, Inst. Pesquisas Tecnológicas S.Paulo, Brasil; J.G.DJANIKIAN, Serrana S.A. de Mineração, Brasil; H.UCHIKAWA, Onoda Cement Co, Ltd, Japan and S.UCHIDA, Onoda Cement Co, Ltd, Japan.

Hydration Charateristics and Porperties of Mixtures of Cement and High Content of Calcium Sulfate

Caractéristique de l'Hydratation et Proprieté du Mélange de Ciment avec Haut Teneur de Sulfate de Calcium

peak was increase of the specific area of the blending component. The calcium sulfate effect on the active hydration of alite is thought to become larger with the increase in it's specific surface area at accelerator period.

3. Hydration Product

A part of powder X-ray Diffraction pattern of each hydrated sample is showed in Fig. 2.
With OPC, the hydrates detected by powder X-ray diffraction were ettringite, monosulfate hydrate and calcium hydroxide. The calcium hydroxide increased with age. With GYP mixture, no monosulfate detected, and ettringite increased with age. On bH mixture, the calcium sulfate dihydrate appeared before one day and increased little after this age. With AN mixture, calcium sulfate dihydrate produced increased with age, but even at the age of 28 days, there remained AN still not hydrated.
Regarding to XRD chart, the following features were recognized. With OPC, the intensity of the diffraction peak was almost the same on (0001) reflection and (10.1) reflection of $Ca(OH)_2$, whereas with the mixing of calcium sulfate, the intensity at (0001) reflection became remarkably great, regardless the kind of calcium sulfate. This shows the orientation of calcium hydroxide, making us estimate that the growth along c axis is smaller than along a axis. According to Berger and Mc Gregor (3) who studied the morphology of calcium hydroxide produced by the hydration of C_3S, the growth along c axis and a axis was different with the kind of additive, and four groups of (I) c/a = 0.5, (II) c/a= 0.5 to 1.5, (III) c/a = 1.5, (IV) irregular, were classified. The result mentioned above corresponds to Group (I), from which it is concluded that the calcium hydroxide formed in the mixture of calcium sulfate and cement has morphology of Group (I).
As for calcium sulfate dihydrate the (020) reflection intensity was very great for GYP mixture, so that intensity ($\bar{2}20$) and ($\bar{2}40$) reflections were about one - third as that of (020) reflection and the intensity of ($\bar{2}02$,022) reflection was comparatively smaller with calcium sulfate dihydrate formed by hydration of AN, aH or bH, on the other hand, the intensity of ($\bar{2}02$) and ($\bar{2}40$) reflections were almost the same as that of (020) reflection, the intensity of ($\bar{2}02$,022) reflection being comparatively larger, indicating that these crystal faces are well developed.

4. Amount of Ettringte and Calcium Hydroxide Formed

Fig. 3 shows the relationship between the amount of various calcium sulfates mixed and the amount of ettringite and $Ca(OH)_2$ at each age.

With OPC alone, the amount of ettringite produced was 5.6% at one day, decreasing slowly by formation of monosulfate hydrate at 3 days or more. When calcium sulfate was mixed, however, the existence of the sufficient amount of SO_3 regardless of the kind of calcium sulfate prevented monosulfate hydrate from being formed, and the amount of ettringite formed changed with the kind and the amount of calcium sulfate mixed.
With bH mixture, more ettringite was formed than in the case of GYP mixture at each age. The amount of ettringite formed in aH mixture at an early age was small, followed by rapid increase at the age of 3 days or more, exceeding the amount for bH mixture at the age of 28 days. In the case of AN mixture, a large amount of ettringite was particulary formed at early age.

On the other hand, the amount of ettringite was largest in the mixture containing 30% of calcium sulfate and decreased with calcium sulfate content increase.

When additive A was used, the amount of ettringite formed increased extremely at early age as shown in the bH mixture, indicating that this additive accelerates the dissolution of alumina from C_3A.
Generally, additives modify the induction period and the hydration of C_3A and C_3S. The additive A used is considered to belong do group (III) (4).
The same trend was observed in the mixture of POZ and calcium sulfate, although more ettringite was generally formed. This is considered that the hydration of interstial phase was accelerated by pozzolan in the pozzolanic cement at early age, while the amount of ettringite formed increased by the reaction of Al_2O_3 contained in pozzolan at later age (5,6).These results show that the amount of ettringite formed in the hardened paste considerably changes with the kind of calcium sulfate. Uchikawa, Uchida, Ogawa and Hanehara (1) studied on the effect of the kind of calcium sulfate on the initial hydration of ordinary portland cement and found that the larger the saturation ratio of $Ca(OH)_2$ and $CaSO_4$ of liquid phase in paste at the time of beginning of ettringite formation, the more closely small ettringite formed on the surface of unhydrated particles, depressing subsequent hydration. The amount of $Ca(OH)_2$ formed for the OPC alone was 6.1, 6.8, 7.8 and 9.7% at 1,3,7 and 28 days respectively.
The dashed line in the drawing indicates the amount of $Ca(OH)_2$ estimated from the amount of calcium sulfate mixed and the amount of $Ca(OH)_2$ for OPC alone.From these results, the early and subsequente hydration of calcium silicate was different with the kind of calcium sulfate. In the case of AN mixture, active hydration of alite and hydration of AN occur at same time, so that the production of calcium sulfate dihydrate appears to reduce the

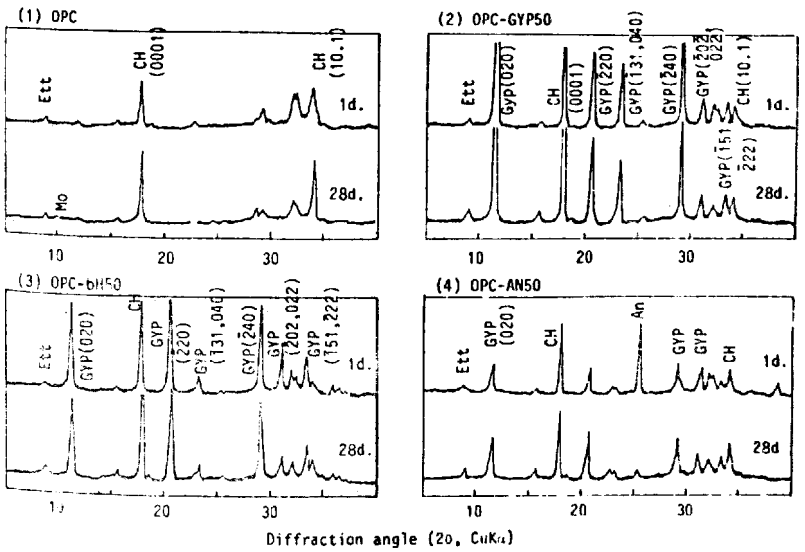

Ett: ettringite, Mo: monosulfate hydrate, GYP: calcium sulfate dihydrate
CH: calcium hydroxide, An: anhydrite

FIG. 2 Powder X-ray pattern of hydrated sample

Y.TEZUKA, Inst. Pesquisas Tecnológicas S.Paulo, Brasil; J.G.DJANIKIAN, Serrana S.A. de Mineração, Brasil; H.UCHIKAWA, Onoda Cement Co, Ltd, Japan and S.UCHIDA, Onoda Cement Co, Ltd, Japan.

Hydration Characteristics and Porperties of Mixtures of Cement and High Content of Calcium Sulfate

Caractéristique de l'Hydratation et Proprieté du Mélange de Ciment avec Haut Teneur de Sulfate de Calcium

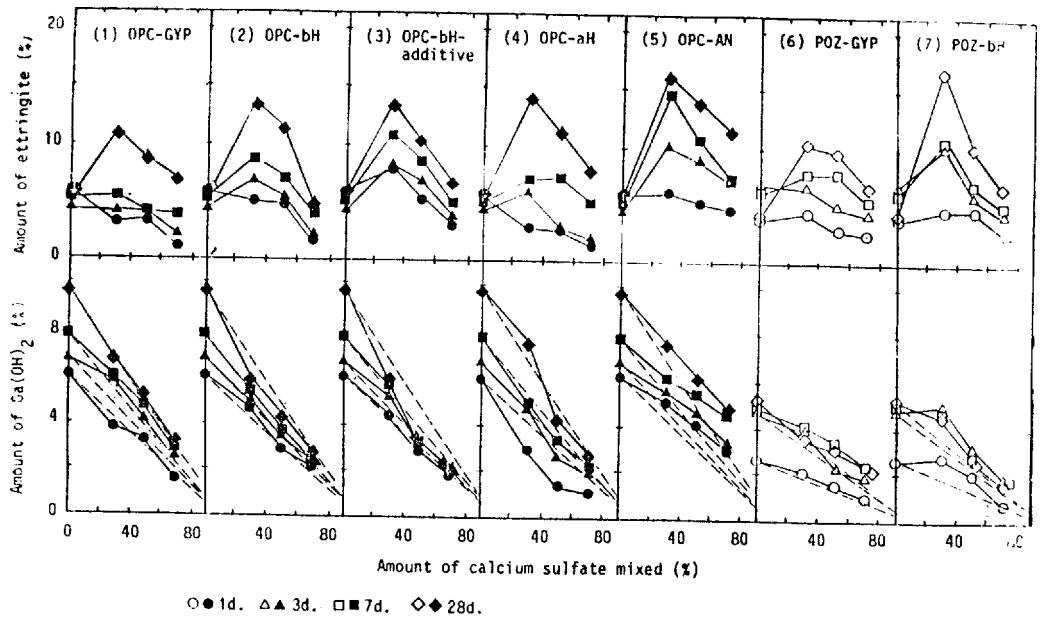

FIG. 3 Amount of ettringite and $Ca(OH)_2$ formed in hardened paste

formation of dense hydrate by hydration of alite.
This trend was reversed in the POZ mixture, considered to be caused by low $Ca(CH)_2$ saturation ratio in liquid phase of the mixture.

5. Change in the Amount of Combined Water

Fig. 4 shows the change in the amount of combined water in various calcium sulfates-OPC mixtures with time. With OPC-GYP mixture, the amount of combined water decreased with the amount of GYP mixed. With bH and aH mixtures, the amount of combined water was very large as compared with GYP mixture. With AN mixture, the amount of combined water at later stage increased more than in the aforementioned two cases, because hydration of AN proceeded after one day. Also, addition of additive A brought increase of the amount of combined water, which well corresponds to the acceleration of initial hydration and subsequent increase in the amount of ettringite formed. A similar result was obtained for the POZ and calcium sulfate mixtures, the amount of combined water, however, was somewhat smaller compared with that in the OPC mixture.

6. Capillary Space and Pore Size Distribution of Hardened Paste

Fig. 5 shows a pore size distribution of OPC and the ratio of capillary space of each mixtures classified into 30 to 60 Å, 60 to 500 Å, 500 Å to 1000 Å and 1000 Å or more in diameter.
The capillary space of OPC alone remarkably decreased with age, accompanying with extreme decrease of pore volume of 1000 Å or more. In comparison, the POZ was associated with a lesser reduction of the capillary space with age. After 28 days, however, the ratio of small pore of 500 Å or less increase with the pozzolanic reaction.
Generally, in the mixture of OPC and calcium sulfate, the capillary space which has ratio of pore of 1000 Å or more in diameter decreased, but the ratio of decrease is smaller than in the case of POZ.
This indicates that the calcium sulfate dihydrate formed by hydration of calcium sulfate makes up a coarse pore structure, leaving large pores over a long period.
Comparison betweem aH and bH mixtures showed no difference in the capilary space, while, the more amount of pore of 1000 Å or more was observed in the aH mixture. This is considered to be caused by smaller specific surface area of aH. The hardened paste of the AN mixture had higher ratio of fine pore than that of aH or bH mixture. This appears to be attributable to the fact that the skeleton structure which is caused by the prodution of calcium sulfate dihydrate is formed simultaneously with hydration of calcium silicate.

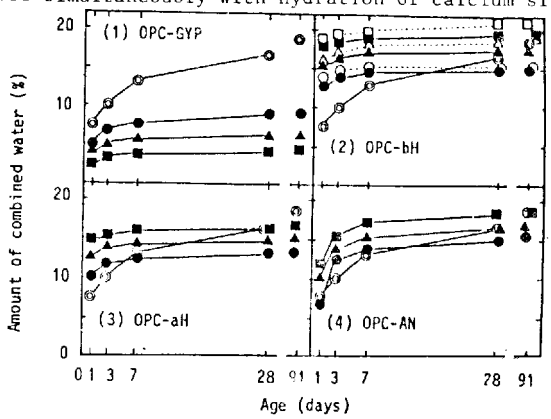

FIG. 4 Amount of combined water in the mixture of calcium sulfate and cement

7. Morphology and Texture of Hydrates in Hardened Paste

Fig. 6 shows scanning electron micrographs of each hardened paste. In the case of GYP mixture, Type I C-S-H (fibrous particle) having 0.1 to 0.2 μm in diameter and 0.5 to 1.0 μm long was formed radially at the age of one day, and part of them was precipitated on the surface of calcium sulfate.

Y.TEZUKA, Inst. Pesquisas Tecnológicas S.Paulo, Brasil; J.G.DJANIKIAN, Serrana S.A. de Mineração, Brasil; H.UCHIKAWA, Onoda Cement Co, Ltd, Japan and S.UCHIDA, Onoda Cement Co, Ltd, Japan.

Hydration Characteristics and Properties of Mixtures of Cement and High Content of Calcium Sulfate

Caractéristique de l'Hydratation et Proprieté du Mélange de Ciment avec Haut Teneur de Sulfate de Calcium

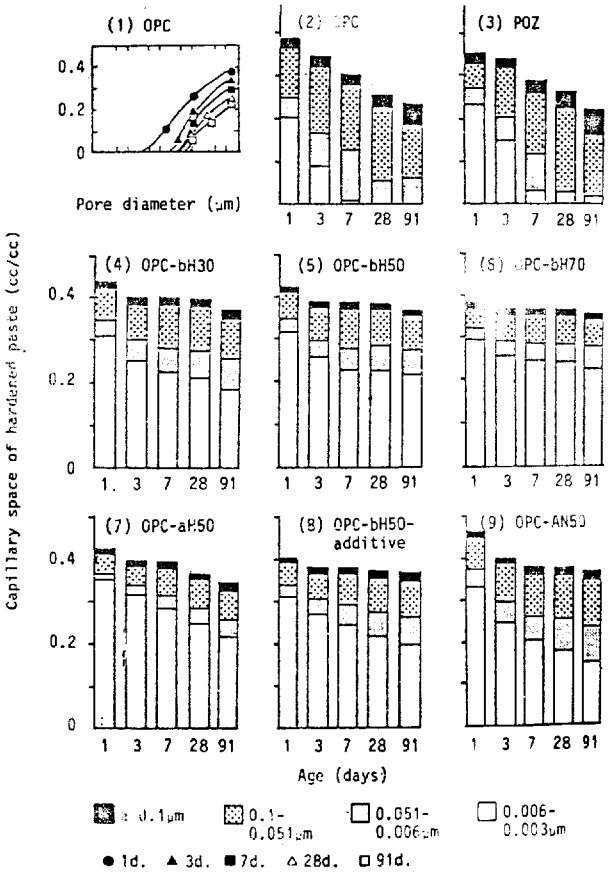

FIG. 5 Capillary space and pore size distribution of hardened paste

The needle-like ettringite grew somewhat greater than C-S-H. At that time, there were seem capillary pore of comparatively large size. The C-S-H grew along the length (c axis) to 0.5 to 2.0 μm at the age of 28 days. Also, the cappilary pore space was embedded with C-S-H containing Type III C-S-H (small equate grain) partially. In the case of bH mixture, the calcium sulfate dihydrate was of the size of about 5 μm in irregular form, while a little C-S-H was precipitated on the surface of the calcium sulfate dihydrate. Type I C-S-H was 0.1 μm in diameter and 0.3 to 0.6 μm long, which was smaller than for the GYP mixture. At the age of 28 days, C-S-H grew to the diameter of 0.1 to 0.2 μm and the length of 0.5 to 2.0 μm filling up the capillary pore spaces. The calcium hydroxide, was of the size of 5 μm and formed a small laminar structure. Part of the calcium sulfate dihydrate grew like prism of 3 μm in thickness and 5 to 10 μm long. The AN mixture developed almost the same texture as calcium sulfate hemihydrate mixture but in a somewhat smaller form of calcium sulfate dihydrate. When additive A was added, the calcium sulfate dihydrate had a small particle size and did not grow much with age.

As explained above, it was observed a difference in the growth of ettringite and calcium sulfate,dihydrate in the texture of hardened paste having different kind of calcium sulfate. The texture in hardened paste containing POZ was similar to that for OPC, with the exception of somewhat larger ettringite grown. These phenomena seem to be attributable to the fact that the low concentration of CaO in liquid phase is maintained as compared with the OPC and calcium sulfate mixture.

8. Setting Time

Fig. 7 shows the setting time of GYP mixture and bH mixture. With OPC-GYP mixture, the initial and final setting time were retarded with the increase in the amount of GYP mixed, because of a small amount of hydrate formed. When additive A was used with this mixture, the initial setting time was accelerated to a abnormal level and the final setting time was retarded very much. These phenomena may be due to acceleration of ettringite formation and delay of active hydration of alite begining.

In the case of POZ-GYP mixture, this trend was almost the same as OPC-GYP misture, except that the final setting time shortened somewhat with the increase in the amount of GYP mixed. Between these two types of mixture, there is a difference in the form of hydrate, indicating that the setting time is affected not only by the amount of hydration but also by the morphology of the hydrate formed.

With OPC-bH mixture with 0.05% of retarder, the initial setting time was considerably delayed as compared with the OPC alone, although tended to accelerate with the increase in the amount of bH mixed. This is considered to be caused by the increase in the amount of free water fixed by hydration of bH. The final setting ocurred earlier than in the case of OPC alone when 30% bH was added, exhibitting the effect of hydration of bH.

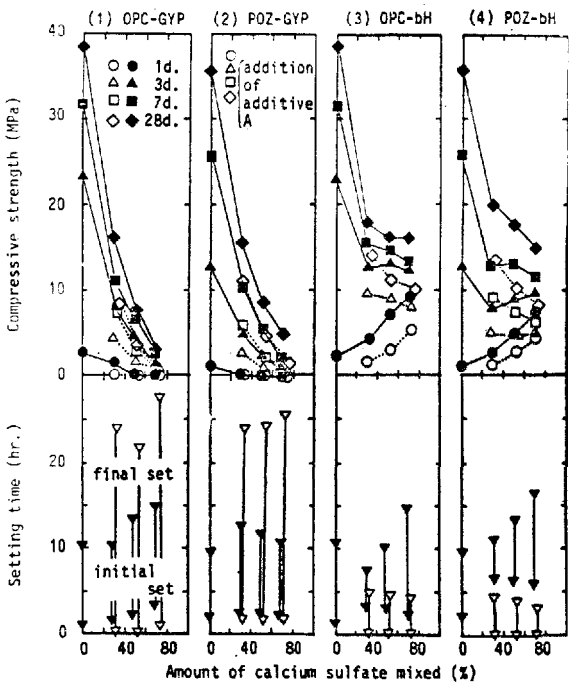

FIG. 7 Setting time and compressive strength of the mixture of calcium sulfate and cement

9. Compressive Strength

Fig. 7 shows the compressive strength of several mixtures. The strength of GYP mixture decreased with the increase in the amount of GYP. The strength of bH mixture, increased up to the age of 3 and 7 days with the increase in the amount of bH. At the 28 days and more, the increase of strength was smaller.

When additive A was added, the strength decreased in

Y.TEZUKA, Inst. Pesquisas Tecnológicas S.Paulo, Brasil; J.G.DJANIKIAN, Serrana S.A. de Mineração, Brasil; H.UCHIKAWA, Onoda Cement Co, Ltd, Japan and S.UCHIDA, Onoda Cement Co, Ltd, Japan.

Hydration Characteristics and Properties of Mixtures of Cement and High Content of Calcium Sulfate

Caractéristique de l'Hydratation et Proprieté du Mélange de Ciment avec Haut Teneur de Sulfate de Calcium

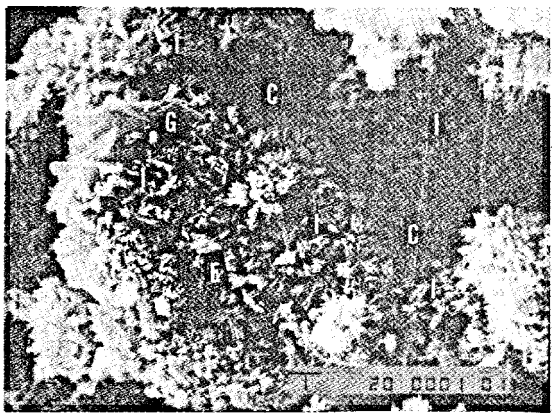

(1) OPC-GYP50 age 1 day

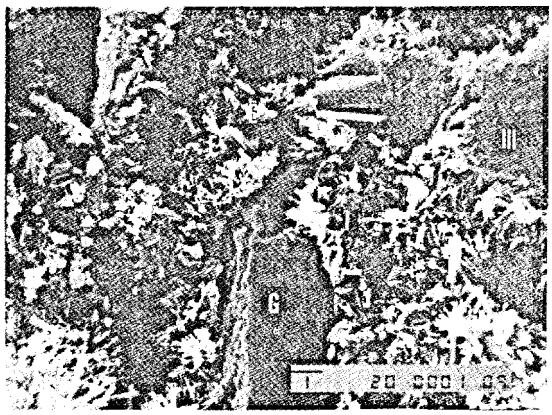

(2) OPC-GYP50 age 28 days

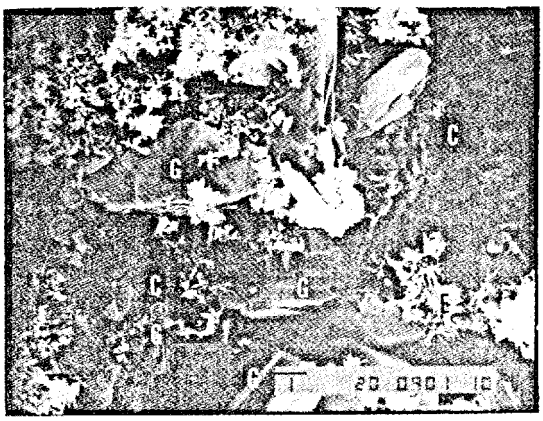

(3) OPC-bH50 age 1 day

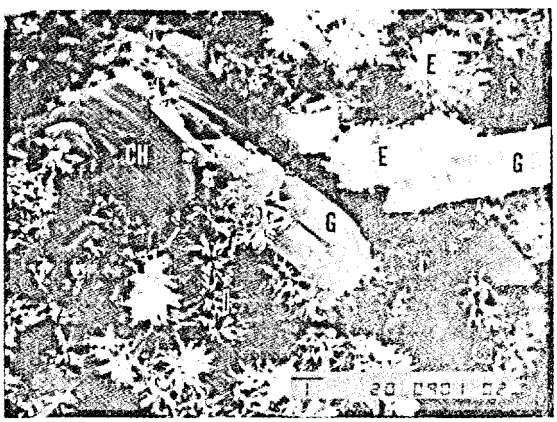

(4) OPC-bH50 age 28 days

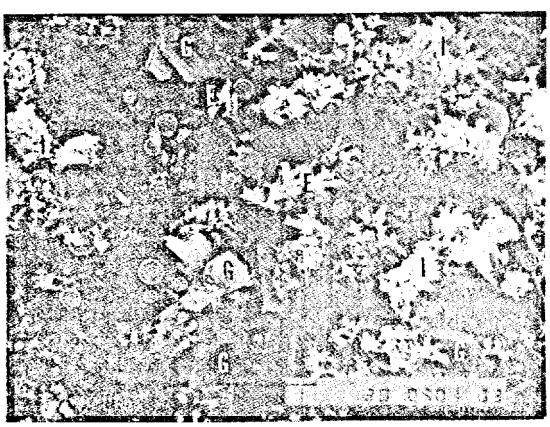

(5) OPC-bH50-additive A age 1 day

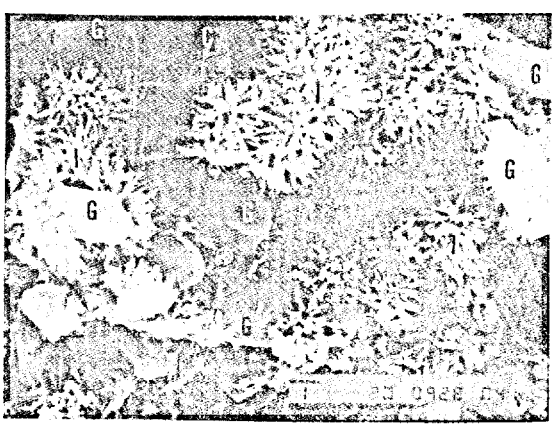

(6) OPC-bH50-additive A age 28 days

E; ettringite, G: calcium sulfate dihydrate, CH: calcium hydroxide
I: Type I C-S-H, III: Type III C-S-H, C: capillary pore

FIG. 6 Scanning electron micrographs of hardened paste

Y.TEZUKA, Inst. Pesquisas Tecnológicas S.Paulo, Brasil; J.G.DJANIKIAN, Serrana S.A. de Mineração, Brasil; H.UCHIKAWA, Onoda Cement Co, Ltd, Japan and S.UCHIDA, Onoda Cement Co, Ltd, Japan.

Hydration Characteristics and Properties of Mixtures of Cement and High Content of Calcium Sulfate

Caractéristique de l'Hydratation et Proprieté du Mélange de Ciment avec Haut Teneur de Sulfate de Calcium

all cases. Low development of strength appears to be related to the extreme acceleration in hydration of calcium sulfate hemihydrate and interstitial phase form a coarse skeleton structure at initial stage, and the delayed hydration of alite prevented subsequent formation of dense structure.

10. Change in Length

Fig.8 shows the change in length of hardened pastes containing cement and calcium sulfate. The expansion was larger for bH mixture than for GYP mixture, and increased extremely with the addition of additive A. Also, the POZ mixture showed a larger increase in expansion than the OPC mixture. These change in length coincides well with the amount of ettringite formed as shown in Fig 3. From this result, it is concluded that the expansion of the mixture depends mainly on the amount of formed ettringite.

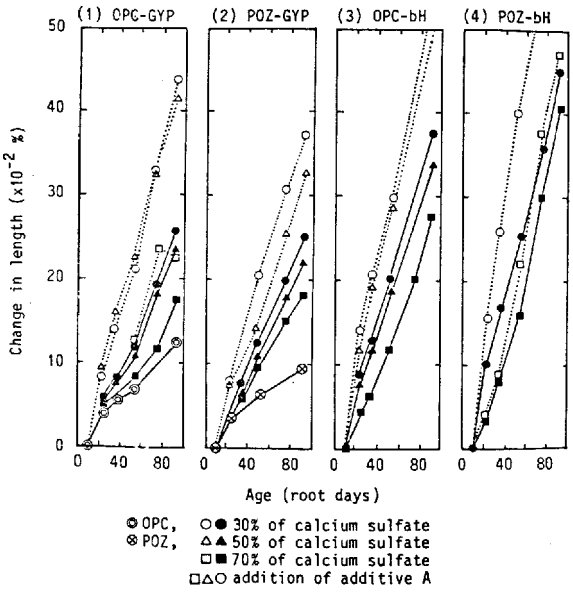

FIG. 8 Change in length of the mixture of calcium sulfate and cement

11. CONCLUSON

1) Hemihydrate of calcium sulfate with and without conventional amount of retarder hydrated actively within 3 hours. Main hydration of anhydrite with an accelerator occured in the coarse of 5-30 hours, indicating that sucessive hydration proceeded slowly over a long time. Vivid hydration of alite in cement was influenced by dissolution rate of calcium sulfate and specific area of them at acceleratory period. The higher dissolution rate and surface area of calcium sulfate, the more the induction period of alite hydration and increase of vivid hydration is shortened and promoted, respectively. Addition of additive A accelerated formation of ettringite and calcium sulfate dihydrate and retarded the alite hydration.

2) The amount of ettringite formed was influenced by the amount and the kind of calcium sulfates, and was large in the sequence of anhydrite, hemihydrate and dihydrate, and of 30%, 50% and 70% of calcium sulfate content. When hemihydrate was mixed, amount of ettringite was larger in POZ mixture than OPC mixture. Addition of additive A brought increase of ettringite formation in all case. Formation of $Ca(OH)_2$ which corresponds to hydration of alite in OPC mixture was the largest in the case of anhydrite, followed by dihydrate and hemihydrate.

3) The amount of combined water at early stage was larger in hemihydrate and anhydrite mixture than OPC alone, but the difference became smaller or was reversed at later stage. The more calcium sulfate content, the more amount of combined water at early stage. This trend was more remarkable in hemihydrate than in anhydrite mixture. Change with age in capillary space of cement-calcium sulfate mixture was small and their capillary space had a large amount of coarse pore of 1000 Å or more.

4) Initial setting time was mainly controlled by increase of viscosity of fresh paste which depended upon the amount of ettringite and calcium sulfate dihydrate produced, and final setting time depended upon vivid hydration of alite. Change in setting time by kind of calcium sulfate mixed and addition of additive A could be explained from hydration characteristic of each mixed component above.

5) Strenght of the mixtures in early stage was strongly dependent on their combined water and in later stage on their capillary space and ratio of coarse pore in it.

6) Change in length corresponded very well to the amount of ettringite formed in the mixture. The more the amount of ettringite, the larger the expansion of hardened paste became.

Reference

(1) U.Uchikawa, S.Uchida, K.Ogawa and Hanehara, Cem. Conc. Res., 14(5), 645-656 (1984)

(2) H.Uchikawa, S.Uchida, K.Ogawa and T.Okamura, to be published in Cemento Gijutsu Nempo.

(3) R.L.Berder and J.D. Mc Gregor, Cem. Conc. Res., 2 (1), 43-55 (1972).

(4) M.F.W.Locher, 7th Inter. Cong. on the Chemistry of Cement IV, 49-54, Paris (1980).

(5) H.Uchikawa, S.Uchida, 7th Inter. Cong. on the Chemistry of Cement III, IV-24- IV29, Paris (1980).

(6) H.Uchikawa, S.Uchida, K.Ogawa, Inter.Symp. on the use of Pulverized Fuel Ash in Concrete, 83-94, April 14-16, Leeds (1982)

DIMAS R. VOLLET - Instituto de Química de Araraquara - UNESP, Araraquara, SP, BRASIL
ALDO F. CRAIEVICH - Centro Brasileiro de Pesquisas Físicas - CNPq, Rio de Janeiro, RJ, BRASIL

STRUCTURE AND KINETICS OF FORMATION OF THE GEL PHASE IN HYDRATED TRICALCIUM SILICATE

SUMMARY

The hydration of tricalcium silicate has been studied by small-angle X-ray scattering (SAXS) at different temperatures. The degree of hydration was determined by quantitative X-ray diffraction analysis (QXDA). The kinetics of setting of the pastes is well described by the Johnson-Mehl equation with n=2, suggesting that the scattering objects (hydrated regions) grow by a diffusion controlled mechanism and have a shape of plates of constant thickness. Features of the SAXS curves from samples, in saturated conditions, are consistent with the lamellar model for the structure of the C-S-H gel.

SUMÁRIO

A hidratação do silicato tricálcico foi estudada mediante a técnica de espalhamento de raios x a baixos ângulos (SAXS), a diferentes temperaturas. O grau de hidratação foi determinado mediante análise quantitativo por difração de raios x (QXDA). A cinética de hidratação das pastas é bem descrita pela equação de Johnson-Mehl com n=2, sugerindo que os objetos espalhadores dos raios x (regiões hidratadas) crescem mediante um mecanismo controlado por difusão e tem forma de placas de espessura constante. As características das curvas de SAXS das diferentes amostras, em condições saturadas, são coherentes com o modelo laminar para a estrutura do gel C-S-H.

Dimas R. Vollet and Aldo F. Craievich

1. INTRODUCTION

The products developed during the hydration of tricalcium silicate (C_3S) and Portland cement have similar properties [1,2]. The basic ones are $Ca(OH)_2$ and a calcium silicate hydrate, called C-S-H, with typical structural features of a poorly crystallized material, often considered as a gel [1]. The fully hydrated paste also contains spaces which are water filled in the fresh paste [1]. These spaces become capilar pores [1] or inter-particles gel pores [3]. Because of their large size, their contribution to small-angle X-ray scattering (SAXS), in the accessible experimental angular range, is negligible.

The C-S-H phase has a characteristic structure containing very small pores, which is about 28% of the hydration products volume [4] and gives an important contribution to SAXS [2,5,6].The small pores are classified as intercrystallite or intracrystallite ones if they are, respectively, external or internal to the "crystals" of the gel particles. The collapse of the interlayer spaces in a lamellar structure, during the drying process, is postulated by many authors [3, 7,8,9,10]. However, there is some controversy about the reversibility of this process and its implications, mainly over the real value of the specific surface of the pastes and the methods for its determination [8,9,10,11].

The specific surface measurements by adsorption methods, and therefore in dry conditions, give values lower than $50m^2/g$ if N_2 is used as adsorbate [8], and of about $200m^2/g$ if water vapour is used [4,7]. The values obtained by Winslow and Diamond [2] by SAXS in D-drying condition, are in agreement with those obtained by water vapour adsorption, under the same conditions but, in saturated conditions, the values are much greater ($\sim 700m^2/g$) than those obtained by adsorption. These authors also showed that the specific surface decreases as drying progresses and that the loss is fully recovered by posterior resaturation, as long as the pastes have not been heated. They tried to associate the different values of the specific surface with the progressive collapse of the interlayers during drying, but verified that it is not at all clear that X-ray scattering measurements could record the interfaces between parallel adjacent layers. They concluded that a layer model is not necessarily appropriate for the C-S-H gel.

In this work, the kinetics of formation of the gel phase, developed during the hydration of C_3S, at several temperatures and the parameters associated with the gel structure of the saturated state and its changes during the drying processes, are studied.

2. EXPERIMENTAL PROCEDURE

Synthetic and microgranulated C_3S was mixed with distilled water in a water/solid weight ratio (w/c) of 0.5, molded into a sealed support and studied by SAXS for different hydration times at constant temperatures. Similar samples were studied by QXDA, using powdered Si as an internal standard and a Guinier chamber. The hydration degree was determined from the decreasing in intensity of a set of diffraction lines of anhydrous C_3S using a microdensitometer with integrator and record system.

The SAXS measurements were carried out using Cukα radiation and Kratky collimation, which gives a "linear and infinite" beam cross-section, a position sensitive X-Ray detector and a multichannel analyser for data recording.

The SAXS data were analysed mainly using Porod's law that holds for two-eletronic density (ρ_1 and ρ_2) systems, which correspond respectively to the ϕ and $(1-\phi)$ fractions of the total volume V. Using a "linear and infinite" beam cross-section, the asymptotic dependence of the scattering intensity, J(h), for such a system, is given by [12]:

$$\lim_{h\to\infty} J(h) = a/h^3 \qquad (1)$$

where

$$a = \lim_{h\to\infty} J(h)h^3 = \pi^2(\Delta\rho)^2 S \qquad (2)$$

is Porod's law constant, $\Delta\rho = \rho_1 - \rho_2$, S is the total interphase area, and h the modulus of the scattering vector defined by $h = 4\pi \sin(\varepsilon/2)/\lambda$, where ε is the scattering angle and λ the incident radiation wavelength.

The SAXS data are often measured in relative units. In this case one determines the J(h)/Q ratio, where Q is the integrated scattering intensity over the reciprocal space, defined by [12]:

$$Q = \int_0^\infty J(h)h\,dh = 4\pi^2\phi(1-\phi)(\Delta\rho)^2 V \qquad (3)$$

From (2) and (3) it follows

$$S/V = 4\phi(1-\phi)a/Q \qquad (4)$$

where S/V is the interphase area per unit volume of the sample.

In addition, from the S/V value one can determine the ℓ_1 and ℓ_2 parameters which represent a mean size of each phase. These parameters are averages of the intersection length, in the respective phases, of lines through all the points in all directions [12]:

$$\ell_1 = 4\phi V/S \;;\quad \ell_2 = 4(1-\phi)V/S \qquad (5)$$

Systematic deviations from Porod's law can occur when there are eletronic fluctuations in the phases (positive deviation) or when the interphase is not well defined (negative deviation) [13]. In the first one, the corresponding intensity component, which is a function of the kind of fluctuations, and the scattering of the ideal two-density system, are simply additive. It results [13]:

$$J(h) = (a/h^3) + b_U/h \qquad (6)$$

$$J(h) = (a/h^3) + b_T \qquad (7)$$

for one-dimensional and tri-dimensional fluctuations, respectively, where the b parameters are related to the magnitude of fluctuations. Two-dimensional fluc-

tuations were not observed in real systems. Tridimensional and one-dimensional fluctuations can be studied through $J(h)h^3$ vs. h^3 or h^2 plots, respectively. In both cases, a linear behavior should be observed in the Porod region. The slope of the straight line gives the b parameter and the extrapolation toward h=0 yields the a parameter.

3. EXPERIMENTAL RESULTS

3.1 SAXS

Fig.1a shows the evolution of SAXS curves for several hydration times at 35°C. Fig.1b shows the time evolution of the scattering intensity for various fixed h values. The time variations are similar for the various h values. The observed intensity increase is related to the paste setting when about 30 per cent of the hydration products is formed. The intensity change is proportional to the amount of the hydrated phase since the submicroscopic porous structure of the resulting C-S-H gel gives most of the contribution to SAXS.

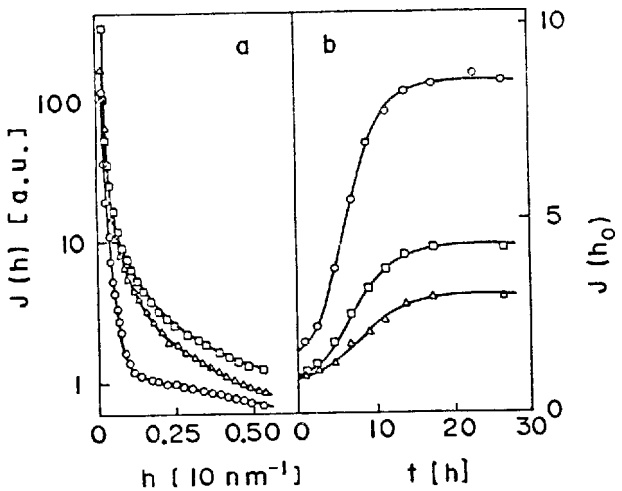

Fig.1: a) SAXS curves for several hydration times
o : 1.0h, Δ : 8.0h, □ : 26h

b) SAXS intensity as a function of hydration time at various h_0 values
o : 0.78nm^{-1}, □ : 1.53nm^{-1}, Δ : 2.14nm^{-1}

Fig.2 shows the time evolution of the C_3S transformed fraction, at 35°C, obtained by QXDA, and the changes in SAXS intensity for fixed h, obtained from samples sealed in different conditions. The second and apparent increase of SAXS for the curve F is not associated with any corresponding evolution in the hydration degree. This intensity change is probably related [6] to an eventual water evaporation process leading to inhomogeneous emptying of the gel porosity and, consequently, to an enhancement of electronic contrast $(\rho_1 - \rho_2)$. This conclusion seems to be confirmed by the analysis of a second sample (curve G) which shows such an effect just when the sealing of the system was removed (time ζ in Fig.2).

The results shown in Fig.2 indicate that the small-angle X-ray scattering intensity at fixed angles, from samples in saturated conditions, can be

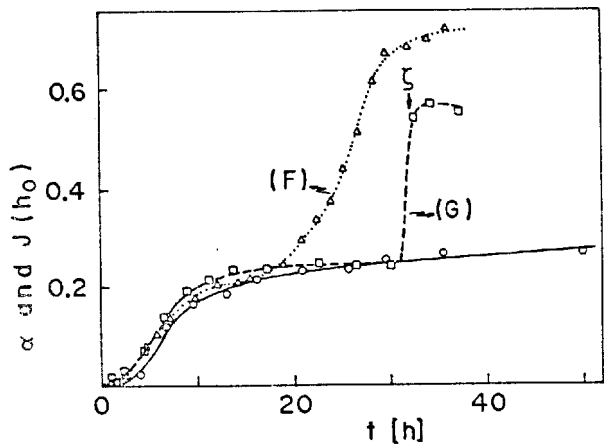

Fig.2: Hydration degree (QXDA) and variation of SAXS intensity at 35°C. o : QXDA, Δ and □ : SAXS intensity under F and G conditions respectively (see text).

used in kinetic studies as a measure of the hydrated fraction.

3.2 Hydration kinetics

Curves like those of Fig.1b were obtained at several temperatures. These curves suggest an analytical form like the Johnson-Mehl equation [14], to describe the SAXS evolution during the pastes setting stage:

$$(J_\infty - J_t) = (J_\infty - J_0)\exp(-k^n t^n/n) \qquad (8)$$

where J_t, J_0 and J_∞ are the scattering intensity values, respectively, at time t, extrapolated to t=0 and corresponding to the apparent upper asymptote. k is an empirical velocity constant and n a parameter that is a function of the phase transformation determinant mechanism [14]. The $\ln\ln[(J_\infty-J_0)/(J_\infty-J_t)]$ vs. ln t plot must be linear in this range, with a slope n. Fig.3 shows it for several temperatures, yielding all of them $n \cong 2$. Then, the k constants were obtained through the $\ln(J_\infty-J_t)$ vs. t^2 plots (Table I).

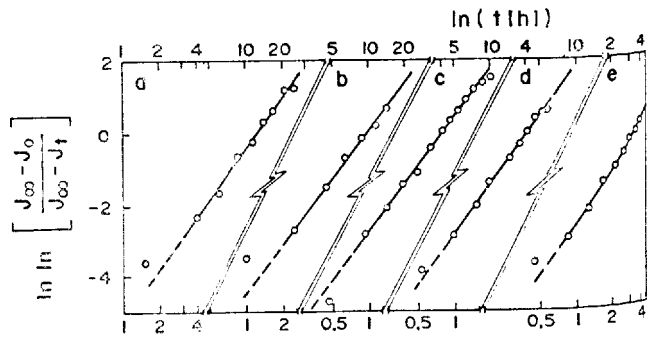

Fig.3: Johnson-Mehl plots at various temperatures. a:25°C (n=2.09); b:35°C (n=2.01); c:44°C (n=2.01); d:52°C (n=2.04); e:65°C (n=2.03).

TABLE I - Empirical velocity constant.

T(°C)	k(h^{-1})	T(°C)	k(h^{-1})
22	0.103	44	0.287
25	0.117	44*	0.283
34	0.198	52	0.442
34*	0.181	65	0.496
35	0.196	65*	0.565

(*) Replica.

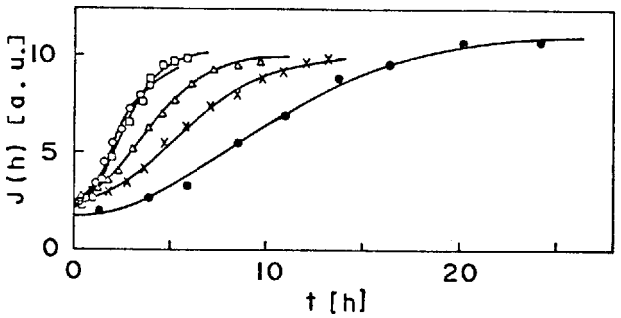

Fig.4: Fitting of Johnson-Mehl equation. •:25°C, x: 35°C, ▲:44°C, ▫:52°C, ○:65°C.

Fig.4 shows the fitting of the Johnson-Mehl function (continuous line) with the experimental data. Excluding the region of higher temperatures, the plot of ln k vs. 1/T is linear (Fig.5), fitting the Arrhenius law k∝exp(-ΔE/RT), where ΔE is the empirical activation energy of the process and R the gas constant. The slope gives ΔE=37.2 KJ/mol.

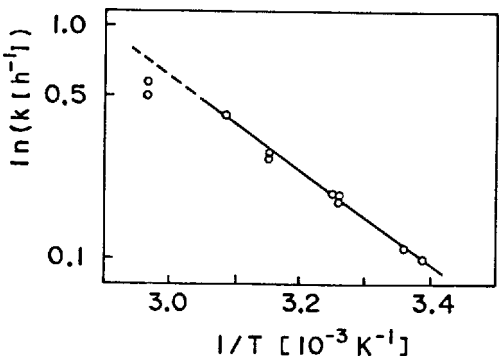

Fig.5: Arrhenius plot for the empirical hydration velocity.

When the transformation occurs by growing of lamellar zones (constant thickness disks), an exponent n=2 in Johnson-Mehl equation, is expected [14].

3.3 Structural parameters and surface area of saturated gels

A positive deviation from Porod's law has been observed in SAXS curves corresponding to every sample in all stages of hydration. Fig.6 shows a typical example, which corresponds to saturated conditions. Fig.7 shows the time evolution of a (surface parameter), b_T (fluctuation parameter), Q and a/Q ratio, during the paste setting at 35°C. There is a close relationship between the hydration degree (Fig.2), Q, which is proportional to the amount of transformated phase, and a, which is proportional to the interphase area [equation (2)].

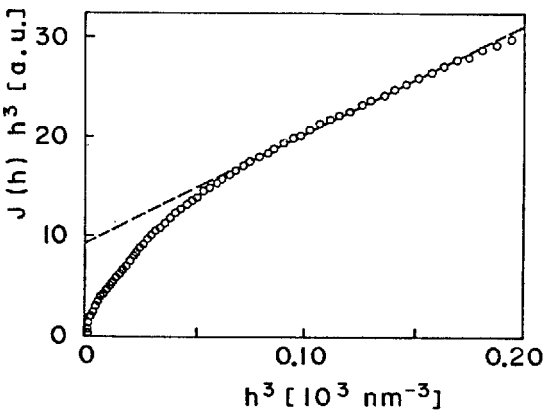

Fig.6: Typical Porod plot indicating a linear region in agreement with equation 7.

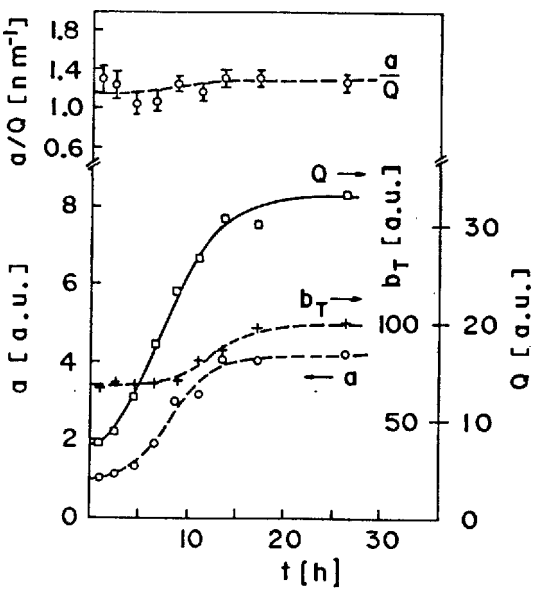

Fig.7: Hydration kinetic parameters. ♦: a/Q ratio, ▫:integrated intensity (Q) (the continuous line represents the Johnson-Mehl function), +: fluctuation parameter (b), ○:surface parameter (a).

The a/Q ratio remains approximately constant. This suggests that the interphase area is approximately equivalent for all gel volume unity formed in this stage. Under these conditions, one may write:

$$\phi_i = \alpha_i \phi_{gel} \quad (9)$$

and

$$a_i = \alpha_i a_{gel} \quad (10)$$

where ϕ_i and a_i are the volume fractions occupied by the gel pores and the surface parameter, respectively, corresponding to the hydration degree α_i and ϕ_{gel} and a_{gel} are the respective values corresponding to total hydration. By using equation (3), (9) and (10) one can extrapolate, from the measured values a/Q_i and α_i, the specific surface S/V for the gel phase (here taken as the whole hydration product and so ϕ_{gel}=0.28) [4]. Equation (4) can be written as follows:

$$(S/V)_{gel} = 4\phi_{gel} \, (1 - \alpha_i \phi_{gel}) \, a_i/Q_i \quad (11)$$

ϕ_{gel} excludes the coarse capillary porosity, which gives no contribution to SAXS, and includes every interlayer space. Equation (11) has not a strong dependence of α_i and errors on this parameter have little influence on the specific surface of the gel.

Table IIa shows the results corresponding to several samples under saturated conditions after the paste setting period. The ℓ_p and ℓ_s parameters, related respectively to the pores and the solid gel particles, obtained from equation (5), are also included in Table II.

TABLE IIa - Results for saturated samples.

Sample	Conditions	α_i	a_i/Q_i (nm^{-1})	$(S/V)_{gel}$ (nm^{-1})	ℓ_p (nm)	ℓ_s (nm)
A	35°C satur.	0.28	1.32	1.36	0.82	2.1
B	25°C satur.	0.32	1.38	1.41	0.79	2.0
C	25°C satur.	0.45	1.47	1.44	0.78	2.0
Z	25°C satur.	0.70	1.53	1.38	0.81	2.1

TABLE IIb - Results for dried samples.

A'	35°C, after removal of the sealing of the system	0.30	0.780	0.800	1.4	3.6
C'	Sample C, 15 days in $CaCl_2$ desiccant	0.45	0.677	0.663	1.7	4.3
WD	D-dried, average of two pastes from ref(2)	0.78-0.86		0.448*	2.5	6.4

(*) Estimated value from the data in Ref.(2).

3.4 Influence of drying

In Fig.8 (a,b) a comparison is made between the SAXS curves for a sample (C, Table IIa) in saturated condition and after 15 days in $CaCl_2$ desiccant (C', Table IIb). The increase in intensity with drying, already cited in sec. 3.1 , is more pronounced in the region of very small angles.

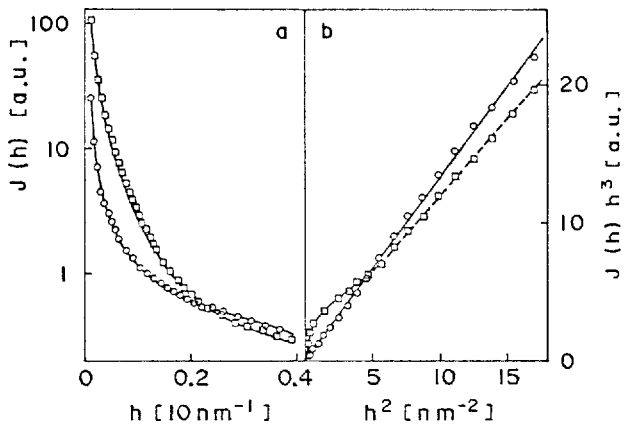

Fig.8: Effects of drying on the SAXS intensity. ○ :saturated state, □ :15 days under $CaCl_2$ desiccant. a) J vs. h plot, b) Jh^3 vs. h^2 plot.

Table IIb shows the changes in the structural parameters associated with the drying process. Because the drying conditions of the samples A' and C' (Table IIb) are not very well defined, only qualitative aspects of this process are discussed from the presented experimental data. $(S/V)_{gel}$ for the desiccated states decreases regarding the saturated condition, while the pores and the solid particle sizes grow. This may occur by a clustering of the particles and pores of the gel. It may also occur that the decreasing in a/Q be caused by changes in contrast due to heterogeneous water evaporation, which could start by the greatest pores. The scattered intensity is proportional to $(\Delta\rho)^2$, so that Q, defined in the whole h space, is more sensitive to contrast variations related to greater pores, than a, defined for $h \to \infty$, where the contribution of these pores is smaller. If the last consideration is correct, the two eletronic density model cannot be applied to middle drying stages.

4. DISCUSSION

4.1 Specific surface

The gel specific surface mean value in saturated conditions (Table IIa) is $1.40 nm^{-1}$. Winslow and Diamond [2], using the same technique for 86%-hydrated cement paste with w/c=0.4, in saturated conditions, obtained 708 $m^2/(g$ ignited at 1050°C) or about 566 $m^2/(D$-dried g). They showed that these values are similar to those of a paste prepared from alita (impure C_3S). Extrapolating to 100% hydration gives 659 $m^2/(D$-dried g). Taking the density $d=2.4 g/cm^3$ [4] one gets $(S/V)_{100\%}=1.58 nm^{-1}$. This value is in good

agreement with that of the present work (Table IIa). The slightly higher value obtained from data of Ref. 2 may be due to the method used to measure the volume which includes the capillary porosity. A lower value of $(S/V)_{100\%}=1.31\ nm^{-1}$ has been obtained [2] for a 78% hydrated paste with w/c=0.3.

According to Powers [4], 79% is the maximum hydration for a w/c=0.3 paste, what would lead to complete elimination of the capillary porosity and consequently the second value would be more representative for the gel. The average value corresponding to the two pastes ($1.45\ nm^{-1}$) is in better agreement with that of the present work.

The D-dried state seems to be well described by a two eletronic density model: empty pores ($\rho=0$) and solid gel particles ($\rho\neq0$). The agreement between the present results and those obtained by Winslow and Diamond [2], in saturated conditions, makes possible the use of their D-dried condition data for the discussion about the features of the dry pastes. From the data of reference [2] (78% and 86% hydrated pastes), we obtained the specific surface at 100% hydration in D-dried conditions, which is equal to $0.448\ nm^{-1}$. From equation (5) this value leads to $\ell_p=2.5$ nm and $\ell_s=6.4$ nm (Table IIb) which are about three times the corresponding values in saturated conditions, indicating a clustering of the gel particles and pores.

4.2 Structural model

Powers [4] postulated a thin sheet of thickness T to describe the colloidal particles of gel of cement pastes in the D-dried state. This shape was suggested by eletron microscopy observations. This author obtained T=3.4 nm from the specific surface measured by water vapour adsorption.

The same result is obtained from our SAXS data. For a thin sheet model we have $T_s=\ell_s/2$ [12], and therefore $\ell_s=6.4$ nm (Table IIb) leads to $T_s=3.2$ nm, in agreement with Powers [4], and $T_p=\ell_p/2=1.25$ nm. Every shape proposed for the particles leads always to the same value for the specific surface, i.e., ... $(S/V) = 4\phi i(1/\ell_i)$; thus their shape must be deduced from other observations.

The hydration kinetic studies (sec. 3.2) lead to a parameter n=2 which suggests that the gel growth is controlled by diffusion. The gel is produced by the formation and lateral growth of plates of constant thickness [14]. Applying this model of plates, the SAXS results (Table IIa) concerning the saturated state, yields $T_s=1.0$ nm and $T_p=0.40$ nm. This would correspond to about one layer of tobermorite type, separated by one or two monolayers of water, on the average.

The dependence on h of the SAXS intensity from saturated samples gives another evidence of the lamellar model. Using a linear and infinite X-ray beam cross-section, a system of infinitely narrow plates, with an infinitely large lateral area A, will scatter according to [12]:

$$\lim_{A\to\infty} J(h)h^3 = \pi^2 A(\Delta\rho)^2 T^2 h^2 \propto h^2 \qquad (12)$$

The $J(h)h^3$ vs. h^2 plot is linear through the origin; Fig. 9 shows it for the saturated sample Z (Table IIa) where equation (12) is verified for a large range of h (until about $3.9\ nm^{-1}$). For $h\geq 3.5/T$, T= minimum plate dimension [15], the classic Porod's law $J(h)\propto 1/h^3$ would also be verified. T=0.65 nm is the minimum sheet thickness that could be accurately measured in the h range for Porod's law fittings like the one show in Fig. 6. Since the obtained value of pore thickness for samples in saturated state was $T_p=0.4$ nm, the linear behaviour of the plot Jh^3 vs. h^3 in the $3.9\ nm^{-1}<h<5.5\ nm^{-1}$ range (Fig. 6) should be considered as an approximated agreement with equation (7). Then the surface parameter a and, consequently, the obtained thicknesses, T_p and T_s, of plates for the saturated state should be taken as approximated values. For a more accurate determination of T_p and T_s of saturated samples, SAXS studies at higher angles would be necessary.

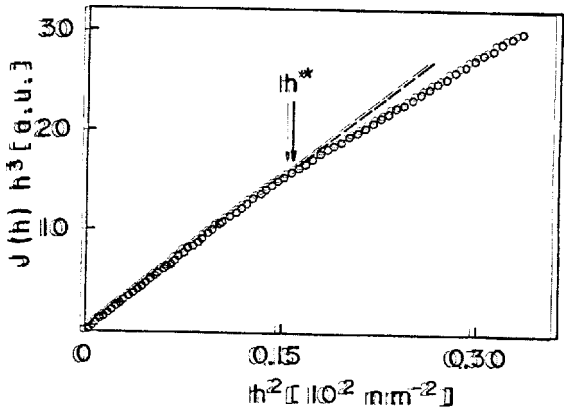

Fig. 9: SAXS intensity from a saturated sample showing the behavior expected from lamellar systems ($h^* = 3.9\ nm^{-1}$).

The experimental thickness of the lamellar particles and pores of the saturated gel ($T_s=1.0$ nm and $T_p=0.40$ nm) are clearly lower than those corresponding to D-dried state ($T_s=3.2$ nm and $T_p=1.25$ nm). This suggests a clustering, by drying, of three elementary layers, on the average, separated by the equivalent clustering of the interlayer spaces in the former saturated state. Some spherical and bigger pores could possibly be present here, even in the previous saturated state, but they may bring a smaller contribution to the specific surface. This contribution could be similar to that recorded by N_2 adsorption.

Water vapour adsorption and SAXS lead to the same surface for D-dried state, suggesting that water records the lateral interfaces of the clustered layers but, in the measurement conditions, it does not recover the interlayer spaces collapsed during the drying precess.

5. CONCLUSION

The parameter n=2 in the kinetic study of the C_3S transformation during hydration and the features of

the small-angle X-ray scattering curves for the saturated conditions [$J(h) \propto 1/h$], allow to conclude that the C-S-H gel exhibits a lamellar morphology.

The increase in T_s and T_p on passing from the saturated to the dry condition indicates that most of the elementary C-S-H lamellas coalesce, increasing the T_s and T_p thickness, without a substantial modification of the global lamellar gel structure observed by eletronic microscopy. The increase in the solid sheet thickness and the clustering of the empty lamellar spaces would lead to a coarser structure without an appreciable change in the total volume of the gel.

REFERENCES

1. T.C. POWERS (1958), "Structure and Physical Properties of Hardened Portland Cement Paste", J.Am. Cer.Soc., 41, 1-6.

2. D.N. WINSLOW and S.DIAMOND (1974), "Specific Surface of Hardened Portland Cement Paste as Determined by Small-Angle X-ray Scattering", J.Am.Cer. Soc., 57, 193-197.

3. M.DAIMON, S.A. EBO-EL-ENEIN, G.HOSAKA, S.GOTO and R.KONDO (1977), "Pore Structure of Calcium Silicate Hydrate in Hydrated Tricalcium Silicate", J. Am.Cer.Soc., 60, 110-114.

4. T.C. POWERS (1964), "Physical Structure of the Portland Cement Paste", in The Chemistry of Cements, by H.F.W. Taylor, Academic Press, London, Vo..I, p.444.

5. D.VOLLET, A.CRAIEVICH and M.REGOURD (1984), "Small Angle X-Ray Scattering from Hydrating Tricalcium Silicate", J.Amer.Cer.Soc., 67, 315-318.

6. D.VOLLET and A.CRAIEVICH (1984), "Structural Transformations in the Hydrated Tricalcium Silicate" (in Port.), Proc. Sixty Brazilian Congress of Materials Science, Rio de Janeiro, T-6, pp. 24-29.

7. R.Sh.MIKHAIL, D.H. TURK and S.BRUNAUER,(1975), "Dimensions of the Average Pore, the Number of Pores, and the Surface Area of Hardened Portland Cement Paste", Cem.Concr.Res., 5, 433-442.

8. P.J. SEREDA, R.F. FELDMAN and V.S. RAMACHANDRAN (1980), "Porosity and Pore-Size Distribution in Ordinary Portland Cement Paste", Proc. Seventy Int. Congr. Chemistry of Cement, Paris, Vol.I, pp VI-1/10-21.

9. S.BRUNAUER, I.ODLER and M.YUDENFREUND (1970), "New Model for Hardened Portland Cement Paste", Highw.Res.Rec., 328, pp 89-101, 105-107.

10. R.F. FELDMAN and P.J. SEREDA (1968), "Model for Hydrated Portland Cement Paste as Deduced from Sorption-Length Change and Mechanical Properties", Mater.Constr., 1, 509-520.

11. R.F. FELDMAN and V.S. RAMACHANDRAN (1971), "Differentiation of Interlayer and Adsorbed Water in Hydrated Portland Cement by Thermal Analysis", Cem.Concr.Res., 1, 607-620.

12. O.GLATER and O.KRATKY (1982), Small-Angle X-ray Scattering, Academic Press, London.

13. W.RULAND (1971), "Small-Angle Scattering of two Phase Systems: Determination and Significance of Systematic Deviations from Porod's Law", J.Appl. Cryst., 4, 70-73.

14. J.BURKE (1965), Kinetics of Phase Transformations in Metals, Pergamon Press, London.

15. H.D. BALE and P.W. SCHMIDT (1984), "Small-Angle X-ray Scattering of Submicroscopic Porosity with Fractal Properties", Phys.Rev.Lett., 53, 596-599.

J.J. Beaudoin and R.F. Feldman, Division of Building Research, National Research Council Canada; J. Baron and M. Conjeaud, Lafarge Coppée Recherche, France

2.2

DEPENDENCE OF DEGREE OF SILICA POLYMERIZATION AND INTRINSIC MECHANICAL PROPERTIES OF C-S-H ON C/S RATIO
INFLUENCE DU RAPPORT C/S SUR LE DEGRÉ DE POLYMÉRISATION DE LA SILICE ET LES PROPRIÉTÉS MÉCANIQUES INTRINSÈQUES DES C-S-H

SUMMARY: Physico-mechanical properties of six C-S-H preparations having C/S ratios of 0.68 to 1.49 and H/S ratios of 1.91 to 6.69 were studied. Characterization of materials included density, surface area and silica polymerization measurements. Some insight as to differences in the nature of the six C-S-H preparations was also obtained from weight and length change versus relative humidity data. A dependence of degree of polymerization on C/S ratio was established. Compacted samples of C-S-H powders were used for mechanical property measurements. Modulus of elasticity (E) or microhardness (H) versus porosity relations were determined. Estimates of the intrinsic (or zero porosity) values of these properties (E_0 and H_0) were made from analyses using different elastic models for porous bodies. The dependence of the intrinsic mechanical properties and other model parameters (shape factors, etc.) on C/S ratio and degree of polymerization were determined. Shape factors associated with two of the models are dependent on C/S ratio. Intrinsic modulus of elasticity and microhardness values are independent of C/S ratio. Results are discussed with respect to possible differences in the microstructure of the C-S-H materials.

Foram estudadas as propriedades físico-químicas de 6 preparações de C-S-H tendo relações de C/S de 0,68 a 1,49, relações de H/S de 1,91 a 6,69. A caracterização dos materiais incluiu densidade, área de superfície específica e medições de polimerização da sílica. Também se obteve algum discernimento quanto às diferenças na natureza das seis preparações de C-S-H, a partir de mudança de peso e comprimento versus dados de umidade relativa. Foi estabelecida uma dependência do grau de polimerização para com a relação C/S. Foram usadas amostras compactadas de C-S-H para medições da propriedade mecânica. Determinaram-se módulos de elasticidade (E) ou microdureza (H) versus relações de porosidade. Foram feitas estimativas dos valores intrínsecos (ou porosidade zero) destas propriedades (E_0 e H_0) a partir de análises usando diferentes modelos elásticos para corpos porosos. Foram determinados a dependência das propriedades mecânicas intrínsecas e outros parâmetros-modelo (fatores de forma, etc.) sobre a relação C/S e grau de polimerização. Os fatores de forma associados com dois dos modelos dependem da relação C/S. O módulo de elasticidade e os valores de microdureza são independentes da relação C/S. Os resultados são discutidos sob o aspecto de possíveis diferenças na microestrutura dos materiais de C-S-H.

J.J. Beaudoin and R.F. Feldman, Division of Building Research, National Research Council Canada; J. Baron and M. Conjeaud, Lafarge Coppée Recherche, France

INTRODUCTION

Calcium silicate hydrates (C-S-H)* form the principal cementing phases in binders for such building materials as portland cement mortar, concrete, certain types of brick and other lime-silica products. The silicate minerals in portland cement (C_3S and C_2S) hydrate to form C-S-H and calcium hydroxide (CH). It is generally held that C-S-H plays an important role in the mechanical behavior of cement systems. Several factors, however, make a quantitative assessment of this role difficult: (i) Hydrated cement contains several other cement phases (aluminates, ferrites, etc.) including CH; (ii) the role of CH has been investigated but is not fully understood (1); (iii) the C/S ratio varies over a wide range, from 0.8 to nearly 3.0 depending on water/solid ratio, temperature and time of curing (2); (iv) the dependence of strength on degree of polymerization of the silicates is not clearly established; (v) the extent to which mechanical properties of the C-S-H solids contribute to the the porous system properties cannot be determined directly in hydrated cements.

Several authors have attributed strength differences of cement products to differences in C/S ratio of the C-S-H present in those products. For example, low strength of autoclaved cement products has been attributed to the presence of αC_2SH (C/S = 2.0) (3).

In order to investigate the contribution of the C-S-H phase alone, it was decided to synthesize C-S-H having a wide range of C/S ratios and to conduct mechanical tests on the material. In addition to mechanical behavior, the importance of the C-S-H phase for volume change and durability is recognized. There is, however, a paucity of data on these characteristics for the C-S-H phase itself. The objective of this investigation was to determine the dependence of the degree of polymerization, adsorption characteristics and intrinsic mechanical properties of C-S-H preparations on C/S ratios.

EXPERIMENTAL

Materials and Preparation

Six C-S-H compositions were produced in aqueous solutions containing variable proportions of sodium metasilicate and calcium oxide. They were dried by washing in acetone and ether. In order to remove the acetone and ether they were first exposed to a stream of dry nitrogen (500 cm^3/min) for four days. Then they were dried in nitrogen atmosphere at 40°C for 24 hours. This was the starting condition for the experimental work.

Characterization

The C/S and H/S ratios are given in Table 1. The C/S ratio was obtained using X-ray fluorescence and flame spectrophotometry. The H/S ratio was calculated from loss on ignition at 1000°C. In spite of the drying treatments, the two C-S-H preparations having the highest C/S ratio had abnormally high ignition loss. The H/S ratios for these preparations are unexpectedly high when compared to published values (2). There is no obvious explanation for this.

No carbonation was detected in the powdered samples. Calcite and vaterite were found in the compact with C/S = 1.26. Aragonite and vaterite were detected in the compact with C/S = 1.17. No unreacted C or S was detected by X-ray diffraction or infrared spectroscopic methods.

Morphology, as revealed by SEM, is broadly divided into two groups according to C/S ratio: C/S = 0.99 - 1.49 and 0.68 - 0.87. C-S-H appears as 50 μm clusters of 1 μm thin foil subparticles in the first group and is representative of Type II cement paste morphology (4). In the second group the subparticles are much smaller and difficult to resolve at the 20nm limit of the SEM. At C/S = 0.68, the subparticles appear as small grains. It could not be determined if the grains were agglomerates of thin foils.

Density values were determined using mass and solid volume measurements determined by helium pyknometric techniques (5). Surface areas of the C-S-H samples were determined using nitrogen adsorption techniques with Numinco-Orr instrumentation. Density and surface area values are given in Table 2.

Silica Polymerization Measurements

The molybdate complexing method developed by Parrott and Taylor was used in this investigation (6). The molybdate complexing reaction curves were obtained on the following:

1) mono-, di- and polysilicic acids. The monosilicic acid was obtained by dissolving 83 mg of anhydrous portland cement in 100 ml of methanolic HCl (0.15 N). The disilicic acid was prepared with 115 mg of hemimorphite instead of 82 mg of anhydrous cement. The polysilicic acid was prepared by reacting 317 mg of anhydrous cement in 15 ml of methanolic HCl (2.0 N) for 20 minutes.
2) powdered and compacted C-S-H samples. The compacts were prepared at pressures ranging from 510 to 1360 MPa.

Two sets of measurements were conducted on powdered C-S-H samples and silicic acids. The second set included measurements on compacts.

Weight and Length Change Isotherms

C-S-H specimens were compacted at 510 MPa in the shape of discs 31.8 mm diameter and 1.27 mm thick. Weight change isotherms were determined using a desiccator method after Kantro et al (7). Equilibration times were at least 30 days for each humidity. Two compacts were used for each C-S-H preparation. For length change measurements specimens were mounted on modified Tuckermann optical extensometers (8). This determined the dimensional changes to a sensitivity of 4×10^{-6} mm/mm. The extensometers were placed in desiccators fitted with optically suitable covers.

*Cement chemistry notation: C = CaO; S = SiO_2; H = H_2O.

Mechanical Properties

Sample Preparation

Specimens were prepared by compacting the various C-S-H powders at pressures up to 1020 MPa. All specimens were circular discs 31.8 mm diameter and 1.27 mm thick.

Porosity Measurement

Porosity was calculated using the apparent volume of the sample and the solid volume directly measured using helium pyknometric techniques (5). Porosity was also determined on some compacted samples by mercury intrusion methods at pressures up to 408 MPa.

Modulus of Elasticity Measurement

The method of measurement consists essentially of measuring the center point deflection of a centrally loaded circular disc supported at three equally spaced edge supports (9). At least three specimens were used for each test condition. All measurements were made in a glove box conditioned at 11% RH.

Microhardness Measurement

Microhardness was determined on compacted C-S-H samples using a Leitz microhardness apparatus with a Vickers indentor (10). The equipment was placed in a conditioned glove box at 11% RH. Up to ten measurements were made on each disc.

RESULTS AND DISCUSSSION

Silica Polymerization

In the molybdate complexing method the analysis of results is based upon the assumption that an individual silicic acid in a mixture of silicic acids is complexed at a rate which is solely dependent upon its degree of condensation, and that the reaction for a silicic acid with a degree of condensation 'i' takes the form:

$$Y = 1 - \exp(-b_i(t-t_i))$$

where Y is the proportion of silica complexed, b_i is the rate constant and t_i the time shift.

The reaction for a mixture of n silicic acids can be then represented by the equation:

$$Y = \sum_{i=1}^{i=h} a \left[1-\exp(-b_i (t-t_i))\right]$$

where a_i is the proportion of silica with the degree of condensation 'i' in the mixture.

In general, the reaction curves ($-\log(1-Y)$ vs. t_i, not shown) for compacts and powdered samples indicate that compaction led to very little difference in the degree of polymerization of the C-S-H, despite large differences in the H/S. The degree of polymerization of the silicates, measured by b_p (the slope of the polymer reaction curve, which increases when degree of polymerization decreases; the polymer fraction refers to silicate chains longer than dimers), is plotted against C/S ratio in Figure 1. The curves in the figure are plotted for data obtained two years apart. This was intended to assess possible aging effects. The degree of polymerization decreases non-linearly with an increase in C/S ratio. The term (b_p) increases slowly, quickly and slightly for the range of C/S ratios, 0.66-1.17, 1.17-1.26, and 1.26-1.49. The decrease in the degree of polymerization can be explained by both the Taylor and the Feldman models, which postulate the omission of silica tetrahedra in the silicate chain and possible replacement by hydroxyl groups (11,8). Omission of tetrahedra increases the effective C/S ratio of the polymer. This is in agreement with results obtained on cement pastes (12,13) and synthetic C-S-H of C/S ratio 0.8 to 1.1 (14), but was not observed on other synthetic C-S-H of C/S ratio 1.14 to 1.55 (15).

Weight Change and Length Change Isotherms

Weight change isotherms are plotted in Figure 2. All isotherms exhibit primary hysteresis. All isotherms except the one for the C-S-H preparation having C/S = 1.26 exhibit secondary hysteresis at lower humidities. Scanning loops start at 11% RH on the desorption branch and rejoin the adsorption branch at 80% RH. Secondary hysteresis is probably due to intercalation of hydrate water and/or aging effects. The preparation having C/S = 1.26 (no secondary hysteresis) has the lowest amount of water held at 11% RH (6%) and has a low N_2 surface area (40 m^2/g). Adsorption on rewetting to 80% RH is reversible. Initiation and completion of intercalation and dissociation processes associated with hydrate water may occur at low humidities (below 11% RH). Thus, irreversibility may not be observed. The C-S-H preparation with lowest C/S ratio loses the largest amount of water at high humidities on desorption, e.g., for C/S = 0.68 there is a 23% weight loss at 80% RH compared to a weight loss of 3-5% for the other preparations. This is an indication that the pore structure is much coarser for the C/S = 0.68 material. These factors will be considered when examining the dependence of mechanical properties on C/S ratio.

Length change versus weight change curves are plotted in Figure 3. The curves are qualitatively similar to the curve for bottle hydrated cement obtained by Feldman (8). The curve for C/S = 0.87 is quantitatively similar. Measurements on drying could not be made below 11% RH as the specimens fractured. The starting condition was 32% RH. The slopes of the length change - weight change curves on desorption (100 - 80% RH) for C-S-H in order of increasing C/S ratio are 7.1, 25.3, 123.3, 38.0, 110.0 and 55.0 $\times 10^{-3}$, respectively. The two preparations with the lowest C/S ratio have the lowest slopes. This may indicate that they have a coarser pore structure than the other preparations, if one ignores possible aging factors. This is supported by pore size distribution data (not presented). Pore size measurements on compacts (510 MPa) indicate that in the fine pore range (pore radii 0.0022-0.0015 µm, the limiting size of the porosimeter) the percentage of pore volume was lowest for the two preparations having the lowest

J.J. Beaudoin and R.F. Feldman, Division of Building Research, National Research Council Canada; J. Baron and M. Conjeaud, Lafarge Coppée Recherche, France

C/S ratio. The high surface area for the C/S = 0.68 material may be related to the presence of micropores not detected by mercury porosimetry.

All the C-S-H samples have large, irreversible shrinkages. Irreversibile shrinkage at 32% RH in order of increasing C/S ratio is as follows: 0.05, 0.11, 0.72, 0.60, 0.42 and 0.58%. The two lowest C/S ratio preparations have the lowest irreversible shrinkages. This may be due to lower amounts of interlayer Ca^{++} and closer proximity of silicate sheets in the C-S-H structure.

Intrinsic Mechanical Properties

Modulus of elasticity (E) and microhardness (H) values were determined on compacted C-S-H samples prepared at different porosities. Mechanical property - porosity data were fitted to several different models, which have been used to describe the dependence of mechanical properties on porosity for a variety of porous systems (16-23). Estimates of intrinsic values of E and H (i.e., zero porosity values, E_0 and H_0) were obtained by extrapolation methods. All the models fit the data reasonably well with one exception. Modulus of elasticity data for the Nielsen model have low values of correlation coefficient for four preparations. H_0 and E_0, regardless of the model used for their estimation, do not correlate well with C/S ratio. The highest values of correlation coefficient for H_0 vs. C/S ratio are 67.4 and 62.7, obtained using the Nielsen and the Knudsen models, respectively. The shape factors "a" (Nielsen model) and "b" (Knudsen model) do depend on C/S ratio. The shape factor, "a", for example, increases to a maximum at C/S = 1.0 and then decreases. This dependence may, however, be a consequence of the effects of compaction on pore shape.

In another approach the modulus of elasticity data for all C/S ratios were treated collectively. The data were fitted to the Balshin model (24) i.e. $E = E_0(1-p)^n$. The regression equation is $E = 34 \times 10^3 (1-p)^{2.7}$, which is very similar to the expression derived from the Powers model (19). Suitable regression curves can be obtained using other models (18-23) in a collective treatment of all the data. The application, however, of the Nielsen and Knudsen models (16,17) does not result in a single curve which describes all the data satisfactorily. Hence, for these models, there is a dependence of the shape factors on C/S ratio. The main conclusion arrived at by treating the data in this way is the same as that obtained with separate data sets for each C/S ratio, i.e. E_0 is independent of C/S ratio and degree of polymerization. The Nielsen and Knudsen models do not predict, as do the others, that the relation E = (p) is independent of C/S ratio.

On the basis of the statistical analysis of the data for all C-S-H preparations, E_0 and H_0 appear to be independent of C/S ratio. However, examination of the data (all models) reveals, for example, that E_0 is nearly always highest for C/S = 1.26. This C-S-H preparation had the highest H/S ratio and reversible characteristics in the adsorption region of the weight change isotherm. The presence of interlayer water in the region (11-100% RH) may contribute to rigidity of the C-S-H if the silicate sheets are held rigidly by this water.

Preparations having C/S = 0.68 also have high E_0 values. This may be due to the absence of interlayer Ca^{++} and closer proximity of silicate sheets. It therefore appears that the degree of polymerization has little effect on E_0. The C-S-H preparation having the highest value of H_0 depends on the predictive model used. The largest value of H_0 (1337 MPa) was estimated by the Nielsen model and was for the preparation having C/S = 1.26.

CONCLUSIONS

1. Degree of polymerization of C-S-H depends on C/S ratio. It decreases as C/S ratio increases.

2. Synthetic C-S-H materials prepared using sodium metasilicate solutions are generally layered systems. Irreversible length and weight change characteristics on exposure to water vapor are due to intercalation processes and aging phenomena.

3. Zero porosity values of modulus of elasticity and microhardness for the C-S-H preparations studied appear to be independent of C/S ratio. As microhardness generally correlates with strength, values for intrinsic strength would appear to be independent of C/S ratio over the range studied.

4. Highest values of modulus of elasticity were obtained for the preparation (C/S = 1.26), which exhibited reversible sorption characteristics in the low pressure region of the water isotherm. Intercalation processes and their effects on the proximity of silicate sheets may have a greater effect on intrinsic mechanical properties than composition and/or degree of polymerization.

REFERENCES

1. J.J. Beaudoin, Cem. Concr. Res. 13 (3), 319-324 (1983).

2. H.F.W. Taylor, "The Calcium Silicate Hydrates", The Chemistry of Cements, Chapter 5, 167-232 (1964), Academic Press, Ed. H.F.W. Taylor.

3. J.J. Beaudoin and R.F. Feldman, Cem. Concr. Res. 5 (2), 103-118 (1975).

4. S. Diamond, Proc. Conf. Hydraulic Cement Pastes - Their Structure and Properties, Univ. Sheffield, UK, 2 (1976).

5. R.F. Feldman, Cem. Technol. 3, 3 (1972).

6. L.J. Parrott and M.G. Taylor, Cem. Concr. Res. 9, 483-488 (1979).

7. D.L. Kantro, S. Brunauer and C.H. Weise, Advances in Chemistry, Series 33, 199 (1962).

8. R.F. Feldman, Proc. V. Int. Symp. Chem. Cem., Tokyo, Part III, Vol. III, 53-66 (1968).

9. P.J. Sereda, R.F. Feldman and E.G. Swenson, High. Res. Bd. Spec. Rpt. 90, 58 (1966).

10. P.J. Sereda, Cem. Concr. Res. 2, 717 (1972).

11. H.F.W. Taylor, Jennite, 1.4 nm Tobermorite and C-S-H gel, Extended Abstracts, Amer. Cer. Soc. 87th Meeting, Cincinnati, 78 (1985).

12. H. Funk, Autoclaved Calcium Silicate Building Products, The Society of Chemical Industry, 122-4 (1967).

13. A. Bentur, R.G. Berger, J.H. Kung, N.B. Milestone, J.F. Young, J. Amer. Cer. Soc. 62 (7,8), 362-6 (1979).

14. H. Uchikawa and R. Furuta, Cement Concr. Res. 11 (1), 65-78 (1951).

15. M. Michaux, D. Ménétrier and P. Barret, C.R. Acad. Sc. Paris, 296, (2), 1043-6 (1983).

16. L.F. Nielsen, J. Amer. Cer. Soc. 67 (2), 93-98 (1984).

17. F.P. Knudsen, J. Amer. Cer. Soc. 42 (8), 376-388 (1959).

18. Z. Hashin and B.W. Rosen, J. Appl. Mech., 223-232 (1964).

19. T.C. Powers, Revue des Matériaux, (544), 79-85 (1961).

20. D.P.H. Hasselman, J. Amer. Cer. Soc. 45, 452 (1962).

21. Z. Hashin, J. Appl. Mech., 143-150 (1962).

22. B. Paul, Trans. Metall. Soc. AIME 218, 36-41 (1960).

23. S.D. Brown, R.B. Biddulph and P.D. Wilcox, J. Amer. Cer. Soc., 47 (7) 320-322 (1964).

24. M.Y. Balshin, Dokl. Akad. Nauk SSSR, 67, 831 (1949).

TABLE 1 - C-S-H COMPOSITION

Composition	C-S-H Designation					
	101	106	107	110	112	113
C/S	0.99	1.26	1.49	0.68	0.87	1.17
H/S *	2.49	6.69	5.53	1.91	2.01	2.58
**	2.36	3.01	2.99	1.79	1.78	2.81

*powdered samples
**compacts

TABLE 2 - DENSITY AND SURFACE AREA OF C-S-H PREPARATIONS

C-S-H	C/S	Density (g/ml)	Surface Area (m^2/g)
101	0.99	2.05	110.7
106	1.26	2.02	40.2
107	1.49	2.03	30.7
110	0.68	2.00	111 9
112	0.87	2.05	56.6
113	1.17	2.07	68.2

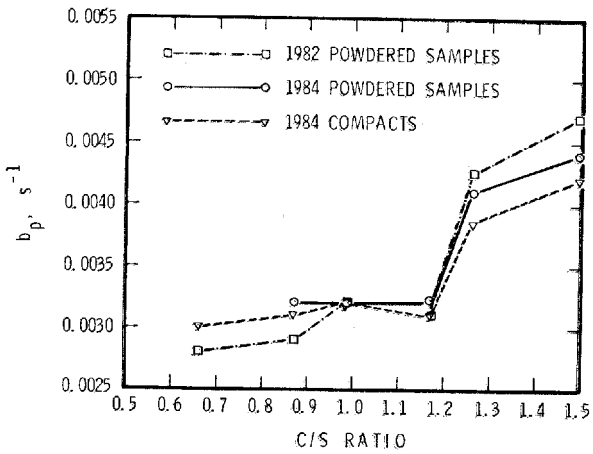

Figure 1. Polymer rate constant "b_p" versus C/S ratio

J.J. Beaudoin and R.F. Feldman, Division of Building Research, National Research Council Canada; J. Baron and M. Conjeaud, Lafarge Coppée Recherche, France

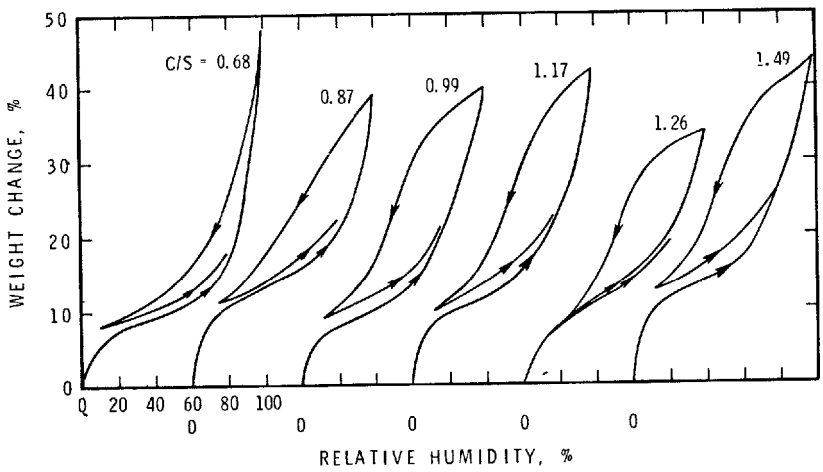

Figure 2. Water adsorption isotherms of C-S-H preparations having different C/S ratios

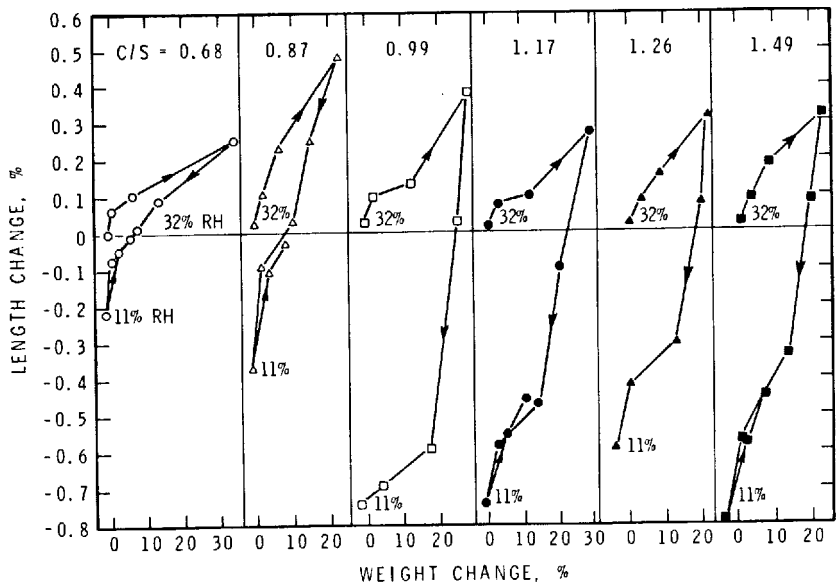

Figure 3. Length change versus weight change curves for C-S-H preparations exposed to water vapor

Lu Ping, Dr.-Eng., Lecturer, Dept. of Materials Science and Engineering, Tongji University, Shanghai, China. 1
Huang Yiun-yuan, Professor, Dept. of Materials Science and Engineering, Tongji University, Shanghai, China.

A STUDY OF THE INTRINSIC PROPERTIES OF HARDENED CEMENT PASTES (HCP)

2.2

SUMMARY The relationship between the intrinsic properties of C-S-H gel in HCP with low porosity and its mechanical behaviour has been investigated. Degree of silicate polymerization (DSP) in this material (compressive strength over 200 MPa) with the additives of several inorganic complex ions and organic silane coupling agents have been analysed by using GPC method. The pore size distributions and non-evaporable water of two series of the samples in which one cured at room temperature and another under hydrothermal condition were determined. Mechanical strength and fracture parameters of the samples were measured. SEM and EMPA were employed to study the microinterface between the grain of still-unhydrated cement and its hydrated products.

Results show that the fracture behaviour of HCP has closs bearing on the DSP of its microstructure at molecular level. The role of additives used is to link-up the inorganic silicate molecules in HCP or to supply coordination ion between them, which results in increasing the DSP of it and improving its intrinsic properties. Both mechanical strength and fracture toughness increase with increasing the DSP (expressed as weight average molecular weight). Furthermore, its brittleness is distinctly decreased. The lower the porosity of HCP is, the stronger the influence of DSP on its mechanical behaviour is. On this basis we have prepared a high strength and low brittleness HCP which is named by us polymerized silicate cement (PSC).

Investigou-se a relação entre as propriedades intrínsecas do gel de C-S-H na pasta de cimento endurecido (HPC) com baixa porosidade, e seu comportamento mecânico. Usando o método GPC foram analisados o grau de polimerização do silicato (DSP) neste material (resistência à compressão acima de 200 MPa) com aditivos de vários íons complexos inorgânicos e agentes de ligação de silane (Si_nH_{2n+2}) orgânico. Foram determinadas as distribuições de tamanho de poro e água não evaporável de duas séries de amostras, uma das quais curada à temperatura ambiente da sala e outra sob condição hidrotérmica. Mediram-se a resistência mecânica e os parâmetros de fratura das amostras. SEM e EMPA foram utilizados para estudo da microinterface entre o grão do cimento ainda não hidratado e seus produtos hidratados.

Os resultados mostram que o comportamento de fratura de HCP tem apoio firme no DSP de sua microestrutura a nível molecular. O papel dos aditivos usados é interligar as moléculas' de silicato inorgânico em HCP ou fornecer íon de coordenação entre elas, do que resulta aumento do seu DSP e melhora de suas propriedades intrínsecas. Tanto a resistência mecânica como a tenacidade à fratura aumentam com o aumento do DSP (expresso como média ponderada do peso molecular). Além disso sua friabilidade decresce distintamente. Quanto menor a porosidade ' de HCP, mais forte é a influência de DSP sobre seu comportamento mecânico. Com esta base preparamos uma HCP de alta resistência e baixa friabilidade que denominamos cimento de silicato polimerizado (PSC).

Lu Ping
Huang Yiun-yuan

INTRODUCTION

In the 7th Congress (Paris) Sereda, Feldman and Ramachandran had discussed the correlation of mechanical behaviour of HCP with its porosity, according to the relationships such as the following /1/:

$$\sigma = \sigma_0 \cdot (1-P)^A \quad \ldots\ldots\ldots\ldots\ldots\ldots \quad (1)$$

$$\sigma = \sigma_0 \cdot e^{-BP} \quad \ldots\ldots\ldots\ldots\ldots\ldots \quad (2)$$

where P - total porosity, σ_0 - intrinsic strength at zero porosity, A,B - constants.
The mechanical strength of porous material is usually recognized to be influenced mainly by its pore structure. The characteristic parameters of pore structure such as total porosity, pore-size distribution, pore geometry etc. have been discussed by many researchers. But the nature of the intrinsic strength (σ_0) has less been investigated. Recently, Odler et al have given these σ_0 values /2/, but have not discussed them in detail. By applying Weibull distribution to the study of pore structure, Huang Yiun-yuan et al have proposed a new expression /3/.

$$\sigma = (K_1 K_2^{K_3+K_4})(K_2^{K_3(W-1)}(1-P)^{K_3W+K_4})\left(\frac{1-P}{1+2P}\right) \quad \ldots\ldots \quad (3)$$

where P - total porosity, W - the factor of relative specific surface area of the pores and $K_1 - K_4$ constants depending on intrinsic properties of HCP, furthermore $K_3 + K_4 \approx 3$. This relationship distinctly shows the factors influencing the mechanical strength at different structural levels involving molecule, micro and mesolevel corresponding to the terms within the first, second and third bracket in eq. (3), respectively. The first term in eq. (3) corresponds to σ_0 in eq. (1) and eq. (2). Beaudoin and Feldman have recently pointed out the important influence of porosity, pore geometry, C-S-H composition, composite behaviour and fracture criteria on strength of porous system /4/.

The aim of this study is to investigate the correlation between the intrinsic properties of HCP and its mechanical behaviour, i.e. the nature of intrinsic strength σ_0, by changing the molecular weight distributions of silicate in C-S-H gel by addition of inorganic complex ions and/or organic silane coupling agents to hydrating cement pastes. The porosity of the specimens used was kept as low as possible in order to approach the ideal zero porosity condition.

EXPERIMENTAL PROCEDURE

Starting materials

HCP with low porosity was prepared according to Roy and Gouda from ordinary Portland cement (ground to a fineness of 5800 cm^2/g Blaine) /5/. The OPC was compacted with W/C ratio of 0.1 at room temperature and under pressures up to 294 MPa (3000 kg/cm^2) to make ϕ1.27 × 1.27 cm cylindrical specimens and 1.4 × 1.4 × 11 cm prisms. The samples cured in water at temperature 20°C for 28 days were labeled by A; the samples cured in water at temperature 20°C for 21 days and then under hydrothermal (95°C) condition for 16 hrs were labeled by B. All samples used were D-dried.

To prepare the samples with complex ions Fe^{++} and Cu^{++}, 15% $FeSO_4$ and $CuSO_4$ solutions were adopted to replace H_2O during compacting. To obtain the samples with silane coupling agents, 2% by weight of VTES ($CH_2 = CH - Si(OC_2H_5)_3$) and MDES ($(CH_3)_2Si(OC_2H_5)_2$) were added to the cement, then the remainder processes were similar to those mentioned above.

Experimental methods

1) GPC
0.2g finely ground sample was derivatized by TMS technique as prescribed by Tamas, Sarkar and Roy (using HMD, DMF and TMCS) /6/. After removing solvent at 105°C the derivatized silicates were evacuated for 3 hrs, then examined by gel permeation chromatography (GPC), without dissolving in THF. The injected volume was 15 µl. The equipment (model NJ-792) is made in China, with two styragel columns (each 1m) and two silicagel columns (each 1m) in series and a differential refractive detector. The flow rate is 1ml/min. This equipment was calibrated by using samples of C_3S, hemimorphite, laumontite and beryl to give derivatized monomer, dimer, cyclic tetramer and cyclic hexamer, respectively. Fig. 1 shows the calibration curve.

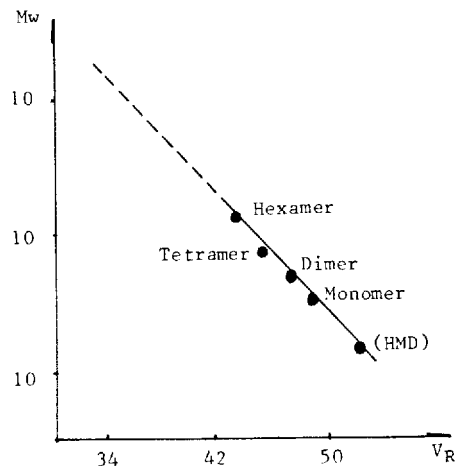

Fig. 1 Calibration Curve

2) Strength and other characterization
Compressive strength and splitting tensile strength were measured in a standard testing equipment on ϕ1.27×1.27 cm specimens. At the same time, the amounts of non-evaporable water of the specimens were measured, and the pore-size distributions of them were determined by mercury porosimetry.

3) Fracture parameters
In this study all calculations and experiments for fracture parameters were carried out from three-point bend specimens (1.4 × 1.4 × 11 cm) with a central notch of 1/2 beam depth on the tensile side. An Instron machine of Model 1122 was employed to determine G_{Ic} (fracture toughness), K_{Ic} (critical stress intensity factor) and B (index of brittleness, defined by the irrecoverable dissipated energy of the specimen during the test up to maximum load) /13/.

4) SEM and EPMA examination
Scanning electron microscopy (SEM) and electron microprobe analysis (EPMA) were applied to some of the samples to compare the microstructures of low porosity HCP with or without additives mentioned above.

RESULTS AND DISCUSSION

1. The role of inorganic complex ions and organic silane coupling agents

According to the calibration curve shown in Fig. 1, the molecular weight distributions of all samples in gel permeation chromatograms have been calculated in order to make comparison with each other. The results of calculation are shown in Table 1.

Table 1. Calculated results of some samples in series A and B

Symb.	Mw	Mn	Mono~	Di~	Tri~	Penta~	Octa~	Poly~
A1	586	436	84.0%	4.3%	0.5%	4.3%	4.6%	1.9%
A2	988	433	77.8%	5.6%	0.3%	3.9%	5.0%	8.7%
A3	877	501	56.3%	12.8%	0.4%	6.1%	7.2%	5.2%
A4	891	509	65.7%	11.0%	0.7%	6.7%	7.7%	7.8%
A5	804	507	65.7%	11.1%	0.7%	8.0%	8.5%	5.4%
B1	822	471	73.2%	6.8%	0.5%	5.4%	7.2%	7.1%
B4	910	509	69.0%	4.9%	0.5%	6.7%	9.9%	8.6%
B6	874	496	71.7%	3.6%	0.6%	6.8%	9.0%	7.8%
B7	920	503	70.0%	5.0%	0.4%	6.2%	9.1%	8.9%

A1, B1: controlled samples;
A2: sample with addition of Fe^{++};
A3: that with Cu^{++}:
A4, B4: that with VTES;
A5, B5: that with MDES;
A6, B6: that with VTES + MDES (1:1) and
A7, B7: that with Fe^{++} + MDES

1) Organic additives
It can be seen from Tab. 1 that after adding VTES and MDES to hydrating cement pastes both the weight average (Mw) and number average molecular weight (Mn) which reflected the molecular weight of TMS-derivatives of silicic acid in samples, were increased. It should be noted that this change of degree of silicate polymerization, especially, the decrease of monomer did not mean progress of hydration as usually did (see Tab. 2 mentioned after). Result of IR measurement of sample A4 indicates that there is a recognizable absorption peak at 1120 cm^{-1} corresponding to stretching vibration of Si_V-O-Si_C bond (where Si_V: silicon atom in VTES, Si_C: that in C-S-H gel). Obviously, Si_V in coupling agent here plays a role to connecting polymers. Analogous interpretation was discussed by Ludwig /7/.

Data of samples B6 and B7 in Table 1 show that the mixture of VTES and MDES did not make Mw and Mn more increase, the reason of which is still not known, ready for further investigation.

2) Inorganic additives
In the process of hydration silicate hydrates of Portland cement can take part in coordination with complex ions. It can be seen from Tab. 1 that after adding Fe^{++} and Cu^{++} monomers in samples decreased, at the same time, dimer, pentamer, octamer and polymer increased. As mentioned above, this must have a close bearing on the growth of chain of silicate anions. It has been obtained from atom-absorption spectrum of the some TMS-derivatized samples that Fe^{++} concentration of sample A1 is 17.23 ppm, but that of sample A2 is 173.10 ppm. This indicates that Fe^{++} ion has stronger ability to form chemical complex.

2. The relationship between DSP and mechanical behaviour of HCP

In this study it is necessary to prepare high strength HCP with low porosity in order to investigate the effect of intrinsic properties of HCP on its mechanical behaviour directly. Furthermore, the factors of strength generation can be closely reflected by index of strength collapse. Tab. 2 shows some experimental results.

Table 2. The physical properties of series A, B

Symb.	Compr. Str. (MPa)	Split. Test (MPa)	Non-evap. H_2O(%)	Total pore Vol. (cm^3/g) 10^2
A1	226.5	13.5	6.7	5.17
A2	313.3	17.2	6.8	4.67
A3	307.8	16.1	6.8	4.72
A4	293.0	18.4	6.6	4.92
A5	280.2	17.3	6.8	4.71
A6	287.1	18.6	7.4	—
A7	255.0	15.2	7.1	—
B1	280.2	15.6	8.3	2.05
B4	321.4	23.2	8.6	1.15
B5	323.6	20.4	8.9	1.55
B6	315.7	21.6	8.7	1.27
B7	332.4	19.7	9.0	1.63

1) Intrinsic properties and mechanical strength
Barnes, Diamond and Dolch have investigated the micromorphology of interfacial zone around aggregate by using SEM and EDXA /8/. Langton and Roy have reported their investigation into interfacial region between HCP and rock, using these technique /9/. In this study, SEM observation on samples A1 and A2 was carried out, as shown in Fig. 2. Both Fig.2a and Fig.2b show some common characteristics of high strength HCP, i.e. besides unhydrated cement grains there are only dense amorpholous precipitates. EMPA were performed along the lines marked in Fig. 2, and the results are given in Fig. 3 and Tab. 3. These lines are so chosen that the state of interficial zone between unhydrated cement grain and its hydrates can be investigated, as such zone is the weak ring in the microaggregate concrete — high strength HCP, which decisively influences the strength of the latter. From the above we can see the following: The place at which the total weight of SiO_2, Al_2O_3, CaO and Fe_2O_3 drops abraptly must be the interfacial layer at microlevel (point 3 in Tab. 3). At a distance 1μ from the interfacial layer (point 4), Si and Ca in samples A1 and A2 were all richened, but the richness of Si in A2 was more than that in A1 and the C/S ratio of A2 was less than that of A1. This is the qualitative indication of the increase of DSP.

In hydrated region beyond point 4 the total weight of four oxides in A2 was more than that in A1, but their degrees of hydration were approximately equal to each other (see Tab. 2), which shows that the structure of A2 was denser than that of A1 due to the effect of Fe ion coordination.

From Tab. 3 it can be estimated that there was a rich-AFt region in the interfacial zone, as having been reported by Ollivier /10/. In this region the structure was most loose in the mass. The thickness of the weak region was about 5μ for A1, as compared with about 3μ for A2. This difference in thickness of weak region had to be reflected in the strength test data,

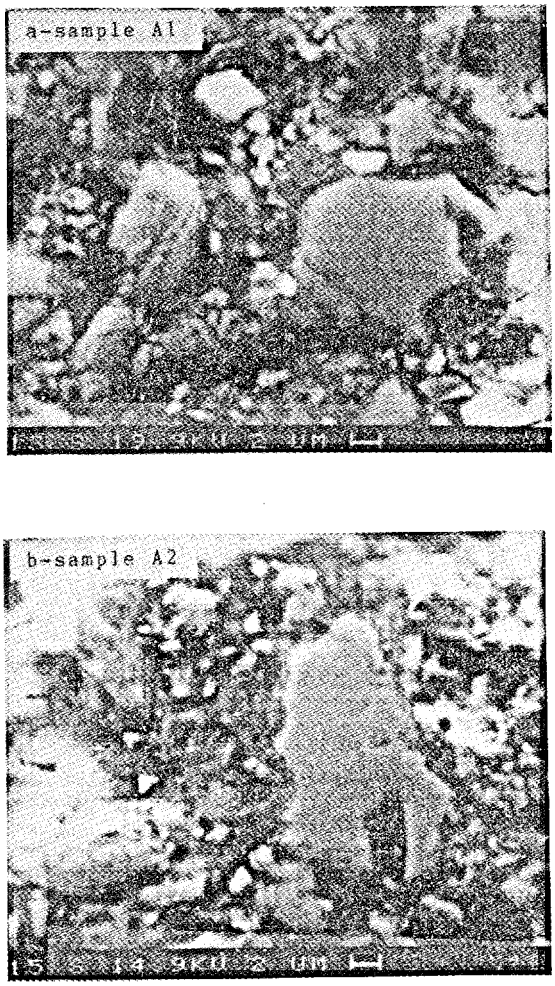

Fig. 2 SEM observation on the samples A1 and A2

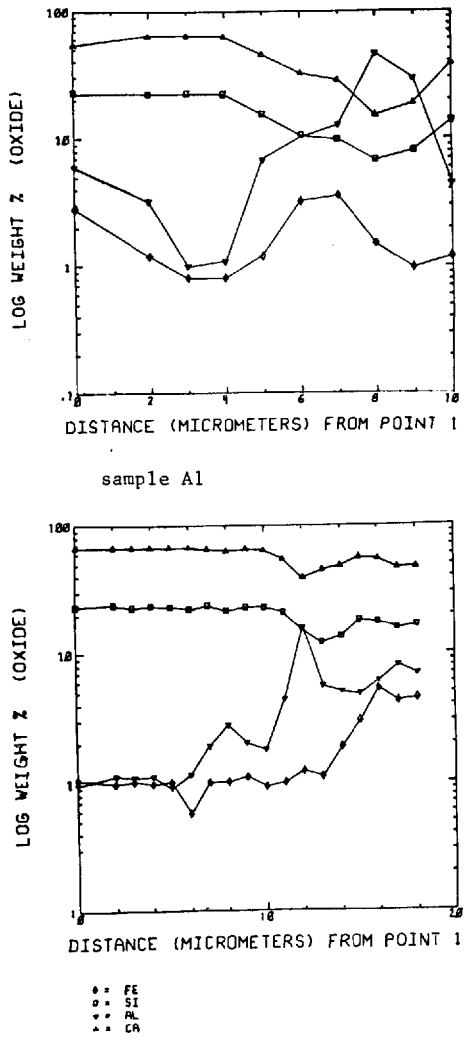

Fig. 3 EMPA of the samples A1 and A2 shown in Fig.2

Table 3. The data of EMPS of samples A1, A2

Point	Fe_2O_3	%(wt)	SiO_2	%(wt)	Al_2O_3	%(wt)	CaO	%(wt)	Total	%(wt)
	A1	A2	A1	A2	A1	A2	A1	A2	A1	A2
1	1.201	1.014	22.213	21.751	3.174	2.800	63.224	64.504	89.812	90.070
2	0.798	1.118	22.572	23.302	0.979	2.040	64.284	66.234	88.634	92.694
3	0.800	0.938	22.347	23.319	1.088	1.783	63.024	64.928	87.260	90.968
4	1.190	1.008	15.506	21.144	6.858	4.453	45.220	55.025	68.774	81.631
5	3.261	1.259	10.664	15.325	10.305	16.362	32.692	39.546	56.921	72.492
6	3.593	1.122	9.995	12.277	12.769	5.679	28.741	46.058	55.098	65.136
7	1.503	1.921	6.770	13.784	46.535	5.125	15.167	48.418	69.976	69.248
8	0.969	3.028	8.037	18.589	29.651	4.885	19.014	56.505	57.672	83.007
9	1.209	5.388	13.918	17.852	4.466	6.217	38.558	55.039	58.151	84.495
10	—	4/305	—	15.686	—	8.189	—	47.214	—	75.394

in which A2 was stronger than A1.

The Tab. 2 and Tab. 3 show that the more the polysilicate in hydrate is, the higher the strength. Uchikawa et al had reported similar results /11/, but they not yet found a regular dependence of the amount of polysilicate in C-S-H gel on the development of strength.

In order to avoid the influence of high porosity on this dependence, we kept the porosity of our samples as low as possible. Furthermore, we have applied the statistical thermodynamics to the study of the intrinsic properties and obtained a theoretical optimum molecular weight distribution which is necessary for the highest strength at zero porosity /12/.

Mw of the samples used were plotted against their compressive strength, as shown in Fig. 4.

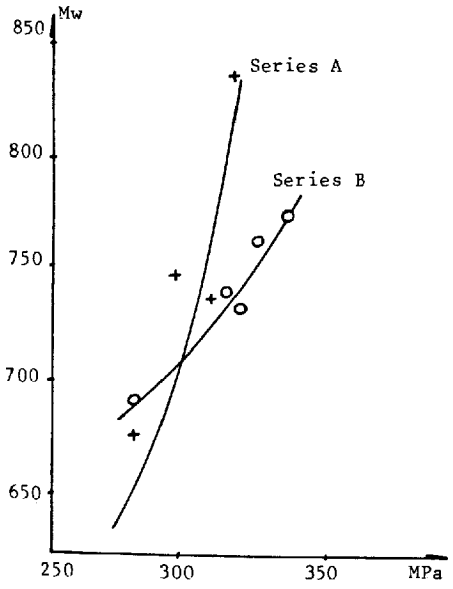

Fig. 4 Relationship between Mw and of series A and B

It can be seen that the slope of curve for series A (samples with relative high porosity) is steeper than curve for series B (samples with relative low porosity). It indicates that the influence of change in Mw on the strength of samples in series A is less than that in series B. So this is the reason why it is difficult to obtain the correlation between Mw and strength at a porosity of common HCP.

2) DSP and fracture parameters of high strength HCP

The calculated results of the three-point slow bend test were shown in Tab. 4.

Because of the additions of complex ions and silane coupling agents, the microstructures of the samples were denser and DSP increased, although their degree of hydration did not distinctly change in each series. The crack in the samples propagated uneasily, which results in the increases of G_{1c} and K_{1c} values to a certain degree.

Imagine that there is a polysilicate in front of a crack-tip, as shown in Fig. 5.

Table 4. G_{1c}, K_{1c} values of series A and B

Samp.	Kc($MN/m^{3/2}$)	Gc(N/m)	Samp.	Kc($MN/m^{3/2}$)	Gc(N/m)
A1	0.62	15.71	B1	1.08	41.52
A2	0.95	30.80	B2	1.20	87.45
A3	0.85	27.40	B3	1.08	51.20
A4	1.00	31.55	B4	0.89	55.56
A5	0.88	34.72	B5	0.91	53.78
A6	0.85	29.20	B6	—	—
A7	0.95	29.92	B7	0.98	47.01

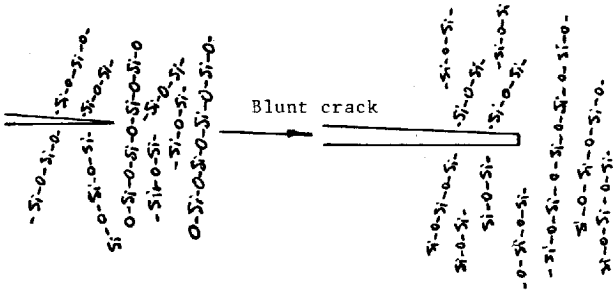

Fig. 5 Crack propagation in high strength HCP

Evidently, in the process of propagating the crack, the primary bond in polysilicate must be broken, and the deformation accompanied with it has to cause the breaking of the secondary bonds between the molecules of lower degree of polymerization in front of it, and between such molecules with it in its vicinity. The result of this process has to form a region of microcracks due to either the splitting of or slipping between molecules, which consumes much more irrecoverable energy than that in high strength HCP without adding Fe^{++} ion.

The change of DSP thus must be responsible for the brittleness of this materials. In terms of definition proposed by Ref. /13/, we have determined the index of brittleness B of the samples A1, A2 and A4, as following:

for A1 B = 3.12
for A2 B = 0.63
and for A4 B = 0.82

It is found that the increase of DSP makes the low porosity HCP not on only develop mechanical strength, but also greatly enhance its ability of producing pseudoplastic strain. Based on this investigation we obtained a high strength and low brittleness HCP in cement based materials. This material is named by us polymerized silicate cement (PSC).

CONCLUSIONS

1. Both pore structure and intrinsic properties of HCP play an important role on its mechanical characteristics. This intrinsic properties can be modified by the DSP in the microstructure of HCP.

2. The DSP can be increased by addition of inorganic complex ions Fe^{++} and Cu^{++} and organic coupling agents VTES and MDES to cement during its hydrating.

Mechanical strength develops with increasing the DSP. The lower the porosity of HCP is, the more sensitive is the influence of the changing of DSP on its mechanical strength.

3. The increase of DSP greating improves its index of brittleness. On this basis, we obtained a high strength and low brittleness HCP which is named by us polymerized silicate cement (PSC).

REFERENCES

1. P.J. Sereda, R.F. Feldman and V.S. Ramachadran, 7th Intern. Conf. on the Cem., Vol.1, VI-1/3, (1980).

2. Huang Yiun-yuan, Ding Wei and Lu Ping, MRS (Material Research Society) Proceeding, (1985) 12. Very High Strength Cement-based Materials.

3. I. Odler et al., Cement and Concrete Research, Vol. 15, p.326, (1985).

4. J.J. Beaudoin and R.F. Feldman, ibid, Vol. 15, p. 105, (1985).

5. D.M. Roy and G.R. Couda, ibid, Vol.2, p.349, (1972).

6. D. Tamas, A.K. Sarkar and D.M. Roy, in "Hydraulic Cement Pastes: Their Structure and Properties", p. 55, (1976).

7. U. Ludwig and K. Sideris, Zement-Kalk-Gips, Vol. 29, p. 463, (1976).

8. Barnes, S. Diamond and Dolch, J. of Am. Ceram. Soc., Vol. 62, p. 21, (1979).

9. C.A. Langton and D.M. Roy, 7th Intern. Conf. on the Chem. of Cem., Vol.3, p.14/22, (1980).

10. J.P. Oilivier, Ph. D. Thesis (1981).

11. H. Uchikawa and K. Furuta, Cement and Concrete Research, Vol. 11, p. 65, (1981).

12. Lu Ping, Ph. D. Thesis. (1985).

13. Huang Yiun-yuan et al, 4th Intern. Conf. Poly. Concrete, p. 429, (1984).

V. Lach, Dpt. of Building Materials, Technical University, Brno, Czechoslovakia

The Formation of $C_2SH(A)$ and C_3SH at the Hydration of Portland Cement

Le formation de $C_2SH(A)$ et C_3SH pendant l'hydratation du ciment portland

SUMMARY: The hydration of Portland cement was studied under hydrothermal conditions. The characteristics of resulting microstrukture were determined by various methods (X-ray diffractometry, microporosimetry, scanning electron microscopy and by mechanical tests). It has stated that the phase composition of microstructure varies significantly with the temperature of autoclaving process (140, 165, 190 and 215°C). The temperature dwell (1, 2 and 4 hrs) did not effect the microstructure in such an extent as the temperature. At 190 and 215°C temperatures, besides common phases CH and C-S-H gel, the basic hydration products $C_2AH(A)$ and C_3SH were formed according to the reaction:

$$m(\text{C-S-H gel}) + nCH \longrightarrow x\ C_2SH(A) + y\ C_3SH$$

High autoclaving temperature effects adversely mechanical properties of hydrated paste. The higher is the crystallinity and basicity of calciumhydrosilicates at the expense of gel and less crystalline ones, the lower is the strength of autoclaved paste. Complete hydration of Portland cement will not occur either at high autoclaving temperature. The specimens places in humid atmosphere after autoclaving increased their strength and reduced microporosity. This effect was smaller at specimens autoclaved at 215°C indicating that just in this case the degree of hydration was highest.

Estudou-se a hidratação do cimento Portland sob condições hidrotérmicas. Através de vários métodos (difratometria de raio X, microporosimetria, microscopia eletrônica de varredura e testes mecânicos), foram determinadas as características da microestrutura resultante. Estabeleceu-se que a composição de fase da microestrutura varia significativamente com a temperatura de autoclave (140, 165, 190 e 215°C). O prolongamento da temperatura (1, 2 e 4 horas) não afeta a microestrutura na mesma extensão que a temperatura por si mesma. A temperaturas de 190 e 215°C, além das fases comuns CH e gel C-S-H, formaram-se produtos básicos de hidratação - $C_2AH(A)$ e C_3SH - de acordo com a reação:

$$m(\text{C-S-H gel}) + nCH \longrightarrow x\ C_2SH(A) + y\ C_3SH$$

Temperatura elevada de autoclave afeta prejudicialmente as propriedades mecânicas da pasta hidratada.

Quanto mais altas a cristalinidade e basicidade dos hidrossilicatos de cálcio à custa de gel e de alguns menos cristalinos, menor a resistência da pasta autoclavada. Nem com alta temperatura de autoclave ocorre a hidratação completa do cimento portland. Os espécimes colocados em atmosfera úmida depois da autoclavagem aumentaram sua resistência e diminuiram a microporosidade. Este efeito foi menor em espécimes autoclavados a 215°C, indicando que justamente neste caso o grau de hidratação foi máximo.

V. Lach, Dpt. of Building Materials, Technical University, Brno, Czechoslovakia

The Formation of $C_2SH(A)$ and C_3SH at the Hydration of Portland Cement

2.2

La formation de $C_2SH(A)$ et C_3SH pendant l hydratation du ciment portland

Introduction

During hydration of Portland cement the formation of basic hydrosilicates $C_2SH(A)$ and C_3SH was observed when the hydration was performed in hydrothermal conditions. Both hydrosilicates were prepared synthetically from β-C_2S or C_3S at 160°C to 350°C (1,2). The $C_2SH(A)$ appears more frequently than C_3SH for example in autoclaved products as in lime sand bricks, slag cement and in similar technical products with relative high lime-to-silica ratio (3,4).

It is to state that both phases originate even during autoclaving of the Portland cement, which is of great effect on the properties of the autoclaved product.

Experimental

The Portland cement used in experiments had the following chemical composition:(%)

Loss of i.	2.82		
SiO_2+u.p.	21.92	MgO	2.22
Al_2O_3	4.98	K_2O	0.81
Fe_2O_3	3.19	Na_2O	0.10
TiO_2	0.23	SO_3	1.05
CaO	62.57	Total	99.89

Specific area of cement was 337 $m^2.kg^{-1}$. Water-cement ratio was 0.30. With this ratio a paste was prepared of which prisms with dimensions 40/40/160 mm were formed. These prisms were placed into humid atmosphere and, after 24 hrs, transferred into autoclave.

The autoclaving temperatureswere: 140, 165, 190 and 215°C
The temperature dwells: 1, 2 and 4 hrs
The temperature rise time lasted 30...40 min., time of cooling 20...25 minutes.

After autoclaving the prisms were removed and tempered for 30 minutes in a vessel with warm water. Then they were placed into humid atmosphere up to the time of tests, namely, after 3, 7 14 and 28 days. Prior to tests the specimens were dried at 50°C.

The phase composition of autoclaved pastes were determined with X-ray diffractometry. In addition to this the microstructure of specimens was still studied with Hg-microporosimetry and scanning electron microscopy.

Mechanical tests were performed in accordance with Czechoslovak Standard ČSN 722117 on the specimens with dimensions 40/40/160 mm.

Results and discussion

The results of analyses of specimens prepared at different conditions were compared and the effect of

- autoclaving temperature
- time of temperature dwell
- time of curing

was determined in regard to the phase composition of specimens, to their microstructure and correlation properties of microstructure, particularly to mechanical strength.

Phase composition

From the X-ray patterns it was found out that the specimens autoclaved at 140 and 165°C do not show differences in diffraction lines against not autoclaved specimens, except for the intensity of some peaks.

The specimens autoclaved at 190 and 215°C differed by increased number of diffraction lines, which were sharper and less diffusive. This is indicative of a growing share of crystalline phases in hydration product. For example 19 lines were found on the diffractogram at the specimens autoclaved at 140°C, while 41 lines were found at specimens autoclaved at 215°C (Fig.1).

At higher temperatures the hydration phases rich in CaO as $C_2SH(A)$ and C_3SH appeared. Because of simultaneus decrease of CH lines intensity with the formation of mentioned phases it is obvious that a reaction between C-S-H gel and CaO occured.

This reaction can be shown schematically as follows:

V. Lach, Dpt. of Building Materials, Technical University, Brno, Czechoslovakia

The Formation of $C_2SH(A)$ and C_3SH at the Hydration of Portland Cement

Lé formation de $C_2SH(A)$ et C_3SH pendant l hydratation du ciment portland

2,2

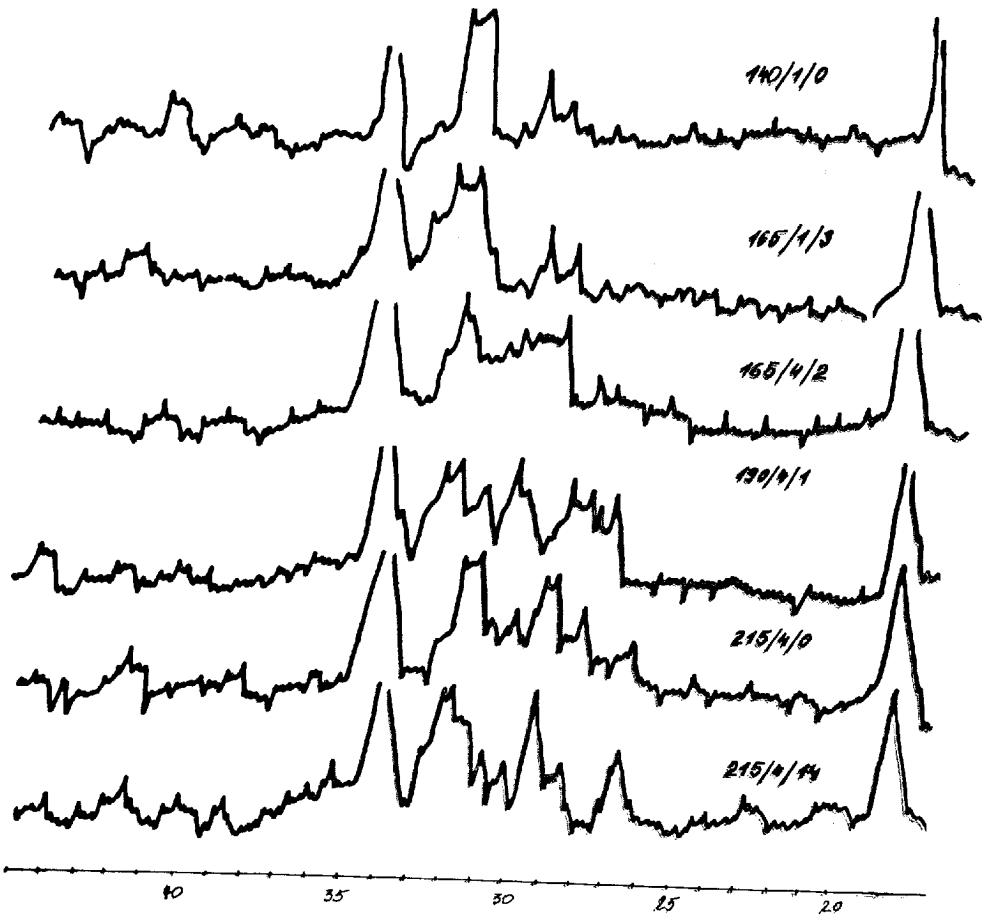

Fig.1 : XRD patterns of autoclaved Portland cement (temperature/dwell/curing)

$$m(\text{C-S-H gel}) + n\ CH \longrightarrow x\ C_2SH(A) + y C_3SH$$

This reaction takes place at higher yield of $C_2SH(A)$ and, according to the conditions in the microregions, with higher or lower formation of C_3SH.

From XRD patterns it follows:

- in hydrothermal processing of Portland cement (without admixtures with SiO_2 content) the $C_2SH(A)$ and C_3SH were formed, particularly at 190 and 215°C, as in the case of processing pure phases of β-C_2S or C_3S,
- in addition to these phases, the usual hydration products as CH, C-S-H gel, C_4AH_{13}, C_3ASH_4 and non-hydrated β-C_2S were found,
- with the time of curing after autoclaving the proportion of cristalline phases increases. Acting in the same manner is even the dwell during autoclaving.

The scanning electron microscopy shows the differences in the microstructure of specimen autoclaved at 190°C after autoclaving and after 14 days of curing (Fig. 2,3).

Since $C_2SH(A)$ and C_3S are referred to have lower binding ability, this feature was followed by the identification of mechanical properties.

Mechanical properties

Mechanical properties of specimens after autoclawing were increasing with the autocleving temperature up to 165°C then, already at 190°C did not grow anymore and, on the contrary, decreased significantly at 215°C (Fig. 4).

V. Lach, Dpt. of Building Materials, Technical University, Brno, Czechoslovakia

The Formation od $C_2SH(A)$ and C_3SH at the Hydration of Portland Cement 2.2

La formation de $C_2SH(A)$ et C_3SH pendant l hydratation du ciment portland

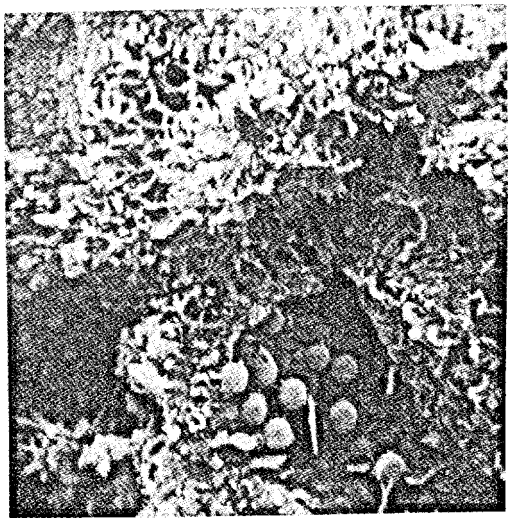

Fig. 2 : Micrograph of specimen autovlaved at 190°C after autoclaving (11000x)

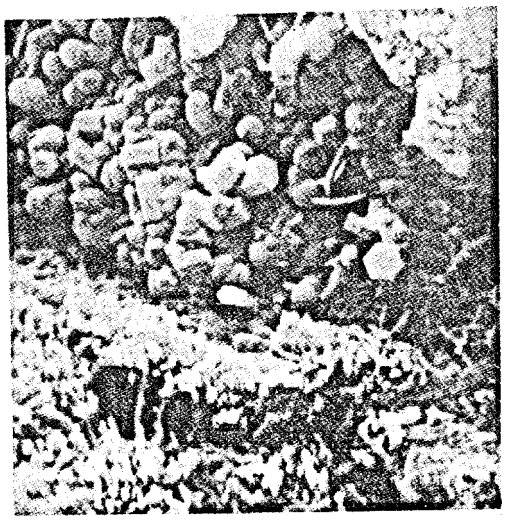

Fig. 3 : Micrograph of specimen autoclaved at 190°C after 14 days of curing

It has been confirmed that phases C_2SH bring about a decrease in compression strength, particularly after autoclaving at 215°C when the relative proportion of both in the microstructure was highest in conformity with X-ray findings.

With the storing time of autocleved specimens in humid atmosphere (to 28 days) their strength kept increasing (Fig. 5, 6, 7). This was dependent on at which tempetature the specimens were autoclaved. The highest increase in strength after storing was shown by specimens autoclaved at 140 and 165°C, lesser increase in strength was found in specimens autoclaved at 190°C. Practically minimum was the increase in strength in the specimens autoclaved at 215°C.

Referring to this could be still added that

- the hydrothermal process did not provoke complete hydration of cement and that some not yet hydrated phases remained in the in specimen, namely β-C_2S,

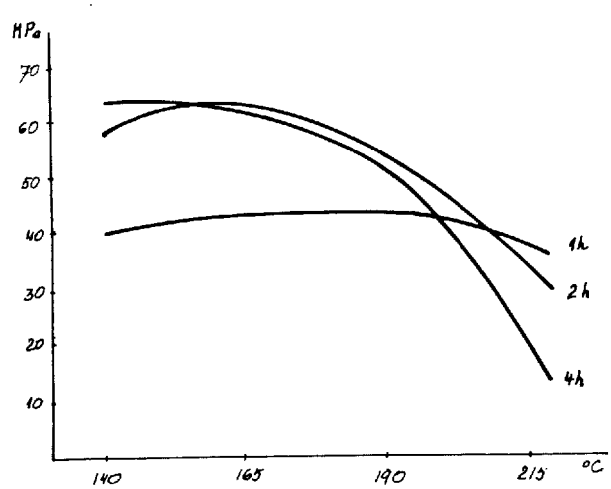

Fig. 4 : Plott of strength against autoclaving temperature and dwell

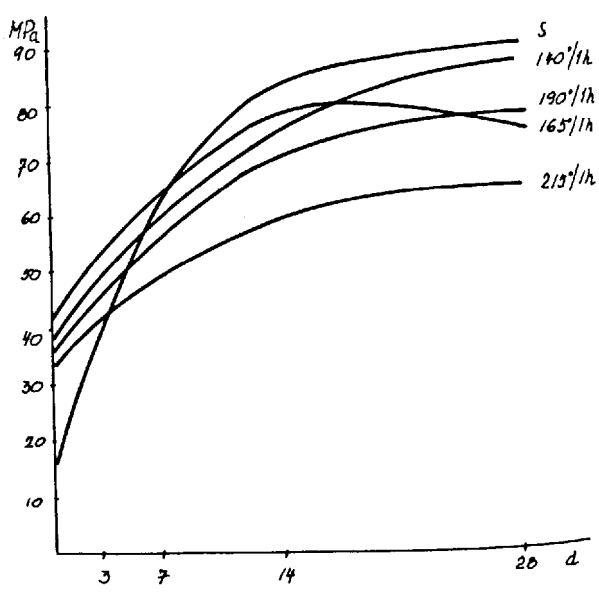

Fig. 5 : Plott of strength against curing time (S - non-autoclaved specimen)

V. Lach, Dpt. of Building Materials, Technical University, Brno, Czechoslovakia

The Formation of $C_2SH(A)$ and C_3SH at the Hydration of Portland Cement

La formation de $C_2SH(A)$ et C_3SH pendant l hydratation du ciment portland

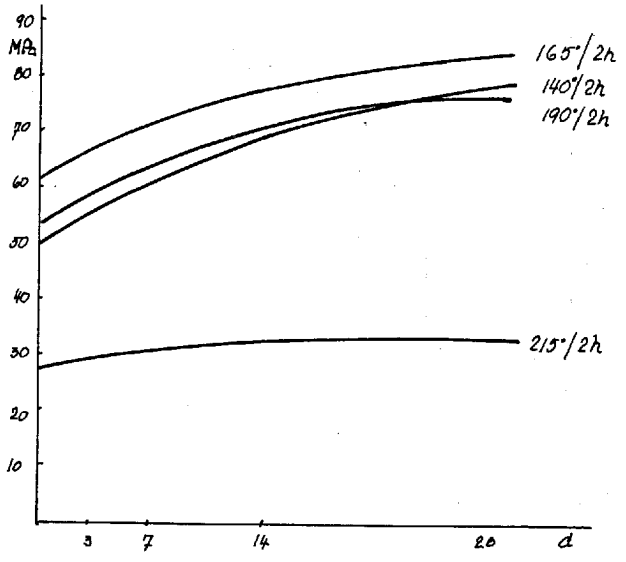

Fig. 6 : Plott of strength against curing time of various specimens

- the increase in strength of specimens during curing is to be ascribed to additional hydration and recovery of microcracks originated due to stress during autoclaving,
- with the autoclaving temperature increase the proportion of crystalline phases grew at the expense of gel phases. The

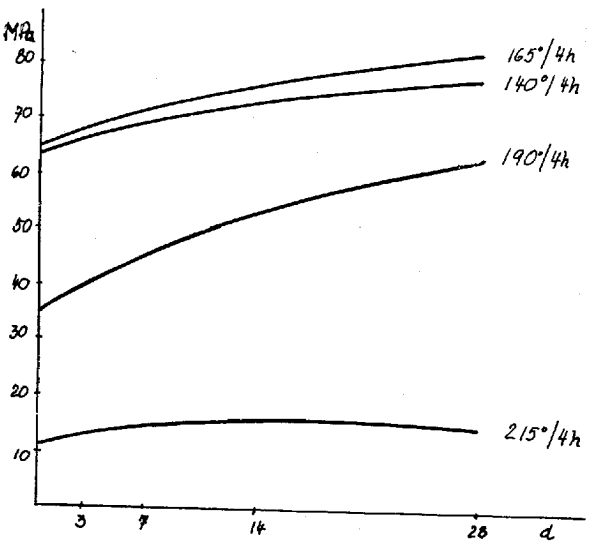

Fig. 7 : Plott of strength against curing time of various specimens

high degree of hydration was achieved at 215°C so that the strength did not increase ary more with the time of curing.

Since the mechanical properties depend on the porosity as well the determination of microporosity was performed.

Microporosimetry

The microstrukcture was investigated with reference the mentioned microporosity.

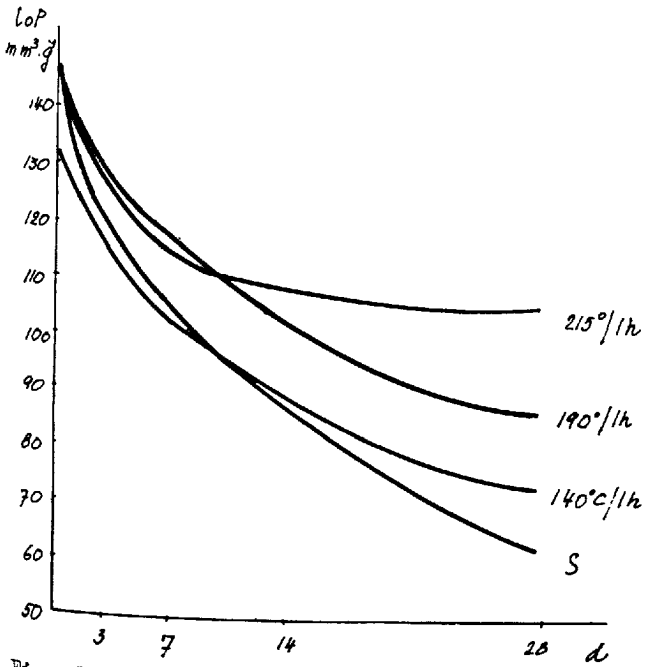

Fig. 8 : Plott of microporosimetry COP against curing time (S-non-autoclaved)

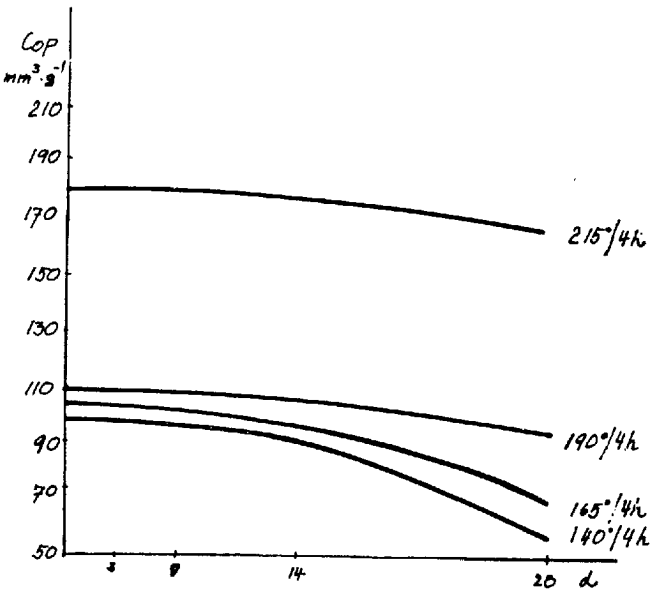

Fig. 9 : Plott of microporosimetry COP against curing time

V. Lach, Dpt. of Building Materials, Technical University, Brno, Czechoslovakia

The Formation of $C_2SH(A)$ and C_3SH at the Hydration of Portland Cement 2.2

La formation de $C_2SH(A)$ et C_3SH pendant l hydratation du ciment portland

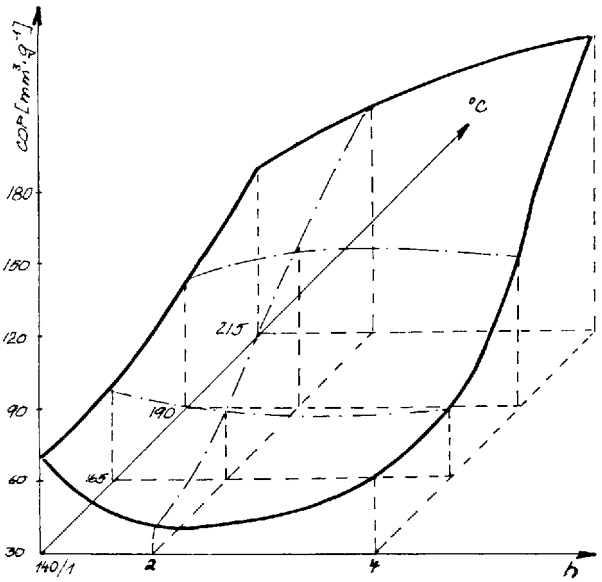

Fig. 10 : Plott of microporosimetry COP against temperature and curing time - 140°C and 28 days

Hg-porosimetry was used with the aid of which micropores and total microporosity (COP) were determined within the range of d = 0.015 ... 15 um. The results of analyses are shown in Figs. 8 - 11.

The pattern of microporosity is in keeping with the mechanical properties of specimens. Reduction in porosity manifested itself most at autoclaving temperatures 140°C and 165°C. At 215°C the autoclaving time caused an increase in microporosity.

Distribution of pores by size showed also certain differences. The biggest volume of pores was in the region of size d = 0.015 to 0.20 um in specimens autoclaved at 140° C and 165°C. At higher temperatures, particularly at 215°C it moves to the region of bigger pores, namely, 0.50 to 2.5 um.

From the results of microporosimetry it follows that

- the total volume of pores COP and distribution of pores change with the temperature and temperature dwell of autoclaving and that certain changes occur even during storing of specimens after autoclaving,

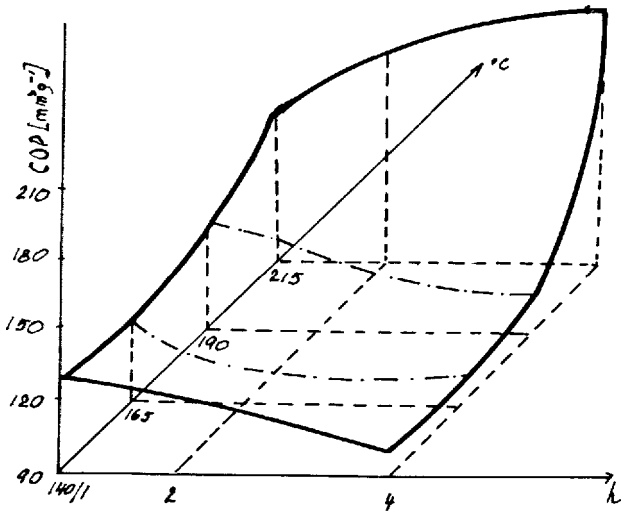

Fig. 11 : Plott of microporosimetry COP against the temperature and curing time - 140°C and 1 day

- the changes in microporosity were in quite good correlation with the strength of specimens. It can be expressed by regression function $COP = - a \sigma_d + b$, where σ_d is the compression strength in MPa, a, b are constant.

  Namely

  for 140°C/ 1 h: $COP = - 1.24 \sigma_d + 184.0$
  for 215°C/ 4 h: $COP = - 1.27 \sigma_d + 198.6$

- the reduction of microporosity with the time of storing of specimens after autoclaving was brought about by additional hydration of calciumsilicates. Pores were filled both by gel and crystalline products, the microporosity was reduced and the number of contacts was increasing. This proces was experienced namely after 140 and 165°C autoclaving temperatures,

- after higher autoclaving temperatures, above all after 215°C, the degree of hydration was high, thus further hydration took place in substantially lesser extent. Since the proportion of crystalline phases and microporosity were high, this made itself felt only by a growth of crystals without any favourable effect on

V. Lach, Dpt. of Building Materials, Technical University, Brno, Czechoslovakia

The Formation of $C_2SH(A)$ and C_3SH at the Hydration of Portland Cement

La formation de $C_2SH(A)$ and C_3SH pendant l hydtatation du ciment portland

2.2

strength.

Conclusion

In the present work the properties of cement paste after autoclaving at 140, 165, 190 and 215°C with various temperature dwell (1, 2 and 4 hrs) were studied.

It has been stated that

- during hydrothermal process changes occur in the phase composition and that the microstrukture of specimens contains high basic hydrosilicates $C_2SH(A)$ and C_3SH,
- this change in phase composition manifests itself adversely on mechanical properties of specimens which are lower in keeping with the proportion of both hydrosilicates,
- the microporosity of specimens correlated with mechanical properties. It increased with temperature and autoclaving time,
- neither in autoclaving the complete hydration of present calciumsilicates will occur, which manifested itself during investigation of properties of specimens placed, after autoclaving, in humid environment for up to 28 days. Porosity was reduced and mechanical strength increased.

REFERENCE

1.- H.F.V. Taylor (1964), "The Chemistry of Cement," Academic Press, London, 213 - 214

H.F.W. Taylor (1969), "The Calcium Silicate Hydrates," Proc., 5th Internat. Symp. Chem. Cement, Tokyo, Vol. 2, 1-26

H.F.W. Taylor (1974), "Crystal Chemistry of Portland Cement Hydration Products," Proc., VIth Internat.Congress Cem.Chem. A princ.peper. II-4-11, 1-45

2.- G.L. Kalousek (1969), "High Temperature Steem Curing of Concrete at High Pressure," Proc., 5th Internat. Symp. Chem. Cement, Tokyo, Vol. 3, 523-540

3.- G. Chiocchio, M. Collepardi and R. Turrizieni (1975), "Substituted Hydrated Calcium Silicates Obtained in Autoclave Hydration," J. Am. Cerem. Soc. 58, 185-188

4.- C.A. Langton, E.L. White, M.V. Gruczech and D.M. Roy (1980), "High Temperature Cements with Geothermal Applications," Proc., VIIth Int.Cong. Chem. Cem., Paris, Vol.III, 145-151

ŠKVÁRA František - Laboratory of Silicate Chemistry, Czechoslovak Academy of Sciences Prague, 166 28 Praha 6 - Suchbátarova 5 - CZECHOSLOVAKIA

Microstructure of Hardened Pastes of Gypsum-free Portland and Slag Cements

The gypsum-free Portland cement (GF) is a system based on ground cement clinker of specific surface 300 to 700 m^2/kg, in which is the gypsum (as setting regulator) replaced by lignine derivate (or sulphonated polyphenolate) plus alkali carbonate (or another salt). Chemical and phase composition of hardened pastes of GF cements (free-flowing pastes, w = 0.20 to 0.25) is similar to the composition of hardened pastes of Portland cements (PC). Hardened GF cement pastes attain a compressive strength of 1 to 9 MPa after 1 to 3 hours, and are composed of crystalline and amorphous patterns featuring the ratios C/S = 1 to 5, and C/A = 10 to 50. In the course of 12 to 24 hours, a dense structure is developed, the morphological character of which does not undergo any further changes through the paste strength increases (to 100 MPa and more after 28 days). This dense structure was not found to contain the crystalline formations typical of hardened PC pastes (portlandite, ettringite). The main component of the binding product in hardened GF cement pastes is a high-lime C-S-H phase (mean C/S ratio = 2.7 $\pm$ 0.1, EDAX analysis) intergrown with very fine $Ca(OH)_2$ and highly dispersed hydroaluminates (cubic and hexagonal).

The gypsum-free slag cement (GFS) is a system based on ground blast furnace slag (300 to 500 m^2/kg, admixed plastificator and alkaline component (hydroxide, silicate). Hardened GFS cement pastes (free-flowing pastes, w = 0.24 to 0.26) attain a compressive strength of 50 to 90 MPa after 28 days, and over 100 MPa after 180 days. These hardened pastes represent a dense microstructure composed of the C-S-H phase intergrown with highly dispersed hydroaluminates and hydroalumosilicates. The composition of hydrated GFS cements is close to the composition of hydrated GF cements, yet the hydrated GFS cements do contain the low-lime C-S-H phase and do not contain $Ca(OH)_2$.

O cimento portland sem gesso (GF) é um sistema baseado em clínquer de cimento moído com superfície específica de 300 a 700 m^2/kg, em que o gesso (como regulador de pega) é substituído por derivado de lenhose (ou polifenolato sulfonado) mais carbonato de álcali (ou outro sal). A composição química e de fase das pastas endurecidas de cimentos GF (pastas sem fluidez, água = 0,20 a 0,25) é semelhante à composição de pastas endurecidas de cimento portland (PC). Pastas endurecidas de cimento GF atingem resistência à compressão de 1 a 9 MPa depois de 1 a 3 horas, e são compostas de exemplares cristalinos e amorfos com relações C/S = 1 a 5, e C/A = 10 a 50. No decorrer de 12 a 24 horas desenvolve-se uma estrutura densa, cujo caráter morfológico não sofre quaisquer alterações adicionais ao longo dos aumentos de resistência de pasta (até 100 MPa e mais, depois de 28 dias). Esta estrutura densa, conforme se constatou, não contém as formações cristalinas típicas das pastas de PC endurecidas (portlandita, etringita). O componente principal no produto ligante nas pastas de cimento GF endurecidas é a fase de C-S-H com alta cal (relação média de C/S = 2,7 $\pm$ 0,1, análise EDAX) entremeado com $Ca(OH)_2$ muito fino e hidroaluminatos altamente dispersos (cúbicos e hexagonais).

O cimento de escória sem gesso (GFS) é um sistema baseado em escória de alto-forno moída (300 a 500 m^2/kg), misturada com fluidificador e componente alcalino (hidróxido, silicato). Pastas de cimento GFS endurecidas (pastas sem fluidez, água = 0,24 a 0,26) atingem resistência à compressão de 50 a 90 MPa depois de 28 dias, e mais de 100 MPa depois de 180 dias. Estas pastas endurecidas representam uma microestrutura densa composta de fase de C-S-H entremeadas com hidroaluminatos e hidrossilicatos altamente dispersos. A composição dos cimentos GFS hidratados é muito próxima da composição dos cimentos GF hidratados, porém os cimentos GFS hidratados contêm fase de C-S-H com baixa cal e não contêm $Ca(OH)_2$.

INTRODUCTION

The Laboratory of Silicate Chemistry of the Czechoslovak Academy of Sciences Prague, has been concerned for a number of years with the problems of inorganic binders based on hydraulically active compounds (clinker, slag, etc.) with a different setting regulator than gypsum[1]. The systems analysis of these gypsum-free binders has shown some of their common characteristics:

a) A greater grinding fineness range than in current cements (300 to 700 m^2/kg in clinker, and 300 to 550 m^2/kg in slag).

b) The presence of alkali activating constituent (carbonate, bicarbonate, silicate, hydroxide) and the plastificator (e.g. sulphonated polyelectrolyte).

c) The alkaline constituent and the plastificator exercise a synergic effect which is a substitution for gypsum acting as the setting retardant.

d) The possibility of working (in some cases necessary because of volume changes) at a low water-cement ratio (up to 0.20) resulting from the synergism of the alkali component and the plastificator.

e) The presence of gypsum in such binders is undesirable mainly for rheological reasons (time-limited liquefying effect at a low water-cement ratio in the presence of gypsum).

f) A fast rise in strength and attainment of higher strengths than in current Portland cements (PC) and slag-Portland ones (SPC).

The gypsum-free binders offer a wide range of options, particularly in combination with other latently hydraulic and active agents.

In this paper, attention is given to the results of the study of microstructure of gypsum-free Portland cements (GF) and gypsum free slag cements (GFS).

The GF cement many be characterized as a system of ground PC clinker of a specific surface of 300 to 700 m^2/kg + plastificator (e.g. the lignine derivate, sulphonated polyphenolate) + alkali carbonete (bicarbonate, etc.)

The GFS cement is a system consisting of the ground blast furnace slag (300 to 550 m^2 kg) + plastificator + alkali hydroxide, silicate.

MATERIALS AND METHODS

The GF cement pastes were prepared by mixing ground clinker with Na-lignin-sulphonate (monosacccharide-free, termed further NaLig) or Na-Fe sulphonated polyphenolate (KORTAN FM, Czechoslovak-made, termed as FeSF), and Na_2CO_3 or $NaHCO_3$ and water. The amount of admixtures varied from 1 to 2.5% by weight. The clinker used originated in the Lochkov, Hranice, or Štramberk Czechoslovak cement factories, and was ground to the specific surface of 300 to 700 m^2/kg in the absence of gypsum, using the grinding admixtures (NaLig, etc.) Chemical and phase clinker composition was given in [2]. The pastes made had at w = 0.20 to 0.25 a freely-flowing character on visual evaluation. For the sake of comparison, commercial PC class 400 of the same factories were used for making lastes of w = 0.35 and the same viscosity.

The GFS cement pastes were made by mixing ground blast furnace slag (300 to 550 m^2/kg), plastificators (NaLig or FeSF) and solution of NaOH or Na-silicate (SiO_2 : Na_2O cca 3). The SiO_2:Na_2O ratio in this experiment varied up to the value of 1.0. The GFS cement pastes contained 1 to 10% of admixtures and had at w = 0.24 to 0.26 a freely-flowing character on sight. Chemical composition of the slags used is given in Tab. 1

Tab.1 Chemical composition of slags(weight %)

	CaO	SiO_2	MgO	Al_2O_3	Fe_2O_3
a)	34.2	39.2	13.2	6.3	0.2
b)	42.2	39.3	5.9	8.3	0.3

The GF and GFS cement pastes were then left in saturated water vapour for 24 hours, until the 28th day in water, and then exposed to the air at a relative humidity of 35-45% and temperature of 22°C. At the prescribed intervals (2 hours to 3 years) the paste sample (sized 2.2.2 cm) were destruction strength-tested and the resultant fragments were used in a further study. The samples were vacuum-dried.

The composition of hard-set pastes was studied by the X-ray analysis, high-pressure Hg-porosimetry (418 MPa) and DTA or DTG analyses. The morphology and composition of the hydration products were SEM and EDAX tested. Using EDAX, the proportional techniques were applied[3], the details of which are described in[4].

RESULTS AND DISCUSSION

The GF cement pastes attain (depending on the specific surface) within 1 to 3 hours since hard-setting the compression strengths of 1 to 9 MPa, and in these hardened pastes are the clinker grains bound by the binding products consisting of crystalline and amorphous structures (Fig. 1).

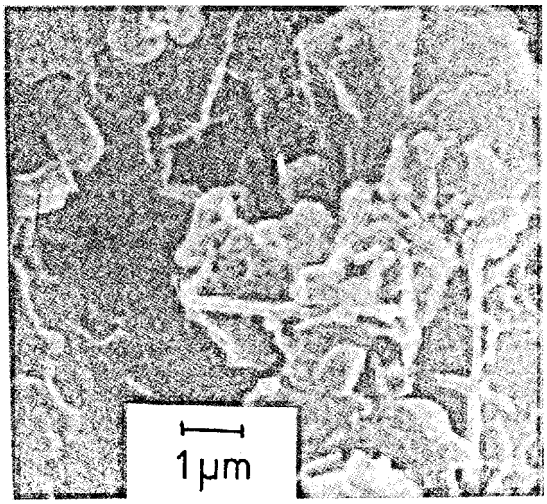

Fig. 1. SEM, paste w=0.23, GF cement 550 m^2 kg +Na_2CO_3+FeSF,2 hours, compr. str. 7.4 MPa

The C/S ratio in these structures ranged from 1 to 5, the C/A from 10 to 50 (direct EDAX analysis). The XRD and TA showed the presence of the C-A-H phase, particularly of the hexagonal C_4AH_n phase. No indices (XRD , TA) typical of the presence of the $C_4A\bar{S}_3H_{32}$ and $C_4A\bar{S}H_{12}$ were found, and the presence of the $C_4A\bar{C}_{0.5}H_{12}$ and $C_4A\bar{C}H_{11}$ (which could be produced theoretically as analogues of the sulphoaluminate hydrates typical of hydrated PC) is uncertain. The results justify a conclusion that the carrier of the initial strengths of the GF cements are, in addition to the C-A-H phase, in the first place the C-S-H phases. This is how the GF cements differ from the sulphoaluminate or fluoroaluminate cements, in which the initial strengths are primarily due to the C-A-H or C-A-S-H phases.

In the following GF cement hydration phase the development of the C-S-H phase is somewhat retarded as a result of the absence of the surface-active agents (particularly of the lignin-sulphonate). After several hours, the microstructure becomes compact in line with the strength development, with strengths attaining 10-40 MPa after 6-12 hours (in relation to specific surface) and as much as 40-80 MPa after 24 hours. The strength development is characterized by an almost violent rise after an initial slower stage. Not later than within 12 to 24 hours will the microstructure of hardened GF cement paste change into a very compact and consistent one (Fig. 2) of a distinct gel character. The morphological appearance will not change in the process of further hydration (and a further increase in strength). The strengths of hard-set GF cement pastes attain the values of 100 to 150 MPa (recorded maximum 245 MPa) after 28 days (depending again on specific surface).

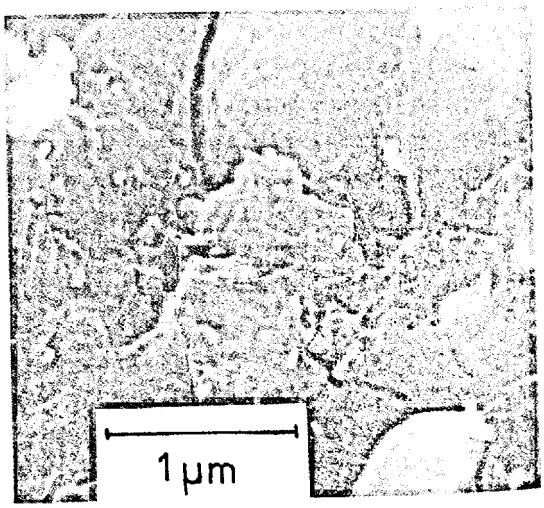

Fig.2. SEM, 24 hours, compression strength 78.6 MPa (comments see Fig. 1).

The major morphological part of hardened GF cement pastes is the C-S-H phase corresponding to C-S-H type III (Diamond[5]). There are no crystalline structure in the compact microstructure, which are typical of hardened PC (columnar portlandite crystals). Morphological appearance of hardened GF pastes was not too dependent on the specific surface of GF cements used. In most EDAX-analysed spots, the C-S-H phase showed the C/S ratio of 2 to 3, and the mean C/S value found in samples of GF cement with the 600-700 m^2/kg specific surface, and hydrated for 3 years (compressive strength 150-210 MPa) was 2.7 ± 0.1. The samples showed sometimes places of local increased concentration Of low frequency with C/S values as much as 7.0, yet not corresponding morphologically to portlandite crystals. This was most likely portlandite slightly interspersed with the C-S-H phase. Distinct portlandite crystals found in hardened PC pastes had invariably a C/S ratio more than 20 -50. The structures of a composition (C/S ratio) close to portlandite in hardened PC were found only in hardened GF cement pastes of a specific surface of some 300 m^2/kg.

All hardened GF cement paste fracture surfaces analysed by EDAX were found (irrespective of GF cement specific surface) other elements (Al, Fe, Na, K). The results obtained show (in keeping with the work by Lachowski[6]) that the phases present in hydrated GF cement may be of variable composition in microsize, and individual phases may contain another elements (Al, Fe) which do not agree with their expected stechiometric composition.

The XRD and TA show that the development of portlandite in the GF takes place later than in PC, and safe portlandite identification is possible only after 2-3 hours of hydration. The portlandite content continued to increase, but was lower than in PC. The presence of the C-S-H phase was XRD discovered after 6-24 hours. The presence of hexagonal C_4AH_n was established since hydration onset, while the cubic C_3AH_6 phase was not found until after 7 days in line with the model experiments by Collepardi[7] on the system C_3A - lignin-sulphonate - Na_2CO_3. The X-ray and TA showed also the presence of hexagonal phases of C_2AH_n, and some results pointed to a slight diffraction of the carbonate-silicate phase, probably tilleyite $Ca_5(Si_2O_7)(CO_3)_2$.

Diffractions of individual clinker minerals were identified throughout the whole period of observation, when a drop in the C_3A intensity appeared. The samples of hardened GF cements after 3 years of hydration (GF of 400-700 m^2/kg spec.surf.) were found by X-ray analysis to contain C_3S up to 8% by weight, and C_2S up to 4%. The percentage of non-hydrated clinker in polished samples of hardened pastes found by a light-microscope was up to 10-12% by volume, and in some cases even more.

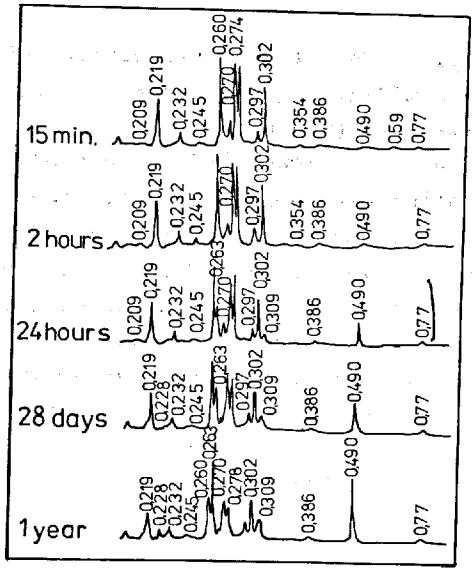

Fig.3. XRD, GF cement 550 m^2/kg, legend see Fig.1.

Lower portlandite content together with a higher C/S ratio suggest a conclusion about a potential shift in the C-S-H phase composition towards a higher C/S in hardened GF pastes processed at a low water-cement ratio . This shift towards higher C/S in hardened PC pastes due to low water-cement ratio and larger specific surface was described e.g. by Jambor[8] and Lachowski[6].

The results of the porosimetric analyses are shown in Fig. 4 for the GF cement pastes and PC class 400 of same rheological qualities.

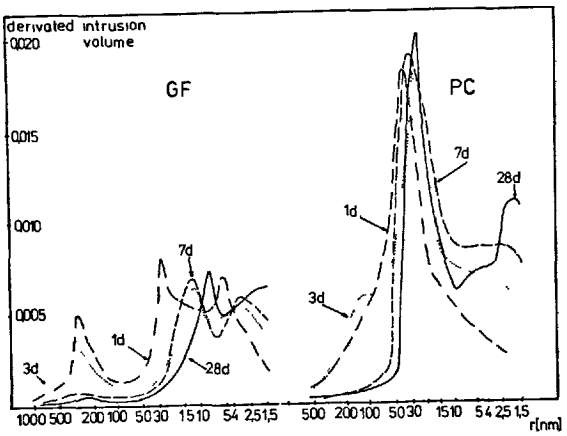

Fig. 4. Pore size distribution, GF cement (550 m^2/kg, Na_2CO_3 + FeSF, w = 0.23); PC class 400 (w = 0.35).

Due to a lower "w", lesser porosity and smaller mean pore size were found in the GF cement, and in the course of hydration the above values declined less than in PC, which shows that a fairly stabile porous structure develops already in the early stages of GF cement hydration. Fig. 5 shows the relationship between cement strength and porosity.

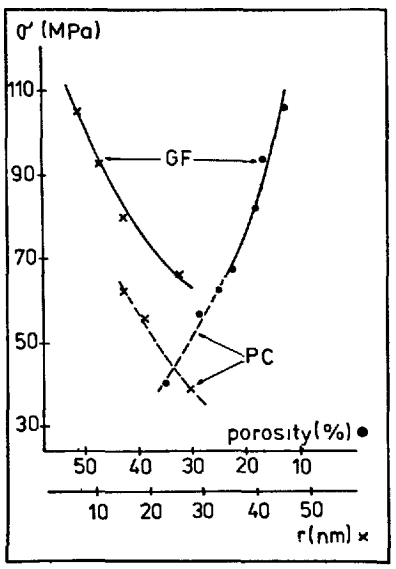

Fig. 5 Compression strength in relation to mean pore size and total porosity for the GF and PC 400 cements (legend see Fig. 4).

There is a similarity in this relationship between GF and PC with regard to total porosity, while a certain difference in the mean pore size effect points to (in line with the EDAX analysis) the fact that apart from the changes in the hydrated GF cement pore structure (in contrast to PC), also a change in the hydration product composition takes place (change in "binding potential", Jambor[8]).

High hydration product density of hardened GF cements follows both from the porosimetric analyses and indirectly from the observation of the effect of aggressive medium on hardened pastes and mortars of GF cements. The corrosion processes in hardened GFs are of a distinctly slower character in comparison with PC, and of prevailing areal nature[3].

The strength development in GFS cements is slower than in GF ones. The GFS compression strength after 24 hours is 10-30 MPa, after 28 days 50-90 MPa (in relation to specific surface and combination of admixtures). The following strength growth is continuous and after 180 days over 100 MPa is attained, after one year under optimum conditions as much as 170 MPa (paste).

Fig. 6 shows the diffractograms (X-ray) for the GFS cement (420 m^2/kg).

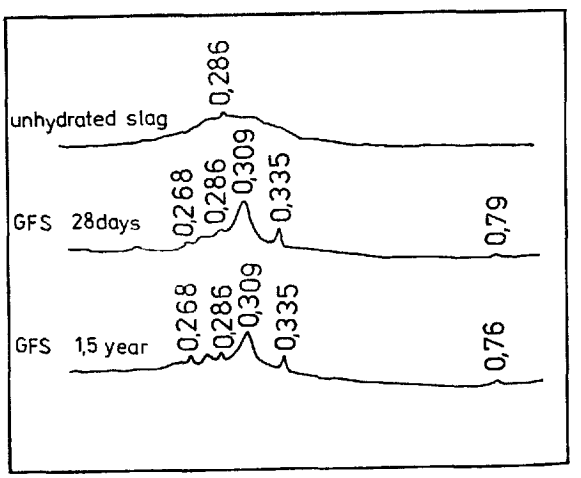

Fig. 6. XRD, GFS cement /420 m^2/kg/ + FeSF + NaOH + Na silicate.

Non-hydrated ground slag features a typical peak (some 0.3 nm) with the only identifiable line belonging most likely to merwinite $Ca_2Mg(SiO_4)_2$. Hydrated GFS cements produce few diffraction lines of low intensity and often of diffusive nature. Identified were the lines corresponding to the C-S-H phase, then slight lines of hexagonal C_4AH_n and the SiO_2 lines. The presence of calcite and thomsonite ($CaNa_2(Al_2Si_2O_8).2.5\ H_2O$) is likely. The presence of another phases described in the slag hydration in the presence of alkali activator (hydroxide, silicate)-Gluchovskij[9] e.g. hydrogranates, gehlenithydrate, gismondite, etc. is unlikely. The portlandite, cubic C_3AH_6 and sulphoaluminate hydrates lines were not observed on X-ray diffractograms.

The results of X-ray analysis are in line with those of TA. Hydrated GFS cement contains C-S-H and C-A-H phases (endothermic effects at 175, 275 and 420°C). Exothermic effects at 825 or 890°C develop as a result of organic GFS part combustion (plastificator) and this effect involves probably the generation of wollastonite or β- C_2S.

The study of the morphological character of fracture surfaces of GFS cements revealed that the matter is of a distinctly gel nature. In the hydration product gel, which is dense and consistent, no crystalline products were found which are typical of hardened PC and SPC (portlandite, ettringite). The C-S-H phase can be assigned morphologically to C-S-H type III[5].

The EDAX analysis showed that the GFS cements studied contained more Al and Mg in the hydrated matter than the GF cements (similarity to hydrated PC comparison). Hydrated GFS cement contains, in addition to Na, S, K, Mg, Fe and Al as its major components also Ca and Si. The mean C/S ratio in hydrated GFS cements was 1.1 ± 0.1, and C/A ratio was cca 10. In hydrated GFS cements, the C/S ratio was found to vary from 2 to 4 in the microsizes. The spots showing a higher C/S did not show the morphological characteristics of portlandite. The results of the porosimetric analysis (Fig. 7) showed a distinct porosity decline in a relative comparison with PC.

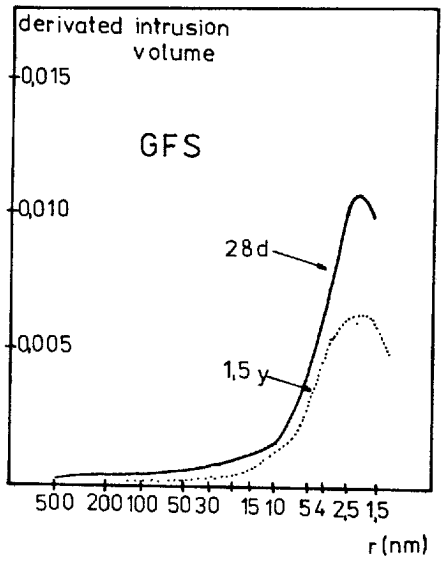

Fig. 7. Pore size distribution in GFS cement (legend see Fig. 6), 28 days, compression strength 90 MPa; 1.5 year - 173 MPa.

The results of a comprehensive analysis of hydrated GFS cements show that their major constituent is the C-S-H phase containing highly dispersible hydroaluminates or hydroalumosilicates. The composition of hydrated GFS cements is close to that of hydrated GF cements with the only exception that the GFS cements contain the low-lime C-S-H phases.

CONCLUSIONS

The results obtained have shown that chemical and phase composition of hardened GF and GFS cement pastes is similar to that of PC and SPC ones. The only significant difference is the absence of sulphoaluminate hydrates in the GF and GFS cements, and in the absence of portlandite in the GFS cement. From the point of morphology, the microstructure of GF and GFS hardened pastes is very compact, and there are no crystalline formations typical of hardened PC and SPC pastes. The hydrosilicate phase of GF and GFS cements may be classified as C-S-H type III[5]. The major constituent of bonding products in hardened GF cement pastes is mostly the hydrosilicates of the type C-S-H II (Taylor) interspersed with very fine $Ca(OH)_2$ and highly dispersed hydroaluminates. The major bonding

component of hydrated GFS cements is the hydrosilicates of a lower C/S ratio and including highly dispersed hydroaluminates and hydroalumosilicates.

The difference in mechanical strength between hardened GF and GFS cements and the PC and SPC ones is obviously the result of the shift towards the products of greater bonding capacities. In our opinion is the absence of crystalline formations (which are typical of hardened PC and SPC pastes) in the GF and GFS hardened pastes, together with a high degree of density and dispersion of all hydration products (in addition to the effect of a lower water-cement ratio) responsible for higher mechanical strengths attained in the gypsum-free Portland and gypsum-free slag cements.

REFERENCES

1) Škvára F., Kolář K., Novotný J., Zadák Z. Bažantová Z.: The cement for use at low temperatures. Proc. 7th Inter. Congress Chem. Cement, Paris 1980, p. V-57, V-61.

2) Škvára F., Kolář K., Novotný J., Zadák Z. Cement pastes and mortars with low water cement ratio. Cem. Concr. Res. 10,253-62 (1980).

3) Diamond S., Young J.F.: SEM-EDAX analysis of cement constituents - some caution. Cem.Concr.Res. 4, 899-914 (1974).

4) Škvára F., Zbuzek B.: The morphology and composition of hardened gypsum-free cements. Silicates (Prague) 27, 215-223, (1983).

5) Diamond S.: Cement paste microstructure - an overview at several levels. Proc. Conf. Hydraulic cement pastes, Sheffield 8-9.4.1976, p. 2-31.

6) Lachowski E.E., Mohan K., Taylor H.F.W., Moore A.E.: Analytical electron microscophy of cement pastes II., J.Amer.Ceram. Soc. 63, 447-452 (1980).

7) Collepardi M., Monosi S., Moriconi G.; Corradi M.: Combined effect of lignosulfonate and carbonate on pure portland cement compounds hydration, Cem. Concr. Res. 10, 455-462, (1980), 12, 271-277, 425-435 (1982), 13, 61-68 (1983), 14 (275-284) 1984.

8) Jambor J.: Influence of water cement ratio on the structure and strength of hardened cement pastes, Proc. Conf. Hydraulic cement pastes, Sheffield, 8-9.4.1980, p. 175-182 (1976).

9) Gluchovskij V.D.: Slag-alkaline cements, concrete and construction, Proc. II. All Union Conf., Kijev, UdSSR, 1984, p. 3-15.

J. Jambor, Institute of Construction and Architecture,
Slovak Academy of Sciences, Bratislava, Czechoslovakia

1

Pore Structure and Strengths of Hardened Cement Pastes

2,2

Structure Poreuse et Resistances des Pâtes de Ciment Durcies

SUMMARY : The pore structure of hardened cement paste has to be considered as an unseparable and integral coproduct of the production processes of the cement paste, which has been developing in a close connection with the hydration process of cement and strength generation of the paste. In addition to the total volume of pores, the pore structure is characterized by the pore size distribution as well as by the shape and space arrangement of pores, too. While the total porosity of the hardened cement paste depends mainly on the amount of mixing water and on the efficiency of compacting process used, its pore size distribution and the shape of pores depend decisively on the properties of cement used as well as on the time and conditions of its curing.

Taking into consideration the origin of pores and their influence on the strength it is useful to distinquish in the hardened cement paste the category of "hydration" micropores the radius of which is below the value of 1 μm and the category of "technological" pores with the radius above 1 μm, but mostly above 10 μm. The size distribution of hydration micropores is a significant characteristic of the maturity degree of the structure and of the binding capacity of hydration products developed in the paste. The technological pores provide the decisive negative influence on the strengths of hardened cement paste and this negative influence increases with growing size of individual pores - in agreement with the Griffith theory.

A new formula expressing the porosity of hardened cement paste as a variable function of its composition and production conditions as well as of its curing time has been derived - on the basis of experimental results. This form of the porosity expression has enabled us to suggest a new formula expressing the relationship between the porosity and the strength of hardened cement paste. These formulae allow to predict the changes of the porosity and strength of the cement pastes in time and they present a basis for the choice of the effective measures leading to the achievement of required properties of hardened cement pastes.

A estrutura do poro na pasta endurecida de cimento deve ser considerada como um co-produto inseparável e integral dos processos de produção da pasta de cimento, que se desenvolveu em estreita conexão com o processo de hidratação do cimento e geração de resistência da pasta. Adicionalmente ao volume total de poros, a estrutura dos poros é caracterizada pela distribuição de tamanho de poro, bem como pela forma e pela disposição espacial dos poros. Enquanto a porosidade total da pasta endurecida de cimento depende principalmente da quantidade de água de mistura e da eficiência do processo de compactação usado, sua distribuição de tamanho de poro e a forma dos poros depende decisivamente das propriedades do cimento usado, bem como do tempo e condições de sua cura.

Levando em consideração a origem dos poros e sua influência sobre a resistência, é útil distinguir na pasta endurecida de cimento a categoria dos microporos de "hidratação" cujo raio é inferior a 1 μm, e a categoria dos poros "tecnológicos", cujo raio é superior a 1 μm, mas muitas vezes é superior a 10 μm. A distribuição de tamanho dos microporos de hidratação é característica significativa do grau de amadurecimento da estrutura e da capacidade de ligação dos produtos de hidratação desenvolvidos na pasta. Os poros tecnológicos proporcionam a influência negativa decisiva sobre as resistências da pasta endurecida de cimento, e esta influência negativa aumenta com o crescimento do tamanho dos poros individuais - de acordo com a teoria de Griffith.

Com base em resultados experimentais foi derivada uma nova fórmula para exprimir a porosidade da pasta de cimento endurecido como uma função variável de sua composição e das condições de produção, bem como do seu tempo de cura. Esta forma de expressão da porosidade nos tornou possível sugerir uma nova fórmula para exprimir a relação entre a porosidade e a resistência da pasta endurecida de cimento. Estas fórmulas permitem a predição de mudanças de porosidade e da resistência das pastas de cimento a tempo, e proporcionam uma base para escolha de medidas efetivas tendentes à obtenção das propriedades requeridas das pastas endurecidas de cimento.

INTRODUCTION

Rational production of concretes and other cement based composites requires to get deeper knowledge of the forming process of their pore structure as well as the relationships between the developed pore structure and their physico mechanical properties.

The early works dealing with relations between the composition and the properties of hardened cement pastes and concretes showed that the mixing water used for their production is the main source of their porosity and further that the strength of these composites decreases very rapidly with increasing porosity. The unfavourable influence of an increasing water-cement ratio on the strength of hardened cement pastes and concretes is expressed by the well-known formulae of R.Feret (1), D.Abrams (2) and J.Bolomey (3), which up to now have been used in various modifications in the design of concrete composition. The decisive negative influence of porosity on the strength follows also from the formulae of T.C.Powers (4), K.K.Schiller (5) and E.Ryshkewitch (6) among others, which have been derived from the results of the theoretical and experimental studies of the hardened cement pastes as well as of the ceramic, vitreous and others porous materials.

The possibility of a wider use of mentioned formulae for the strength's prediction of cement composites is, however, very limited. Various cement composites with the same value of total porosity may possess very different relative volumes of binding hydration products and in this connection also a very distinct pore structure differing especially by pore size distribution and by morphological properties of pores. These differences in the pore structure result in significantly different strengths of cement composites - in spite of their similar total porosity. Unlike the ceramic and vitreous pore material, the porosity and the pore structure of cement composites are not stable and they change in time - in dependence on their curing conditions. Hence, the same value of total porosity in various cement composites may have different significance from the point of view of their strength and on principle it is not possible to suggest a generally valid formula expressing the strength - porosity relationship of various cement composites without simultaneously taking into consideration their composition and the conditions of their production (7,8).

The aim of this contribution is to analyze more profoundly the process of the formation of the porosity and pore structure, as well as their relationship to the strength of cement composites.

EXPERIMENTAL RESULTS

In support of the following considerations about the formation process of the porosity and pore structure of cement composites - in dependence on their composition and production conditions - the test results of the basic physico mechanical and structural properties of the selected cement pastes with various water-cement ratios are given in Table I.

Three cement types i.e.high strength portland cement -HSPC class 550, a portland cement -PC class 400 and a portland slag cement -PSC class 325, were used for the production of the investigated pastes. The cement pastes with low water-cement ratios and with relatively high strengths were used for these tests, too. An effective compaction of the pastes with low water-cement ratios has been provided by pressing process. The test specimens of the cylindrical shape with a diameter of 32 mm and a height of 30 mm were used. The test specimens were cured in usual way -i.e.24 hours at a relative humidity of 99% and then submerged in water at 20°C. The specimens were tested in their original - saturated state as well as after their drying at 100°C. The test results of the specimens in dry state are given in Table I.

The usual test methods for the determination of the physico mechanical properties of specimens were used. The pore structure analyzes were made by using a Carlo Erba high pressure mercury porosimeter of model 70 H. The pore size distribution in the investigated pastes is presented in Table I in a simplified form only - i.e.by the value of "average" pores radius. This is the median of the cummulative pore size distribution curve. This value characterizes the pore size distribution and allows at least approximately to compare very quickly the pore size distribution in various cement composites. The specific surface of the tested pastes was determined by BET method and nitrogen was used as the sorption gas. The values of bound water in the binding hydration products given in Table I were determined by the complex thermal analysis and are identical with the ignition loss in the temperature range of 100 to 450°C. These values show at least approximate relative amount of the binding hydration products developed in the tested pastes (9).

ORIGIN AND CHANGES OF POROSITY

The main cause of the origin of pores in the cement composites is the mixing water used for their production and the air voids, which remaine in the fresh mix after its compaction. The total porosity could be increased by various pores, internal flaws of the pore structure and by the micro - craks created additionally in the hardened cement composites due to bleeding, drying-shrinkage, local chemical changes and re-crystalization of some phases, temperature gradients and thermal expansion, etc (7).

The results given in Table I confirm that the total porosity of the cement composites diminishes with time period of their curing - i.e. with the proceeding hydration process of the cement. It is due to

TABLE I

Paste No	Paste w/c	Compaction	Air voids in fresh paste /approx./ %	Curring time at 20°C days	Unit weight g.cm^{-3}	Compression strength MPa	Density g.cm^{-3}	Total porosity %	Pores with radius R = 3.75 - 7500 nm: Pores volume cm^3.g^{-1}	Pores volume %	Average pores radius nm	Specific surface m^2.g^{-1}	Bound water in hydration products %
High strength Portland cement 550													
1	0.30	rammed	-	1	1.789	84.90	2.831	36.8	0.11570	20.7	39	3.539	7.7
2				28	1.830	96.12	2.780	34.2	0.10035	18.4	32	4.506	9.2
3				90	1.859	131.17	2.665	30.2	0.08733	16.2	25	6.716	11.5
4	0.20	pressed at 27.2 MPa	-	1	2.010	103.42	2.943	31.5	0.08607	17.3	77	3.420	5.7
5				28	2.041	135.21	2.852	28.5	0.07790	15.9	42	3.692	7.2
6				90	2.068	174.20	2.770	25.3	0.06335	13.1	32	4.890	8.7
7	0.15	pressed at 48.0 MPa	0.5	1	2.126	126.12	2.950	27.9	0.07385	15.7	148	3.216	5.4
8				28	2.157	196.20	2.848	24.3	0.06497	14.0	38	2.727	6.7
9				90	2.189	254.56	2.786	21.5	0.05573	12.2	22	3.387	7.3
10	0.10	pressed at 81.6 MPa	1.2	1	2.243	144.24	2.937	23.6	0.06331	14.1	271	1.956	4.8
11				28	2.254	224.22	2.858	21.3	0.05368	12.1	28	3.975	5.9
12				90	2.260	282.56	2.817	19.8	0.04509	10.2	20	3.667	6.4
Portland cement 400													
13	0.30	rammed	-	1	1.782	44.28	2.826	37.0	0.13162	23.8	173	2.472	5.6
14				28	1.840	96.23	2.635	30.2	0.10428	19.2	55	3.996	8.0
15				90	1.855	114.32	2.583	28.2	0.09032	16.8	47	5.182	8.7
16	0.10	pressed at 81.6 MPa	1.3	1	2.237	107.51	2.919	23.4	0.07973	17.7	420	1.962	3.5
17				28	2.262	212.72	2.829	20.0	0.05923	13.4	42	3.760	5.4
18				90	2.270	240.20	2.811	19.3	0.05279	12.0	36	4.702	5.7
Portland - slag cement 325													
19	0.30	rammed	-	1	1.722	31.81	2.787	38.2	0.16101	28.0	280	2.726	4.6
20				28	1.795	76.24	2.617	31.4	0.13036	23.4	54	4.672	7.3
21				90	1.826	101.60	2.534	28.0	0.10871	19.7	42	6.307	8.4
22	0.10	pressed at 81.6 MPa	1.6	1	2.209	112.38	2.875	23.2	0.09124	19.8	510	2.522	3.6
23				28	2.215	179.20	2.794	20.7	0.07088	15.7	35	3.315	4.9
24				90	2.252	243.56	2.754	18.2	0.05639	12.7	30	3.993	5.5

the greater volume of the hydration products in comparison with the volume occupied in the mix by hydrated cement before its hydration. Provided no microcraks and additionally created pores in the hardened cement composite are present, its total porosity in every stage of its hardening may be expressed by formula

$$P = P_o - \Delta V_{hp} \qquad (1)$$

where P_o - is the "theoretical" initial porosity, the value of which is given by the sum of the volumes of mixing water - V_w and air voids -V_v in a volume unit of the composite immediately after its compaction - i.e. $P_o = V_w + V_v$.

ΔV_{hp} - is the difference between the volume of the developed hydration products - V_{hp} and the volume share occupied by the hydrated cement in its original unhydrated state in the volume unit of the composite - V_{hc} -i.e. $\Delta V_{hp} = V_{hp} - V_{hc}$. This difference corresponds to the volume increase of the solid phases in the volume unit of the composite due to the hydration process.

The volume of the hydration products developed in the composite and the subsequent decrease of its porosity is a function mainly of the time period and the conditions of composite hardening, of the value of w/c and of the cement type used. Our test results of a great number of hardened cement pastes made of portland cements with different w/c ratios and cured for different time period in water at 20°C showed, that the volume increase of the solid phases due to the cement hydration - ΔV_{hp} in the volume unit of hardened cement pastes may be roughly expressed by

$$\Delta V_{hp} = A.w/c - \frac{B}{\sqrt{T + \frac{B}{A.w/c}}} \qquad (2)$$

where A - is a coefficient depending on the cement composition, the value of which in case of portland cements is approximately 68.4; the product A. w/c is then the maximum possible volume increase of the solid phases that may be achieved in the cement pastes with given w/c - after their long term curing in water at 20°C.

B - is a coefficient depending mainly on the class and fineness of cement; its value for portland cements of class 400 is approximately 17.1.

T - is time period of curing in water at 20°C in days.

The formulae (1) and (2) allow to predict the changes of the porosity of hardened cement pastes - in dependence of their curing time. The analysis of these formulae shows the significance of individual factors which decisively influence the porosity, pore structure and strength of the cement composites. They show that the porosity of the cement composite may change during its hardening only within the limits, that are given by its composition and its initial porosity - P_o. The use of these formulae allow also to explain some apparent discrepancies in the relations between the porosity and strength of hardened cement pastes. So the expression of the porosity of the cement pastes Nos 8 - 10 by using the formula (1) shows, that the cement paste No 8 contains an approximately 6-times greater volume of the hydration products than the cement paste No 10. This explains the 52 MPa higher compressive strength of the paste No 8 at approximately the same porosity of both pastes (7,10).

SIZE OF PORES AND ITS INFLUENCE ON STRENGTH

The size of pores in the current dense cement composites varies usually within the pores with the radius below 1 nm (10^{-9} m) up to pores with the radius of 100 μm (10^{-4} m) and some-times even more. Some authors categorized the pores in the cement composites according to their size (4,11,12). Taking into consideration the process of the formation of pores of different size as well as their possible influence on the strength we take it as useful to distinquish two categories of pores in cement composites.

a/ "Hydration" micropores, the radius of which is mostly below the value of 1 μm. The size distribution and the shape of this category of pores depend decisively on the type and on the volume of the hydration products developed in the paste (7,13).

b/ "Technological", pores with the radius above 1 μm. The air pores as well as the flaws of the structure and microcracks generated in the composite additionally belong mostly in this category of pores, too.

The size of all pores in the cement composites diminishes with their proceeding hydration process. This is confirmed also by the values of the average pore radius of the same cement pastes but after different time of their curing, which are given in Table I. These results show that the rate of the decrease of the value of average pores radius during the curing time, depends on the total porosity of the composite, but above all on the activity of the used cement and on the conditions of curing. Generally the value of average pores radius depends decisively on the volume and also on the type of hydration products developed in the composite. Hence, the low value of the average pores radius is a significant characteristic of the "maturity" degree and the stability of the composite pore structure as well as of its strength (7,9,13).

With increasing size of pores - at the same total porosity - the strength of the cement composites drops. This is confirmed also by the comparison of the values of the compression strength, total porosity and of average pores radii exhibited by pairs of cement pastes Nos 5 and 7, further more Nos 8 and 10, Nos 9 and 11 and others, which are given in Table I.

Hence the most unfavourable influence on the strength produce the technological pores - especially of larger size - even when they are present in a relatively small number in the cement composite. This involves the mechanism of the failure of cement composites under stress, which is explained by the Griffith theory (14). The pores of larger size in the cement composite under stress may act as centres for the formation and propagation of the failure cracks and the failure of the test specimen takes place on a considerable lower level of the acting load. Our approximate calculations showed that the critical pores size, at which the pores may act as centres for the formation of failure cracks, is approximately 70 μm in the cement composites with a compressive strength of 50 MPa and approximately 28 μm in the composites with a compressive strength of 100 MPa. The technological pores of these sizes are present also in well prepared cement composites - especially in the initial stage of their hardening.

POROSITY - STRENGTH RELATIONSHIP

As stated above, the relationship between strength and porosity of cement composites cannot be satisfactorily expressed without considering the main factors affecting the pore structure of the composite. Taking this into account and using the results of tests of cement pastes given in Table I as well as the test results given in our further works we have come to the following formula, which we believe to express with sufficient accuracy the relation between the compression strength of a hardened cement composite - S and its posority :

$$S = K \frac{\sqrt{P_o - P}}{w/c \cdot P} \qquad (3)$$

where P - is the total porosity in the time of test

P_o - is the initial porosity as it has been defined above

K - is coefficient, the value of which depends on the type and activity of cement, on the curing conditions, on the dose of cement in a volumen unit of the composite and also on the type of test specimens.

On the basis of results given in Table I the coefficient K in equation (3) was found to have the value of 260 for cement pastes made of cement HSPC 550, further the value of 205 for cement pastes of cement PC 400 and the value of 180 for cement pastes of cement PSC 325.

The formula (3) shows that the strength of cement composites is proportionate to the cement activity and to the volume of developed hydration products - expressed by the difference $P_o - P$. It is indirectly proportionate to the values of w/c and total porosity of the composite. The internal structure of its formula corresponds to the real process of strengths generation in the cement composites and that's why it has on principle a wide validity.

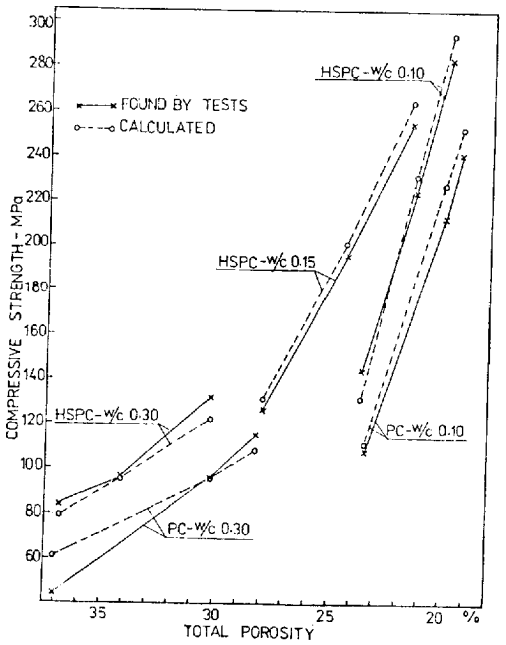

Fig.1 - Relationship between compressive strength and total porosity of hardened cement pastes prepared of cement HSPC 550 and PC 400 with different water -cement ratios.

The comparison of the experimental and calculated values of the compression strength of the tested cement pastes confirms a satisfactory occuracy of this formula. This is demonstrated also by the graphical representation of the compression strength - porosity relationship of cement pastes made of cement HSPC 550 and PC 400, which is presented in Fig.1. The difference between the experimental and calculated values of the compression strength do not mostly exceed 7%, being within the range of errors of experimental measurements. Major differences have been found only in the case of cement pastes Nos 13 and 19, by which the experimental values of compression strength were significantly lower than the calculated values. This disagreement is obviously due to the presence of larger pores in this pastes. These could not be eliminated in the course of one day curing by the developed hydration products and became active as centres for failure cracks in the sense of Griffith's theory.

CONCLUSION

The results proved a close relationship between the strength of cement composites and their pore structure, which in addition to the total volume of pores is characterized by the relative share of pores of different size, by their shape and their arrangement in space, too. The pore structure of the cement composite develops as an unseparable part of the cement hydration and of the hardening process of the composite. Its properties depend on the same factors as the relative volume and properties of developed hydration products and the strength generation of the composite. The dose od the mixing water and the volume of the air pores in a volume unit of the composite mix immidiately after its compaction are the factors which influence decisively the total volume of pores in the cement composite and substantially determine the limits within which the total porosity of the composite may vary in the various stages of its hardening. The type and the activity of used cement, as well as the time and the conditions of curing of the composite - or precisely the kind, binding capacity and the volume of hydration products developed in a volume unit of the hardened composite - are the main factors affecting the value of total porosity in its given limits - in dependence on achieved hardening stage as well as the pore size distribution and hence the degree of the maturity and the strength of the pore structure.

Considering the development process of the pore structure of cement composites new formulae expressing the decrease of the porosity in time and furthemore , the relationship between the compression strength and the pore structure have been suggested. The satisfactory accuracy of these formulae consist in their internal structure, which correspond to the process on the pore structure development and of the strength generation in the cement composites. These formulae represent a basis for the choice of effective technological measures to be taken in order to acquire the desired pore structure and high strengths of the cement composites or for the prediction of their strengths development in time.

REFERENCES

1.- R.Feret (1897).Bull.Soc.d'Encouragement, 1'Indust.Nati.II, 1604, Paris.

2.- D.Abrams (1918)"Design of concrete mixture". Struc.Mater.Res.Lab., Lewis Inst. Bull. No 1, Chicago.

3.- J.Bolomey (1935) "Granulation et prévision de la résistence probable des bétons". Travaux, 17.

4.- T.C.Powers (1958) "Structure and physical properties of hardened Portland cement paste". J.Am.Ceram.Soc. 41, pp. 1-6.

5.- K.K.Schiller (1958) "Porosity and strength of brittle solids". In: Mechanical properties of nonmetalic brittle materials. Ed.H.Walton, pp.35-49, Butterworth Sci.,London.

6.- E.Ryshkewitch (1953) "Compression strength of porous sintered alumina and zirconia". J.Am.Ceram.Soc. 36, pp.65-68.

7.- J.Jambor (1979) "Composition, structure and physico mechanical properties of silicate composite building materials". In: Proc.II. Nat.Conf.Mechanics and Technology of Composite Materials, Publish. BAN, Sofia.

8.- G.Fagerlund (1973) "Strength and porosity of concrete". In : Pore Structure and Properties of Materials. Int.Symp. Prague, Part II, pp.D 51-D 73. Publish. Academia, Prague.

9.- J.Jambor (1976) "Influence of water-cement ratio on the structure and strength of hardened cement pastes". In: Hydraulic cement pastes : their structure and properties. Proc.Conf., pp.175 - 188. Publish. Cement and Concr. Ass.,London.

10.- J.Jambor (1973) "Influence of phase composition of hardened cement paste on its pore structure and strength". In : Pore Structure and Properties of Materials. Int.Symp.Prague, Part II, pp. D 75-D 96. Publish. Academia, Prague.

11.- F.H.Wittmann (1979) "Micromechanics of achieving high strength and other superior properties". In : Proc.Workshop on High Strength Concrete, s.p. Shah; Ed.Univ.Illinois, Chicago Circle, Chicago III.

12.- K.Kendall; A.J.Howard; J.D.Birchall (1983) "The relation between porosity, microstructure and strength and the approuch to advanced cement based materials ". Phil.Trans.R.Soc.London,A. 310, pp. 139-153, London.

13.- Della M.Roy; G.R.Gouda (1973) "High strength generation in cement pastes". Cement and Concrete Res.,Vol.3,pp.807.

14.- A.A.Griffith (1920) :Phil.Trans.Roy. Soc., A. 211, pp.163-198, London.

Torben Knudsen, Technical University of Denmark, Lyngby, Denmark.

The dispersion model for hydration of Portland cement. II. The influence of fineness (*)

SUMMARY: A danish grey Portland cement clinker was ground in a laboratory rotary tube-mill to specific surfaces (Blaine) in the range 200-600 m^2/kg. The hydration at 20°C of the ground clinker was followed by measurement of chemical shrinkage, and the linear part of the dispersion model were fitted to the hydration curves to obtain the parameters: t_o, t_{50} and P_∞. The prediction of the model, that t_{50} depends in a simple way on r_o:

$$t_{50} = r_o/k$$

was verified for these samples. t_{50} is the reaction-time to reach 50% hydration, k is the rate-constant corresponding to a linear kinetic reaction mechanism, and r_o is the fineness-constant found by fitting the particle size distributions of the ground clinker samples with the equation (Rosin-Rammler):

$$F(r) = 1 - \exp(-r/r_o)$$

SUMÁRIO

Um clínquer de cimento portland dinamarquês foi moído em moinho rotatório de laboratório para a obtenção de superfícies específicas (Blaine) na faixa de 200-600 m^2/kg. A hidratação do clínquer moído foi seguida por medidas de retração química, e a parte linear do modelo de dispersão foi ajustada para as curvas de hidratação para obter o parâmetro = t_o, t_{50} e P_∞. A predição do modelo, que t_{50} depende de uma forma simples em r_o:

$$t_{50} = r_o/k$$

foi verificada para estas amostras. t_{50} é o tempo de reação para obter 50% da hidratação, k é a constante de velocidade correspondente a um mecanismo de reação cinético linear e r_o é a constante de finura determinada ao ajustar as distribuições do tamanho de partículas das amostras de clínquer moído com a equação (Rosin-Rammler)

$$F(r) = 1 - \exp(-r/r_o)$$

(*) The first part of this survey with the following sub-title "I. General concepts" is quoted at the end in the list of references under no.6.

Torben Knudsen, Technical University of Denmark, Lyngby, Denmark.

The dispersion model for hydration of Portland cement. II. The influence of fineness (*)

INTRODUCTION

The increase in reaction rate for solid state reactions with increasing fineness of material is a well-known general rule. The increase in hydration rate of Portland cements during the latest decades has (together with other factors) been achieved through prolonged grinding of the clinkers, thereby providing the cements with larger specific surface areas.

In mathematical modelling of the hydration performance of Portland cements some workers in the field have pointed to the risc of an oversimplification by merely using the limited information contained in the specific surface area or the average grain size. Taplin was probably the first to stress the importance of incorporating the entire particle size distribution (psd) curve in works about mathematical modelling of cements hydration (1). In most of his work in the field of hydration psd has been incorporated in a numerical way, whereas a recent article treats the problem of joining kinetics with psd in a more comprehensive mathematical fashion (2). In the work of Bezjak et al. concerned with hydration mechanism of cements and single phases, the entire psd is used in the numerical calculations of hydration performance, in order to compare to experimental hydration curves (3). Knudsen made a first attempt to develop an analytical model of hydration by considering a linear hydration mechanism and using a Rosin-Rammler psd (with n=1) (4), and later demonstrated by numerical examples and the use of this model the necessity of taking the psd into consideration in works on modelling hydration (5). Recently Knudsen presented a simple analytical model of hydration (the dispersion model) which covers both linear, parabolic and joined kinetics of hydration (6). This model was tested on experimental hydration curves, mainly obtained by chemical shrinkage measurements with varying water/cement-ratio, temperature and admixtures (7,8).

The aim of this paper is to demonstrate the validity of the equation:

$$t_{50}=r_o/k \qquad (1)$$

expressing the influence of fineness on the hydration rate, as predicted by the linear part of the dispersion model (4,6).

The fact that the time constant t_{50} in the linear dispersion model comes out as a simple function of the fineness constant r_o does not contradict the argument that the entire psd is needed in mathematical modelling of hydration. As shown in the theoretical part of the paper it is the simplicity of the formal basis chosen in the derivation of the dispersion model that leads to the simpel relation (1) between t_{50} and r_o.

THEORETICAL PART

The linear part of the dispersion model contains the adjustable parameters t_o, t_{50} and P_∞:

$$\alpha \equiv P/P_\infty = (t-t_o)/(t-t_o+t_{50}) \qquad (2)$$

P is a measured property depending proportionally on the degree of hydration and P_∞ is this property at degree of hydration $\alpha=1$. $t-t_o$ is reaction time measured from the onset of the main reaction t_o and t_{50} is the reaction time needed to reach 50% of the ultimate hydration.

In the derivation of the linear dispersion model the reaction of a single grain with size r was assumed to follow the kinetic equation:

$$\alpha(r,t) = \exp(-r/kt) \qquad (3$$

and the psd for Portland cements was approximated by a Rosin-Rammler equation:

$$F(r) = 1 - \exp(-r/r_o) \qquad (4$$

By integrating over all grain sizes:

$$\alpha(t)=\int_o^\infty \alpha(r,t)\,dF(r)=t/[t+(r_o/k)] \qquad (5$$

The dispersion model for hydration of Portland cement.
II. The influence of fineness (*) 2.2

was arrived at.

Now combining eq.(5) and eq.(2), the equation (1) relating fineness and hydration rate can be derived.

EXPERIMENTAL PART

Materials

The material used was a danish grey clinker with the potential phase composition: C_3S: 46.3%, C_2S: 26.7%, C_3A: 10.1% and C_4AF: 11.8%. The content of free lime was 0.7% and eqv. Na_2O was 0.58%.

Clinkers were crushed to - 2 mm, and ground in a rotary tube-mill containing porcelain balls, for 1-10 hours.

The specific surface areas were measured by the traditional airpermeability apparatus, according to ASTM, C 204-55.

The psd of the ground clinker samples were found by sedimentation in absolute alcohol with a little strontium chloride added as a peptisizer. The Andreasen pipette apparatus was used, and measurements carried out according to a danish standard F-1975.

Determination of t_{50} and r_o.

The hydration performance of clinker samples with varying fineness was measured by following the chemical shrinkage of small paste samples as described in (7,8). Water/cement-ratios of 0.5 and 1.0 were chosen and sedimentation was avoided due to flash set of the paste samples. Exceptionally long dormant periods were found for water/cement-ratio 1.0 due to excess water and lack of calcium sulfate.

The hydration curves obtained (20°C), giving the amount of chemical shrinkage as a function of time, were fitted with eq.(2) by means of a computer program HYDFIT 1. The computer program uses the reciprocal form of (2):

$$1/P = 1/P_\infty + (t_{50}/P_\infty)/(t-t_o) \qquad (6)$$

and determines t_{50} and P_∞ by linear regression for running values of t_o. The regression result with the minimum deviation from the experimental points was considered the best estimate of the three adjustable parameters: t_o, t_{50} and P_∞. In these calculations the early part of the hydration curve (~15%) was excluded, since the dispersion model can not handle this accelleratory part of the hydration curve.

The value of r_o in (4) was determined by fitting a Rosin-Rammler equation (allowing n to take on values different from unity) to the obtained psd curves:

$$F(r) = 1 - \exp\left[-(r/r_o)^n\right] \qquad (7)$$

The values determined of n were found to lie in the range 0.85-1.15 with an average close to 1. The values of r_o found were lying in the range 12.0-35.6 µm, decreasing with increasing grinding times.

RESULTS AND DISCUSSION

19 samples in all of grey clinker were ground, as earlier described, with grinding times chosen between 1 and 10 hours and psd were determined for all of these samples. Only 4 are shown in fig.1 as an illustration of the curves obtained. It can be seen from the figure, that by fitting with the simpler Rosin-Rammler equation (4), with n=1, a reasonable approximation to the experimental points is obtained, with deviations not larger than a couple of percent.

The hydration curves for the same selected samples are shown in figure 2. The curves have the typical S-shape, when plotted along a log-t axis where t is reaction time. Also shown are the results of fitting with the linear part of the dispersion model. The accuracy of the fits are at the same level as that obtained in fig.1. Finally fig. 3 demonstrates the relationship found between t_{50} and r_o. The graph contains 51 points, the results of 2-4 determinations of t_{50} for each sample (because of the limited resolution on the graph not all points show up). It can be seen that repeated determinations of t_{50} typically vary about 10%. Thus a linear rela-

The dispersion model for hydration of Portland cement.
II. The influence of fineness (*) 2.2

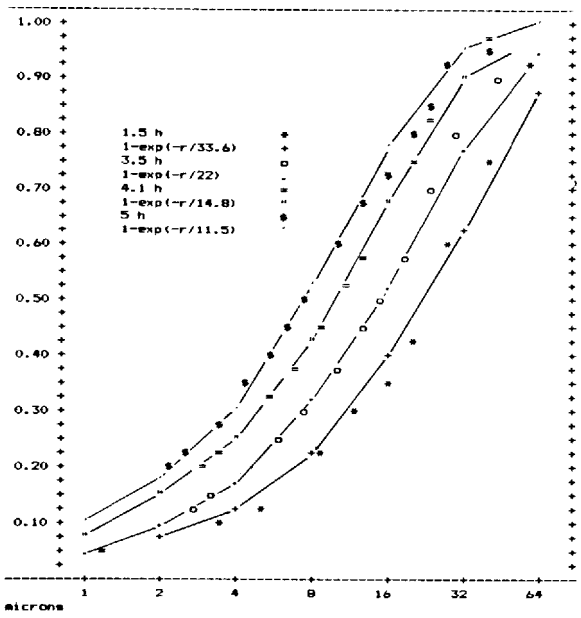

Fig.1. The accumulative particle size distribution of 4 clinker samples ground for 1.5, 3.5, 4.1 and 5 hours, compared to the results of fitting with Rosin-Rammler eq.(4).

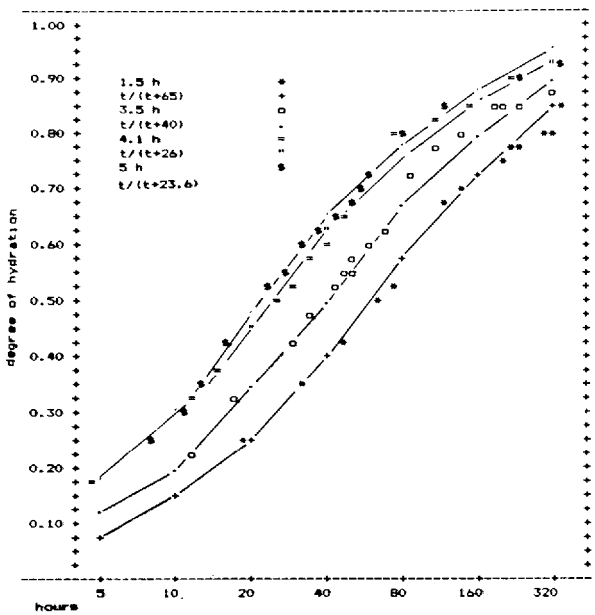

Fig.2. Hydration curves for the 4 clinker samples in fig.1 as found by chemical shrinkage measurements, compared to the results of fitting with the linear part of the dispersion model eq. (2). Plotted times are reaction times: $t-t_o$.

tion between t_{50} and r_o, as predicted from eq.(1) is proven for these clinker samples, within the accuracy of the t_{50}-determination. It can be seen that water/cement-ratio does not influence this relationship significantly.

The value of t_o, as determined by fitting with the linear dispersion model, differs greatly for these samples depending on water/cement-ratio. Dormant periods were found for W/C=0.5 to be 6±2 hours whereas for W/C=1.0, t_o was typically determined to 25±5 hours. Additions of gypsum up to 5% reduced t_o for the W/C=1.0 samples to approximately 5 hours. This demonstrates the significant effect of gypsum in promoting the onset of the main reaction.

Ultimate values of chemical shrinkage were found to lie in the range 4.0-5.0 ml/100 g cement with a tendency for W/C = 0.5 to lie in the lower part of this range. Thus the average of P_∞ found for these clinker samples is significantly less than for the corresponding cements, which are found to lie in the range 5.0-5.5 ml/100 g in reference (7). The difference is partly dur to the large water demand of the ettringite produced during cement hydration.

The slope of the regression line in Fig. 3 leads to a determination of the rate constant k in eq.(1): k = 0.54 µm/h.

The only approximate validity of eq.(4) as a model for actual psd-curves can clearly be seen from the fact that eq.(4) does not allow a determination of a specific surface area. This is only of secondary importance in modelling hydration because each size class contribute to the total degree of hydration with its weight content and not with its surface area content. But even small deviations in the finest size classes from the underlying true psd, may lead to large errors in the calculation at the total specific surface area, since the major part of the specific surface area is posseded by the finest 5-10% of the material.

Torben Knudsen, Technical University of Denmark, Lyngby, Denmark.

The dispersion model for hydration of Portland cement.
II. The influence of fineness (*)

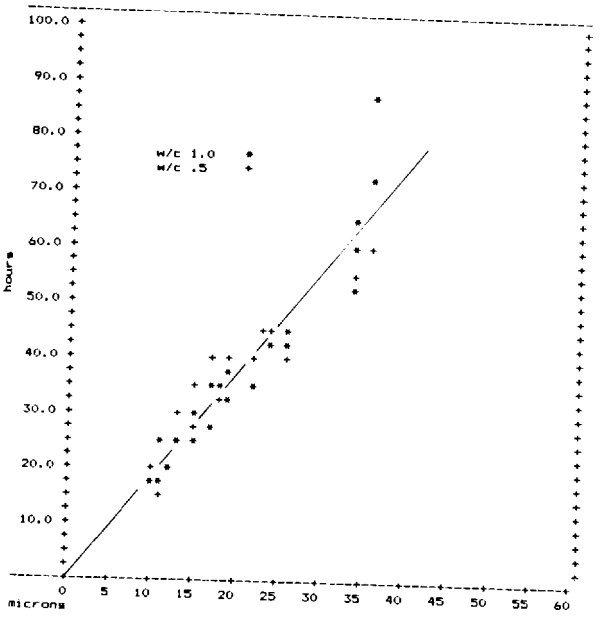

Fig.3. The time constant t_{50} (hours) plotted as function of r_o (microns) for 19 clinker samples hydrated a W/C: 0.5 and 1.0.

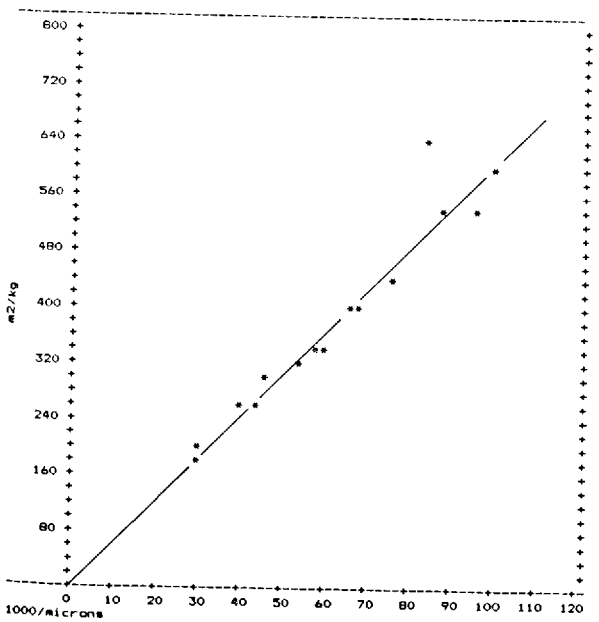

Fig.4. The specific surface area (m^2/kg) plotted as function r_o^{-1} (1000/microns) in eq.(4) for clinkers ground for 1-10 hours.

Since the Blaine surface of a cement is a standard method of defining fineness, the relation between this and r_o is given in fig. 4 for the clinker samples investigated in this work. A linear relation is obvious from the plot between Blaine surface and r_o^{-1}. From this a relation between t_{50} and Blaine surface may be derived giving:

$$t_{50}\ (h) \times \text{Blaine}\ (m^2/kg) = 11 \cdot 10^3 \qquad (8)$$

According to M.Geiker et al (7) an ordinary Portland cement with a Blaine surface close to 280 m^2/kg gave an average t_{50}, (depending somewhat on the W/C-ratio) of 31 hours. According to eq.(8) t_{50} is 39 hours for a clinker of the same Blaine surface. This shows that the relation (8) does only apply with approximation to cements. Ignoring the value of the constant in eq.(8) we get:

$$(t_{50})_1/(t_{50})_2 = (\text{Blaine})_2/(\text{Blaine})_1 \qquad (9)$$

From reference (7) and (8), t_{50}-values for a rapid and a normal hardening Portland cements may be found, leading to:

$$(t_{50})_{rapid}/(t_{50})_{ordinary} = 22/31 = 0.71$$

and

$$(\text{Blaine})_{ord}/(\text{Blaine})_{rap} = 280/380 = 0.74$$

a result comparing favorably to eq.(9).

For cements hydrating according to a parabolic kinetic mechanism (6) a different relation between t_{50} and r_o is predicted by the dispersion model:

$$t_{50} = r_o^2/k \qquad (10)$$

The form of eq.(10) is equivalent to eq. (1) except for r_o being raised to the second power. The implication of this is, that the influence of fineness on cements reacting according to a parabolic kinetic mechanism is more pronounced than for linear cements. The validity of eq(10) has not been experi-

The dispersion model for hydration of Portland cement.
II. The influence of fineness (*) 2.2

metally verified.

CONCLUSION

Ordinary Portland cement clinker was ground to fineness in the range 200-600 m^2/kg. Their rates of hydration were calculated as t_{50}, by fitting the linear part of the dispersion model to hydration curves obtained by measureing chemical shrinkage as a function of time. Values of t_{50} were found to be related to r_o by:

$$t_{50} = r_o/k$$

demonstrating the validity of the prediction of the linear dispersion model for hydration of cements.

Since the rate constant k is dependent on factors like temperature, admixtures etc, the value of k = 0.54 µm/h found in this paper applies only to the particular samples investigated.

A direct proportionallity was found between the specific surface area measured as Blaine surface and r_o^{-1} for the clinker samples.

For cements reacting according to a linear kinetic mechanism, and differing only in their psd's, hydration rates (as defined by t_{50}) are expected to be inversely proportional to their Blaine surfaces.

ACKNOWLEDGEMENT

The experimental work was carried out by Søren Bang Larsen as part of his M.Sc. graduation work. This and supplementary work concerned with the influence of certain admixtures on the hydration performance of cements (9) is highly acknowledged by the author of his paper.

REFERENCES

1. J.H. Taplin, 5th International Symposium on the Chemistry of Cement, Tokio 1968, Vol. II, p. 249, p. 337 and p. 421.

2. J.H. Taplin, J.C.S.Faraday I, 76, 2229 (1980).

3. A. Bezjak and I. Ielenic, Cement and Concrete Research, 10, 553 (1980).

4. T. Knudsen, 7th International Congress on the Chemistry of Cement, Paris 1980, I-170.

5. T. Knudsen, Engineering Foundation Conference, Henniker, New Hampshire 1982.

6. T. Knudsen, Cement and Concrete Research, 14, 622 (1984).

7. M. Geiker and T. Knudsen, Cement and Concrete Research, 12, 603 (1982).

8. M. Geiker, Ph.D. thesis, Danish Technical University, The Institute of Mineral Industry, 1983.

9. S. Bang Larsen, M.Sc. report, Danish Technical University, The Institute of Mineral Industry, 1983 (in danish).

E. Henderson and J.E. Bailey, Dept. Ceramics, Glasses and Polymers, University of Sheffield, Sheffield, U.K.
In part: Department of Materials Science and Engineering, University of Surrey, Guildford, U.K.

Structure and Morphological Aspects of Calcium Silicate Hydrates.
la Structure et les Aspects Morphologiques de Calcium Silicate Hydrates.

Abstract

The structure at the micro and molecular level of a variety of calcium silicate hydrates (CSH) have been compared. These studies show that by carrying out model experiments, it is possible to monitor their structure in the transmission electron microscope (TEM). Various CSH precipitates have been prepared in a model system, by hydrolysis of $(C_2H_5O)_4Si$ at an organic aqueous interface; with C/S ratios ranging from 0.8 to 1.9 and having various crystallinities. These usually tend to have a foillike microstructure typical of CSH(1). The hydrolysis reaction was investigated by following concentration changes in the aqueous layer, and by examining the interfacial material in the TEM. At low $(C_2H_5O)_4Si$ concentrations a ca 4 nm thick layer of amorphous CH forms; subsequently ca 10^2–10^3 nm² regions containing a honeycomb of foils develop, which gradually grow to cover the entire interfacial region. High resolution TEM of these foils indicates formation of material of complex microstructure some 10^2–10^3 nm in extent, but only ca 1 nm thick. In certain regions, double foils ca 2 nm or less apart, extending over distances of up to ca 10^2 nm have been observed; indicative of incipient short range ordering.

The detailed microstructure observed for the CSH obtained in the above model system, has been compared with material formed in the C-S-H system and by hydration of C_3S. In certain preparations TEM has revealed material that is foil-like with a ca 1 nm thickness, but which is generally multilayered with individual layers spaced ca 1.5 - 3.0 nm apart. Although the structure has been referred to as foillike a fibre-like character cannot yet be ruled out.

TEM studies of the microstructure of CSH precipitates prepared from a variety of sources indicates that they have a directionally orientated layered atomic structure related to a backbone CaO_x polyhedra rather than any 3-dimensional silicate framework-like structure.

SUMÁRIO

A estrutura em um nível micro e macromolecular de uma variedade de silicatos de cálcio hidratado (CSH) foram comparados. Estes estudos mostram que fazendo-se experimento modelo é possível monitorar as suas estruturas em um microscópio eletrônico de transmissão (TEM). Vários precipitados de CSH foram preparados em um sistema modelo, pela hidrólise de $(C_2H_5O)_4Si$ em uma interface orgânica aquosa, com relação C/S variando de 0.8 a 1.9 e tendo várias cristalidades. Estas tendem a ter uma microestrutura em forma de chapa, típico do CSH (1). A reação de hidrólise foi investigada com o acompanhamento das mudanças de concentrações na camada aquosa, e examinando o material interfacial num TEM.

Com baixas concentrações de $(C_2H_5O)_4Si$ uma camada de aproximadamente 4 nm de CH amorfo é formada subsequentemente regiões com 10^2–10^3 nm² contendo ninho de abelha nas chapas, se desenvolve, e finalmente cresce até cobrir a região interfacial inteiramente. Análise de alta resolução com TEM destas chapas indica formação de material com microestrutura complexa com 10^2–10^3 nm em extensão, mas com aproximadamente apenas 1 nm de espessura. Em certas regiões, foram observadas chapas duplas distantes aproximadamente 2 nm, ou menos, extendendo sobre distâncias de até aproximadamente 10^2 nm, indicando um incipiente arranjo de curta extensão.

A microestrutura detalhada observada para o CSH obtido no sistema modelo acima, foi comparado com material formado no sistema CSH e pela hidratação do C_3S. Em certas preparações, o TEM revelou material parecido com chapas de aproximadamente 1 nm de espessura, mas que tem geralmente várias camadas, com camadas individuais distantes aproximadamente 1.5-3.0 nm. Embora a estrutura tenha sido referida como parecida com chapas, o caracter de fibra não pode ser descartado.

Estudo com TEM da microestrutura dos precipitados de CSH preparados com uma variedade de fontes indicam que eles tem uma estrutura atômica direcionalmente orientados em camadas relacionadas a um poliedro de CaO_x e não de qualquer arranjo estrutural tridimensional de silicato.

E. Henderson and J.E. Bailey, Dept. Ceramics, Glasses and Polymers, University of Sheffield, Sheffield, U.K.
In part: Department of Materials Science and Engineering, University of Surrey, Guildford, U.K.

2.2

Structure and Morphological Aspects of Calcium Silicate Hydrates.
la Structure et les Aspects Morphologiques de Calcium Silicate Hydrates.

Abstract

The structure at the micro and molecular level of a variety of calcium silicate hydrates (CSH) have been compared. These studies show that by carrying out model experiments, it is possible to monitor their structure in the transmission electron microscope (TEM). Various CSH precipitates have been prepared in a model system, by hydrolysis of $(C_2H_5O)_4Si$ at an organic aqueous interface; with C/S ratios ranging from 0.8 to 1.9 and having various crystallinities. These usually tend to have a foil-like microstructure typical of CSH(1). The hydrolysis reaction was investigated by following concentration changes in the aqueous layer, and by examining the interfacial material in the TEM. At low $(C_2H_5O)_4Si$ concentrations a ca 4 nm thick layer of amorphous CH forms; subsequently ca 10^2-10^3 nm^2 regions containing a honeycomb of foils develop, which gradually grow to cover the entire interfacial region. High resolution TEM of these foils indicates formation of material of complex microstructure some 10^2-10^3 nm in extent, but only ca 1 nm thick. In certain regions, double foils ca 2 nm or less apart, extending over distances of up to ca 10^2 nm have been observed; indicative of incipient short range ordering.

The detailed microstructure observed for the CSH obtained in the above model system, has been compared with material formed in the C-S-H system and by hydration of C_3S. In certain preparations TEM has revealed material that is foil-like with a ca 1 nm thickness, but which is generally multilayered with individual layers spaced ca 1.5 - 3.0 nm apart. Although the structure has been referred to as foil-like a fibre-like character cannot yet be ruled out.

TEM studies of the microstructure of CSH precipitates prepared from a variety of sources indicates that they have a directionally orientated layered atomic structure related to a backbone CaO_x polyhedra rather than any 3-dimensional silicate framework-like structure.

Introduction

A typical Portland cement contains C_3S (60%), β-C_2S (20%), C_3A (10%), the ferrite phase (C_4AF) (5%) and gypsum (5%). The calcium silicates on hydration produce an amorphous calcium silicate hydrate, of variable composition, but with a C/S ratio usually in the range 1.5 to 2.0, and crystalline CH(1). The mature cement paste contains roughly 70% calcium silicate hydrate (C-S-H), 20% CH and 10% aluminate and sulphoaluminate hydrates (2). The major component is therefore the C-S-H and is consequently of great importance in relation to the overall mechanical properties and durability characteristics of concrete, mortars, etc. containing Portland cements. In spite of this its micro and molecular structure remains uncertain.

Most microstructural and indirect surface area studies indicate a two dimensional layer-like structure (3), and various models have been proposed to demonstrate how this situation might arise (4). To elucidate more detailed molecular and microstructural characteristics various synthetic C-S-H have been prepared and studied with particular reference to possible structural relationships between these and the hydrates in Portland cement pastes (5,6). The majority of synthetic preparations are generally regarded, from x-ray diffraction evidence, to have some overall two dimensional layer-like structure, reminiscent of the crystal structure of the mineral tobermorite (2,7); the basic structure of which is based on CaO_x polyhedral layers sandwiched between long chain silicate $(Si_3(O/OH)_9)$ groups (8). Other non-layered structures have been proposed for both synthetic C-S-H gels and the hydrates in Portland cement pastes (9,10). Sing et al (9) have proposed a non-layered structure for C-S-H, based on a three dimensional silicate framework, whose intrinsic negative charge is balanced by ancillary calcium counterions. Another structural type not based on tobermorite has been proposed by Grudemo (10) for the hydrate in paste hydrated Portland cement. Recently a more complex microheterogeneous structure for the C-S-H present in Portland cement pastes has been proposed by Taylor (11). In this model, such sub-crystalline order as exists may only be confined to the neighbourhood of small fragments of Ca-O layers, perhaps some tens of Angstrom long and only rarely parallel; with attached low molecular weight silicate groups. These regions are dispersed in a completely amorphous matrix, containing Ca^{2+}, H_2O and polysilicate anions, some 50 nm in size (11).

In view of the above uncertainties concerning the basic structure of the C-S-H present in Portland cement pastes, and the relationships between this, and the synthetic hydrates of various compositions and crystallinities; we have studied C-S-H formed in a model two phase system. By using this approach it has been possible to distinguish micro and molecular detail within the hydrates using transmission electron microscopy.

Experimental

The interfacial material was prepared by using a two phase system, consisting of an aqueous $Ca(OH)_2$ solution and an organic layer of hexane containing $(C_2H_5O)_4Si$. To minimise instability at the interface, during addition of the $(C_2H_5O)_4Si$ and to ensure early

homogeneity, the organic silicate was first dissolved in 25% of the total hexane used. This was then run down the wall of the partially sealed container from a pipette. The hydrolysis process was followed by determining concentration changes in the aqueous phase using a standard conductivity cell and Wayne Kerr AC autobalancing bridge B642, see figure 1. At suitable hydrolysis times ca 90% of the organic layer was removed by vacuum suction through a glass capillary. Under an atmosphere of nitrogen, either a formvar or carbon coated copper microscope grid was carefully passed through the interfacial layer. The grids were immediately placed in a vacuum desiccator over SiO_2 gel and pumped for 10 min to approximately 0.1 torr. In the instance of the formvar coated grids, a very thin film of carbon was deposited using an Edwards coating unit. The grids were then examined in a Philips 400T transmission electron microscope. The interfacial material was analysed either by a Link System x-ray analyser 860 Series II (University of Surrey) or EDAX analyser system (University of Sheffield).

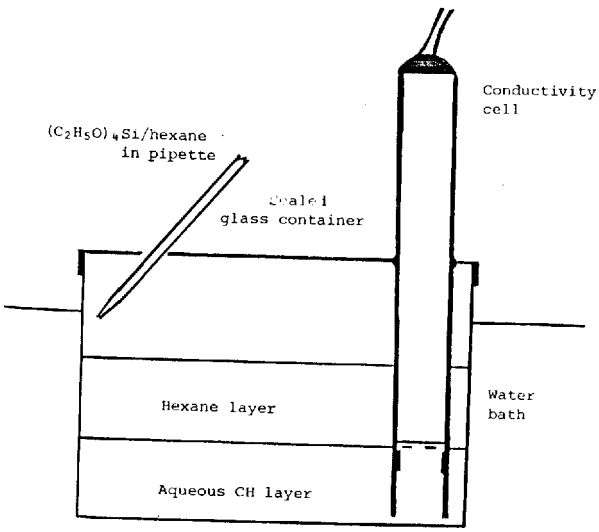

Figure 1. Schematic diagram of apparatus used to study the interfacial hydrolysis of $(C_2H_5O)_4Si$.

Other non-interfacial C-S-H were prepared by mixing CH and BDH Ltd precipitated SiO_2 with distilled water (H_2O/solid = 5). The specimen examined by TEM was left for 32 days at 100°C in a Digestion bomb. The paste recovered was first washed in an excess of acetone, then vacuum dried in a desiccator over SiO_2 gel. A specimen, with an overall C/S molar ratio of 1.7, was prepared for examination in the TEM by making a dilute suspension of the hydrate in 2-propanol. A drop of this was run onto a carbon coated Cu grid, which was then vacuum dried over SiO_2 gel.

Results and Discussion

A model two phase system was used to prepare various types of interfacial material for our TEM studies into the micro and molecular structure of C-S-H. The system chosen was found to be capable of not only producing hydrate material in a format most suitable for detailed TEM, but also of providing a reasonably controlled reaction interface for investigating the hydrolysis reaction:-

$$(C_2H_5O)_4Si + Ca(OH)_2 \rightarrow xCaO.SiO_2yH_2O + C_2H_5OH \quad \ldots\ldots \quad 1$$

The overall reaction was studied by following the decrease in electrical conductivity of the aqueous phase as CH is consumed. The conductivity scale was calibrated using known concentrations of CH; estimates of the average thickness of the interfacial film can then be made, when used in combination with:-

1) Compositional analysis of the interfacial layer.
2) The surface area of the interface.

If the above data are combined; a decrease in conductivity of 0.002 mS has been estimated to represent the formation of a ca 4 nm thick layer of CH, or ca 8 nm thick layer of C-S-H, of composition 1.5 $CaO.SiO_2.H_2O$.

Typical conductivity curves for the hydrolysis reaction at two $(C_2H_5O)_4Si$ concentrations are presented in figure 2. At low $(C_2H_5O)_4Si$ concentrations, the following hydrolysis scheme has been defined for initial interfacial CaO to SiO_2 molar ratios greater than 5:-

1) Formation of a coherent ca 4 nm thick layer of amorphous CH.
2) Formation of islands in the CH layer, ca 80 nm^2 in area, of C-S-H with C/S ratios ranging from ca 0.8 to >2.
3) Growth of these islands until the surface is covered by C-S-H of a honeycomb microstructure.
4) Thickening of the C-S-H film.

At higher $(C_2H_5O)_4Si$ concentrations, with initial C/S molar ratios less than 5, more complex behaviour was observed.

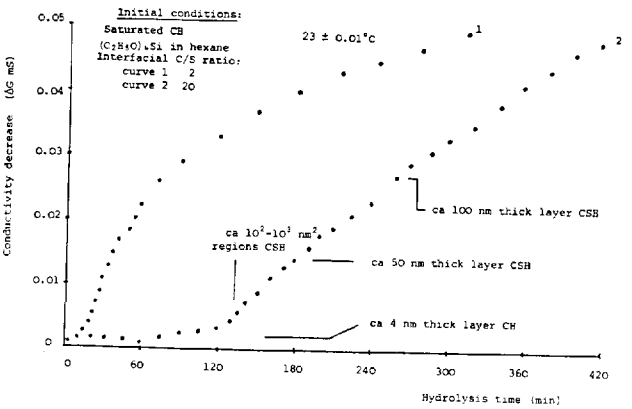

Figure 2. Electrical conductivity changes within the aqueous phase as a function of hydrolysis time.

A range of initial C/S ratios have been investigated, using CH solution of various concentrations, including supersaturated, using appropriate $Ca(NO_3)_2$ and NaOH solutions. The results pertaining to the formation of C-S-H are summarised in Table 1.

The overall effect of changing the experimental conditions on the composition and crystallinity of C-S-H are:-

1) Decreasing the initial C/S ratio results in earlier formation of an interfacial film of C-S-H with a typical foil-like microstructure.
2) The average C/S ratio is ca 1.8 for the C-S-H formed at an initial interfacial C/S ratio is 20. This decreases steadily to around 1 at the lower initial interfacial C/S ratio of 0.4. At the lowest initial ratio studied of 0.1, nonfoil-like C-S-H with a C/S ratio of 0.51 was formed.
3) At the high initial C/S of 20 an unstable microcrystalline C-S-H was formed using saturated CH solution. However, at all lower initial interfacial C/S ratios, using saturated or supersaturated CH, a generally amorphous C-S-H was formed. These

Table 1

Effect of experimental variables on the formation of interfacial C-S-H films.

Conc^{n}. of CH (factor of saturated)[1]	Hydrolysis time (h)	TEM analysis: as C/S molar ratio	Crystallinity: amorphous (a) microcrystalline (mc)
Initial interfacial C/S molar ratio of 20[5]			
1.5	1	∿4	a
1.0	0.16	∿90	a
1.0	0.50	∿50	a
1.0	1	∿40	a
1.0	4	1.91	mc[3]
1.0	8	1.77	mc
Initial interfacial C/S molar ratio of 5			
1.5	0.33	∿4[2]	a
1.5	1	∿3[2]	a
1.2	0.33	∿4[2]	a
1.0	0.16	>90	a
1.0	0.33	∿15	a
1.0	0.5	1.5-3	a
1.0	1	4	a
1.0	4	1.75	a
1.0	8	1.70	a
0.5	2	1.94	mc
0.2	2	1.65	mc
Initial interfacial C/S molar ratio of 2			
1.5	0.33	1.55	a
1.2	1	1.65	a
1.0	0.16	∿2[2]	a
1.0	0.33	∿3[2]	a
1.0	0.5	1.77	a
1.0	1	1.54	mc/a
0.5	2	1.94	mc
Initial interfacial C/S molar ratio of 1			
1.0	0.16	∿2[2]	a
1.0	0.5	∿2[2]	a
1.0	1	1.35	a
1.0	3	0.90	a
0.5	3	1.25	mc
Initial interfacial C/S molar ratio of 0.4			
1.0	0.16	∿2[2]	a
1.0	0.5	1.77	a
1.0	1	1.05	a
1.0	4	1.30	a
0.8	4	1.13	a
0.6	4	0.90	mc/a
0.5	4	1.05	mc
0.4	4	0.98	mc
0.2	4	1.05	mc
0.05	4	<0.05[4]	a
Initial interfacial C/S molar ratio of 0.1			
1.0	4	0.51[4]	a

Suffixes

[1]CH concentration given as factor of solubility at 23°C

[2]Variable composition [3]Unstable in electron beam

[4]Nonfoil-like in character

[5]Initial C/S ratio, defined as the ratio of number of equivalent CaO and SiO_2 species at the interface

typically contained two diffuse rings in electron diffraction centred at 0.30 nm and 0.21 nm, see Table 2. At lower CH concentrations, below 50% of saturated, various microcrystalline varieties of C-S-H with C/S ratios ranging from 0.98 to 1.94 are formed, see Table 2. These usually contain up to a maximum of 12 well defined electron diffraction rings.

Table 2

Selected area electron diffraction of interfacial films.

Interfacial CH film		Crystalline CH
band range d_{hkl} (nm)	band centre d_{hkl} (nm)	X-ray diffraction data (12) d_{hkl} (nm)
0.332-0.318 (s)	0.325	0.311 (m)
0.281-0.273 (s)	0.297	0.263 (vvs)
0.201 (w)	0.201	0.193 (ms)
0.187 (w)	0.187	0.179 (ms)

Interfacial C-S-H films				C-S-H(I) X-ray diffraction data (12)
amorphous		microcrystalline		
C/S = 0.8	C/S = 1.5	C/S = 0.91	C/S = 1.60	
d_{hkl} (nm)	d_{hkl} (nm)	d_{hkl} (nm)	d_{hkl} (nm)	d_{hkl} (nm)
				1.25 (vs)
0.330-0.278 (s)	0.327-0.275 (s)	0.315 (s)	0.312 (s)	0.307 (vs)
		0.285 (s)	0.280 (w)	0.280 (s)
				0.24 (w/d)
0.242-0.180 (w)	0.235-0.175 (w)			0.21 (w/d)
		0.183 (m)	0.185 (m)	0.183 (s)
		0.171 (w)	0.710 (w)	0.167 (mw)
		0.140 (vw)	0.141 (vw)	0.140 (w)
		0.120 (vvw)	0.121 (vvw)	0.123 (vw)
		0.113 (vvw)	0.115 (vvw)	0.117 (vw)
		0.105 (vvw)	0.103 (vvw)	0.111 (w)
				0.107 (vw)

The amorphous CH film has d -spacings somewhat greater than those of crystalline CH, indicating an overall expansion of the lattice, no doubt due to the disorder present. For the microcrystalline C-S-H the d-spacings observed are close to those obtained by x-ray diffraction for C-S-H (I)(12). The major difference is the absence of any detectable basal reflection at ca 1.2 nm, due presumably to the mode of formation of our interfacial C-S-H.

The interfacial material collected during stages 2 and 3 of the hydrolysis sequence described earlier, has been examined in some detail at high magnification in the TEM. A variety of C-S-H compositions, either amorphous or microcrystalline has been examined, and within the resolution achieved (ca 0.3 nm) no difference in molecular character was detected. With regard to the important molecular level features, we have observed within thin regions of the interfacial C-S-H films, foils ca 1 nm thick extending some 10^2-10^3 nm, see arrowed regions in figures 3 and 4. In certain regions double foils, also ca 1 nm thick, but ca 2 nm and less apart were also observed, see double arrows in figure 3. This represents the first direct observation at the molecular level of a highly orientated 2-dimensional layered structure. No evidence was obtained for a 3-dimensional silicate framework-like structure as proposed by Sing et al (9)for synthetic C-S-H prepared from sodium silicate and CH.

Although our C-S-H films are synthetic preparations, no evidence has been obtained to support the micro-heterogeneous structure of the C-S-H present in paste hydrated Portland cement, proposed by Taylor (11).

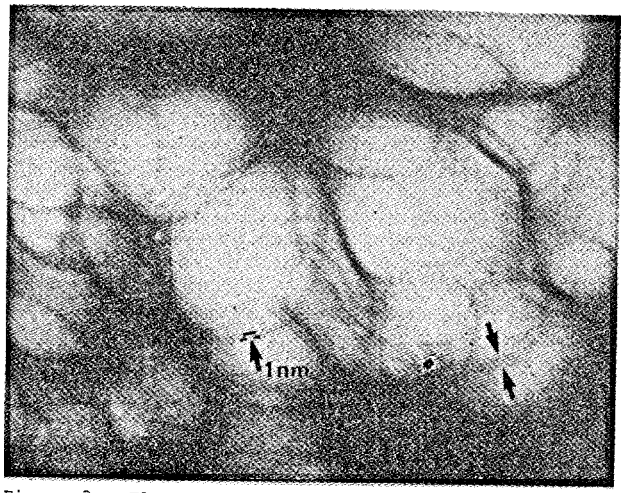

Figure 3. Electron micrograph of microcrystalline C-S-H (C/S = 1.65); initial C/S ratio of 20.
Magnification x 380000

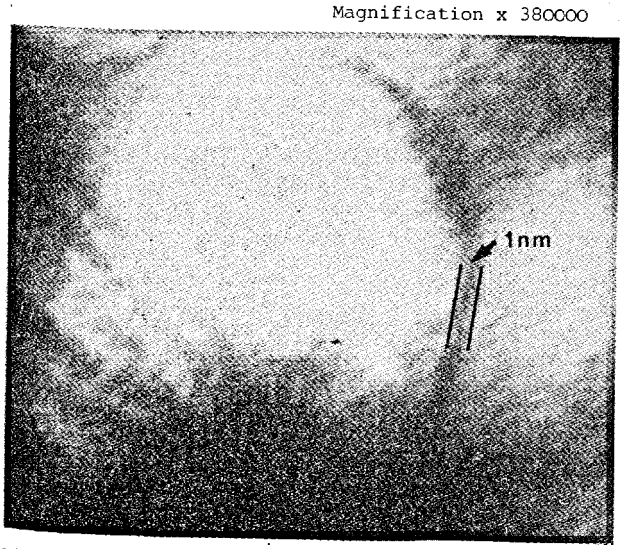

Figure 4. Electron micrograph of amorphous C-S-H (C/S = 0.90); initial C/S ratio of 5.
Magnification x 2600000

No evidence for microheterogeneous regions on the tens of Angstrom scale was obtained, when the sheet itself was examined at high magnification. Instead the film is generally featureless with only substructure on the 0.5-1 nm scale, related to the phase contrast image (13) being observed.

A foil-like structure of the type directly observed in our present studies is shown schematically in figure 5. This is derived from that proposed by Beaudoin et al (3). These strongly orientated structures contain a core layer of CaO_x polyhedra, sandwiched between silicate groups, reminiscent of the layers in crystalline tobermorite (8). The attached silicate groups are not, however, of infinite length as found in tobermorite, but considerably shorter. Typically Si_2O_7, Si_5O_{16}, Si_8O_{25}, etc chains have been found in both paste hydrated C_3S (14) and Portland cement (15,16), and in various synthetic C-S-H preparations (5,17). The thickness of the layer shown in figure 5, containing CaO_x polyhedra and short chain length silicate groups, can be estimated from the known bond lengths of 0.235 nm for Ca-O and 0.27 nm for Si-O (18). A layer of this type was estimated to be 1.1 nm thick, very close to the ca 1 nm directly observed for the foil thickness in our investigations. This estimate is also very similar to that found for an equivalent single layer in the crystal lattice of tobermorite (8).

The double foils ca 2 nm and less apart observed in the high magnification TEM, are also shown schematically in figure 5. These are probably due to incipient short range ordering in a direction at right angles to the sheet, i.e. in the "c-cell direction". Such foils represent only a very small percentage of the overall field of view, and are not parallel even over the scale of a few nanometres, see figure 3. The degree of ordering in this direction therefore appears to be extremely low. The lack of any significant ordering in this direction is confirmed by the absence of a basal reflection, in any of the electron diffraction patterns obtained of our interfacial preparations, see Table 2. This absence of such ordering in these interfacial C-S-H is probably related to the micro-environment at the interface. Intermolecular forces appear to be operating in such a way as to inhibit ordering in a direction at right angles to the sheet, even for microcrystalline hydrates. The weaker long range Van der Waals forces, operating over 2 nm or so between neighbouring foils, appear to be incapable, in general, of overcoming the intermolecular hydrogen bonds, between the H_2O and C_2H_5OH molecules in the inter-foil region at the interface. As a consequence only a statistically insignificant number of foils are ca 2 nm or less apart.

A non-interfacial C-S-H preparation with a C/S ratio of 1.7 has also been examined in the TEM and significantly micro and molecular detail has again been observed. A low magnification micrograph clearly reveals the pseudo-hexagonal microstructure, formed by what, at this level of magnification, appears to be material of a fibre-like character, see figure 6. Although the general microstructure appears to be highly directionally orientated; conventional 'microspot' selected area diffraction, to spot size 40 nm, was consistent with a generally amorphous C-S-H with 2 broad bands centred at 0.31 nm and 0.19 nm. At higher magnification the apparent fibre-like microstructure is now observed to be foil-like, reminiscent of the C-S-H interfacial foils, except in being much straighter, see figure 7. High magnification TEM has again revealed foils ca 1 nm thick, extending over 10^2-10^3 nm, see arrowed region in figure 7. In addition, these foils are multilayered in character, some 2-4 nm apart, with up to at least six layers. This multilayered microstructure is probably the reason why various C-S-H of this high C/S ratio, designated C-S-H(II) are thought to be fibre-like in character (19).

The ca 1 nm thick foils present in the non-interfacial hydrate, are significantly straighter and multilayered in character, compared in the doublets and highly curved ca 1 nm foils present in interfacial C-S-H of the same composition. These differences in microstructure are probably related to the difference in microenvironment between the two preparation routes. However, in spite of these, C-S-H with the same basic molecular character are formed, retaining the ca 1 nm foil thickness typical of a CaO_x polyhedral layer

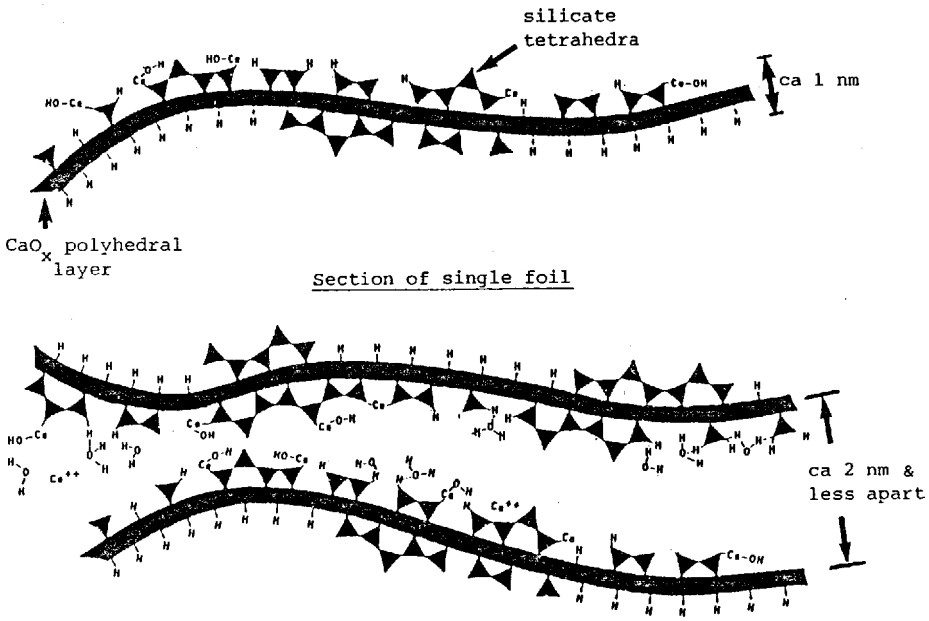

Figure 5. Schematic representation of the C-S-H foils observed in the transmission electron microscope.

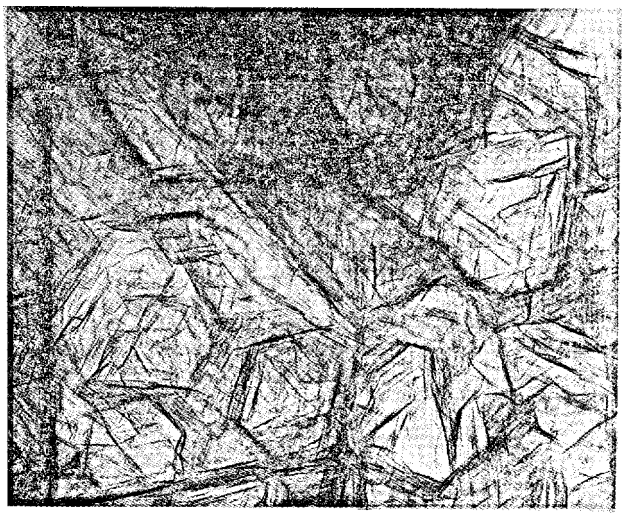

Figure 6. Electron micrograph of C-S-H (C/S = 1.7); prepared from a C/S paste, left for 32d at 100°C. magnification x 38000

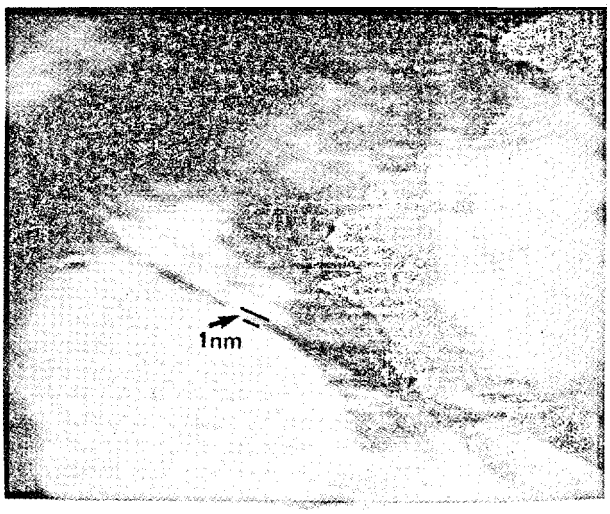

Figure 7. Electron micrograph of C-S-H (C/S = 1.7); prepared from a C/S paste, left for 32d at 100°C. magnification x 1000000

sandwiched between silicate chains as shown in figure 5. The basic molecular features are therefore retained, independently of the mode of formation, the composition or degree of order. This strongly suggests that the C-S-H in paste hydrated Portland cement has a similar basic molecular structure to that directly observed in the TEM, in these studies using a model two phase system or CaO/SiO_2 paste.

Conclusions

By using a model two phase system it has been found possible to, not only prepare a wide variety of C-S-H, but produce interfacial hydrates of an appropriate format to characterise their micro and molecular structure in the transmission electron microscope. Dependent on experimental conditions various amorphous or microcrystalline hydrates, with C/S molar ratios ranging from ca 0.8 to 1.9 were prepared. The majority of these C-S-H were found by TEM to have a typical crumbled foil microstructure.

In particular hydrate preparations more detailed TEM has revealed their micro and molecular structural character. The presence of ca 1 nm foils extending to 10^2-10^3 nm along the sheet have been directly observed in both amorphous and microcrystalline hydrates, with

compositions in the range C/S = 0.9 to 1.75. The ca 1 nm thick foils appear to represent the basic core structure of these hydrates, consisting of a CaO_x polyhedral sheet sandwiched between short chain silicate groups. The presence of double ca 1 nm foils ca 2 nm and less apart, extending over 10^2-10^3 nm are indicative of incipient short range ordering at right angles to the sheet.

The non-interfacial C-S-H (C/S = 1.7) was thought to have a fibre-like microstructure when examined at low magnification. However, more detailed microscopy revealed the actual character of this hydrate at a micro and molecular level. Highly directionally orientated foils ca 1 nm thick extending some 10^2-10^3 nm were observed. Instead of doublets, multilayered C-S-H foils between ca 2 nm and 4 nm apart, consisting of up to 6 layers, were also observed. In spite of the overall highly directionally orientated character of these foils, conventional electron diffraction contained but two diffuse bands typical of amorphous materials. The thickness of these ca 1 nm foils, like similar but more highly curved interfacial C-S-H foils, is again consistent with a basic structural core, consisting of a CaO_x polyhedral sheet sandwiched between silicate groups. The difference in foil character, between the interfacial C-S-H, where they are high curved and the highly directionally orientated non-interfacial hydrate foils, is probably related to the great difference in preparative conditions, rather than to any basic change in their overall sheet-like molecular structure.

The retention of this foil-like molecular level structure, containing CaO_x polyhedral sheets sandwiched between silicate groups of various types; independent of mode of formation, composition or degree of order, strongly suggests that the C-S-H in paste hydrated Portland cement, could well, also contain this basic highly orientated layer-like molecular structure.

Acknowledgements

One of the authors, EH, would like to thank Blue Circle Industries PLC, Research Division, Greenhithe, Kent, U.K. for their permission to participate in The Royal Society/SERC Industrial Fellowship scheme and also these bodies for the award of a 2 year fellowship. He would also like to thank many colleagues at the Universities of Surrey and Sheffield for their help in using the TEM and ancillary equipment and for many useful discussions.

References

1. D.D. Double, "New Developments in understanding the chemistry of cement hydration", In: Technology in the 1990's: Developments in Hydraulic Cements, The Royal Society (London), p.53, 1983.
2. S. Diamond, Proc. Conf. Hydraulic Cement Pastes: Their Structure and Properties, Sheffield 1976.
3. V.S. Ramachandran, R.F. Feldman and J.J. Beaudoin Concrete Science, Heyden & Son Ltd., 1981.
4. H.M. Jennings, "The Developing Microstructure in Portland Cement", In: Advances in Cement Technology (Ed. S.N. Ghosh) Pergamon Press, p.349, 1983.
5. H. Stade, Z. Anorg. Allg. Chem. 470, 69, 1980.
6. H.F.W. Taylor, 5th ISCC, Tokyo, Vol.11, 1, 1968.
7. R.H. Smith, P. Bayliss and B.R. Gamble, Cem. Concr. Res., 2, 559, 1972.
8. S.A. Hamid, Z. fur Kristographie, 154, 189, 1981.
9. F.G.R. Gimblett, Z. Mohm. Amin and K.S.W. Sing, 7th ISCC, Paris II, 11-225, 1980.
10. A. Grudemo, Rilem-d'INSA Symp. Toulouse, November 1972, CBI rapporter 9:75.
11. H.F.W. Taylor, Prog. Eng. Found. Conf., New Hampshire (Ed. J. Shalny) p. 107, 1979.
12. H.F.W. Taylor, The Chemistry of Cements, Vol.2, Academic Press, 1964.
13. D.J. Smith, W.O. Saxton, J.R.A. Cleaver and C.J.D. Catto, J. of Microscopy, 119(1), 19, 1980.
14. J. Hirljac, Z.-Q. Wu and J.F. Young, Cem. Concr. Res., 13, 877, 1983.
15. B.R. Currell, H.R. Midgeley, M. Montecinos and J.R. Parsonnage, Cem. Concr. Res., 15, 889, 1985.
16. N.J. Claydon, C.M. Dobson, G.W. Groves, C.J. Hayes and S.A. Rodger, Proceeding 35, The Chemistry and Chemically Related Properties of Cement, Brit. Ceram. Soc., p.55, 1984.
17. H. Stade and W. Wicker, Z. Anorg. Allg. Chem., 466, 55, 1980.
18. J. Klinowky and A.L. Mackay, "Silicate Structures and Methods for their Analysis", In: Structure and Performance of Cements (Ed. P. Barnes), Applied Sci. Publ. Ltd., p.1, 1983.
19. H.F.W. Taylor, "The Chemistry of Cement Hydration", In: Progress in Ceramic Science (Ed. J.E. Burke), Pergamon Press, p.89, 1961.

N.B. Eden and J.E. Bailey
Department of Ceramics, Glasses and Polymers, University of Sheffield, S10 2TZ, England.

2.2

Crack Tip Processes and Fracture Mechanism in Hardened Hydraulic Cements
Les procédes de formation d'un bout de felure et le mécanisme de fracture dans les ciments hydrauliques et durs

Summary

A major problem in examining crack tip processes in hardened cement paste is that, although sufficient resolution is obtained in the scanning electron microscope, this technique involves desiccation of the cement and consequent microstructural damage. Such a drawback can be overcome by the use of optical microscopy, though it generally gives insufficient resolution, this being limited to above 1 μm.

To examine cracks finer than this, it is necessary to improve the resolution of the reflected light microscope. This is possible by utilizing the transluscence of cement pastes, and the ability of fine cracks, about 0.1 μm wide to scatter transmitted light. By reducing the diameter of the illuminating beam to within the field of view, concentration may be focussed on the area immediately around the beam, where light is being transmitted through the sample, perpendicular to the beam. If a crack, about 0.1 μm or more wide, is present in this "diffuse illumination" zone, then light will be scattered by the crack, resulting in an easily observable change in light intensity either side of the crack.

By the use of this technique in conjunction with a straining stage, it is possible to observe the processes occurring at the crack tip as the load on the sample is increased and to observe changes in crack tip processes in wet or partially dried cement pastes during ageing, and when the pastes are modified. Complex changes occur in the "process zone" where fracture develops ahead of a notch or flaw, and these have a direct effect upon the mechanical properties of the cement.

This paper describes the diffuse illumination optical microscopy technique, and examines the observations made on normal and modified hydraulic cements.

Um problema relevante no exame dos processos de formação de trinca em pasta de cimento endurecido está no fato de que, embora se tenha solução por intermédio de microscópio eletrônico de varredura, esta técnica implica em dessecação do cimento, e conseqüentemente em dano microestrutural. Este inconveniente pode ser evitado com o uso de microscopia ótica, apesar de o mesmo proporcionar resolução insuficiente por estar limitado a acima de 1 μm.

Para examinar trincas de grandeza menor que esta é necessário melhorar a resolução do microscópio de luz refletida. Isto é possível aproveitando-se a translucidez das pastas de cimento, e a aptidão das trincas finas (com abertura de 0,1 μm) para dispersar luz transmitida. Reduzindo o diâmetro do facho de luz para dentro do campo de visão, a concentração pode ser focalizada na área imediatamente circunvizinha do facho, onde a luz está sendo transmitida através da amostra, perpendicular ao facho. Se houver uma trinca com abertura de cerca de 0,1 μm ou mais nesta área de "iluminação difusa", então a luz será dispersa pela trinca, dando como resultado uma alteração facilmente observável na intensidade da luz nas laterais da trinca.

Com o emprego desta técnica conjugada a um estágio de esforço, é possível observar-se os processos que ocorrem no traçado da trinca quando é aumentada a carga sobre a amostra, e observar as mudanças nos processos da trinca em pastas de cimento úmidas ou parcialmente secas durante o envelhecimento, e quando as pastas são modificadas. Há mudanças complexas na "zona de processo" em que se desenvolve a fratura à frente de um entalhe ou falha, e elas têm um efeito direto sobre as propriedades mecânicas do cimento.

Este artigo descreve a técnica de microscopia ótica de iluminação difusa, e examina as observações feitas em cimentos hidráulicos normais e modificados.

1. Introduction

This paper reports observations of stable crack growth in hydrated Portland cement based materials, and these are discussed both in terms of previous observations and detailed fracture mechanics principles.

Diamond (1) has reported a study by scanning electron microscopy (SEM) of cracking in dry Portland cement paste, from which the following observations may be drawn:

1) After "initial" loading, a relatively long, narrow crack was formed, about 30 μm wide at the notch tip and extending about 10 mm into the specimen. The width of the crack gradually diminished to about 3 μm near its tip, at which point it became difficult to separate from the general inhomogeneity of the paste.

2) In macroscopic terms, cracking was long, narrow parallel-sided and unbranched. On a finer scale, it tends to zig-zag somewhat at a scale of approximately 60 μm, and is sometimes discontinuous near the crack tip.

Higgins and Bailey (2) made similar observations on wet cement pastes, using an extension of optical microscopy which will be described in Section 3 of this paper. In macroscopic terms, their observations were similar to those of Diamond above, but the cracking was much finer, of the order of 1 μm wide and up to 1 mm in length, and appears to correspond to the very tip of the cracks described by Diamond, where fracture is still taking place. The fracture mechanics of this process will be outlined in the next Section.

2. Theory

2.1 Cracking in brittle or semi-brittle materials

Before assessing the importance of the observations in this paper, it is first necessary to consider in more detail the use of notched specimens for the study of crack growth in brittle or semi-brittle materials.

Figure 1 shows a single edge notched beam (SENB) specimen together with a typical load/deflection curve for a brittle material, such as glass, using a very stiff testing machine.

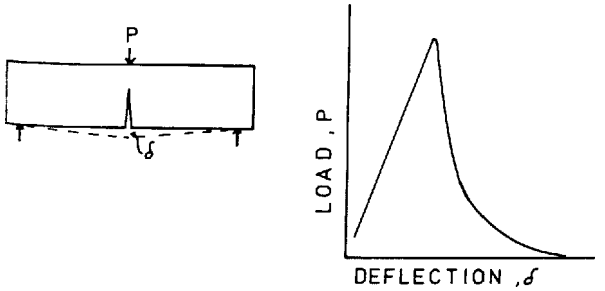

Fig. 1. SENB specimen and typical load/deflection curve for very brittle material (after Nakayama (3)).

The curve is essentially linear elastic up to the peak load, point A. After this point, the shape of the load/deflection curve depends upon the hardness of the testing machine (3,4). If it is sufficiently hard, i.e. there is negligible stored strain energy, then energy for crack formation must come from that within the specimen. It is thus possible to choose the specimen dimensions such that, once the crack has started to propagate, there is insufficient elastic strain energy stored in the specimen for the crack to propagate in an unstable manner right across the specimen. Thus stable crack growth is obtained, with the position of the crack front being dependent upon the deflection imposed by the testing machine.

It must be emphasized that the "stability" of this cracking is a consequence of the conditions of the test, not of the fracture mechanism of the specimen material itself. Were there sufficient energy stored in the specimen and/or testing machine at point A, then catastrophic failure could occur, though the curve up to this point would still be linear (i.e. there is no cracking prior to point A).

Let us now consider the case where the load/deflection curve prior to point A is non-linear, as in figure 2.

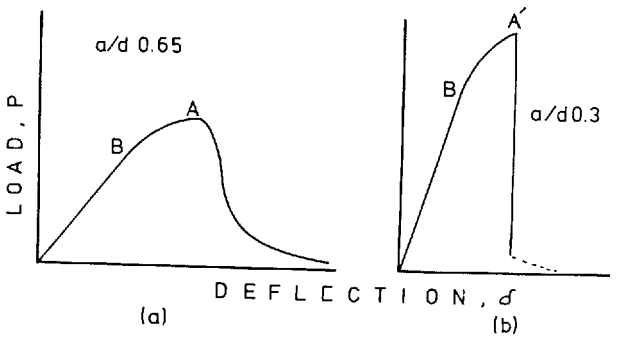

Fig. 2. Non-linear behaviour prior to development of peak load in SENB test on cement paste. (a) "stable" crack configuration, (b) unstable crack configuration.

Up to point B, the curve appears to be linear, but then departs from linearity and continues under increasing load, until point A´ is reached. Once again, after this point the stability of the cracking depends upon the test configuration. In figure 2a, the notch is sufficiently deep to provide stable fracture, whereas at low notch/depth ratios, figure 2b, too much energy is stored and a catastrophic or near-catastrophic failure results. In both cases, however there is still non-linearity before peak load, and this is a function of the fracture mechanism of the material, not of the "stability" of the test geometry.

The case of non-linear elasticity can be discounted in the case of cement paste, since it is known that the stiffness of a specimen unloaded between ponts B and A´ on figure 2 is lower than when tested for the first time. Brown (5) showed that a crack could be grown through a notched beam of cement paste by repeatedly loading and unloading just prior to failure. After each loading step, the crack had advanced by between 1 and 1.5 mm.

Direct observation of crack growth during this stable extension period is of great value in considering the fracture mechanics of the paste, and Higgins and Bailey (2) found that very fine cracks could be

seen to grow up to about 1 mm in length before catastrophic failure occurred.

In terms of fracture mechanics, this can be seen as the growth of a "process zone", which develops to a critical size at which unstable fracture may proceed if there is sufficient energy available from the test geometry.

2.2 Fracture mechanics

One of the main uses of fracture mechanics is providing engineers with mathematical tools to design against catastrophic failures if the correct materials performance parameters are known. One of the main uses of linear elastic fracture mechanics (LEFM) is in the measurement of such performance parameters. Here we are primarily concerned with predicting the effect of flaws which are not inherent in the structure of the material itself.

However, even though linear elastic fracture mechanics can be used to measure the performance parameters of almost any solid material, given the correct specimen size, this does not necessarily indicate the applicability of LEFM to the processes occurring in the immediate vicinity of the advancing crack front.

As an example, figure 3 shows crack length/failure stress curves predicted by two different fracture mechanics theories for three materials, glass, Portland cement paste and steel.

Griffith

$$\sigma = \frac{2E\gamma}{\pi a} \qquad \ldots\ldots(1)$$

$$(2\gamma = Gc)$$

Dugdale

$$\delta_c = \frac{8\,\sigma y\, a}{\pi E} \ln\left[\sec\left(\frac{\pi\,\sigma}{2\sigma y}\right)\right] \qquad \ldots\ldots(2)$$

$$\delta_c = \frac{G_c}{\sigma y} = \frac{2\gamma}{\sigma y}$$

Both equations can be rearranged to obtain a relationship between the crack length, a, and failure stress, σ, of a large specimen. In each case, both curves are calculated from the same materials parameters of Young's modulus (E), fracture surface energy (γ) or critical strain energy release rate (G_c) and yield stress (σy), as detailed in Table 1.

Table 1. Fracture mechanics parameters for the three materials in figure 3

Material	Young's modulus E, GPa	Yield stress σy, MPa	Fracture energy 2γ or G_c, J/m^2
Glass (4,6)	71	7.1×10^3*	8 (2γ)
Portland cement paste (7)	26	12	7.6 (2γ)
Steel (8)+	210	500	1×10^5 (G_{1c})

Notes: * calculated as $\sigma y \simeq E/10$ (9)
+ ductile fracture at room temperature.

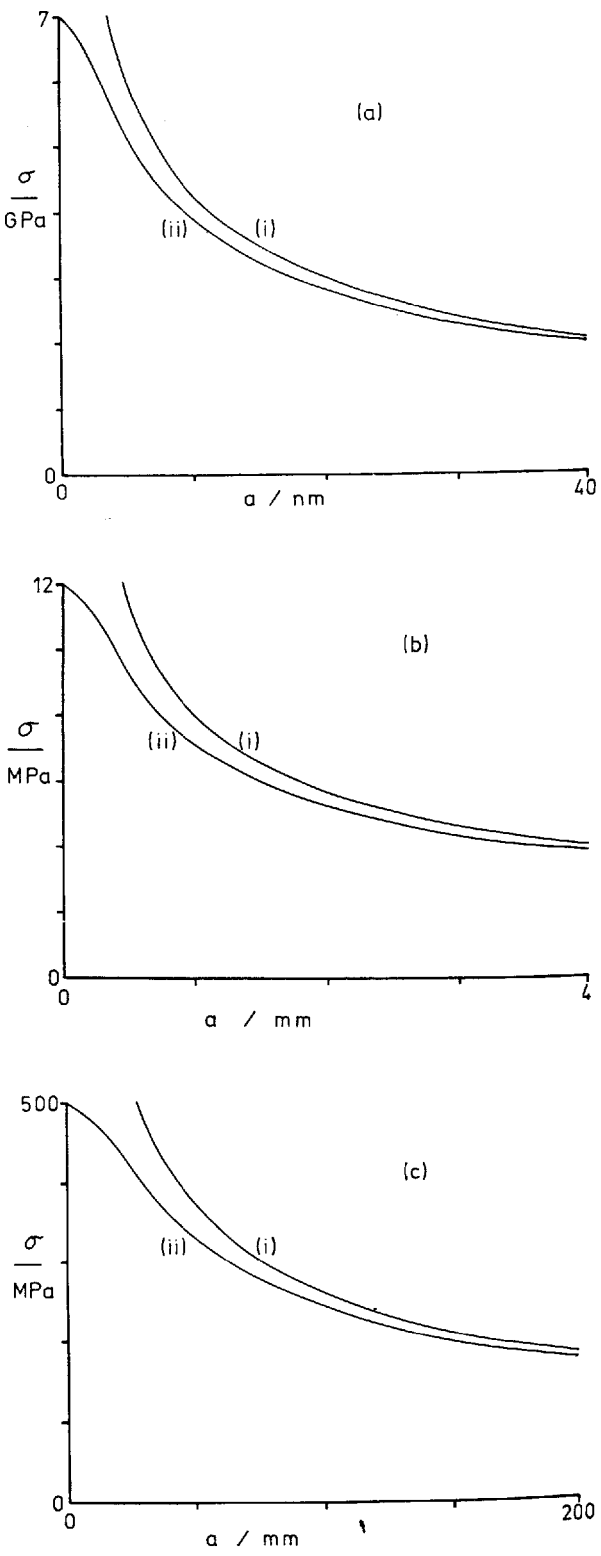

Fig. 3. Crack length/failure stress curves calculated from (i) Griffith and (ii) Dugdale equations, for a) glass, b) Portland cement paste and c) steel (plane stress).

Strictly, glass is the only material in this example for which the application of the Griffith equation is correct, as the term γ in this case should relate to the thermodynamic surface energy of the material. In the case of steel, if only the thermodynamic surface energy were used in the Griffith equation, the predicted failure stress would be several orders of magnitude lower than actually observed. Both Radjy (10) and Diamond (11) have noted that the fracture surface energy of cement paste cannot be explained in terms of thermodynamic surface energy alone. It is also important to note that G_c of the steel was measured using LEFM and very large specimens (8).

The form of the curves in each case is identical, as is the near coincidence of the Griffith and Dugdale curves towards the right of each diagram. Note however the very different scale on each part of the diagram. The coincidence of the two curves should not be taken as meaning that the predictions of both are interchangeable. For instance, figure 3c does not indicate that the strength of steel, 500 MPa, is limited by flaws of 27mm in size, as predicted by the "Griffith" curve, neither does figure 3a indicate the presence of "flaws" of 4 nm in a "perfect" glass specimen, as this is too close to the size of the structural elements of the material for the theory to be applicable (12). Likewise, the coincidence of the two curves in the case of cement paste is not sufficient reason to postulate the existence of flaws of about 0.5 to 1 mm, as previously suggested (13,14).

3. Experimental Method

3.1 Hydrated Materials preparation

White Portland cement was used for this study to improve the resolution of the technique.

De-aired pastes were made, as described before (7), at a water/cement ratio of 0.33. Manufacture of polymer modified cements is also detailed elsewhere (15) and a volume fraction of 64% cement was used. The polymer is hydroxypropyl methyl cellulose (HPMC).

All specimens were cut from plates using a water-cooled diamond saw, and notched using a fine diamond tipped slitting disc to give a notch root radius of about 100 μm. The surface to be observed was polished wet on 1200 grade "wet and dry" paper. All testing was carried out with the specimens saturated with water which had previously been used to cure the same cement.

3.2 Diffuse optical illumination

In conventional reflected light microscopy, the area of specimen illuminated is larger than that observed, to give an even illumination. In the "diffuse illumination" technique (2), the diameter of the incident beam is stepped down to within the field of view, as shown in figure 4a.

Because cement paste is slightly translucent, light penetrates the sample below the incident beam and is scattered across and back out of the specimen by the many interefaces within its structure, resulting in a zone of "diffuse" illumination around the incident beam.

Extremely fine cracks have the ability to transmit light, rather than reflect it; hence the need for etching when examining glass surfaces for hairline cracks (16). It has been shown (17) that for this to occur, the crack width must be of the order of one tenth of the wavelength of the light, e.g. about 0.1 μm for visible light. Above this value, light is scattered by the crack. Figure 5 shows both diagramatically and pictorially the effect of the presence of a crack in the diffuse illumination zone.

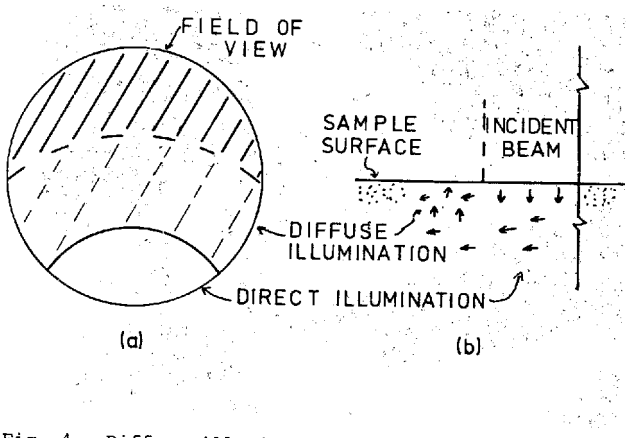

Fig. 4. Diffuse illumination of cement specimen a) plan view, b) cross section.

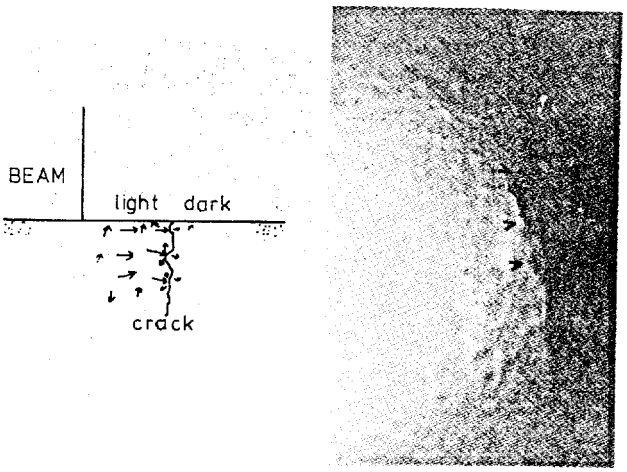

Fig. 5. Effect of a crack in the diffuse illumination zone.

Because the resolution of the light microscope is limited to the wavelength of visible light, approximately 1 μm, it can be seen that the diffuse illumination technique can be used to "image" cracks of between about 0.1 and 1 μm, which are not visible under normal illumination (2,18). In excess of 1 μm, the crack can be seen under normal illumination as a very fine line.

3.3 Optical microscope straining stage

Figure 6 shows the straining stage, used in conjunction with the microscope, to obtain load/deflection data during the test. It consists of a double-screw actuator, giving fine and coarse adjustment, which transmits load via a miniature load cell to the specimen. Deflection of the specimen is monitored by an LVDT, mounted on the side of the stage. The entire specimen can be kept submerged in water throughout

the test.

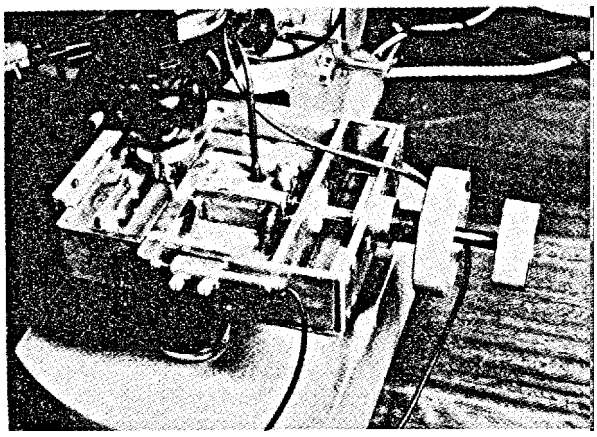

Fig. 6. Optical microscope and straining stage.

4. Results and Discussion

4.1 Macroscopic nature of cracking

The observation that fracture proceeds by a single crack (1,2) is confirmed by the present study. Occasional crack branching occurs, usually when the crack meets a large unhydrated grain, but the branches tend to rejoin, as shown in figure 7.

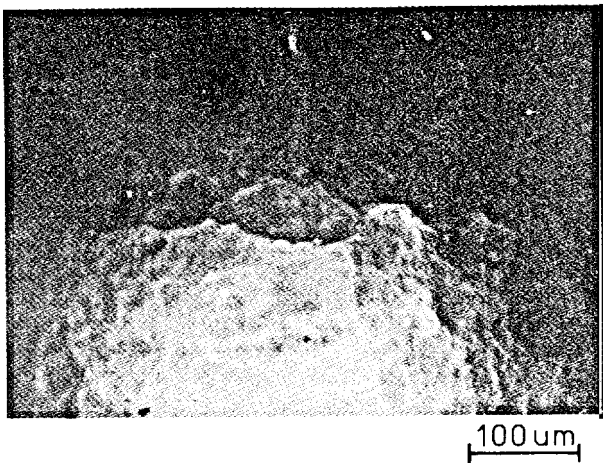

Fig. 7. Crack branching in Portland cement paste.

Near the tip of the crack, it is often seen that the visible cracking is disjointed, figure 8.

Though these observations are generally comparable to those of Diamond (1), it should be noted that, because of the width of cracking, Diamond's observations must have been made in a post-peak load regime, where stability is provided by the test geometry, i.e. after point A´ in figure 2 or its equivalent for the compact tension specimen used. Because an instrumented straining stage has been used in the present study, it is known that the cracking observed here is formed during the rising portion of the load/deflection curve, i.e. between points B and A´ of figure 2. These observations therefore relate to the development of the process zone prior to failure.

A further point must be made here regarding the resolution of the mechanical testing and microscope techniques. Although the departure from linearity is

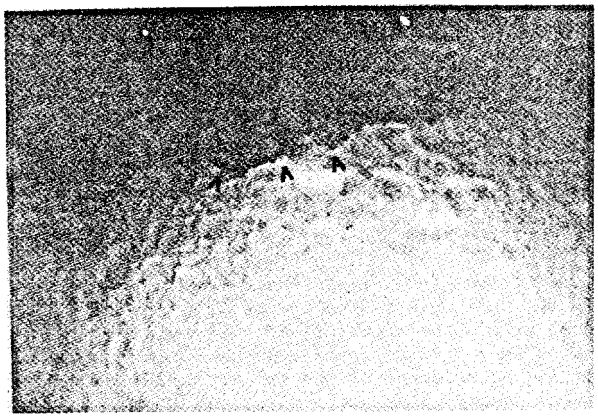

Fig. 8. Disjointed cracking close to crack tip.

easily visible on load/deflection curves, the strain required for initial de-bond of hydrate particles may be so small that it produces negligible additional deformation of the test piece, and may therefore be occurring at an earlier point than point A´ in figure 2. Also, as particles within the hydrate structure move apart graudally, they are unlikely to form a "clean" break, on a sub-micron scale, and substantial de-bonding may take place before there is sufficient separation (∿ 0.1 μm) for light to be scattered by the new interface. Fracture processes may therefore be occurring ahead of the portions of cracking visible even under diffuse illumination.

4.2 Process zone development

The onset of visible cracking at notch tip can be observed, as in figure 9.

The load, expressed as percentage of maximum, at which this occurs is dependent upon the composition of the specimen (e.g. paste or polymer modified) and also upon age. Chanda and Bailey (18) found that changes in the flexural strength and notched load/displacement curves for Portland cement and blended pfa/Portland cement could be correlated by using the tied-crack model (19) to explain changes in the process zone parameters as the cements were aged.

In this study, it has been found that the onset of cracking occurs at a higher proportion of peak load in older pastes than in young ones. For instance 8 day old pastes were observed to start cracking at about 70% of peak load, whereas 28 day pastes typically strted at 90 to 95% of peak load. The former is shown in figure 9.

The onset of cracking in wet polymer modified pastes was found to occur at much lower loads, often below 40% of the peak load. The notched load/ deflection curves of these materials become more markedly curved as the polymer content is increased (20). Furthermore, time effects have been found to occur during observation of these cracks. Higgins and Bailey (2) found that specimens of 6 weeks old paste loaded to 95% of maximum load often failed after several minutes while the photograph was being taken. The effect is much greater in polymer modified cements.

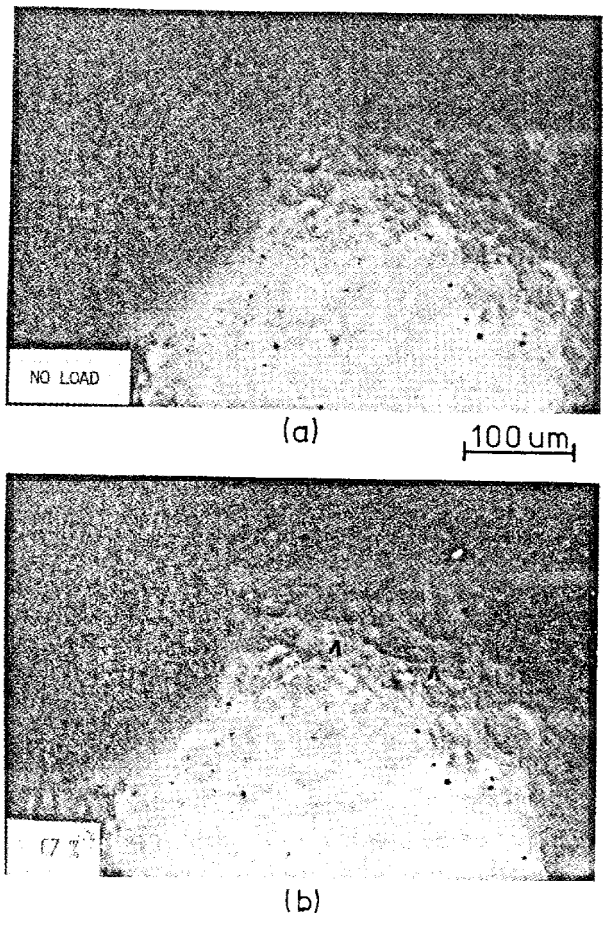

Fig. 9. Notch a) without load, b) onset of cracking (arrowed). Material: white P.C. paste, w/c 0.33 8 days old.

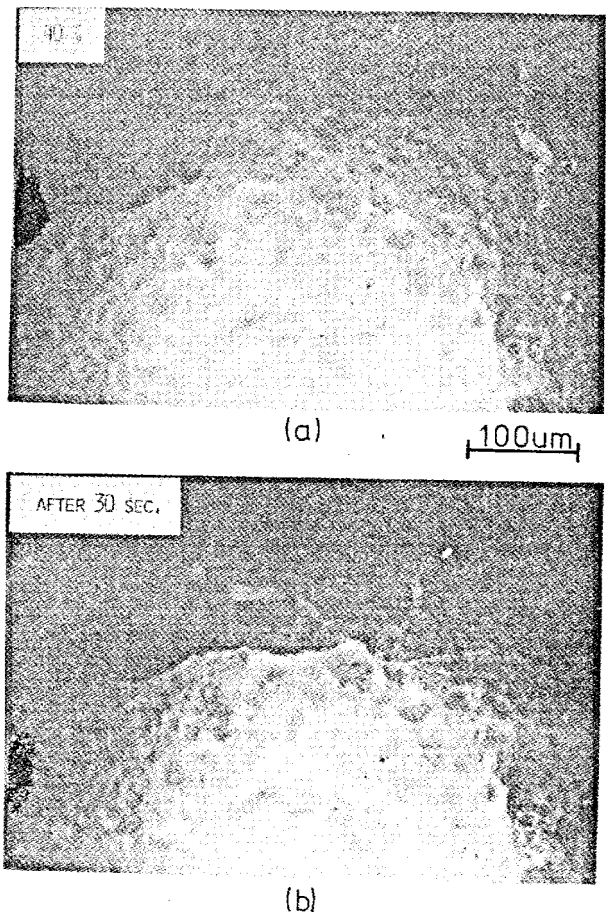

Fig. 10. Crack advancement with time in a 64/1% by volume OPC/HPMC polymer modified cement.

Figure 10 shows the end of a crack at 40% of maximum load, together with the same area after 30 seconds, during which period the crack advanced considerably and the load dropped by about 5%.

This suggests a considerably enhanced creep mechanism in these cements, at least in the wet state, which may be attributable to visco-elastic deformation of the polymer (15). Such a phenomenon has obvious connotations with regard to the effect of strain rate on crack development and flexural strength.

Although it is possible by this method to monitor the position of the crack tip, as load is increased, it has not yet proved possible to obtain reliable crack growth curves because of this significant time effect.

4.3 Model of Fracture

The fracture mechanics of these cements can be analysed using a "tied-crack" model (19), which indicates that the very fine (0.1 to 1 μm wide) cracking observed by the diffuse illumination technique is not completely separated. That is to say, there are forces across the crack which give rise to the stable cracking described in Section 2.

A fibrillar pull-out model has been proposed (15, 19) to explain this phenomenon, both for normal and polymer modified cements. It has been challenged (21) on the grounds that pull-out regions are not easily visible on fracture surfaces, though the nature of the surfaces may be such that direct SEM observation of pull-out is not possible (22).

Furthermore, the adoption of some microstructural model is still required to explain the partial bonding which must occur across crack faces to produce stability of cracking.

A number of authors (10, 23-25) have suggested that the bonding in hydrated Portland cement consists primarily of physical bonds between the colloidal, sheet-like hydrate particles, and the most direct interpretation of the results of this study and those preceding it is that fracture occurs by the parting of these hydrates, primarily by shear across the interface where bonding is weak. There may be some use for this model in predicting creep behaviour, though this

has not yet been attempted by the present authors.

5. Conclusions

1) Stable cracking of Portland cement materials is observed to proceed in a single, relatively straight, path.

2) Fracture mechanics indicate that this stable crack growth is the formation of a process zone, which grows to a characteristic size before failure occurs.

3) The process zone can be described mathematically in terms of a "tied-crack" model.

4) The most direct interpretation of this is that fracture of Portland cement materials occurs by the parting of two-dimensional hydrate particles, primarily by shear across their interfaces.

References

1. S. Diamond. Proc. 7th Int. Congr. on the Chemistry of Cements, Paris, 1980, Editions Septima, Paris 1980, Vol III, p VI-114.
2. D.D. Higgins and J.E. Bailey, Conf. on Hydraulic Cement Pastes, Sheffield, Cement and Concrete Association, U.K., 1976, 283-96.
3. J. Nakayama, J. Amer. Ceram. Soc., 48, 1965, 583-87.
4. R.W. Davidge, G. Tappin, J. Mater. Sci., 3, 1968, 165-173.
5. J.H. Brown, Mag. Concr. Res., 24, 1972, 185-196.
6. G.W.C. Kaye and T.H. Laby, "Tables of Physical and Chemical Constants", Longman, London, 14th Ed., 1973.
7. N.B. Eden and J.E. Bailey, J. Mater. Sci., 19 1984, 150-158.
8. J.F. Knott, "Funamentals of Fracture Mechanics", Butterworths, London, 1973.
9. B.R. Lawn and T.R. Wilshaw, "Fracture of Brittle Solids", Cambridge University Press, Cambridge, U.K., 1975.
10. F. Radjy, J.Amer. Concr. Soc., 57, 1974, 88-89.
11. S. Diamond, Materials Research Scoiety, Proceedings 42, MRS, Pittsburg, 1985, 233-243.
12. A.A. Griffith, Phil. Trans. R. Soc., Lond., A221, 1920, 163-198.
13. J.P. Birchall, A.J. Howard and K. Kendall, Nature, 289, 1981, 388.
14. N. McN. Alford, J.D. Birchall, A.J. Howard and K. Kendall, J. Mater. Sci., 19, 1985, 1134.
15. N.B. Eden and J.E. Bailey, J. Mater. Sci., 19 1984, 2677-2690.
16. F.M. Ernsberger, in "Fracture Mechanics of Ceramics", Vol. 1.1, Ed. R.D. Bradt et al, Plenum Press, New York, 1974.
17. E.E. Hall, Physical Review, 15, 1902, 73.
18. J.E. Bailey, S. Chanda and N.B. Eden, IVth Int. Symp. on the Fracture of Ceramics, Virginia Polytechnic Institute, June 1985, Proceedings in press.
19. D.D. Higgins and J.E. Bailey, J. Mater. Sci., 11, 1976, 1995.
20. N.B. Eden and J.E. Bailey, Materials Research Society, Proceedings, 42, MRS, Pittsburg, 1985, 79-87.
21. N. McN. Alford, J.D. Birchall, G.W. Croves and K. Kendall, Discussion of ref 15. J. Mater. Sci., 20, 1985, 3418.
22. N.B. Eden and J.E. Bailey, Reply to ref. 21, ibid, p.3419.
23. D. McLean, in "Structure Solid Mechanics and Engineering Design, Part I", ed. M. Te'Eni, Wiley Interscience, London, 1971, 13-25.
24. F. Wittmann, ibid, 295-300.
25. P.J. Sereda, R.F. Feldman and E.G. Swanson, Highway Research Board Spec. Rep. No.90, 1966, 58-73.

K. L. SCRIVENER, Department of Metallurgy & Materials Science, Imperial College, Prince Consort Road, London SW7 2BP, UK.

A STUDY OF THE MICROSTRUCTURE OF TWO OLD CEMENT PASTES

SUMMARY: The microstructure of two old cement pastes has been examined by backscattered electron (bse) imaging of flat polished sections in the SEM. One paste has been hydrated under carefully controlled conditions for 23 years. The other is of a cement made by William Aspdin and first came into contact with water in 1848. The bse imaging technique allows the different phases and porosity in the pastes to be distinguished at a resolution of about 0.1 μm.

Many features of the original cement can be deduced from the microstructure of the pastes. Many relicts of original cement grains can be distinguished, indicating the original particle size distribution of the cement and water/cement ratio of the paste. This study indicates that the net movement of most ionic species during hydration is very small and provides evidence for an *in situ* reaction mechanism during the latter stages of hydration.

Através de imagem eletrônica retro-dispersa (bse) de seções polidas planas em SEM, foi examinada a microestrutura de duas pastas envelhecidas de cimento. Uma pasta fora hidratada sob condições cuidadosamente controladas durante 23 anos. A outra é de um cimento feito por William Aspdin e entrou em contato com a água pela primeira vez em 1848. A técnica de imagem bse permite que sejam distinguidas as diferentes fases e porosidade nas pastas, numa resolução de cerca de 0,1 μm.

A partir da microestrutura das pastas podem ser deduzidas muitas propriedades do cimento original. Podem-se distinguir muitos resquícios dos grãos do cimento original, indicando a distribuição original de tamanho de partícula do cimento e a relação água/cimento da pasta. Este estudo indica que o movimento líquido de grande parte das espécies iônicas durante a hidratação é muito pequeno e fornece evidência para um mecanismo de reação "in situ" durante os estágios finais de hidratação.

INTRODUCTION

The use of backscattered electrons (bse) to image flat polished surfaces in the SEM [1,2,3] is an invaluable technique in the study of the microstructure of cement pastes. The intensity of electrons backscattered increases monotonically with atomic number (or average atomic number for compounds); thus in cement pastes: anhydrous material appears bright; calcium hydroxide light grey; C-S-H and other hydration products dark grey and porosity black.

Fig 1 shows a typical bse image from an 69 day old paste; the bright unhydrated cores of the original cement grains can be seen surrounded by dense inner C-S-H, whilst extensive regions of calcium hydroxide can be seen in the originally water filled space.

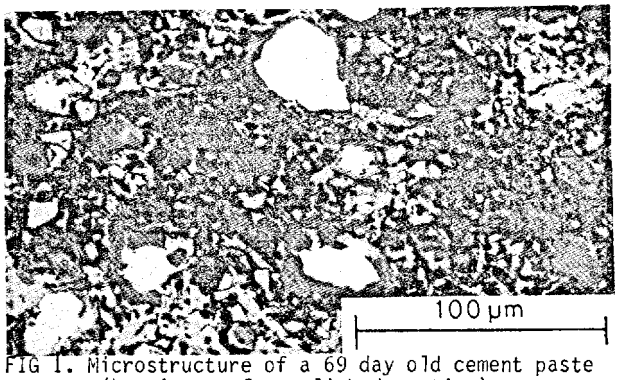

FIG 1. Microstructure of a 69 day old cement paste (bse image of a polished section)

This paper describes the study of two cement pastes using this technique. One is a 23 year old paste which has been previously studied in the electron microprobe by Taylor & Newbury [4]. The other dates from 1848.

MATERIALS

The 23 year old paste was prepared from a type I portland cement (Bogue composition, C_3S - 45%, C_2S - 28%, C_3A - 12.6%, C_4AF - 7.3%, $CaSO_4$ - 2.7%) at the Portland Cement Association Research and Development Laboratories, USA. The original w/c ratio was 0.45 and it was stored moist at 25°C for 23 years. Further details can be found in references 4 & 5.

The other sample has an unusual history [6]. In 1848 a sailing barge containing barrels of cement ran ashore off Sheerness on the Isle of Sheppy, UK. The partially hydrated barrels of cement were retrieved and used to build the 'Ship-on-the-Shore' inn, from whence this sample came. The original cement was manufactured by William Aspdin and is a 'meso-Portland cement' consisting of some alite, but predominantly belite in a matrix of C_3A and C_4AF [6]. The cement was initially hydrated with salt water. Although the initial w/c ratio is unknown, the volume occupied by actual cement grains in a typical cement/air mixture is approximately 40% which is roughly the same as the volume occupied by cement grains in a paste mixed at a w/c ratio of 0.5, so the initial w/c ratios of the two pastes are not dissimilar. Although the sample is 138 years old it has not been stored under controlled conditions, so the extent to which subsequent hydration might have occured over the years is unclear.

EXPERIMENTAL

Sections of the paste were polished to ¼µm with diamond paste on lapping cloths. The polished sections were coated with carbon and examined in a JEOL 35CF scanning electron microscope equipped with a solid state bse detector.

RESULTS AND DISCUSSION

23 Year Old Paste

Use of the bse technique allowed large areas of the paste to be examined. Some 100 areas about 0.1mm² were recorded photographically many of which were also examined at higher magnifications. The micrographs presented here show features which could be found throughout the microstructure.

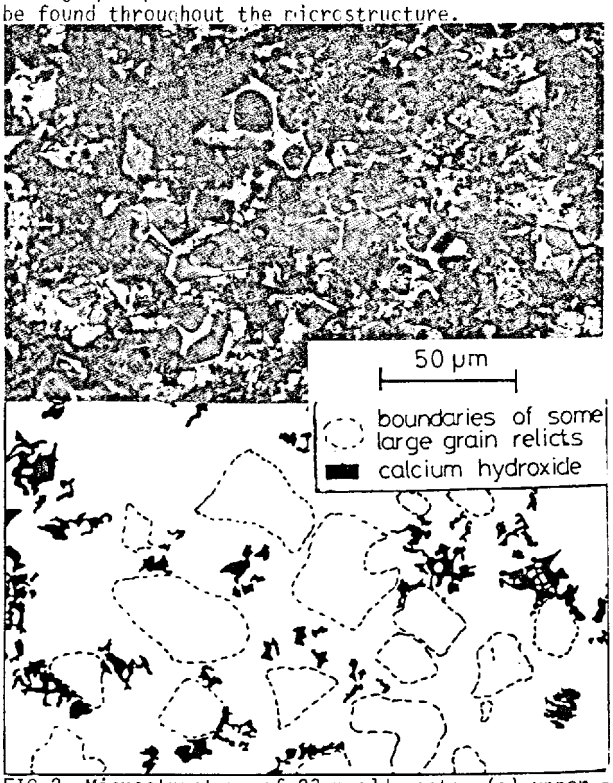

FIG 2. Microstructure of 23yr old paste, (a),upper - bse image, (b),lower - identification of some principal features.

Figure 2 shows a general view of the microstructure, the brightest areas are regions of high iron concentration, corresponding to the ferrite phase in the original cement (these features will be discussed in more detail subsequently).

The light grey ragged areas are calcium hydroxide (CH). The distribution of CH is very similar to that seen in much younger pastes (e.g. Fig 1); this observation supports the idea that CH nucleates in the originally water-filled spaces and grows from relatively few nuclei.

The absence of any other regions (apart from those with a high iron concentration) brighter than those of CH indicates that the calcium silicates have completely hydrated, as found by Taylor & Newbury [4] using X-ray diffraction. The relatively homogeneous mid-grey areas correspond to dense 'inner' C-S-H which indicate the shape of the original alite and

belite crystals. The size, shape and distribution of these relicts indicate the particle size distribution of the original cement with a fair number of grains being 50μm or larger.

Evidence for 'in-situ' hydration

Closer examination of the hydrated belite grains (Fig 3) shows a pattern of striations reminiscent of the twin structure of anhydrous belite [7,8]. This suggests that the belite has hydrated via an 'in-situ' or topochemical mechanism. Following a study of naturally occuring C-S-H, such a mechanism was proposed by McConnell [9] in 1955 and was also suggested by Funk [10] after studying synthetic β-C_2S.

Several relicts of grains about 20μm in size appear to have originally been predominantly alite. On examination (Fig 4) three regions of C-S-H can be distinguished within these relicts.

At the extreme edge is a thin layer (clearest along the lower edge of the grain in Fig 4) ~0.5μm thick with a fibrous appearance corresponding to the early, outer product formed during the main heat evolution peak by a 'through-solution' mechanism. In pastes examined after only some 12-24 hours hydration it has been found that this product forms as a shell separated by about 1μm from the underlying anhydrous core [2,11,12,13]. Grains smaller than about 3μm hydrate completely by this mechanism to leave small empty shells of C-S-H, which acount for much of the porosity in the 1-3μm range seen on polished surfaces.

Inside this outer layer is a more dense region of C-S-H formed through solution, by dissolution of the anhydrous core and deposition of product on the inside of the separated hydrate shell until the gap between shell and core disappears [2,11].

The innermost region is also dense and homogeneous and is only distinguishable from the surrounding region by a line of discontinuity. This product is probably formed by a slow 'in-situ' mechanism as proposed for belite. Taylor [14,15] has noted that the number of oxygen atoms per unit volume is approximately the same in C-S-H as in C_3S and has suggested that in-situ replacement of C_3S by C-S-H occurs by the counter-diffusion of H^+ ions inwards and Ca^{2+} ions and some silicon outwards.

Reaction of the ferrite phase

The regions of high iron content often show two levels of brightness (Fig 5). The size of these regions is too small for any difference in composition to be determined by energy dispersive X-ray analysis (EDXA) quantitatively. However, qualitatively, the outer, darker region has a higher iron and lower aluminium concentration (relative to calcium), whilst the inner, brighter region has a lower iron and higher aluminium concentraton. This evidence suggests that the inner region may be unreacted ferrite phase, with the outer region being amorphous ferric hydroxide formed as the aluminium and calcium leach out and react.

Comparision of results with those of Taylor & Newbury

The results presented here confirm the deductions made by Taylor & Newbury from the X-ray dot maps they obtained, and illustrate the improved resolution of the bse technique over X-ray mapping. Relicts of the original grains, areas of calcium hydroxide and areas

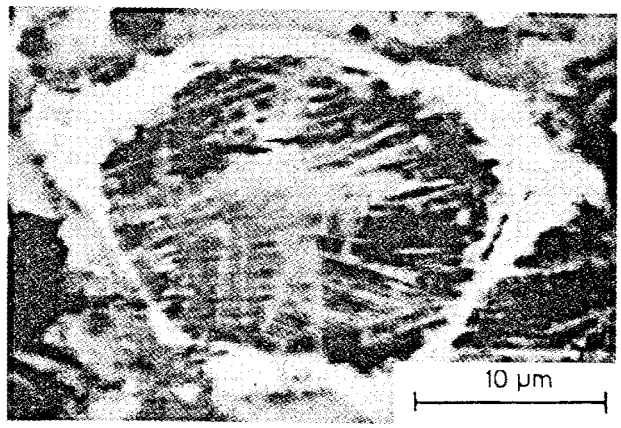

FIG 3. Relict of belite grain (bse image)

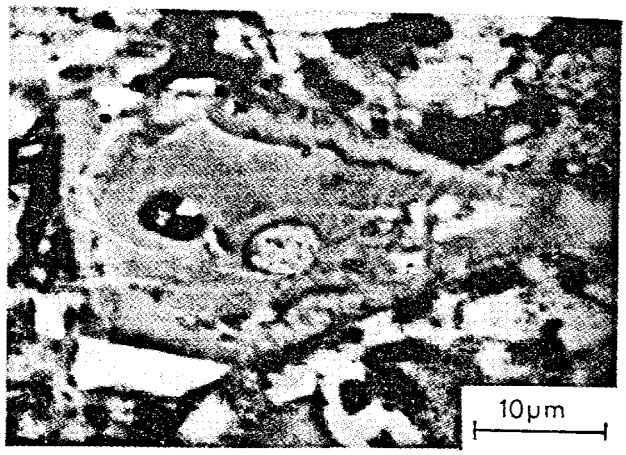

FIG 4. Relict of grain which was predominantly alite (bse image)

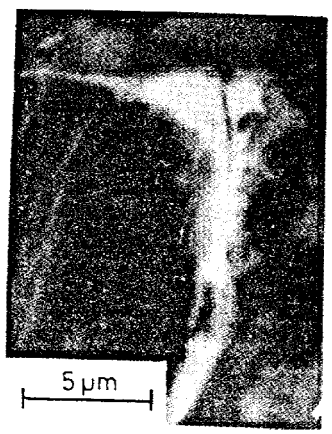

FIG 5. Iron rich area (bse image)

rich in iron can all be clearly identified from the same micrograph which can be aquired relatively rapidly. In addition, several new features can be identified, such as the fine structure within the relicts of the belite and alite grains.

The bse technique cannot, however, provide detailed chemical analyses. Although the variation in bse coefficent with atomic number is known, the effect of the structure and porosity of a compound on this coefficent is unclear.

Aspdin Cement Paste

Fig 6 shows a view of the microstructure at fairly low magnification. Several anhydrous cores can be seen, some almost 0.5mm in size. Such cores have also been observed by optical microscopy in thin sections of a sample from the same source, by Blezard [6] and in thin sections from a concrete specimen, also made by Aspdin, examined by Idorn and Thaulow [16]. Despite the uncertain hydration conditions, a considerable amount of reaction has taken place. Fig 7 shows the relict of a smaller grain in which the calcium silicate phases have completely reacted leaving a 'skeleton' of apparently unreacted ferrite phase. Fig 8 shows a larger grain with a hydrated rim some 30μm thick.

Despite the presence of some very large grains in the original cement, there appears to have also been a considerable amount of fine material (<5μm). Fig 9 shows an area which has resulted from the hydration of this fine material. Much of the porosity in the 1-3μm range has resulted from the rapid hydration of small grains leaving hollow shells of C-S-H.

In contrast to the other paste there are no massive areas of calcium hydroxide apparent in this paste. The small amount of alite in the original paste is probably the main reason for this, although Idorn and Thaulow [16] found that crystalline calcium hydroxide was abundantly precipitated in the concrete they examined. Some areas of calcium hydroxide can be identified, as at the bottom of the relict grain in Fig 7. Even this region is far less distinct than in the other paste, which may be as a result of partial carbonation.

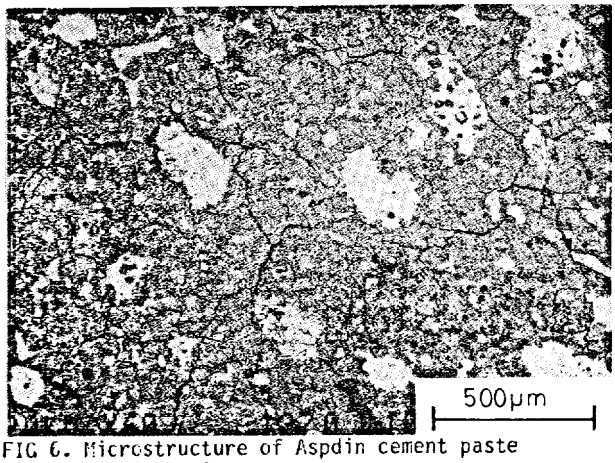

FIG 6. Microstructure of Aspdin cement paste (bse image)

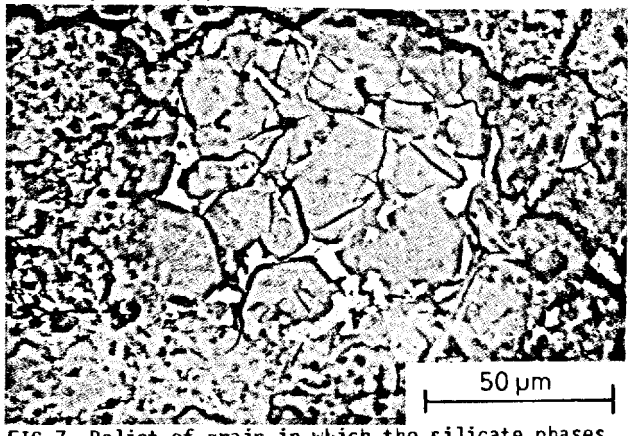

FIG 7. Relict of grain in which the silicate phases have hydrated (bse image)

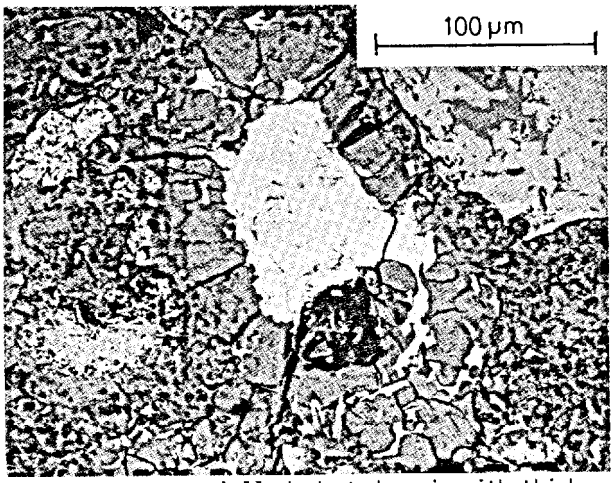

FIG 8. Large, partially hydrated grain with thick reaction rim (bse image)

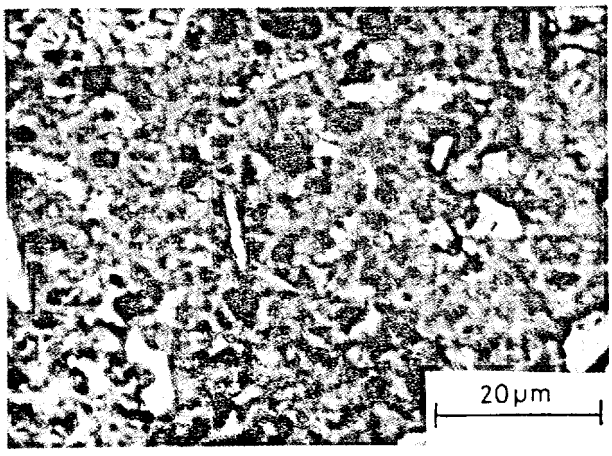

FIG 9. Microstructure of area where fine grains have hydrated (bse image)

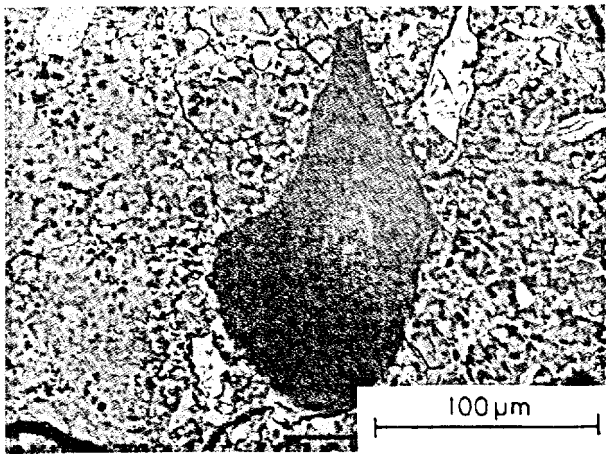

FIG 10. Dark particle of silica introduced during grinding of the original cement (bse image)

Another notable difference between this paste and the other is the lack of any structure in the hydrated belite relicts. This is to be expected as the firing temperature of the Aspdin cement was much lower than that of modern cements so the $\alpha \rightarrow \alpha' \rightarrow \beta$ transition, which produces the twinned structure, would not have occurred.

Fig 9 shows a small dark particle of silica. Blezard [6] has identified such features in a sample from the same source as being introduced during grinding. It is interesting that there has been no noticable reaction of this particle despite the age of the sample.

CONCLUSIONS

The results presented for these two cement pastes illustrate the use of backscattered electron images of polished surfaces in the study of cement.

In both pastes the approximate boundaries of many of the original cement grains can be identified despite their age and the fact that the 23yr old paste has hydrated virtually completely. Thus, the use of the bse technique enables much to be deduced about the original particle size distribution of a cement (and possibly the original water to cement ratio used) even in very old samples.

The fine striations in the relicts of belite grains and the structure of the C-S-H in the relicts of the alite grains in the 23yr old paste, provide strong evidence that the later stage of hydration occurs by a slow 'in-situ' mechanism.

In the 23yr old paste there is some evidence that partial reaction of the ferrite phase has occurred, but without significant migration of the Fe ions. The does not appear to have been any reaction of this phase in the Aspdin paste.

ACKNOWLEDGEMENTS

The author would like to acknowledge the Science and Engineering Research Council for financial support. Thanks are also due to Prof. H. F. W. Taylor through whom the 23yr old specimen was obtained and for helpful discussions, to Dr. L. G. Mallinson of Taylor Woodrow Construction Ltd. through whom the Aspdin specimen was obtained and to Prof. P. L. Pratt for helpful discussions and advice.

REFERENCES

1. K. L. Scrivener & P. L. Pratt, (1984), 'Backscattered Electron Images of Polished Cement Sections in the Scanning Electron Microscope' Proc. 6th Int. Conf. on Cement Microscopy, Albuquerque, pp145-155.
2. K. L. Scrivener, (1984), 'The Development of Microstructure During the Hydration of Portland Cement', PhD Thesis, University of London.
3. K. L. Scrivener, (1985) 'The Use of Backscattered Electron Imaging in the Study of Cement and Concrete' Proc. Engineering Foundation Conf., Cement Manufacture & Use, Henniker, in press.
4. H. F. W. Taylor & D. E. Newbury, (1984), 'An Electron Microprobe Study of a Mature Cement Paste', Cem. Concr. Res., 14, pp565-573.
5. W. Lerch & C. L. Ford, (1948) J. Amer. Concr. Inst., 19, p745
6. R. G. Blezard, (1981), 'Technical Aspects of Victorian Cement' Chemistry & Industry, 19th September 1981, pp630-636.
7. F. Hofmanner, (1975), 'Microstructure of Portland Cement Clinker', "Holderbank" Management and Consulting Ltd, May
8. G. W. Groves, (1981), 'Twinning in β-Dicalcium Silicate', Cem. Concr. Res., 12, pp615-625.
9. J. D. C. McConnell, (1955), 'The Hydration of Larnite (β-Ca_2SiO_4) and Bredigite (α'-Ca_2SiO_4) and the Properties of the Resulting Gelatinous Mineral Plombierite', Miner. Mag., 30, pp672-680
10. H. Funk, (1960), 'Two Different Ways of Hydration in the Reaction of β-Ca_2SiO_4 with Water at 25 to 120°C', Proc. 4th Int. Symp. Chem. Cement, Washington, 1 pp291-295 (Nat. Bur. Stands. Monograph 43, 1962).
11. K. L. Scrivener, 'Observations of "Separated Hydrate Shells" Formed During the Hydration of Portland Cement', to be published.
12. B. J. Dalgleish, P. L. Pratt & E. Toulson, (1981), 'Fractographic Studies of Early Hydration Products in Cement Pastes', Cem. Concr. Res., 11, pp729-739.
13. P. L. Pratt & A. Ghose, (1983), 'Electron Microscope Studies of Portland Cement Microstructure During Setting and Hardening' Phil. Trans. R. Soc. Lond., A310, pp93-103.
14. H. F. W. Taylor, (1984), 'The Reactions of Cement Compounds with Water' Proc. 10th Int. Symp. Reactivity of Solids, Dijon, in press, Elsevier Science Publishers, Amsterdam
15. H. F. W. Taylor, (1985), 'Some Aspects of Cement Hydration Mechanisms' as ref. 3 in press.
16. G. M. Idorn & N. Thaulow, (1983), 'Examination of 136 Years Old Portland Cement Concrete', Cem. Concr. Res., 13, pp739-743.

A. Negro, L. Montanaro, A. Bachiorrini - Dipartimento di Scienza dei Materiali e Ingegneria Chimica, Politecnico di Torino, Italia.

SUR L'HYDRATATION DE LA PHASE FERRITE EN PRESENCE DE CHAUX ET GYPSE
ON THE HYDRATION OF FERRITE PHASE IN THE PRESENCE OF LIME AND GYPSUM

Resumé

En general on admet que la phase ferrite du ciment est constituée d'une solution solide désignée par $C_2(A_nF_{n-1})$ ou $0<n<0,7$.
A partir de trois composants de cette solution solide C_6A_2F, C_4AF, et C_6AF_2 additionés de $Ca(OH)_2$, $CaSO_4.2H_2O$ et de poudre silicieuse on a preparé des mortiers dont le rapport eau/solide était 0,3.
Les expansions enregistrées durant les vingthuit jours d'hydratation de ces trois mortiers ont été comparées aux expansions de deux mortiers de référence constitués par C_3A, $Ca(OH)_2$ et $CaSO_4.2H_2O$ pour le premier et par C_3A dopé avec 5% de Fe_2O_3, $Ca(OH)_2$ et $CaSO_4.2H_2O$ pour le deuxième.
On a pu observer que l'expansion des mortiers à base de phase ferrite est fonction de sa teneur en Al_2O_3 et que cette expansion est beaucoup plus faible que celle-la des mortiers à base de C_3A. Pour ces derniers l'expansion diminue lorsque l'on passe du C_3A au C_3A dopé.
La cinétique d'hydratation des mortiers a été suivie en évaluant (à l'aide de l'analyse calorimétrique différentielle) la quantité d'ettringite formée au cours du temps. On constate qu'il existe un relation entre l'expansion des mortiers et leur teneur en ettringite.
D'aprés ces résultats, il semble que la faible teneur en ettringite et la plus faible expansion presentée par les ferrites, par rapport au C_3A, soit due non seulement à leur mediocre réactivité mais aussi à la formation de composés ferriques amorphes qui entraîne un ralentissement de l'hydratation.

Em geral se admite que a fase de ferrita do cimento é constituída de uma solução sólida apresentada por $C_2(A_nF_{n-1})$, em que $0<n<0,7$.

A partir de três componentes desta solução sólida - C_6A_2F, C_4AF e C_6AF_2 - com adição de $Ca(OH)_2$, $CaSO_4.2H_2O$ e de pó silicoso, foram preparadas argamassas com relação água/sólido igual a 0,3.

As expansões registradas durante os 28 dias de hidratação destas três argamassas foram comparadas com as de argamassas de referência, constituídas por C_3A, $Ca(OH)_2$ e $CaSO_4.2H_2O$ para a primeira, e por C_3A dopado com 5% de Fe_2O_3, $Ca(OH)_2$ e $CaSO_4.2H_2O$ para a segunda.

Pôde-se observar que a expansão das argamassas à base de fase ferrita é função de seu teor de Al_2O_3 e que esta expansão é muito mais fraca que a das argamassas à base de C_3A. No caso destas últimas a expansão diminue quando se passa de C_3A para C_3A dopado.

A cinética de hidratação das argamassas foi acompanhada através de avaliação (por intermédio de análise calorimétrica diferencial) da quantidade de etringita formada ao longo do tempo. Constata-se que existe uma relação entre a expansão das argamassas e seu teor de etringita.

De acordo com tais resultados, parece que o baixo teor de etringita e mais a baixa expansão apresentada pelas ferritas, em relação ao C_3A, se deva não apenas à sua reatividade medíocre, mas também à formação de compostos férricos amorfos que ocasionam uma retardação da hidratação.

Introduction

En étudiant l'action exercée par le gypse au cours de l'hydratation des ciments, les chercheurs se sont intéressés plus particulièrement à la réaction entre aluminate tricalcique et gypse, aux sulfo-aluminates de calcium hydratés, à leur rôle au cours de la prise et du durcissement.

Par contre, moins de recherces ont été consacrées à l'interaction du gypse avec la phase ferrite, une solution solide indiquée généralement par $C_2(A_nF_{1-n})$ où $0 < n < 0,7$; cela est dû, peut être, à la supposition que la phase ferrite et l'aluminate tricalcique ont un comportement analogue.

La présente recherche a pour but d'évaluer l'expansion des ferrites, lorsqu'elles sont hydratées en présence de gypse et de chaux, de comparer cette expansion à celle de l'aluminate tricalcique et de déterminer le rôle joué par le fer pendant l'hydratation.

Partie experimentale

Partant de produits pur pour analyse ($CaCO_3$, Al_2O_3 et Fe_2O_3) nous avons synthétisé à 1350°C:

- Trois composés de la solution solide: C_6AF_2, C_4AF, C_6A_2F.
- C_3A.
- C_3A dopé avec du fer.

Le C_3A a servi pour comparer son expansion avec celle des ferrites; le C_3A dopé pour vérifier si la diversité de la réactivité des ferrites par rapport au C_3A (1) est à imputer non seulement à une différence substantielle de composition et de structure cristalline, mais aussi à la présence de fer en solution solide.

Nous avons donc réalisé un C_3A dans lequel 4,5% de Al_2O_3 ont été substitués par Fe_2O_3: Burnett et Scharp (2) ont vérifié que cette substitution est possible sans que se produise un changement dans la structure de l'aluminate.

La pureté de tous les composés synthétisés, broyés jusqu'à obtenir une surface spécifique B.E.T. d'environ 1,5 m^2/g, a été contrôlée par diffractométrie des rayons X. L'aluminate tricalcique pur et l'aluminate tricalcique dopé présentaient tous deux une maille élémentaire cubique au paramètre a_o=1,526 et a_o = 1,528 Å respectivement.

Nous avons donc réalisé deux mélanges à partir des ferrites et des aluminates avec $CaSO_4.2H_2O$ et $Ca(OH)_2$.

Pour le premier mélange utilisé pour les mesures dilatométriques, nous avons réspecté les proportions indiquées par Schwiete et coll. (3): le gypse a été additionné en une quantité telle que les ions sulfate produisent, à la suite de l'hydratation, du monosulfoaluminate hydraté en tant que produit final unique.

Dans le second mélange employé quant à lui pour les mesures calorimétriques, la quantité de gypse était pour tous les échantillons de 15%. Il a fallu opérer avec une quantité de gypse plus réduite pour provoquer, dans des temps brefs, la transformation ettringite ⟶ monosulfoaluminate, afin que l'appareillage puisse mesurer l'évolution de la chaleur de cette réaction.

De plus nous avons additionné 15% de quartz finement broyé tous les mélanges. En effet, Molten et Stein (4) ont montré l'influence de celui-ci sur la cristallisation de l'ettringite et, de plus, il nous a semblé plus judicieux d'opérer avec des mortiers plutôt qu'avec des pâtes.

L'évolution du dégagement de chaleur produit par l'hydratation des mortiers a été suivie par calorimétrie (calorimètre à flux Karmazsin-Murat (5)).

Nous avons utilise un rapport E/S égal à l'unité a fin d'assurer un bon contact entre l'eau et le solide.

Les variations dimensionnelles ont été mesurées par dilatométrie (dilatomètre Netzsch) d'après une metodologie décrite précédemment (6) sur des mortiers de même consistance: c'est à dire avec un rapport E/S = 0,3 pour les mortiers préparés avec les ferrites et E/S = 0,4 pour ceux préparés avec les aluminates.

Tous ces essais ont été effectués à 25°C.

Sur une partie des mortiers utilisés pour les mesures dilatométriques (6) nous avons suivi le processus d'hydratation par analyse calorimétrique différentielle (DSC). Les surfaces du pic endothermique de l'ettringite et du monosulfoaluminate hydraté, calculées par un ordinateur associé à l'appareil de mesure, sont exprimées en J/g.

La morphologie des produits d'hydratation a été observée au microscope électronique à balayage.

Resultats et discussion

Les résultats de l'analyse calorimétrique concordent avec ceux obtenus par Collepardi et coll. (7): dans le cas des ferrites, les courbes de flux thermique signalent un dégagement de chaleur peu de temps après le contact du solide et de l'eau. Aucun autre déga-

gement de chaleur n'a été enregistré pendant les premiers deux jours d'hydratation.

Dans le cas des aluminates, en plus du dégagement initial de chaleur, dû à la mise en contact du solide avec l'eau, apparaît un second pic calorimétrique, caractérisé par la valeur t_o correspondant au début du pic calorimétrique (Figure 1).

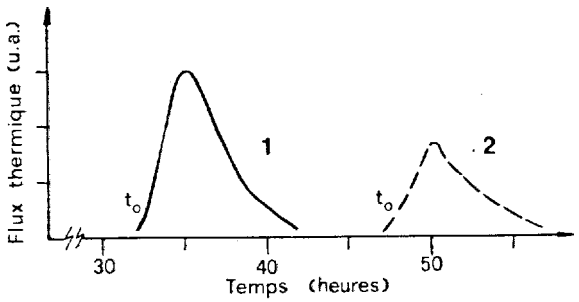

Fig. 1 - Courbes de flux thermique pour le C_3A (1) et le C_3A dopé (2).

Etant donné que, pour le C_3A et pour le C_3A dopé, les valeurs de t_o se situent respectivement à 32 et à 47 heures, nous en déduisons que la présence du fer dans le réseau de l'aluminate augmente la période d'induction de la conversion ettringite ⟶ monosulfoaluminate.

Les courbes "vitesse-degré d'avancement" (8) ont été obtenues à partir des courbes de flux thermique (Figure 2); l'examen de ces dernières permet de constater que la présence de fer diminue la vitesse maximale de conversion de $C_6A\bar{S}_3H_{32}$.

Nos résultats corroborent ceux de Burnett et Scharp (2). Ces derniers ont en effet montré que l'introduction de fer dans la structure du C_3A détermine une action retardatrice significative sur la réactivité de l'aluminate, lorsqu'il est hydraté en présence de gypse.

La Figure 3 présente les courbes d'expansion des trois ferrites en fonction du temps: elle est plus importante pour C_6A_2F, C_4AF et C_6AF_2 ayant des comportements plus proches. Cette différence devient encore plus évidente après 28 jours d'hydratation. Après cette période l'expansion est encore en cours, alors que dans le cas de C_3A, elle s'achève en un laps de temps mineur.

La Figure 4 présente l'allure des mêmes courbes pour les aluminates. Après 28 jours d'hydratation l'expansion, désormais terminée, est environ 10 fois supérieure à celle des ferrites à la même échéance.

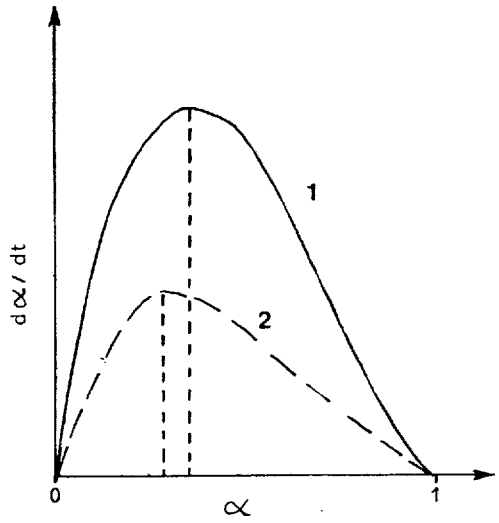

Fig. 2 - Courbes "vitesse-degré d'avancement" pour le C_3A (1) et le C_3A dopé (2).

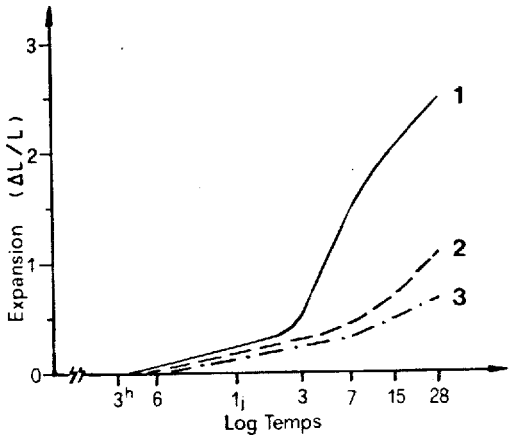

Fig. 3 - Courbes d'expansion presentée par C_6A_2F (1), C_4AF (2) et C_6AF_2 (3).

De plus nous constatons que, dans la periode considerée, la présence du fer dans le réseau du C_3A réduit l'effet d'expansion.

Les différences observées entre les ferrites et les aluminates s'expliquent par la quantité d'ettringite formée (Figures 5 et 6): la teneur en ettringite, produite par la réaction entre les ferrites et le gypse après 28 jours, est plus faible de celle formée après 6 heures d'hydratation dans le cas du C_3A et du C_3A dopé.

En observant la Figure 4, nous pouvons constater que l'expansion des ferrites après 28 jours est comparable a celle des aluminates après 6 heures.

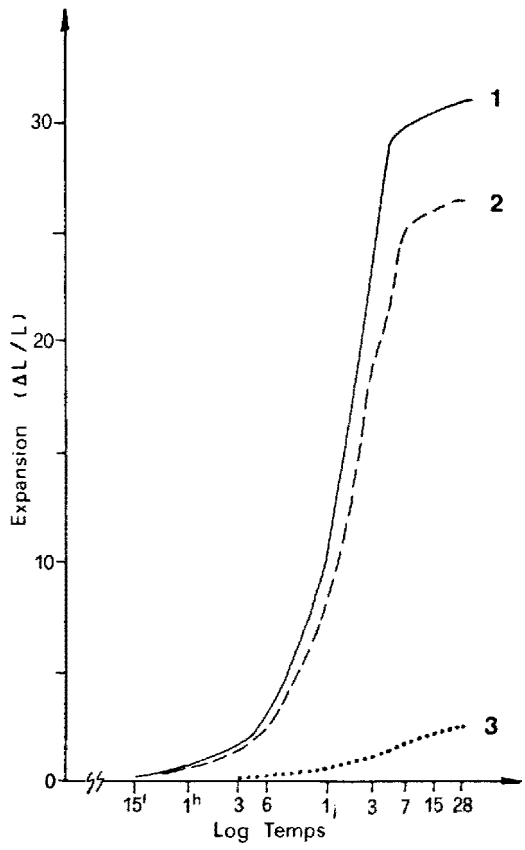

Fig. 4 - Comparaison de l'expansion presentée par le C_3A (1), le C_3A dopé (2) et par le ferrites (valeur moyenne (3)).

Après trois mois, dans les mortiers à base de ferrite, la quantité d'ettringite est encore faible et sa formation encore en cours (Figure 5), contrairement aux aluminates (Figure 6). Dans ces derniers, l'ettringite commence sa conversion en monosulfoaluminate après 3 jours d'hydratation pour le C_3A et après 7 jours pour le C_3A dopé.

La Figure 7 presente la morphologie des différents produits d'hydratation. L'aspect des cristaux d'ettringite formés par réaction de l'aluminate tricalcique (Figure 7a-7c), est semblable à celui que décrit Mehta (9-11): au début, ces cristaux apparaissent mal formés (ettringite colloidale) mais, avec le temps, ils acquièrent l'aspect de courts prismes.

Les produits d'hydratation des ferrites se présentent dès le début comme des amas nodulaires très compacts (Figure 7d) et, contrairement à ce qui est observé pour

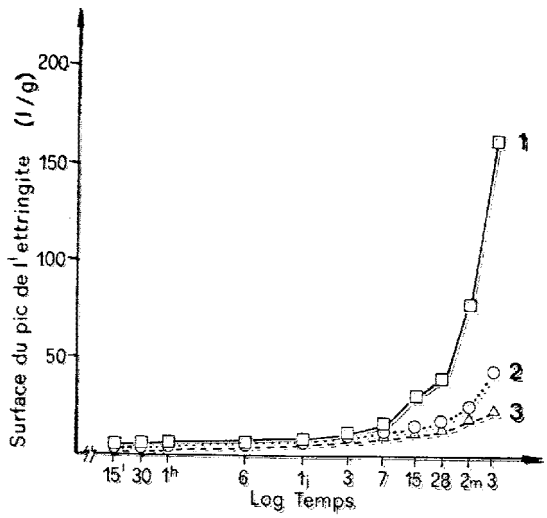

Fig. 5 - Evolution de la teneur en ettringite formée en fonction du temps pour C_6A_2F(1), C_4AF(2) et C_6AF_2(3).

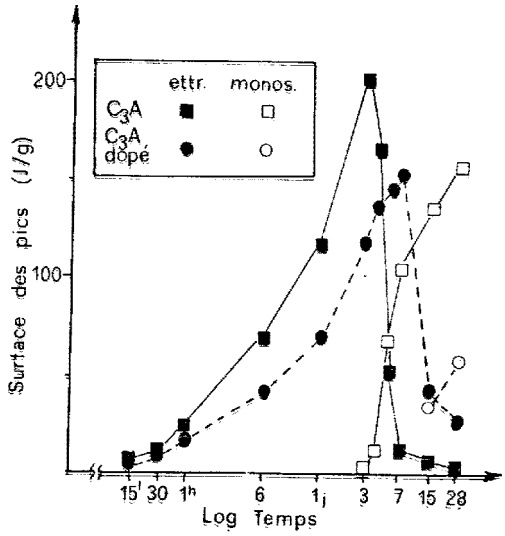

Fig. 6 - Evolution de la teneur en ettringite et en monosolfoaluminate formés en fonction du temps pour le C_3A et le C_3A dopé.

le C_3A, nous ne constatons par la suite aucune évolution morphologique (Figure 7e-7f), si bien qu'aucun faciès n'est relevable à 28 jours. Il faut aussi remarquex que dans les mélanges contenant du C_3A les hydrates tendent à revêtir entièrement les grains de l'aluminate, partiellement ceux de l'agrégat siliceux et à laisser découverts les cristaux de gypse (Figure 7g), dans le cas de mélanges

contenant des ferrites, les hydrates tendent à revêtir rapidement et de façon absolument indifférente tous les grains de départ (Figure 7h).

L'ensemble de ces résultats nous invite à penser que la présence de fer dans le réseau du C_3A détermine, par rapport au C_3A pur, un retard significatif dans la formation d'ettringite, dans la conversion ettringite → monosulfoaluminate et dans la vitesse de cette réaction: l'expansion du système est diminuée en présence de fer.

De plus le fer provoque un effet analogue dans le cas des ferrites. La différence de comportement du fer et de l'aluminium, pendant l'hydratation de la phase ferrite en présence de gypse, a été signalée par de nombreux chercheurs (12-15).

Après avoir vérifié que l'hydratation du système C_4AF + gypse, se traduirait, dans la phase trisulfatée, par un rapport A/F del-l'ordre de 4, alors que dans le produit de départ il n'etait que de 1, Tenoutasse (12) conclut que le fer excédentaire s'y trouve sous forme d'hydroxyde colloidal. De Keyser

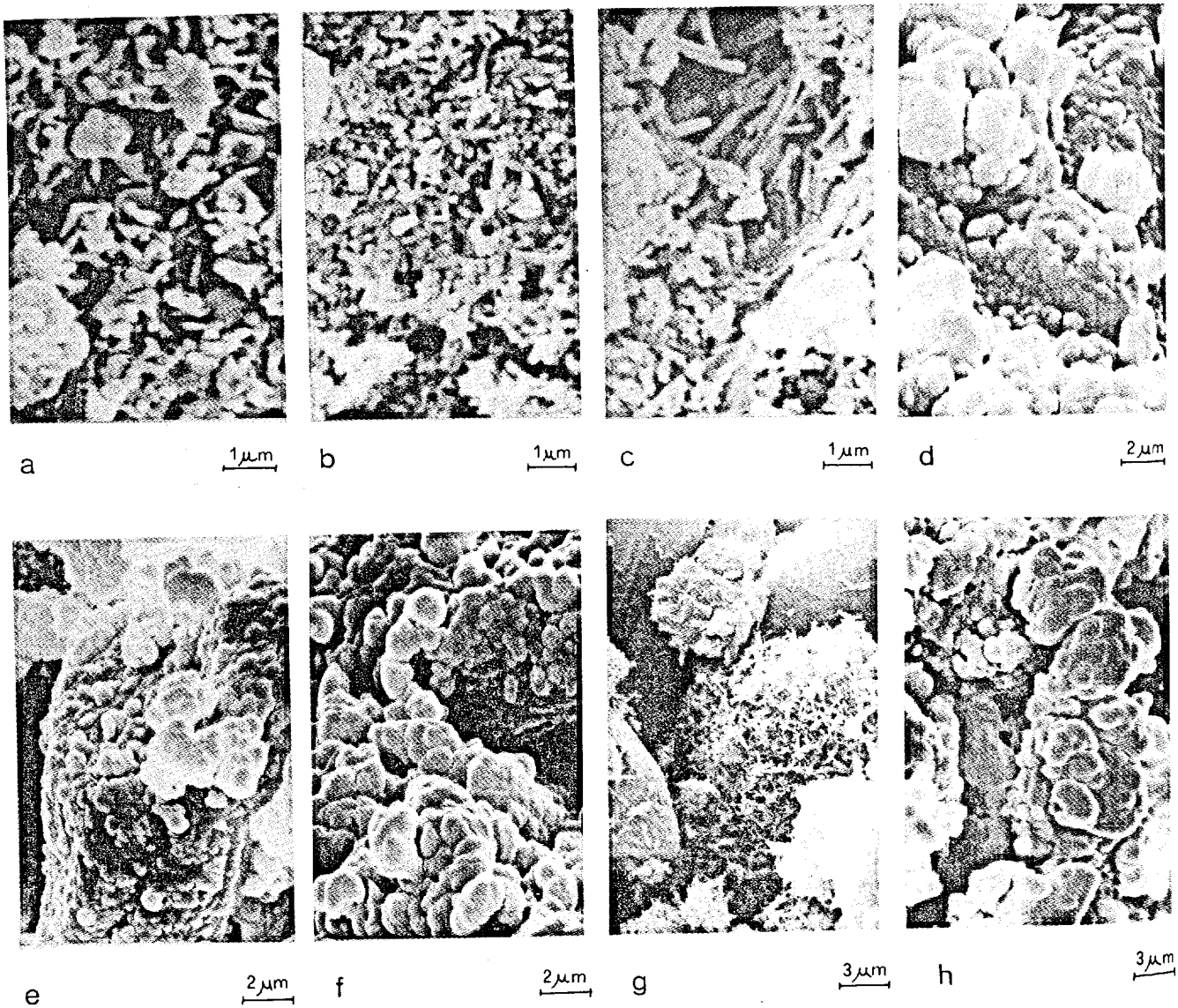

Fig. 7 - Morphologie des différents produits d'hydratation.
Ettringite formée par hydratation de C_3A après: 15 minutes (a), 6 heures (b) et 3 jours (c). Ettringite formée par hydratation de C_4A_2F après: 1 heure (d), 7 jours (e) et 28 jours (f). Revêtement des differents grains après hydratation de 1 jour d'un mélange contenant du C_3A (g) et d'un mélange contenant de la ferrite (h).

et coll. arrivent aux mêmes conclusions (13).

De même, Ramachandran et Beaudoin (14) avancent l'hypothèse de la formation d'un oxyde ferrique hydraté.

Jawed et coll. (15) en hydratant le C_4AF en présence de gypse ont mis en évidence que la couche d'ettringite formée est suffisamment dense pour empêcher l'hydratation ultérieure.

Plus récemment, Fukuhara et coll. (16) en se servant de la diffraction des rayons X, M.E.B., E.D.A.X, ont identifié, pendant les premières périodes d'hydratation du système C_4AF + gypse, deux phases: la première était de l'ettringite contenant du fer, et l'autre était constituée de particules à l'état amorphe.

Soit Tenontasse (17) que Fukuhara (18) s'accordent à dire que cette réaction est contrôlée par un processus diffusionnel.

En fonction des résultats obtenus et des données de la littérature, nous pouvons supposer que pendant l'hydratation des ferrites le solide libère des ions ferriques, qui se transforment en un hydroxyde amorphe; cet hydroxyde, parallèlement à l'ettringite, recouvre aussi bien les grains de ferrite que ceux de gypse et détermine une couche dense qui limite la progression de l'hydratation.

Conclusions

Les résultats obtenus nous permettent d'avancer les conclusions suivantes:

- L'expansion des ferrites se situe, après 28 jours d'hydratation, à un dizième environ de celle des aluminates;
- L'expansion et la formation d'ettringite, dans le cas des ferrites, sont encore en cours après 28 jours d'hydratation, alors qu'elles s'achèvent, pour l'aluminate tricalcique, ou bout de quelques jours;
- L'introduction de fer dans le réseau du C_3A en ralentit l'hydratation et en diminue l'expansion;
- La présence de fer dans le réseau des composés examinés se traduit en cours d'hydratation par la formation de composés amorphes du fer. Ces derniers recouvrent les grains des réactifs et, en même temps que l'ettringite, ralentissent l'hydratation et, par conséquent, l'expansion.

Bibliographie

1) F.M. Lea (1970), "The chemistry of cement and concrete", pag. 182, E. Arnold Ltd., London.
2) N.C. Burnett et J.H.Sharp (1984), "Hydration of doped tricalcium aluminate", J. Mat. Sci. 19, 1980-1990.
3) H.E. Schwiete, U. Ludwig et P. Jäger, (1964), "Untersuchungen im system $3CaO.Al_2O_3 - CaSO_4 - CaO - H_2O$", Zement Kalk Gips 17, 229-236.
4) C.L.M. Molten et H.N. Stein, (1977), "Influence of quartz surfaces on the reaction $C_3A + CaSO_4.2H_2O$ + water", Cem. Concr. Res. 7, 291-296.
5) E. Karmazsin et M. Murat (1978), "Study of a 'solid + liquid -- solid' reaction (hydration of calcium sulfate hemihydrate) by simultaneous isothermal calorimetry and electrical resistivity measurement", Cem. Concr. Res. 8, 553-558.
6) A. Negro et A. Bachiorrini (1982), "Expansion associated with ettringite formation at different temperatures", Cem. Concr. Res. 12, 677-684.
7) M. Collepardi, S. Monosi et G. Moriconi (1979), "Tetracalcium aluminoferrite hydration in the presence of lime and gypsum", Cem. Concr. Res. 9, 431-437.
8) M. Murat et E. Karmazsin (1977), "Cinetique d'hydratation des sulfates de calcium semihydratés. Essai d'interpretation des courbes vitesse-degré d'avancement", Coll. Intern. Rilem "Sulfates de calcium et materiaux dérivés", St. Rémy -les-Chevreuse, II-6, 217-236, M. Murat et M. Foucault Editeurs.
9) P.K. Mehta (1969), "Morphology of calcium sulfoaluminates hydrates", J. Amer. Ceram. Soc. 52, 521-522.
10) P.K. Mehta (1973), "Mechanism of expansion associated with ettringite formation", Cem. Concr. Res. 3, 1-6.
11) P.K. Mehta (1976), "Scanning electron micrographic studies on ettringite formation", Cem. Concr. Res. 6, 169-182.
12) N. Tenoutasse (1966), "Influence du gypse sur l'hydratation de la phase ferrite des ciments portland", Rev. Mat. Constr. 604, 18-26.
13) W.L. De Keyser et N. Tenoutasse (1968), "The hydration of the ferrite phase of cement", V I.C.C.C., Tokio, vol. II, 379-386.
14) V.S. Ramachandran et J.J. Beaudoin (1976) "Significance of water/solid ratio and temperature on the physico-mechanical characteristics of hydrating C_4AF", J. Mat. Sci. 11, 1893-1910.
15) J. Jawed, S. Goto et R. Kondo (1976), "Hydration of tetracalciumaluminoferrite in presence of lime and sulfates", Cem. Concr. Res. 6, 441-454.
16) M. Fukuhara, S. Goto, K. Asaga, M. Daimon, R. Kondo, Y. Ono (1980), "Behaviour of Fe component in the hydration of C_4AF with gypsum during ettringite for-

ming period", Yogyo-Kyokai-Shi 88, 436-440.

17) N. Tenoutasse (1966), "L'action du gypse sur l'hydratation de la phase ferrite. Aspect cinétique", Rev. Mat. Constr. 614, 452-458.

18) M. Fukuhara, S. Goto, K. Asaga, M. Daimon et R. Kondo (1981), "Mechanism and kinetics of C_4AF hydration with gypsum", Cem. Concr. Res. 11, 407-414.

Nous remercions Md.me A.A. Fournier de l'E.N.S.M. de St. Etienne pour la revision du texte.

Le travail a été accompli avec la contribution du M.P.I..

K. Isozaki, Denki Kagaku Kogyo Co., Ltd, Japan and K. Nakagawa, Denki Kagaku Kogyo Co., Ltd, Japan.

Behavior of ettringite in high strength hardened cement paste

Conduite d'ettringite dans la pâte de ciment durci de haute résistance

SUMMARY: The morphology of ettringite and hydrate structure in high strength hardened cement pastes made with normal portland cement containing Type II anhydrous calcium sulfate (anhydrite) at long term water curing were investigated by SEM observation, mercury pressure porosimetry and powder X-ray diffractometry.

The added amounts of anhydrite to normal portland cement were varied from 0 to 20 wt%. The water to cement ratio of the paste specimens was 0.3. After precuring at 20°C, they were steam cured at 65°C for 4 hrs and immersed in water at 20°C for forty months.

By addition anhydrite, ettringite in the high strength hardened cement paste at forty months of age was found to be stable and monosulfate hydrate was not detected even in the cement of 5 wt% anhydrite addition. The average shape of ettringite was a needlelike form of 0.2 to 0.8 μm in diameter and 2 to 6 μm in length. A number of ettringite crystals were concentrated in small voids and some of them were sintered together, growing into a large crystal. These phenomena appear to depend on the amount of unreacted anhydrite and the compactness of the matrix of cement paste.

Investigou-se, utilizando observação SEM, porosimetria de pressão de mercúrio e difratometria de raio-X de pó, a morfologia da etringita e a estrutura do hidrato em pastas endurecidas de cimento de alta resistência, feitas com cimento portland comum contendo sulfato de cálcio anidro Tipo II (anidrito), com longo tempo de cura.

As quantidades de anidrito adicionadas ao cimento portland comum variaram de 0 a 20% em peso. A relação água/cimento dos espécimes de pasta foi de 0,3. Depois de pré-cura a 20°C, eles foram curados em vapor a 65°C por 4 horas e imersos em água a 20°C por 40 meses.

Pela adição de anidrita, constatou-se que a etringita na pasta endurecida de cimento de alta resistência aos 40 meses de idade era estável e não foi detectado hidrato monossulfato nem mesmo no cimento com adição 5% de anidrito, em peso. A forma média da etringita era semelhante à agulha de 0,2 a 0,8 μm de diâmetro e 2 a 6 μm de comprimento. Numerosos cristais de etringita estavam concentrados em pequenos vazios e alguns deles estavam sinterizados juntamente, crescendo num grande cristal. Estes fenômenos parecem depender da quantidade de anidrito que não reagiu e da compacidade da matriz da pasta de cimento.

1. INTRODUCTION

Ettringite displays many different shapes and has remarkably effect on the characters of cement stones in the case of expansive cement, quick hardening cement or high strength cement. In expansive cement of a calcium sulfoaluminate system, colloidal or amorphous ettringite is said to have the ability to expand at an early period and the contribution of ettringite to early strength development is researched in ultra rapid or quick hardening cements. But the operative mechanism of ettringite is not well understood. Especially the behavior of ettringite at long term period is rarely reported.

The effects of ettringite giving rise to expansive, quick hardening or high strength cement stones should be studied in relation to hydrate structures having different mechanical strengths. In this paper, the hydrate structure and morphology of ettringite in normal portland cement paste admixed with Type II anhydrous calcium sulfate (anhydrite) at long term age are studied from the viewpoint of high strength hardened cement paste.

2. EXPERIMENTAL

Table I shows the chemical and mineral compositions of normal portland cement. In Table II, there are shown anhydrite amounts in normal portland cement.

Table I
Chemical composition and mineral composition of normal portland cement
(wt%)

Chemical composition		Mineral composition	
CaO	64.6	C_3S	51.1
SiO_2	22.1	C_2S	24.9
Al_2O_3	5.0	C_3A	7.8
Fe_2O_3	3.2	C_4AF	9.7
SO_3	2.0	$CaSO_4.2H_2O$	4.3

Table II
Added amounts of anhydrite to normal portland cement
(wt%)

Mix No.	Added amount of anhydrite
1	0
2	5
3	7
4	10
5	13
6	15
7	20

The paste specimens (4x4x16 cm beam) were prepared at a water to cement ratio of 0.3. The curing cycle was a precuring period of 4 hrs at 20°C, the rate of temperature rise, 65°C for 4 hrs and then natural cooling. After accelerated curing, the specimens were cured in water at 20°C for forty months.

The mixing ratios of anhydrite to normal portland cement were 0, 5, 7, 10, 13, 15 and 20 wt%.

The mechanical strength, powder X-ray diffraction patterns, evaporable water, non-evaporable water, morphology of hydrate (by SEM) and pore size distribution (by mercury pressure porosimeter) were measured. (1)

3. RESULTS AND DISCUSSION

3-1. MECHANICAL STRENGTH AND HYDRATE STRUCTURE

The 7 wt% addition of anhydrite showed a maximum compressive strength. (Fig. 1) Generally, the addition of anhydrite to normal portland cement accelerates the strength development more than pure normal portland cement. As shown in the previous report (1), this is caused by the increase in non-evaporable water, decrease in pore volume and strengthened structure.

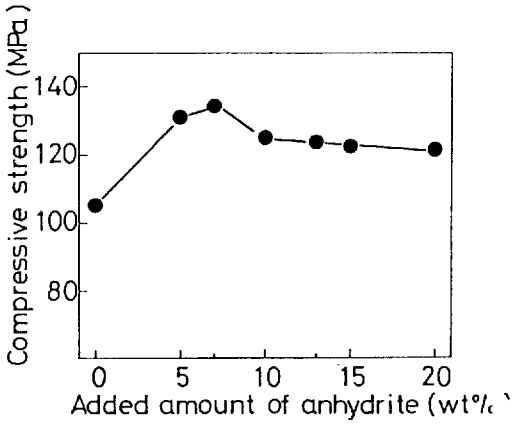

Fig. 1 Effect of added anhydrite on strength development.

The relations between the non-evaporable water, the compressive strength and the total pore volume are not solved. The difference between the pure normal portland cement and the normal portland cement admixed with anhydrite is relatively large. The behavior of ettringite influences the character of cement stone. The author calls it ettringitic cement stone.

The total pore volume of the 5 and 7 wt% addition of anhydrite is smaller than that of the pure normal portland cement, but in the range of over 10 wt% addition, the total pore volume is larger. The pore volume of 7.5 to 25 nm radii remarkably increases. (Fig. 2)

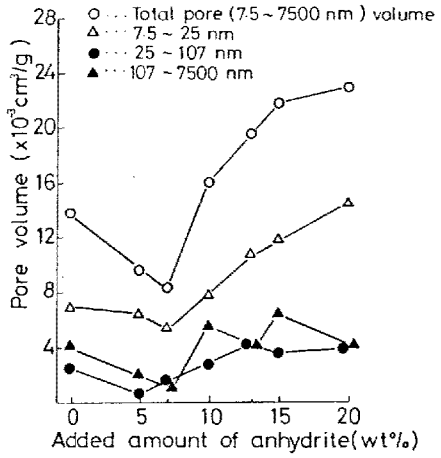

Fig. 2 Effect of added anhydrite on pore size distribution.

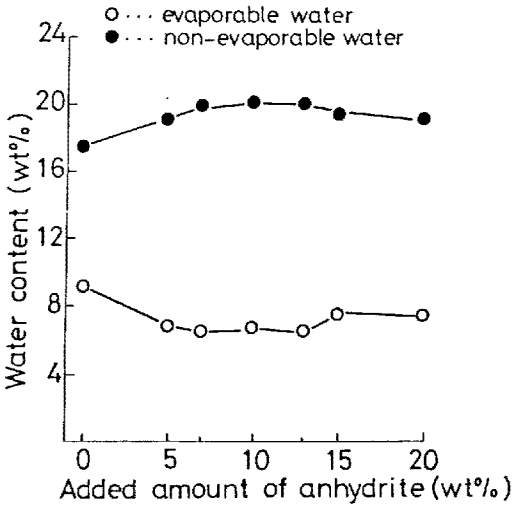

Fig. 3 Effect of added anhydrite on evaporable water* and non-evaporable water.**
* Treated by D-dry method for 48 hrs
** Heated at 1000°C for 1 hr

This phenomenon is related to the expansive effect of ettringite in producing capillary pores. However, the compressive strength of normal portland cements admixed with anhydrite are larger than that of the pure normal portland cement and the relation between the total pore volume and compressive strength in normal portland cements admixed with anhydrite is clear.

The amount of non-evaporable water of the normal portland cements admixed with anhydrite are larger than that of the pure normal portland cement, but the relation between the non-evaporable water and compressive strength is complicated. The morphology of ettringite and ill-crystalline C-S-H gel or intrinsic strength of hydrates should also be considered. (Fig. 3)

3-2. MORPHOLOGY OF ETTRINGITE

The morphology of ettringite in normal portland cements admixed with anhydrite at a long term period varies. This fact indicates the heterogeneity of the matrix of cement stone. Cement paste is composed of cement particles and water. Furthermore, cement particles consist of calcium silicates, calcium aluminate, calcium aluminum ferrite and gypsum. The dispersed state of these groups is a very important factor for the morphology of ettringite. We think that the matrix of cement paste is very heterogeneous from the standpoint of micro structure.

The morphology of ettringite is divided into a few types from SEM observations as follows.

Table III
Classification of ettringitelike hydrates

Type	Explanation of morphology
I	In relatively large voids, the form is acicular (0.1-0.2 μm in diameter x 3-4 μm in length). The crystal grows in the liquid phase of a void by a solution reaction. (Fig. 4)
II	In relatively small voids, the form is needlelike (0.2-0.8 μm in diameter x 2-6 μm in length). The number of crystals is great and they are concentrated in the void. Some of them are sintered together and grow into a large crystal. Crystal growth partially progresses by a solid-solid reaction. (Fig. 5)
III	A giant hydrate in a platelike form is present. It is 5-10 μm in width and 30-50 μm in length. It is doubtful whether the hydrate is ettringite. It seems to be calcium hydroxide. (Fig. 6)

Type II ettringite was observed at various times. The shape of ettringite appears to be average in the high strength hardened cement paste made with normal portland cement containing anhydrite at a long term period.

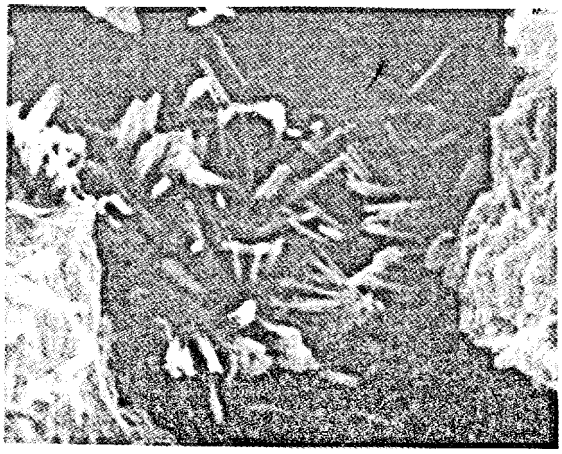

1 μm

(A) Mix No. 3

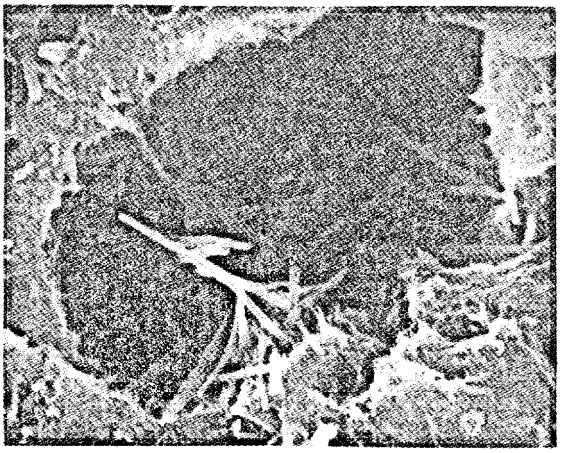

1 μm

(B) Mix No. 5

Fig. 4 Type I ettringite

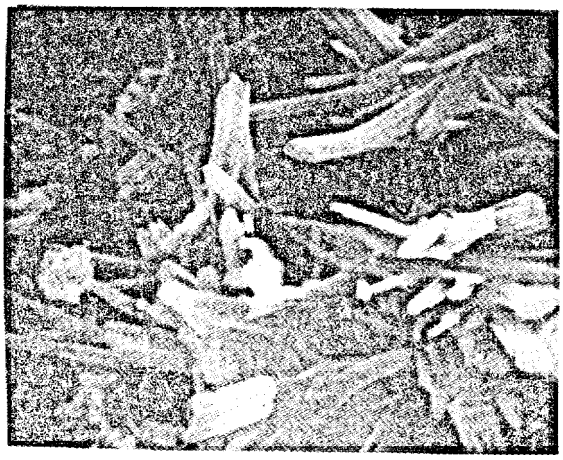

1 μm

(A) Mix No. 4

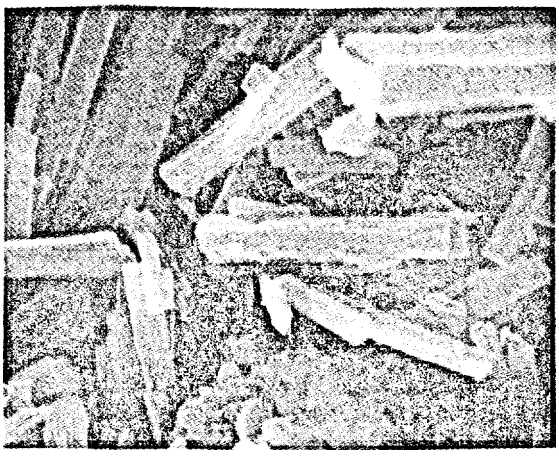

1 μm

(B) Mix No. 6

Fig. 5 Type II ettringite

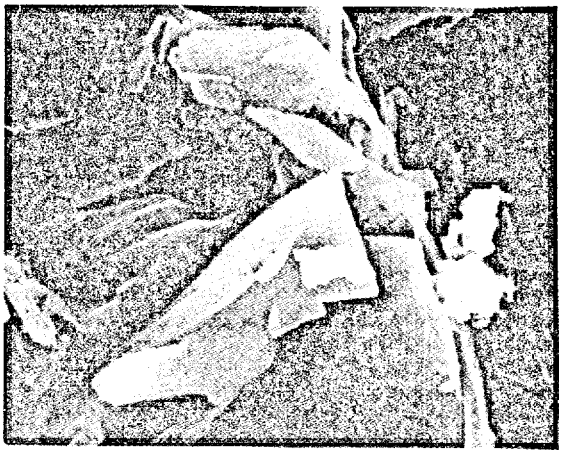

5 μm

(A) Mix No. 2

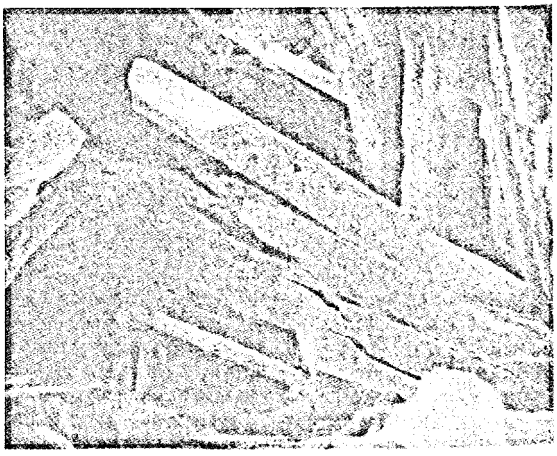

5 μm

(B) Mix No. 7

Fig. 6 Type III hydrate

3-3. BEHAVIOR OF ETTRINGITE IN HIGH STREHGTH HARDENED CEMENT PASTE

The morphology of ettringite indirectly reveals the characters of cement minerals and the reaction conditions. The shape of ettringite formed by the reaction between C_3A (C_4AF) and anhydrite (gypsum) in normal portland cement admixed with anhydrite is different from those of ettringite in expansive or quick hardening cement (1), (2). In expansive cement containing calcium sulfoaluminate, colloidal or amorphous ettringite which is converted to fine crystals after a while is said to have the ability of expansion of cement stone at an early period (3). The reaction is mainly topochemical. The crystal growth of hydroxide may also have effects on the expansion of cement stone. The contribution of ettringite to early strength development is shown in regulated set cement or quick hardening cement (4). But the behavior of ettringite in these special cements at long term age has been scarcely reported, especially in high strength cement.

The effects of ettringite in high strength hardened cement paste are described as follows.

(a) Ettringite has much bound water which contributes to making the matrix of cement paste dense.
(b) Ettringite crystal fills voids in the matrix of the cement paste. (Type I, II)
(c) The crystal growth of ettringite gives rise to expansion of the cement paste. (Type II)

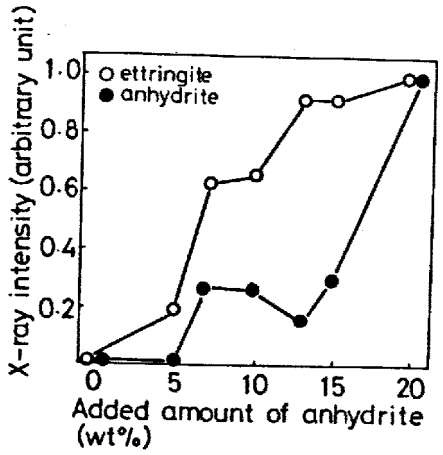

Fig. 7 Amounts of ettringite and unreacted anhydrite. X-ray intensity = $I_{No.x}/I_{No.7}$

These properties of ettringite at long term age in normal portland cement admixed with anhydrite should be influenced by the following factors.

(a) Chemical composition of cement (SO_3/Al_2O_3 ratio is most important.)
(b) Amounts of unreacted anhydrite and calcium aluminate
(c) Compactness of hardened cement paste (Degree of C_3S hydration and water to cement ratio)
(d) Initial curing conditions
(e) Change of curing method (for example, water curing —— air curing)

The necessary amount of anhydrite for the chemical stability of ettringite is more than 20 wt% that of normal portland cement. Otherwise, ettringite must convert to monosulfate hydrate at a later age. However, it takes a much longer time for the reaction to proceed because of the heterogeneous solid. Especially, in the case of low water to cement ratio, this tendency is remarkable. Monosulfate hydrate could not be recognized even in the normal portland cement admixed with 5 wt% anhydrite. Normal portland cement contains 3-5 wt% gypsum; however, ettringite formed at an early period immediately converted to monosulfate hydrate. The difference in the rate of conversion reaction is very large. The phenomenon appears to depend on the amount of unreacted anhydrite and the compactness of the hardened cement paste matrix. (Fig. 7)

The crystal growth of Type II ettringite greatly influences the properties of cement stone. This is largely related to the amount of unreacted anhydrite inducing expansive phenomenon in long term age. Type II ettringite crystals are produced together in a small void but there is no space for them to grow in. Therefore they tend to make the matrix of cement paste spread out. There are two ways for ettringite crystals to grow:

(a) Each crystal grows by a solution reaction.
(b) Some crystals sinter together by a solid- solid reaction.

4. CONCLUSIONS

(1) The average shape of ettringite in the high strength hardened cement paste made with normal portland cement containing anhydrite at forty months of age in water curing is a needlelike and 0.2-0.8 μm in diameter and 2-6 μm in length.

(2) A number of ettringite crystals are concentrated in a small void. Some ettringite crystals are sintered together and grow into a large crystal.

(3) Monosulfate hydrate could not be recognized even in the normal portland cement of 5 wt% anhydrite addition.

2.2

REFERENCES

1.- K. Nakagawa, K. Isozaki and Y. Watanabe (1980), "Hydration and strength of normal portland cement admixed with anhydrous calcium sulfate" Proc. 7th Inter. Symp. Chem. Cement, Paris, II 192 -197.

2.- K. Isozaki, K. Nakagawa and Y. Watanabe (1978), "Studies on the strength of high ettringitic cement stones steam cured at normal pressure" CAJ Review of the 32nd General Meeting, 42-43.

3.- J. Isogai, A. Saito and M. Takahashi (1977), "On the expansion due to hydration of hardened cement paste with calcium sulfoaluminate admixture" CAJ Review of the 31st General Meeting, 43-45.

4.- K. Isozaki S. Sakamaki and K. Nakagawa (1980), "Application of activated calcium aluminate clinker to quick hardening cement" Proc. 7th Inter. Symp. Chem. Cement, Paris, V 214-219.

W. KURDOWSKI and K. MISKIEWICZ, University of Mining and Metallurgy, 30-059 Cracow, al. Mickiewicza 30, POLAND

$Ca_3SiO_4Cl_2$ hydration under hydrothermal conditions.

L'hydratation de $Ca_3SiO_4Cl_2$ dans les conditions hydrothermales.

ABSTRACT : The calcium chlorosilicate samples and the mixtures of calcium chlorosilicate with mole ratio of silica to chlorosilicate being 1 and 2, were hydrated at 200°C and 240°C for 48, 96, 192 and 384 hours. It was estabilished that the hydration products of $Ca_3SiO_4Cl_2$ consist of tobermorite, xonotlite and basic calcium chlorate. This last, in the amorphous form is not detectable by X-ray diffraction. A short time of reaction results in predominant content of tobermorite, which thereafter is slowly transformed to xonotlite. The addition of active silica alters the phase composition of products. The mixture of $Ca_3SiO_4Cl_2$ and SiO_2 with mole ratio of silica to chlorosilicate being 1 gives xonotlite and basic calcium chloride. Some quantities of tobermorite and CSH phase initially formed turn quickly into xonotlite. Also in this case the basic calcium chloride is not detectable by X-ray diffraction. An increase in silica addition up to the mole ratio of SiO_2 to $Ca_3SiO_4Cl_2$ being 2 brings about the formation of CSH phase of different degree of crystallinity, it means from rather poor crystalline CSH up to tobermorite. In this case the calcium chloride is randomly distributed among the hydrates. The hydration products of this mixture tend to pass slowly into gyrolite. It was established that during the hydration of calcium chlorosilicate and its mixtures with silica under hydrothermal conditions, chlorine does not form any stable compounds with the calcium silicate hydrates. On the other hand calcium chloride influences the stability of calcium silicate hydrates. For example, the transformation of CSH phase into gyrolite seems to be sluggish. The stability of tobermorite phase is also markedly influenced. Chlorine is probably adsorbed on the CSH phase surface, because it is easily rinsed out by use of ethyl alcohol. After rinsing, about 0.6 weight per cent of chlorine remains in the CSH phase.

A 200°C e 240°C por períodos de 48, 96, 192 e 384 horas, foram hidratadas amostras de clorossilicato de cálcio e misturas de clorossilicato de cálcio com relação molar de sílica para clorossilicato de 1 e 2. Estabeleceu-se que os produtos de hidratação de $Ca_3SiO_4Cl_2$ consistem de tobermorita, xonotlita e clorato básico de cálcio. Este último, em forma amorfa, não é detectável por difração de raio X. Uma reação de curta duração dá como resultado uma predominância de teor de tobermorita que, a seguir, transforma-se lentamente em xonotlita. A adição de sílica ativa altera a composição de fase dos produtos. A mistura de $Ca_3SiO_4Cl_2$ e SiO_2, com relação molar de sílica para clorossilicato igual a 1, dá xonotlita e cloreto básico de cálcio. Algumas quantidades de tobermorita e de fase de CSH formado, rapidamente se transformam em xonotlita. Também neste caso o cloreto básico de cálcio não é detectável por difração de raio X. Um aumento na adição de sílica até a relação molecular de SiO_2 para $Ca_3SiO_4Cl_2$ igual a 2, ocasiona a formação de fase de CSH com grau diferente de cristalinidade, ou seja de CSH com cristalinidade bastante pobre até tobermorita. Neste caso o cloreto de cálcio é distribuído aleatoriamente entre os hidratos. Os produtos de hidratação desta mistura tendem a passar lentamente para girolita. Estabeleceu-se que durante a hidratação do clorossilicato de cálcio e de suas misturas com sílica sob condições hidrotérmicas, o cloro não forma quaisquer compostos estáveis com os hidratos de silicato de cálcio. Por outro lado, o cloreto de cálcio influencia a estabilidade dos hidratos de silicato de cálcio. Por exemplo, a transformação da fase de CSH em girolita parece ser vagarosa. A estabilidade da fase de tobermorita também é influenciada acentuadamente. O cloro provavelmente é adsorvido na superfície da fase de CSH, porque é facilmente enxaguado com o uso de álcool etílico. Depois de enxaguado, cerca de 0,6% em peso de cloro permanece na fase de CSH.

W. KURDOWSKI and K. MIŚKIEWICZ, University of Mining and Metallurgy, 30-059 Cracow, al. Mickiewicza 30. POLAND

1. INTRODUCTION

Calcium chlorosilicate $Ca_3SiO_4Cl_2$ is a phase forming at about 600°C in the system $CaO-SiO_2-CaCl_2$ /1, 2, 3/. The investigations we have carried out previously /4/ indicated that calcium chlorosilicate reacts vigorously with water, dissoloving congruently. At a temperature of 20°C and water/anhydrous sample ratio of 1, CSH phase and basic calcium chloride $CaCl_2.Ca(OH)_2.H_2O$ are formed. At higher water/anhydrous sample ratio, viz. 10, the composition of hydrates includes CSH and $Ca(OH)_2$, as under these conditions basic calcium chloride is wholly dissolved. Interesting results of the studies on the reaction of chlorosilicate with water at room temperature determined us to extend the experiments and to embody with them the hydration process of $Ca_3SiO_4Cl_2$ under hydrothermal conditions. The present work contains a description of these experiments.

2. MATERIALS USED

Calcium chlorosilicate $Ca_3SiO_4Cl_2$ - was synthesized starting from a mixture of calcium carbonate, amorphous silica and calcium chloride with molar ratio 2:1:1, in a laboratory furnace. The temperature and the time of synthesis were 800°C and 2 hours, respectively. Chlorosilicate thus obtained was pulverized in a Fritch agate mill to a specific surface area of 3000 cm^2/g. SiO_2 - was used in the form of silica gel "Aerosil 200", which is characterized by a high specific surface.

3. INVESTIGATION METHODS

The phase composition of the products of calcium chlorosilicate hydration under hydrothermal conditions was determined using a Philips X-ray diffractometr and an UR-20-type infra - red absorption spectrometr. The thermal analysis of the samples was performed using a V. Paulik, J. Paulik and L. Erdey derivatograph. The microstructure of selected sample fractures was observed using a Tesla scanning electron microscope. The assessment of the conceivable binding of chlorine by hydration products was realized with a method described by Tenoutasse /5/.

4. EXPERIMENTAL RESULTS

The hydrothermal processing was used with calcium chlorosilicate as well as its blends with 1 mole and with 2 moles of amorphous silica. In this way three blends with molar CaO/SiO_2 ratios 3, 1.5 and 1 have been obtained. Taking into consideration the presence of the chlorine in the calcium chloride phase, the CaO/SiO_2 molar ratio will be, of course, lower and will amount 2, 1 and about 0.63, respectively /Table 1/. These blends have been subjected to a hydrothermal processing at temperatures 200°C and 240°C in saturated steam. The samples were held in these conditions for 24, 48, 96, 192 and 384 hours. An examination of the phase composition of the blends on hydrothermal processing demonstrated that the calcium chlorosilicate was fully reacted as soon as after 24 hours.

Table 1 - Composition of samples

Phase content in molar ratios	Sample		
	A	B	C
$Ca_3SiO_4Cl_2$	1	1	1
SiO_2-Aerosil	0	1	2

The first sample, A, contained a mixture of 10 Å - and 11 Å - tobermorite. The X-ray diffraction pattern, shown in Fig. 1, do not exhibit other lines. On the other hand the thermal curve, shown in Fig. 2, evidences the A sample to give endothermic effects at 145°, 440° and 565°C, respectively, which can be attributed to particular decomposition stages of basic calcium chloride.

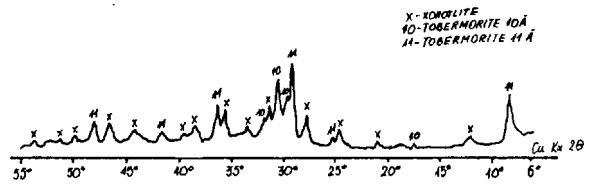

Fig. 1 - X-ray examination of sample A, temp. 200°C, 24 hours.

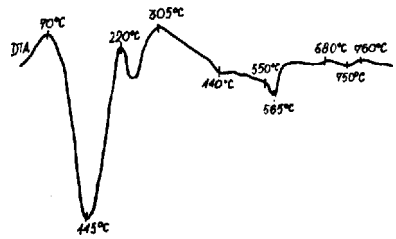

Fig. 2 - DTA curve of sample A, temp. 200°C, 24 hours.

Remaining thermal effects can be identified with the decomposition of tobermorite phases. The infra-red spectrum reveals also small absorption maxima at 1415 and 1450 cm^{-1}, attributed to OH^- bonds, which denotes the occurrence of calcium hydroxide in the sample. In Figs 3 and 4 the picture of the sample under scanning microscope is shown after 24 and 384 hours of hydrothermal treatment at 240°C. The crystals of tobermorite and xonotlite are visible. On the other hand the microscopic observations did not exhibit the presence of amorphous phases, which should be formed in substantial amount by the basic calcium chloride. This phenomenon can be tried to explain only by the adsorption of calcium chloride on calcium silicate hydrates /6/. The autoclaved B sample, being a blend of calcium chlorosilicate with amorphous silica in a 1:1 molar ratio gives on the X-ray diagram the diffraction lines which are characteristic for xonotlite. The position of these lines indicates a slight displacement

towards higher angles of about 0.01 Å /Fig. 5/.

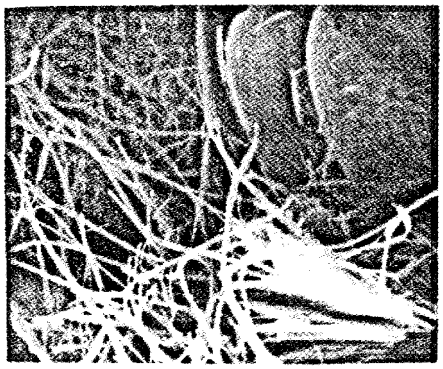

Fig. 3 - SEM micrograph of sample A, temp. 240°C, 24 hours, 10 000 X, xonotlite and tobermorite.

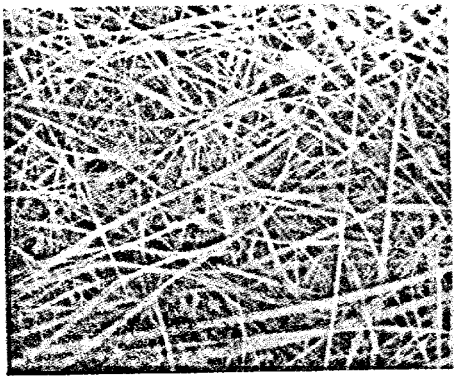

Fig. 4 - SEM micrograph of sample A, temp. 240°C, 384 hours, 10 000 X, xonotlite.

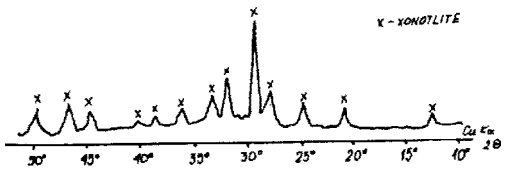

Fig. 5 - X-ray examination of sample B, temp. 200°C, 24 hours.

On the other hand on the thermal curve, shown in Fig. 6, endothermic peaks at temperatures 140° and 170°C and an exothermic effect at 710°C additionally occur. The effect at 140°C and diffused effects at 590°C can be attributed to amorphous basic calcium chloride, whereas the peaks : endothermic one and exothermic another, at 170°C and 710°C, respectively - to CSH phase. The occurrence of OH groups as well as of the CSH phase are confirmed by infra-red absorption spectra. The presence of OH groups is evidenced by absorption bands at about 1415 and 1450 cm^{-1}, respectively, while the presence of CSH phase by the bands at 470, 665, 870, 990 and 1230 cm^{-1}, respectively. The microphotograph shows well crystallized xonotlite crystals. Also the presence of needles of CSH phase and of anhydrous calcium chloride can not be excluded /Fig. 7/.

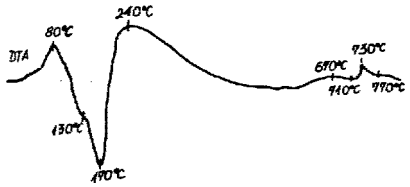

Fig. 6 - DTA curve of sample B, temp. 200°C, 24 hours.

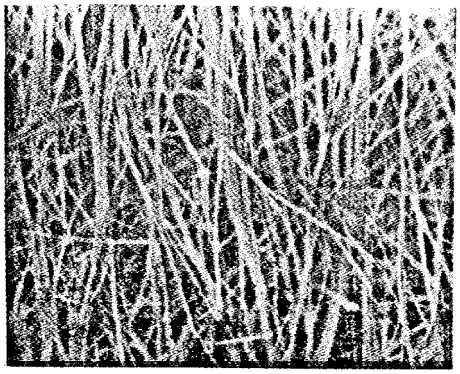

Fig. 7 - SEM micrograph of sample B, temp. 240°C, 24 hours, 10 000 X, xonotlite.

The sample C was a blend of calcium chlorosilicate and amorphous silica with molar ratio of 1:2. The X-ray diagram of this blend on hydrothermal processing at 200°C shows the diffraction lines typical for CSH phase. For longer reaction times gyrolite starts to appear in the sample ; it seems to be a stable phase under these conditions for this blend. However even in the sample subjected to a hydrothermal treatment at 240°C for 96 hours three phases occur together : CSH, tobermorite and gyrolite /Fig. 8/. The thermal curve /Fig. 9/ gives the effects typical for a mixture of 11 Å - tobermorite, CSH and gyrolite; also the presence of basic calcium chloride cannot be excluded /a shoulder on the curve at 440°C/.

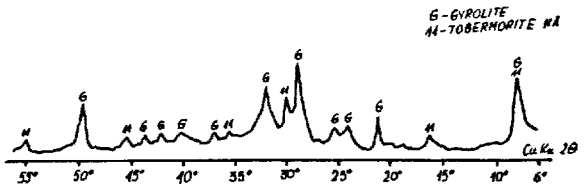

Fig. 8 - X-ray examination of sample C, temp. 240°C, 96 hours.

It is very probable that - similarly as in other samples - calcium silicate is adsorbed on the surface of the grains of calcium silicate hydrates. In order to elucidate this

W. KURDOWSKI and K. MIŚKIEWICZ, University of Mining and Metallury, 30-059 Cracow, al. Mickiewicza 30, POLAND

Table 2 - Phase composition of samples

Sample with molar ratio		$Ca_3SiO_4Cl_2$					$Ca_3SiO_4Cl_2$:SiO_2 1:1					$Ca_3SiO_4Cl_2$: SiO_2 1:2				
time /h/		24	48	96	192	384	24	48	96	192	384	24	48	96	192	384
temperature	200°C	T10 T11 CSH? CCH	T10 T11 CCH	T10 T11 CCH	X T10 T11 CCH	X T11 CCH	X T11 CSH CCH	X T11 CSH CCH	X T11 CSH CCH	X T11 CSH CCH	X CSH CCH	T11 CSH C	T11 CSH G C	T11 G CSH C	G CSH C	G CSH C
	240°C	T10 T11 CSH? CCH	T10 T11 CCH	T10 T11 CCH	X T11 CCH	X T11 CCH	X T11 CSH CCH	X T11 CSH CCH	X CSH CCH	X CSH CCH	X CSH CCH	T11 G CSH C	T11 G CSH C	T11 G CSH C	G CSH C	G CSH C

T10 - 10 Å tobermorite ; T11 - 11 Å tobermorite ; X - xonotlite ; G - gyrolite ; CCH - $CaCl_2.Ca/OH/_2.H_2O$; CSH - CSH /I/ ; C - $CaCl_2 \cdot nH_2O$

problem the samples A and B, after 24 hours of hydration in an autoclave at 200°C have been rinsed with absolute alcohol. It has been found, that almost whole calcium chloride get leached out from both samples. In sample B after rinsing small amounts of vaterite appeared, which evidences a non-complete protection of the preparation against the influence of CO_2 from the atmosphere during rinsing operation. The X-ray diffraction pattern of both samples on rinsing did not undergo any changes. This trial confirmed the supposition of an adsorptive binding of calcium chloride in the samples.

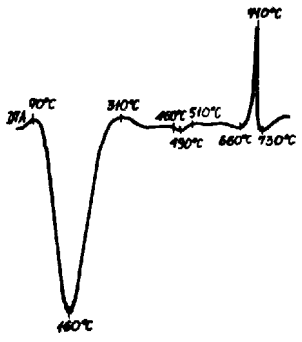

Fig. 9 - DTA curve of sample C, temp. 240°C, 96 hours.

5. CONCLUSIONS

- The behaviour of sample A in the process of autoclaving is consistent with investigation results of other authors on $CaO-SiO_2-H_2O$ system, of course if the reduction of CaO/SiO_2 ratio in consequence of the formation of $CaCl_2.Ca/OH/_2.H_2O$ will be taken into account. It means, that in result of autoclaving sample A, calcium chlorosilicate without addition, gives tobermorite, passing into xonotlite phase. The course of the process of calcium chlorosilicate reaction with water under hydrothermal conditions can be schematically written :

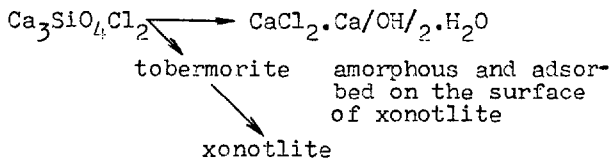

- Sample B, a blend of calcium chlorosilicate with amorphous silica with 1:1 molar ratio, gives xonotlite, which corresponds to a CaO/SiO_2 ratio of 1:1. The course of the process can be schematically written :

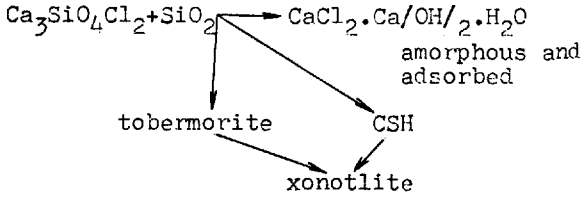

- Sample C, a blend of calcium chlorosilicate with amorphous silica with CaO/SiO_2 molar ratio of 1:2, gives gyrolite as the product of autoclaving, with intermediate formation of tobermorite and CSH. The presence of chloride ions seems to retard the transition of CSH phase into gyrolite /Fig.10/.



The course of the process can be schematically written :

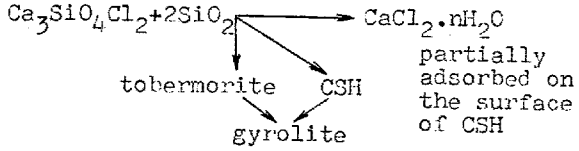

- Calcium chloride appears to form no crystalline phase in the autoclaving process. Under these conditions it is adsorbed on the surface of calcium silicate hydrates. It can be readily leached out in absolute alcohol. A high specific surface area of calcium silicate hydrates creates favourable conditions for the adsorption and even for chemisorption of chlorine /7/. Estimatively it seems probable, that in C sample after rinsing remains about 0.6 weight per cent of chlorine. This chlorine can entry in the lattice of hydrated calcium silicates /7/.

6. REFERENCES

1.- W. KURDOWSKI, Silicates Industr., 30, 500 /1965/.

2.- R. CZAYA, Zeitschr. f. allg. Chemie, 375, 124 /1970/.

3.- R. CZAYA, Kristall. u. Technik, 5, No 4, K 9 /1980/.

4.- W. KURDOWSKI and K. MIŚKIEWICZ, Cem. Concr. Res., 15, No 5, 785 /1985/.

5.- N. TENOUTASSE, Int. Symp. Admixtures for Mortars and Concrete, RILEM, Rapport No V/15, 251, Brussels 1967.

6.- V.S. RAMACHANDRAN, Matériaux et Constructions, Vol. 4, No 9, 3 /1971/.

7.- V.S. RAMACHANDRAN, Canadian Journal of Civil Engineering, Vol. 5, No 2, 213 /1978/.

O. Z. Cebeci, Department of Civil Engineering,
King Abdulaziz University, Jeddah, Saudi Arabia

Hydration and Porosity of Cement Paste Cured in Warm and Dry Envirnment

SUMMARY: The effect of simultaneous changes in the temperature and the relative humidity of the curing media on the hydration and porosity of pure cement paste was investigated. Two different temperatures, 17 and 37 C, were maintained during mixing as well as in the three different curing media; in lime saturated water, 75%, and 33% relative humidity. The degreees of hydration and mercury intrusion pore size distributions of the hardened pastes were determined at various ages from one to ninety days. The results indicated that the deficiency in the relative humidity of the environment, rather than the increase in the hydration temperature, is the dominant factor affecting the parameters investigated in this study. The cement pastes hydrated at lower humidity attained lower ultimate degree of hydration and greater porosity, particularly in macropores, as compared to the pastes hydrated in water.

Realizou-se investigação sobre o efeito de mudanças simultâneas de temperatura e de umidade relativa do ambiente de cura na hidratação e porosidade de pasta de cimento puro. Foram mantidas duas temperaturas diferentes, 17 e 37°C, durante o amassamento e nos três diferentes ambientes de cura: em água saturada de cal, umidade relativa de 75% e de 33%. As pastas de cimento endurecido foram submetidas a exame em várias idades, de 1 a 90 dias, para determinação dos graus de hidratação e distribuição de tamanho de poro por intrusão de mercúrio. Os resultados indicaram que deficiência na umidade ambiental relativa, mais do que o aumento da temperatura de hidratação, é o fator preponderante que afeta os parâmetros investigados neste estudo. As pastas de cimento hidratado com umidade mais baixa apresentaram grau limite mais baixo de hidratação e porosidade maior, particularmente em macroporos, em comparação com as pastas hidratadas em água.

O. Z. Cebeci, Department of Civil Engineering.
King Abdulaziz University, Jeddah, Saudi Arabia

Hydration and Porosity of Cement Paste Cured in Warm and Dry Envirnment

INTRODUCTION

The process of cement hydration is influenced by a number of chemical and physical parameters which may vary from one laboratory investigation to another. These parameters are naturally varied by the widely different ambient conditions under which concrete is produced and they are intentionally altered and controlled, to some advantage, by various concrete production techniques.

The variations in the chemical and physical parameters result in the formation of hydration products which differ in chemical composition, physical structure and porosity, thereby, largely control the properties and behavior of hardened cement paste, mortar and concrete (1-3)

Hydration temperature in hot weather concreting is naturally higher than that in cold weather concreting, and in accelerated curing technology the temperature of concrete elements are further elevated. The rates of chemical reactions are accelerated by increasing temperature and this is known to be true for the hydration of calcium silicates and Portland cement. Within the range of ambient temperatures encountered in concrete construction sites the stoichiometry of hydration is essentially unaffected although the composition, morphology and the micro- structure of the products change somewhat (4-7). The effects of temperatures above 100 C, as encountered in autoclaving, are quite different and are out of the scope of this work.

The temperature dependence of cement hydration is influenced by the extent, or the degree, of hydration. Increased temperature of hydration results in more rapid initial rates and the difference in the degree of hydration between warm and cold pastes decreases with time (1,3-7). Ultimately, the difference is small, and even though some workers have reported the warmer pastes attaining a greater ultimate degree of hydration (1,4,8-10) others have found the colder hydration resulting in a higher percentage (1,4,11-15).

The degree of hydration of calcium silicate or Portland cement pastes are measured by a number of methods including the determination of the heat of hydration and the water of hydration, or the non-evaporable water content, and by the quantitative X-ray diffraction techniques. Brunauer and Kantro (12) consider the former two techniques as indirect and unreliable due to the changes in the composition of the calcium silicate hydrates in the course of hydration. However, Lea (1) has reported that the results of the different methods are reasonably similar, and Berger et al (16) have employed the latter two methods without differentiating

The effect of hydration temperature on the pore structure of calcium silicate hydrates was investigated by several workers who analysed pore size distribution and surface area measurements obtained from adsorption data (15,17-19). Considering that the results of these analysis give an inadequate characterization of much of the pore structure of hardened cement paste, Diamond (10) employed mercury intrusion porosimetry in his work on cement pastes hydrated in lime saturated water at 6 and 40 C. Diamond reported the degree of hydration, density, total porosity and pore size distribution of the specimens and concluded that " Initially, the pastes hardened at low temperatures have much coarser pore size distributions, but by a month the differences are small. After a year the distributions are identical except in the range below several hundred A, where the pastes hydrated at the low temperature show a negligible content of pores." (10).

The results of water and nitrogen adsorption and mercury intrusion porosimetry tests were combined by Bentur (22) who concluded that the tricalcium silicate pastes which were hydrated at 4 and 25 C had similar, but not identical, pore structure. Increasing the hydration temperature to 65 C caused coarsening of the pore structure which was exhibited by an increase in macropore volume at the expense of mesopore and micropore volumes. These changes were not accompanied by changes in total porosity, suggesting that the shifts in pore structure are the result of rearrangement of the growing hydration products rather than change in their volume (22).

While the above investigators explored the effect of temperature on the hydration and porosity of cement paste the specimens were kept in water or 100% relative humidity. In many practical cases, particularly in hot and dry environment, the cement paste in hardening concrete can not be kept saturated for prolonged periods. It is known that hydration of cement practically stops below about 80% internal relative humidity (1-3). When partial drying occurs during hydration

originally water-filled spaces empty and deposition of hydration products cannot then occur in such spaces (13). Verbeck and Helmuth (13) stated that differences in the pore size distributions would be expected depending upon whether the paste was saturated or allowed to dry; however, relevant data has not been reported.

In the present work, the effect of simultaneous changes in the temperature and the relative humidity of the curing media on the hydration and porosity of pure cement paste was investigated. Two different temperatures, 17 and 37 C, were maintained during mixing as well as in the three different curing media; in lime saturated water, 75% and 33% relative humidity. The degrees of hydration and mercury intrusion pore size distrubutions of the hardened pastes were determined at various ages from one to ninty days.

EXPERIMENTAL METHODS

The cement used in this study was a commercial ordinary Portland cement of 335m2/kg specific surface. The oxide composition was 20.37% SiO_2, 5.52% Al_2O_3, 3.78% Fe_2O_3, 61.71% CaO, 2.51% MgO and 2.42% SO_3. Insoluble residue was 0.45% and the ignition loss was 2.30%.

Distilled water and cement were mixed at a water/cement ratio of 0.6 while keeping all materials and equipment at 17 or 37 C within ±2 C. Mixing was done under vacuum in order to avoid entrapped air bubbles (23), and the pastes were cast into cylindrical molds (discs) 12mm in diameter and 3mm in height. The molded pastes with uncovered tops were immediately placed in humidity-temperature cabinets controlled at 75% and 33% relative humidity and 17 and 37 C. The specimens were demolded the next day and some of those kept in the 75% relative humidity cabinets were placed in lime saturated water at 17 and 37 C while others were kept in the cabinets.

At the end of the curing periods a number of hardened cement paste discs were removed from the curing water and cabinets, they were oven-dried at 105±5 C, and kept in desiccators until further testing.

The specimens of various ages were ignited at 1050±50 C to determine the non-evaporable water content. The ratio of this to the nonevaporable water content of the paste completely hydrated with excess water in a ball-mill indicates the degree of hydration of the specimen.

The pore size distributions of the specimens were determined by mercury intrusion porosimetry; now a widely used technique which is capable of measuring the widest range of pore sizes. This method is particularly useful in comparative studies rather than in the analysis of complex (non-cylindrical) pore geometries (24).

The mercury porosimeter used in this work was capable of exerting a maximum pressure of 414 MPa, thereby intruding pores as small as 2.1 nm in diameter when the contact angle of mercury on hardened cement paste is taken as 117° (10).

The oven-dried hardened cement paste discs were broken into four quarters, and one quarter from four discs were collected and tested in the porosimeter. For each different set of specimens another test was run on four more quarters collected from four other discs. Thus, the pore size distribution curves reported in this work generally represent the average of eight samples.

RESULTS AND DISCUSSION

The degrees of hydration of the cement pastes cured in lime saturated water (reported as 17 C-W and 37 C-W curves in Fig. 1) indicate that higher temperature increases the early hydration rate. After about 10 days the paste hydrated at lower temperature attains greater degree of hydration although the difference at the end of 90 days is only 4%. This observation is in line with several earlier reports (1, 4,8-10).

When the relative humidity of the curing medium is reduced to 75% and 33% hydration practically ceases within 14 days. In 75% relative humidity greater degree of hydration is attained throughout 90 days of curing at the higher temperature It is implied that the initial greater hydration accomplished under these conditions has played a dominant role in determining the ultimate degree of hydration. The reverse is true when the relative humidity is only 33%; the higher initial hydration is not high enough, whereas the slower loss of moisture from the cooler paste allows it to attain a greater degree of hydration after about 5 days.

Another important result illustrated in Fig. 1 is that the differences, or the reductions, in the relative humidity of the curing media, rather than the differences

in hydration temperature, are more influencial in determining the degree of hydration of the cement paste. Regardless of the curing temperature, the pastes kept at 33% relative humidity are hydrated only about half as much as those cured in water.

The mercury intrusion pore size distributions of the pastes hydrated for 7, 28, and 90 days are presented in Fig. 2. Naturally, the pastes cured at below saturation humidity have greater pore volume than those hydrated in water. Regardless of the curing period and temperature, the lower is the relative humidity the larger is the total pore volume intruded. Moreover, it should be noted that the deficiency in the relative humidity has increased particularly the volume of pores greater than 0.030μm in diameter, defined as macropores (25). This indicates the lack of hydration and deposition of products in these pores since they are subject to greater loss of capillary water by evaporation.

Table 1, obtained from Fig.1, shows the changes in the total intrusion and macro-porosity under different conditions for various periods. With increasing age, the pastes hydrated in water at 17 C or 37 C show a reduction in total intrusion, as well as in the volume and volume percentage of macropores.

Table 1. Total intrusion and macroporosity of hydrated cement pastes

Curing Period and Conditions	Total Intrusion, cm^3/g	Macroporosity cm^3/g	% of total intrusion
7d/W/17 C	0.248	0.176	71
28d/W/17 C	0.227	0.143	63
90d/W/17 C	0.205	0.128	62
7d/75%/17 C	0.270	0.218	81
28d/75%/17 C	0.259	0.236	91
90d/75%/17 C	0.242	0.231	95
7d/33%/17 C	0.276	0.263	95
28d/33%/17 C	0.265	0.258	97
7d/W/37 C	0.260	0.178	68
28d/W/37 C	0.242	0.164	67
90d/W/37 C	0.223	0.131	59
7d/75%/37 C	0.287	0.260	91
28d/75%/37 C	0.284	0.270	94
90d/75%/37 C	0.271	0.264	97
7d/33%/37 C	0.293	0.282	96
28d/33%/37 C	0.291	0.282	97

In the pastes hydrated in 75% and 33% relative humidity the volume percentage of macropores increases as curing time and temperature increase. The volume of the macropores also increases with increasing hydration temperature. However, the volume of the macropores of the pastes hydrated in 75% relative humidity increases as time increases from 7 to 28 days, and then decreases slightly at 90 days of hydration. The total- and macro-porosity of the cement pastes hydrated in 33% relative humidity, and particularly at the higher temperature, show little or no change beyond 7 days.

The above analysis confirms that "we may thus expect differences whether the paste was kept saturated,.. or allowed to dry..." (13). The present work has shown that when a cement paste is allowed to dry the macroporosity is altered more than the total intrusion. Furthermore, the influence of the deficiency in the relative humidity on the pore size distribution of hardened cement paste is substantially greater than the effect of the increase in the hydration temperature.

CONCLUSION

The decrease in the relative humidity of the curing media (from saturation to 75% and 33%) predominantly influences the hydration and porosity of hardened cement paste whereas the increase in the hydration temperature (from 17 to 37 C) has a less pronounced effect.

The degrees of hydration reached in cement pastes cured at 75% and 33% relative humidity are only about two-thirds and one-half, respectively, of that attained in the pastes hydrated in lime saturated water for 90 days. The pastes cured at 17 C in water and in 33% relative humidity hydrate slower initially, but reach higher ultimate degrees of hydration than the corresponding warmer pastes. Hydration in 75% relative humidity results in higher initial as well as ultimate degree of hydration in the warmer pastes.

The deficiency in the humidity of curing increases the volume of pores intruded by mercury in hydrated cement pastes. The increase is more pronounced in the volume of pores greater than 0.030μm in diameter. This is accountable by the fact that, if drying occurs during hydration, larger pores empty due to evaporation of capillary water, and hydration products cannot be deposited in such spaces.

O. Z. Cebeci, Department of Civil Engineering,
King Abdulaziz University, Jeddah, Saudi Arabia

4

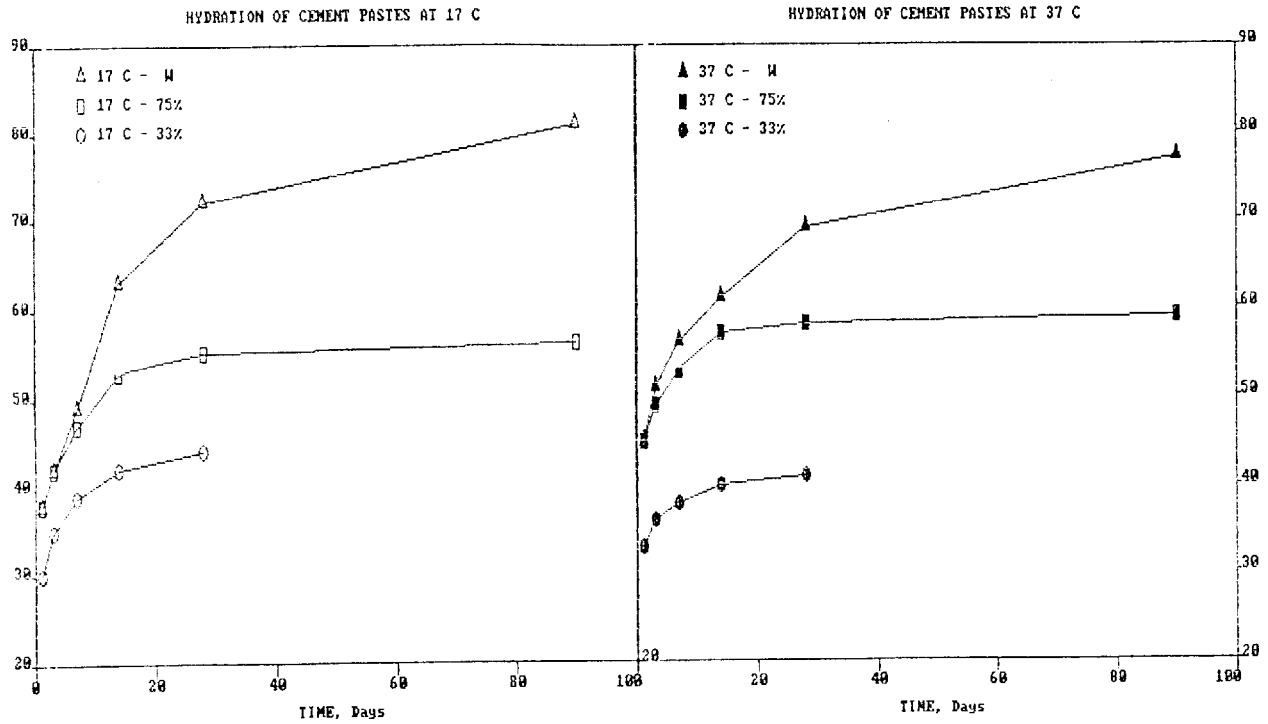

FIGURE 1 - Degrees of hydration of Portland cement pastes hydrated at different temperatures and relative humidities.

ACKNOWLEDGEMENT

This paper is based upon work supported by the College of Engineering of King Abdulaziz University, Jeddah, Saudi Arabia, under Grant No. 02-110.

REFERENCES

1. - F.M. LEA (1970), " The chemistry of cement and concrete, 3rd ed. ", Edward Arnold Publishers Ltd., London.

2. - A.M. NEVILLE (1981), "Properties of concrete, 3rd ed.", Pitman Books Ltd., London.

3. - S. MINDESS and J.F. YOUNG (1981), "Concrete", Prentice-Hall, Inc., Englewood Cliffs, New Jersey.

Alan D. Buck, Geologist, Concrete Technology Division, Structures Laboratory, U.S. Army Engineer Waterways Experiment Station, Vicksburg, Mississippi, USA 39180-0631

Relationships Between Ettringite and Chloroaluminate, Strength, and Expansion in Paste Mixtures.

SUMMARY: As part of a study of cementitious mixtures for underground sealing and isolation of nuclear wastes, there was concern about the stability of ettringite and tetracalcium aluminate dichloride-10-hydrate (chloroaluminate) and the effects of the stability of these phases on such factors as strength and expansion of candidate mixtures. Therefore, a series of paste mixtures using a portland cement, plaster of paris, and two levels of water content with or without the presence of fly ash, ground granulated iron-blast furnace slag, silica fume, or natural pozzolan were made; four mixtures contained sodium chloride instead of plaster of paris were also made.

Specimens from these mixtures were stored at different temperatures and monitored at different ages up to one year for phase composition by X-ray diffraction (XRD), for compressive strength, and for restrained expansion.

The most significant finding was that since loss of ettringite crystallinity at about 100°C, as determined by XRD, did not affect either compressive strength or expansion significantly, the thermal stability of ettringite in this temperature range need not be a concern for repository sealing use of cementitious mixtures. Other findings were:

a. Some ettringite was destroyed at about 75°C while that in other mixtures persisted to about 100°C. The higher stability seemed to relate to impurity, but this could not be definitely proved by XRD.

b. If a long-term source of alumina is available and other necessary ingredients are present, new ettringite may continue to form for at least a year.

c. Once ettringite had been destroyed by heat, it did not tend to reform under moist storage conditions at room temperature.

d. When ettringite was destroyed by heat, tetracalcium aluminate monosulfate-12-hydrate (monosulfoaluminate) did not replace it. Instead there was sometimes formation of hydrogarnet after heating to 100°C.

e. Conversion of ettringite to chloroaluminate in the mixtures containing salt ranged from none to complete at 23°C with some coexistence for a year. In no case did ettringite replace chloroaluminate.

Como parte de um estudo de misturas cimentosas para vedação subterrânea e isolação de rejeitos nucleares, foi levantada a questão da estabilidade da etringita e do dicloreto-10-hidrato de aluminato tetracálcico (cloroaluminato) e dos efeitos da estabilidade destas fases sobre fatores tais como resistência e expansão das misturas concorrentes. Por isso foi feita uma série de misturas de pasta usando-se um cimento portland, plaster de paris, e dois níveis de teor de água com ou sem a presença de cinza volante, escória de alto forno de ferro granulada moída, microsílica, ou pozolana natural. Também foram feitas quatro misturas contendo cloreto de sódio em vez de plaster de paris.

Espécimes destas misturas foram guardados a temperaturas diferentes e monitorados em diferentes idades até 1 ano, através de difração de raio X (XRD) no que tange à composição de fase, resistência à compressão e expansão restringida.

A tendência mais significativa foi que, uma vez que a perda de cristalinidade da etringita a cerca de 100°C, conforme determinação por XRD, não afetou significativamente nem a resistência à compressão nem a expansão, a estabilidade térmica da etringita nesta faixa de temperatura não é necessariamente um problema para o uso de misturas cimentosas na vedação de depósitos. Outras tendências foram:

a. Parte da etringita foi destruída a cerca de 75°C, enquanto a de outras misturas perdurou até cerca de 100°C. A estabilidade maior pareceu estar relacionada com a impureza, mas isto não pôde ser definitivamente provado por XRD.

b. Se houver disponibilidade de fonte de alumina a longo prazo e outros ingredientes necessários estiverem presentes, pode continuar a haver formação de etringita nova por pelo menos um ano.

c. Uma vez destruída a etringita pelo calor, ela não tem tendência a se refazer sob condições de armazenagem úmida à temperatura da sala.

d. Tendo sido a etringita destruída pelo calor, o monossulfato-12-hidrato de aluminato tetracálcico (monossulfoaluminato) não a substitui. Ao invés houve algumas vezes formação de hidrogranada após aquecimento a 100°C.

e. A conversão de etringita em cloroaluminato nas misturas contendo sal foi de zero a completa a 23°C, com alguma coexistência por um ano. Em nenhum caso a etringita substituiu o cloraluminato.

INTRODUCTION

Present plans for underground disposal of nuclear wastes in the U.S. call for the use of expansive hydraulic cementitious systems to seal off access to these wastes. Since these sealing materials are expected to experience elevated temperatures of up to about 100°C there was concern about the possible effect of such temperature on the products that produce the expansion (ettringite, chloroaluminate*). Therefore, work was done to study the stability of these phases and the effects of their destruction on such parameters as compressive strength and expansion (Buck, Burkes, and Poole, 1985).

While ettringite has been the subject of many investigations and much discussion, these have generally concentrated on different treatments of one phase or cement system (Kalousek and Adams 1951, Jones 1960, Turriziani 1964, Schweite and Ludwig 1968, Roberts 1968, Mather et al 1978, Taylor and Roy 1980, Ghorab et al 1980, Ogawa and Roy 1981, and Mehta 1972). In general, these indicate that ettringite is stable to about 100°C at atmospheric pressure and that it is usually replaced by tetracalcium aluminate monosulfate-12-hydrade and some form of calcium sulfate when it is destroyed by heat. Higher pressure will raise the decomposition temperature (Ogawa and Roy 1981) and vacuum will lower it (Ghorab et al 1980); Burkes (unpublished) has also found the decomposition temperature is lower in a vacuum. The present work tends to differ from other work in that only a few things were done to a variety of cement systems that might well be used in a nuclear waste isolation sealing project. Compressive strength and restrained expansion were determined concurrently with observation of decomposition with temperature elevation.

Considerably less work has been done on the behavior of chloroaluminate in a cement-containing system (Jones 1960, Turriziani 1964, Schweite et al 1968, Roberts 1968, Lea 1971, and Benstead 1977). less work was done with chloroaluminate than with ettringite.

MATERIALS

Materials used in the ettringite work were as follows: (a) Portland cement (RC-BCHSR). This was a Class H highly sulfate-resistant oil-well cement. Major characteristics were that the calculated C_3A** content was low (3 percent) and the cement was coarse (2100 cm^2/g or 210 m^2/kg by the air permeability test). (b) Plaster (AD-661(2 and 3). This was a nonretarded alpha form of $CaSO_4$ $1/2H_2O$. It was used to produce an expansive cementitious system. (c) Blending materials. Each of the following six materials was used in an amount to replace 30 percent of the cement on a solid volume basis. (1) AD-643(2). Granulated iron blast-furnace slag from Maryland. (2) AD-513. Class C fly ash from Colorado. (3) AD-629). Class C fly ash from Wisconsin. (4) AD-628). Class F fly ash from California. (5) AD-518). Natural volcanic glass from California. (6) AD-536(3). Silica fume from Alabama.
(d) Each combination of materials was batched and mixed twice. Once with the amount of distilled water to produce normal consistency as determined by ASTM C 187. Once with enough water to combine with all of the alumina in the cement and the blending material to form ettringite plus enough additional water to allow for the hydration of the remaining cementitious solids at a water to solids ratio of 0.2.

Finally, four mixtures were made using salt (NaCl) to replace the plaster so that expansive product would be chloroaluminate rather than ettringite, these mixtures were checked by XRD only. These included one with no pozzolon plus ones with ashes AD-513 or AD-628 or slag, all with enough water for normal consistency. The mixture with ash AD-513 (3B(2)) was repeated so strength and expansion tests could be made.

PROCEDURE

Ettringite study. Preliminary experimentation indicated that test temperatures 23, 50, and 75°C would be satisfactory; the first 24 hours was always to be at 23°C. During the work, the 50°C temperature was changed to 100°C when it was found that 75°C was not high enough to assure destruction of ettringite in most of the mixtures.

Both cubes (ASTM C 109) (2 by 2 by 2 in) and restrained expansion bars (ASTM C 806) (2 by 2 by 10 in.) were cast from each mixture and Teflon vials were filled for curing at three temperatures (four in one case) and testing to 1 year at 12 different ages. The cubes were to be broken for compressive strength, the bars were measured for length change and the vial samples were examined by XRD. The hardened paste in each vial was removed intact, sawed longitudinally, and cut to a 2-in. length if needed. After minimal grinding with alcohol and abrasive, these sawed surfaces were examined by XRD to provide quantitative peak intensity data on ettringite, gypsum, and calcium hydroxide (CH) by peak height intensities. The following seven XRD peaks were covered by XRD if present: 9.7-Å * (ettringite), 7.6-Å (gypsum), 7.3-Å (unhydrated cement), 5.9-Å (unhydrated cement and plaster (?)), 5.6-Å (ettringite), 4.9-Å (CH), and 4.7-Å (ettringite). When it is not possible to make the XRD examination of a vial sample at the scheduled time, the sample was placed in methanol and kept in a freezer until it could be examined. It has been found that this procedure will effectively preserve such a sample for extended periods without significant change. In addition to this XRD examination of vial specimens, two special XRD examinations were made. They included: (a) Addition of an internal standard (hornblende) to ground portions of 28-day-old Mixture 14 (fume) paste and to 21-day-old Mixture

*Tetracalcium aluminate dichloride-10-hydrate.

**C = CaO, A = Al_2O_3.

16 (ash 628) paste. The 9.7-Å ettringite peak of these powders was then examined using modified diffractometer settings to provide better determination of this peak position for each paste was then corrected by use of the internal standard hornblende peak at 8.418-Å . This was done to determine if there was a detectable XRD difference between ettringite stable at 75°C (ash) and ettringite whose crystallinity was destroyed at 75°C fume). (b) Vial samples of paste Mixtures 12 (no admixture) and 17 (no admixture) were placed in distilled water at about 23°C (73°F) when they were 56 and 42 days old, respectively. Both had been in the 100°C environment and both had had the routine XRD examinations to that time. These two mixtures differ only in water content. They were given limited XRD examination during this new storage condition after 7, 14, 30 days, and about 5-1/2 months. The intent was to see if the ettringite changed at the 100°C storage would reform or new phases would form since recognizable new calcium-aluminate sulfate phases had not been formed after initial storage at 100°C.

A control mixture was made each time a test mixture was made and specimens from the control batch were tested for strength only. This provided a measure of reproducibility for quality assurance purposes and data were not collected beyond 28 days. Since fewer specimens were needed, this control mixture was made in a smaller mixer. Calculations indicated no significant effect on cube strength due to use of a different mixer. However, the water content of the control mixture was reduced from a water to cementitious materials ratio of 0.27 and 0.28 to accompany Mixtures 2 and 3, respectively, to 0.22 to accompany all other mixtures. Once the 0.22 value was used, this meant the control mixture was then the same as Mixture 12.

The cubes and bars were demolded after the first 24 hr; the vials were not demolded until they were used. All of these specimens were kept in plastic bags which were placed in polyethylene containers. The containers which held the bars, cubes, and vials, which were to be stored at elevated temperatures, were immersed in hot water of the desired temperature to within 2 to 3 in. of the top. The moisture conditions were not always as intended. This was particularly troublesome with materials stored at 100°C.

Chloroaluminate phase. A few experimental mixtures were made to select elevated test temperatures in addition to the reference 23°C. Since it was obvious that the decomposition temperature of the chloroaluminate was above 100°C (Lea 1971), it was necessary to include both temperature and pressure in these considerations. Test temperatures of 130°C and 170°C were selected along with 0.17 and 0.69 megapascals (25 and 100 psi), respectively, for use in autoclaves. Four mixtures were made and vials were filled for periodic XRD examination. No cubes or bars were made from them due to lack of storage space in the autoclaves. One mixture was repeated to measure strength and length change.

RESULTS

XRD examination at early ages of a paste made with portland cement and water showed that ettringite crystallinity was destroyed at a temperature of 75°C. This was the basis for starting the work using 23°, 50°, and 75°C. When other work using portland cement, water, and plaster with or without some of the pozzolans showed that the ettringite was stable at 75°C, this was the basis for changing from 50° to 100°C so the test temperatures were 23°, 75°, and 100°C. Since this change was not made until Mixture 12 was cast, 10 mixtures were tested at a maximum temperature of 75°C and 5 mixtures were tested at both 75° and 100°C.

The presence and relative amounts of ettringite were determined by the presence and intensity of the 9.7-Å peak by XRD. A similar procedure was used to monitor both gypsum (7.6-Å) and C.H (4.9-Å) , but these data are not included in detail. In general, ettringite was destroyed at 75°C for mixtures of cement and water only and for mixtures containing cement, plaster, water, and silica fume (mixtures 10 and 14). It was always destroyed for the five mixtures tested at 100°C by an age of 14 days; these included two with no fly ash, slag, natural pozzolan, or fume; two with fly ash (AD-628,629); and one with the silica fume. In no case was there any replacement recognizable by XRD of ettringite by tetracalcium aluminate monosulfate-12-hydrate (monosulfoaluminate) as had been expected. Nor was there significant reformation of ettringite or any formation of sulfoaluminate when samples of two paste mixtures (Nos 12, 17) that had been heated at 100°C were kept in water at room temperature for 5-1/2 months and examined by XRD.

Destruction of ettringite at 75°C in a low-sulfate paste consisting only of portland cement and water and in a low alumina paste of portland cement, plaster, silica fume, and water and its persistence above this temperature in the other 13 pastes that contained abundant sulfate and alumina or just sulfate suggested stabilization perhaps by a compositional variation (Diamond and Lochowski, 1983). If so, it did not produce any definite detectable crystal lattice shift as determined by position of the 9.7-Å XRD peak. In general, use of two levels of water did not affect the ettringite content.

The increase in amount of ettringite to an age of one year, when testing stopped, for all paste mixtures except those two (Nos 10, 14) containing silica fume demonstrated how long this reaction may occur under favorable circumstances. This was generally true at 23°, 50°, and 75°C. This was also interpreted as showing that alumina was being obtained from the glassy portion of the fly ashes, slag, and natural pozzolan, over this time period.

Compressive strength data were less satisfactory largely because of variation in storage conditions. However, there were usually gains with

*Angstrom (Å)x0.1 equals nonometres

increasing age and higher temperature and there was no recognizable effect of ettringite destruction on strength. The same sort of conclusion was reached for the restrained expansion data.

Typical XRD, compressive strength, and restrained expansion data are shown in abbreviated Tables 17 (A, B, C), 13 (A, B, C) and 9 A, B, C); the numbering system for these tables is the same as that used in the original report (Buck, et al 1985).

The results for chloroaluminate were less satisfactory. However, XRD did indicate that chloroaluminate was destroyed at 170°C and 0.69 megapascal (100 psi) but not at 130°C and 0.17 megapascal (25 psi).

For the four mixtures made with salt instead of plaster, chloroaluminate ranged from not present in the cement, salt, and water mixture to coexistence with ettringite in the mixture made with fly ash AD-628 to preferential replacement of ettringite in the mixtures made with fly ash AD-513 and with the slag.

CONCLUSIONS

The most significant finding was that destruction of ettringite at 100°C did not appear to have detrimental effects on compressive strength or volume stability of the paste mixtures studied. Therefore, there should be no concern about destruction of it in expansive cementitious systems that may be used for repository sealing applications.

While fewer results were available for the effects of destruction of chloroaluminate on similar properties, the same conclusion would seem warranted.

Subsidary findings included: (a) agreement with previous work about temperature stability of these phases, (b) formation of additional ettringite in some of these pastes, especially those containing fly ash, for at least one year, (c) some ettringite was destroyed at 75°C while other was stable at that temperature, (d) there was no recognizable formation of sulfoaluminate.

REFERENCES

Benstead, J., 1977, "Chloroaluminates and the Role of Calcium Chloride in Accelerated Hardening of Portland Cement," pp 171-175, World Cement Technology, Vol 8, No. 5.

Buck, A. D., J. P. Burkes, Toy S. Poole, 1985, "Thermal Stability of Certain Hydrated Phases in Systems Made Using Portland Cement," U.S. Army Engineer Waterways Experiment Station Miscellaneous Paper SL-85-7, Vicksburg, MS.

Diamond, S., and E. E. Lochowski, 1983 "Investigation of the Composition and Morphology of Individual Particles of Portland Cement: 2. Calcium Sulfoaluminates," Cement and Concrete Research, Vol 13, pp 335-340, Pergamon Press, N.Y.

Ghorab, H. Y., D. Heinz, V. Ludwig, T. Meskendahl, and A. Wolter, 1980, "On the Stability of Calcium Aluminate Sulphate Hydrates in Pure Systems and in Cements," pp 469-503 in Seventh Inter-national Congress on the Chemistry of Cement, Vol IV, Principal Reports, Paris, France.

Jones, F. E., 1960, "Hydration of Calcium Aluminates and Ferrites," pp 204-246, in Chemistry of Cement, Proceedings of th Fourth International Symposium, Washington, Vol 1, Washington, D.C.

Kalousek, G. L. and M. Adams, 1951, "Hydration Products Formed in Cement Pastes at 25 to 175°C," Journal of the American Concrete Institute, Vol 23, No. 1, pp 77-90, (Proceedings, Vol 48, Title No. 48-7).

Lea, F. M., 1971, "The Chemistry of Cement and Concrete," 3rd ed., pp 232-233, Chemical Publishing Co., N.Y.

Mather, K., J. P. Burkes, G. S. Wong, and R. E. Reinhold, 1978, "Effects of Accelerated Curing on Hydration Products of Cement and Cement-Fly Ash Pastes," U.S. Army Engineer Waterways Experiment Station, CE, Miscellaneous Paper C-78-11, Vicksburg, MS.

Metha, P.K., 1972, "Stability of Ettringite on Heating," Journal of the American Ceramic Society, Vol 55, pp 55-56.

Ogawa, K. and D. M. Roy, 1981, "C_4A_3S Hydration, Ettringite Formation, and Its Expansion Mechanism: I. Expansion; Ettringite Stability," pp 741-750, Cement and Concrete Research, Vol 11, Pergamon Press, N.Y.

Roberts, M. H., 1968, Supplementary Paper II-29, "Calcium Aluminate Hydrates and Related Basic Salt Solid Solutions," pp 104-117 in Proceedings of the Fifth International Symposium on the Chemistry of Cement, Part II, Tokyo, Japan.

Schweite, H. E. and U. Ludwig, 1968, Principal Paper "Crystal Structures and Properties of Cement Hydration Products (Hydrated Calcium Aluminates and Ferrites)," pp 37-78, in Proceedings of the Fifth International Symposium on the Chemistry of Cement, Part II, Tokyo, Japan.

Standard Test Method for Compressive Strength of Hydraulic Cement Mortars (Using 2-in. or 50-mm Cube Specimens), ASTM C 109, Vol 04.01, Cement, Lime Gypsum, 1985, Annual Book of ASTM Standards, American Society for Testing and Materials, Philadelphia, PA.

Ibid., "Standard Test Method for Restrained Expansion of Expansive Cement Mortar," ASTM C 806.

Taylor, H. F. W. and D. M. Roy, Sub-Theme II-2, 1980, "Structure and Composition of Hydrates," pp II-2-1 through II-2-13 in Seventh Inter-national Congress on the Chemistry of Cement, Vol I, Principal Reports, Paris, France.

Turriziani, R., 1946, "The Calcium Aluminate Hydrates and Related Compounds," pp 260-262, in the Chemistry of Cements, Taylor, H. F. W. (ed.), Vol 1, Chapter 6, Academic Press, N.Y.

Table 17A
Stability and Persistence of Ettringite and Gypsum in Cement, Plaster, and Water Mixture* by X-Ray Diffraction**

Age	Temperature, °C 23	50	75	100
24 hr - Ettringite	5	--	--	--
Gypsum	2	--	--	--
7 day - Ettringite	9	13	13	6
Gypsum	4	4	4	ndt
90 day - Ettringite	16	20	17	nd
Gypsum	3	3	nd	nd
365 day - Ettringite	20	25	20	nd
Gypsum	Trace	nd	nd	nd

*Cast 17 made 15 July 1982; w/s was 0.34.

Table 13A
Stability and Persistence of Ettringite and Gypsum in Cement, Plaster, Fly Ash AD-629, and Water Mixture* by X-Ray Diffraction

Age	Temperature, °C 23	75	100
24 hr - Ettringite	11	--	--
Gypsum	16	--	--
7 day - Ettringite	15	42	Tr
Gypsum	11	9	ndt
90 day - Ettringite	33	43	nd
Gypsum	7	3	nd
365 day - Ettringite	48	53	Tr
Gypsum	7	2	nd

* Cast 13 made 5 July 1982; w/s was 0.43.

Table 9A
Stability and Persistence of Ettringite and Gypsum in Cement, Plaster, Fly Ash AD-628, and Water Mixture* by X-Ray Diffraction**

Age	Temperature, °C 23	50	75
24 hr - Ettringite	5	--	--
Gypsum	14	--	--
7 day - Ettringite	10	22	25
Gypsum	13	13	21
90 day - Ettringite	15	21	16
Gypsum	13	11	7
365 day - Ettringite	24	33	29
Gypsum	18	9	7

*Cast 9 made 23 June 1982; w/s = 0.34.

**Peak intensity values are in net chart units; 9.7- and 7.6-Å peaks.

†Not detected.

Table 17B
Compressive Strengths of Paste Cubes at Different Temperatures and Ages

Temperature °C	Control Mixture *	Compressive Strengths (psi)*** at Ages Shown Below, days 1	7	28	90	270	365
23	Avg**	6480	10,040	12,190	--	--	--
	Test Mixture †						
	Avg**	1710	4,040	6,070	7690	8370	†††
75	Avg**	n.d.††	4,300	7,980	7750	8600	†††
100	Avg**	n.d.	4,660	5,870	5020	5950	†††

* Normal consistency paste of cement and plaster; same as cast 12.
** Each value for the control mixture is the average for three 2- by 2-in. cubes; values for the test mixture are averages for two or three cubes.
***Divide by 145.03894 to obtain megapascals.
† Cast 15 July 1982; cement, plaster, and excess water.
†† Not determined.
†††No cubes remained.

Table 17C
Restrained Expansion of Bars Cured 24 hr at 23°C and Then Stored at 23°C and Other Temperatures

Test Mixture No. 17*	Temperature °C	Restrained Expansion of Single Bars at Ages Shown Below, % 1 (23°C)	2	7	28	90	180	365
Bar 58	23	0.004	0.006	0.006	0.023	-0.081	-0.087	-0.066
Bar 61	75	-0.001	0.011	-0.008	0.020	0.031	0.041	0.017
Bar 71	100	0.001	0.005	0.133	0.014	0.232	0.199	0.020

* Cement, plaster, and water for normal consistency.

Table 13B
Compressive Strengths of Paste Cubes at Different Temperatures and Ages

Temperature °C	Control Mixture *	Compressive Strengths (psi)*** at Ages Shown Below, days 1	7	28	90	180	270	365
23	Avg**	7210	11,600	12,190	--	--	--	--
	Test Mixture †							
	Avg**	780	2,350	3,380	3890	4780	5150	6190
75	Avg**	n.d.††	7,120	9,160	7050	8170	7750	7430
100	Avg**	n.d.	2,760	8,070	2330	2340	3140	2100

* Normal consistency paste of cement and plaster; same as cast 12.
** Each value for the control mixture is the average for three 2- by 2- 2-in. cubes; values for the test mixture are for one, two, or three cubes.
***Divide by 145.03894 to obtain megapascals.
† Cast 5 July 1982; cement, plaster, fly ash AD-629, and excess water.
†† Not determined.

Table 13C
Restrained Expansion of Bars Cured 24 hr at 23°C and Then Stored at 23°C and Other Temperatures

Test Mixture No. 13*	Restrained Expansion of Single Bars at 1 (23°C)	Temperature °C	Ages Shown Below, % 2	7	28	90	180	365
Bar 31	0.002*	23	0.030	0.042	0.086	0.123	0.169	0.250
Bar 78	0.004	75	0.064	0.093	0.194	0.218	0.230	0.217
Bar 80	0.011	100	0.063	0.081	0.159	0.073	0.063	0.046

* Cement, plaster, fly ash AD-629, and excess water.

Table 9B
Compressive Strengths of Paste Cubes at Different Temperatures and Ages

Temperature °C	Control Mixture *	Compressive Strengths (psi)*** at Ages Shown Below, days 1	7	28	90	180	270	365
23	Avg**	5920	8840	10,950	--	--	--	--
	Test Mixture †							
	Avg**	1530	2980	5,020	6700	7,410	9,150	8,000
50	Avg**	n.d.††	5770	10,170	9830	10,100	11,480	13,580
75	Avg**	n.d.	8140	10,380	6700	9,720	9,850	11,790

* Normal consistency paste of cement and plaster; same as cast 12.
** Each value for the control mixture is the average of three 2- by 2- by 2-in. cubes; values for the test mixture are for one, two, or three cubes.
*** Divide by 145.03894 to obtain megapascals.
† Cast 9 made 23 June 1982; normal consistency mixture of cement, plaster, and fly ash AD-628.
†† Not determined.

Table 9C
Restrained Expansion of Bars Cured 24 hr at 23°C and Then Stored at 23°C and Other Temperatures

Test Mixture No. 9*	Restrained Expansion of Single Bars at 1 (23°C)	Temperature °C	Ages Shown Below, % 2	7	28	90	180	365
Bar 21	0.004	23	0.008	0.016	0.020	0.030	0.015	0.099
Bar 29	-0.005**	50	0.005	0.078	0.127	0.229	0.254	0.379
Bar 42	-0.005	75	0.016	0.057	0.032	0.278	0.142	0.193

* Cement, plaster, fly ash AD-628, and water for normal consistency.

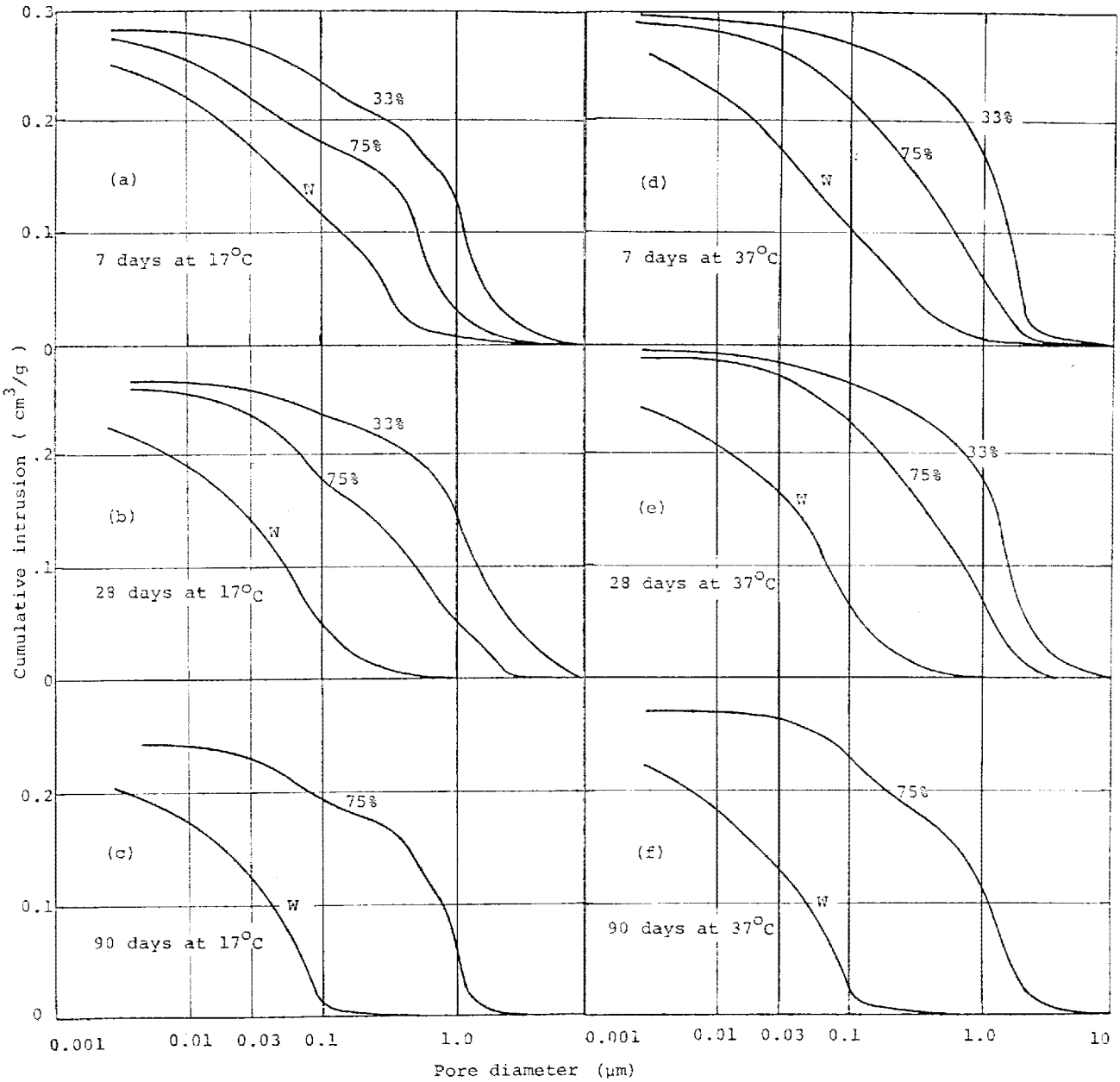

FIGURE 2 - Pore size distributions of Portland cement pastes hydrated at different temperatures and relative humidities.

4. - I. SOROKA (1979), "Portland cement paste and concrete", The Macmillan Press Ltd., London.

5. - J. SKALNY and J.F. YOUNG (1980), "Mechanisms of Portland cement hydration", Proceedings, Seventh International Conference on the Chemistry of Cement, Paris, Vol. I, pp. II-1/3-45, Editions Septima, Paris.

6. - H.F.W. TAYLOR and D.M. ROY (1980), "Structure and composition of hydrates", Proc. 7th Int. Conf. on the Chemistry of Cement, Paris, Vol. I, pp. II-2/1-13, Editions Septima, Paris.

7. - P. BARNES, Ed. (1983), "Structure and performance of cements", Applied Science Publishers, London.

8. - L.H. TAPLIN (1962), "The temperature dependence of the hydration rate of Portland cement paste", Australian Journal of Applied Science, 13(2)164-171.

9. - I. ODLER and J. GEBAUER (1966), "Cement hydration in heat treatment", Zement-Kalk-Gips, 55(6)276-281.

10. - S. DIAMOND (1973), "Pore structure of hardened cement paste as influenced by hydration temperature", Proc. RILEM /IUPAC Int. Symp. Pore Structure and Properties of Materials, Prague, Vol. I, pp. B-73-88.

11. - D.L. KANTRO, S. BRUNAUER, and C.H. WEISE (1961), "Development of surface in the hydration of calcium silicates" Advances in Chemistry Ser.,33,199-219.

12. - S. BRUNAUER and D.L. KANTRO (1964), "The hydration of tricalcium silicate and ß-dicalcium silicate from 5 to 50 C", in Chemistry of Cements, Ed. H. F.W. Taylor, Academic Press, London, pp. 287-309.

13. - G.J. VERBECK and R.H. HELMUTH (1968), "Structures and physical properties of cement paste", Proc. 5th Int. Symp. on the Chemistry of Cement, Tokyo,Vol. III, pp. 1-32.

14. - I. ODLER and J. SKALNY (1973), "Hydration of C_3S at elevated temperatures", J. Appl. Chem. Biotechnol., 23(9)661-67.

15. - A. BENTUR, R.L. BERGER, J.H. KUNG, N.B. MILESTONE and J.F. YOUNG (1979), "Structural properties of calcium silicate pastes: II, Effect of curing temperature", J. Amer. Ceram. Soc., 62 (7-8)362-66.

16. - R.L. BERGER, A. BENTUR, N.B. MILESTONE and J.H. KUNG (1979), "Structural properties of calcium silicate pastes: I, Effect of the hydrating compound", J. Amer. Ceram. Soc., 62(7-8)358-362.

17. - J. SKALNY and I. ODLER (1972), "Pore structure of hydrated calcium silicates: III, Influence of temperature on the pore structure of hydrated tricalcium silicate", J. Colloid Interface Sci., 40(2)199-205.

18. - J. SKALNY and I. ODLER (1972), "Pore structure of calcium silicate hydrates", Cem. Concr. Res., 2(4)387-400.

19. - M. COLLEPARDI (1973), "Pore structure of hydrated tricalcium silicate", Proc. Int. Congr. Colloid and Surface Chem (IUPAC), Prague, Vol. I, B25-49.

20. - P.J. SEREDA, R.F. FELDMAN, and V.S. RAMACHANDRAN (1980), "Structure formation and development in hardened cement pastes", Proc. 7th Int. Congr. Chemistry of Cement, Paris, Vol. I, pp. VI-1/3-44, Editions Septima, Paris.

21. - V.S. RAMACHANDRAN, R.F. FELDMAN, and J.J. BEAUDOIN (1981), "Concrete Science", Heyden and Sons Ltd., London.

22. - A. BENTUR (1980), "Effect of curing temperature on the pore structure of tricalcium silicate pastes", J. Colloid Interface Sci., 74(2)549-59.

23. - O.Z. CEBECI (1981), "Pore structure of air-entrained hardened cement paste", Cem. Concr. Res., 11(2)257-65.

24. - O.Z. CEBECI (1980), "The intrusion of conical and spherical pores in mercury intrusion porosimetry", J. Colloid Interface Sci., 78(2) 383-88.

25. - I.U.P.A.C. (1972), Manual of Symbols and Terminology, Appendix 2, Part 1, Colloid and Surface Chemistry, Pure Appl. Chem., 31, 578.

L. CHPYNOVA,
V. ILIOUKHINE,
M. SANITSKI,
S. MELNIK, Institut polytechnique de Lvov, Institut de cristallographie de Moscou, URSS

1

2.2.

PHENOMENES CRISTALLOCHIMIQUES INTERVENANT DANS L'HYDRATATION DES MINERAUX DU CIMENT

Les auteurs ont examiné les facteurs cristallochimiques déterminant l'activité d'hydratation des minéraux du ciment. Ils ont montré l'influence qu'exercent l'anisotropie des liaisons chimiques dans les polyèdres de la structure et l'insaturation des efforts de valence dans les anions sur l'hydratation des minéraux du clinker. Ils ont montré la possibilité de formation, lors de l'hydratation de C_3S, d'hydrosilicates d'une haute basicité, analogues structuraux de l'hydroxyde de calcium.

Pour les silicates de calcium, les processus déterminant le mécanisme d'hydratation sont: la polycondensation des tétraèdres de SiO_4 dans les hydrosilicates, la lixiviation de $Ca(OH)_2$ et sa cristallisation dans les pores sous forme de portlandite; pour les aluminates et les alumoferrites de calcium: la protonisation de tous les O^{2-} et le passage de Al^{3+} et de Fe^{3+} de la coordination IV en VI avec destruction totale de la structure cristalline du minéral du départ.

Os autores examinaram os fatores cristaloquímicos que determinam a atividade de hidratação dos minerais do cimento. Eles mostraram a influência exercida pela anisotropia das ligações químicas nos poliedros da estrutura e pela insaturação dos esforços de valência nos aníons sobre a hidratação dos minerais do clínquer. Mostraram a possibilidade de formação, quando da hidratação do C_3S, de hidrossilicatos com basicidade alta, análogos estruturais do hidróxido de cálcio.

Quanto aos silicatos de cálcio, os processos que determinam o mecanismo de hidratação são: a policondensação dos tetraedros de SiO_4 nos hidrossilicatos, a lixiviação de $Ca(OH)_2$ e sua cristalização nos poros sob a forma de portlandita;quanto aos aluminatos e ferroaluminatos de cálcio: a protonização de todos os O^{2-} e a passagem de Al^{3+} e de Fe^{3+} da coordenação IV em VI com destruição total da estrutura cristalina do mineral de origem.

L. CHPYNOVA,
V. ILIOUKHINE,
M. SANITSKI,
S. MELNIK

Le principal composant des ciments largement utilisés dans la construction, est l'oxyde de calcium. En état pur, ce dernier entre énergiquement en réaction mutuelle avec l'eau et dégage une importante quantité de chaleur d'hydration (65 kJ/mole) en un court laps de temps ce qui entraîne la destruction de la structure du ciment durci et rend faible sa résistance (de 0,3 à 0,5 MPa). Il est possible d'affaiblir l'activité chimique du CaO grâce à l'évacuation de la chaleur d'hydratation, à l'utilisation d'adjuvants chimiques et à une mollification forcée de la masse de l'oxyde de calcium par de petits ions à forte polarisation (1,2).

L'utilisation de deux premières voies de baisse de l'activité du CaO, l'addition d'adjuvants composés de bouillie alcool-levure, de carbonate de sodium et d'acide borique en combinaison avec l'évacuation de la chaleur d'hydratation grâce au gâchage de la pâte à -15 °C ont permis de porter la résistance de la pierre calcaire à 40 MPa. En ce qui concerne la troisième voie, on l'utilise dans le procédé technologique de production des ciments de calcium. Pendant la cuisson de ces derniers, on introduit dans le réseau du CaO de petits ions tels que Si^{4+}, Al^{3+}, Fe^{3+} et d'autres ce qui donne une fixation partielle ou complète de l'oxygène par les éléments intégrés. Cela permet de limiter la vitesse du processus de protonisation et d'établir l'activité du liant obtenu.

Pour définir l'essence cristallochimique du processus d'hydratation des ciments, il est nécessaire d'examiner l'interaction des minérais de clinker et de l'eau durant l'établissement de la structure cristalline des phases d'hydratation. Le résultat de telles réactions est l'apparition de cristallohydrates avec un système de liaisons d'hydrogène. Aussi, l'activité hydraulique des liants est-elle déterminée par la capacité des composés de permettre, durant la réaction avec H_2O, l'établissement des contacts grâce à la liaison d'hydrogène. Du point de vue de la cristallochimie, il s'agit de la possibilité d'attirer les anions en tant que donneurs dans le système de liaisons d'hydrogène ce qui est conditionné par les facteurs d'ordre structural: anisotropie des liaisons chimiques dans les polyèdres structuraux, sous-saturation des efforts de valence sur les anions et leur action combinée (3).

Pour apprécier les facteurs cristallochimiques déterminant l'activité d'hydratation des minérais de ciment, on a utilisé les identifications précisées des structures cristallines de C_3S, β - et de γ - C_2S, C_3A, C_4AF, C_2F. Sur la base des données cristallographiques ont été calculés les efforts de valence V_{ij} transmis par le j-cation à l'i-anion ainsi que les bilans formel et local de valence des structures cristallines des minérais de ciment.

Dans les structures cristallines des minérais de ciment actifs, les polyèdres de coordination sont sensiblement déformés ce qui fait qu'à l'intérieur des polyèdres structuraux se manifeste l'anisotropie des liaisons chimiques et se produit une variation de la résistance des forces de liaison unitaires cation-anion. Par exemple, dans un tétraèdre idéalisé de SiO_4 les efforts de valence entre Si-O se répartissent de façon régulière et constituent 1,000. Cependant, dans un tétraedre réel de SiO_4 à structure cristalline de β - C_2S, les efforts de valence, grâce à une différence de distance entre Si-O, se redistribuent entre les anions, et la valeur de l'anisotropie des liaisons chimiques constitue dans un tel tétraèdre 0,149 tandis que la dispersion des valeurs de l'énergie de la force de liaison unitaire est égale à 66 kJ.

Dans le cadre d'une seule structure cristalline des minérais de ciment, la force de la liaison entre Ca-O est considérée comme l'élément le plus faible étant donné que les valeurs moyennes des efforts de valence des cations et de la résistance des forces unitaires de liaison sont de 2 à 4 fois plus faibles dans les Ca-polyèdres que dans les

complexes tétraédriques de SiO_4 et autres. Il existe une interdépendance entre les caractéristiques énergétiques de la liaison chimique existant dans les Ca-polyèdres et l'indice de coordination de Ca: un accroissement de ce dernier entraine une réduction de l'énergie des forces de liaison unitaires et, par conséquent, une augmentation de l'activité d'hydratation du minérai comme le montre la série α-, α'-, β-, γ-C_2S (4).

Une analyse du bilan local des valences révèle la présence d'anions d'oxygène qui sont sous-saturés et sursaturés par les efforts de valence des cations. C'est pour les ions sous-saturés d'O^{2-} que paraissent les plus probables la chimisorption de molécules d'eau et la participation dans les liaisons d'hydrogène.

L'influence des facteurs cristalochimiques sur la vitesse d'hydratation est montrée dans γ- et β-C_2S pris à titre d'exemple. Dans les Ca-octaèdres de la structure de γ-C_2S les forces de liaison sont très proches entre elles (les caractéristiques énergétiques des forces de liaison unitaires varient entre 169 et 206 kJ). Cette structure se caractérise par une saturation formelle complète des anions d'oxygène et une activité d'hydratation minimale. Le passage de γ à β-C_2S augmente l'anisotropie des liaisons chimiques (ΔE = 116 kJ) et la sous-saturation des atomes d'oxygène (où convergent les Capolyèdres à une coordinence de 7 et 8) ce qui favorise finalement son activité.

La principale cause de l'activité d'hydratation élevée de C_3S par rapport à β-C_2S doit être attribuée à la conservation dans le réseau de C_3S de la cinquième partie des atomes d'O qui ne se trouvent pas sous écran de silicium (ne sont pas liés à Si^{4+}) et que des murs en Ca-polyèdres contenant des tétraèdres de SiO_4 réunissent en un seul massif tridimensionnel ainsi qu'à un déséquilibrage local de la structure. Un accroissement du rapport molaire de SiO_2 dans les silicates de calcium amène à la formation d'éléments structuraux tels que des diorthogroupes dans la rankinite on des chaînes dans la wollastonite CS. La commensurabilité des arêtes des Ca-polyèdres et des radicaux composés de silicates qui possèdent des liaisons de siloxane Si-O-Si conditionnent l'élimination des propriétés liantes des cilicates de calcium à faible basicité.

Au moment où commence l'hydratation du principal minérai de clinker C_3S il se produit une dissolution congruente de ce dernier à la surface des grains et a lieu la formation de riches solutions alcalines à une forte concentration d'ions d'OH^-. De gros complexes d'hydrates $Ca(OH)_n^{2-n}$ se cristallisent sous la forme d'un très dense assemblage hexagonal d'OH-groupes où les cations de calcium occupent une moitié des vides octaédriques, une des couches de l'assemblage étant complètement remplie et l'autre, vide. La solution comporte des ions de $(SiO_4)^{4-}$ qui s'intègrent dans la structure du $Ca(OH)_2$ pendant la cristallisation de ce dernier.

Dans la structure cristalline du $Ca(OH)_2$ le couche remplie de calcium possède deux vides tétraédriques avec les coordonnées du centre (1/3, 2/3, z où z = 0,85) tandis que la couche non remplie en possède un vide octaédrique dont le centre a les coordonnées (0, 0, 1/2) et deux vides tétraédriques (1/3, 2/3, z où z = 0,65). Dans ces vides tétraédriques formés par des groupes hydroxyles peut s'intégrer le Si^{4+} ce qui s'accompagne du remplacement simultané de quatre ions d'OH^- par quatre ions d'O^2. Dans le premier cas d'isomorphisme le vide tétraédrique est formé par des OH-groupes éloignés l'un de l'autre de 2,99 Å (côté de tétraèdre). Alors la distance du centre du tétraèdre à son sommet constitue 1,83 Å, et le rayon de la sphère inscrite dans le tétraèdre est de 0,61 Å. Etant donné que les OH-groupes ne se touchent pas entre eux, le rayon du vide tétraédrique est encore plus grand (de l'ordre de 0,80 Å), c'est-à-dire que dans ce vide peuvent s'intégrer

librement les cations de Si^{4+} dont le rayon ionique est de 0,39 Å. Dans ce cas il est possible qu'il se forme l'hydrocilicate de calcium à la composition de $Ca_4[SiO_4](OH)_4$ avec la participation de quatre OH groupes appartenant à quatre mailles élémentaires différentes de $Ca(OH)_2$. Comme le montrent les calculs (5), la variation d'intensité des lignes sur les diffractogrammes de $Ca(OH)_2$ dans le cas de l'isomorphisme avec intégration est faible par rapport à celle enregistrée dans le cas de portlandite pure.

Dans les silicates, la distance entre Si-O varie généralement dans les limites de 1,54 à 1,69 Å. Dans les cas que nous sommes en train d'examiner, elle constitue 1,83 et 2,10 Å, c'est-à-dire, les anions sont éloignés l'un de l'autre à des distances supérieures à la valeur du côté qui ferme le SiO_4 potentiel et, donc, le principe géométrique de commensurabilité exige une nouvelle réunion de "molécules" de SiO_2. Pour les structures à enveloppe d'hydrate, elle se réalise sous la forme d'un diorthogroupe statique de Si_2O_7 (6). Il se produit alors une reconstruction de la structure de $Ca(OH)_2$. De nouveaux hydrocilicates qui se forment sont également instables tout en conservant les éléments structuraux de l'hydroxyde de calcium ce qui est enregistré par de différentes méthodes d'étude. Sur les spectres infrarouges ce changement s'exprime par un déplacement progressif de la bande d'absorption des tétraèdres de SiO_4 dans le sens d'accroissement des nombres d'onde, sur les dérivatogrammes par un déplacement des effets endothermiques dans le sens d'augmentation des températures et sur les diffractogrammes, par la formation et une augmentation ininterrompue de trois halos portant une rangée de lignes accentuées dans les domaines 20 jusqu'à 14, de 26 à 36° et de 50 à 52°.

Les résultats des études de spectroscopie infrarouge, des études thermiques et radiographiques ainsi que les données de calcul citées doivent être considérés comme preuve de la justesse du processus indiqué de dissolution congruente du silicate tricalcique accompagnée de la formation d'hydrocilicates de calcium ayant la structure de l'hydroxyde de calcium. Les processus déterminant le mécanisme ultérieur de l'hydratation du C_3S sont: polycondensation des tétraèdres de SiO_4 dans les hydrocilicates de calcium, lixiviation du $Ca(OH)_2$ et sa cristallisation dans des pores sous la forme de portlandite (1,2).

La plus haute réactivité du C_3A parmi les minérais de clinker durant le processus d'hydratation est due à une brusque anisotropie des liaisons dans les Ca-polyèdres et un déséquilibrage local de la structure: 2/3 des atomes d'O deviennent sous-saturés et ceux d'O(3) et d'O(5) le sont à un assez haut niveau. En même temps, les atomes en pont d'O(1) et d'O(2) sont sursaturés et leur participation dans les liaisons d'hydrogène exige une reconstruction de la structure cristalline. Le mécanisme d'hydratation des aluminates de calcium est déterminé par deux processus: protonisation de tous les O^{2-} et passage de l'Al^{3+} de la coordination IV à la coordination VI. Il en résulte une destruction complète de la structure cristalline des minérais de départ tandis que les couches de portlandite de la composition de $[(Ca_2Al(OH)_6]^+$ jouent le rôle de formateurs de structure pendant la formation des phases hydratées.

L'activité d'hydratation des ferrites et des alumoferrites de calcium s'explique avant tout par une métastabilité de la coordination tétraédrique des atomes de fer dans le C_2F, d'aluminium et de fer dans les alumoferrites de calcium et par une sous-saturation des atomes d'oxygène dans ces complexes (7). Les différences entre les structures électroniques de Fe^{3+} et d'Al^{3+} font que le caractère de formation des hydrates des ferrites et des alumoferrites de calcium diffère avec l'âge de durcissement: les produits d'hydratation de C_2F - les hydroferrites de calcium - sont des hydrates instables du point de vue de la structure et se décomposent en $Ca(OH)_2$

et en hétite α-FeOOH; la substitution d'une partie d'ions de Fe^{3+} par ceux d'Al^{3+} dans leur composition stabilise les phases cubiques et hexagonales des alumoferrites hydratés de calcium.

REFERENCES

I. Формирование и генезис микроструктуры цементного камня./ Л.Г. Шпынова, В.И. Чих, М.А. Саницкий и др. - Львов, Изд-во "Вища школа", 1981, 160 с.
2. Л.Г. Шпынова, Белов Н.В., Саницкий М.А. Кристаллохимический аспект гидратации цемента. - В сб.: Гидратация и твердение вяжущих. Львов, 1981, с. 4-9.
3. Шпынова Л.Г., Илюхин В.В., Саницкий М.А. Кристаллохимические факторы гидратационной активности цементных минералов. - Докл. АН УССР, сер. Б, 1983, № 2, с. 58-61.
4. Гидросиликаты кальция. Синтез монокристаллов и кристаллохимия./ Н.В. Илюхин, В.А. Кузнецов, А.Н. Лобачев, В.С. Бакшутов. - М.: Наука, 1979. - 184 с.
5. Шпынова Л.Г., Белов Н.В., Мельник С.К. Роль структуры портландита в формировании цементного камня. - Кристаллография, 1980, т. 25, № 6, с. 1188-1193.
6. Белов Н.В. Очерки по структурной минералогии. - М.: Недра, 1976. - 344 с.
7. Шпынова Л.Г., Саницкий М.А. Гидратационная активность ферритов и алюмоферритов кальция. - Украинский химический журнал, 1983, т. 49, № 11, с. 1138-1142.

SUB-THEME/SOUS-THÈMEM 2.3

Bond: paste-aggregate, paste-reinforcement and paste-fibres. Adhérence: pâte-granulat, pâte-armature et pâte-fibres.

Chairman/Président:

J. P. Skalny
W. R. Grace, & CO., Research Division
Columbia, Maryland, U.S.A.

Principal Reporter/Rapporteur Principal:

F. Massazza
Italcementi, S. p. A.
Laboratorio Chimico Centrale
Bergamo, Italy

P.J.M. Monteiro, Grupo de Cimento Portland Paraiso, Brasil; P.K. Mehta, University of California at Berkeley, U.S.A.

Improvement of the Aggregate-Cement Paste Transition Zone by Grain Refinement of Hydration Products

AMELIORATION DE LA ZONE DE TRANSITION DU GRANULAT-PÂTE DE CIMENT PAR REDUCTION DES GRAINS DES PRODUITS D'HYDRATATION

SUMMARY: The weakest component in hardened portland cement concrete is generally the aggregate-cement paste transition zone, and one of the primary causes of this weakness is the presence of very large crystals of calcium hydroxide with c-axis preferrentially oriented in a direction normal to the aggregate surface. It is expected, therefore, that everything else remaing the same, the strength of a concrete would be improved by grain refinement, i.e. replacement of large crystals by smaller ones.

Three case studies where the transition zone is improved by grain refinement are described in this paper. Two of those studies show how grain refinement is achieved when the composition of the cement is suitably modified. One case study shows how a similar effect is achieved by chemical interaction between the aggregate and cement hydration products.

SUMÁRIO

O componente mais fraco em um concreto endurecido de cimento portland é, geralmente, a zona de transição entre o agregado e a pasta de cimento; uma das causas principais deste fenômeno é a presença de grandes cristais de hidróxido de cálcio com o eixo preferencialmente orientado com uma direção perpendicular à superfície do agregado. Portanto, é de se esperar que, mantendo-se constante os outros parâmetros, a resistência do concreto pode ser melhorada através de refinamento do tamanho dos cristais, isto é, substituição de cristais grandes por cristais menores.

Este artigo descreve três casos onde a zona de transição é melhorada através de refinamento do tamanho dos cristais. Dois desses casos demonstram como o refinamento dos cristais é obtido quando a composição do cimento é modificada adequadamente. O terceiro caso mostra como um efeito similar é obtido pela interação química entre o agregado e os produtos da hidratação do cimento.

Introduction

The control of microstructure to achieve desired behavior is at the heart of materials engineering today. For instance, metallurgists obtain the desired toughness or strength of a metal by a precise tailoring of the microstructure. This has not been possible with concrete because of the highly complex microstructure which cannot be easily determined and controlled.

There is a strong motivation to study the transition zone between aggregate and cement paste because it is often the phase where microcracks first develop (1). The microstructure of the solid hydration products in the transition zone is different from the bulk matrix, mainly due to a higher water/cement ratio caused by internal bleeding (2).

The surface effect produced by the aggregate result in a cement paste with a higher w/c ratio in the transition zone, causing the development of a different crystal morphology as compared to that of the bulk matrix. The microstructure of the transition zone for a portland concrete at early ages is diagrammatically represented in Fig. 1. The cement grains dissolve to ions that easily diffuse to the higher water-cement ratio paste around the aggregate interface. These ions precipitate larger crystals with a better developed morphology than the matrix because due to a higher porosity in the transition zone, there is more space available for crystal growth. The calcium hydroxide crystals thus formed have a preferential orientation, with the c-axis perpendicular to the aggregate surface.

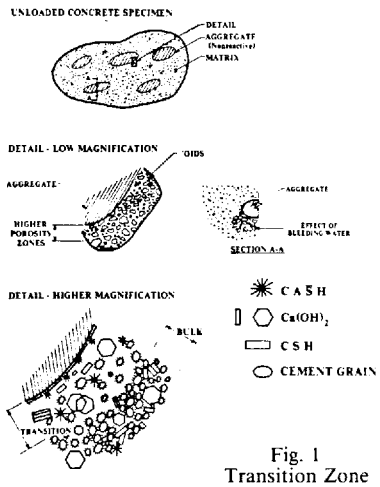

Fig. 1
Transition Zone

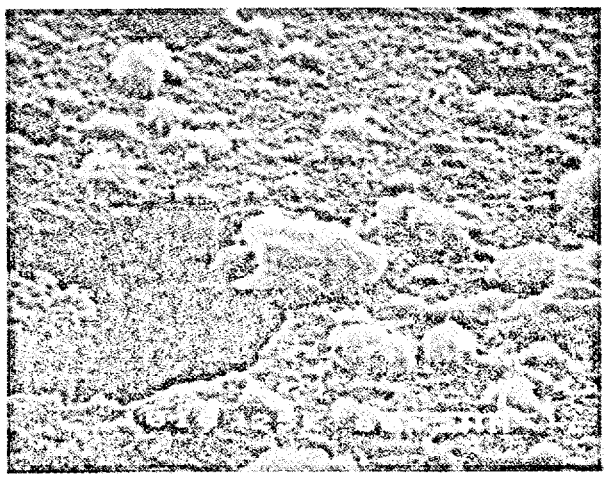

Fig. 2
Typical Morphology of the Hydration Products over the Aggregate

Fig. 2 shows the typical morphology of the hydration products over the aggregate surface. The flat dark zone is the aggregate surface; the reticular products are CSH, and the lumps are composed of cement grains surrounded by hydration products. The topology resembles a lake (aggregate), a valley (CSH), and hills (outer products of cement hydration). This picture is reversed on the cement paste side producing a plateau, a valley, and a depression respectively. The plateau, shown in Fig. 3, is formed by a film of calcium hydroxide (CH) oriented with the c-axis normal to the aggregate surface. The valley is constituted of CSH, and the depression is the empty zone produced either by natural porosity or by pull-out of cement grains surrounded by hydration products.

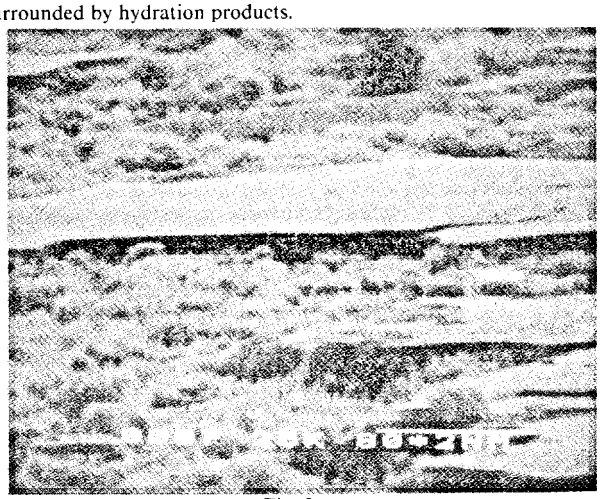

Fig. 3
Interface Morphology on the Cement Paste Side

Being in direct contact with the aggregate surface, the calcium hydroxide crystals form almost a continuous film with c-axes normal to the surface. This phenomenon has been reported by many researchers, including: Farran and Maso (3), Buck and Dolch (4), Hadley (5), Barnes (6), and Grandet and Ollivier (7). Fig. 4 is a scanning electron micrograph showing how cracks develop parallel to the sheet-structure of CH demonstrating that this cleavage plane can be problematic if higher strengths are to be achieved.

It follows, therefore, that the strength characteristic of a portland cement would be enhanced if large grains of calcium hydroxide present in the transition zone are either eliminated or reduced in size (i.e. undergo grain refinement). In this paper the results of three case studies involving grain refinement are described. The first case study describes the grain refinement that occurs when a portland-pozzolan cement containing condensed silica fume is used. The second case study describes the grain refinement when, instead of portland

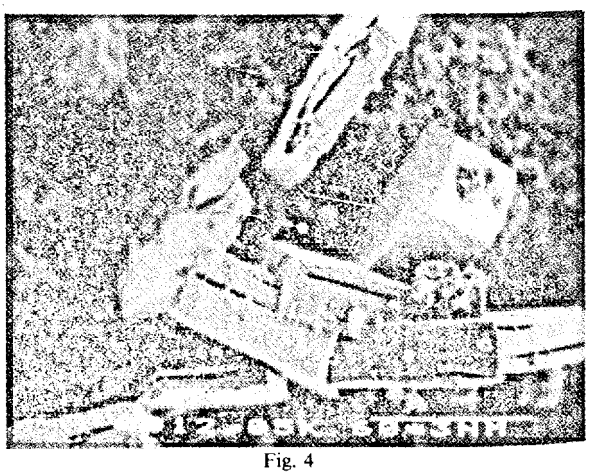

Fig. 4
Cracking in CH Crystals

cement, a Type K cement is used. It may be noted that Type K cement is a modified portland cement containing $C_4A_3\bar{S}$, which reacts with calcium hydroxide and calcium sulfate to form ettringite. The third case study describes the grain refinement which takes place when, instead of silicious rock, carbonate aggregate is used.

Transition Zone with Cement Containing Silica Fume

The use of silica fume in fresh concrete introduces a series of beneficial effects: it increases cohesion and reduces bleeding and segregation. Some of these parameters have a major influence in the development of the transition zone microstructure. It should be noted that typically silica fume has an average particle size of less than 1/100 of that the anhydrous cement grain, therefore its introduction will affect the physical arrangement of the system, particularly near the aggregate surface where a higher porosity exists. Also the pozzolanic nature of the silica fume will influence the microstructure of the transition zone, because in this region a large amount of calcium hydroxide would have been consumed by the pozzolanic reaction.

Based on a X-ray diffraction method (7) for determination of the transition zone thickness, the transition zones for both systems with and without silica fume were measured. Fig. 5 shows that a remarkable decrease of the transition zone thickness occurs when silica fume is used. Evidently this decrease is associated with both the pozzolanic reaction and a local reduction of water/cement ratio (thus reducing the differences between water/cement ratios of the bulk cement paste and the transition zone cement paste).

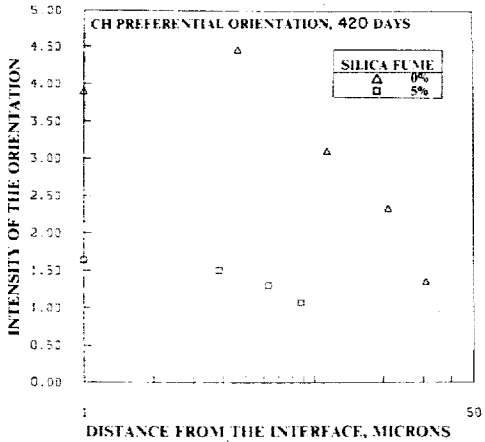

Fig. 5
CH Preferential Orientation Over the Transition Zone

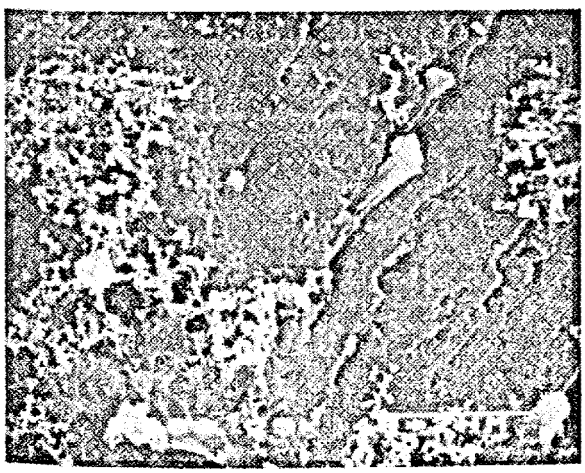

Fig. 6
Pozzolanic Reaction on the CH Film

Some silica fume particles react quickly during the early stages of hydration while others are only partially dissolved at the test age. Continued pozzolanic reaction with the CH film, forming CSH on top of the film, is shown by the scanning electron micrograph in Fig. 6. However, some silica fume particles, or their pseudomorphs, appear to get engulfed in the CH film. The effect of these particles on the mechanical behavior of the film is not known, although it might be anticipated that these particles will reinforce the film. The scanning electron micrograph in Fig. 7 shows the silica fume particles around a crack (probably due to shrinkage) in the film. It can be seen that the particles are fairly well distributed and that they bridge the crack at various points. This process consumes energy, and therefore the particles play a toughening role on the film. However, it should be noted that this is a local toughening effect; the global toughness of the specimen will depend on a variety of other factors such as the size of flaws, the morphology of crystals, etc.

In summary, the addition of silica fume to cement paste seems to have the following effects on the transition zone: First, less free water is accumulated at the interface during the casting of the specimens. Secondly the pozzolanic reaction between CH and silica fume causes a reduction in transition zone and thus the preferential orientation of CH crystals is considerably reduced.



Fig. 7
Silica Fume Particles Embedded on the CH Film

Transition Zone with Type K Cement

Many researchers have observed that at a given water/cement ratio the compressive strengths of Type K cement concrete is often higher than the corresponding of portland cement concrete. For instance, Polivka and Willson (8) reported that with concretes of water/cement ratios within the range 0.4 to 0.65, the compressive strength was higher when a Type K cement was used instead of Type I portland cement. Monteiro and Mehta (9) investigated the possibility that the higher strength of the Type K cement concrete compared to the portland cement concrete at a give water/cement ratio may be due to formation of a stronger transition zone in the former case.

In the case of portland cement, large CH crystals with a preferential orientation form a continuous film in direct contact with the aggregate surface (Fig. 3); whereas in the case of Type K cement small CH crystals are precipitated with a random orientation on the top of a discontinuous CH film (Fig. 8).

In summary, for expansive cement the precipitation of ettringite either in individual crystals or in bunches over the aggregate surface prevents the formation of a continuous CH film. A few small CH crystals with a preferential orientation are still present, however the deposition of CH crystals with a random orientation on their top probably reduces the facility of cracks to propagate in this zone. Both the high concentration of ettringite and the CH grain refinement in the interfacial zone may explain the reported higher mechanical strength of Type K cement compared to Type I portland cement.

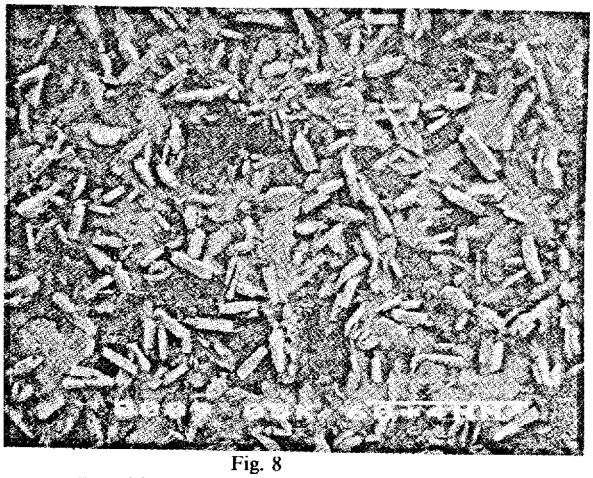

Fig. 8
Transition Zone with a Type K Cement

Transition Zone with Carbonate Rock as Aggregate

The carbonate-cement paste interface has been investigated by researchers since Farran (10) pointed out a reaction between this aggregate and that the cement paste. He discovered that there was a corrosion of the calcite surface and the bond between calcite or dolomite and cement paste was better than the bond with other mineral aggregates.

A possibility of reaction in the calcite aggregate-cement paste interface exists when the aluminate phases from cement enter into a chemical reaction with the carbonate phase of the aggregate. Lyubimova and Pinus (11), and Schwiete et al. (12) originally postulated this reaction. Later on Cussino and Pintor (13), and Cussino et al. (14) showed in the presence of water a reaction between calcite and C_3A or C_4AF produces $C_3A.CaCO_3.11H_2O$. More recently Grandet and Ollivier (15) reported the formation of $C_3A.CaCO_3.11H_2O$ by the reaction between $C_3A.1/2CO_2.12H_20$ and carbonate ions produced by dissolution of calcium carbonate. They also showed the "corrosion" of the calcite surface in contact with cement paste.

On this subject a brief report of recent work by Monteiro and Mehta (16) is given next. The etching of the calcite can be observed as shown in Fig. 9. The imprint of this etching can be seen on top of the CH film in Fig. 10. These micrographs show without any doubt that there is a chemical reaction between the carbonate rock and the cement paste matrix. From the micrographs it appears that the reaction is particularly intense where there is direct contact between the aggregate and the CH film; no reaction between the calcite and the aluminates could be observed by scanning electron microscopy.

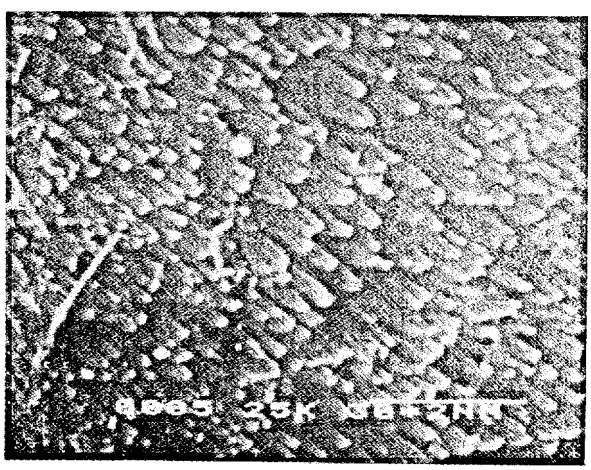

Fig. 9
Etching of the Calcite

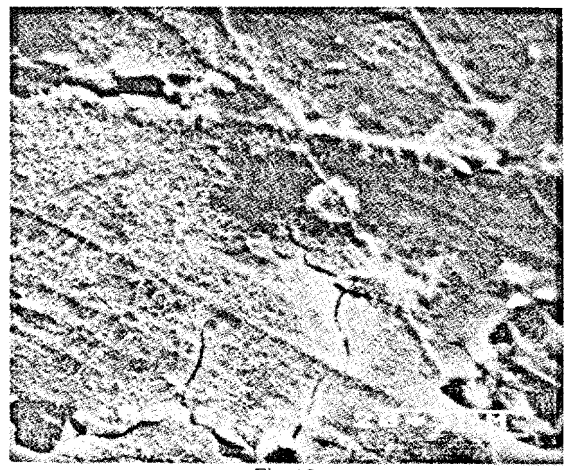

Fig. 10
Imprint of the Calcite Etching on the CH Film

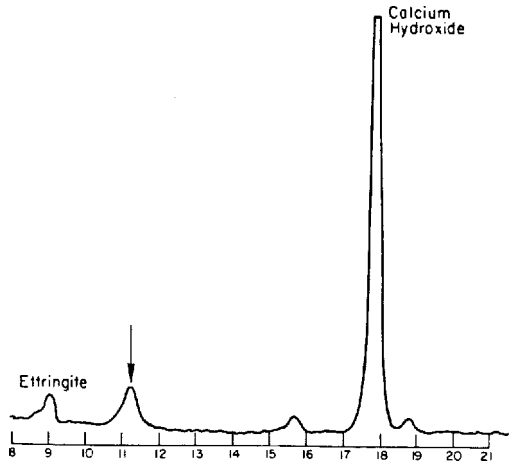

Fig. 11
XRD Analysis of the Interface with Portland Cement

Also a detailed XRD analysis of the transition zone from 1 day to over 1 year was performed. A typical XRD analysis of the interface is presented in Fig. 11. The peak at 11.2° 2θ ($Cu-K\alpha$) should be noted. Grandet and Ollivier (15) reported a peak at 11.6° 2θ ($Cu-K\alpha$) and proposed that it was due to calcium hydrocarboaluminate. In this work, however, for all the specimens investigated the peak was found to occur at 11.2° 2θ. Also, it should be mentioned that in no case any peak due to the $C_4A.\frac{1}{2}CO_2.12H_2O$ was obtained.

Since the authors suspected the bond strengthening to be due to an interaction between CH and calcite rather than due to the formation of carboaluminates hydrates it was decided to study the transition zone between marble aggregate and an alite cement (which contained no aluminate phase).

It was confirmed that the corrosion reaction reported between marble and portland cement also developed when alite cement was used instead of portland cement. The micrograph shown in Fig. 12 demonstrates that the calcite etches in the same way when alite cement was used.

Again with alite cement an extensive XRD analysis was performed on the transition zone from 1 day to 220 days. A typical XRD diagram is shown in Fig. 13. It is important to note the presence of the same peak (11.2° 2θ) which occurs when portland cement is used; therefore the traditional explanation of this peak being due to a calcium carboaluminatehydrate is not satisfactory.

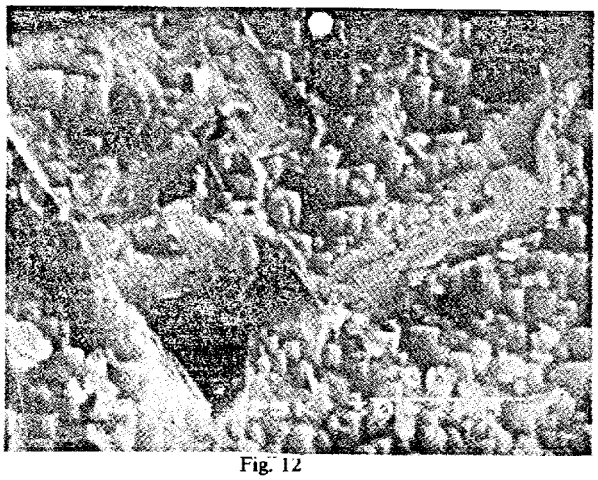

Fig. 12
Etching of Calcite Cast Against Alite Cement Paste

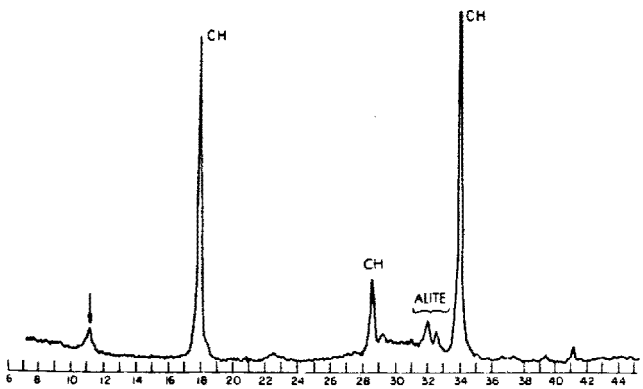

Fig. 13
XRD Analysis of the Interface with Alite Cement

It was speculated by the authors (16) that instead of a calcium carboaluminatehydrate it is probable that the interaction product in the transition zone is a calcium carbonate-calcium hydroxide complex. It is a known fact that reaction products of the composition $Mg_4(OH)_2CO_3.3H_2O$ and $Mg_2(OH)_2CO_2.3H_2O$ do exist, but the existence of corresponding products containing calcium are difficult to synthesize because of experimental difficulties. However, Schimmel (17,18) was able to prove the existence of a basic calcium carbonate with 1.5 molecules of crystallized water, $Ca_3(OH)_2(CO_3)_2.1.5H_2O$. His work showed that the X-ray pattern was extremely sensitive to the amount of crystallized water, and when the crystallized water was evaporated, the second highest peak was at 11.4° 2Θ, which is very close to the one obtained by the authors (16). The small difference in XRD diffraction peaks can be attributed to different amounts of crystallized water. Therefore it is proposed that the interaction product from the dissolutions of calcite and CH is composed of small crystals of basic calcium carbonate with a variable content of crystallized water, $Ca_3(OH)_2(CO_3)_2.xH_2O$. In conclusion, the improved mechanical strength of portland cement-carbonate rock system is due to replacement of large CH crystals in the transition zone with small crystals of a basic calcium carbonate, as shown in Fig. 14.

Conclusions

Metallurgists have been controlling and improving the quality of their products for years by applying the knowledge of crystal size effects on mechanical behavior. In concrete technology, this is still a farfetched goal, however some important qualitative guidelines can be established. In the case of Type K cement, for instance it has been suggested that the increase of mechanical strength of concrete is caused by grain refinement of the calcium hydroxide in combination with a higher concentration of ettringite in the transition zone. In the case of modified portland cement containing silica fume, the admixture acts as an activating site for hydration which causes an overall densification and grain refinement in the matrix particularly the transition zone. The transition zone improvement obtained when carbonate rocks are used, can also be considered as a case of grain refinement because the dissolution of large crystals of CH and of calcium carbonate originates a network of smaller crystals of a basic calcium carbonate.

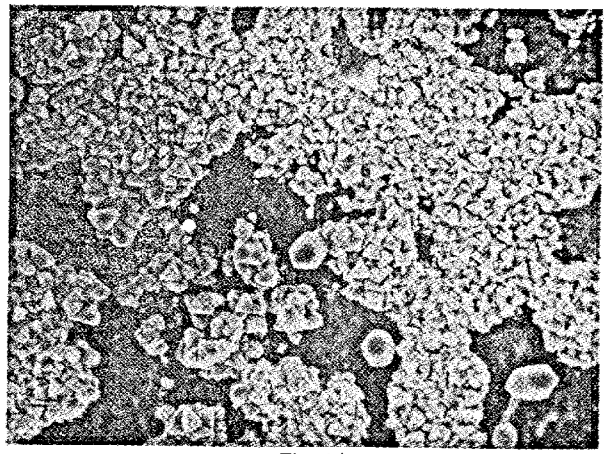

Fig. 14.
Small Crystals on Top of the CH Film

References

1. P.J.M Monteiro, "Microstructure of Concrete and Its Influence on the Mechanical Properties". Ph.D. Thesis, University of California at Berkeley (1986).
2. P.K. Mehta, "Concrete: Structure, Properties, and Materials". Prentice-Hall (1985).
3. J.C. Farran and J.C. Maso, Revue Mater. Constr. 587-588 (1964).
4. A.D. Buck and W.L. Bolch, J. Am. Concr. Inst. 63 , 775 (1966).
5. D.H. Hadley "The Nature of the Paste-Aggregate Interface" Ph.D Thesis. Purdue University, (1972).
6. B. Barnes "Morphology of the Paste-Aggregate Interface" Ph.D Thesis, Purdue University, (1975).
7. J. Grandet and J.P. Ollivier, 7th. Intl. Congress on the Chemistry of Cement, Volume III, VII-85, Paris (1980).
8. M. Polivka and C. Willson, "Properties of Shrinkage-Compensating Concretes", ACI Publication No. SP-38. 227 (1973).
9. P.J.M. Monteiro and P.K. Mehta, CCR, 16 , 111 (1986).
10. J. Farran ,Revue Mater. Constr. Trav. Publ. 490,491,492 (1956).
11. T.Y. Lyubimova and E.R. Pinus, Colloid J. USSR., 24 , 491, (1962).
12. H.E. Schwiete, U. Ludwig and J. Albeck, Wiss. Z. Tech. Univ. Dresden, 17 , 1587, (1968).
13. L. Cussino and G. Pintor, Il Cemento, 4 , 255, (1972).
14. L. Cussino, M. Murat and A. Negro, Il Cemento, 73 , 77, (1976).
15. J. Grandet and J.P. Ollivier, Cement and Concrete Research, 10, 759, (1980).
16. P.J.M Monteiro and P.K. Mehta, CCR, 17 , No. 2, (1986).
17. G. Schimmel, Nature, 57 , 38, (1970).
18. G. Schimmel, Phys. Blutter, 5 , 213, (1970).

P. KITTL, Researcher and Head of the Electron Microscopy Laboratory, Engineering and Materials Science Department, IDIEM, Faculty of Physical and Mathematical Sciences, University of Chile, P.O.Box 1420, Santiago, Chile.
G. DIAZ, Researcher of the Engineering and Materials Science Department, IDIEM, Faculty of Physical and Mathematical Sciences, University of Chile, P.O. Box 1420, Santiago, Chile.

1

2.3

COMPATIBILITY OF COPPER FIBRE WITH COMPACTED CEMENT AND LOW THERMAL-SHOCK FATIGUE THEREOF.
COMPATIBILITÉ DE LA FIBRE DE CUIVRE AVEC LE CIMENT COMPACTÉ, ET LA FATIGUE CORRESPONDANTE SOUS LE FAIBLE CHOC THERMIQUE.

SUMMARY: This investigation refers to a composite that contained 4% by weight of copper fibre 0.16 mm in diameter and 18 mm long, mixed with commercial cement having a water/cement ratio of 0.04 and compacted by compression to 35 MPa; thereafter the composite was kept in a moist room during 7 days. In this way there is obtained a material whose strength amounted to about 19 - 24 MPa and that admitted high deformation between brittle fracture of the matrix and final collapse. About 150 samples of compacted copper - fibre cement composite were prepared and subjected to thermal shock between 283°K and 373°K, completing 3000 cycles that caused no rupture but a reduction in mean strength. Fatigue curves were drawn for every 500 - cycle period, and a comparison was carried out with pure compacted cement paste. Dimensional stability as well as corrosion resistance were checked through long-range immersion in hot water (368°K). At last the inclusion of short ductile copper-fibres randomly distributed within a brittle cement matrix was able to block the thermal-fatigue process. This property is atributed to the fact that the different expansion-coefficients of cement and of copper produce microcracks and the high deformation admitted by the copper fibres. Evidence of this, supplied by scanning electron microscopy, is gathered through the comparison of samples with and without copper fibres.

SUMÁRIO

Esta investigação se refere a um composto que continha 4% em peso de fibras de cobre com 0.16 mm de comprimento misturados com cimento comercial, tendo uma relação água/cimento de 0.04 e compactado por compressão de 35 MPa; depois o composto foi mantido numa câmara úmida durante 7 dias. Desta forma, foi obtido um material cuja resistência foi de cerca de 19-24 MPa e que admitia uma alta deformação entre a fratura frágil da matrix e o colapso final. Cerca de 150 amostras do composto fibra de cobre-cimento foram preparadas e submetidas a um choque térmico entre 283K e 373K, completando 3.000 ciclos que não causaram ruptura alguma mas uma redução na resistência média. Curvas de fadiga foram traçadas para cada período de 500 ciclos e uma comparação com pasta pura de cimento compactado foi realizada.

Estabilidade dimensional assim como resistência à corrosão foram verificadas através de longa imersão em água quente (368K). Finalmente, a inclusão de fibras curtas ducteis de cobre aleatoriamente distribuídas na matrix frágil de cimento foi capaz de bloquear o processo de fadiga térmica. Esta propriedade é atribuída ao fato de que os diferentes coeficientes de expansão do cimento e do cobre produzem microfissuras e à alta deformação admitida pelas fibras de cobre. Evidência disto, demonstrada por microscópio eletrônico de varredura, é apresentada através de comparação de amostras com e sem fibras de cobre.

INTRODUCTION

The fibre-reinforced cement composites have been studied previously[1, 2]. However, to the authors' knowledge no information is existing about studies using one of the most ductile fibres, namely copper fibres; but some work has been made by the authors[3, 4] about load transmission between fibres and matrix, and the obtainment of the best proportion and size for a short ductile copper fibre randomly dispersed in the cement matrix. Copper fibre has a thermal expansion coefficient quite different from that of cement, and microcracks can be formed in the matrix; these microcracks can stop the propagation of some fatigue cracks. The main object of this work is getting the mechanical and direct microscopical evidence of this fact.

EXPERIMENTAL METHODS

The matrix was made using commercial portland cement without additives and having the following composition, by weight: 20.02% S, 7.56% A, 3.02% F, 61.60% C, and 1.80 % M; specific surface of 310 m^2/kg, and a retention of 13.6% on a moist 45 μm sieve. The fibres used are made of 99.9% pure electrolytic copper having a density of 8.9 g/cm^3, an elongation of 15% prior to fracture, a diameter of 0.16 mm, and a maximum ultimate tensile stress σ_{fu} = 400 MPa. The coefficient of thermal expansion was 12 x 10^{-6}°C^{-1} for cement, and 16.9 x 10^{-6}°C^{-1} for copper.

The cement mixed with 4% by weight of water and with copper fibres was introduced in a rectangular steel mould 0.055 x 0.020 m at the base thereof, and compacted applying a pressure of 35 MPa in order to get samples 5.5 x 2.00 cm at the base thereof and about 0.40 cm high. This pressure was sufficient to produce a good cohesion to the end of avoiding handling problems. The specimens were then kept in a moist room at 295°K for 24 h. In order that the hydration may proceed as much as possible, the specimens were immersed in water till saturation and thereafter they were placed again in the moist room for 7 days. The hydration process was ended by placing the specimens in an oven at 373°K for 24 h to get dry specimens, and then these were stored in a dessicator till testing time.

The neat cement paste and the copper-fibre cement composite were subjected to thermal cycling through immersion in water so that their extreme temperatures varied between 283°K and 373°K. Each heating and cooling cycle lasted two minutes, namely one minute at 283°K and one minute at 373°K. The sudden temperature difference between the inside of the sample and its external boundary originates alternating stresses[5] within the fibrocement, thus producing fatigue. In order to observe the accumulated fatigue, during each 500-cycle period and till compelting 3000 cycles there were randomly removed cement paste and fibrocement specimens which were then broken through the 3-point bending test using a Monsanto tensiometer. Maximum stress at fracture was computed using the wellknown expression $\sigma = (3/2)(PL/bh^2)$ with L=3.80 cm and b=2.00 cm, h being measured in each case.

Dimensional stability was checked by means of immersion in hot water at 373°K during 50 hours for copper-fibre cement composite and during 100 hours for neat cement paste. Corrosion resistance was observed using optical microscopy in specimens over two years old, of each one of the 500-cycle periods.

Some specimens of neat cement paste and of fibrocement were selected and analysed using scanning electron microscopy (SEM), with 3000 cycles and with zero cycles. The observation was made on fracture and polished surfaces. Polished surfaces were prepared through grinding with emery paper, and were finished by polishing them with micropolish of 0.05 μm A plus water.

ANALYSIS OF RESULTS AND DISCUSSION

The difference in thermal-expansion coefficients of cement and of copper can originate microcracks able to modify thermal fatigue because they can stop the propagation of fatigue cracks and modify the mean strength. This analysis is less relevant in steel-fibre reinforced cements inasmuch as the corresponding thermal-expansion coefficient of 12 x 10^{-6}°C^{-1} has a value similar to that of cement. The specimens were tested in the dry state, for the zero cycle at 7 days of hydration. However, in many instances fatigue response of some composites depends on matrix behaviour more directly[6]. In addition, fatigue accumulated in neat-cement paste was analysed.

In cement fatigue[7] the first 3×10^3 cycles of stress are those that count because it is during these initial cycles that main fatigue originates.

During the first 3×10^3 cycles, fracture resistance is reduced to 90%, and if we take into account that after 10^7 cycles fracture strength is reduced to 59% we may conclude that the first 3000 cycles are decisive.

Figure 1 shows low thermal-shock fatigue for neat-cement paste and for copper-fibre cement compo site. The lower full-line curve represents the behaviour of mean fracture-strength of the paste and its dependence on cycle number, while the upper full-line curve represents the same thing for the composite. Qualitatively both curves obey the same phenomenon; during the first 500 cycles a reinforcement is observed for both materials, but it impro ves the mechanical strength of the reinforced material more than the neat cement, in comparison with this characteristic at the time of manufacture, cycle zero. During the following cycles and upon reaching the maximum strength the weakening process of specimens is started, i.e. fatigue has begun. It is probable that an increase in microcracks number is produced during the first 500 cycles. However the inclusion of short copper fibres randomly distributed within the cement matrix has been able to block the fatigue process, as shown by the fact that the fibrocement curve is not parallel to the cement-paste curve and extends far above the same. The dash-line curve represents the expected behaviour of the fibrocement, i.e. only the reinforcement, which is shown by this curve running parallel to the cement-paste curve. In reference (4) there is shown a typical load/deflection diagram for cement without and with reinforcement, and according to which, upon a 10% weakening through matrix ruptu re, the composite withstands 10 times more deformation without further weakening, and ends with a ductile fracture shows in the Figures 2 and 3 by means of SEM. This last behaviour corresponds to plastic deformation of the fibres and to their extraction from the matrix, which means that the fibres were capable to absorb fatigue, inasmuch as fa tigue implies that some cracks propagate owing to the singularities in the elastic field, but these propagating cracks are doing so without weakening the material because the fibres have adapted themselves to crack propagation through plastic deformation and they are still resisting; this process ends when the crack reaches a microfissure at an oblique angle thereto. That is to say, it could be possible to decrease fatigue with non-reinforcing fibres if there is microfissure production. Besides, as low thermal-shock fatigue progresses the presence of fibres originates microcracks that do not necessarily constitute some disadvantage in brittle composites[8], as may be seen in the present instance. The constitution of microcracks may lead to an important increase in composite though - ness and, in particular, materials propending to microfissuration are perhaps the only sort of engineering materials that are suitable under conditions requiring high resistance to thermal shock and hence good resistance to thermal fatigue.

The neat-cement paste and the copper-fibre cement composite samples submerged in water at 373°K, are keeping their volumetric variation around 2%, registered from the first 10 hours till completing 100 hours and 50 hours, respectively, thus showing a high dimensional stability in both materials.

Optical-microscopy observations of copper-fi bres in samples over two years old showed no corrosion, and the same result is obtained through immer sion in water at 373°K for 50 hours.

Figures 4 - 10 allow to observe, by means of SEM, the fracture and polished surfaces of neat-ce ment paste and of copper-fibre cement composite. With zero cycles there were observed only a few cracks in the neat-cement paste (Figs. 4, 5); but in the copper-fibre cement composite a few cracks were observed in the cement matrix, and many ones near the copper fibres (Figs. 6, 7). With 3000 cycles many cracks were observed in the neat-cement paste (Figs. 8, 9) but the same few ones in the copper-fibre cement composite (Fig. 10). Consequently the presence of copper fibres stopped the thermal-fatigue cracks in the cement matrix.

CONCLUSION

The copper fibres were able to absorb thermal fatigue, stopped the thermal-fatigue crack and the cracks can propagate without weakening the cement matrix because the fibres undergo some plastic deformation that adapts them to this process that ends when the crack reaches some microfissure at an oblique angle thereto.

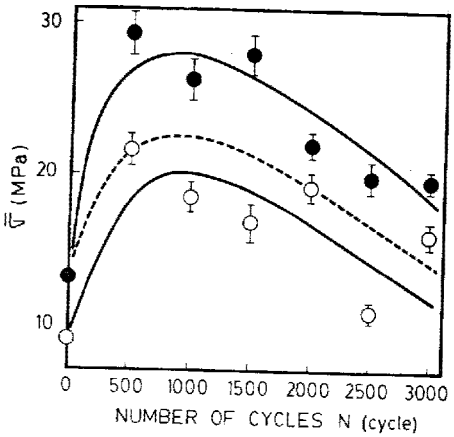

Fig. 1 Variation of mean fracture-strength as a function of cycle number. ○ : neat cement paste; ● : copper-fibre cement composite. Bars indicate standard deviation.

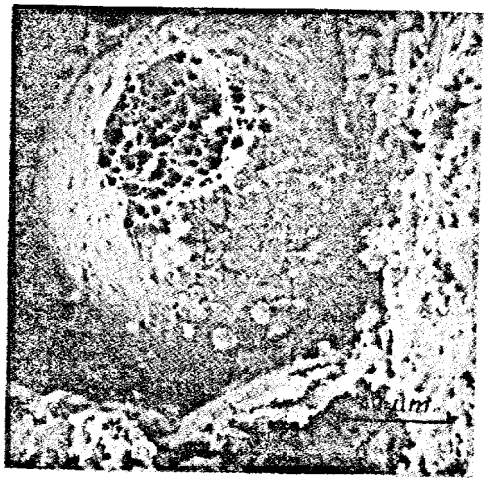

Fig. 2 SEM of fracture surface of copper-fibre cement composite with zero cycles, showing normal ductile fracture.



Fig. 3 SEM of fracture surface of copper-fibre cement composite with 2500 cycles, showing oblique ductile fracture.

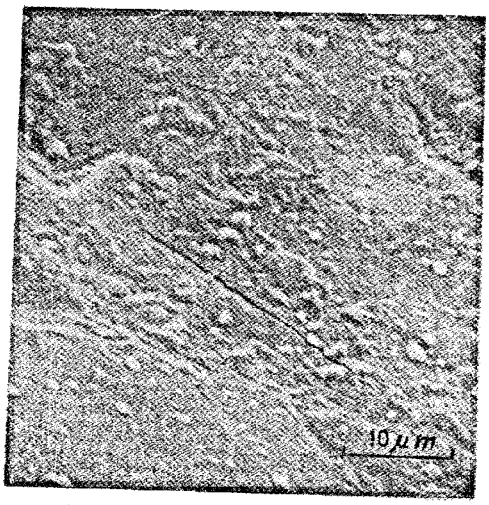

Fig. 4 SEM of polished surface of neat-cement paste with zero cycles.

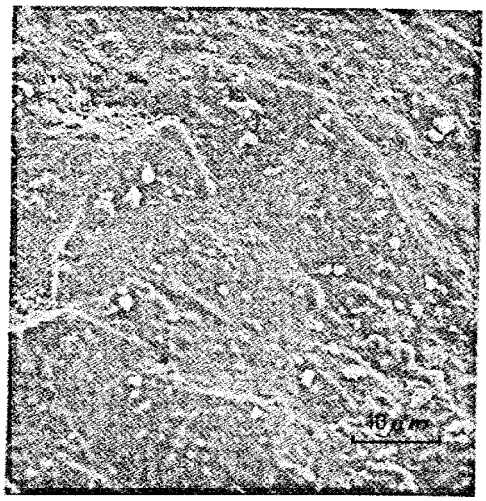

Fig. 5 SEM of polished surface of neat-cement paste with zero cycles.

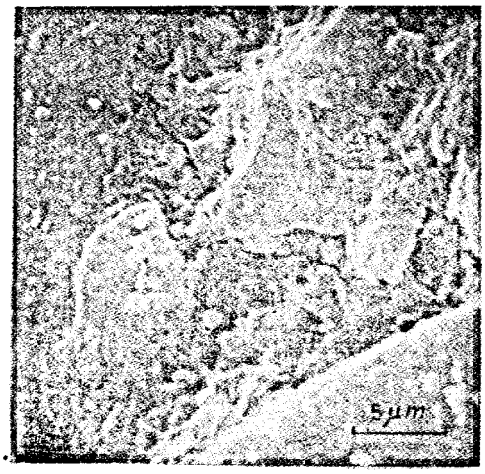

Fig. 6 SEM of polished surface of copper-fibre cement composite with zero cycles, showing crack near copper fibre.

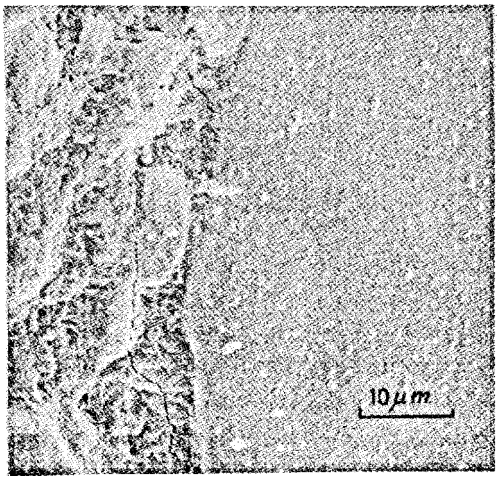

Fig. 7 SEM of polished surface of copper-fibre cement composite with zero cycles, showing cracks near copper fibre.

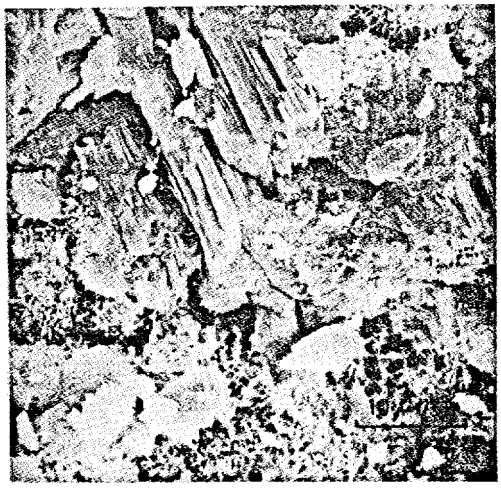

Fig. 8 SEM of fracture surface of neat-cement paste with 3000 cycles, showing typical portlandite and tobermorite as hydration products, and crack.

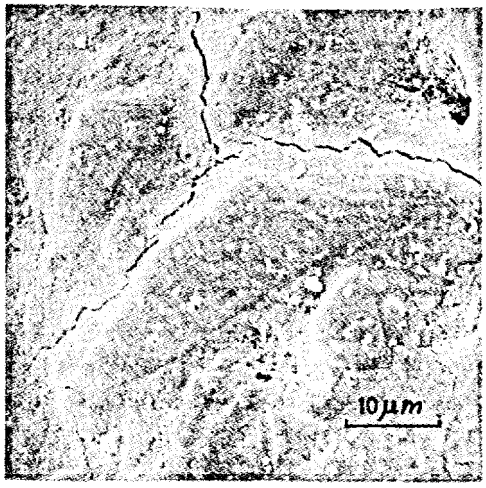

Fig. 9 SEM of polished surface of neat-cement paste with 3000 cycles, showing many cracks among puzzolanic particles.

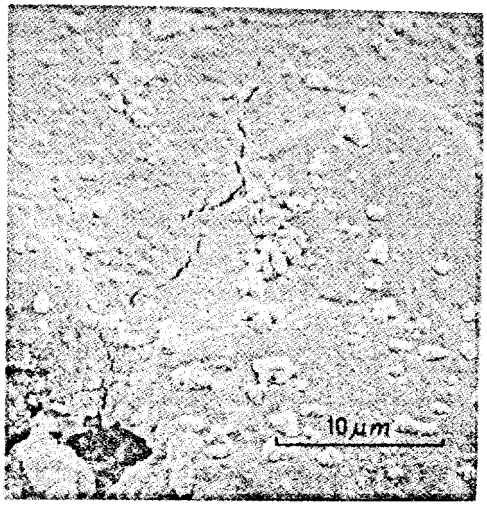

Fig. 10 SEM of polished surface of copper-fibre cement composite with 3000 cycles, showing cracks.

ACKNOWLEDGEMENTS

The authors wish to thank the Department of Investigation and Libraries of the University of Chile for its Grant N° 12292/8512 covering a part of the funds for this work. They are also grateful to Professor A. Lamana, Director of the IDIEM, for his constant encouragement, and to Raymond Toledo for his assistance in the redaction of the manuscript.

REFERENCES

1.- SWAMY, R.N., MANGAT, P.S. and RAO, C.V.S.K.; The Mechanics of Fiber Reinforcement of Cement Matrices. Publication SP-44, Am. Concr.Inst., Detroit, 1974, pp. 1 - 28.

2.- MAJUMDAR, A.J.: Properties of Fibre Cement Composite. Fibre Reinforced Cement and Concrete. RILEM Symposium, 1975, pp. 279 - 313.

3.- KITTL, P. and GALLEGUILLOS, E: Statistical Analysis of Decohesion in a Cu Wire/Cement Interface. Res Mech. Lett., 1 (1981), pp. 445 - 449.

4.- KITTL, P., GALLEGUILLOS, E. and DIAZ, G.: Properties of Compacted Copper-Fibre Reinforced Cement Composite. Int. J. Cem. Comp. Lightweight Concr. 7 (1985), pp. 193 - 197.

5.- GLANDUS, J.C. and BOCH, P.: Influence of the Size Factor on the Thermal Shock Resistance of Ceramic Samples. Int. J.Thermophys., 2 (1981), pp. 89 - 101.

6.- REIFSNIDER, K.: Fatigue Behaviour of Composite Materials. Int. J. Fract., 16 (1980), pp. 563-583.

7.- RAITHBY, K.D.: Behaviour of Concrete under Fatigue Loading. In: Developments in Concrete Technology - 1, ed. by F.D. Lydon, Applied Science Publishers Ltd., London, 1979.

8.- SINGH, J.P., HASSELMAN, D.P.H., SU, W.M., RUBIN, J.A. and PALICKA, R.: Observations on the Nature of Microcracking in Brittle Composites. J. Mater. Sci., 16 (1981), pp.141-150.

Chen Zhi-Yuan and Zhang Xio-Zhong, Department of Materials Science and Engineering,
Tong-Ji University, Shanghai, China

Investigations on the Zinc/Hydrated-Cement-Paste Interfacial Zone

Une recherche sur l'interface entre le zinc et la pâte de ciment hydratée

SUMMARY: The comprehensive research on Zinc/Hydrated Cement Paste interfacial zone were studied by using XRD, SEM, EPM and DSC. It was found that the thickness of the interfacial zone amounts to about 70 μm at a w/s ratio 0.29. In the whole interfacial zone a new hydrate $Ca(Zn(OH)_3)_2 . 2H_2O$, is present which can be found mainly in the region 0-10 μm from the interface. With increasing distance from the interface the quantity of $Ca(OH)_2$ decreased and its degree of orientation became low. After the adding five percent silica fumes the quantity of $Ca(Zn(OH_3)_2.2H_2O$ in the interfacial zone decreased and it became detectable only in the region 0-30 μm from the interface. Both the quantity of the CSH phase and the cleavage strength increased. A structure model of the Zinc/Hydrated-Cement-Paste interfacial zone is proposed, and the process and mechanism of formation of the interfacial zone is discussed.

Desenvolveu-se pesquisa abrangente sobre a zona interfacial de Zinco/Pasta de Cimento Hidratado, usando-se XRD, SEM, EPM e DSC. Constatou-se que a espessura da zona interfacial é de cerca de 70 μm com uma relação A/S igual a 0,29. Em toda a zona interfacial há a presença de um novo hidrato $Ca(Zn(OH)_3)_2.2H_2O$, o qual pode ser encontrado principalmente na região de 0-10 μm a partir da interface. Aumentando a distância da interface, diminui a quantidade de $Ca(OH)_2$ e seu grau de orientação tornou-se baixo. Depois da adição de 5% de microssílica, a quantidade de $Ca(Zn(OH)_3)_2.2H_2O$ na zona interfacial diminui e tornou-se detectável apenas na região de 0-30 μm a partir da interface. Aumentou tanto a quantidade de fase de CSH como a resistência à clivagem. Propõe-se um modelo de estrutura da zona interfacial Zinco/Pasta de Cimento Hidratado e se discute o mecanismo de formação da zona interfacial.

Chen Zhi-Yuan and Zhang Xio-Zhong, Department of Materials Science and Engineering, Tong-Ji University, Shanghai, China

Investigations on the Zinc/Hydrated-Cement-Paste Interfacial Zone

Recently more and more attention has been paid to the structure of the interfacial zone between cement paste and aggregate and its modification. The efforts in this area have been concentrated on the study of the interfacial zone between cement paste and rocks (1.2). In the field of prestress and reinforced concrete, zinc coated steel reinforcement is being used, however the structure of the zinc-cement paste interface has been studied only in a limited extent (3). Within this paper data on the structure of the interfacial zone between Zn and cement paste, as determined by XRD, SEM, DSC, EPM and its modifications brought about by silica fume additions are reported.

Experiments

Materials
Zinc plate: purity 99.995%.
Cement: Ordinary portland cement of the following oxidic composition: CaO 61.4%, SiO_2 18.3%, Al_2O_3 6.60%, Fe_2O_3 5.29%, MgO 1.88%, SO_3 1.80%. Ignition loss 1.8%, and with a spec. surface area of 220 m^2/kg (Blaine).

Silica fume: A material with 94.7% SiO_2 and a BET_{N_2} spec. surface area of 26 m^2/g.

Preparation of the samples

In order to eliminate the effect of mechanical interlocking forces on the cleavage strength of the Zn/cement paste composites, the surface of the zinc plate was polished with an alumina polishing powder (1 µm in size) to a mirror-like surface.

The type, size and preparation of Zn/cement paste composite samples, and the calculations of the cleavage strength of the composite samples, were described in our previous paper (4). The only difference consisted in using a zinc instead of an aggregate surface.

Results and Discussion

I. The distribution of $Ca(Zn(OH)_3)_2.2H_2O$ and of other hydrates of cement in the interfacial zone.

After the samples were cleavage at the age required, the cleavage surface of zinc plate always stickes a layer of hydrates about 25-30 µm in thick. Both cleavage faces were used for XRD, EPM, SEM and DSC studies. The XRD diagrams of both sides of the composite interface showed two strong diffraction peaks with d=3.10Å belonging to Calcium hydroxyzincate $Ca(Zn(OH)_3)_2.2H_2O$ with strong orientation, as shown in Fig. 1. This findings is in line with that of G. Arugie et.al. (5) who detected the compound after immersing zinc plates in to saturated lime solution. We do the similar experiments confirmed it and believe that the $Ca(Zn(OH)_3)_2.2H_2O$ formed within the zinc/cement paste interface is the product of a reaction between zinc and $Ca(OH)_2$ formed in the hydration of the cement.

The distribution of the phase $Ca(Zn(OH)_3)_2.2H_2O$ within interfacial zone analyzed. To do so, only the second strongest peak d = 6.25 Å could be used due to an overlapping of the strongest peak d = 3.12 Å with a peak of $Ca(OH)_2$ d = 3.11 Å. The obtained results for 3 and 28 day old pastes with and without silica fume are shown in Fig. 2. (7 day similar to 28days.) From Fig. 2 it is apparent that the distance from the zinc surface in which $Ca(Zn(OH)_3)_2.2H_2O$ is still detectable

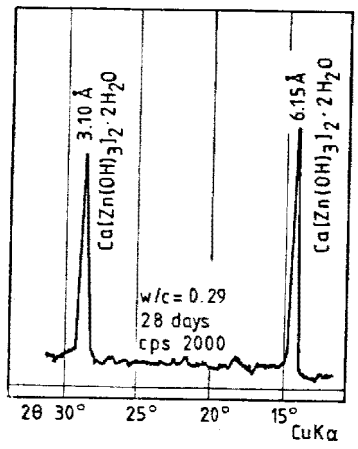

Fig. 1: The XRD diagram of a composite sample on the zinc side

increased with hydration time. On the other hand the intensity of the pertinent peak in the vicinity of the zinc surface declined with hydration time. This decline in peak intensity does not imply necessarily a decrease in the amount of the calcium zincate present as such changes may also be brought about by alterations in the orientation of the $Ca(Zn(OH)_3)_2.H_2O$ crystals in the vicinity of the zinc surface. In the presence of silica fume the intensity of the Ca-zincate peak declined apparently indicating the formation of smaller amounts of this compound due to a decreased supply of calcium hydroxide.

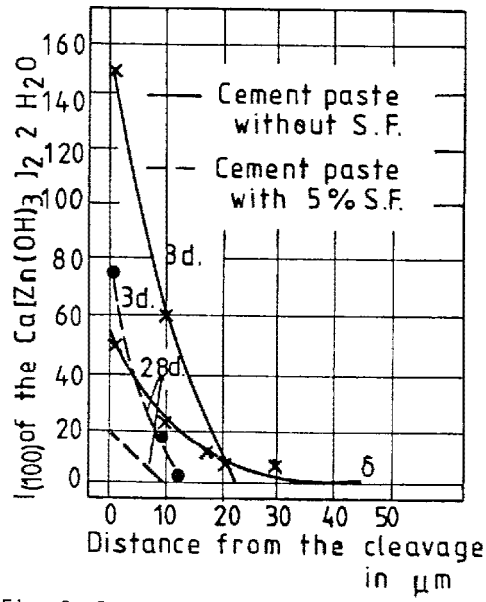

Fig. 2: $I_{(100)}$ of the $Ca(Zn(OH)_3)_2.2H_2O$ vers the distance from the cleavage

Fig. 3 shows the obtained Zn-line scanning data at the Zn/cement paste interface. The obtained data indicate a Zn diffusion distance of about 70 µm after 28 days of hydration for both plain cement pastes as well as those with silica fume added.

Chen Zhi-Yuan and Zhang Xio-Zhong, Department of Materials Science and Engineering,
Tong-Ji University, Shanghai, China

Investigations on the Zinc/Hydrated-Cement Paste Interfacial Zone

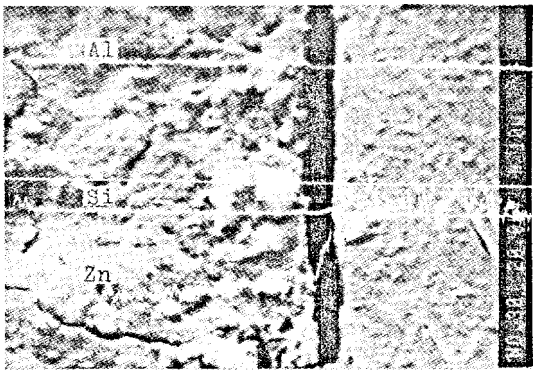

Fig. 3: Line scanning of EPM on the Zn/cement paste interface

The morphology of the zinc/hydrated-cement-paste interface was studied by SEM. The pertinent SEM pictures are shown in Fig. 4. The only product detected at the zinc surface was large quantity of $Ca(Zn(OH)_3)_2.2H_2O$ crystals, formed as dense layer, as shown in Fig. 4 (a). The morphology of calcium hydrxyzincate becomes apparent from picture 4b. The fibrous CSH phase at the interface can be seen in Fig. 4c. After adding 5% silica fume, the amount of the CSH phase increased and became dense as shown in Fig. 4d. $Ca(OH)_2$ appeared in form of very small grains and was present only in pores of the paste as show in Fig. 4e (without silica fume), and f (with 5% silica fume). Ettringite was not detected on the cleavage surface.

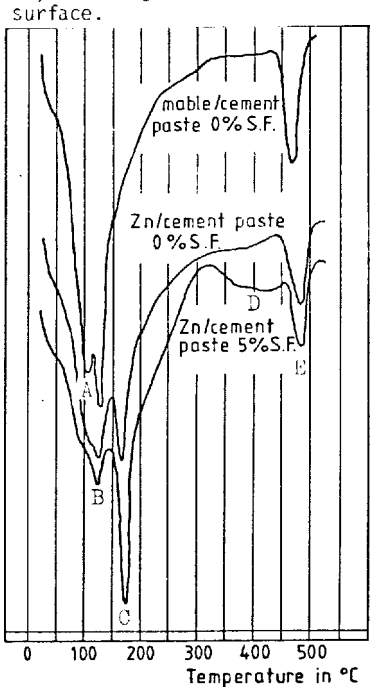

Fig. 5: The typical DSC curves

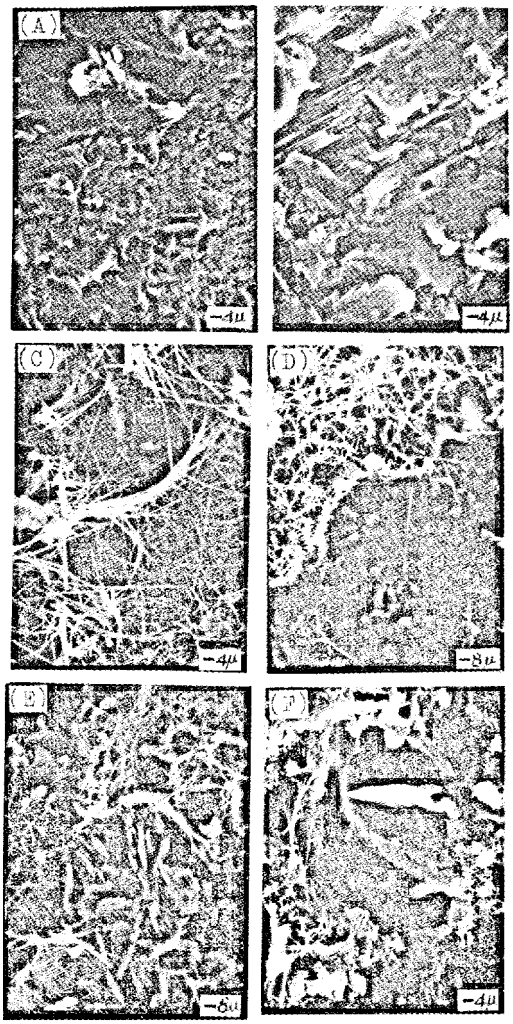

Fig. 4: Micrograph of the interface of zinc/ hydrated-cement-paste under SEM, after 7 days hydration

Fig.4.

For the study of the distribution of the interfacial zone differential scanning calorimetry was employed. Some typical DSC curves of the first layer within the interfacial zone are shown in Fig. 5. The peaks A,B, D and E represent the phases CSH, ettringite, calcium-silicate-hydrate and $Ca(OH)_2$ respectively. As the peak C at 175 °C is absent within the first layer of a cement paste in the marble cement paste interface, we believe that it belongs to the phase $Ca(Zn(OH)_3)_2.2H_2O$ We assume that the thermoeffect related to this peak is due to the loss of two mols of crystalline water from this compound. For semiquantitative evaluation of the DSC-recordings the method described in Fig. 6. It shows an uneven distribution of the phases involved within the zinc-cement paste contact zone. In samples with silica fume added the amounts of $Ca(OH)_2$ were lower while those of the CSH phase higher. $Ca(Zn(OH)_3)_2.2H_2O$ was detectable only within the range of 0-30 μm from the cleavage interface and its amount declined with increasing distance. The results are in line with those found by XRD and EPM. The decision to attribute the peak A and D to calcium silicate hydrate phases is based on a parallel studies an hydrated pure tricalcium silicate in which similar peaks were also

Chen Zhi-Yuan and Zhang Xio-Zhong, Department of Materials Science and Engineering, Tong-Ji University, Shanghai, China

Investigations on the Zinc/Hydrated Cement Paste Interfacial Zone

detectable. An addition of 5% silica fume to the cement paste resulted in a decrease of the amount of CSH phase (peak A) after 28 days, but the peak D increased. The typical curve can be found in Fig. 5. The total amount of the calcium silicate hydrates were increased. It is favour to improve the bond strength.

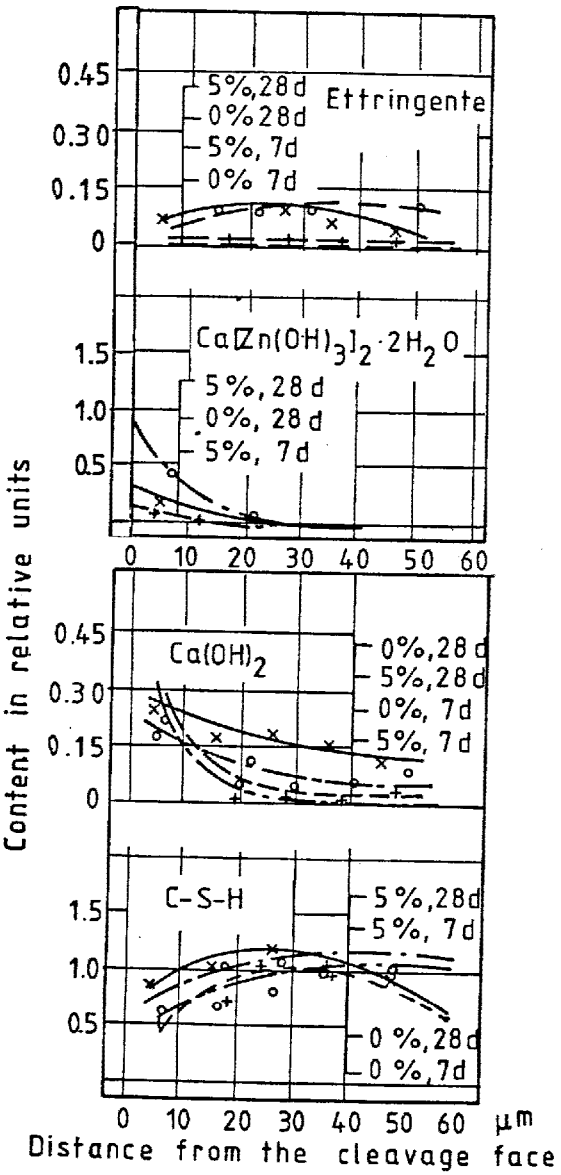

Fig. 6: The distribution of hydrates of cement in the interfacial zone (w/c = 0.29, 7 and 28 days)

II. The mechanism of the formation of the zinc/cement paste interfacial zone and its structural model

Summarizing the results of XRD, EPM, SEM and DSC, the following mechanism of the formation of the zinc/cement paste interfacial zone and its structure is proposed.

After mixing with water, the process of cement hydration at the contact with the zinc surface is initially similar as that in the bulk cement paste. At the same time, the ions Ca^{2+}, OH^- and Zn^{2+} diffuse into the water film adsorbed on the zinc plate and react with each other to form calcium hydroxyzincate ($Ca(Zn(OH)_3)_2 \cdot 2H_2O$). A fraction of Zn^{2+} dissolved from the zinc plate diffuses deeper towards the cement paste and reacts here chemically with Ca^{2+} and OH^- to produce again $Ca(Zn(OH)_3)_2 \cdot 2H_2O$. Due to the formation of large quantities of $Ca(Zn(OH)_3)_2 \cdot 2H_2O$, the degree of supersaturation of $Ca(OH)_2$ decreases and thus, additional amounts of $Ca(OH)_2$ must enter the liquid phase. As the result of chemical reactions among these phases, a dense layer of crystalline $Ca(Zn(OH)_3)_2 \cdot 2H_2O$ about 10 μm thick forms within adsorbed water film at the Zn surface. With an increasing thickness and densification of this layer, the diffusion of Zn^{2+}, Ca^{2+} and OH^- gets gradually more difficult, and the rate of $Ca(Zn(OH)_3)_2 \cdot 2H_2O$ formation declines.

In addition to Ca-zincate the interfacial zone also contains of calcium hydroxide. This phase crystallizes in the vicinity of the zinc surface in larger amounts than in the bulk material due to a larger space for available crystallization in this region. The $Ca(OH)_2$ appears to be intergrown with CSH phase within the zone.

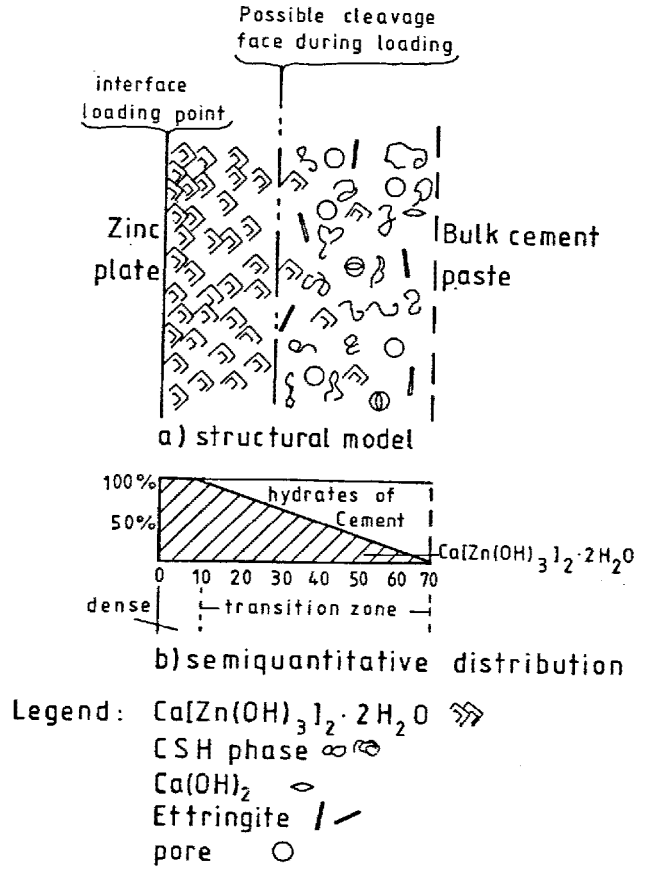

Fig. 7: A structural model of the interfacial zone of zinc/cement paste

The absence of distinct ettringite crystalls close to the interface may be explained by the dense structure present here. Fig. 7 shows schematically the structure of the interfacial zone. According to this concept, the cleavage path that develops under mechanical loading of the interfacial zone progresses along the contacting face between the sub-dense layer and the more porous bulk of the cement paste.

III. Relationship between the structure of the interfacial zone and the mechanical behavior

As mentioned above a dense layer of $Ca(Zn(OH)_3)_2.2H_2O$ about 10 µm thick forms at the zinc surface within the interfacial zone. The cohesion between the metallic surface and this layer is probably brought about by a combination of chemical bonds, van der Waals forces and mechanical interlocking. The latter phenomenon develops, however, only after the zinc surface is partially corroded by the fresh paste. Of those the chemical bonding seems to be the main factor reponsible for adhesion. On the other hand, due to the fact that the surface of the zinc plate was polished, the mechanical interlocking probably plays only a minor role in developing the bond. In spite of its lower density the structure of the sub-dense layer is not too different from the dense one. Consequently the cohesion between these two layers seems to be rather good. On the other hand the interface between the sub-dense layer and the bulk paste appears to be most prone to failure due to the existing structurak differences of these materials.

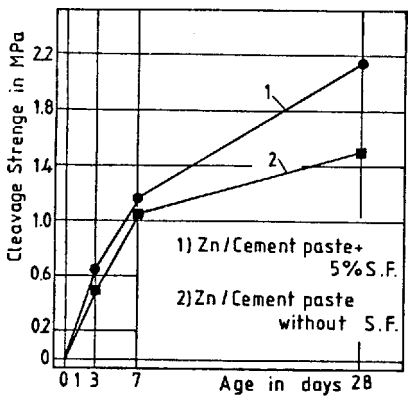

Fig. 8: The cleavage strength of the composite samples

From Fig. 8 the gradual increase of the cleavage strength with age is apparent. This strength increase was obviously due to the progressing hydration and thus to an increase of the amount of hydration products and a densification of the hydrated material formed.

Conclusions

1. In the course of hydration a region of particular morphology and structure develops at the zinc/portland cement paste interface. This region consists of a dense layer about 10 µm thick containing mainly crystals of $Ca(Zn(OH)_3)_2.2H_2O$ located in the immediate vicinity of the zinc surface and a neighboring "sub-dense" layer containing, beside the cement hydration products, still distinct amounts of the above calcium zinc hydrate.
2. The mechanism of the formation of the interfacial zone can be explained by a "through-solution" mechanism, on the basis of which the calcium, sulfate, aluminate and silicate ions migrate to the water film adsorbed on zinc surface and, therefore, the hydrates get precipitated there. A structure model of Zn/cement interfacial zone is proposed, which indicates the possible cleavage face during loading.
3. 5% silica fume added to the cement paste densified the interfacial zone and thus increase the cleavage strength of the composite samples.

Acknowledgement

The authors gratefully acknowledge Professor Dr.-Ing. I. Odler for his helpful discussion and the work of Mr. Zhao Wei-Min in helping to carry out the experiments.

References

1. B.D. Barnes, S. Diamond and W.L. Dolch: "Micromorphology of the interfacial zone around aggregates in portland cement mortar". J. Am. Cer. Soc., Vol. 62, No. 1-2, pp. 21-24 (1979).
2. C.A. Langton, D.M. Roy: "Morphology and Microstructure of cement paste/Rock interfacial regions. 7th Int. Congress on Chem. Cem., Vol. III, pp. VIII-127/132, Paris(1980).
3. P.J.M. Monteiro and P.K. Mehta: Ettringite Formation on the Aggregate-Cement paste interface, Cem. Concr. Res., Vol. 15, pp. 378-380 (1985).
4. Chen Zhi-Yuan and Zahng Xiao-Zhong. Distribution of $Ca(OH)_2$ and of the CSH phase in the Oolithic Marble/Hydrated Cement Paste Interfacial Zone. 8th Int. Congr. Chem. Cem. in press.
5. G. Arliguie, J. Grandet and R. Duval: Study of the Contact zone between Zinc and Portland Cement Paste. 7th Int. Congr. Chem. Cem., Vol. IV, pp. VII-22/27, Paris (1980).

Chen Zhi-Yuan and Zhang Xio-Zhong, Department of Materials Science and Engineering, Tong-Ji University, Shanghai, China 1

Distribution of $Ca(OH)_2$ and of the CSH phase in the Oolithic Marble/Hydrated Cement Paste Interfacial Zone 2.3

La distribution de $Ca(OH)_2$ et de la phase CSH dans l'interface entre le marbre oolithique et la pâte de ciment hydratée

SUMMARY: DSC and GPC were used to determine the distribution of the CSH-phase and of $Ca(OH)_2$ in the Oolithic Marble/Hydrated-Cement-Paste interfacial zone and the degree of polymerization of the CSH phase. The specimens studied were tested at 3,7 and 28 days. It was found that in the interfacial zone the amount of $Ca(OH)_2$ is increased as compared to bulk material. The distribution of the CSH phase was found to be inhomogeneous. With increasing age the degree of of polymerization increased. The degree of polymerization of CSH phase in the interfacial zone is higher than that in the bulk cement paste. After adding 5% silica fume the quantity of $Ca(OH)_2$ in the interfacial zone decreased while that of CSH phase increased. The degree of polymerization increased both in the interfacial zone and in the bulk cement paste. The cleavage strength of the interfacial zone increased too.

Usando DSC e GPC, determinou-se a distribuição da fase de CSH e de $Ca(OH)_2$ na zona interfacial de mármore oolítico/pasta hidratada de cimento e o grau de polimerização da fase de CSH. Os espécimes estudados foram testados aos 3, 7 e 28 dias. Constatou-se que na zona interfacial a quantidade de $Ca(OH)_2$ é maior em comparação com o material granelado. Verificou-se que não é homogênea a distribuição da fase de CSH. Com o aumento da idade, aumenta o grau de polimerização. O grau de polimerização da fase de CSH na zona interfacial é mais alto do que na pasta de cimento. Depois da adição de 5% de microssílica, a quantidade de $Ca(OH)_2$ na zona interfacial diminui, enquanto a fase de CSH aumentou. O grau de polimerização aumentou tanto na zona interfacial como na pasta de cimento. Também aumentou a resistência à clivagem na zona interfacial.

Chen Zhi-Yuan and Zhang Xio-Zhong, Department of Materials Science and Engineering, Tong-Ji University, Shanghai, China

Introduction

The structure of the interfacial zone between calcareous aggregate and cement paste has been studied by several investigators (1-5). Recently Monteiro and Mehta published data on the distribution of ettringite in the interfacial zone, using a commercial portland cement and a granite aggregate (6), while similar data on the distribution of the CSH phase and portlandite have not been published yet. The latter two phases, however, may affect the bond strength between cement paste and aggregate significantly.

The present authors studied the quantitative distribution of CSH phase and $Ca(OH)_2$ within the interfacial zone, and the degree of polymerization of CSH phase, using differential scanning calorimetry (DSC) and gel permeation chromatography (GPC). In addition to that the effect of silica fume addition on the structure of the interfacial zone was also investigated.

1. Experimental

1.1. Materials

a) Marble: Blackish Jade Marble with Oolite structure;

b) Cement: Ordinary portland cement of the following oxidic composition: CaO 61.4%, SiO_2 18.3%, Al_2O_3 6.60%, Fe_2O_3 5.29%, MgO 1.88%, SO_3 2.46%, L.O.I. 1.80%. Its specific surface area was 220 m^2/kg (Blaine).

c) Silica fume: The used materials had a SiO_2 content of 99.7% and a specific surface area of 25 m^2/g (BET, N_2).

1.2. Testing procedures

For cleavage strength determination 20x20x10 mm cube-shaped specimens were employed. They consisted of two identical halves of marble and cement paste The surface of aggregate contacted with cement paste was polished to a mirror-like finish to eliminate possible interlocking effects. The cement paste was made with w/s = 0.29. After casting, the compositie samples were kept over water at 20 ± 2 °C for 24 hours, then demolded and kept under water (20 ± 2 °C) until testing. The bond strength of the composite samples was determined by cleavaging at the interface. The bond strength (σ) was calculated according to the formula:

$$\sigma = 2P/\pi a^2$$

where P: applied force in N;
a: side length of the composite cube in mm.

After cleavaging the composite sample at the required age, the cement paste part of it was immersed into absolute ethanol and subsequently ethyl ether to stop the hydration and then stored in ethyl alcohol until testing to prevent carbonization.

For further testing subsequent layers of material about 10 µm thick were scraped of the sample and analyzed individually. The amount of material needed for DSC testing was about 1 mg and the temperature rate employed 20 °C/min. Due to a partial overlapping of parts of the peak areas of CSH phase and ettringite in the DSC diagram the quantitative evaluation was made in a way as shown in Fig. 1. The existing peaks were identified by comparing them with similar peaks obtained with pure materials determined under identical experimental conditions.

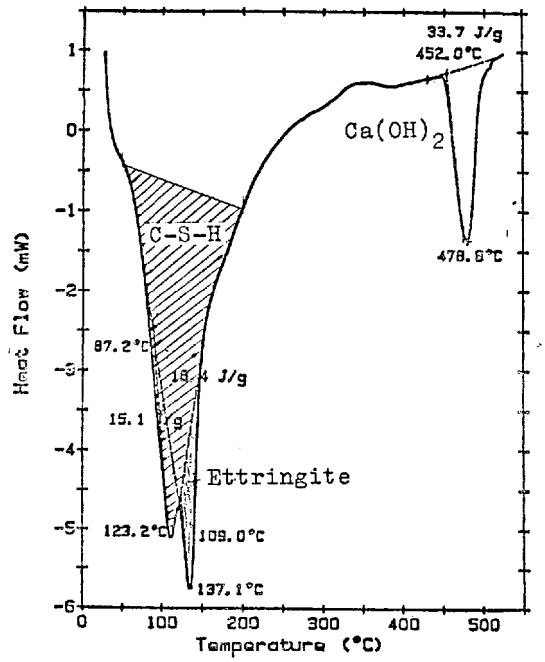

Fig. 1: Typical DSC curve

In addition, the obtained material was studied by X-ray diffraction and gel permeation chromatography. The latter determination was made in a way as described in (7).

2. Results

2.1. Phase distribution within the interfacial zone

The distribution of the individual phases within the interfacial zone as determined by DSC is shown in Fig. 2. It shows the distribution of the CSH-phase, ettringite and $Ca(OH)_2$ within in the interfacial zone at different ages. The figure shows both data for plain OPC and OPC with 5% silica fume added. The results are given in relative units. Due to a partial overlapping of the pertinent peaks, the data obtained for the CSH-phase and ettringite have to be considered just as semiquantitative ones.

The distribution of $CaCO_3$ within the interfacial zone is given. Here, the obtained values were obtained by X-ray diffraction, shown in Fig. 3.

2.2. Degree of polymerization of the CSH-phase

The degree of polymerization of the CSH-phase within the interfacial zone was measured by GPC. The data obtained are summarized in Table I. Here the parameter $\bar{M}n$ indicates the number average of the molecular weight and the parameter $\bar{M}w$ the weight average of the molecular weight. The individual fractions represent monomer, dimer and polymer forms of SiO_2.

Chen Zhi-Yuan and Zhang Xio-Zhong. Department of Materials Science and Engineering, Tong-Ji University, Shanghai, China

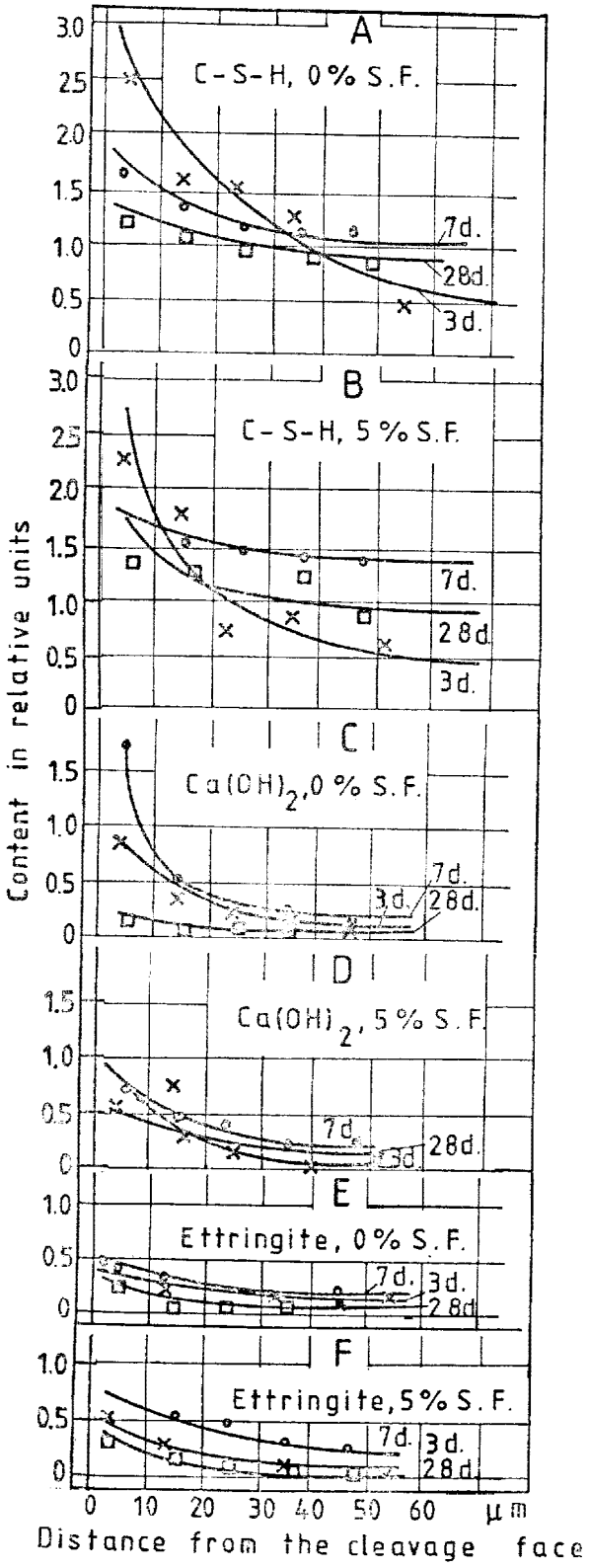

Fig. 2: The distribution of hydrates of cement in the interfacial zone (w/c = 0.29)

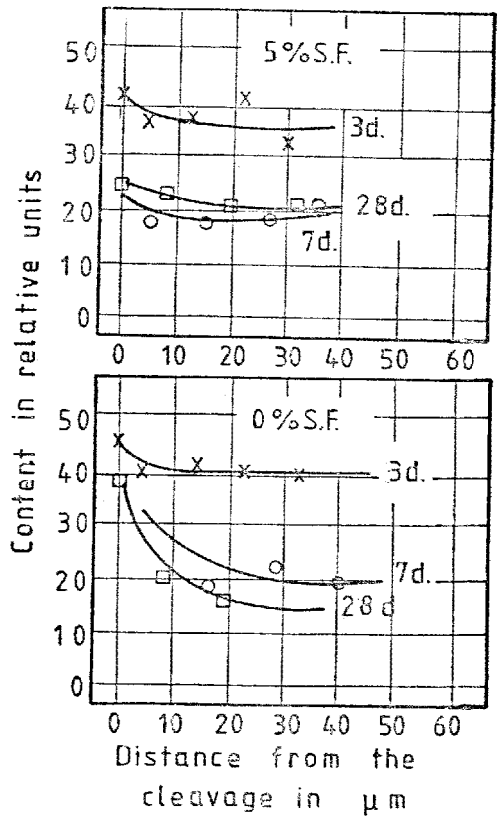

Fig. 3: The distribution of $CaCO_3$ measured by XRD

Table I: The polymerization of CSH phase of cement paste

Location	Age days	$\bar{M}n$	$\bar{M}w$	$\bar{M}n/\bar{M}w$	Mono- %	Di- %	Poly- %
Interfacial zone	7	226.5	114.9	2.79	54.5	6.30	39.2
Bulk	7	559.8	459.1	1.73	62.5	11.7	25.7

2.3. SEM of the interface

The morphology of both side of the interface was studied by SEM. Fig. 3 shows the corrosion of marble by the liquid phase of cement paste after contacting with it for one day. In Fig. 3, the right side shows the original polished marble surface; and the left the corroded surface, in which the round circles are the oolite structure formed by amorphous calcium carbonate.

2.4. Development of cleavage strength within the interfacial zone

The cleavage strength of the cubic composite sample of marble/cement paste with and without 5% silica fume is shown in Fig. 6 as functions of hydration time. From the obtained data a positive effect of silica fume addition of cleavage strength is apparent.

Chen Zhi-Yuan and Zahng Xio-Zhong, Department of Materials Science and Engineering, Tong-Ji University, Shanghai, China

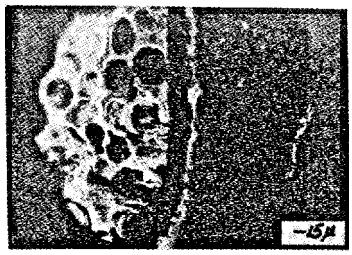

Fig. 4: The morphology of the marble before and after contacting with cement paste

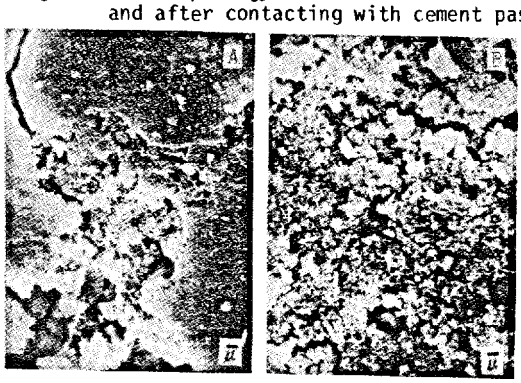

Fig. 5: SEM of the cement paste
A) without silica fume
B) with 5% silica fume

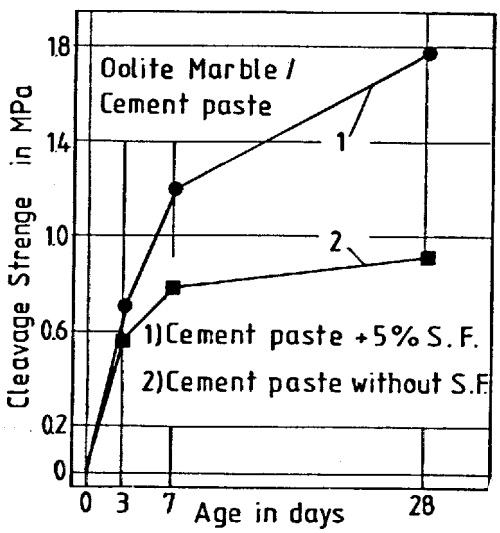

Fig. 6: The development of cleavage strength

3. Discussion

3.1. The distribution of hydrates within the interfacial zone

From the obtained data an inhomogeneous distribution of the individual phases within the interfacial zone between oolithic marble and cement paste is apparent. There is evidence that larger quantities of hydrate phases are located closer to the marble surface, apparently at the expense of the non-hydrated material. We believe that this uneven distribution is due to the presence of a water film and along with it to an absence of cement grains at the aggregate surface at the beginning of the hydration process. This point of view is in line with that proposed by Maso (1). Thus it may be assumed that the hydrate phases in the vicinity of the marble surface have been formed by a diffusion of the ions involved, from regions more distant. Another factor affecting the structure of the interfacial zone is the migration of Ca^{2+} and CO_3^{2-} ions from the marble surface towards the cement paste. There is an evidence that the oringinal polished surface was corroded by contacting with cement paste only one day as showing in Fig. 4. It can prove that the marble was dissolved by and entered into the liquid phase of the cement paste. Both factors result in the uneven, distribution of the phases present in the vicinity of the marble surface. The reasons for the decrease of $Ca(OH)_2$ content in the vicinity of the marble surface after longer hydration time is not obvious. The reasons for the decrease of the intensity of the peak belonging to the CSH-phase in the vicinity of the marble surface after longer hydration time is not obvious either. It may be speculated that this change may be related to changes in the degree of polymerization taking place parallely.

From the fact that in the cleavage tests the separation occured consistently along the marble-paste interface, it has to be concluded that this region is the weakest link in the system studied. This finding is in line with previous observation on systems with a variety of surfaces combined with OPC pastes.

An addition of silica fume resulted in an alteration of the structure of the interfacial zone and parallel to it in an expected decrease of the $Ca(OH)_2$ content. This may be the reason for the observed cleavage strength increase.

The distribution of $CaCO_3$ in the interfacial zone is shwon in Fig. 3. Expectedly the amount of $CaCO_3$ increased in the close vicinity of the marble surface indicating a diffusion of the CO_3^{-2} ions into the paste. A relative decrease of the amount of $CaCO_3$ within may explained by a gradual filling of the interfacial space with additions phases especially CSH-phase and $Ca(OH)_2$.

3.2. The polymerization of CSH-phase in the interfacial zone

The obtained data revealed difference in the degree of polymerization of the CSH phase within the interfacial zone and the bulk material. The degree of polymerization of the former is higher than that in the bulk. We assume that the existing differences were brought about by parallel differences in the c/s ratio of the CSH phase formed and/or by differences in the degree of packing of the material. Surprisingly, such differences in the degree of polymerization were not observed obviously in the presence of silica fume. But after adding silica fume, the amount of monomer decreases significantly either in the interfacial zone or in the bulk cement paste

due to the $Ca(OH)_2$ absorption by silica fume and formation of CSH. The monomer content decreases as the silica fume acts as a coupling agent which accelerates the conversion of the monomer into a dimer or polymer.

3.3. Modification of the marble/cement paste interfacial zone by addine silica fume

After adding silica fume the cleavage strength is improved. Fig. 6 shows that the cleavage strength can be increased significantly by adding 5% silica fume. At 28 days, the cleavage strength of composite samples with 5% silica fume in the cement paste increase approxinately twice, compared with the sample without silica fume. We realized that it due to the structure of the interfacial zone changed. From the Fig. 5a and 5b, we can find after adding 5% silica fume the $Ca(OH)_2$ film formed at closely contacting with marble surface is disapped and shows the roughly cleavage surface, it may increase the bond in the interface of marble/cement paste. Furthermore, from the data mentioned above we know that after adding 5% silica fume the $Ca(OH)_2$ decreases largely in the vicinity of the marble surface, while the amount of CSH gel increases slightly compared to that without silica fume. It indicates that the silica fume not only increases the amount of CSH but also acts by dispersion of fine particle to improve the structure and density of the paste.

Conclusion

1.
The distribution of the hydrates of cement pastes in the interfacial zone between the oolite marble and the cement paste is inhomogeneous. Much layer quantities of CSH and $Ca(OH)_2$ and large quantities of ettringite are present in the vicinity of the marble surface than further away from it.

2.
The degree of polymerization of the CSH phase in the interfacial zone is higher than that in the bulk cement paste.

3.
Adding 5% silica fume increases the amount of CSH-phase and decrease that of $Ca(OH)_2$ in the interfacial zone, thus improving the bond strength between cement paste and marble.

Acknowledgements

The authors gratefully acknowledge Professor Dr.-Ing. I. Odler for his helpful discussion and the work of Dr. Lu Ping and Mr. Zhao Wei-Min in helping to carry out the GPC experiment and DSC separately.

References

1. J.C. Maso: The bond between aggregates and hydrated cement paste. 7th International Congress on the Chemistry of Cement. Vol. 1, pp. VIII-1/3-15, Paris (1980).

2. L. Struble, J. Skalny and S. Mindess: A review of the cement-aggregate bond", C.C.R. Vol. 10, No. 2 pp. 277-286 (1980).

3. D.H. Hadley: The Nature of the Paste-Aggregate Interface. Ph.D. Thesis. Purdue University (1972).

4. B. Barnes: Morphology of the Paste-Aggregate Interface. Ph. D. Thesis, Purdue University (1975).

5. J. Grandet and J.P. Ollivier. 7th Internat. Congress on Chemistry of Cement. Vol. III, pp. VII-85, Paris (1980).

6. P.J.M. Monteiro and P.K. Mehta: Ettringite formation on the aggregate-cement paste interface. C.C.R. Vol. 15, pp. 378-380 (1985).

7. F.D. Tamas, A.K. Sarkar and D.M. Roy: Effect of variables upon the silylation products of hydrated cements. Proceedings of the Conference held at Sheffield on Hydraulic Cement Paste: Their Structure and Properties, pp. 55-72 (1976).

Wu Xuequan, Han Sufen, Bian Qinghan, Tang Mingshu,
Nanjing Institute of Chemical Technology, Nanjing, China.

1

Effect of Pretreatment of Aggregate Surface on the Properties of Concrete

2.3

ABSTRACT: It has been known that the interfacial zone is the weakest region of the concrete, which is more porous than in the matrix of cement paste and is characterized by the large oriented portlandite crystals. Potential microcracks may also exist in this region due to drying shrinkage and volume changes during hydration. These cracks tend to develop and propagate preferentially along the interfacial zone under external load and then penetrate through the matrix of cement paste, resulting in the failure of the concrete. In order to improve the properties of concrete, the composition and structure of the interfacial zone have to be modified, which may be realized by pretreating the aggregate with special reagents and methods to form an reactive surface, which will then react with the cement paste, resulting in enhancement of bond strength between cement paste and aggregate through the combination of physical, chemical and mechanical interlocking effects. Sulphuric acid solution, alum solution, acidized sodium silicate solution and acidized cement suspension etc. were used to pretreat the aggregates (siliceous, calcareous and dolomitic). The compressive and flexural strength of mortar bars and concrete bars were determined to evaluate the effect of pretreatment of aggregate on the properties of concrete. It is conclued from experimental results that both compressive and flexural strength were increased. The water permeability of mortar pies made from treated aggregates was lower than for control one, indicating the formation of a denser interfacial zone. The composition in the contact zone was examined by X-Ray diffraction.

Sabe-se que a zona interfacial é a região mais fraca do concreto, por ser mais porosa do que na matriz da pasta de cimento, e é caracterizada pelos grandes cristais orientados de porlandita. Nesta região também podem existir microfissuras potenciais devido à retração por secagem e às mudanças de volume durante a hidratação. Estas fissuras tendem a se desenvolver e propagar de preferência ao longo da zona interfacial, sob carga externa, e então penetrar através da matriz da pasta de cimento, resultando na ruptura do concreto. Com a finalidade de melhorar as propriedades do concreto devem ser feitas modificações na composição e estrutura da zona interfacial; tais modificações podem ser feitas pelo pré-tratamento do agregado com reagentes e métodos especiais para formação de uma superfície reativa. Esta superfície reagirá então com a pasta de cimento, dando como resultado um aumento da resistência da aderência entre pasta de cimento e agregado, por intermédio de combinação de efeitos bloqueadores físicos, químicos e mecânicos. Foram empregadas solução de ácido sulfúrico, solução de alúmen, solução de silicato de sódio acidificado e suspensão de cimento acidificado, etc., para pré-tratamento de agregados (silicosos, calcários e dolomíticos). Determinou-se a resistência à compressão e à flexão de barras de argamassa e de concreto, para avaliação do efeito do pré-tratamento do agregado sobre as propriedades do concreto. A partir dos resultados experimentais se concluiu que ambas as resistências, à compressão e à flexão, aumentaram. A permeabilidade dos corpos de prova feitos com agregados tratados foi menor que a do corpo de prova de referência, indicando a formação de uma zona interfacial mais densa. A composição na zona de contato foi examinada por difração de raio X.

1. INTRODUCTION

It has been known that the interfacial zone between cement paste and aggregate is the weakest region of the concrete for both mechanical properties and durabilities.

It is generally observed that the cracks tend to develop and propagate preferentially along the interfacial zone under external load and then penetrate through the matrix of cement paste, eventually leading to the failure of the concrete (1-4). Lyubimova (5) measured the microhardness across the cement paste-aggregate contact zone and found that the microhardness in the interfacial region is much lower than that in both cement paste and aggregate. Farran (6) found that there is a chromatic ring appearing in the interfacial zone when impregnating a dried and vacuated mortar with an organic dye solution for a certain time, indicating that this region is less dense.

By using SEM examination of acetate film replicas, Farran et al (7) described an aureole of hydrated paste surrounding the calcite aggregate, where cement hydration products were less dense than in the mass of the cement paste. They also found that the cement grains from the aureole had a greater tendency to pull away with the acetate film than did grains from the mass of cement paste, suggesting that the aureole provided less mechanical resistance.

Our previous experimental results demonstrated that the water permeability of a mortar pie made from acid activated slag is much lower than for unactivated one, while the only difference between them is the composition and structure of the interfacial zone, which indicates that the interfacial zone of the former is denser.

Maso (1) suggested that the surface of aggregates may adsorb water during the mixing in concrete processing, forming a several micrometers water film. There are only a few cement particles existing in such water film, while the hydrates in this region are formed by diffusion of the solved ions from the cement paste. The W/C ratio in this region is much higher than that in the bulk paste, resulting in an adequate space for crystal growth. Besides, oriented portlandite may be formed due to the surface effect of aggregates. In short, the interfacial zone is characterized by the large oriented portlandite crystals and higher porosity as well as lower bond strength. If the aggregate is soluble, the solved ions may take part in the reaction and the products could fill in the pores and cracks in the contact zone, resulting in a stronger bond strength. Furthermore, due to drying shrinkage, bleeding, volume changes during hydration and air introduced during mixing, cracks and pores at the cement-aggregate interface have been observed even prior to the application of any external load (8).

The above point of view might be used to explain the reason that why the interfacial zone becomes the weakest region of the concrete.

Grandet (9-10) measured the preferred orientation of $Ca(OH)_2$ near the boundary by X-Ray diffraction and found that the thickness of the interfacial zone is about 40-50 micrometers, depending on the nature of the aggregates and on the W/C ratio.

In order to improve the properties of the concrete, the composition and the structure of the interfacial zone should be modified, in other words, the bond strength between cement paste and aggregate has to be enhanced. Although the effect of the bond strength on concrete strength is a subject of controversy, however, there seem to be a relationship between bond strength and concrete strength as well as durability (7). Since the bond is a result of mechanical interlocking of cement hydration products with the aggregate surface and chemical reaction between aggregate and cement paste, the enhancement of bond strength may be realized by promoting the mechanical and chemical effects.

Massazza (11) reported that very strong silica-lime bond existing in the autoclaved concrete may be related principally to the epitaxic intergrowth of C-S-H crystalline deeply embeded in the sites of corroded surfaces of quartz grains. Such bond may be considered as a kind of ideal bond in the concrete.

Lybimova (12) has suggested to treat the sand by 10% HCl and water, and following activation of it by the saturated solution of $Ca(OH)_2$. Such treatment makes far better crystallization of C-S-H, resulting in the increase of mortar strength.

According to USA patent No. 395222 (13), the treatment of fly ash by 10% HCl, concrete strength in the age of 72 hours has been increased almost 2 times. The acid treated ash was not washed with water, therefore, the increase of concrete strength in the earlier dates is possible to relate with acceleration of cement hydration and hardening by the chlorides.

By preactivation of grains surface of aggregates made from blast-furnace and phospheric slags with dilute sulphuric acid, Ayapov (14) found that the adhesion strength of slag aggregates with cement paste increases 1.4-1.6 times. The author suggested that the new growth in the form of silica gel on grain surface of activated aggregates quickly reacted with hydrolysed calcium oxide of cement, forming C-S-H gel, and calcium hydrosulphoaluminate is also present in the interfacial zone.

Various studies have been performed to modify the interfacial zone by means of different ways based on different principles. However, it is believed that the most feasible and effective way of the modification of the interfacial zone is by pretreating the aggregate surface with special reagents and methods to form an active surface, which will then react with the cement paste, resulting in enhancement of bond strength between cement paste and aggregate through the combination of physical, chemical and mechanical interlocking effects. Besides, a new technique called "aggregate coating process" in concrete manufacture has been developed in Japan and China. By coating the aggregate grains with a low W/C ratio cement slurry, the bond strength as well as the concrete strength are increased or the cement expenditures are lowered. It is clear that the interfacial zone is denser in this case owing to the lower moisture content, while the composition in the interfacial zone seems to be no changes.

In this paper, various reagents were used to treat the inert aggregates according to the principles of both activating and coating process.

2. EXPERIMENTAL

Portland cement (grade 525) was used as the binder. For the preparation of mortar bars, silica sand from Ping-Tan beach or ground limestone (0.15-2 mm) was used as the fine aggregate, the ratio of cement to aggregate was 1:2.5, and the W/C ratio was 0.44. The concrete bars were composed of the same silica sand (0.3 mm, fine aggregate) and crushed dolomite (5-8 mm, coarse aggregate). The composition of the concretes are given in Table 1.

TABLE 1: Composition of concretes

	grade 500	grade 200
525 Ptl cement	1.00	1.00
Fine aggregate	1.00	2.85
Coarse aggregate	2.00	3.42
Water	0.36	0.6

The compressive and flexural strength were determined according to chinese national standard. The dimension of the specimen for both mortar bars and concrete bars were 4X4X16 cm.
The aggregate was mixed first with treating solution for 3 minutes to form a well distributed liquid film on the surface of aggregate grains. The volume of the solution was 20-30% of the total water consumption, when the amount of the solution was more than 30%, which may result in a high W/C ratio in the interfacial zone; while less than 20%, which may be not enough to wet out all the surface of the aggregate. After that, the cement was added and mixed with treated aggregate to form a low W/C ratio cement slurry surrounding the surface of the aggregate. Finally, the rest of the water was added in and mixed with the mixture. The mould with freshly mixed mortar or concrete bars was cured in a fog room, after 24 hours, the specimen were removed from the mould and then cured in water at 20°C until desired dates.
The composition of the solutions used for pretreatment were as follows:

No.1 Dilute sulphuric acid (code L)
H_2SO_4 : H_2O = 5.3 ml : 100 ml
No.2 Alum solution (code K)
Alum : H_2O = 14.7 g : 100 ml
No.3 Sulphuric acid and alum solution (code LK)
H_2SO_4 : alum : H_2O = 5.3 ml : 14.7 g : 100 ml
No.4 Acidized sodium silicate solution (code W)
H_2SO_4 : water glass : H_2O = 2.75 ml : 6.9 ml : 100 ml
(water glass used is a kind of industrial product of sodium silicate, which solid content is 35% and S/N ratio is 3.1)
No.5 Alum and water glass solution (code KW)
Alum : water glass : H_2O = 11.7 g : 6.9 ml : 100 ml
No.6 Sulphuric acidized cement suspension (code LO)
H_2SO_4 : cement : H_2O = 2 ml : 5 g : 100 ml

The water permeability of mortar pies made from treated and untreated aggregates were measured under low pressure by using a home made appratus.
The composition of the interfacial zone was examined by X-Ray diffraction.

3. RESULTS AND DISCUSSIONS

Various tests have been performed, while some of them with better effects are given fere.
The compressive and flexural strength of siliceous mortar bars are illustrated in figure 1. Sample "S" represents the control one. It is clear that both compressive and flexural strength of mortar made from treated silica sand are higher than for untreated one. The growth rate of compressive strength after 3, 7, and 28 days are 13-42%, 17-27% and 11-22% respectively; while 12-31%, 12-19% and 7-19% for flexural strength increment. It is conclued that the increment of compressive strength is higher than that of flexural strength and the increment of early strength is higher than for the strength at later dates.
Sample SLK shows a distinct increasement in early strength, the compressive and flexural strength of which after 3 days increases by 41.9% and 31% respectively. Meanwhile, sample SW shows the similar results. This could be explained in part as the acceleration of cement hydration and hardening by alkali sulphate.

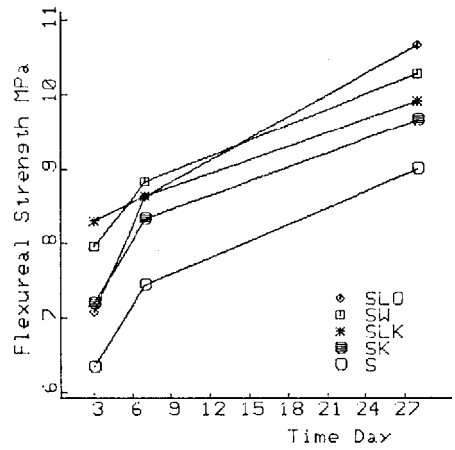

(a) Flexural strength

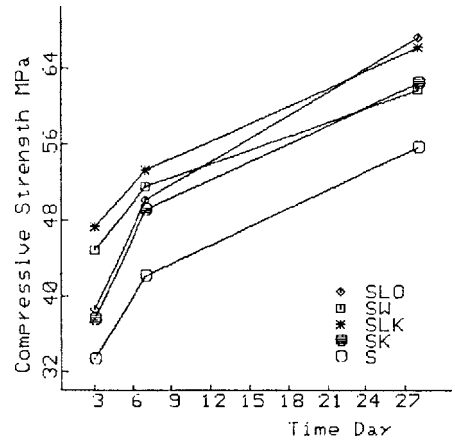

(b) Compressive strength

FIG. 1: Compressive and flexural strength of siliceous mortar vs curing time

The reactive silica gel (in sample SW) and alumina gel (in sample SK and SLK) may quickly react with $Ca(OH)_2$ derived from cement paste to form calcium hydrosilicate and calcium hydroaluminate (the later may further react with gypsum to form calcium hydrosulphoaluminate). These hydrates could fill in the pores and cracks in the interfacial zone, resulting in a denser structure. Thus, the bond strength as well as concrete strength could be enhanced due to the modification of the composition ans structure of the interfacial zone.
Comparing with sample SK, sample SLK is more effective on the improvement of the strength owing to the higher acidity, which may be favorable for the acceleration of hydration. Besides, the acidized surface of silica sand is more reactive. It is suggested that there are silic-hydroxy radical (-Si-OH) on the silica surface, resulting in the hindrance to the reaction with $Ca(OH)_2$. The following reaction might

Wu Xuequan, Han Sufen, Bian Qinghan, Tang Mingshu,
Nanjing Institute of Chemical Technology, Nanjing, China.

occur during acidization:

$$-Si-OH + H^+ = -Si- + H_2O$$

The free valence bond of silicon could make the reaction between silica and calcium hydroxide easier. The above Lybimova's (12) tests may be used to support this suggestion.

It is noted that, for sample SLO, the strength after 28 days is the highest in all case, although the increment of early strength is less obvious. The development of the strength within 7 to 28 days is faster than the others, which is illustrated by the slope of the curve (see Fig. 1). It is believed that the sulphuric acidized cement suspension is composed of gypsum, silica gel, alumina gel, ferric gel and hydrates of cement. The species are favorable for the hydration of cement and for the formation of a denser interfacial zone.

Figure 2 shows the effects of pretreatment of calcareous aggregate on the mortar strength.

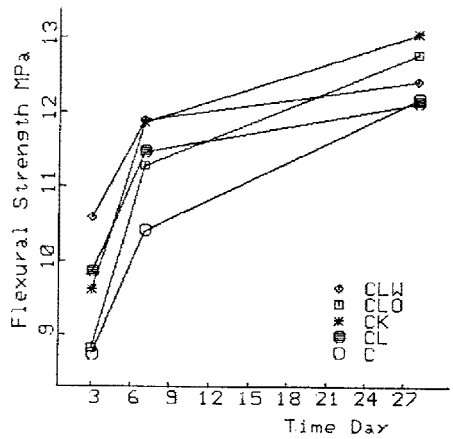

(a) Flexural strength

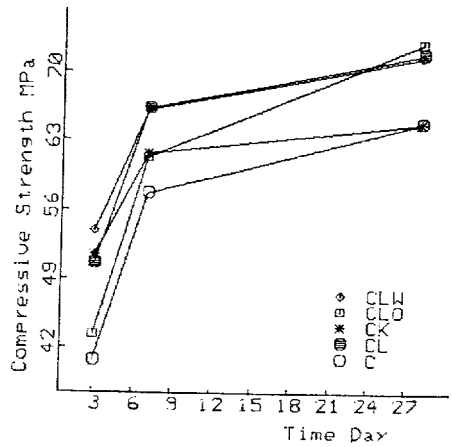

(b) Compressive Strength

FIG. 2: Compressive and flexural strength of calcareous mortar vs curing time

Sample C is the control one. Sample CLW represent that, the ground limestone is treated first by dilute sulphuric acid in a minute and then by water glass solution. The composition of "LW" solution is the same with that of "W" (No.4).

Both compressive and flexural strength of mortar bars made from treated limestone is higher than for untreated one. For compressive strength, the growth rate after 3, 7, and 28 days are 7-33%, 6-15% and 0-12% respectively; while 10-21%, 8-14% and 0-7% for flexural strength. Indeed, the absolute values of strength increment for calcareous mortar are also considerable and similar to that for siliceous mortar, although the relative increment is lower, because the control sample C possesses higher strength level in comparison with sample S.

Sample CK is characterized by higher flexural strength; while sample CL and CLW by higher compressive strength.

It is clear that, the calcite could react with sulphuric acid forming gypsum. Besides, some corrosion cavities may be formed on the grain surface, which provide a space for embedment of hydrates. This supposal may be supported by the fact that, the sample CLW possesses higher strength owing to the embedment of C-S-H, derived from the reaction of silica gel and $Ca(OH)_2$. Nevertheless, the effect of alkali sulphate is unnegligible.

The feature of sample CLO are similar to that of sample SLO.

Figure 3 shows the development of concrete strength within half year.

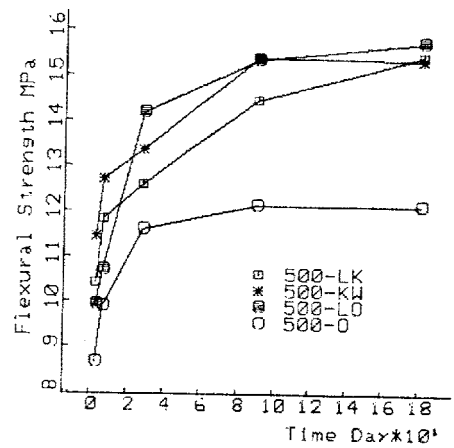

(a) Flexural strength for grade 500

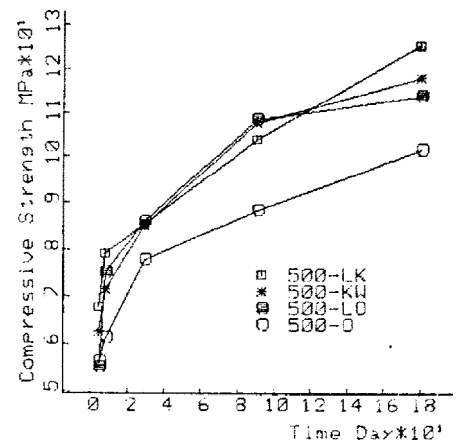

(b) Compressive strength for grade 500

Wu Xuequan, Han Sufen, Bian Qinghan, Tang Mingshu,
Nanjing Institute of Chemical Technology, Nanjing, China.

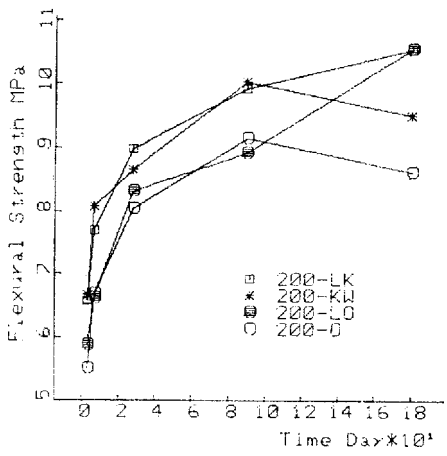

(c) Flexural strength for grade 200

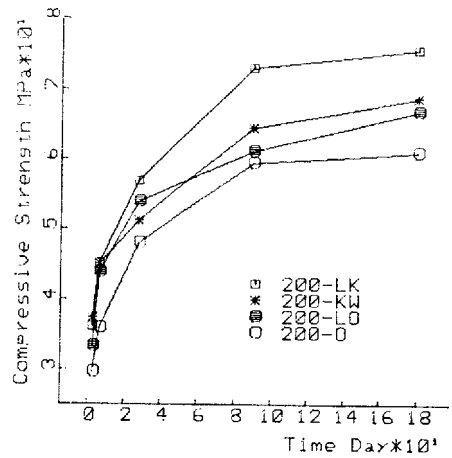

(d) Compressive strength for grade 200

FIG. 3: Compressive and flexural strength of concrete (grade 500 and 200) vs curing time

Sample 500-0 and 200-0 represent the control one of concrete grade 500 and 200 respectively. It can be seen first that, the values of concrete strength are much higher than the designed values, for instance, the compressive strength of concrete bars after 28 days are 78.8 and 47.9 MPa for sample 500-0 and 200-0 respectively, while the designed values are only 49 and 19.6 MPa, which may be attributed to the smaller size of the coarse aggregate (5-8 mm). However, the strength of concrete made from treated aggregates are still higher than for untreated one in all case, for example, the increment of compressive and flexural strength after 180 days are 11-22% and 27-30% respectively for concrete grade 500; while 10-24% and 10-23% for grade 200. The increment of flexural strength of concrete grade 500 is higher than that of compressive strength as contrasted with the case of silica and calcite mortar strength, which is valuable for concrete, because the flexural strength is generally low in concrete material. Among all samples, it seems that, sample LK produce either higher early strength or higher strength at later dates. But unfortunately, the treating solution LK is acidic, which could attack the concrete mixer and react with the remainder in the mixer, resulting in the reduction of concentration of the solution and interference to the pretreating process. So that, acidic pretreating reagents may not be expected in practice, unless above problems could be solved. However, the solution KW is neutral, and LO is somewhat basic. Both of them also generate better results and may preferably be accepted by the concrete manufacturer.

It is concluded that, the effect of pretreatment of aggregate with above reagents on mortar or concrete strength is positive. Nevertheless, the results are derived from our preliminary tests in laboratory; the real effect in construction site needs to be tested further, in other words, the optimum composition and concentration of the pretreating solution have to be studied in accordance with the realistic condition, such as the composition of concrete, the nature and size of aggregates and so on.

In order to eliminate the influence of impurities from experimental results, chemical pure reagents were used, but for economic consideration, industrial reagents even waste products without harm to the quality of concrete could be used.

The effect of pretreatment of aggregate on the composition and structure of interfacial zone were studied as follows:

The water permeability of mortar pies made from treated or untreated aggregates were measured under low pressure by using a home made apparatus. The mortar pies (ϕ7X1 cm) are composed of portland cement and ground limestone as fine aggregate, the A/C ratio is 4.0 and W/C ratio is 0.625.

Figure 4 shows the water permeability of mortar pie treated with silica gel solution is much lower than for untreated one, indicating the former is denser in microstructure of the interfacial zone.

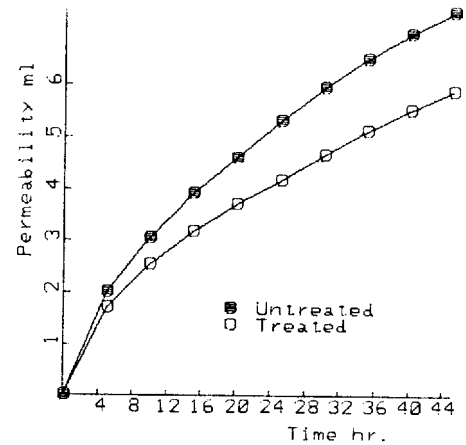

FIG. 4: Water permeability of mortar pie vs testing time

The above pretreating solutions contain some reactive components, such as, silica gel, alumina gel and sulphates, which may generally be used as admixtures for accelerating the hydration and hardening of cement. In order to verify the effect of these solutions on the modification of interfacial zone, the same solution used as admixture instead of aggregate pretreating reagent was mixed together with cement, aggregate and the rest of the water. By comparing the mortar strength derived from these two different procedyres, it is found that, both compressive and flexural strength of mortar made from silica sand

treated by solution LK are higher than that of the siliceous mortar with admixture solution LK. For instance, the growth rate of compressive strength after 3, 7 and 28 days are 16.04%, 23.26% and 11.83% respectively; while 7.05%, 10.7% and 7.25% for flexural strength increment, although the mortar strength in the later case is still higher than for control one. The fact give a evidence for the effect of pretreatment of aggregate on the modification of interfacial zone.

By using X-Ray diffraction, the composition and the prefered orientation of $Ca(OH)_2$ were examined. When a calcite aggregate was treated with solution LO and alum, the degree of orientation of $Ca(OH)_2$ is 1.04 (on the surface of cement paste side of the interface and calculeted by equation: $I = I_{(001)}/0.74/I_{(101)}$); while 2.01 for the control one, indicating the prefered orientation of $Ca(OH)_2$ is eliminated. Besides, the amount of portlandite is decreased to 83% (estimated by the intensities of diffraction peaks), showing 17% $Ca(OH)_2$ has been consumed to form hydrates. C-S-H gel is probably present, but the peaks were difficult to define. Ettringite was also found. In short, the composition of the interfacial zone could be modified by the pretreatment of aggregate.

4. CONCLUSION

4.1 By pretreating the inert aggregate with special reagents, the mortar strength and concrete strength could be increased, and the composition and structure of interfacial zone have been modified, result-in a denser interface, which is favorable for the properties of concrete.

4.2 The mechanism of pretreatment of aggregate may be explained as the aggregate surface is activated, and then react with cement paste to form hydrates, which might fill in the pores and cracks. Meanwhile the W/C ratio in the interfacial zone is reduced in accordance with coating process. In short, the improvement of the properties of concrete is a result of the combination of physical, chemical and mechanical interlocking effects.

4.3 In order to obtain the best effects, optimum composition and concentration of the pretreating solution have to be studied further according to the composition of concrete and the nature and size of the aggregates.

REFERENCES

1. J. Glurlich, The effect of microcracking in time dependent deformations and long term strength of concrete. International conference on the structure of concrete, cement and concrete association, 1968, 82-92, London.

2. M. Regourd, Microstructures et proprietes des ciments, mortiers et betons, ciments, betons, plastres, chaux, No. 734, 1/82.

3. S. Mindness and S. Diamond, A device for direct observation of cracking of cement paste and mortar under compressive loading within a scanning electron microscope, Cem. Concr. Res. Vol 12 (1982).

4. Wu Zhong-wei, Liu Bao-yuan, Xie Song-shan, Interfacial zone in cement-based composite material, Proceeding of international symposium on bond between cement pastes and other materials, A28-A32, 17-19th, Nov. 1982, Toulouse, France.

5. T. Yu. Lyubimova and E. R. Pinus, Crystallization structure in the contact zone between aggregate and cement in concrete, Colloid, J. USSR, 24(5), 491-498 (1962).

6. J. Farran, Contribution mineralogigue e l'etude de l'adherence entre les constituants hydrates des ciment et les materiaux emropes, Revue des materiaux de construction, no. 490-492 (1956).

7. L. Struble and J. Skalny, A review of the cement aggregate bond, Cem. Concr. Res. Vol. 10, 277-286 (1980).

8. J. C. Maso, The bond between aggregate and hydrated cement paste, 7th International congress on the chemistry of cement, Vol. I, VII 1/3-15, Paris, 1980.

9. J. Grandet, J. P. Ollivier, Orientation of hydration products near aggregate surface, idem, Vol. III, VII 63-68.

10. J.Grandet, J. P. Ollivier, New method for the study of cement-aggregate interfaces, idem Vol.III VII 85-89

11. F. Massazza and M. Pezzuoli, Cement paste-quartz bond in autoclaved concretes, idem, Vol.III, VII 16-21.

12. Lyubimova, Vliyanie sostoyaniya poverhnosti kvartsevogo zapelnitel'a na kristallizatsionnoe tverdenie tsementa i svoistva tsementnogo kamnya v zone kontakta, "Kolloidnyi zhurnal", V. 29, No.4, 1964, P.546.

13. USA Patent CI 106-97 (C04B,7/02) No. 395222, filed 10.04, 1974 (Ser. No. 459587), Patented 27.04, 1976
Bainton John W. Addition of acidulated pozzolan to concrete and concrete products.

Wang Jia, Liu Baoyuan, Xie Songshan, Engineers; Wu Zhongwei, Professor, Consultant
Research Institute of Building Materials, Beijing, China

IMPROVEMENT OF PASTE-AGGREGATE INTERFACE BY ADDING SILICA FUME

SUMMARY: The mean size and orientation index of CH and AFt crystals in interface layer between portland cement paste and calcite aggregate are determined by X-ray diffractometer. The effective fracture energy and microhardness at interface and concrete strength as well are also investigated.

By adding 5% wt. silica fume into cement paste, the mean size and orientation index of CH crystal are reduced and much denser structure of interface layer with higher micro-hardness and fracture energy is obtained. The increase of concrete compressive strength amounts to more than 10%.

The explaination of silica fume effects on the paste-aggregate interface is also proposed.

Por difratometria de raio-X se determinou o tamanho médio e o índice de orientação dos cristais de CH e AFt na camada interfacial entre a pasta de cimento portland e o agregado de calcita. Foram também investigadas a energia efetiva de fratura e a microdureza na interface, e a resistência do concreto.

Com a adição de 5% em peso de microssílica na pasta de cimento, foram reduzidos o tamanho médio e o índice de orientação do cristal de CH e se obteve estrutura mais densa da camada de interface com microdureza e energia de fratura mais altas. O aumento da resistência do concreto à compressão é da ordem de mais de 10%.

Também se dá a explicação dos efeitos do fumo de sílica sobre a interface pasta-agregado.

Wang Jia, Liu Baoyuan, Xie Songshan, Engineers; Wu Zhongwei, Professor, Consultant
Research Institute of Building Materials, Beijing, China

INTRODUCTION

Research results show that there are some imperfections in interface layer between portland cement paste and aggregate, such as orientation and large size of crystals, large porosity and pore size. So the interface layer is believed to be a weak part in concrete structure, and must be improved in order to get better properties of concrete.

In this paper, the mean size and orientation index of CH and AFt crystals in interface layer between portland cement paste and calcite aggregate are determined by X-ray diffractometer. The effective fracture energy and microhardness at interface and concrete strength as well are also investigated.

Adding silica fume into cement paste can reduce the mean size and orientation index of CH crystal and obtain much denser structure. The reason is that the particles of silica fume play the same part as nuclei in early period of hydration, then the active SiO_2 in silica fume reacts with CH crystals and C-S-H gel is formed. As the structure of interface layer is improved with adding silica fume, both effective fracture energy and microhardness at interface are improved, hence the properties of concrete.

EXPERIMENTAL PROCEDURE

One type of portland cement and one type of silica fume are used in this study. Their chemical compositions are given in Table 1.

Table 1 Chemical compositions of portland cement and silica fume

	CaO	SiO_2	Al_2O_3	Fe_2O_3	SO_3	MgO	K_2O	Na_2O	TiO_2	P_2O_3	Ignition loss
portland cement	63.26	19.94	5.79	4.98	2.44	1.08	0.48	0.11	0.28	-	1.92
silica fume	1.15	74.93	3.41	1.88	-	3.30	1.20	0.61	0.09	0.14	12.43

Calcite aggregate and water reducing agent named UNF are also used.

The determination of mean size of CH and AFt crystals is based on Scherrer equation.[1] The orientation index of CH crystal is defined and determined by the same way as reference (2) and (3). The test specimen used for measurement of effective fracture energy[4] of interface is shown in Fig.1.

The mix proportion of concrete for determination of strength is listed in Table 2.

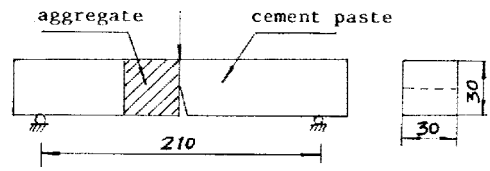

Fig.1 Determination of effective fracture energy by slow-bending method
($\frac{a}{d}$=0.4, a=crack length, d=specimen height)

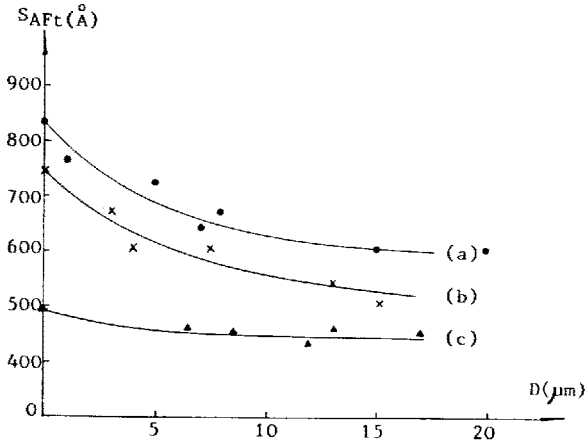

Fig.2 Mean size of AFt in interface layer with respect to interfacial distance (28 days)
(a) W/C = 0.40 (b) W/C = 0.30
(c) W/C = 0.23

RESULTS

The mean size of AFt crystal normal to plane (110) in interface layer between porltand cement paste and calcite agregate is shown by curves in Fig.2. The mean size of AFt crystal decreases with the interfacial distance from the aggregate surface on which the biggest one lies. Beyond the range of 5-15 um from the interface crystal mean size is almost the same. Both

Wang Jia, Liu Baoyuan, Xie Songshan, Engineers; Wu Zhongwei, Professor, Consultant
Research Institute of Building Materials, Beijing, China

Table 2 Concrete mix proportion

No.	silica fume (%)	cement (kg/m^3)	coarse aggregate (kg/m^3)	fine aggregate (kg/m^3)	water (kg/m^3)	UNF (%)
0-0	0	510	1312	392	195	0.5
0-2	2	500	1312	392	195	0.6
0-5	5	486	1312	392	195	0.8
0-10	10	464	1312	392	195	1.0

mean size and range of variation decrease with W/C ratio. When W/C ratio is 0.40, the mean size of AFt crystal varies from 840 Å to 560 Å. When W/C ratio is 0.30, it varies from 740 Å to 510 Å, and W/C is 0.23, from 500 Å to 450 Å.

The mean size of CH crystal normal to plane (001) in interface layer is shown by curves in Fig.3, similar to those in Fig.2. The mean size of CH crystal is much larger than that of AFt crystal. It is also shown that adding silica fume into cement reduces the mean size of CH crystal.

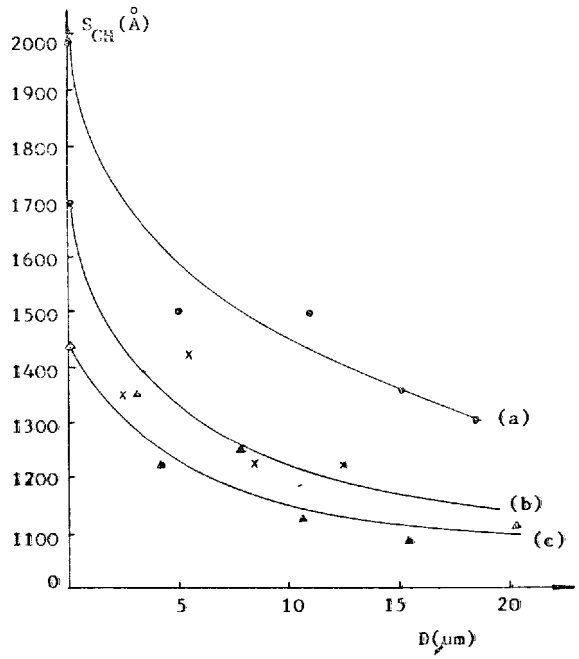

Fig.3 Mean size of CH in interface layer with respect to interfacial distance (7days)
(a) W/C = 0.30
(b) W/C = 0.30, 5% silica fume, 0.5% UNF
(c) W/C = 0.23

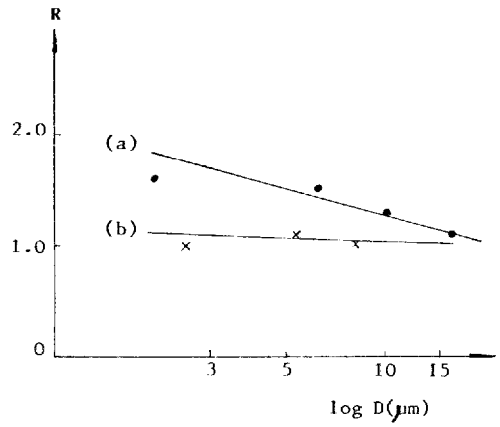

Fig.4 Effect of silica fume on the orientation index of CH at same W/C (7 days)
(a) W/C = 0.30, 0.5% UNF
(b) W/C = 0.30, 5% silica fume, 0.5% UNF

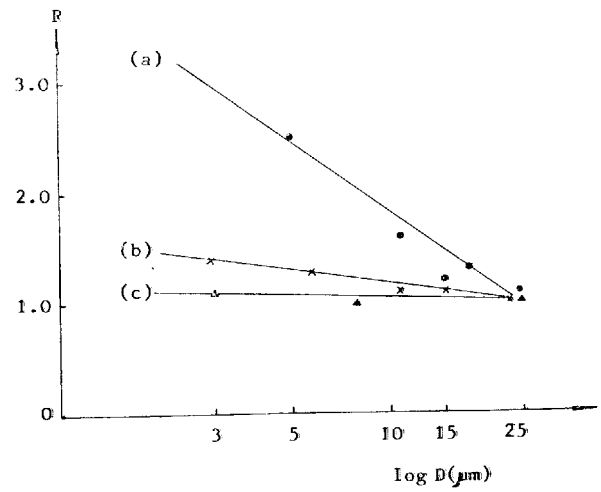

Fig.5 Effect of silica fume on the orientation index of CH at same flow (7 days)
(a) W/C = 0.30
(b) W/C = 0.39, 5% silica fume
(c) W/C = 0.47, 10% silica fume

Wang Jia, Liu Baoyuan, Xie Songshan, Engineers; Wu Zhongwei, Professor, Consultant
Research Institute of Building Materials, Beijing, China

The orientation indices of CH crystal under the conditions of maintaining same W/C and same flow when adding silica fume are given in Fig.4 and Fig.5. Whether at same W/C ratio or same flow, adding 5% wt. silica fume or above can make the CH crystals in interface layer disorientated, namely, the orientation index of CH approaches to 1.0. Fig.6 also shows the effect of silica fume content on the orientation index of CH crystal at the interfacial distance 1 μm [$R_{(D=1\,\mu m)}$].

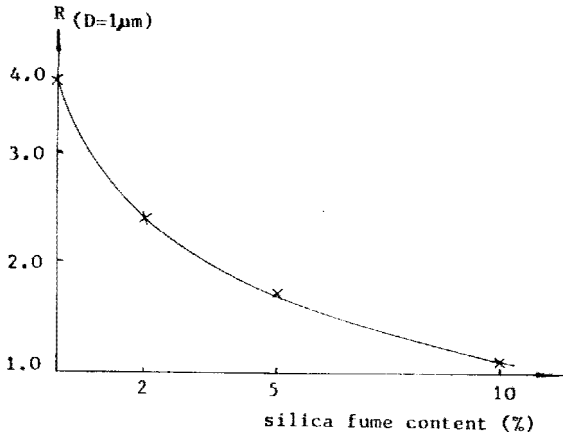

Fig.6 Relation between silica fume content and orientation index of CH at interfacial distance 1 μm

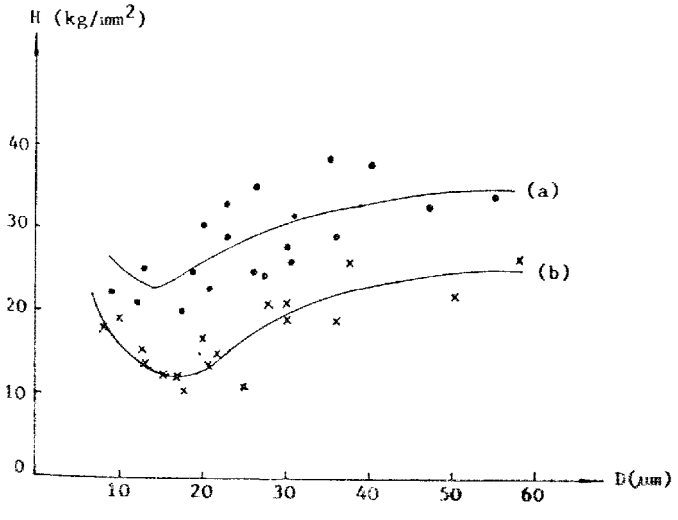

Fig.7 Microhardness in interface layer (32 days)
(a) 0% silica fume
(b) 5% silica fume

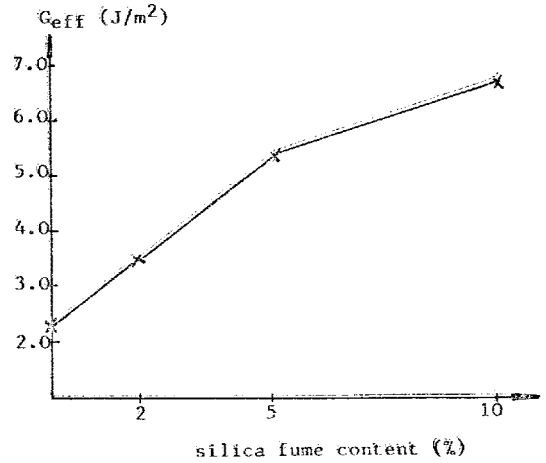

Fig.8 Relation between effective fracture energy of interface and silica fume content (28 days)

The microhardness and effective fracture energy at interface layer are given in Fig.7 and Fig.8. The data of concrete strength are shown in Table 3. It is found that by adding 5% wt. or more silica fume into cement, higher microhardness and effective fracture energy are obtained and increase of concrete compressive strength amounts to more than 10%.

Table 3 Concrete strength

No.	Silica fume (%)	Modulus of rupture kg/cm²		Compressive strength kg/cm²	
		7 days	28 days	7 days	28 days
0-0	0	35.9	44	415	570
0-2	2	35.1	50	490	637
0-5	5	42.3	52	501	632
0-10	10	41.5	50	466	653

DISCUSSION

Reduction of initial setting time and free water content during the early hydration stage due to large water requirment was believed by some authors to be responsible for decreasing the orientation index of CH crystal by adding silica fume. This explanation may not be true. The results given in Table 4 show that initial setting time is almost the same at different silica fume contents. Moreover, the results

mentioned above also show that the orinetation index of CH crystal decreases with silica fume content at same W/C or same flow. Therefore the influence of water requirement can be ignored.

Table 4 Relation between content of silica fume and initial setting time

Silica fume (%)	Sandard consistency (%)	Initial setting	Final setting
0	23.75	2:33	3:35
5	24.00	2:42	4:25
10	25.00	2:45	4:42

A hypothesis is proposed that during early hydration stage of portland cement containing silica fume, very fine particles of silica fume play the same part as nuclei, on which CH germs attach. With the process of hydration, the active SiO_2 in silica fume reacts with CH crystal and produces C-S-H gel, which causes the reduction of both pores size and porosity, as shown in Table 5. The photographs of scanning electronic microscope shown in Fig.9 also prove that adding silica fume gets a denser structure of interface layer. Because the mean crystal size reflects the size of space in which it grows, the smaller the space for crystal to grow, that is the smaller the pore, the samller will be the mean crystal size. Addition of silica fume and low W/C ratio reduce both pore size and porosity, which restrict the growth of crystal. Consequently, the mean crystal size decreases.

Table 5 Effect of silica fume on the pore size distribution of cement paste (28 days)

Silica fume (%)	Most probable diameter of pore (Å)	Per cent of pores with diameter below 250 Å (%)
0	342	38.7
5	250	75.6

The particles of silica fume in interface layer interfere the orinetation of CH crystals. CH crystals no longer grow on the surface of aggregate with the plane (001) parallel to it, instead they grow on the surface of silica fume particles. Furthermore, the reaction between SiO_2 and CH crystals reduces the amount of CH crystal orientated in interface layer. These are the main reason why the orientation index of CH crystals decreases when adding silica fume. The different growth patterns of CH crystals with and without silica fume addition are schematically shown in Fig.10.

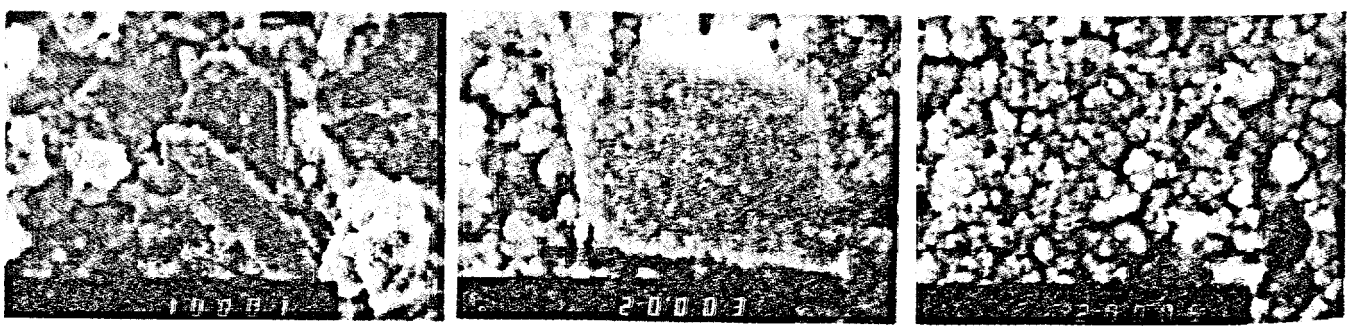

(a) (b) (c)

Fig.9 SEM photographs of interface layer (3 days)
(a) without silica fume (1000 X)
(b) 5% silica fume (2000 X)
(c) 20% silica fume (2000 X)

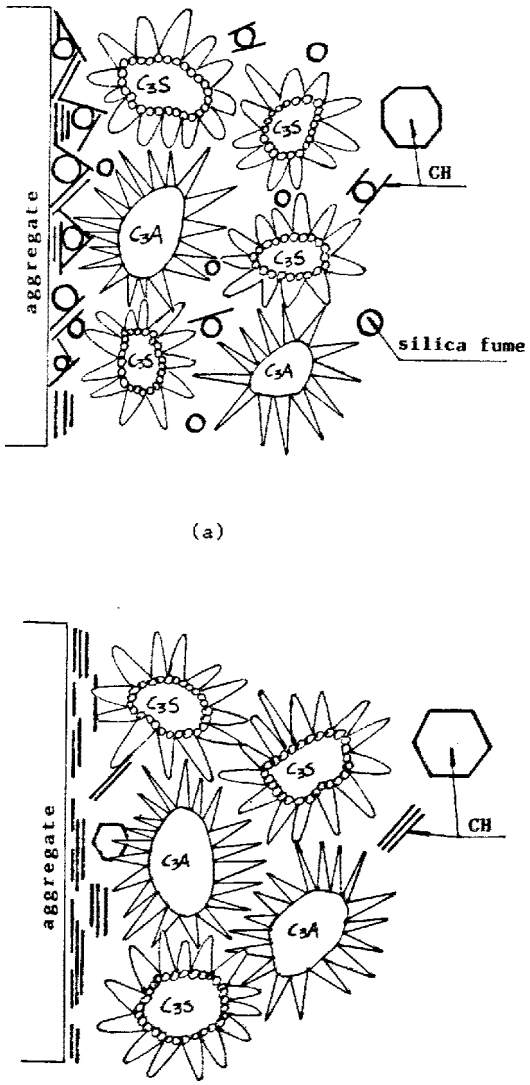

Fig.10 Different growth patterns of CH crystals (Schematic)
(a) with silica fume
(b) without silica fume

After adding silica fume, the mean size and orientation index of CH in interface layer decrease. The structure of interface layer is improved. Therefore, effective fracture energy and microhardness at interface and the strength of concrete as well are improved.

The mean crystals size determined by X-ray diffractometer can also be used to evaluate the structure of interface layer as the orientation index of CH crystal. Having a better knowledge of the porosity and pore size in interface layer, one can visualize the structure of interface layer.

CONCLUSION

(1) The mean size of AFt and CH normal to plane (110) and (001) respectively in interface layer between portland cement paste and calcite aggregate are determined by X-ray diffractometer, the former varies within the range of 400-900 Å, while the latter within the range of 1000-2000 Å. The mean size of crystals decreases with interfacial distance from the aggregate surface on which the biggest one lies. Beyond the range of 5-15 μm from interface the mean size of crystals is almost the same.

(2) Adding silica fume into portland cement decreases the mean size and orientation index of CH crystal. The active SiO_2 in silica fume reacts with CH crystals and produces C-S-H gel. So the interface structure between paste and aggregate is improved by adding silica fume.

(3) As the result of improvement of interface structure with addition of silica fume, the effective fracture energy and microhardness at interface increase, the strength also increases an amount more than 10%.

REFERENCE

(1) H.P. Klug, L.E. Alexander; X-ray Diffraction Procedures for Polycrystalline and Amorphous Materials, A Wiley-Inter-Science, 1974

(2) J.P. Ollivier, J. Grandet; 7th Inter. Congr. on Chem. of Cement, Paris, Vol.III, Part VII-85 (1980)

(3) Wu Zhongwei, Liu Baoyuan, Xie Songshan; Liasons Pates de Ciment Materiaux Associes, Colloque International, Toulouse France, A.28 (1982)

(4) P.E. Petersson, Cement and Concrete Research, Vol.10, p.78 (1980)

K. L. SCRIVENER & P. L. PRATT, Department of Metallurgy & Materials Science, Imperial College, Prince Consort Road, London SW7 2BP, UK.

A preliminary study of the microstructure of the cement/sand bond in mortars

SUMMARY: Two electron optical techniques have been used to study the microstructure of the interface between sand and cement in mortars. These are the examination of fracture surfaces using secondary electrons and back-scattered electron (bse) imaging of flat polished surfaces, both in the SEM.

This study shows that a surface layer of C-S-H forms around the sand grains during the first day of hydration by a through solution mechanism. The concentration of AFt (ettringite) also appears to be higher in the interfacial region.

There is no evidence for the formation of an epitaxial layer of calcium hydroxide around the sand grains. Some crystals of calcium hydroxide grow adjacent to the sand grains and may tend to be oriented with their C-axes parallel to the surface of the sand. These large crystals tend to predominate on fracture surfaces due to the ease with which calcium hydroxide cleaves along its basal plane.

The relative movement of the sand and cement grains during mixing, and possibly settling of the sand grains before the cement paste sets, may lead to regions of low paste density around the sand grains and to areas of localised bleeding at the interface in which large calcium hydroxide crystals precipitate.

Através de utilização de duas técnicas de óptica eletrônica se estudou a microestrutura da interface entre areia e cimento em argamassas. Estas duas técnicas são o exame das superfícies de fratura usando imagem de elétrons secundários e imagem de elétron retro-dispersa (bse) de superfícies polidas, ambas no SEM.

Este estudo mostra que a camada de superfície de C-S-H se forma ao redor do grão de areia durante o primeiro dia de hidratação por um mecanismo direto de solução. A concentração de AFt (etringita) também parece ser maior na região interfacial.

Não há evidência de formação de uma camada epitaxial de hidróxido de cálcio ao redor dos grãos de areia. Alguns cristais de hidróxido de cálcio crescem adjacentes aos grãos de areia e podem tender a serem orientados com seus eixos - C paralelos para a superfície da areia. Há tendência de predominância dos cristais grandes sobre as superfícies de fratura, devido à facilidade com que o hidróxido de cálcio cisalha ao longo do seu plano de base.

O movimento relativo dos grãos de areia e de cimento durante a mistura, e possivelmente a acomodação dos grãos de areia antes que a pasta de cimento dê pega, pode levar a regiões de baixa densidade de pasta ao redor dos grãos de areia e a áreas de exudação localizadas na interface, nas quais grandes cristais de hidróxido de cálcio se precipitam.

INTRODUCTION

An understanding of the nature and properties of the bond between cement paste and aggregate or sand is essential to the understanding of the properties and behaviour of concretes and mortars.

Struble et al [1] have reviewed work on the nature and properties of the cement aggregate bond; they conclude that there is evidence of epitaxial growth of certain hydration products on the surface of the aggregate. However there appears to be considerable controversy as to the details of this epitaxial growth.

From the study of the contact zone between cement and glass surfaces [2] and of the interfacial zone around aggregates in Portland cement mortar [3], Barnes, Diamond and Dolch proposed that a duplex film is formed at the aggregate surface. The part of this duplex film in contact with the agggregate surface was reported to be $Ca(OH)_2$ preferentially orientated with c-axis normal to the surface of the aggregate, with the outer part of the duplex film being a layer of C-S-H gel [2]. Beyond the duplex film large well-formed crystals of $Ca(OH)_2$ with their c-axes roughly parallel to the surface, were observed [3].

Several workers have used the specimen configuration developed by Farran [4] in which cement paste is cast onto a large flat piece of aggregate (all sealed within the same container). This configuration facilitates examination of the morphology of the interfacial region in the SEM when the specimen is fractured parallel to the interface. The concentration and orientation of phases in the interfacial region can also be analysed by the technique developed by Grandet and Ollivier [5,6]; which involves successive abrasion of the cement paste side of the interface surface, followed by examination by X-ray diffraction analysis of the compounds on the surface. This technique has shown that there is a preferred orientation of the $Ca(OH)_2$ crystals up to 50μm or more from the interface [6,7,8]. Increased concentrations of ettringite in the interfacial zone have also been reported [6,8,9].

It is not however clear whether these gross changes, occurring over several tens of microns, will be present in concretes and mortars with a realistic size range, particle shape and concentration of aggregate and sand. This paper presents the results of a preliminary investigation into the microstructure of the interfacial region in mortars. In addition to the examination of fracture surfaces, backscattered electron (bse) images of polished sections have also been studied. The bse images clearly reveal the different cement phases at fairly high resolution (∿50nm) and allow extensive areas of random sections to be examined [10,11,12].

MATERIALS & EXPERIMENTAL

In this preliminary study mortars were prepared from ordinary Portland cement and a commercial sand in order to simulate practical conditions as closely as possible.

The cement was obtained through The Cement & Concrete Association, UK. The composition by Bogue and by quantitative X-ray diffraction analysis (QXDA) is given in table 1.

TABLE 1

	C_3S	C_2S	C_3A	C_4AF	$C\bar{S}$	Free CaO
Bogue	59.0	13.7	8.5	9.4	4.6	1.1
QXDA	67	15	5	6	-	

The development of microstructure during the hydration of this cement has been reported elsewhere [11] and is similar to the reported microstructural development of other OPCs (e.g. [13])

The sand came from the Thames Valley, UK. It was graded from 710-120μm. Mineralogically it was a Sublithic Aranite (i.e. 75-95% quartz). Grains other than quartz were not examined in the microstructural study. The sand was dispersed on an aluminium stub and examined in the SEM, a typical micrograph is shown in fig 1. The roughness of the particles varies considerably, some grains being fairly smooth, whilst others have many crevices.

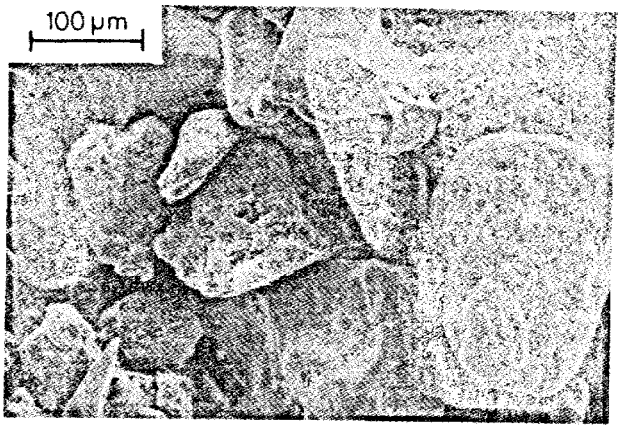

FIG 1. Sand grains (secondary electron image, SEI)

The mortar was mixed with a water to cement ratio of 0.5 and a sand to cement ratio of 1:1. The sand to cement ratio is lower than would be found in practice (∿3:1), but it was found difficult to avoid excessive void formation around the sand grains at higher ratios in the small specimens. The mortar was mixed for 3 minutes and then cast into small polythene tubes (1cm wide x 3cm high). At appropriate times after mixing the samples were freeze-dried. After fracture surfaces had been prepared, the samples were resin impregnated to facilitate the preparation of polished sections. Sections 2mm thick were cut from the impregnated samples with a diamond slitting wheel. These were polished to 1μm using diamond pastes on lapping cloths. The fracture surfaces were sputter coated with gold and the polished sections were coated with carbon for examination in the scanning electron microscope (a JEOL 35CF fitted with a split ring, solid state backscattered electron detector).

RESULTS AND DISCUSSION

Observations of Fracture Surfaces

Fracture surfaces were examined from specimens of between 1 and 30 days in age. Fig 2 shows the microstructure of a 4 day old specimen, which is typical of the the appearance of all the mortars at this low magnification. Many sand grains are exposed on the surface and many areas where a sand grain has broken away at the sand/cement interface can also be seen. Such projected areas of interfacial fracture were found, using an image analyser, to constitute 47% of the total area. The area occupied by sand grains on a random section would be about 31%. Thus it is clear that the bond between the sand and cement is an area of weakness in the structure at this age.

Fig 3, from a 1 day old mortar, shows in greater detail an area where a sand grain has broken away. The areas which were in contact with the sand grain are fairly smooth, but do not appear to have a crystalline morpholgy as would be expected of calcium hydroxide. In the central region the surface layer has broken away with the sand grain. A high density of AFt (ettringite) rods can be seen in this area, much higher than is observed on a fracture surface of the plain cement paste. To the upper left of this region can be seen a grain whose hydrate shell has broken away to reveal its separated anhydrous core. Such feature, often refered to as 'Hadley grains', were first observed in such interfacial regions [2,3], but can be found throughout cement pastes [11,13,14,15,16]

Fig 4, also from a 1 day old mortar, shows the surface of a grain on the fracture surface (i.e. the complementary case to fig 3). In some areas the surface layer remains attached to the sand grain. The morphology of the product which has formed on the surface of the grain is the same as that of the hydrates seen around cement grains in plain cement pastes and around the cement grains in fig 3; namely that of early C-S-H (Diamond Type I [17]) and AFt (ettringite). This product can also be seen in the cracks and crevices in the surface of the sand grain.

The suface layer is shown at higher magnification in fig 5. This micrograph is from a 4 day old mortar, but is identical to that observed at younger ages. A small hexagonal crystal (arrowed), probably of calcium hydroxide, can be observed on the inner edge of the layer. However, this in no sense constitutes a continuous layer; neither is there any sign of a calcium hydroxide layer on the sand grain surfaces (e.g. fig 4).

Large calcium hydroxide crystals were frequently seen near the edges of sand grains. In almost all cases the basal cleavage plane ran perpendicularly (c-axis parallel), or nearly so, to the interface, as found by Barnes et al [3]. Fig 6 shows an exceptional instance in which a large $Ca(OH)_2$ crystal has grown with its basal plane nearly parallel to the surface of the sand grain (c-axis perpendicular). Even in this case, several other $Ca(OH)_2$ crystals can be seen with grossly different orientations. Many areas could be found where there was no calcium hydroxide in the interfacial region.

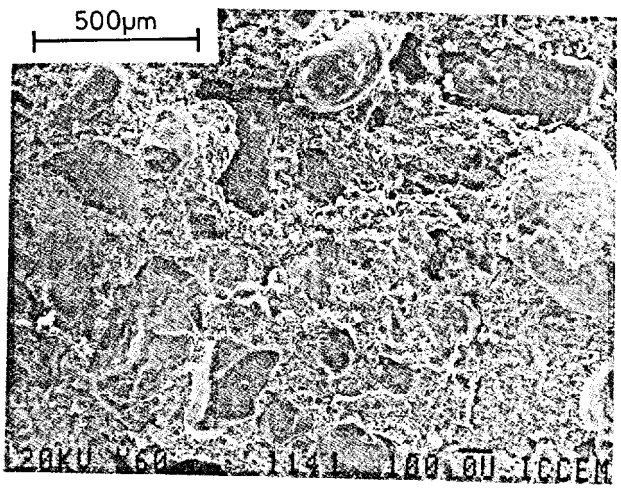

FIG 2. Microstructure of fracture surface at low magnification (4 day old mortar, SEI)

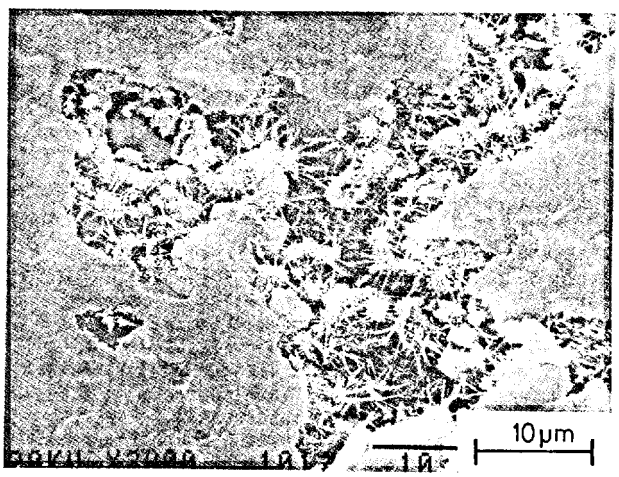

FIG 3. Area of fracture surface where sand grain has broken away (1 day old mortar, SEI).

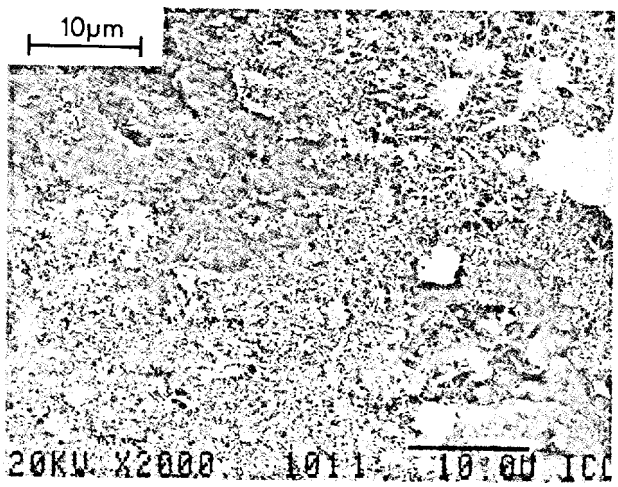

FIG 4. Surface of sand grain exposed on the fracture surface (1 day old mortar, SEI)

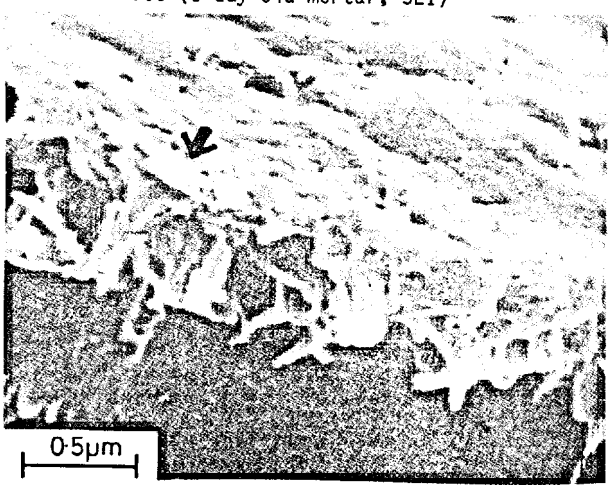

FIG 5. Detail of surface layer with possible $Ca(OH)_2$ crystal arrowed (4 day old mortar, SEI)

On the fracture surface of mortars at older ages the densification of the cement microstructure is apparent, as observed in the study of plain cement pastes; cleavage of calcium hydroxide tending to dominate the fracture path increasingly as hydration continues. As the hydration time increased the fracture around the sand grains followed the interface more closely, so fewer areas in which the surface layer remained attached to the surface of the sand grains were observed. The surface layer of C-S-H which formed on the sand grains during the first day of hydration did not appear to grow or thicken further.

Observations of polished surfaces using bse

A typical microstructure of a 1 day mortar is shown in fig 7. The area fraction of sand particles in this section by image analysis is 30%, very close to that expected for a random section. Several extensive areas (mid-grey) of calcium hydroxide are visible, in some cases these are adjacent to the sand grains, but none of the grains is surrounded by a continuous layer.

Fig 8 shows a single sand grain in greater detail. By image analysis, the volume fraction of $Ca(OH)_2$ in a plain paste of the same cement was found to be 14±1% [18]. For this particular grain $Ca(OH)_2$ is adjacent to the boundary for about 20% of its length. This one result is not statistically significant and a more detailed analysis would be needed to discover if there is a tendancy for $Ca(OH)_2$ to grow preferentially in the interfacial region. To the right and lower edges of this sand grain there is a region, some 20-30μm thick, where the paste appears to be less dense. This could have arisen during mixing as the large sand particle swept through the paste or could have been caused by settling before the paste set.

The edge of a sand particle is shown in more detail in fig 9. There is a thin layer of C-S-H (dark grey) along the entire length of this edge, even where a large crystal of $Ca(OH)_2$ (light grey) has grown close to the sand grain. The c-axis (which is perpendicular to the cracks along the basal cleavage plane) of this $Ca(OH)_2$ crystal is roughly parallel to the surface of the sand grain. This was found to be the case generally, although the roughness and angularity of the sand meant that the orientation of the surface of the sand to the adjacent $Ca(OH)_2$ varied considerably. The large crack through this $Ca(OH)_2$ demonstrates the ease with which this phase

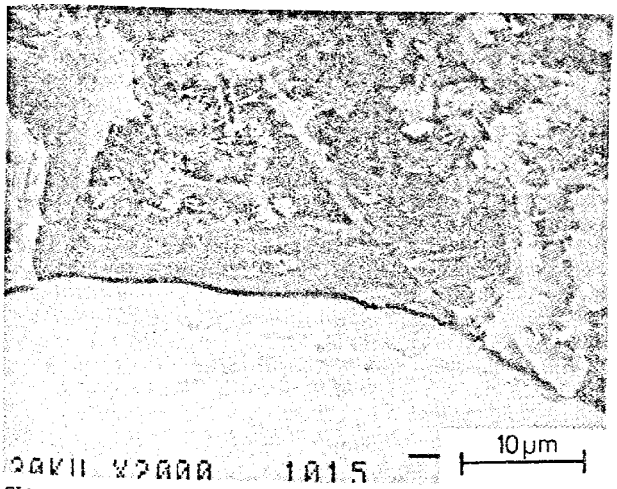

FIG 6. Calcium hydroxide crystal growing close to the surface of a sand grain, with various orientations (1 day old mortar, SEI)

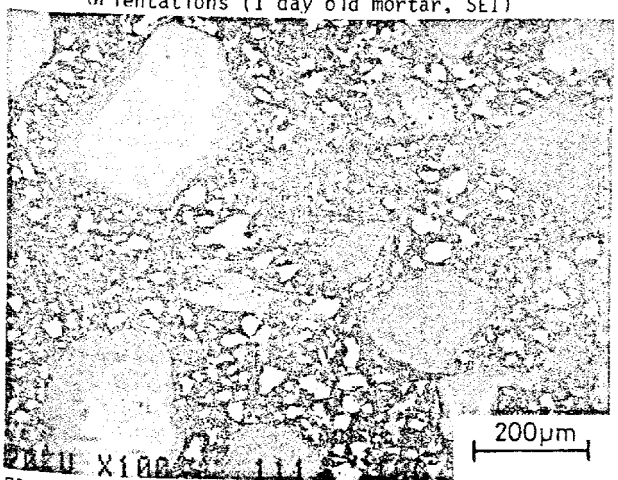

FIG 7. Microstructure of a polished surface of a 1 day old mortar (bse image)

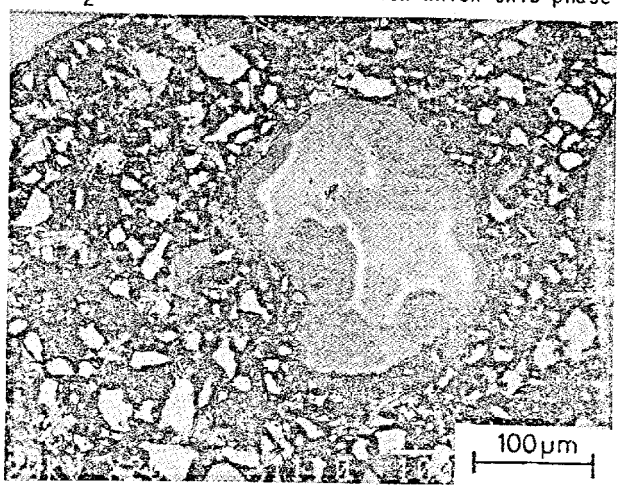

FIG 8. Microstructure of a sand grain and the surrounding paste (1day old mortar, bse image)

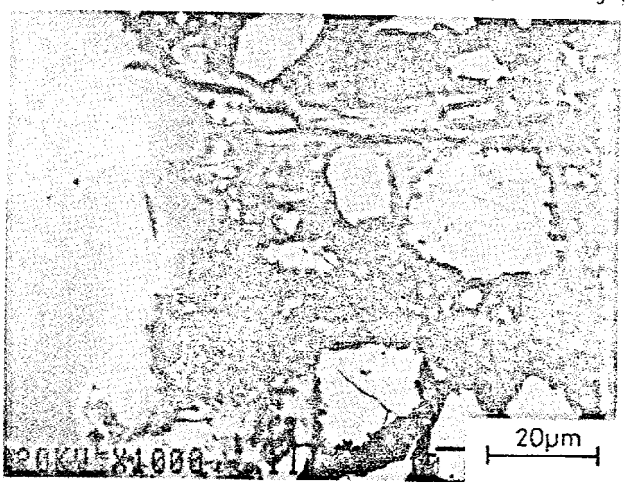

FIG 9. Detail of microstructure at edge of sand grain (1day old mortar, bse image)

cleaves along the basal plane, and thus tends to predominate on fracture surfaces at later ages.

Figs 10 & 11 illustrate interesting formations of calcium hydroxide in the vicinity of sand grains. Fig 10 is a bse image of a 1 week old mortar with a sand to cement ratio of 3:1. A pronounced layer of calcium hydroxide has formed along one side of the grain (that uppermost in the micrograph, although the orientation of the sand grain during setting and curing is not known). It is thought that this layer of $Ca(OH)_2$ has formed where localized bleeding has taken place. Similarly, fig 11 shows a large region of $Ca(OH)_2$ which has formed where two sand grains are very close together, again a region in which localized bleeding would be likely. This micrograph is of an 85 year old concrete and illustrates how $Ca(OH)_2$ crystals which nucleate during the early stages of hydration may persist indefinitely.

In specimens of the configuration described in the introduction (where a block of cement is cast directly onto the flat surface of a block of aggregate) it is possible that localized bleeding might occur along the interface and lead to anomalous results.

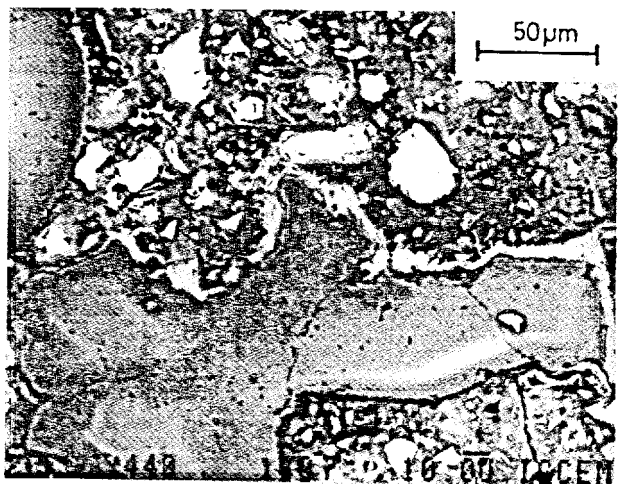

FIG 10. Sand grain and surrounding paste in a 1wk old mortar (bse image)

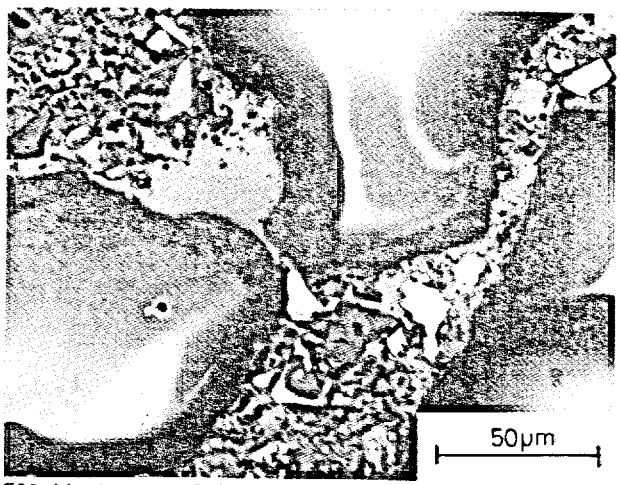

FIG 11. Large calcium hydroxide crystal between two sand grains in an 85 year old concrete. (bse image)

CONCLUSIONS

The present work confirms that the cement/sand interface is an area of weakness in the strucure of mortars. It also illustrates the value of the backscattered electron (bse) imaging technique in the study of the microstructure of the cement/aggregate bond.

During the first day of hydration a layer of C-S-H, about 0.5μm thick, forms on the surface of the sand grains by a through-solution mechanism. Interestingly the same phenomenon is observed on the surface of fly-ash particles in cement/pfa blends [19]. This surface layer cannot be considered to be epitaxial, as this term implies a strict orientation relationship between two crystalline phases.

A much higher concentration of AFt (ettingite) is observed in the interfacial region. This might be due to the preponderance of small cement particles near the interface, on the surface of which more interstitial material is exposed. AFt is also formed on the surface layer of product around the sand grains, confirming that it is precipitated through solution in agreement with Monterio and Mehta [8].

Beyond this surface layer, some large crystals of calcium hydroxide may form adjacent to the sand particles, these tend to predominate on fracture surfaces due to the ease of cleavage along the basal plane of calcium hydroxide. The orientation of these crystals varies considerably, although there may be some preference for the c-axis to be aligned parallel to the surface of the grain as noted by Barnes et al [3].

There are several instances where sand particles are bordered by regions of paste with a lower density of cement particles, especially those greater than 10μm in size (equivalent to a higher local w/c ratio). Such regions are usually present only to one side of the sand grains and it is thought they arise as the large sand grains are swept through the paste during mixing. Exceptionally large or extensive crystals of calcium hydroxide can often be found where local bleeding would have been likely. These last two conclusions illustrate the importance of studying realistic mortars and concretes.

ACKNOWLEDGEMENTS

The authors would like to acknowledge the financial support of the Materials Committee of the Science and Engineering Research Council, UK for this work.

REFERENCES

1. L. Struble, J. Skalny & S. Mindess, (1980), 'A Review of the Cement-Aggregate Bond' Cem. Concr. Res., 10, pp277-286.
2. B. D. Barnes, S. Diamond & W. L. Dolch, (1978), 'The Contact Zone Between Portland Cement Paste and Glass "Aggregate" Surfaces', Cem. Concr. Res., 8, pp233-243.
3. B. D. Barnes, S. Diamond & W. L. Dolch, (1979), 'Micromorphology of the Interfacial Zone Around Aggregates in Portland Cement Mortar' J. Am. Ceram. Soc., 62, pp21-24.
4. J. Farran, (1956), 'Contribution minéralogique à l'étude de l'adhérence entre les constituants hydratés des ciment et les matériaux enrobés' Revue des matériaux de construction, n° 490-491-492.

5. J. Grandet & J. P. Ollivier, (1980),
'Nouvelle méthode d'étude des interface ciment-granulats'
7th Int. Cong. on the Chemistry of Cement, Paris, III, ppVII-85 - VII-89
6. J. P. Ollivier, (1981),
'Contribution à l'étude de L'hydration de la pâte de ciment Portland au Voisinage des Granulats'
Thesis Toulouse.
7. J. Grandet & J. P. Ollivier, (1980),
'Orientation des hydrates au contact des granulats',
7th Int. Cong. on the Chemistry of Cement, Paris, III, ppVII-63 - VII-68
8. P. J. M. Monterio & P. K. Mehta, (1985),
'Ettringite Formation on the Aggregate-Cement Interface',
Cem. Concr. Res. 15, pp378-380.
9. P. J. M. Monterio, J. C. Maso & J. P. Ollivier, (1985)
'The Aggregate-Mortar Interface'
Cem. Concr. Res. 15, pp953-958.
10. K. L. Scrivener & P. L. Pratt, (1984),
'Backscattered Electron Images of Polished Cement Sections in the Scanning Electron Microscope'
Proc. 6th Int. Conf. on Cement Microscopy, Albuquerque, pp145-155.
11. K. L. Scrivener, (1984),
'The Development of Microstructure During the Hydration of Portland Cement',
PhD Thesis, University of London.
12. K. L. Scrivener, (1985)
'The Use of Backscattered Electron Imaging in the Study of Cement and Concrete'
Proc. Engineering Foundation Conf., Cement Manufacture & Use, Henniker, in press.
13. B. J. Dalgleish, P. L. Pratt & E. Toulson, (1981)
'Fractographic Studies of Early Hydration Products in Cement Pastes',
Cem. Concr. Res., 11, pp729-739.
14. K. L. Scrivener,
'Observations of "Separarted Hydrate Shells" Formed During the Hydration of Portland Cement',
to be published.
15. B. D. Barnes, S. Diamond & W. L. Dolch, (1978),
'Hollow Shell Hydration of Cement Particles in Bulk Cement Pastes',
Cem. Concr. Res., 8, pp263-272.
16. P. L. Pratt & A. Ghose, (1983),
'Electron Microscope Studies of Portland Cement Microstructure During Setting and Hardening'
Phil. Trans. R. Soc. Lond., A310, pp93-103.
17. S. Diamond, (1976),
'Cement Paste Microstructure - an Overview at Several Levels',
in Hydraulic Cement Pastes: their Structure and Properties", (Cement & Concrete Association), pp2-30.
18. K. L. Scrivener & A. Crumbie,
unpublished work.
19. A. Ghose & P. L. Pratt, (1981),
'Studies of the Hydration Reactions and Microstructure of Cement-Flyash Pastes',
In Proc. Symp. Effects of Fly ash Incorporation in Cement & Concrete, Boston, Materials Research Society, pp82-91.

G. ARLIGUIE et J. GRANDET
Laboratoire de Génie Civil (I.N.S.A-U.P.S.) Avenue de Rangueil
31077 TOULOUSE cédex (France)

Durabilité de la liaison acier galvanisé - pâte de ciment Portland
Durability of the bond between galvanized steel and Portland cement paste.

2.3

RESUME : Des armatures galvanisées sont parfois utilisées dans le béton lorsque les constructions se trouvent dans un milieu agressif. La liaison entre l'armature et la pâte de ciment Portland est essentiellement assurée par une pellicule continue d'hydroxyzincate de calcium résultant de l'action des ions Ca^{2+} et OH^- sur l'hydroxyde de zinc. Dans ce travail, on étudie la durabilité de cette pellicule en présence de chlorures, de gaz carbonique et également sa stabilité thermique. On montre l'excellent comportement de cette liaison.

Freqüentemente se usam armaduras galvanizadas no concreto quando as construções se encontram em meio agressivo. A ligação entre a armadura e a pasta de cimento Portland é garantida essencialmente por uma película contínua de hidrozincato de cálcio resultante da ação dos íons Ca^{2+} e OH^- sobre o hidróxido de zinco. Neste trabalho se estuda a durabilidade desta película em presença de cloretos, de gás carbônico, e ainda sua estabilidade térmica. Mostra-se o comportamento excelente desta ligação.

INTRODUCTION

Des armatures galvanisées peuvent être utilisées en béton quand des conditions agressives existent. De nombreux rapports techniques ont souligné la tenue très satisfaisante des aciers galvanisés dans des constructions exposées à divers milieux marins (1,2). Cependant, ces essais ont été effectués sans que le comportement de la liaison entre l'acier galvanisé et le béton soit totalement éclairci. Des recherches précédentes (3) ont montré que cette liaison se différencie des autres liaisons existant dans le béton (granulat-pâte de ciment) car elle conduit à la formation d'un composé d'interaction, l'hydroxyzincate de calcium.

Dans cette communication, nous rappelons le mécanisme de formation de cette liaison, puis nous étudions la durabilité de la pellicule d'hydroxyzincate de calcium.

FORMATION DU CONTACT ZINC-PATE DE CIMENT PORTLAND

La galvanisation à chaud consiste à obtenir un revêtement par immersion de l'acier, préalablement préparé en surface, dans du zinc en fusion à une température comprise entre 440 et 460°C. Dans la majorité des cas, la couche externe (appelée êta) est une couche de zinc pur.

Le comportement de l'acier galvanisé sera, au moins au premier stade, celui du zinc.

Lors du contact entre une armature galvanisée et la pâte de ciment Portland, on peut observer les phénomènes suivants (4) :

- dissolution superficielle du zinc avec diffusion d'une partie des ions zinc dans la pâte de ciment encore fluide,

- réaction avec les ions présents dans la solution interstitielle ; l'interaction entre les ions zinc et hydroxyles entraîne la précipitation de l'hydroxyde de zinc $Zn(OH)_2$. Ce composé se forme non seulement sur la surface du métal mais aussi sur les grains de ciment proches, provoquant ainsi un retard d'hydratation de la pâte.

- transformation de $Zn(OH)_2$ en hydroxyzincate de calcium par action des ions Ca^{2+} et OH^- produits par l'hydratation des grains de ciment non perturbés.

Finalement, l'hydroxyzincate de calcium recouvre progressivement les armatures et assure la liaison avec la pâte de ciment.

STABILITE DE L'HYDROXYZINCATE DE CALCIUM

Nous avons examiné des plaques d'acier galvanisé enrobées dans un béton et soumises à une exposition atmosphérique pendant six ans.

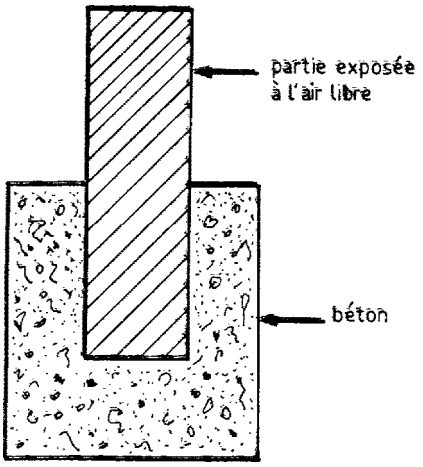

(a) schéma : position de l'armature dans le béton

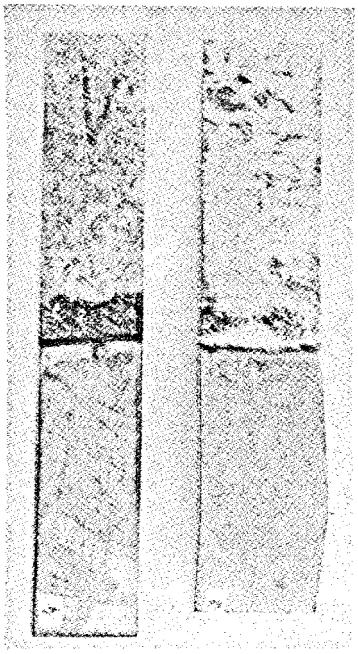

(b) aspect des plaques après extraction

FIGURE 1

Les éprouvettes métalliques étaient enrobées dans le béton sur une certaine longueur, l'autre partie étant exposée à l'air libre (schéma, figure 1). La séparation entre la plaque et le béton est très difficile. Des amas de pâte adhèrent au métal et ne peuvent être détachés sans altérer la surface. Ceci témoigne de l'excellent accrochage entre les deux matériaux.

A l'intérieur même du béton, l'armature semble peu attaquée ; sur les rares zones où l'épaisseur de mortier accroché est faible, l'analyse par diffractométrie des rayons X révèle la présence d'hydroxyzincate de calcium et d'oxyde de zinc.

A l'interface mortier-atmosphère, on observe une formation de rouille due à une usure du revêtement de galvanisation provoquée par les différentes manipulations de l'éprouvette. Cependant, il faut remarquer que dans l'utilisation habituelle du béton armé, une telle interface n'existe pas.

ETUDE DE LA DURABILITE DE L'HYDROXYZINCATE DE CALCIUM

1 - Echantillons utilisés

1 -1- Obtention de l'hydroxyzincate de calcium en poudre

Nous avons pu synthétiser ce composé au laboratoire de deux façons.

- action de la chaux sur l'hydroxyde de zinc

Nous avons ajouté, dans un excès d'eau, des quantités croissantes de chaux à de l'hydroxyde de zinc (lui-même préparé par action d'une base sur un sel de zinc). La transformation de $Zn(OH)_2$ en hydroxyzincate de calcium s'effectue dès que la concentration en chaux est suffisante, selon la réaction :

$$2\ Zn(OH)_2 + 2\ OH^- + Ca^{2+} + 2\ H_2O \rightarrow Ca\ Zn(OH)_{3\ 2}.2H_2O$$

Les réactifs de départ étant peu solubles, il est difficile, si les quantités ne sont pas rigoureusement stoechiométriques, d'isoler l'hydroxyzincate de calcium.

- action de la chaux sur le sulfate de zinc :

$$3\ Ca(OH)_2 + 2\ ZnSO_4 + 4\ H_2O \longrightarrow$$

$$Ca\ Zn(OH)_{3\ 2}.2H_2O + 2CaSO_4.2H_2O$$

Nous obtenons un mélange d'hydroxyzincate de calcium et de gypse. Il est alors aisé d'obtenir l'hydroxyzincate de calcium pur par lavage à l'eau déminéralisée qui dissout le gypse.

Le diffractogramme X caractéristique de ce composé est représenté par la figure 2.

1 -2- Fabrication d'éprouvettes mixtes

Nous avons confectionné des éprouvettes mixtes obtenues par coulage d'une pâte de ciment Portland sur la face polie d'un cylindre de zinc et conservées à 20°C et 100 % d'humidité relative. Au moment de l'observation, les deux parties sont séparées mécaniquement au niveau de l'interface. Les deux surfaces de rupture sont alors analysées par diffractométrie des rayons X.

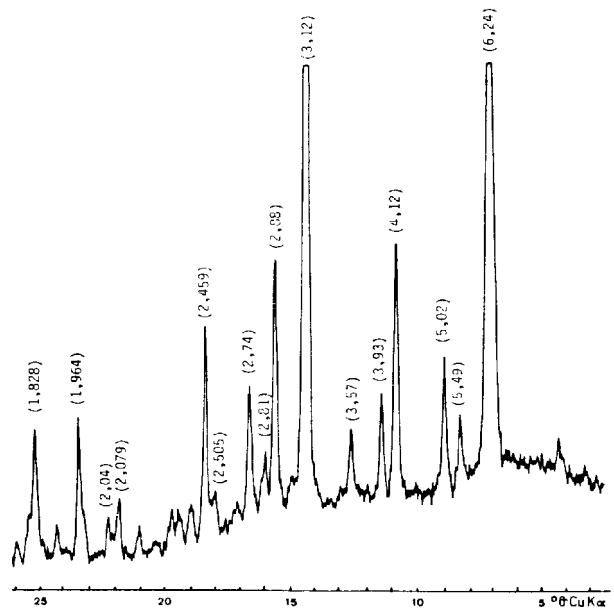

FIGURE 2

Enregistrement diffractométrique caractéristique de l'hydroxyzincate de calcium. ( ) distances réticulaires en Å.

2 - Action du gaz carbonique

La pénétration du gaz carbonique à l'intérieur du béton est un des facteurs qui conduit à la corrosion des armatures en acier non galvanisé.

Une éprouvette mixte zinc-pâte de ciment Portland est séparée après une durée de contact de 1 mois. La surface du métal est recouverte d'hydroxyzincate de calcium. Nous l'avons laissée à l'air libre durant plusieurs mois. L'analyse par diffractométrie des rayons X ne fait apparaître aucune modification du diffractogramme.

Nous avons traité de la même façon un échantillon en poudre obtenu par synthèse : aucune altération n'a été constatée.

L'hydroxyzincate de calcium est donc très stable dans un milieu contenant du gaz carbonique.

3 - Action des chlorures

La présence de chlorures dans un béton provoque la corrosion par piqûres des armatures en acier.

Comme précédemment, nous avons utilisé une éprouvette de zinc déjà recouverte d'hydroxyzincate de calcium. Nous l'avons immergée dans une solution d'hydroxyde de calcium contenant 35 g/l de chlorure de calcium afin de simuler la phase interstitielle du béton pollué par des chlorures. Après un mois d'immersion, l'analyse par diffractométrie des rayons X ne met pas en évidence de réaction entre l'hydroxyzincate de calcium et la solution.

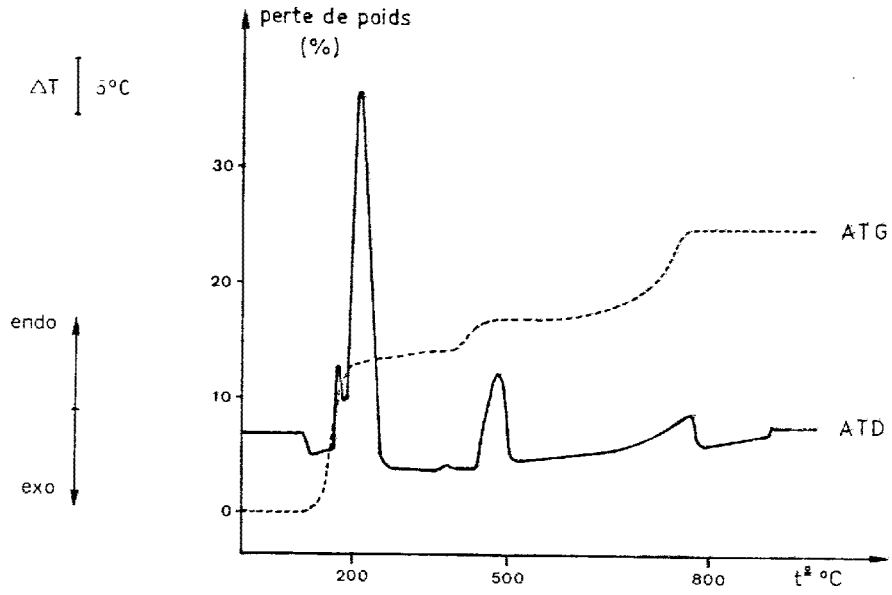

masse échantillon = 80 mg ; référence = alumine ;
600°C/heure dans l'air

FIGURE 3

Analyses thermique différentielle et thermogravimétrique simultanées de l'hydroxyzincate de calcium.

4 - Stabilité thermique

Les analyses thermique différentielle et thermogravimétrique simultanées sont représentées sur la figure 3. D'après les diagrammes que nous avons obtenus, il semble que la décomposition de l'hydroxyzincate de calcium se fasse selon le processus suivant :

- entre 150 et 190°C : départ progressif de l'eau d'hydratation,
- entre 190 et 200°C : décomposition de $Zn(OH)_2$,
- vers 480°C : décomposition de $Ca(OH)_2$.

La température de dissociation de l'hydroxyde de zinc est plus élevée que lorsqu'il est pur (160-170°C).

Nous avons ensuite examiné par diffractométrie des rayons X et par microscopie à balayage (figure 4) des échantillons d'hydroxyzincate de calcium ayant subi des traitements thermiques de 3 heures aux températures suivantes :

200°C - 280°C - 380°C - 450°C - 600°C - 850°C.

La forme externe des cristaux reste inchangée jusqu'à 450°C, température largement supérieure à celle où le produit ne présente plus le diffractogramme caractéristique de l'hydroxyzincate de calcium (200°C). L'oxyde de zinc, produit final de la décomposition thermique, ne cristallise qu'après la décomposition de la chaux.

Nous avons ajouté de l'eau à un échantillon ayant subi un traitement de 3 heures à 300°C. Le produit d'hydratation réformé est l'hydroxyzincate de calcium.

En conclusion, la stabilité thermique de l'hydroxyzincate de calcium est suffisante pour la majorité des applications du béton armé.

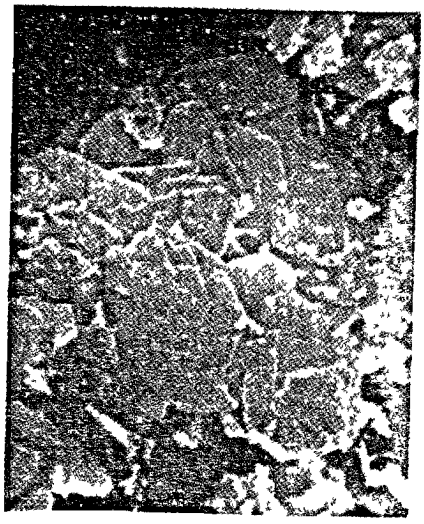

(a) CZH 2,5 µm



(b) 380°C 2,5 µm



(c) 850°C 2,5 µm

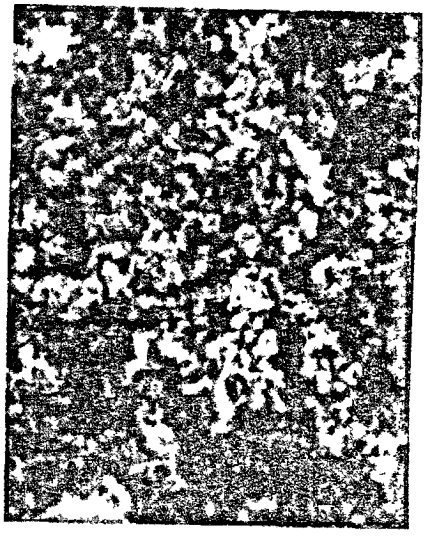

(d) ZnO 2,5 µm

FIGURE 4

Traitements thermiques de l'hydroxyzincate de calcium (CZH)

CONCLUSION

L'hydroxyzincate de calcium, constituant majeur de la liaison zinc-pâte de ciment Portland, présente une bonne stabilité vis-à-vis des agents corrosifs les plus fréquents pour une armature d'acier : le gaz carbonique et les chlorures. La stabilité thermique de ce composé est meilleure que celle de nombreux hydrates de la pâte de ciment (sulfoaluminates de calcium et aluminates de calcium hydratés).

Les armatures galvanisées présentent donc une durabilité supérieure à celle des armatures d'aciers dans les ambiances particulièrement agressives.

BIBLIOGRAPHIE

(1) - D. STARK et W. PERENCHIO. (1975) "The performance of galvanized reinforcement in concrete bridge decks". Construction technology laboratories. project ZE - 206.

(2) - KRAVCHENKO et ALEKSEEV. "Construction en béton armé avec armatures recouvertes de zinc". Béton i Zelezobeton, U.R.S.S., juin 1981, n°6, 25.

(3) - G. ARLIGUIE et J. GRANDET "Etude du contact zinc-pâte de ciment Portland". 7ème congrès international de la Chimie des ciments, Paris (FRANCE), juillet 1980. volume III, thème VII, pages 22 à 27.

(4) - G. ARLIGUIE et J. GRANDET. "Formation de l'auréole de transition entre la pâte de ciment Portland et le zinc". Colloque international Liaisons pâte de ciment - matériaux associés, Toulouse (FRANCE), novembre 1982.

G. FRIGIONE, Cementir, Cementerie del Tirreno S.p.A., Naples, Italy.
B. MARCHESE, Department of Materials and Production Engineering, University of Naples, Italy.
R. SERSALE, Department of Materials and Production Engineering, University of Naples, Italy.

1

MICROCRACKINGS PROPAGATION IN FLEXURAL LOADED PORTLAND AND HIGH SLAG CEMENT CONCRETES

2.3

SUMMARY: An account of the results attained examining the flexural behaviour, until rupture occurs, of a series of reinforced beams and of unreinforced specimens manufactured with high blast furnace slag cement and Portland cement concretes, stored either at ambient temperature or steam cured, has been given by the Authors.

It has been emphasized that the structural elements manufactured with high slag cement concrete show, as a rule, cracking patterns characterized by progressively more numerous cracks, of moderate width, slowly growing with stress, whereas Portland cement concrete elements show a nearly constant number of cracks, of width swiftly growing with the stress. Steam curing abates the above mentioned differences, even if the crack patterns remain qualitatively unchanged.

The influence of the choice of cement type and of maturation procedure on the durability of plain and reinforced concrete structures has been pointed out and the differences of the cracking patterns of the two types of binder are discussed in terms of a higher bond strength at the paste-aggregate interface in the high slag cement than in Portland cement concretes.

Os autores informam sobre os resultados obtidos no exame do comportamento flexional, até que ocorre ruptura, de uma série de vigas armadas, e de corpos de prova não armados, feitos com concretos de cimento de escória de alto forno e cimento portland, armazenados tanto em temperatura ambiente como curados a vapor.

Enfatizou-se que os elementos estruturais preparados com concretos de cimento de alta escória apresentam, em regra, modelos de trinca caracterizados por trincas progressivamente mais numerosas, de abertura moderada, lentamente crescentes com a tensão, enquanto os elementos de concreto de cimento portland apresentam um número quase constante de trincas, cuja abertura cresce rapidamente com a tensão. A cura sob vapor reduz as diferenças mencionadas acima, mesmo que os modelos de trinca permaneçam quantitativamente inalterados.

Ressalta-se a importância da escolha do tipo de cimento e processo de maturação sobre a durabilidade de estruturas simples e armadas de concreto, e se discutem as diferenças dos modelos de trinca dos dois tipos de ligante, em termos de uma resistência mais alta de aderência na interface de pasta-agregado nos concretos com cimento de alta escória do que nos com cimento portland.

G. FRIGIONE
B. MARCHESE
R. SERSALE

INTRODUCTION

The behaviour of cement concrete under loading is an essential factor for the long-range forecast of the structures durability and, at the same time, a datum of considerable importance for the designer. Despite the very large amount of valuable contribution that has been given (1 - 9) to the study of the concrete deformation by external loading, the mechanism of crack growth through the hardened cement paste, mortar or concrete, is not yet very well understood (10). Further attention should be paid indeed to the study of the paste - aggregate interface, which appears to be the weakest part of the heterogeneous concrete system, in order to ascertain if the microcracks or microvoids which initiate during setting and hardening, bridging one another with increasing stress and beginning to form continuous crack patterns, develop in plain and reinforced concrete primarily along the interfaces between the individual aggregate particles and the surrounding cement paste or mortar matrix.

To this end a wide experimental investigation on models and structures of reinforced concrete has been started (11), in order to examine its structural behaviour as a function of the type of cement and of the curing procedure. In this paper the account is restricted to the results of a comparative examination of the microcrackings progress until the specimens are completely disrupted, for beams both of reinforced high slag cement (SC) concrete and of Portland cement (PC) concrete, as well for unreinforced specimens manufactured with the same blend used for the beams, tested after three months.

The investigation appears to be of particular interest since the microcrackings propagation process influences structures durability to a great extent. Cracking and crack widths, shape and distribution of the cracks promote in fact, in a different way, corrosion phenomena of the reinforcement as well as the concrete decay, allowing the penetration of foreign aggressive ions and providing space for the deposition of corrosion products (12). It is therefore imperative to bear in mind that, together with other parameters, the width and the distribution of the cracks both share in the enhancement of the above mentioned phenomena.

EXPERIMENTAL

First of all, two similar series of beams have been prepared, each consisting of eight elements with rectangular section 15x30x320 cm, reinforced with two inferior bars, 16 mm diameter, of Fe B 44 k steel (13). One series has been manufactured with SC concrete and the other with PC concrete. Four elements of each series have been cured at ambient temperature (20 ± 2 °C) and the remaining four elements have been steam cured according to the following thermal cycle: four hours pre-curing, two hours from 20 to 80 °C, two hours at 80 °C, slow cooling. The SC has been manufactured by simultaneous grinding of clinker (28 %) and slag (70 %), with 2% gypsum addition. PC has been prepared with the same clinker used for manufacturing SC, with 4 % gypsum addition, Table I.

Table I : Characteristics of the Cements.

	Slag Cement (SC)	Portland Cement (PC)
Blaine Surface Area, m^2/kg	365	367
Set:		
Initial, hours - min	3.50	2.40
Final, hours - min	5.00	3.50
Strength:		
Flexural 7 ds, MPa	5.0	6.0
Compressive 7 ds, MPa	21.8	24.0
Flexural 28 ds, MPa	8.4	8.2
Compressive 28 ds, MPa	42.5	47.7

Table II : Characteristics of the Concretes

Cement Content		370
Aggregate Content:		
Crushed Basalt	15 / 30	870
Crushed Basalt	5 / 15	520
Crushed Siliceous Sand	0.15 / 5	560
Natural Sand	0 / 0.5	540
Slump		11.5
Compressive Strength of Concrete Cured at 20 °C (28 days):		
Made with Slag Cement		31.0
Made with Portland Cement		34.4
Compressive Strength of Concrete Steam Cured (28 days):		
Made with Slag Cement		38.0
Made with Portland Cement		42.0

Beyond the two series of beams, cylindrical (15.5x30.2 cm) and rectangular (10x10x40 cm) unreinforced specimens of the same blend used for the beams, Table II, have been prepared and stored either at ambient temperature or steam cured.

The beams were loaded, applying the solicitation in a quasistatic way, in four-point, Fig. 1. All details about conditions of the testing and obtained results are given in (11). Beams have been cracked and the crack pattern has been obtained by means of an optical micrometer, with reference to position, height and width of the individual fissures, Fig. 1. It is to be

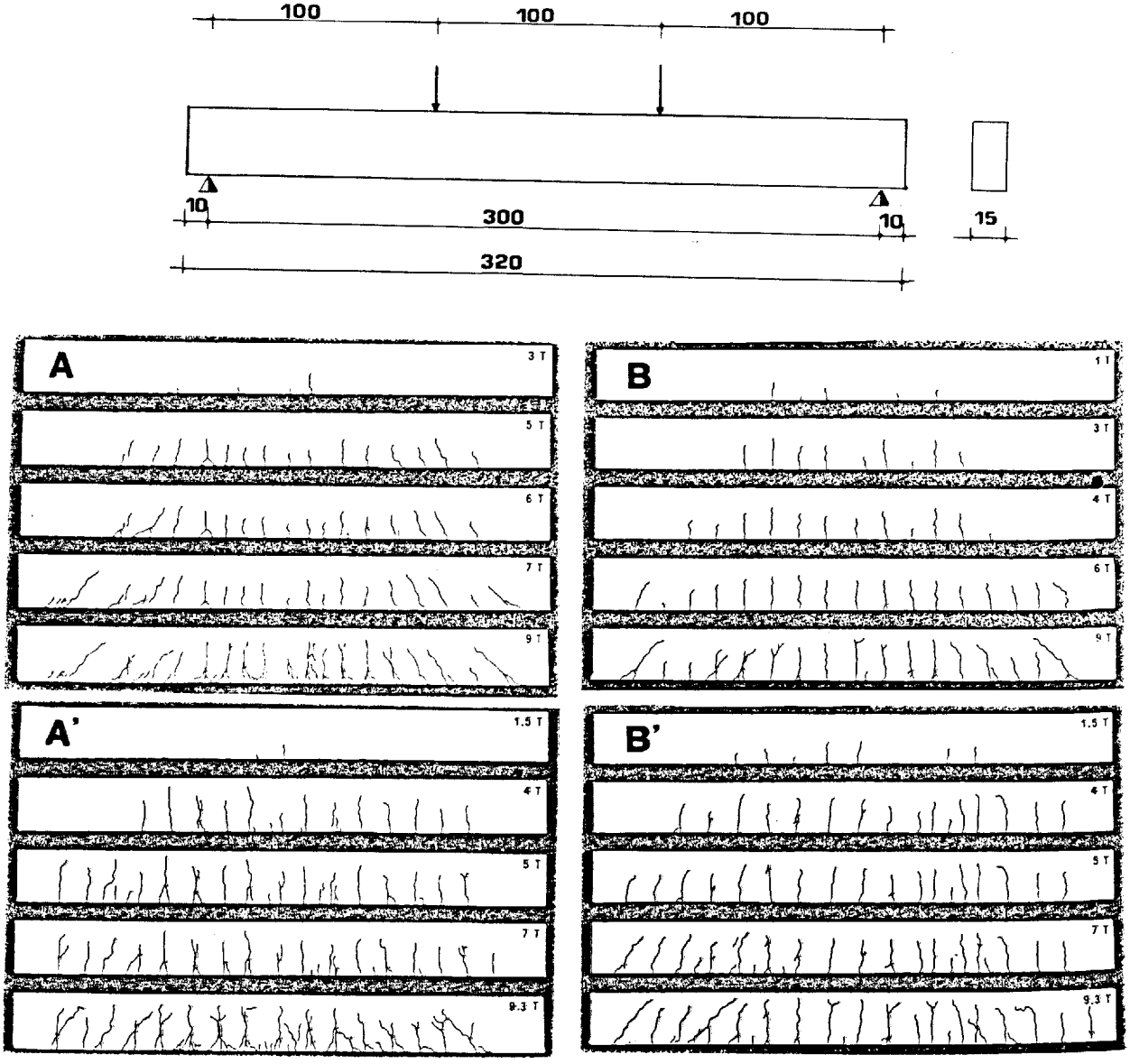

Fig. 1: Cracking patterns of reinforced beams as a function of the load.
A = SC, at ambient temperature cured,
A' = SC, steam cured,
B = PC, at ambient temperature cured,
B' = PC, steam cured.

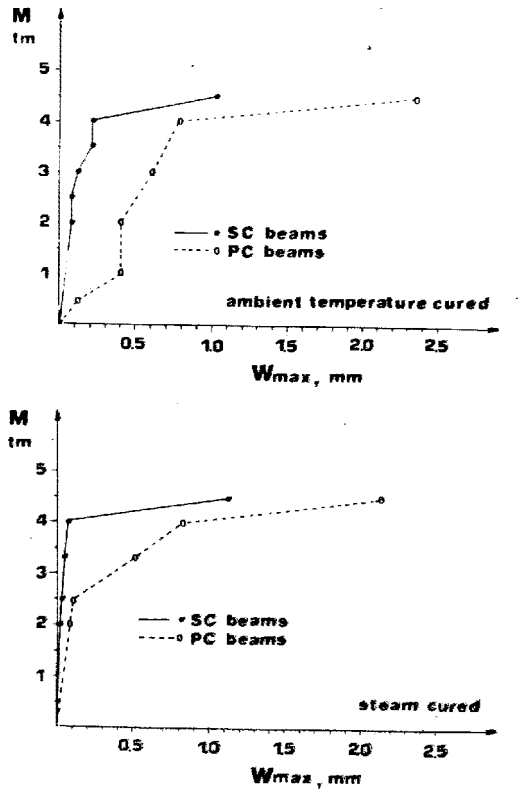

Fig. 2 : Progress of the widest fissure as a function of the load (T = ton).

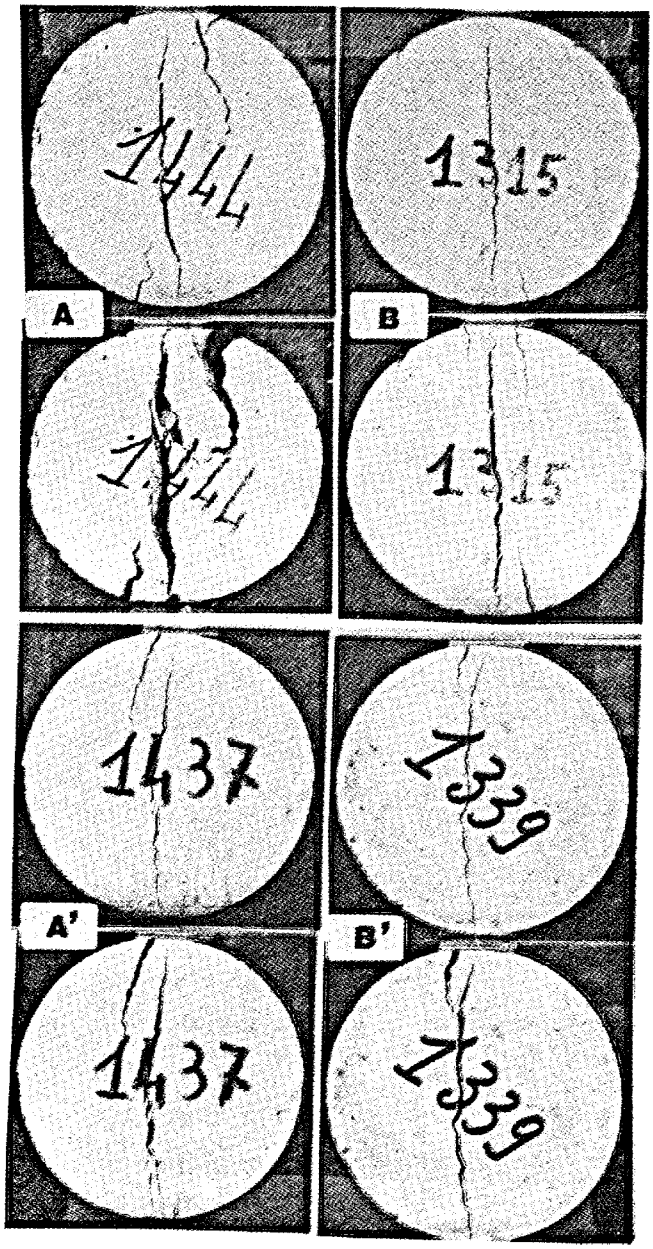

Fig. 3 : Crack map on the terminal surface of cylinders during the splitting test.
A, A', B, B' as Fig. 1.

noticed that the structural elements prepared with SC concrete show, as a rule, crack patterns characterized by fissures progressively more numerous, but with moderate width, slowly growing with the stress. In contrast, the number of fissures in the structural elements prepared with PC concrete appears to be nearly constant, of width swiftly growing with the stress. The maturation at ambient temperature particularly enhances the phenomenon, whereas steam curing has a lowering action, even if the cracks course remains qualitatively unchanged.

Since the crackings behaviour is strictly related to the possible attack or degradation of the structure, the course of the largest width of the fissures as a function of the stress has been examined, too. To this end, for each level of the load, corresponding to a determined moment M, the widest fissure (W_{max}) has been identified, which, as a rule, appeared to be also the deepest one, almost always localized inside the central part of the beam, even if such a localization varied, in general, with the stress.

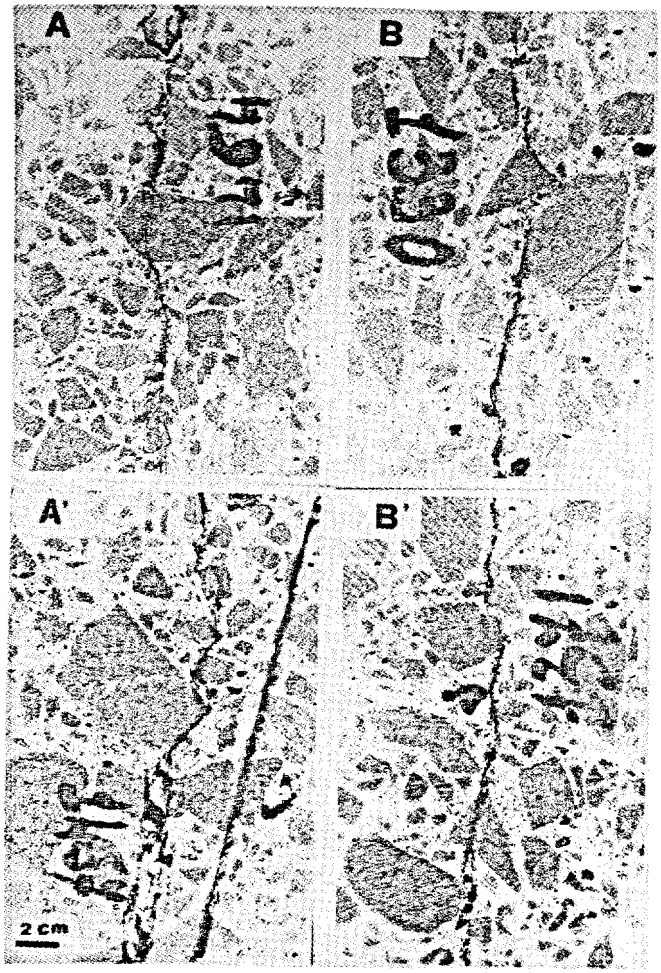

Fig. 4 : Macrographs of cross section of the specimens after splitting tests.
A, A', B, B' as Fig. 1.

The $M - W_{max}$ course both for the series of beams and for the maturation procedures is reported in Fig. 2. It is to be noticed that the width W_{max} appears to be definitely smaller for the beams prepared with SC concrete than for beams with PC concrete, whose fissures appear sometimes to be more than twice as large. Stress being the same, W_{max} values are moreover considerably lower for steam cured specimens.

Taking into account that as regards structures durability it is more effective to lower the width of the fissures, rather than their number, the choice either of the type of cement or of the curing procedure appears to be of considerable importance. A limitation of the crack width is in fact demanded both for reasons of esthetics and of protection against corrosion. The admissible limit values are above all very important for the utilization of great steel strengths since an increased limitation of the crack widths is accompanied by a decrease of the utilizable steel stress (14). In consideration of this premisses, the results obtained through the investigation on the beams have been confirmed by means of mechanical tests and macrographic examination of the crack progress on a series of unreinforced specimens, manufactured with the same blend used for the beams. The macrographs of SC and PC concrete cylindrical specimens matured either at ambient temperature or steam cured, have been reported in Fig. 3, during and after the splitting test (15). The macrographs confirm that specimens manufactured with SC concrete show a higher number of fissures in comparison to those of PC specimens and that the steam curing procedure significantly abates such a difference.

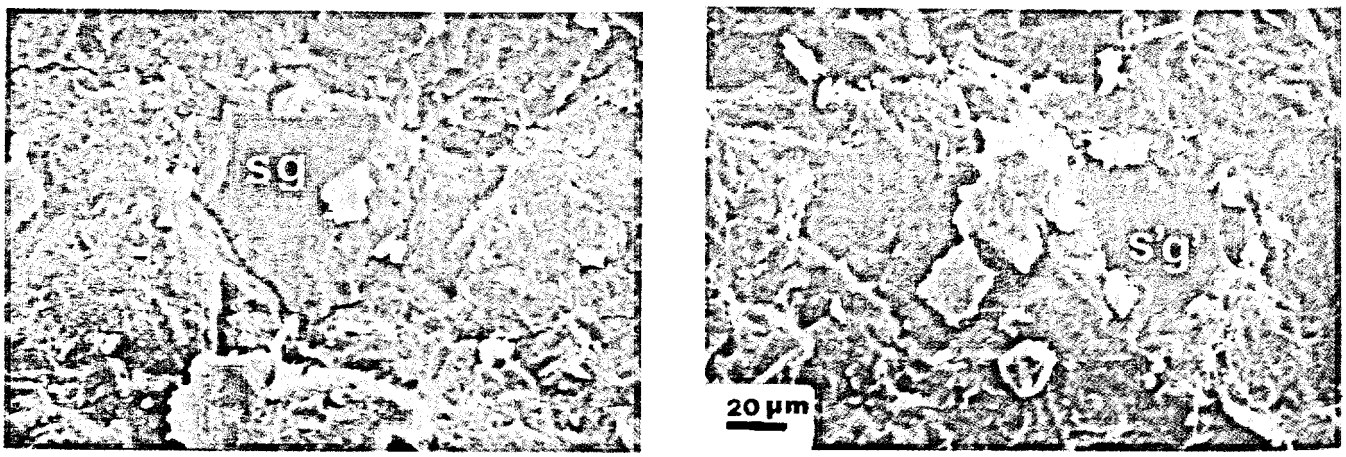

Fig. 5 : SEM twin fracture surfaces of SC pastes one year old, (s g = unhydrous slag grain).

The polished cross sections of the split semi-cylinders, moreover give evidence that the fracture in the SC concrete also involves the aggregate particles, some of them appearing clearly cracked, while the fracture of PC concrete specimens primarily involves the paste-aggregate interface, running along the contour of the individual particles, Fig. 4. This would suggest the existance of a better adhesion paste-aggregate in SC than in PC concretes.

To save space macrograph results of the longitudinal sections of rectangular unreinforced specimens, flexural cracked, are not reported. As has been already emphasized with the cylindrical specimens, in SC concrete specimens the fracture propagates also through the aggregate particles, rather than primarily at the paste-aggregate interface, as in the case of PC concrete specimens, cured at ambient temperature.

The examination of the fracture surfaces allows one to calculate the percentage of fractured aggregates, approximately above 10 mm in size, in comparison to that of the unaltered ones (16). Values indicate that the percentage of the fractured particles lies around 50% for SC concrete and 35% for PC concrete, for specimens cured at 20 ± 2 °C.

In order to investigate the fracture propagation at a microscopic level, the twin fracture surfaces of one year old SC pastes have been observed. Fig. 5 a shows that the fracture path runs through the hydration products, being hindered by the unhydrated slag grain, at the center of the image. At the same time, a smooth and wide surface of the same grain detaches from the hydration products, as is demonstrated by the replica left on the corresponding surface in Fig. 5 b. This indicates that other factors locally present, attributable to the nature, the shape and the lay of fracture surfaces and deriving from the presence of unhydrated grains, can affect the fracture path.

DISCUSSION AND CONCLUSION

The whole of the experimental results and of the deductions that reasonably can be drawn, strengthen the considerable influence of the choice of the type of binder, as well of the ageing procedure, on the durability of reinforced and plain concrete. The comparative examination of the cracking progress of the structural element, in fact, emphasized a different crack map in the high slag cement concrete elements in comparison to the Portland cement ones, particularly for the maturation at ambient temperature. Slag cement concrete specimens show, indeed, fissures progressively more numerous, but of moderate width and slowly growing with the stress, so that the possible degradation of the structure is reduced. Portland cement concrete specimens show instead an almost constant number of fissures, but their width swiftly increases with the stress.

A possible interpretation of the different behaviour, however, supported by the complementary investigations, might be advanced assuming a better cohesion of the matrix in the blast furnace slag cement in comparison to that in the Portland cement concrete structures, a cohesion to be probably related also to the higher compactness of the C-S-H in the high slag cements, poor in hydrated lime (17). In the Portland cements, a remarkable influence on the paste-aggregate bond strength is to be attributed to calcium hydroxide, depending on its morphology and orientation properties (18). The interfacial region can in fact consist of more densely and orientated growths of $Ca(OH)_2$ than are found in bulk paste and this must have implications regarding the nucleation of microcracking around aggregate particles or reinforcement in concrete. The virtual absence of calcium hydroxide in high blast furnace slag cements (19) could therefore explain the higher adhesion paste-aggregate and explain the microcracking propagation preferentially through the aggregate particles. On the contrary, a lower bond strength paste-aggregate in the Portland cement specimens would promote a fracture propagation primarily along the interfaces.

In the blast furnace slag cement concretes maturated either at ambient temperature or steam cured, as well in Portland cement concretes steam cured, paste-aggregate bonding being stronger, individual aggregate particles could act as crack arrestors, causing the formation of numerous potential failure planes before rupture occurs. In the Portland cement concretes matured at ambient temperature, paste-aggregate bonding being weaker, once a potential failure plane is developed, it could continuously grow in an almost flat plane, so causing failure.

Besides all this, the slag cement paste better than Portland cement one, might be regarded as a "micro-aggregate concrete" (20). In fact, the unreacted slag micro-particles with their peculiar shape, could represent a barrier against the microcrackings propagation, thus obliging frequent interruption to fracture progress and preventing the crackings widening. The higher number of fracture surfaces would then enhance a wides distribution of the fracture energy, favouring a more ductile behaviour.

Accelerating the hydration process by means of steam curing, accomodation and orientation of calcium hydroxide at the interfacial regions of the Portland cement concretes become more difficult, minimizing the differences in the behaviour shown by the two types of cement.

REFERENCES

1. HSU T.T.C., SLATE F.O., STURMAN G.M. and WINTER G. (1963),"Microcracking of Plain Concrete and Shape of the Stress - Strain Curve", Journal of the Am. Concr. Inst., Vol. 60, n° 2, pp 209 - 224.

2. SLATE F.O., OLSEFSKI S. (1963), "X - Rays for Study of Internal Structure and Microcracking of Concrete", Journal of the Am. Concr. Inst., Vol. 60, n° 5, pp 575 - 588.

3. TAYLOR M.A., BROMS B. B. (1964), "Shear Bond Strength Between Coarse Aggregate and Cement Paste or Mortar", Journal of the Am. Concr. Inst. Vol. 61, n° 8, pp 939 - 957.

4. MORINO K. (1980), "Properties of bond between various types of rock aggregate and cement paste", Transactions of the Japan Concrete Institute, Vol. 2, pp 109 - 116.

5. MAZARS J. (1981), "Evolution de la microfissuration dans les bétons: formation de fissures", Beton n° 398, pp 23 - 42.

6. SHRIVE N.G. (1983), "Compression testing and cracking of plain concrete", Magazine of Concrete Research, Vol. 35, n° 122, pp 27 - 39.

7. CARRASQUILLO R.L. (1984), "Cracking and Failure: Mechanism of high Strength Concrete subjected to biaxial State of Stress", Proc. 6th Int. Conf. on Cement Mocroscopy, (Albuquerque, USA, March 26-29 1984) pp 344 - 359.

8. NALLATHAMBI P., KARIHALCO B.L., HEATON B.S. (1984) "Effect of specimen and crack size, water / cement ratio and coarse aggregate texture upon fracture toughness of concrete", Magazine of Concrete Research, Vol. 129, n° 129; pp 227 - 236.

9. ELIGEHAUSEN R., SAWADE G. (1985), "Verhalten von Beton auf Zug",Betonwerk + Fertigteil - Technik (5) pp 315 - 322.

10. MINDESS S. (1983), "Mechanical Performance of Cementitious Systems". In "Structure and Performance of Cements", Ed. Bartos P., Applied Science Publishers (London) pp 319 - 363.

11. GIANGRECO E. et alii (1985), "Indagine sperimentale comparativa sul comportamento a fessurazione e rottura di travetti in cemento armato". Report Istituto Tecnica delle Costruzioni, Università di Napoli, pp 1 - 56.

12. DARWIN D., MANNING D.G., HOGNESTAD E., BEEBY A.W. RICE P.F., GHOWRWAL A.Q. (1985), "Debate : Crack width, cover and corrosion", Concrete International, Vol. 7, n° 5, pp 20 - 35.

13. UNI 6407

14. SCHIESSL P. (1975), "Admisible crack width in reinforced concrete structures" In "Behaviour in service of concrete structures". Colloquium Inter Association, Tome II, Liege, pp 739 - 753.

15. BS 1881 - 1970.
ASTM C 496 - 71 (1979).

16. CONJEAUD M., LELONG B., CARIOU B. (1980),"Liaison pâte de ciment Portland - Granulats naturels", 7th Int. Congress on the Chem. of Cement, Paris, III, pp VII-6 - 11.

17. REGOURD M. (1980), "Structure et comportement des Hydrates des Ciments au Laitier", 7th Int. Congr. on the Chem. of Cement, Paris, I, pp III - 2/9-2/26.

18. BARKER A.P. (1984), "Structural and mechanical characterization of calcium hydroxide in set cement and the influence of various additives", World Cement Technology, Vol. 15, n° 1, pp 25 - 31

19. SERSALE R. (1983), "Aspects of the chemistry of additions". In "Advances in Cement Technology"Ed. Ghosh S.N., Pergamon Press, (Oxford) pp 537 - 567.

20. HUI - ZEHN L. (1982), "Morphology of interface between zeolite aggregate and cement paste". In: "Bond in Concrete", Ed. Bartos P., Applied Science Publishers, (London) pp 34 - 39.

P. BARTOS, Paisley College of Technology, Paisley, Scotland, U.K. 1

Bond in Cements Reinforced with Bundles of Fibres
Adherence dans les ciments armes avec les faisceaux de fibres 2.3

SUMMARY: Bundles of short wires or strands of fibres are used in manufacture of cement based composites but individual fibres are expected to separate during manufacture and disperse uniformly throughout the matrix in order that maximum efficiency of the reinforcement is achieved. Glass reinforced cement represents a case in which the fibres remain in bundles and form the basic reinforcing elements even in a finished composite.

Investigation of pullout failure mechanism of glass fibre strands embedded in cement-based matrices indicates that intermediate modes of failure occur apart from the complete pullouts or tensile fractures of the strand. The intermediate modes of failure include a combined mode in which certain fibres fracture in tension and the rest pull out and a telescopic mode in which pullouts and fractures occur in stages. The energy absorption during these types of failure is very high and significantly contributes to the pseudo-ductility of a young glass reinforced cement.

Types of fibres and matrices, age and exposure conditions change the fibre-matrix and fibre-fibre bond. Increased bond especially when combined with a decrease of glass fibre strength due to chemical attack or other damage changes the mode of pullout failure and causes embrittlement of the composite.

The principle of telescopic pullout failure of bundles of fibres offers a new way to improvement of both strength and toughness of a brittle matric composite provided the fibre-matrix and fibre-fibre bond are controlled over the expected service life of the composite. Development of special fibre bundles as reinforcement is proposed.

Malhas de arames curtos ou telas de fibras são usadas na manufatura de compostos baseados em cimento, mas espera-se que fibras individuais se separem durante a manufatura e se dispersem uniformemente pela matriz para que se consiga o máximo de eficiência de armação.Cimento reforçado com vidro representa um caso em que as fibras permanecem em conjunto e formam os elementos básicos de reforço mesmo num composto acabado.

Investigação do mescanismo de ruptura à tração de malhas de fibra de vidro embebidas em matrizes com base de cimento indica que acontecem formas intermediárias de ruptura, à parte de "pullouts" completas ou fratura de tração da malha. As formas intermediárias de ruptura incluem uma forma combinada em que certas fibras se fraturam por tensão e o resto se desligam, e uma forma telescópica em que "pullouts" e fraturas acontecem em estágios. A absorção de energia durante estes tipos de rompimento é muito alta e contribui significativamente para a pseudo-dutibilidade de um cimento novo reforçado com vidro.

Tipos de fibras e matrizes, idade e condições de exposição mudam a ligação fibra-matriz e fibra-fibra. Aumento da ligação, especialmente quando combinada com uma diminuição da resistência da fibra de vidro devido a ataque químico ou a outro dano, muda a forma de rompimento por "pullouts" e causa friabilização do composto.

O princípio de rompimento por desligamento telescópico de malhas de fibras oferece um modo novo para melhora da resistência e dureza de um composto de matriz friável, desde que a ligação fibra-matriz e fibra-fibra seja controlada durante o tempo de vida esperado do composto. Propõe-se o desenvolvimento de malhas de fibra especial como reforço.

INTRODUCTION

Fibre reinforced cements and concretes (FRC) are usually reinforced with short fibres. Manufacturing processes differ but the principal aim of all is a uniform dispersion of the fibrous reinforcement. Bundles of fibres or wires are also used instead of individual fibres, the main reasons being their easier incorporation into the cement matrix and, namely in case of glass fibres, a more convenient form for their manufacture and a better protection from damage during handling and production processes. During manufacture of a FRC the bundles are expected to break up as much as possible into individual fibres evenly distributed throughout the matrix. Uniform distribution of single fibres is considered desirable because only then the maximum efficiency and complete utilisation of the fibres can be achieved.

The separation into individual fibres is not always complete. Examples are asbestocement and glass reinforced cement (GRC). Asbestos fibres occur naturally as a 'fibrous mass' and despite being subjected to forcible separation during manufacture of the composite the very thin fibres remain in substantial bundles even in the finished product. The fibres are so well bonded together that the 'bundles' behave as solid, irregular and rough-surfaced reinforcing elements. Glass fibres are supplied as strands containing approx. 200 fibres each. The degree of disintegration of single fibres depends on the GRC production method and on the coating (size) of fibres which is used for their protection. Examination of sections of GRC indicated that strands split into smaller bundles but the number of individual fibres separating was very small. A bundle of fibres remains the basic reinforcing element in GRC. This is widely recognised but although investigations into microstructure of glass fibre strands especially after ageing are being carried out very little is known about their failure mechanism. In this paper the pullout modes of failure of glass strands are examined and the complexity of the process together with the influence of ageing are indicated.

The results are considered from the point of view of durability of GRC, especially its toughness and a new approach, based on specific development of the bundles of fibres as reinforcement is suggested for improvement of the GRC and other brittle-matrix composites.

BASIC CHARACTERISTICS OF BOND

In FRC reinforced with discontinuous fibres the external loads are transferred to the reinforcement through the cement matrix (Fig. 1). Bond which permits the load transfer consists of an adhesive, elastic bond q_c which is mobilised first, and frictional bond q_f which resists fibre displacement once the maximum q_a has been reached and the interface debonded. A non-linear distribution of adhesive bond and a uniform distribution of frictional bond are normally assumed. Such a simplified distribution is shown on Fig. 1. It should be noted that if the bond strength ($Q = \max q_a$) were small the reinforcement could debond partially or completely before cracking of the matrix. When matrix cracks the bond distribution changes significantly and the reinforcement is subjected to pullout (1).

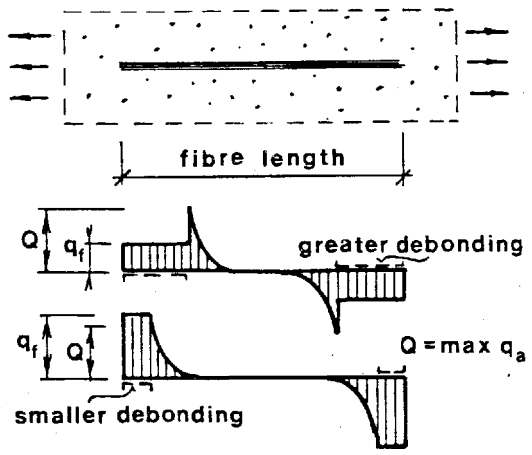

Fig. 1 Bond distribution, uncracked matrix. Effect of high and low frictional bond on debonding.

The degree of bonding is important:

(a) No fibre-matrix bond exists. The reinforcement is not utilised at all.
(b) There is good fibre-matrix bond but no bond between the fibres in a bundle. Only the fibres in contact with the matrix are utilised.
(c) There is bond both between the fibres and the matrix and between the fibres in the bundle. In this case the relative magnitude of the bond matters.

If the fibre-fibre bond were much stronger than the fibre-matrix bond the bundle would behave as a 'solid' single reinforcing element which would contribute to the composite properties according to the fibre-matrix bond only.

If the fibre-fibre bond were significantly less than the fibre-matrix bond the inner fibres would contribute partially to the strength of the composite. Intermediate modes of failure, partial pullout and fracture could occur.

The mechanism of pullout failure of a single fibre has been previously analysed in detail (2). It can be also applied to the pullout of a bundle. Depending on the relative magnitudes of adhesive and frictional fibre-matrix bond and on the tensile strength of the bundle overall, the following modes of pullout failure and corresponding critical embedment lengths are identified:

(a) Pullout following an instantaneous complete debonding. $L < L_p$.
(b) Pullout following a gradual debonding. $L_p \leq L < L_c$.
(c) Tensile fracture following a gradual debonding $L_c \leq L < L_t$.
(d) Tensile fracture without any previous debonding. $L < L_t$.

Diagram on Fig. 2 shows a special case in which the magnitude of adhesive and frictional bond and the strength of reinforcement are such that all four modes of failure occur. In many cases the original lengths L_p, L_c, L_t merge or do not exist, e.g. if the tensile strength of the fibre were greater than the debonding force (O-a-d) for all embedment lengths.

the critical length L_r would not occur.

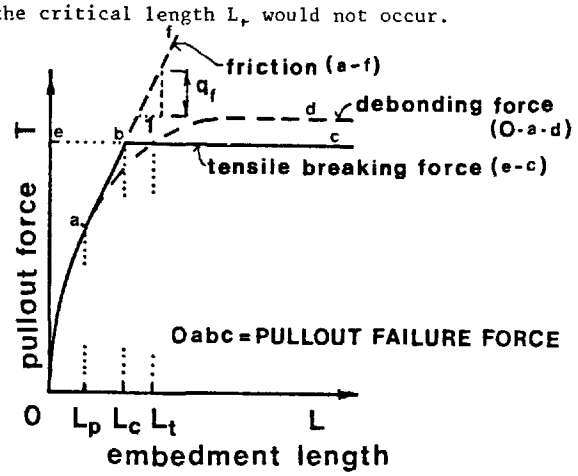

Fig. 2 Ultimate pullout force as a function of embedment length.

TELESCOPIC AND COMBINED FAILURES OF GLASS STRAND

An extensive programme of pullout tests (Fig. 3) was carried out for different combinations of matrices, glass fibres, curing conditions and age. Very many pullout force-extension diagrams were obtained. Part of the quantitative results has been used previously for quantitative assessment of bond using methods developed by the author (1,2,3). The shapes and other features of the force-extension diagrams were examined, compared with the condition of the strands after each test and the following modes of failure were identified:

(1) Complete tensile fracture of the whole strand. Typical curve is shown on Fig. 4.

(2) Complete pullout of the whole strand. The magnitude of the drop in pullout force after the peak had been reached indicated the strength of frictional bond (Fig. 5a). The lesser the drop the greater was the friction until it overshadowed the adhesive bond and dominated the pullout (Fig. 5b). Differences in static and dynamic friction and transverse strain variations often caused the stick-slip movement reflected as the saw-tooth shape of the pullout curve (Fig. 5b).

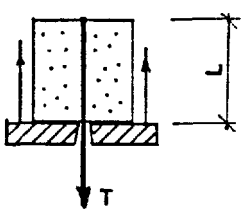

Fig. 3 Pullout test

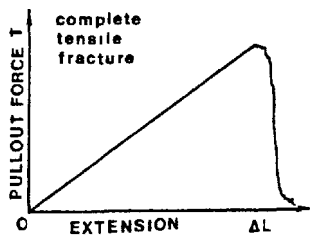

Fig. 4 Tensile failure

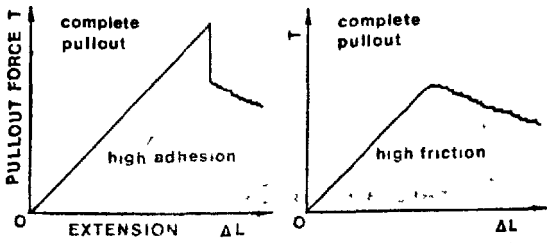

Fig. 5ab Complete pullouts

(3) Intermediate failure mode.
In a significant proportion of tests neither a complete fracture nor a complete pullout occurred. These intermediate modes were separated further into two types:

(i) Combined pullout and tensile failure.
In this case the outer fibres of the strand were weak and/or much better bonded to matrix than to the internal fibres which remained strong. The outer fibres fractured while the inner fibres pulled out. Typical curve is on Fig. 6.

(ii) Telescopic failure.
In this case the pullout force was sufficient to break the fibre-matrix adhesive bond and to commence the pullout. The frictional fibre-matrix bond permitted the pullout but the friction caused damage to the outer fibres which then fractured. The remaining 'core' fibres took on the pullout force and continued to pull out until the frictional fibre-fibre bond caused enough damage and another layer of the fibres failed in tension. Typically the telescopic failures occurred in two or three stages as shown on curve on Fig. 7. Depending on strength of bond and on embedment length more gradual telescopic failures were also observed.

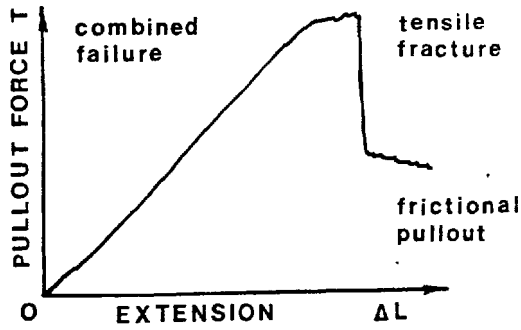

Fig. 6 Combined failure

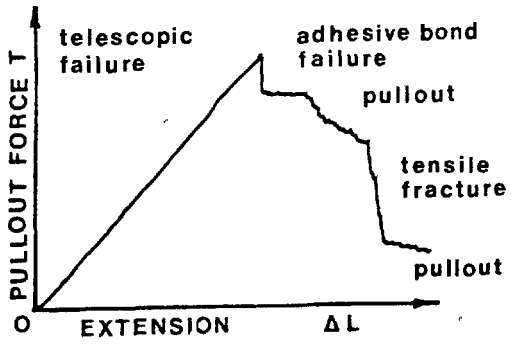

Fig. 7 Telescopic failure

Bond in FRC composite changes with age and curing. Strength of the matrix depends on similar parameters and strength of fibres is not always independent of age and environment either. The possibility of a reduction of strength of glass fibres in an alkaline cement is well known but recent report has indicated that even thin metallic fibres can change their basic mechanical properties once embedded in a cement

matrix (4).

The pullout tests revealed the effects of ageing, Figs. 8a and 8b show the example on E-glass strands embedded in ordinary portland cement paste.

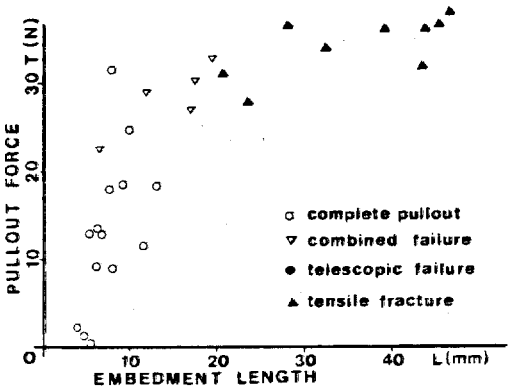

Fig. 8a Ultimate pullout force-embedment length diagram. OPC, w/c = 0.4, E-glass, air cure 50% R.H., 20°C, 28 days.

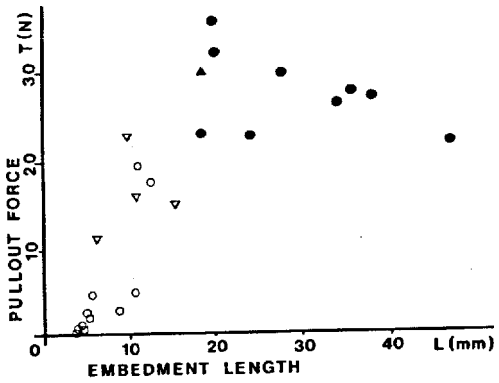

Fig. 8b As above; 90 days.

Matrices other than plain OPC were tested. High alumina cement (HAC) paste at w/c = 0.35 and a polymer modified OPC paste with a solid acrylic polymer content of 20% by mass of cement w/c = 0.35 were used in combination with E-glass and two types of alkali resistant (AR1, AR2) glass fibres.

Intermediate modes of pullout failure were observed for all combinations of fibres and matrices and curing conditions. There was never a clear transition from complete pullouts to complete tensile fractures as the embedment length increased. Diagram on Fig. 8a is a typical example. The telescopic modes of failure were identified only on specimens tested at the age of 90 days or more. The incidence of telescopic failures depended strongly on the type of glass and matrix used. Excluding the complete pullouts which were observed for short embedment lengths the following were approximate proportions of telescopic failures observed at the age of 90 days:

OPC/e-glass ..... 65%. HAC/E-glass 5%
OPC/AR1&AR2-glass .. 50% HAC/AR1-glass .. 15%
PPC/E-glass & AR1-glass .. none

The acrylic polymer (PPC) increased all bond so much that only extremely short embedment lengths produced a pullout or a combined failure (Fig. 9).

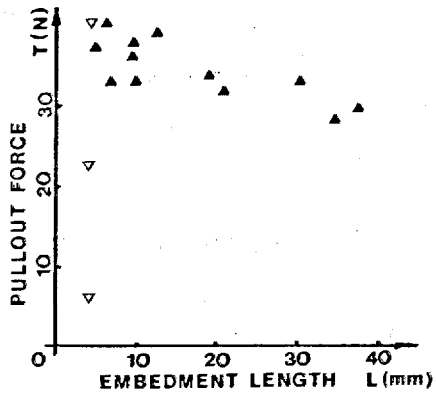

Fig. 9 Ultimate pullout force-embedment length diagram. PPC matrix, 90 days, air as for 8a.

The HAC also improved fibre-matrix and fibre-fibre bond.

Wet curing increased bond considerably and in case of AR2 fibres (a more recent version of the AR1 fibres having different coating) the complete pullouts were entirely eliminated and the incidence of telescopic pullouts was reduced (Figs. 10a,b).

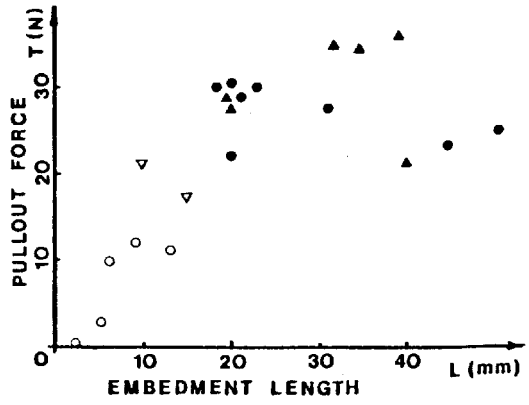

Fig. 10a Ultimate pullout force-embedment length diagram. OPC, w/c = 0.4, AR2-glass, air cure 50% R.H., 20°C, 180 days.

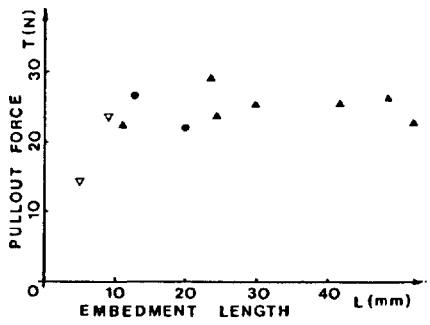

Fig. 10b As above, cured in water 20°C, 180 days.

BOND AND DURABILITY OF GRC

GRC represents a brittle matrix reinforced with brittle fibres and its toughness relies entirely on its pseudo-ductile behaviour. The pseudo-ductility depends on pullouts and intermediate failures of the fibre bundles.

In an unaged GRC the fibre-matrix bond is relatively low and the fibres are strong. The fibre-fibre bond is also relatively low. At this stage many strands fail by pullouts and intermediate modes of failure, both pullouts and tensile fractures are preceded by gradual debonding. The composite exhibits considerable pseudoductility and toughness. Initial ageing increases bond and mechanical properties of the composite may improve while the pseudoductility is generally maintained.

Ageing of GRC improves bond overall. The build-up of fibre-fibre frictional bond is important, if sufficiently high it eliminates all intermediate modes of pullout failure. Together with increased fibre-matrix frictional bond this change alone reduces the pseudoductility and fracture energy of the composite. If the strength of the fibres were also reduced the critical embedment length L_c would be greatly reduced and the length L_t would occur for a short fibre embedment. In such a case the pseudoductility is lost entirely and the toughness and impact resistance of the GRC is reduced close to that of a plain matrix.

The increase of the fibre-fibre frictional bond which is assumed to be caused by deposition of cement hydration products initially 'activates' the inner fibres of the strand. At early ages this can cause a better utilisation of the strand and off-set temporarily the loss of strength of the peripheral fibres affected by the alkali attack.

A total loss of the effect of fibre length on the properties of GRC with AR-fibres after 10 years has been reported by Majumdar and Singh (5). Bentur and Diamond (6) tested E-glass/OPC specimens which cracked without any significant fibre-matrix debonding. Both reports have provided further evidence that ageing, natural or artificial increased greatly the bond overall. Had there been no change of bond and the fibres were weakened the strength of the composite would have decreased but some pseudoductility would have been retained. The results published agreed with predictions made using relationships between individual and simultaneous effects of changes of bond and fibre strength previously developed (1,2).

Acrylic polymers are now increasingly used for modification of OPC matrix, additions of 10%-15% by mass of cement improve very considerably both fibre-matrix and fibre-fibre bond. The improved adhesive bond leads to a better utilisation of the strand and a higher strength of the polymer-modified GRC, the PGRC. The PGRC also maintains its strength better even if aged in water (7). The bond is so improved that the incidence of intermediate failures and pullouts is greatly reduced and the unaged PGRC has lower toughness than ordinary GRC (Fig.11), both with AR fibres.

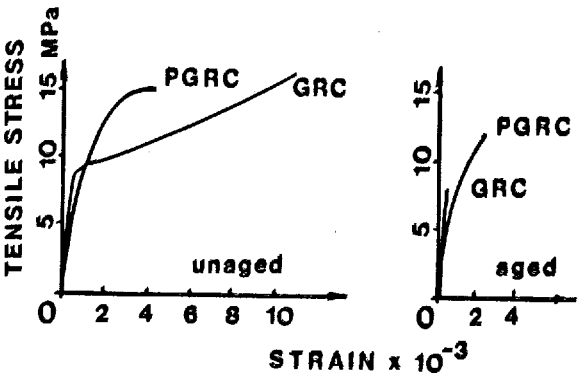

Fig.11 Tensile stress-stress diagrams of GRC and PGRC; unaged : 28d in 65% R.H., 20°C; aged : as above + 70 d. in water at 50°C. (7).

Ageing of PGRC increases the bond further and frictional bond becomes significant. The ultimate strain capacity of the PGRC is also reduced but the long-term value is greater than that of the GRC, mainly because of the polymer content of the composite. Fig. 11 indicates that the tensile stress and ultimate tensile strain of aged PGRC are improved but still far from satisfactory from the practical design application point of view. A considerable scope for improvement exists.

DISCUSSION OF METHODS FOR IMPROVEMENT OF BOTH STRENGTH AND TOUGHNESS OF FRC

Properties of FRC depend strongly on bond for the composite action between fibrous reinforcement and cement matrix. For brittle, low tensile strength matrices such as hardened cement paste fibres of high strength and stiffness are usually selected. If well bonded and dispersed as single fibres such a reinforcement increases strength of the resulting composite which, however, remains very brittle with only a very small or no improvement of its ultimate strain capacity over that of the matrix alone. In case the same fibres are not bonded well to the matrix, pullouts occur and the high strength and stiffness of the fibres is not fully utilised. The composite exhibits pseudoductility and improved ultimate strain capacity but the potential composite strength is not achieved.

The loss of toughness of GRC with age has important commercial consequences and as a result a considerable research development has been aimed at its improvement. Bijen (8) has recently reviewed this work and indicated that greatest effort was concerned with development of:

(a) More alkali resistant glass fibres,
(b) Special impermeable coating and coating which changed the affinity of glass to hydration products.
(c) Additions of polymers penetrating the strands and preventing deposition of hydration products between the fibres.
(d) Reduction of alkalinity of matrix, special cements and blended cements, microsilica, etc.

The generally low level of appreciation of bond is notable, it is often not understood that even if no reduction of fibre strength occurred high bond associated with strong cement matrices would lead to very low toughness in the long term.

A considerable market exists for composites based on relatively inexpensive matrices such as hardened cement which would have both strength and toughness much better than the matrix alone.

Several systems for such composites are possible and some have been already tried.

Reinforcing fibres with very thick coatings which provided two interfaces, a weak and a strong one when incorporated into brittle matrix can be made. The production costs of such 'hybrid" fibres are so high that the method does not appear to have been used in a practical composite.

Morley et al (7) proposed 'duplex' reinforcement which consisted of very thin tubes with helically crimped wires inside them. The shear bond at the internal interface adjusted itself according to the strain of the composite. The 'duplex' fibres were tried but did not find practical application.

More than one type of single fibre reinforcement can be used to satisfy the strong and weak bond requirement. However, the maximum fibre content which can be incorporated into cement matrix is low and varies according to the fibres. Single fibres designed to increase strength usually require longer length and the resulting high aspect ratio often reduces the practical fibres content. Uniform dispersion of two different fibres is also complicated by their tendency to segregate.

CONCLUSIONS

Investigation of pullout failures of glass fibre strands embedded in cement matrices revealed the existence and significance of intermediate modes of pullout failure. The energy absorption of the fibre bundles failing in a combined or telescopic mode was usually greater than when complete pullouts or complete tensile fractures of the bundles were recorded.

The changes of bond associated with continuing hydration of cement matrix gradually reduced or eliminated the complete pullouts or intermediate failures of the embedded glass fibre strands. The bond, if sufficiently increased, could cause a loss of pseudo-ductility of a FRC composite with stiff strong fibres even if the fibre strength remained unaffected.

The investigations indicated the considerable potential of bundles of fibres to act as reinforcement which can improve both strength and toughness of a brittle matrix composite. The potential lies in the capacity of bundled fibrous reinforcement to fail in the telescopic mode when subjected to pullout force. A specifically designed bundle of fibres in which the perimeter fibres are well bonded to or anchored into the matrix and the inner, core fibres are bonded enough to pull out, or pull-out and fracture, even after long ageing will contribute both to strength and toughness of the composite. Such new system appears particularly applicable to FRC composites based on new macro-defect-free and densified microsilica high-strength cement matrices.

The results emphasise the importance of fibre-matrix and fibre-fibre bond including the relative magnitude of adhesive and frictional bond on the fracture mechanism of a FRC composite reinforced with fibre bundles such as GRC. Significant progress has been achieved by other researchers in identification and assessment of microstructures of interfacial regions of cement based composites. However, it is suggested that in such research not only changes in properties of constituent materials of the composites but the bond characteristics and their implication should be considered as well.

CURRENT AND FUTURE RESEARCH PROPOSED

A new programme aimed at a development of special bundled fibre reinfocement for reinforcement of brittle matrices, especially cement based ones has been commenced. The current first stage concentrates on fundamental behaviour of bundles containing varying numbers of metallic fibres of different diameters and on development of an appropriate theoretical model. A specially designed SEM stage which permits observations of pullouts on specimens up to 100 mm long has been installed and successful pilot tests have been carried out. A parallel programme orientated more towards development of different bundle configurations and compositions for potential practical composites is being planned.

REFERENCES

1. - P. BARTOS (1981) "Bond in fibre reinforced cement and concretes", Intl.J.ofCem.Composites, Vol.3, No.3, pp.159-177.

2. - P. BARTOS (1980) "Analysis of pullout tests on fibres embedded in brittle matrices", J.Mat.Sci. Vol.15, No.12, pp.3122-3128.

3. - P. BARTOS (1982) "Bond in concrete", Proc.Intl. Conf. on Bond in Concrete, Paisley, Scotland, pp.60-72, Elsevier Applied Science, London, 1982.

4. - C.K. JOLLY (1985) "The stiffness and strength of small diameter steel fibres in cementitious composites", 3rd Intl.Conf. on Composite Structures, Paisley, Scotland, Sept.9-11, 1985.

5. - B. SINGH, A.J. MAJUMDAR (1985) "The effect of fibre length and content on durability of glass reinforced cement - ten year results", J.Mat. Sci., Lett., Vol.4, pp.967-971.

6. - A. BENTUR, S. DIAMOND (1984) "Fracture of glass fibre reinforced cement", Cem. & Con. Res., Vol.14, pp.31-42.

7. - M. JACOBS (1985) "Durability of PGRC : Design implications", 5th Biennial Congress of GRCA, Darmstadt, Oct. 16-18, 1985.

8. - J. BIJEN (1985) "A survey of new developments in glass composition, coatings and matrices to extend service life to GFRC", Intl.Symp. on Durability of glass fibre reinforced concrete, Chicago, USA, Nov.12-15, 1985.

9. - J.G. MORLEY, R.S. MILLAN (1974) "The application of self-adjusting interfaces to the design of fibrous composites", J.Mat.Sci., Vol.9, pp. 1171-1182.

Abla Gráfica e Editora Ltda.
Rua Júlia Lopes de Almeida, 15 e 15-A
Telefones: 253-6054, 253-6296, 253-6329
Rio de Janeiro – RJ

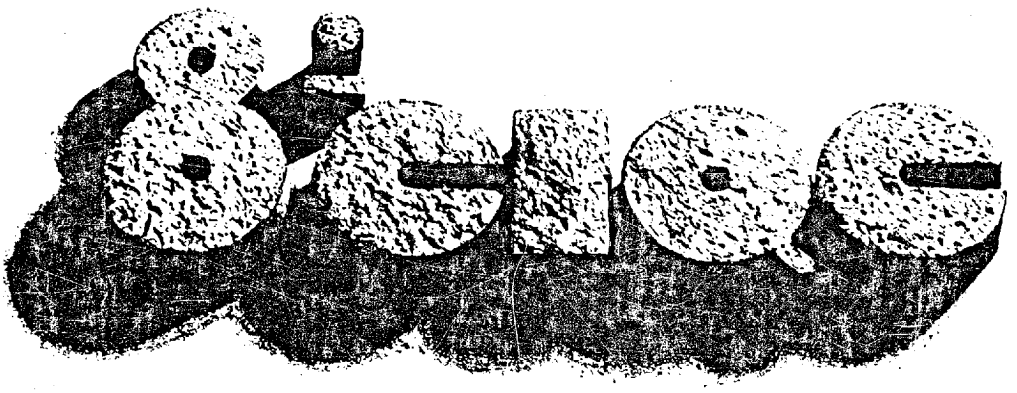

8.º Congresso Internacional de Química do Cimento

8th International Congress on the Chemistry of Cement

8e Congrès International de la Chimie des Ciments

Communications
THEME 3
Volume IV

22-27 de setembro de 1986
Rio de Janeiro — Brasil

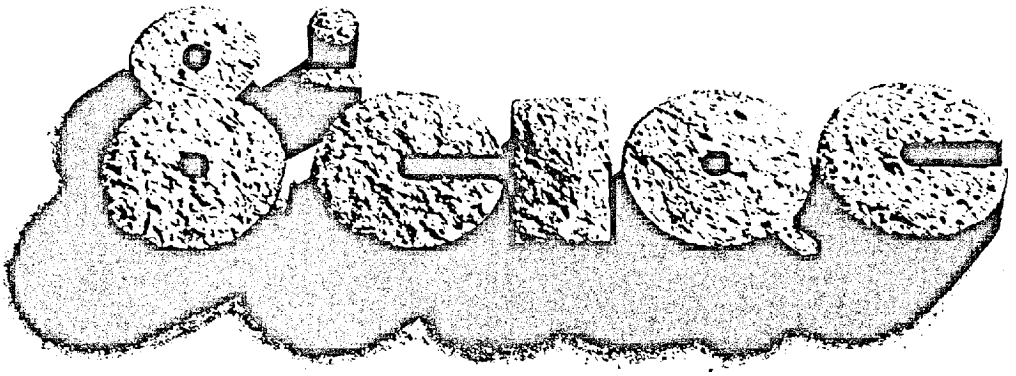

8.º Congresso Internacional de Química do Cimento

8th International Congress on the Chemistry of Cement

8e Congrès International de la Chimie des Ciments

Communications
THEME 3
Volume IV

22-27 de setembro de 1986
Rio de Janeiro — Brasil

Não é permitida a reprodução dos Anais sem prévia autorização da Comissão Organizadora do Congresso.

The Proceedings are not to be reprinted without a previous permission of the Organizing Commission of the Congress.

La reproduction des Annales est interdite sans, au-devant, l'autorisation de la Commission d'Organisation du Congrès.

• • •

A substância e a forma de apresentação dos trabalhos que compõem os Anais do Congresso são de exclusiva responsabilidade de seus autores.

The substance and the form of presentation of the papers that compound the Proceedings of the Congress are exclusive responsability of their authors.

Le fond et la forme de publier les travaux qui composent les Annales du Congrès sont d'exclusive responsabilité de leur auteurs.

Secretaria Geral do 8º CIQC:
Rua da Assembléia, 10 - 40º and. - Gr. 4001
Tel.: 221-6562 – Telex: (021) 33191
20011 Rio de Janeiro – RJ – Brasil

Apoio financeiro da

finep FINANCIADORA DE ESTUDOS E PROJETOS

ORGANIZING COMMISION:

PRESIDENT:	JOSÉ ERMÍRIO DE MORAES FILHO	BRASIL
EXECUTIVE VICE-PRESIDENT:	PAULO MÁRIO FREIRE	BRASIL
TECHNICAL DIRECTOR:	FRANCISCO DE ASSIS BASÍLIO	BRASIL
ADMINISTRATIVE DIRECTOR:	JOÃO BATISTA MENESCAL FIUZA	BRASIL
DIRECTORS:	ALBERTO LUIZ GONÇALVES SOARES	BRASIL
	ENRIQUE GUNTHER DREWES	BRASIL
	EPAMINONDAS MELO DO AMARAL FILHO	BRASIL
	MARCÍLIO DE BRITO	BRASIL
	NEWTON GOULART	BRASIL

SCIENTIFIC COMMITTEES:

- SOUTH AMERICA:
  - PRESIDENT:

FRANCISCO DE ASSIS BASÍLIO	BRASIL
ALVARO AUGUSTO ALVES PINTO	BRASIL
DANTE E.J. VERONELLI	ARGENTINA
FLEMING OEST	BRASIL
HANS BUCHER	BRASIL
JOÃO GASPAR DJANIKIAN	BRASIL
LUIZ ROBERTO MARTINS DE MIRANDA	BRASIL
MARIA DAS GRAÇAS JAQUÁ	BRASIL
MARIA LUIZA MOREIRA DE MORAES	BRASIL
NEY JOSÉ DE SOUZA E SILVA	BRASIL
PABLO KITTL D.	CHILE
PAULO RODRIGUES	BRASIL
ROBERTO R. COELHO	BRASIL
YASUKO TESUKA	BRASIL
YUSHIRO KIHARA	BRASIL

- NORTH AND CENTRAL AMERICA, AND FAR EAST:
  - PRESIDENT:
  - MEMBERS:

JAN P. SKALNY	U.S.A.
DELLA M. ROY	U.S.A.
GEOFFREY FROHNSDORFF	U.S.A.
GERARD G. LITVAN	CANADA
HIROSHI UCHIKAWA	JAPAN
J. FRANCIS YOUNG	U.S.A
JORGE MARIO VILLASENOR	MEXICO
R.E. OBERHOLSTER	SOUTH AFRICA
SIDNEY DIAMOND	U.S.A.
S.W. TRESOUTHICK	U.S.A.
WU ZHONG-WEI	CHINA

- EUROPE, ASIA AND AFRICA:
  - PRESIDENT:
  - MEMBERS:

JEAN PAUL MERIC	FRANCE
C. CHARRETON	FRANCE
FRANCO MASSAZZA	ITALY
FRANÇOIS LE BEL	FRANCE
FRIEDRICH W. LOCHER	WEST GERMANY
F. YAGIZ	TURKEY
H.W.W. POLLITT	ENGLAND, U.K.
JOSE CALLEJA	SPAIN
J. TALLABER	HUNGARY
LABO KADA ABOUBACAR	NIGERIA
O.P. MTCHEDLOV-PETROSSIAN	U.S.S.R.
P. DUTRON	FRANCE
RENATO BUCCHI	ITALY
S.K. CHOPRA	INDIA
T.V. KOUZNETSOVA	U.S.S.R.
WIESLAW KURDOWSKI	POLAND

INDEX

AUTHORS'NAMES/NOMS DES AUTEURS	SUB-THEMES/SOUS-THÈMES
A	
ADDEL-REHIM, H.A.A.	3.3
AITCIN, P.C.	3.1
AMBROISE, J.	3.1 – 3.3
ANDREEV, V.V.	3.3
ANDRONESCU, E.	3.3
ATZENI, C.	3.2
B	
BACHIORRINI, A.	3.3 (2)
BAILEY, J.E.	3.2
BANFILL, P.F.G.	3.3
BARRET, P.	3.3
BATTAGIN, A.F.	3.1
BELLINA, G.	3.1
BENSTED, J.	3.3
BERGER, R.L.	3.2
BHATTY, M.S.Y.	3.1
BOJENOV, P.I.	3.2
BOMBLED, J.P.	3.1 (2) – 3.2
BORLERA, M.L.	3.3
BRISI, C.	3.3
C	
CARLES-CIBERGUES, A.	3.1
CHATTERJEE, A.K.	3.1
CHENG, HAN QI	3.1
CIOFFI, R.	3.2
CUSSINO, L.	3.3
D	
DERDACKA-GRZYMEK, A.	3.3
DJABAROV, N.B.	3.3
DJUREKOVIC, A.	3.1 – 3.2
DRON, R.	3.1
E	
EDEN, N.B.	3.2
EL-JAZAIRI, B.	3.3
ELOLA, A.I.	3.2
F	
FOURNIER, A.A.	3.3
FUKAYA, K.	3.1 – 3.2
G	
GAIDJOUROV, P.	3.3
GAROFANO, R.	3.3
GEGOUT, P.	3.2
GEORGE, C.M.	3.3
GEORGESCU, M.	3.3

GHOSH, R.	3.3
GOMA, F.	3.3
GOVOROV, A.A.	3.1
GILL, S.M.	3.1
GRANDET, J.	3.2
GRIGOR'EV, B.A.	3.2
GRZYMEK, J.	3.3
GU, Z.Z.	3.2
GUILHOT, B.	3.3
GUSTAW, K.	3.2
H	
HALSE, Y.	3.2 – 3.3
HANEHARA, S.	3.2
HANNA, B.	3.2
HARRISON, A.M.	3.2
HASABA, S.	3.1
HEBLE, A.S.	3.3
HORNAIN, H.	3.2
HOSEK, J.	3.3
HU, KE-YONG	3.3
I	
IIJIMA, Y.	3.2
ISHIKAWA, Y.	3.2
IWANCIW, J.	3.3
J	
JENSEN, H.-U.	3.2
JI, SHANG-XING	3.3
JIPING, CHENG	3.1
JIZHI, XU	3.3
JUNGAN, XUE	3.3
K	
KAWAMURA, M.	3.1
KOIBUCHI, K.	3.2
KOLAR, K.	3.3
KOLLEK, J.J.	3.2
KONIK, Z.	3.3
KONISHI, E.	31. – 3.2
KORNEEV, V.I.	3.3
L	
LAXMI, S.	3.3
LIQUN, YANG	3.1
LIU, YIN-JIANG	3.3
M	
MACDOWELL, J.F.	3.3
MALEK, R.I.A.	3.2 (2)
MALOLEPSZY, J.	3.1 (2)
MANDAL, P.K.	3.3
MARCHESE, B.	3.2
MARCIALIS, A.	3.2
MASSIDDA, L.	3.2
MENETRIER-SORRENTINO, D.	3.1 – 3.3 (2)
MIZUKAMI, Y.	3.2
MORAES, M.L.M.	3.3
MORTUREUX, B.	3.1 – 3.2
MUDBHATKAL, G.A.	3.3
MURAT, M.	3.1 – 3.3 (2)
N	
NEGRO, A.	3.3
NIKIFOROV, U.V.	3.3
NOUDELMAN, B.I.	3.3
NOVOTNY, J.	3.3
O	
OGAWA, K.	3.2
OLLIVIER, J.P.	3.2
OPOCZKY, L.	3.2
OSBAECK, B.	3.1
OUDJIT, M.N.	3.1

P	
PAI, B.V.B.	3.3
PARAMESWARAN, P.S.	3.1 – 3.3
PÉRA, J.	3.1 – 3.3
PETRI, M.	3.1
POPOVIC, K.	3.1
POULATOV, Z.P.	3.3
PRATT, P.L.	3.2 – 3.3
PURI, A.	3.3
PUZALSKI, M.	3.3
Q	
QIZHONG, SHENG	3.1
R	
REGOURD, M.	3.2
RÉVAY, M.	3.3
ROSZCZYNIALSKI, W.	3.2
ROY, D.M.	3.2 (2)
S	
SAKAKIBARA, Y	3.3
SANNA, U.	3.2
SANTORO, L.	3.3
SAQOUT, S.	3.3
SATO, K.	31 – 3.2
SERSALE, R.	3.2
SHKOLNICK, Y. SH.	3.1
SHIYUAN, HUANG	3.1
SILSBEE, M.	3.2 (2)
SILVA, M.G.P.	3.3
SILVEIRA, M.	3.3
SORRENTINO, F.P.	3.3
SOUSTELLE, M.	3.3
STOK, A.	3.3
SUBBA RAO, V.V.	3.3
SZATURA, L.	3.2
SZTEINBERG, A.S.	3.2
T	
TAKANO, Y.	3.2
TAYLOR, H.F.W.	3.2
TEOREANU, I.	3.3 (2)
THURET, B.	3.2
TORII, K.	3.1
TORRENT, R.J.	3.2
TRIVIÑO, F.	3.3
TANG, T.F.	3.2
U	
UCHIDA, S.	3.2 (2)
UCHIKAWA, H.	3.2 (2)
UKRAINCIK, V.	3.1
V	
VALENTI, G.L.	3.2 – 3.3
VAQUIER, A.	3.1
VARMA, S.P.	3.2
VINCZE-SZÉKELY, I.	3.2
VOLANT, J.	3.2
W	
WANG, SHAN-BA	3.2 – 3.3
WANG, W.J.	3.2
WENHAO, CHEN	3.3
WINTER, N.B.	3.2
X	
XIANYU, XU	3.1
XUELI, TONG	3.3

Y	
YAMAZAKI, Y.	3.3
YAOZHONG, XI	3.3
YIYU, ZHANG	3.3
YUE, M.L.	3.2
YUJI, WANG	3.1
Z	
ZARIS, C.	3.2
ZHOU, B.W.	3.2
ZONGHAN, LOU	3.1
ZOUBEKHIN, A.P.	3.3

CONTENTS/TABLE DE MATIÈRES

THEME/THÈME 3
BLENDED AND SPECIAL CEMENTS/CIMENTS SPÉCIAUX ET CIMENTS AVEC ADDITIONS.

Chairman/Président: V.I. KUSCHIDI (U.S.S.R.) – Secretary/Secrétaire: Y. KIHARA (Brasil)

SUB-THEME/SOUS-THÈME 3.1
Characteristics and Activation of Blending Components.
Caractéristiques et Activation des Composants des Matières d'Addition.

Chairman/Président: R. BUCCHI (Italy) – Principal Reporter/Rapporteur Principal: M. REGOURD (France)

Pages	Authors (Countries)/Auteurs (Pays)	Titles of Papers/Titres des travaux
17	A.F. Battagin (Brasil)	The use of microscopy for estimating the basicity of slags in slag-cements.
22	P.C. Aitcin (Canada), A. Carles-Cibergues, M. Oudjit, A. Vaquier (France)	Influence des éléments autres que Si sur la réactivité des fumées de silice.
30	Lou Zonghan, Xu Xianyu, Yang Liqun, Sheng Qizhong (China)	Dissociation of aluminium from slag glasses and formation of ettringite.
36	Wang Yuji (China)	The effect of hydration products in steam treated steel slag (O.C.S.) on the hydration of steel slag-portland blended cement.
41	Huang Shiyuan, Cheng Jiping (China)	The evaluation of pozzolanic reactivity of fly ashes.
46	Han Qi Cheng (China), B. Osbaeck (Denmark)	Effects of fly ash grinding on the hydration and strength development of fly ash cements.
	M. Murat, J. Ambroise, J. Péra (France)	Les différents procédés d'activation des minéraux argileux permettant d'élaborer des liants pouzzolaniques à résistances optimales.
60	D. Menetrier-Sorrentino (France)	Particle size distribution in blended cements.
66	J.P. Bombled (France)	Différents moyens d'actovatopm des materiaux potentiellement pouzzolaniques. Application aux liants chaux-pouzzolane.
74	J.P. Bombled, G. Bellina, B. Mortureux (France)	Détermination des courbes granulométriques te des aires massiques des constituants de mélanges cobroyés: applications aux fillers et aux laitiers.
81	R. Dron (France)	Structure et reactivité du laitier granulé.
86	P.S. Parameswaran, A.K. Chatterjee (India)	Alkali activation of indian blast furnace slags.
92	M. Kawamura, K. Torii, S. Hasaba (Japan)	Reaction process and microstruture in compacted fly ashes and fly ash-chemical additive mixtures.
98	K. Sato, E. Konishi, K. Fukaya (Japan)	Hydration of blast furnace slag particle.
104	J. Malolepszy (Poland)	Activation of synthetic melilite slags by alkalies.
108	J. Malolepszy, M. Petri (Poland)	High strength slag-alkaline blinders.
112	F. Gomà (Spain)	Generalized method for the determination of the composition of portland cement mixtures with additions.

118	M.S.Y. Bhatty (U.S.A.)	Properties of blended cements made with portland cement, cement kiln dust, fly ash, and slag.
128	A.A. Govorov (U.S.S.R.)	Certains aspects de la structure des laitiers granulés.
133	Y.Sh. Shkolnick (U.S.S.R.)	Physicochemical principles of the hydraulic activity of blast furnace slags.
137	K. Popovic, A. Djurekovic, V. Ukraincik (Yugoslavia)	Blended and special cements incorporating condensed silica fume.

SUB-THEME/SOUS-THÈME 3.2
Effect of Blending Components on Hydration and Structure Formation.
Effets des Composants des Matières d'Additions dans l'Hydratation et dans la Formation de la Structure.
Chairman/Président: J. CALLEJA (Spain)
Principal Reporter/Rapporteur Principal: H. UCHIKAWA (Japan)

Pages	Authors (Countries)/Auters (Pays)	Titles of Papers/Titres des travaux
145	A.I. Elola, A.S. Szteinberg, R.J. Torrent (Argentina)	Effect of the addition of blastfurnace slag on the physical and mechanical properties of mortars cured at high temperatures.
150	Z.Z. Gu, B.W. Zhou, M.L. Yue, T.F. Tang, W.J. Wang (China)	Effect of cement composition on the strength contribution of fly ash.
158	Shan-Ba Wang (China), R.L. Berger (U.S.A.)	Effect of $Ca(OH)_2$ and $CaSO_4.2H_2O$ on the strength of flyash cement pastes.
163	N.B. Eden, J.E. Bailey (England, U.K.)	Effect of polymer modifications on the mechanical properties of calcium silicate and calcium aluminate cements.
170	A.M. Harrisson, N.B. Winter (England, U.K), H.F.W. Taylor (Scotland, U.K.)	An examination of some pure and composite portland cement pastes using scanning electron microscopy with X-ray analitical capability.
176	Y. Halse, H.-U. Jensen, P.L. Pratt (England, U.K.)	The effect of the curing temperature on the pozzolanic reaction in flyash blended cement.
183	J.J. Kollek, S.P. Varma, C. Zaris (England, U.K.)	Measurement of OH^- ion concentrations of pore fluids and expansion due to alkali-silica reaction in composite cement mortars.
190	J.P. Bombled (France)	Rheologie du béton frais: Influence de l'ajout de fillers aux ciments.
197	P. Gegout, H. Hornain, B. Thuret, B. Mortureux, J. Volant, M. Regourd (France)	Texture et performance des ciments fillerisés.
204	J.P. Ollivier, J. Grandet, B. Hanna (France)	Action d'un fluidifiant et d'une fumée de silice condensée réactive aux courtes échéances sur la liaison gros granulat-mortier.
210	L. Opoczky, I. Vincze-Székely, L. Szatura (Hungary)	Research on making cements of improved sulfate resistance and watertightness.
218	B. Marchese (Italy)	Interfacial microstructural alterations of mature blast furnace cement pastes.
224	C. Atzeni, A. Marcialis, L. Massidda, U. Sanna (Italy)	Effect of fine mineral admixtures on the properties of hardened cement pastes.

228	G.L. Valenti, R. Cioffi, R. Sersale (Italy)	Behaviour of italian fly ash in portland cement mortars.
233	Y. Takano, Y. Mizukami (Japan)	Influence of calcium sulfate on hardng of cement paste mixed with humic acid.
239	K. Sato, E. Konishi, K. Fukaya, K. Koibuchi, Y. Ishikawa, Y. Iijima (Japan)	Properties of very fine blast furnace slag prepared by classification.
245	H. Uchikawa, S. Uchida, S. Hanehara (Japan)	Effect of character of glass phase in blending components on their reactivity in calcium hydroxide mixture.
251	H. Uchikawa, S. Uchida, K. Ogawa (Japan)	Influence of character of blending component on the diffusion of Na and Cl in ions hardened blended cement paste.
257	W. Roszczynialski, K. Gustaw (Poland)	Activity of fly ashes used as a pozzolanic admixture to cement.
263	M. Silsbee, R.I.A. Malek, D.M. Roy (U.S.A.)	Composition of pore fluids extruded from slag-cement pastes.
270	R.I.A. Malek, M. Silsbee, D.M. Roy (U.S.A.)	Zeta-potential and rheological behaviour of slag pastes.
276	P.I. Bojenov, B.A. Grigor'ev (U.S.S.R.)	Ciments multicomposants à base des laitiers de métallurgie des métaux non ferreux.
279	A. Djurekovic (Yugoslavia)	Hydration of alite and C_3A and changes of some structural characteristics of cement pastes by addition of silica fume.

SUB-THEME/SOUS-THÈME 3.3
Special Cements. Calcium Aluminate and Other No-Silicate Cementes. Ciments Spéciaux. Ciments à Base d'Aluminates Calciques et Autres Ciments sans Silicates

Chairwoman/Président: T.V. KOUZNETSOVA (U.S.S.R.)
Principal Reporter/Rapporteur Principal: W. KURDOWSKI (Poland)

Pages	Authors (Countries)/Auters (Pays)	Titles of Papers/Titres des travaux
289	M.G.P. Silva, M.L.M. de Moraes, H.A.A. Abdel-Rehim (Brasil)	The effect of the hemihydrated and dihydrated cristalline forms of calcium sulphate on the thickening time, rheological properties and compressive strength of the oil well cement slurries.
295	N.B. Djabarov (Bulgaria)	Expansive cement with hydroxyde expanding phase on admixture's basis.
301	Shan-Ba Wang, Shang-xing Ji, Yin-Jiang Liu, Ke-Young Hu (China)	Effect of alkali on the expansive properties of sulfoaluminate cement pastes.
306	Xue Jungan, Tong Xueli, Chen Wenhao, Xu Jizhi, Xi Yaxhong, Zhang Yiyu (China)	Study on high self-stress aluminate cement.
312	J. Hosek, K. Kolar, J. Novotny (Czechoslovakia)	Shrinkage problem of quick-settinng cement.
317	Y. Halse, P.L. Pratt (England, U.K.)	The development of microstruture in high alumina cement.
322	S.M. Gill, P.F.G. Banfill, B. El-Jazairi (England, U.K.)	The effect of superplasticisers on the hydration of aluminous cement.

328	J. Bensted (England, U.K.)	Infrared spectral examination of oilwell cements.
334	D. Menetrier-Sorrentino, C.M. George, F.P. Sorrentino (France)	the stting and hardening characteristics of calcium aluminate cements: studies of the systems $C_{12}A_7$-C_3A and $C_{12}A_7$ - CA.
339	D. Menetrier-Sorrentino, P. Barret, S. Saqout (France)	Investigations on the system MgO-$MgCl_2$-H_2O, and hydration of Sorel cement.
344	J. Péra, J. Ambroise, M. Murat, M. Silveira (France)	Ciments à base de laterites thermiquement activées. Rôle des oxydes de fer dans le developpement des resistances mecaniques.
351	M. Révay (Hungary)	A summary of experiences on estimating the expectable changes of strength of concretes made with high alumina cement.
357	S. Laxmi, P.K. Mandal, R. Ghosh, V.V. Subba Rao (India)	Development of a fast setting high strength cement composite.
364	G.A. Mudbahatkal, P.S. Parmeswaran, A.S. Heble, B.V.B. Pai, A.K.Chatterjee (India)	Non-alitic cement from calcium sulphoaluminate clinker – Optimisation for high-strength and low-temperature application.
371	M.L. Borlera, C. Brisi (Italy)	Stability of the compound C_5A_3 in the system CaO-Al_2O_3.
376	A. Bachiorrini, A. Negro (Italy), B. Guilhot, M. Murat, M. Soustelle, A.A. Fournier (France)	Influence de la calcite sur l'hydratation de l'aluminate monocalcique. Corrélation entre les résultats expérimentaux et la thermodynamique du système.
383	A. Bachiorrini, L. Cussino (Italy)	Hydratation en milieur pur et en solution sulfate du ciment alumineux en presence d'aggrégat siliceux ou calcaire.
389	L. Santoro, R. Garofano, G.L. Valenti (Italy)	Calcium sulphoaluminate made from phosphogypsum and its hydration properties.
395	Y. Yamazaki, Y. Sakakibara (Japan)	The mecanism of expansive pressure development with the hydration of CaO.
401	J. Grzymek, A. Derdacka-Grzymek, Z. Konik, M. Pyzalski, A. Stock, J. Iwanciw (Poland)	The effect of synthesis and cooling conditions on phase properties of the $C_{12}A_7$.
407	I. Teoreanu, M. Georgescu, A. Puri (Romania)	The influence of some additions on the hydration and hardening of tricalcium aluminate.
412	I. Toreanu, E. Andronescu (Romania)	Le comportement, dans le processus de durcissement, des certaines compositions su systeme $3CaO.SiO_2$ – $2CaO.SiO_2$ – $2BaO.Sio_2$. Ciment fondu: comme eviter leur degradation des résistances mécaniques.
417	F. Triviño (Spain)	Hydrogarnet-gehlenite hydrate cements from CaO-Al_2O_3-SiO_2 glasses.
423	J.F. MacDowell (U.S.A.)	Ciments sur la base des hydrogenats et des hydrocarboaluminates de calcium.
429	V.I. Korneev, V.V. Andreev, U.V. Nikiforov (U.S.S.R.)	Ciment d'alinite résistant aux sulfates.
433	Z.P. Poulatov, B.I. Noudelman (U.S.S.R.)	Particularités des phénomènes de formation de minéraux et d'hydratation des ciments décoratifs et en haute teneur de fer.
438	P. Gaidjourov (U.S.S.R.)	Nouveaux aspects de la chimie physique du ciment portland blanc.
443	A.P. Zoubekhin (U.S.S.R.)	

THEME/THÈME 3

Blended and special cements. Ciments spéciaux et ciments avec additions.

Chairman/Président :

V. I. Kuschidi
Institute Niicement
Moscow, U.S.S.R.

Secretary/Secrétaire :

Y.Kihara
Associação Brasileira de Cimento Portland, São Paulo, Brasil

SUB-THEME/SOUS-THÈME 3.1

Characteristics and activation of blending components.

Caractéristiques et activation des composants des matières d'addition.

Chairman/Président :

R. Bucchi
Italcementi, S.p.A.
Bergamo, Italy.

Principal Reporter/Rapporteur Principal:

M. Regourd
C.E.R.I.L.H.
Paris, France

ARNALDO FORTI BATTAGIN, Research Mineralogist, Departament of Physicochemistry, Associação Brasileira de Cimento Portland, SP, Brazil.

THE USE OF MICROSCOPY FOR ESTIMATING THE BASICITY OF SLAGS IN SLAG-CEMENTS
L'UTILISATION DE LA MICROSCOPIE OPTIQUE POUR L'EVALUATION DE LA BASICITÉ DU LAITIER DANS LES CIMENTS AUX LAITIERS

ABSTRACT: Many countries require or suggest in their specifications for slag-cements the use of chemical moduli calculated from the chemical composition of the slags.

Based on this fact, this paper deals with an attempt of correlating, by means of the linear regression analysis, the refractive index of granulated blastfurnace slags to the most usual chemical moduli employed in the quality control of slags.

The investigation of 30 samples of slags from different origins shows a good correlation between the refractive index and $\frac{C + M + 1/3A}{S + 2/3A}$, $\frac{C}{S}$, $\frac{C + M}{S}$, $\frac{C + M + A}{S}$. The correlation coefficient r ranges from 0.96 to 0.99.

Simultaneously, r values of 0.91, 0.80 and 0.87 were obtained in this investigation correlating the refractive index of the slags to the compressive strength of slag-cements at 7, 28 and 90 days, respectively.

Besides its quickness, the method may be applied for estimating the moduli of slags in slag-cements samples were the application of chemical method requires previous and laborious separation of the slag.

Muitos países exigem ou sugerem em suas especificações para cimentos com escórias, o uso de módulos químicos calculados em função da composição química das escórias.

Baseado nesse fato, este trabalho trata de uma tentativa de correlacionar, por meio de análise de correlação linear, o índice de refeação das escórias granuladas de alto forno com os módulos químicos empregados no controle de qualidade das escórias.

A investigação de 30 amostras de escórias de diferentes origens mostrou boa correlação entre o índice de refração e $\frac{C + M 1/3A}{S + 2/3A}$, $\frac{C}{S}$, $\frac{C + M}{S}$, $\frac{C + M + A}{S}$. O coeficiente de correlação r variou de 0,96 a 0,99.

Simultâneamente, valores de r de 0,91, 0,80, 0,87 foram obtidos nesta investigação correlacionando o índice de refração das escórias e a resistência à compressão de cimento-escória a 7, 28 e 90 dias, respectivamente.

Além de sua rapidez, este método pode ser aplicado para avaliação dos módulos das escórias em amostras de cimento-escória enquanto que a aplicação do método químico requer prévia e trabalhosa separação da escória.

1 INTRODUCTION

Granulated blast-furnace slags, by-products of pig iron manufacture, have potential hydraulic properties, that is, setting and hardening take place when water is added. However, their hydration reactions are so slow that this would limit their commercial application if activators weren't used.

The free hydrated lime arising from the hydration of the silicates of the cement (C_3S and C_2S) acts mainly as an activator when slag is blended to the clinker.

The hydraulic activity of slags depends mainly on their chemical composition (function of iron ore characteristics, of fluxes and of operational conditions in the blast-furnace) and on their vitrification degree (function of the quenching condition).

There are several methods to investigate the slag activity and generally they are based on its chemical composition, its structure and its own hydration. The most current methods of slag quality control are based on its chemical composition. In fact, many authors have studied the correlation between slag chemical moduli and slag-cement compressive strengths (1). Based on this fact, many countries require or suggest in their specifications for slag-cements the use of chemical moduli calculated from the chemical composition of slags. West Germany (2) and Spain (3) require $\frac{C + M + A}{S} > 1$ and Japan (4), $\frac{C + M + A}{S} > 1{,}4$.

In France, there are no requirements, but it is recommended to use slags that fulfil $\frac{C}{S} > 1$. Other chemical indexes are suggested in English and Indian standards.

Through NBR 5735/80 (5), Brazil specifies $\frac{C + M + 1/3A}{S + 2/3A} \geq 1$, similar to the old American Specification for slags used in slag-cements, but there are studies of standard commitees with the aim of adopting $\frac{C + M + A}{S} > 1$, similar to the German Standard. According to the European Commitee of Normalization (6), the index $\frac{C + M}{S}$ will be adopted, in the future, in Europe.

Although, for a long time, chemical moduli have been used to control the basicity of slags, they have an inconvenience due to the time spent to carry out chemical analysis. The problem is greater for cement consumers that rarely have the slag utilised in slag-cement manufacture.

The observance of a close relation between the chemical composition and the refractive index of granulated blast-furnace slags shows that the determination of the latter, by means of a polarizing microscope, may give information concerning the basicity of the slag. This principle has been already applied to the quality control of glasses in Glass Technology or to the classification of volcanic rocks in Petrography.

2 EXPERIMENTAL PROCEDURE

2.1 Sample Preparation and Methodology

In order to elucidate the correlation between the chemical composition and the refractive index of slags, thirty samples have been selected from the four largest Brazilian siderurgics and from other plants, that use vegetal coal instead of coke as fuel. These samples are typical of a wide range of Brazilian industrial production.

Table 1 shows, the chemical composition.

Samples were powdered and the fraction 63-53μm has been selected and analysed by microscopy. Refractive indexes were measured by *Feck's Line Method* by means of an index of refraction liquids set, with 0,002 accuracy. Table 2 shows both the refractive index values and chemical moduli calculated from the chemical composition.

2.2 Results

By means of the linear regression analysis, several correlation coefficients were obtained between the refractive index and different chemical moduli.

Evaluation of results were based on calculating the standard error of predicted value, defined as:

$$E = \sqrt{\frac{\sum_{i}^{N} (F_c - F_{ch})_i^2}{N - 2}}, \quad \text{where}$$

E = Standard error of predicted value

F_c = Function value, obtained from the calibration curve

F_{ch} = Function value, obtained from the chemical composition

N = Number of samples

TABLE 1 - Chemical Composition of Slags

Sample / Compound	1	2	3	4	5	6	7	8	9	10	11	12	13	14	15	16	17	18	19	20	21	22	23	24	25	26	27	28	29	30
SiO_2	37.79	39.07	46.30	38.12	42.25	46.20	42.59	39.55	55.03	43.97	50.51	40.07	34.10	34.51	34.74	35.32	44.90	39.44	36.08	33.48	34.83	34.66	32.80	37.64	32.58	34.56	32.77	35.33	34.70	34.67
Al_2O_3	14.82	14.08	9.96	19.44	15.74	12.29	11.43	17.45	11.12	13.21	8.39	13.65	15.45	11.43	14.27	21.80	17.27	12.31	12.06	13.46	13.26	12.89	14.86	15.44	16.85	13.30	14.92	12.12	12.33	14.98
Fe_2O_3	0.79	1.99	1.49	1.30	0.44	1.20	1.11	0.79	1.75	0.40	0.68	2.53	0.73	0.94	0.88	0.88	3.08	4.34	0.51	0.46	0.52	0.36	0.48	1.41	0.73	0.52	0.56	0.56	0.50	0.90
TiO_2	0.76	0.72	0.26	0.62	0.16	0.25	0.20	0.30	0.19	0.16	0.28	0.21	0.49	0.48	0.47	0.57	-	0.69	0.43	0.53	0.53	0.42	-	0.44	-	0.55	-	0.43	0.53	0.49
P_2O_5	0.02	0.08	0.01	0.02	0.005	0.01	0.01	0.02	0.01	0.01	0.01	0.03	0.02	0.02	0.02	0.03	-	0.14	0.07	0.03	0.01	0.03	-	0.05	-	0.05	-	0.05	0.02	0.01
CaO	39.77	33.77	35.35	34.97	36.48	33.98	39.28	29.48	24.49	34.89	32.77	35.07	40.68	44.29	39.78	35.36	28.82	33.40	43.16	41.99	43.24	41.85	40.57	40.90	42.70	43.68	40.45	42.44	43.32	39.88
MgO	2.30	3.74	4.60	1.63	2.10	1.88	2.10	8.67	2.07	3.67	2.18	1.95	6.57	7.21	6.65	2.77	5.83	3.85	5.78	7.69	5.20	7.55	5.56	5.62	5.93	5.30	5.44	7.02	6.52	6.62
Na_2O	0.28	0.11	0.20	0.12	0.09	0.20	0.12	0.12	0.17	0.12	0.17	0.19	0.21	0.20	0.32	0.12	0.30	0.17	0.21	0.14	0.16	0.15	0.18	0.13	0.10	0.13	0.17	0.20	0.16	0.20
K_2O	1.03	1.54	1.53	1.88	1.76	2.96	2.00	1.94	2.22	1.86	2.45	1.94	0.66	0.53	0.82	1.98	1.30	1.89	0.52	0.66	0.61	0.56	0.80	0.65	0.54	0.61	0.92	0.54	0.62	0.86
Mn_3O_4	2.14	4.93	0.18	1.86	0.64	0.22	1.02	0.78	2.17	0.85	2.34	0.64	0.86	0.60	0.78	0.96	-	3.62	0.77	0.86	0.90	0.75	-	1.04	-	0.80	-	0.70	0.87	0.77
SO_3	0.09	0.01	0.02	0.02	0.01	0.03	0.15	0.03	0.03	0.02	0.22	-	-	-	0.12	0.08	-	0.03	0.04	0.06	0.03	0.04	-	0.03	-	0.04	-	-	-	-
S	0.10	0.09	0.19	0.10	0.10	0.08	0.10	0.06	0.03	0.07	0.10	0.08	0.23	0.11	0.22	0.17	0.15	0.07	0.90	1.13	1.06	1.20	1.20	1.02	1.34	0.78	1.13	1.00	0.93	1.05

TABLE 2 - Chemical Moduli and Refractive Index of Slags

Sample	N	$\frac{C+M+\frac{1}{3}A}{S+2/3A}$	$\frac{C+M+A}{S}$	$\frac{C+M}{S}$	$\frac{C}{S}$
1	1,629	0,99	1,51	1,11	1,05
2	1,625	0,87	1,32	0,96	0,86
3	1,609	0,82	1,08	0,86	0,76
4	1,615	0,84	1,47	0,96	0,92
5	1,613	0,83	1,29	0,91	0,86
6	1,603	0,73	1,04	0,78	0,74
7	1,617	0,90	1,24	0,97	0,92
8	1,611	0,86	1,41	0,96	0,74
9	1,571	0,48	0,68	0,48	0,45
10	1,613	0,81	1,18	0,88	0,79
11	1,599	0,67	0,86	0,69	0,65
12	1,615	0,85	1,26	0,92	0,88
13	1,645	1,18	1,84	1,39	1,19
14	1,653	1,31	1,82	1,49	1,28
15	1,645	1,16	1,74	1,34	1,15
16	1,619	0,91	1,70	1,08	1,00
17	1,611	0,72	1,16	0,77	0,64
18	1,623	0,87	1,26	0,88	0,80
19	1,651	1,20	1,69	1,35	1,20
20	1,653	1,28	1,89	1,58	1,35
21	1,651	1,21	1,77	1,40	1,25
22	1,649	1,24	1,80	1,43	1,22
23	1,651	1,20	1,86	1,41	1,24
24	1,647	1,18	1,84	1,38	1,22
25	1,651	1,24	2,01	1,49	1,31
26	1,651	1,23	1,80	1,40	1,26
27	1,645	1,19	1,86	1,40	1,23
28	1,651	1,23	1,74	1,40	1,20
29	1,649	1,26	1,79	1,44	1,25
30	1,645	1,15	1,77	1,34	1,15

Definitive curves were obtained after the elimination of individual values that presented differences twice bigger than the standard error of predicted value (E), that is, a level of significance near 5% was adopted.

Figures 1 to 4 show the calibration curves.

The experimental research suggests that not only it is possible to predict the value of chemical moduli from calibration curves, but also to calculate the refractive index of a slag from its chemical composition. In this case, a linear multiple regressive analysis was applied to correlate the refractive index to the most chemical oxides. Table 3 shows complete equation parameters. The correlation coefficient is equal to 0,9975.

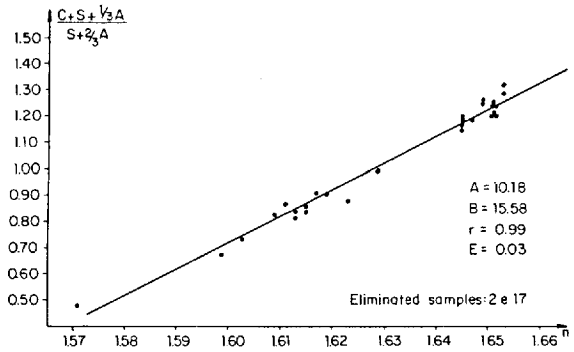

FIGURE 1 - Relation between the refractive index and $\frac{C+M+\frac{1}{3}A}{S+\frac{2}{3}A}$

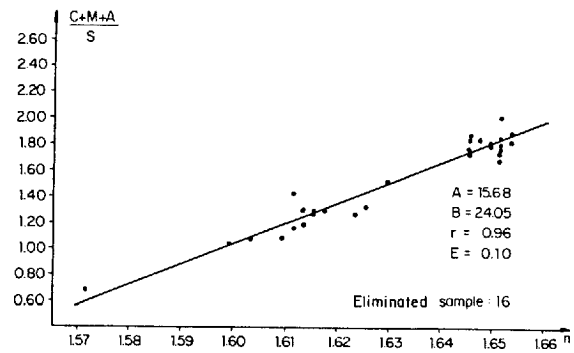

FIGURE 2 - Relation between the refractive index and $\frac{C+M+A}{S}$

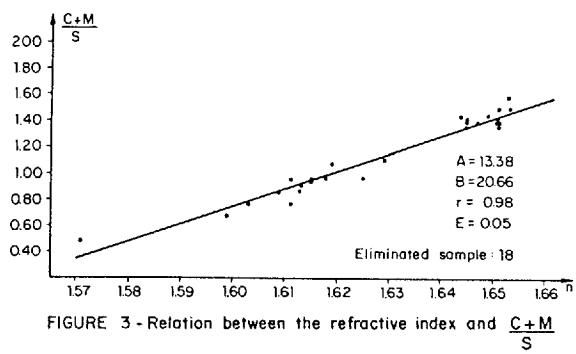

FIGURE 3 - Relation between the refractive index and $\frac{C+M}{S}$

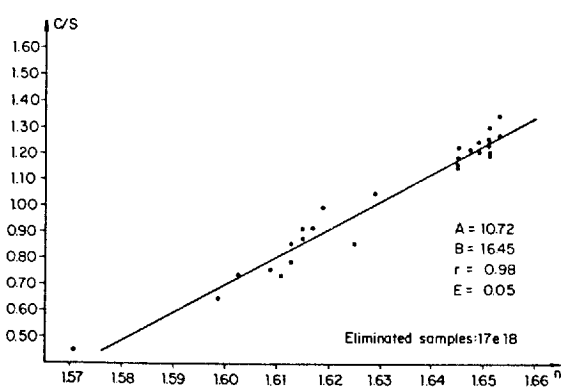

FIGURE 4 - Relation between the refractive index and C/S

TABLE 3 - EQUATION PARAMETERS OF MULTIPLE LINEAR CORRELATION BETWEEN CHEMICAL COMPOSITION AND REFRACTIVE INDEX OF SLAGS

PARAMETER	COEFFICIENT VALUE
Refractive Index (Dependent Variable)	1
SiO_2	$- 0.1656 \times 10^{-2}$
Al_2O_3	$- 0.4397 \times 10^{-3}$
TiO_2	- 0.0043
P_2O_5	+ 0.0312
CaO	$+ 0.2080 \times 10^{-2}$
MgO	$+ 0.1573 \times 10^{-2}$
Na_2O	+ 0.0195
K_2O	$- 0.3664 \times 10^{-3}$
Mn_2O_3	$+ 0.1475 \times 10^{-2}$
S	0.0041
Constant	1.6076
r	0.9975
r^2	0.9950

From a general point-of-view it can be seen that CaO, MgO, Na_2O, Mn_2O_3, S and P_2O_5 contribute to increase the refractive index value, while SiO_2, Al_2O_3, TiO_2 and K_2O contribute for its decrease.

This fact may elucidate why $\frac{C + M + A}{S}$ resulted in the worst correlation with the refractive index. Al_2O_3 contributes to decrease the refractive index and was considered at the same level of CaO and MgO that have an opposite effect on the refractive index value.

The importance in knowing the refractive index from the slag chemical composition, is assigned to the possibility of previous selecting of samples for the adjustement of calibration curves.

2.3 Correlation Between Slag Refractive Index and Slag-Cement Compressive Strength

In order to investigate any correlation between slag refractive index and slag-cement compressive strength, 12 out of 30 samples were selected. From these samples, 12 laboratory slag-cements were made under standarded conditions as showed in Table 4.

Compressive strengths of mortars (cylinder) were obtained according to Brazilian Method - NBR 7215 (7) at ages of 7, 28 and 90 days. Results are in Table 5.

Table 6 shows results of the linear regression analysis.

TABLE 4 - LABORATORY CEMENTS CHARACTERISTICS

SLAG CONTENT (in mass)	60 %
CALCIUM SULPHATE CONTENT (in mass)	2.5 %
BLAINE FINENESS (m^2/kg)	399 to 413
CLINKER	The same for all laboratory cements

TABLE 5 - COMPRESSIVE STRENGTH OF SLAG-CEMENT MORTAR

SLAG-CEMENT	COMPRESSIVE STRENGTH (MPa)		
	7 days	28 days	90 days
1	12.3	22.8	34.3
4	14.3	25.2	34.5
5	11.5	29.5	37.9
6	10.9	25.5	37.3
7	11.5	30.9	39.3
8	13.0	27.5	34.1
10	10.7	26.1	34.6
11	9.9	24.9	34.4
12	11.7	23.1	35.1
13	22.5	36.7	48.9
14	20.6	38.3	49.1
15	21.9	41.3	49.1
no slag	23.6	30.5	36.9

TABLE 6 - EQUATION PARAMETERS OF THE LINEAR CORRELATION BETWEEN THE SLAG REFRACTIVE INDEX AND SLAG-CEMENT MORTAR COMPRESSIVE STRENGTH

COMPRESSIVE STRENGTH	PARAMETER VALUE			
	Coefficient A	Coefficient B	Number or samples	Correlation coefficient
7 days	242.25	- 378.57	12	0.91
28 days	286.85	- 435.81	12	0.80
90 days	309.22	- 462.36	12	0.87

Results of tests, made under standarded conditions, show the great influence of the slag refractive index value on the slag-cement compressive strength at the largest possible number of invariable parameters. As refractive index depends directly on the slag chemical composition , it is shown once again the influence of slag chemical characteristics on the cement quality. Although the determination of slag refractive index doesn't have any practical importance in the evaluation of industrial slag-cements, where many factors are acting simultaneously, its determination will be very profitable with regards to the selection of appropriate slags as addition to the cement.

3 CONCLUSIONS

Basicity characteristics of slags, used in the cement industry, can be easily evaluated through a very simple and quick method. This method consists on predicting slag basicity ratios as $\frac{C}{S}$, $\frac{C + M + A}{S}$, $\frac{C + M}{S}$ by means of correlation curves between these parameters and the slag refractive index, measured under polarizing microscope . Experimental values of r ranging from 0.95 to 0.99 showed the good correlation between the chemical composition and the refractive index of slags.

In addition, the method proved to be advantageous due to the fact that it can be applied to slag-cement samples, where chemical methods are limited, requiring previous and laborious slag separation.

Finally, the significative influence of slag refractive index values on laboratory slag-cement compressive strength results showed, by it turn, the importance of chemical composition on slag hydraulicity, because the slag refractive index depends mainly on its chemical composition.

References

1 DEMOULIAN, E. et alii - *Influence de la composition chimique et de la texture des laitiers sur leur hydraulicité*. Proc VIIth Int. Symp. Chemistry of Cement, vol. 2 III 89-94, Paris, 1980.

2 DEUTSCHER NORMENAUSSCHUSS - *Portland, Einsenportland, Hochofen und Trasszement: Begriffe , Bestandteile, Anforderungen, Lieferung; DIN 1164*. In Schumacher, W. - *Neue Normen im Beton und Stahlbetonbau*, v. 1, p. 99-101, Verner Verlag, Dusseldorf, 1972.

3 VIRELLA BLODA, A. - 7º Congresso Internacional de la Quimica de los Cementos - Tema III - *Estructura de las escórias. Hidratacion de los cementos de escórias*. Cemento-Hormigón , 51(565), p. 1042, dic, 1980.

4 JAPANESE INDUSTRIAL STANDARD (JIS). *Portland Blast-Furnace Slag Cement*. JIS R 5211/1979.

5 ASSOCIAÇÃO BRASILEIRA DE NORMAS TÉCNICAS (ABNT). *Cimento portland de alto-forno*, NBR 5735/80.

6 CALLEJA CARRETE, J. *Adiciones y cementos com adiciones Cemento-Hormigón*, Barcelona, 54(594):439-59, may 1983.

7 ASSOCIAÇÃO BRASILEIRA DE NORMAS TÉCNICAS (ABNT). *Ensaio de cimento portland*, NBR 7215/82.

P.C. AITCIN, University of Sherbrooke, Sherbrooke, Québec, Canada
A. CARLES-GIBERGUES, M.N. OUDJIT, A. VAQUIER, Laboratoire de Génie Civil, Toulouse, France.

Influence des éléments autres que Si sur la réactivité des fumées de silice.
Influence of elements (Si, Al, K, Na, Ca, Cl, C) on the reactivity of condensed silica fumes. 3.1

Les fumées de silice condensées sont utilisées en Génie Civil, notamment pour la fabrication de bétons à hautes et très hautes résistances.

Cette étude montre que ces matériaux ont des réactivités très différentes qui les rendent donc plus ou moins intéressants.

Nos essais ont porté sur 20 fumées de silice d'origines très diverses: fabrications de silicium, d'alliages Fe - Si à 50, 75 et 90%- d'alliages Fe - Cr - Si, Si Mn.

Après étude de la composition physico-chimique nous suivons leur solubilisation dans l'eau pure. Nous déterminons ensuite la réactivité des fumées de silice vis-à-vis de la chaux en suspension diluée mais aussi en pâte. Enfin nous évaluons leur activité pouzzolanique pour la fabrication de ciments Portland avec ajout.

Les résultats ont montré que la finesse ne joue pas un rôle primordial; de même le taux de silice, dans la majorité des cas, n'est pas le facteur prédominant de la réactivité des fumées de silice. Ce sont essentiellement les éléments étrangers (autres que Si) qui sont à considérer. En premier lieu, l'existence de carbone imbrulé bloque la dissolution de la silice pendant une période d'autant plus grande que le taux d'imbrulé est élevé. L'aluminium freine également la dissolution de la silice. Par contre il conduit en présence de chaux dans le cas des fumées de silice qui renferment des sulfates, à la formation d'aluminates ou de sulfoaluminates de calcium qui viennent renforcer la cohésion des CSH. Les alcalins et alcalino terreux jouent également un rôle important dans la réactivité des fumées de silice: par leur action sur le pH ils influencent la solubilité de la silice. Lorsque les fumées de silice sont ajoutées à des CPA ces alcalins (le potassium surtout) accélèrent l'hydratation du silicate tricalcique.

Dans certains cas les chlorures, présents en faibles quantités, expliquent l'accélération de la prise des pâtes (fumées de silice + ciment).

Nous concluons en insistant sur le fait que d'autres recherches effectuées au Laboratoire de Génie Civil de Toulouse ont confirmé les résultats exposés dans cette publication: en particulier l'importance du rôle des imbrulés.

Os fumos condensados de sílica são utilizados na engenharia civil, notadamente na fabricação de concretos com resistências altas e muito altas.

Este estudo mostra que tais materiais têm reatividades diferentes, que os tornam, portanto, mais ou menos interessantes.

Nossos ensaios se basearam em 20 fumos de sílica de origens muito diferentes: fabricações de silício, de ligas Fe-Si com 50, 75 e 90%, de ligas Fe-Si, Si Mn.

Após estudo da composição físico-química, prosseguimos com sua solubilização em água pura. Determinamos a seguir a reatividade dos fumos de sílica diante de cal em suspensão diluída, e também em pasta. Por fim, avaliamos sua atividade pozolânica para a fabricação de cimentos portland com aditivo.

Os resultados mostraram que a finura não desempenha papel primordial; do mesmo modo, na maioria dos casos o teor de sílica não é o fator predominante da reatividade dos fumos de sílica. Essencialmente são os elementos estranhos (que não a Si) que devem ser considerados. Em primeiro lugar, a existência de carbono não queimado bloqueia a dissolução da sílica durante um período tanto maior quanto mais elevado for o teor de carbono não queimado. Também o alumínio dificulta a dissolução da sílica. Ao contrário, em presença de cal, no caso de fumos de sílica que contêm sulfatos, leva à formação de aluminatos ou de sulfoaluminatos de cálcio que vêm reforçar a coesão dos GSH. Os materiais alcalinos e alcalino-terrosos também exercem um papel importante na reatividade dos fumos de sílica: pela sua ação sobre o pH, eles influenciam a solubilidade da sílica. Quando os fumos de sílica são adicionados aos CPA, estes alcalinos (sobretudo o potássio) aceleram a hidratação do silicato tricálcico.

Em certos casos os cloretos, presentes em quantidades pequenas, explicam a aceleração da pega de pastas (fumos de sílica + cimento).

Concluímos insistindo no fato de que outras pesquisas realizadas no Laboratório de Engenharia Civil de Toulouse confirmaram os resultados expostos neste artigo: em particular a importância do papel dos não-queimados.

I - INTRODUCTION

Les fumées de silice condensée (CSF) obtenues dans les fours qui élaborent du silicium pur ou allié sont utilisées dans la fabrication des bétons de ciment Portland en raison de leur caractère pouzzolanique.

Cette étude a été entreprise sur 18 fumées de silice d'origines variées pour déterminer leurs différences de réactivité vis-à-vis de la chaux (réaction pouzzolanique) susceptibles d'apparaître en raison de leurs diversités de composition.

II - MATERIAUX ETUDIES

Les 18 échantillons sont répertoriés dans le tableau I en fonction :

1 - de leur pays d'origine : Allemagne de l'Ouest (A), Canada (C), France (F), Suède (S), U.S.A. (US) ;

2 - de la nature du métal ou de l'alliage produit : silicium pur (1), ferro silicium 75 (2), ferro-silicium 50 (3), calcium silicium (4), silico manganese (5), fer chrome silicium (6).

Sur ce même tableau sont indiquées les masses volumiques apparentes (mva) et les surfaces spécifiques mesurées par adsorption BET (S).

TABLEAU I - ECHANTILLONS ETUDIES - CARACTERISTIQUES PHYSIQUES

Echantillon	1	2	3	4	5	6	7	8	9	10	11	12	13	14	15	16	17	2'
Pays d'origine	F	C	F	F	F	F	F	F	F	A	S	C	US	US	A	US	US	F
Fabrication du four	1	1	2	2	2	2	2	2	2	2	2	2	3	3	4	5	6	1
mva,(kg/m^3)	125	275	140	175	200	185	470	375	600	240	-	220	330	240	475	480	355	
S,($10^3.m^2/kg$)	-	23,9	19,4	-	23,3	23	21	12	18,2	17,9	13,8	-	-	-	9,9	7,5	15,7	

L'examen des résultats amène à faire les remarques suivantes :

(i) l'état de division de tous les échantillons est toujours très poussé mais la variation de surface spécifique est beaucoup plus importante (de 7,5 à 23,9 $m^2.g^{-1}$) que celle rapportée dans la littérature (1) ;

(ii) la masse volumique apparente varie, elle aussi, dans une plage beaucoup plus étendue que celle qui était indiquée (1).

On notera que les CSF 7, 9, 15, 16 possèdent naturellement des masses volumiques apparentes aussi élevées que celles atteintes sur d'autres CSF après un traitement de densification. Ceci constitue un élément favorable pour la valorisation de ces CSF denses dont le coût de transport est abaissé.

III - ESSAIS EFFECTUES

La composition chimique a été déterminée par microfluorescence X pour les éléments majeurs, à l'exception du soufre dosé, par gravimétrie sous forme de sulfate ; les traces ont été dosées par fluorescence X.

La constitution minéralogique a été déterminée par DRX, éventuellement complétée par analyse thermique (étude de la récristallisation).

Le comportement dans l'eau pure a été étudié en milieu dilué (rapport eau/solide = 100), agité faiblement, à température ordinaire (20 ± 0,5°C), entre 1 et 100 jours. Les solutions ont été analysées par spectrométrie d'absorption atomique, colorimétrie potentiométrie.

La capacité de fixation de la chaux a été déterminée de deux façons différentes :

a - par mesure chimique dans des suspensions diluées (liquide/solide = 100) d'eau initialement saturée en chaux ;

b - par analyse diffractométrique de pâtes CSF chaux (eau/solide = 0,75 ; solide constitué de 48 % de CSF, 48 % de chaux éteinte, 4 % d'anatase).

Certaines conclusions tirées de ces essais ont été validées par des mesures de résistances mécaniques de mortiers dont le liant est un mélange : 85 % de ciment Portland + 15 % CSF.

IV - RESULTATS DES ESSAIS

IV - 1- Composition chimique

Elle est reportée sur les tableaux II (éléments majeurs) et III (traces).

L'examen du tableau II montre que l'on regroupe sous une même dénomination des matériaux ayant des compositions chimiques très différentes : on remarque, en particulier, que la teneur en impuretés, c'est-à-dire en oxydes autres que la silice, s'élève jusqu'à 77 % (échantillon 16) et dépasse 10 % dans 8 cas sur 17.

On peut donc déjà s'attendre à ce que la réactivité des CSF soit sous la dépendance des impuretés dès lors qu'elles représentent une partie parfois importante du matériau.

P.C. AITCIN, A. CARLES-GIBERGUES, M.N. OUDJIT et A. VAQUIER

TABLEAU II - COMPOSITIONS CHIMIQUES DES CSF (ELEMENTS MAJEURS)

oxydes, %	1	2	2'	3	4	5	6	7	8	9	10	11	12	13	14	15	16 (*)	17 (**)
SiO_2	93.0	95.8	91.5	90.5	93.0	85.1	85.0	87.9	70.8	81.2	92.2	88.0	92.1	90.7	91.9	57.5	23.0	73.6
Al_2O_3	.3	.5	.1	.8	.3	.3	.7	.8	2.1	.8	.5	1.2	.3	.3	.5	1.0	6.4	3.8
Fe_2O_3	.3	.0	.2	.9	.3	.8	1.4	1.3	2.0	1.6	.7	1.9	.6	.7	.4	.5	3.9	1.0
CaO	.4	.4	.45	.3	.4	2.6	.4	.4	1.1	.1	.2	.4	.2	.2	.4	24.6	15.0	.8
MgO	.5	.5	.7	1.7	.5	1.0	.7	.7	1.1	2.4	1.7	2.7	1.3	1.2	1.4	4.0	3.0	17.0
K_2O	.6	1.0	1.85	1.2	.5	1.0	2.6	.8	1.3	2.9	1.1	1.7	2.0	1.2	1.0	2.7	9.1	1.0
Na_2O	.2	.0	.2	.4	.2	.3	.5	.2	.3	.5	.2	.4	.2	.2	.2	.6	1.0	.3
SO_3	.7	.3	.3	.4	.7	.6	1.5	1.5	2.6	.4	.1	.4	.3	.2	.0	1.1	4.6	.1
P_2O_5	-	.0	-	-	-	-	-	-	-	-	.0	.0	.0	.0	.0	.1	.15	.0
Cl^-	.2	.0	-	.0	.2	.4	.3	.3	2.5	.6	-	.0	.2	2.0	.0	.5	.2	.1
p.f. (1000°C)	3.9	.9	4.7	3.8	3.9	7.7	6.1	6.0	16.4	10.0	3.0	3.1	3.0	3.8	3.7	7.9	7.5	2.2
C (500°C)	1.4	.6	2.0	.1	1.6	4.1	1.6	3.0	7.0	5.0	1.0	.0	-	.2	.6	-	-	.2

(*) Le CSF 16 renferme, en outre : MnO 0,26,9 %.

(**) Le CSF 17 renferme 1 % de Cr (tableau III)

TABLEAU III - COMPOSITIONS CHIMIQUES DES CSF (ELEMENTS TRACES) (*)

éléments, ppm	Ba	Sb	Sn	Cd	Mo	Sr	Rb	Pb	Br	As	Ge	Zn	Cu	Ni	Mn	Cr	Ti	B	Ga
CSF 2	50	0	0	0	0	30	0	10	20	0	10	1300	50	20	150	0	0	10	10
3	0	0	20	0	0	20	0	300	30	0	5	1300	250	30	1200	20	20	20	10
5	0	200	70	0	0	30	0	4000	30	0	20	0	1000	50	2000	20	20	20	10
9	0	20	250	0	0	30	0	800	1000	100	20	1300	400	10	1000	20	20	50	20
10	0	0	20	0	0	20	200	500	30	0	5	400	150	20	500	20	20	10	10
11	50	20	100	0	20	200	200	200	0	20	10	500	350	50	1000	1000	30	20	20
12	0	0	30	0	0	0	100	1200	30	0	10	1500	150	20	400	30	20	20	10
13		150	1500	0	10	100	100	4000	20	0	70	4000	800	20	1700	70	20	20	20
14	0	20	200	0	0	30	100	1500	0	0	10	700	400	30	700	200	20	20	20
15	350	0	20	0	0	100	300	250	50	0	5	500	150	10	2500	20	20	10	10
16	2500	20	0	70	500	3500	350	10000	0	5000	0	3000	600	100	tab.11	250	300	20	0
17	0	20	10	0	0	100	100	1500	0	0	5	3000	120	100	1500	10000	50	10	20

(*) Analyses effectuées au Laboratoire de Minéralogie-Cristallographie - Université Paul Sabatier - Toulouse.

Par ailleurs l'étude des traces (tableau III) souligne que certains CSF renferment des taux non négligeables d'éléments (Pb, Zn) connus comme retardateurs de prise des ciments Portland ou d'éléments toxiques (As, Pb) susceptibles de créer des problèmes de pollution des nappes phréatiques en cas de stockage à l'air libre, sans précaution particulière.

IV -2- Constitution minéralogique

Tous les CSF, à l'exception du 16, sont essentiellement formés par un verre siliceux : le diagramme de DRX est caractérisé par un halo important, centré à 4,05 Å dans la majorité des cas.

A cette phase vitreuse s'ajoute une phase cristallisée : celle-ci comporte presque toujours un carbure de silicium (dans 15 cas sur 18). Voici, ci-après, les autres espèces cristallines identifiées avec indication du nombre de CSF qui en renferment.

sylvite KCl : 12 - quartz : 11 -
fer métallique : 8 - ferro silicium : 5 -
arcanite, K_2SO_4 : 2 - Mg Cr_2 O_4 : 1.

D'autres minéraux ont été rencontrés, dans les CSF 15 et 16 : ils seront examinés plus loin.

Nous avons tenté de mieux définir la phase vitreuse des CSH au moyen des caractéristiques suivantes :

- caractéristiques géométriques (a, b, c) (*) du halo de diffraction de rayons X ;
- température de recristallisation mesurée dans un essai d'analyse thermogravimétrique au cours duquel est également déterminée la teneur en carbone;
- nature des produits de recristallisation (Cr : cristobalite, E : enstatite, M : magnétite, P.w : pseudowollastonite , V).

(*) a : équidistance en A, correspondant au maximum du halo ;

b : rapport de la hauteur du halo (au-dessus de la ligne de fond continu) à sa largeur ;

c : rapport de l'aire du halo vitreux à la somme des aires de ce halo et des pics de diffraction (dans l'intervalle 5 - 35°θCo).

Les paramètres b et c sont fonction du matériau mais aussi des conditions expérimentales : ils n'ont donc qu'une valeur comparative.

Les résultats sont reportés sur le tableau IV.

Il apparaît que les CSF 15 et 16 sont très différents des autres échantillons aussi bien par l'importance réduite de la phase vitreuse que par sa nature.

CSF 15 - Le halo du verre est centré à une valeur (3,85 Å) différente de l'équidistance de 4,05 A caractérisant la réflexion (101) de la cristobalite. Si l'on admet, comme l'ont proposé DIAMOND (2) et d'autres auteurs par la suite (3), que le déplacement de ce maximum vers les faibles équidistances traduit un enrichissement de la phase vitreuse en calcium, ceci pourrait indiquer que le verre de ce CSF ne renferme pas seulement de la silice mais aussi du calcium. La recristallisation de ce CSF (chauffage à 1000°C) n'entraîne, d'ailleurs, la formation que de faibles quantités de cristobalite : il apparaît essentiellement de la pseudo-wollastonite.

La fraction cristallisée de ce CSF est voisine de 25 % ; à côté de minéraux déjà identifiés dans les autres CSF (carbure de silicium, quartz, calcite) existent des quantités importantes de chaux éteinte et d'un silicate probablement bicalcique (*). La chaux éteinte constitue, en moyenne, 9,5 % du matériau ; quant au silicate présumé il représente de 5 à 7 %.

CSF 16 - Ce CSF est largement cristallisé.

La fraction vitreuse ne provoque qu'un halo peu marqué, centré sur une distance réticulaire de 2,55Å.

La phase cristallisée renferme :

- d'une part un sel soluble, l'arcanite K_2 SO_4, qui représente 10 % du matériau ;
- d'autre part un système complexe d'oxydes de manganèse (notamment MnO_2) et de silicates manganocalciques.

(*) l'identification de ce minéral qui est détruit par traitement à l'acide salycylique demande à être confirmée.

TABLEAU IV - CARACTERISTIQUES DES VERRES DES CSF

Echantillon	1	2	2'	3	4	5	6	7	8	9	10	11	12	13	14	15	16	17
a, en Å	4,05	4,05	4,05	4,05	4,05	4,05	4,05	4,05	4,05	4,05	4,05	4,05	4,05	4,05	4,05	3,85	2,55	4,05
b	1,3	1,3	1,4	1,1	1,3	1,2	1	1,2	/	1	1,3	1,2	1,2	1,2	1,2	0,4	/	0,75
c, %	96	99	93	99	95	90	90	98	/	91	99	99	98	97	99,5	62	32	97
température de cristallisation, en °C	930	> 1000	845	915	860	855	845	960	845	1025	> 1000	> 1000	> 1000	> 1000	> 1000	880	/	870
produits de cristallisation	Cr.	Cr.	Cr.	Cr.	Cr.	Cr.	Cr.	Cr.	Cr.	Cr.	Cr.	Cr.	Cr.	Cr.	V	Pw,Cr.	/	V,E,M,

IV -3- Comportement dans l'eau pure

L'examen des résultats et, spécialement de ceux enregistrés après 4 jours de traitement, montre des comportements variables d'un CSF à l'autre (figure 1 (*)).

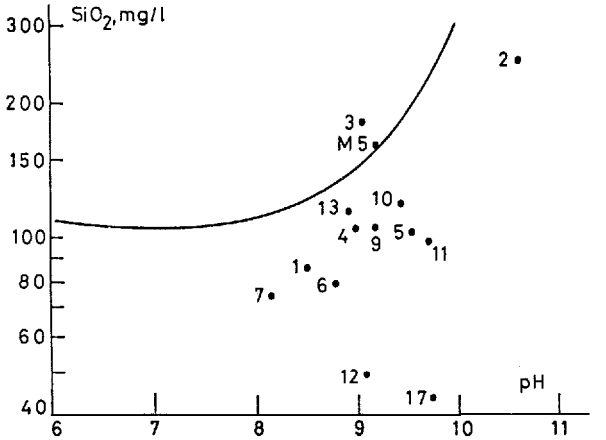

Figure 1 - Teneurs en silice et pH des filtrats (4j).

On constate tout d'abord que les pH des filtrats varient largement de 6,6 à 12.

On observe que la solubilité de la silice ne dépend pas exclusivement du pH, car 4 CSF seulement ont leurs points figuratifs de la concentration en SiO_2 dissoute situés sur la courbe théorique : les autres sont nettement en dessous.

Cette sous saturation est probablement explicable par l'influence des impuretés (ions dissous, carbone) : effectivement les analyses chimiques des filtrats montrent qu'ils renferment sodium, potassium et calcium sous forme de chlorures et sulfates. Par ailleurs les CSF riches en carbone sont toujours très en dessous de la courbe théorique (échantillons 5, 8,).

IV -4- Fixation de la chaux en suspension diluée

La vitesse de fixation de la chaux varie elle aussi très largement d'un CSF à l'autre. C'est ce qui apparait dans le tableau V ou figurent les quantités de chaux, I et I , fixées respectivement après 4 et 16 jours de traitement (I et I sont exprimés en mg de Ca $(OH)_2$ par gramme de CSF).

TABLEAU V - FIXATION DE LA CHAUX PAR LES CSF APRES 4 ET 16 JOURS.

CSF, n° / indice	16	8	15	1,6	2, 10, 11, 12, 13, 14,	17	3	5
I_4	0	31	15	76	130	132	85	24
I_{16}	68	78	109	144	152	155	148	141

(*) les résultats suivants complètent la figure 1 libération de SiO_2 nulle pour les CSF 8, 15 et 16 dont les pH valent respectivement 6,6 - 12 et 11,4.

Compte tenu du rapport CSF/eau de chaux, choisi (10) la fixation complète de la chaux apportée correspond à un indice I = 159.

A titre comparatif signalons que cette valeur est effectivement atteinte en 7 jours par une silice pure M5, de surface spécifique (BET) 200 m /g.

Il apparait, à la lecture de ces résultats, un classement net en deux groupes :

- CSF peu réactifs : 8, 15 et 16 ;

- CSF réactifs : tous les autres avec une légère restriction concernant le CSF 5 pour la valeur basse de I_4.

IV -5- Fixation de la chaux en pâte

Le dosage, par diffractométrie de rayons X, de la chaux restante dans les pâtes nous a permis de tracer les courbes de fixation de la chaux en fonction du temps. Elles sont représentées sur la figure 2.

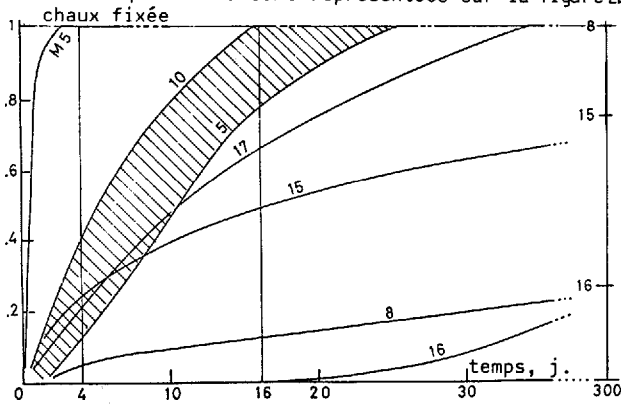

Figure 2 - Fixation de la chaux par les CSF (en g.CH/g.CSF)

Le classement des réactivités en suspension diluée se retrouve, à peine modifié, dans le cas des pâtes : le CSF 16 est très peu réactif, les CSF 8 et 15 sont peu réactifs. Le CSF 17 est légèrement retardé dans son action.

Nous avons reporté dans le tableau VI les quantités i_4, i_{16} et i_{300} de chaux fixées après 4, 16 et 300 jours (exprimées en mg. de $Ca(OH)_2$ par g. de CSF).

En comparaison, la silice pure, étalon, fixe la totalité de la chaux (i = 1000) en 3 jours.

En règle générale la silice des CSF fixe la chaux sous forme de CSH. Nous avons observé deux exceptions :

- avec le CSF 16 il n'apparaît pas de CSH mais seulement de faibles quantités d'ettringite ;

- avec le CSF 17 un aluminate tétracalcique apparaît en plus de CSH.

TABLEAU VI - FIXATION DE LA CHAUX PAR LES CSF APRES 4, 16 ET 300 JOURS.

CSF / indice	16	8	15	17	autres CSF
i_4	0	60	240	210	166 - 350
i_{16}	0	125	480	650	770 - 980
i_{300}	270	1000	670	1000	1000

V - INTERPRETATION DES RESULTATS

Les divers essais effectués ont montré que les différents CSF ont des aptitudes largement variables à libérer de la silice puis à fixer la chaux.

On peut penser que la capacité de fixation de chaux sous forme de CSH est liée à l'existence d'une phase vitreuse, donc facilement soluble, riche en silice ou même purement siliceuse ; bien évidemment un état de division poussé favorise cette réaction.

Dans nos expériences la teneur en verre siliceux est connue, par excès, à partir des données de l'analyse chimique, dès lors que la DRX a établi que le CSF est vitreux : le taux de verre est pris égal au taux de silice lorsque le halo de diffraction, centré à 4,05 Å, indique une composition proche de la cristobalite et que le chauffage du CSF provoque effectivement la cristallisation en cristobalite et tridymite.

Par ailleurs nous retiendrons comme indice d'activité pouzzolanique l'indice i_{16}, du tableau VI.

V -1- Cas du CSF 16

Ce cas est discuté séparément car ce matériau est le seul a avoir montré une inertie presque totale. Il libère peu de silice en solution, ne fixe que très peu de chaux et ne forme pas de CSH.

Les échantillons de pâte : (CSF 16 + chaux) n'ont toujours pas durci après 1 an de conservation.

Ce CSF n'est donc ni pouzzolanique ni hydraulique. Son inactivité est liée à plusieurs causes. Tout d'abord, sa pauvreté en silice (23 %); ensuite son caractère faiblement vitreux (l'indice c = 32 % est très inférieur aux valeurs > 90 % de la majorité des autres CSF). Enfin, le centrage du halo de diffraction X à 2,55 Å indique qu'il s'agit d'un verre non siliceux.

V -2- Influence de la teneur en silice vitreuse sur l'activité pouzzolanique

L'examen de la figure 2 et du tableau VI montre que l'on peut distinguer trois groupes dans les CSF (excepté CSF 16) et la silice de synthèse M5 en ce qui concerne la cinétique de fixation de la chaux.

1 - Silice de synthèse M5 : très active puisque la totalité de la chaux est fixée au bout de 3 jours.

2 - CSF 8, 15 et 17 : peu réactifs, compte tenu de ce que la fixation complète de la chaux demande plus d'un mois.

3 - Autres CSF : manifestent de légères différences mais fixent toute la chaux dans un délai moyen de 20 jours.

Etant donné que tous ces CSF sont caractérisés par un halo de diffraction X centré à 4,05 Å (avec quelques restrictions pour CSF 15) on peut supposer que tous leurs verres sont siliceux. Dans ce cas, on est amené à se demander si les différences enregistrées dans la vitesse de fixation de la chaux ne sont pas imputables aux différences de teneurs en silice.

La figure 3 montre, qu'à l'exception de CSF 8, il existe une relation de proportionnalité entre l'indice i_{16} et la teneur, S, en silice. Compte tenu de cette conclusion nous avons tracé l'évolution avec le temps des quantités de chaux fixée rapportées au contenu en SiO_2 de chaque CSF (figure 4). On constate que les CSF 15 et 17 se rangent dans le même fuseau que les autres CSF et que seul le CSF 8 est toujours situé très en dessous.

Les vitesses moyennes de fixation de la chaux, exprimées en mg $Ca(OH)_2/g.SiO_2/jour$, s'établissent aux valeurs suivantes :

- silice M5 : 825
- CSF 8 : 4,8
- autres CSF : 52 à 69.

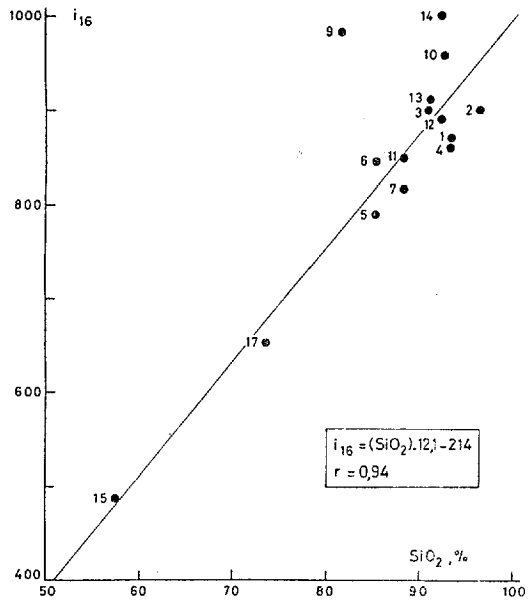

Figure 3 - Influence de la teneur en SiO_2 sur la fixation de chaux (i_{16})

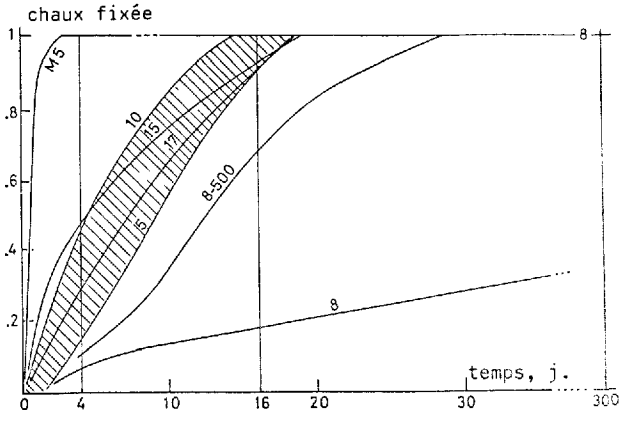

Figure 4 - Fixation de la chaux par les CSF (en $g.CH/g.SiO_2$)

V -3- Influence de la surface spécifique sur l'activité pouzzolanique

Pour savoir si ce défaut de réactivité est imputable au facteur surface spécifique nous avons tracé le graphe $i_{16}/g.SiO_2$ = f (surface spécifique). Il apparait qu'il n'y a pas de corrélation significative entre ces deux quantités (coefficient de corrélation r = 0,29 pour un ajustement linéaire) et que, là encore, le CSF 8 est situé très en dessous du nuage de points représentatifs des CSF.

V -4- Influence des impuretés sur le comportement des CSF

Dans une étude précédente (4), l'un de nous a mis en évidence en étudiant sept CSF d'origine française, le rôle des impuretés sur la réactivité des fumées de silice vis-à-vis de l'eau, de la chaux et des ciments Portland.

Dans le cas présent il est apparu que les impuretés expliquent également les particularités du comportement du CSF 8 et, aussi, du CSF 15.

1 - Rôle du carbone - La très faible réactivité du CSF 8 est imputable à sa teneur élevée en carbone. Ceci a été établi en comparant les comportements du CSF brut, d'une part, et du CSF privé de la presque totalité de son carbone imbrûlé par chauffage à 500°C, pendant 1 heure (*) d'autre part. Il en est, en effet, résulté :

- une solubilité dans l'eau pure largement facilitée : la silice dosée dans les filtrats, après 1 jour, passe de 0 mg/l à 70 mg/l ;

- une accélération du processus de fixation de la chaux dont le terme est atteint en 45 jours au lieu de 210 jours ;

- une suppression de son rôle retardateur de la prise et du durcissement des pâtes ou mortiers de ciment Portland auxquels il est incorporé.

Ce dernier point est à développer. Alors que le remplacement de 15 % du ciment Portland d'un mortier par le CSF 6 ne modifie que très peu la cinétique d'hydratation, l'introduction de cette même quantité de CSH 8 retarde très fortement les réactions d'hydratation; ceci est mis en évidence aussi bien par calorimétrie que par dosage (DRX) des minéraux. On constate, par exemple, un retard de 6 jours dans l'apparition de la portlandite. La conséquence pratique est un abaissement considérable des résistances mécaniques des mortiers (**) aux jeunes âges, visible sur la figure 5.

La plus grande partie de ce retard est annulée lorsque on emploie du CSF 8 chauffé à 500°C.

On peut penser que le carbone contenu dans cette fumée de silice est fortement fixé sur les grains du matériau : il constitue un écran qui réduit la surface libre que présente ce CSF à l'eau ou aux solutions intersticielles des pâtes. Ceci entraîne un ralentissement de la dissolution directement responsable de l'abaissement de la vitesse de fixation de la chaux.

(*) désigné par 8 - 500 sur les figures 4 et 5.

(**) mortiers conformes à la norme AFNOR P15:403

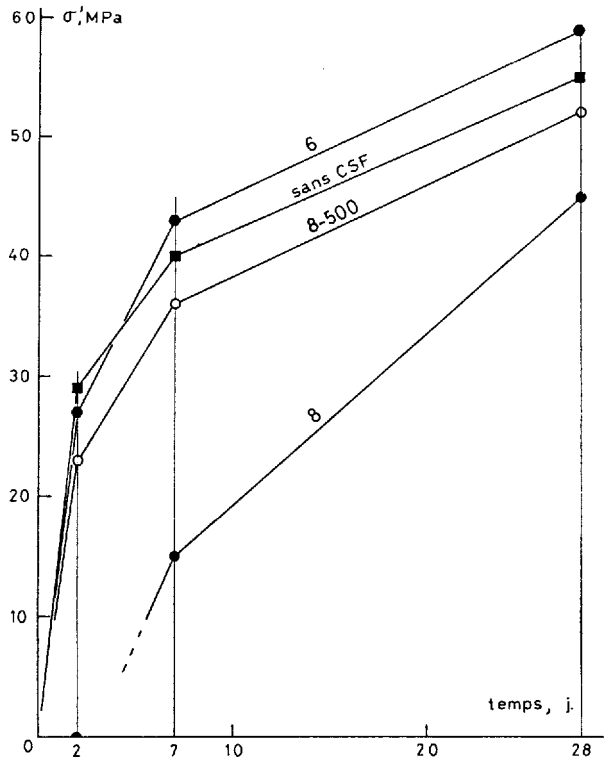

Figure 5 - Influence des CSF sur le durcissement des mortiers.

Concernant les réactions dans les pâtes de ciment Portland, si l'on admet avec BACHE (5) que les particules de CSF entourent les grains de ciment, elles constituent un écran qui réduit l'interface C_3S-eau de gâchage et retarde ainsi l'hydrolyse du C_3S. Cet effet retardateur est donc supprimé si l'on permet la dissolution rapide du CSF, en éliminant donc le carbone.

Le rôle du carbone est facile à montrer pour le CSF 8 où il est abondant : 7,0 %. Bien que moins indiscutable il existe également dans d'autres CSF. C'est ainsi que l'ajout de CSF 9 (qui renferme 5,0 % de C) accroît le délai de manifestation du flux maximum (enregistré en calorimétrie adiabatique) qui passe de 14 h pour le mortier de ciment Portland pur à 14 h 30 ; au contraire l'ajout de ce même CSF 9, mais préalablement chauffé 1 h à 500°C, réduit ce délai à 10 h. On observe alors un effet accélérateur de l'hydratation du ciment Portland, déjà cité par de nombreux auteurs, et qui a été également trouvé avec le CSF 3 lui-même pauvre en carbone (0,1 %) : délai mesuré de 10 h également.

2 - Rôle du calcium - Nous avons déjà vu que la capacité réduite de fixation de chaux par le CSF était explicable par la teneur réduite (57,5 %) en SiO_2. Il est apparu que sa surface spécifique plus basse que la moyenne observée pour les autres CSF (9,9 m^2/g) n'a que peu d'influence sur sa réactivité. Ces conclusions ne s'opposent pas à celles qu'avait formulées M. REGOURD (6) dans son étude d'un CSF issu d'une fabrication d'alliage Ca-Si.

Il nous apparait opportun d'apporter ici une précision concernant le rôle du calcium. Celui-ci est une impureté majoritaire de ce CSF : 24,6 % en CaO. Cet élément est essentiellement sous forme de $Ca(OH)_2$ et d'un silicate bicalcique probablement.

On peut donc envisager que ce CSF, par réaction de ces deux derniers minéraux avec sa phase vitreuse en présence d'eau, manifeste des propriétés hydrauliques. C'est ce que nous avons effectivement constaté. Le suivi, par DRX, de l'hydratation d'une pâte de (CSF 15 + eau pure) montre que :

- la chaux éteinte est consommée en 10 jours ;
- le silicate bicalcique n'est que peu réactif ;
- le verre est hydrolysé ;
- une phase CSH se forme, décelable par DRX au bout de 7 jours;
- de l'ettringite apparaît aussi, en faible quantité, dès le deuxième jour.

VI - CONCLUSIONS

1 - Les 18 CSF étudiés ont des propriétés physiques extrêmement variables : surfaces spécifiques (BET) comprises entre 7 et 24 m^2/g, masses volumiques apparentes s'étalant de 125 à 600 kg/m^3.

2 - Leurs compositions chimiques manifestent aussi de grandes variations : la teneur en impuretés (autres que SiO_2) va de 4 à 77 %. Dans ce dernier cas (CSF 16 : 23 % de SiO_2 seulement) la dénomination CSF est injustifiée.

3 - La dissolution des CSF par l'eau pure ainsi que leur activité pouzzolanique, exprimée en tant que fixation de chaux, dépendent essentiellement de leur contenu en silice vitreuse. C'est pourquoi tous les CSF examinés sont pouzzolaniques à l'exception du CSF 16 qui est inerte.

4 - La vitesse moyenne de la réaction pouzzolanique ne varie que très peu pour les CSH (à l'exception du CSF 8) et ne semble pas dépendre de la surface spécifique.

5 - La très faible vitesse observée pour le CSF 8 est attribuable à la présence de carbone qui abaisse fortement les surfaces de contact entre verre de SiO_2 et milieu ambiant : l'élimination de ce carbone rehausse la vitesse de réaction à un niveau (57,5) compris dans le domaine des autres CSF (52-69).

6 - L'existence de ce CSF 8 attire spécialement l'attention sur la variabilité de composition des CSF provenant d'un même four (ici, les CSF 6,7, 8 et 9).

7 - Certaines impuretés peuvent transformer le comportement d'un CSF : le calcium rend le CSF 15 simultanément hydraulique et pouzzolanique comme cela a déjà été observé (3) sur une cendre volante particulière.

BIBLIOGRAPHIE

(1) V.M. MALHOTRA - "Condensed silica fume. An introduction" in : Condensed silica fume. P.C. Aitcin éditeur, Université Sherbrooke, 1983.

(2) S. DIAMOND - "On the glass present in low-calcium and high-calcium flyashes". Cement and Concrete Research, vol. 13, n°4, pp 45964.

(3) P.C. AITCIN, F. AUTEFAGE, A. CARLES-GIBERGUES, A. VAQUIER - "Comparative study of the cementitious properties of different flyashes" - 2nd Inter. Conf. on the use of flyash, silica fume, slag and natural pozzolans in Concrete. Madrid, april 1986.

(4) M.N. OUDJIT - "Reactivité des fumées de silice condensée en présence de chaux ou de ciment Portland". Thèse Docteur Ingénieur, I.N.S.A. Toulouse, 1986.

(5) H.H. BACHE - "Densified ultra fine particles based material". 2ème Conf. Internat. Superplastifiants dans le béton, Ottawa, juin 1981.

(6) M. REGOURD - "Pozzolanic reactivity of condensed silica fume" in : Condensed silica fume. P.C. Aitcin éditeur, Université de Sherbrooke, 1983.

LOU Zonghan, Professor, XU Xianyu, YANG Liqun and SHENG Qizhong, Lecturers

Zhejiang University, P. R. China

Dissociation of Aluminium from Slag Glasses and Formation of Ettringite*

ABSTRACT: In the $CaO-Al_2O_3-SiO_2$ system 24 slag glasses were melted. The investigations on them were carried out by means of various techniques. The emphases of the investigations were laid on the dissociation reaction of aluminium and the formation of ettringite under alkaline conditions. Following conclutions can be drawn.

1. In the solution with different pH value, aluminium will exist in the form of AlO_2^- or Al^{3+} or $Al(OH)_3$. They have an important effect on the activity of the slag glass.

2. Al^{3+} ions in the slag glasses is fourfold coordinated. After the slag glass is attacked by acid or alkali, the coordination state of Al^{3+} ion is transformed from fourfold to sixfold coordination, and bridging oxygen in glass network changes into non-bridging oxygen. The two changes are presented by the changes of the electron binding energy of Al2p and O1s. They indicate the destruction of the structure of the glass network.

3. After the slag glass is attacked by alkaline solution, the hydrate products, ettringite and C-S-H gel, will form rapidly by the surface reaction between the slag glass and alkaline solution. They will promote the dissociation of the slag glass.

No sistema $CaO-Al_2O_3-SiO_2$ se fez a fusão de 24 vidros de escória. Por intermédio de diversas técnicas foram realizadas investigações sobre eles. Nas investigações foi dada ênfase à reação de dissociação de alumínio e à formação de etringita sob condições alcalinas. Podem ser tiradas as seguintes conclusões:

1. Na solução com valor de pH diferente, o alumínio existirá sob a forma de AlO_2^- ou Al_3^+ ou $Al(OH)_3$. Eles têm efeito importante sobre a ativação do vidro de escória.
2. Íons Al^{3+} nos vidros de escória são coordenados quatro vezes. Depois que o vidro de escória é atacado por ácido ou álcali, o estado de coordenação do íon Al^{3+} é transformado de coordenacão quádrupla para sêxtupla, e oxigênio de ligação na rede de vidro se muda em oxigênio de não-ligação. As duas mudanças são apresentadas pelas alterações da energia de ligação do eléctron de Al2p e Ols. Elas indicam a destruição da estrutura da rede de vidro.
3. Depois que o vidro de escória é atacado por solução alcalina, os produtos do hidrato, etringita e gel C-S-H, se formarão rapidamente pela reação de superfície entre o vidro de escória e a solução alcalina. Eles promoverão a dissolução do vidro de escória.

Dissociation of Aluminium from Slag Glasses and Formation of Ettringite*

3.1

Blastfurnace slags are the most useful latent hydraulic materials. They are added into cement in percentages of 20-85%. There still have been being many attempts to find more effective ways to ultilize them. Slags essentially are the glasses in $CaO-Al_2O_3-SiO_2$ system. So, we try to interpret the hydration mechanism of slag glass in cement paste through the research on $CaO-Al_2O_3-SiO_2$ glass.

According to our previous work, the curves of iso-weight-loss of the $CaO-Al_2O_3-SiO_2$ glass attacked by alkali are shown in Fig. 1, and it can be found that Al_2O_3 is the important factor which affects the activity of the slag glass/1/. Besides, the main difference among the slags from different countries and steel factories lies in the difference of the content of Al_2O_3 in the slags/2/. Therefore, this paper is concerned with the dissociation of Al_2O_3 from slag glass and the formation of ettringite, which is in close relation with the dissociation of Al_2O_3. This is an important problem in the study on the hydration mechanism of the slag cement.

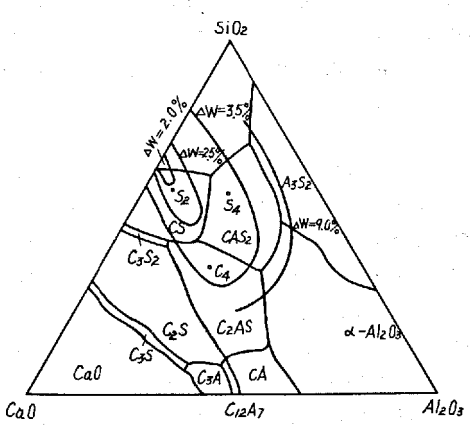

Fig. 1 Curves of iso-weight-loss of the glasses

1. The Dissociation of Al_2O_3 from Slag Glasses in the Attacking Solutions with Different pH Values

Three glasses were chosen for the determination of weight loss of glass attacked by acid or alkaline medium. They are S_2 in the phase field of CS, S_4 in that of CAS_2 and C_4 in that of C_2AS. Their compositions are listed in Table 1.

Table 1. Chemical compositions of glasses

No.	Weight per cent (%)			Mole per cent (%)		
	CaO	Al_2O_3	SiO_2	CaO	Al_2O_3	SiO_2
S_2	37.12	7.60	55.28	39.96	4.50	55.54
S_4	26.95	21.30	51.75	30.99	13.47	55.54
C_4	34.80	30.90	34.30	41.52	20.28	38.20

The method of determination of weight loss of glass is as follows. Glass grains (-40+60 mesh) were attacked in the solutions (W/S=50:1) with different pH values for 8 hrs. at 80°C, then filtered and washed with acid and then acetone, then dried until constant weight. After determination, the content of Al_2O_3 in the filtrate was determined by AA.

The results of two determinations are shown in Fig. 2 and Fig. 3. From these results, it can be found that the change of the weight loss with pH value is in the almost same regularity. There are two turns in the curves of weight loss at pH≒3 and pH≒11. The weight loss of glass increases obviously when pH<3 or pH>11, and keeps unchange and a little value when 3<pH<11 (Fig. 2). The relationship between the content of Al_2O_3 in filtrate and pH value is just the same(Fig.3).

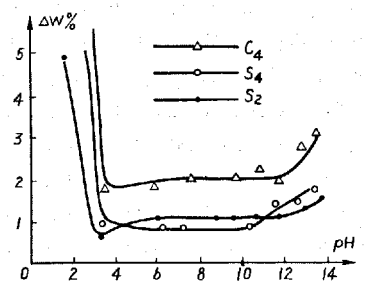

Fig. 2 Weight losses of glasses under different pH value condition

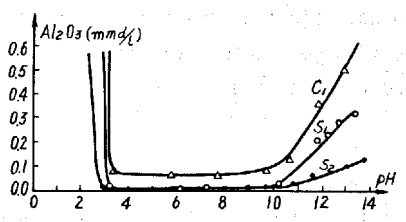

Fig. 3 Variation of concentration of Al_2O_3 with pH values in attacking aq. solutions

Aluminium is typical amphotere. In the solutions with different pH, there are 3 equilibria respectively. They are $Al^{3+}+3OH^- \rightleftharpoons Al(OH)_3$ (in neutral solution), $Al(OH)_3+3H^+ \rightleftharpoons Al^{3+}+3H_2O$ (in acid solution), $Al(OH)_3+OH^- \rightleftharpoons AlO_2^-+2H_2O$ (in alkali solution).

* This research is financed with Science Funds of Chinese Academy of Science.

The relationship between the stability of $Al(OH)_3$, Al^{3+} AlO_2^- and pH value has been calculated (Fig. 4) according to the principle of thermodynamics. The result, which is consistent with that of A. Paul/3/, indicates that Al^{3+}, AlO_2^-, $Al(OH)_3$ are stable when pH<3.2, pH> 10.7 and 3.2<pH<10.7.

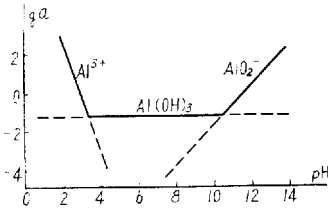

Fig. 4 Stability of Al_2O_3 in aq. solutions at different pH value (25°C)

In the aq. solution, the reaction,

$$Al_2O_3(glass)+3H_2O \rightleftharpoons 2Al(OH)_3,$$

will take place on the surface of glass grains. In acid solution, $Al(OH)_3$ formed reacts with H^+ immediately to form Al^{3+}; in alkaline solution, $Al(OH)_3$ formed reacts with OH^- immediately to form AlO_2^-; the dissociation of Al_2O_3 and the corrosion of glass are promoted by the transformation of $Al(OH)_3$ to Al^{3+} or AlO_2^-, so the weight loss increases. In the solutions with 3.2<pH<10.7, $Al(OH)_3$ is stable; the reaction is ease to get equilibrium because of lower solubility of $Al(OH)_3$. Moreover, $Al(OH)_3$ adheres to the surface of glass as gel, so the corrosion of glass is inhibited.

Thus it can been seen that the weight loss of glass, the content of Al_2O_3 in filtrate and the way Al_2O_3 exists in aq. solutions regularly vary with pH values, and there is a good interrelation among the three of them. The results of glass C_4 is shown in Fig. 5.

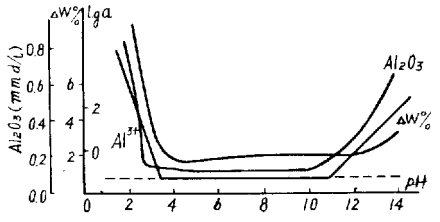

Fig. 5 Stability of Al_2O_3 and the corresponding weight loss and content of Al_2O_3 in aq. solutions.

The above is chiefly on aluminium in $CaO-Al_2O_3-SiO_2$ glass, aluminium is the most unstable in this case. If there is a little aluminium in the glass, its effect is secondary but the effect of silicon will be dominant/3/. It has been confirmed by our previous work/4/.

All the discussions above are on the dissociation of glass in the attacking solutions with different pH values. They have indicated the effects of the concentrations of OH^- or H^+. The hydration of slag glass in cement paste is essentially the dissociation of the slag glass by the attacking of OH^-.

2. The Change of the Coordination State of Al^{3+} Ion in Slag Glass in the Attacking Process

Our previous work/5/ has indicateed that in $CaO-Al_2O_3-SiO_2$ glass, Al^{3+} ion is in fourfold coordination, and after being attacked by extract from cement paste, the coordination state of Al^{3+} ion is transformed into sixfold coordination. To investigate the change of the coordination state of Al^{3+} ion in attacking process, the coordination state of Al^{3+} ion in the glass surface layer was determined on glass C_4 by means of XPS.

Glass C_4 grains (-170+360 mesh) were attacked in the solutions (W/S=250:1) with different pH values for 1 hr. at 60°C, then washed with absolute alcohol and dried. The pH values of the solutions are listed in Table 2. The XPS measurements were carried out with KRATOS ES-300 Electron Spectrometer. The thickness of the analyzed layer is about 25Å. α-Al_2O_3 and Albite were chosen as the reference materials of sixfold and fourfold coordinated Al^{3+} ion respectively. the results of the determination are shown in Fig. 6, Fig. 7 and Table 3.

Table 2. pH values of attacking aq. solutions

No.	C_4-1	C_4-2	C_4-3	C_4-4	C_4-5	C_4-6
pH	1.72	3.47	8.17	11.36	12.66	13.54

The electron binding energy of Al2p and O1s can be calculated according to the equation of

$$E_b=E_kC1s+E_bC1s-E_k.$$

All the electron kinetic energy and binding energy of

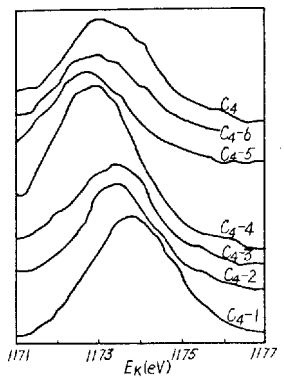

Fig. 6 Variation of Al2p spectra as function of pH values for glass C_4

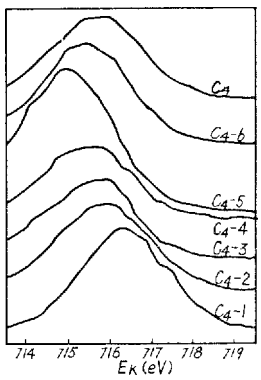

Fig. 7 Variation of O1s spectra as function of pH values for glass C_4

Table 3. Data of XPS measurements

Samples	Kinetic energy (eV)			Binding energy (eV)	
	C1s	Al2p	O1s	Al2p	O1s
α-Al_2O_3	960.10	1170.74		74.70	
Albite	962.25	1172.85		74.40	
C_4	962.25	1173.15	715.70	74.10	531.55
C_4-1	963.50	1173.90	716.39	74.60	532.15
C_4-2	962.70	1173.40	715.95	74.30	531.75
C_4-3	962.65	1173.55	715.80	74.10	531.85
C_4-4	962.10	1172.90	715.55	74.20	531.55
C_4-5	962.25	1172.70	715.05	74.55	532.20
C_4-6	962.55	1172.80	715.40	74.75	532.15

the samples are listed in Table 3. The chemical shifts of the electron binding energy of Al2p and O1s in slag glasses are listed in Table 4. The relationship between the chemical shifts of binding energy of Al2p and O1s electrons and pH values of the solutions are shown in Fig. 8 and Fig. 9.

From the results above, it can be found that there is no or a little chemical shift of Al2p electron binding energy by comparing the samples attacked by weak acid or weak alkali with glass C_4; being attacked by strong acid (pH≒1.72) or strong alkali (pH>12), the chemical shift of Al2p electron binding energy of the samples increases obviously compared to glass C_4, and the values of binding energy of them are almost same as that of α-Al_2O_3 (74.7 eV). So, it can be confirmed that in the surface layer of these glasses, the coordination state of Al^{3+} ion has been transformed from fourfold

Table 4. Chemical shifts of XPS spectra for C_4 samples

Samples		C_4	C_4-1	C_4-2	C_4-3	C_4-4	C_4-5	C_4-6
Chemical shift (eV)	Al2p	0	0.5	0.2	0.0	0.1	0.45	0.65
	O1s	0	0.6	0.2	0.3	0.0	0.65	0.60

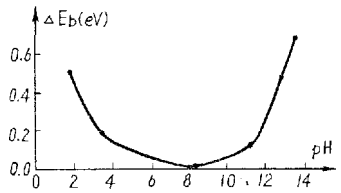

Fig. 8 Variation of the chemical shift of Al2p spectra with pH values of solutions

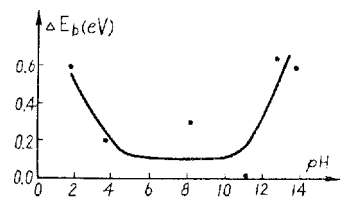

Fig. 9 Variation of the chemical shift of O1s spectra with pH values of solutions

to sixfold coordination.

The relationship between the chemical shift of O1s electron binding energy and pH value is just same as the case of Al2p. The reason may be as follows. In unattacked glass C_4, the network modifier near the non-bridging oxygen is Ca^{2+} ion. In the glass C_4 attacked by strong acid or strong alkali, Al^{3+} ion in surface layer is transformed from fourfold to sixfold coordinated, i.e., from network former to modifier. So, the number of non-bridging oxygen in glass structure increases, and the network modifier connected with them is Al^{3+} ion. This transformation will cause the decrease of electron-density around the nucleus of the non-bridging oxygen, so the electron binding energy of O1s will increase.

This research indicates that when slag glass is attacked by acid or alkali, the charging neutrality in glass structure is broken due to the diffusion of Ca^{2+} and H^+ or the bonding-broken effect of OH^- on the bridging oxygen. In this case, fourfold coordinated Al^{3+} ion

will occupy the space of network modifier, Ca^{2+}, and be transformed to sixfold coordinated Al^{3+} ion. These changes are presented in XPS spectra by the chemical shifts of the peaks of both Al2p and O1s electron binding energy. The values of the chemical shifts are regularly related to pH values of the attacking solutions. The transformations of fourfold coordinated Al^{3+} ion to sixfold coordinated Al^{3+} ion and bridging oxygen to non-bridging oxygen indicate the break of glass network and dissociation of slag glass. "The activity" of blast-furnace slag in cement paste does mean these essential changes by the act of OH^-.

3. The Surface Reaction of Slag Glass and Its Hydrate Products

Slag glass dissociates in alkaline solution, so there exist many ions in the solution and they will form some new hydrate products on the surface of the glass. The thick honeycomb-like film can be found on the surface of glass attacked by NaOH by means of SEM (Fig. 10). By means of XRD, it can be confirmed that this film is C-S-H gel with a little $Ca(OH)_2$ and $CaCO_3$ (Fig. 11).

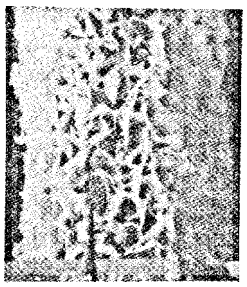

Fig. 10 Surface morphology of the glass attacked by NaOH.

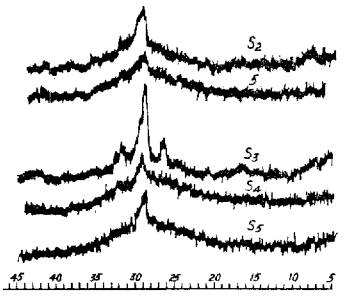

Fig. 11 XRD patterns of residues of glass after being attacked by NaOH.

Our previous work has proved that Al_2O_3 dissociates most easily from glass attacked by alkali, and gather generously on the surface of the glass. It can be shown in the results of EDXA on the surface and matrix of the glass (Fig. 12)

In the slag cement paste, there exist many ions in its liquid, such as Ca^{2+}, AlO_2^-, Si^{4+}, SO_4^{2-}, OH^- and CO_3^{2-}. They will interreact to form various hydrate products.

Under this condition, ettringite can form rapidly, i.e.,

$$3CaO\cdot Al_2O_3\cdot 3CaSO_4\cdot 31H_2O \rightleftharpoons 6Ca^{2+}+2AlO_2^-+3SO_4^{2-}+4OH^-+29H_2O.$$

According to our experiments/6/,

$$K_{sp}=(Ca^{2+})^6\cdot(SO_4^{2-})^3\cdot(AlO_2^-)^2\cdot(OH^-)^4=1.1\times10^{-40},$$

so it can form very easily and is very stable. Ettringte can be observed very easily by means of SEM (Fig.13).

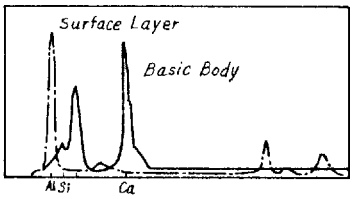

Fig. 12 Surface and matrix EDXA patterns of glass C_2 attacked by NaOH



Fig. 13 Morphology of ettringite formed by the reaction of glass and SO_4^{2-}, OH^-, etc. (x5000)

By the interface of Portland or supersulphated cement paste and C_2 glass rod, the crystal of ettringite can be found by means of SEM (Fig. 14).

The surface reaction of slag glass and the formation of the hydrate products are the direct results of the dissociation of slag glass under the condition of alkali attacking. Meanwhile, these results will promote the dissociating process of slag glass too.

4. Conclusions

From the investigation above, following conclusions can be drawn.

1). In the solutions with different pH values, aluminium will exist in the form of AlO_2^- or Al^{3+} or $Al(OH)_3$. They have an important effect on the activity of the slag glass.

2). Al^{3+} ion in the slag glasses is fourfold coordinated. After slag glass is attacked by acid or alkali, the coordination state of Al^{3+} ion is transformed from fourfold to sixfold coordination, and bridging oxygen in glass network changes into non-bridging oxygen. The two changes are presented by the changes of the



a) Glass C_2 in supersulphated cement paste (x10000)



b) Glass C_2 in Portland cement paste (x10000)

Fig. 14 Morphology of ettringite by the interface of cement paste and C_2 glass rod.

electron binding energy of Al2p and O1s. There is a good interrelation between them and the activity of the slag glass.

3). After the slag glass is attacked by alkaline solution, the hydrate products, ettringite and C-S-H gel, will form rapidly by the surface reaction between the slag glass and alkaline solution. They will promote the dissociation of the slag glass.

The hydration mechanism of blastfurnace slag glass in cement paste has been summing up as "alkaline activating" and "sulphate activating". Our research indicates that a important part of "alkaline activating" is the transformations of fourfold coordinated Al^{3+} ion to sixfold coordinated Al^{3+} ion and bridging oxygen to non-bridging oxygen, which make the network structure broken; "sulphate activating" is the formation of ettringite by the reaction of Ca^{2+}, $SO_4^{=}$, OH^- and AlO_2^- which dissociates from the slag glass in the solution. Factually, there is no so-called "sulphate activating".

REFERENCES:

1. ZHEJIANG UNIVERSITY, NANJING INSITITUTE OF GLASS FIBRE, "The Alkali Resistance of the Glass in $CaO-Al_2O_3-SiO_2$ System", 1982, (unpublished)
2. B. STARLING, "Portland Slag Cement", 6th Int. Congr. Chem. Cem., Moscow, 1956
3. A. PAUL, "Chemical Durability of Glasses: A Thermodynamic Approch", J. Material Science, 12, (1977) pp. 2246-2268
4. QIZHONG SHENG, "Behavior of Aluminium in $CaO-Al_2O_3-SiO_2$ Glasses during the Alkali Attack Process", M.Sc. Thesis, Zhejiang University, 1984, pp. 53-54
5. DUNSHI GE, "Structural Transformation of $CaO-Al_2O_3-SiO_2$ Glass during Alkali Attack Process", 1982, (unpublished)
6. FEIPENG ZHANG, ZHIFA ZHOU, ZONGHAN LOU, "Solubility Product and Stability of Ettringite", 7th Int. Congr. Chem. Cem., Paris, 1980

WANG YUJI, Lecturer, Department of Materials Science and Engineering Tongji University, Shanghai, China. 1

THE EFFECT OF HYDRATION PRODUCTS IN STEAM TREATED STEEL SLAG (O.C.S.) ON THE HYDRATION OF STEEL SLAG - PORTLAND BLENDED CEMENT

3.1

SUMMARY: Steam treatment can be used effectively in processing oxygen converter steel slag (O.C.S.) in order to facilitate the quick and complete hydration of f-CaO in it, to eliminate its unstability due to expension and to retain the reactivity of silicate minerals in it to great extent. Thus under appropriate control of processing conditions, the steam treated steel slage can be used to produce high quality steel slag - portland blended cement. Pressure and time used in steam treatment mainly controls the degree of hydration and characteristics of hydrated products of f-CaO and silicate minerals in steel slag. In this paper the effects of steam treated steel slag obtained under different steam pressures for different times on the hydration of steel slag - portland blended cement are discussed.

The morphology and amount of $Ca(OH)_2$ and hydrated silicate are different in steel slag treated under different pressure and for different times. Irregular round particles of $Ca(OH)_2$ were found under lower pressure and shorter time. With the increase of pressure and time, crystallize of $Ca(OH)_2$ enlarges in size and gradually has its regular hexagonal form. The silicate hydrates is chiefly fibrous and needle like with high CaO/SiO_2 ratio.

When the treated steel slag is used for making blended cement, the hydrates formed in the process of steam treatment, will decrease the rate of hydration of the cement in earlier stages, but promote the hydration of the unhydrated particles of blended cement in later stage and increase the density of hardened cement paste. Obviously it will be beneficial to medium and long term strength development and more suitable to use the treated slag for making blended cement from portland cement steel slag and blast furnace slag.

The optimum condition of steam treatment for steel slag is found to be 1-3 atm. pressure of saturated steam for a time below of 3 hours.

O tratamento a vapor pode ser usado eficazmente no processamento de escória por conversor de oxigênio (O.C.S.), a fim de facilitar a rápida e completa hidratação de f-CaO no mesmo, para eliminar sua instabilidade devido à expansão e para reter a reatividade dos minerais de silicato em grande quantidade nele. Assim, sob controle apropriado das condições de processamento, a escória de aço tratada a vapor pode ser usada para produzir escória de aço-cimento portland blendado de alta qualidade. Pressão e tempo usados no tratamento a vapor controlam particularmente o grau de hidratação e as características dos produtos hidratados de f-CaO e minerais de silicato na escória de aço. Neste artigo são discutidos os efeitos da escória de aço tratada a vapor, obtida sob diferentes pressões de vapor por períodos diferentes de tempo, sobre a hidratação da escória de aço - cimento portland blendado.

A morfologia e a quantidade de $Ca(OH)_2$ e de silicato hidratado são diferentes na escória de aço tratada sob pressões diferentes e tempos diferentes. Foram encontradas partículas redondas irregulares de $Ca(OH)_2$ sob pressão mais baixa e tempo mais curto. Com o aumento da pressão e do tempo, o cristal de $Ca(OH)_2$ aumenta em tamanho e gradativamente adquire sua forma hexagonal regular. Os hidratos de silicato são principalmente fibrosos e em forma de agulha, com alta relação de CaO/SiO_2.

Quando se utiliza a escória de aço tratada para se fazer cimento blendado, os hidratos formados no processo de tratamento a vapor diminuirão a velocidade de hidratação do cimento nos estágios iniciais, mas promovem a hidratação das partículas não hidratadas do cimento blendado no estágio final, e aumentam a densidade da pasta endurecida de cimento. É claro que isto é favorável para o desenvolvimento da resistência a médio e longo prazos, e mais conveniente para a utilização de escória tratada para a fabricação de cimento blendado a partir de cimento portland, escória de aço e escória de alto forno.

Constatou-se que a condição ótima para tratamento a vapor de escória de aço é de 1 - 3 atmosferas de pressão de vapor saturado, por um período de tempo inferior a 3 horas.

INTRODUCTION

The principal minerals in the oxygen converter's steel slag are C_3S, C_2S and its P_2O_5 - bearing solid solutions, C_2F and its Al_2O_3 - bearing solid solutions, f-CaO and its FeO - bearing solid solutions, Ro phase ((Fe, Mn, Mg)O), etc. In these four kinds of mineral, the unstability of volume expansion of the steel slag largely results from the hydration of f-CaO. Hence high content of f-CaO in the slag is an obstruction to the comprehensive application of steel slag. Generally speaking, before the steel slag is to be used, it is necessary to be treated so that it is stable and granulated (1).

The author had ever expressed in another paper (1) that in order to eliminate the unstable mineral f-CaO in steel slag and to retain the reactivity of silicate minerals to the greatest extent, it was better to adopt the steam treatment method than the water immersion method. When steel slag was soaked in water, the free lime in it formed Ca(OH) within the original interstices through the liquid phase reaction, which reduced its porosity and was disadvantageous to further hydration of f-CaO. As there was a lot of water there, the hydration of silicates in the slag was accelerated. With the duration of water immersion, the hydration of silicates increased. When steel slag was exposed to the steam, the solution of CaO and the movement of Ca^{++} ions was hindered and the hydration reaction directly took place on the surface of the CaO grains. This was a topochemical reaction wedging the crystal grains. The expansion stress produced in parts, enabled the slag to crack to pieces, which was advantageous to further hydration of f-CaO. But as there was less water there, the condition under which a great quantity of silicates hydrated was not formed. When the two main performance factors - the stability and the hydraulic activity of the steel slag both are considered at some time the steam method should be used in the treatment of the slag. In order to shorten the period of treatment, saturated steam under certain pressure was used, the hydration of silicates was accelerated with increasing pressure of steam. In order to get an optimum treatment condition, in this paper the effects of hydrates formed under various pressures of steam on the reactivity of steel slag are discussed.

EXPERIMENTAL

In this investigation, the original materials used were: (1) the oxygen converter steel slag from Workshop No. 3, Shanghai Steel Plant No. 1; (2) the portland cement clinker from Nanhui Cement Works of Shanghai. Their chemical and mineralogical compositions are shown in Table 1 and Table 2 respectively.

Table 1. Chemical Compositions (in wt %)

material	SiO_2	Al_2O_3	Fe_2O_3	FeO	CaO
steel slag	9.55	0.89	12.35	14.75	52.19
clinker	22.2	5.1	3.2	/	65.1

material	MgO	f-CaO	P_2O_5	CaO/SiO_2
steel slag	3.63	14.4	1.54	5.46
clinker	1.4	0.65	/	2.93

Table 2. Mineralogical Compositions (in wt %)

material	C_3S	C_2S	C_3A	C_4AF	C_2F	RO
steel slag	35.31	0.74	/	4.25	18.62	19.88
clinker	53	24	8	10	/	/

The steel slag and the cement clinker were crushed to a particle size smaller than 10 mm, then treated under the different conditions (Table 3).

Table 3. Different Treatment Conditions

treatment conditions		original sample	soaked in water			
			1 week	2 weeks	3 weeks	4 weeks
No.	steel slag	1-01	1-11	1-12	1-13	1-14
	clinker	2-01	2-11	2-12	2-13	2-14

	placed in steam									
	1atm 2h	1atm 4h	1atm 8h	3atm 1h	3atm 2h	3atm 3h	8atm 1h	15atm 1h	20atm 1h	20atm 2h	20atm 3h
	1-21	1-22	1-23	1-31	1-32	1-33	1-41	1-51	1-61	1-62	1-63
	2-21	2-22	2-23	2-31	2-32	2-33	2-41	2-51	2-61	2-52	2-63

Both treated steel slag and cement clinker were analysed chemically, studied by SEM, IR, DTA, TG and XRD, and their physical and mechanical properties were also tested respectively.

RESULTS AND DISCUSSION

1. SEM observation of treated steel slag and portland cement clinker

SEM micrographs of steel slag treated under different conditions are shown in Fig. 1.

When the steel slag was soaked in water, it would form numerous thick fibrous C-S-H gel and less quantity of circular or irregular $Ca(OH)_2$ particles. When the slag was stored in steam (P=1 atm, T=100°C. RH= 96% respectively), a lot of circular or irregular $Ca(OH)_2$ particles and small quantity of C-S-H gel were found in the sample. The fibrous and bunch-like C-S-H gel increased with the duration of treatment. While the slag was stored in steam under 3 atm. pressure the thick and regular $Ca(OH)_2$ formed. The structure of the crystal became perfect as treatment period was prolonged. At that time, C-S-H gel was wormy-like and in gelatinous state. In steam under higher pressure, C-S-H increased in quantity. Its morphologies were needle-like, bunch-like, fibrous, etc.. And $Ca(OH)_2$ was mainly thick crystal of sexangular, clinkers treated under different condition various appearances of C-S-H were observed, such as, lamelar, plate-like, fibrous, pipy, columned, needle-like, flower-like, tobermorite, etc. (Fig. 2). The results indicate that C-S-H would vary in composition and morphology with pressure of steam. Generally, in lower pressure steam, the morphology of C-S-H gel is greatly lamelar, and in higher pressure steam, is needle-like and fibrous. It is possible that the difference in morphology of C-S-H gel which closely relates to the pressure of steam, results from the difference in



A. In water for 1 week

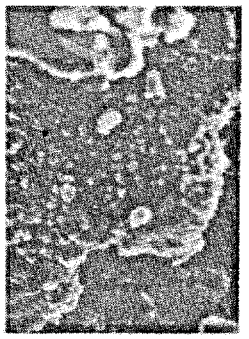

B. In 1atm of steam for 2h



C. In 1atm of steam for 8h

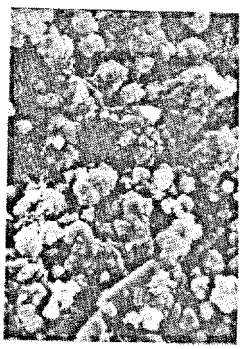

D. In 3atm of steam for 2h

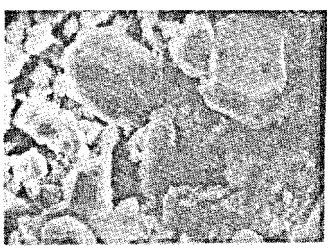

E. In 3atm of steam for 3h



F. In 15atm of steam for 1h

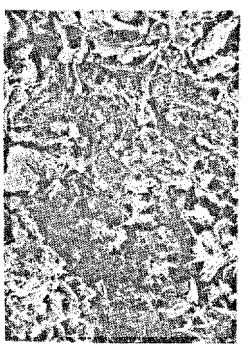

G. In 20atm of steam for 1h

Fig. 1 SEM micrographs of steel slag treated under different conditions



A. In water for 1 week



B. In steam under 1atm pressure for 8h



C. In steam under 3atm. pressure for 3h

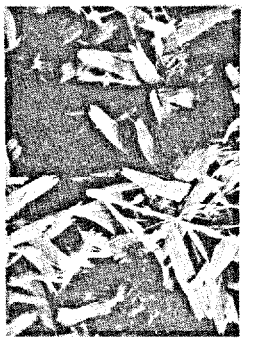

D. In steam under 3 atm. pressure for 1h



E. In steam under 20 atm. pressure for 2h

Fig. 2 SEM micrographs of clinker treated under different conditions

ratio of CaO/SiO_2 of the gel. According to F.M. Lea (2), as ratio of $CaO/SiO_2 < 1.5$, the gel is lamelar CSH (I); as ratio of $CaO/SiO_2 > 1.5$, it is fibrous CSH(II). Form this, it might be considered that when treated in low pressure steam, clinker would form CSH(I) with low CaO/SiO_2 ratio, and that in higher pressure steam, CSH(II) with high CaO/SiO_2 ratio would be produces.

Since C-S-H produced from high basic steel slag treated in steam under various pressures was mainly fibrous and needle-like, it might be CSH(II) with high CaO/SiO_2.

2. Hydration of f-CaO and silicate minerals in steel slag treated under different conditions

In order to determined the degree of hydration of f-CaO and reactive silicates in the steel slag treated under different conditions, the amount of Ca(OH) by TG. The results and calculated degree of hydration of f-CaO and silicates are shown in Table 4.

Table 4. Degree of Hydration (%)

No.	f-CaO %	$Ca(OH)_2$ %	$Ca(OH)_2$ produced % from f-CaO	$Ca(OH)_2$ produced % from Silicates	Degree of Hydration % f-CaO	Degree of Hydration % Silicates
original sample	14.4					
1-22	4.8	15.42	12.69	2.73	66.7	10.59
1-33	1.5	33.85	17.03	16.82	89.6	65.22
1-51	0.6	39.50	18.22	21.28	95.8	82.53

It can be seen from Table 4 that various treatments for the elimination of f-CaO in the slag caused hydration of not only f-CaO, but also silicate minerals. In steam under 1 atm. pressures f-CaO hydrated quickly, but silicates did much slow. With increasing the pressure of steam, the hydration of silicates was greatly accelerated. When the pressure of steam grew to 15 atm. for 1 hour, the degree of hydration of silicates was 82.53%.

3. The properties of cement produced from treated steel slag

In making blended cement, the steel slag treated in steams under different pressures for different periods, and mixed with blast furnace slag, portland cement clinker and gypsum in the proportion of 30:30:35:5, and then ground to a fineness with specific surface area 3200-3500 cm^2/g, the blended cement pastes with 24% water were moulded to form cubes of $2\times2\times2$ cm^3 for strength tests and cakes for soundness tests.

The experimental results are shown in Table 5.

Table 5. Properties of Cement made from Treated Steel Slag

No.	soundness		compressive strength MPa		
	boiled	autoclaved	7d	28d	90d
1-01	unevenness	/	80.3	114.0	102.5
1-11	unevenness	/	36.8	78.8	105.9
1-12	unevenness	/	36.9	88.3	120.6
1-13	evenness	evenness	29.5	81.8	108.4
1-14	evenness	evenness	24.8	69.3	89.8
1-21	evenness	evenness	85.1	123.8	126.0
1-22	evenness	evenness	79.5	105.0	118.0
1-23	evenness	evenness	77.4	110.8	123.5
1-31	evenness	evenness	77.3	111.9	111.3
1-32	evenness	evenness	79.4	111.9	151.5
1-33	evenness	evenness	83.8	114.6	149.5
1-41	evenness	evenness	67.0	92.5	95.1
1-51	evenness	evenness	87.7	108.3	119.3
1-61	evenness	evenness	79.6	90.0	137.5
1-62	evenness	evenness	65.9	97.0	105.3
1-63	evenness	evenness	82.5	113.2	112.1

It can be seen from Table 5 that the results of soundness test of cements made from steel slag treated in steam under various pressures were all qualified, but cements made from steel slag soaked in water, only those whose soaking duration over half a month, their soundnesses could be improved. For the mechanical proporty, the strengths of cements made from steel slag soaked in water for different periods always lie in the lowest range of strength date in our study, while those for cements made from steel slag treated in steam under 1-3 atm. pressure for 1-3 hours lie in the highest range. These results are in accord with the SEM analysis above. However here occured an interesting phenomenon — the degree of hydration of silicates in steel slag treated in steam over 15 atm. pressure was up to more than 80%, but the hydraulic activity of the blended cement made from it as a whole was still high, not influenced by the presence of the treated slag in it. This is probably due to the following:

A) The pipy fibrous C-S-H from treated slag facilitates the diffusion of water and solutes through the its pores and thus it is advantageous to the hydration of the whole cement. Principles of this process were discussed by Double et al and Brunauer et al.

B) The volume expansion due to the hydration of f-CaO in steel slag during treatment, results cracks and defects in the interior of the treated mass, which provides the proper space for the growth of calcium silicate hydrates and crystal $Ca(OH)_2$. Both hydrates grow crosswise and mixedly (Fig. 3).

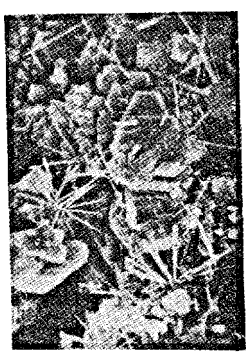

Fig. 3. Steel slag treated in steam under 20 atm. pressure

But, at the same time, crystals of $Ca(OH)_2$ mixed with fibrous C-S-H gel will block the free space between them and prevent water to move towards non-hydrated particles. To sum up: The activity of the steam treated steel slag is very low because of the hydration of silicates in it, but certain quantity of pipy fibrous C-S-H produced will facilitate further hydration of blended cement made from steel slag and portland cement clinker; The existence of a great deal of $Ca(OH)_2$ crystals will hinder the hydration of the cement in the early stage; However, crystals of $Ca(OH)_2$ formed in later stage will fill in the interstices of sub-hexagonal structure formed by the fibrous C-S-H gel resulting in the compact structure;

Besides, when the blended cement is made from steel slag, blast furnace slag and portland cement clinker, as a basic exciter, all Ca(OH) performs an obvious exciting function in hydration of blast furnace slag. When the abovementioned factors are functioning together, for cement made from steel slag treated in steam of under various pressure there is not very obvious, sharp change in its mechanical properties. Of course, when the pressure of steam in treatment is too high and the period of treatment is overlong the strength of cement will descend. Table 6 gives the strength of the mortar of blended cement made from steel blast furnace slag and portland cement clinker. It can be seen from Table 4-6 that it is appropriate to treat steel slag in 1-3 atm of steam.

Table 6. Strength of mortar of blended cement

No.	proportion %				fineness %	consistency %	soundness
	steel slag	blast furnace slag	clinker	gypsum			
1-22	23	23	50	4	5.8	27	
1-33	23	23	50	4	7.1	27	evenness
1-51	23	23	50	4	5.0	27	

set time hours-minutes		bending strength Mpa		compressive strength Mpa	
initial	final	7d	28d	7d	28d
3-10	4-40	7.6	9.8	32.9	52.2
3-00	4-30	7.7	10.4	31.0	51.4
3-18	5-18	7.0	10.4	27.9	49.3

4. Manufacture and applications of the blended cement
It was successful that treated steel slag and blast furnace slag were used as compound admixture in manufacture of blended cement. Its performance, range and method of application and properties of the concrete are identical with those of the blast furnace slag cement. This blended cement is good in the resistance to permeate, wear and corrosion, and it is low in heat of hydration. Fig. 4 gives photos of auditorium, factory buildings, road, bridge, etc. built with concretes from this blended cement made from steel slag, blast furnace slag and portland cement clinker.



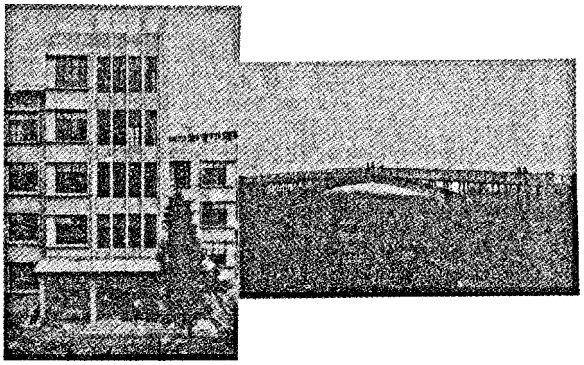

Fig. 4 Photos of auditorium, factory house, road, bridge, etc. built of this blended cement

CONCLUSIONS

1. In the steel slag treated in steams under different pressures for different periods, the Ca(OH) and C-S-H formed in them are of different morphologies and quantities. When the pressure of steam is low and the period of treatment is short, the crystal of Ca(OH) is irregular, circular. With the prolongation in period of treatment and increase of pressure of steam, the amount of Ca(OH) crystal increased and the size enlarged, the crystals gradually changed from round into regular hexagonal. Calcium silicate hydrates are largely of fibrous, needle-like.

2. In the blended cement made from steam treated steel slag, because of the effects of hydrates which are different in quantity and morphology produced during the treatment of the slag on hydration of cement, the early hydration rate will decrease. But the further hydration in interior will be promoted, the compactness of the hardened cement paste will increase, so the strength at middle and later stages will increase.

3. It is better to treat steel slag in 1-3 atm of steam, since under this condition the most of f-CaO in the slag has hydrated but the degree of hydration of its silicates is low.

REFERENCES

1. Wang Yuji, Du Tiazhen, "The Effect of Different Technical Treatment on Hydration of f-CaO and Silicates in the Oxygen Converter Steel Slag."

2. F.M. Lie, "The Chemistry of Concrete and Cement."

HUANG SHIYUAN, Shanghai Institute of Building Materials, Shanghai, China
CHENG JIPING, Wuhan University of Technology, Wuhan, China

THE EVALUATION OF POZZOLANIC REACTIVITY OF FLY ASHES

SUMMARY: The reaction degree of fly ashes with $Ca(OH)_2$ and water at ambient temperatures measured by a chemical method based on determination of the quantity of dissolved substances in fly ashes in hydrated fly ash - $Ca(OH)_2$ pastes was found to be well correlated with the strength of the fly ash - $Ca(OH)_2$ and the fly ash -cement pastes, which proves the pozzolanic reactivity of fly ashes does directly contribute to the strength of fly ash cement pastes and concretes.

The pH value of the liquid in fly ash suspension in deionized water seems to have a good correlation with the reaction degree of fly ashes used in the present test. Measurement of the pH value of fly ash suspension under a certain condition might be a simple way for comparatively evaluating the pozzolanic reactivity of fly ashes.

Verificou-se que o grau de reação das cinzas volantes com $Ca(OH)_2$ e água, a temperaturas ambientes, medido por método químico baseado na determinação da quantidade de substâncias dissolvidas em cinzas volantes nas pastas de cinza volante-$Ca(OH)_2$ está relacionado com a resistência das pastas de cinza volante-$Ca(OH)_2$ e cinza volante-cimento, o que prova que a reatividade pozolânica das cinzas volantes contribui diretamente para a resistência de pastas e concretos de cimento de cinza volante.

O valor do pH do líquido em suspensão de cinza volante em água desionizada parece ter uma boa correlação com o grau de reação das cinzas volantes usadas no presente ensaio. A medição do valor do pH de suspensão de cinza volante sob determinada condição pode ser um modo simples de avaliacão comparativa da reatividade pozolânica de cinzas volantes.

1. INTRODUCTION

Pozzolanic reactivity or chemical activity of fly ashes is the index of the reaction degree of fly ashes with $Ca(OH)_2$ and water at ambient temperatures as defined by K. Takemoto and H. Uchikawa [1].

Numerous test methods have been suggested for the assessment of the pozzolanic property of fly ashes. ISO method evaluates the pozzolanility by the $Ca(OH)_2$ concentration in the liquid of cement - pozzolana suspension. Some methods are based on determination of the amount of soluble substances in fly ashes during alternating acid - alkali or acid treatment. Raask and Bhaskar [2] have devised a rapid method based on the measurement of electrical conductance of the fly ash samples dispersed in dilute solution of hydrofluoric acid. Soviet standard GOST 6269-63 uses the lime-binding capacity of pozzolana as its activity.

However, no so good correlation has been found between the strength of the fly ash - cement system and the test results of the pozzolanic reactivity of fly ashes carried out by some devised methods. Therefore, K. Takemoto and H. Uchikawa concluded "strength which is one of the representative properties of pastes, is strongly influenced by the kinds, shapes, sizes and distribution of hydration products and pores, has not so good correlation with the degree of reaction".[1]

In the present paper, the pozzolanic reactivity, i.e. the degree of reaction of fly ashes was measured by chemical analyses in the fly ash - $Ca(OH)_2$ pastes at various ages, and attempts were made to correlate the reaction degree with the strength of fly ash - $Ca(OH)_2$ and fly ash - cement pastes.

2. EXPERIMENTAL METHODS AND MATERIALS

2.1 Materials and specimen preparation

Seven fly ashes selected from various power stations in China have been used for testing with chemical compositions and surface areas shown in Table 1, which may represent most fly ashes produced by power stations using anthracite and bitumious coal in China. Fly ashes from subbituminous and lignite coal have not been selected to be used for testing and are not covered in the present paper.

Fly ashes dried at 100°C for 12 hours were stored in a desiccator for use. Chemically pure CaO was used. Pure clinker cement used was made in Hua Xin Cement Plant.

The fly ash-CaO ratio of the mixtures was the same 4:1 for all fly ash - CaO paste specimens and the fly ash - cement ratio was 3:7 for all fly ash - cement paste ones. For getting the results comparable, the pastes were prepared with the same water - solid ratio of 0.65 for fly ash - CaO pastes and 0.30 for fly ash - cement pastes so as to exclude the apparent influence of water - solid ratio on strength.

Pastes were cast into moulds 20 mm in diameter and 25 mm high, vibrated and cured at the room temperature.

Strength test and chemical analyses were made for pastes cured for definite ages. The samples taken out from the center of fractured fly ash - Ca(OH) specimens, immersed in ethyl alcohol of 99% concentration, extracted flushed by alcohol and then dried in a vaccum desiccator under a vaccum pressure of 200 mm Hg and 60 C for six hours were chemically analysed.

2.2 Measurement of content of dissolved substances

The samples weighing precisely 5 grams were dissolved in the 2N HCl solution, poured into a beaker of the volume of 300 ml with continuous agitation, submerged in a thermostatic bath at 80°C with agigation and filtered 15 - 20 minutes later. The beaker was flushed by water of 80°C three times, so that all the remains in the beaker would be flushed through the funnel. The precipitation above the filter paper flushed by 2% Na_2CO_3 solution of 80°C three times and water of 80°C other three times were placed in a cup together with the filter paper.

The cup was burnt at 950 C for half an hour, cooled and taken out from the furnace, cooled to room temperature in a desiccator and weighed.

he content of dissolved substances in percentage will be

$$S = \left(1 - \frac{G_1}{G}\right) \times 100\%$$

where G_1 - the weight of remains after burning (g)
G - the weight of the sample (g)

2.3 Calculation of the reaction degree of fly ash

The reaction degree of fly ash was calculated by the following expression:

$$d_t = \frac{S_t - S_{th}}{F}$$

Table 1. Chemical composition and surface area of fly ashes tested

No.	Place of production	Chemical Composition								Soluble*		Surface area (cm^2/g)
		SiO_2	Al_2O_3	Fe_2O_3	CaO	MgO	K_2O	Na_2O	IL	SiO_2	Al_2O_3	
1	Nanning	46.84	36.26	6.88	2.64	0.19	0.82	1.56	5.17	0.15	0.19	5425
2	Zhuzhou	57.48	25.35	3.12	1.12	1.12	2.49	2.39	9.08	0.30	0.05	2398
3	Wuhan	51.85	27.58	6.75	2.82	0.91	1.63	0.94	7.24	0.30	0.12	3449
4	Kunming	54.49	19.69	8.91	4.13	0.96	—	—	10.88	0.14	0.04	3370
5	Zhenzhou	61.15	19.11	8.68	2.80	2.41	3.06	1.60	1.08	0.26	0.14	1955
6	Beijing	50.87	29.39	9.32	2.88	0.80	1.30	1.45	4.23	0.24	0.14	4406
7	Shanghai	53.82	30.06	6.99	2.61	0.93	1.00	1.50	7.02	0.28	0.10	3697

* measured by colorimetry

where S_t - the content of dissolved substances in fly ash at the age t

S_{4h} - the content of dissolved substances in fly ash at first 4 hours after mixing, which we assign conditionally as the start point of measurement

F - weight fraction of fly ash in the fly ash - $Ca(OH)_2$ mix, in this case being 0.75

2.4 pH value measurement

The pH value were measured in a 1:20 fly ash - water suspension at the first 10 minutes.

3. RESULTS AND ANALYSES

The reaction degree of seven fly ashes were measured from 7 to 180 days, which ranges between 1.5 and 4% at 7 days and 7 and 20% at 180 days (Fig. 1). It can be seen that the pozzolanic reaction still keeps comparatively high rate at 180 days.

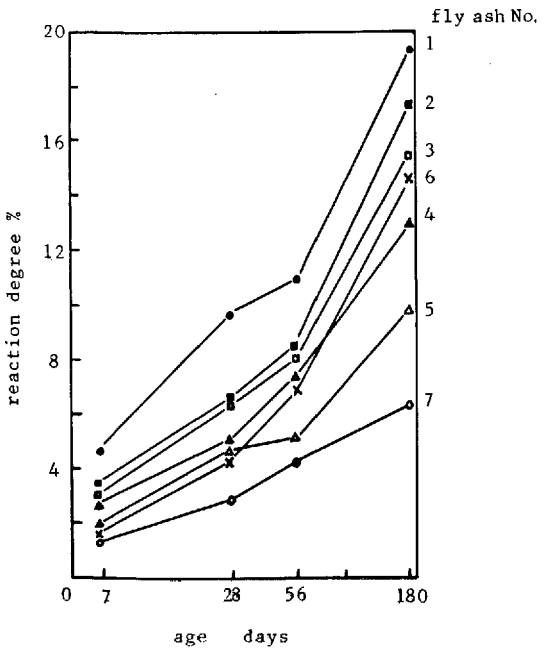

Fig. 1 The reaction degree of fly ashes in fly ash - $Ca(OH)_2$ pastes with ages

The strength development of fly ash - $Ca(OH)_2$ and fly ash - cement pastes was shown in Figs. 2 and 3, and the plots of the strength of fly ash - $Ca(OH)_2$ and fly ash - cement pastes against the reaction degree of fly ashes were illustrated in Fig. 4 and 5 respectively.

By analysing the results shown in Figs. 1-5, it can be seen that both the strengths of fly ash - $Ca(OH)_2$ and fly ash - cement pastes correlate rather well with the reaction degree of fly ashes, which indicates the reaction degree does contribute to the strength. Very little contribution of fly ash - $Ca(OH)_2$ reaction can be found to the strength of pastes as the degree of reaction of fly ash is less than 6-7% under the condition of the present test. As the reaction degree

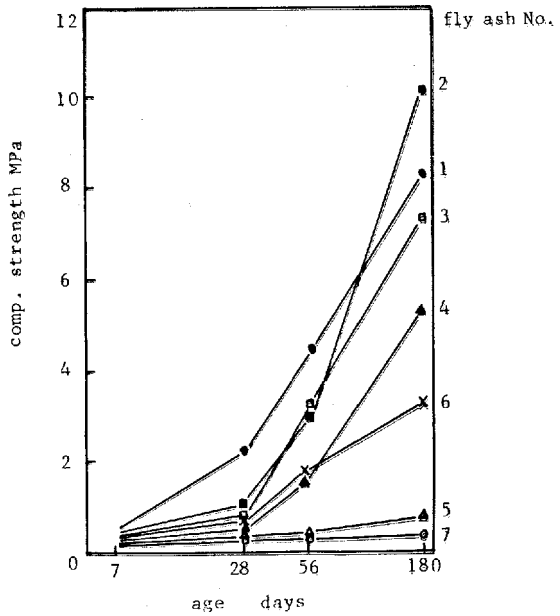

Fig. 2 Strength development of fly ash - $Ca(OH)_2$ pasts

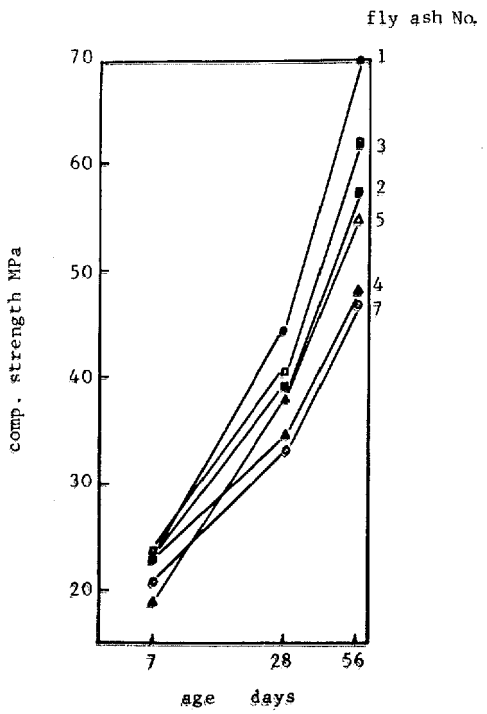

Fig. 3 Strength development of fly ash - cement pastes

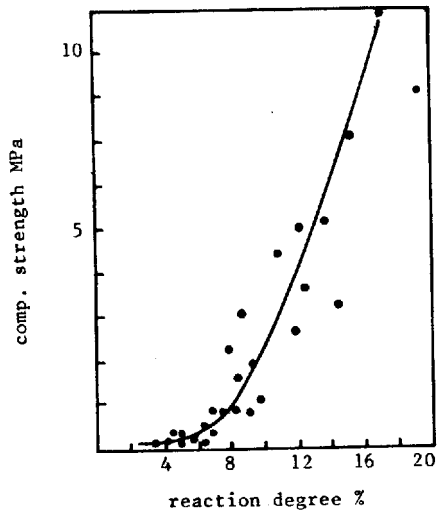

Fig. 4 Relationship between the strength of fly ash - $Ca(OH)_2$ pastes and the reaction degree of fly ashes

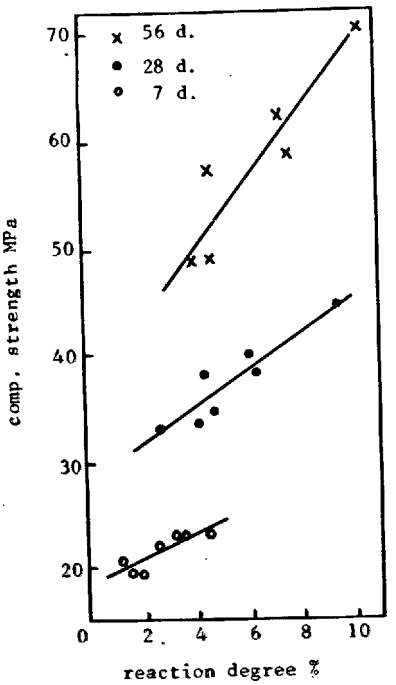

Fig. 5 Relationship between the strength of fly ash - cement pastes and the reaction degree of fly ashes

is more than 6-7%, the contribution to the strength begins to dramatically increase with the increase of reaction degree (Fig. 4). The reaction degree of fly ashes tested with exception of fly ash No. 1 is below 6-7% before 28 days (Fig. 1), which may explain why fly ash pays little contribution to the fly ash cement pastes or concretes at early ages and fly ash cement has a high strength potential at later ages.

Although the reaction degree of fly ashes in fly ash - Ca(OH) pastes chemically measured by the present method can reflect the chemical activity of fly ashes, the method is rather time consuming and is naturely not suitable for practical use.

It was found that the pH value of the liquid in the fly ash suspension in deionized water had a good correlation with the reaction degree (Fig. 6). The reaction degree of fly ashes at early ages is in the same order as the pH value of the fly ash suspension.

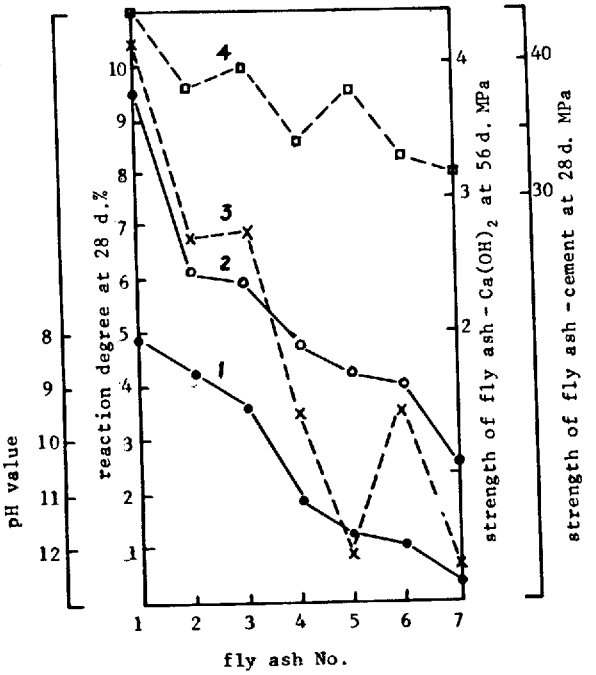

Fig. 6 Relationship between pH value, reaction degree, strength of fly ash - Ca(OH) pastes and strength of fly ash cement pastes

1 - pH value,
2 - reaction degree,
3 - strength of fly ash - Ca(OH) ,
4 - strength of fly ash - cement

The less the pH value, the more the reactivity of fly ash is. However, it should be noticed that the role indicated above did not apply to lignite coal ashes, which usually contained a large amount of calcium, having some self binding property. It should be further pointed out that a pH value alone seems to be in some cases not precise enough to evaluate the pozzolanic reactivity. For example, the pH value of fly ash No. 3 ground for 1 hour increases from

original 9.3 to 9.5, whereas its reaction degree does not decrease but greatly increases in comparison with that of unground one. That is because the surface area of ground fly ash greatly increases. Therefore, the surface area, an important factor influencing the reaction rate should also be taken in consideration.

Nevertheless, the measurement of pH value of the liquid in fly ash suspension under a certain condition may be a very simple and rapid method for comparative assessment of the pozzolanic reactivity of fly ashes.

4. DISCUSSION

The mechanism of the reaction in the system pozzolana-$Ca(OH)_2$ -H_2O has been studied by some authors and reviewed by K. Takemoto and H. Uchikawa as follows[1] :

After mixing pozzolana and $Ca(OH)_2$ with water, the liquid is saturated with $Ca(OH)_2$ in the short time. Pozzolana grains are protonically attacked by water in high caustic solution dissociating the SiOH group on the surface of grains to SiO_4^{4-} and H^+ leaving negatively charged grains. Ca^{2+} is adsorbed on the surface of grains and alkalies in pozzolana dissolve into the liquid phase remaining a thin amorphous Si, Al - rich layer on the surface of pozzolana grains, and AlO_2 in the layer gradually begin to dissolve and combine with Ca^{2+} to increase the thickness of the layer. The subsequent reaction is mainly caused by the diffusion of atomic groups through the denser layer of hydrates formed between pozzolana and $Ca(OH)_2$.

According to the mechanism mentioned above, the pozzolanic reactivity of fly ashes is considered to be determined by the richness of the Si and Al layer and the surface area of fly ash grains. The pH value of fly ash suspension may reflect the richness of the Si, Al layer. The less the pH value, the Si, Al richer the layer is, and the more the Ca^{2+} will be attracted on the surface to react.

An interesting experiment made by Cheng Jiping might serve as a side proof of this mechanism. The ability of adsorbing water reducers of type sulphonated naphthalene-formaldehyde condensate (SNF) and type lignosulphonate was measured for six kinds of fly ashes with different pH values. These water reducers dissociate negatively charged polar groups, which tend to be adsorbed on the surface of solid, and positive ionic groups in water. Results show the exact correspondence of the order of the amount of adsorbed reducer with that of the pH value of fly ashes as it is expected (Fig. 7). The less the pH value, the more the Ca^{++} is adsorbed as mentioned above, but on the contrary, the less the negatively charged polar groups of water reducers should be adsorbed on the surface of fly ashes

5. CONCLUSIONS

5.1 The reaction degree of fly ashes measured by a chemical method based on determination of the quantity of dissolved substances in fly ashes in hydrated fly ash - $Ca(OH)_2$ pastes well correlates with the strength of the fly ash - $Ca(OH)_2$ and fly ash cement pastes.

5.2 The pH value of the liquid in fly ash suspension in deionized water was found to have some correlation with the reaction degree of fly ashes. Measurement of pH value of fly ash suspension might be taken as a simple and rapid method for comparative evaluation of the pozzolanic reactivity of fly ashes under a certain condition.

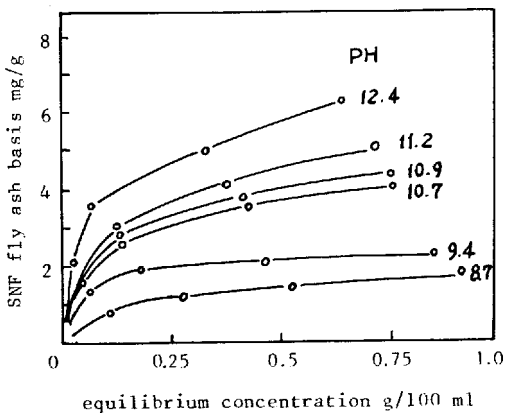

Fig. 7 Adsorption isotherms of water reducer SNF on fly ashes with different pH values

REFERENCES

1. K. Takemoto and H. Uchikawa, Hydration of pozzolanic cement, Proceedings of 7th International Congress on Cement Chemistry, 1982.

2. E. Raask, Pulverised fuel ash constituents and surface characteristics in concrete applications, International Symposium on the Use of PFA in Concrete, 1982.

3. Cheng Jiping, Thesis for master degree, Wuhan Institute of Building Materials, 1984.

Han Qi Cheng * and Bjarne Osbaeck,
F.L. Smidth & Co. A/S, R&D Dept., Copenhagen, Denmark.

Effects of Fly Ash Grinding on the Hydration and Strength Development of Fly Ash Cements.

Effets du Broyage des Cendres Volantes sur l'Hydratation et le Développement des Résistances des Ciments aux Centres Volantes.

SUMMARY: A coarse fly ash with a specific surface of about 200 m^2/kg (Blaine) was ground to 450 m^2/kg and 650 m^2/kg, and the three materials were tested in fly ash Portland cement mixés with 10, 20 and 30% fly ash. Setting, heat development, flowability of mortar, strength development and lime consumption were determined. The finer grinding of the fly ash resulted in improved flowability of mortar and substantial improvements in strength development characteristics. The strength results are compared with the information on the hydrating system obtained by calorimetry and thermal analyses, and suggestions to the factors behind the contribution to stength from the fly ash are given.

Moeu-se uma cinza volante com superfície específica de cerca de 200 m^2/kg (Blaine) até 450 m^2/kg e 650 m^2/kg, e os três materiais foram testados em misturas de cimento portland de cinza volante com 10, 20 e 30% de cinza volante. Foram determinados: pega, desenvolvimento de calor, fluidez da argamassa, desenvolvimento da resistência e consumo de cal. A moagem mais fina da cinza volante resultou em melhora da fluidez da argamassa e em melhoras substanciais nas características de desenvolvimento da resistência. Os resultados de resistência são comparados com a informação sobre o sistema hidratante obtido por calorimetria e análises térmicas, e são feitas sugestões para os fatores de contribuição da cinza volante para a resistência.

* Permanent Address: Shanghai Research Institute of Building Sciences, Shanghai, China.

Introduction

When fly ash is used as a partial replacement for Portland cement in mortar or concrete the contribution from the fly ash to the strength development and other properties will be dependent on fly ash characteristics among which the fineness has been found to be a dominant one. Differences in fineness of fly ash is usually a result of different sources of coal, different fineness of the coal powder used for combustion and different burning and ash collection methods. However, the fineness of the fly ash can also be influenced by grinding the ash (1,2).

The contribution to strength from the fly ash is generally related to pozzolanic properties, i.e. its ability to react with lime to form C-S-H-gel. Other aspects should, however, also be considered, especially when the effect of grinding fly ash is evaluated (2,3,4).

The purpose of the present study is to investigate how grinding of a fly ash affects its physical characteristics and how this influences its contribution to the strength development and other properties of fly ash - Portland cement mixes of different fly ash content.

Experimental

Materials

The fly ash (PFA) used was collected at a Danish power plant using a coal of Australian origin. The ash has a rather high SiO_2-content and a fairly low content of residual carbon (Table 1). Physically it is characterized by a low density and by being relatively coarse (Table 2).

The clinker used was an ordinary Portland type (Table 1). The gypsum was a natural quality, but used in a 50% dehydrated form to simulate conditions in practice.

TABLE 1

Chemical Composition of Starting Materials

%	Clinker	Gypsum	PFA
SiO_2	21.3	1.27	66.3
Al_2O_3	5.65	0.32	22.7
Fe_2O_3	2.88	0.20	3.98
CaO	65.6	34.9	0.56
MgO	1.16	0.79	0.26
MnO	0.04	0.00	0.09
TiO_2	0.29	0.05	0.94
P_2O_5	0.17	0.02	0.23
K_2O	0.70	0.08	1.43
Na_2O	0.33	-	0.09
SO_3	0.43	47.2	0.06
L.O.I	1.29	14.9	3.19
C	-	-	2.66
Free CaO	2.66		0.00
Total sulphur	0.17		0.04
Soluble K_2O	0.37		0.005
Soluble Na_2O	0.10		0.002
C_3S	52		
C_2S	22		
C_3A	10.1		
C_4AF	8.8		

TABLE 2

Physical Properties of Reference Cement and PFAs

		Portland cement	PFA-0	PFA-1	PFA-2
Density	(kg/m^3)	3130	2030	2340	2470
Specific surface (Blaine)	(m^2/kg)	324	217	448	646
	(10^3 m^2/m^3)	1014	441	1048	1596
Sieve residues (Air jet)	125 µm (%)	0	10.2	0	0
	90 " "	0.4	18.3	0	0
	45 " "	18.4	42.2	2.2	0.2
	20 " "	52.0	68.6	38.0	9.0
Particle size distibution (CILAS)	125 µm (%)	0.0	10.2	0.0	0.0
	64 " "	5.5	30.8	0.6	0.3
	32 " "	30.5	57.4	15.4	0.3
	16 " "	54.4	75.9	45.7	20.5
	8 " "	71.3	87.0	67.9	52.1
	4 " "	82.3	93.5	82.4	71.6
	2 " "	89.3	96.3	91.7	86.2
RR-parameters	$d_{50\%}$ (µm)	16	39	13	8
	n	0.92	1.00	1.15	1.12
Bulk density of powder (DIN 53.194)	Loose (kg/m^3)	1300	865	780	727
	Compact. (kg/m^3)	1825	1109	1168	1082
	Loose (m^3/m^3)	0.415	0.426	0.333	0.294
	Compact. (m^3/m^3)	0.583	0.546	0.499	0.438

Grindings

The PFA as received, designated PFA-0, was ground in a laboratory ball mill to two fineness levels (Blaine): One of about 450 m^2/kg (PFA-1) and one of about 650 m^2/kg (PFA-2). Physical data of the three materials were determined and their general appearance was evaluated by scanning electron microscopy.

The clinker was ground to ordinary Portland cement fineness in the same mill with 4% of the 50% dehydrated gypsum, and physical data of resulting cement was determined.

Cement Blends

PFA-cements containing 10, 20 and 30% PFA were prepared from each of the three PFA-products by blending them intimately with the Portland cement in a powder blender.

With the pure Portland cement this gave 10 cements whose properties were examined.

Properties of cements

The setting characteristics of the cements were determined by the Vicat method.

The strength development was determined according to the ISO-RILEM-method with testing at the following ages (at 20°C water curing): 1, 3, 7, 28, 56, 91 and 365 days.

The flow behaviour of the mortar mixes (3 parts Standard ISO-sand to 1 part cement to 0.50 part water all by weight) was tested using the ASTM-flow table, and the bleeding behaviour was tested on the same mortar mixes by weighing the amount of water being expelled from a 400 ml mortar sample during the first 4 hours after water addition.

The density of the fresh mortar and of the mortar prisms after demoulding was determined and used for calculating the air content of the materials.

The $Ca(OH)_2$ in the mortar prisms was determined at the ages of strength measurement by grinding the fragments from the strength test with acetone, drying the powder at 40°C and determining the weight losses up to 880°C by thermogravimetric analysis. As carbonation takes place during storage of the prisms and during preparation of the specimens for TGA, converting some of the $Ca(OH)_2$ to $CaCO_3$, the loss between 440 and 510°C usually being designated to $Ca(OH)_2$ dehydration was expected to give too low an estimate on the $Ca(OH)_2$ that had actually been produced.

Consequently, an alternative estimate of the potential $Ca(OH)_2$-content including the loss between 510 and 880°C, mainly associated with decarbonation of $CaCO_3$, was also calculated.

To get information on the early hydration behaviour of the cement conduction calorimetry on cement pastes (25°C and W/C = 0.5) was performed recording the rate of heat liberation in the first 24 hours.

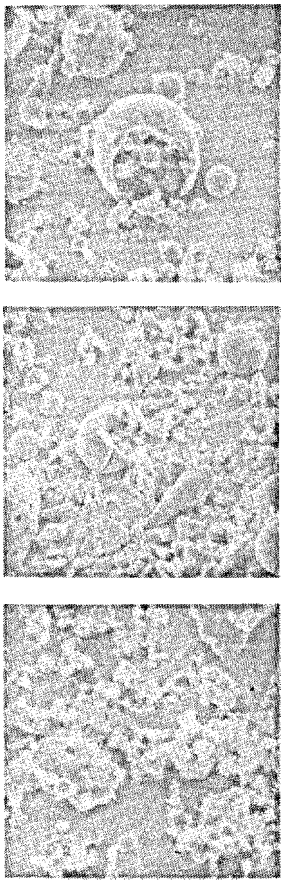

FIG. 1

Scanning electron micrographs of the fly ash sample as received (PFA-0, top) and after grinding (PFA-1, centre, and PFA-2, bottom). (Width of photos corresponds to 110 µm).

Results

Physical properties

The physical properties recorded for the reference cement and the three fly ash samples are found in table 2. The marked increase in density on grinding due to the reduction of the inherent porosity of the material should be noted. Further grinding of the fly ash indicated a limiting density value of 2530 kg/m^3. Due to the differences in density of the materials the specific surfaces are also expressed on volume basis.

The particle size distribution (PSD) as found by LASER granulometry of the ash as received has a shape similar to ball mill ground clinker. The PSD, however, tends to get more narrow with grinding, probably due to the fact that the coarse particles also tend to have higher porosity and therefore are more easily ground. (Cenospheres and porous carbon particles are more abundant among the coarse particles).

The fly ash products were examined by scanning electron microscopy (Fig. 1). In the ground products sharp-edged fragments of spheres and cenospheres are found, but a part of the smaller spherical particles seems to have survived the grinding.

In table 2 is listed the bulk density of the powders loosely packed and after compaction on a shock table. As for the specific surface a value based on volume seems more rational for comparisons. It is seen that the bulk density of the fly ash powder (on volume basis) falls substantially with grinding.

TABLE 3

Properties of Cement-Paste - Water Requirements and Setting Times

PFA-content	0%	10%			20%			30%		
PFA-No	-	0	1	2	0	1	2	0	1	2
Density (kg/m^3) of cement	3130	2970	3080	3050	2850	2960	2990	2710	2840	2880
Wt.% water	28.5	30.5	30.5	30.0	31.0	30.5	30.0	33.0	32.5	31.5
Vol.% water	89	91	94	92	88	90	90	89	92	91
Initial set (H:M)	3:50	4:40	3:50	3:50	4:30	4:30	4:40	5:10	5:00	5:00
Final set (H:M)	5:10	6:00	5:50	5:50	6:20	6:00	5:50	7:40	6:40	6:30

Water Requirement and Setting

The water requirements and setting times of the cement blends evaluated in paste (Vicat procedure) are shown in table 3. On weight basis the fly ash cements seem to have higher water requirements than the pure Portland cement, but evaluated on volume basis the difference is negligible for the PFA-0-cements while a slightly higher water demand is indicated for cements based on ground PFA. The setting time is in general 1-2 hours longer for the fly ash cements than for the pure cement. Within the fly ash cements setting times are prolonged with increased addition and shortened with increased fineness of the ash.

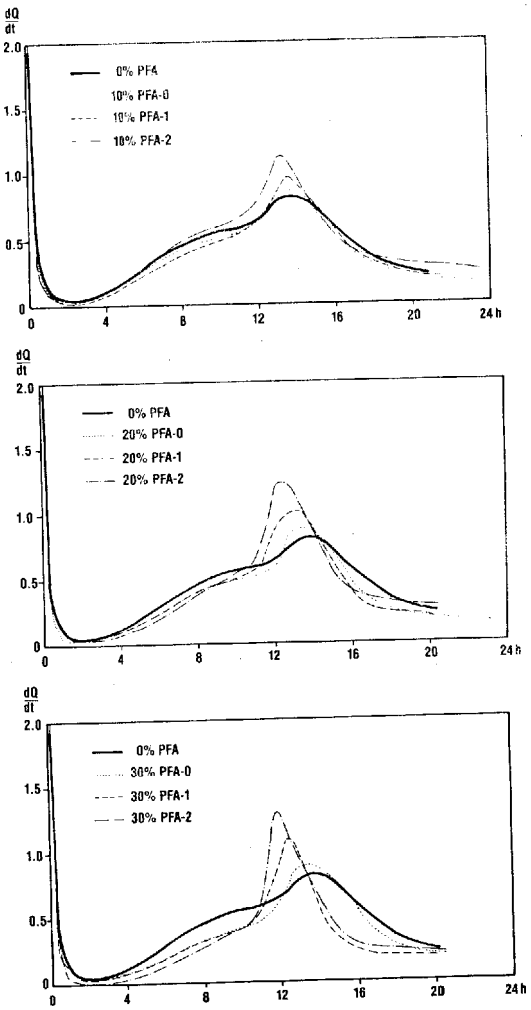

FIG. 2

Rate of heat development of the fly ash - Portland cements determined by conduction calorimetry (Arbitrary scale). Pastes of W/C = 0.5. Temperature: 25°C. 0-24 hours.

Conduction Calorimetry

The heat development of the fly ash-Portland cement blends as measured by conduction calorimetry is shown in figure 2. For the first 10 hours (initial and second peak) a reduction in heat intensity almost proportional to the amount of intermixed fly ash is found. A remarkable effect is, however, seen on the third peak, which is associated with the rapid reaction of the C_3A phase after depletion of the gypsum in the system. It is strongly enhanced and tends to occur earlier when fly ash is present, and both effects are fortified by increasing the fineness as well as the amount of fly ash in the system.

TABLE 4

Properties of Fresh Mortar (ISO-RILEM)
(Sand : Cement (PC+PFA) : Water = 3 : 1 : 0.5)

PFA-content		0%	10%			20%			30%	
PFA-No		-	0	1	2	0	1	2	0	1	2
Limiting density (kg/m^3)		2306	2286	2294	2296	2265	2280	2286	2246	2268	2276
Measured density (kg/m^3)		2186	2183	2198	2212	2185	2206	2218	2152	2218	2233
Entrained air (Vol.%)		5.2	4.5	4.2	3.7	3.5	3.2	3.0	4.2	2.2	1.9
% Flow (ASTM flow table)		131	117	131	134	112	128	131	107	131	131
Bleeding (Wt.%)	1 h	0.70	0.72	0.67	0.61	0.73	0.66	0.61	0.88	0.81	0.55
	2 h	1.16	1.28	1.25	1.11	1.30	1.16	1.09	1.35	1.24	0.87
	3 h	1.49	1.61	1.56	1.39	1.54	1.47	1.36	1.45	1.36	1.05
	4 h	1.55	1.68	1.63	1.49	1.61	1.52	1.45	1.48	1.36	1.07

Properties of Fresh Mortar

The air content, flow and bleeding tendency of ISO-RILEM-mortar prepared with the 10 cements are shown in table 4.

The air content is reduced with increasing amount of fly ash in the cement and with increasing grinding of the fly ash.

The flowability of mortars with ground fly ash additives is similar to the pure cement mortar, while cements based on the fly ash as received have a substantially lower flow. The flowability is further decreased with increased amount of this fly ash.

The bleeding tendency forms the following pattern:
Increased fly ash fineness results in decreased bleeding. Increased fly ash addition tends to enhance bleeding at first (1 h results), but reduces bleeding markedly later on (3 and 4 h results). The bleeding of the pure cement mortar falls somewhere in the middle of the PFA-cement bleeding tendencies.

TABLE 5

Density and Strength of Mortar Prisms (ISO-RILEM)

PFA-content		0%	10%			20%			30%		
PFA-No		-	0	1	2	0	1	2	0	1	2
Density (kg/m^3)		2252	2234	2267	2268	2213	2265	2269	2194	2260	2269
Entr.air (%)		2.3	2.3	1.2	1.2	2.3	0.7	0.7	2.3	0.4	0.3
Total air (%)		2.3	2.7	1.3	1.3	3.3	1.0	0.8	3.7	0.8	0.4
Flexural Strength (MPa)	1 d	2.6	2.5	2.8	2.8	2.0	2.2	2.5	1.5	2.0	2.1
	3 d	5.3	4.6	5.0	5.2	4.1	4.7	5.0	3.3	4.1	4.4
	7 d	6.3	5.8	5.9	6.0	5.1	5.5	5.5	4.7	5.2	5.6
	28 d	7.3	6.8	7.1	7.0	5.7	6.9	6.8	5.4	6.2	6.5
	56 d	7.8	7.5	7.6	8.2	7.1	7.7	8.1	6.2	7.2	8.0
	91 d	8.1	7.3	7.7	8.3	7.1	7.7	8.1	6.5	7.9	8.2
	365 d	8.6	8.8	9.5	9.4	8.5	9.0	9.2	8.5	9.6	9.8
Compressive Strength (MPa)	1 d	9.9	8.6	9.9	10.2	7.1	8.3	9.2	5.4	6.8	7.9
	3 d	26.4	22.7	24.3	25.3	17.8	22.3	23.3	14.4	18.2	20.8
	7 d	35.4	31.6	33.4	34.0	25.7	29.0	30.5	21.1	24.8	26.9
	28 d	46.2	41.0	43.8	45.3	35.6	42.3	42.4	29.5	35.2	38.8
	56 d	52.3	47.1	52.2	53.2	43.7	50.0	52.9	36.1	45.5	51.0
	91 d	55.3	50.7	56.2	58.9	46.8	53.9	57.1	41.2	51.3	57.7
	365 d	57.8	62.2	69.5	72.7	59.8	72.2	74.8	57.0	70.2	74.4

Strength Development

The results of flexural and compressive strength measurements are compiled in table 5 together with estimates of the amount of entrained and total air in the mortar prisms at the time of demoulding (1 day at 20°C).

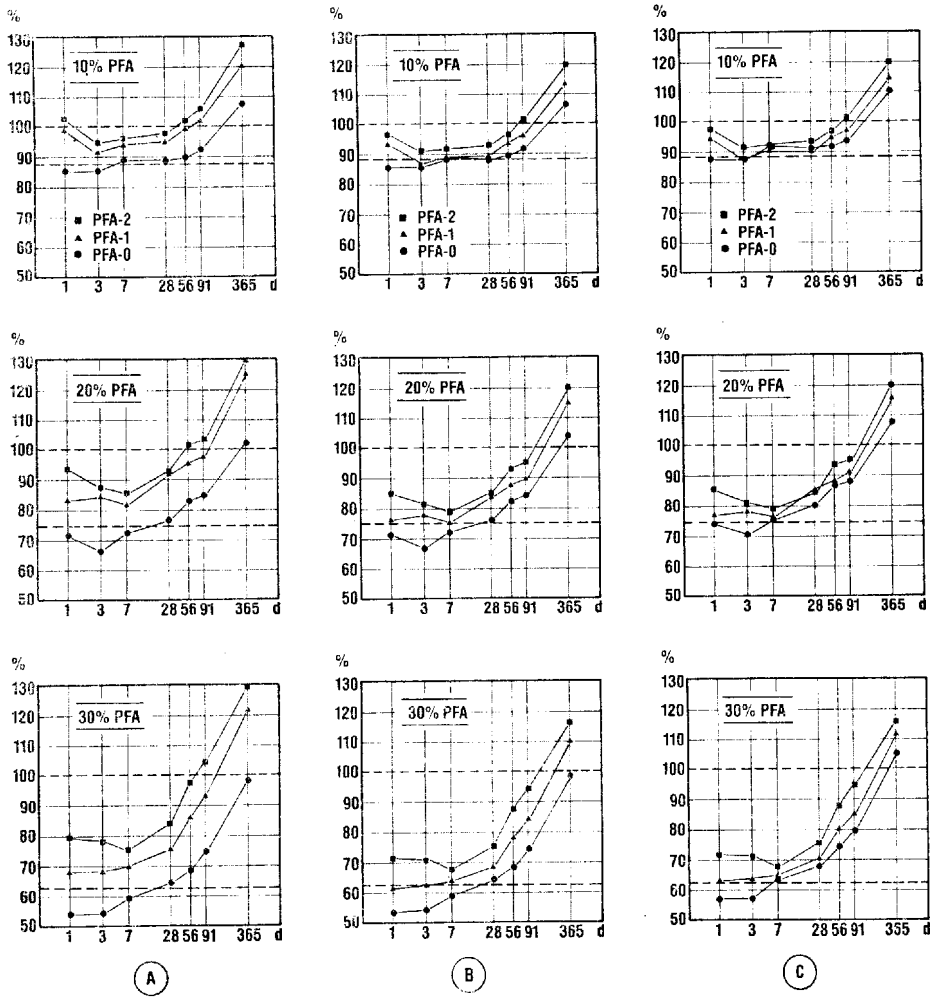

FIG. 3

Strength of PFA-Portland cement blends in percentage of strength of pure Portland cement.
Based on compressive strength of mortar prisms (ISO-RILEM-method).
A: As measured. B: Corrected to zero % entrained air.
C: Corrected to zero % total air.
(Lower dashed line in the plots is the level of relative strength with an inert substitution of Portland cement as estimated from Ferets formula (3). Indicates expected strength level due to change in water-to-Portland cement-ratio as brought about by simple dilution).

The air content is calculated from the measured densities of the prisms and limiting densities calculated from the densities of the materials used in the mortar. The total air includes the pores in the fly ash particles.

As the amount of air influences the strength results, corrections have been made to eliminate these influences (3). Correction of compressive strength values to zero air content has been performed by the expression $\sigma_0 = \sigma \cdot \exp(0.05 \cdot a)$, where σ_0, σ and a is strength at zero per cent air, strength as measured and air percentage, respectively.

The relative strength (compressive) of PFA-cements to pure Portland cement has been calculated applying both values as measured and corrected values, and the results are plotted in figure 3.

From the results the following observations can be stated:

- Increased dosage of PFA decreases early strength and increases late strength when compared with unblended cement. The cross-over varies between 1 month and 1 year depending on amount and fineness of the ash.

- The onset of a marked growth in relative strength traditionally connected with a pozzolanic reaction of the PFA takes place after between 1 and 3 weeks (at 20°C) depending primarily on the fineness of the ash.

- The "dormant level" of untreated fly ash is close to the estimated inert level, but is markedly increased by increased grinding of the ash. This difference is, however, reduced when corrections for different air contents are made.

$Ca(OH)_2$-Content of Mortars

The change in $Ca(OH)_2$-content of mortar with time is shown in figure 4. The lower group of curves is based on the loss directly connected with dehydration of $Ca(OH)_2$, while the upper group includes the $CaCO_3$-loss converted to the equivalent amount of $Ca(OH)_2$. All losses are normalized to Portland cement basis for easier comparison. The results indicate that the $Ca(OH)_2$-consumption by PFA becomes significant between 7 and 28 days of hardening (at 20°C). After 28 days an actual decline in $Ca(OH)_2$-content takes place, being more pronounced with higher content and higher grinding fineness of the PFA.

Discussion

When fly ash is ground, three major changes in its physical character take place:

1) Its fineness is increased,
2) there is an increase in density due to the crushing of hollow particles and
3) there is a change in particle shape away from the predominantly spherical shape.

The spherical character of most of the particles in a fly ash has often been claimed to be an important factor in the workability improvements or water reduction possibility when using fly ash in concrete, though, convincing experimental evidence is hard to find in the literature. In the present study the amount of water (on volume basis) to attain a paste of normal consistency (Table 3) does not change much, neither with fly ash grinding nor with level of replacement. A small increase when using ground fly ash can, however, be claimed, but this could also be due to the higher fineness (increased importance of surface forces) of these materials. If we turn to the mortar results (Table 4) we find an appreciable reduction in flow when we use the fly ash as received and it is reduced further with increased replacement.

Replacements with ground fly ash on the other hand do not change the flow significantly.

An interpretation of these results is, however, complicated by the fact that the volumetric ratio of water to cementitious mate-

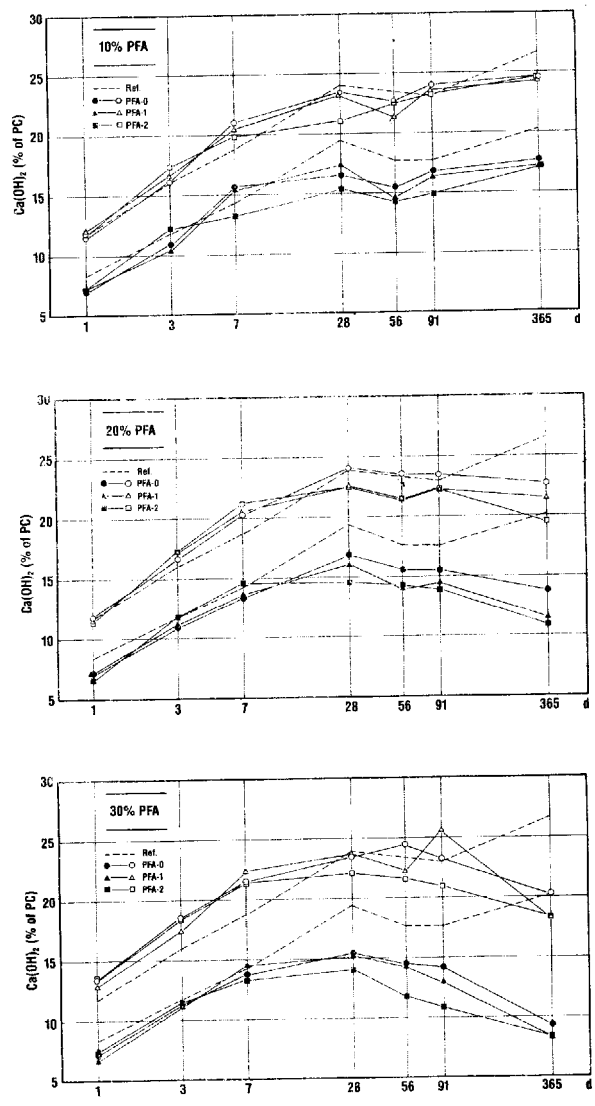

FIG. 4

$Ca(OH)_2$-content on Portland cement basis as function of time. Measured on ISO-RILEM-mortar by thermogravimetric analysis.

The curves represent values for 10% (top), 20% (centre), and 30% (bottom) replacements with PFA-0 (as received), PFA-1 (ground) and PFA-2 (ground).

Lower group of curves in each plot is based on loss between 440 and 510°C ($Ca(OH)_2$-dehydration) while the upper group is based on this loss plus the high temperature loss between 510 and 880°C (mainly $CaCO_3$-decarbonation), converted to equivalent $Ca(OH)_2$-amounts.

rial is not the same in the mixes due to differences in density of the fly ashes and constant water-to-cement-ratio (by weight) procedure used, and by the fact that the mortar has ended up with different amounts of air which will also effect the flow behaviour.

The bleeding tendency (Table 4) of the fly ash cements is significantly reduced with increased grinding of the fly ash. Again it is impossible to say whether this is due to the higher fineness of the powder or the changes in particle shape brought about by the grinding.

The setting is slightly retarded with increasing amount of fly ash, probably merely due to the dilution of the Portland cement. That this retardation is diminished by finer grinding of the fly ash could be explained by the fact that the Portland cement hydration is enhanced by dilution with fly ash and more so the finer it is. This has been indicated by the calorimetric investigation, which has further indicated that it is apparently the reaction of the aluminate phase (3rd peak in the rate curve) that for some reason is enhanced.

This enhancement of the Portland cement hydration, sometimes referred to as "a filler effect", can probably also explain part of the improvements in early strength brought about by finer grinding of the fly ash. (Figure 3. Strength corrected to zero per cent air).

However, as can be seen from figure 3, a large part of the improvement in early strength as measured can actually be explained by changes in initial porosity of the mortar. Finer grinding of the fly ash tends to decrease the amount of entrained air in the mortar. This is shown in the fresh mortar (Table 4) as well as in the mortar prisms at the time of demoulding (Table 5), this supporting similar results reported earlier (3). A possible explanation for this effect is that the residual carbon in the fly ash acts as an absorbent for organic impurities in the sand or cement, organic impurities that would otherwise increase air entrainment in the mortar. By finer grinding and increased fly ash dosage the effectiveness of this carbon absorbent will increase.

Another effect to be considered is the reduction in internal porosity of the fly ash by grinding. The effect of this change on the initial porosity of the mortar can be read from table 5 by comparing the two columns "entrained air" and "total air", the latter being "entrained air" plus fly ash porosity.

The expected effect on strength, assuming that 1% of air will introduce a 5% reduction in strength whether this air is entrained or inherent pores in fly ash particles, can be evaluated in figure 3.

The main effect of fly ash on the strength development of fly ash - Portland cement blends is, of course, the pozzolanic reaction, i.e. the reaction between $Ca(OH)_2$ and ash to produce C-S-H-gel. This becomes a dominant factor for strength from about 1 to 4 weeks or longer. Here the rapid rise from the level of simple dilution takes place. That there is a close connection between the increase in strength development and the consumption in lime is obvious when comparing figures 3 and 4.

Conclusions.

Grinding of fly ash can lead to a substantial increase of strength of fly ash Portland cement mixes at all ages from 1 day onwards. The increase in strength contribution from the fly ash on grinding can apparently be traced back to several sources:

- An enhancement of the rapid aluminate reaction taking place after the induction period.
- An increased pozzolanic reaction corresponding to the consumption of lime in the system.
- A decreased content of air entrained in the mortar tests specimens.
- A reduced intrinsic porosity of the fly ash itself.

It would appear useful to distinguish between these (and possible other) factors affecting strength when strength measurements are used as a means of following hydration reactions or as a means of evaluating fly ash quality for practical purposes.

Acknowledgements

The present work was accomplished when the first-mentioned author as a UNIDO fellow was carrying out a training programme at F.L. Smidth & Co. A/S, Copenhagen. The financial support from UNIDO is gratefully acknowledged.

Additionally, both authors want to thank the technical staff of the R&D laboratories of F.L. Smidth for their guidance and assistance in carrying out the experimental work involved.

References

(1) M. Venuat: Revue des Mat. de Constr. No. 506, 309-317 (1957)

(2) B. Osbaeck: Proc. of Mat.Res.Soc. Ann. Meeting Boston, Nov. 1981, Symp. N, 280-288 (1981)

(3) B. Osbaeck: Cem. Concr. Res. 15, 53-64 (1985)

(4) A. Carles-Gibergues et A. Vaquier - Ciments, Bétons, Plâtres, Chaux No. 752, 46-50 (1985)

M. Murat, J. Ambroise et J. Péra, Institut National des Sciences Appliquées de Lyon, Laboratoire des Solides et Matériaux Minéraux, Bât. 404, 20, Av. Albert Einstein, F-69621 Villeurbanne Cedex (France).

3.1

Les différents procédés d'activation des minéraux argileux permettant d'élaborer des liants pouzzolaniques à résistances optimales.
The different activation processes of clay minerals to obtain pozzolanic binders with optimal strengths.

Résumé. L'utilisation des minéraux argileux comme matières premières dans le domaine des matériaux ou liants spéciaux utilisables en construction nécessite différents procédés d'activation :

- L'activation chimique qui consiste à associer au minéral argileux (argile crue ou argile calcinée) un réactif susceptible de fournir, en solution, des espèces chimiques (ions OH^- et Ca^{2+}) capables de réaliser l'attaque du feuillet argileux puis la précipitation d'hydrates minéraux dont la microstructure et l'arrangement cristallin conduisent au phénomène de consolidation. L'hydroxyde de calcium est l'exemple type de l'activateur chimique.

- L'activation thermique qui consiste, par calcination de certains types d'argiles dans le domaine des moyennes températures, à réaliser la désorganisation plus ou moins totale de la structure cristalline : on obtient ainsi des pouzzolanes de synthèse dont le processus de de consolidation par voie hydraulique nécessite l'emploi d'un activateur chimique, mais est beaucoup plus rapide que dans le cas de minéraux argileux non activés thermiquement.

- L'activation mécanique par broyage, qui conduit à la formation de sites superficiels réactifs, donc à une augmentation de la vitesse de consolidation.

Ces trois procédés d'activation sont illustrés par les travaux des auteurs dans le domaine concerné, l'objectif étant d'obtenir des résistances mécaniques optimales à court terme.

A utilização de minerais argilosos como matérias primas na área de materiais e ligantes especiais, utilizáveis em construção, precisa de diferentes processos de hidratação:

- A ativação química, que consiste em associar ao mineral argiloso (argila crua ou argila calcinada) um reativo capaz de fornecer, em solução, espécies químicas (íons OH^- e Ca^{2+}) aptas a realizarem o ataque à lâmina argilosa após a precipitação dos hidratos minerais, cuja microestrutura e arranjo cristalino levam ao fenômeno de consolidação. O hidróxido de cálcio é o exemplo típico de ativador químico.
- A ativação térmica, que consiste na realização, por calcinação de determinados tipos de argilas em ambientes de temperaturas médias, a desorganização mais ou menos total da estrutura cristalina: desta forma se obtêm pozolanas sintéticas, cujo processo de consolidação por meio hidráulico precisa de um ativador químico, mas é muito mais rápida do que no caso de minerais argilosos não ativados termicamente.
- A ativação mecânica por moagem, que leva à formação de sítios superficiais reativos, e consequentemente a um aumento da velocidade de consolidação.

Estes três processos de ativação são ilustrados por trabalhos dos autores neste campo, tendo por objetivo obter resistências mecânicas ótimas a curto prazo.

1. INTRODUCTION.

Les minéraux argileux sont des matières premières abondantes appartenant à la famille des phyllosilicates (1) dont la structure type est constituée d'un empilement bidimensionnel de couches de tétraèdres de silice SiO_4 et de couches d'octaèdres d'alumine AlO_6 certains atomes d'oxygène étant remplacés par des groupements hydroxyles OH. Le nombre et le mode de superposition des couches de silice et d'alumine, la substitution totale de l'aluminium par du magnésium dans la couche octaédrique, ou les substitutions partielles de Si, Al ou Mg par des cations de valences différentes, conduit à une famille de minéraux très complexe dont certains présentent une capacité d'échange d'ions et une instabilité de l'équidistance interfoliaire. Mais les minéraux argileux les plus courants restent la kaolinite, les montmorillonites, les micas, et à moindre titre, les vermiculites, les chlorites, le chrysotile, le talc, etc...

Les minéraux argileux se rencontrent couramment soit à l'état de roches spécifiquement argileuses, soit comme constituants de roches calcaires (marnes), de bauxites ou de nombreux sols et terres dont les latérites. En dehors de leur utilisation dans l'élaboration des "crûs" de cimenterie ou des tuiles et briques (terres cuites), ces minéraux font l'objet d'un renouveau d'intérêt pour la fabrication de matériaux à propriétés spécifiques (liants pouzzolaniques de synthèse) ou dans l'élaboration de structures pour le Génie-Civil (construction en terre) dans l'optique des économies d'énergie et de matières premières. De telles utilisations nécessitent cependant l'emploi de procédés d'activation (chimique, thermique, ou mécanique) permettant de réaliser la consolidation du minéral argileux en des temps acceptables.

2. LES DIFFERENTS PROCEDES D'ACTIVATION.

2.1. L'activation chimique.

L'addition, au mélange eau + argile, de certaines substances minérales jouant le rôle d'activateurs chimiques est nécessaire si on veut réaliser la consolidation par voie chimique, c'est-à-dire favoriser la dégradation chimique de l'alumino-silicate (qui passera ainsi lentement en solution) puis la germination et la croissance d'hydrates dont l'établissement de la microstructure sera favorable au développement de propriétés mécaniques (2).

Ces activateurs chimiques doivent obéir à deux critères fondamentaux :

a) être susceptibles de réaliser l'attaque chimique du solide de départ et de faire passer ainsi certaines espèces en solution (silice et alumine le plus souvent, éventuellement oxydes de fer, de magnésium, selon la nature du minéral argileux) ;

b) favoriser, de par leur composition chimique, la précipitation des hydrates (généralement des silicates, des aluminates ou des alumino-silicates de cations alcalino-terreux) à partir de la solution sursaturée résultant de l'attaque chimique précédemment citée.

Ces deux aspects de la dissolution non congruente (phénomène de dissolution-précipitation) n'excluent pas une étape initiale d'adsorption-désorption des cations alcalino-terreux sur les groupements silanols Si-OH (et éventuellement sur les groupements aluminols Al-OH) présents initialement à la surface du solide ou créés dès que celui-ci est placé dans un milieu aqueux. On aurait alors la succession de phénomènes suivants :

$$2\ (Si\text{-}OH) + M^{2+} \rightleftarrows (Si\text{-}O)_2M + H_2O$$

phénomène mis en évidence dans le système SiO_2-CaO-H_2O (3), puis concernant la couche tétraédrique de silice :

$$SiO_2 + H_2O \rightleftarrows H_4SiO_4 \qquad (pH < 9,6)$$

$$H_4SiO_4 \rightleftarrows H_3SiO_4^- + H^+ \qquad (9,6 < pH < 12,7)$$

$$H_3SiO_4^- \rightleftarrows H_2SiO_4^{2-} + H^+ \qquad (pH > 12,7)$$

et concernant la couche octaédrique :

$$Al(OH)_3 + OH^- \rightleftarrows [Al(OH)_4]^- \quad (pH\ basique)$$

puis la précipitation de CSH (phénomène prédominant pour la kaolinite) ou d'aluminates de calcium hydratés (phénomène prédominant pour la montmorillonite) (2) à partir de la solution sursaturée.

Dans l'état actuel des choses il ne semble pas qu'une modélisation de ces phénomènes ait été présentée. On doit cependant supposer, compte-tenu de la lenteur du processus de consolidation par précipitation d'hydrates, que l'étape limitative est la dissolution du minéral argileux.

Le rôle d'activateur chimique est particulièrement bien rempli par des substances susceptibles de se dissocier en solution aqueuse pour fournir des ions hydroxyles OH^- et des cations alcalino-terreux : comme dans le cas de l'attaque "hydroxylique" des laitiers (4), les ions hydroxyles réalisent la dégradation lente de la structure alumino-silicatée de l'argile de départ ; les cations alcalino-terreux favorisent la précipitation des hydrates, ces cations alcalino-terreux étant généralement absents dans les argiles les plus courantes qui sont dioctaédriques (kaolinite, illite, montmorillonites).

On voit donc là tout l'intérêt d'activateurs chimiques, basiques (et en particulier la chaux, éventuellement la

magnésie) ou de substances susceptibles d'évoluer dans le milieu réactionnel en fournissant un produit de réaction basique : c'est le cas du ciment portland artificiel qui libère de la chaux ou portlandite $Ca(OH)_2$ jouant le rôle d'activateur chimique, et qui fournit parallèlement du silicate de calcium hydraté (CSH) jouant son propre rôle au niveau du processus de consolidation de l'ensemble.

La soude Na(OH), souvent utilisée comme activateur chimique des laitiers (4) n'est certainement pas l'activateur le mieux adapté au cas de la consolidation des minéraux argileux, le calcium ou le magnésium étant des éléments alcalino-terreux présents en quantité assez notable dans les laitiers, mais absents dans les minéraux argileux courants dioctaédriques.

La cinétique de consolidation chimique des minéraux argileux bruts est cependant très lente, d'où l'utilisation parallèle assez courante d'un compactage dynamique permettant d'assurer le développement d'une certaine cohésion mécanique à court terme.

Nous nous sommes donc intéressés plus spécialement à la voie "activation thermique" pour transformer préalablement les minéraux argileux bruts en solides à réactivité beaucoup plus élevée. Mais cette opération n'exclue en rien la nécessité d'une activation chimique pour réaliser la consolidation mais la cinétique de formation des hydrates sera très nettement améliorée, l'étape lente (dégradation de la structure du minéral avec passage en solution de l'alumine et de la silice) devenant une étape moins limitative pour l'ensemble du processus dans le cas des argiles thermiquement activées. Le développement des résistances mécaniques à court terme est alors très nettement amélioré.

2.2. L'activation thermique.

La dissociation thermique ou réaction de "déshydroxylation" de certains minéraux argileux dioctaédriques (kaolinite, illite, montmorillonite), trioctaédriques (chrysotile, talc) ou des chlorites, dans le domaine de température 600-900°C, conduit à des phases dites "transitoires" caractérisées par un désordre cristallin plus ou moins prononcé (1,5,6), donc plus réactives que le minéral de départ. Nous appellerons ces phases transitoires des Argiles Thermiquement Activées (A.T.A.). Le cas le plus typique d'une activation thermique est celui associé à la déshydroxylation de la kaolinite qui conduit à la formation d'une phase transitoire, le métakaolin, selon une réaction du type :

$$\left\{\begin{array}{c} Al_2O_3 \cdot 2SiO_2 \cdot 2H_2O \\ \text{ou} \\ Si_2O_5Al_2(OH)_4 \\ \text{(kaolinite)} \\ \text{(dioctaédrique)} \end{array}\right\} \rightarrow Al_2O_3 \cdot 2SiO_2 + 2H_2O \text{ vap.}$$

(Métakaolin)

L'état de désorganisation du réseau cristallin du métakaolin est clairement mis en évidence par l'allure du spectre d'absorption infrarouge (Fig. 1) ou du diagramme de diffraction des rayons X (Fig. 2).

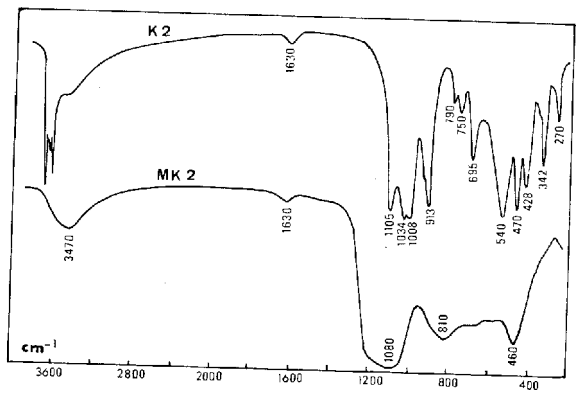

Fig. 1
Spectres infrarouges comparés d'une kaolinite (K2) et du métakaolin (MK2) obtenu par activation thermique à 750°C.

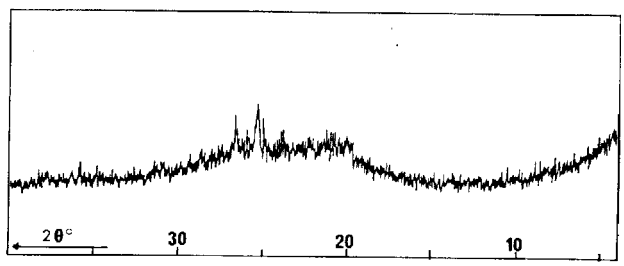

Fig. 2
Diagramme de diffraction X du métakaolin MK2.

Le métakaolin $Al_2O_3 \cdot 2SiO_2$ (noté ici MK) va donc présenter une réactivité bien supérieure à celle de l'argile de départ (kaolinite) lors d'une réaction d'hydratation réalisée à la température ambiante en présence d'un activateur chimique calcique et basique tel que l'hydroxyde de calcium : la consolidation du mélange "Métakaolin (MK) - Hydroxyde de Calcium (CH) - Eau" est beaucoup plus rapide que celle des meilleures pouzzolanes naturelles (7) et conduit à la formation de CSH_1 de Taylor (8), de géhlénite hydratée C_2ASH_8 et de faibles quantités d'aluminate tétracalcique hydraté C_4AH_{13} (9-11).

Les différentes recherches que nous avons effectuées dans ce domaine ces quatre dernières années (11-21) nous ont permis d'aboutir aux principaux résultats suivants :

a)L'optimisation des résistances en com-

pression pure (Rc) à 28 jours de liants préparés à partir d'argiles thermiquement activées (ATA), pour des conditions données de conservation des éprouvettes, résulte essentiellement du choix de la valeur du rapport massique "A.T.A./Activateur chimique". Ce rapport, noté MK/CH pour le système Métakaolin/Hydroxyde de Calcium, est de 3 si on part d'une kaolinite pure (Fig. 3) (19, 20). Il est aussi voisin de 3 pour l'illite et la montmorillonite (19, 21). Dans ces conditions toute la chaux est consommée à 28 jours et les résistances n'évoluent que très lentement au delà de cette échéance.

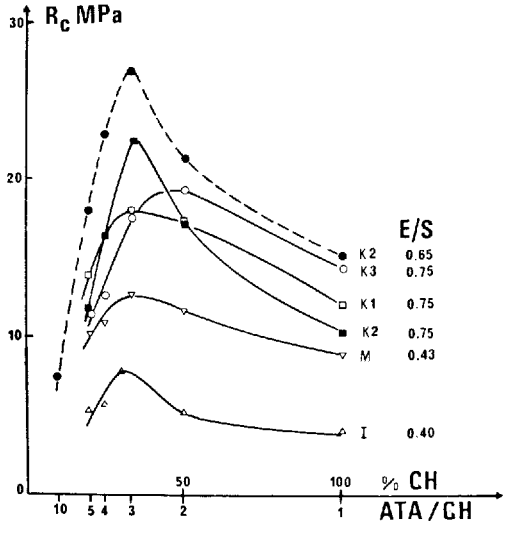

Fig. 3
Variation de la résistance en compression de liants "ATA-Chaux" en fonction de la quantité de chaux CH ajoutée ou du rapport massique ATA/CH
K2 : kaolinite pure
K1-K3 : kaolins impurs
M : montmorillonite du Wyoming
I : illite

b) La meilleure activation thermique pour la kaolinite est obtenue par calcination dans le domaine de température 700-800°C (11, 14, 15, 22, 23). Au delà de 850-900°C commence à se manifester un phénomène de recristallisation lente du solide en phases haute-température mullite ou spinelle (11, 24), ce qui diminue la réactivité avec la chaux. Mais le domaine de température dans lequel doit être effectuée la calcination diffère selon le type de minéral argileux concerné comme l'illite (22), les chrysotiles à grande surface spécifique (6) et surtout les montmorillonites dont la deshydroxylation peut se manifester en deux étapes à des températures variables entre 680°C et 920°C en fonction de la nature des substitutions (25, 26).

c) Si on compare la réactivité des minéraux argileux thermiquement activés à celle des minéraux bruts (17, 21), on trouve des ordres décroissants différents :
Kaolinite > Montmorillonite > Illite >> Micas cristallisés
pour les argiles thermiquement activées, et:
Montmorillonite > Illite > Kaolinite
pour les argiles brutes (27).

Pour les premières c'est l'ordre décroissant de l'état de désorganisation du réseau cristallin de la "phase transitoire"; pour les secondes c'est l'ordre décroissant des capacités d'échange ionique.

d) Par ailleurs avec la condition (MK/CH)=3, la réactivité des métakaolins est d'autant meilleure que la kaolinite elle-même est mal cristallisée, ce qui présente un intérêt certain pour la valorisation des kaolins contenant des oxydes de fer ou comportant des substitutions Al-Fe dans la couche octaédrique, phénomène qui diminue leur état de cristallinité (28, 29).

e) Le rôle des ions hydroxyles OH^- en solution dans l'activation chimique du métakaolin a été clairement mis en évidence en comparant l'action de l'hydroxyde de calcium, du carbonate de calcium et du gypse, activateurs qui apportent tous les ions calcium nécessaires à la précipitation des hydrates mais l'emploi de carbonate de calcium seul ou de gypse seul ne conduit à aucun phénomène notable de consolidation, laquelle ne se manifeste qu'en associant calcite ou gypse à la chaux : on observe alors la formation simultanée de CSH et respectivement de carboaluminate de calcium hydraté $C_4A\bar{C}H_{12}$ ou d'ettringite $C_6A\bar{S}_3H_{32}$ mais les résistances à 28 jours sont toujours inférieures à celles obtenues dans le cas d'une activation avec $Ca(OH)_2$ seule, à rapport massique Métakaolin/activateur donné (19, 20).

Nous avions soulevé par ailleurs le problème de l'activation par la magnésie dans le cas de fabrication d'un activateur par calcination de dolomie (15) : il semble que cela conduise à des résultats intéressants (30) mais une étude systématique doit être faite dans ce domaine.

L'association d'une activation thermique et d'une activation chimique conduit donc à une consolidation rapide avec l'obtention de résistances mécaniques à court terme bien supérieures à celles obtenues en utilisant l'activation chimique seule.

Un autre procédé de traitement thermique consiste à traiter à l'autoclave le minéral argileux brut additionné de l'activateur chimique : on réalise alors la dissolution de l'alumino-silicate et la cristallisation des hydrates en conditions hydrothermales. Bien que très séduisant, ce procédé qui a été mis à profit par exemple pour la valorisation des latérites (31), ne sera pas discuté dans cette communication.

2.3. L'activation mécanique par broyage.

Le broyage mécanique des matières premières a essentiellement pour rôle de séparer ou de libérer les espèces minéralogiques dans un mélange, de réduire la granulométrie et d'augmenter la surface spécifique des solides. Un autre aspect très important du broyage est la création de nouvelles surfaces susceptibles de présenter des sites ou espèces superficielles jouant un rôle très important au niveau de la réactivité (32)

On sait que le broyage mécanique des minéraux argileux peut conduire à des modifications très sensibles de la structure (33, 34) mais il ne semble pas y avoir de données actuelles concernant l'application de ce procédé d'activation pour améliorer la consolidation à froid des argiles brutes.

Suite à d'autres travaux auxquels a participé l'un d'entre nous dans le domaine de l'activation des solides par broyage : gypse (35), anhydrite (36), aluminate monocalcique (37), nous avons été conduits à entreprendre quelques recherches sur la consolidation du système "Métakaolin-Hydroxyde de calcium-Eau", les deux solides de départ ayant été préalablement broyés séparément ou ensemble (à charge totale en masse et à temps fixés) dans un broyeur à boulets.

Les résultats tous récents obtenus par J. AMBROISE (non publiés) à ce sujet ont mis en évidence deux faits importants :

a) La vitesse de consolidation du métakaolin est nettement améliorée par broyage sans que l'on note de variations sensibles dans l'évolution de la granulométrie (la kaolinite de départ est très fine, $\bar{d} < 10\,\mu m$) ou de la surface spécifique de l'échantillon, ce qui laisse supposer la formation d'espèces superficielles réactives au cours du phénomène de comminution. Ces espèces peuvent résulter :

. Soit de la création de défauts ou désordres locaux superficiels,
. Soit de la rupture des liaisons, par exemple de la couche tétraédrique Si-O-Si avec formation de sites actifs (38, 39) :

$$\equiv Si\text{-}O\text{-}Si \equiv \rightarrow \equiv SiO^{\bullet} + {}^{\bullet}Si \equiv$$

qui conduisent à la formation de groupes silanols en présence d'eau vapeur ou liquide, ou d'une séparation partielle des couches tétraédrique et octaédrique avec création de nouvelles surfaces comportant des sites réactifs résultant de la rupture des liaisons Si-O-Al.

b) Le broyage provoque par contre une baisse faible mais cependant sensible de la réactivité de l'hydroxyde de calcium.

Ces résultats laissent à penser qu'il est probablement plus judicieux de soumettre l'argile à l'opération de broyage après activation thermique plutôt qu'avant dans la mesure où la calcination est effectuée sur des grains de dimensions pas trop élevées pour ne pas ralentir de façon notable la cinétique de déshydroxylation. Le cobroyage métakaolin-chaux n'est pas recommandé.

3. CONCLUSION.

La consolidation des minéraux argileux à froid et en milieu aqueux (pâte) nécessite la mise en oeuvre d'une activation chimique réalisable par addition au milieu réactionnel, de composés basiques, généralement alcalino-terreux ; ceci conduit à la précipitation d'hydrates consécutive à une dégradation de la structure alumino-silicatée avec passage des espèces en solution. Mais le phénomène est très lent et le développement des résistances mécaniques très limité. On peut alors faire appel à une activation thermique du minéral de départ en réalisant la deshydroxylation à température modérée (600-900°C), ce qui confère à ce dernier une structure cristallographiquement désorganisée donc très réactive : la consolidation à froid à l'aide d'un activateur chimique basique en milieu aqueux est alors beaucoup plus rapide comme en attestent les travaux effectués sur la kaolinite, l'illite ou la montmorillonite. Mais tous les minéraux argileux et en particulier les micas bien cristallisés ne sont pas forcément concernés par le phénomène d'activation thermique. On doit signaler aussi que l'activation thermique des minéraux argileux peut conduire à des matériaux très prometteurs : leur association par exemple au ciment portland permet d'améliorer très nettement la durabilité des fibres de verre E utilisées comme agent de renforcement (40, 41) ; de même l'association "Métakaolin-Chaux" est un meilleur activateur chimique que la chaux seule pour la stabilisation des sols à froid (42, 43).

Le broyage (activation mécanique) des minéraux argileux préalablement activés thermiquement accélère encore le processus de consolidation, probablement par formation d'espèces superficielles réactives.

Références.

(1) - S. CAILLERE, S. HENIN et M. RAUTUREAU, "Minéralogie des Argiles", Masson, Paris, 1982, 2 volumes.

(2) - A. LE ROUX, Bull. de Liaison du L.C.P.C., Fr., 1969, (40), 59-96.

(3) - R. DRON, Thèse, Paris, 1984. Rapport L.C.P.C. N° 3514 (février 1984).

(4) - D. MENETRIER, Thèse, Dijon, 1977.

(5) - L. LEMAITRE, A.J. LEONARD and B. DELMON, Bull. Minéral., 1982, 105-501-507.

(6) - M. della FAILLE, C. de KIMPE et J.J. FRIPIAT, Silic. Ind. (Belg.), 1966, 31, 469-73.

(7) - M. FOURNIER and J. M. GEOFFRAY, Bull. Liaison Lab. Ponts et Chaussées, 1978, 93, 70-78.

(8) - H.F.W. TAYLOR, "The Chemisty of Cement", Academic Press, London and New-York, 1964, Vol. 1., p. 167-232.

(9) - H.F.W. TAYLOR, Ibid., Vol. 2, p. 75-81.

(10) - R. TURRIZIANI and G. SCHIPPA, Ricerca Scient., Ital., 24, (2), 366-74.

(11) - M. MURÁT and A. BACHIORRINI, Bull. Minéralogie, 1982, 105, 543-55.

(12) - M. MURAT, Cem. Concr. Res., 1983, 13, 259-66.

(13) - M. MURAT, Cem. Concr. Res., 1983, 13, 511-18.

(14) - M. MURAT and C. COMEL, Cem. Concr. Res., 1983, 13, 631-37.

(15) - M. MURAT, Entropie (Fr.), 1983, 110, 82-85.

(16) - M. MURAT, J. AMBROISE and J. PERA, Int. RILEM/CIB Symp. on appropriate Building Materials for low-cost Housing - Naïrobi (Kenya), Nov. 7-14, 1983, Chapman and Hall, London, 1983, Sect. II, p. 117-26.

(17) - M. MURAT, J. AMBROISE, J. PERA, J.P. BASTIDE, C.R, Acad. Sci., Fr., 1984, 1179-81.

(18) - J. PÉRA, M. MURAT, J. AMBROISE et D. BOISSIER, C.R. Acad. Sci., 1984, 299, Ser. II, 1251-54.

(19) - J. AMBROISE, Thèse INSA de Lyon (France), 1984.

(20) - J. AMBROISE, M. MURAT and J. PERA, Cem. Concr. Res., 1985, 15, 83-88.

(21) - J. AMBROISE, M. MURAT and J. PERA, Cem. Concr. Res., 1985, 15, (2), 261-68.

(22) - J.A. FORRESTER, "Lime and Alternative Cements", Proceed. of a one-day Meeting on Small Scale Manufacturing of Cementitious Materials, R. Spence Ed. Intermediate Technology Publication Ltd., London, 1974, p. 53-59.

(23) - A.A. HAMMOND, Int. RILEM/CIB Symp. on appropriate Building Materials for low-cost Housing, Naïrobi, Kenya, Nov. 7-14, 1983, Chapman and Hall, London, 1983, Sect. II, p. 73-83.

(24) - G.W. BRINDLEY and NAKAHIRA, J. Amer. Ceram. Soc., 1959, 42, (7) 311-14 ; 1959, 42, (7), 314-18 ; 1959, 42, (7) 319-24.

(25) - N. TRAUTH et J. LUCAS, Bull. Gr. Fr. Argiles 1967, XIX, (2), 11-24.

(26) - F. CHANTRET, A. DESPRAIRIES, P. DOUILLET, C. JACOB, M. STEINBERG et N. TRAUTH, Bull. Gr. Fr. Argiles, 1971, XXIII, 141-72.

(27) - M. ALBENQUE, L. COLLON, S. LOREC, J.P. BOMBLED, B. MORTUREUX, M.REGOURD and J. VOLANT, Rev. Mat. Construc., Ciments-Bétons-Plâtre-Chaux, 1982, 737, 217-25 et 738, 291-96.

(28) - O. LIETARD, Thèse, Nancy, 1977.

(29) - M. M. MESTDAGH, L. VIELVOYE and A.J. HERBILLON, Clay Minerals, 1980, 15, 1-13.

(30) - V.D. LOUNG et O. HENNING, Baustoffindustrie, Dtsch., Ser. A, 1985, 28 (3), 76-8

(31) - T. RINGSHOLT, Tech. Report n° 11, U.N., Indonesia U.N. Development Programme, Universitetsbiblioteket Lund, 1976, 124 p. et "Le Latorex", L'Ind. Ceram, Fr., 1978, (722), 733-36.

(32) - J.P. MERIC, "La Fragmentation", FNB Collège Int. pour la Construction, Paris, 1980, p. 263-79.

(33) - T. HENMI et N. YOSHINAGA, Clay Minerals, 1981, 16, 139-49.

(34) - R.E. GRIM, "Clay Mineralogy," Mac. Graw-Hill, 1968, p. 469-71.

(35) - A. BACHIORRINI, A. NEGRO et M. MURAT, Rev. Mat. Constr., Ciments-Bétons-Plâtre-Chaux, 1976, 703, 347-53.

(36) - M. MURAT et A. EL. HAJJOUJI, Thermochimica Acta, 1985, 85, 119-22.

(37) - A. FOURNIER, J.P. LECOMPTE, B. GUILHOT, M. SOUSTELLE, M. MURAT, A. BACHIORRINI et A. NEGRO, Cem. Concr. Res., 1985, 15, (2) 269-75.

(38) - J.B. DONNET, Bull. Soc. Chim. Fr., 1970, N° Spécial, p. 3364.

(39) - J. FRIPIAT, J. CHAUSSIDON et A. GELLY, "Chimie-physique des phénomènes de surfaces. Applications aux oxydes et aux silicates", Masson, Paris, 1971, p. 326

(40) - J. AMBROISE, M. MURAT, J. PERA, Verres et Réfractaires, Fr., 1985, n° 6 (in press). et comm. au congrès Int.

GRFC, Chicago, Nov. 1985.

(41) - J. AMBROISE, J. PERA et M. MURAT
Comm. à ce congrès.

(42) - H. TAIBI, Thèse, INSA de Lyon, 1985.

(43) - H. TAIBI, J. AMBROISE, M. MURAT,
J. PERA et J. TUSET, Sem. Rég. sur
l'Habitat Spontané et l'Habitat économique, UNESCO et CEBTP, Addis-Abeba,
18-21 Nov. 1985.

D. MENETRIER - SORRENTINO, Chargée de Recherche au C.N.R.S., en détachement à LAFARGE COPPEE RECHERCHE, France

PARTICLE SIZE DISTRIBUTION in BLENDED CEMENTS

REPARTITION GRANULOMETRIQUE des CONSTITUANTS d'un CIMENT COMPOSE

SUMMARY : In cement containing mineral additions, and processed by cogrinding, the individual characteristics of the clinker and of the filler are not reached. A direct measure would be much more rewarding, since it would allow an accurate knowledge of the contribution of each component to the final properties of cement.

Among them, is the fineness of both constituents and our study is concerned with the fineness of Portland cement containing calcareous filler.

We have developed a simple method allowing the obtention of the full granulometric curves of both the clinker and the filler. It is divided in 2 main steps :

- determination of the complete granulometric curve of the blended cement and gathering of all the granulometric fractions,
- precise analysis of the CO_2 contained in each fraction.

It has been checked, using 3 cements of known granulometry and then applied on 3 industrial cogrinded cements.

The most important result is that such cements contain :

- a large amount of fine grains of limestone,
- a large part of rough grains of clinker ($>$ 45 microns).

These large size grains are not easily hydrated, consequently they do not take part in early strength development. This means that the clinker is not at best used, and that a better control of the granulometric distribution of both the clinker and the mineral addition would result in an improvment of the properties of these blended cements.

Em cimentos contendo adições minerais, e processados por moagem conjunta, não se conseguem as características individuais do clínquer e do "filler". Uma providência direta seria muito mais vantajosa, uma vez permitiria um conhecimento acurado da contribuição de cada componente para as propriedades finais do cimento.

Entre elas está a finura de ambos os componentes, e nosso estudo aborda a finura de cimento portland contendo "filler" calcário.

Desenvolvemos um método simples que permite a obtenção de curvas granulométricas plenas de ambos, clínquer e "filler". Divide-se em duas etapas:

- determinação da curva granulométrica completa do cimento blendado e reunião de todas as frações granulométricas;
- análise exata do CO_2 contido em cada fração.

O método foi checado, usando-se 3 cimentos de granulometria conhecida e aplicando-os então em três cimentos industriais moídos em conjunto.

O resultado mais importante é que tais cimentos contêm:

- uma grande quantidade de grãos finos de calcário;
- uma grande parte de grãos grossos de clínquer (> 45 mícrons).

Estes grãos grandes não se hidratam facilmente, em conseqüência do que eles não participam do desenvolvimento da resistência inicial. Isto significa que o clínquer não está sendo usado de forma ótima, e que um melhor controle da distribuição granulométrica do clínquer e do aditivo mineral resultaria em melhora das propriedades destes aditivados blendados.

D. MENETRIER - SORRENTINO, chargée de Recherche au C.N.R.S., en détachement à LAFARGE COPPEE RECHERCHE, France

INTRODUCTION

Portland cements containing an high level of mineral addition have received a great deal of attention in France, for many years, and their marketing is developing quickly : 16.5 millions of tons, out of the 23 millions produced in 1983, contain mineral fillers (from 5 to 35 %). They are termed C.P.J. while ordinary Portland cements are termed C.P.A.*

Among the currently used fillers (pozzolanas, flyashes, slags, alone or mixed), the most important one is limestone : 7.7 millions of tons in 1983. This is in relation with the recognition of such cements by French standarts in 1979.

The paper entitled "Developing of hydraulic activity of clinker in Portland cements containing calcareous filler addition", presented by R. GUYOT, B. CARIOU, R. RANC, at the present congress, briefs the situation, and supplies scientific arguments showing the real interest of these cements (1).

Its final conclusion, (which can be translated by : "the importance of knowing and controlling the true fineness of the clinker in the cement, must be pointed out because it is the determining element of the quality of the C.P.J. containing calcareous addition"), introduces well and at the same time justifies, the present investigation.

As a matter of fact, since industrial cement C.P.J. are processed by cogrinding, the individual characteristics, and especially the fineness, of both constituents (clinker, filler) are not known.

We must add that, it is also of high value to assess the fineness of limestone because, on one hand, the presence of very fine grains is favourable to the early strength development and to the rheology of fresh concrete, and on the other hand, the filler is not completely unreactive and the formation of monocarboaluminate may occur rapidly.

From this, we perceive the interest in determining the detailed grain size distribution of each constituent, and not only their global fineness, this is the main objective of the present work.

MATERIALS

Two types of cements have been used :

- three industrial cements : C, L and F,

- laboratory cements : 3 cements have been prepared in our research laboratory, with a composition and a blaine specific surface close of that of the industrial cements. They have been obtained by simply mixing (without grinding) the clinker and the filler, previously ground at a desired and known fineness. The same clinker has been used to prepare all three cements, while limestone is the one utilized to manufacture the industrial cements as C, L and F.

Two percentages of filler have been tested (15 and 27 %), however, since the basic results of our study are not dependent on the proportion of the filler, we will give only those obtained with 15 % filler.

* Please, note : CPA = OPC
CPJ = Composite (or blended) cement

EXPERIMENTAL PROCEDURE

1 - First trials

We have assumed that it would be possible to separate quantitatively the clinker from the filler, in a first step, and to determine the particle size distribution of each part in the second one, similarly to what has been done on slags for example. However, methods involving dense liquors or chemical dissolution appeared invalid : it is impossible to separate chemically $CaCO_3$ from the clinker, and dense liquors only work properly in a narrow particle size range (32-63 µm).

In such a situation, we have been obliged to reverse the order of the experimental steps, i.e. to start with the granulometric analysis of the C.P.J., and to determine then the relative proportion of $CaCO_3$ on each fraction of grains collected during the grain size analysis. The methods of grain size analysis are not all suitable to do this : most of those recently developed supply a neat curve, but they do not give back the separated fractions of the grains. So, we have needed to look at the methods capable of returning the grains once their granulometric size distribution was achieved.

We have been unsucessful in using a sub-sieve sizer (due to large errors in the small size fractions), and an optical microscope, but have fulfilled our objective with the following method. We must point out here, that an equivalent research has been conducted at CERILH : their method involves Andreasen pipettes, and quantitative X-Ray diffraction analysis to determine the proportion of $CaCO_3$ (3).

2 - Method developed

Our method includes two successive steps :

- granulometric analysis of the C.P.J., and collection of the separated fractions,
- quantitative determination of the $CaCO_3$ content in each fraction.

21 - Grain size distribution in C.P.J.

The full curve is obtained by combining both techniques of sieving and sedimentation with Andreasen pipettes.

Experimentally, this is realized in the following way : a first fractionnement is operated at 63 µm, under alcohol and vigourous shaking. Both parts are dried at 110 °C and weighted. The oversize ($>$ 63 µm) fraction is submitted to classical sieving, while the undersize ($<$ 63 µm) is investigated by Andreasen pipettes. We will not detail the method, but just mention that its principle is based on the application of the Stokes law, and binds the sedimentation time with the diameter of the particles (2).

For one given cement, 12 fractions are thus gathered : 4 are provided by sieving, and 8 by the pipettes. Each experiment with pipettes has been made in triplicate and has shown the good reproducibility of the method.

Ten grams of cement are suspended in 200 ml of absolute ethylic alcohol containing 5 ml of a 0.1.N $CaCl_2$ solution, as dispersive agent. Samples of 10 or 20 ml are removed at intervals of time, dried, and precisely weighted. Using the Stokes law the percentage of particles passing through a given diameter, is calculated.

We have checked the validity of this part of our method (sieving + pipettes), by comparing the results

obtained at first on a regular C.P.A. and then on C.P.J., with different methods (laser, sedigraph) : we observed a good agreement (4).

22 - $CaCO_3$ determination

The amount of CO_2 contained in each fraction is determined precisely with a calcimeter.

3 - S.E.M. Studies

The industrial cements have been comparatively observed with the laboratory made cements, in a scanning electron microscope, with the same magnifications (X 500 and X 1000) and adequate preparation of the specimens (dispersion, impregnation...).

EXPRESSION of the WHOLE RESULTS

Tables and graphs

We will first give a few key-explanations in order to understand the results in the recapitulative table 1.

TABLE 1 : Granulometric Analysis on the Industrial C.P.J. L.
I - Andreasen pipettes

	CPJ			$CaCO_3$	Clinker
d [µm]	cumulative % passing	CO_2 %	$CaCO_3$ %	cumulative % passing	
(1)	(2)	(3)	(4)	(5)	(6)
1.0	2.8	15.45	37.8	7.2	2.0
1.5	5.5	20.60	50.4	18.6	3.2
3.7	14.2	19.95	48.8	46.4	8.5
6.0	20.9	18.45	45.1	63.5	13.4
10.0	30.3	14.75	36.1	73.5	22.7
16.0	41.2	12.05	29.5	81.7	34.1
25.0	54.0	10.05	24.6	89.4	47.9
32.0	64.2	8.85	21.7	93.5	59.1
45.0	72.5	7.70	18.8	91.9	69.1

II - Sieving

Sieves opening [µm]	Fraction analyzed [µm]	CPJ			$CaCO_3$	Clinker
		cumulative % passing	CO_2 %	$CaCO_3$ %	Cumulative % passing	
(7)	(8)	(9)	(10)	(11)	(12)	(13)
63	< 63	88.6	6.5	16.0	95.1	87.5
80	63-80	92.9	2.65	6.40	97.0	92.2
100	80-100	96.	2.85	7.00	98.4	95.5
	> 100	99.4	3.00	7.34	100	99.2

It is divided in two parts : the upper part is concerned with the Andreasen pipettes, the lower part with sieving :

- The experimental data resulting from one method or the other, are not of the same type : in the case of the pipettes, the available data are the weight percent of particles (column 2) passing through a given diameter (equivalent spherical diameter, col.1) while with the sieves, they are the weight of the fraction of particles (col. 8) sized between the opening diameter of two sieves (col. 7).To get the cumulative weight percent, it is necessary to add the successive results (col. 9).

From the twelve values expressed in columns 2 and 9 it is possible to draw the full grain size distribution curve of the C.P.J. (dash line curve, fig. 1).

- The experimental values of the CO_2 content are in columns 3 and 10. The percentage of $CaCO_3$ contained in each sample results from the ratio of these values over the CO_2 content of the concerned C.P.J. (around 15 %) (col. 4 and 11).

From all of these, the respective grain size distribution of the clinker and of the filler may be assessed separately : the cumulative weight percent of the filler (col. 5 and 12) are calculated by multiplying line by line, the results of col. 2, with those of col. 4, and the results of col. 9 with these of col. 11 while the cumulative weight percent of the clinker (two last columns, 6 and 13) are obtained by a simple substraction between the weight percent of the C.P.J. and the filler, at a same equivalent spherical diameter.

Here again, the twelve experimental values allow us to get the complete granulometric curves of the filler and the clinker (fig. 1).

Numerical examples

1 - Validation of our method

The laboratory made cements are very helpful to check the validity of the method we have developed : indeed, since they result from a simple blend - without grinding - of both constituents of C.P.J., the individual characteristics (fineness, grain size distribution) may be determined directly on the clinker and on the filler themselves, before their blend. If these results fit well with those obtained with our method, this will prove its validity. We have applied our method on the 3 laboratory cements, and observed a very good agreement with results obtained directly (4).

2 - Comparative results on C.P.J. L.

The granulometric curves of the industrial 45 R C.P.J. L. are comparatively represented in fig. 1, with those obtained on the equivalent laboratory made cement (fig. 2) ; the difference appear immediately. They are corroborated by the visual observation of the two following photographs taken at a same magnification (X 500) of these two types of cements, fig. 3,4. The well contrasted grains are clinker, the ill contrasted ones are grains of limestone : the difference between the particle size of both clinkers is obvious. Qualitatively, the same type of results has been obtained with C.P.J. C and C.P.J. F ; the most pronounced differences are with C.P.J. F.

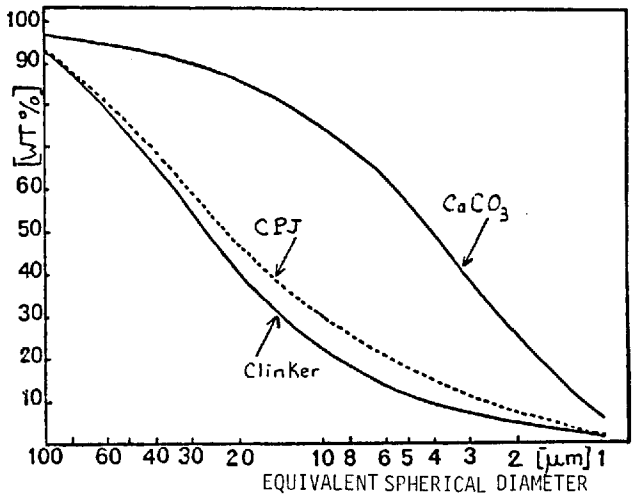

Fig. 1 : Particle size distribution of the industrial C.P.J. L., and of its constituents.

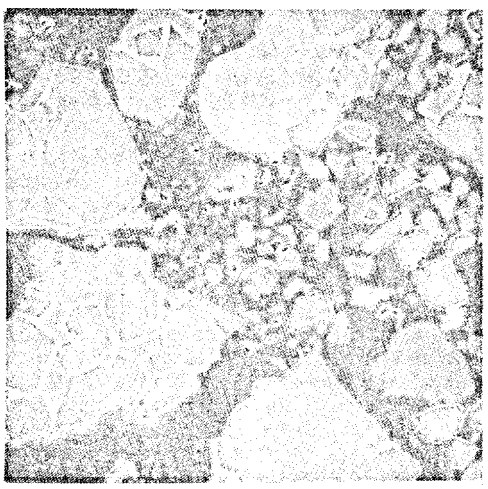

Fig. 3 : S.E.M. observation of the industrial C.P.J. L., (X 500)

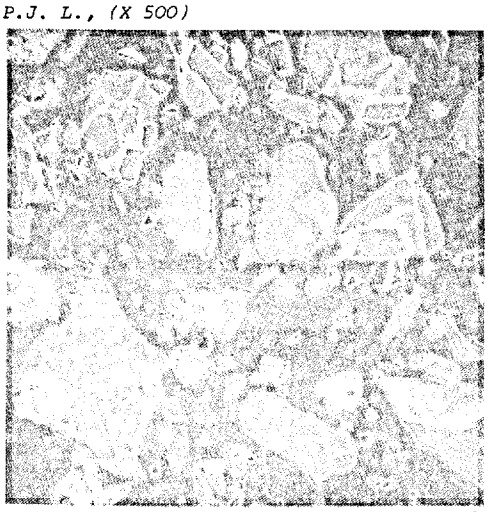

Fig. 4 : Comparative observation of the Labo. made C.P.J. L. (X 500).

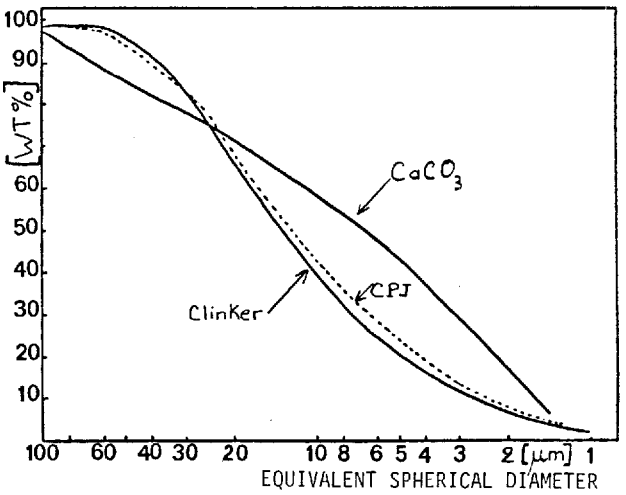

Fig. 2 : Particle size distribution of the Lab. C.P.J. L., and of its constituents.

POINTS of PECULIAR INTEREST ; DISCUSSION

After this overall presentation, we will now focuse on few selected points, highlighting the results : they are expressed in tables 2 and 3, and in fig. 5.

TABLE 2 : Comparative results between industrial and Laboratory-made.

	Industrial			Lab. Made		
CPJ C	Filler (1)	Clinker (2)	CPJ (3)	Filler (4)	Clinker (5)	CPJ (6)
Median (µm)	7.5	21	19	14.5	13	13
< 10 µm (%)	54		31	46	40	40.8
Fraction 1-2 µm	12			11.5		
> 45 µm	14.2	20.1	19.2	29.3	4.9	10.3
B.S.S. [cm2.g-1]			3885	5050	4035	4175
CPJ L						
Median (µm)	4.1	26	21.5	6.8	13	12
< 10 m (%)	74	22.5	30	58	40	43
Fraction 1-2 µm	18.5			12.5		
>45 µm (%)	8.1	30.9	27.5	16.3	6.3	7.8
B.S.S. [cm2.g-1]			3750	5000	4035	
CPJ F						
Median (µm)	2.7	30	24	11.5	13	13
< 10 µm (%)	74	21	29	48.5	40	41.5
Fraction 1-2 µm	32			18.5		
>45 µm	7.3	35.1	30.9	36	6.5	8.8
B.S.S. [cm2.g-1]			4047	5000	4035	

D. MENETRIER - SORRENTINO, chargée de Recherche au C.N.R.S., en détachement à LAFARGE COPPEE RECHERCHE, France

TABLE 3 : Percent of filler and clinker contained in the < 4 µm fraction. Comparative results.

CPJ	Industrial			Lab. Made		
	Passing % (1)	$CaCO_3$ % (2)	Clinker % (3)	Passing % (4)	$CaCO_3$ % (5)	Clinker % (6)
C	14.22	43.04	56.96	19.43	26.09	73.90
L	14.17	48.83	51.17	17.85	28.01	72.0
F	17.40	52.40	47.60	18.0	28.48	71.52

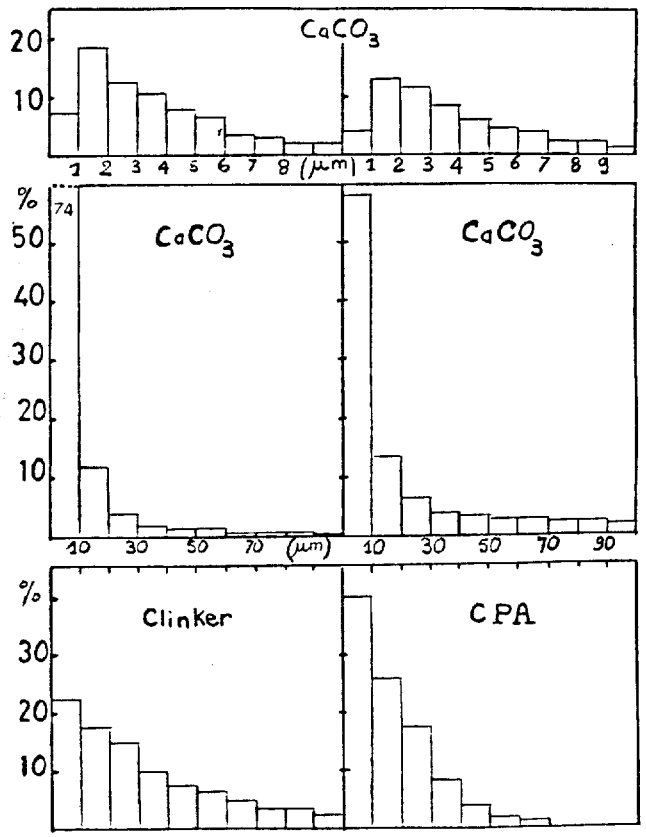

Fig. 5 : Histograms of the industrial C.P.J. L. and of its constituents.

From them, the following remarks can be made :

- the median in laboratory made cements is almost constant for the clinker and the C.P.J. (col. 5 and 6, table 2) : the reproducible value of 13 µm obtained for the clinker was expected, in fact, since the same clinker has been used to prepare those cements. This proves indirectly that our method is correct,

- the medians of the industrial cements are higher than their twin - laboratory made ones : 19, 21.5 and 24 µm for the C.P.J. (col. 3), compared with 13 µm (col. 6). For the clinker, 21, 26 and 30 µm (col.2) compared with 13 µm, and we point out here, the increasing values obtained, among the industrial C.P.J. (21 to 30 µm),

- the median of limestone is always smaller in industrial cements (first column) than in Laboratory made cements (col. 4) and we note the opposite evolution of the filler in industrial cements (7.5, 4.1., 2.7 µm) to that one observed for the clinker,

- the second line of each part of table 2, is concerned with the percent of particles passing through 10 µm : in the Lab made cements C and F, the values obtained for the filler and the clinker are relatively close (46 against 40 %, and 48.5 against 40 %), but the great differences of values observed on the industrial cements between the clinker and the filler are striking : 54 µm against 26.5 µm for C.P.J. C, 74 µm and 22.5 µm for C.P.J. L, 74 and 21 µm for CPJ F,

- results in table 3, expressing the relative proportion of the clinker and the filler, constituting the smallest fraction of the grains (< 4 µ), evidence this also.

1 - The general trend is that Lab. made cements yield higher values (col. 4) than the industrial C.P.J. ones (col. 2).
2 - The proportion of limestone in Lab. made cements is relatively constant (26-28 %, col.5) while the proportion of limestone in industrial CPJ varies much more and is very high (43 to 52.5 %, col. 2). We recall that the global value is close to 15 %.

- another way of expressing results is to present them as histograms (fig. 5). We have established the population of limestone between 0 and 10 µm, and noticed that they all show a maximum between 1 and 2 µm (table 2) ; the industrial C.P.J. F has the most pronounced maximum with 32 %,

- looking now at the opposite part of the granulometric curve, i.e. the large size grains, the results complement and corroborate those obtained for the lower part of the curve : the fraction of the clinker not passing through 45 µm in all three Lab. made cements, is small, and around 5 %. On the contrary, the corresponding values for the industrial cements are high, and show large discrepancies - 20,1 µm for C.P.J. C., 30.9 µm for C.P.J. L., and 35.1 µm for C.P.J. F.. This is a clear indication that clinker is not optimally ground in coground C.P.J. cements.

CONCLUSIONS

We have developed an accurate and simple method involving traditional techniques - in order to dermine the respective grain size distribution of the clinker and the calcareous filler, both the constituents of C.P.J. cements, in the particular case, where they are industrially produced by cogrinding.

Our method has been tested at first on 3 Laboratory-made cements, since the grain size distribution could be determined on each of the constituent, by direct method, before the blend was realized : it appeared successful.

Three industrial C.P.J. have then been investigated.

The most striking results concerning the industrial C.P.J. which are expressed comparatively in the tables, photographs and figures, may be summarized as follows :

- the calcareous filler contains an high amount of very small grains, and the median ranges between 2.7 and 7.5 µm,

- the clinker contains on the contrary, a large proportion of large size grains, as indicated, eg, by the percent of particles above 45 µm : 20.1, 30.9 and 35.1 µ. Those grains are not easily hydrated, and do no take part in the development of early strength.

Thus, cogrinding is not the most well adapted process, in the case where the filler of the C.P.J. cement is calcareous, since it partially counteracts the beneficial effects brought by the addition of limestone.

REFERENCES

1 - R. GUYOT, R. RANC, B. CARIOU, Utilisation de la Potentialité Hydraulique du Clinker dans les Ciments Portland avec Ajout de Filler Calcaire. Séminaire 2. Present congress.

2 - C.A. JOUENNE, Traité de Céramiques et Matériaux Minéraux. Septima Ed. PARIS (1975).

3 - B. MORTUREUX, J.P. BOMBLED, Broyage Simultané d'un Mélange de Clinker et de Roche Calcaire. Rapport CERILH (1985).

4 - D. SORRENTINO, Finesse des Fillers Calcaires dans les C.P.J. Rapport interne LAFARGE (1985).

AUTEUR : J.P. BOMBLED (C.E.R.I.L.H. - PARIS/FRANCE)

SUJET : **Différents moyens d'activation des matériaux potentiellement pouzzolaniques. Application aux liants chaux-pouzzolane.**

1

Various activation means of potentially pozzolanic materials: Application to lime-pozzolana cements.

3.1

RESUME

Les matériaux potentiellement pouzzolaniques, devant permettre la fabrication dans les P.E.D., de liants à bas coûts type chaux-pouzzolane, sont soit des matériaux argileux, soit des sols latéritiques, des bauxites éventuellement, des roches volcaniques ou sédimentaires (gaize, kieselguhr), voire des sous-produits industriels ou des déchets agricoles (cendres de riz, de mil, de bagasse, ...) : tous ces matériaux sont riches en oxydes acides, silice, alumine et fer qu'il faut rendre réactifs en présence de chaux avec formation de liaisons et de résistances mécaniques.

Les moyens d'activation de ces matériaux silico-alumineux sont de plusieurs natures : mécaniques (surbroyage), rhéologiques (serrage, réduction d'eau) et surtout chimiques (adjuvants utilisés soit sur matériaux crus, soit sur matériaux cuits) ou thermiques; l'activation thermique peut se faire soit à "basse" température (étuvage, autoclavage) soit à température plus élevée, généralement comprise entre 400 et 900 °C, et dans ce cas, on peut encore "activer" le traitement thermique par des adjuvants de cuisson.

Il existe pour la calcination de chaque matériau une température optimale de traitement. Parmi les actions chimiques les plus efficaces, on peut noter les traitements sulfatiques, sodiques et sodo-sulfatiques et parfois aluminate ou silicate de Na, déjà préconisés pour les laitiers et les cendres volantes. Un des objets de ce travail a été non seulement de mettre en relief l'action séparée de chaque mode d'activation mais aussi de les conjuguer : des résultats intéressants ont été observés sur une latérite et sur une kaolinite.

Enfin, il était intéressant de comparer les propriétés de ces liants chaux-pouzzolane à celles des ciments traditionnels et de fixer les limites d'emploi où ils pourraient les remplacer.

Os materiais potencialmente pozolânicos aptos a permitir nos P.E.D. a fabricação de ligantes de baixo custo tipo cal-pozolana, são quer materiais argilosos, quer solos lateríticos, eventualmente bauxitas, rochas vulcânicas ou sedimentares (gaize, kieselghur), às vezes sub-produtos industriais ou refugos agrícolas (cinzas de arroz, bagaço, ...): todos estes materiais são ricos em óxidos ácidos, sílica, alumina e ferro, que devem ser tornados reativos em presença de cal com formação de ligações e de resistências mecânicas.

Os meios de ativação destes materiais são de naturezas diversas: mecânicas (supermoagem), reológicas (compactação, redução de água) e sobretudo químicas (adjuvantes utilizados seja com os materiais crus, seja com materiais cozidos) ou térmicos; a ativação térmica pode ser feita tanto sob temperatura "baixa" (secagem em estufa , autoclavagem), seja sob temperatura mais elevada, geralmente compreendida entre 400 e 900°C e, neste caso, pode-se ainda "ativar" o tratamento térmico por meio de adjuvantes de coccão.

Para a calcinação de cada material há uma temperatura ótima de tratamento. Entre os tratamentos químicos mais eficazes, podemos notar os tratamentos sulfáticos, sódicos e sodo-sulfáticos, e às vezes aluminato ou silicato de Na, já preconizado para as escórias e cinzas volantes. Um dos escopos deste trabalho foi não somente colocar em relevo a ação separada de cada forma de ativação, mas também conjugá-las: foram observados resultados interessantes com uma laterita e uma caolinita. Enfim, era interessante comparar as propriedades destes ligantes cal-pozolana com as dos cimentos tradicionais e fixar os limites de utilização em que os primeiros poderiam substituir os últimos.

1. INTRODUCTION

Dans les pays en développement, les importants besoins en ciment destinés en grande partie à la construction de logements, liés à l'expansion démographique, peuvent être réduits dans une certaine mesure par le choix convenable des procédés de construction, par une réduction raisonnable des exigences et des dosages et enfin grace à des liants de remplacement généralement pouzzolaniques.

A cause des grandes distances et de l'incidence des prix des transports, le coût du ciment y est toujours très élevé (~ 20 % de la construction contre ~ 2 % en France)il est par conséquent généralement avantageux d'y incorporer le plus possible de composants locaux peu coûteux tels que fillers, déchets divers et pouzzolanes.

Ces pouzzolanes n'existant pas partout à l'état naturel (d'origine soit volcanique, soit sédimentaire) il faut avoir recours à des déchets industriels ou agricoles (cendres de balle de riz par exemple), voire activer des roches potentiellement pouzzolaniques : ce sont ces moyens d'activation que nous nous proposons d'examiner ici.

2. GENERALITES

2.1. POUZZOLANICITE

On sait que la réaction pouzzolanique est une véritable attaque de la silice et de l'alumine par la solution calcique à pH élevé avec dissolution et recristallisation des silicates de Ca hydratés, voire d'ettringite en présence de sulfates.

Il faut néanmoins un état suffisamment instable et un contact intime entre les éléments acides et la solution calcique pour que l'on puisse considérer l'existence de silice ou d'alumine "solubilisables".

Si la pouzzolanicité peut se repérer par des tests physico-chimiques de fixation de la chaux celle-ci n'est pas suffisante pour prévoir l'acquisition des résistances mécaniques : il faut toujours confirmer les tests chimiques par des essais mécaniques.

2.2. RECENSEMENT DES MOYENS D'ACTION

La séquence des phénomènes qui constituent l'hydratation et la prise d'un liant hydraulique est rappelée dans le tableau I avec les moyens théoriques d'action à chaque niveau : mouillage, floculation, pénétration ou attaque, hydrolyse, dissolution, solvation, diffusion des ions hydratés, sursaturation et précipitation.

On peut noter dans le tableau la fréquence d'apparition de la température, de la surface du contact solide-liquide et d'adjuvants potentiels. .

On pourra espérer agir à chaque stade et par différents moyens.

Il ressort par conséquent que pour activer les réactions pouzzolaniques on pourra avoir recours :

- à des traitements thermiques.
- à des moyens chimiques (adjuvants)
- à des procédés mécaniques (surbroyage)
- éventuellement à des moyens "rhéologiques" (réduction de teneur en eau, serrage,...).

Tableau I

Phase de l'hydratation	Phénomènes physico - chimiques	Action physique ou chimique efficace	Intervention possible en fabrication	Intervention possible à l'utilisation
Mouillage	Tension superficielle de l'eau.	Inutile (les ciments sont hydrophiles)	-	-
Floculation (ou défloculation)	Potentiel électrocinétique de l'interphase .	Adjuvants ioniques	-	Défloculants ou fluidifiants pour réduire les espaces intergranulaires.
Pénétration	Viscosité de l'eau	Température	-	Chauffage
	Surface d'action	Accroissement de la surface ext Défauts et failles int. des grains .	Broyage Trempe	-
Hydrolyse	Surface d'action	idem	Broyage ou trempe	-
	Affinités chimiques	ions convenables "catalyseurs"	Teneur en C3A	Adjuvants
Dissolution	Forces de séparation des ions Agitation thermique Surface d'action "Solvants"	Constante diélectrique . Température . Défaut de cristaux . Ions convenables	- - Broyage, trempe -	- . Chauffage - . Adjuvants
Diffusion	Agitation thermique Dimensions des ions Gradient de concentration	. Température . Concentration, dosages.	- -	- Chauffage E/C et serrage
Précipitation et Cristallisation	Sursaturation . Germination . Morphologie des cristaux.	Ions convenables, température Architecture réticulé (accueil de cristallisation) Concentrations	- Fillers -	Adjuvants, chauffage Germes, fillers . E/C et serrage.

Ces différents moyens seront étudiés séparément, ou dans certains cas conjugués comme le montre le schéma des différents chemins possibles du plan d'essais ci-dessous.

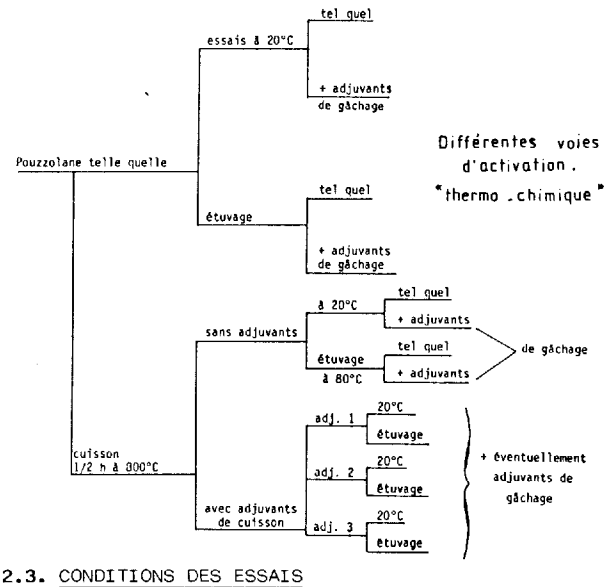

2.3. CONDITIONS DES ESSAIS

La plupart des essais ont été effectués sur des échantillons choisis parmi les matériaux suivants :

- Kaolin d'Arvor (France) et une argile illitique.
- Bauxite riche et pauvre en silice (Guinée et France).
- Latérites de Côte d'Ivoire et du Niger
- Basalte du Massif Central (France).
- Pouzzolane de Volvic (France).
- Silice fossile (Kieselguhr)
- Silice ultra-fine de dépoussiérage sidérurgique (fumées de silice)
- Quartz broyé à plusieurs finesses de mouture .

Pour chacun des matériaux on pourra :

(a). Soit utiliser le matériau potentiellement pouzzolanique tel quel (cru),

(b). Soit le soumettre à un traitement thermique (cuisson), avec ou sans adjuvants de cuisson.

A partir de là, et dans chaque cas, on pourra agir avec les différents moyens, et les conjuguer comme indiqué ci-dessus.

Outre des mesures de fixation de chaux (essai Chapelle) effectués systématiquement, la plupart des résultats exposés ci-après concernent des pâtes pures à consistance normale (E/s $\simeq$ 0,25) contenant 80 % de matériau pouzzolanique et 20 % de Ca (OH)2, teneur trouvée optimale dans des essais antérieurs; les éprouvettes ont été conservées en milieu humide et rompues en compression à 28 jours , sauf pour l'étuvage (40 h).

3. ACTIVATION THERMIQUE A TEMPERATURE ELEVEE (>400 °C)

Il s'agit de conférer une activité pouzzolanique à des matériaux qui le sont potentiellement ou encore dont la pouzzolanicité est peu marquée (Fig. 4).

3.1. MODIFICATIONS APPORTEES PAR LES TRAITEMENTS THERMIQUES A TEMPERATURE ELEVEE

L'élévation de température, et éventuellement la trempe, induisent certaines transformations qui se conjuguent plus ou moins dans l'effet pouzzolanique:

- Déshydroxylation des matériaux argileux qui libère sans doute des sites disponibles à d'autres liaisons ultérieures.

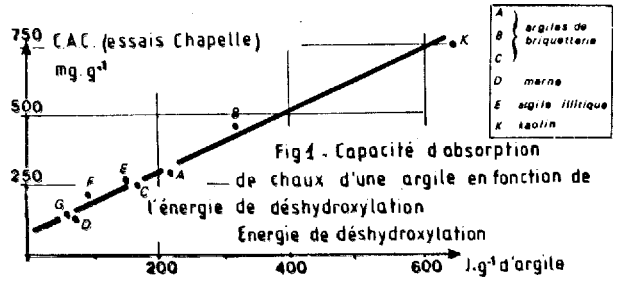

Fig 1 - Capacité d absorption de chaux d'une argile en fonction de l'énergie de déshydroxylation
Energie de déshydroxylation

- Des transformations cristallographiques. L'activité maximale de l'effet pouzzolanique correspond généralement à la disparition d'un état cristallin (s'il existait préalablement) plus ou moins bien architecturé et au "basculement" vers un état désordonné où les éléments réacquièrent une certaine individualité. En revanche, quand la température continue à croître, une réorganisation s'amorce.

- Création de surfaces nouvelles soit par microfissuration (qui favorise en outre la pénétration de la solution intersticielle calcique), soit aussi par la disparition d'éléments peu stables quand la température s'élève (eau libre, matières organiques, CO_2, SO_3,...). L'expérience montre que selon les matériaux traités et suivant les températures atteintes, le traitement thermique peut se révéler utile ou inutile voire néfaste; on note par exemple une diminution de la surface BET au delà d'une certaine température sans doute par suite d'un début de recristallisation et d'une amorce de frittage surtout si des éléments fondants sont présents et le favorisent.

3.2. TEMPERATURE OPTIMALE DE CALCINATION

L'expérience montre que la pouzzolanicité est généralement obtenue, et c'est le cas pour la plupart des argiles, par la chauffe à une température optimale pour laquelle les résistances mécaniques présentent un maximum (Fig. n° 2 et 3).

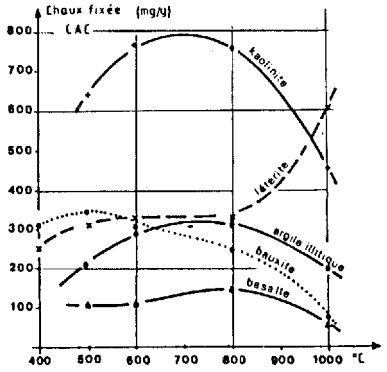

Fig 2
- Chaux fixée en fonction de la température de traitement de l'argile.

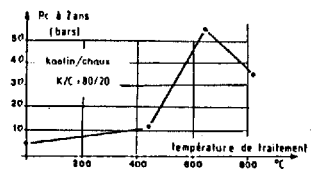

Fig 3. Résistance et traitement thermique. (LONGUET)

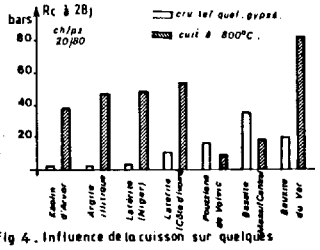

Fig 4. Influence de la cuisson sur quelques matériaux.

Un certain nombre d'auteurs indiquent pour les températures optimales de calcination des argiles, les valeurs suivantes :

- pour les kaolinites 600 °C à 800 °C (Longuet, Murat)
- Pour les Illites ~ 550 °C } (Roberton)
- Pour les Smectites ~ 650 °C }
- Pour les Bauxites 250 à 350 °C (Lea)

de même pour une pouzzolane italienne ~ 800°C (Massazza)

Notons que les températures de traitement optimales correspondant aux résistances en compression maximales sur des pâtes pouzzolane-chaux 80-20, apparaissent un peu différentes, ce qui laisse penser que d'autres facteurs peuvent intervenir : vitesse de chauffe, condition de refroidissement (trempe), pureté du matériau (fondants alcalins) dimension de l'échantillon traité...

La figure n° 5 montre les résultats obtenus en analyse thermique différentielle par BAIN sur quelques matériaux, ici aussi, comparés aux maximums de la figure n° 2, on observe un décalage d'environ 100 °C par rapport aux pics de déshydroxylation.

3.3. DUREE DU TRAITEMENT

Non seulement la température de cuisson, mais la durée du traitement semblent jouer un rôle, la cinétique du phénomène étant évidemment

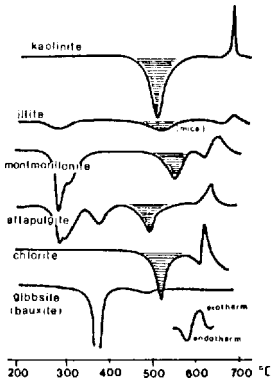

Fig 5 . ATD sur plusieurs argiles. (BAIN)

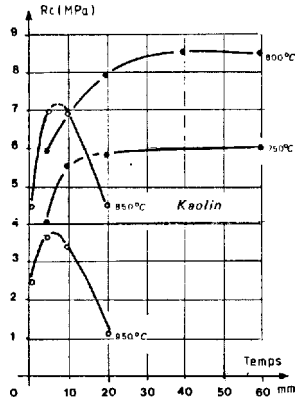

Fig 6. Influence de la température et de la durée de cuisson sur les résistances en compression . (d'après Forrester)

liée à la puissance de chauffe, à la dimension du creuset, à la quantité de matériau traité, et à l'inertie thermique, au rapport surface/volume de l'échantillon, etc...

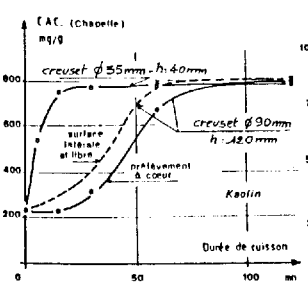

Fig 7 . Vitesse de déshydroxylation et dimension de l'échantillon .

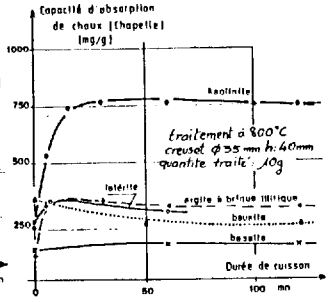

Fig 8. CAC et durée de traitement .

Les figures n° 6, 7 et 8 illustrent ces remarques et en particulier l'influence de la dimension de l'échantillon et de son inertie thermique, dans certains cas pour de petites quantités, la déshydroxylation peut s'effectuer très rapidement puisque sur la figure n° 6 le maximum s'observe entre 5 et 10 minutes. Ces renseignements pourront être utiles pour la mise au point d'une fabrication ou celle du matériel de traitement et prévoir les débits des installations.

3.4. INFLUENCE D'ADJUVANTS DE CUISSON

La présence de certains ions devrait pouvoir modifier la cinétique de l'activation par la température et améliorer les résultats obtenus sur les résistances mécaniques en pâte pouzzolane-chaux.

Les principaux adjuvants de cuisson qui ont été essayés sont les suivants :

- Chlorures de Na et Ca
- Nitrates de Na, Ca, K et Fe
- Sulfates de Na, Ca et K
- Carbonates de Na et Ca
- Aluminate, silicate, borate, fluosilicate, fluorure et hydroxyde de Na.

La teneur adoptée, sans doute trop élevée, dans ces essais préliminaires a été de 10 % du poids de pouzzolane. On verra sur les figures suivantes que les adjuvants de cuisson qui ont été le plus souvent efficaces sont la soude, le silicate de Na, le nitrate de K et parfois le carbonate et le fluorure de Na (Planche 9).

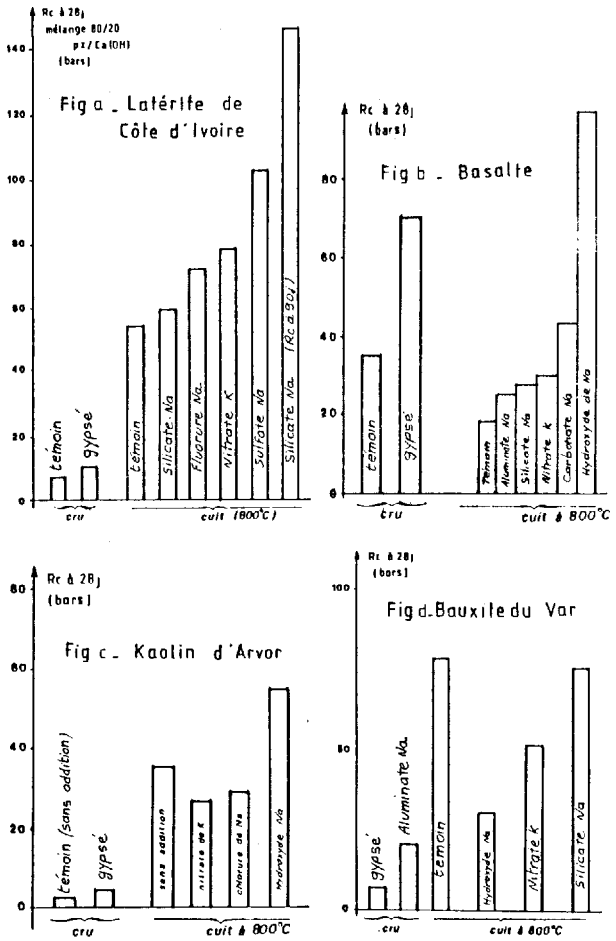

Planche 9 . Cuisson avec additions

Sur la planche n° 9, relative à quatre matériaux potentiellement pouzzolaniques, on a consigné aussi les résistances obtenues avec le matériau cru, tel quel, ce qui permet de mettre en relief le gain obtenu par la cuisson avec divers adjuvants de cuisson; les résultats sont très marqués avec la latérite, un peu moins avec le kaolin et parfois médiocres avec d'autres matériaux (basalte par exemple).

4. ACTIVATION THERMIQUE A BASSE TEMPERATURE. (étuvage)

Le cycle adopté pour la plupart des essais est rappelé fig (a) de la planche n° 10. ce traitement a été effectué soit sur le matériau cru, soit sur le matériau cuit (sans adjuvant de cuisson) à 800 °C : les figures (b), (c) et

(d) de la même planche illustrent l'importance de l'étuvage quand le matériau est déjà actif (basalte tel quel, latérite ou kaolin cuits à 800 °C), mais agit peu dans le cas contraire.

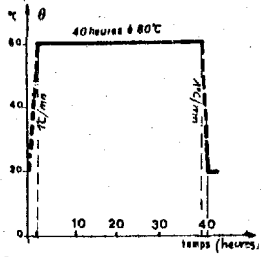

Fig a. Cycle d'étuvage adopté

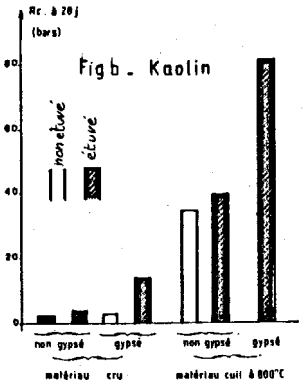

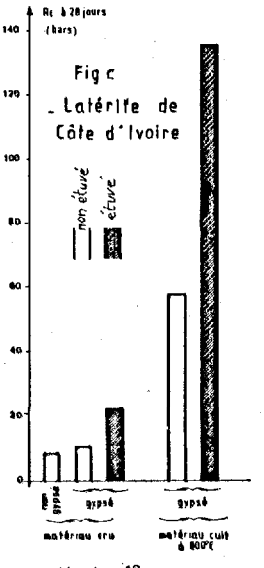

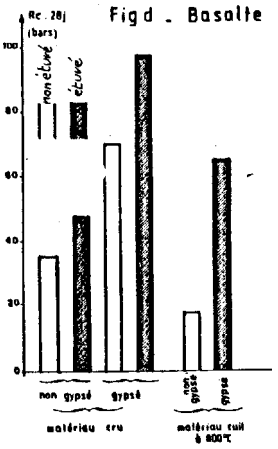

Planche 10

Activation basse température (étuvage 40h à 80°C)

Notons enfin que si l'étuvage permet parfois d'augmenter sensiblement les résistances des matériaux actifs, la présence de sulfate de Ca sous forme de gypse par exemple, apporte aussi une augmentation sensible des résistances (les doublent souvent) dans la plupart des cas; ceci nous amène déjà à l'activation chimique.

5. ACTIVATION CHIMIQUE PAR ADJUVANTS DE GACHAGE

Le rôle de ces adjuvants devrait être avant tout de faciliter ou d'accélérer la dissolution de la silice et de l'alumine : la figure (a) de la planche 11 rappelle l'influence des ions alcalins et du pH sur la solubilité de SiO_2 et Al_2O_3.

5.1. RESULTATS SUR MATERIAUX CRUS

Les figures de la planche 11 concernent seulement des pouzzolanes crues telles quelles. On peut y voir l'influence générale des sulfates, et du gypse en particulier, sur des matériaux divers tels que la latérite, bauxite et Kieselguhr.

Dans la plupart des cas on note l'action de la soude, du carbonate de Na et parfois du silicate et de l'aluminate de Na; On voit qu'il s'agit toujours de bases fortes ou de sels de

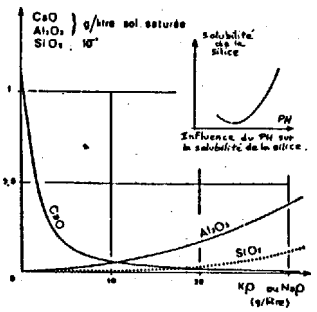

Fig a. Influence des alcalins sur la solubilité de CaO, SiO_2 et Al_2O_3.

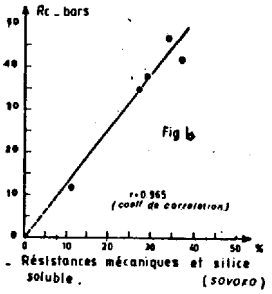

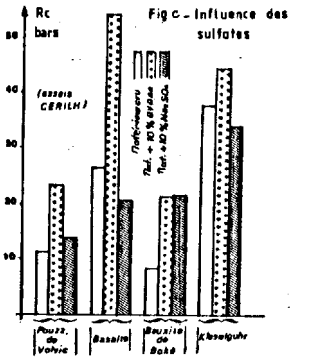

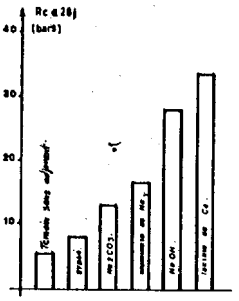

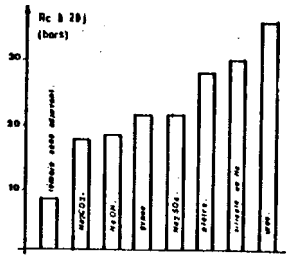

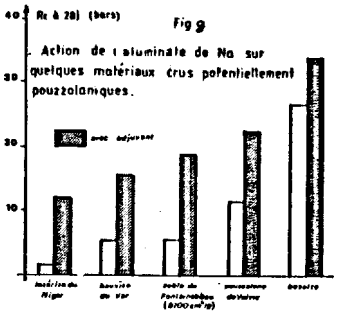

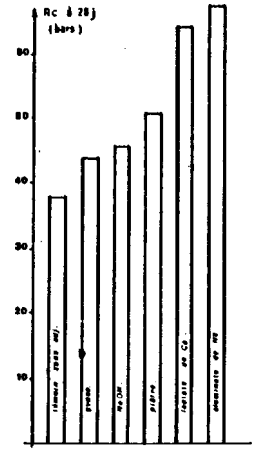

Planche 11

Pouzzolanes crues activation chimique.

bases fortes et d'acides faibles (signalons que l'aluminate de Na est un bon accélérateur des ciments aux cendres).

Nous verrons plus loin (Cf. 5.3.2.) les résulats obtenus sur les matériaux potentiellement pouzzolaniques crus pour lesquels on a couplé les adjuvants chimiques et l'étuvage.

5.2. ACTIVATION CHIMIQUE PAR ADJUVANTS DE GACHAGE SUR MATERIAUX CUITS

La planche 12 ci-après illustre l'action des adjuvants de gâchage sur des matériaux potentiellement pouzzolaniques cuits à 800 °C : On retrouve l'intérêt du sulfate et du silicate de Na et

et surtout de la soude.

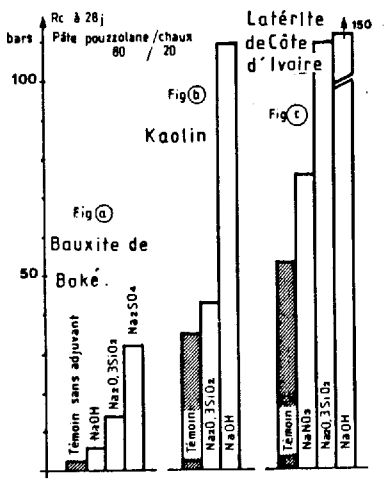

Planche 12 . Activation chimique par adjuvants de gâchage, de matériaux cuits à 800°C .

5.3. EFFETS CONJUGUES THERMO-CHIMIQUES

5.3.1. Couplage adjuvants de cuisson et étuvage

Les résultats obtenus avec trois matériaux sont consignés sur la planche 13; si l'adjuvant de cuisson présente l'intérêt déjà signalé sur la planche 9, l'étuvage permet d'obtenir évidemment plus vite les résistances même s'il existe un manque à gagner final.

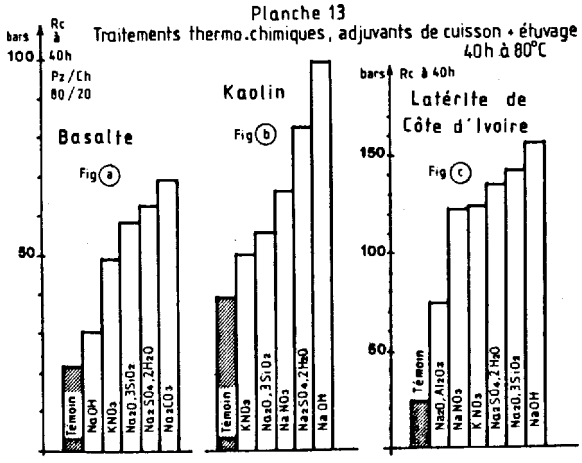

5.3.2. Couplage adjuvants de gâchage et étuvage

La planche 14 regroupe les résultats obtenus par le couplage des adjuvants de gâchage et de l'étuvage soit sur des matériaux crus, soit sur des matériaux cuits à 800 °C.

5.3.3. Résultats globaux

La presque totalité des couplages efficaces est regroupée, pour le kaolin et la latérite de Côte d'Ivoire, sur les histogrammes des figures 15 et 16.

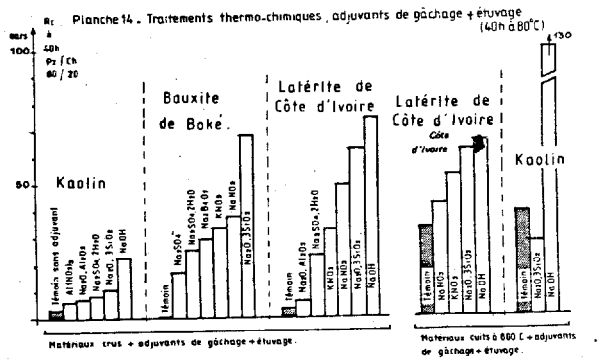

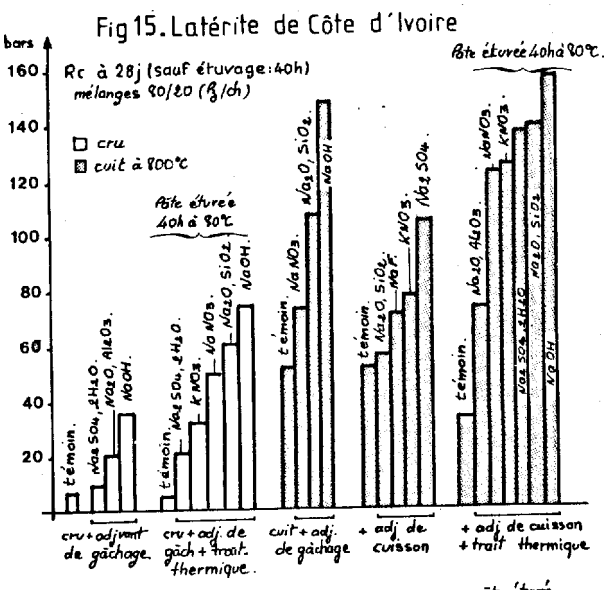

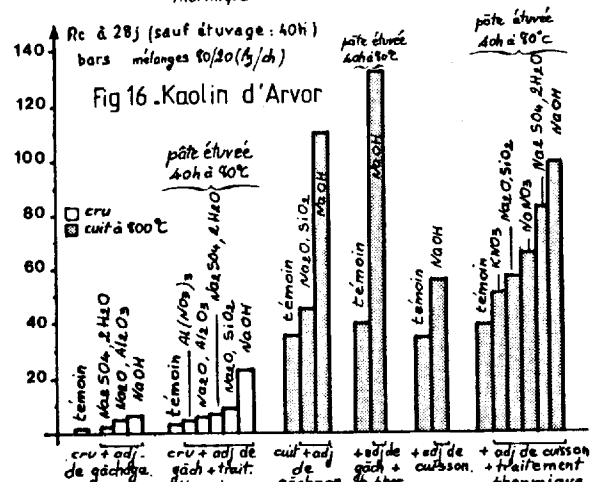

Dans les deux cas regroupés sur les figures précédentes, on peut mesurer l'étendue des gains possibles : ainsi pour ces deux matériaux où l'on part de résultats très faibles, pour le témoin cru initial gâché sans adjuvant, on peut multiplier par plus de 30, voire même de 50 la résistance en compression à 28 jours (des gains encore très supérieurs seraient obtenus avec ces matériaux pouzzolaniques évidemment pour des échéances plus éloignées).

Malheureusement, ces traitements peuvent être coûteux en énergie, en investissement, en frais d'exploitation et leurs couplages en série risquent parfois d'anihiler le bénéfice escompté et surtout de dépasser le coût de fabrication du clinker ou du ciment Portland : Un bilan est à faire pour chaque matériau et dans chaque situation.

6. AUTRES MODES EVENTUELS D'ACTIVATION

Nous avons vu en 2.2. que l'on pouvait "activer" l'action pouzzolanique par des actions d'ordre mécanique tel que le surbroyage qui crée des surfaces nouvelles d'échange et le serrage qui rapproche les éléments à liaisonner. De même sans doute l'intérêt de germes (fillers calcaires).

Les figures 17 à 20 illustrent ces différentes actions; insistons en particulier sur l'importance du serrage énergique pour ce type de liant.

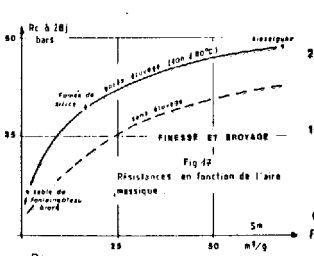

Fig 17
Résistances en fonction de l'aire massique

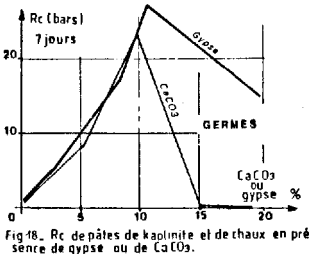

Fig 18. Rc de pâtes de kaolinite et de chaux en présence de gypse ou de $CaCO_3$.

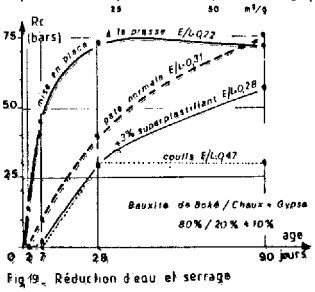

Fig 19. Réduction d'eau et serrage

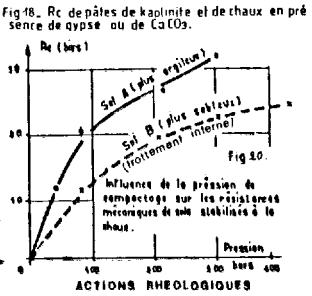

Fig 20. Influence de la pression de compactage sur les résistances mécaniques de sols stabilisés à la chaux.

La figure n° 18 montre un maximum voisin de 10 % pour le sulfate, valeur d'ailleurs adoptée dans les différents essais précédents.

7. REMARQUES SUR LES LIANTS CHAUX-POUZZOLANES

7.1. EFFETS COMPARES DU SECHAGE, DE LA CARBONATATION ET DE L'ACTION POUZZOLANIQUE

Dans les pays à climat chaud et sec, l'évaporation de l'eau et la carbonatation de la chaux peuvent précéder l'action pouzzolanique qui exige une cure humide très prolongée ce qui peut être considéré comme une sujetion.

La figure n° 21 permet de comparer les résistances obtenues pour quelques matériaux par les trois actions séparées.

7.2. INFLUENCE DE LA CARBONATATION PARTIELLE PREALABLE DE LA CHAUX DES LIANTS CHAUX-POUZZOLANES

La chaux ayant une très grande affinité pour le CO_2, les chaux industrielles sont toujours peu ou prou carbonatées : l'expérience montre qu'un peu de CO_3Ca (ou d'incuits) < 5 à 8 % peut ne pas être néfaste (germes); c'est ce qu'illustre la figure n° 22.

7.3. TENEUR EN CHAUX DES LIANTS CHAUX-POUZZOLANES

L'expérience montre que la teneur optimale en $Ca(OH)_2$ des liants chaux-pouzzolanes est voisine de 20 % du mélange (Fig. 23) : c'est ce que nous avons adopté pour tous les essais dans ce travail.

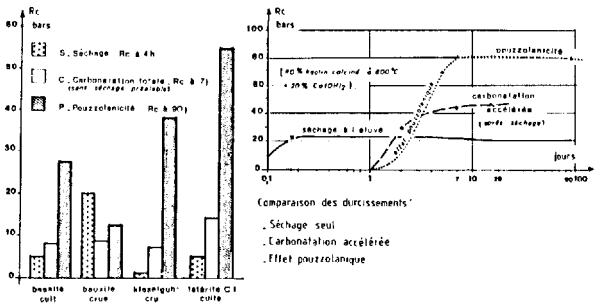

Fig 21. Comparaison des trois modes de durcissement pour 4 matériaux potentiellement pouzzolanique + chaux(80/20)(essais en pâte pure).

7.4. VITESSE DE DURCISSEMENT DES LIANTS CHAUX-POUZZOLANES

Si ces liants peuvent avoir un intérêt économique (à vérifier), il faut préciser que leur vitesse de durcissement est très lente comparée à celle du Portland même fortement fillérisé (Figure n° 24) et qu'ils ne peuvent remplacer les ciments Portland dans tous leurs emplois.

7.5. REMARQUE SUR L'INTERET ECONOMIQUE

Le coût énergétique et économique des différents moyens d'activation, surtout s'ils sont conjugués, risque de devenir très vite prohibitif : il faut évidemment dans chaque cas et dans chaque pays, et pour chaque matériau, effectuer un bilan aussi complet que possible; la relation ci-dessous donne une idée de la série d'éléments à considérer.

Par exemple pour l'énergie consommée :

$$E = \underbrace{\alpha C_1}_{\text{calcin. pouzz. artif. (p.ex. argile)}} + \underbrace{(1-\alpha) C_2}_{\text{cuisson de la chaux (pour des liants chaux/pouz.}} + \underbrace{k C_3 \frac{\Delta S}{1000}}_{\text{surbroyage (par rapport au Portland)}} + \underbrace{\alpha' C_4 d}_{\text{transport}} + \underbrace{\frac{k}{x}(C_5+C_6)}_{\text{traitement thermique du béton}} + \underbrace{\sum \beta_i C_i}_{\text{adjuvants de cuisson ou de gâchage}}$$

Il ne faut pas oublier de comparer aussi les solutions "clinker" qui sont :

- soit les bétons maigres à faible dosage en ciment (y compris sol ciments et bétons de terre) (Fig. 25).

- Soit les ciments Portland fortement fillérisés.

La première solution est plus économique en terme de broyage et de transport.

8. CONCLUSION

S'il existe un certain nombre de moyens pour activer des matériaux potentiellement pouzzolaniques ou pour "exciter" des pouzzolanes "peu nerveuses", il est non moins certain que le coût de ces traitements risque de faire perdre l'intérêt misé sur les liants à forte teneur en pouzzolanes

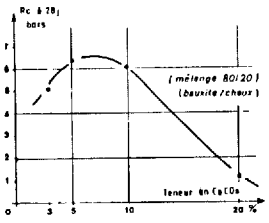

Fig 22. Impuretés des chaux
Influence de la carbonatation
avant la mise en œuvre.

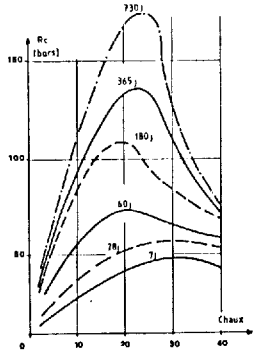

Fig 23. Influence du dosage en chaux sur les performances mécaniques. (LCPC)

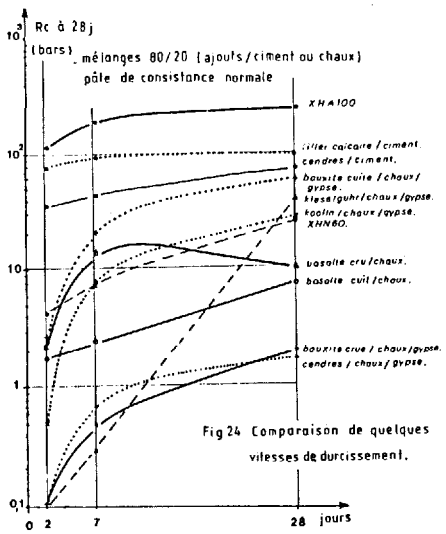

Fig 24 Comparaison de quelques vitesses de durcissement.

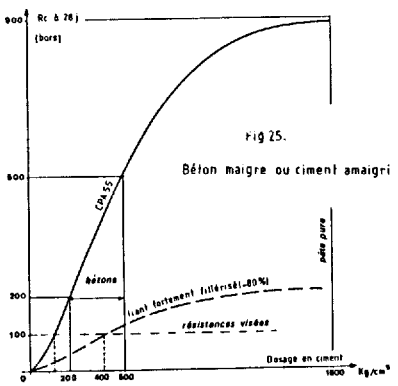

Fig 25.

Béton maigre ou ciment amaigri

et en particulier les liants pouzzolanes-chaux (théoriquement plus faciles à produire que les Portland par les PED), d'autant plus que les propriétés de ces liants sont loin d'égaler celles des Portland naturels, il est presque toujours apparu que la fabrication de pouzzolanes artificielles coûte à tous égards à peu près aussi cher que l'élaboration du clinker. Ces clinkers peuvent être utilisés pour la fabrication de ciments fortement fillérisés, mais il est souvent plus logique et plus économique (broyage, transport...) de préconiser des bétons maigres, à faible dosage en ciment (ou des bétons de terre et des sols-ciments) généralement très suffisants pour la plupart des besoins dans l'habitat local.

AUTEURS : J.P. BOMBLED, G. BELLINA et B. MORTUREUX. (C.E.R.I.L.H. - PARIS/FRANCE)

SUJET : **Détermination des courbes granulométriques et des aires massiques des constituants de mélanges cobroyés : applications aux fillers et aux laitiers.**

Particule size distribution and specific surface measurements of components of cogrinded blended cements : application to fillers and slags.

3.1

RESUME

Lors du broyage simultané (ce qui est le cas habituel en cimenterie), d'un mélange de clinker et d'un autre constituant (filler, laitier, pouzzolanes,...) pour fabriquer des ciments composés (CPJ des normes Françaises par exemple), il peut être utile de connaître les répartitions granulométriques et les aires massiques particulières de chacun des constituants; En effet, celles-ci peuvent jouer un rôle important sur les propriétés des mortiers et des bétons soit à l'état frais, soit à l'état durci.

Pour des matériaux cristallisés, par exemple la calcite des fillers calcaires, la méthode d'analyse granulométrique proposée résulte du couplage de la sédimentométrie à la pipette d'Andreasen et du dosage des constituants par diffraction des rayons X, dans les fractions granulaires séparées; les résultats présentés confirment l'intérêt de cette procédure et le degré de précision espéré.

Ce type de méthode peut être étendu à des matériaux non cristallisés à condition de trouver un élément marqueur dans l'un des constituants et de pouvoir disposer d'une méthode d'analyse suffisamment sensible car les teneurs à doser sont généralement très faibles.

Ainsi, pour le laitier, on a choisi comme élément caractéristique le Manganèse, lequel a été dosé dans chaque fraction par absorption atomique.

Pour la détermination des aires massiques (surfaces spécifiques) particulières, on peut avoir recours soit à des relations plus ou moins empiriques basées sur la composition granulométrique (relation de Kilhstedt), soit à des relations fondées sur le rapport des broyabilités des différents composants (formules de Bombled) : l'accord trouvé entre les valeurs obtenues par ces différentes méthodes s'est révélé généralement satisfaisant.

Quando da moagem simultânea (o que é comum na indústria cimenteira) de uma mistura de clínquer e de outro componente ("filler", escória, pozolana, ...) para fabricação de cimentos compostos (CPJ das Normas Francesas, por exemplo), pode ser útil o conhecimento da distribuição granulométrica e das superfícies específicas individuais de cada um dos componentes. De fato, estas características podem exercer um papel importante sobre as propriedades das argamassas e dos concretos seja em estado fresco, seja endurecido.

Para materiais cristalizados, por exemplo a calcita dos "fillers" calcários, o método de análise granulométrica proposto resulta da conjunção da sedimentometria com pipeta de Andreasen e da dosagem dos componentes por difração de raio-X, nas frações granulares separadas; os resultados apresentados confirmam o interesse deste procedimento e o grau de exatidão esperado.

Este tipo de método pode ser estendido a materiais não cristalizados, com a condição de haver um elemento marcante num dos componentes, e de se poder contar com um método de análise suficientemente sensível, já que os teores a serem dosados geralmente são baixos.

Assim, para a escória, escolhemos como elemento característico o Magnésio, que foi dosado em cada fração por absorção atômica.

Para determinação das superfícies específicas individuais, podemos ter recursos seja com relações mais ou menos empíricas baseadas na composição granulométrica (relação de Kilhstedt), seja com relações baseadas nas relações das aptidões de moagem dos diferentes componentes (fórmulas de Bombled): a conformidade encontrada entre os valores obtidos por estes diferentes métodos revelou-se geralmente satisfatória.

1. INTRODUCTION

Le broyage simultané de deux matériaux de broyabilités différentes fournit un mélange dont la composition granulométrique et l'aire massique (surface spécifique) globales diffèrent évidemment de celles de chacune des constituants pris séparément.

Or, le cas d'un tel broyage simultané est habituel en cimenterie où l'on broie toujours le clinker avec une addition de gypse et, pour les ciments composés, avec des proportions variées d'ajouts divers, laitiers, cendres, pouzzolanes et plus récemment fillers généralement calcaires.

Comme un grand nombre des propriétés des ciments ou des bétons (réactivité, maniabilité, déformabilité, variations dimensionnelles ...) peuvent varier notablement en fonction des finesses particulières des divers constituants, il est utile d'essayer d'avoir une idée précise de la granulométrie ou de la surface de chacun.

Il y a plusieurs années, nous avions examiné ce problème uniquement sous l'angle des aires massiques et plutôt dans le cas des mélanges clinker-laitier. Dans cette étude, nous nous sommes attachés à étudier la répartition granulaire, le calcul des surfaces spécifiques particulières ayant surtout servi de moyens indirects de vérification.

2. PRINCIPE DE LA METHODE D'ANALYSE GRANULOMETRIQUE PROPOSEE

2.1. POSITION DU PROBLEME

La séparation des différentes phases d'un mélange après broyage simultané, par exemple par liqueurs denses, est non seulement très difficile, mais entachée de telles erreurs que les résultats sont généralement inutilisables.

Dans ces conditions, nous avons pensé qu'il était préférable d'inverser l'ordre des opérations et d'effectuer d'abord la séparation granulométrique sur le mélange en analysant ensuite les fractions séparées.

Nous avons ainsi cherché à coupler l'analyse granulométrique par sédimentation à la pipette d'Andréasen et l'analyse par une méthode suffisamment sensible, car les quantités prélevées peuvent être relativement faibles (< 100 mg) et d'analyser les constituants dans le prélèvement.

Pour des constituants cristallisés, nous avons choisi l'analyse par diffraction des rayons X et dans le cas contraire, c'est-à-dire si le matériau mélangé au clinker est amorphe ou vitreux (laitier par exemple) on a cherché une analyse par un élément marqueur peu présent dans les clinkers, manganèse par exemple dans les laitiers, l'analyse étant effectuée par absorption atomique ou par spectométrie plasma.

2.2. SEDIMENTATION A LA PIPETTE D'ANDREASEN

Le schéma de l'appareil utilisé au C.E.R.I.L.H., et ses dimensions, sont rappelés sur la figure n° 1. Rappelons le principe de l'essai :

La poudre étudiée est dispersée dans un liquide (pour les ciments généralement de l'éthanol) avec ou sans défloculant (Cl_2Ca avec l'alcool) et après une agitation prolongée on effectue des prélèvements à des temps convenablement choisis, écoulés à partir du temps initial correspondant au début du repos de la suspension.

Le rapport $\frac{C_i}{C_o}$ de la concentration trouvée au temps t_i à la concentration initiale C_o donne la proportion des grains, inférieurs à la dimension $\emptyset$ calculée pour cette durée par la loi de STOKES :

$$V = \frac{g}{18} \frac{\emptyset^2}{\eta_\theta} (\rho_s - \rho_l) = \frac{H}{t_i} \qquad (1)$$

H = Hauteur de chute

η_θ = Viscosité du liquide à la température θ de l'essai.

ρ_s et ρ_l = Masses volumiques du solide et du liquide de la suspension.

d'où :

$$\emptyset_{\mu m} = \frac{10000}{\sqrt{k}} \sqrt{\frac{H}{t_i}} \quad \text{avec } k = 54{,}5 \frac{\rho_s - \rho_l}{\eta_\theta} \qquad (2)$$

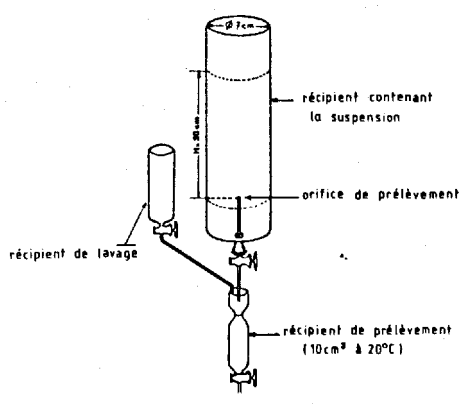

Fig1 . Pipette d'Andreasen CERILH .

La sédimentométrie à la pipette d'Andréasen se prête bien pour l'analyse granulométrique et les séparations dans l'intervalle 1-50 μm.

Le problème est, à ce stade, d'analyser dans chaque prélèvement la quantité de chacun des composants du mélange. Ces analyses ne sont pas faciles pour plusieurs raisons :

- d'abord la quantité prélevée, surtout vers les éléments fins, ne dépasse généralement pas quelques dizaines de mg.

- ensuite, les matériaux analysés peuvent contenir les mêmes éléments (clinker et laitier par exemple).

Pour la recherche de fillers calcaires l'analyse chimique est exclue et la faible quantité prélevée dans la sédimentation à la pipette classique interdit l'emploi de la thermogravimétrie, on a donc dû avoir recours au dosage de la calcite par diffraction des rayons X.

Ce procédé est malheureusement inutilisable pour des matériaux non cristallisés comme les laitiers, on a eu recours au dosage d'un élément marqueur comme le Mn .

3.1

2.3. GRANULOMETRIE DES CONSTITUANTS A PARTIR DES DOSAGES EFFECTUES DANS LES PRELEVEMENTS

Nous connaissons la concentration initiale en ciment dans la suspension et la teneur en ajout de ce ciment; l'analyse des prélèvements nous indique la proportion de chacune des phases dans le prélèvement pour un temps de sédimentation t_i donc pour une dimension de coupure connue $\emptyset_i$. Une simple opération nous permet de calculer, pour chaque composant du mélange, le taux de passant cumulé pour le diamètre équivalent $\emptyset_i$.

Si on appelle :

α = teneur en ajout du ciment (filler, laitier)
β = Concentration en ciment dans la pipette d'Andréasen (masse de ciment/volume liquide).
v = Volume de suspension prélevé à chaque temps.
a_i = Masse de solide prélevé au temps t_i.
$\emptyset_i$ = Dimension de coupure.
X_A = Teneur en ajout dans le prélèvement a_i.

On aboutit aux relations suivantes :

- Granulométrie de l'ajout (% $< \emptyset_i$)

$$\tau_a = \frac{X_a}{\alpha} \cdot \frac{a_i}{\beta v} \qquad (3)$$

- Granulométrie du clinker (% $< \emptyset_i$)

$$\tau_c = \frac{1 - X_a}{1 - \alpha} \cdot \frac{a_i}{\beta v} \qquad (4)$$

Ce sont ces formules qui seront appliquées quel que soit le mode de dosage de X_a dans le prélèvement.

3. COUPLAGE SEDIMENTATION/DIFFRACTION DES RAYONS X : APPLICATION AUX CIMENTS CONTENANT DES FILLERS

Les résultats de la sédimentation à la pipette d'Andréasen pour un ciment contenant 75 % de clinker et 25 % de filler calcaire sont groupés dans le tableau I ci-dessous :

Tableau I
(Pipette d'Andréasen)

N°	TEMPS DE SEDIMENTATION	$\emptyset$ (μ) DU FILLER	$\emptyset$ (μ) MOYEN	$\emptyset$ (μ) DU CLINKER	m (mg)	% PASSANT CUMULE
1	1'	59,8	55,7	54,1	76,7	68,4
2	2'	42,0	39,1	38,0	66,5	59,3
3	3'	34,0	31,7	30,8	60,1	53,6
4	5'	26,1	24,3	23,7	56,4	50,3
5	10'	18,1	16,9	16,4	45,9	40,9
6	30'	10,5	9,9	9,5	34,1	30,4
7	1 h	7,4	6,9	6,7	29,1	26,0
8	2 h	5,4	4,8	4,6	23,7	21,1
9	5 h	3,3	3,0	2,9	17,7	15,7
10	40 h	1,5	1,4	1,4	8,6	7,7
11	119 h	1,06	0,98	0,94	4,1	3,7

Des échantillons issus des prélèvements ont été analysés soit à l'aide d'une chambre photographique GUINIER équipée d'un porte échantillon spécial pour de très faibles masses, soit à l'aide d'un diffractomètre.

3.1. DIAGRAMMES A LA CHAMBRE GUINIER

Les micro-densimétrages de ces diagrammes mettent en évidence la variation des proportions relatives de calcaire et de clinker dans les différentes fractions : on peut noter que les tranches correspondant aux particules les plus fines sont très nettement enrichies en CO_3 Ca.

Les conditions d'obtention de ces diagrammes, non parfaitement reproduisibles, (épaisseur de l'échantillon, temps de pose, traitement photo, ...) ne permettent pas d'apprécier directement la proportion de calcaire ou de clinker présent dans un échantillon : Une même teneur en clinker et en calcaire dans deux échantillons différents peut donner des intensités (hauteurs) de raies différentes; mais les intensités relatives des raies des différentes phases sont conservées.

C'est donc l'intensité relative des raies des phases du clinker et de la calcite qui doit être comparée : pour une même intensité des raies de CO_3Ca, l'intensité des phases du clinker (C_3S et C_3A) diminue dans les fractions fines (Fig. 2).

Fig2. Diffraction des rayons X.

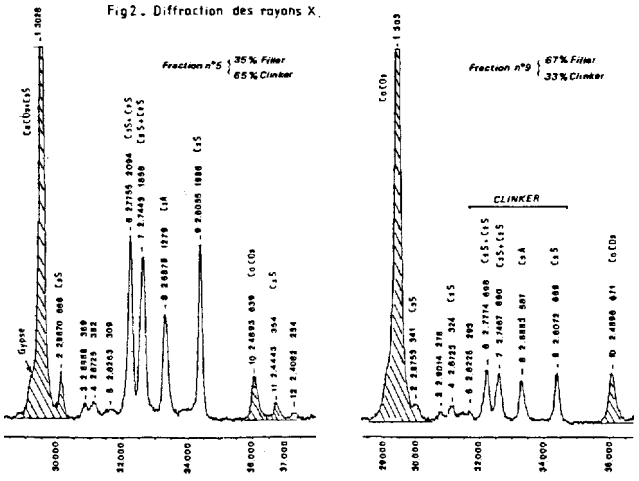

Dans d'autres cas, pour une intensité comparable des raies des phases du clinker, l'intensité des raies de CO_3Ca augmente nettement vers les fractions les plus fines.

Remarque : L'analyse des phases des différentes tranches granulométriques montre une variation de la composition de la fraction clinker : la teneur en C_3A par rapport au C_3S augmente dans les fractions fines; l'effet est visible sur les diffractogrammes des prélèvements n° 8 et 9; dans cette dernière fraction correspondant aux particules < 3 μm, la teneur en C_3A est de 17 % environ au lieu de 12 % sur l'ensemble du clinker.

3.2. ESSAI D'ANALYSE QUANTITATIVE

A titre de vérification de la méthode, des mesures précises d'intensité ont été effectuées sur les échantillons n° 1, 3, 5, 7, 8 et 9 du tableau I, à l'aide d'un diffractomètre SIEMENS muni d'un traitement numérique des données; les prélèvement 10 et 11 n'ont pu être analysés par cette technique en raison de trop faible quantité de matière. Les valeurs des intensités cumulées de raies sont indiquées dans le tableau II ci-après.

Tableau II.
(Mesures d'intensités D.R.X.)

FRACTION N°	1	3	5	7	8	9
Raies $CaCO_3$ + C_3S à 3,035 Å (n. d'impulsions = aire de la raie)	46 752	51 098	53 687	63 011	62 031	62 947
Raies du clinker C_3S + C_2S + C_3A dans le domaine 31,5 - 35 °	70 847	66 096	61 730	39 801	32 556	19 376
Raie de $CaCO_3$ (2,49 Å)	3 713	4 205	4 552	6 219	6 608	6 121
$\frac{I\ CaCO_3\ 2,49\ Å}{I\ clinker}$	0,052	0,064	0,074	0,156	0,203	0,316
$\frac{I(CaCO_3 + C_3S)\ 3,035\ Å}{I\ clinker}$	0,660	0,773	0,870	1,58	1,90	3,25
% $CaCO_3$	25	29	35	50	56	67
% Clinker	75	71	65	50	44	33

On peut noter la progression de la teneur en CO_3Ca dans les prélèvements successifs, c'est-à-dire en allant vers les éléments fins et a contrario la décroissance de la teneur en clinker. On peut noter que la proportion de CO_3Ca atteint 50 % dans la fraction n° 7 ($\varnothing \leqslant 7\,\mu m$) et dépasse ce chiffre dans les fractions plus fines (rappelons que la teneur initiale en calcaire est de 25 %).

Les proportions relatives de clinker et de CO_3Ca dans les différentes fractions ont été calculées à partir du principe fondamental de l'analyse par DRX. Le rapport des intensités des raies de deux phases présentées dans un mélange est proportionnel au rapport de concentration de ces deux phases.

Les six échantillons du tableau II servant de repères, il est possible d'estimer les portions relatives de calcaire et de clinker dans toutes les tranches, soit par interpolation (prélèvements n° 2, 4 et 6) soit par extrapolation (échantillons n° 10 et 11); c'est ce qui est résumé dans le tableau III suivant.

Tableau III
Proportions clinker/filler

FRACTION N°	1	2	3	4	5	6	7	8	9	10	11
Clinker	75	73	71	69	65	59	50	44	33	22	10
$CaCO_3$ (Filler)	25	27	29	31	35	41	50	56	67	78	90

3.3. GRANULOMETRIE DU FILLER CALCAIRE ET DU CLINKER COBROYES

Les résultats permettent de tracer la courbe de répartition granulométrique des deux composants connaissant celle du mélange. En appliquant les relations (3) et (4) données en 2.3 on obtient les résultats numériques corrigés dans le tableau IV et qui ont permis de tracer les courbes granulométriques de la figure n° 3 ci-après.

Tableau IV

ECHANTILLON i	1	2	3	4	5	6	7	8	9	10	11
Masse de filler au temps t_i	19,2	18,0	17,4	17,5	16,1	14,0	14,6	13,3	11,9	6,7	3,7
% filler passant	68,4	64,1	62,2	62,4	57,3	49,9	51,9	47,3	42,3	2	13,2
Diamètre équivalent (μm)	59,8	42,0	34,0	26,1	18,1	10,5	7,4	5,4	3,3	1,5	1,06
Masse de clinker au temps t_i	57,5	48,6	42,7	38,9	29,8	20,1	14,6	10,4	5,8	1,9	0,4
% clinker passant	68,4	57,7	50,7	46,3	35,5	23,9	17,3	12,4	6,9	2,2	0,5
Diamètre équivalent (μm)	54,1	38,0	30,8	23,7	16,4	9,5	6,7	4,6	2,9	1,4	0,94

Fig. 3.
Granulométrie du mélange et de chacun de ses deux constituants.

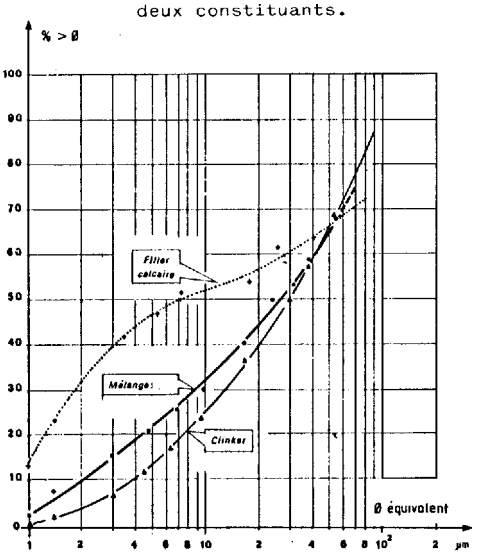

4. CAS D'AJOUT NON CRISTALLISE : APPLICATION AUX CIMENTS CONTENANT DU LAITIER

Comme il a été dit plus haut, c'est ici sur un procédé résultant du couplage de la sédimentométrie et de l'analyse d'un élément marqueur par absorption atomique que nous avons fondé cette deuxième partie de la méthode, la suite de l'exploitation des résultats restant inchangée.

4.1. ANALYSE DES PRELEVEMENTS PAR ABSORPTION ATOMIQUE

Le manganèse est un élément présent dans les laitiers en quantité non négligeable et ne figure qu'en très faible teneur dans les clinkers.

La quantité d'extrait sec provenant des prélèvements à la pipette est habituellement comprise entre 5 et 100 mg; comme la teneur en Mn des laitiers peut être l'ordre de 0,4 %, il en résulte que pour des ciments contenant 25 % de laitier, ce sont des proportions en moyenne quatre fois plus faibles qu'il faut généralement doser soit, en valeur absolue, entre 5 et 100 μg.

La raie d'absorption du Mn est située à 279,5 nm; la limite de détection est de l'ordre de 0,003 μg par ml de solution à analyser. Cet élément est néanmoins assez sensible aux interactions chimiques en absorption atomique.

La courbe d'étalonnage de l'appareil utilisé dans ces essais est reportée sur la figure n° 4 ci-dessous.

Fig. 4.
Etalonnage du Dosage du Mn par absorption atomique.

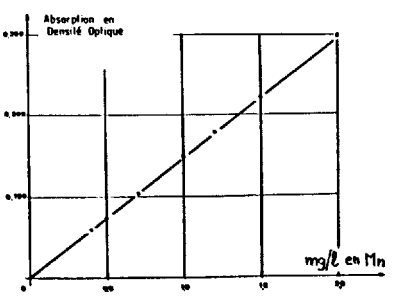

4.2. DETERMINATION DE X_a

On commence par doser le Mn respectivement dans le laitier et dans le clinker seul soit λ et γ.
On dose ensuite le Mn de chaque prélèvement, la mise en solution étant faite par attaque HCL puis filtrage (une addition de lanthane a été faite pour atténuer l'effet de matrice et les interactions entre éléments).

A partir du dosage en Mn obtenu, un calcul simple aboutit à la relation suivante pour les teneurs en laitier et en clinker du prélèvement considéré :

$$X_a = \frac{\tau_i - \gamma}{\lambda - \gamma} \; 100 \qquad (5)$$

$$X_c = (1 - X_a)\; 100 \qquad (6)$$

avec :
τ_i (%) = teneur totale en Mn dosée dans le prélèvement effectué au temps t_i.
λ (%) = teneur en Mn du laitier seul.
γ (%) = teneur en Mn du clinker seul.

4.3. APPLICATION

Un mélange contenant 25 % de laitier et 75 % de clinker a été cobroyé et soumis à la séparation granulométrique par sédimentation.

Par ailleurs, la teneur en Mn des composants était la suivante :

- laitier : = 0,423 %
- clinker : = 0,030 %

Le tableau V résume les résultats obtenus pour les différents prélèvements.

Tableau V
Teneur en laitier des prélèvements

N° prélèvement	1	2	3	4	5	6	7	8	9
$\emptyset_L$ (µm)	57,5	40,2	33,0	25,5	17,5	10,5	6,8	4,2	1,5
% Mn τ_i (%)	0,120	0,117	0,108	0,107	0,106	0,102	0,094	0,090	0,068
X_L (%)	22,9	22,1	19,8	19,6	19,3	18,3	16,3	15,3	9,7
$\emptyset_c$ (µm)	54,5	38,5	31,2	23,6	17,0	9,5	6,5	3,7	1,3
X_c	77,1	77,9	80,2	80,4	80,7	81,7	83,7	84,7	90,3

Toutes les valeurs relatives au laitier ont été reportées sur le graphique de la figure n° 5 ci-contre.

En appliquant les relations (3) et (4) on obtient les valeurs du tableau VI.

Tableau VI.
Répartition granulométrique.

	N° prélèvement	1	2	3	4	5	6	7	8	9
Mélange	$\emptyset_m$	55,8	39,2	31,8	24,4	17,1	9,8	6,6	3,9	1,4
	% < $\emptyset_m$	84,5	74,4	67,4	60,4	51,2	39,8	27,6	16,2	3,5
Laitier	$\emptyset_L$	57,5	40,2	33,0	22,5	17,5	10,5	6,8	4,2	1,5
	% < $\emptyset_L$	77,4	65,9	53,5	47,3	39,6	29,2	18,0	9,9	1,3
Clinker	$\emptyset_c$	54,5	38,5	31,2	23,6	17,0	9,5	6,5	3,7	1,3
	% < $\emptyset_c$	86,9	77,2	72,0	64,7	55,1	43,3	30,8	18,3	4,2

Fig. 5. Teneurs en Mn et en laitier suivant la granulométrie.

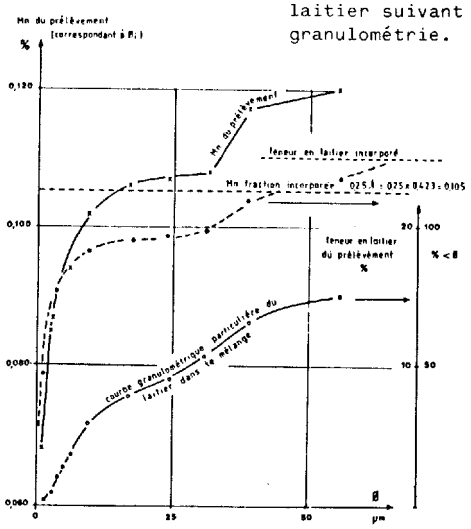

Les valeurs du tableau VI ont permis de tracer les courbes granulométriques de la figure n° 6 : on peut voir la nette différence imputable à l'écart des broyabilités; cette différence se retrouve aussi dans les aires massiques que l'on peut calculer.

Fig. 6. Répartitions granulométriques particulières des constituants cobroyés.

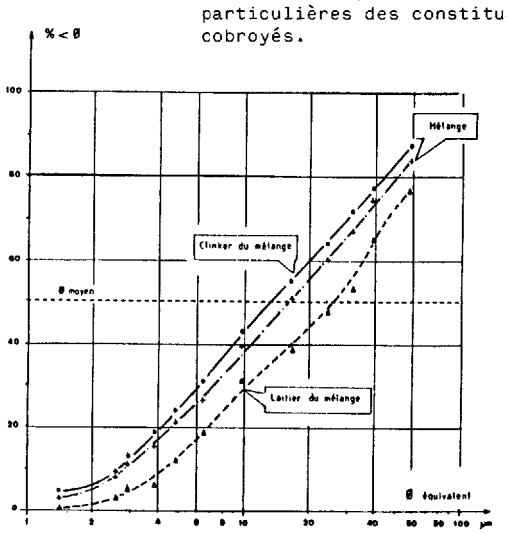

5. CALCUL DES AIRES MASSIQUES PARTICULIERES DES COMPOSANTS DES MELANGES COBROYES

Rappelons que l'on peut calculer l'aire massique particulière de chaque composant, soit à partir d'un point caractéristique de la courbe granulométrique (relation de Kilhstedt par exemple) soit à partir de la surface globale et du rapport des broyabilités (formules de Bombled).

5.1. DETERMINATIONS A PARTIR DE LA COURBE GRANULOMETRIQUE

Un certain nombre de relations permettent de calculer une aire massique approchée à partir d'une courbe granulométrique (ou d'un point

caractéristique de celle-ci). Nous avons regroupé dans le tableau VII quelques formules pouvant être utilisées, avec leurs coefficients, ainsi que les aires massiques particulières calculées pour les deux constituants du ciment contenant 25 % de filler calcaire étudié en 3.3.

Rappelons quelques caractéristiques de ce ciment :

- Aire massique globale Blaine : $S_T = 4\ 200\ cm^2 g^{-1}$.
- Teneur en filler calcaire : $\alpha = 0{,}25$
- Broyabilité du calcaire : B_F 160 $cm^2 j^{-1}$
- Broyabilité du clinker : B_E 70 $cm^2 j^{-1}$

Tableau VII

Méthodes		Relations appliquées	Valeurs des constantes et des coefficients adoptées (par le CPJ étudié)	Aire massique calculée (cas du CPJ de la fig. n°3) cm²/g Filler (et gypse)	Clinker
Calculs à partir de la granulométrie (courbes figure n° 3)	Découpage de la courbe granulométrique et somme des aires élémentaires calculées	$S = \frac{k}{\rho} \Sigma \frac{x_i}{\theta_i}$	k théorique ~6* (pratique ~7)	8 100	2 900
	Relation empirique pour les ciments (Vénuat)**	$S = k' x_7$	$k' \simeq 110$ x_7 étant la fraction<7 µm	10 500	2 100
	Relation de Kilstedt en minéralurgie*	$S = \frac{K}{\rho\sqrt{\theta_r}}$	pour les ciments* K ≈ 500 si $\theta_r = \theta_{50}$ (ou K ≈ 775) (si $\theta_r = \theta_{80}$)	7 140	2 890
Calculs à partir de la surface globale et de la broyabilité	Formules de Bombled** Calcul à partir de la surface globale S_T et du rapport des broyabilités	$S_F = \frac{S_T}{\alpha+(1-\alpha)\frac{B_C}{B_F}}$ $S_C = a\, S_T \frac{B_C}{B_F}$	B_C = 70 cm²/joule B_F = 160 cm²/joule α_F = 0,25 S_T = 4200 cm²/g	7 370	3 190

* Publication technique CERILH n° 161

** Publication technique CERILH n° 162

ρ: masse volumique du produit concerné.

x_i: pourcentage pondéral de grains ayant pour diamètre θ_i.

5.2. DETERMINATION A PARTIR DU RAPPORT DES BROYABILITES (Formules de Bombled)

Dans la publication technique CERILH déjà citée, nous avons donné, pour des mélanges binaires voire polyphasés, des relations pour calculer les aires massiques particulières des constituants connaissant l'aire massique globale du mélange S_T, le rapport des broyabilités des constituants B_1 et B_2 et la proportion α et $1-\alpha$ de chacun dans le mélange binaire :

$$S_1 = \frac{S_T}{\alpha + (1-\alpha)\frac{B_2}{B_1}} = a\, S_T \qquad (7)$$

$$S_2 = a \frac{B_2}{B_1} S_T = b\, S_T \qquad (8)$$

La figure n° 7 donne, pour deux rapports de broyabilité, les valeurs des coefficients a et b en fonction de α.

Nous avons, par conséquent, ajouté les valeurs calculées par cette méthode à celles du tableau VII obtenues à partir de la granulométrie.

Par ailleurs, dans le tableau VIII, ci-après, nous regroupons les résultats obtenus avec le mélange clinker-laitier étudié en 4.3.

Fig.7. Coefficient a et b des formules de Bombled.

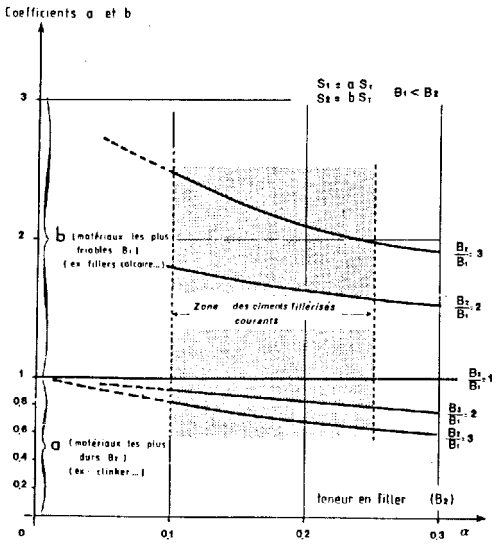

Tableau VIII

Méthodes	Relations appliquées	Valeurs des constantes adoptées	Aires massiques particulières clinker	laitier
A partir des courbes granulométriques (Kilstedt)	Relation de Kilstedt (minéralurgie) $S = \frac{K}{\rho\sqrt{\theta_r}}$	pour les ciments K ≈ 500 si $\theta_r = \theta_{50}$ *	4200	3230
A partir du rapport des broyabilités (Bombled)	$S_C = \frac{S_T}{\alpha+(1-\alpha)\frac{B_L}{B_C}} = a\, S_T$ $S_L = a\, S_T \frac{B_L}{B_C}$	B_C = 70 cm2/J B_L = 55 " α_L = 0,25 " S_T = 3800 cm2/g ****	4050	3150

* relevées sur les courbes de la figure n° 5

**** cas du ciment étudié ci-dessus

La concordance des résultats est très bonne, ce qui apparaît comme une confirmation indirecte de la validité des granulomètries déterminées par la méthode proposée.

A part la deuxième relation du tableau VII, au demeurant très empirique, on peut noter une excellente concordance entre tous les résultats obtenus.

A titre d'exemple, et pour fixer les idées, nous donnons dans le tableau IX ci-après les aires massiques calculées pour le filler calcaire et le clinker dans le cas d'un rapport de broyabilité $\frac{B_F}{B_C} = 2$ (valeur assez fréquente pour beaucoup de roches calcaires utilisées comme filler en cimenterie) et pour une aire massique globale de 4 000 $cm^2 g^{-1}$, valeur proche également de celle de ce type de ciment, et ceci pour différentes teneurs en filler.

Tableau IX

$\frac{B_F}{B_c} = 2$						
	Clinker	0,90	0,85	0,80	0,75	0,70
	Filler	0,10	0,15	0,20	0,25	0,30
aires massiques en $cm^2 g^{-1}$	Clinker S_c	3 640	3 480	3 330	3 200	3 080
	Filler* S_F	7 280	6 960	6 640	6 400	6 150

*y compris gypse

Notons que pour le ciment fillérisé étudié en 3.3., le clinker peut n'être broyé qu'aux trois quarts de la surface et le filler presque au double de l'aire massique mesurée globalement sur le ciment.

Dans le cas d'un calcaire très friable (pour fixer les idées $B_F \simeq 300$ $cm^2 j^{-1}$) et d'un clinker très dur ($B \simeq 65$ $cm^2 j^{-1}$) et pour une teneur en filler ne dépassant pas 15 % on trouverait pour S_F des valeurs voisines de 12 000 $cm^2 g^{-1}$ et seulement 2 500 $cm^2 g^{-1}$ pour la partie clinker : Ceci peut présenter évidemment des conséquences nombreuses sur les propriétés de ces ciments (réactivité, maniabilité, variations dimentionnelles).

6. PRECISION DE LA METHODE

On peut admettre, en simplifiant que l'erreur commise sur une détermination est la somme de celle commise en sédimentométrie et de celle résultant de l'analyse des prélèvements.

Fig. 8. Pipette d'Andréasen.
Relation entre la dispertion des résultats et la dimension des grains.

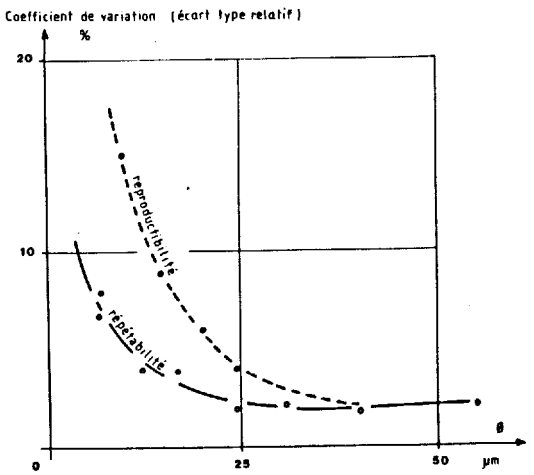

Pour la sédimentométrie, la précision varie avec la dimension analysée ; les courbes de la figure n° 8 illustrent ce fait d'une part en répétabilité au sein d'un même laboratoire et d'autre part en reproductibilité par les moyennes des valeurs obtenues sur une dizaine d'années dans les campagnes d'essais interlaboratoires CERILH; On voit que le coefficient de variation peut évoluer entre $\simeq 1$ et 20 % quand la dimension des grains analysés varie de 50 à 2 μm. En absorption atomique, on peut calculer en répétabilité des coefficients de variation d'environ 0,1 %; elles seraient de l'ordre de 0,5 à 3 % en reproductibilité.
Pour ce qui est de la diffraction des rayons X, on admet des coefficients de variation voisins de 5 % avec les moyens actuels.

7. CONCLUSION

L'analyse granulométrique des composants plus ou moins cristallisés grâce au couplage de la sédimentométrie à la pipette d'Andréasen et l'analyse des phases par diffraction des rayons X a permis de résoudre dans ce domaine relativement facilement le problème ardu de la connaissance des finesses particulières des composants d'un mélange cobroyé.

L'extension aux matériaux non cristallisés, dans le cas où l'on peut trouver un élément marqueur présent quasi uniquement dans l'un des composants, devrait permettre, grâce aux couplages avec la spectrométrie plasma ou l'absorption atomique, de résoudre la plupart des problèmes; resterait à essayer l'application à un grand éventail de matériaux cobroyés.

Le calcul des aires massiques particulières soit à partir du rapport des broyabilités soit à partir de la répartition granulométrique a donné des résultats suffisamment concordants pour fournir une vérification indirecte de l'exactitude probable des courbes granulométriques trouvées.

8. BIBLIOGRAPHIE SOMMAIRE

- J.P. BOMBLED — Etude du broyage de mélanges clinker laitier. RMC n° 593 - février 1965. Publication technique CERILH n° 162.

- J.P. BOMBLED — Mesures de finesses dans l'industrie des liants hydrauliques. RMC n°s 628 et 629, janvier et février 1968. Publication CERILH n° 191.

- B. MORTUREUX, H. HORNAIN, M. REGOURD — Liaison pâte de ciment-filler dans les ciments composés. Colloque International R.I.L.E.M. Liaison pâtes de ciment-Matériaux associés. Novembre 1982, Toulouse (FRANCE)

- M. PINTA — Spectrométrie d'absorption atomique. Masson Ed. 1971.

R. DRON - LABORATOIRE CENTRAL DES PONTS ET CHAUSSEES
58, Bd Lefebvre - 75015 PARIS - FRANCE

STRUCTURE ET REACTIVITE DU LAITIER GRANULE

STRUCTURE AND REACTIVITY OF GLASSY SLAGS

RESUME: La structure du laitier vitreux résulte du figeage, au moment de la trempe, de la structure du laitier fondu. Celle-ci peut être décrite par dénombrement des espèces acido-basiques de la silice.

Les concepts de l'acido-basicité, appliqués aux silicates liquides du système CaO-MgO $-Al_2O_3-SiO_2$, ont permis de faire ce dénombrement en fonction de la composition et le niveau de basicité du milieu a pu être déterminé expérimentalement sur des verres synthétiques par exploitation de la spectrométrie Raman.

La silice se comporte comme un acide tétrafonctionnel, la chaux et la magnésie comme des bases fortes, et l'alumine comme une base faible, dans le domaine de composition des laitiers de hauts fourneaux.

La réactivité hydraulique des laitiers peut être mesurée par détermination de leur solubilité dans une solution de soude à pH 12,6. L'étude sur verres synthétiques montre que cette solubilité varie proportionnellement au rapport $\frac{CaO.Al_2O_3}{(SiO_2+Al_2O_3)^2}$ et l'étude sur laitiers industriels qu'elle est corrélée de façon satisfaisante avec la résistance mécanique de mortiers à base de laitier moulu et de chaux.

A estrutura da escória vítrea é resultado da fragmentação, no momento da têmpera, da estrutura da escória fundida. Isto pode ser descrito como classificação das espécies ácido-básicas da sílica.

Os conceitos de ácido-basicidade, aplicados aos silicatos líquidos do sistema CaO-MgO $-Al_2O_3-SiO_2$, permitiram fazer-se esta classificação em função da composição, e o nível de basicidade do meio pôde ser determinado experimentalmente em vidros sintéticos com utilização de espectrometria Raman.

A sílica se comporta como um ácido tetrafuncional, a cal e a magnésia como bases fortes, e a alumina como uma base fraca, no campo de composição das escórias de altos fornos.

A reatividade hidráulica das escórias pode ser medida por determinação de sua solubilidade em uma solução de soda com pH de 12,6. O estudo dos vidros sintéticos mostra que esta solubilidade varia proporcionalmente em relação a $\frac{CaO.Al_2O_3}{(SiO_2+Al_2O_3)^2}$ e o estudo das escórias industriais mostra que a solubilidade está correlacionada de fôrma satisfatória com a resistência mecânica das argamassas à base de escória moída e cal.

INTRODUCTION

L'intervention d'un facteur structural dans la manifestation du pouvoir hydraulique du laitier s'impose à l'esprit par une évidence triviale :
- à l'état vitreux, le laitier est réactif et donne naissance à des composés hydratés doués de propriétés liantes,
- à l'état cristallisé, il est inerte.

Il ne fait donc aucun doute que cette différence de comportement est étroitement liée à l'existence, à l'état solide, de deux structures possibles, l'une périodique suivant les règles de la cristallographie l'autre caractérisée par l'absence d'ordre à longue distance, et donc de réseau cristallin, ce qui n'exclut pas un ordre local contrôlé par la compensation des charges électriques et la coordinence des divers éléments.

La grande similitude des spectres infra-rouge ou Raman des verres silicatés et de ceux du liquide qui leur a donné naissance par refroidissement suggère que la structure d'un verre est une image de la configuration instantanée du liquide |1|. La connaissance de l'état vitreux passe donc par la caractérisation de la structure des silicates fondus.

LE PROBLEME DE LA STRUCTURE DES SILICATES LIQUIDES

Les silicates fondus ont un caractère ionique qui est attesté par leur conductivité électrique élevée. Le bilan des charges électriques montre que dans un binaire dont le rapport molaire CaO/SiO_2 est inférieur à 2, la charge négative par atome de silicium est inférieure à 4 et que par conséquent, l'existence exclusive d'ions monomères SiO_4^{4-} ne peut être envisagée. Cette remarque a été à l'origine de deux démarches théoriques mettant en jeu des équilibres entre diverses entités résultant de la polymérisation de l'anion orthosilicate.

La première est celle de Toop et Samis |2| qui proposèrent de considérer l'équilibre entre trois formes de l'atome d'oxygène, selon qu'il porte 2 charges électriques, (ion libre O^{2-}) ou une seule (oxygène non pontant O^-), ou aucune, étant lié à deux atomes de silicium (oxygène pontant O°) :

$$O^{2-} + O^\circ \rightleftharpoons 2\ O^-$$

La seconde théorie est due à Masson |3| et fait intervenir la polymérisation de l'ion SiO_4^{4-} par des équilibres de la forme :

$$SiO_4^{4-} + SiO_4^{4-} \rightleftharpoons Si_2O_7^{6-} + O^{2-}$$

$$Si_2O_7^{6} + SiO_4^{4-} \rightleftharpoons Si_3O_{10}^{8-} + O^{2-}$$

etc.

L'application de la loi d'action de masse à ces équilibres permet de calculer la répartition des espèces en fonction de la composition, qui apparait comme le facteur déterminant.

L'un et l'autre de ces modèles reposent en fait sur une analyse statistique des configurations basée sur des hypothèses de probabilité ne tenant pas compte des contraintes énergétiques. Ni l'un ni l'autre ne sont d'autre part transposables aux systèmes à plus de deux constituants. Leur discussion détaillée nous a amené à proposer une approche plus générale |4|, s'appuyant sur les concepts de l'acido-basicité, et faisant intervenir la notion d'espèces acido-basiques conjuguées et celle de pO^{2-}, qui est la transposition du pH dans les milieux aprotoniques.

THEORIE ACIDE-BASE DES SILICATES FONDUS

On considère la silice comme un polyacide tétrafonctionnel, dont les espèces successives sont :

$$SiO_2,\ SiO_{2,5}^{-},\ SiO_3^{2-},\ SiO_{3,5}^{3-} \text{ et } SiO_4^{4-},$$

qu'on désigne par les symboles

X , Y , E , Z et S

et qui représentent les entités présentes dans le réseau anionique formé par les enchainements d'atomes de silicium et d'oxygène

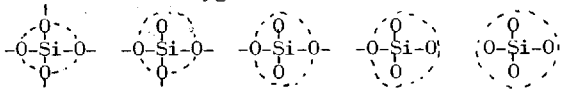

L'écriture de la loi d'action de masse relative aux quatre équilibres acide-base :

$$X + 1/2\ O^{2-} \rightleftharpoons Y \qquad E + 1/2\ O^{2-} \rightleftharpoons Z$$

$$Y + 1/2\ O^{2-} \rightleftharpoons E \qquad Z + 1/2\ O^{2-} \rightleftharpoons S$$

introduit quatre constantes K_1, K_2, K_3 et K_4 dont la connaissance permet de calculer les concentrations de chaque espèce pour une composition binaire donnée, compte tenu des bilans de masse et de charge électrique.

La résolution du système introduit la quantité F telle que

$$F = \sqrt{O^{2-} \cdot O^\circ}$$

dans laquelle O^{2-} est le nombre d'ions oxygènes libres et O° le nombre d'oxygènes pontants.

Le logarithme de F a les propriétés du potentiel de basicité pO^{2-} ou encore de la fonction H_o de Hammet telle que

$$H_o = pK_a + \log \frac{B}{A}$$

où A et B sont les concentrations de deux espèces acido-basiques conjuguées.

L'exploitation des données d'activité disponibles dans la littérature montre que cette théorie rend compte de l'expérience à condition de choisir les 4 constantes en progression géométrique de raison 4 (pK_a en progression arithmétique de pas 0,6).

La fonction H_o fixant les balances acido-basiques de tout couple présent dans le milieu, la théorie est applicable aux systèmes multi-constituants, et en particulier au laitier fondu, qui contient, outre la silice et la chaux, de l'alumine et de la magnésie.

UTILISATION DES DONNEES SPECTRALES

Comme toute échelle de potentiel chimique, la fonction H_o de Hammet n'est définie qu'à une constante additive près. On peut s'affranchir de cette constante en choisissant un état de référence correspondant par convention à

$$H_o = pK_a + \log \frac{B}{A} = 0$$

La fonction d'acidité s'écrit alors :

$$H_o = \log \frac{B}{A} - \log\left(\frac{B}{A}\right)_{ref} = \log \frac{B}{A} \Big/ \left(\frac{B}{A}\right)_{ref}$$

On peut donc avoir une mesure de H_o si l'on dispose d'une méthode permettant de connaître la valeur relative des rapports de concentration d'espèces acido-basiques conjuguées. C'est le cas de la spectroscopie Raman.

ETUDE DES VERRES DE LA FAMILLE DES LAITIERS PAR SPECTROSCOPIE RAMAN

Le massif haute fréquence des spectres Raman des verres silicatés est la résultante de cinq bandes de profil gaussien caractéristiques des cinq types possibles d'environnement oxygène des atomes de silicium. Elles correspondent donc très exactement aux cinq espèces acido-basiques que nous avons définies. L'intensité de ces bandes est, pour un spectre donné, proportionnelle aux abondances des dites espèces avec un coefficient de réponse variable selon l'espèce, et non accessible en valeur absolue. D'un spectre à l'autre, on ne peut déterminer que la valeur relative des rapports d'intensité, et donc d'abondance, mais il se trouve que c'est ce double ratio qui intervient dans la définition de la fonction d'acidité. La seule difficulté pratique est la décomposition du massif en gaussiennes, ce travail étant facilité par le fait que les bandes élémentaires sont stables en position et en largeur.

L'étude des verres de la famille des laitiers a été effectuée sur des verres quaternaires synthétiques $CaO-MgO-Al_2O_3-SiO_2$ obtenus par fusion à 1600 °C de mélanges d'oxydes, suivie d'une trempe à l'air de perles centimétriques, dans lesquelles sont taillés les cubes nécessaires à l'obtention des spectres Raman. La rapidité du refroidissement nous autorise à penser que la structure du verre est proche de celdu verre originel.

Les spectres ont été obtenus grâce à l'obligeance de B. Piriou sur un spectromètre Raman à excitation laser à double monochromateur pHO CODERG, sous polarisation VV. La bande haute fréquence est décomposée en gaussiennes élémentaires par ajustements successifs et la grandeur H_o est déterminée par les rapports des intensités des bandes à 980 et 910 cm^{-1}, caractéristiques des deux espèces prépondérantes, E et Z, c'est à dire SiO_5^{2-} et $SiO_{3,5}^{2-}$, par référence au rapport correspondant dans le verre de métasilicate de calcium CS.

On a testé 18 compositions regroupées en 4 séries dont une série ternaire sans magnésium, de stoechiométrie Ca = Al + Si, et la série correspondante avec substitution de 1 atome de magnésium à 1 atome de calcium (par exemple C_7AS_5 et C_6MAS_5). Deux autres séries font varier le rapport Ca+Mg/Al+Si de part et d'autre de 1. La série pseudo-binaire CS-CMS avait été préalablement explorée par P. Mc Millan et B. Piriou [5].

RESULTATS EXPERIMENTAUX

On donne à titre d'exemple Fig.1 les spectres Raman des verres de la série $C_{n+1}MAS_n$ qui sont caractéristiques de l'évolution du profil en fonction de la composition. La comparaison de ces spectres avec ceux de la série correspondante $C_{n+2}AS_n$ montre qu'ils sont superposables pour une même valeur de n. Cela signifie que dans le verre, et par conséquent dans le produit fondu, le calcium et le magnésium jouent le même rôle modificateur du réseau silicaté. On peut donc représenter les résultats dans un diagramme pseudo-ternaire dans lequel la chaux et la magnésie sont confondues.

Le calcul de la grandeur H_o, conduit comme il est dit plus haut, donne l'évolution en fonction de la composition, sa valeur croissant de façon régulière dans le champ étudié (Fig. 2).

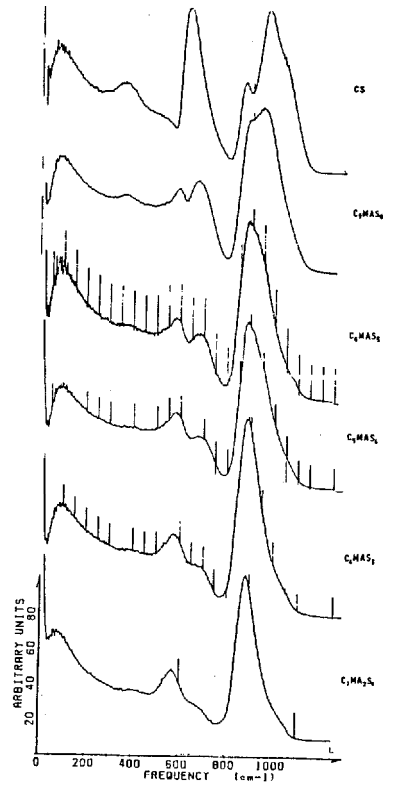

Fig. 1

Spectres Raman des verres Ca+Mg = Al+Si

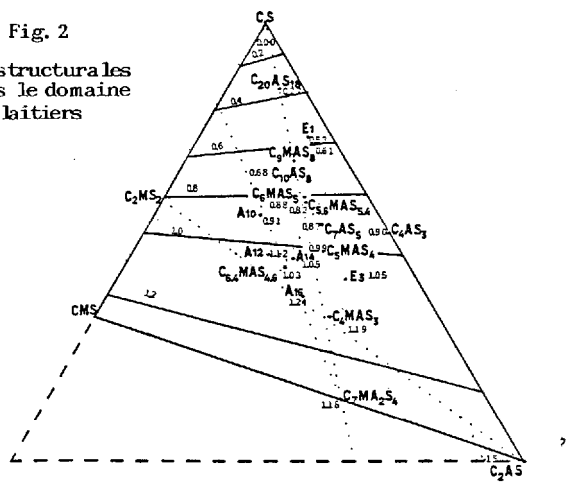

Fig. 2

Isostructurales dans le domaine des laitiers

Les lignes d'égales valeurs de H_o sont des isostructurales puisqu'elles correspondent à une même répartition des différentes espèces silicatées. Le réseau qu'elles forment a une configuration rayonnante autour d'un pôle situé à gauche de la figure au niveau de C_2MS_2. Leur inclinaison conduit à attribuer à l'aluminium un caractère cationique, l'espèce prépondérante dans le domaine exploré étant AlO^+. Les espèces anioniques du type AlO_2^- ne peuvent apparaitre qu'après neutralisation des quatre acidités potentielles de la silice, donc en milieu très basique où la silice est entièrement sous forme SiO_4^{4-}.

CONCLUSION DE L'ETUDE STRUCTURALE

La structure du laitier vitreux est caractérisée par un sous-réseau anionique silicaté formé d'enchainements d'éléments E (SiO_3^{2-}) compris entre des bifurcations tridirectionnelles Y ($SiO_{2,5}^{-}$) et des terminaisons Z ($SiO_{3,5}^{-}$). La liaison entre les atomes de silicium et les atomes d'oxygène pontants ou non pontants a un caractère covalent.

Les ions calcium, magnésium et aluminium (AlO^+) forment un sous-réseau cationique sans liaisons internes imbriqué au précédent par l'attraction coulombienne.

L'ensemble des deux sous-réseaux forme le réseau vitreux dont les noeuds sont occupés par les atomes de silicium, de calcium, de magnésium et d'aluminium reliés entre eux par des atomes d'oxygènes par l'intermédiaire, selon les cas, de liaisons covalentes fortes, ou électrovalentes de moindre énergie, qui constituent des points faibles du réseau.

ETUDE DE LA RÉACTIVITE DES VERRES DE LA FAMILLE DES LAITIERS

L'hydratation du laitier vitreux a lieu suivant un mécanisme de dissolution-précipitation. Elle ne se produit que si la solution interstitielle est basique, ce qui indique clairement que l'attaque est hydroxylique.

L'énergie libre du processus global dépend de la solubilité relative des réactifs (produit anhydre et activants) et des produits de la réaction, c'est à dire des hydrates. Plus précisément, elle est de la forme:

$$\Delta G^\circ = RT \text{ Log } \frac{P_2}{P_1}$$

dans laquelle P_1 et P_2 sont les produits de solubilité étendus à l'ensemble des composés de départ, dont le laitier anhydre, et à l'ensemble des composés finaux, avec des exposants correspondant à la stoechiométrie de la réaction.

Les composés hydratés qui se forment par hydratation du laitier (C-S-H, aluminate tétracalcique, ettringite) de même que les activants (hydroxyde de calcium, gypse) ont une nature invariable et par conséquent un produit de solubilité défini et indépendant du laitier. Il s'ensuit que l'énergie libre de dissolution-précipitation ne dépend que de la solubilité de la phase anhydre, le laitier en l'occurrence.

Les différences de réactivité entre divers laitiers peuvent donc être appréciées par la mesure de leur solubilité, à condition de fixer le pH de la phase aqueuse. Dans la pratique, sa valeur est déterminée par l'équilibre de dissolution de l'hydroxyde de calcium et est proche de 12,6. Par ailleurs, pour atteindre la solubilité vraie, il importe de se placer dans des conditions telles que la précipitation des hydrates ne soit pas amorcée. Cet impératif interdit l'emploi d'une solution saturée de chaux comme liqueur d'attaque, la haute concentration en ions calcium entrainant une précipitation quasi immédiate des ions silicate à l'état de C-S-H. C'est ce qui nous a amené à choisir comme milieu une solution de soude 0,04 N, qui a le même pH que l'eau de chaux saturée. Une étude cinétique préalable nous a permis de fixer les conditions opératoires de telle façon que l'équilibre de dissolution soit pratiquement atteint et que la précipitation ne soit pas amorcée.

On opère de la façon suivante :

On pèse 2,5 g de laitier broyé à la finesse de 3000 cm^2/g environ, qu'on place dans un erlenmeyer en acier inox On ajoute 250 ml d'une solution de soude 0,04 N, on ferme et on agite magnétiquement la suspension pendant 10 minutes. On laisse reposer 5 minutes et on filtre sur filtre millipore. On conserve la solution pour analyse et on répète l'opération 6 fois de suite sur le même échantillon. Les solutions sont analysées séparément de façon à tester la reproductibilité qui est excellente. Les moyennes sont calculées pour chaque échantillon en éliminant les déterminations aberrantes éventuelles.

Les essais ont été pratiqués sur l'ensemble des verres synthétiques préparés pour l'étude par spectroscopie Raman.

RESULTATS

Pour un verre donné, la dissolution est quasi congruente en ce qui concerne la chaux, l'alumine et la silice, c'est à dire que leur répartition pondérale dans le verre et dans la solution sont voisines, avec toutefois un léger enrichissement relatif de la solution en alumine pour les verres ternaires C-A-S et un léger appauvrissement pour les verres quaternaires C-M-A-S. Par contre, la magnésie a un taux de solubilisation systématiquement nul.

La solubilité, chiffrée par la somme des concentrations en CaO, Al_2O_3 et SiO_2 en solution, varie de façon très importante avec la composition du verre. L'examen détaillé des résultats expérimentaux [4] montre qu'elle dépend de trois facteurs, qui sont les rapports molaires des constituants du verre :

$$\frac{Al}{Al+Si} \qquad \frac{Ca}{Ca+Mg} \qquad \frac{Ca+Mg}{Al+Si}$$

dont le produit est :

$$R = \frac{Al.Ca}{(Al+Si)^2}$$

ce rapport variant, dans notre expérimentation, conduite sur 18 compositions, de 0 à 0,5.

On constate que la solubilité varie de façon pratiquement proportionnelle à R (Fig. 3).

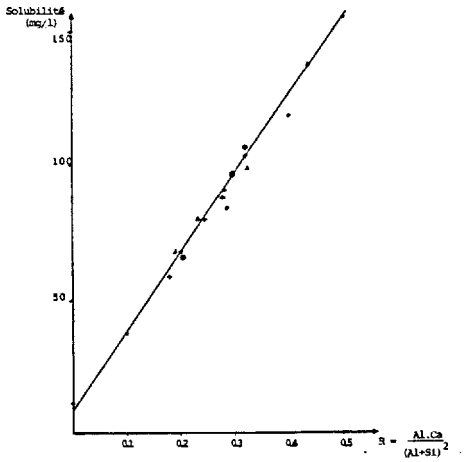

Fig. 3

Solubilité des verres S = f (R)

Compte tenu du fait que les masses moléculaires de CaO, SiO_2 et 1/2 Al_2O_3 sont voisines, une bonne corrélation est également obtenue si l'on prend le rapport massique

$$R' = \frac{Al_2O_3.CaO}{(Al_2O_3+SiO_2)^2}$$

dans lequel CaO, Al_2O_3 et SiO_2 sont les teneurs pondérales des trois oxydes dans le laitier.

MECANISME DE L'ATTAQUE HYDROXYLIQUE.

La forme de l'expression de la solubilité des verres montre que la réactivité du laitier est déterminée par l'abondance des sites cationiques AlO^+, qui constituent des centres d'affinité pour les solutions basiques, lorsqu'ils sont dans un environnement d'ions Ca^{2+}.

On peut proposer le mécanisme suivant pour la propagation de l'attaque :

A l'interface verre-solution, ces sites subissent une attaque hydroxylique et l'aluminium est solubilisé sous forme d'un ion $AlO_4H_4^-$.

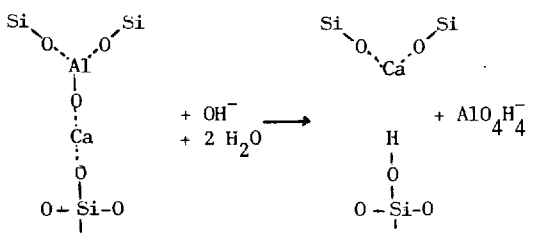

Cette élimination induit un site acide Si-OH qui est immédiatement ionisé à l'état de Si-O$^-$, dans lequel la charge négative n'est pas compensée. Si ce silicium appartient à une terminaison de chaine (espèce Z), il tend à passer en solution sous la forme $SiO_4H_2^{2-}$, ce qui provoque un déséquilibre de sens contraire et par suite le passage en solution d'un ion Ca^{2+}, et ainsi de suite. Cette solubilisation alternée des ions silicate et calcium est possible tant que la solution n'est pas saturée en ces espèces et que les sites silicium concernés constituent des terminaisons de chaines, qui sont ainsi progressivement amputées. L'attaque s'arrête quand elle arrive à un élément Y de bifurcation de chaines.

Les ions Mg^{2+} ne constituent pas, comme les ions Ca^{2+}, des éléments de propagation, car au moment du déséquilibre de charge, ils fixent un ion OH^- au lieu de passer en solution.

CONCLUSION

La réactivité des laitiers vitreux est due à leur solubilité dans les solutions basiques, très supérieure à celle des hydrates auxquels ils donnent naissance. On rend compte de leur tendance à la solubilisation par la considération de la structure en chaines ramifiées du sous-réseau anionique silicaté, de l'existence de sites aluminium de caractère cationique, et d'une propagation de l'attaque par passage en solution alterné d'ions silicate et d'ions calcium, le magnésium constituant un élément d'interruption de la réaction.

Cette réactivité peut être mesurée par la solubilité du laitier dans une solution de soude 0,04 N.

Elle peut, de façon plus simple, être chiffrée par l'indice

$$R' = \frac{Al_2O_3.CaO}{(Al_2O_3+SiO_2)^2}$$

dont on a montré par ailleurs |4| qu'il est en bonne corrélation avec les résistances mécaniques.

Un laitier est de qualité acceptable quand son indice de réactivité est supérieur à 0,18. Pour les laitiers granulés français, R' est compris entre 0,20 et 0,30.

REFERENCES

1 - P. RICHET et Y. BOTTINGA, Verres, liquides et transition vitreuse, Bull. Minéral., 106, 1983, 147-168.

2 - G.W. TOOP et C.S. SAMIS, Activities of ions in silicate melts, Trans. Met. Soc. AIME, 224 (5), 1962, 878-887.

3 - C.R. MASSON, An approach of the problem of ionic distribution in liquid silicates, Proc. Roy. Soc., A 287 (1409), 1965, 201-221.

4 - R. DRON, Structure et réactivité des laitiers vitreux, Thèse de Doctorat d'Etat, Univ. Paris VI, Rapport des Laboratoires, Publ. LCPC, Paris, 1984.

5 - P. Mc MILLAN et B. PIRIOU, Raman spectroscopic studies of silicate and related glass structure, Bull. Minéral., 106, 1983, 57-75.

ALKALI ACTIVATION OF INDIAN BLAST FURNACE SLAGS

P.S. Parameswaran, A.K. Chatterjee
The Associated Cement Companies Ltd.,
Central Research Station, Thane 400604, INDIA.

ABSTRACT :

Development of alkali-activated slag for use as a cementing material has been attempted quite extensively during the last two decades. In keeping with this trend the R&D Division of the Associated Cement Cos. Ltd., (India), carried out a systematic study on the alkali-activation of Indian blast furnace slags of composition 30-35% lime, 20-24% alumina, and 7 - 9% magnesia. Studies have also been conducted on the activation of slag-flyash (60:40) blends. Sodium hydroxide and sodium sulphate individually, as well as three component admixtures of hydrated lime, sodium carbonate and sodium sulphate have been tried as activators.

In the present article the mortar properties of various blends have been reported along with strength development patterns. The hydration characteristics of such blended cements at various ages have also been highlighted.

A semifield trial conducted with a patch of concrete pavement laid with such alkali activated slag cement and its durability over a time period of six years have been specifically highlighted to reflect on the performance evaluation of such blended cements. The broad ideas on the problems and prospects of commercialisation of such blended cements in the environment prevailing in the developing countries like India have been presented.

SUMÁRIO

O desenvolvimento de escória ativada por álcalis para uso como material cimentício foi tentado extensivamente durante as duas últimas décadas.

Segundo esta tendência, a divisão de pesquisa e desenvolvimento da Associated Cement Co. Ltd (Índia) realizou um estudo sistemático da ativação por álcalis de escórias de alto forno indianas com composição 30-35% de cal, 20-21 de óxido de alumínio e 7-9% de óxido de magnésio. Estudo referente à ativação de misturas escórias-cinzas volantes (60:40) foram também conduzidos. Hidróxido de sódio e sulfato de sódio, assim como três aditivos de cal hidratado, carbonato de sódio e sulfato de sódio foram tentados como ativadores.

No presente artigo, as propriedades das argamassas provenientes de várias misturas são apresentadas, assim como o padrão de desenvolvimento da resistência. As características da hidratação de tais cimentos compostos em várias idades foram também discutidas.

Um teste parcial de campo foi conduzido com pavimento de concreto no qual foi utilizado o cimento de escória ativada por álcalis, e a sua durabilidade ao longo de seis anos foi especialmente estudada para refletir a avaliação do desempenho de tais cimentos misturados. As idéias gerais dos problemas e perspectivas de comercialização de tais cimentos misturados no ambiente existente em países em desenvolvimento como a Índia são apresentados.

INTRODUCTION

The Indian blast furnace (bf) slags differ from similar slags in other countries in having either higher alumina content or lower lime or both as seen in Table 1.

Ref.: Metallurgical Slags Potential for Conservation for Energy and material resources for Building Materials. S.Laxmi and P K Mandal CRI.

Country	SiO_2 %	CaO %	MgO %	Al_2O_3 %
USSR	30-40	30-50	2-14	5-7
USA & CANADA	33-42	36-47	1-16	6-16
AUSTRALIA	33-38	39-44	1-4	15-19
JAPAN	31-40	38-45	2-8	13-17
SOUTH AFRICA	30-36	30-40	8-21	9-16
WESTERN EUROPE & YUGOSLAVIA	30-38	33-47	2-10	9-18
INDIA	27-39	30-40	0-17	17-33

Other minor components (TiO_2, MnO, FeO, S, Na_2O, K_2O) together constitue about 5%.

Table 1:Comparative Chemical Analysis of Foreign and Indian Slags.

About 7.4 million tonnes of such slag is generated per year in India, of which about 3.5 million tonnes is reported to be available in granulated form for use in the cement industry.

The primary mode of utilisation of the available granulated bf slag in India is as an admixture in the manufacture of blended cement (PSC). The next possible use of this slag as a raw mix component is not popular due to the difficulties of availability of granulated bf slag and problems of grinding of the air cooled bf slag.

The third possible use of the slag as an activated binder by itself has been an object of R & D in India quite in keeping with the global trend. The present paper is intended to highlight the salient findings of a course of investigation conducted by the Research & Development Division of The Associated Cement Cos.Ltd., the largest manufacturer of Cement in India.

2. DEVELOPMENTAL APPROACH :

One of the basic characteristics of the granulated bf slag is its glass content. In order to ascertain its effect on alkali activation, four different slags of varying glass contents were subjected to activation by using the same dosage of sodium hydroxide (Table 2).

Mix : 1 : 2 Mortar

	NaOH %	Glass Content %	Compressive Strength kg/cm² 1 D	3 D	7 D	28D	91D
Slag I	5	85	221	297	343	371	489
Slag II	5	88	208	272	297	389	490
Slag III	5	90	278	358	386	450	480
Slag IV	5	75	194	285	324	348	450

Table 2:Effect of Glass Content on Slag Activation.

It is evident from the Table that the response of a slag to activation is, to a great extent, related to its glass content. Considering the commercial availability of the slag and the data furnished in Table 2, slags with glass content of minimum 85% were chosen for further developmental studies. The slags finally used in the present investigation are analysed in Table 3.

	Slag I %	II %	III %
SiO_2	32.3	31.0	33.4
Al_2O_3	20.7	21.2	22.8
Fe_2O_3	0.4	1.6	1.1
Mn_2O_3	0.9	1.3	3.2
CaO	31.3	34.3	31.3
MgO	8.7	7.7	5.6
SO_3	-	0.1	0.1
'S'	0.9	0.8	0.7
I.R.	3.6	1.0	1.0
L.O.I.	0.9	-	-

Table 3 : Chemical composition of Slags used for investigation.

The next basic consideration for development was the sensitivity of the specific surface of ground bf slag and activator dosages in the strength development of activated binder (Figure 1).

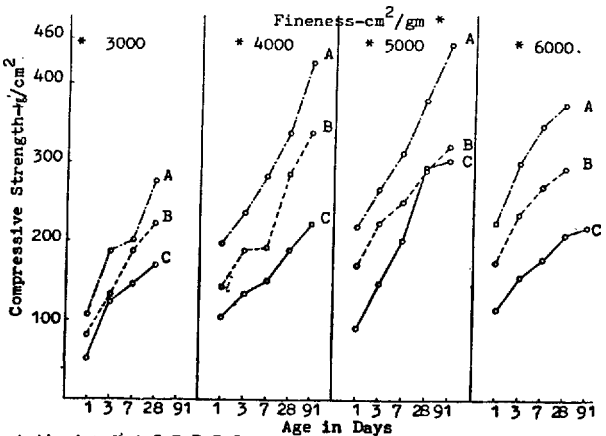

Activator % A-5,B-3,C-2.
FIG. 1:Effect of Fineness of Slag and Activator Dosage .

Appreciably lower strengths particularly at early ages with coarsely ground slags(3000-4000cm^2/g) indicated the need for higher surface area at least in the range of 5000-6000cm^2/g. Simultaneously, important was the optimisation of the activator dosage. Significant increase in strength with increase in activator dosage from 3 to 5% indicated the futility of lower dosages.

2.1 Selection of Activators

Based on chemical principles the selection of activators was restricted to alkalies, lime and sulphate. The ultimate objective was to select in place of caustic NaOH, such activators that could be easily handled and used in the large scale production process without sacrificing the primary objective of strength development, commercial availability was also taken as one of the criteria for selection. Effects of different activators, when used singly or in combination, are shown illustratively and not exhaustively in Table 4.

	Compressive Strength kg/cm^2			
	1 D	3 D	7 D	28 D
Sodium Silicate	Soft	6	41	158
Na_2SO_4	Soft	21	69	254
Na_2CO_3	Soft	34	53	69
Hydrated Lime	Soft	Soft	No Strength	
Na_2SO_4+Hyd.Lime	141	172	175	217
l_1%Na_2CO_3+m_1%Na_2SO_4 +n_1% Hyd.Lime	112	123	125	151
l_2%Na_2CO_3+m_2%Na_2SO_4 +n_2% Hyd.Lime	145	177	217	246
l_3%Na_2CO_3+m_3%Na_2SO_4 +n_3% Hyd.Lime	259	286	317	388
l_4%Na_2CO_3+m_4%Na_2SO_4 +n_4% Hyd.Lime	228	246	248	307
l_5%Na_2CO_3+m_5%Na_2SO_4 +n_5% Hyd.Lime	320	393	399	406
l_6%Na_2CO_3+m_6%Na_2SO_4 +n_6% Hyd.Lime	259	286	317	388

(l_1% to l_6%) are various percentages of (m_1% to m_6%) individual components in the (n_1% to n_6%) Mixture.

Table 4:Strength inducing characteristics of Activators /proportions.

From an exhaustive study of this kind, it was finally concluded that for the slags under consideration, an activator mix of (1% Na_2CO_3+m%Na_2SO_4+n% Hyd. Lime is practically as effective as the optimum dosage of NaOH. The comparative strength data are furnished below :

Activator	Compressive Strength,kg/cm^2				
	1 D	3 D	7 D	28D	91 D
NaOH	290	372	409	481	548
3 Component Mix	330	369	466	500	559

Further investigations were carried out with the activated binder prepared by intergrinding of the 3 component solid activators mix with slag.

3. CONCRETE FROM ACTIVATED SLAG BINDER :

Before preparing and evaluating the concrete properties of activated slag binder, it was ascertained to what extent the normal relation of strength Vs. water/cement ratio holds good for the slag binder. The relation for slag binder as compared with OPC is shown in Fig. 2 which confirm by and large, the normality of the relation for the slag binder.

Fig. 2

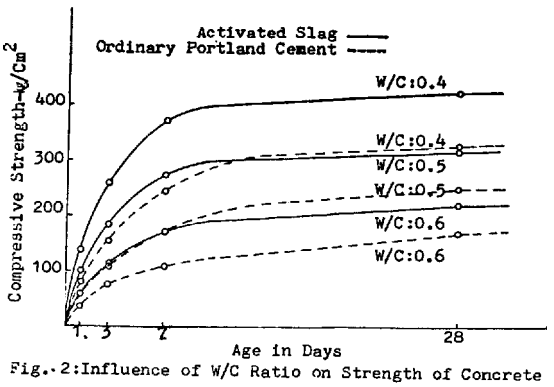

Fig.2:Influence of W/C Ratio on Strength of Concrete

Subsequently, bulk lots of concrete were prepared using varying proportions of the activator slag binder of the composition developed by the authors. The normal features of increasing concrete strength with increasing binder content in concrete (Fig.3) was clearly observed.

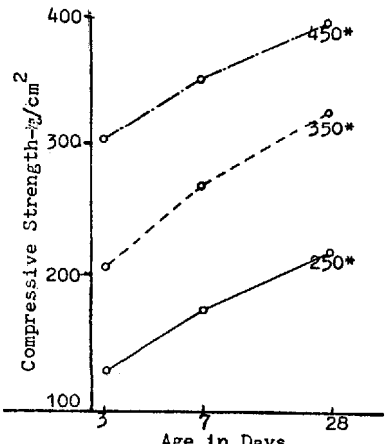

Fig.3:Activated Slag Content Vs Strength on Concrete

However, in the case of slag concrete, the strength rise beyond 28 days was only marginal, although this rising trend in strength could be seen upto one year of age.

3.1 Comparison of OPC and Slag Concrete.

Concrete batches were prepared with the slag binder containing 3 component activator of our design. Parallelly concretes were prepared from a slag binder containing an optimum dosage of caustic NaOH as well as from OPC of following properties. The compartive concrete properties are presented in Table 5. Some salient observatons are highlighted below :

- Between the slag binders with two different activators, one of our design with 3 component activators mix possesses better workability. With NaOH activated slag binder the concrete shows stiffening and slump loss within 10 min.
- Early age strength is better in slag concretes as compared to OPC concrete.
- Strength rise with age is poorer in slag concretes, when compared wth OPC concrete.
- No strength retrogression is observed in Slag concretes upto 6 years of age.

Binder	Activator & Dosage	W/C	Compressive Strength kg/cm^2 1 D	3 D	7 D	28 D
OPC	-	0.457	95	145	170	265
Slag	NaOH %	0.457	114	216	220	255
Slag	1%Na_2CO_3+ m%Na_2SO_4+ n%Hyd.Lime	0.457	-	210	271	327

Binder	Activator & Dosage	W/C	Compressive Strength kg/cm^2 90D	180D	365D	6 yrs.
OPC	-	0.457	300	350	435	485
Slag	NaOH %	0.457	255	280	310	325
Slag	1%Na_2CO_3+ m%Na_2SO_4+ n%Hyd.Lime	0.457	344	-	390	400

SLAG CONCRETE	CEMENT CONCRETE
Binder/Aggregate ratio 1:5.96	Cement/Aggregate ratio 1:5.41
Binder/M^3 = 350 kg.	Cement/M^3 = 360 kg.

3.2 Field Trial Slag Concrete

In order to ascertain the climatic effects on the slag concrete, a small pavement area measuring 2 m x 0.6 m was laid with about 0.2 m^3 of slag concrete of the following design. The mixes were designed as per ACI.

Details of Concrete Mix :

Binder content	: 350 kg/M^3
Binder aggregate ratio	: 1:5.96
Water cement ratio	: 0.46
Aggregate size	: 25 mm m.s.a.
Type of aggregate	
Coarse	: Crushed basalt Agg.
Fine	: Natural sand
Workability	: Medium
Slump	: 25 mm
Compacting Factor	: 0.88
Compressive Strength, kg/cm^2	
3 Days	: 210
7 Days	: 225
28 Days	: 255
90 Days	: 265

The climatic conditions to which the experimental pavement is kept exposed are :

Temp. fluctuations	: 16 - 38 ^oC
Humidity	: 35 - 90 %
Rainfall	: 2000 - 2600 mm

However, this particular stretch of concrete is exposed to direct sunlight. The concrete road is being subjected to normal vehicular traffic including heavy loaded trucks.

The experimental patch has so far withstood well a time span of 6 years without any apparent deterioration. The performance of the patch is monitored by Non-destructive testing. The photographs of Slag Concrete and OPC Concrete Road are shown below :

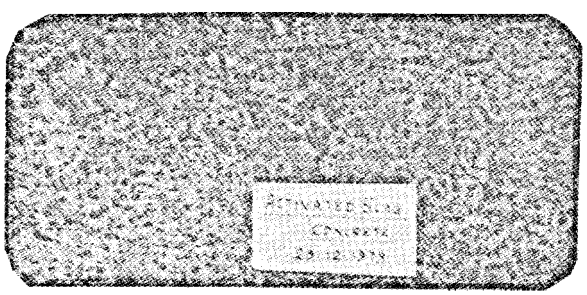

ACTIVATED SLAG CONCRETE ROAD

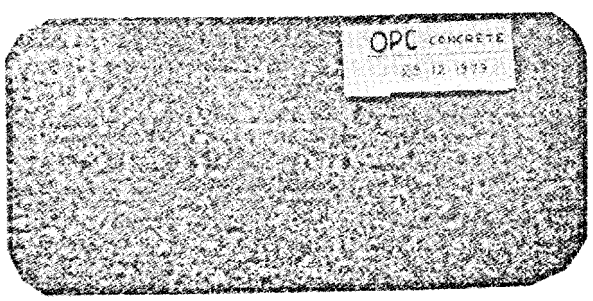

OPC CONCRETE ROAD

4. EXPLORATION OF SLAG-FLY ASH COMPOSITIONS :

After having developed an acceptable activated slag binder, an attempt was made to explore the possibility of activation of slag-fly ash blends through a similar route. The composition of fly ashes considered is given in Table 6.

	Fly Ash I	Fly Ash II
Chemical Composition %		
SiO_2	62.4	60.5
Al_2O_3	22.6	23.3
Fe_2O_3	7.0	7.2
CaO	1.9	5.7
MgO	0.3	0.6
LOI	3.9	1.6
Na_2O	0.3	0.36
K_2O	1.2	0.3
Lime Reactivity	55	70

Table 6:Chemical Composition of Fly Ash used in Studies.

The Slag fly ash blends prepared were examined microscopically for homogenity prior to use. The microphotographs of Slag and Slag+ fly ash blends are shown below :

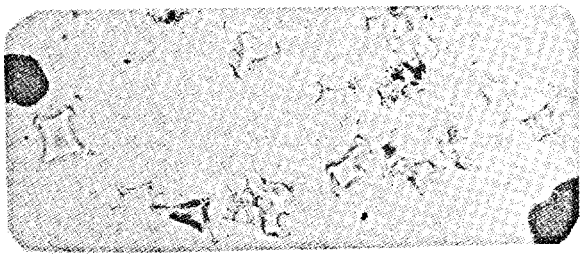

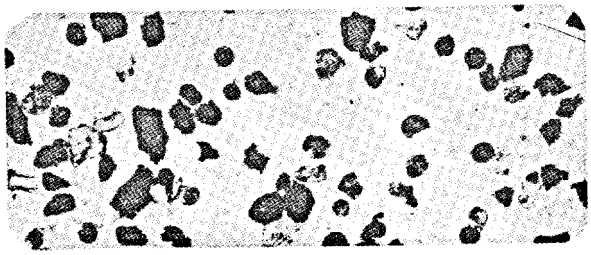

The activation results of slag-fly ash blends of 60:40 ratio are presented in Fig. 4(a) to (d). It may be observed from the figures that the slag alone gives better strength characteristics than slag-fly ash blends. The compressive strength obtained of 60:40 ratio blends of slag of fineness (6000 cm^2/gm)+ pozzolana(PFA) is equivalent to strength

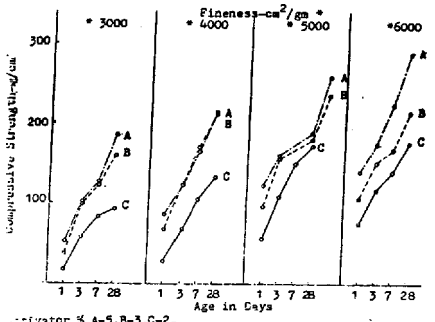

Activator % A-5,B-3,C-2.
Fig.4(a): Effect of Fineness ,Activated Dosage on Slag (III)-Pozzolana (I PFA) Blends.

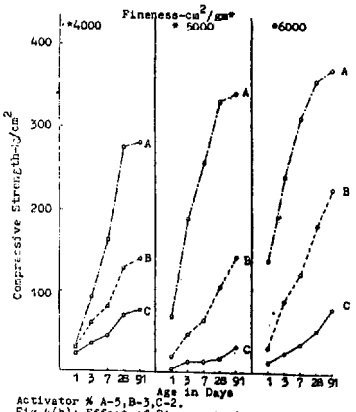

Activator % A-5,B-3,C-2.
Fig.4(b): Effect of Finess, Activated Dosage on Slag(III)-Pozzolana (II PFA) Blends.

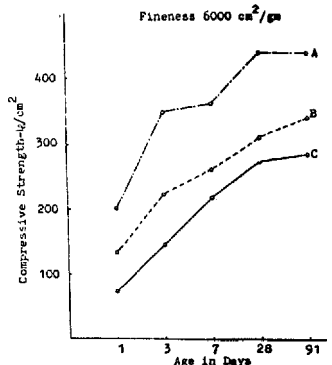

Activator% A-5,B-3,C-2.
Fig.4(c): Effect of Activator Dosage on Slag (I)-Pozzolana (II PFA) Blends.

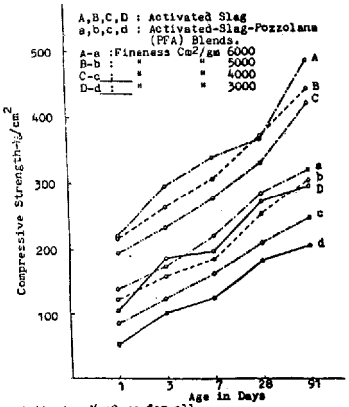

Activator % :Same for all
Fig. 4(d): Comparison between Activated Slag Vs. Activated Slag Pozzolana(PFA)Blends at various Fineness.

obtained on activated slag fineness of 3000 cm^2/gm. Fly ash from various sources showed similar trend in strength pattern. It is possible to produce a medium strength binder using slag fly ash blends.

In India about 20 million tonnes of fly ash is available as a waste product from Thermal Power Stations. The cost of fly ash is lower than granulated slag. As per the investigation, 40% of slag could be replaced by fly ash for obtaining medium strength concrete for construction of roads ,etc. In other words, slag-fly ash interground with the three component activator could be used effectively for non-load bearing structures.

Indian fly ashes are less reactive and more angular in shape as could be observed from the above photograph. Because of the angular shape of the fly ash, no improvement in workability of fly ash blends is noticed. This is contrary to the trend observed in foreign fly ashes which are rounded in shape.

5. PROGNOSIS FOR COMMERCIALISATION :

So far, alkali activators single or two component type, have been reported. This paper reports on the development of a three component activator based on commercially available chemicals. The 3 component solid activators lend themselves for easy handling and accurate dosing; the activator can be uniformly dispersed during normal intergrinding process, without any special arrangement.

For equivalent binder content, the slag binder attains better early strength characteristics. The cost of the activated processed slag will be around Rs.400/- to Rs.500/- per ton, whereas the cost of ordinary cement works out to be around Rs.600/- per ton used for these tests. On the basis of the strength data, the cost of slag concrete will be cheaper than the normal OPC concrete.

For every ton of clinker produced, 0.3 ton of coal is consumed. Hence, the use of activated slag for manufacturing a hydraulic binder will help to preserve about 2.1 million ton of coal, if entire quantity of slag generated about 7 million tons is utilised for this purpose.

Finally, the use of three component activator-cum-ground slag binder, might pose limitations where natural aggregates suspected to be alkali-reactive are met with.

Slag fly ash activated blends could be used for producing medium strength concrete. With the present availability of 7 million tons of slag a cheap binder of 11 million tons could be produced with the utilisation of 4.2 million tons of fly ash.

The cost of slag fly ash binder works out around Rs.350/- to Rs.380/- per ton. This will be cheaper by 37% to 42% compared to OPC.

The use of activated slag fly ash blend may also reduce the risk of alkali aggregate reaction.

Thus the three component activator mixture developed by author, could be profitably used for manufacture of hydraulic binder with added advantage of cost reduction and utilisation of industrial waste.

M. Kawamura, Faculty of Eng., Kanazawa University, Japan, K. Torii, Faculty of Eng., Kanazawa University, Japan and S. Hasaba, Faculty of Eng., Kanazawa University, Japan

Reaction Process and Microstructure in Compacted Fly Ashes and Fly Ash-Chemical Additive Mixtures

Processus de réaction et microstructure des comprésses cendres volantes et cendres volantes-additions chimique mélange

SUMMARY : This study mainly aims at clarifying the relationships between unconfined compressive strength and reactions taking place in compacted fly ashes and fly ash-chemical additive mixtures. The effects of chemical composition and physical properties of fly ashes, curing temperature, curing period and type of chemical additive on hardening characteristics of compacted fly ashes and fly ash-chemical additive mixtures were investigated. Reaction process, microstructure and surface features of fly ash particles in hardened compacted fly ashes and fly ash-chemical additive mixtures were elucidated by SEM observation, X-ray diffraction analysis, differential thermal analysis and pore size distributions determined by the mercury penetration porosimeter. A relatively small amount of free lime and anhydrite as well as the glassy phase were confirmed by the X-ray diffraction diagrams obtained for the fly ashes used. It was found that the presence of free lime and anhydrite in the fly ashes produced ettringite crystals on the surfaces of fly ash particles. The development of strength in the compacted fly ashes and fly ash-chemical additive mixtures closely related to the amount of ettringite and to the changes in microstructure by the formation of ettringite, although the degree of hardening was significantly influenced by the type of fly ashes used. Influences of the addition of $Ca(OH)_2$ and $CaSO_4 \cdot 2H_2O$ on the amount of ettringite produced in the compacted fly ash-chemical additive mixtures were also investigated. The addition of even a small amount of $Ca(OH)_2$ and $CaSO_4 \cdot 2H_2O$ was found to promote the formation of ettringite in compacted fly ash- chemical additive mixtures. With regard to reactions occurring in the compacted fly ash-$Ca(OH)_2$-$CaSO_4 \cdot 2H_2O$ system, it was found that the pozzolanic reaction products such as C-S-H gel, C_4AH_{13} and C_2ASH_8 as well as ettringite were produced at later ages by which most of the gypsum added had been consumed to produce ettringite.

Este estudo tem por objetivo principal esclarecer as relações entre resistência à compressão não confinada e reações que ocorrem em cinzas volantes e misturas de cinza volante-aditivo químico compactadas. Foram investigados os efeitos da composição química e das propriedades físicas da cinza volante, da temperatura de cura, do período de cura, e do tipo de aditivo químico, sobre as características de endurecimento de cinzas volantes e de misturas de cinza volante-aditivo químico compactadas. Através de observação por SEM, análise por difração de raio-X, análise termodiferencial e distribuições de tamanho de partícula por porosímetro de penetração de mercúrio, foram elucidados o processo de reação, as características de microestrutura e de superfície de partículas de cinza volante, em cinzas volantes e misturas de cinza volante-aditivo químico compactadas. Pelos gráficos de difração de raio-X das cinzas volantes usadas, confirmou-se uma quantidade relativamente pequena de cal livre e anidrito, bem como fase vítrea. Constatou-se que a presença de cal livre e anidrito nas cinzas volantes produziu cristais de etringita nas superfícies das partículas de cinza volante. O desenvolvimento da resistência nas cinzas volantes e nas misturas de cinza volante-aditivo químico ficou estreitamente relacionado com a quantidade de etringita e com as mudanças na microestrutura por formação de etringita, embora o grau de endurecimento tenha sido influenciado significativamente pelo tipo de cinzas volantes usadas. Também foram investigadas influências exercidas pela adição de $Ca(OH)_2$ e $CaSO_4.2H_2O$ sobre a quantidade de etringita produzida nas misturas compactadas de cinza volante-aditivo químico. Verificou-se que a adição até mesmo de pequena quantidade de $Ca(OH)_2$ e $CaSO_4.2H_2O$ enseja a formação de etringita nas misturas compactadas de cinza volante-aditivo químico. Com relação às reações que ocorrem no sistema compactado de cinza volante-$Ca(OH)_2$-$CaSO_4.2H_2O$, constatou-se que os produtos da reação pozolânica, tais como gel C-S-H, C_4AH_{13} e C_2AS_8, bem como etringita, ocorreram nas idades finais, sendo que a maior parte do gesso adicionado foi consumida para produzir etringita.

M. Kawamura, Faculty of Eng., Kanazawa University, Japan, K. Torii, Faculty of Eng., Kanazawa University, Japan and S. Hasaba, Faculty of Eng., Kanazawa University, Japan

INTRODUCTION

The fly ashes produced from the pulverized bituminous and sub-bituminous coals exhibit a hardening property when they are compacted at an appropriate moisture content. The characteristics of reactions and hardening processes in compacted fly ashes and fly ash-chemical additive mixtures are very important for utilizing fly ash as a material for base course and as a fill in embankment.

The major phases of fly ashes are glassy SiO_2, Al_2O_3 component and minerals such as quartz, mullite and a magnetite and so on. In addition to these phases, small amount of free lime and anhydrite is present in bituminous fly ashes. When usual bituminous fly ashes are compacted at an appropriate moisture condition, the compacted fly ashes exhibit a slowly hardening property. The hardening property of compacted fly ashes is supposed to be derived from the free lime and anhydrite contained in fly ashes (1,2). However, the chemical reactions responsible for the hardening in compacted fly ashes are not fully understood.

The glassy phase of fly ash in concrete or mortar is dissolved by the alkali hydroxide pore solution (3). The most important reaction product which precipitates in other sites than on the fly ash spheres is calcium silicate hydrate (3). On the other hand, the chemical reactions of fly ash particles in compacted fly ashes and fly ash-chemical additive mixtures take place in the situations greatly different from those under which fly ash particles in concrete or mortar exist. Hence, it may be possible that the reaction products other than calcium silicate hydrate also contribute to the development of strength in compacted fly ashes and fly ash-$Ca(OH)_2$ mixtures.

The objective of this paper is to reveal the characteristics of reaction process and microstructure in compacted fly ashes and fly ash-chemical additive mixtures. The reaction process and features of microstructure in a compacted fly ash with and without chemical additives were elucidated by scanning electron microscope observation, X-ray diffraction analysis, differential scanning calorimetry-thermogravimetry analysis and pore size distribution measurements. The relations between strength development and reaction process in the compacted materials are discussed.

MATERIALS AND EXPERIMENTAL PROCEDURE

The bituminous fly ashes used in this study are discharged from a power station in Japan in which pulverized domestic coals are burning. The chemical composition and physical properties of three fly ashes used are presented in Table 1. It is confirmed by X-ray diffraction analysis that the major component of these fly ashes are glass, quartz and mullite, and that small amount of free lime and anhydrite are contained.

The chemical additives added to fly ashes are hydrated lime ($Ca(OH)_2$), gypsum ($CaSO_4 \cdot 2H_2O$) and ordinary Poltland cement. The additive content ranges from 2.5 % to 10 % by weigtht of dry fly ash samples. Hydrated lime (or Portland cement):gypsum ratios are 1 and 3.

Table 1 Chemical composition and physical properties of fly ashes

	Flyash A	Flyash B	Flyash C
Ig.Loss %	1.9	3.2	5.7
SiO_2 "	54.7	48.5	54.2
Al_2O_3 "	27.0	26.5	27.9
Fe_2O_3 "	6.5	6.2	6.1
CaO "	4.4	3.9	3.7
MgO "	1.9	1.5	2.5
Na_2O "	1.7	2.2	0.2
K_2O "	1.2	1.2	0.4
SO_3 "	0.9	0.7	—
Specific gravity	2.27	2.21	2.18
Specific surface area (Blain), cm^2/g	3390	3140	2980
Specific surface area (BET), m^2/g	2.1	2.1	1.5

Fly ash samples and additives were mixed in a dry state and then the distilled water by the amounts of which correspond to the optimum moisture content of the compacted fly ash samples was added. Cylindrical specimens of 5 cm in diameter and 10 cm in height were statically compacted by an oil jack to equal the maximum dry density of a fly ash sample or a fly ash-additive mixture. Specimens were cured at 20℃ in sealed vinyl sacks and the unconfined compressive strength test was conducted at the ages of 7 days, 14 days, 28 days and 90 days. The strain rate was held at 1 % / min. during loading.

Ground samples for powder X-ray diffraction and differential scanning calorimetry-thermogravimetry (DSC-TG) were preserved in the vaccum desiccator for 24 hours at 20℃. A quantitative analysis of ettringite formed in compacted fly ashes and fly ash-additive mixtures was carried out by measuring accumulated counts at $2\theta=9.1°$ for 40 seconds.

The pore size distributions of various compacted samples which had been freeze-dried for 24 hours at -55℃ were determined with the mercury penetration porosimeter.

REACTION PROCESS IN COMPACTED FLY ASHES AND FLY ASH-ADDITIVE MIXTURES

The reaction process in a compacted fly ash was pursued by X-ray diffraction analysis and DSC-TG analysis. As shown in Fig. 1, X-ray diffraction peaks for free lime at $2\theta=37.3°$ and for anhydrite at $2\theta=25.5°$ diminish with age until 7 days. Fig. 1 shows that the height of a peak for ettringite at $2\theta=9.1°$ slowly increases with age. The process of formation of ettringite in a compacted fly ash is also indicated in DSC curves shown in Fig. 2. Namely, an endothermic peak for ettringite at approximately 110℃ gradually increases with age. These X-ray diffraction and DSC-TG results obviously show that one of the major reaction products formed in the compacted fly ashes is ettringite. Ettringite in the compacted fly ashes may be formed as a result of the reaction in which the glassy Al_2O_3 component of the fly ash, free lime and anhydrite take part.

X-ray diffraction diagrams of compacted fly ash-hydrated lime mixtures given in Fig. 3 show that the amount of ettringite formed is considerably increased by the addition of hydrated lime. Furthermore, it is

M. Kawamura, Faculty of Eng., Kanazawa University, Japan, K. Torii, Faculty of Eng., Kanazawa University, Japan and S. Hasaba, Faculty of Eng., Kanazawa University, Japan

noteworthy that the pozzolanic reaction products such as $C_4A \cdot 0.5CO_2 \cdot 12H_2O$ ($2\theta=10.7°$) and C_2ASH_8 ($2\theta=7.0°$) coexist with ettringite after 28 days. These pozzolanic reaction products are considered to be produced by a slowly continueing reaction of the fly ash with hydrated lime.

When gypsum is added along with hydrated lime, the reaction for the formation of ettringite is promoted as pointed out by some workers (4,5). Especially, at the hydrated lime : gypsum ratio of 1, the reaction for the formation of ettringite rapidly proceeds after the age of 14 days until either hydrated lime or gypsum added is completely consumed, as shown in Fig. 4. It is interesting to note that there is no difference in the age when the reaction for the formation of ettringite starts between the compacted fly ash with and without the additives. This result indicates that decomposition of the glass phase in the fly ash takes place at early ages even in compacted fly ash without the additives as well as in compacted fly ash-additive mixtures.

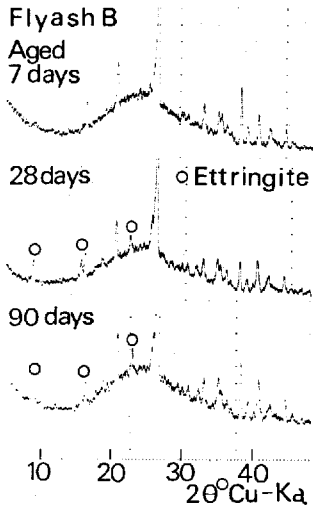

Fig. 1 X-ray diffraction diagrams of a compacted fly ash

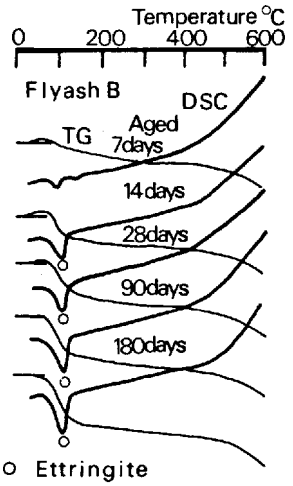

Fig. 2 DSC-TG curves for a compacted fly ash

X-ray diffraction diagrams of compacted fly ash-Portland cement mixtures given in Fig. 5 show that the amount of ettringite formed by the age of 7 days is greater than that of other compacted fly ash-additive mixtures. However, the increase in the amount of ettringite after 7 days is not significant in the mixtures containing Portland cement. Furthermore, X-ray diffraction diagrams of compacted fly ash-Portland cement-gypsum mixtures given in Fig. 6 show that the reaction for the formation of ettringite in the mixtures is not so remarkable as that in compacted fly ash-hydrated lime-gypsum mixtures. A relatively large amount of gypsum exists in the mixtures even at the age of 90 days.

RELATION BETWEEN COMPRESSIVE STRENGTH AND THE AMOUNT OF ETTRINGITE IN COMPACTED FLY ASHES AND FLY ASH-ADDITIVE MIXTURES

The relations between compressive strength and the amount of ettringite determined by X-ray diffraction analysis for each compacted mixture are shown in Fig. 7, Fig. 8 and Fig. 9. The compressive strength of the compacted fly ashes is approximately proportional to the amount of ettringite regardless of type of fly ash and curing conditions (Fig. 7).

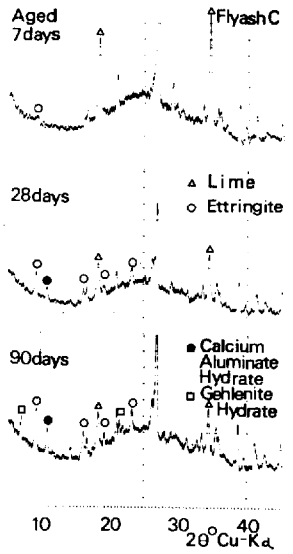

Fig. 3 X-ray diffraction diagrams of compacted fly ash-hydrated lime mixtures (lime content:10%)

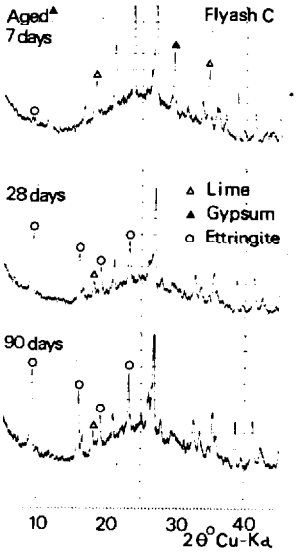

Fig. 4 X-ray diffraction diagrams of compacted fly ash-hydrated lime-gypsum mixtures (lime·gypsum ratio=0.1, lime:gypsum ratio=1)

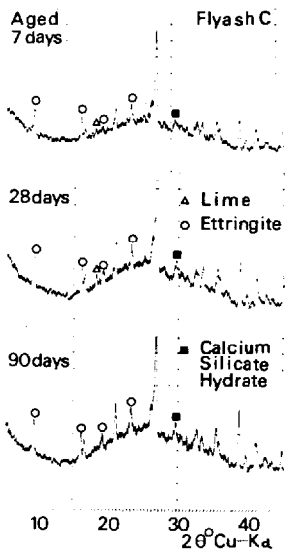

Fig. 5 X-ray diffraction diagrams of compacted fly ash-Portland cement mixtures (cement content:10%)

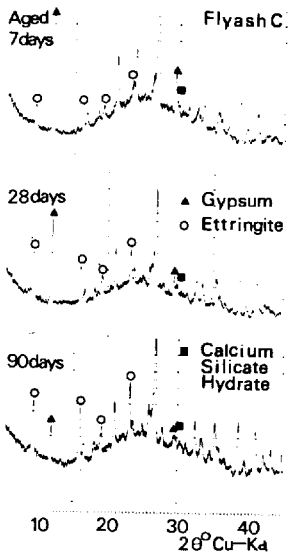

Fig. 6 X-ray diffraction diagrams of compacted fly ash-Portland cement-gypsum mixtures (cement·gypsum ratio=0.1, cement:gypsum ratio=1)

M. Kawamura, Faculty of Eng., Kanazawa University, Japan, K. Torii, Faculty of Eng., Kanazawa University, Japan and S. Hasaba, Faculty of Eng., Kanazawa University, Japan

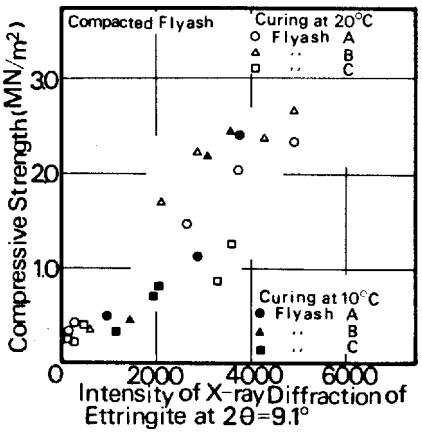

Fig. 7 Relation between compressive strength and the amount of ettringite produced in the compacted fly ashes

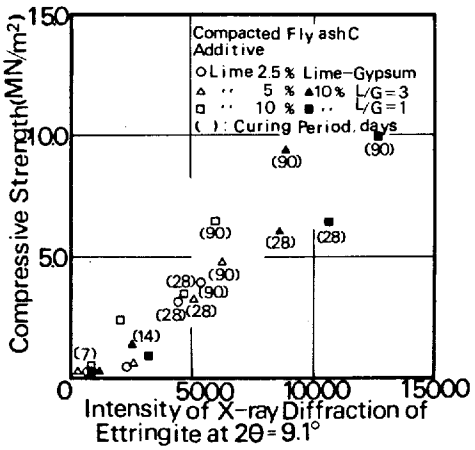

Fig. 8 Relation between compressive strength and the amount of ettringite produced in the compacted fly ash-hydrated lime and fly ash-hydrated lime-gypsum mixtures

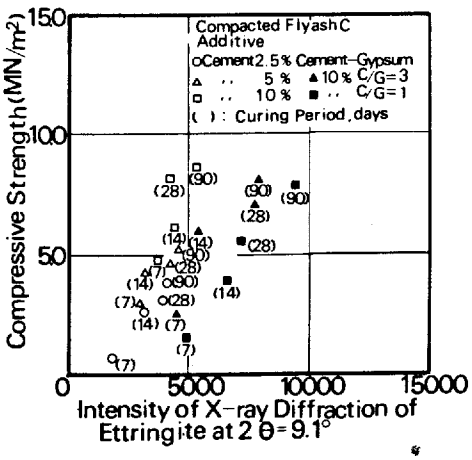

Fig. 9 Relation between compressive strength and the amount of ettringite produced in the compacted fly ash-Portland cement and fly ash-Portland cement-gypsum mixtures

The compressive strength of compacted fly ash-hydrated lime and fly ash-hydrated lime-gypsum mixtures also linearly increases with increasing the amount of ettringite, as shown in Fig. 8. These results indicate that the amount of ettringite produced is closely related to the strength development of compacted fly ashes and fly ash-hydrated lime-gypsum mixtures. However, there is a poor correlation between compressive strength and the amount of ettringite produced in compacted fly ash-Portland cement mixtures, as shown in Fig. 9. This fact shows that the hydration products of Portland cement other than ettringite play an important role in the strength development of compacted fly ash-Portland cement mixtures.

RELATION BETWEEN COMPRESSIVE STRENGTH AND PORE SIZE DISTRIBUTIONS IN COMPACTED FLY ASHES AND FLY ASH-ADDITIVE MIXTURES

The pore size distributions of compacted fly ash-hydrated lime (or Portland cement)-gypsum mixtures at the age of 28 days are shown in Fig. 10. It is clear that the peak of pore size distribution of compacted fly ash-hydrated lime-gypsum mixtures shifts toward smaller diameter with decreasing total pore volume. Accordingly, a relatively large strength of compacted fly ash-hydrated lime-gypsum mixtures is found to be due to the subdivision of spaces among fly ash particles by the formation of ettringite. The total pore volume of compacted fly ash-Portland cement mixtures is less by about 20 % than that of compacted fly ash-hydrated lime mixtures. As shown in Fig. 11, the compressive strength of compacted fly ashes and fly ash- additive mixtures tends to be inversely proportional to the total pore volume.

SEM OBSERVATIONS OF REACTION PRODUCTS IN COMPACTED FLY ASHES AND FLY ASH-ADDITIVE MIXTURES

As shown in Fig. 12, fly ash particles in compacted fly ash B do not show any significant change on their surface at 7 days. However, as shown in Fig. 13, fine products are found on the surfaces of fly ash particles at 28 days. These fine products appear to connect the fly ash particles, leading to the strength development of the compacted fly ashes.

As shown in Fig. 14, plate-like products coexist with fine ettringite crystals after 28 days in the compacted fly ash-hydrated lime mixtures. On the other hand, no ettringite crystals are found on the surfaces of fly ash particles in the 7 days old compacted fly ash-hydrated lime-gypsum mixtures, as shown in Fig. 15. However, it is found from Fig. 16 that ettringite formation actively progresses after 14 days. Especially, at the hydrated lime : gypsum ratio of 1, a great number of needle-like ettringite crystals of 5 μm to 10 μm long are seen to protrude from the individual fly ash particles. As shown in Fig. 17, the compressive strengths of the mixtures prepared at the hydrated lime : gypsum ratio of 1 are considerably greater than those for fly ash-hydrated lime mixtures after 28 days. The greater strength attained at the hydrated lime : gypsum ratio of 1 seems to be attributable to the production of large amounts of ettringite. At the hydrated lime : gypsum ratio of 3, plate-like products are also observed along with needle-like ettringite crystals at the vicinity of fly ash particles at 90 days, as shown in Fig. 18.

M. Kawamura, Faculty of Eng., Kanazawa University, Japan, K. Torii, Faculty of Eng., Kanazawa University, Japan and S. Hasaba, Faculty of Eng., Kanazawa University, Japan

3.1

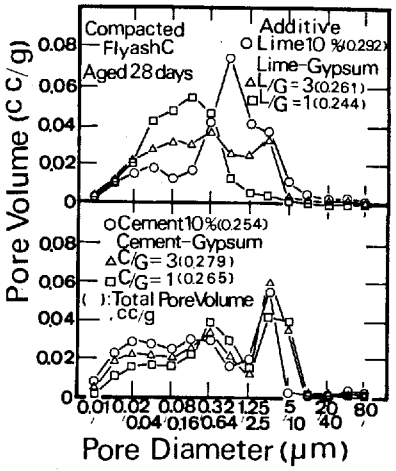

Fig. 10 Pore size distributions of the compacted fly ash-additive mixtures

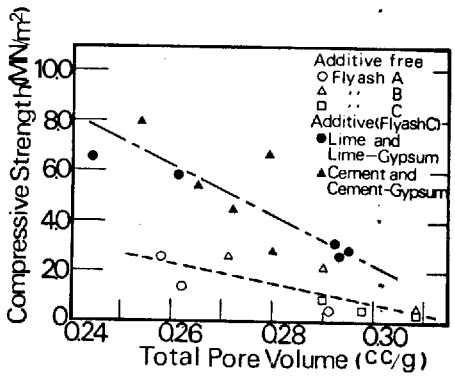

Fig. 11 Relations between compressive strength and total pore volume in the compacted fly ash mixtures with and without the additives

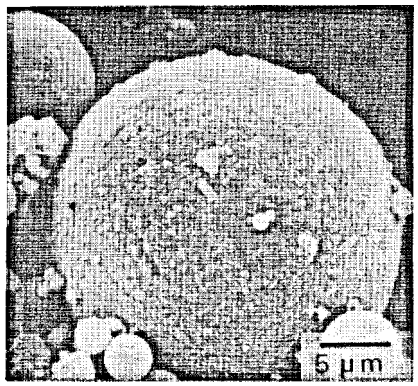

Fig. 12 Scanning electron micrograph of a fly ash sphere in the compacted fly ash B at 7 days

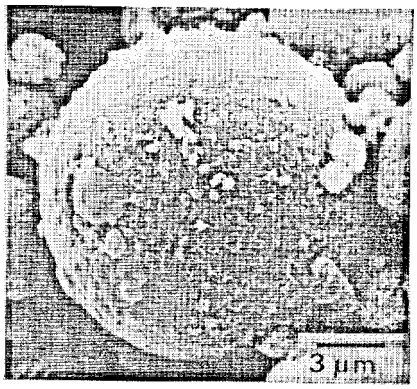

Fig. 13 Scanning electron micrograph of a fly ash sphere in the compacted fly ash B at 28 days

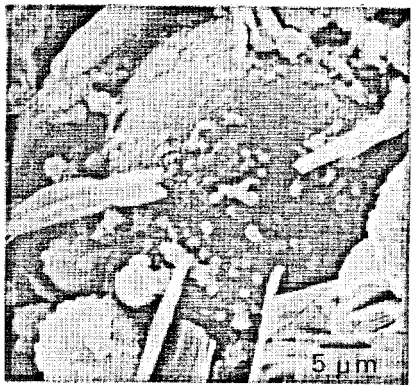

Fig. 14 Scanning electron micrograph of the fracture surface of a compacted fly ash C-hydrated lime mixture specimen at 28 days (lime content:10%)

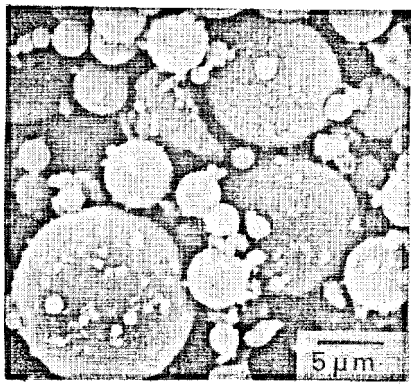

Fig. 15 Scanning electron micrograph of the fracture surface of a compacted fly ash C-hydrated lime-gypsum mixture specimen at 7 days (lime·gypsum ratio =0.1, lime:gypsum ratio=1)

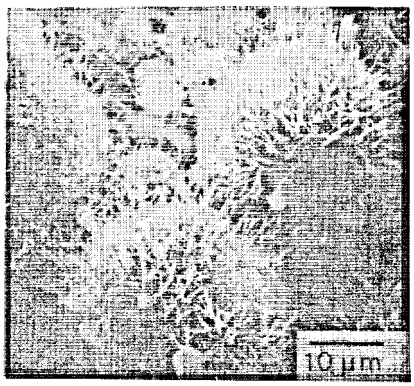

Fig. 16 Scanning electron micrograph of fly ash spheres in the compacted fly ash C-hydrated lime-gypsum mixtures at 28 days (lime·gypsum ratio=0.1, lime:gypsum ratio=1)

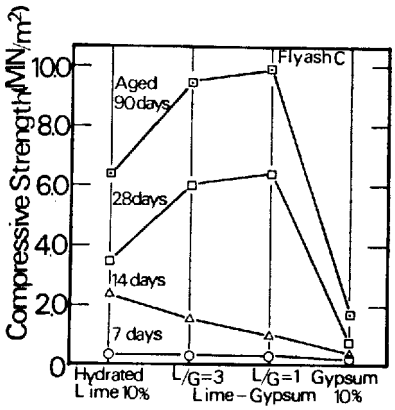

Fig. 17 Compressive strength of the compacted fly ash C-additive mixtures (additive content: 10%)

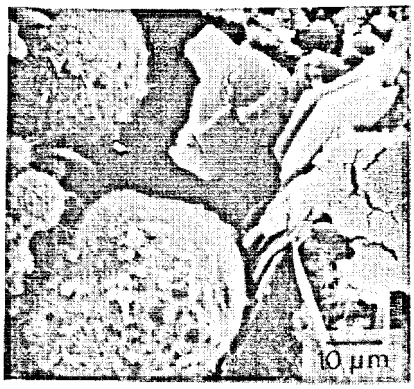

Fig. 18 Scanning electron micrograph of the fracture surface of a compacted fly ash C-hydrated lime-gypsum mixture specimen at 90 days (lime·gypsum ratio =0.1, lime:gypsum ratio=3)

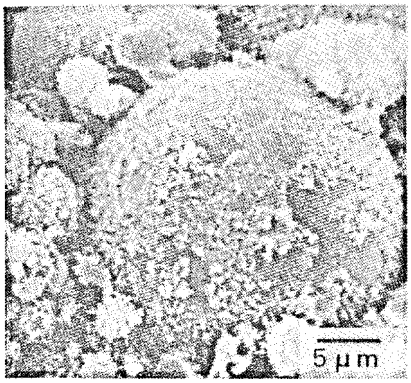

Fig. 19 Scanning electron micrograph of a fly ash sphere in the compacted fly ash C-Portland cement mixtures at 7 days (cement content:5%)

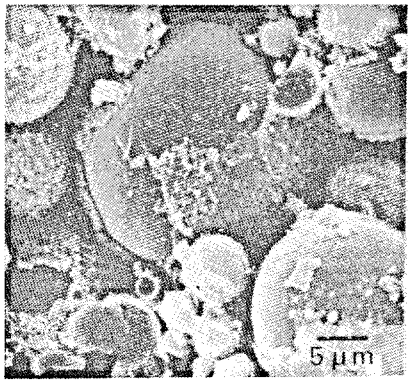

Fig. 20 Scanning electron micrograph of the fracture surface of a compacted fly ash C-Portland cement mixture specimen at 28 days (cement content:10%)

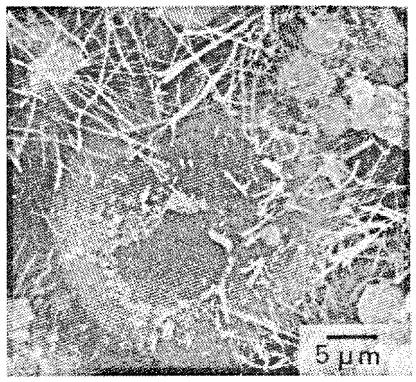

Fig. 21 Scanning electron micrograph of the fracture surface of a compacted fly ash C-Portland cement mixture specimen at 28 days (cement content:10%)

As shown in Fig. 19, surfaces of fly ash particles in compacted fly ash-Portland cement mixtures are covered with dense layers which appear to be composed of fine products. The exterior layers on fly ash particles are often seen to be peeled off, as shown in Fig. 20. Needle-like ettringite crystals are also found at the vicinity of fly ash particles in the mixtures, as shown in Fig. 21.

CONCLUSIONS

From the results obtained in this study, it was confirmed that one of the major reaction products in compacted fly ashes was ettringite and that the chemical reaction of fly ashes in compacted fly ashes was considerably different from the pozzolanic reaction in concrete or mortar containing fly ash. The major results obtained are as follows ;

(1) The compacted fly ashes exhibited a hardening property. This hardening property was found to be derived from free lime and anhydrite contained in the fly ashes. The reaction for the formation of ettringite actively occurred in the compacted fly ashes.

(2) The addition of hydrated lime and gypsum effectively promoted the formation of ettringite in the compacted mixtures. In compacted fly ash-hydrated lime-gypsum mixtures, the pozzolanic reaction products as well as ettringite were also produced by the reaction of fly ashes with hydrated lime occurring over long terms after the gypsum added had been consumed by the reaction for the formation of ettringite.

(3) The strength of compacted fly ash-hydrated lime and fly ash-hydrated lime-gypsum mixtures closely related to the amount of ettringite determined by X-ray diffraction analysis and to the changes in pore size distributions. However, there was a poor correlation between strength and the amount of ettringite in compacted fly ash-Portlan cement mixtures.

(4) The needle-like crystals of ettringite produced on the surfaces of fly ash particles appear to contribute to the strength development of compacted fly ash mixtures by the densification of their structure.

REFERENCES

1.- R.C. JOSHI and M.A. WARD (1980), Cementituous Fly Ashes - Structural and Hydration Mechanisms, Proc. of 7th Int. Congress on Chemistry of cement , Vol.3, pp. 78-83.

2.- H.B. SUTHERLAND, T.W. FINLAY and I.A. CRAM (1968) , Engineering and Related Properties of Pulverized Fuel Ash, Journal of the Institute of Highway Engineers, Vol. 5, No. 6, pp. 19-27.

3.- S. DIAMOND (1981), The characterization of Fly-ashes, Proc. Symp. N Materials Research Society Annual Meeting, Ed. by S. Diamond, pp. 12-23.

4.- S. OHSAGA, K. ASAGA et al. (1985), Quantitative Determination of Fly Ash in the Hydrated Fly Ash -$CaSO_4 \cdot 2H_2O$-$Ca(OH)_2$ System, Cement and Concrete Research, Vol. 15, pp. 357-366.

5.- M. DAIMON, O. YAMAGUCHI et al. (1982), Hydration of Fly Ash in Presence of Gypsum, Review of 36th General Meeting of Cement Association of Japan, pp. 45-46.

K.SATO, E.KONISHI and K.FUKAYA, Nippon Kokan K.K., Kawasaki, JAPAN

Hydration of blast furnace slag particle
Hydratation de particule de laitier de haut fournau

SUMMARY: It is most practical to evaluate the hydraulic reactivity of water granulated blast furnace slag in terms of the strength of hardened body. In order to make the extensive use of slag, however, it is important to investigate the hydration properties of individual particles. Hydration properties mainly investigated here were the change in the amount of hydration and the thickness of hydrated layer with time, and the effect of alkaline activator. We examined the hydration of ground commercial slag with various particle sizes. Experiment was carried out as follows: samples with five different particle sizes (3.27, 4.05, 5.86, 8.66 and 13.36 μm by volume mean diameter) were prepared. They were hydrated in suspension with the water-slag ratio of 10 with NaOH, $Ca(OH)_2$ or ordinary Portland cement as alkaline activator. The amount of hydration of the slag under such an alkali-condition was measured by determining the soluble part of the hydration product using salicylic acid-acetone-methanol solution, and also by loss on ignition.
The following results were obtained. The thickness of hydrated layer of particle did not depend on the particle size, that is, the hydration reactivity had nothing to do with particle size and the rate of hydration was actually in proportion to the total surface area. It was suggested, on the other hand, that each alkaline activator show the characteristic effect on the hydration of each sample. Some of these results were supported by further experiments.

É muito prático avaliar a reatividade hidráulica de escória de alto forno granulada em água, em termos de resistência do corpo endurecido. Contudo, para ampliar a utilização da escória, é muito importante investigar as propriedades de hidratação das partículas individuais. As propriedades da hidratação estudadas particularmente aqui foram a mudança na quantidade de hidratação e a espessura da camada hidratada em função do tempo, e o efeito do ativador alcalino. Examinamos a hidratação de escória comercial moída com vários tamanhos de partícula. As experiências foram realizadas conforme a seguir: amostras com cinco diferentes tamanhos de partícula (3,27 - 4,05 - 5,86 - 8,66 e 13,36 μm por diâmetro médio de volume) foram preparadas. Elas foram hidratadas em suspensão com relação água/escória de 10, e tendo como ativador NaOH, $Ca(OH)_2$ ou cimento portland comum. A quantidade de hidratação da escória sob tal condição alcalina foi medida por determinação da parte solúvel do produto de hidratação, usando-se solução de ácido salicílico-acetona-metanol, e também por perda ao fogo.

Os resultados obtidos foram os seguintes. A espessura da camada hidratada não depende do tamanho da partícula, isto é, a reatividade de hidratação nada tinha a ver com o tamanho da partícula, e a velocidade de hidratação era realmente proporcional à área total de superfície. Por outro lado, sugeriu-se que cada ativador alcalino apresenta um efeito característico sobre a hidratação de cada amostra. Alguns destes resultados foram reforçados por experiências adicionais.

1. INTRODUCTION

The hydraulic hardening property as well as other properties of water granulated blast furnace slag (hereafter referred to as slag) has been widely used for cementing materials.

Recently, there are efforts to fully utilize these properties through fineness control[1].

Here, the authors examine the hydraulic reaction with respect to the particle size of slag to acquire more information on the reaction than ever before.

The particle size distribution and the hydraulic reactivity under several kinds of alkaline activators at relatively early stages of reaction were measured.

From the results obtained, the thickness of the reacted layer of the slag particles was calculated.

State of the reacted surface was also examined by means of AES.

2. EXPERIMENTAL

2.1 Materials and Preparation

The chemical compositions of slag and ordinary Portland cement (hereafter referred to as OPC) used are shown in Table 1.

Table 1. Chemical compositions of slag and OPC (wt.%)

	Ig.loss	Insol	SiO_2	Al_2O_3	Fe_2O_3	CaO	MgO	SO_3	Na_2O	K_2O	TiO_2	P_2O_5	MnO	S
slag	+0.1	0.1	35.4	12.9	0.3	41.8	6.1	0.0	0.26	0.38	1.65	0.00	0.42	1.0
OPC	1.1	0.1	21.2	5.1	3.0	63.1	2.1	2.2	0.40	0.44	0.43	0.07	0.09	-

Besides OPC, guaranteed reagents of NaOH and $Ca(OH)_2$ were used as alkaline activators.

The slag was pulverized to a Blaine specific surface area of 3720 cm^2/g with a ball mill, then separated into 5 samples (denoted as A, B, C, D, and E in order of fineness, particle size distributions and specific surface area are shown in Fig. 3 and Table 3 respectively) by use of a forced vortex type centrifugal classifier.

The particle size distributions were measured by the microscopic method (Image analysis). In this method, the slag powders were dispersed over a slide-glass in a neoprene toluene solution by ultrasonic waves, and the data on each individual particle was computer-processed to get its diameter of the circle of equal projected area giving the particle size distribution.

2.2 Quantitative Determination of Reacted Slags

Sample slag (10g) was hydrated at 20±1°C in 3 different alkaline solutions for 3, 7, and 14d, all with slag-water ratio of 0.1.

Used alkaline solutions were as follows.

(i) 0.1N NaOH aq.soln.

(ii) saturated $Ca(OH)_2$ soln.

(iii) 10g OPC mixed and stirred in 100g water

Sealed polyethylene bottles were used as reaction vessels to prevent carbonation.

With regard to (iii) above mentioned, reaction of 10g OPC alone in 100g water was also carried out as a standard for the determination of reacted slag in a slag-OPC mixture.

After a specified time, the solutions were filtered and the residues were washed with acetone to stop hydration, then D-dried[2] (equivalent vapor pressure = 5×10^{-4} mmHg).

Samples thus obtained were then stirred in a salicylic acid-acetone-methanol solution (hereafter referred to as SAM)[3] to dissolve the hydrated parts for quantitative determination of the reacted slag, and also measured for loss on ignition at 700°C for 1 h.

The amount of hydration of OPC alone (standard) was also quantitatively measured in the same manner.

From this result, rate of reaction and loss on ignition for slag in a slag-OPC mixture were obtained.

The rate of reaction was calculated assuming the soluble part in SAM to be the reacted part, where loss on ignition was taken into consideration.

2.3 Evaluation of the Thickness of the Hydrated Layer

The thickness of the hydrated layer with respect to each sample slag was evaluated as follows making use of the particle size distribution and the rate of hydration.

(1) Particle size (with max. diameter, Dn, by Image analysis) is divided into n portions ($0 \sim D_1$, $D_1 \sim D_2$, ..., $D_{n-1} \sim D_n$).

(2) Assuming the middle value of each portion as the representative diameter, the representative radius of each portion becomes $D_1/4$ ($\equiv r_1$), $(D_1+D_2)/4$ ($\equiv r_2$), ..., $(D_{n-1}+D_n)/4$ ($\equiv r_n$).

(3) The thickness, δ, is obtained by the solution of following equation.

$$R = \sum_{k=1}^{n} M_k \left\{ 1 - \left(1 - \frac{\delta}{r_k} \right)^3 \right\}$$

$$= \left(\sum_{k=1}^{n} \frac{M_k}{r_k^3} \right) \delta^3 - 3 \left(\sum_{k=1}^{n} \frac{M_k}{r_k^2} \right) \delta^2 + 3 \left(\sum_{k=1}^{n} \frac{M_k}{r_k} \right) \delta$$

where M_1, M_2, ..., M_n are the contents (weight ratio) of each portion, and R the rate of reaction measured.

2.4 AES Analysis

AES coupled with Ar ion milling was performed on the surface of the hydrated slag particles (sample E) to obtain the compositional profile of the hydrated surface.

A Perkin-Elmer SAM-600 was used with the electron beam voltage and current of 3 kV and 4×10^{-8} A respectively.

The voltage and current of ion beam were 3 kV and 2 ∿ 3 μA respectively.

In this analysis, sample particles were lightly pressed against an indium plate for fixation and electric conductivity.

Changes in Auger spectra were examined for NaOH-activated samples (3, 7, and 14d) and $Ca(OH)_2$-activated sample (14d) with ion milling times of 0, 2, 5, 10, 20, 30, 40, 50, 80, and 120 minutes.

3. RESULTS AND DISCUSSIONS

3.1 Rate of Hydration and Non-evaporable Water

Changes in the non-evaporable water content (determined by ignition of D-dried samples at 700°C for 1 h) and the rate of reaction for each slag are shown in Fig. 1 and Fig. 2 respectively.

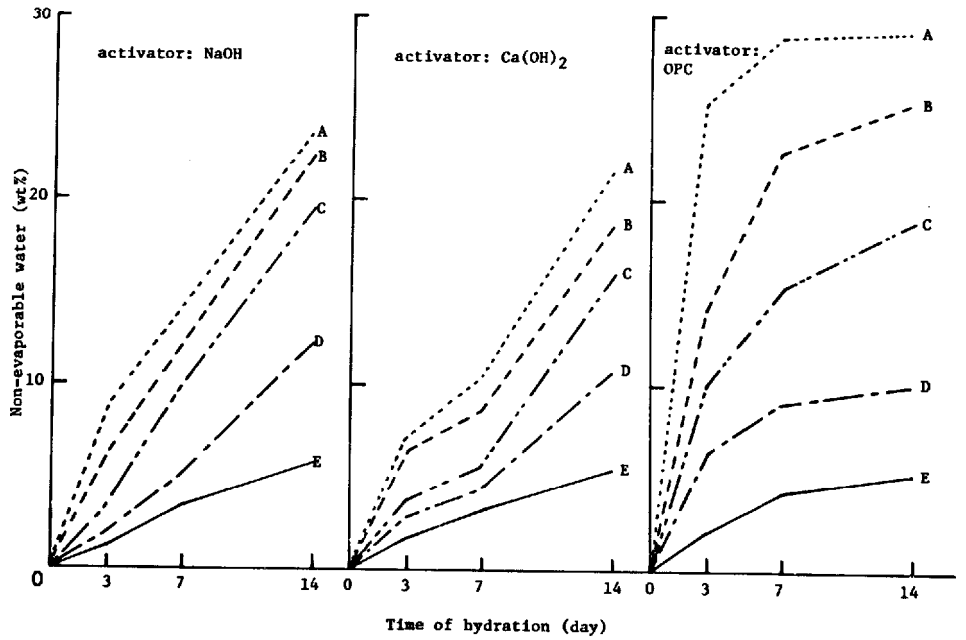

Fig. 1. Non-evaporable water content (loss on ignition)

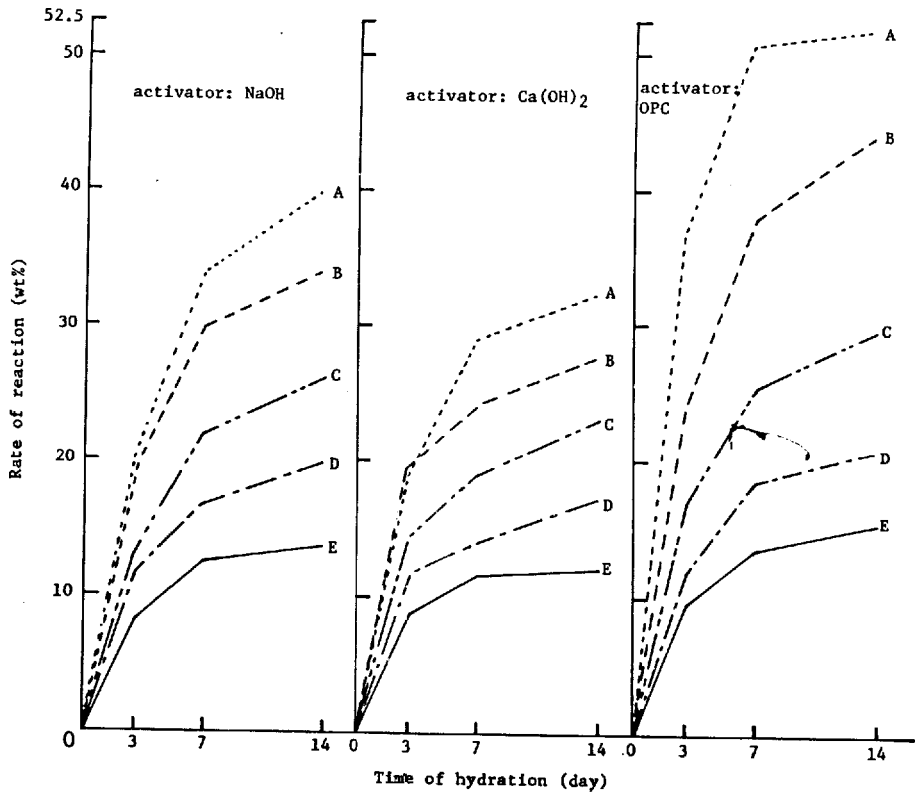

Fig. 2. Change in rate of reaction with time

3.1

As shown in Fig. 1, tendencies of increase in non-evaporable water content are nearly the same for NaOH-activated samples and $Ca(OH)_2$-activated ones, however, in the case of $Ca(OH)_2$-activation, the rate of increase temporarily slows down during the period from 3d to 7d.

On the other hand, OPC-activated samples show very large non-evaporable water contents which are especially large in the cases of fine samples and early stages.

Concerning the rate of hydration, as shown in Fig. 2, activating effect of NaOH is superior to that of $Ca(OH)_2$, and OPC shows the highest effectivity even from very early stage.

3.2 Factors Influencing the Slag Hydration

(1) Particle size

Figure 3 shows the particle size distributions (by Image analysis) of sample slags before hydration.

The thickness of the reacted layer was evaluated through the method mentioned in 2.3 using the particle size distributions (Fig. 3) and the rate of reaction (Fig. 2).

In this case, particle diameters mentioned in 2.3 (1) were chosen as D_1=1, D_2=2, ..., D_{10}=10, D_{11}=12, D_{12}=15, D_{13}=20, and D_{14}=25 (n=14).

The results are shown in Table 2.

As shown in Table 2, the thickness of the hydrated layer changes with the kind of used activators, but the difference in the thickness among samples of various fineness is not significant.

From these data, it may be deduced that the thickness of the reacted layer has nothing to do with particle size.

The thickness for $Ca(OH)_2$-activated samples are approximately 0.13 μm at 3d, 0.17 μm at 7d, and 0.2 μm at 14d.

This result is in fine agreement with that for paste-hydration reported by Daimon, et al[4].

This agreement implies that the difference in reaction environment (suspension form or paste form) does not affect hydration.

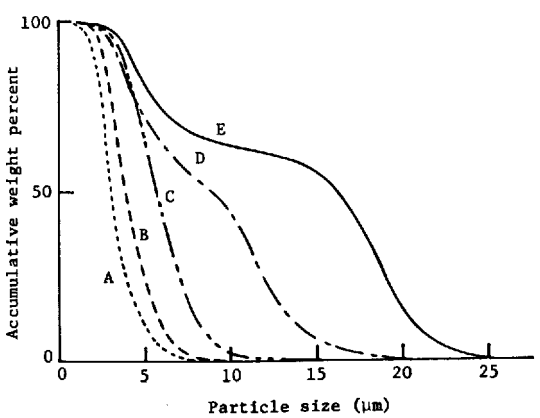

Fig. 3. Particle size distributions of slags

(2) Surface area

Based on the result of particle size analysis, the specific surface area of each slag (before hydration) was calculated. The result is shown in Table 3.

The reacted amount with respect to a unit surface area was obtained by dividing the rate of reaction by the calculated specific surface area. The result is shown in Fig. 4.

As shown in Fig. 4, slags with various fineness show almost equal reacted amount for unit surface area regardless of the kind of activator; the amount of reaction is practically dependent only on the total surface area.

The reacted amounts for the fine samples, however, tend to be a little smaller than those for coarse ones in the cases of NaOH and $Ca(OH)_2$-activation, and the increase in the reacted amount for sample E tends to slow down at later stage.

The reason for this seems to be due to the change in reaction area caused by the agglomeration of particles.

Such tendencies were not shown in the case of OPC-activation.

Table 2. Thickness of the reacted layer (μm)

activator	slag	3d	7d	14d
NaOH	A	0.13	0.18	0.23
	B	0.12	0.20	0.24
	C	0.13	0.20	0.25
	D	0.13	0.19	0.23
	E	0.13	0.21	0.23
$Ca(OH)_2$	A	0.10	0.16	0.18
	B	0.12	0.17	0.18
	C	0.13	0.17	0.22
	D	0.13	0.16	0.20
	E	0.13	0.18	0.20
OPC	A	0.21	0.32	0.34
	B	0.16	0.27	0.33
	C	0.16	0.25	0.30
	D	0.14	0.21	0.24
	E	0.15	0.24	0.26

Table 3. Specific surface area of slags obtained from particle size analysis

slag	A	B	C	D	E
specific surface area (cm^2/g)	7200	5610	3860	2780	2330

3.1

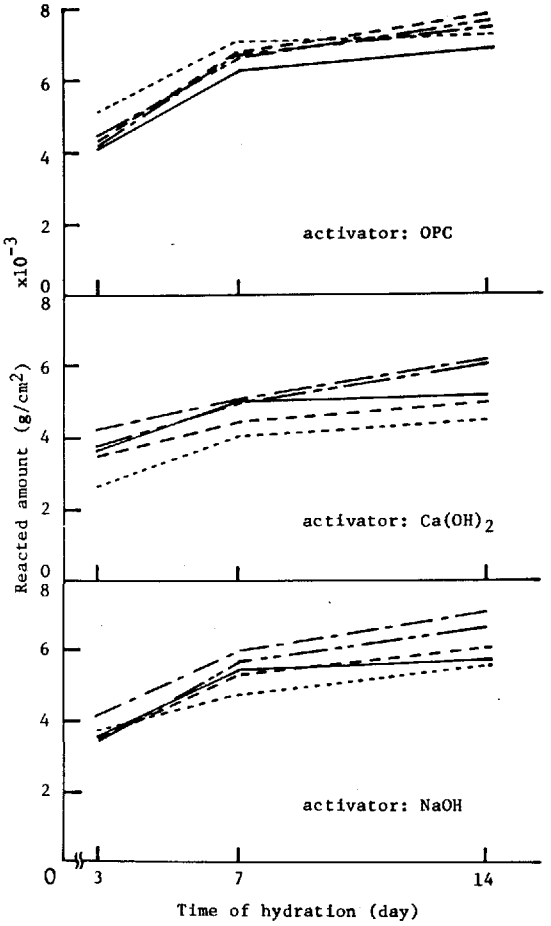

Fig. 4. Reacted amount for a unit surface area

(----------A, - - - - - - B, —— - - —— C
—— - —— D, ———— E)

(3) Alkaline activator

There is no difference between NaOH and $Ca(OH)_2$ in the activating effect up to 3d, however, the effect of NaOH becomes greater on and after 7d.

On the other hand, OPC has a superior activating effect especially in the early stage.

Higher effectivity of OPC could be due to the active release of $Ca(OH)_2$ accompanying its hydration and the acceleration of ion mobility.

This corresponds with the effectivity of OPC-originated $Ca(OH)_2$ on slag hydration especially high in the early stage reported by Matsukawa, et al[5].

3.3 State of the Hydrated Surface

Figure 5 shows the changes in Ca/Si ratios obtained from AES (peak-to-peak height) with ion milling time.

Here, ion milling time corresponds to the depth below the surface.

The Ca/Si ratios for the near surface are considerably small especially after 7d of hydration, which suggests the presence of a SiO_2-enriched layer resulting from the leaching of Ca.

The Ca/Si ratios take sudden increase with the process of ion milling.

The peak of the Ca/Si ratio was shifted to longer ion milling time (deeper below surface) with the process of hydration.

As shown in Fig. 5, peak positions are 20, 30, and 40 minutes in terms of ion milling times for 3, 7, and 14d samples respectively.

The Ca/Si ratios for 14d samples remained quite low up to 20 min of ion milling time.

In the case of $Ca(OH)_2$-activation (14d), the ratio increased away from the near surface to have a peak at about the same depth as NaOH-activation.

With regard to 3d sample, ion milling of 40 ∿ 50 min was required for the Ca/Si ratio to equal that of inner part (unhydrated part), and 50 ∿ 80 min was required in the cases of 7 and 14d samples.

The rate of material removed can be taken to be about 30 Å/min[6]. With this rate, ion milling times of 40, 50, and 80 min correspond to the depth below surface of 0.12, 0.15, and 0.24 μm respectively.

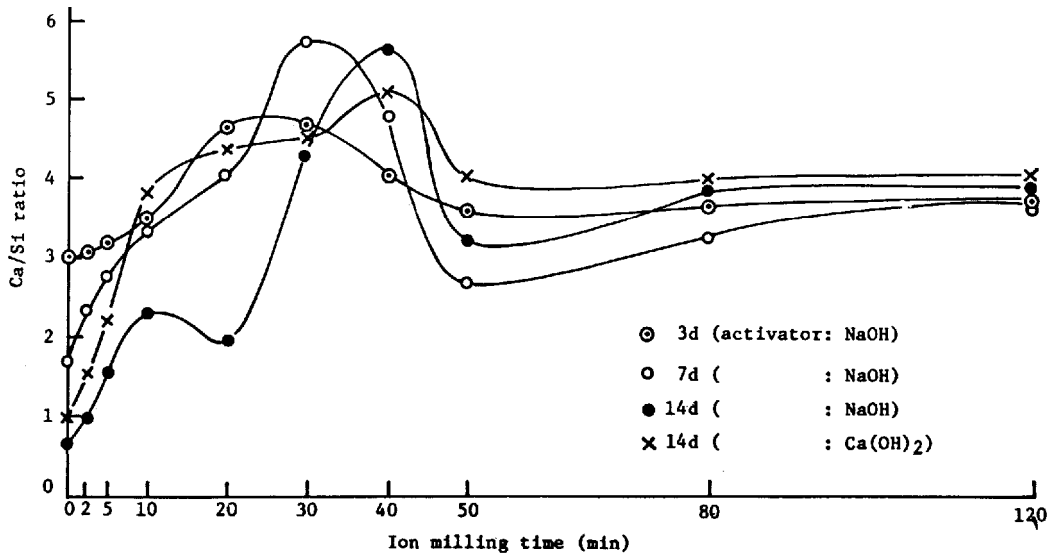

Fig. 5. Change in Ca/Si (by peak-to-peak height) with ion milling time

4. CONCLUSION

Slag powders of various particle size distributions prepared by classification were suspension-hydrated to examine the factors affecting the hydration of slag particles (e.g. particle size, surface area, kind of alkaline activator).

Obtained results can be summarized as follows.

(1) Thickness of the hydrated layer on slag particles are independent of particle size, that is, reactivity of slag particle has nothing to do with the particle size.

(2) The rate of hydration of slag powder is actually dependent only on the total surface area.

(3) Each alkaline activator has the characteristic effect on slag hydration. The difference between NaOH and $Ca(OH)_2$ in activating capacity is not noticeable up to 3d, but the effectivity is greater with NaOH after 7d. On the other hand, activating effect by OPC is far greater especially in the early stages.

(4) AES coupled with ion milling on the hydrated surface shows that Ca content decreases at near surface, and the peak of Ca/Si ratio is shifted inside with the process of hydration. Changing profile of Ca/Si ratios with ion milling time (depth) depend on the kind of alkaline activator.

REFERENCES

1. K. Sato, E. Konishi, K. Fukaya, K. Koibuchi, Y. Ishikawa and Y. Iijima, "Properties of very fine blast furnace slag prepared by classification", 8th Int. Cong. Chem. Cem., Rio de Janeiro, 1985, submitted.
2. L.E. Copeland, J.C. Hayes, ASTM Bull., No.194, 70 (1953)
3. R. Kondo and S. Ohsawa, Proc. 5th Inter. Symp. Chem. Cement, Tokyo Vol. IV, 255 (1968)
4. S.A. Abo-EI-Enein, M. Daimon, S. Ohsawa and R. Kondo, Cement and Concrete Research, 4, 299 (1974)
5. M. Matsukawa, K. Sato and K. Fukaya, Revew of the 39th general meeting of The Cement Association of Japan, 1985, Lecture No.129
6. D.E. Clark, M.F. Dilmore, E.C. Ethridge and L.L. Hench, J.Am. Ceram. Soc., 59 [1-2] 62 (1976)

J. MAŁOLEPSZY, University of Mining and Metallurgy, Cracow, Poland

Activation of synthetic melilite slags by alkalies.
L'activation alcaline des laitiers mélilitiques synthétiques.

SUMMARY : The investigations of the Polish granulated blast furnace slags have shown that the glassy and crystalline melilite is the main phase in these slags. The object of the research was to determine the influence of different alkaline additions on the hydration process of melilite slags. Three melilite slags with variable ratio of C_2MS_2 to C_2AS were applied. Na_2CO_3 and NaOH served as the activators of the hydration of synthetic slags. The investigations of the strength properties of hardened melilite pastes shoved that there are close relations between the chamical composition of the slag and used acivator. As activator Na_2CO_3 is especially suitable for activation of the slags rich in C_2MS_2, and NaOH for the slags rich in C_2AS. The slags containing the largest amount of C_2AS gained the highest strength of 110 MPa. The X-ray and microscopic investigations revealed that the hydrogarnets, calcium hydrosilicates of CSH type, $CaCO_3$ and sodium zeolites are the newly formed products. The amount of crystalline phases occuring in hardened melilite pastes depends on the time and conditions of hardening. Autoclaving provokes an elargement of the amount of well-developed crystals of newly formed products.

A investigação de escórias polonesas de alto forno, granuladas, mostraram que a melilita vítrea e cristalina é a fase principal destas escórias. O objeto desta pesquisa foi determinar a influência de adições alcalinas diferentes sobre o processo de hidratação de escórias de melilita. Foram utilizadas três escórias de melilita com relação variável de C_2MS_2 para C_2AS. Os ativadores da hidratação das escórias sintéticas foram Na_2CO_3 e NaOH. As investigações relativas às propriedades de resistência de pastas de melilita endurecidas mostraram que há relações estreitas entre a composição química da escória e o ativador usado. Como ativador, Na_2CO_3 é especialmente adequado para ativação de escórias ricas em C_2MS_2, e NaOH para escórias ricas em C_2AS. As escórias contendo maior quantidade de C_2AS atingiram resistência máxima de 110 MPa. As investigações por raio-X e microscopia revelaram que hidrogranadas, hidrossilicatos de cálcio de tipo CSH, $CaCO_3$ e zeolitos de sódio são os produtos formados por último. A quantidade de fases cristalinas que ocorrem nas pastas endurecidas de melilita depende do tempo e das condições de endurecimento. A autoclavagem provoca um aumento da quantidade de cristais bem desenvolvidos dos produtos recentemente formados.

1. INTRODUCTION

The properties of binding materials obtained from granulated blast furnace slags depend not only on the type of slag, but on the additions introduced in the grinding process and on the method of preparation of mortars and concretes too. Portland cement clinker quicklime and gypsum are commonly used additions. As the usual practice dry granulated slag is fed into a grinding mill with the activators. The obtained materials are characterized in many cases by very slow rate of strength development in initial period of hardening /1-4/. The materials obtained from granulated slags containing considerable amount of alumina may be the exception to the rule. The growing economic crisis in the world induces investigations on new technologies of binding materials. These technologies should consider low energy-consuming materials in comparison with the commonly produced cements /5-6/. The lovest energy consumption is required for the production of binding materials containing no Portland cement clinker. In the case of activation of granulated slags by small amounts of alkalies /NaOH, Na_2CO_3, liquid glass/ the obtained binding materials are characterized by very low energy consumption and high early as well as ultimate strength /7-10/. The tests made on Polish granulated blast furnace slags showed, that they have low hydraulic properties. The slags contain, as an essential component, melilite phase both in glassy and crystalline form. From the available literature one would conclude, that melilite glasses were activated practically only by $Ca(OH)_2$ and $CaSO_4$ /11-12/. Our investigations on the activation of melilite glasses by alkalies have shown that it is possible to obtain the binding materials with different properties /13/. In this paper the results of investigations of compound composition and texture of hardened melilite pastes are presented.

2. EXPERIMENTAL

2.1. Characteristic and preparation of samples.

Three slags of melilite series were synthesized. The conventional compound composition was, as follows :

Slag I 20% C_2AS + 80% C_2MS_2
Slag II 40% C_2AS + 60% C_2MS_2
Slag III 60% C_2AS + 40% C_2MS_2

The slags were prepared from sodium carbonate, alumina oxide, silica gel and magnesium hydroxide of the highest purity, covering an area of calculated chemical compositions. The mixtures were fused for 30 min at the maximum temperature. The completely fused masses were quenched with large amounts of water. The chemical composition of obtained slags was confirmed. The results of the investigations are given in Table 1.

Table 1 : Determined chemical composition of the slags used in the tests

Constituent	Content in slag [%]		
	I	II	III
CaO	41,2	41,2	41,0
MgO	39,5	5,8	5,8
Al_2O_3	7,4	14,8	22,3
SiO_2	11,9	35,2	30,9

The degrec of ritrification and compound composition of synthetic slags were determined by means of Reichert microscope. Fractions of glass and crystalline phases in the tested slags were determined using povder preparations. Content glass phases in slags was elevateing 80%.
In synthesized slags the crystalline phase was formed by melilite crystals of several microns. X-ray examinations confirmed the results of the observations of the slags under microscope.

2.2. Effect of Na_2CO_3 and NaOH on the strength properties of hardened pastes.

The synthetic slags were ground in agate mill to a fineness of 3200 cm^2/g, measured according to the Blaine method. Sodium carbonate and sodium hydroxide were used as activators. The activation was carried out in two manner. In the first case the both activators used in different amounts. The addition of 5 per cent of sodium carbonate was applied, it is equivalent of 2,9% Na_2O. The amount of this activator was selected in accordance with the results of our investigations /15/. The amount of sodium hydroxide was 3,8 per cent-equivalent of 2,9% Na_2O.
In the second case only NaOH was applied for activation of slags. The amounts of activator were variable and related to Al_2O_3 content in tested slags. The amount of NaOH was applied in a proportion to make the molar ratio $Na_2O/Al_2O_3 = 1$. Such amount of the activator makes that theoretically total amount of Al_2O_3 in slags reacts with NaOH to form sodium hydroaluminosilicates.
The powdered slags were mixed with water at a slag/water ratio of 0,3. The pastes were formed into cylinders of 2 cm high and 2 cm diameter, and vibrated for 2 min. The cylinders were steam cured and autoclaved. The conditions of steam curing were, as follows temperature - 80°C, time - 6hrs. The cylinders were autoclaved for a period of 2 hrs at 180°C.
The compressive strength and compound composition were tested employing the cylinders made from hardened slag pastes.
The results of compressive strength test are given in Tables 2 and 3.

Table 2 : Strength data of slag pastes activated by addition of 5% Na_2CO_3 and 3,8% NaOH

Type of heat treatment	Slag	Compressive strength /MPa/ after steam curing		at 28 days	
		Na_2CO_3	NaOH	Na_2CO_3	NaOH
Steam curing	I	41,3	15,5	51,4	21,7
	II	36,8	19,8	46,6	27,6
	III	25,2	27,8	29,6	37,5
Autoclaving	I	46,6	33,8	58,5	40,9
	II	39,8	38,9	48,5	46,3
	III	36,7	52,7	41,3	59,3

Table 3 : Strength data of slag pastes activated by NaOH at $Na_2O/Al_2O_3 = 1$

Slag	Strength of pastes /MPa/ steam cured		autoclaved	
	after treatment	at 28 days	after treatment	at 28 days
I	36,8	45,9	70,9	80,6
II	47,2	56,4	87,6	95,6
III	53,6	61,4	95,3	109,8

2.3. Effect of added activators on the compound composition of hardened slag pastes

In the order to elucidate the reason of the differences in strength properties of slag pastes the compound composition was investigated by means of X-ray diffraction method and scanning electron microscope. In the case of activation of slags I, II and III by sodium carbonate the greatest amount of newly formed compounds was stated in hardened paste prepared from slag I. In this sample considerable amounts of calcite /d=3,03; 2,48/, thomsonite /d=2,95 ; 2,68; 3,30/, hydrogarnet /d=2,73 ; 3,26/, CSH phase /d=3,07 ; 1,83/ and small amounts of sodium zeolites /d=3,40 ; 1,63/ were observed. The smallest amount of newly formed crystalline compounds occured in slag III, as practically calcite /d=3,03/, CSH /d=3,07/ and hydrogarnet /d=2,75/ only were identified. The investigations of compound composition of the slags activated by NaOH revealed that the greatest amount of newly formed phases occured in the hardened paste made from slag III. The characteristic lines of sodium zeolites /d=7,62 ; 6,02 ; 4,38 ; 3,65/, thomsonite /d=2,98 ; 2,85 ; 3,30/, calcite /d=3,03/ CSH /d=3,07/ and hydrogarnet /d=2,75/ were noticed.
The results of the investigations by means of scanning electron microscope are given in the Figures.

3.1

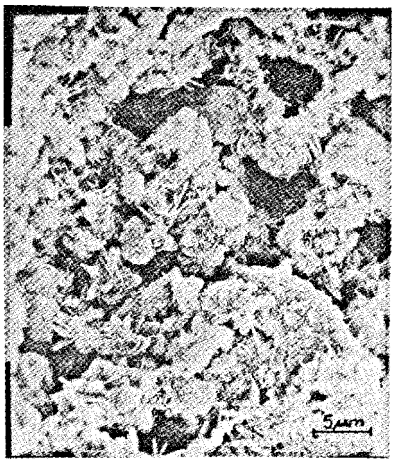

Fig. 1 - Slag paste I /Na_2CO_3 as activator ; steam cured/ at 28 days of hardening.

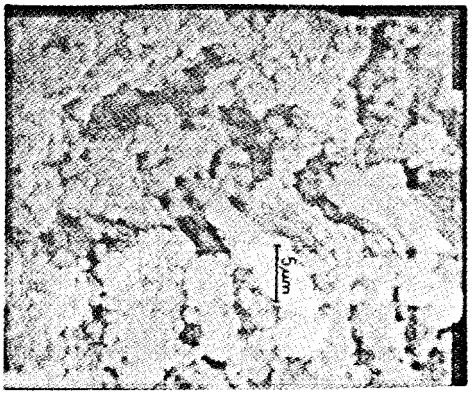

Fig. 2 - Slag paste III /Na_2CO_3 as activator; steam cured/ at 28 days of hardening.

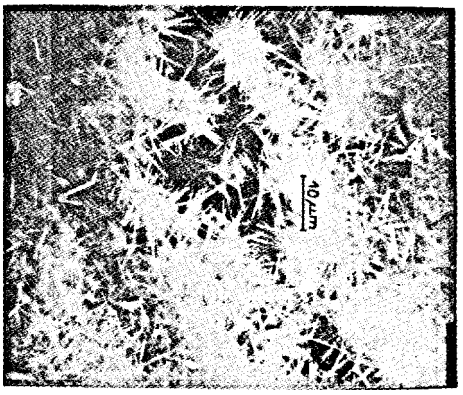

Fig. 3 - Slag paste I /Na_2CO_3 as activator , autoclaved cured/.

3. DISCUSSION

The investigations revealed that the compressive strength of hardened slag pastes depend first of all on the type of the alkaline activator. The rate of strength development is affected by the conditions and period of hardening and by quantity of activator. The autoclaved pastes made from the slag III with NaOH as activator attained the highest strength of 110 MPa. It is concluded that Na_2CO_3 is especially suitable for activation of melilite slags rich in C_2MS_2 and NaOH -

for activation of melilite slags rich in C_2AS. The differences in the strength properties of hardened slag pastes result first of all from the different degrees of promotion of the reaction of slag with activator. The results of X-ray investigations demonstrated that the pastes attaining the high compressive strength are characterized by larger amount of newly formed products in comparison with the melilite pastes of lower strength. The research carried out by means of scanning electron microscope have shown that at early age of hardening of slag pastes the gel phase is the main product. The well - developed crystals occured only occasionally. Calcite is the first crystalline phase. Prolonged period of hardening or hydrotermal treatment cause that the amount of crystalline phases considerably increases. It has been stated, that the crystals characterized by fibrous habit /probably they are sodium zeolites/ appeared in small amounts and first of all in the pores. On the basis of the realized research and the literature data /14, 15/ it may be concluded, that efficiency of the influence of the activator depends on the structure of melilite glass and thereby on the ratio of C_2MS_2 to C_2AS in the slag.

4. REFERENCES

1. - P. BUDNIKOW , Granulowanyje domiennyje szłaki i szłakowyje ciemienty,Moskwa 1953.
2. - F. SCHRØDER, 5-th Intern. Symp. on the Chem. of Cement, Tokyo 1968 vol. IV, 149-179.
3. - W. SATARIN, 6-th Intern. Symp. Chem. of Cement, Moskwa 1974 vol. III 45-56.
4. - I. TEOREANU, M. GEORGESCU, A. PURI, 7-th Intern. Symp. on the Chem. of Cement, Paris 1980 vol. III 99-104.
5. - P.K. MEHTA, World Cement Technology 1980, 5, 144-147.
6. - W. KURDOWSKI, L. TACZUK, Cement Wapno Gips 1983, 10-11, 271-273.
7. - W.D. GŁUCHOWSKI, Gruntosilikati worobi i konstrukcji, Kijów 1968.
8. - W.D. GŁUCHOWSKI, Baustoffindustrie 1974, 3, 9-12.
9. - W.D. GŁUCHOWSKI, Bieton-Żelazobieton 1975, 5, 8-11.
10. - J. MAŁOLEPSZY, 8.Intern. Baustoff und Silikattagung "Ibausil", Weimar 1982 vol. I 158-164.
11. - K. STEPIEŃ, Cement Wapno Gips 1973, 3 80-83.
12. - A.A. GORROW, 7-th Intern.Symp. on the Chem. of Cement, Paris 1980, vol. III 7-12.
13. - A. DERDACKA, J. MAŁOLEPSZY, Cement Wapno Gips, 1980, 8-9, 217-220.
14. - P.W. KRIWIENKO, II Wsiochsojuznaja Konferencja, Kijów 1984, 10-16.
15. - W. SATARIN, 6-th Intern. Symp. of the Chem. of Cement, Moskwa 1974 vol. III 45-56.

J. MAŁOLEPSZY and M. PETRI, University of Mining and Metallurgy, Cracow, Poland

High strength slag-alkaline binders.

Matariaux liants en laitier alcalinisé de haute resistance.

SUMMARY : There have been studied two binders prepared from the blast furnace slag with Blain's surface area about 3200 cm^2/g, activated by water-glass or Na_2CO_3. Quantities of alkaline additions in both causes were 3% Na_2O in proportion to slag. Sand mortar samples were made with water/solid state ratio 0.3. Theirs mechanical properties as: compressive strength, bending strength, Young's modulus, and scale effect were determinated. Structurs were investigated by SEM and mercury porosimetry. It was shown, that material made of slag-water glass binder assure the high strength, especially compresive strength.

Foram estudados dois materiais ligantes a partir de escória de alto forno, com área de superfície Blaine de cerca de 3.200 cm^2/g, ativados por agua-vidro ou Na_2CO_3. As quantidades de adições alcalinas em ambos os casos foram de 3% de Na_2O em relação à escória. Amostras de argamassa de areia foram preparadas com relação água/sólido igual a 0,3. Foram determinadas suas propriedades mecânicas, como resistência à compressão, resistência à flexão, módulo de Young, e efeito de escala. A investigação das estruturas foi feita por SEM e porosimetria de mercúrio. Ficou demonstrado que material feito com ligante de "vidro de escória - água" garante a alta resistência, especialmente a resistência à compressão.

1. INTRODUCTION

A conventional production of Portland cement is very energy-consuming ; price increase of fuels and electric energy being the reason of additional cost of the production of this material. Reduction of the energy consumption can be obtained by means of dry clinker production. Other way of saving energy may be attained by modifying the mineralogical composition of clinker to lower the burning temperature of initial material mixture of about 1200°C /1, 2/. A large economy of energy is effecting by using the hydraulic clinkerlss binders /3/. Activation of glassy calcium and magnesium aluminosilicates is one of the ways of getting such binders, the theoretical basis of which has been described by Głuchowski /4/. This binder is of very beneficial features, for instance high strength, freeze resistance and chemical carrosion resistance /5-9/. Basic materials to obtain such binders there are the granular blast furnace slag as well as the slags of non-ferrous metallurgy. In the production of slag-alkaline binders the energy-consuming processes such as preparation and burning of basic mixture, are negligible. This technology makes also possible to obtain rapid-hardening cements, drilling cements and others /10, 11/. In this paper the results of microstructure studies and utilitarian properties are presented.

2. EXPERIMENTAL

2.1. Conditions of mortar preparation.

A weakly-alkaline granular blast furnace slag of specific surface of 3200 cm^2/g was used to mortar preparation. The sodium carbonate and water-glass of silicate module of 1.0 was the activating agent. The mortar was prepared from the standard sand and slag of 3:1 ratio. The water-binding coefficient amounted to 0.30. The content of the activator was : 5% Na_2CO_3 with respect to slag ; 15% water-glass with respect to slag. The formed beams of 20x20x100 mm dimensions were low-pressure infused for 4h at the temperature 80°C and then dry stored for 28 days.

2.2. Mechanical properties.

Destructive determinations of mechanical properties of the studied material were performed, i.e. bending strength /σ_b/, compressive strength /σ_c/ and Youngs' modulus /E/. The samples of 20x20x100 mm dimensions were bended in the three-point system with spacing bearings of 50 mm and after that the half-sample, 20x20x50 mm, were compressed. The results are collected in the table 1.

Table 1

Material	Determination	N	$\bar{X}$ /MPa/	σ^2	Variation as: $\frac{\sigma}{\bar{x}}\cdot 100$	
slag + +water glass	σ_b	77	21,94	13,58	16,8	10,7*
	σ_c	156	101,38	497,43	22,0	
	E	77	$1.76\cdot10^4$	$1.03\cdot10^7$		
slag + +Na_2CO_3	σ_b	94	13,44	2,54	11,8	12,9*
	σ_c	181	37,53	17,99	11,3	
	E	94	$1.10\cdot10^4$	$1.78\cdot10^6$		

*Values were calculated from "m" constant in the Weibull's equation

From the results constant function parameters formulating the probability of material rupture /S/ at given distribution of stresses /σ/ over a volume /V/ have been evaluated. The measurements of the bending strengths both materials were correlated with Weinbull's equation /12/.

$$S = 1-\exp /-VK /\sigma - \sigma_u/^m/$$

where σ_u, k, m, are the characteristic constants . A statistical theory of fracture /WLT/ assumes that probability of brittle failure depends on the localized stress in the point where the most important defects of microstructure appear. These defects are subject to statistical distribution, which is in good agreement with Weinbull's equation for majority of experimental data. The larger is specimen, the higher is probability of finding a primary element of weak strength what results in weaker strength of specimen in total. In Batdorf's opinion /13/ the micro-cracks in the material are responsible for cracking and Weinbull's equation is the cracking density function. The WLT theary is limited to incidental stresses of stretching type or to combination of non-axial stretching and compression. In Fig. 1 and 2 a distribution function in the system of coordinates is presented

$$\log\log\frac{1}{1-s} = m\log/\sigma - \sigma_u/ + \log V + \log k + \log\log e$$

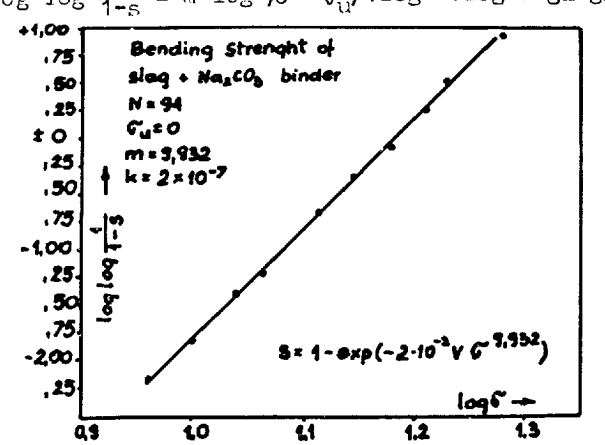

Fig. 1 - Distribution vs bending strength in slag + Na_2CO_3 material.

3.1

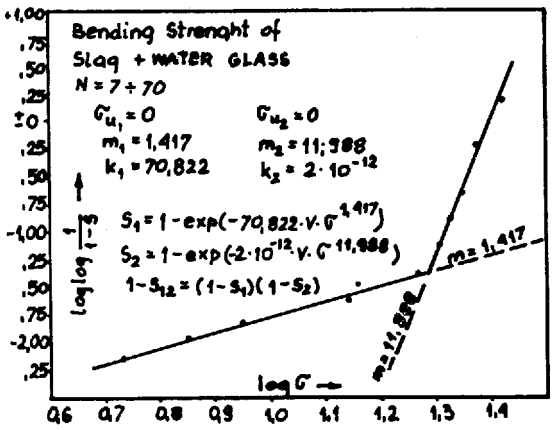

Fig. 2 - Distribution vs bending strength in slag + water glass material.

For both water-glass and Na_2CO_3 activated materials the σ_u attains value of 0 what means that the rupture can appear at any positive value of tensile stress. For the material obtained from the water-glass activated slag a distribution function is composite one and can be expressed by two distribution equations, S_1 and S_2. A rupture probability, S_{12}, for the material of such a distribution function can be calculated /14/ as : $/1-S_{12}/ = /1-S_1//1-S_2/$. The above observation proves that two kinds of defects appear in the material obtained from the water-glass activated slag and each one is described by different distribution function. The "m" constant in the Weinbull's equation is a measure of variation of material strength. For $\sigma_u = 0$ a coefficient of variation for homogeneous state of stress calculated as $/ \frac{\sigma}{\bar{\sigma}} \cdot 100/$ is independent of sample volume and is defined by the "m" exponent.

2.3. Microstructure

X-ray analysis of phase composition has shown that in the material obtained from the Na_2CO_3 activated slag the reaction products are : CSH phase, calcite and zeolite-type minerals, thomsonite mainly. Using a water-glass as the activator the same reaction products are obtained, but a stage of the slag reaction is higher and consequently the higher is content of CSH phase and zeolites. The SEM observation of the fracture surfaces are shown in the Fig. 3-6. Microphotograph /Fig. 3/ shows a typical range occupied by the reaction products /of gel character/, and irregular microstructure with clearly visible micro-cracks.



Fig. 3 - Fracture surface of slag + Na_2CO_3 material.

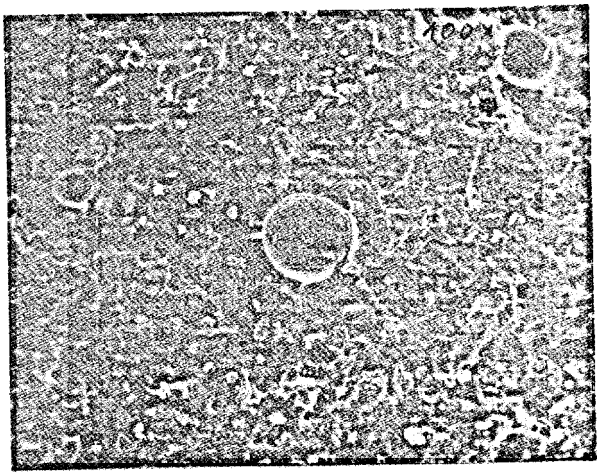

Fig. 4

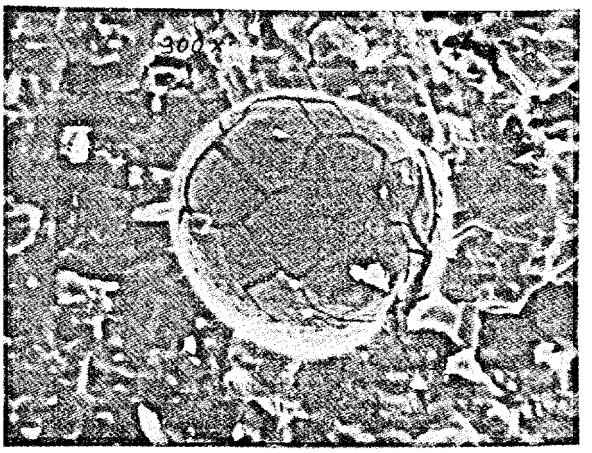

Fig. 5

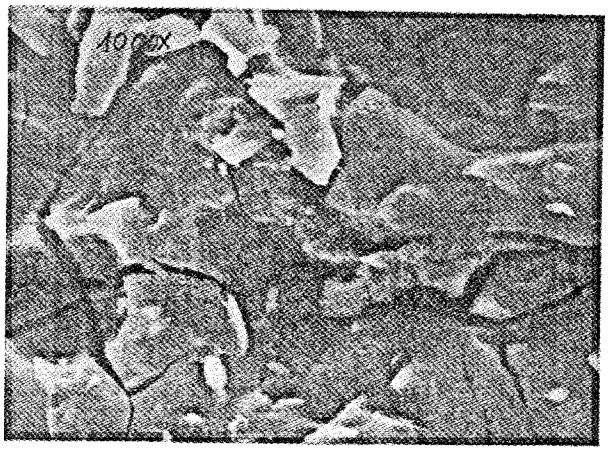

Fig. 6

Figures 4, 5, 6 - Fracture surfaces of slag + water-glass material.

The reaction products of slag and water--glass are more compoct. It is possible to distinguish the two kinds of microstructure defects, i.e. micro-cracks and spherical pores of 25-160 /um. This observation is in agreement with the results of mechanical properties measurements. A determination of porosity and distribution of pore size /Fig. 7/ has shown that these two materials differ mainly with the general porosity but the distribution of pore size is close to each other.

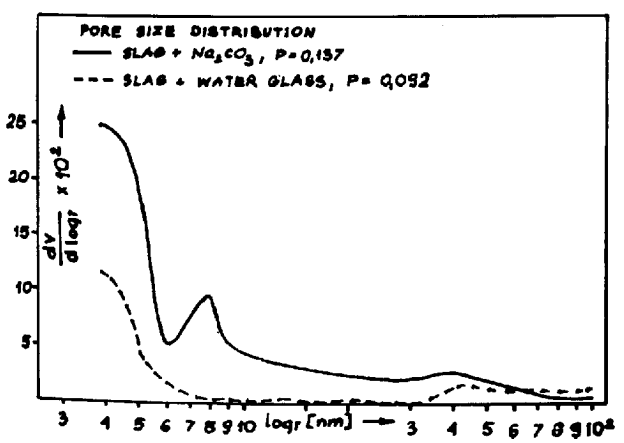

Fig. 7 - Pore size distribution curves of both slag-alkaline materials.

It can be assumed that pores identified by porosimetry are those observed on micro-photographs as micro-craks. The large, spherical pores existing in the material slag--water-glass have not been detected by means of mercuric porosimetry because of their large size.

3. CONCLUSIONS

The kind of activator is of great importance with respect to microstructure and mechanical properties of the slag-alkaline binders. Much higher values of $_c$, $_b$ and E can be obtained in the case of water-glass activation of slag. Characteristic features of this material consist on two kinds of micro-defects ; micro-cracks and spherical pores which have different effects on its mechanical properties. Neverthelss, the more compact structure of CSH gel and smaller porosity assure the high strength, especially compression strength.

4. REFERENCES

1.- P.K. MEHTA, World Cement Technology,4, /1980/.

2.- W. KURDOWSKI and L. TACZUK, Cement Wapno Gips, 10,11, p.271-273, /1983/.

3.- P.A. BUDNIKOV, Granulovany domennye shlaky y shlakovye cementy, Moskva /1953/.

4.- W.D. GŁUCHOWSKI, Gruntosylykatny Vyroby y Konstrukcy, Kiev /1967/.

5.- W.D. GŁUCHOWSKI and G.S. ROSTOVSKAYA, Beton zelazobeton, 6 /1975/.

6.- W.D. GŁUCHOWSKI, Cement Wapno Gips 4, /1976/.

7.- J. MAŁOLEPSZY, 8 Intern. Baustoff und Silikattagung, Sektion 1, Weimar /1982/.

8.- T. KUTTI, R. MALINOWSKI and M. SREBNIK, Silicates Industriels, 6, p.149-153, /1982/.

9.- K.C. NARANG and CHOPRA, Silicates Industriels, 9, p. 175-182, /1983/.

10.-W.D. GŁUCHOWSKI, II Wsyes Konf.Shlako. Cementy, Betony y Konstrukcye, p.3-9, Kiev, /1984/.

11.- J. MAŁOLEPSZY and J.DĘJA, Cement Wapno Gips, 10,11, p. 300-303, /1983/.

12.-W. WEIBULL, A statistical theory of the strength of materials, Ingeniörsvetenskapsakademiens, Handlingar nr 151,Stockholm /1939/.

13.-S.B. BATDORF, Fundamentals of the statistical theory of fracture, in Vol. 3, Fracture Mechanics of Ceramics, Ed. R.C. Bradt, D.P.H. Hasselman, F.F. Lange, Plenum Press /1978/.

14.-W. WEIBULL, The phenomen of rupture in solids, Ingeniörsvetenskapsakademiens, Handlingar nr 153, Stockholm /1939/.

F.GOMA Doctor of Chemistry Science
Laboratori de recerca química del Departament de Construcció de
L'ESCOLA TÈCNICA SUPERIOR D'ARQUITECTURA DE BARCELONA -

Generalized method for the determination of the composition of Portland cement mixtures with additions .

Méthode généralisée pour la determination de la composition des ciments Portland avec constituants secondaires.

GENERALIZED METHOD FOR THE DETERMINATION OF THE COMPOSITION OF PORTLAND CEMENT MIXTURES WITH ADDITIONS

SUMMARY

We describe a new method for the determination of the composition of Portland cement mixtures with active additions and the identification of the type of addition.

This method enables us to classify a Portland cement or Portland cement with active additions,whatever this addition may be, and it is specially suitable for discriminating the type of slag when there are slags present.

Descrevemos um novo método para a determinação da composição de misturas de cimento portland com adições ativas, e a identificação do tipo de adição.

Este método nos permite classificar um cimento portland ou um cimento portland com adições ativas, qualquer que seja esta adição, e é especialmente adequado para identificar o tipo de escória, quando há presença de escórias.

Generalized method for the determination of the composition of Portland cement mixtures with additions

INTRODUCCTION

The presence of active additions in cements as a secondary components raises the need for disposing of analytical methods which can solve their compositions

The methods existing nowadays,based on more or less selective dissolutions,are useful for determining,in a quantitative way,with strong limitations in many cases,it must be known in advance which one it is.

CRITICAL ASPECTS OF THE EXISTING METHODS

Of all the methods used to obtain a separation between the clinker and the active additions,only the ones based on selective attacks in an acid or alkaline medium are really worthy of interest :

As regards to the acid medium,we have studied the dissolutions in weak acids in an aqueous medium,such as the use of the monochlorine-acetic acid (1),ascorbic acid,etc,and we have obtained good results with the 10% PO_4H_3 in water when cold,which we have used for first time.Under these circumstances,we have found that the medium also attacks in a considerable degree the active addition.

Substituting the water by an alcoholic medium such as methanol and salicilic acid,applied for the first time to these analysis by P.LUXAN (2),and the modification of the previous procedure by means of the introduction of a strong acid,such as hydrochloric acid,has succeeded in reducing in a noticeable way the undissolved residue of the clinkers,but also attacks a considerable degree the active addition,and it not having become a selective attack. The interferences of the gypsum and $CaCO_3$ oblige us to accept practical "correction factors".

As regards to the alkaline medium,the method used to separate the clinker from the slags by means of an ethylene-diamino-tetracetic attack in the presence of triethanolamine with a pH of nearly 11 (3) has given good results when the slags are of siderurgical origin

We still do not know which is the behaviour of other types of slags different from the siderurgical ones, such as those coming from other metallurgical processes,in this attack dissolution. Slags which are more and more used.

During our experimental works on these separations,we have noticed that the $CaCO_3$ leaves a great amount of residues within the usual attack period, as well as it varies depending on the type of calcareous; that the pH has a remarkable influence,depending on the type of slag,on the residue. We have been able to demonstrate that this attack dissolution solves above all remarkable quantities of volcanic pozzuolana , of calcareous materials and about 50% in the case of the fly ashes of the sulpho-calcic type,etc.

In conclusion,we are still far from having a really selective dissolution for the analysis of the components of a given cement.

The methods based on the determination of the complete chemical analysis of the sample,knowing the components previously,such as the method applied by K.KIRTSCHIG (4) to the concrete analysis,have not given good results because, according to our criteria on the analysis of silicates exposed in different works (5),(6),(7),there is not enough exacteness and accuracy in many methods of analysis and,above all,in the determination of the silica specially by conventional gravimetry.

The application of our works in the chemical quantitative analysis of the aforementioned silicates and our idea of analysing the "soluble fractions of these mixtures"have enabled us to find a new way that we are explaining here.

BASES FOR THE NEW METHOD OF ANALYSIS

1-In the quantitative silica determination

The methods of analysis used for the silica determination until now,result in the highest statistical deviations. The use of our modified and simplified (7) gravimetric method has reduced those deviations which were mainly due to the temperatures and to the acid concentration of the extraction and washing dissolutions.

2- About the knowledge of the solubility curves in dissolution of 10% hydrochoric acid when cold.

In one of our previous works (8),we had studied the shape of the solubility curves of active additions belonging to different types in this dissolution depending on the time. The dissolution is practically complete in 15 minutes. Under these conditions,the clinker,the gypsum and the limestone are completely solved. The reason why we have chosen this dissolution is that it completely solved this components within 15 minutes when cold. Under these conditions the silicic acids which pass to the dissolution have a low polymerization degree and the insoluble gels do not practically appear.

3- About the knowledge of the composition of the soluble fraction of active additions.

Their chemical compositions of their soluble fraction, under the mentioned conditions,are different enough to enable their identification. In a certain geographical cement consumption area, the active additions are quite scant,therefore,their identification is possible,as we shall see.

The Portland cement, without secondary components,is completely soluble and therefore the composition of its soluble fractions"coicides" with its chemical composition of oxides. The technological development of the clinkerization and the technical and energetic requirements of the present Portland raw mixes,followed by means of the clinkerability curves (9),have caused that their compositions are more close to one another. The method is based on the knowledge of the chemical compositions of the main oxides :SiO_2,CaO ,(Al_2O_3 + Fe_2O_3) of the soluble fraction, that is, of the proportion of the sample which is solved into the medium of aforementioned attack dissolution,when the results are

referred to the proportion of the sample which is solved in percentage and not (referred) to the total mass of the original sample.

DESCRIPTION OF THE METHOD OF ANALYSIS OF THE SOLUBLE FRACTIONS.

The representative sample,deironed and homogenized in a vibratory dish according to the method described in (5),are reduced to a maximum grain size of 63μm with a uniform granulometric distribution and with a constant fraction <10μm as less as possible (10).

We take 3 g. of dry sample and it is placed into a small dish to be made thin out into 3 or 4 ml. of distilled water,breaking up,at the same time,any agglomeration of particles by means of a flat glass rod.

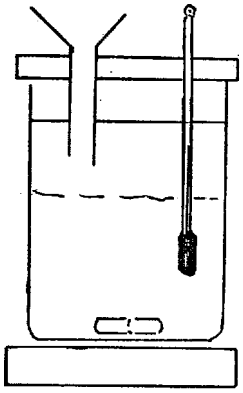

Fig. nº 1
Reactor used

The product so"made thin out" is poured,with the help of the minimum possible amount of water (10 ml)and "very slowly"(within a period not shorter than 1 minute)into a mass of 130 ml.of 10% hydrochloric acid when cold, (T^{o} < 20ºC) in a device like the one shown by Fig. nº 1, during 15 minutes.

Then,it is filtered with a medium paper filter and washed with cold water until the calcium ion is eliminated.

The dissoluble washed residue into the filter is incinerated and calzined and determined its percentage gravimetrically .

Determination of the soluble silica by own methode(7)

The liquid obtained filtered,with its washing waters, are poured into a porcelain dish of about 250 ml. of capacity and it is evaporated by dryness under epiradiated heat.The temperature of material must be 170º ∓5ºC. The dry product is treated with 5 ml.of concentrated hydrochloric acid and evaporated to dryness.When we have reached the dry state,the dehydration is still continued for 30 minutes.

Then, when it is cold ,is treated with 5 ml. of acetic anhidride, it is evaporated to dryness again,prolongating then,the dehydration under epiradiated heat during 30 minutes at 170 ºC ∓ 5ºC.

The residue is extracted,"when cold" (temperature less than +5ºC),with 5 ml. of hydrochloric acid 1:1 (with little ice of distilled water).After 20 minutes of digestion,it is filtered through a fine-medium texture filter paper,it is washed with"cold water",incinerated ,calcined at 1.200 ºC and weighed.

The silica which passes to the solution under these conditions is a "minimum and constant" quantity of less than 1 mg.(7) which can be taken into account and it is not necessary to recover it .

The silicas obtained from these attacks are very pure and there is no need to determine its purity with the usual attack of the sulphuric and hydrofluoric acids,unless there are additions which contain iron in an important quantity.

The silica extraction filtering is gauged at 250 ml. We take three aliquot parts of 50 ml. and determine in each of them one of the following oxides : CaO ,Fe_2O_3 and(Fe_2O_3 +Al_2O_3) using the complexometrics methods of our systematic quantitative analysis procedure for silicates (11),(12),which provides certain general and particular conditions which are explained hereafter and which have enabled us to reach a higher accuracy and reproductibility degree,something which we require for this method.

GRAPHICAL PROCEDURE DESIGNED TO IDENTIFY THE MATERIALS PRESENT

We have designed a graphical representation of these compositions of the soluble fraction,having added up to 100% the content of the four soluble components oxides : SiO_2,+CaO + R_2O_3, (R_2O_3 being =Al_2O_3 +Fe_2O_3) This way makes it possible to identify the nature and the origine of the addition which composes the mixture and determine the content of the same with sufficient accuracy,in most of the cases.
We represent the ternary composition point on a ternary diagram composed of an equilateral triangle in which the highest vertex corresponds to 100% of SiO_2, the lowest left-hand vertex corresponds to 100% of CaO , and the lowest right-hand vertex to 100% of R_2O_3 , as the one shown by figure nº 2 .

The analysis of the soluble fraction of a binary mixture gives a location point for its representation on the ternary diagram SiO_2,CaO,R_2O_3, which is necessarily found in the composition line: from composition of (clinker +gypsum) ⟶ to composition of addition. Precisely the addition that composes the mixture.

The direction of this line shows the area of the composition of the soluble fraction of the composing addition.

The proportionality of the distances of the composition point of the mixture at the ends of the segment,which represent the compositions of the soluble fractions of the components,refers to these compositions,and not,to the chemical compositions of the whole sample . The proportionality ratio to the integral compositions of the samples,as it is logical,is a different fonction.

However,we have seen that it is more practical and accurate to carry out the calculation of the binary mixture,starting directly from the insoluble residues of the mixture and of their components by means of a simple equation system, when the addition residue is higher than 10% approximately.

When the addition has a low residue,similar to the value of the cement residue,it is not possible to calculate it using the values of the residues.

Generalized method for the detrmination of the composition of Portland cement mixtures with additions. 3.1

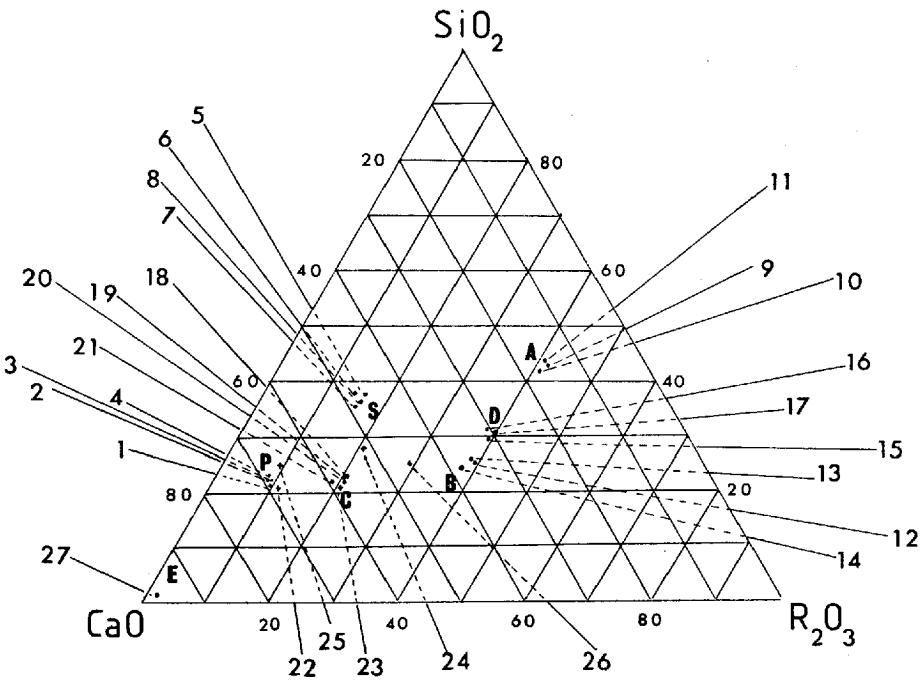

Fig. nº 2

Composition of the main oxides of the soluble fractions in 10% hydrochloric acid when cold of the additions and mixtures in Catalonia .

Then,the values of their soluble fractions are very similar to the total chemical compositions and can be calculated directly by a graphical ratios for the ternary diagram.

That is the interesting case when the siderurgical slag is present . In our Laboratory,we use a triangular diagram 500 mm. high,in order to obtain a good accuracy when reading the mm.

By this way,we obtain a graphic system in which each ternary composition has a "biunivocal correspondence" depending on the three main components ,or else , said with other words, each point represents a unique ternary ratio or "Ternary Modules" of the three compo - nents.

EXPERIMENTAL DETERMINATIONS

We are including hereaftersome of the results obtai - ned in our laboratory with cement and active additions samples of a known composition coming from Catalonia.

All these samples have been prepared using the homoge- nizing procedure of the vibrating dish which has been noted previously.

In the following table I we show the composition of the soluble fractions corresponding to diferent Portland cements in the dissolution of 10% hydrochloric acid when cold .

In the next table II are given the compositions of the soluble fractions in the same dissolution and conditions of typical active additions from Catalonia.

TABLE I

Cements without addition	Insoluble residue in ClH 10%	Soluble oxides referred to soluble fraction of the sample % SiO_2	CaO	Al_2O_3	Fe_2O_3	reference on the diagram	
A	0,4	19,5	64,3	5,4	3,3	1	
B	0,3	20,0	64,2	4,7	3,5	2	P
C	0,5	19,6	63,8	5,1	3,5	3	
D	0,6	20,7	62,5	5,7	2,1	4	

Its maximum granulometric size has been < 63 μm and the fraction < 10 μm was constant near to 5% for all sam - ples.

We prepared samples with known proportions of cement-1 with the active additions studied .They have been homogenized and analysed with this method and have been the same granulometric conditions .

In the next table III there are the results obtained in this mixtures .

CHARACTERISTICS OF THE METHOD AND APLICATIONS

This method is specialy suitable when the insoluble residue of the sample or the addition is low as it is the case when there are soluble slags in the dissolution of 10% hydrochloric acid .

The experimental observation of the results obtained and verified on the drawn diagram gives us, in rela - tion to the cements of our area, the following data:

Generalized method for the determination of the composition of Portland cement mixtures with additions. 3.1

TABLE II

Different samples of same material.	Characteristics of additions	% Insoluble residue in ClH 10% cold	Soluble oxides referred to soluble fraction of the sample %. SiO_2	CaO	Al_2O_3	Fe_2O_3	reference nº on the diagram.	
1	siderurgical	1,3	33,3	39,6	12,9	1,2	5	
2	slag	0,9	33,1	40,7	12,1	0,6	6	S
3	"	1,0	33,0	44,6	13,2	1,7	7	
4	"	0,7	33,8	44,0	14,9	1,0	8	
5	pozzuolana	69,0	33,1	11,4	16,0	15,1	9	
6	of Girona	63,4	34,9	14,9	19,0	14,2	10	A
7	Catalonia	66,7	33,6	12,2	17,3	13,6	11	
8	basalt rock	82,4	11,6	16,5	15,8	3,1	12	
9	" "	82,1	12,0	17,1	14,7	3,6	13	
10	" "	81,4	12,3	20,4	14,0	5,1	14	B
11	metallurgical	81,6	19,8	20,8	20,9	5,9	15	
12	slag "	81,9	20,1	20,2	19,4	5,2	16	D
13	" "	82,5	18,5	19,3	19,4	5,5	17	
14	fly ashes	46,6	19,6	57,3	15,8	4,6	18	
15	sulpho-calcic	48,0	20,8	52,8	14,5	4,2	19	
16	" "	47,1	21,0	54,3	14,9	4,3	20	C
17	" "	46,0	20,5	57,0	15,0	4,3	21	
18	Calcareous	1,1	1,2	54,9	0,52	0,35	27	E

TABLE III

Samples nº	% Composition reference on diagram.	% Insoluble residue in ClH 10% cold	Soluble oxides referred to soluble fraction of the sample % SiO_2	CaO	Al_2O_3	Fe_2O_3	Reference nº on diagram	% proportions found in analysis	Characteristic of additions
1	80 cement - 1 20 addition-20	10,0	19,8	62,3	6,4	3,5	22	79,4 20,6	sulpho-calcic fly ashes
2	80 cement - 1 20 addition-14	16,2	16,1	52,4	7,5	5,4	23	80,5 19,5	basalt rock
3	60 cement - 1 40 addition-10	26,4	25,7	44,3	9,2	9,5	24	58,3 41,7	pozzuolana Girona
4	90 cement - 1 10 addition- 6	0,46	20,9	58,3	6,1	3,0	25	12,2 (*) 87,8	siderurgical slag
5	30-cement - 1 70-addition-15	56,9	19,7	33,9	16,2	5,1	26	30,4 69,6	metallurgical slag

(*) Graphical calculation
segment point mixture ⟶ point slag 41,4 mm.
" " " ⟶ " cement 5,7mm.

1-All Portland cements without addition from different origen give a narrow location area,very limited, point x (fig. nº 2) being the one which can be considered as the equidistant centre. This point is useful,technically ,when the type of cement used is not known.

2-The different types of additions studied given location areas on the diagram that are sufficiently isolated to be able to be identified very easily.

3-A specially interesting possibility offered by this method we propose,is that of being able to know with certainty whether a mixture,morter or

concrete has or has not any addition o secondary components . The composition of its soluble fraction,under our attack conditions,falls within the area of the Portland cements for Portland cements without addition

Its most suitable and important application is for mixtures that contain slags and other materials that are soluble into all mediums into which clinkers are also soluble,and, therefore, they are a serious interference for all of them,as we have seen in the critical explanation of the background.

When the sample of the addition is not known or is not available,and it is slag,the procedure already mentioned in this work (3), is specially interesting here Based on the attack at pH 11,5 by means of ethylenediamino-tetracetic in the presence of triethanolamine, is specially useful for separating the addition from the cement applied to about 5 to 10 grammes of sample for isolating previously a sufficient amount of slag or addition for determining the composition of their soluble fraction (with reduction previously its granulometric size) and locate it on the ternary diagram. The situation of its composition point on the diagram makes it possible to know and determine the kind of addition.

When there are,in the mixtures,considerable quantities of calcareous material, it is necessary to deduct the quantity of CaO which stochiometrically corresponds to the quantity of CO_2 determined by the difference in weight that the sample undergoes by calcination from temperatures ranging between 650º and 950º C , which are reached thanks to a good stabilization, and determining their values until getting a controlled weight constant, preferably in a platinum crucible.

In the cases we have studied, in which we know or have the materials which make up the mixture, and when this is a binary one, the errors range within $\mp$ 1,5% in the percentage composition .

CONCLUSION

We have tried to give a method of a general type which makes it possible to undertake the study of the agglomerating materials and furnishes fuller information on the type of addition which makes up the sample.

For all the reasons exposed, this method seems to be able to verify the absence of additions and it could be an interesting criterion for the teams working within the rules committees.

With the application of the results of our researches on the chemical analysis of the silicates ,we think that we have found a way which can be widely applied and which makes it easier to study and know the new types of hydraulic agglomerates .

REFERENCES

1- G.BABACHEV, M.PETROVA "Chemical analysis of gyp - sum -cement pozzuolana binder" Tsement 1978(7),16

2- Mª.P.LUXAN "Metodo de valoración cuantitativo de las adiciones de tipo silíceo presentes en el cemento" Monografia nº 369 I.E.T.c.c 1982 MADRID

3-E.DEMOULIAN , C.VERNET "Determination de la teneur en laitier dans les ciments par dissolution selectiva" 7º Congrés International de la Chemie des ciments Vol II -III 151-1980 -PARIS.

4-K.KIRTSCHIG "cálculo para el análisis del hormigón" Zement-Kalk-Gips nº 10 -477-485; 1969.

5-F.GOMA "Sobre la determinació gravimètrica de la sílice" Tesi Doctoral -Departament d'analisi química de la UNIVERSITAT DE BARCELONA Desembre 1975.

6-F.GOMA "Nuevo método gravimétrico para la determinación de sílice en silicatos atacables por ácido" Materiales de Construcción nº 164. p 1-23 .I.E.T.c.c 1976- MADRID

7-F.GOMA "Nuevo método gravimetrico para la determinación de la sílice en materiales silíceos" .Cemento -Hormigón nº 505 marzo 1976.

8-F.GOMA "Método para determinar el contenido de cemento y adiciones en el hormigón fresco.Importancia de la relación SO_3/cemento " Working Sessions W 10-8-4 ,1-10 -1983. LONDRES.

9-F.GOMA "Generalized clinkerability function" 7º Congrès International de la Chemie des Ciments Vol II ;I-67 -72. 1980. PARIS.

10-F.GOMA "Proposta de mètodes per a determinar el contingut de ciment i addicions en el formigó fresc" Publicació de la Secretaria General del Departament de Política territorial i Obres Públiques -La Generalitat de Catalunya -1984.

11-F.GOMA " Anàlisi química de silicats" Departament de Química analítica-Universitat de Barcelona (en preparació.)

Dr. Muhammad S. Y. Bhatty, Portland Cement Association, Skokie, Illinois, U.S.A. 1 1

Properties of Blended Cements Made With Portland Cement, Cement Kiln Dust, Fly Ash, and Slag 3.1

3.1

ABSTRACT

Binary, ternary, and quaternary blended cements were prepared from one portland cement, three cement kiln dusts, two fly ashes (ASTM Class F and C) and one slag. On the basis of their chemical composition, kiln dusts were relatively classified as: 1) low alkali-low chloride-moderate sulfate, 2) low alkali-low chloride-high sulfate, and 3) high alkali-high chloride-low sulfate. The amount of kiln dust used in the blends was fixed at a level of 10% by weight while the amount of fly ash and slag was varied from 10% to 30% and 10% to 40% by weight, respectively, in the blends. All the materials that were added replaced cement.

Blended cements were tested for compressive strength, drying shrinkage, autoclave expansion, sulfate expansion, and alkali-aggregate expansion. The type of kiln dust used was found to influence the properties of blended cements with or without the addition of fly ash and/or slag.

Test results indicate that properly designed blended cements can be prepared that have properties comparable to that of portland cement. These cements can provide the construction industry with a useful and cost effective product. They are also energy efficient and can reduce environmental concerns by utilizing waste and by-product materials of various industries.

Foram preparados cimentos com adição binária, ternária e quaternária, a partir de um cimento portland, três pós de forno de cimento, duas cinzas volantes (Classes F e C ASTM), e uma escória. Com base em sua composição química, os pós de forno foram classificados relativamente como: 1) sulfato moderado - baixo álcali - baixo cloro; 2) baixo álcali - baixo cloro - sulfato alto; 3) álcali alto - cloro alto - sulfato baixo. A quantidade de pós de forno usada nas blendagens foi fixada num nível de 10% em peso, enquanto a quantidade de cinza volante e escória variou de 10% a 30% e de 10% a 40% em peso, respectivamente, nas blendagens. Todos os materiais empregados substituíram cimento.

Os cimentos blendados foram submetidos a testes de resistência à compressão, contração de secagem, expansão em autoclave, expansão de sulfato e expansão de álcali-agregado. Constatou-se que o tipo de pó de forno utilizado influencia as propriedades dos cimentos blendados com ou sem adição de cinza volante e/ou escória.

Os resultados do teste indicam que cimentos blendados adequadamente projetados podem ser produzidos com propriedades comparáveis às do cimento portland. Estes cimentos podem fornecer à indústria de construção um produto útil e de custo conveniente. Também economizam energia e podem atender às necessidades ambientais pela utilização de materiais de rejeito e sub-produtos de várias indústrias.

Dr. Muhammad S. Y. Bhatty, Portland Cement Association, Skokie, Illinois, U.S.A. 2

Properties of Blended Cements Made With Portland Cement, Cement Kiln Dust, Fly Ash, and Slag 3.1

INTRODUCTION

Industrial waste and by-product materials are accumulating at an increasingly rapid rate and efforts are underway in many parts of the world to find economical and environmentally safe procedures to utilize these materials for beneficial purposes. Examples of such materials that are being and can be used in the construction industry are slag, fly ash, silica fume, recycled concrete, cement kiln dust, lime kiln dust, etc. The use of fly ash and slag in concrete is reasonably well documented in the literature. However, only recently there has been some interest in evaluating the use of cement kiln dust as a construction material. (1-6) Other uses of kiln dust are also reported in the literature. (7-17)

Kiln dust is a by-product which is generated in the production of portland cement clinker. The composition of kiln dust is similar to the cement kiln raw feed but in many kiln dusts the amounts of alkalies, chlorides, and sulfates are considerably higher. Dusts may also contain other materials such as free lime, clinker, and raw feed minerals. Because a major portion of kiln dust is composed of partially calcined calcite, the cement industry makes every effort to return as much kiln dust as possible to the kiln without exceeding acceptable levels of alkali and sulfate in the cement. This saves disposal costs and conserves energy.

However, it was reported that 60% of the cement manufacturing plants in the United States cannot return the dust to the kiln because of its high alkali content. (18) Cement containing alkali content greater than 0.60% as equivalent Na_2O can influence the durability of concrete due to alkali-aggregate reaction if a potentially reactive aggregate is present. Therefore, to use some kiln dusts, a modification of the cement-kiln dust system (for example, addition of other materials) may be needed.

The beneficial effect of some fly ashes and slag additions to cement to control alkali-aggregate expansion and certain other properties are well known but low early strengths produced are sometimes not desirable. Addition of some kiln dusts to cement may produce deleterious expansion resulting from alkali-aggregate reaction but most cement-kiln dust blends produce higher early strengths than cement alone. It was found that deleterious alkali-aggregate expansion can be prevented by using a combination of kiln dust and slag or fly ash while still avoiding the early strength loss. (3,6)

Since preliminary studies carried out by the author (3,5,6) and other research workers (1,2,4) showed promising results for some concrete properties such as compressive strength, the research program was extended to study other properties that can influence the durability of concrete. This paper reports and compares the properties of mortars made with blended cements containing cement-kiln dust, cement-kiln dust-slag, cement-kiln dust-fly ash, cement-slag-fly ash, and cement-kiln dust-slag-fly ash combinations. The properties studied are compressive strength, autoclave expansion, drying shrinkage, sulfate expansion, and expansion due to alkali-aggregate reaction.

EXPERIMENTAL

The materials used for making the blends for this study were an ASTM Type I portland cement, three kiln dusts, two fly ashes (ASTM Class F and Class C), and one granulated blast furnace slag. Kiln dusts were classified according to the relative amounts of alkali, chloride, and sulfate present in dusts and were designated as: 1) low alkali-low chloride-moderate sulfate (Dust S); 2) low alkali-low chloride-high sulfate (Dust H); and 3) high alkali-high chloride-low sulfate (Dust L). The chemical composition and other pertinent data of all materials used in this study including the classification of dusts are presented in Table 1. Phases present in dusts are reported in Table 2.

Exact composition of blends are reported in appropriate tables along with the test results. In order to make the blends, materials were accurately weighed and blended in a pebble mill. The amount of kiln dust in the blends was fixed at a level of 10% by weight, but the amount of slag and fly ash in the blends was varied from 10-40% and 10-30% by weight, respectively. All the materials that were added replaced cement. Binary, ternary, and quaternary blends were made. Blends were tested for the following properties and the deviations from the ASTM test procedure for each test are also noted. The main purpose of this study was to make relative comparison of the blends rather than obtaining the absolute values.

1. Compressive strength, ASTM Test C 109, using a fixed water to solid (W/S) ratio of 0.45.

2. Drying shrinkage, ASTM Test C 596, using a fixed W/S ratio of 0.45.

3. Autoclave expansion, ASTM Test C 151, using a fixed W/S ratio of 0.45

4. Alkali-aggregate reactivity, ASTM Test C 227, using a fixed W/S ratio of 0.45. Beltane opal was used as reactive aggregate.

5. Sulfate expansion, ASTM Test C 1012 using a fixed W/S ratio of 0.45.

   In this test mortar bars were placed in mixed sulfate solution when companion mortar cubes (ASTM C 109) achieved a compressive strength of at least 3000 psi, at 73°F and 100% relative humidity. No accelerated curing was carried out as specified in the ASTM procedure. Also, technical grade chemicals were used instead of reagent grade chemicals.

RESULTS AND DISCUSSION

Binary, ternary, and quaternary blends were made from cement, kiln dust, fly ash, and slag. Binary blends consisted of a combination of cement with kiln dust or slag or fly ash. Ternary blends consisted of a combination of cement and kiln dust with slag or fly ash. Some ternary blends were also made from cement, slag, and fly ash. Quaternary blends consisted of cement, kiln dust, fly ash, and slag.

Dr. Muhammad S. Y. Bhatty, Portland Cement Association, Skokie, Illinois, U.S.A. 3

Properties of Blended Cements Made With Portland Cement, Cement Kiln Dust, Fly Ash, and Slag 3.1

3.1

Table 1a - Chemical Analysis and Other Relevant Data on Cement, Kiln Dust, Fly Ash, and Slag (wt. %)

Components	Material Designation						
	Cement	Kiln Dust			Slag	Fly Ash ASTM Class F	Fly Ash ASTM Class C
		S	H	L			
SiO_2	21.4	14.7	15.5	15.4	35.6	56.0	31.1
Al_2O_3	5.1	3.31	3.84	2.65	9.4	22.0	17.0
Fe_2O_3	3.5	2.04	2.13	1.51	0.8	11.02	5.6
CaO	64.6	49.3	51.7	41.9	40.91	8.7	29.0
MgO	2.1	1.03	1.59	1.35	10.9	1.71	3.79
SO_3	1.7	3.07	11.1	0.25	3.2(a)	0.64	4.77
Na_2O	0.23	0.23	0.22	0.23	0.16	1.75	3.17
K_2O	0.46	2.6	2.5	4.9	0.38	0.91	0.37
Total Alkalies(b)	0.53	1.94	1.86	3.45	0.41	2.34	3.41
TiO_2	0.26	N.D.(c)	N.D.	N.D.	N.D.	N.D.	N.D.
P_2O_5	0.11	N.D.	N.D.	N.D.	N.D.	N.D.	N.D.
L.O.I.	1.1	23.43	10.5	34.06	+1.34	2.01	0.28
CL	N.D.	0.24	0.26	3.47	N.D.	N.D.	N.D.
Free Lime	0.7	10.43(d)	21.72(d)	3.0(d)	N.D.	1.23(d)	1.08(d)
$CaCO_3$(e)	N.D.	50.94	22.65	64.68	N.D.	N.D.	N.D.
Insol. Residue	0.07	11.62	9.82	14.58	0.3	N.D.	N.D.
Blaine CM^2/g	3261	5108	4894	4385	5485	6124	8137

Dust Classification S = Low alkali-low chloride-moderate sulfate
H = Low alkali-low chloride-high sulfate
L = High alkali-high chloride-low sulfate

(a) Total sulfur as SO_3 (b) Equivalent as Na_2O (c) Not Determined
(d) Determined by Modified Franke Method (19) (e) Determined by Thermogravimetric Analysis

Table 1b - Calculated Compound Composition of Cement, wt. %

C_3S	53.5
C_2S	21.0
C_3A	7.5
C_4AF	10.7

Table 2 - XRD Analysis of Kiln Dusts

Dust	Phases*
S	$CaCO_3$, CaO, SiO_2, $CaSO_4$(tr)**, $K_3Na(SO_4)_2$?, K_2SO_4(tr)
H	$CaCO_3$, CaO, $CaSO_4$, SiO_2
L	$CaCO_3$, SiO_2, KCl, CaO, K_2SO_4(tr)

*Phases are listed in decreasing order of intensity of peaks, with due consideration to other factors such as composition.

**tr = Traces ? = may be present

Test results are reported in Tables 3 through 9 and each test will be discussed separately.

Mortar Compressive Strength

Compressive strengths of blends were determined at 1, 7, 28, 90 days, and one year (Tables 3 through 6). Strengths are also reported as percent of values for cement alone at each age.

Binary blends made with all three dusts showed significantly higher strengths at 1 day but strengths generally decreased at 7, 28, and 90 days compared to cement alone (Table 3). However, at one year, strengths were comparable to cement alone. Binary slag blends, on the other hand, showed lower strengths at 1 day compared to cement, and as the amount of slag in the blends increased from 10% to 40%, decrease in strengths became more significant (Table 3). From 28 days to one year, binary blends containing 10% slag showed comparable strengths to cement but for other blends containing 20% to 40% slag, significantly higher strengths were obtained. Thus, the increase in the slag content resulted in progressively higher strengths at later ages. Binary fly ash blends made with ASTM Class F fly ash behaved differently from blends made with ASTM Class C fly ash (Tables 4 and 5). One day strengths for Class F fly ash blends were significantly lower than cement alone but strengths of blends made with Class C fly ash were generally comparable to cement. At 90 days and one year, strengths of blends made with either fly ash were generally higher than cement alone.

Addition of slag (by replacing cement) to cement-kiln dust blends reduced 1 day strengths compared to cement-kiln dust blends irrespective of the kiln dust used (Table 3). With the increase in the amount of slag from 10% to 40% in ternary blends, 1 day strengths generally decreased but strengths at later ages generally increased for all the kiln dusts

studied. Looking from another direction, addition of 10% of any kiln dust to cement-slag blends improved the strengths significantly at one day compared to cement-slag blends.

Ternary blends made with cement, kiln dust and either Class F or C fly ash (Tables 4 and 5) generally behaved the same way as that of ternary slag blends discussed above. The major difference in behavior was noted with respect to the time it took for fly ash blends to overtake or approximately produce the same strengths as that of cement. This time increased to 90 days for Class F fly ash blends and to one year for Class C fly ash blends compared to 7 or 28 days for the slag blends. Ternary blends made with kiln dusts and either fly ash produced comparable strengths at later ages. In general, the ternary slag blends developed better strengths than ternary Class F fly ash or Class C fly ash blends at later ages. Also, ternary Class F fly ash blends produced slightly better strengths at later ages than ternary Class C fly ash blends.

Ternary blends made from Class F fly ash and slag (Table 6) produced relatively poor strengths at early ages compared to most of the ternary blends discussed above; however, strengths improved considerably at later ages. Increase in the amount of slag in this ternary system produced lower strengths at early ages but higher strengths at later ages.

Quaternary blends made from kiln dust S, Class F fly ash, and slag (Table 6) generally behaved similarly to ternary blends made from cement, Class F fly ash, and slag, and ternary blends made with cement, kiln dust S, and either Class F or C fly ash. Significantly lower strengths of quaternary blends at early ages can probably be attributed to considerably reduced cement content in the blends as well as to dust S which consist of relatively small amounts of accelerators such as alkali, chloride, and sulfate.

Compressive strengths determined for blends of the same composition using 1-inch paste cubes (5) generally showed lower strengths compared to mortar cubes made according to ASTM C 109 procedure when cement alone was used as a reference in the two methods and the same W/S ratio was used.

Mortar Drying Shrinkage

Drying shrinkage of blends was measured at 4, 11, 18, and 25 days. The results are presented in Tables 3 through 6. Drying shrinkage of binary kiln dust blends depended on the type of kiln dust used (Table 3). Drying shrinkage of binary blends containing kiln dusts S and L increased compared to cement alone but decreased for blends containing kiln dust H. Binary slag blends showed mixed results. Drying shrinkage was similar to cement alone for binary

Table 3 - Properties of Blended Cements Made with Cement, Kiln Dust, and Slag

Blend	Blend Composition Wt. %			Autoc. Expan.	Drying Shrinkage %				Compressive Strength psi				
	C	KD	SL	%	4d	11d	18d	25d	1d	7d	28d	90d	1Y
1	100	0	0	0.087	0.056	0.096	0.112	0.115	1320(100)	4920(100)	6030(100)	6150(100)	6830(100)
		Dust S											
2	90	10	0	0.099	0.065	0.112	0.130	0.137	1540(117)	4380(89)	5280(88)	5430(88)	6870(101)
4	80	10	10	0.108	0.070	0.113	0.123	0.132	1490(113)	4710(96)	5800(96)	6000(98)	7250(106)
5	70	10	20	0.120	0.072	0.117	0.132	0.136	1250(95)	4800(98)	6300(105)	6990(114)	7800(114)
53	60	10	30	0.120	0.073	0.114	0.129	0.134	1170(89)	5110(104)	6810(113)	7370(120)	8380(123)
54	50	10	40	0.127	0.075	0.120	0.136	0.142	1030(78)	5370(109)	7300(121)	7960(129)	8850(130)
		Dust H											
16	90	10	0	0.090	0.040	0.068	0.085	0.088	1880(142)	4430(90)	5540(92)	6290(102)	6680(98)
18	80	10	10	0.094	0.041	0.070	0.088	0.091	1610(122)	4510(92)	6070(101)	7080(115)	7480(110)
19	70	10	20	0.095	0.047	0.079	0.093	0.099	1520(115)	4880(99)	6280(104)	6770(110)	7130(104)
61	60	10	30	0.098	0.050	0.081	0.097	0.100	1550(117)	5130(104)	7020(116)	7980(130)	8630(126)
62	50	10	40	0.093	0.049	0.079	0.096	0.097	1230(93)	4970(101)	6690(111)	7600(124)	8550(125)
		Dust L											
10	90	10	0	0.117	0.064	0.110	0.133	0.140	1850(140)	4130(84)	5300(88)	5420(88)	6660(98)
12	80	10	10	0.106	0.063	0.112	0.137	0.147	1610(122)	4270(87)	5640(94)	5930(96)	6820(100)
13	70	10	20	0.119	0.066	0.114	0.138	0.143	1530(116)	4890(99)	5820(97)	6320(103)	7000(102)
57	60	10	30	0.123	0.067	0.107	0.132	0.138	1480(112)	5060(103)	6360(105)	6910(112)	7850(115)
58	50	10	40	0.115	0.063	0.105	0.132	0.142	1340(102)	5310(108)	6350(105)	6820(111)	8180(120)
8	90	0	10	0.079	0.058	0.102	0.112	0.115	1270(96)	4600(93)	6170(102)	6310(103)	7030(103)
9	80	0	20	0.090	0.067	0.108	0.120	0.123	1190(90)	4910(100)	7000(116)	7760(126)	7530(110)
51	70	0	30	0.086	0.063	0.104	0.113	0.114	1060(80)	4750(97)	7400(123)	7860(128)	7950(115)
52	60	0	40	0.081	0.083	0.116	0.126	0.130	980(74)	4680(95)	7740(128)	8670(141)	8910(130)

Key for abbreviations used in this table.
C = cement KD = kiln dust SL = slag Autoc. Expan. = Autoclave Expansion
Dust S = Low alkali - low chloride - moderate sulfate
Dust H = Low alkali - low chloride - high sulfate
Dust L = High alkali - high chloride - low sulfate
Figures in parentheses represent compressive strengths as % of values for cement.

blend containing 10% slag; it increased for blends containing 20% slag but decreased slightly for blends containing 30% slag; a definite increase was observed for blends containing 40% slag. Binary blends containing 10% Class F fly ash had similar drying shrinkage as that of cement alone (Table 4). Increase in the amount of Class F fly ash to 20% and 30% in blends produced a decrease in drying shrinkage. On the other hand, binary blends made with Class C fly ash showed similar drying shrinkage as that of cement alone (Table 5).

Ternary blends appear to follow somewhat similar trends as that of binary blends. For example, ternary blends made with any of the kiln dusts and either slag or Class F or C fly ash (Tables 3 through 5) showed increase in shrinkage for blends containing dusts S and L but a decrease in shrinkage for blends containing dust H compared to cement alone. Ternary blends containing dust L and either Class F or C fly ash consistently showed higher shrinkage compared to their counterparts made with dusts S and H. Highest shrinkage was obtained for blends containing dust L and Class C fly ash. From the limited amount of data available for ternary blends made with slag and Class F fly ash (Table 6), it was noted that an increase in the combined amount of fly ash and slag content showed a slight decrease in drying shrinkage.

Quaternary blends also showed mixed results for drying shrinkage. A blend containing 40% of combined amounts of Class F fly ash and slag showed lower shrinkage than cement alone.

Test results indicated that binary and ternary blends containing dust H, which is a high sulfate dust, showed lower shrinkage than cement alone but opposite behavior was observed when dust L, which is a high chloride dust, was present in binary and ternary blends.

Autoclave Expansion

The results of autoclave expansion of blends are shown in Tables 3 through 6. The type of kiln dust in the binary cement-kiln dust blends influenced the autoclave expansion. Binary blends containing kiln dust H showed autoclave expansions comparable to cement alone but higher expansions were noted for dusts S and L (Table 3). Binary slag blends produced lower or comparable autoclave expansions to cement alone. Expansion steadily decreased with an increase in the amount of Class F fly ash in the binary cement-Class F fly ash blends (Table 4) but for binary blends containing Class C fly ash (Table 5), expansion was comparable to cement alone.

Ternary blends containing cement, kiln dust and slag produced higher expansions than cement alone (Table 3). Expansion was significantly higher for ternary blends containing slag and kiln dust S or L but only sightly higher for blends containing slag and kiln dust H compared to cement alone. No consistent trend was observed for expansions when the amount of slag was increased from 10% to 40% in these blends.

Addition of Class F fly ash to binary kiln dust blends generally proved beneficial (Table 4). Ternary blends made with cement, kiln dust, and Class F fly ash generally produced lower expansions than comparable cement-kiln dust blends. Increase in the amount of Class F fly ash in these ternary blends generally decreased expansion but opposite was the case for Class C fly ash blends (Table 5).

Significantly lower expansions were obtained for ternary blends containing Class F fly ash and slag (Table 6) compared to cement alone as well as other ternary blends. Quaternary blends made with the addition of kiln dust to these ternary blends pro-

Table 4 - Properties of Blended Cements Made with Cement, Kiln Dust, and ASTM Class F Fly Ash

Blend	Blend Composition Wt. %			Autoc. Expan.	Drying Shrinkage %				Compressive Strength psi				
	C	KD	FF	%	4d	11d	18d	25d	1d	7d	28d	90d	1Y
1	100	0	0	0.087	0.056	0.096	0.112	0.115	1320(100)	4920(100)	6030(100)	6150(100)	6830(100)
		Dust S											
2	90	10	0	0.099	0.065	0.112	0.130	0.137	1540(117)	4380(89)	5280(88)	5430(88)	6870(101)
22	80	10	10	0.093	0.062	0.100	0.121	0.132	1260(95)	3750(76)	5240(87)	6380(104)	ND
23	70	10	20	0.103	0.052	0.092	0.109	0.116	880(67)	3620(74)	5190(86)	6500(106)	7410(108)
78	60	10	30	0.082	0.057	0.088	0.102	0.112	850(64)	3090(63)	5060(84)	6410(104)	7720(113)
		Dust H											
16	90	10	0	0.090	0.040	0.068	0.085	0.088	1880(142)	4430(90)	5540(92)	6290(102)	6680(98)
33	80	10	10	0.074	0.041	0.059	0.072	0.078	1560(118)	4180(85)	5410(90)	6190(101)	7180(105)
34	70	10	20	0.067	0.033	0.058	0.070	0.076	1180(89)	3790(77)	5240(87)	6500(106)	7740(113)
79	60	10	30	0.064	0.034	0.057	0.068	0.074	1430(108)	3230(66)	5190(86)	6730(109)	8090(118)
		Dust L											
10	90	10	0	0.117	0.064	0.110	0.133	0.140	1850(140)	4130(84)	5300(88)	5420(88)	6660(98)
28	80	10	10	0.108	0.063	0.108	0.131	0.140	1690(128)	4210(86)	5400(90)	6330(103)	ND
29	70	10	20	0.110	0.065	0.105	0.126	0.137	1530(116)	4020(82)	5300(88)	6920(113)	7880(115)
80	60	10	30	0.103	0.061	0.104	0.126	0.135	1410(107)	3560(72)	5320(88)	6480(105)	7390(108)
26	90	0	10	0.081	0.058	0.098	0.115	0.125	1100(83)	4460(91)	5900(98)	6590(107)	7400(108)
27	80	0	20	0.063	0.050	0.082	0.094	0.100	980(74)	3880(79)	5460(91)	6800(111)	8130(119)
77	70	0	30	0.053	0.048	0.073	0.082	0.087	820(62)	3300(67)	5000(83)	6740(109)	8280(121)

See Table 3 for details of abbrevations.
FF = ASTM Class F Fly Ash.
ND = Not Determined

duced higher expansions in most cases than cement alone.

Autoclave expansion of blends appears to have some similarities to that of drying shrinkage of blends. Although most of the ternary blends containing dust showed higher autoclave expansions than cement alone, the blends containing dust L, which is a high chloride dust, generally produced higher expansions than blends containing high sulfate dust H.

It should be noted that autoclave expansions are well below the ASTM C 150 specification of 0.8% in all cases.

Alkali-Aggregate Reactivity

The potential alkali-aggregate reactivity of blends was investigated using ASTM C 227 test procedure at a fixed W/S ratio of 0.45. The aggregate used consisted of 95% Ottawa sand and 5% Beltane opal. Beltane opal has been used as a reactive aggregate in a number of previous studies (6). The cement used contains a total alkali content of 0.53% as sodium oxide equivalent and is considered a low alkali cement according to ASTM C 150 specifications. When other materials were added to the cement, the alkali content of the blends exceeded 0.60%. It should be noted that a major portion of alkali in dust L is probably present as chloride salt. Total alkali content (as equivalent Na_2O) of blends and mortar bar expansions of blends at 3 and 6 months are shown in tables 7 through 9.

Binary blends made with cement and slag or Class F fly ash showed lower expansions at 3 and 6 months than ASTM limit of 0.05%, and 0.1%, respectively, at these ages (Tables 7 and 8). However, binary blends made with Class C fly ash showed much higher expansions when the amount of fly ash in the blend was 20% and 30% (Table 9).

Alkali-aggregate expansions of ternary blends made with different kiln dusts and slag were similar to cement alone, binary kiln dust, and binary slag blends (Table 7). Addition of 10% Class F fly ash to all cement-kiln dust blends produced expansions greater than those for cement alone at 3 and 6 months (Table 8). Increase in Class F fly ash content to 20% and 30% in ternary blends reduced the expansions significantly to well below the ASTM limits. Similar ternary blends made with Class C fly ash behaved differently. In most of these blends, addition of Class C fly ash increased the expansion significantly compared to cement alone and cement-kiln dust blends (Table 9). For some blends expansions were much higher than ASTM limit at addition levels of 20% and 30% of fly ash C.

Previous results have shown that in a ternary blend made from cement, kiln dust and slag, the amount of slag up to 20% was not sufficient to prevent alkali-aggregate expansion for some blends (6). Therefore, higher amounts of slag may be needed. In practice, slag content of 40% is probably the minimum amount used. In this study, however, the amount of slag from 10% to 40% reduced the alkali-aggregate expansion for any ternary blend made with kiln dust compared to cement.

It is also noted that kiln dust is not the only material in a binary or ternary blend that can influence the alkali-aggregate expansion. Different cements with the same kiln dust can produce different expansion not only due to differences in alkali content but other compositional variations (6).

Table 5 - Properties of Blended Cements Made with Cement, Kiln Dust, and ASTM Class C Fly Ash

Blend	Blend Composition Wt. %			Autoc. Expan.	Drying Shrinkage %				Compressive Strength psi				
	C	KD	FC	%	4d	11d	18d	25d	1d	7d	28d	90d	1Y
1	100	0	0	0.087	0.056	0.096	0.112	0.115	1320(100)	4920(100)	6030(100)	6150(100)	6830(100)
		Dust S											
2	90	10	0	0.099	0.065	0.112	0.130	0.137	1540(117)	4380(89)	5280(88)	5430(88)	6870(101)
37	80	10	10	0.110	0.054	0.104	0.120	0.131	1190(90)	3710(75)	4890(81)	5630(92)	ND
38	70	10	20	0.124	0.053	0.099	0.120	0.131	860(65)	3580(73)	4640(77)	5520(90)	6830(100)
82	60	10	30	0.158	0.049	0.101	0.119	0.135	790(60)	3100(63)	4530(75)	5200(85)	6280(92)
		Dust H											
16	90	10	0	0.090	0.040	0.068	0.085	0.088	1880(142)	4430(90)	5540(92)	6290(102)	6680(98)
47	80	10	10	0.092	0.040	0.072	0.082	0.097	1720(130)	4260(87)	4840(80)	6000(98)	7110(104)
48	70	10	20	0.107	0.040	0.074	0.085	0.098	1330(101)	3780(77)	4960(82)	5560(90)	6740(99)
83	60	10	30	0.135	0.039	0.073	0.087	0.101	1450(110)	3830(78)	4970(82)	5930(96)	7360(108)
		Dust L											
10	90	10	0	0.117	0.064	0.110	0.133	0.140	1850(140)	4130(84)	5300(88)	5420(88)	6660(98)
43	80	10	10	0.117	0.067	0.113	0.138	0.154	1730(131)	4030(82)	5330(88)	5570(91)	6510(95)
44	70	10	20	0.132	0.070	0.125	0.142	0.166	1740(132)	4070(83)	4930(82)	5750(93)	6680(98)
84	60	10	30	0.150	0.056	0.117	0.146	0.169	1600(121)	3760(76)	4920(82)	5770(94)	7270(106)
41	90	0	10	0.082	0.054	0.089	0.107	0.113	1270(96)	4730(96)	5730(95)	6570(107)	7200(105)
42	80	0	20	0.081	0.046	0.091	0.109	0.122	1390(105)	4210(86)	5440(90)	6270(102)	7120(104)
81	70	0	30	0.095	0.055	0.092	0.108	0.117	1200(91)	3950(80)	5240(87)	5690(93)	6910(101)

See Table 3 for details of abbreviations.
FC = ASTM Class C Fly Ash
ND = Not Determined

Dr. Muhammad S. Y. Bhatty, Portland Cement Association, Skokie, Illinois, U.S.A. 7

Properties of Blended Cements Made With Portland Cement, Cement Kiln Dust, Fly Ash, and Slag 3.1

Table 6 - Properties of Blended Cements Made with Cement, Kiln Dust, ASTM Class F Fly Ash and Slag

Blend	Blend Composition Wt. %				Autoc. Expan.	Drying Shrinkage %				Compressive Strength psi				
	C	KD	FF	SL	%	4d	11d	18d	25d	1d	7d	28d	90d	1Y
1	100	0	0	0	0.087	0.056	0.096	0.112	0.115	1320(100)	4920(100)	6030(100)	6150(100)	6830(100)
		Dust S												
65	80	0	10	10	0.062	0.064	0.099	0.114	0.119	1050(80)	4320(88)	6200(103)	7230(118)	8130(119)
66	70	0	10	20	0.061	0.067	0.097	0.107	0.114	930(70)	4090(83)	7110(118)	8160(133)	9330(137)
67	70	0	20	10	0.052	0.052	0.085	0.095	0.105	1040(79)	3920(80)	5890(98)	6760(110)	7630(112)
68	60	0	20	20	0.068	0.058	0.081	0.086	0.097	775(59)	3480(71)	6270(104)	8210(133)	9300(136)
69	70	10	10	10	0.103	0.054	0.095	0.114	0.122	1150(87)	4230(86)	5980(98)	7000(114)	7730(113)
70	60	10	10	20	0.097	0.058	0.104	0.119	0.131	740(56)	4210(86)	6470(107)	7780(127)	9350(137)
71	60	10	20	10	0.100	0.055	0.092	0.102	0.113	760(58)	3750(76)	5640(94)	7060(115)	8490(124)
72	50	10	20	20	0.061	0.041	0.073	0.088	0.097	850(64)	3880(79)	5580(93)	6880(112)	8080(118)

See Tables 3 and 4 for details of abbreviation.

Mortar Sulfate Expansion

Length change of the mortars made from different blends was measured up to one year for most blends. Data are reported at 3, 6, 9 months and one year. Expansion of 0.1% at one year can be considered a conservative limit.

At 9 months and one year, sulfate expansion for cement alone was 0.09% and 0.263%, respectively. Addition of kiln dust to cement significantly reduced expansion at one year. Binary slag blends containing 10% and 20% slag showed significantly higher expansion at one year but as the amount of slag in blends increased to 30% and 40%, the expansion decreased significantly to a safe level (Table 7). Binary blends containing Class F fly ash showed much lower expansion than cement alone at one year (Table 8). For binary blends containing Class C fly ash, data are only available for 9 months and expansion at 9 months is considerably less than cement alone (Table 9).

Ternary blends made with cement, kiln dust, and slag showed much lower expansions at one year when the amount of slag was increased to 30% and 40% (Table 7). At addition levels of 10% and 20% slag, ternary blends made with kiln dust L had comparable expansion to cement alone at one year, but similar blends made with dusts S and H showed significantly lower expansions. Ternary Class F fly ash blends produced significantly lower expansion than cement (Table 8). Similar behavior was observed for ternary Class C fly ash blends at 9 months.

Table 7 - Properties of Blended Cements Made with Cement, Kiln Dust and Slag

Blend	Blend Composition Wt. %			Total Alkali in Blend as Equiv Na_2O	Alkali-Aggregate Expansion % of Length at one Day		Sulfate Expansion % of Length at one Day			
	C	KD	SL	wt. %	3M	6M	3M	6M	9M	1Y
1	100	0	0	0.53	0.016	0.032	0.014	0.034	0.090	0.263
		Dust S								
2	90	10	0	0.67	0.016	0.018	0.019	0.025	0.033	0.095
4	80	10	10	0.66	0.017	0.015	0.017	0.021	0.028	0.059
5	70	10	20	0.65	0.017	0.017	0.016	0.025	0.023	0.039
53	60	10	30	0.64	0.017	0.017	0.019	0.019	0.018	0.031
54	50	10	40	0.62	0.020	0.019	0.018	0.020	0.020	0.030
		Dust H								
16	90	10	0	0.66	0.015	0.015	0.020	0.026	0.032	0.055
18	80	10	10	0.65	0.016	0.018	0.018	0.023	0.025	0.045
19	70	10	20	0.64	0.018	0.020	0.019	0.024	0.023	0.039
61	60	10	30	0.63	0.023	0.025	0.018	0.024	0.022	0.033
62	50	10	40	0.62	0.022	0.025	0.020	0.021	0.020	0.030
		Dust L								
10	90	10	0	0.82	0.020	0.023	0.024	0.034	0.076	0.174
12	80	10	10	0.81	0.022	0.024	0.027	0.033	0.086	0.254
13	70	10	20	0.80	0.020	0.022	0.025	0.030	0.067	0.219
57	60	10	30	0.79	0.021	0.024	0.015	0.020	0.020	0.031
58	50	10	40	0.77	0.027	0.025	0.017	0.023	0.023	0.037
8	90	0	10	0.52	0.012	0.014	0.019	0.035	0.136	0.557
9	80	0	20	0.51	0.017	0.016	0.023	0.032	0.140	0.598
51	70	0	30	0.49	0.018	0.016	0.021	0.022	0.025	0.080
52	60	0	40	0.48	0.020	0.019	0.020	0.026	0.027	0.063

See Table 3 for details of abbreviations.

Table 8 - Properties of Blended Cements Made with Cement, Kiln Dust, and ASTM Class F Fly Ash

Blend	Blend Composition Wt. %			Total Alkali in Blend as Equiv Na_2O wt. %	Alkali-Aggregate Expansion % of Length at one Day		Sulfate Expansion % of Length at one Day			
	C	KD	FF		3M	6M	3M	6M	9M	1Y
1	100	0	0	0.53	0.016	0.032	0.014	0.034	0.090	0.263
		Dust S								
2	90	10	0	0.67	0.016	0.018	0.019	0.025	0.033	0.095
22	80	10	10	0.85	0.058	0.061	-	0.023	0.027	0.035
23	70	10	20	1.03	0.019	0.023	0.012	0.021	0.026	0.041
78	60	10	30	1.21	0.014	0.017	-	0.017	0.025	0.034
		Dust H								
16	90	10	0	0.66	0.015	0.015	0.020	0.026	0.032	0.055
33	80	10	10	0.84	0.058	0.065	0.012	0.022	0.028	0.043
34	70	10	20	1.03	0.019	0.023	0.010	0.019	0.025	0.036
79	60	10	30	1.21	0.012	0.016	0.012	0.018	0.022	0.034
		Dust L								
10	90	10	0	0.82	0.020	0.023	0.024	0.034	0.076	0.174
28	80	10	10	1.00	0.102	0.107	0.014	0.023	0.029	0.046
29	70	10	20	1.18	0.039	0.044	-	0.023	0.032	0.040
80	60	10	30	1.37	0.025	0.029	0.021	0.029	0.035	0.050
26	90	0	10	0.71	0.015	0.018	0.011	0.022	0.036	0.063
27	80	0	20	0.89	0.024	0.029	0.017	0.028	0.043	0.073
77	70	0	30	1.07	0.020	0.023	0.022	0.030	0.036	0.050

See Table 3 and 4 for details of abbreviations.

Table 9 - Properties of Blended Cements Made with Cement, Kiln Dust, and ASTM Class C Fly Ash

Blend	Blend Composition Wt. %			Total Alkali in Blend as Equiv Na_2O wt. %	Alkali-Aggregate Expansion % of Length at one Day		Sulfate Expansion % of Length at one Day		
	C	KD	FC		3M	6M	3M	6M	9M
1	100	0	0	0.53	0.016	0.032	0.014	0.034	0.090
		Dust S							
2	90	10	0	0.67	0.016	0.018	0.019	0.025	0.033
37	80	10	10	0.96	0.016	0.018	0.011	0.025	0.034
38	70	10	20	1.25	0.094	0.147	0.013	0.028	0.038
82	60	10	30	1.54	0.084	0.098	0.013	0.029	0.037
		Dust H							
16	90	10	0	0.66	0.015	0.015	0.020	0.026	0.032
47	80	10	10	0.95	0.045	0.060	0.013	0.029	0.036
48	70	10	20	1.24	0.085	0.095	0.016	0.031	0.038
83	60	10	30	1.53	0.111	0.126	0.015	0.030	0.038
		Dust L							
10	90	10	0	0.82	0.020	0.023	0.024	0.034	0.076
43	80	10	10	1.11	0.080	0.126	0.018	0.032	0.042
44	70	10	20	1.40	0.119	0.145	0.018	0.033	0.043
84	60	10	30	1.69	0.089	0.096	0.021	0.037	0.044
41	90	0	10	0.82	0.035	0.051	0.013	0.032	0.062
42	80	0	20	1.11	0.140	0.218	0.015	0.034	0.060
81	70	0	30	1.39	0.158	0.197	0.012	0.029	0.045

See Tables 3 and 5 for details of abbreviations.

Since the ASTM test procedure used for sulfate expansion is relatively new, limited data are available in the literature, but it is believed that a number of research workers are now using this test procedure. Therefore, in the next few years, a considerable amount of empirical data will be available. In the meantime, the results of this study suggest that some blended cements of selected compositions could reduce the sulfate expansion compared to cement with or without kiln dust addition.

CONCLUSION

Since earlier studies of kiln dust blended cements showed encouraging results on compressive strength, time of initial set, workability, and alkali-aggregate expansion, the research program was

extended to include other properties that can influence the durability of concrete. The conclusions of this study with respect to strength development of kiln dust blended cements are generally similiar to earlier studies in which the same blend compositions were used. Similarities in alkali-aggregate expansion behavior were also observed.

The main conclusion of this study is, as in previous studies, that blended cements, comparable to portland cement, containing materials such as kiln dust, fly ash, and slag can be produced for use in the construction industry.

Based on these tests, conclusions on specific properties of blended cements are as follows:

Binary blends made from cement and kiln dusts developed higher strengths compared to cement alone at 1 day, but strengths became comparable to cement alone at one year.

Most ternary blends made from cement, high sulfate or high chloride kiln dust and slag or Class F and Class C fly ash developed significantly higher strengths than cement alone at 1 day. One year strengths of most ternary blends were higher than cement.

At later ages, ternary blends containing kiln dusts and slag produced higher strengths than ternary blends containing kiln dusts and either Class F or Class C fly ash.

Quaternary blends made from cement, kiln dust containing moderate sulfate content, slag and Class F fly ash produced significantly lower 1-day strength but higher strength at one year than cement alone.

Autoclave expansions of binary cement-kiln dust blends were higher than cement alone, but lower expansions were obtained for most binary cement-fly ash blends and for cement-slag blends.

All ternary blends made with cement, kiln dusts, and slag or fly ash showed higher autoclave expansion than cement alone except the ternary blends made with cement, high sulfate dust, and Class F fly ash.

Drying shrinkage of binary and ternary blends made with high sulfate dust was lower than cement alone and other comparable binary and ternary blends. Some quaternary blends produced lower shrinkage than cement alone.

Alkali-aggregate mortar bar expansions of binary cement-kiln dust, cement-slag and cement-Class F fly ash blends were comparable to cement alone and significantly below the ASTM limit of 0.1% at six months. Binary cement-Class C fly ash blends showed much higher expansions at one year when these blends contained 20% and 30% Class C fly ash.

Alkali-aggregate expansions of ternary blends containing cement, kiln dust and slag behaved similarly to binary kiln dust and binary slag blends. Most ternary blends containing Class F fly ash meet the ASTM limit of 0.1% at six months, but some ternary blends containing Class C fly ash did not.

Binary blends containing cement and kiln dust showed lower sulfate expansion than cement alone. Sulfate expansion of binary blends made with cement and slag decreased with increase in the amount of slag. Ternary blends made with cement, kiln dust, and slag behaved similarly.

At addition levels of 10%, 20%, and 30% of Class F fly ash in binary cement-fly ash blends, sulfate expansion was significantly lower than cement alone at one year. Similar results were obtained with Class C fly ash at 9 months. Ternary blends made with cement, kiln dust and either Class F or C fly ash also behaved similarly to the respective binary blends made with Class F or C fly ashes.

At addition levels of 10% and 20% in binary and ternary blends, fly ashes were much better inhibitors of sulfate expansion than slag but at higher addition levels both fly ashes and slag behaved similarly in reducing the expansion significantly compared to cement alone.

ACKNOWLEDGEMENTS

The author expresses his appreciation to the members of the review committee of the Portland Cement Association's General Technical Committee for their helpful comments, to S. W. Tresouthick for his valuable discussions, to R. A. Helmuth and P. Klieger for reading the manuscript, to J. Patrick for the experimental work and to S. L. Ito for her assistance in the preparation of the final manuscript.

REFERENCES

1. Ravindrarajah, R.S., "Usage of Cement Kiln Dust in Concrete," International Journal of Cement Composites and Light-Weight Concrete, Vol. 4, No. 2, May 1982, pp 95-102.

2. Daugherty, K.E. and Funnell, J.E., "The Incorporation of Low Levels of By-Products in Portland Cement and the Effects on Cement Quality," Cement, Concrete, and Aggregates, CCAGDP, Vol. 5, No. 1, Summer 1983, pp 14-20.

3. Bhatty, M.S.Y., "Use of Cement Kiln Dust in Blended Cements," World Cement, Vol. 15, No. 4, 1984, pp 126-128, 131-134.

4. Sprouse, J.H., "Cements, Mortars, and Concretes," U.S. Patent 4,451,295, May 29, 1984.

5. Bhatty, M.S.Y., "Kiln Dust Cement Blends Evaluated," Rock Products, Vol. 88, 1985, pp 47-52.

6. Bhatty, M.S.Y., "Use of Cement Kiln Dust in Blended Cements -- Alkali-Aggregate Reaction Expansion," World Cement, Vol. 16, No. 10, 1985, pp 386, 388-390, 392.

7. Greening, N.R. et al, "Disposal and Utilization of Waste Kiln Dust from the Cement Industry," Environmental Protection Agency, EPA-670/2-75-043, May 1975.

8. Sell, N.J. and Fischback, F., "Cement Dust: Pollutant and Profit Thief," Rock Products, Vol. 79, No. 6, 1976, pp 78-82.

9. Cohen, S.M., "Processing of Waste Kiln Dust," IEEE Cement Industry Technical Conference, Toronto, May 1980, pp 1-18.

10. Gartner, E.M., "Leaching of High Alkali Dust without Discharge of Leachate," Portland Cement Association, Internal Report, 1979.

11. McCoy, W.J. and Kriner, R.W., "Use of Waste Kiln Dust for Soil Consolidation," Portland Cement Association, Internal Report, 1971.

12. Miller, C.T. et al, "Use of Cement-Kiln Dust and Fly Ash in Pozzolanic Concrete Base Courses," Transportation Research Board Record No. 754, 1980, pp 36-41.

13. Spinola, A.A., "Treatment of Acid Waste Waters with Cement-Kiln Flue Dust," Portland Cement Association, Internal Report, 1971.

14. Wheller, W.E. and Oltjen, R.R., "Cement Kiln Dust in Complete Diets for Finishing Steers and Growing Lambs," Journal of Animal Science, Vol. 48, No. 3, 1979, pp 658-665.

15. Ward, G.M. et al, "Cement Kiln Dust in Finishing Lamb Diets," Journal of Animal Science, Vol. 49, No. 3, 1979, pp 637-640.

16. Carrol, D.M. et al, "Cement Kiln Flue Dusts for Soil Liming," Agronomy Journal, Vol. 56, 1964, pp 373-376.

17. Nagai, S., "Special Masonry Cement having a High Slag Content," Proceedings, Fourth International Symposium on Chemistry of Cement, (Washington, D.C. 1960), Monogram No. 43, National Bureau of Standards, Washington, D.C., 1964, Vol. II, pp 1043-1055.

18. Davis, T.A. and Hooks, D.B., "Disposal and Utilization of Waste Kiln Dust from the Cement Industry," U.S. Environmental Protection Agency, EPA-670/2-75-043, May 1975.

19. Pressler, E.E., et al, "Investigation of Franke Method of Determining Free Calcium Hydroxide and Free Calcium Oxide," Analytical Chemistry, Vol. 28, 1956, p. 896: Portland Cement Association, Research Bulletin 62.

A.A. GOVOROV, Institut de chimie colloidale et de chimie de l'eau, Kiev, URSS

CERTAINS ASPECTS DE LA STRUCTURE DES LAITIERS GRANULES

Les données des diagrammes d'equilibre du système $CaO-MgO-Al_2O_3-SiO_2$, de la composition chimique et du calcul de la composition minéralogique potentielle des laitiers vitreux synthétiques ont permis de déterminer les teneurs en S+A en moles % délimitant différents types technologiques et structuraux de laitiers, lesquels diffèrent également par les spectres IR, la vitesse de passage en solution de la silice dans l'eau, les produits d'hydratation hydrothermale et l'intensité de durcissement hydrothermal des coulis. Le rôle prépondérant des phases cristallines primaires potentielles et des éléments subcristallins potentiels prédominants correspondants se trouve confirmé.

Os dados de diagramas de equilíbrio do sistema $CaO-MgO-Al_2O_3-SiO_2$, a composição química e o cálculo da composição mineralógica potencial de escórias vítreas sintéticas permitiram a determinação dos teores de S+A em % molecular delimitando diferentes tipos tecnológicos e estruturais de escórias, as quais igualmente diferem pelos espectros de raio X, velocidade de passagem em solução de sílica em água, produtos de hidratação hidrotérmica e intensidade de endurecimento hidrotérmico das corridas. Confirma-se o papel preponderante das fases cristalinas primárias potenciais e dos elementos subcristalinos potenciais correspondentes que predominam.

L'on sait que la teneur relative en CaO, MgO, Al_2O_3, SiO_2 des laitiers constitue l'un des principaux facteurs de leur activité hydraulique et sert de critère pour son appréciation. Si l'on ne tient compte que de ces quatre oxydes en égalant leur somme à 100 %, il s'avère que la teneur en S + A ne dépasse pas 40 moles % dans les laitiers de fours Martin et ceux de la production d'alliages ferreux, est comprise entre 40 et 50 moles % dans les laitiers de haut fourneau et ceux de la production électrothermique du phosphore, dépasse 50 moles % dans les laitiers acides d'aciéries, de cubilot, et ceux de la production du nickel et du cuivre. La relation entre la teneur des quatre oxydes mentionnées et les particularités structurales des laitiers granulés est importante pour l'explication des différences d'activité hydraulique.

La structure et les propriétés des laitiers granulés dépendent:

a/ de leurs éléments structuraux subcristallins, essentiellement constitués de groupes de tetraèdres (SiO_4) et (AlO_4);

b/ des phases cristallines potentielles, surtout primaires, dépendant de la proportion et du degré d'ordre de répartition des divers éléments subcristallins.

En partant des diagrammes d'équilibre du système quaternaire CaO-MgO-Al_2O_3-SiO_2 pour des teneurs en MgO de 0, 5, 10, 15 % mass. (1) nous avons relevé (tableau 1) les diverses phases cristallines primaires potentielles du domaine des laitiers de ce système, en les disposant selon la composition chimique de ceux-ci. L'on voit que pour des teneurs en S + A inférieures à 40 moles % avec peu de MgO le silicate primaire potentiel est théoriquement C_2S, et avec beaucoup de MgO c'est C_3MS_2. Pour S + A compris entre 40 et 50 moles % le silicate primaire potentiel doit être la rankinite, ou C_2S, ou la pseudowollastonite aux basses teneurs en alumine et magnésie, soit la mélilite (géhlénite), ou C_2S aux basses teneurs en magnésie, soit la mélilite, ou la merwinite, ou la forstérite aux teneurs élevées en magnésie. Pour S + A compris entre 50 et 60 moles % le silicate primaire potentiel doit être la pseudowollastonite, ou la mélilite, ou l'anorthite aux basses teneurs en magnésie, soit le pyroxene, ou la forstérite aux teneurs élevées. Pour S + A supérieur a 60 moles % le silicate primaire potentiel doit être la pseudowollastonite, ou la wollastonite, ou le pyroxène, ou l'anorthite, ou la forstérite, ou la tridymite.

Ainsi la cristallisation primaire de mélilite dans les laitiers quaternaires considerés n'est théoriquement possible que dans ceux contenant 40-60 moles % S + A, celle de C_2S ou C_3MS_2 - que dans ceux contenant moins de 50 moles % S + A, celle de l'anorthite - que dans ceux contenant plus de 50 moles % S + A.

Afin d'évaleur la teneur en différents produits de cristallisation potentiels dans ces laitiers quaternaires nous avons appliqué la methode proposée par (2). Les resultats de nos calculs effectués pour 33 laitiers synthetiques sont graphiquement representés sur la fig. 1, qui montre que dans les laitiers contenant 40-50 moles % S + A la phase cristalline potentielle prédominante doit être la mélilite (géhlénite), ou la rankinite; dans les laitiers contenant 50-60 moles % S + A - ce doit être la pseudowollastonite; dans ceux contenant 60-65 moles % S + A - l'anorthite ou le pyroxène; dans ceux contenant plus de 65 moles % S + A - la tridymite.

Ces résultats s'accordent avec les donénées précédentes du tableau 1 obtenues à partir des diagrammes d'equilibre. Ils permettent d'admettre que dans les laitiers considérés contenant 40-50 % moles % S + A l'élément structural subcristallin prédominant est le groupe (Si_2O_7) ou ($SiAl_2O_7$), dans ceux contenant 50-60 moles % S + A - - le groupe (Si_3O_9), dans ceux contenant 60-65 moles % S + A - les chaînes anorthitique ($Si_2Al_2O_8$) ou pyroxènique (SiO_3), dans ceux contenant plus de 65 moles % S + A - le réseau de tetraèdres de la silice.

Tableau 1

Les phases cristallines primaires potentielles du domaine des laitiers du systeme $CaO-MgO-Al_2O_3-SiO_2$

S+A mol.%	A/S mol.	Teneur en MgO, % mass. 0	5	10	15
30-40	0-0,1	C_3S	C_2S	$C_2S;C_3MS_2$	$C_2S;C_3MS_2;M$;
	0,1-0,2	C_2S	C_2S	$C_2S;C_3MS_2$	$C_2S;C_3MS_2;M$;
	0,2-0,3	C_2S	C_2S	$C_2S;C_3MS_2$	$C_3MS_2;M$;
	0,3-0,5	C_3S	C_2S	$C_2S;C_3MS_2$	$C_3MS_2;MA;M$
40-50	0-0,1	$C_2S;C_3S_2;\alpha CS$	$C_2S;mel;\alpha CS$	$C_3MS_2;mel$	$C_3MS_2;mel;CMS_2$
	0,1-0,2	$C_2S;C_3S_2;\alpha CS;C_2AS$	$C_2S;mel$	$C_3MS_2;mel$	$C_3MS_2;mel;M_2S;MA$
	0,2-0,3	$C_2S;C_2AS$	$C_2S;mel$	$C_3MS_2;mel;MA$	$C_3MS_2;MA;M_2S$
	0,3-0,5	$C_2S;C_2AS$	$C_2S;mel$	$C_3MS_2;mel;MA$	MA
50-60	0-0,1	αCS	αCS	$\alpha CS;\beta CS;mel;CMS_2$	$CMS_2;S$
	0,1-0,2	αCS	$\alpha CS;mel;CAS_2$	$mel;CMS_2;CAS_2$	$CMS_2;M_2S$
	0,2-0,3	$\alpha CS;C_2AS;CAS_2$	$mel;CAS_2$	$mel;CAS_2;MA$	$M_2S;MA$
	0,3-0,5	$C_2AS;CAS_2$	$mel;CAS_2;MA$	$mel;CAS_2$	MA
60-70	0-0,1	$\alpha CS;S$	$\beta CS;CMS_2;S$	$S;CMS_2$	$S;CMS_2$
	0,1-0,2	$\alpha CS;CAS_2$	$\beta CS;CMS_2;CAS_2$	$CMS_2;CAS_2$	$CMS_2;S;M_2S$
	0,2-0,3	$\alpha CS;CAS_2$	CAS_2	CAS_2	$M_2S;MA$
	0,3-0,5	CAS_2	$CAS_2;MA$	$CAS_2;MA$	MA

Ainsi ces teneurs en S+A délimitent non seulement différents types technologiques de laitiers, mais également leurs divers types structuraux, caracterisés par la prédominance de différents éléments structuraux subcristallins.

Sur la fig. 2 nous avons représenté par des points les raies des spectres IR d'absorption obtenus pour une centaine de laitiers, et disposés selon leur teneur en S+A en moles %. L'on voit que la position de la raie d'intensité maximale diffère selon l'élément structural subcristallin prédominant dans le laitier. Ainsi pour les laitiers contenant 30-40 moles % S+A avec A/S inférieur à 1 ce maximum se situe dans l'intervalle 920-940 cm^{-1}, et correspond, de toute évidence, aux vibrations du groupe (SiO_4), tandis qu'avec A/S = 1-2 ce maximum se situe près de 900 cm^{-1} et est dû aux groupes de tetraedres (AlO_4). Le maximum d'intensité de la bande d'absorption IR pour les laitiers contenant 40-50 moles % S+A se situe dans l'intervalle 940-990 cm^{-1}, sa fréquence augmentant avec la teneur en S+A des laitiers, ce qui semble dû au remplacement des groupes (Si_2O_7) par ceux (Si_3O_9), comme le montre la fig. 1. Les laitiers contenant 50-65 moles % S+A donnent deux maxima dans les intervalles 1000-1020 et 1080-1090 cm^{-1} qui correspondent probablement aux groupes (Si_3O_9) et au réseau de tetraèdres siliciques. Les laitiers contenant plus de 65 moles % S+A ne donnent plus que le maximum 1080-1090 cm^{-1} correspondant aux vibrations du réseau silicique.

Ces différences dans les éléments structuraux subcristallins prédominants des laitiers contenant diverses teneurs en S+A se répércutent évidemment sur la vitesse de passage en solution de leur silice sous l'action de l'eau. Cela est bien visible sur la fig. 3, montrant la relation entre la

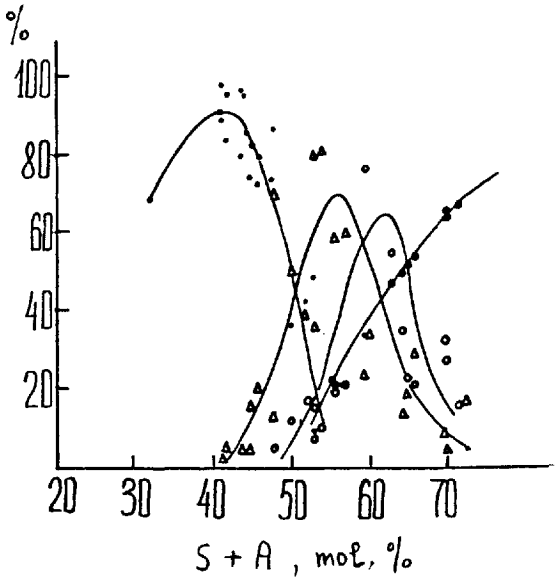

Fig. 1. Teneurs calculées des différents produits de cristallisation potentiels dans les laitiers $CaO-MgO-Al_2O_3-SiO_2$ en fonction de leur teneur en $SiO_2+Al_2O_3$:
(·) pour $C_2AS+C_3S_2+C_2MS_2$
(△) - αCS
(○) - CAS_2+CMS_2
(●) - S

teneur en S+A des laitiers et la fraction de leur silice se trouvant en solution après échauffement en autoclave jusqu'à diverses temperatures, suivi d'un refroidissement immediat. La silice en solution était dosée par la méthode photocolorimétrique du complexe silicomolybdique.

Il ressort de la fig. 3 que le maximum de silice en solution s'observe: pour les laitiers contenant près de 40 moles % S+A - après autoclavage à 100 °C, pour les laitiers contenant près de 50 moles % S+A - après autoclavage à 150-200°, pour les laitiers contenant plus de 50 moles % S+A - après autoclavage à 250°. Cela s'accorde avec l'accroissement du nombre de tetraèdres siliciques par élément structural subcristallin et, par consequent, avec l'accroissement de sa stabilité à l'attaque hydrolythique. En outre la teneur de silice en solution augmente avec

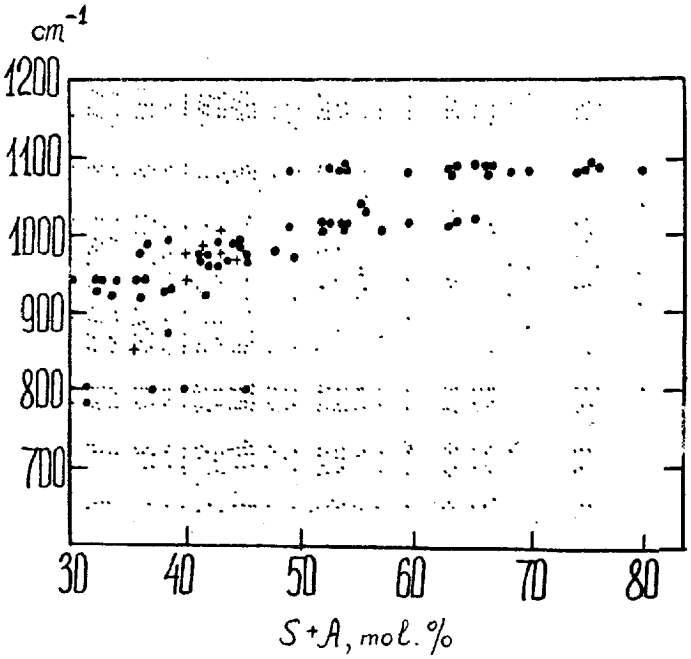

Fig. 2. Spectres IR des laitiers disposés selon leur teneur en $SiO_2+Al_2O_3$ Les raies sont représentées par des points. Les cercles noirs représentent les maxima d'intensité observés pour les laitiers synthétiques, les croix (+) - ceux pour les laitiers réels

A/S des laitiers, surtout ceux contenant 30-40 moles % S+A. Dans les deux cas l'augmentation de silice en solution est liée à celle du déficit en calcium, lequel est nécéssaire à la recombinaison de la silice dans les hydrosilicates de calcium. Ce déficit est dû dans le premier cas à la diminution de la basicité des laitiers avec l'accroissement de S+A et dans le second, à la plus rapide recombinaison du calcium avec les éléments structuraux contenant (AlO_4). (3).

Les diagrammes X ont mis en évidence la cristallisation hydrothermale d'hydrates de C_2S dans le cas des laitiers avec 30-45 moles % S+A, d'hydrogrenats - avec 30-60 moles % S+A, de la tobérmorite - avec 48-65 moles % S+A, de la gyrolite - avec 60-80

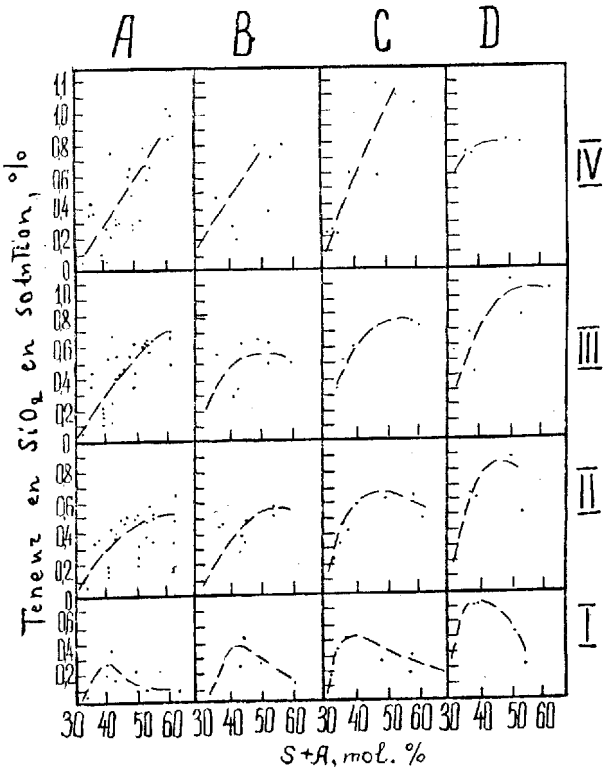

Fig. 3. Teneur en silice du laitier se trouvant en solution après échauffement à l'autoclave jusqu'à 100° (I), 150° (II), 200° (III), 250° (IV) des laitiers synthétiques contenant diverses teneurs en $SiO_2+Al_2O_3$ et diverses valeurs de Al_2O_3/SiO_2 égales à moins de 0,1 (A) 0,1-0,3 (B), 0,3-0,6 (C), 0,6-1,0 (D)

moles % S+A, d'anorthite hexagonale - avec 55-70 moles % S+A, d'anorthite - avec 55-80 moles % S+A. Il en resulte que les éléments structuraux siliciques subcristallins des phases hydratées sont proches de ceux des laitiers d'origine.

Les coulis de laitiers synthétiques et réels avec 30-40 moles % S+A atteignaient en durcissant le maximum de résistance après autoclavage à près de 100 °C, ceux avec 40-50 moles % S+A - à pres de 200°, ceux avec 50-60 moles % S+A - à près de 250°.

Tout ce qui vient d'être exposé confirme le rôle prépondérant des phases cristallines primaires potentielles et des éléments structuraux subcristallins prédominants, comme facteurs essentiels de l'activité hydraulique des laitiers granulés.

BIBLIOGRAPHIE

1. S. Solacolu, P. Balta. Les propriétés hydrauliques des laitiers de haut fourneau du systeme $MgO-CaO-Al_2O_3-SiO_2$ contenant du manganèse et du soufre. Revue des matériaux de constr., 1964, n° 583, 95-110.
2. M. Gourdin. Composition minéralogique potentielle des laitiers vitrifiés de haut fourneau. Ciments Béton Plâtre Chaux, 1980, n° 727, p. 363-365.
3. A.A. Govorov, E.V. Djouss, F.D. Ovtcharenko. L'influence du $Ca(OH)_2$ sur l'hydratation hydrothermale des laitiers. C.R. Acad. Sci. de la RSS d'Ukraine, 1983, n° 7, p. 35-38.

Y.Sh. SHKOLNICK, Ural Iron and Steel Institute, USSR 1

PHYSICOCHEMICAL PRINCIPLES OF THE HYDRAULIC ACTIVITY OF BLAST FURNACE SLAGS

3.1

The mechanism of slag hydratation and conditions of hydrate phase formation is considered in terms of oxygen forms in slags.

It is shown that slag hydraulic activity increases owing to the directional crystallization of active phases, chemical and thermal depolymerization of the glassy structure, and also owing to the use of water soluble additions adsorbed on the surface charges of slag grains during granulation.

In addition the cooling of slag melts during granulation should be carried out by inert gases, which would reduce the losses of sulphide sulphur having a favourable effect on the slag hydratation process.

Estuda-se o mecanismo de hidratação da escória e as condições da formação da fase de hidrato, em termos de formas de oxigênio nas escórias.

Mostra-se que a atividade hidráulica da escória aumenta devido à cristalização direcional de fases ativas, despolimerização química e térmica da estrutura vítrea, e também devido ao uso de adições solúveis em água, adsorvidas nas cargas de superfície dos grãos de escória durante a granulação.

Adicionalmente, o resfriamento das fusões de escória durante a granulação deverá ser feito por meio de gases inertes, que reduzirão as perdas de sulfato, já que o enxofre tem um efeito favorável sobre os processos de hidratação da escória.

3.1

The extension of the production of blast furnace slags for cement industry and the increase of the slag hydraulic activity during granulation is an important problem which is to be solved with due regard for the analysis of interrelations between the blast furnace slag structure and binding properties along with the slag vitrification behaviour and other factors. The binder hydratation process is accompanied by the Me-O bond break which depends in particular on the magnitude of the Me-O unit bond energy and the cation coordination number relative to oxygen [1].

On the basis of the approach to the binder solution mechanism in terms of the Me-O bond break during the oxide ion protonization and OH^- nucleophilic attack onto Me^{2+}, we may consider the equations of slag solution mechanisms with regard to the oxygen forms present in slags (double-fixed O^- realized in the Si-O-Si bond, mono-fixed O^- realized in the Si-O-Me bond, and "free" O^2 realized in the Si-O-Me bond) and the conditions of hydrate phase formation.

With the double-fixed oxygen present in slags the reaction proceeds according to the following equation:

a) $\equiv Si-O-Si \equiv + HOH \longrightarrow 2\ (\equiv SiOH)$

With the mono-fixed oxygen present the equation has the following form:

b) $\equiv Si-O-Me-O-Si \equiv + (2(HOH) \longrightarrow 2(\equiv SiOH) + Me^{2+} + 2OH^{-2}$

And in the case of the "free" oxygen present the reaction takes a form

c) $\equiv Si-O-Me...O...Me-O-Si \equiv + 3(HOH) \longrightarrow 2(\equiv SiOH) + 2Me^{2+} + 4HOH^-$

Assuming that for the formation, for instance, of CSH per SiOH bond it is necessary to have both a Ca^{+2} cation and an OH^- ion, we can see that for the "b" case (mono-fixed oxygen) the concentration of Ca^{2+} and OH^- ions at the initial stages is insufficient for the formation of the mentioned types of hydrate phases. And only with the beginning of the polymerization processes of hydroxylated silicon-oxygen complexes, formed due to an earlier leaching of Ca^{2+} from the surface, the Ca^{2+} and OH^- concentration necessary for each Si-O-Si-OH bond is ensured.

In view of the long duration of these processes, it becomes clear that for their acceleration it is necessary to make the low-basic silicates, and slags in particular, more active by introducing alkaline or alkaline-earth components into the hydrated system. For the case of high-basic silicates ("c" variant) the Ca^{2+} and OH^- concentration necessary for the CSH formation is ensured by the interaction of the binder with water.

From the analysis it is clear that the hydraulic activity of the slag glassy phase rises with the augmentation of the degree of silicon-oxygen complex depolymerization and decrease of the Me-O unit bond energy, the thermal structure depolymerization proceeding rather with the increase of the melt cooling rate than with the increase of the melt superheat above T_ℓ. In this case a melt structure, having many small chain fragments containing end atoms of oxygen or end groups of O-Me, is observed.

As it is known the Me-O unit bond energy is determined by the coordination number and the amount of orbital overlapping which characterizes the bond of ionicity degree, the latter having a considerable effect on the intensity of interaction between minerals and water.

There is some evidence that the slag transformation from a crystalline state into a glassy one increases the ionicity degree of a Me-O bond, and that accounts for a greater hydraulic activity of glassy slags in comparison with crystalline ones of the equivalent composition. These assumptions are based on the results in [4], where it is shown by the positron annihilation method that the SiO_2 transformation from a crystalline state into a glassy one is accompanied by an increase of the Si-O bond covalency.

In the case of Si-O-Me fragments an increase of the Si-O bond covalency results in "drawing-off" the electron cloud from oxygen to silicon, thus increasing the Me-O bond of ionicity.

The experience of using granulated blast furnace slags in cement industry has shown that slag activity depends not only on the glass content, but on the crystalline phase presence as well.

In connection with this it is clear that for solving the problems of slag granulation it is necessary to prevent the formation of inert compounds during slag cooling.

In this context it has been shown [1] that in order to raise the activity of slags with Mo >1 the granulation should be carried out at the lowest temperatures possible (below T_ℓ), and in the case of slags with Mo <1 the temperatures should be above T_ℓ.

The surface of glassy slags is non-uniform and has a set of various adsorption centres. The IR-spectroscopy and diffuse reflection examination of the lignosulphate adsorption from water solutions on slags with various Al_2O_3 contents has shown that along with physical adsorption there occurs also chemisorption, the excess charges formed as a result of the aluminium coordination number mismatch being most likely adsorption centres.

The calculation carried out by the method [3] has shown that in presence of Al (IV) and Al (VI) in slags a positive charge equal unity, which might serve as an adsorption centre, e.g. for anion surface-active agents, is generated on the slag surface in the aluminium region.

This allows to granulate slags rather by water solutions containing various surface-active and other water soluble additions, which might be adsorbed on the surface charges of the slag particles, than by process water. It should be noted that the surface adsorption activity of the slag particles, formed during the crushing of coarse grains into smaller ones in the course of their cooling in water, is rather high on account of the formation on them of a great amount of uncompensated surface charges (similar to charges formed on the clinker surface during crushing).

An examination of slag portland cement, carried out on the slags granulated by lignosulphate water solutions and industrial waste water containing calcium and sodium chlorides, has shown, for the former case, an increase in the slag portland cement strength due to a plasticizing action of the lignosulphate molecules adsorbed on the slag surface, and, for the latter case, an increase in the strength due to an activating effect of the chlorides, also adsorbed on the slag surface.

As it is known, modern methods of producing granulated slags provide cooling them by water. As a result, the hydrolysis of calcium sulphide occurs, sulphur transferring into gaseous and water phases. According to [4], total sulphur losses during slag granulation might be up to 20-30 % of the initial sulphur content in the melt. As for the effect of sulphide sulphur on slag hydratation processes, there exists some controversy mainly because of the differences in slag producing methods.

We have carried out a detailed study of the problem in question, different amounts of S^{2-} being introduced into slag along with maintaining its basicity (CaO/SiO_2). It has been found that sulphur within its solubility range (up to 2-2.5 % for S^{2-}), exerts a favourable influence on the hydraulic activity of slags; a further increase in its content has no effect on hydratation processes.

This might be attributed to the features of S^{2-} entering the slag glass structure. So, within the solubility range sulphur forms Si-O-Ca-S groups, in which the binding energy between silicon-oxygen complexes and calcium cations is reduced because of a more covalent character of the Ca-S bond in comparison with the Ca-O bond.

As the amount of sulphur in blast furnace slags is in this range, the use of water for cooling the slag results in its desulphuration and, therefore, in some loss of activity.

In view of this it seems desirable to use air or, still better, inert gases for cooling slag melts. This, along with the improvement of the quality of granulated slags due to the reduction of sulphide sulphur losses, contributes to environmental problems owing to a lesser evolution of noxious sulphuric gases with water steam into atmosphere

REFERENCES

1. Школьник Я.Ш. - Цемент, 1985, № 2, с. 14-15.
2. Тарасов В.В. - Проблемы физики стекла, М., Стройиздат, 1979, с. 255.
3. Tanabe K., Siniyoschi T. - Shibotak, Bull. Chem. Soc. Jap., 1064 (1974).
4. Будников П.Н., Григорьев В.С. и др. - Строительные материалы, 1968, № 3, с. 13-15.

K.Popović, A.Djureković, V.Ukrainčik - Civil Engineering Institute - ZAGREB YUGOSLAVIA

BLENDED AND SPECIAL CEMENTS INCORPORATING CONDENSED SILICA FUME

CIMENTS COMPOSES CONTENANT DES FUMEES DE SILICE.

SUMMARY

Procedure for industrial use of condensed silica fume (c.s.f.) as a pozzolanic admixture to portland cement have been investigated and developed.

Transport and handling as well as the problems of increased water requirement and drying shrinkage of cements containing c.s.f. have been solved or significantly reduced without need of (super) plasticizers, when the predensed dust or intergrinding of c.s.f. pellets with portland cement clinker was applied.

Testing of laboratory and industrially produced cements has shown that the addition of 5-15% of condensed silica fume:

- increases efficiency of cement in concrete strength development,
- enables simultaneous satisfying of the contradictory requirements for strengths and heat of hydration in low-heat cements,
- improves durability of cement paste and mortar in sulfate environment.

Investigou-se e se desenvolveu processo para utilização industrial de microsílica (c.s.f.) como mistura pozolânica para cimento portland.

Problemas de transporte e manipulação, bem como problemas de aumento da necessidade de água e de contração de secagem dos cimentos contendo c.s.f., foram resolvidos, ou significativamente minimizados sem necessidade de (super) fluidificantes, quando se aplicou pó pré-condensado ou moagem conjunta de peletes de c.s.f. e clínquer de cimento portland.

Cimentos produzidos em laboratório e em escala industrial mostraram que a adição de 5 a 15% de fumo condensado de sílica:

- aumenta a eficiência do cimento no desenvolvimento da resistência do concreto,
- possibilita o atendimento simultâneo de requisitos contraditórios para resistências e calor de hidratação em cimento de baixo-calor,
- melhora a durabilidade da pasta e da argamassa de cimento em ambiente sulfatado.

K. Popovic, A. Djurekovic, V. Ukraincik - Civil Engineering Institute - ZAGREB
YUGOSLAVIA

INTRODUCTION

Approximately 30,000 tons of condensed silica fume have been collected yearly in yugoslav ferro-silicon plants. Only a part of it is used as an admixture to concrete in order to improve the durability against chemical agression,[1] but broader application was not possible earlier since its inconvenient physical characteristics (bulk density approx. 250 kg m^{-3}, and BET spec. surface approx. 20 m^2 g^{-1}) cause problems in handling and transport. In addition to this the beneficial effect is reduced by negative influence of c. s.f. in original very fine form on the water requirement of cement and concrete,so the use of (super) plasticizers in necessary. (2-8).

Agglomeration of c.s.f. in pellets with addition of water or predensing of original fine dust in ball mill solves the problems of transport and handling in consequence of increasing bulk density up to 600 kg m^{-3} and formation of fine particle agglomerates, and these two forms seem to be suitable for use as a pozzolanic admixture. The following experiments have been proceeded to find out the influence of different forms of c.s.f. on physical properties, heat of hydration,strength development and sulfate resistance of portland cement.

EXPERIMENTS AND RESULTS

1. Basic properties of cements incorporating condensed silica fume

Different cement samples have been produced:
- by addition of original very fine silica dust (BET surface 20 m^2g^{-1}) to portland cement,
- by addition of ground pellets of c.s.f. to portland cement,
- by addition of predensed dust to portland cement,
- by laboratory and industrial intergrinding of PC-clinker and c.s.f. pellets.

For these experiments ordinary portland cement clinker of following mineral composition (Bogue) was used:
C_3S 55.8%, C_2S 18.7%, C_3A 9.7%, C_4AF 9.0%.
The most significant characteristics and properties of those cements are shown in tables 1 and 2. Properties of concrete prepared with these cements are shwon in table 3.

Table 1 - Water for standard consistency (Vicat) %

Silica fume content (%)	Form of silica fume and way of addition			
	Comparative (ordinary portland)	Original dust added to separately ground cement	Ground pellets added to separately ground cement	Intergrinding of pellets and clinker
0	27.3	-	-	-
3		28.3	27.5	
5		28.7	27.8	
7		29.7	28.7	26.5
9		30.7	29.2	
15		32-34*	29.5	27.3

* High thixotropy

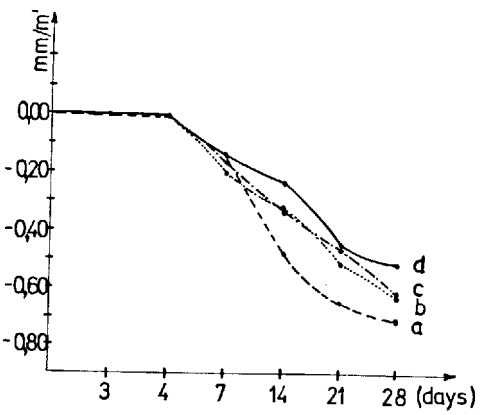

Fig.1 - Drying shrinkage of cement mortar containing different forms of condensed silica fume

a) portland cement with addition of 15% silica fume in original dust form
b) portland cement containing 15% of silica fume: 7.5% of pellets interground with PC clinker and additional 7.5% added in a form of predensed dust
c) portland cement with addition 15% of silica fume in a form of ground pellets
d) pure portland cement - comparative

Table 2 - Physical and mechanical properties of cements containing silica fume

Silica fume Content	Form and way of addition	Spec.surf. Blaine $cm^2\ g^{-1}$	Water for standard consistency Vicat (%)	Consistenty by flow-table (cm)	Strength (MPa) 3 days flexur.	3 days compr.	28 days flexur.	28 days compr.	Drying shrinkage 28 days ($mm\ m^{-1}$)
0	(comparative)	3,330 (cement)	27.3	11.5	6.5	27.1	8.9	46.9	0.502
7.5	original dust added to comparative	30.000 (dust)	29.7	11.3	5.8	28.7	8.9	62.0	0.661
15			32-34*	10.7	5.7	27.1	8.1	56.3	0.700
7.5	ground pellets added to comparative	8.500 (dust)	28.7	10.1	6.4	27.7	8.4	50.1	0.474
15			29.5	10.5	5.8	25.9	8.2	46.7	0.596
7.5	industrial inter grinding pellets with PC-clinker	3.890 (cem+dust)	26.5	12.0	7.2	31.4	9.8	51.5	0.549
15	additional 7.5% of dust added to cement interground wit 7.5% pellets	4.300 (cem+dust)	27.3	12.4	7.4	31.3	9.2	57.6	0.610

* High thixotropy

Table 3 - Composition and properties of concrete with silica fume

Cement	Content (kg/m^3) cem	c.s.f.	total cementitious	w/c	slump (cm)	density ($\frac{kg}{dm^3}$)	Pore content (%)	Compressive strength (MPa) 7 d	28 d	90 d	Efficiency* 28 days of total cementitous	pure PC (clinker)
C- 1	300	-	300	0.58	6.5	2.33	2.4	23.6	29.6	32.8	0.99	0.99
C- 2	277.5	22.5(7.5%)	300	0.61	7.0	2.33	2.5	26.0	33.8	37.3	1.12	1.22
C- 3	275	45 (15 %)	300	0.65	6.5	2.30	2.6	26.4	37.6	36.4	1.25	1.36
C- 1	300	-	300	0.58	7.0	2.33	2.4	23.6	29.6	32.8	0.99	0.99
C- 4	276	24 (8%)	300	0.63	7.0	2.32	2.4	23.0	33.5	36.1	1.12	1.21
C- 5	255	45 (15%)	300	0.68	6.5	2.28	2.6	22.1	32.7	33.9	1.09	1.28

* Efficiency = $\frac{\text{Strength}}{\text{Cement content}}$ $\left(\frac{dN/mm^2}{kg/m^3} \right)$

C- 1 Ordinary Portland cement

C- 2 C-1 containing 7.5% c.s.f. (industrially interground pellets)

C- 3 C-2 containing additional 7.5% c.s.f. in the form of predensed dust; (total c.s.f. content = 15%)

C- 4 C-1 containing 8% of c.s.f. in the form of predensed dust

C- 5 C-1 containing 15% of c.s.f. in the form of predensed dust.

K. Popovic, A. Djurekovic, V. Ukraincik - Civil Engineering Institute - ZAGREB YUGOSLAVIA

2. Sulfate resistance of cements containing condensed silica fume

Two procedures have been used to ascertain sulfate resistance of cements containing c.s.f. in comparison with sulfate resistant cements defined by standards. Results are presented in figure 2 (Koch-Steinegger[9] test) and in table 4 (ASTM C 452 - expansion test).

Table 4 - Sulfate expansion of cement mortar ASTM C 452

Cement composition	Expansion at 14 days
Ordinary portland cement (C_3A=9.7 %)	0.075 %
Ordinary portland containing 7% c.s.f. (interground pellets)	0.054 %
Ordinary portland containing 12% c.s.f. (interground pellets)	0.035 %
Sulfate resistant cement (yugoslav standard) C_3A=0.2%	0.015 %
Moderate sulfate resistance (ASTM Typ II) C_3A=6.2%	0.048 %

Note: JUS B.C1.014 requirement for C_3A max. 3.5%

ASTM Typ II requirement for C_3A max 8%

ASTM Typ V (high sulfate resistance)- requirement for C_3A max. 5%

ASTM C 150 - requirement for sulfate expansion at the age of 14 days max. 0.045%.

3. Influence of c.s.f. on heat of hydration

The property of c.s.f. that increases cement strengths in later periods of hydration owing to its intensive pozzolanic activity was used for simultaneous achievement of two contradictory properties required for low-heat cement: certain level of strengths together with limited heat of hydration. Blended portland cements containing originally 50 per cent of fly ash or 55 per cent of blast furnace slag were used in these experiments. The results obtained are presented in table 5.

4. In order to explain different properties of various forms of c.s.f. SEM was used. The most significant SEM micrographs are presented in figures 3, 4 and 5.

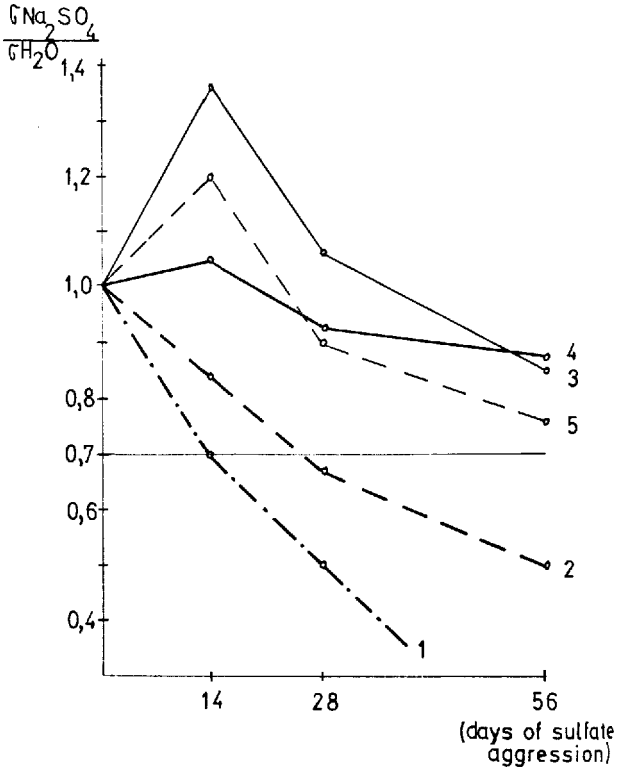

Fig.2 - Koch-Steinegger test for sulfate resitance: ratio between strength for mortar samples exposed to 10% Na_2SO_4 solution and samples stored in water

1) Ordinary portland cement C_3A (Bogue) 9.7%
2) Ordinary portland containing 7% of c.s.f. added by intergrinding pellets
3) Ordinary portland containing 12% of c.s.f. added by intergrinding pellets
4) Ordinary portland containing 10% of c.s.f. in original dust form
5) Sulfate resistant cement - C_3A (Bogue) 3.2%

$\frac{\sigma Na_2SO_4}{\sigma H_2O}$ ratio min. 0.7 at 56 days for sulfate resistant cement

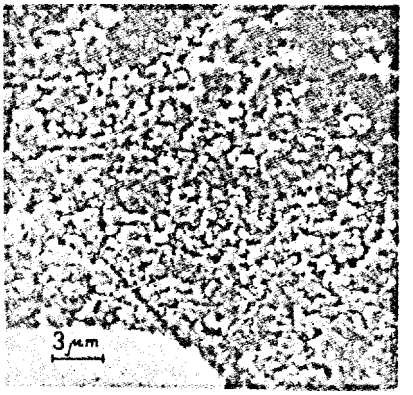

Fig.3- SEM micrograph of original silica dust; separated very fine (approx. 0.5 μm) particles can be seen



Fig.4 - SEM of predensed silica fume; original fine particles are agglomerated in (5-15 μm) grains.

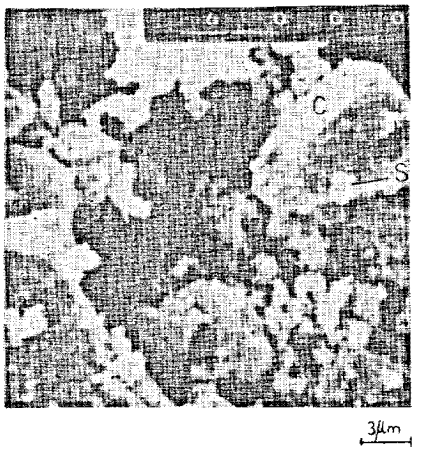

Fig.5 - Cement mix produced by intergrinding PC clinker and c.s.f. pellets; Clinker grains of approx. 10 μm and c.s.f. agglomerates of approx. 1-3 μm can be seen.
C - clinker grain, S - silica grain

Table 5. Influence of c.s.f. on the properties of low-heat cements

Cement composition (%)			c.s.f.* content	Strength (MPa)				Heat of hydration (J/g)	
				7 days		28 days		7 days	28 days
Clinker	Gypsum	Admixture		flexur. min	compr. min	flexur. min	compr. min	max 250**	max 295**
			yugoslav standard requirement	3.0	14.0	4.0	25.0		
47	3	50(Fly Ash)	0	3.6	16.3	4.5	23.0	242	283
44.6	2.9	47.5	5.0	4.4	16.2	5.5	28.6	221	270
42.3	2.7	45	10.0	4.4	16.1	5.9	29.2	243	237
40	5	55 (B.F. slag)	0	5.2	20.5	8.3	36.9	247	311
33	5	55	7	5.0	18.8	8.7	36.4	218	277
37	5	51	7	5.1	21.4	9.1	44.4	242	291

* Added in fine dust form to ground cement

** Method of solution

K. Popovic, A. Djurekovic, V. Ukraincik - Civil Engineering Institute - ZAGREB YUGOSLAVIA

DISCUSSION

It is obvious that replacement of small portion of PC clinker with predensed c.s.f. or intergrinding of agglomerated pellets with PC clinker has positive influence on cement properties. Although some previous experiments[10] showed that specific surface of predensed dust is approximately one half of the original fine dust surface (for ground pellets even one third of dust) and that pozzolanic activities of thesetwo forms are reduced in the same proportion, the increase in cement later strengths is still significant. In additon to this, the water requirement and drying shrinkage of such cements are not so high as those caused by very fine original silica dust.

The greater suitability of agglomerated pellets and of predensed dust for application in cement (higher bulk density) and more acceptable properties of cements incorporating such forms of c.s.f. can be explained by the presence of agglomerated silica particles in predensed dust and in pellets. SEM micrographs (figures 3, 4 and 5) confirm this presumtion. The agglomeration reduces active surface of silica particles and their water requirement consequently. It seems, however, that the bonds between silica particles in agglomerated grains are not so strong to hinder proper pozzolanic reaction which contributes to strength and durability of hydrated cement paste.

Effects on concrete properties, especially better efficiency in strength development makes these cements more valuable and, at the same time, cheaper due to energy saving for clinker burning. The cement production using intergrinding c.s.f. pellets is present in yugoslav practice for two years.

Testing the performance of portland cements produced by intergrinding c.s.f. pellets with ordinary PC clinker has showed that such cements exhibit similar or even better sulfate resistance than sulfate resistant cements defined by standards (ASTM Typ II and Typ V, DIN or JUS).
Previous experiments[1] with very fine original silica dust have shown the same results, but applying of c.s.f. in fine dust form is not convenient for broad application and,especially for this purpose of corrosion preventing needs use of water reducers.

ASTM C 452 expansion test gives preference to low C_3A sulfate resistant type of portland cement because only chemical influence of c.s.f. on durability is included. Physical influence i.e. reduced porosity/permeability of PC paste can not be evaluated by this method.

Possibility of using c.s.f. for blended low-heat cement production is very important, since difficulties in achieving the required properties are often present as can be seen from table 5. Industrial pilot grinding of low-heat cement incorporating c.s.f. was undertaken recently in order to confirm the promising laboratory results.

REFERENCES:

1. Popović,K., Ukrainčik,V., Djureković,A., Improvement of Mortar and Concrete Durability By the Use of Condensed Silica Fume , Durability of Building Materials, 2 (1984) 171.
2. Asgeirsson,H. and Gudmundsson,G., Pozzolanic activity of silica dust. Cement and Concrete Research, 9, (1979) 249-252
3. Bache,H.H., Densified cement/ultra-fine particle-based materials. 2nd Int.Conf.on Superplasticizers in Concrete, Ottawa, (1981)
4. Gutt,W. and Nixon,P.J., Use of waste materials in the construction industry. Materiaux et Construction, 12 (1979) 255-299
5. Traetteberg,A., Silica fume as a pozzolanic material. Il Cemento, 75 (1978) 369-376
6. Jahren,P., Use of Silica Fume in Concrete, ACI SP-79 Vol.II, (1983) 625-642
7. Sellevold,E.J., Radjy,F.F., Condensed Si ica Fume in Concrete - Water Demand and Strength velopment, ACI SP-79, Vol II, (1983) 677-694
8. Mehta,P.K., Pozzolanic and Cementitious By-Pr cts as Mineral Admixtures for Concrete. ACI SP- Vol.I, (1983) 1-46.
9. Koch,A. and Steinegger,H., Ein Schnellprüfverfahren für Zemente auf ihr Verhalten Sulfatangriff Zement-Kalk-Gips, 7 (1960) 317-324
10. Popović,K., Ukrainčik,V., Djureković,A., Silica Fume from Ferro-Alloys as a Pozzolanic Admixture to Cement, Kemija u industriji, 34 (1985), 575 (in Croatian).

SUB-THEME/SOUS-THÈME 3.2

Effect of blending components on hydration and structure formation.

Effets des composants des matières d'additions dans l'hydratation et dans la formation de la structure.

Chairman/Président :

J. Calleja
Instituto Español del Cemento y sus Aplicaciones (IECA)
Madrid, Spain

Principal Reporter/Rapporteur Principal:

H. Uchikawa
Onoda Cement CO., Ltd.
Tokyo, Japan

A.I. ELOLA, Mrs., A.S. SZTEINBERG, Miss, R.J. TORRENT, Dr.
Building Dept., Instituto Nacional de Tecnología Industrial (INTI), Buenos Aires, Argentina.

"EFFECT OF THE ADDITION OF BLASTFURNACE SLAG ON THE PHYSICAL AND MECHANICAL PROPERTIES OF MORTARS CURED AT HIGH TEMPERATURES". 3.2

SUMMARY: Compressive strength, non-evaporable water content and pore size distribution were studied on mortar specimens cured at 20, 40 and 80° C for different periods, after a delay of 1 day at 20°C. A portland cement and a slag cement, prepared from the same clinker, were used.

The experimental results are discussed with reference to the effect of curing temperature on the acceleration of the hydration process of both cements and on changes in pore structure. The influence of the amount of combined water and pore size distribution on the strength is also discussed.

Both cements showed differentiated behaviours when the curing temperature was raised from 40 to 80°C. No significant differences in behaviour were detected between portland cement mortars cured at 40 and at 80°C, whilst for slag cement a higher rate of strength development, coupled with a refinement of the pore structure was observed at 80°C. Also, slag cement, when cured at high temperature, showed a different strength-pore structure relation than that found for portland cement cured at normal and high temperatures.

SUMÁRIO

A resistência à compressão, quantidade de água não-evaporável e distribuição do tamanho de poros foram estudadas em corpos de prova de argamassa curadas a 20, 40 e 80°C por diferentes períodos, após uma espera de 1 dia a 20° C. Um cimento portland e um cimento de escória, preparados a partir do mesmo clínquer, forma utilizados.
Os resultados experimentais foram discutidos com referência ao efeito da temperatura de cura na aceleração do processo de hidratação de ambos cimento e às mudanças de estrutura dos poros. A influência da quantidade de água combinada e da distribuição do tamanho de poro na resistência sãotambém discutidas.
Ambos cimentos mostraram comportamentos diferenciados quando a temperatura de cura foi aumentada de 40 a 80°C. Não foram detectadas diferenças significativas de comportamento entre as argamassas de cimento portland curadas a 40 e 80°C, enquanto para o cimento de escória uma maior velocidade de desenvolvimento da resistência, associada ao refinamento da estrutura dos poros foram observadas a 80°C. Também, cimento de escória, quando curado a alta temperatura, mostrou uma diferente relação resitência-estrutura de poros,em relação a aquela verificada para um cimento portland à temperaturas ambientes e altas.

1. INTRODUCTION.

Curing at elevated temperatures is a well known and widely used method of accelerating the setting and hardening of both portland and blastfurnace slag cements (1). High temperature treatments, as those applied in the precast industry, are specially beneficial for blastfurnace slag cements that show, generally, a low rate of reaction at normal temperature. The influence of the curing temperature is also relevant for mass concrete structures, as a consequence of the slow dissipation of the heat of hydration of the cement.

This work is part of an investigation aimed at studying the behaviour of slag cements cured at above-normal temperatures and at relating the engineering properties observed with changes in the internal structure of the material.

It is known that high temperature curing (up to 100°C) has only a slight influence on the phase composition of the newly formed compounds; on the other hand, the hydrothermal treatment of cement paste exerts a considerable influence on its physical structure, as for example the change of its pore structure (2).

The object of this paper is to study the evolution of compressive strength, non-evaporable water content and pore size distribution with age and curing temperature, as well as to analyse the interrelation between those variables, for mortar specimens made of portland and slag cement.

2. EXPERIMENTAL PROCEDURE.

Two cements were used in this investigation, one a portland cement and the other a blastfurnace slag cement. Both cements were prepared in the laboratory from the same clinker and gypsum, with and without the addition of ground granulated blastfurnace slag at the mixer. Details of the grinding and blending techniques used can be found elsewhere (3).

The chemical and physical characteristics of the clinker and the slag used are reported in Table I.

The cement employed were proportioned by weight as follows:

Portland Cement: Clinker:gypsum:slag = 95:5:0

Slag Cement: Clinker:gypsum:slag = 32.5:5:62.5

Two sets of mortar prisms, made according to the ISO-RILEM-CEMBUREAU procedure, were cast using the portland cement and the slag cement, respectively. The specimens were kept in their moulds for 24 hours in a room at 20°C; after demoulding, they were placed in three water baths, kept at temperatures of 20, 40 and 80°C, for different periods of time, as indicated below:

For 20°C: 2, 6, 13 and 27 days

For 40°C: 6, 20, 56 and 137 hours

For 80°C: 2, 4.5, 15, 29 and 72 hours

After being removed from the bath, the specimens were allowed to reach the room temperature and tested in bending and in compression; in this paper only the compressive strength results are discussed. One set of mortar prisms for each cement were tested immediately after demoulding, at the age of 1 day. From the three specimens cast, only two were actually tested (four halves in compression), whilst the remaining one was treated as described below.

TABLE I
Characteristics of the clinker and the slag

	CLINKER	SLAG
Insol. Residue (g/100 g)	0,11	2,83
SiO_2 "	23,0	32,5
Al_2O_3 "	4,78	13,5
Fe_2O_3 "	3,55	3,80
Mn_2O_3 "	-	0,45
CaO "	64,6	41,5
MgO "	0,65	5,10
Na_2O "	0,08	0,32
K_2O "	1,00	0,39
SO_3 "	0,18	0,17
S^{2-} "	-	0,94
Free CaO "	0,49	-
LOI "	2,32	-
C_3S "	48,4	-
C_2S "	29,4	-
C_3A "	6,7	-
C_4AF "	10,8	-
BLAINE (m^2/kg)	366	369

The hydration process of the remaining specimen was stopped by removing the free water with solvent, and the following determinations were made:

a) Non-evaporable water content by loss of ignition at 900°C.

b) Pore size distribution in the range 37.5-75000 Å (pore radius), by high pressure mercury porosimetry

3. TEST RESULTS.

The gain in mortar compressive strength with age for curing temperatures of 20, 40 and 80°C is presented in Figs. 1a) and 1b), for portland and slag cements, respectively.

The increase with age of the non-evaporable water content (Wn), regarded as a measure of the total amount of hydration products (4), for the different curing temperatures is shown in Figs. 2a) and 2b) for portland and slag cements, respectively.

In order to trace changes in pore structure with age, curing temperature and cement type, a representative value of the pore size distribution had to be chosen. The percentage by volume of pores having radii smaller than 1000 Å (P1000) was selected, as suggested by other authors . This value is considered as a conventional boundary between small pores and medium-large pores (5).

Figs. 3a) and 3b) show the variation of P1000 with age and curing temperature for portland and slag cement.

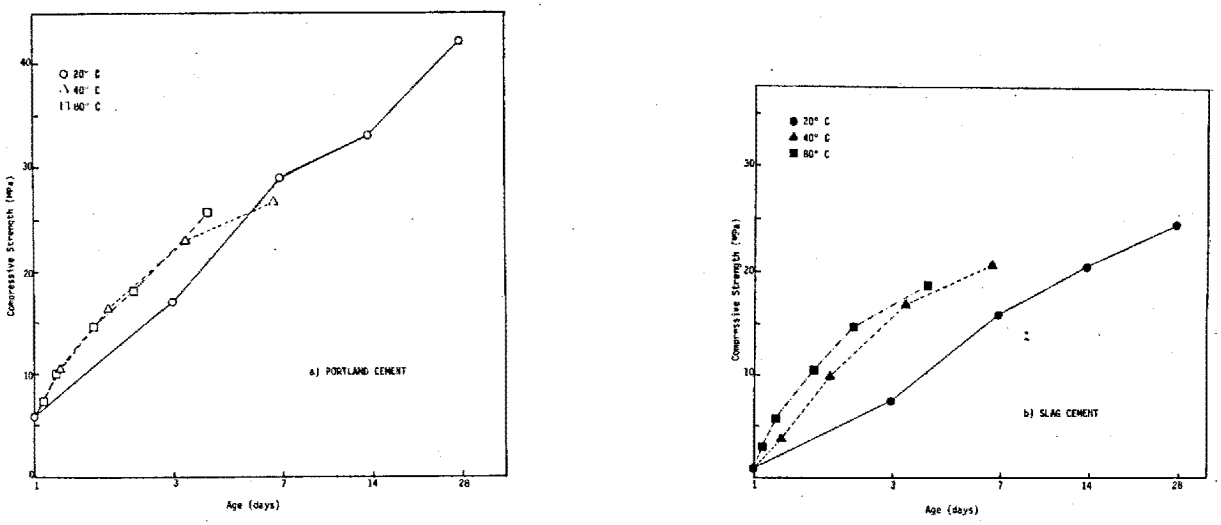

Fig. 1 - Development of compressive strength of mortars cured at 20, 40 and 80°C for a) Portland Cement and b) Slag Cement.

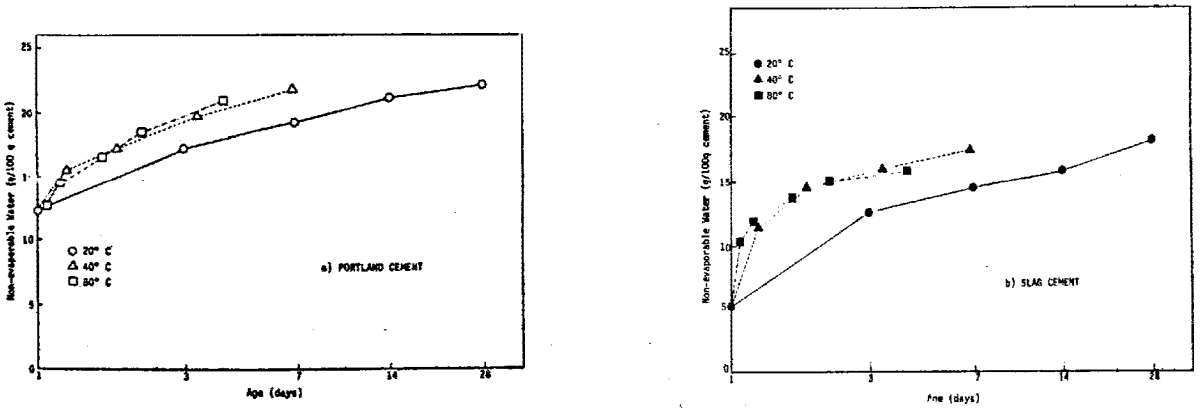

Fig. 2 - Increase in content of non-evaporable water with age for specimens cured at 20, 40 and 80°C, for a) Portland Cement and b) Slag Cement.

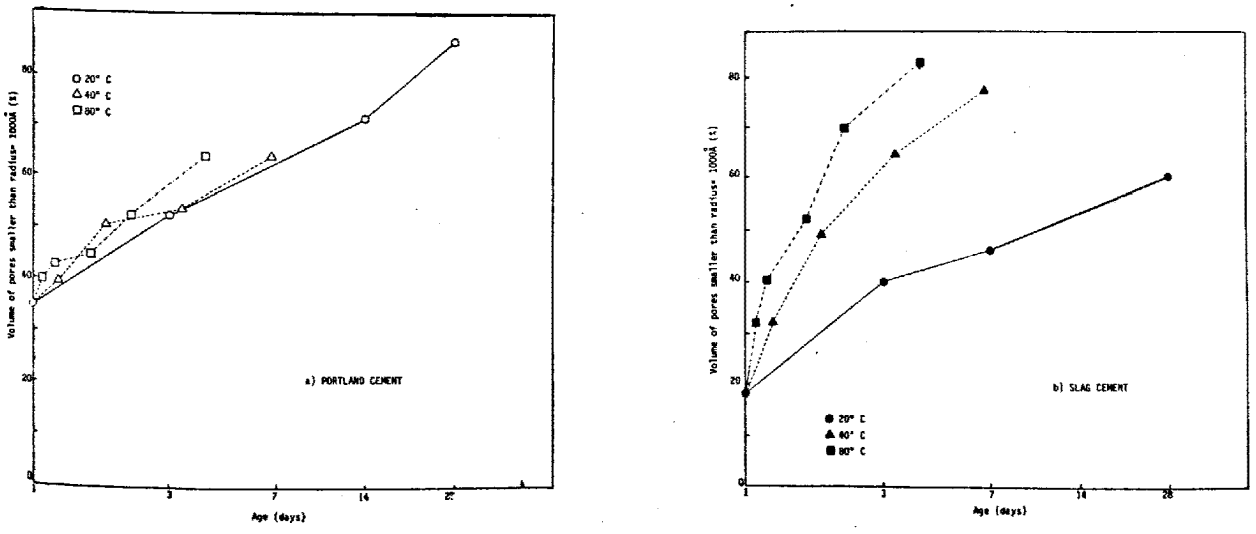

Fig. 3 - Change in the percentage (by volume) of pores having radii smaller than 1000 Å with age and curing temperature, for a) Portland Cement and b) Slag Cement.

4. DISCUSSION.

From Figs. 1a) and 1b) it can be seen that, as was to be expected, the strength development is accelerated by curing at higher temperatures. However, for portland cement (Fig. 1a), a similar strength gain was observed for curing temperatures of 40 and 80°C, whilst for slag cement the mortars cured at 80°C showed some acceleration with respect to those cured at 40°C. This behaviour of the portland cement is attributed to the delay of 1 day before applying the thermal treatment, since in a parallel research important accelerations were observed between 40 and 80°C, for the same materials, after shorter delays.

The evolution of Wn with age and temperature (Figs 2a and 2b) is similar to that of the strength, except by the fact that, in this case, conversely to what happened for the strength of slag cement, no significant distinction can be made between the curves for 40 and 80°C.

From Fig.3a) it can be seen that, for a given age, a slightly finer pore structure exists in portland cement mortars cured at temperatures above 20°C. In the case of slag cement mortars, Fig. 3b), curing at higher temperatures leads to a drastic increase in the fineness of the pore structure, for a given age. Comparing Figs. 3a) and 3b), it is observed that, even though the pore size distribution of slag cement mortars cured at 20°C is coarser than that for portland cement mortars, after short periods under higher curing temperatures the situation is reversed.

In order to study the effect of both Wn and P1000 on mortar compressive strength, Figs. 4a), 4b) and 5 are presented. Fig. 4a) shows that, for Wn values higher than 17%, the strength of portland cement mortars cured at 20°C was higher than for mortars cured at higher temperatures, containing the same amount of non-evaporable water. This effect was not observed for slag cement mortars, as shown in Fig. 4b).

The pattern observed in Fig. 4a) can be explained by the change in morphology and microstructure taking place when the material is cured at above-normal temperatures (6). For slag cement mortars, the relation between strength and Wn is quite independent of the curing temperature, thus indicating that no significant change in morphology occurs at high temperatures.

Fig.5 shows the relation between strength and percentage by volume of pores having radii smaller than 1000 Å, both for portland and slag cement mortars. It can be seen that a single relation exists between strength and P1000 for portland cement mortars cured at all temperatures; this relation also applies for slag cement mortars cured at 20°C. However, for slag cement mortars cured at higher temperatures the strength values measured are lower, for a given pore size distribution than for portland cement mortars. This fact indicates that the very fine pore structure observed in slag cement mortars cured at above-normal temperatures (Fig.3b) is not reflected in an increase in strength of similar magnitude.

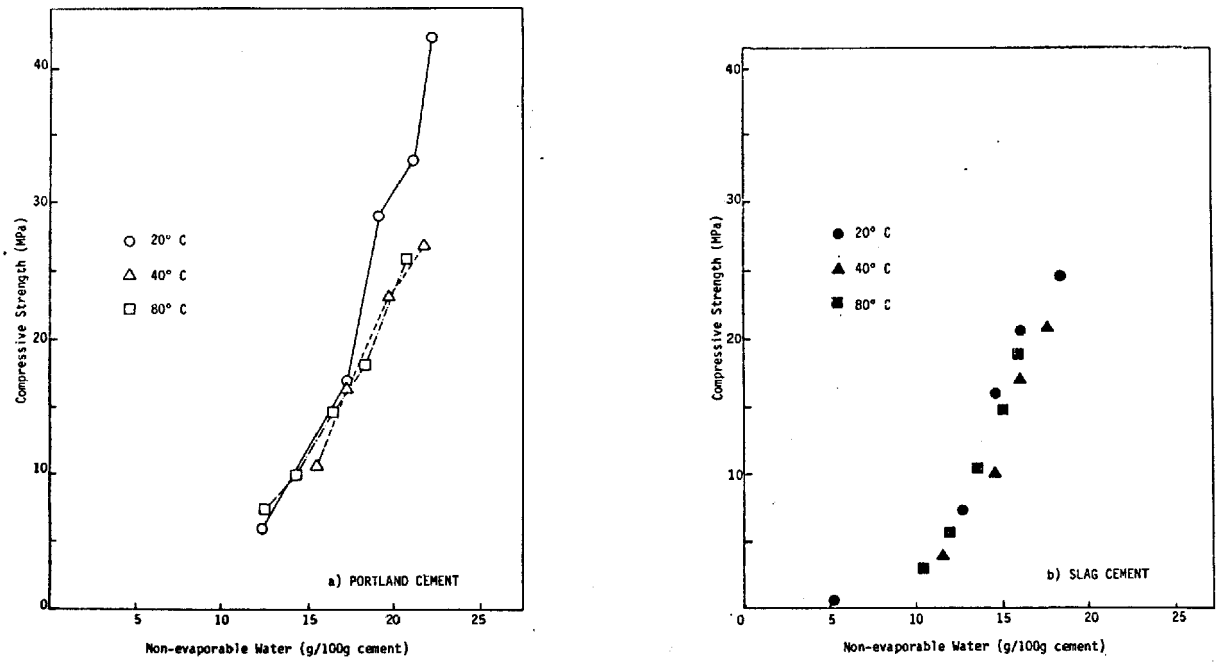

Fig.4 - Relation between compressive strength and content of non-evaporable water for mortar specimens cured at 20, 40 and 80°C, for a) Portland Cement and b) Slag Cement.

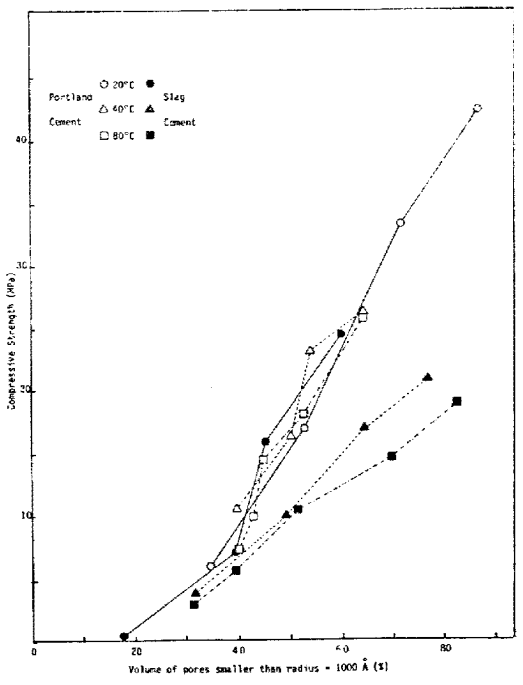

Fig.5 - Relation between compressive strength and percentage (by volume) of pores having radii smaller than 1000 Å.

5. CONCLUSIONS.

The particular curing conditions applied to the specimens produced an acceleration of the reaction rate for above-normal curing temperatures, expressed both by a more rapid strength development and by a higher rate of increase in non-evaporable water content.

For the portland cement no significant acceleration of the reaction rate was found between mortars cured at 40 and 80°C, as measured either by strength development or by content of non-evaporable water.

For the slag cement, some acceleration in strength development was observed in specimens cured at 80°C with respect to those cured at 40°C; this effect was not accompanied by a similar acceleration in the increase in non-evaporable water content.

It was found that curing at higher temperatures leads to a strong refinement of the pore structure of slag cement; this effect was not observed for portland cement.

The different strength behaviour of slag and portland cement when the curing temperature was raised from 40°C to 80°C can be explained by the change in pore structure mentioned in the previous paragraph.

For portland cement and for the same amount of non-evaporable water (degree of hydration), specimens cured at 20°C showed higher strengths than those cured at higher temperatures, probably due to changes introduced in the morphology of the hydration products by the high temperature curing. This effect was not observed in slag cement, which suggests that such changes do not occur for this type of cement.

A unique strength-pore structure (measured by P1000) relation was found for portland cement mortars cured at all temperatures and for slag cements cured at 20°C, whilst slag cement mortars cured at 40 and 80°C followed a different relation.

REFERENCES.

1 - Regourd,M., "Structure et comportement des hydrates des ciments au laitier". VII Congres Intern. de la Chimie des Ciments, Vol.I, III 2/9, Paris, 1980.

2 - Butt,Yu., Kolbasov,V.M. and Timashev,V.U., "High temperature curing of concrete under atmospheric pressure". V Intern. Symp. on the Chemistry of Cement, Vol. III, 437, Tokyo, 1968.

3 - Longo,A., Torrent,R.J., "Methods of addition of blastfurnace slag: their effect on the compressive strength of mortars and concrete". 2nd Intern. Conf. on the use of Fly Ash, Silica Fume, Slag and Natural Pozzolans in Concrete, Madrid, april 21-26 1986.

4 - Odler,I., Judenfreund,M., Skalny,J. and Brunauer, S., "Hardened portland cement paste of low porosity". Part III. Cement & Concr. Res., Vol.2, pp. 463-480, 1972.

5 - Lach,V. and Rosova,M., "The development of porosity in hydrated paste and water cement ratio". VII Congres Intern. de la Chimie des Ciments, Vol. IV, 776, Paris, 1980.

6 - Taylor,H.F.W. and Roy,D.M., "Structure et composition des hydrates". VII Congres Intern. de la Chimie des Ciments, Vol.I, II 2/1, Paris, 1980.

Z.Z. Gu, B.W. Zhou, M.L. Yue, T.F. Tang, W.J. Wang
Shanghai Research Institute of Building Sciences, Shanghai, China

Effect of Cement Composition on the Strength Contribution of Fly Ash

Summary: Being used as an addition of cement, fly ash can not only save energy and cut down cost but also improve certain properties of cement. The study of effect of cement composition on strength contribution of fly ash may give scope to the potential pozzolanicity of fly ash and promote the utilization of fly ash in cement and concrete. 17 samples of clinker with different composition were collected, and the samples were prepared with adequate gypsum and ground to same fineness. Mortar specimens were prepared with the above 17 cements and the same cements but replaced by 30% typical fly ash respectively, and strength were tested at the fixed ages. Regressive analyses were used to clarify the correlation between cement composition and strength contribution of fly ash, which is expressed by the mortar strength ratio between specimens with and without fly ash. It indicates that owing to the difference of cement composition the strength ratio at 28 days ranges from 0.65 to 0.90. Obviously, cement composition significantly influences the strength contribution of fly ash. Regressive analysis shows that strength contribution of fly ash is positively affected by K_2O, KH and C_3S, negatively affected by $CaSO_4$ and C_2S in cement. An equation is put up to illustrate the correlation between cement composition and fly ash strength contribution based on which an optimum clinker composition might be selected for the manufacture of fly ash cement.

Usada como aditivo do cimento, a cinza volante pode não apenas economizar energia e reduzir custo, mas também melhorar certas propriedades do cimento. Estudar o efeito da composição do cimento sobre a contribuição da cinza volante para a resistência, pode ensejar o aproveitamento do potencial pozolânico da cinza volante e promover sua utilização em cimento e concreto. Foram colhidas 17 amostras de clínquer com composição diferente; elas foram preparadas adequadamente com gesso e moídas com a mesma finura. Prepararam-se corpos de prova de argamassa com os 17 cimentos acima, e com os mesmos cimentos com substituição de 30% por cinza volante típica, respectivamente. As resistências foram testadas nas idades estabelecidas. Usou-se análise regressiva para esclarecer a correlação entre composição do cimento e contribuição da cinza volante para a resistência, sendo esta contribuição expressa pela relação entre a resistência dos corpos de prova de argamassa com e sem cinza volante. O resultado indica que, devido à diferença de composição do cimento, a relação da resistência aos 28 dias varia de 0,65 a 0,90. Obviamente a composição do cimento tem influência significativa sobre a contribuição da cinza volante para a resistência. A análise regressiva mostra que a contribuição da cinza volante para a resistência é relativamente afetada por K_2O, KH e C_3S de forma positiva; e por $CaSO_4$ e C_2S do cimento, de forma negativa. Formula-se uma equação para ilustrar a correlação entre a composição do cimento e a contribuição da cinza volante para a resistência, baseada na qual se pode escolher uma composição ótima do clínquer para a fabricação de cimento de cinza volante.

Introduction

Using fly ash as the addition of cement can not only save energy and cut down cost but also improve certain proporties of cement, eg. lowering the heat of hydration, improving sulphate and sea water resistance and lessen alkali-aggregate reaction, etc. As miniral mixture of concrete, the strength contribuion of fly ash is affected by its quality, chemical and miniral compoition of cement, curing condition, etc. Research on the influence of the quality of fly ash (1) (2) (3) (4) (5) (6) (7) and curing condition (2) (8) (9) (10) (11) to the strength contribution of fly ash in concrete have already been done enormously and reached rather identical views. On the influence of cement composition, Davis (12), Stingley and Peyton (13) and Rsukayama and Miyoshi (14) pointed out that the strength contribution of fly ash is better with OPC than that with other kinds of cement. Brink and Halstead (15) and Timms and Grieb (16) stated that the reaction rate of fly ash with cement was related to the alkali content of cement. Kovacs (17) reported that S.M=2.5, I.M=1.6--1.7 is the suitable clinker composition for fly ash cement when lime saturation factor is 0.9. Dalziel (18) believed that the influence of cement composition on fly ash cement strength is smaller than that on OPC, and it is unnecessary to select a special composition for fly ash cement. Therefore, in order to clarify these problems, it is required to carry out a systematic research project. It is known that the cement composition is quite complicated, as Kokubu (19) declared that the clinker composition suitable to fly ash cement was very difficult to be clearly understood. Nevertheless, this paper, as a part of the whole project, is only a preliminary study and the auther hope it could be conductive to the further understanding of this problem.

Material and Procedure

It is almost imporssible to directly find out the effects of each component of cement on the strength contribution of fly ash, for the cement composition is too complicated. Therefore, 17 typical clinker were collected, ground to the same fineness, i.e. specifice surface area was equal to $3100\pm100 cm^2/g$. The gypsum content was the same as that in the factories. Two series of 4x4x16cm mortar specimen were made with the same fall-table spread and the cement/sand ratio of 1:2.5. One was OPC mortar, the other 30% of cement was replaced with fly ash Strength were tested after standard curing ($20^{\circ}C$, 90%RH) for 7, 28 and 90 days. The cement composition is shown in table 1 and fly ash in table 2. The 45μm S.R. of fly ash was 14.7% and water requirement was 96%. The strength of OPC/PFA mortar or its ratio over OPC mortar were used to represent the suitability of the cement composition. Monadic and multivariate regressive analyses were carried out among each component of cement and strength or strength ratio to explore the effects of each component of cement and find out an appropriate way for evaluating the suitability of cement.

Experimental Results

The strength of OPC and OPC/PFA mortar and their strength ratio are given in table 3 and figure 1. The results shows that the 7 and 28 days strength were all decreased for the replacement of cement with 30% fly ash, but the strength reduction at 28 days was much smaller than that of 7 days. While at 90 days, the strength are nearly the same in average, and increased for some cements, of which, the composition might be suitable for fly ash cement. The results also showed that the influence of cement composition on strength of fly ash cement is remarkable. For the fly ash cement, the strength of a suitable cement is reduced only by 10% at 28 days and increased by 15% at 90 days.

Table 4 shows the result of monadic regression between cement composition and

Table 1 Cement Composition

	X_1	X_2	X_3	X_4	X_5	X_6	X_7	X_8	X_9	X_{10}	X_{11}	X_{12}
	$CaSO_4$ %	f-CaO %	Alkal. Equal. %	K_2O %	Na_2O %	C_3S %	C_2S %	C_3A %	C_4AF %	KH	N	P
Max.	5.7	2.9	1.09	1.17	0.52	59.8	32.4	14.0	17.1	0.94	2.28	2.41
Min.	3.5	0.4	0.19	0.12	0.10	34.6	10.9	3.3	9.1	0.82	1.76	0.87
Aver.	4.4	1.1	0.54	0.50	0.21	45.5	24.3	7.8	14.4	0.87	1.92	1.30

Table 2 Chemical Composition of fly ash (%)

LOI	CaO	MgO	SiO_2	Al_2O_3	Fe_2O_3	SO_3
2.8	5.06	1.1	50.6	28.1	10.3	0.6

Table 3 Strength of Mortars (MPa)

Curing age	OPC			OPC/PFA			Strength Ratio		
	Max.	Min.	Aver.	Max.	Min.	Aver.	Max.	Min.	Aver.
7d.	55.0	27.2	46.9	40.9	19.3	30.7	0.77	0.53	0.66
28d.	70.6	37.0	62.1	56.5	31.6	48.1	0.90	0.65	0.78
90d.	76.1	43.3	67.2	74.6	46.4	66.6	1.13	0.86	1.00

strength contribution of fly ash. With 17 samples, the critical corrilation coefficient for the significance level of 0.05 is 0.482. Compare it with the data of regressive analyses, the K_2O (or/and equevalent Na_2O), C_3S and KH of cement are directly proportional to the strength of fly ash cement, while $CaSO_4$, C_2S are inversely proportional to that.

The result of all parameters multivariate regressive analyses of the strength of OPC/PFA mortar and cement composition turned out to be equation (1), (2), (3), and the comparison between the calculated value and test results are plotted in figure (2), (3), (4).

Equation (4), (5), (6) are the result of multivariate regression among strength ratio of 7, 28 and 90 days and cement composition respectively, and the calculated results were compared with test result in figure (5), (6), (7).

3.2

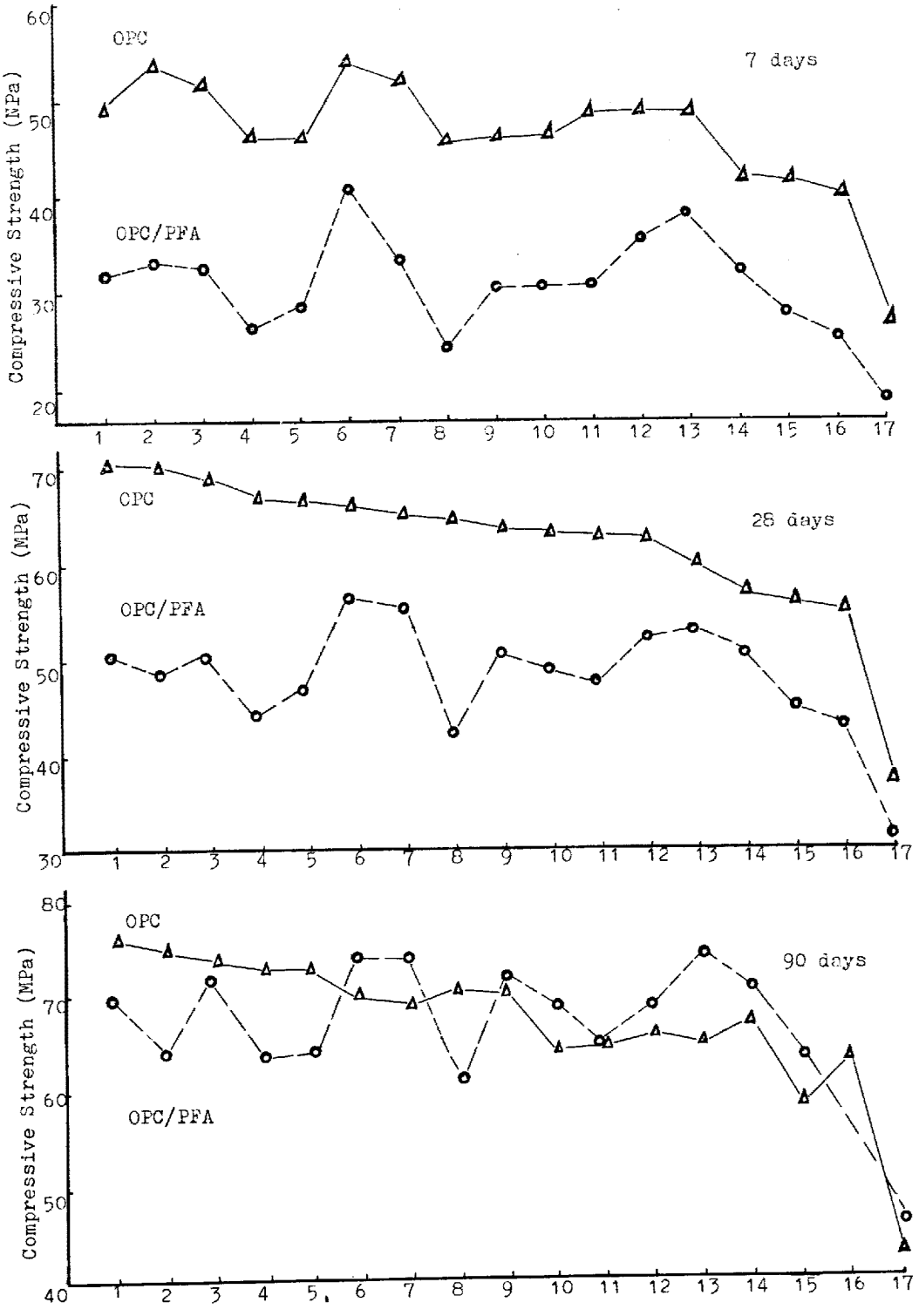

Figure 1 Compressive Strength of OPC and OPC/PFA

Table 4 Monadic Correlative Coefficients

Cement Composition		OPC			OPC/PFA			Strength Ratio		
No.	Parameter	7d.	28d.	90d.	7d.	28d.	90d.	7d.	28d.	90d.
X_1	$CaSO_4$	-0.40	-0.39	-0.38	-0.33	-0.50	-0.49	0.03	-0.03	-0.01
X_2	f-CaO	-0.47	-0.54	-0.46	-0.27	-0.28	-0.24	0.21	0.34	0.30
X_3	Alkal. Equal.	-0.53	-0.74	-0.77	-0.25	-0.34	-0.39	0.38	0.58	0.56
X_4	K_2O	-0.53	-0.76	-0.80	-0.13	-0.32	-0.36	0.55	0.65	0.64
X_5	Na_2O	-0.27	-0.33	-0.34	-0.29	-0.19	-0.22	-0.07	0.19	0.17
X_6	C_3S	0.50	0.46	0.53	0.60	0.55	0.51	0.24	0.04	-0.13
X_7	C_2S	-0.51	-0.38	-0.45	-0.69	-0.55	-0.50	-0.37	-0.13	0.03
X_8	C_3A	0.17	0.02	-0.08	0.19	0.09	-0.03	0.04	0.06	0.05
X_9	C_4AF	-0.23	-0.09	-0.05	-0.26	-0.25	-0.16	-0.08	-0.15	-0.09
X_{10}	KH	0.49	0.41	0.48	0.63	0.54	0.50	0.31	0.09	-0.08
X_{11}	N	-0.32	-0.31	-0.34	-0.38	-0.19	-0.12	-0.16	0.17	0.28
X_{12}	P	0.17	0.13	0.00	0.13	0.14	0.15	-0.05	-0.03	0.17

$$Y_{S7}=-585.4-7.70X_1-5.20X_2-875.28X_3+582.49X_4+899.89X_5-4.646X_6-0.264X_7-1.015X_8-1.044X_9 +1024.1X_{10}-3.86X_{11}+6.60X_{12} \quad (1)$$

$$Y_{S28}=-665.8-8.84X_1-5.77X_2-1119.3X_3+739.29X_4+1148.2X_5-5.177X_6-0.081X_7-2.050X_8-2.253X_9 +1181.5X_{10}-0.63X_{11}+8.83X_{12} \quad (2)$$

$$Y_{S90}=-846.7-10.30X_1-49.7X_2-1414.0X_3+930.90X_4+1436.41X_5-6.631X_6+0.889X_7-3.023X_8 -2.861X_9+1491.8X_{10}+9.18X_{11}+10.53X_{12} \quad (3)$$

$$Y_{SR7}=-12.3756-9.4871X_1-1.2678X_2-8.5377X_3+5.8661X_4+8.7714X_5-7.7424X_6+1.7571X_7-3.1235X_8 -2.1304X_9+19.9634X_{10}-2.2370X_{11}+6.4472X_{12} \quad (4)$$

3.2

$$Y_{SR28}=-17.6673-1.1830X_1-2.1026X_2-6.4204X_3+4.4699X_4+6.8202X_5-1.1038X_6+2.4157X_7 -4.4367X_8-3.5933X_9+27.9407X_{10}-1.1565X_{11}-9.2360X_{12} \quad (5)$$

$$Y_{SR90}=-21.1860-1.6674X_1-3.9668X_2-8.5672X_3+5.5037X_4+8.8171X_5-0.1390X_6+2.1246X_7 -3.6630X_8-1.8533X_9+31.1116X_{10}+1.5905X_{11}+1.3041X_{12} \quad (6)$$

Where,

Y_{S7}, Y_{S28} and Y_{S90}: the compressive strength of fly ash cement at 7, 28 and 90 days (MPa)

Y_{SR7}, Y_{SR28} and Y_{SR90}: the strength ratio of fly ash cement at 7, 28 and 90 days

X_1, X_2,.....X_{11} and X_{12}: cement composition as in table 1

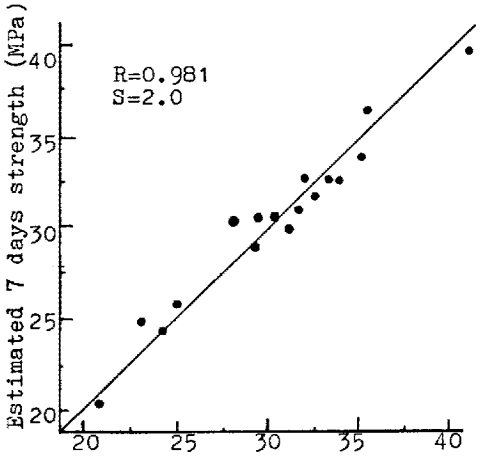

Figure 2

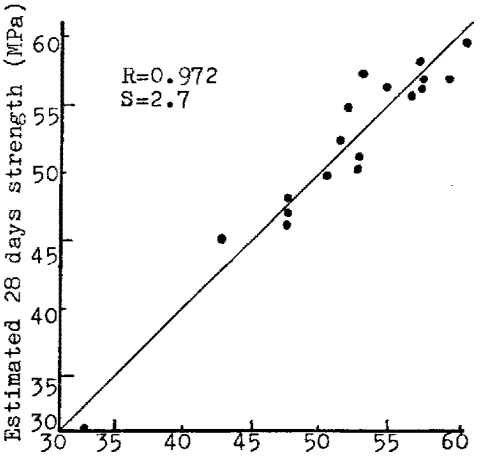

Figure 3

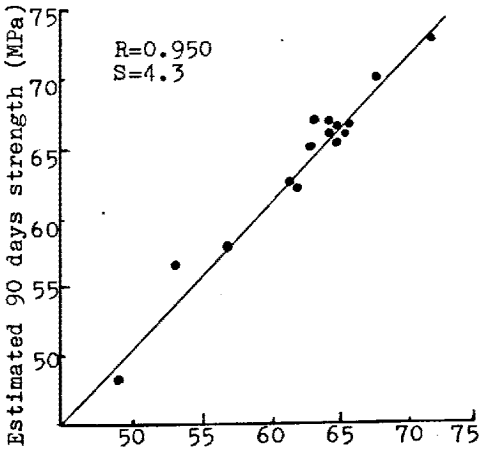

Figure 4

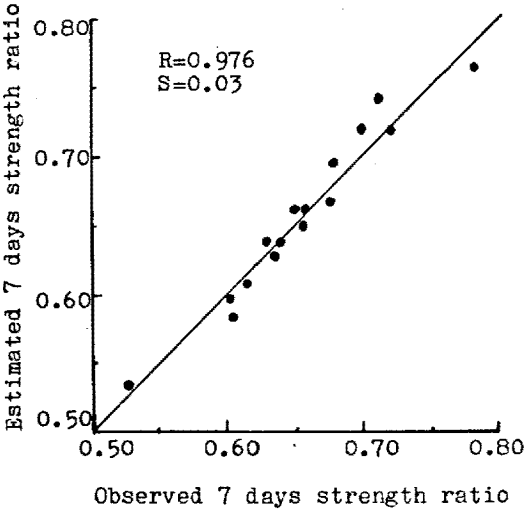

Figure 5

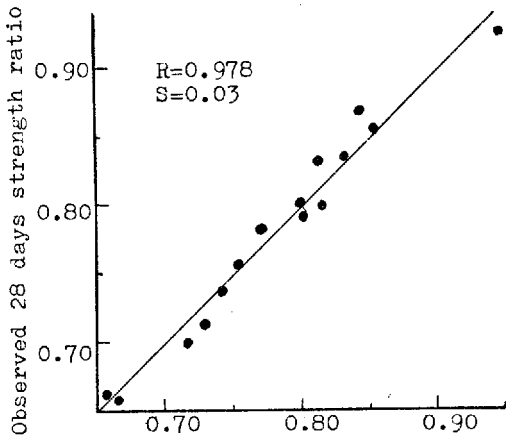

Figure 6

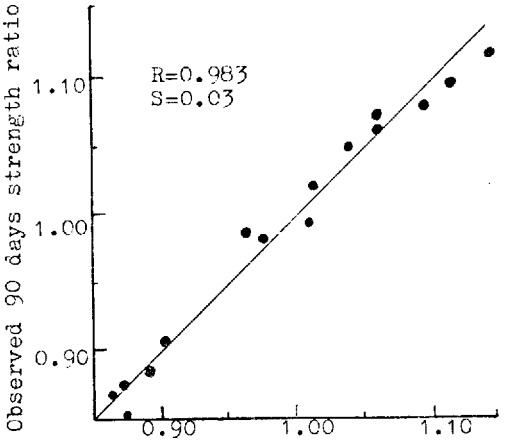

Figure 7

Discussion

From figure 1, it is evident that with the addition of 30% fly ash, the fluctuation of 28 days strength were notably reduced comparing with OPC mortar as was similar to Dalziel (18) conclusion. But the result also shows that the strength reduction of fly ash cement changes greatly due to the difference of cement composition. At 28 days, for example, the strength of OPC sample No.6 and No.8 are approximately the same, but, the OPC/PFA strength of No.6 is 14MPa higher than that of No.8. Therefore, it would be worthwhile to develop a special cement which is suitable for fly ash cement production.

In table 4, the OPC strength is in direct proportion of its C_3S content, and the correlation coefficient was notable increased with the addition of fly ash. It indicates that the C_3S is beneficial to the strength contribution of fly ash. A higher C_3S content usually means a higher KH, so the latter should be beneficial to the strength contribution of fly ash either. Table 4 also shows the correlation coefficient between KH and strength growes with the addition of fly ash. .The higher rate of hydration of C_2S and more released $Ca(OH)_2$ promoted the pozzolanic reaction of fly ash. OPC especially RHPC contains more C_2S, so that they are reported to be more suitable for fly ash addition. The inverse correlation coefficient between C_2S and the strength expanded for the adding of fly ash, it means the C_2S is disadvantageous to the strength contribution of fly ash. Because the hydration rate of C_2S is very slow at earlier ages, the pozzolanic reactivity could not be activated. Although C_3A and C_4AF hydrate quickly, they don't release $Ca(OH)_2$ so that they have no use for the reaction of fly ash. For this reason, there is no correlations between the strength contribution of fly ash and either of the two. The f-CaO in cement is harmful, as table 4 shows, it is inversely proportional to strength, but its harmfulness was lowered by the pozzolanic reaction, when fly ash was used. The K_2O in cement was also in inverse proportion of OPC strength, but with fly ash, the inverse correlation coefficient was much smaller, as hinted that K_2O might be beneficial to the strength contribution of fly ash. It is known to all that other than existing as K_2SO_4, the K_2O in clinker mainly changes C_2S to $KC_{23}S_{12}$, which hydrates more rapidly than C_2S. Because the hydration rate of C_2S was accelerated by K_2O,

when fly ash was added, it is also helpful to the pozzolanic reaction. Besides, K_2O can increase the solubility of acidic oxiedes in fly ash, so it can increase the pozzolanic reaction, either. In addition to existing as Na_2SO_4, Na_2O chiefly forms NC_8A_3, which don't release $Ca(OH)_2$ when hydrating, so that Na_2O is not related to the strength contribution of fly ash. Brink and Halstead (15), Timms and Grieb (16) had briefly pointed out the influence of alkali, but actually, what affected was K_2O, the data in table 4 has comfirmed it. In the case of this experiment, $CaSO_4$ is in inverse proportion of the strength contribution of fly ash at 28 and 90 days, it might result from that the Al_2O_3 in fly ash had speeded up the transformation of AFt to AFm.

It is manifested in figure (2), (3) and (4) that the strength calculated with equation (1), (2) and (3) are quite close to the test result. Therefore, under the limitation of this experiment, these equations can be used to evaluate the suitability of clinker for fly ash cement. For the same reason, the strength contribution of fly ash in different OPC can be evaluated with equation (4), (5) and (6).

Conclusion

Cement composition has evident effects on the strength contribution of fly ash, so that to find out a cement with porper composition has practical significance in the production of fly ash cement. The KH and C_3S are directly proportional to the strength of fly ash cement, while inversely are C_2S and $CaSO_4$. Although K_2O is in inverse proportion of OPC strength, yet it is beneficial to the strength contribution of fly ash. Thus, the disadvantagious of K_2O can be reduced by the addition of fly ash. Under the limitation of this experiment, the multivariate regressive equation can be used to evaluate the suitability of different ordinary portland cement for the production of fly ash cement with good accuaacy.

References

1. N. Fratimi, Ann., Chim., 39, 41, (1949)
2. F.M. Lee, Cem., Tech., 4, 1, (1973)
3. E. Raask, 7th Int. Symp. Chem. Cem., Paris (1980)
4. M. Raverdy, F. Brivot, A.M. Paillere and R. Dron, 7th Int. Symp. Chem. Cem., Paris (1980)
5. Z.Z. Gu, M.L. Le, X.L. Wu, W.J. Wang, J.F. Wu, "Study on the Activity of Fly Ash" Jour. Chin. Soc., 10, 2, (1982)
6. P.L. Owens and J. Waddicor, Int. Symp. of the Use of PFA in Conc., U. K., (1982)
7. K. Takemoto and H. Uchikawa, 7th Int. Symp. Chem. Cem., (1980)
8. P.L. Owens and F.G. Buttler, 7th Int. Symp. Chem. Cem., (1980)
9. R.K. Dhir, J.C.L. Munday and L.T. Ong, Concrete, 15, 6,(1981)
10. S. Nagataki, E. Sakai and Mueda, Int. Symp. of the Use of PFA in Conc., U. K., (1982)
11. J.A. Dalziel, 7th Int. Symp. Chem. Cem., (1980)
12. R.E. Davis, Symp. on the Use of Pozz. Mater. and Conc., Spec. Tech. Publ., No.99, ASTM, 3--15, (1949)
13. W.M. Stingley and R.L. Peyton, Highway Research Record, No.73, Symp. on Fly Ash in Conc., Highway Research Board, 26--31, (1965)
14. R. Tsukayama and Miyoshi, Review of the 22nd General Meeting, Cem. Assoc. of Japan, 117--121, (1968)
15. R.H. Brink and W.J. Halstead, Proc. ASTM, 56, 1161--1206, (1956)
16. A.G. Timms and W.E. Grieb, Proc. ASTM, 56, 1139--1157, (1956)
17. R. Kovaos, 7th Int. Symp. Chem. Cem. Paris (1980)
18. J.A. Dalziel, Int. Symp. of the Use of PFA in Conc., U. K., (1982)
19. M Kokubu, 5th Int. Symp. Chem. Cem. Tokyo, (1968)

Shan-Ba Wang, Wuhan Institute of Building Materials,Wuhan,China
R.L Berger University of Illinois,Urbana,Illinois,U.S.A

Effect of $Ca(OH)_2$ and $CaSO_4 2H_2O$ on the strength of flyash cement pastes

Effet de $Ca(OH)_2$ et de $CaSO_4.2H_2O$ sur la résistance des pâtes du ciment aux cendres volantes

Summary: The effect of CH and $C\bar{S}H_2$ added to flyash cement pastes on the strengths was studied by strength test combining with QXDA,thermal analysis and SEM as well as Trimethylsililation method.

The addition of CH decreases the strength of flyash cement paste even at 90 days although it increases the reaction degree of flyash.

Gypsum added to flyash cement paste decreases the strength at early ages but increases the strength at later ages. All gypsum added is consumed up at 28 days,therefore,the contribution of gypsum added is limited within 28 days. The contribution of gypsum to strength lies in the formation of ettringite in the capillary and densification of the structure of the paste.Gypsum combining with small amount of CH added contributes more to strength of the paste at later ages.

The reactivity of flyash is very low,only 7-12% reaction degree at 60 days,which is probably associated with only 8% monomer in silica acid of flyash. After addition of CH and $C\bar{S}H_2$, the monomer decreases,and dimer and polymer increase in flyash cement paste at 60 days.

The strength of flyash cement paste,whether CH and $C\bar{S}H_2$ are added or not,are lower than that of portland cement paste even at 90 days if same w/s ratio is used.

Através de teste de resistência, combinado com QXDA, análise térmica e SEM, bem como pelo método de trimetilsililação, estudou-se o efeito do CH e $C\bar{S}H_2$, adicionado a pastas de cimento de cinza volante, sobre as resistências.

A adição de CH diminui a resistência da pasta de cimento de cinza volante mesmo aos 90 dias, embora ela aumente o grau de reação da cinza volante.

A adição de gesso à pasta de cimento de cinza volante diminui a resistência nas idades iniciais, mas aumenta-a nas idades finais. Todo o gesso adicionado é consumido até aos 28 dias; portanto, a contribuição do gesso adicionado está limitada ao período de 28 dias. A contribuição do gesso para a resistência consiste na formação de etringita nos capilares e na densificação da estrutura da pasta. O gesso, em combinação com pequena quantidade de CH adicionado, contribui adicionalmente para a resistência da pasta nas idades finais.

A reatividade da cinza volante é muito baixa, grau de reação de apenas 7 - 12% em 60 dias, o que provavelmente está associado com os apenas 8% de manômero no ácido silícico da cinza volante. Depois da adição de CH e $C\bar{S}H_2$, o manômero diminui, e aumentam o dímero e polímero na pasta de cimento de cinza volante aos 60 dias.

A resistência da pasta de cimento de cinza volante, com ou sem CH e $C\bar{S}H_2$, é inferior à da pasta de cimento portland mesmo aos 90 dias, se tiver sido usada a mesma relação a/s.

Shan-Ba Wang, Wuhan Institute of Building Materials, Wuhan, China
R.L Berger University of Illinois, Urbana, Illinois, U.S.A

Effect of $Ca(OH)_2$ and $CaSO_4.2H_2O$ on the strength of flyash cement pastes

Effet de $Ca(OH)_2$ et $CaSO_4\ 2H_2O$ sur la résistance des pâtes du ciment aux cendres volantes

1. Introduction

Numerous papers on the investigation of flyash have been published recently, some papers dealed with the properties of flyash /1-3/, some were on pozzolanic reaction of flyash /4-7/. K.Takemoto et al /8/ reviewed the works on hydration of pozzolanic cements including the flyash cement at the 7th International Symposium on the Chemistry of Cement.

Many papers pointed out that the utilization of flyash "lubricated" the particles of the concrete mixture, allowing the water demand of the mixture to be reduced. Besides, it acted as "precipidate sites" for hydrates of portland cement as well as reacted with CH to form CSH gel.

Huang Shiyan /4/ pointed out that flyash was actually non-reactive at early ages and the addition of gypsum could accelerate the pozzolanic reaction between CH and flyash and increase the strength of the paste after 28 day age.

Some works published was studied by using water solid ratio (w/s) by weight. As well known, flyash has less specific gravity than that of portland cement, therefore, if same w/s ratio by weight is used, flyash cement will have less capillary pore than that of pure portland cement paste, which will influence the strength significantly.

In the present papers same w/s ratio by volume was used to eliminate the effect of the difference of origenal capillary in the pastes. The investigation was focused on the effect of CH and $C\bar{S}H_2$ added on the strength of the pastes, because both CH and $C\bar{S}H_2$ in flyash cement paste are not enough for flyash reacting completely to form CSH gel and AFM or AFT phase. According to calculation, 11% $C\bar{S}H_2$ of the mixture has to be added to the cement for 25% of the flyash added in the mixture to hydrate in our experiments in which 70% portland cement is mixed with 30% flyash by weight (65%:35% by volume). If 50% and 100% of flyash in the minture react completely with CH and $C\bar{S}H_2$, 7.7% CH+ 22% $C\bar{S}H_2$ and 31% CH+44%$C\bar{S}H_2$ have to be added.

2. Materials and experiments

Portland cement Type 1 was supplied by Cement and Concrete Reference Laboatory. The chemical and potential mineralogical composition (calculated by Bogue formula) were listed in table 1 and table 2.

Table 1. Chemical composition of portland cement

SiO_2	Al_2O_3	Fe_2O_3	CaO	MgO	SO_3	Na_2O	K_2O
20.46	5.30	2.12	63.16	3.96	2.58	0.23	o.95

Table 2. Potential mineralogical composition of portland cement

C_3S	C_2S	C_3A	C_4AF	f-CaO	MgO	$C\bar{S}H_2$	K_2O
50.23	20.62	10.46	6.41	1.27	3.90	5.53	0.95

The fineness of cement is 3689 cm/g(Blaine), 87% particles pass through No.325 sieve.

flyash was from American Flyash Company. The chemical composition is as follows:

SiO_2	Al_2O_3	Fe_2O_3	CaO	MgO	Na_2O
50.83	29.37	13.83	1.65	0.86	1.82

79.7% particles pass through No.325 sieve.

Chemical grade reagent CH and $C\bar{S}H_2$ were used.

The pastes of portland cement, flyash cement, flyash cement+CH, flyash cement+$C\bar{S}H_2$ and flyash cement+CH+$C\bar{S}H_2$ were prepared by w/s ratio 1:1 by volume to keep the initial capillary pore in nearly the same level for all pastes. All mixture were blended in a bowl handly and mixed in a Hobort mixer for 1 minute. Afteradding water, the mixtures were mixed at low, middle and high speeds for 30,30 and 60 secconds respectively. The portland cement flyash ratio of all mixture were kept in 65:35 by volume(70:30 by weight). Different amount of CH, $C\bar{S}H_2$ and CH+$C\bar{S}H_2$ were added to the mixture respectively. 1' dia. by 2' high cylinders were prepared and cured in 40°C water until the ages for compressive strength test. 1'x1'x1' cubes were prepared for thermal analysis at 105°C to determine the total porosity. The ignition losses of hydrated products and CH contents of the samples were determined at 300,400,600 and 950°C.

QXDA was run for checking the phase composition and the contents of ettringite, C_3S and $C\bar{S}H_2$ quantitatively. The ratio of the peak intensities were determined by weighing the paper of the peak area at 9.1°2θ for ettringite, 11.7°2θ for $C\bar{S}H_2$, 51.8°2θ for C_3S and 42.9°2θ for internal standard MgO.

GPC analysis were carried out by the method of J.F Young /9/.

The samples were observed by SEM but the picture were not present here for spaces liminted.

3. Results and discussions

Fig.1 shows the effect of the amounts of CH added to cement on the compressive strengths of the pastes.

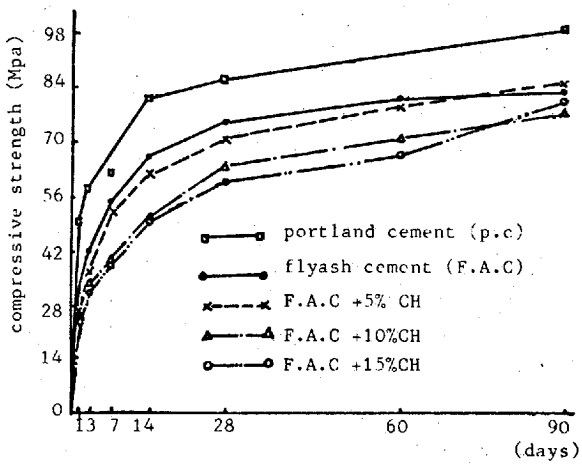

Fig.1 Effect of CH added on the strengths of flyash cement pastes

The strength decreases with the addition of CH at early ages, even at 90 days only the paste with 5% CH addition catches up with flyash cement paste. The more CH addition, the lower compressive strength at early ages. Huang Shiyan /4/ believed that flyash was non-reactive actually at early ages. We find that the strengths of flyash cement are the function of the contents of portland cement in the mixture at early

Shan-Ba Wang, Wuhan Institute of Building Materials,Wuhan,China
R.L Berger University of Illinois,Urbana,Illinois,U.S.A

Effect of $Ca(OH)_2$ and $CaSO_4\ 2H_2O$ on the strength of flyash cement pastes

Effet de $Ca(OH)_2$ et $CaSO_4\ 2H_2O$ sur la résistance des pâtes du ciment aux cendres volantes

ages. Most of flyash particles do not react with CH, their surface are still smooth without any change by SEM observation at early ages. At 28 days some flyash particles reacted,but some still do not. Even at 60 days we still find some holes in which flyash particles are pulled out when the samples are broken. The reacted degree of flyash was calculated from the difference between theoretical and actual CH contents of various pastes at 60 days,and the result was showed in Fig.2.

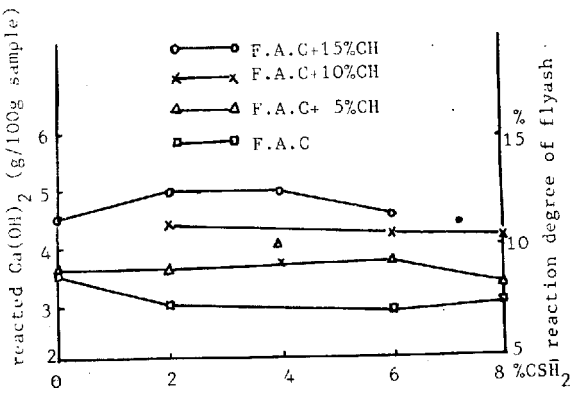

Fig.2 The effect of CH and $C\bar{S}H_2$ addition on reaction degree of flyash

The actual CH contents were measured from thermal analysis,the theoretical contents of CH were calculated from CH content of portland cement paste and the percentage of portland cement in flyash cement. For calculation briefly,it is assumed that portland cement in all pastes has same hydration degree in same ages. If we assume that SiO_2 and Al_2O_3 in flyash react with CH and $C\bar{S}H_2$ stochiometrically and forming ettringite or AFM or AFt or C_3AH_6,the reaction degree of flyash can be calculated from CH reacted in the pastes. It seems that CH added increases reaction degree of flyash,for example,from 7% of non-addition of CH to about 12% by addition of 15% CH at 60 days. Because only about 10% of CH added reacts with flyash,90% of the CH added exists as fine aggregate which is the weakness of the paste according to the report of S.B Williamson /10/. The more CH in the paste,the less percentage hydration products in the pastes. This is the reason that the strength of the paste with CH addition is lower than that with CH addition even at 60-day age. F.G Butter and E.J Walker /5/ stated that pozzolanic reaction of flyash could not proceed to a point which would cause the PH of the pore fluids to drop to a dangerous level. We believe that the addition of CH may keep the pore solution of the paste at higher CaO concentration (higher PH value) even at later age, which is favorable to pozzolanic reaction of flyash, therefore,the reaction degree of flyash increases with the amounts of CH addition.

The effect of $C\bar{S}H_2$ on the strengths of the pastes is showed in Fig.3.We can find that the strengths of the pastes with 2%,4% and 6% $C\bar{S}H_2$ addition catch up with that of flyash cement at 14 to 28 days and surpass to that of flyash cement at 60 days. The paste with 8% $C\bar{S}H_2$ addition catches up with that of flyash cement at 60 days.During 3 to 14 days,the strengths of the pastes with 2%,4% and 6% $C\bar{S}H_2$ increase rapidly,which is contributed by the formation of ettringite at the capillary between the particles. QXDA curve in Fig.4

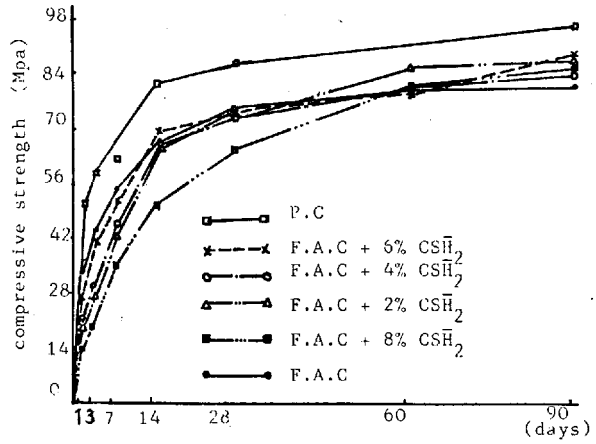

Fig.3 Effect of the amount of $C\bar{S}H_2$ on the compressive strength of the pastes

showed that most of ettringite were formed before 14 days,which coincided with the increase of strength curve in Fig.3. $C\bar{S}H_2$ was consumed up at 28 days showed in Fig.4,indicating that the contribution of $C\bar{S}H_2$ to strength was limited within 28 days.Fig.5 showed that the contents of ettringites in the pastes increased with the amounts of $C\bar{S}H_2$ added. We believe that the

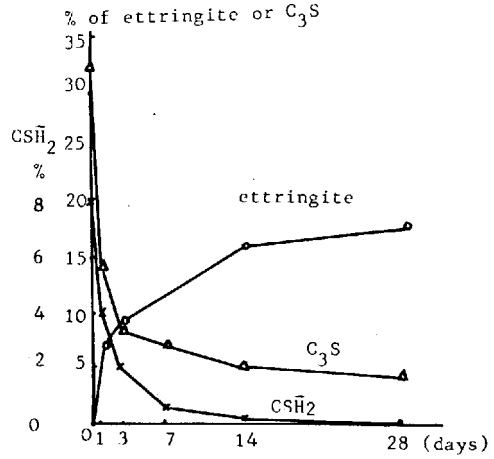

Fig.4 QXDA curves of C_3S,ettringite and $C\bar{S}H_2$ of the paste with 8% $C\bar{S}H_2$ addition,at 60 days

higher strength of the paste with $C\bar{S}H_2$ added at later ages stems from both: the reaction of $C\bar{S}H_2$ with C_3A or with Al_2O_3 from flyash to form ettringite in the capillary and the pozzolanic reaction of flyash with CH to form $C\bar{S}H$ gel at later age,which contributes a denser structure to the paste.

The effect of CH+$C\bar{S}H_2$ on the strength of flyash cement paste is illustrated in Fig.6. The decrease of the compressive strength is much more than that added CH or $C\bar{S}H_2$ alone. This is the combination of both negative effect of CH and $C\bar{S}H_2$ to the strength. The strengths of all pastes catch up that of flyash cement

Shan-Ba Wang, Wuhan Institute of Building Matreials,Wuhan,China
R.L Berger University of Illinois,Urbana,Illinois,U.S.A

Effect of $Ca(OH)_2$ and $CaSO_4\ 2H_2O$ on the strength of flyash cement pastes

Effet de $Ca(OH)_2$ et $CaSO_4\ 2H_2O$ sur la résistance des pâtes du ciment aux cendres volantes

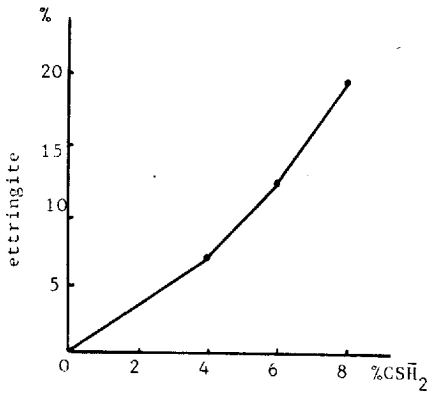

Fig.5 The content of ettringite as the function of the amount of $C\bar{S}H_2$ added (60 days age by QXDA)

paste at 28 to 40 days and surpass that of flyash cement paste at 60 days. This is attributed to the combination effect of both the formation of ettringite by addition of $C\bar{S}H_2$ and more CSH gel formed by flyash reaction with CaO of higher CaO concentration in pore solution by addition of CH.Because of the addition of CH, the non-evaporable water in the pastes measured at 950°C includes the water by dehydration of CH,we measure the non-evaporable water at 300° C which is representative of most non-evaporable water of the hydrates which are main contributor to the strength except CH. The curve profile of non-evaporable water showed in Fig.7 is similar to strength curves above. Because the pastes with 4%,6% and 8% $C\bar{S}H_2$ addition have 8%,12% and 19% ettringite at 60 days respectively and ettringite loses more water molecues at 300°C than that of other hydrates,therefore we conclude again that the major contribution of $C\bar{S}H_2$ to the strength is to form ettringite in the capillary at early age,thereby the CSH formed by pozzolanic reaction of flyash at later age densifies the structure of the paste.

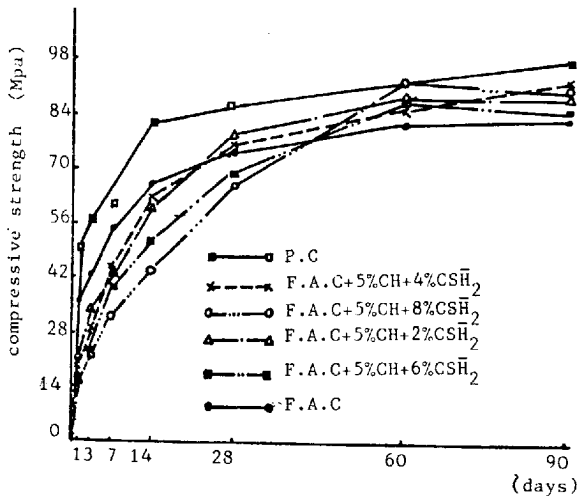

Fig.6 Effect of 5% CH + $C\bar{S}H_2$ added on the strength of the paste

From Fig.1 to Fig.6 we find that the strengths of

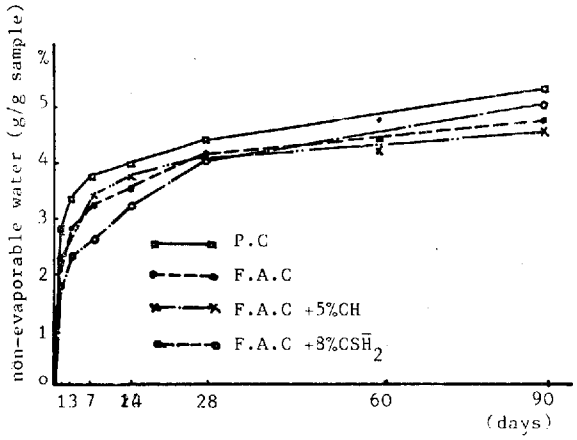

Fig.7 Non-evaporable water contents (at 300 C) of several samples as function as hydration ages

flyash cement pastes,whether CH and $C\bar{S}H_2$ are added or not,are lower than that of pure portland cement even at 90 days if w/s ratio by volume is used,which is origenated from the lower activity of flyash cement and hence higher porosity in the pastes of flyash cement. The origenal porosity of all pastes are 50%,but at 60 days the total porosities of portland cement, flyash cement,flyash cement with 5%,10% and 15% CH addition are 29.2%, 31.6%, 36.1%, 36.7% and 37.2% respectively. H.Uchikawa /11/stated that capillary space was increased with the blending ratio of flyash,and total porosity increased about 2% to 6% with the blending amount of flyash. In our experiments,the non-evporable water in portland cement,flyash cement,flyash cement+5%CH,flyash cement+8%$C\bar{S}H_2$ pastes obtained from 105 to 300°C at 90 days are 5.4%,4.8%,4.6% and 5.2% respectively,which is in agreement with the results of the strength.

The results of TMS of some pastes are showed in Fig.8 and table 3.

Table 3. The effect of CH and $C\bar{S}H_2$ added on the derivatization of some flyash cement pastes (60 days samples)

	Mo.	Di.	Pe.	Oct.	Te.	Do.
Flyash	8	31	15	10	15	21
Flyash cement	39	34	12	5	6	4
Flyash cement+5%CH	27	37	15	7	8	6
Flyash cement+8%CSH̄	29	39	12	6	8	6
Flyash cement+5%CH +8%CSH	12	38	16	10	12	12

Mo.---monomer Di.---dimer
Pe.---pentamer Oct.--octamer
Te.---tetradecamer Do.---docosamer

There exists only 8% monomer in the silica acid of flyash,while dimer and polymer equal to about 90%. Small amount of monomer probably is responsible for lower reactivity of flyash. After addition of CH and $C\bar{S}H_2$, monomer decreases and polymer increases in flyash cement pastes compared with the paste without CH and $C\bar{S}H_2$ addition at 60 days.Especially in the paste with addition of both CH and $C\bar{S}H_2$, monomer is much less and polymer is more greater than that of the paste with the addition of CH or $C\bar{S}H_2$ alone. It is uncertain to confirm the higher strength of the paste with addition of CH and $C\bar{S}H_2$ to be related with more polymer in the paste. More works are needed to understand the source of polymer because we do not known

Shan-Ba Wang,Wuhan Institute of Building Materials Wuhan,China
R.L Berger University of Illinois,Urbana,Illinois,U.S.A

Effect of $Ca(OH)_2$ and $CaSO_4\ 2H_2O$ on the strength of flyash cement pastes

Effet de $Ca(OH)_2$ et $CaSO_4\ 2H_2O$ sur la résistance des pâtes du ciment cendres volantes

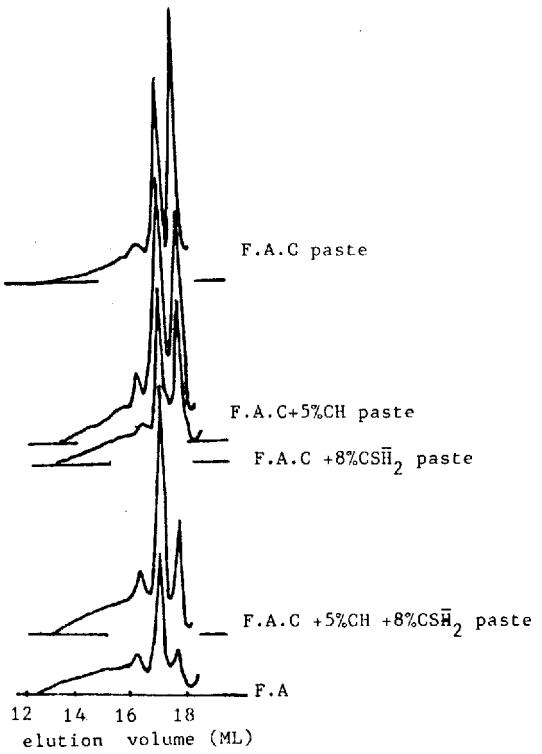

Fig.8 Gel permeation chromatogram of derivatized hydrated flyash cement pastes showing the effects of CH and $C\bar{S}H_2$ added (60 days samples)

that they are from unreactive flyash or from the hydration products of portland cement and flyash.

4. Conclusions

Some conclusions can be drawn from above results and discussions:

1). The strengths of flyash cement pastes,whether CH and/or $C\bar{S}H_2$ added or not, are lower than that of portland cement paste even at 90 days if same w/s ratio by volume is used.

2). The addition of CH decreases the strength of flyash cement paste even at 90 days.

3). Gypsum added to flyash cement paste decreases the strength at early ages but increases the strength at later ages. All gypsum added is consumed up at28 days. The contribution of gypsum to the strength lies in the formation of ettringite in the capillary and densification of the structure of the paste. Gypsum combining with small amount of CH added contributes more to the strength at later ages due to increase of the reaction degree of flyash by addition of CH to mantain higher PH value in pore solution.

4). The reactivity of flyash is very low, only 7-12% reaction degree takes place at 60 days,which is probably associated with 8% monomer in flyash.

5). After addition of CH and $C\bar{S}H_2$, the monomer in flyash cement paste decreases,dimer and polymer increases.

References

1/. Sun Baozhen et al. Journal of the Chinese Silicate Society Vol. 10, No.1,1982
2/. Guo Cheng zhou et al: Journal of the Chinese Silicate Society Vol. 10, No.2,1982
3/. D.G Montgomery et al; Cem. Conc. Res. Vol.11, No. 4 pp 591-593, 1981
4/. Huang Shiyan: Journal of Wuhan Institute of Building Materials No.2 pp 151-168, 1982
5/. F.G Butter and E.J Walker: The rate and extent of reaction between calcium hydroxide and pulverised fuel ash , Symposium on the application of PFA in concrete pp 71-81, 1981
6/. J.G Cabraya: Mineralogy and Morphology of the C_3A-PFA system, Symposium on the application of PFA in concrete, pp 111-120,1981
7/. K,Ogawa et al: Cem. Conc. Res. Vol.10 No.6 pp683-693, 1980
8/. K.Takemoto et al: 7th I.C.C.C Vol.1 Theme VI-2 Paris, 1980
9/. J.F Young: Trimethyl sililation manual
10/. R.B Williamson: The solidification of portland cement
11/.H.Uchikawa et al: Influence of the properties of flyash on the fluidity and the structure of flyash cement paste, Symposium on the application of PFA in concrete, pp83-94,1981

N.B. Eden and J.E. Bailey
Department of Ceramics, Glasses and Polymers, University of Sheffield, Sheffield S1O 2TZ, England.

Effect of Polymer Modifications on the Mechanical Properties of Calcium Silicate and Calcium Aluminate Cements. 3.2
L'effect de modifications d'un polymère sur les propriétés mécaniques des ciments en silicate calcique et alumine calcique.

Summary

The new polymer modified cements, also known as "NIMS" or "MDF" cement have been found to be complex new materials, many of which cannot be said to be mere extensions of conventional hydraulic cement materials. Mechanical properties depend markedly upon the combination of polymer type and cement type, with certain combinations, such as Calcium Aluminate cement/Poly Vinyl Acetate/Alcohol copolymer being of particularly high mechanical strength when processed in the correct manner.

In the calcium silicate, or Portland cement system, different polymers such as poly acrylamide and hydroxypropyl methyl cellulose may be used to produce materials with varying properties.

It is clear that the polymers affect the hydration reaction to varying degrees, depending on their own reactivity, and this may lead to a complex polymer/hydrate gel or even a chemically cross-linked polymer, rather than hydrate particles alone being the main binding agent.

Evidence is presented here for some of the microstructural features of these cements which affect mechanical properties. In particular detailed attention is given to the fracture processes involved during mechanical failure.

Os novos cimentos polímeros modificados também chamados "NIMS" ou "MDF" conforme se constatou, são novos materiais complexos, muitos dos quais não se pode dizer que são meras extensões dos materiais do cimento hidráulico convencional. As propriedades mecânicas dependem acentuadamente da combinação do tipo de polímero e do tipo de cimento, tendo certas combinações - como cimento de aluminato de cálcio/acetato de polivinil/copolímero de álcool - resistência mecânica particularmente elevada quando processados de maneira correta.

No silicato de cálcio, ou sistema de cimento portland, podem ser usados diferentes polímeros, como poliacrilamida e celulose-metil-hidroxipropil, para produzir materiais com propriedades diferentes.

É claro que os polímeros afetam a reação de hidratação em vários graus, dependendo de sua própria reatividade, e isto pode levar a um gel complexo polímero/hidrato ou mesmo a um polímero, ligados transversalmente de forma química, mais do que se partículas de hidrato sozinhas fossem o principal agente ligante.

Neste trabalho se tornam evidentes algumas características microestruturais destes cimentos, que afetam as propriedades mecânicas. Dá-se atenção detalhada em particular aos processos de fratura envolvidos durante a ruptura mecânica.

1. Introduction

This paper presents results on the mechanical properties of polymer modified calcium silicate (Portland) and calcium aluminate cements.

These cements were originally termed "macro-defect free" cements (1) as it was believed that their superior mechanical properties were primarily due to the removal of large air-bubble defects, which were thought to act as flaws obeying the Griffith (2) equation. This was, however, contrary to the conclusions of an extensive study of the fracture mechanics of Portland cement paste (3) where it was found that the failure stress-notch size relationship was better fitted by an equation which included in it a value for the yield stress, predicting that there was a limiting, or "intrinsic" strength which could not be exceeded merely by removing flaws. It was subsequently shown (4) that removal of air bubble defects did not substantially improve the flexural strength; the mean flexural strength was increased by approximately 15% and the scatter in results considerably decreased but the maximum flexural strength remained the same. It was concluded from this study that, even though the air bubbles did act as flaws, their effect was not the same as that of sharp flaws in a linear elastic medium, as required for the Griffith analysis. Alford et al (5) suggested that there may be other flaws present, but there is no clear microstructural evidence of the existence of such flaws of sufficient size to account for the low flexural strength (about 15 MPa) even in the absence of air bubbles. The simplistic Griffith model was later modified (6) by the addition of empirical equations relating Young's modulus and fracture surface energy to porosity.

Rodger et al (7) have studied the Portland cement/poly acrylamide (PAAm) and calcium aluminate cement/poly vinyl acetate - alcohol (PVAAl) systems, and have proposed that in both cases the hydration reaction and the products thereof, are chemically modified by the polymer. When PVAAl is introduced into the calcium aluminate system, it is seen from infra-red studies that the polymer hydrolyzes to become poly vinyl alcohol, the acetate groups combining with a small amount of calcium, whilst x-ray diffraction suggests that production of conventional crystalline hydrates is heavily suppressed. The authors proposed that the material was bound together by a poly vinyl alcohol gel cross-linked with metal ions from a small amount of cement hydration.

In the case of Portland cement/PAAm system it was similarly proposed that the polymer first hydrolyzes at the high pH produced early in the hydration reaction, to form poly acrylic acid which is then cross-linked by metal ions to form the binding agent; apparently conventional hydrates are also present (8).

2. Experimental Method

2.1 Preparation of materials

Full details of the mixing, pressing and curing of the polymer modified cements have been given elsewhere (9). In all cases, the dry powdered polymer was mixed with the anhydrous cement, and the water then added during mixing in a planetary mixer. When a uniform crumble had thus been obtained, it was fed onto a laboratory twin roll mill and rolled until a dough was formed. This was then folded and passed through a wider nip to obtain the desired thickness of plate.

The plates were pressed between "melinex" non-stick films, at a pressure just sufficient to begin deforming them, and left at room temperature under pressure for up to 24 hours.

Pressure was then released and the non-stick film peeled off. Portland cement preparations were then submerged for the desired period in curing baths filled with water which had previously been used to cure the same cement. This was to prevent excess leaching of alkalis. Calcium Aluminate cement plates were left to dry to ambient humidity immediately after removal from the press.

2.2 Testing Procedures

The plates were cut into bars using a water-cooled diamond tipped saw. The bars were then tested in three point bending either in the water-saturated, ambient dried or oven-dried condition. All testing was carried out at room temperature, and the test procedures have been described elsewhere (4).

Flexural strength and Young's modulus (initial tangent modulus) were measured on bars nominally 6 mm or 3 mm thick x 12 mm wide, tested in 3-point bend over a span of 180 mm or 80 mm respectively. The high span/depth ratios were chosen to minimise errors in the measurement of the modulus (4). Fracture surface energy was calculated from slow-bend tests on notched bars, 6 mm deep x 12 mm wide, span 50 mm and nominal notch/depth ratio of 0.65. In all cases, this produced a fully stable fracture.

A conduction calorimeter was used to follow the hydration of Portland cement at 21°C with and without polymer additions. A water/cement (w/c) ratio of 0.15 was used, and all mixing was carried out prior to placing a small ($\sim$ 10g) sample in the calorimeter cell. Unless otherwise stated, the mixing included passing the crumble repeatedly through a twin roll mill until a uniform product was obtained. Rate of heat evolution was calculated on the basis of the weight of dry cement in the sample.

3. Results and Discussion

3.1 Calorimetry

The rates of heat evolution for various OPC/polymer mixes are shown in figures 1 to 3.

The rolling process has had a marked effect on the hydration of the cement in the absence of the polymer. This is likely to be due to an improved wetting of the anhydrous cement surface. Though some friction would inevitably have occurred between cement grains, the mill nip of 1.3 mm was over ten times greater than the maximum particle size, and the milling was carried out gently to avoid this problem. No temperature rise was noted during milling, and the sample size was small compared with the mill capacity. There is an almost complete lack of a dormant period, particularly after rolling. This may be due to the low water content, which is rapidly saturated with calcium.

Total heat evolved was not affected by rolling, this being (at 48 hrs) 116 kJ/kg for the rolled cement and 117 kJ/kg for the hand mixed one.

Figures 2 and 3 show that the addition of the polymers retards the hydration, though by differing extents.

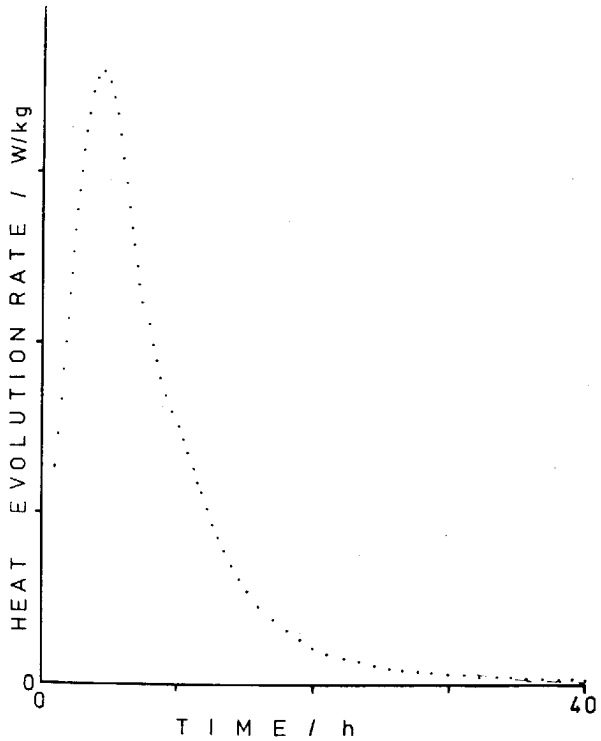

Fig.1. Effect of twin-roll milling on rate of heat evolution from OPC, w/c 0.15. (no polymer additions).

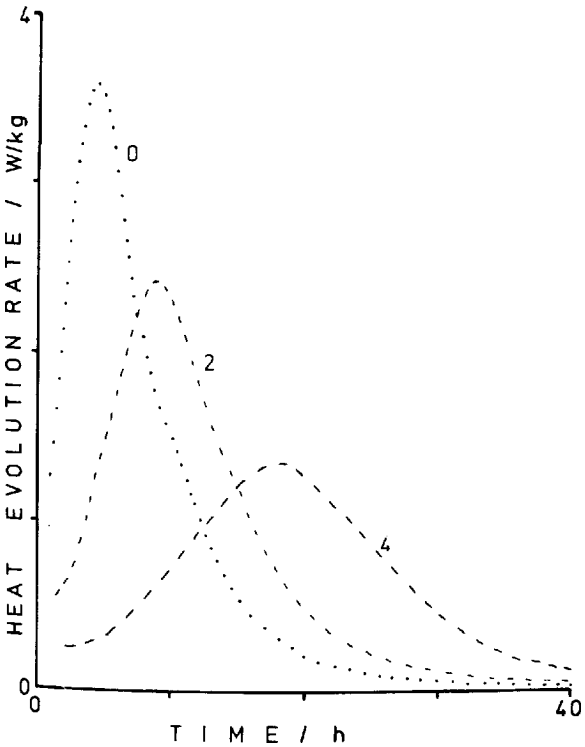

Fig. 2. Effect of addition of hydroxy propyl methyl cellulose on the rate of heat evolution from OPC, w/c 0.15. Small figures are wt.% polymer addition, based on weight of cement.

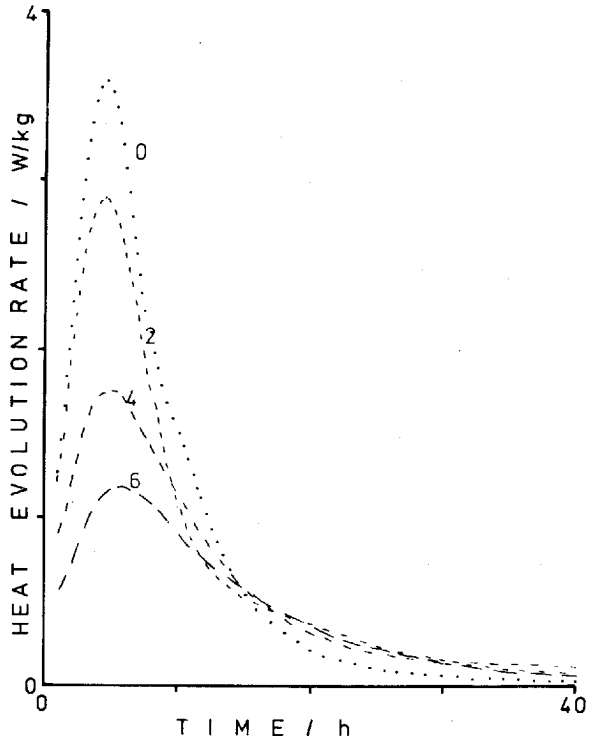

Fig.3. Effect of addition of poly acrylamide on the rate of heat evolution from OPC, w/c 0.15. Small figures as for Fig.2.

Retardation is likely to occur due to the hydrophilic nature of the polymers, i.e. water is physically bound to the polymer, and is therefore less mobile than in the bulk liquid state. Transport of other ions will also be inhibited.

Chemical effects from the different polymers must also be expected. The cellulose molecule is made up of glucose rings, and the retarding effect of HPMC may be likened to the effect of sugars (10), though of a far less radical nature.

The polycrylamide has a much less drastic effect upon hydration rate, as, in the initial stages, it has not hydrolised to form polyacrylic acid, and is not therefore in a suitable form to complex calcium ions.

No additional heat evolution peaks were found to occur in the Portland cement system, in contrast to studies on calcium aluminate cement (8).

A reduction in the total heat evolved during hydration was noted as the polymer content was increased, as shown in table 1.

Table 1. Effect of polymer additions on total heat evolved after 48 hours, in kJ/kg

	Polymer addition, wt.%			
	0	2	4	6
HPMC	116	109	96	-
PAAm		105	86	68

A similar effect is seen with both polymers; although the reaction has not completely stopped after 48 hours, figures 2-3, the rate is extremely low at this point, and the reduction in total heat evolved most probably reflects the increasing amount of water bound by the polymer gel. It should be noted here that the water available for reaction in these calorimetric studies is limited to the amount used for mixing, which is not the case where the material is allowed to cure under water (9).

The apparent degree of hydration can be calculated from the calorimetric data if a nominal average heat of hydration for the whole cement is assumed. This is only an approximate calculation, as the heats of hydration of the component minerals vary widely (11). However, it is useful to gain some understanding of the amount of cement consumed, and we take a value of about 490 kJ/kg for a typical Portland cement (11). Taking the "4%" mixes from table 1 which correspond approximately to mix of 64%/6% by volume (9), the degrees of hydration of OPC/HPMC and OPC/PAAm are 20% and 18% respectively. The former is somewhat lower than the value of 26% calculated previously for a 64/6 OPC/HPMC from simple bound water measurements (9).

An analogy has been drawn by Rodger et al (7) between these OPC/PAAm cements and certain dental cements containing ion-leachable glass and poly acrylic acid (12). However, the proportioning of these cements (13) is such that the polymer and glass are present in comparable proportions, whereas much less polymer is used in the cements under consideration here. It can be seen from the model proposed (7) that one calcium ion is bound by two monomer units of the polymer in the case of polymer-cement adhesion and by four monomer units in the case of polymer-polymer cross linking. Assuming, as a conservative estimate, that one calcium ion combines with two monomer units, then, given the respective molecular or atomic weights of PAAm and Ca as 71 and 40, we may calculate that calcium amounting to 1.1% of the weight of the polymer is required, or 1.6% expressed as CaO. Assuming a CaO content of 65% of the cement, this can also be expressed as about 2.4% of the weight of the anhydrous cement for a material containing 4% polymer.

Some 25% of the hydration products of Portland cement normally occur as Calcium Hydroxide and it can be seen that, at a degree of hydration of about 18% there is more than enough free calcium available without taking any from the calcium silicate hydrates which form the main binding agent in Portland cement pastes. It may be this free calcium which would otherwise crystallize as Calcium Hydroxide, that has been identified by Sinclair and Groves (8) as separate from the definable calcium silicate hydrates.

3.2 Mechanical Properties

3.2.1 Portland Cement

The mechanical properties of Portland cement modified with hydroxy propy methyl cellulose have been documented elsewhere (9). It was found that full densification of the cement could be obtained at a polymer content of about 1% by total volume, or 0.7% of the weight of the cement. As the polymer content was increased, the dry (ambient humidity) flexural strength was observed to increase markedly, whilst initial tangent modulus remained constant, as expected from the constancy in porosity. Changes in flexural strength were found to be brought about by the toughening action of the polymer, not by improved flaw removal, as the flexural strength was observed to increase by the same extent as the fracture surface energy (14). This cannot be explained in terms of the simplistic porosity model (6).

Figure 4 shows the evolution of flexural strength, Young's modulus (initial tangent modulus) and fracture surface energy for a mix of 64% OPC/6% PAAm by volume.

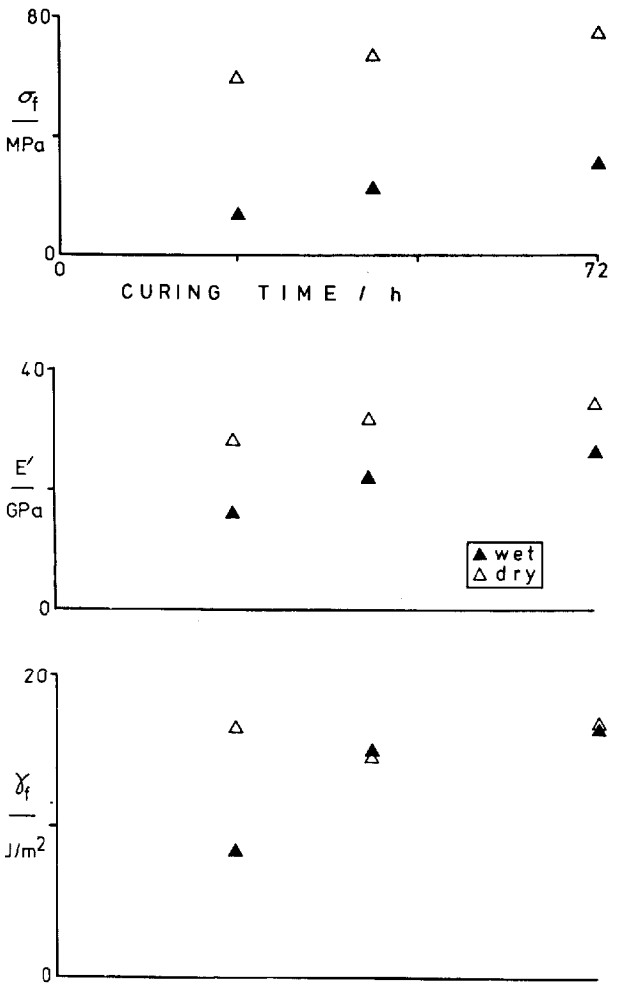

Fig. 4. Mechanical properties of a 64/6 (% by volume) OPC/PAAm polymer modified cement. a) wet, as cured, b) dried at ambient humidity.

In the OPC/HPMC system studied previously (9,14) the fracture surface energy and flexural strength were linked directly through fracture mechanics, as the results suggested that the flexural strength was a close approximation to the yield stress in the Dugdale/Barenblatt equation.

The initial tangent modulus in both systems appears to develop in a similar manner. However, in this study it can be seen from figure 4 that, particularly in the dry state, the fracture surface energy appears to be unaffected by curing time, whereas there is a steady increase in flexural strength between 24 and

72 hours.

This indicates that some changes may be taking place in the process zone parameters as the cement is cured. Further information can be gained from the load/deflection behaviour of notched and unnotched beams.

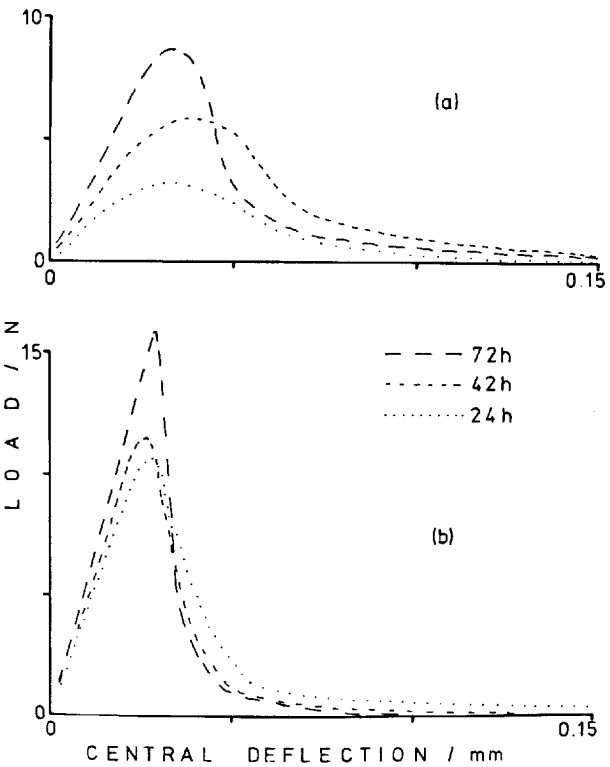

Fig. 5. Notched bar load/deflection curves for 64/6 OPC/PAAm . a)wet, as cured, b) dried to ambient humity. Small figures are curing times in hours.

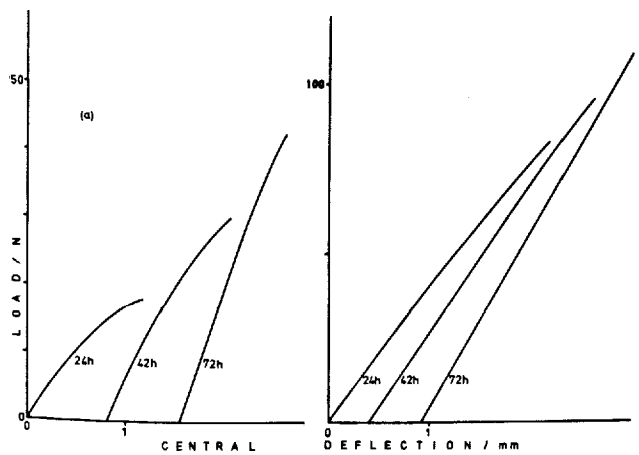

Fig. 6. Unnotched bar load/deflection curves for 64/6 OPC/PAAm. Notes as for Fig. 5.

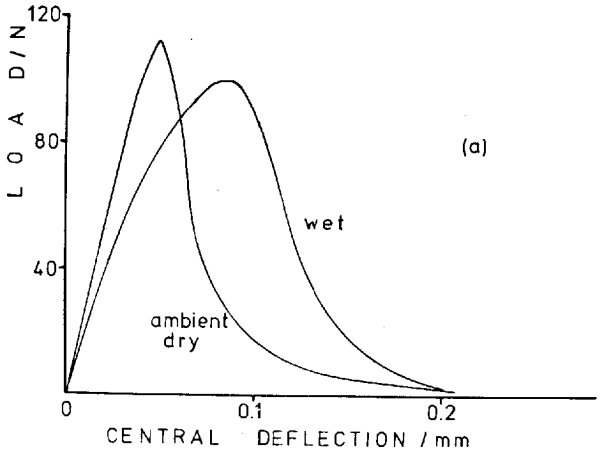

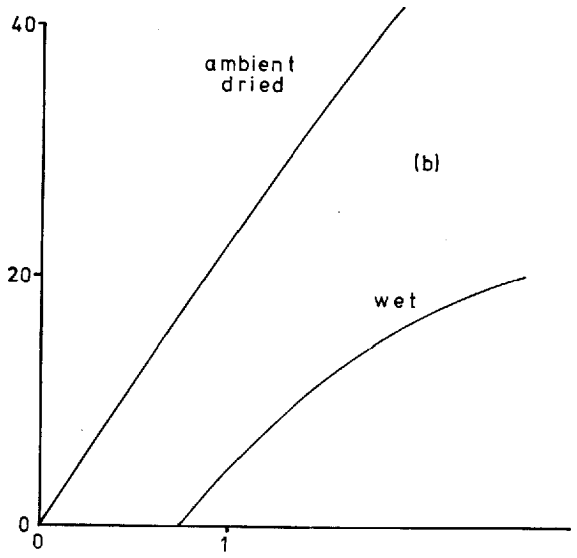

Fig. 7. Wet and dry load/deflection curves for a 3 day old 64/6 OPC/HMPC polymer modified cement. a) notched bar, a/d ∿ 0.65, b) unnotched bar.

Figures 5 and 6 show typical load/deflection curves for the two tests (i.e. notched and unnotched bars) in both moisture states.

By comparison, figure 7 shows the same curves for a 3 day old 64/6 OPC/HPMC mix.

In all cases, curvature of the load/deflection curve is very marked in the wet state. The degree of curvature reduces with increasing curing time, and this is more marked for the PAAm materials than for those made with HPMC (9).

Removal of water leads to a large reduction in curvature; again, this is more marked at later ages in the PAAm materials than the HPMC. Indeed, after 72 hrs curing, the dry PAAm material is essentially linear to failure, even in the notched test. This is indicative of increasing brittleness, and a greater variation is found in the flexural strength tests.

with coefficient of variation rising from typically below 6% for the dry HPMC materials, to over 12% for the more brittle PAAm materials. Such an embrittled state is not found in the cements made with cellulose derivatives until they are oven-dried (14).

We now turn to consider the process of fracture in terms of the microstructure of the hydrated cement described in more detail elsewhere in this conference by the present authors.

The calcium silicate hydrates formed by Portland cement are sheet-like, consisting of layers of calcium hydroxide with silica tetrahedra in-between (15). It is proposed that fracture occurs primarily by the sliding apart of such layers, and that in the polymer modified cements, the interlayer adhesion is improved by the presence of polymer (9), at least when it is dried.

Thus the stiffness of the material is dependent primarily upon the anhydrous grains and hydrated particles, whilst the yield stress, and hence fracture surface energy and flexural strength, depends upon the state of the polymer (i.e. wet or dry) and the bond between the polymer and the hydrates. Calculations based on the hydrate surface visible in the SEM at high water contents gave good agreement with mechanical test data for OPC/HPMC materials (9), though the details of the model have been challenged (16) on the grounds that such "fibrillar" growths are not visible on the fracture surfaces of polymer modified cements.

Nevertheless, it seems likely that the OPC/PAAm materials are bound together by conventional hydrates and a modified acrylic gel, as suggested by Rodger et al (7), though the amount of calcium required to saturate the gel can be obtained from the excess left after conventional hydration. We would therefore envisage a fracture mechanism similar to that in OPC/HPMC, save that the adhesion between polymer and hydrates may be enhanced, due to chemical bonding between the carboxyl groups on the polymer and metal ions on the hydrate surfaces, and the calcium-modified polymer will be more rigid due to linkage between polymer chains and also due to the hard, rather brittle, nature of the polymer. Thus the yield stress may be enhanced, but slippage may occur over smaller distances, leading to a material which is slightly stronger but more brittle, with less stable cracking and hence less curvature of the load/deflection curve, as noted above.

3.2.2 Calcium Aluminate cement

Calcium Aluminate cements hydrate in a very different manner to Portland cement. The conventional hydrates are generally crystalline, and can easily be studied using x-ray diffraction. Rodger et al (7) have shown that the formation of such crystalline hydrates is strongly suppressed by the presence of large amounts of polymer (e.g. 5 to 10% by weight). Indeed, when conventional hydrates are formed by immersing polymer modified CA cement in water at 80°C (after it has been hydrated and dried), strength is drastically and irreversibly lost.

Table 2 compares flexural strength and modulus for similarly proportioned polymer modified cements made from OPC and PAAm and from Secar 71 (CA) cement and PVAAc. Both contain 64% cement, 10% polymer by volume , and were cured for 3 days at 20°C in a sealed environment, the first 24 hours being under a pressure of approximately 3 MPa.

Table 2. Comparison of properties of OPC/PAAm and CA/PVAAC cements

	Flex. strength σ_f, MPa		Initial tangent modulus E´, G Pa	
	ambient dry	80°C	ambient dry	80°C
OPC/PAAm	77	78	30	34
CA/PVAAc	101	150	27	50

It is clear that, far from being embrittled by drying at 80°C, as is the case in the OPC system, the Secar 71 material has improved considerably. This is due to densification of the material, which occurs mainly during the oven-drying stage. Such a densification process is virtually absent from the OPC system, as is clear from the small change in modulus.

The calcium aluminate based materials generally maintain a greater degree of non-linear load/deflection behaviour, at a given state of drying, than similar materials in the OPC system. This is shown in figure 8. These two states are broadly similar, in terms of load/deflection behaviour, to the "wet" and "dry" states for the OPC based materials described in the previous section and elsewhere (9,14). However,

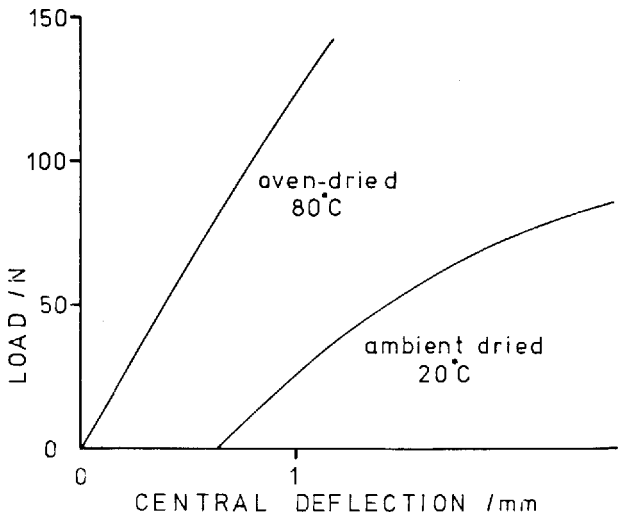

Fig. 8. Load/deflection behaviour in unnotched flexure of a 64%/10% by volume CA/PVAAc cement a) ambient dried, b) oven dried at 80°C.

there is considerably less water present in the polymer, and the large degree of curvature cannot be explained in terms of the viscosity of a wet polymer, as is the case for the OPC/HPMC system (9). Rather, it is likely that the polymer is playing a more direct role in the transfer of stress throughout the system.

In the case of the calcium aluminates, the polymer or modified polymer gel plays a much greater role in the stress-strain behaviour, since the strain in the polymer gel is not restrained by the stiffness of the

hydrates, as is probably the case in Portland cement. This results in two effects:

1) The polymer is free to contract and hence aid densification when it is de-hydrated.

2) The modulus of the CA based materials is lower than anticipated from porosity-modulus curves for Portland cement.

Helmuth and Turk (17) studied pastes of tricalcium silicate which had been aged for several months, and obtained an exponential porosity-modulus relationship which has been shown to agree with moduli measured in the OPC/HPMC system (9). Such a curve predicts a zero porosity modulus of about 80 MPa, which is significantly higher than the 50 MPa measured on CA/PVAAl materials of virtually zero porosity (6).

It is therefore clear that the calcium aluminate based materials behave in a manner quite different from the calcium silicate system. Whether a "tied-crack" fracture model can be applied to these materials, with the yield stress being governed by the nature of the hydrate/polymer gel is as yet unknown.

4. Conclusions

1. The mechanical properties of polymer modified cements are influenced by the polymer content, water content, and the nature of any polymer/cement interaction.

2. The effect of reaction between the polymer and hydrates in the calcium silicate system may be limited due to the presence of conventional hydrates, but in the case of calcium aluminates may radically change the nature of the binding agent.

3. In all practical cases, load/deflection behaviour is seen to be non-linear, and where full linearity is induced by excessive drying, this leads to increased brittleness.

4. The polymer plays a major role in the mechanical properties, and improvements in, for example, durability, will come through a better understanding of the role of the polymer throughout the life of the material.

References

1. J.D. Birchall, A.J. Howard and K. Kendall, Nature, 289, 1981, 388.
2. A.A. Griffith, Phil. Trans. R. Soc. Land, A221, 1920, 163-198.
3. D.D. Higgins and J.E. Bailey, J. Mater. Sci., 11, 1976, 1995.
4. N.B. Eden and J.E. Bailey, J. Mater. Sci., 19, 1984, 150-158.
5. N. McN. Alford, J.D. Birchall, A.J. Howard and K. Kendall, J. Mater. Sci., 19, 1985, 1134.
6. K. Kendall, A.J. Howard and J.D. Birchall, Phil. Trans. R. Soc. Lond., A310, 1983, 139-153.
7. S.A. Rodger, S.A. Brooks, W. Sinclair, G.W. Groves and D. Double, J. Mater. Sci., 20 , 1985 , 2853-2860.
8. W. Sinclair and G.W. Groves, J. Mater. Sci., 20, 1985, 2846-2852.
9. N.B. Eden and J.E. Bailey, J. Mater. Sci., 19, 1984, 2677-2690.
10. J.D. Birchall and N.L. Thomas, Cem. Concr. Res., 13, 1983, 830-842.
11. F.M. Lea, "The Chemistry of Cement and Concrete", Edward Arnold, London, 1970.
12. A.D. Wilson and S. Crisp, Br. Polym. J., 7, 1975, 279-296.
13. J. Elliott, L. Holliday and P.R. Hornsby, Br. Polym. J., 7, 1975, 297-306.
14. N.B. Eden and J.E. Bailey, Materials Research Soc., Proc. 42, MRS, Pittsburg, 1985, 79-87.
15. R.F. Feldman, in "Concrete Science" by V.S. Ramachandran, R.F. Feldman and J.J. Beaudoin, Heydon, London, 1981, p.5.
16. N. McN. Alford, J.D. Birchall, G.W. Groves and K. Kendall, J. Mater. Sci., 20, 1985, 3418.
17. R.A. Helmuth and P.M. Turk, Symposium on the Structure of Portland Cement (Highways Research Board S.P. 90, Washington, D.C. 1966), pp. 135-144.

A.M. HARRISSON and N.B. WINTER, Blue Circle Industries PLC, Research Division, Greenhithe, Kent.
and H.F.W. TAYLOR, Dept of Chemistry, Aberdeen University

AN EXAMINATION OF SOME PURE AND COMPOSITE PORTLAND CEMENT PASTES USING SCANNING ELECTRON MICROSCOPY WITH X-RAY ANALYTICAL CAPABILITY

Examination des pâtes de ciments, pûres et composites, par
la microscopie electronique à balayage avec analysateur aux rayons-X

SUMMARY: Pastes of Portland cements alone or with pulverised fuel ash (pfa, fly ash) or granulated blastfurnace slag, and aged from 3 days to 6 months, were examined using scanning electron microscopy with microanalytical capability. In any one paste, the C-S-H composition was found to vary only in minor respects between different regions, such as space occupied initially by alite or belite, or adjacent to $Ca(OH)_2$ or to unreacted pfa or slag, where present. In pastes not made with pfa or slag, the C-S-H typically had a Ca/Si ratio of about 2.0, and Al/Ca about 0.06, with some variation among cements. In those made with pfa or slag, the Ca/Si ratios were lower; e.g. in a 6 month old paste with 40% replacement of cement by pfa, Ca/Si was about 1.6 and in a similar paste with 40% slag, it was about 1.8. The C-S-H in the pastes made with pfa was also more aluminous. The product formed in space initially occupied by slag was high in CaO, SiO_2, Al_2O_3 and MgO, and was possibly an intimate mixture of C-S-H with other phases. In all the pastes, the AFm phase was low in SO_3 compared with monosulphate, ($[Ca_2Al(OH)_6]_2SO_4.6H_2O$). In those made with pfa, it was also high in Al_2O_3. For the pastes made with and without pfa or slag, the Ca/Si ratios found for the C-S-H in this work are higher than those found in some other recent electron optical investigations. The higher values agree better with ones calculated from contents of $Ca(OH)_2$ and unreacted anhydrous phases obtained using other techniques.

SUMÁRIO

Pastas de cimento portland puras ou com cinzas volantes (pfa, fly ash) ou com escória granulada de alto-forno, com idades de 3 dias a 6 meses, foram examinadas usando-se microscópio eletrônico de varredura com capacidade de microanálise.

Em qualquer pasta, foi verificado que a composição do C-S-H variava pouco entre as vârias regiões, tais como os espaços ocupados inicialmente pela alita ou belita, ou adjacente ao $Ca(OH)_2$ ou ao pfa ou escória, quando presentes. Em pastas que não tinham pfa ou escória, o C-S-H tinha, tipicamente, uma relação Ca/Si de cerca de 2.0, e uma relação Al/Ca de cerca 0.06 com alguma variação entre os cimentos. Naqueles que tinham pfa ou escória, a relação Ca/Si, era menor; por exemplo, em uma pasta de 6 meses com 40% de substituição de cimento por pfa, a relação Ca/Si era de cerca de 1.6 e numa pasta similar com 40% de escória, era de 1.8. O C-S-H nas pastas com pfa, era, também, mais aluminoso. O produto formado no espaço inicialmente ocupado pela escória era alto em CaO, SiO_2, AL_2O_3 e MgO, e era possivelmente uma mistura íntima de C-S-H e outras fases. Em todas as pastas, a fase AFm era baixa em SO_3, comparada ao monosulfato, ($[Ca_2Al(OH)_6)]_2SO_4.6H_2O$). Nas pastas com pfa, era também alto o Al_2O_3. Para as pastas com ou sem pfa ou escória, as relações Ca/Si encontradas para o C-S-H neste trabalho foram maiores que o encontrado em outras investigações eletro-ópticas. Os valores maiores concordam com os calculados pelo conteúdo de Ca $(OH)_2$ e fases anidras que não reagirem, utilizando-se outros métodos.

A.M. HARRISSON and N.B. WINTER, Blue Circle Industries PLC, Research Division, Greenhithe, Kent.
and H.F.W. TAYLOR, Dept of Chemistry, Aberdeen University

1. INTRODUCTION

In recent years there have been a number of electron optical studies of the hydrated phases in Portland cement pastes with and without pfa or slag. For example, Rayment and Majumdar[1] collected a set of results of cement hydrate analyses which suggested a Ca/Si ratio of about 2.7 in the outer hydrate and about 2.0 in the inner product. The outer hydrate is almost certainly a mixture with CH and AFm phase. Rayment[2] gave evidence that the presence of pfa lowered the Ca/Si ratio. Earlier, Stuke and Majumdar[3] had found a bimodal distribution of results for Ca/Si ratios. These were interpreted as showing a different composition for inner and outer product C-S-H. Lachowski and co-workers[4,5] used an analytical electron microscope to obtain analyses of ground fragments of hydrates in OPC pastes at early and mature ages. Their results suggested a decrease in Ca/Si ratio with time.

This paper gives the results obtained from a range of pure and composite cement pastes, using a scanning electron microscope with X-ray microanalytical capability.

2. EXPERIMENTAL

Three Portland cements, two samples of pfa and one of ground granulated blastfurnace slag were used. Table 1 gives the bulk chemical analyses of these materials. Both pfa samples consisted largely of glass, with some mullite, quartz and iron oxides. The slag consisted almost entirely of glass. One of the pfa cements (BQ) was prepared by blending Portland cement and pfa in a ratio 72:28. For the other (AP) the ratio was 60:40. The slag cement was blended in the proportion cement to slag 60:40. Table 2 details the paste samples studied. Polished sections were analysed in an ISI DS 130 SEM, with a PGT energy dispersive X-ray detector and System IV analyser. All specimens were coated with 30 nm of carbon by evaporation, measured using an oscillating quartz crystal. Most analysis points were selected visually, though a few were collected arbitrarily on a grid pattern.

All analyses were carried out at an accelerating voltage of 15 KV which was considered to be a satisfactory compromise resulting in acceptable X-ray spatial resolution and sufficient excitation of the Fe Kα line. At each point analysed, X-rays were collected for 100 seconds. A beam current of 0.7 nA measured in a Faraday cup on the edge of the sample holder was used throughout in order to minimise errors in dead time correction. A total of 619 analyses were made, including 90 of anhydrous phases.

3. RESULTS AND DISCUSSION

3.1 Unreacted clinker phases

Limited data were obtained for unreacted clinker phases of cements B and C, and are given in Table 3, together with the results for cement A, which we have reported previously[6]. A number of belites gave low totals, typically around 97% and in Table 3, this lower total group is presented separately. At present, we do not fully understand the reason for this effect.

3.2 Hydration products in OPC pastes

3.2.1 General

For each paste, a preliminary survey of the results was made by plotting the ratios Al/Ca against Si/Ca for individual analyses. All analyses for a given paste were plotted except those which clearly included some anhydrous material. These were taken to be any with a total above 85%. The plots were often annotated by using different kinds of points to indicate either microstructural type, or to mark analyses particularly high in Mg, S or Fe. Fig.1 is a typical example.

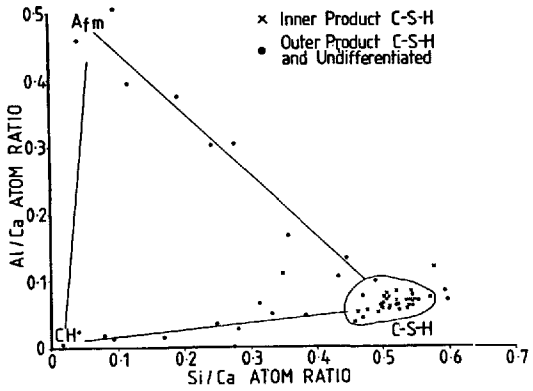

Fig. 1 Analyses from Paste C91

For all the OPC pastes, most of the analyses lay either near to a composition taken to be that of the C-S-H (Si/Ca 0.5, Al/Ca 0.06), or near to lines joining that composition to the origin, or to a composition near Si/Ca $\sim$ 0.05, Al/Ca $\sim$ 0.5. It was presumed that the latter composition was that of the AFm phase and that points near to the line between it and the C-S-H composition represented mixtures of these phases. Points near to the line between the C-S-H composition and the origin were similarly taken to represent mixtures of C-S-H and CH. With few exceptions, analyses of what was clearly recognised as inner product of either alite or belite proved to be of substantially pure C-S-H. Of the analyses of what was considered to be outer product or of uncertain microstructural affiliation, some were also of substantially pure C-S-H, but others were mixtures of C-S-H with AFm phase or CH or, rarely, both. Spots of pure AFm phase were relatively uncommon; from a total of 283 analyses of hydration products of OPC pastes, only 13 were found, of which 7 were of 3 day old pastes. Areas of CH of various dimensions were also found, and were presumed to form parts of the outer product.

3.2.2 C-S-H in OPC Pastes

For each paste, a group of analyses was selected that appeared to represent substantially pure

C-S-H. The boundary used to define it on the plot of Al/Ca against Si/Ca was arbitrarily chosen for each paste; Fig.1 illustrates it for a typical case. Table 4 gives the results.

For all the OPC pastes, the mean Si/Ca ratio of the C-S-H was between 0.50 and 0.53 (a Ca/Si ratio of 1.89 to 2.00). The most significant compositional differences between the pastes are in the mean Mg/Ca ratios, which were higher for the pastes of cement C (0.07 - 0.08) than for those of the other cements (0.02 - 0.03). The Mg/Ca ratios correlate with the MgO contents of the cements, and, probably more directly with those of the alites they contain. The mean Al/Ca ratios were also slightly higher for the pastes of cement C, while the mean K/Ca ratios were highest for the pastes of cement B and lowest for those of cement A; these differences, too, reflect ones in the compositions of the cements. It must be borne in mind that, in an OPC paste that has not been dried, the Na and K are very largely contained in the pore solution. When the paste is dried, as it must be in order to analyse it in the SEM, they are deposited as the solution evaporates, and are to be found largely in the C-S-H.

For a given cement, there is no clear indication that the C-S-H composition changes with time, except that the S/Ca ratio decreases with time for cements A and C, though not for cement B. This difference between the cements possibly reflects differences in the sulphate contents of the belites. For any normal Portland cement, the sulphate available for incorporation in the hydration products is provided mainly by the gypsum and alkali sulphates, and is thus available from an early stage of reaction; it is spread increasingly thinly as more and more hydration products are formed. The belite in cement B was notably high in SO_3 (0.7%), and this would be expected to have counteracted this tendency.

Table 4 also gives the results for inner and outer product separately for paste C at 91 days. The differences in composition were small, but the inner product had a higher Mg/Ca ratio and lower K/Ca and S/Ca ratios than the outer product. The outer product compositions used were those which were considered to contain no AFm or CH phases. The Mg probably came largely from the alite and belite, while the S and K entered the C-S-H mainly from the pore solution, partly during sample preparation.

3.2.3 AFm Phases in OPC Pastes

Table 5 includes results of 13 analyses of what appeared to be substantially pure AFm phase in the OPC pastes. All were low in Fe, and the individual analyses corresponded fairly closely to formulae in the $[Ca_2Al(OH)_6](SO_4)_n(OH)_{(1-2_n)}.xH_2O$ series, with minor replacement of sulphate by silicate, Ca by Mg, and Al by Fe. The small contents of Na and K could have been deposited from the pore solution. Of the replacements, that of sulphate by silicate is the most substantial.

Some analyses were presumed to represent mixtures of AFm phase with C-S-H. In order to compare the compositions of the pure AFm described above, and that mixed with C-S-H, a composition for C-S-H, equal to the mean for the pure C-S-H in that paste, was removed from the analysis of the mixture. There were 17 analyses remaining after this procedure which could be called AFm. The compositions were close to those of the pure AFm, but tended to have higher ratios of S/Ca. In 4 cases, the compositions were equal within experimental error to that of monosulphate. The mean of these 17 analyses is included in Table 5.

3.2.4 Regions High in Iron

The procedure described above for subtracting the contribution from C-S-H was applied to all analyses of hydrated material having Fe/Ca ratios >0.05. From all the OPC pastes, there were 17 such analyses, and in all but 2 of these 10% or more of the Ca could not be attributed to C-S-H. The results for these 15 analyses, after subtracting the contributions attributable to C-S-H, are given in Table 5. In only 4 cases were the Al/Ca ratios outside the range 0.45 to 0.55; there were no significant correlations, either positive or negative, between the Mg/Ca, Al/Ca, S/Ca and Fe/Ca ratios. These results do not favour the view that any substantial fraction of the iron entering the hydration products goes into an AFm phase.

3.2.5 Other Results for OPC Pastes

Analyses relatively high in Mg but low in Fe (Mg/Ca > 0.1 and Fe/Ca <0.05) were examined. There were only 8, of which 7 were from pastes of the relatively Mg rich cement C. Three had been identified as inner product, and the others as outer product or uncertain. The Mg/Ca ratios were 0.10 - 0.23; in other respects, 7 of the analyses were typical ones of C-S-H and the other a typical one of C-S-H mixed with AFm phase. For 6 analyses from pastes of cement C that appeared to be of C-S-H apart from their Mg/Ca ratios, the Si/Ca ratios were 0.49 - 0.55, which is normal for the C-S-H from this cement; the ratios of Si to (Ca + Mg) were 0.44 - 0.50. This suggests that Mg in excess of some quite small amount does not replace Ca in C-S-H, but occurs in a separate phase, which is, however, closely mixed with it.

Twenty one analyses from the OPC pastes gave compositions that lay either well inside the triangles linking the C-S-H, AFm and CH compositions on the plots of Al/Ca against Si/Ca, or near to the lines joining the AFm and CH compositions. These were examined by deducting contributions from C-S-H as for the mixtures containing AFm phase, but accepting only those analyses that, after carrying out this subtraction, had Al/Ca ratios of 0.20 - 0.45. The analyses thus corrected for C-S-H had Al/Ca ratios fairly evenly spread over the range accepted and S/Ca ratios of 0.09 - 0.33, with a mean of 0.17. With a few exceptions, S/Ca tended to increase with Al/Ca, from about 0.1 at Al/Ca = 0.3 to about 0.25 at Al/Ca = 0.45. Ettringite

has Al/Ca = 0.33 and S/Ca = 0.5. Either ettringite, or an AFt phase lower in sulphate, could have been a constituent in some of the spots giving these analyses, but on the whole, the evidence suggests that most were mixtures of C-S-H, AFm phase and CH.

3.3 Hydration Products in Pfa Cement Pastes

3.3.1 General

As with the OPC pastes, a preliminary survey was made for each paste by plotting Al/Ca against Si/Ca for all analyses with totals below 85%. The results were broadly similar to those for OPC pastes but, except with the 3 day old paste, the C-S-H compositions were somewhat different and a significant number of points lay outside the triangle joining the compositions of C-S-H, CH and AFm phase with Al/Ca 0.5, Si/Ca 0.05. Fig. 2 shows an example.

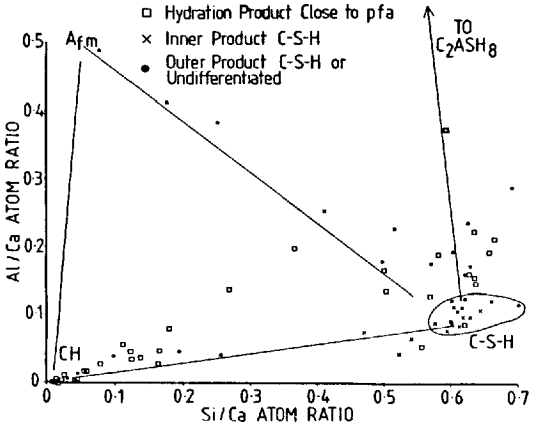

Fig.2 Analyses from paste BQ 91

3.3.2 Products Formed near to Pfa Residues

A number of other analyses of material near to residual pfa particles gave compositions with Si/Ca ratios near to that of the C-S-H in the same paste but of significantly higher Al/Ca ratio. The group of analyses shown in Fig. 2 with Si/Ca 0.62, Al/Ca 0.18 illustrates this. Such material is probably either inner product of pfa or outer product formed close to pfa. A possible interpretation of these analyses is that they represent mixtures of C-S-H and stratlingite (C_2ASH_8), the C-S-H being of somewhat higher Si/Ca and Al/Ca ratios than that formed elsewhere in the microstructure. Stratlingite is an AFm phase that has been detected in XRD in pfa cement pastes made with high proportions of pfa and hydrated for sufficiently long times. This interpretation is tentatively indicated in Fig.2. The analyses in this group were notably high in K (K/Ca typically 0.06). This concentration is probably too high to have come from the pore solution, and the relatively high concentrations found near to pfa suggest this to be a source. The K is more likely on structural grounds to be in the C-S-H than the stratlingite.

3.3.3 C-S-H. in Pfa Cement Pastes

As with the OPC pastes, the inner products of the alite and belite were essentially pure C-S-H. The C-S-H from other parts of the microstructure, apart from that near to the pfa residues discussed in the previous section, did not appear to differ significantly from it in mean Si/Ca and Al/Ca ratios. The C-S-H in the 3 day old paste did not differ significantly in Si/Ca and Al/Ca ratios from that in the paste of the same age made from the same cement without pfa. That in the two older pfa cement pastes showed a progressive increase with time in mean Si/Ca and mean Al/Ca ratios, attributable to the pozzolanic reaction. In all cases, S/Ca was low; this reflects the low SO_3 contents of the unreacted cements.

It is apparent that the presence of pfa affects the composition, not only of the C-S-H formed close to it or as its own inner products, but also that of the C-S-H formed as inner product of alite or belite, albeit to a lesser extent. The pozzolanic reaction also leads to the formation of additional C-S-H not only in space occupied previously by pfa or pore solution, but also in space previously occupied by CH. Some analyses were made of CH which lay close to pfa and was often mixed with C-S-H. Fig.2 shows that the line joining the composition of C-S-H formed from pfa to the CH composition lies in a more Al-rich position than that joining clinker inner product C-S-H to CH. This may suggest that C-S-H forming as a result of CH reacting with pfa has a higher Al/Ca ratio than that formed as inner product of alite or belite.

3.3.4 Other Results for Pfa Cement Pastes

Table 5 includes results for substantially pure AFm phase found in pfa cement pastes. Most are for relatively large crystals, up to 20 μm wide and 5 μm thick, that were found in paste AP 180. The compositions are quite near to those of the pure AFm phase in the OPC pastes, but the S/Ca ratios were lower which is attributable, as in the case of C-S-H, to the lower SO_3 content of the original cements. The mean (Si+S)/Ca ratio was 0.13, with all but one value between 0.09 and 0.15. Other results for the pfa cement pastes were analogous to those for the OPC pastes. Analyses were obtained which corresponded to AFm phase of similar composition to that described above, mixed with C-S-H, together in some cases with additional Fe or Mg or both. The compositions, after deducting the C-S-H, had Al/Ca ratios in some cases significantly above 0.5, perhaps attributable to the presence of stratlingite.

3.5 Hydration Products in Slag Cement Pastes

Reactions rims around the larger slag grains were barely detectable in secondary or backscattered electron images of the 28 day old slag cement paste (AS28), but the 180 old paste (AS180) showed well developed rims up to 10 μm wide. Fully reacted relicts of smaller grains were also abundant. A considerable proportion of the slag must nevertheless have been hydrated at 28 days because the C-S-H inner product formed from clinker grains

A.M. HARRISSON and N.B. WINTER, Blue Circle Industries PLC, Research Division, Greenhithe, Kent.
and H.F.W. TAYLOR, Dept of Chemistry, Aberdeen University

differed in composition from that formed from the same cement without slag (A28) and was close to that formed from the slag cement at 180 days (Table 4). In the latter paste there was a matrix apparently of C-S-H closely mixed with AFm phase, in which were embedded the partly and fully reacted slag grains mentioned above, together with relics of clinker phases, regions of CH, occasional unreacted clinker phases, and occasional aggregates of AFm crystals up to 30 μm in size.

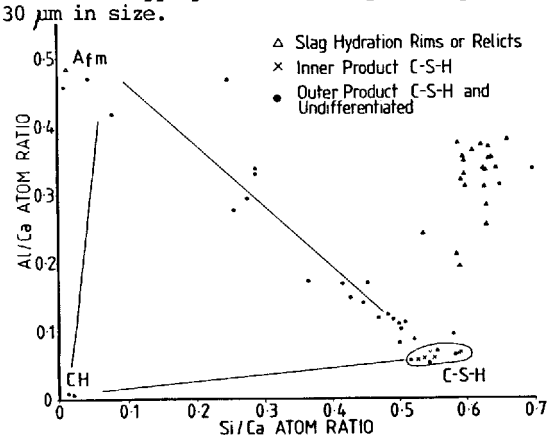

Fig.3 Analyses from Paste Al80

In Fig.3 Al/Ca ratios are plotted against Si/Ca ratios for the 180 day old slag cement paste. The slag rims and relics contained substantial amounts of MgO, Al_2O_3, SiO_2 and CaO; this agrees with an observation by Regourd[7]. Compared with the unreacted slag the Al/Ca and Mg/Ca ratios (0.34 and 0.66 respectively) were higher, but the Si/Ca ratio (0.62) was lower. These analyses might be interpreted in various ways. If it is assumed that the material includes some C-S-H, then it must also contain some aluminate phase. Hydrated magnesium aluminates of the hydrotalcite group have been detected in slag cements by XRD[8]. If it is further assumed that the C-S-H is of similar composition to the other C-S-H in the same paste, then another silicate phase must be present, since the Si/Ca ratio of the material is higher than that of the C-S-H. It is, however, possible that the C-S-H formed in the slag rims and relics may be of a different Ca/Si ratio to that formed elsewhere in the paste, and so the possible presence of a further magnesium silicate hydrate phase is not confirmed.

4. CONCLUSIONS

(i) Inner product C-S-H compositions varied with the composition of the clinker phases.
(ii) The composition was further influenced by the addition of pfa or slag. In the case of pfa the Al/Ca and Si/Ca ratios were increased. In the case of slag, the Si/Ca ratio was increased.
(iii) With the addition of pfa, it is likely that stratlingite was formed. With slag addition, a hydrotalcite-type phase, and possibly another magnesium silicate hydrate were formed.
(iv) The AFm phase contained very little Fe, suggesting the presence of another Fe-rich hydrated phase.

REFERENCES

1. D.L. Rayment and A.J. Majumdar (1982) "The Composition of the C-S-H phases in Portland Cement Pastes", Cem. & Conc. Res. 12, 753-764.

2. D.L. Rayment (1982) "The Effect of Pulverised Fuel Ash on the C/S Molar Ratio and Alkali Content of Calcium Silicate Hydrates in Cement", Cem. & Conc. Res 12, 133-140.

3. M.S. Stuke and A.J. Majumdar (1976) "The Composition of the Gel Phase in Portland Cement Paste", Hydraulic Cement Pastes, their Structure and Properties, Cement and Concrete Association, Slough.

4. E.E. Lachowski, K. Mohan, H.F. Taylor and A.E. Moore (1980) "Analytical Electron Microscopy of Cement Pastes: II Pastes of Portland Cements and Clinkers", J. Am. Ceram. Soc. 63, 447.

5. E.E. Lachowski, K. Mohan, H.F. Taylor, C.D. Lawrence and A.E. Moore (1981) "Analytical Electron Microscopy of Cement Pastes: III Pastes Hydrated for Long Times", J. Am. Ceram. Soc. 64, 319.

6. A.M. Harrisson, H.F.W. Taylor and N.B. Winter (1985) "Electron Optical Analyses of the Phases in a Portland Cement Clinker, with some Observations on the calculation of Quantitative Phase Composition", Cem. and Conc. Res. 15, 775-780.

7. M. Regourd (1980) "Structure and Behaviour of Slag Portland Cement Hydrates", VIII Int. Congress Chem. Cement, Paris, Principal Paper.

8. G. Mascalo and O. Marine (1980) "MgO-bearing Phases in the Hydration Products of Slag Cement", VIII Internat. Congress Chem. Cement. Paris, II.

	Na_2O	MgO	Al_2O_3	SiO_2	SO_3 **	K_2O	CaO	TiO_2	Mn_2O_3	Fe_2O_3	Other	Loss +	Total	Spec. Sfce. *	+45 μm Residue	LSF	SR	A/F	Free CaO
OPC A	0.19	1.3	5.4	20.6	2.7	0.38	65.3	0.27	0.07	3.0	0.5	1.9	101.6	330	11.6	95.9	2.45	1.80	0.7
B	0.31	1.4	5.4	20.2	3.0	0.93	63.9	0.27	0.07	3.4	1.0	1.4	101.3	448	8.7	94.7	2.30	1.59	1.2
C	0.06	3.0	5.8	19.8	2.3	0.43	63.8	0.24	0.12	3.4	0.5	0.8	100.2	375	14.1	96.3	2.15	1.71	1.2
PFA P	1.20	1.6	27.3	51.2	0.90	3.9	1.3	0.96	0.04	9.3	0.22	2.6	100.5	373	5.4				
Q	0.80	1.7	26.7	48.7	0.93	3.6	2.5	0.97	0.07	10.3	0.4	3.2	99.9	348	5.0				
Slag S	0.39	8.4	10.8	34.0	0.13	0.41	43.2	0.64	0.56	0.90	1.8	3.0	104.2	477	3.5				

* m^2kg^{-1}, Lea and Nurse method
** Total S as SO_3 except slag where S^{2-} = 1.2%
\+ Includes C (P = 1.5%, Q = 2.3%)

Table 1. Chemical and Physical Characteristics of the starting materials

A.M. HARRISSON and N.B. WINTER, Blue Circle Industries PLC, Research Division, Greenhithe, Kent.
and H.F.W. TAYLOR, Dept of Chemistry, Aberdeen University

Designation	Type	Ingredients and Proportions		SO_3(%)	Curing Time	Curing Temperature	No. of Analyses
		Cement	Pfa or Slag		days	°C	
A 28	OPC	A(100%)		2.7	28	25	81
A 180	OPC	A(100%)		2.7	180	25	57
B 3	OPC	B(100%)		3.0	3	20	18
B 91	OPC	B(100%)		3.0	91	20	33
C 3	OPC	C(100%)		2.3	3	20	40
C 91	OPC	C(100%)		2.3	91	20	54
AP 180	PFA	A(60%)	P(40%)	2.0	180	25	51
BQ 3	PFA	B(72%)	Q(28%)	2.4	3	20	27
BQ 91	PFA	B(72%)	Q(28%)	2.4	91	20	90
AS 28	SLAG	A(60%)	S(40%)	1.7	28	25	13
AS 180	SLAG	A(60%)	S(40%)	1.7	180	25	65

Table 2. Details of the Pastes

Oxides (%)	Na_2O	MgO	Al_2O_3	SiO_2	SO_3	K_2O	CaO	TiO_2	Mn_2O_3	Fe_2O_3	Other	Total*	No. of Analyses
Cement A													
Alite	0.0(0)	0.6(1)	1.0(3)	25.8(3)	0.0(0)	0.0(0)	72.6(5)	0.0(0)	0.0(0)	0.4(2)	0.1(1)	100.3(8)	32
Belite	0.0(0)	0.3(4)	2.1(7)	31.8(13)	0.2(4)	0.9(3)	63.2(8)	0.3(1)	0.0(0)	0.8(2)		99.7(10)	21
Aluminate	0.9(8)	1.4(5)	31.3(12)	4.2(8)	0.0(0)	0.6(3)	56.0(12)	0.2(2)	0.0(0)	5.0(9)		99.6(8)	14
Ferrite	0.0(0)	3.9(5)	22.1(18)	3.8(9)	0.1(1)	0.3(1)	47.4(8)	1.6(10)	0.5(3)	19.6(15)		99.2(11)	17
Cement B													
Alite	0.5(1)	0.9(1)	1.2(2)	24.6(4)	0.0(1)	0.3(0)	70.6(10)	0.0(0)	0.6(2)	0.6(2)		98.8(11)	11
Belite+	0.6(1)	0.5(3)	2.0(5)	30.4(1)	0.7(6)	0.6(2)	61.0(16)	0.1(1)	0.0(0)	0.9(2)		96.7(18)	10
Belite	0.5(1)	0.5(1)	2.0(3)	31.0(5)	0.7(2)	0.6(2)	62.9(4)	0.1(1)	0.0(0)	0.9(1)		99.1(7)	3
Aluminate	2.3(4)	1.4(1)	28.1(11)	5.0(8)	0.0(0)	1.4(6)	54.8(10)	0.0(1)	0.0(0)	5.5(10)		98.7(17)	5
Ferrite	0.8(2)	3.5(5)	20.4(21)	4.0(11)	0.2(4)	0.4(2)	47.9(10)	1.2(4)	0.1(2)	20.5(11)		98.9(15)	8
Cement C													
Alite	0.5(1)	1.6(1)	1.3(2)	24.9(3)	0.1(1)	0.3(0)	69.7(6)	0.0(0)	nd	0.4(2)		98.7(7)	13
Atom Ratios	Na	Mg	Al	Si	S	K	Ca	Ti	Mn	Fe			
Cement A													
Alite	.00	.01	.02	.33	.00	.00	1.00	.00	.00	.00			
Belite	.00	.01	.04	.47	.00	.02	1.00	.00	.00	.01			
Aluminate	.03	.04	.62	.07	.00	.01	1.00	.00	.00	.06			
Ferrite	.00	.11	.51	.08	.00	.01	1.00	.02	.01	.29			
Cement B													
Alite	.01(0)	.02(0)	.02(0)	.33(1)	.00(0)	.01(0)	1.00	.00(0)	.00(0)	.01(0)			
Belite+	.02(0)	.01(1)	.04(1)	.47(2)	.01(1)	.01(0)	1.00	.00(0)	.00(0)	.01(0)			
Belite	.01(0)	.01(0)	.04(1)	.46(1)	.01(1)	.01(0)	1.00	.00(0)	.00(0)	.01(0)			
Aluminate	.08(1)	.04(0)	.57(2)	.09(1)	.00(0)	.03(1)	1.00	.00(0)	.00(0)	.07(1)			
Ferrite	.03(1)	.10(1)	.47(5)	.08(2)	.00(1)	.01(0)	1.00	.02(1)	.00(0)	.30(2)			
Cement C													
Alite	.01(0)	.03(0)	.02(0)	.33(1)	.00(0)	.01(0)	1.00	.00(0)	.00(0)	.00(0)			

* Any discrepancies in the totals arise from rounding.
\+ Totals < 98%
Standard deviations on final digits are in parentheses.

Table 3. Analyses of Clinker Phases

Cement	Curing Time	Mean Atom Ratios Relative to Ca									No. of Analyses
		Na	Mg	Al	Si	S	K	Fe	Ca/Si(mean)	Total(%) as oxides	
A	28	.01(1)	.02(2)	.06(2)	.50(2)	.03(1)	.01(1)	.02(1)	2.00(7)	73(3)	31
A	180	.01(1)	.02(1)	.05(1)	.50(2)	.01(1)	.01(2)	.01(1)	2.02(9)	73(4)	22
B	3	.01(1)	.02(1)	.05(0)	.53(2)	.03(1)	.02(1)	.01(0)	1.90(8)	70(5)	11
B	91	.01(1)	.03(1)	.05(1)	.52(2)	.03(1)	.02(1)	.02(1)	1.93(8)	66(2)	17
C	3	.01(1)	.08(4)	.07(1)	.52(3)	.03(2)	.02(1)	.02(1)	1.93(13)	56(6)	16
C	91	.01(1)	.07(2)	.07(1)	.53(3)	.01(1)	.01(0)	.02(1)	1.90(10)	67(3)	32
AP	180	.01(1)	.03(3)	.12(2)	.64(3)	.00(1)	.01(0)	.02(1)	1.57(8)	76(4)	32
AS	28	.01(1)	.03(2)	.06(1)	.57(0)	.02(0)	.01(0)	.01(0)	1.74(1)	75(3)	4
AS	180	.02(1)	.03(1)	.06(1)	.56(2)	.01(1)	.01(1)	.01(1)	1.79(8)	71(2)	9
BQ	3	.01(1)	.03(2)	.04(1)	.51(3)	.00(0)	.03(0)	.02(1)	1.95(10)	59(2)	7
BQ	91	.01(1)	.03(2)	.10(2)	.61(3)	.01(1)	.03(1)	.02(1)	1.63(8)	70(3)	17
C Inner C-S-H	91	.01(1)	.07(1)	.07(2)	.52(3)	.01(0)	.01(1)	.02(1)	1.92(2)	68(3)	20
C Outer C-S-H	91	.01(1)	.04(2)	.07(2)	.40(2)	.03(1)	.02(1)	.02(0)	2.03(6)	61(2)	4

Standard deviations on final digits are in parentheses
Mean Ti/Ca and Mn/Ca both <.01

Table 4. C-S-H Compositions

Cement	Phase(s)	Mean Atom Ratios Relative to Ca									No of analyses
		Na	Mg	Al	Si	S	K	Fe	Total	f(Ca)	
A+B+C	a	.02(2)	.01(1)	.50(5)	.05(2)	.12(4)	.01(1)	.01(1)	67(5)	1	13
A+B+C	b	.03(4)	.03(2)	.51(5)	[.05]	.17(5)	.02(3)	.03(3)		.66(2)	17
A+B+C	c	.05(4)	.35(7)* .11	.48(10)	[.05]	.09(6)		.31(17)		.58(20)	15
AP+BQ	a	.02(1)	.02(1)	.52(3)	.07(2)	.07(2)	.01(0)	.03(2)	67(7)	1	6

* Mean is 0.35, median 0.11
Phases are as follows:
a - Pure AFm.
b - AFm calculated by removing C-S-H from mixtures.
c - AFm plus Fe phase, calculated by removing C-S-H.

f(Ca) - Fraction of total Ca not attributed to C-S-H.
[ ] - Assumed value.
Standard Deviations on the final digits are in parentheses.

Table 5. Analyses of AFm and associated phases

Y. HALSE, H-U. JENSEN & P. L. PRATT, Department of Metallurgy & Materials Science,
Imperial College, Prince Consort Road, London SW7 2BP, England.

The effect of the curing temperature on the pozzolanic reaction in flyash blended cement

SUMMARY: An ordinary Portland cement and a blended cement containing 30% flyash were hydrated at temperatures of 8 °C, 20 °C and 40 °C. The heat evolution during the first two days hydration was measured by conduction calorimeter. The $Ca(OH)_2$ content was measured by thermogravimeter and in the blended cements the maximum content was reached after 10 days at 20 °C hydration. At 8 °C this maximum was delayed until 28 days whereas at 40 °C it was advanced to 2 days. The decrease of $Ca(OH)_2$ content in the blended cements corresponded to the augmentation of strength by the flyash. The development of microstructure has been studied to further understanding of the pozzolanic reaction at various hydration temperatures.

Um cimento portland comum e um cimento aditivado contendo 30% de cinza volante foram hidratados a temperaturas de 8°C, 20°C e 40°C. Mediu-se a evolução de calor durante os primeiros dois dias de hidratação, utilizando-se calorímetro de condução. Por termogravimetria mediu-se o teor de $Ca(OH)_2$: nos cimentos aditivados o máximo foi alcançado depois de 10 dias de hidratação a 20°C. A 8°C este máximo foi retardado até 28 dias, enquanto a 40°C foi antecipado para 2 dias. A diminuição de $Ca(OH)_2$ nos cimentos aditivados correspondeu ao aumento de resistência pela cinza volante. Foi estudado o desenvolvimento da microestrutura, para compreensão adicional da reação pozolânica em várias temperaturas de hidratação.

INTRODUCTION

The curing temperature affects the rate of strength development in concrete (1) in two distinct ways. The early strength is increased at higher curing temperatures up to 50 °C, due to the increased rate of hydration, but at later ages the strength is decreased at the higher temperatures. This decrease is thought to be caused by a non-uniform distribution of hydration products leaving weak zones in the form of increased capillary porosity in the cement. Lowering the temperature to 4 °C slows the initial rate of hydration and reduces the early strength but the ultimate strength is higher.

The purpose of this paper is to examine the effect of curing temperature on the hydration mechanisms, microstructure and strength of OPC cured at 8-10 °C, 20 °C, and 40 °C. Using the same cement, the influence on the pozzolanic reaction with a low lime class F flyash is examined.

EXPERIMENTAL METHODS AND MATERIALS

The cement, D44, was an OPC supplied by the Cement and Concrete Association. The oxide composition of the cement is given in Table 1 and the phase compositions determined by quantitative X-ray analysis and by Bogue in Table 2.

Table 1 Oxide compositions %

Cement	SiO_2	Al_2O_3	Fe_2O_3	CaO	Na_2O	K_2O
D44	21.5	4.8	2.0	64.6	0.2	0.7

Cement	MgO	SO_3	P_2O_5	TiO_2	Mn_2O_3	Free lime
D44	1.9	2.7	0.1	2.27	0.06	1.1

Table 2 Phase compositions by QXRA and Bogue

	C_3S	C_2S	C_3A	C_4AF	Hemi-hydrate
QXRA	69	22	5.5	3	2.0
Bogue	54	20	7	6	-

The flyash, from Fiddlers Ferry power station, had a low lime content of 3.4%, a low loss on ignition of 3.2%, low soluble alkali and SO_3 content and a high silica glass content of 80%. The crystalline content was 8.3% mullite, 7.4% magnetite, and 3.8% quartz. The particle size distribution was similar to that of the cement in the fine range but contained a larger percentage by weight of particles greater than 10 μm in size.

The pastes for all experiments were mixed at a w/s ratio of 0.45, cast in cylindrical moulds, sealed and cured. For curing at 20 °C and 40 °C the moulds were kept sealed and immersed in a water-bath. For 8 °C and 10 °C the specimens were demoulded after 24 hours and immersed in saturated lime-water. Hydration was stopped at appropriate times by freeze-drying. The flyash cement mixtures contained 30% by weight of f.f.a.

Specimens for the scanning electron microscope for back-scattered electron (bse) imaging were prepared by cutting a flat surface from the cross-section of the mould and polishing this with diamond paste. The back-scattered detectors were manufactured by JEOL and fitted to a JSM 35 microscope. Fracture surfaces were prepared for secondary electron imaging. Samples for thermogravimetric analysis (TGA) for the $Ca(OH)_2$ content were prepared by grinding in an agate mill for 10 mins. Analyses were performed between 20 °C and 800 °C in an atmosphere of nitrogen. Strength was measured in compression on small cubes 0.5" in size.

Heats of hydration were measured in a Wexham Instruments isothermal conduction calorimeter, using 10 g samples hand-mixed in a polythene bag outside the calorimeter.

EXPERIMENTAL RESULTS

(a) Heat of hydration

The heat output during the hydration of the neat and blended cement pastes is shown in Fig.1 for temperatures of 20 °C, 40 °C and 10 °C. Increasing the temperature to 40 °C advances and enhances the hydration substantially, while decreasing to 10 °C extends the induction period, broadens the peaks and lowers the peak rate of heat output substantially. The positions and heights of peak 2 for alite hydration and of peak 3 for the aluminate phase are summarised in Table 3.

Table 3 Heats of hydration

10 °C

	D44	Blend
Peak 2	1.7 W/kg, 14 hrs	1.8 W/kg, 16 hrs
Peak 3	1.7 W/kg, 22 hrs	1.9 W/kg, 23 hrs

20 °C

	D44	Blend
Peak 2	3.5 W/kg, 8 hrs	3.7 W/kg, 10 hrs
Peak 3	3.5 W/kg, 11 hrs	3.8 W/kg, 13 hrs

30 °C

	D44	Blend
Peak 2	10.1 W/kg, 3 hrs	11.2 W/kg, 4 hrs
Peak 3	11.4 W/kg, 5 hrs	13.0 W/kg, 7 hrs

This behaviour for the neat cement paste is similar to that reported by earlier workers (2). The small shoulder on peak 3 at 40 °C, occurring after 8-12 hours, is not easily observed at 10 °C but some trace appears after 40-50 hours hydration. The principal effects of the flyash on the heat output of the blends are the retardation and enhancement of peaks 2 and 3. The enhancement of peak 3 is somewhat greater than that of peak 2.

The total heat output at 40 °C increases rapidly for the first 10 hours and is almost constant after 40 hours. At 20 °C the initial increase lasts for 20 hours, the output continuing to rise more slowly

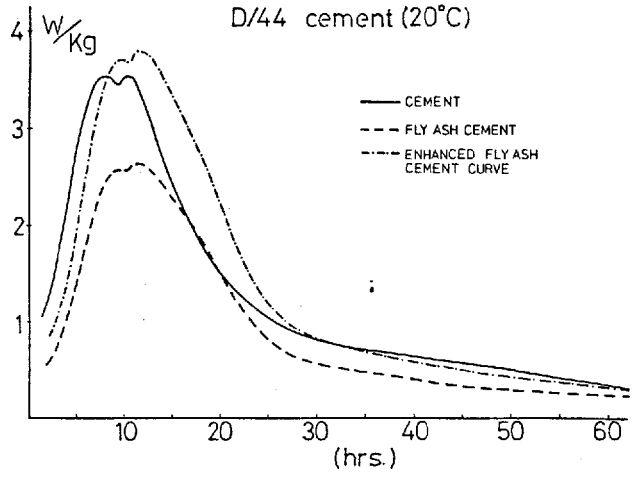

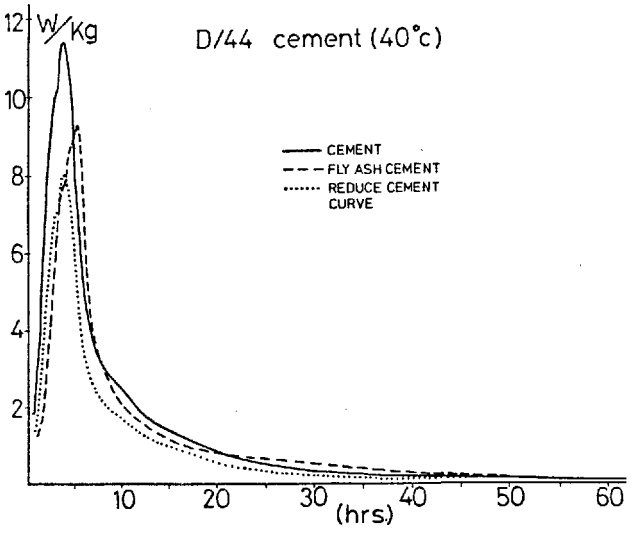

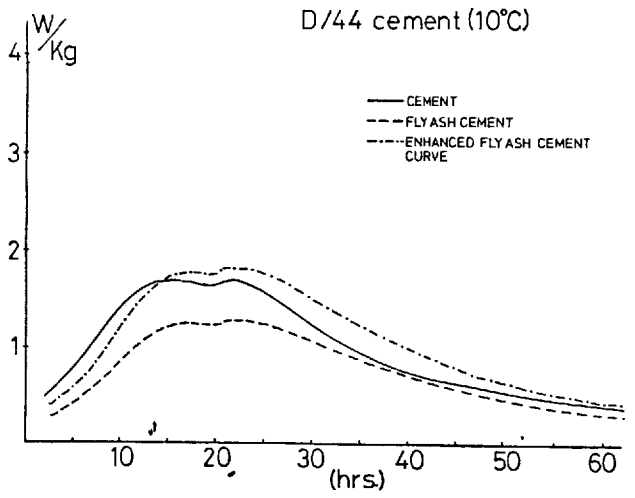

FIG.1 Heats of hydration at 10 °C, 20 °C and 40 °C

and eventually crossing that for 40 °C after about 7 days. At 10 °C the initial increase lasts for 45 hours and continues to rise more slowly up to 60 hours.

After 60 hours, the effect of adding the flyash is to increase the total heat output /g cement by 10% at 10 °C rising to 25% at 40 °C. Despite the initial retardation, clearly the flyash has enhanced the amount of hydration in the first 2-3 days at all temperatures.

(b) The rate of formation and consumption of CH

The weight of CH per ignited weight of cement at 800 °C is plotted against the time of hydration in Fig.2 for the neat cement pastes. Here the curve for 20 °C rises more slowly than at 40 °C but crosses the latter after 7-14 days and continues to rise steadily thereafter. At 8 °C the onset of the formation of CH is delayed and the curve always lies below that at 20 °C at least up to 90 days.

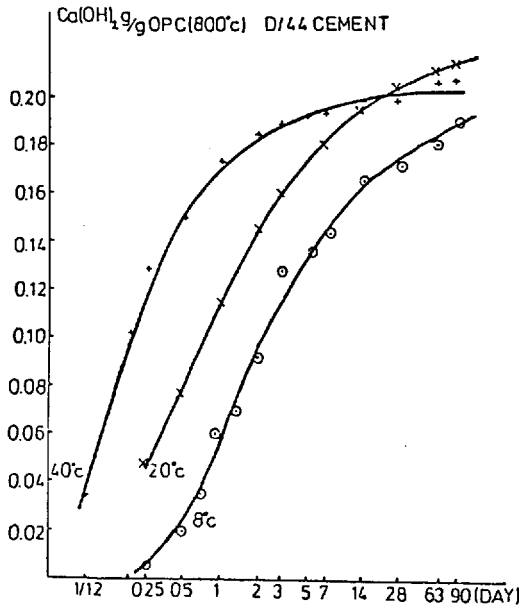

FIG.2 Formation of CH in neat cement pastes

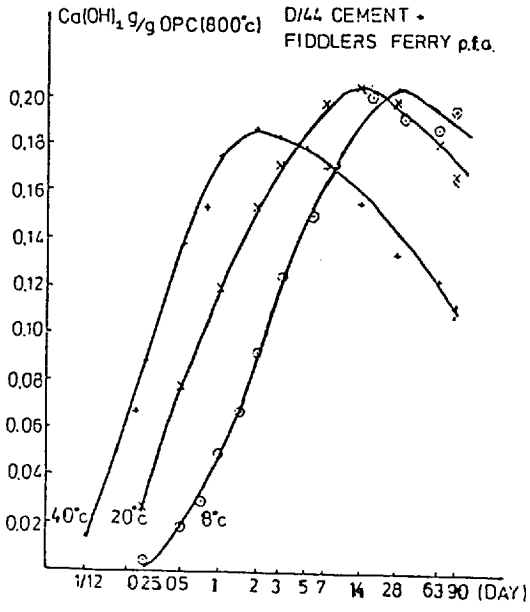

FIG.3 Formation of CH in flyash blends

The effect of adding flyash is shown in Fig.3. At all three temperatures the formation of CH is increased above that of the neat cement, in agreement with the heat of hydration, and all three curves pass through a peak which occurs at later times at lower temperatures. The height of the peak is lowest at 40 °C although the maximum occurs after only 2 days, compared with 10 days at 20 °C and 28 days at 8 °C. After 90 days of hydration, 39% of the CH has reacted with the flyash at 40 °C, compared with 20% at 20 °C and only 10% at 8 °C.

(c) Development of compressive strength

The development of compressive strength with time at 20 °C in the neat cement paste shows an anomaly, Fig.4, in the form of a plateau between 28 and 90 days which is believed to be real. The plateau is less obvious in the flyash blend although the best fit line could be drawn to include one between 28 and 63 days. Thereafter there is a marked increase in the strength due to the pozzolanic reaction between CH and the flyash with the curves crossing between 90 and 180 days.

At 40 °C, Fig.5, the plateau in the neat cement pastes occurs between 7 and 14 days, with a maximum in the strength at 28 days followed by a decline. In the flyash blend a small change in slope occurs between 7 and 14 days with a plateau between 28 and 63 days. The strength of the blended paste equals that of the neat cement at 63 days.

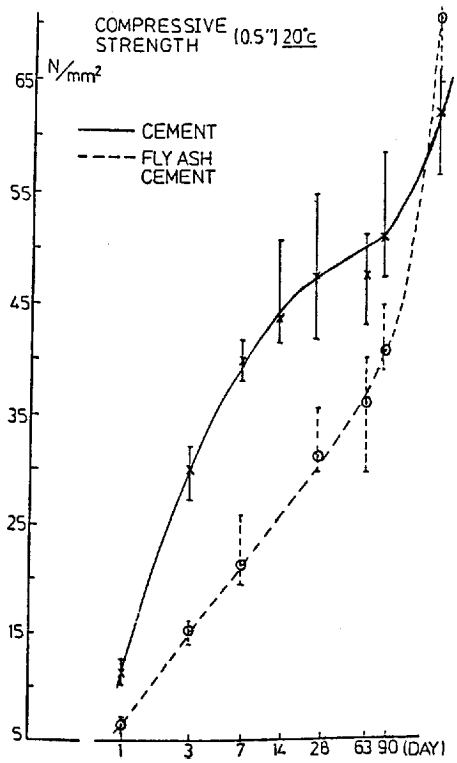

FIG.4 Development of cube strength at 20 °C

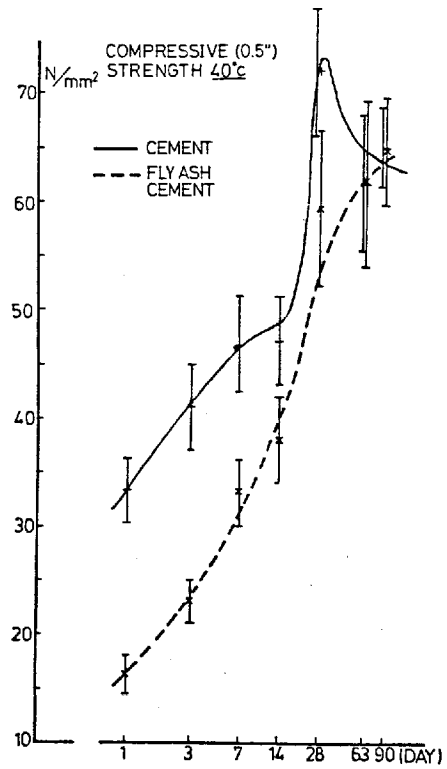

FIG.5 Development of cube strength at 40 °C

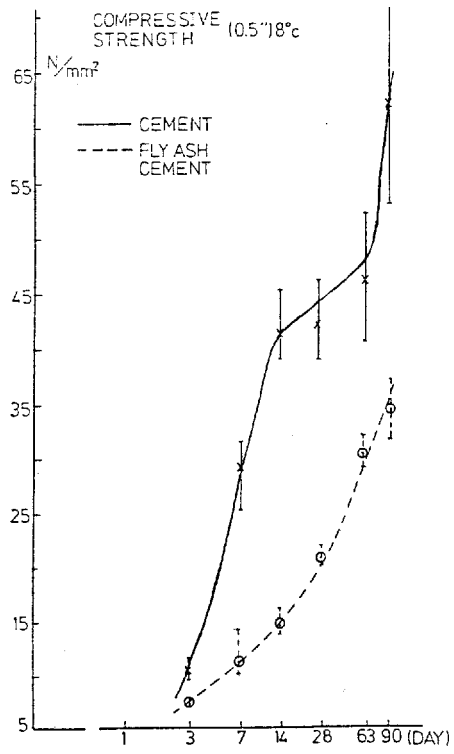

FIG.6 Development of cube strength at 8 °C

At 8 °C, Fig.6, there is a plateau between 14 and 63 days for the neat cement with a steep rise thereafter. Between 14 and 63 days the strength at 8 °C is almost equal to that at 20 °C, and by 90 days it is larger by about 20%. The flyash blend shows a small change in slope between 63 and 90 days but the strength is always much below that of the neat paste for the first 90 days.

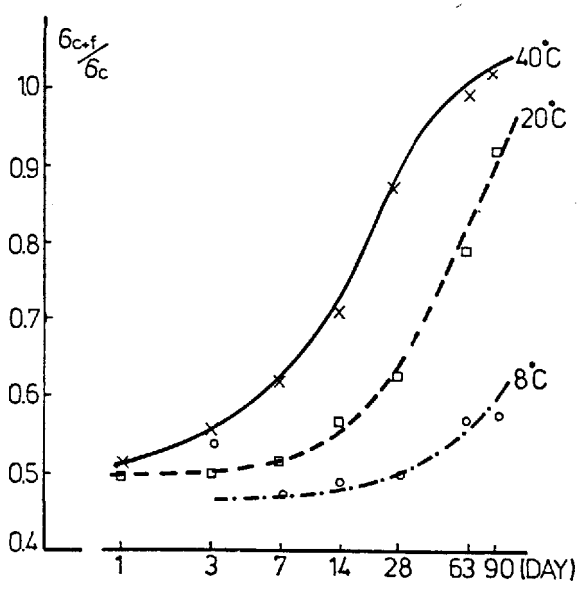

FIG.7 Strength ratio for neat and blended pastes

The contribution of the pozzolanic reaction to the strength of the blended pastes can be estimated by taking the ratio of the strength of the blend to that of the neat cement paste, Fig.7. At 40 °C this contribution starts as early as 2 days, compared with 10 days at 20 °C and 28 days at 8 °C. By 90 days at 40 °C with 39% of the flyash consumed, this contribution is decreasing in importance, although it continues to increase at the lower temperatures.

(d) The development of microstructure

Some features of the development of microstructure in D44, with and without flyash, at 20 °C have been described in an earlier publication (3). To relate these to the microstructures found at 8 °C and at 40 °C it is convenient to adopt the designations proposed by Dalgleish, Pratt and Toulson (4) of "early product" formed during initial wetting and the induction period, of "middle product" formed during peaks 2 and 3 of the calorimeter output and of "late product" formed by slower processes over long periods of time. Table 4 shows how these periods are related at the different temperatures for D44 cement.

Table 4 Products of hydration

Temperature	Early	Middle	Late
8 °C	0-4 hrs	4-40 hrs	40 onwards
20 °C	0-2 hrs	2-24 hrs	24 onwards
40 °C	0-½ hrs	½- 8 hrs	8 onwards

(i) Early product

In the scanning electron microscope, short rods of AFt are seen to form a discontinuous layer over the surface of both cement and flyash particles. This involves the dissolution of gypsum and of the aluminate phases on the surface of the cement particles. These react nearby in the solution to form crystals of AFt which fall back onto the surface (4,5) during drying.

(ii) Middle product

During the acceleratory period the surfaces of both cement and flyash particles become covered with small crystals of CH and Type I C-S-H, engulfing the short rods of AFt. Again this is a through-solution reaction because C-S-H appears on the surface of all the flyash particles as well as on the cement. A shell of these hydration products builds up on the cement particles during peak 2, leading to a separation between the dissolving core and the shell outside it in the form of a Hadley grain. These are frequent features on the fracture surface of specimens broken about half-way through the middle period, after 2 hours at 40 °C, 12 hours at 20 °C or 24 hours at 8 °C. They become more obvious after peak 3 when renewed hydration of C_3A takes place, with the appearance of rods of ettringite 2-3 μm in length growing out through the shell into the water-filled space between the particles. As they grow, these leave behind the spaces inside the shell from which the aluminate has dissolved. After 6 hours at 40 °C, X-ray results show that all of the calcium sulphate has been consumed by the aluminate phase and the AFm phase starts to appear. Differential thermal analysis confirms this after 12 hours and large hexagonal platelets of AFm appear in the microstructure. This coincides with the shoulder on the

calorimeter curve at 10 hours. Small hexagonal platelets of AFm have been found as early as 6 hours inside hollow shells where the concentration of sulphate ions is likely to be low. At room temperature AFm was found both in the microstructure as large hexagonal platelets and by X-ray after 48 hours. A broad but small peak can be seen in the calorimeter curve between 40 and 60 hours.

(iii) Late product

During this period small cement grains are fully hydrated while larger ones continue to hydrate by two different mechanisms:

- the cores continue to dissolve slowly as water diffuses in through the shells. Ca-ions diffuse out through the shell to precipitate as CH crystals in the original water space. C-S-H precipitates on the inside of the shells, thckening them in the inwards direction (6). Depending upon the space available, the size of the grain and the porosity of the shell, the grain may hydrate completely to fill the shell or even to leave a hole in the centre.
- if the grain is very large the inward thickening shell may fill the available space before hydration is complete. Then a second mechanism of hydration takes place (7), with an *in situ* conversion of alite to C-S-H involving diffusion of protons inwards and Ca and Si outwards.



FIG.8 Areas of CH in 90 day old (a) cement and (b) flyash blend at 40 °C

When the pozzolanic reaction gets under way in the flyash blends, dissolution of the glassy phase takes place beneath the earlier shell of hydration products, leaving the characteristic gap which often is revealed on fracture surfaces. Part of the C-S-H product of the pozzolanic reaction is precipitated on the inside of this shell in the form of a porous honeycomb especially at 40 °C. Complete conversion of the smaller flyash particles is found after 63 days at this temperature, whereas the larger particles dissolve to reveal crystalline phases. The amount of CH visible on a flat polished surface is reduced substantially, Fig,8, in agreement with the thermogravimetric results and with our earlier observations at 20 °C (11). Part of the pozzolanic C-S-H must form in the space left by the dissolution of CH.

DISCUSSION

Influence of curing temperature on neat cement pastes

(a) Increased temperature

In agreement with the earlier work of Regourd et al (2) the effect of increasing the curing temperature is to accelerate the hydration of OPC pastes. The mechanism of hydration does not appear to be altered greatly, with similar microstructures appearing at equivalent times as judged by the calorimeter curves. At 40 °C the rate of hydration decreases after 7 days and the degree of hydration becomes less than that at 20 °C. This is believed to be due to a dense layer of C-S-H forming around the alite slowing down the subsequent hydration (8). At the same time the size of the CH crystals is smaller because of the decrease of CH solubility with increasing temperature (9), and our results suggest that they are not only smaller and more numerous but that they have a more angular morphology with less intergrowth and a higher degree of perfection even at late ages. C_2S hydration is reported to be accelerated more than that of C_3S at higher temperatures (10) and this could account for the plateau found in the development of compressive strength. A possible explanation for the plateau at room temperature is the slowing down of C_3S hydration after 28 days, in agreement with X-ray observations, followed by the continued hydration of C_2S which is known to contribute most strongly to the strength at late ages. At 40 °C the plateau is advanced to 7 days in keeping with the greater acceleration of C_2S. Careful inspection of the 40 °C curve in Fig.2 shows a small increase in the rate of formation of CH, as might be expected for enhanced hydration of C_2S.

(b) Decreased temperature

Lowering the temperature to 8-10 °C slows the initial rate of hydration as expected (1) and the plateau in the compressive strength is a little earlier than that at 20 °C although at almost the same strength level. The most obvious difference is the marked increase in strength between 63 and 90 days. The only difference in the microstructure was the compactness and the extent of the intergrowth of CH around all the other phases. A quantitative study of this may throw more light upon the mechanism of strengthening. For the moment it seems that, at a given w/c ratio, space is filled more slowly and more uniformly at low temperatures, in agreement with the reduced capillary porosity found by Bentur et al (8).

Influence of curing temperature on the pozzolanic reaction

The pozzolanic reaction is accelerated significantly with increasing temperature as judged by the change in the amount of CH present and by the effect of flyash upon the compressive strength. The highest 28 day strength for the blend is found with curing at 40 °C but, by 180 days, curing at 20 °C gives higher strengths than at 40 °C. Curing at 8 °C appears to slow down both the formation of CH from the cement and its consumption in the pozzolanic reaction. Even at 90 days the compressive strength of the blend is only just over one half of the neat cement paste.

ACKNOWLEDGEMENTS

The authors are grateful to the Marine Technology Directorate of SERC for financial support for this work and to Dr K Scrivener for valuable discussions and help with the bse imaging.

REFERENCES

1. S. Mindess and J. F. Young, "Concrete", Prentice-Hall, New Jersey, 1981.
2. M. Regourd, B. Mortureux, E. Gautier, H. Hornain and J. Volant, 7th International Congress on Cement Chemistry, Vol.II, III-105, Editions Septima, Paris, 1980.
3. Y. Halse, D. J. Goult and P. L. Pratt, Proc. Brit. Ceram. Soc., 36, 403, 1984.
4. B. J. Dalgleish, P. L. Pratt and E. Toulson, J. Mat. Sci., 17, 2199, 1982.
5. K. L. Scrivener and P. L. Pratt, Proc. Brit. Ceram. Soc., 36, 207, 1984
6. P. L. Pratt and A. Ghose, Phil. Trans. R. Soc. London A, 310, 83, 1983.
7. H. F. W. Taylor, Proc. 10th Int. Symp. Reactivity of Solids, Dijon; Elsevier, Amsterdam, in press.
8. A. Bentur, R. L. Berger, J. H. Kung, N. B. Milestone and J. F. Young, J. Amer. Ceram. Soc., 62, 362, 1979.
9. J. P. Boyer, MSc thesis, Univ. of Illinois, 1976.
10. V. Lach and J. Bures, 6th International Congress on Cement Chemistry, Vol.II, 73, Moscow, 1974.
11. K. L. Scrivener, K. D. Baldie, Y. Halse and P. L. Pratt, Mat. Res. Soc. Symp. Proc., 42, 39, 1985.

J.J. Kollek, S.P. Varma, C. Zaris Blue Circle Industries PLC, Research Division Greenhithe, Kent 1

MEASUREMENT OF OH^- ION CONCENTRATIONS OF PORE FLUIDS AND EXPANSION DUE TO ALKALI-SILICA REACTION IN COMPOSITE CEMENT MORTARS

3.2

Mesure des Concentrations d'Ions OH^- intervenant dans les Fluides Interstitiels et Expansions due à la Reaction Alcali-Silice dans les Mortiers de Ciment Composé

SUMMARY: Pore fluid was extracted from mortars based on Portland and composite cements and their OH^- ion concentrations were determined.

Mortar bars for expansion studies were prepared according to a modified ASTM C227-81 procedure containing opal as the reactive aggregate.

The results indicate that additives of the types covered in this investigation release varying amounts of alkalis into the pore fluid dependent upon their type, their alkali content and their reactivity. Pfa's, in general, suppress the OH^- ion concentration but not always the damaging bar expansion even at 30% substitution level. Bfs's invariably contribute to the OH^- ion concentration but exhibit a beneficial effect on bar expansion at higher levels of substitution. Natural pozzolanas with a high alkali content contribute to the OH^- ion concentration to a level at which damaging bas expansion occurs even with low alkali Portland cements. Zeolitic natural pozzolana is an effective suppressant of alkalinity and damaging bar expansion.

Extraiu-se o fluido intersticial de argamassas à base de cimentos portland e de cimentos compostos, e foram determinadas suas concentrações de íons OH^-.

Foram preparados prismas de argamassa destinados aos estudos de expansão, de acordo com o método ASTM C227-81, e que continham opala como agregado reativo.

Os resultados indicam que os constituintes secundários dos tipos especificados nesta investigação liberam quantidades diferentes de álcalis no fluido intersticial, em função de seu tipo, de seu teor de álcali e de sua reatividade. Os c.v. em geral suprimem a concentração de íon OH^-, mas nem sempre anulam a expansão nociva do prisma, mesmo a um nível de substituição de 30%. As escórias de alto forno contribuem invariavelmente para a concentração de íons OH^-, mas apresentam um efeito favorável sobre a expansão do prisma a níveis mais elevados de substituição. As pozolanas naturais, com alto teor de álcali, contribuem para a concentração de íons OH^- até um nível em que a expansão nociva do prisma acontece mesmo com cimentos portland com baixo teor de álcali. A pozolana natural zeolítica se constitui em supressor eficaz da alcalinidade e da expansão nociva do prisma.

1. INTRODUCTION

Concern is felt about the damage to Portland cement concrete resulting from alkali-silica reaction. While the basic phenomena underlying this damaging reaction are now sufficiently well understood, practically acceptable solutions to the problem are not always easily attainable. One solution, which has considerable practical potential and a long-standing history of usage, is the partial replacement of cement by materials such as blast furnace slags (bfs), pulverised fuel ashes (pfa) and natural pozzolanas (np) in appropriate proportions. The wide appeal of this solution stems from the ready availability of these materials and their comparative cheapness.

More recently, however, doubt has emerged concerning the effectiveness of some of these materials in preventing the alkali silica reaction particularly in relation to their potential for the release of alkalis. Pfa's have been known to contain over 4.6% eq. Na_2O alkali, bfs's 1.8% and np's as high as 8.0%. As these materials hydrate, do the alkalis enter into the pore fluid thus raising the OH^- ion concentration or, as has been suggested, does the gel formed in such systems accommodate the additional alkali released?

The alkali level of additives is known to influence, if not fundamentally determine, their reactivity and hence influence their contribution to strength development. The user may have to choose between using a reactive, potentially damaging additive or selecting a less reactive material which will reduce the risk of alkali silica reaction occurring. He may want to reach a compromise, given the necessary information.

2. A BRIEF BACKGROUND

For simplicity the alkali silica reaction may be written using cement chemist's notation as follows:

$$N(K)H + S \longrightarrow N(K)\text{-}S\text{-}H$$

Three conditions must be satisfied:- there must be reactive silica, sufficient quantity of pore fluid and the pore fluid OH^- ion concentration must be above a certain threshold level. In a situation where reactive silica is present and moisture conditions are reasonably constant, the problem reduces largely to considerations of the OH^- ion concentration of the pore fluid only.

If cement replacement materials are used, which in their most part contain water insoluble alkalis only, the questions which arise are:-

1. Do they then act as straight diluents in proportion to their Portland cement replacements level in their effect on the pore fluid alkalinity?

2. Do they contribute to the alkalinity of the pore fluid as they enter pozzolanic or latent hydraulic reactions?

3. Do they contribute to the alkalinity of the the pore fluid in excess of that contributed by the Portland cement which they have replaced and thereby raise the probability of deleterious alkali silica reaction occurring?

Diamond[1], found that for their most part pfa's acted as inert diluents but recognised that they can vary considerably in availability of alkalis and in reactivity.

Glasser et al[2], found that partial replacement of a high alkali cement with low or high alkali pfa reduces pore fluid alkalinity while a low alkali cement with a high alkali pfa increases alkalinity.

Nixon et al[3], found that partial replacement of Portland cement with low alkali pfa was more effective in reducing deleterious concrete expansion than high alkali pfa, implying a differential effect by the two pfa's on the pore fluid.

The work described in this paper seeks to add quantitative information to the discussion of these problems, and thereby add to our knowledge concerning the most effective actions to minimise the risk of alkali silica reaction causing damage.

3. EXPERIMENTAL

The experimental work involved in this investigation comprised two types of test: pore fluid composition analysis and mortar bar expansion measurements using various ratios of cement to additive.

3.1 Materials

Three works-produced Portland cements were used as reference cements: high alkali cement (HC) 0.92% eq. Na_2O, low alkali cement (LC) 0.34% eq. Na_2O and medium alkali cement (MC) 0.68% eq. Na_2O. Their chemical analyses are given in Table 1.

Table 1 - Chemical analyses and some physical properties of Portland cements

Oxide, %	HC	LC	MC
SiO_2	20.2	19.8	19.9
IR	(0.91)	(0.50)	(0.73)
Al_2O_3	5.4	5.8	6.4
Fe_2O_3	3.4	3.4	2.2
Mn_2O_3	0.07	0.12	0.04
P_2O_5	0.10		0.23
TiO_2	0.27		0.30
CaO	63.9	63.8	64.9
MgO	1.4	3.0	1.2
SO_3	3.0	2.3	2.9
LOI	1.4	0.8	1.5
K_2O	0.93	0.43	0.51
Na_2O	0.31	0.06	0.34
Na_2O eq.	(0.92)	(0.34)	(0.68)
C_3S	52.0	54.0	53.3
C_2S	18.7	16.1	16.9
C_3A	8.6	9.6	13.3
C_4AF	10.4	10.4	6.7
Free lime	1.2	1.2	1.3
Specific surface m^2/kg	448	375	334
45 μm residue	9.6	13.6	15.6
Apparent particle density kg/m^3	3130	3180	3130

IR - Insoluble residue
LOI - Loss on ignition
Values in parentheses are not included in total

Two pfa's were used of widely different alkali contents: a high alkali pfa (H-pfa) 3.17% eq. Na_2O and a low alkali pfa (L-pfa) 0.97% eq. Na_2O. Their chemical and physical characteristics are given in Table 2. In their physical properties the two pfa's were roughly equivalent although the high alkali ash had a higher glass content. The pfa's were used at cement replacement levels of 14%, 28%, 42% and 56%.

Table 2 Chemical analyses and some physical properties of pulverised fuel ashes and blast furnace slags

Oxide %	L-pfa	H-pfa	H-bfs	L-bfs	M-bfs
SiO_2	50.7	48.7	31.0	36.8	33.6
IR	(79.7)	(74.6)	(0.4)	(0.31)	(0.30)
Al_2O_3	31.5	26.7	16.0	11.2	13.4
Fe_2O_3	6.5	10.3	1.5	0.4	1.5
Mn_2O_3	0.07	0.07	0.83	0.83	0.85
P_2O_5	0.78	0.38	<0.01	0.02	0.01
TiO_2	1.3	0.97	1.0	0.99	0.54
CaO	2.7	2.5	36.3	40.0	40.4
MgO	1.3	1.7	11.0	7.7	8.3
SO_3	0.27	0.93	0.16	0.13	0.05)
S			1.1	0.97	0.82)
C	(2.7)	(2.3)			
LOI	3.4	3.2	0.4**	0.6**	0.4**
K_2O	1.2	3.6	0.65	0.47	0.52
Na_2O	0.18	0.80	0.56	0.35	0.33
Na_2O eq.	(0.97)	(3.17)	(0.99)	(0.66)	(0.67)
Cl	0.004	0.003	0.06	0.01	0.01
Specific surface m^2/kg	342	358	384	397	394
45 μm residue	7.3	5.3	2.1	6.2	6.5
Apparent particle density kg/m^3	2230	2380	2910	2920	2930
Crystallinity Index*	36	23	0	11	0
Hydraulic Index***			2.0	1.6	1.8

IR - Insoluble residue
LOI - Loss on ignition
Values in parentheses are not included in total.

* by X-ray diffraction
C.I.= $\frac{\text{Area under peaks} \times 100}{\text{Total area}}$ in range 12-38° 2θ, Cu K_α radiation
** in nitrogen
*** Hydraulic Index = $\frac{C + M + A}{S}$

Three bfs's were used having a range of reactivity and alkali content. High reactivity granulated bfs (H-bfs), 0.99% eq. Na_2O, medium reactivity granulated bfs (M-bfs), 0.67% eq. Na_2O and low reactivity pelletised bfs (L-bfs), 0.66% eq. Na_2O. Their chemical and physical characteristics are given in Table 2. The slags were ground to nominally the same surface area and used at cement replacement levels of 23%, 46%, 69% and 92%.

Four np's were used which were selected on the basis of their geographic diversity of source and considerable usage rather than specifically different chemical and physical properties: IP,8.07% eq.Na_2O, CP, 6.77% eq. Na_2O, MP 6.92% eq.Na_2O and MPZ, 1.80% eq. Na_2O. Their chemical analyses and some physical properties are given in Table 3. Mineralogically, MPZ is a zeolite while the other three np's are mainly of glass composition. The np's were used at cement replacements levels of 14%, 28% and 42%.

3.2 Pore fluid composition analysis.

The apparatus used for pore fluid extraction was similar to that used by Longuet et al[4], Barneyback and Diamond[5] and elsewhere and need not be described here. The mortar specimens were prepared using mix proportions of cement:sand:

Table 3 Chemical analyses and some physical properties of natural pozzolanas

Oxide %	MPZ	CP	IP	MP
SiO_2	68.9	69.8	52.3	73.0
IR	(44.9)	(87.9)	(67.7)	(87.4)
Al_2O_3	12.3	13.7	16.8	11.9
Fe_2O_3	1.5	1.8	4.5	2.1
Mn_2O_3	0.06	0.09	0.17	0.05
P_2O_5	0.02	0.08	0.18	0.01
TiO_2	0.16	0.23	0.46	0.14
CaO	4.0	1.8	9.3	1.0
MgO	1.0	0.6	1.8	0.2
SO_3	0.05	0.12	0.33	0.11
LOI	9.5	3.9	4.2	3.2
K_2O	1.6	3.9	7.4	4.3
Na_2O	0.75	4.2	3.2	4.1
Na_2O eq.	(1.80)	(6.77)	(8.07)	(6.92)
Cl	0.004	0.006	0.055	0.004
Specific surface m^2/kg	1600	550	618	570
45 μm residue	5.8	7.2	6.8	7.6
Apparent particle density kg/m^3	2200	2400	2580	2410
Crystallinity Index*	100	25	57	28

IR - Insoluble residue
LOI - Loss on ignition
Values in parentheses are not included in total.

* by X-ray diffraction
C.I. = $\frac{\text{Area under peaks} \times 100}{\text{Total area}}$ in range 12-38° 2θ, Cu K_α radiation

water = 1:2.25:0.5 and were stored in air-tight containers at 20°C until testing at ages varying from 3 to 365 days. At test, the specimens were subjected to a load of 2000 kN which corresponds to a pressure of 640 MN m^{-2}. The pore fluid was collected and analysed for Na^+, K^+ and Ca^{2+} concentration by atomic absorption spectrometry and OH^- ion concentration by volumetric analyses against 0.1M HCl using methyl red as indicator.

3.3 Mortar bar expansion tests

The method used was that specified in ASTM C227 with the only difference that the storage temperature for the bars was fixed at 20°C. The reactive silica was Beltane opal crushed and screened to lie in the size range 150-300 microns. The pessimum level of opal addition was determined from the following[6]:

$$\% \text{ opal} = \% \text{ water soluble alkalis}/0.067$$

and was used in all combinations of cement and additive. Apart from the control at zero level of opal addition, three additional levels, one lower and two higher than the calculated pessimum, were also used. Thus, five sets of bars (two bars in each set) were used for each mix comprising the various combinations of cement and additive. Expansions were monitored at regular intervals up to one year. Failure was recorded when the bar expansion exceeded 0.1%.

4. RESULTS AND DISCUSSION

The bar expansion data for the three Portland cements at various mix proportions with additives are given in Tables 4A, 4B and 4C. The maximum OH^- ion concentration and the pessimum percentage of opal are also given.

Since the Na^+, K^+ and Ca^{2+} ion concentrations are not central to the objectives of this paper, only

OH^- ion concentrations of the pore fluid are presented in figures 1,2,2A,3,3A,4 and 4A.

The pore fluid OH^- ion concentration of the pure cements as a function of hydration time is shown in figure 1. Maxima were reached within 10 to 28 days. Thereafter, the concentration decreased slowly hinting at alkali re-absorption by the hydration products. MC cement which has a higher proportion of water insoluble or combined alkalis than the other two cements released the OH^- ions less rapidly.

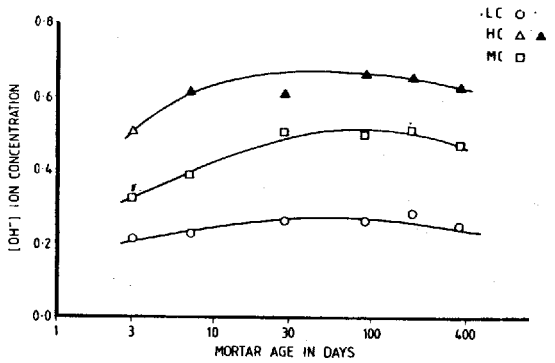

Fig.1 OH^- ion concentration of pore fluid in mortar made from three works Portland cements. Corresponding expansion bar test results superimposed; failure indicated in bold characters.

A similar pattern of change in the OH^- ion concentration with time as for the pure cements was observed for the composite cements but the results are not presented in this paper. The OH^- ion concentration at 180 days hydration has been arbitrarily selected for comparison purposes between the range of additives, their level of addition and expansion failure of mortar bars.

The effects of partial replacement of high alkali cement HC and low alkali cement LC by the two pfa's is given in figure 2. It is evident that in the case of the high alkali cement HC, both pfa's had a marked suppressing effect on the pore fluid alkalinity, the L-pfa, not surprisingly, having a stronger suppressive effect than the H-pfa. Evidently, the pfa's are not only acting as diluents but, moreover, as positive suppressants of alkalinity.

However, despite the large reduction in alkalinity the corresponding mortar bars have failed up to the 42% H-pfa and 28% L-pfa replacement levels respectively.

The effect of partial replacement of low alkali cement LC with pfa is distinctly different from that of the high alkali cement HC replacement. With the low alkali cement LC the H-pfa contributes to the alkalinity although not to the threshold level of mortar bar failure at 180 days.

The results in figure 2A, which illustrate the effect of the partial replacement of medium alkali cement MC by the two pfa's, do not fall into the neat correlation of OH^- ion concentration and expansion bar failures established in figure 2. Here the expansion bars based on the pure MC cement remained sound while those based on partial replacement with L-pfa have failed up to the 14% level and those with H-pfa have failed up to the 42% level and this despite a marked reduction in the recorded OH^- ion concentration. Clearly, some other factor is interacting. This does, however, illustrate the importance of tests in establishing the innocuousness of some combinations of cement and pfa.

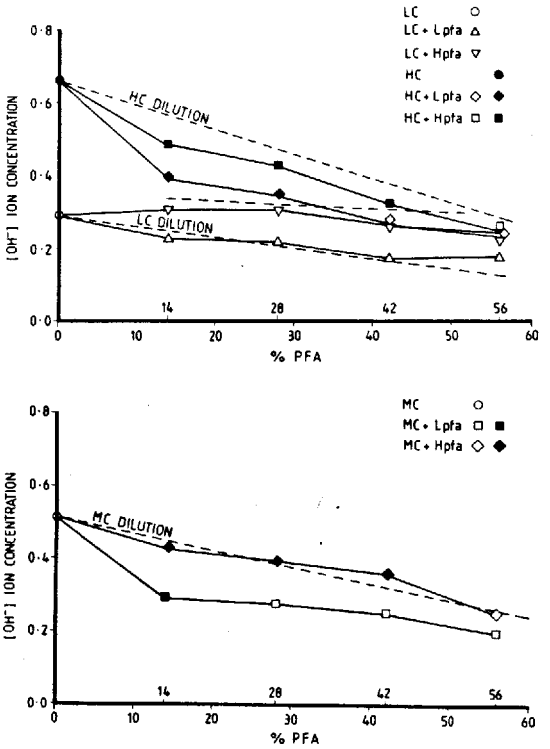

Figs 2 and 2A OH^- ion concentration of pore fluid in mortar made from three works Portland cements with progressive substitution by two pfa's. Corresponding expansion bar test results superimposed; failure indicated in bold characters.

The combined results in figures 2 and 2A suggest that, provided the pore fluid OH^- ion concentration of pfa extended cements is less than 0.3M at 180 days, a deleterious expansion with Beltane opal is unlikely to occur.

In contrast to pfa, bfs was found to be invariably a net contributor to the alkalinity of pore fluid in all combinations of Portland cement and bfs. The extent of its contribution is not only dependent on its own anhydrous alkali content but also on its reactivity as determined by its contribution to strength development. This is demonstrated by reference to M-bfs and L-bfs in Table 2 and figures 3 and 3A, indicating that they have virtually the same anhydrous alkali content but contribute significantly different pore fluid alkalinities. Also, M-bfs's contribution to the 28 day strength (not reproduced here) has greatly exceeded that of the L-bfs.

3.2

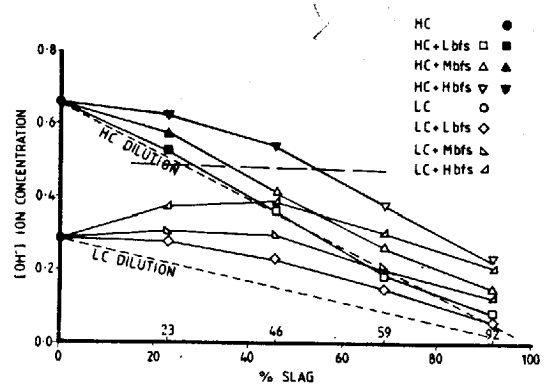

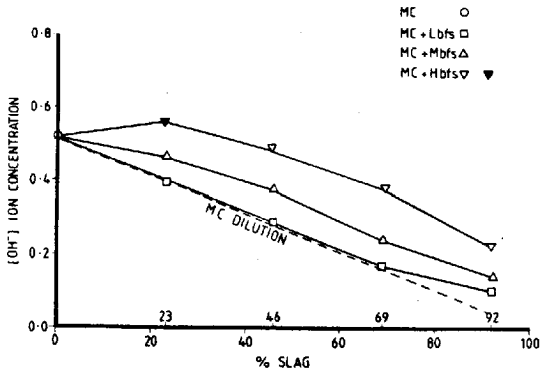

Figs 3 and 3A OH^- ion concentration of pore fluid in mortar made from three works Portland cements with progressive substitution by three bfs's. Corresponding expansion bar test results superimposed; failure indicated in bold characters.

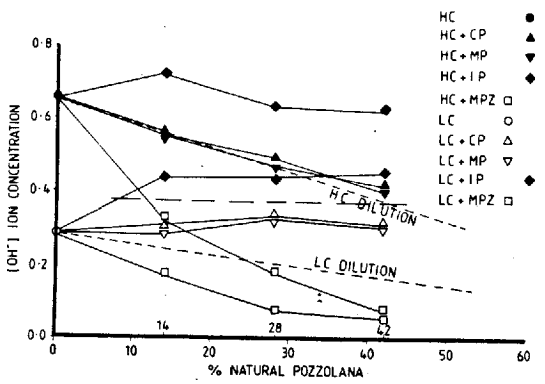

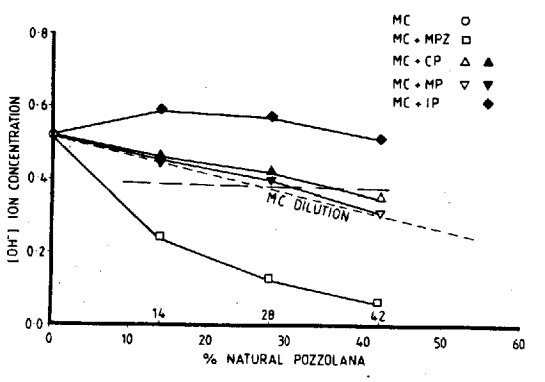

Figs 4 and 4A OH^- ion concentration of pore fluid in mortar made from three works Portland cement with progressive substitution by four natural pozzolanas. Corresponding expansion bar test results superimposed; failure indicated in bold characters.

A closer look at figure 3 reveals that at a 50% replacement of low alkali cement LC with H-bfs the contribution by the bfs to the total alkalinity is about twice that of the Portland cement component.

Figure 3A gives a vivid demonstration of the rôle which H-bfs can play where a substitution of 23% for medium alkali cement MC has resulted in a failure of the mortar bar whereas the pure MC cement mortar bar exhibited no failure.

The effect of partial replacement of Portland cement by four different natural pozzolans on the OH^- ion concentration is illustrated in figures 4 and 4A. The partial replacement of high and medium alkali cements HC, MC by natural pozzolana has an additive effect with IP, neutral effect with CP and MP and a negative effect with MPZ on the pore fluid alkalinity. In combination with low alkali cement LC, however, the first three pozzolanas increase the OH^- concentration whereas MPZ decreases it.

The very strong alkalinity suppressive effect of MPZ, is not only interesting but could have significant practical implications. It may also be relevant to note that its contribution to strength development is considerable.

The results obtained on mortar bars made from natural pozzolana containing cements are given in Tables 4A, 4B and 4C and are superimposed on figures 4 and 4A. It will be seen that the correlation of bar failures with OH^- ion concentration is very good and that the threshold level separating the failed from the sound bars lies at 0.4M.

It is important to note that three of the four natural pozzolanas in this investigation have no alleviating effect on the deleterious alkali-Beltane opal reaction, not even at high substitution levels. This may have far-reaching practical implications in regions where reactive aggregates occur. However, it must be emphasised that reactive aggregates of the Beltane opal type are unlikely to be encountered in many parts of the world.

5. CONCLUSIONS

5.1 The technique of pore fluid extraction and analysis is useful in the study of the effect of cement composition upon the potential for alkali silica reaction.

5.2 Pfa's on the whole have a suppressive effect on the OH^- ion concentration of the pore fluid of

high alkali Portland cement but high alkali pfa's make a small positive contribution when combined with low alkali cement. Despite this suppressive effect on the OH^- ion concentration, the addition of even 30% of pfa may not be sufficient to eliminate the damaging alkali-silica reaction based on Beltane opal. An OH^- ion concentration of 0.3M appears to be a threshold for damaging reaction at 180 days with pfa composite cements.

5.3 Bfs's invariably contribute to the OH^- ion concentration of Portland cement. This contribution depends on the alkali content of the bfs and on its reactivity. The damaging effect of alkali-silica reaction can be effectively reduced at higher levels of cement substitution. An OH^- ion concentration of 0.5 M appears to be a threshold for damaging reaction at 180 days with bfs composite cements.

5.4 Natural pozzolanas with a high alkali content are ineffective suppressants of damaging alkali-silica reaction based on Beltane opal and can, in fact, raise the OH^- ion concentration of even a low alkali Portland cement to a level at which damaging reactions occur. A natural pozzolana of the zeolite type was found to be an effective suppressant of OH^- ion concentration and of damaging alkali-silica reaction. An OH^- ion concentration of 0.4 M appears to be the threshold for damaging reaction at 180 days with natural pozzolana composite cements.

REFERENCES

1. Diamond, S. "Effects of two Danish fly ashes on alkali contents or pore solutions of cement-flyash pastes" Cement and Concrete Research, Vol 11, No.3, pp 383-394 (1981).

2. Glasser, F.P. and Marr, J. "The effect of mineral additives on the composition of cement pore fluids" British Ceramic Society, Proceedings 35, pp 419-429, (1984).

3. Nixon, P.J. and Gaze M.E. "The Effectiveness of fly ashes and granulated blastfurnace slags in preventing aar" Proceedings of Conference: Alkalis in Concrete, Copenhagen June 1983.

4. Longuet, P., Burglen, L. and Zwewer, A. "La Phase Liquide du Ciment Hydrate" Revue des Materiaux, Vol 1, pp 35-41, (1973).

5. Barneyback, R.S. Jr. and Diamond, S."Expression and analysis of pore fluids from hardened cement pastes and mortars" Cement and Concrete Research, Vol 11, pp 279-285 (1981).

6. Hobbs, D.W. "Influence of pulverised fuel ash and granulated blastfurnace slag upon expansion caused by the alkali-silica reaction" Magazine of Concrete Research, Vol 34, No. 119, pp 83-94, (1982).

Table 4A Bar expansion data of composite high alkali cement

Mix Proportions	OH^- ion concentration M, max.	% opal pessimum	failure in time [days]										% expansion at 180 days
			7	14	28	42	56	70	90	120	180	365	
HC	.67	8.1	o	F									1.168
+14% L-pfa	.58	7.6	o	F									1.629
+28%	.40	6.6	o	o	F								1.310
+42%	.35	6.0	o	o	o	o	o	o	o	o	o	o	.012
+56%	.24	4.0	o	o	o	o	o	o	o	o	o	o	.017
+14% H-pfa	.61	7.9	o	F									2.146
+28%	.44	6.6	o	o	F								1.392
+42%	.40	6.0	o	o	F								1.195
+56%	.30	4.8	o	o	o	o	o	o	o	o	o	o	.018
+23% L-bfs	.56	6.9	o	o	F								1.700
+46%	.38	5.2	o	o	o	o	o	o	o	o	o	o	- .007
+69%	.21	3.0	o	o	o	o	o	o	o	o	o	o	- .028
+92%	.10	1.2	o	o	o	o	o	o	o	o	o	o	- .012
+23% M-bfs	.63	6.8	o	o	F								1.236
+46%	.49	5.1	o	o	o	o	o	o	o	o	o	o	- .016
+69%	.29	3.0	o	o	o	o	o	o	o	o	o	o	- .025
+92%	.15	1.3	o	o	o	o	o	o	o	o	o	o	- .024
+23% H-bfs	.69	5.5	o	o	F								1.722
+46%	.57	5.1	o	o	o	o	o	o	F				.900
+69%	.38	3.4	o	o	o	o	o	o	o	o	o	o	- .019
+92%	.22	2.1	o	o	o	o	o	o	o	o	o	o	- .032
+14% IP	.77	7.3	o	F									2.322
+28%	.71	6.5	o	o	F								2.120
+42%	.63	5.5	o	o	F								1.680
+14% CP	.63	7.3	o	F									2.481
+28%	.53	6.3	o	o	F								2.000
+42%	.46	5.1	o	o	o	o	o	F					0.479
+14% MP	.65	7.0	o	F									2.408
+28%	.52	6.1	o	o	F								1.476*
+42%	.47	4.9	o	o	o	F							.937*
+14% MPZ	.37	7.1	o	o	o	o	o	o	o	o	o	o	- .016
+28%	.22	6.4	o	o	o	o	o	o	o	o	o	o	- .006
+42%	.11	5.7	o	o	o	o	o	o	o	o	o	o	- .002

F = failure is indicated at expansion >0.1% * at 90 days

Table 4B Bar expansion data of composite low alkali cement

Mix Proportions	OH^- ion concentration M, max.	% opal pessimum	failure in time [days] 7	14	28	42	56	70	90	120	180	365	% expansion at 180 days
LC	.29	3.7	o	o	o	o	o	o	o	o	o	o	-.019
+14% L-pfa	.28	2.5	o	o	o	o	o	o	o	o	o	o	-.020
+28%	.24	2.6	o	o	o	o	o	o	o	o	o	o	-.015
+42%	.19	2.2	o	o	o	o	o	o	o	o	o	o	.007
+56%	.18	2.0	o	o	o	o	o	o	o	o	o	o	.003
+14% H-pfa	.35	3.4	o	o	o	o	o	o	o	o	o	o	-.013
+28%	.31	3.3	o	o	o	o	o	o	o	o	o	o	-.017
+42%	.26	3.0	o	o	o	o	o	o	o	o	o	o	-.016
+56%	.24	2.8	o	o	o	o	o	o	o	o	o	o	.016
+23% L-bfs	.30	3.0	o	o	o	o	o	o	o	o	o	o	-.025
+46%	.24	2.4	o	o	o	o	o	o	o	o	o	o	-.019
+69%	.16	1.4	o	o	o	o	o	o	o	o	o	o	-.031
+92%	.09	0.4	o	o	o	o	o	o	o	o	o	o	-.027
+23% M-bfs	.32	2.8	o	o	o	o	o	o	o	o	o	o	-.025
+46%	.30	2.1	o	o	o	o	o	o	o	o	o	o	-.032
+69%	.22	1.3	o	o	o	o	o	o	o	o	o	o	-.024
+92%	.14	0.5	o	o	o	o	o	o	o	o	o	o	-.041
+23% H-bfs	.43	2.6	o	o	o	o	o	o	o	o	o	o	-.028
+46%	.41	2.0	o	o	o	o	o	o	o	o	o	o	-.029
+69%	.33	1.3	o	o	o	o	o	o	o	o	o	o	-.034
+92%	.21	0.6	o	o	o	o	o	o	o	o	o	o	-.034
+14% IP	.44	3.3	o	o	o	o	o	o	o	F			.630
+28%	.59	3.4	o	o	o	o	o	F					1.273
+42%	.51	3.4	o	o	o	o	o	o	o	F			.826
+14% CP	.31	3.3	o	o	o	o	o	o	o	o	o	o	-.018
+28%	.40	2.8	o	o	o	o	o	o	o	o	o	o	-.015
+42%	.31	2.4	o	o	o	o	o	o	o	o	o	o	-.027
+14% MP	.31	3.0	o	o	o	o	o	o	o				-.012*
+28%	.40	2.4	o	o	o	o	o	o	o				-.014*
+42%	.34	2.0	o	o	o	o	o	o	o				-.019*
+14% MPZ	.19	1.2	o	o	o	o	o	o	o	o	o	o	-.032
+28%	.12	1.9	o	o	o	o	o	o	o	o	o	o	-.002
+42%	.07	2.4	o	o	o	o	o	o	o	o	o	o	-.007

F = failure is indicated at expansion >0.1% * at 90 days

Table 4C Bar expansion data of composite medium alkali cement

Mix Proportions	OH^- ion concentration M, max.	% opal pessimum	failure in time [days] 7	14	28	42	56	70	90	120	180	365	% expansion at 180 days
MC	.52	4.5	o	o	o	o	o	o	o	o	o	o	-.011
+14% L-pfa	.47	4.3	o	o	o	o	o	F					.812
+28%	.37	3.6	o	o	o	o	o	o	o	o	o	o	-.013
+42%	.29	3.3	o	o	o	o	o	o	o	o	o	o	.009
+56%	.22	3.1	o	o	o	o	o	o	o	o	o	o	.017
+14% H-pfa	.49	4.3	o	o	o	o	F						1.503
+28%	.43	4.2	o	o	o	o	F						1.126
+42%	.37	3.7	o	o	o	o	o	o	F				.642
+56%	.27	3.4	o	o	o	o	o	o	o	o	o	o	.014
+23% L-bfs	.42	3.1	o	o	o	o	o	o	o	o	o	o	-.028
+46%	.30	2.2	o	o	o	o	o	o	o	o	o	o	-.016
+69%	.18	0.5	o	o	o	o	o	o	o	o	o	o	-.014
+92%	.11	0.3	o	o	o	o	o	o	o	o	o	o	-.023
+23% M-bfs	.48	3.4	o	o	o	o	o	o	o	o	o	o	-.024
+46%	.38	2.4	o	o	o	o	o	o	o	o	o	o	-.021
+69%	.25	1.4	o	o	o	o	o	o	o	o	o	o	-.022
+92%	.15	0.6	o	o	o	o	o	o	o	o	o	o	-.039
+23% H-bfs	.64	3.4	o	o	o	o	o	F					1.034
+46%	.50	2.7	o	o	o	o	o	o	o	o	o	o	-.019
+69%	.40	1.7	o	o	o	o	o	o	o	o	o	o	-.033
+92%	.23	1.1	o	o	o	o	o	o	o	o	o	o	-.041
+14% IP	.67	4.2	o	o	o	F							1.841
+28%	.61	4.1	o	o	o	F							1.646
+42%	.56	3.7	o	o	o	o	F						1.240
+14% CP	.55	4.2	o	o	o	F							1.879
+28%	.45	3.7	o	o	o	o	o	o	F				.461
+42%	.38	3.0	o	o	o	o	o	o	o	o	o	o	-.018
+14% MP	.52	4.6	o	o	o	F							1.615
+28%	.44	3.8	o	o	o	o	F						.193*
+42%	.39	3.1	o	o	o	o	o	o	o				-.003*
+14% MPZ	.30	3.9	o	o	o	o	o	o	o	o	o	o	-.026
+28%	.14	3.6	o	o	o	o	o	o	o	o			.006*
+42%	.09	4.3	o	o	o	o	o	o	o	o			.009*

F = failure is indicated at expansion >0.1% * at 90 days

AUTEUR : J.P. BOMBLED (C.E.R.I.L.H. - PARIS/FRANCE)

SUJET : **Rhéologie du béton frais : Influence de l'ajout de fillers aux ciments.**

Rheology of fresh concrete : Influence of filler addition in the cements.

3.2

RESUME

Les principales composantes de la maniabilité des bétons frais sont la cohésion et la viscosité de la pâte interstitielle formée par l'eau et les éléments les plus fins du ciment et par le filler; celle-ci joue un rôle lubrifiant à l'égard du frottement interne résultant de l'enchevêtrement des granulats les plus gros. La cohésion est non seulement liée à la finesse (où les fillers, de grande broyabilité jouent un rôle), mais aussi au degré de floculation de la pâte interstitielle lequel peut être modifié par les éléments rapidement solubles ou des adjuvants.

La présence des fillers joue par conséquent par leur action sur la cohésion et sur le pouvoir lubrifiant, surtout par la géométrie des grains (dimension, forme, état de surface). Toutes choses égales, l'influence des fillers est surtout liée à la nature de la roche dont ils sont issus, à sa broyabilité et à la présence éventuelle de matériaux phyliteux (argiles) ainsi évidemment qu'à leur teneur dans les ciments.

Quand leur action est sensible, elle va toujours dans le sens d'une amélioration de la cohésion, donc de la stabilité des bétons frais (lutte contre ressuage et ségrégations) et généralement une meilleure lubrification; l'influence sera d'ailleurs d'autant plus sensible qu'il pourra y avoir dans la granulométrie du béton un certain déficit en éléments fins ou ultra fins (dosage en ciment trop faible, mouture grossière du liant,...). D'une façon générale, l'exigence en eau des bétons de ciments fillérisés, à caractéristiques rhéologiques égales, n'est pas différente de celle des ciments Portland fabriqués avec le même clinker.

Un autre point assez important est le rôle des conditions de broyage, cobroyage ou broyage séparé (nous avons donné une méthode d'analyse granulométrique ou de calcul des aires massiques particulières des composants de mélanges cobroyés) : Les différences sont évidemment fonction de l'écart des broyabilités entre clinker et filler.

Enfin, en ce qui concerne la prise, les fillers calcaires peuvent participer aux réactions et, dans le cas des clinkers riches en C_3A et pour des grandes finesses de mouture, on peut observer un effet pseudo-accélérateur dû aux fillers. Par ailleurs, les ciments contenant des fillers calcaires se sont révélés plus sensibles au froid que les Portland de même origine.

Os principais componentes da maniabilidade dos concretos frescos são a coesão e a viscosidade da pasta intersticial, formada pela água e os elementos mais finos do cimento e pelo "filler"; este exerce um papel lubrificante em relação ao atrito interno resultante da acomodação dos agregados mais grossos. A coesão está ligada não somente à finura (na qual os "fillers", de grande facilidade de moagem, exercem um papel), mas também ao grau de floculação da pasta intersticial, a qual pode ser modificada por elementos rapidamente solúveis ou por adjuvantes.

Consequentemente, a presença dos "fillers" influi por sua ação sobre a coesão e o poder lubrificante, sobretudo pela geometria dos grãos (dimensão, forma, estado da superfície). A influência dos "fillers" está ligada sobretudo às rochas de que são originários, à sua aptidão de moagem e à eventual presença de materiais filitosos (argilas), assim como ao seu teor nos cimentos.

Quando sua ação é sensível, ela se manifesta sempre no sentido de uma melhora da coesão, portanto da estabilidade dos concretos frescos (combate à exsudação e (segregações) e geralmente uma lubrificação melhor; a influência será ainda mais sensível na medida em que houver na granulometria do concreto um certo déficit de elementos finos ou ultrafinos (dosagem muito fraca de cimento, moagem grossa do ligante...). De um modo geral, a necessidade de água dos concretos com cimentos "filerizados", com características reológicas iguais, não é diferente da dos cimentos portland fabricados com o mesmo clinquer.

Outro ponto bastante importante é o papel das condições de moagem, moagem simultânea ou moagem separada (damos um método de análise greanulométrica ou de cálculo das áreas de massa particulares dos componentes de moagens simultâneas): as diferenças evidentemente são função da diversidade de aptidões de moagem entre clinquer e "filler".

Por fim, no que diz respeito à pega, os "fillers" calcários podem participar das reações e, no caso de clínqueres ricos em C_3A e no de grandes finuras de moagem, pode-se observar um efeito pseudo-acelerador devido aos "fillers". Além disso, os cimentos contendo "fillers" calcários se mostraram mais sensíveis ao frio que os portand de mesma origem.

1. INTRODUCTION

1.1. POSITION DU PROBLEME

Un des moyens efficaces pour réduire le coût énergétique dans la fabrication des ciments a été le plus souvent de lui incorporer des ajouts en profitant généralement pour valoriser des sous produits ou des déchets industriels (laitier, cendres, ...).

Par ailleurs, les normes Françaises actuelles (et sans doute bientôt au niveau Européen) ont prévu la possibilité de comprendre parmi ces ajouts des fillers plus ou moins inertes; ce type de ciment s'est beaucoup développé ces dernières années en France.

Toutefois, l'apparition de ces "nouveaux" ciments a parfois fait craindre aux utilisateurs la détérioration de certaines caractéristiques parmi lesquelles l'exigence en eau ou la maniabilité des bétons frais.

Dans ces conditions, le laboratoire du CERILH a entrepris de nombreuses études dont certaines ont porté sur l'influence de la présence des fillers sur les propriétés rhéologiques des pâtes, mortiers et bétons frais : c'est la synthèse de ces résultats que nous donnerons ci-dessous :

1.2. ROLE ET PLACE DES FILLERS

Ajoutés aux composants des liants, les fillers peuvent jouer plusieurs rôles :

- Rôle de "remplissage" (origine du mot filler); c'est-à-dire complément de la courbe granulométrique déficitaire en éléments fins.

- Rôle de "colmatage" en bouchant les capillaires pour empêcher la percolation de l'eau (ce rôle est tenu par les hydrates dans le béton durci).

- Rôle rhéologique par leur action sur les propriétés de la pâte interstitielle interposée entre les granulats, c'est ce que nous verrons plus loin.

- Rôle actif éventuellement suivant sa nature, le filler peut intervenir dans l'hydratation (carbo-aluminates, pouzzolanicité des silices ultrafines, germes de cristallisation, points d'ancrage des hydrates, ...).

2. GENERALITES

2.1. RAPPEL DES CARACTERISTIQUES RHEOLOGIQUES ET DES COMPOSANTS DE LA MANIABILITE DES BETONS FRAIS

Le terme maniabilité recouvre des qualités souvent contradictoires telles que :

- L'aptitude à l'écoulement et au remplissage du moule avec le minimum d'énergie.

- L'aptitude au serrage pour atteindre la compacité maximale, gage des performances mécaniques et de la durabilité.

- L'aptitude à conserver l'homogénéité (lutte contre la sédimentation ou les ségrégations) sans laquelle aucune qualité ne peut être atteinte.

Les composantes de la maniabilité sont :

•(a) un élément statique lié à la résistance au cisaillement, elle même somme de la cohésion et de la part statique du frottement (Coulomb) dû à l'enchevêtrement des gros granulats.

•(b) Une composante dynamique, intervenant pendant l'écoulement, liée à la part dynamique du frottement lui même modifié par l'effet lubrifiant dû à la pâte interstitielle (Figure n° 1).

En associant la loi de Coulomb au critère de Bingham on aboutit pour la contrainte d'écoulement à une relation de la forme :

$$F = C + K(\eta)\,tg\varphi + \eta G \qquad (1)$$

Cohésion de la pâte — Frottement interne — Viscosité de la pâte interstitielle.

$k(\eta)$ tenant compte du pouvoir lubrifiant.

Ajoutons qu'une vibration énergique supprime localement la cohésion et atténue le frottement interne rendant le corps pseudo Newtonien.

Rappelons que l'on peut définir (Bombled) une plasticité intrinsèque de la pâte interstitielle par le rapport de ses deux coefficients rhéologiques.

$$\tau_i = \frac{f}{\eta} \quad (\text{en } s^{-1}) \qquad (2)$$

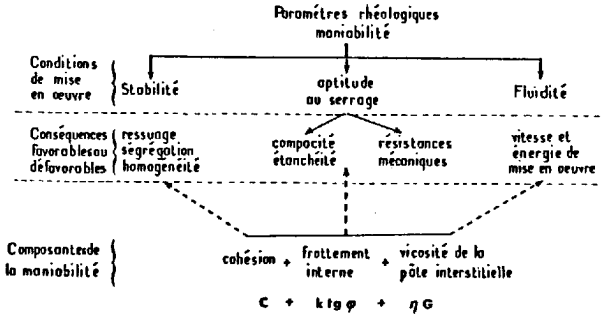

Fig. 1. Comportement du béton frais.

Même si elles ne sont pas rigoureuses, ces représentations ont l'intérêt de faire ressortir les éléments importants qui sont en résumé:

- La cohésion apportée par la pâte interstitielle liée à la granulométrie, à la floculation, à la teneur en eau (Figure n° 2).

- Le frottement interne dû essentiellement à l'enchevêtrement des gros granulats lequel "amplifie" la cohésion dans une certaine mesure.

- Le pouvoir lubrifiant et la viscosité de la pâte interstitielle liée aux dosages (eau et fines) et à la géométrie des grains .

En résumé, pour atténuer les frottements il faut non seulement assez de "graisse" (pâte interstitielle) mais aussi une fluidité adaptée de ce lubrifiant pour éviter le "grippage" (effet de squelette) : Un béton mal dosé en élément fin voit généralement ce défaut compensé (généralement mal) par une exigence en eau plus élevée.

En pratique, les fillers joueront essentiellement sur le couple cohésion/lubrification.

2.2. QUELQUES FACTEURS INFLUENTS

Que ce soit sur la cohésion ou sur le pouvoir lubrifiant, on peut réduire, en simplifiant, les principaux facteurs influents à trois, dont deux peuvent intéresser les fillers :

- La géométrie des grains (dimension, aire volumique, forme, état de surface, espaces inter-granulaires, nombre de points de contact...)

- La floculation (charges électriques, dissymétries, hétérogénéités, ions de surface et dissous) et ses conséquences rhéologiques (seuil de cisaillement, thixotropie).

- La quantité d'eau interstitielle et sa composition (ions, adjuvants, ...) qui conditionnent le comportement rhéologique de la pâte et du béton. (Figure n° 2).

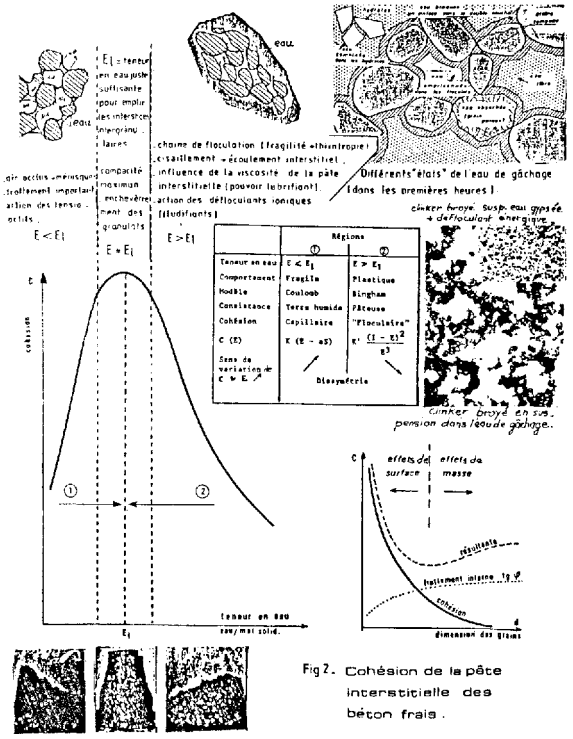

En résumé, cohésion ,viscosité et frottement interne sont les trois grandeurs qui peuvent, en simplifiant, caractériser le béton frais.

2.3. ELEMENTS CARACTERISTIQUES INFLUENTS DES FILLERS

D'une façon générale, les éléments qu'il peut être utile de connaître sur les fillers, ou sur leur roche d'origine et qui pourront, nous le verrons plus loin, intervenir et influer sur la rhéologie des bétons frais seront principalement :

- La broyabilité de la roche
- La porosité de la roche
- La surface BET du filler
- La teneur en silice
- La teneur en alumine et en argile
- La teneur en CO_3Ca (éventuellement en dolomie)
- La teneur en sels plus ou moins solubles (sulfates,alcalins,...)

Toutes ces grandeurs ne sont évidemment pas indépendantes (par ex. silice et broyabilité, alumine, alcalis, BET et matériaux argileux...etc).

2.3.1. Eléments des fillers influant sur la cohésion de la pâte et du béton

Ce sera le nombre de points de contact où s'éxercent des forces de liaison donc la dimension des grains (et la floculation) donc la teneur en éléments fins et par conséquent :

- La broyabilité et les conditions de broyage (mode, agglomérabilité ...)

- L'inclusion d'éléments très fins ou plus friables (matériaux argileux surtout).

2.3.2. Facteurs liés aux fillers pouvant intervenir sur le pouvoir lubrifiant de la pâte interstitielle

Formes et état de surface des grains (constitution minéralogique de la roche), cristalinité, angularité, rugosité, ...

2.3.3. Composants des fillers pouvant jouer sur la floculation

- Composition de la roche de base (silice, dolomie) impuretés (matières organiques) sels solubles (sulfates, sulfures,chlorures, ...)

- Présence d'argiles (décelée par exemple par la méthode au bleu de méthylène).

Pour illustrer ce qui précède la figure 3 (a) et (b), montre l'influence des argiles, vue par la teneur en Al_2O_3 et par la surface BET, sur la plasticité intrinsèque des pâtes de ciment.

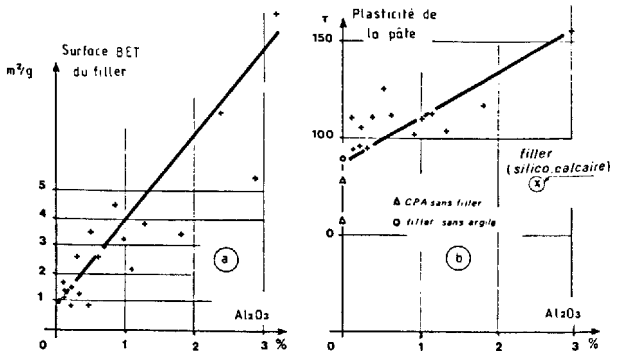

Fig 3. BET et plasticité de la pâte en fonction de l'Al_2O_3 (argiles) dans les fillers

2.3.4. Différentes actions des fillers sur les pâtes mortiers et bétons à l'état frais

Ces effets peuvent être d'ordre mécanique ou relever d'actions physico-chimiques :

- Action mécaniques : complément granulométrique pour certains modes de broyage, (meule, jet, ...); colmatages des canalicules et diminution du ressuage (figure n°11).

- Effets physico-chimiques par leur fraction argileuse et par les sels solubles,certains éléments peuvent participer à la floculation ou a contrario à la défloculation (alcalis); les calcaires peuvent participer à l'hydratation (carboaluminates) ou enfin pour les ultra fins jouer le rôle de colloïde protecteur en s'adsorbant sur les grains avec ses conséquences (vitesse de dissolution, de prise,...).

3. FILLERS ET PATE INTERSTITIELLE DES BETONS FRAIS

3.1. INFLUENCE DE LA BROYABILITE DE LA ROCHE DE BASE DU FILLER

Nous avons montré à maintes reprises l'influence prépondérante des éléments fins sur les propriétés rhéologiques des bétons frais; or toutes choses égales par ailleurs la teneur en éléments fins et ultra fins est avant tout liée à la broyabilité de la roche de base du filler.

L'étude en laboratoire d'un certain nombre de matières premières de caractéristiques minéralogiques assez variées a permis de tracer les histogrammes de la figure n° 4 et les courbes de la figure n° 5.

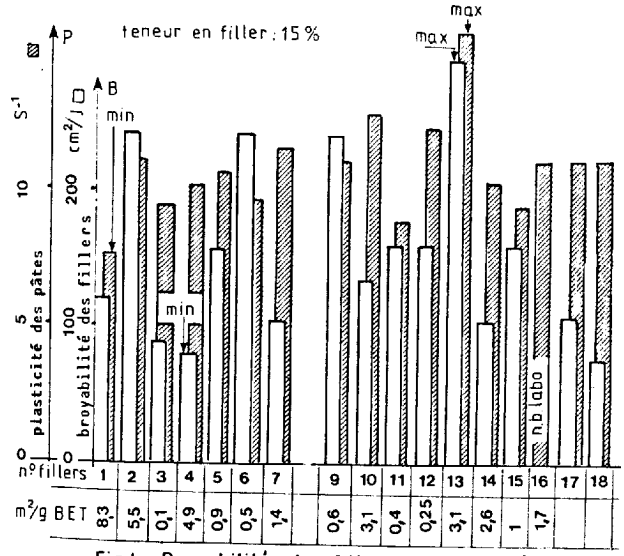

Fig 4 - Broyabilité des fillers et plasticité des pâtes de ciment fillérisé

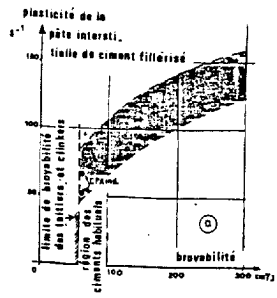

Fig 5 - Relation entre la broyabilité du filler et la plasticité des pâtes de CPA fillérisé.

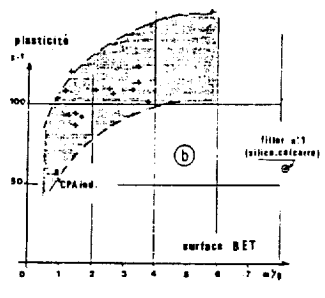

Fig 5 - Relation entre l'aire massique BET du filler broyé et la plasticité des pâtes du CPA fillérisé.

On peut noter que dans tous les cas, la présence de fillers accroît peu ou prou la plasticité comparée à celle du Portland pur témoin et l'on peut voir que cette plasticité de la pâte croît avec la broyabilité et avec la surface BET du filler broyé (ici peut intervenir aussi la présence de fractions argileuses): Broyabilité, porosité, surface BET et teneur en argile, voire en éléments floculants, sont les éléments qu'il faut considérer parmi d'autres dans le choix des fillers pour les ciments.

3.2. REMARQUES SUR LE BROYAGE ET LA GRANULOMETRIE

Dans la plupart des cas, le broyage du clinker et du filler se fait ensemble (cobroyage) et la finesse particulière de chacun des constituants est fonction de sa broyabilité et on peut avoir des granulométries très différentes si le clinker et la roche de base du filler ont des broyabilités très éloignées.

3.2.1. Granulométries particulières d'un clinker et d'un filler cobroyés

Nous avons donné dans une autre communication à ce Congrès, comment obtenir l'analyse granulométrique de matériaux cobroyés. La figure n°6 illustre la différence de granulométrie entre un clinker et un filler calcaire cobroyés.

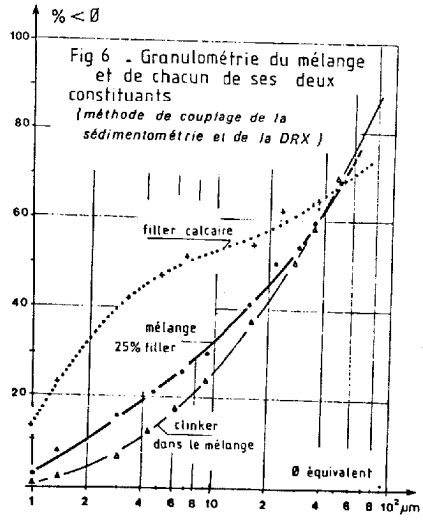

De même, en tenant compte du rapport des broyabilités, on peut calculer (formules de Bombled) les surfaces spécifiques de chaque composant; Le tableau I illustre les différences que l'on peut observer pour des teneurs variables en filler et une surface spécifique globale de 4 000 $cm^2 g^{-1}$.

Tableau I

$\frac{B_F}{B_C} = 2$	Clinker	0,90	0,85	0,80	0,75	0,70
	Filler	0,10	0,15	0,20	0,25	0,30
aires massiques en $cm^2 g^{-1}$	Clinker S_C	3 640	3 480	3 330	3 200	3 050
	Filler* S_F	7 280	6 960	6 640	6 400	6 150

*y compris gypse

On peut conclure que pour un calcaire très friable et un clinker très dur ($B_F / B_C > 4$) et pour des teneurs en filler ne dépassant pas 15% du ciment, nous trouverons pour S_F des valeurs voisines de 12000 $cm^2 g^{-1}$ et pour le clinker seulement 2 500 $cm^2 g^{-1}$, ce qui peut avoir des répercutions non seulement sur la plasticité mais aussi sur la réactivité.

3.3. REMARQUES SUR LE POTENTIEL ELECTRONEGATIF ET LA FLOCULATION

Le C_3A et la chaux sont électro-positifs, le C_3S, les fillers siliceux et calcaires sont plus ou moins électro-négatifs : plus le potentiel est élevé, plus on tend vers un état de dispersion et inversement lorsqu'il tend vers zéro (figure 7).

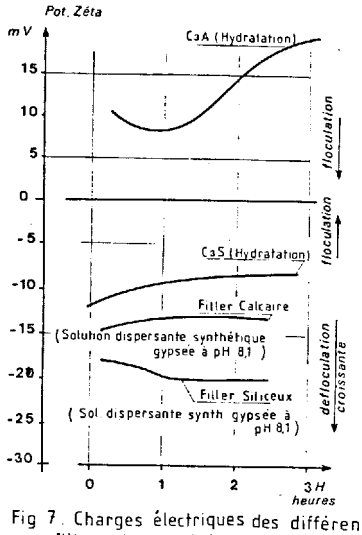

Fig 7. Charges électriques des différents fillers et des minéraux du clinker

Les conditions de broyage, séparé ou simultané, qui comme on l'a vu, jouent sur la finesse particulière semblent peu influer sur le taux de floculation : celui-ci est un peu plus faible pour les ciments fillérisés que pour les Portland.

4. ETUDE DE LA PATE INTERSTITIELLE DES BETONS DE CIMENTS FILLERISES

- Cohésion et seuil de cisaillement.

L'étude de la cohésion et du seuil de cisaillement des pâtes de ciment fillérisés comparées à celle des pâtes de ciment Portland pures (fabriquées avec le même clinker) montre qu'il y a généralement peu de différence, du moins tant que la teneur en filler reste inférieure à 10 ou 15 %.

Il y a généralement plus de différences entre le Portland de même classe mais d'usines différentes qu'entre le Portland et les ciments contenant des fillers de la même usine.

La figure n° 8 schématise le sens de la variation de cohésion et du seuil de cisaillement quand varient différents facteurs liés aux fillers.

- Pouvoir lubrifiant.

De même, pour la viscosité plastique et le pouvoir lubrifiant (figure n° 9) où influe beaucoup la finesse et les éléments ultra-fins, (figure n° 10).

Les petits grains de fillers peuvent venir s'interposer entre les grains plus gros et plus rugueux du clinker et modifier la viscosité de la pâte qui elle même fait effet de "graissage" quand elle vient s'interposer entre les granulats au sein du béton, cette action lubrifiante est limitée (trop de graisse n'apporte plus rien);et aussi la viscosité doit se placer dans une fourchette optimale.

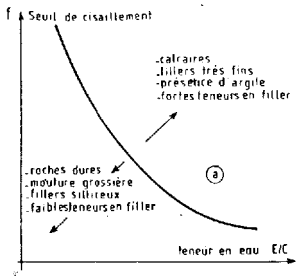

Fig 8. Sens de l'action des fillers sur le seuil de cisaillement

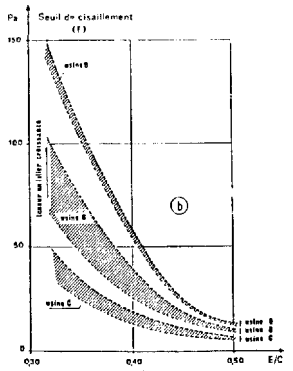

- Variation du seuil de cisaillement en fonction du rapport E/C

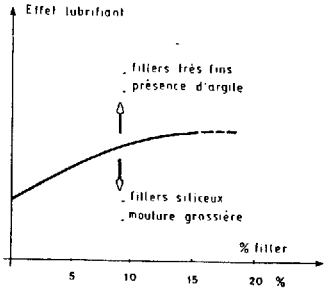

Fig 9. Effet lubrifiant (schéma)

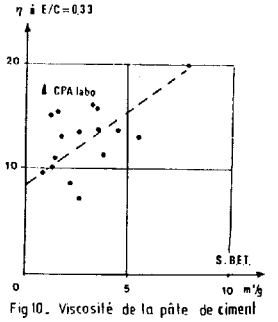

Fig 10. Viscosité de la pâte de ciment fillérisé et surface BET du filler

- Pouvoir de rétention d'eau et ressuage.

D'une façon générale, les pâtes de ciment fillérisé ont un ressuage (et une vitesse de ressuage) plus faible (figure n° 11) que celui des Portland.

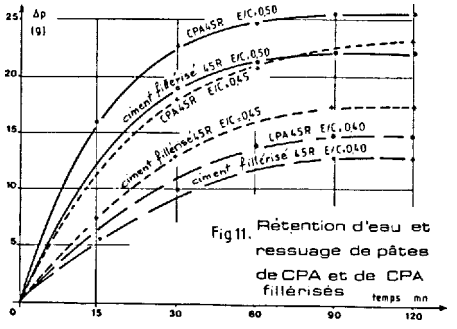

Fig 11. Rétention d'eau et ressuage de pâtes de CPA et de CPA fillérisés

- Action des fluidifiants.

En ce qui concerne les fluidifiants de synthèse, il n'apparaît pas de différence significative entre le Portland et le ciment fillérisé fabriqué avec le même clinker; le classement de l'efficacité des différents produits est le même.

Les figures 12 (a) et (b) montrent l'évolution du potentiel zéta et la baisse d'efficacité sur la défloculation pour le CPA et le ciment fillérisé de la même usine avec trois fluidifiants commerciaux différents.

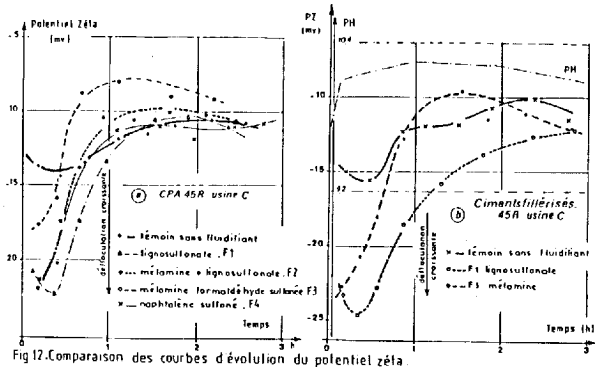

Fig 12. Comparaison des courbes d'évolution du potentiel zéta

4. INFLUENCE DES FILLERS SUR LE COMPORTEMENT RHEOLOGIQUE DES MORTIERS ET BETONS FRAIS

4.1. CAS DU MORTIER NORMAL

Le mortier AFNOR ayant un déficit de cohésion et une prédominance du frottement (masqués par d'énergiques moyens de serrage) l'apport d'éléments fins par les fillers ne peut que faire augmenter l'un et diminuer l'autre donc aller dans le sens favorable. En pratique, les différences observées sont généralement très faibles. Les courbes de principe de la figure 13 (a) et (b) illustrent les sens de variation généralement observés.

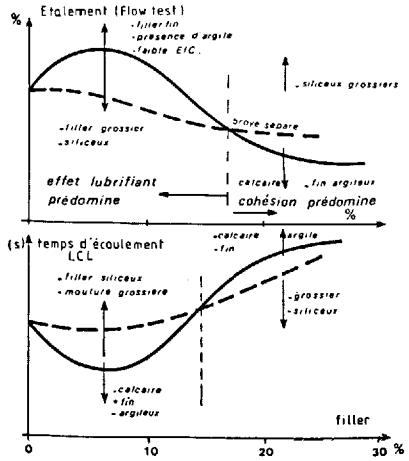

Fig 13. Tendance de l'action des fillers sur la plasticité du mortier normal.

4.2. ESSAIS SUR BETONS DE REFERENCE

Les fuseaux de la figure n° 14 relatifs à 10 ciments contenant de 10 à 25 % de fillers provenant des 6 usines (dont on donne aussi les résultats avec les Portland fabriqués avec les mêmes clinkers) montrent deux populations pour lesquelles, à part une exception, la présence de filler a été relativement peu sensible sur la maniabilité.

L'examen détaillé des courbes montre qu'il y a généralement une légère augmentation de la cohésion pour les bétons de ciments fillérisés par rapport à ceux de ciments Portland purs de la même usine; Le pouvoir lubrifiant est aussi le plus souvent amélioré (surtout

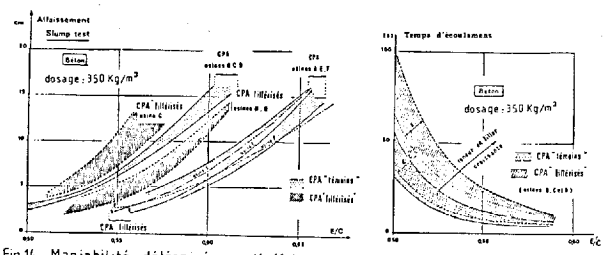

Fig 14. Maniabilité déterminée par l'affaissement (a) au cône d'Abrams (b) - Mesures au maniabilimètre LCL.

pour les bétons trop faiblement dosés en ciment) sauf pour les fillers silico-calcaires ou siliceux (angularité des grains).

Le schéma de la figure n° 15 fait ressortir quelques tendances de l'action limitée des fillers dans le cas du slump test.

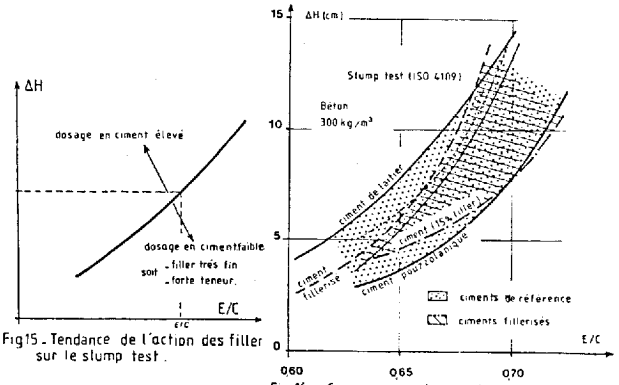

Fig 15. Tendance de l'action des fillers sur le slump test.

Fig 16. Comparaison de ciments fillérisés et de quelques ciments "de référence"

4.2.1. Exigence en eau à caractéristiques égales

L'expérience a montré que la réponse à cette question dépendait souvent des éléments considérés, par exemple:

- La réponse peut être différente entre pâte, mortier et béton car la cohésion, le frottement et le pouvoir lubrifiant y ont des incidences différentes.

- La réponse peut être différente pour un même matériau selon le choix des moyens de mesure de l'état rhéologique : étalement, écoulement, pénétration, essais statiques, dynamiques (chocs, vibrations, pressions, ...) car on y mesure pas la même grandeur, ou la conjugaison dans la même proportion, des mêmes grandeurs.

Ceci doit toujours inciter à quelque prudence dans nos conclusions.

Globalement, la présence du filler dans des proportions même élevées n'apparaît pas (sauf cas exceptionnel d'un filler argileux, intérêt de l'essai au bleu) susceptible de modifier l'exigence en eau des bétons comparée à d'autre liants (Fig. 16).

4.2.2. Remarques

- Présence de fillers et dosage en ciment du béton

Les fillers calcaires tendent à augmenter l'action des éléments fins, à accroître la cohésion et à améliorer la lubrification, ils se sont révélés d'autant plus utiles qu'il pourrait y avoir déficit en éléments ultra-fins et c'est la cas des dosages trop parcimonieux en ciment (qui ont

d'ailleurs d'autres inconvénients, notamment sur la durabilité) ou encore quand il s'agit des ciments broyés trop grossièrement et dans ce cas il y a toujours intérêt à des teneurs raisonnables en éléments très fins (broyabilité élevée, présence d'une fraction argileuse, ...).

- Fillers et évolution de la maniabilité

Les exemples de la figure n° 17, montrant pour des bétons au repos ou des bétons constamment malaxé (malaxage énergique) la position des ciments à 15 et 20 % de filler calcaire par rapport à celle des Portland provenant du même clinker, ne permettent de mettre en relief aucune action des fillers.

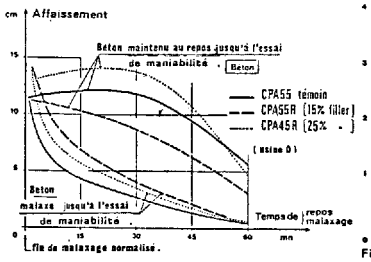

Fig 17 . Evolution de la maniabilité .

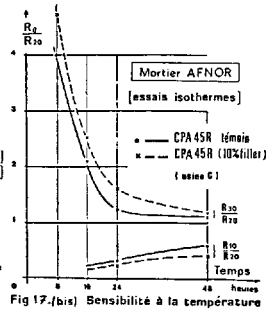

Fig 17 (bis) Sensibilité à la température aux jeunes âges .

- Présence des fillers et action des fluidifiants

Etant donnée la grande aire massique des fillers, surtout s'ils ont une grande broyabilité, il était à craindre qu'ils puissent annihiler l'action d'adjuvants en les adsorbant et en les bloquant : En pratique, le classement de l'action des différents adjuvants fluidifiants est le même pour les Portland et les ciments fillérisés du même clinker.

- Influence des conditions de broyage (séparé ou cobroyage)

Nous avons vu les différences notables qu'il peut y avoir sur la granulométrie et la surface spécifique du filler et du clinker cobroyés : en réalité ces ciments seront le reflet des broyabilités; ceci étant bien connu maintenant, l'expérience n'a pas montré de répercussions très grandes sur le plan rhéologique dans les cas habituels (teneur et broyabilité).

5. PRESENCE DE FILLER ET PRISE

Dans de nombreux cas (surtout pour les teneurs modérées $\leqslant$ 15 %) il y a peu de différence sur les temps de prise Vicat, mais parfois sur la partie des courbes qui précède. En revanche pour des clinkers très réactifs et des ciments finement moulus (Fig. n° 18 (a)) il y a un effet pseudo-accélérateur sans doute en liaison avec la formation de carbo-aluminates (figure n° 19).

Il en résulte que l'éventail des ciments fillérisés couvre pour les temps de prise celui des Portland (figure n° 18 (b)).

L'effet pseudo-accélérateur est encore visible sur les courbes des figures 20 (a) et (b) montrant l'influence des conditions de broyage sur la vitesse de prise.

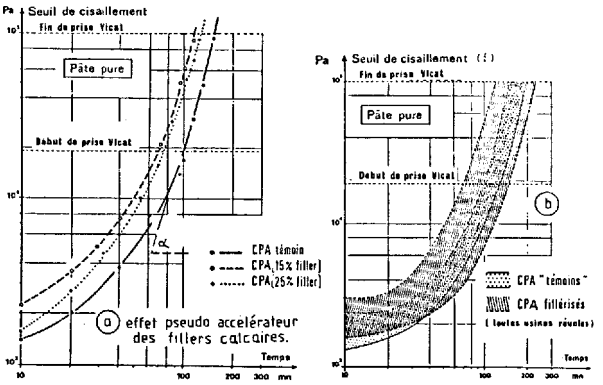

Fig 18 . Etude des pâtes au rhéographe Bombled.

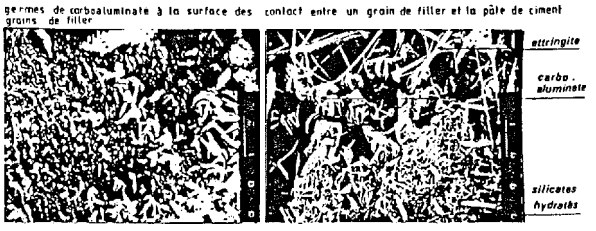

Fig 19 . Microstructure des pâtes de ciment. (formation de carboaluminates)

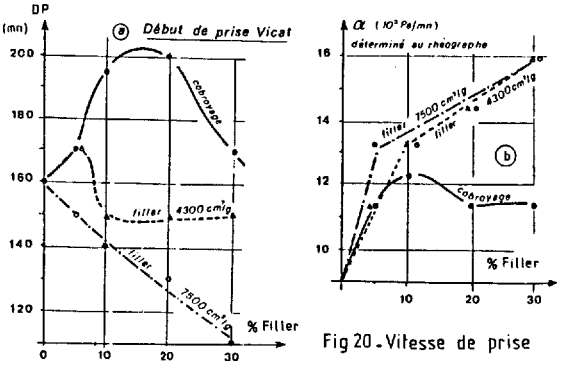

Fig 20 . Vitesse de prise

6. CONCLUSION

Globalement la présence de fillers (dans le domaine étudié $<$25 %) n'apporte pas de différences sensibles sur le comportement rhéologique des bétons frais, exigence en eau et action des fluidifiants sont inchangées. Quand il y a quelque influence cela va dans le sens d'une plus grande cohésion, d'une meilleure plasticité et parfois vers une pseudo-accélération de la prise.

P. GEGOUT, H.HORNAIN, B.THURET, B.MORTUREUX, J.VOLANT, M.REGOURD
CERILH - PARIS - FRANCE

TEXTURE ET PERFORMANCE DES CIMENTS FILLERISES
TEXTUREAND PERFORMANCE OF FILLER CEMENTS.

RESUME Une étude des variations texturales et mécaniques a été menée sur des pâtes pures et des mortiers de CPA et de CPJ - L'influence de la nature du clinker et de la nature, de la granulométrie et de la quantité de l'ajout est étudiée en fonction du temps.

Les distributions poreuses des pâtes des ciments fillérisés reproduisent avec un décalage d'échéance les distributions des pâtes de CPA. La résistance en compression est proportionnelle au carré de la diminution de porosité, et la relation est indépendante de la nature et de la quantité d'ajout. Cependant, et plus particulièrement aux courtes échéances, les cinétiques de développement des résistances sont très influencées par la nature du clinker composant le ciment.

L'étude des variations de résistance en compression en fonction du module d'élasticité dynamique longitudinal montre que la relation entre les deux paramètres dépend également de la nature du ciment. La présence d'un ajout quelconque modifie la réponse initiale obtenue et à résistance égale, le module d'élasticité du matériau augmente avec la quantité et la dimension des grains de l'ajout.

En ce qui concerne le filler calcaire, l'étude au MEB et en DRX de ces grains met en évidence des liaisons superficielles de ceux-ci avec les C-S-H et $Ca(OH)_2$. Pour les fortes teneurs en filler, on note un effet accélérateur sur l'hydratation de C_3A et C_3S, associée à une consommation partielle du filler. Simultanément, on constate la formation de carboaluminate de calcium et un accroissement relatif du taux de $Ca(OH)_2$.

Realizou-se um estudo das variações de textura e mecânicas, com emprego de pastas puras e argamassas de CPA e CPJ. Em função do tempo, estudou-se a influência da natureza do clínquer, e da natureza, granulometria e quantidade de aditivo.

As distribuições porosas das pastas de cimentos filerizados reproduzem, com uma defasagem de limite, as distribuições das pastas de CPA. A resistência à compressão é proporcional ao quadrado da diminuição da porosidade, e a relação independe da natureza e da quantidade de aditivo. Entretanto, e mais particularmente com limites exíguos, as cinéticas de desenvolvimento das resistências são muito influenciadas pela natureza do clínquer componente do cimento.

O estudo das variações da resistência à compressão, em função do módulo da elasticidade dinâmico longitudinal, mostra que a relação entre os dois parâmetros depende igualmente da natureza do cimento. A presença de qualquer aditivo modifica a resposta inicial obtida e, com resistência igual, o módulo de elasticidade do material aumenta com a quantidade e a dimensão dos grãos do aditivo.

Com relação ao "filler" calcário, o estudo com MEB e DRX destes grãos põe em evidência as ligações superficiais destes com os C-S-H e $Ca(OH)_2$. Com teores elevados de "filler", nota-se um efeito acelerador sobre a hidratação do C_3A e do C_3S, associado a um consumo parcial do "filler". Simultaneamente se constata a formação de carboaluminato de cálcio e um crescimento relativo do teor de $Ca(OH)_2$.

1. INTRODUCTION

L'intérêt économique et technique des ciments à ajouts n'est plus à démontrer. La raréfaction des constituants traditionnels (cendres, laitiers) mais aussi la possibilité d'atteindre de bonnes performances mécaniques avec des fillers, et surtout des fillers calcaires aisément disponibles justifie leur utilisation croissante.

Les travaux effectués jusqu'ici sur les ciments fillérisés ont essentiellement porté sur la maîtrise et l'amélioration des caractéristiques rhéologiques et des résistances effectives.

L'objet de la présente étude, effectuée sur des liants expérimentaux, est de mettre en évidence les modifications apportées par les fillers à un ensemble plus large de propriétés des matériaux durcis et de les relier aux caractéristiques de leurs textures.

2. CONDITIONS EXPERIMENTALES

Cette étude a été effectuée sur deux clinkers et deux fillers calcaires. Les compositions minéralogiques des clinkers diffèrent essentiellement par les teneurs en C_3A et C_2S (tableau 1). Le clinker riche en C_3A est référencé n°1.

Les fillers calcaires ont une teneur en $CaCO_3$ supérieure à 98%. Il s'agit d'un marbre (noté M) et d'une craie (notée C) broyés chacun à deux finesses différentes. L'éventail de finesses ainsi obtenu s'étend de 1000 à 12000 cm^2/g. (Fig.1). Un filler siliceux (quartz noté Q) a été utilisé comme ajout témoin. Sa finesse est de 3700 cm^2/g.

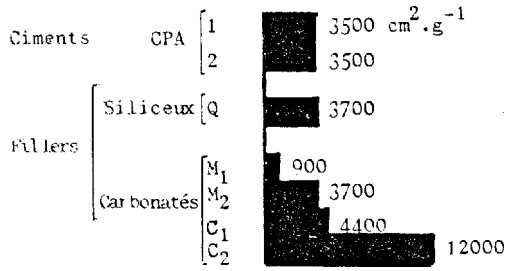

Fig.1 - Surface spécifique des composants

phase / clinker	C_3S	C_2S	C_3A	C_4AF	CaO libre
1	58	20	11,5	7	1,5
2	60	27	2	9,5	

Tableau 1 - Composition des clinkers (% en poids) Analyse quantitative par diffraction des rayons X

A partir des produits broyés séparément, ont été préparés deux CPA et des mélanges CPA-filler, les proportions de ce dernier variant de 15 à 60% .

Des éprouvettes de pâte pure ou de mortier ont été confectionnées selon la norme NF.P.15-401; les rapports pondéraux e/c étaient 0,3 pour les pâtes et 0,5 pour les mortiers. Quelques pâtes ont été gâchées à e/c = 0,43 et 0.35.

Après conservation dans l'eau à 20°C, le module d'Young est mesuré sur 9 éprouvettes 4 x 4 x 16 cm à partir des fréquences de résonance en flexion. Le prisme de valeur médiane est utilisé pour les examens physicochimiques de texture. La résistance mécanique en compression est déterminée sur les 8 autres.

Les valeurs des modules et résistances présentées plus loin sont donc les moyennes de 8 et 16 déterminations, respectivement.

Le sigle C.P.E.J. sera employé dans ce qui suit pour distinguer les liants élaborés pour cette étude des C.P.J industriels normalisés (E = expérimental).

3. EVOLUTION COMPAREE DES RESISTANCES EN COMPRESSION DES CPEJ AUX FILLERS

Soient Ro et Re les résistances en compression respectives du CPA et du CPEJ. Les figures 2 et 3 représentent l'évolution au cours du temps du rapport Re/Ro pour la série 1 (CPEJ à base de CPA 1) et la série 2 (CPEJ à base de CPA 2).

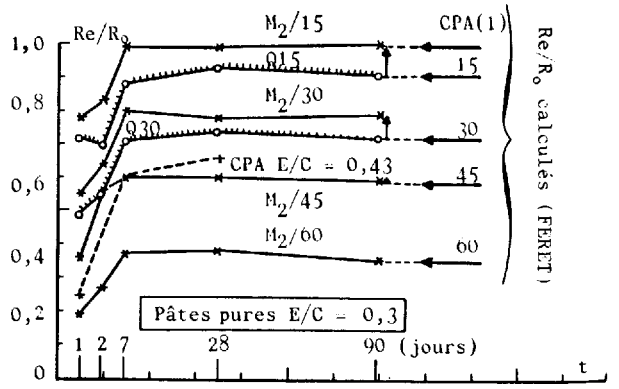

Fig.2 - Evolution du rapport R_e/R_o pour la série 1

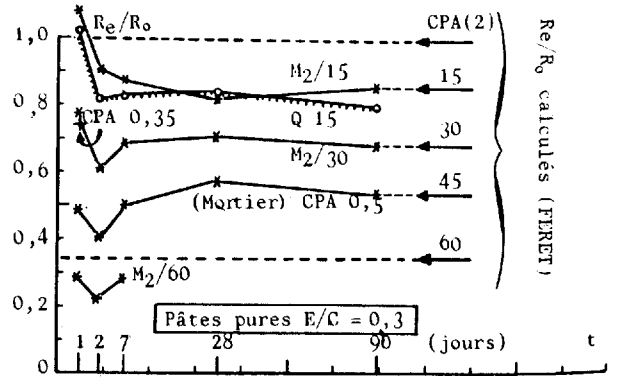

Fig.3 - Evolution du rapport R_e/R_o pour la série 2

On remarque sur les courbes des figures 2 et 3, deux parties bien distinctes de part et d'autre de l'échéance à 7 jours.

Après 7 jours : le rapport $R_e R_o$ s'établit à une valeur constante. Pour la série 1, ce rapport est légèrement supérieur à celui obtenu lorsque Re est calculé avec la relation de FERET. L'écart diminue linéairement avec la teneur en filler pour s'annuler à 60% d'ajout. Les courbes obtenues avec différents fillers montrent que la granulométrie et la composition du filler interviennent peu.

Pour la série 2, les rapports R_e/R_o se confondent avec ceux calculés à partir de la relation de FERET. Les fillers calcaires semblent avoir pour cette dernière série, le même effet qu'une charge inactive, alors que pour la série 1, ils contribuent légèrement aux résistances.

Dans tous les cas cependant, et indépendemment du pourcentage de filler, la résistance en compression reste essentiellement liée au rapport eau/CPA dans le ciment composé (loi de FERET), le filler se comportant en partie comme le sable d'un mortier.

Avant 7 jours : Pour la série 1, le rapport Re/Ro est nettement inférieur au palier obtenu à partir de 7 jours. Les CPEJ aux fillers, calcaires et quartz, présentent des cinétiques de développement des résistances tout à fait semblables.

Pour la série 2, les courbes présentent une allure inverse de la série 1. Le sens des perturbations entraînées avant 7 jours dépend donc de la nature du CPA constituant le mélange et non de celle du filler (calcaires ou quartz).

4. RELATION RESISTANCE-POROSITE (Fig.4)

Les porosités des pâtes pures et des mortiers ont été déterminées par injection de mercure sous pression sur des échantillons traités par cryosublimation sous vide jusqu'à équilibre avec la pression de vapeur de la glace à -40°C.

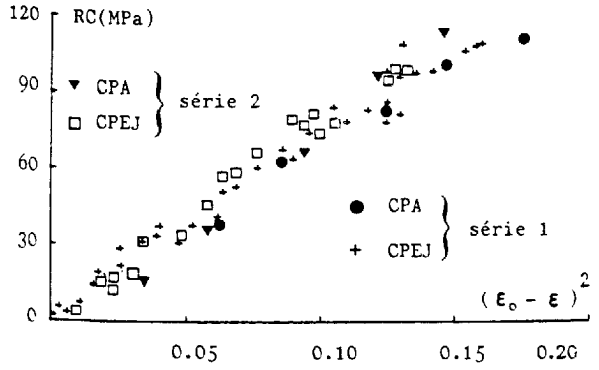

Fig.4- Relation porosité-résistance pour les deux séries de ciments.

Les comparaisons portent sur des pâtes de résistance, donc de porosité, sensiblement égales. Dans ces conditions, les distributions poreuses sont presque identiques.

On note toutefois un léger déplacement de la distribution vers les pores de moindres dimensions en présence de filler calcaire (M_2) pour la série 1.

En première approximation, on observe pour chaque série, une relation biunivoque entre la résistance en compression et la porosité pour toutes les pâtes pures des ciments composés ou non à toutes les échéances.

Diverses relations entre la résistance en compression et la porosité ont été publiées (GRANJU & MASO, ODLER , POWERS ....). Appliquées à notre étude, ces relations ont donné des corrélations sensiblement équivalentes. Dans le cas présent, une relation $R_e = k(\varepsilon_o - \varepsilon)^n$ a été trouvée, où ε_o représente la porosité volumique initiale et ε la porosité à une échéance donnée. Le coefficient de corrélation le plus significatif a été obtenu pour une valeur de n proche de 2 ($0,9 < r < 0,99$) pour la série 1.

ε_o peut être considéré comme constant. La différence ($\varepsilon_o - \varepsilon$) représente l'accroissement de volume solide au cours de l'hydratation. La résistance en compression semble donc être proportionnelle au carré de l'accroissement du volume de solide formé, pour une porosité initiale donnée.

5. RELATION ENTRE LE MODULE D'ELASTICITE ET LA RESISTANCE EN COMPRESSION

Au cours du temps, le module d'Young et la résistance en compression évoluent dans le même sens. Qu'il s'agisse de pâtes pures ou de mortiers, l'augmentation de la teneur en ajout entraîne, à résistance égale, une augmentation du module E comme le montre la figure 5.

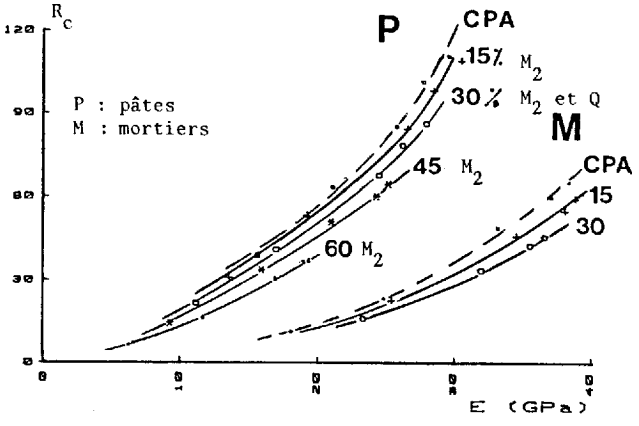

Fig. 5 - Module-résistance : rôle de la teneur en ajout.

Pour les deux types de matériaux la pente des courbes s'abaisse d'autant plus qu'il y a d'ajout dans le ciment.

Pour les mortiers, les courbes, entre 1 et 90 jours peuvent être assimilées à des droites.

A titre indicatif, la relation linéaire obtenue à partir des mesures effectuées sur 120

prismes de mortier de CPA 1 réparties sur 15 échéances entre 1 et 90 jours, donne un coefficient de corrélation compris entre 0,97 et 0,99 au seuil de signification de 99%.

Ces observations portent sur des gâchées de même rapport e/c (0,3 pour les pâtes, 0,5 pour les mortiers). Dans ce cas, le rapport eau/CPA augmente proportionnellement avec la quantité de filler dans le CPEJ.

La figure 6 met en évidence l'influence de l'ajout de filler pour un rapport eau/CPA identique (0,43 pour les pâtes pures, 0,60 pour les mortiers).

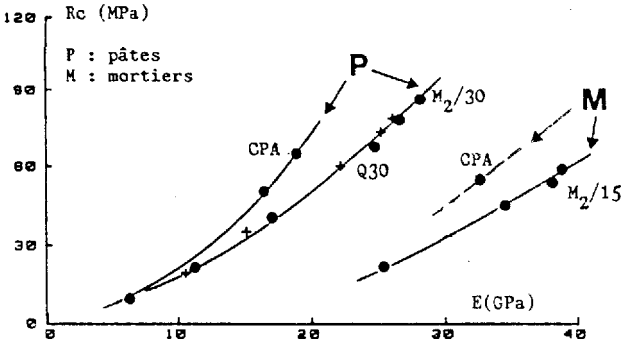

Fig.6 - Module-résistance - Influence de l'ajout pour un rapport eau/CPA identique (pâtes pures 0,43, mortiers 0,6).

L'eau et le filler ont donc un effet opposé à résistance égale, le module du matériau augmente lorsque :

. le rapport eau/CPA diminue
. la quantité d'ajout augmente

Ceci explique les faibles écarts entre 2 courbes de la figure 5, les deux effets se compensant partiellement.

La nature de l'ajout quant à elle n'entraîne pas de différences significatives (Figure 6), les grains d'ajout ayant des modules peu différents. Ces modules sont (HIRSCH, 1962) proches de celui de l'anhydre mais très différents de celui des hydrates (GRANJU et MASO, 1980).

Dans la gamme des finesses étudiées (entre 1000 et 12000 cm^2/g) la finesse joue un rôle relativement limité.

On constate cependant, à résistance égale, que plus le filler est fin, plus faible est le module du matériau, toutes choses égales par ailleurs (Figure 7).

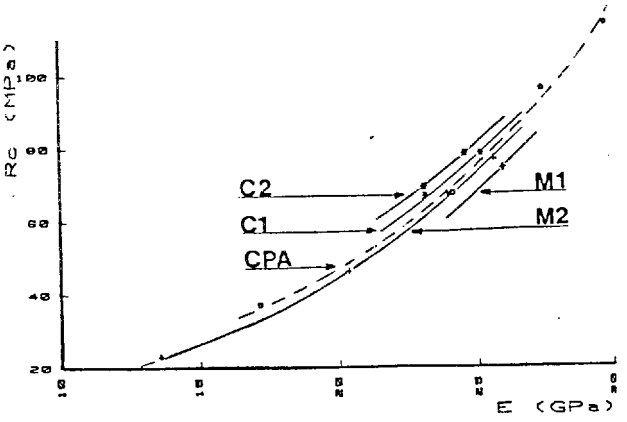

Figure 7.- Module-résistance : Influence de la finesse du filler. (Ciment n°2 + 30% de filler à des finesses différentes)

Si l'on compare sur la figure 6, la pâte pure et le mortier de CPA, on constate un écart important entre les deux courbes (d'autant plus important que le rapport e/c est différent). Le mortier peut-être considéré de ce point de vue comme une pâte pure contenant 75% d'un ajout, très grossier de surcroît (finesse de l'ordre de 300 cm^2/g environ).

Les travaux de HIRSCH (1962) et les remarques de ISHAI (in DOUGILL et al, 1962) font ressortir que le module d'élasticité d'un béton est fonction de 3 facteurs :

. la teneur en granulats
. le module des granulats
. le module de la pâte de ciment, elle même dépendante de l'âge et du rapport e/c.

Les résultats observés sur les fillers confirment ces observations : d'un point de vue strictement mécanique, les fillers se comportent, dans les pâtes pures ou dans les mortiers, comme les granulats d'un béton : à résistance égale, le module du matériau durci (modules des hydrates), dépend de la nature du liant, des proportions d'eau (rapport e/c) et d'ajout (quantité de filler), ainsi que de la taille des grains de celui-ci.

6. CARACTERISATION MINERALOGIQUE DES PATES DE CIMENTS FILLERISES.

6.1 Taux d'hydratation de C_3S et C_3A

Les mesures effectuées par D.R.X indiquent, pour la série 1, une tendance à l'accélération de l'hydratation en présence de filler calcaire.

Cette observation publiée par MORTUREUX et al (1982) est confirmée par les examens au microscope optique et au M.E.B de sections polies sur lesquelles ont été déterminées par comptage les volumes d'anhydre restant après 2 jours et 28 jours d'hydratation. Les résultats de ces comptages sont donnés dans le tableau 2.

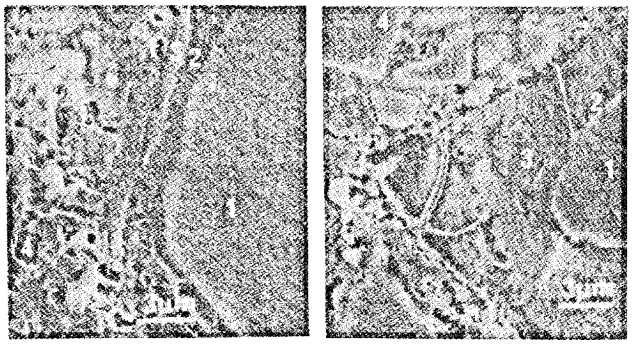

a b

Fig.8 - M.E.B - section polie a) 0% filler b) 60% filler. 1. C_3S 2. C-S-H pseudomorphique 3. $Ca(OH)_2$ 4. Filler

Composition		2 jours	28 jours
CPA 1		30 %	26 %
M2	15 %	33	25
	30	33	15
	45	31	-
	60	-	15
Q	15 %	-	22
	30	30	19

Tableau 2
Volume d'anhydre après deux et vingt huit jours d'hydratation.

Les variations sont surtout sensibles à 28 jours, notamment pour les très fortes teneurs en fillers calcaires.

Le taux d'hydratation plus élevé dans les pâtes fillérisées se traduit également par l'existence d'une zone de C-S-H pseudomorphique autour des noyaux de C_3S encore anhydres, d'autant plus large que la teneur en filler est élevée (Figures 8a et 8b).

6.2 Distribution de $Ca(OH)_2$

Les mesures comparatives par DRX montrent un accroissement très net de l'intensité relative des pics de $Ca(OH)_2$ lorsque la teneur en ajout calcaire ou quartzeux augmente. L'évolution de l'intensité relative de la raie à 4.90 Å en fonction du temps et de la quantité de filler est illustrée par la Fig.9 où l'intensité de $Ca(OH)_2$ du CPA est prise égale à 1.

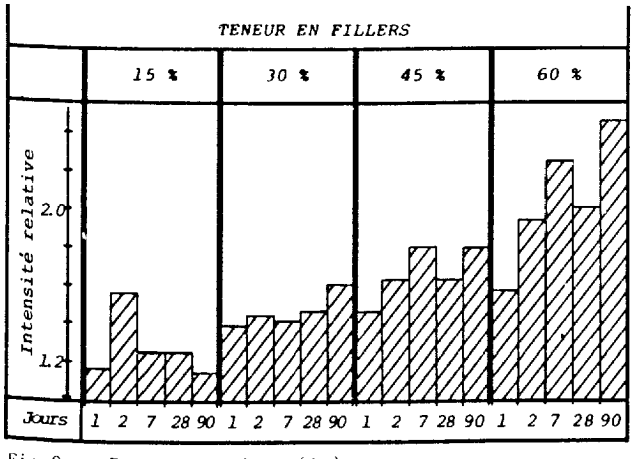

Fig.9.- Examen DRX de $Ca(OH)_2$.

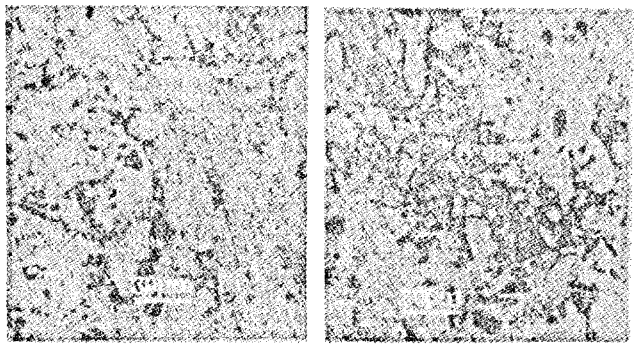

a b

Fig. 10 - Microscopie optique. Section polie attaquée au borax. Distribution de $Ca(OH)_2$ (noir) a)0% filler b) 60% filler .

Les accroissements observés sont dus à une augmentation effective du taux de portlandite et vraisemblablement aussi aux differences de distribution et de taille des cristaux dont la contribution au rayonnement peut varier. L'observation de sections polies au microscope optique montre une distribution relativement homogène de petits cristaux dans les pâtes sans fillers (Fig.10 a).

Dans le cas des fortes teneurs en ajout, la chaux est en cristaux plus gros groupés en amas (Fig.10 b). La densité de cristaux par unité de longueur déterminée au microscope par la méthode des sécantes aléatoires, est une image de la dispersion de $Ca(OH)_2$. Les résultats suivants ont été obtenus sur les pâtes du CPA numéro 1 :

Filler 0% $\quad \bar{N}_c = 380$ cm-1
Filler 30% $\quad \bar{N}_c = 300$ cm-1
Filler 60% $\quad \bar{N}_c = 240$ cm-1

($\bar{N_c}$ = nombre moyen de cristaux interceptés par unité de longueur de sécante).



Fig.11- $Ca(OH)_2$ en section polie M.E.B.

1. $Ca(OH)_2$
2. Filler

Dans tous les cas $Ca(OH)_2$ cristallise en éléments de contours variables, dentelés en section. Il constitue une phase de remplissage "pontant" les grains de fillers entre eux, notamment dans les pâtes à forte teneur en fillers au contact desquels il précipite (Fig. 11).

Au M.E.B. il se présente sous son faciès habituel en cristaux massifs clivés.

6.3 Composition et texture des C-S-H

Les C-S-H pseudomorphiques autour des noyaux de C_3S anhydres ont été dosés par E.D.S à l'échéance de 28 jours. Les résultats indiquent une diminution du rapport molaire CaO/SiO_2 lorsque la teneur en filler augmente. Dans les pâtes de CPA n°1 (riches en C_3A) contenant 0%, 30% et 60% de fillers calcaires, les rapports C/S moyens mesurés sont respectivement égaux à $2,1 \pm 0,2$, $1,8 \pm 0,15$ et $1,6 \pm 0,1$.

La dispersion est beaucoup plus importante dans les ciments sans fillers dans lesquels les zones de C-S-H pseudomorphiques sont étroites et où les interférences avec les phases adjacentes sont à craindre.

Les examens fractographiques au M.E.B n'ont pas mis en évidence de différences significatives en ce qui concerne la morphologie des C-S-H en présence ou en l'absence d'ajout calcaire. La texture est granuleuse, parfois fibreuse dans les produits peu compacts (échéances courtes ou fortes teneurs en fillers).

6.4 Cristallisation des aluminates hydratés

Deux types d'aluminates sont détectés par DRX : ettringite et monocarboaluminates de calcium. L'ettringite donne des pics nets dès 1 jour dans les pâtes de ciment au clinker n°1 en présence et en l'absence de fillers calcaires.

Dans les pâtes de ciment au clinker n°2 les pics, de très faible intensité, n'apparaissent qu'après 28 jours.

Les observations au M.E.B. donnent un résultat apparemment contradictoire : l'ettringite en fines aiguilles est visible dès les premiers jours dans les pâtes du ciment n°2.

Bien que plus abondante d'après la DRX, elle est paradoxalement difficilement observable dans les pâtes du ciment n°1 où elle peut être finement cristallisée et masquée par les C-S-H.

Les carboaluminates, très peu visibles au M.E.B , ne sont détectés nettement par DRX qu'après 7 jours dans les pâtes de CPEJ à base de clinker n°1. Les pics apparaissent plus tardivement et sont très peu intenses dans le cas des CPEJ au clinker n°2.

Des microcristaux en plaquettes hexagonales qui sont vraisemblablement des phases du type Afm sont également observés au M.E.B dans les empreintes laissées par des grains de ciment déchaussés. Ces cristaux sont mis en évidence surtout aux courtes échéances dans toutes les pâtes de ciment, en présence ou en l'absence de fillers calcaires . (Fig.12)

6.5 Liaisons hydrates - Fillers calcaires

La formation de carboaluminates de calcium traduit l'aptitude à réagir des ajouts calcaires. Cette réactivité se manifeste par une consommation plus ou moins importante du filler suivant la nature minéralogique du calcaire et la composition du ciment. La réactivité du filler calcaire entraîne également la formation de liaisons avec les hydrates du ciment par l'intermédiaire en particulier de microcristaux de $Ca(OH)_2$ orientés sur $CaCO_3$ et d'autres phases mal définies.

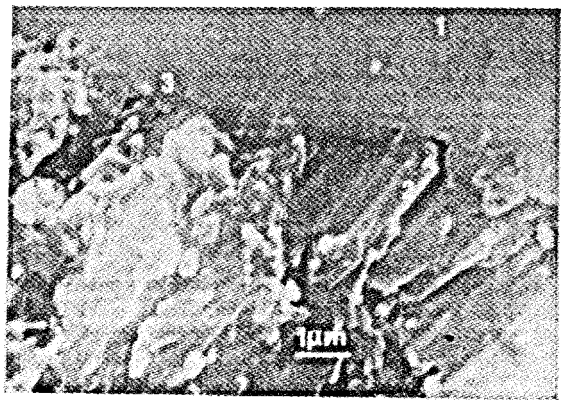

Fig. 12 - M.E.B. Liaison pâte de ciment durcie-filler calcaire - 1) filler 2) $Ca(OH)_2$ 3) C-S-H.

6.6 Fissuration

L'examen des éprouvettes de pâte pure soumises au traitement de dessiccation par cryosublimation révèle un maillage de microfissures superficielles. En comparant les diverses pâtes aux mêmes échéances on constate que le phénomène tend à s'atténuer pour les teneurs croissantes en filler.

Les rôles relatifs des teneurs en hydrates et des retraits consécutifs, et, par ailleurs, de la présence d'inclusions de filler restent à évaluer.

7. DISCUSSION

Nous avons observé que l'adjonction de fillers à un clinker de ciment Portland modifie sensiblement un ensemble varié des caractéristiques des pâtes ou mortiers correspondants.

Les modifications observées peuvent être classées en 3 catégories suivant qu'elles dépendent ou non essentiellement de la nature du clinker, de celle du filler, ou de la quantité de filler.

La nature du clinker détermine, pour l'essentiel, le sens de la modification de la cinétique du développement des résistances en présence de fillers aux courtes échéances, les résistances à long terme, la nature des hydrates formés (aluminates).

La nature du filler conditionne sa contribution aux résistances à long terme. intervient dans la formation de carboaluminates et dans les liaisons pâte-filler (CO_3Ca), mais ne modifie pratiquement pas les relations résistance en compression - module - porosité ni la cinétique de développement des résistances à court terme. Elle peut avoir une influence sur l'hydratation du clinker mais agit peu sur la quantité et la répartition de la chaux.

La quantité de filler, indépendamment de sa nature est le principal facteur déterminant les propriétés mécaniques à une échéance donnée. Elle conditionne le volumme d'hydrates formés et modifie la relation résistance-module des pâtes de C.P.E.J de e/c donné.

Le rapport e/CPEJ, constant, entraîne cependant un rapport e/clinker qui, dans les mélanges fillérisés, croît proportionnellement à la quantité

de filler. Or l'augmentation de e/c retarde l'acquisition des résistances des pâtes des deux CPA (fig. 2 : E/C = 0,3 et E/C = 0,43 et fig. 3 : E/C = 0,3 et E/C = 0,35). Donc le comportement différent des deux séries de CPEJ, avant 7 jours, ne s'explique pas uniquement par l'augmentation du rapport e/clinker.

En effet, une analyse plus fine de la relation résistance-porosité ne permet pas de distinguer les CPEJ (1) de leur CPA : la cinétique de développement des résistances est donc liée à celle du développement du volume des hydrates. Pour la série (2) par contre, les rapports $Re/(\varepsilon_0 - \varepsilon)^2$ du CPA aux courtes échéances sont légèrement mais systématiquement inférieurs à ceux des CPEJ (figure 4). Dans ce cas, la cinétique du développement initial des résistances des CPEJ 2 serait liée à la qualité des liaisons et la nature des hydrates et non à leur quantité.

8. CONCLUSION

Prenant comme base de comparaison une pâte pure de CPA, les caractéristiques des pâtes et mortiers de ciments fillérisés apparaissent tributaires :

- en premier lieu, du rapport e/(clinker du mélange fillérisé).
- en second lieu, de l'association clinker-filler.

Il sera sans doute possible dans l'avenir de distinguer un nombre limité d'associations types filler-clinker-gypse de comportement similaire en tenant compte de facteurs tels que : teneur en C_3A et rapport C_2S/C_3S du clinker, taux de gypse.

Concernant l'avenir des ciments fillérisés, la présente étude confirme que pour des teneurs en filler de 15 %, les performances mécaniques mais aussi la texture poreuse de leurs pâtes durcies, peuvent être équivalentes, voire plus favorables pour certaines échéances, comparées aux pâtes de leur CPA de base.

9. REMERCIEMENTS

Nous remercions vivement C.COGNET, P. NOEL et M. FOURRE, Techniciens au Département Microstructures, pour leur collaboration.

10. BIBLIOGRAPHIE

- DOUGILL JW., ISHAI O., PAUW A., MEYERS BL., HIRSCH TJ. (1962) Modulus of Elasticity of Concrete Affected by Elastic Moduli of Cement Paste Matrix and Aggregate. Discussion of a Paper by TJ. HIRSCH. J. amer. Concr. Inst. 59,9, 1363-5.
- GRANJU JL., MASO JC. (1980) Module de Déformation Longitudinale des Pâtes de Ciment Portland Conservées dans l'Eau. Cem. Concr. Res. 10, 6,731-738.
- HIRSCH TJ. (1962) Modulus of Elasticity of Concrete Affected by Elastic Moduli of Cement Paste Matrix and Aggregate. J. amer. Concr. Inst. 59,3, 427-452.
- HORNAIN H., MORTUREUX B., REGOURD M., (1982) Aspect Physico-Chimique et Mécanique de la Liaison Pâte de Ciment-Granulat. Colloque International RILEM, Toulouse 17-19 nov., C 56 - C 65.
- KENDALL K., HOWARD AJ. and BIRCHALL FRS. (1983) The Relation Between Porosity Microstructure and Strength and the Approach to Advanced Cement-Based Materials. Phil. Trans. R. Soc. Lond, A 310, 139-153.
- MORTUREUX B., HORNAIN H., REGOURD M., (1982) Liaison Pâte de Ciment-Filler dans les Ciments Composés. Colloque International RILEM , Toulouse, 17-19 nov., A 64 - 72.
- ROSSLER M., ODLER I. (1985) Investigations on the Relationship Between Porosity, Structure and Strength of Hydrated Portland Cement Pastes . Cem. Concr. Res. 15,2, 320.330.
- WITTMAN F.H. (1982) Structure and fracture Mechanics of Concrete - Seminaire "Mécanique de la rupture". I.T.B.T.P., St-Rémy-les-Chevreuse, 8-11 juin.

J.P. OLLIVIER, J. GRANDET, B. HANNA
Laboratoire de Génie Civil I.N.S.A.-U.P.S., Avenue de Rangueil
31077 TOULOUSE Cedex - France

Action d'un fluidifiant et d'une fumée de silice condensée réactive aux courtes échéances sur la liaison gros granulat-mortier

Effect of superplasticizer and reactive condensed silica fume on the mortar-coarse aggregate bond

RESUME. L'utilisation d'un naphtalène sulfonate ne modifie pas l'orientation des cristaux de portlandite dans un mortier de ciment Portland au voisinage d'un gros granulat mais par contre les cristaux se développent de façon isolée à l'interface. La fumée d'une silice réactive aux courtes échéances diminue fortement cette orientation préférentielle aussi bien en l'absence qu'en présence de fluidifiant. La cristallisation de l'ettringite dans la zone interfaciale indique que dans les mortiers avec fluidifiant la silice comble la porosité et empêche la formation d'un gradient de teneur en eau. Il en résulte une consolidation de l'interface mortier-gros granulat qui doit contribuer à expliquer l'augmentation de résistance et la fragilisation des bétons confectionnés avec des fluidifiants et de la fumée de silice.

A utilização de um naftaleno sulfonado não modifica a orientação dos cristais de portlandita numa argamassa de cimento portland na proximidade de um agregado grosso, mas, ao contrário, os cristais se desenvolvem de forma isolada na interface. O fumo de sílica reativo , em limites reduzidos, diminui grandemente esta orientação preferencial, tanto na presença como na ausência de fluidificante. A cristalização da etringita na zona interfacial indica que, nas argamassas com fluidificante, a sílica enche a porosidade e impede a formação de um gradiente de teor de água. Resulta daí uma consolidação da interface de argamassa-agregado ' grosso que deve contribuir para explicar o aumento de resistência e a fragilização dos concretos confeccionados com fluidificantes e fumo de sílica.

I - INTRODUCTION

L'étude du comportement mécanique des bétons durcis de très haute résistance fabriqués à partir de ciment portland, de fluidifiant et de fumée de silice condensée fait apparaître une rigidification importante par rapport aux bétons de ciment portland traditionnels. Le résultat s'explique peut être par une modification de la texture des CSH formés (1) mais aussi, peut être, par la consolidation de l'auréole de transition.

Pour clarifier cette dernière hypothèse nous avons entrepris d'analyser l'influence d'un couple fluidifiant (naphtalène sulfonate)-fumée de silice sur la formation de l'auréole de transition dans un béton. Celui-ci est modélisé par une éprouvette mixte constituée d'un granulat de marbre plan poli contre lequel est coulé un mortier. Nous présentons uniquement des résultats aux courtes échéances jusqu'à 28 jours.

II - MATERIAUX UTILISES - METHODES EXPERIMENTALES

Le ciment choisi est un ciment portland de la classe 55R (norme NF C 15.301) de surface spécifique 310 m^2/kg. Sa composition chimique est indiquée au tableau I.

La fumée de silice retenue est très réactive aux jeunes âges (2). Ses caractéristiques physiques et chimiques sont également présentées au tableau 1. Le dosage est 10 % en poids de ciment.

Le fluidifiant utilisé est un naphtalène sulfonate dosé à 4 % en poids de ciment. Il est introduit aux 2/3 du temps total de malaxage des mortiers.

La granularité du sable calcaire est indiquée au tableau II.

Le mortier est confectionné avec un dosage liant/sable = 1,5 ce qui correspond à l'ordre de grandeur retenu dans la préparation des bétons de haute résistance dosés à 700 kg de ciment/m^3 de béton.

Les éprouvettes mixtes sont conservées dans un moule étanche. Après la rupture qui se produit au voisinage immédiat de l'interface, le mortier est analysé par diffraction de rayons X depuis la surface de rupture jusqu'à coeur selon la méthode d'abrasion progressive (3). Cette technique permet de quantifier la variation de l'orientation préférentielle des cristaux de portlandite au voisinage du gros grain ainsi que les variations de teneurs en constituants anhydres ou hydratés cristallisés.

Nous avons montré par ailleurs (4) que la formation de l'auréole de transition dans les pâtes pures de ciment était fortement influencée par la teneur en eau de gâchage donc par les propriétés rhéologiques avant prise. Le choix des mortiers utilisés ici a donc été effectué après leur étude au maniabilimètre LCL. Les résultats présentés à la figure 1 montrent que la fumée de silice dispersée par le naphtalène sulfonate a un rôle fluidifiant.

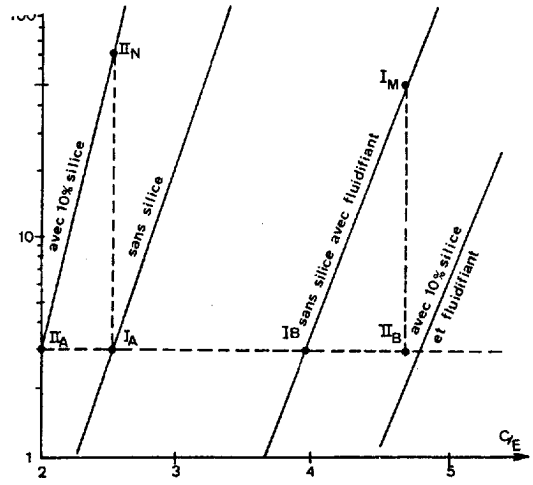

Figure 1 - Maniabilité des mortiers pour éprouvettes mixtes

	SiO_2	Na_2O	MgO	Al_2O_3	CaO	MnO	K_2O	Fe_2O_3	SO_3	C	Perte au feu
Ciment	22,4	0,2	4,3	6,15	59,1	0	0,8	3,3	1,3	-	2,45
Fumée de silice	93,4	0,4	1,9	0,8	0,3	-	1,3	0,9	0,7	0,1	3,9

Tableau I - Composition chimique du ciment et de la fumée de silice

Classe granulaire [mm]	0,08-0,16	0,16-0,315	0,315-0,63	0,63-1,25	1,25-2,5
% pondéral	12	12	8	14	54

Tableau II - Granularité du sable utilisé

La croissance cristalline des hydrates dans l'auréole de transition étant influencée par la vitesse d'hydratation (4), nous avons étudié ce paramètre par calorimétrie adiabatique. Afin de limiter les dégagements de chaleur les essais ont été effectués avec des mortiers 1/3. Dans ces conditions, les teneurs en eau des mortiers testés en calorimétrie différent de celles retenues pour la confection des éprouvettes mixtes. Nous avons toutefois choisi les valeurs des teneurs en eau à partir du même type d'essais de maniabilité dont les résultats sont rapportés à la figure 2.

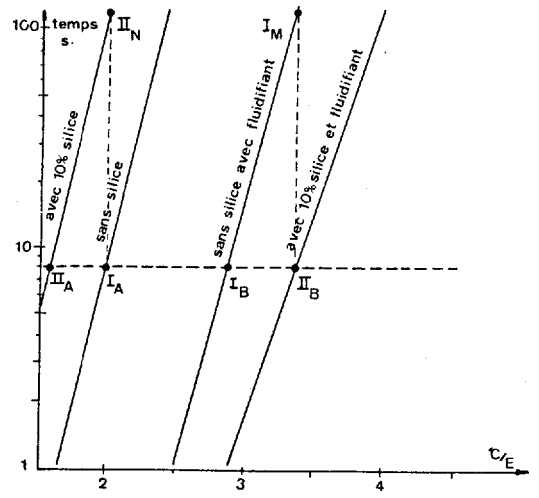

Figure 2 - Maniabilité des mortiers pour calorimétrie

III - FORMATION DE L'AUREOLE DE TRANSITION DANS LES MORTIERS PREPARES SANS FLUIDIFIANT

La croissance particulière des hydrates au voisinage d'un gros grain est due à l'existence d'un effet de paroi. Dans le cas des ciments portland elle est principalement influencée par la vitesse d'hydratation, le contrôle de la réaction du C_3A et les possibilités de diffusion des ions vers le gros grain (4).

L'étude de l'hydratation des mortiers I_A et II_A par calorimétrie adiabatique met en évidence le rôle accélérateur de la silice (figure 3). La figure 4 représente les variations des quantités de C_3S en fonction de la distance au gros grain mesurées par diffraction de rayons X (DRX) et rapportées à la même quantité de ciment portland. La silice accélère vivement l'hydratation du C_3S dans les quelques premières dizaines de microns au voisinage de l'interface. On peut noter que la teneur en C_3S croît depuis l'interface vers le coeur du mortier sur une profondeur dont l'ordre de grandeur est la dizaine de microns ce qui correspond à l'effet de surface entre les grains de ciment et le gros grain puis diminue ensuite. L'enrichissement relatif en C_3S de la zone de contact s'explique par un autre effet de paroi entre les grains de sable et le gros grain contre lequel le mortier est coulé.

La mesure de la quantité d'aluminates hydratés dans l'auréole de transition (figure 5) montre que les sulfates ne contrôlent pas efficacement l'hydratation du C_3A au voisinage du gros grain dans les mortiers II_A ce qui s'explique par la forte teneur en eau utilisée pour leur gâchage (5).

La croissance de la portlandite dans l'auréole de transition peut être représentée au moyen des courbes de la figure 6 qui caractérisent l'orientation préférentielle des cristaux en fonction de la distance au gros grain dans les trois mortiers I_A, II_A et II_N.

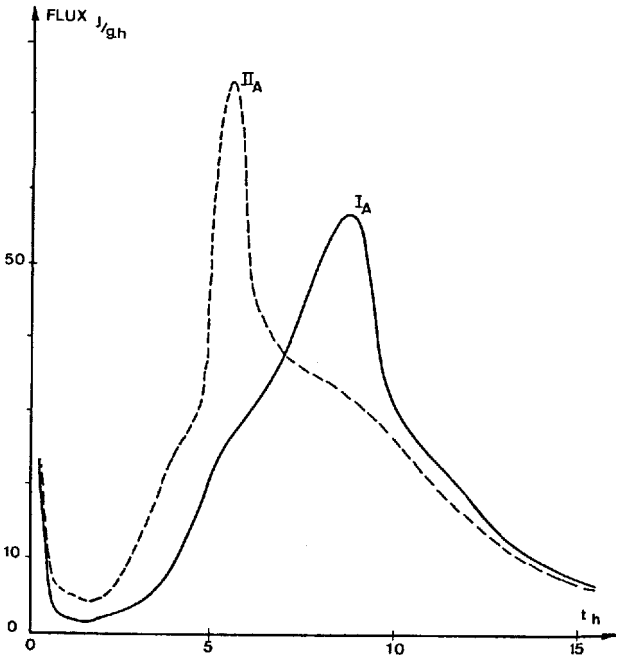

Figure 3 - Hydratation adiabatique des mortiers sans fluidifiant

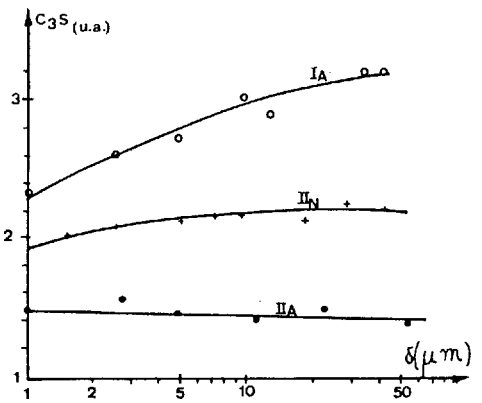

Figure 4 - Répartition du C_3S dans l'auréole de transition sans fluidifiant

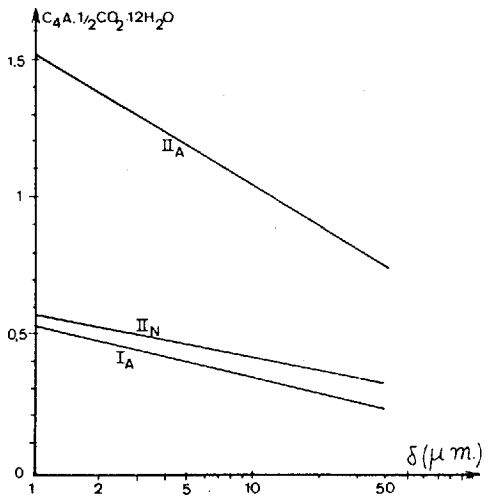

Figure 5 - Répartition de l'aluminate hydraté dans l'auréole de transition sans fluidifiant

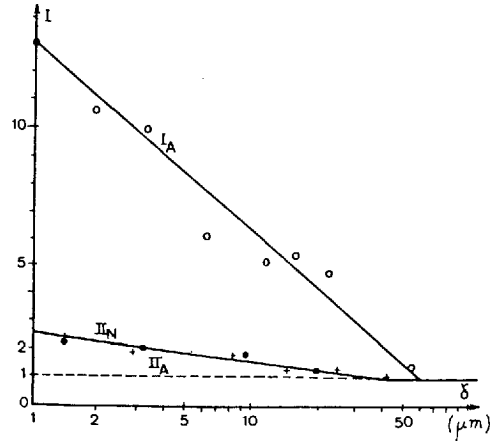

Figure 6 - Orientation préférentielle des cristaux de portlandite dans l'auréole de transition sans fluidifiant

La faible orientation des cristaux de portlandite au voisinage d'un gros grain dans les mortiers II_A peut être expliquée par :

- la présence de silice qui peut jouer un rôle de germe de cristallisation et un rôle de remplissage contrariant ainsi la croissance anisotrope des cristaux ;

- l'accélération de l'hydratation qui conduit à un remplissage plus rapide des vides intergranulaire dans l'auréole de transition ;

- la formation d'aluminates de calcium hydratés en quantité dans l'auréole de transition ce qui constitue un facteur propice à la désorientation des cristaux de portlandite (5).

Dans le cas des mortiers II_N, les cristaux de CH sont également peu orientés par rapport au gros grain. Aux deux premiers éléments d'analyse cités précédemment on peut ajouter la diminution de la fluidité du mortier II_N par rapport au mortier I_A. Les possibilités de migration des ions Ca^{++} sont ainsi diminuées et la croissance des cristaux de portlandite au voisinage du gros grain est moins rapide.

IV - FORMATION DE L'AUREOLE DE TRANSITION DANS LES MORTIERS AVEC FLUIDIFIANT

En l'absence de silice, le fluidifiant utilisé retarde l'hydratation du ciment dans les mortiers préparés à même maniabilité (courbes I_A et I_B de la figure 7). Sur la même figure les courbes calorimétriques relatives aux mortiers I_M et II_B confirment l'accélération de l'hydratation causée par la silice choisie.

Le développement des cristaux de portlandite au voisinage d'un gros grain dans les mortiers I_B, II_B et I_M peut être analysé au moyen des courbes de la figure 8. Alors que la diminution de la teneur en eau conduit à une plus faible orientation préférentielle des cristaux de portlandite à l'interface en l'absence de fluidifiant (5), on observe ici une forte orientation par rapport au gros grain dans le mortier I_B. Avec le fluidifiant, la variation de la quantité d'ettringite en fonction de la distance au gros grain (figure 9) indique qu'un gradient de teneur en eau peut encore s'établir au voisinage de l'interface (5,6). Le retard d'hydratation et la fluidité des mortiers permettent alors la diffusion des ions Ca^{2+} vers l'interface. Les cristaux de portlandite se développent de façon isolée (figure 10) avec leur plan (00.1) parallèle à la surface du gros grain. Leur croissance n'est pas contrariée par la présence d'aluminates hydratés puisqu'avec la faible quantité d'eau de gâchage utilisée l'hydratation du C_3A est bien contrôlée.

Dans le cas des mortiers I_M l'orientation préférentielle est un peu plus faible que dans les mortiers I_B (la teneur en eau diminue, l'hydratation est plus rapide et le mortier est moins fluide). Les cristaux de portlandite se développent encore de façon isolée à l'interface (figure 11) et on peut également observer des dépôts de forme particulière, peut être dus à la migration et à la saturation du fluidifiant au voisinage du gros grain.

La silice choisie occasionne une désorientation des cristaux de portlandite (courbe II_B de la figure 8) que l'on peut expliquer par un remplissage partiel des vides intergranulaires du ciment au voisinage du gros grain et par l'accélération de l'hydratation.

On peut enfin noter que l'adhérence entre les mortiers contenant de la silice et les gros grains est élevée. La face de rupture, côté gros grain, présente après 28 jours un film compact d'hydrates (figure 12a) ou des décohésions intragranulaires (figure 12b) qui témoignent de la qualité des liaisons interfaciales.

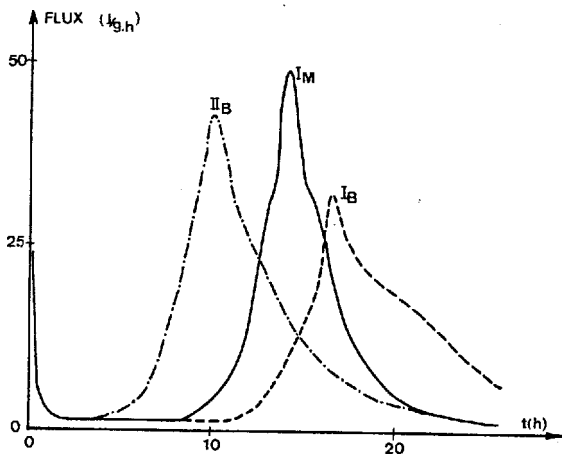

Figure 7 - Hydratation adiabatique des mortiers avec fluidifiant

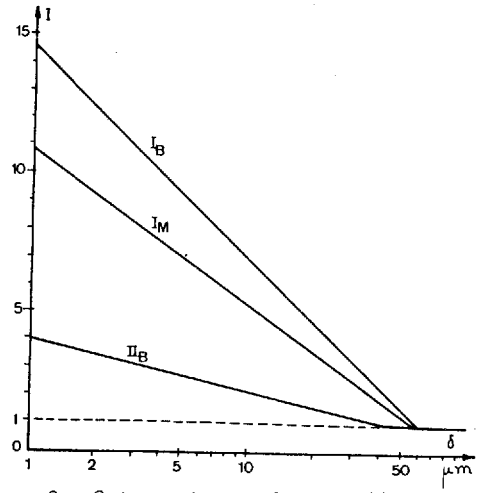

Figure 8 - Orientation préférentielle des cristaux de portlandite dans l'auréole de transition avec fluidifiant

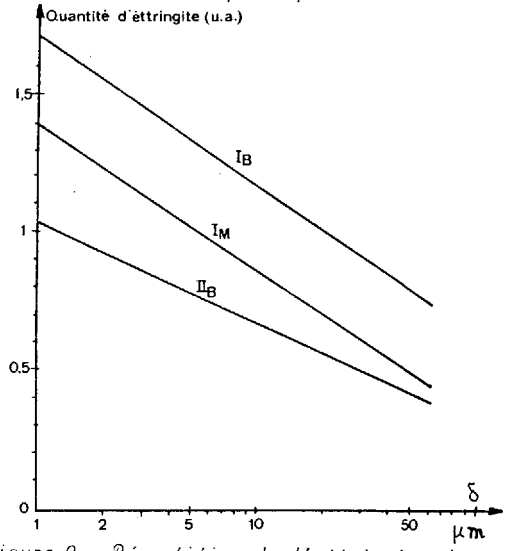

Figure 9 - Répartition de l'ettringite dans l'auréole de transition avec fluidifiant

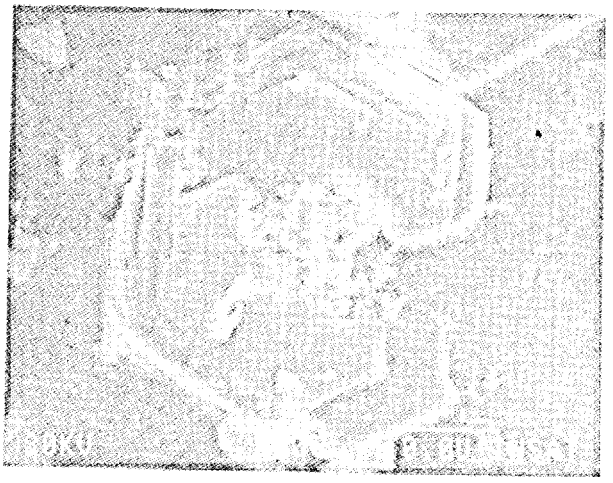

Figure 10 - Cristallisation de la portlandite au voisinage du granulat dans un mortier I_β sans silice préparé avec 4 % de fluidifiant (7 jours)

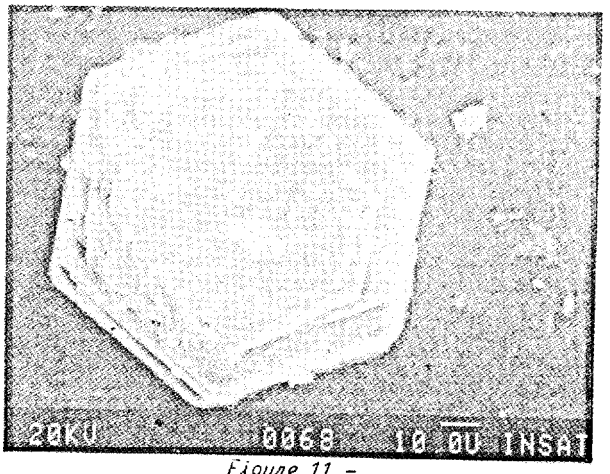

Figure 11 -

Figure 11 - Cristallisation de la portlandite au voisinage du granulat dans un mortier I_M sans silice préparé avec 4 % de fluidifiant (7 jours)

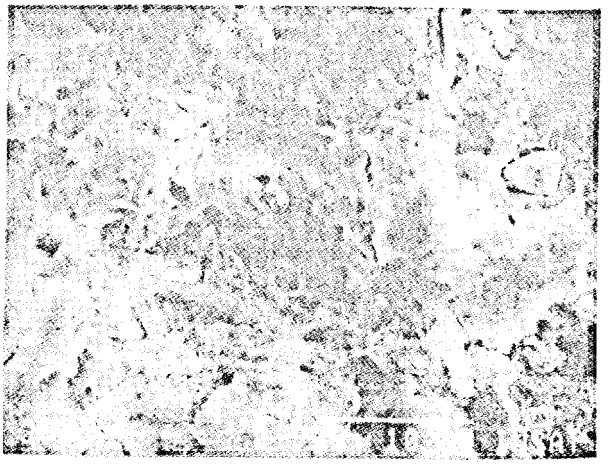

Figure 12a - Faces de rupture d'une éprouvette mixte II_β âgée de 28 jours (face mortier)

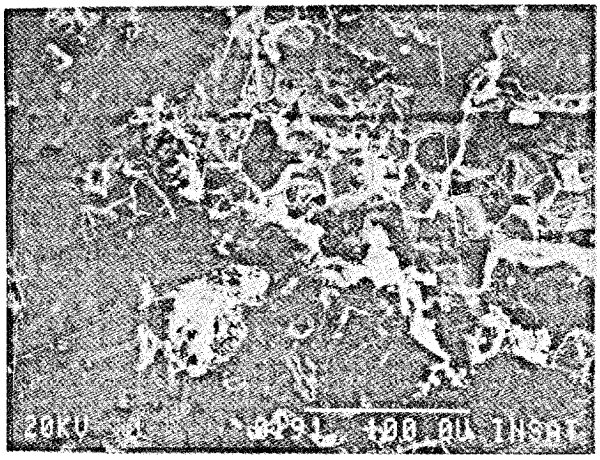

Figure 12b - Faces de rupture d'une éprouvette mixte II_β âgée de 28 jours (face granulat)

V - CONCLUSION

En présence de fumée de silice condensée la structure de l'auréole de transition est modifiée. Avec ou sans fludifiant les cristaux de portlandite se développent avec une faible orientation préférentielle au voisinage des gros grains. Les particules de silice contribuant par ailleurs à combler une partie de la porosité élevée de l'auréole de transition. On peut alors penser que cette addition minérale joue un rôle bénéfique sur les propriétés mécaniques de la zone de liaison entre granulat et mortier.

BIBLIOGRAPHIE

(1) M. REGOURD, B. MORTUREUX, E. GAUTIER
Hydraulic reactivity of various pozzolanas. 5th Int. Symposium on technology of concrete, Monterrey, N.L. Mexico, march 1981.

(2) P.C. AITCIN, A. CARLES-GIBERGUES, N. OUDJIT, A. VAQUIER
Influence des éléments autre que Si sur la réactivité des fumées de silice. Congr. Int. Chimie des Ciments, Rio, 1986.

(3) J. GRANDET, J.P. OLLIVIER
Nouvelle méthode d'étude des interfaces ciment-granulat. 7ème Congrès Int. de la Chimie des Ciments. VII.85, Paris, 1980.

(4) J.P. OLLIVIER, J. GRANDET
Processus de formation de l'auréole de transition. Colloque Int. Liaisons pâtes de ciment-matériaux associés, Toulouse, novembre 1982.

(5) J.P. OLLIVIER
Contribution à l'étude de l'hydratation de la pâte de ciment portland au voisinage des granulats. Thèse d'Etat, Toulouse, 1981.

(6) P.J.M. MONTEIRO, P.K. MEHTA
Ettringite formation on the aggregate - cement paste interface. Cem. Concr. Research, vol. 15, n° 2 1985.

L.Opoczky, I.Vincze - Székely, L. Szatura Central Research and Design Institute for Silicate Industry,P.O.Box 112.Budapest,Hungary

3.2

RESEARCH ON MAKING CEMENTS OF IMPROVED SULFATE RESISTANCE AND WATERTIGHTNESS
RECHERCHE POUR LA REALISATION DU CIMENT Á HAUTE RESISTANCE SULFATIQUE ET HYDROPHOBE

SUMMARY:Using the silica fume by-product occuring in ferro-silicon-alloy plants cement andconcrete of high compressive- and flexural strength as well as of improved sulphate resistance and watertightness were made.The mechanism of action of silica fume has been examined in a complex way by instrumental analytical methods. It was shown that the action of silica fume is the consequence of chemical and physical processes. On the one hand the silica fume reacts with the $Ca/OH/_2$ of cement hydration resulting in the for - mation of a large amount of CSH-phase in the capillary pores. On the other hand the high surface area hydrogel forming during the hardening of cement compacts by itself the pore structure of cement stone. As a result of the above effects a system of improved strength and chemical resistance is formed.

Utilizando microsílica, sub-produto de fábricas de liga ferro-sílico, foram preparados cimento e concreto de alta resistência à compressão e à flexão, bem como de alta resistência sulfática e hidrofóbica. Foi examinado o mecanismo de reação da microsília numa forma complexa, por intermédio de métodos analíticos instrumentais. Ficou demonstrado que a ação da microsílica é conseqüência dos processos químico e físico. Por outro lado, o fumo de sílica reage com o $Ca(OH)_2$ da hidratação do cimento, tendo como resultado a formação de grande quantidade de fase-CSH nos poros capilares. E mais, o hidrogel com grande área de superfície, em formação durante o endurecimento do cimento, compacta por si mesmo a estrutura de poro da pedra de cimento. Como resultado dos efeitos acima, forma-se um sistema melhorado de resistência e químico.

L.Opoczky, I. Vincze - Székely, L. Szatura

INTRODUCTION

In Hungary there are a lot of problems due to the sulfate content of ground water. The application of the so called sulfate resistant /AM=0,64-1,0/cements was not always proved to be effective.
According to the literature /1-3/by add - ing of silica fume - occuring in some factories as waste product - corrosion resistance of cement and concrete can be highly improved.
The aim of this work was to study the influence of silica fume on the hydraulic, physical and chemical properties of cement and to develop improved sulfate resistant and watertight cement.

EXPERIMENTAL MATERIALS AND INVESTIGATION METHODS

In our experiments the following materials were used:
- sulfate resistant industrial cement /C/ /C_3S=42,89%,C_2S=27,27%,C_3A= 4,40% , C_4AF= 18,26%, AM= 0,91 /,
- silica fume with the characteristics listed in Table 1.

Characteristics of Silica Fume

Chemical composition %		Density /g/cm^3/	Specific surface area/BET/ /m^2/g/	Amorp- hous phase	Mineralogical composition Crystal- line	Grain size %	Pozzolanic reaction mg CaO/g	Solubility %	
SiO_2	87 - 90	2,18	12 - 13	~90	SiC	>90 µm 7,40	425 - 450 /fly ash	in 10% HCl	3,70
low Al_2O_3						>10 µm 47,28	50-130/ /tuff-trass 80-150/	in 10% H_2SO_4	0,35
Fe_2O_3								in 10%lactic acid	4,70
alkali						<1 µm 11,94			

Table 1 .

Silica fume is a very active material with high amount of amorpous SiO_2 and with high fineness and very fine grain size distribution.It can be seen from Fig.1 that silica fume has a high pozzolanic activity,that is a high reaction rate is characteristic to its pozzolanic reaction,which deviates by a great extent from the appropriate data of fly ash.

Cements with various amount of silica fume were prepared in laboratory ball mill and pilot plant homogenizer,respectively.

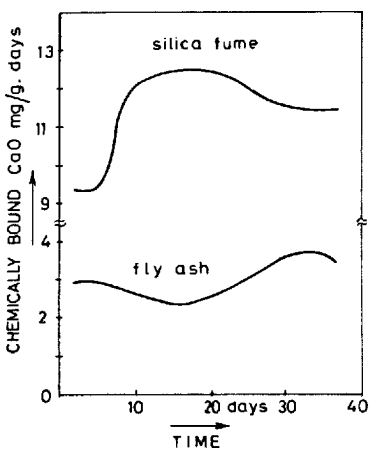

Fig.1.

Pozzolanic activity

Strength,sulfate resistance,watertightness etc. tests were carried out with cements in mortar and concrete.The water demand of mortar and concrete was determined on the basis of their consistency.It was stated that by adding silica fume, the water demand of mortar and that of the concrete was increased, therefore to ensure the appropriate workability, some plasticizing agents must be added to the cement. The optimum amount of the plasticizer is depending on the amount and fineness of silica fume and on the mineralogical composition of the cement.

Sulfate resistance was studied by two methods: by sulfate expansion /4/ and by the change of the strength.

The investigation of watertightness was carried out according to MSZ 4715/3 standard in concrete at 0,1;0,4 ;0,8 and 1,6 MPa water pressure.

The following amounts of cement were used in concrete: 265, 300 and 350 kg/m^3, respectively.

Study of the influence of silica fume on the hydraulic and physico-chemical properties of cement pastes was carried out by X-ray diffraction,thermal analysis , SEM,porosity and hydration heat measurements at 0,45 v/c.The heat of hydration was determined in isothermal calorimeter.

EXPERIMENTAL RESULTS

In Fig.2 the strength, in Figs.3 and 4. the sulfate resistance /sulfate expansion and the change of strength,resp./ are shown for a standard cement (C) and for cements containing 15 and 25% silica fume and 0,15-0,20% plasticizer (P)(SFC(15) and SFC (25)).In Fig.3 the requirements of the sulfate expansion fitting to the MI 523/7-78 standard is also shown.

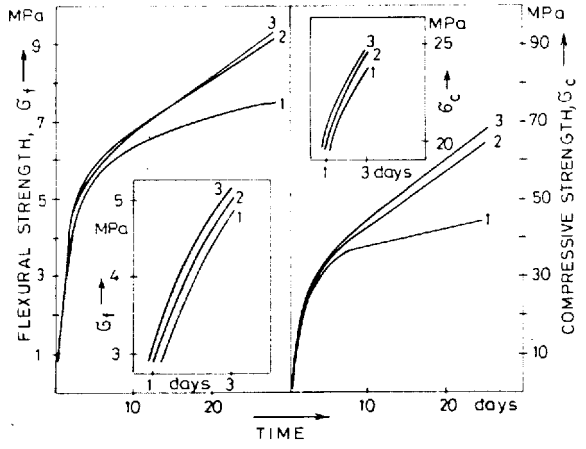

Fig. 2.
Strength of cements
1. Standard cement (C)
2. C+15 % silica fume +0,15 % P
3. C+25 % silica fume +0,20% P

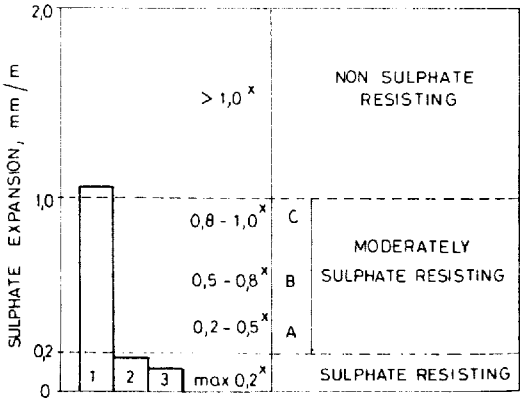

x MI 523/7 - 78 (Standard)

Fig. 3.
Sulfate resistance of cements
1. Standard cement (C)
2. C+15 % silica fume +0,15 % P
3. C+25 % silica fume +0,20 % P

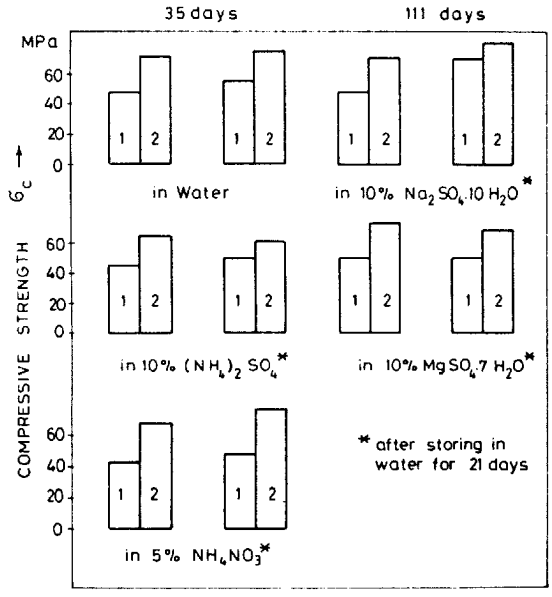

Fig. 4.

Sulfate resistance of cements

1. Standard cement (C)
2. C + 15 % silica fume + 0,15 % P

It can be stated that the strength of the cement is increased by 20-40% , while the sulfate resistance by 80-90% by the effect of adding 15 and 25% silica fume and 0,15-0,20 % plasticizer.It is worth to note the high flexural strength of cement with silica fume.

The good data of strength measured in mortar have been proved by the investigation of concrete, too /Fig. 5./.

The evaluation of the watertightness tests made in concrete has shown,that the cement with silica fume has an enhanced watertightness compared with that of the standard cement /Fig. 6./.

According to MSZ 4719 standard the concrete can be considered as watertight if following the exposure to given water pressure the water penetration does not exceed 1/3 of the specimen thickness which is 40 mm for standard specimens.

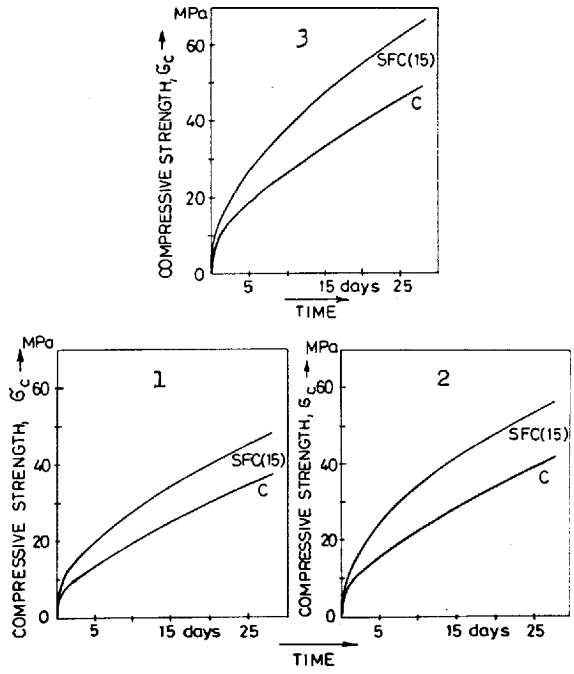

Fig. 5.

Strength of concrete

Cement content in concrete:

1 - 265 kg m^{-3}
2 - 300 kg m^{-3}
3 - 350 kg m^{-3}

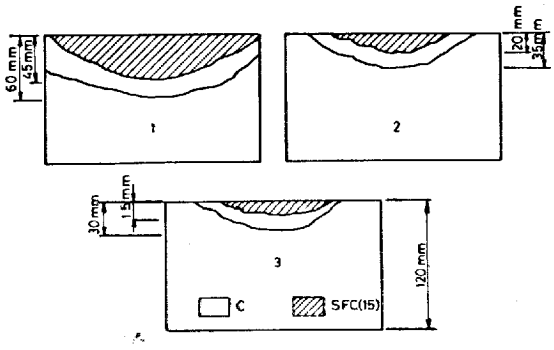

Fig. 6.

Watertightness of concrete

Cement content in concrete:

1 - 265 kg m^{-3}
2 - 300 kg m^{-3}
3 - 350 kg m^{-3}

Derivatographic curves are shown in Fig.7 for the standard cement and for the SFC(15) respectively.Silica fume reacts with $Ca/OH/_2$ formed at the hydration of cement, and as a result a calcium silicate hydrate /CSH/ phase is occuring /at 1053 and 1133 K,resp./.The formation of CSH is evident even after 3 days /Fig. 7/.

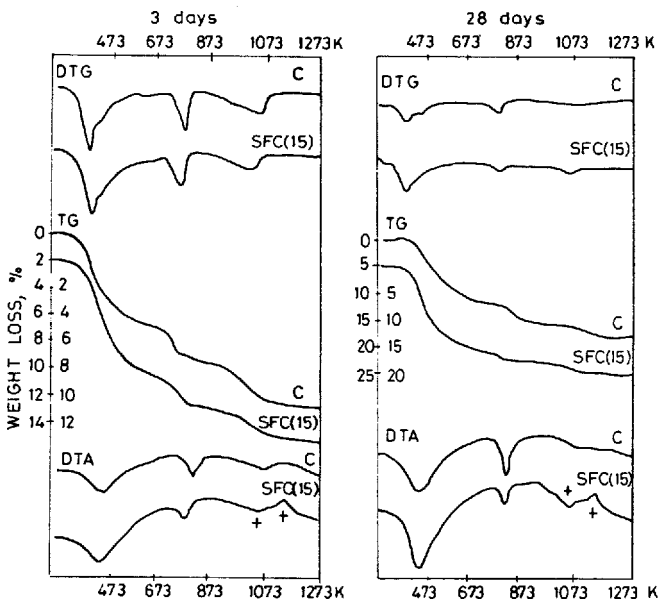

Fig. 7.
DTA - DTG curves of cements

The amount of the chemically bound water of cements with silica fume is the same at the beginning, then after an age of 28 days it is higher than that of the standard cement /Table 2/.
This is related to the ability of the silica fume to accelerate the hydration of cement and by the reaction between $Ca/OH/_2$ and silica fume high amount of CSH hydro-gel is formed.

Chemically bound water, %		
Age /days/	Type of cement C	SFC (15)
3	12,9	11,6
7	15,0	14,7
28	18,0	19,5
90	19,4	20,0

Table 2.
Chemically bound water of cement pastes

The decrease of the $Ca/OH/_2$ content /at 0,492 nm/ and the formation of CSH /at 0,182 and 0,305 nm/can be recorded by X-ray diffraction,too /Fig.8/.

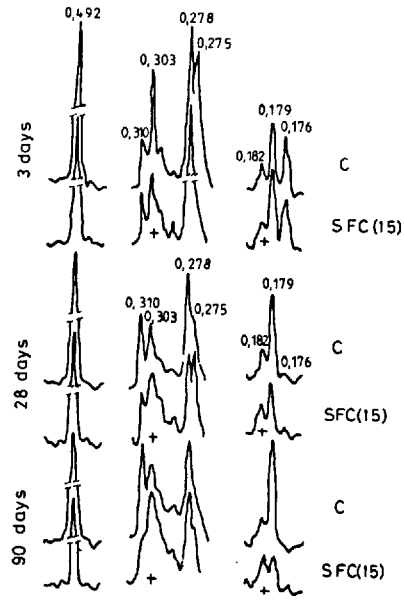

Fig. 8 .

X-ray diffraction patterns of cements

During the hydration of cement with silica fume CSH phase is occuring first in form of islands of small equant grains /at 3 days/, then it exhibits /at 7 and 28 days,resp./elongated and fibrous morphology /Fig.9/.

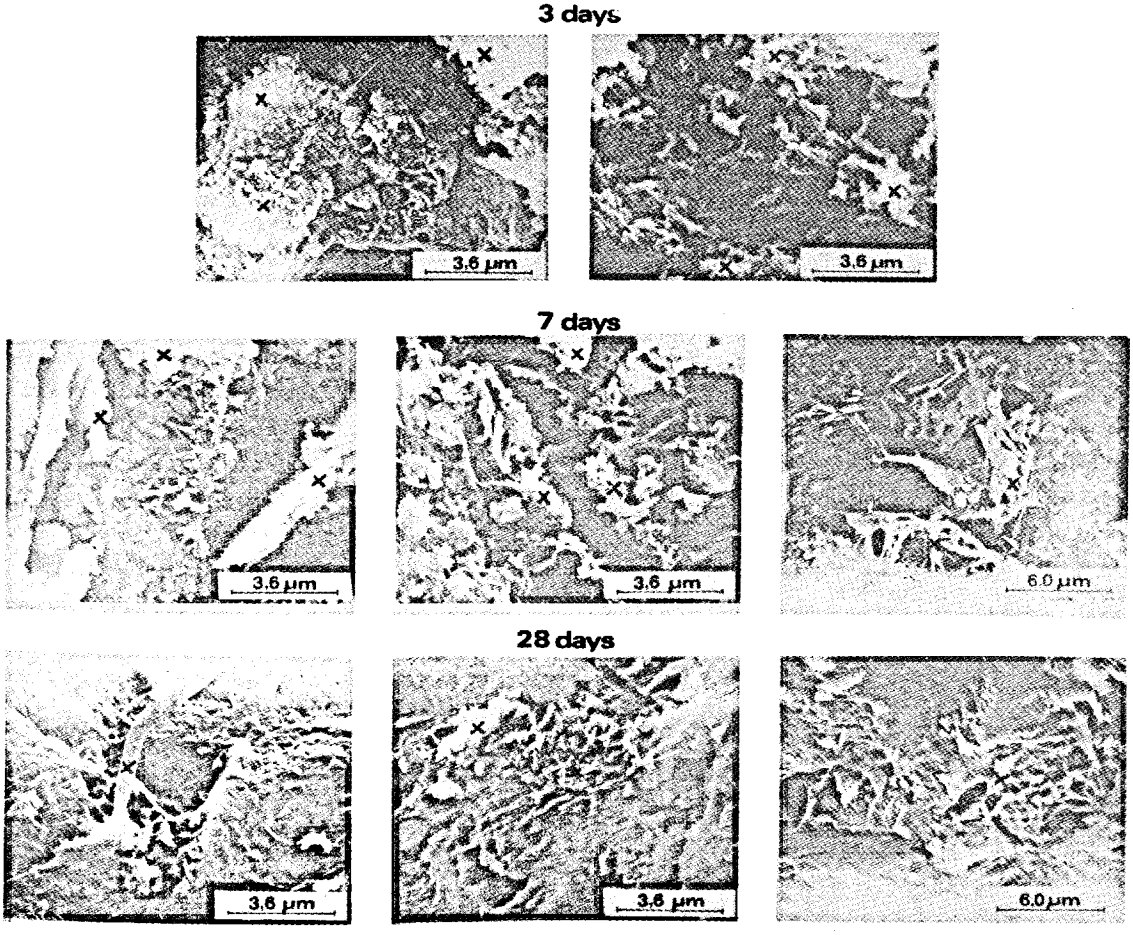

x CSH

Fig. 9.

Scanning electronmicrographs of hardened cement pastes

According to Fig.10 the heat of hydration for cement with silica fume is higher than that of the standard cement, but the exo - therm peak characteristic to the hydra - tion of alite is shifted to longer time period.The place and the height of this peak is influenced also by the plasticizer /Fig. 10/.

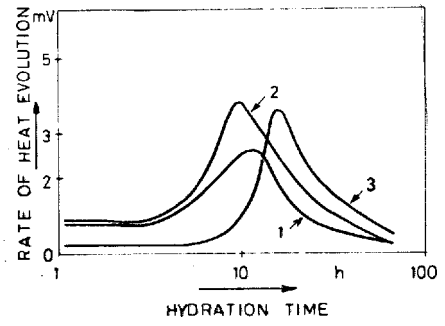

Fig.10.

Heat evolution curves in hydration of cements

1. Standard cement (C)
2. C + 15 % silica fume
3. C + 25 % silica fume + 0,20 % P

Porosity of cement pastes with silica fume is lower than that of the standard cement and the characteristic pore size is shifted from 100 nm to 10 nm/Fig. 11/.

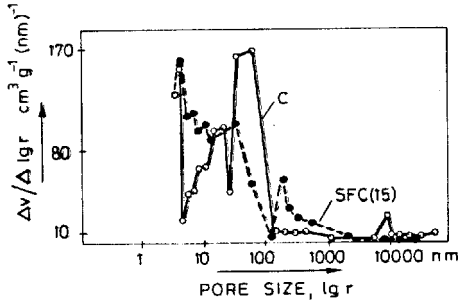

Fig.11.

Pore size distribution curves of hardened cement pastes measured by mercury penetration method

CONCLUSIONS

It was verified by these investigations that by applying silica fume - occured as waste material in ferro silicon producing plants cement and concrete with high compressive and flexural strength and with enhanced sulfate resistance and water - tightness can be produced.

By adding appropriate amount of plasticizer to the cement, the amount of silica fume can be increased up to 25 % without decreasing the strength of the cement.

The influence of silica fume on the cement is different from that of the common pozzolanic materials /like fly ash, trass/ .

At the explanation of the reaction mechanism of it, the chemical and physical effects must also be taken into account.

Silica fume is an amorphous material having high "total" specific surface area and consisting of particles with submicron size - as a consequence very high pozzo - lanic activity and reaction rate are characteristic to it. The hydration pro - cess of cement is accelerated by silica fume because even at the early stage of hardening Ca^{2+} ions are adsorbed by it and high specific surface area is ensured for the formation of hydrates.Due to the reaction between silica fume and $Ca/OH/_2$, high amount of calcium-silicate-hydrate /CSH/ is formed in some capillary pores thus compacting the pore structure of the cement stone.At the initial stage of hardening the CSH phase is grainy, later it exhibits elongated and fibrous morphology.Silica fume - in the presence of water and appropriate plasticizer or moistening agent- is converted into a jelly,plastic hydrogel,then during the hardening of cement it is converted into a rigid,coherent

structure /xerogel/.
Capillary pores are filled by hydrogel with high specific surface area, so it becomes watertight therefore the penet - ration of corrosive material is preven - ted.The strength of cement stone is en - hanced by the hardened geleous structure. The stability of silica gel structure is increased by some cations /like Mg^{2+} , Ca^{2+},etc./.

REFERENCES

1. Traetteberg,A /1978/:Silica fumes as pozzolanic material Il Cemento , 3, pp. 369.
2. Popovic, K. - Ukraicik, V. - Djureko - vic, A. /1984/: Improvement of mortar and concrete durability by the use of condensed silica fume Durability of Building Materials,2, pp. 171.
3. Buil, M. - Paillére, A.M. - Roussel, B. /1984/ : High strength mortars conta - ining condensed silica fume Cement and Concrete Research,14, pp. 693.
4. Kovács, R. - Medgyesi, I. - Révay, M. /1978/ : Problems of Testing Cements for their Sulfate Resistance /in Hungarian/ Építőanyag, 5 . pp. 186

B. MARCHESE, Professore, Dipartimento di Ingegneria dei Materiali e della Produzione, Facolta' di Ingegneria Universita' di Napoli, Piazzale Tecchio, 80125 Napoli, ITALIA

INTERFACIAL MICROSTRUCTURAL ALTERATIONS OF MATURE BLAST FURNACE CEMENT PASTES

SUMMARY: Microstructural modifications of reinforced blast furnace cement pastes at crack surfaces and steel/cement paste interfaces were examined. After curing 6 months in tap fluent water specimens were loaded in flexion in order to create microcracks in paste and then immersed for 3 years in static sea water.
Morfologies of typical localized regions by scanning electron microscopy (SEM) were identified and their comparative elemental compositions by energy dispersion X-ray spectrometry (EDXRA), like "finger prints", determined.
Crystalline and hydrated phases of bulk cement paste by X-ray diffraction (XRD) and thermogravimetry (TG) analyses were detected.
No macroscopical alterations of preexisting cracks have been evidenced.
The preformed calcite patina on external surface was able only slightly to transform in aragonite.
At cracks internal surfaces reaction of mature paste with sea water gave 2nd generation products: altered forms of C-S-H, aragonite, calcite and, in some cavities, still CH and modified ettringite.
At steel/paste interface, porous and dense regions formed the paste surfaces. The dense ones seemed to be constituted by a Ca-rich layer as calcite and aragonite. In certain areas diffusion of Mg, Cl, and Fe in discrete amounts were registered.

SUMÁRIO

Foram examinadas as modificações mocroestruturais nas superfícies das fissuras e nas interfaces aço-pasta de cimento em pastas de cimento com escória armadas. Após uma cura de 6 meses em água corrente, os corpos de prova foram carregados à flexão para criar microfissuras nas pastas, e então foram submersas por 3 anos em água marítima. As morfologias das regiões típicas foram identificadas por microscópio eletrônico de varredura (SEM) e as composições elementares foram determinadas como por "impressão digital" usando expectrometria de dispersão de raios X (EDXRA). As fases cristalinas e hidratadas da pasta foram determinadas por difração de raios X (XRD) e termogravimetria (T. G). Nenhuma alteração microscópica das fissuras pré-existentes foi evidenciada. Uma pátina pré-existente de calcita nas superfícies externas apenas transformou-se um pouco em aragonita.

Nas superfícies internas das fissuras, reações da pasta madura com água do mar origina, uma segunda geração de produtos: formas alteradas de C-S-H, aragonita, calcita e, em algumas cavidades, ainda CH e etringita modificada.

Na interface aço/pasta, regiões porosas e densas formaram a superfície da pasta. A região densa parecia ser constituído por uma camada rica em Ca como calcita e aragonita. Em certas áreas, a difusão de Mg, Cl e Fe em quantidades discretas foram registradas.

INTRODUCTION

In steel reinforced concrete the cement paste is required to perform a double role: those of mechanical strength and chemical resistance. It is on this dichotomy that the durability of the cement paste rests, in answer to the demands made upon it both by the external environment and from within the paste itself.
Cement paste works at interfaces different both in nature and size: paste/paste, paste/aggregate, paste/steel, paste/environment (1,2,3).
It is well known that both aggregate and steel surfaces are the preferential growth sites of hydrate phases, calcium hydroxide, CH, in particular. The paste/steel interfacial region is enriched with CH up to as much as 40% of the global content of mature Ordinary Portland Cement, OPC, paste (4). In consequence its resistance to fracture is recognizably dependent in part on the crystalline state of the CH and on its distribution, see for example (5,6).
Moreover, it has been shown that the chemical resistance too is correlated with the microstructure of paste regions in contact with steel (7,8) and other materials (9).
Cracks present in the paste generate new surfaces, wich are usually propagating along a mechanically weaker path (10,11). They are most dangerous because they put the interior of the paste in contact with the external environment. When they reach the surface of the steel reinforcement they annul both the chemical and mechanical protection of the paste. As a result the nature and thickness of the cover and the features of the cracks: width, length, branching, direction, etc., become important (12).
A fruitful study of the morphological features of the crack surfaces has been made with SEM (10). Distinct morphologies of numerous phases were also evidenced and associated with compositional data by EDXRA (4, 13, 14).
In the present work the interfacial regions of a slag-rich cement paste were examined after a long contact with sea water. The aim was to know the degree of modification by both outward facing surfaces and those of the paste and steel which were found, owing to the presence of the cracks, to be in contact with sea water.

EXPERIMENTAL

Two 3-years old pastes at w/c = 0.33, one from a commercial Portland cement with low content of Al_2O_3, OPC, and the other from a commercial Portland cement formed by the same clinker and 70% slag, SC, were investigated.
Prismatic specimens, 1x1x6 cm, reinforced with a steel fibre having a circular cross section of 3 mm diameter positioned at center and longitudinally were confectioned. Steel surfaces were polished with 300 and 600 grit abrasive and washed with acetone. After 24 hours in 100% RH they were immersed in tap water for six months.
After curing two specimens of SC and OPC reinforced pastes, separated by two glass cylinders, were loaded in flexion, Fig.1, until cracks in paste were visually observed.Then they were kept for 3 years in natural sea water renewed each month.
Fractions of bulk mature pastes were ground and analyzed by DTA, TG, and XRD.
A Cambridge Stereoscan 100 scanning electron microscope, SEM, together with a Link system energy dispersive X-ray analyser, EDXRA, was used.
The energy range for "windows", in EV, were as follows:
960-1100 for NaKα ; 1160-1320 for MgKα and MgKβ ; 1360-1560 for AlKα and AlKβ; 1600-1900 for SiKα and SiKβ; 2160-2420 for SKα , 3500-3860 for CaKα and 6160-6620 for FeKα (13). The counts were accumulated simultaneously until a predetermined gross value of 20000 in the CaKα "window".
The net integrated intensity ofthe radiation of each element was related to one of CaKα ,Pinchin, Tabor (4).

RESULTS AND DISCUSSION

At the centre of Fig. 2A, the external surface II shows three cracks, parallel to each other and transversally set to the steel fibre. Starting from the surface, the zone of maximum deformation, they advance inside the paste leaving traces on the other external surfaces I and III. These cracks become narrowwer and narrowwer and in correspondence with the steel fibre split into two, going in a longitudinal direction. The flexion of the steel fibre has also generated shorter cracks at the extremities, which slope at less than 45° to the axis of the fibre. After curing in water, Fig 2B, the state of the cracks does not seem to have altered as regards their number and width. Rather one notices a partial filling.
Bulk paste constitution can be deduced from thermal analysis and XRD data. DTA profile reveals the presence of three phases: a C-S-H like phase, a CH one, and a $CaCO_3$ one, Fig 3. The three phases are responsable respectively for the large endothermic peak that reaches 265 °C, and the two much smaller ones in the 457-577 °C and 577-724 °C intervals. From the TG curve the corresponding losses of weight in respect to the weight of the sample at 900 °C are 13.9%, 2.5% and 2.5%. The considerable amount of the C-S-H phase is attributable to a greater hydration of the slag grains.
In Fig 4 XRD patterns of bulk paste show a not very intense peak attributable to calcite, and two others still weaker at 11.3 and 31.2 2 attributable to gypsum. On the surface the paste presents a layer of calcite and, in minimum quantity, aragonite. The calcite patina, preformed during immersion in fresh water, is only partly transformed into aragonite (16). Aragonite, however, constitutes the major part of the encrustation on the brass screws, Fig 1. Some peaks can be attributed to those of calcite, but of anomalous intensity. The morphological characteristics of the encrusted surfaces are highlighted by SEM micrographs. The bunched fibrous shapes may be considered representative of aragonite deriving from sea water, Fig 5, (17).

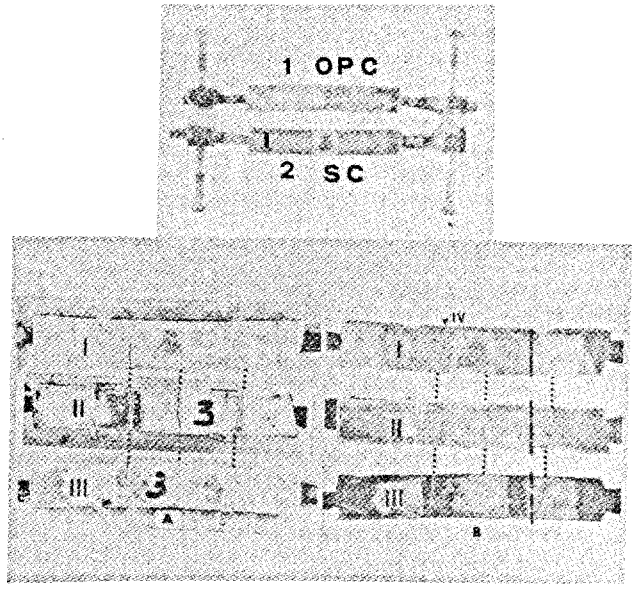

Fig.1 - 1=OPC and 2=SC pastes specimens, 3 years cured in sea water.

Fig.2 - Surfaces I, II, and III of SC paste cured A= in tap water for 6 months, and B= for further 3 years in sea water. The right high risk zone was cut and examined.

Fig.3 - DTA and TG profiles for bulk mature paste.

Fig.4 - Densitometric traces of XRD guinier patterns for: 1= coating of brass screw surface; 2= coating of paste; and 3= bulk paste.

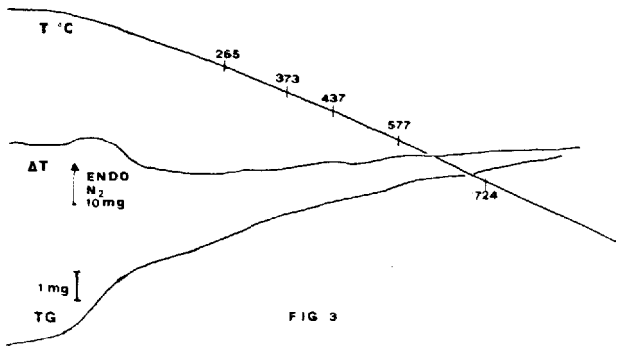

FIG 3

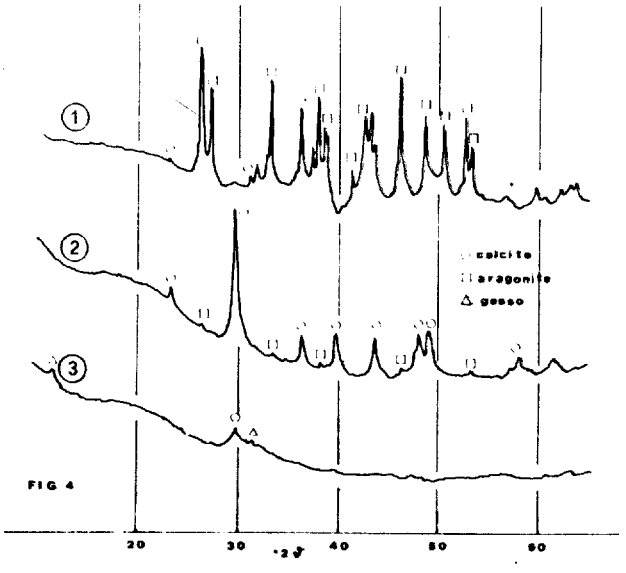

FIG 4

The internal surfaces of a crack show a "plenitudo" of morphologies. The zone reported in Fig 6 is that nearer the external surface indicated as IV in Fig 2B. On the rigth of Fig 6B, the surface layer reveals irregular shaped grains, probably the relicts of slag grains covered with calcite. These would be responsible for the discrete amounts of Al and Si shown by the EDXRA data,see Table 1.
An intermediary layer of brucite (16) is not visible even though a notable Mg content is present. It is to be noted that the porosity of the patina diminishes considerably towards the interior.
The most internal zones of cracks show flattened areas surrounded by fibrous forms and granular ones, Fig 6A. The former, probably "pseudomorphs" of slag grains, show a honeycomb or reticulated structure, Fig 6D, and are rich in Al, region 2, Table 1. The bunched fibrous forms, Fig 6E, are not attributable to ettringite, because of their size and low S content, region 3, and also because ettringite is not stable in sea water. Presumably they are made of aragonite, mainly because of their shape (17), even if EDXRA signals other elements. Actually their distribution suggests than they derive from the zones rich in Ca, that is cement paste, which initially wrap round the slag grains, Fig 6A.
The granular forms, partly separated from the paste, show a notable Ca, Mg, and Si content. Ellipsoid forms, the sole fish type, are also present, on the left of Fig 6D and at the centre of Fig 6F. With enlargment they show transversal grooves on the surface. The Si content is very high, and the Al content is considerable. Their shape means they belong to marine fauna.
The paste/pore interface is the most suitable site for the growth of regular, large size crystalline forms, owing to the wide space available. Hexagonal lamellar forms, even 0.5 mm in size, have been recognized as CH crystals, but are not reported here.
The fibrous forms, such as those in Fig 7, protrude like 100 μm long sticks, 2 μm diameter, with the ends truncated. As may be deduced from EDXRA data, the Al content excludes attribution to Taumasite (17). The element ratio between Al and S would also exclude both ettringite and monosulphate (17).

3.2

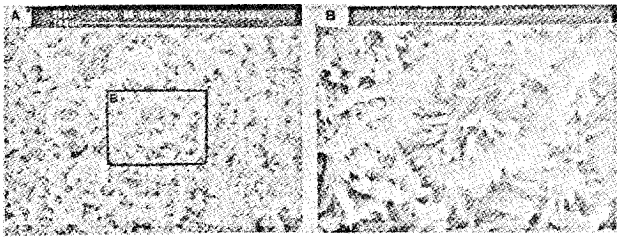

Fig.5 - Aragonite deposit on the brass screw surfaces. B= enlargement of area marked in A.

Fig.6 - Internal surface of a crack far, A, and near, B, the no. IV external surface. C, D, and E are magnifications of the areas marked in A.

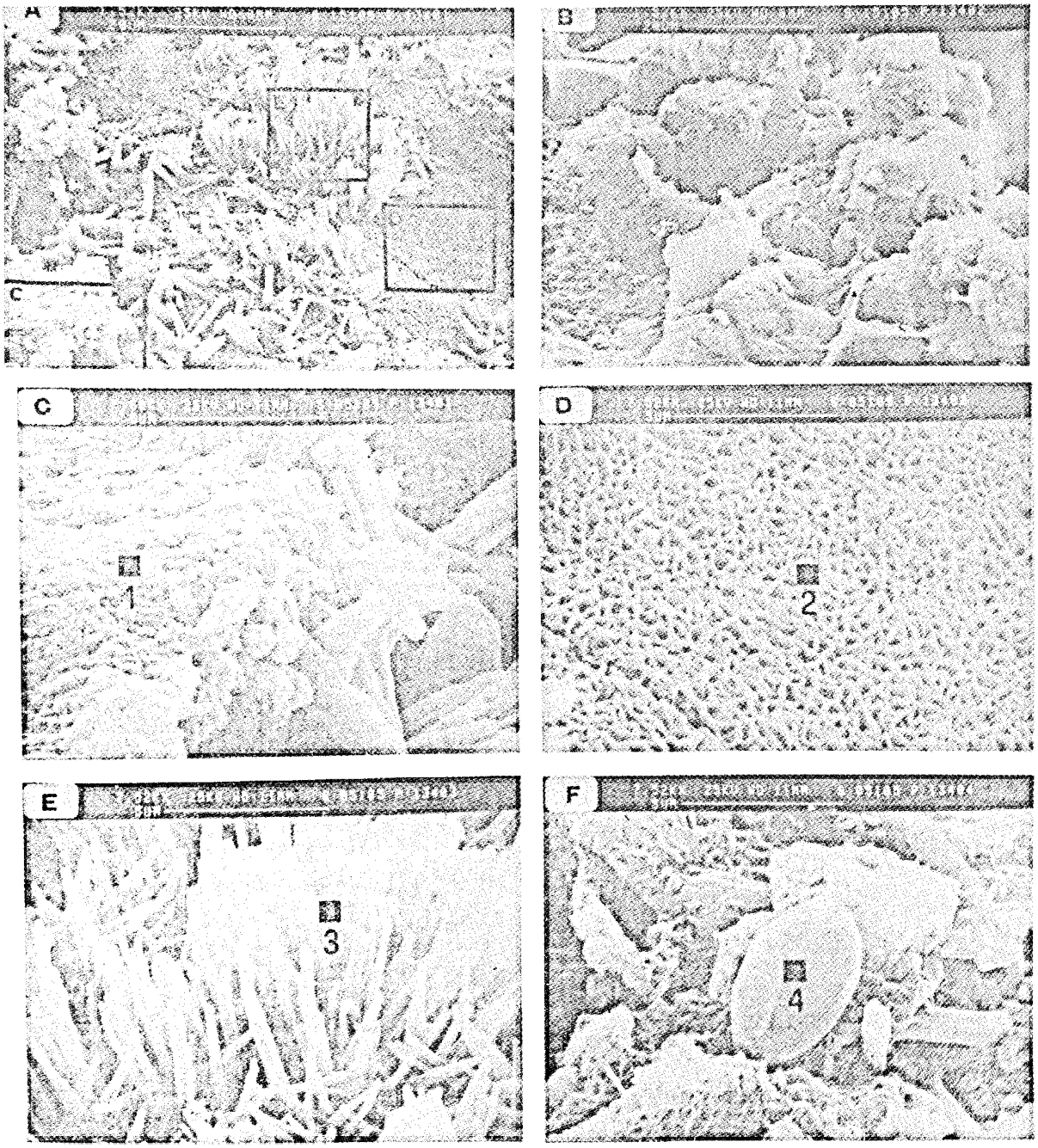

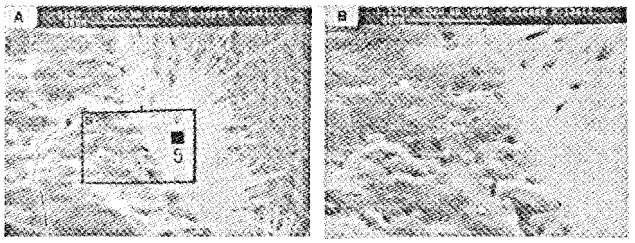

Fig.7 - Paste/pore interface. B is a magnification of area marked in A.

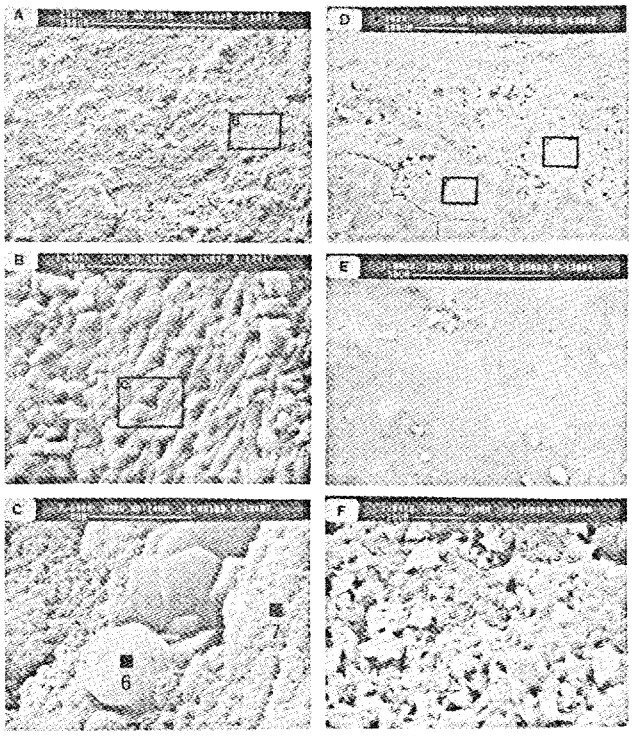

Fig.8 - Paste/steel interface. A= paste surface groove; D= matching steel surface. B,C and E, F are magnifications of aras marked in A and in D, respectively.

TABLE 1. Peak area ratios($x10^{-3}$) by EDXRA for the regions of interfaces in Figs. 6,7,and 8. N.D.= not determined for the interference of Au peak.

FIG.	REGION	Na/Ca	Mg/Ca	Al/Ca	Si/Ca	S/Ca	Cl/Ca	Fe/Ca
6A	general area	1	8	47	333	105	87	55
6B	general area	0	360	509	1890	236	972	690
6C	spot 1	38	203	214	429	N.D.	149	372
6D	spot 2	0	169	333	683	N.D.	479	229
6E	spot 3	0	32	165	277	N.D.	134	285
6F	spot 4	0	213	575	4853	N.D.	814	1104
7A	spot 5	0	121	254	1032	1128	243	99
8A	general area	9	709	157	1222	1693	1333	153
8C	spot 6	0	103	0	353	N.D.	36	2037
8C	spot 7	0	2217	75	4410	N.D.	1199	33082

Attribution is most likely to be to a Si-ettringite, Mehta type 1, with paste of Al O substituted by SiO (18).
At the paste/steel interface the characteristic reddish-browwn colour of rust is visible to the naked eye, both on the paste and the steel.
SEM micrographs show an irregular, but compact, surface, Fig 8. The element ratio Fe/Ca is very high, and the S/Ca and Mg/Ca ratios are also notable, see Table 1.
The area delineated in Fig 8A is less rich in Si and Cl. At higher magnification, it shows sparse polyhedric grains in a mass of much smaller grains. The largest, such of those in Fig 8C, can be considered calcite grains, because of their shape and the low content of other elements. The base mass is characterised by a high content of Mg, Si, Cl, and Fe. The morphology reveals a high degree of crystallinity, but it is not possible distinguish characteristic crystalline shapes. It is probable that these neoformations derive from alterations in the thin layer of CH initially deposited on the steel surface (19, 20, 21).
Even the matching steel surface shows irregularity and dishomogeneity, Fig 9. Both the "smooth" zones, Fig 9B, and the granular ones, Fig 9C, are typical of a layer in decomposition. Elemental analyses show the highest content of Fe and so it is not possible to obtain ratios in respect to Ca.

CONCLUSIONS

Contact between static sea water and mature blast furnace cement paste has not presented apparently noticeable alterations after long ages. The pre-cracking pattern, for example, has not revealed changes in the number and width of the cracks. These are found to be filled by products deriving from both the solution and the paste.

A thick layer of aragonite has been deposi ted by the sea water on the brass surface. A much thinner layer, however, is present on the outer surface of the cement paste. In this case the formation of aragonite has been hindered by the layer of pre-existing calcite. When cracks form in mature paste, the sea water penetrates in its interior and rouses the latent chemical reactivity in

correspondence with the two internal surfaces of the fracture.

The degree of sea water attack will depend on the volume made available by the cracks and the renewal capacity regulating the saturation. In such highly variable conditions the hydrate phases making up the mature paste react with the sea water to form alteration products.

The most characteristic second generation products observed have been: Honeycombe or reticulated C-S-H, leaf-shaped aragonite, granular Ca-rich forms. Flat fish shaped forms are also visible, presumably of an organic nature. Hexagonal lamellae of CH and fibres of ettringite, type I, are still visible in pre-existing cavities. The presence of Mg, Cl, and even Fe, is due to a certain diffusion of the sea water in the interior.

The crack that forms at the paste/steel interface consists of two quite distinct surfaces which react differently with sea water. The paste surface shows a typical compact cristalline microstructure where Mg, Si,Cl, and Fe are present in notable quantities. Sensible larger grains of calcite are distributed in it. It is probable that their growth occurred in pre-existing microcracks.

The steel matching surface shows compact areas beside extremely porous ones both indicative of a high degree of corrosion.

ACKNOWLEDGEMENT

The Author wishes to thank Mr A. Annetta for his technical assistance.

REFERENCES

Only papers published dating from the 7th Congress in Paris (1980) are reported.

1.BOND IN CONCRETE,ed.Bartos,Applied Science Publ.,London,1982.

2.COLLOQUE INTER.LIAISONS PATES DE CIMENTS MATERIAUX ASSOCIES,Ed. Laboratoire de Genie Civil, Tolouse,France,nov.1982.

3.BENTUR A.,DIAMOND S.:"Crack Patterns in Steel Fiber Reinforced Cement Paste" Mater. et Construc. 18 49-56 1985.

4.PINCHIN D.J.,TABOR D.:"Interfacial Phenomena in Steel Fibre Reinforced Cement I: Structure and Strength of Interfacial Region" Cem.Concr.Res. 8 15-24 1978, ref 9 in (3).

5.BARKER A.P. :" Structural and Mechanical Characterization of CH in Set Cement and the Influence of Various Additives" World Cement 15 25-31 1984.

6.ARLIGUIE G.,GRANDET J.,OLLIVIER J.P.:"Orientation de la portlandite, dans les mortiers et betons de ciment Portland" Mater. et Constr. 18 263-267 1985.,

7.MASO J.C.:"La liaison entre les granulats et la pate de ciment hydrate" 7th Int.Cong.Chem.Cem. Paris Rapport principal, sous-theme VII-1 1980.

8.TASHIRO C.,TATIBANA S.:"Bond Strength between C3S Paste and Iron Copper or Zinc Wire and Microstructure of Interface" Cem.Concr.Res. 13 377-382 1983.

9.LANGTON C.A.,ROY D.M.:"Morphology and Microstructure of Cement Paste/Rock Interfacial Regions" 7th Int.Cong. Chem.Cem.,III,VII 127-132 1980.

10.BENTUR A.,DIAMOND S.,MINDESS S.:"Cracking Processes in Steel Fiber Reinforced Cement Paste" Cem.Concr.Res. 15 331-342 1985.

11.PAGE C.L.:"Microstructural Features of Interfaces in Fibre Cement Composites" Composites 13 140-144 1982.

12."Debate: Crack Width, Cover and Corrosion" Concrete Intern. 7 20-35 1985.

13.MARCHESE B.:"IL contributo della SEM allo studio delle paste di cemento.Nota IV." Il Cemento 80 107-120 1983.

14.MARCHESE B.:"Morphology and Composition of Twin Fracture Surfaces of A Crack in PC Paste" Cem.Concr.Res. 13 435-440 1983.

15.MARCHESE B.:"Microstruttura delle fessurazioni nelle paste mature di cemento di altoforno" in "I Materiali per l'ingegneria" Atti 1 Convegno ASMI ott 1983 Milano p.497-504 ed Pitagora,Bologna.

16.CONJEAUD M.L.:"Mechanism of Sea Water Attack on Cement Mortar" in "Performance of Concrete in Marine Environment" Pub.SP-65 ACI Detroit p.39-62 1980.

17.REGOURD M.:"Physico-chemical Studies of Cement Pastes, Mortars,and Concretes Exposed to Sea Water" as (16) p.63-83.

18.MEHTA P.K.:"Mechanism of Sulfate Attack on Portland Cement Concrete-Another Look" Cem. Concr. Res. 13 401-406 1983.

19.MARCHESE B.:"Morfologia e composizione delle microlesioni alla interfaccia acciaio/pasta di cemento" Convegno AITEC Parma ott. 1985, to be published in Il Cemento.

20.MONTEIRO P.J.M., GJORV O.E., MEHTA P.K.:"Microstructure of the Stel-cement Paste Interface in the Presence of Chloride" Cem. Concr.Res. 15 781-784 1985.

21.ZIMBELMANN R.:"A Contribution to the Problem of Cement-Aggregate Bond" Cem.Cocr.Res. 15 801-808 1985.

C. ATZENI, A. MARCIALIS, L. MASSIDDA, U. SANNA
ISTITUTO DI CHIMICA APPLICATA E DI METALLURGIA - UNIVERSITA' DI CAGLIARI - ITALY

EFFECT OF FINE MINERAL ADMIXTURES ON THE PROPERTIES OF HARDENED CEMENT PASTES.
POROSITY-STRENGTH RELATIONSHIPS

L'EFFET DES ADJUVANTS MINERAUX FINES SUR LES PROPRIETES DE PATES DURCIES DE CIMENT.
RELATIONS POROSITE-RESISTANCE

SUMMARY : The effect of fine mineral admixtures on the porosity of hardened cement pastes and the relationships with their strength properties have been examined. An ordinary Portland cement and a variety of blends with admixed pozzolan (10% and 20% by weight), fly-ash (20%) and a finely ground siliceous sand (20%) were tested. Cylindrical specimens prepared from pastes having w/c ratio = 0.25 (using a superplasticizer) and 0.30, were cured at 25°C for between 1 and 90 days.

The obtained mechanical strengths were correlated with the pore structure of the different systems. In order to allow for pore size distribution a parameter, called mean distribution radius r_m, was defined. Introducing this parameter into the function

$$R = \frac{R_c(1-X_v)}{\sqrt{r_m}}$$

together with total porosity X_v and characteristic strength of the system R_c, the overall mechanical results of the systems examined can be correlated with a single expression.

Foram examinados o efeito de misturas minerais finas sobre a porosidade de pastas endurecidas de cimento e as relações com suas propriedades de resistência. Foram testados um cimento portland comum e uma variedade de adições com mistura de pozolana (10 e 20% em peso), cinza volante (20%) e areia silicosa moída finamente (20%). Foram preparados corpos de prova cilíndricos, com pastas com relação água/cimento = 0,25 (usando-se superfluidificante) e 0,30, os quais foram curados a 25°C de 1 e 90 dias.

As resistências mecânicas obtidas estavam correlacionadas com a estrutura porosa dos diferentes sistemas. Para permitir a distribuição de tamanho de poro, definiu-se um parâmetro a que se chamou raio de distribuição médio r_m. Introduzindo este parâmetro na função

$$R = \frac{R_c(1-X_v}{\sqrt{r_m}}$$

juntamente com a porosidade total X_v e a resistência característica do sistema R_c, os resultados mecânicos globais dos sistemas examinados podem ser correlacionados com uma expressão única.

INTRODUCTION

Very high mechanical strengths can be achieved in cement pastes prepared with costly techniques such as high pressure compaction, high temperature curing, polymer impregnation and fibre reinforcement.

In recent years it has emerged that high strength cements can be obtained simply by introducing mineral admixtures of suitable fineness such as, for instance silica fume.

Furthermore it has been recognized that a knowledge of the pore structure of the cement materials and the means of controlling it are fundamental factors in enhancing the performance of a material which is becoming increasingly topical as far as energy cost and versatility are concerned (1).

The effect of volume and morphology of voids on the mechanical strength of a pore structure has been studied on theoretical models adopting, for instance, Griffith's approach (2). However the results achieved thereby are not always applicable to cement systems having a highly complex pore distribution and morphology.

Several authors (3-7) have expressed the dependence of compressive strength of cement systems as a function of total porosity of the paste using empirical relations. In this regard Odler and Rössler (8-9) have recently published a more comprehensive study: the authors have defined a linear dependence of total porosity on strength and have examined moreover the effect on strength of three pore classes.

The present work is concerned with the modifications induced in the pore structure of hardened cement pastes by the addition to ordinary Portland cement of mineral fines, comprising some of pozzolanic reactivity.

Strength is studied in relation to total pore volume and in addition a function is defined in which strength properties depend not only on total pore volume but also on a new parameter related to pore distribution defined as mean distribution radius.

EXPERIMENTAL

The systems studied were ordinary Portland cement (OPC) with admixed pozzolan from Sacrofano (P) (10% and 20%), fly ash (FA), residuum of burning coal dust in an electric power station (20%) and a finely ground siliceous sand (S) (20%).

The chemical and physical characteristics of these materials are given in Table 1. Pastes with water/cement (w/c) ratio of 0.25 and 0.30 (0.35 for the mix with 20% pozzolan) were prepared, using an electromechanical stirrer, in accordance with Italian standards for plastic mortars. In the systems with w/c ratio of 0.25 a superplasticizer was added in the dosage of 3% by weight. For each test ten cylindrical specimens (diameter 30 mm, length 50 mm) were prepared and subsequently vibrated for 2 minutes. Curing (1,3,7,14,28 and 90 days) was carried out at 25°C with relative humidity of over 95%.

Table 1 - Chemical and physical characteristics of the materials

		Portland Cement	Sacrofano Pozzolan	Fly Ash	Siliceous Sand
SiO_2	%	22.4	86.5	64.0	96.0
Al_2O_3	%	4.8	2.3	13.0	0.9
Fe_2O_3	%	2.2	0.2	2.1	1.8
CaO	%	62.1	0.8	7.6	-
MgO	%	1.7	-	1.8	-
Na_2O	%	0.6	0.1	0.6	0.4
K_2O	%	0.3	0.5	1.0	0.1
SO_3	%	3.6	-	3.0	-
Lo.I.	%	4.5	9.6	5.4	-
S.W. ($kg/m^3 \cdot 10^3$)		3.0	1.9	2.2	2.5
SS Blaine (m^2/kg)		390	2660	586	592
SS B.E.T ($m^2/kg \cdot 10^3$)		1.6	61	1.9	1.3

The specimens were then subjected to uniaxial compression tests and porosity was measured with a mercury porosimeter over the range 37-7500 nm.

RESULTS AND DISCUSSION

Compressive strengths versus curing time of specimens with w/c ratio of 0.25 and 0.30 are plotted in Figs. 1a and 1b respectively. For the system containing 20%

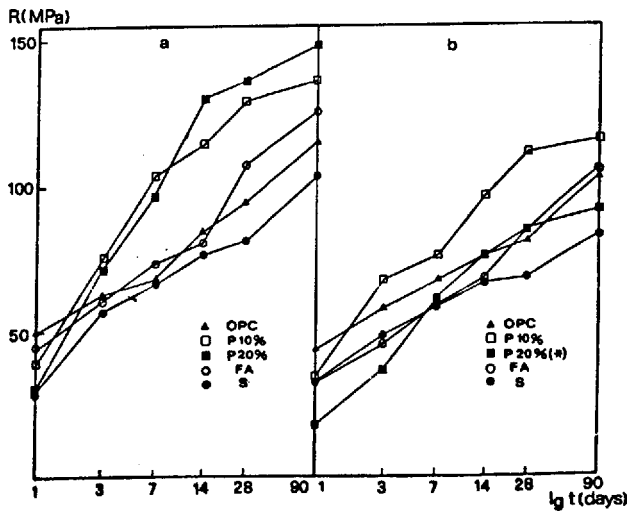

Fig.1 - Compressive strength vs curing time
a) w/c = 0.25
b) w/c = 0.30 ; (*) w/c = 0.35

pozzolan the w/c ratio had to be increased to 0.35 to achieve the same degree of workability due to its large specific surface (2660 m^2/kg Blaine).

The influence of the admixtures in the development of strength differed considerably.

The effect of admixed ground sand, with or without superplasticizer, on the strength of the hardened specimens proved negative. In fact for identical w/c ratios strengths obtained were consistently lower than those of pure cement. Thus the sand has the sole function of inert matter with the result that, for the same degree of hydration, the number of interparticle linkages decreases and strength likewise.

The effect exerted by the two pozzolanic admixtures (pozzolan and fly-ash) is more complex. Initially, after 24 hours hydration, they were observed to weaken the structure; however, after just three days curing the specimens containing pozzolan - quicker to react than ash - yielded strengths higher than pure cement. The mechanical properties of the fly-ash mix improved with curing time and after 90 days strengths about 10% higher than for pure cement were observed.

Under identical conditions the admixtures with 10% and 20% pozzolan yielded increments of about 17% and 30% respectively. A similar trend was observed in the mixes without superplasticizer with the exception of that containing 20% pozzolan where the w/c ratio was increased, as mentioned, to 0.35. In this case obviously the favourable effect of the pozzolanic reaction is neutralized by the different porosity created by the higher water content of the paste.

These findings are corroborated by the results of the porosimetric analysis of the different specimens shown in the histograms of Figs.2 and 3 where the size distribution of the voids is divided into 20 fractions thus allowing a more comprehensive interpretation of the mechanical results.

One common feature that emerged appears to be the continuous reduction of total pore volume with the advancement of hydration. Thus in line with the approach adopted by Hasselman (6-7), subsequently resumed by Rössler and Odler (8), a simple linear relationship may be used to correlate compressive strength with percentage of voids. These correlations, shown in Fig.4, hold true for all the systems and allow to obtain, by extrapolating the regression lines to zero porosity, different values of characteristic strength (R_c).

The attempt to define the contribution of each class of pores within the system in the development of strength appears much more arduous. Examination of Figs.2 and 3 reveals that in all cases prolonged hydration results in a decrease in total porosity as well as a shift of pore size towards smaller dimensions. The further advancement of hydration produces finally a reduction in the amount of the same small pores as the interparticle space is gradually occupied by the gel formed in the hydration reaction.

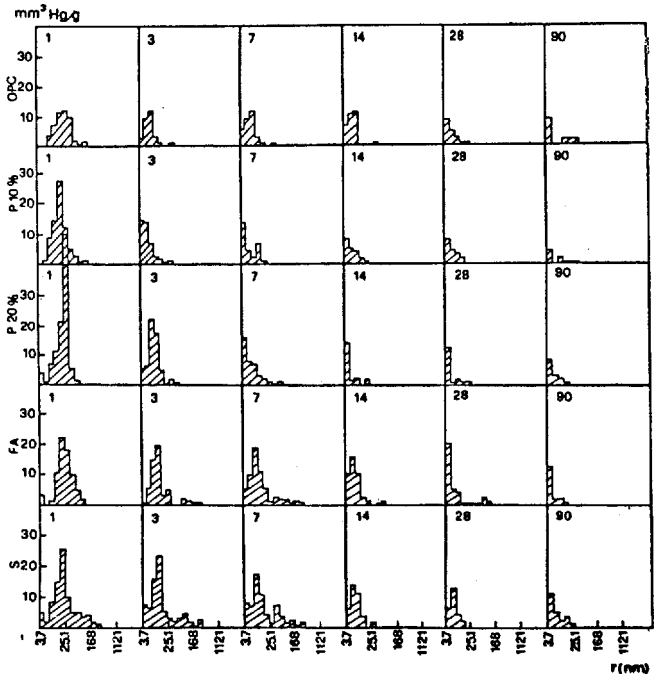

Fig.2 - Pore size distribution in the systems hydrated with w/c = 0.25

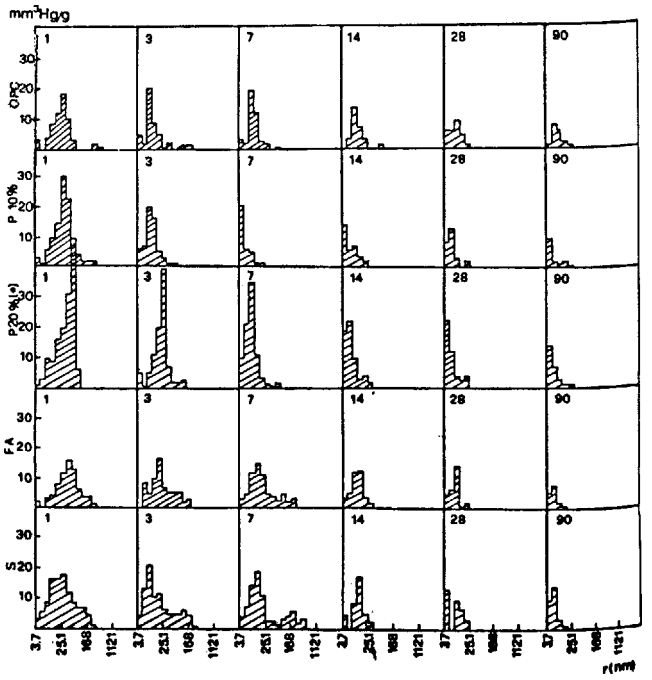

Fig.3 - Pore size distribution in the systems hydrated with w/c = 0.30; (*) w/c = 0.35

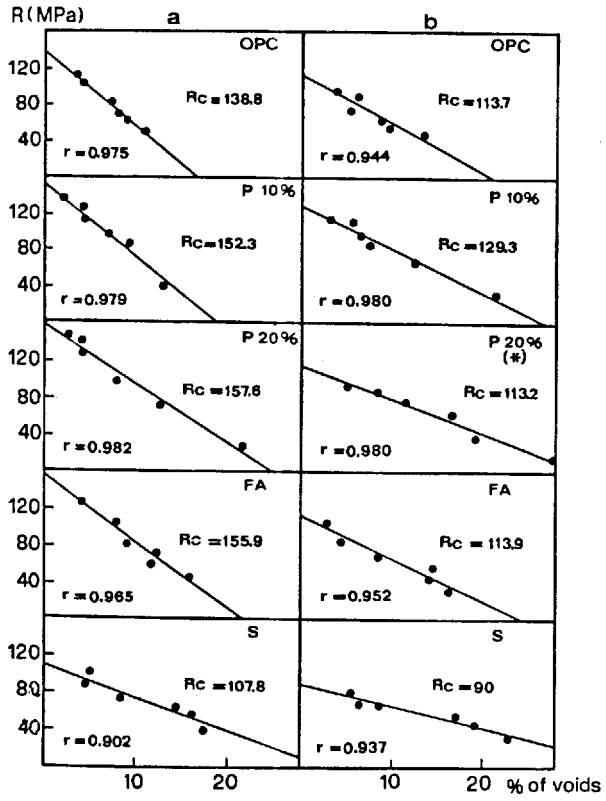

Fig.4 - Strength vs total porosity
a) w/c = 0.25
b) w/c = 0.30; (*) w/c = 0.35

Without a suitable chemical-physical model it is difficult to select the particular pore classes for a more accurate correlation of the strengths. One parameter of porosity that takes into account pore size distribution can be defined as the mean distribution radius r_m (nm):

$$\ln r_m = \frac{\Sigma V_i \ln r_i}{\Sigma V_i}$$

where V_i is the volume of the ith class and r_i the mean radius of the ith class.

The above parameter, in conjunction with total porosity, expressed as a fraction of the voids X_v, and characteristic strength can be used to define the following function:

$$R = K \cdot \frac{R_c(1-X_v)}{\sqrt{r_m}}$$

which enables a unique correlation of the mechanical data obtained for all the systems examined here.

The results of correlation with the above function are shown in Fig.5.

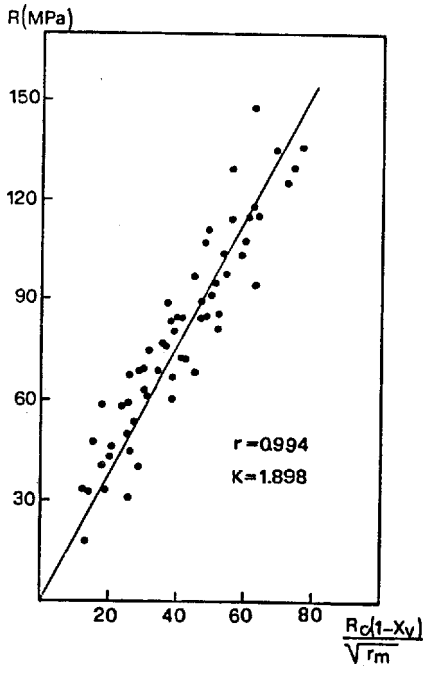

Fig.5 - Compressive strength vs porosity relation containing the distribution parameter.

CONCLUSIONS

The admixing of pozzolanic fines to ordinary Portland cement results in a marked improvement in the mechanical strengths of the hardened products prepared with identical w/c ratios as pure cement.

Strength is enhanced due to the modification of the pore system which brings about a reduction in total porosity as well as a more rapid shift of the most abundant classes towards smaller sizes.

Mechanical strengths can be correlated using a relation which incorporates, besides the characteristic strength of the system and the percentage of porosity, a parameter related to distribution, defined as mean pore radius.

This correlation is independent of type of system and w/c ratio.

REFERENCES

(1) G. FROUHNSDOFF, J. SKALNY (1983), Phil. Trans. R. Soc., London, A 310, 17.
(2) A.A. GRIFFITH (1920), Phil. Trans. R. Soc., London, A 221, 163.
(3) E. RYSKEWITCH (1953), J. Amer. Ceram. Soc, 36, 65.
(4) W. DACKWORTH (1953), J. Amer. Ceram. Soc., 36, 68.
(5) K.K. SCHILLER (1959), in "Mechanical Properties of non Metallic Materials", WALTON (Ed.), Batterworths Sc. Pub., London, 35.
(6) D.P.H. HASSELMANN (1962), J. Amer. Ceram. Soc., 45, 452.
(7) D.P.H. HASSELMANN (1963), J. Amer. Ceram. Soc., 46, 564.
(8) M. ROESSLER, I. ODLER (1985), Cem. Concr. Res., 15, 320.
(9) I. ODLER, M. ROESSLER (1985), Cem. Concr. Res., 15, 101.

G.L. Valenti, R. Cioffi and R. Sersale
Dipartimento di Ingegneria dei Materiali e della Produzione, Università di Napoli, Italy

Behaviour of Italian Fly Ash in Portland Cement Mortars.

Comportement des Cendres Volantes Italiennes dans les Mortiers de Ciment Portland.

SUMMARY: A wide programme of coal utilization for power generating industry is at present in progress in Italy. This programme is based both on the construction of new coal burning power stations and on the conversion from oil fired to coal fired plants.

In 1980, before the start of the above mentioned programme, the amount of coal burnt was about $5x10^6$ tons. In 1984 it rose to $8.2x10^6$ tons. In the beginning of the 1990's consumption of about $30x10^6$ tons of coal is expected. As a consequence of above, the problem of fly ash disposal and utilization is of great actuality in our country.

In this view, chemical and mineralogical composition, glass content, density, moisture content, fineness and particle size distribution of some typical fly ashes are examined and their influence on the mechanical behaviour of portland cement mortars is discussed. Particle size distribution and calcium oxide content seem to be the main factors that influence the performance of the fly ash in portland cement - fly ash mortars.

It is concluded that Italian fly ashes generally show fair pozzolanic behaviour.

No momento existe na Itália um amplo programa para utilização de carvão na indústria de geração de energia. Este programa se baseia tanto na construção de novas usinas geradoras com queima de carvão, como na transformação de usinas a óleo para carvão.

Em 1980, antes do início do atual programa, a quantidade de carvão queimado era de cerca de 5×10^6 t. Em 1984 esta quantidade subira para $8,2 \times 10^6$ t. Espera-se que no início da década de 90 este consumo seja em torno de 30×10^6 t. Em consequência, o problema do que fazer com a cinza volante disponível é muito atual em nosso país.

Sob este ponto de vista se examina a composição química e mineralógica, o teor de vidro, a densidade, o teor de umidade, a finura e a distribuição de tamanho de partícula de algumas cinzas volantes típicas, e se discute sua influência sobre o comportamento mecânico de argamassas de cimento portland. Parece que a distribuição de tamanho de partícula e o teor de óxido de cálcio são os fatores principais que influenciam a performance da cinza volante nas argamassas de cimento portland - cinza volante.

Conclui-se que as cinzas volantes italianas têm, de um modo geral, um comportamento pozolânico excelente.

G.L. Valenti, R. Cioffi and R. Sersale
Dipartimento di Ingegneria dei Materiali e della Produzione, Università di Napoli, Italy.

Introduction

In 1980 the electric energy produced in Italy was 146,856 Gwh. That generated by combustion of traditional fuels (oil, coal, natural gas) was 72.8%. Oil burning accounted for 81.5%, coal 12.3% and natural gas 6.2%. Coal in the amount of $5x10^6$ tons was used. After this year ENEL, the National Electricity Generating Board, has started a wide programme of coal ilization, based both on the construction of new coal-burning power stations and on the transformation of oil fired plants. In 1983 the percentage of traditional thermoelectric energy obtained from oil burning decreased to 71.0%, that derived from coal rose to 18.5%. The amount of burnt coal was $7x10^6$ tons. The coal used was almost entirely imported: 43% from South Africa, 40% from United States, 14% from Poland, 2% from Australia, 1% from Soviet Union.

In 1984 coal in the amount of $8.2x10^6$ tons was used.

In the beginning of the 1990's consumption of about $30x10^6$ tons of coal per year is expected. As a consequence of above, the problem of fly ash disposal and utilization is of great actuality in our country.

On the basis of the experience of nations which traditionally use coal as primary source of energy, the principal utilization of fly ash concerns the fields of blended cements and concrete, where fly ash is employed as pozzolanic addition to portland cement and as its partial replacement, respectively. At present the amount of fly ash utilized in Italy is about 1% of the cement production. That does not only depend on the fact that our country is a strong cement producer (about $40x10^6$ tons per year) and a weak coal consumer, but also on the circumstance that Italy is rich in natural pozzolans. It is expected, however, that soon a strong incentive for fly ash utilization will arise not only from the increased production, but also from the interest of the community towards an adequate disposal, considering the impact that such a problem has on the safeguard of the environment.

The aim of this work is to correlate the chemical and physical properties of some fly ashes produced in Italy with their technical behaviour when mixed with portland cement. At present in our country there are no specifications concerning fly ash sampling and testing for specific uses, but only specifications indicating the requirements of portland pozzolan cements and then, indirectly, of binders containing fly ash as admixture to portland cement. Even if it is clear that modifications of the existing regulations have to be proposed and new specifications have to be defined on the basis of the experiences made in other countries, in this research the evaluation of the technical behaviour of the mixtures containing fly ash is largely based on the methods currently employed in Italy.

Experimental

Five samples of fly ash supplied by ENEL were investigated: one derived from South African coal, two from American coal, two from Polish coal, and are designated as Fly Ash No.1,2 and 3,4 and 5, respectively.

Chemical composition was evaluated through X-ray fluorescence, flame atomic absorption and gravimetric analysis (for sulfates). Loss on ignition (l.o.i.) was determined by heating to constant weight at 750°C. Mineralogical composition was evaluated by means of X-ray diffraction analysis. The glass content was estimated as the ash fraction soluble in a 2 wt.% HF solution using the method of Murat and coworkers (1). Density measurements were performed by helium pycnometry. Moisture content was determined by drying to constant weight at 110°C. Specific surface (Blaine) was measured by an air permeabilitymeter. Particle size distribution was evaluated by laser diffraction and sieve analyses.

For mechanical tests a high strength portland cement having a Blaine fineness of 399.0 m^2kg^{-1}, supplied by Cementir S.p.A., was utilized. The chemical composition (wt.%) of portland cement was the following: SiO_2 20.8; Al_2O_3 6.4; Fe_2O_3 2.9; CaO 62.3; MgO 1.6; Na_2O 0.5; K_2O 0.7; SO_3 3.2; l.o.i. 1.9. Sixteen mixes were prepared: a control containing only portland cement; 15 containing the five ashes and the pozzolan, each at 3 levels of partial cement replacement: 10; 20; 30 wt.%. The cement or cement+ash-sand-water mix ratios were 1:3:0.5. From each mix 9 prisms, 40x40x x160 mm, were obtained. From each specimen broken by flexure two half-specimens were generated for compressive strength tests.

Results and discussion

The chemical composition of the fly ashes is shown in Table 1. It can be seen that fly ashes generated by coals of different origin have different compositions. L.o.i. is a reflection of the efficiency of the combustion process rather than an intrinsic characteristic of fly ash: thus the unusually high value observed for Fly Ash No.1 is probably due to imperfect combustion.

In regards to the mineralogical composition, the main crystalline components found in all ashes are: quartz, mullite, hematite. Fly Ash No.1 contains calcium oxide. Fly Ashes No.4 and 5 contain magnetite and calcium oxide. In Fly Ash No.1 the main reflection for mullite is more intense than that for quartz. Compared to Fly Ash No.1, Fly Ashes No.2-5 have a higher quartz/mullite ratio.

The values of glass content, density, moisture content, specific surface (Blaine), <45μm fraction (sieve analysis) are listed in Table 2. The finding that fly ashes with similar <45μm fractions have considerably different values of Blaine fineness is in part due to a diversified particle size distribution. This clearly appears from Fig.1 showing the cumulative percentage volume of particles, in the normalized 2-176 μm range,

G.L. Valenti, R. Cioffi and R. Sersale
Dipartimento di Ingegneria dei Materiali e della Produzione, Università di Napoli, Italy

with dimensions lower than the diameter reported in abscissa. In the range 2-45μm Fly Ashes No.1 and No. 4 are respectively richer and poorer in the smaller particles than other ashes.

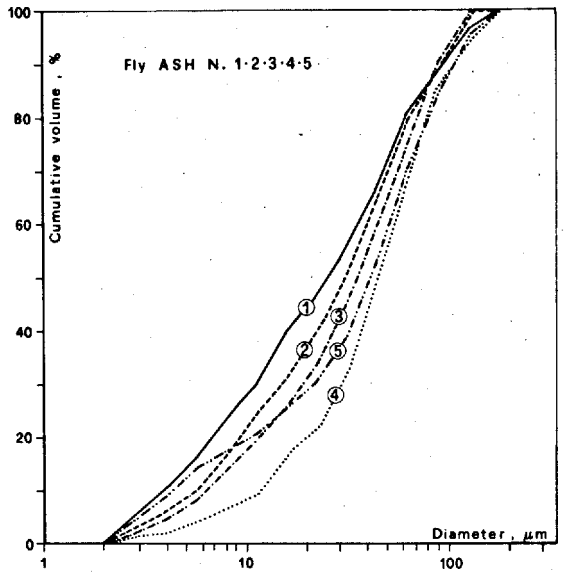

Fig.1 - Cumulative data of the particle size distribution of Fly Ashes.

Table 3 shows the sieve analysis data, expressed as weight fractions, in the range 45-250μm. Data shown in Fig.1 are thus confirmed and a further indication is obtained: that the difference between the >45μm fractions of Fly Ashes No.4 and 5 is pratically concentrated in the fraction having particles larger than 250μm.

Table 1 - Chemical Composition of Fly Ashes, % .

	Fly Ash No.				
	1	2	3	4	5
SiO_2	42.74	50.23	49.97	46.27	44.50
Al_2O_3	28.49	26.99	26.83	21.05	22.03
Fe_2O_3	4.61	6.31	6.32	10.22	9.49
MnO	0.03	0.03	0.03	0.15	0.15
TiO_2	1.47	1.42	1.43	1.01	1.00
CaO	9.33	1.81	1.89	6.34	7.22
MgO	2.12	1.14	1.20	4.11	4.40
Na_2O	0.59	0.66	0.53	0.93	1.03
K_2O	0.81	2.51	2.47	2.23	2.34
SO_3	0.75	0.90	0.79	1.87	1.13
l.o.i.	12.94	6.91	7.02	3.97	3.92

Table 2 - Physical Properties of Fly Ashes.

	Fly Ash No.				
	1	2	3	4	5
Glass content,%	64	73	75	63	67
Density,Kg m^{-3}	2380	2300	2290	2370	2370
Moisture content,%	0.1	0.2	0.3	0.9	0.1
Specific surface (Blaine), m^2Kg^{-1}	606.0	332.0	349.0	192.5	302.0
<45μm fraction,%	75.4	74.8	70.6	46.0	51.9

Table 3 - Sieve Analysis of Fly Ashes, %.

Size range, μm	Fly Ash No.				
	1	2	3	4	5
> 250	1.6	2.8	3.4	9.9	3.4
180-250	3.1	1.8	2.2	5.5	6.5
125-180	4.1	2.3	3.0	6.8	7.5
90-125	4.4	3.3	4.1	7.8	8.5
63-90	5.4	6.2	7.1	11.3	11.0
45-63	6.0	8.8	9.6	12.7	11.2
< 45	75.4	74.8	70.6	46.0	51.9

Tables 4,5 and 6 show the flexural and compressive strengths of portland cement-fly ash mortars at 3,7, 28 days, for percentage of cement replacement equal to 10,20 and 30%, respectively. Strength values lower than minimum limits required by the Italian standards are underlined.

From the overall examination of the mechanical properties the following indications can be achieved:

a) the behaviour of the portland cement-fly ash mixtures is better at flexion than at compression;
b) Fly Ash No.1 shows a better behaviour and Fly Ash No.4 the worst one, while the other ashes do not behave much differently one from another.

These indications are more evident when the curing time is longer and as the percentage of cement replacement is higher. Fly Ash No.1 is the only one that shows, in some occasions, higher or equal strengths with respect to those shown by cement without addition. This happens respectively for values of compressive strengths at 7 and 28 days, at a 10% replacement level, and for values of flexural strength, at 28 days, which increase together with the percentage of replacement.

G.L. Valenti, R. Cioffi and R. Sersale
Dipartimento di Ingegneria dei Materiali e della Produzione, Università di Napoli, Italy.

Table 4 - Flexural and compressive strengths of portland cement-fly ash mortars (percentage of cement replacement: 10 wt.%).

Mortar made with:	Flexural Strength MPa			Compressive Strength MPa		
	3d	7d	28d	3d	7d	28d
No addition	5.8	6.9	7.6	31.1	37.2	45.5
Fly Ash No.1	5.3	6.2	7.6	29.4	37.0	45.7
Fly Ash No.2	5.3	6.2	7.4	27.4	32.8	41.1
Fly Ash No.3	5.3	6.2	7.2	28.4	35.1	42.7
Fly Ash No.4	5.0	5.9	6.8	25.0	32.0	39.9
Fly Ash No.5	5.2	6.1	7.4	27.8	33.5	41.1

Table 5 - Flexural and compressive strengths of portland cement-fly ash mortars (percentage of cement replacement: 20 wt.%).

Mortar made with:	Flexural Strength MPa			Compressive Strength MPa		
	3d	7d	28d	3d	7d	28d
No addition	5.8	6.9	7.6	31.1	37.2	45.5
Fly Ash No.1	4.9	5.9	7.7	26.1	33.1	42.8
Fly Ash No.2	4.6	5.8	7.3	24.5	30.6	40.1
Fly Ash No.3	4.4	5.9	7.1	24.3	30.4	39.7
Fly Ash No.4	4.6	4.8	6.2	23.5	24.9	32.4
Fly Ash No.5	4.5	5.8	7.2	24.7	31.3	37.7

Table 6 - Flexural and compressive strengths of portland cement-fly ash mortars (percentage of cement replacement: 30 wt.%).

Mortar made with:	Flexural Strength MPa			Compressive Strength MPa		
	3d	7d	28d	3d	7d	28d
No Addition	5.8	6.9	7.6	31.1	37.2	45.5
Fly Ash No.1	3.9	5.3	8.0	21.8	27.4	40.1
Fly Ash No.2	4.1	5.5	6.9	21.5	25.1	35.5
Fly Ash No.3	4.0	5.0	7.0	21.5	25.5	34.8
Fly Ash No.4	4.2	3.9	5.4	20.5	19.0	25.7
Fly Ash No.5	3.9	4.6	6.6	21.6	24.3	32.3

Concerning the influence of chemical and physical properties of these fly ashes on the mechanical characteristics of the corresponding cement mortars, first of all it has to be pointed out that Fly Ashes No. 2 and 3 promote a similar behaviour. Furthermore Fly Ashes No.2 and 3 have similar characteristics in terms of chemical composition, glass content, fineness and particle size distribution. It is thus confirmed what is found in literature (2-7) about the importance that these factors have on fly ash reactivity.

Within the ranges of the examined values for each of the above mentioned factors, particle size distribution and calcium oxide content seem to be the main parameters that influence the performance of fly ash in portland cement-fly ash mortars.

Fly Ashes No.4 and 5, similar except for particle size distribution, show a very different behaviour thus evidentiating the important role played by such factor. Fly Ash No.4 determines inferior mechanical properties because of a coarser particle size distribution under 45μm and higher residue with respect to 250μm (9.9 versus 3.4%).

The strength contribution rate of Fly Ash No.5 is similar to that of Fly Ashes No.2 and 3, in spite of a less favourable particle size distribution. Furthermore Fly Ashes No.2 and 3 have the highest amount of silica, silica+alumina (77%), silica+alumina+iron oxide (83%) and of glass phase. The mechanical behaviour of Fly Ash No.5 is probably due to a higher calcium oxide content (7.2 versus 1.8%). As a matter of fact, according to Mehta (8) an aluminosilicate glass containing more calcium is more reactive. The free lime content of Fly Ash No.5, determined by Franke method, is about 0.8%.

The highest l.o.i., the lowest values of the silica and of $SiO_2+Al_2O_3+Fe_2O_3$ contents and a $SiO_2+Al_2O_3$ amount as well as a glass content lower than the ones of Fly Ashes No.2 and 3, do not prevent Fly Ash No.1 from being superior to others. This is predominantly due to a larger concentration of the smaller particles in the range 2-45μm.

However, it must not be considered that particle size distribution alone, whatever are the Fly Ash characteristics, regulates the mechanical behaviour of portland cement-fly ash mortars. In fact, the compressive strengths, at 28 days of curing, of 3 mortars (20% replacement of cement), each containing one of three fractions of Fly Ash No.5 ground in a laboratory mill for 20,40 and 60 minutes, are respectively: 38.7, 39.5 and 40.0 MPa. Fig.2 shows the particle size distribution of such fractions indicated as B,C and D respectively, together with that of the generating Fly Ash No.5 indicated as A. Going from A (Table 5) to B, from B to C, and from C to D the gains of strength are: 2.6; 2.2; 1.3%, respectively. Therefore, within the examined kinds of particle size distribution, the strength contribution due to this parameter acquires progressively less importance as the

particle size distribution shifts towards greater contents of smaller particles.

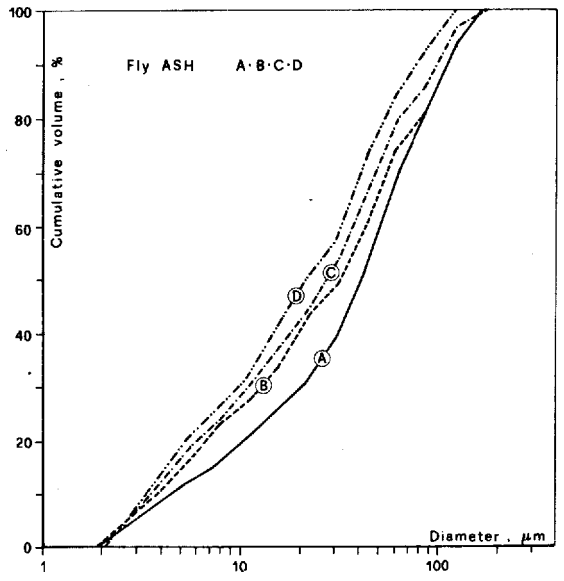

Fig. 2 - Cumulative data of the particle size distribution of ground fractions of Fly Ash No.5.

Furthermore Fly Ash C has a particle size distribution practically equal to Fly Ash No.1 (Figs.1 and 2) while it promotes an eight percent lower compressive strength (Table 5). This behaviour is probably due to the different calcium oxide content.

Conclusions

Italian fly ashes, when employed as partial replacement of portland cement in normally cured mortars, generally show a quite satisfactory pozzolanic behaviour.

Within the ranges of the examined values for each of the chemical and physical properties of fly ash, particle size distribution has a dominant influence on the performance of fly ash in portland cement-fly ash mortars. This influence becomes less strong as the particle size distribution shifts towards greater content of smaller particles.

Calcium oxide content also plays a substantial role, while the other parametersare of no majr importance.

Acknowledgements

This work has been carried out with the financial support of Progetto Finalizzato Energetica, Sottoprogetto Carbone-Idrogeno, CNR-ENEA, contract No. 84.2946.59.'

The Authors wish to express their gratitude and appreciation to Dr.Eng. C.Sandrelli and Dr.Eng. M.Puccio - Centro Ricerche Ceneri - ENEL and to Dr.Prof. G.Frigione - CEMENTIR S.p.A. for contributing to the success of this work.

References

1. M. Murat, Y. Arnaud, M. El Moussaouiti and C. Comel, (1984) "Détermination des teneurs en alumino-silicates cristallisés et amorphes dans les cendres volantes et les mullites synthétiques", Silicates Industriels, Vol.49, No.6, 127-135.
2. R. Sersale, (1980) "Structure et charactérisation des pozzolanes et des cendres volantes", 7e Congrès International de la Chimie des Ciments, Editions Septima, Paris, Vol.I, IV-1/3 - IV-1/21.
3. K. Takemoto and H. Uchikawa (1980) "Hydratation des ciments pouzzolaniques", ibidem, Vol.I, IV-2/1 -- IV-2/29.
4. J. Beretka and T. Brown, (1976) "Properties and pozzolanic behaviour of Australian fly ash",Journal of the Australian Ceramic Society, Vol.12, 13-19.
5. J. Calleja, (1983) "Cenizas, cementos y hormigones con cenizas", Cemento Hormigon, No.597, 707-730 and No.598, 827-850.
6. P.K. Mehta, (1983) "Pozzolanic and cementitious by-products as mineral admixtures for concrete - A critical review", ACI Special Publication SP 79 (Editor: V.M.Malhotra), Vol.1, 1-46.
7. S. Diamon , (1984) "The utilization of fly ash", Cement and Concrete Research, Vol.14, 455-462.
8. P.K. Mehta (1985) "Influence of fly ash characteristics on the strength of portland-fly ash mixtures", ibidem, Vol.15, 669-674.

YUKIO TAKANO, Senior Research Chemist, Research Department,
YUKIO MIZUKAMI, Research Chemist, Chichibu Cement Co., Ltd., JAPAN

Influence of Kind of Calcium Sulfate on Hardening of Cement Paste Mixed with Humic Acid

SUMMARY: The influence of the kind of calcium sulfate on the hardening of cement paste mixed with humic acid was studied mainly with reference to the saturation ratio of $[Ca^{2+}]\cdot[SO_4^{2-}]$ and $[Ca^{2+}]\cdot[OH^-]^2$ in the liquid phase of three types of high SO_3 cement paste containing gypsum, β-hemihydrate and anhydrite II respectively.
Comparison of the saturation ratio of $[Ca^{2+}]\cdot[SO_4^{2-}]$ in the liquid phase at the initial age of the three types of cement paste mixed with humic acid shows that the saturation ratio of the cement paste containing anhydrite II is smallest due to the slow dissolving speed of anhydrite II. Also, the cement paste containing anhydrite II has the highest amount of humic acid dissolved in the liquid phase for its smallest Ca^{2+} concentration in the liquid phase.
As a result, it seems that when 5% humic acid is added to the cement paste containing anhydrite II, the amount of humic acid adsorbed on the initial hydrate of C_3Ass increases and conversion and crystallization of the initial hydrate is prevented, therefore, the hydration of C_3Ass is retarded.
Furthermore, an increased amount of humic acid adsorbed on alite reduces the rate of Ca^{2+} elution from alite. Therefore, $[Ca^{2+}]\cdot[OH^-]^2$ saturation ratio is unable to reach the maximum value before 7 days in age, resulting in extreme retardation of hydration of alite.
The cement containing β-hemihydrate or gypsum, on the other hand, began to hydrate vividly even mixed with 5% humic acid.
A stabilization experiment on peat based on this knowledge shows that the cement mainly comprising anhydrite II with a small amount of β-hemihydrate is more suitable to peat stabilization than the cements used with gypsum, β-hemihydrate and anhydrite II individually.

Estudou-se a influência do tipo de sulfato de cálcio sobre o endurecimento da pasta de cimento misturada com ácido húmico, relativamente à relação de saturação de $Ca^{2+}).(SO_4^{2-})$ e $(Ca^{2+}).(OH^-)^2$ na fase líquida de três tipos de pasta de cimento com SO_3 alto, contendo gesso, β-semihidrato e anidrito II, respectivamente.

A comparação da relação de saturação de $(Ca^{2+}).(SO_4^{2-})$ na fase líquida em idade inicial dos três tipos de pasta de cimento misturada com ácido húmico mostra que a relação de saturação da pasta de cimento contendo anidrito II é a menor, devido à velocidade lenta de dissolução do anidrito II. A pasta de cimento contendo anidrito II também tem a maior quantidade de ácido húmico dissolvido na fase líquida, devido à menor concentração de Ca^{2+} na fase líquida. Como resultado, parece que quando são adicionados 5% de ácido húmico à pasta de cimento contendo anidrito II, a quantidade de ácido húmico adsorvido no hidrato inicial de C_3Ass aumenta, e a conversão e cristalização do hidrato inicial são impedidas, retardando-se, portanto, a hidratação de C_3Ass.

E mais: um aumento da quantidade de ácido húmico adsorvido em alita reduz a velocidade de elução de Ca^{2+} da alita. Portanto, a relação de saturação de $(Ca^{2+}).(OH^-)^2$ não basta para atingir o valor máximo antes da idade de 7 dias, dando como resultado uma grande retardação da hidratação da alita.

Por outro lado, o cimento contendo β-semihidrato ou gesso começa a hidratar-se acentuadamente, mesmo misturado com 5% de ácido húmico.

Uma experiência de estabilização com turfa, à base deste conhecimento, mostra que o cimento contendo principalmente anidrito II com uma pequena quantidade de β-semihidrato é mais adequada para estabilização da turfa do que os cimentos usados com gesso, β-semihidrato e anidrito II individualmente.

YUKIO TAKANO, Senior Research Chemist, Research Department,
YUKIO MIZUKAMI, Research Chemist, Chichibu Cement Co., Ltd., JAPAN

INTRODUCTION

In recent years, cement of high SO_3 type has come to be used more and more widely in Japan. In solidifying soil with cement, the influence of an organic matter such as humic acid on the hydration of cement is pointed out as an important problem.(1) The influence of organic matters on the hardening of cement has been the subjects of many researches mainly relating to saccharide and lignosulfonate salt.(2), (3) Very few of them concerns the study of the relationship with the kind of calcium sulfate although some of them refers to the relationship with the amount of calcium sulfate.

We are empirically aware that the high SO_3 cement using anhydrite suitable for stabilization soil containing a small amount of organic matters has less effect of peat stabilization than the high SO_3 cement using hemihydrate or gypsum.

We have conducted a study of the influence of the kind of calcium sulfate on the hardening of cement paste of high SO_3 type mixed with humic acid mainly by analysis of the liquid phase effective for study of initial hydration. At the same time, study was made about the kind of calcium sulfate desirable for the high SO_3 cement for peat stabilization.

SAMPLE AND EXPERIMENT

High SO_3 type cement

The chemical composition of clinker and gypsum are shown in Table 1. The clinker is burnt in a practical rotary kiln, and the gypsum is made by desulfurization of waste gas and contain no silicofluoride or phosphate. The Blaine specific surface area of gypsum was 1440 cm^2/g. The β-hemihydrate and anhydrite II were obtained by heating gypsum for 12 hours at 120°C and for two hours at 800°C respectively.

Table 1 Chemical composition of clinker and gypsum.

Sample	Chemical composition (%)									
	ig. loss	insol.	SiO_2	Al_2O_3	Fe_2O_3	CaO	MgO	SO_3	Na_2O	K_2O
Clinker	0.1	0.0	22.7	4.8	3.4	65.9	1.2	0.6	0.50	0.63
Gypsum	20.1	0.7	0.1	0.7	0.5	31.8	0.3	44.8	0.04	0.00

The clinker alone was ground up to 3190 cm^2/g in Blaine specific surface area, and the three kinds of calcium sulfate each 10% were added to prepare three types of high SO_3 cement.

In this report, the high SO_3 cement prepared by use of gypsum, β-hemihydrate and anhydrite II are designated by G, H and A respectively.

Humic acid

In this study, the reagent humic acid obtained from peat was used.

Hydration of cement paste

Humic acid of 0, 1, 2 and 5% were added to the three types of cement and hydrated at 20°C with the water cement ratio of 3 assuming the peat stabilization. In order to prevent separation of cement from liquid phase, a cylindrical container 60 mmøx 100 mm containing cement paste was rotated at the rate of 4 turns per minute.

Determination of ionic concentration in liquid phase

The paste hydrated up to predetermined age was filtered, and the liquid phase was collected, so that the dissolved amount of humic acid and the concentration of Ca^{2+}, $R^+(Na^+ + K^+)$, SO_4^{2-} and OH^- were determined. For the collection of the liquid phase from the stabilized peat, the pressure method was used.

Quantitative analysis of ettringite and $Ca(OH)_2$

The hydrate obtained when collecting the liquid phase was dried by the D-Drying method after stopping the hydration with acetone. The ettringite was determined by the XRD method and $Ca(OH)_2$ by the solvent extraction method.

RESULT AND DISCUSSION

Hydration of cement paste

Amount of humic acid dissolved

Humic acid is not dissolved in pure water but in alkali such as NaOH solution. With Ca^{2+}, however, it is said to precipitate in the form of calcium salt. Fig. 1 shows the relationship between the Ca^{2+} concentration and the dissolved amount of humic acid at the initial age of nine types of cement paste covering 1, 2 and 5% of humic acid added and three types of cement.

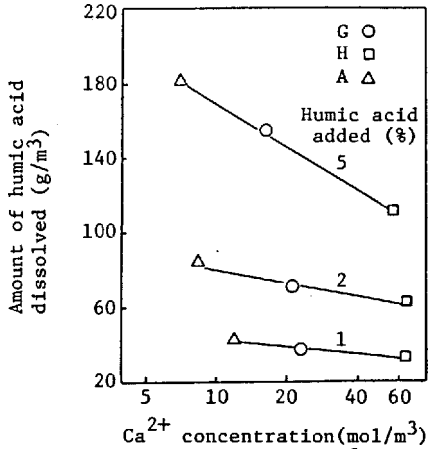

Fig. 1 Relation between Ca^{2+} concentration and amount of humic acid dissolved at 2 minutes after mixing.

YUKIO TAKANO, Senior Research Chemist, Research Department,
YUKIO MIZUKAMI, Research Chemist, Chichibu Cement Co., Ltd., JAPAN

The dissolved amount of humic acid has the linear relationship with log Ca^{2+}. By cement type, cement A with smaller Ca^{2+} concentration was accompanied by a greater dissolved amount of humic acid, and when 5% humic acid was added, humic acid was dissolved at the rate of 180 g/m^3.

$[Ca^{2+}]\cdot[SO_4^{2-}]$ and $[Ca^{2+}]\cdot[OH^-]^2$ Saturation ratio of liquid phase

By use of the ionic concentration in the liquid phase of cement paste shown in Fig. 2, $[Ca^{2+}]\cdot[SO_4^{2-}]$ and $[Ca^{2+}]\cdot[OH^-]^2$ saturation ratio was calculated by the method of Kondo, et al.(4) Fig. 3 shows the relationship between $[Ca^{2+}]\cdot[SO_4^{2-}]$ and $[Ca^{2+}]\cdot[OH^-]^2$ saturation ratio in the liquid phase at initial age and the amount of humic acid mixed. Fig. 4, on the other hand, shows the time dependency of the $[Ca^{2+}]\cdot[SO_4^{2-}]$ saturation ratio and Figs. 5 and 6 the time dependency of $[Ca^{2+}]\cdot[OH^-]^2$ saturation ratio.

Fig. 3 shows that the $[Ca^{2+}]\cdot[SO_4^{2-}]$ saturation ratio in the liquid phase at initial age is dependent to a large measure on the type of cement involved, without humic acid, cement H being largest, followed by cement G and A in that order. When humic acid is mixed, $[Ca^{2+}]\cdot[SO_4^{2-}]$ saturation ratio decreased at higher rate for cement A than for cement G and H. When 5% humic acid is added, for instance, $[Ca^{2+}]\cdot[SO_4^{2-}]$ saturation ratio declined for one-third of cement G and one-tenth of cement H, and remains far from the saturation level.

The retardation of C_3Ass hydration due to an organic admixture is caused, according to Milestone(5), by the fact that organic molecules are entered into the crystal lattice of hexagonal hydrate to stabilize

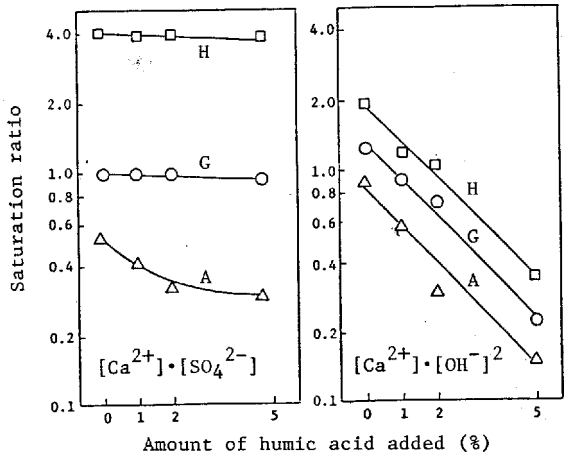

Fig. 3 $[Ca^{2+}]\cdot[SO_4^{2-}]$ and $[Ca^{2+}]\cdot[OH^-]^2$ saturation ratio in liquid phase at 2 minutes after mixing.

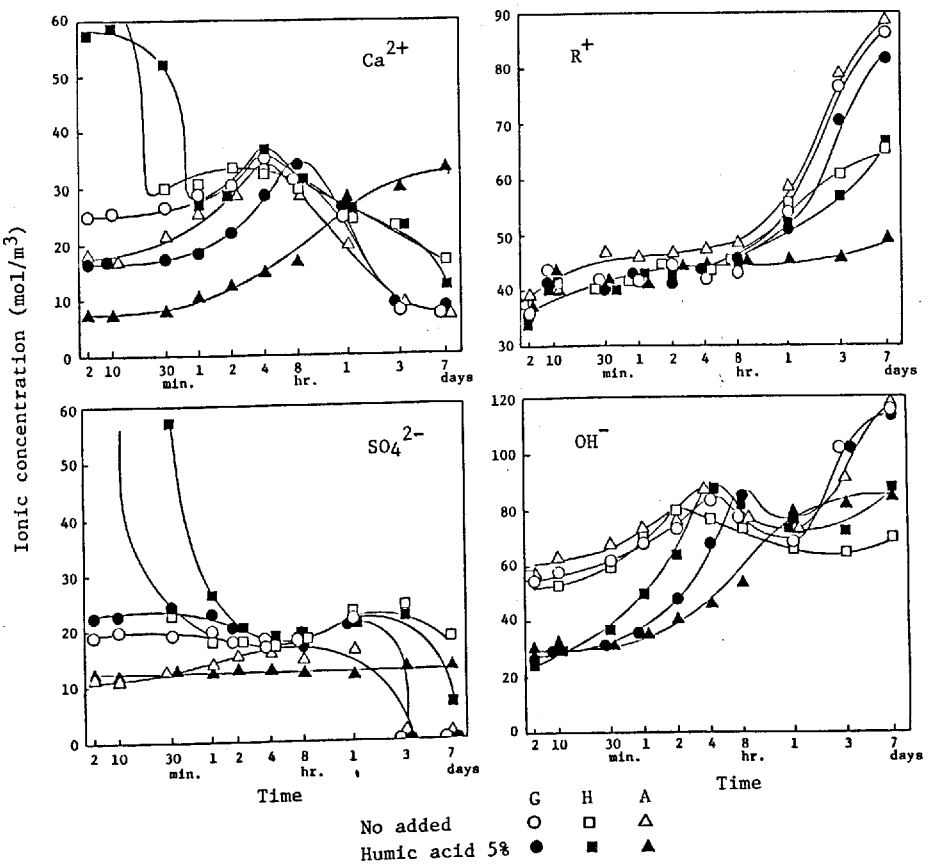

Fig. 2 Change of each ionic concentration in liquid phase.

YUKIO TAKANO, Senior Research Chemist, Research Department,
YUKIO MIZUKAMI, Research Chemist, Chichibu Cement Co., Ltd., JAPAN

the hexagonal hydrate. It seems that if the amount of dissolved humic acid is great with low $[Ca^{2+}]\cdot[SO_4^{2-}]$ saturation ratio as is seen when the 5% humic acid is added to cement A, more humic acid is adsorbed on fine hydrate formed at the initial age of $C_3As\bar{s}$ hydration, with the result that crystallization and conversion of initial hydrate are hampered, thus retarding hydration of $C_3As\bar{s}$ greatly.

This retardation ends with the decrease in the dissolved amount of humic acid and the rise in $[Ca^{2+}]\cdot[SO_4^{2-}]$ saturation ratio, but continued up to the age of 7 days in the case of 5% humic acid was added to cement A. With respect to the time dependency of saturation ratio, it is interesting to note as shown Fig. 4 that the saturation ratio is sharply reduced by the precipitation of secondary gypsum for cement H and the stable saturation ratio of cement G at saturation level and the saturation ratio for cement A is very low., Especially in the case of cement A, the dissolving speed of anhydrite is so slow that it takes a long time before $[Ca^{2+}]\cdot[SO_4^{2-}]$ saturation ratio reaches saturation level, and with 5% humic acid is added, it takes 7 days before $[Ca^{2+}]\cdot[SO_4^{2-}]$ of saturation in spite of very little consumption of $CaSO_4$ for $C_3As\bar{s}$ hydration, indicating that the dissolving speed of anhydrite was reduced greatly by the adsorption of humic acid thereon.

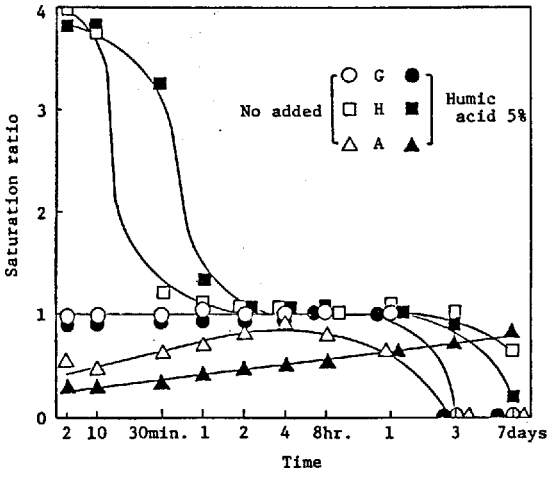

Fig. 4 Change of $[Ca^{2+}]\cdot[SO_4^{2-}]$ saturation ratio in liquid phase of cement paste.

The $[Ca^{2+}]\cdot[OH^-]^2$ saturation ratio at initial age, like $[Ca^{2+}]\cdot[SO_4^{2-}]$ saturation ratio, is smallest for cement A as shown Fig. 3. With the addition of humic acid, $[Ca^{2+}]\cdot[OH^-]^2$ saturation ratio is remarkably reduced for every type of cements, and it declines down to 0.15 with the addition of 5% humic acid to cement A. At initial age, the $[Ca^{2+}]\cdot[OH^-]^2$ saturation ratio depends on the kind of calcium sulfate added to cement and free lime of cement.(6), (7)

The rise of $[Ca^{2+}]\cdot[OH^-]^2$ saturation ratio is considered to concern with elution of Ca^{2+} from alite.(8) It may be that the rate at which the $[Ca^{2+}]\cdot[OH^-]^2$ saturation ratio rises decreases as the elution of Ca^{2+} from alite is hampered as a result of adsorption of humic acid thereon. Therefore, as apparent from Fig. 5, the addition of humic acid lengthens the time before $[Ca^{2+}]\cdot[OH^-]^2$ saturation ratio reaches a maximum value.

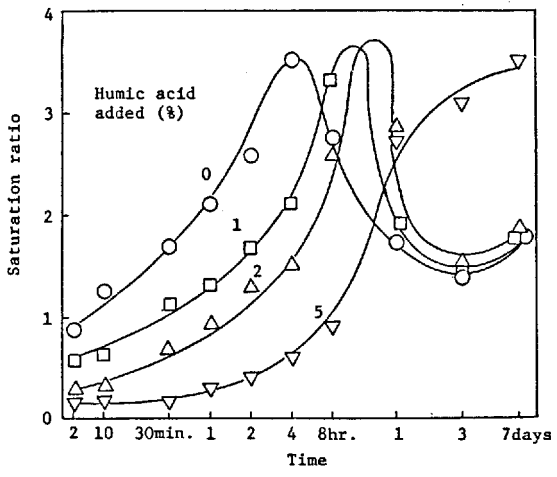

Fig. 5 Change of $[Ca^{2+}]\cdot[OH^-]^2$ saturation ratio in liquid phase of A cement paste.

In the case where humic acid of 5% is added to cement A, $[Ca^{2+}]\cdot[OH^-]^2$ saturation ratio at initial age declines down to 0.15 and more humic acid remains dissolved with an increased adsorption thereof on alite, with the result that the $[Ca^{2+}]\cdot[OH^-]^2$ saturation ratio rises so slowly that it is not before 7 days in age that it reaches a maximum value. It is known that there is some relationship between the advent of a maximum value of $[Ca^{2+}]\cdot[OH^-]^2$ saturation ratio in the liquid phase and vivid hydration of alite,(4), (6) and it is apparent that the addition of humic acid retards the hydration of alite. On the other hand, for cement G and H, as apparent from Fig. 6, even with the addition of 5% humic acid, $[Ca^{2+}]\cdot[OH^-]^2$ saturation ratio reached a maximum 4 to 8 hours in age, starting vivid alite hydration.

Young(9) made comments on the mechanism of retarding the hardening of cement paste by an organic admixture by classifying the process into 1) adsorption, 2) complexation, 3) precipitation, and 4) nucleation control, from the viewpoint of extension of the induction period. The third classification has often been cited for the retarding mechanism by the humic acid since humic acid is liable to precipitate in the form of calcium salt.(2) This theory however, may not be satisfactory in view of the fact that the retarding action by humic acid acts more strongly on cement A small in Ca^{2+} concentration as compared with cement H which is larger in initial Ca^{2+} concentration producing more calcium salt of humic acid.

YUKIO TAKANO, Senior Research Chemist, Research Department,
YUKIO MIZUKAMI, Research Chemist, Chichibu Cement Co., Ltd., JAPAN

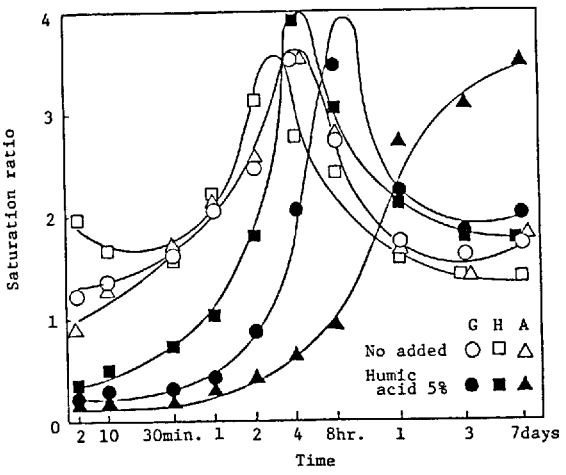

Fig. 6 Change of $[Ca^{2+}]\cdot[OH^-]^2$ saturation ratio in liquid phase of cement paste.

Our present experiment indicates that, as has been explained in the past, the explanation of the retarding mechanism by humic acid based on the first theory is more rational. More specifically, the adsorption of humic acid on cement causes a reduced elution rate of Ca^{2+}, retarding the advent of a maximum value of $[Ca^{2+}]\cdot[OH^-]^2$ saturation ratio, therefore, hydration of alite is retarded.

Amount of Hydration Products

Fig. 7 shows the change of the amount of ettringite and $Ca(OH)_2$ formed in the cement paste with 5% humic acid. $Ca(OH)_2$ is not detected in either cement substantially before 2 hours in age. This may be related to the fact that the $[Ca^{2+}]\cdot[OH^-]^2$ saturation ratio in the liquid phase has not yet exceeded saturation level.

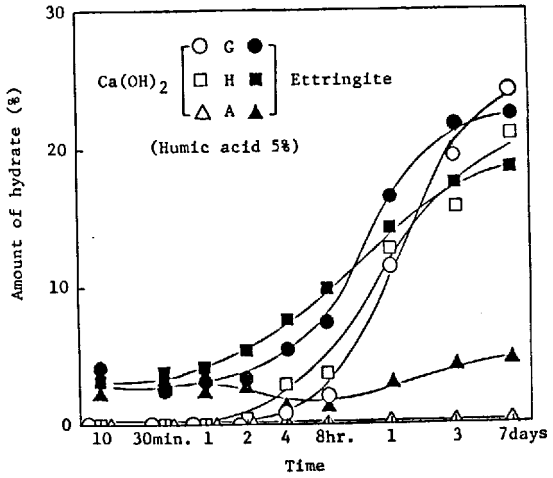

Fig. 7 Change of amount of hydrate formed in cement paste with 5% humic acid.

In the case of cement H and G, $Ca(OH)_2$ increases at about 4 hours in age. The time when $Ca(OH)_2$ sharply increases almost coincides with the time the $[Ca^{2+}]\cdot[OH^-]^2$ saturation ratio in the liquid phase reaches the maximum, indicating the start of vivid hydration of alite. About 3% ettringite is formed at initial age, and it begins to increase somewhat earlier than $Ca(OH)_2$.

In the case of cement A, on the other hand, though a small amount of ettringite is formed, substantially no $Ca(OH)_2$ is detected before 7 days in age, indicating an extreme retardation of hydration of cement paste.

Stabilization of Peat

The hydration of cement paste with anhydrite is retarded extremely with the increase in the amount of humic acid added, according to the hydration test of paste, probably for the reason that the dissolving speed of anhydrite is slow and therefore the initial $[Ca^{2+}]\cdot[SO_4^{2-}]$ saturation ratio is small. On the other hand, we have experienced that the high SO_3 cement with anhydrite is effective for the stabilization of soil containing little organic matters.

Securing the initial $[Ca^{2+}]\cdot[SO_4^{2-}]$ saturation ratio with a small amount of hemihydrate, we conducted a peat stabilization test using high SO_3 cement (abbreviated as AH) mainly comprising anhydrite. The same test was conducted on cements G, H and A.

The sample peat used was a soil containing much organic matters and water as shown in Table 2. This peat was mixed with 30% cement, and the unconfined compressive strength obtained is shown in Fig. 8.

Table 2 Character of peat.

Moisture content (%)	664
Liquid limit (%)	465
Plastic limit (%)	157
Plasticity index	308
Humic acid (%)	24.6
Fulvic acid (%)	6.8

AH cement displayed superior strength as expected, which reached the unconfined compressive strength about 7 times that of cement A by 3 days in age and more than four times that of cement A by 7 days in age. The strength obtained by cement H, by contrast, was higher than that of the other types of cement on the first day, while it declined below that of cement G and AH by 3 days in age. This may be explained in relation to the amount of $Ca(OH)_2$ and ettringite produced in the paste experiment.

The time dependency of the $[Ca^{2+}]\cdot[SO_4^{2-}]$ and $[Ca^{2+}]\cdot[OH^-]^2$ saturation ratio in the liquid phase collected for each age from a stabilized peat is shown in Fig. 9. In the case of AH cement, the $[Ca^{2+}]\cdot[SO_4^{2-}]$ is oversaturated at 1.6 in saturation ratio by

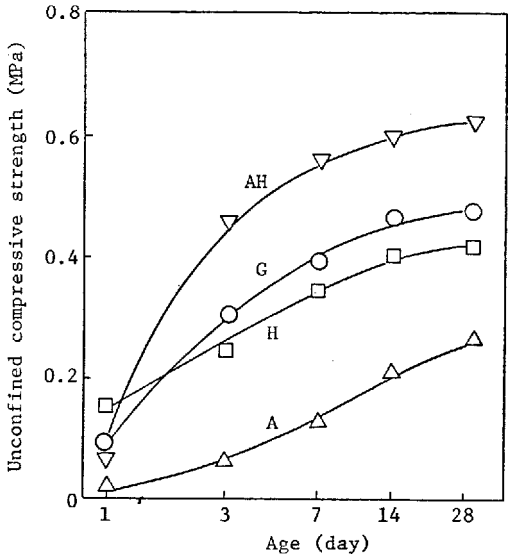

Fig. 8 Unconfined compressive strength of stabilized peat.

the effect of hemihydrate at initial age, but came to settle at 0.8, with less humic acid remaining dissolved with the exception of cement H. The $[Ca^{2+}]\cdot[OH^-]^2$ saturation ratio also reached a maximum during the period 24 to 48 hours in age, indicating a smooth progress of hydration of cement paste.

The $[Ca^{2+}]\cdot[SO_4^{2-}]$ saturation ratio of cement A, on the other hand, is as low as 0.2 to 0.4, and the $[Ca^{2+}]\cdot[OH^-]^2$ saturation ratio neither failed to reach a maximum before three days in age, in a trend similar shown by the result of the paste test.

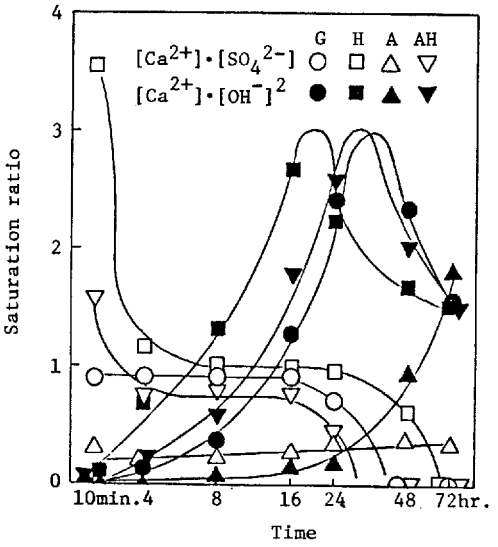

Fig. 9 Change of $[Ca^{2+}]\cdot[SO_4^{2-}]$ and $[Ca^{2+}]\cdot[OH^-]^2$ saturation ratio in liquid phase of stablized peat.

CONCLUSION

The influence of humic acid on the hardening of high SO_3 cement paste greatly depends on the dissolving speed of calcium sulfate added to cement of high SO_3 type, and the cement using anhydrite II is extremely hampered in hardening. The high SO_3 cement using both anhydrite II and β-hemihydrate is more suitable for peat stabilization than the cements using gypsum, β-hemihydrate and anhydrite II individually.

ACKNOWLEDGEMENT

We wish to express ours thanks to the top management and Mr. O. Suzuki, Manager of Research Department and Mr. M. Tanaka, Chief Chemist of Chichibu Cement Co., Ltd., for invaluable advices and useful suggestion and allowing us to publish this paper.

REFERENCES

1.- M. OBA, K. FUJISAKI, I. KOJIMA (1966), "On the effect of soil organic matter on the herdening of cement", Semento Gijutsu Nenpo, 20, 231-237.
2.- S. SUZUKI, S. NISHI (1959), "Influence of saccharides and other organic additives on the hydration of portland cement" Semento Gijutsu Nenpo, 13, 160-170.
3.- RENE' J. BAUSET (1968), "Abnormally delayed setting of a low-heat portland cement with lignosulphonate admixtures", Fifth Intern. Symp. Chemistry of Cement, Tokyo, Vol. IV, 53-57.
4.- W. KONDO and K. FUJII (1974), "Occurrence of supersaturated solution with respect to $Ca(OH)_2$ in portland cement paste", J. Cer. Assoc. of Japan, 82(6), 333-336.
5.- N.B. MILESTONE (1977), "The effect of glucose and some glucose oxidation products on the hydration of tricalcium aluminate", Cem. Concr. Res., 7, 45-52.
6.- H. UCHIKAWA, S. UCHIDA, K. OGAWA (1984) "Influence of $CaSO_4 2\cdot H_2O$, $CaSO_4 1/2\cdot H_2O$ and $CaSO_4$ on the initial hydration of clinker having different burning degree", Cem. Concr. Res., 14, 645-656.
7.- H. UCHIKAWA, K. OGAWA, S. UCHIDA (1985), "Influence of character of clinker on the early hydration process and rheological property of cement paste", Cem. Concr. Res., 15, 561-472.
8.- P. FIERENS, J.P. VERHAEGEN (1976) "Hydration of tricalcium silicate in paste-kinetics of calcium ions dissolution in the aqueous phase", Cem. Concr. Res., 6, 337-342.
9.- J.F. YOUNG (1972) "A review of the mechanisms of set-retardation in portland cement pastes containing organic admixtures", Cem. Concr. Res., 2, 415-433.

K.SATO, E.KONISHI and K.FUKAYA, Nippon Kokan K.K., Kawasaki, JAPAN
K.KOIBUCHI, Y.ISHIKAWA and Y.IIJIMA, Dai-ichi Cement Co., Ltd., Kawasaki, JAPAN

Properties of very fine blast furnace slag prepared by classification
Propriété de la poudre très fine de laitier de haut fournau préparée par la classification 3.2

SUMMARY: The hydraulic hardening capacity of granulated blast furnace slag can be drastically improved by making it finer. In this study, two grades of very fine slag were obtained by classifying ground commercial slag. The slag powders thus obtained had the Blaine surface area of more than 8000 cm^2/g. Investigation was carried out as Portland blast furnace cement on very fine slag. The mortar strength and shrinkage, the resistance of hardened paste to the expansion due to the alkali-aggregate reaction and the Cl^--permeability were measured with hardened mortar. For the slag particles less than 5 μm in diameter, the mortar strength was much higher than that of ordinary Portland cement (OPC). Even when the particle sizes were less than 10 μm, mortar strength was also higher than that of OPC after 7 days onwards. The tendency of shrinkage was closely similar to the case with slag of normal fineness. Moreover, the use of very fine slag was remarkably effective in preventing the expansion due to the alkali-aggregate reaction. It is still effective in the resistance to expansion when the slag of normal fineness was used, or the fineness of slag is not an important factor in the resistance to expansion.
The Cl^--permeability of hardened paste is very small: after soaking in sea water, the concentration of Cl^- ion in the hardened paste was found lower than that of OPC subjected to the same conditions. It is concluded that slag powder prepared by the classification practically applicable to producing such very fine slag has excellent properties as a cementitious material.

A capacidade de endurecimento hidráulico da escória granulada de alto forno pode ser drasticamente melhorada, refinando-a. Neste estudo, foram obtidos dois graus de escória muito fina por meio de classificação de escória comercial moída. Os pós de escória obtidos desta forma tinham área de superfície Blaine superior a 8.000 cm^2/g. Desenvolveu-se estudo como cimento de escória de alto forno com escória muito fina. A resistência e retração da argamassa, a resistência da pasta endurecida à expansão, devida à reação álcali-agregado e a permeabilidade Cl^- foram medidas com argamassa endurecida. No caso de partículas de escória com diâmetro menor que 5 μm, a resistência da argamassa foi muito mais alta que a de cimento portland comum (OPC). Mesmo quando os tamanhos de partícula eram menores que 10 μm, as resistências da argamassa também foram mais altas que as do cimento portland comum depois de 7 dias e mais. A tendência de retração foi estreitamente semelhante à do caso de escória com finura normal. Além disso, o uso de escória muito fina foi notavelmente eficaz na prevenção da expansão, devido à reação álcali-agregado. Ela é ainda eficaz na resistência à expansão quando se usou escória com finura normal, ou a finura da escória não é um fator importante na resistência à expansão. A permeabilidade da pasta endurecida ao Cl^- é muito pequena: depois de embebida em água do mar, verificou-se que a concentração de íon Cl^- na pasta endurecida era menor que a de cimento portland comum submetido às mesmas condições. Concluiu-se que pó de escória, preparado por classificação, de aplicação prática na produção de escória muito fina, tem propriedades excelentes com material cimentoso.

K.SATO, E.KONISHI and K.FUKAYA, Nippon Kokan K.K., Kawasaki, JAPAN
K.KOIBUCHI, Y.ISHIKAWA and Y.IIJIMA, Dai-ichi Cement Co., Ltd., Kawasaki, JAPAN

1. INTRODUCTION

In the recent years in Japan, durability of concrete has been a matter of great concern as the deterioration of concrete structure due to the alkali-aggregate reaction or chloride damage drew more social attention.

The addition of water granulated blast furnace slag or fly ash is reported to be effective in preventing the alkali-aggregate reaction and the chloride damage [1),2),3)], however the low early-stage strength caused by this addition has been a big problem.

Focusing on the use of water granulated blast furnace slag because of its economy and stable quality, the authors found that the early-stage strength as well as other properties such as durability could be improved by making the fineness of slag very high.

The very fine slag used here could be obtained practically by classification following the usual pulverization process.

In the present study, the hydraulic hardening capacity, effectiveness in preventing the alkali-aggregate reaction, and the durability against sea water of the very fine slag obtained mainly by the process mentioned above were examined.

2. EXPERIMENTAL

2.1 Preparation of Samples

Chemical compositions of the slag powder (Blaine specific surface area 3700 cm^2/g, denoted as S) and ordinary Portland cement (denoted as OPC) are shown in Table 1.

Table 1. Chemical compositions of slag and OPC (wt%)

	Ig.loss	Insol	SiO_2	Al_2O_3	Fe_2O_3	CaO	MgO	SO_3	Na_2O	K_2O	TiO_2	P_2O_5	MnO	S
slag	+0.1	0.1	35.4	12.9	0.3	41.8	6.3	0.0	0.26	0.38	1.65	0.00	0.42	1.0
OPC	1.1	0.1	21.2	5.1	3.0	63.1	2.1	2.2	0.40	0.44	0.43	0.07	0.09	-

The very fine slag powder was prepared by classifying the ordinary slag powder S with a forced vortex type centrifugal classifier or by pulverizing S with a ball mill.

In the case of the classification process, very fine slag powders having Blaine specific surface area of about 5000 cm^2/g, 6000 cm^2/g (denoted as S20), 8000 cm^2/g (denoted as S10), 12000 cm^2/g, and 15000 cm^2/g were obtained at cut sizes of 25μm, 20μm, 10μm, 5μm, and 3μm respectively.

In the pulverization process, slag powders of about 5000 cm^2/g, 6000 cm^2/g, 7000 cm^2/g , and 8000 cm^2/g (Blaine) were obtained by using diethylene glycol as a grinding aid.

Figure 1 shows the particle size distributions of two slag powders prepared by different processes having about the same fineness (approximately 8000 cm^2/g).

The particle size distributions were measured by means of the Coulter Counter method.

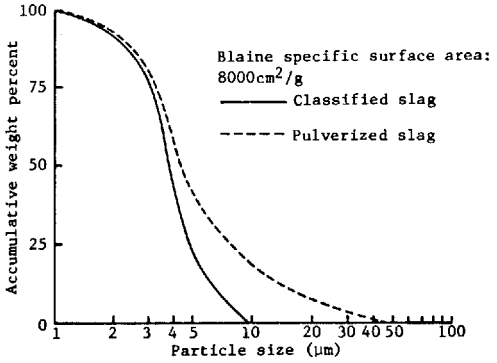

Fig. 1. Particle size distributions

2.2 Quality Tests for Trial Cements Prepared with Very Fine Slag

Setting and mortar strength tests were carried out for the trial cements (compounding ratios are shown in Table 2) according to JIS R5201.

In addition, the trial cements No.6, 11, and 17 were subjected to the shrinkage test according to the JCA (The Cement Association of Japan) method.

Table 2. Blaine specific surface area of materials (cm^2/g) and compounding ratios of trial cements (wt%)

Materials	Blaine (cm^2/g)	Compounding ratios (wt%) OPC	Slag	No.
Classified slag	5000	60	40	1
	6000	80	20	2
		60	40	3
		40	60	4
	8000	80	20	5
		60	40	6
		40	60	7
	12000	60	40	8
	15000	60	40	9
Pulverized slag	3700	80	20	10
		60	40	11
		40	60	12
	5000	60	40	13
	6000	60	40	14
	7000	60	40	15
	8000	60	40	16
OPC	3200	100	0	17

2.3 Effectiveness of the Very Fine Slag in Preventing the Alkali-Aggregate Reaction

The slag powders S and S10 were used for the alkali-aggregate reaction test.

Here, the amounts of slag powders contained in the trial cements were 0, 20, 40 and 60% by weight.

Used aggregates were of Yamagata and Kagawa prefecture origin which were supposed to be very alkali-reactive under highly alkaline conditions.

Chemical compositions of the aggregates are shown in Table 3.

Table 3. Chemical compositions of aggregates (wt%)

	ig.loss	SiO_2	Al_2O_3	Fe_2O_3	CaO	MgO	Na_2O	K_2O	MnO
Kagawa	2.2	65.8	15.8	3.0	3.9	2.6	3.07	2.04	0.02
Yamagata	0.6	54.9	18.8	8.2	9.8	3.9	2.17	0.55	0.17

The alkali-aggregate reaction was tested according to ASTM C227 (mortar bar method), but 0.5N NaOH aq.soln. was used as mixing water in order to accelerate the reaction. In the case of OPC, tap water was also used for comparison.

2.4 Durability of Very Fine Slag Based Mortar in Sea Water

Durability against sea water was tested by measuring the Cl^--permeation depth in the hardened bodies soaked in sea water. The depth of Cl^--permeation was measured with $AgNO_3$ as an indicator (color development method [4]). Trial cements used here were the same with those prepared for the alkali-aggregate reaction test mentioned before. Specimens of size 4 x 4 x 16cm were prepared according to JIS R5201 but with water-cement ratio of 0.5. The specimens were cured in 20°C tap water for 7 days (standard curing) then cured in 20°C sea water. Here, Cl^- concentration of the sea water was 2.04%. The surfaces of the specimens except both ends were coated with paraffin in order that only both ends of the specimens come into contact with sea water. After reaching a fixed age, specimens were cut perpendicular to both ends.

$AgNO_3$ aq.soln. (0.1N) was sprayed on the surface to produce AgCl (white precipitate) which indicates the extent of Cl^--permeation. Depth of Cl^--permeation was measured also by means of EPMA, and pore size distributions were measured by means of mercury porosimetry for the 6 months-soaked specimens.

3. RESULTS AND DISCUSSIONS

3.1 Quality of Cement Prepared with the Very Fine Slag

Results of setting test and mortar strength test are shown in Table 4.

Table 4. Setting time and strength

No.	Water amount (%)	Setting time: Initial (hr-min)	Setting time: Final (hr-min)	Compressive strength (MPa): 3d	7d	28d	Bending strength (MPa): 3d	7d	28d
1	30.5	3-02	4-37	11.3	20.4	53.5	3.2	4.3	9.0
2	29.5	3-00	4-30	14.1	25.5	50.6	3.3	5.8	7.8
3	31.0	2-52	4-20	12.0	21.8	59.4	3.2	4.5	8.3
4	35.0	3-12	4-52	10.0	21.1	49.9	2.6	4.3	7.4
5	29.0	2-59	3-50	17.2	28.1	48.7	4.1	5.9	7.8
6	32.0	2-54	3-55	13.7	25.9	58.3	3.4	5.2	8.8
7	36.5	3-06	4-46	12.0	24.5	53.9	3.4	5.2	8.8
8	33.0	2-06	2-59	18.8	33.6	55.3	4.2	6.1	7.7
9	35.0	1-40	2-35	21.4	37.8	48.0	4.4	6.1	6.3
10	28.5	3-00	3-59	11.6	20.5	39.7	3.2	4.1	6.7
11	28.0	3-26	4-38	10.2	17.2	40.5	3.1	4.1	7.1
12	30.0	4-01	5-04	6.1	13.9	38.3	2.0	3.3	6.5
13	29.0	3-10	4-08	11.5	20.6	48.7	3.4	4.7	7.4
14	29.2	2-49	3-34	12.3	23.2	51.2	3.4	5.1	7.8
15	29.5	2-54	3-33	12.9	23.8	51.5	3.3	5.1	7.7
16	29.5	2-44	3-08	13.6	26.9	49.4	3.5	5.8	8.3
17	28.5	2-40	3-36	12.5	22.1	39.4	3.1	4.8	6.7

a. Setting

Slag contents being equal, finer slag requires more water for normal consistency and shorter setting time.

As slag content increases, required water and setting time increase.

These tendencies are shown both by the classified slag and the pulverized one.

b. Mortar Strength

Figure 2 shows the relation between fineness of slags and compressive strength of trial cements containing the slags by 40 wt%.

Figure 3 shows the relation between slag contents and compressive strength.

Comparing the strength development of the classified slag and pulverized one, as shown in Fig. 2, both slags show the same early-stage (3d, 7d) strength development which are proportional to their fineness.

With regard to 28d strength, however, strength due to classified slag is apparently higher than that due to pulverized one.

Both slags show their maximum strength at about 7000 cm^2/g.

As shown in Fig. 3, with ordinary slag powder (S, 3700 cm^2/g), higher slag content gives lower early-stage strength, however, 28d strength is the same with that of OPC as long as slag content is kept within 60%.

On the other hand, with classified slag, early-stage strength is best with S10 (8000 cm^2/g) while later-stage strength is best with S20 (6000 cm^2/g).

The strength of the classified slag is generally higher than that of OPC and considerably higher than ordinary slag's. Optimum content of the classified slag is estimated to be 20% for early stage and 40 - 60% for later stage.

c. Shrinkage

The results of the shrinkage tests are shown in Fig. 4. The mortar shrinkage for slags were a little larger than that for OPC, however S and S10 show almost the same shrinkage.

3.2

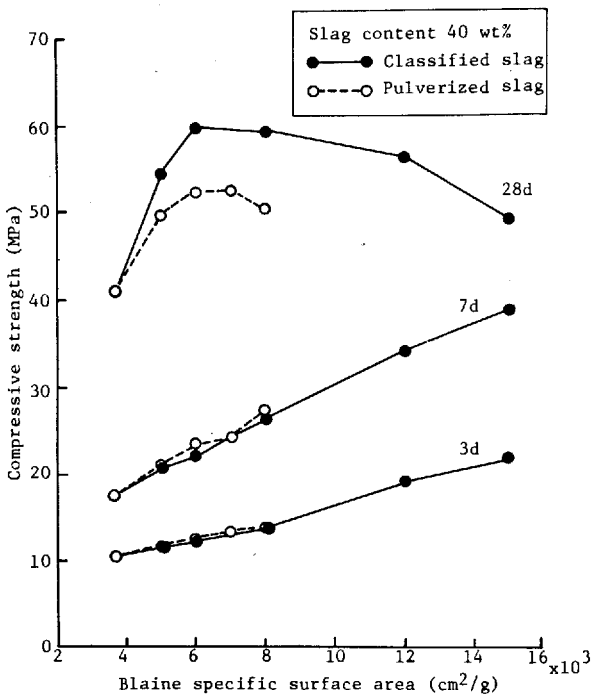

Fig. 2. Fineness of slag and compressive strength

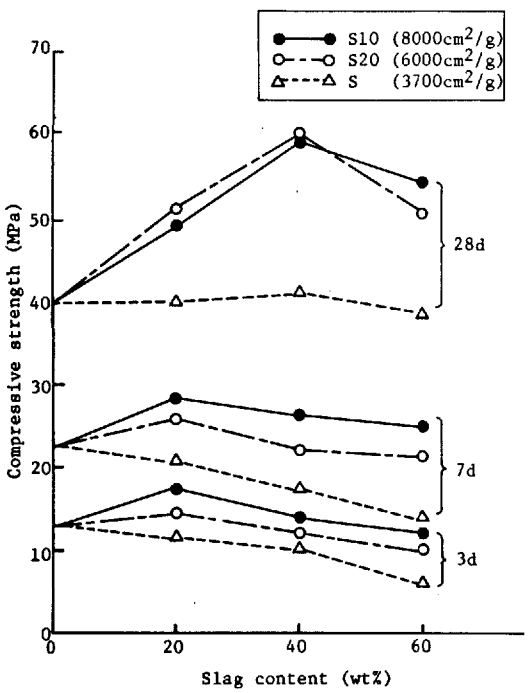

Fig. 3. Slag content and compressive strength

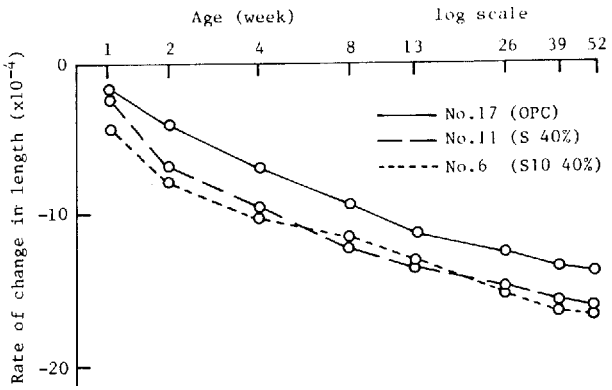

Fig. 4. Shrinkage

3.2 Effectiveness in Preventing the Alkali-Aggregate Reaction

Figure 5 shows the relation between age and the expansion of mortar bars.

As shown in Fig. 5, the addition of slag is apparently very effective in retarding expansion and this effectiveness is especially clear with a slag content of 60%.

The classified slag (S10) shows a higher effectivity than the ordinary slag (S).

When tap water was used as mixing water, the expansion for the OPC-aggregate (Yamagata) combination exceeded the ASTM standard (0.1% at 6 months) while that for the OPC-aggregate (Kagawa) combination did not.

3.3 Durability of Very Fine Slag Based Hardened Mortar in Sea Water

Figure 6 shows the relation between sea water curing time and the depth of Cl^--permeation.

It is apparent that the higher the slag content, the shallower the permeation depth, and that the addition of classified slag (S10) is very effective.

Figure 7 shows the results of EPMA which are in fine agreement with the results shown in Fig. 6.

Figure 8 shows the pore size distributions of hardened mortars cured in sea water which are apparently different between the slag based mortars and the OPC mortar.

However, difference in pore size distribution is not remarkable between S and S10 based mortars.

Improvement of durability against sea water by the addition of S10 is considered to be due to its high reactivity with free $Ca(OH)_2$ and compactness of the hardened body.

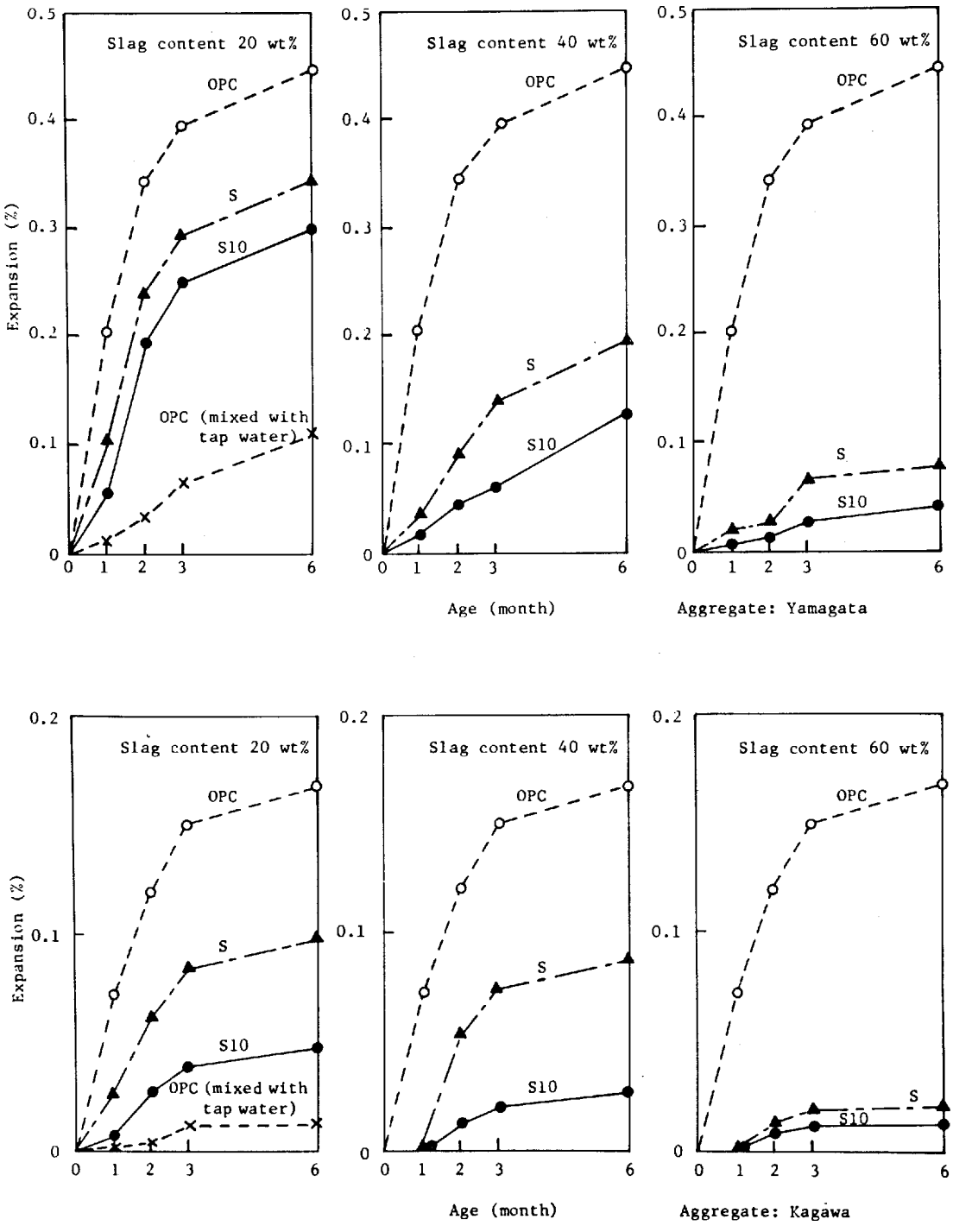

Fig. 5. Expansion of mortar bars

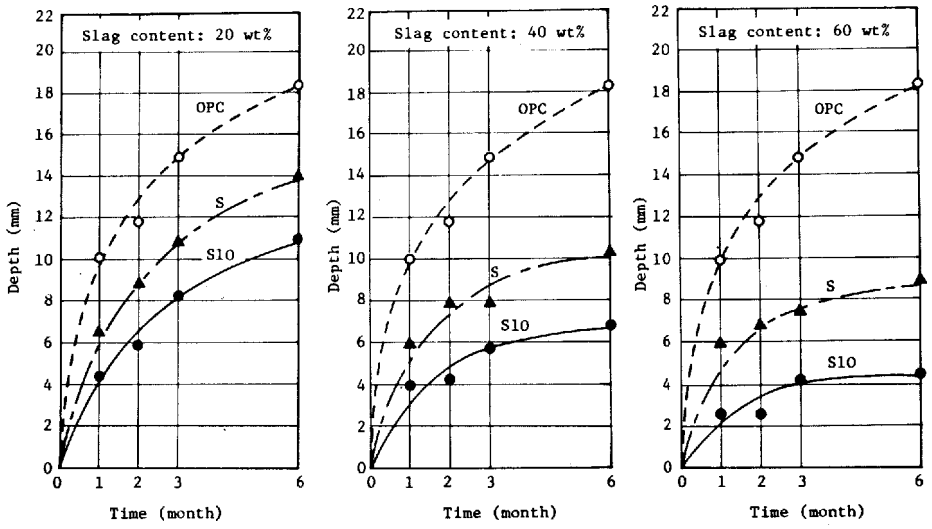

Fig. 6. Cl^--permeation depth in sea water cured mortars

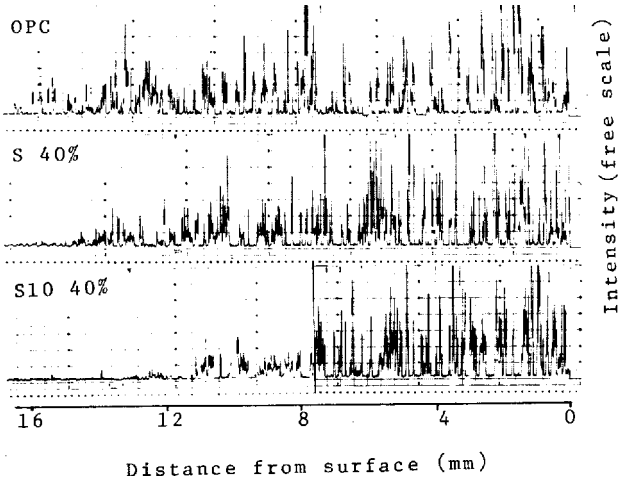

Fig.7. Cl^- concentration profile in mortars (EPMA)

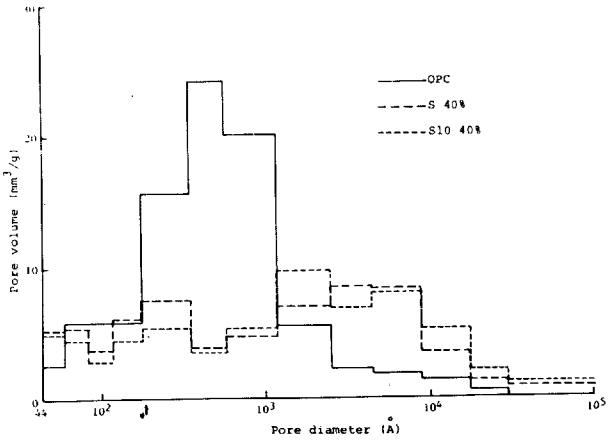

Fig. 8. Pore size distributions of hardened mortars (44Å-10^5Å)

4. CONCLUSION

Water granulated blast furnace slag powder used for Portland blast furnace cement usually has a Blaine specific surface area of about 4000 cm^2/g in Japan.

In the present study, properties of very fine slag powder produced by classifying ordinary slag powder were examined. Obtained results can be summarized as follows.

1) Use of the very fine slag can improve low early-stage strength of slag based cement giving very good later-stage strength development as well.
2) The very fine slag produced by the classification process shows higher later-stage strength in comparison with the slag produced by the pulverization process, with a maximum strength at about 7000 cm^2/g.
3) Shrinkage with very fine slag produced by the classification process is equal with that with the ordinary slag.
4) Effectiveness of classified slag in preventing the alkali-aggregate reaction is more remarkable than that of ordinary slag especially when slag content reaches 60 wt%.
5) Cement based on the classified slag has an excellent durability against sea water (resistance to Cl^--permeation).

The authors hope that more studies on the very fine slag mentioned above will be carried out with emphasis on improvement of concrete durability and high use of slag for a wider and better use of slag.

REFERENCES

1. Cement and Concrete Association Working Party, Minimizing the Risk of Alkali-Silica Reaction, Guidance Note (1983)
2. K. Kobayashi, H. Uchikawa and H. Kasami, Japan Concrete Institute, 22 [5], 4 (1984)
3. O.E.Gjorv, ACIJ., 68, 60 (1971)
4. S. Goto, M. Tsunetani, H. Yanagida and R. Kondo, Journal of the Ceramic Society of Japan, 87, 126 (1979)

Hiroshi UCHIKAWA, Doctor of Engineering, General Manager, Central Research Laboratory, Shunichiro UCHIDA, Manager, Cement Chemistry Section and Shunsuke HANEHARA, Senior Research Chemist, Onoda Cement Co., Ltd.

Effect of Character of Glass Phase in Blending Components on their Reactivity in Calcium Hydroxide Mixture

SUMMARY: Characterization of 6 slags, 6 fly ashes, 3 silica fumes and 2 rice husk ashes was performed in order to obtain the relation between character of glass phase and pozzolanic reactivity of blending component.

Slags with lower content of crystalline phase and higher ratio of monomer/dimer has higher pozzolanic reactivity. Fly ashes with larger amount of glass phase and higher glass basicity has higher pozzolanic reactivity. Silica fumes and rice husk ashes shows pozzolanic reactivity corresponding to their specific surface area and glass phase content.

It is reconfirmed that simple but effective method for pozzolanic reactivity evaluation of blending component is amount of NaOH (pH=13) soluble SiO_2 for slag and acid soluble $SiO_2+Al_2O_3$ for the other blending component, respectively.

Efetuou-se a caracterização de 6 escórias, 6 cinzas volantes, 3 microsílicas e 2 cinzas de casca de arroz, com a finalidade de se obter a relação entre o caráter da fase de vidro e a reatividade pozolânica do componente de adição.

Escórias com teor mais baixo de fase cristalina e maior relação de manômero/dímero' têm maior reatividade pozolânica. Cinzas volantes com maior quantidade de fase de vidro e maior basicidade vítrea têm reatividade pozolânica mais alta. Microsílica e cinzas de casca de arroz apresentam reatividade pozolânica correspondente à sua área de superfície específica e teor de fase de vidro.

Reconfirma-se que um método simples mas eficaz para avaliação da reatividade pozolânica de componente de adição é a quantidade de SiO_2 solúvel em NaOH (pH = 13) para escória, e de $SiO_2+Al_2O_3$ solúvel em ácido para o outro componente de blendagem, respectivamente.

1. INTRODUCTION

Various kinds of blending components are mixed with portland cement and widely used from the viewpoint of improving properties of paste, mortar and concrete as well as saving energy and resources. It is necessary that pozzolanic reactivity of blending component is grasped exactly and conveniently so as to produce and supply the blended cement having excellent quality.

In this paper, the chemical composition and structure of glass phase in blending component which mainly controls pozzolanic reactivity were analysed and the relationship between their characters and the pozzolanic reactivity of blending components in calcium hydroxide mixture was studied.

2. SAMPLE

Four kinds of blending components (17 samples) were used in this study. These were 6 slags, 6 fly ashes, 3 silica fumes and 2 rice husk ashes.

3. EXPERIMENT

3.1 Characterization of glass phase in blending component

(1) Amount and chemical composition of glass phase Amount of glass phase in each blending component was calculated from content of each crystalline phase determined by XRD. Chemical composition was directly measured by EPMA.

(2) Structure of glass phase Infrared spectrum of ν_3 stretching vibration of Si-O bond, fraction of bridged oxygen which bonds to silicon, peak position of halo of glass and condensation degree of silicate ion was analysed and measured by FT-IR, chemical shift of ^{29}Si with FT-NMR, XRD and TMS method, respectively.

(3) Determination of soluble part of blending component Amount of CaO, SiO_2 and Al_2O_3 of all slags and fly ash #6 eluted by 0.1N NaOH solution of which pH corresponds that of saturated $Ca(OH)_2$ solution was measured. Soluble part in the other blending components to 10% Na_2CO_3 solution after treated in hot conc. HCl was determined as acid soluble part.

3.2 Measurement of pozzolanic reactivities of blending components

(1) Preparation of hydrated sample 5% $Ca(OH)_2$ as activator was added to each slag. The other blending components were mixed with $Ca(OH)_2$ at 1.1 mol ratio of $CaO/(SiO_2+Al_2O_3+Fe_2O_3)$, respectively. Each mixture of slag, fly ash, silica fume and rice husk ash was mixed with water solid ratio of 0.4, 0.45, 0.65 and 0.55, respectively and cured at 313°K for 1, 7 and 28 days.

(2) Measurement of hydration degree of blending component in $Ca(OH)_2$ mixture Hydration reactivity of each blending component was evaluated from its hydration degree, amount of combined water and reacted $Ca(OH)_2$. Amount of slag reacted was determined by XRD after heating and recrystallizing hydrated sample at 1223°K for half an hour. For the other components, amount of reacted SiO_2 and Al_2O_3 at each hydration time was obtained by the method for dissolving with 5% Na_2CO_3 solution after treated with 1+100 HCl. Amount of combined water and reacted $Ca(OH)_2$ was measured by ignition loss and DSC method, respectively.

4. RESULT AND DISCUSSION

4.1 Amount and chemical composition of glass phase and kinds of crystalline phase

(1) Slag Important characters of each blending component are shown in **Table 1.** Content of glass phase in slags varied from 72 to 100% and melilite which was a solid solution of gehlenite (C_2AS) and akermanite (C_2MS_2) was observed as crystalline phase. Basicity ($CaO+MgO+Al_2O_3/SiO_2$) of 6 Japanese slags used was from 1.84 to 1.89. Slags poor in crystalline phase had almost constant basicity ratio in each particle and its position and were microscopically homogeneous in chemical composition. The glass phase in them had the same basicity as a whole. On the other hand, the basicity of glass phase in slag with over 10% crystalline phase was decreased less than 1.80. X-ray image of Al and basicity on the surface of polished slag with melilite measured by EPMA with ultra-high speed wide area multi analyser is shown in **Fig. 1.** Initial crystallized melilite which located at the center of crystalline phase had high basicity ratio shifted to gehlenite side. On the boundary between melilite and glass phase, melilite had lower basicity than that at center but higher than glass phase, which had less Al_2O_3 content than glass phase of slag as a whole. It had a low basicity and its chemical composition shifted to akermanite side. Therefore glass phase in slag rich in crystalline phase turns to low basicity and the variation of chemical composition in it becomes larger.

(2) Fly ash Crystalline phase of fly ash was from 15 to 35%. Quartz and mullite was observed as crystalline phase in each fly ash. Fly ash #4 and 6 had magnetite and C_3A, respectively. Total basicity of fly ashes except #6 was from 0.5 to 0.6. Fly ash #6 with 27% CaO differed virtually from the other fly ashes. This type of fly ash (high calcium fly ash) is classified as class C fly ash in ASTM. SiO_2, Al_2O_3, Fe_2O_3 and CaO in glass phase of each fly ash was 70.0-27.1%, 31.2-7.1, 29.8-0.5 and 34.7-1.0, respectively. There was a large difference of chemical composition among fly ash particles except fly ash #4. Mean basicity of glass phase in Fly ash #1, 2, 3, 4 and 5 is from 0.5 to 0.84. Fly ash with more glass phase content had higher basicity. Variation of composition in glass phase in fly ash particle is considered to be caused by difference in amount of quartz and mullite in fly ash. Glass phase rich in Fe_2O_3 was observed in fly ash #4. Glass phase in fly ash #6 (high calcium fly ash) was almost same level of basicity as slag.

(3) Silica fume Silica fume is a by-product of fabrication of silicon and ferrosilicon in arc furnaces and is condensed in the fine amorphous form. Silica fume #2 and 3 had a few percent of quartz as an impurity. Amount of SiO_2 in silica fume reached to more than 85% and the mean diameter was less than 100 nm. Silica fume #2 and 3 were contaminated with 5% of Na_2O+K_2O. They had large specific surface area of 20 m^2/g and spherical shape. Silica fume #1 has BET specific surface area of 13m^2/g corresponding to half of #2 and 3.

(4) Rice husk ash Rice husk ashes contained cristobalite and tridymite as crystalline phase and amount of SiO_2 reached to more than 90%. Rice husk ash #1 had 20% of glass phase, which was 1/3 of #2. Since Rice husk ash #2 had amorphous carbon having large specific surface area, it had larger BET specific surface area than #1.

Table 1 Characters of blending components and their glass phase

		slag						fly ash						silica fume			rice husk ash	
		#1	#2	#3	#4	#5	#6	#1	#2	#3	#4	#5	#6	#1	#2	#3	#1	#2
Chemical composition (%)	SiO_2	33.4	34.2	34.4	34.4	34.4	34.4	59.3	58.3	59.2	44.9	60.1	33.6	85.9	90.3	86.4	94.5	90.7
	Al_2O_3	15.0	14.7	13.2	13.1	15.9	14.5	25.0	24.1	24.8	18.1	28.6	22.0	1.0	0.2	0.1	0.3	0.4
	Fe_2O_3	0.9	0.8	0.7	0.8	0.2	0.2	4.3	4.6	4.3	21.9	2.9	6.4	1.7	4.1	3.0	0.1	0.2
	CaO	42.3	41.5	43.1	42.8	41.4	42.6	2.8	3.5	4.4	6.2	4.2	27.1	0.4	0.8	0.8	0.6	0.6
	MgO	6.0	6.6	7.1	6.9	6.1	6.7	1.6	1.5	0.9	1.2	1.3	4.5	1.9	0.3	0.3	1.0	1.0
Basicity ratio	C+M+A/S	1.89	1.84	1.84	1.83	1.84	1.85	0.50	0.50	0.51	0.57	0.57	1.60					
Amorphous phase (%)	SiO_2	33.4	34.0	34.5	34.4	35.2	35.3	50.5	43.9	41.2	45.2	45.5	32.4					
	Al_2O_3	15.0	14.6	13.1	13.2	14.2	12.6	20.5	18.5	16.9	22.1	25.6	18.8					
	Fe_2O_3	-	-	-	-	-	-	6.8	10.3	8.5	24.6	4.8	5.7					
	CaO	42.3	41.9	43.2	43.1	41.9	41.7	3.8	7.8	12.6	4.5	9.9	28.8					
	MgO	6.0	5.8	7.4	7.4	5.9	7.4	1.4	3.6	4.2	1.1	2.5	3.9					
Basicity ratio	C+M+A/S	1.89	1.83	1.85	1.85	1.76	1.77	0.51	0.68	0.81	0.61	0.84	1.59					
Content of glass phase (%)		100	100	99	98	85	72	64	70	71	72	67	86	100	97	98	18	56
melilite(quartz)(%)		0.0	0.0	1.3	1.7	15.1	26.9	(17)	(14)	(13)	(7)	(13)	(5)	(0.0)	(3)	(2)	Cr(58)	Cr(44)
merwinite(%)		-	-	-	-	-	1.5	Mu(19)	(16)	(16)	(6)	(20)	(2)	-	-	-	Tr(24)	-
											Mg(15)		C_2A(7)					
Specific surface area	Blaine(cm^2/g)	4980	5050	5020	4960	5030	5070	3190	3840	3840	2810	2990	3730	carbon free			-	-
	BET (m^2/g)	1.08	1.15	1.18	1.10	1.23	1.22	0.84	1.38	2.09	0.38	0.49	0.60	(5)	(21)	(21.8)	(0.8)	(1.1)
Acid insoluble part (dissolution with 10% Na_2CO_3 solution after treated in hot conc.HCl) (%)		-	-	-	-	-	-	84.6	83.2	87.3	58.4	77.4	37.8	-	-	-	93.2	86.0
Acid soluble	SiO_2							4.5	4.8	5.4	6.7	7.6	15.3	13.1	18.4	17.7	4.4	11.3
	Al_2O_3							2.3	2.5	3.1	4.9	4.9	21.3					
	$SiO_2+Al_2O_3$							6.8	7.3	8.5	11.6	12.5	36.6	13.1	18.4	17.7	4.4	11.3
	$SiO_2+Al_2O_3$/BET							16.6	16.6	18.9	22.3	26.6	64.2	1.3	0.9	0.8	5.7	10.3
Basic soluble part (elution into 0.1 N NaOH solution)(%)																		
	CaO	0.50	0.48	0.58	0.56	0.45	0.41											
	SiO_2	0.29	0.28	0.32	0.33	0.26	0.24											
	Al_2O_3	0.20	0.18	0.19	0.20	0.16	0.12											
	$SiO_2+Al_2O_3$	0.49	0.46	0.51	0.53	0.42	0.36											

Note; Mu: mullite, Mg: magnetite, Cr: cristobalite, Tr: tridymite.

4.2 Analysis of structure of glass phase

(1) Structure of glass phase estimated by XRD method
In stead of the diffraction, x-ray scattering by particular atomic couples appeared as x-ray halo of broad peak was measured. Typical halo of blending components by XRD is shown in **Fig. 2.**

Peak position of halo of fly ashes except high calcium fly ash, silica fumes and rice husk ashes appeared at 22° (2θ, Cukα) as well as quartz glass. It is known that its peak position of quartz glass coincides with maximum peak for α-cristobalite (111=0.40nm). The structure of blending component above mentioned seems to be related to that of α-cristobalite.

Slag showed the peak of halo at about 32° coincided with maximum peak of melilite (211=0.28nm). It showed that there is a symmetry of melilite in the structure of glass phase in slags. The peak position of fly ash #6 was same as that of slags and melilite was observed after heated at 1223°K for half an hour. Diamond (1) said structure of glass phase in class C fly ash was closely related to glass of $C_{12}A_7$. In this study, however, glass phase in high calcium fly ash corresponding to ASTM class C coincided with that of slag.

According to x-ray small angle scattering measurement of domain size in the range from 1 to 1000nm, there was no scattering in all slags and high calcium fly ash. This result suggests that the glass phase in these blending components consists of random arrangement of atoms in stead of agglomeration of fine crystallite.

(2) Condensation degree of silicate ions in glass phase determined by IR, NMR and TMS method. Since blending components used in this experiment were mainly composed of glass phase as shown in **Table 1,** NMR and TMS data of each blending component could be considered to reflect the character of glass phase. It is well known that ν_s stretching vibration of Si-O bond makes a strong absorption at 1100 cm^{-1} in

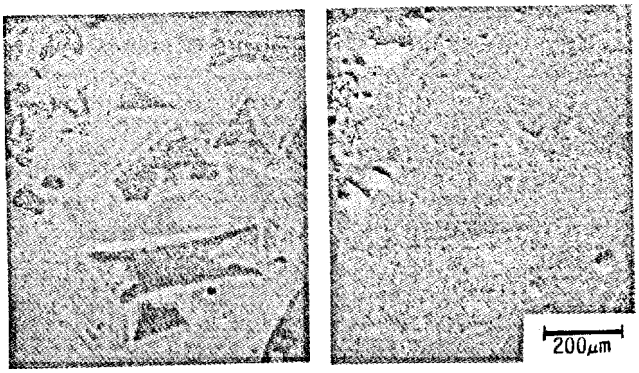

	Al_2O_3 content	Basicity (C+M+A)/S
white	more than 65%	more than 2.2
pink	30-	2.0 -
red	15-	1.9 -
yellow	10-	1.85-
green	7-	1.8 -
light blue	5-	1.75-
blue	3-	1.65-
black	less than 3%	less than 1.65

Fig. 1 X-ray map of Al and $(CaO+MgO+Al_2O_3)/SiO_2$ ratio on the polished surface of slag grain rich in crystalline phase by EPMA with ultra-high speed wide area multi analyser

infrared spectrum and this absorption peak shift towards higher wave number as the condensation degree of silicate ions increases (2). The peak position of each blending component by IR is shown in **Fig. 3.** All slags and fly ash #6 had a peak at about 960cm^{-1}. While the other blending components had a peak at about 1100cm^{-1}. The condensation degree became larger in the order of slag, high calcium fly ash: ordinary fly ash: rice husk ash, silica fume.

The fraction of bridged and nonbridged oxygen bonded to silicon was obtained by peak shift of ^{29}Si (3). As shown in **Fig. 4,** each peak position of slag #4, slag

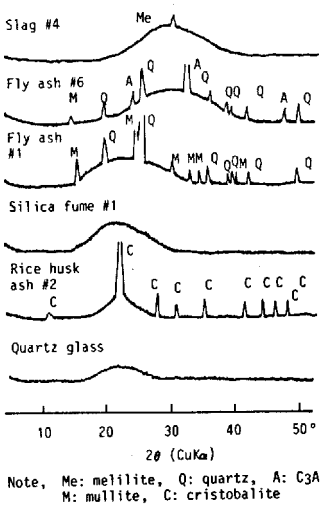

Fig. 2 Typical halo profile of blending component by XRD

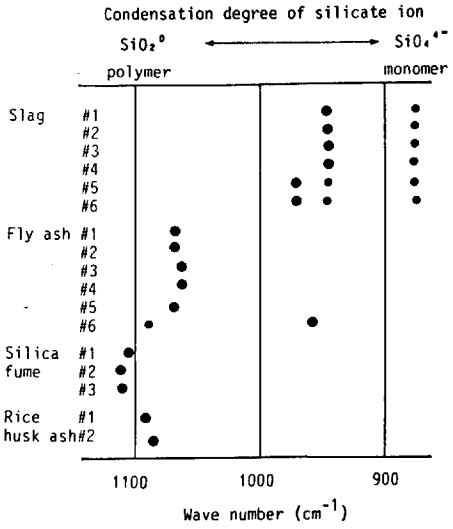

Fig. 3 Peak position of infrared absorption spectrum of blending component

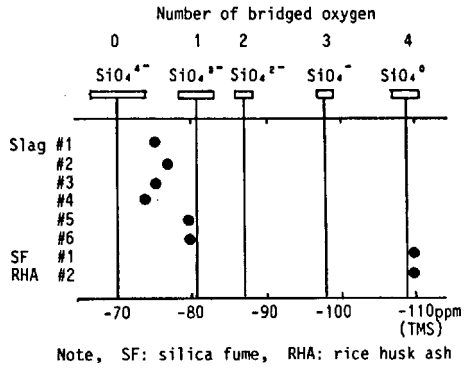

Fig. 4 Chemical shift of ^{29}Si in blending component by FT-NMR

#3 and 1, slag #2, and slag #5 and 6 appeared at -73, -75, -77 and -80ppm, respectively. Fraction of monomer having no bridged oxygen among four was decreased in this turn. The peak position of silica fume and rice husk ash appeared at -110ppm coinciding with that of quartz glass with huge condensation degree of silicate ions.

Fig. 5 shows the fraction of monomer, dimer, trimer and polymer of silicate ion in slags, fly ash #6 and typical other blending components analysed by TMS method. Most of silicate ion in slag were made up of monomer and dimer. Among slags, slag #5 and 6 with more amount of melilite had smaller fraction of monomer than the other slags. Content of monomer turned to about 50% in slag #3 and 4 with about 2% melilite. They were larger than slag #1 and 2 without melilite. Fly ash #6 had more polymer than slags. These results were closely related to condensation degree measured by NMR. As for the other blending components, fly ash #1 had 1% of monomer+dimer and silica fume and rice husk ash had no monomer, dimer and trimer at all. This result was corresponded with that of IR.

4.3 Amount of soluble CaO, SiO_2 and Al_2O_3 of blending components

Since blending components used were mainly composed of glass phase as shown in **Table 1**, Date of soluble amount of each blending component could be also considered to reflect the character of glass phase. Weakly bonded SiO_2 and Al_2O_3 with comparatively high reactivity in blending component was easily dissolved by Na_2CO_3 solution after boiled in conc. HCl (acid soluble part). Acid insoluble part and acid soluble SiO_2 and Al_2O_3 per weight and per specific surface area of blending components except slags are shown in **Table 1**. Although amount of soluble SiO_2+Al_2O_3 per weight in fly ash, silica fume and rice husk ash was 6.8-36.6%, 13.1-17.7 and 4.3-11.3, respectively, fly ash had largest acid soluble part per specific surface area because Al ion in fly ash acts as reducer of silicate chain in glass phase. This result well corresponded with the result of IR. Acid soluble part per specific surface area reflects structural difference of glass phase in blending component.

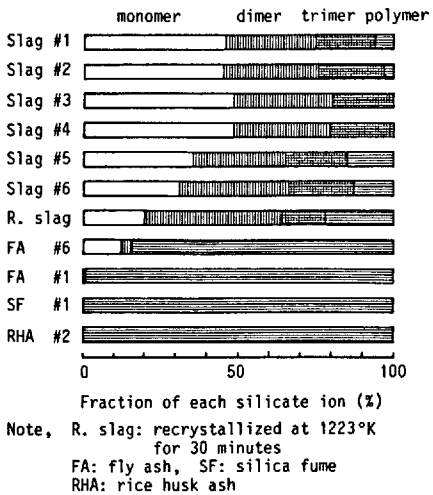

Fig. 5

The kind and amount of silicate ion in blending component by TMS

Considering that the hydration of slag is based on the elution of the chain structure of SiO_4^{4-} and AlO_4^{5-} in slag by the attack of OH^-, the difference of amount of blending component eluted by alkali solution is considered to be related with its reactivity. Amount of SiO_2, Al_2O_3 and CaO dissolved by 200 times of 0.1N NaOH solution with pH 13 at 293°K for 10 minutes was measured modifying the method of Dron (4). Amount eluted from slag #5 and 6 with more than 10% crystalline phase was the smallest as shown in **Table 1**. Slag #3 and 4 containing about 2% melilite had larger elution amount than slag #1 and 2 without melilite. As for slags with less 5% melilite, elution amount from slags did not always varied according to their glass content.

Fig. 6 shows the relation between amount of SiO_2 eluted and condensation degree of silicate ions among slags used, synthesized melilite, gehlenite and akermanite. Synthesized gehlenite containing monomer of silicate ion had larger dissolution amount than synthesized akermanite with dimer. Amount of SiO_2 eluted from each synthesized crystal was linearly

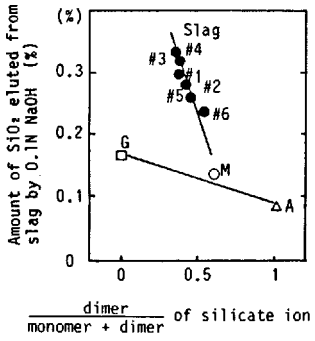

Fig. 6

The relationship between amount of SiO_2 eluted and condensation degree of silicate ion

increased with the decrease of dimer/(dimer+monomer) of silicate ion. Amount of SiO_2 eluted from slag #3 having nearly same basicity level of glass as synthesized melilite was about 2.5 times as large elution as it and larger than synthesized high basicity gehlenite. The relation between dimer/(dimer+monomer) ratio of slags used and synthesized crystal and eluted SiO_2 is shown in **Fig. 6.** This fact suggests that amount of SiO_2 eluted was larger in glass phase than in crystalline phase and closely related to dimer/(dimer+monomer) ratio in slag.

4.4 Pozzolanic reactivity of blending component

(1) Slag The hydration degree and combined water of slags are shown in **Fig. 7.** Hydration degree of slag #5 and 6 with high crystalline phase content was small. That of slags with less than 5% crystalline phase, however, was not related to content of glass phase. The hydration degree of slag was related to the amount of SiO_2 eluted by 0.1N NaOH solution coinciding with the pH of $Ca(OH)_2$ saturated solution as shown in **Fig. 8.** In the other words, the condensation degree of silicate ions could be estimated by the amount of SiO_2 eluted by 0.1N NaOH solution and it is considered to correspond to the pozzolanic reactivity of slag.

(2) Fly ash, silica fume and rice husk ash The amount of combined water and hydration degree calculated by reacted $SiO_2+Al_2O_3$ are shown in **Fig. 7.** When much amount of Al-bearing hydrates was produced in the mixture, amount of combined water was remarkably increased in spite of same hydration degree. On the other hand, amount of reacted $Ca(OH)_2$ could not be estimated in case of blending components rich in CaO. Hydration degree estimated from reacted $SiO_2+Al_2O_3$, therefore, is considered to be suitable for the measurement of reactivity of blending component by selecting appropriate solvent.

High calcium fly ash had high combined water but the reactivity based on reacted $Ca(OH)_2$ and reacted $SiO_2+Al_2O_3$ could not be exactly evaluated. Hydration degree of its glass phase could be measured after recrystallizing method of slag and was lower than slags. Ordinary fly ashes containing higher glass phase content and basicity had higher reactivity. Hydration degree of fly ash #4 with relatively low basicity was high. It is considered that glass phase of fly ash rich in Fe_2O_3 serves to decrease the condensation degree of silicate ions and thereby its reactivity is improved in spite of low basicity.

Since silica fume and rice husk ash hardly contained Al_2O_3, hydration degree could be evaluated by reacted $Ca(OH)_2$ and reacted SiO_2. Reactivity of silica fume and rice husk ash was dominantly controlled by specific surface area and content of glass phase.

The relationship between acid soluble part and hydration degree is shown in **Fig. 8.** Except silica fume, acid soluble part of each blending component was well correlated to its hydration degree. Takemoto and Uchikawa (5) reported the reaction rate of pozzolanic materials was proportional to square of its specific surface area. Since the specific surface area of

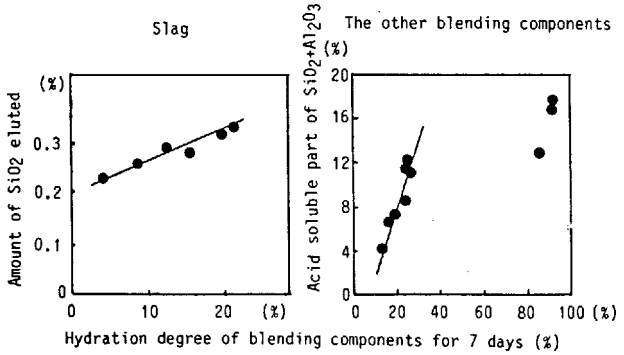

Fig. 8 The relationship between hydration degree and amount of SiO_2 eluted of slag and acid soluble part of $SiO_2+Al_2O_3$ of the other blending component

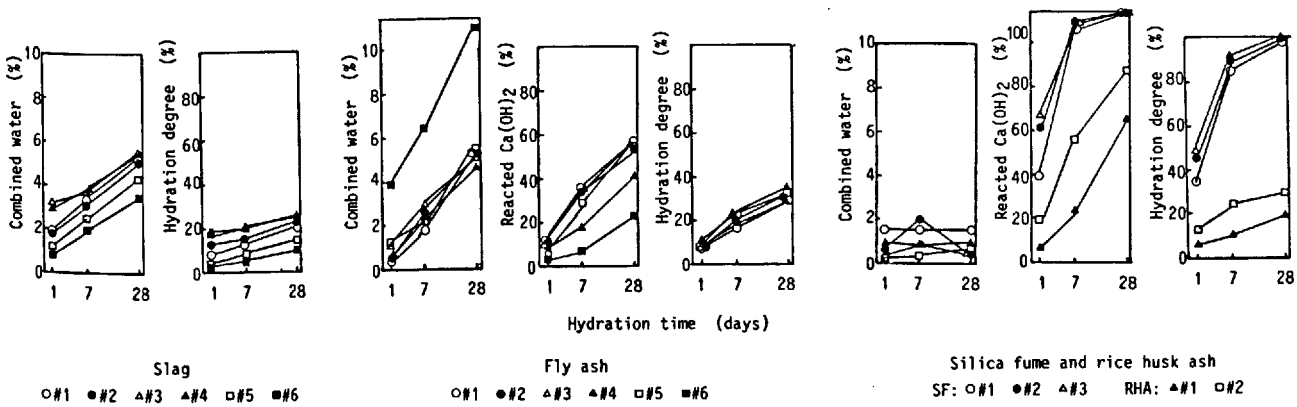

Fig. 7 Amount of combined water, reacted $Ca(OH)_2$ and hydration degree of blending component with hydration time (313°K)

silica fume was about 10 times larger than that of the other blending components, silica fume is considered to indicate higher hydration degree in spite to lower content of acid soluble part per weight.

5. CONCLUSION

Following results were obtained by the studies on the effect of character of glass phase in blending components on their pozzolanic reactivities in calcium hydroxide mixture.

(1) Amount of glass phase in slags, fly ashes, silica fumes and rice husk ashes was 70-100, 65-85, 97-100 and 20-60%, respectively. The chemical composition of glass phase in slag having more than 95% was almost as same as that of overall slag. The basicity of glass phase in slag with less than 95% glass phase, however, was lowered and it was slightly poor in Al_2O_3 and rich in SiO_2 and MgO. Mean basicity of glass phase in fly ash was from 0.51 to 1.59 and this value differed greatly from each particle and its position in each particle as well as kind of fly ash. The basicity of glass phase in high calcium fly ash was almost the same as that in slag. Silica fumes and rice husk ashes were remarkably rich in SiO_2 and contained crystalline phase such as quartz, cristobalite and tridymite depending on the produced condition. The former had large specific surface area, especially.

(2) The structure of glass phase in slags and high calcium fly ash was related to melilite, while the ordinary fly ashes, silica fumes and rice husk ashes was related to α-cristobalite. The glass phase in slag and high calcium fly ash did not consist of agglomeration of fine crystallite judging from x-ray small scattering. The shift of Si-O adsorption peak measured showed the condensation degree is larger in order of slags and high calcium fly ash, ordinary fly ashes, rice husk ashes and silica fumes. Slags composed mainly of dimer and monomer of silicate ion and ratio of monomer/dimer was decreased with increasing crystalline phase. Its value of slag with more than 95% glass phase was about 1.2. High calcium fly ash was richer in monomer than ordinary fly ashes. Silica fumes and rice husk ashes contained only polymer.

(3) As for slags, amount of SiO_2 eluted by 0.1N NaOH solution varied according to crystalline phase content, basicity and ratio of monomer/dimer. The higher the content of glass phase, basicity and ratio of monomer/dimer, the larger amount of SiO_2 was eluted by 0.1N NaOH solution.

(4) As for fly ashes, silica fumes and rice husk ashes, amount of $SiO_2+Al_2O_3$ dissolved into 10% Na_2CO_3 solution after treated in hot conc. HCl varied depending on their specific surface area, glass phase content, basicity and condensation degree of silicate ions. The amount of $SiO_2+Al_2O_3$ dissolved per specific surface area of blending components is considered to correspond to their basicity and condensation degree of silicate ion. It became larger in order of fly ashes with higher basicity, rice husk ashes and silica fumes. On the other hand, the amount of $SiO_2+Al_2O_3$ dissolved per weight was larger in order of silica fumes, fly ashes and rice husk ashes.

(5) Slags with lower content of crystalline phase and higher ratio of monomer/dimer had higher pozzolanic reactivity. The reactivity of slag seems to correspond to amount of SiO_2 eluted by 0.1N NaOH solution. The larger the amount of glass phase and the higher the basicity in their glass phase, the larger amount of fly ashes reacted. Amount of silica fumes and rice husk ashes reacted varied according to their specific surface area and glass phase content. Hydration degree of fly ashes, silica fumes and rice husk ashes is corresponding to their acid soluble $SiO_2+Al_2O_3$ per weight.

6 REFERENCE

(1) S. DIAMOND (1980), "On the glass present in low calcium and in high calcium flyashes", Cem. Conc. Res., **13**, 459-464

(2) T. YANAGESE and Y. SUGINOHARA (1970), "Studies on consititution of vitreous silicate by infrared absorption spectra", Trans. Japan Inst. Metals, **11**, 400-403

(3) E. LIPPMMA, M. MAGI, A. SAMOSON, E. ENGELHARDT and A.R. GRIMMER (1980), "Structural studies of silicates by solid-state high-resolution ^{29}Si", J. Am. Chem. Soc., **102**, 4889-4893

(4) R. DRON (1979), "Structure des silicates fondus: interpretation statistique de la theorie de Masson" and "Theorie statistique des silicates fondus à forte et moyenne teneurs en silice", C.R. Acod. Sc., Paris, à paraître

(5) K. TAKEMOTO and H. UCHIKAWA (1980), "Hydration of pozzolanic cement", 7th Intern. Cong. Chem. Cem., I, IV 2/1 - 2/29

Hiroshi UCHIKAWA, Doctor of Engineering, General manager, Central Research Laboratory,
Onoda Cement Co., Ltd.
Shunichiro UCHIDA, Manager, Cement Chemistry Section, Central Research Laboratory,
Onoda Cement Co., Ltd.
Kenji OGAWA, Senier Research Chemist, Cement Chemistry Section, Central Research Laboratory,
Onoda Cement Co., Ltd.

INFLUENCE OF CHARACTER OF BLENDING COMPONENT ON THE DIFFUSION OF NA AND CL IONS IN HARDENED BLENDED CEMENT PASTE

SUMMARY: Relationship between composition, structure and diffusion coefficient of Na^+ and Cl^- through hardened blended cement paste was studied in order to clarify the effect of blending component on the depression of concrete deterioration by alkali aggregate reaction and by chloride attack to reinforcement.

The diffusion of alkalies and chlorine was strongly influenced by the porosity and pore structure of hardened cemet paste. The composition and structure of hydrate produced, zeta potential of pore surface and continuity of pore is also related to the diffusion coefficient of alkalies and chlorine ion through hardened cement paste.properties.

Reduction of total porosity and shift of capillary pore size distribution to smaller side is effective to reduce the diffusion coefficient of these ions as well as the formation of low C/S C-S-H.

Estudou-se a relação entre composição, estrutura e coeficiente de difusão de Na^+ e Cl^- na pasta de cimento aditivado, com o fim de esclarecer o efeito do componente de adição sobre a depressão de deterioração do concreto, por reação do agregado alcalino e por ataque de cloreto à armação.

A difusão de álcalis e cloro foi fortemente influenciada pela porosidade e estrutura do poro da pasta endurecida de cimento. A composição e estrutura do hidrato produzido, o potencial zeta da superfície do poro e a continuidade do poro também estão relacionados com o coeficiente de difusão de íon de álcali e cloro através das propriedades da pasta endurecida de cimento.

A redução da porosidade total e mudança da distribuição de tamanho do poro capilar para menor tamanho, efetivamente reduzem o coeficiente de difusão destes íons, bem como a formação de C-S-H com baixa relação C/S.

Toyosu 1-1-7, Koto-ku Tokyo, JAPAN

H. UCHIKAWA
S. UCHIDA
K. OGAWA

1. INTRODUCTION

The deterioration and damage of concrete and steel reinforced concrete by alkali aggregate reaction and by chloride attack has recently become serious problem on the durability of concrete. Substitution of slag and fly ash for part of portland cement is recommended for one of the solution of these problems and it is proved effective in many experiments.

In this paper, influence of the addition of blast-furnace slag, fly ash and silica fume on the diffusion coefficient of Na and Cl ions was studied in order to clarify the mechanism of the depression of alkali aggregate reaction and by chloride attack by the blending component.

2. SAMPLE

Chemical composition and specific surface area of ordinary portland cement (OPC) and three kinds of blending component used are shown in **Table 1.**

3. EXPERIMENTAL METHOD

3.1 Preparation and characterization of hardened paste

Blended cements prepared from various amount of fly ashes and slags, 10% of silica fume were mixed at water with water cement ratio of 0.3, 0.4, 0.6 and cured in plastic vessel for two months at 318°K. After predetermined time, hardened paste was D-dried. Then, produced hydrates was analysed by DSC and EPMA, total porosity estimated by ig. loss of hardened paste, pore volume and pore size distribution of hardened paste was determined by mercury penetration and nitrogen adsorption method, analysis of composition of hydrate, especially C-S-H, Na and Cl ion distribution in hardened paste after diffusion test was also measured by EPMA.

3.2 Measurement of diffusion coefficient of Na and Cl ion in hardened paste and zeta potencial of hardened cement paste powder

Diffsion coefficient of each ion at 293°K was measured using diffusion cell (1) as shown in **Fig. 1.** Na and Cl ions concentration in distilled water side was measured at constant interval by flame photometry and spectrophotometry using $Hg(SCN)_2$, respectively. Zeta potential of hardened paste powder was measured by streaming potential method.

4 RESULT AND DISCUSSION

4.1 Composition and structure of hardened paste

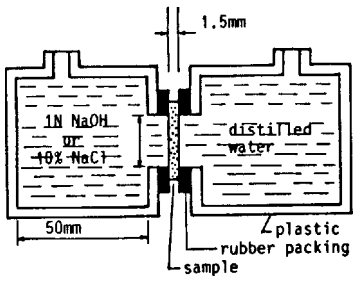

Fig. 1 Diffusion cell

4.1.1 Amount of hydrates and chemical composition of C-S-H

Hydrates detected by XRD were mainly AFm and $Ca(OH)_2$. The amount of these hydrates in hardened cement paste are shown in **Fig. 2.** Dotted line shows amount of hydrates per unit weight of ordinary portland cement for reference calculated from mixing ratio of it. The amount of $Ca(OH)_2$ in hardened blastfurnace slag cement paste was almost same as that of fly ash cement paste and was decreased with the increasing amount of blending components added. On the other hand, the amount of AFm was increased both in blast-furnace slag cement and ordinary fly ash cement paste compared with that in OPC paste, though there were remarkable difference in degree. Fly ash cement paste with 20% high calcium fly ash had more amount of AFm than with ordinary fly ash cement paste and had small amount of cubic aluminate hydrate. In silica cement paste with 10% of silica fume, the amount of AFm and $Ca(OH)_2$ was remarkably small comparing with fly ash cement paste with 10% of ordinary fly ash.

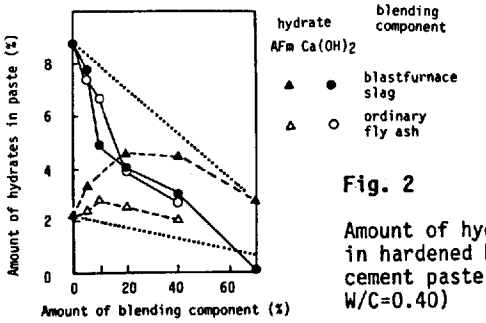

Fig. 2 Amount of hydrates in hardened blended cement paste (318°K, W/C=0.40)

Table 2 shows the chemical composition of C-S-H formed in hardened cement paste. C/S ratio of C-S-H

Table 1 Chemical composition of ordinary portland cement and blending component used.

	ig. loss	SiO_2	Al_2O_3	Fe_2O_3	CaO	MgO	SO_3	Na_2O	K_2O	Total	Blaine(cm^2/g)
ordinary portland cement	0.5	21.9	5.6	3.2	64.3	1.9	2.0	0.2	0.7	100.3	3,240
ordinary fly ash	1.6	58.3	24.1	4.6	3.5	1.5	0.1	1.7	0.5	95.9	3,840
high calcium fly ash	1.3	33.6	22.0	6.4	27.1	4.5	2.1	1.6	0.5	99.1	3,730
blastfurnace slag	0.4	31.6	15.0	0.4	40.7	7.6	0.0	0.5	0.5	96.7	5,980
silica fume	4.0	86.4	0.1	3.0	0.8	0.3	-	0.2	0.8	95.6	21.8(BET m^2/g)

Table 2 Chemical composition of C-S-H in hardened cement paste determined by EPMA (318°K, age 2 months)

	C/S	C/A	C/(S+A)	Na_2O(%)	K_2O(%)
OPC	1.90	0.07	1.72	0.03	0.33
FC	1.32	0.19	1.19	0.25	0.78
SC	1.43	0.22	1.12	0.33	0.32
BC	1.65	0.32	1.32	0.15	0.28

OPC: ordinary portland cement paste
FC: fly ash cement with 40% of ordinary fly ash
SC: silica cement with 10% of silica fume
BC: blastfurnace slag cement with 40% slag

in hardened paste became lower in the order of OPC, blastfurnace slag cement with 40% slag, silica cement with 10% of silica fume and fly ash cement with 40% of ordinary fly ash. In the C/(S+A) ratio, the order of SC and FC are in versed. Fly ash cement with high calcium fly ash showed almost the same C/S ratio of C-S-H as blastfurnace slag cement. C-S-H formed in blended cement paste tend to have more amount of Al and alkali ions than those in OPC.

4.1.2 Pore structure and texture

Fig. 3 shows total porosity and capillary pore volume ratio of each size range of hardened blended cement paste with different amount of blending component added. Fly ash blended cement paste with ordinary fly ash had larger total porosity and pore volume ratio of 5-50nm in diameter than OPC and they increased with increasing fly ash content. On the other hand, blastfurnace slag cement with slag up to 40% had smaller total porosity and larger pore volume ratio less than 5nm. However, blastfurnace slag cement with 70% of slag tended to have larger total porosity and pore volume ratio less than 5nm. In case of silica cement with 10% of silica fume, total porosity and pore volume ratio less than 5nm increased compared with OPC. Total porosity of fly ash cement with 20% of high calcium fly ash decreased and pore volume ratio less than 5nm and more than 100nm increased compared with fly ash cement with same content of ordinary fly ash. When mixed with different W/C, especially pore volume ratio more than 100nm remarkably changed as reported by Mehta et al (2).

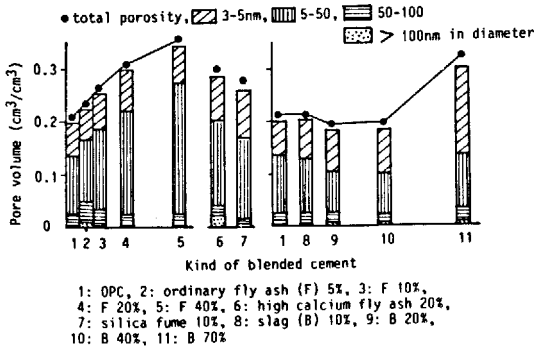

Fig. 3 Total porosity and pore volume ratio of each capillary pore size range of hardened blended cement paste (318°K, W/C=0.40)

The pore size distribution of gel pore in hardened cement paste with ordinary fly ash and blastfurnace slag measured by N_2 adsorption method is shown in **Fig. 4.** Maximum peak at about 1 nm in radius (2nm diameter), which corresponds to average distance between C-S-H solid surface decreased in fly ash cement but it was increased in blastfurfnace slag cement. It is probably considered to be caused by the formation of more dense structure by low C/S C-S-H in former and the increase in amount of C-S-H in latter. Pore size distribution of gel pore of 10% silica fume blended cement was comparatively similar to blastfurnace slag cement.

Fig. 5 shows back scattering image on the polished surface of hardened blended cement paste. OPC had

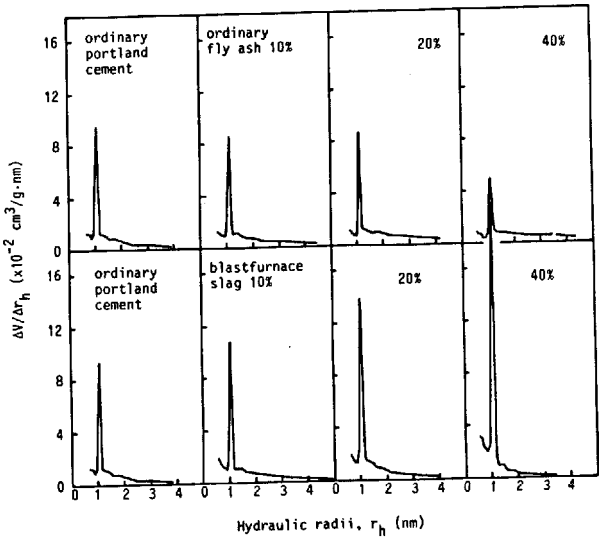

Fig. 4 Pore size distribution of gel pore in hardened blended cement paste with blastfurnace slag and fly ash measured by N_2 adsorption method (318°K, W/C=0.40)

dense C-S-H around alite and large layer aggromeration of $Ca(OH)_2$ crystal. Blastfurnace slag cement had dense C-S-H complicated with AFm. While, fly ash cement paste contained fine sized C-S-H around fly ash and locally produced $Ca(OH)_2$ and AFm phase, and silica fume cement was rich in C-S-H and poor in Al-bearing hydrate.

4.2 Diffusion coeffitient of Na and Cl ions through hardened paste

4.2.1 Relationship between diffusion coefficient and water cement ratio of paste

As shown in **Fig. 6**, the diffusion coefficient of Na ion become larger with increase of water cement ratio. The diffusion coefficient through OPC paste was the largest and showed almost the same tendency as through blastfurnace slag cement paste with 40% slag against increase of W/C ratio. While, fly ash cement had smaller diffusion coefficient than the former two and its increase rate against W/C was small.

4.2.2 Diffusion coefficient of Na and Cl ions through hardened blended cement paste

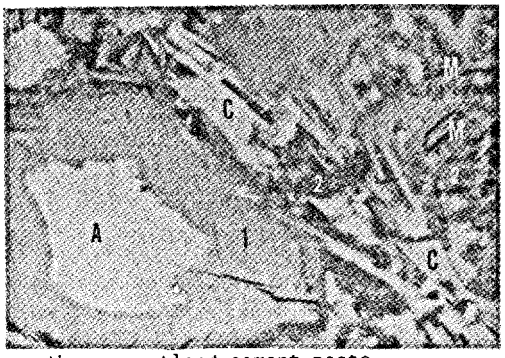

ordinary portland cement paste



blastfurnace slag cement paste

A: alite
C: $Ca(OH)_2$
F: fly ash
H: hydrated slag grain
M: AFm
S: unhydrated slag
1: dense C-S-H around alite
2: C-S-H filling hydration space



fly ash cement paste with ordinary fly ash

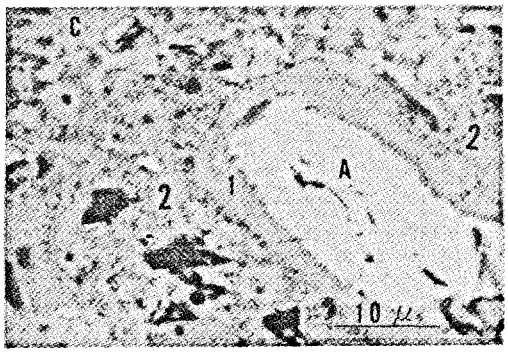

silica cement paste with silica fume

Fig. 5

Back scattering image of the polished surface of hardened blended cement paste.

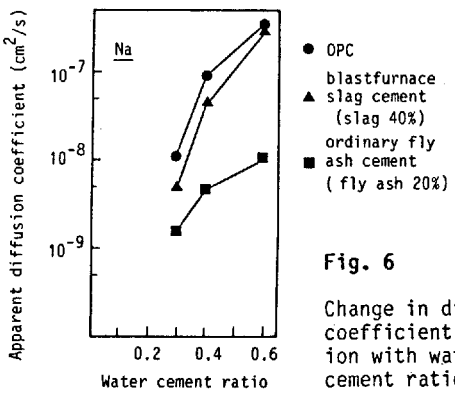

Fig. 6

Change in diffusion coefficient of Na ion with water cement ratio

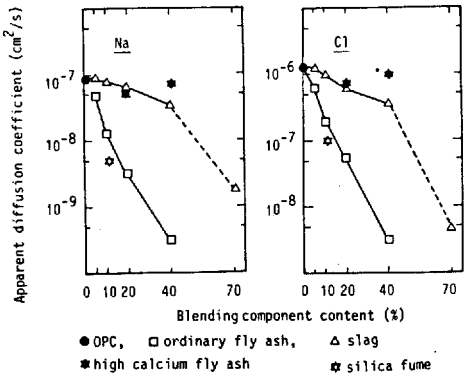

Fig. 7 Diffusion coefficient of Na and Cl ions through blended cement paste with different amount of blending component (318°K, W/C=0.40).

Fig. 7 shows diffusion coefficient of Cl and Na ions through hardened cement paste with different amount of blending component. Effect of fly ash on the diffusion coefficient seemed to be different fromthat of blastfurnace slag. When compared with same level of blending component, diffusion coefficient of each ion became smaller in the order of fly ash cement with high calcium fly ash, blastfurnace slag cement, fly ash cement with ordinary fly ash and silica cement with silica fume. In every case, the diffusion coefficient of Cl ion was larger than that of Na ion in spite of kind of blending component and its blended amount.

4.3 Relationship between diffusion coefficient and structure and composition of hardened paste

4.3.1 Relationship between total porosity and diffusion coefficient

Fig. 8 shows relationship between total porosity and diffusion coefficient of Cl and Na ions of hardened paste. Diffusion coefficient of each ion seemed to be mainly determined by W/C ratio without influence of kinds of blending component and its blended amount. The diffusion coefficient of Cl ion was about ten times as large as that of Na ion. The hardened paste after diffusion test had much amount of Fredel salt but no $Ca(OH)_2$. Large value of diffusion coefficient of Cl is considered to be caused by production of large pore eluting Ca ion from hydrates in hardened cement paste.

4.3.2 Relationship between pore size distribution and diffusion coefficient

In fly ash cement with ordinary fly ash, diffusion of ions appears to become difficult with increasing pore volume ratio of 5-50 nm in size in spite of its high

total porosity. On the other hand, in case of blastfurnace slag cement, the diffusion coefficient became smaller with increase in pore volume ratio less than 5nm. Fly ash cement paste with high calcium fly ash

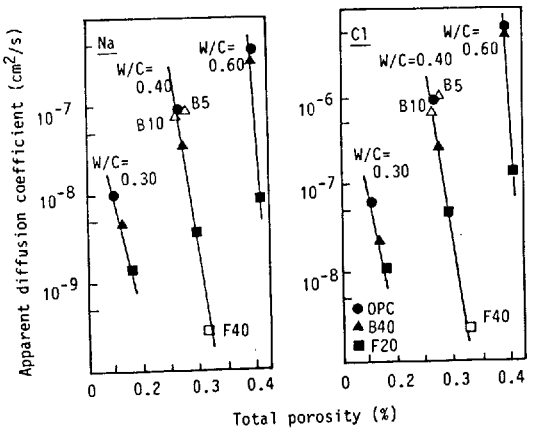

Fig. 8 Relationship between total porosity and diffusion coefficient of Na and Cl ions (318°K, W/C=0.40, B5: blastfurnace cement with 5% blastfurnace slag, F20: fly ash cement with 20% of ordinary fly ash).

containing large capillary pore more than 100nm had large diffusion coefficient. Capillary pore is considered to have more contribution than gel pore to the reduction of diffusion coefficient. Continuity of capillary pore also influences the diffusion coefficient of these ions.

4.3.3 Relationship between composition and surface properties of hydrate and diffusion of ions

(1) Na and Cl distribution of hardened cement paste after a diffusion test **Fig. 9** shows corrected Na concentration distribution of hardened cement paste after a diffusion test. Gradient of alkali concentration from the NaOH solution side towards the distilled water side was larger in the order of OPC, blastfurnace slag cement, ordinary fly ash cement. Alkali concentration of alkali solution side became higher in that order and that of the distilled water side became lower in that order. Since the diffusion of ion proceeded in the constant rate, it is considered that blastfurnace slag cement and fly ash and silica fume blended cement have resistance to the diffusion of alkali ion. Na concentration of the distilled water side is higher than original level and its trend is inhanced in blended cement paste. It is also, therefore, suggested that blended cement paste have larger holding capacity of alkali permeated than OPC paste.

Cl ion distribution showed similar trend to that of Na ion, but it depended strongly upon the amount of Al-bearing hydrate.

(2) Zeta potential of hardened cement paste powder Fly ash and blastfurnace slag showed negative zeta potential in water suspension (3). OPC ordinally with negative potential by the adsorption Ca^{2+}, Na^{+} and K^{+}, charged to positive and become larger with time (4). **Fig. 10** shows zeta potential of hardened paste powder measured by 1N NaOH solution streaming method. The zeta potential was high in the order of fly ash cement, blastfurnace slag cement and OPC, turning from negative to positive value with time in the latter two. This indicates that fly ash cement paste prevent alkali ions from diffusing by electric repulsion more than blastfurnace slag cement.

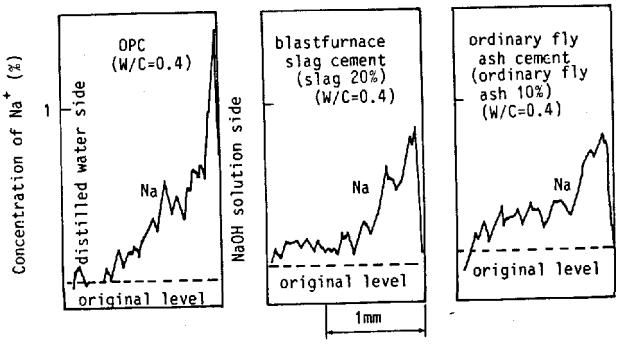

Fig. 9 Distribution of Na^{+} in cross section of hardened cement paste after diffusion test

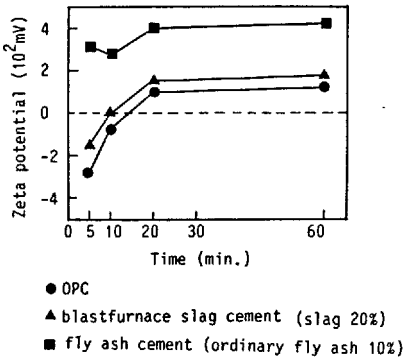

Fig. 10 Change of zeta potential of hardened paste powder

(3) Chemical composition of C-S-H in hardened paste

It is well known that specific surface area of C-S-H generally become higher with lower C/S ratio. Therefore, one of the reason why blended cement, especially ordinary fly ash cement and silica fume blended cement have higher effect on the reduction of diffusion of alkali than OPC is considered to be the formation of low C/S C-S-H with high specific surface area and capable of adsorbing much alkalies.

K ion is considered to show similar behavour of Na ion for diffusion of ion through hardened cement paste.

5. CONCLUSION

(1) The amount of $Ca(OH)_2$ in matured hardened blastfurnace slag cement was approximately same as in fly ash cement paste with ordinary fly ash and decreased with increasing blended amount. AFm content in the former was about two times in the latter and was larger than in OPC. Fly ash cement paste with high calcium fly ash had much amount of AFm and small amount of cubic aluminate hydrate. Silica fume blended cement paste was smaller in amount of $Ca(OH)_2$ and AFm.

C/S ratio of C-S-H formed was lower in the order of OPC, blastfurnace slag cement, fly ash cement with ordinary fly ash, silica fume cement, when same

amount of blending component was added. Low C/S C-S-H contained larger amount of Al and alkalies.

(2) Fly ash cement paste with ordinary fly ash had larger total porosity and pore volume ratio of 5-50nm than OPC and they increased with increasing fly ash amount. Blastfurnace slag cement paste with slag up to 40% showed smaller total porosity and larger porevolume ratio less than 5 nm than OPC. Both total porosity and pore volume ratio less than 5nm became large in blastfurnace slag cement with 70% content of slag and silica fume blended cement paste. Fly ash cement paste with high calcium fly ash had much more pore volume ratio larger than 100nm than with ordinary fly ash. Maximum peak of gel pore size distribution which corresponds to average distance between C-S-H solid surface decreased with the formation of more dense structure of low C/S C-S-H in ordinary fly ash cement and increased with the increase in amount of C-S-H in blastfurnace slag cement.

(3) When compared with same level, the diffusion coefficient of each ion through hardened paste became smaller in the order of OPC and fly ash cement with high calcium fly ash, blastfurnace slag cement, fly ash cement with ordinary fly ash and silica cement with silica fume. Capillary pore and its continuity had more contribution than gel pore to the reduction of diffusion coefficient. The diffusion of Cl ion proceeded same manner as alkali ions but diffusion coefficient of Cl ion was about ten times as large as that of Na ion.

(4) Low C/S C-S-H with high specific surface area serve to adsorb or incorporate much amount of alkali into it and to prevent movement of alkali through hardened paste by electric repulsion. This fact is confirmed from the results of alkali concentration distribution in hardened paste after diffusion test and zeta potential of hardened paste powder in NaOH solution.

REFERENCES

(1) R.F.M. BAKKER (1981), "About the cause of the resistance of blastfurnace slag cement concrete to the alkali silica reaction", Proc. 5th Int. Conf. on Alkali Aggregate Reaction in Concrete, Cape Town, S252/29.

(2) P.K. MEHTA and D. MANMOHAN (1980), "Pore size distribution and permeability of hardened paste", 7th Int. Cong. Chem. Cem. Paris, III, VII-1-VII-5.

(3) H. UCHIKAWA, S. UCHIDA and K. OGAWA (1982), "Influence of fly ash characteristics on the rheological properties of fresh fly ash cement paste", Pro. Mat. Res. Soc., Concrete rheology, Boston, Nov. 1-4, 203-214.

(4) H. UCHIKAWA, S. UCHIDA and K. OGAWA (1982), "Influence of organic additives on the rheological properties of fly ash cement paste", Pro. Mat. Res. Soc., Concrete rheology, Boston, Nov. 1-4, 192-202.

W. ROSZCZYNIALSKI and K. GUSTAW, University of Mining and Metallurgy, Cracow, Poland 1

Activity of fly ashes used as a pozzolanic admixture to cement. 3.2
Activité des cendres volantes utilisées comme l'addition pouzzolanique pour ciments.

SUMMARY : Some physical and chemical properties of fly ashes and their pozzolanic activity as well as their influence on hydration and properties of the hardened cement binder have been studied. Both ground and unground fly ash, and fly ash fractions collected in different sections of a power plant duster were used. Samples were prepared by the two methods : /I/ simultaneous grinding of cement and fly ash, and /II/ mixing of the ground and unground fly ash with cement. Pure Portland cement was used as a reference sample. It has been found that the ashes show certain pozzolanic activity. Their addition to the Portland cement modifies its properties and particularly resistance to sulphate corrosion and heat of hydration. The influence of fly ash on the mechanical strength of the cement depends on the ratio of the all constituants of the cement mixture, way of its preparation, phase composition of the ash and its grain size. The mechanical strength of the cement with the additive of the fly ash after long time of its storing is the best proof of the pozzolanic activity of the fly ash used.

Foram estudadas algumas propriedades físicas e químicas de cinzas volantes e sua atividade pozolânica, bem como sua influência sobre a hidratação e as propriedades do ligante cimentoso endurecido. Foram utilizadas tanto cinza volante moída e não moída, como porções de cinza volante coletadas em diferentes seções de um pulverizador de usina de força. Dois métodos foram usados para preparação de amostras: 1) moagem simultânea de cimento e cinza volante, e 2) mistura de cinza volante moída e não moída ao cimento. Como amostra de referência usou-se cimento portland comum. Constatou-se que as cinzas volantes apresentam certa atividade pozolânica. Sua adição ao cimento portland modifica sua propriedade e particularmente a resistência à corrosão por sulfato e o calor de hidratação. A influência da cinza volante sobre a resistência mecânica do cimento depende da relação de todos os constituintes da mistura de cimento, forma de sua preparação, composição de fase da cinza e sua granulometria. A resistência mecânica do cimento com aditivo de cinza volante, após longo tempo de armazenagem, é a melhor prova da atividade pozolânica da cinza volante usada.

1. INTRODUCTION

Various special methods for determining the pozzolanic activity of fly ashes bring not always correlated results and very often do not characterize this activity unequivocally. It is therefore difficult to decide whether a given type of fly ashes can be applied as addition to cements. The problem arizing from this difficulty can be solved by a complex method consisting in determining the influence of the fly ash addition on the process of hardening and investigating the properties of cements in conneetion with some properties of fly ashes used.

2. DETERMINATION OF PHYSICAL AND CHEMICAL PROPERTIES OF FLY ASHES.

2-1. Chemical analysis.

The results of chemical analysis create the possibility to determine the type of fly ashes and bring information about the content of undesired components as e.g. carbon /loss on ignition at 450°C/. Carbon content above 3% renders the fly ash unapplicable as a pozzolanic addition to cement/1/.

2-2. Granulometric composition.

Table I illustrates the grain composition of a given fly ash sample as well as the grain composition of fractions obtained from different sections of electrofilters.

Table 1

Kind of fly ash sample	Specific surface		Granulometric composition /%/					
	according to Blaine /cm^2/g/	according to BET /m^2/g/	>60 /um	60-30 /um	30-15 /um	15-10 /um	10-5 /um	5-0 /um
Mean sample	3140	16.1	24.7	25.2	28.3	9.7	7.1	5.0
Sample from 1^{t} sect. of electrofilters	2370	12.4	30.1	42.3	14.5	7.1	4.1	1.9
Sample from 2^{d} sect. of electrofilters	3090	19.1	14.5	20.3	26.4	14.3	15.2	9.3
Sample from 3^{d} sect. of electrofilters	4760	24.5	8.1	10.1	27.1	17.7	20.4	16.6
Ground sample	4350	22.8	2.1	18.5	36.9	20.0	13.4	9.1

The results obtained for a mean sample ground 30 minutes in a normalized laboratory mill are also included.

The correlation between the granulometry of fly ashes and their pozzolanic activity is clearly seen especially in the case of the mechanically ground sample because of the fact that owing to the destruction of the glassy surface layer covering the grains their internal more active part becomes rendered accessible.

2-3. Phase composition.

Microscopy and X-ray phase analysis bring a semi-quantitative information about the content of not active crystalline components as haematite, magnesite, calcite, quartz, belite, anhydrite, rutile a.o. The content and mean diameter of pozzolanic active particles can be also approximately determined.

3. INVESTIGATION OF HYDRATION OF CEMENTS CONTAINING FLY ASH ADDITIONS.

Investigations of hydration of cements were performed for the following cements :

cement 1 - 95% clinker + 5% gypsum

cement 2 - 52% clinker + 3% gypsum + 45% ground fly ash

cement 3 - 52% clinker + 3% gypsum + 45% not ground fly ash

Fly ash additives were mixed with separately ground cement.

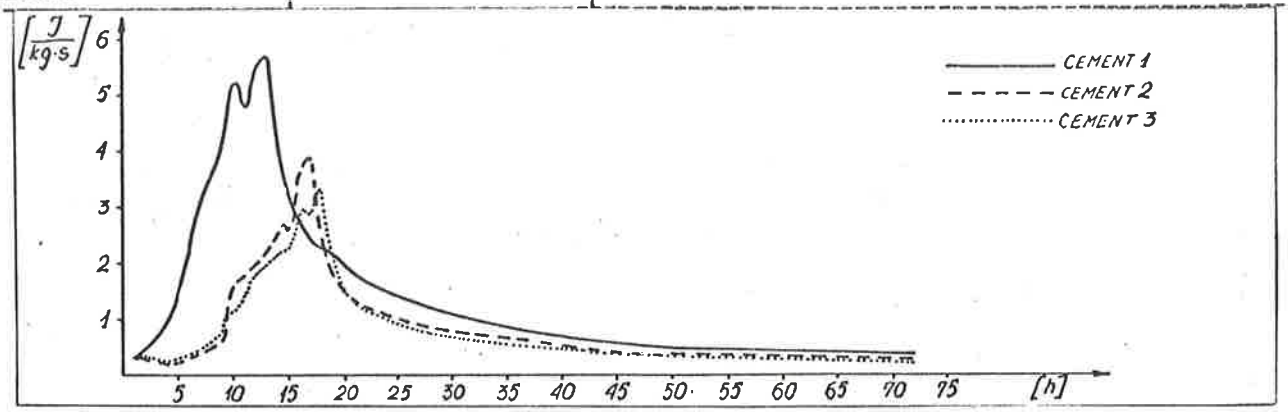

Fig. 1 - Heat evolution during hydration of cements.

3-1. Heat of hydration.

The results of colorimetric investigations are presented in Fig. 1. The colorimetric curves indicate that a fly ash addition diminishes the rate of heat evolution and simultaneously retards the appearance of the maximal heat effects corresponding to the hydration of alite and C_3A. The retarding influence of fly ashes exerted on the hydration process is due to the content of SO_3 /ca 1%/ and of elementary carbon /ca 2.5%/. Cements containing ground fly ash addition reach the moment of maximal heat evolution earlier than those containing not ground addition. Also in the time period between 20 and 72 hours of hydration the rate of heat evolution and therefore also the rate of chemical reaction are greater in the case of ground fly ash addition. In the first 10 hours of hydration the rate of heat evolution in the case of cements containing not ground additions is a little greater what can be possibly ascribed to low homogenous distribution of carbon particles.

3-2. Phase composition of cement pastes.

The results of DTA and X-ray investigations in the period between 1 and 90 days of hydration have brought the proof that the fly ash addition increases the rate of hydration of clinker phases and binds the calcium hydroxide. The influence of fly ashes consisting in increasing the rate of hydration can be explained by the so called "effect of small particles" /2/. The binding of calcium hydroxide leading to formation of hydrated calcium silicates and aluminates is the fundamental pozzolanic reaction. The determination of the rate of this reaction can be thus very usefull in characterizing the pozzolanic activity of fly ashes. Fig. 2 illustrates the influence of fly ash addition on the $Ca/OH/_2$ - content in hydrated cements.

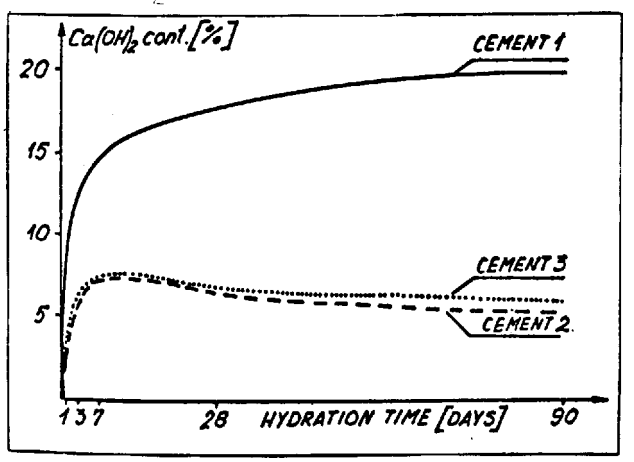

Fig. 2 - $Ca/OH/_2$ content in cement pastes in function of time.

3-3. Porosity of cement pastes.

Fig. 3 illustrates the relation between the decrease of total porosity of pastes containing fly ash addition and their compressive strength.

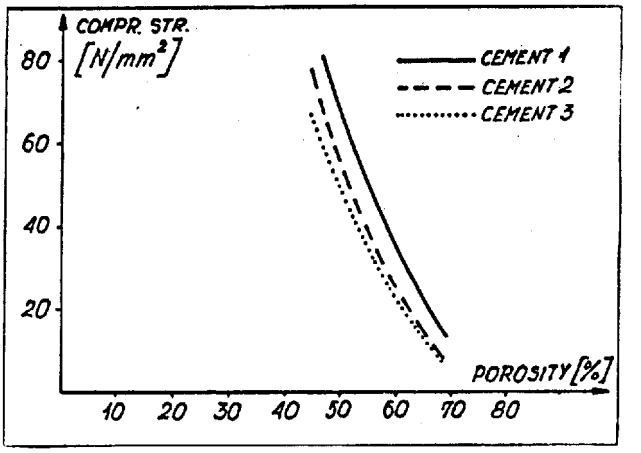

Fig. 3 - Compressive strength in function of porosity of cement pastes.

For given values of porosity the past containing ground addition exhibits greater compressive strengths than that containing not ground addition, but smaller than in the case of paste without ash addition. The compressive strength of cement pastes does not depend only on their total porosity but also on the type of hydrating phases and on the shape and distribution of pores /3/.

4. INVESTIGATIONS OF PROPERTIES OF CEMENTS WITH FLY ASH ADDITION.

Investigations of properties of cements containing fly ash additions bring the most significant information about the pozzolanic activity and can be considered to be the most important criterion of the applicability of this fly ash in cement manufacture. Most reliable data are obtained in the result of compressive strength determinations especially after long periods of hardening.

4-1. Fundamental physical properties of cements containing fly ash additions.

Physical properties of cements containing fly ash additions determined using the normalized methods are presented in Table 2.

The results obtained for ashes from different sections of electrofilters show that with decreasing mean grain diameter the mechanical strength increases.

Best mechanical strength were observed after grinding the all cement components /Portland clinker, gypsum and fly ash/ together in one mill charge. Introduction of already ground fly ash lowers the initial strength stronger than the introduction of not ground addition. The positive effect of previous grinding is

Table 2

Fly ash additive	Normal consistency /% H_2O/	Set /h,min/		Strength /N/mm^2/									
				Bending					Compressive				
		Initial	Final	3days	7days	28days	90days	1year	3days	7days	28days	90days	1year
-	26.5	2^{50}	4^{30}	5.7	8.4	9.3	9.7	10.0	21.6	35.4	47.6	62.0	67.2
15%MS-X	29.5	3^{30}	5^{10}	6.1	7.9	9.9	10.1	10.6	24.2	34.4	49.1	64.5	71.1
15%S1-X	29.5	3^{30}	5^{15}	5.9	7.8	9.7	10.0	10.4	23.7	33.7	48.8	64.4	70.8
15%S2-X	29.0	3^{25}	5^{05}	6.4	8.1	9.9	10.1	10.7	25.0	36.0	49.3	65.0	71.3
15%S3-X	29.0	3^{25}	5^{00}	6.5	8.1	9.9	10.3	10.8	25.5	37.2	49.2	65.2	71.3
15%GS-O	30.5	3^{40}	5^{25}	5.6	7.2	9.7	10.1	10.8	18.9	31.3	41.4	55.3	65.3
15%US-O	29.0	3^{20}	4^{50}	5.8	7.8	9.8	10.0	10.2	20.5	34.1	40.5	53.8	60.0
45%MS-X	33.5	4^{45}	7^{35}	3.5	4.6	7.5	10.1	10.4	12.4	18.2	30.3	49.9	66.6
45%S1-X	34.0	5^{05}	8^{00}	3.0	4.1	7.0	9.7	9.9	11.4	17.3	29.5	48.7	65.1
45%S2-X	32.5	4^{20}	7^{05}	3.8	5.1	8.0	10.2	10.5	13.5	19.1	31.0	50.8	67.0
45%S3-X	32.5	4^{15}	6^{45}	4.4	5.5	8.5	10.8	11.0	13.9	20.2	32.7	52.8	69.1
45%GS-O	34.5	5^{00}	7^{40}	2.9	4.0	6.8	9.9	10.6	9.9	14.8	25.8	47.0	59.7
45%US-O	33.0	4^{30}	7^{20}	3.0	3.8	5.8	9.8	9.7	11.2	15.7	24.8	41.4	53.3

MS - mean sample ; S1 - sample from 1st section of electrofilters ; S2 - sample from 2nd section of electrofilters ; S3 - sample from 3rd section of electrofilters ; GS - ground sample ; US - unground sample ; X - simultaneous grinding all cement components ; O - mixing fly ash and cement

observed not earlier than after 7-28 days of hydration. This agrees with results obtained in determining the heat of hydration /3-1./.

The results presented in Table 3 illustrate the decrease of compressive strength during storage in dry-air conditions. This proves that the presence of liquid phase is indispensable for proper proceeding of the pozzolanic reaction.

Table 3

Fly ash additive	Strength after storage in dry-air conditions /N/mm^2/			
	Bending		Compressive	
	28 days	1 year	28 days	1 year
-	10.3	9.4	50.6	56.5
15%MS-X	9.8	9.6	46.6	51.4
45%MS-X	7.1	8.0	28.2	38.4

4-2. Special properties of cements modified by fly ash additions.

Pozzolanic additions decrease the heat of hydration and increase the resistivity to corrosion especially with respect to sulphates. The influence of fly ash addition on the heat of hydration is illustrated by Table 4, and the resistivity to sulphate corrosion by Fig. 4.

Table 4

Time of hydration /h/	Heat evolution /J/g/		
	pure cement	cement with 45% ground fly ash add.	cement with 45% unground fly ash add.
1	2.85	1.01	1.07
6	22.19	5.25	6.45
12	116.77	30.10	25.82
24	229.88	120.66	111.78
36	273.38	154.67	141.82
48	300.58	172.98	160.91
60	320.23	191.29	174.88
72	335.66	203.16	185.86

As it can be seen from the presented results the fly ash addition diminishes the hydration heat mainly in the period of some very first hours of hydration. After 36 hours in the case of 45% content of ground ash and after 72 hours in the case of 45% content of not ground ash the total heat of hydration was

lowered to 45% in comparison with that for cement without ash additions.

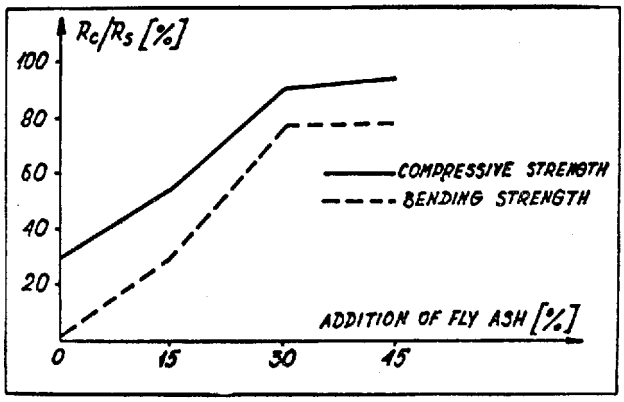

Fig. 4 - Influence of the fly ash addition on the resistivity of cement to sulphate corrosion.
R_s - strength after 3 years storage in standard conditions
R_c - strength after 3 years storage in 2% $MgSO_4$ solution

The results presented in Fig. 4 prove that the fly ash addition increases the resistivity to sulphate corrosion. To protect effectively against this corrosion the addition of fly ash shall amount to not less than 30%.

5. SPECIAL METHODS FOR DETERMINING THE POZZOLANIC ACTIVITY OF FLY ASHES.

Basing on results discussed in 2, 3 and 4 the authors consider the ASTM - method /4/ to be the best suitable chemical method and the method proposed by Fratini and Lea /5,6/ the best physical method for determining the pozzolanic activity. The results obtained using the ASTM method are presented in Table 5, those obtained according to Fratini in Table 6.

Table 5

Kind of fly ash sample	Content of active components /%/	
	SiO_2	Al_2O_3
Mean sample	19.13	6.53
Sample from 1st sect. of electrofilters	18.42	6.25
Sample from 2nd sect. of electrofilters	19.93	6.62
Sample from 3rd sect. of electrofilters	20.99	6.98
Ground sample	20.07	6.41

Table 6

Kind of cement	Compressive strength /N/mm²/		
	R_s	R_p	$R_p - R_s$
Pure cement	35.4	40.4	5.0
Cement+45% MS-X	18.2	42.9	24.7
Cement+45% S1-X	17.5	39.8	22.3
Cement+45% S2-X	19.1	44.0	24.9
Cement+45% S3-X	20.2	45.5	25.3
Cement+45% GS-O	14.8	35.8	21.0
Cement+45% US-O	15.7	30.4	14.7

R_s - strength after 7 days storage in standard conditions
R_p - strength after 3 days storage in standard conditions and 4 days storage in water at 50°C

Other indications as in Table 2

These results are very good correlated with those obtained after long-time determinations /Table 2/ which best characterize the pozzolanic activity of fly ashes. The ASTM method brings the results faster but the Fratini method also allows to forsee the order of magnitude of mechanical strength after very long hardening periods.

6. CONCLUSIONS

The obtained results prove that the most reliable determination of pozzolanic activity of fly ashes consists in parallel application of the ASTM and the Fratini method ; additional determination of the carbon content in ashes can be also very usefull.

7. BIBLIOGRAPHY

1.- F. MASSAZZA, Structure of pozzolana and fly-ash and the hydration of pozzolanic and fly-ash cements, 7th International Congress on the Chemistry of Cement, Vol. IV, Paris 1980, 85-91.

2.- Z.B. ENTIN, E.T. YASHINA, G.G. LEPSHENKOVA and N.Z. RYAZANTSEVA, On the Hydration and Hardening of Cement with Fly-ash Addition, 6th International Congress on the Chemistry of Cement, Vol. III, Moscow 1976, 95-98.

3.- J. JAMBOR, Relations between phase composition, over-all porosity and strength of hardened lime-pozzolana pastes, Magazine of Concrete Research, 1963, Nr 45, 131-142.

4.- ASTM C 593-69, Standard Specificacion for Fly-Ash and other Pozzolans for use with Lime, Washington 1969.

5.- F.M. LEA, The chemistry of cement and concrete, Academic Press, London 1956, 373-413.

6.- F.M. LEA, The testing of pozzolanic cements, Cement Technology, 1973, Nr 1, 21-25.

M. Silsbee, R.I.A. Malek and D.M. Roy, Materials Research Laboratory, The Pennsylvania State University, University Park, PA 16802 USA

Composition of Pore Fluids Extruded From Slag-Cement Pastes

SUMMARY

The hydration of cement pastes prepared from several different cements has been studied by pore fluid expression. The effect of replacement of a portion of the cement by blast furnace slags was explored. The chemistry of pore fluids is important not only because of this role in the hydration of cement but also with respect to the passivation of steel in concrete and in alkali-aggregate reactions.

In general the results of pore solution studies were found to be quite sensitive to many factors. For instance expression pressure, curing conditions, and post expression handling of the expressed liquids have all been found to affect the final results.

Additions of the relatively silica rich slags to the portland cement lead to a partial neutralization of the pore fluids. Primarily through a reduction of the alkali present resulting in a lowering of the pH by 0.5. However, the lower pH values observed are still adequate for passivation of steel.

Por meio de expressão de fluido de poro, estudou-se a hidratação de pastas de cimento preparadas com diversos cimentos diferentes. Explorou-se o efeito da substituição de uma porção de cimento por escórias de alto forno. A química dos fluidos de poro é importante, não só por seu papel na hidratação do cimento, mas também em relação à passivação do aço no concreto e às reações no álcali-agregado.

Em geral os resultados dos estudos da solução de poro foram considerados bastante sensíveis a muitos fatores. Por exemplo, a pressão para expressão, as condições de cura, e o manuseio dos líquidos expremidos após a expressão, afetam - conforme se constatou - os resultados finais.

Adições de escórias, relativamente ricas em sílica, ao cimento levam a uma neutralização parcial dos fluidos de poro. Primeiramente por meio da redução do álcali presente, resultando em diminuição de 0,5 no pH. Contudo, os valores de pH mais baixos observados ainda são adequados para passivação do aço.

J. Silsbee, R.I.A. Malek and D.M. Roy, Materials Research Laboratory, The Pennsylvania State University, University Park, PA 16802 USA

INTRODUCTION

Studies of the hydration processes involved in hydrating cement pastes are generally hampered by uncertainties about the nature of the aqueous phase. In 1973 Longuet (1) stimulated renewed interest in the nature of the aqueous phase by expressing pore fluids from hardened cement pastes. Since that time Diamond (2), Glasser and Marr (3) and others have made significant contributions to the general understanding of cement/hydration chemistry using similar devices. Combining the results of this recent work with earlier studies (eg. [Flint and Wells-calcium-silicate solutions; 1934 (4), Kalousek, soda-lime-silica solution; 1944 (5)] should lead to a better understanding of the processes involved.

Interest in the aqueous portion of hydrating cement pastes extends beyond hydration processes to concerns about alkali-aggregate reactions and the passivation of steel in concretes. This study examines the effects of major substitution of ground granulated blast-furnace slag on the properties of cement paste pore solutions.

EXPERIMENTAL

Pore fluids were expressed from samples that had been cured for times ranging from a few hours to several months at pressures up to 275 MPa. Except where otherwise noted pressure was applied in ~14MPa increments with pauses to allow fluid to escape. In general two sets of curing conditions were employed 1) 25°C over water and 2) 38°C in a controlled humidity chamber.

Due to the relatively small quantities of fluid collected during these studies special sample preparation techniques (6) were employed prior to carrying out an analysis of the fluids. Samples for cation analysis were diluted using 5% v/v HCl solution. Three to 6 ml of the HCl solution was placed in a 7 ml plastic scintillation vial and the sample added in 100µL increments utilizing an MLA automatic pipette equipped with disposable plastic tips. Further dilutions were performed in Pyrex volumetric flasks as necessary (note: additional HCl was added as necessary to maintain the low pH state of the samples.

Cation determinations were performed on a DC plasma emission spectrometer*. The instrument was calibrated with aqueous standards containing 1% v/v HCl. A typical analytical run consisted of 10-15 samples and five standards. Analysis of each standard was performed twice, immediately prior to the unknowns and immediately after, to compensate for any instrumental drift.

Sample preparation for anion analysis follows much the same pattern as for cation determinations with the exception that all dilutions were performed with deionized water. The anion determinations were performed utilizing Ion Exchange Chromatography**. Separation was accomplished using a fast run anion separator (HPIC-AS3 with A6B guard column). Samples were injected through a 0.2µm syringe filter.

Standards for both the anion and cation analysis were made by serial dilution of 1000µg/mL stock solutions obtained from J.T. Baker Co. or Alfa Inc.

Chemical analysis and Blaine specific surface area values for the starting raw materials used in this work are shown in Table I.

Experimental Variations

As part of this study a systematic attempt to determine the effects of experimental conditions on the results of pore solution studies was made. A batch prepared from Type I (I-09) cement with 0.50 w/c was cast into 1 inch diameter x 2 inch height cylindrical molds and allowed to cure for 24 hrs at 25°C in an atmosphere saturated with water vapor. In addition a specimen was prepared by casting the paste directly into a plastic vial. The vial was subsequently sealed and allowed to cure at 25°C. The remaining samples with one exception were demolded after 24h and set to cure over deionized

TABLE I: Chemical Analysis and Other Characteristics of the Materials Used in this Work (wt.%)

	(I-09)	(I-13)	(B66)	(S37)	II-04
CaO	62.98	62.7	40.61	43.7	63.12
SiO_2	19.80	20.2	34.3	36.3	21.0
Al_2O_3	5.74	6.2	10.2	9.7	4.02
Fe_2O_3	2.17	2.1	0.67	0.6	3.33
SO_3	2.55	3.30	**	**	2.52
S	-	-	1.31	-	-
MgO	3.13	2.50	11.4	8.2	3.86
Na_2O	0.19	0.21	0.19	0.30	0.23
K_2	0.78	1.23	0.45	0.50	0.44
LOI	1.40	1.04	---	---	1.06
(a)	3.18	3.10	1.18	1.18	3.01
(b)	3.63	3.53	1.79	1.67	3.38
(c)	0.70	1.02	0.49	0.63	0.52
(d)	0.97	1.47	0.64	0.80	0.67
(e)	330	402	550	*	3790

(a) Index of Neutrality (c/s)
(b) Index of Hydraulicity (C+M+A/S)
(c) Total Alkali (Na_2O) Equiv.
(d) Total Alkali (Na+K)
(e) Blane Specific Surface Area (m^2/g)
* Blane specific surface area was not determined due to extreme fineness of samples. BET surface area was 9.26 m^2/g
** Gain on ignition indicates the existence of sulfur as S or S^{2-} rather than SO_3
I-09 - MRL code for Type I cement from Lone Star
I-1B - MRL code for Tye I high alkali cement obtained via Atlantic Cement Co.
B-66 - MRL code for Newcem Slag from Atlantic Cement Co.
S-37 - MRL code for granulated blast furnace slag dust from Purfleet
II-04 - MRL code for Type II/I cement from Atlantic Cement Co.

*Model IIIb from Beckman/Smith-Kline
**Dionex Model 2010,

water at 25°C. One sample was immediately placed in a solution saturated with $Ca(OH)_2$ and allowed to cure at 25°C.

The analyses of the pore fluids expressed from these samples after 7 days of curing are shown in Table II and are treated in Figures 1 and 2. Table II and Figure 1 summarize the effect of pressure on the pore fluids expressed from hardened cement pastes. Also included in Table II are the results from a determination in which the pressure was rapidly increased to 275MPa prior to the extraction effort. The lower ionic strength exhibited by this sample would tend to suggest a simple filtration effect caused by the collapse of the pore matrix. Laschenko and Loganina (7) reported a similar effect which they attributed to the presence of two liquids in the cement pastes. They labeled these liquids a) dispersion and b) gel liquids.

TABLE II: Pressure Effect on Pore Fluids (conc. in moles/L)

pressure interval (kpsi)	Ca	K	Na	Si	Al	SO_4
0-20	3.0	315	109	7.5	0.63	
20-30	2.6	330	117	9.3	0.37	3.54
30-40	2.4	345	122	9.6	0.15	3.75
40-50	0.5	258	130	7.12	0.26	6.77
0-20	3.0	315	109	7.5	0.63	
0-30	0.62	248	126	8.4	0.26	2.76
0-40	0.62	445	139	6.7	0.32	3.33
rapid* increase	0.50	240	96	4.8	0.30	3.96
Unfilt.	0.62	353	130	7.1	0.3	-
Filt.	2.74	322	126	6.4	0.52	-
with 1/2 drop conc. HCl (after filtering)						
Unfilt.	1.62	222	109	4.27	0.1	-
Filt.	4.12	212	104	3.92	0.2	-
$Ca(OH)_2$ cured	4.24	107	63	2.4	0.2	0.78
plastic cured	3.12	297	126	1.2	0.3	2.97
'moist' cured	0.62	445	139	4.8	0.3	3.33
$Ca(OH)_2$	14.6	26	9.2	0.5	<0.1	0.02
water	3.4	16	5.9	0.9	<0.1	0.06
deionized water	<.002	.003	.004	.025	.003	0.07

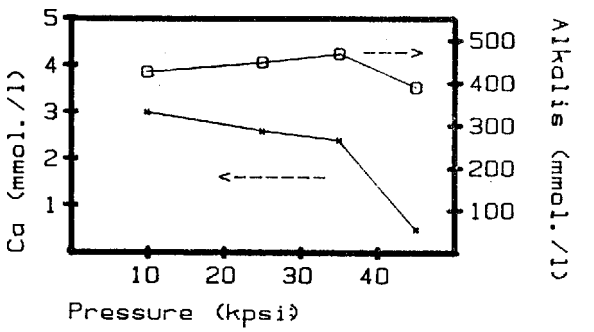

Figure 1. Variation of Ca and alkali concentration with pressure data from Table II.

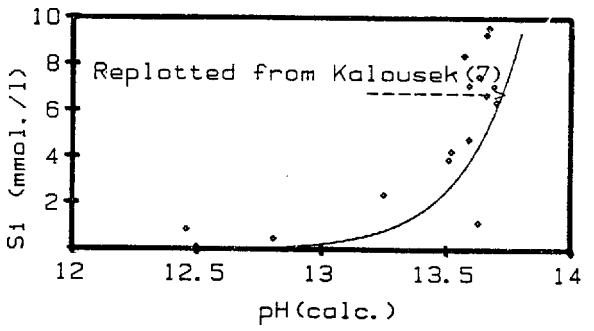

Figure 2. Variation of Si content with calculated pH in pore fluids. The pH was calculated on the basis of $OH-Na^{+}+K^{+}+2*Ca^{2+}$.

Also explored in Table II, the effect of post-expression treatment on the resulting analysis. In this case two samples were split into havles with one of the halves being passed through a 0.2μm syringe filter. One set of samples was then acidified using concentrated HCl (1/2 HCl in ~0.6mL of fluid). In general filtering lead to a slight decrease in ionic strength. The effect of immediate acidification was a more dramatic decrease in ionic strength.

The next section of Table II examines the effect of curing conditions on the pore solutions. Both the sample cured in saturated $Ca(OH)_2$ and the sample cured in a sealed vial exhibit significantly lower ionic strengths than the sample cured in a moist atmosphere (normal conditions for this study). This raises the possibility that interactions with the storage solutions may be playing a significant role in the pore solution. The last section of Table II contains the analyses of the two storage solution along with typical results from the deionized water used in preparing them. The ability of these storage solutions to act as leachants is strongly suggested by these results.

The silica concentrations found in these solutions are surprisingly high when compared with those found by other investigators (3). Figure 2 is intended to explore a possible explanation for this

relationship. The pH values were calculated on the basis of [OH] = [$^-$Na] + [K] + 2 x [$^-$Ca]. This method offers the advantage of avoiding placing a glass pH electrode in these highly alkaline fluids. The solid line in Figure 2 is a best fit line based on data from Kalousek's (5) study of soda-calcia-silica gels. The line is intended to represent an upper limit for Si concentrations in solutions in contact with soda-calcia-silica gels and crystalline $Ca(OH)_2$. While this does not offer a clear explanation of the silica concentrations it does suggest that the nature of the (substituted) C-S-H gel formed may be playing a role. It may be that in many cements a 'quasi' crystalline C-S-H gel is formed while in this case the C-S-H formed was closer to a true gel, and of much higher silica content. Perhaps the leaching effect of the storage solution plays a role in this phenomenon. However further work in this area is indicated to reach a definitive conclusion on this subject.

Early Ages

A limited study of fluids extracted from pastes during the very early period of hydration was also included as part of this study (1/2-24h). A typical set of results is shown in Figure 3. For times up to 7h the liquid was collected by centrifuging the sample and passing the supernatant fluid through a 0.2μm syringe filter. The 12h and 24h samples were collected using pore expression.

28 Day Studies

The batch proportions and curing temperatures for the mixtures used in this portion of this investigation are shown in Table III. As can be seen from Figure 4 the alkali levels in this pore fluid climb rapidly and by 7 days nearly all the alkalis present in the mixture are contained in the pore fluids. Potassium levels were always much higher than sodium. These levels then remain fairly constant or show a slight decline over the period of the test.

Additions of slag always lowered the alkali levels substantially from that found in the 'pure' cements. Figure 5 provides a comparison of these levels. The plot shown as Figure 6 suggests that this is partly due to the variation in the alkali contents of the original mixes. However, the slag containing mixes enjoy an advantage at the later

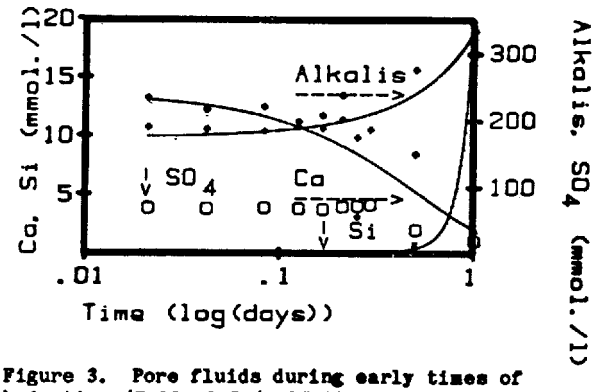

Figure 3. Pore fluids during early times of hydration (I,09-,0.5w/c,25°C)

TABLE III: Mix Proportions and Curing Temperatures

S-01	0.35 I-09, 0.65 B-66, 0.5 w/c, 38°C
S-03	I-09, 0.5 w/c, 25°C
S-04	0.5 I-09, 0.5 B-66, 25°C
S-05	I-13, 0.5 w/c, 25°C
S-06	0.5 I-13, 0.5 B-66, 15°C
S-07	0.5 I-09, 0.35 B-66, 0.15 S-37, 25°C, 0.4 wt% A=3*
S-09	I-09, 0.5 w/c, 25, 38°C
S-10	0.35 I-09, 0.65 B-66, 25, 38°C
S-11	II-04, 0.5 w/c, 25, 38°C
S-12	0.35 I-13, 0.65 B-66, 0.5 w/c, 25, 38°C
S-13	I-09, 0.4 wt% NaCl, 0.5 w/c, 25, 38°C
S-14	0.35 I-09, 0.65 B-66, 0.4 wt% NaCl, 0.5 w/c, 25, 38°C
S-15	II-04, 0.4 wt% NaCl, 0.5 w/c, 25, 38°
S-16	0.35 I-13, 0.65 B-66, 0.4 wt% NaCl, 0.5 w/c, 25, 38°C

*A-3 -Mighty 150, KAO Chemicals, sulf. napth

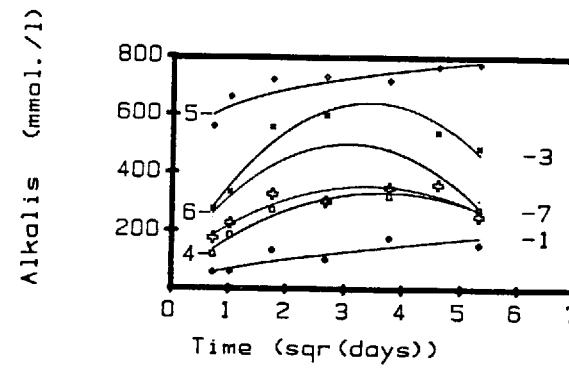

Figure 4. Alkali level in pore solutions. (The numbers refer to the mix numbers in Table III).

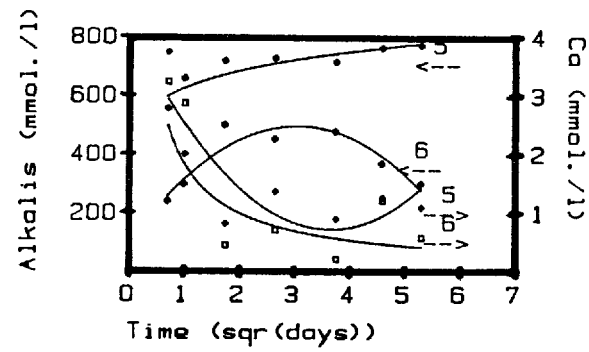

Figure 5. Comparison of alkali and calcium levels in the pore fluids of a slag-cement vs. portland cement. (The numbers refer to the mix numbers in Table III).

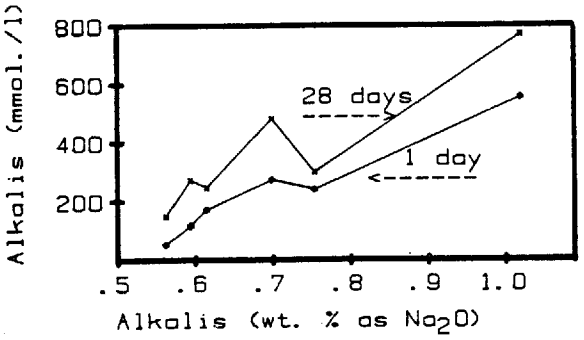

Figure 6. Relationship of alkali levels of pore fluids and total akalis (as Na_2O) of mixes.

times, while the alkali contents of the cement pore solution remained high.

The calcium concentration in the pore fluids quickly drops to near millimolar levels. Calcium levels in the slag containing mixes generally are somewhat lower than for the corresponding 'pure' cement mixes. This can be attributed to two effects 1) lower calcium content of the mixes and 2) increased consumption of the calcium by the relatively silica-rich slag-cement mixtures, the latter believed to be dominant.

Sulfate levels drop quickly from the high levels found immediately after mixing. In slag-cement mixtures the sulfate levels then remained relatively constant. However, in the portland cement mixtures the sulfate levels tended to pass through a minimum and then increase. This phenomenon is demonstrated in Figure 7. This behavior suggests early ettringite formation (low $SO_4^=$ in solution) followed by release of sulfate to solution along with Ca and Al. The aluminum levels would then be limited by C_2AH_x solubility.

In addition to those already discussed cation analysis for Ba, Fe, Mg, and Sr were also carried out. With the exception of Sr they all remained at

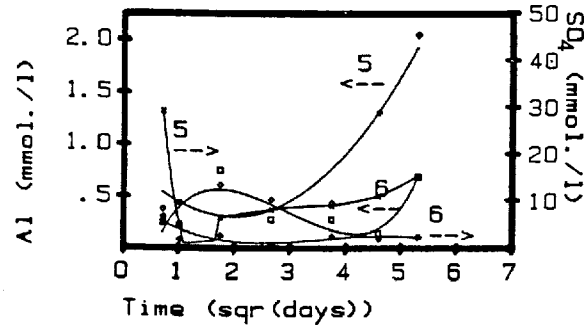

Figure 7. Comparison of aluminum and sulfate levels in the pore fluids of a slag-cement vs. portland cement. (The numbers refer to the mix numbers in Table III).

low ppm levels with Sr occasionally reaching tens of ppm. Anion determinations were also routinely carried out for NO_2^-, NO_3^-, $PO_4^=$ and Cl^- with only Cl^- levels reaching significant proportions (100 ppm).

EFFECTS OF NaCl ADDITIONS

The maintenance of high pH values in the pore fluids of concrete is desirable for the protection of steel by passivation. Soluble chlorides, at levels as low as 0.4% by weight of cement (8), are capable of inducing pitting corrosion of steel in spite of the high pH levels normally maintained.

Therefore to examine the effect of blast-furnace slag on these two phenomena a series of eight batches was prepared (S-09-S-16 in Table III). Two sets of specimens were prepared from each batch and one set cured over de-ionized water at 25°C, the other at 38°C. Pore fluids were then extracted from these samples at times up to six months. The results are presented in Tables IV-VII and Figures 8-11.

The pH values of the pore solutions obtained from the salt free mixes are plotted against the square root of time in Figures 8 and 9. Since mild steel has been observed (8) to acquire a passivation layer when immersed in alkali solutions with pH values in excess of ca. 11.5 the reduction in pH caused by additions of blast furnace slag is not likely to cause major deleterious effects. Figure 10 compares the Cl^- retained in the pore fluids for the various mixes. In all cases, the slag-cement mixtures contained much lower chloride levels in the pore solution then the portland cement mixes. Figure 11, a plot of the overall c/s ratio of the mixes vs. %Cl^- retained in the pore fluids suggests that the c/s ratio plays a major role in the ability

TABLE IV: Analysis of Pore Fluids from Salt-Free Specimens Cured at 25°C

Mix	Curing time (months)	Concentrations (mmole l) Na^+	K^+	Ca^{2+}	SO_4^{2+}	Cl^-
S-09-25	1	139	358	2.1	3.0	.48
	2	130	345	2.6	2.4	.68
	3	144	279	.4	3.3	1.35
	6	113	169	.2	2.5	.59
S-10-25	1	91	166	.2	3.2	1.70
	2	67	115	1.87	2.1	.28
	3	78	102	.2	1.2	.38
	6	78	90	.1	2.8	.65
S-11-25	1	183	187	.3	2.1	.48
	2	139	192	1.6	3.4	.73
	3	178	187	.2	3.8	1.30
	6	130	113	.7	2.6	.25
S-12-25	1	87	166	2.2	5.1	2.12
	2	70	151	.1	5.1	-
	3	88	120	.1	1.6	1.55
	6	80	104	.2	2.8	.54

M. Silsbee, R.I.A. Malek and D.M. Roy, Materials Research Laboratory, The Pennsylvania State University, University Park, PA 16802 USA

TABLE V: Analysis of Pore Fluids from Samples Containing .4% by Weight of Solids, NaCl cured at 25°C

Mix	Curing time (months)	Concentrations (mmole l) Na^+	K^+	Ca^{2+}	SO_4^{2+}	Cl^-
S-13-25	1	204	286	.5	8.1	53.88
	2	257	315	.5	4.1	20.02
	3	222	230	2.0	4.1	18.33
	6	265	240	3.9	5.7	22.00
S-14-25	1	135	115	.4	10.5	13.54
	2	178	107	.2	3.3	8.74
	3	139	82	.3	2.4	6.77
	6	122	72	.1	2.9	8.03
S-15-25	1	270	179	.5	3.6	20.88
	2	239	162	1.9	4.5	14.46
	3	470	221	.3	7.5	32.72
	6	209	113	1.1	9.8	21.44
S-16-25	1	170	159	.3	4.8	18.05
	2	157	143	.4	8.5	22.00
	3	170	107	.2	6.9	11.56
	6	135	90	.2	9.8	10.72

TABLE VI: Analysis of Pore Fluids from Salt-Free Speciments Cured at 38°C

Mix	Curing time (months)	Concentrations (mmole l) Na^+	K^+	Ca^{2+}	SO_4^{2+}	Cl^-
S-09-38	1	120	0345	.1	6.3	.79
	2	152	389	2.7	12.4	.20
	3	157	284	.5	15.2	.4
	6	148	243	.6	16.56	1.07
S-10-38	1	109	176	.1	8.2	.96
	2	87	153	.4	8.8	2.68
	3	86	97	.1	2.4	.48
	6	68	64	.1	2.4	.31
S-11-38	1	161	197	.6	5.4	1.10
	2	135	169	2.5	5.1	.32
	3	98	138	.2	3.3	.87
	6	152	130	1.4	7.0	.23
S-12-38	1	104	194	.2	9.69	1.13
	2	83	171	.1	3.3	.36
	3	148	138	.9	5.5	.84
	6	89	105	.2	5.8	.59

TABLE VII: Analysis of Pore Fluids from Samples Containing .4% by wt of Solids NaCl, Cured at 38°C

Mix	Curing time (months)	Concentrations (mmole l) Na^+	K^+	Ca^{2+}	SO_4^{2+}	Cl^-
S-13-38	1	3?	4?	.2	24.0	62.05
	2	257	253	.4	7.9	35.54
	3	204	199	1.72	6.4	27.08
	6	222	194	.2	15.0	36.67
S-14-38	1	93	74	.3	7.7	18.62
	2	183	118	.2	9.4	11.85
	3	148	97	.2	3.44	8.18
	6	130	79	.3	3.5	9.87
S-15-38	1	270	171	.4	9.3	38.08
	2	239	151	.4	10.9	26.80
	3	322	164	.4	15.2	33.57
	6	226	110	3.4	11.6	20.87
S-16-38	1	165	143	.4	4.8	12.69
	2	196	174	.3	5.0	10.15
	3	387	289	1.5	19.5	40.34
	6	174	107	.5	5.9	12.97

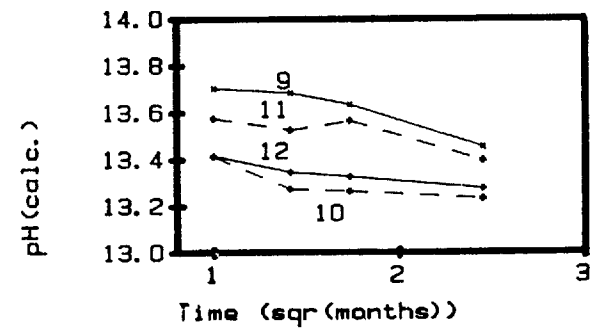

Figure 8. The pH of salt free specimens cured at 25°C. The pH calculated on the basis of $Na^+ + K^+ + 2\ Ca^{2+}$. (The numbers refer to the mix numbers in Table III).

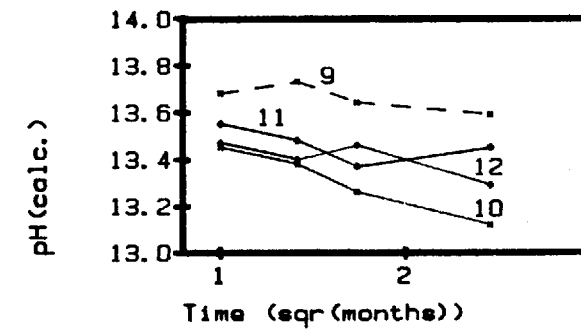

Figure 9. The pH of salt free specimens cured at 38°C. The pH calculated on the basis of $Na^+ + K^+ + 2\ Ca^{2+}$). (The numbers refer to the mix numbers in Table III).

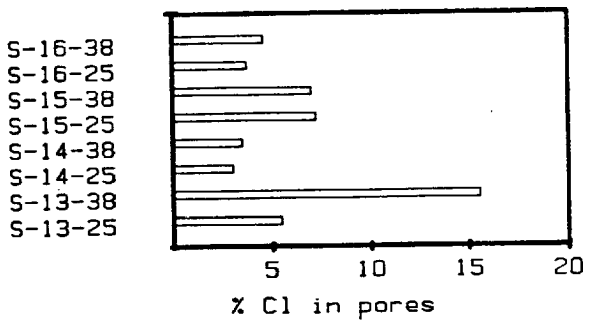

Figure 10. Percentage of available Cl^- remaining in pore fluids. Assuming the chemical composition of the total evaporable water to be identical with that of the expressed pore fluids.

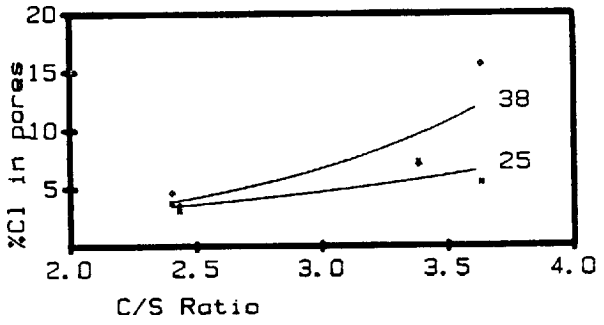

Figure 11. The % Cl^- retained in pore fluids vs. the overall c/s ratio of the mixes.

of the cement pastes to retain Cl^- in the pore fluids.

The lower c/s ratios (slag-containing mixtures) apparently fixed much of the Cl^- in the solid phase, leaving much less available in the pore solution for reaction with reinforcement.

Additionally, in related studies it has been shown that the diffusion rates of ions through blast-furance slag-containing pastes are much lower than for portland cement pastes (9,10) diminishing the rate of penetration of harmful species from the environment.

REFERENCES

1. P. Longuet et al., 'La Phase Liquide du Ciment Hydrate,' Revue des Materiaux 1, 35-41 (1973).

2. S. Diamond, 'Effects of Two Danish Flyashes on Alkali Contents of Pore Solutions of Cement-Flyash Pastes,' Cem. Con. Res. 11, 383-394 (1984).

3. F.P. Glasser and J. Marr, 'The Effect of Mineral Additives on the Composition of Cement Pore Fluids,' British Ceramic Proceedings 35, 419-419 (1984).

4. E.P. Flint and L.S. Wells, 'Study of the System $CaO-SiO_2-H_2O$ at 30 C and of the Reaction of Water on the Anhydrous Calcium Silicates,' Bureau of Standards Journal of Research 12, 751-783 (June 1984).

5. G.L. Kalousek, 'Studies of Portions of the Quaternary System Soda-Lime-Silica-Water at 25 C,' Journal of Research of the National Bureau of Standards, 32, 285-302 (1944).

6. Private Communications, Mr. Scott Atkinson.

7. Translated from Zhurnal Prikladni Khimii, 47, 645-647 (March 1974).

8. C.L. Page and O. Vennesland, 'Pore Solution Composition and Chloride Binding Capacity of Silica Fume Cement Pastes,' Materiaux et Constructions 16, 19-25 (1983).

9. A. Kumar and D.M. Roy, 'Pore Structure and Ionic Diffusion in Admixture Blended Portland Cement Systems,' (this symposium, 1986).

10. C.L. Page, N.R. Short, A.E.I. Tarras, 'Diffusion of Chloride Ions in Hardened Cement Pastes,' Cem. Concr. Res. 11, 395-406 (1981).

R.I.A. Malek, M. Silsbee, D.M. Roy*, Materials Research Laboratory, *Also, Dept. of Materials Science and Engineering, The Pennsylvania State University, University Park, PA 16802, USA

ZETA-POTENTIAL AND RHEOLOGICAL BEHAVIOR OF SLAG CEMENT PASTES

SUMMARY: Among the generally favorable properties of fine particulate slag is its apparent ability to develop and maintain adequate dispersion when intermixed with cement. In addition, adequate dispersion may enhance the slag particles' reactivity by exposing higher surface areas to the hydration process. The zeta (ζ) potential value can give an estimation of the likely state of dispersion when water is added. It can also be used to estimate the effectiveness of a particular superplasticizer in deflocculation of slag and slag/cement particles in a paste.

The ζ-potentials of different slags were determined using the microelectrophoresis technique with and without intermixture with cement and superplasticizer. The early stage rheological properties including mortar flow, yield stress, and viscosity were determined for slag/cement mixes. Also, the particle size and shape distributions have been determined for different slag types. An intercorrelation between those properties has been attempted.

It has been found that cement imposes its own surface characteristics on the slag particle surfaces. Different slags were found to possess different degrees of agglomeration which correlate with degree of hydration and rheological properties of slag/cement pastes. Furthermore, the particle size and shape distribution were found to affect the rheological properties and hydration process of slag/cement pastes through generating various degrees of particle packing. Details of the investigation and the effects of other variables are discussed.

Entre as propriedades gerais favoráveis da escória finamente particulada acha-se sua aparente habilidade para desenvolver e manter uma adequada dispersão quando misturada com cimento. E mais, a dispersão adequada pode aumentar a reatividade das partículas de escória pela exposição de uma maior superfície específica ao processo de hidratação. O valor do potencial zeta (ζ) pode dar uma estimativa do provável estado de dispersão quando se faz a adição de água. Ele pode também ser usado para avaliar a eficiência de um superfluidificante particular na defloculação das partículas de escória e escória/cimento numa pasta.

Foram determinados os potenciais zeta de escórias diferentes com o uso de técnica de microeletroforese, com e sem intermistura com cimento e superfluidificante. As propriedades reológicas no estágio inicial, incluindo fluidez da argamassa, tensão limite, e viscosidade, foram determinadas nas misturas de escória/cimento. Também foram determinados nos diferentes tipos de escória o tamanho de partícula e as distribuições de forma. Tentou-se uma intercorrelação entre essas propriedades.

Verificou-se que o cimento impõe suas próprias características de superfície às superfícies de partícula de escória. Constatou-se que escórias diferentes possuem graus diferentes de aglomeração, que correspondem ao grau de hidratação e às propriedades reológicas das pastas de escória/cimento. Além disso, verificou-se que o tamanho de partícula e a distribuição de forma afetam as propriedades reológicas e o processo de hidratação das pastas de escória/cimento, pela geração de vários graus de ajuntamento de partículas. São discutidos detalhes da investigação e os efeitos de outras variáveis.

R.I.A. Malek, M. Silsbee, D.M. Roy*, Materials Research Laboratory, *Also, Dept. of Materials Science and Engineering, The Pennsylvania State University, University Park, PA 16802, USA

INTRODUCTION

The measurement of the ζ-potential of different cementitious materials has attracted recent attention and the results have been applied to understanding particle characteristics and behavior in slurries with water and in the presence of other materials. The studies extended from portland cement and clinker components (1-7) to the effects of chemical admixtures on cements (8-10), other cementitious materials and intermixtures with cement, e.g., ground granulated blast-furnace slag (11,12), and fly ash (13).

The ζ-potential value can be used to predict the degree of agglomeration or flocculation of slag particles in a suspension. The particle size distribution and shape distribution can give an estimate of the degree of initial agglomeration, but the zeta potential can give much better estimation of the likely state when water is added. Thus in a system containing particles of many different sizes collisions will occur in different combinations among small particles, among large and small particles, and the large particles among themselves. As the conglomerate of a large particle and a small particle is still large, collisions between small and large particles do not change the number of large particles, but they do decrease the number of small one. Thus, the finer fraction of the particles plays an important role in affecting the extent of agglomeration. The particle size distribution is not the only factor that affects this process, but also the particle shape. Thus, anisodimensional particles have relatively larger collision diameters combined with a relatively larger diffusion constant than the isodimensional particles which will result in a higher probability of collision and flocculation. In addition, the extent of agglomeration will be inversely proportional to the magnitude of the potential barrier between stable and flocculated systems. Under similar circumstances, the height of this barrier is a function of the surface potential and concentration.

In the present investigation, the ζ-potential of granulated blast-furnace slags of different fineness and from different sources (different properties) were measured on suspensions of slag or mixtures of slag and cement in water. The effects of superplasticizers on granulometry and workability of slag cement pastes were also evaluated. Some rheological properties were determined and correlated with ζ-potential values. An attempt is made to transfer effectively the ζ-potential values into meaningful results in field concrete.

MATERIALS AND METHODS

Granulated blast-furnace slags from different sources and of different characteristics were used in the present investigation. The slags were supplied by Atlantic Cement Co. [designated NEWCEM, PSU numbers B63, B66 and B66A (550 m^2kg^{-1}], by Civil and Marine Ltd., U.K. [four different finenesses: 400, 440, 500, and 550 m^2kg^{-1}, designated EN400, EN450, EN500 and EN550, respectively], and by Frodingham Cement Co., Ltd., U.K. [designated Cemsave Scunthorpe]. We also investigated the effects of different weathering conditions and duration of exposure on surface characteristics and behavior of slag particles in slurries intermixed with cement. Although this is not the main purpose of the present paper, ζ-potential values of some of the samples included in that study will be presented here as they relate to the other findings included in this paper. Those samples are designated 853-1, 853-4, and S-456. Bulk chemical compositions and surface areas of the slags are presented in Table I. ASTM Type-I cement [designated I-09] was used for preparation of mixtures with slags. The chemical composition of I-09 cement is shown also in Table I.

TABLE I. Chemical and Spectrochemical Analysis of Slags and Cement.

Sample Number	EN Slag	Atlantic Slag B66	Atlantic Slag B63	Other Slags S-456	Other Slags 853-1	Other Slags 853-4	Cement I-09
SiO_2	36.3%	34.3%	34.7%	36.0%	34.66%	34.14%	20.00%
Al_2O_3	9.7	10.2	10.7	9.6	10.91	11.09	5.64
TiO_2	0.7	0.48	0.51	—	—	—	0.24
Fe_2O_3	0.6	0.67	0.41	1.24	0.37	0.45	2.45
MgO	8.2	11.4	11.9	8.4	9.76	12.20	3.21
CaO	42.7	40.61	39.37	44.5	41.46	39.10	61.37
MnO	0.6	0.510	0.39	—	—	—	0.065
SrO	—	0.05	0.04	—	—	—	0.30
BaO	—	0.05	0.05	—	—	—	0.02
Na_2O	0.3	0.19	0.25	0.12	0.23	0.22	0.26
K_2O	0.5	0.45	0.5	0.28	0.39	0.39	0.95
P_2O_5	0.3	0.02	<0.5	—	—	—	0.27
SO_3	—	—	—	—	—	—	2.53
S	*	1.31	*	1.33	1.26	1.22	—
L.O.I.	+1.7*	*	+1.34*	+1.89*	+1.12*	-0.21	2.30
Totals	99.9%	100.24%	100.36%	—	—	—	99.61%
Blaine m^2kg^{-1}	(550)	(550)	(550)	(552)	(547)	(612)	(350)

*These samples gained weight on heating, indicating the existence of sulfur as S or S^{2-} rather than SO_3.

Mineralogical constitutions have been determined for different slags using x-ray diffraction. All slags are mainly composed of pyrosilicate glass with a small degree of crystallinity (melilite and merwinite).

Electrokinetic Studies

The electrophoresis technique was followed to measure the electrophoretic mobility ($cm^2/V \cdot S$) of the charged particles. A Zeta-Meter (ZM-77 manufactured by Zeta-Meter, Inc., 1720 First Avenue, New York, NY 10028) was used. Suspensions in deionized water were used at room temperature. From the electrophoretic mobilities, zeta-potentials were calculated according to the relationship:

$$ZP = 4\pi\eta(T)/D(T) \times EM$$

where ZP = zeta-potential in electrostatic units, $\eta(T)$ = viscosity of the suspending liquid at temperature (T), D(T) = dielectric constant of the suspending liquid at temperature (T), and EM = electrophoretic mobilities at actual temperature (T).

When a voltage is imposed across the electrophoretic cell, frictional heat is generated by the moving ionic species, causing the temperature of the liquid to rise continuously. If the rate of temperature rise is too high, thermal turbulence of the suspended particles makes the measurement inaccurate. The rate of temperature rise depends on the specific conductance of the suspending medium as well as the applied voltage. The specific conductance of each suspension was measured prior to zeta-potential determination, and a maximum

recommended voltage was applied, to minimize the temperature rise at a particular specific conductance value. The applied voltage, however, was found in some cases to require further reduction to maintain the particle velocity in the range ≤0.5 micrometer per second in order to eliminate the 'human factor' in creating measurable errors while tracking particles. In spite of the above experimental precautions, a slight temperature rise could not be eliminated. The temperature of each suspension was measured before and after each zeta-potential determination and the average temperature was used to find the corresponding viscosity and dielectric constant of the suspending liquid. A temperature rise of 1 to 2°C was detected in the present measurements where the average velocity of up to 30 particles was determined over a period of time not exceeding one minute. An error in zeta-potential values of ±2% is thereby due to this temperature approximation.

Rheological/Viscosity Studies

Samples of EN slag, along with various other ground slags were tested for their rheological behavior. Detailed measurements were made with a concentric-cylinder viscometer (Haake-Rotovisco). The procedures used are standard (14) and will not be discussed here. Mixtures consisted of slag, 50:50 (weight) slag + Type I portland cement, and the latter slag + cement mixture with 0.5 wt.% of superplasticizer, all at 0.4 w/c (water/solids) ratios.

Additionally, mortar flow measurements were made according to ASTM C 109 and ASTM C 230 standard procedures.

Solid Phases Examination

The starting materials were characterized by XRD. A Phillips 3600 automated diffraction unit equipped with CuKα source was used to obtain XRD patterns. The operating voltage was 40 KV at 30 mA current and step scans of 0.02 degrees with counting times of 0.30 seconds were used.

Particle Size Distribution

Particle size distribution was determined using a sedimentation method (Sedigraph 5000D manufactured by Micrometrics), which measures the sedimentation rates of particles dispersed in a liquid in terms of the Stokesian or equivalent spherical diameter, in micrometers (μm). The instrument determines by means of a finely collimated beam of x-rays, the concentration of particles remaining at decreasing sedimentation depths as a function of time. To minimize the time required for analysis, the position of the sedimentation cell is continuously changed so that the effective sedimentation depth is inversely related to the elapsed time. The cell movement is synchronized with the X-axis of the X-Y recorder to indicate the equivalent spherical diameters corresponding to the elapsed time and instantaneous sedimentation depth.

RESULTS AND DISCUSSION

Zeta-Potential

First, the dependence of zeta-potential on concentration of slag in water was determined. It was found (Fig. 1) that the magnitude of the ζ-potential of a particular slag/deionized water suspension (#B63) decreases with increasing slag concentration. The ζ-potential tends to reach a certain limiting value at a concentration of <0.5 g/100 ml, while measurements made beyond 0.75 g/100 ml were difficult because of the excessive coagulation. Thus a concentration of 0.5 g/100 ml could be considered a critical concentration for ζ-potential measurement that can correlate with the performance of slag in a slurry. From Fig. 1 the strongly negative zeta potential of the slag is apparent, as in previously reported work, although it becomes less negative with increasing slag concentration. In contrast, the cement (I-09) is barely negative initially, undergoes a charge reversal and becomes positive with increased concentration. The specific conductance of the liquid in contact with both powders similarly increases with concentration of solids, reflecting an increasing concentration of electrolytes in the solution, which interact with the particle surfaces and change the zeta potential. Furthermore, in mixtures of slag with cement, the effect of adsorbed ions dissolved from other materials and from the cement on the zeta-potential influences the extent of agglomeration, which could be evaluated at such critical concentrations.

Second, the effectiveness of admixtures such as superplasticizers in inducing dispersive action on particles and their efficiency in preventing agglomeration was investigated. The ζ-potential value at the point of starting agglomeration appears to be a reproducible and significant value when

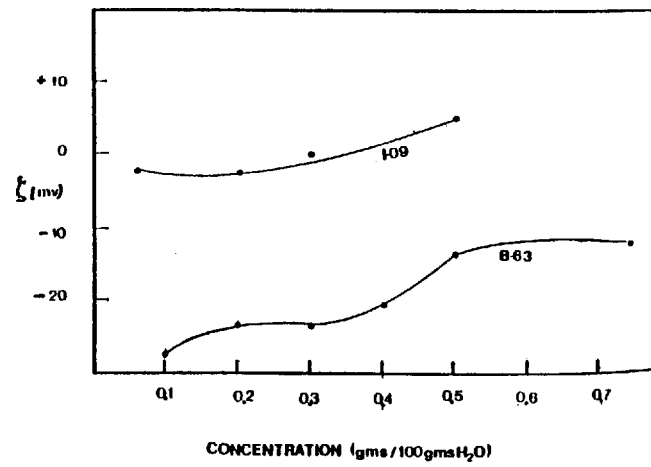

FIG. 1. Concentration dependence of ζ-potential of slag (B63) and Type-I cement (I-09) at 25°C.

comparing values obtained with added superplasticizer. The use of the concentration at the point of starting agglomeration makes it possible to evaluate:

R.I.A. Malek, M. Silsbee, D.M. Roy*, Materials Research Laboratory, *Also, Dept. of Materials Science and Engineering, The Pennsylvania State University, University Park, PA 16802, USA

(1) degree of agglomeration,
(2) dispersive efficiency of a superplasticizer,
(3) effect of foreign ions, and
(4) effect of particle size distribution.

Thus, using different slags in the same range of fineness (e.g., 550 m^2/kg), enables comparison with respect to the above variables, using the ζ-potential determined at the critical concentration. Nevertheless, the use of more dilute suspensions (giving higher ζ-potential values) may also be important for comparing the different surface characteristics of slags.

Table II contrasts the zeta potentials of several slags from different lots. Also given are the larger magnitude zeta potentials determined at lower concentrations (0.05 g/100 ml), for four of the materials. The values indicate that B63 is the least agglomerated, whereas B66A is maximally agglomerated. A less agglomerated slag may be more workable as will be discussed later.

TABLE II. Zeta Potential (mV) of Different Atlantic Slag.

	0.05 g/100 ml	0.05 g/100 ml deionized water
B-66	—	-4.97 (normal)
B66A	—	+2.26 (maximum agglomeration)
853-1	-17.43	-4.66 (normal)
853-4	-18.03	-4.45 (normal)
S-456	-20.96	-4.30 (normal)
B-63	(-27.5)	-13.20 (minimum agglomeration)

Additional measurements were made on the various particle suspensions in deionized water. The measurements reported were after 15 min., with results as summarized:

(1) The zeta-potential becomes more negative as the fineness of a particular slag is increased at a pH of 10 (Fig. 2).

(2) The addition of a sulphonated naphthalene formaldehyde condensate superplasticizer (#A3) to slags has little effect on low surface area slag but has a more pronounced effect on high surface area ones (Fig. 3). This phenomenon appears to be related to the adsorption mechanism in conjunction with the available surface area. The 550 m^2/kg EN slag is comparable to the NEWCEM (B63) Atlantic slag.

(3) The two NEWCEM slags (B66 and B66A) seem to have different surface characteristics (Fig. 4). The ζ-potential is less negative, and for B66A the surface has a slightly positive potential in water, or with a low percentage of superplasticizer.

(4) When different slags were mixed with cement (Type I), they were found to assume surface characteristics which are closer to that of cement alone (Fig. 5). It is thus concluded that the cement, by affecting the solution chemistry, modifies the surface characteristics of slag. This differs slightly from the results of previous studies with Type I/II (moderately low-C_3A) cement/slag mixtures (11) from which it may be concluded that the cement composition is important as well in affecting the slag zeta potential. The current zeta potential measurements correlate with viscosity measurements, as discussed later.

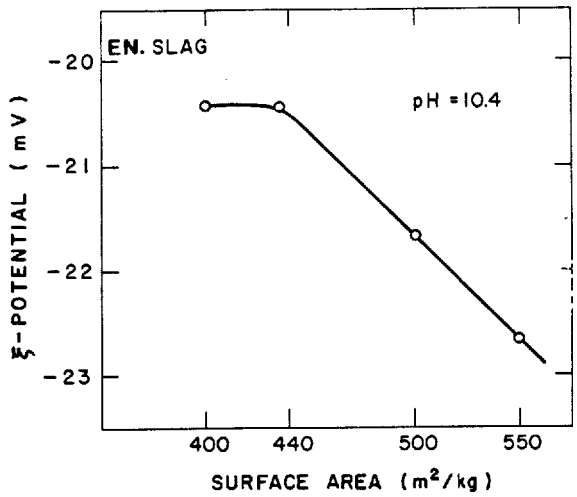

FIG. 2. Surface area dependence of ζ-potential of a slag at 25°C without addition of superplasticizer.

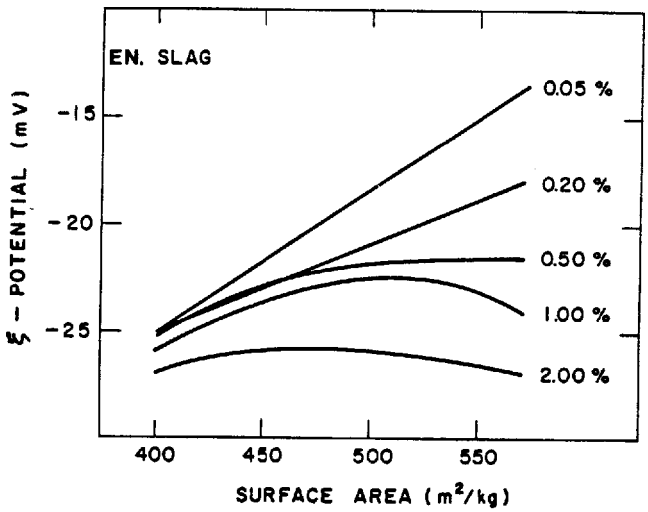

FIG. 3. Surface area dependence of ζ-potential of a slag at 25°C with superplasticizer content.

(5) A critical concentration of the superplasticizer of about 0.5% was found to be sufficient to produce an effective superplasticizing effect to all slags used when mixed with the Type I cement. Thus, it could be extrapolated to assume that using 0.5-1.0% superplasticizer would be enough to produce effectively workable paste with any type of cement.

Viscosity/Rheology

The results of rotational viscometer and other measurements reflect some thixotropic character and are summarized in Table III. The data were assumed to fit an equation of the form:

R.I.A. Malek, M. Silsbee, D.M. Roy*, Materials Research Laboratory, *Also, Dept. of Materials Science and Engineering, The Pennsylvania State University, University Park, PA 16802, USA

$$C = \tau y + c\dot{\gamma}$$

where C = measured shear stress; τy = apparent yield stress; c = constant; $\dot{\gamma}$ = shear rate. The data in Table III reveal that slag exhibits a nearly linear dependence on surface area for τy. This appears to

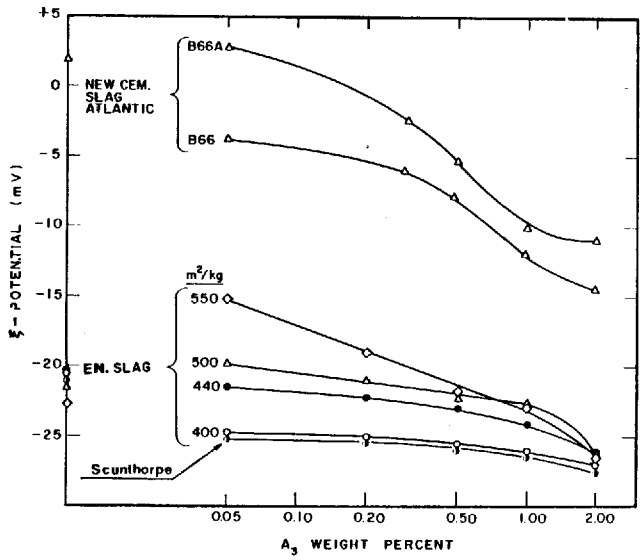

FIG. 4. Variation of ζ-potential of different slags as a function of concentration of the added superplasticizer.

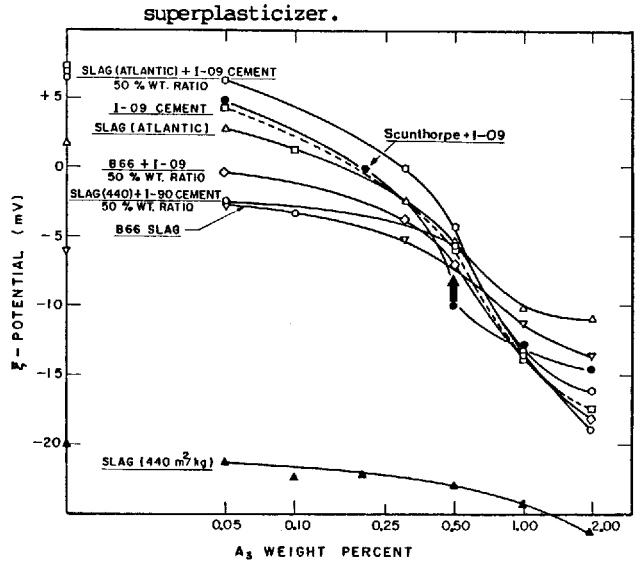

FIG. 5. Variation of ζ-potential of different slags in mixtures with Type I cement as a function of the superplasticizer concentration.

be related to the favorable particle packing in mixtures made with high surface area slag (finer particles), which results in better flow. In this way, the high surface area slag (550 NEWCEM) appears to generate the most favorable rheology of the blends investigated. It appears desirable to have different particle size distributions of the portland cement and slag.

TABLE III. Yield stresses (τy) of 0.4 w/c ratio slag, slag-cement, and slag-cement-superplasticizer mixtures (Pa).

	15 min.		1 hr.		2 hr.	
	c	τy	c	τy	c	τy
			slag			
EN 400	0.21	79.70	0.24	60.70	0.28	86.02
EN 450	0.36	91.11	0.32	99.87	0.23	97.23
EN 500	0.33	111.11	0.28	94.0	0.61	121.86
EN 550	0.23	75.71	0.34	120.86	0.43	136.86
			(1:1) slag + I-09			
EN 400	0.17	92.83	0.13	70.60	0.13	67.79
EN 450	0.14	63.74	0.13	60.47	0.27	68.97
EN 500	0.13	67.05	0.13	45.16	0.26	84.83
EN 550	0.15	63.52	0.14	62.65	0.14	62.65
			(1:1) slag + I-09 + A-3*			
EN 400	0.11	42.3	0.21	77.14	0.16	74.1
EN 450	0.25	48.35	0.13	39.58	0.09	40.07
EN 500	0.20	44.08	0.21	495.4	0.25	49.63
EN 550	0.14	38.36	0.1	65.61	0.14	84.87
I-09	0.13	45	0.16	29.4	0.14	65
B-66	0.16	76	0.23	77	0.31	88
B-66A	0.82	77	0.25	48	0.65	77
Scunthorpe	0.07	28	0.11	21	0.28	44
B-66 + I-09 (1:1)	0.12	49	0.18	65	0.72	30.1
B-66A + I-09 (1:1)	0.214	70	0.20	47	0.29	40
Scunthorpe + I-09 (1:1)	0.16	46	0.09	56	0.09	59.5
B63 + I-09 (1:1)	—	26	—	39	—	48.5

*Sulphonated naphthalene formaldehyde condensate.

Mortar Flow

Mortar flow measurements were made on the various slags, in comparison with mortars made of Type I portland cement. The results (measured by ASTM C 109 and C 230 standard procedures) are given in Table IV. It can be seen that in all cases, the mortar flow values of the slag + Type I cement mixture are substantially greater than those of the Type I cement alone. This indicates the ability of slag particles to improve workability of cement mortars and concretes.

ζ-Potential—Workability Relationship

Although no well established relationship exists between values of ζ-potential and workability of a cementing material/water system, the dependence of workability on ζ-potential is evident if all other factors are kept constant. The other factors of workability on D-potential is evident if all other factors are kept constant. The other factors include but are not limited to fineness, temperature, particle size and shape distribution, magnitude of solid surface-aqueous medium interaction (chemical composition and crystallinity of solid materials) and presence of additives or admixtures. It is one of our major research objectives to establish such a relationship between

TABLE IV. Mortar flow test results.

	% flow*
EN 400	69
EN 450	68
EN 500	70
EN 550	65
Scunthorpe	63.5
B-66	110
B-63	103
I-09**	35.5

*Slag cement mortars. 1:1 slag:cement, 1:2.75 fine solids:sand, w/c = 0.485.
**Cement mortar. 1:2.75 cement:sand, w/c = 0.485.

ζ-potential and workability. The results in this area are not yet finalized but as an approximation high (negative) ζ-potential materials should be more workable when mixed with water. For example, the slag type B-63 was found to have maximum negative D-potential (Table II), indicating minimum agglomeration and presumably good workability in concrete. A systematic study has been made to evaluate the viscosity of pastes and workability (flow) of mortars made of this particular slag in comparison to other slags of the same fineness. The flow test result on sample (B63) showed a value of 103% (Table IV) which is relatively equivalent to B66 slag but higher than the EN slag of equal fineness (550 m^2/kg). Viscosity test results (Table III) indicate clearly the low yield stress of B63 relative to the other slags of comparable fineness.

In an attempt to understand the causes for such differences in surface characteristics, a comparison was made between the three slags with respect to particle size distribution, chemical composition and degree of crystallinity. The particle size distributions of 550 m^2/kg surface area slags (EN 550, B63and B66) were very similar. This rejects the possibility of particle size dependence of the workability for the same fineness slags and thus the workability should be related to extent of agglomeration which, according to our procedure could be estimated by ζ-potential measurements. Chemical compositions (Table I) do not indicate major differences between different slags.

The x-ray diffraction patterns indicated variable degree of crystallinity in different slags. Thus, although B-63 slag is essentially completely amorphous, B-66 contains very little, < about 1% crystalline material whereas the EN slag has≤7% crystallinity. Crystalline materials are mainly melilite and merwinite. The small variations in crystallinity do not explain adequately the differences in workability.

CONCLUSIONS

Slag particle characteristics were monitored in an aqueous suspension (ζ-potential) and in a slurry or paste (viscosity). In both cases the effects introduced by intermixing with portland cement were determined. Three basic findings were derived from this study:

(1) The ζ-potential value of slag particles reflects its agglomeration tendency, the more negative its value the more dispersed (less agglomerated) the slag. Thus it appears possible to transfer ζ-potential values to predicting concrete workability. Thus a highly negative ζ-potential slag (less agglomerated) was found to exhibit favorable workability (low yield stress, high flow).

(2) In addition, ζ-potential values were found to be correlated with other physical properties of slag particles, i.e., fineness and surface characteristics. It was also used to calculate optimum superplasticizer concentrations necessary to produce desired workability.

(3) In this study, we also found that desirable workability could be attained in a mixture by blending different particle sizes of both slag and cement.

ACKNOWLEDGEMENTS

Partial financial support from Atlantic Cement Co. (now Blue Circle, Inc.); Civil and Marine Ltd.; Frodingham Cement Co., Ltd.; and Oy Lohja Co. is much appreciated.

REFERENCES

1. K. Suzuki,T. Nichikawa, K. Kato, and S. Ito, Cem. Concr. Res. 11, 759-769 (1981).
2. L. Nagele and P. Ney, ibid. 12, 535-536 (1982).
3. H.N. Stein, J. Coll. Int. Sci. 28, 203-213 (1968).
4. H. Nagele, Cem. Concr. Res. 15, 453-462 (1985).
5. M.E. Tadros, J. Skalny and R.S. Kalyoncu, J. Amer. Cer. Soc. 59 (7-8), 344-347 (1976).
6. M.E. Tadros, W.Y. Jackson and J. Skalny, J. Colloid Interface, No. 4, 211-223 (1976).
7. A. Zelwer, 7th Int. Cong. Chem. Cem., Paris, Vol. II, pp. 147-152 (1980).
8. D.M. Roy and M. Daimon, ibid., pp. 242 (1980).
9. M. Daimon and D.M. Roy, Cem. Concr. Res. 8, 753-764 (1978).
10. Ibid., 9, 102-110 (1979).
11. X. Wu and D.M. Roy, in 'Concrete Rheology', Ed. J. Skalny, pp. 215-222, Materials Res. Soc. Proceedings (1982).
12. Wu Xuequan and D.M. Roy, Cem. Concr. Res. 14, 521-528 (1984).
13. R.I.A. Malek and D.M. Roy, in 'Fly Ash and Coal Conversion By-Products: Characterization, Utilization and Disposal I', Eds. G. McCarthy and R. Lauf, pp. 41-50, Materials Res. Soc. Proceedings, Vol. 34 (1985).
14. E.L. White and D.M. Roy, Concrete Rheology, Ed. Jan Skalny, pp. 108-119; Proc., Symposium M, Materials Res. Soc. (1982).

P.I. BOJENOV,
B.A. GRIGOR'ÉV, Institut des ingénieurs du batiment de Léningrad, URSS

CIMENTS MULTICOMPOSANTS A BASE DES LAITIERS DE METALLURGIE DES METAUX NON FERREUX

Le clinker de ciment portland est un système multicomposant. Tous les ciments à sa base sont également multicomposants. L'augmentation de la multicomposition complique les processus de l'hydratation, se fait sentir sur les propriétés des mélanges de mortier et de béton (notamment sur la rhéologie), exerce une influence sur la formation des propriétés de construction techniques de la pierre et sur les caractéristiques de fonctionnement des produits et des structures.

L'augmentation de la multicomposition des ciments avec introduction des produits secondaires, y compris les laitiers de métallurgie des métaux non ferreux, permet de résoudre les problèmes pratiques importants concernant un plus grand rendement du ciment par tonne de clinker et ceux de diminution de la capacité d'absorption de l'énergie au cours de la production (car ces laitiers ont déjà subi le traitement thermique). Cette augmentation permet également d'améliorer la densité et la résistance à la gelée des bétons, leur résistance à la corrosion dans les différents milieux agressifs et d'élever le degré de serrage des matériaux de remplissage et de renforcer le travail de la couche intermédiaire entre les agrégats et la pierre de ciment.

Les aspects particuliers concernant le problème des ciments multicomposants avec les exemples de réalisation industrielle sont aussi examinés.

O clínquer de cimento portland é um sistema multicomposto. Todos os cimentos em sua base são igualmente multicompostos. O aumento da multicomposição complica os processos de hidratação, se manifesta nas propriedades das misturas de argamassa e de concreto (especialmente sobre a reologia), exerce influência sobre as propriedades técnicas de construção de concreto e sobre as características de funcionamento dos produtos e das estruturas.

O aumento da multicomposição dos cimentos com introdução de produtos secundários, aí incluídas as escórias de metalurgia de metais não ferrosos, permite a solução de problemas práticos importantes, relativos a um maior rendimento do cimento por tonelada de clínquer, e os problemas de diminuição da capacidade de absorção de energia no decurso da produção (porque as escórias já sofreram o tratamento térmico). Este aumento igualmente permite melhorar-se a densidade e a resistência do gel dos concretos, sua resistência à corrosão em diferentes meios agressivos, elevar o grau de compactação dos materiais de enchimento, e reforçar o trabalho da camada intermediária entre os agregados e o concreto.

Também são examinados os aspectos particulares referentes ao problema dos cimentos multicompostos, com os exemplos de realização industrial.

Les laitiers provenant du traitement pyrométallurgique de l'agglomérat cupro-nickélique présentent des systèmes complexes contenant les oxydes: K_2O, Na_2O, CaO, MgO, FeO, Al_2O_3, Fe_2O_3, SiO_2, S, Ni, CuO, Co.

Le clinker de ciment Portland présente également un système complexe qui comprend K_2O, Na_2O, CaO, MgO, MnO, Al_2O_3, Cr_2O_3, Fe_2O_3, SiO_2, TiO_2, P_2O_5.

Les laitiers se distinguent du clinker par une teneur élevée en oxydes de fer (jusqu'à 61%), en silice (jusqu'à 47%) et par une teneur diminuée en oxyde de calcium (1,1-9,0%). Les laitiers granulés dans l'eau se composent du verre (jusqu'à 85%) et des phases cristallines: olivines, diopsides, montitshellites, fayalites, augites.

Les laitiers en état cristallisé contiennent 7-30% de verre, les minéraux mentionnés, ainsi que les sulfures et autres composés. Les laitiers granulés comme les laitiers cristallisés ne montrent pas une activité hydraulique indépendante. Cependant, une grande échelle de leur production (jusqu'à quelques millions de tonnes sur un combinat) et une grande consommation d'énergie pendant la production pyrométallurgique obligent à chercher les procédés d'utilisation des laitiers, y compris en qualité du constituant du mélange de ciment cru. Une teneur élevée en composés de fer dans les laitiers donne une base pour leur utilisation au lieu des résidus de pyrite et des poussières de gueulard. Selon les données de P'iatshev /I/, les processus de formation du clinker dans le cru contenant les laitiers de nickel et autres laitiers s'écoulent plus intensivement par rapport aux crus ordinaires. Le volume d'utilisation des laitiers nécessaire pour ce but n'est pas grand et constitue I-5% de la masse.

Un grand rendement d'utilisation des laitiers est obtenu en cas de leur utilisation au lieu de l'argile. Dans ce cas, la quantité de constituants du mélange cru diminue, l'humidité du schlamm se réduit de quelques pour-cent et la consommation d'énergie pour sécher et calciner le schlamm diminue aussi.

Il apparaît perspectif de résoudre le problème d'augmentation d'activité des laitiers et de leur utilisation en vue de produire les ciments mixtes. L'activité hydraulique indépendante des laitiers est attendue en cas de leur basicité amenée jusqu'aux valeurs assurant la formation du silicate bicalcique et l'obtention des autres phases entourant les grains C_2S favorisant l'hydratation du laitier broyé. L'obtention du C_2S peut être assurée au stade de formation de la matière fondue et au moyen de saturation en chaux du laitier après la séparation de ce dernier de la matte. Le premier procédé est plus acceptable du point de vue technologique. Les études de laboratoire et et les essais industriels montrent qu'il n'est pas utile d'assurer une fixation complète de la silice en C_2S è cause de la diminution du rendement des fours.

Cependant, la conversion de la fusion de l'agglomérat sulfure-cupro-nickélique avec un flux acide (grès) à la fusion avec un flux basique (calcaire), en cas de garantie de la teneur en CaO dans le laitier dans des limites de 25-30%, permet non seulement de diminuer les pertes des métaux non ferreux de 12-15%, mais d'obtenir également un laitier s'activant sous l'influence du clinker, de l'anhydride et des autres matières. Le laitier de nickel acide obtenu traditionellement agit, selon les essais effectués, comme un adjuvant inerte. Le laitier calcaire absorbait trois fois plus de CaO de la solution saturée de l'hydroxyde de calcium par rapport au laitier acide. Le dégagement calorifique lors de la dissolution du laitier calcaire dépasse de six fois le dégagement calorifique du laitier acide. Les essais mentionnés montrent qu'il existe une interdépendance entre la capacité réactionnelle des laitiers et la quantité d'oxyde de calcium dans la composition du laitier. Sur la base du laitier obtenu se-

lon la technologie proposée, on a préparé les ciments mixtes avec la teneur en laitier de 25 à 70%. Pour obtenir ces ciments, on a utilisé le clinker avec une activité de 30 MPa.

Les essais montrent que le laitier de nickel possède une broyabilité diminuée par rapport au clinker. Le rendement des broyeurs diminue dans ce cas de 7-15%.

Les ciments obtenus avaient, en fonction de la composition, la densité normale dans des limites de 25-30% et les temps de prise ordinaires (début de prise 2-15 - 4-30, fin de prise 3-25 - 6-00 h, min).

Les résultats des essais mécaniques montrent que les ciments sur la base du laitier de nickel (comme la plupart des ciments mixtes) développent lentement la résistance au premier temps de durcissement (3 et 7 jours). Après cela, la résistance par rapport aux ciments de clinker purs est égalisée vers 28 jours de durcissement.

Une attention particulière est attirée par les ciments "anhydrite - laitier - clinker" contenant jusqu'à 25% de clinker type 30 MPa qui vers 28 jours de durcissement possèdent une activité dépassant 30 MPa.

Les essais des massifs des bétons à grains fins préparés à partir des mélanges fluides de béton basés sur les ciments mixtes à laitiers calcaires et de nickel montrent que ces bétons, d'après la résistance, la déformabilité et l'anticorrosion, ne cèdent pas aux bétons sur la base du ciment de clinker pur et parfois dépassent ces derniers.

L'utilisation du ciment Portland de laitier à fabrication industrielle pour la fabrication des bétons montre que ceux-ci, aux dosages analogues de ciment, peuvent être utilisés pour la production des éléments et des structures dont la résistance et les autres propriétés ne cèdent pas aux bétons sur la base du ciment sans additions et dont la résistance à la gelée dépasse ces derniers plus de deux fois. Par exemple, les éprouvettes de béton sur la base du ciment Portland de laitier ont subi 523 cycles de gel et dégel sans endommagement apparent et perte de masse, tandis que les éprouvettes sur la base du ciment de clinker pur n'ont subi que 250 cycles de gel et dégel. Ce fait peut être expliqué par les particularités du mécanisme de l'hydratation des ciments mixtes et de la formation de structure du béton qui exercent une influence sur le serrage de l'agrégat et de l'armature par la pierre de ciment. V.K. Bojenov a montré expérimentalement /2/ que les ciments mixtes sur la base du ciment Portland et du schlamm de néphéline (jusqu'à 80%) avaient une plus grande valeur de serrage par rapport aux ciments sans additions.

Bibliographie

I. Использование шлаков цветной металлургии в производстве цемента / Пьячев В.А. - Цементная промышленность. Серия I: Обзор. инф. ВНИИЭСМа, 1985, выпуск I, 53 с.
2. Боженов П.И. Технология автоклавных материалов - Л.: Стройиздат, 1978, 367 с.

HYDRATION OF ALITE AND C_3A AND CHANGES OF SOME STRUCTURAL CHARACTERISTICS OF CEMENT PASTES BY ADDITION OF SILICA FUME

1

L'HYDRATATION DES ALITES ET DE C_3A ET LES MODIFICATIONS DES CARACTERISTIQUES DE LA STRUCTURE DANS LES PÂTES DE CIMENT CONTENANT DES FUMEE DE SILICA

3.2

DUREKOVIĆ ANDRIJA, Scientific Assistant, Civil Engineering Institute, Zagreb, Yugoslavia

SUMMARY

Three cement pastes with the equal w/c ratio fo 0,68 have been prepared for the investigation of alite and C_3A hydration in the presence of silica fume: one ordinary portland cement paste and two pastes in which the OP-cement was replaced with 5 and 10 % of c.s.f.

The degree of alite and C_3A hydration at various ages ranging from 1 to 28 days were determined by quantitative X-ray difraction.

Paralel to this the compressive strength, pore size distribution, free lime content and changes in the degree of silica plymerisation of hardened pastes have also been estimated.

Obtained results show that silica fume causes acceleration of alite and some retardation of C_3A hydration process. These effects as well as detected structural changes in relation with added amount of silica fume have been considered.

SUMÁRIO

Três pastas de cimento com relação água/cimento constante e igual a 0,68 foram preparadas para a investigação da hidratação da alite e C_3A na presença de microsílica: uma pasta de cimento portland e duas pastas nas quais o cimento portland foi substituído por 5 e 10% de microsílica. O grau de hidratação da alita e do C_3A em várias idades de 1 a 28 dias foi determinado por análise quantitativa de raios X.

Paralelamente foram determinados em pasta de cimento endurecido a resistência à compressão, a distribuição do tamanho dos poros, o conteúdo de cal livre e as mudanças no grau de polimerização da sílica.

Os resultados obtidos indicam que a microsílica causa uma aceleração do processo de hidratação da alita e retardamento do C_3A. Estes efeitos assim como as mudanças estruturais devidas às adições de microsílica foram considerados.

INTRODUCTION

Silica fumes are the by-products from the silicon-metal and ferrosilicon alloys production.Such by-products,called also microsilica, silica dust or condensed silica fume,are pozzolanic materials more reactive than natural pozzolans or fly ashes.Initial investigations on the effect of silica fume were caried out in the early fifties (1) and practical use report of silica fume dated from 1968.(2).Silica fumes from both productions- the silicon-metal and ferrosilicon industries- are X-ray amorphus and contain more than 85% SiO_2.But the approach to silica fume as the uniform product is not valid (3). A typical value for its specific surface obtained by the adsorption measurements is about 20 m^2/g (4).The partical size analysis shows individual spheres ranging from 0,01 to 0,3 μm with about 70% < 0,1 μm /1000 Å/ (5,6). By use of silica fume in concrete the most of concrete's properties will be improved:spectacular compressive strengths have been achieved (7,8,9);high efficience in prevention of alkali-aggregate reaction is obtained when a reactive aggregate and alkali-rich cement were used (10); the chemical attack resistance and freezing-thawing resistance have been increased (11,12,13,14). Microstructural studies of cement matrix containing silica fume have shown the presence of CSH low in calcium but containing alumina and alkalies (12).The same study reported about a strong cement-aggregate bond.The C/S value of the calcium silicate hydrates,which are formed as a result of pozzolanic reaction of silica fume,was found to be in the range range from 0,9 to 1,3 (12,15,16).Such products has been reported to be of less dense from similar products originated by portland cement hydration (16,17) causing large pores volume reduction/with radius 0,1 μm/ (4).Large pore volume reduction was also registrated by testing the field silica fume-concrete samples (18).Silica fume pozzolanic activity has been investigated by different methods.In the papers presented results are conflicting,qualifying this activity as to be small(15,19),medium (20),strong or very good (13,16). Results of the hydration reactions in portland cement-silica fume blends,investigated by conduction calorimetry,were recently published (21).After studying in calcium hydroxide solution one model for silica fume hydration mechanism has been proposed (22).

Although a number of studies on silica fume in cement paste have been made,the effect of silica fume on hydration chemistry has not been fully elaborated.The present work was therefore undertaken.

EXPERIMENTAL

The materials used in this work were an ordinary portland cement and the silica fume from ferrosilicon alloys production.

Chemical composition of starting materials are given in Table 1.The cement with a fineness of 3800 cm^2/g,density of 3,09 g/cm^3,has had the following QXRD determined compcsition: 60% C_3S, 17% C_2S , 8% C_3A and 5% C_4AF.Trace compounds containing in the used silica fume have already been described before (13).

Table 1: Chemical composition of starting materials (percent by weight)

Compounds	Ordinary portland cement	Silica fume from ferrosilicon production
SiO_2	19,65	86,92
Al_2O_3	5,50	2,26
Fe_2O_3	3,10	1,42
$CaO_{Tot.}$	61,88	1,15
MgO	1,70	0,60
SO_3	3,40	0,61
P_2O_5	-	-
MnO	-	0,09
Na_2O	0,38	0,48
K_2O	0,98	1,50
L.o.i.	1,57	4,80
CaO_{free}	1,12	-
Ins.residue	1,15	

Three mixes were prepared from those materials using water/(cement+silica fume) ratio of 0,65 : one pure portland paste (marked PC) and two pastes in which the cement was replaced by 5 weight percent of silica fume (marked 5P) and 10 weight percent of silica fume (marked 10P). Cement,silica fume and destilled water were weighed and hand mixed in the open beakers.To minimize the bleeding the pastes were periodically mixed until the setting has just begun.Then they were cast into plastic molds of two different sizes (one cylinder size for the strength determination and second size for other measurements) and kept for the time up to 20 hrs in a humid box. Afterwards,the molds were carefully stripped away and samples placed under lime water for the remaining hydration time. Casting and curing were done at $20^o \pm 3^oC$.

Determination of hydration degree of alite and C_3A

After definite hydration time of 1,3,7 and 28 days the slices from the main specimens of each hardened cement paste were cut off and crushed into small pieces. The hydration was stopped by milling and washing with aceton and finally by drying for 48 hrs in vacuum generated by using a rotary pump (23).In such way prepared samples were stored until measuring in a desiccator over silica-gel and KOH. Samples were examined quantitatively by X-ray diffraction using a Philips 1130 diffractometer that utilized a Cu (Kα) radiation source with a graphite monochromator in the diffracted beam by a kilovoltage constant potential at 35 and miliamperage at 20.A proportional detector and strip chart recorder were also used. The scan rate was equivalent to 1/8 degree two-theta for unhydrated samples and to

1/4 degree two-theta for hydrated samples.The region from 25 to 35 and from 49 to 53 degrees two-theta was scaned.Suprapur,fine pulverized,calcium fluoride (from "Merck",W.Germany) as internal standard for X-ray intensities was used.For monoclinic alite as well as for tricalcium aluminate in the three cement pastes,concerning fundamental principles of the QXRD-analysis (24,25,26),the degree of hydration at different ages was determined by applying equation :

$$(\alpha)_t = 1 - \frac{(1-Lo)\ (Ii/Is)_t}{(1-Lt)\ (Ii/Is)_o}$$

with following meaning:

$(\alpha)_t$ degree of hydration of i-th compound at time t

Lo,t Loss on ignition of samples after hydration time o and t

$(Ii)_{o,t}$ Intensity of analytical diffraction maximum belonging to i-th compound for hydration time o and t

$(Is)_{o,t}$ Intensity of 28,3 degree two-theta maximum of calcium fluoride in the samples for hydration time o and t.

The hydration degree of tricalcium aluminate was determined from the intensity of 440 diffraction maxima,while the intensity of alite diffraction maxima $I_A(620,040)$ itself served for determination of the degree of alite hydration.

Free lime content and loss on ignition

Differential thermal and thermogravimetric analysis has been employed to detect the variations in the free lime content and the loss on ignition of hydrated cement pastes. The amount of calcium hydroxide was determined by measuring abrupt weight loss in the temperature range from 510° to 600°C.The weight loss curves were recorded between 20° and 1000°C using a MOM-derivathograph (Budapest,Hungary) which utilizes Al_2O_3 as a control material at heating rate of 10 degrees Celsius per minute. Portions of 500 mg "aceton stopped" samples of 1,3,7 and 28 days age were analysed.The preparation of samples has been already described in this paper.

Silicate structure changes

The structure of silicate anions and their changes during hydration in cement pastes were investigated by the use of molybdate method (27,28).The changes after 1,3,7 and 28 days hydration time were analysed.The silicomolybdate complex is formed at 25°C by mixing 20 ml of standard ammonium molybdate solution and 500 ml of 0,1 N HCl solution of cement paste samples.SiO_2 concentration in that 0,1N HCl solution was ~1mg/50ml . The formation of yellow coloured silicomolybdate complex was being monitored continuously by syphoning the reaction mixture through a flow-through cell in a "Perkin Elmer Coleman Junior II" spectrophotometer set at 410 nm. The spectrophotometer output was recorded graphically on a 10 inch xt-recorder. Before,after and sometimes during a run the zero stability of spectrometer plus recorder was checked by use of suitable blanks. Details of used procedure can be found elsewhere (29).
Total silica content and insoluble residue of hardened cement paste s were estimated by standard chemical methods (30).

Pore size distribution

The influence of silica fume on the porosity of hardened cement paste has been determined by mecrury intrusion method. Experiments were conducted on a "Carlo Erba 70" porosimeter working up to 200 MPa and measuring pore radius down to 3,75 nm. After hydration time of 1, 3,7 and 28 days the slices of 8-9 mm depth were cut off from the main pastes specimens and subjected to an organic solvent replacement treatment.For 7 days period the specimens were placed in dioxan,afterwards for 7 days in water-free ethanol and finally the samples were dried at 20°C for 48 hrs in vacuum made by using a rotary pump. Such treatment was done in order to minimize the pore structure changes that can occur during a drying of samples (31).The analysed size of samples were from 0,8 to 1,0 gram.

Compressive strength

Compressive strength of hardened cement pastes was determined by using a "Tonnindustrie" testing machine.At each age 4 specimens of 30 mm I.D. and 50 mm length were tested in saturated surface-dry condition.The specimens were tested at each age of 1,3,7 and 28 days.

RESULTS AND DISCUSSION

The hydration degrees of alite and tricalcium alumirate determined at different time of reaction in the cement pastes,with and without presence of silica fume are given in Figure 1 and Figure 2.

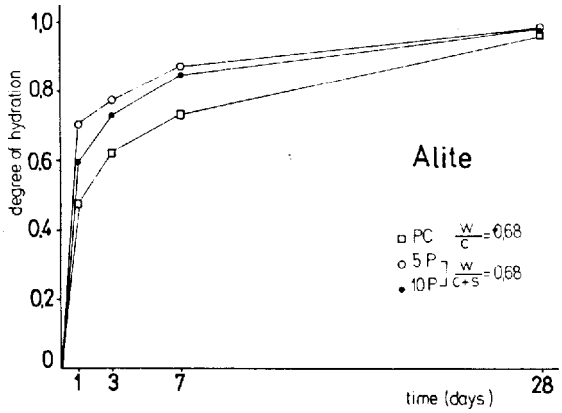

Figure 1: The hydration degree of alite at different ages of the cement paste samples PC,5P,10P.

As the results in Figure 1 show,the hydration degree of alite in the cement pastes containing silica fume was higher for the entire 28-days period than the degree of alite hydration in the pure PC-paste.This acceleration was very strong manifested after hydration time of 1,3 and 7 days. Lower conversion of alite detected in the cement paste with higher silica fume content (10%) from the paste with 5% of silica fume

should be related to the more difficult water transport through the formed hydration product layers.

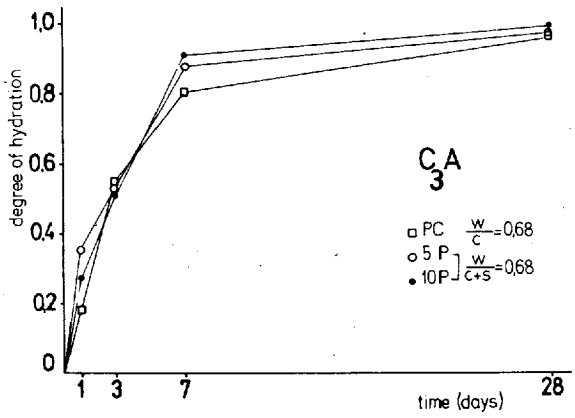

Figure 2: The hydration degree of C_3A at different ages of the cement paste samples PC, 5P and 10P.

The results presented in Figure 2 show the following: If silica fume was included into cement paste, C_3A hydration after 1 day was accelerated but afterwards in the age of 3 days the relative retardation was observed. At 3-days age the determined degrees of tricalcium aluminate in all three investigated pastes were nearly of the same level. Later, it was detected that the hydration of C_3A accelerated agin, but it is not clear why the highest determined C_3A-conversion occured in the paste with 10% of silica fume. It seems to be very likely that hydration of alite as well as C_3A in the cement paste containing silica fume could be influenced by many factors, sometimes of opposite action: By intensive consumption of calcium and sulphate ions as reported by Grutzeck and coauthors (22) and Stein and Stevels (32), by big surface of silica fume which is electrical charged (33), by forming of secondary CSH products of lower density than CSH products formed in the pure OPC-paste (16,17).
The results of free calcium hydroxide contents, determined by TGA method, in the paste samples after different hydration time as well as the results of their ignition losses are listed in Table 2.

Time of hydration (days)	PC		5P		10P	
	CaO free (%)	L.o.i. (%)	CaO free (%)	L.o.i. (%)	CaO free (%)	L.o.i. (%)
1	11,91	15,76	11,00	16,44	10,00	16,67
3	14,50	19,90	13,80	20,00	12,25	20,40
7	15,80	22,55	14,05	22,60	12,69	21,41
28	16,55	24,14	15,27	24,44	13,42	24,30

Table 2: Free lime content (expressed as CaO) and loss on ignition at different hydration time in cement paste samples PC, 5P and 10P.

The results show that the lime diminishing continue also at the age of 7 and 28 days of hydration. In view of this fact it should be concluded that alite hydration acceleration takes place not predominantly caused by hydrolysis equilibrium shift due to pozzolanic lime consumption.
The obtained results of silicate condensation changes shown in Figure 3,4 and 5 can be also used for pozzolanic activity valuing of silica fume.

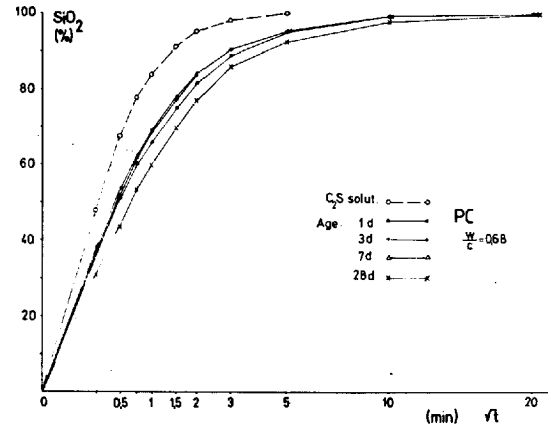

Figure 3: Molybdate-complexation curves of PC paste samples at different hydration time. C_2S-solution as monosilicate anion standard.

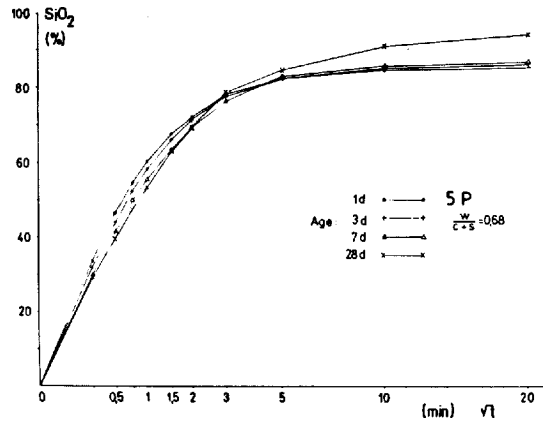

Figure 4: Molybdate-complexation curves of 5P paste samples at different hydration time.

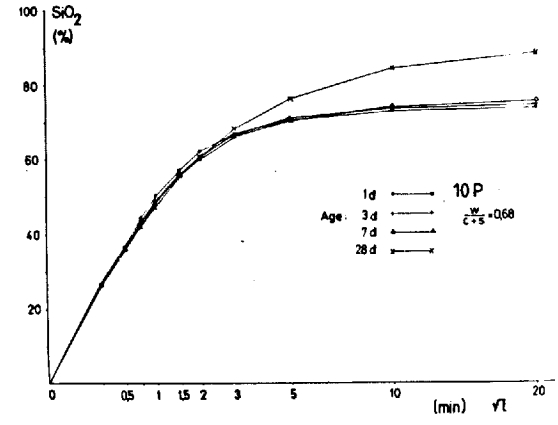

Figure 5: Molybdate-complexation curves of 10P paste samples at different hydration time.

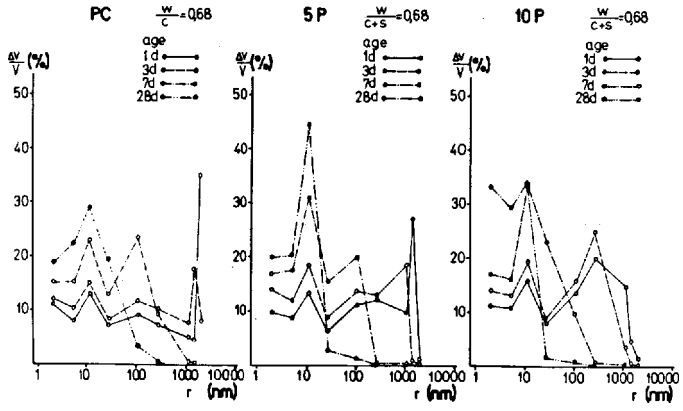

Figure 6: The pore size distribution in the paste samples PC,5P and 10P at different hydration time - the pore shares Δv/V are plotted versus the entrance pore share radius r.

After pozzolanic reaction the insolubility of silica fume in 0,1 N HCl will be changed. The extent of the insolubility change may be judged from the total silica fume hydrolytical decomposition determined at the end of molybdate complexation reaction and the same is determined by the total SiO_2 content bonded into silicomolybdate complex. It is evident from the Figure 4 and Figure 5 that silicates hydrolytical decomposition in the cement paste containing silica fume increases with hydration progress. Total silicates hydrolytical decomposition obtained after nearly finished complexation was higher in the pastes containing 5% of silica fume compared to the same in the pastes with 10% of silica fume. But totaly converted SiO_2 during pozzolanic reaction from 1 to 28 days was higher in the 10P paste (about 16 % SiO_2 converted) than in the 5P paste (about 8,5 % SiO_2 converted). In another words the pozzolanic activity of silica fume was stronger in the 10P cement paste. Identical conclusion can be made after considering the results of insoluble residue given in Table 3.

Time of hydration (days)	PC (%)	5P (%)	10P (%)
1	0,29	3,49	6,46
3	0,22	2,50	5,06
7	0,17	1,61	4,27
28	0,18	0,74	1,10

Table 3: Results of insoluble residue in the paste samples PC,5P and 10P at different time of hydration.

At the Figure 3,4 and 5 attention should be paid to a significant reduction of S'_{90}-value by the increasing of replaced cement part by silica fume. It should be noted that S_{90}-value is predominantly caused by the scope of mono- and disilicate fraction of the hydrochloric acid soluble silicate anions.

The results of mercury porosimetry are presented in Figure 6 where the volume pore shares Δv/V (%) are plotted versus the entrance pore share radius r. It is shown that hydration progress in the cement pastes shifts a maximum of the pore fraction to the smaller pore radius. After 28 days of hydration a very small fraction of the pores with a radius over 50nm (500 Å) has been detected in the pastes containing silica fume. Similar results were found in other reports (4,18) on the cement pastes and field concretes.

The presence of silica fume in the cement paste provided also, after hardening, its compressive strength as shown in Figure 7.

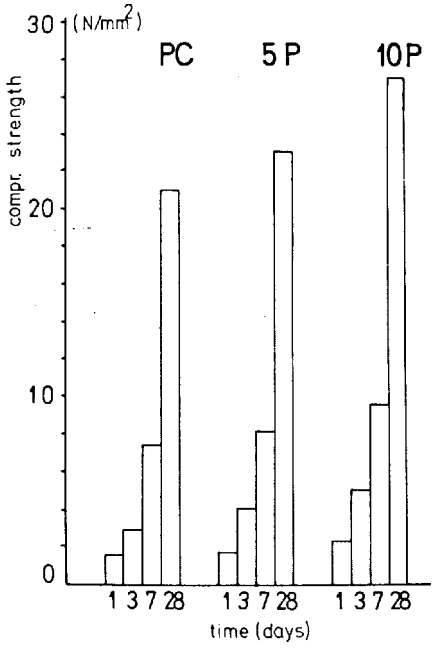

Figure 7: Compressive strengths of hardened cement paste samples PC,5P and 10P at different ages.

The highest value of strength as shown in Figure 7 has been determined in the 28-days

paste containing 10% of silica fume.

CONLUSION REMARKS.

In this work it has been found out:
-In the cement paste containing silica fume the acceleration of alite hydration has been detected at all observed stages of reaction. The tricalcium aluminate acceleration of hydration was relatively retarded at the 3-days age cement paste including silica fume.
-The results obtained by the molybdate methode indicate that after 28 days of hydration in the cement paste containing silica fume a significant part of silica fume was still hydrolyticaly undecomposable. These results can be used for evaluation of silica fume pozzolanic activity.
-The results of the mercury porosimetry show a "refinement" in the pore size distribution in similar way as reported in previously published research works. At all tested ages the compressive strengths of hardened cement-silica fume blends were increased in comparing with them of the pure hardened cement pastes.

Acknowledgements
The author is gratefull to Mr Ir Lenart Earbič and to the technicians from "Salonit-Anhovo" for their help and obliging by the use of mercury technique.
The author wish also to thank to Missis Biserka Konečny for her valuble assistance by the chemical analysis of the samples.

REFERENCES

1.Fernhardt,C.J.,"SiO_2dust as a cement additive"(Norwegian),Betongen idåg.17 årg.,No 2 (1952) 29-53

2.Markestad,A.,"Addition of SiO_2-dust in concrete"(Norwegian),Nordic concrete research congress,1968.

3.Jahren,P.,"Use of silica fume in concrete",ACI SP-79,Vol II (1983) 625-642

4.Mehta,P.K.,Gjørv,O.E.,"Properties of portland cement concrete containing fly ash and condensed silica fume",Cem.Concr.Res.,Vol 12 (1982) 587-595

5.Olsen,W.C.,"Kompaktering av silikatstøv-Mikroanalyske studier av kompaktert støv",Chr.Michelsens Institutt,mr 790802/SEM 203/ II&III,Bergen,April 1980.

6.Fesil Silica,Elkem Calc,Technical Bulletin,June 1980.

7.Bürge,T.A.,(1971)"High strength cement composites", CH-Patent 574680,A-Patent 31 24 90.

8.Bürge,T.A.,"High strength lightweight concrete with condensed silica fume",ACI SP-79,Vol II(1983) 731-745

9.Bache,H.H.,"Densified cement/Ultra fine particle-based materials",2nd Int.Conf. on superplasticizers in concrete",June 10-12,1981.Ottawa,Canada (1981)

10.Asgeirsson,H.,Gudminudsson,G.,"Pozzolanic activity of silica dust",Cem.Concr.Res.,Vol 9 (1979)249-252

11.Traetteberg,A.,"Frost action in mortar blended cement with silica dust",ASTM STP 691-Proc.of the 1st Int.Conf.:Durability of Build.Mater. and Component, Ottawa 1978. (1980) 536-548

12.Regourd,M.,Mortureux,B.,Aitcin,P.C.,Pinsonneault,F., "Microstructure of field concretes containing silica fume".Proc.4th Int.Conf. on cement microscopy,Las Vegas,NV,April 1982.pp 249-260

13.Popović,K.,Ukrainčik,V.,Đureković,A.,"Study on improving concrete durability by use of condensed silica fume",1st Int.Conf.on the use of fly ash,silica fume,slag and other mineral by-products in concrete, July 31-Aug. 5,1983.Montebello,Quebec,Canada.

14.Feldman,R.F.,Huang Cheng-yi.,"Resistance of mortars containing silica fume to attack by a solution containing chlorides",Ce.Concr.Res.,Vol 15 (1985) 411-420

15.Traetteberg,A.,"Silica fumes as a pozzolanic material",Il Cemento,Vol 75 (1978) 369-376

16.Regourd,M.,Mortureux,B.,Gautier,E.,"Hydraulic activity of various pozzolanas",Proc.5th Int.Symp.on concrete technology,Monterey,March 1981.;Universidad Autonom de Neuovo Leon,Monterey,Mexico,1981.ppl-14

17.Mehta,P.K.,"Sulphate resistance of blended portland cements containing pozzolanas and granulated blast furnace slag",ibid,1981.pp 35-50

18.Delage,P.,Aitcin,P.C.,"Influence of condensed silica fume on the pore-size distribution of concretes", Ind.Eng.Chem.Prod.Res.Dev.,22 (1983) 286-290

19.Chatterji,S.,Thaulow,N.,Christensen,P.,"Puzzolanic activity of byproduct silica-fume from ferro-silicon production",Note from Cem.Concr.Res.,Vol 12(1982) 781-784

20.Scheetz,B.,Grutzeck,M.,Strickler,D.W.,Roy,D.M.,"Effect of composition of additives upon microstructures of hydrated portland cement composites",Proc.3rd Int.Conf.on cement microscopy.Houston,USA,1981.pp307-318

21.Huang Cheng-yi,Feldman,R.F.,"Hydration reactions in portland cement-silica fume blends",Cem.Concr.Res., Vol 15 (1985) 585-592

22.Grutzeck,M.W.,Atkinson,S.,Roy,D.M.,"Mechanism of hydration of condensed silica fume in calcium hydroxide solution",ACI SP-79 Vol II (1983) 643-664

23.Kalausek,G.L.,Kopanda,J.E.,"Approach to fundamentals of concrete strength",Cem.Concr.Res., Vol 1 (1971) 63-73

24.Euw,v.M.,"Quantitative analysis of portland cement clinker by X-rays" (French),Silicates Ind.,23 (1958) 643-649

25.Kantro,D.L.,Copeland,L.E.,Weise,C.H.,Brunauer,S., "Quantitative determination of major phases in portland cement by X-ray diffraction methods",J.Res.Dev. Lab.,Portland Cem.Assoc.,6,(1),20-40 (1964) PCA Res. Dept.Bull.166

26.Jelenić,I.,Bezjak,A.,Bujan,M.,"Hydration of B_2C_3-stabilized α'- and β-modifications of dicalcium silicate",CemConcr.Res.,Vol 8 (1978) 173-180

27.Weitz,E.,Franck,H.,Schuchard,M.,"Ueber die Kieselsaeure und die Silikate",Chemikerztg.,20 (1950)256

28.Thilo,E.,Wieker,W.,Stade,H.,"Ueber die Beziehungen zwischen dem Polymerisationgrad silikatischer Anionen und Reaktionsvermoegen mit Molybdaensaeure",Z. anorg.allgm.Chem.,340 (1965)261-276

29.Đureković,A.,Bezjak,A.,Jelenić,I.,"Variation of the degree of polymerization of silica and of the C/S-ratio in hardened cement paste in the presence of NH_4NO_3 "(In German),Proc.Int.Colloq.Materials Science and Restoratin,Techn.Akademie Esslingen,Esslingen,W.Germany,1983.pp 205-208

30. JUS B.C8.C20 ; BS 4550:Part 2:1970

31. Litvan, G.G., "Variability of the nitrogen surface area of hydrated cement paste", Cem. Concr. Res., Vol 6 (1976) 139-144

32. Stein, H.N., Stevels, J.M., "Influence of silica on hydration of C_3S", Jour. Appl. Chem., 14 (1964) 338-356

33. Đurekovič, A., Popovič, K., unpublished results.

SUB-THEME/SOUS-THÈME 3.3

Special cements. Calcium aluminate and other no-silicate cements.

Ciments spéciaux. Ciments à base d'aluminates calciques et autres ciments sans silicates.

Chairman/Président :

T. V. Kouznetsova
Mendeleyev Institute of Chemical Technology, Moscow, U.S.S.R.

Principal Reporter/Rapporteur Principal:

W.Kursdowski
Academy of Mining and Metallurgy Institute of Building Materials and Refractories, Krakow, Poland

M.G.P. SILVA (PETROBRÁS's Research and Development Center - Brazil)
M.L.M. de Moraes (PETROBRÁS's Research and Development Center - Brazil)
Hosam A.A. ABDEL - REHIM (PETROBRÁS's Research and Development Center - Brazil)

The effect of the hemihydrated and dihydrated cristalline forms of the calcium sulphate on the thickening time, rheological properties and compressive strength of the oil well cement slurries.
L'effet des formes cristallines hémihydratés et dihydratés du sulfate de calcium sur le temps de pompabilité, les propriétés rhéologiques et la résistance à la compression des pâtes de ciment pour forages pétroliers.

SUMARY

In the cement slurries used in oil wells, the most important physical properties are: thickning time, rheological properties and compressive strength.

In this study, the effect on these parameters of the hemihydrated and dihydrated crystalline forms of the calcium sulphate present in the cement was determined.

An analytical method was developed to determine the concentrations of the crystalline forms of the calcium sulphate using a high power X-ray diffractometer.

It was shown, in this type of cement, that an increase in the concentration of the hemihydrate caused a higher shift in the values of the principal physical properties than the dihydrate.

SUMÁRIO

Nas pastas de cimento utilizadas em poços de petróleo, as propriedades físicas mais importantes são: tempo de espessamento, propriedades reológicas e resistência à compressão.

Neste estudo determinou-se o efeito sobre estes parâmetros das formas cristalinas hemidratada e diidratada do sulfato de cálcio presentes no cimento.

Foi desenvolvido um método analítico para determinar as concentrações das referidas formas cristalinas do sulfato de cálcio utilizando-se um difratômetro de raios X de alta potência.

Verificou-se, neste tipo de cimento, que um aumento na concentração do hemiidrato causou um maior incremento nos valores das principais propriedades físicas do que aquele obtido com o diidrato.

INTRODUCTION

It is of the utmost importance that cements for oil well cementing be highly uniform, such that the systems obtained therefrom exhibit a predictable and reproducible behavior, which will greatly speed up the work involved in designing the cement slurries to be utilized in those operations.

However, gypsum dehydration resulting from the raise in temperature during the milling process, according to:

$$CaSO_4.2H_2O \xrightarrow[120-130^oC]{} CaSO_4.1/2H_2O + 3/2H_2O$$

contributes to increase the number of variables influencing the rheological properties and parameters, the thickening time and compressive strength of the slurries for this type of application.

Through laboratory tests utilizing a rotational coaxial viscosimeter, a consistometer for high pressures and temperatures, and a hydraulic press, the variations of the main properties and parameters of slurries prepared with class "G" cement containing different $CaSO_4.2H_2O$ and $CaSO_4.1/2H_2O$ concentrations were determined.

Chemical analysis of the dihydrated and hemihydrate crystalline forms of calcium sulphate was carried out by a method utilizing a high power X-ray diffractometer.

EXPERIMENTAL PART

Analysis of the Calcium Sulphate Crystalline Forms Present in the Cement

Analysis of $CaSO_4.2H_2O$ and $CaSO_4.1/2H_2O$ in class "G" cements for use in oil wells could be carried out by using thermogravimetric techniques or X-ray diffraction. Such techniques have not produced satisfactory results, since the dihydrated and the hemihydrated phases of gypsum are present in small amounts, close to the methods' detection limits.

Preconcentration tests, following the recommendations of Tabikh and Mehta, have been attempted, with a subsequent evaluation by X-ray diffraction. In this way detection of gypsum and/or hemihydrate is possible; this procedure, however, has also been abandoned, due to low repeatability and the gelling process during the preconcentration step.

The alternative chosen was high-power X-ray diffraction. Such technique utilizes a rotating anode and operates at up to 12 kW power. The equipment used was the Rotaflex-Rigaku model X-ray diffractometer, with a rotating copper anode, a graphite monocromator and pulse height discriminator. Conditions were 40 kV, 80 mA, scanning velocity $1/2^o$/min, 5 mm/min chart speed, 400 cps scale.

The peak height of the hemihydrated and dihydrated crystalline forms of calcium sulphate was correlated to the content thereof present in the cement samples.

SAMPLE PREPARATION

Different cement samples were prepared in the laboratory, from the generating clinkers of three class "G" cements, designated as cement 1, cement 2 and cement 3.

Cement samples prepared from the same clinker differ from one another by the added gypsum concentration, as well as the crystalline form thereof.

With respect to this material, during the preparation of the first samples, the presence of particles of a size greater than the 200 mesh average was found. This fraction, because it was greater than 100 mesh in diameter, made gypsum homogenization in the clinker difficult.

To avoid the possible influence of these larger gypsum particles in the small cement samples, the calcium sulphate was reground, such that all of the material passed the 325 mesh sieve.

The hemihydrated form of calcium sulphate was obtained by placing the gypsum in a THELCO vacum oven during at least 3 hours, at a temperature of 140^oC. As soon as the partially dehydrated material returned to room temperature, it was immediately blended to the clinker, in plastic containers.

A small fraction of the so prepared cement was subjected to high resolution X-ray diffraction, to confirm the presence of $CaSO_4.1/2H_2O$, with the remaining portion being promptly used in preparing slurries for the thickening time, rheology and compressive strength tests.

The chemical and physical characteristics of the clinkers which generated the cements 1, 2 and 3, and gypsum utilized in the preparation of these cements are set forth in Tables I and II, respectively.

Procedures

- Preparation of Cement Slurries

The cement samples containing different $CaSO_4.2H_2O$ and $CaSO_4.1/2H_2O$ concentrations were added to water at the rate of 44% relative to the weight of the cement, with the aid of a Waring blender, of 1 liter capacity. During the first fifteen seconds, they were stirred at 150 rev./sec, and in the last thirty-five seconds, at 200 rev./sec.

- Determination of the Rheological Properties and Parameters

After the previously described procedure, the slurries were subjected to stirring in the atmospheric consistometer at the ro-

tational velocity of 2.5 rev./sec for a 20 minute period, at a temperature of 26.6°C, or they were heated at a 1.25°C/min rate, to a temperature of 51.6°C. At the end of this period, the cement slurries were poured into the sample thermal cup, previously heated to test temperature, and the rheological tests were carried out at once.

TABLE I
CHEMICAL COMPOSITION OF CLINKERS (Wt%)

SAMPLE NUMBER	1	2	3
CaO	64.10	60.20	60.10
SiO_2	21.10	20.20	20.30
Al_2O_3	4.81	4.84	4.84
Fe_2O_3	5.80	6.40	6.30
SO_3	1.10	1.20	1.00
MgO	1.50	1.10	1.60
Na_2O	0.18	0.20	0.21
K_2O	0.22	0.47	0.49
Mn_2O_3	0.11	0.08	0.09
P_2O_5	0.19	0.13	0.13
TiO_2	0.20	0.24	0.24
SrO	0.16	0.18	0.18
Free CaO	0.74	1.33	1.46
BLAINE (m^2/kg)	284	285	278
① WET SCREEN ANALYSES	74.30	82.69	81.73
LOSS ON IGNITION	0.68	0.89	0.62
INSOLUBLE RESIDUE	0.28	0.20	0.29
②			
C_3S	58.2	46.20	46.0
C_2S	16.6	22.80	23.5
C_3A	2.4	2.0	2.1
C AF	17.6	19.4	19.1

NOTES :

① PASSING U.S. STD. Nº 325 SIEVE (45 μm).

② CALCULATED BY BOGUE FORMULAS.

TABLE II
GYPSUM CHARACTERISTICS (Wt%) .

$CaSO_4 . 2H_2O$	75.3
ANHYDRITE	NEGLIGIBLE
LOSS AT 110° C	11.0
LOSS AT 500° C	17.0
LOSS AT 60° C ,HUMIDITY	0.48

- Equipment

A Fann V.G. Model 35A, direct reading rotational viscosimeter, which permits measuring the shear stress at several shear rates, was used. This apparatus comprises a concentrically aligned external cylinder (or rotor) and another, internal cylinder (or bob), the latter being attached to a spring, which measures the torque that is exerted on it, caused by rotation of the rotor when immersed in the cement slurry. The rotor-bob combination employed was R_1-B_1 and a spring factor of 1.

Rheological determinations on the cement slurries at 26.6°C and 51.6°C were carried out at the following rotational velocities: 10.0; 5.0; 3.3; 3.0; 1.67; 1.0; 0.5; 0.10 and 0.05 rev./sec with 20 second intervals between readings and following a decreasing order of velocities.

The rheological calculations were made based on the Bingham model, from a linear relationship between shear stress and shear rate. The terms describing this model are: yield point (YP) and plastic viscosity (PV), its basic equation being:

$$Ss = YP + (PV).(SR),$$

wherein:

Ss = shear stress, Pa
YP = yield point, Pa
PV = plastic viscosity, Pa.S
SR = shear rate, s^{-1}

In figures 1, 2 and 3, the variation in yield point of the class "G" cement slurries for use in oil wells, with different $CaSO_4.2H_2O$ and $CaSO_4.1/2H_2O$ contents, both at 21.6°C and 51.6°C is shown. The latter temperature corresponds to the application of this cement type at 2,440 m depth, according to "Schedule 5" of the American Petroleum Institute recommendations for oil well cement testing (A.P.I. Spec. 10).

The rheological curves presented in Figures 4 and 5, relating to the slurries prepared from a commercial "Class G" cement sample, were plotted from the readings obtained on the above-mentioned viscosimeter, with the following rotational velocities being employed: 10; 5; 3.33; 3.0; 1.67; 1.50; 1.0 and 0.5 rev./sec. One curve relates to the cement sample without any previous treatment, and the other one, to the sample that was heated to cause dehydration of the $CaSO_4.2H_2O$ contained therein.

- Thickening Time Determinations

The slurries prepared from cements 1 and 2 were subjected to the high pressure and temperature consistometer, according to "Schedule 5-API SPECIFICATION", wherein well bottom simulation conditions are as follows: a 35,600 kPa pressure and a 52°C temperature. The results presented in Figure 6 correspond to the time required for the slurries to reach 100 consistency units, from which value onwards they would not be pumpable within the well.

The potenciometric mechanism and the measuring circuit for the consistency indicating voltages were calibrated by the weight method. This type of calibration establishes equivalent torque values for several consistency levels as defined from the following equation:

$$T = 78.2 + 20.02\ B_c$$

wherein:

T = torque, g.cm
B_c = Bearden Slurry Consistency Units

COMPRESSIVE STRENGTH

Cements 1 and 2, comprising dihydrated and hemihydrated calcium sulphate contents ranging from 2 to 3% were blended with water (w/c = 0.44), according to the previously described procedure, and the resulting slurries were cast in cubic molds, to yield 50.8 mm edge specimens. Thereafter, the molds containing the specimens were cured in a water-bath at a temperature of 37.7°C for the 8 and 24-hour periods.

After curing the molds were removed from the bath 45 minutes before testing, and placed in a water-bath held at 27 ± 3°C for 35 minutes. The specimens were broken in a hydraulic press, using a loading rate comprised within the range of from 6,900 kPa to 13,800 kPa.

RESULTS AND DISCUSSION

Influence on the Rheological Parameters of the Slurries

To ascertain the effect of the hemihydrated and dihydrated crystalline forms of calcium sulphate on the rheological parameter values of the slurries, twelve cement samples were initially prepared from the clinker used to prepare cement 1. These samples differ from one another with respect to the content and crystalline form of the added calcium sulphate.

Figure 1 shows that, regardless of the test temperature, the slurries showing the highest yield point values were those cements that contained the hemihydrated form.

It is also found that when the cement has a 3% calcium sulphate content, there is a decrease in the difference between the yield points of the slurries prepared from hemihydrate and dihydrate, that is, the hemihydrate presence influence is lower at this concentration than at 2% addition.

At the 4% concentration, the influence of $CaSO_4.1/2H_2O$ is again greater than it was in the cements containing 2% and 3% of this partially dehydrated sulphate.

As shown in Figure 2, the yield points of the slurries prepared from the clinker used to prepare cement 2 confirm the tendency of the hemihydrate-containing cements to produce slurries with a higher inertia to motion. It is further found, at the 26.6°C and 51.6°C temperatures, that at the 3% concentration, the effect of the hemihydrate relative to the dihydrate is smaller than at 2,4 and 5% concentration.

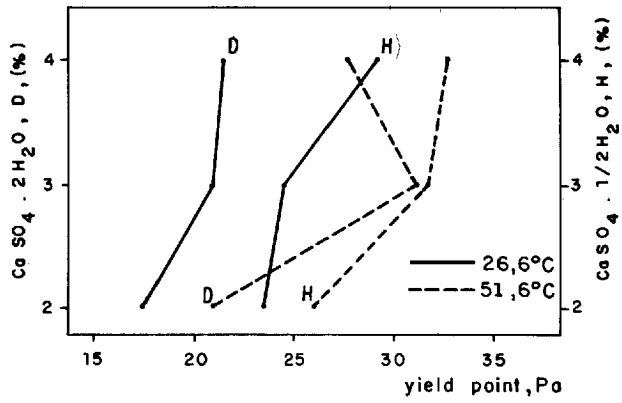

FIG. 1—RHEOLOGY— CIM. 1

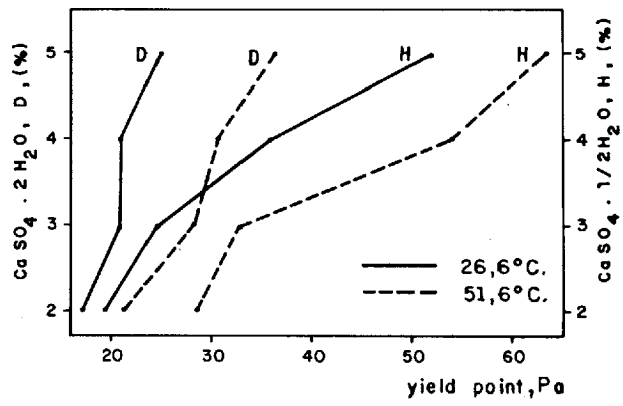

FIG. 2—RHEOLOGY— CIM. 2

Figure 3 shows that, at a temperature of 26.6°C, the addition of 3% calcium sulphate to the clinker used in preparing cement 3, did not change the yield point value, whether this compound was in the hemihydrated or dihydrated form.

At this same temperature, it is further found that for concentrations higher than 3%, the influence of the hemihydrate is manifested by the increase in yield point of the slurries.

At the 51.6°C temperature there was practically no influence of the hemihydrated phase. There was a reversion of the tendencies at the 3 and 5% concentrations, i.e.,

the dihydrate slightly increased the slurries' yield point.

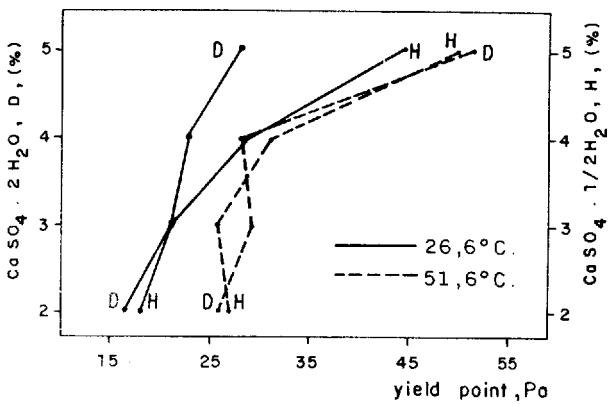

FIG. 3 – RHEOLOGY – CIM. 3

To corroborate the fact that the hemihydrate-containing cements have higher yield points, a class "G" commercial cement sample was heated for 3 hours at a temperature of 140°C. X-ray diffraction analyses showed that all of the sample's gypsum had been converted into $CaSO_4.1/2H_2O$.

Figures 4 and 5 show that, for the same shear rate, the slurries prepared from the hemihydrate-containing cement, in addition to greater yield points, also exhibited higher readings on the FANN Viscosimeter, that is, higher apparent viscosities, when subjected to the rheology test.

As regards the influence of the hemihydrate on the plastic viscosity of the slurries prepared with cements 1, 2 and 3, it was found that at the 26.6°C temperature, this crystalline form of the sulphate tends to make slurries more viscous. However, at the 56.6°C temperature, an adverse behaviour was sometimes observed. This occurred with cement 2, when 3, 4 and 5% $CaSO_4.1/2H_2O$ amounts were added to the clinker from which this cement was made.

Based on the heretofore performed tests, using the FANN viscosimeter, no evidence has been found that the hemihydrate, when present in the cement, causes an increase in the gellation tendency of the slurries.

Influence on Thickening time

The consistency tests performed under the API Schedule 5 temperature and pressure conditions, with cements 1 and 2 show, as presented in Figure 6, that the presence of hemihydrate delays thickening of the slurries.

However, at contents higher than 4%, and at temperature of 56.6°C, it has been found that hemihydrate presence did not interfere with the thickening time of slurries.

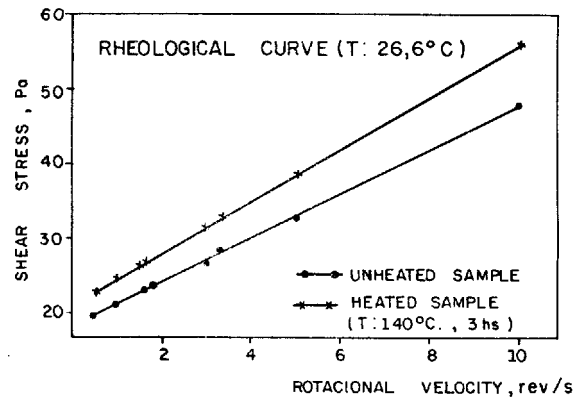

FIG. 4 – CEMENT SLURRIES PREPARED WITH CLASS G CEMENT SAMPLE.

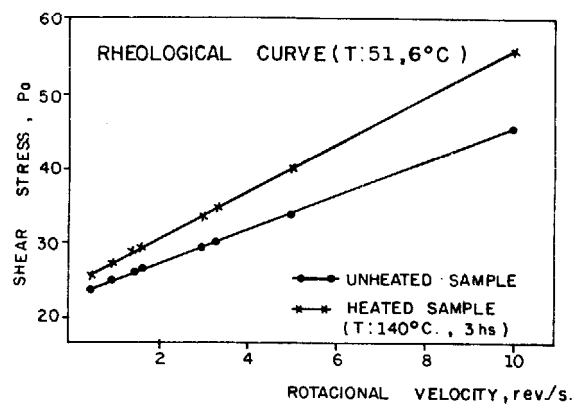

FIG. 5 – CEMENT SLURRIES PREPARED WITH CLASS G CEMENT SAMPLE.

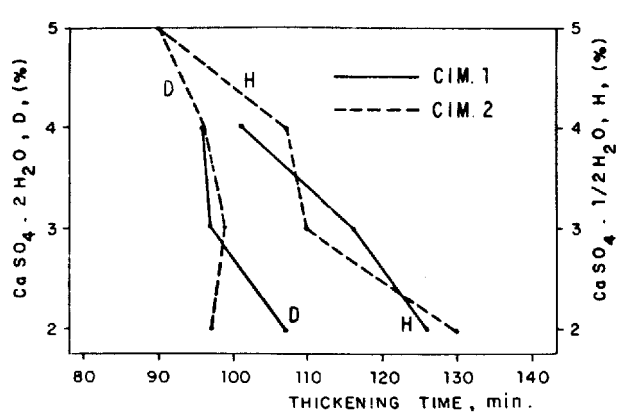

FIG. 6 — THICKENING TIME
Sch: 5

Influence on Compressive Strength

Addition of hemihydrate calcium sulphate to the clinkers of the cements 1 and 2 provided specimens with a greater compressive strength than those originating from these same cements, but containing the calcium sulphate in its dihydrated form.

Figures 7 and 8 show these results after 8 and 24 hours curing time, respectively.

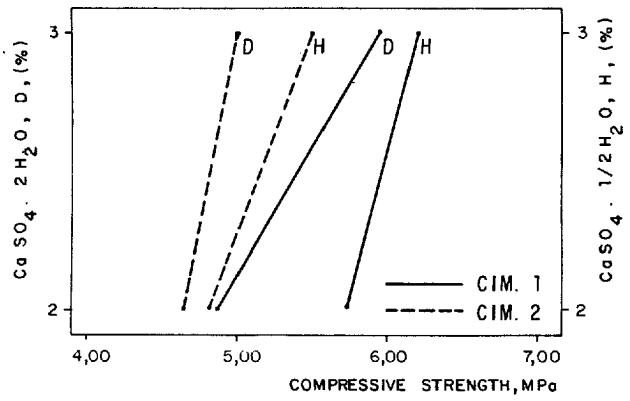

FIG. 7 — COMPRESSIVE STRENGTH
CURING TIME: 8 h; T: 37,7 °C, P: atmos.

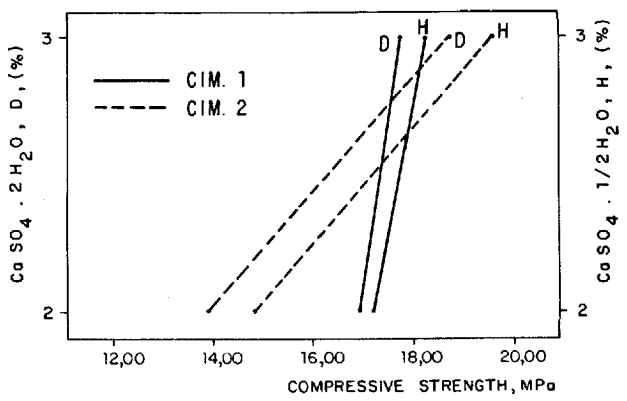

FIG. 8 — COMPRESSIVE STRENGTH
CURING TIME: 24 h; T: 37,7 °C, P: atmos.

CONCLUSIONS

Conclusions as to the effects of the calcium sulphate hemihydrate in concentrations ranging between 2 and 5% (w/w) in class "G" cement samples for oil well cementations are as follows:

- $CaSO_4.1/2H_2O$ raises the yield point of slurries and may also cause an increase in plastic viscosity. A significant increase in apparent viscosity was observed in all samples.

- It could not be concluded that the hemihydrate favors the increase of the gel strength of the slurries.

- Slurry thickening time is delayed as a result of hemihydrate presence at concentrations of up to 4% (w/w).

- Compressive strength is increased, when the cement contains calcium sulphate in its hemihydrated form.

BIBLIOGRAPHY

CALLEJA, J. Puntos de vista sobre el contenido de yeso de los cementos Portland. Revista Materiales de Construcción, 120, Oct. Nov. Dic. 1965.

HELMUTH, R.A. Structure and rheology of fresh cement paste. In: INTERNATIONAL CONGRESS ON THE CEMENT CHEMISTRY. 7. Paris, 1980. v. 1, VI-O.

LUDWING, U. The influence of various sulphates on the setting and hardening of cements. Zement-Kalk-Gips, 1964. p. 81-90, 109-119, 175-180 (Translation).

GREENBERG, S.A. and MEYER, L.M. - Rheology of fresh Portland cement pastes. Influence of Calcium Sulphates. Highway Research Record, 1963, nº 3, p. 9-19.

API SPECIFICATION 10, First Edition. American Petroleum Institute, Washington, D.C. (1982).

N. B. Djabarov, Bulgarian Academy of Sciences-Central Laboratory of Physico-Chemical Mechanics, Sofia, Bulgaria

1

Expansive Cement With Hydroxyde Expanding Phase on Admixture's Basis

Ciment expansé avec une phase expansive d'hydroxyde à la base d'un ajout

3.3

SUMMARY: At the previous 7th International Congress on the Chemistry of Cement - Paris, 1980 was reported about a complex admixture for expansive cement with hydrosulfoaluminate (ettringite) expanding phase. This study treats the further development of expansive cements on admixture's basis. A new chemical admixture for obtaining expansive cement with hydroxyde expanding phase was elaborated. The cement with that expanding mechanism possess good plasticity and workability, great expansion with high strength and selfstressing etc.

According to the needs of construction and prefabrication, by means of the new admixture, ordinary cements are modified in shrinkage compensating, expansive and selfstressing cements with hydroxyde expansive mechanism.

The expansion and selfstressing of the modified cements can be precisely regulated. Depanding on the admixture's quantity the wished value of deformation and selfstressing is obtained.

The high technical qualities of the new expansive cement discover large possibilities for introduction in constructions and prefabrication, where shrinkage compensating or selfstressing, higher crack resistance, deminished water leakage etc are needed.

No 7º Congresso Internacional da Química do Cimento - Paris, 1980, relatou-se sobre uma mistura complexa para cimento com uma fase expansiva de hidrossulfoaluminato (etringita). O presente estudo aborda o desenvolvimento posterior de cimentos expansivos à base de aditivo. Foi elaborado um novo aditivo químico para obtenção de cimento expansivo com fase expansiva de hidróxido. O cimento com aquele mecanismo expansivo possui boa plasticidade e trabalhabilidade, grande expansão com alta resistência e auto-estressante, etc.

De acordo com as necessidades de construção e de prefabricação, por meio do novo aditivo os cimentos comuns são modificados em cimentos compensadores da retração, expansivos e auto-estressantes com mecanismo expansivo de hidróxido.

A expansão e o auto-estressamento dos cimentos modificados podem ser regulados com precisão. Dependendo da quantidade de aditivo, obtém-se o valor desejado de deformação e auto-estressamento.

As altas qualidades técnicas do novo cimento expansivo abrem grandes possibilidades para sua introdução em construções e pré-fabricação, em que há necessidade de compensação da contração ou auto-estressamento, alta resistência à fissura, vazamento reduzido de água, etc.

Expansive and selfstressing cements at present are mainly based on hydrosulfoaluminate (ettringite) expanding mechanism. For it's realization three components are needed: aluminate, sulfate and calcium. A great variety of the aluminate components is characterizing the different expansive cements. Components as: aluminous cements, different Ca-aluminates (C_3A, $C_{12}A_7$, CA, CA_2) or slags containing these minerals, Ca-sulfoaluminate ($C_3A_3C\bar{S}$) or clinker with high percentage of that mineral, thermal activated alunite, different aluminium salts etc are used. At the previous 7th International Congress on the Chemistry of Cement, Paris'80 /1/ was reported about a high quality expansive cement with complex admixture containing special Al-salts.

They are also known expansive cements with hydroxyde or this combined with ettringite expanding mechanism, but they are less compared to these based on hydrosulfoaluminate phase. For expansive agents are proposed: calcined by 800-900°C dolomite or magnesite /2/, byproducts of MgO (periclase) for hydrothermal treated cements and concretes/3, 4/, silica-organic compound introduced in cement and CaO in the mixing water/5/, carefully calcined (900-950°C) and sized MgO for mass concrete /6/, calcined by high temperature (1500°C) CaO + $C\bar{S}$ and with or without $C_3A_3C\bar{S}$ /7/ or special clinkers, containing: Ca-alumoferrites + CaO /8/, C_3S + CaO /9/, $C_3A_3C\bar{S}$ + $C\bar{S}$ + CaO + C_2S /10/, $C_{11}A_7 \cdot CaF_2$ + CaF_2 + anhydrite + CaO /11/.

In spite of its simplicity - only one component (MgO or CaO) instead of three - the hydroxyde expanding mechanism has not be till now largely employed for expansive cements. Very few of these cements were introduced industrial in the constructional practice and they are actually such with combined expanding mechanism /10/. The reason for not using hydroxyde phase independently seems to be the difficult regulation of MgO and CaO qualities like expanding agents. Their reactivity with water is strongly influenced from the temperature of calcination and other technological conditions.

Based on former experience /3, 4, 1 etc/ in the Central Laboratory of Physico- Chemical Mechanics by the Bulgarian Academy of sciences was created a new admixture with hydroxyde expanding mechanism only. This additive can be obtained by an easy realizable technology from ordinary row materials and as believed also with good economical profit. The admixture's composition ansures the oxyde + water reaction to be realized by normal temperature and at a definite period of structure development of the hardening cement stone. It is the time when some strength is already acquired in order to withstand the pressure of the growing hydroxyde crystals. At the same time the structure has retained still sufficient plasticity, so that the expansion will not interrupt the integrity of hardened cement. Thus the admixture ansures optimal conditions an ordinary cement to be modified in expansive or selfstressing cement.

To illustrate the qualities of the new cements with hydroxyde expanding phase are given some experimental data.

For the investigations are used four basic cements: three ordinary portland cements, marked OPC, OPC_1, OPC_2 and one sulfateresistant - SRC. They are modified in expansive cements (EC) or selfstressing cements (SC) by means of different admixture's quantities. With supplementary mark "x" is indicated some increased additive's amount for expansion rise.

The experimental results and their discussion are given in four parts.

1. Setting time

The known expansive cements are usualy quick setting which is limiting their field of application. Therefore it is important to obtain such type of cements with normal setting time.

In table 1 are compared the initial port-

land (OPC) and the expansive and selfstressing cements on its basis (EC, EC*, SC). Setting time is determined by standard Vicat method.

Table 1
Setting time of cements

Cement type	Mixing water for standard plasticity /%/	Setting time /hours-minutes/	
		Initial	Final
OPC	24,1	1-30	3-11
EC	24,4	2-37	3-12
EC*	26,1	2-26	2-45
SC	27,2	2-20	2-45

Expansive cements EC, EC*, SC with the new admixture have retarded initial setting and unchanged or by increased additive's quantity (EC*, SC) little accelerated final setting. With such normal setting time the proposed expansive cements are giving the possibility to overcome the technological difficulties caused by the quick setting of the prevailing part of known expansive and selfstressing cements especially with hydrosulfoaluminate phase. Thus will be ansured larger introducing of these special cements in constructions.

2. Free expansion and strength at different demoulding ages

On table 2 are given the linear free (unrestrained) expansion and on table 3-strength of hardened standard mortar (1:3) and W/C ratio 0,5. The specimens 40/40/160 mm are prepared according RILEM-CEMBUREAU method. The expansion is measured on the unmoulded prisms by means of micrometer. Specimens unmoulding is done after 6.30 and 18.30 hours followed by hardening in water at about 20°C.

By means of the new admixture with hydroxyde expanding phase from the basic OPC are obtained expansive and selfstressing cements with relatively high plasticity (flow test). Their deformation and strength properties can be well regulated with the additive's quantity. The expansion is manifested by normal temperature within the first days of hardening and there after the mortar volume is remaining stable. By testing on cement stone or mortar with higher cement content the expansion's size is several times greater compared to the standard mortar 1:3 used in present investigations.

Table 2
Free (unrestrained) linear expansion of cement-sand mortar 1:3

Cement type	Flow test /mm/	Expansion /%/ at age /days/		
		1	3	28
	Demoulding after 6.30 h			
EC	186	0,976	0,989	0,989
SC	198	2,381	2,528	2,528
	Demoulding after 18.30 h			
EC	188	0,086	0,096	0,096
SC	188	0,471	0,962	0,962

Table 3
Compressive strength of cement-sand mortar 1:3

Cement type	Flow test /mm/	Strength /MPa/at age/days/		
		1	7	28
	Demoulding after 6.30 h			
EC	186	5,1	19,0	23,5
SC	198	2,7	7,8	9,5
	Demoulding after 18.30 h			
EC	188	11,1	28,3	35,7
SC	188	7,7	13,7	18,0

Compared to the known expansive cements with hydroxyde expanding mechanism the new one has much greater expansion. For example the described cements are expanding only 0,18-0,4 % tested on cement stone /2/, 0,02-0,05 % on mortar 1:2 /5/ and 0,088 - 0,555% on cement stone and increased temperature

($32^{o}C$). Expansion by /3, 4/ is similar to that in the present investigations, but with the new admixture the great deformation is achieved at normal temperature. By /3, 4/ is needed hydrothermal treatment and rise in temperature. So the new development has important technological advantages.

In relation to the high expansion's value in unrestrained conditions the hardened mortars have also good strength properties, which are constantly improving in the course of time.

Early demoulding is leading to 2,6 - 10,3 times greater expansion respectively for SC and EC. Corelated with the high unrestrained deformation the strength of same cements for 28 days age is 1,9 - 1,5 times decreased. These experimental results point out the importance of the strength characteristics of hardening mortar at the beginning of the free (unrestrained) deformation and the mutual dependency between strength and expansion during the whole hardening process.

3. Free expansion and strength by different curing conditions

With different amounts of the admixture initial OPC_1, OPC_2 and SRC are changed in EC_1, SC_1, SC_2 and SC_3. Testing is carried out according to the same method used in part 2 (see above). Demoulding is done after 18.30 hours and curing is at about $20^{o}C$ in water or on the air with moistening in the initial period.

On tables 4 and 5 are to be seen the linear free (unrestrained) expansion and strength respectively.

Experimental results are proving the high effectiveness of the admixture to modify different ordinary portland and other types of cements in expansive and selfstressing cements. By all of them mortar plasticity is relatively high and near to that of ordinary cements. On the contrary known expansive and especially selfstressing cements with hydrosulfoaluminate phase have usually very worsened rheological characteristics.

Table 4

Free (unrestrained) linear expansion of cement-sand mortar 1:3

Cement type	Flow test /mm/	Expansion /%/ at age /days/ 1	3	28
		Water curing		
EC_1	184	0,082	0,108	0,108
SC_1	179	0,657	0,904	0,904
SC_2	161	0,232	0,534	0,534
SC_3	163	0,336	0,510	0,510
		Air curing		
EC_1	184	0,094	0,113	0,112
SC_1	181	0,696	0,983	0,978
SC_2	177	0,237	0,584	0,574
SC_3	163	0,301	0,479	0,467

Table 5

Compressive strength of cement-sand mortar 1:3

Cement type	Flow test /mm/	Strength/MPa/ at age/days/ 1	7	28
		Water curing		
EC_1	184	7,6	-	39,0
SC_1	179	6,3	-	27,2
SC_2	161	12,6	21,1	27,7
SC_3	163	10,4	22,4	30,2
		Air curing		
EC_1	184	7,4	-	41,5
SC_1	181	5,5	-	23,3
SC_2	177	12,8	17,6	23,2
SC_3	163	11,6	19,4	24,7

In accordance with the used admixture's amount and specimens demoulding age of 18.30 hours the free expansion has reached the desired size for the different initial cements in the limits from 0,1 to 0,98 %.

The expansion of tested cements by the two different curing conditions is practically the same. Differences at 3 days age, when

the expansion is completed, are no more than -6 to +9 %. By air hardening in later age and suspended moistening the expansion is little deminished which is usual for these curing conditions.

By raising the expansion's degree the difficulties to keep stable strength's grow with time are well known. The problem is most difficult by the selfstressing cement. Experimental data from these investigations are showing steadily strength's increase of the new cements including such with great expansion and selfstressing.

The strengths by air hardening are similar or some what decreased compared to those by water curing. Differences between them at 28 days are from -18 to +6 %.

4. Restrained expansion and selfstressing

The selfstressing is tested on cement-sand mortar 1:1 specimens 40/40/160 mm with restrained expansion by means of dynamometric frames. The used cements SC and SC_a are based on OPC and the new admixture in two variants. Demoulding is done after 6.30 hours followed by water curing at about 20°C.

On table 6 is given free and restrained expansion (linear) of the hardening mortars and on table 7 - selfstressing and strength by free expansion at different ages.

Experimental data are making evident the good selfstressing qualities of cement with the proposed additive containing hydroxyde expanding phase. By increasing admixture's quantity the selfstressing can reach much higher value but the used in this case method and dynamometric frames are with limited possibilities to test higher selfstressing.

The ratio free/restrained expansion for SC and SC_a is 6,27-6,30 and 5,93 respectively. This ratio is characterizing to which extent the chemical energy is transformed in expansion's work in restrained conditions compared to the free expansion. The ratio's values by these investigations are better towards those of the greater part of known selfstressing cements with hydrosulfoaluminate expanding mechanism. The determined ratio here is nearer to that of cement with expanding agent periclase (MgO) /3, 4/. In contrast to it selfstressing with the new admixture is obtained without hydrothermal treatment, which has great technical and economical advantages.

Table 6

Free and restrained linear expansion of cement-sand mortar 1:1

Cement type	Flow test /mm/	Free/restrained expansion /%/ at age /days/			
		3	4	28	40
SC	155	2,051	2,059	2,059	2,059
		0,327	0,327	0,327	0,327
SC_a	175	1,792	1,892	1,892	1,892
		0,302	0,319	0,319	0,319

Table 7

Selfstressing and compressive strength of expansive cement-sand mortar 1:1

Cement type	Selfstressing by restrained expansion /MPa/ at age /days/				Strength by free expansion /MPa/, age/days/	
	3	4	28	40	3	28
SC	60,2	60,2	60,2	60,2	27,6	43,0
SC_a	55,6	58,7	58,7	58,7	28,2	45,5

By summarizing the carried out investigations becomes evident that the proposed admixture is a very efficient expanding agent, which is based on the simple principle of hydroxyde expanding mechanism successfully realized by normal temperature. The expansive and selfstressing cements on the new amixture's basis have high technical qualities which discover large possibilities for their introduction in constructions and prefabrication, where shrinkage

compensating or selfstressing, higher crack resistance, deminished water leakage etc are needed.

REFERENCES

1.- N.B. Djabarov, Y.T. Simeonov (1980),"Ciment expansé composé d'un ciment normal et d'un ajout complexe", Communications 7e Congrès International de la Chimie des Ciments, Vol.III, Paris, V-88-V-93.

2.- P.P. Budnikov, Z.S. Kossyreva (1952), "Expansive cement without hydrosulfoaluminate building"(in Russian),Cement, No. 4, 11.

3.- W. Slatanov, N. Djabarov (1960),"Further investigations on selfstressed concrete by means of MgO expansion"(in German), Silikattechnik, No. 10, 470-473.

4.- V. Slatanov, N. Djabarov (1961),"L'autocontrainte des bétons par l'hydratation du periclase MgO", Revue des matériaux No. 544, 30-33.

5.- A.E. Sheikin, T.Y. Yakub (1966),"Shrinkage compensating portland cement" (in Russian), Strojisdat, Moscow.

6.- P.K. Mehta, D. Pirtz, G.J. Komandant (1980),"Magnesium oxide additive for producing selfstress in mass concrete", Communications 7th International Congress on the Chemistry of Cement, Vol. III, Paris, V-6-V-9.

7.- U. Yamazaki, H. Kamiaka, S. Kobayashi (1980),"Role of expansive additive CaO in expansive cement",Communications 7th International Congress on the Chemistry of Cement, Vol. III, Paris,V-220-V-223.

8.- Y. Konde, M. Sato,"Expansive additive", Jap. Patent No. 55-49020/1972, publ. 09.12.1980.

9.- T. Kawano, K. Hitotsuya, T. Mori(1974), "The role of $CaSO_4$ in(Alite-CaO-$CaSO_4$-interstitial substance) system expansive component for cement",Proc. of the 6th Int.Congress on the Chemistry of Cement, Moscow.

10.-P.K. Mehta, M. Polivka (1974),"Expansive cements", Proc. of the 6th Int.Congress on the Chemistry of Cement,Moscow.

11.-Y. Suzukawa, W. Kobayashi, Sh.Okabayashi, H. Ichinose, "Expansive cement additive and cementitious material added therewith", US Pat. 4452637/1983, publ. 05.06.1984.

Shan-Ba Wang, Shang-xing Ji, Yin-Jiang Liu and Ke-Yong Hu
Wuhan Institute of Building Materials, Wuhan, China

Effect of alkali on the expansive properties of sulfoaluminate cement pastes

Effet de l'alcali sur les propriétés de l'expansion des pâtes du ciment sulfoalumineux

SUMMARY: The effect of alkali (NaOH) on expansive properties of sulfoaluminate cement pastes was studied by measurement of expansion value, XRD as well as liquid phase analysis.

NaOH increase compressive strengths of the pastes in early ages but decreases the strength at later ages. NaOH accelerates the formation of ettringite and content of ettringite in the pastes increases with increasing NaOH concentration. The ettringite formed even in PH=13.3 environment(0.7 M NaOH solution) is not amorphous but crystalline. The concentration of CaO in liquid phase decreases and the concentration of Al_2O_3 increases with increasing NaOH concentration. The expansion of the paste increases as NaOH concentration increases The expansion caused by ettringite formed in higher PH value but lower CaO concentration solution is greater than that in lower PH value but higher CaO concentration solution;the higher NaOH concentration, the more ettringite and the greater expansion. Therefore, the expansion of ettringite does not always depend on CaO concentration but depends on PH value in pore solution within the paste. We conclude that it is better to be related the expansion with PH value than that with CaO concentration if alkali is present in the paste.

Por meio de adição do valor de expansão, XRD e análise de fase líquida, estudou-se o efeito do álcali (NaOH) sobre as propriedades expansivas de pastas de cimento de sulfoaluminato.

NaOH aumenta as resistências à compressão das pastas nas idades iniciais, mas as diminui nas idades finais. NaOH acelera a formação de etringita, e o teor de etringita nas pastas aumenta com o aumento de concentração de NaOH. A etringita formada até mesmo em ambiente com pH = 13,3 (solução de 0,7 M NaOH) não é amorfa, mas cristalina. A concentração de CaO na fase líquida diminui, e a concentração de Al_2O_3 aumenta com o aumento de concentração de NaOH. A expansão da pasta aumenta na medida em que aumenta a concentração de NaOH. A expansão causada pela etringita, formada em solução com valor mais alto de pH e concentração mais baixa de CaO, é maior do que a formada em solução com valor de pH mais baixo e concentração mais alta de CaO. Quanto maior a concentração de NaOH, mais etringita e maior a expansão. Portanto, a expansão da etringita nem sempre depende da concentração de CaO, mas depende do valor de pH na solução porosa dentro da pasta. Concluímos que é melhor que a expansão esteja relacionada com o valor de pH do que com a concentração de CaO se há presença de álcali na pasta.

Shan-Ba Wang, Shang-xing Ji, Yin-jiang Liu and Ke-Yong Hu
Wuhan Institute of Building Materials, Wuhan, China

Effect of alkali on the expansive properties of sulfoaluminate cement pastes

Effet de l'alcali sur les propriétés de l'expansion des pâtes du ciment sulfoalumineux

1. Introduction

Alkali(Na_2O+K_2O) is an important minor-component in cements. When cement comes to contact with water, alkali sulfates pass to water rapidly, the alkali in silicate and aluminate also dissolves to the liquid phase with proceeding of cement hydration. Data from Longuet et al /1/ showed that low alkali cement gave rise to alkali concentration of the order of 0.2M. Normal cement, with higher alkali contents might give pore solution of 0.7M or even higher within a month or so. F.M Locher /2/ pointed out that the PH of the pore solution within a high alkali cement pastes might reach a value of 12.9 in two minutes, and 13.7 or higher after 28 days. The addition of gypsum apparently has little effect on PH value. The OH concentration found by Longuet et al /1/ are of the order of 15 times greater than the concentration of saturated $Ca(OH)_2$. H.E Vivian/3/ found that the presence of alkali decreased the solubility of $Ca(OH)_2$. The decreased solubility would change the rate of nucleation and crystallization. Ershov et al /4/ noted that alkali accelerated the formation of ettringite, but Schwiete et al concluded that crystalline ettringite could be formed only in PH=11.5 to 11.8; if PH reached 12.5 to 12.8, non-crystalline materials with composition similar to ettringite was formed. J.E Bailey found /6/ the existence of both crystalline and non-crystalline ettringites in portland cement paste and synthetic system. K.Ogawa et al /7/ found that NaOH accelerated the hydration of $C_4A_3\bar{S}$ and the formation of ettringite, but the expansion of the paste was less than that of the paste without alkali because of the dense structure.

In present paper the expansion of sulfoaluminate cement paste affected by NaOH was study by expansion measurement, strength test, XRD and liquid phase analysis.

2. Materials and experiments

The chemical composition of sulfoaluminate clinker is listed in table 1.

Table 1. the chemical composition of sulfoaluminate clinker

SiO_2	Fe_2O_3	Al_2O_3	CaO	MgO	SO_3	K_2O	Na_2O	Loss
9.30	2.71	30.67	42.55	1.99	11.0	0.08	0.29	0.86

Chemical grade gypsum was used.

Sulfoaluminate cement was manufactured by the mixture of clinker-gypsum ratio 74:26 by weight and ground to less 80μ.

Three kinds of NaOH solution were prepared. The concentrations and PH values are as follows:

Table 2. PH values and concentrations of HaOH solution

concentrations of NaOH	0.06M	0.2M	0.7M
PH values	12.50	12.98	13.28

10x10x60 MM samples were prepared by water-cement ratio(w/c) 0.36 by weight and cured at 20±2 C fog room for 24 hours. After demoulding the lengths of the samples were determined, then the samples were measured at regular intervals.

20x20x20 mm cubic samples were prepared by using distilled water and three kinds of NaOH solution by w/c ratio of 0.36 by weight and cured at 20±2 C, then measured the compressive strength at I,3,7,14 and 28 days.

XRD was carried out for 7-day and 28-day samples.

40:I of water: cement paste at different age was stirred and the filtrates were used for analyzing chemical composition of Liquid phase.

3. Results and discussions

Fig.1 shows the effect of the concentrations of NaOH solutions on the expansions of sulfoaluminate cement pastes. We find that all pastes occur some expansions whether mixed by distilled water or by NaOH solution. The expansion of the paste prepared with 0.06M NaOH solution (abreviate as So.06) is similar to that of the pastes prepared with distilled water (abreviate as So). there is not any difference between them. The expansion of the sample prepared with 0.2M NaOH solution (abbreviate as So.2) is similar to that of So at the early age but greater than that of So at later age. The sample prepared with 0.7M NaOH solution has less expansion than So at 5 days but catches up with and surpasses the expansions of So, So.06, So.2, after 5 days and cracked at 8 days.

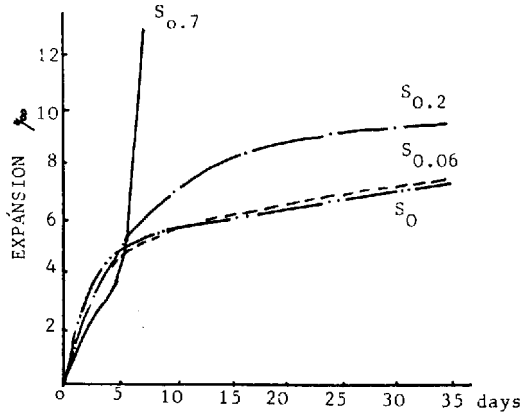

Fig.1 Effect of concentrations of NaOH solutions on expansions of the pastes
So-the paste prepared with distilled water
So.06--the paste prepared with 0.06M NaOH solution
So.2--the paste prepared with 0.2M NaOH solution
So.7--the paste prepared with 0.7M NaOH solution
(same below)

The effect of the concentrations of NaOH solution on the compressive strength is showed in Fig.2 in which the early strengths and maximum strengths of So.06, So.2 and So.7are greater than that of So. From the cuves we find a trend that the strengths of all pastes increase with curing age and drop down after reaching maximal strength. The higher NaOH concentration, the shorter age of reaching maximal strength dropping. The maximal strengths and the ages attaining to maximal strengths for So, So.06, So.2 and So.7 are 50 Mpa 64 Mpa, 68 Mpa, 62 Mpa and 14, 7,7 and 3 days respectively. After that ages the strengths of all pastes decrease, the decreased order is So.7, So.2, So.06 and So. The strength of So.7 lowers to less than that of So at 14 days and drops to 41% of its maximal strength at 28 days.

Shan-Ba Wang, Shang-xing Ji, Yin-Jiang Liu and Ke-Yong Hu
Wuhan Institute of Building Materials, Wuhan, China

Effect of alkali on the expansive properties of sulfoaluminate cement pastes

3.3

Effet de l'alcali sur les propriétés de l'expansion des pâtes du ciment sulfoalumineux

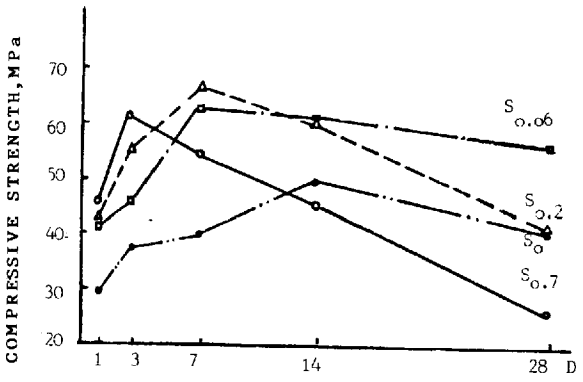

Fig.2 Effect of concentrations of NaOH solutions on compressive strengths of the pastes

From Fig.1 and Fig.2 we can conclude that the higher compressive strength and less expanstion are occurred in sulfoaluminate cement pastes at early hydration ages but less strength and greater expansion,at later ages. This is attributed to the acceleration of $C_4A_3\bar{S}$ hydration and the formation of ettringite.K.Ogawa/7/ believed that NaOH accelerated the hydration of $C_4A_3\bar{S}$. Our results show the acceleration of ettringite formation and increase of expansion of sulfoaluminte cement pastes in the presence of NaOH solution. As we know, sulfoaluminte cement clinker consists mainly of $C_4A_3\bar{S}$ and β-C_2S. Skeikin/8/ noted that alkli accelerated C_2S hydration. K.K Kuataev et al /9/ reported significant increase in the hydration of β-C_2S and C_3S by addition of $SiO_2$with Na_2O or K_2O. In our experiments, more ettringite would be formed in the pastes in the presence of NaOH solution due to the acceleration of $C_4A_3\bar{S}$ and β-C_2S. It has to be pointed out that the expansion at one day was restrained in mould,therefore the pastes prepared with NaOH solution have dense structure and higher early strength, and shorter curing age is needed to obtained maximal strength compared with the paste without presence of NaOH solution. The contribution of ettringite to strength is different at different ages. In early age the skeleton of the structure of the paste is constructed by ettringite and the structure is densified by $Al(OH)_3$ and CSH gel. Because of dense structure and higher strength, the pastes expand small even more ettringite is formed this period. But the effect of ettringite formed is different after the paste reaching to dense structure and the maximal strength, the paste will be exerted a expansive force by the formation of ettringite. Therefore, the higher NaOH solution concentration, the more ettringite formation, the greater expansion, the shorter age of strength decrease and the greater strength decrease. For exsample, So.7 expands gentle compared with So before 5 days, thereon expands rapidly, which coincides with that the strength reaches maximum at 3 days and lowers at 7 days, whereas So hydrates slowly compared with So.7, and the strength and the expansion are gentle. The maximal strength of So occurs at 14 days and the slope of the curve of strenght dropping is less than that of So.2 and So.7, which is in coincidence with the gentle expansion curve. It is the evidence that the intensity of the peaks belong to ettringite enhances with the concentration of NaOH (see Fig.3). For example, the ratio of the intensity of the peaks belong to ettringite is 1:1.15:1.6:3.1 for So:So.o6:So.2:So.7. A great amount of ettringite is an evidence of acceleration of $C_4A_3\bar{S}$ hydration, because Al^{+++} ions in ettringite can be obtained only from the hydration of $C_4A_3\bar{S}$.

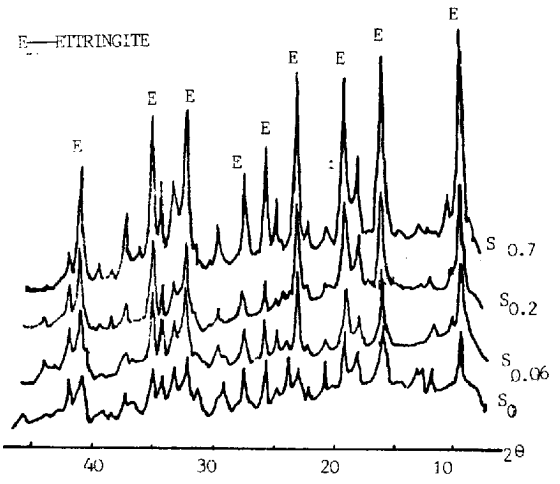

Fig.3 XRD diagrams of the pastes prepared with NaOH solutions different concentration

Fig.4 shows the influence of NaOH concentration on the expansion of $C_4A_3\bar{S}$+8$C\bar{S}H_2$+6CaO Compact. The result proves again that expansions increase with the concentration of NaOH,especially at later age.

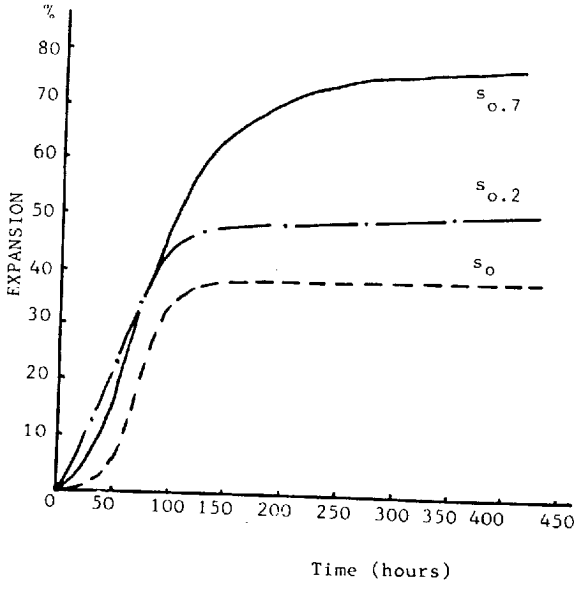

Fig.4 Effect of concentrations of NaOH solution on expansion of compacts of $C_4A_3\bar{S}$+8$C\bar{S}H_2$+6CaO

It should be pointed out that ettringite is not amorphous but crystalline even in the presence of 0.7M NaOH solution (PH=13.3) , the sharper and stronger peaks at 9.1°,15.78° and 22.92° 2θ belong to ettringite gives evidence.

Fig.5 and table 3 show the chemical composition of

Shan-Ba Wang , Shang-xing Ji, yin-Jiang Liu and Ke-Yong Hu
Wuhan Institute of Building Materials, Wuhan, China

Effect of alkali on the expansive properties of sulfoaluminate cement pastes

Effet de l'alcali sur les propriétés de l'expansion des pâtes du ciment sulfoalumineux

liquid phase, in which the concentration of CaO is depressed and the concentration of Al_2O_3 is increased with the NaOH concentration. CaO concentration drops to 0.07g/L from 0.3g/L and Al_2O_3 concentration increases to 0.35g/L from 0.07g/L at one day if NaOH concentration increases to 0.7M from zero. Same trend occurs at other curing ages. This result is similar to the effect of alkali on the solubility of C_3A reported by G.Y Shin /10/. The acceleration of ettringite formation is associated with increase of Al_2O_3 concentration in presence of NaOH, because higher concentration of Al_2O_3 contributes more Al ions to form ettringite.Besides, OH^- ions probably participates in the chemical reaction of forming ettringite According to A.E Moor and H.F.W taylor /11/, ettingite has the formula $\{Ca_6[Al(OH)_6]_2\cdot 24H_2O\}\,3(SO_4)\cdot 2H_2O$,the

Table 3. The concentration of CaO and Al_2O_3 in Liquid phase of the pastes (mg/L)

	1D		3D		7D		14D		28D	
samples	CaO	Al_2O_3	CaO	Al_2O_3	CaO	Al_2O_3	CaO	Al_2O_3	CaO	Al_2O_3
So	360	70	540	58	425	49	320	12	408	-
S0.06	300	80	425	69	369	82	185	49	302	47
S0.2	140	170	212	126	225	167	99	56	277	67
S0.7	70	350	94	226	139	238	14	108	128	197

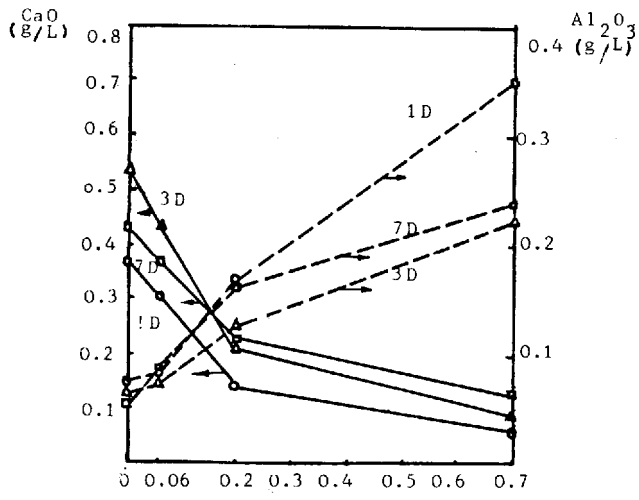

Fig.5 Effect of concentrations of NaOH solutions on chemical composition of the liquid phase in the pastes

columns $\{Ca_6[Al(OH)_6]_2\cdot 24H_2O\}^{6+}$ are based on $[Al(OH)_6]^{3-}$ octahedra running along c axis, each $[Al(OH)_6]^{3-}$ linked to each of its neighbours through three Ca ions, the latter are 8-coordinated by 4 H_2O molecures and 4 OH^- groups (see Fig. 6). There are two H_2O molecures and three SO_4 in the channels of the columns.$[Al(OH)_6]^{3-}$ octahedra consists of Al^{III} and OH^- ions. The increase of Al^{III} and OH^- ions concentration is favorable for forming $[Al(OH)_6]^{3-}$,i.e, favorable for forming the column of ettringite, and hence favorable for forming nuclei of ettringite. Therefore more ettringite are formed and more expansions are produced inthe paste. Most reseacher believed that the expansion of ettringite was associated with the CaO concentration in liquid phase where the ettringite was formed, and the higher CaO concentration in liquid phase,the greater expansion in the paste. It is true if there is not any alkali in cement. In this case, higher CaO concentration is equal to higher PH value in liquid phase. Unfortunately,cement always contain some alkalies, in this case higher PH value is not equal to higher CaO concentration in the pore solution within the cement paste. In our experiments the expansion caused by ettringite formed in higher PH value but lower CaO concentration solution is greater than that in lower PH value but higher CaO concentration solution. From the results that the higher NaOH concentration,the PH value and lower CaO concentration, the greater expansion,we conclude that it is better to relate the expansion of ettringite with PH value than that with CaO concentration. NaOH contributes more OH^- ions and Al^{III} ions due to increase of solubility of Al_2O_3 in the presence of NaOH,which is favorable to form $[Al(OH)_6]^{3-}$,and favorable to form ettringite. If NaOH concentration increase,the concentration of OH^- ions and Al^{+++} ions increase,the ettringite and expansion increase in the paste.

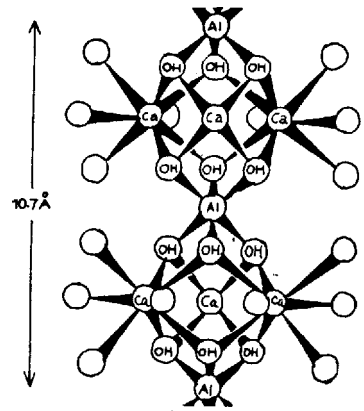

Fig. 6 Part of a single column of ettringite
(after A.E Moor and H.F.W Taylor /11/)

5.Conclusions

From above results and discussions,some conclusions can be drawn:

1). NaOH accelerates the formation and expansion of etteingite in sulfoaluminate cement paste and $C_4A_3\bar{S}+8C\bar{S}H_2+6CaO$ compact, therefore we have to consider the effect of alkali on the soundness of sulfoaluminate cement during the hydration.

2).NaOH increases the strengths of sulfoaluminate cement paste at early ages but decreases the strength at later ages.

3).The ettringite formed even in PH=13.3 environment (0.7 M NaOH solution) is not amorphous but crystalline.

Shan-Ba Wang, Shang-xing Ji, Yin-Jiang Liu and Ke-Yong Hu
Wuhan Institute of Building Materials, Wuhan, China

Effect of alkali on the expansive properties of sulfoaluminate cement pastes

Effet de l'alcali sur les propriétés de l'expansion des pâtes du ciment sulfoalumineux

4).As NaOH concentration increases,CaO concentration decreases and Al_2O_3 concentration increases,ettringite and expansion of the paste increase. We conclude that it is better to be related the expansion of ettringite with PH value than that with CaO concentration because the expansion of ettringite does not always depend up CaO concentration but depends upon PH value in the liquid phase. The higher PH value,the lower CaO concentration and the greater expansion in sulfoaluminate cement paste in the presence of NaOH.

Reference

1/,2/,8/,9/ cited from I.Jawed and J.Skalny: Cem. Concr. Res. Vol.8,No.1, pp37-52,1978
3/,4/ cited from J.Salny and J.F Young: Hydration of pure portland cement 7th ICCC, Paris,1980
5/,6/ cited from J.E Bailey: On the structure of some precipitated Calcium Alumino-Sulphate hydrates J. Mater. Sci. (17) 1982
7/ K.Ogawa and D.M Roy: Cem. Concr. Res. Vol.12, No.2, pp247-256, 1982
10/ G.Y Shin and F.P Glasser; Cem. Concr. Res. Vol.13, No.3, pp 366-376, 1983
11/ A.E Moor and H.F.W Taylor: Crystal structure of ettringite ACTA. Cryst. B266 p386 1970

Xue Jungan, Senior Engineer, Vice Director, Cement Research Institute;
Tong Xueli, Engineer; Chen Wenhao, Senior Engineer; Xu Jizhi, Xi Yaozhong, Zhang Yiyu, Engineers
Research Institute of Building Materials, Beijing, China

STUDY ON HIGH SELF-STRESS ALUMINATE CEMENT

SUMMARY: At present the self-stress (SS) values of SS cement produced at home and abroad are 2.0-4.0 MPa for SS silicate cement and 4.5-6.0 MPa for SS aluminate cement and SS sulfo-aluminate cement.
High SS aluminate cement of SS value 7.0-10.0 MPa has been produced. The development of this cement is based on a study into the expansive characteristics of ettringite under semi-saturated CaO concentration and also on the practice in the production of ordinary SS aluminate cement. XRD and DTA have been employed in the study of the hydration products and the rate of hydration. Results show that the hydration products of high SS aluminate cement are similar to those of ordinary SS aluminate cement. They are ettringite and hydro-alumina gel. However, the rate of hydration of the high SS aluminate cement is higher than that of the ordinary SS aluminate cement. According to the study on pore size distribution of the hardened pastes, the most probable radius of the high SS aluminate cement paste is slightly larger than that of the ordinary SS aluminate cement but smaller than that of SS silicate cement. Its resistance to water permeation is still satisfactory. High SS aluminate cement and high pressure water pipes made from this cement have been produced in batches. Concrete pipes of inside diameter 720 mm passed the 3.0 MPa water pressure inspection test. The destructive water pressure for the ones of inside diameter 950 mm has reached 2.2 MPa. The SS value of concrete for these penstocks reached 8.0 MPa. The results of their experimental use at four small hydropower stations with water heads of 100-200 m for a period of 2-5 years are good. In December, 1983, the high SS aluminate cement and the penstocks made from it were approved by a technical appraisal committee.

Atualmente os valores de auto-estressamento (SS) de cimento SS produzido regionalmente e externamente são de 2,0 - 4,0 MPa para cimento SS de silicato, e 4,5 - 6,0 MPa para cimento SS de aluminato e cimento SS de sulfoaluminato.

Foram produzidos cimentos de aluminato com alto SS, com valores de SS de 7,0 - 10,0 MPA. O desenvolvimento deste cimento está baseado num estudo das características expansivas da etringita sob concentração semi-saturada de CaO, e também na prática de produção de cimento de aluminato SS comum. Foram empregados XRD e DTA no estudo dos produtos de hidratação e da velocidade de hidratação. Os resultados mostram que os produtos de hidratação do cimento de aluminato com alto SS são semelhantes aos do cimento de aluminato SS comum. Estes produtos são etringita e gel de hidro-alumina. Contudo, a velocidade de hidratação do cimento de aluminato com alto SS é maior do que a do cimento de aluminato SS comum.

De acordo com o estudo da distribuição de tamanho de poro das pastas endurecidas, o raio mais provável da pasta de cimento de aluminato com alto SS é ligeiramente maior que o do cimento de aluminato SS comum, mas menor que o do cimento de silicato SS. Sua resistência à permeabilização por água é ainda satisfatória.

Cimento de aluminato com alto SS e manilhas de alta pressão feitas com este cimento forma produzidos em bateladas. Manilhas de concreto com diâmetro interno de 720 mm resistiram a teste de inspeção com pressão de água de 3,0 MPa. A pressão destrutiva de água para manilhas com diâmetro interno de 950 mm foi atingida a 2,2 MPa. O valor SS do concreto para estas adutoras foi de 8,0 MPa. Os resultados do seu uso experimental em quatro pequenas usinas hidrelétricas com carga de água 100 - 200 m, por um período de 2 - 5 anos, foram satisfatórios. Em dezembro/83 o cimento de aluminato com alto SS e as adutoras feitas com ele foram aprovados por uma comissão técnica de avaliação.

INTRODUCTION

At present, self-stress value of several kinds of SS cement produced in our country is 2-6 MPa, (1), (2), (3) while the actural SS value of the SS cement concrete used in abroad is about 3.5 MPa (4), (5), (6), (7). Studies have been made in collaboration with Shanghai White Cement Mill to develop high SS aluminate cement. High-pressure pipes made from this cement have been used in a small hydroelectric station with 100-200 m water head for 5-7 years.

DEVELOPMENT AND PERFORMANCE OF THE CEMENT

1. The concept and the selection of raw materials

Aluminate clinker-gypsum system is selected according to theoretical studies (8), (9) on the expansive characteristics of ettringite under semi-saturated CaO concentration and to the practice in the production of SS aluminate cement. It is possible to obtain a compact hardened cement paste of well-matched strength and expansion and high SS value so long as an adequate amount of ettringite and hydro-alumina gel are formed at a definite rate.

The chemical composition and mineral composition of the aluminate clinker are listed in Table 1.

The SO_3 content of gypsum dihydrate used exceeds 40%.

2. Study on the technological factors affecting SS value

1) Alkalinity coefficient (Am) of aluminate clinker

With the increase in the alkalinity coefficient, the ratio of CA/CA_2 in the clinker is increased, the rate of hydration becomes higher and the SS value rises (Fig.1).

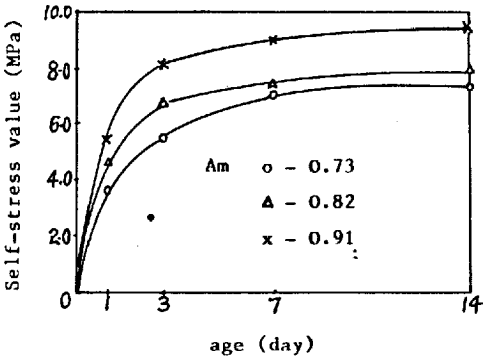

Fig.1 Effect of alkalinity coefficient (Am) of clinker on SS value of cement

2) SO_3 content in cement

With the increase in SO_3 content the SS value and free expansion are increased (Fig.2, 3) but the strength is to a certation extent lowered.

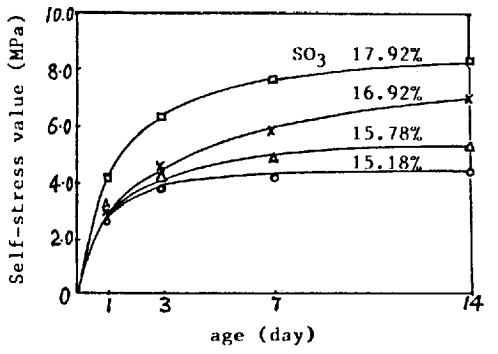

Fig.2 Effect of SO_3 content in cement on SS value

Table 1 Chemical composition, alkalinity coefficient (Am) and mineral composition of aluminate clinker

Chemical composition (%)						Am and mineral composition (%)						
SiO_2	Al_2O_3	Fe_2O_3	TiO_2	CaO	MgO	Am	CA	CA_2	C_2AS	CT	C_2F	MA
2.29 | 5.04	54.29 | 56.93	2.29 | 2.90	2.02 | 3.34	33.34 | 34.79	0.28 | 0.81	0.83 | 0.96	45.95 | 70.41	5.73 | 19.13	13.32 | 23.03	3.43 | 5.68	3.89 | 4.93	0.99 | 2.86

3.3

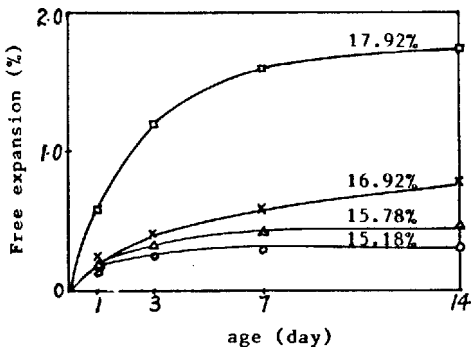

Fig.3 Effect of SO_3 content in cement on free expansion

3) water curing temperature

The higher the water curing temperature is, the faster the cement hydrates. At a water curing temperature of 40°C high SS value can be obtained in 7 days.

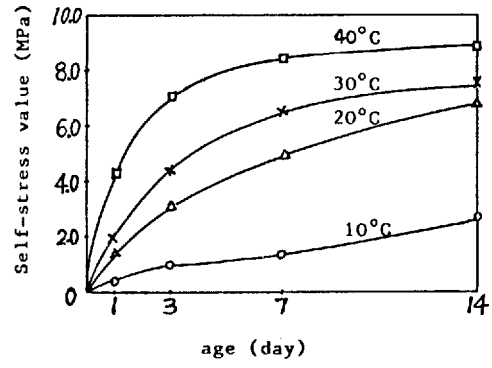

Fig.4 The affect of water-curing temperature on SS value

3. Cement performance

1) quality indexes

The initial setting time of such a cement should not be earlier than 30 minutes and the final setting time should not be later than 3 hours.

Its 1:2 plastic mortar after 14 days water curing at 40°C should have a SS value of 7-10 MPa, a free expansion of less than 3.0% and a compressive strength of no less than 30 MPa. The performance of a batch of 1400 ton high SS aluminate cement produced is up to the standards mentioned above (Table 2).

2) long-term stability in volume

The specimens that had been water-cured for 14 days at 40°C were placed in water at a constant temperature of 20°C for long-term curing of 2-5 years. As compared with the values at 14 days, the SS values at 2-5 years have increased by 0.3-0.7 MPa and free expansion has increased by 0.13-0.19% (Table 3).

3) resistance to permeation

1:2 mortar conical disk and concrete pipe sections of Ø140 mm were prepared for permeation resistant test, and no leakage were noted under water pressure of 4 MPa.

4) dry shrinkage

SS is reduced by 25% after 6-month natural drying and can be restored after water recuring to above 90% of the value obtained at 14 days. However, after drying for two years, the SS value is reduced by 40% and does not increase after recuring in water.

Table 2 Performance of high SS aluminate cement produced by factories

Number of specimens	Setting time		Self-stress value (MPa)				Free expansion (%)				Compressive strength (MPa)			
	initial	final	1d	3d	7d	14d	1d	3d	7d	14d	before water curing	3d	7d	14d
6029	1:03	1:54	5.2	6.8	8.2	8.3	0.61	1.18	1.84	2.15	15.9	44.0	43.4	55.0
6022	1:38	2:38	5.4	7.8	8.4	8.6	0.71	1.56	2.17	2.34	8.0	42.5	47.0	46.5
6027	1:22	1:42	4.8	7.4	8.7	9.7	0.54	1.06	1.53	1.87	14.5	50.0	46.8	51.5

3.3

Table 3 Long-term volume stability of high SS aluminate cement

Number of specimen	Self-stress value (MPa)						Free expansion (%)					
	14d	1y	2y	3y	4y	5y	14d	1y	2y	3y	4y	5y
6029-1	8.3	8.8		8.8		8.9	2.15	2.34		2.34		2.34
6029-3	8.2	8.4				8.5	2.43	2.55		2.56		2.56
80-20	8.4	9.1	9.1				2.20	2.36	2.36			
M-49	8.6			9.1	9.3		2.70			2.69	2.68	

4. Materials science study on the hardened paste of high SS aluminate cement

1) phase composition and rate of hydration

The XRD shows that hydration products of high SS aluminate cement paste are ettringite and hydro-alumina gel. They are the same as the hydration products of ordinary SS aluminate cement. The height of XRD characteristic peaks of hardened pastes were compared to assess the change in the amount of various phases. The characteristic peaks chosen are: ettringite - 9.8 Å; dihydrate gypsum - 7.6 Å; hydro-alumina gel - 4.83 Å; and CA - 2.29 Å (see Fig.5). It can be seen that as hydration progresses, the ettringite and the hydro-alumina gel are increased while CA and dihydrate gypsum are reduced. Moreover, most of the hydration takes place within 7 days. This agrees with the rate of growth of SS value of this cement. Besides, by comparison of the test specimens cured in 20°and 40°C water, it can be noted that curing in water of 40°C will accelerate the formation of ettringite and hydro-alumina gel, and bring self-stress into play earlier, and the ultimate SS value of this cement is higher.

2) texture of hardened paste

Pore size distribution of the paste at various ages of water curing at 40°C is determined by using mercury porosimetry. The results show that the texture of hardened paste is getting denser with the increase of SS value (Fig.6).

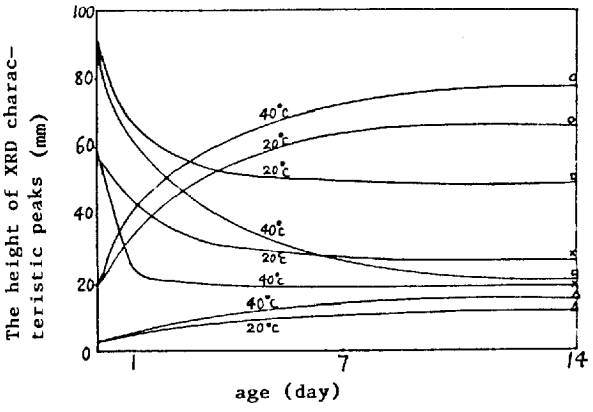

Fig.5 XRD of hardened cement paste for water curing at 20°C and 40°C
o - ettringite Δ - hydro-alumina gel
□ - gypsum x - CA

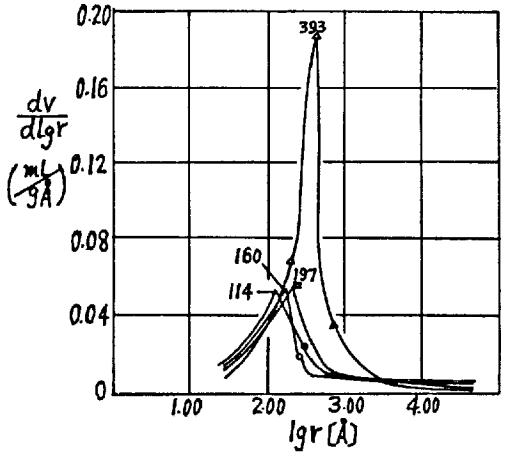

Fig.6 Pore size distribution of hardened cement at different ages
Δ - before water curing □ - 1 day
o - 7 days ● - 14 days

3.3

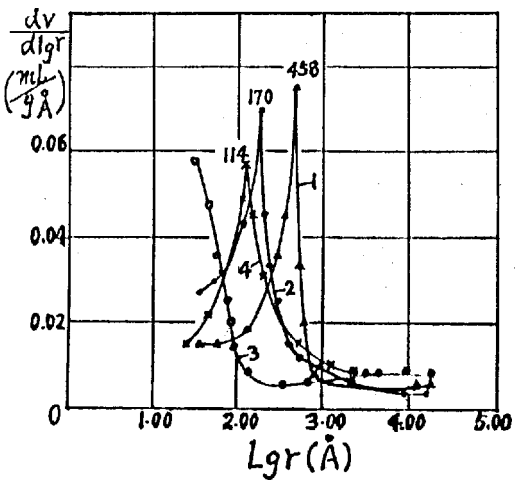

Fig.7 The pore size distribution of four hardened cement pastes

1. ordinary portland cement, three months
2. SS silicate cement, 28 days
3. SS aluminate cement, 28 days
4. SS high aluminate cement 14 days

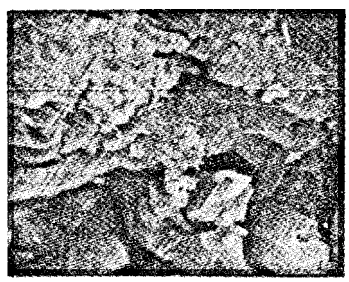

(a)

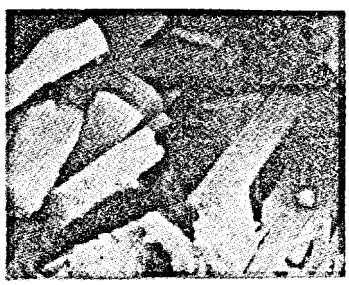

(b)

Fig.8 The texture of high SS hardened aluminate cement paste in 5 years (SEM x 2000)

From Fig.7, the density of high SS aluminate cement is lower than that of ordinary SS aluminate cement, but higher than that of ordinary portland cement and self-stress portland cement. SEM observation (Fig.8) of the fractured surface of 5 years old hardened paste shows that hydro-alumina gel grains are seen filling up the space between ettringite particles (Fig.8 a). The grains, < 0.1 μm across, exist as aggregate. The morphology of ettringite particles in the pores is clearly discernible (Fig.8 b).

DISCUSSION

A large amount of ettringite and alumina gel are formed in the hydration of high SS aluminate cement. As the two compounds form in the same chemical reaction under semi-saturated CaO concentration, the strength development of the hardened paste is in harmony with the development of expansion. The texture of the paste becomes denser with the hydration and high self-stress value is produced. The fact that hydration products remain unchanged over a long period of time and that the increase in late age expansion remains low, suggest that the hardened paste of this cement has a good long term stability.

APPLICATION OF HIGH SS ALUMINATE CEMENT

1. Development of penstock

Penstocks of Ø720 mm and Ø950 mm with water pressure of 1.8-3.0 MPa have been developed by the Research Institute of Building Materials in collaboration with a related designing institute and penstock factory. The actual SS value of conduits has reached 8 MPa. The conduits that have been dried in the atmosphere may be used after recuring in water for a period of time.

2. Examples of application of pipe-lines

High SS aluminate cement concrete pipes of Ø500, Ø720 and Ø950 mm have been used at 3 hydropower stations with 100 - 200m water head for 5-7 years. The performance is satisfactory.

CONCLUSION

1. SS value of high SS aluminate cement prepared with certain aluminate clinker and appropriate amount of gypsum and cured in water at 40°C for 14 days attains 7-10 MPa.

2. Materials science study indicates that ettringite and hydro-alumina gel in the high SS aluminate cement paste are formed in the same chemical process under semi-saturated CaO. In this case, the strength development of the hardened paste is in harmony with the development of expansion. The texture of the paste becomes denser with the hydration and high self-stress value is produced.

3. High-pressure conduits of Ø500-Ø950 mm with water pressure of 1.8-3.0 MPa can be made from high SS aluminate cement. They are applicable to samll hydroelectric station as conduit pipe-lines with 100-200 m water head.

REFERENCES

1. JC 218-79, Self-stress Portland Cement (Standard Issued by the State Administration of Building Materials Industry)

2. JC 214-78, Self-Stress Aluminate Cement (Standard Issued by the State Administration of Building Materials Industry)

3. Ji Q/shi S 180-182, Self-Stress Sulfo-Aluminate Cement (Local Standard Issued by Heber Province)

4. V.V. Mikhailov, I.V. Kravchenko, Proceedings of the Fourth International Symposium on the Chemistry of Cement, Washington, 1960, Vol.2, 927(1962)

5. V.V. Mikhailov, Klein, Symposium on Expansive Cement Concrete, ACI Pub, SP-38, 415(1972)

6. M. Polivka, Klein, Symposium on Expansive Cement Concrete, ACI Pub, SP-438(1972)

7. P.K. Mehta, M. Polivka, Preceedings of the Sixth International Symposium on the Chemistry of Cement, Moscow, 1974, 3, 158(1976)

8. Xue Jungan, Chen Wenhao, Tong Xueli, Zhao Yuping and Xu Jizhi, 7th International Congress on the Chemistry of Cement, Vol.III V-33 (1980, Paris)

9. Cement Research Institute, Research Institute of Building Materials, Journal of the Chinese Silicate Society, Vol.VI, No.1-2, 15(1978)

J.HOSEK, K.KOLAR, J.NOVOTNY, Faculty of Civil Engineering, Technical University in Prague, Czechoslovakia.

SHRINKAGE PROBLEM OF QUICK-SETTING CEMENT

SUMMARY: The modification of portland cement investigated in laboratories of Technical University in Prague enables to regulate the rate of hardening in very wide range. By the combination of ligninderivates with alkalicarbonates applied during the grinding of clinker we obtain a very fine cement and both plastification and acceleration effects.

To verify if the fineness and new chemical composition provoke also excessive shrinkage, showed to be a serious experimental problem. The existing methods are not suitable for measuring of rapid rate of hardening.

The principaly new method using the rubber bellows as the lost mould and combination of LVDT transducers with strain gauges enables to follow the course and variation of volume changes, temperature gradient and internal stresses during hardening of cements with different proportion of components.

The actual extent of shrinkage is the result of combined effect of thermal expansion and volume changes due to rigid structure formation. The rapid transition from quasiliquid to solid state affects the early shrinkage of clinker-ligninderivate-alkalicarbonate system.

A modificação de cimento portland, investigada em laboratórios da Universidade Técnica de Praga, permite regular-se a velocidade de endurecimento em escala muito ampla. Com a combinação de lignoderivados com carbonatos alcalinos, aplicados durante a moagem do clínquer, obtemos um cimento muito fino e os efeitos de plastificação e aceleração.

Para verificar se a finura e a composição química nova provocam retração excessiva, defrontamo-nos com um problema experimental sério. Os métodos existentes não são adeqüiados para medição da velocidade rápida de endurecimento.

Principalmente o novo método que usa foles de borracha como molde perdido e uma combinação de transdutores LVDT e medidores de deformação, nos permitem seguir o curso e variação de mudanças de volume, gradiente de temperatura e tensões internos durante o endurecimento de cimentos com diferentes proporções de componentes.

A grandeza real da retração é o resultado do efeito combinado da expansão térmica e das mudanças de volume, conseqüentes da formação da estrutura rígida. A rápida transição do estado quase-líquido para o sólido afeta a retração inicial do sistema clínquer-lignoderivado-carbonato alcalino.

J.HOSEK, K.KOLAR, J.NOVOTNY, Faculty of Civil Engineering, Technical University in Prague, Czechoslovakia.

INTRODUCTION

Quicksetting cements of Czechoslovak production belongs to the category of modified ordinary portland cements. The modification is realized in the phase of clinker grinding process by addition of ligninderivates in combination with salt of alkaline metals instead of gypsum (1, 2).

An intensification effect of ligninderivates enables to achieve extremely fine sizes of cement particles under 5 μm at relatively low energy costs (Fig. 1).

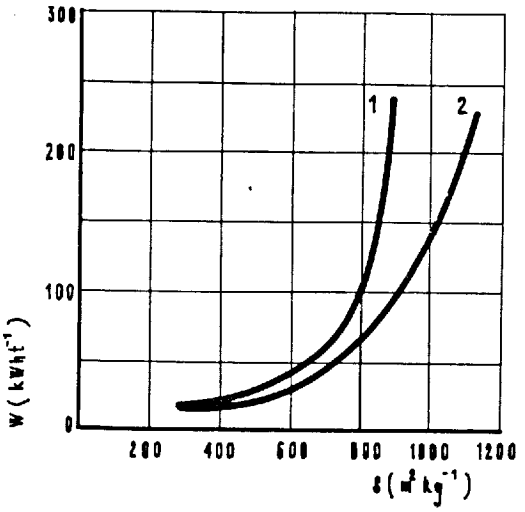

Fig. 1 - Dependence of the grinding energy W on the specific surface S

1 - cement clinker

2 - with active ingredient system

Hardening is accelerated by finer grinding in such rate (Tab. I), that without adding suitable types of alkaline salts the concrete mixtures are not workable (Fig. 2).

The high initial strength developed by cement at early ages and the relative decrease with rising w/c ratio is shown in Table II. The effect of fineness, gypsum absence (3) and chemical additives on the rate of hardening is evident.

TABLE I

Specific surface $m^2\ kg^{-1}$	Setting time (min.)	
	initial	final
274	355	595
475	75	110
680	35	40
851	7	8

Tab. I - Setting time by Vicat needle test at the same doses sodium ligninsulfonate and sodium carbonate

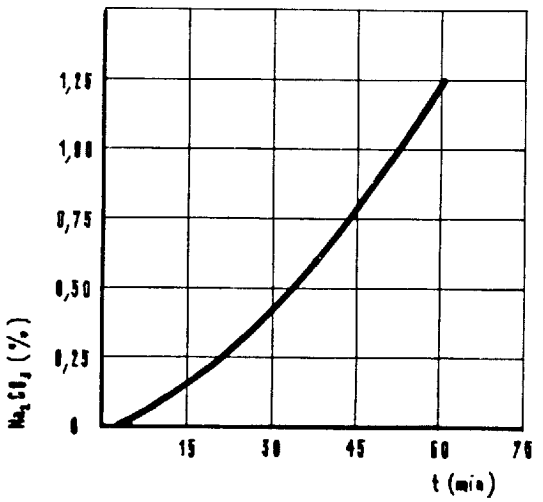

Fig. 2 - Initial setting time of the cement (650 $m^2 . kg^{-1}$) at a constant dose of sodium ligninsulfonate and different amount of sodium carbonate

With regard to the strength properties and further advantages of pastes mortars and concretes made from this cement as are rheological behaviour, adhesion and higher resistance to the action of aggressive chemical agents, the first applications has been directed towards the injection technique, reconstruction works and protective layers. For this plan it has been necessary to get information about the contraction during hardening.

J.HOSEK, K.KOLAR, J.NOVOTNY, Faculty of Civil Engineering, Technical University in Prague, Czechoslovakia.

According to the valid ideas about the hydration process just chemical composition and fineness of the cement are the main factors affecting the early shrinkage yields to stresses and cracks in structure (4, 5).

TABLE II

Time h	Compressive strength (MPa)		
	w = 0,23	w = 0,26	w = 0,29
3	1,4	0,9	0,6
6	4,5	2,1	1,3
24	26,7	24,4	14,8
48	40,0	36,2	27,5
72	43,7	38,7	29,7

Tab. II - Rate of strength development, cement paste (cement 650 $m^2 \cdot kg^{-1}$), sodium ligninsulfonate (1,0 %) + sodium carbonate (0,8 %) + condensation product of sulfonated phenols and formaldehyde (0,5 %)

METHODS OF SHRINKAGE MEASUREMENT

Present methods of shrinkage measurement do not make possible to get a reliable picture about the complete time-course of volume changes during hardening process. Regarding to the rapid transition of water-cement system from quasiliquid paste to the solid state, it is impossible to use dilatometers with the beginning of measuring after removal of test samples out of mould, when the main part of quicksetting cements shrinkage is already finished.

Errors appear also within the measuring in the split mould with moving clips or with sunk probes (6) because adhesive forces (skin friction) restrained the free movement to develope the stresses

$$\sigma_s(t) = \varepsilon_s(t) \cdot E(t) \qquad (1)$$

where deformation ε_s and modulus of elasticity E are time-dependent quantities.

Even though the theoretical analysis is very difficult because of the experimental troubles to evaluate the changes of above named quantities, we can estimate the limits of ultimate strain for concrete if the mould does not resist the deformation: for the case of bond failure in the moment when tension stresses approaches to the tensile strength, for possible values of adhesive forces σ_{ad} = 0,2; 0,1; 0,05; 0,01 $N.mm^{-2}$ the correspondent dimensional changes of concrete element would reach the value ε_s = 0,06; 0,05; 0,04; 0,03 ‰ which is more than quarter of whole concrete shrinkage in moisture atmosphere.

With regard to these facts we tried to measure the volume changes of cement mixtures on principle in a new way, using the rubber bellows as a "lost mould" (7). The resistance of bellows shape to longitudinal deformation is insignificant (1/180 value of cylinder with the same parameters). It has been verified experimentally that the bellows mould 160 mm high, of diameter 70 mm, made from rubber 40°Sh affects the 1 ‰ deformed concrete by the force of 0,0208 N, which develops in the concrete body a fully negligible tension $5,4 \cdot 10^{-6}$ $N \cdot mm^{-2}$.

The testing equipment (Fig. 3) consists of fixing bench which partly prevents the deviation of rubber mould in horizontal direction, partly serves as a base for fixing the LVDT transducers.

The rubber mould is provided with removable thin metallic plate for connection with tested sample. The contact between the inductive sensors without its own directive force and sample is interposed just through this plate.

The Data-advision system Autolog 900 fy Peekel has been used for direct recording of volume changes.

J.HOSEK, K.KOLAR, J.NOVOTNY, Faculty of Civil Engineering, Technical University in Prague, Czechoslovakia.

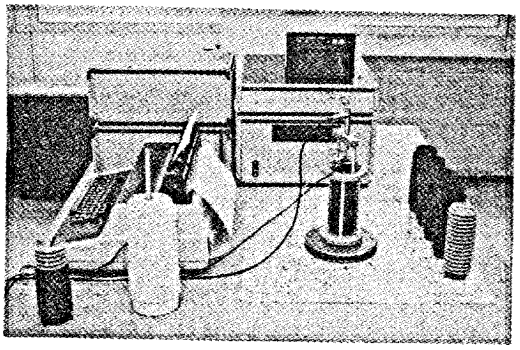

Fig. 3 - Volume changes measurement by the method of lost mould

Measurement range of LVDT transducers was 20 mm and sensitivity 0,0013 mm. The hydration heat of the investigated mixtures has been measured as a change of temperature by Cu-Ko termocouples and the shrinkage stresses by couple of tubular strain-gauges isolated against water penetration. The second strain-gauge was a compensation to heat effects: it was located inside the cylindrical box so that the values corresponded to the heat effect only.

EXPERIMENTAL

Cement mixtures were always compacted by vibration in rubber bellows moulds of the following size: high h = 160 mm, internal diameter d_1 = 50 mm, external diameter d_2 = 70 mm. Immediately after 2 min. vibration the termocouple and straingauges were immersed into the tested mixture through the gap between mould and metallic plate. On the end the inductive sensor was touched to the plate. All procedure keeps 5 to 6 minutes.

Originally made measurement, concentrated on time recording of the shrinkage only, did not enable to read off the beginning of the hardening. Therefore it has been extended by the simultaneous recording of the temperature and tension. In this combination the characteristic curves of many different mixtures based on quicksetting cement were realized.

The record of cement pastes with three fixed water/cement ratio w = 0,23; 0,26; 0,29 is shown in Fig. 4.

The characteristic of quicksetting cement: specific surface 650 $m^2 . kg^{-1}$, active ingredient system see Tab. II.

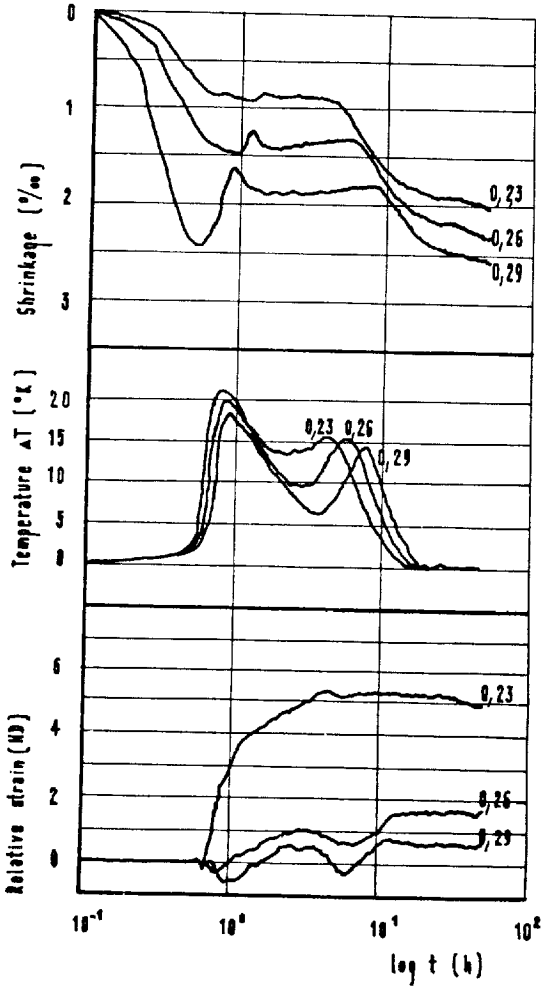

Fig. 4 - Time dependence of volume changes, heat of hydration and shrinkage stresses for cement pastes of different w/c ratio

J.HOSEK, K.KOLAR, J.NOVOTNY, Faculty of Civil Engineering, Technical University in Prague, Czechoslovakia.

DISCUSSION

From the experimental results it is evident that gypsum free cement of high specific surface 650 $m^2 . kg^{-1}$, with active system ligninsulfonan - sodium carbonate starts to hydrate very shortly after mixing. The rapid hardening is caused by the changes in chemical composition and by fineness of the clinker. The heat evolution at ordinary temperature characterized by the first peak nearly corresponds with the setting time of these cements which indicates abudant formation of aluminate hydrates.

High strength after a few hours of hardening is probably produced by means of special chemical additives and depends also on the w/c ratio.

For the estimation of the beginning of structure shrinkage has the main importance the lower diagram on the Fig. 4 which indigates the origin of tensile stresses tending to pull the capillary walls in rigid structure closer together. It has to be the moment of the transition of quasiliquid cement paste to the solid cement stone.

The actual extent of the shrinkage is the result of combined thermal expansion which develops the compressive stresses and volume changes due to forming an integral capillary system accompanied by tensile stresses. It leads to the decreased early shrinkage.

This fact and rapid growth of strength at early age explain why no cracking occure due to hardening. That the shrinkage of this type quicksetting cement composition is in the limits of ordinary cement has been proved by the field experiences.

CONCLUSIONS

From the results obtained in this study the following conclusions could be derived:

1) Method of rubber bellows-lost mould makes possible to follow the volume changes of quicksetting cement mixtures during the whole hydration process.

2) Simultaneous measurement of hydration heat and rise of internal tension is necessary for determination of the beginning of rigid structure formation.

3) Mixture on the base of gypsum free quicksetting cement when regulating system ligninsulfonate-sodium carbonate is used shrink in the limits of ordinary portland cement.

BIBLIOGRAPHY

1.- J.NOVOTNÝ, K.KOLÁŘ, F.ŠKVÁRA, Z.ZADÁK, Z.BAŽANTOVÁ (1979), Stavivo 57, No.2, 44-49.

2.- K.KOLÁŘ, F.ŠKVÁRA, J.NOVOTNÝ, Z.ZADÁK, V.ŠATAVA, J.ŽEŽULKA, Z.BAŽANTOVÁ, V.WEISS, US Patent 4, 168.985 (1989)

3.- W.LERCH, Proc.ASTM 46 (1948), 1252

4.- A.A.RAHMAN, D.D.DOUBLE, Cem.and.Conc.Res. (1982) 12, 33.

5.- W.CZERNIN, Cement Chemistry and Physics for Civil Engineers (1980), New York.

6.- L.BRULL, K.KOMLOŠ, Proc.of the Europ. Conf. on Building Materials (1981), 13-18.

7.- J.HOŠEK, Stavební výzkum (1986), 4, in press.

Y. HALSE & P. L. PRATT, Department of Metallurgy & Materials Science, Imperial College, Prince Consort Road, London SW7 2BP, UK.

The development of microstructure in high alumina cement

SUMMARY: The development of the microstructure in the early hydration of high alumina cement under various conditions has been investigated and the associated changes in hydration products have been determined. The first week of hydration of neat cement in tap water at 8 °C, produces mainly alumina gel together with the crystalline hydrate CAH_{10}. After 4 months hydration, small amounts of conversion product (C_3AH_6) have been detected, but the gel has not yet changed to crystalline AH_3. When the cement is hydrated in tap water at temperatures of 23 °C and 40 °C, the conversion reaction starts after 7 days and 12 hours respectively. The alumina gel structure also varies with hydration temperature.

The microstructure development suggests that the bonding starts earlier at 8 °C and 40 °C than at 23 °C, whereas the rate of the hydration increases with temperature.

The rate of hydration in seawater at 8 °C is retarded compared with that in tap water. CAH_{10} and alumina gel are the initial products and C_4AH_{13} has been detected after 12 hours.

Foi investigado o desenvolvimento da microestrutura na hidratação inicial de cimento alto-aluminoso sob várias condições, e foram determinadas as mudanças associadas nos produtos de hidratação. A primeira semana de hidratação do cimento puro em água natural a 8°C produz principalmente gel de alumina juntamente com o hidrato cristalino CAH_{10}. Depois de 4 meses de hidratação, foram detectadas pequenas quantidades de produto de conversão (C_3AH_6), mas o gel ainda não se mudara em AH_3 cristalino. Quando o cimento é hidratado em água natural a temperaturas de 23°C e 40°C, a reação de conversão começa depois de 7 dias, e 12 horas, respectivamente. A estrutura do gel de alumina também varia com a temperatura de hidratação.

O desenvolvimento da microestrutura sugere que a ligação começa mais depressa a 8°C e a 40°C do que a 23°C, enquanto a velocidade de hidratação aumenta com a temperatura.

A velocidade de hidratação em água marinha a 8°C é retardada em comparação com a da água natural, CAH_{10} e gel de alumina são os produtos iniciais, e depois de 12 horas foi detectado C_4AH_{13}.

INTRODUCTION

HAC is not a suitable material for building construction, because of weakening caused by the conversion reaction of the cement products (1,3). On the other hand, in contrast to ordinary Portland cement, the material is very resistant to sulphate attack (2).

The phase that is concerned in the early stage of hydration is CA, the hydration process usually being represented (2) as

Temperature	Reaction
< 23 °C	$CA \rightarrow CAH_{10}$ + alumina gel
23-25 °C	$CA \rightarrow C_2AH_8$ + alumina gel
> 35 °C	$CA \rightarrow C_2AH_8$ + alumina gel
	$\rightarrow C_3AH_6 + AH_3$ (Gibbsite)

Both CAH_{10} and C_2AH_8 have a metastable hexagonal crystal structure converting to cubic C_3AH_6 crystals under warm and moist conditions. The conversion involves an increase in porosity due to the difference in density of the reactant and product, causing a dramatic decrease in the strength (3).

In this paper the changes in the microstructure during hydration at temperatures between 0 °C and 40 °C have been observed in a scanning electron microscope, so that some knowledge of the development of the bonding of the pastes, and of the conversion reaction, can be obtained. In order to characterise the hydration products, the hydrated pastes have been examined using X-ray diffraction and DTA methods.

MATERIAL

HAC and ordinary Portland cement have substantially different oxide compositions, the typical ranges being shown in Table 1.

Table 1 Chemical compositions in HAC and OPC

Oxides	HAC (wt %)	OPC (wt %)
CaO	35-39	65-69
Al_2O_3	37-41	2-7
SiO_2	3.5-5.5	20-25
Fe_2O_3	9-12	0.25-3.5
FeO	4-6	-
TiO_2	1.5-2.5	0.2
MgO	0.5-1	0.4-2

The phases present in HAC have not all been well established, but the dominant one is monocalcium aluminate (CA). Table 2 shows typical phase compositions in HAC.

Table 2 Phase compositions in HAC

Composition	Wt (%)
CA	60
C_2AS	5-20
Pleochroite (C_3A_2F)	5-15
$C_{12}A_7$, Ferrite phase, FeO, C_2S	5-30

EXPERIMENTAL METHODS

a) Preparation of specimens

The cement was mixed with either tap water or seawater at w/c = 0.4 and sheared by hand using a spatula for about 3 minutes. The paste was cast into cylindrical polystyrene bottles which were stored in a temperature controlled water bath, the tap water specimens at 40 °C, 23 °C, and 8 °C, the seawater paste at 8 °C.

b) Microscope sample preparation

The hardened pastes were removed from the water bath at various ages and broken by tension to obtain a fracture surface, which was then coated with gold for SEM examination using secondary electron imaging. Other specimens were prepared with cut and polished flat surfaces for back-scattered electron (b.s.e.) imaging.

c) X-ray diffraction

The X-ray powder samples were prepared by hand-grinding in an agate mortar. The diffractomer traces were obtained with a Philips PW 1710 system using Cu-K_α radiation.

d) DTA analysis

The DTA was carried out on about 40 mg of sample, using a Stanton Redcroft model 780. The analyses were performed between 30 °C and 550 °C in a nitrogen atmosphere with a heating rate of 10 °C/min, and a gas flow rate of 50 ml/min.

RESULTS AND DISCUSSION

The phase distribution in the anhydrous HAC grains is very different from that in OPC since the former is produced via a crystallization process from the liquid phase. The back-scattered image (Fig.1) shows that most of the grains are multiphase with some 50% of CA (dark grey colour) and a mixture of other minor phases (light colour). There are also some single phase grains which are either CA or pleochroite.

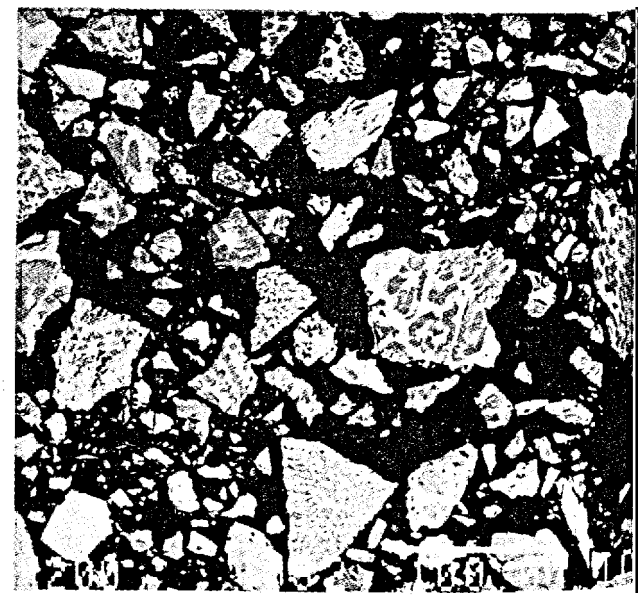

FIG.1 B.s.e. image of unhydrated HAC

a) Hydration at 8 °C in tap water

CAH_{10} is the only crystalline product found by X-ray but the major hydrate phase is alumina gel, as has been shown by DTA. Crystalline AH_3 (Gibbsite) has not been detected in the 4 months old sample, however small amounts of cubic C_3AH_6 have been found. The initial product, after 2 hours hydration, is mainly alumina gel which is very difficult to observe under the microscope. The bonding between the particles builds up quickly after 4 hours hydration when large amounts of gel and small hexagonal platelets have been formed (Fig.2). The gel appears in a short spikey form due to the effects of drying. As time goes by, the hexagonal plates grow in number and size to form a radiating spheroidal cluster, while the gel becomes much more dense, losing its earlier rod-like appearance after 6 hours (Fig.3), although long gel rods can still be observed in the porous areas.

After 9 hours, Fig.4 shows that there are many Hadley grains, consisting of shells of hydration product separated from the anhydrous core within them. Part of this separation in the grains on the right of Fig.4 is due to the opening of drying shrinkage cracks. Part may be caused by shrinkage of the gel material in the shell away from the core. The central grain at the bottom and the two grains on the left of the figure show clearly that early hydration involves dissolution of the CA preferentially from the surface of the multi-phase grains and precipitation of hydration products in the original water-filled space outside the shells. The shells are stabilised by the crystalline hexagonal products trapped in the gel and, once formed, the gap between shell and core remains a feature of the microstructure for the first 24 hours. Preferential dissolution of the CA is very evident in the large grain on the lower right hand side of this figure, leaving a stepped and serrated surface on the hydrated core.

After 7 days hydration, the fracture surface appears featureless so that little information on the microstructure can be obtained in this way.

b) Hydration at 23 °C in tap water

More crystalline phase is produced at 23 °C than at 8 °C, the dominant hydrate being CAH_{10}, but after 12 hours small amounts of C_2AH_8 were found and C_3AH_6 was found by X-ray diffraction after 7 days. Alumina gel is still the major hydration product, and probably has a similar structure to that produced at 8 °C, judged by their similar decomposition temperatures of 130 °C.

The microstructure is very similar to that at low temperature, until 4 hours hydration when large amounts of fibrous alumina gel were observed on the surface of the cement grains (Fig.5). The paste fell to pieces during fracture, indicating that the bonding between particles is very weak and hence that the onset of bonding is slower than at low temperature.

Between 4 and 6 hours, the size of the dried gel fibres increased rapidly, in contrast to the 8 °C sample, indicating that the rate of hydration is faster at 23 °C. After 6 hours hydration, the hardness of the paste increases significantly as

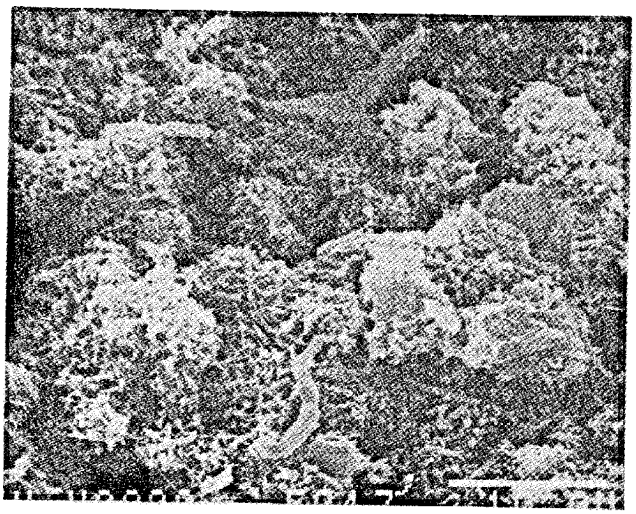

FIG.2 4-hour hydration at 8 °C, tap water

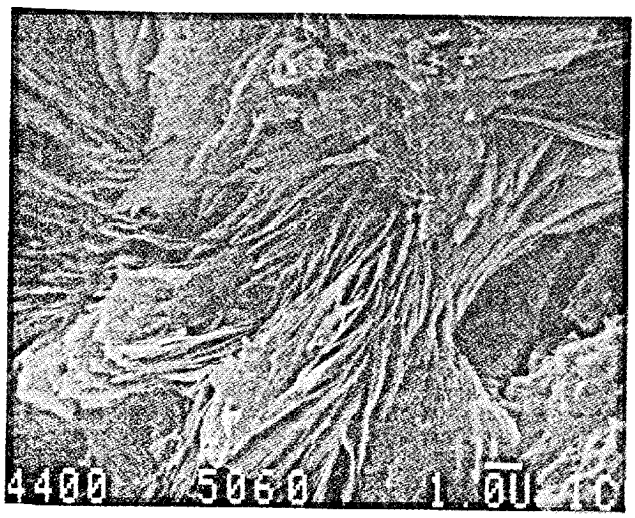

FIG.3 6-hour hydration at 8 °C, tap water



FIG.4 9-hour hydration at 8 °C, tap water

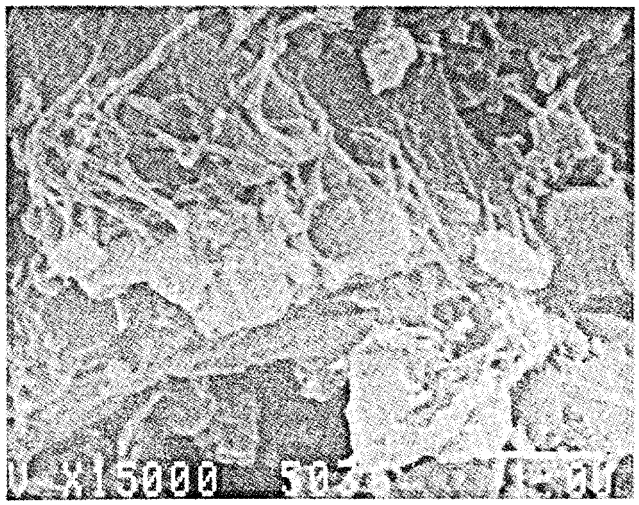

FIG.5 4-hour hydration at 23 °C, tap water

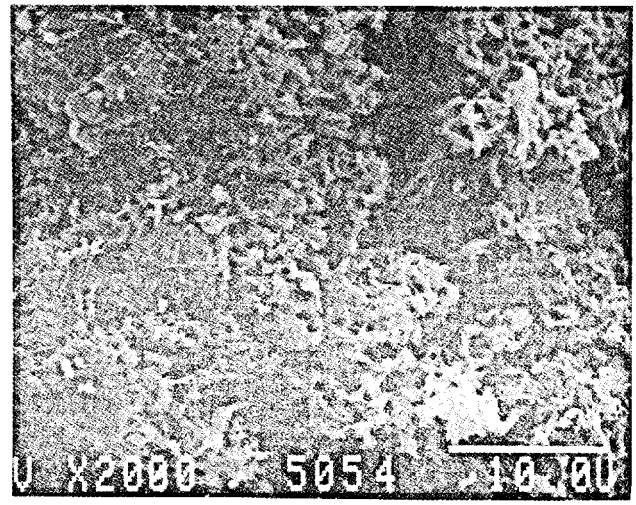

FIG.6 6-hour hydration at 23 °C, tap water

large amounts of hydrates form (Fig.6). The separated shell structure was not often seen in samples hydrated at this temperature. To reveal the gap between the shell and core on a fracture surface, the crack must pass through the shell and not around it. This implies that the bonding between neighbouring shells must be stronger than within the shells themselves. At 23 °C the additional crystalline phase in the form of small hexagonal plates is a possible source of increased strength in the shell, forcing the cracks to run between the shells and making it less easy to see the gap.

c) Hydration at 40 °C in tap water

X-ray results show that the initial crystalline hydrates are mainly β-C_2AH_8 with very small amounts of CAH_{10} and Gibbsite. After 12 hours CAH_{10} disappears and C_3AH_6 is found, indicating that conversion has already started at this early age.

The DTA results indicate that the alumina gel formed at 40 °C has a lower decomposition temperature (90 °C) than that formed at either 8 °C or 23 °C (130 °C), suggesting that they have different structures.

After 2 hours hydration, the surface of the grains is fully covered by a fine structure of alumina gel (Fig.7). The hardness of the paste increases significantly after 4 hours hydration. Fig.8 shows that the microstructure at this age consists of Hadley grains and hexagonal plates, and that there is less amorphous gel than at the lower temperatures. The microstructure of the dried alumina gel (Fig.9) in this sample is very different from those formed at the lower temperatures; it is more compact and does not have the fibre-like appearance. By 2 days, the conversion reaction has already started, causing the paste to become crumbly (Fig.10); spheroidal particles of C_3AH_6 can be seen both inside and outside the Hadley grains and thin flaky plates of Gibbsite can easily be observed.

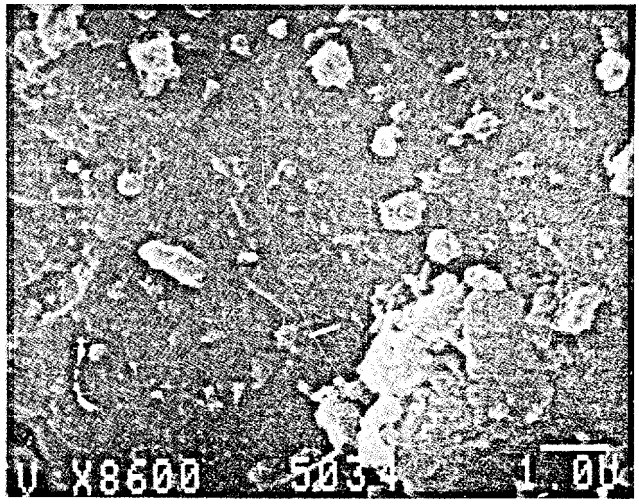

FIG.7 2-hour hydration at 40 °C, tap water



FIG.8 4-hour hydration at 40 °C, tap water

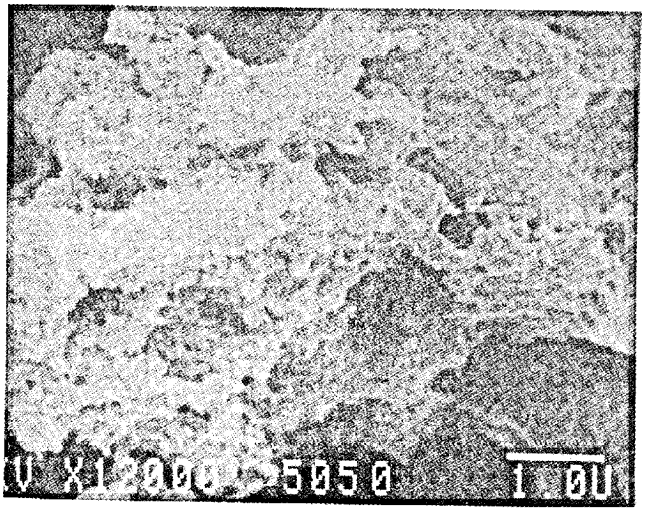

FIG.9 4-hour hydration at 40 °C, tap water

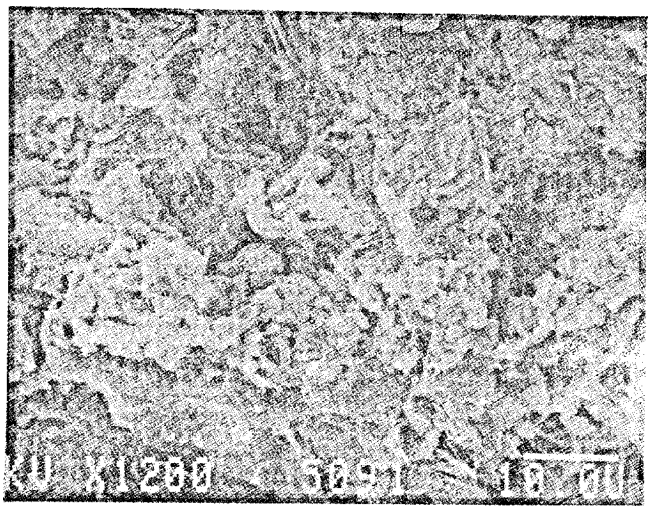

FIG.10 2-day hydration at 40 °C, tap water

d) Hydration at 8 °C in seawater

The amounts of crystalline hydrate (CAH_{10}) and alumina gel formed within the first 4½ hours are less than those formed in the tap water sample; this is due to the retardation effect of the seawater on the hydration (4). After 12 hours hydration, small amounts of C_4AH_{13} can be detected by X-ray.

Fig.11 shows that very little gel has formed after 4½ hours with seawater compared to that with tap water, although the decomposition temperatures are similar. The gel material becomes fibrous after 6 hours (Fig.12), and indeed the microstructure is very similar to that of the tap water sample at the same temperature.

CONCLUSIONS

1. The amount of alumina gel decreases as the temperature of the hydration increases. DTA results show that the alumina gel formed at 40 °C has a lower decomposition temperature than that formed at the lower temperatures.

2. The onset of bonding at 8 °C and 40 °C in tap water is earlier than at 23 °C, but the rate of reaction increases with temperature.

3. Seawater has a retarding effect on the hydration of HAC.

REFERENCES

1. A.M. Neville, High alumina cement concrete, Construction Press, Lancaster, England (1975).

2. F.M. Lea, The chemistry of cement and concrete, Edward Arnold Ltd, London (1976).

3. H.G. Midgley, The mineralogy of set high-alumina cement, Trans.Brit.Ceram.Soc., 66, 161 (1967).

4. P.L. Domone, private communication.

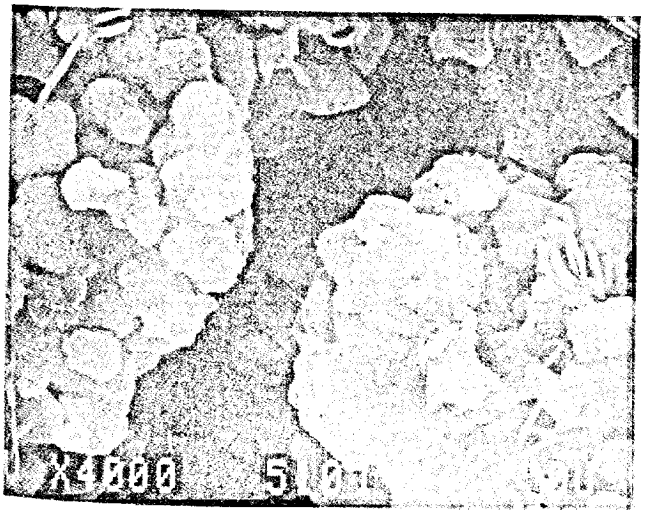

FIG.11 4½-hour hydration at 8 °C, seawater



FIG.12 6-hour hydration at 8 °C, seawater

S.M. GILL, P.F.G. BANFILL, B. EL-JAZAIRI*
School of Architecture and Building Engineering, University of Liverpool, P.O. Box 147, Liverpool L69 3BX,
* FEB (Great Britain) Ltd., Swinton Hall Road, Swinton, Manchester M27 1DT, U.K.

THE EFFECT OF SUPERPLASTICISERS ON THE HYDRATION OF ALUMINOUS CEMENT
L'EFFET DES ADJUVANTS SUPERPLASIFIANTS SUR L'HYDRATATION DU CIMENT ALUMINEUX

SUMMARY

The use of superplasticisers to produce aluminous cement mixes at low water content is an attractive proposition which is hindered by their retarding effects. In order to examine the possibility of overcoming the retardation the influence of two superplasticisers and an accelerator, both singly and in combination, on Ciment Fondu has been systematically studied.

The setting time of cement pastes was determined by the Vicat needle penetrometer and the kinetics of hydration studied in a conduction calorimeter.

The strength of mortar cubes was monitored by ultrasonic pulse velocity which was correlated with compressive strength in a subsidiary series of tests.

Both superplasticisers have a severe retarding effect at 5°C and 20°C, extending the time to the main heat evolution peak by up to 60 hours depending on the concentration used. At 30°C both admixtures overcome the well known retardation which occurs at this temperature in plain Ciment Fondu pastes and at 40°C slight acceleration occurs. The severe retardation at low temperatures may be overcome by simultaneous use of a lithium salt accelerator.

O uso de superfluidificantes para produzir misturas de cimento aluminoso com baixo teor de água é uma proposição atraente que encontra obstáculo em seus efeitos retardadores. A fim de examinar a possibilidade de afastar o obstáculo da retardação, foram submetidos a estudo sistemático dois superfluidificantes e um acelerador, separadamente e em combinação, com cimento Fondu.

O tempo de pega das pastas de cimento foi determinado por penetômetro de agulha de Vicat, e a cinética de hidratação estudada num calorímetro de condução.

Monitorou-se a resistência dos cubos de argamassa por velocidade de pulso ultrassônico, que foi correlacionada com a resistência à compressão numa série subsidiária de testes.

Ambos os superfluidificantes têm um efeito retardador muito grande a 5°C e a 20°C, dilatando o tempo do pico principal de evolução de calor em até 60 horas, dependendo da concentração usada. A 30°C, ambas as misturas superam a conhecida retardação que ocorre a esta temperatura em pastas de cimento fondu e a 40°C uma ligeira aceleração ocorre. A retardação severa a baixas temperaturas pode ser eliminada pelo uso simultâneo de um acelerador de sal de lítio.

INTRODUCTION

The use of superplasticisers with Portland cement is now well established enabling the production of extremely workable mixes or of mixes with significantly reduced water content. Superplasticised aluminous cement mixes with similar characteristics are an attractive proposition. Highly workable mixes could be used where high early strength or improved chemical resistance is required whilst reduction of water content to less than 0.40 water/cement ratio (w/c) significantly reduces the rate of conversion (1). Previous studies on such systems have however shown the tendency for unacceptable set retardation (2).

The hydration of Ciment Fondu will not be described in detail in this paper since much work has already been reported (3-7). A major feature however is the effect of temperature, since, unlike Portland Cement, the products of hydration are not the same at all temperatures. Hydration of Ciment Fondu may be described in terms of the hydration of CA, its major constituent (typically 50%), but there is disagreement over the temperature ranges for the formation of each hydrate (8,11) and over the hydration reactions. At low temperatures (<20°C) CAH_{10} is formed, above approximately 30°C the products of hydration are C_3AH_6 and alumina gel. The equations given below are not established but represent a possible reaction scheme (4):

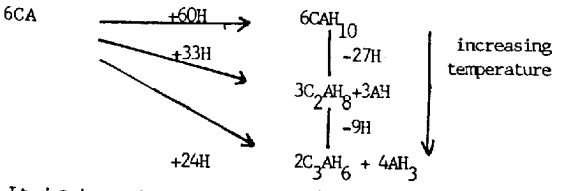

It is important not to neglect the influence of other phase components such as $C_{12}A_7$, CA_2, C_2AS, C_4AF and other minor constituents. Variation in Ciment Fondu composition further complicates understanding of the processes involved. The main manifestation of all this complexity is that the hydration rate slows above about 20°C until 30°C at which temperature the rate starts to increase rapidly. This behaviour causes delayed setting of pastes and concretes (6,7).

This paper describes a systematic study of the influence of 2 superplasticisers and an accelerator, both singly and in combination, on the setting, hydration and strength development of Ciment Fondu at temperatures between 5 and 40°C.

While the mortar test programme described here will eventually provide strength data over a much longer period, at the time of preparing this paper results were available up to 28 days.

EXPERIMENTAL PROCEDURES

MATERIALS

Cement: Ciment Fondu from one production batch was used for all tests on pastes and mortars. The chemical composition and physical properties are given in Appendix 1.

Superplasticisers: S1 sulphonated naphthalene resin, S2 development product. (Admixture dosages in % by weight of cement.) Accelerator: Lithium salt.
Water: Deionised water used in all experiments.

CONDUCTION CALORIMETRY

Tests were carried out using Oxford Conduction Calorimeter (Calox) units. This type of calorimeter is capable of giving information on the heat evolution from the instant when cement and water first come into contact. As the reaction proceeds, and heat is evolved the small temperature difference across thermocouples between the experimental chamber and a heat sink produces an emf which is detected by a potentiometric chart recorder. The voltage output is also fed to a solid state memory recorder which converts the readings to digital form. The recorder stores the voltages in this form at preset intervals of 5 minutes and can store 1024 values which are subsequently transferred through an interface to an Apple III microcomputer. For pastes which show considerable acceleration, data can be taken from the chart output at shorter intervals and added to the stored data. This ensures that the peak in rate of heat evolution is well defined. A suite of computer programs was written for the Apple III microcomputer to process and analyse the results.

For plain pastes runs were made over the range of 5 to 45°C at 5°C intervals. An additional test at 27°C was made to provide a comparison with results obtained by French workers (11). Runs were also made on pastes containing various admixture combinations. A total of 14 combinations, listed in Table 1, were all tested at 5, 30 and 40°C. All tests were carried out using 12g of cement at both 0.30 and 0.40 w/c.

It should be noted that only a limited amount of the data produced can be reported in a paper of this length.

SETTING TIMES

The Vicat needle penetrometer was used to measure the initial setting time of pastes with the following accelerator dosages at 5, 20, 30 and 40°C w/c and at 20°C only at 0.30 w/c:

0, 0.01, 0.075, 0.05, 0.01, 0.5, 1.0, 2.0%.

STRENGTH DEVELOPMENT

PUNDIT equipment was used to monitor the ultrasonic pulse velocity (UPV) of 70.7 mm cubes of 1:1½ cement:sand mortar stored in water at 5, 20, 30 and 40°C. A total of 12 mixes, detailed in Table 1, were tested at each of the four temperatures. Four cubes were cast from each mix, 2 of which are tested for compressive strength at randomly chosen ages to enable the correlation between UPV and strength to be investigated. Great care was taken to ensure that materials were stored at the appropriate temperature prior to mixing. Immediately after casting the moulds and their contents were placed inside plastic bags in water at the correct temperature. The exception to this was that cubes cast at 20°C were cured in air in the laboratory, covered with plastic sheeting to prevent drying. Cubes were demoulded as soon as possible, typically 6 hours after casting though considerably longer for some mixes. The first UPV readings were taken 24 hours after casting. Other test ages are 2, 3, 7, 14, 21, 28 days, 2, 3, 6, 12, 18 months.

UPV testing is advantageous since the same specimen is repeatedly checked thus eliminating the effects of variability between samples tested to destruction.

TABLE 1. MIX DETAILS FOR PASTES AND MORTARS.

Paste	Mortar	Admixture Dosage (%) Super-plasticiser. S1	S2	Accelerator
P1	M1	0	0	0
P2	M3	0.3	0	0
P3	-	0.6	0	0
P4	M4	1.0	0	0
P5	M5	0	0.3	0
P6	-	0	0.6	0
P7	M6	0	1.0	0
P8	M2	0	0	0.25
P9	-	0	0	0.1
P10	-	0	0	1.0
P11	M7	0.3	0	0.025
P12	M8	1.0	0	0.025
P13	M9	0	0.3	0.025
P14	M10	0	1.0	0.025

RESULTS

HYDRATION OF PLAIN PASTE

A typical graph obtained from calorimetry testing is shown as Figure 1. The effect of temperature on the hydration of plain paste at 0.30 w/c is shown on Figure 2. The method of presentation used is that of Wilding, Walter and Double (13). The pattern of results at 0.40 w/c is very similar.

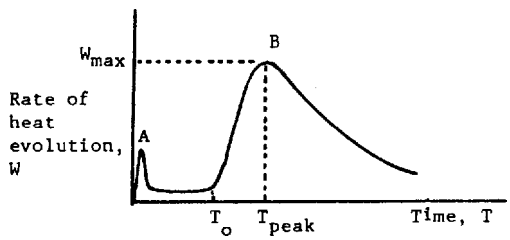

FIGURE 1 - Variation of rate of heat evolution with time in conduction calorimeter.

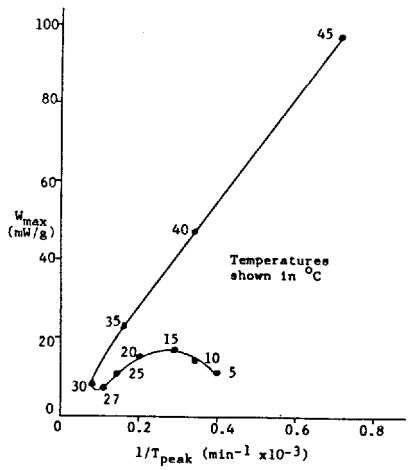

FIGURE 2 - Effect of temperature on heat evolution.

HYDRATION AND SETTING OF PASTE CONTAINING ACCELERATOR ALONE

Figure 3 shows the results of Vicat testing. Results obtained from calorimetry testing showed that a second distinct peak in rate of heat evolution was produced by some mixes, as shown in Figure 4, though the highest peak is not always the second to occur. This leads to difficulties in interpretation of results. Throughout this report, W_{max} and T_{peak} refer to the highest peak present.

Values of Vicat initial set and T_{peak} are given in Table 2.

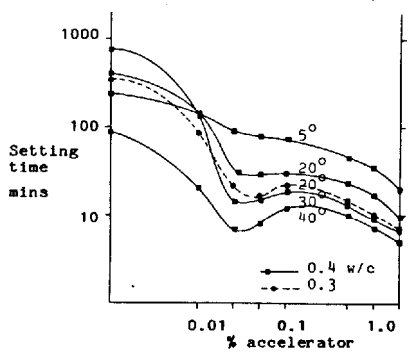

FIGURE 3 - Effect of accelerator on Vicat initial setting time.

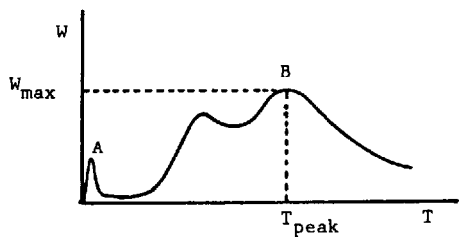

FIGURE 4 - Double peaks observed in conduction calorimeter with certain mixes (see Table 3).

TABLE 2. CORRELATION OF VICAT INITIAL SET WITH CALORIMETER T_{peak}

Temperature	%Accelerator	Vicat Initial Set (Minutes)	T_{peak}	Number of peaks
5°C	0	240	250	1
w/c 0.40	0.025	90	120	1
	0.1	75	115	2
	1.0	35	50	1
20°C	0	350	495	1
w/c 0.30	0.025	22	140	2
	0.1	23	30	2
	1.0	10	17	2
20°C	0	395	435	1
w/c 0.40	0.025	32	150	2
	0.1	30	30	2
	1.0	17	22	2
30°C	0	745	1290	1
w/c 0.40	0.025	14	250	2
	0.1	19	16	2
	1.0	9	10	2
40°C	0	85	290	1
w/c 0.40	0.025	7	9	1
	0.1	12	10	2
	1.0	7	6	2

EFFECT OF SUPERPLASTICISERS ALONE AND WITH ACCELERATOR

Calorimetry

Several mixes produced more than one peak in the rate of heat evolution as shown in Figure 4. Table 3 summarises the peak pattern.

TABLE 3. EFFECT OF SUPERPLASTICISERS AND ACCELERATOR ON CALORIMETER OUTPUT.

MIX	5°C	20°C	30°C	40°C
P2	P	P	Pp	PP
P3	P	P	Pp	Pp
P4	P	P	P	Pp
P5	P	P	pp	P
P6	Pp	P	Pp	P
P7	P	P	P	P
P11	Ppp	PP	PP	P
P12	Ppp	P	Pp	Pp
P13	Ppp	Ppp	PP	P
P14	Pp	P	Ppp	pP

P denotes one major peak. PP denotes 2 major peaks;
Pp denotes one major and one considerably smaller peak, etc.,.

Figure 5 summarizes the acclerating/retarding action of the admixtures. The vertical axis of this figure shows the ratio of the time to W_{max} for the particular combination of admixture and temperature to the time to W_{max} for the plain paste at the same temperature i.e.:

$$X = \frac{T_{peak\ (admixture)}}{T_{peak\ (control)}}$$

Deviation of the curve above X = 1 signifies retardation, below X = 1 acceleration.

Strength Development

For the 48 results obtained up to 28 days the relationship between UPV (v) and compressive strength (f) is:

$$f = 0.0019\ v^{7.3} \quad \text{(correlation coefficient = 0.93)}$$

This is shown on Figure 6 together with the upper and lower 95% prediction intervals.

Figures 7-10 show the changes in UPV occurring up to 28 days after casting.

DISCUSSION

PLAIN PASTE

During the hydration of Ciment Fondu heat is evolved as shown in Figure 1. The initial peak A is thought to be due to wetting of solids, chemical dissolution and partial hydration occurring when water first comes into contact with cement (14). This is followed by a dormant period whose length is determined by temperature, water content and chemical composition. After this dormant period, the rate of heat evolution increases rapidly at T_o until a clearly defined peak, B, is seen.

The well known delay affect around 30°C is confirmed in Figure 2. Above 30°C the relationship between W_{max} and $1/T_{peak}$ is linear and corresponds to the acceleration of a single hydration reaction (the formation of C_3AH_6) by increasing temperature (13). Between 5 and 30°C the behaviour is more complex, due possibly to interactions in the simultaneous production of several hydrates. The maximum delay in hydration occurred at 30°C as compared to the 27°C reported by Murat et al for pure CA (11).

ACCELERATED PASTES

Figure 3 illustrates the dramatic effect of the lithium salt accelerator on setting time. At dosages exceeding only 0.01% by weight of cement the 30°C delay is masked and setting times decrease consistently with increasing temperature. As dosage increases, a minimum setting time is observed at about 0.025%; this effect being more noticeable as temperature increases. Setting times were longer at higher paste water content. This behaviour may be explained by the longer time required to achieve the saturated solution from which initial hydrate precipitation occurs.

An attempt was made to correlate the Vicat initial setting time with parameters obtained from the calorimetry results; for example, T_o, T_{peak}, or T_{cum}, the time at which a predetermined cumulative amount of heat has been evolved. The onset of bulk precipitation of hydrates (and hence production of heat) is said to correspond with the time at which measureable mechanical resistance begins to develop in the paste (6). However, a difficulty in establishing the correlation is caused by the presence of multiple peaks for many mixes. It thus proved to be impossible to produce a quantitative relationship between setting time and any of the 3 parameters listed above. DTA results have led to the suggestion that the first peak is due to the formation of a calcium aluminate hydrate gel and the second to a more stable monocalcium aluminate decahydrate (15). Further work on the chemical differentiation between these peaks is planned as a later stage of this research. Additional problems arise in correlating setting time with calorimetry results because of the different patterns of heat evolution when forming different hydrates and in the interpretation of Vicat results in fundamental terms. Inspection of the data in Table 2 shows that the time to initial set is normally slightly less than T_{peak}. This confirms the findings of Casson et al (16).

Relatively little work has been carried out on the mechanism of lithium salt accelerators. Rodger and Double (17) propose that formation of lithium aluminate promotes nucleation of calcium aluminate hydrates. This was confirmed by Crepaz and Raccanelli (18) by solution analysis studies.

EFFECT OF SUPERPLASTICISERS

The presence of multiple peaks in heat evolution again causes difficulty in interpretation. Times to the maximum rate of heat evolution were used to prepare Figure 5 which clearly shows the dramatic effect of temperature on superplasticised mixes.

At 5°C mixes without accelerator all exhibit retardation. 1.0% S2 causes a 16 fold increase in T_{peak} over the control mix. This corresponds to a setting time of approximately 60 hours. Addition of 0.025% accelerator is sufficient to overcome the retardation for all except the 1.0% S2 mix. At 20°C the behaviour is similar though retardation is less marked and 0.3% S1 causes slight acceleration. At 30 and 40°C all mixes are accelerated.

Sulphates retard the hydration of Ciment Fondu at room temperature (19), and the behaviour of S1 and S2 which contain 5% and 15% w/w free sodium sulphate, respectively, may perhaps be attributed to this. Further work is planned to increase the understanding of this aspect.

It may be expected that mortar mixes containing admixtures would show early differences in UPV in accordance with the acceleration/retardation of hydration. Figures 7-10 show however that this is

3.3

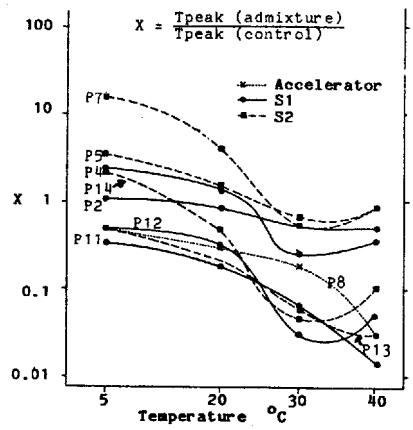

FIGURE 5 - Effect of temperature on T_{peak} of pastes.

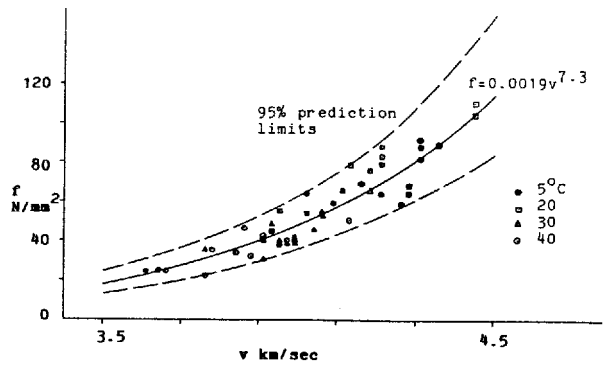

FIGURE 6 - Relationship between UPV and strength for 70.7 mm mortar cubes.

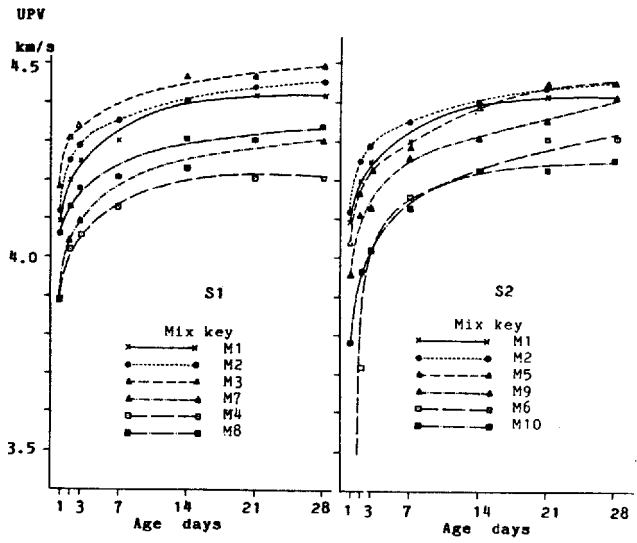

FIGURE 7 - UPV/Age relationship for mortars at 5°C.

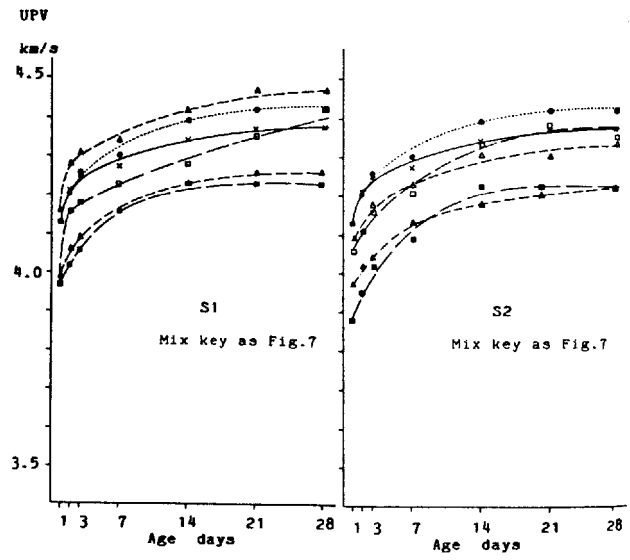

FIGURE 8 - UPV/Age relationship for mortars at 20°C.

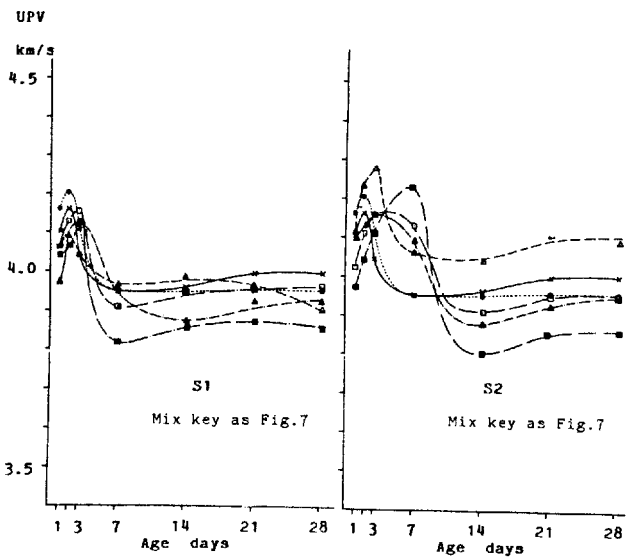

FIGURE 9 - UPV/Age relationship for mortars at 30°C.

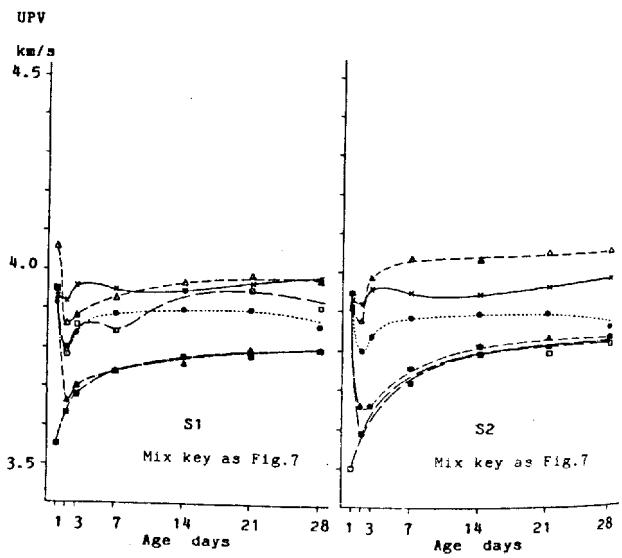

FIGURE 10 - UPV/Age relationship for mortars at 40°C.

not always so, although the extreme retardation of the 1.0% S2 mix is reflected in very low early UPV.

There is an obvious difference between the UPV/age relationships at 5, 20°C and those at 30, 40°C. The mixes at 5 and 20°C all exhibit a steadily increasing trend in UPV with age up to 28 days. At 30°C there is the same initial rapid increase in UPV but a maximum is reached after between 2 and 7 days. At 40°C the maximum is reached before 1 day, thereafter UPV decreases before increasing again. This behaviour is characteristic of the conversion reactions of CAH_{10} and C_2AH_8 to C_3AH_6 and AH_3 (6).

Another trend which is clearly visible from figures 7-10 is that mixes containing a superplasticiser in combination with accelerator show reduced UPV values at all ages. These low values are accompanied by low compressive strengths. Thus there is a very complex pattern of behaviour since setting and early hydration is accelerated whilst strength is reduced. Further testing is planned to enable confirmation of hydrates produced which should provide an indication of the mechanisms in operation.

Whilst there is reasonable overall correlation between UPV and strength, there are as yet insufficient results at each temperature to confirm that this correlation holds true for all hydration temperatures and hence for different hydrate compositions.

CONCLUSIONS AND FURTHER WORK.

1. The considerable retardation of the hydration of Ciment Fondu at around 30°C has been confirmed. The relationship between W_{max} and $1/T_{peak}$ is linear above 30°C which is taken to mean that the hydration reaction remains the same above this temperature. Below 30°C the situation is very complex with the parallel formation of more than one hydrate.
2. A lithium salt accelerator is extremely efficient in overcoming the retardation at 30°C.
3. Superplasticisers retard the hydration of Ciment Fondu at 5 and 20°C but accelerate slightly at 30 and 40°C. The retardation is tentatively ascribed to the presence of free sulphate in the admixtures.
4. The retardation by superplasticisers may be overcome by simultaneous use of the lithium salt accelerator.
5. The hydration kinetics of Ciment Fondu pastes containing superplasticisers are highly complex with some combinations, particularly at higher temperatures, producing double peaks in the rate of heat evolution.
6. Use of the PUNDIT apparatus to monitor the ultrasonic pulse velocity through Ciment Fondu mortar cubes provides a valuable indication of changes occurring in the samples with time. There is a good general correlation with the compressive strength of the cubes which enables the variation in strength with time to be determined with economy in terms of the effort involved in specimen preparation and storage.
7. Mortar strength continues to increase up to 28 days at 5 and 20°C but at 30 and 40°C it passes through a substantially lower strength before increasing slowly. The 28 day strengths at 30 and 40°C are about half those at lower temperatures. Both superplasticisers, the accelerator and combinations affect the variation in strength with time in different ways.

This paper has reported a preliminary stage in a substantial research programme. Other aspects under investigation are the effects of superplasticisers on flow properties, on changes in hydrate composition with time and consequently on mechanical properties. When complete it is hoped that more progress can be made in interpreting some of the complex effects described in this paper.

ACKNOWLEDGEMENTS

The authors gratefully acknowledge the financial assistance of the Science and Engineering Research Council and the provision of materials by the Lafarge Aluminous Cement Co Ltd.

REFERENCES

1. H G MIDGLEY, A MIDGLEY (1975), Mag.Con.Res. 27, 59.
2. D H QUON, V M MALHOTRA (1981), in "Developments in the use of superplasicisers", ACI SP 68-10,173.
3. F M LEA (1970), "The chemistry of cement and concrete", Edward Arnold, London.
4. K M PARKER, J H SHARP (1982), Trans. J. Brit. Ceram. Soc. 81, 35-42.
5. B COTTIN (1971), Cem.Conc.Res. 1, 177-186.
6. C M GEORGE (1983), in "Structure and performance of cements", ed P. BARNES, Applied Science, Lond.
7. T D ROBSON (1962), "High alumina cements and concretes", Contractors Record Ltd, London.
8. K MISHIMA (1968), Proc. 5th Int. Symp. Chemistry of Cement, Tokyo 3, 167-174.
9. A C TSEUNG, K G CARRUTHERS (1963), Trans. Brit. Ceram. Soc. 62, 305-309.
10. B COTTIN (1971), Cem. Conc. Res. 1, 273-284.
11. M MURAT et al (1980), C.R. Acad. Sci. Paris, 291, Series C, 113-115.
12. P J FRENCH, N G J MONTGOMERY, T D ROBSON, (1970), Meeting of British Ceramic Society.
13. C R WILDING, A WALTER, D D DOUBLE (1984), Cem. Concr. Res. 14, 185-194.
14. R MAGNAN (1970), Bull. Am. Ceram. Soc. 314-315.
15. H G MIDGLEY (1985), Private communication.
16. R B CASSON et al (1982), Proc. Symp. "Concrete rheology", Boston.
17. S A RODGER, D D DOUBLE (1984), Cem. Conc. Res. 14, 73-82.
18. E CREPAZ, A RACCANELLI (1975), Ind. Ital. Cem. 35, 761-768.
19. V S RAMACHANDRAN, R FELDMAN, J J BEAUDOIN (1981), "Concrete science", Heyden, London.

APPENDIX

Properties of the Ciment Fondu

Setting time (BS 915): Initial	280 min
Final	293 min
90 μm residue (%)	3.8
Surface Area (Blaine) (m^2/kg)	276
Chemical Composition (%):	

SiO_2	Al_2O_3	Fe_2O_3	FeO	TiO_2	CaO	Na_2O	K_2O	SO_3	CO_2
4.14	28.67	10.43	5.63	1.98	38.5	0.06	0.04	0.19	0.42

JOHN BENSTED, BP Research Centre, Exploration and Production Division
Chertsey Road, Sunbury-on-Thames, Middlesex, TW16 7LN, UK.

INFRARED SPECTRAL EXAMINATION OF OILWELL CEMENTS

EXAMEN PAR SPECTROSCOPIE INFRAROUGE DES CIMENTS POUR PUITS DE PETROLE

SUMMARY: Examination of the infrared spectra of oilwell cements can provide a quick and convenient method of ascertaining the forms of calcium sulphate present and whether any aeration (including prehydration) has taken place, which can affect the quality of the cement during downhole cementing operations. Calcium sulphate dihydrate (gypsum) and/or its dehydration products are identified from the shapes and positions of the sulphate bands in the spectral regions 1050 - 1200 cm^{-1} and 650 - 680 cm^{-1}, and of the water bands at 1600 - 1700 cm^{-1} and above 3400 cm^{-1}. Aeration is identified from the effects of both prehydration and carbonation. Prehydration can be found from the presence of hydrate bands over and above those identified for the small quantities of calcium sulphate present in the cements (especially above 3300 cm^{-1}), and also from any changes observed in the expected shapes and positions of the main silicate absorption bands centred upon ca. 930 cm^{-1}. Carbonation is revealed by increased carbonate bands in the spectral regions 1350 - 1500 cm^{-1} and 850 - 900 cm^{-1}. If the spectra show excessive amounts of calcium sulphate present in the hemihydrate/solubte anhydrite form and/or evidence of significant aeration, indicating possible quality problems in practice, then the cementing behaviour of the oilwell cements concerned should be evaluated by established API Spec 10 or other appropriate procedures, for confirmation of whether the practical performance is likely to be poor or not.

O exame dos espectros infravermelhos de cimentos para poço de petróleo pode proporcionar um método rápido e conveniente de avaliação das formas de sulfato de cálcio presentes e se houve alguma aeração (inclusive pré-hidratação), que podem afetar a qualidade do cimento durante as operações de cimentação do poço. O di-hidrato de sulfato de cálcio (gesso) e/ou seus produtos de desidratação são identificados a partir das formas e posições das bandas de sulfato nas regiões espectrais 1050 a 1200 cm^{-1} e 650 - 680 cm^{-1}, e a partir das bandas de água a 1600 - 1700 cm^{-1} e acima de 3400 cm^{-1}. A aeração é identificada a partir dos efeitos tanto da pré-hidratação como da carbonatação. A pré-hidratação pode ser constatada pela presença de bandas de hidrato acima e abaixo daquelas identificadas pelas quantidades menores de sulfato de cálcio presentes nos cimentos (especialmente acima de 300 cm^{-1}), e também por quaisquer mudanças observadas nas formas e posições esperadas das bandas principais de absorção do silicato centradas sobre ca. 930 cm^{-1}. A carbonatação é revelada pelo aumento de bandas de carbonato nas regiões espectrais 1350 - 1500 cm^{-1} e 850 - 900 cm^{-1}. Se os espectros apresentarem quantidades excessivas de sulfato de cálcio presente na forma semi-hidrato/anidrito solúvel e/ou evidência de aeração significativas,indicando possíveis problemas práticos de qualidade, então o comportamento de cimentação dos cimentos de poço de petróleo concernentes deverão ser avaliados de acordo com a Spec 10 API ou outros processos apropriados, para confirmar se a performance prática tem possibilidade de ser deficiente ou não.

JOHN BENSTED, BP Research Centre, Exploration and Production Division
Chertsey Road, Sunbury-on-Thames, Middlesex, TW16 7LN, UK.

INTRODUCTION

Oilwell cements are primarily employed for sealing the annular space between the drilled out borehole and the steel casing that is placed down the hole for facilitating further drilling and later for carrying any oil or gas formed. The quality of oilwell cements is very important for being able to complete cementing jobs successfully [1-4]. Oilwell cements should be able to be pumped down the casing and back up the annulus, filling the latter before they thicken up. In practice, a setting or thickening time of 3-4 hours is usually sufficient for completing the cementing operation and allowing sufficient time for delays. These cement slurries normally contain a number of additives for producing a satisfactory cementing job for given well conditions. In the specification[5], the thickening time is regulated; viz Class G and H basic oilwell cements must thicken between 90 and 120 minutes so that consistent cementing properties can be obtained. If the cements are too reactive, the slurries will thicken up too quickly to permit successful cementing of wells. If they are insufficiently reactive, thickening may be too long for completing the cementing job efficiently. Excessive exposure to the atmosphere may cause aeration (a combination of prehydration and carbonation)[6], which generally lowers the reactivities of the cements, giving rise to longer thickening times and poorer compressive strength development.

Infrared spectroscopy should be able to be used as a preliminary aid in determining whether there might be quality problems in a number of instances with oilwell cements, since the forms of calcium sulphate present, which affect early hydration behaviour, and the presence of wavebands due to hydrates and carbonates can be identified[7-9]. Accordingly, a number of oilwell cements were investigated by infrared spectroscopy and appropriate comparisons made with their cementing properties, in order to evaluate the usefulness of the technique for such characterisation.

EXPERIMENTAL PART

Infrared spectra of a number of Class G and Class H cement samples were recorded on a Perkin-Elmer 582 infrared spectrophotometer over the wavenumber range 200 - 4000 cm^{-1} using both the potassium bromide disc and the Nujol mull techniques. Comparisons were made with infrared spectra obtained for the different forms of calcium sulphate and for various carbonates[7-9]. API Schedule 5 thickening time determinations on these cements were carried out using a Chandler Pan - American type thickening time tester[5].

RESULTS AND DISCUSSION

The results obtained are illustrated by reference to particular Class G and Class H cements examined in Figure 1. The main infrared wavebands for the different forms of calcium sulphate are given in Table 1 and illustrated in Figure 2. In practice with cements, it is not easy to differentiate between the hemihydrate and soluble anhydrite forms of calcium sulphate. However, since soluble anhydrite is a quasi-zeolitic variety of hemihydrate of the composition $CaSO_4$ 0.001 - $0.5H_2O$, such differences between the two spectra are not so important from the viewpoint of establishing whether extensive dehydration of the gypsum has occurred in the grinding process during cement manufacture. The API Schedule 5 thickening times determined for these cements are shown in Table 2.

The Class H cement designated A in Figure 1 shows, from the disposition of the sulphate wavebands in the regions 650 - 680 cm^{-1} and 1050 - 1200 cm^{-1} and of the small wavebands from water in the regions 1600 - 1700 cm^{-1} and 3500 - 3650 cm^{-1}, a preponderance of calcium sulphate in the hemihydrate/soluble anhydrite form. There were no significant carbonate or other hydrate water wavebands, demonstrating a lack of carbonation and prehydration in this cement. These results indicated that there had been a substantial dehydration of the gypsum during clinker-gypsum grinding in the manufacturing process. The Schedule 5 thickening time of this cement was 88 minutes, which was just below the minimum of 90 minutes required for Class H cement in API Spec 10 [5]. Hemihydrate/soluble anhydrite has a much higher solubility than gypsum[10] and the extra sulphate ions in solution (with respect to gypsum), as well as enhancing early formation of ettringite[11], also accelerate hydration of the tricalcium silicate (alite) phase[12]. Hence, too high a clinker-gypsum grinding temperature leading to considerable gypsum dehydration was a key factor in producing an enhanced reactivity with this particular cement. However, the reverse situation cannot necessarily be inferred as a generalisation for all oilwell cements. If gypsum dehydration is detected in a cement, then that cement may not necessarily be too reactive, since other factors also influence reactivity, viz surface area, form and quantity of alite present etc. Nevertheless, gypsum dehydration can produce premature stiffening (or false set) downhole, caused mainly by rehydration to gypsum, which may not always be eliminated by the slurry mixing process[12]. The presence of extensively dehydrated gypsum does indicate a potential problem with oilwell cement slurries, which can be checked out by appropriate thickening time measurements[5].

Another sample of the Class H cement, designated B in Figure 1, which had been exposed to the atmosphere, revealed some significant changes in its infrared wavebands compared with those

JOHN BENSTED, BP Research Centre, Exploration and Production Division
Chertsey Road, Sunbury-on-Thames, Middlesex, TW16 7LN, UK.

present for cement A. More gypsum relative to hemihydrate was found and, from the presence of clear wavebands in the regions 850 - 900 cm^{-1} and particularly 1350 - 1500 cm^{-1}, which could be ascribed to carbonates like calcite[9], as well as increased hydrate water bands above 3400 cm^{-1}, it was clear that extensive aeration had taken place. The action of moist carbon dioxide had thus resulted in some prehydration coupled with carbonation. The Schedule 5 thickening time of this cement was 118 minutes, which was just within the maximum value of 120 minutes for Class H cement stipulated by API Spec 10 [5]. This cement had a lowish reactivity, which is a common consequence of aeration[6]. However, in this instance the reactivity of the cement was still within the specification. The effects of aeration on oilwell cement quality and the need to avoid unnecessary exposure of cement to the atmosphere prior to usage have been discussed elsewhere[6].

The Class G cement designated C in Figure 1 shows a more complex disposition of wavebands from calcium sulphate, indicative of a mixture of gypsum, hemihydrate/soluble anhydrite and insoluble anhydrite. Carbonate bands due to calcite were prominent, but the absence of other hydrate water bands indicated a lack of prehydration and suggested that these calcite bands were due to a calcitic impurity in the cement (probably in the gypsum component) and not to the effects of aeration. Gypsum dehydration to hemihydrate/soluble anhydrite had only been slight. The insoluble anhydrite must have been present as such in the gypsum component of the cement, otherwise had it arisen from excessive dehydration of gypsum during clinker-gypsum grinding in the manufacturing process (where the temperature would need to have exceeded ca. 200°C) no residual gypsum or significant quantities of hemihydrate/soluble anhydrite would have remained as such. These results were confirmed from the Schedule 5 thickening time investigation (Table 2) where the thickening time was a very acceptable 105 minutes and showed a lowish maximum consistence of 14Bc during the first 15 - 30 minutes of the Schedule 5 test. From this particular examination, it should be made clear that the mere presence of calcite should not be regarded as necessarily indicating that aeration of a cement has taken place. Indeed with cement C there was no evidence for any significant aeration having taken place.

A sample of this Class G cement, designated D in Figure 2, which had been exposed to the atmosphere for three days, revealed enhanced gypsum wavebands relative to those of hemihydrate/soluble anhydrite, with the insoluble anhydrite wavebands remaining as such. The carbonate bands were enhanced and there was evidence of prehydration. Some slight changes in the main silicate absorption bands which were centred at ca 940 cm^{-1} instead of 925 - 930 cm^{-1}, indicative of some silicate phase hydration, were also apparent. The thickening time was 126 minutes, outside the API Spec 10 limit of 120 minutes, showing the expected diminished reactivity as a result of aeration. This cement had undergone a greater degree of aeration than cement B had.

CONCLUSION

From these results, it is clear that infrared spectroscopy can play a useful, though limited, role in the characterisation of oilwell cements by demonstrating qualitatively the different calcium sulphate forms present (quantitative work is not possible owing to extensive band overlap), whether carbonates are present and, for a given source whether aeration (prehydration plus carbonation) of the cement is likely to have occurred or not. In the worst cases of aeration, the main silicate wavebands centred on 925 - 930 cm^{-1} are visibly affected as well. Such an infrared spectroscopic examination is no substitute for the usual quality examination of oilwell cements, but can be a valuable supplement to it and, for a given source of supply, can act as an indicator of whether a detailed examination of a particular sample is necessary for the purposes intended. In this way the infrared method can enhance and simplify available testing techniques.

BIBLIOGRAPHY

1. - D.K. Smith: (1976) 'Cementing' Society of Petroleum Engineers of AIME, New York, Dallas.

2. - K.-H. Arens and M. Akstinat: (1982) Bundesministerium für Forschung und Technologie - Forschungsbericht T82-112. Verbesserung der Ringraumzementation in tiefen und übertiefen Bohrungen - Teil 2: Tiefbohrzemente und Additive. Fachinformationszentrum, Energie-Physik-Mathematik-GmbH, Karlsruhe.

3. - J. Bensted, P.E. Haynes, E. Henderson, A. Jones and T.B. Smallwood: (1983) Chemical aspects of oilwell cementing, in 'Special Publication No. 45: Chemicals in the Oil Industry'. (Editor: P.H. Ogden) pp 42 - 60. The Royal Society of Chemistry, Burlington House, London.

4. - Dowell Schlumberger: (1984) 'Cementing Technology'. Nova Communications Ltd., London.

5. - API Spec 10, Second Edition, June 1984. American Petroleum Institute, Washington DC.

6. - J. Bensted: (1984) Effects of aeration on the properties of Class G oilwell cement, in 'British Ceramic Proceedings

JOHN BENSTED, BP Research Centre, Exploration and Production Division
Chertsey Road, Sunbury-on-Thames, Middlesex, TW16 7LN, UK.

No. 35: The Chemistry and Chemically-Related Properties of Cement". (Editor: F.P. Glasser). pp 317 - 337. British Ceramic Society, Stoke-on-Trent.

7. - J. Bensted and S.P. Varma: (1974) Some applications of infrared and Raman spectroscopy in cement chemistry. Part 2. Portland cement and its constituents. Cement Technology 5 (4), 378-382.

8. - ibid. (1974) Part 3. Hydration of Portland Cement and its constituents. Cement Technology 5 (5) 440-450.

9. - J. Bensted and S.P. Varma: (1977) Infrared and Raman spectroscopy in cement chemistry - miscellaneous applications. World Cement Technology 8 (1), 16-20.

10. - J. Bensted: (1975) Un esame dell' anidrite solubile/An examination of soluble anhydrite II Cemento 72 (3), 139-145.

11. - J. Bensted: (1982) Effects of the clinker-gypsum grinding temperature upon early hydration of Portland cement. Cement and Concrete Research 12 (3), 341-348.

12. - J. Bensted: (1983) Hydration of Portland Cement, in 'Advances in Cement Technology'. (Editor: S.N. Ghosh) pp 307-347. Pergamon Press, Oxford, New York, Toronto.

TABLE 1 - Main Infrared Wavebands for Calcium Sulphate Forms

WAVEBAND (cm^{-1})				ASSIGNMENT
GYPSUM	HEMIHYDRATE	SOLUBLE ANHYDRITE*	INSOLUBLE ANHYDRITE	
			593 s	
602s	602 vs	602 vs	612 s	ν_4, SO_4
667s	660 s	665 s	675 s	
1004 vw	1008 vw	1008 vw		
		1012 vw	1012 vw	ν_1, SO_4
	1094 s	1092 s		
1120 vs	1115 s	1115 s	1130 s	ν_3, SO_4
1145 vs	1155 vs	1155 vs	1158 vs	
1623 s	1623 s			ν_2, H_2O
1688 m				
3410 s				ν_1, H_2O
3500 w	3560 m			
3555 m	3615 s			ν_3, H_2O

vs = very strong, s = strong, m = medium, w = weak, vw = very weak.
* = minimal water content.

TABLE 2 - API Schedule 5 Thickening Times

CEMENT DESIGNATION	TYPE	THICKENING TIME (minutes)	MAXIMUM CONSISTENCE DURING 15 - 30 MINUTES OF SCHEDULE 5 THICKENING (Bc)
A	Class H, fresh	88	15
B	Class H, aerated	118	11
C	Class G, fresh	105	14
D	Class G, aerated	126	10

API Spec 10 Limits: Schedule 5 Thickening Time: 90 - 120 minutes
Maximum Consistence during first 15 - 30 minutes of Schedule 5 Thickening: 30 Bc.

JOHN BENSTED, BP Research Centre, Exploration and Production Division
Chertsey Road, Sunbury-on-Thames, Middlesex, TW16 7LN, UK.

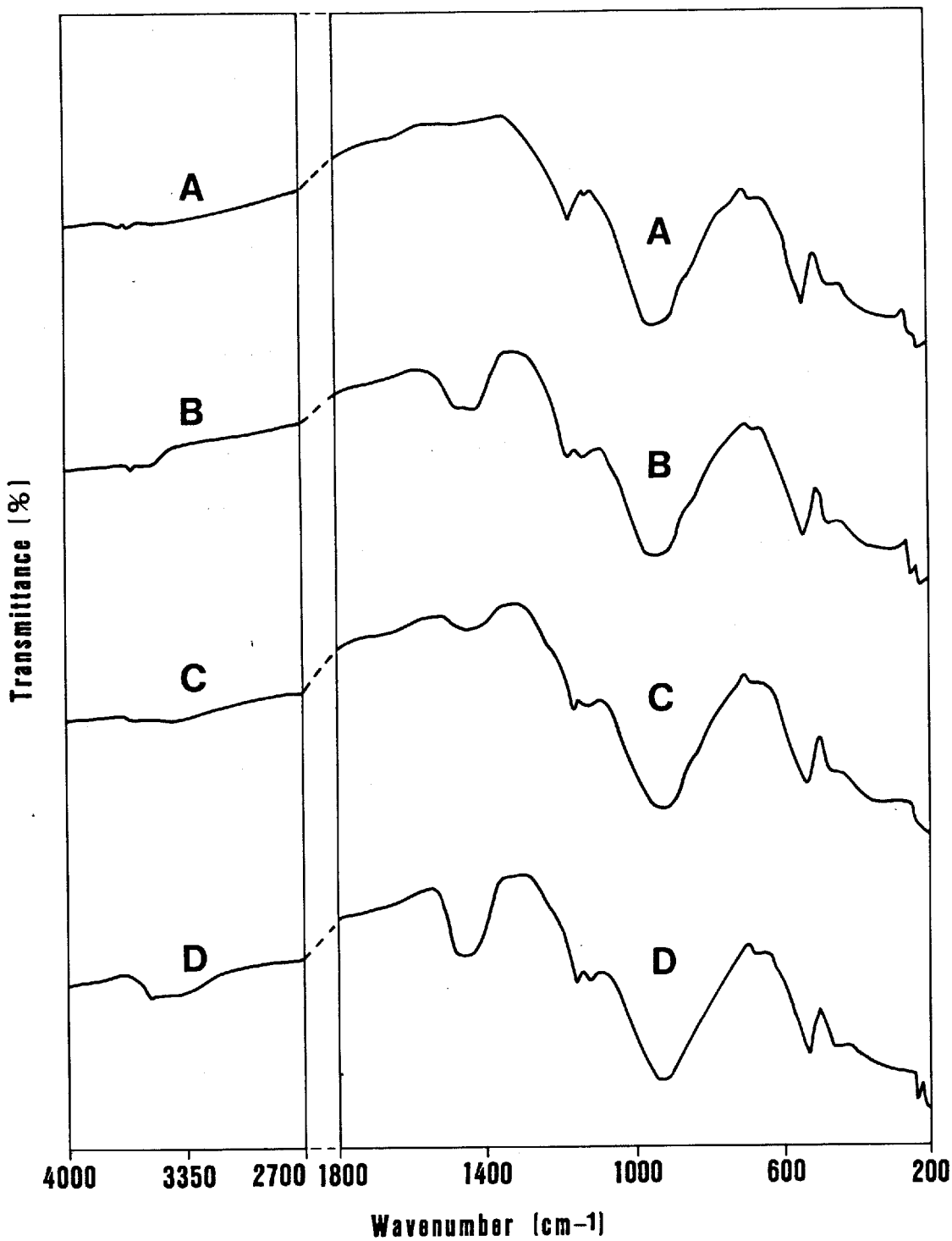

Fig. 1 - Infrared spectra of oilwell cements A-D:
A) Class H fresh, B) Class H aerated, C) Class G fresh, D) Class G aerated

JOHN BENSTED, BP Research Centre, Exploration and Production Division,
Chertsey Road, Sunbury-on-Thames, Middlesex, TW16 7LN, UK.

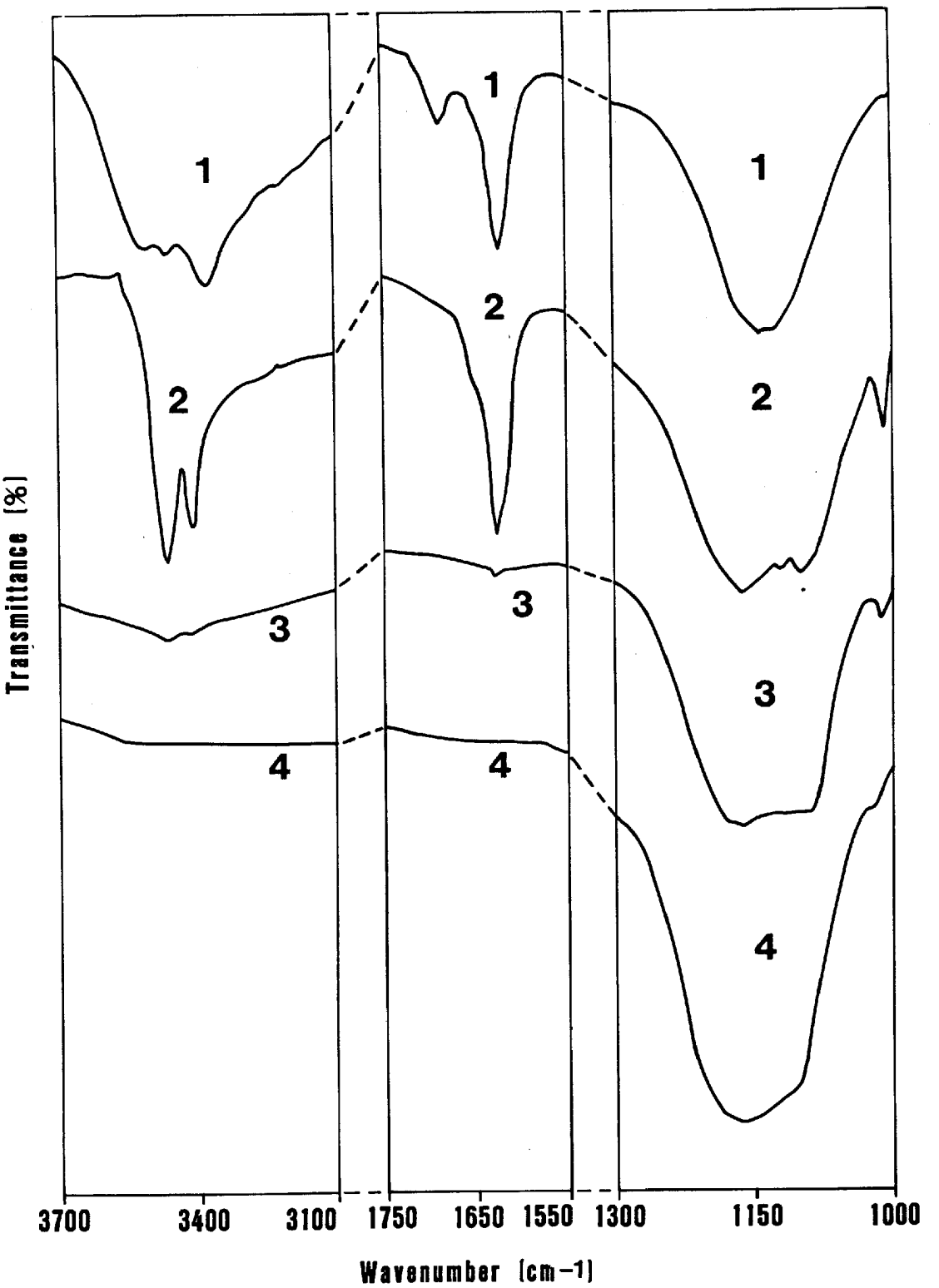

Fig. 2 - Infrared spectra of calcium sulphate forms in KBr disc media:
1) gypsum, 2) hemihydrate, 3) soluble anhydrite, 4) insoluble anhydrite.

D. MENETRIER-SORRENTINO (LAFARGE COPPEE RECHERCHE France)
C.M. GEORGE (LAFARGE CALCIUM ALUMINATE NORFOLK U.S.A.)
F.P. SORRENTINO (LAFARGE COPPEE RECHERCHE)

3.3

The SETTING and HARDENING CHARACTERISTICS of CALCIUM ALUMINATE CEMENTS : STUDIES of the SYSTEMS $C_{12}A_7$-C_3A and $C_{12}A_7$-CA

CARACTERISTIQUES de PRISE et de DURCISSEMENT des CIMENTS à BASE d'ALUMINATES de CALCIUM : ETUDE des SYSTEMES $C_{12}A_7$-C_3A et $C_{12}A_7$-CA

SUMMARY : the setting and hardening characteristics of experimental cements produced by fusion in the C_3A-$C_{12}A_7$ systems have been studied. At various ages conductimetric, calorimetric, XRD and penetrometry tests were made. The amount of reacted water was also determined. Rapid setting occurs in cement rich in both $C_{12}A_7$ and C_3A by precipitation of C_2AH_8. Set times are longer in $C_{12}A_7$-CA cements : CAH_{10} is the principal hydrate. After 4 hours all the cement pastes show equivalent strengths and the same amount of hydration. The rate of hydration and strength development of the rapid setting cement is low between 4 hours and 28 days. The other cements hydrate continuously over this period and 28 days strengths increase with setting time and CA content. These effects are related to the dissolution kinetics of the different cements (which warrants, further study) and the ratio of calcium to aluminate ions in solution, which depends on the composition of the anhydrous calcium aluminates.

Foram estudadas as características de pega e endurecimento de cimentos experimentais produzidos por fusão nos sistemas C_3A-$C_{12}A_7$. Em várias idades foram realizados testes condutimétricos, calorimétricos, XRD e penetrometria. Também foi determinada a quantidade de água reagida. Dá-se pega rápida em cimento rico em $C_{12}A_7$ e C_3A por precipitação de C_2AH_8. Os tempos de pega são mais longos em cimentos $C_{12}A_7$-CA: o hidrato principal é CAH_{10}. Depois de 4 horas, todas as pastas de cimento apresentam resistência equivalente e a mesma quantidade de hidratação. A velocidade de desenvolvimento da hidratação e resistência do cimento de pega rápida é baixa entre 4 horas e 28 dias. Os outros cimentos se hidratam continuamente no decorrer deste período e as resistências aos 28 dias aumentam com o tempo de pega e o teor de CA. Estes efeitos estão relacionados com as cinéticas de dissolução dos diferentes cimentos (o que justifica estudo adicional) e a relação de íons de cálcio para aluminato em solução, que depende da composição dos aluminatos de cálcio anidros.

D. MENETRIER-SORRENTINO (LAFARGE COPPEE RECHERCHE France)
C.M. GEORGE (LAFARGE CALCIUM ALUMINATE NORFOLK U.S.A.)
F.P. SORRENTINO (LAFARGE COPPEE RECHERCHE France)

INTRODUCTION :

The growing interest in a variety of cements displaying different setting times and rates of hardening used for engineering construction, maintenance and repair has prompted us to investigate the mechanisms of setting and of strength development.

Methods of accelerating cementitious binders, include mixing together Portland and aluminous cements, finer grinding of cements, the use of chemical additives for example. A review of these methods has already been published (1).

In a previous study (2,3), we investigated the reactions taking place with water in cements based on C_3S-CA and C_2S-$C_{12}A_7$. The present work concerns the systems $C_{12}A_7$ and $C_{12}A_7$-C_3A.

EXPERIMENTAL PROCEDURES and RESULTS

Cements were prepared from natural raw materials (bauxite and limestone) by fusion at 1450 °C followed by slow cooling. Compositions were chosen to cover the range C_3A + $C_{12}A_7$ to CA + $C_{12}A_7$.

The chemical and mineralogical compositions obtained are shown in Table 1.

The calculated phase compositions suppose that the cements are totally crystalline and that there is no solid solution. XRD was used to determine the percentage of $C_{12}A_7$ formed. Qualitatively speaking, the results can be considered coherent if the absence of C_2S is due to the formation of silica containing glass.

Quantitatively, in the C_3A-$C_{12}A_7$ zone the observed concentration of $C_{12}A_7$ is of the same order as that calculated. By contrast, it is very much lower than that calculated in the zone CA-$C_{12}A_7$. This may be explained by the fact that liquidus temperatures in this zone are lower thus encouraging the formation of more vitreous material during cooling. The amount of crystalline $C_{12}A_7$ is thus diminished.

The samples were ground in such a manner that we were able to select the cements produced to have all the same fineness measured by the Blaine method.

Setting times were measured at a constant water/cement ratio of 0.4

We chose for further study, the fastest setting composition (1 minute), the longest setting composition (90 minutes), and one sample each from the $C_{12}A_7$-CA zone (45 minutes), and the $C_{12}A_7$-C_3A zone (60 minutes) close to the frontier between these two zones.

Thus we have :

$C_{12}A_7$-CA zone, sample no. 1; set, 1 minute

$C_{12}A_7$-CA zone, sample no. 5; set, 45 minutes

$C_{12}A_7$-CA zone, sample no. 9; set, 90 minutes

$C_{12}A_7$-C_3A zone, sample no. 6; set, 60 minutes

The hydration of these cements was studied using conductimetry, isothermal microcalorimetry, XRD, measurement of the amount of bound water and penetrometry tests.

Table 1. Chemical and Mineralogical Analyses of Experimental Cements

No.	CaO	Al_2O_3	SiO_2	Fe_2O_3	FeO	MgO	TiO_2	Phase Composition, % calculated		observed
1	50.87	43.19	1.41	0.65	0.35	0.41	2.83	$C_{12}A_7$	63	62
								C_3A	28	present
								C_2S	4	not detected
2	49.75	43.44	1.27	0.70	0.30	0.25	2.85	$C_{12}A_7$	67	63
								C_3A	24	present
								C_2S	4	n.d.
3	49.04	44.33	1.32	0.75	0.45	0.30	2.90	$C_{12}A_7$	73	90
								C_3A	18	present
								C_2A	4	n.d.
4	48.76	44.05	1.59	1.10	0.15	0.24	2.89	$C_{12}A_7$	74	88
								C_3A	16	present
								C_2S	5	n.d.
5	47.87	45.94	1.55	0.90	0.50	0.29	2.89	$C_{12}A_7$	85	93
								C_3A	6	present
								C_2S	4	n.d.
6	45.83	47.14	2.02	0.75	0.75	0.34	2.99	$C_{12}A_7$	81	47
								CA	8	n.d.
								C_2S	6	n.d.
7	45.63	46.20	2.04	0.65	1.10	0.32	2.99	$C_{12}A_7$	81	60
								CA	7.1	present
								C_2S	6	n.d.
8	44.50	47.39	2.37	1.00	0.85	0.30	3.01	$C_{12}A_7$	71	44
								CA	17	present
								C_2S	6	n.d.
9	43.51	48.07	2.86	0.80	1.25	0.34	2.98	$C_{12}A_7$	60	24
								CA	27	present
								C_2S	8	n.d.

CONDUCTIMETRY

Measurements were made at a water/cement ratio of 0.5 and the results are shown in table 2 and figure 1.

TABLE 2

Sample No.	Time to peak maximum (min - sec) First peak	Second Peak	Set Time (minutes)	Conductivity m. Siemens . cm^{-1} 1st Peak	2nd Peak
1	0' 45	1' 25	1	2,78	2,91
5	1' 50	3' 20	45	2,43	2,66
6	2' 35	4' 00	60	2,42	2,62
9	3' 20	5' 00	90	2,54	2,62

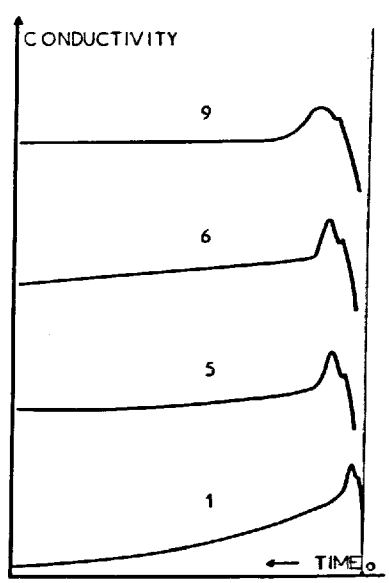

FIGURE 1

D. MENETRIER-SORRENTINO (LAFARGE COPPEE RECHERCHE France)
C.M. GEORGE (LAFARGE CALCIUM ALUMINATE NORFOLK U.S.A.)
F.P. SORRENTINO (LAFARGE COPPEE RECHERCHE France)

Figure 1 shows that the passage of ions into solution follows a similar pattern in all 4 samples. Table 2 shows that the peaks in conductivity appear earlier the faster the setting time of the cement.

MICROCALORIMETRY

The results obtained are shown in table 3 and figures 2 and 3.

Table 3 : Microcalorimetry data on Cements.

Sample No.	Set time (minutes)	Time to first peak (min.-sec.)	ΔH (15 min.) J/gm.	Time to second peak (hrs.-min.)	Δ H (24 hrs.) J/gm.
1	1	4' 30	93	1 - 35	418
5	45	1' 15	17	3 - 45	466
6	60	1' 00	12.3	2 - 35	410
9	90	1' 15	1.3	3 - 50	415

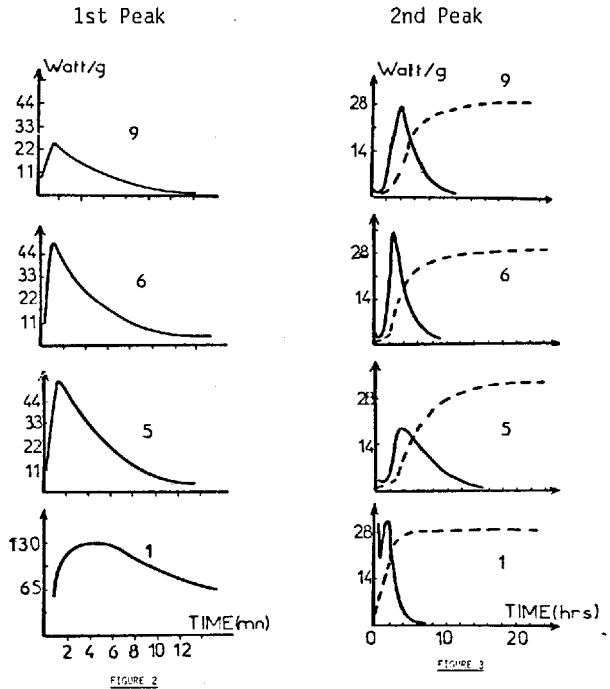

FIGURE 2

FIGURE 3

All cements display two peaks in heat evolution and the same total heat of hydration after 24 hours. Sample no 1 has a different shape of its first peak, which is spread over a period of 4 to 5 minutes.

There is no correlation between the time at which the first peak appears and the setting time of the cements, whereas setting time and the amount of heat associated with the first peak are inversely related.

MEASUREMENT of BOUND WATER, PENETRATION RESISTANCE and XRD EXAMINATION

Bound water is estimated by measuring the loss on ignition after the free water has been removed from the samples by washing with acetone and drying with ether. The results are shown in figure 4.

Penetrometer results are given in figure 5 and the XRD data on the $C_{12}A_7$ present is shown in figure 6.

All these results are plotted as a function of time in a semi-logarithmic form.

The hydrates formed, detected by XRD, are shown in table 4.

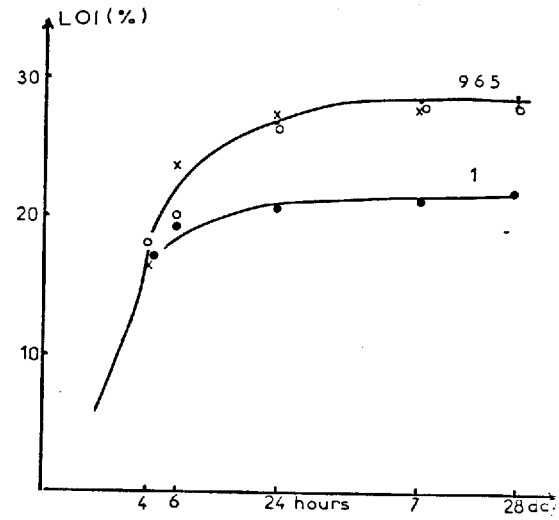

FIGURE 4

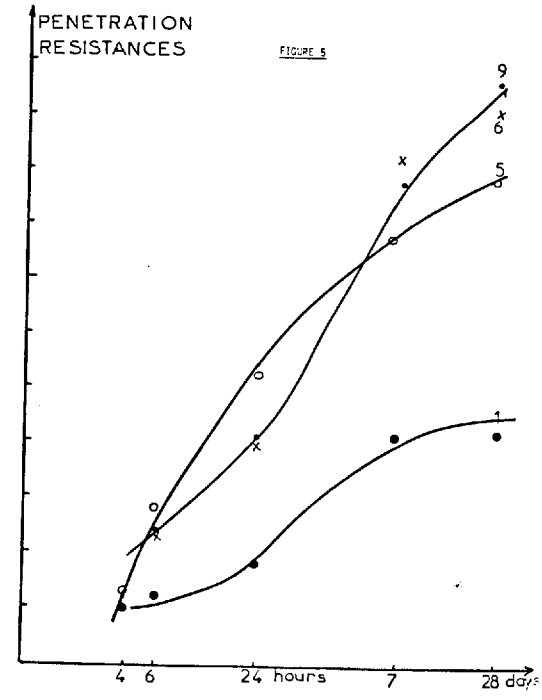

FIGURE 5

Table 4. Hydrates Formed as a Function of Hydration Time

Sample No.	Hydrate Type	6 hrs.	24 hrs.	7 days	28 days
1	C_2AH_8	strong	very strong	very strong	medium
	CAH_{10}	very weak	---	---	---
	C_3AH_6	---	very weak	weak	medium
5	C_2AH_8	medium	medium	strong	medium
	CAH_{10}	very weak	very weak	weak	very weak
	C_3AH_6	---	---	very weak	medium
6	C_2AH_8	medium	medium	medium	medium
	CAH_{10}	medium	medium	medium	very weak
	C_3AH_6	---	very weak	very weak	weak
9	C_2AH_8	medium	medium	medium	weak
	CAH_{10}	very strong	very strong	very strong	strong
	C_3AH_6	---	---	---	very weak

D. MENETRIER-SORRENTINO (LAFARGE COPPEE RECHERCHE France)
C.M. GEORGE (LAFARGE CALCIUM ALUMINATE NORFOLK U.S.A.)
F.P. SORRENTINO (LAFARGE COPPEE RECHERCHE France)

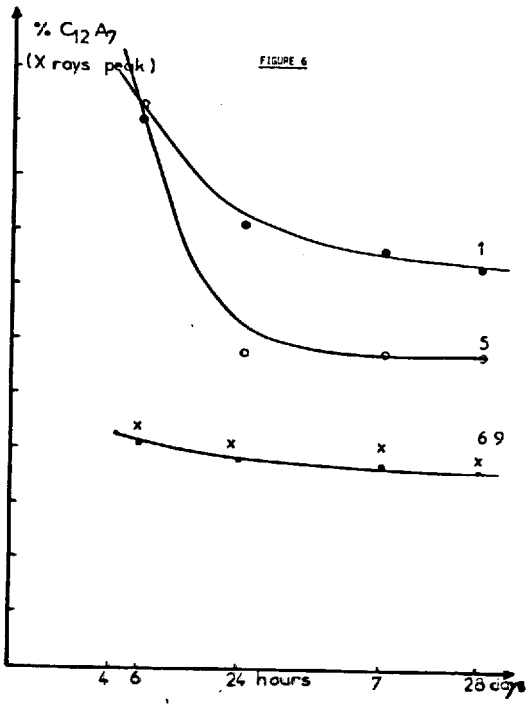

The results for LOI and for penetration resistance distinguish the very rapid setting cement (no 1) which has combined with much less water and shows lower strengths than the other cements.

The consumption of $C_{12}A_7$ during hydration indicated by the XRD data of figure 6 splits the cements into two categories corresponding to the two different mineralogies : $C_{12}A_7$ - C_3A and $C_{12}A_7$ - CA.

DISCUSSION

When calcium aluminates are put in contact with water calcium and aluminate ions pass into solution. In the case of CA, a metastable equilibrium is reached after about 2 hours with 20.5 X 10-3 moles/litre of calcium ions and 17.8 moles/litre of aluminate ions (4).

There then follows a dormand period of several hours which increases with the purity of the CA. Evnetually CAH_{10} precipitates and some C_2AH_8.

In the case of $C_{12}A_7$, the calcium and aluminate ions reach $25.0X10^{-3}$ moles/litre and 19.1×10^{-3} moles/litre respectively in about 30 minutes, at which point C_2AH_8 precipitates.

In general, ions pass into solution more rapidly and precipitation of hydrates occurs earlier the greater the C/A ratio of the anhydrous materials. This is related to the solubility products constants of the hydrates (5).

CAH_{10}, log. K_{sp} = -8.0 ; C_2AH_8, log K_{sp} = 13.75 ;
C_3AH_6, log. K_{sp} =-22.3 ; C_4AH_{19}, log K_{sp} =-25.5

In the case of the cements studied in this work the very rapid set (hydrate precipitation) of sample no 1 can be attributed to the dissolution of $C_{12}A_7$ accompanied by dissolution of C_3A to rapidly attain a ratio of calcium to aluminate ions of 2 and exceed the solubility limit of C_2AH_8.

In the case of sample no. 5, the amount of C_3A present is small and the other samples lie in the $C_{12}A_7$-CA zone. The beginning of hydrate precipitation (set) is thus progressively delayed as the ratio of calcium to aluminate ions in solution decreases.

It may also be supposed that the less lime rich calcium aluminates dissolve less rapidly.

The appearance of C_2AH at later ages is due to metastability of the hexagonal hydrates (CAH_{10}, C_2AH_8, C_4AH_{19}) with respect to this hydrate.

Support for the above description is given in figure 7 where the percentage of $C_{12}A_7$ measured in the samples is plotted agains the total CaO content. The amount of $C_{12}A_7$ is greatest in samples 5 and 6 and lower in sample 9 due to the formation of CA and lower in sample 1 due to the formation of C_3A. On the same figure the heat evolved during the first 15 minutes of reaction is also shown. It is quite low in samples 5, 6 and 9 which all have setting times well in excess of 15 minutes. On the contrary, sample 1, with a setting time of 1 minute has evolved nearly 25 % of its total heat of hydration due to hydrate precipitation.

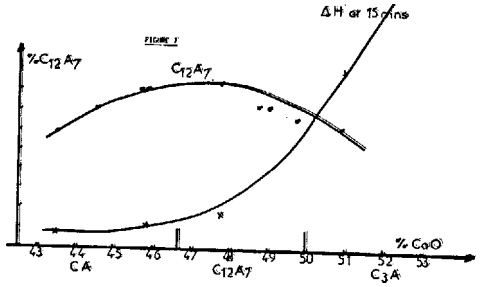

The penetrometer tests correlate well with the measurements of LOI. After 4 hrs, all samples have reacted with about 18 % of the available water and display the same strength. Beyond this age, samples 5, 6 and 9 continue to hydrate and increase in strength whereas sample 1 shows much smaller changes.

The ultimate penetration resistance (28 days) increases as the setting time increases. This cannot be explained by the degree of hydration alone (LOI) and is most likely to be a fonction both of hydrate morphology and the density of the hydrates formed which is generally greater the higher the ratio of C/A.

CONCLUSIONS

The use of conductimetry, microcalorimetry, XRD, penetrometry and measurement of bound water on a number of experimental cements in the $C_{12}A_7$-C_3A and $C_{12}A_7$-CA systems enables differences in their setting hardening characteristics to be at least partially explained.

Rapid setting is associated with cements rich in $C_{12}A_7$ and C_3A which dissolve rapidly, and quickly exceed to solubility of the C_2AH_8 hydrate. Cements containing $C_{12}A_7$-CA were the longest setting cements studied in this work. As the amount of C_3A in these cements diminishes and the amount of CA increases the predominant hydrate found becomes CAH_{10} which has a much higher solubility product than C_2AH_8 and is precipited less rapidly.

The long term strengths of the cements investigated increase as their setting times increase and their early strengths diminish.

This can be explained to some degree from a knowledge of densities of the different hydrates and is also probably related to their morphology and degree of cristallinity.

To achieve a greater understanding of the hydration characteristics of these typical calcium aluminate cements, sutdies are needed of the rate of dissolution in water and the interactions occurring between the different ionic species in solution which influence the nature and timing of hydrate precipitation.

REFERENCES

1 - KURDOWSKI W., SORRENTINO F.
Special Cements - Chapter 10 in "Structure and Performance of Cements", Colt Barnes, Applied Science Publisher, 1983.

2 - COTTIN B., Certaines interactions entre C_3A et C_3S lors de l'hydratation des ciments Portland. 7th International Congress on the Chemistry of Cement, Paris, 1980.

3 - COTTIN B. et al
Fast Setting Cement - Mechanism of Hydration. American Ceramic Society Congress, Cincinnati, 1982.

4 - BERTRANDIE D.
Cinétique de Formation d'Hydrates dans des solutions obtenues à partir de Ciments Alumineux. These, 13 JUIN 1977. Dijon.

5 - NIKUSHCHENKO, V.M. et al
Determination of the Standard Free Energy of Formation of Calcium Aluminates. Cement Concrete Research vol. 3. pp. 625, 1973.

D. MENETRIER-SORRENTINO, Chargée de Recherche au CNRS, en détachement à LAFARGE COPPEE RECHERCHE, France 1
P. BARRET, Laboratoire de Recherche sur la Réactivité des Solides, DIJON, France - S. SAQOUT

INVESTIGATIONS on the SYSTEM MgO - $MgCl_2$ - H_2O, and HYDRATION of SOREL CEMENT
RECHERCHES sur le SYSTEME MgO - $MgCl_2$ - H_2O - et HYDRATATION du CIMENT de SOREL 3.3

SUMMARY : Magnesium oxychloride cement, also termed Sorel cement (1), is made by mixing powered MgO with concentrated aqueous solutions of $MgCl_2$.

The hydration kinetics develop in several successive or overlapping steps, and hardening of the pastes occurs with the formation of hydrates containing two or three of the constituents. From this, it is clear that the understanding of the behaviour of Sorel cement, and more precisely its behaviour against water attack, goes necessarely with an accurate knowdledge of the solubility curves of the hydrates formed in the MgO - $MgCl_2$ - H_2O system.

Our work is mainly directed to answer this question and contains two basic parts : one, kinetic, is intended to seize the steps of the reaction (4 have been evidenced), the other is devoted to the precise establishment of the equilibrium phase diagram. Four hydrates are susceptible to form at 25 °C ; their solubility products have been determined, but more stricking is the position of their solubility curves in the diagram, prompting us to express an unfavourable opinion about the outdoor use of such a cement.

O cimento de oxicloreto de magnésio, também chamado cimento de Sorel, é feito com mistura de MgO pulverizado com soluções aquosas concentradas de $MgCl_2$.

A cinética de hidratação se desenvolve em vários estágios sucessivos ou sobrepostos, e o endurecimento das pastas se dá com a formação de hidratos contendo dois ou três constituintes. Daí se torna claro que a compreensão do comportamento do cimento de Sorel, e mais precisamente do seu comportamento contra o ataque de água, pressupõe necessariamente um conhecimento acurado das curvas de solubilidade dos hidratos formados no sistema MgO-$MgCl_2$-H_2O.

Nosso trabalho pretende principalmente resolver esta questão, e contém duas partes básicas: uma, cinética, tenciona dimensionar as etapas da reação (4 foram evidenciadas); a outra se volta para o estabelecimento preciso do diagrama de fase de equilíbrio. Quatro hidratos podem formar-se a 25°C; seus produtos de solubilidade foram determinados, mas o mais notável é a posição de suas curvas de solubilidade no gráfico, levando-nos a emitir uma opinião desfavorável a respeito do uso de tal cimento ao ar livre.

D. MENETRIER-SORRENTINO, Chargée de Recherche au C.N.R.S., en détachement à LAFARGE COPPEE RECHERCHE, France 2
P. BARRET, Laboratoire de Recherche sur la Réactivité des Solides, DIJON, France S. SAQOUT

INTRODUCTION

In our attempt to develop a new type of composite material constituted by a mat of ordinary E-glass fibers, impregnated with a fluid paste of Sorel cement (2), we have been led to undertake a basic study on this cement (3).

The composite samples had a bad behaviour, when kept out of doors (small pieces were peeling off, cracks were appearing) and they eventually fell appart.

Similar problems have previously been observed, and several solutions have been proposed, many of them as patents (see examples quoted in the report on Special Cements, this congress). We must however point out that, although a wide variety of products has been tested very few works have a scientific basis, and are devoted to determine the exact reason why this cement offers a poor resistance to weathering. In such a situation, we have conducted a thorough and systematic study of the $MgO-MgCl_2-H_2O$ system, since Sorel cement is made of MgO and aqueous solutions of $MgCl_2$. Among all the studies dealing with this cement, two only have led to the establishment of the equilibrium phase diagram of the $MgO - MgCl_2 - H_2O$ system, both of them being by SORRELL et al,[2] (4, 5). But, large discrepancies appear in the position of the curves ; the authors could not choose between them and they also made the activity of MgO responsible for the problems encountered with Sorel cement. If we agree on the fact that MgO plays an important role and that a good quality MgO is a necessary condition, its careful selection is however not sufficient alone.

EXPERIMENTAL PROCEDURE

A series of mixturescontaining MgO, $MgCl_2$, H_2O in different proportions have been prepared. The compositions have been calculated in order to cover all the parts of the diagram of interest for Sorel cement.

The experiment consists, in fact, first in preparing the solution of $MgCl_2$ of desired concentration and placing it in a thermo regulated cell. Once the electrical conductibility (χ) of the solution and its pH are stable, the weighted amount of MgO is added and reaction initiates.

We have worked out this study along two principal axis : a kinetic one, an a thermodynamic one (equilibrium state), what makes one of its originalities. Another one is the experimental procedure, we have developed.

Kinetic steps of the reaction are followed in one hand, by continuously recording the electrical conductibility and the pH of the liquid phase, and in the other hand, by performing analysis on samples collected at selected times in the reacting vessel. After separation of the liquid and solid phase by filtration, and drying of the solid by ethylic alcohol, Mg^{2+}, Cl^- and OH^- are quantitatively determined on the liquid phase, while solid phases are characterized using X-ray diffraction, infrared spectroscopy, S.E.M., ...

Parallel experiments have been conducted with an isotherm Calvet calorimeter.

Once reaction has gone to completion, the same series of analysis are applied to the mixture. This gives, for each composition studied, a couple of values (liquid phase, solid phase).

RESULTS, DISCUSSION

Both aspects of our study are in close connection, however to be clear, will be handled separately.

Kinetic study : whatever composition under investigation, the shape of the curves showing the evolution of χ and pH of the solution is unique (fig. 1) ; the numerical values are however different.

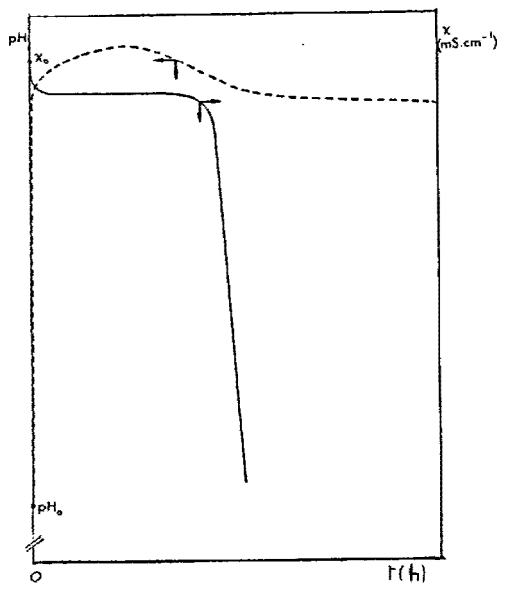

FIG.1 : Kinetic study of the reaction MgO + $MgCl_{2aq}$: evolution of χ and pH of the liquid phase.

Exception made with compositions leading to the formation of pure $Mg(OH)_2$, the curves obtained for Mg^{+2} and Cl^- are also typical (fig. 2).

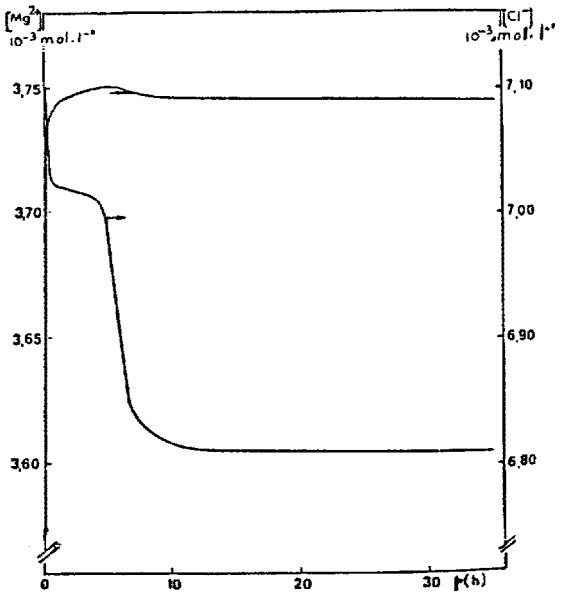

FIG. 2 : Evolution of Mg^{+2} and Cl^- concentrations, in the liquid phase .

D. MENETRIER-SORRENTINO, Chargée de Recherche au C.N.R.S. , en détachement à LAFARGE COPPEE RECHERCHE, France 3
P. BARRET, Laboratoire de Recherche sur la Réactivité des Solides, DIJON, France - S. SAQOUT

This is valid only in the case of the formation of one type of hydrate, otherwise the curves are more complex.

The observation of these 4 curves allows us to say that the reaction proceeds through 4 main steps :

1 - The initial, very short period (few min.), is characterized by a rapid increase of pH and Mg^{2+} concentration. The Mg^{2+} increase is relatively small (0.1 to 0.25 mol.l^{-1}) compared to the pH one whose magnitude (1 to 2 units) depends on the pH of the $MgCl_2$ solution, at instant zero.

2 - During the second step, pH and Mg^{2+} variations are small, however positive, which makes the liquid slightly supersaturated with respect to the hydrates.

π shows a plateau, as also observed with other classical cements (6). However, at the contrary to these cements, for which it is difficult to give a conclusive answer on the exact origin of the plateau - (induction period of the hydrates or steady state having a kinetic origin resulting from a competitive process between hydrates precipitation and MgO dissolution) - the analytical data available in this case, allow to bring a conclusion : since the total amount of Cl^- ions is introduced at t = 0, in the form of $MgCl_2$ solution, the variation of stationnary level of Cl^- is directly related to the precipitation rate of the hydrates or to their induction period : fig. 2 shows that Cl^- presents a plateau, so, this second period, is the nucleation period of the hydrates.

3 - π and Cl^- concentration decrease promply : this indicates a massive precipitation of the hydrates. Mg^{2+} and pH vary slowly, because, during this period unreacted particles of MgO dissolve, and supply the solution with Mg^{2+}.

4 - Hydrates continue being formed, but at a slower rate; the cement paste is hard, and the reaction goes on, to reach its equilibrium state.
This sequence of steps is confirmed by the calorimetric curves (3). When only one type of hydrates is formed, the thermogram looks typically like those obtained with regular cements : an initial sharp peak of short length is followed by a period of low heat evolution, then a massive exothermic peak occurs, connected with the intensive hydrates precipitation. If two hydrates are formed successively two main peaks are observed ; they are more or less well separated, depending on the beginning time of precipitation of the second hydrate.

Thermodynamic study : the collection of all the points representing the values obtained on the liquid phases, at equilibrium, allow to define the solubility curves of the hydrates, and the points representing the corresponding solid phases, delineate the separated regions of the phase diagram, as shown in fig. 3.
The existence of 4 hydrates has been confirmed, and from the left to the right part of the diagram, we have :

- $Mg(OH)_2$
- 5 $Mg(OH)_2.MgCl_2.8H_2O$ termed 5.1.8. or phase 5
- 3 $Mg(OH)_2.MgCl_2.8H_2O$ termed 3.1.8. or phase 3
- $MgCl_2.6H_2O$

FIG. 3 : Equilibrium phase diagram of system MgO - $MgCl_2$ - H_2O at 25°C.

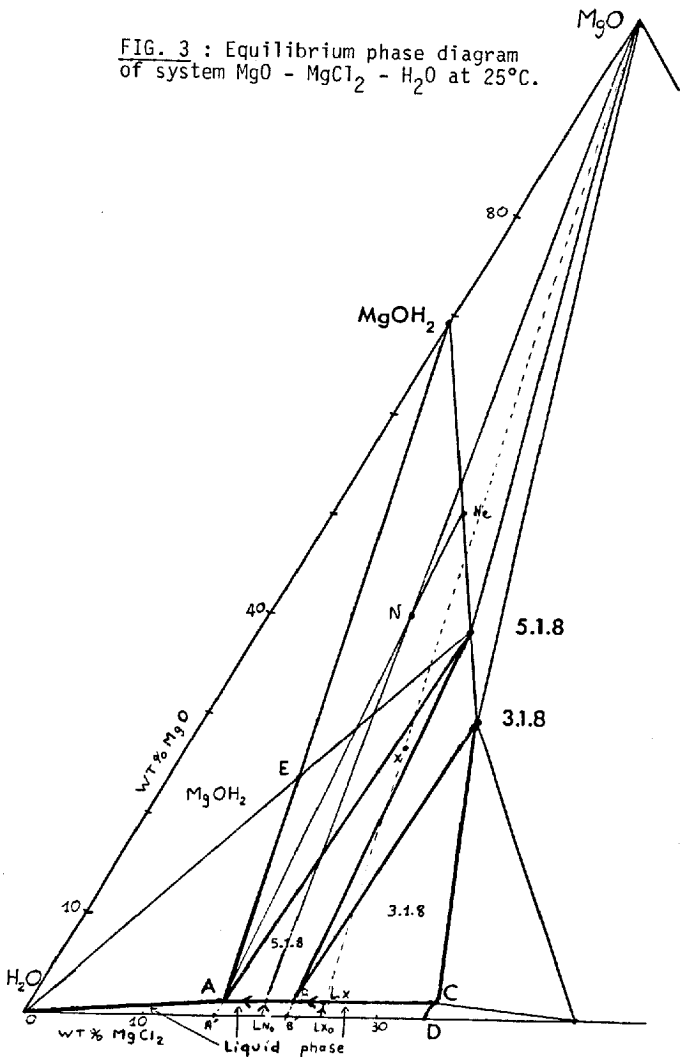

The solubility product of each hydrate has been determined by calculation based on, liquid phase analysis, ionic strength, the activity coefficients and using the equation of the hydrate decomposition. Values are respectively $5.82.10^{-11}$ for $Mg(OH)_2$, $7.33.10^{-54}$ for 5.1.8. and $3.9.7.\ 10^{-31}$ for 3.1.8.[2] However, although there is undoubtedly an interest in knowing them ; we must be very careful, since their very low values could easily result in a misinterpretation. The numerical values of the solubility, expressed as MgO and $MgCl_2$ are much more adequate to reflect the reality : for 5.1.8., MgO is around 10 g. l^{-1}, and $MgCl_2$ ranges from 205 to 270 g.l^{-1}, what is extremely high.

Several results can be drawn from this diagram : one part is, what can regularly be expected, another one has a precise meaning concerning Sorel cement. We present few examples :

- the equilibrium state, of a given mixture may be predicted qualitatively (nature of the solid phases) and quantitatively (proportions of the solid phases, concentration of the liquid phase), by the simple knowledge of the composition of the initial mix

D. MENETRIER-SORRENTINO, Chargée de Recherche au C.N.R.S., en détachement à LAFARGE COPPEE RECHERCHE, France 4
P. BARRET, Laboratoire de Recherche sur la Réactivité des Solides, DIJON, France - S. SAQOUT

($MgO + MgCl_2 Sol.$). As illustration, let's take a composition commonly used to prepare Sorel cement pastes : 40 % MgO, 12.3 % $MgCl_2$, 47.6 % H_2O ; it is represented by point N, fig.3 (weight percent). The corresponding aqueous solution of $MgCl_2$ is 20, 60% (point LN_0), and according to the basic rule in use in the phase diagram these three points N, LN_0 (liquid phase) and MgO (solid phase) form a straight line. When the hydration reaction will be over, the global composition will still be represented by N, but the solid phase will be N_e (5.1.8. + $Mg(OH)_2$) and the liquid phase will be located in A (invariant point of intersection of the solubility curves of $Mg(OH)_2$ and 5.1.8.).Note that the three points are again on line.

- The transitory precipitation of one hydrate, and its subsequent disappearance, finds also a theoretic explanation : point X, eg is located in the region of formation of the unique phase 5.1.8., however, due to the position of its corresponding initial liquid phase (point Lx_0), we see that 3.1.8. will form first (point Lx) and then will get transformed into 5.1.8., while the remaining MgO will react with $MgCl_2$, to form additional 5.1.8.

- The stability of hydrate 5.1.8. has been questioned by several authors, who noticed its conversion into 3.1.8. (4, 7, 8). This may possibly mean that 5.1.8. is metastable with respect to 3.1.8., otherwise said, the solubility curve of 3.1.8. would lie under that of 5.1.8. one, in the region where 5.1.8. is expected to be stable. To check if such an hypothesis is valid, we have tried to approach the solubility curves of phase 5 by a different way. The experiment consists of the dissolution of 5.1.8. - previously prepared in large quantities - in solutions ranging from pure water to saturated $MgCl_2$ solutions. The apparently strange results - $Mg(OH)_2$ or 5.1.8. or their mixture, and even 3.1.8., were obtained - are however in conformity with the phase diagram. Three types of results are possible :

1 - If 5.1.8. is placed in pure water, or in solutions containing less than 16.4 % $MgCl_2$ - point A' -, it will dissolve and then form either pure $Mg(OH)_2$, or $Mg(OH)_2$ + 5.1.8. This depends on the proportion of 5.1.8. (solid) compared to that of the liquid phase one : if the mixture is diluted, then its representative point - necessarely lying on the H_2O - 5.1.8. line - will be located on this side of point E, i.e. in the $Mg(OH)_2$ region. If the mixture is 5.1.8. rich, the point will be beyond point E, in the region where $Mg(OH)_2$ + 5.1.8. coexist.

2 - If the concentration of the $MgCl_2$ solution is higher than 22.1 % (B') 3.1.8. or a mixure of 3.1.8.+ 5.1.8. may appear.

3 - If the concentration of the $MgCl_2$ solution is between 16.4 and 22.1 % it is the only case where the dissolution of 5.1.8. will finally result in the re-precipitation of 5.1.8., in other words, its preservation. This makes the previous hypothesis unvalid : 5.1.8. has been kept, precisely in the region where its stability was questioned, and the exact reason of its conversion, into phase 3, has still to be found.

Explanation of the behaviour of Sorel cement, out of doors

We have now sufficient information to deal with our most important point, the instability of Sorel cement with respect to water. As said above, a paste contains usually a mix of $Mg(OH)_2$ + 5.1.8. (point N_e), and sometimes unreacted MgO. If rain-water comes into contact with this paste, $Mg(OH)_2$ will not be greatly modified - its solubility is very low -, but 5.1.8. will be dissolved.

The situation is partially the one explained in §1, with this difference that, in the previous case, the system was closed and the liquid phase had a finite volume. In this opposite case, we are dealing with running water-, the system is open. 5.1.8. which undergoes a dissolution, will supply the liquid phase with Mg^{2+}, Cl^- and OH^- ions, so its representative point will move along the straight line H_2O - 5.1.8., and, as seen in fig.3, it will be immediatly supersaturated with respect to $Mg(OH)_2$. This liquid phase will run away, fresh rain-water will come into contact with the paste, and 5.1.8. will progressively be destroyed.

Depending on the rate of leaching $Mg(OH)_2$ may or not have enough time to re-precipitate on the surface of the paste.

This theoritical prediction has - unfortunatly - been fully confirmed experimentally, thanks to a test we have especially developed, and called "rain-water simulation test". A thin piece of hydrated paste, is submitted to a flow of pure water, in defined conditions (flow-rate, position of the sample...) ; the liquid then enters a conductimetric cell with circulation - thus indicating the rate of dissolution -, and a second vessel containing a pH and Cl^- specific electrode, also rendering an account of the instantaneous dissolution rate. Complete results of this test are given elsewhere (2), but they can be summarized in three points :

1 - 5.1.8. dissolves continuously and at a steady rate, apart from an initial short period,

2 - the total amount of solid dissolved during one test, lasting 8 hours, is high, and may reach several per cent. Repeated tests on the same sample show the same trend,

3 - X-Ray diffraction analysis of the residual surface of the paste show that it is ill-crystallized $Mg(OH)_2$.

Equivalent results would be obtained with the second main hydrate 3.1.8.

This leads to express an unfavourable opinion about the outdoor use of Sorel cement and to question the validity of patents on its water-resistance (5.1.8. solubility is around 200 g. l^{-1}).

CONCLUSIONS

Our study, which is original in several ways (kinetic study along with thermodynamic study development of special experimental procedure ...) has allowed :

- a better understanding of the mechanisms of hydration of magnesium oxychloride cement : the reaction proceeds through 4 main steps.

- the establishment of the full equilibrium phase diagram of the system MgO - $MgCl_2$ - H_2O at 25 °C. From this, the instability of Sorel cement paste,

when kept out of doors, has found an explanation.

However, thanks to its numerous qualities, and even superiorities with respect to other cements, we can reasonably predict new developments to this cement, for indoor uses. The renewed interest brought to it, is already detectible through the high number of publications and patents published during the last 6 years (see principal report on Special Cements this congress).

ACKNOWLEDGEMENTS

The authors are thankful to D.G.R.S.T. for its financial support (grant 81 P 0630).

REFERENCES

1 - S. SOREL, Sur un Nouveau Ciment Magnésien, C.R. Acad. Sc. Paris 65, 102-104 (1867).

2 - D. MENETRIER-SORRENTINO, Rapport D.G.R.S.T., Matériaux P.079, 81 P 0630, Recherche du Contrôle de la Tenue aux Intempéries d'un Matériau Composite Fibres de Verre - Ciment à l'Oxychlorure de Magnésium (1984).

3 - S. SAQOUT, Contribution à l'Etude du Diagramme Ternaire MgO - $MgCl_2$ - H_2O à 25°C, thèse Dijon (France) (1983).

4 - C.A. SORRELL, C.R. ARMSTRONG, Reactions and Equilibrium in Magnesium Oxychloride Cements, J. Amer. Ceram. Society, 59, 51 (1976).

5 - L. URGWONSE, C.A. SORRELL, The System Mgo - $MgCl_2$ - H_2O, at 23 °C, J. Amer. Ceram. Society 63, 501, (1980).

6 - P. BARRET, D. MENETRIER, D. BERTRANDIE, Cem. Concr. Research, 4, 545 - 556 (1974).

7 - B. MATKOVIC et al. Development of Strength in Cements. Report no. FHWA/RD - 80/128 (1981).

8 - Y. BIANCO, Formation des Chlorures Basiques du Magnésium, C.R. Acad. Sc. Paris, 232, 1108 (1951).

J. Péra, J. Ambroise, M. Murat et M. Silveira. Institut National des Sciences Appliquées de Lyon. Laboratoire des Solides et Matériaux Minéraux Bât. 404., 20, Avenue Albert Einstein. F. 69621 Villeurbanne Cedex (France).

Ciments à base de latérites thermiquement activées. Rôle des oxydes de fer dans le développement des résistances mécaniques.

Cements of thermally activated laterites. Role of iron oxides on the strength development.

Résumé. Les auteurs montrent que les latérites thermiquement activées à 750°C s'avèrent être des pouzzolanes de synthèse de premier choix pour l'élaboration de liants économiques dans les pays en développement. Après calcination, les latérites donnent une phase cristallographiquement désorganisée qui réagit en présence de chaux et d'eau pour donner un liant atteignant des résistances en compression de l'ordre de 30 MPa à une échéance de 28 jours. Ces résistances sont très intéressantes pour des sols à teneur assez peu élevée en kaolin (30 à 55 %) par rapport à des liants pouzzolaniques de synthèse obtenus à partir d'un kaolin pur (35 MPa).

En outre, le rapport massique (latérite calcinée/chaux) conduisant aux résistances optimales est en général de 4, ce qui est particulièrement intéressant pour des régions comme l'Afrique sub-saharienne où les latérites sont très abondantes et l'approvisionnement en chaux ou en clinker assez difficile.

On constate par ailleurs que la présence d'oxydes de fer dans des sols assez pauvres en kaolinite pure est un facteur favorable dans le développement des résistances mécaniques des produits d'activation thermique traités à la chaux. En effet, celles-ci croissent avec le rapport (Kaolinite + Oxydes de fer)/(Quartz). L'étude menée par les auteurs a d'autre part clairement mis en évidence le rôle néfaste du quartz à partir d'un certain seuil (environ 50 %).

Os autores mostram que as lateritas ativadas termicamente a 750°C constituem pozolanas de síntese de primeira categoria para elaboração de ligantes econômicos em países em desenvolvimento. Após calcinação, as lateritas dão uma fase desorganizada cristalograficamente, que reage em presença de água para dar um ligante que atinge resistências à compressão da ordem de 30 MPa ao final de 28 dias. Estas resistências são muito interessantes para solos com teor bastante baixo de caolim (30 a 55%) em relação aos ligantes pozolânicos sintéticos obtidos a partir de um caolim puro (35 MPa).

Além disso, a relação de massa (laterita calcinada/cal), que leva às resistências, ótimas, em geral é igual a 4, o que é particularmente interessante para regiões como o sub-Saara na África, onde há grande abundância de lateritas e o suprimento de cal ou clinquer é muito difícil.

Por outro lado se constata que a presença de óxidos de ferro em solos muito pobres em caolinita pura é um fator favorável para o desenvolvimento das resistências mecânicas dos produtos de ativação térmica tratados a cal. Com efeito, estas crescem na razão de (caolinita + óxidos de ferro)/(quartzo). O estudo feito pelos autores, por outro lado, evidenciou o papel prejudicial do quartzo a partir de um certo limite (cerca de 50%).

I. INTRODUCTION.

Le problème d'approvisionnement en ciment des pays en développement se pose aujourd'hui avec beaucoup d'acuité à cause des investissements gigantesques nécessaires, des infrastructures pratiquement inexistantes et de la maitrise de matières premières différentes de celles qu'on rencontre par exemple en Europe (1). Par ailleurs si, en Europe, les liants ne représentent que 1 à 2 % du coût de la construction, ils peuvent en revanche atteindre 10 à 30 % du prix de l'habitat économique.

La fabrication d'un liant pouzzolanique à partir de latérites calcinées à moyenne température s'avère être une solution intéressante à ce problème puisqu'elle permet à la fois d'économiser le calcaire (assez peu abondant en Afrique sub-saharienne) et de valoriser des matériaux abondants comme les latérites. En effet, le rapport chaux/pouzzolane qui conduit aux résistances mécaniques optimales est de 1/4 alors que la fabrication de clinker requiert 80 % de calcaire et 20 % d'argile (2 à 8).

L'étude présentée ici porte sur six latérites kaoliniques (le pourcentage de kaolinite variant de 33 à 55 %) et une kaolinite française impure servant de référence. C'est une extension des recherches menées ces dernières années au laboratoire sur l'élaboration de liants pouzzolaniques de synthèse à partir de kaolinites thermiquement activées dans le domaine de température (600-800°C) (3, 9 à 16).

II. DONNEES CONCERNANT LES LATERITES.

2.1. Formation et composition des latérites.

Le phénomène de latérisation est un processus de formation des sols spécifique aux régions tropicales chaudes et humides. Il s'agit d'une altération de la roche mère dont la caractéristique essentielle réside dans une mise en solution puis un départ de la silice, phénomène de lessivage, accompagnés d'un enrichissement en fer et en alumine sous forme de sesquioxydes Fe_2O_3 et Al_2O_3.

Le tableau I donne les éléments majeurs entrant dans la composition minéralogique des latérites

2.2. Déshydratation des argiles et des latérites (3).

2.2.1. Déshydratation des argiles.

La réactivité hydraulique des produits de déshydroxylation (ou de déshydratation) des argiles est liée à leur caractère de "phase cristallographiquement désorganisée". La formation de ces phases désorganisées est tributaire de la nature de l'argile de départ.

Les principaux minéraux argileux susceptibles de conduire à ces phases désorganisées sont essentiellement :

- la kaolinite, le talc et la montmorillonite selon Sabatier,
- le talc, la vermiculite, le chrysotile et la kaolinite selon Lemaître.

Les argiles ne donnant pas de phases désorganisées par déshydroxylation sont essentiellement la pyrophyllite et la muscovite.

L'existence d'une phase transitoire désorganisée peut être détectée sur les courbes ATD par l'existence vers 900-1100°C d'un pic exothermique traduisant un phénomène de recristallisation (Fig. 1).

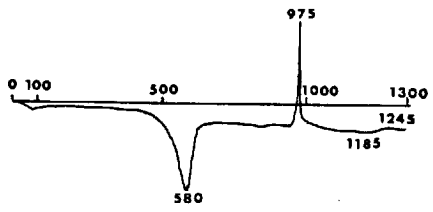

Figure 1. Courbe d'analyse thermique différentielle du kaolin (17).

La décomposition du kaolin entre 600 et 900°C se fait suivant la réaction :

$$\underset{\text{kaolin}}{Al_2O_3.2SiO_2.2H_2O} \rightarrow \underset{\substack{\text{métalaolin} \\ \text{cristallographiquement} \\ \text{amorphe}}}{Al_2O_3.2SiO_2} + 2\ H_2O\ \text{vap.}$$

TABLEAU I
Minéraux entrant dans la composition des latérites.

Eléments	Hydroxydes et oxydes de fer	Hydroxydes et oxydes d'aluminium	Minéraux argileux
communs	goethite limonite hématite	gibbsite boehmite (plus rare)	kaolinite halloysite (plus rare)
rares	maghémite magnétite illiménite	corindon diaspore	illite montmorillonite

2.2.2. Déshydration des latérites

Ces matières premières contiennent des minéraux argileux (kaolinite, halloysite, montmorillonite) et des oxydes de fer ou d'aluminium. La déshydroxylation des minéraux argileux se ramène à ce qui a été dit précédemment.

La boehmite ainsi que la gibbsite présentes dans les latérites conduisent à des phases désorganisées à moyenne température ; ces phases recristallisent en corindon au delà de 1000°C.

$$AlOOH \text{ (boehmite)} \xrightarrow{450\text{-}580^\circ C} Al_2O_3\gamma \rightarrow \delta \rightarrow \theta$$

$$Al(OH)_3\gamma \text{ (gibbsite)} \xrightarrow{300^\circ C} \begin{matrix} Al_2O_3\gamma \rightarrow Al_2O_3 K > 1000^\circ C \\ AlOOH\gamma \rightarrow Al_2O_3\gamma \rightarrow \delta \end{matrix} \rightarrow \theta \xrightarrow{> 1000^\circ C} \text{corindon}$$

La déshydratation des hydroxydes de fer ne conduit pas à des phases désorganisées mais une activité hydraulique de ces oxydes n'est pas exclue si leur état de cristallisation est mauvais.

III. RESULTATS EXPERIMENTAUX ET INTERPRETATION.

Les caractéristiques des produits étudiés figurent dans le tableau II.

Les produits sont calcinés pendant cinq heures à une température de 750°C dans un réacteur à lit fixe. La caratérisation des produits avant et après cuisson est effectuée par diffraction des rayons X. La figure 2 montre la désorganisation parfaite de la kaolinite contenue dans la latérite de Yaoundé (notée C) après activation thermique à 750°C. Sur cette figure, est clairement mise en évidence la présence de quartz, de gibbsite, d'oxyde de fer et de goethite.

Les produits activés thermiquement sont mélangés à de l'hydroxyde de calcium dans des proportions massiques "Latérite calcinée/Chaux" variant de 1 à 5. Le liant est obtenu par mélange avec de l'eau dans un malaxeur RILEM type 32. Le taux de gâchage retenu a conduit aux résistances mécaniques optimales ; il correspond à une ouvrabilité limite soit la consistance normale définie par la norme NFP15-402. Les éprouvettes utilisées sont des micro-cylindres de 2 cm de diamètre et d'élancement 2.

Pendant le début de l'hydratation, les éprouvettes sont conservées dans les moules en plexiglass à l'abri de l'air à 20°C. Le démoulage intervient à 7 jours ; les échantillons sont alors placés sous eau (norme NFP15-401, pâte pure). Les résistances en compression sont déterminées après séchage pendant 24 heures à 50°C, au vingt-huitième jour sur une population de 6 éprouvettes pour chaque rapport"Latérite calcinée/Chaux", avec une dispersion inférieure à 10 %.

TABLEAU II
Origine et caractéristiques des sols étudiés.

Numérotation	SM1	SM2	SM3	SM4	G	C	K
Origine	Bamako Sotuba (Mali)	Bamako Bako-Djikoroni (Mali)	Bamako Djikoroni Para (Mali)	Bamako Kalabankora (Mali)	environs Libreville (Gabon)	Carrière IRIC Yaoundé Cameroun	Société SIKA (Hostun) France
Perte au feu	10,20	6,2	10,3	6,5	15,1	11,6	8,12
SiO_2	61,17	63,74	75,5	65,93	48,15	48,56	66,87
Al_2O_3	17,39	19,40	12,84	17,15	13,61	22	23
TiO_2	1,30	1,15	1,16	0,89	0,91	1,07	0,27
Fe_2O_3	7,61	4,40	3,73	2,36	17,94	9	0,85
CaO	0,40	0,61	0,29	0,99	0,59	0,048	0,30
MgO	0,41	0,26	0,19	1,51	0,57	0,50	traces
Na_2O	0,27	0,22	0,29	0,68	0,68	0,013	0,07
K_2O	0,89	0,67	0,48	0,79	0,48	0,04	0,23
% kaolinite calculée (*)	44	49	33	43	34	55	63
% Quartz	41	41	60	46	32	23	37

(*) En supposant que l'alumine contenue est entièrement sous forme de kaolinite. En fait, une partie du fer dans ces minéraux est substituée en couche octaédrique donc les % de kaolinite calculés sont par défaut.

3.3

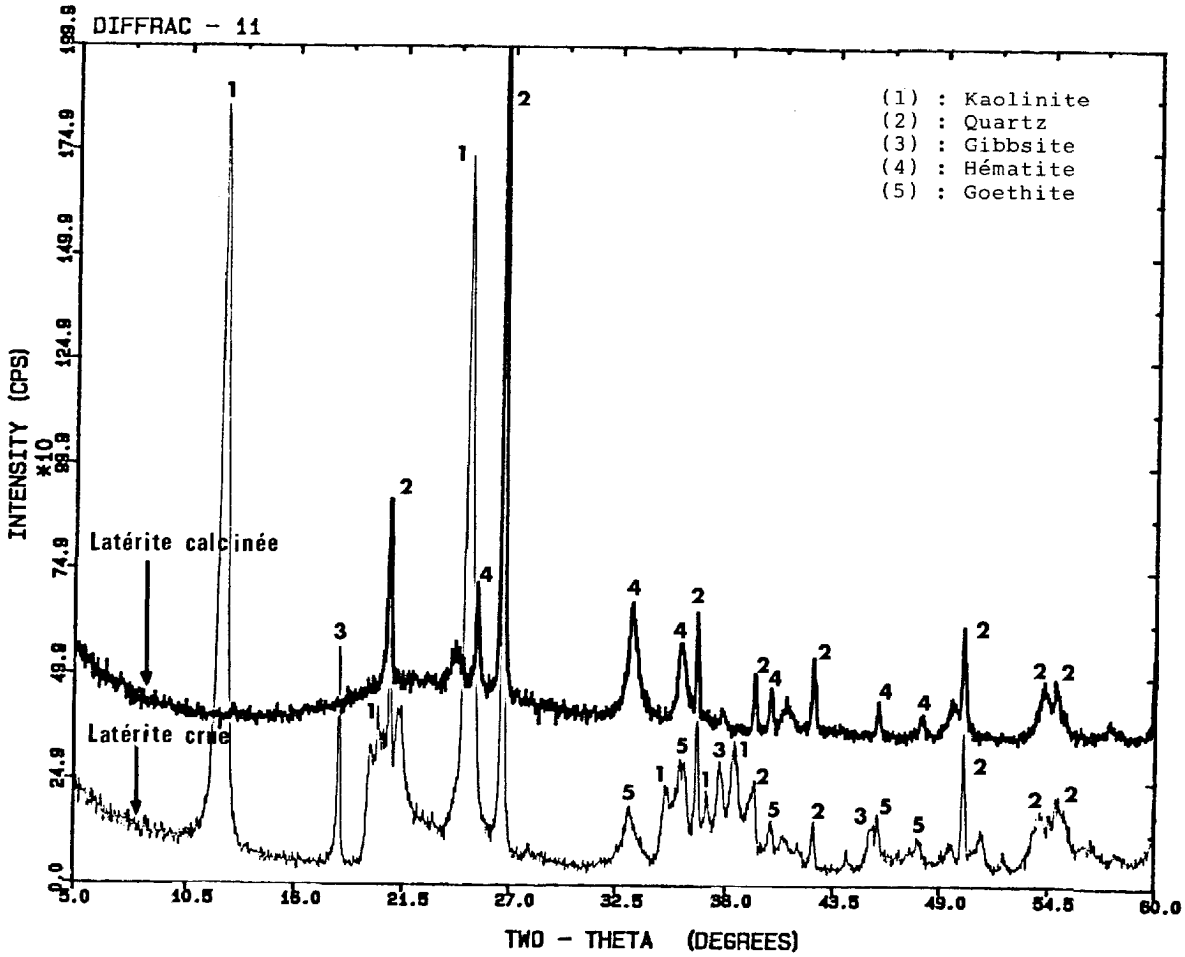

Figure 2. Diffractogrammes X de la latérite du Cameroun (C) et de son produit de cuisson. Pour faire la comparaison, un décalage de zéro a été nécessaire.

Les résultats obtenus sur la latérite du Cameroun (C) et trois des sols maliens (SM1, SM2, SM3) sont comparés à ceux issus de l'élaboration d'un liant à partir de kaolinite pure (notée K_2) sur la figure 3.

Sur cette figure, on voit parfaitement que le rapport "Latérite calcinée/Chaux" conduisant aux résistances optimales est égal à 4 dans la plupart des cas. Ce résultat a été confirmé par les résultats obtenus à partir de la latérite du Gabon et du sol malien SM4.

Il semble également que l'état de désorganisation de la phase transitoire issue de la cuisson à 750°C du minéral de départ est d'autant plus marqué que l'état de cristallinité de ce minéral est plus mauvais. Ce phénomène est clairement apparu dans le cas des kaolinites et des latérites que nous avons étudiées (4, 13, 14). Les conditions de formation géologique de ces dernières ont conduit le plus souvent à un phénomène de substitution partielle de l'aluminium de la couche octaédrique du feuillet de kaolin par du fer, ce qui est un facteur défavorable

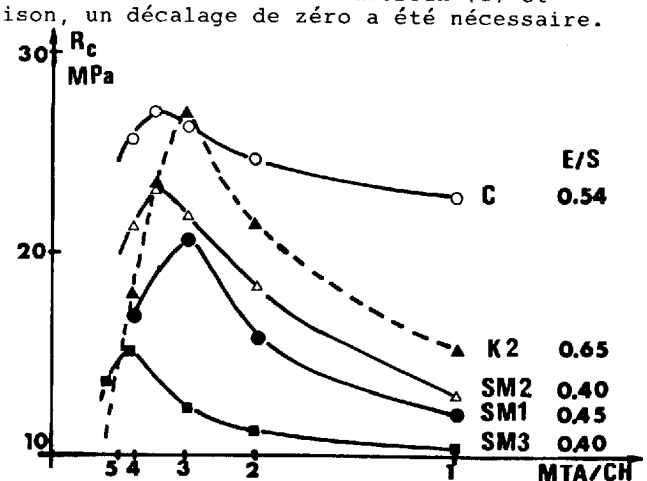

Figure 3. Variation de la résistance en compression à 28 jours (sur pâte pure) en fonction du rapport "Minéral thermiquement activé/Hydroxyde de calcium" (MTA/CH).

C : Latérite du Cameroun
K_2 : Kaolinite pure
SM : Latérites du Mali
E/S : Taux de gâchage

pour la cristallinité mais par contre très favorable si l'on désire valoriser localement ces sols dans le domaine des ciments pouzzolaniques de synthèse, comme en attestent les niveaux de résistance mécanique (15 à 27 MPa) obtenus à l'échéance de 28 jours pour des sols à teneur assez peu élevée en kaolin (33 à 55 %) (Fig. 3).

Pour mettre en évidence le rôle joué par les oxydes et hydroxydes de fer dans le développement des résistances (R_c) de ces liants, nous avons considéré le rapport A défini comme suit :

$$A = \frac{\text{Kaolinite + Oxydes de fer}}{\text{Quartz}}$$ (Tableau III)

TABLEAU III.

Relation entre le rapport A et la résistance R_c.
Les proportions de kaolinite, d'oxydes de fer et de quartz ont été calculées en considérant que la somme de ces trois éléments faisait 100 %.

Minéral de départ / %	SM_1	SM_2	SM_3	SM_4	G	C	K
Kaolinite	47,5	51,9	34,1	47,1	40,5	63,2	63
Oxydes de fer	8,2	4,7	3,9	2,6	21,4	10,3	1
Quartz	44,3	43,4	62	50,3	38,1	26,5	36
A	1,26	1,30	0,61	0,99	1,62	2,77	1,78
R_c (MPa)	21	23	15	20	26	27	18

La figure 4 donne l'évolution de la résistance R_c en fonction d'une part du rapport A et d'autre part du pourcentage de quartz.

Il est ainsi clairement mis en évidence (Fig. 4), le rôle bénéfique de la présence d'oxydes de fer dans les latérites sur le développement des résistances. En effet, si on se réfère au kaolin K contenant 63 % de kaolin et 1 % d'oxydes de fer, on s'aperçoit que des sols contenant moins de kaolin (SM1, SM2, SM4, G, et C) mais plus d'oxydes de fer ont des résistances supérieures. Seul le sol SM3 présente une résistance plus faible, mais il contient également beaucoup plus de quartz. Le rôle néfaste de ce dernier est également illustré sur cette figure. Le quartz, inerte vis à vis de la réaction d'hydratation, joue plutôt le rôle de granulat et le liant obtenu est plus un mortier qu'une pâte pure de liant pouzzolanique. Ceci est particulièrement vrai pour une proportion de quartz supérieure à 50 %.

IV. CONCLUSION.

L'élaboration de ciments pouzzolaniques de synthèse à partir de latérites calcinées à 750°C est sans doute une voie de développement intéressante dans l'optique des économies d'énergie et de matières premières. Il suffit en effet d'une proportion en masse de 20 % de chaux pour l'activation chimique de ces pouzzolanes. Cette chaux peut être soit de l'hydroxyde de calcium sous forme de chaux éteinte $Ca(OH)_2$ directement produite (c'est ce qui a été le cas pour notre étude) soit de la portlandite $Ca(OH)_2$ issue de l'hydratation du ciment portland artificiel (6,7).

Les latérites comportant du kaolin et une proportion minimale de 10 % d'oxydes de fer semblent être les plus aptes à être transformées en pouzzolanes de synthèse à condition que leur teneur en quartz soit inférieure à 50 %.

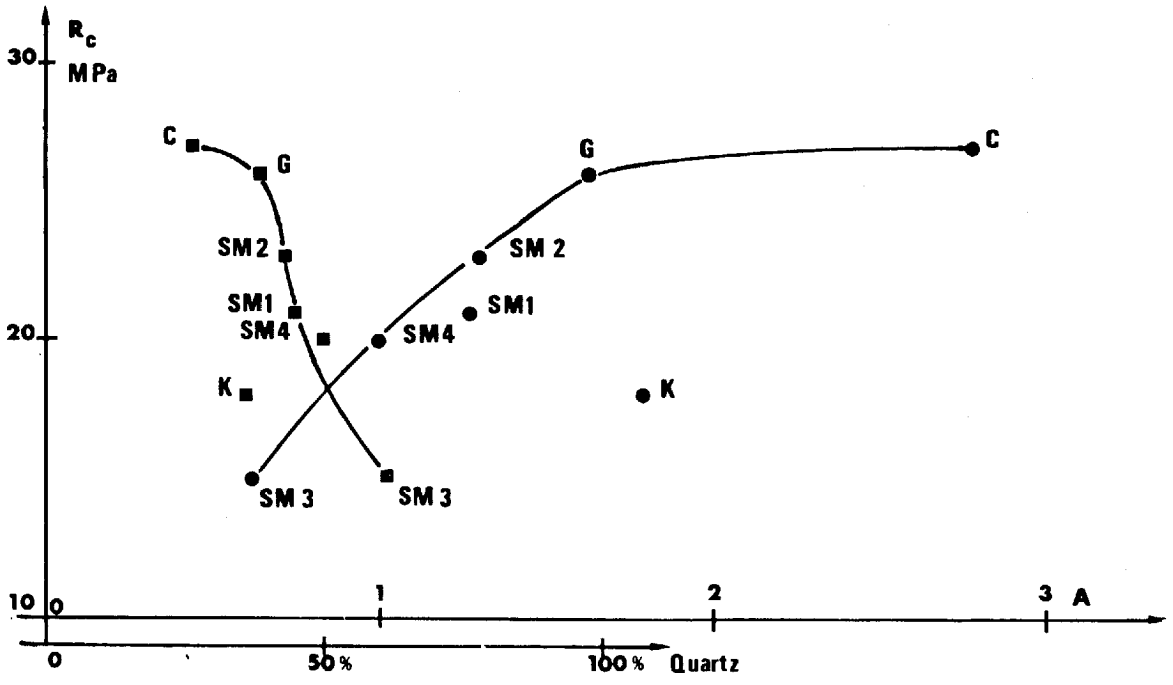

Figure 4. Evolution de la résistance R_c enfonction du rapport A et de la proportion de quartz.

Références.

(1) - MERIC J.P. "L'industrie du ciment dans les pays en voie de développement". Revue des Matériaux de Construction, Fr., 1981, 730, p. 137-138.

(2) - FORRESTER J.A., "Burntclay pozzolanas" in "Lime and alternative cements". Proceed of one day meeting on small scale manufacturing of cementitions materials, edited by K. SPENCE, Intermediate Technology Publications, London, 1974, P. 53-59.

(3) - AMBROISE J., "Elaboration de liants pouzzolaniques à moyenne température et étude de leurs propriétés physico-chimiques et mécaniques". Thèse de Doctorat ès Sciences. Lyon, 2 juillet 1984.

(4) - AMBROISE J.,MURAT M. and PERA J., "Hydration and Hardening of calcined clays and related minerals. V-Extension of the research and general conclusions". Cem. Concr. Res., 15, 1985, p. 261-268.

(5) - AMBROISE J., BACOT J., MURAT M. et PERA J., "Valorisation de la latérite en tant que matériau de construction dans un habitat économique". Premier Congr. Intern. de Géoméchanique des Sols Tropicaux et Saprolitiques, Brasilia (Brésil), 1985, Ed. ISSFME, Vol. II, (1985), p. 395-406.

(6) - SILVEIRA M., "Elaboration de liants pouzzolaniques à base de clinker et de latérites thermiquement activées". Thèse (en préparation).

(7) - MESSI A., "Eléments de toitures économiques à base de latérites calcinées à moyenne température". Thèse (en préparation).

(8) - GNIEWEK J., "Liants pouzzolaniques à base de montmorillonites thermiquement activées. Extension à des sols tropicaux". Thèse de Doctorat ès Sciences (en préparation).

(9) - MURAT M., "Activation thermique des argiles en réacteur solaire - Etude des ciments de métakaolin". Rapport final de recherche PIRDES-CNRS, Paris, Janv. 82, 78 p.

(10) - MURAT M. , "Hydration reaction and hardening of calcined clays and related minerals. I. Preliminary investigation on metakaolinite". Cem. and Concr. Res., 1983, 13 (2) p. 259-66.

(11) - MURAT M., ibid. "II Influence of the mineralogical properties of the raw-kaolinite on the reactivity of metakaolinite". Cem. and Concr. Res. 1983, 13 (4), p. 511-18.

(12) - MURAT M. and COMEL C. ibid. "Influence of calcination process of kaolinite on the reactivity of metakaolinite". Cem. and Concr. Res., 1983, 13 (5), p. 631-37.

(13) - AMBROISE J., KANTE M., MURAT M. et PERA J., "Elaboration de ciments pouzzolaniques par décomposition thermique de kaolinite à moyenne température. Extension à des sols tropicaux kaoliniques". Colloque "Nouveaux matériaux en construction et génie-Civil", Rennes, 20-22 oct. 1983, Actes du colloque, p. 31-39.

(14) - MURAT M., AMBROISE J. PERA J. et BASTIDE J.P., "Influence des caractéristiques cristallochimiques sur les propriétés pouzzolaniques des minéraux argileux thermiquement activés". C.R., Acad. Sci., 1984, 299, Sér. II, (17), 1179-81.

(15) - PERA J. MURAT M., AMBROISE J. et BOISSIER D., "Effet pouzzolanique du métakaolin. Corrélation entre le développement des résistances mécaniques et la nature des hydrates formés". C.R. Acad. Sci., 1984, 299, Sér. II, (17), 1251-54.

(16) - AMBROISE J., MURAT M.,and PERA J., "Hydration reaction and hardening of calcined clays and related minerals. IV- Experimental conditions for strength improvment on metakaolinite minicylinders". Cem. and Concr. Res., 1985, 15, (1), 83-88.

(17) - JOUENNE C.A., "Traité de céramiques etmatériaux minéraux", 650 p. Editions SEPTIMA-Paris 1975.

M.Révay Central Research and Design Institute for Silicate Industry,P.O.Box 112. Budapest, Hungary

3.3

A SUMMARY OF EXPERIENCES ON ESTIMATING THE EXPECTABLE CHANGES OF STRENGTH OF CONCRETES MADE WITH HIGH ALUMINA CEMENT

RESULTATS DES ESSAIS EN VUE DES PREVISIONS DE L'EVOLUTION DES RESISTANCES DES BETONS DE CIMENTS A FORTE TENEUR EN ALUMINE.

SUMMARY: The strength of high alumina cement concretes- following an increase due to hydration - is decreasing when the conversion of primary compounds increases their porosity. The subsequent carbonization may cause a slight increase of strength. The possible /expectable/ decrease of strength as well as the change of strength as a function of time of high alumina cement concretes can be estimated on the basis of reaction kinetical considerations based on phase composition investigations carried out by thermoanalytical methods. By the examination of several hundred concrete specimens it could be stated that the majority of the high alumina cement concretes in Hungary had showed the the minimal strength at the mid of the seventies. The maximal rate of strength decreasing can be dated to the mid of the sixties.

As resistências de concretos de cimento de alta alumina - em seguida a um aumento devido à hidratação - têm um decréscimo quando a conversão dos compostos primários aumenta sua porosidade. A carbonização subsequente pode causar um ligeiro aumento da resistência. A diminuição possível (esperável) da resistência, bem como a alteração da resistência, em função do tempo, de concretos de cimento alto-aluminoso, podem ser estimadas com base em considerações de cinética de reação, apoiadas em investigações de composição de fase realizadas por métodos termoanalíticos. Pelo exame de algumas centenas de corpos de prova de concreto, foi possível estabelecer-se que a maioria dos concretos de cimento alto-aluminoso na Hungria apresentou a resistência mínima em meados dos anos 70. O índice máximo de decréscimo de resistência pode ser datado em meados dos anos 60.

In Hungary, in the years preceding the II.world war a plurality of projects were built by using alumina cement/1-3/. In particular, in the sixties and seventies with the majority of these projects considerable drop of strength and damages could be observed.
As it is well known, drop of strength is caused by the conversion of the instable calcium-aluminate hydrates /CAH_{10}, C_2AH_8/ of large molar volume primarly formed in course of hydratation of the calcium-aluminates /CA, CA_2, $C_{12}A_7$/ contained in the alumina cement into stable compeunds of considerably smaller molar volume /C_3AH_6, AH_3/, resp. by the considerable increase of porosity, taking place as a consequence of the aforementioned conversion ./1-6/.

Accordingly, when making a decision in matters of said buildings, in addition to the result of tests directed to statics and strength, data relating to the chemical condition of the material of the material is also to be considered.

In course of an earlier conference we already reported on the testing methods having been alaborated for the determination of the chemical state./7/. The essence of said testing method lies in that the concrete sample in its original state and after having been subjected to an autoclave treatment is examined by using the DTA method, thereafter, on basis of the qualitative and quantitative changes occuring under the influence of autoclave treatment, the three most important state characteristics of the concrete made with alumina cement namely the extent of hydratation /D_h/, conversion /D_c/ and carbonization /D_{carb}/ are calculated. In knowledge of these data, as well as of porosity and cement content of the concrete and changes in molar volume taking place in course of partial processes /D_h, D_c, D_{carb}/ / see table 1/, expectable future changes in porosity can be calculated.

Figure 1

Correlation strength/porosity in case of CA specimens stored under different circumstances

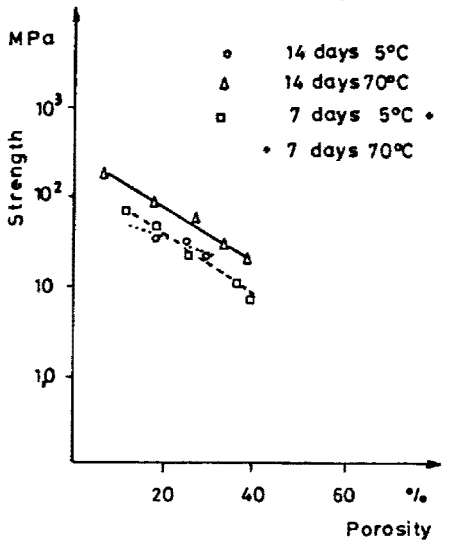

According to our examination, similarly to some other materials, /5,6,7/, the known exponential relationship

$$R = R_o e^{-bP} \qquad /1/$$

/wherein R:strength, P:porosity, R_o and b:constants/ is also valid for the hardened calcium-aluminates and concretes made with alumina cement, in such a manner that from porosity /Pc/belonging to complete conversion the possible minimal strength /Rmin/ of the concrete, from the porosity belonging to the complete carbonization the "final" strength /Rf/ of the concrete can be determined. The knowledge of these data can be of utmost importance in view of decisions being in connection with the future of valuable buildings.

Table 1 Processes of CA conversion

Chemical reaction	Volume of solid phases cm^3/mol		
	Prior to reaction	After reaction	Change
$CA + 10H = CAH_{10}$	52,68	198,24	+145,56
$CA + 5\frac{1}{2}H = \frac{1}{2}C_2AH_8 + \frac{1}{2}AH_3$	52,68	122,90	+ 70,22
$CA + 4H = \frac{1}{3}C_3AH_6 + \frac{2}{3}AH_3$	52,68	92,92	+ 40,24
$CAH_{10} = \frac{1}{3}C_3AH_6 + 1/2AH_3 + 1/2H$	198,24	82,16	-116,08
$C_2AH_8 = 2/3C_3AH_6 + 1/3AH_3 + 3H$	181,22	121,27	- 59,95
$C_3AH_6 + 3CO_2 = 3CaCO_3 + AH_3 + 3H$	149,60	166,97	+ 17,37

For the sake of order it should be mentioned that under the influence of carbonization following conversion porosity decreases, at the same time, although to a slight extent, strength is increasing. It goes without saying that this statement does not relate to the carbonization taking place immedia - tely after hydration and generally under the influence of alkaline catalysis, in course of which porosity increases and strength simultenously decreases. On basis of several tests the experience was gained, in so far as at the majority of the Hungarian alumina cements a significant conversion was taking place, however, carbonization was less.

Reaction-kinetic characteristics of conversion were examined on synthetic calcium-aluminate hydrates / CAH_{10} and C_2AH_8/ -after having subjected them to hydrothermal treatments of different temperature and dwelling time - also by DTA-methods.

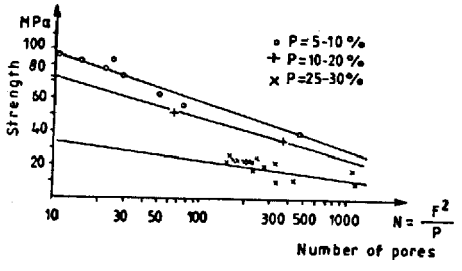

Figure 2

Conversion of CAH_{10} at different temperatures, plotted in a co-ordinate system corresponding to the reaction kinetically primary reaction $\log /1-D_c/ - \mathcal{T}$

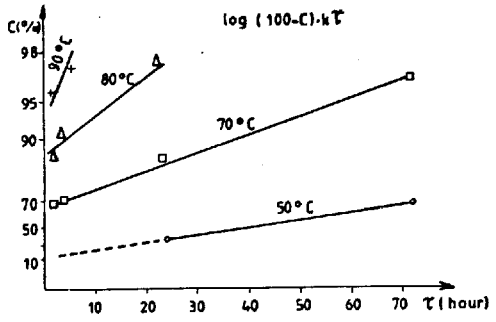

Figure 3

Relationship $\log k - \frac{1}{T}$ /Arrhenius equation/

It can be seen that conversion can be described with a good approximation with the reaction-kinetically primary equation, while the dependence of the rate constant on temperature corresponds to the Arrhenius equation.

From the aforementioned relationship it becomes obvious, that "half-period" of the conversion of CAH_{10} - compliance with our examination- amounts at 90 C^o not more than 2 minutes, at 30 C^o 73 days, at 10 C^o 19 years .Applying the relationship for the Hungarian buildings made of concrete with alumina cement, supposing a useful life of 40 to 50 years and an average temperature of 15 C^o, we obtain a conversion of 80 to 95 % being in good compliance with experiences having been gained in practice.

Summing up what has been said, change of the strength values of concretes prepared with alumina cement in dependence of time can be described as follows: Due to porosity reducing effect of hydratation /D_h/ strength will increase as long as said effect is larger than the effect of porosity increase caused by conversion, having an opposite sign. Thereafter porosity increases as long as reching the maximal value.

Possible maximal value of porosity / as a consequence, minimum of strength/are determined by the mineral composition of cement, conditions of concrete preparation, first of all cement content and w/c factor, while the minimal strength belonging to maximal porosity is influenced in particular by enviromental effects / first of all ambient temperature and moisture content /. Strength minimum will be the less, and occurs with the least possible delay, the higher is the rate of the conversion resulting in increased porosity. As already detailed earlier /7-9/, this phenomenon can be explained by the fact that with identical porosity at a higher rate of conversion the number of pores will increase.
As a matter of fact, pores are nothing else, than faults interrupting continuity of the material, accordingly, when the quantity of pores increases, strength will be less even with identical porosity.

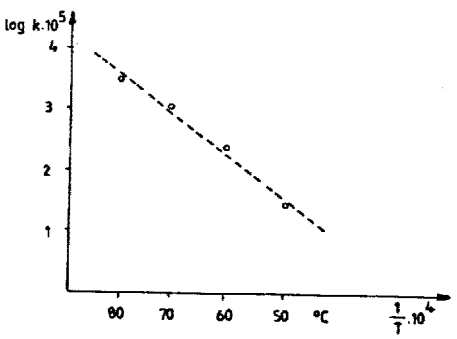

Figure 4
Relationship between number of pores and strength

The change of the size and number of pores, respectively does not influence the fundamental tendencies of change of strength of concretes prepared with alumina cement. According to aforementioned the change of strength with time of an average concrete prepared with alumina cement can be seen in Figure 5, wherein single processes being determinant in respect to the individual phases of hardening are also indicated.

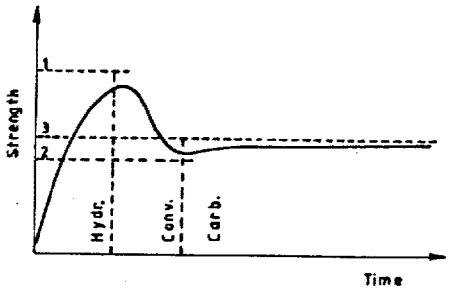

Figure 5
Changes of strength of concretes made with a usual alumina cement

On basis of the results having been obtained in course of several DTA examinations, it can be stated that for the majority of Hungarian concretes made with alumina cement the conversion is /80 to 95 %/, while carbonization is less /60 to 80%/ and hydration is practically of full extent.
In course of repeated chemical examination we had the opportunity to study the changes of conversion and carbonization in dependence of time on the concretes of some buildings. We could state that we were not mistaken in considering the processes as kinetically primary reactions. Starting from this supposition, we determined the rate constant of chemical reactions for some definite cases. Based on the average values thereof the integrated form of rate equation of chemical reactions for Hungarian circumstances is, as follows:

$$W_c = /1-D_c/e^{-0,46\tau} \qquad /2/$$

$$W_{carb} = /1-D_c/\cdot e^{-0,07\tau} \qquad /3/$$

Wherein τ stands for time /year/

As from the data of Table 1 it can be calculated that unit conversion is causing o,57-fold increase in porosity and unit carbonization leads to a o,18-fold reduction of porosity, for the change of porosity in dependence of time, using the average velocity constants, the following relationship can be described /4/

$$\Delta p = o,57/1-D_c/e^{-o,46\tau} - o,18/1-D_{carb}/e^{-o,07\tau}$$

From the equation it becomes obvious that a period -reckoned from the time of examination- needed for complete stopping of porosity increase and strength reduction /Δ p=o/ is

$$\tau_1 = \frac{1,15+\ln\frac{1-D_c}{1-D_{carb}}}{o,39} \quad /year/ \qquad /5/$$

In case if the concrete is in the phase of strength decrease τ_1 has positive sign, while when reaching the minimal concrete strength the sign will be negative.
The first derivative of the equqtion /5/ gives the time of strength drop of maximal rate, i.e, the inflexion point of the strength-curve: /6/

$$\Delta p' = -o,26/1-D_c/e^{-o,46\tau} + o,o1/1-D_{carb}/e^{-o,07\tau}$$

Wherefrom

$$\tau' = \frac{-3,26+\ln\frac{1-D_c}{1-D_{carb}}}{o,39} \quad /year/ \qquad /7/$$

Hystogrammes in Figures 6-7 show the results of the calculations having been performed on several hundreds of concrete specimens.

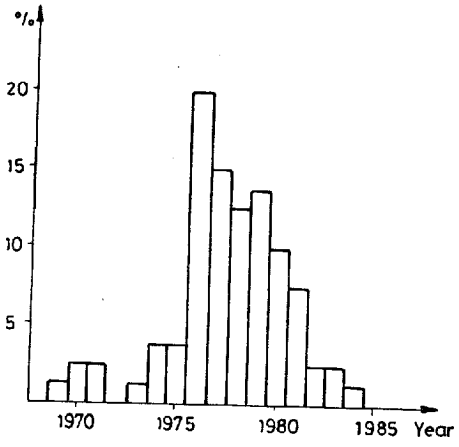

Figure 6

Time of reaching the minimal strength /year/

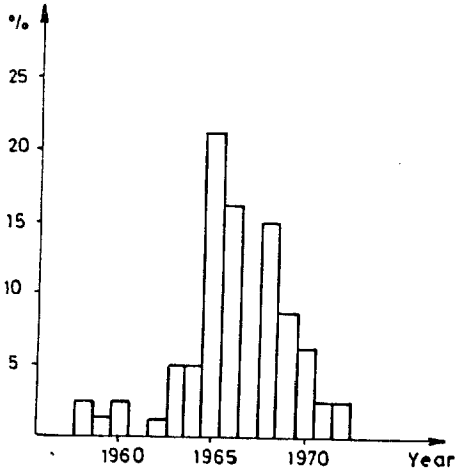

Figure 7

Time of strength drop taking place with maximal rate

As it can be well seen, the process of strength drop of the concretes examined was finished in the greater part till the middle of seventies, while the maximal decrease in strength could be observed so about 1o years ago. Nowdays the strength stopped, the more, in

certain cases a certain increase in strength of some procents could be observed /carbonization/

References

1. Talabér,J.:Építőanyag 8 /5/ p161-174, /6/ p:202-213, /8/ p:295-308, /9/ p:349-356. 1956.
2. Talabér,J.:Proc 6 Int Congr on the Chem. Cem. V:III, p:124-133. Moscow
3. Révay,M.: Proc.6. Int.Congr.on the Chem. Cem. V:III, p:146-148, Moscow
4. Kühl,H.: Zement Chemie Berlin VEB Verlag Technik 1958
5. Midgley, H.G.: Trans Br. Ceram.Soc. 66 /4/ p:161-189, 1967.
6 George,C.M.· Proc.7. Int. Congr. on the Chem. Cem. Parizs,1980.
7 Révay,M.+ Wagner,Zs.: Thermochimica Acta /31/ p: 365-374. 1979.
8 Talabér,J.- Révay,M.- Wagner, Zs : Proc.II Eur.Symp. on Thermal Anal Edit. D. Dollimore Heyden and Son Ltd. p·498-500. 1981.
9. Révay,M + Wagner,Zs.: Építőanyag 37 /11/ p:321-330. 1985.

S. LAXMI, P.K. MANDAL, R. GHOSH
National Council for Cement and Building Materials
M-10, South Extension Part - II, New Delhi - 110 049, INDIA.

1

V.V. SUBBA RAO
Director, Department of Scientific & Industrial Research,
Ministry of Science and Technology, Govt. of India,
Technology Bhavan, New Mehrauli Road, New Delhi - 110 016, INDIA.

3.3

Development of a Fast Setting High Strength Cement Composite

DEVELOPPLMENT DE PRISES RAPIDES DE CIMENTS COMPOSES DE HAUTE RESISTANCE.

SUMMARY: A fast setting, high strength cement composite for special applications was developed based on Ordinary Portland Cement, High Alumina Cement and other cement additives. The composite sets within 15 minutes and yielded strengths of the order of 10 and 23 N/mm² at 1 and 2 h respectively and 45 and 70 N/mm² at 8 and 24 h respectively. It also gave an expansion of 0.2 percent at 3 d and a pull out strength of 12 tonnes with 12.5 mm bar.

Studies on setting, hydration, pore structure, microstructure and expansion characteristics have indicated that formation of ettringite and stratlingite are mainly responsible for fast setting and high strength development at very early ages, and ettringite provides for the desired expansion. Studies on rate of heat evolution during hydration and X-ray diffraction patterns of hydration products at different ages have indicated that hydration takes place in two stages. The first stage in within 15 minutes during which mainly hydration of aluminate phases take place. This is followed by an induction period of about 5 minuts after which hydration of silicate phases take place, most of which is achieved within 120 minutes, followed by a slow and steady rate of hydration. The high strength achieved may also be attributed to a significant reduction in porosity to as low as 6.5 percent and near absence of macropores in the system. Effect of fineness, w/c ratio, curing temperature, etc. on compressive strength have also been studied.

The cement composite developed has great potentials of application in mining, tunnelling, emergency repairs of dams, water retaining structures, airports and emergency construction of defence installations etc.

Desenvolveu-se um composto de cimento de pega rápida e alta resistência, para aplicações especiais, baseado em cimento portland comum, cimento alto-aluminoso e outros aditivos de cimento. O composto da pega dentro de 15 minutos e atinge resistências da ordem de 10 e 23 N/mm² a 1 e 2 horas, respectivamente, e 45 e 70 N/mm² a 8 e 24 horas, respectivamente. Apresentou também expansão de 0,2% a 3 dias, e uma resistência de aderência de 12 t com barra de 12,5mm.

Estudos sobre pega, hidratação, estrutura de poro, microestrutura e características de expansão indicaram que a formação de etringita e estralingita é a principal responsável pela pega rápida e desenvolvimento de alta resistência nas idades mais iniciais, e que a etringita proporciona a expansão desejada. Estudos sobre a velocidade de evolução do calor durante a hidratação e análise de difração de raio-X dos produtos de hidratação em diversas idades indicaram que a hidratação acontece em duas etapas. A primeira etapa dentro de 15 minutos, durante os quais ocorre principalmente a hidratação das fases de aluminato. Esta fase é seguida por um período de indução de cerca de 5 minutos, depois do que se dá a hidratação das fases de silicato, grande parte da qual se completa dentro de 120 minutos, seguindo-se uma velocidade lenta e uniforme de hidratação. A alta resistência atingida pode também ser atribuída a uma redução significativa da porosidade para menos de 6,5%, e à quase ausência de macroporos no sistema. Também foram estudados os efeitos da finura, da relação a/c, da temperatura de cura, etc., sobre a resistência à compressão.

O composto de cimento desenvolvido tem grande potencialidade de aplicação em mineração, túneis, reparos de emergência de represas, estruturas para retenção de água, aeroportos e construção de emergência de instalações de defesa, etc.

INTRODUCTION

Fast setting, high strength cementitious materials are requiried for special application areas like installing anchor bolts for strengthening or reinforcing members in rock formations in mining and tunnelling, structural bodies in emergency repairs of dams, airports, water retaining structures, machinery installations and emergency construction of defence installations etc.

A fast setting, high strength, expansive type cement composite has been developed based on High strength Ordinary Portland Cement (OPC), High alumina cement (HAC), Calcium anhydrite, calcium chloride and graded sand. The composite sets within 15 minutes and gives compressive strengths of the order of 10 and 23 N/mm^2 at 1 and 2 h respectively and 45 and 70 N/mm^2 at 8 and 24 h respectively (1-3).

In contrast to portland cement where the major cohesive hydration product is colloidal C-S-H gel with small amounts of crystalline calcium hydroxide and aluminate hydrates, the hardening of the composite is associated with the formation of an interlocking structure of calcium silicate hydrates, crystalline aluminate hydrates (mainly CAH_{10}, C_2AH_8, C_4AH_{13}), ettringite, C_2ASH_8, calcium chloroaluminate, portlandite and gibbstite etc. Presence of substantial quantities of alumina gel contribute to the consolidation of the microstructure.

This paper describes studies on various physico-mechanical properties, work performance, chemical interactions among the ingredients during hydration, pore structure and microstructure of the cement composite.

EXPERIMENTAL

MATERIALS

Raw Materials : The rawmaterials used for the preparation of cement composite were High strength Ordinary Portland Cement conforming to IS:8112-1976, High Alumina Cement conforming to IS:6452-1972, fused calcium chloride and sand were of commercial origin. Anhydrous calcium sulphate was prepared by calcining commercial grade calcium sulphate at 350°C - 380°C for 4-5 h. Physical properties of raw materials are given in Table I. Sand was ground to pass 425 μm sieve.

Fast setting, High strength cement composite : Various trial mixes (CC-1 to CC-6) were prepared to achieve fast setting and high strength development characteristics (Table II). Cement composite CC-5 was considered as most appropriate composite due to minimum contents of high alumina cement, calcium chloride and anhydrite, The cement composite was then prepared by integrinding all ingredients except sand in a batch type ball mill to a fineness of 485 m^2/kg (Blaine) and then blending with fine graded sand (CC-6).

TABLE - I

PHYSICAL CHARACTERISTICS OF THE RAW MATERIAL

Material	Fineness m^2/kg	Compressive Strength N/mm^2			
		1d	3d	7d	28d
High strength Ordinary Portland Cement	420.0	24	33	51	61
High Alumina Cement	350.6	35	65	-	-

	Sieve Analysis	
	Sieve No.	Percent passing
Sand (-425 μm)	300 μm	58
	150 μm	35
	90 μm	26
	45 μm	10

TABLE - II

COMPRESSIVE STRENGTH OF DIFFERENT COMPOSITE MIXES

Cement Composite	W/C	Compressive Strength, N/mm^2				
		1h	2h	6h	1d	3d
(CC-1)	0.25	Nil	Nil	4.7	28.7	-
(CC-2)	0.30	Nil	Nil	5.9	36.4	-
(CC-3)	0.30	Nil	1.0	8.0	39.0	-
(CC-4)	0.30	1.0	3.3	10.0	40.1	-
CC-5)	0.20	12.0	28.0	45.0	77.5	-
(CC-6)	0.21	10.1	21.0	41.1	75.5	82.2

RESULTS

Conduction Calorimetry : Heat evolution profile for fast setting, high strength cement composite (CC-5) has been shown in Fig. 1. The curve is characterised by two rate peaks, first being within 15 minutes and the second between 80 to 120 minutes indicating that the hydration in early stages takes place in two stages. Heat evolution in the first stage is attributed to heat of wetting of $CaCl_2$, calcium sulphate anhydrite, high alumina cement etc., and an exchange of ionic species initiates between the solid and liquid phase. The high solubility of some of the components lead to a rapid increase in ion concentration of the liquid phase with respect to CA, C_3A, $C\bar{S}$ and $CaCl_2$, leading to large amount of heat evolution, which results in acceleration of early hydration. However, it is difficult to characterize, early hydration products morphologically. After that the rate of heat evolutin diminishes very quickly during 15-80 minutes. During the induction period Ca^{2+} concentration of the liquid phase reaches supersaturation with respect to $Ca(OH)_2$ and consequently nucleation and

growth of both C-S-H and $Ca(OH)_2$ begin. During this time most of the C_3A and CA have been consumed by sulphates to form ettringite.

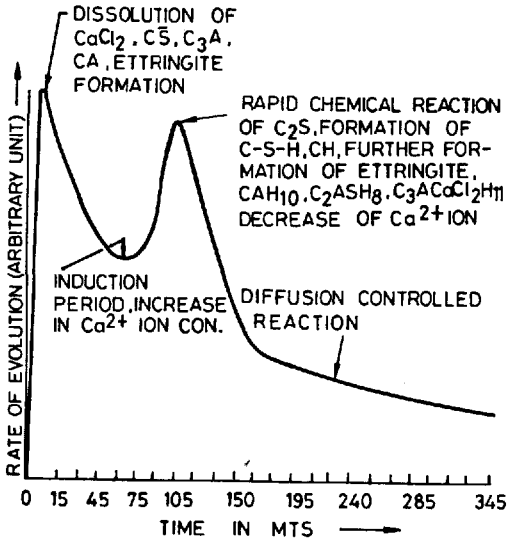

Fig. 1 : Calorimetric curve for cement composite (CC-5).

After reaching a minimum, the heat evolution rate begins to increase to the second rate peak which occures after 1-2 h of hydration. This peak is attributed to the early hyration of alite and further ettringite formation (4). Presence of adequate amount of sulphate ions in the system under study prevents monosulphate formation which is confirmed by the non appearence of the third peak.

In contrast to above in the case of High strengh Ordinary Portland Cement hydration there are generally two rate peaks and third rate peak occurs only occasionally (5). The first rate peak appears within 1h and is due to the contribution of dissolution of sample and hydration of free lime. The second rate peak appears after 10-14 h of hydration and is attributed to early hydration of alite and formation of ettringite. The appearance of third rate peak is attributed to formation of monosulphate.

X-ray Diffraction : X-ray diffractograms of anhydrous cement composite and hydrated specimens at various ages are shown in Fig. 2. Formation of ettringite has been identified in all hydrated samples beyond 6 minutes hydration. Presence of CAH_{10}, needle shaped ettringite $C_3ACaCl_2H_{11}$, C_2ASH_8, C_3AH_6, AH_3, C_2AH_8 and $Ca(OH)_2$ have been identified in specimens hydrated for 30 minutes and more. However, formation of above hydration products are more pronounced in specimen of 1h hydration.

Scanning Electron Microsocopy : Scanning electron micrographs and EDAX of hydrated samples (Fig. 3) at 1h, 6h and 1 d have indicated formation of needle shaped ettringite at early ages and formtion of a dense matrix beyond 6h hydration. Well crystallized silicate hydrates are visible at 1d.

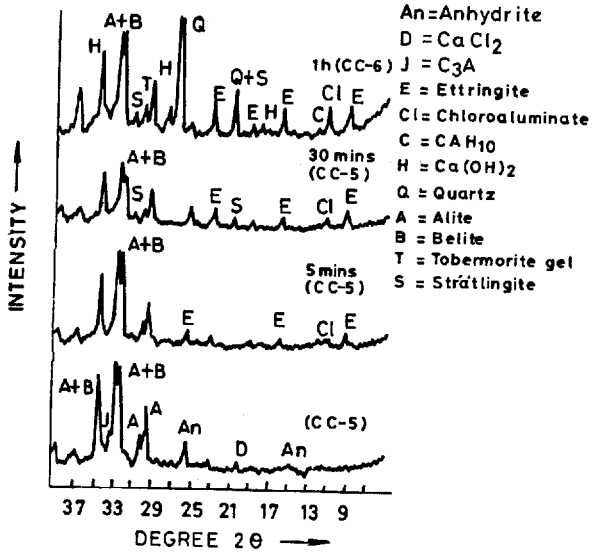

Fig. 2 : XRD curves of anhydrous and hydrated composite (CC-5).

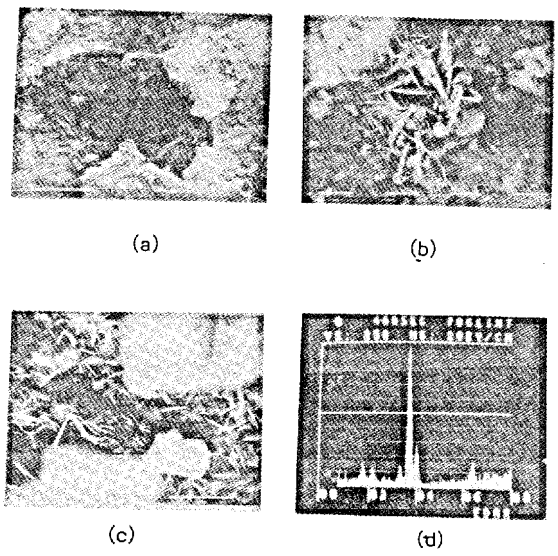

Fig. 3 : SEM and EDAX of hydrated cement composite

a/ 1h hydration
b/ 6h hydration
c/ 1d hydration
d/ EDAX of position X of 3 (c)

Hardening and Strength Development : Cement composite indicated hardens within 15 minutes (Table -III).

TABLE - III

PERFORMANCE CHARACTERISTICS OF DIFFERENT BATCHES OF CEMENT COMPOSITE

Sample No.	Fineness* m^2/kg	Hardening time (min)	W/C	Compressive Strength, N/mm^2					
				2h	4h	7h	1d	3d	7d
CC-6 (A)	482	≃ 15	0.22	21.0	31.5	42.0	65.0	70.0	75.0
CC-6 (B)	488	≃ 15	0.22	19.0	-	41.0	-	72.0	-
CC-6 (C)	475	≃ 15	0.23	18.0	-	39.5	-	66.0	-
CC-6 (D)	482	≃ 15	0.22	18.0	-	40.0	70.0	-	-
CC-6 (E)	479	≃ 15	0.22	21.6	-	-	75.5	82.2	-

* without sand

The effect of fineness of the cement composite (without sand) was studied and the data is presented in Table IV.

TABLE - IV

EFFECT OF FINENESS OF CEMENT COMPOSITE ON COMPRESSIVE STRENGTH

Sample No.	Fineness* m^2/kg	W/C	Compressive Strength, N/mm^2		
			2h	7h	3d
CC-6	427	0.25	7.0	31.5	67.0
CC-6	470	0.20	23.0	46.0	71.0
CC-6	500	0.20	24.0	44.0	-

* without sand (CC-5)

It is evident that optimum strength development is obtained at the fineness of the order of 470 m^2/kg and there is no specific advantage of further grinding. However, studies on particle size distribution (Fig. 4) have indicated that the majority of particles are in the range of 3-12 μm. The presence of fine perticles is also responsible for fast setting.

Compressive strength development of cement composite was determined at the ages of 2, 4, 7h and 1, 3 and 7d and the data is presented in Table III. It is evident from the data that the compressive strength of the order of 18-21 N/mm^2 at 2h, 39-42 N/mm^2 at 7h and above 65 N/mm^2 are obtained at 1d and after.

Effect of water-cement (w/c) ratio on the compressive strength development of the cement composite was studied and the data is presented in Table V.

TABLE - V

EFFECT OF W/C RATIO ON COMPRESSIVE STRENGTH

Sample No.	Fineness* m^2/kg	W/C ratio	Compressive Strength N/mm^2		
			2h	7h	7d
CC-6	482.0	0.25	14.5	36.0	88.0
		0.23	17.5	37.0	85.0
		0.22	22.0	44.0	84.0
		0.20	23.0	46.0	81.5

*without sand (CC-5)

It is evident from the data that the optimum strength development is achieved for w/c ratio between 0.20-0.22 and that w/c ratio beyond 0.23 reduces strengths at early ages i.e. upto 7h, beyond which the effect is insignificant.

Pull out test of the cement composite has indicated pull out strength of 12 tonnes with 12.5 mm tor steel bar at 6h.

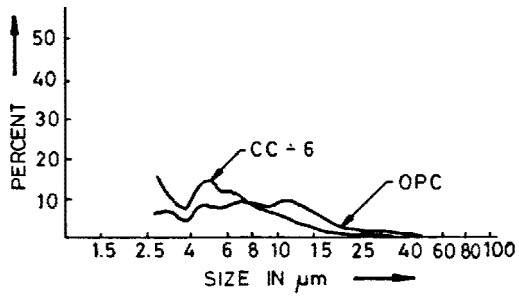

Fig. 4 : particle size distribution (population) of OPC and cement composite (CC-5).

Thermal Stability : Thermal stability of hardened cement composite was established by monitoring the compressive strength development at 50°C and 100°C which was also considered desirable due to presence of High alumina cement in the composite (Table VI).

TABLE - VI

EFFECT OF CURING TEMPERATURE ON COMPRESSIVE STRENTH

Sample No.	Temperature of curing	Compressive strength N/mm^2		
		6h	1d	3d
CC-5	27°C air curing :RH 65%	41.1	75.5	82.2
	50°C water curing	58.0	72.8	72.0
	100°C water curing	54.3	70.5	71.0

It is evident from the data that with the increase in curing temperature ther is an increase in compressive strength upto 6h but no significant change is observed beyond 1d.

Expansion : The cement composite is of expansive type and expansion characteristics of the composite upto 4 months are presented in Fig. 5. A maximumof 0.2 percent expansion was observed in the hardened cement composite, most of which is obtained in 3d and no significant expansion is observed beyond 1 month.

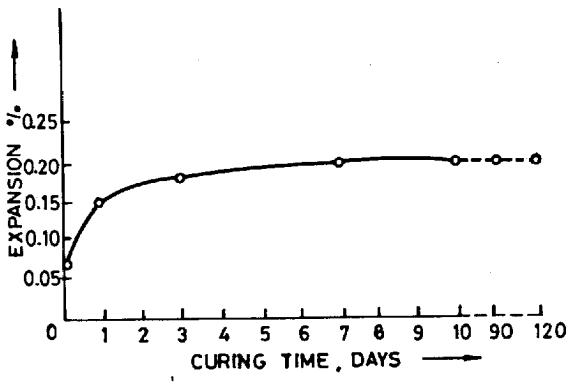

Fig. 5 : Expansion characteristics of CC-6 at 27°C in water

Porosity and pore size Distribution : The percentage porosity of hydrated cement composite specimens at different ages (1h, 2h, 4h, 6h, 1d, 3d, 7d, and 28d) are given in Table VII.

TABLE - VII

POROSITY OF HYDRATED CEMENT COMPOSITE

Sample No.	Age of curing	W/C	Percent Porosity
CC-6 (a)	1h	0.23	17.83
CC-6 (b)	2h	0.23	18.08
CC-6 (c)	4h	0.23	13.72
CC-6 (d)	6h	0.23	11.11
CC-6 (e)	1d	0.23	9.04
CC-6 (f)	3d	0.23	8.72
CC-6 (g)	7d	0.23	9.08
CC-6 (h)	28d	0.23	6.50

The data indicates that the porosity gradually decreases as the hydration progresses. The total porosity is 17.83 percent after 1h hydration which decreases to 6.50 percent after 28d hydration. The decrease in porosity is attributed to the decrease in total number of pores due to filling by the hydrated products at later stages of hydration.

The higher values of porosity at early ages i.e. 17.83 percent at 1h and 18.08 percent at 2h are due to formation of needle shaped ettringite, simultaneously which increases the volume of semihydrated sample and presence of pores in the matrix. At the later stages these pores are filled by the tobermorite gel and other hydration products. Almost equal porosities at 1 and 7d indicate that the major part of the hydration reactions gets completed within 1d.

The cement hydration products in the presence of $CaCl_2$ exhibit a higher amount of micropores (6). The pore size distribution curve (Fig. 6) indicates that in all the samples studied, most of the pores are distributed in the range 0.02 μm to 0.10 μm which are micropores. It is also evident from Fig. 6 that the percent distribution of micropores is more at early ages of hydrtion as compared to 1d hydration indicating that micropores have greater role on strength development as the 'wide pores' are already filled up by the graded inert filler (Sand) used in the composite. Thus the macropores are filled by the inert filler and micropores are filled by the hydrated products.

Feldman and Beaudsin (7) found that strength is controlled by porosity but that morphology (crystal bonding and product density) is also important. Optimum strength development is obtained with a dense, well crystallized material (8). Presence of High alumina cement in the composite leads to the formation of CAH_{10} during hydration, which is a very dense material at very low w/c ratio. Alumina gel appears in the composite cement paste as an amorphous material and fills up the spaces between crystals of other hydrates resulting into decreased porosity (9) leading to high strength development.

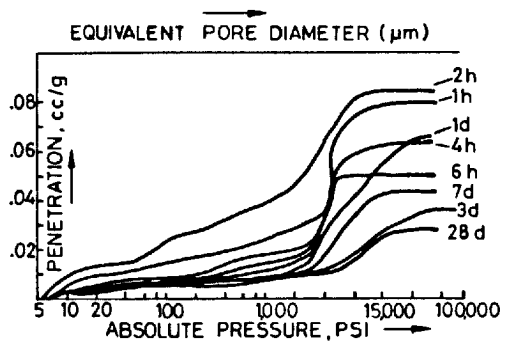

Fig. 6 : Pore size distribution of hydrated cement composite.

Corrosion Measurement : The pH of the pastes of hardened cement composite ground with small quantities of distrilled water at various ages of hardening upto 1 year remained constant at 13.1. The high alkalinity indicates that the cement composite is capable of providing excellent protection to reinforcement against corrosion, even in the presence of small amount of chloride.

A typical set data of galvanostatic studies has indicated, no incidence of corrosion in the steel rod in one year water curing at 27°C (Fig. 7). Similarly, no loss of weight in the steel rod was observed with time in Clark's solution in weighing method (10).

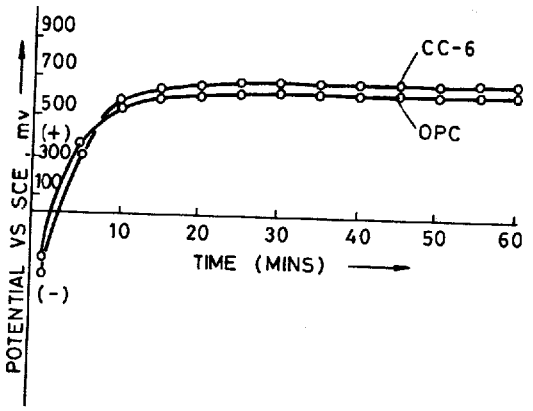

Fig. 7 : Typical set of corrosion measurement.

DISCUSSION

Cement composite (CC-6) based on high strength OPC, High alumina cement, $CaCl_2$, anhydrite and graded sand has been considered most appropriate based on early strength development characteristics. A - compressive strength of the order of 10 N/mm^2 45 N/mm^2 and 70 N/mm^2 is obtained after 1h, 8h and 1d respectively and an expansion of 0.2 percent in 3d provides extra advantage during anchoring. Other combinations fail to attain high strength at early ages i.e. 1 - 2h.

The hydration of the present cement composite under study is a sequence of overlapping chemical reactions among cementitious components, anhydrite, gypsum, calcium chloride and water leading to continuous cement paste stiffening and hardening. The disssolution of calcium chloride, high alumina cement and anhydrite lead to high rate of heat evolution during initial stage. The high temperature environment enables very quick hydration of C_3A, CA and C_3S phases resulting into formation of compounds whose solubilities are lower than those of the anhydrous composite minerals, thus leading to the precipitation of colloidal and crystalline hydrates which form the hardened paste. It is reported that presence of substantial quantitites of $C\bar{S}$ in a mixture of 75 percent aluminous and 25 percent portland cement gives a fast setting and very high compressive strength due to rapid formation of ettringite (11). However, in the system under study relatively small dosage of high alumina cement (< 20 percent) and high content of OPC (> 60 percent) havebeen used to make very fast setting high strength cement composite. The formulation is thus both economical and capable of yeilding superior performance (3). The strength development at early ages have been attributed to combined action of $CaCl_2$, $C\bar{S}$ and aluminates.

A small addition of $CaCl_2$ to portland cement is known to accelerate the setting and hardening characteristics of the cement (12, 13). This is mainly attributed to the action of $CaCl_2$ on the silicate phases. The reaction between aluminates, gypsum and anhydrite is accelerated in the presence of $CaCl_2$ (14, 15).

Monochloroaluminate hydrate, $C_3A.CaCl_2H_{11}$ forms after most part of gypsum is consumed in the reaction with C_3A to form ettringite. Converision of ettringite to monosuphoaluminate is remote due to presence of excess of SO_4^{2-} ions in the system, which is confirmed by absence of XRD peak at 9.9° 2θ.

In the OPC-CA-$C\bar{S}$-$CaCl_2$-H_2O system relatively higher amounts of $Ca(OH)_2$ is released at early ages of hydration in the presence of $CaCl_2$ leading to formation of substantia quantities of C_4AH_{13} XRD peaks at 31.2° and 36.7°, 2 θ) resulting into better strength development at early ages.

The increase of temperature due to dissolution of $CaCl_2$, anhydrite and high alumina cement does not result into conversion of CAH_{10} to C_3AH_6 due to low w/c ratio (0.23) and as the cement composite hydrates the amount of free water reduces gradually and eventually no free water is remaining in the matrix. Thus conversion of CAH_{10} to C_3AH_6 is inhibited to large extent at higher temperatures. At the same time the presence of $CaCl_2$, CA and anhydrite in the system enhances the formation of C-S-H gel from OPC (major constituent) which in turn reacts with metastable aluminate hydrates (CAH_{10} and C_2AH_8) leading to possible formation of stratlingite (C_2ASH_8) which contributes to the high strength before they are converted to C_3AH_6.

The XRD data has indicated the presenc of ettringite within 5 minutes of hyderation. Presence of ettringite, CAH_{10} (12,36°, 6.22°, 25.01°, 2 θ), $C_3A.CaCl_2H_{11}$, (11.21°, 22.57°23.10°, 2 θ), (31.16°, 7.01° and 21.25°, 2 θ), C_2ASH_8, C_4AH_{13} (31.2° and 36.7° 2 θ) at 30 minutes and 1h hydration are clearly visible indicating accelerated hydration in the system.

The combinations (CC-1 to CC-4) do not provide substantial strength development at 1-2h indicate that presence of $CaCL_2$, anhydrite and CA alone or below the optimum dosage does not provide for strength development at very early ages. A combination of $CaCl_2$, High alumina cement and anhydrite behaves as a 'Super accelerator' in the system which extraordinarily increases the kinetics of hydration from 5 minutes and contribute towards high strength within one hour (10 N/mm^2), which is clear from conduction calorimetic rate peaks indicating the early hydration and formation of hydration product at a very early age.

Porosity and pore size distribution data has clearly indicated formation of a very desnse structure attributing to high strength development. This is also supported by SEM studies, wherein electron micrographas at 6 h hydration has indicated dense morphology (Fig. 3). No deterioration in the crystal matrix has been observed at higher curing temperatures upto 100°C.

CONCLUSION

1. A fast setting high strength expansive type cement composite based on High strength Ordinary portland cement, High alumina cement, anhydrite, graded sand and $CaCl_2$ has been developed.

2. The cement composite sets within 15 minutes and give rise to strength of the order of 10, 23, 45 and 70 N/mm^2 at 1, 2, 8 and 24h respectively. The composite is thermally stable, expansive type and provides for a pull out strength of 12 tonnes at 6h.

3. Conduction calorimeter, XRD and SEM data indicate that high strengths at early ages have been achieved due to accelerated hydration of aluminate and silicate phases, formation of ettringite and stratlingite in less than 10 and 30 minutes and formation of highly impermeable matrix.

4. A Combination of $CaCl_2$, High alumina cement and anhydrite in optimum ratio act as a super accelerator.

5. The cement composite developed has great potential of application in mining, tunelling emergency repair of dams, water retaining structures, air ports and emergency construction of Defence installations.

ACKNOWLEDGEMENT

The work described here was carried out as a part of the R&D programme of the national Council for Cement and Building Materials, and the authors are grateful to Dr. H.C. Visvesvarya, Chairman and Director General of the Council for his permission to communicate this work.

REFERENCES

1.- V.V. SUBBA RAO, S. LAXMI, P.K. MANDAL and R. GHOSH, A process for the preparation of fast setting and high early strength cement composte, Indian Patent, Application No. 549/Del '83 dt: 10.8.1983.

2.- Development of fast setting, high strength cement grout material for roof bolting in coal mines, Cement Research Institute of India, January, 1984.

3.- V.V. SUBBA RAO, S. LAXMI and P.K. MANDAL. Fast setting, high strength cement composite for mining, tunnelling and other special applications - Technology Digest, Cement Research Institute of India, Nov. 1984.

4.- H.E. SCHWIETE and E. NIEL, Zement-Kalk-Gips, 18(4), p 157 (1965).

5.- J.A. FORRESTER, Cement Technology, 1(3) p 95 (1970).

6.- M. COLLEPARDI, Proc. Inter. Symp on pore structure and properties of materials, RILEMIUPAC, Prague, pp B-25-B-49 September (1973).

7.- R.F. FELDMAN and J.J. BEAUDOIN, Cem. Concr. Res, 6, 369 (1976).

8.- S. CHATTERJEE and J.W. LESNIKOFF, Trans. Brit. Ceram. Soc. 67, 171 (1968).

9.- M. YUDENFREUND, K.M. HANNA, J. SKALNY, I OLDER and S. BRUNAUER, Cem. Concr. Res., 2, 731 (1972).

10.- K. TUUTTI, Corrosion of Steel in Concrete, Swidish Cement and Concrete Research Institute Stockhom p 219 (1982).

11.- W. KURDOWSKI and F. SORRENTINO, Structure and Performance of Cement, Edited by P Barnes, (Applied Science Publishers Limited) p 486 (1983).

12.- V.S. RAMACHANDRAN, Mat. et. Const., 4, 3, (1971).

13.- A TRAETTEBERG and V.S. RAMACHANDRAN, App. Chem. Biotechnol, 24, 157 (1974).

14. A TRAETTEBERG and P.J. SAREDA, VI Inter, Cong. Chem. Cement, Moscow, Supp. paper, Section II, (1974).

15.- B. JANOSNE and B. GIYORGS, Kozlekedesi Dokumentacios Vallalat, Budapest, p 105 (1972.).

NON-ALITIC CEMENT FROM CALCIUM SULPHOALUMINATE CLINKER - OPTIMISATION FOR HIGH-STRENGTH AND LOW-TEMPERATURE APPLICATION

3.3

G.A. Mudbhatkal, P.S. Parmeswaran, A.S. Heble, B.V.B. Pai, and A.K. Chatterjee,
The Associated Cement Companies Ltd.,
Central Research Station, Thane 400 604, INDIA.

SUMMARY :

Cements from calcium sulphoaluminate clinkers have been in the forefront of research all over the world in the recent past. Varieties of products have been reported with various phase combinations like $C_4A_3\overline{S}$ and β-C_2S, $C_4A_3\overline{S}$ and C_3S, $C_4A_3\overline{S}$ and C_4AF, etc., with or without $CA/C_{12}A_7$, C_2AS, $CaSO_4$ and $CaO/Ca(OH)_2$. Because of variations in phase assemblages the resultant product properties have also varied.

In our development of a similar family of products the emphasis has been laid on optimisation of phase assemblge with $C_4A_3\overline{S}$, β- C_2S and $CaSO_4$ towards high strength and low temperature concreting applications. In this context the products characteristics with varying A/S and A/$\overline{S}$ ratios and firing temperature range has been studied for the optimisation of our targetted product quality.

The hydration reaction of the product from a few hours to a few years have been studied under normal ambient conditions. The hydration characteristics of the product under low temperature conditions have been compared.

The application properties of the product by designing high-strength concrete and their comparison with equivalent ordinary Portland cement concrete have been highlighted. Case studies of actual constructions under normal and low temperature conditions have been dealt with.

Em passado recente, em todo o mundo, os cimentos de clínqueres de sulfoaluminato de cálcio têm sido objeto principal de pesquisa. Foram reportadas muitas variedades de produtos com diversas combinações de fase, como $C_4A_3\overline{S}$ e β-C_2S, $C_4A_3\overline{S}$ e C_3S, $C_4A_3\overline{S}$ e C_4AF, etc. com ou sem $CA/C_{12}A_7$, C_2AS, $CaSO_4$ e $CaO/Ca(OH)_2$. Por causa das variações nos agrupamentos de fases, também variaram as propriedades do produto resultante.

Em nosso desenvolvimento de uma família semelhante de produtos, foi dada ênfase à otimização da reunião de fase com $C_4A_3\overline{S}$, β-C_2S e $CaSO_4$ no sentido de aplicações em concretagem de alta resistência e temperatura baixa. Neste contexto foram estudados os produtos característicos com relações variáveis de A/S e A/$\overline{S}$ e faixa de temperatura de queima para otimização da qualidade do nosso produto em objetivo.

Foi estudada a reação de hidratação do produto desde poucas horas até alguns anos sob condições ambiente normais. Foram comparadas as características de hidratação do produto sob condições de baixa temperatura.

Foram esclarecidas as propriedades de aplicação do produto para projetos de concreto de alta resistência e sua comparação com concreto equivalente de cimento portland comum. Também foram abordados estudos de caso de construções reais sob condições de temperatura normal e baixa.

INTRODUCTION:

In the quest for low energy cements, non-alitic cements (NAC) have an important role to play. Ordinary Portland Cements (OPC) containing C_3S as an essential phase need a high temperature for clinkerisation, whereas it is well known that NAC largely containing $C_4A_3\bar{S}$ phase can be produced at lower temperatures. This reduction of clinkering temperature can help in reducing the specific heat consumption substantially, and at the same time may lead to additional savings in power due to decreased gas volumes or higher throughput for the same installed power. Further, the softer non-alitic clinker lends itself to grinding with lower energy consumption.

In addition to the energy advantage, the NAC have the additional property of being able to set early and develop good strengths at even early ages. This property lends the cement for use in a good many circumstances like urgent repairs, precast concrete products, and in cold weather applications.

The present paper aims at reporting the optimisation of composition of such NAC for high strength and low-temperature concreting and a few field trials.

2. SUMMARY OF LITERATURE DATA :

A rapid scan of the published literature on the subject shows that a wide variety of compositions have been tried in the past and the characteristics of the products studied by the different authors are briefly summarised in TABLE-1. It is noticeable from the table, that the proportion of $C_4A_3\bar{S}$ in various compositions varies over a wide range - from as little as 15% to 64%. Similarly, the range of β-C_2S varies from 16% to 60%, while the amount of CS spreads over 4 to 22%. At the same time, the phase assemblage present in their products also differs - one composition has upto 9% free lime, another upto 40% C_4AF, the third CA upto 20% and the fourth $C_{12}A_7$ upto 10%.

Ignoring, for the present, the variations in compressive strengths that may arise due to variations in test procedures, the three-day strengths achieved, range from 75 to 450 Kg/Cm^2 depending upon the phase composition of the product. One-day strengths in the range of 250-350 Kg/Cm^2 have been reported by two authors while the highest 7 day strength reported is 750 Kg/Cm^2.

3. OPTIMISATION OF PRODUCTION PARAMETERS:

On the basis of the information available so far, it was decided to optimise some of the parameters, so as to obtain clinker with firing at a low temperature, say between 1200-1300°C. The compositional parameters that were decided to be varied initially, were A/S, $A/\bar{S}$; two different temperatures of firing 1200°C and 1300°C were to be adopted.

Raw materials used were limestone, bauxite, clay and gypsum. The chemical composition of these ingredients is given in TABLE-2. These materials were suitably proportioned after requisite preparation in the laboratory mills.

For each temperature of 1200°C and 1300°C with LSF*=1.0,(i)three A/S ratios of 2.0,2.5 and 3.0 and (ii)three $A/\bar{S}$ ratios of 3.6,3.8 and 4.0, were adopted for proportioning the raw materials.

*$LSF=C/0.7(F+T+\bar{S})+0.55A+1.87\bar{S}$ (Ref.4)

4.LABORATORY TRIALS:

The proportioned batches of materials were nodulised and oven dried, and then were fired in a laboratory electric furnace; the soaking period of the nodules being in the range of 30-40 minutes at the firing temperature. The nodules were taken out of the furnace and air cooled.

The properties of the products fired as above are presented in TABLE-3.(The strength values reported in the table are those of cement produced by grinding clinker with constant proportion of gypsum). At a firing temperature of 1200°C, the composition of A/S=2.5, $A/\bar{S}$=3.8 and LSF 1.0 has shown better strengths, while for firing temperature of 1300°C, the composition based on A/S=2.0 and $A/\bar{S}$=3.8 has shown better strength. As the main objective was to study cement produced with the lowest energy consumption, the composition with A/S=2.5, $A/\bar{S}$=3.8 and LSF=1.0, was considered for further evaluation. Studies of the product fired at different temperatures have been presented in Fig. A.

The technique adopted to study the reaction sequence has been as follows : First pellets were prepared and after air-drying and oven drying, were fired to temperatures of 800°C to 1350°C. The change in the dimensions of the pellets were measured and the computed percentages are given in Fig.A. There is shrinkage initially upto 1000°C, due to decarbonation and decomposition of clay minerals; then there is expansion upto 1200°C, which can be attributed to the formation of Sulphoaluminate phases. Beyond 1200°C shrinkage is observed again due to the transition to liquid phase. These phenomena are also corroborated by the XRD analysis - Fig.A gives four of the phases observed, the

sulphoaluminate peak reaches the maximum at 1250°C, remaining stable till 1350°C. Similarly, it can be seen from the figure, maximum strengths are attained at 1250°C.

Of the other phases, C_2AS (Gehlenite) is increasing till 1100°C. Then it decreases and at 1250°C it completely disappears. As regards Belite, it is more or less uniform from 1000°C, but the peaks are not well defined because it is not well crystallised.

5. HYDRATION :

The hydration characteristics of of NAC were studied by hydrating the cement with 0.4 W/C ratio. The XRD results of hydration products are given in Fig. B. It is observed that 55 percent of the $C_4A_3\bar{S}$ is hydrated in eight hours, forming Ettringite which is responsible for the high early strength. This hydration of $C_4A_3\bar{S}$ continues and the extent is 80,90 and 95 percent at one, three and seven days as seen in Fig. B and C. No mono-sulphate hydrate was detected. The other hydration products such as C_3AH_6, C_4AH_{13} and $C_3A\bar{C}H_{12}$ ($\bar{C}=CaCO_3$) have also been identified.

6. PROPERTIES OF CEMENT :

The clinker as produced hitherto is ground along with the appropriate dosage of calcium sulphate, to a surface of 5000cm^2/gm and the physico-mechanical characteristics have been presented in TABLE -4.

7. PILOT PLANT PRODUCTION :

The pilot plant production utilised various raw materials, like limestone, hydrated lime, diaspore, bauxite, kyanite, clay, and gypsum (both mineral and chemical) appropriately mixed to reach the requisite raw material composition. The raw mix was nodulised in pans and dried in ovens before being fed to the 1 Ton/day kiln. So far over 50 to 60 Tons of the cement has been produced on pilot plant scale, using LDO as fuel.

Full scale plant trials were also carried out in a rotary kiln of 1.5M dia., 55M length, using furnace oil as fuel, using the facilities at one of our Cement Works. About 30 Tons material was produced as a trial lot.

The physical characteristics of the pilot plant produced cement are given in TABLE-4.

8. FIELD TRIALS :

All new cements need a proper evaluation of their performance in the field so as to become acceptable as commercial products.

The cement produced in Pilot Plant has been evaluated for typical concrete properties and Table-5 presents a comparison of NAC concrete properties along with concrete produced from OPC, conforming to Indian Standards. It is seen that high early strength concrete can be produced using the same quantity of cement and the 3 day strengths are nearly twice, while the 28 day strength is almost identical.

As a case study, a prototype structure was constructed partially over 4 years ago. The roof and beams were cast about nine months back - a special feature being the removal of the shuttering in a relatively short period of about seven days, compared to a normal period of three weeks. The concrete columns cast over four years ago, are in sound condition. Long term strength patterns are given in TABLE-6. From the data, the gradual gain in strength upto 4 years is confirmed and no retrogression in strength development is observed at any age within this period.

To evaluate the use of cement under low temperatures, concrete and mortar cubes were prepared and cured under slightly sub-zero temperatures. The heat of hydration in the first few hours(45-50 Cal/gm in 24 hrs.) has been able to overcome the effect of low temperatures and the TABLE-7 gives details of the strength development. In the actual field also, this cement has been tried out for producing concrete in sub-zero conditions.

In one trial in the forward areas near Leh Himalayas, tests under identical conditions gave concrete strengths of 160-250 Kg/Cm^2 at 3 days with the NAC while the OPC concrete strengths were around 60 Kg/Cm^2, while in another trial the respective values were 208 Kg/Cm^2 and 31 Kg/Cm^2

Preliminary studies also have shown that NAC produced has good sulphate resistance properties. Accelerated corrosion resistance tests have revealed superior properties in comparison with normal Portland cements, as shown in Fig. D.

Trials of Precasting of a number of types of concrete, like flooring tiles, columns, lintels have also been carried out with a large improvements in turnover.

9. CONCLUSIONS :

NAC have shown good promise both in economic production and field applications. It can become a useful variety of cement, with further all round development.

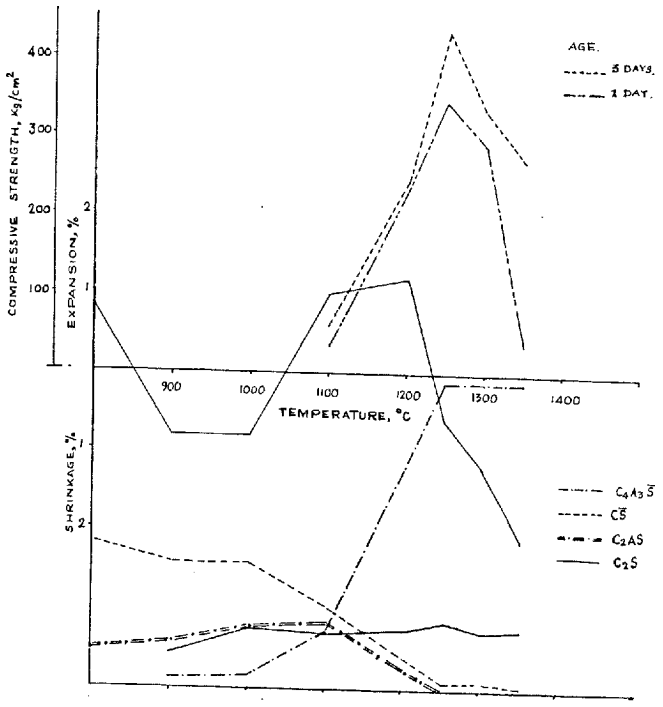

FIGURE-A

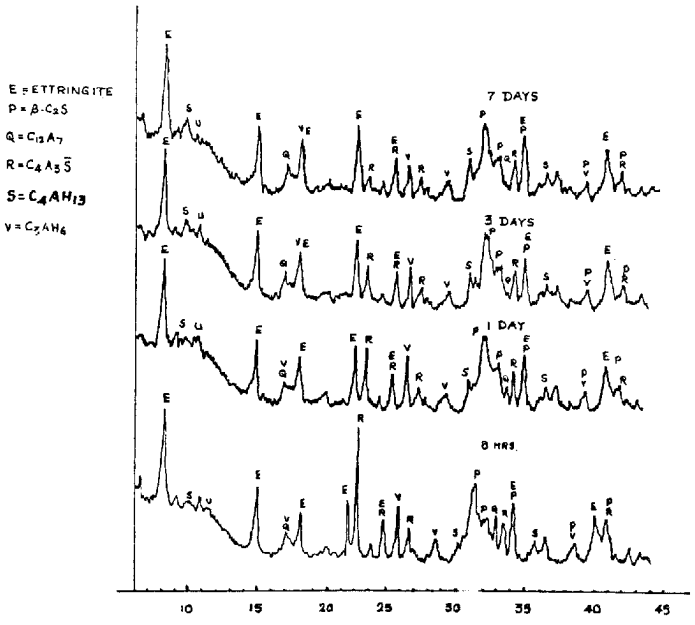

FIGURE-B : XRD PATTERNS OF HYDRATED PASTES OF NAC

TABLE 1

Data on Sulphoaluminate based Cements as available in Published Papers

Phases								Compressive Strength Kg/cm^2				Reference	Remarks
$C_4A_3\bar{S}$	C_2S	CA	$C_{12}A_7$	C_4AF	CS	CaO	Others	1 D	3 D	7 D	28 D		
15.5	60.3	5.7	8.2	-	-	-	-	-	75	115	220	(1)Pg.114/116	
14.7	58.0	7.4	9.8	-	-	-	-	-	140	220	265		
28.8	40.8	20.0	-	-	8.7	-	1.7	280	320	380	550	(2)Pg.33/34	
42.6	42.0	6.3	-	-	4.5	-	2.5	-	360	430	750		
38.7	32 8	19.0	-	-	8.1	-	1.4	310	500	580	600		
54.3	34 2	6 0	-	-	3.9	-	1.5	-	450	650	650		
54.0	32.0	-	-	5	-	9	-	-	-	-	-	(3)Pg.154	Clinker Cement
41.0	32.0	-	-	4	22 0	-	-	-	175	244	407		
64 35	16.09		-	-	19.56*			245	305	345	360	(4)Pg.384	*Gypsum
50.74	33.83	-	-	-	15.43*	-	-	250	305	295	330		
20.00	25.00	-	-	40	15.00	-	-	343	364	369		(5)Pg.10/12	
20.00	30.00	-	-	30	20.00	-	-	279	336	346			
15.66	67.47	-	-	2.92	7.72	-	-				-	(6)Pg.7	
28.34	38.80	-	-	7.96	12.43	6.13	-	376	390	620	720		Clinker + 10%Gyps.

Note: The unit of strength values have been converted uniformly to Kg/Cm^2, where a different unit was used by the author

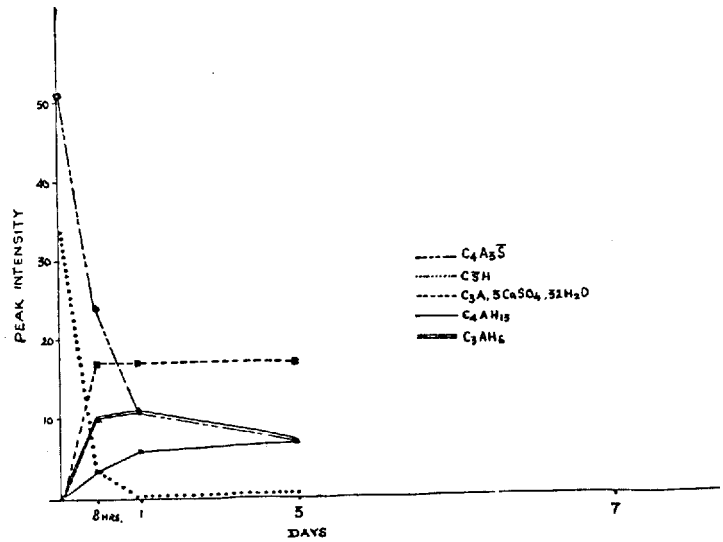

FIGURE-C: IDENTIFICATION OF HYDRATED PHASES OF NAC BY XRD

TABLE 2

Raw Materials : Chemical Analysis

Material	S	A	F	C	LOI	S	$\overline{S}$
Limestone	1.7	2.2	0.5	52.8	41.9	-	-
Raw Bauxite	0.1	63.9	1.9	0.5	30.2	-	-
Clay	42.0	39.0	2.5	1.0	10.5	-	-
Gypsum (Chemical)	0.6	0.6	0.2	40.5	2.5	51	1.0
Gypsum (Mineral)	0.2	2.4	1.0	26.5	18.0	32	19.5

TABLE 3

Relation of Compressive Strength(Kg/cm^2) with Compositional Changes and Firing Temperatures.

a. Sintering Temperature 1200°C

S. No.	A/S $\overline{A/S}$		3.6	3.8	4.0
		Days	Compressive Strength (Kg/cm^2)		
1	2.0	1	115	145	165
		3	120	170	180
2	2.5	1	125	235	250
		3	210	245	260
3	3.0	1	170	145	110
		3	130	95	165

b. Sintering Temperature 1300°C

1	2.0	1	285	485	220
		3	480	525	320
2	2.5	1	395	290	315
		3	410	330	370
3	3.0	1	355	310	355
		3	450	485	490

Note: The A/S and $A/\overline{S}$ Modulii indicated in the Table pertain to the composition of clinker/raw materials. The strength values are those of cement obtained by grinding clinker and a constant proportion of gypsum.

TABLE 4

Physical Characteristics of Non-Alitic Cements

S. No.	Characteristics	Range
1	Specific Gravity	2.80 - 2.85
2	Fineness - Blaine cm^2/gm	4500 - 5000
3	Consistency %	25 - 27
4	Setting Time	
	Initial - Minutes	30 - 40
	Final - Minutes	50 - 70
5	Compressive Strength Kg/cm^2	
	1 Day	300 - 350
	3 Day	330 - 380
	7 Day	390 - 440
	28 Day	450 - 500
6	Tensile Strength (Kg/cm^2) (Modulus of Rupture)	
	1 Day	60 - 70
	3 Day	60 - 70
	7 Day	60 - 70
	28 Day	60 - 70
7	Soundness Expansion by Autoclave Method (%)	Nil

TABLE 5

Strength Development at Early Ages

Type of Cement	Cement Content Kg/M^3	Compressive Strength (Kg/cm^2) 1 D	3 D	7 D	28 D
Non-Alitic Cement	300	180	185	190	230
	400	270	280	320	320
	500	370	390	400	490
Ordinary Portland Cement	300	60	120	150	230
	400	80	150	190	290
	500	120	210	260	395

TABLE 6

Long Term Strengths of NAC Concrete

S.No.	Age	Compressive Strength
	days	Kg/cm^2
1	1	140
2	3	220
3	7	230
4	28	270
5	91	310
6	180	340
7	1460 (4 Years)	360

Note : Values in S.No. 1 to 6 are cube strengths, while that in S.No.7 is the Rebound Test hammer result.

TABLE 7

Strength Development at Low Temperature

	Temperature of		Compressive Strength			Remarks
	Mixing ^oC	Curing ^oC	Kg/cm^2			
			1 D	3 D	7 D	
Mortar 1:1 Mix	27	27	410	454	480	Non-alitic cement
"	15	-5	31	50	100	"
"	10	-5	30	40	110	"
Concrete 1:2:4 Mix	27	27	370	390	440	"
"	27	-5	35	35	40	"
"	15	-5	15	20	40	"
"	27	-5	-No Strength-			Ordinary Portland Cement

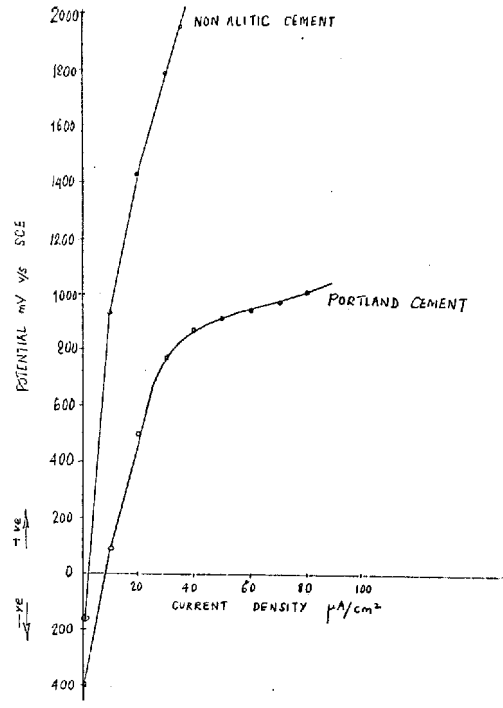

FIGURE-D

REFERENCES:

1. V.N.VISHWANATHAN, S.J.RAINA and A.K.CHATTERJEE(1978), " An exploratory investigation on Porsal Cement ", World Cem.Tech 9, 109-118.

2. K.IKEDA(1980) "Cement along the join $C_4A_3\bar{S}-C_2S$",Proc. 7th Int. Cong. on Chemistry of Cem, Vol II Theme III 31-36

3 G.SUDOH,T.OHTA, and H.HARADA, (1980), " High Strength Cement in the CaO $Al_2O_3-SiO_2-SO_3$ System and its application ", Proc. 7th Int. Cong. on Chemistry of Cem.,Vol. III, Theme V 152-157.

4. DENG JUN-AN, GE WEN-MIN, SU MU-ZHEN, LI XIU-YING,(1980), " Sulfoaluminate cement series", Proc.. 7th Int. Cong. on Chemistry of Cem, Vol. IV Theme V, 381-386.

5. P.K.MEHTA,(1977). " U.S. Patent 4, 036, 657 ".

6. I.V. KRAVCHENKO , V.A. KHARLAMOV, T.V.KUZNETSOVA, L.L.ASTANSKII(1978), " Rapid hardening belite cement "

LUCCO BORLERA MARIA, BRISI CESARE, Dipartimento di Scienza dei Materiali e Ingegneria Chimica del Politecnico di Torino, Italy.

1

Stability of the compound C_5A_3 in the system $CaO-Al_2O_3$

Sur la stabilité du composé C_5A_3 dans le système $CaO-Al_2O_3$

3.3

SUMMARY - The behaviour of the compound C_5A_3 heated in presence of gaseous atmospheres of variable composition is examined. This in the aim to clarify its stability conditions and its equilibrium relationships in the solid state with the dodecacalcium heptaaluminate $C_{12}A_7$.

Heated in air with a normal moisture content C_5A_3 changes very quickly into a mixture of $C_{12}A_7$ with little CA. The reaction is coupled to a small increase of mass and its rate is largely affected by variations of the contact surface solid-gas. The compound C_5A_3 remains instead unaltered if heated in a flow of very dry nitrogen or oxygen; the presence of low quantities of water vapour is however sufficient to obtain a fast transformation to the heptaaluminate. On the contrary the phase $C_{12}A_7$ decomposes into a mixture of C_5A_3 with little C_3A when heated in contact of very dry nitrogen or oxygen. C_5A_3 can be obtained also directly by reaction in the solid state of mixtures of CA and C_3A, this provided the reaction is performed in conditions of extremely low partial pressures of water vapour.

These results show that the presence of water, and consequently of hydroxyl groups, is essential for the stability of the phase $C_{12}A_7$, which so results extraneous to the true binary system $CaO-Al_2O_3$. The compound C_5A_3 appears instead a real equilibrium phase of the system.

Examina-se o comportamento do composto C_5A_3 aquecido em presença de atmosferas gasosas de composição variável. Com isto se pretende esclarecer as condições de estabilidade e suas relações de equilíbrio no estado sólido com heptaaluminato dodecacálcico $C_{12}A_7$.

Aquecido em ar com um teor normal de umidade, C_5A_3 muda-se muito rapidamente numa mistura de $C_{12}A_7$ com pouco CA. A reação está associada a um pequeno aumento de massa e sua velocidade é grandemente afetada por variações da superfície de contato sólido-gás. O composto $C_{12}A_7$, ao invés, permanece inalterado se aquecido numa corrente do nitrogênio ou oxigênio muito secos; contudo, a presença de poucas quantidades de vapor de água é suficiente para obter-se uma transformação rápida para heptaaluminato. Ao contrário, a fase $C_{12}A_7$ se decompõe numa mistura de C_5A_3 com pouco C_3A, quando aquecido em contato com nitrogênio ou oxigênio muito secos. C_5A_3 pode também ser obtido diretamente pela reação em estado sólido de misturas de CA e C_3A, desde que a reação se realize em condições de pressões parciais extremamente baixas de vapor d'água.

Estes resultados demonstram que a presença de água, e conseqüentemente de grupo de hidrais é fundamental para a estabilidade da fase $C_{12}A_7$, que resulta extrôneo à sistema binário verdadeiro $CaO-Al_2O_3$. O composto C_5A_3 aparece como a fase de equilíbrio real do sistema.

LUCCO BORLERA MARIA, BRISI CESARE

INTRODUCTION

The compound C_5A_3 was first identified by Aruja (1) who obtained it through crystallization in nitrogen atmosphere of melted masses of suitable composition. Subsequently, it was prepared by several other researchers, but always under such conditions wich had led to the belief that it was a phase of non equilibrium. Hence the term of unstable C_5A_3, that is often used to indicate this compound in the chemistry of cement.

The reaction at high temperature in presence of air of mixtures of calcium oxide and aluminium oxide with molar ratio 5/3 in fact never leads to the formation of C_5A_3 and gives rise instead to the formation of the so-called dodecacalcium heptaaluminate, $C_{12}A_7$, accompanied by small amounts of monocalcium aluminate. This is probably due to the fact that water and oxygen produce a stabilizing effect on this phase by becoming part of the crystal lattice in the form of hydroxylic (2,3,4) or peroxidic groups (5,6). The phase assumes so a composition corresponding to the formula $C_{12-x}A_7.xCa(O,OH)_2$.

Some researches we have recently performed (7) made it possible to prove that in environments with a very low partial pressure of oxygen and water vapour, C_5A_3 can be obtained both through direct reaction in the solid state between C_3A and CA, and as a transformation product of $C_{12}A_7$, which heated under these conditions, gives just rise to a mixture of C_5A_3 with little C_3A. This seems to show that C_5A_3 is a phase of true equilibrium of the calcium oxide-alumina system totally free from extraneous substances, this at least at temperatures lower than 1280°C.

To further clarify the problem we have now studied the behaviour of C_5A_3 when heated in gaseous atmospheres of various compositions.

EXPERIMENTAL PART AND DISCUSSION

Pure C_5A_3 was prepared using the following technique. Solutions of calcium nitrate and aluminium nitrate of stoichiometric composition were evaporated with the previous addition of about 15% of tartaric acid. The product obtained in this manner was then heated in air for two hours at 700°C, getting so a mass amorphous to X-rays, which was subsequently kept for six hours in a current of very pure hydrogen (H_2O+O_2 < 5 ppm) at 1200°C. The X-ray powder pattern performed on the resulting material displayed only the lines typical of C_5A_3 (8). We looked also for the possible presence of peroxidic oxygen, that was found to be nil or at least not analytically detectable.

A first sample of C_5A_3, ground till passing totally through a sieve with mesh opening of 150 micrometers, was heated for increasing periods of time in ambient air at a temperature of 1100°C. X-ray examination made it possible to ascertain that under these conditions it tends to change into the phase $C_{12}A_7$ with the simultaneous formation of a little CA. The phenomenon evolves very rapidly: after 15 minutes the transformation already involves about 50% of the initial C_5A_3 and after 30 minutes increases to 80%, to reach almost the completion after one hour.

At 1200°C the transformation is even faster and it is nearly complete after only

15 minutes of heating.

The phenomenon is accompanied by a modest, but clearly detectable, increase of mass. For the product totally transformed in $C_{12}A_7$ plus CA at 1200°C this increase was found to be 0.72%. In the material obtained in this way we observed the presence of an excess of oxygen of 0.09%.

The amount of water (obviously bound in the form of hydroxyl groups) held by the $C_{12}A_7$ heated at high temperatures varies, as does the amount of excess oxygen, as a function of several factors: in addition to temperature the other variables that come into play include cooling speed, porosity, specific surface of the specimens and maybe also air moisture.

In the case of samples cooled down rapidly from 1200°C the water content is found to be in any case close to 0.70% in mass (6). On this basis we may calculate for the product being considered a composition that corresponds with good approximation to the formula:

$$C_{11.38}A_7 \cdot 0.54Ca(OH)_2 \cdot 0.08CaO_2$$

The transformation from C_5A_3 to a $C_{12}A_7$ with the above composition can therefore be represented by the reaction:

$$5\ C_5A_3 + 1.08\ H_2O + 0.08\ O_2 \longrightarrow$$

$$\longrightarrow 2(C_{11.38}A_7 \cdot 0.54Ca(OH)_2 \cdot 0.08CaO_2) + CA$$

which involves an increase in mass of 0.75% in respect to the initial C_5A_3; a value that, within the limits of experimental error and the approximation of the formulae, is in very good agreement with the result experimentally obtained and above indicated.

All the tests mentioned so far were carried out on C_5A_3 in form of fine powder; other experiments instead were performed using cylinders of C_5A_3 measuring about 10 mm in diameter and 5 mm in height, obtained by pressing at 2.10^8 Pa the amorphous material from the decomposition of nitrates and subsequent sintering at 1200°C in a hydrogen flow. The specimens prepared in this way displayed an apparent density close to 75% of the theoretical density.

In this case too, heating in air leads to the transformation of C_5A_3 into a mixture of $C_{12}A_7$ and little CA, but the phenomenon is much slower than with the powders; after 15 minutes at 1100°C, for instance, the transformation involved only about 8% of the material, and this percentage rose to about 25% after one hour, compared with the values of 50 and 95%, respectively.

These results provide further confirmation of the fact that the transformation of C_5A_3 into $C_{12}A_7$ and CA is not a simple phenomenon of decomposition internal to the calcium oxide-alumina system, but is the consequence of a reaction between the pentacalcium trialuminate and some constituents of air (water vapour and oxygen) and, as such, its speed is markedly affected by the extension of the solid-gas contact surface.

Another series of tests was performed by heating at 1200°C the powdered C_5A_3 in a flow of very pure nitrogen ($O_2 < 2$ ppm, $H_2O < 5$ ppm): the compound remained completely unaltered even with rather long (50 hours) heating periods. On the other hand, few hours of heating at 1200°C in a current of slightly moist nitrogen are sufficient to produce a nearly total transformation into the mixture of $C_{12}A_7$ and CA. This con-

firms the influence of the hydroxyl groups on the stability of dodecacalcium heptaaluminate.

Heating experiments in a flow of nitrogen with a very low oxygen and water vapour content were also performed on samples of $C_{12}A_7$ obtained through rapid cooling in air from 1200°C and thus containing at the start little quantities of water and excess oxygen. Under these conditions the heptaaluminate is no longer stable and it changes into a mixture of C_5A_3 with little C_3A: after 15 hours the unaltered fraction amounted to about 10% of the initial product. The breakdown of the crystal lattice of $C_{12}A_7$ is obviously connected with the gradual loss of the excess oxygen and water.

In order to ascertain whether oxygen alone is sufficient to make the structure of $C_{12}A_7$ stable even in the total or nearly total absence of hydroxyl groups, another series of tests was carried out heating the $C_{12}A_7$ obtained in air for increasing periods of time at 1200°C in a current of oxygen with extremely low moisture content (H_2O < 5 ppm). With relatively short heating times $C_{12}A_7$ remains unchanged and it even shows an increase in the content of excess oxygen. In a sample heated for seven hours, for example, the excess oxygen was found to be about 0.4% by mass. But if the heating period is extended, the $C_{12}A_7$ gradually begins to decompose, giving rise as usual to the formation of C_5A_3 and little C_3A. This phenomenon is relatively slow and the transformation is not fully completed even after 50 hours.

The results of this last series of tests show that unlike what is sometimes believed, oxygen alone is not sufficient to stabilize the lattice of dodecacalcium heptaaluminate; this at least at a temperature of 1200°C and with an oxygen pressure of 101.325 Pa (1 atm). These results, in fact, should be in our opinion interpreted in this manner. Relatively short heating periods cause the elimination of a considerable proportion of water and this favours, as was already known (6), the introduction of peroxidic groups. As heating continues in very dry oxygen, the content of water withheld by the product decreases, till it reaches values that are not sufficient to the persistence of the structure of the heptaaluminate and the latter changes into C_5A_3.

The fact that oxygen by itself is not sufficient to stabilize the structure of $C_{12}A_7$ is also confirmed by the observation that C_5A_3 heated in dry oxygen does not display any tendency to change into $C_{12}A_7$, even over a wide variety of heating times (1 to 50 hours). Even in the case of heating in oxygen current the presence of moisture traces leads anyway to the rapid formation of the heptaaluminate.

The transformation of $C_{12}A_7$ into C_5A_3 through heating in environments with very low partial pressure of water vapour at temperatures elevated, but still rather far from the melting temperatures, is another proof of the fact that the so-called dodecacalcium heptaaluminate does not belong to the true binary calcium oxide-alumina system, but it still does not demonstrate that the compound C_5A_3 is a phase thermodynamically stable. In fact, it might represent only a product of transition towards a situation of greater equilibrium, such as, for instance, as some authors have suggested (3), a mechanical mixture of C_3A and CA.

In order to gain a better understanding of this problem we performed a number of tests, in which mixtures of C_3A and CA in suitable proportions, were heated at 1200°C in a flow of very dry nitrogen or oxygen.

In the products treated in this manner we always observed, along with a certain amount of the starting substance still unaltered, the presence of C_5A_3 in percentages increasing with the increase of the heating time. On the other hand the formation of $C_{12}A_7$ was never observed. These experiments, as well as similar tests performed in a hydrogen current (7), prove that C_5A_3 - at least at 1200°C - is a phase thermodynamically more stable even in respect to mixtures of C_3A and CA, and therefore it may be assumed to be a phase of true equilibrium of the $CaO-Al_2O_3$ system.

CONCLUSIONS

C_5A_3, when heated in air with normal moisture content, is transformed very quickly into the phase $C_{12}A_7$, or more precisely into $C_{12-x}A_7 \cdot xCa(O,OH)_2$.

The compound remains unaltered if it is heated even for long periods of time at 1200°C in a flow of nitrogen or oxygen with very low moisture content. On the contrary the transformation takes place easily if che heating is performed in a current of slightly moist gas.

The phase $C_{12}A_7$ heated in a flow of very dry nitrogen or oxygen tends to change into C_5A_3. In a current of oxygen this transformation takes place more slowly and at first there is even a further fixation of excess oxygen on the part of $C_{12}A_7$.

The results referred above show that the presence of water traces and hence of hydroxyl groups, is indispensable for the stability of the structure of dodecacalcium heptaaluminate and that, although this phase might absorb even considerable amounts of excess oxygen in the form of peroxidic groups, these alone are not sufficient to allow its stability. It is therefore confirmed that $C_{12}A_7$ is not a stable phase of the true binary system calcium oxide-alumina.

In addition to starting from $C_{12}A_7$, C_5A_3 can also be obtained, with a direct reaction in the solid state, by heating at 1200°C in a flow of very dry nitrogen or oxygen stoichiometric mixtures of C_3A and CA. Thus C_5A_3 is found to be - at least at 1200°C - thermodynamically mor stable than the mixture of the two compounds mentioned above and therefore may be regarded in all likelihood as a phase of true equilibrium of the calcium oxide-alumina system.

REFERENCES

1) Aruja E., Acta Cryst., 10, 337 (1957).

2) Jeevaratnam J., Glasser F.P., Dent Glasser L.S., J.Am.Ceram.Soc.,47, 105 (1964).

3) Nurse R.W., Welch J.H., Majumdar A.J., Trans.Brit.Ceram.Soc., 64, 323 (1965).

4) Nurse R.W., Welch J.H., Majumdar A.J., Trans.Brit.Ceram.Soc., 64, 409 (1965).

5) Imlach J.A., Dent Glasser L.S., Glasser F.P., Cement Concrete Res., 1, 57 (1971).

6) Brisi C., Lucco Borlera M., Il Cemento 80, 155 (1983).

7) Lucco Borlera M., Brisi C., Il Cemento 81, 13 (1984).

8) A.S.T.M.: X-ray Powder Data File, Card 11-357 (1957).

A. Bachiorrini, B. Guilhot, M. Murat, A. Negro, M. Soustelle, A.A. Fournier

INFLUENCE DE LA CALCITE SUR L'HYDRATATION DE L'ALUMINATE MONOCALCIQUE. CORRELATION ENTRE LES RESULTATS EXPERIMENTAUX ET LA THERMODYNAMIQUE DU SYSTEME.

HYDRATION OF MONOCALCIUM ALUMINATE WITH CALCITE. RELATION BETWEEN EXPERIMENTAL RESULTS AND THE THERMODYNAMICAL STUDY OF THE CaO Al_2O_3-CO_2-H_2O SYSTEM

La confrontation de l'étude thermodynamique et des résultats expérimentaux obtenus par les auteurs concernant l'action de la calcite sur l'hydratation de l'aluminate monocalcique à 20°C met en évidence les points suivants:

- L'analyse thermodynamique du système CaO - Al_2O_3 - CO_2 - H_2O a montré que les phases hydratées formées ont une stabilité croissante, dans l'ordre $C_4A\bar{C}H_{11}$, C_2AH_8 et CAH_{10}.

- Les vitesses de précipitations expérimentales de ces hydrates varient dans l'ordre inverse comme en attestent les résultats obtenus par calorimètrie isotherme. Ceci entraîne lors de la précipitation de ces phases l'ordre d'apparition suivant (si la vitesse de passage de CA en solution devient faible) : CAH_{10}, C_2AH_8 puis $C_4A\bar{C}H_{11}$.

- La géométrie du milieu réactionnel (surtout en pâte) peut conduire à des gradients de concentration qui entraînent une dissolution de tous les hydrates dans une zone et la reprécipitation dans une autre zone.

Tout se passe alors comme si on dissolvait des cristaux de CAH_{10} dans une région pour former du carboaluminate hydraté dans une autre (au voisinage de la calcite).

A confrontação do estudo temodinâmico e dos resultados experimentais obtidos pelos autores, relativamente à ação da calcita sobre a hidratação do aluminato monocálcico a 20°C, põe em evidência os seguintes pontos:

- A análise termodinâmica do sistema CaO-Al_2O_3-CO_2-H_2O mostrou que as fases hidratadas formadas têm uma estabilidade crescente, na sequência $C_4A\bar{C}H_{11}$, C_2AH_8 e CAH_{10}.

- As velocidades de precipitações experimentais destes hidratos variam na ordem inversa, conforme o atestam os resultados obtidos por calorimetria isotérmica. Isto ocasiona, quando da precipitação destas fases, a seguinte ordem de aparecimento (se a velocidade de passagem de CA em solução se torna lenta): CAH_{10}, C_2AH_8, depois $C_4A\bar{C}H_{11}$.

- A geometria do meio reacionário (sobretudo em pasta) pode levar a gradientes de concentração que ocasionam uma dissolução de todos os hidratos numa zona e a precipitação noutra zona.

Tudo acontece então como se fossem dissolvidos cristais de CAH_{10} numa região para se formar carboaluminato hidratado em outra (na vizinhança da calcita).

I - Introduction

Les premiers travaux concernant l'interaction entre les pâtes de ciment et les granulats calcaires ont été effectués par Farran (1), il y a une trentaine d'années.

Le cas des ciments alumineux a fait l'objet de recherches plus récentes (2-11), orientées essentiellement vers l'amélioration des résistances mécaniques en limitant la conversion des hydrates hexagonaux (CAH_{10} et C_2AH_8) en hydrate cubique (C_3AH_6).

L'objet de ce travail est d'examiner l'apparition des différentes phases au cours de la réaction et de les corréler avec l'analyse thermodynamique.

II - Stabilité thermodynamique

Nous avons entrepris une étude mathématique sur la stabilité thermodynamique des différentes phases en présence dans le système quaternaire $CaO-Al_2O_3-H_2O-CO_2$ à 20°C (12-13). Ce calcul est fondé sur l'existence dans la solution aqueuse de cinq types d'ions à savoir :

$$AlO_2^-,\ Ca^{++},\ CO_3^{--},\ OH^-,\ H^+$$

Les solides susceptibles d'être stables dans nos conditions expérimentales sont au nombre de six :

$$CaCO_3,\ Al(OH)_3,\ Ca(OH)_2,\ CAH_{10},\ C_2AH_8$$

et enfin $C_4A\bar{C}H_{11}$

Le système est alors déterminé à l'aide de cinq équations :

- la neutralité électrique dans la solution,
- le produit ionique de l'eau,
- l'équilibre entre le gaz carbonique et la solution,
- les deux dernières équations dépendent des phases solides en équilibre avec la solution ce qui conduit alors, si nous nous fixons comme paramètres invariants la pression du gaz carbonique (P), au-dessus de la solution ainsi que le nombre de moles de $CA(N_{CA})$ et de chaux (N_C) passées en solution, à 22 cas d'équilibre possibles que nous pouvons décomposer en trois catégories :

a) aucun solide ne précipite : 1 cas
b) un seul solide précipite : 6 cas
c) deux solides précipitent : 15 cas

Nous ne connaissons pas, à priori, pour une valeur déterminée de P, N_C, N_{CA}, le ou les solides en équilibre avec la solution. Nous avons donc opéré par une méthode de balayage sur les 22 cas possibles à l'aide d'un programme informatique pour les déterminer.

Les phases stables peuvent être représentées dans un diagramme à trois dimensions (P, N_C, N_{CA}) ou plus simplement dans des diagrammes plans isobares ou à nombres de moles de $CaCO_3$ constants où sont délimités les domaines de stabilité des différents hydrates solides. Nous avons pu déduire de cette approche mathématique que le seul hydrate stable dans les conditions de notre étude est CAH_{10} et que si celui-ci précipite en présence d'un deuxième solide, la masse de ce dernier reste constante quand les masses de produits introduits varient.

Nous observons que l'apparition de C_2AH_8 à température ambiante ainsi que celle du carboaluminate hydraté $C_4A\bar{C}H_{11}$ quand nous sommes en présence de CO_2 ou de $CaCO_3$ ne peuvent résulter que de sursaturations par rapport à CAH_{10}.

Nous avons ainsi pu vérifier mathématiquement que la présence de $C_{12}A_7$ dans le CA se traduit par un accident dans la partie croissante de la courbe conductimétrique sous forme d'un petit palier ce qui est en accord avec nos résultats expérimentaux. Ce calcul nous a aussi permis d'expliquer l'ensemble des "vagues" constituant dans certains cas (sursaturation en chaux donc présence de $C_{12}A_7$) le palier dit de "sursaturation".

Ces "vagues" correspondent donc à une succession d'hydrates métastables qui précipitent puis se redissolvent avant l'apparition de l'hydrate stable CAH_{10}.

Tous les calculs ont été effectués en milieu dilué (domaine d'application de la loi de Debye-Hückel) et la transposition à l'hydratation en pâte devra être faite avec précaution. Cependant, quel que soit le rapport E/S, la concentration des ions de la phase aqueuse est toujours faible car tous les produits solides du système ont une faible solubilité.

3.3

III - Résultats expérimentaux. Nature des phases obtenues :

Trois techniques expérimentales ont été utilisées pour étudier la nature des phases formées au cours de l'hydratation du système $CaCO_3$-Al_2O_3, à savoir :

- diffraction des rayons X
- microscopie électronique à balayage
- calorimètrie isotherme.

*Observation par diffraction des rayons X :

Les essais ont été réalisés sur des pâtes de monoaluminate et de carbonate dont l'évolution a été stoppée à diverses échéances par la méthode la plus appropriée (14).

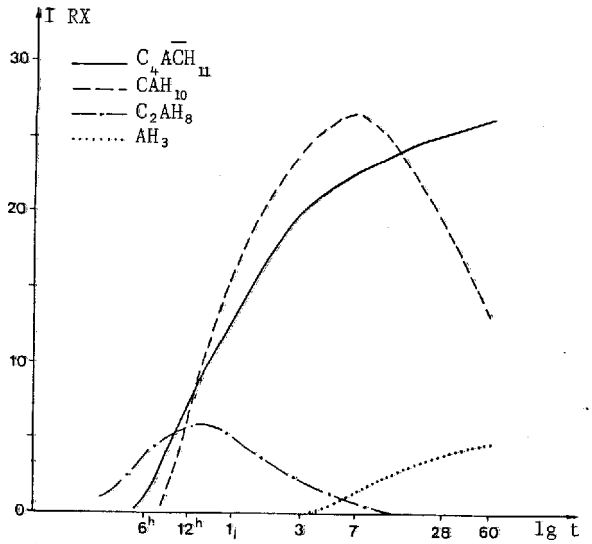

Figure 1 : Evolution comparative des quantités d'hydrates en fonction du temps

L'évolution comparative des quantités d'hydrates en fonction du temps (figure 1) met clairement en évidence la précipitation et la dissolution de C_2AH_8 et celle de CAH_{10}, décalées dans le temps, simultanées à l'apparition du carboaluminate puis de la gibbsite cristallisée (10). Ces résultats sont en accord avec ceux d'Hakim (8).

*Microscopie électronique à balayage :

Les essais ont porté sur l'interface cristal de calcite-pâte de CA en cours d'hydratation. Aux premières échéances de précipitation se forment essentiellement les hydrates hexagonaux CAH_{10} et C_2AH_8 (cliché 1).

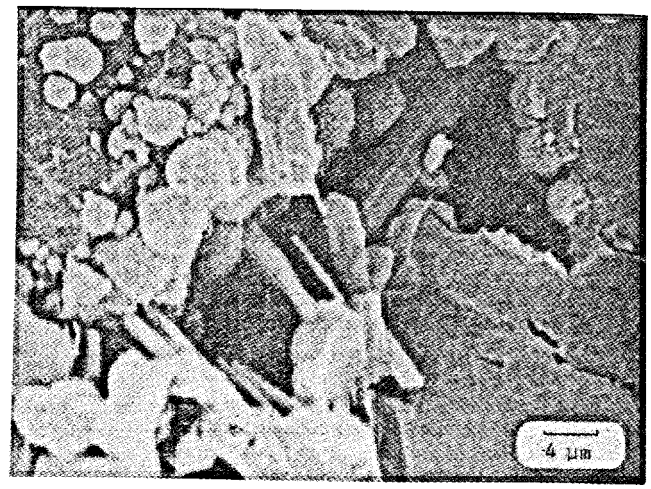

Cliché 1 : cristaux tabulaires de C_2AH_8 et cristal aciculaire de CAH_{10} dans la pâte (en contact avec de la calcite).

Une observation analogue avait été faite en trempant une lame de calcite dans une solution obtenue par dissolution de CA (cliché 2) (15).

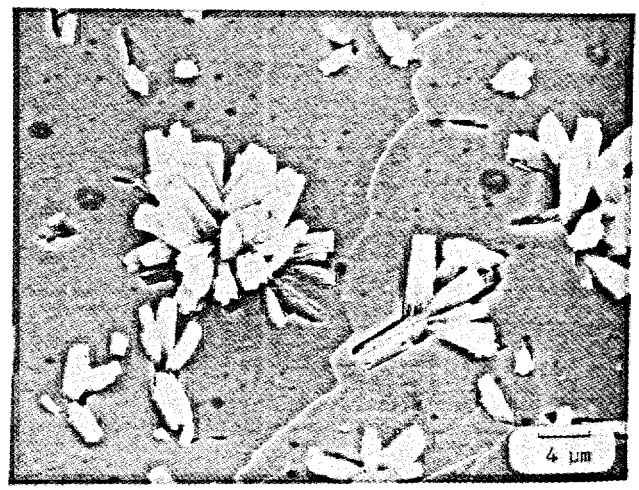

cliché 2 : cristaux de CAH_{10} émergeant des figures de dissolution de la calcite.

Nous observons, dans un deuxième temps la dissolution des hydrates précédemment formés au contact de la pâte (clichés 3 et 4) et la précipitation au contact de la calcite, de cristaux de carboaluminate hydraté $C_4\bar{A}CH_{11}$ (cliché 5) comme le montrent les analyses par spectrométrie de rayons X en dispersion d'énergie.

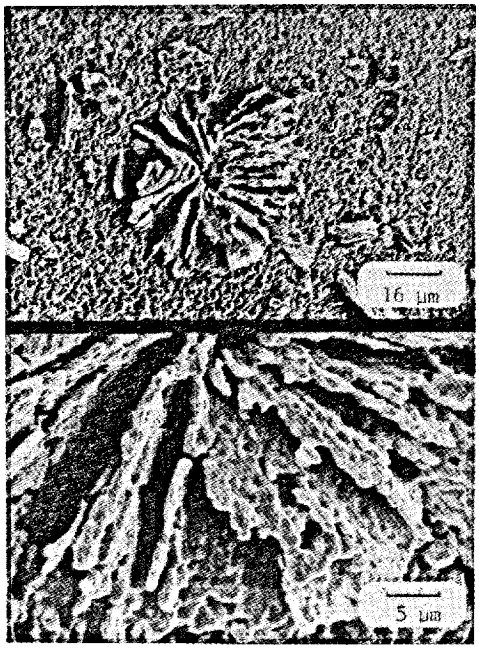

cliché 3 : dissolution de cristaux tabulaires de C_2AH_8

Le M.E.B. montre que les évolutions moyennes mises en évidence par diffraction des rayons X sont en fait localisées en des points bien précis du mélange.

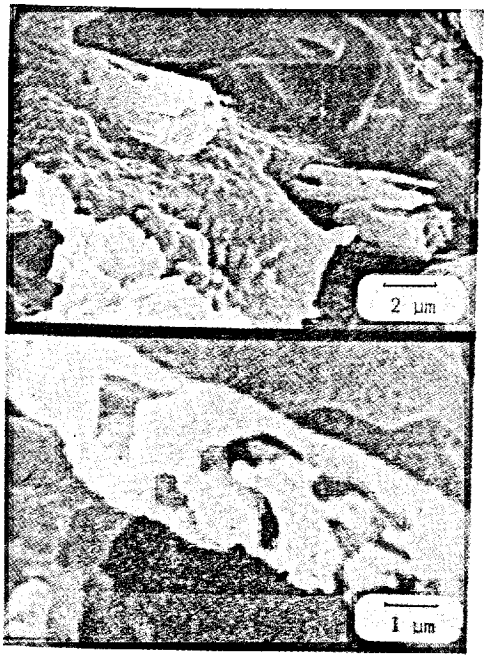

cliché 4 : dissolution de CAH_{10}

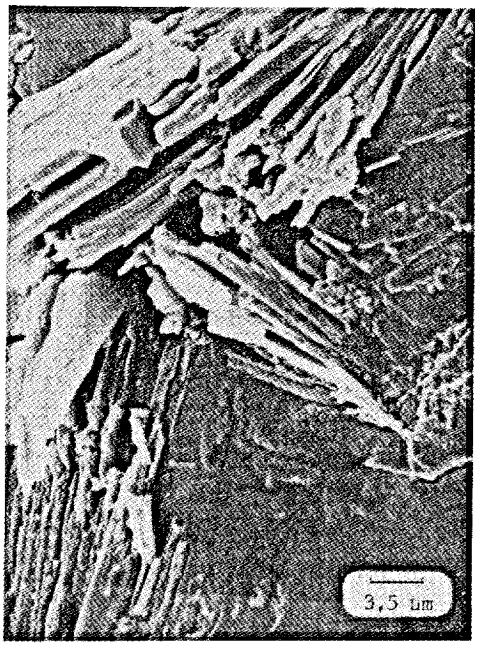

cliché 5 : précipitation de cristaux tabulaires de $C_4A\overline{C}H_{11}$ au contact de la calcite

*Cinétique d'évolution du système par calorimétrie isotherme :

La figure 2a présente l'allure des courbes de flux de chaleur en fonction du temps associée à l'évolution du système pour différents pourcentages de carbonate mélangés au CA. Ces courbes sont en fait des courbes de vitesse en fonction du temps. L'évolution observée n'est pas due à un effet de dilution dans lequel le carbonate de calcium aurait un rôle inerte comme c'est le cas lors de l'ajout de silice (figure 2b). On voit nettement que la présence de carbonate favorise la précipitation simultanée des nouvelles phases et ce à des échéances plus courtes qu'en milieu pur (16).

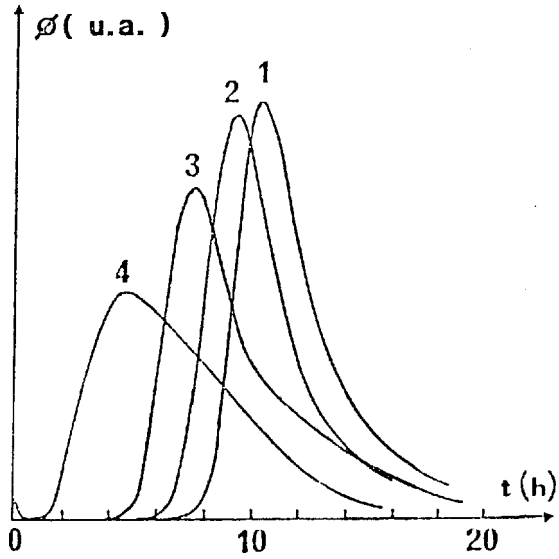

figure 2a : variation du flux thermique observé en calorimétrie isotherme au cours de l'hydratation de CA pur et de mélanges $CA/CaCO_3$ C. Erba

CA pur (1)
90/10 (2)
82,6/17,4 (3)
50/50 (4)

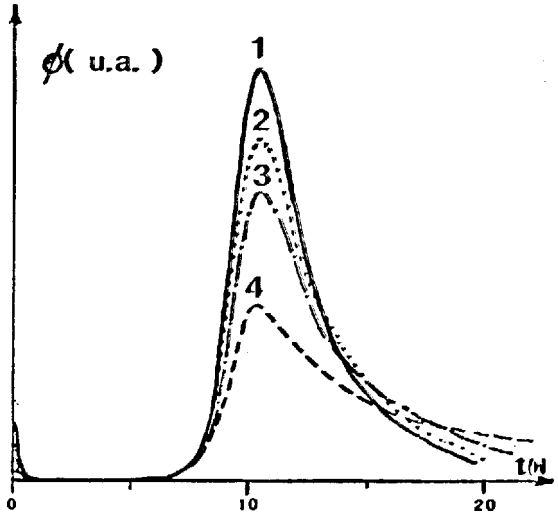

figure 2b : variation du flux thermique Ø en fonction du rapport CA/S

$S = SiO_2$ CA pur (1)
CA/S 90/10 (2)
82,6/17,4 (3)
50/50 (4)

IV - Corrélation des résultats expérimentaux avec la thermodynamique des systèmes :

La phase aqueuse, quel que soit le rapport E/S, est toujours à faible concentration en ions car tous les produits solides du système ont une faible solubilité.

L'étude thermodynamique prend comme hypothèse le fait que les concentrations sont uniformes (E/S élevé), ce qui n'est pas forcément vérifié dans le cas des pâtes car le modèle ne peut être appliqué qu'en chaque point de l'espace ce qui conduit à tenir compte des gradients de concentration des différents ions.

On a montré que la vitesse de germination des phases hydratées était accélérée par la présence d'une surface de calcite. Donc, dans un premier temps, on formera ces hydrates.

Si on admet que les vitesses de précipitation sont des fonctions croissantes des concentrations des ions réactants, en un point de l'espace, à un instant t_1 la vitesse de précipitation des phases est fonction d'une part de la concentration en carbonate de calcium pour le monocarboaluminate hydraté, et d'autre part indépendante de la concentration en CO_3^{--} pour CAH_{10} et C_2AH_8 (figure 3).

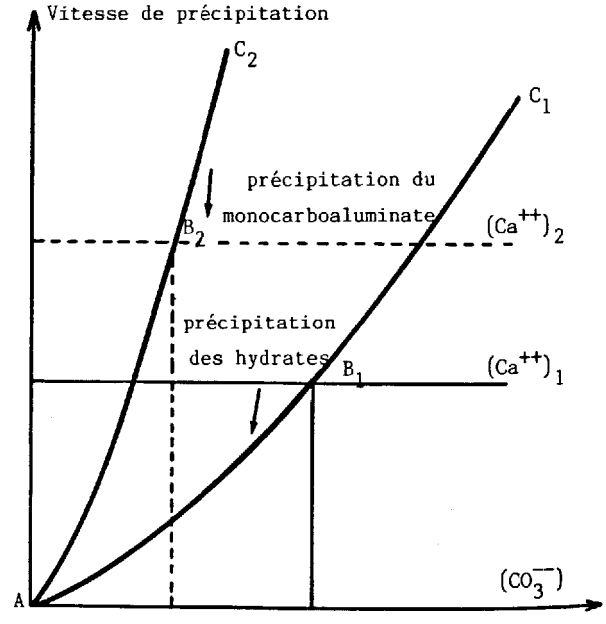

Figure 3 : Evolution de la vitesse de précipitation des hydrates

Appelons C_1 la concentration limite en Ca^{++} donnée à l'instant t_1 à partir de laquelle la vitesse de précipitation du monocarboaluminate devient supérieure à celle de précipitation de CAH_{10} et C_2AH_8. Dans l'intervalle AB_1, les hydrates CAH_{10} et C_2AH_8 précipiteront, dans l'intervalle B_1C_1, ce sera $C_4A\overline{C}H_{11}$.

A un instant t_2, la concentration en Ca^{++} a changé, modifiant les vitesses d'où les nouveaux intervalles correspondants AB_2 et B_2C_2.

A l'interface eau/calcite, la concentration en ions CO_3^{--} est celle donnée par le produit de solubilité de la calcite. Lorsqu'on s'éloigne de l'interface cette concentration diminue suivant un profil de diffusion à un instant donné t_i.

La variation du profil de concentration en CO_3^{--} va être telle que la région de l'espace pour laquelle cette concentration sera supérieure à C_i va augmenter et dans cette région, on assistera à la précipitation du monocarboaluminate. Cette précipitation du carboaluminate entraîne une forte consommation d'ions calcium, d'où l'existence d'un gradient de calcium entre l'interface eau/monocarboaluminate et l'interface eau/aluminate hydraté. Cette diminution de la concentration en ions Ca^{++} entraîne la dissolution des hydrates formés antérieurement (figure 4).

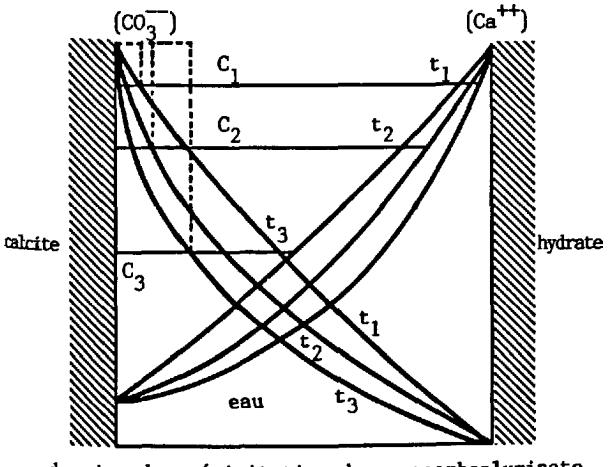

— domaine de précipitation du monocarboaluminate

Figure 4 : allure des gradients de concentrations locaux

Quand E/C augmente, les concentrations aux interfaces restent identiques, mais la distance entre les interfaces augmente. Cette interprétation de nos résultats expérimentaux est cohérente avec les diagrammes thermodynamiques des domaines de stabilité de CAH_{10} et C_2AH_8 (13) qui montrent que la diminution de la concentration en ions Ca^{++} même liée à une augmentation de la concentration en ions CO_3^{--} entraîne la dissolution de ces hydrates.

V - Conclusion

La présence du calcaire lors de l'hydratation de l'aluminate monocalcique modifie profondément l'évolution du système.

Ceci se traduit par :

- l'apparition d'une nouvelle phase à savoir : le monocarboaluminate
- la modification de la cinétique de précipitation des hydrates.

La cause profonde de ces phénomènes provient des gradients de concentration dans la solution dus à des hétérogénéités du milieu créés par l'apparition d'interfaces eau/calcite.

Les processus révélés suggèrent l'importance de l'origine du carbonate de calcium et son état de division dans le comportement global du système.

L'agitation et l'augmentation du rapport eau/solide, en atténuant ces gradients, diminuent les effets du carbonate liés aux concentrations locales ce qui n'est pas le cas dans les conditions normales d'emploi.

BIBLIOGRAPHIE

1 J. FARRAN Rev. Mat. Const., 1956, 490-91, 153
Rev. Mat. Const., 1956, 492, 191
Sil. Ind., 1957, 4, 447, 528, 595

2 M. COLLEPARDI, A. MARCIALIS, R. TURRIZIANI
II Cemento, 1972, 69, 179

3 A. NEGRO, L. CUSSINO, A. BACHIORRINI
II Cemento, 1978, 75, 285

4 L. CUSSINO, A. NEGRO
Proc. VII, J.S.C.C., Vol III, V-62-67, Paris (1980), Ed. Septima

5 A. NEGRO, A. BACHIORRINI, L. CUSSINO
Aluminates de calcium - Séminaire International - Torino Sept. 1982, 219-230

6 A. BACHIORRINI, M. MURAT, A. NEGRO
Liaisons-pâtes de ciment matériaux associés - Coll. Int. Toulouse Nov. 1982
Communication A1

7 M. PEREZ MENDEZ, F. TRIVINO VASQUEZ
Cem. Conc. Res., 1984, 14(2), 161

8 M.F. HAKIM
Thèse Toulouse 1984

9 H.G. MIDGLEY
Clay Minérals 1984, 19, 857

10 A. BACHIORRINI
Thèse Lyon 1985

11 C.H. FENTIMAN
Cem. conc. Res., 1985, 15(4), 622

12 M. SOUSTELLE, B. GUILHOT, A.A. FOURNIER, M. MURAT, A. NEGRO
Cem. Conc. Res., 1985, 15(3), 421

13 M. SOUSTELLE, B. GUILHOT, A.A. FOURNIER, M. MURAT, A. NEGRO
Cem. Conc. Res., 1985, 15(4), 655

14 A. BACHIORRINI, B. GUILHOT
Cem. Conc. Res., 1982, 12(5), 559

15 A. NEGRO, A. BACHIORRINI, M. MURAT
Cristallisation, déformation, dissolution des carbonates Bordeaux, Nov. 1980, 345

16 M. MURAT, A. NEGRO, A. BACHIORRINI
C.R. Acad. Sci. Paris 1980, Série C, 291, 287

A. Bachiorrini - Dipartimento di Scienza dei Materiali e Ingegneria Chimica, Politecnico di Torino, Italia.
L. Cussino - Ricerca e Sviluppo UNICEM SpA, Casale Monferrato, Italia.

HYDRATATION EN MILIEU PUR ET EN SOLUTION SULFATE DU CIMENT ALUMINEUX EN PRESENCE D'AGREGAT SILICEUX OU CALCAIRE.

ALUMINA CEMENT HYDRATION IN PURE WATER AND IN SULPHATE SOLUTION IN THE PRESENCE OF SILICEOUS OR CALCAREOUS AGGREGATE.

Resumé

Les auteurs ont suivi l'hydratation en milieu pur, des pâtes, mortiers et bétons de ciment alumineux et d'agrégat siliceux ou calcaire jusqu'à 5 ans (7 ans pour les bétons) et simultanement ils ont suivi l'hydratation en presence d'ions sulfate de mortiers alumino-siliceux et alumino-calcaires.
Les mesures de résistance mécanique, de porosité et de variation de dimension des éprouvettes ainsi que l'analyse calorimétrique différentielle et l'analyse aux rayons X des produits d'hydratation prouvent que la substitution de l'agrégat siliceux par un granulat calcaire augmente la stabilité de dimension des éprouvettes et entraîne une amélioration de l'évolution dans le temps de leurs propriétés mécaniques et de leur résistance à l'attaque sulfatique à cause de la variation de la cinétique l'hydratation provoquée par la réaction entre le calcaire et le ciment alumineux.
Cette variation de cinétique comporte la conversion des hydrates hexagonaux en $C_4A\bar{C}H_{11}$ et empêche, durant des ans, la formation de C_3AH_6.
A cause du plus grand volume molaire de $C_4A\bar{C}H_{11}$ on observe une progressive diminution de porosité surtout dans la zône de contact ciment - granulat. Les essais sur pâtes ont démontré soit qu'il est l'évolution de la macroporosité (pores avec rayon supérieur à 10.000 Å) à jouer un rôle primordial sur l'évolution des propriétés mécaniques, soit qu'un rapport eau/ciment très faible peut être également très favorable.

Sumário

Os Autores seguiram a hidratação em meio puro, de pastas, argamassas e concretos de cimento aluminoso e agregados silicosos ou calcáreos até 5 anos (7 anos para os concretos) e simultaneamente seguiram a hidratação na presença de ions sulfato de argamassas alumino-silicosas e alumino-calcáreas.

As medidas de resistência mecânica, de porosidade e de variação de dimensão dos corpos de prova, bem como a análise calorimétrica diferencial e análise de raios X dos produtos de hidratação, provam que a substituição do agregado silicoso por um agregado calcáreo aumenta a estabilidade das dimensões dos corpos de prova e acarreta uma melhora da evolução no tempo de suas propriedades mecânicas e de sua resistência ao ataque sulfático, por causa da variação na cinética da hidratação provocada pela reação entre o calcáreo e o cimento aluminoso.

Esta variação de cinética inclui a conversão dos hidratos hexagonais em $C_4A\bar{C}H_{11}$ e impede, durante anos, a formação do C_3AH_6.

Devido ao maior volume molar do $C_4A\bar{C}H_{11}$ observa-se uma progressiva diminuição da porosidade, sobretudo na zona de contato cimento-agregado. Os ensaios em pastas demonstraram, ou que a evolução da macroporosidade (poros com raio superior a 10.000 Å) exerceu um papel primordial sobre a evolução das propriedades mecânicas, ou que um fator água/cimento muito baixo pode ser igualmente favorável.

Introduction

Il est notoire que le béton préparé avec du ciment alumineux présente une résistance mécanique notable à court terme, mais aussi une bonne résistance à l'attaque sulfatique, au gel et au dégel.

Mais en concomitance avec la conversion des hydrates hexagonaux en hydrate cubique, on observe généralement une diminution de résistance mécanique et une augmentation de porosité telles qu'elles rendent le béton sensible à l'agression chimique.

En 1967 déjà, Midgley (1) et plus tard Cottin et Reif (2) avaient conclu que la chute de résistance n'était due qu'à l'augmentation de porosité et à la libération d'eau associées à la réaction de conversion des hydrates hexagonaux. Récemment, Rettel et coll. (3) ont démontré que l'hydratation du CA se fait de façon pulsante, c'est-à-dire que seule l'eau libérée par la conversion des hexagonaux et par la cristallisation du gel d'alumine permet un avancement de l'hydratation du CA. De plus, ces auteurs soutiennent que l'augmentation de porosité du béton est due à la cristallisation du gel bien plus encore qu'à la conversion hexagonaux-cubique.

Mehta et Lesnikoff (4) sont persuadés que la perte de résistances mécaniques est due aussi à la variation, à la suite de la conversion, de la surface spécifique des hydrates. Mais tous ces auteurs s'accordent pour dire qu'un rapport initial eau/ciment très bas (inférieur à 0,3) devrait garantir l'absence d'importantes diminutions des résistances mécaniques sans par ailleurs empêcher la conversion.

Toutefois, étant donné que réduire sous 0,3 le rapport eau/ciment dans un béton à base de ciment alumineux est très difficile, voire impossible, les différents chercheurs ont préféré essayer de provoquer une réduction et même l'annulation du phénomène de conversion. C'est ainsi qu'il a été proposé d'ajouter au béton frais divers additifs tels que sels inorganiques, tensioactifs, polysaccharides ou encore alcools polyoxhydryliques (5), ou bien la "fillérisation" du ciment avec $C_4A_3SO_3$ (6-7) ou encore le traitement de maturité du béton à 80°C (8).

En 1978, Negro et coll. signalaient que le $CaCO_3$ empêchait, à moyen terme du moins, la conversion des hydrates hexagonaux en hydrate cubique avec formation de $C_4A\bar{C}H_{11}$ (9).

De plus on a pu vérifier que l'influence du carbonate de calcium se prolonge dans le temps en exerçant un effet bénéfique sur les propriétés mécaniques des bétons et des mortiers (10).

Ces observations on été récemment confirmées par les travaux de Pérez Méndez et coll. (11) et de Hakim (12), mais mises en question par Midgley (13) et, partiellement, par Fentiman (14).

C'est pourquoi il ne semble pas superflu de présenter les résultats les plus significatifs obtenus en poursuivant l'étude de l'influence du carbonate du calcium sur l'hydratation du CA et sur les conséquences qu'elle exerce aussi bien sur l'évolution des propriétés mécaniques que sur la résistance à l'attaque sulfatique des bétons à base de ciment alumineux.

Partie expérimentale

Pour nos expérimentations nous avons utilisé deux ciments alumineux en vrac de même provenance. L'analyse chimique des deux ciments et celle des agrégats utilisés sont indiquées dans le Tableau 1.

Tableau 1 - Analyse chimique des matériaux utilisés

Oxydes	Ciment		Agrégat		
			Siliceux		Calcaire
	N. 1	N. 2	Mortier	Béton	
SiO_2	2,65	3,29	86,60	73,60	0,70
Al_2O_3	40,50	40,63	5,08	6,94	0,18
Fe_2O_3	12,77	11,40	2,13	1,78	0,14
FeO	3,88	3,63	-	-	-
TiO_2	1,95	1,85	-	-	-
CaO	36,60	37,21	1,64	5,23	54,80
MgO	0,54	0,18	0,29	5,27	0,43
K_2O	0,05	0,04	1,27	1,19	0,02
Na_2O	0,05	0,06	1,26	1,55	0,05
SO_3	0,05	0,25	0,00	0,00	0,00
p.a.f.	0,60	1,01	0,85	3,59	42,85

Les alcalins contenus dans les agrégats ne présentent aucune caractéristique de solubilité ni dans l'eau ni dans une solution aqueuse de chaux. Avec le ciment n° 1 nous avons réalisé les éprouvettes suivantes:
A - Eprouvettes cubiques de 15 cm de large, de béton avec granulat siliceux roulé: Ø max 20 mm; courbe granulométrique continue; ciment; 350 kg/m^3; E/C = 0.54; Slump 10 cm;

tassement par table vibrante; masse volumique = 2,43.

B - Eprouvettes de béton avec granulat calcaire concassé de mêmes caractéristiques que les éprouvettes A, exepté: E/C = 0,60 et masse volumique = 2,41.

A' - Eprouvettes de béton avec granulat siliceux comme pour A. Le liant, au lieu d'être seulement du ciment alumineux, se compose d'un mélange à 75/25 respectivement de ciment alumineux et poudre de calcaire à surface Blaine de 5000 cm^2/g; liant 350 kg/m^3; E/C = 0,51 (*), Slump 12 cm; masse volumique = 2,40.

C - Eprouvettes de 4 x 4 x 16 cm en mortier plastique type ISO, fabriqué avec du sable siliceux conformément aux Normes italiennes.

D - Eprouvettes en mortier plastique comme en C, en utilisant du sable calcaire de granulometrie identique à celle du sable normale.

C' - Eprouvettes en mortier plastique comme en C et donc avec du sable siliceux, mais en utilisant comme liant un mélange à 75/25 respectivement de ciment alumineux et poudre de calcaire broyé à environ 5000 cm^2/g de surface Blaine.

C" - Eprouvettes en mortier plastique comme en C' en substituant dans le mélange du liant le sable siliceux broyé à environ 4000 cm^2/g de surface Blaine.

E - Eprouvettes 4 x 4 x 16 cm de pâte normale, conformément aux normes italiennes, dans lesquelles le ciment pur a été substitué par un mélange 50:50 de ciment et sable siliceux broyé jusqu'à 4000 cm^2/g de surface Blaine; rapporto E/C = 0,26 (*).

F - Eprouvettes de pâte normale comme pour E, mais en utilisant comme "filler" l'agrégat calcaire broyé jusqu'à 5000 cm^2/g de surface Blaine. Rapport E/C = 0,22 (*).

G - Eprouvettes de pâte normale comme pour E, mais en utilisant du ciment pur; rapport E/C = 0,24.

Avec le ciment n° 2 nous avons réalisé les éprouvettes suivantes.

H et H' - Eprouvettes en mortier plastique come en C.

I et I' - Eprouvettes en mortier plastique comme en D.

(*) A noter que pour les éprouvettes A', E et F où le ciment est "fillérisé", le rapport indiqué E/C doit s'entendre comme: Eau/(Ciment+Filler).

Pour les échantillons A, B et A' nous avons travaillé sur une periode de 7 ans, pour les autres de 5 ans.

Conformément aux Normes italiennes, les éprouvettes de béton après démoulage, ont été conservées dans une chambre conditionnée à 20°±1°C et une humidité relative superieur ou égale à 90%; les éprouvettes de mortier (excepté les H' et I') et les éprouvettes de pâte ont été conservées dans l'eau. Les éprouvettes de mortier H' et I' ont été conservées dans l'eau pendant les premiers 28 jours seulement; par la suite le traitement s'est poursuivi dans une solution à 3% en poids de Na_2SO_4; cette solution était renouvelée chaque mois.

Les pâtes ont été étudiées pour contrôler l'effet du bas rapport E/C (eau/ciment) sur les propriétés mécaniques.

Avec les éprouvettes A' et C' nous avons voulu vérifier si une addition au ciment de 25% de calcaire finement broyé provoquait, avec les années, un effet positif sur les résistances mécaniques tant des bétons que des mortiers.

A chaque échéanche parallèlement aux essais mécaniques, nous avons effectué l'analyse par diffractométrie des rayons X et l'A.T.D. pour déterminer les phases qui se formaient au cours de l'hydratation.

De plus, pour les échantillons C,D,E,F et G nous avons procédé aux analyses prosimétriques, alors que pour les échantillons H, H', I et I' nous avons contrôlé les valeurs d'expansion en fonction du temps de conservation.

Résultats et discussion

Les résultats des essais mécaniques à la compression sont indiqués dans le Tableau n. 2.

Il en ressort que l'utilisation de l'agrégat calcaire en substitution de la silice, ou bien la "fillérisation" du ciment alumineux avec du calcaire exerce un effet positif sur les caractéristiques mécaniques des échantillons conservés pendant de longues périodes car, si nous n'obtenons pas toujours l'annulation du phénomène de rétrogradation des résistances mécaniques (comme c'est le cas pour le mélange F), nous obtenons toutefois un décalage sensible dans le temps et, ce qui est bien plus important, une réduction considerable de son intensité. En effet, alors qu'en présence d'un agrégat siliceux, la résistance mécanique commence à diminuer après 28-90 jours de traitement et comporte, à 7 ou 5 ans, une perte de 50-70%

par rapport à la valeur maximale, en présence d'agrégat (ou de "filler") calcaire, la rétrogradation ne s'observe qu'après 1 ou 2 ans, et ne dépasse pas un général des pointes de 20% de la valeur maximale (échantillon D), se situant en moyenne sur des valeurs de 5 a 10%. La comparaison entre les valeurs indiquées au Tableau 2 dans les colonnes C' et C" de même que E et F montre combien l'effet du calcaire diffère par rapport au matériau siliceux, s'il est utilisé comme "filler" du ciment alumineux. Les valeurs concernant l'échantillon G confirment qu'un rapport eau/ciment très bas minimise avec les années les pertes de résistance mécanique.

Tableau 2 - Evolution des résistances mécaniques à la compression des éprouvettes examinées

Age	Eprouvettes														
	A	B	A	C	D	C	C	E	F	G	H	H'	I	I'	
1j	53	54	45	67	49	58	57	49	76	64	60	60	47	47	MPa
28j	73	72	56	89	73	74	67	85	112	85	85	85	73	73	"
90j	68	80	58	90	75	85	70	62	110	75	-	-	-	-	"
180j	63	80	71	89	81	89	69	59	108	94	90	66	82	70	"
1 a	55	85	70	84	82	88	59	48	108	105	85	67	84	71	"
2 a	53	87	72	73	80	85	53	38	111	105	75	59	80	65	"
5 a	39	76	62	37	66	84	34	26	110	102	42	34	76	61	"
7 a	29	71	64												

L'ensemble de ces résultats confirme ceux qui ont déjà été présentés précédemment (10) mais incite en même temps à une plus grande prudence en ce qui concerne l'extrapolation à des échéances de l'ordre de dizaines d'années sur l'effet nettement positif exercé par le calcaire.

L'examen aux rayons X a mis en évidence pour tous les mortiers et les bétons contenant de l'agrégat siliceux, la formation initiale de CAH_{10}, C_2AH_8 et AH_3 et la transformation ensuite des deux premiers en C_3AH_6 et gibbsite. Pour la pâte E, la vitesse de conversion en hydrate cubique du C_2AH_8 s'est révélée si élevée que seule l'A.T.D. a permis de relever la formation en traces au cours des premiers mois d'hydratation (15).

Pour tous les échantillons contenant du calcaire, nous observons, par contre la formation de CAH_{10} et de $C_4A\bar{C}H_{11}$ et AH_3 déjà aux premières échéances, alors que C_3AH_6 n'apparaît que après 2 années de conservation (Figure 1) et en petites quantités seulement. La présence da C_2AH_8 n'a pas été relevée, étant donné sa vitesse de conversion élevées en carboaluminate hydraté (15).

L'analyse par A.T.D. corrobore les données apportées en diffractométrie des rayons X en permettant d'observer la présence de gel d'alumine et confirme la marche pulsante de l'hydratation du CA (3). Le phénomène de la disparition et réapparition du gel en des temps successifs a été particulierement marqué pour la pâte de ciment alumineux pur (Figure 2); cela en corrélation évidente avec le bas rapport E/C.

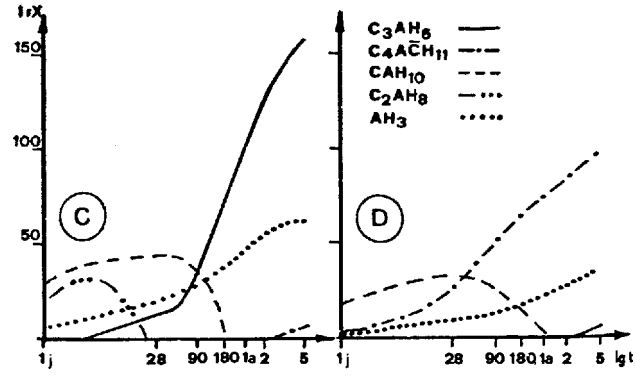

Figure 1 - Variation de l'intensité des pics de diffraction des rayons X en fonction du temps de traitement des mortiers C et D.

L'étude de la porosité ouverte des mortiers et des pâtes a permis de mettre en évidence qu'en substituant l'inerte siliceux avec du calcaire, on obtenait, en fonction du temps de traitement, une évolution différente du volume total des pores (qui diminuait en présence de calcaire et augmentait en présence de silice), mais aussi de la répartition même des pores. En effet dans les échantillons contenant du calcaire, c'est

surtout le volume des pores de grand rayon qui diminue, alors que le contraire se produit en présence d'inerte siliceux. Ayant choisi arbitrairement comme limite inférieure des macropores la valeur de 10000 Å de rayon, nous avons traité les données porosimétriques comme le présente le Tableau n. 3. La comparaison entre les Tableaux 2 et 3 fait ressortir de façon évidente que la résistance mécanique à la compression dépend de la porosité totale, mais cette relation de dépendance est bien plus étroite, si l'on se refère à la macroporosité seulement (les échantillons D et F sont symboliques).

Smolczyk et coll. (16) étaient arrivés à des conclusions analogues, c'est-à-dire à une dépendance étroite entre macroporosité et propriétés mécaniques des bétons ordinaires.

En examinant les résultats du Tableau 2 relatifs aux échantillons H, H', I et I'; nous pourrions croire que l'agrégat calcaire n'exerce qu'un effet bénéfique indirect pur la résistance à l'attaque sulfatique, car dans les deux cas, nous observons une perte de résistance mécanique variant entre 27 et 20% de la valeur correspondance de l'échantillon conservé dans l'eau. Les diagrammes des valeurs moyennes d'expansion des échantillons que présent la Figure 3, indique toutefois que l'agrégat calcaire augmente non seulement la stabilité dimensionnelle des échantillons hydratés normalement, mais qu'il favorise une limitation de l'expansion ultérieure provoquée par l'attaque sulfatique.

Nous avons donc pu confirmer que la présence d'un granulat calcaire limite fortement, si elle n'empêche pas, la conversion des hydrates hexagonaux en aluminate cubique en faveur de leur conversion en carboaluminate. Cela implique de plus une évolution différente de la porosité totale des échantillons et, surtout, de leur macroporosité (qui tend à diminuer au lieu d'augmenter avec les années) à laquelle s'associe une évolution différente de la résistance à la compression (qui continue à croître même au-delà des

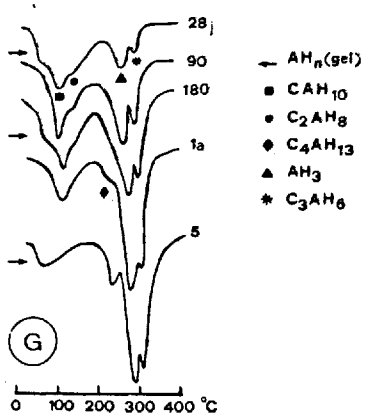

Figure 2 - Courbe ATD de l'échantillon G.

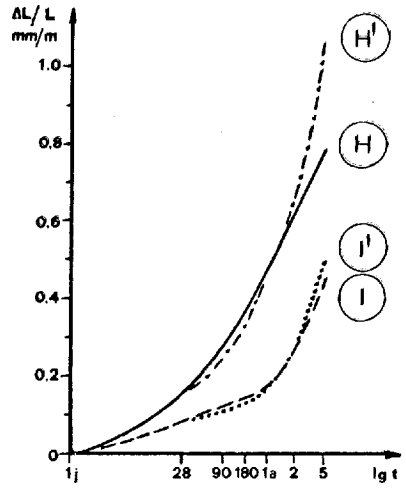

Figure 3 - Evolution de l'expansion en fonction du temps de conservation dans l'eau (H et I) ou en solution sulfatique (H' et I').

Tableau 3 - Evolution de la porosité totale (PT) et de la macroporosité (MP) en fonction du temps de cure

Age	Echantillons										
	C		D		E		F		G		
	PT	MP	PT	MP	PT	MP	PT	MP	PT	MP	
1 j	135,9	45,2	140,7	50,3	138,5	43,1	120,8	25,0	132,0	33,4	mm^3/g
28 j	52,7	15,9	65,9	22,4	83,5	13,0	91,7	4,4	31,4	10,2	"
90 j	-	-	-	-	124,8	20,0	79,3	5,0	36,1	21,3	"
1 a	66,6	17,8	38,3	18,0	148,3	25,0	60,4	5,0	35,2	2,0	"
5 a	68,8	53,4	36,9	24,9	166,6	32,2	54,0	5,1	38,3	2,2	"

premiers mois de traitement) et une augmentation de la stabilité dimensionnelle et de la résistance à l'attaque sulfatique.

Etant donné que la transformation des hydrates hexagonaux en carboaluminate est fortement conditionnée par la surface spécifique du carbonate qui doit réagir (15) pour augmenter les propriétés mécaniques à long terme d'un mortier ou d'un béton alumineux, il peut même se révéler plus avantageux de "filléríser" le ciment avec du calcaire très finement broyé, plutôt que de substituer l'agrégat siliceux avec de l'agrégat calcaire. Ce résultat est nettement confirmé par les données des colonnes C et C' du Tableau n. 2. Du reste, en examinant les bétons B et A', on note que, bien que la résistance du béton A' soit plus basse en valeur absolue (moindre teneur en ciment) la perte de résistance à 7 ans est de 11%, alors que dans le béton B elle atteint 18%.

De plus, contrairement à ce qu'affirme Midgley (13) les effets positifs de l'agrégat calcaire à température ambiante et pour n'importe quelle granulométrie, ne sont pas d'une brève durée mais persistent pendant des années.

Conclusions

Le recours au calcaire comme agrégat ou bien comme "filler" du ciment permet la préparation de bétons et de mortiers alumineux, dans lesquels la résistance à la compression et à l'attaque sulfatique reste élevée même aux longues échéances. En effet, le calcaire en réagissant avec le ciment donne lieu à la formation de carboaluminate, ce qui empêche ou limite fortement la formation de C_3AH_6 et diminue la porosité du béton.

Bibliographie

1) H.G. Midgley (1967) "The mineralogy of set high alumina cement" Trans. Brit. Ceram. Soc. 66, 161-187.
2) B. Cottin, P. Reif (1971) "Paramètres physiques régissant les propriétés mécaniques des pâtes pures de liants alumineux" Rev. Matér. Constr. n° 661, 293-305.
3) A. Rettel, W. Gessner, D. Müller (1985) "On the hydration of $CaAl_2O_4$ at various temperatures" Brit. Ceram. Trans. J. 84, 25-28.
4) P.K. Mehta, G. Lesnikoff (1971) "Conversion of $CaO.Al_2O_3$ to $3CaO.Al_2O_3.6H_2O$" J. Amer. Cer. Soc. 54, 210-212.
5) T.D. Robson (1962) "High alumina cement and concretes" J. Wiley and Sons N.Y..
6) P.K. Mehta (1969) "Successful prevention of loss of strength in concrete made with high alumina cement" Proc.V I.S.C.C. Vol. II, 148-151 (Tokyo).
7) M. Collepardi, A. Marcialis, R. Turriziani (1972) "The influence of $4CaO.3Al_2O_3.SO_3$ on the hydration of monocalcium aluminate" Il Cemento 69, 179-188.
8) V.S. Ramachandran, R.F. Feldman (1973) "Hydration characteristics of monocalcium aluminate at low water/solid ratio" Cem. Concr. Res. 3, 729-750.
9) A. Negro, L. Cussino, A. Bachiorrini (1978) "The hydration of monocalcium aluminate in presence of quartz and calcium carbonate" Il Cemento 75, 285-290.
10) L. Cussino, A. Negro (1980) "Hydratation du ciment alumineux en présence d'agrégat siliceux et calcaire" Proc. VII I.S.C.C. Vol. III, V-62-67 (Paris).
11) M. Pérez Méndez, F. Trivino Vàsquez (1984) "Study of the strenght developed by stable carbonate phases in high alumina cement" Cem. Concr. Res. 14, 161-169.
12) M.F. Hakim (1984) "Etude de l'hydratation du ciment alumineux associé à des granulats calcaires, consequences sur les propriétés mécaniques" Thèse INSA de Toulose.
13) H.G. Midgley (1984) "Measurement of high alumina cement-calcium carbonate reactions using DTA" Clay Minerals 19, 857-864.
14) C.H. Fentiman (1985) "Hydration of carbo-aluminous cement at different temperatures" Cem. Concr. Res. 15, 622-630.
15) A. Bachiorrini (1985) "Interactions physico-chimiques entre l'aluminate monocalcique et différents carbonates au cours de la réaction d'hydratation" Thèse, Université de Lyon.
16) H.G. Smolczyk, H. Romberg (1976) "The influence of the curing time and storing condition on the hardening and the pore size distribution of concrete" Tonind. Ztg. 100, 349-357 et 381-390.

Nous remercions Md.me A.A. Fournier de l'E.N.S.M. de St. Etienne pour la revision du texte.

Ce travail a été accompli avec la contribution du C.N.R. Cont. n. 84.02663.59.

L. Santoro, Dipartimento di Chimica, Università di Napoli, Italy; R. Garofano, Dipartimento di Chimica, Università di Napoli, Italy; G.L. Valenti, Dipartimento di Ingegneria dei Materiali e della Produzione, Università di Napoli, Italy.

Calcium Sulphoaluminate Made from Phosphogypsum and its Hydration Properties.

Sulphoaluminate de Calcium obtenu de Phosphogypse et ses Proprietes d'Hydratation.

SUMMARY: The synthesis of calcium sulphoaluminate from stoichiometric mixtures of phospho- or pure gypsum, calcium carbonate and aluminium oxide has been investigated.

The use of phosphogypsum in the raw mix allows the synthesis to be performed at temperatures and times considerably lower than those required when pure gypsum is employed. In fact in the case of phosphogypsum the synthesis goes to completeness within times ranging from 30 to 90 minutes at temperatures from 1000 to 1100°C. On the other hand, the use of pure gypsum requires times ranging from 3 to 10 hours and temperatures from 1200 to 1350°C.

Mixtures of calcium sulphoaluminate, phospho- or pure gypsum and calcium hydroxide in stoichiometric ratio to form ettringite only, have been paste hydrated at 25°C and up to 7 days. The influence of the nature of gypsum employed and the synthesis temperature on the hydration properties of calcium sulphoaluminate is examined and discussed.

The main experimental techniques used to follow the processes of synthesis and hydration are X-ray diffraction and thermal analyses, as well as solvent extraction followed by chemical titration.

Investigou-se a síntese de sulfoaluminato de cálcio a partir de misturas estequiométricas de fosfogesso ou de gesso puro, carbonato de cálcio e óxido de alumínio.

O uso de fosfogesso na mistura crua permite que a síntese seja feita a temperaturas e tempos consideravelmente mais baixos do que os requeridos quando se uso gesso puro. De fato, no caso de fosfogesso a síntese se completa em períodos de tempo que vão de 30 a 90 minutos, a temperaturas de 1.000 a 1.100°C. Por outro lado, o uso de gesso puro exige períodos de 3 a 10 horas e temperaturas de 1.200 a 1.350°C.

Misturas de sulfoaluminato de cálcio, fosfogesso ou gesso puro e hidróxido de cálcio, em relação estequiométrica para formar apenas etringita, foram hidratadas em pasta a 25°C e até 7 dias. Examina-se e discute-se a influência da natureza do gesso empregado e da temperatura de síntese sobre as propriedades de hidratação do sulfoaluminato de cálcio.

As principais técnicas experimentais usadas para acompanhar os processos de síntese e hidratação são difração de raio X e análises térmicas, bem como extração de solvente seguida de titulação química.

L. Santoro, Dipartimento di Chimica, Università di Napoli, Italy; R. Garofano, Dipartimento di Chimica, Università di Napoli, Italy; G.L. Valenti, Dipartimento di Ingegneria dei Materiali e della Produzione, Università di Napoli, Italy.

INTRODUCTION

It is well known that cements containing calcium sulphoaluminate $C_4A_3\bar{S}$(°) may have various applications(1-3). Depending mainly on the rate of formation of ettringite and other hydrated phases, as well as their relative amounts, a series of cements with different performances, that is rapid hardening (4), expansive and self-stressing (5-7) cements, can be obtained.

Furthermore, $C_4A_3\bar{S}$ bearing clinkers allow a substantial energy saving to be achieved in their manufacture inasmuch as they are obtained at burning temperatures considerably lower than those required by ordinary Portland clinkers.

Another important aspect to be taken into account is the possibility of utilizing many industrial by-products as raw materials. One of them is phosphogypsum(FG).

Wide applications of this by-product have been proposed and practised in the field of binding materials(8-13). Moreover its use has also been suggested for the manufacture of cements containing $C_4A_3\bar{S}$(14-15).

The aim of this work is to study the synthesis of $C_4A_3\bar{S}$ from stoichiometric mixtures of FG, $CaCO_3$ and Al_2O_3 at different temperatures. Furthermore the hydration properties of this $C_4A_3\bar{S}$ when paste hydrated together with phospho- or pure gypsum in stoichiometric ratio to form ettringite only have been investigated. For the sake of comparison, the behaviour of a $C_4A_3\bar{S}$ made from pure gypsum has also been investigated.

(°)Common cement chemistry nomenclature is used herein: C=CaO; A=Al_2O ; $\bar{S}$=SO_3; H=H_2O.

EXPERIMENTAL

The FG employed in the experimental work has been supplied by Montedison S.p.A.(Italy). Its chemical composition is shown in Table I. Other reagents were analitical grade $CaCO_3$, Al_2O_3, $Ca(OH)_2$ and $CaSO_4.2H_2O$.

Table I

Phosphogypsum composition, wt%	
Loss on ignition	22.9
CaO	34.3
SO_3	40.0
P_2O_5	1.8
SiO_2	1.4
F	1.2
Na	0.8

The synthesis of $C_4A_3\bar{S}$ has been carried out by firing in a muffle furnace mixtures(100g in weight) of phospho- or pure gypsum, Al_2O_3 and $CaCO_3$ in the stoichiometric ratio for the reaction:

$$3CaCO_3 + 3Al_2O_3 + CaSO_4.2H_2O \longrightarrow 3CaO.3Al_2O_3.CaSO_4 + 3CO_2 + 2H_2O \quad (1)$$

The fractional conversion has been found by determining the unconverted lime concentration following the Franke method(16). The nature of the reaction products has been ascertained by means of X-ray diffraction analysis.

The hydraulic properties of the various samples of $C_4A_3\bar{S}$ prepared from phospho- or pure gypsum at different temperatures have then been tested by adding CO_2-free water to stoichiometric mixtures of the sulphoaluminate, phospho- or pure gypsum and hydrated lime according to the reaction:

$$3CaO.3Al_2O_3.CaSO_4 + 8(CaSO_4.2H_2O) + 6Ca(OH)_2 \longrightarrow 3(3CaO.Al_2O_3.3CaSO_4.32H_2O) \quad (2)$$

The water/solid ratio was 1.0 and the ageing times were 1, 3, 6, 24, 72 and 168 hours. The curing temperature was 25°C. At the end of each pre-fixed ageing time the reaction

was stopped by grinding under acetone followed by washing with ether. The samples were then stored in a desiccator in the presence of P_2O_5.

Hydration products were qualitatively characterized by means of both thermal and X-ray diffraction analyses, and quantitative data were obtained by determining the amount of unreacted lime by the Franke method(16). Non-evaporable water was determined by ignition at 1000°C.

RESULTS AND DISCUSSION

Synthesis of $C_4A_3\bar{S}$

Figs 1 and 2 show the amount of unconverted lime, in terms of percentage of the initial quantity in the raw mix, as a function of time for the systems containing FG and pure gypsum, respectively. It is clearly evident the enormous difference between the two systems inasmuch as the use of FG in the raw mix allows the synthesis to be performed at temperatures and times considerably lower than those required when pure gypsum is employed. As seen in Fig. 1, in the case of FG, the synthesis goes to completeness within times ranging from 30 to 90 minutes when the temperature decreases from 1100 to 1000°C.

On the other hand, Fig. 2 shows that the use of pure gypsum requires 10 hours at 1200°C for the conversion to be more than 99.5%. At higher temperatures, namely 1250, 1300 and 1350°C, total conversion is reached after 9, 5 and 3 hours, respectively.

X-ray diffraction analysis has shown that, besides $C_4A_3\bar{S}$, only $C_{12}A_7$ is formed in traces, which are slightly more evident in the case of FG(17).

The acceleration of the synthesis due to the presence of FG is more marked than that which can be deduced comparing the results of Figs 1 and 2 inasmuch as the following considerations must be taken into account:

a) pure gypsum is finer than FG, as the residues on the 325 mesh sieve were 0 and 32%, respectively;

b) in the case of pure gypsum the samples were ground to pass the 325 mesh sieve between two consecutive firings.

The mechanism by which FG impurities are able to speed considerably up the synthesis is considered to be related to their fluxing and/or mineralizing properties. The specific role of the impurities is still under investigation, with the purpose of ascertaining

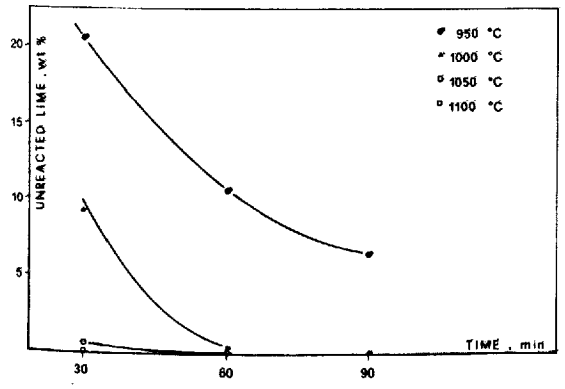

Fig. 1 - $C_4A_3\bar{S}$ synthesis data for systems containing FG.

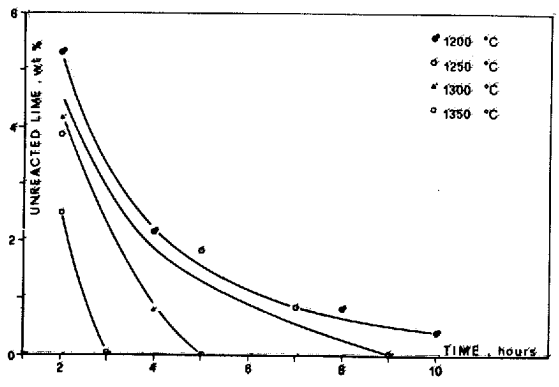

Fig. 2 - $C_4A_3\bar{S}$ synthesis data for systems containing pure gypsum.

L. Santoro, Dipartimento di Chimica, Università di Napoli, Italy; R. Garofano, Dipartimento di Chimica, Università di Napoli, Italy; C.L. Valenti, Dipartimento di Ingegneria dei Materiali e della Produzione, Università di Napoli, Italy.

whether they simply decrease the melting point or accelerate the process by catalyzing a solid state reaction within the liquid phase.

Hydration of $C_4A_3\bar{S}$

Some of the samples of $C_4A_3\bar{S}$ have been mixed with phospho- or pure gypsum and hydrated lime in stoichiometric ratio to form ettringite only. The mixtures have been paste hydrated in order to investigate the influence of the nature of the gypsum employed and the synthesis temperature on the hydration properties.

The mixtures to be hydrated are identified by a code of the type X_YZ where:
X can be F or G depending on whether phospho- or pure gypsum is used for the synthesis of $C_4A_3\bar{S}$, respectively;
Y refers to the synthesis temperature and in case of FG is equal to 1, 2, 3 for 1000, 1050, 1100°C, respectively, while in the case of pure gypsum is equal to 1, 2, 3, 4 for 1200, 1250, 1300, 1350°C, respectively;
Z can be F or G depending on whether phospho- or pure gypsum is added to $C_4A_3\bar{S}$ in the mixture to be hydrated.

X-ray diffraction and differential thermal analyses have shown that, for the compositions tested and up to 168 hours of hydration at 25°C, ettringite only forms(17). The fractional conversion of the reagents into ettringite is determined by analysing the cured samples for unreacted lime content.

Fig. 3 shows the amount of unconverted lime, in terms of percentage of the initial quantity in the mixture to be hydrated, as a function of time for the systems F_1F and F_3F. It is seen that $C_4A_3\bar{S}$ reactivity does not depend on the synthesis temperature, at least in the range 1000-1100°C. At the longest curing time examined the residual lime content is about 50%.

Fig. 4 shows the same results for the systems G_1G and G_4G. Early ages data indicate that, in this case, the sulphoaluminate reactivity decreases as the synthesis temperature increases from 1200 to 1350°C. This may be due to the favourable effect of temperature on the cristallites growth process. Later ages data are not significantly different for the two systems; furthermore, the fractional conversion is slightly higher than that of Fig. 3.

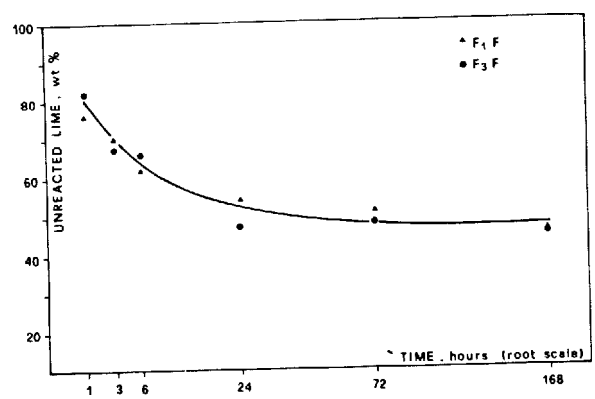

Fig. 3 - Hydration data for systems of composition F_1F and F_3F.

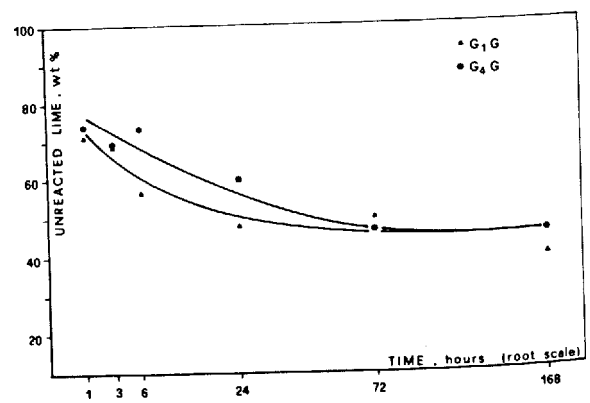

Fig. 4 - Hydration data for systems of composition G_1G and G_4G.

In order to examine how hydration is influenced by the type of gypsum added to a sulphoaluminate of given origin and synthesis temperature, the behaviour of the systems G_4F and F_3G has been studied and compared to that of the systems G_4G and F_3F, as shown in Fig. 5.

The system G_4F hydrates more rapidly than G_4G, due to a catalytic activity of FG impurities. The observed enhancement of ettringite formation agrees with previous findings on different systems. In fact it has been reported(18) that the impurities present in FG accelerate the ettringite formation in the early stages of Portland cement hydration. Similarly, when compared to pure gypsum, FG appears to be a more efficacious activating agent of granulated blast-furnace slag with regard to the ettringite formation (13). The fact that the enhancing effect has been observed in systems very different from each other, means that the catalytic activity is an intrinsic property of FG impurities.

The comparison between the systems F_3F and F_3G does not show significant differences. Evidently, within the concentration limits relative to these two systems, the impurities play a constant role.

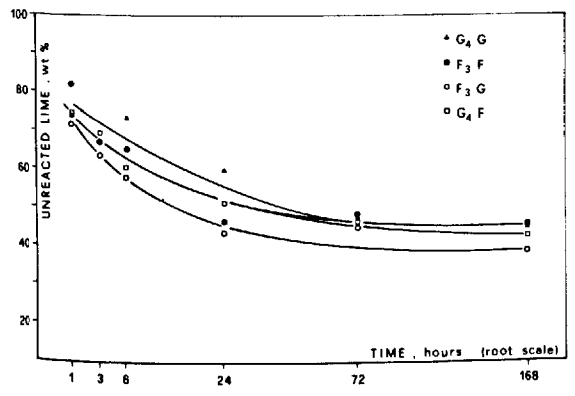

Fig. 5 - Hydration data for systems of composition G_4F, F_3G, G_4G and F_3F.

CONCLUSIONS

The use of phosphogypsum instead of pure gypsum in the formation of calcium sulphoaluminate $C_4A_3\bar{S}$ allows considerable reductions of the temperature and time required for the synthesis.

As far as the formation of ettringite is concerned, the behaviour of mixtures of $C_4A_3\bar{S}$, phospho- or pure gypsum and calcium hydroxide does not reveal major difference.

Finally, the following considerations can be made:

a) the reactivity of $C_4A_3\bar{S}$ made from phosphogypsum does not depend on the synthesis temperature in the range 1000-1100°C;

b) the reactivity of $C_4A_3\bar{S}$ made from pure gypsum decreases, at early ages, as the synthesis temperature increases from 1200 to 1350°C;

c) phosphogypsum impurities exhibit an intrinsic catalytic activity.

REFERENCES

1-P.K. Mehta and M. Polivka(1974), "Expansive Cements", Proc. of the Sixth Int. Congress on the Chemistry of Cement, Moscow, 1974, Principal Paper, 3-45.

2-W. Kurdowski(1980), "Ciments Expansifs", 7e Congrés Int. de la Chimie des Ciments, Editions Septima, Paris, 1980, Vol. I, Rapports Principaux, V-2/1—V-2/10.

3-T.V. Kouznetsova and I.V. Kravtchenko (1980), "Le Róle des Aluminates et des Sulfoaluminates de Calcium dans l'Elaboration de Propriètès de la Pierre de Ciment", ibidem, Vol. II, II-198—II-202.

4-G. Sudoh, T. Ohta and H. Harada(1980), "High Strength Cement in the $CaO-Al_2O_3-SiO_2-SO_3$ System and its Application",

ibidem, Vol. III, V-152—V-157.

5-A. Klein and G.E. Troxell(1958), "Studies of Calcium Sulfoaluminate Admixtures for Expansive Cements", Proc. ASTM, Vol. 58, 986-1008.

6-M. Kokubu(1973), "Use of Expansive Components for Concrete in Japan", ACI Publ. N° SP-38, 353-378.

7-T.V. Kouznetsova(1979), "Chimie et Technologie des Ciments Expansifs et Contraints", Tsement N° 2, 10-11(en russe).

8-W. Gutt and M.A. Smith(1971), "The use of Phosphogypsum as a Raw Material in the Manufacture of Portland Cement", Cem. Technol., March-April 1971, 41-50.

9-A.A. Tabikh and F.M. Miller(1971), "The Nature of Phosphogypsum Impurities and their Influence on Cement Hydration", Cem. Concr. Res., Vol. 1, 663-678.

10-P.K. Mehta and J.R. Brady(1977), "Utilization of Phosphogypsum in Portland Cement Industry", Cem. Concr. Res., Vol. 7, 537-544.

11-J. Berekta, D.N. Crook and G.A. King(1981), "Physico-chemical Properties of By-product Gypsum", J. Chem. Tech. Biotechnol., Vol. 31, 151-162.

12-L. Santoro, G.L. Valenti and G. Volpicelli(1984), "Application of Differential Scanning Calorimetry to the Study of the System Phosphogypsum-Lime-Aluminium Hydroxide-Water", Thermochim. Acta, Vol. 74, 35-44.

13-G.L. Valenti, L. Santoro and G. Volpicelli(1984), "Hydration of Granulated Blast-furnace Slag in the Presence of Phosphogypsum", Thermochim. Acta, Vol. 78, 101-112.

14-I. Teoreanu and M. Muntean(1983), "Expansive Sulphate Aluminate Cements", Cem. Concr. Res., Vol. 13, 711-720.

15-P.K. Mehta(1980), "Investigation on Energy-saving Cements", World Cem. Technol., May 1980, 166-177.

16-F.A. Shelb and U. Ludwig(1978), "Investigations Relating to the Determination of Calcium Hydroxide by the Franke Method", Zement-Kalk-Gips, Vol. 10, 510-515(in german).

17-R. Garofano(1985), "Synthesis and Hydration Properties of Calcium Sulphoaluminate Made from Phosphogypsum", Graduation Thesis in Chemistry, University of Naples, Italy(in italian).

18-J. Bensted(1979), "Early Hydration Behaviour of Portland Cement Containing Chemical By-product Gypsum", World Cem. Technol., December 1979, 404-410.

Y.Yamazaki, Nihon Cement Co.Ltd.,Japan and Y.Sakakibara,Nihon Cement Co.Ltd., Japan.

The Mechanism of Expansive Pressure Development with The Hydration of CaO

SUMMARY: Cao has been used for expansive cements and demolition agents. For the purpose of making more clear of the mechanism of expansive pressure developed by the hydration of CaO, expansive pressure development and pore volume changes with the hydration of CaO were meseared at the high external restraint. These hydrated specimens of CaO were examined with Photomicroscope, SEM,XRD and DTA.

Micro-crystallite of Ca(OH)2 generated and aggrgated on the surface of CaO grains and crystals. The expansive pressure was developed by tne enlargement of aggregated massive Ca(OH)2 on the CaO particle. The maximum expansive pressure value reached to 9000 N. The inner vacant volume in the hydrated sample of CaO continuously increased from the time molding to the time in which the expansive pressure developed up to 9000 N. It is important for the develment of expansive pressure to increase the porosity in the hydration of CaO.

Usou-se CaO como componente de expansão em cimentos expansivos e agentes de demolição. Com a finalidade de esclarecer melhor o mecanismo de pressão expansiva desenvolvido pela hidratação de CaO, mediu-se o desenvolvimento da pressão expansiva e as mudanças de volume de poro com hidratação de CaO sob alta limitação externa. Estes espécimes hidratados de CaO foram examinados com fotomicroscopia, SEM, XRD, TG-DRA e EPMA.

Gerou-se micro-cristal de $Ca(OH)_2$ e se agregou à superfície dos grãos de CaO e cristais. A pressão expansiva se desenvolveu por crescimento do $Ca(OH)_2$ maciço agregado sobre partícula de CaO. O tamanho do cristal de $Ca(OH)_2$ foi de algumas centenas de Å mesmo a 7 dias a 25°C. O valor máximo de pressão expansiva atingido foi de 90 MPa. O volume de vazio interno na amostra hidratada cresceu continuamente desde a ocasião da moldagem até a época em que a pressão expansiva se desenvolveu atingindo 90 MPa. É Importante para o desenvolvimento da pressão expansiva o aumento da porosidade na hidratação de CaO.

Y.Yamazaki, Nihon Cement Co. Ltd.,Japan and Y.Sakakibara, Nihon Cement Co. Ltd. Japan.

1. Introduction

Lime is used as one of the good expansive components of expansive cements and demolition agents. Many studies about the expamsive action have been done. There are some hypotheses under each experimental condition. These are roughly classified to two groups. One of them is crystal growth or recrystalization theory[1][2] based on the formation of hexagonal plate or hexagonal prism crystal of a few μm Ca(OH)2. The other is dusting or swelling theory[3][4] based on the formation of micro crystal of Ca(OH)2. However, there has been no general agreement on the suitable mechanisms by which the expansion pressure takes place. Especially, there has been scarcely discussed the mechanism of expanssive pressure development with the hydration of CaO under a condition of high external restraint and low water ratio.

This paper reports the mechanism of expansive pressure development with the hydration of CaO by measuring of expansive pressures and inner vacant volumes generated by the hydration of a hard-burned quick lime. The quick lime was mixed with additives and water, and then filled in a thick carbon steel pipe. The hydrated samples were observed by XRD,TG-DTA,Photomicroscope,SEM,and EPMA for analyzing the hydration process,the texture and the crystal forms.

2. Experimental procedure

2-1. Materials

A comercial hard-burned quick lime was used. The crystal sizes of CaO were 1～60μm. The quick lime was pulverized to 2500cm2/g (Blaine) in specific surface area The chemical compositions of the quick lime are shown in Table 1.

Table 1. Chemical compositions of the quick lime used

ig.loss	insol	SiO_2	Al_2O_3	Fe_2O_3	CaO	MgO	SO_3	Na_2O	K_2O	TiO_2	Total
1.5	0.2	3.0	1.0	0.2	92.0	1.6	0.3	0.03	0.05	0.04	99.92

And then it was mixed with a silica powder and a water reducing retarder as shown in Table 2.

Table 2. Proportions of Materials Mixed

Lime	Silica powder	Retarder
90	9	1

The retarder used was a powder type containing a formaline condensation product of sodium β-naphtalenesulfonate.

2-2. Measuring methods

Fig.1 shows the special equipment for measuring the expansive pressure and the inner vacant volume of the hydrated sample developed by the hydration of the quick lime in a thick carbon steel pipe.

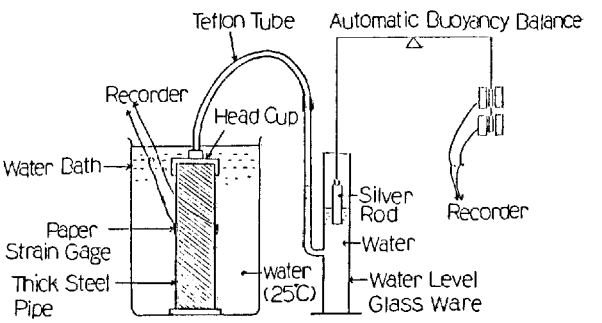

Fig. 1. The equipment for measuring the expansive pressure and the inner vacant volume of the hydrated sample of the quick lime in the steel pipe

The mixed materials was mixed at water/solid ratio of 0.28 and filled into the carbon steel pipe of wall thickness 5.1mm,external diameter 48.6mm,and length 200mm and then set as shown Fig.1. The pipe was cured in water at 25℃.

The magnitude of the expansive pressure assosiated with the hydration of CaO is calculated from equation(1).

The inner vacant volume generating in the hydrated sample is calculated from atomospheric pressure changes in the steel pipe by the use of Boyle and Charles's Law.

Y.Yamazaki, Nihon Cement Co. Ltd.,Japan and Y.Sakakibara, Nihon Cement Co. Ltd. Japan.

$$P = \frac{E}{2-\nu} \cdot \frac{h_0^2 - h_1^2}{h_1^2} \cdot \varepsilon_\theta \quad (1)$$

P = the expansive pressure (N)

E = the elastic factor of the steel (2.06×10^7 N)

ν = the poasson ratio (0.3)

h_0 = the outer radius of the pipe

h_1 = the inner radius of the pipe

ε_θ = the expansive strains of circumferential direction

At each age, hydrated samples were picked from the central part of the pipe which was cut by a diamond cutter. These samples were treated by freezed dry at -40°C and at atomosphere 1 Pa and used for following measurements. Only amounts of free water remained in samples were obtaine from the difference of the weight loss between non-dried samples and dried samples at 100°C. Hydration ratio of CaO at each age was calculated from the weight loss of samples caused by dehydration of Ca(OH)2 and decomposition of CaCO3 in DTA. The crystallite size of Ca(OH)2 was calculated using Scherrer's formula and Warren's method[5] for the harf width of XRD peaks which were found at 2θ=18.1 and 50.8 with Cu Kα corresponding to (001) and (110) plane of Ca(OH)2 lattice, respectively. The texture and the crystal form of hydrated samples were observed by SEM,Photomicroscope and EPMA.

3. Results

Fig.2 shows the relationships between an elapsed time and the expansive pressure or the volume expansion of steel pipe or the inner vacant volume ratio generated by the hydration of the quick lime under the high restrained condition with the carbon steel pipe at 25°C.
The expansive pressure reached about 5000 N at 24 hours and about 9000 N at 168 hours. The inner vacant volume in the hydrated samples continuously increased until 168 hours and was far larger as compared with the volume expansion of the steel pipe.

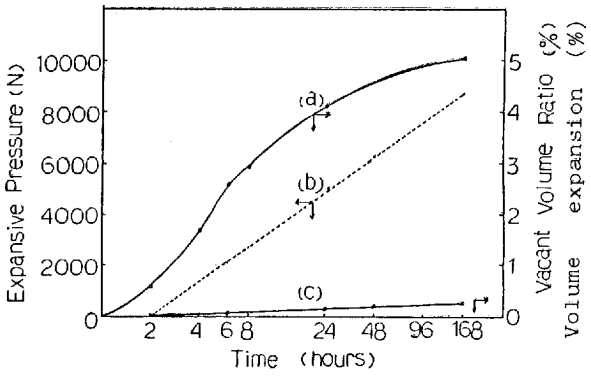

Fig. 2, The relationships between an elapsed time and the expansive pressure, the volume expansion of the steel pipe and the inner generated vacant volume ratio

(a) : Vacant volume ratio
(b) : Expansion pressure
(c) : Steel pipe volume expansion

Fig.3 shows the results of the measurement of free water amounts remaining in the samples and hydration ratio of CaO at each age.

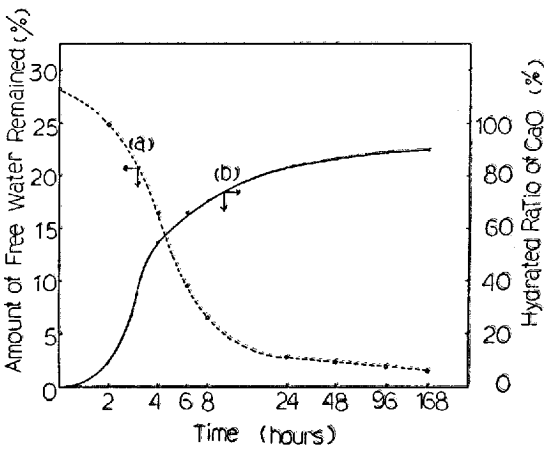

Fig. 3, Free water amounts and hydration ratio of CaO in the hydrated samples at each age

(a) : Free water amount
(b) : Hydrated ratio of CaO

Hydration ratio of CaO was about 90% and free water existed about 1.5% even at 168 hours.

Y.Yamazaki, Nihon Cement Co. Ltd.,Japan and Y.Sakakibara, Nihon Cement Co. Ltd. Japan.

Fig.4 shows the relationships between the elapsed time and the crystallite size of Ca(OH)2 associated with hydration of the quick lime in the pipe.

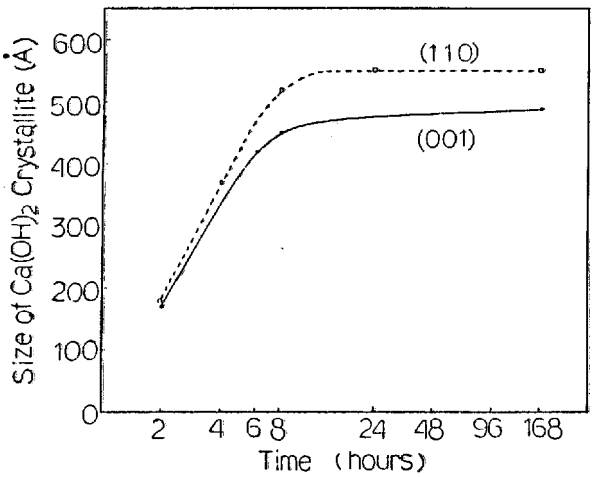

Fig. 4 The relationships between the elapsed time and the crystallite size of Ca(OH)2 generated in the hydrated samples

It became larger till 8 hours and didn't almost grow after that. The final crystallite size was about 500 Å and about 600 Å for (001) and (110) plane, respectively.

Fig.5 was the SEM's micrograph of the hydrated samples at each age.

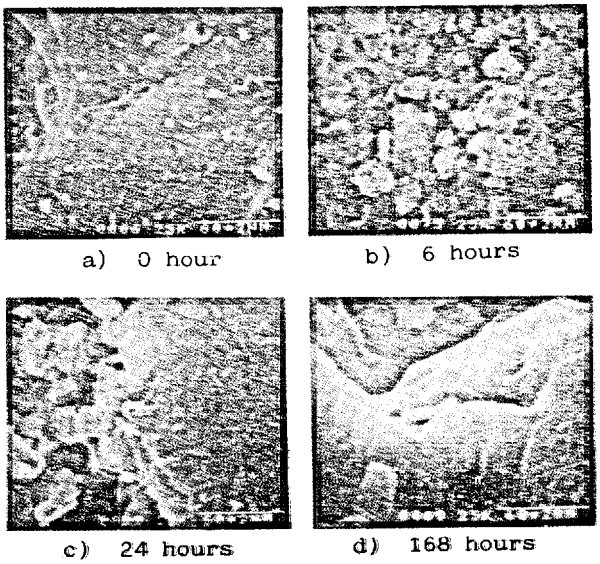

Fig. 5. SEM's micrograph of the hydrated samples

The texture of the hydrated sample was the more compacted the longer curing time.

Fig.6 was the photo micrograph about the thin sections of the hydrated sample at 48 hours. It was found that uncombined CaO crystal remained. The rim around CaO was crearly visible.

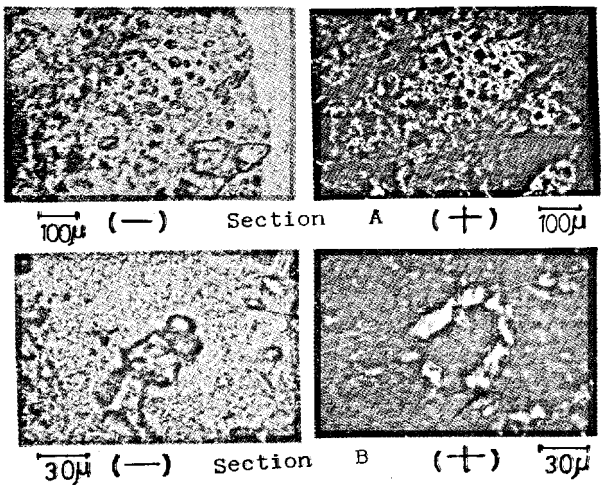

Fig. 6. Photomicrograph of the thin sections of the hydrated sample at 48 hours

Fig.7 was the EPMA's micrograph about the polished section of the hydrated samples at 48 hours.

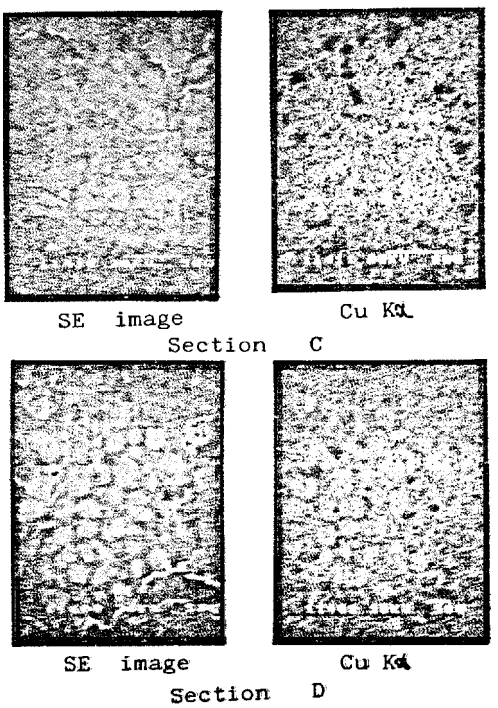

Fig. 7. EPMA's micrograph of the polished section of the hydrated samples at 48 hours

Y.Yamazaki, Nihon Cement Co. Ltd.,Japan and Y.Sakakibara, Nihon Cement Co. Ltd. Japan.

From Fig.7, it was revealed that the quick lime dusted and was massively surrounded by micro crystal Ca(OH)2.

Fig.8 shows photos of SEM observation in high magnification on the massive Ca(OH)2 compacted by the hydration of CaO at one day and seven days.

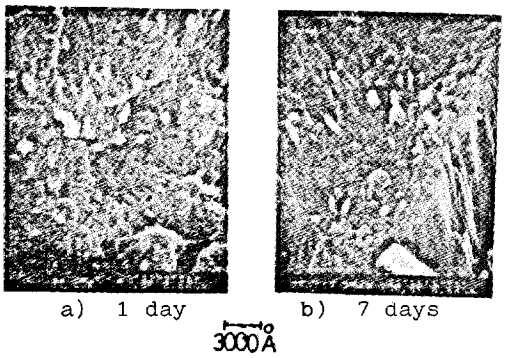

Fig. 8. SEM's micrograph of the massive $Ca(OH)_2$ in the hydrated sample at each age

The massive Ca(OH)2 consisted of smaller micro crystal Ca(OH)2 than about 1000 Å. There was little difference in the crystal size of Ca(OH)2 between at one day and at seven days.

4. Discussion

The hydration of the hard-burned quick lime progresses even under the condition of high external restraint about 9000 N as shown in Fig.2. Fig.9 shows the relations of the expansive pressure developed and the inner vacant volume generated in the hydration of the quick lime. In this fact, it is suggested that the expansive pressure is generated by an increase not only in solid volume but also in pore volume even at the high expansive pressure same as at usual expansive pressure in the case of expanssive cement.[6]

From Fig.3, the increases of both volumes are mainly obtained by the produce of Ca(OH)2 associated with the hydration of the unconbined CaO remained in the hydrated samples.

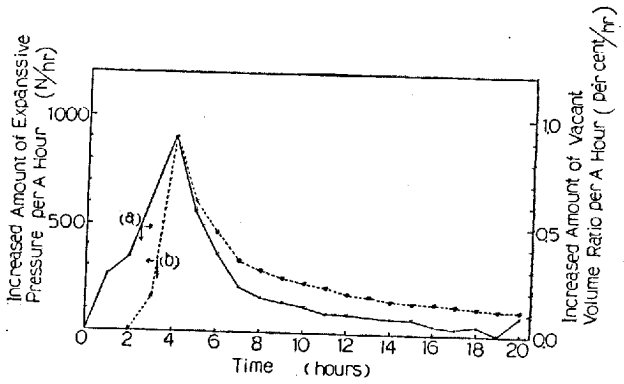

Fig. 9. Increased amount of the expansive pressure and the vacant volume per one hour in the hydrated samples

(a) : Vacant volume ratio

(b) : Expansive pressure

It is found that the quick lime grains change to the state like dusting and that the vacant space increases within six hours age from Fig.5. This fact is coresponding to remarkable increase of the inner vacant volume within six hours age as shown in Fig's 2 and 9. It is considered that the inner vacant pore distribution changes to the smaller size by the larger expansive pressure and that the hydrated sample is ccompacted with age as seen in Fig. 5.

It seems that Ca(OH)2 firstly occurs in the matorix from the hydration of fine and active lime in early stage and that the rims of Ca(OH)2 is formed around the coarse and the dusted lime as shown in Fig's 6 and 7. In this case, as Richards' model[7] for ettringite expansion, the enlargement of the thickness of the rims contributes to the development of the expansive pressure espcialy after one day. The same phenomena about ettringite formation with hydration of $C_4A_3\bar{S}$ has been discussed by Ogawa and Roy.[8]

The crystal form of Ca(OH)2 in this report is massive and irregular as previously observed in expansive cement.[9][10] Ca(OH)2 crytals of hexagonal plate and hexagonal prism with size a few μm was produced as shown in Fig. 10 when the same mixed materials mixed with water/ratio 5.

Y.Yamazaki, Nihon Cement CO. Ltd.,Japan and Y.Sakakibara, Nihon Cement Co. Ltd. Japan.

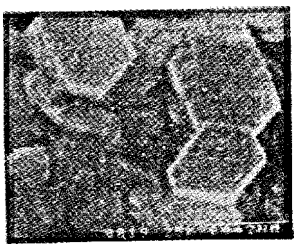

7 days

Fig. 10. SEM's micrograph of $Ca(OH)_2$ generated in the hydration of the quick lime with water/solid ratio 5

But they were not found in this study. Therefore, it is difficult to support the opinion that the expansive pressure of the hydration of CaO is caused by the growth of Ca(OH)2 crystal of hexagonal plate and prism. Because the hydration process of CaO is one based on the topochemical growth of crystals of Ca(OH)2 in actual low water/solid ratio.

As observed in Fig's 4 and 8, the crystallite size of Ca(OH)2 is very small with diameter some hundred Å. This result supports the presumption discussed in okushima's report.[2] And it was not detected in DTA of this study though the existence of amorphous Ca(OH)2 has been reported by Takashima[11] and Brunauer.[12]

5. Conculusion

1) The hydration of CaO continues under high external restraint and the expansive pressure associated with the hydration developes to about 9000 N.
2) The inner vacant volume is generated with the hyddration of CaO even though the hydration product is compacted by the expansive pressure.
3) The texture of hydrated sample of CaO is mostly composed of aggregates of irregular massive Ca(OH)2 of which crystallite size is some hundreds Å.
4) The expansion with the hydration of CaO mainly depend on the elongation of the micro crystal Ca(OH)2 rim around CaO uncombined after dusting.

Acknowledgements

The authors extend their thanks to Mr. M.Sawamura and Mr.H.Moriya, Nihon Cement Co. Ltd., for granting permissions to publish this paper, and to Dr.N.Kawada, Nihon Cement Co.,Ltd., for his guidances. Furthermore thanks are due to Mr.H.Sibazaki, Nissei Sangyo Co.,Ltd., Mr.M.Hashimoto and Mr.T.Matsu, Nihon Cement Co.,Ltd., for their assistances in microscopy.

References

1) Chatterji S. and Jeffery J.M., Mag. Concrete Research Vol.18, No55 (1966), pp65-68
2) M.Okushima, R.Kondo, H.Muguruma and Y.Ono, Proc. 5th Int. Symp. Chemistry of Cement, Tokyo, Vol.3 (1968), 419
3) Ramachandran V.S., Sereda P.J., and Feldman R.F., Nature Vol.201, No.4916, 18 January (1964), pp288-289
4) Mehta P.K., Cement and Concrete Research, Vol.3, No.1 (1973), pp96-97
5) B.E. Warren and B.L. Averbach, J. Appl Phys., Vol.21 (1950), 595
6) Y.Yamazaki, H.Kamiaka and S.Kobayashi, Proc. 6th Int. Symp. Chemistry of Cement, Mosscow, Vol.3 (1974)
7) C.W.Richards and R.A.Helmuth, National Science Fundation Technical Repot No. 191, (1975)
8) K.Ogawa and D.M.Roy, Cement and Concrete Research, Vol.12, No.1 (1982), pp101-109
9) M.Sato,etc, (in Japanese), Semento Gijutsu Nenpo, Vol.24, (1975),pp118-121
10) Y.Yamazaki, H.Kamiaka and S.Kobayashi, Proc. 7th Int. Symp. Chemistry of Cement, Paris, Vol.3, (1980),pp.V220-V223
11) S.Takashima, (in Japanese), Semento Gijutsu Nenpo, Vol.10,(1956), pp51-56
12) S.Brunauer and S.A.Greenberg, Proc. 4th Int. Symp. Chemistry of Cement, Washington, Vol.1, (1960), 138

J.Grzymek, A.Derdacka-Grzymek, Z.Konik, M.Pyzalski, A.Stok and J.Iwanciw
Academy of Mining and Metallurgy, Krakow, Poland.

The effect of synthesis and cooling conditions on phase properties of the $C_{12}A_7$ 3.3

Effets des conditions de cuisson et de refradissement sur les propriétés de $C_{12}A_7$

SUMMARY: The $C_{12}A_7$ was synthesized at different temperatures in oxidizing and reducing atmosphere in the superkanthal furnace.
Samples with the furnace were cooled slowly, rapidly air cooled and refrigerated in the liquid nitrogen.
Moreover the $C_{12}A_7$ was synthesized in chamber of the "Setaram" type thermoanalyser in vacuum.
The samples were examined by DTA and TG method /in vacuum/ and roentgenografic and were observed using optical and scanning microskopes.
The investigations confirmed the existence of phase variants of the $C_{12}A_7$.
It was explained that the amount and structure of these phases depend on synthesis as well as on cooling conditions.
The polycrystal of the $C_{12}A_7$ consisting of isotropic and anisotropic phases was obtained.
Phoenomena of polymorphic transitions of $C_{12}A_7$ phase were observed by scanning microscope and on DTA curves.
Two polymorphic variants were obtained - cubic crystal variant α $C_{12}A_7$ and anisotropic variant γ $C_{12}A_7$. It was stated that polymorphic transition occurs at 1473 K temperature.

Faz-se a síntese de $C_{12}A_7$ sob diferentes temperaturas em atmosfera oxidante e redutora em forno superkantal.

Amostras e forno forma esfriados lentamente, resfriados rapidamente a ar, e refrigerados em nitrogênio líquido.

Além disso o $C_{12}A_7$ foi sintetizado a vácuo em câmara de termoanalisador tipo "Setaram". As amostras foram examinadas por método DTA e TG, em vácuo, e roentgenografia e foram observadas por microscópios óticos e de varredura.

As investigações confirmaram a existência de variantes de fase do $C_{12}A_7$.

Ficou esclarecido que a quantidade e estrutura destas fases dependem da síntese e das condições de resfriamento.

Conseguiu-se o policristal de $C_{12}A_7$ consistindo de fases isotrópicas e anisotrópicas. Por intermédio de microscópio de varredura e curvas de DTA, observaram-se fenômenos de transições polimórficas da fase de $C_{12}A_7$.

Foram obtidas duas variantes polimórficas - variante $\alpha C_{12}A_7$ de cristal cúbico, e variante anisotrópica $\gamma C_{12}A_7$. Definiu-se que a transição polimórfica se dá à temperatura de 1473K.

J.Grzymek, A.Derdacka-Grzymek, Z.Konik, M.Pyzalski, A.Stok and J.Iwaniw
Academy of Mining and Metallurgy, Krakow, Poland.

INTRODUCTION

To this day is a certain amount of questionable problems relating to properties and structure of $C_{12}A_7$.
Many controversial statements with regard to properties, structure and polymorphic variations of $C_{12}A_7$ are in literature.
Our investigations carried out for several last years proved that the phase transitions of $C_{12}A_7$, beside of the transition βC_2S into γC_2S, are of great importance for self-disintegration process.
It was observed that the obtainment of self-disintegrating powders containing $C_{12}A_7$, that decomposes at different rate in the aqueous solution of carbonate sodium, depends on the temperature and atmosphere of burning the sinters and cooling conditions.
On this ground one could consider that the $C_{12}A_7$ in these powders appears in different polymorphic variants /1/.
The authors investigations were carried out in order to explain this phenomenon and to determine the influence of conditions of the synthesis and cooling on the properties of $C_{12}A_7$ as well as the temperature of polymorphic transition.

THE INFLUENCE OF TEMPERATURE AND ATMOSPHERE OF THE SYNTHESIS AS WELL AS COOLING CONDITIONS ON THE PROPERTIES OF $C_{12}A_7$ PHASE.

$C_{12}A_7$ was synthesized from row mixture of $CaO:Al_2O_3$ ratio corresponding to 0,84 in a superkanthal furnace at the following temperatures: 1623, 1673, 1723, 1773 and 1823 K in oxidizing and reducing atmosphere /2/.
The samples, after air quenching and slow cooling with the furnace, were investigated using: X-Ray mehod, optical microscope, differential thermal analysis-DTA as well as underwent leaching using aqueous soda solution.
X-Ray diffraction studies were made using "Philips" X-Ray diffractometer, microscopic observations in transmitted polarized light the universal "Reichert-MeF-2" microscope and differential thermal analysis-DTA using the "Setaram" 6-24 type apparatus.
The investigations of the $C_{12}A_7$ samples, using the "Philips" X-Ray diffractometer, in the range of 20° - 70° 2Θ revealed peaks corresponding to the isotropic regular phase of $C_{12}A_7$ and their values of "d" in Å accorded well with the data given in the catalogues.
The patterns in the range of 70° - 130° 2Θ were also obtained and the additional peaks were found. This pekas are not tabulated for the isotropic phase of $C_{12}A_7$.
The microscopic observations of microsections revealed that the $C_{12}A_7$ samples are not homogenous but composed both optically isotropic and anisotropic phases.
The isotropic phase forms colourless crystals of irregular shape sometimes isometric characteristic for the cubic $C_{12}A_7$.
The anisotropic phase forms predominantly the skeleton structure composed of irregular or prismatic crystals.

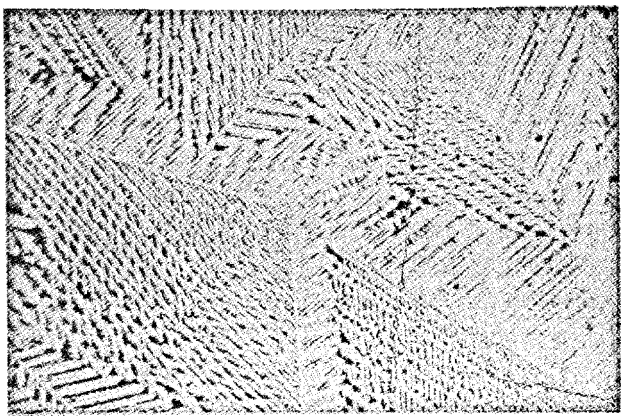

Fig.1. $C_{12}A_7$ synthesized in the oxidizing atmosphere at 1773 K, rapidly cooled. Average image. The rectangular prisms composed of the isotropic and anisotropic phase. Nic.II. 75 x.

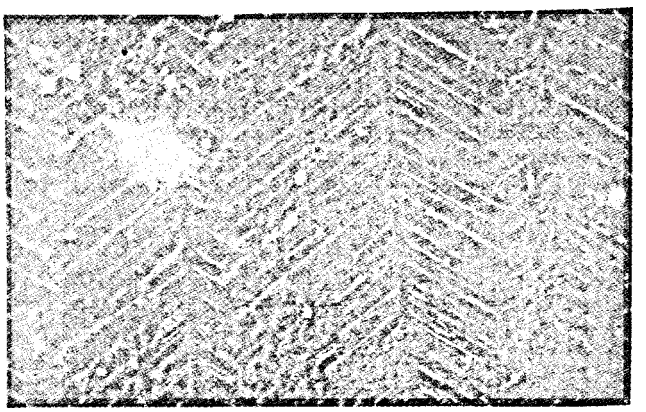

Fig.2. $C_{12}A_7$ synthesized in the oxidizing atmosphere at 1773 K, rapidly cooled. Average image. The rectangular prisms composed of the isotropic and anisotropic phase. Nic. +. 75 x.

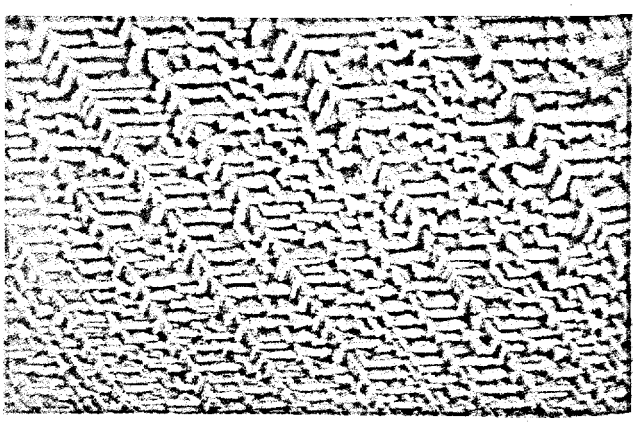

Fig.3. $C_{12}A_7$ synthesized at the oxidizing atmosphere at 1323 K, rapidly cooled. Average image. Isotropic and anisotropic phase. Nic. II. 75 x.

J.Grzymek, A.Derdacka-Grzymek, Z.Konik, M.Pyzalski, A.Stok and J.Iwanciw
Academy of Mining and Metallurgy, Krakow, Poland.

The $C_{12}A_7$ samples synthesized at lower temperatures are of monolithic structure..
In the main isotropic phase there are non-uniformly spaced inclusions of the anisotropic phase skeleton crystals.
At the higher temperatures the anisotropic phase crystallizes on the grain boundaries of isotropic phase forming the skeleton or prismatic crystals rather uniformly spaced.
The $C_{12}A_7$ samples synthesized at 1773 K and 1823 K and cooled rapidly have visible prismatic structure and consist of rectangular prisms composed of isotropic and anisotropic phases. The anisotropic phase of $C_{12}A_7$ may be of low or high birefrigence/ Fig. 1-3 /
The low-birefrigence phase is cryptocrystalline. One may consider that the cryptocrystalline anisotropic phase is intermediate one between the isotropic and anisotropic of high birefregence. As it follows from the aluminium oxide leaching from $C_{12}A_7$ using the 12 % aqueous soda solution, the samples synthesized at higher temperatures lixiviate better at 313 K and synthesized at lower temperatures lixiviate better at 333 K.
The differential thermal analysis-DTA was made using $C_{12}A_7$, sample synthesized at 1823 K and rapidly cooled. On the DTA curves are visible 4 endothermic peaks in the range of 1605 - 1785 K.
The results of studies point out that the investigated sample is not homogenous.
The differential thermal analysis- DTA study - was made also using the $C_{12}A_7$ sample synthesized at 1623 K and rapidly cooled.
The sample in the platinum concible was heated up to 1803 K in an argon atmosphere with constant rate of 10 K/min. and was stored at above mentioned temperature for15 min. and then cooled to 293 K also with constant rate of 10 K/min. /Fig.4./.

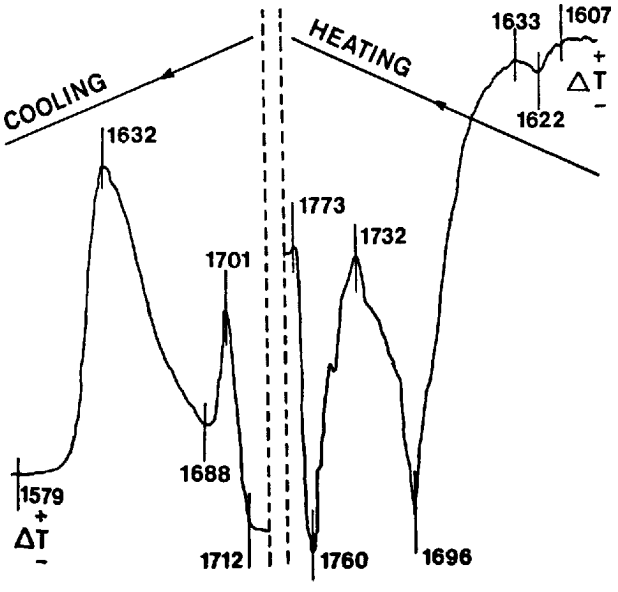

Fig.4. DTA-curve $C_{12}A_7$. Temp./K/.

This way a polycrystal about 9 mm long was obtained from liquid phase. /Fig.5./

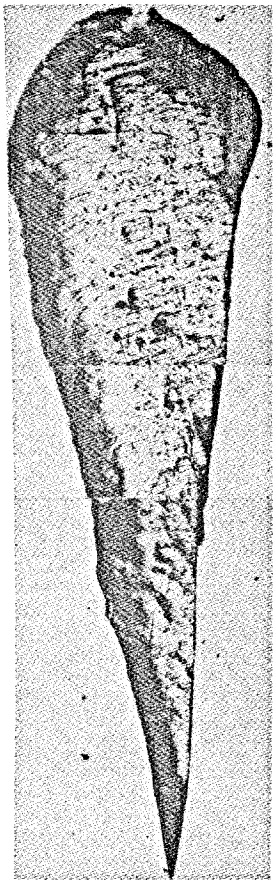

Fig.5. Policrystal $C_{12}A_7$.
Mic. II. 30 x.

The microscopic observations of this polycrysta were made in transmitted polarized light /without microsections/.
The observations revealed that the polycrystal is composed of both optical isotropic and anisotropic phases.
Subsequently the mixture of CaO : Al_2O_3 ratio corresponding to 0,94 was synthesized at 1673 K in oxidizing atmosphere and after taking out of the furnace at 1673 K was refrigerated in liquid nitrogen. The X-Ray examination of the sample revealed that it is phase of $C_{12}A_7$. On the X-Ray photography made in the range of 20^0 - 70^0 2 θ only reflections from regular isotropic $C_{12}A_7$ appear.
Furthermore the higher background due to the glassy phase of the sample occurs.
From microscopic observations it is evident that $C_{12}A_7$ is composed of both optical isotropic and anisotropic phases.
The sample refrigerated in the liquid nitrogen is characterized by the smaller crystal habit of anisotropic phase in comparison with the sample air cooled.
The $C_{12}A_7$ synthesized at 1673 K in oxidizing atmosphere and then rapidly air cooled was examined under the scanning elektron microscope.
The sample was exposed on the electron beam action during 20 minutes. In the dark spots formed during this operation "bulges" appeared, then they enlarged and cracked. On the surface a transversal crack was visible.
The phenomenon observed by using scanning microscope was photographed /Fig. 6 - 9/.
In the opinion of authors this phenomenon it is probably due to the $C_{12}A_7$ polymorphic transition.
The $C_{12}A_7$ synthesized at 1673 K and then air quenched was examined by thermogravimetric method in vacuum. The examination in a vacuum reveals the weight loss of 1,45 % during the heating up to 1673Kand 80 % of this weight loss takes place in the range of 1363 K - 1373 K.

J.Grzymek, A.Derdacka-Grzymek, Z.Konik, M.Pyzalski, A.Stok and J.Iwanciw
Academy of Mining and Metallurgy, Krakow, Poland.

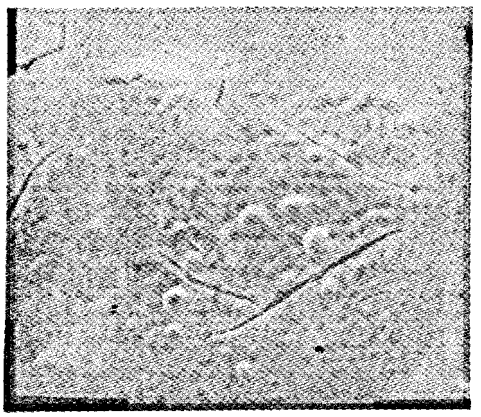

Fig.6. SEM. $C_{12}A_7$ synthesized at 1673 K in an air atmosphere. The surface before an electron beam action. 6000 x.

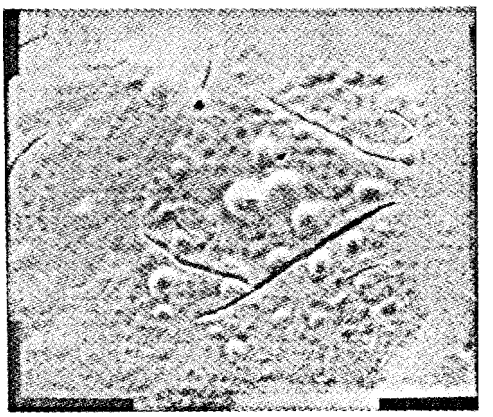

Fig.7. SEM. $C_{12}A_7$ synthesized at 1673 K in an air atmosphere. The surface after 20 min. exposure. The new "bulge", its growth and crack is visible. 6000 x..

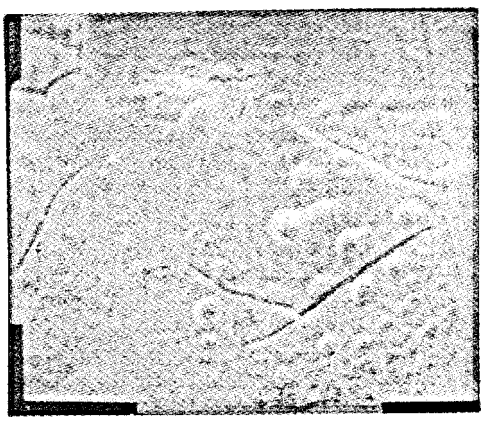

Fig.8. SEM. $C_{12}A_7$ synthesized at 1673 K in an air atmosphere. The surface after 20 min. exposure with the transversal crack. 6000 x.



Fig.9. SEM. $C_{12}A_7$ synthesized at 1673 K in an air atmosphere, fragment of Fig.8 with magnification. 19 000 x.

$C_{12}A_7$ SYNTHESIS IN VACUUM.

The mixture of CaO : Al_2O_3 weight ratio equal to 0,94 was heated with constant rate of 10 K/min. up to 1823 K in vacuum of 3.10^{-2} - 2.10^{-4}.
The sample was stored at 1823 K for 30 min. and then cooled to 293 K with constant rate of 8 K/min. /4/.
The DTA curve /Fig. 10/ for the sample show one exothermic peak in the range of 1588 K-1548 K and position of his maximum is at 1573 K. Two broaded small exothermic peaks can be also observed in the range of 1418 K-1353 K and one small exothermic peak in the range of 818 K - 733 K.
the shape of the DTA curve presented in Fig. 10 can suggest the polymorphic transition of $C_{12}A_7$..
The volume increase of 3 % seems to confirm the above statement. The sample synthesized in "Setaram" chamber was examined both by X-Ray and microscopic method.

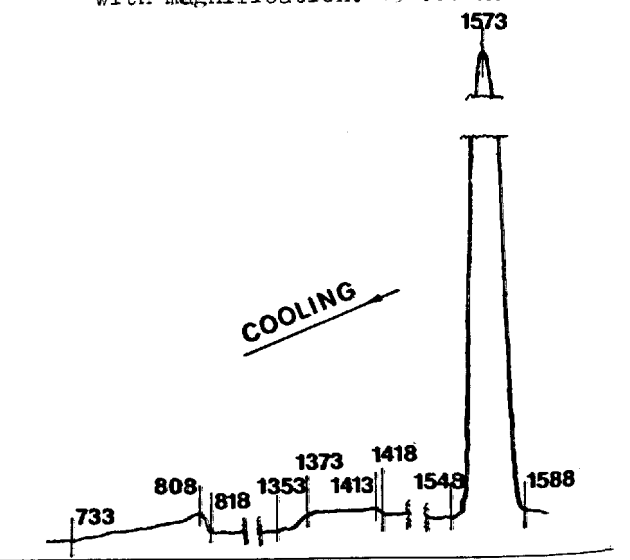

Fig. 10.DTA curve of $C_{12}A_7$ synthesized in vacuum.

J.Grzymek, A.Derdacka-Grzymek, Z.Konik, M.Pyzalski, A.Stok and J.Iwanciw
Academy of Mining and Metallurgy, Krakow, Poland.

The X-Ray result of this sample is diffe - rent from the result of regular $C_{12}A_7$ phase. The "d" values do not correspond to the regular $C_{12}A_7$ phase.
The "d" values as well as the peak intensities of this phase are shown in the table 1.

Table 1. X-Ray diffraction pattern of $C_{12}A_7$ phase syntesized in vacuum "d" values and peak intensities.

d	I/I_1	d	I/I_1	d	I/I_1
5.11	3	2.1438	7	1.6387	5
3.3510	4	2.0826	19	1.6189	3
3.1426	54	1.9906	21	1.5914	7
2.9094	40	1.9271	11	1.5536	3
2.8801	24	1.8361	4	1.5455	9
2.6905	5	1.7923	4	1.5409	8
2.5693	100	1.7815	11	1.4662	5
2.4669	13	1.7163	29	1.4467	7
2.4442	28	1.6757	2	1.4214	11
2.3383	13	1.6480	4	1.3597	4

The microscopic observations of microsections in transmitted polarized light revealed that the sample is of crystalline structure and consist of anisotropic plate-like and prismatic coarse crystals /Fig.11, 12/.

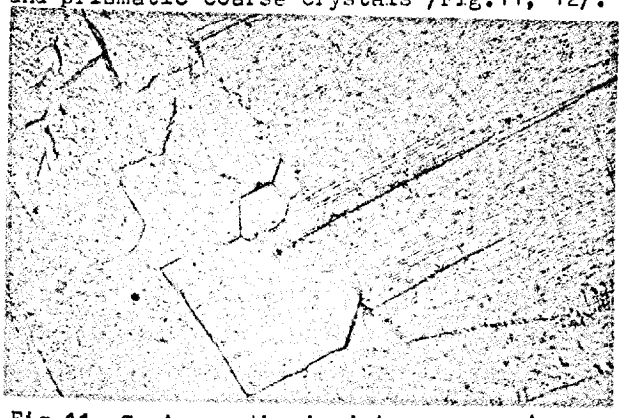

Fig.11. $C_{12}A_7$ synthesized in vacuum. Average microstructure. Coarse crystals of anisotropic phase. Nic.II. 75 x.



Fig.12. $C_{12}A_7$ synthesized in vacuum. Average microstructure. Coarse crystals of anisotropic phase. Nic.+. 75 x.

The observations of the sample under scan - ning elektron microskope SEM revealed that the sample has plate-like and prismatic structure of anisotropic phase crystals. /Fig.13, 14/.

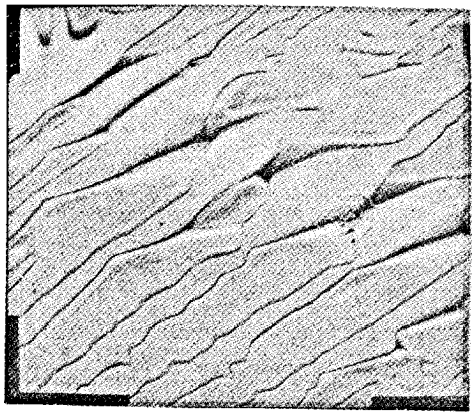

Fig.13. SEM. $C_{12}A_7$ synthesized in vacuum. Anisotropic phase crystals of prismatic habit. 5000 x.

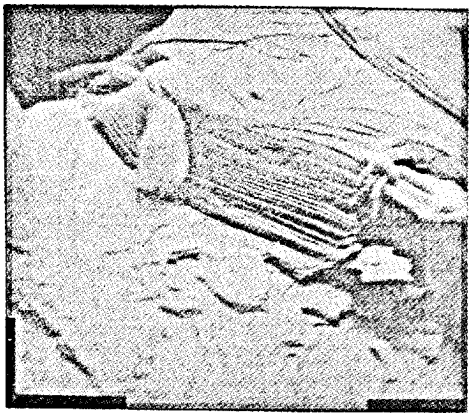

Fig.14. SEM. $C_{12}A_7$ synthesized in vacuum. Anisotropic phase crystals of plate-like habit. 5000 x.

ASSIGNATION OF TEMPERATURE OF POLYMORPHIC TRANSITION $\gamma \rightarrow \alpha$ $C_{12}A_7$.

The results of investigations obtained hitherte revealed that it is possible to obtain two different $C_{12}A_7$ phases from mixture of CaO : Al_2O_3 ratio correspondig to 0,94 according to conditions of the synthesis and cooling.
We determined first phase as α $C_{12}A_7$ phase with peaks corresponding to the regular $C_{12}A_7$ phase and second anisotropic phase as γ and her "d" values in Å are shown in the table 1.
The obtainment of two seperate α and γ $C_{12}A_7$ phases and two broaded small exotermic peaks on the DTA curve in the range 1418 - 1353 K for the sample synthesized in vacuum permitted to make a hypothesis that it is the temperature of polymorphic transition $\gamma \rightarrow \alpha$.

J.Grzymek, A.Derdacka-Grzymek, Z.Konik, M.Pyzalski, A.Stok and J.Iwanciw
Academy od Mining and Metallurgy, Krakow, Poland.

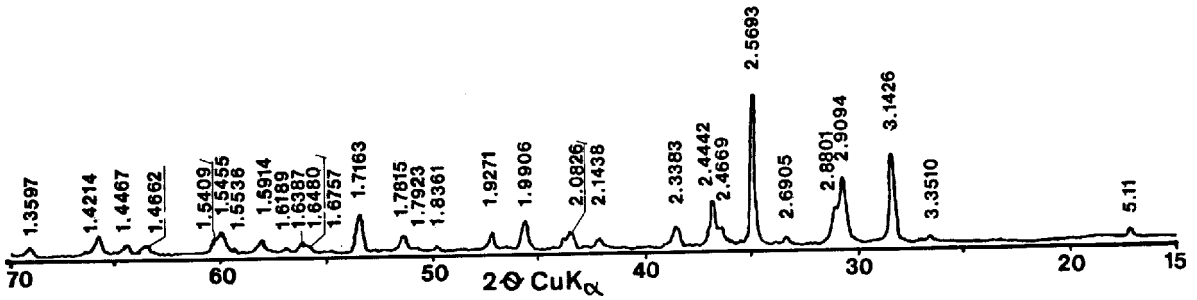

Fig. 15. X-Ray diffraction pattern γ $C_{12}A_7$.

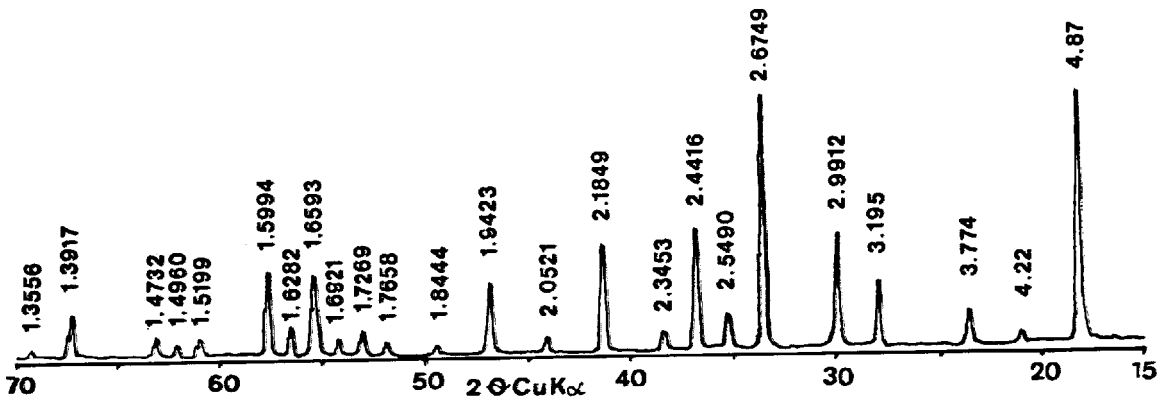

Fig. 16. X-Ray diffraction pattern α $C_{12}A_7$.

The anisotropic phase γ $C_{12}A_7$, for which the result is showed in Fig. 15, was roasted in a superkanthal furnace during 1 h at the temperature of 1473 K and then after taking out of the furnace was air cooled.
The obtained sample was X-Ray examinated and results of the examination accorded with α $C_{12}A_7$ regular phase /Fig. 16/.
Therefore one should state that α and γ are polymorphic variants of $C_{12}A_7$ and that 1673K is the temperature of transition of polymorphis variant $\gamma \rightarrow \alpha$.

CONCLUSIONS

1. The investigation confirmed the existence of $C_{12}A_7$ two polymorphic variants: regular polymorphic variant - α $C_{12}A_7$ and anisotropic polymorphic variant - γ $C_{12}A_7$. In the opinion of authors the regular variant α $C_{12}A_7$ with published in literature "d" values in Å is the mixture of the isotropic and anisotropic phases and thise one last, in all probability, is not charakterized by properties of anisotropic phase determined by us γ .
2. It was stated that the temperature of 1473 K is the temperature of polymophic transition $\gamma \rightarrow \alpha$ $C_{12}A_7$.

REFERENCES

1. Grzymek J. et al., "Method for obtaining aluminium oxide" United States Patent, No-4149898, 1979.
2. Grzymek J., Derdacka-Grzymek A., Konik Z., Stok A., Gawlicki M., "The complex production of aluminium oxide and iron from laterite raw materials applying the calcium aluminates polymorphism", Light Metals, AIME, 1985.
3. Grzymek J., Derdacka-Grzymek A., Konik Z., Stok A.,Pyzalski M. "Bedeutung der polymorphen Umwandlung des Kalziumaluminats $C_{12}A_7$ als Grundlage des Komplexverfahrens zur Gewinnung von Portlandzement, Eisen und Tonerde", Baustoffindustrie 1985,3, /Mai/.
4. Grzymek J., Derdacka-Grzymek A., Konik Z., Stok A., Pyzalski M., Iwanciw J. "Some physicochemical properties of $12CaO.7Al_2O_3$ phase in relation to Al_2O_3 production from self-disintegrating sinters". Article will be publish in Light Metals, AIME, 1986.

Ion Teoreanu, Maria Georgescu and Annemarie Puri, Polytechnical Institute Bucharest, Romania. 1

The influence of some additions on the hydration and hardening of tricalcium aluminate 3.3

L'influence de quelques additifs sur l'hydratation et durcissement de tricalcium aluminate

SUMMARY: In this paper are examined the hydration and hardening processes of tricalcium aluminate (C_3A) with additions of 10% $CaSO_4 \cdot 2H_2O$ and 0.2% dimethylterephtalate (DMTP).

Differential thermal analysis, diffractometry and electron microscopy are used in this study in order to obtain data concerning the influence of the above mentioned additions on the interaction rate of tricalcium aluminate with water. The composition, texture and morphology of the resulting hydrated products are examined, too.

Measurements of mechanical strength are used for the characterisation of binding properties in the C_3A-water and C_3A-water-additions systems.

Neste trabalho são examinados os processos de hidratação e de endurecimento do aluminato tricálcico (C_3A) com adições de 10% de $CaSO4.2H_2O$ e 0,2% de dimetiltereftalato (DMTP).

Neste estudo foram usadas análise termodiferencial, difratometria e microscopia eletrônica, a fim de se obter dados concernentes à influência das adições mencionadas acima sobre a velocidade de interação do aluminato tricálcico com a água. Também foram examinadas a composição, textura e morfologia dos produtos hidratados resultantes.

As medições da resistência mecânica são usadas para a caracterização das propriedades do ligante nos sistemas C_3A-água e C_3A-água-adições.

Ion Teoreanu, Maria Georgescu, Annemarie Puri

1. Introduction

The energetic interaction of C_3A with water can be retarded by adding relatively large amounts of gypsum, sodium or calcium lignosulphonate, sodium gluconate, some oxides or hydroxides a.o. /1-6/. This additions have also modified the kinetics of the conversion processes of the hydrated compounds resulted.

The present work is focused on obtaining data concerning the influence of gypsum associated with an organic compound on the hydration, conversion and hardening processes in the C_3A-water system.

2. Working procedure

Tricalcium aluminate has been synthesized by reacting a stoichiometric mixture of chemically pure $CaCO_3$ and Al_2O_3 fired four hours at 1350°C. The formation of C_3A has been checked by determining the amount of free CaO and by X-ray diffractometry. After three succesive runs at 1350°C, done under the same conditions, no more free CaO has been found, and the diffraction pattern showed the lines of C_3A only.

The tricalcium aluminate thus prepared has been ground with 10% $CaSO_4.2H_2O$ and 0,2% DMTP down to Blaine surface areas between 2500-3000 cm^2/g.

The informations concerning the hydration and conversion processes in the systems with and without additions, have been obtained by the following techniques: X-ray diffractometry, DTA and electron microscopy. The measurements of mechanical strength have provided informations on the changes in the hardening process of C_3A due to the use of gypsum in association with DMTP.

3. Results and discussion

X-ray diffraction and DTA show that the respective rates of the interaction between C_3A and water and of the conversion of the resulted hydrocompounds are affected

After the first half hour of hydration, the products noted are the hexagonal hydroaluminates C_2AH_8 and C_4AH_{13} (Fig.1a). From the diffraction patterns given in the same figure, in the early hours of the hydration process are deduced relatively small rates of hydration and conversion as compared to the system without any addition - Fig.2a. This conclusion is in agreement with the following fact: the mortars prepared from these masses stiffen later than the masses without addition - namely after about 3 hours from their casting.

Later, after one day of hydration, sharp diffraction interferences characteristic to tricalcium hexahydroaluminate (C_3AH_6) appear in the system without additions, they can be seen even after three hours of hydration (see figures 1b and 2b). No ettringite is seen in the samples, mainly due to the small amount of gypsum.

On the DTA curves (Fig.3) made after hydration durations of 1 to 28 days, endoeffects assigned both to cubic hydroaluminate (C_3AH_6 at 310-320°C and 460-470°C) and to hexagonal hydroaluminates (at 100-125°C, 190-220°C and 740-750°C) are seen. The effect at 740-750°C can be assigned to partly carbonated hexagonal hydroaluminate phases /5/. Comparing the TG curves to those obtained for the reference system (whithout addition), wich are given in Fig.4, it is rendered clearly visible that a smaller amount of cubic hydroaluminate is present in the case of the system with gypsum and DMTP additions. The retardation effect exerted by DMTP on the conversion of hexagonal hydroaluminates into cubic ones is proven by this observation, too.

The TEM micrographs given in Fig.5 show that the binder hardened in the presence of gypsum and DMTP additions has finer crystals than the reference system, whose micrographs are given in Fig.6.

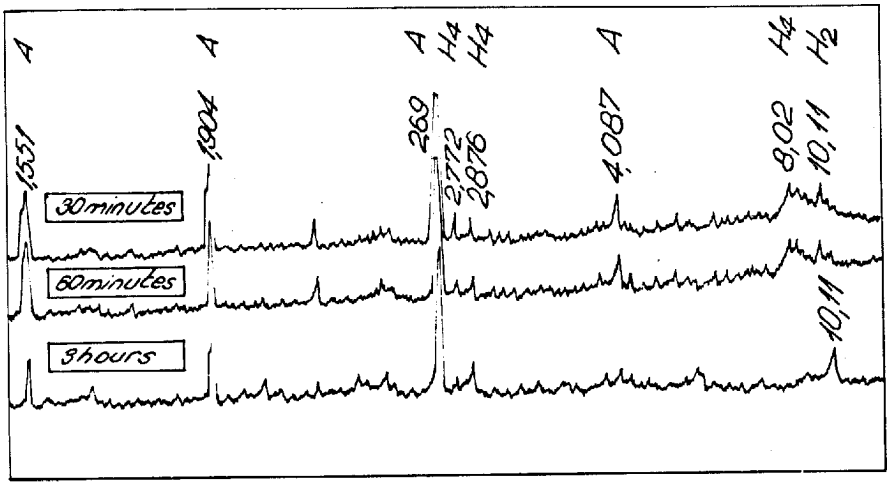

Figure 1 X-ray diffraction patterns of tricalciumaluminate hydrated with 10% $CaSO_4.2H_2O$ and 0.2% DMTP:
a) 30 minutes to 3 hours;
b) 1 to 28 days;
A - C_3A;
H_2 - C_2AH_8;
H_4 - C_4AH_{13};
C - C_3AH_6;
M - $C_3A\overline{C}S\overline{H}_{12}$.

a

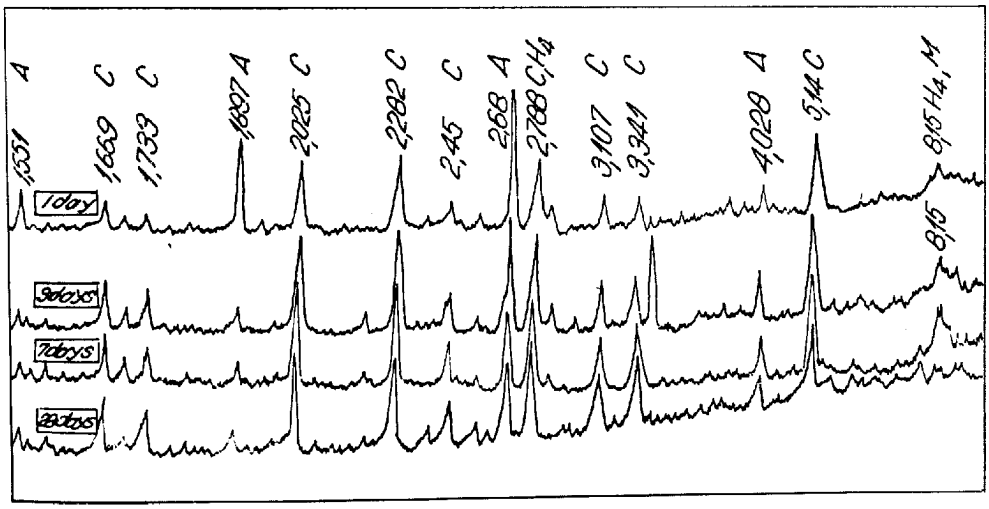

b

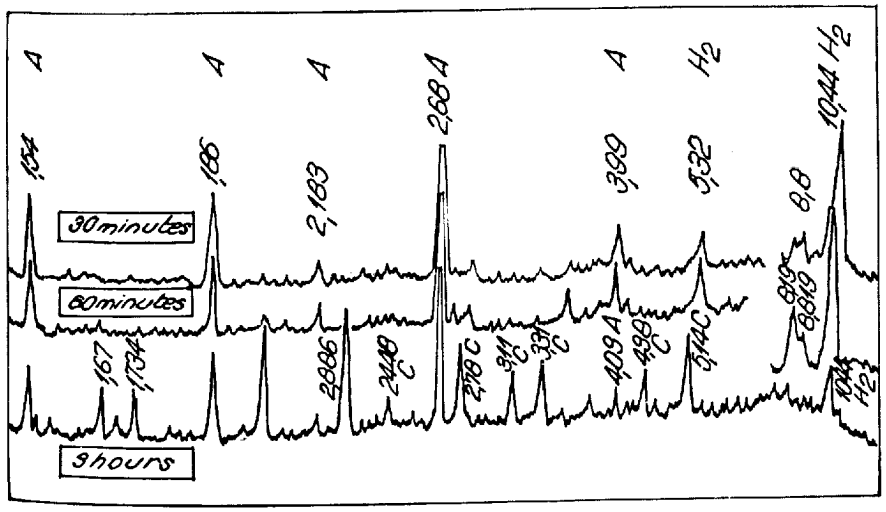

Figure 2 X-ray diffraction patterns of hydrated tricalciumaluminate:
a) 30 minutes to 3 hours;
b) 1 to 28 days.

a

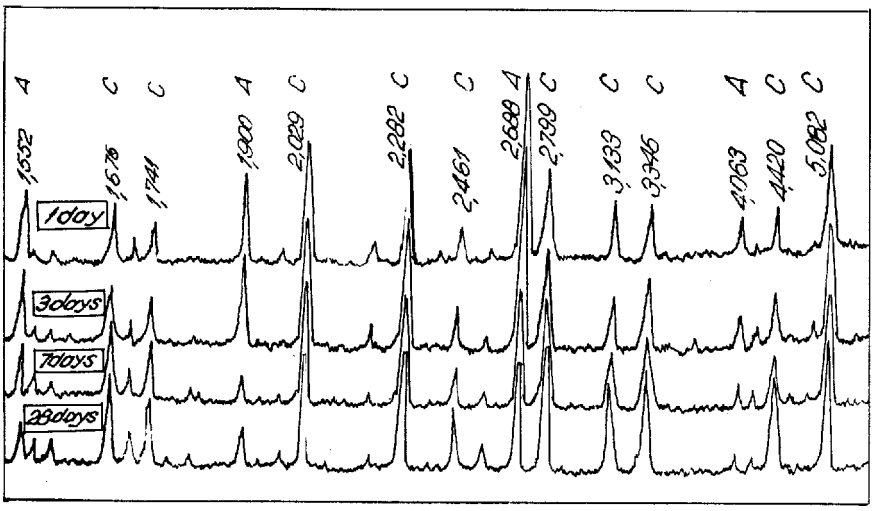

Figure 2b

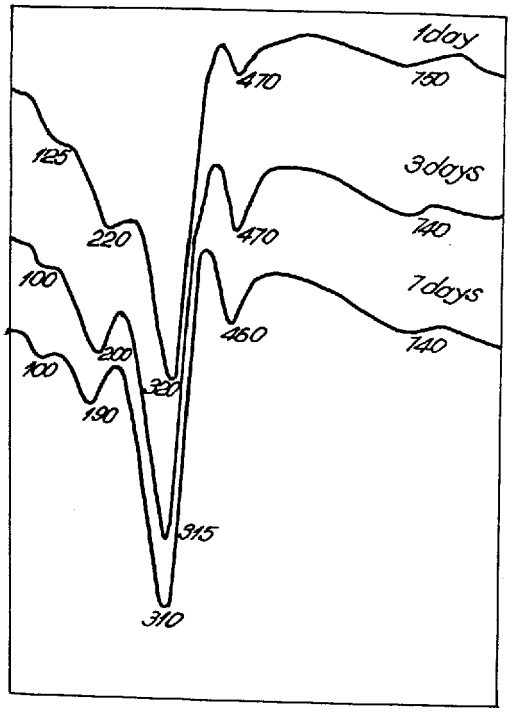

Figure 3 DTA curves of C_3A with 10% gypsum and 0,2% DMTP, hydrated 1 to 7 days.

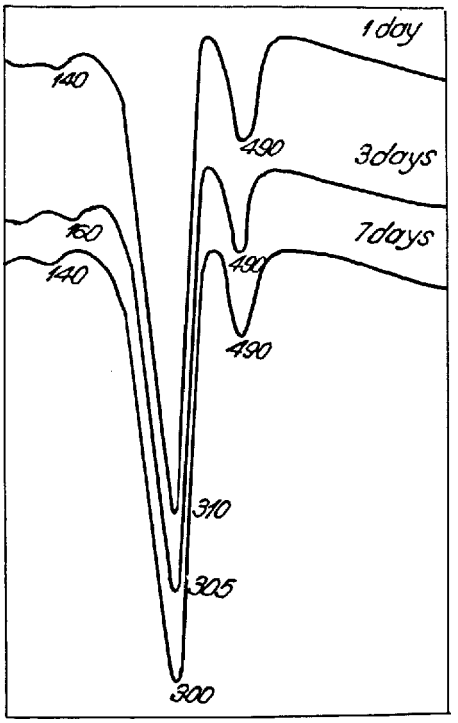

Figure 4 DTA curves of 1 to 7 days hydrated C_3A.

The changes in the kinetics of the process, in the composition, texture and morphology of the systems are finally reflected in the strength of the respective mortars. If gypsum and DMTP additions are used in the C_3A-H_2O system, outstanding values of mechanical are noted, even after a single day of hardening. This values steadily increase with time, regardless of the environment, as seen in table 1. The exposure to air is more favourable from the viewpoint of the hardening process than the exposure to a humid environment, but the relative differences are less important.

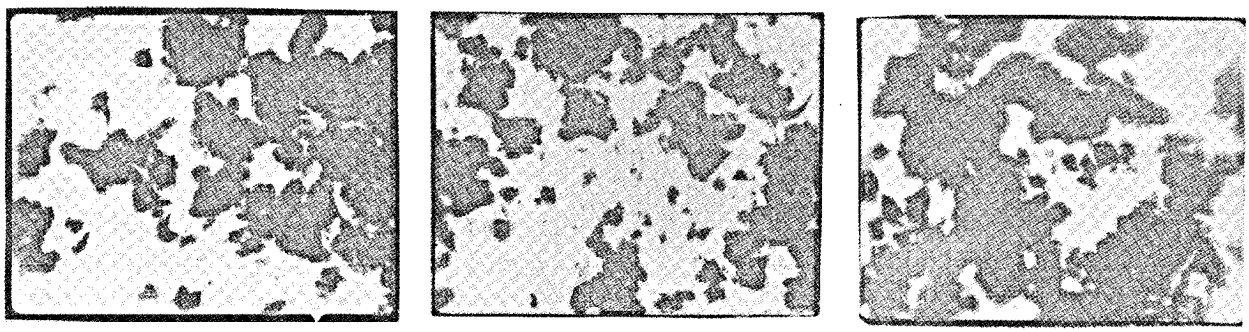

a b c

Figure 5 TEM micrographs of C_3A with 10% gypsum and 0,2% DMTP, hydrated 1 day (a), 3 days (b) and 7 days (c).

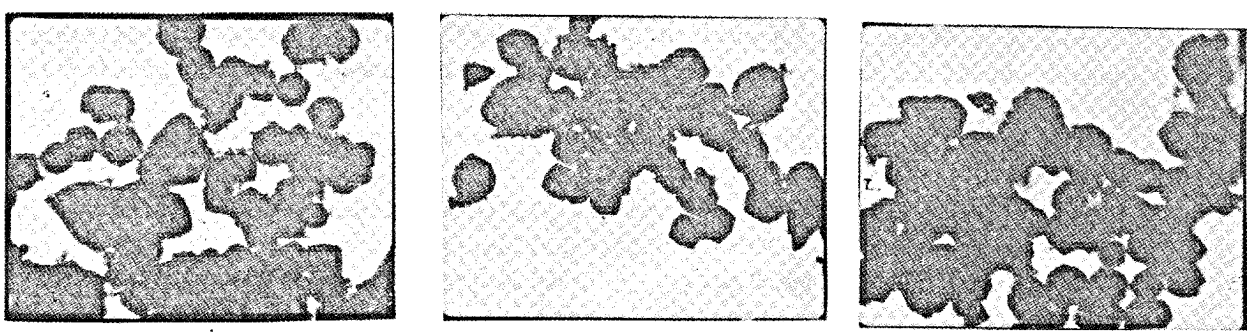

a b c

Figure 6 TEM micrographs of C_3A hydrated 1 day (a), 3 days (b) and 7 days (c).

Table 1 Compressive strength of C_3A-based hardened mortars with and without additions

type of environment	investigated system	water binder ratio	Blaine surface area (cm^2/g)	Compressive strength in daN/cm^2 on cubes with l=1,5cm, after:			
				1 day	3 days	7 days	28 days
humid	C_3A-water	1,o	299o	0	0	0	10,5
	C_3A-additions--water	0,90	3080	53,0	72,0	142,0	175,0
air	C_3A-water	0,85	2550	12,5	11,5	25,0	27,5
		1,0	2990	-	8,0	11,0	14,0
	C_3A-additions--water	0,85	2620	55,0	153,0	186,5	278,0
		0,90	3080	67,0	-	187,0	294,0

References

1. G.I.Shin, F.P.Glasser - Cem.and Concr. Res. 13,(3),366,1983
2. S.Chatterji - Proc. of the 7th Congress on the Chem. of Cement, Paris, vol.4, p.595, 1981
3. V.M.Kolbasov a.o. - idem 2, p.455
4. S.Chatterji - Indian Concr. Journal 41, p.161, 1967
5. S.Monosi, G.Moriconi, M.Collepardi - Cem. and Concr. Res. 13,(4),568,1983
6. C.Tashiro, J.Oba - Cem. and Concr. Res. 9,(2),253,1979.

Ion Teoreanu,Ecaterina Andronescu, Institute Politechnique Bucharest,Roumanie. 1

Le comportament,dans le processus de durcissement,des certaines compositions du système $3CaO.SiO_2$ - $2CaO.SiO_2$ - $2BaO.SiO_2$

The behaviour of certain compositions belonging to the $3CaO.SiO_2$ - $2CaO.SiO_2$ - $2BaO.SiO_2$ system, during hardening thereof. 3.3

SOMAIRE:Le système $3CaO.SiO_2$ - $2CaO.SiO_2$ - $2BaO.SiO_2$ présente une importance essentielle pour les ciments silicates, de calcium et baryum.
Les compositions considerés dans le système $3CaO.SiO_2$ - $2CaO.SiO_2$ - $2BaO.SiO_2$ ont été analysées sous l'aspect de la formation des phases minéralogiques et de leur réactivité par rapport à l'eau.
La formation des phases minéralogiques a été evaluée à l'aide de la diffractométrie à rayon X.
En tant que phases , ont été mises en évidence le silicate tricalcique et solutions solides de silicate dicalcique - silicate dibaryque.
La formation des solutions solides $2CaO.SiO_2$ - $2BaO.SiO_2$ détermine une augmentation du degré de désordre de la structure, avec effets positifs sur l'activité hydraulique .
L'activité hydraulique a été évaluée par déterminations de : la conductivité electrique en suspensions aqueuses , la resistance mécanique et le degré de hydratation.
Les résultats obtenus permetent l'appréciation du comportament liant des certaines compositions appartenant au système $3CaO.SiO_2$ - $2CaO.SiO_2$ - $2BaO.SiO_2$.

O sistema $3CaO.SiO_2$ - $2CaO.SiO_2$ - $2BaO.SiO_2$ é essencialmente importante para os silicatos de cimento de cálcio e de bário.

As composições consideradas no sistema $3CaO.SiO_2$ - $2CaO.SiO_2$ - $2BaO.SiO_2$ foram analisadas sob o aspecto da formação de fases mineralógicas e de sua reatividade em relação à água.

A formação das fases mineralógicas foi avaliada por meio de difratometria de raio X.

No que se refere às fases, foram evidenciados o silicato tricálcico e soluções sólidas de silicato bicálcico - silicato dibárico.

A formação das soluções sólidas $2CaO.SiO_2$ - $2BaO.SiO_2$ determina um aumento do grau de desordem da estrutura, com efeitos positivos sobre a atividade hidráulica.

A atividade hidráulica foi avaliada através de determinações de: condutividade elétrica em suspensões aquosas, resistência mecânica e grau de hidratação.

Os resultados obtidos permitem a apreciação do comportamento ligante de certas composições pertencentes ao sistema $3CaO.SiO_2$ - $2CaO.SiO_2$ - $2BaO.SiO_2$.

ION TEORBANU, ECATERINA ANDRONESCU

The behaviour of certain compositions belonging to the $3CaO.SiO_2$ - $2CaO.SiO_2$ - $2BaO.SiO_2$ system, during hardening thereof. 3.3

Le comportament, dans le processus de durcissement, des certaines compositions du système $3CaO.SiO_2$ - $2CaO.SiO_2$ - $2BaO.SiO_2$

INTRODUCTION

Le système $3CaO.SiO_2$ - $2CaO.SiO_2$ - $2BaO.SiO_2$ (C_3S - C_2S - B_2S) présente une importance essentielle pour les ciments silicatiques de calcium et baryum.

Dans le cadre du système C_3S - C_2S - B_2S, le silicate dicalcique et le silicate dibarique forment par substitution isomorphique des cristaux mixtes, en composition $mCaO$. $nBaO$. SiO_2, où $m + n = 2$ /1-4/.

La substitution des atomes de calcium, dans le reseau de l'orthosilicate de calcium, par des atomes de baryum, conduit à l'accomplissement de la stabilisation des changements en haute température du silicate dicalcique /1,4/.

RESULTATS EXPERIMENTAUX ET LEUR INTERPRETATION

Pour mettre en évidence l'évolution des propriétés liantes dans le système C_3S - C_2S - B_2S, on a considéré les compositions ternaires, présentées en pourcentages oxydiques et minéralogiques dans le Tableau Nr.1.

no.	Composition oxydique (% Gr)			Composition minéralogique (% Gr)		
	CaO	BaO	SiO_2	C_3S	C_2S	B_2S
1	62,51	8,36	29,13	45	45	1o
2	55,52	16,72	27,76	4o	4o	2o
3	48,58	25,o8	26,34	35	35	3o
4	67,8o	4,18	28,o2	47,5o	47,5o	5
5	58,6o	8,36	33,o4	-	9o	1o
6	66,32	8,36	25,32	9o	-	1o
7	56,81	16,72	26,46	55	25	2o

Les compositions présentées dans le Tableau Nr.1 ont été obtenues à partir de $CaCO_3$, $BaCO_3$ et SiO_2 (non-cristallin), tous de haute pureté (au-dessus de 99,8%). A partir des mixtures dosées conformément au Tableau Nr.1 et homogénéisées d'une manière appropriée, on a réalisé, par compression à 1loo - 12oo daN/cm^2, des compositions qui ont été traités thermiquement dans l'intervalle de température de 135o à 145o°C. maintenus à la température maxima à 0 jusqu'à 4 heures, après quoi ils ont été refroidis rapidement.

Après chaque traitement thermique, on a poursuivi la formation des phases minéralogiques, par diffraction des rayons X et on a déterminé par analyse chimique le contenu en oxyde de calcium libre.

Les compositions traitées thermiquement pendant 4 heures à 145o°C ont présenté les moindres valeurs d'oxyde de calcium non-lié (au-dessous de 1%), raison pour laquelle elles ont été choisies en vue de tester le comportement liant.

Il est bien connu que les propriétés liantes d'un ciment sont en dépendance de son degré de dispersion et de sa composition en phases. En ce qui concerne leur état de dispersion, les compositions ternaires considérées dans le système C_3S-C_2S-B_2S ont été ramenées aux surfaces spécifiques Blaine, contenues dans l'intervalle à valeurs de 4135 - 4245 cm^2/g. La composition en phases a été analysée par mesurages de la diffraction des rayons X, à l'aide d'un diffractomètre Karl-Zeiss Jena TUR-M-62. Les résultats obtenus ont mis en évidence, dans toutes les compositions considérées, la présence de deux phases; en silicate tricalcique et en solutions solides de α'-silicate dicalcique. Dans les cristaux mixtes de α'-C_2S (ss), la substitution des atomes de calcium par des atomes de baryum pro-

que la déformation de la cellule élémentaire du α'-C_2S, c'est à dire son allongement selon l'axe "a", comme il en ressort des données présentées dans le Tableau Nr.2.

Dans le Tableau Nr.2, on a fait inscrire les dimensions de la cellule élémentaire pour $\alpha'C_2S$ (indexées dans /5/, comme aussi celles correspondantes aux cristaux mixtes (à proportions variables de B_2S) :

Tableau Nr.2

Composition	Paramètres de la cellule élémentaire /Å/		
	a	b	c
α'-C_2S	1o,73	18,41	6,75
1	11,o7	18,4o	6,74
2	11,47	18,37	6,71
3	12,o5	18,3o	6,6o

Le comportement des compositions ternaires étudiées, concernant la capacité d'interaction avec l'eau et de développement de certaines structures résistantes de durcissement est mis en évidence, d'une manière corroborée, par :

- mesurages de conductivité électrique des suspensions aqueuses;
- déterminations des degrés de hydratation;
- évaluation des résistances mécaniques à la compression.

La conductivité électrique des suspensions aqueuses, déterminée avec le conductimètre type OK - 1o2/1 RADELKIS - HUNGARY, est presentée dans la figure Nr.1.

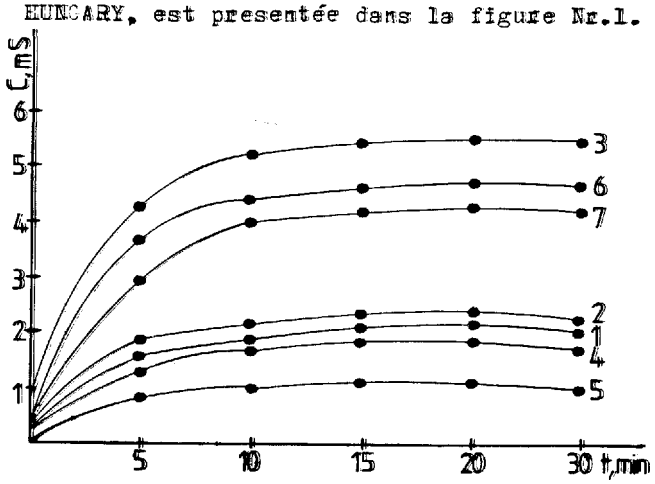

Fig.1 - La conductivité électrique des suspensions aqueuses

Les résultats obtenus mettent en évidence des croissances importantes de la conductivité des suspensions aqueuses, en particulier dans les premières 15 minutes s'ensuivant après la dispersion dans l'eau déionisée de la composition pulvérulent.

En ce qui concerne la réactivité, les compositions examinées peuvent être réparties en trois catégories :

- les compositions 3,6 et 7 - les plus reactives;
- les compositions 2,1 et 4 - avec une réactivité intermédiaire;
- la composition 5 - moine réactive

La répartition par groupes des sept compositions précitées a été justifiée soit par le contenu élevé en Ba^{2+} (la composition 3), soit par la valeur importante du silicate tricalcique dans leur composition (6,7) dans le cas des compositions plus réactives, comme asussi par la grande proportion d'orthosilicate de calcium (5) dans le cas de la composition moine réactive.

Le degré de hydratation a été déterminé par des mesurages roentgénographiques, effectués après 1,3,7 et respectivement 21 jous à partir de la réalisation des pâtes avec le rapport eau/liant; o,4.

Les résultats obtenus sont présentés graphiquement dans la figure Nr.2.

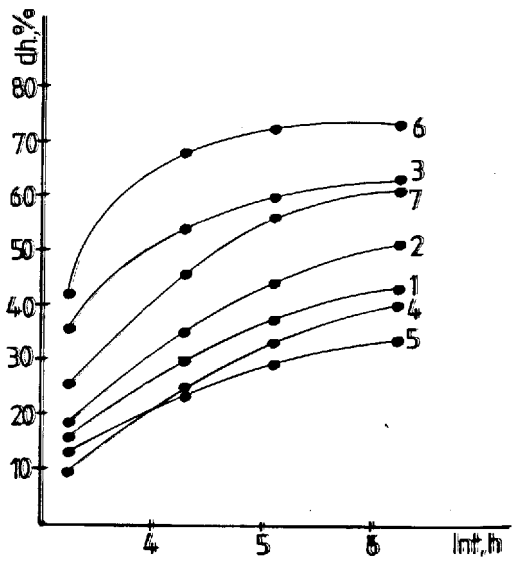

Fig.2 -La variation du degré de hydratation

ION TEOREANU , ECATERINA ANDRONESCU

3.3

Suite aux données enregistrées,on peut faire les affirmations suivantes:
- le plus important degré de hydratation a été observé à la composition 6, conséquence de son contenu élevé en silicate tricalcique;
- pour les compositions 3 et 7, après 21 jours de durcissement, on obtient des degrés de hydratation rapprochés, malgré leur différentiation en ce qui concerne les compositions (voir le Tableau Nr.1);il en ressort que la proportion plus élevée en B_2S - comme solution solide avec C_2S de la composition 3- fait balancer la baisse du contenu en C_3S par rapport à la composition 7(dans les limites où cette baisse a eu lieu);
- pour toutes les autres compositions on peut constater un parallélisme distinct avec les résultats des déterminations de la conductivité électrique - mesurage de l'intensité de l'hydrolyse initiale en suspensions aqueuses de liants.

Le comportament mécanique a été évalué par déterminations de résistance mécanique à la compression, sur microéchantillons avec ϕ=2omm et h=2omm,réalisés à partir des mortiers normaux (la granulométrie du sable o,16-o,25mm),conservés en atmosphère humide.

Les valeurs des résistance mecaniques à la compression sont représentées dans Fig.3.

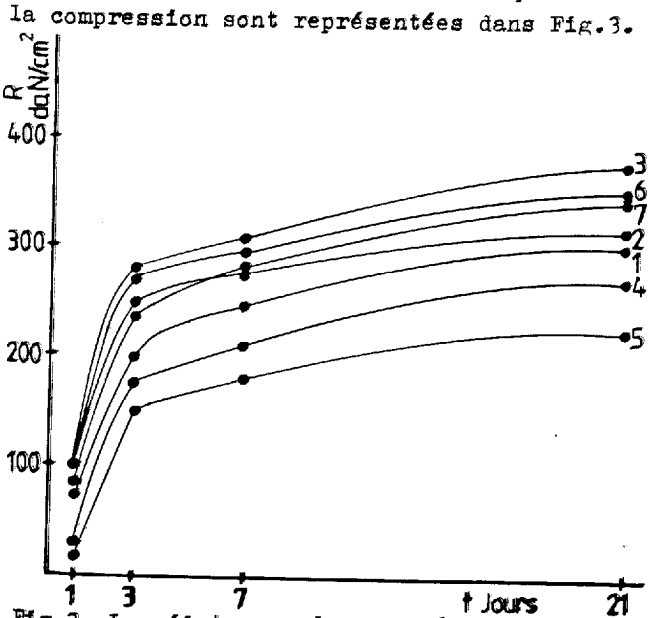

Fig.3.-La réistance mécanique à la compression

Les résultats enregistrés mettent en évidence d'importantes croissances des résistances mécaniques, particulièrement dans les premiers 7 jours de durcissement.

Les plus grandes résistances mécaniques , après 21 jours, ont été obtenues pour les compositions 3,6 et 7 , succédées aux différences de plus en plus importantes par les compositions 2 , 1 , 4 et 5.

Le comportament mécanique différencié est en rélation avec la composition minéralogique et avec la structure des phases presentes.

De cette manière , les compositions 6 et 7 juissent d'un contenu élevé en silicate tricalcique , mais aussi de la présence positive du Ba^{2+} dans le reseau $\alpha C'$ de l'orthosilicate de calcium. Le rôle positif du Ba^{2+} ressort d' une manière convaincante du comportement général de la composition 3 (avec le contenu le plus élévé en Ba^{2+}) , l'effet favorable du Ba^{2+} représentant en fait une totalisation de plusieurs effets.

D'une part , le Ba^{2+} intervient dans le processus de synthèse des phases minéralogiques , par la formation d'une phase intermédiaire siliceuse - riche en Ba^{2+} - qui facilite les processus de diffusion , probablement à l'aide des structures "dérangées", à grande concentration de défauts /1,4/.

D'autre part , le Ba^{2+}, par son intégration en cristaux mixtes avec l'orthosilicate de calcium, joue aussi un double rôle positif :

- il détermine la stabilisation plus réactive de la forme α'-C_2S et mène à la réalisation des cristaux mixtes , dont la structure présente une grande concentration de défauts, fait qui apporte son contribution à la croissance de la réactivité / 1/ ;
- en même temps, la présence du

Ba^{2+} détermine une cinétique accélérée des processus de hydratation-hydrolyse, en urgentant la formation des hydro-silicates et le durcissement du système liant.

CONCLUSIONS

Les recherches effectuées ont eu en vue la mise en évidence des propriétés liantes dans le système C_3S - C_2S - B_2S, les corrélations de celles-ci avec la composition des masses afférentes, y compris les applications à la production des certains ciments spéciaux.

Les résultats obtenus ont démontré que l'intégration du Ba^{2+} - par substitution isomprphe du Ca^{2+} dans le reseau de l'orthosilicate de calcium - en stabilisant C_2S (ss) dans la forme α', en tant que structure réactive, apporte son contribution à l'accroissement de la cinétique de durcissement des liants synthétisés. Ce comportement est ressorti de la réactivité chimique accrue par rapport à l'eau, exprimée par des mesurages de la conductivité électrique des suspensions aqueuses, par l'évaluation du degré de hydratation et aussi des résistances mécaniques à la compression.

Les résultats obtenus ont mis en évidence le rôle determinant de la composition minéralogique et de la structure des phases présentes, comme aussi la possibilité de pouvoir obtenir - par des modifications adéquates concernant les caractéristiques précitées - des ciments à haute résistance mécanique.

REFERENCES

1. D.Ziemer, K.H.Jost: Silikattechnik 30, 175-179 (1979)
2. D.Stavrakeva : Stroit.Mat.i.Silik. Prom. 23, 1,5, (1982)
3. D.Stavrakeva : Stroit.Mat.i.Silik. Prom. 24, 3,9-11, (1983)
4. R.G.Grebensnikov, A.Toropov : Izv.Akad.Nauk, SSSR, Otdel.Khim.Nauk 201 4, 545-55 (1962)
5. M.Regourd : Proc.5-th.Int.Symp. Chem. Cement,Tokyo,44-48, (1968)

F. TRIVIÑO, Docteur de Sciences Chimiques, CSIC Institut Eduardo Torroja (Madrid) España

CIMENT FONDU COMME EVITER LEUR DEGRADATION DES RESISTENCES MECANIQUES
ALUMINOUS CEMENT: HOW AVOID DEGRADING OF MECANIQUE RESISTENCE

SUMARY: The strength of aluminous cement specimens decreases all the time crystaline structure transforms the hexagonal system into cubic one. Such a transformation appears in a variable way as temperature changes.

The strength decrease may be avoided by different methods. Here two processes are examinated in which the thermal treatment is limited to the plastic phase of cement setting, and the strength increases as a consequence of the formation of calcium aluminate carbonate hydrates. The first process is made by mixing aluminous cement with calcium carbonate up to twenty per cent, and the second one corresponds to the thermal treatment in a CO_2 atmosphere.

Tests are fulfilled on both specimens 4 x 4 x 16 cm of cement pastes and silica mortars. Results show the strength variations as functions of temperature and duration of thermal treatment for different humidity conditions. Hence optimum processes have been proposed.

A resistência do corpo de prova de cimento aluminoso diminui todas as vezes que a estrutura cristalina se transforma de sistema hexagonal em cúbico. Esta transformação aparece de maneira variável quando a temperatura se altera.

A diminuição da resistência pode ser evitada por diferentes métodos. Aqui são examinados dois processos nos quais o tratamento térmico é limitado à fase plástica da pega do cimento, e a resistência aumenta em consequência da formação de hidratos de carboaluminato de cálcio. O primeiro processo consiste na mistura de cimento aluminoso com carbonato de cálcio até 20%, e o segundo corresponde ao tratamento térmico numa atmosfera de CO_2.

Foram testados corpos de prova de 4 x 4 x 16 cm, de pastas de cimento e de argamassas de sílica. Os resultados mostram que as resistências variam em função da temperatura e duração do tratamento térmico em diferentes condições de umidade. Por isso foram propostos os processos ótimos.

1. EFFET DE L'ADDITION DE CALCAIRE AU CIMENT FONDU

1.1. Experimental

Avec des proportions variables de CaCO de 0%, 15%, et 20% et du ciment fondu, des éprouvettes prismatiques de 4 x 4 x 16 cm furent confectionnées.

Trois types de traitement furent effectués:

1. Les éprouvettes sont placées en chambre humide. On procède à les démouler 19 heures après leur préparation.
2. Le ciment, l'eau et les moules sont chauffés à 50ºC. Une fois que les éprouvettes et les moules sont confectionnés, ils sont maintenus à 50ºC pendant 19 heures. On procède à démouler les éprouvettes, qui sont placées pendant 24 heures en chambre humide.
3. Les éprouvettes démoulées, qui étaient restées à 50ºC sont introduites dans un récipient hermétique (fig. nº 1) à 50ºC et sont traitées avec CO_2 à une pression de 0,14N pendant 5 heures. Ce temps ayant pris fin, elles sont introduites en chambre humide pendant 19 heures.

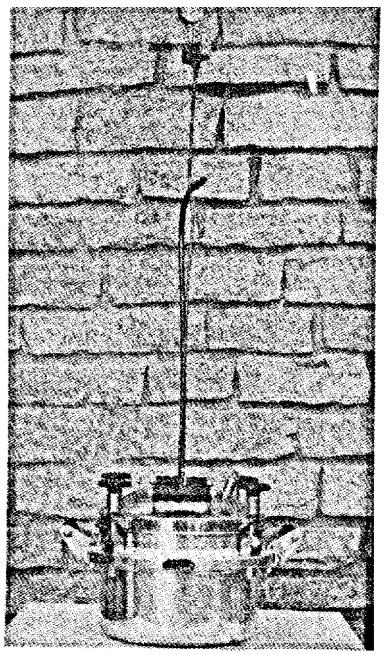

Fig. 1

1.2. Resultats

Les résultats de rupture à compression et à flexion, ainsi que ceux obtenus des difractogrammes des rayons X, des intensités relatives des composés: CA, CAH_{10}, C_3AH_6, AH_3, cC, cC_4AH_{12} sont utilisés pour confectionner les graphiques de la figure nº 2.

1.3. Interpretation et Conclusions

1.- La résistance à compression, dans les trois traitements, augmente si le contenu de $CaCO_3$ augmente.

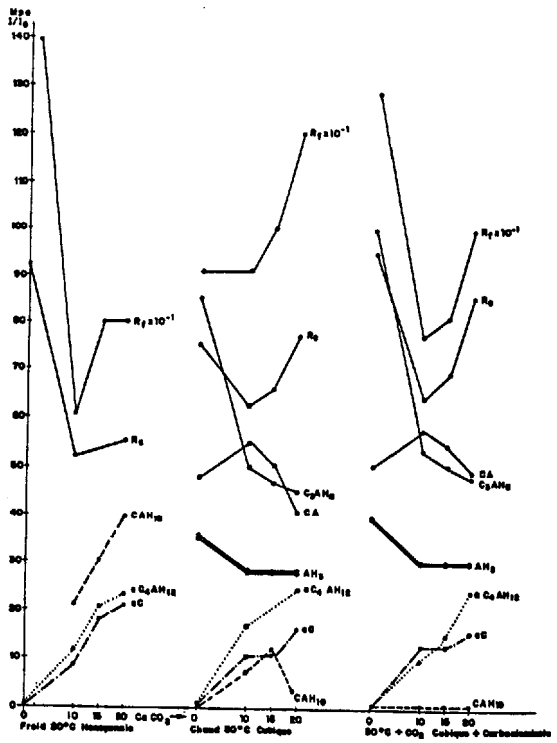

FIG. 2

2. La résistance à compression augmente-pour 20% de $CaCO_3$, en effectuant les traitments thermique et de CO_2.
3. Il y a, à réaliser le traitement thermique, une diminution de la résistance à compression -lorsqu'il n'y a pas d'adition de calcite- à cause de la réaction de $CA \longrightarrow CAH_{10} \longrightarrow C_3AH_6$, diminuant le CAH_{10} et le CA, qui remonte au moyen d'un traitement avec CO_2 avec passage partiel de $C_3AH_6 \longrightarrow CC_4AH_{12}$ et autres carboaluminates calciques hydratés.
4. La concentration de AH_3 se maintient dans les difractogrammes -ce qui indique la croissance proportionnelle- si la quantité de $CaCO_3$ augmente, c'est à dire, 10, 15 et 20% respectivement.
5. Si on effectue les traitements à 50ºC avec CO_2, la concentration de $CaCO_3$ détectée dans les difractogrammes diminue, ce qui indique que lorsque les échantillons sont chauffés, le $CaCO_3$ réactionne avec les aluminates, c'est pourquoi, rien qu'avec le traitement thermique, on obtient déjà la formation des carboaluminates calciques hydratés sans qu'il soit nécessaire d'ajouter CO_2, et en conséquence on obtient l'augmentation des résistances mécaniques.

   Las résistances à flexion diminuent avec le traitement thermique et tendent à se récupérer par carbonatation avec CO_2, ce qui indique que le type de

cristaux produits par le traitement thermique (pentagones dodécaèdres du C_3AH_6) offre une plus petite résistance à la flexion que les hexagonels du CAH_{10}, produits par le traitement à 20ºC, et aussi que les cristaux de carboaluminate calcique hydratés sous forme d'aiguilles (provoqués par la réaction avec le $CaCO_3$ ou avec le CO_2) que favorisent les résistances à flexion. Et finalement, lorsque des cristaux de calcite se forment (rhomboèdres), les résistances à flexion diminuent à nouveau. De cette façon les résistances à flexion augmentent par traitement thermique au chaud lorsque la concentration de $CaCO_3$ augmente dans le mélange et/ou si l'on traite les mélanges plus riches en $CaCO_3$ avec CO_2 (effet synergique) par formation de carboaluminates.

2. ETUDE DU TEMPS DE TRAITEMENT AVEC ADITION DE CALCITE

2.1. Experimental

Comparaison entre deux types de traitement.

1. Les éprouvettes prismatiques de 4 x 4 x 16 cm confectionnées avec ciment alumineux et 20% de $CaCO_3$, avec une relation eau-ciment de 0,235%, traitées à 20ºC en chambre humide pendant 2, 4 et 14 jours.

2. Eprouvettes égales aux premières, curées à 50ºC avec CO_2, à 2, 3, 4, 6, 9 et 14 jours.

2.2. Resultats

Les résultats apparaissent dans la figure nº 3.

Dans les deux cas on observe une augmentation des résistances à flexion et à compression avec un temps supérieur aux précédents et une chute dans les résistances à flexion entre 9 et 14 jours, dues au passage de carboaluminates à carbonate calcique, par décomposition des précédents avec le carbonique. De ce qui vient d'être dit, on peut déduire que la formation de carbonate calcique par météorisation implique une récupération des résistances à flexion initiales et une montée des résistances à compression.

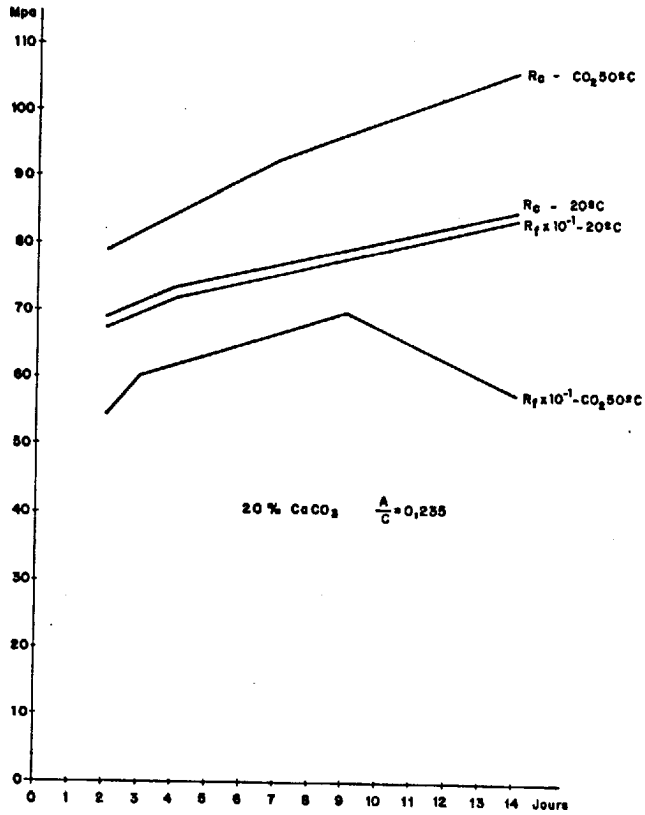

FIG. 3

3. MORTIERS SILICIQUES

3.1. Preparation des eprouvettes

Dans un malaxeur normalisé, d'après le RC-75, 1.500 grs de sable silicique normalisé, 500 gr de ciment alumineux et 214 ml. d'eau déionisée furent mélangés. Une partie du mortier fut placée dans un moule, avec trois empreintes prismatiques de 4 x 4 x 16 cm situé sur une machine à secousses normalisée, d'après le RC-75.

3.2. Le traitement des eprouvettes

Le moule couvert avec une lame en plastique (pour éviter l'ensablement superficiel) est placé dans un autocuiseur (fig. 1) où sont effectués les traitements au chaud ou à température ambiante avec CO_2. Les moules, ou seulement les éprouvettes démoulées sont séparés avec des liteaux, pour éviter le contact entre eux et avec l'eau qui se trouve quelques fois au fond de l'autocuiseur. Le couvercle de l'autocuiseur a une soupape de sûreté qu'il faut ouvrir pour retirer.

Dans le couvercle il y a aussi un tuyau pour l'accès des gaz, et un manomètre (fig. 1).

Les traitements effectués avec les éprouvettes de mortier alumineux on été les suivants:

1. $2h^{105ºC}CO_2 - H_2O$	2 Eprouvettes
2. $5h^{105ºC}CO_2 - H_2O - 5h^{105ºC} - 2h^{105ºC}CO_2$	2 "
3. $2h^{105ºC}CO_2 - H_2O - 14h^{20ºC} - 5h^{105ºC}CO_2$	2 "
4. $7h^{105ºC}CO_2 - H_2O - 2h^{20ºC} - 7h^{105ºC}CO_2$	2 "
5. $5h^{105ºC} - H_2O - 10h^{105ºC}CO_2 - H_2O$	6 "
6. $72h^{85ºC}CO_2 - H_2O$	3 "
7. $72h^{70ºC}CO_2 - H_2O$	6 "
8. $19h^{95ºC}CO_2 - H_2O$	6 "
9. $72h^{80ºC}$ - (cubique) Patron	1 "
10. $72h^{20ºC}$ - (hexagonale) Patron	2 "

3.3. Resultats

La porosité des éprouvettes a été mesurée; dont le résultat a été:

P_1 = Poids de l'éprouvette déssechée à 105ºC - jusqu'à pesée constante
P_2 = Poids de l'éprouvette saturée d'eau
P_3 = Poids sous l'eau de l'éprouvette saturée d'eau

Nous appelons porosité le cotient entre le colume des pores ouverts, $P_2 - P_1$ et le (volume apparent) $P_2 - P_3$:

$$\text{Porosité} = \frac{(P_2 - P_1)}{P_2 - P_3} = 100$$

Les intensités relatives de CA dans 2θ = 29,96º pour cuivre = 1,54 Å; C_3AH_6 dans 2θ = 17,20º; du AH_3 dans 2θ = 18,27º; du $CaCO_3$ dans 2θ = 29,40º; du cC_4AH_{12} dans 2θ = 11,64º et dans CAH_{10} dans 2θ = 6,17º ont été mesurées.

L'augmentation du poids des éprouvettes fût mesuré; elles pesaient de l'ordre de 595 à 610 gr et oscillait de 0 à 15 gr au maximum.

Ont été analysés: le contenu en CO_2, la perte au feu, l'eau à 110ºC et l'eau combinée, dont il n'y a pas de données, n'ayant pas trouve de corrélations. Les données obtenues sont représentées dans la fig. 4.

Lorsqu'on observe les résultats des traitements 9e (cubique) et 10e (Hexagonal), nous trouvons que dans le cas du nº 9 cubique, les résistances à flexion et à compression et le contenu de CA diminuent et les teneurs en C_3AH_6 et en AH_3 augmentent. La diminution des résistances mécaniques, de la conversion de l'exagonal au cubique, peut être compensées par carbonatation, comme le traitement nº 3 indique.

Dans la fig. 4 on peut observer que le traitement nº1 est insuffisant en tant que temps de carbonatation, étant donné que la teneur en C_3AH_6 est grande et petite en cC. Le traitement nº 2 n'augmente pas les résistances mécaniques puisque, pendant la deuxième étape du traitement la température s'élève à 110ºC, l'éprouvette se dessèche et absorbe mal le CO_2. Les caractéristiques des composants produits sont similaires à celles du 1er cas. Le traitement nº 3 améliore les résistances mécaniques atteignant des valeurs pratiquement égales aux initiales , avec le même temps de carbonatation et une deuxième étape du traitement à une température plus basse (20º). Dans les difractogrammes on observe une descente du C_3AH_6, une élévation de la teneur en $CaCO_3$, ayant comme résultat l'augmentation du poids de l'éprouvette.

Avec le traitement nº 4, le temps de carbonatation augment (7 heures), le résistance à flexion cependant diminue, la résistance à compression augmente légèrement, et la teneur en $CaCO_3$ et C_3AH_6 s'abaisse, ce qui veut dire qu'il n'est pas rentable par rapport au précédent.

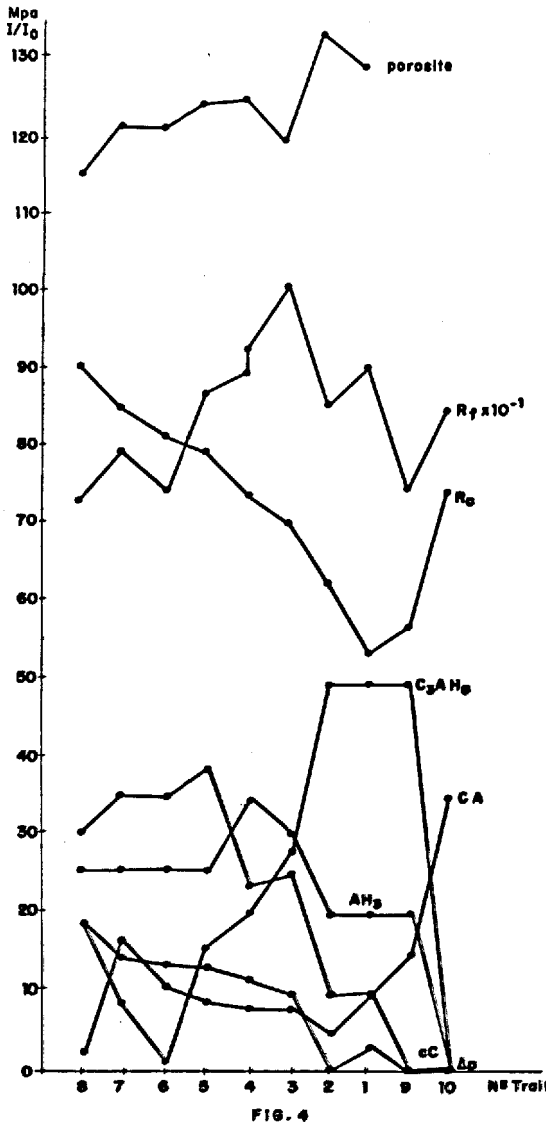

FIG. 4

Le traitement nº 5 donne le maximum de $CaCO_3$, une diminution conséquence du C_3AH_6 qui se décompose, une augmentation de la résistance à compression et une diminution de la résistance à flexion. Dans ce cas, le temps de carbonatation est aussi inférieur au précédent. Les résistances à flexion diminuent et les résistances à compression augmentent lorsqu'il y a formation de carbonate calcique.

Les traitements nºs 6 et 7, très longs (72 heures), arrivent à des résistances plus grandes à compression mais avec des résistances à flexion semblables à celles de forme cubique qui, d'après les difractogrammes, disparaît lorsque la température du traitement avec CO_2 est de 85ºC, et il en reste un peu lorsque le traitement avec CO_2 est effectúe à 70ºC.

Finalement, le traitement qui a donné les meilleurs résultats en tant que résistance à compression, c'est le traitement nº 8. Dans celui-là, la carbonatation s'effectue durant 19h à 95ºC avec CO_2 à 0,14 MPa en milieu humide, et le traitement se poursuit sans CO_2 en milieu humide, pendant 43 heures, à 110ºC. Dans ce cas l'aluminate calcique disparaît complètement, et la formation de calcite est plus faible que dans le cas précédent; l'éprouvette à une augmentation de poids relatif très forte (18 grammes), c'est à dire 3% réel de l'augmentation du poids, il y a formation de quelque C_3AH_6 après la carbonatation - avec le CA qui restait avec le traitement avec CO_2, en chauffant l'éprouvette à nouveau-. La résistance à compression est remarcable, 90 MPa, bien que la flexion descende à 7,2 MPa; la porosité du mortier est la plus basse obtenue.

3.4. Observations

- Lorsque les éprouvettes sont curées sous l'eau, la résistance à compression descend et la résistance à flexion augmente, ce qui, dans la pratique,n'est pas utilisable; mais il faut en tenir compte pour obtenir des résultats comparatifs.
- L'augmentation de poids dans les éprouvettes s'avère la méthode plus simple et plus économique à prouver le degré de carbonatation des éprouvettes, et il est en relation avec l'augmentation des résistances à compression, étant donné que cette formation est due à la formation de calcite, aragonite et/ou vatérite.
- Pendant l'hydratation du ciment alumineux à 20ºC, une partie de l'aluminate calcique rest toujours sans s'hydrater. Si le temps d'hydratation au chaud a été suffisant, tout l'aluminate monocalcique est hydraté.

Si la carbonatation a duré et a été suffisante, il ne doit pas rester d'aluminate tricalcique hexahidraté car celui-là doit se décomposer, par carbonatation, en aragonite, vatérite, calcite, alumine et/ou hydroxides d'aluminium.

A fin de trouver les conditions optimales du traitement, dans un temps raisonnable, une autre série d'éprouvettes prismatiques de 4 x 4 x 16 cm fût préparée avec: 500 gr de ciment alumineux, 1.500 gr de sable normalisé et 220 ml d'eau déionisée. Les moules des trois éprouvettes fût chauffé à 100ºC ainsi que le ciment, l'eau et le sable. La température du moule des éprouvettes fût maintenue à l'intérieur du cuiseur pendant 4 heures. Elles furent ensuite démoulées et soumises aux traitements et aux cures suivants:

1. 24 heures à 100ºC avec eau et CO_2 curé 24 heures sous eau
2. 28 heures à 20ºC avec eau et CO_2 curé 24 heures à l'air
3. 24 heures à 20ºC avec eau et CO_2 curé 24 heures à l'air
4. 24 heures 100ºC avec eau et CO_2 curé 24 heures chambre humide
5. 24 heures 100ºC avec eau et CO_2 curé 24 heures à l'air

Les résultats des résistances mécaniques à flexion et compression se trouvent dans la figure nº 5.

On observe l'augmentation des résistances à flexion lorsque la curé est effectuée sous l'eau ou avec humidité à saturation. De toute façon notre opinion est que les augmentations de la résistance mécanique, de quelque 2 MPa, ne se produisent pasen réalité, car les ouvrages ne subissent pas ces conditions d'humidité, donc, les résultats sont fictifs. La résistance à compression la plus élevée se trouve dans les deux derniers traitements qui impliquent un temps élevé de 24 heures de carbonatation.

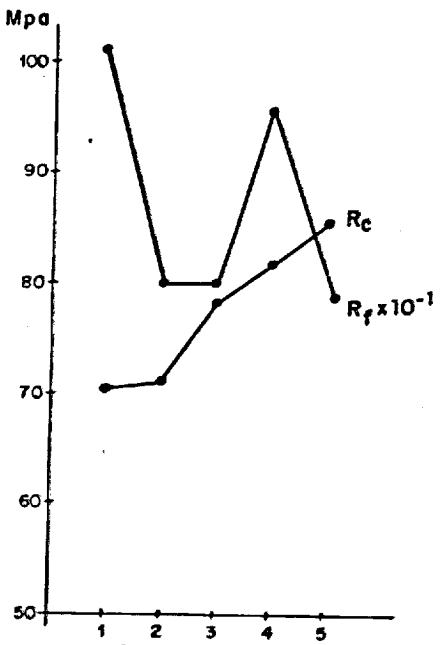

FIG.5

La carbonatation pourrait être effectuée industriellement en utilisant les gaz de combustion qui se perdent très souvent sans utilisation ultérieure dans de nombreuses industries; de même les températures employées peuvent être obtenues avec les gaz industriels entre 80ºC et 100ºC qui se perdent dans de nombreux procès, tels que fusions de fer et autres métaux, centrales thermiques, chauffage, fabrication de ciments, de fer, de sucre, en général de tout procès industriel qui comporte une combustion, surtout dans les cas ôu la récupération de chaleur n'est pas effectuée avec efficacité.

Les procès, en général implique une accélération des phénomènes qui se succèdent d'une façon naturalle

dans l'hydratation di ciment alumineux tout au long de plusieurs années..Si on accélère ces procès, les réactions intermèdes sont évitées, avec une économie d'eau consumée, ce qui bénéficie les résistances mécaniques et empêche leur dégradation. Il y a une série de réactions qui, même étant thermodinamiquement stables au contact avec le gaz carbonique de l'air, cessent de l'être; ce qui produit une augmentation des résistances mécaniques et une diminution dans les résistances à flexion, mais toujours plus petites que celles produites par une conversion à travers l'aluminate calcique deca-hydraté.

BIBLIOGRAPHIE

1º.- On the carbonation mechanism of calcium aluminate hexahydrate in hydrated high alumina-cement. Suppementary paper Section III - III - 4 The VI International Congres on the chemistry of cemert Set. 1974. Moscow.

2º.- Estudio de las transformaciones del cemento aluminoso hidratado mediante las técnicas de di - fracción de Rayos X, Espectrometría Infrarroja y Análisis Térmico. Influencia del anhídrido carbónico, temperatura, humedad y adición de caliza en polvo. T. Vázquez, F. Triviño, A. Ruiz de Gauna. Materiales de Construcción nº 157 43-70. 1975 nº 158, 1-48. 1975. Monografía número 334. Julio 1976.

3º.- On the carbonation mechanism of calcium aluminato hexahydrate in hydrated hig alumina cement. Research working papers nº 31. Noviembre 1975. I.E.T.c.c. (Madrid-33).

4º.- Nuevo procedimiento de fabricación de elementos prefabricados de hormigón de cemento aluminoso que no experimentan transformaciones perjudiciales. Patente nº 423.305. C.S.I.C. España 1974.

5º.- Study of stabilized phases in high alumina cement mortars. M. Pérez, T. Vázquez, F. Triviño. Cement and Concrete Research. Vol. 13 759-770 1983. Vol. 14 1-10 - 1984.

6º.- Aspectos físico-químicos y estabilización de los aluminatos cálcicos resultantes de la hidratación del cemento aluminoso. M. Pérez Méndez, Fernando Triviño. Informes de la Construcción nº 332. 1981.

J. F. MacDowell, Corning Glass Works, Sullivan Park FR-53, Corning, New York 14831 USA

Hydrogarnet-Gehlenite Hydrate Cements from $CaO-Al_2O_3-SiO_2$ Glasses

Ciments de Granate Hydrate-Hydrate de Gehlénite des Verres du Système $CaO-Al_2O_3-SiO_2$

SUMMARY: Calcium aluminosilicate glasses within a composition region between 45% and 55% CaO, 12% and 26% SiO_2, and 22% and 40% Al_2O_3 formed hydraulic cements containing hydrogarnet C_3AH_6 and gehlenite hydrate (C_2ASH_8). The glasses were ground to about 10-15 microns average particle size and a uniform specific surface area of 3500 to 5000 cm^2/g and cured without activators. The majority of glass cements within the area studied formed a mixture of hydrogarnet solid solution with silicate (grossular) garnet [$C_3AS_xH_{(6-2x)}$] and gehlenite hydrate [C_2ASH_8]. The latter phase was dominant in cements with greater than 20 wt. % SiO_2 and the former phase dominant in cements with less than 15% SiO_2.

Although C_2AH_8 "superhydrate" was observed first during 25°C cure of the lower SiO_2 (<15%) compositions, hydrogarnet was the dominant phase before the final set. At higher SiO_2 (>15%) levels, both hydrogarnet and gehlenite hydrate formed directly.

Scanning electron microscopy indicates that hydration of the higher SiO_2 glass cement grains proceeds linearly to completion, indicating a hydration mechanism involving simultaneous precipitation of the intergranular material to gehlenite hydrate vis a vis the through-solution mechanism normally postulated for high alumina cements.

Moderate compressive strengths (5-15M psi), high porosities (20-30%), and excellent thermal and chemical stability characterize the predominantly hydrogarnet cements, where as high strengths (15-25M psi), very low porosities (1 to 10%) and instability above 100°C are characteristics of the gehlenite hydrate cements.

Evaluation of these cements for commercial use is suggested.

Vidros de aluminossilicato de cálcio com uma região de composição entre 45-55% de CaO, 12 - 26% de SiO_2 e 22 - 40% de Al_2O_3 formaram cimentos hidráulicos contendo hidrogranada C_2AH_6 e hidrato de gelenita (C_2ASH_8). Os vidros foram moídos até um tamanho médio de partícula de 10-15 mícrons e a uma área de superfície específica de 3.500 a 5.000 cm^2/g, e curados sem ativadores. A maioria dos cimentos de vidro na área estudada formaram uma mistura de solução sólida de hidrogranada com granada de silicato (grossular) [$C_3AS_xH_{(6-2x)}$] e hidrato de gelenita (C_2ASH_8). A última fase era dominante em cimentos com mais de 20% em peso de SiO_2, e a primeira era dominante em cimentos com menos de 15% de SiO_2.

Embora o "superhidrato" C_2AH_8 fosse observado primeiro durante a cura a 25°C das composições com SiO_2 mais baixo (<15%), a hidrogranada era a fase dominante antes da pega final. Com índices mais altos de SiO_2 (>15%), houve formação direta de ambos, hidrogranada e hidrato de gelenita.

A microscopia eletrônica de varredura indica que a hidratação dos grãos de cimento de vidro com SiO_2 mais alto se processa linearmente até completar-se, indicando um mecanismo de hidratação que envolve precipitação simultânea de material intergranular em hidrato de gelenita, vis-a-vis com o mecanismo de trans-solução normalmente postulado para cimentos de alta alumina.

Resistências moderadas à compressão (5-15M psi) porosidades altas (20-30%), e excelente estabilidade térmica e química caracterizam os cimentos predominantemente de hidrogranada, enquanto resistências altas (15-25M psi) porosidades muito baixas (1 a 10%) e instabilidade acima de 100°C são características dos cimentos de hidrato de gelenita.

Sugere-se a avaliação destes cimentos para uso comercial.

I. Introduction

Since the late 1960's, the structural (load-bearing) uses of calcium aluminate cements have been severely restricted or banned in most countries of the world. These CA-based high alumina cements carry a stigma of unreliability that originates from several catastrophic failures in England and on the Continent.[1] The failures were traced to chemical instability of the first-formed hydrate phases, CAH_{10} and C_2AH_8, which tend to "convert" over time to C_3AH_6 (hydrogarnet) and AH_3 (gibbsite), releasing considerable water during the process. The conversion can be accompanied by up to 50% densification, increases in porosity, and dramatic losses in strength.[2]

Although several means have been devised to reduce the chances or extent of conversion (e.g., reducing the w/c ratio, organic additions, curing and maintaining use temperatures below 30°C), structural use of high alumina cements (HAC) is still considered a poor risk.[3]

The underlying logic in the current study is that C_3A-based cements should, from a purely chemical standpoint, form the higher hydrates (CAH_{10} and C_2AH_8) much less readily than the commercial CA-based varieties. In other words, compositional restrictions of the same type as when lower water content tends to limit conversion to higher hydrates should prevail when, at the C_3A ratio, there is always sufficient CaO available to form the stable C_3AH_6 phase.

To further assist the kinetics of hydrogarnet formation in the C_3A-based cements, but to decrease the overall rate of hydration to a manageable level, the author chose to center this study of cement formation and hydraulic activity around $CaO-Al_2O_3-SiO_2$ glasses along the C_3A-S compositional tie-line.

Perhaps the most significant consequence of this study was the discovery of stable gehlenite hydrate cements that did not require activators for their formation. Locher[4] extensively studied hydration of $CaO-Al_2O_3-SiO_2$ glasses and concluded: 1) activators such as portland cement clinker, gypsum, or $Ca(OH)_2$ were required to produce practical rates of hydration in glasses near the gehlenite stoichiometry, and 2) a major gehlenite hydrate constituent of strength could only be inferred because of the conversion of gehlenite hydrate to hydrogarnet by the excess lime in the activators.

In the current study, stable gehlenite hydrate cements were formed directly from glass cements without activators. Furthermore, some of these cements displayed high early strength and an unusually dense structure. A rather broad compositional range of glass cements were found that cured to a mixture of the two hydrated phases, hydrogarnet (HG) and gehlenite hydrate (GH).

II. Experimental

To obtain inclusion-free glass, one kilogram of oxide batch was 1) dry ballmilled to achieve homogeneity, 2) melted in 500 cc 80 platinum-20 rhodium crucibles at 1550-1650°C for 2 hours, and 3) quenched between water-cooled steel rollers or poured into cold tap-water (drigaged).

The quenched ribbon or drigage cullet was then crushed in a Bico crusher and ballmilled in a #1 Jar using 7/8" Al_2O_3 cylinders for about 8 hours to an average particle diameter of between 8 and 15 microns. Specific surface area (Blaine) was measured on selected glass powders and varied between 3500 and 5000 cm^2/g.

Raw materials used for the glass melts with their respective oxide equivalents are as follows:

Batch Material	Oxide
Supersil (-200 mesh) Sand	SiO_2
Alcoa A-14 Alumina	Al_2O_3
Limestone, Glass Stone #1	CaO
Titanox 3020 (National Lead)	TiO_2
Zircoa Standard Grade Zirconia	ZrO_2

Routine evaluations of hydraulic activity of the glass powders were accomplished by mixing 25 g with 7.5 to 10 ml of cold tap water (0.3 to 0.4 w/c ratio) using a stainless steel spatula in a flat polyethylene dish (with vibration).

The 5 cm x 5 cm x 0.5 cm neat cement squares were cured one week (unless otherwise noted) in a humidity chamber at ~25°C and >90% relative humidity.*

The square samples were initially broken by hand using finger pressure and a relative figure of merit was assigned for strength.

Compressive strengths were determined on the stronger compositions by 1) curing 25 g of cement with 7.5-10 ml. H_2O in cylindrical polyethylene capsules about 2.1 cm in diameter x 3.6 cm in height, and 2) breaking the neat cylinders in a Tinius Olsen Electomatic testing machine at a load rate of 0.125 cm/minute. X-ray diffraction analysis was performed routinely on the cement samples that displayed appreciable hydraulic activity. These routine analyses were performed using Cu Kα radiation (λ = 0.15418 nm) at 0.5 degrees/minute and chart scale at 2.5 cm per degree. Silicon, with its (111) peak at 2θ = 28.465° was used as an internal standard.

DTA and scanning electron microscopy were used as an aid to determining crystalline and gel phases present and in correlating composition and properties with microstructure.

Results and Discussion

Figure 1 shows the area of the $CaO-Al_2O_3-SiO_2$ system that was investigated for hydraulic activity. The 1600°C liquidus isotherm and the 3)% SiO_2 tieline were arbitrarily chosen as limits for our studies. There are three principal degrees of glass stability shown:

I. Greater than 2/3 of the melt could be quenched to a glass in a 1 cm thick patty when poured on a cold steel plate.

II. More than 1/3, but less than 2/3, of the melt could be quenched to a glass.

III. Less than 1/3 of the melt remained glassy under the above conditions.

*To eliminate the strong exothermic effect upon the temperature of certain fast-setting cements, curing was selectively accomplished by squeezing the pastes between two 0.5 cm thick steel or aluminum metal plates.

Figure 2 locates the principal area of hydraulic activity found during this study.

Glasses higher in SiO_2 than the enclosed polygon displayed little or no hydraulic activity. In all cases, the cements were cured without the benefit of accelerators or activators such as lime or alkali.

Hydraulic activity was judged on the basis of compressive strength - all cements within the enclosed area having at least 200 Kg/cm^2 compressive strength. Glass cement paste compositions within the lower area marked HG produced hydrogarnet solid solution as the major crystalline phase, whereas in area GH, gehlenite hydrate was the dominant crystalline phase.

HYDROGARNET CEMENTS

Pure C_3A melts did not form glass even upon rapid quenching, and hydrated much too rapidly to mix thoroughly with water before initial set. Even with up to 10 wt. % SiO_2, these highly reactive powders produced such a severe exotherm that steam was given off - sometimes for a minute or more. Set retarders such as sucrose or Plastiment* slowed the hydration, but the cured cements did not meet our strength requirement of 200 Kg/cm^2.

Between about 10 and 15 wt. % SiO_2, on the C_3A-SiO_2 tie line, glasses were formed readily, and cements containing large amounts of HG could be cured in less than 10 minutes.

C_3AH_6 is the most stable phase in high alumina cements, and is commonly formed as a result of "conversion" from CAH_{10} or C_2AH_8. Flint et al[5] postulated and Shoji[6] demonstrated that there is extensive solid solution between C_3AS_3 (glossular garnet) and C_3AH_6 (hydrogarnet). The general formula is $C_3AS_{\gamma}H_{(6-2\gamma)}$. Foreman worked out the structure of hydrogarnet and revealed that the SiO_4 tetrahedron of garnet can be isomorphously replaced by a H_4O_4 tetrahedron in hydrogarnet as illustrated in Figure 3.

This remarkable substitution is believed to be the reason that hydrogarnet retains much of the stability and durability of its anhydrous counterpart. Rodingite, a metasomatic rock found bordering areas of intense metamorphism of ultramafic materials, consists largely of hydrogarnet solid solution formed by alteration of serpentinite via removal of MgO and FeO and penetration by high lime waters.[8] As an indication of its resistance to weathering, rodingite generally stands out in positive relief in contrast to the surrounding rock species.

HG solid solution with silicate garnet was observed to occur in the cements of this study. Based upon the relationships developed by Shoji[6] where water content of HG ss is correlated with the position of the (420) x-ray reflection, the hydrogarnets synthesized during this study contained from 0.3 to 0.9 moles of SiO_2 per unit formula. [$C_3AS_{0.3}H_{5.4}$ to $C_3AS_{0.9}H_{4.2}$] depending upon the SiO_2 content of the glass cement.

Table I gives the compositions, curing times, compressive strengths, and major crystalline hydrates present after one week curing of the HG cements in Figure 2. It is seen that setting times vary inversely with SiO_2 and CaO content, and that compressive strengths seem to increase as the ratio of GH to HG increases. Figure 4 is a composite XRD trace of Compositions 2, 7, and 12, showing the shift from essentially pure HG cement in Composition #2 to pure GH in #12.

Figure 5 is a composite DTA curve comparing the major water endotherms of cements synthesized from pure C_3A (Composition #1 in Table I), pure CA (the basis for most commercial HAC cements), and $C_3AS_{0.7}$ (Composition #2)

All three curves have deep C_3AH_6 absorptions at from 350-375°C, but only the CA cement has the doublet AH_3 (gibbsite) peak immediately preceeding the hydrogarnet peak, and a CAH_{10} peak at about 100°C. Both the hydrated C_3A and Composition #2 show only one major peak, and thus show no evidence of a significant conversion event.

To eliminate the effect of the high temperature exotherm on the primary phase assemblage of C_3A-based cements during curing, a technique whereby the fluid uncured cement pastes were squeezed between two thick aluminum or steel slabs was employed. In most compositions containing less than 15% SiO_2, the first (albeit minor) phase to form during curing was C_2AH_8, but within 30 minutes to 2 hours, these broad embryonic peaks disappeared, and only HG remained.

*Sika Chemical Corp., Lyndhurst, N.J

FIGURE 1
CaO-Al_2O_3-SiO_2 SYSTEM: GLASS FORMATION BELOW 30% SiO_2

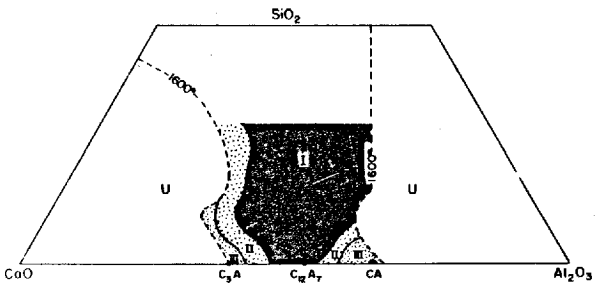

U = > 1600°C LIQUIDUS
I = > 2/3 GLASS
II = 1/3 - 2/3 GLASS
III = < 1/3 GLASS

FIG. 2.
COMPOSITION AREA STUDIED

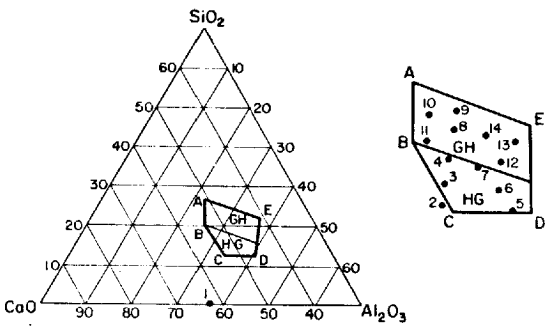

FIGURE 3.

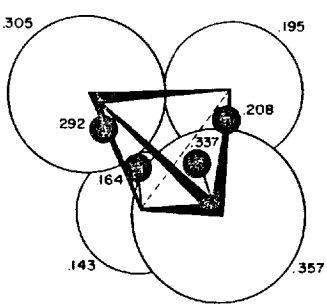

H_4O_4 TETRAHEDRON (AFTER FOREMAN[7])

TABLE I

HYDROGARNET CEMENTS

Composition Number	Wt. % SiO_2	Wt. % Al_2O_3	Wt. % CaO	Initial Set(min.)	Relative Strength	Compressive Strength (kg/cm^2)	% Porosity	Cryst. Phases
1	-	37.7	62.3	<0.1	-	-	-	C_3AH_6
Mole Ratio	0	1	3					
2	12.9	32.9	54.2	1	5	930	-	C_3AH_6
	0.7	1	3					
3	15.0	32.0	53.0	3	5	790	27.4	C_3AH_6, (C_2ASH_8)
	0.8	1	3					
4	18.2	30.9	51.0	6	7	-	-	C_3AH_6, C_2ASH_8
	1	1	3					
5	12.0	40.0	48.0	25	6	860	25.3	C_3AH_6, C_2ASH_8
	.5	1	2.2					
6	14.7	37.4	48.0	5	7	1000	20.7	C_3AH_6, C_2ASH_8
	.7	1	2.3					
7	17.0	34.0	49.0	7	5	790	-	C_3AH_6, C_2ASH_8
	.9	1	2					

FIGURE 4
X-RAY DIFFRACTION PATTERNS OF THREE HYDRAULIC CEMENTS
■ = $C_3AS_{0.5}H_5$ □ = C_2ASH_8

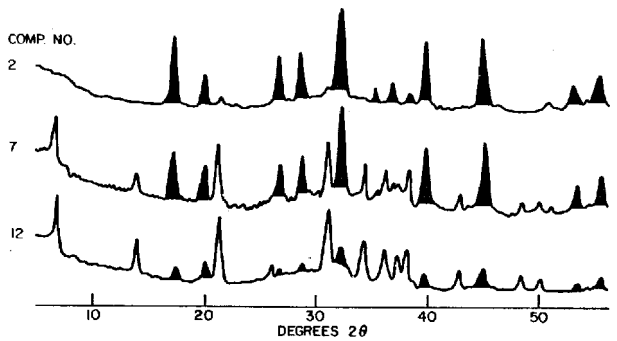

FIGURE 5
DIFFERENTIAL THERMAL ANALYSIS CURVES OF C_3A (#1), CA, AND $C_3AS_{0.7}$ (#2) CEMENTS.

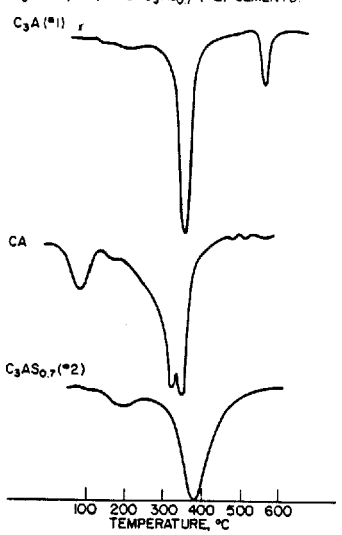

Figure 6 is a composite XRD trace, showing the curing of a 0.5 cm sample of cement paste. It can be seen that HG is the only phase present at all curing stages. From the position of the (420) peak, the composition of the hydrated #2 cement is $C_3AS_{0.7}H_{4.6}$. Thus, all of the available SiO_2 appears to have participated in forming the garnet-hydrogarnet solid solution phase. Apparently, only a very small exotherm and consequent heating of these C_3A-based cements is required to provide solubility of the higher hydrate phases and to cause direct precipitation of the stable HG.

FIGURE 6.
X-RAY DIFFRACTION STUDY OF GLASS CEMENT #2 ($C_3AS_{0.7}$) DURING CURING

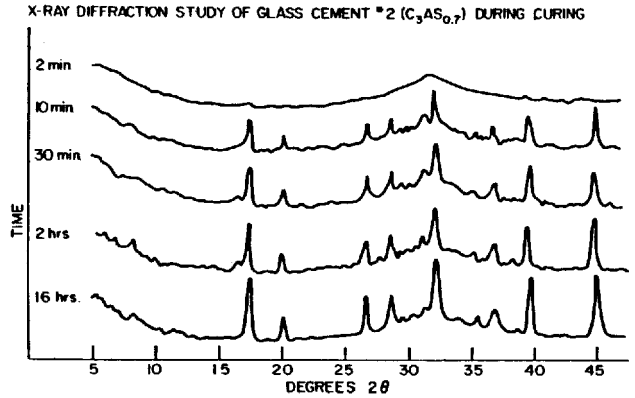

Figure 7 is an SEM (polished and etched) of cured Composition #3 glass cement revealing a structure rather typical of high alumina cements with a dense zone of hydration immediately surrounding each anhydrous core. The intergranular zone is only partially filled with a network of crystals and thus contains considerable porosity. The structure of this hydrogarnet cement is very stable and durable. Even after boiling 24 hours in water, this structure remains intact. Chemical durability is also excellent, as will be discussed subsequently.

Progressing in Figure 2 from the C_3A to the C_2A ratio and lower, the tendancy to form higher hydrates such as C_2AH_8 during the initial curing stages increases dramatically.

The pastes begin to acquire higher strengths in general as SiO_2 content is increased and as GH becomes the dominating phase.

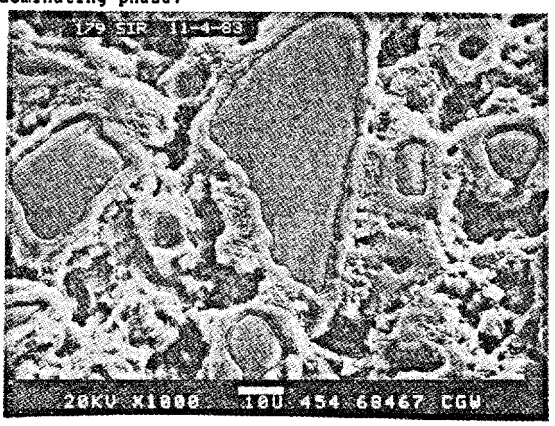

FIGURE 7 - S.E.M. of Cement No. 3 - Polished and Etched

GEHLENITE HYDRATE CEMENTS

Robson,[9] Glasser,[10] and Lea[11] all refer to gehlenite as a hydraulically inactive and therefore undesirable phase in high alumina cements. Kiel and Gille,[12] Zur Strassen,[13] Locher,[4] and Teoreanu and Georgescu,[14] however, all found that certain $CaO-Al_2O_3-SiO_2$ glasses could be hydrated with the aid of various "activators", principally lime and alkali, to form fairly strong cements. Without activators, these authors concluded that there is little significant hydraulic activity. Locher[4] was forced to infer that the major hydrogarnet phase he observed was a direct result of the breakdown of GH in the presence of his $Ca(OH)_2$-containing activator.

In the present study, the author has been able to form dense, strong, GH cements directly from $CaO-Al_2O_3-SiO_2$ glasses without the use of additives or activators.

In Figure 2, the upper area designated GH contains glass cement compositions that hydrate predominatly to C_2ASH_8. It can be seen in Table II that 1) compressive strengths, and 2) curing times both increase as compared to the hydrogarnet pastes in the lower SiO_2 section of the ABCDE diagram in Figure 2. Note also that TiO_2 and ZrO_2 additions to the ternary were made to Compositions #15, 16, and 17. These oxides seem to promote the uniform crystallization of C_2ASH_8 as described in the following paragraphs.

Figure 8A is a scanning electron micrograph of cement Composition No. 17, polished only, with a 0.4 water/cement ratio. Note the dense structure with almost total lack of pores. Figure 8B is the same composition, polished and then etched for 6 minutes with 1% EDTA + 5% NaOH solution revealing a laminar or mica-like matrix structure surrounding the unreacted portions of the glass cement grains. A micrograph at higher magnification is also included in Figure 8B to further elucidate the laminar structure.

Figure 9 contrasts the structure of Cement No. 16 with 0.4 w/c (9A) to the same composition having 0.8 w/c ratio (9B). The anhydrous glass cement grains in 9A appear to have disappeared into the matrix of gehlenite hydrate in 9B - as though they had been completely hydrated and were simply relicts of their original anhydrous parents. Figure 10 compares the XRD pattern of the

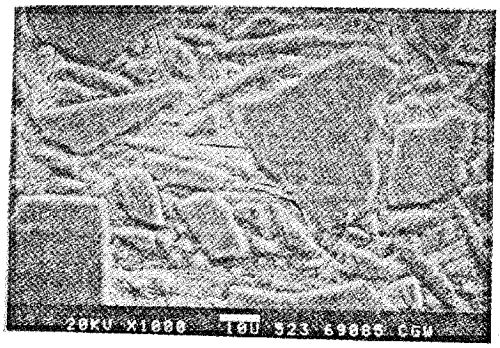

A. Polished only

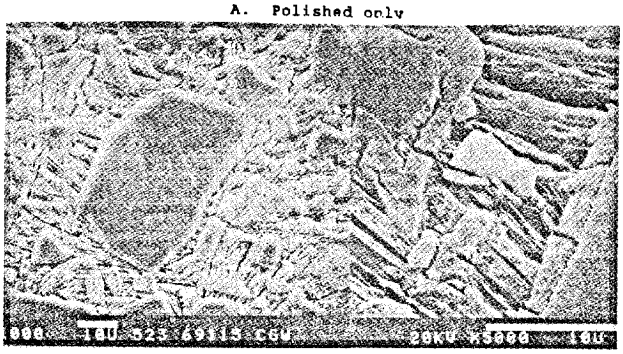

B. Etched

FIGURE 8 - S.E.M.s of Gehlenite Hydrate Cement Comp. #17, W/C ratio - 0.4

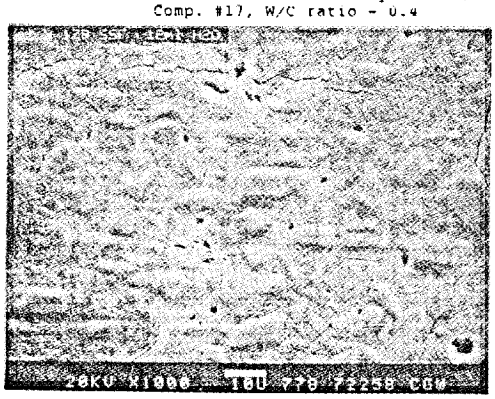

A. 0.4 W/C Ratio

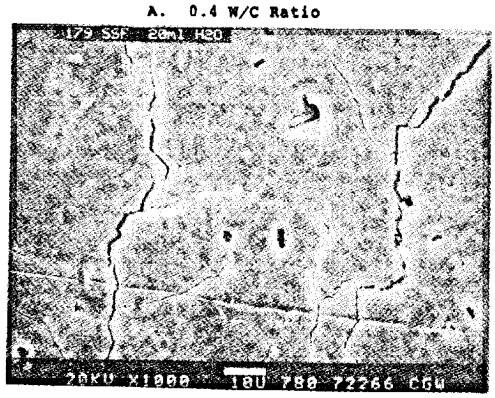

B. 0.8 W/C ratio

FIGURE 9 - S.E.M.s of Gehlenite Hydrate Cement No. 16, polished only

TABLE II.

GEHLENITE HYDRATE CEMENTS

Composition Number	Wt. % SiO_2	Al_2O_3	CaO		Initial Set(min.)	Relative Strength	Comp. Strength (kg/cm^2)	% Porosity	Cryst. Phases
8	21.7	29.5	48.7		100	9	-	-	C_2ASH_8, C_3AH_6
Mole Ratio	1.3	1	3						
9	23.4	28.9	47.7		300	8	-	-	C_2ASH_8, (C_3AH_6)
	1.4	1	3						
10	23.2	26.3	50.6			7	-	-	C_2ASH_8
	1.5	1	3.5						
11	20.0	27.5	52.5		18	7	-	-	C_2ASH_8, (C_3AH_6)
	1.2	1	3.4						
12	17.7	36.1	46.2		45	9	-	11.5	C_2ASH_8, (C_3AH_6)
	0.8	1	2.3						
13	20.0	36.0	44.0		45	6	1140	-	C_2ASH_8
	.8	1	2.2						
14	21.0	33.0	46.0		200	5	-	16.4	C_2ASH_8, C_3AH_6
	1.1	1	2.5						
15	15.7	33.3	45.8	5.2 TiO_2	45	10	1100	5.6	C_2ASH_8
	0.8	1	2.5	0.2					
16	18.5	35.0	42.3	4.2 ZrO_2	120	10	1200	-	C_2ASH_8
	0.9	1	2.2	0.1					
17	16.2	34.1	41.5	8.3 ZrO_2	240	10	1360	1.6	C_2ASH_8
	0.8	1	2.2	0.2					

FIG 10
XRD PATTERNS OF GLASS CEMENT NO 16 AT 0.4 AND 0.8 WATER/CEMENT RATIOS

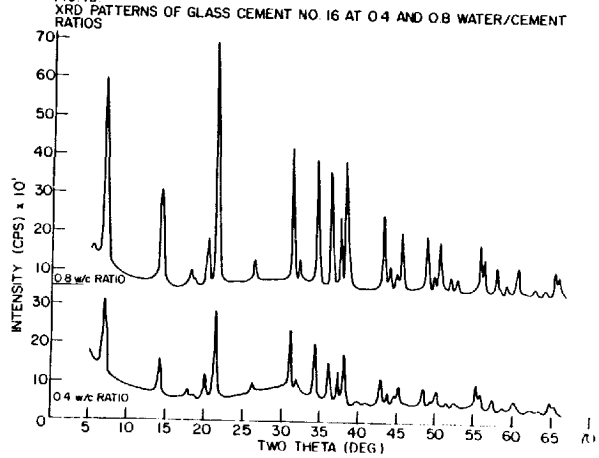

samples shown in Figure 9 (GH cement No. 16) with 0.4 (9A) and 0.8 (9B) w/c ratios. The reflection amplitudes clearly indicate that the crystallinity of the paste with the higher proportion of water is much higher - over 2 x the lower water cement. Further, the apparent lack of anhydrous cement grains in the 0.8 w/c sample (Figure 9B) and the absence of a glassy "halo" (about 30° 2θ) in Figure 10 (0.8 w/c) are convincing evidence for the almost total hydration of the original glass cement particles! There is reason to speculate that this nearly complete hydration would normally not be observed in cements that hydrate via a "direct" mechanism. In fact, a decrease in hydration rate as direct hydration progresses would be expected from a lengthening of the water diffusion path (the solid hydrate material surrounding each grain) as the thickness of the hydration layer increases. The "indirect" or "through-solution" mechanism, on the other hand, is equally unlikely to produce a very dense cement with high w/c ratio because one would expect that some of the water would be partitioned from that which forms a liquid envelope around the anhydrous grain. The almost total lack of porosity in these gehlenite hydrate cements leads the author to speculate that the original void space between particles was filled with a hydrated "gel" that formed via solution-deposition. Further, after a rather long incubation or ripening period, the gel spontaneously crystallized to C_2ASH_8 after becoming supersaturated or "ripened". It appears that solution of the anhydrous grain occurs in a virtually linear fashion until the gel is supersaturated. Then, presumably the interstices could be completely filled during an almost simultaneous crystallination of the gel, thus making possible the formation of a truly monolithic essentially void-free cement.

Hydrogarnet and Gehlenite Hydrate Cements Compared

Figure 11 is a composite of mercury porosimetry curves of four cements made during this study, one with a CA base, #2 ($C_3AS_{0.7}$), #12 (GH with some HG), and #17 (pure GH). The figure contrasts the relatively high (~30%) porosities of HG cements vs. the low porosities (high densities) of the GH cements (1.6 and 11.5%).

Stability of GH cements seems to be excellent near normal ambient temperatures, but they appear to lose some water near 100°C. HG cements, on the other hand, do not begin losing water at an appreciable rate until well over 200°C. Figure 12 is a composite DTA curve showing the phase distribution of a mixed HG-GH cement before and after treatment at 105°C and 250°C. The GH largely disappears after the 105°C treatment for 3 days, whereas the HG phase remains unchanged, even after a 250°C treatment. After boiling for 24 hours in water, the GH cements begin to break down to form HG cements.

FIGURE 11
Hg POROSIMETRY CURVES FOR FOUR CEMENTS

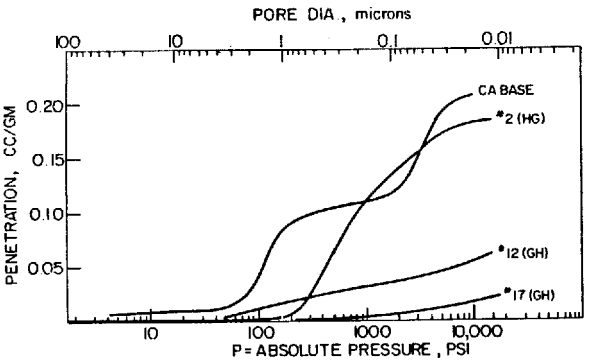

FIGURE 12
DTA CURVES OF NO. 14 CEMENT BEFORE & AFTER HEATING

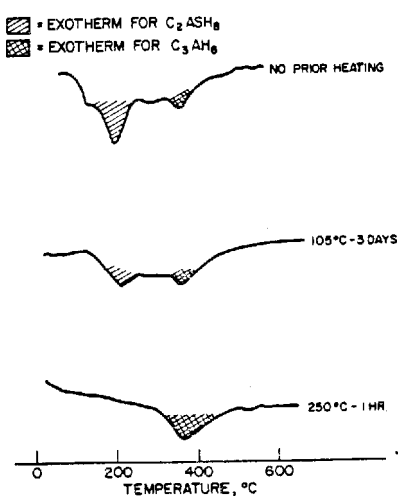

IV. Summary and Conclusions

A region of Glass Cement compositions was found during this study that appear to be novel and may become commercially useful. Single and mixed phase cements were made which developed high compressive strengths during set periods ranging from one minute to one day.

The principal attraction of the HG-silicate solid solution cements is their high thermal and chemical stability and their reluctance to form the unstable higher hydrates. It is judged that, even during adverse conditions of placement, sufficient heat from exothermic reactions would be available to form hydrogarnet directly from the C_3A-based cements. The dense structure of the slower reacting GH cements and their propensity toward complete hydration given available water summarizes their most remarkable features. Whether the stability of GH at high temperatures is sufficient for commercial consideration remains a question that seems worth answering. Perhaps the most compelling reason for commercial evaluation of these cements is their high SiO_2 content vs. commercial HAC and thus their potentially lower batch cost. Of course, the effect of impurities (especially iron) upon properties, must be studied before cost estimates can be established.

The inherent uniformity and predictability of the properties of glass vs. crystalline cements also provide a valid reason for further study. With a view toward potential commercialization, the author filed a U.S. patent application in January of 1985.[15]

Of course, on the negative side, the lower Al_2O_3 content of these cements may be a limiting factor in their application as monolithic refractories.

Further research should include the effect of large proportions of aggregate upon the properties of these cements. High sheer mixing, low w/c ratios, and the additions of micro-silica also seem likely subjects for further study of these fascinating glass cements.

Acknowledgements

The author is deeply grateful to his technologist, Mr. R. L. Andrus, for accomplishing most of the work described in this paper with diligence and skill. Thanks also to those in the Technical Services and Melting Services groups in Corning Glass Works R&D Division. Dr. W. R. Prindle also contributed his ideas, interest, and support to this investigation.

REFERENCES

1. A. M. Neville, "High Alumina Cement Concrete," Construction Press, Ltd., Hornby, Lancaster, England, 201 pgs. (1975)

2. H. C. Midgley, "The Mineralogy of Set High Alumina Cement," Trans. Brit. Cer. Soc., 66 (4) pp. 161-187 (1967)

3. C. Bradbury, P. M. Callaway and D. D. Double, "The Conversion of High Alumina Cement/Concrete," Mat. Sci. and Eng., 23, 43-53 (1976)

4. F. W. Locher, "Hydraulic Properties and Hydration of Glasses in the System $CaO-Al_2O_3-SiO_2$," Fourth Int'l. Symp. on the Chemistry of Cements," Washington, D.C. (1960)

5. E. P. Flint, H. F. McMurdie, and L. S. Wells, "Hydrothermal and X-Ray Studies and the Relationship of the Series to Hydration Products of Portland Cement," Jour. Res. Nat'l. Bur. Stand., 26, 13-33 (1941)

6. T. Shoji, "$Ca_3Al_2(SiO_4)_3$-$Ca_3Al_2(H_4O_4)_3$ Series Garnet: Composition and Stability," Jour. Mineral. Soc. Japan, 11, 359-372 (1974) (in Japanese)

7. D. W. Foreman, Jr., "Neutron and X-Ray Diffraction of $Ca_3Al_2(D_4O_4)_3$, a Garnetoid," Jour. Chem. Phys. 48, 3037-3041 (1968)

8. B. Mason, "Larnite, Scawtite and Hydrogrossular from Tokatoka, New Zealand," Am. Mineral., 42, 379-392 (1957)

9. T. D. Robson, "High Alumina Cements and Concretes," Wiley, London, p. 36 (1962)

10. F. P. Glasser, "Application of the Phase Rule to Cement Chemistry," Phase Diagrams - Materials Science and Technology - Volume II, Chapt. V, pg. 158.

11. F. M. Lea, "The Chemistry of Cement and Concrete," Third Edition, Chemical Pub. Co., N.Y., pgs. 56, 506 (1971)

12. F. Keil and F. Gille, "Hydraulic Properties of Basic Glasses with the Gehlenite and Ackermanite Composition," Zement-Kalk-Gips, 2 [12], pgs. 229-232 (1949)

13. H. Zur Strassen, "Die Chemischen Reaktionen bei der Zementerhärtung," Zement-Kalk-Gips, 11, 137-143 (1958)

14. I. Teoreanu and M. Georgescu, "Chemical Studies and X-Ray Analysis of the Hydration of Vitreous Gehlenite in the Presence of Activators," Bulletin of the Polytechnic Institute of Bucharest, 32, [6], pgs. 1-8 (1970)

15. J. F. MacDowell, "$CaO-Al_2O_3-SiO_2$ Glass Hydraulic Cements," U.S. Patent Applic. No. 695355, Jan 28, 1985

V.I. KORNEEV,
V.V. ANDREEV,
U.V. NIKIFOROV, Institut Technologique Lensovet, Giprocement,
Léningrad, U.R.S.S.

CIMENTS SUR LA BASE DES HYDROGRENATS ET DES HYDROCARBOALUMINATES DE CALCIUM

Les hydrogrenats de calcium $C_3AS_xH_{6-2x}$, où x = 0,01-0,25 et les hydrocarboaluminates de calcium $C_3A \cdot CaCO_3 \cdot H_{II}$ sont des produits secondaires prevenant de la production de l'alumine servant d'une source de matière crue perspective pour obtenir à leur base des ciments spéciaux.

L'introduction dans le ciment des hydrogrenats et des hydrocarboaluminates de calcium ou des composés obtenus à leur base (mayenites, fluoroaluminates et sulfoaluminates de calcium) assure la formation dirigée de la composition et de la quantité des phases hydratées dans la pierre de ciment. On observe l'augmentation du degré d'hydratation des minéraux de clinker et l'acroissement de la quantité des hydrosilicates à basse basicité et de l'ettringite. Cela permet de produire les ciments Portland à haute résistance, durcissement rapide et à autocontrainte.

Les ciments alumineux à durcissement super-rapide peuvent être obtenus en cas de l'utilisation des phases sulfoaluminates, fluoroaluminates et hydroaluminates synthétisées sur la base des hydrogrénats et des hydrocarboaluminates de calcium.

Os hidrogranadas de cálcio $C_3AS_xH_{6-2x}$, onde x = 0,01 - 0,25, e os hidrocarboaluminatos de cálcio $C_3A.CaCO_3.H_{11}$ são produtos secundários provenientes da produção de alumínio e servem de fonte de matéria crua em perspectivas, para obtenção de cimentos especiais à base dos mesmos.

A introdução no cimento de hidrogranadas e de hidrocarboaluminatos de cálcio, ou de compostos obtidos com eles (maienitas, fluoraluminatos e sulfoaluminatos de cálcio) garante a formação dirigida da composição e a quantidade de fases hidratadas na pedra de cimento. Observa-se aumento do grau de hidratação dos minerais de clinquer e o crescimento da quantidade de hidrossilicatos de baixa basicidade e de etringita. Isto permite a produção de cimentos portland de alta resistência, endurecimento rápido e de autocontração.

Os cimentos aluminosos de endurecimento super-rápido podem ser obtidos em caso de utilização de fases sulfoaluminatos, fluoraluminatos e hidroaluminatos sintetizados à base de hidrogranates e hidrocarboaluminatos de cálcio.

V.I. KORNEEV,
B.B. ANDREEV,
Yu.V. NIKIFOROV

Les hydrogrenats de calcium $C_3AS_xH_{6-2x}$ et les hydrocarboaluminates de calcium $C_3A{\cdot}CaCO_3{\cdot}H_{II}$ sont des sous-produits de la fabrication de l'alumine (les pâtes d'hydrogrenats) comprennent de 16% à 24% Al_2O_3 [1].

L'utilisation des hydrogrenats et des hydrocarboaluminates de calcium dans la composition des ciments est basée sur les processus de déshydratation thermique avec formation des hydrocarboaluminates et aluminates actives, de synthèse à haute température des aluminates de calcium et de ses dérivés, aussi que sur les processus de leur interaction avec les sulfates de calcium avec formation des hydrosulfoaluminates de calcium [2].

L'étude des processus de dissociation thermique des hydrogrenats de calcium dans le domaine de température de 573-1373K a mis en évidence la formation successive de trois groupes de composés lors du chauffage, dont chacun peut servir de base pour la production des liants spéciaux et utilisables aux travaux de génie civil.

Au cours de la déshydratation des hydrogrenats de calcium ayant la composition $C_3A{\cdot}S_xH_{6-x2}$, se forment les produits partiellement déshydratés de formules suivantes: $C_3AS_xH_{1,5-2x}$, où x n'est pas supérieur à 0,5 et de $C_3AS_xH_{1,5-x}$, où x est égal à 0,5-1,2.

L'augmentation de la température du traitement thermique jusqu'à 873K mène à la déshydratation complète des hydrogrenats de calcium avec formation de $C_{12}A_7$.

La cuisson des hydrogrenats de calcium à teneur plus élévée en silice à 973-1173K provoque la formation de gehlénite et de l'aluminate tricalcique (10-15%). Lors du traitement thermique des hydrogrenats de calcium à 1373K ont lieu la formation de mayenite (93-95%), de même que du silicate bicalcique 1-3%, de CaO - 1,5-2,5% [3].

Les résultats expérimentaux se trouvent en bonne concordance avec ceux du calcul thermodynamique de la valeur du potentiel isobarique-isothermique ΔG°_T du processus de décomposition thermique de l'hydrogrenat de calcium $C_3AS_{0,2}H_{5,6}$ dans la gamme de température 673-1073K [4].

Les résultats du calcul thermodynamique de la décomposition thermique de l'hydrogrenat de calcium $C_3A{\cdot}S_{0,2}H_{5,6}$ ont permis d'établir que le processus de décomposition thermique suit préférablement les réactions avec formation de $C_{12}A_7$, CaO, C_2S et H_2O. La formation du produit partiellement déshydraté de type $C_3AH_{1,5}$ avec élimination de la silice à l'état libre s'est avérée possible à la température supérieure à 700K. Thermodynamiquement l'élimination de la silice en état libre ou en forme de silicate bicalcique s'est avérée préférable par rapport à la formation du gehlénite ou d'anorthite.

L'analyse théorique des conditions de formation des hydrogrenats de calcium partiellement déshydratés, de l'aluminate tricalcique a permis d'élaborer des liants, pouvant être utilisés pour la préparation des mélanges de fonderie moulés en métallurgie des métaux ferreux et non ferreux. Ces ciments de fonderie assurent les délais admissible de viabilité des mélanges de moulage, les caractéristiques de résistance nécessaires (résistance à la compression après 1 et 3 heures du durcissement - pas moins de 0,8 MPa et après 48 heures - jusqu'à 2 MPa), l'éboulement diminué et la résistance residuaire plus basse. Outre cela les dégagements toxiques pendant la fabrication des moules et leur coulage en métal sont exclues [5].

L'utilisation des compositions contenant de l'aluminium à base des hydrogrenats et d'hydrocarboaluminates de calcium s'est manifestée efficace comme constituant de cristallisation assurant l'alliage d'hydratation des ciments, c'est à dire la formation orientée de la composition et de la quantité des phases hydratées en pierre de ciment durci. L'efficacité des ajouts s'augmente suivant la séquence suivante: $C_3AS_{0,25}H_{5,5} \longrightarrow C_3AS_{0,1}H_{5,8} \longrightarrow C_3ACaCO_3{\cdot}H_{II} \longrightarrow C_3AH_6 \longrightarrow C_3A$. Il a été établi que

l'introduction de 0,5-1% d'ajouts susnommés au ciment augmente le degré de l'hydratation des minéraux de clinker et la quantité de l'ettringite et des hydrosilicates à basse basicité de type tobermoritique. Une partie industrielle du ciment à base du ciment portland normal avec ajout de 1,0-1,5% de la pâte d'hydrogrenat a été fabriquée. La composition de phase de la pâte a été la suivante: aluminates de calcium hexagonaux - 30-35%; hydrocarboaluminates de calcium - 25-30%; hydrogrenats de calcium à teneur en silice jusqu'à 0,1 mole - 20%. La part de l'aluminium dans l'ajout fait en moyenne 15,4%.

Les résultats d'essais ont révélé la possibilité de fabrication du ciment à prise rapide de marque "500" ayant des propriétés du liant sans retrait à partir du clinker normal de marque "400".

Ainsi, à l'âge déjà de 3 jours la réistance à la compression est de 5 MPa supérieure à celle, établie par la norme pour le ciment portland à prise rapide de type "500" au dilatement libre de 0,08%. Le ciment obtenu a été utilisé dans la fabrication du béton. Les résultats des essais complexes de tels bétons ont mis en évidence que la résistance des échantillons de béton après le traitement thermique humide à 85°C suivant la séquence 3+3+5+2 à l'âge de 1 jour fait en moyenne 38 MPa, qui est de 10 MPa supérieure à celle citée dans la norme pour le béton de type "400" et de 5 à 7 MPa dépasse la résistance des bétons à base du ciment portland "500".

A l'âge de 28 jours la résistance du béton avec ajout spécial d'hydrogrenat atteint 48 MPa, ce qui est de 8 MPa supérieure à celle mentionnée dans la norme - GOST- et de 3 à 5 MPa dépasse celle du béton à base du ciment sans ajouts de type "500". Les résistances citées autorisent d'admettre que l'utilisation de tel ciment permettra de diminuer le temps du traitement thermique humide et d'abaisser de 20-30 kg le débit du ciment pour 1 m^3 du béton [6].

L'addition de la pâte d'hydrogrenat influence de même manière les propriétés du ciment portland de laitier. L'addition de l'ajout à teneur en hydrocarboaluminate de calcium pas moins de 30% assure le gain de la résistance de 10 à 12 MPa aux trois premiers jours du durcissement, ce qui fait possible l'obtention du ciment portland de laitier à prise rapide.

Il a été démontré par les résultats des recherches physico-chimiques que l'amélioration des caractéristiques du ciment dûe à l'addition de la pâte d'hydrogrenat et d'hydrocarboaluminate, de même que l'augmentation du degré d'hydratation des minéraux de ciment est liée avec la formation supplémentaire de l'ettringite, abaissant la déformation de retrait et optimisant la structure de la pierre de ciment.

L'étude des processus de l'interaction des hydrogrenats de calcium avec des composés sulfateux (gypse dihydraté, gypse semihydraté, anhydrite, phosphogypse) a permis d'établir que le processus de l'interaction des constituants dans le système depend généralement de la teneur en silice dans l'hydrogrenat de calcium, de type de la composante sulfateuse et de la température ambiante.

En fonction des conditions de la synthèse, l'ettringite $C_3A \cdot 3CsH_{31}$ possède une morphologie différente (aiguilles, écailles, cavités sur la surface des grains de l'hydrogrenats de calcium), et sa teneur peut varier dans un large gamme de 0 jusqu'à 100% au cours de 28 jours du durcissement dans les conditions normales. Les hydrogrenats de calcium à basse teneur en silice (jusqu'à 0,1 mole) réagissent avec du gypse le plus intensivement. Pratiquement la teneur en silice dans l'hydrogrenat de calcium dépassant 0,25 mole n'engendre pas la formation de l'ettringite.

Les lois révélées de la formation de l'ettringite au cours de l'interaction des hydrogrenats de calcium et de leur produits du traitement thermique et chimique avec les sulfates de calcium ont servi de base à l'élaboration des ciments expansifs (ciments à autotension "НЦ"), du ciment pour la fab-

rication des objets en amiante ciment et al.

Il a été établi qu'à l'utilisation des pâtes d'hydrogrenat à teneur en silice dans l'hydrogrenat de calcium ne dépassant 0,1 mole, la fabrication du ciment expansif "НЦ-20" nécessite l'introduction de 5-15% de la pâte d'hydrogrenat et cette quantité est augmentée de 5 à 10% pour la fabrication du ciment "НЦ-40".

A partir des clinkers à forte teneur en alites et en aluminates on peut obtenir les ciments à grande énergie d'autotension, bien qu'en principe n'importe quel clinker de ciment portland normal est valable pour la fabrication des ciments expansifs "НЦ".

Les ciments expansifs "НЦ" avec presque le même contenu des additions, obtenues au cours du traitement thermique et chimique des hydrogrenats de calcium à haute teneur en silice (0,2-0,25 mole), répondent aussi aux exigences de la norme sur le ciment expansif "НЦ-20" et "НЦ-40". Des ciments expansifs à base de la pâte d'hydrogrenat ont été utilisées pour la réalisation de divers travaux. Il est à noter la maniabilité des mortiers de béton et de ciment, le temps de prise normal, la haute qualité des objets et des travaux [7]. L'utilisation des pâtes d'hydrogrenat dans la composition du ciment pour la fabrication des objets en amiante ciment (tôles et tubes) se manifeste bien efficace. Lors du durcissement de la masse en amiante ciment à base de ce liant l'utilisation de l'effet d'autotension, dû à la formation de l'attringite dans le système durcissant, s'avère possible. Cela permet d'améliorer la qualité des objets en amiante ciment par l'utilisation plus complète des propriétés armantes de l'amiante.

Les pâtes d'hydrogrenat présentent une source perspective en matières premières pour la fabrication à leur base des ciments portlands expansifs à haute résistance, à prise rapide et des ciments de laitier, des ciments portlands pour l'industrie d'amiante ciment et d'autres liants spéciaux.

BIBLIOGRAPHIE

I. Шморгуненко Н.С. , Сизяков В.М. Научно-технический прогресс в производстве глинозема. - М.: Цветные металлы, 1981, № 8.
2. Сизяков В.М., Корнеев В.И., Андреев В.В. Химико-технологические основы переработки гидрогранатовых и гидрокарбоалюминатных шламов. - Алма-Ата: Наука. В кн.: Щелочная металлургия цветных металлов, 1981.
3. Корнеев В.И., Сизяков В.М., Андреев В.В. и др. О составе продуктов термической диссоциации гидроалюминатов и гидрогранатов кальция. - М.: Цветные металлы, 1980, № 2.
4. Андреев В.В. О термической диссоциации гидрогранатов кальция. Ж.П.Х., 1982, № 2.
5. Борсук П.А., Корнеев В.И., Кузнецов В.Г., Кузьмин Б.А. Самотвердеющие смеси на основе алюминатного цемента и СДБ. - М.: Литейное производство, 1982, № 8.
6. Корнеев В.И., Андреев В.В., Никифоров Ю.В. и др. Быстротвердеющие и высокопрочные портландцементы со специальными добавками. - Л.: Цемент, 1983, № 3.
7. Корнеев В.И., Андреев В.В., Сизяков В.М. Напрягающий цемент из попутных продуктов производства глинозёма. - Л.: Цемент, 1979, № 12.

Z.P. POULATOV,
B.I. NOUDELMAN, NIIstromproekt, Tachkent, URSS

CIMENT D'ALINITE RESISTANT AUX SULFATES

3.3

Les résultats de recherches sur la résistance à la corrosion des ciments d'alinite ayant des compositions diverses dans les solutions de sels sulfatés de Na et de Mg.

On montre la possibilité praticable d'obtention de ciments d'alinite ayant une haute résistance aux sulfates selon la voie à basse température.

On met en évidence que la résistance aux sulfates des ciments d'alinite ne dépend que du contenu en chloraluminates et en ions de chlore résiduels.

Lors de la solidification il se forme plus de gypse combiné dans les hydrosulfoaluminates de calcium, qu'en cas de ciment portland classique résistant aux sulfates.

São apresentados resultados de pesquisas sobre a resistência à corrosão de cimento de alinita, tendo composições diversas nas soluções de sais sulfatados de Na e de Mg.

Mostra-se a possibilidade prática de obtenção de cimentos de alinita tendo alta resistência aos sulfatos em baixas temperaturas.

Evidencia-se que a resistência aos sulfatos dos cimentos de alinita não depende senão do teor de cloroaluminatos e de íons residuais de cloro.

Quando da solidificação, forma-se mais gesso combinado nos hidrosulfoaluminatos de cálcio do que no caso de cimento portland clássico resistente aos sulfatos.

Une des orientations promettant de contribuer à la baisse des dépenses de combustible et d'énergie dans l'industrie du ciment est la mise en oeuvre du procédé industriel de fabrication du clinker à basse température dont les principes ont été mis au point en URSS.

La mise en production du procédé de fabrication du clinker à basse température ouvre de larges possibilités d'extension de la création de nouveaux matériaux de construction et d'articles de qualité supérieure assurant un accroissement du niveau d'industrialisation et une baisse des dépenses d'énergie, de la consommation de matériaux et du coût de la construction.

Une des particularités du ciment obtenu à basse température est la présence dans sa composition de minéraux contenant du chlore (alinite, chloraluminate de calcium et autres) qui diffèrent par leurs propriétés des minéraux entrant dans la composition du clinker de ciment Portland.

L'étude des principales propriétés techniques des ciments d'alinite représente un grand intérêt scientifique et pratique.

Dans la présente communication on trouvera les résultats des études de la résistance à la corrosion des mortiers et des bétons de ciment d'alinite au cours de leur durcissement dans des solutions magnésiennes-sulfatiennes et dans des conditions naturelles en présence de sols très minéralisés et d'eaux souterraines.

Les essais de résistance à la corrosion des ciments d'alinite ont été réalisés suivant les méthodes d'Anstett, de V.V. Kind, la méthode mise au point par l'Institut de chimie de l'Académie des sciences de la République Socialiste Soviétique d'Ouzbékistan et le NIIJB ainsi que par des mesures d'allongements linéaires.

Il a été utilisé 10 lots de ciments d'alinite préparés sur la base des clinkers fabriqués à basse température en laboratoire (série HЦ) et dans des fours industriels de la cimenterie pilote d'Akhangaran (série OЦ). En qualité d'échantillons de référence on a utilisé le ciment Portland résistant aux sulfates de la cimenterie d'Akhangaran.

Les ciments soumis à l'essai avaient une composition chimique différente. La quantité d'alinite variait dans les limites de 55 à 85 %, de chloraluminate dans les limites de 3 à 8 % et celle de chlore restant constituait de 2,41 à 5,06 % (tabl. 1).

Les résultats des essais ont démontré qu'au cours de leur durcissement dans des solutions des sulfates de sodium et de magnésie pendant une période ne dépassant pas 30 mois, tous les ciments d'alinite (sauf ceux des séries HЦ-5 et HЦ-6) ne cessaient d'accroître leur résistance sans manifester d'indice de destruction. A tous les délais, les coefficients de stabilité sont très hauts (de 0,85 à 1,23) (tabl. 2). En ce qui concerne les échantillons du ciment Portland résistant aux sulfates qui ont été soumis aux essais à titre de comparaison, ils ont manifesté vers le 12-e mois de durcissement une baisse de la résistance, le coefficient de stabilité ayant diminué à 0,74.

Les ciments d'alinite HЦ-5 (à teneur élevée en Cl^-) et HЦ-6 (à teneur élevée en chloraluminate) ont manifesté selon les prévisions une faible résistance à la corrosion en comparaison avec les autres ciments d'alinite. Ces ciments mis dans une solution de sulfate de sodium ont fait preuve vers le 12-e mois d'une baisse des indices de résistance.

L'étude du durcissement des échantillons de ciment d'alinite dans des milieux magnésiens-sulfatiens à l'aide des méthodes physico-mécaniques, physico-chimiques et d'analyse chimique a permis d'établir que:

- les ciments d'alinite de composition chimique et minéralogique normalisée possèdent une haute résistance à la corrosion pendant le durcissement dans des milieux magnésiens-sulfatiens;
- la résistance à la corrosion des ciments d'alinite dépend exclusivement de la teneur du ciment en chloraluminate de calcium et en chlore-ion restant. Si la teneur du ciment alinitique en chloraluminate de calcium

Tableau 1

Composition chimique et minéralogique potentielle des ciments utilisés

Ciments	Teneur en oxydes, %								Composition minéralogique, % (potentielle)			
	Pertes à feu	SiO_2	Al_2O_3	Fe_2O_3	CaO	MgO	SO_3	Cl	Alinite	C_2S	Chloraluminate	C_2F
D'alinite НЦ-I	2,57	21,56	4,11	4,75	60,06	1,68	2,44	2,85	66	23	3	8
D'alinite НЦ-2	2,48	21,55	3,98	4,50	61,18	1,78	2,23	2,41	72	17	4	7
D'alinite НЦ-3	2,00	21,36	4,71	3,75	60,38	1,93	2,62	2,80	62	23	5	5
D'alinite НЦ-4	1,89	21,72	4,18	4,74	59,84	1,70	2,48	2,47	55	28	4	9
D'alinite НЦ-5	5,23	20,68	4,55	4,71	57,66	2,06	2,54	5,06	85	6	3	7
D'alinite НЦ-6	2,56	22,66	6,55	2,37	59,30	2,09	2,39	3,02	64	26	8	1
D'alinite ОПЛ-I	2,08	22,06	5,04	4,82	59,94	1,56	0,62	2,69	58	27	6	8
D'alinite ОПЛ-4	1,03	22,00	5,15	4,25	63,31	1,24	0,83	3,10	68	21	5	6
D'alinite ОПЛ-5	1,68	22,00	5,18	3,84	63,92	1,09	0,68	3,02	67	22	6	3
D'alinite ОПЛ-6	1,45	23,57	5,44	4,28	61,88	2,05	0,22	2,90	64	28	6	2
D'Akhangaran résistant aux sulfates	1,21	21,60	4,59	4,95	61,12	2,41	1,92	-	$\frac{C_3S}{47}$	$\frac{C_2S}{27}$	$\frac{C_3A}{4}$	$\frac{C_4AF}{15}$

Tableau 2

Résistance à la corrosion de différents ciments d'alinite en durcissement dans les solutions à 0,9 % de Na_2SO_4 et à 0,5 % de $MgSO_4$ (échantillons de 1x1x6 cm au rapport eau/ciment de 0,40)

Ciments	Limite de flexion, MPa														
	Durcissement dans l'eau					Solution à 0,9 % de Na_2SO_4					Solution à 0,5 % de $MgSO_4$				
	Mois														
	1	3	6	12	30	1	3	6	12	30	1	3	6	12	30
D'Akhangaran résistant aux sulfates	6,1	7,5	9,1	9,7	10,8	6,3	7,2	8,6	8,6	8,6	6,0	7,4	7,7	7,2	7,0
D'alinite НЦ-3	6,7	7,4	9,1	9,6	10,6	7,0	8,3	9,7	9,9	10,5	7,5	8,3	8,9	9,2	9,1
D'alinite НЦ-5	6,3	6,6	8,0	8,3	8,4	6,1	7,8	9,0	8,5	7,8	6,2	6,7	7,8	8,0	8,2
D'alinite НЦ-6	5,9	8,0	9,0	9,6	10,1	6,7	7,7	8,3	8,0	7,6	5,7	7,4	7,9	8,0	7,6
D'alinite ОПЛ-I	6,8	8,1	9,2	9,4	9,9	8,4	9,3	9,9	10,2	10,7	6,6	8,9	9,1	9,0	8,7
D'alinite ОПЛ-4	6,2	9,6	9,8	9,4	9,5	7,2	9,7	9,6	9,4	9,6	6,1	8,2	8,8	9,6	9,1
D'alinite ОПЛ-5	8,2	9,3	9,7	10,1	10,2	8,6	9,4	9,7	10,2	10,3	7,9	9,2	9,9	11,0	11,1
D'alinite ОПЛ-6	7,3	8,7	9,2	9,4	9,6	8,0	9,0	9,3	9,4	10,0	7,2	9,1	9,8	10,2	10,4

est élevée (plus de 5 %), les échantillons manifestent d'importants allongements linéaires pendant le durcissement dans la solution de sulfate de calcium aussi bien que dans celle de sulfate de magnésie et lorsqu'il s'agit de la teneur élevée en chlorions (plus de 3 %), des allongements linéaires importants ne sont observés que dans la solution de sulfate de magnésie (fig. 1);

- dans les échantillons des ciments d'ali-

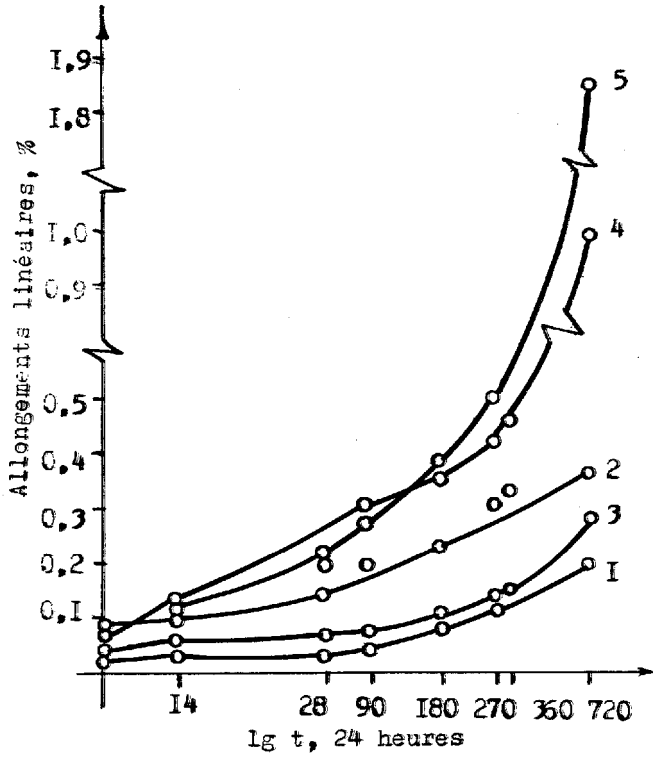

Fig. 1. Allongements linéaires des ciments d'alinite durcis dans la solution à 1 % de $MgSO_4$.
1 - Ciment Portland d'Akhangaran résistant aux sulfates;
2 - Ciment d'alinite HI-3;
3 - Ciment d'alinite HI-4;
4 - Ciment d'alinite HI-5;
5 - Ciment d'alinite HI-6;
6 - Ciment d'alinite HI-3 + 30 % de laitier de phosphore;
7 - Ciment d'alinite HI-3 + 30 % de gliège

nite qui durcissent dans des solutions des sulfates de calcium et de magnésie il se forme beaucoup plus de gypse lié à l'hydrosulfaluminate de calcium que dans les échantillons de ciment Portland résistant aux sulfates. En revanche, l'accumulation du gypse libre se produit plus intensivement dans les échantillons de ciment Portland résistant aux sulfates;

- malgré le fait que dans les échantillons de ciments d'alinite on observe une plus grande vitesse d'accumulation de l'hydrosulfaluminate et d'importants alon-

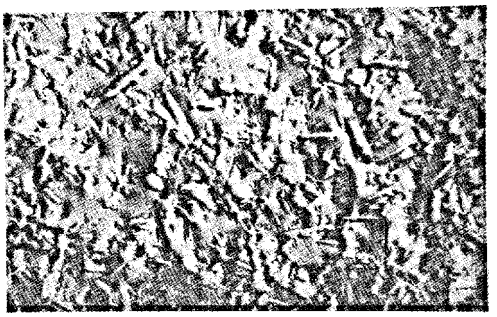

Fig. 2. Photographie au microscope électronique du mélange d'alinite (80 %) et de chloraluminate (20 %) hydraté dans l'eau durant 6 heures en présence d'ions de SO_4^{2-}

gements linéaires en cas de durcissement dans des milieux agressifs, leur haute résistance à la corrosion est due à ce que les minéraux à alumine du ciment d'alinite (alinite, chloraluminate) sont répartis d'une façon régulière dans tout le volume de l'échantillon grâce à quoi l'hydrosulfaluminate qui se forme se répartit également de façon régulière dans le volume du ciment en durcissement. Dans le ciment durci d'alinite, é la place des essaims d'agrégats de cristaux fibreux et aciculaires se forment sous l'aspect de sphérolithes et se répartissent de façon régulière de petits cristaux aciculaires d'hydrosulfaluminate. Dans ce cas, la dilatation est tridimensionnelle et à la place des phénomènes destructifs on constate un accroissement de densité et de dureté du ciment durci;

- lorsqu'on introduit du laitier de phosphore et de gliège dans le ciment d'alinite, sa résistance aux sulfates augmente proportionnellement à la quantité d'additif. Les influences positives du gliège et du laitier de phosphore sur la résistance aux sulfates du ciment d'alinite commencent à se manifester à 15 % d'additif et deviennent particulièrement efficaces à une quantité

de 30 à 40 % d'additif. Le laitier de phosphore et le gliège introduits dans le ciment d'alinite réduisent également d'une manière brusque les allongements linéaires des échantillons de mortiers ciment-sable lorsqu'ils durcissent dans des solutions agressives à haute concentration.

P. GAIDJOUROV, Institut polytechnique de Novotcherkassk, U.R.S.S.

PARTICULARITES DES PHENOMENES DE FORMATION DE MINERAUX ET D'HYDRATATION DES CIMENTS DECORATIFS ET EN HAUTE TENEUR EN FER

3.3

L'auteur a étudié l'influence qu'exercent les diverses conditions de la cuisson et du refroidissement sur la formation de la composition par phases, de la structure, et les caractéristiques du clinker du ciment Portland blanc. Il a établi que les conditions réductrices locales d'une cuisson basées sur la conversion du gaz naturel et un refroidissement brusque du clinker, ainsi que des additions organiques, accroissent le coefficient de réflexion du ciment. L'auteur a dégagé les lois régissant la variation de la chromaticité du clinker suivant l'état de valence des cations fer. En partant des données d'une analyse thermogravimétrique différentielle, il a calculé les paramètres cinétiques de la dissociation thermique de $CaCO_3$. Les cations fer divalents Fe^{2+} qui résultent de la cuisson réductrice accélèrent la décarbonisation, réduisent la viscosité de la phase liquide du clinker, d'où l'intensification du processus de formation du clinker.

Les courbes thermocinétiques représentatives de l'hydratation des ciments décoratifs contenant des additifs complexes caractérisent le degré de combinaison des aluminates de calcium donnant de l'ettringite aux premiers stades de durcissement, ce qui modifie la structure de la pierre de ciment, en favorisant son tassement. Ce phénomène améliore les caractéristiques d'utilisation des ciments décoratifs.

La composition par phases, la structure et l'activité d'hydratation du clinker d'un ciment à haute teneur en fer sont déterminées par les conditions de la cuisson (la température et l'état de gaz).

O autor estudou a influência exercida pelas diversas condições da queima e do resfriamento sobre a formação da composição de fases, sobre a estrutura, e as características do clinquer de cimento portland branco. Estabeleceu que as condições redutoras locais de uma queima, baseadas na conversão do gás natural, e um resfriamento brusco do clinquer, bem como adições orgânicas, aumentam o coeficiente de reflexão do cimento. O autor determinou as leis que regem a variação da cromaticidade do clinquer de acordo com o estado de valência dos catíons ferro. Partindo de dados de uma análise termogravimétrica diferencial, ele calculou os parâmetros cinéticos da dissociação térmica de $CaCO_3$. Os catíons ferro bivalentes Fe^{2+}, resultantes da cocção redutora, aceleram a descarbonização, reduzem a viscosidade da fase líquida do clinquer, donde a intensificação do processo de formação do clinquer.

As curvas termocinéticas, representativas da hidratação dos cimentos decorativos contendo aditivos complexos, caracterizam o grau de combinação dos aluminatos de cálcio que dão etringita nos primeiros estágios de endurecimento, o que modifica a estrutura do concreto, e favorecem sua acomodação. Este fenômeno melhora as características de utilização dos cimentos decorativos.

A composição de fases, a estrutra e atividade de hidratação do clinquer de um cimento com alto teor de ferro são determinadas pelas condições de queima (temperatura e estado de gás).

Pour intensifier la blancheur du clinker dans la technique de fabrication du ciment Portland blanc, on utilise avec succès des milieux réducteurs gazeux locaux créés à l'aide d'injecteurs dont on équipe le four pour y introduire des mélanges gaz-vapeur. Le contact du clinker incandescent avec le mélange de gaz naturel et de vapeurs d'eau amorce un processus de conversion $CH_4+H_2O=CO+2H_2$ durant lequel a lieu un dégagement d'agents réducteurs actifs. Ce processus est accompagné de réactions de réduction qui se déroulent dans le clinker en cuisson grâce aux impuretés organiques contenues dans les composants argileux.

Les conditions réductrices de cuisson et un brusque refroidissement du clinker contribuent à obtenir une composition de phase et une structure optimales ce qui augmente considérablement le facteur de réflexion du ciment Portland blanc. Des cations bivalents de fer Fe^{2+} formés pendant la cuisson réductrice déterminent un teint bleu-clair du clinker à la place du vert foncé typique pour le clinker de cuisson oxydante. Ceci s'explique par le fait que les cations bivalents Fe^{2+} ont une configuration électronique $3d^6$ où toutes les d'orbitales sont remplies ce qui fait que la transition électronique d'une d'orbitales à une autre est impossible. En revanche, dans le cas de la cuisson oxydante, les cations trivalents Fe^{3+} dont la configuration électronique est $3d^5$ ont une d-orbitale libre ce qui conduit à une fission des niveaux des d-orbitales. Ces particularités font que les composés des cations bivalents de fer sont incolores tandis que ceux des cations trivalents sont fortement colorés (1).

Une inégalité des cations Fe^{3+} et Fe^{2+} en valeur énergétique influe différemment sur la dissociation thermique de $CaCO_3$ ainsi que sur la structure et les propriétés de la phase liquide du clinker. La cinétique de la réaction de décarbonisation thermique du composant brut peut être décrite à l'aide de l'équation suivante (2):

$$\frac{d\eta}{dm} = A\cdot\exp\left(\frac{E}{RT}\right)\cdot(1-\eta);\quad -\frac{dm}{d\tau} = K\cdot m^n$$

où $\eta = \dfrac{m_o - m}{m_o - m_f}$ est le taux de décarbonisation; m_o est la masse de l'échantillon avant la réaction; m_f est la masse finale de l'échantillon après la réaction; m est la valeur actuelle de la masse de l'agent de dissociation vers un moment τ ; A est le facteur préexponentiel (dépend de la structure de la matière); E est l'énergie d'activation; R est la constante des gaz; T est la température; n est l'ordre de la réaction; K est la constante de la vitesse de réaction.

Le calcul des paramètres cinétiques E, n, A, K est basé sur l'utilisation de la courbe de température ainsi que des courbes différentielle thermogravimétrique et différentielle thermographique (fig. 1). Les résultats de l'analyse différentielle thermogravimétrique (ADT) montrent que la cuisson réductrice réduit à l'encontre de la cuisson oxydante ordinaire, de 373 K la période d'induction de la dissociation thermique de $CaCO_3$ et de 333 K sa température de décarbonisation finale. Dans le cas de la cuisson oxydante, l'énergie d'activation E = 39,7 kcal/mole, l'ordre de la réaction n = 0,82 et le facteur préexponentiel A = 2,5 mn^{-1}·mole tandis que dans celui de la cuisson réductrice les paramètres cinétiques E et n diminuent et constituent 28,4 kcal/mole et 0,41 respectivement et le paramètre A augmente à 3,8 mn^{-1}·mole ce qui accélère le processus de décarbonisation du mélange de ciment brut.

La figure 2 montre la variation du degré de décarbonisation du calcaire en fonction des additifs à utiliser: oxyde de fer ou charbon ainsi qu'en fonction de la température de cuisson. Une baisse du degré de décarbonisation du $CaCO_3$ par suite d'une augmentation de sa teneur en charbon s'explique par le fait qu'à l'intérieur des granules de la matière en cuisson se forme une quan-

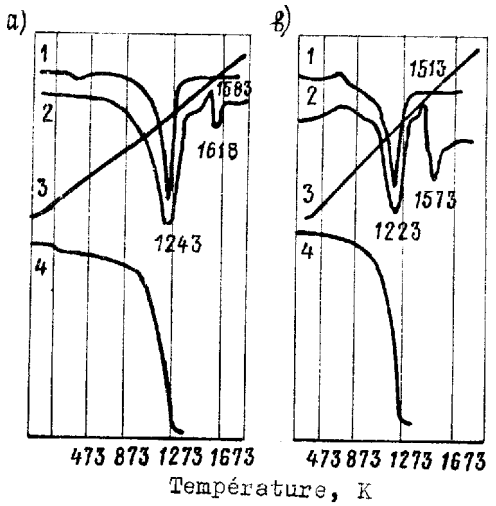

Fig. 1. Courbes de l'ADT: a - cuisson oxydante; b - cuisson réductrice; 1 - courbe différentielle thermogravimétrique; 2 - courbe différentielle thermographique; 3 - courbe de température; 4 - courbe de perte de poids

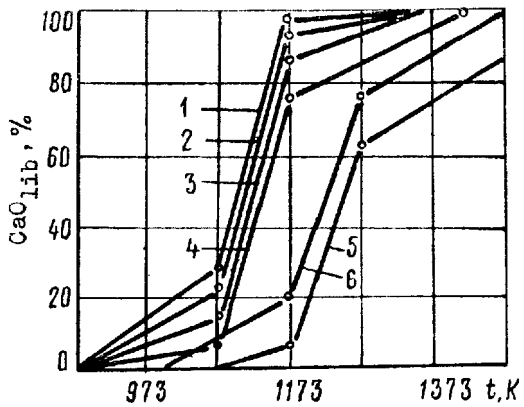

Fig. 2. Variation du degré de décarbonisation du $CaCO_3$ en fonction du nombre d'additifs de charbon ou d'oxyde de fer et en fonction de la température de cuisson (temps de cuisson - 60 mn): 1 - $CaCO_3$ pur; 2 - $CaCO_3$+5% Fe_2O_3+ +1 % de charbon; 3 - $CaCO_3$+0,5 % de charbon; 4 - $CaCO_3$+1 % de charbon; 5 - $CaCO_3$+3 % de charbon; 6 - $CaCO_3$+5 % Fe_2O_3

tité supplémentaire de CO_2 grâce à la combustion du charbon ce qui provoque une hausse de la pression partielle du gaz carbonique. Une baisse considérable (supérieure à 10 fois) du degré de décarbonisation du calcaire additionné de 5 % de Fe_2O_3 en comparaison avec le $CaCO_3$ pur est due à la formation de ferrites de calcium qui a lieu à des températures relativement basses (de 973 à 1073 K). Il en résulte que des formations structurales pleines se forment à la surface des particules du carbonate de calcium ce qui ralentit la diffusion du CO_2. Cependant, une introduction du charbon dans le calcaire ferreux provoque la réaction réductrice $2Fe_2O_3 + C = 4FeO + CO_2$. L'oxyde ferreux qui se forme réagit activement avec le $CaCO_3$ en donnant lieu à une création de phases métastables intermédiaires ce qui contribue à la diffusion du CO_2 à travers la couche superficielle friable de la matière carbonatée en cuisson.

L'étude des propriétés de la phase liquide représente un intérêt particulier pour la technique du ciment Portland blanc à teneur faible en oxydes de fer pour cette raison que le mélange brut s'y trouve difficile à s'agglomérér. Les cations trivalents Fe^{3+} qui possèdent une capacité élevée de polariser les anions d'oxygène du milieu, représentent des anions formateurs de complexes dans le clinker fondu tandis que les cations bivalents Fe^{2+} y jouent le rôle d'ions modificateurs. Les cations de fer Fe^{2+} dont l'énergie de liaison Me - O est beaucoup plus faible que celle des cations Fe^{3+}, réduisent la viscosité du clinker en fusion. Dans la phase liquide du clinker du ciment Portland blanc, le coefficient de diffusion des ions Ca^{2+} constitue $3,3 \cdot 10^{-5}$ cm^2/s pour la cuisson oxydante à 1723 K et $14,8 \cdot 10^{-5}$ cm^2/s pour la cuisson réductrice.

Une large introduction des ciments décoratifs dans l'industrie du bâtiment nécessite une élaboration de méthodes efficaces visant à accroître leur résistance à l'efflorescence. Un accroissement sensible de la résistance à l'efflorescence s'obtient grâce à une addition combinée dans la composition des ciments décoratifs d'adjuvants hydrauli-

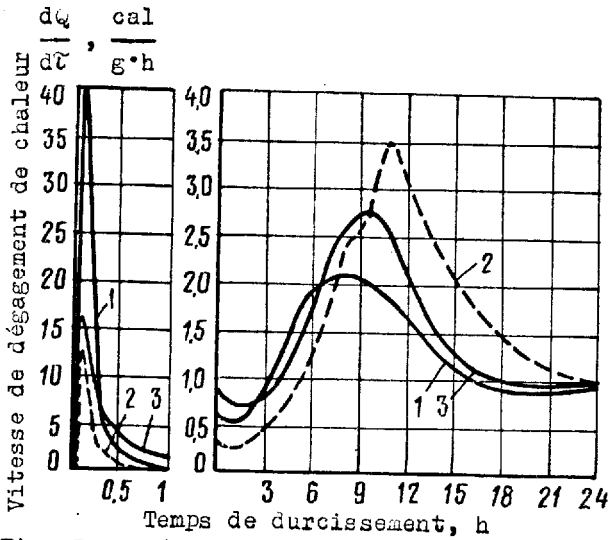

Fig. 3. Cinétique de dégagement de chaleur par les ciments décoratifs: 1 - sans additifs; 2 - additionné de diatomite; 3 - additionné de diatomite et de sulfaluminosilicate

ques, sulfaluminosiliciés et organosiliciés (3). Le processus d'efflorescence est déterminé par la composition minéralogique du clinker, la structure du ciment durci et les conditions d'hydratation. L'essence physico-chimique de ce processus qui est celui de diffusion, est conditionnée par la densité du ciment durci et non pas par sa teneur en hydroxyde de calcium. Les courbes thermocinétiques (fig. 3) montrent qu'une variation de la vitesse de dégagement de chaleur au cours de l'hydratation du ciment décoratif additionné de diatomite et de sulfaluminosilicate est conséquente d'une augmentation allant à 2,5 fois du degré de fixation de l'aluminate tricalcique dans l'ettringite au premier stade de durcissement. Ceci conduit à des modifications de la structure du ciment durci en améliorant son compactage et, par là, en assurant sa résistance à l'efflorescence.

Ces derniers temps, on procède à des recherches poussées dans le domaine de la synthèse et de l'utilisation des ciments ferreux pour la granulométrie sans cuisson des concentrés de minérais de fer (4). L'utilisation des ciments ferreux à ces fins dans la sidérurgie permet d'économiser le combustible ainsi que de perfectionner la technique de préparation des matières crues à l'élaboration de fonte en haut fourneau. Les matières crues à utiliser pour obtenir ce ciment sont les concentrés de minérais de fer et les roches carbonatées (calcaire, craie). Les mélanges crus sont calculés d'après le degré de saturation CH = 0,8 - 1,1 et le module alumineux P = 0,1 - 0,2. Les matières principales entrant dans le clinker du ciment ferreux sont la ferrite bicalcique C_2F, les aluminoferrites de calcium type $C_2A_xF_{1-x}$ et la bélite C_2S. La cuisson du clinker s'effectue dans les milieux oxydant et réducteur à 1423 K.

Grâce au rôle déterminant qu'elle joue dans la formation de la structure et de la composition de phase de la solution d'alumoferrite solide, la nature du milieu gazeux de la cuisson exerce une influence considérable sur les indices de résistance des aluminoferrites de calcium. Ainsi, une cuisson à faible effet réducteur contribue à une augmentation de l'activité d'hydratation de la solution solide. Une augmentation du degré de réduction dans les échantillons soumis à l'essai conduit à une baisse brusque de la résistance des aluminoferrites de calcium. Ceci s'explique par le fait que pendant une cuisson à haut degré de réduction il se produit une destruction des aluminoferrites de calcium

$$2CaO \cdot xAl_2O_3 \cdot (1 - x)Fe_2O_3 +$$

$$+ CO \longrightarrow 5CaO \cdot 3Al_2O_3 + CaO + Fe + CO_2$$

L'addition de SiO_2 en quantité de 2 % à la ferrite bicalcique dans la gamme des températures de cuisson de 1373 à 1473 K n'altère pas les indices de résistance du minéral C_2F. Ce fait révèle la limite de solubilité de la silice dans la ferrite bicalcique. Une triple baisse de la résistance des échantillons étudiés de C_2F contenant plus de 2 % de SiO_2 est observée à une température de plus de 1473 K. Cela s'explique par ce que dans le domaine de hautes tempé-

ratures, le C_2F devient instable en présence de SiO_2 et se décompose: $2CaO \cdot Fe_2O_3 + SiO_2 = 2CaO \cdot SiO_2 + Fe_2O_3$. A cause de ce phénomene, la cuisson du clinker de ciment ferreux s'effectue à une température relativement basse de 1423 K.

Les particularités structurales des échantillons hydratés de la ferrite bicalcique sont étudiées dans l'ouvrage (5). Pour évaluer l'activité d'hydratation des ferrites de calcium des compositions C_2F, CF et CF_2, on a calculé les degrés de liaison ionique et les valeurs géométriques moyennes de l'électronégativité de ces minéraux. Une basse valeur numérique de l'électronégativité $\bar{E}N$ = 0,143 eV de la ferrite bicalcique et, en même temps, un haut degré ionique de la liaison chimique $\bar{E}$ = 81 % déterminent une haute activité d'hydratation du ciment ferreux et les conditions de son durcissement.

CONCLUSIONS

1. Des conditions réductrices locales de la cuisson à la base de la conversion du gaz naturel et un brusque refroidissement du clinker ainsi que la présence d'additifs organiques augmentent considérablement le facteur de réflexion du ciment Portland blanc.

2. Les cations bivalents Fe^{2+} formés dans un milieu réducteur accélèrent le processus de dissociation thermique de $CaCO_3$, diminuent la viscosité du bain fondu de clinker ce qui intensifie le processus de clinkérisation.

3. L'utilisation d'additifs minéraux et organosiliciés dans la composition des ciments décoratifs contribue au compactage du ciment durci ce qui assure sa résistance à l'efflorescence.

4. La composition de phase, la structure et l'activité d'hydratation du clinker du ciment ferreux sont déterminées par le milieu thermique et gazeux de la cuisson.

REFERENCES
(en russe)

1. Карапетьянц М.Х., Дракин С.И. Строение вещества. М., Высшая школа, 1978, с. 218-223.
2. Аллахвердов Г.Р., Степин Б.Д. О новом варианте определения кинетических характеристик по данным термогравиметрического анализа. - Журнал физической химии АН СССР, 1969, т. XШ, вып. 9, с. 2268-2272.
3. Сибирякова И.А., Сыркин М.Я., Щеткина Т.Ю. Особенности получения и твердения декоративных шлакопортландцементов. - Цемент, 1979, № II, с. 13-14.
4. Гайджуров П.П., Зубарь Г.С., Уварова И.В. Влияние температуры синтеза на процесс гидратации двухкальциевого феррита. - Изв. вузов. Химия и химическая технология, 1982, т. 25, вып. 9, с. 1124-1126.
5. Шпынова Л.Г. и др. Формирование и генезис микроструктуры цементного камня. Львов, Вища школа, 1975, с. 63-76.

A.P. ZOUBEKHIN, Institut polytechnique de Novotsherkassk, URSS

NOUVEAUX ASPECTS DE LA CHIMIE PHYSIQUE DU CIMENT PORTLAND BLANC

Les régularités physico-chimiques nouvelles sont mises en évidence pour le changement du coefficient de réflexion (CR) et de chromaticité des minéraux et du clinker du ciment portland blanc (CPB) en cas des teneurs complexes et élevées en oxydes de fer, de titane et de manganèse. Le degré différent de diminution du coefficient de réflexion (CR) des phases siliceuses et des C_3A est établi en fonction de l'état cristallochimique des additions de Ti, Mn, et Fe dans les solutions solides et en fonction des conditions de cuisson et de refroidissement.

Dans les conditions d'oxydation, la diminution du coefficient de réflexion (CR) des minéraux augmente de la façon suivante:

Ti^{4+} — Mn^{4+} — Fe^{3+} —C_3S, b-C_2S;

Fe^{3+} — $Ti^{4}{}_{+}$ — Mn^{4+} — C_3A.

Dans les conditions de réduction, le degré de diminution du coefficient de réflexion (CR) des minéraux augmente dans les séries:

Mn^{2+} — Ti^{3+} — Fe^{2+} (partiellement Fe^{3}) — C_3S;

$M_n{}^{2+}$ — Ti^{2+} — Ti^{3+} — b-C_2S;

Ti^{3+} — Mn^{2+} — Fe^{3+} (partiellement Fe^{2}) — C_3A.

Sur la base des régularités établies, les auteurs ont argumenté scientifiquement les procédés efficaces de neutralisation de l'influence colorifique du complexe des additions Fe, Ti et Mn. Ces procédés sont confirmés par les résultats d'obtention du ciment portland blanc (CPB) à partir des matières premières ayant la teneur élevée en ces additions.

São colocadas em evidência as novas regularidades físico-químicas para alteração do coeficiente de reflexão (CR) e de cromaticidade dos minerais e do clínquer do cimento portland branco (CPB) em caso de teores complexos e elevados de óxido de ferro, titânio e magnésio. O grau diferente de diminuição do coeficiente de reflexão (CR) das fases silicosas e de C_3A é estabelecido em função do estado cristaloquímico de Ti, Mn e Fe nas soluções sólidas e em função das condições de queima e resfriamento.

Nas condições de oxidação, a diminuição do coeficiente de reflexão (CR) dos minerais aumenta da seguinte forma:

Ti^{4+} — Mn^{4+} — Fe^{3+} — C_3S, b-C_2S

Fe^{3+} — Ti^{4+} — Mn^{4+} — C_3A

Nas condições de redução, o grau de diminuição do coeficiente de reflexão (CR) dos minerais aumenta nas séries:

Mn^{2+} — Ti^{3+} — Fe^{2+} (parcialmente Fe^{3}) — C_3S

Mn^{2+} — Fe^{2+} — Ti^{3} — b-C_2S

Ti^{3+} — Mn^{2+} — Fe^{3+} (parcialmente Fe^{2}) — C_3A

Com base em regularidades estáveis, os autores argumentaram cientificamente sobre os processos eficazes de neutralização da influência cromática do complexo de adições Fe, Ti e Mn. Estes processos são confirmados pelos resultados de obtenção de um cimento portland branco (CPB) a partir de matérias primas com alto teor destas adições.

Un problème très important qui s'impose dans la théorie et la technique du ciment Portland blanc (CPB) est la neutralisation de l'effet colorant des additifs. Malgré un nombre important de travaux consacrés à ce problème, on n'a pas étudié jusqu'à présent la question de changement de la blancheur et de la chromaticité du CPB contenant un ensemble d'additifs colorants en quantité élevée.

A côté des oxydes de Fe et Mn, le clinker du CPB contient toujours des oxydes de titane. Le TiO_2 et ses autres composés sont, de règle, incolores ce qui, notamment, a servi de base pour obtenir le blanc de titane et des revêtements d'émail blancs.

On estimait (1,2) qu'une introduction de TiO_2 dans le mélange brut de CPB contenant des oxydes de Fe et Mn augmentait la blancheur du clinker par suite de l'accroissement de la coordination d'ions de fer et de manganèse. Cependant, un accroissement de la coordination d'ions colorants ne constitue pas un facteur déterminant dans la coloration des verres (3) et des minérais de ciment (4). En outre, la pareille conclusion est un résultat de l'étude de la blancheur des clinkers contenant les Fe_2O_3 et Mn_2O_3 en quantités de 0,2 et 0,05 % en masse respectivement, la quantité additionnée de TiO_2 étant de 0,05 % en masse. Les éléments indiqués ont été obtenus dans un milieu oxydant avec le refroidissement dans l'eau. Pour ce qui est des clinkers industriels du CPB, leur teneur en Fe_2O_3 atteint 0,6 % et dans certains cas 1,0 % (5) et celle en TiO_2, 0,3 % (6). Les aspects physico-chimiques de variation du facteur de réflexion (FR) du clinker dans ces conditions n'ont jamais été étudiés. Dans le présent ouvrage sont établies de nouvelles lois physico-chimiques de l'influence des oxydes de Fe, Mn et Ti qu'ils exercent tant individuellement qu'en combinaison en quantité élevée dans de différentes conditions de cuisson et de refroissement sur le FR du clinker de CPB et ses phases. Comme on l'a constate, les variations du FR des phases du silicate et du C_3A ne sont pas identiques ce qui est prédéterminé par l'état cristallochimique des ions colorants dans la structure des solutions solides de minérais (tabl. 1).

Dans le milieu oxydant, la baisse du FR des minérais croît en présence des séries d'ions:

$Ti^{4+} \longrightarrow Mn^{4+} \longrightarrow Fe^{3+}$ - C_3S, β-C_2S;

$Fe^{3+} \longrightarrow Ti^{4+} \longrightarrow Mn^{4+}$ - C_3A.

Le milieu réducteur fait varier l'influence des ions (en fonction de leur valence) sur le degré de baisse du FR des minérais lequel croît dans les séries:

$Mn^{2+} \longrightarrow Ti^{3+} \longrightarrow Fe^{2+}$ (partiellement Fe^{3+}) - C_3S;

$Mn^{2+} \longrightarrow Fe^{2+} \longrightarrow Ti^{3+}$ - β-C_2S;

$Ti^{3+} \longrightarrow Mn^{2+} \longrightarrow Fe^{3+}$ (partiellement Fe^{2+}) - - C_3A.

En présence d'oxydes de titane aussi bien que de ceux de manganèse au sein des structures C_3S et β-C_2S mises dans un milieu oxydant, il se produit dans les sous-réseaux anioniques de $Si^{4+} \rightleftarrows Ti^{4+}$ des substitutions isovalentes qui n'aboutissent pas à la défectuosité de la structure électronique. Etant donné que le Ti^{4+} ne possède pas de d-électrons, de telles substitutions n'amènent pas à l'apparition de bandes de transfert de la charge et à une baisse sensible du FR des phases des silicates. Dans le C_3A ont lieu des substitutions hétérovalentes $4Al^{3+} \rightleftarrows 3Ti^{4+}$ qui conduisent à une défectuosité de la structure électronique et à l'apparition de bandes de transfert de la charge ce qui a pour conséquence une plus importante baisse du FR, surtout en cas d'une teneur élevée en TiO_2 allant à 1 %. Dans le milieu réducteur de synthèse, le Ti^{4+} se réduit au Ti^{3+} ce qui influe sur la nature de formation des solutions solides: elle devient hétérovalente dans les C_3S et β-C_2S et isovalente dans le C_3A. Dans ce cas, grâce aux phénomènes physico-chimiques indiqués, la baisse du FR croît rapidement dans les minérais silicieux et diminue sensiblement dans le C_3A.

Tableau 1

Degré de baisse du FR des solutions solides de minérais à additifs colorants et sa valeur en fonction des transformations cristallochimiques

Minérais	Milieu de cuisson et de refroidissement	Baisse du FR par rapport aux minérais sans additifs, % abs. et types des substitutions dans la structure du minérai pour les teneurs en*, % en masse					
		Oxydes de titane		oxydes de manganèse		oxydes de fer	
		0,25	1,0	0,1	0,25	0,25	1,0
C_3S	oxydant	0,1	5,0	6,6	10,8	23,6	41,6
		$Si^{4+} \rightleftarrows Ti^{4+}$		$Si^{4+} + Ca^{2+} \rightleftarrows Mn^{4+} + Mn^{2+}$		$Si^{4+} + Ca^{2+} \rightleftarrows 2Fe^{3+}$ $3Si^{4+} \rightleftarrows 3Fe^{3+} + Fe^{3+}$	
β-C_2S	-"-	0,0	4,1	6,5	10,6	9,4	30,5
		$Si^{4+} \rightleftarrows Ti^{4+}$		$Si^{4+} + Ca^{2+} \rightleftarrows Mn^{4+} + Mn^{2+}$		$3Ca^{2+} \rightleftarrows 2Fe^{3+}$	
C_3A	-"-	2,6	19,2	9,7	38,2	1,2	4,1
		$4Al^{3+} \rightleftarrows 3Ti^{4+}$		$4Al^{3+} \rightleftarrows 3Mn^{4+}$ u $Ca^{2+} \rightleftarrows Mn^{2+}$		$Al^{3+} \rightleftarrows Fe^{3+}$	
C_3S	réducteur ($CO:CO_2$) = I:I)	9,1	18,0	1,0	6,5	21,5	39,5
		$3Si^{4+} \rightleftarrows 4Ti^{3+}$		$Ca^{2+} \rightleftarrows Mn^{2+}$		$Ca^{2+} \rightleftarrows Fe^{2+}$ $Si^{4+} + Ca^{2+} \rightleftarrows 2Fe^{3+}$	
β-C_2S	-"-	1,0	15,5	0,0	0,1	0,0	16,6
		$3Si^{4+} \rightleftarrows 4Ti^{3+}$		$Ca^{2+} \rightleftarrows Mn^{2+}$		$Ca^{2+} \rightleftarrows Fe^{2+}$	
C_3A	-"-	0,0	3,6	2,4	5,0	0,0	7,8
		$Al^{3+} \rightleftarrows Ti^{3+}$		$Ca^{2+} \rightleftarrows Mn^{2+}$		$Ca^{2+} \rightleftarrows Fe^{2+}$	$Al^{3+} \rightleftarrows Fe^{3+}$ $Ca^{2+} \rightleftarrows Fe^{2+}$

* A la synthèse de minérais, les oxydes ont été introduits sous la forme de TiO_2, Mn_2O_3, Fe_2O_3

Comme on le sait (7), les oxydes de titane renforcent leur effet colorant en combinaison avec d'autres additifs colorants. Nous avons établi qu'en présence de TiO_2 en combinaison avec le Fe_2O_3 dans les minérais de clinker, le FR diminue de 20 à 23 % en comparaison avec celui des minérais ne contenant que le Fe_2O_3. Cela étant, la couleur croît d'intensité et vire du blanc et du jaune clair au brun (tabl. 2). Conformément à la théorie de chromaticité des matériaux inorganiques (7), l'intensification de la couleur est due à un fort déplacement du bord de la bande d'absorption grâce à un transfert de la charge du côté des ondes longues et à un brusque accroissement d'intensité du maximum d'absorption à environ 9000 cm^{-1}. La présence de liaisons entre les polyèdres par l'intermédiaire de leurs faces et des arêtes, en particulier, entre les polyèdres du C_3S ainsi qu'une réduction incomplète du Fe^{3+} au Fe^{2+} font diminuer brusquement le FR ce qui est causé également par la formation de complexes colorants hétérovalents type $Ti^{4+} - O^{2-} - Fe^{3+}$, Ti^{4+}, $Ti^{4+} - O^{2-} - Fe^{2+}$ et $Fe^{3+} - O^{2-} - Fe^{2+}$. Des processus analogues se déroulent dans les β-C_2S et C_3A mais à un moindre degré compte tenu des particularités de leurs réseaux cristallins.

Sous un effet combiné des oxydes de Fe, Mn et Ti, les processus physico-chimiques

3.3

Tableau 3

Valeur du FR des clinkers en fonction de la teneur en oxydes de Fe, Ti et Mn et des procédés de fabrication

Composition calculée du clinker, % en masse	Teneur, % en masse			FR, % abs. pendant la cuisson et le refroidissement			
				oxydants		réducteurs	
	Fe_2O_3	TiO_2	Mn_2O_3	à l'air	dans l'eau	en milieu réducteur	dans l'eau
C_3S - 65	0,59	-	-	70,3	81,6	73,0	86,9
C_2S - 24	0,59	0,25	-	65,2	72,5	67,4	80,2
C_3A - 10 C_2F - 1	0,59	0,25	0,25	28,8	54,1	46,4	74,6

Tableau 2

Valeur du FR et couleurs des minérais en fonction de la teneur en oxydes de fer et de titane

Minérai	Teneur en oxydes, %		FR, % abs. et couleur du minérai pendant la cuisson et le refroidissement			
			oxydants		réducteurs	
	Fe_2O_3	TiO_2	à l'air	dans l'eau	en milieu réducteur	dans l'eau
C_3S	0,5	-	58,9 jaune	73,4 jaunâtre-clair	71,0 jaunâtre clair	77,0 blanc à teint jaune
	0,5	0,5	35,9 gris-brun	79,5 jaunâtre-rosâtre	49,5 brun clair	78,5 blanc à teint rose
β-C_2S	0,5	-	74,9 jaune clair	78,4 blanc à teint jaune	86,4 blanc	79,0 blanc
	0,5	0,5	54,2 jaune clair	65,6 crème	52,7 grisâtre-jaunâtre	56,4 brun clair
C_3A	0,5	-	90,0 blanc	89,6 blanc	91,8 blanc	90,8 blanc
	0,5	0,5	69,3 crème	82,2 blanc	65,6 jaunâtre	78,1 blanc à teint crème

pareils s'intensifient encore davantage grâce à une manifestation de tout un ensemble de transformations cristallochimiques dans les minérais (tabl. 1). Le résultat de ces processus est une brusque chute de FR des clinkers contenant 0,59 % de Fe_2O_3 et une quantité élevée de TiO_2 et Mn_2O_3 allant à 0,25 %. Les données obtenues (tabl. 3) montrent qu'en cas de teneur combinée en oxydes de Fe et Ti en quantités indiquées comme c'est le cas des clinkers industriels de CPB (6), le FR des clinkers diminue de 4,1 et 9,1 % dans le milieu oxydant et de 5,6 et 6,7 % dans le milieu réducteur. Le FR des clinkers diminue dans un degré encore plus grand: de 41,5 et 17,5 % et de 26,6 et 12,3 % respectivement dans le cas de la teneur combinée en oxydes de Fe, Ti et Mn. Il n'est possible d'obtenir le CPB dans ce cas qu'

en combinant la cuisson réductrice laquelle neutralise l'effet colorant des oxydes de manganèse et, partiellement, des oxydes de fer (dans les phases de silicate) avec un brusque refroidissement du clinker dans l'eau assurant une répartition dirigée des additifs de Fe et Ti dans les phases les moins colorées (C_3A et phase vitrifiée). Ceci permet d'obtenir un CPB de haute qualité à partir des matières premières à teneur combinée élevée en oxydes de fer, de manganèse et de titane.

REFERENCES

1. Ротыч Н.В. Влияние окислов некоторых переходных элементов на структуры и свойства белого портландцемента. - Автореф. дисс. канд. техн. наук, Новочеркасск, 1966. - 20 с. (en russe).
2. Технология белого портландцемента./Грачьян А.Н., Гайджуров П.П., Зубехин А.П., Ротыч Н.В. - М.: Стройиздат, 1970. - 72 с. (en russe).
3. Химическая технология стекла и ситаллов./ Под ред. Павлушкина Н.М. - М.: Стройиздат, 1983. - 432 с. (en russe).
4. Зубехин А.П., Китаев В.В. Структура железосодержащих фаз клинкера белого портландцемента и механизм повышения его коэффициента отражения. - Известия Сев.-Кавк. научного центра высшей школы, сер. Технические науки, 1982, № 4, с. 78-83 (en russe).
5. Зубехин А.П. Эффективные способы обжига и отбеливания клинкера при получении декоративных цементов. - М.: ВНИИЭСМ, 1979. - 60 с. (en russe).
6. Фомичева О.И., Бойкова А.И., Зубехин А.П. Физико-химические особенности процесса отбеливания маложелезистых клинкеров. - Цемент, 1984, № 6, с. 12-15 (en russe).
7. Коцик И., Небрженский И., Фандерлик И. Окрашивание стекла. - М.: Стройиздат, 1983. - 211 с. (en russe).

Abla Gráfica e Editora Ltda.
Rua Júlia Lopes de Almeida, 15 e 15-A
Telefones: 253-6054, 253-6296, 253-6325
Rio de Janeiro – RJ



8.º Congresso Internacional de Química do Cimento

8th International Congress on the Chemistry of Cement

8e Congrès International de la Chimie des Ciments

Communications
THEME 4
Volume V

5-

22-27 de setembro de 1986
Rio de Janeiro — Brasil

Verein Deutscher Zementwerke e.V.
4 Düsseldorf 30, Tannenstraße 2
16. MRZ. 1988

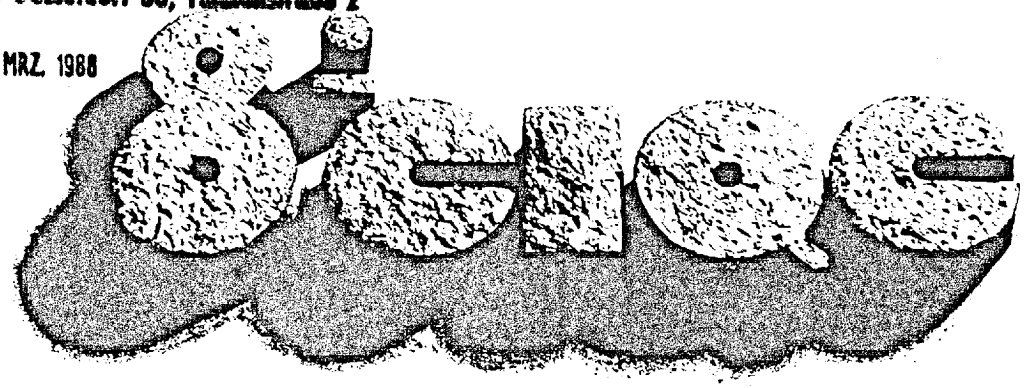

8.º Congresso Internacional de Química do Cimento

8th International Congress on the Chemistry of Cement

8e Congrès International de la Chimie des Ciments

Communications
THEME 4
Volume V

22-27 de setembro de 1986
Rio de Janeiro — Brasil

Não é permitida a reprodução dos Anais sem prévia autorização da Comissão Organizadora do Congresso.

The Proceedings are not to be reprinted without a previous permission of the Organizing Commission of the Congress.

La reproduction des Annales est interdite sans, au-devant, l'autorisation de la Commission d'Organisation du Congrès.

• • •

A substância e a forma de apresentação dos trabalhos que compõem os Anais do Congresso são de exclusiva responsabilidade de seus autores.

The substance and the form of presentation of the papers that compound the Proceedings of the Congress are exclusive responsability of their authors.

Le fond et la forme de publier les travaux qui composent les Annales du Congrès sont d'exclusive responsabilité de leur auteurs.

Secretaria Geral do 8º CIQC:
Rua da Assembléia, 10 - 40º and. - Gr. 4001
Tel.: 221-6562 – Telex: (021) 33191
20011 Rio de Janeiro – RJ – Brasil

Apoio financeiro da

finep FINANCIADORA DE ESTUDOS E PROJETOS

ORGANIZING COMMISION:

PRESIDENT:	JOSÉ ERMÍRIO DE MORAES FILHO	BRASIL
EXECUTIVE VICE-PRESIDENT:	PAULO MÁRIO FREIRE	BRASIL
TECHNICAL DIRECTOR:	FRANCISCO DE ASSIS BASÍLIO	BRASIL
ADMINISTRATIVE DIRECTOR:	JOÃO BATISTA MENESCAL FIUZA	BRASIL
DIRECTORS:	ALBERTO LUIZ GONÇALVES SOARES	BRASIL
	ENRIQUE GUNTHER DREWES	BRASIL
	EPAMINONDAS MELO DO AMARAL FILHO	BRASIL
	MARCÍLIO DE BRITO	BRASIL
	NEWTON GOULART	BRASIL

SCIENTIFIC COMMITTEES:

- SOUTH AMERICA:
  - PRESIDENT:

FRANCISCO DE ASSIS BASÍLIO	BRASIL
ALVARO AUGUSTO ALVES PINTO	BRASIL
DANTE E.J. VERONELLI	ARGENTINA
FLEMING OEST	BRASIL
HANS BUCHER	BRASIL
JOÃO GASPAR DJANIKIAN	BRASIL
LUIZ ROBERTO MARTINS DE MIRANDA	BRASIL
MARIA DAS GRAÇAS JAQUÁ	BRASIL
MARIA LUIZA MOREIRA DE MORAES	BRASIL
NEY JOSÉ DE SOUZA E SILVA	BRASIL
PABLO KITTL D.	CHILE
PAULO RODRIGUES	BRASIL
ROBERTO R. COELHO	BRASIL
YASUKO TESUKA	BRASIL
YUSHIRO KIHARA	BRASIL

- NORTH AND CENTRAL AMERICA, AND FAR EAST:
  - PRESIDENT:
  - MEMBERS:

JAN P. SKALNY	U.S.A.
DELLA M. ROY	U.S.A.
GEOFFREY FROHNSDORFF	U.S.A.
GERARD G. LITVAN	CANADA
HIROSHI UCHIKAWA	JAPAN
J. FRANCIS YOUNG	U.S.A
JORGE MARIO VILLASENOR	MEXICO
R.E. OBERHOLSTER	SOUTH AFRICA
SIDNEY DIAMOND	U.S.A.
S.W. TRESOUTHICK	U.S.A.
WU ZHONG-WEI	CHINA

- EUROPE, ASIA AND AFRICA:
  - PRESIDENT:
  - MEMBERS:

JEAN PAUL MERIC	FRANCE
C. CHARRETON	FRANCE
FRANCO MASSAZZA	ITALY
FRANÇOIS LE BEL	FRANCE
FRIEDRICH W. LOCHER	WEST GERMANY
F. YAGIZ	TURKEY
H.W.W. POLLITT	ENGLAND, U.K.
JOSE CALLEJA	SPAIN
J. TALLABER	HUNGARY
LABO KADA ABOUBACAR	NIGERIA
O.P. MTCHEDLOV-PETROSSIAN	U.S.S.R.
P. DUTRON	FRANCE
RENATO BUCCHI	ITALY
S.K. CHOPRA	INDIA
T.V. KOUZNETSOVA	U.S.S.R.
WIESLAW KURDOWSKI	POLAND

INDEX

AUTHORS'NAMES/NOMS DES AUTEURS	SUB-THEMES/SOUS-THÈMES
A	
ABBOTT, J.H.	4.2
ABDUL-MAULA, S.	4.2
ALDRIDGE, L.P.	4.2
ALKSNE, V.I.	4.2
ALKSNIS, F.F.	4.2
ALONSO, C.	4.3
ANDRADE, C.	4.3
ARPAIA, M.	4.3
B	
BAJZA, A.	4.2
BAROVSKI, N.	4.1
BERNAUDAT, F.	4.1 (2)
BLUNK, G.	4.1
BOZHINOV, G.	4.1
BRIVOT, F.	4.2
C	
CANJIANO, S.	4.3
CHIAPPINI, R.	4.1
CIGNA, R.	4.3
COPPETTI, G.	4.3
CZAJA, J.	4.3
D	
DAVIES, G.	4.3
DEDONG, LI	4.2
DIMIC, D.	4.2
DROLJC, S.	4.2
DRON, R.	4.2
E	
F	
FUKUSHIMA, Y.	4.3
G	
GASPAR-TÉBAR, D.	4.2
GEGOUT, P.	4.1
GHORAB, H.Y.	4.2
GONZÁLEZ-VILA, V.	4.2
GOUTIÈRE, G.	4.1
GUNKEL, P.	4.1
GUOKUANG, SUN	4.2
H	
HEINZ, D.	4.2
HORNAIN, H.	4.1 (2) – 4.2
I	
J	
JAIN, N.K.	4.1
JOE, Y.	4.2

K	
KADLECEK, VI.	4.3
KARYS, J.	4.3
KATAOKA, N.	4.3
KISHAR, E.A.	4.2
KOBAYASHI, S.	4.3
KOBAYASHI, W.	4.3
KOELLIKER, E.	4.2
KOTANI, H.	4.2
KOURBATOVA, I.I.	4.3
KRISHNAMOORTHY, S.	4.1
KUMAR, A.	4.1
KVARTSKHAVA, K.	4.2
L	
LAMEILLE, J.-M.	4.1
LARIONOVA, Z.M.	4.3
LAWRENCE, C.D.	4.1
LICASTRO, P.H.	4.3
LUDWIG, U.	4.2 (2)
M	
MACÍAS, A.	4.3
MALEK, R.I.A.	4.3
MARION, A.M.	4.1
MEHR, S.	4.2
MILESTONE, N.B.	4.2
MODRY, S.	4.3
MORALES, R.T.	4.2
MULLICK, A.K.	4.3
N	
NAGAOKA, S.	4.3
NAKANO, K.-I.	4.3
O	
OBERHOLSTER, R.E.	4.3
OBERSTE-PADTBERG, R.	4.2
ODLER, I.	4.2
P	
PANTSKHAVA, I.	4.2
PETIT, J.-C.	4.1
Q	
R	
REGOURD, M.	4.1 (3)
REVERTEGAT, E.	4.1 (2)
ROUSEKOVA, I.	4.2
ROY, D.M.	4.1 – 4.3
S	
SAGRERA-MORENO, J.L.	4.2
SAMUEL, G.	4.3
SANTOS, P.	4.3
SHIZAWA, M.	4.2
SINHA, S.K.	4.3
SMOLCZYK, H.-G.	4.1
ST. JOHN, D.A.	4.2
T	
TASHIRO, C.	4.3
TENOUTASSE, N.	4.1
TEODORU, G.	4.1
THURET, B.	4.1
TOGNON, G.P.	4.3
TSILOSSANI, Z.	4.2
TSUTSUMI, Y.	4.3
TURRIZIANI, R.	4.3
U	

V	
VERNET, C.	4.2
VISVESVARAYA, H.C.	4.3
VOLANT, J.	4.2
VRANA, O.	4,2
W	
WASON, R.C.	4.3
WISNIEWSKI, J.	4.3
X	
Y	
YUPING, ZHAO	4.2
Z	
ZÜRZ, A.	4.2

CONTENTS/TABLE DE MATIÈRES

THEME/THÈME 4
INFLUENCE OF CEMENT IN THE DURABILITY OF CONCRET/INFLUENCE DU CIMENT DANS LA DURABILITÉ DU BÉTON

Chairman/Président: G. WISCHERS (West Germany) – Secretary/Secrétaire: H.R.E. BUCHER (Brasil)

SUB-THEME/SOUS-THÈME 4.1
Pore Structure, Permeability and Diffusivity as Related to Durability.
Structure des Pores, Perméabilité et Diffusibilité en Liaison avec la Durabilité.

Chairman/Président: R.E. OBERHOLSTER (South Africa)
Principal Reporter/Rapporteur Principal: R.F. FELDMAN (Canada)

Pages	Authors (Countries)/Auteurs (Pays)	Titles of Papers/Titres des travaux
15	N. Tenoutasse, A.M. Marion (Belgium)	Relationship between microstructure and durability of blended cement.
22	G. Bozhinov, N. Barovsky (Bulgaria)	To the analysis of the pore structure of cement stone.
29	C.D. Lawrence (England, U.K.)	Measurements of permeability.
35	E. Revertegat, F. Bernaudat (France)	Rôle de la porosité dans la durabilité des liants hydrauliques.
41	F. Bernaudat, E. Revertegat (France)	Modelisation des phénomènes de transport dans les mécanismes d'alteration d'une pâte de ciment.
47	P. Gegout, H. Hornain, B. Thuret, M. Regoud (France)	Résistance au gel des ciments aux fillers calcaire.
53	H. Hornain, M. Regourd (France)	Microfissuration des bétons.
60	J.-M. Lameille, R. Chiappini, G. Goutière, J.-C. Petit, M. Regourd (France)	Relation entre la lixiviation d'éléments tracés (Cs, Sr et Co), et la microstrusture au cours du vieillissement d'un mortier a base de CPA.
67	S. Krishnamoorthy, N.K. Jain (India)	Influence of blending flyash with portland cement on the pore structure changes of portland cement mortars cured in NaCl solutions.
73	A. Kumar, D.M. Roy (U.S.A.)	Pore structure and ionic diffusion in Admixtures blended portland cement systems.
80	G. Teodoru (West Germany)	Influence des conditions de durcissement sur la durabilité de la pâte de ciment et du béton.
85	G. Blunk, P. Gunkel, H.-G. Smolczyk (West Germany)	On the distribution of chloride between the hardening cement paste and its pore solution.

SUB-THEME/SOUS-THÈME 4.2

Mechanism of Cement Paste Degradation due to Chemical and Physical Processes. Mécanisme de la Dégradation de la Pâte de Ciment due aux Processus Chimiques et Physiques.

Chairman/Président: G.G. LITVAN (Canada) – Principal Reporter/Rapporteur Principal: D.M. ROY (U.S.A.)

Pages	Authors (Countries)/Auteurs (Pays)	Titles of Papers/Titres des travaux
93	Zhao Yuping, Li Dedong, Sun GuoKuang (China)	Investigation into the carbonation of autoclaved aerated concrete.
99	A. Bajza, I. Rousekova, O. Vrana (Czechoslovakia)	Corrosion of hardened cement pastes by NH_4NO_3 solutions.
104	H.Y. Ghorab, E.A. Kishar (Egypt)	The stability of the calcium sulfoaluminate hydrates in aqueous solutions.
110	R. Oberste-Padtberg (France)	Degradation of hydrated cements by chloride brines.
115	R. Dron, F. Brivot (France)	Contribuition à l'étude du gonflement ettringitique.
121	C. Vernet (France)	Évolution de la microstructure des bétons au cours du test ASTM de gel-degel.
128	J. Volant, H. Hornain (France)	Évolutions des résistances mécaniques et de la microstructure de bétons traités jusqu'à 1100°C.
135	M. Shizawa, Y. Joe, H. Kotani (Japan)	Influence of ionic species on alkali-aggregate reaction.
141	N.B. Milestone, D.A.St. John, J.H. Abbott, L.P. Aldridge (New Zeland)	CO_2 corrosion of geothermal cement grouts.
145	D. Gaspar-Tébar, J.L. Sagrera-Moreno, V. González-Vila (Spain)	Contribuition à l'étude de la résistance chimique des ciments. Comportement mécanique-résistant d'un ciment portland (C_3A, calculée = 0%) aux divers solutions agressives.
151	R.T. Morales (Spain)	The sulphate resistant portland cement are not ultimate answer to the problem of sulphate attack.
159	E. Koelliker (Switzerland)	Skins of calciumcarbonate and their significance for the corrosion of concrete.
165	Z. Tsilossani, I. Pantskhava, K. Kvartskhava (U.S.S.R.)	Contraintes internes dans le béton et sa durabilité.
170	F.F. Alksnis, V.I. Alksne (U.S.S.R.)	Sur le rôle de la phase siliceuse dans les processus de destruction de la pierre de ciment dans les millieux de sulfate.
175	A. Zürz, I. Odler, S. Abdul-Maula (West Germany)	Thermal decompositon of hydrated cement pastes.
181	U. Ludwig, S. Mehr (West Germany)	Destruction of historical buildings by de formation of ettringite or thaumasite.
189	D. Heinz, U. Ludwig (West Germany)	Mechanism of subsequent ettringite formation in mortars and concretes after heat treatment.
195	D. Dimic, S. Droljc (Yugoslavia)	The influence of alite content on the sulphate resistance of portland cement.

SUB-THEME/SOUS-THÈME 4.3
Compatibility of Cement Paste with Aggregates and Reinforcements, Including Electrochemical Corrosion.
Compatibilité de la Pâte de Ciment avec les Granulats et les Armatures, y Compris la Corrosion Életrochimique.

Chairman/Président: R. CIGNA (Italy) – Principal Reporter/Rapporteur Principal: R. TURRIZIANI (Italy)

Pages	Authors (Countries)/Auteurs (Pays)	Titles of Papers/Titres des travaux
203	Vl. Kadlecek, S. Modry (Czechoslovakia)	Effect of degree of compatibility of cement and aggregates on concrete durability under conditions of higher temperatures action.
208	H.C. Visvesvaraya, A.K. Mullick, G. Samuel, S.K. Sinha, R.C. Wason (India)	Alkali reactivity of granitic rock aggregates.
214	M. Arpaia, R. Cigna, R. Turriziani (Italy)	Corrosion behaviour of TAD, diffused reinforcement concrete tubes.
220	G.P. Tognon, S. Cangiano, G. Coppetti (Italy)	Thermomechanical compatibility of aggregates in autoclaved very high strength concretes.
226	C. Tashiro, Y. Fukushima (Japan)	Effect of zinc oxide admixture on corrosion inhibition of iron in cement mortar contaning sea water.
231	W. Kobayashi, N. Kataoka, Y. Tsutsumi (Japan)	On the behaviour of alkali in alkali-aggregate reaction.
237	K.-I. Nakano, S. Kobayashi, S. Nagaoka (Japan)	Influence of reactive aggregate and alkali compounds of expansion of alkali-slica reaction.
243	J. Wisniewski, J. Karys, J. Czaja (Poland)	Protection chimico-potentiostatique de l'armature dans le béton.
249	G. Davies, R.E. Oberholster (South Africa)	Chemical and swell properties of the alkali-silica reaction product.
256	C. Andrade, C. Alonso, P. Santos, A. Macías (Spain)	Corrosion behaviour of steel during accelerated carbonation of solutions which simulate the pore concrete solution.
263	R.I.A. Malek, P.H. Licastro, D.M. Roy (U.S.A.)	The compatibility between an expansive grout and its restraining environment.
268	Z.M. Larionova, I.I. Kourbatova (U.S.S.R.)	Première hydratation des ciments et formation de gel au contact avec des aggrégats.

THEME/THÈME 4

Influence of cement in the durability of concrete. Influence du ciment dans la durabilité du béton.

Chairman/Président:

G. Wischers
Forschungsinstitut der Zementindustrie, Dusseldorf, West Germany.

Secretary/Secrétaire:

H. R. E. Bucher
Associação Brasileira de Cimento Portland, São Paulo, Brasil

SUB-THEME/SOUS-THÈME 4.1

Pore structure, permeability and diffusivity as related to durability.

Structure des pores, perméabilité et diffusibilité en liaison avec la durabilité.

Chairman/Président:

R. E. Oberholster
National Building Research Institute
Pretoria, South Africa

Principal Reporter/Rapporteur Principal:

R. F. Feldman
Division of Building Research
National Research Council
Ottawa, Ontario, Canada

N. TENOUTASSE and A.M. MARION

Relationship between Microstructure and Durability of Blended Cement

RELATIONSHIP BETWEEN MICROSTRUCTURE AND DURABILITY OF BLENDED CEMENT

N. TENOUTASSE, S.A. REDCO, Research, Engineering and Development Company, c/o ETERNIT N.V., 2920 KAPELLE-OP-DEN-BOS (Belgium) and U.L.B. (Brussels University), Department of Industrial and Solid State Chemistry, Avenue F.D. Roosevelt 50, 1050 BRUSSELS (Belgium)
A.M. MARION, U.L.B. (Brussels University), Department of Industrial and Solid State Chemistry, Avenue F.D. Roosevelt, 1050 BRUSSELS (Belgium)

SUMMARY

The influence of Belgian PFA (Powder Fly Ashes) substitution (10 to 80 %) on the hydration of OPC (Ordinary Portland Cement) was studied.

Scanning Electron Microscopy (SEM) and Energy Dispersive Analysis of X-Rays (EDAX) were used in this investigation.

The hydration time varies from three days to two years.

The release of alkalis from pure PFA has been investigated by Atomic Absorption Spectrometry.

The SEM data concerning OPC + PFA mixtures, at different hydration periods, demonstrate the pozzolanic activity of PFA and the deep heterogeneity of the pozzolanic reaction. After one year of hydration, some PFA particles seem to be intact, whereas others are completely reacted.

The authors propose an original mechanism for the understanding of the attack of PFA particles by $Ca(OH)_2$ generated by cement hydration. The presence of a new well crystallized compound (hexagonal shape) in the long time hydrated fly ash cement allows us to propose some original explanation with regard to the beneficial effect of fly ash substitution in preventing harmful alkali aggregate reaction.

Estudou-se a influência das PFA belgas (Cinzas Volantes em Pó), em adições de 10 a 80%, sobre a hidratação de OPC (cimento portland comum).

Na investigação se utilizou microscopia eletrônica de varredura (SEM) e análise dispersiva de raio - X (EDAX).

O tempo de hidratação varia de três dias a três anos.

Usando espectroscopia de absorção atômica, investigou-se a liberação de álcali das PFA puras.

Os dados de SEM relativos às misturas de OPC + PFA, em diferentes períodos de hidratação, demonstram a atividade pozolânica de PFA e a heterogeneidade profunda da reação pozolânica. Depois de um ano de hidratação, algumas partículas de PFA parecem estar intactas, enquanto outras reagiram completamente.

Os autores propõem um mecanismo original para o entendimento do ataque às partículas de PFA por $Ca(OH)_2$ gerado pela hidratação do cimento. A presença de um composto novo bem cristalizado (de forma hexagonal) no cimento de cinza volante hidratado há longo tempo, permite-nos propor uma explicação original com relação ao efeito benéfico da substituição de cinza volante para prevenção da reação prejudicial do agregado alcalino.

N. TENOUTASSE and A.M. MARION

Relationship between Microstructure and Durability of Blended Cement

INTRODUCTION

Direct economy factors coupled with an increasing awareness of the need to protect the environment and conserve energy have combined to focuse attention on the use of fly ash in concrete.

Fly ash is considered by some authors to be effective in reducing expansion due to alkali aggregate reactivity (1, 2). It is now admitted that alkalis react simultaneously with both reactive aggregate and pozzolanes, in amount that are directly proportional to their surface area (3).

However, the exact mechanism by which mineral admixtures are able to reduce expansion is still imperfectly understood.

The quantity of OPC that can be replaced should be carefully considered. Furthermore, fly ash must be readily reacted by alkalis, have a fine particle size and contain negligible amounts of soluble alkalis. Indeed, some investigators (4, 5) have pointed out that it is the soluble alkali and not the total alkali content of the fly ash, which plays a role in increasing the alkali-silica reactivity.

In that field, the authors obtained interesting chemical data concerning the solubility behaviour of alkalis from Belgian fly ashes, in different conditions (6).

The question related to "the PFA alkali development" in blended cement can, to some extent, be elucidated by SEM-EDAX examination of such a long period hydrated cement.

MATERIALS AND METHODS

The cement used in this study was an OPC ASTM Type I ; its specific surface was 2500 cm^2/g (ASTM C 204 : Standard Test Method of Fineness by Air Permeability Apparatus). The mineralogical composition is : 60.1 % C_3S, 9.4 % C_2S, 8.9 % C_3A, 9.9 % C_4AF and 3.5 % $CaSO_4$; the Na_2O and K_2O contents are respectively 0.30 % and 0.39 %.

PFA 4 has been selected because of its chemical composition (Table 2) which symbolizes that of fly ash commonly produced by Belgian power stations. Belgian fly ashes are in the class F category of ASTM C 618-80 : their SO_3 and lime contents are very low. The K_2O and Na_2O contents of PFA 4 are respectively 0,71 % and 2.21 %.

Mullite, quartz and magnetite are the main crystalline components of PFA 4. The microstructure of cement containing from 0 to 80 % PFA 4 was investigated by SEM coupled with EDAX, for hydration times from three days to two years.

The alkali release of PFA 4 was studied by atomic absorption spectrometry.

RESULTS AND DISCUSSIONS

Characterization of fly ashes

A previous work (7) reported some interesting data concerning the solubility of PFA alkali oxides in water, and lime saturated solutions. These results allow us to propose a different location for the two alkali oxides (Na_2O-K_2O).

The release of alkali from PFA was checked in OPC and OPC + 25 % PFA 4, by analyzing the chemical composition of the pore fluid, from 5 minutes to 8 hours.

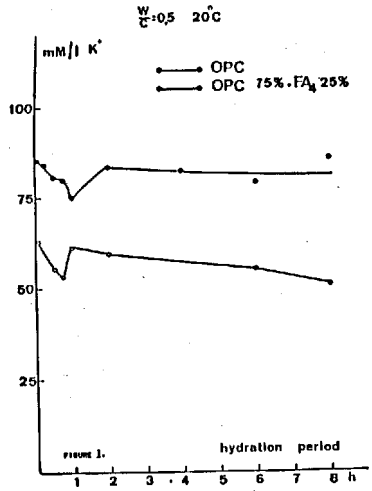

figure 1.

As it can be seen in *figure 1*, the replacement of 25 % of OPC by PFA leads to a lower K_2O content in the liquid phase. This observation suggests that the K^+ concentration in the aqueous phase is only due to cement, and hence, confirms the low solubility of K_2O from PFA ; indeed, it seems that alkalis are more easily released from cement than from PFA 4. This fact is interesting and reassuring with regard to the use of cement blended with PFA ; indeed, the K_2O content in PFA 4 is relatively higher than OPC.

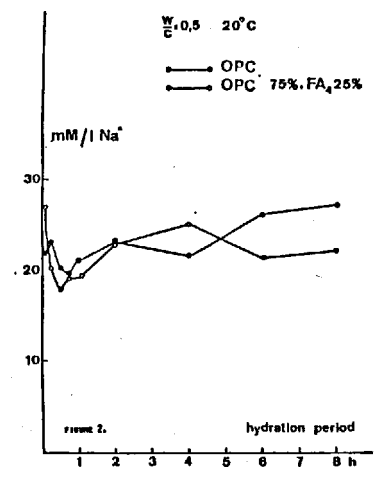

figure 2.

Figure 2 presents the solubility behaviour of Na_2O in pure and blended cements (25 % PFA 4). PFA 4 releases some sodium into solution, but no significant change is observed between the two concentration profiles.

SEM AND EDAX EXAMINATIONS

Characterization of the pozzolanic reaction

The pozzolanic reaction involving the glassy phase of the PFA particles and the $Ca(OH)_2$ generated by cement hydration has been investigated by SEM coupled with EDAX.

The examination of cement blended with low and high PFA contents (10 to 80 %) by SEM, has permitted to observe, after 14 days, the pozzolanic activity of some PFA particles : they exhibit at their surface typical constitutive mullite crystals *(Figure 3)*. However, it is important to note that, as well as the amount of free lime, the mechanical performances of such a blended cement do not permit to conclude to a significant pozzolanic reaction at this age.

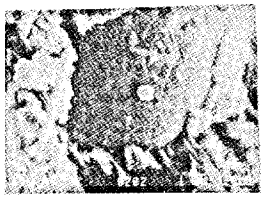

Figure 3.
OPC + 20 % PFA 4
(14 days)

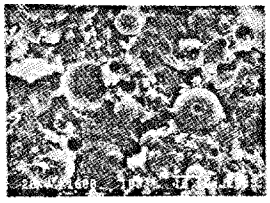

Figure 4.
OPC + 10 % PFA 4
(2 years)

It is surprising to note, even in the case of low PFA blended cement (10 %) the persistence of fly ash particles intact, after two years of hydration *(Figure 4)*.

These data demonstrate the profound heterogeneity of the pozzolanic reaction : each PFA particle presents an intrinsic pozzolanic behaviour which is conditioned by its "thermal history". The cooling process in the burning zone promotes the inhomogeneous distribution of chemical compounds in fly ash particles, as demonstrated by the authors for both alkali oxides (6).

The pozzolanic reaction appears as an erosion of the vitreous phase of the PFA particles ; among mullite crystals, quartz and in some cases, small radial crystals become observable on the surface of the reacted particle as demonstrated respectively on *figures 5* and *6*.

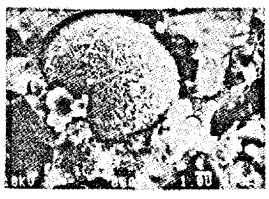

Figure 5.
OPC + 80 % PFA 4
(60 days)

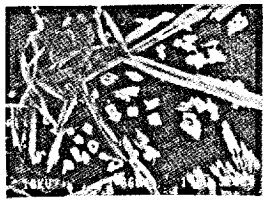

Figure 6.
OPC + 60 % PFA 4
(120 days)

As the reaction progresses, macropores become apparent at the surface of PFA particles *(Figure 7)*.

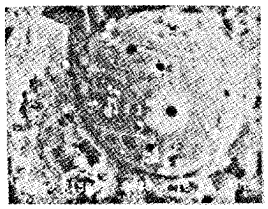

Figure 7 - OPC + 20 % PFA 4 (1 year)

Those macropores are formed during the cooling process of PFA and generally are not observable at the surface of unattacked particles *(Figures 8 and 9)*.

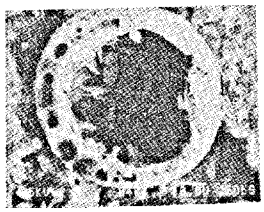

Figure 8.
OPC + 40 % PFA 4
(150 days)
UNATTACKED PARTICLE



Figure 9.
OPC + 20 % PFA 4
(120 days)
ATTACKED PARTICLE

In the ultimate stage of the reaction, the particles are desintegrated *(Figure 10)*.

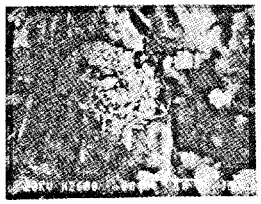

Figure 10 - OPC + 50 % PFA 4 (9 months)

PRODUCTS OF THE POZZOLANIC REACTION

The pozzolanic reaction promotes the massive formation of CSH *(Figure 11)*. In some cases, when the PFA particle is entirely reacted, a CSH colony follows the exact shape of the original PFA particle *(Figure 12)*. EDAX reveals the presence of non negligible amounts of aluminium in CSH : this observation demonstrates well the pozzolanic reaction between the silico-aluminous vitreous phase of PFA and $Ca(OH)_2$.

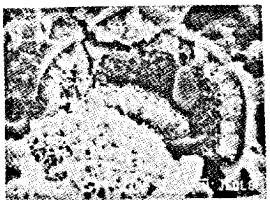

Figure 11.
OPC + 30 % PFA 4
(120 days)

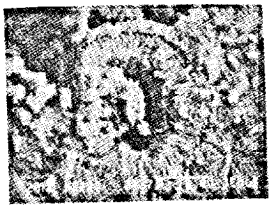

Figure 12.
OPC + 10 % PFA 4
(1 year)

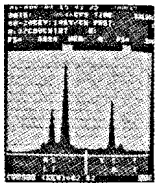

Chemical composition 1.

After long hydration periods, SEM does not point out any trace of mullite crystals in the cement paste, whereas X-rays diffraction exhibits typical mullite spectrum lines. The hypothesis of such residual crystals embedded in CSH matrix has to be considered, mullite behaving then probably like an active site for the microcrystallization of CSH gel.

Calcium monosulfoaluminate (MSA), better crystallized than in pure paste, is observed after long hydration period of PFA cements *(Figure 13)*. Probably alumina from both PFA and OPC react concommitantly to form such crystals.

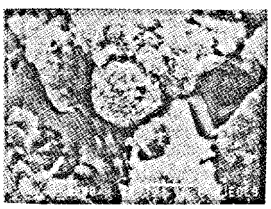

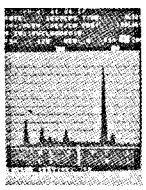

Figure 13.
OPC + 10 % PFA 4
(2 years)

Chemical composition 1.

The most exciting microscopical results concern the presence of well crystallized plates (apparently in the hexagonal system) in PFA blended cement *(Figure 14, 14(a), 14(b))*. The morphology reminds that of $Ca(OH)_2$ and/or MSA, but EDAX shows high silica and alumina amounts and an appreciable K content. The number of these plates seems to be proportional to the PFA content of the hardened paste.

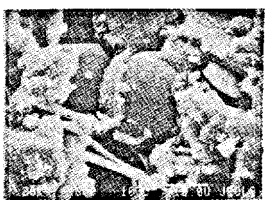

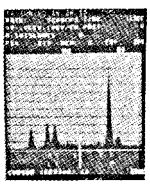

Figure 14.
OPC + 30 % PFA 4
(2 years)

Chemical composition 1.



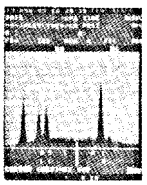

Figure 14(b).
OPC + 20 % PFA 4
(2 years)

Chemical composition 1.

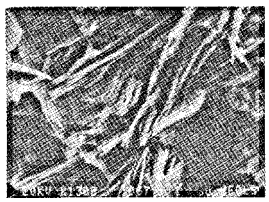

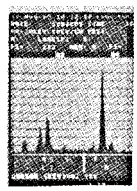

Figure 14(b).
OPC + 80 % PFA 4
(2 years)

Chemical composition 1.

The identification by EDAX of both Si and S in some of these hexagonal plates *(Figure 15)* suggests the formation of solid solution between MSA and that compound.

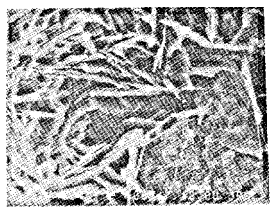

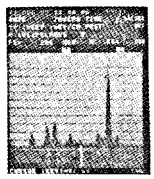

Figure 15.
OPC + 30 % PFA 4
(2 years)

Chemical composition 1.

The most interesting observation is related to the amount of potassium of this crystalline compound which demonstrates that PFA alkalis are kept in hydrated products resulting from the pozzolanic reaction.

It is well known that many of the PFA materials have some sorptive capacity for sodium and especially for potassium (8).

These microscopical data could permit to establish a closed relationship between the pozzolanic reaction and the alkali aggregate reaction. Indeed, the existence of this pozzolanic reaction product with such a morphology which reminds quite enough that of some alkali aggregate reaction products, allows us, to some extent, to better understand the beneficial effect of PFA in this "concrete disease". There is clearly a variety of alkali aggregate reaction rather than a single one : the reaction product can contain aluminium and iron originally associated to impurities in the reactive aggregate, and its calcium content is variable. This calcium content derives from $Ca(OH)_2$ and even CSH gel crystals in the vicinity of the alkali aggregate sites.

Some authors found (9) that in "reactive concrete containing PFA", the amount of calcium in reaction product was considerably greater than that of concrete without PFA. It can be suggested (10) that PFA acts so as to bring about an increase of the amount of $Ca(OH)_2$ in the vicinity of silica reactive surface (including PFA particles themselves, and directly siliceous reactive aggregates) ; $Ca(OH)_2$ could be distributed more uniformly throughout the PFA-OPC system.

So the PFA does not inhibit alkali-silica reaction, but facilitates the mobilization of calcium into reactive siliceous particles, leading to the formation of gels with high calcium concentration.

It is well known that when the alkali-silica complex reacts with $Ca(OH)_2$, it forms the white opaque non swelling calcium-alkali-silica complex (4). The favourable effect of PFA particles in the alkali aggregate reaction could be resumed as follows. Their pozzolanic activity, which allows them to "attract" and/or to react with $Ca(OH)_2$, associated with their ability to fix alkalis, contributed to the formation of a stable compound : a calcium hydroxide - alkali hydroxide - silica reaction product which does not absorb water.

MECHANISM OF POZZOLANIC REACTION

Microscopical examination of cement blended with PFA allows the authors to propose some original mechanism that better explain the pozzolanic reaction.

Previous comment has suggested that some siliceous phase with pozzolanic properties can promote the better dispersion of $Ca(OH)_2$ throughout the cement paste. Closely related to this hypothesis, the existence of some "active sites" at the external and internal surfaces of the PFA particles should be considered.

Throughout those data, a model could be proposed for the pozzolanic reaction mechanism, involving the following steps.

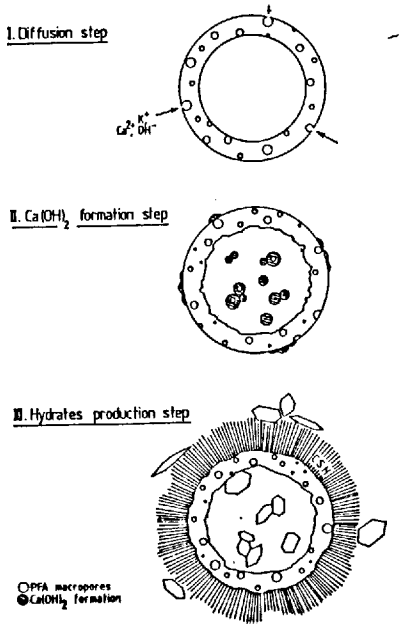

The first step (I) consists in the diffusion of the aqueous phase through the cement paste and/or the macropores of the PFA particles, into the active sites.

The second step (II) is the precipitation of $Ca(OH)_2$ on the active site (internal and external) to form circular $Ca(OH)_2$ masses.

The reaction between these masses and the silico-aluminous vitreous phase of PFA particles constitutes the third step of the pozzolanic reaction. This leads to the formation of CSH gel containing aluminum (and potassium in some cases), and to well crystallized calcium silico-aluminate containing potassium.

The reaction model is perfectly illustrated by SEM micrographs. *Figures 16* and *16(a)* show the formation of $Ca(OH)_2$ at internal and external sites of a PFA particle. The macropore through which the calcium saturated aqueous phase has diffused can be observed in the centre of some $Ca(OH)_2$ masses *(Figure 16(b))*.

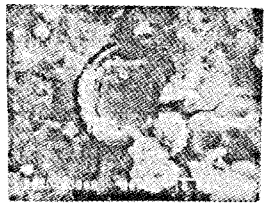

Figure 16.
OPC + 40 % PFA 4
(60 days)

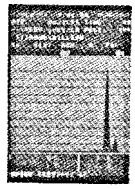

Chemical composition 1.



Figure 16(a).
OPC + 30 % PFA 4
(60 days)

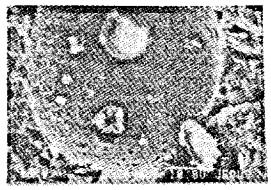

Figure 16(b).
OPC + 40 % PFA 4
(120 days)

The reaction progresses, promoting CSH formation *(Figure 17)* and crystal development, inside *(Figure 18)* as well as outside *(Figure 19)* of the PFA particle.

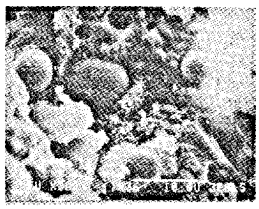

Figure 17.
OPC + 80 % PFA 4
(2 years)

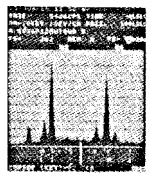

Chemical composition 1.

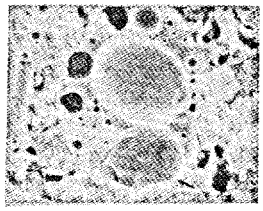

Figure 18.
OPC + 40 % PFA 4
(2 years)

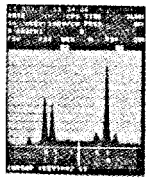

Chemical composition 1.

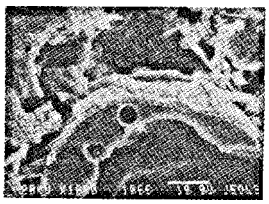

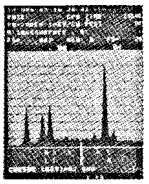

Figure 19. *Chemical composition 1.*
OPC + 60 % PFA 4
(2 years)

As it can be seen in *Figure 20*, when the sample is prepared for microscopical examination, some of the circular $Ca(OH)_2$ masses can be removed from the PFA particles, and it is easy to observe the "replica" of these formations, resulting from the pozzolanic reaction.

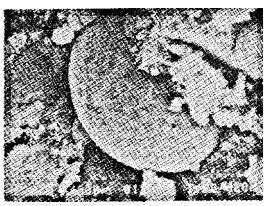

Figure 20 - OPC + 30 % PFA 4 (90 days)

CONCLUSIONS

1. During the early stages of hydration, no significant alkali release is observed in cement blended with low PFA content, in comparison with OPC. This confirms the very low solubility of alkalis from PFA 4.

2. During this investigation, the authors have found significant differences between fly ash particles. Indeed, we have found some particles that are never acting even after two years and other ones that present a pozzolanic reaction very early.

   Concerning the mechanism of pozzolanic reaction, according to classical pictures, fly ash acts as a so-called "pozzolan" ; it reacts with calcium-hydroxide liberated by C_3S and C_2S hydrations.

   According to S. DIAMOND, actually we have not enough data to understand this phenomenon (11).

   For the first time, the authors have proposed a mechanism for the pozzolanic reaction between PFA particles and calcium hydroxide in a cement matrix.

   This mechanism can be summarized through the following steps :

   a) diffusion step
   b) $Ca(OH)_2$ formation step
   c) hydrates production step

3. The presence of some well crystallized hydrates containing significant amounts of potassium has been observed by the SEM-EDAX examination of cement blended with PFA.

It is probably the generation of such a reaction product that could better explain the beneficial effect of the PFA particles namely preventing the harmful alkali aggregate reaction ; however, more data are needed to confirm this hypothesis.

ACKNOWLEDGEMENT

This paper reports results that are a part of a research contract between I.R.S.I.A. (Institut pour l'Encouragement de la Recherche Scientifique dans l'Industrie et l'Agriculture, Brussels) and C.R.I.C. (Centre National de Recherches Scientifiques et Techniques pour l'Industrie Cimentière, Brussels) devoted to the study of blended cements.

The authors gratefully acknowledge I.R.S.I.A. for their financial support.

REFERENCES

(1) BERRY E.E. and MALHOTRA V.M., "Fly Ash for Use of Concrete - A critical review", ACI Journal, Vol. 2, No. 3, March-April 1982, pp. 59-73.

(2) DIAMOND S., "Effect on two Danish Fly Ashes on Alkali Content of Pore Solution of Cement - Fly Ash Parts", Cement and Concrete Research, Vol. II, 1981, 383-394.

(3) VIVIAN H.E., "The Process of Alkali Aggregate Reaction, Water Absorption, Reacted Aggregate Swelling, Expansion of Mortar and Concrete and Pozzolan Behaviour", Proceedings of the 6th International Conference on Alkalis in Concrete, Copenhagen, 1983, pp. 187-194.

(4) OSBAECK P., SMIDTH F.L., "Alkalis and Cement Strength", Proceedings of the 6th International Conference on Alkalis in Concrete, Copenhagen, 1983, pp. 93-100.

(5) MEHTA P.K., "Pozzolanic and Cementitious By-products as Mineral Admixtures for Concrete - A critical review", Proceedings of the Conference on Fly Ash, Silica Fume, Slag and Other Mineral By-products in Concrete, Vol. I, pp. 1-45.

(6) TENOUTASSE N. and MARION A.M., "Mechanism of Hydration of Cement Blended with PFA", to be published in ASTM publications.

(7) TENOUTASSE N. and MARION A.M., "Influence of Fly Ashes on the Structure of OPC and Pure Calcium Silicates", Proceedings of the British Ceramic Society Meeting on the Chemistry and Chemically Related Properties of Cement, London, April 1984, pp. 359-374.

(8) MARR J. and GLASSER F.P., "Effect of Silica, PFA and Slag Additives on the Composition of Cement Pore Fluid", Proceedings of the 6th International Conference on Alkalis in Concrete, Copenhagen, 1983, pp. 239-242.

(9) DIAMOND S., "Alkali Reaction in Concrete - Pore Solutions Effects", Proceedings of the 6th International Conference on Alkalis in Concrete, Copenhagen, 1983, pp. 155-166.

(10) KAWAMURA M., TAKEMOTO K. and HASABA S., "Application of quantitative EPXA analyses and Microhardness Measurements to the Study of Alkali-silica Reaction Mechanism", Proceedings of the 6th International Conference on Alkalis in Concrete, Copenhagen, 1983, pp. 167-174.

(11) DIAMOND S., "The Characterization of Fly Ashes", Proceedings of Symposium on Effects of Fly Ash Incorporation in Cement and Concrete, Boston, November 1981, pp. 12-19.

G. BOZHINOV, N. BAROVSKY

TO THE ANALYSIS OF THE PORE STRUCTURE OF CEMENT STONE

4.1

A L'EGARD DE L'ANALYSE DE LA STRUCTURE POREUSE DU CIMENT DURCI

SUMMARY

The genesis and development in time of the pore space in cement pastes are analysed in terms of the up-to-date concepts on the hardening and structure formation of cement stone.

A physical model is involved to define and illustrate the main pore structure characteristics (total and partial pore volumes, gel and capillary pores etc.). On this basis some classification schemes of pores are considered as well.

The role and influences of some technological factors (mineral composition and Blaine fineness, water/cement ratio, conditions and duration of hardening) on the pore volume changes in time are discussed using respective analytical relations and experimental data.

On the basis of the analysis presented one can obtain more detailed information about the physical nature of the pore structure of cement stone and substantial role in the synthesis of the physico-chemical and mechanical properties of cement concretes.

SUMÁRIO

A gênese e desenvolvimento do espaço ocupado pelos poros nas pastas de cimento ao longo do tempo são analisados em termos atualizados de endurecimento e formação da estrutura da pasta.

Um modelo físico é proposto para definir as características principais dos poros (volume total e parcial dos poros, poros capilares e do gel etc.). Nesta base, alguns esquemas de classificação dos poros são também considerados.

A importância e influência de alguns fatores (composição mineral, e finura Blaine, relação água/cimento e condições e duração de endurecimento) na mudança de volume dos poros ao longo do tempo são discutidas usando-se relações analíticas e dados experimentais.

Com base na análise apresentada, podem-se obter informações mais detalhadas sobre a natureza física da estrutura dos poros na pasta de cimento e sua importância fundamental na síntese das propriedades físico-químicas e propriedades mecânicas do concreto.

INTRODUCTION

THE CEMENT STONE, THAT IS THE HARDENED CEMENT PASTE, IS A TYPICAL POROUS BODY. ITS PROPERTIES DEPEND TO A GREAT EXTENT ON THE STRUCTURE OF THE PORE SPACE. THE TERM "PORE STRUCTURE" HAS BEEN DEFINED COMPLETELY BY ZAGAR (1) AS A COMPLEX PROPERTY OF THE SOLID MATERIALS CONTAINING VOIDS BIGGER THAN MOLECULAR DIMENSIONS. IT INCLUDES THE VOLUME OF THE VOIDS /POROSITY/, THEIR SURFACE, GEOMETRICAL AND FUNCTIONAL MORPHOLOGY, SIZE DISTRIBUTION AND SOME PARAMETERS TAKING INTO ACCOUNT THE SHAPE AND SPATIAL DISTRIBUTION OF PORES.

PORE STRUCTURE HAS BEEN A SPECIAL SUBJECT OF INVESTIGATION BY MANY AUTHORS FROM VARIOUS POINTS OF VIEW. IRRESPECTIVE OF SO MUCH ATTENTION TO THE PROBLEM THE PHYSICAL NATURE OF THE PHENOMENA THAT CAUSE OR ATTEND TO THE ORIGIN AND DEVELOPMENT OF THE PORE STRUCTURE IN TIME IS STILL NOT CLEAR AND THIS SEEMS TO SUSTAIN A PERMANENT INTEREST.

IN THIS PAPER AN ATTEMPT IS MADE TO DISCUSS THE ORIGIN OF THE PORES IN THE HARDENING CEMENT PASTE AND TO EVALUATE APPROXIMATELY THE PORE VOLUMES ON THE BASIS OF A SIMPLIFIED PHYSICAL MODEL PROPOSED.

ORIGIN OF THE PORE SPACE IN CEMENT STONE

IT IS USUAL TO START WITH THE STATE OF THE FRESH CEMENT PASTE, WHICH IS REGARDED AS A THICK SUSPENSION OF THE CEMENT PARTICLES IN MIXING WATER (2). THE STRUCTURE OF SUCH A SYSTEM IS CHARACTERISED BY THE VOLUME CONCENTRATION OF THE CEMENT PARTICLES IN THE SOLUTION, THEIR SIZE DISTRIBUTION, INTERPARTICAL FORCES AND ADSORBTION OF WATER ON THE SOLID SURFACES. A TYPICAL FLOCULENT STATE IS ALSO INHERENT TO CEMENT PASTE (3).

IMMEDIATELY AFTER MIXING THE CEMENT WITH WATER THE ABSOLUTE VOLUME OF THE CEMENT PASTE CONSISTS OF THE VOLUMES OF THE CEMENT /CEMENT GRAINS ASSUMED UNPOROUS/, MIXING WATER AND POSSIBLY AIR VOIDS. THE LATTER TWO VOLUMES FORM THE SO CALLED "FREE VOLUME" OF THE CEMENT PASTE, WHICH IS INITIALLY AVAILABLE FOR THE CEMENT HYDRATION PRODUCTS TO GROW IN (4). DURING THE PROCESS OF HYDRATION THIS VOLUME INCREASES AT THE EXPENSE OF THE REACTING PORTIONS OF CEMENT AND WATER. ON THE OTHER HAND PART OF IT IS SIMULTANEOUSLY FILLED BY THE HYDRATION PRODUCTS FORMED AT THE TIME CONSIDERED. IN THIS CONTEXT IT MAY BE REASONABLE TO THINK THAT THE WATER CONTENT IN THE PASTE IS ONE OF THE MAIN SOURCES OF THE PORE SPACE AND THAT THE STATE OF WATER IN THE HARDENING SYSTEM SHOULD PLAY AN IMPORTANT ROLE.

THE HYDRATION PRODUCTS THAT ARISE AS A RESULT OF THE CHEMICAL REACTIONS BETWEEN CEMENT COMPOUNDS AND WATER ARE PRESENTED IN GENERAL BY TWO TYPES OF SUBSTANCES (5): POORLY CRYSTALLIZED MATTER, THAT IS THE CALCIUM SILICATE HYDRATES /C-S-H GEL/ BEING THE PREDOMINANT PHASE AND, PARTLY, THE CALCIUM ALUMINATE HYDRATES /C-A-H GEL/; AND RELATIVELY WELL-CRYSTALLIZED PHASES, SUCH AS CALCIUM HYDROXIDE AND ETTRINGITE. ALL OF THE HYDRATION PRODUCTS ARE OF VARIOUS DIMENSIONS AND MORPHOLOGY WITH MORE OR LESS EXTENSIVE INTERLOCKING OF THE PARTICLES AND SPECIFIC

PROPERTIES OF THE LIQUID PHASE IN THE HARDENING SYSTEM. IN THE COURSE OF TIME THE INITIAL FREE VOLUME IN THE CEMENT PASTE IS GRADUALLY FILLED BY THESE PRODUCTS, THE STRUCTURE OF THE PASTE BECOMES INCREASINGLY DENSER. THE INITIAL LABILE STRUCTURE OF THE PASTE IS STEP-BY-STEP CONVERTED INTO A CONDENSED MACHANICALLY STABLE STRUCTURE OF CEMENT STONE.

AS KNOWN, THE ABSOLUTE VOLUMES OF THE HYDRATES ARE LARGER THAN THOSE OF THE INITIAL UNHYDRATED GRAINS /SWELLING/, BUT SMALLER THAN SUMMARY ABSOLUTE VOLUMES OF THE CEMENT GRAINS AND WATER REACTED /CONTRACTION OF THE SYSTEM/. WHEN THE WATER-CEMENT RATIO EXCEEDS THE VALUE THAT CORRESPONDS TO THE STOICHIOMETRY OF THE REACTIONS THE INITIAL VOLUME OF THE PASTE DOES NOT PRACTICALLY CHANGE DURING THE PROCESS OF HYDRATION (6). AS A RESULT CONTRACTING PORES ORIGINATE PERFORCE.

ANOTHER REASON, MAY BE MORE IMPORTANT, TO FORM PORE SPACE IS RELATED TO THE MORPHOLOGY AND DISTRIBUTION OF THE SOLID PARTICLES INTO THE HARDENING SYSTEM. THE COMPLEX INTERNAL STRUCTURE OF THE HYDRATES WITH EXREMELY DEVELOPED SURFACE AREA AND SORPTION ABILITY TO WATER, BOND CAPACITY, MUTUAL DISTRIBUTION AND COHERENCE OF THE PARTICLES PREDETERMINE THE CONDITIONS THAT A TYPICAL PORE STRUCTURE SHOULD FORM. IN THIS CONTEXT SOME PECULIARITIES CONCERNING THE STATE OF WATER IN THE HARDENING SYSTEM SHOULD BE MENTIONED (7). A PART OF THE MIXING WATER IN HARDENING CEMENT PASTE IS CHEMICALLY COMBINED IN THE HYDRATION PRODUCTS /WITH BASIC OR SECONDARY VALENCES/, ANOTHER PART IS ADSORBED ON SOLID SURFACES AND A PART REMAINS OUTSIDE THE FORCE FIELDS OF SOLID SURFACES /CAPILLARY WATER/. THESE SORTS OF WATER DIFFER IN DENSITY, AND THUS IN SPECIFIC VOLUMES, BOND FORCES TO SOLID PHASE AND VOLATILITY. THE SEPARATION OF THE CHEMICALLY COMBINED WATER FROM THE ADSORBED AND CAPILLARY WATER IS DISCUSSED BY POWERS (8) ON THE BASIS OF SOME EXPERIMENTS UNDER SPECIAL DRYING CONDITIONS AND THE TERMS NON-EVAPORABLE WATER AND EVAPORABLE WATER ARE INVOLVED TO DESIGNATE THESE TWO CLASSES OF WATER RESPECTIVELY. ACCORDING TO THIS CONSIDERATION IN A HARDENED CEMENT PASTE THE SPACE OCCUPIED BY THE VOLUME OF THE EVAPORABLE WATER SHOULD CORRESPOND TO THE TOTAL VOLUME OF THE PORES, THE LATTER CONSISTING OF GEL PORES AND CAPILLARY PORES. SUCH A CLASSIFICATION OF PORES SEEMS TO BE ACCEPTABLE FOR THE AUTHORS BECAUSE IT IS BASED ON THE PHYSICAL NATURE OF THE MATERIAL. IN ADDITION, KONDO AND DAIMON (9) DIFERENTIATE THE GEL PORES INVOVING THE TERMS INTER CRYSTALLITE AND INTRACRYSTALLITE PORES. IN PORE STRUCTURE ANALYSIS SOME AUTHORS OFTEN USE THE TERMS MICRO-, MESO- AND MACROPORES TO DENOTE THE SIZE RANGE /APPROXIMATE RADII/ OF THE PORES.

IT MAY BE CONCLUDED THAT, IRRESPECTIVE OF SOME DISTINCTIONS AND CONTRADICTIONS IN THE APPROACH TO THE PROBLEM, THE TOTAL PORE VOLUME IN A WATER SATURATED HARDENING CEMENT PASTE DIRECTLY CORRESPONDS TO THE SPACE OCCUPIED BY THE EVAPORABLE WATER. THAT IS, THE TOTAL PORE VOLUME MAY BE PRESENTED AS A DIFFERENCE BETWEEN THE TOTAL VOLUME OF THE

HARDENED PASTE AT A GIVEN TIME AND THE ABSOLUTE VOLUME OF THE SOLID PHASE AT THE SAME TIME IF THE AIR CONTENT IS NEGLECTED. IN SOME CASES THE CONTRACTION POROSITY NEEDS TO BE CONSIDERED ESPECIALLY AND THE CONTRACTING PORES ARE TO BE TREATED AS A SEPARATE FRACTION OF THE TOTAL PORE VOLUME (10). IN SUCH CASES IT IS NECESSARY TO SPECIFY ADDITIONALLY FRACTIONAL PORE VOLUMES.

A SIMPLIFIED MICRO-STRUCTURE MODEL OF CEMENT STONE

TO ANALYSE THE PROPERTIES OF THE HARDENING CEMENT PASTE IT IS USUAL TO INVOLVE MORE OR LESS SIMPLIFIED MODELS WHICH PRESENT AT LEAST THE MAIN STRUCTURE PECULIARITIES OF THE REAL MATERIAL. KONDO AND DAIMON (9) HAVE USED A PERTINENT MODEL OF C-S-H GEL TO DIFFERENTIATE THE GEL STRUCTURE. GRANJU AND MASO (11) HAVE PROPOSED A PHYSICAL MODEL FOR EVALUATION OF THE CEMENT PASTE MICRO-STRUCTURE AND STRENGTH LAW. THE AUTHORS OF THIS PAPER SUGGEST A SIMPLIFIED PHYSICAL MODEL OF THE HARDENING CEMENT PASTE /FIG.1/ TO DERIVE THE TOTAL AND FRACTIONAL PORE VOLUMES.

THE BASIC CONCEPT OF THIS MODEL IS THAT THE PORE STRUCTURE GENESIS AND DEVELOPMENT IN TIME RELATE TO THE INITIAL STATE OF THE CEMENT PASTE AND FOLLOW THE HYDRATION PROCESS OF THE CEMENT IRRESPECTIVE OF THE INHERENT MECHNISM THROUGH WHICH THE HYDRATION PRODUCTS ARISE. IT IS SUPPOSED THAT THE CONTRACTION IS INDUCED MAINLY BY THE C-A-H GEL HYDRATES AND OCCUPY A PART OF THE INTER-GEL PARTICLE WATER FILLED SPACE AND

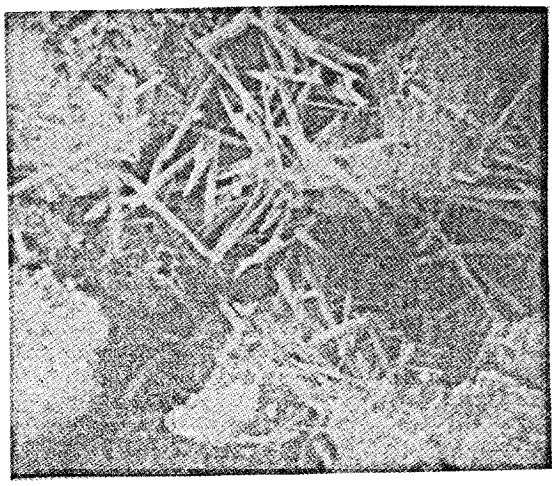

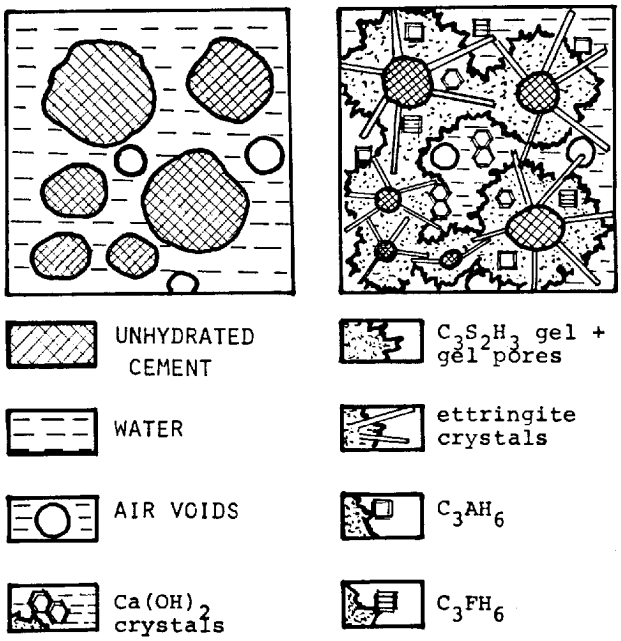

FIG.1. STRUCTURE OF CEMENT STONE AND ITS PHYSICAL MODEL

A PART OF THE CAPILLARY PORE SPACE. THE GEL PORES ARE RELATED TO THE C-S-H GEL WATER. THE VALIDITY OF THE MODEL IS RESTRICTED BY THE FOLLOWING CONDITIONS:

- PURE CLINKER CEMENT USED, WITH GYPSUM ADDITIVE ONLY;
- GLASS-TUBE HYDRATION AND HARDENING OF CEMENT PASTE /ABSENCE OF SHRINKAGE OR SWELLING/ AT ROOM TEMPERATURE;

- THE HYDRATION OF CLINKER COMPOUNDS DOES NOT DIFFER ESSENTIALLY FROM THE HYDRATION OF THE CORRESPONDING PURE MINERALS AND THE PRINCIPLE OF ADDITIVITY /SUPERPOSITION OF EFFECTS/ OF THE COMPOUNDS TO THE PROPERTIES CONSIDERED IS APPLICABLE;
- GYPSUM ADDITIVE IS REACTED COMPLETELY WITH C_3A TO FORM ETTRINGITE DURING THE EARLY STAGE OF HYDRATION;
- THE TERM "GEL" IS RELATED TO C-S-H GEL;
- POSSIBLE AIR CONTENT IN CEMENT PASTE IS NEGLECTED.

TO USE THIS MODEL IN PORE STRUCTURE ANALYSIS OF CEMENT STONE THE INITIAL INFORMATION ON MINERAL COMPOSITION OF THE CEMENT / % MASS CONTENT OF CLINKER COMPONENTS, THAT IS C_3S, C_2S, C_3A, C_4AF, FREE C, M AND GYPSUM/ AND WATER-CEMENT RATIO /BY WEIGHT/ ARE NECESSARY. THE CHEMICAL REACTIONS BETWEEN CLINKER COMPOUNDS AND WATER ARE SUPPOSED ACCORDING TO THE SCHEMES (12):

(I) $2C_3S + 6H = C_3S_2H_3 + 3CH$;

(II) $2C_2S + 4H = C_3S_2H_3 + CH$;

(IIIA) $C_3A + 3(C\bar{S}H_{0,5}) + 29,5H = C_3AC\bar{S}H_{31}$;

(IIIB) $C_3A^* + 6H = C_3AH_6$;

(IV) $C_4AF + 2CH + 10H = C_3AH_6 + C_3FH_6$;

(V) $C + H = CH$;

(VI) $M + H = MH$;

WHERE THE WELL KNOWN ABBREVIATED SYMBOLS ARE USED. IN REACTION (IIIB) C_3A^* CORRESPONDS TO THE REMAINDER OF C_3A, AFTER THE REACTION (IIIA) HAS BEEN COMPLETED.

BEARING IN MIND THE MOLECULAR MASS OF THE REACTANTS, THE MASS AND THE ABSOLUTE VOLUMES OF THE HYDRATES PRODUCED BY UNIT MASS OF THE COMPOUND THE CORRESPONDING AMOUNT OF CHEMICALLY COMBINED WATER MAY BE CALCULATED (12). THEN INVOLVING THE DEGREE OF HYDRATION (m_i^t) OF THE INDIVIDUAL COMPONENTS IN THE CEMENT (13) TO A GIVEN TIME "t", IT IS POSSIBLE TO ESTIMATE APPROXIMATELY THE ABSOLUTE VOLUME OF THE SOLIDE PHASE (v_s^t) IN A UNIT VOLUME OF HARDENED CEMENT PASTE, I.E.:

(1) $$v_s^t = v_{s,o}^t + v_{s,h}^t \quad (cm^3/cm^3);$$

WHERE $v_{s,o}^t$ AND $v_{s,h}^t$ ARE THE ABSOLUTE VOLUMES OF THE NON-HYDRATED AND HYDRATED PARTS OF THE CEMENT AT THE TIME "t", RESPECTIVELY. THE VALUES $v_{s,o}^t$ AND $v_{s,h}^t$ MAY BE OBTAINED BY SUMMARISING THE ABSOLUTE VOLUMES REFERING TO THE INDIVIDUAL COMPOUNDS AND HYDRATES, I.E.:

(1a) $$v_{s,o}^t = c_o \sum v_{o,i}(1 - m_i^t) \quad (cm^3/cm^3);$$
$$v_{o,i} = g_{o,i}/d_{co,i} \quad (g/cm^3) ;$$

(1b) $$v_{s,h}^t = c_o \sum g_{o,i} v_{h,i}^t m_i^t \quad (cm^3/cm^3) ;$$
$$v_{h,i}^t = g_{h,i}^t / d_{ch,i} \quad (cm^3/cm^3) ;$$

WHERE: c_o IS QUANTITY OF CEMENT IN 1 cm^3 INITIAL CEMENT PASTE (g/cm^3); $g_{o,i}$ - MASS OF THE "i" - COMPOUND IN 1g CEMENT (g/g); $g_{h,i}^t$ - MASS OF THE " i - HYDRATE" RELATED TO 1g OF THE COMPOUND (g/g); $d_{co,i}$ AND $d_{ch,i}$ - SPECIFIC GRAVITIES (g/cm^3); $v_{o,i}$ - ABSOLUTE VOLUME OF THE " i"-COMPOUND (cm^3/g); $v_{h,i}^t$ - ABSOLUTE VOLUME OF THE " i- HYDRATE" (cm^3/g); m_i^t - DEGREE OF HYDRATION OF THE "i"- COMPOUND AT THE TIME "t", DEFINED AS THE RELATION OF THE MASS OF THE "i"-COMPOUND, IN CEMENT, REACTED AT THE TIME "t" TO THE INITIAL MASS OF THE SAME COMPOUND.

IF THE INITIAL UNIT VOLUME ($1cm^3$) OF THE

CEMENT PASTE REMAINS UNCHANGEABLE IN TIME, THEN THE TOTAL PORE VOLUME MAY BE DEFINED:

(2) $$v_p^t = 1 - v_s^t \ (cm^3/cm^3);$$

WHERE v_s^t IS THE ONE PRESENTED IN EQUATION (1).

IN ADDITION, THE PARTIAL VOLUMES OF GEL PORES ($v_{p,g}^t$) AND CONTRACTING PORES ($v_{p,con}^t$) IN UNIT VOLUME OF THE HARDENED CEMENT PASTE MAY ALSO PRESENTED. PROPOSING THAT THE VOLUME OF GEL PORES CORRESPONDS TO AMOUNT OF GEL WATER SORBED AT THE GIVEN TIME "t", THEN

(3) $$v_{p,g}^t = c_o(s_g^t/d_{g,w})\sum_{(i)} g_{o,i} g_{h,i}^t m_i^t \ \left(\frac{cm^3}{cm^3}\right)$$

WHERE THE INDEX "i" DILATES ON THE SILICATE COMPOUNDS (C_3S AND C_2S) AND C-S-H GEL ONLY; s_g^t - MASS OF THE SORBED WATER PER 1G C-S-H GEL (g/g); $d_{g,w}$ - DENSITY OF GEL WATER (g/cm^3). THE VALUE OF s_g^t IS MEASURED EXPERIMENTALLY.

THE VOLUME OF CONTRACTING PORES CAN BE CALCULATED APPROXIMATELY USING THE AVERAGE VALUES OF THE COEFFICIENT OF CONTRACTION AND DEGREE OF HYDRATION OF CEMENT (10):

(4) $$v_{p,con}^t = q m_c^t c_o \ (cm^3/cm^3);$$

WHERE "q" IS COEFFICIENT OF CONTRACTION (0,09 - 0,15 cm^3/g); m_c^t - DEGREE OF HYDRATION OF CEMENT.

IT SEEMS TO BE MORE PERSPECTIVE TO DESCRIBE THE CONTRACTING PORE VOLUME INVOLVING THE INDIVIDUAL PARAMETERS k_i, m_i^t AND n_i^t OF THE CEMENT COMPOUNDS (n_i^t IS THE MASS OF THE CHEMICALLY COMBINED WATER PER 1G COMPOUND):

(4a) $$v_{p,con}^t = c_o \sum k_i g_{o,i} m_i^t \left(\frac{1}{d_{co,i}} + \frac{n_i^t}{d_w}\right) \left(\frac{cm^3}{cm^3}\right);$$

WHERE: k_i - COEFFICIENT OF VOLUME CONTRACTION (12) RELATING THE REACTIONS (I)-(VI) (cm^3/cm^3); d_w - DENSITY OF WATER (g/cm^3).

ON THE BASIS OF THE RELATIONS (2), (3) AND (4a) THE CAPILLARY PORE VOLUME IS CALCULATED:

(5) $$v_{p,c}^t = v_p^t - v_{p,g}^t - v_{p,con}^t \ (cm^3/cm^3).$$

THUS, AT A GIVEN TIME OF HYDRATION THE FOLLOWING RELATION WOULD BE VALID TO A CERTAIN EXTENT OF APPROXIMATION:

(6) $$v_s^t + v_{p,g}^t + v_{p,con}^t + v_{p,c}^t = 1 \ (cm^3).$$

THIS RELATION MAY BE USED TO CHECK THE CALCULATED PORE VOLUMES.

EXPERIMENTAL PROCEDURE AND RESULTS

PURE CLINKER CEMENT IS USED WITH MINERAL COMPOSITION (g/g): C_3S = 0,500; C_2S = 0,244; C_3A = 0,081; C_4AF = 0,096; FREE C = 0,007; M = 0,012 AND GYPSUM 0,060.

SERIES OF CEMENT PASTE ARE PREPARED VARYING THE WATER-CEMENT RATIO - 0,30, 0,35, 0,40, 0,45 AND 0,50. THE SAMPLES ARE CAST IN GLASS TUBES PLUGGED TIGHTLY TO AVOID WATER EVAPORATION, HARDENED AT ROOM TEMPERATURE AND TESTED AT 1, 3, 7, 28 AND 180 DAYS AFTER MIXING. THE CHEMICALLY COMBINED WATER IS MEASURED USING DTA TECHNIQUE. THE TOTAL PORE VOLUME IS ESTIMATED ON THE BASIS OF THE BULK DENSITY AND SPECIFIC GRAVITY OF CEMENT STONE. THE PORE SIZE DISTRIBUTION IN LIMITS OF 5 - 10^4 NM IS MEASURED BY USING MERCURY INTRUSION POROSIMETRY FOR EVALUATION OF THE CONTRACTING AND CAPILLARY PORES. SORBTION ABILITY IS MEASURED BY MEANS OF WATER SORBTION METHOD.

THE KINETICS OF THE FRACTIONAL PORE VOLUMES

IN TIME UP TO 180 DAYS (CALCULATED DATA) IS GRAPHYCALLY ILLUSTRATED IN FIG.2.

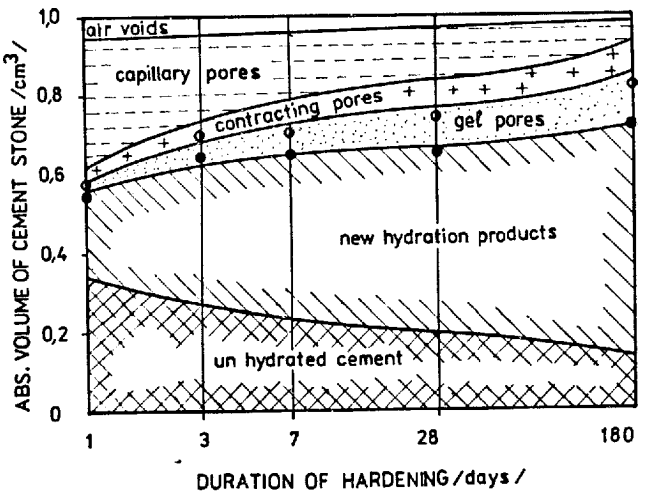

FIG.2. KINETICS OF FRACTIONAL PORE VOLUMES IN CEMENT STONE.

THE DATA CONFIRM THE GENERAL TENDENCY OF PORE STRUCTURE DEVELOPMENT IN TIME-GRADUAL DECREASING OF THE TOTAL PORE SPACE WITH THE INHERENT REDISTRIBUTION OF THE FRACTIONAL PORE VOLUMES, THAT IS INCREASING OF THE VOLUMES OF GEL AND CONTRACTING PORES AND DECREASING OF THE VOLUMES OF CAPILLARY PORES AND INITIAL AIR VOIDS.THIS RESULTS ARE IN ACCORDANCE WITH THE BASIC CONCEPT OF THE PHYSICAL MODEL INVOLVED. IN PARTICULAR, A VERY GOOD AGREEMENT WITH THE EXPERIMENTAL DATA IS OBTAINED WITH RESPECT TO THE TOTAL PORE VOLUME /BLACK POINTS IN FIG.2/,WHILE THE QUANTITATIVE ESTIMATION OF THE FRACTIONAL VOLUMES CALCULATED NEEDS ADDITIONAL EXPERIMENTAL CORROBORATION /BLACK AND WHITE POINTS IN FIG.2/

CONCLUSION

THE SIMPLIFIED PHYSICAL MODEL OF THE HARDENING CEMENT PASTE STRUCTURE IS A RELIABLE BASE TO ESTIMATE THE ORIGIN AND DEVELOPMENT OF PORE STRUCTURE IN TIME. THE RELATIONS DERIVED FROM THE MODEL PERMIT TO DIFFERENTIATE THE PORE SPACE INTO FRACTIONAL PORE VOLUMES /GEL, CONTRACTING AND CAPILLARY/. THE ACCURACY OF THE RELATIONS IS PROVED EXPERIMENTALLY. THOSE RELATIONS TO THE FRACTIONAL VOLUMES NEED ADDITIONAL MORE PRECISE EXPERIMENTS TO BE CONFIRMED.

REFERENCES

1.L.ZAGAR, Proc.of Int.Symp."Pore Str. and Prop.of Mat.",Part I, Acad.Prague, 1973.
2.R.HELMUTH, 7 Int.Congr.on Chem. of Cem., Vol.III, Paris, 1980.
3.T.C.POWERS, The Properties of Fresh Concrete, John Wiley, New York, 1968.
4.Y.SIMEONOV,G.BOZHINOV,N.BAROVSKY, "Phys.-chem. Mechanics",No.2,1976 (in Bulgarian).
5.L.E.COPELAND,D.L.KANTRO, 5 Int.Cong. on Chem.of Cement, Tokyo, 1968.
6.A.V.VOLZHENSKII,"Build.Mat."No.7,1979
7.L.E.COPELEND,G.I,VERBEK, 6 Int. Cong. on Chem.of Cem.,Moskow, 1974.
8. T.C.POWERS,Chem.of Cements,Moskow,1969.
9.R.KONDO,M.DAIMON, 6 Int.Cong.on Chem. of Cement, Moskow, 1974.
10.G.I.GORCHAKOV,et al.,Improvement of Frost-resistance of Concrete, Moskow,1965(in Rus.).
11.J.I.GRANJU,J.C.MASO,"Cement and Concrete Research",Vol.14, No.2, 1984.
12.A.V.VOLZHENSKII,"Concrete and Reinforced Concrete",No.3,1969 (in Russian).
13.Z.N.LARIONOVA, Structure and Properties of Cement Stone and Concrete, Moskow,1971 (in Russian).

C D Lawrence. Cement and Concrete Association. United Kingdom.

MEASUREMENTS OF PERMEABILITY

Le mesurage de la perméabilité

Summary: This paper describes the design and proving trials for one particular permeability cell. Gas permeability and diffusivity measurements on dried concretes are relatively undemanding on permeability cell performance and they typically can be completed in a few hours; water permeability measurements require several days for completion and have been shown to be satisfactory only after further developments of the cell. The most important parameters controlling gas permeability are the relative humidity and the degree of curing of the concrete. For water permeability, previous drying history has equally as great an influence as degree of curing. Preliminary data on Portland cement concretes and concretes containing pulverized-fuel ash or granulated blastfurnace slag as partial replacements, are included in the report.

Este artigo descreve o projeto e as provas experimentais de uma célula particular de permeabilidade. As medições de permeabilidade ao gás e de difusividade em concretos secos relativamente não sobrecarregam muito a performance da célula de permeabilidade e podem tipicamente ser completadas em poucas horas; medições de permeabilidade à água exigem vários dias para se completarem e se mostraram satisfatórias apenas depois de desenvolvimentos adicionais da célula. Os parâmetros mais importantes de controle de permeabilidade ao gás são a umidade relativa e o grau de cura do concreto. No caso de permeabilidade à água, a história de secagem prévia tem igualmente uma influência tão grande quanto o grau de cura. No relatório se incluem dados preliminares sobre concretos de cimento portland e concretos contendo cinza pulverizada de combustível ou escória granulada de alto forno como substituições parciais.

Introduction

The Darcy equation relating flow rate to imposed pressure gradient provides the most direct approach to measurement of concrete permeability. The large number of studies that have been published utilizing this Darcy procedure, mostly using water flow, have resulted in relatively few standard methods, however.

The most often quoted standard procedure for permeability measurement is an indirect one which examines the penetration of water under pressure into a concrete surface[1]. After an arbitrary period of time, the concrete is broken open and the depth of penetration, judged by the staining from excess water oozing from the concrete, is measured and converted to a permeability value by an approximate formula.

An Indian standard for water permeability[2] is based on the Darcy equation but utilises mortar specimens cast within the permeability cell. An East German standard for gas permeability[3] based on the Darcy equation is available for concrete; this standard makes use of a rubber seal which is pressed against the curved face of cylindrical specimens by pneumatic pressure. A West German standard for gas permeability of ceramic materials[4] also utilises a pneumatic pressure seal, as does a very similar British Standard[5].

The present study has developed the above permeability cell designs and has increased the size of the specimen to 150 mm diameter x 50 mm height, with a view to testing concretes containing up to 20 mm diameter aggregate.

Permeability Cell Design

Details of the permeability cell developed in this study are illustrated in Figure 1. A medium soft plasticised polyvinyl chloride (PVC) collar is pressed against the curved surface of the concrete specimen to form a seal. Pneumatic pressure is employed using a vehicle wheel inner tube. An inflation pressure of 5 bar can be held and was found to be sufficient to form a satisfactory seal for use with fluid pressure heads up to 2.5 bar. More recently, a cold-cast polyurethane rubber has been employed instead of PVC.

Theoretical analyses of the effects of variation in seal pressure on the deflection of the 20 mm thick steel end plates and the resulting changes in cell volume, which might be important when measurements of water permeability are being undertaken, have demonstrated that even a 10% change in seal pressure has a negligible effect.

Gas permeability

The arrangement for measuring gas (oxygen) permeability is shown in Figure 2; the gas flow rate is measured by means of a soap bubble flow meter. An extensive series of tests have been conducted to establish that the seal is satisfactory. It was found that, using a gas pressure head of 1 bar, a seal pressure as low as 1.25 bar prevented gas flow past an impermeable aluminium blank. Changing seal pressure from 3 to 6 bar produced no change in flow rate through a concrete specimen subjected to a pressure head of 2.5 bar.

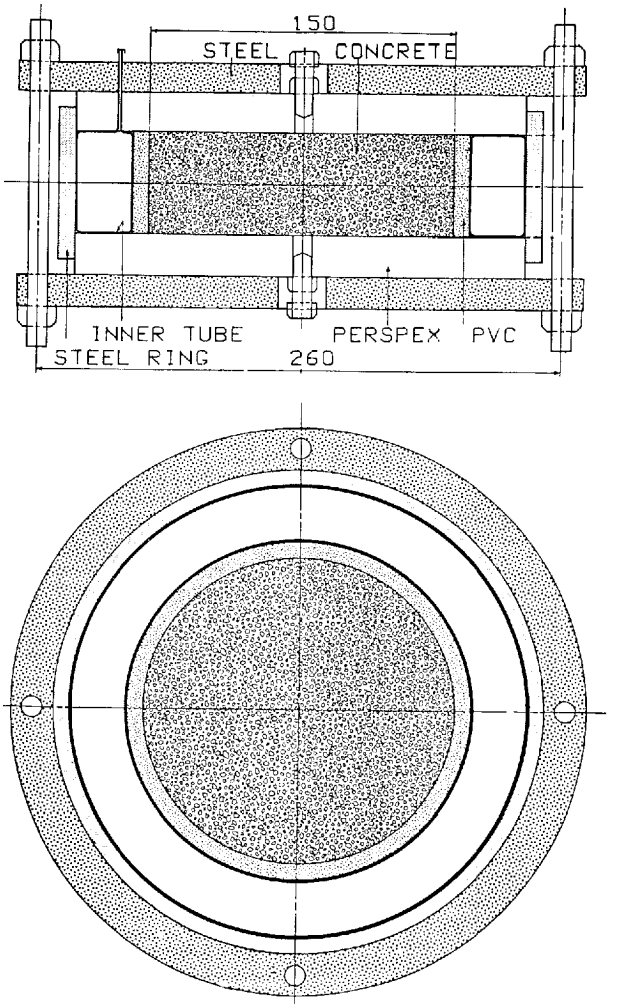

Figure 1: CACA permeability cell

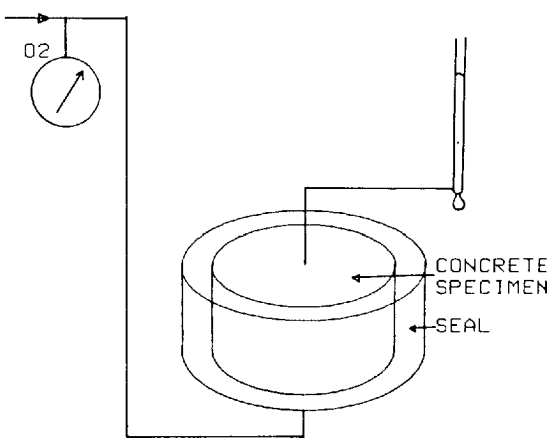

Figure 2: Measurement of oxygen permeability

The conversion of gas flow rate to gas permeability takes account of the compressibility of gases and the increasing volume flow rates which occur in passing through the specimen. Typical data are presented in Figure 3. The reproducibility of permeability data from 150 mm diameter cores cut from two concrete slabs is presented in Figure 4. 50 mm slices were cut from the middle region of each of the cores and then conditioned at 55% Relative Humidity and 20°C for several weeks.

The relative humidity of specimens has a major influence on gas permeability, and specimens must be carefully equilibrated before test. The effect of the period of time for conditioning is illustrated in Figure 5: it appears that 4 weeks allows a satisfactory estimate of gas permeability to be made for the normal range of concrete qualities.

Mix 2369 (700 x 700 x 200 mm slab)

(01) 1.73		(02) 1.58
(11) 1.21	(12) -	(13) -
(21) -		(22) .78, 1.02
(31) -	(32) 1.15	(33) 1.46
(41) 1.4		(42) -

Average $1.29 \pm 0.31 \times 10^{-16}$ m²

Mix 2385 (700 x 700 x 200 mm slab)

(01) 2.41		(02) -
(11) -	(12) -	(13) -
(21) 1.78		(22) 1.68
(31) 2.07	(32) 1.81	(33) 1.84
(41) -		(42) 2.40

Average $2.00 \pm 0.30 \times 10^{-16}$ m²

Figure 4: Reproducibility of oxygen permeabilities on 150 mm diameter cores from two slabs

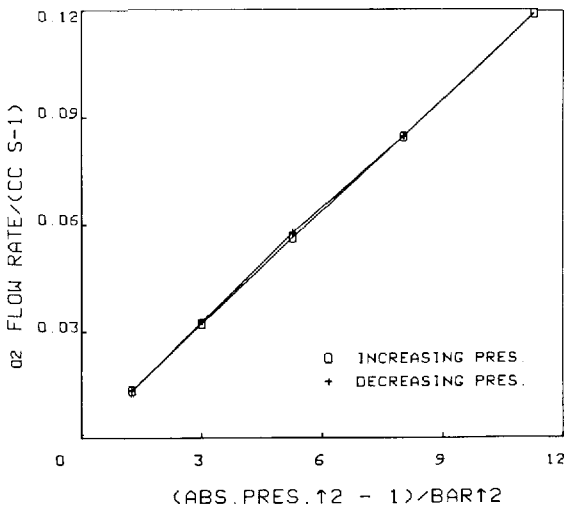

Figure 3: Typical oxygen flow data

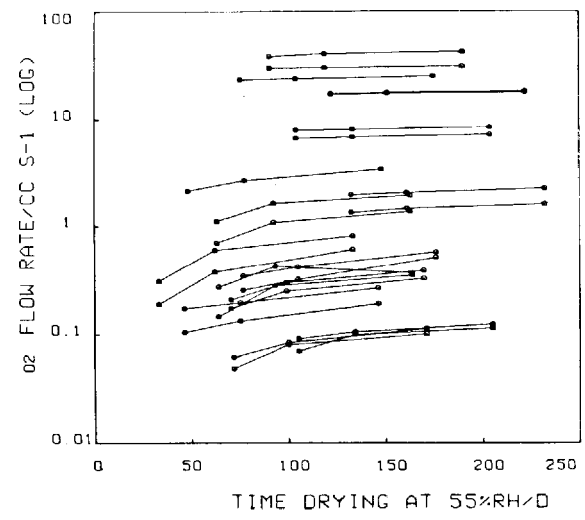

Figure 5: Effect of time drying on oxygen flow rate at 2 bar pressure

A short series of tests on different cement types has been conducted, Table 1. Figure 6 shows the relationship between oxygen permeability and compressive strength for concretes cured at 20°C under water. To a good approximation, there is a single relationship between strength and permeability for concretes containing either Portland cement or those with partial replacements of ground granulated blastfurnace slag or pulverised-fuel ash. It is interesting to speculate on the modifications to pore size distribution found for concretes with secondary cement additions and the relative insensitivity of permeability to these reported changes.

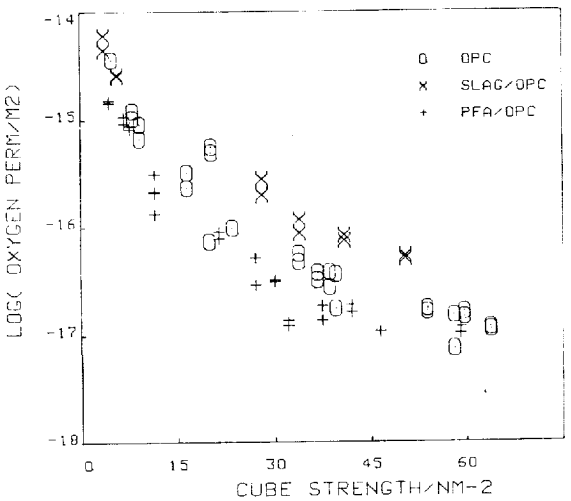

Figure 6: Relationship between oxygen permeability and cube strength

Table 1 Concrete mix proportions and cube strengths

Mix Number	Mix composition/kg m^{-3}				Free water /PC	Free water /Total cem.	Air %	Slump /mm	Cube strengths /N mm^{-2}		
	PC D51/52	Pfa/slag	Total Cem.	Total water					1 d	28 d	56 d
	Slag blends (D51 OPC)										
3724	364	-	364	183	0.47	0.47	-	-	16.5	53.7	59.5
3738	182	182	364	187	0.95	0.47	0.3	40	5.8	40.7	50.3
3759	277	-	277	186	0.62	0.62	0.4	37	8.1	33.6	38.4
3776	140	140	280	187	1.23	0.62	0.25	24	3.7	28.0	33.8
3792	199	-	199	185	0.86	0.86	0.65	18	4.8	20.2	23.4
	Pfa blends (D52 OPC)										
3836	279	-	279	187	0.62	0.62	0.3	75	9.1	36.5	39.3
3809	182	98	280	185	0.94	0.61	0.1	173	4.5	21.4	27.0
3850	217	115	332	184	0.78	0.51	0.2	135	6.8	30.0	37.3
3901	367	-	367	183	0.46	0.46	-	35	19.9	57.9	63.6
3883	234	127	361	185	0.74	0.48	0.2	155	7.6	32.0	41.9
3890	278	149	427	184	0.62	0.40	0.3	77	11.5	46.4	58.9

Oxygen diffusivity

An outline of the flow system employed to measure oxygen diffusivity is shown in Figure 7. Similar procedures have been described by Ludwig[6] and by Tuutti[7]. The permeability cell is similar to that for gas permeability, with a modification to allow gas entry and exit at each of the flat faces of the specimen. A further modification became necessary when it was discovered that slight absorption of oxygen was taking place by the PVC seal material; a polyurethane rubber material proved a satisfactory replacement. The commercially available device for measuring small concentrations of oxygen in the nitrogen gas stream is an electrochemical cell containing a heated zirconium oxide diaphragm; an oxygen level of 0.00002% can be measured on the most sensitive scale of the instrument. Floating ball gas flow meters were employed in the flow system.

Specimens were conditioned in the same way as for the gas permeability measurements, and a single relationship was observed between oxygen permeability and oxygen diffusivity, when specimens were conditioned at 55% RH, Figure 8.

Oxygen diffusivity measurements allow examination of denser specimens than can be studied by oxygen permeability, and data have been obtained on water saturated concretes in the range 1 to 50 x 10^{-13} m^2s^{-1}.

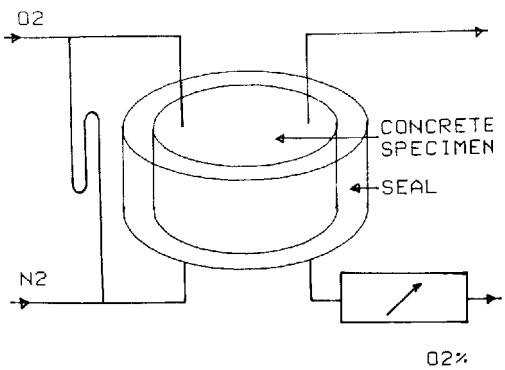

Figure 7: Measurement of oxygen diffusivity

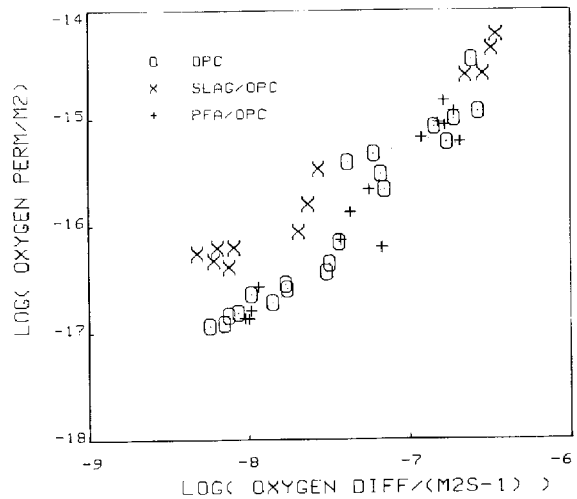

Figure 8: Relationship between oxygen permeability and diffusivity

Water permeability

The large number of studies of water permeability in the literature have been recently reviewed[8]. Figure 9 shows the layout for the present determination of the water permeability of concretes. Again, a similar permeability cell is employed, but because of the long period of time required to complete this measurement, additional precautions are

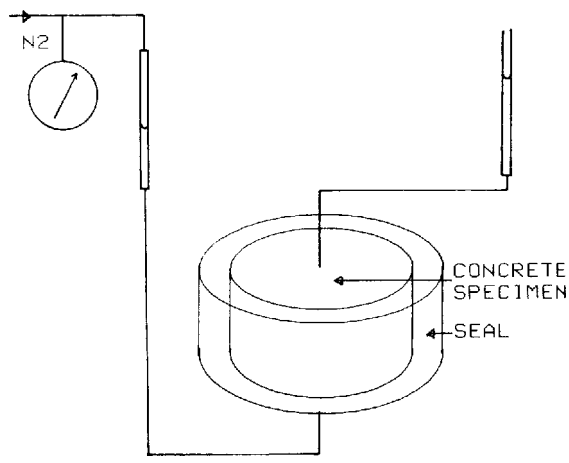

Figure 9: Measurement of water permeability

necessary for satisfactory results. In addition to using a polyurethane rubber seal having upper and lower edge faces that are cast smooth to form a watertight seal against the perspex discs, it has been found necessary to wrap a coarsely woven nylon cloth around the pressurised inner tube in order to release the very small quantities of pressurised gas which diffuse through the wall of the inner tube and otherwise interfere with the water flow through the specimen.

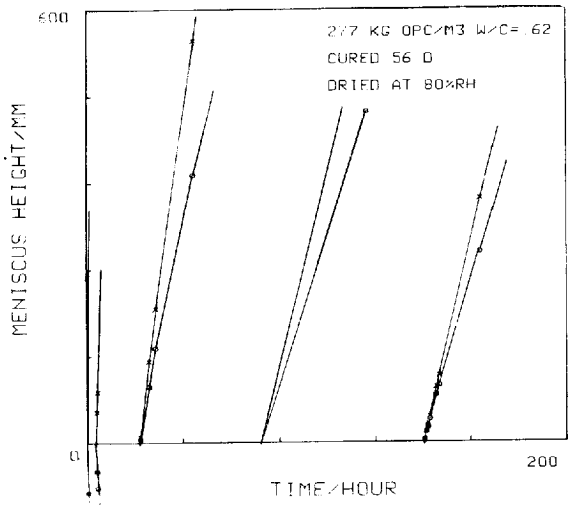

Figure 10: Water meniscus height measurements; —x— inflow, —o— outflow

Table 2 Water permeabilities for concrete mix 3776: 280 kg cementitious/m^3 (140 OPC + 140 SLG), w/c = 0.61

Specimen Age days	Water permeability/(10^{-13} ms^{-1}) (average of inflow and outflow data)				
Specimen No.	8	9	10	11	12
10	93	152	159	247	181
11/12	28	57	52	56	63
14/19	8	15	10	13	14
21/24	8	11	7	7	12
24/26	6	7	7	6	6
26/35	3.2	11	3.5	3.0	4.1
37/42	2.1	1.6	6.6	2.5	1.3
39/44	1.3	1.1	1.4	1.7	2.1
47	-	-	-	-	-
48/52	-	-	-	-	-

Inflow and outflow rates of water are measured by following the movement of water menisci in glass standpipes. Typical experimental results are shown in Figure 10, and Table 2 illustrates the water permeability values calculated for replicate specimens of young concrete. Specimens are vacuum saturated before placing in the permeability cell, however slow swelling of partially dried hydrates is indicated from the large fall in water permeability over a period of several weeks, when predried specimens are examined.

Discussion

The techniques developed for measuring oxygen permeability, oxygen diffusivity and water permeability have proved to be satisfactory, within our laboratory. The easiest procedure examined is that of oxygen permeability. However, a collaborative programme under the aegis of Cembureau[9] has shown poor agreement between different laboratories; it appears that gas permeability is exceptionally sensitive to the exact curing procedure adopted in each laboratory and further work is being undertaken to ellucidate this point. Oxygen diffusivity measurements can provide a more sensitive test for very dense or water saturated concretes. Water permeability measurements are the most difficult of the three to perform and occasionally continue to provide data which is difficult to interpret; these data provide an interesting way of following microstructural changes during water storage, however.

References

1. Deutsche Normen. DIN 1048: 1978. Prufverfahren fur Beton.

2. Indian Standard IS 2645: 1975. Specification for integral cement water proofing compounds.

3. Fachbereich-Standard (DDR) TGL 21094/12: 1975. Prufung des Erharteten Betons. Bestimmung der spezifischen Gasdurchlassigkeit.

4. Deutsche Normen. DIN 51088 (1963). Bestimmung der spezifischen Gasdurchlassigkeit feuerfester steine.

5. British Standard BS 1902. Refractory Materials Part 3. General and textural properties. Section 3.9. Determination of permeability to gases (1981).

6. G M Darr and U Ludwig. Determination of permeable porosity. Materials and Structures, 6, 185-190 (1973).

7. K Tuutti. Corrosion of steel in concrete. Swedish Cement and Concrete Research Institute (1982).

8. C D Lawrence. Water permeability of concrete. Cement and Concrete Association. PP/423 (1985).

9. H Grube and C D Lawrence. Permeability of concrete to oxygen. RILEM Seminar: Durability of Concrete Structures under Normal Outdoor Exposure. Hanover (1984).

E. REVERTEGAT , F. BERNAUDAT
Ingénieurs au DRDD/SESD - CEA Fontenay-aux-Roses - FRANCE

ROLE DE LA POROSITE DANS LA DURABILITE DES LIANTS HYDRAULIQUES

Influence of porosity on durability of cement pastes

RESUME

Les liants hydrauliques sont utilisés dans les stockages des déchets radioactifs pour la fabrication de l'infrastructure, des conteneurs, et des matrices d'enrobage.

Pour justifier une durabilité sur 300 ans de ces liants, deux types d'essais sont menés en parallèle :

- mise en évidence des interactions chimiques entre les pâtes de ciment et diverses solutions agressives (chlorure, sulfate, acides carboniques et humiques)
- détermination des paramètres régissant le transport des ions en solution dans la pâte de ciment et, en particulier, mesure des coefficients de diffusion.

On s'est particulièrement attaché à relier les paramètres mesurés à la porosité et à la répartition du diamètre des pores.

Les premiers résultats concernent les ciments CPA et CLC, agressés par des solutions ($|Cl^-|$ = 20 ; 2,0 ; 0,2 g l^{-1}) à pH = 13 et 11, 5.

Initialement les pores du ciment CLC sont plus fins que ceux du Portland même pour une porosité totale plus grande.

Après 6 mois d'agression à pH = 11,5 et pour $|Cl^-|$ = 20 g l^{-1}, la fraction de CaO lixiviée est cinq fois plus faible pour le ciment CLC que pour le ciment CPA ; corrélativement, la porosité du ciment Portland augmente de 62 % et celle du CLC seulement de 18 %. Dans le cas du ciment CPA, le départ de la chaux entraîne l'apparition d'un domaine poreux, pour lequel les diamètres des pores sont compris entre 0,06 µm et 0,90 µm.

A pH = 13, le CLC présente peu de modifications alors que la porosité du CPA se bouche (- 13 %) par formation de chloroaluminates sans lixiviation de la chaux.

Ces résultats expérimentaux seront utilisés pour modéliser l'altération chimique des liants hydrauliques.

Sumário

Os ligantes hidráulicos são utilizados na estocagem de rejeitos radioativos para a fabricação da infraestrutura, de containers e de matrizes de envolvimento.

Para justificar uma durabilidade de 300 anos desses ligantes, dois tipos são realizados em paralelo:

- por em evidência as interações químicas entre as pastas de cimento e as diversas soluções agressivas (cloretos, sulfatos, ácidos carbônico e húmico);
- determinação de parâmetros que regem o transporte dos íons em solução na pasta de cimento e, em particular, a medida dos coeficientes de difusão.

Procurou-se especialmente associar os parâmetros medidos à porosidade e aos diferentes diâmetros dos poros.

Os primeiros resultados referentes aos cimentos CPA e CLC, atacados por soluções de ($|Cl^-|$ = 20; 2,0; 0,2 g l^{-1}) pH = 13 e 11,5.

Inicialmente os poros do cimento CLC são menores do que os de Portland mesmo para uma porosidade total maior.

Após 6 meses de ataque com pH = 11,5 e para $|Cl^-|$ = 20 g l^{-1}, a fração de CaO lixiviada é cinco vezes mais fraca para o cimento CLC do que para o cimento CPA; correlativamente, a porosidade do cimento Portland aumenta de 62% e a do CLC somente 18%; a saída da cal acarreta o aparecimento de uma região porosa, para a qual os diâmetros dos poros estão compreendidos entre 0,06 µm e 0,90 µm.

Com pH = 13, o CLC apresenta poucas modificações enquanto que a porosidade do CPA se colmata (-13%) pela formação de cloroaluminatos sem lixiviação da cal.

Esses resultados experimentais serão utilizados para modelisar a alteração química dos ligantes hidráulicos.

1) INTRODUCTION

Un programme d'étude a été entrepris au Service **d'Etude des Stockages de Déchets,** en collaboration avec **l'Agence Nationale de la Gestion des Déchets,** dans le but d'appréhender et de modéliser les mécanismes d'altérations chimiques et la cinétique de détérioration des bétons de conteneurs, utilisés dans les stockages de surface de déchets nucléaires de faible et moyenne activité.

Les eaux d'infiltration, en contact avec les conteneurs, contiennent des ions (chlorure, sulfate, acides carboniques et humiques) susceptibles d'agresser la pâte de ciment et dont les concentrations varient au cours du temps. L'étude du vieillissement est menée en prenant en considération soit les recommandations CEMBUREAU (1) soit pour les chlorures les teneurs rencontrées dans l'eau de mer ou les eaux naturelles.

La méthode utilise une approche simplificatrice ; chaque mécanisme intervenant dans le processus complexe de dégradation chimique de la pâte de ciment est étudié indépendamment des autres. Cette approche facilite l'exploitation des résultats dans une démarche de modélisation.

Pour ce faire deux types d'essais ont été menés en parallèle :

- la mise en évidence de phénomènes d'interactions chimiques entre une pâte de ciment (type CPA ou CLC) et une solution aqueuse contenant un ion agressif, à différentes concentrations et pour deux valeurs de pH
- la détermination des coefficients de diffusion des ions agressifs dans chaque pâte de ciment.

Les recherches menées, jusqu'à présent, sur l'attaque d'un liant hydraulique par les chlorures ont été centrées soit sur la corrosion de l'acier dans le béton armé soit sur les mécanismes d'attaque à forte concentration (2). Les résultats, présentés par la suite, tentent de rattacher l'évolution de la porosité totale et de la distribution diamétrale des pores dans la pâte, aux phénomènes de diffusion des chlorures.

2) CONDITIONS EXPERIMENTALES

2.1 Conditions expérimentales concernant l'étude des mécanismes d'interactions chimiques.

Des plaquettes rondes de 4 mm d'épaisseur et de 70 mm de diamètre ont été réalisées à l'aide de deux ciments type CPA et CLC de rapport E/C = 0,37, conservées 3 mois dans une eau saturée en chaux. Les plaques sont ensuite immergées dans des bacs d'une contenance de 50 litres à raison, pour chacun des bacs, de 16 éprouvettes par type de ciment.

La concentration en ions Cl^-, introduits sous forme de NaCl, est respectivement de 0 - 0,2 - 2 et 20 g l^{-1}. Les concentrations sont contrôlées tout au long de l'expérimentation et maintenues constantes. Pour chaque concentration deux valeurs de pH sont étudiées : pH = 11,5 et pH = 13. L'équilibre du pH est réalisé soit par passage sur colonne de résine échangeuse d'ions, pour les faibles concentrations en chlorure soit par ajout de l'acide correspond pour les fortes concentrations.

Les éprouvettes sont constamment agitées, afin d'améliorer le renouvellement de la solution agressive à leur contact. Le tout est parfaitement étanché afin d'éviter les phénomènes de carbonatation.

A chaque échéance : (0 - 1 - 3 - 6 mois) les mesures et analyses suivantes ont été réalisées sur les éprouvettes: - résistance mécanique en flexion - porosité au mercure et à l'eau - teneur en $Ca(OH)_2$ par thermogravimétrie - analyse chimique des éléments par fluorescence X - profil de diffusion du chlore par microanalyse électronique - étude microstructurale par diffraction des rayons X et microscopie électronique à balayage.

2.2 Conditions expérimentales concernant l'étude de la diffusion

L'étude est réalisée en cellule de diffusion (figure 1) sur des éprouvettes de 4 mm et 1,5 mm d'épaisseur.
Le pH de la solution dans chaque compartiment est égal à 13. Le compartiment " amont " contient une concentration fixe en ions Cl^- (0,2 - 2 ou 20 g l^{-1}). La teneur en ions chlorure qui diffusent dans le compartiment " aval " est analysée par chromatographie en phase liquide.

3) EVOLUTION DE LA POROSITE SOUS L'INFLUENCE DES INTERACTIONS CHIMIQUES

On observe pour les deux pâtes de ciment le même comportement global. La porosité totale augmente d'autant plus que la valeur du pH est faible et que la concentration en ions Cl^- est élevée (figures 2 et 3).

A titre d'exemple, on constate après un séjour de 6 mois :

- une augmentation de la porosité totale de 46% pour le témoin CPA et de 26% pour le témoin CLC, tous deux lixiviés à pH = 11,5
- une augmentation de 62% pour l'échantillon CPA et seulement de 18% pour l'échantillon CLC, tous deux immergés dans une solution à 20 g l^{-1} d'ions Cl^- à pH = 11,5.

On peut noter que l'effet du pH est moins important sur le ciment CLC et que, pour un temps d'attaque donné, sa variation de porosité est plus faible, bien que la porosité initiale de la pâte CLC soit plus grande que celle de la pâte CPA (respectivement égale à 32% et 25%).

3.1 Comportement des pâtes de ciment en présence de solutions chlorées à pH = 11,5

3.1.1. Pâte de ciment CPA

L'augmentation de la porosité est essentiellement due à la solubilisation et à la lixiviation de la chaux $Ca(OH)_2$ (figure 4) mise en évidence sur les spectres de diffraction des rayons X et par l'analyse thermogravimétrique. La perte de $Ca(OH)_2$, exprimée en masse de CaO, est de 38% pour le témoin après 6 mois d'immersion et de 100% pour l'échantillon immergé dans une solution à 20 g l^{-1} de Cl^- après la même échéance (76% au bout de 3 mois). Une fraction de $Ca(OH)_2$ est utilisée pour former des chloroaluminates et une fraction est lixiviée (17% de la teneur en CaO totale de l'échantillon a disparu au bout de 6 mois pour le témoin, 28% pour l'échantillon en contact avec la solution fortement chlorée).

Parallèlement et progressivement, apparaît sur les histogrammes de porosité, un domaine poreux pour lequel les diamètres de pores sont compris entre 0,06 µm et 0,90 µm, domaine inexistant sur le témoin à t = 0 (figure 5).

Les spectres de porosité (figure 5) mettent également en évidence :

- une augmentation globale de la fine porosité inférieure au diamètre 0,06µm. Cette augmentation est surtout perceptible pour les échéances de 6 mois (+ 11% pour les éprouvettes qui ont séjourné dans une solution à 20 g l^{-1} de Cl^-)

- un déplacement de l'intensité des familles vers les pores les plus fins.

Ces deux phénomènes, d'autant plus importants que la teneur en chlorure de la solution est élevée, sont probablement la conséquence d'une part de l'évolution de l'hydratation du ciment et d'autre part d'un subdivision du milieu poreux par réarrangement structural (apparition de chloroaluminates au détriment des aluminates hydratés du ciment et de la chaux).

On a mis en évidence, sur les spectres de diffraction des rayons X, l'instabilité de l'ettringite à pH =11,5 même en l'absence de chlorure ; elle ne semble donc pas réagir directement avec les ions Cl^-.

Malgré l'apparition abondante des chloroaluminates aucun bouchage des diverses familles de pores n'est observé. Les cristaux trouvent la place nécessaire à leur développement dans les cavités laissées par les produits lixiviés.

3.1.2 Pâte de ciment CLC

La porosité totale mesurée par pesée, (figure 3) augmente peu par rapport à celle du ciment CPA et de façon identique pour chaque série d'échantillons (+ 25% à l'échéance de 6 mois). Pour les échantillons conservés dans la solution à 20 g l^{-1} d'ions Cl^-, l'augmentation de la porosité est la plus faible (+ 18% à 6 mois), en accord avec le développement des chloroaluminates dans un domaine poreux peu modifié par une faible lixiviation de la chaux.

En effet les mesures par fluorescence X mettent en évidence un taux de lixiviation (teneur en CaO totale disparue de l'éprouvette) nettement inférieure pour le ciment CLC,comparativement au ciment CPA, pour un temps d'agresssion identique. Il en est de même pour les variations de $Ca(OH)_2$ déterminées par thermogravimétrie.

Les valeurs correspondant à l'échéance de 3 mois sont présentées dans le tableau 1.

	Témoin		0,2 g.l^{-1} [Cl^-]		2 g.l^{-1} [Cl^-]		20 g.l^{-1} [Cl^-]	
	CaO de $Ca(OH)_2$	CaO total	CaO de $Ca(OH)_2$	CaO total	CaO de $Ca(OH)_2$	CaO total	CaO de $Ca(OH)_2$	CaO total
CPA	- 1,1 g	- 2,0 g	- 1,2 g	- 2,5 g	- 1,5 g	- 2,7 g	- 2,4 g	- 3,8 g
	- 34 %	- 13 %	- 37 %	- 17 %	- 47 %	- 18 %	- 75 %	- 25 %
CLC	- 0,3 g	- 0,6 g	- 0,4 g	- 0,6 g	- 0,4 g	- 0,7 g	- 1,2 g	- 0,9 g
	- 25 %	- 7 %	- 33 %	- 7 %	- 33 %	- 8 %	- 100 %	- 11 %

Tableau 1 : Pertes de CaO total et de CaO provenant de la chaux $Ca(OH)_2$ pour l'échéance de 3 mois et pour les deux ciments, dans différentes solutions agressives de chlorure, à pH = 11,5.

Pour comparer rigoureusement les mesures réalisées sur les deux ciments, il est nécessaire de se reporter aux quantités réelles de chaux qui ont réagi et non aux pourcentages calculés à partir d'échantillons de composition initiale différente, c'est-à-dire :

- pour le ciment CPA :
  14,9 g de CaO total (53% en poids)
  3,2 g de CaO sous forme de $Ca(OH)_2$ (15%)
- pour le ciment CLC :
  8,5 g de CaO total (34% en poids)
  1,2 g de CaO sous forme de $Ca(OH)_2$ (6%)

En présence de chlorure le ciment CLC voit disparaître plus rapidement sa faible quantité de chaux libre, cette disparition est de 100% à trois mois pour la plus forte solution chlorée, contre 75% pour le ciment CPA. Les autres hydrates de constitution étant moins solubles, l'attaque du ciment CLC sera ensuite ralentie.

On peut remarquer que potentiellement au temps t = 0 l'éprouvette de CLC possède suffisamment de $Ca(OH)_2$ (1,2 g) pour réagir de la même façon que le ciment CPA (par exemple dans la solution à 0,2 g l^{-1} d'ions Cl^-) ; or seule une faible fraction disparait (0,4 g). Il est probable, et nous l'avons constaté lors des essais de diffusion (§ 4), que l'ion Cl^- diffuse beaucoup plus difficilement dans une pâte de ciment CLC.

A l'inverse du ciment CPA, à pH = 11,5, en présence de chlorure, l'ettringite visible sur les spectres de diffraction des rayons X, est présente au moins jusqu'à trois mois pour tous les échantillons et jusqu'à 6 mois pour la solution à 20 g l^{-1} de Cl^-. Les monosulfoaluminates, qui sont initialement plus abondants que dans le ciment CPA, se déstabilisent pour donner du C_4AH_{13}, puis des chloroaluminates en quantité également supérieure à celle observée dans le ciment CPA. Le sulfate libéré, lors de cette transformation, pourrait alors diffuser plus difficilement à travers la pâte de CLC, et réagir avec les monosulfoaluminates restants pour redonner de l'ettringite. Celle-ci en effet a été observée au microscope électronique à balayage, préférentiellement sur les bords des éprouvettes.

Compte-tenu de la faible lixiviation de la chaux, de la formation d'ettringite, et de l'apparition plus importante des chloroaluminates, la porosité du ciment CLC dans la classe 0,90 µm$<\emptyset<$0,06 µm varie peu (figure 6). Cette famille de pores est égale à 2% ($|x/V|.100$) pour l'échantillon au temps t = 0. Quelle que soit l'attaque, l'augmentation de cette classe de pores est de l'ordre de 2% ($|\Delta x/V|.100$) pour tous les échantillons, V étant le volume poreux total de l'échantillon témoin au temps t = 0.

Comparativement, pour le ciment CPA, la variation de cette classe de pores, dont la valeur est égale à 3% au temps t = 0, est représentée dans le tableau 2 :

	1 mois	3 mois	6 mois
Témoin	+ 9 %	+ 13 %	+ 14 %
[Cl^-] = 0,2 g.l^{-1}	+ 7 %	+ 14 %	+ 14 %
[Cl^-] = 2 g.l^{-1}	+ 10 %	+ 15 %	+ 17 %
[Cl^-] = 20 g.l^{-1}	+ 18 %	+ 27 %	+ 29 %

Tableau 2 - Evolution de la porosité dans la classe $0,90 < \emptyset < 0,06$ µm pour la pâte de ciment CPA à pH =11,5

Enfin le déplacement des familles de pores vers les pores les plus fins par cloisonnement de l'espace (figure 6) est beaucoup plus visible que dans le cas du ciment CPA attaqué par les chlorures. Par exemple, pour une solution à 20 g l^{-1} d'ions Cl^-, la répartition par rapport au témoin initial (t = 0) est la suivante :

- pour 0,06 µm $> \emptyset >$ 0,01 µm : - 30%
- pour 0,01 µm $> \emptyset >$ 0,003 µm : + 53%

La division de la porosité vient probablement de la présence des chloroaluminates formés qui se logent dans une structure peu lixiviée, alors que dans le cas du ciment CPA ils auraient tendance à remplir les pores laissés vides par le départ de $Ca(OH)_2$. Nous verrons (§ 3.2) que l'hydratation du laitier et des cendres semble nettement ralentie lorsque le pH de l'eau interstitielle diminue en équilibre avec l'eau de contact.

3.2 Comportement des pâtes de ciment en présence de solutions chlorées à pH = 13.

Les cinétiques de transformation des hydrates sont très ralenties dans les deux ciments. Les analyses par fluorescence X montrent que la quantité de CaO total lixiviée

n'est pas significative, c'est-à-dire en dessous de la précision des mesures, et toujours inférieure aux valeurs obtenues pour la solution à pH = 11,5.

La comparaison entre les deux ciments reste valable à pH = 13 comme à pH = 11,5, quant à la variation de $Ca(OH)_2$ déterminée par thermogravimétrie. La diminution est de l'ordre de 0,4 - 0,5 g exprimée en CaO pour les échantillons CPA à 6 mois ($\simeq$ 16%) et de l'ordre de 0,3 g ($\simeq$ 25%) pour les échantillons CLC. Ces résultats signifient qu'il n'y a pas eu lixiviation de la chaux, mais réaction de celle-ci pour former des chloroaluminates dans le cas du ciment CPA, et probablement réaction pour hydrater les produits siliceux dans le cas du ciment CLC, car pour celui-ci l'apparition des chloroaluminates est très faible.

L'ettringite visible sur les spectres de diffraction X est toujours présente quel que soit le ciment ; il n'y a pas eu solubilisation.

Il en résulte pour la pâte de ciment CPA une porosité totale (figure 2) constante sauf dans le cas où $[Cl^-]$ est égal à 20 g l^{-1} pour lequel on observe une légère diminution (-13% à l'échéance de six mois). Cette diminution est vraisemblablement due à l'apparition de chloroaluminates qui ne trouvent pas, comme dans le cas des échantillons maintenus à pH = 11,5, un espace créé par la lixiviation de la chaux et de l'ettringite. Elle s'accompagne d'un déplacement de la porosité vers les pores les plus fins (décalage du pic maximum de 0,040 µm à 0,024 µm) significatif, lorsque les volumes de toutes les familles de pores diminuent, d'un cloisonnement du domaine poreux (figure 7).

Dans le cas du ciment CLC la porosité totale est pratiquement constante pour tous les échantillons (figure 3). Bien que cette porosité totale soit supérieure à celle du ciment CPA (31% pour le CLC et 25% pour le CPA), la distribution des familles de pores se localise plus dans le domaine des petits pores. Le pic maximum est situé à 0,016 µm pour le ciment CLC et à 0,040 µm pour le ciment CPA au temps t = 0 (figure 8).

De plus, grâce aux histogrammes de porosité, l'évolution des domaines poreux en fonction de la cinétique d'hydratation du ciment CLC, a pu être mise en évidence. Il est bien connu qu'un ciment au laitier et aux cendres s'hydrate sur une période plus longue que celle d'un ciment Portland et bien au-delà des trois mois de cure. Ce phénomène se traduit parfaitement sur les spectres de porosité (figure 9). Entre le témoin t = 0, c'est-à-dire après trois mois de cure, et l'échantillon conservé six mois dans une solultion à pH = 13, sans agression, les familles de pores se déplacent vers les domaines de pores fins, avec un translation du pic maximum de 0,016 µm à 0,008 µm, sans variation notable de la porosité totale. Il y a subdivision du milieu poreux par apparition d'hydrates C.S.H.(essentiellement). La présence d'ions chlorure dans les solutions à pH = 13 semble ralentir l'hydratation des produits siliceux. Le déplacement du pic maximum est inexistant. Le même phénomène est constaté lorsque le pH de la solution est abaissé. A six mois, sans agression, les variations des volumes poreux, par rapport au témoin t = 0, correspondant aux deux familles de pores fins sont respectivement, pour les deux pH :

	$[Cl^-]$=0 ; pH=11,5	$[Cl^-]$=0 ; pH = 13
- 0,06 µm > Ø > 0,01 µm	- 9%	-30%
- 0,01 µm > Ø > 0,003 µm	+32%	+59%

4) MESURE DES COEFFICIENTS DE DIFFUSION

En complément indispensable aux diverses mesures effectuées pour étudier l'attaque chimique d'un ciment par une solution agressive, des essais de diffusion des ions Cl^- et SO_4 ont été réalisés. A ce jour, seuls les résultats concernant le ciment CPA et les chlorures sont exploités ; dans le cas du ciment CLC aucune diffusion significative n'a été observée au bout de 41 semaines. La courbe théorique (quantité cumulée en fonction du temps) superposée aux résultats expérimentaux (figure 10) permet de déterminer le coefficient de diffusion effectif (D_e) et la porosité apparente (ε_a) à partir de l'intersection de l'asymptote avec l'axe des temps (ti = temps de décalage) et de la pente de cette même asymptote. Le coefficient de diffusion est donné par :

$$De = \frac{l.P}{C_1}$$

l = épaisseur de l'échantillon

C_1 = concentration itiale en Cl^- dans la chambre " amont "

La porosité apparente est donnée :

$$\varepsilon_a = \frac{6.De.ti}{l^2}$$

Les différents essais ont fourni un coefficient de diffusion effectif de l'ordre de 8.10^{-13} m^2/s dans tous les cas, ces valeurs sont en moyenne plus faibles que celles rencontrées dans la littérature (1.10^{-12} à 5.10^{-12} m^2/s) [3]. Par contre la porosité apparente (ou le taux de retard égal au rapport porosité apparente/porosité réelle) croît fortement lorsque la concentration en chlorure décroît (ε_a = 0,60 pour 20 g l^{-1} de Cl^-, ε_a = 12 pour 0,2 g l^{-1}). Cela suggère un phénomène d'adsorption non linéaire ou une absorption chimique dans les hydrates du ciment.

5) CONCLUSION

La principale dégradation observée dans une pâte de ciment CPA, soumise à l'agression d'une eau chlorée, ne sera pas due à l'apparition des chloroaluminates, mais à une augmentation de la porosité engendrée par la solubilisation de l'ettringite et essentiellement de la chaux. Ce phénomène de solubilisation et de lixiviation de $Ca(OH)_2$ est d'autant plus important que le pH de l'eau de contact est faible et que la concentration en ions Cl^- est élevée ; dans ce cas les C.S.H présentent un aspect alvéolaire. Par contre, les ions chlorures qui migrent à l'intérieur du béton, dans une eau interstitielle de pH voisin de 13, vont former seulement des chloroaluminates qui bouchent la porosité, du moins pour les fortes concentrations en chlorure (20 g l^{-1}).

Pour une pâte de ciment CLC les différences essentielles de comportement avec la pâte de ciment CPA sont les suivantes :

- une distribution de pores à l'origine plus fine et qui ne pourra que s'accentuer lors de l'hydratation progressive de produits siliceux. En conséquence le ciment CLC possède un chemin diffusionnel, pour les ions agressifs ou radioactifs, plus fin que le ciment CPA
- une quantité de $Ca(OH)_2$ à l'origine plus faible et qui ne peut que décroître lors de l'hydratation. En conséquence un ciment soumis à l'action des chlorures étant essentiellement affecté par la disparition de la chaux, le ciment CLC sera plus résistant qu'un ciment CPA
- après attaque, l'augmentation de la porosité totale est nettement inférieure (+ 18% au lieu de 62% pour les ciments CPA à l'échéance de six mois dans une solution à 20 g l^{-1} de Cl^-). La quantité de chaux qui réagi avec les chlorures et qui s'est lixiviée est nettement moins importante que celle d'un ciment CPA

- absence d'un domaine poreux entre 0,06 µm et 0,90 µm, observé sur les ciments CPA après attaque, et qui a été attribué à la lixiviation de la chaux
- bien qu'un retard dans l'hydratation des produits siliceux a été observé à pH = 11,5 un début de cloisonnement de la fine porosité apparaît pour les fortes concentrations en chlorure. Ce phénomène est probablement dû à l'apparition abondante de chloroaluminates dans une structure peu lixiviée. Pour le ciment CPA il y a à la fois cloisonnement et augmentation de la fine porosité, sous la double action de l'apparition des chloroaluminates et de la lixiviation importante de la chaux et de l'ettringite.

Lorsque les ions Cl^- seront véhiculés dans une eau interstitielle de pH = 13 la modification de la matrice du ciment CLC sera pratiquement inexistante. Il n'existe donc pas une barrière " protectrice ", comme dans le ciment CPA, qui pourrait freiner la lixiviation des radioéléments vers l'extérieur du béton. Reste à savoir comment évoluera cette " barrière " lorsqu'elle sera atteinte par le front de dégradation.

Un modèle mathématique global qui couple la formation des précipités lié aux équilibres chimiques dans l'eau, les modifications de la porosité et les processus de diffusion, est en cours de développement. Les données expérimentales ponctuelles en pH et en concentrations permettront de le vérifier et de l'extrapoler afin de prévoir à long terme, l'évolution d'un béton au contact de l'eau souterraine dans un site de stockage de déchets.

REFERENCES

[1] " Use of concrete in Agressive Environments " CEMBUREAU RECOMMANDATION U.D.C. 389.6.666.94.620.193 - 25/27 january 1979

[2] M. CONJEAUD, " Mécanisme d'attaque des ciments Portland par $CaCl_2$ " Calcium Aluminates, Séminaire international, TURINO (Italie) 1982, p. 171

[3] S. GOTO, D.R. ROY " Diffusion of ions through hardened cement pastes " Cement and Concrete Research Vol 11 - pp. 751-757 - 1981

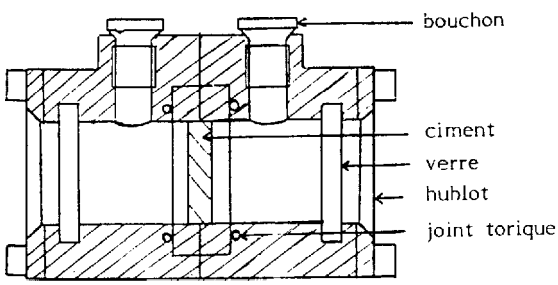

Figure 1 : Cellule de diffusion pour une rondelle de ciment (lucoflex)

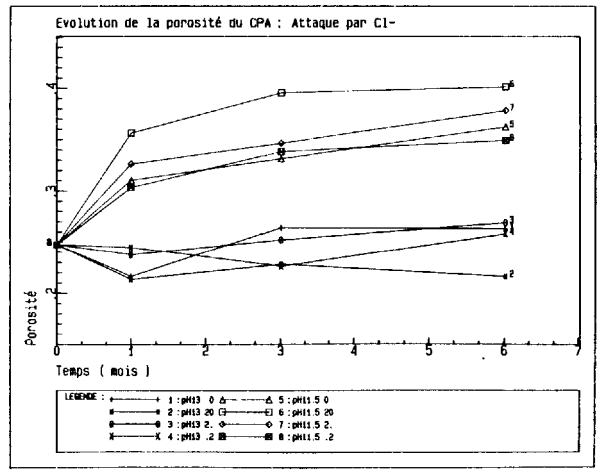

Figure 2

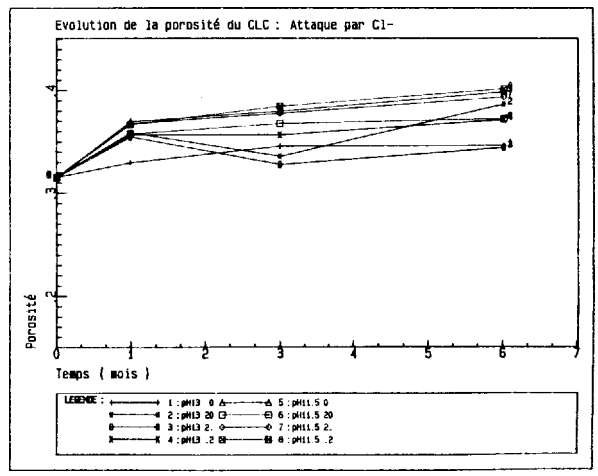

Figure 3

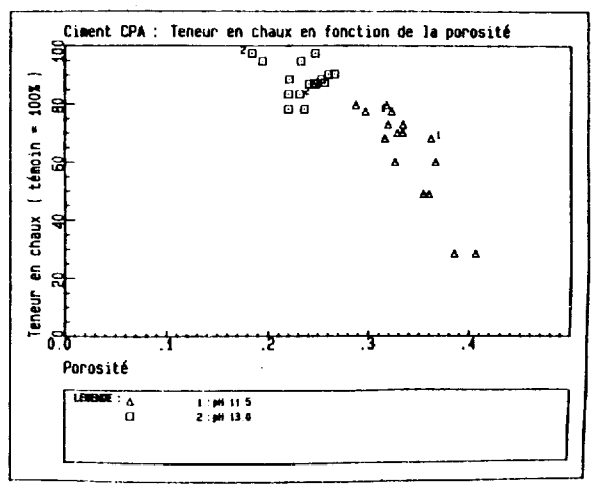

Figure 4

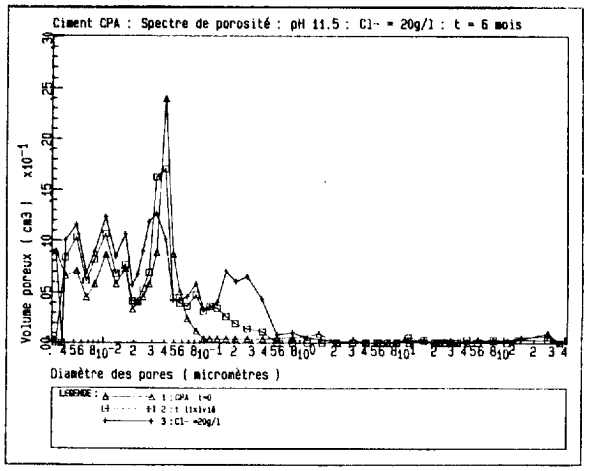

Figure 5

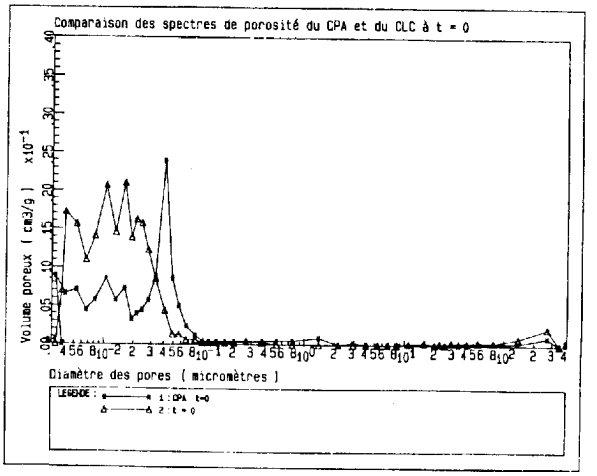

Figure 8

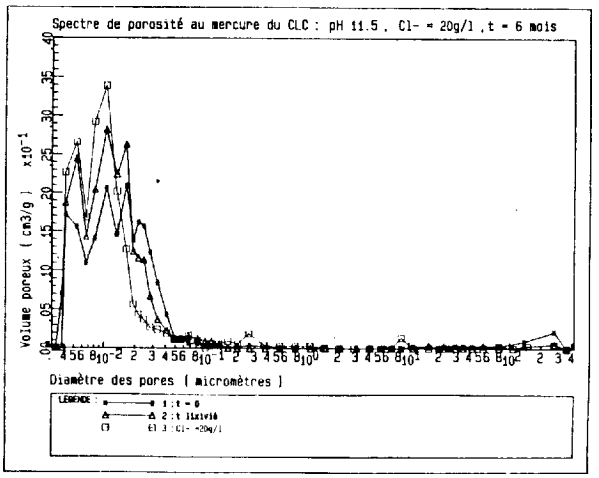

Figure 6

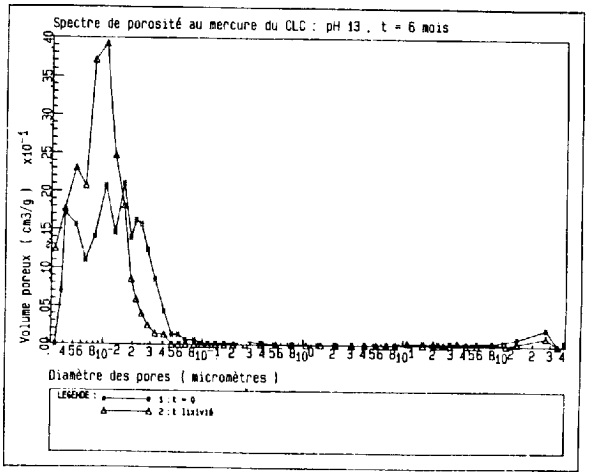

Figure 9

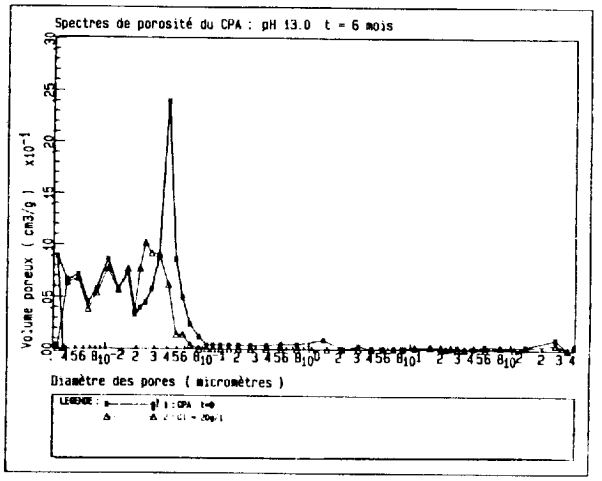

Figure 7

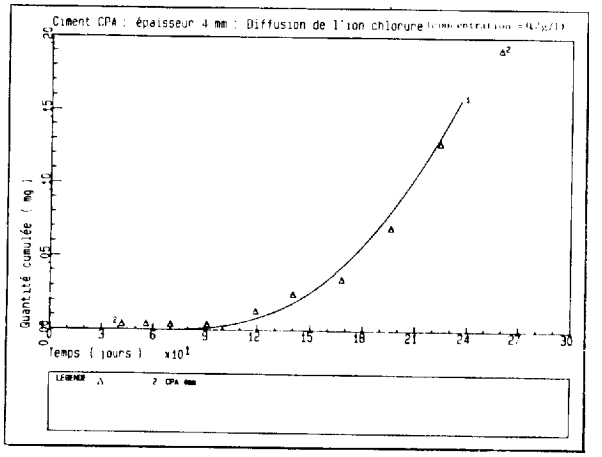

Figure 10

F. BERNAUDAT , E. REVERTEGAT
Ingénieurs au DRDD/SESD - CEA Fontenay-aux-roses - FRANCE

MODELISATION DES PHENOMENES DE TRANSPORT DANS LES MECANISMES D'ALTERATION D'UNE PATE DE CIMENT

Modelisation of transport phenomena in alteration processes of cement pastes

RESUME

Les phénomènes d'altération d'un liant hydraulique en présence d'eau chargée d'ions sont très importants dans le cadre d'un stockage de déchets radioactifs dont la durée de vie est de trois cents ans.

L'étude de la durabilité des liants hydrauliques possède un aspect expérimental et un aspect prédictif par le biais de la modélisation.

Dans un premier temps, il est montré, pour les ciments CPA que les expériences menées en cellules de diffusion peuvent être interprétées par un phénomène de diffusion avec épuisement de la source. Cependant, des écarts à la loi de diffusion apparaissent au bout d'un certain temps. Bien que plus poreux, le ciment type CLC ne permet qu'une diffusion très limitée des chlorures. Dans ce cas, ainsi que dans celui des sulfates, la loi de diffusion de Fick semble en défaut.

D'autres phénomènes, d'ordre chimique sont à prendre en compte. Un code qui calcule un équilibre chimique dans l'eau interstitielle, en prenant en compte un certain nombre d'espèces en solution et de phases solides a été développé. La porosité est liée aux variations de quantité de précipités.

Un second module du code résout l'équation de Fick, écrite pour un milieu dont la porosité varie dans le temps et l'espace.

Le code complet vérifie tout d'abord que l'équilibre chimique est réalisé dans les solutions de trempage (essais d'agression ou de diffusion) et dans l'eau interstitielle. Puis le calcul proprement dit commence en réalisant à chaque pas de temps :

- un calcul de diffusion
- un équilibre chimique
- un réajustement de la porosité.

Après recalage sur les résultats expérimentaux, le code permet de prédire le comportement d'un liant hydraulique sur la durée de vie d'un stockage, soit 300 ans.

Sumário

Os fenômenos de alteração de um ligante hidráulico em presença d'água carregada de íons são muito importantes no quadro da estocagem de resíduos radioativos cuja duração de vida é de trezentos anos.

O estudo da durabilidade dos ligantes hidráulicos possui um aspecto experimental e um aspecto de predição com o auxílio da modelisação.

Em um primeiro tempo, mostra-se, para os cimentos portland, que as experiências realizadas em células de difusão podem ser interpretadas por um fenômeno de difusão com esgotamento da fonte. Entretanto, afastamentos à lei de difusão aparecem no fim de um certo tempo. Se bem que mais poroso o cimento de escória não permite senão uma difusão muito limitada de cloreto. Neste caso,bem como no dos sulfatos, a lei de difusão de Fick parece em falta.

Outros fenômenos, de ordem química devem ser levados em conta. Um código que calcula um equilíbrio químico na água intersticial, levando em conta um certo número de espécies em solução e de fases sólidas foi desenvolvido. A porosidade está ligada às variações das quantidades precipitadas.

Um segundo módulo do código resolve a equação de Fick, escrita para um meio cuja porosidade varia no tempo e no espaço.

O código completo verifica inicialmente que o equilíbrio químico é realizado em soluções de têmpera (ensaios de agressão ou de difusão) e na água intersticial. Em seguida, o cálculo propriamente dito começa realizando a cada intervalo de tempo:

- um cálculo de difusão
- um equilíbrio químico
- um reajustamento da porosidade.

Após recalibração sobre os resultados experimentais, o código permite predizer o comportamento de um ligante hidráulico sobre a duração da vida de uma estocagem, de 300 anos.

I) INTRODUCTION

L'utilisation des liants hydrauliques dans les stockages de déchets radioactifs nécessite la connaissance du comportement à long terme de ces matériaux, d'une part vis-à-vis de l'eau extérieure et des ions agressifs qu'elle est susceptible de véhiculer, d'autre part du déchet lui-même que les barrières ouvragées sont censées retenir pendant sa durée de vie. Il faut préciser dans ce qui précède ce que signifie "long terme". En effet les déchets stockés dans des conteneurs en béton ont une demi-vie maximale de l'ordre de 30 ans. Leur nuisance est estimée durer 10 fois la demi-vie, soit 300 ans. Le béton du conteneur doit donc résister aux agressions externes et assurer le confinement pendant cette durée.

Une approche expérimentale a été entreprise au Service d'Etude de Stockages de Déchets (Cen-Fontenay aux-Roses). Elle se décompose en trois séries d'essais : des essais d'attaque de pâtes de ciment par des ions agressifs (ciments CPA et CLC, attaque par des ions chlorure et sulfate) ; des essais en cellule de diffusion permettant de mesurer le coefficient de diffusion d'ions agressifs. Ces deux premières séries d'essais ont été menées au Laboratoire des Bétons et Revêtements. La troisième série d'essais a permis de mesurer les paramètres du transport des éléments radioactifs tels que le césium, et l'eau tritiée. Elle a été menée au Laboratoire d'Etude des Transferts, au CEN de Fontenay-aux-Roses.

Pour apprécier la durabilité d'un ciment ou d'un béton sur une durée de 300 ans, il est nécessaire, de simuler, en se replaçant dans la situation d'un stockage, le comportement à l'aide d'un modèle mathématique après avoir par une approche expérimentale, déterminé les différents phénomènes qui entrent en jeu et leur importance relative.

Dans un premier temps, nous avons cherché à interpréter les expériences de diffusion par un modèle simple faisant intervenir un transport par loi de Fick dans un milieu poreux. Dans les cas où un transfert a pu être détecté, on montre qu'un phénomène d'adsorption-désorption quelquefois réversible se superpose à la diffusion, et cela même pour l'eau tritiée. De plus, le régime permanent qui est atteint au cours de ces essais n'est qu'apparent. Au bout d'un temps assez long après le passage en régime permanent, les points expérimentaux ne s'alignent plus sur la courbe théorique. Ce phénomène semble assez général. Dans d'autres cas, la seule loi de Fick, même avec adsorption réversible, ne permet pas d'expliquer les résultats. Un autre modèle a donc été développé. Celui-ci fait intervenir à la fois des phénomènes de transport par diffusion (avec ou sans adsorption) et des équilibres chimiques dans la solution interstitielle de la pâte de ciment. L'équation de diffusion a été modifiée de façon à tenir compte des variations de porosité dues à la formation ou à la disparition de précipités. Les équations "chimiques" sont résolues par une méthode de Newton-Raphson. L'ensemble permet d'interpréter aussi bien des essais de diffusion que des essais d'agression. Il permettra par la suite de prévoir le comportement à long terme d'un liant hydraulique dans un stockage de déchets radioactifs.

II) LE MODELE DE DIFFUSION DES IONS

Le modèle qui a été développé jusqu'à présent suppose que les ions ou les molécules, sont transportées dans l'eau interstitielle par une diffusion suivant la loi de Fick ; c'est à dire que le flux de particules est proportionnel au gradient de concentration : [1] , [2]

$$\vec{J} = - D_x \frac{\partial c}{\partial x} \qquad (1)$$

On suppose en outre qu'une fraction de particules se trouve adsorbée sur les parois des pores et que cette adsorption est linéaire et instantanée, c'est à dire que si F est la quantité adsorbée par unité de masse de matériau, F est relié à la concentration C par une loi du type : [3].

$$F = K_d . c \qquad (2)$$

le coefficient K_d est appelé coefficient de partage.

L'introduction de ce coefficient suppose en outre que l'adsorption est réversible. Avec ces conditions, l'équation générale du transport s'écrit :

$$D_x^* \frac{\partial^2 c}{\partial x^2} = \frac{\partial c}{\partial t} \qquad (3)$$

avec

$$D_x^* = \frac{D_x}{1 + \rho . K_d \frac{1-\theta}{\theta}} \qquad (4)$$

et les conditions aux limites suivantes :

$c = C_0$ pour $x = 0$ $\forall t$ (5)
$c = 0$ pour $x = 1$ $\forall t$ (6)

ρ = masse volumique de la pâte de ciment
θ = porosité cinématique du ciment.

En posant $D_e = \theta . D_x$, coefficient de diffusion effectif, l'équation précédente s'écrit :

$$D_e \frac{\partial^2 c}{\partial x^2} = (\theta + \rho K_d (1 - \theta)) \frac{\partial c}{\partial t} \qquad (7)$$

Le coefficient $(\theta + \rho K_d (1-\theta))$ étant appelé "porosité apparente". Plus ce paramètre est grand devant la porosité réelle et plus le matériau a une grande capacité de rétention.

Les hypothèses qui conduisent à ce formalisme, posent cependant un problème. L'introduction d'un phénomène d'adsorption se traduit au niveau formel par l'introduction d'une porosité apparente supérieure à la porosité réelle. Pour remonter au K_d, il est nécessaire de connaître, par un autre moyen, la porosité réelle (ou du moins la fraction de cette porosité qui participe au transport). Or, un ciment très poreux comme le CLC (porosité $\varepsilon \simeq 32$ %) ne laisse pratiquement rien diffuser alors qu'un CPA ($\varepsilon \sim 25$ %) donne un résultat tout à fait interprétable. Cela tient entre autres au diamètre moyen des pores, très fins, typiquement inférieurs à 0,01 µm dans le cas du CLC, ce qui fait qu'une très faible partie du réseau poreux participe à la diffusion.

Cela dit, aucun modèle, linéaire, de Langmuir ou de Freundlich[3] ne se justifie pleinement et notre choix a été guidé ici par la simplicité.

III. INTERPRETATION DES EXPERIENCES DE DIFFUSION

Les calculs ont été menés à partir de l'équation (3) pour interpréter des expériences, menées d'une façon classique en cellule de diffusion. Une lame de ciment est placée entre deux solutions. L'une d'elles, dite solution "amont" contient un ion ou une molécule dont on veut connaître le coefficient de diffusion dans les pores du ciment. L'autre est appelée solution "aval". Elle ne contient pas la particule étudiée. Celles-ci diffusent de la solution amont vers la solution aval, qui est dosée et renouvelée à des intervalles de temps déterminés. Le dosage s'effectue par chromatographie en phase liquide ou par comptage si l'élément étudié est un émetteur γ.

La solution "amont" n'a jamais été renouvelée, ce qui entraîne un épuisement progressif de la quantité de particules disponibles. On a été amené à tenir compte dans les calculs de ces conditions car certaines expériences ont montré qu'une fraction importante de la quantité initiale a traversé la lame de ciment à la fin de l'essai. On serait conduit sans cette correction à sous-estimer le coefficient de diffusion.

a) Diffusion de l'eau tritiée

Les expériences ont été menées sur un grand nombre de matériaux. Les éprouvettes avaient des épaisseurs de 0,3 à 0,6 cm et un diamètre de 58mm. Nous ne retenons ici que les résultats concernant les pâtes pures à base de ciment de type CPA et CLC. Les résultats sont montrés dans le tableau I. Les figures 1a, 1b, 1c, 1d, montrent la validité des calages du calcul numérique sur les résultats expérimentaux. Le résultat le plus intéressant concerne le taux de retard qui est pratiquement égal à 1 dans le cas du CLC et qui prend une valeur comprise entre 2,5 et 4 pour le CPA.

Epaisseur / type de ciment	0,30 cm (CPA) 0,35 cm (CLC)	0,60 cm (CPA et CLC)
CPA	$D_x^* = 1{,}7.10^{-12}$ m²/s $\alpha = 1{,}0$ $D_e = 1{,}7.10^{-12}$ m²/s (figure 1a)	$D_x^* = 2{,}3.10^{-12}$ m²/s $\alpha = 0{,}6$ $D_e = 1{,}4.10^{-12}$ m²/s (figure 1b)
CLC	$D_x^* = 3{,}2.10^{-12}$ m²/s $\alpha = 0{,}27$ $D_e = 8{,}6.10^{-13}$ m²/s (figure 1c)	$D_x^* = 2{,}4.10^{-12}$ m²/s $\alpha = 0{,}32$ $D_e = 7{,}8.10^{-13}$ m²/s (figure 1d)

Tableau I

Interprétation des expériences de diffusion d'eau tritiée : Valeur des coefficients de diffusion (D_x^*) effectifs (D_e) et des porosités (α) calculées à partir du modèle de diffusion de Fick avec adsorption linéaire

De ce résultat, il ressort que le coefficient de diffusion apparent du CPA est plus faible que celui du CLC alors que le coefficient de diffusion effectif D_e est plus important pour le CPA ($\sim 1{,}6.10^{-12}$ m²/s) que pour le CLC ($\sim 8{,}0.10^{-13}$ m²/s).

L'étude de la porosité par différentes méthodes expérimentales a montré que les pâtes pures à base de CLC utilisées pour les essais étaient plus poreuses que les pâtes à base de CPA. Cependant la porosité y est plus fine. Cela pourrait expliquer le fait que le coefficient de diffusion effectif soit plus faible dans le cas du CLC. Par contre, pour les raisons exposées ci-dessus (pores plus fins, porosité totale plus importante), on pourrait penser que le CLC présente une surface spécifique plus importante, donc une capacité d'adsorption plus grande. L'expérience montre qu'il n'en est rien. Il reste à essayer de relier ce phénomène à d'autres paramètres physiques, structuraux, ou chimiques qui distinguent les deux types de ciment.

b) Diffusion d'ions agressifs (Cl^- et SO_4^{2-})

L'étude de l'agression du ciment par les ions chlorure et sulfate comprend des essais de diffusion en cellule. La solution "amont" de la cellule n'est pas renouvelée. Elle s'appauvrit donc en élément diffusant. L'interprétation est faite à l'aide du même modèle que précédemment, mais en remplaçant la condition à la limite (5) par :

$$C_o(t) = C_o(t=0) - \int_o^t \frac{q(\tau)}{V}\, d\tau \qquad (8)$$

V est le volume de la chambre "amont" de la cellule

q(t) est le débit transitant dans la lame de ciment

Les résultats de calcul montrent, en ce qui concerne le CPA et les ions chlorure, que l'on peut encore modéliser le phénomène de transport par une loi de Fick avec taux de retard. Deux faits distinguent cependant ces expériences de celles qui ont été menées avec l'eau tritiée :

- Lorsque l'expérience a été menée pendant un temps assez long, les courbes de débit cumulé s'écartent progressivement de la courbe calculée, sans que cela puisse être attribué à un épuisement de la source. Cela est particulièrement sensible dans le cas du chlorure à concentration de 20 g/l. Ce phénomène pourrait être dû à une modification de structure, elle-même liée à des réactions chimiques à cinétique lente dans le ciment.

- Le taux de retard croît lorsque la concentration en ions chlorure diminue. Là encore, il se peut qu'un équilibre chimique impose l'adsorption ou la précipitation sous forme solide, d'une certaine quantité de chlore. Cette consommation peut freiner considérablement la diffusion dans le cas où la concentration initiale est faible (0,2 g/l). Son influence est beaucoup moindre dans les autres cas (2 g/l et 20 g/l de Cl^-).

Les résultats de calcul concernant le CPA et les ions Cl^- sont consignés dans le tableau 2.

C_o = 20 g/l	C_o = 2.0 g/l	C_o = 0,2 g/l
$D_e = 5.10^{-13} m^2/s$ $\alpha = 0,6$	$D_e = 8,1.10^{-13} m^2/s$ $\alpha = 3,5$	$D_e = 9,7.10^{-13} m^2/s$ $\alpha = 12$

Tableau 2

Diffusion de l'ion chlorure dans le CPA. Résultats obtenus à l'aide du modèle de diffusion avec adsorption linéaire.

Les autres essais concernent la diffusion de l'ion sulfate dans le CPA et la diffusion des deux ions Cl^- et SO_4^{2-} dans le CLC. Les expériences ont démarré depuis plus de 6 mois. Dans aucun des cas le régime permanent n'a été atteint et bien souvent aucune concentration n'est même détectée dans le compartiment "aval" de la cellule (CLC). Dans le cas où on a pu mesurer les quantités transitant dans l'échantillon, les courbes obtenues (corrigées des valeurs obtenues pour les témoins n'ont pas du tout l'aspect théorique d'une courbe obtenue à l'aide du modèle de diffusion (figures 2a, b, c, d).

IV. LE MODELE DE DEGRADATION D'UN CIMENT

Les résultats précédents montrent que, si la diffusion de l'eau tritiée peut fort bien être représentée par un modèle tel que celui qui est décrit plus haut, il n'en est pas de même pour le transport des ions tels que les chlorures et les sulfates.

Il semble que, même dans des conditions de pH élevé, des réactions chimiques mettant en jeu les ions agressifs aient lieu et ont une influence très importante sur le transport de ces ions. Un modèle général de dégradation d'un ciment qui prendra en compte la diffusion et les interactions chimiques est en cours d'écriture. Ce modèle pourra servir à interpréter à la fois les essais de diffusion et les essais d'attaque chimique.

Le modèle résout simultanément et à chaque pas de temps :

- Une équation de diffusion, pour chaque espèce en solution dont on aura déterminé le coefficient de diffusion et le taux de retard,
- Un système d'équations que l'on peut diviser en deux types :
  - . des équilibres chimiques
  - . des équations de conservation.

Le code déterminera, en fonction de la quantité de précipités formés ou disparus, la variation de la porosité. Pour cette raison, il a fallu modifier l'équation de diffusion qui prend la forme :

$$\frac{\partial}{\partial x}\left(D\varepsilon \frac{\partial c}{\partial x}\right) = \frac{\partial}{\partial t}(\varepsilon c) \qquad (9)$$

afin de tenir compte des variations spatiales et temporelles de la porosité.

Les équations représentant des équilibres chimiques sont du type :

$$\prod_j C_j^{x_{ij}} = K_i \qquad (10)$$

Les équations de conservation sont de la forme

$$\sum_j x_{ij} C_j + \sum_k x_{ik} S_k = Q_i \qquad (11)$$

ou C_j représente la concentration de l'espèce j

S_k est la quantité de la phase solide k,

les x_{ij} et x_{ik} sont des coefficients stœchiométriques,

les K_i sont les constantes d'équilibres,

Q_i est la quantité initiale en élément i.

L'ensemble de ce système non linéaire est résolu numériquement par la méthode de Newton-Raphson. Les nouvelles concentrations sont réutilisées au pas de temps suivant pour l'équation de diffusion (9).

V. CONCLUSION

La compréhension des phénomènes d'altération à long terme d'un ciment nécessite l'étude des phénomènes de transport des différents éléments (eau et ion agressifs) intervenant dans ce processus.

Le transport de l'eau peut se modéliser par une loi de diffusion de type loi de Fick, avec un taux de retard dans le cas du ciment de type CPA. Par contre, le transport des ions chimiquement agressifs fait intervenir vraisemblablement des équilibres chimiques entre la solution interstitielle et les différents constituants solides. Le modèle global, réalisant le couplage entre ces deux types de mécanismes devra se recaler sur les résultats expérimentaux, en particulier ceux concernant l'évolution dans le temps de la porosité d'un ciment placé dans des conditions d'agression.

REFERENCES BIBLIOGRAPHIQUES

[1] CRANK J.
The matematics of diffusion (2nd edition)
Clarendon Press, Oxford (1973)

[2] LEDOUX E., de MARSILY G.
Transport de masse et d'énergie en milieu poreux. Rapport LHM/RD/76/16
Ecole des Mines de Paris (1976)

[3] GOBLET P.
Modélisation des transferts de masse et d'énergie en aquifère. Thèse de D.I.
Ecole des Mines de Paris (1980)

[4] POMMERSHEIM J., CLIFTON J.
Prediction of concrete service life.
Matériaux et construction. 01/85 pp. 21-30

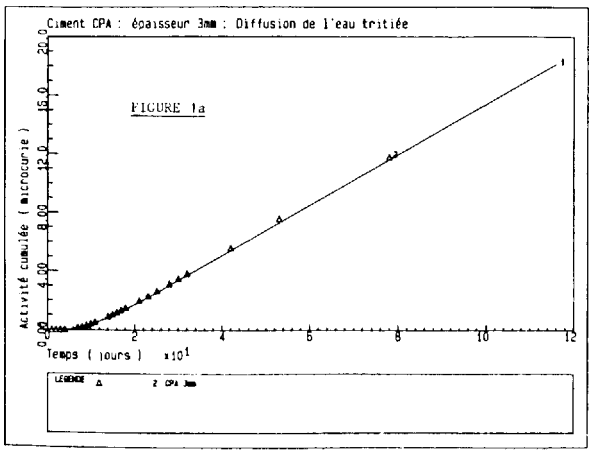

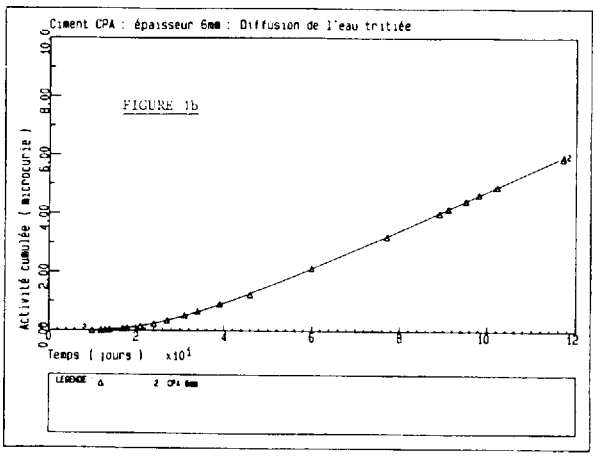

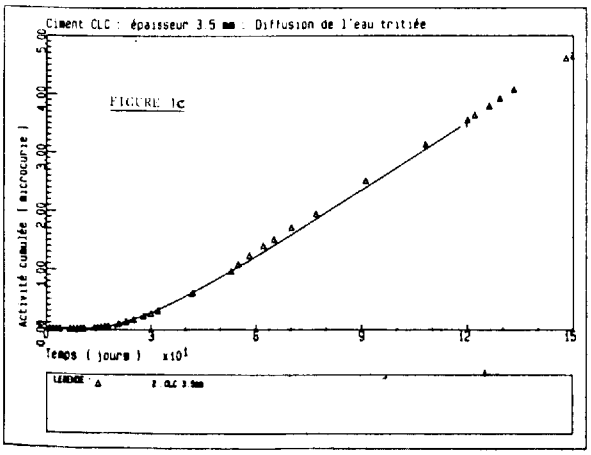

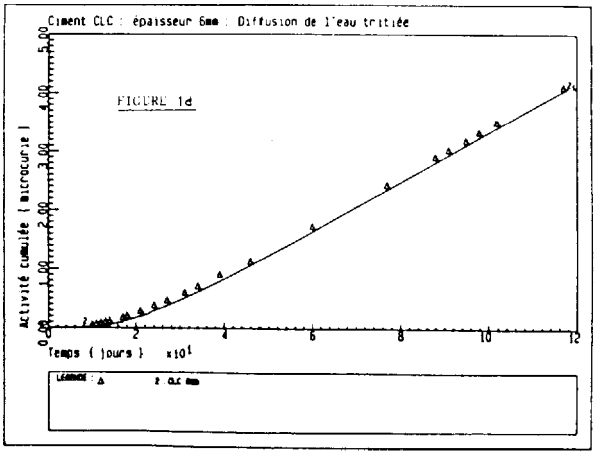

Figures 1 a, b, c, d, : Interprétation des essais de diffusion d'eau tritiée

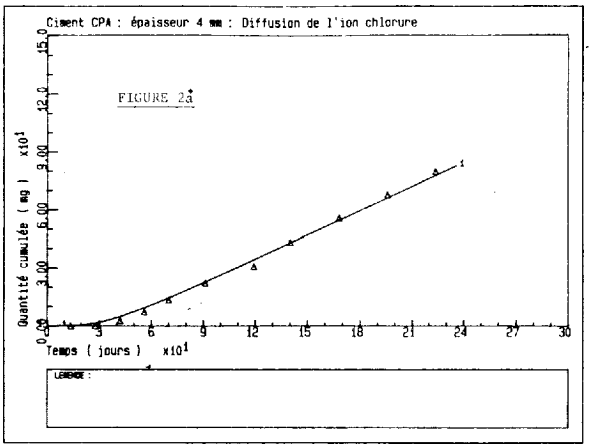

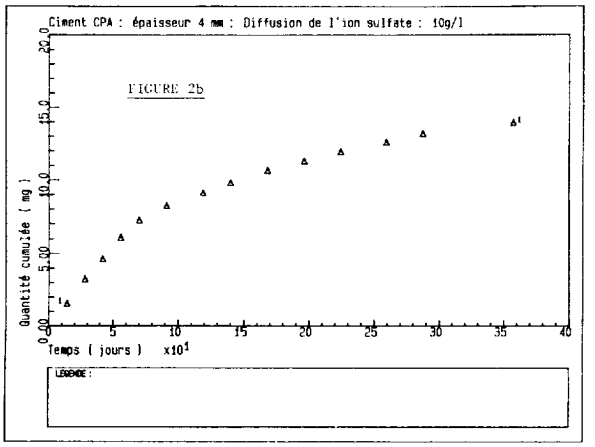

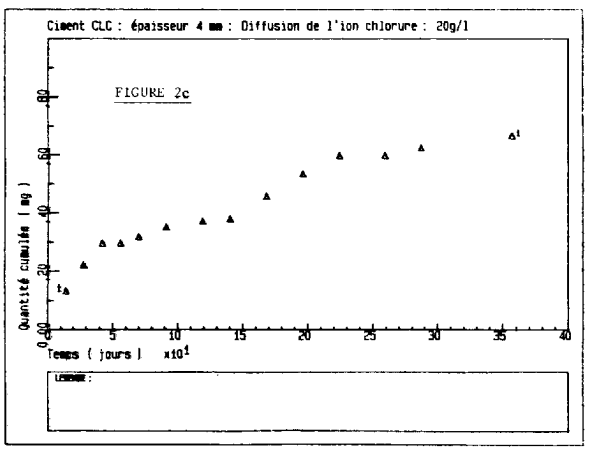

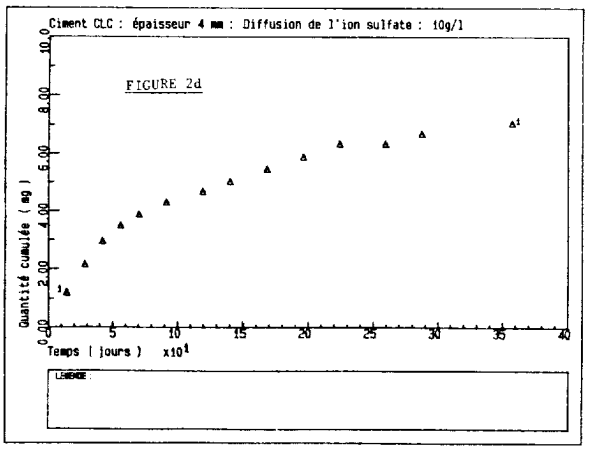

Figures 2 a, b, c, d

Essais de diffusion d'ions agressifs.
Le trait plein sur la figure 2 a est le résultat du calcul numérique.

P. GEGOUT, H. HORNAIN, B. THURET, M. REGOURD
C.E.R.I.L.H. - Paris - FRANCE

Frost resistance of limestone filler cements
Résistance au gel des ciments aux fillers calcaires.

RESUME

Des mortiers de CPJ expérimentaux, préparés à partir d'un ciment Portland et d'un filler calcaire (15 % et 30 % de filler) gâchés à différents rapports Eau/CPEJ ont été soumis à des cycles gel-dégel. Les facteurs d'espacement des bulles d'air $\bar{L}$ ont été déterminés avant la mise au gel et le $\bar{L}$ critique ($\bar{L}cr$) a été déduit des mesures d'expansion linéaire. Au rapport E/CPEJ = 0,5, $\bar{L}cr$ diminue de 420 à 180 μm quand le taux de filler passe de 0 à 30 %, mais à E/CPEJ = 0,42, le $\bar{L}cr$ est voisin de 350 μm dans tous les cas. L'addition de 1% d'entraîneur d'air réduit le $\bar{L}$ à 100 μm dans tous les mélanges. Les résistances en compression (après 300 cycles gel-dégel) en fonction de $\bar{L}$, accusent une chute dès le passage par le $\bar{L}cr$.

Argamassas de CPJ experimentais, preparadas a partir de um cimento Portland e de um "filler" calcário (15% e 30% de "filler") misturadas com diferentes relações água/CPEJ foram submetidas a ciclos de gelo-degelo. Os fatores de espaçamento das bolhas de ar $\bar{L}$ foram determinados antes da congelação e o $\bar{L}$ crítico ($\bar{L}cr$) foi deduzido das medidas de expansão linear.

Na relação água/CPEJ, $\bar{L}cr$ diminui de 420 a 180 µm quando a porcentagem de "filler" passa de 0 a 30%, mas para água/CPEJ = 0,42, o $\bar{L}cr$ é próximo a 350 µm em todos os casos. A adição de 1% de incorporador de ar reduz o $\bar{L}$ a 100 µm em todas as misturas. As resistências à compressão (após 300 ciclos de gelo-degelo) em função de $\bar{L}$, acusam uma queda desde a passagem pelo $\bar{L}cr$.

1. INTRODUCTION

Les ciments avec ajouts représentent une part importante de la production des liants hydrauliques. Ceux contenant des fillers calcaires sont de plus en plus souvent mis en oeuvre en France. Leur utilisation rationnelle nécessite que soit bien connu leur comportement. L'objet de cette étude est de caractériser l'influence de ce type d'ajout sur la tenue au gel des mortiers.

Les nombreux travaux, notamment de POWERS (1 à 5) et de LITVAN (6 à 9) ont clairement mis en évidence que les mouvements de l'eau dans le béton étaient en grande partie responsables des dégradations du matériau par le gel.
L'utilisation d'adjuvants entraîneurs d'air qui permettent de développer dans le béton un réseau de bulles jouant le rôle de "vases d'expansion" est un moyen efficace de lutter contre les effets du gel. M. PIGEON (10 à 12), reprenant la théorie de la pression hydraulique de POWERS, a montré qu'il existait un espacement critique (noté $\bar{L}cr$) entre les bulles d'air en deça duquel le béton devenait résistant au gel et que $\bar{L}cr$ était fonction de la vitesse de refroidissement.

2. CONDITIONS EXPERIMENTALES

2.1. Préparation des échantillons

Deux ciments, notés CPEJ 15 et CPEJ 30 contenant respectivement 15 % et 30 % de filler calcaire, ont été préparés par mélange d'un CPA industriel et d'un calcaire (98 % $CaCO_3$) broyés séparément à 3 500 et 3 700 cm^2/g respectivement.

Des prismes de mortiers 4 x 4 x 16 cm ont été gâchés avec différents rapports E/C dans le but de comparer leur comportement soit à E/C constant, soit à E/(CPA contenu dans le mélange) constant. (Tableau 1).

Tableau I

% Fillers \ E/C	0,60	0,50	0,425	0,420
0 (CPA)	0,60	0,50	-	-
15	-	0,59	0,50	-
30	-	0,71	-	0,60

Rapport eau/(CPA du mélange) en fonction du taux de filler dans le mélange et du rapport E/C

Des quantités variables d'entraîneur d'air (0 (témoin), 0,2 - 0,4 - 0,6 - 0,8 - 1 et 2 g/l) ont été ajoutées à l'eau de gâchage afin d'obtenir des quantités d'air différentes et des bulles plus ou moins espacées, ($\bar{L}$ plus ou moins grand). Neuf prismes par dosage en entraîneur d'air et par ciment ont été confectionnés et conservés dans l'eau à 20 °C.

Après 7 jours, le module d'Young a été déterminé à partir des mesures de résonance en flexion, sur les 9 prismes de chaque série. Le prisme présentant la valeur médiane a été sélectionné pour les comptages de bulles d'air et le calcul de $\bar{L}$. Les 8 autres prismes ont été conservés dans l'eau à 20 °C jusqu'à 105 jours.

A 105 jours, 4 prismes sur 8, présentant le module d'Young le plus proche de la valeur médiane de la population à cette échéance, sont introduits dans l'enceinte de gel; les 4 autres servent à mesurer les résistances mécaniques en compression.

2.2. Gel des échantillons

Les conditions de gel ont été les suivantes:

	Milieu	T°C finale	Durée
Gel	Air	- 20 °C	3 h
Dégel	Eau	+ 20 °C	1 h

La vitesse de refroidissement est de l'ordre de 10 °C/heure; la durée d'un cycle gel-dégel est de 4 heures. Les prismes ont subi 300 cycles au total. Les variations dimensionnelles (gonflement ou retrait) ont été mesurées tout au long du traitement.

2.3. Détermination du facteur d'espacement des bulles d'air $\bar{L}$

La technique des traversées linéaires dont les principes sont décrits dans la norme ASTM C 457-82 a été utilisée. Le facteur d'espacement moyen, $\bar{L}$, est calculé en faisant l'approximation que toutes les bulles sont des sphères de même diamètre réparties uniformément. Le calcul utilisé par POWERS (1), qui ne tient pas compte de la distribution réelle donne vraisemblablement des valeurs de $\bar{L}$ un peu supérieures aux valeurs réelles.

Les résultats, illustrés par la figure 1, montrent que l'allure des courbes $\bar{L}$ en fonction de la concentration en entraîneur d'air est sensiblement la même pour tous les mélanges testés : $\bar{L}$ diminue d'abord rapidement quand la concentration augmente et se stabilise autour de 100 μm à partir de 0,8 à 1 g/l d'adjuvant.

La précision des mesures de $\bar{L}$ dépend de la teneur en air et du nombre de traversées effectuées. Elle varie entre 10 et 50 μm environ suivant le cas.

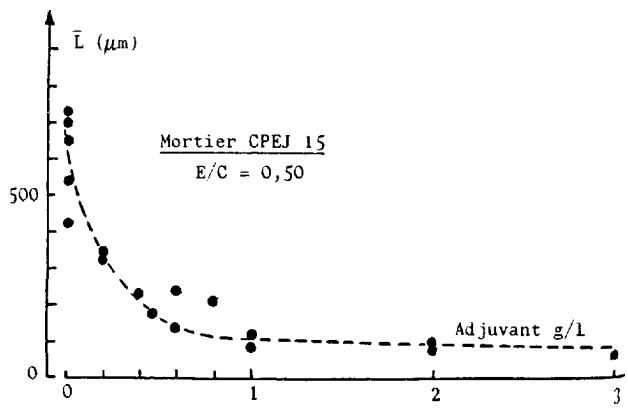

Figure 1
Variation de $\bar{L}$ en fonction de la concentration en entraîneur d'air- Exemple: Mortier CPEJ 15

3. DETERMINATION DES $\bar{L}$ CRITIQUES ($\bar{L}cr$) (Fig.2).

Le $\bar{L}cr$ est une valeur conventionnelle définie comme le $\bar{L}$ au-delà duquel un matériau donné ne résiste pas aux conditions de gel imposées.

PIGEON (1984), dans ses essais sur l'influence de la vitesse de gel, avait défini le $\bar{L}cr$ comme le $\bar{L}$ au-delà duquel le gonflement était supérieur à 150 $\mu m/m$ après 300 cycles de gel-dégel.

Nos conditions expérimentales beaucoup plus sévères entraînant une dégradation très importante des éprouvettes après 300 cycles, le $\bar{L}cr$ a été déterminé après 100 cycles seulement. A cette échéance, les mesures de gonflement sont beaucoup moins dispersées, et permettent la comparaison recherchée des différents ciments.

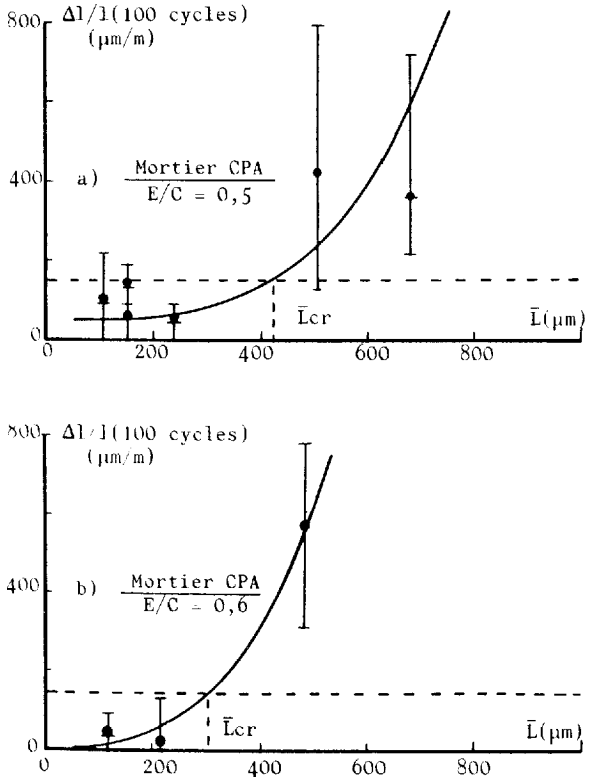

Figure 2

Détermination graphique du $\bar{L}cr$ des mortiers de CPA après 100 cycles de gel-dégel pour E/C = 0,5 et 0,6.

Le tableau 2 rassemble les valeurs de $\bar{L}cr$ estimées pour le CPA et les 2 CPEJ. Ces valeurs sont déterminées graphiquement, comme indiqué sur les figures 2 a et b, où on a fait figurer l'écart absolu des mesures de gonflement.

Composition		$\bar{L}cr$
Ciment	E/C	
CPA	0.50	420 ± 50
	0.60	300 ± 90
CPEJ 15	0.50	300 ± 80
	0.425	350 ± 50
CPEJ 30	0.50	180 ± 50
	0.42	380 ± 80

Tableau II

Valeurs de $\bar{L}cr$ pour les différents ciments et pour des E/C variables.

4. INFLUENCE DU FILLER SUR LE COMPORTEMENT AU GEL

La figure 3 montre que le $\bar{L}cr$ diminue lorsque la teneur en filler augmente pour un rapport E/C identique.

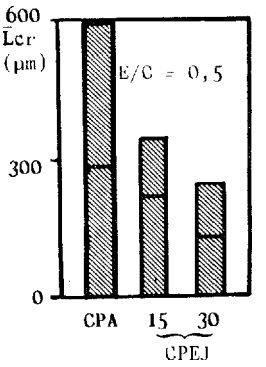

Figure 3

Variation du $\bar{L}cr$ en fonction du pourcentage de filler dans le ciment. Les 2 traits horizontaux représentent les valeurs basse et haute du $\bar{L}cr$ et donnent une idée de la dispersion.

Toutefois, cette représentation peut être trompeuse dans la mesure où l'accroissement de la teneur en filler correspond à une augmentation de la quantité d'eau rapportée à la quantité de CPA proprement dit dans le mélange fillérisé ("E/CPA">E/C). Les rapports "E/CPA" dans les mortiers de CPEJ 15 et de CPEJ 30 sont en réalité respectivement égaux à 0,59 et 0,70 . Les variations de $\bar{L}cr$ enregistrées sont dues davantage à l'augmentation du rapport "E/CPA" qu'à l'ajout des fillers.

En effet, pour un même ciment, les variations de E/C entraînent des comportements au gel très différents qui sont en relation avec la quantité d'eau "déstabilisée" mobilisable au cours du gel.

Indépendamment de la quantité de filler, l'augmentation du rapport E/C pour chacun des ciments entraîne une diminution du $\bar{L}cr$ (Figure 4).

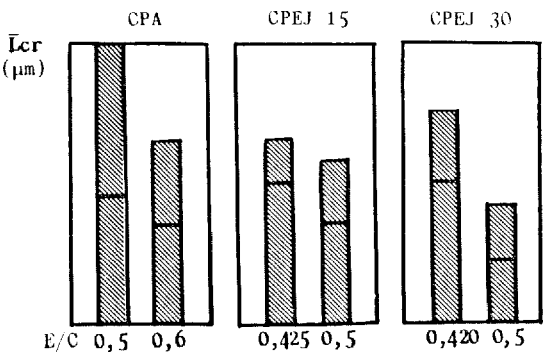

Figure 4

Influence du rapport E/C sur le $\bar{L}cr$ des différents ciments.

Ainsi, pour mettre en évidence l'influence propre du filler, il faut comparer ces ciments à E/CPA identique. Il est possible compte-tenu des E/C utilisés (tableau I) de comparer entre-eux:

- CPA et CPEJ 15 à "E/CPA" = 0,5
- CPA, CPEJ 15, CPEJ 30 à "E/CPA" = 0,6

La figure 5 présente alors une allure très différente de la figure 3.

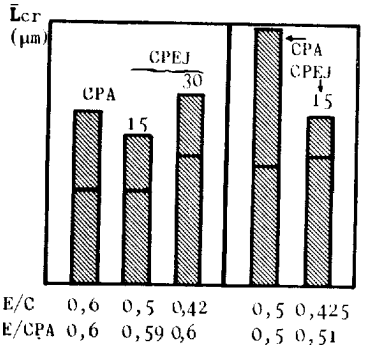

Figure 5

Influence du pourcentage de filler sur le $\bar{L}cr$ pour un rapport E/CPA identique.

La comparaison effectuée dans ces conditions fait ressortir le strict effet du filler. Il apparaît que ce dernier n'a aucune influence néfaste sur la tenue au gel. Le CPEJ 30 semble même se comporter un peu mieux que le CPA correspondant.

Toutes choses égales par ailleurs, il semble donc que le rapport E/C soit prépondérant dans la tenue au gel des materiaux durcis. Les CPEJ sont défavorisés par rapport aux CPA lorsqu'on travaille à E/C égal; ils renferment alors une quantité d'eau congelable plus grande, proportionnelle au pourcentage de filler dans le CPEJ.

5. INFLUENCE DES FILLERS SUR LE COMPORTEMENT MECANIQUE PENDANT LE GEL

5.1. Résistances avant gel

Les résistances en compression des mortiers ont été mesurées avant gel (à 105 jours) et après 300 cycles de gel-dégel.
La figure 6 montre qu'à âge égal et à même E/C les mortiers témoins, sans entraineur d'air, sont d'autant moins résistants qu'ils contiennent plus de filler.

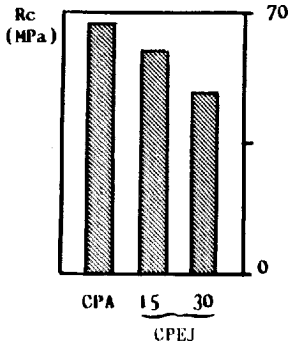

Figure 6

Résistances à 105 jours en compression des mortiers en fonction du pourcentage de filler à E/C constant =0,5. Ciments témoins sans entraineur d'air.

Dans ces conditions, les contraintes mécaniques engendrées par le gel affecteront plus facilement les mortiers de CPEJ moins résistants au moment de leur mise au gel.

L'examen particulier de l'influence du rapport E/C sur la résistance avant gel des mortiers indique que dans tous les cas, l'augmentation de ce rapport a pour effet de diminuer les résistances à échéance donnée (Fig. 7).

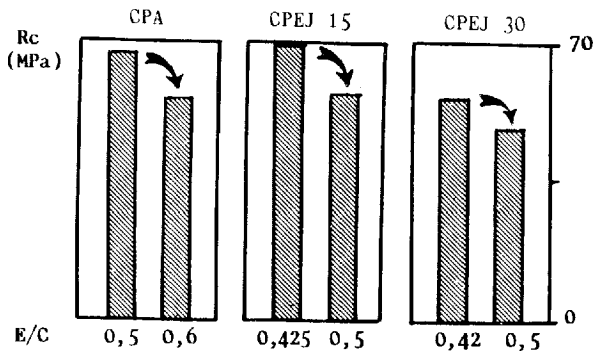

Figure 7

Influence du E/C sur la résistance avant gel des mortiers de CPA et CPEJ témoins sans entraîneur d'air

Par contre, lorsque les mortiers sont gâchés avec un E/CPA identique, ils présentent à 105 jours la même résistance quelle que soit la proportion de filler (fig. 8).

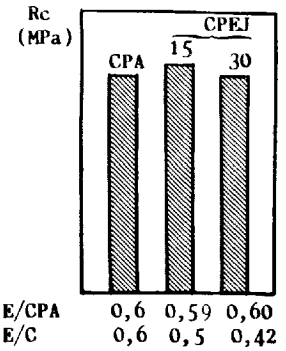

Figure 8

Résistances en compression du CPA et des CPEJ à 105 jours, pour un "E/CPA" identique.
Mortiers témoins sans entraîneur d'air.

La correction des E/C en fonction du pourcentage de filler que contient un ciment composé, permet donc de rétablir des résistances comparables à celles des CPA.

5.2. Résistances après gel

L'introduction d'entraîneur d'air provoque naturellement au-delà d'un certain dosage, une baisse des résistances mécaniques à 105 jours, (Fig. 9).

Cet effet pourrait être considéré comme néfaste à première vue. Cependant, on constate sur la figure 9, que tous les mortiers ayant suffisamment d'entraîneur d'air et présentant des $\bar{L}$ inférieurs au $\bar{L}cr$, ont des résistances avant et après gel quasiment égales.

Au-delà de la zone du $\bar{L}cr$, les résistances après gel chutent fortement comparativement aux résistances avant gel.

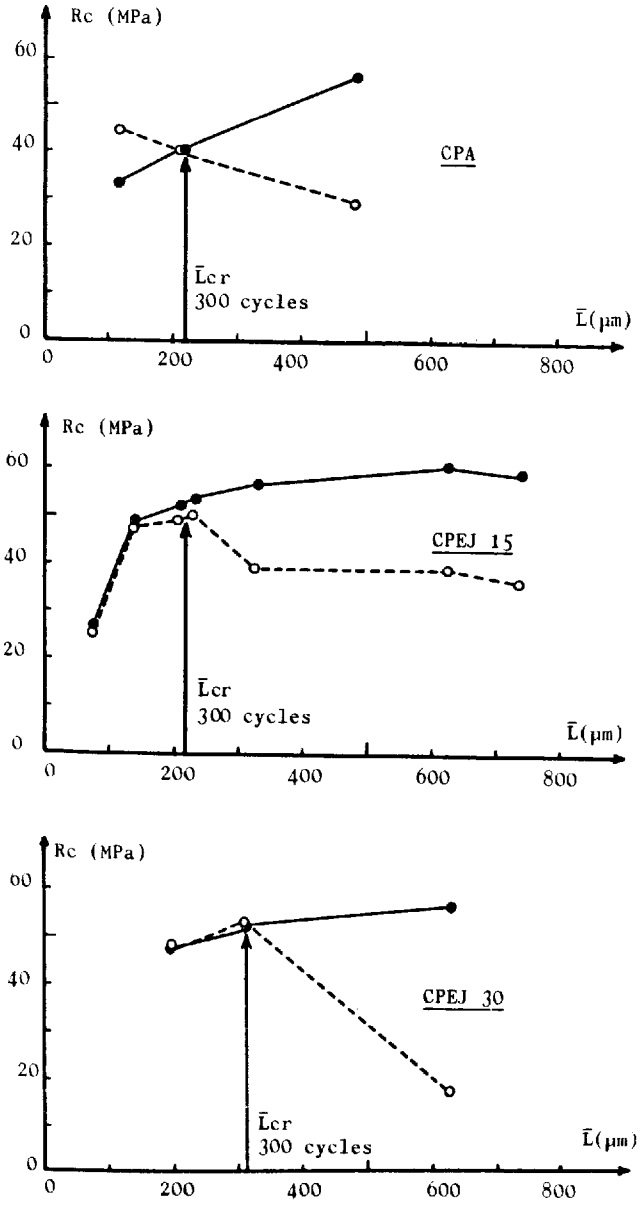

Figure 9

Résistances avant et après gel en fonction de $\bar{L}$. Les résistances après gel sont mesurées après 300 cycles. La flèche représente le $\bar{L}$cr estimé à 300 cycles.

● avant gel ○ après gel

6. CONCLUSIONS

Les principaux résultats obtenus sur le comportement de mortiers de ciments fillérisés expérimentaux ont permis de mettre en évidence les points suivants :

Avant gel :

- A E/C égal, les résistances mécaniques diminuent quand la teneur en filler augmente.

- La diminution des résistances est due, dans ce cas, à l'accroissement de la proportion d'eau disponible relativement à la quantité de CPA proprement dit dans le ciment fillérisé. Pour un rapport E/C constant, le rapport "E/CPA" augmente avec la teneur en filler.

- Une correction du rapport E/C tenant compte de l'excès d'eau engendré par la présence de filler, permet d'obtenir des résistances comparables à celles des CPA.

Après gel :

- L'addition d'entraîneur d'air permet d'introduire dans les mortiers un réseau de bulles susceptibles d'améliorer leur comportement au gel.

- En fonction du rapport E/C et de la teneur en filler, il est possible de déterminer un espacement moyen critique des bulles d'air, noté $\bar{L}$cr, au-delà duquel le mortier devient gélif dans les conditions expérimentales choisies.

- Pour un même ciment, $\bar{L}$cr diminue quand E/C augmente.

- De même, à E/C égal, $\bar{L}$cr diminue quand le pourcentage de filler augmente.

- Toutefois la correction du E/C tenant compte de l'excès d'eau apporté par la présence de filler permet d'obtenir des $\bar{L}$cr, donc des résistances au gel, comparables à celles des CPA.

- L'abaissement des résistances mécaniques dans le cas des fortes teneurs en air entraîné, ($\bar{L}$ faible), n'a pas d'incidence néfaste sur la tenue au gel des mortiers dont les $\bar{L}$ restent inférieurs aux $\bar{L}$cr.

REMERCIEMENTS

Nous tenons à remercier de leur contribution à ce travail, L.J. HOLLEBECQ, ingénieur et G. SCEMAMA, technicien au Département Bétons, ainsi que E. ZWIANZEK, technicien au Département Microstructures.

BIBLIOGRAPHIE

* * *

1. **POWERS T.C.** (1949) : "The Air Required of Frost-Resistant Concrete" Proc. Highway Res. Board, 29, 1-28.

2. **POWERS T.C.** (1954) : "Void Spacing as a Basis for Producing Air Entrained Concrete" J.A.C.I. 25, 741-760, P.C.A., Bull. 58.

3. **POWERS T.C.** (1955) : "Basic Considerations Pertaining to Freezing and Thawing Tests" A.S.T.M. Proc, 55, P.C.A., Bull. 58.

4. **POWERS T.C.** (1975) : "Freezing Effects in Concrete" A.C.I., SP 47, 1 - 11.

5. **POWERS T.C. HELMUTH R.A.** (1953). "Theory of Volume Changes in Hardened Portland Cement Paste During Freezing". P.C.A. Bull 46. Proc. Highway Res. Board, 32, 285 - 297.

6. **LITVAN G.G.** (1973) : "Frost Action in Cement Paste" Mat. and Struct. 34, 293 - 300.

7. **LITVAN G.G.** (1974) : "Design for Frost Durability" 2° Intern CIB/RILEM Symp. Rotterdam, 4, 1-4.

8. **LITVAN G.G.** (1980) : "Freeze Thaw Durability of Porous Building Materials " A.S.T.M. STP 691, 455-463.

9. **LITVAN G.G.** (1981) : "Frost Action in Porous Systems" Séminaire Altération des Bétons et des Pierres - Col. international des Sciences de la Construction, Saint-Rémy-les-Chevreuse.

10 **PIGEON M.** (1984) : "La microstructure et la Résistance au gel des ciments et bétons" Thèse Doc. Ing Université P et M Curie, Paris.

11 **PIGEON M. LACHANCE M.** (1981) : "Critical Air-Void Spacing Factors for Concretes Submitted to Slow Freeze-Thaw Cycles". J.A.C.I. 78 (4) 282-291.

12 **PIGEON M. PREVOST J. SIMARD J.M.** (1984) : "Freeze Thaw Durability as Freezing Rate". A paraître dans J.A.C.I.

H.HORNAIN et M.REGOURD - CERILH - PARIS - FRANCE

MICROFISSURATION DES BETONS
MICROCRACKING OF CONCRETE

Les techniques microscopiques et stéréologiques ont été appliquées à l'observation et à la quantification du réseau microfissural de bétons. Trois niveaux de structure sont considérés : échelle centimétrique (interfaces pâte-granulats)observées au stéréo-microscope aux grandissements 10 à 50 , échelle millimétrique (interfaces pâte-sable, anhydres, $Ca(OH)_2$),observés au microscope optique en lumière réfléchie sur sections polies et sur répliques aux grandissements 100 à 500 , échelle micrométrique (C-S-H, $Ca(OH)_2$, sulfo-aluminates hydratés), observés au M.E.B. aux grandissements 1000 à 10.000 . Les techniques sont appliquées à l'étude de deux bétons avant et après chargement : un béton de granulats silico-calcaires et un béton de granulats légers.

Les résultats permettent de caractériser l'état initial des deux bétons avant chargement et leur différence de comportement à la rupture. Ils mettent également en évidence le caractère d'objet fractal du béton où le processus de fissuration présente une certaine homothétie aux différentes échelles. Une tentative de mesure de la dimension fractale de la surface de fracture des bétons est effectuée.

As técnicas microscópicas e estereológicas foram aplicadas à observação e à quantificação da rede de microfissuras do concreto. Três níveis de estrutura são considerados: escala centimétrica (interface pasta-agregado) observadas no estéreo-microscópio com aumento de 10 a 50; escala milimétrica (interface pasta-areia, anidros, $Ca(OH)_2$) observadas no microscópio ótico com luz refletida sobre seções polidas e sobre réplica com aumentos de 100 a 500; escala micrométrica (C-S-H, $Ca(OH)_2$) sulfo-aluminatos hidratados) observadas no MEV com aumentos de 1.000 a 10.000. As técnicas são aplicadas ao estudo de dois concretos antes e após carregamento: um concreto com agregado silico-calcário e um concreto com agregados leves.

Os resultados permitem caracterizar o estado inicial dos dois concretos antes do carregamento e suas diferenças de comportamento à rutura. Eles põem, igualmente, em evidência o caráter de objeto fractal ao concreto onde o processo de fissuração apresenta uma certa homotética nas diferentes escalas. Uma tentativa de medida da dimensão fractal da superfície de fratura dos concretos é efetuada.

1. INTRODUCTION

A l'échelle microscopique le béton est un matériau composite hétérogène qui, dans les conditions normales de mise en oeuvre, renferme toujours des discontinuités assimilables à des microfissures ou "défauts" au sens de Griffith. Ces discontinuités sont liées aux conditions de mise en place, d'environnement, de chargement, mais aussi au mode même de structuration et d'évolution du liant hydraté au sein du réseau de granulats (1, 2, 3).

Au-delà d'un certain seuil de contrainte locale ou globale (contrainte interne d'origine physico-chimique ou contrainte externe d'origine mécanique) des microfissures peuvent se développer à partir des discontinuités préexistantes. La coalescence des microfissures en fissures plus importantes peut entraîner la dégradation progressive du béton ou, suivant la géométrie et les conditions de chargement, sa rupture brutale quand la fissure atteint une certaine dimension critique (4).

Dans le cadre d'une recherche coordonnée par l'AFREM (Association Française de Recherches et d'Essais sur les Matériaux de Construction) sur l'origine et le mécanisme de la microfissuration (5), le CERILH, en partant des travaux antérieurs de SLATE (6), DHIR et SANGHA (7) et plus récemment de STROEVEN (8), a étudié la microfissuration de bétons avant et après chargement à l'aide des techniques microscopiques : microscopie optique et microscopie électronique à balayage (M.E.B).

Les phénomènes de fissuration se situant à différents niveaux de structure (9), les observations ont été effectuées à 3 échelles :

- niveau de structure I : échelle centimétrique qui est celle du béton proprement dit et qui correspond à la dimension des plus gros granulats (1 à 20 mm). Le volume élémentaire représentatif considéré est de l'ordre de 1 dm^3. Les examens se font sur plaques polies de béton 10 x 10 cm, aux grandissements 4 à 40 à l'aide d'une loupe binoculaire qui permet l'observation des distributions et orientations préférentielles des granulats, des interfaces ...

- niveau de structure II : échelle millimétrique qui est celle du mortier comprenant les grains de sable associés à la pâte de ciment et ses inclusions (interfaces, anhydres, $Ca(OH)_2$ ...). Le volume élémentaire représentatif est de l'ordre de 1 cm^3. Les examens sont effectués au microscope optique ou au M.E.B à des grandissements compris entre 300 et 1000 environ. Ils nécessitent la préparation de sections polies, de lames minces ou de répliques.

- niveau de structure III : échelle micrométrique qui est celle de la pâte de ciment durcie et des hydrates proprement dits (assemblage des C-S-H, $Ca(OH)_2$, aluminates). Le volume élémentaire représentatif est de l'ordre de 1 mm^3. Les examens sont réalisés au M.E.B sur fractures.

2. TRAITEMENT PREALABLE DES ECHANTILLONS

Le problème essentiel est de trouver une technique de préparation qui conserve le béton dans son état initial sans induire de microfissurations accidentelles. Or l'observation microscopique, qu'elle soit directe ou indirecte (réplique) nécessite un traitement préalable de la surface à examiner : polissage, découpage, éventuellement dessiccation et imprégnation. Ces opérations peuvent engendrer des contraintes mécaniques, donc des microfissures. Il est possible de s'affranchir plus ou moins des risques dûs aux contraintes mécaniques proprement dites en prenant un certain nombre de précautions : échantillons suffisamment épais, sciage ménagé, polissage progressif. Par contre les inconvénients liés à la dessiccation accidentelle et à l'élimination de l'eau sont plus difficiles à maîtriser. La déshydratation préalable des échantillons destinés aux observations microscopiques (lumière réfléchie et M.E.B) a pu être obtenue de différentes façons :

- sèchage à l'air ou à l'étuve : ce traitement qui peut modifier la microstructure de la pâte de ciment et qui provoque un retrait important est à proscrire.

- cryosublimation ou lyophylisation : la transformation suffisamment rapide de l'eau en glace se fait sans augmentation notable de volume et la sublimation lente de la glace est moins dommageable pour l'échantillon que le passage direct liquide → vapeur. Cette technique qui est utilisable pour les petits échantillons ne donne pas satisfaction dans tous les cas et n'est pas adaptée au traitement des gros échantillons.

- échange progressif eau-solvant-résine. La méthode empruntée aux biologistes permet de fixer et d'imprégner un matériau hydraté en remplaçant très progressivement l'eau par une résine époxy par l'intermédiaire d'un solvant (oxyde de propylène). Cette méthode encore à l'étude, ne semble pas induire de microfissurations accidentelles. Son principal inconvénient est la durée importante du traitement (plusieurs jours).

3. TECHNIQUES DE VISUALISATION ET D'OBSERVATION DES MICROFISSURES

3.1 Par coloration du béton

Cette technique est destinée à caractériser la microfissuration des bétons au niveau de structure I. La préparation des échantillons comporte les opérations suivantes : découpage à la scie diamantée sous eau de plaquettes de 1 cm à 1,5 cm d'épaisseur, suivant des directions repérées; polissage mécanique sur émeri 250 et 400 dans l'eau; badigeonnage à l'aide d'une solution alcoolique d'un colorant (rouge Irgacete par exemple) insoluble dans l'eau; séchage ménagé du colorant à l'air (environ 5 à 10 min.); polissage progressif sur émeris 600, 800 et 1000 jusqu'à élimination de l'excès de colorant qui ne subsiste que dans les microfissures et les zones poreuses du béton. La diffusion du colorant dans ces zones et la détermination du moment où le polissage doit être arrêté sont deux difficultés de la méthode. Sauf pendant la période courte de séchage du colorant, le béton est toujours maintenu en présence d'humidité et les risques de microfissuration par dessiccation sont faibles tout au moins au niveau de structure considéré. Après polissage, le comptage des microfissures est effectué par la méthode des sécantes aléatoires décrite plus loin, soit directement sous le microscope, soit à partir de photographies représentatives dont le réseau microfissural

a été reproduit sur calque.

3.2 Par imprégnation de résine

La méthode surtout utilisée pour caractériser le niveau de structure II peut aussi être utile à la préparation d'échantillons de grande dimension. Les prélèvements préalablement déshydratés à l'aide de l'une des techniques décrites au §2, sont imprégnés d'une résine (époxy, méthyl-métacrylate, ...) puis polies et éventuellement attaquées par un réactif sélectif qui permet d'augmenter les contrastes en lumière réfléchie. Ceux-ci sont encore améliorés par une très légère métallisation des sections polies qui peuvent alors être également observées au M.E.B. L'utilisation de pigments fluorescents incorporés à la résine d'imprégnation peut être avantageuse si l'on dispose d'un microscope optique équipé d'une source U.V (10).

3.3 Par fractographie au M.E.B et au stéréomicroscope.

L'examen au M.E.B des surfaces de fracture obtenues par des essais de traction, flexion ou compression permet la caractérisation du faciès des hydrates et de leur mode de rupture, l'étude fine des interfaces pâte de ciment-granulat, l'observation du mode de rupture des granulats (rupture trans ou intergranulaire) et autres inclusions.

A une échelle plus grossière la stéréomicroscopie peut présenter un certain intérêt pour l'étude qualitative et quantitative des surfaces de rupture des bétons.

3.4 Par répliques

Cette technique d'observation indirecte récemment développée par l'équipe de l'INSA de Toulouse (11) présente deux avantages majeurs: la réplique est obtenue sur le matériau en l'état (sans dessiccation préalable) d'une part; elle permet de suivre directement l'évolution de la fissuration aux différents stades du chargement d'autre part. Elle nécessite toutefois le polissage préalable de la surface à répliquer et ne permet que l'observation des phénomènes superficiels. La technique, également utilisée au CERILH, consiste à presser un film de "biodène" (acétyl-cellulose) (environ 1,5 cm x 3 cm) préalablement imbibé d'acétate de méthyle sur la zone à observer. Après évaporation du solvant le biodène est décollé puis observé soit au microscope optique en transmission ou en réflexion, soit au M.E.B. après métallisation à des grandissements ne dépassant pas 1000. Afin de "nettoyer" la surface à répliquer il peut être nécessaire de réaliser plusieurs empreintes successives avant d'obtenir la réplique définitive. Par ailleurs, les observations au M.E.B sont effectuées avec des tensions d'accélération n'excédant pas 10 kV afin de ne pas détériorer le film plastique. Deux exemples d'empreintes observées au M.E.B et au microscope optique par transmission sont donnés figures 1 et 2.

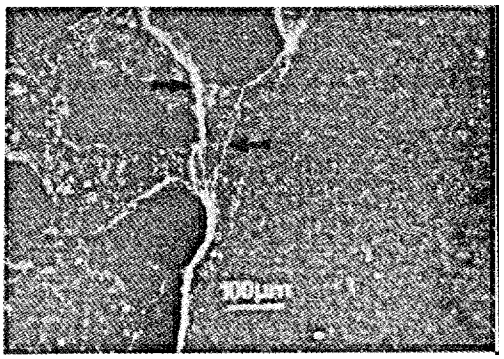

Fig.1 - Réplique observée au MEB.

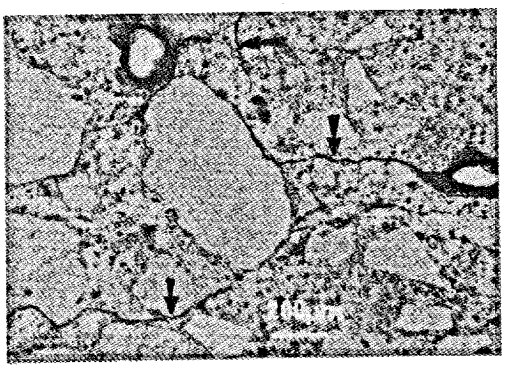

Fig.2 - Réplique observée au microscope optique par transmission

4. QUANTIFICATION DU RESEAU MICROFISSURAL DES BETONS

La stéréologie permet de relier les propriétés statistiques quantitatives des structures tridimensionnelles à celles des structures bi-dimensionnelles. A l'inverse elle permet de reconstruire certains aspects de l'espace 3D à partir de l'analyse quantitative d'images planes. Ainsi les microfissures des bétons, qui en section apparaissent sous forme d'éléments linéaires, peuvent être caractérisées quantitativement par simple comptage de leurs intersections avec un réseau de sécantes aléatoires ou orientées.



Fig.3 - Principe de mesure du nombre d'intersections des microfissures $P_L(\theta)$ avec une sécante orientée faisant un angle θ avec une direction déterminée.

La méthode proposée par SALTIKOV (12) et utilisée par P.STROEVEN (8, 13) pour étudier les aspects micromécaniques du comportement du béton, permet de déterminer les paramètres suivants: le nombre moyen d'intersections $\bar{P}_L$ par unité de longueur de sécante. $\bar{P}_L$ représente en quelque sorte la "densité" de microfissures dont on peut déduire la surface spécifique par l'équation : $S_V = 2\ \bar{P}_L$ qui, dans le cas d'une structure où les microfissures ont une orientation préférentielle suivant un plan déterminé, devient : $S_V = (2-\pi/2)\ P_{L//} + \pi/2\ P_{L\perp}$ où $P_{L//}$ et $P_{L\perp}$ correspondent aux deux directions, parallèle et perpendiculaire, au plan considéré. La règle des projections totales établit par ailleurs que la valeur $\bar{P}_L(\theta)$ prise suivant la direction θ, est égale à la longueur totale L_A des éléments linéaires (traces de microfissures dans le plan) projetée sur une droite perpendiculaire au réseau de sécantes : $\bar{P}_L(\theta) = L_A$ proj. Cette méthode dite des sécantes orientées dans un plan, permet également de déterminer la "rose des nombres d'intersections" qui traduit les anisotropies de distribution des microfissures. P_L est alors mesuré suivant différentes directions du plan. Dans le cas des structures isotropes $\bar{P}_L$ est indépendant de θ. On peut alors établir une relation entre $\bar{P}_L$, L_A et S_V :

$$\frac{\pi}{2}\ \bar{P}_L = L_A = \frac{\pi}{4}\ S_V$$

Il est possible encore de calculer un degré d'orientation et un espacement moyen des microfissures pour lesquels nous renvoyons à la littérature spécialisée. (8, 12, 13, 14).

5. APPLICATION A L'ETUDE DE BETONS

5.1 Matériaux testés

Deux bétons ont été étudiés : un béton de granulats silico-calcaires 3,15-10 mm, dosé à 350 kg CPA/m^3 et gâché avec un rapport E/C = 0,57 d'une part, un béton de granulats légers (schiste expansé) dosé à 350 kg CPA/m^3 et de E/C = 0,525 d'autre part. Les deux bétons enduits d'une résine d'étanchéité ont été conservés à température ambiante pendant $\sim$1 an. Leur état de microfissuration a été étudié avant chargement et après chargement en flexion trois points à déformation contrôlée. Les prismes 10 x 10 x 40 cm ont été déformés de manière anélastique sans rupture. Les courbes effort-déformation correspondantes obtenues par M.TERRIEN (15) sont reproduites figure 4.

Des essais complémentaires de rupture non contrôlée en flexion trois points ont également été réalisés.

5.2 Microfissuration avant chargement

5.2.1 Niveau de structure I.

Les valeurs de $\bar{P}_L$ sont égales à 2,0 cm^{-1} et à 1,3 cm^{-1} respectivement dans le béton silico-calcaire et le béton de schistes expansés.

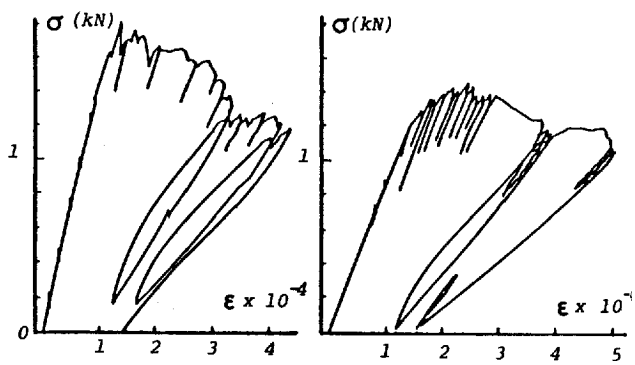

Fig. 4 - Courbe effort-déformation du béton silico-calcaire (à gauche) et du béton de granulats légers (à droite) (communiquées par M.TERRIEN (15).

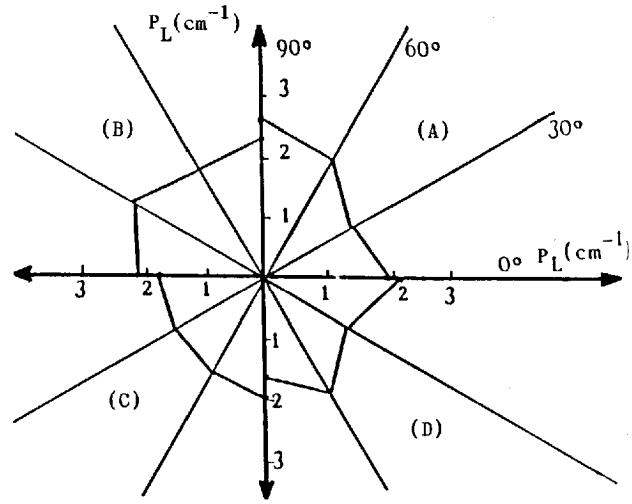

Fig. 5 - "Rose" des intersections. Béton de granulats silico-calcaire avantchargement (comptage sur 4 échantillons différents A, B, C, D).

L'examen de plaques 10 x 10 x 1,5 cm préparées suivant la technique décrite au § 3.1 montre que dans les deux bétons des zones de moindre cohésion assimilables à des fissures se manifestant par la pénétration ou la diffusion du colorant, existent aux interfaces pâte de ciment durcie-granulats. Leur quantification par la méthode des sécantes orientées montre que leur distribution est plus ou moins isotrope (Fig.5) mais que leur "densité" est plus faible dans le béton de granulats légers comme l'indiquent les valeurs de $\bar{P}_L$.

La différence est due à une meilleure liaison entre le liant hydraté et les granulats de schistes expansés.

5.2.2. Niveau de structure II.

L'examen au microscope optique au grandissement 500 révèle que la pâte de ciment renferme des inclusions diverses (petits grains de sable, noyaux de clinker anhydre, $Ca(OH)_2$) et que des microfissures se sont déjà formées. Celles-ci joignent souvent des inclusions entre elles. Il s'agit principalement de microfissures de retrait dont une partie a pu être induite par le traitement préalable de déshydratation. Les

aspects sont très voisins dans les deux bétons à cette échelle d'observation où les comptages donnent des valeurs de $\bar{P}_L$ de l'ordre de 1,2 cm^{-1}.

5.2.3. Niveau de structure III

Les examens fractographiques au M.E.B montrent que la pâte de ciment proprement dite comporte à ce niveau de nombreuses discontinuités dues au mode de formation et d'assemblage des hydrates qui laissent subsister une microporosité relativement importante. On note que des microfissures "naturelles" telles que celles constituées par les clivages de $Ca(OH)_2$ peuvent exister. Par ailleurs, l'observation particulière des interfaces confirme la présence de zones de moindre cohésion (auréole de transition) (3).

5.3 Microfissuration après chargement

5.3.1. Niveau de structure I

Les observations ont été effectuées sur des sections 10 x 10 x 1 cm découpées dans la zone tendue, perpendiculairement au plan de contrainte et préparées suivant la technique du § 3.1. Elles mettent en évidence dans les deux bétons la formation d'une fissure principale sous forme d'une bande étroite microfissurée, de quelques centaines de microns de largeur, tortueuse souvent oblique par rapport à la direction de contrainte. Dans le cas du béton silico-calcaire la fissure principale qui s'est propagée sur environ 3/5 de l'épaisseur du prisme, est constituée de tronçons plus ou moins discontinus branchés ou parallèles contournant généralement les granulats et orientés parallèlement à la contrainte (Fig.6).

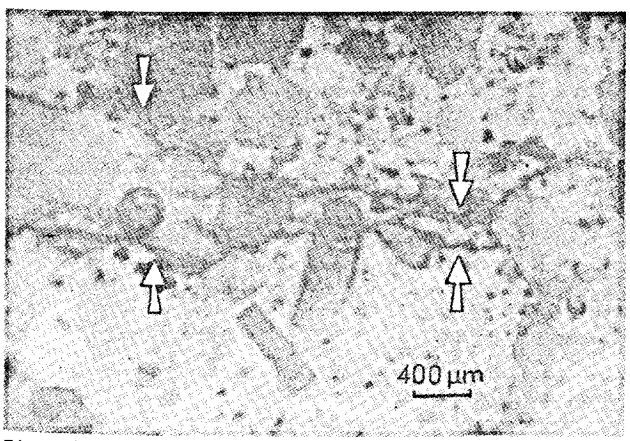

Fig. 6 - Béton silico-calcaire après chargement. Bande endommagée. Microfissures nettes.

La rupture y est rarement transgranulaire sauf localement où les granulats étaient préfissurés. Dans le cas du béton de granulats légers, la fissure principale, qui s'est développée sur 2/5 de l'épaisseur du prisme est également surtout intergranulaire. Elle présente un aspect différent de celui observé dans le béton silico-calcaire. Dans ce dernier la trace des différentes microfissures constituant la fissure principale est nette et bien dessinée. Elle apparaît plus diffuse dans le béton de granulats légers (Figure 7). Cet aspect paraît correspondre à un micro-endommagement de la pâte de ciment proprement dite sur le trajet de la fissure.

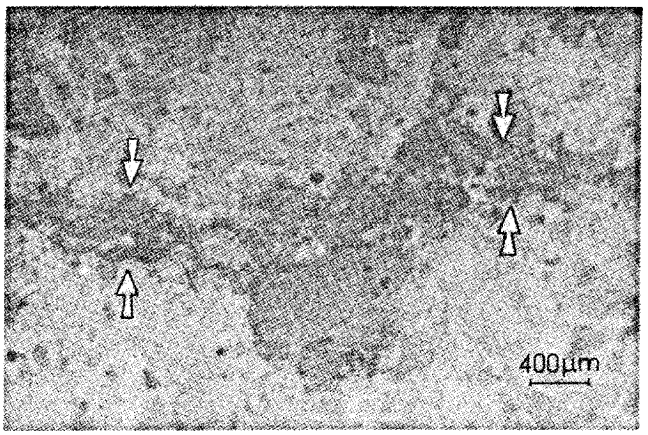

Fig. 7 - Béton de granulats légers après chargement. Bande endommagée - microfissuration "diffuse"

Les déterminations quantitatives ne révèlent pas d'accroissement significatif de la densité de microfissures par rapport à l'état initial, la contribution de la fissure principale au nombre total de microfissures restant faible. De même l'orientation des microfissures parallèlement à la direction de contrainte n'est sensible que dans une zone très étroite de part et d'autre de la fissure principale.

5.3.2 Niveau de structure II (fig. 8 et 9).

L'examen de sections polies prélevées dans la bande endommagée montre que les microfissures se propagent le long des petits grains de sable qu'elles contournent pour progresser ensuite dans la pâte de ciment où elles peuvent subir des déviations importantes par les micro-inclusions (noyaux anhydres, fines). Le mode de propagation à l'échelle du mortier et de la pâte de ciment paraît homothétique de celui du béton. Dans le cas du béton de schistes expansés l'existence d'un micro-endommagement de la pâte de ciment, se traduisant par des fissures très fines contournant plus ou moins les micro-inclusions et ayant parfois un aspect "en chapelet" semble confirmée.

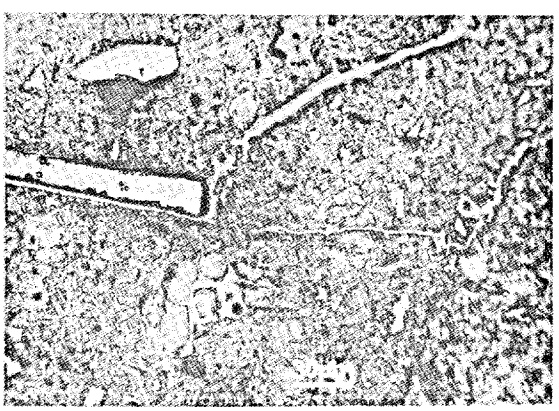

Fig.8 - Béton silico-calcaire après chargement
1. pâte de ciment
2. sable
3. Clinker

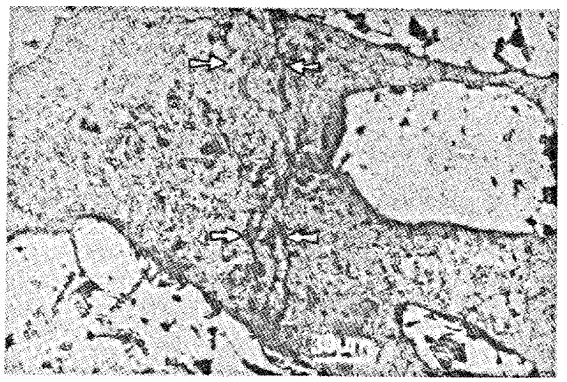

Fig. 9 - Béton de granulats légers
Micro-endommagement de la pâte de ciment.

5.3.3. Niveau de structure III (fig. 10)

Les examens au M.E.B à fort grandissement de surfaces de fractures prélevées sur le trajet de la fissure principale montre que, d'une façon générale, les microfissures présentent une forte tortuosité en relation avec le mode de rupture souvent interparticulaire des hydrates : leur progression semble se faire davantage par décohésion au niveau des interfaces entre particules hydratées (C-S-H) plutôt que par rupture de ces dernières sauf dans le cas de composés clivés tels que Ca(OH)2.

Les vides capillaires en tant qu'amorces possibles de microfissures ainsi que les inclusions dures en tant qu'obstacles à la microfissuration, interviennent également dans le processus de rupture.

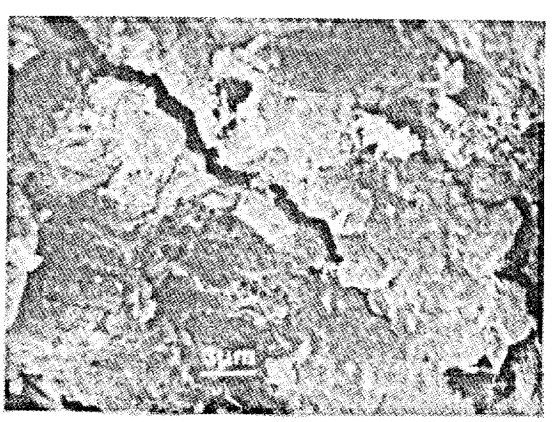

Fig.10 - Béton de granulats légers.
M-E-B. Mode de fracture interparticulaire des C-S-H.

5.4 Discussion des résultats

Les observations des niveaux de structure I et II ont montré que la déformation contrôlée conduit à la formation d'une bande endommagée de faible largeur correspondant à une fissure plus ou moins discontinue formée de tronçons parallèles ou branchés, suivant généralement les interfaces. Ceci traduit la nature progressive de l'endommagement qui par ailleurs, est un peu différent dans les deux bétons testés.

Son aspect plus diffus dans le béton de granulats légers dont les propriétés mécaniques (module d'Young en particulier) sont plus proches de celles de la pâte, semble en relation avec une propagation par microfissurations successives de plus faible amplitude que dans le béton silico-calcaire. Ceci paraît confirmé par l'enregistrement des émissions acoustiques effectué par M.TERRIEN (15) sur les mêmes éprouvettes en charge : un plus grand nombre d'évènements accoustiques de plus faible amplitude sont mis en évidence dans le béton de schistes expansés.

Sous chargement contrôlé la fracture des deux bétons est essentiellement intergranulaire. Toutefois, des essais complémentaires dans des conditions de rupture instable montrent qu'elle devient à 75% transgranulaire dans le béton de granulat léger contre 30% dans le béton silico-calcaire.

La comparaison des aspects de la rupture à différentes échelles indique qu'il existe une certaine homothétie entre les différents niveaux de structure du béton. Le mortier d'enrobage des gros granulats d'une part et la pâte de ciment durcie avec ses micro-inclusions (fines, noyaux anhydres) d'autre part se comportent comme des "micro-bétons" du point de vue de la propagation des fissures. Cette "self-similarité" propre aux objets fractals (16) peut être exploitée pour étudier les processus de rupture.

Ce type d'exploitation actuellement à l'étude, a fait l'objet de premiers essais destinés à caractériser la surface de rupture des bétons par leur dimension fractale D qui est une image de leur irrégularité ou rugosité.

L'application aux deux bétons étudiés ici, rompus de manière non contrôlée en flexion trois points donne des valeurs de D égales à 2,67 et 2,87 respectivement pour le béton silico-calcaire et le béton de schistes expansés.

Ces valeurs obtenues par la méthode des "slit islands" due à MANDELBROT (16) correspondent à une forte irrégularité des surfaces de rupture. Cette irrégularité serait plus forte dans le cas du béton de granulat léger. Les représentations log (surface des "iles") en fonction de log (périmètre des "iles") permettant de calculer D sont données fig. 11.

Si l'objet est fractal le graphe obtenu doit être une droite dont la pente D'=D-1.

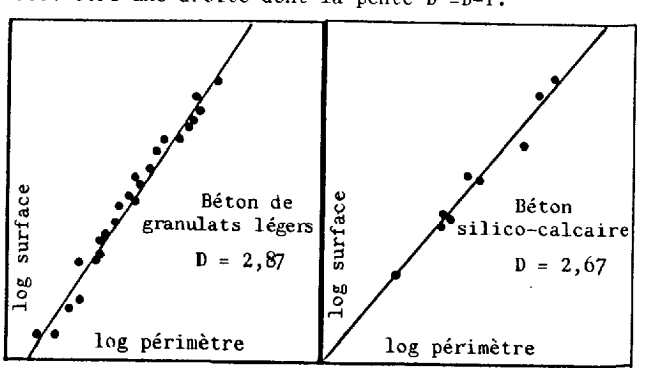

Fig. 11- Détermination de la dimension fractale D par la méthode des "slit -islands". (Niveau de structure I).

Remerciements

Nous tenons à remercier Monsieur J.P COMMENE pour sa contribution importante à la mise au point des différentes techniques d'observation et de quantification des micro-fissures.

Nous remercions également Monsieur M.TERRIEN du Laboratoire de Mécanique des Solides de l'Ecole Polytechnique qui a réalisé les essais de déformation contrôlée des bétons étudiés.

Cette étude fait partie du programme de recherche "Progrès dans la Construction par la maîtrise de la fissuration des bétons hydrauliques" financé par le Ministère de la Recherche et de la Technologie, le Ministère de l'Urbanisme et du Logement et le Syndicat National des Fabricants de Ciments et de Chaux.

6. BIBLIOGRAPHIE

1. M. REGOURD (1982) "Microstructures et propriétés des ciments, mortiers et bétons". Ciments, bétons, plâtre, chaux N° 734 , 41-48.

2. J. BARON (1982) "Déformations, contraintes et ruptures dans le béton avant tout chargement" Séminaire "Mécanique de la rupture", St Rémy-les-Chevreuse.

3. MASO J.C (1980) "La liaison entre les granulats et la pâte de ciment hydraté" Sous-thème VII - 1, 7e Congrès International de la Chimie des Ciments, Vol I., Rapport principal Paris, 1980, VII - 1/3 à VII - 1/14.

4. ZIEGELDORF S. "Phenomenological aspects of the fracture of concrete" Fracture Mechanics of concrete, ed. by F.H WITTMANN, 1983, Elsevier Science publishers B.V, Amsterdam , 31-41.

5. AFREM (1985) "Progrès dans la Construction par la maîtrise de la fissuration des bétons hydrauliques". Thème I "Origine et mécanisme de la microfissuration" Rapport final. A paraître.

6. SLATE F.O (1983) "Microscopic observation of cracks in concrete, with emphasis on techniques developed and used at Cornell University, Fracture Mechanics of Concrete, ed. by F.H. WITTMANN, 1983, Elsevier Science publishers B.V., Amsterdam, 75-83.

7. DHIR R.K., SANGHA C.M (1974) "Development and propagation of microcracks in plain concrete" Mater. Constr. Vol.7, N° 37, 17-23.

STROEVEN P. (1973) "Some aspects of the micromechanics of concrete", Ph. D. Thesis, Delft.

8. F.H. WITTMANN (1983) "Structure of concrete with respect to crack formation" Fracture Mechanics of Concrete, ed. by F.H. WITTMANN, Elsevier Science publishers B.V. Amsterdam ,83-74.

9. KNAB L.I., WALKER H.H, CLIFTON J.R. (1984) "Fluorescent thin sections to observe the fracture zone in mortar". J.C.C.R., Vol 14, 3, 334-339.

11. J.P. OLLIVIER (1985) "A non destructive procedure to observe the microcracks of concrete by scanning electron microscopy", J.C.C.R., Vol.15, n° 6. 1055 - 1060.

12. SALTIKOV S.A. (1976) "Stereometrische Metallographie" VEB Deutschen Verlag für Grundstofferindustrie, Leipzig.

13. STROEVEN P. (1979) "Geometric probability approach to the examination of microcracking in plain concrete". Journ. of Mater. Sci., 14, 1141 - 1151.

14. FISCHMEISTER H.F (1975) "Determination of pore structure by stéréological Measurements" chalmers University of Technology, S-402 20 Gothenburg (Suède)

15. M.TERRIEN (1985) "Etude de la microfissuration du béton en traction par émission acoustique" Rapport final AFREM "Progrès dans la construction par la maîtrise de la fissuration des bétons hydrauliques". Thème I. "Origine et mécanisme de la microfissuration".

16. B.B. MANDELBROT (1982)" The fractal geometry of nature" W.H FREEMAN ed.

J-M. Lameille, R. Chiappini, G. Goutière, J-C. Petit, et M. Regourd

Influence of the aging of cementitious (OPC) radwaste matrix on the leaching rates of trace elements (Cs, Sr and Co).

Relation entre la lixiviation d'éléments traces (Cs, Sr et Co) et la microstructure au cours du vieillissement d'un mortier à base de CPA.

RÉSUMÉ:

Certains déchets radioactifs sont solidifiés dans des matrices cimentées à base de ciment Portland artificiel (CPA) en vue de leur stockage. La sûreté de ces stockages doit être assurée sur des périodes $\gtrsim$ 300 ans, ce qui nécessite de prédire les variations des relâchements de radioactivité. A long terme, celles-ci sont vraisemblablement reliées au vieillissement des matrices qui reste mal connu. Le travail présenté ici porte, dans le cas particulier d'un mortier gâché avec une solution boratée, sur les relations existant entre les relâchements de certains radioéléments (60Co, 90Sr et 137Cs) sous l'action du lessivage par l'eau et l'évolution des caractéristiques cristallochimiques et microstructurales de la matrice.

Nous avons abouti aux conclusions suivantes: le bore a peu d'influence sur la microstructure et sur les évolutions des propriétés physiques de la matrice (porosité, résistances mécaniques etc...), qui restent modérées au moins pendant deux ans. Par contre, les taux de relâchement d'activité évoluent considérablement pendant cette période. La cinétique de lixiviation des radioéléments, dont la majeure partie (~ 70%) est incorporée dans les hydrates, est contrôlée par une combinaison de plusieurs phénomènes : à court terme la fraction libre en solution (donc ~ 30%) est relâchée par simple diffusion de Fick. Par contre à long terme, les transformations cristallochimiques correspondant à des dissolutions-cristallisations complexes des hydrates notablement accélérées par la température gouvernent le passage des radioéléments dans le liquide interstitiel et autorisent leur diffusion vers la solution exterieure. Nous avons pu préciser les sites de piégeage des radioéléments dans les hydrates qui contrôlent leur relâchement à long terme : le césium est faiblement retenu dans les C-S-H et la chaux et s'incorpore préférentiellement dans les hydrates alumineux. De plus, le strontium, faiblement retenu dans les silicates, est piégé dans les sulfoaluminates. Enfin, le cobalt est retenu en grandes proportions dans le solide lors de l'hydratation par la formation d'un composé propre du type hydroxychlorure de cobalt.

Sumário:

Alguns rejeitos radioativos são solidificados dentro de matrizes cimentadas com base de cimento Portland artifical (CPA) tendo em vista sua estocagem. A segurança dessas estocagens deve ser assegurada para período $\gtrsim$ 300 anos, o que necessita predizer as variações das liberações de radioatividade. A longo prazo, estas são possivelmente associadas ao envelhecimento das matrizes que continuam mal conhecidos. O trabalho apresentado aqui relaciona, no caso particular de uma argamassa preparada com uma solução boratada, sobre as relações existentes entre as liberações de certos radioelementos (60 Co, 90 Sr e 137 Cs) sob a ação da lavagem pela água e a evolução das características cristaloquímicas e microestruturais da matriz.

Nós chegamos às conclusões seguintes: o boro tem pouca influência sobre a microestrutura e sobre as evoluções das propriedades físicas da matriz (porosidade, resistências mecânicas, etc...) que ficam moderadas ao menos durante dois anos. Ao contrário, as taxas de liberação de atividade evoluem consideravelmente durante este período. A cinética da lixiviação dos radioelementos, cuja maior parte (~ 70%) é incorporada aos hidratos, é controlada por uma combinação de vários fenômenos: em prazo curto, a fração livre em solução (portanto ~30%) é liberada por simples difusão Fick. Ao contrário, em prazo longo, as transformações cristaloquímicas correspondentes à dissoluções cristalizações complexas dos hidratos notavelmente acelerados pela temperatura, governam a passagem dos radioelementos no líquido intersticial e permitem sua difusão para a solução exterior. Nós podemos precisar as regiões de captação dos radioelementos nos hidratos que controlam a sua liberação a longo prazo: o césio é fracamente retido nos C-S-H e a cal e se incorpora de preferência nos hidratos aluminosos. Além disso, o strôncio, fracamente retido nos silicatos, é captado pelos sulfoaluminatos. Enfim, o cobalto é retido em grandes proporções no sólido por ocasião da hidratação para a formação de um composto próprio do tipo hidroxicloreto de cobalto.

I. Introduction

Le ciment Portland artificiel (CPA) est utilisé pour l'immobilisation de certains déchets radioactifs en vue de leur stockage. En général, il s'agit de déchets de faible et moyenne activité. Compte tenu des constantes de désintégration de certains radioéléments contenus dans ces déchets, il est nécessaire d'assurer la sûreté des stockages sur de très longues durées. Par exemple, le césium 137, qui est un produit de fission, a une période de 30 ans. Un stockage d'environ 300 ans, soit 10 périodes, est ainsi nécessaire afin de diminuer la radioactivité initiale des déchets par un facteur de 1000 qui permet alors une banalisation du site.

Il se pose donc le difficile problème de la durabilité de la matrice cimentée incorporant les déchets nucléaires sur des durées inaccessibles directement à l'expérience au laboratoire. De telles échéances n'ont pas été étudiées par les cimentiers dont les préoccupations concernant la durabilité des liants hydrauliques (Calleja, 1980) vont en général au maximum jusqu'à quelques dizaines d'années (rôle de la garantie décennale dans les travaux publics).

Au cours de ce travail nous avons étudié, dans le cas particulier des "concentrats" boratés d'évaporateur, les relations entre les relâchements de radioactivité et l'évolution des caractéristiques physiques et microstructurales de la matrice. Ces déchets particuliers résultent de la purge du circuit primaire de refroidissement des centrales électronucléaires et se présentent sous forme de solutions boratées qui servent de liquide de gâchage d'un liant dont la formulation spéciale (voir ci-dessous) est à base de CPA.

On pouvait a priori craindre deux types d'altération affectant le confinement des radioéléments : soit la destruction directe de la matrice due aux différentes agressions physiques et chimiques susceptibles d'affecter ce matériau dans les conditions de stockage; soit des modifications minéralogiques, structurales ou texturales qui, sans affecter l'intégrité du liant lui-même, pourraient conduire à une augmentation excessive des relâchements de radioactivité. Ceci nous a conduit à étudier le rôle des caractéristiques physico-chimiques (microstructure, minéralogie etc...) sur la lixiviation de deux radioéléments essentiels de ce type de déchets (137 Cs et 60 Co).

Notre travail comportait donc deux séries d'expériences menées en parallèle : sur une matrice cimentée simulée, nous avons tout d'abord étudié les variations avec le temps de la lixiviation de 137 Cs et 60 Co en fonction de l'évolution de ses caractéristiques microstructurales, qui traduisent son "vieillissement". Sur des systèmes simples, constitués des principaux composants du CPA, mis en contact avec des solutions diluées de césium, strontium et cobalt, nous avons étudié les partages solide/liquide durant l'hydratation. Nous avons cherché à identifier la forme chimique sous laquelle étaient incorporés ces éléments afin d'interpréter les caractéristiques de leurs lixiviations : substitution en traces dans le réseau des minéraux habituels des liants ou cristallisation de composés spécifiques.

II. Protocole expérimental

Le concentrât d'évaporateur utilisé dans notre étude est une solution contenant principalement des borates de sodium (~ 25000 ppm de bore) et quelques autres ions en très faible quantité (voir Lameille, 1984). La radioactivité de ce concentrât est due essentiellement à 137 Cs, 90 Sr, 60 Co. Afin de mener l'étude de vieillissement nous avons reconstitué un concentrât synthétique inactif. Pour uniformiser les deux types d'étude (vieillissement et lixiviation), ce concentrât synthétique a également été utilisé pour l'étude des relâchements de radioactivité; nous avons alors dû le doper avec des activités en 137 Cs et en 60 Co de 20 µCi. Nous n'avons pas pu étudier le 90 Sr qui, étant un émetteur ß pur, aurait posé des problèmes analytiques difficiles dans le cadre de notre travail.

La formule de l'enrobé est intermédiaire, du point de vue de la teneur en ciment, entre celle d'une pâte pure et celle d'un mortier. Pour 1000 kg de ciment, on ajoute 750 kg de sable, 400 l de concentrât et 60 kg de chaux ce qui donne un rapport eau/ciment de 0,4. La chaux introduite sert à stabiliser les borates sous forme calcique et donc à diminuer leur effet retardateur.

Pour l'étude du vieillissement, nous avons reconstitué (très schématiquement) un site de stockage. Les éprouvettes sont des parallélépipèdes rectangles de dimensions 2 x 2 x 16 cm placées sous une couverture de deux centimètres d'argile, recouverte par 2 cm d'eau. L'argile est un mélange de kaolinite et de montmorillonite, et l'eau est faiblement minéralisée (en $mg.l^{-1}$) :

Ca^{2+} : 37,7; K^+ : 22; NH_4^+ : 0,28; Na^+ : 16,1;

SO_4^{2-} : 36,3; NO_3^- : 0,1; PO_4^{3-} : 0,1; Cl^- : 25;

F^- : 0,7

En plus d'une étude en "temps réel" à 10°C (température interne du site) qui sert de référence, nous avons choisi d'accélérer les cinétiques tout en évitant de dégrader trop brusquement et artificiellement la matrice. Ceci a été réalisé en augmentant la température de conservation des éprouvettes jusqu'à 60°C. A chaque échéance, nous avons mesuré sur les différentes éprouvettes les paramètres physiques suivants : résistances mécaniques en compression, porosités, masses et gonflements. La microstructure est étudiée au moyen d'un microscope électronique à balayage (MEB), d'une microsonde électronique et de la diffraction des rayons X.

Les éprouvettes dopées au césium 137 ou au cobalt 60 sont des orthocylindres carottés de 2 cm. Elles sont ensuite stockées à 10°C, 40°C

ou 60°C pendant un temps donné, puis lixiviées à 10°C dans de l'eau déminéralisée. Les lixiviations sont menées en dynamique c'est-à-dire avec renouvellement de l'eau, selon un test normalisé par l'AIEA : 3 fois la première journée, chaque jour la première semaine, chaque semaine le premier mois, chaque mois le premier semestre et enfin tous les semestres. Un enrobé n'ayant pas subi de vieillissement (lixivié immédiatement après la cure en atmosphère humide) sert de référence. Les mesures de radioactivité dans les lixiviats sont effectuées au moyen d'un spectromètre γ muni d'un détecteur NaI ou GeLi.

Lors des expériences d'hydratation de composés simples, nous avons étudié la rétention de chaque élément trace au cours des hydratations de C_3S, de $C_3S + C_3A$ puis de $C_3S + C_3A +$ gypse avec un rapport e/s ~ 10. La filtration est effectuée sur filtre millipore de 0,45 µm et l'hydratation est stoppée par trois lavages à l'éther et par cryosublimation. Le solide est ensuite examiné au cours du temps au moyen de diverses techniques physiques d'analyse complémentaires (MEB, DRX, microsonde électronique et ionique etc...); La solution est analysée soit par volumétrie et par absorption atomique. Cette partie de notre travail faisant l'objet d'une communication spécialisée (Lameille et coll., 1986) n'est pas développée ici.

III. Résultats sur la lixiviation des radio éléments

1. Cas du césium

Les courbes de relâchement d'activité après des cures de 1, 4 et 6 mois à 10 °C (voir figures 1, 2 et 3) sont très comparables. La fraction d'activité relâchée (F_r) tend vers une valeur d'environ 30% pour des temps d'expérience supérieurs à 250 jours. Il est donc vraisemblable que la structure de la matrice et que la quantité de césium contenue dans la solution interstitielle (donc le coefficient de partage de cet élément entre les phases solide et liquide) varient peu pendant ce laps de temps. Malgré la mauvaise linéarité des courbes au delà de ~ 40 jours, il est cependant possible d'estimer le coefficient de diffusion du césium à ~ 10^{-9} $cm^2.s^{-1}$, en se basant sur le modèle de diffusion hors d'un cylindre fini (Crank, 1975). Après 12 mois de cure, le coefficient de diffusion ainsi calculé diminue d'un facteur ~ 2. Les résultats obtenus pour des cures à 40°C sont comparables; on note toutefois une légère diminution du césium contenu dans l'eau interstitielle (~ 25%). En revanche, pour des cures supérieures à 6 mois à 60°C, on observe des modifications très nettes des caractéristiques de lixiviation : les courbes présentent une bonne linéarité jusqu'à 200 jours, le coefficient de diffusion apparent chute d'un facteur ~ 8 et la fraction d'activité relâchée tend vers une valeur voisine de 20%. Ces caractéristiques n'évoluent plus jusqu'à 24 mois.

Les taux de lixiviation varient de 4 à 18 10^{-3} $g/cm^2/j$ (à 2 jours) et de 1 à 5,7 10^{-4} $g/cm^2/j$ (à 150 jours). Ces valeurs sont compatibles avec celles rencontrées habituellement dans la littérature.

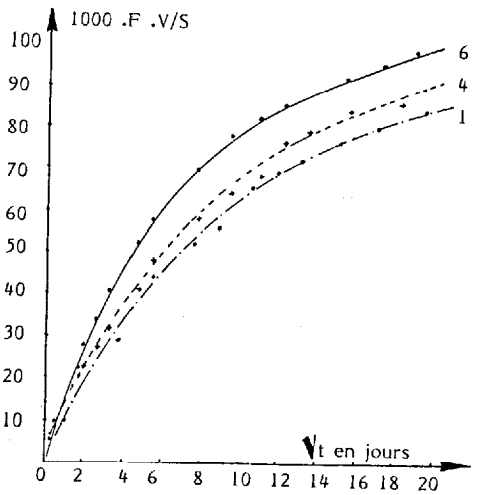

Figure 1 : courbes de lixiviation du césium en fonction du temps, pour des vieillissements à 10°C durant :-·-1 mois,··· 4 mois et — 6 mois.

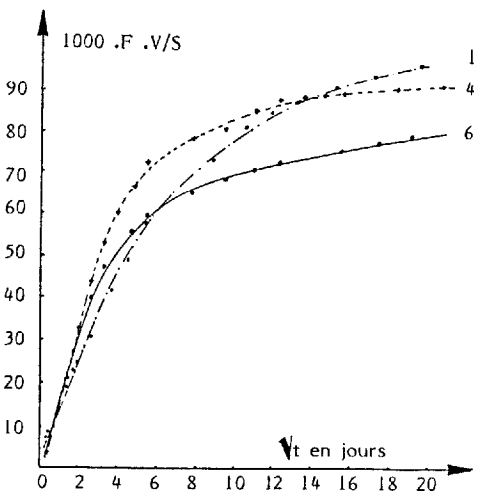

Figure 2 : courbes de lixiviation du césium en fonction du temps, pour des vieillissement à 40°C durant :-·-1 mois,···4 mois et — 6 mois.

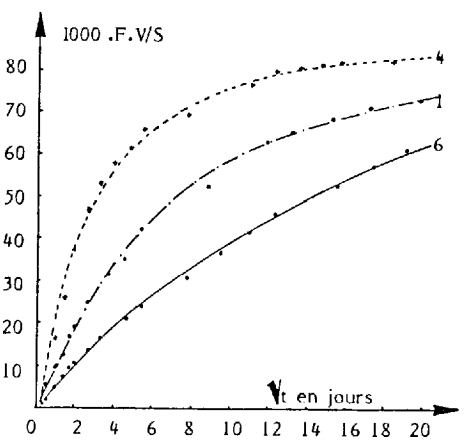

Figure 3 : courbes de lixiviation du césium en fonction du temps, pour des vieillissement à 60°C durant :-·-1 mois,··· 4 mois et — 6 mois.

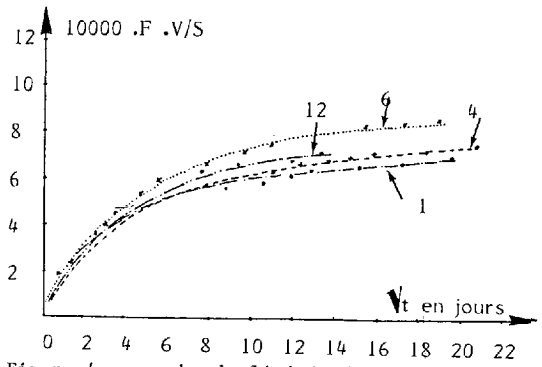

Figure 4 : courbe de lixiviation du cobalt en fonction du temps, pour des vieillissements à 10°C durant :—·—1 mois,---4 mois,·····6 mois et —··—12 mois.

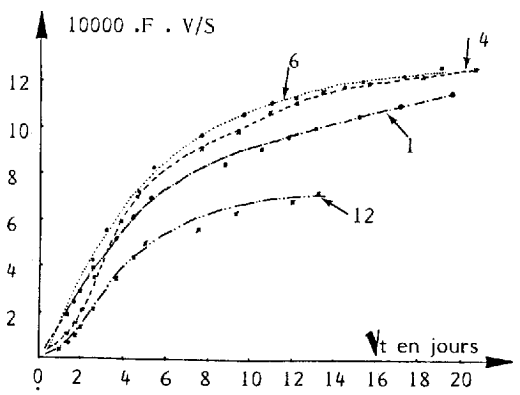

Figure 5 : courbe de lixiviation du cobalt en fonction du temps, pour des vieillissements à 40°C durant :—·—1 mois,----4 mois,·····6 mois et —··—12 mois.

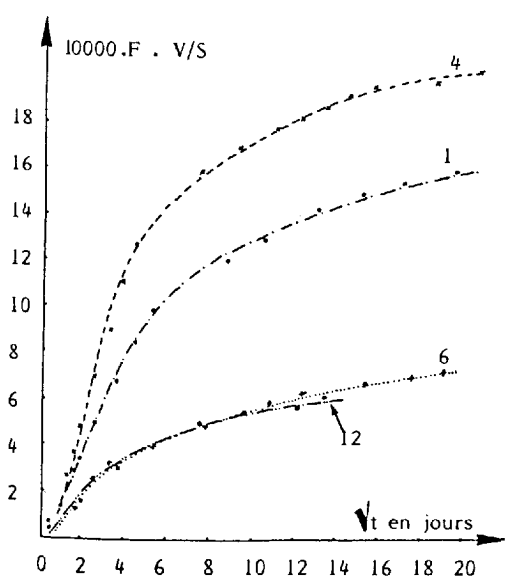

Figure 6 : courbe de lixiviation du cobalt en fonction du temps, pour des vieillissements à 60°C durant :—·—1 mois,----4 mois,·····6 mois et —··—12 mois.

2. Cas du cobalt

Comme dans le cas précédent, les courbes de relâchement d'activité après des cures de 1, 4 et 6 mois à 10 °C (voir figures 4, 5 et 6) sont également comparables. De plus, F_r est constante et tend vers une valeur d'environ 0,2%. Ces résultats confirment ceux obtenus avec le césium et reflètent une faible évolution de la matrice jusqu'à 6 mois à cette température. Après 12 mois de cure, les relâchements de cobalt diminuent légèrement mais F_r reste constante. A 40°C, les courbes de relâchement d'activité sont à nouveau comparables entre elles jusqu'à 6 mois; par contre F_r augmente jusqu'à 0,3%. Après 12 mois de cure, les caractéristiques de lixiviation du cobalt deviennent très voisines de celles obtenues à 10°C. Par contre à 60°C, F_r augmente avec le temps de cure jusqu'à 4 mois pour ensuite diminuer d'un facteur ~ 3 entre 4 et 6 mois et rester stable au delà.

IV. Résultats sur le vieillissement de la matrice cimentée

Dans ce travail, l'échantillon ayant subi une cure de 28 jours en atmosphère humide et à température ambiante sert de référence. Sa résistance mécanique est de 56 MPa et le volume total de porosité est de $7{,}2.10^{-2}$ $cm^3.g^{-1}$. La pâte observée au MEB présente des hydrates peu cristallisés. De plus, la sonde ionique montre que le bore est réparti de façon homogène. Par ailleurs, la diffraction des rayons X n'a pas permis de mettre en évidence des cristallisations spécifiques mais la damburite et la datolite (Freund, 1973), qui sont des borosilicates susceptibles de se former, ne peuvent être détectés car leurs raies caractéristiques se superposent à celles de la portlandite. On ne peut conclure sur la nature du constituant incorporant le bore dans la matrice, mais cet élément pourrait se présenter sous forme de borate de calcium stable. Cette matrice est donc très comparable à un mortier normal à base de CPA 55. Les variations des résistances mécaniques (figure 7) et des volumes totaux de porosité (figure 8) en fonction du temps de vieillissement, à différentes températures, montrent que le volume de porosité diminue lorsque la résistance mécanique augmente. En fait, pendant les premiers mois de stockage l'hydratation se poursuit et les volumes de porosité diminuent alors que les résistances mécaniques en compression augmentent; ensuite les phénomènes de vieillissement apparaissent au bout de temps variables en fonction de la température.

Le calcul des taux d'hydratation après 12 mois de vieillissement, basé sur les spectres de diffraction des rayons X, montre que l'hydratation maximale est obtenue à 40°C. De manière inattendue, l'échantillon conservé à 60°C est le moins hydraté mais ses hydrates sont cependant mieux développés qu'aux autres températures. Dans le cas de l'ettringite, qui est le seul hydrate alumineux bien cristallisé identifiable en diffraction des rayons X, on constate qu'à 60°C ce minéral a complètement disparu après 6 mois de vieillissement alors qu'à 10°C et 40°C il est encore présent à 12 mois.

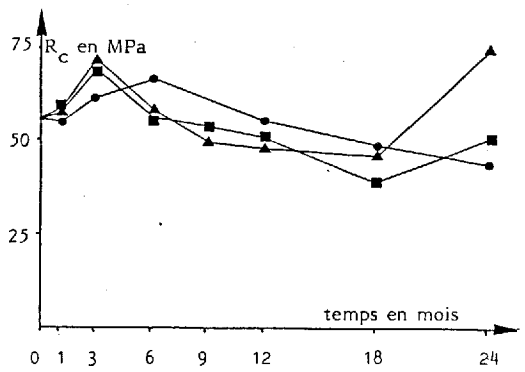

Figure 7 : variations des résistances mécaniques en compression en fonction du temps de vieillissement à différentes températures, ●10°C, ▲40°C, ■60°C.

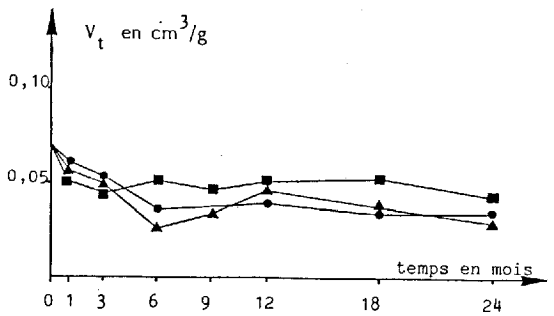

Figure 8 : variation des volumes totaux de la microporosité en fonction du temps de vieillissement à différentes températures, ●10°C, ▲40°C, ■60°C.

La figure 9 rassemble des micrographies au MEB de pâtes de ciments conservées à 10°C, 40°C et 60°C pendant 12 mois; on note que la compacité augmente lorsque la température diminue. Bien que les expériences de lixiviation conduites en parallèle n'aient été menées que sur des échantillons vieillis au maximum 12 mois, il est cependant intéressant de noter au delà d'un an les évolutions suivantes de la microstructure (Chiappini et coll., 85) : entre 12 et 18 mois, les variations se font dans le même sens pour toutes les températures; entre 18 et 24 mois à 40°C et 60°C, les résistances mécaniques augmentent de façon importante alors que les volumes totaux de porosité diminuent; par contre, à 10°C les évolutions sont faibles. Les pâtes de ciment conservés à 40°C et 60°C sont très hétérogènes mais avec des hydrates mieux développés qu'à 10°C.

V. Résultats sur la rétention de Cs, Sr et Co dans les hydrates des composés simples du CPA

Nous rappelons ici brièvement nos principaux résultats qui sont exposés en détails par ailleurs (Lameille et coll., 1986).

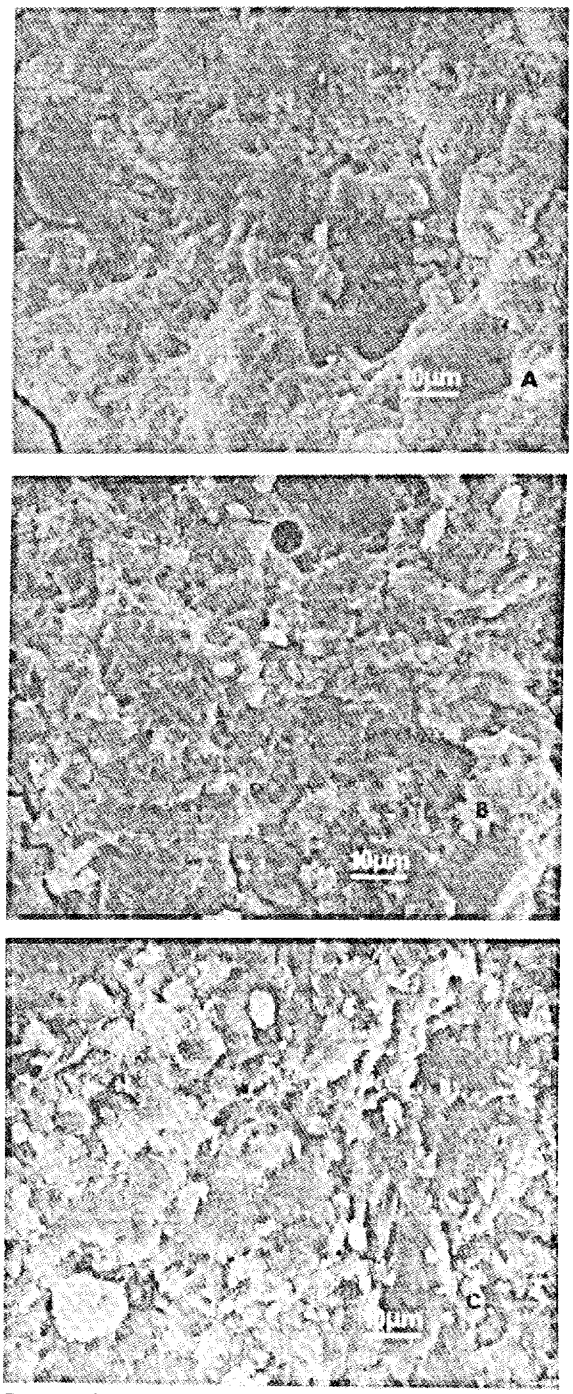

Figure 9 : micrographies au MEB de surfaces de fractures des échantillons après 12 mois de vieillissement à 10°C (A), 40°C (B), 60°C (C).

1. cas du césium

Lors de l'hydratation du C_3S seul, le césium reste en solution pendant la phase d'induction de l'hydratation du C_3S. Les phénomènes d'adsorption sur les surfaces sont donc négligeables. Puis le césium se fixe partiellement dans les hydrates (12 % à 48 heures). Cette fixation a lieu pendant la précipitation

des silicates hydratés de calcium (notés C-S-H) et de la portlandite. On peut interpréter cette rétention par la formation d'un composé du type Si-O-Cs, par analogie avec les composés qui se forment avec d'autres alcalins, par exemple le sodium (Regourd et coll., 1983). Durant l'hydratation d'un mélange C_3S + C_3A (80 et 20%), on constate que la rétention du césium dans les hydrates augmente, pour atteindre 24% au bout de 48 heures. Notons que le taux de fixation de 24% est atteint dès les premières heures, ce qui permet de penser que, dans ce cas, la rétention du césium est liée à la formation des aluminates hydratés de calcium qui cristallisent plus rapidement que les C-S-H. Dans le cas de l'hydratation du mélange ternaire, C_3S + C_3A + gypse (76, 19 et 5 %), la rétention du césium est un peu plus faible qu'en l'absence de gypse (18% à 48 heures). Là encore, la formation des hydrates alumineux semble jouer un rôle important. Pour expliquer la baisse du taux de rétention, remarquons que dans le cas du mélange binaire, il existe des ions aluminiques en solution qui sont éliminés par ajout de gypse. Pour tester cette hypothèse, nous avons ajouté durant l'hydratation du mélange gypsé, une solution de chlorure d'aluminium à 2.10^{-2} mole.l^{-1}. La fraction de césium fixée dans les hydrates augmente effectivement de 18 à 22%.

En conclusion, ces expériences nous ont permis de mesurer les coefficients de partage du césium dans les trois cas étudiés :

C_3S	K_{Cs} = 3,7
C_3S + C_3A	K_{Cs} = 5,5
C_3S + C_3A + gypse	K_{Cs} = 4,2

2. cas du strontium

Le strontium est faiblement retenu (~ 5%) après 48 heures d'hydratation du C_3S. Cette rétention ne semble pas augmentée par la présence de 20% de C_3A. Par contre l'ajout de gypse au mélange augmente rapidement la rétention pour atteindre ~ 16% à 48 heures. Celle-ci pourrait donc être liée à la formation de sulfoaluminates de calcium (ettringite). A la sonde ionique, on détecte la présence de strontium dans la couche d'hydrates autour des grains de C_3A. On peut donc penser que le strontium se substitue au calcium, ce qui est logique puisque ces deux éléments ont des rayons ioniques voisins. Les coefficients de partage que nous avons évalués sont les suivants :

C_3S	K_{Sr} = 1,7
C_3S + C_3A	K_{Sr} = 0,6
C_3S + C_3A + gypse	K_{Sr} = 3,4

3. cas du cobalt

on constate une forte rétention du cobalt dans le solide et simultanément l'apparition d'ions calcium en solution due à la dissolution du C_3S. il faut noter que pour la fraction granulométrique la plus fine (diamètre < 25 µm), 85% du cobalt sont retenus dans le solide après 4 heures d'hydratation seulement. L'observation des grains hydratés au MEB montre la formation en surface d'hydrates bien cristallisés donnant à la sonde de Castaing des signaux Co et Cl. L'étude de ces solides en diffraction des rayons X montre qu'ils ont une structure proche de celle d'un hydroxychlorure de fer de formule $Fe^{2+}_{3,6}$, $Fe^{3+}_{0,9}$, $(O, OH, Cl)_9$. Le cobalt et le fer ayant des rayons ioniques proches on peut penser que le produit cobalté formé a une formule du type Co^{2+}_x, Co^{3+}_y, $(O, OH, Cl)_z$. Cet hydroxychlorure se décompose presque totalement en 50 jours à 60°C; le cobalt semble alors s'incorporer dans les CSH en substitution du calcium.

VI. Discussion

La principale observation de cette étude est qu'il n'existe pas de lien directe entre les variations, au cours du vieillissement, des caractéristiques macroscopiques de la matrice cimentée (résistances mécaniques, porosité, texture etc...) et les taux de lixiviation du césium et du cobalt. En fait, cette matrice se comporte comme un CPA classique du fait que le borate de sodium est stabilisé par de l'hydroxyde de calcium et que sa teneur dans la formulation est maintenue à une valeur suffisamment faible (< 25.000 ppm dans la solution de gâchage). Compte tenu des concentrations en radioéléments introduites (Cs : ~ $4,1\ 10^{-3}$ ppm; Co : ~ $1,6\ 10^{-3}$ ppm), il est vraisemblable que les composés incorporant effectivement ces radioéléments représentent une très faible fraction de la masse totale de la matrice. Il est donc normal que la formation et/ou l'évolution au cours du temps de ces composés n'induisent pas de modifications des propriétés macroscopiques de la matrice.

Par contre, les caractéristiques de lixiviation de ces éléments sont directement liées à la forme chimique sous laquelle ils sont présents. En particulier, les courbes de lixiviation suggèrent l'existence de deux étapes : dans un premier temps la fraction des radioéléments restée dans l'eau interstitielle (~ 30%) est relâchée par diffusion; cette fraction est déterminée par le coefficient de partage solide/liquide lors de la prise du ciment. Ceci se produit lorsque les conditions physico-chimiques sont peu agressives. La durée de cette première étape, qui est effectivement observée expérimentalement, diminue lorsque la température de vieillissement des échantillons augmente. Par exemple à 60°C, cette étape dure pratiquement 1 an. La deuxième étape correspond soit à une transformation des composés incorporant le radioélément soit à leur corrosion par la solution lorsque celle-ci est suffisamment agressive.

Précisons maintenant les comportements spécifiques du césium et du strontium :

1. cas du césium

Nous avons déjà noté que le coefficient de diffusion D de cet élément diminuait au cours du temps bien que la porosité variât peu. Ce résultat pourrait s'expliquer par une augmentation de la tortuosité de la matrice due à un meilleur

développement des hydrates, observé en particulier après 6 mois à 60°C où D chute d'un ordre de grandeur alors que la cristallisation des CSH est nettement observable au MEB. Il pourrait également s'agir de la transformation des aluminates en leur forme stable C_4AH_{13}. Le fait que l'ettringite ait totalement disparu après un vieillissement de 6 mois à 60°C, laisse penser que cette transformation est terminée à la fin de cette période; cela expliquerait que l'on ne constate aucun changement à cette température entre 6 et 12 mois. Comme nous l'avons indiqué en V., le césium est préférentiellement retenu dans les aluminates et la réduction de la fraction maximale lixiviée pourrait s'expliquer par un piégeage d'une partie du césium contenu dans l'eau interstitielle, lors de la recristallisation des aluminates. A 40°C, les variations sont beaucoup moins importantes, mais commencent à s'amorcer au delà de 12 mois de vieillissement.

2. cas du cobalt

Les expériences de rétention nous ont permis de mettre en évidence la formation d'un hydroxychlorure de cobalt instable, ce qui explique qu'en augmentant le temps de vieillissement le taux de lixiviation du cobalt croisse. Par ailleurs l'augmentation de température accélère la dégradation du composé cobalté et augmente donc la quantité lixiviable de cet élément. Au delà de 6 mois à 60°C, ce taux diminue alors que l'hydroxychlorure s'est vraisemblablement totalement décomposé. Nous suggérons que le cobalt contenu dans l'eau interstitielle peut réagir avec les CSH. En effet, les calculs thermodynamiques effectués par Lameille (1984) montrent que l'échange cobalt-calcium se produit facilement dans un composé du type 2 CaO, SiO_2, 2 H_2O. La valeur du coefficient de distribution est $\sim 1{,}6\ 10^{19}$ ce qui confirme l'échelle d'affinité fournie par Perruchot (1982) pour les alcalino-terreux et les éléments de transition sur les gels de silicates magnésiens.

VII. Conclusion

Comme nous l'avions supposé, la température induit des variations microstructurales importantes de la matrice. Toutefois, les taux de lixiviation observés ne peuvent être directement corrélés à ces modifications physiques mais plutôt aux formes chimiques de rétention des radioéléments. La température influe également fortement sur la transformation au cours du temps de ces composés. Par exemple, la transformation des aluminates en leur forme stable induit le piégeage d'environ 10% de césium supplémentaire et, après 6 mois à 60°C, ~ 80% du césium se trouve dans les aluminates. A long terme, seule leur transformation ou leur destruction sous l'action de l'environnement peut permettre la libération du césium. De même la fraction du cobalt piégé dès la prise est ~ 99,8%; la destruction de l'hydroxychlorure formé initialement entraîne l'incorporation de cet élément dans les CSH qui gouverneront donc son relâchement à long terme.

Toutefois, compte tenu des périodes de temps (300 ans) sur lesquelles une évaluation du relâchement des radioéléments doit être effectuée, il est nécessaire de poursuivre ce type d'étude sur des durées beaucoup plus longues (plusieurs années), au moins jusqu'à ce qu'un état stationnaire soit observé. L'identification des composés dans lesquels s'incorporent les divers radioéléments, ainsi que la connaissance de leurs propriétés thermodynamiques, est un élément clef d'une telle étude. Par conséquent, le confinement des déchets nucléaires dans des matrices à base de ciment est un problème auquel la chimie des ciments, et en particulier des éléments traces, doit apporter une contribution décisive.

Si certains radioéléments sont associés à des composés spécifiques et habituellement constitutifs des liants hydrauliques, on peut proposer l'utilisation de la méthodologie développée dans ce travail pour suivre les diverses transformations minéralogiques qui traduisent le vieillissement de ces matériaux.

Références

J. CALLEJA (1980). Durabilité. 7ème Cong. Intern. Chim. Cem, 1 (VII-2), 1-50.

R. CHIAPPINI, G. GOUTIERE, J.M LAMEILLE (1985). Etude du devenir des déchets contenus dans les concentrâts d'évaporateurs enrobés dans une matrice ciment à base de CPA 55. Rapport interne CEA, RCP/DE n° 005-85.

R. CRANK (1975). Mathematics of diffusion. Oxford University Press.

E. FREUND (1973). Hydrothermal crystallisation of boron containing zeolites, borosilicates and borogermanates. DIC, Imperial College of Science and Technology, London.

J.M. LAMEILLE et J.C. PETIT (1982). Etude bibliographique de la lixiviation des effluents radioactifs dans les ciments. Rapport interne CEA. RCP/DE n° 005/82.

J.M. LAMEILLE (1984). Etude du rôle de la durabilité d'une matrice cimentée sur le relâchement d'éléments traces : application au stockage de déchets nucléaires. Thèse de 3ième cycle, Université de Paris VI.

J.M. LAMEILLE, G. GOUTIERE, J.C. PETIT et M. REGOURD (1986). Retention of cesium, strontium and cobalt in the hydrates of C_3S, C_3A and gypsum. Soumis à J. Amer. Ceram. Soc.

A. PERRUCHOT et F. DELBOVE (1982 a). Etude thermodynamique des échanges d'ions entre gels silicatés (A-B)-SiO_2- mH_2O et solution aqueuse (A^{2+}, B^{2+}) d'élément de transition. Clay Minerals, 17, 421-432.

M. REGOURD (1983). Chemical corrosion of mineral bulding materials. Intern. Coll. Mat. Sci. Restor., Esslingen.

S. KRISHNAMOORTHY,
Professor, Civil Engineering, Indian Institute of Technology, New Delhi, India

N.K. JAIN,
Scientist, National Council for Cement and Building Materials,
M-10, N.D.S.E. Part - II, New Delhi - 110 049, INDIA.

Influence of Blending Flyash with portland Cement on the Pore Structure Changes of Portland Cement Mortars Cured in NaCl Solutions.

INFLUENCE DES CENDRES VOLANTES, AJOUTEES AUX CIMENTS, SUR LES CHANGEMENTS DANS LA STRUCTURE DES PORES DANS LES MORTIERS CONSERVES DANS DES COLUTIONS DE NaCl.

SUMMARY : The paper presents the results of experimental investigations carried out on small-sized portland cement mortar prism specimens cured in 3 and 6 percent sodium chloride solutions for periods upto one year. The specimens were cured in the respective solutions after 24 hours of casting. Two portland cement samples and their blends with 25 percent fly ash were used to cast the specimens.

The specimens were tested for compressive strength at specified ages and representative portions of the specimens were tested for determining the pore structure using mercury intrusion porosimetry and minerals formed by X-ray diffractometry (XRD).

The pore size changes have been analysed for discrete range of pore sizes and such analysis of pore sizes revealed that certain pore size ranges increased under attack of sodium chloride. Such a deteriorating mechanism through changes in pore structure is arrested when fly ash is blended with portland cement. The reasons for the changes in structure have been postulated as due to formation of chemical compounds as identified in X-ray diffractograms.

It is concluded that even though in absolute terms the compressive strength of fly ash blended portland cement mortars is somewhat less than that of cement mortars without fly ash, the rate of deterioration due to NaCl attack is low to none when fly ash is blended to portland cements.

O trabalho apresenta os resultados de investigações experimentais realizadas em corpos de prova prismáticos pequenos de argamassa de cimento portland, curados em soluções de 3 e 6% de cloreto de sódio por períodos de até 1 ano. Os corpos de prova foram curados nas soluções respectivas após 24 horas da moldagem. Foram usadas amostras de dois cimentos portland e suas adições com 25% de cinza volante para a moldagem dos corpos de prova.

Os corpos de prova tiveram sua resistência à compressão testada em idades especificadas e parte representativa deles foi testada para determinação da estrutura de poro por meio de porosímetro de intrusão de mercúrio, e os minerais formados foram determinados por difratometria de raio-X (XRD).

As mudanças de tamanho de poro foram analisadas para determinação de faixa de tamanhos de poro, e tal análise de tamanhos de poro revelou que determinadas faixas de tamanho de poro aumentaram sob ataque de cloreto de sódio. Tal mecanismo de deterioração atuante nas mudanças de tamanho de poro é sustado quando se faz a adição de cinza volante com o cimento portland. Admitiu-se que as mudanças na estrutura são devidas à formação de compostos químicos, conforme identificados nos difratogramas de raio-X.

Concluiu-se que apesar de em termos absolutos, a resistência à compressão das argamassas de cimento portland aditivado com cinza volante ser algo menor que a das argamassas de cimento sem cinza volante, o índice de deterioração devido ao ataque de NaCl é de baixo a nenhum quando a cinza volante é aditivado aos cimentos portland.

INTRODUCTION

The effect of penetration of chloride on hardened cement paste and concrete has been studied by Gjorv and Vennesland (1), Midgley and Illston (2), Smolczyk (3), Kawadkar and Krishnamoorthy (4). These studies have highlighted that chloride can have a deteriorating influence on portland cement concrete besides the activation of embedded steel which may lead to its corrosion. The deterioration of cement concrete has been attributed to the reaction of chloride with products of hydration leading to formation of water soluble compounds. These chemical compounds have been identified as Friedel's salt and calcium chloride. Massaza (5) suggested that penetration of chloride ions in cement concrete is significantly affected by the nature of pores and the type of cement.

The addition of reactive silicious materials in the form of pozzolanas is known to introduce changes in the nature of pore structure and total pore volume of hardened cement pastes (6). With this in view, the effect of addition of pulverised fuel ash (fly ash) to a few portland cements has been investigated in order to determine the nature of changes in pore sizes of the hardened cement paste and consequent influence on durability of mortar specimens made with these cements.

EXPERIMENTAL

Two portland cements were used. The chemical analysis and calculated Bogue's compositions are given in Table 1. One of the cement had a very low C_3S content while the other had 33% C_3S content. The other two cements, C and D, were prepared by blending 25 percent fly ash with cements A and B respectively. Mortar specimens were prepared using a mix proportion 1:3. Standard sand, conforming to IS:650-1966, was used. Distilled water with a water cement ratio of 0.4 was used for casting, in order to avoid chloride contemination. The specimens were cast using 40 x 40 x 160 mm steel moulds. These were kept under wet hessian for 24 hours and then kept in tap water, 3% and 6% sodium chloride solutions for curing periods of 7, 28, 90, 180 and 365 days respectively.

TABLE - 1

CHEMICAL ANALYSIS OF THE CEMENTS

Chemical compound	A	B	C	D
LOI	1.25	3.86	4.42	4.95
SiO_2	26.54	23.17	31.20	30.00
Fe_2O_3	2.06	1.93	3.41	2.47
Al_2O_3	4.81	5.32	8.83	8.91
CaO	60.42	62.24	46.59	50.00
MgO	2.11	1.96	1.80	1.60
SO_3	1.97	1.96	1.95	1.58
Na_2O	0.25	0.11	0.26	0.13
K_2O	0.61	0.41	0.91	0.67
Bogue's Compound Composition				
C_3S	3.63	33.1	-	-
C_2S	73.80	41.50	-	-
C_3A	9.25	10.80	-	-
C_4AF	6.27	5.87	-	-

TEST METHODS

The specimens were tested for flexural strength and the broken specimens were further tested for compressive strength. Three specimens were tested for an average test result.

Small representative samples of mortars were taken out from the broken specimens and were treated with acetone and dried at 105°C in an incubator. They were preserved in a vaccum desicator to arrest further hydration. Mercury porosimetry measurements were carried out on these samples in an 'AMINCO' porosimeter with pressures upto 407 MPa.

X-ray diffractograms were obtained with powdered samples which passed through 45 μm sieve, on Phillips Diffractometer PW-1120. A standard platinum reference was used in order that the peak heights of any compound can be expressed with relation to that of the standard platinum.

RESULTS AND DISCUSSIONS

Compressive Strength

The compressive strength of portland cement mortar specimens made with the four cements and cured in 3% and 6% NaCl solutions relative to that of tap water cured specimens (of the same age) are given in Table 2.

TABLE - 2

RELATIVE COMPRESSIVE STRENGTH WITH RESPECT TO WATER CURED CEMENT MORTAR SPECIMENS (%)

Curing Solution		3% NaCl				6% NaCl		
Cement	A	B	C	D	A	B	C	D
Age in days								
90	83	87	88	85	82	91	83	81
180	84	86	88	84	80	86	84	84
365	80	81	88	83	73	81	88	82

It is evident from the results that the cement mortars cured in NaCl solutions had relatively lower strength compared to mortars cured in tap water. It is also observed that loss of strength is relatively more in cement A as compared to cement B. This may be due to lower C_3S content of cement A which produces a weaker mortar matrix. Addition of fly ash has resulted in an improved quality of mortar, as is evident from relatively lower loss of strength in case of mortar

made with fly ash blended cements (cements C and D) when cured in sodium chloride solutions.

Flexural Strength

The test results of flexural strength did not show any significant effect of curing in NaCl solutions, though there was some reduction in the strength for all cements studied.

Mercury Porosimetry Measurements

Mortars cured in tap water

In order to appreciate the pore size changes, graphs were plotted between logarithm of mean pore size and incremental penetration of mercury in cm^3/g (Figure 1). The mean pore size represents a range of pore sizes and the entire incremental penetration of mercury through this range is assumed to take place at this mean pore size. It is observed that there are certain mean pore sizes in which maximum mercury penetration occurs and these can be called dominant mean pore sizes. For mortars made with cement A (Figure 1a) the dominant pore size goes on reducing upto an age of 28 days when cured in tap water and then it becomes more or less constant at 350 Å beyond this age. For mortars made with cement B and cured in tap water such a dominant mean pore size is observed at 750 Å (Figure 1b). Such dominant mean pore sizes are also observed at 350 Å for mortars made with cement C (Figure 1c) and D (figure 1d). It has also been observed that effect of addition of fly ash on dominant mean pore size is significant in cement D where a reduction in dominant mean pore size is observed from 750 Å (cement B) to 350 Å (cement D).

Mortar cured in NaCl solutions

Mean pore size plots against incremental penetrat of mercury were also plotted for all the four cen

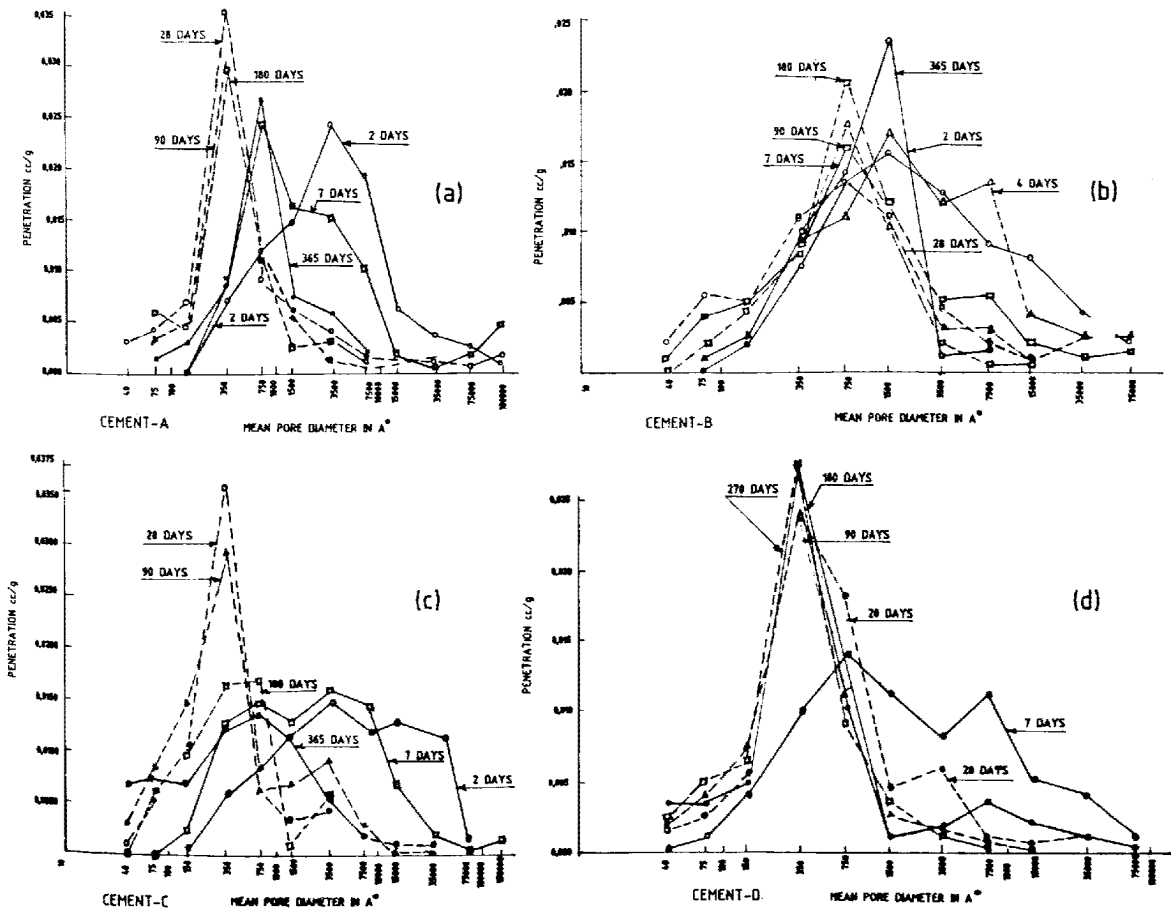

Fig. 1 : PENETRATION OF MERCURY AGAINST MEAN PORE DIAMETER IN CEMENT MORTARS CURED IN TAP WATER

mortars cured in 3% and 6% NaCl solutions and are given in Figures 2 and 3 respectively. It is noted, from Figure 2a, which is for mortars made with cement A, that the dominant mean pore size peak shifted from 350 Å to 750 Å at the age of 180 days and 365 days. A secondary dominant mean pore size is also seen at 7500 Å. These features indicate that, at later ages, there is some dissolution of the hydrated cement compounds, probably in the form of leaching of calcium hydroxide. For cement B (Figure 2b) a similar behaviour is seen except that the secondary dominant mean pore size is observed at 3500 A at 180 and 365 days. Figures 2c and 2d, for mortars made with cement C and D, show that the dominant mean pore size remained at 350 A even upto 365 days of curing in 3% NaCl solution, though a small secondary dominant mean pore size at a higher size is discernible. Such a characteristic suggests that addition of fly ash results in a more stable structure of the hardened cement paste which is not attacked by the NaCl solution.

Similar conclusions can be made from the corresponding plots for cement mortars made with these portland, and blended cements cured in 6% NaCl solution (Figure 3). The beneficial effects of addition of fly ash has been confirmed.

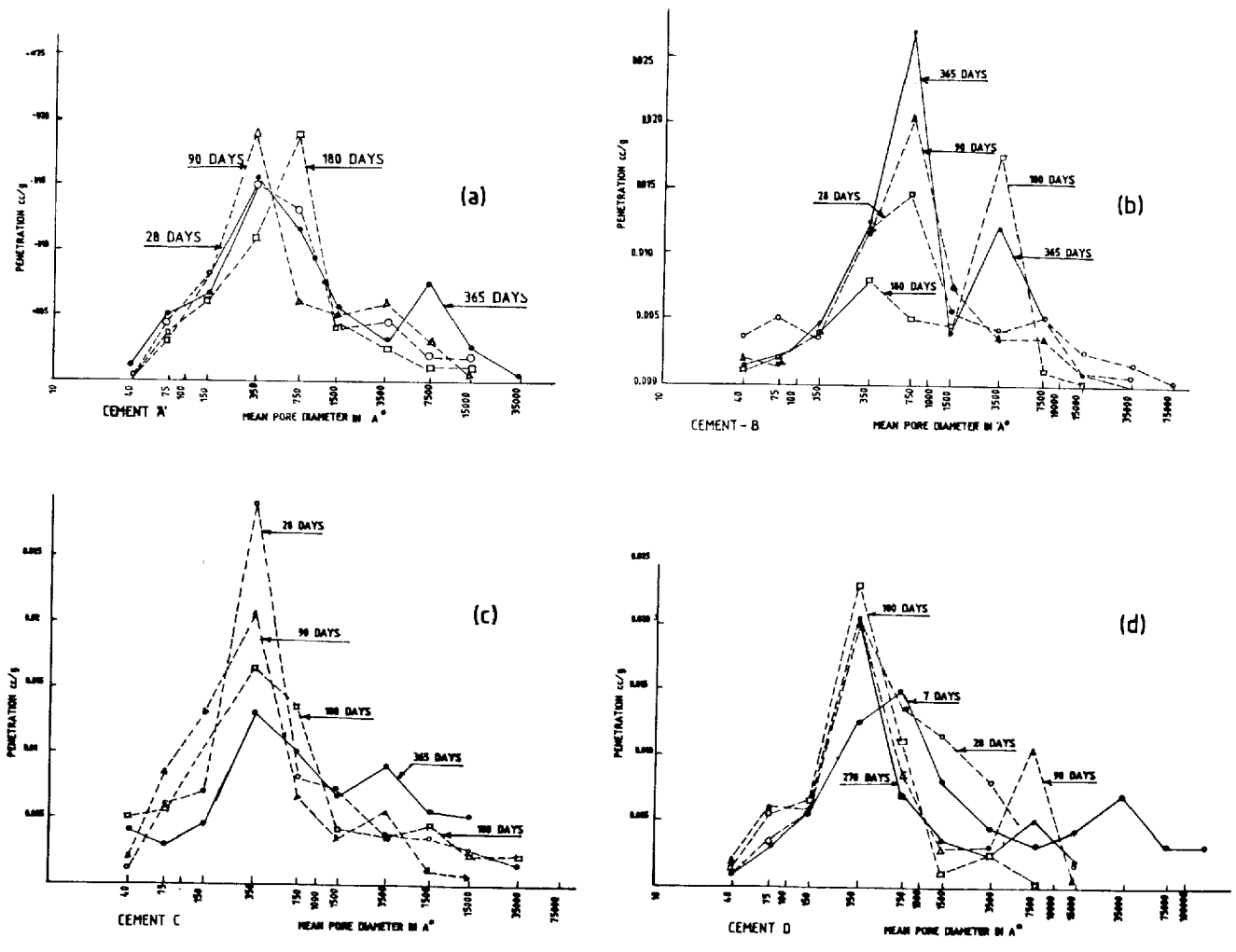

Fig. 2 : PENETRATION OF MERCURY AGAINST MEAN PORE DIAMETER IN CEMENT MORTARS CURED IN 3% NaCl SOLUTION

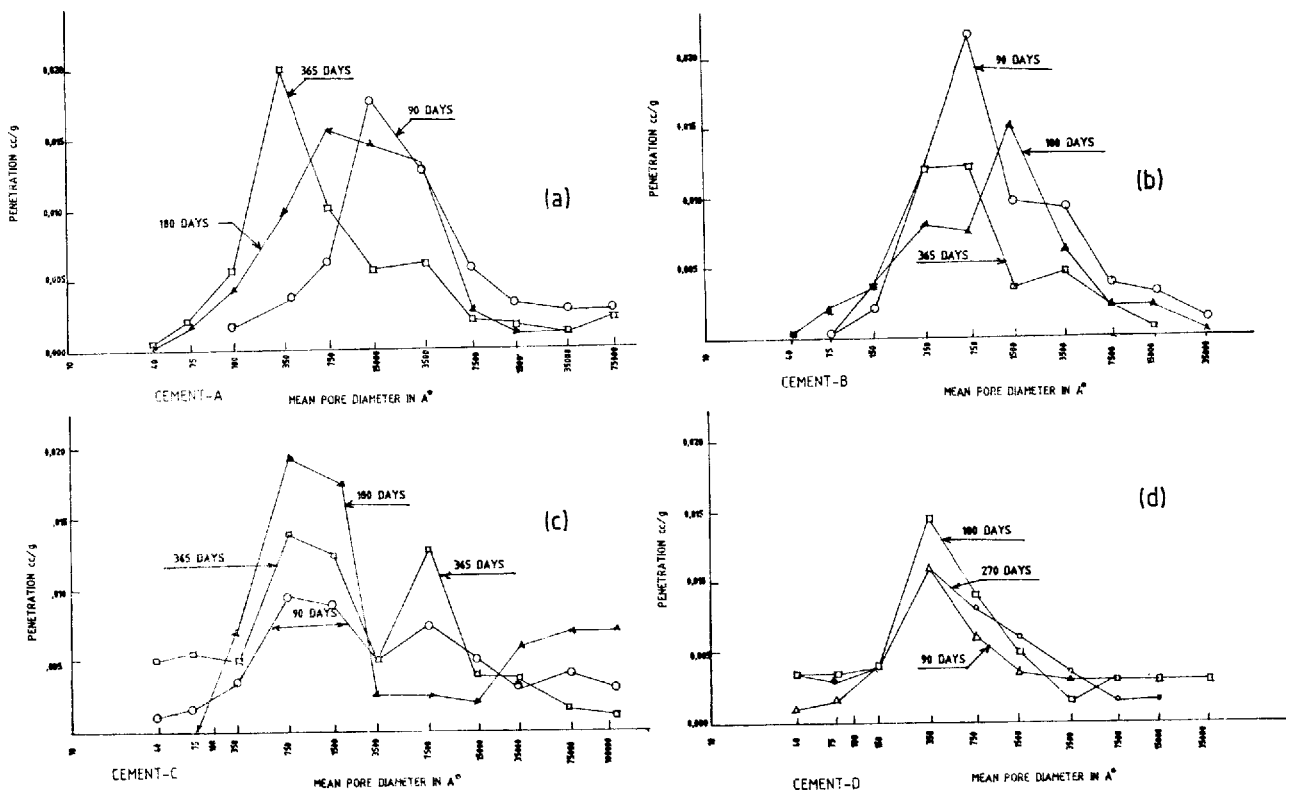

Fig. 3 : PENETRATION OF MERCURY AGAINST MEAN PORE DIAMETER IN CEMENT MORTARS CURED IN 6% NaCl SOLUTION

X-ray Diffraction Analysis

X-ray diffractograms for cement mortars cured in tap water, 3% NaCl solution are given in Figure 4 for the four cements. It can be seen from X-ray diffractograms for mortars made with cements A and B and cured in tap water, that a large quantity of $Ca(OH)_2$ is produced as observed at 2 θ angle of 18.1°. The formation of calcium chloroaluminate is observed when these cement mortars are cured in NaCl solutions. The quantity of $Ca(OH)_2$ is seen to reduce considerably. The reduction of $Ca(OH)_2$ would be due to formation of chloroaluminate and $CaCl_2$, (which would have leached out). This would explain the reason for the increase of large-sized pores of these mortars as observed in mercury porosimetry plots.

The X-ray diffractograms for specimens made with fly ash blended cements C and D (Figures 4c and 4d) show the presence of only small quantities of $Ca(OH)_2$. Since $Ca(OH)_2$ would have been consumed in pozzolanic action with fly ash and part of it would have been reacted to form calcium chloroaluminate ($C_3A.CaCl_2.10H_2O$), the possibility of leaching out of soluble products, as such, are less in hydrated cement paste of these cements.

CONCLUSION

The following conclusions are drawn :

i/ The sodium chloride attck on ordinary portland cement mortars results in increase of large-sized pores due to dissolution of hardened cement paste caused by the formation of $CaCl_2$ and $C_3A.CaCl_2.10H_2O$

ii/ The blending of fly ash with these cements inhibits

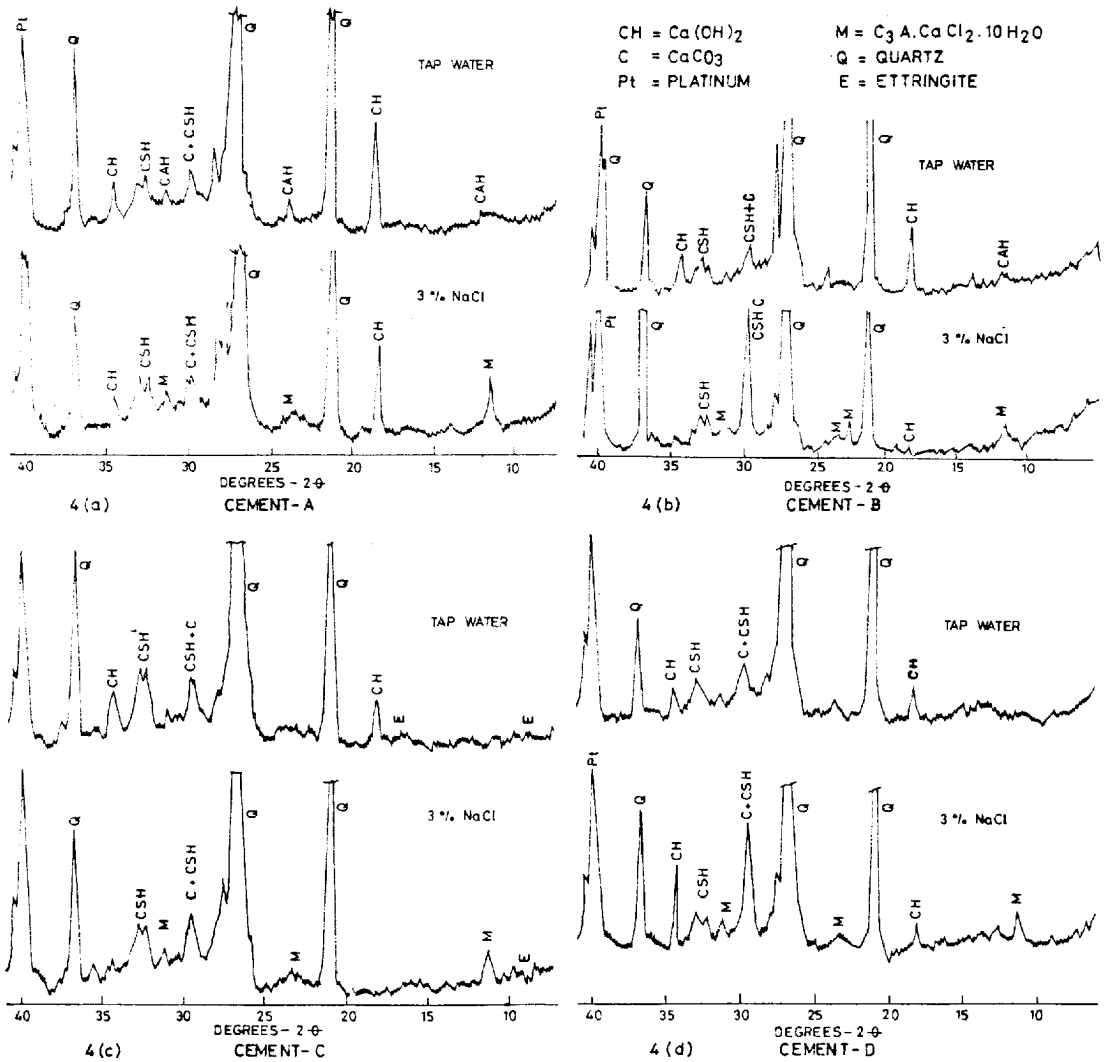

Fig 4. XRD'S FOR MORTAR SAMPLES CURED IN WATER AND 3 % NaCl SOLUTION (365 DAYS)

the formation of lager size pores when cured in NaCl solutions. This results in a lower relative loss of strength of mortars made with such blended cements.

ACKNOWLEDGEMENT

This paper is based on the experimental work relating to Doctoral Thesis of one of the authors NKJ carried out at the National Council for Cement and Building Materials. The authors are grateful to Dr. H.C. Visvèsvaraya, Chairman and Director General of the Council for his encouragement and permission to carry out the studies. This paper is communicated with his permission.

REFERENCES

1.- GJORV, O.E., and VENNESLAND, "Diffusion of chloride ion from sea water into concrete", Cement and Conrete Research Vol. 9, pp. 229-238 (1979).

2.- MIDGLEY, H.G. and ILLSTON, J.M., "Effect of chloride penetration on the properties of hardened cement pastes", Int. Symp. on Chem. of Cement, Paris, VII-101 (1980).

3.- SMOLCZYK, H.G. "Chemical reactions of strong chloride solutions with concrete", Proc. of Vth Int. Sympo. on Chem. of Cement, Tokyo III-31 (1968).

4.- KAWADKAR, K.G. and KRISHNAMOORTHY. S. "Behaviour of cement concrete under common salt both under hydrostatic and atmospheric pressures", Cement and Concrete Research, Vol. 2 pp 103-113 (1981).

5.- MASSAZZA, F. COSTA, U., "Aspects of the pozzolanic activity and properties of pozzolanic cements". Il Cemento, Vol. 1, pp 3-17 (1979).

6.- MEHTA, P.K. "Studies on blended portland cements containing santorin earth", Cement and Concrete Research, Vol. 11, pp. 507-511 (1981).

Amitabba Kumar and Della M. Roy*, Materials Research Laboratory and *Department of Materials Science and Engineering, The Pennsylvania State University, University Park, PA 16802, USA

PORE STRUCTURE AND IONIC DIFFUSION IN ADMIXTURE BLENDED PORTLAND CEMENT SYSTEMS

SUMMARY: Diffusion mechanisms of ionic species and their relationship to basic material properties have been investigated in water-saturated, hardened cementitious materials. Granulated blast furnace slag, ultra-fine amorphous silica, fine-grained quartz, and low calcium fly ash have been blended with ordinary portland cement to provide a variety of cementitious matrices, generally reducing ionic diffusivity. Porosity and pore structure of hardened pastes formulated from the above have been evaluated using mercury intrusion porosimetry. The effective coefficients for Cl^- and Cs^+ have been measured across water-saturated disks of hardened cement pastes using a new technique.

Water-to-cement or water-to-solid ratios during mixing vary from 0.30 to 0.40, while curing and diffusion were carried out between 27° and 60°C in samples cured up to ages of one year. Non-evaporable water content, bulk density, and total porosity have been measured, and limited scanning electron microscopy studies of polished sections have also been conducted.

The fractional porosity, ε, and the median or modal pore size, r, have been found to be related to the effective diffusion coefficient, D_{eff}, of ions in water-saturated hardened cement pastes. The general relationship is given by $D_{th}/D_{eff} = C_1\varepsilon C_2 r C_3$, where D_{th} is the diffusion coefficient of an ion at infinite dilution in water and C_1, C_2 and C_3 are constants. Decreasing the water content during paste mixing results in lower ionic diffusion coefficients and porosites. Hardened pastes of cement blended with blast furnace slag and amorphous silica show increased ionic diffusion with increase in curing and diffusion temperature. Higher temperature causes increased reactions of fly ash and crystalline silica blends, which leads to lower effective ionic diffusion. Blast furnace slag blends exhibit low Cl^- and Cs^+ diffusion coefficients. Fly ash and amorphous silica blending result in low Cs^+ diffusion, while crystaline silica blending leads to low ionic diffusion at later ages, compared to the parent hardened paste. Hardened cement pastes behave as electronegative semipermeable membranes, retarding the cation preferentially over the anion. The lower effective diffusion of ions in admixture blended portland cement pastes has important application in corrosion problems and nuclear waste management.

Foram investigados o mecanismo de difusão de espécies iônicas e sua relação com propriedades básicas do material, em materiais cimentosos endurecidos em água saturada. Escória granulada de alto forno, sílica amorfa ultra-fina, quartzo granulado fino e cinza volante com baixo cálcio foram aditivados com cimento portland comum, para obtenção de variedade de matrizes cimentosas, geralmente redutoras da difusividade iônica. Foram avaliadas a porosidade e a estrutura de poro de pastas endurecidas preparadas com as misturas acima, usando-se porosimetria de intrusão de mercúrio. Foram medidos os coeficientes efetivos para Cl^- e Cs^+ através de discos de pastas endurecidas de cimento, saturados em água, com emprego de uma nova técnica.

As relações água/cimento e água/sólido durante a mistura variam de 0,30 a 0,40, enquanto a cura e a difusão foram realizadas entre 27 e 60°C, com amostras curadas por períodos de até um ano. Foram medidos o teor de água não evaporável, densidade em massa, e porosidade total, e foram feitos estudos limitados de microscopia eletrônica de varredura em seções polidas.

Constatou-se que a porosidade fracionária, ε, e o tamanho médio ou modal de poro, r, estão relacionados com o coeficiente de difusão efetiva, D_{eff}, de íons em pastas endurecidas de cimento em água saturada. A relação geral é dada por $D_{th}/D_{eff} = C_1\varepsilon C_2 r C_3$, onde D_{th} é o coeficiente de difusão de um íon em diluição infinita em água, e C_1, C_2 e C_3 são constantes. Diminuindo o teor de água durante o amassamento da pasta, tem-se como resultado coeficientes mais baixos de difusão iônica e porosidades. As pastas endurecidas de cimento ativado com escória de alto forno e sílica amorfa apresentaram difusão iônica aumentada com o aumento na temperatura de cura e de difusão. Temperatura mais alta causa reações maiores das adições de cinza volante e de sílica cristalina, o que leva à difusão iônica efetiva mais baixa. A adição de escória de alto forno apresenta coeficientes baixos de difusão de Cl^- e Cs^+. A adição de cinza volante e de sílica amorfa resulta em baixa difusão de Cs^+, enquanto a adição de sílica cristalina proporciona baixa difusão iônica nas idades finais, comparada com a pasta endurecida de referência. As pastas endurecidas de cimento se comportam como membranas eletronegativas semi-permeáveis, retardando o cátion preferencialmente sobre o aníon. A difusão efetiva mais baixa de íons na mistura de pastas de cimento portland aditivado tem importante aplicação nos problemas de corrosão e no gerenciamento de lixo nuclear.

Amitabha Kumar and Della M. Roy*, Materials Research Laboratory and *Department of Materials Science and Engineering, The Pennsylvania State University, University Park, PA 16802, USA

INTRODUCTION

The diffusion of ions and the permeability of fluids across a porous cementitious matrix are, intuitively, related to the volume of pores and the size and interconnectivity of these pores. The basis for such a statement lies in the fact that if the diffusion and permeability of ions and fluids were not related to the pores in a porous matrix but to the solid part, the observed rates of diffusion of $\sim 10^{-12}$ m^2/sec at room temperature in porous cementitious materials would instead resemble that of atomic diffusion in polycrystalline ceramics of $\sim 10^{-17}$ m^2/sec or lower. The permeability of water through water saturated cementitious materials has been shown to be related to the porosity and pore size distribution (1,2). In the case of ionic diffusion in water saturated porous cementitious materials, the diffusion coefficients for moderately sized, singly charged cations generally range between 10^{-11} and 10^{-13} m^2/sec (3-5) while the diffusion coefficients for these ions in pure water is $\sim 10^{-9}$ m^2/sec (6). The obvious question thus arises as to why the diffusion is retarded through the matrix. One of the factors contributing to the decrease is the smaller area through which the ions may migrate in a porous matrix viz. the area of the pores. This area factor may explain a two- or three-fold decrease in the diffusion coefficient of an ion across a porous matrix as compared to that in the pure phase. It was pointed out earlier that the observed decreases are generally much larger than two- or three-fold, in the vicinity of 10^2 to 10^4 times. Considering recent evaluations (4,5,7-9) the probable reason for such a large retardation arises from the constriction and tortuosity of the pore path through which an ion migrates in a water saturated porous matrix. The ion-wall interaction leads to a substantial decrease in diffusion. Recent papers elucidating this point have been published (10,11).

To understand the effects of porosity and pore size distribution on the diffusion of ions in cementitious materials, a variety of matrices have been created using portland cement and admixtures. The diffusion of cesium chloride across these matrices has been studied at different temperatures so as to evaluate the dependence of ionic diffusion on porosity parameters. It is felt that such a basic and systematic approach could be used towards a fundamental understanding in the design of materials that may be used to retard diffusion of ions. Such a retardation in diffusion leads to corrosion resistance and in the development of sealing materials for nuclear waste applications.

EXPERIMENTAL

A Type I portland cement (ASTM classification) was used for the entire study. Pastes were formulated with the neat cement and with admixture blends. Ground granulated blast furnace slag, low calcium fly ash, fine grained amorphous silicon dioxide and fine crystalline quartz were used as admixtures. The latter two are usually called silica fume and Min-u-Sil*. The chemical composition and some physical properties of these materials are listed in Table 1. The blast furnace slag has a high MgO content while the fly ash has a high K_2O content. Silica fume and Min-u-Sil are almost entirely made up of SiO_2.

Each composition was cured at 27°, 38° and 60°C. Mold cure, subsequent cure and diffusion studies were carried out at these three temperatures, on pastes formulated following ASTM C 305 mixing procedures. A superplasticizer, sodium salt of naphthalene sulphonate formaldehyde condensate was used to give better workability at the lower water ratios. Superplasticizer content was maintained at 0.331% solids as this was found to give a workability equal to that of a mixture with a water to solid ratio 0.5 more than a mixture not containing superplasticizer.

The pastes were cast into thin disks either 1.7 or 3.2 mm high and 3.5 cm in diameter in an acrylic-teflon mold shown in Fig. 1. The molds were

Table 1. Chemical Composition of Starting Materials.

Materials	Type I/II Cement I-06	Blast Furnace Slag B-64	Fly Ash B-86	Min-u-Sil
SiO_2	20.2	32.7	48.9	99.7
Al_2O_3	3.92	10.0	27.4	0.1
TiO_2	0.20	0.48	1.3	0.02
Fe_2O_3	3.48	0.86	11.0	0.03
MgO	4.56	11.0	0.93	<0.01
CaO	64.88	42.04	2.70	---
MnO	0.080	0.48	0.04	---
SrO	0.05	0.05	0.09	---
BaO	0.08	0.05	0.12	---
Na_2O	0.17	0.25	0.23	---
K_2O	0.49	0.55	2.45	---
P_2O_5	0.14	<0.05	0.38	---
SO_3	2.46	---	0.40	---
S	---	1.28	---	---
LOI**	1.58	Negative***	3.6****	0.16
Sr ppm	---	75	---	---
Ba ppm	---	77	---	---
Total	102.29	99.79	99.5	100.02

*LOI represents loss on ignition at 100°C.
**Negative LOI indicates presence of sulfide.
***LOI at 750°C.

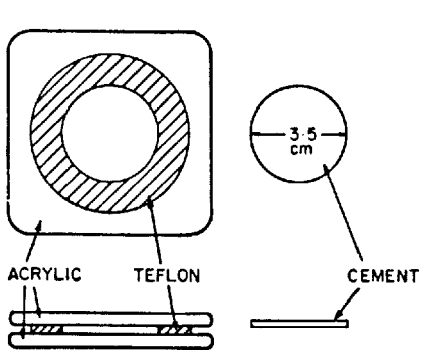

Fig. 1. Mold for preparation of diffusion specimens.

*Min-u-sil is a trade name of the Pennsylvania Glass Sand, 300 Penn Center, Pittsburgh, PA.

vibrated for one minute on a vibrating table, bound with rubber bands, and cured under deionized water for 24 hours. Following the initial cure, the hardened paste disks were demolded and cured for the required time in saturated calcium hydroxide solution. The diffusion of cesium chloride across these disks was studied after 7, 28, 90, 180, and 365 days of curing. Four disks of each thickness were used at each age. One day before the start of the diffusion experiment eight disks, four of each thickness, were removed from the curing baths, washed in deionized water and polished on both surfaces with SiC paper. Four hundred followed by 600 grit paper was used so as to obtain disks either 1.68 ± 0.05 or 3.18 ± 0.05 mm in thickness. The disks were sealed onto small plastic petri dishes to render a diffusion cell filled with saturated calcium hydroxide solution on the inside, as described elsewhere (12,17). One thin (1.68 ± 0.05 mm) and one thick (3.18 ± 0.05 mm) disk cell were removed from the bath each week and the entire solution in the cell was analyzed for its Cs^+ and Cl^- contents. Cs^+ was analyzed using atomic absorption techniques while Cl^- was determined using a specific ion electrode. In this manner a concentration profile for the sink side of the hardened cement paste disk was obtained as a consequence of the diffusion of CsCl across the disk.

Mercury porosimetry studies were carried out on hardened cement paste disks identical to those used for diffusion studies. These porosimetry studies were carried out on samples cured up to the start of the diffusion studies. Prior to mercury intrusion, the samples were freeze dried at -80°C and ~10 mTorr pressure (2.67 Pa). The porosity and pore size distribution between 7.5 μm and 1.9 nm was measured using mercury at pressures up to 386 MPa and calculated, assuming the contact angle between mercury and freeze dried cement to be 140°.

CALCULATION OF DIFFUSION COEFFICIENT

The diffusion experiments yielded concentrations of Cs^+ and Cl^- on the sink side of the water saturated hardened cement paste disk after various times of diffusion. The source concentration of CsCl was maintained at 0.05M by using a large supply bath as compared to the small volume of the petri dish. The diffusion coefficient was calculated in the following manner. Consider a membrane as depicted in Fig. 2. The boundary conditions for the diffusion of ions across this membrane are also detailed in Fig. 2. The source concentration remains constant at C, while the sink concentration, C_2, is initially at zero and is ~C_1

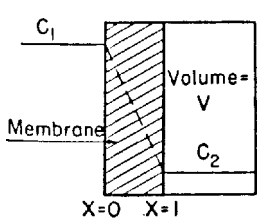

At X = 0
C = C_1 at $t \geq 0$
At X = l
C = C_2 = 0 at $0 \leq t \leq t_o$
C = C_2 = f(t) at $t > t_o$

Fig. 2. Theoretical representation of the diffusion across a HCP disk describing boundary conditions.

at infinite time. Solution to this problem is given by

$$D = [Vl/A \cdot 1/(t-t_o)]\ln(1/[1-C_2/C_1])$$

where D = effective diffusion coefficient, m^2/sec; V = volume of sink, m^3; l = thickness of membrane or disk, m; A = area of membrane or disk exposed to diffusant, m^2; t = time of diffusion, sec; t_o = time at which first ion is detected in the sink, lag time, sec; C_1 = concentration of source; g/L; C_2 = concentration of sink, g/L.

This equation was solved using known values for V, A and l. Average 'l' values for a series of samples, viz. for different times of diffusion, were used. The values of $\ln[1/1-C_2/C_1]$ at different times, t_1, t_2, etc., were least square fitted so as to optimize the value of D and t_o. If it was observed that the value of t_o, the lag time after which the ion of interest was first detected in the sink, appeared unreasonable when the theoretical and experimental data were compared, then an average value for D was computed assuming t_o to be zero. At least 70% of the entire data fit the least square method.

ANALYSIS OF MERCURY POROSIMETRY DATA

It was mentioned earlier that the porosity and pore size distribution of the freeze-dried hardened cement paste disks were measured using mercury porosimetry. The pore sizes in this range have been reported so as to effectively describe the distribution by an 'average' parameter. Generally the pore size are described by reporting the critical pore radius (12). The critical pore radius is the radius at which the maximum value of dV/dP, the differential of the volume intrusion with respect to the intrusion pressure is observed. The second description which has been incorporated here is the pore radius at which 50% of the pore volume is observed in the pore size range considered above, which may also be described as the median pore radius. In most cementitious materials the critical pore radius and the median pore radius have similar values. Properties of different cementitious compositions may be contrasted by comparing the porosity, median pore radius or the critical pore radius.

The mercury porosimetry measurement results for the three temperatures 27, 38 and 60°C are given in Tables 2, 3, and 4, respectively.

RESULTS AND DISCUSSION

The results from porosimetry studies have been listed in Tables 2, 3, and 4. The results of diffusion studies at various temperatures for the different compositions are listed in Tables 5 and 6 for Cl^- and Cs^+ diffusion respectively. These data are for measurements conducted on thin disk (1.68 ± 0.05mm) samples. More elaborate data regarding thick disk (3.18 ± 0.05 mm) values, error values and standard deviations are provided elsewhere (12).

Considering the porosimetry results for ordinary portland cement pastes, it is observed that the porosity decreases by 3 up to 5 percentage points with a 0.05 lowering in the w/c ratio, in

Amitabha Kumar and Della M. Roy*, Materials Research Laboratory and *Department of Materials Science and Engineering, The Pennsylvania State University, University Park, PA 16802, USA

Table 2. Porosity and Median Pore Size for Type I Portland Cements Blended with Various Admixtures and Cured at 27°C.

Composition (by wt.)	Age (Days)	Porosity (%) w/s 0.40	w/s 0.35	w/s 0.35 + SP	w/s 0.30 + SP	Median Pore Size (nm) w/s 0.40	w/s 0.35	w/s 0.35 + SP	w/s 0.30 + SP
Type I Portland Cement	7	27.0	25.0		21.0	12.5	13.5		9.2
	28	22.5	20.0			17.5	13.0		
	90	22.0	17.0			16.0	10.5		
	180	----	----	14.0	10.5	----	----	6.7	5.4
	365	20.0	16.0	14.8	12.3	13.0	15.0	7.7	13.0
35% Type I PC + 65% Blast Furnace Slag	7		21.5		15.5		13.5		4.6
	28		12.2		14.0		2.75		2.60
	90		9.5		7.0		2.3		2.45
	180		8.0		4.5		2.35		2.3
	365		5.5		6.0		2.4		3.0
90% Type I PC + 10% Silica Fume	7	27.5				9.5			
	28	24.5				8.0			
	90	22.5		19.0		5.8		4.1	
	180	21.0				4.2			
	365	22.2		16.0		10.0		4.1	
75% Type I PC + 12.5 5μm Min-u-Sil	90		20.0		16.5		7.5		5.5
	180		18.0		14.5		8.0		4.9
+ 12.5% 10μm Min-u-Sil	365		23.0		18.0		9.0		11.0
70% Type I PC + 30% Fly Ash	7		26.7		25.5		28.0		14.0
	28		25.0		19.0		11.0		8.0

*SP: Superplasticizer - 0.331% of solid content in paste samples at 90 and 180 days have been over-cured up to 10% of the curing time in a few cases. Comparisons between those over-cured and cured for exact duration indicates that the discrepancy is negligible.

Table 3. Porosity and Median Pore Size for Type I Portland Cements Blended with Various Admixtures and Cured at 38°C.

Composition (by wt.)	Age (Days)	Porosity (%) w/s 0.40	w/s 0.35	w/s 0.35 + SP	w/s 0.30 + SP	Median Pore Size (nm) w/s 0.40	w/s 0.35	w/s 0.35 + SP	w/s 0.30
Type I Portland Cement	7	27.0	24.0		21.5	12.5	12.0		9.2
	28	23.5	22.0			14.0	15.0		
	90	24.5	19.0			19.0	12.5		
	180			16.5	12.8			7.5	5.4
	365	27.0	18.0	17.0	13.6	17.5	14.0	8.8	12.5
35% Type I PC + 65% Blast Furnace Slag	7		19.0		14.5		13.5		3.7
	28		11.5		12.5		2.75		2.65
	90		10.0		6.5		2.45		2.45
	180		8.0		5.7		2.40		2.55
	365		6.0		4.5		2.50		2.65
90% Type I PC 10% Silica Fume	7	27.7				8.0			
	28	27.5				7.5			
	90	24.0		20.5		6.2		4.1	
	180	23.0				4.2			
	365	22.0		16.5		8.0		4.2	
75% Type I PC + 12.5% 5μm Min-u-Sil + 12.5% 10μ m Min-u-Sil	90		20.5		17.0		8.5		5.5
	180		19.5		16.5		8.5		5.0
	365		23.5		18.5		10.0		9.0
70% Type I PC + 30% Fly Ash	7		26.6		25.0		29.0		10.0
	28		26.0		21.3		9.2		6.4

bearing with previous work (1). Increasing the curing time leads to decreases in porosity, the differential being greatest at 27°C and least at 60°C, in the range 7 to 365 days of curing. the median pore size increases with age at the higher w/c ratios and always increases between 6 months and 1 year of hydration. It is presumed that the pore structure and interconnectivity of pores of portland cement pastes alters substantially even at ages up to 1 year in a water saturated atmosphere. Even though the porosity decreases, the structure that develops through later hydration is more 'open'.

Comparing blast furnace slag blended pastes and the parent portland cement pastes, it is clear that the porosities of blast furnace slag blended hardened pastes are lower and the pore sizes considerably finer than the portland cement pastes. The pore sizes of silica fume blended pastes are

Table 4. Porosity and Median Pore Size for Type I Portland Cements Blended with Various Admixtures and Cured at 60°C.

Composition (by wt.)	Age (Days)	Porosity (%) w/s 0.40	w/s 0.35	w/s 0.35 + SP	w/s 0.30 + SP	Median Pore Size (nm) w/s 0.40	w/s 0.35	w/s 0.35 + SP	w/s 0.30 + SP
Type I Portland Cement	7	29.5	25.0		21.4	12.5	9.0		7.0
	28	26.0	22.0			17.5	13.5		
	90	29.0	24.5			20.0	17.5		
	180			22.0	15.5			11.0	6.2
	365	26.0	22.6	19.5	18.8	17.5	12.5	9.8	11.0
35% Type I PC + 65% Blast Furnace Slag	7		17.0		9.5		11.0		2.9
	28		12.0		11.0		2.95		2.85
	90		10.0		6.0		2.60		2.70
	180		8.0		5.5		2.50		2.75
	365		8.0		5.5		2.70		2.65
90 Type I PC + 10% Silica Fume	7	25.5				5.8			
	28	27.5				6.7			
	90	25.0		21.0		6.2		4.1	
	180	25.5				4.6			
	365	28.5		20.5		8.0		9.8	
75% Type I PC + 12.5% 5μ Min-u-Sil + 12.5% 10 μm Min-u-Sil	90		21.5		18.5		5.1		3.4
	180		19.0		13.5		3.3		3.1
	365		13.5		10.0		3.0		2.75
70% Type I PC + 30% Fly Ash	7		27.9		25.5		12.0		6.2
	28		28.5		23.5		7.5		6.1

finer compared to the parent portland cement pastes but the porosities are nominally higher. Portland cements blended with Min-U-Sil behave in a manner similar to the present paste at 27°C but at 60°C the blends have lower porosity and finer pores as compared to the parent. The results obtained for pastes hardened at 38°C follow the trend of finer pore size distribution and lower porosity for the Min-U-Sil blended portland cement pastes. Fly ash blended portland cement pastes indicate slightly higher porosities at 7 and 28 days but the pore size distributions observed in the 28 day samples show a greater number of finer pores especially at 0.35 w/s for the fly ash blends over the ordinary portland cement paste.

In general the addition of mineral admixtures to portland cement leads to a decrease in pore size or an increase in the fraction of porosity in the finer pore range of 15 nm or less. The porosity may increase through this incorporation as in silica fume and fly ash cases but the increase in porosity is only in the quantity of finer pores. The results are quite in bearing with those of previous evaluation of similar systems (13). The effect of the increase in finer pore content indirectly leads to an increase in the tortuosity or interconnectivity of the pores. A migrating ionic species within a fine pore matrix has to traverse an anfractuous path to penetrate a small part of the matrix whereas, if the pores are large the migrating species may penetrate with alacrity. Thus a tentative and reasonable conclusion with regard to diffusion in blended portland cement matrices is to expect a slower migration of ions due to the larger tortuosity of the matrix through the presence of a larger number of finer pores.

The relevance of the previous discussion is observed from the impact it has on the diffusion of ions in water saturated hardened cement pastes. It is apparent, from a consideration of the experimentally determined diffusion coefficients presented in Tables 5 and 6, that the diffusion of Cl^- and Cs^+ is affected by the presence of admixtures within a portland cement paste. The water content of the paste and the temperature of

Amitabha Kumar and Della M. Roy*, Materials Research Laboratory and *Department of Materials Science and Engineering, The Pennsylvania State University, University Park, PA 16802, USA

Table 5. Effective Diffusion Coefficients for Cs^+ Diffusion Across Water Saturated Hardened Cement Paste Disks of Blended Portland Cement.

		Effective Diffusion Coefficient, m^2/sec, $x10^{13}$											
Composition:		Ordinary Portland Cement (OPC)			OPC + Blast Furnace Slag			OPC + Silica Fume (90:10) wt.%		OPC + Min-U-Sil (75:12.5:12.5) wt.%		OPC + Fly Ash (70:30) wt.%	
Temp. (°C)	Age (Days)	0.40 w/c	0.35 w/c	0.35+SP** w/c	0.30+SP w/c	0.35 w/s	0.30+SP w/s	0.40 w/s	0.35+SP w/s	0.35 w/s	0.30+SP w/s	0.35 w/s	0.30+SP w/s
27	7	28.5	22.2	——	7.66	2.32	<0.9	2.31	——	——	——	163	167
	28	23.0	16.2	87.9	8.88	42.3	2.25	<0.8	<0.4	——	——	68.8	37.8
	90+	43.7	13.0	22.5	5.84	2.48	5.26	1.47 (av)	1.19	125	38.7	——	——
	180+	47.3	8.19	15.2	2.33	1.14	1.68	7.44	3.59	74.4	37.2	——	——
	365	22.7	8.49	18.1 (av)	4.35	1.61	11.7	1.08	1.22	101	45.0	——	——
38	7	43.6	31.4	——	21.9	0.842	1.87	1.35	——	——	——	79.0	92.2
	28	85.8	51.9	95.8	27.2	95.5	9.36	<0.7	1.76	——	——	13.6	4.55
	90+	121	55.7	110	34.7	13.9	1.77	1.15 (av)	8.75	338	120	——	——
	180+	139	47.2	69.7	18.1	0.353	12.2	<0.7	8.00	122	88.7	——	——
	365	154	49.1	99.7 (av)	21.8	5.45	18.0	1.42	4.02	186	24.3	——	——
60	7	1020	903	——	255	<1.1	56.4	3.68	——	——	——	135	8.21
	28	1590	1730	1380	1950	<36.8	1.14	177	319	——	——	16.2	5.54
	90+	4610	1740	3330	968	61.6	3.06	116 (av)	43.6	579	102	——	——
	180+	1310	1950	6340	580	3.57	3.17	241	80.2	71.4	40.8	——	——
	365	*	2040	1570 (av)	843	14.5	28.1	685	137	278	24.6	——	——

*Bad Data. ——No data. (av) Average of two different samples.
+Reported age of samples cured for 90 and 180 days vary from 90 to 100 days and 180 to 200 days.
**SP: Superplasticizer: Sodium Salt of Naphthalene Sulphonate Formaldehdye Condensate.

Table 6. Effective Diffusion Coefficients for Cl^- Diffusion Across Water Saturated Hardened Cement Paste Disks of Blended Portland Cement.

		Effective Diffusion Coefficient, m^2/sec, $x10^{13}$											
Composition:		Ordinary Portland Cement (OPC)			OPC + Blast Furnace Slag			OPC + Silica Fume (90:10) wt.%		OPC + Min-U-Sil (75:12.5:12.5) wt.%		OPC + Fly Ash (70:30) wt.%	
Temp. (°C)	Age (Days)	0.40 w/c	0.35 w/c	0.35+SP** w/c	0.30+SP w/c	0.35 w/s	0.30+SP w/s	0.40 w/s	0.35+SP w/s	0.35 w/s	0.30+SP w/s	0.35 w/s	0.30+SP w/s
27	7	113	88.2	——	66.6	27.9	20.6	17.9	——	——	——	103.0	97.4
	28	110	75.1	60.0	56.9	9.62	8.61	4.35	2.9	——	——	55.8	43.8
	90+	75.8	44.2	57.2	36.8	4.87	2.08	5.92 (av)	1.12	67.7	50.4	——	——
	180+	74.5	50.4	61.3	21.4	1.83	1.21	1.92	2.18	70.6	43.4	——	——
	365	58.6	45.7	47.5 (av)	27.6	1.37	<0.7	3.65	<1.0	77.5	53.8	——	——
38	7	92.0	77.1	——	57.3	42.9	29.5	13.7	——	——	——	66.6	64.4
	28	227	129.0	156	87.1	18.2	9.07	15.6	7.62	——	——	13.5	13.4
	90+	89.4	63.7	81.1	64.7	15.7	1.74	11.2 (av)	8.16	112	59.4	——	——
	180+	78.5	58.2	84.6	44.0	12.9	1.73	16.7	10.3	250	47.0	——	——
	365	104	84.3	85.0 (av)	79.0	4.07	1.69	23.0	5.24	110	39.1	——	——
60	7	200	106	——	96.9	55.2	46.0	42.6	——	——	——	13.9	12.5
	28	303	181	127	314	32.1	23.8	49.6	102	——	——	12.4	10.7
	90+	317	286	623	217	41.5	6.58	80.3 (av)	60.9	73.7	29.3	——	——
	180+	337	451	701	311	11.0	2.04	132.0	50.9	4.99	34.1	——	——
	365	*	171	285	*	8.66	7.22	141.0	61.8	8.45	<0.8	——	——

*Bad Data. ——No data. (av) Average of two different samples.
+Reported age of samples cured for 90 and 180 days vary from 90 to 100 days and 180 to 200 days.
**SP: Superplasticizer: Sodium Salt of Naphthalene Sulphonate Formaldehdye Condensate.

hydration and diffusion also have a significant effect on the diffusional characteristics of a given cement paste.

Considering diffusion results for hardened ordinary portland cement pastes in Tables 5 and 6 it is clear that an increase in water content of a paste mix increases the effective diffusion coefficient (D_{eff}) of Cl^- and Cs^+ ions. The results at 27°C for this material are schematically shown in Fig. 3. The effect of increasing the water content leading to an increase in D_{eff} for Cl^- and Cs^+ is to be expected in the light of increased porosity and median pore radius data listed in Tables 2, 3, and 4, as suggested by the previous discussions. Similar arguments may be extended to blast furnace slag and silica fume samples, in line with previous work (5). An interesting comparison may be made between the D_{eff} Cl^- values for blast furnace slag and ordinary portland cement hardened pastes with a w/c of 0.30. As depicted in Fig. 4, increasing the age of a sample of ordinary portland cement at 27° or 38°C leads to a slight decrease in D_{eff} Cl^- while 60°C curing results in an increase in Cl^- diffusion with age. The increase is attributed to a coarser pore structure with age. There is an increase in D_{eff} Cl^- with age between 180 and 365 days at 27° or 38°C for the same pastes and is also attributed to a coarser structure, while comparable blast furnace slag pastes show a sharp decrease in D_{eff} Cl^- with age except for the 27°C paste sample indicating a slight increase at 1 year age. The latter exception is attributed to an increase in porosity and median pore size, as given in Table 2. Blast furnace slag in portland cement effectively retards the diffusion of Cl^-, especially at later ages and higher temperatures. The results for Cs^+ are not as straight forward though the decrease in diffusion of the ion is definitely diminished by the slag blended paste.

The effective diffusion coefficients of Cl^- and Cs^+ in silica fume blends are lower than those for hardened pastes of pure portland cement. There is an increase in D_{eff} for Cl^- and Cs^+ at later ages, viz. at least 100 days, for the fume blends just as in the ordinary portland paste cases. This is again attributed to a coarser pore structure developed with age as noted from the porosimetry data. The Cs^+ diffusion across silica fume blends is exceptionally low and makes this a positive candidate for sealing materials to be used for Cs^+ containing nuclear waste materials. The use of crystalline siliceous material, Min-U-Sil results in D_{eff} values quite similar to the neat paste at 27° and 38°C, or sometimes a larger diffusion coefficient. A different perspective evolves when considering D_{eff} values obtained for Min-U-Sil

Amitabha Kumar and Della M. Roy*, Materials Research Laboratory and *Department of Materials Science and Engineering, The Pennsylvania State University, University Park, PA 16802, USA

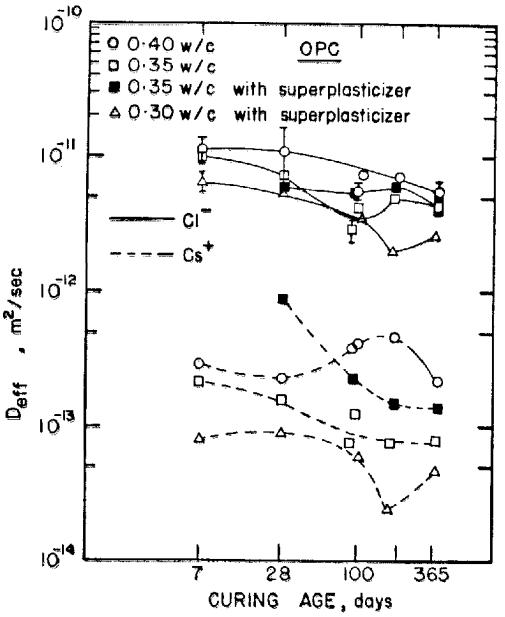

Fig. 3. Effect of water/cement ratio on Cs^+ and Cl^- effective diffusion coefficients for hardened portland cement pastes.

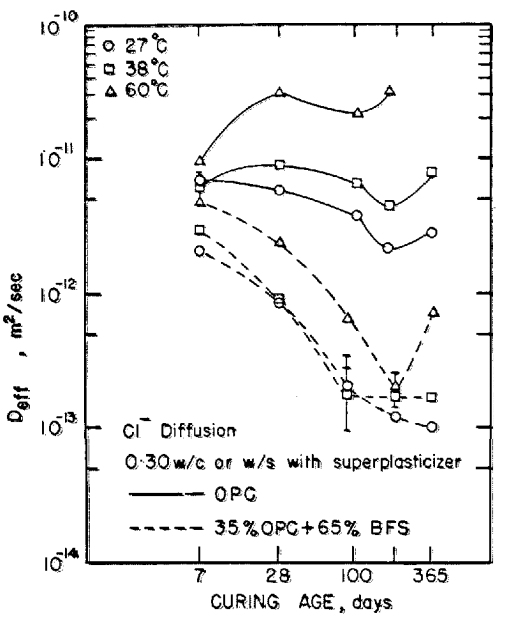

Fig. 4. Comparison of effective diffusion coefficients for Cl^- between blast furnace slag blended and ordinary cement hardened pastes.

blends at 60°C cured over 90 days. D_{eff} values are smaller than for the neat pastes. Porosimetry results indicate that the porosity and pore sizes of the Min-U-Sil blended pastes at 60°C are smaller than those for comparable neat pastes. The higher temperature of 60°C, compared to 27° or 38°C, apparently results in a reaction of the crystalline silica with the portland cement to produce a more dense structure resulting in a retardation of the diffusion of ions across the matrix. Since silica fume is amorphous it reacts with calcium hydroxide from the cement at the lower temperature of 27° to produce the denser structure but Min-U-Sil, being crystalline, requires thermal activation and prolonged curing to create the fine structure and low porosity required to diminish ion migration rates. On this basis it is suggested that portland cement blended with siliceous pozzolanas or mineral admixtures will result in a denser pore structure and it is a question of temperature and time before which the blended material is able to effectively retard the diffusion of ions (14).

In the studies with fly ashes the diffusion of Cl^- is extremely low in fly ash blends compared with neat paste at relatively early ages of 7 and 28 days at temperatures of 38° and 60°C while it is comparable at 27°C. The D_{eff} for Cs^+ at 27°C and early ages is higher in the fly ash blends over neat pastes. At 38°C, the fly ash blends retard Cs^+ over the neat paste at 28 days age. At 60°C, the fly ash blends retard Cs^+ over the neat paste. The porosimetry data indicates that the fly ash blends are more porous at all temperatures but have a finer pore size distribution at later ages and higher temperatures. In summary, it is observed that the blending of mineral admixtures with portland cements leads to a modified pore structure generally being of a riner size distribution than in neat pastes. The resulting material is able to retard the diffusion of anions and cations. The effectiveness depends on degree of reaction, and age, temperature and nature of the admixture and the quality used. On this basis it was proposed that a model relating the pore structure, porosity and effective diffusion coefficients be set up. Since the effective diffusion in water saturated media is dependent on the diffusion coefficient at infinite dilution in pure water (D_{th}) a relationship between D_{th} and D_{eff} may be related to porosity and pore sizes. However, additional factors may control the relationship between D_{th} and D_{eff}. Supposing all factors except the area available for ion migration remain the same then the ratio between the theoretical and effective diffusion coefficients is given by

$$\alpha = \frac{D_{th}}{D_{eff}} = \frac{A_{th}}{A_{eff}} = \frac{A_{ac}}{A_p} \qquad (1)$$

Here, A_{ac} is the actual membrane area exposed to the migrating ion while A_p is the cross sectional pore area within the membrane. Secondly, consider an ion moving across a path length X. Assuming Fick's Laws for diffusion apply (3,15),

$$X = k/Dt \qquad (2)$$

is the migration path in time t. If l_{ac} is the actual membrane width while l_p is the average pore length and $[l_p/l_{ac}]$ is the tortuosity, q, of a pore path, or the degree by which the pore path exceeds the actual membrane width. Then

$$\alpha = \frac{D_{th}}{D_{eff}} = [\frac{l_p}{l_{ac}}]^2 = \frac{A_{ac}}{A_p} \cdot q^2 \qquad (3)$$

when all factors excluding pore size and porosity do not affect ionic diffusion.

Now, porosity, ε, is defined as the ratio of the void or pore volume to the actual external volume of the porous medium. Thus

$$\varepsilon = \frac{V_p}{V_{ac}} = \frac{A_p \cdot l_p}{A_{ac} \cdot l_{ac}} = \frac{A_p}{A_{ac}} \cdot q \qquad (4)$$

Combining (3) and (4),

$$\alpha = q^3/\varepsilon \qquad (5)$$

ε is easily obtained for most materials but q is difficult to obtain. Assuming all pores are of the same size and cylindrical, it may be assumed that (16),

$$q = C_a r^{C_b} \qquad (6)$$

r is the 'average' or median pore size and C_a and C_b are constants. Combining (5) and (6),

$$\alpha = [C_a r^{C_b}]^3/\varepsilon \quad \text{or} \quad \alpha = C_1 \varepsilon^{C_2} r^{C_3} \qquad (7a,b)$$

C_1, C_2, and C_3 are constants. The exponent to ε, C_2, has been introduced for correlation between ε and r. The general relationship proposed in equation (7b) between the theoretical, effective and porosimetry parameters was examined for the set of data provided in the table of results. Values for C_a and C_b were generated for the neat portland cement pastes and $C_a = 10.3 \pm 2.6$ and $C_b = -0.41 \pm 0.13$ for Cl^- diffusion and $C_a = 4.6 \pm 2.5$ and $C_s = -0.62 \pm 0.08$ for Cs^+ diffusion were obtained over the temperature range of 27° to 60°C. Considering equation (7b), multivariate regression was used to predict C_1, C_2, and C_3 values. The predicted values of D_{eff} for Cl^- using computed C_1, C_2 and C_3 values were good to within 60-90% of the experimental values over the entire range of materials and temperatures. Using C_a and C_b values to predict a tortuosity, q, and then compute D_{eff} for Cs^+ or Cl^- yielded fair results. The computed and experimental values at lower temperatures for Cl^- were within a factor of 2 though the values were more random at 60°C. The correlations for Cs^+ were not as good but in all cases the experimental and computed D_{eff} values were within a factor of three, in good agreement, as the range of D_{eff} values for Cl^- range over three orders of magnitude and that for Cs^+ over four (12).

CONCLUSIONS

The porosity and pore size distribution of a hardened portland cement paste have considerable influence over the ionic diffusion characteristics of the matrix. The possible model and the actual relationship have been outlined above. The simple method to measure the diffusion of ions across hardened cement pastes has provided reasonable insight into the mechanisms of diffusion. The cation is generally retarded as compared to the anion and the portland cement matrix may thus be considered an electronegative membrane. The use of low water contents and blending with mineral admixtures leads to lower ionic diffusion. The use of small quantities of amorphous siliceous admixtures is rather advantageous even at room temperature but higher temperatures are required so as to generate sufficient activation for reaction and pore structure modification when using crystalline or mineral admixtures. Low cost sealing materials may be designed using blast furnace slag or fly ash where high levels of portland cement replacement are possible yet yielding low diffusion matrices.

ACKNOWLEDGEMENTS

The authors acknowledge support of NSF grants CPE-8112821 and DMR 8418160. Thanks are due to Mr. S. Atkinson for solution analyses and Dr. W.P. Freeborn for assistance in experimental design.

REFERENCES

1. P.K. MEHTA and D. MANMOHAN, Proc. 6th Int. Congr. Chemistry of Cement, Vol. III, Theme VII, 1-5, Editions Septima, Paris (1980).
2. B.K. NYAME and J.M. ILLSTON, Proc. 6th Int. Congr. Chemistry of Cement, Vol. III, Theme VI, 181-185, Editions Septima, Paris (1980).
3. H. USHIYAMA and S. GOTO, Proc. 6th Int. Congr. Chemistry of Cement, Moscow, 2(1), 331-337, Stroyizdat, Moscow (1974).
4. S. GOTO and D.M. ROY, Cem. Concr. Res. 11(5), 751-757 (1981).
5. C.L. PAGE, N.R. SHORT, and A. EL TARRAS, Cem. Concr. Res. 11, 395-406 (1981).
6. Handbook of Electrochemical Constants, R. Parsons, Butterworths Scientific Publications, Table 79, 85 (1959).
7. H.G. MIDGLEY and J.M. ILLSTON, Cem. Concr. Res. 14, 453-614 (1984).
8. H.G. SMOLCYZK, Betonwerk und Fertigteil-Technik, Heft 12, page numbers unknown (7 pp.) (1984).
9. A. ATKINSON and A.K. NICKERSON, AERE Harwell, DOE Report No. DOE/RW/83, 137 pp.
10. K. ANDERSSON, B. TORSTENFELT, and B. ALLARD, Scientific Basis for Nuclear Waste Management 3, 235-242, Ed. J.G. Moore, Plenum Press, NY (1981).
11. R. HEITANEN, T. JAAKOLA, and J.K. MIETTINEN, 8th Int. Symp. Scientific Basis for Nuclear Waste Management, Boston, MA (Nov. 26-30, 1984).
12. A. KUMAR, Diffusion and Pore Structure Studies in Cementitious Materials, PhD Thesis in Solid State Science, The Pennsylvania State University, University Park, PA 16802 (1985).
13. P.K. MEHTA and O.E. GJØRV, Cem. Concr. Res. 12(5), 587-595 (1981).
14. D.M. ROY and K.M. PARKER, Proc. CANMET/ACI 1st Int. Conf. on the Use of Fly Ash, Silica Fume, Slag and Other Mineral By-Products in Concrete, Vol. I, 397-414, ACI SP-79, Ed. V.M. Malhotra, ACI, Detroit (1983).
15. M. COLLEPARDI, A. MARCIALIS, and R. TURRIZIANI, J. Am. Ceram. Soc. 55(10), 534-535 (1972).
16. P.V. PATEL and J.B. BUTT, Industrial Engineering Chemistry, Proc. Des. Dev. 14(3), 298-304 (1975).
17. A. KUMAR and D.M. ROY, J. Am. Cer. Soc. (1986).

Dr.-Ing. George TEODORU, Cologne, West Germany
Chargé de Cours à l'Ecole Supérieure
des Sciences Appliquées de Cologne

Influence des conditions de durcissement sur la durabilité de la pâte de ciment et du béton

Influence of hardening conditions on the durability of cement paste and concrete

RESUME: L'étude présente les recherches sur des composants minéralogiques purs du ciment Portland, sur des ciments et bétons, en vue d'expliquer la contradiction entre très hautes résistances mécaniques obtenues à la fois avec de très basses vitesses de propagation des ultrasons sur des bétons ayant durci à l'autoclave.
Les résultats viennent compléter les recherches précédentes /2/ sur des suspensions de ciment, sections minces et sections polies, et d'autre part à l'aide du microscope électronique sur des "répliques" contrastées avec du platine.
Afin d'obtenir des informations basées sur une répartition aléatoire des phénomènes remarqués à microéchelle, en dehors des mesures de vitesse et atténuation des ultrasons, on a recouru à des critères de durabilité, basés sur la variation du module d'élasticité dynamique et du décrément logarithmique.
On peut conclure qu'une haute résistance mécanique n'est pas un indice suffisant pour un béton durable mais c'est surtout sa structure qui est déterminante, et pour le béton autoclavé, cette structure possède plus de défauts que dans le cas du durcissement dans des conditions standard.

Sumário: O estudo apresenta as pesquisas sobre os componentes mineralógicos puros do cimento portland, sobre os cimentos e concretos, tendo em vista explicar a contradição entre muito altas resistências mecânicas obtidas ao mesmo tempo com baixas velocidades de propagação de ultrasons sobre concretos endurecidos em autoclave.

Os resultados vêm completar as pesquisas precedentes (2) sobre suspensões de cimento, seções delgadas e seções polidas, e por outro lado com auxílio do microscópio eletrônico sobre "réplicas" com contraste de platina.

Afim de obter informações baseadas numa repartição aleatória dos fenômenos notados em microescala, além das medidas de velocidade e atenuação dos ultrasons, recorreu-se à critérios de durabilidade, baseados sobre a variação do módulo de elasticidade dinâmico e do decréscimo logarítmico.

Pode-se concluir que uma alta resistência mecânica não é um índice suficiente para um concreto durável mas é sobretudo a sua estrutura que é determinante, e para o concreto autoclavado, esta estrutura possui mais defeitos que no caso de endurecimento em condições normais.

1. INTRODUCTION

La durabilité du béton dépend de sa structure physique, de sa composition chimique et elle diffère par rapport à la nature du milieu environnant qui exerce des actions destructives mécaniques-physiques et chimiques après la mise en service du bâtiment. L'évolution de la structure hétérogène du béton dans le temps est longue.Cette évolution est fort influencée par la composition minéralogique du liant utilisé. C'est pour cela que l'étude microscopique est commencée au niveau de ces composants. Basé sur des études précédentes /1/, on a choisi pour conditions de durcissement, l'autoclavage.

2. RECHERCHES MICROSCOPIQUES

2.1. Le silicate tricalcique

Les fig. 1 et 2 montrent l'aspect de l'hydratation du silicate tricalcique dans une suspension aqueuse à 20°C, l'une après 45 minutes, l'autre après 24 h. Dès le commencement on constate que les particules réagissent avec l'eau et à leur surface commence une cristallisation. Après 24 h,de grands cristaux d'hydroxyde de calcium sont à signaler dans la phase aqueuse et plus petits à la périphérie des granules, cristaux ayant un contour arrondi, parfois fragmentés, rarement un contour parfait.

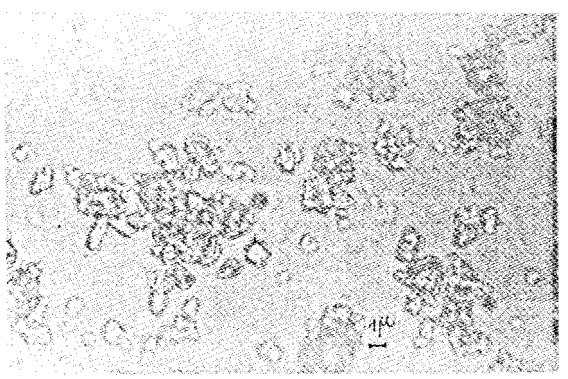

Fig. 1 Suspension de silicate tricalcique après 45 min. à 20°C.

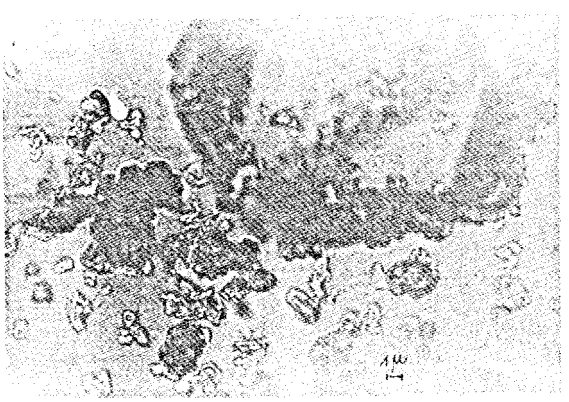

Fig. 2 Suspension de silicate tricalcique après 24 h à 20° C.

Les particules de silicate tricalcique sont entourées des films de nouveaux silicates hydratés, à ce moment très dispersés, invisibles au microscope optique, contenant moins d'oxyde de calcium que le silicate d'origine /1/. La fig. 3 présente l'aspect de la suspension de silicate tricalcique après autoclavage. Il est caractéristique après 6 h la formation de grands "éventails" vigoureux ayant comme point de départ les granules de silicate tricalcique.Le champ reste presque vide, ou peuplé par de petits fragments.

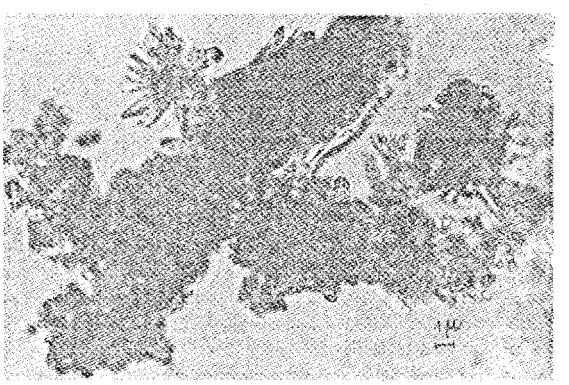

Fig. 3 Suspension de silicate tricalcique 6 h après autoclavage à 185° C.

Le développement des cristaux après traitement est réduit, le processus étant presque terminé à ce moment-là. On a remarqué,et la fig. 3 confirme cela, la présence dans les suspensions après l'autoclavage de moins nombreux cristaux de portlandite.

2.2 Le silicate dicalcique

La fig. 4 montre la suspension de silicate dicalcique hydratée à 20° C, très semblable aux fig. 1 et 2. Les cristaux d'hydroxyde de calcium y sont aussi présents.

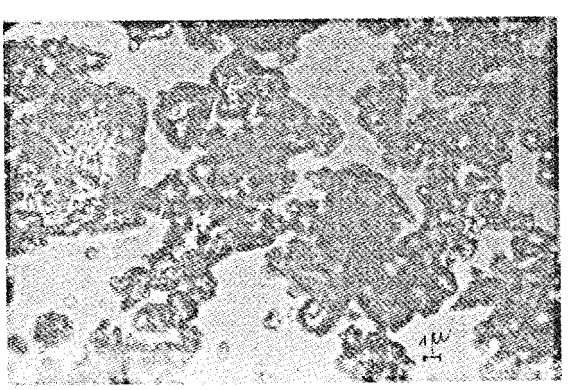

Fig. 4 Suspension de silicate dicalcique après 45 min. à 20° C.

Les fig. 5 et 6 présentant la suspension de silicate dicalcique l'une après 6 h,l'autre après 24 h, montrent que l'autoclavage a fortement augmenté la vitesse d'hydratation, plus que dans le cas du silicate tricalcique. C'est une constatation qui est confirmée

aussi par l'action favorable de l'autoclavage sur les résistances en compression par rapport aux résistances à 28 jours de durcissement des pâtes de silicate dicalcique pur. Dans le cas des pâtes de silicate tricalcique pur on avait enregistré le contraire: les résistances en compression après autoclavage sont inférieures à celles obtenues après 28 jours de durcissement normal /2/.

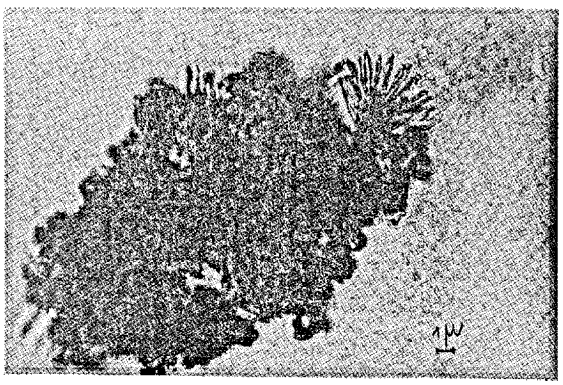

Fig. 5 Suspension de silicate dicalcique 6 h après autoclavage à 185° C.

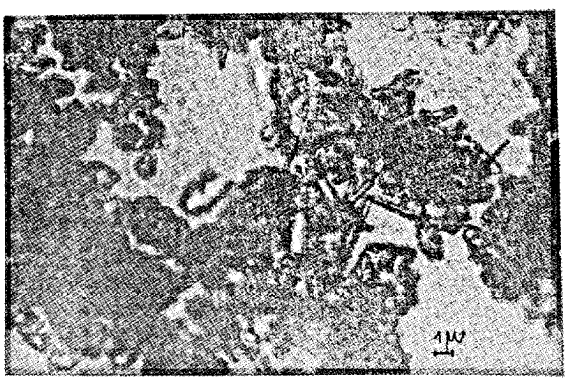

Fig. 6 Suspension de silicate dicalcique 24 h après autoclavage à 185° C.

2.3 L'aluminate tricalcique

La comparaison des fig. 7 et 8 faites l'une après 45 min. et l'autre après 6 h à 20° C



Fig. 7 Suspension d'aluminate tricalcique après 45 min. à 20° C.

sur une suspension d'aluminate tricalcique avec les fig. 9 et 1o prises après autoclavage, montre l'effet défavorable de ce traitement freinant l'hydratation. Les résistances en compression après autoclavage étaient

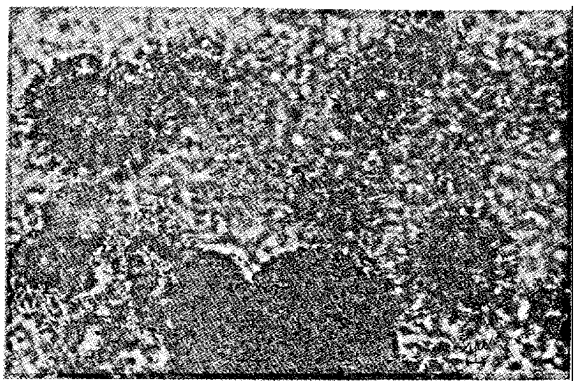

Fig. 8 Suspension d'aluminate tricalcique après 6 h à 20° C.

presque nulles /2/. Intéressant est la présence des couches successives de néoformations (fig.8) autour des granules d'aluminate tricalcique qui parlent aussi pour une très grande vitesse de réaction avec l'eau. A mesure que la température s'accroit, les aluminates de calcium hydratés deviennent instables et se transforment dans des produits

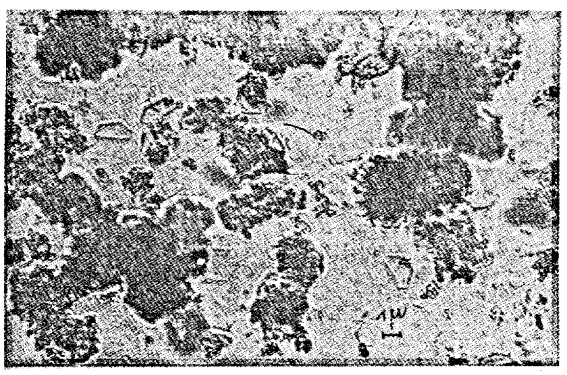

Fig. 9 Suspension d'aluminate tricalcique 6 h après autoclavage à 185° C.

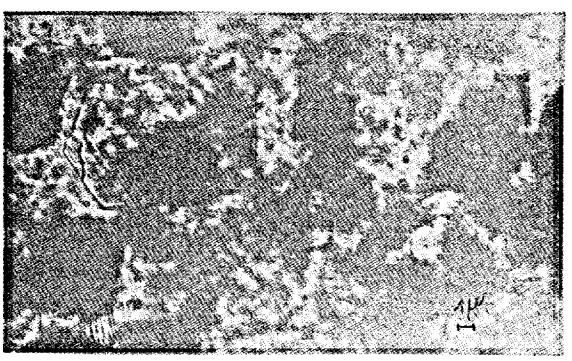

Fig. 1o Suspension d'aluminate tricalcique 24 h après autoclavage à 185° C.

moins riches en oxyde de calcium ce qui amène la cristallisation des quantités appréciables d'hydroxyde de calcium. Ce fait semble être bien mis en évidence par la fig.10. Du point de vue structure (mise en évidence par la vitesse de propagation des ultrasons) et résistance en compression,l'influence la plus défavorable est exercée par l'autoclavage sur l'aluminate tricalcique (tableau I en /2/).

2.4 L'aluminoferrite tétracalcique

Sous le traitement en autoclave l'aluminoferrite tétracalcique s'hydrate plus intensément que dans le cas du durcissement à 20° C et donne de grandes quantités d'hydroxyde de calcium et d'hydroxyde de fer.

2.5 Suspensions de ciment

Les résultats ci-dessus sont obtenus sur les substances chimiques pures isolées, tandis que les composants minéralogiques du clinker de ciment sont des solutions solides, dans lesquelles prédomine un certain composant chimique (silicate tricalcique/dicalcique, aluminate tricalcique ou aluminoferrite tétracalcique). Dans le ciment ces composants minéralogiques ne se trouvent pas isolés mais tous ensemble, et l'hydratation se produit en présence des quantités assez importantes de gypse - qui influence surtout la réaction des aluminates - et des alkalis. Pour cela, on a poussé les recherches à l'aide du microscope optique sur des suspensions de ciment, sections minces et sections polies et d'autre part, à l'aide du microscope électronique sur des "répliques" contrastées avec du platine. Les fig. 11 et 12 présentent l'aspect typique de la suspension de ciment RIM 200 (un ciment à HRI) traitée à 90° C après 4 h par comparaison avec la même suspension traitée en autoclave, après 72 h.

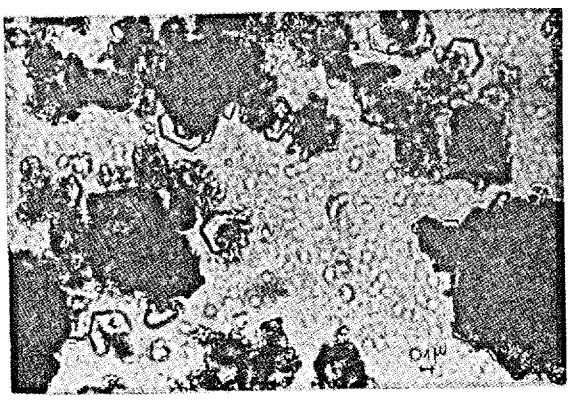

Fig. 11 Suspension de ciment RIM 200, 4 h après traitement à 90° C.

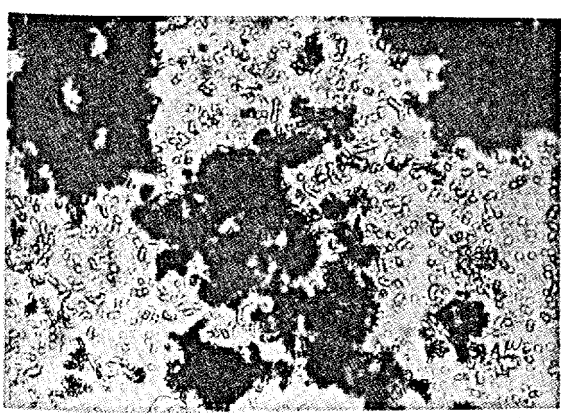

Fig. 12 Suspension de ciment RIM 200 72 h après autoclavage à 185° C.

3. ESSAIS A ULTRASONS

Quoiqu'on se donne toujours la peine de saisir des aspects représentatifs de la structure examinée, par suite du champ réduit de l'examen microscopique - surtout celui du microscope électronique - les conclusions tirées sur la structure et les résistances des pâtes de ciment n'ont qu'une valeur limitée, pour le béton encore plus limitée, parce que la fraction fine du granulat peut modifier profondément les propriétés du ciment. Cette modification est tellement profonde, que dans le béton ne se trouve plus le ciment initial, mais un ciment composé, dont les propriétés diffèrent de celles du ciment simple. C'est pour cela qu'on a utilisé aussi une méthode capable à donner des informations plus globales sur un grand volume de béton caractérisé par une répartition aléatoire des phénomènes remarqués à microéchelle. A l'aide de la vitesse de propagation longitudinale et atténuation des ultrasons on a obtenu des indications qualitatives et quantitatives sur la structure des bétons traités à l'autoclave /3/ qui laissent entrevoir l'existence des défauts de structure. Basé sur ces essais, on a pu conclure que les très grandes résistances en compression (70-90 N/mm^2) obtenues pour le béton autoclavé en même temps avec de basses vitesses des ultrasons (3,5-3,9 km/sec tandis que pour le béton durci dans des conditions normales les vitesses sont de l'ordre de 4,5-4,9 km/sec) ne sont pas à expliquer seulement par la porosité ou par la répartition dimensionelle des pores (taille plus petite des pores pour les résistances plus élevées) /4/.

4. ESSAIS DE DURABILITE

Les recherches ont porté sur la détermination sur des prismes de béton 10x10x55 cm^3 après saturation à l'eau,de la variation du:

- module d'élasticité dynamique (E_d) par l'excitation des oscillations longitudinales
- décrément logarithmique (δ_1) des oscillations forcées de la courbe de résonance (par mesurage de la largeur de bande pour $A = 0,5, A_r$ et $A = 0,707 A_r$)
- décrément logarithmique (δ_2) des oscillations libres mesuré de la courbe de décroissance des amplitudes,

suite à l'exposition aux cycles de gel-dégel.

Dans la méthode basée sur le décrément logarithmique, on avait déjà établi un critère de durabilité /5/: un béton doit être considéré comme résistant aux "x" cycles de gel-dégel, si:

(1) $$\frac{\delta x}{\delta o} \leqslant 1{,}50$$

A cause de l'espace, de tous les résultats obtenus on présente seulement le comportement de deux compositions de béton traitées à l'autoclave (A1 et A2) et durcies dans des conditions standard (S1 et S2), c'est-à-dire 7 jours dans l'eau et 21 jours à l'air (20°C et 65 % humidité relative).

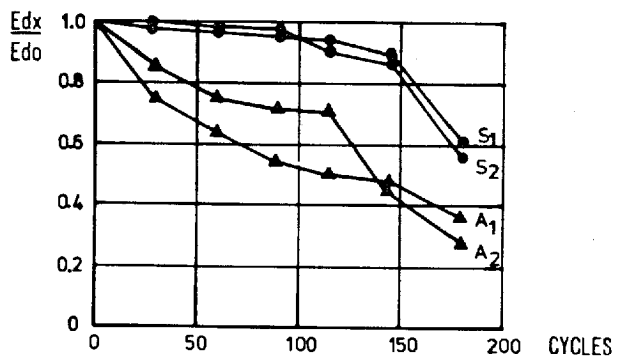

Fig. 13 Variation de $\frac{Edx}{Edo}$ fonction des cycles de gel-dégel.

Le critère accepté pour la variation du module d'élasticité dynamique est:

(2) $$\frac{Edx}{Edo} \geqslant 0{,}85$$

Le module d'élasticité dynamique après "x" cycles de gel-dégel ne doit pas marquer des pertes plus grandes que 15 % par rapport à la valeur initiale après 28 jours de durcissement et saturation dans l'eau afin de prouver la gélivité Gx. La fig. 13 montre pour le béton standard une gélivité G150 tandis que pour celui autoclavé à peine G25.

5. CONCLUSIONS

a) Les recherches microscopiques sur les composants minéralogiques purs ont mis en évidence que l'autoclavage exercite une influence favorable sur leur vitesse d'hydratation à l'exception de l'aluminate tricalcique. L'influence la plus favorable semble correspondre pour le silicate dicalcique. Ces faits sont d'ailleurs confirmés par les résistances mécaniques et vitesses des ultrasons (tableau I /2/).

b) Les recherches microscopiques sur des ciments ont montré pour l'autoclavage que les formations cristallines possèdent des dimensions beaucoup plus petites que celles obtenues par les traitements hydrothermiques sans pression et par conséquent un grand degré de dispersion, ce qui mène à un haut niveau d'énergie potentielle de surface (voir aussi les recherches à l'aide du microscope électronique en /2/).

c) L'effet favorable de l'autoclavage sur le béton se manifeste par l'activation du SiO_2 du sable fin quartzeux, avec formation de plus grandes quantités de CSH-phases de basicité réduite du type tobermorite ayant de meilleures qualités liantes que les phases à haute basicité. En même temps la quantité de portlandite libre est plus réduite ce qui laisse entrevoir un meilleur comportement du béton autoclavé à l'agression chimique. La liaison du SiO_2 du granulat avec les CH, CSH du ciment a, dans le cas de l'autoclavage, un caractère chimique, témoigné par le fait que, contraire aux bétons durcis dans des conditions standard, l'humidité n'influence plus les résistances mécaniques.

Les vitesses élevées des ultrasons pour le béton durci dans des conditions standard sont à attribuer aux néoformations jouissant dans ce cas d'une compacité élevée qui améliore la transmission acoustique mais pas les résistances mécaniques.

On peut conclure qu'une haute résistance mécanique du béton autoclavé n'est pas un indice suffisant pour un bon comportement au gel-dégel, mais c'est sa structure surtout qui est déterminante.

6. BIBLIOGRAPHIE

1.- G. TEODORU (1983) "Einfluß der Hydrothermalbehandlung auf den Beton", Zement-Kalk-Gips International Nr. 1 pp. 35-42.

2.- G. TEODORU (1980) "Structures et résistances mécaniques sous des traitements hydrothermiques", 7e Congrès de la Chimie des ciments, Paris vol. IV pp. 318-323.

3.- G. TEODORU (1984) "Is Compactness of Hydrothermally-Treated Concrete Less Important?", Fall Convention of ACI, Open Session, New York, Concrete International Nr. 10 p. 68.

4.- G. TEODORU (1985) "Mechanical Strength-Property of Concrete at Early Ages as Reflected by Schmidt Rebound Values, Ultrasonic Pulse Velocity and Ultrasonic Attenuation", Symposium "Properties of Concrete at Early Ages", Chicago p. 53.

5.- G. TEODORU (1984) "A New Durability Criterion", 3e Colloque International sur la durabilité des matériaux et des éléments de construction, Helsinki vol. 3 pp. 411-421.

On the Distribution of Chloride between the Hardening Cementpaste and Its Pore Solution

4.1

Investigation of the liquid phase of setting and hardening cementpastes under influence of chloride. Extraction of pore solution by compressing hardened cementpastes at pressures up to 500 N/mm^2 (MPa). Investigation of the influences of the type of chloride salt, and the time of hydration on the binding of chloride to the hydration products of several portland cements and blastfurnace slag cements, and of the pure cementminerals C_3S and C_3A.

While the high concentration of the sulfateions and calciumions, which dominate in the solution at the first time of hydration disappear from the liquid phase during the time between 6 hours and 2 days, the alkalies of the cement dissolve furtheron as hydroxide hereby rising the pH up to values of more than 13.0. The liquid phase of the hardened cementpaste then consists of a strong alkalihydroxide solution containing low residual concentrations of calcium and sulfate and the unbound proportion of free chloride.

The binding of chloride is determined markedly by adsorption processes. C_3A and granulated blastfurnace slag as cement-components promote the chloride binding. But more essential is the influence of other parameters such as the amounts of alkali and sulfate in the hardened paste and the quantity and the type of the influencing chloride.

SUMÁRIO

É investigada a fase líquida durante a pega e endurecimento de pastas de cimento sob a influência de cloretos. Extração da solução existente nos poros através de compressão das pastas endurecidas de cimento com pressões de até 500 N/mm^2 (MPa) é realizada. São investigadas as influências dos tipos de cloreto, e o tempo de hidratação para a união dos cloretos aos produtos de hidratação dos diversos cimentos portland e cimentos com escória de alto forno, e dos minerais puros C_3S e C_3A.

Enquanto a alta concentração de ions de sulfato e cálcio, que dominam na solução durante as primeiras horas de hidratação, desaparecem da fase líquida durante o tempo entre 6 horas e 2 dias, os álcalis do cimento dissolvem-se como hidróxido portanto aumentando o pH até a valores superiores a 13,0. A fase líquida da pasta de cimento endurecida então consiste de uma forte solução álcali-hidróxido contendo baixas concentrações residuais de cálcio e sulfato e uma porção não ligada de cloretos livres.

A ligação dos cloretos é determinada marcadamente pelo processo de absorção. C_3A e escória granulada de alto forno como componentes do cimento promovem a ligação dos cloretos. Entretanto, mais essencial é a influência de outros parâmetros tais como o aumento de álcali e sulfato na pasta endurecida e a quantidade e tipo de cloreto existente.

Particularly in cementpaste containing chloride the composition of pore solution is very important for the protection of the reinforcement against corrosion. Even though a considerable part of chloride is bound by the hardened cementpaste /1/, it should be assumed that in the pore solution a remnant remains dissolved which, however, can cause a considerable concentration because of the little quantity of this solution. In the course of setting and hardening the hydration processes cause far-reaching changes in the liquid phase of the hardening cementpaste. Only since it has been achieved to squeeze this pore solution out of the hardened cementpaste at pressures up to 500 N/mm² /2/ the composition of the liquid phase during the whole hydration process could be investigated /3/4/.

Fig. 1 and 2 demonstrate the typical process of concentrations as it was found in the pore solution of hardening cementpaste during a period up to one year /4/.

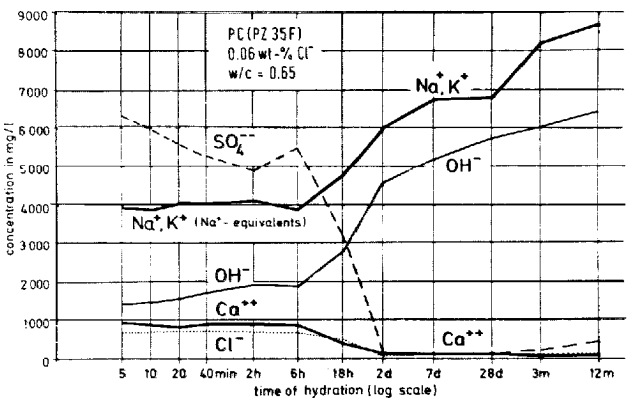

Fig. 1: Composition of the pore solution of the paste in relation to the time /4/

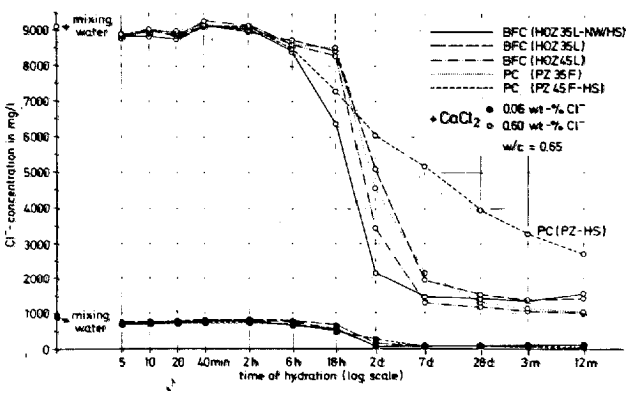

Fig. 2: Concentration of chloride in the pore solution of the paste in relation to the time /4/

Whereas during the time between 6 hours and 2 days the concentrations of SO_4^{--}, Ca^{++} and Cl^- (0.06 wt-%) nearly disappear the alkali- and OH-ions continue to dissolve and the pH-value rises up to more than 13.0. So the pore solution of the hardened cementpaste is a strong 0.2 n to 0.4 n alkalihydroxide solution in which KOH dominates. According to its low solubility in alkalihydroxide solution $Ca(OH)_2$ exists in traces only. Except from the available amount of water (w/c-value, degree of hydration) the alkalinity of the pore solution is dependent on the content of soluble alkalies in the cement. It is important for the protection of the reinforcement against corrosion that the high alkalinity of the relative low quantitiy of pore solution is preserved by the much larger available supply of CaO in the hardening cementpaste.

Whereas the chloride that is bound during the hydration can be investigated by means of the analysis of pressed out pore solution, it is more difficult to establish the amount of bound chloride that later on has been penetrated into the hardened cementpaste. Fig. 3 shows that chloride penetrates hardening cementpaste only very slowly. Blastfurnace slag cements with more than 40 wt-% granulated slag (H 40 to H 70) prove to have an extraordinarily high diffusional resistance against chloride /5/. Furthermore the figure demonstrates that the amount of penetrated chloride decreases constantly with the depth of penetration.

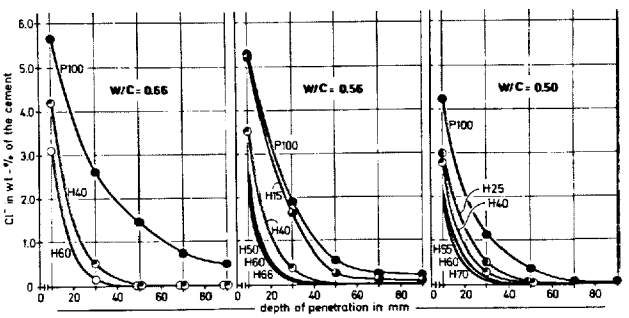

Fig. 3: Distribution of chloride in concretes after a storage of 1 year in a 3 molar NaCl solution /5/
(P 100 = PC, H 15 to H 70 = cements containing indicated contents of granulated blastfurnace slag)

To avoid a concentration gradient during the investigation of the dissolved and bound chlorides the routes of diffusion had to be kept as short as possible. This can be obtained by storing hardened cementpaste after hydration for 28 days in a crushed state (0.5 to 1 mm) in a solution of chloride.

4.1

Experiments

Several portland and blastfurnace slag cements as well as the pure clinker minerals C_3S and C_3A were investigated. The C_3A was mixed with $CaSO_4.2H_2O$ and $Ca(OH)_2$ in the mole ratio 1 : 1 : 0.3. The cements or the clinker minerals were treated to pure pastes and hydrated for 28 days. The w/c-value was 0.60 for the cements and the C_3S and 0.90 for the mixture of C_3A. The chloride contents varied between 0.2 and 3.0 wt-%, referring to material without loss of ignition.

According to the two kinds of chloride influence on the cementpaste - during the hydration and in a later on diffusion - two different attempts were made:

1) The addition of the chloride to the mixing water and the analysis of the dissolved chloride in the pressed out pore solution (pore solution tests).

2) Crushing and screening of test specimens free from chloride to a grain size of 0.5 to 1 mm, storage of the granulated material in a solution of chloride for 28 days, investigation of the bound chloride by measuring the decrease of the concentration of chloride in this solution (diffusion tests).

The testing parameters are described in Tab. 1. The cements in this table are a German "PZ 35 F" with 10 wt-% C_3A (PC) and a German "HOZ 35 L" with 66 wt-% granulated blastfurnace slag (BFC).

material	w/c	age	salt	influence of the chloride: before hardening	influence of the chloride: after hardening
C_3A + gypsum + $Ca(OH)_2$ 1 : 1 : 0.3 mole ratio	0.90	28 days	$CaCl_2$ and NaCl	chloride in the mixing water	storing of granulate 0.5 to 1mm in Cl^--solution
C_3S	0.60				
PC	0.60			(pore solution tests)	(diffusion tests)
BFC	0.60				

Tab. 1: Test parameters

Results

Fig. 4 and 5 show the content of bound chloride in dependence on the given total chloride of the clinker minerals and the two cements. The contents refer to material without loss of ignition. The dotted straight lines represent the values which would be obtained if the whole chloride is bound.

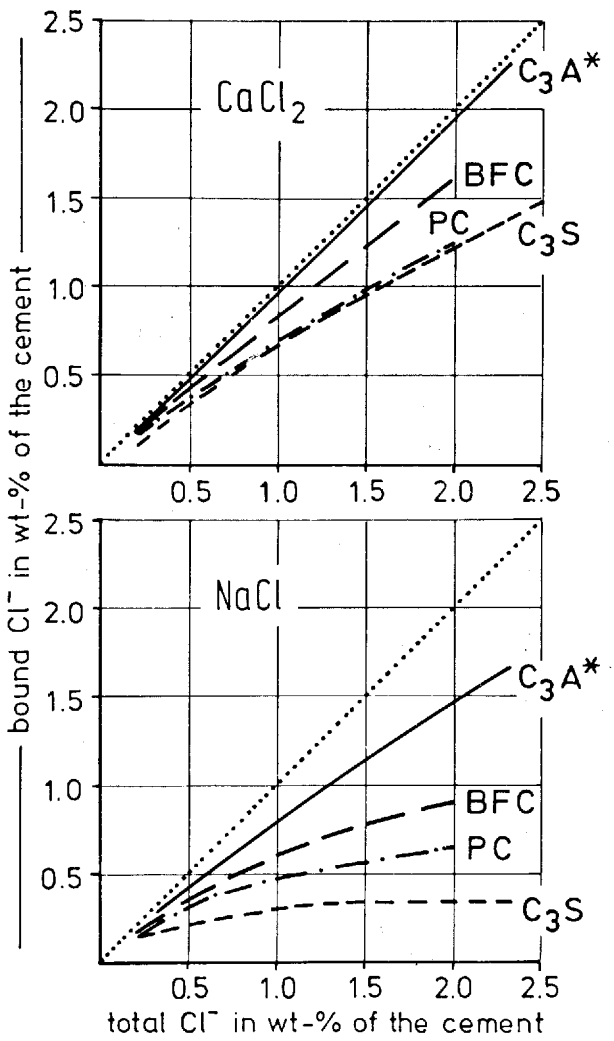

Fig. 4: Pore solution tests
Relation of the bound chloride to the total content of chloride
* Mixture with $CaSO_4.2H_2O$ and $Ca(OH)_2$

The mixture of C_3A binds most chloride in all experiments. This very high binding capacity of the aluminate depends on the chemical reaction to poorly soluble Friedels' salt $C_3A.CaCl_2.nH_2O$ /6/. In this special case Friedels' salt formed mixed phases with other hydrates of the family of the AFm-phases (aluminatehydrate-monophases) /7/, as the x-ray investigation showed. The experiments with C_3S prove that the chloride in the cements is bound not only chemically by the aluminates but also to a high extent by silicatehydrates. In this case mainly adsorption processes have to be assumed. Accordingly the chloride binding of the cements ranges between the clinker minerals C_3A and C_3S, that means chloride is bound by the hardening cementpaste by means of poorly soluble aluminates as well as by binding to the silicatehydrates.

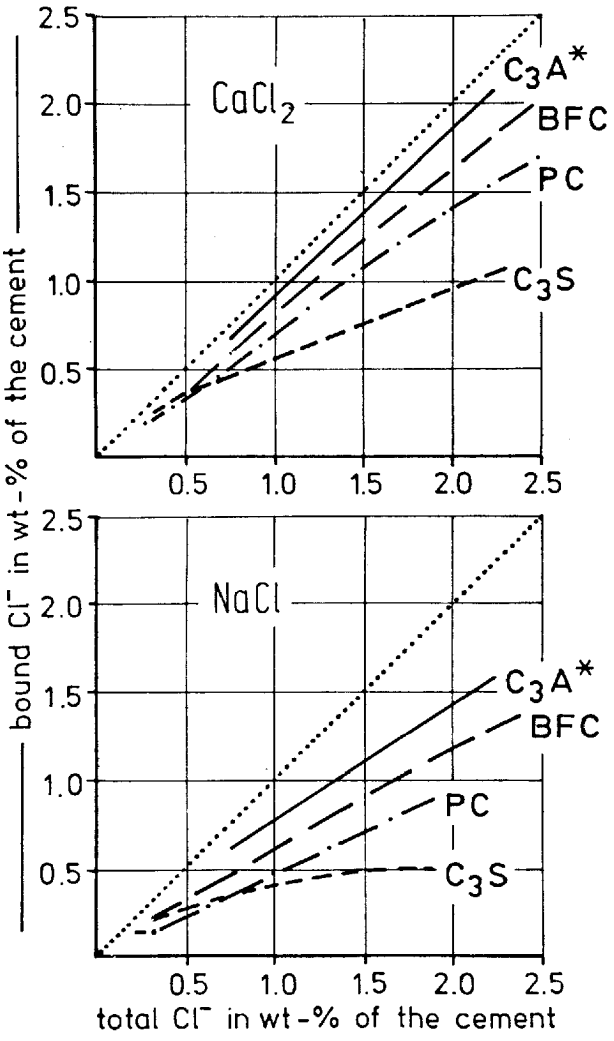

Fig. 5: Diffusion tests
Relation of the bound chloride to the total content of chloride
* Mixture with $CaSO_4.2H_2O$ and $Ca(OH)_2$

In the range of lower contents up to 1 wt-% Cl^- the different types of reaction of the chloride, that is the reaction during the hydration or the reaction depending on the later on diffusion into the hardened paste, have only little influence on the chloride binding of the investigated cements or clinker minerals. For higher contents up to 2 wt-% the binding capacity of the cements and C_3S for NaCl during the hydration (pore solution tests) decreases considerably in comparison with the later on reaction (diffusion tests). This can also be seen in the strongly flatening curves for both cements during the pore solution tests with NaCl. For $CaCl_2$ this tendence can to a less degree only be recognized for the PC. In contrast to the cements C_3S and the mixture of C_3A are found to bind even a little more chloride from $CaCl_2$-solution during hydration than in a later on influence.

As also stated by other authors /8/9/ the content of bound chloride and thereby also the composition of the pore solution are to a great extent dependent on the type of reacting salt. Fig. 4 and 5 show that in all investigated samples less chloride was bound from NaCl-solutions than from $CaCl_2$-solutions. According to the type of influence C_3S binds not more than 0.3 or 0.5 wt-% Cl^- from NaCl-solution. For the $CaCl_2$-solutions the inclination of the curves proves that the binding capacity of C_3S up to 1 wt-% bound chloride is not yet exhausted. Accordingly in the presence of NaCl more chloride remains in solution than in the presence of $CaCl_2$. At the same time, however, the pH-value of the pore solution - in contrast to the solution without chloride - is increased by NaCl and decreased by $CaCl_2$. Tab. 2 demonstrates the ranges of Cl^-- and OH^--concentrations, which remain in the pore solutions if 1.0 wt-% Cl^- is added to the mixing water.

materials	w/c	added chlorides					
		$CaCl_2$			NaCl		
		Cl^- mg/l	OH^- mg/l	Cl^-/OH^-	Cl^- mg/l	OH^- mg/l	Cl^-/OH^-
C_3A + gypsum	0.90	800	1300	0.7	4900	8800	0.6
BFC	0.60	3400	2800	1.2	7900	6400	1.2
PC	0.60	7700	4200	1.8	12400	9100	1.4
C_3S	0.60	7600	500	15.2	15200	1700	8.9

Tab. 2: Cl^- and OH^--concentrations in the pore solutions of the specimens with 1.0 wt-% Cl^- in the cement after 28 days hydration.

According to other authors /10/11/ not only the value of chloride concentration is important for the steelcorrosion but the relation of Cl^-/OH^-. Only if the value of 1.2 is surmounted, corrosion has to be taken into consideration. As the ratios of Cl^-/OH^- in table 2 demonstrate the disadvantage of higher chloride concentrations for NaCl with regard to corrosion processes is thus balanced by the higher alkalinity. The corrosion effect of $CaCl_2$-solution accordingly has to be regarded either as the same or even as less favourable.

The test results show that there is no limit to the critical chloride content valid for all cements, below which the whole chloride were bound and therefore corrosion induced by chloride were not to be expected. In contrast to this chloride is never completely bound and thereby removed from the pore

solution but there always remains a low residual concentration that also increases with increasing content of total chloride. In Fig. 6 the development of chloride concentrations in the pore solution with increasing total content of $CaCl_2$ is shown (pore solution test). The dotted line shows the concentrations which would be obtained if all chloride remains in solution. Even for low total contents no range is recognizable for the cements where a constantly low concentration indicates the formation of the poorly soluble Friedels' salt, as it is the case for the mixture of C_3A for contents up to 2.0 wt-%, with regard to the mixture. The only possible explanation is that the surely existing chemical binding during the formation of Friedels' salt is overlapped by the adsorbative binding to the silicatehydrates.

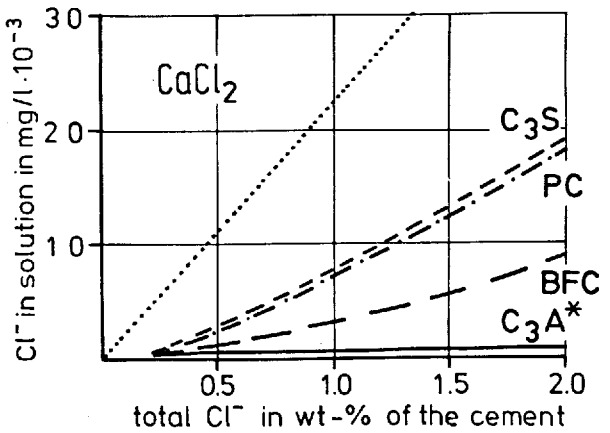

Fig. 6: Pore solution tests
Concentration of chloride in the pore solution in relation to the total content of chloride
*) Mixture with $CaSO_4.2H_2O$ and $Ca(OH)_2$

The higher chloride concentrations of pore solutions in the presence of higher concentrations of hydroxylions point to a negative influence of OH^--ions on the chloride binding, whereby the concentration of OH^--ions depends decisively on the content of dissolved alkali of the cementpaste. This influence obviously can be stronger than the negative influence of the sulfate /9/. Tab. 3 shows the influences of equivalent additions of sulfates and alkalihydroxide on the chloride binding respectively the contents of the pore solutions. The values are given for a PZ 35 F with constant addition of 0.4 wt-% Cl^- as NaCl. Compared with the pore solution without addition a calcium sulfate addition increases the soluble chloride only a little. The addition of the equivalent quantity of NaOH, however, increases the soluble chloride by about one third. Finally when Na_2SO_4 is added the dissolved chloride is even doubled. Since both additions, Na_2O and Na_2SO_4, increase the OH^--concentration in the same range it can be assumed that in the case of Na_2SO_4 both anions, OH^- and SO_4^{--}, decrease the binding of chloride. The ratio Cl^-/OH^- nearly stays unchanged.

additions / solution	without addition (only NaCl)	addition to the cement (with NaCl) $CaSO_4$ 1.36 wt-%*)	Na_2O 0.62 wt-%*)	Na_2SO_4 1.42 wt-%*)
Cl^- mg/l	2900	3200	4100	5700
OH^- mg/l	7200	7200	11800	12100
Cl^-/OH^-	0.40	0.44	0.35	0.47

*) 0.10 mol/kg cement

Tab. 3: Cl^- and OH^--concentrations in the pore solutions of a PC with 0.4 wt-% Cl and different additions after 28 days hydration
(w/c = 0,50, NaCl and the other additions in the mixing water)

Discussion

The pore solution of hydrated cement essentially consists of an alkalihydroxide solution with pH-values above 13. Calciumions are to be found in the alkaline solution only in minor remaining concentrations according to the poor solubility of $Ca(OH)_2$ in strong alkalihydroxide solutions.

A high amount of the chloride is bound by the hardened cement paste in a non-corrosive form. Here the type of salt, the soluble alkalies and sulfates of the cement as well as the time of binding are of main influence. Chloride from NaCl-solution is bound less than from $CaCl_2$-solution. Increasing concentrations of OH^- and SO_4^{--} markedly lessen the bound amount of the chloride. Chloride penetrating the hardened cement paste in the range of minor total amounts up to 1 wt-% Cl^- of the cement is bound in similar quantities and in the range of higher amounts, especially in case of NaCl it is even bound in higher quantities than the chloride being introduced before hydration.

In the binding capacity of hardened cementpaste to chloride apart the aluminatehydrates also the silicatehydrates are involved, which bind considerable amounts of chloride too. It can be assumed that in the case of the silicatehydrates the adsorptional binding dominates the chemical binding. A confirmation for the assumption of adsorptional processes is seen in the fact that the concentrations of chloride in

the pore solution of the hardened cement-paste steadily increase with the total amount of chlorid. There is no limit for the concentration which otherwise would indicate the development of a poorly soluble compound by chemical reaction of the chloride.

References

/1/ Richartz, W.: Die Bindung von Chlorid bei der Zementerhärtung
Zement-Kalk-Gips 22 (1969) no. 10, p. 447/456

/2/ Longuet, P., L. Burglen and A. Zelwer: La Phase liquide du ciment hydraté
Révue matériaux construction (1973) no. 676, p. 35/41

/3/ Barneybeck, R. S., and S. Diamond: Expression and analysis of pore fluids from hardened cement pastes and mortars
Cement and Concrete Research 11 (1981), p. 279/285

/4/ Gunkel, P.: Die Zusammensetzung der flüssigen Phase erstarrender und erhärtender Zemente
Beton-Informationen 23 (1983) no. 1, p. 3/8

/5/ Brodersen, H. A.: Zur Abhängigkeit der Transportvorgänge verschiedener Ionen im Beton von Struktur und Zusammensetzung des Zementsteins
Dissertation RWTH Aachen (1982)

/6/ Schwiete, H. E., U. Ludwig and J. Albeck: Bindung von Calciumchlorid und Calciumsulfat bei der Hydratation der aluminatisch-ferritischen Klinkerbestandteile
Zement-Kalk-Gips 22 (1969) no. 5, p. 225/234

/7/ Smolczyk, H.-G.: Die Ettringit-Phasen im Hochofenzement
Zement-Kalk-Gips 14 (1961) no. 7, p 277/284

/8/ Page, C. L., and O. Vennesland: Pore solution composition and chloride binding capacity of silica-fume cement pastes
Matériaux et Constructions 16 (1983) p. 19/25

/9/ Smolczyk, H.-G.: Flüssigkeit in den Poren des Betons - Zusammensetzung und Transportvorgänge in der flüssigen Phase des Zementsteins
Beton-Informationen 24 (1984) no. 1, p. 3/10

/10/ Hausmann, D. A.: Steel corrosion in concrete
Materials Proctection 6 1967 Nov., p. 19/25

/11/ Tuutti, K.: Corrosion of steel in concrete
Cement- och betonginstitutet, forskning 4.82, Stockholm 1982

SUB-THEME/SOUS-THÈME 4.2

Mechanism of cement paste degradation due to chemical and physical processes.

Mécanisme de la dégradation de la pâte de ciment due aux processus chimiques et physiques.

Chairman/Président:

G. G. Litvan
Division of Building Research
National Research Council
Ottawa, Ontario, Canada

Principal Reporter/Rapporteur Principal:

D. M. Roy
Materials Research Laboratory the
Pennsylvania State University
University Park, PA, U.S.A.

ZHAO YUPING, LI DEDONG AND SUN GUOKUANG
Research Institute of Building Materials, Beijing, People's Republic of China

INVESTIGATION INTO THE CARBONATION OF AUTOCLAVED AERATED CONCRETE (AAC)

SUMMARY: IR, XRD, mercury intrusion porosimetry and SEM have been employed to study the behavior of three types (cement-lime-sand, cement-slag-sand and cement-lime-flyash) of AAC carbonated in various environments. The rate of carbonation of different varieties of calcium silicate hydrate is found to be closely related to their crystallinity. The difference in the rate of carbonation of different AAC as determined by IR quantitative analysis is accounted for by the difference in their content of tobermorite and C-S-H.

Different carbonation conditions differ greatly in their influence on the strength property of AAC. Artificial carbonation where R.H. and CO_2 are both high has an adverse effect on the strength of all the three types of AAC. However, exposure in natural environment for one to two years results in an increase in the strength of some of them. Mercury intrusion porosimetry has shown that artificial carbonation of AAC leads to a drop in the percentage of its smaller gel pores and an increase in that of larger ones.

SEM-EDAX shows calcium carbonate builds up in large amounts in the air pores of all the AAC carbonated in high R.H. and high CO_2 environment. However, no such aggregation is observed for samples after two years of outdoor exposure. The authors have ascribed this to the different carbonation mechanisms involved in the varied carbonation conditions.

Com utilização de IR, XRD, porosimetria de intrusão de mercúrio e SEM, estudou-se o comportamento de três tipos de AAC (cimento-cal-areia, cimento-escória-areia e cimento-cal-cinza volante) carbonatados em vários ambientes. Constatou-se que o índice de carbonatação das diferentes variedades de hidrato de silicato de cálcio está estreitamente relacionado com sua cristalinidade. A diferença do índice de carbonatação dos diversos AAC, conforme determinada por análise quantitativa IR, é atribuída à diferença do seu teor de tobermorita e C-S-H.

As condições diferentes de carbonatação variam grandemente em sua influência sobre a propriedade de resistência dos AAC. A carbonatação artificial, em que tanto a umidade relativa como CO_2 são altos, tem um efeito adverso sobre a resistência dos três tipos de AAC. Contudo, a exposição em ambiente natural por um ou dois anos resulta num aumento da resistência de alguns deles. A porosimetria de intrusão de mercúrio mostrou que a carbonatação artificial de AAC leva a uma redução na porcentagem de seus poros menores de gel e a um aumento nos maiores.

SEM-EDAX mostra formação de carbonato de cálcio em grandes quantidades nos poros de ar de todos os AAC carbonatados em ambiente de alta umidade relativa e alto CO_2. Entretanto, tal agregação não é observada em amostras depois de dois anos de exposição ao tempo. Os autores atribuíram isso aos mecanismos diferentes de carbonatação envolvidos nas condições variadas de carbonatação.

ZHAO YUPING, LI DEDONG AND SUN GUOKUANG
Research Institute of Building Materials, Beijing, People's Republic of China

1. INTRODUCTION

An investigation has been conducted on the basis of a research into the autoclaved aerated concrete /1/.

The characteristics of three types of AAC, i.e. cement-lime-sand, cement-slag-sand and cement-lime-flyash in the course of carbonation have been studied. Also, different carbonation conditions are compared with respect to their effect on the properties of AAC.

IR was used to determine quantitatively the amount of $CaCO_3$ in AAC carbonated for different time period. It is concluded that the crystallinity of the hydration products of different types of AAC is chiefly responsible for the difference in their rate of carbonation.

Different carbonation conditions differ greatly in their influence on the strength property of AAC. The strength retrogression of AAC in artificial carbonation is found related to the rate of carbonation.

SEM has revealed that in artificial carbonation where R.H. and CO_2 content are both high calcium carbonate builds up in large amounts in the air pores. Such phenomenon is not observed in samples carbonated in outdoor exposure for two years. This may be ascribed to the difference in the carbonation process involved in the varied carbonation conditions.

2. EXPERIMENTAL

2.1 Materials

Three types of AAC samples were taken from plant products and cut into 10x10x10 cm cubes. The proportion of the samples and their autoclaving pressure are given below.

Type of AAC	Proportion	Autoclaving pressure
cement:lime:sand	12.5:27.5:60	12
cement:slag:sand	18.0:32.0:50	15
cement:lime:flyash	10.0:17.0:70*	8

*with 3% gypsum

2.2 Conditions for carbonation

Samples for strength test in artificial carbonation were placed in a chamber where the relative humidity and CO_2 concentration were conditioned manually.

Samples were also stored in natural environment for strength tests. Year round temp. -20°C — +40°C, relative humidity 41 — 77%.

Other carbonation tests have also been conducted, the conditions of which are given in the text.

2.3 Detecting equipments

X-ray diffractometer — Rigaku D/Max III
SEM-EDAX — Shimazu ASM-SM
Infrared spectrometer — Perkin Elmer 683, Scanning range 4000-200 cm^{-1}
Mercury porosimeter — 3000 atm.

3. RESULTS AND DISCUSSIONS

3.1 The evolution of the hydration products and the structure of AAC in the course of carbonation

The main hydration products of AAC are tobermorite and ill-crystallized C-S-H. In the surroundings containing CO_2 the hydration products decompose, forming calcium carbonate which exists chiefly in the form of calcite. μ-$CaCO_3$ and aragonite are also found in small amounts. XRD is not effective enough to offer information on the whereabout of SiO_2 after the sample has been carbonated. However, infrared spectroscopy may give a clue to its solution.

The kinetic process of the carbonation of AAC was studied using IR. Fig.1 shows the infrared diagrams of a C-L-S AAC sample carbonated in a chamber (R.H. 90%, CO_2 65-90%) for various periods. The shift of the absorbing peak from 965 cm^{-1} to 1045 cm^{-1} indicates the gradual replacement of tobermorite and C-S-H by SiO_2 gel. In the fully carbonated samples where 11.3, 3.08 and 2.97 Å characteristic peaks for tobermorite and C-S-H do not exist in XRD, the 965 cm^{-1} IR absorbing peak is entirely replaced by the 1045 cm^{-1} peak. The IR curves of C-S-S and C-L-F samples in the course of carbonation change in a similar way.

ZHAO YUPING, LI DEDONG AND SUN GUOKUANG
Research Institute of Building Materials, Beijing, People's Republic of China

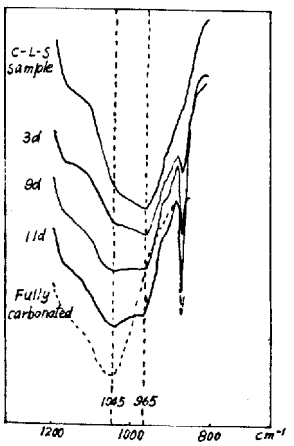

Fig.1 The IR diagram of C-L-S sample in the course of carbonation

SEM observation shows that AAC retains its network structure after carbonation, which Sauman referred to as "pseudomorphism" /2/. But since the observation is confined to a very small area, the morphology of particles and pore characteristics may differ from time to time. Thus it is difficult to get a clear idea of the change in network stucture from SEM observation alone.

The authors determined the pore size distribution of the three types of AAC before and after carbonation with a 3000 atm mercury porosimeter. AAC particles were crushed to 90-250 μm to avoid possible interference air pores may bring about.

Fig.2 shows the histograms of the pore size distribution of AAC. The pores from 2.5 to 5500 nm are divided into 15 groups arbitrarily according to their size and the volume percentage of each group is indicated in the ordinate. The difference in the composition of pores of the three AAC is clearly shown.

It is worth noting that for all the three types of AAC, carbonation leads to a drop in the percentage of small pores and an increase in larger ones. The authors ascribes this to the contraction of particles when Ca ions leave them and also to the fact that in artificial carbonation where R.H. and CO_2 content are high, $CaCO_3$ mainly precipitate in the air pores outside the network structure (see Fig.5).

3.2 The rate of carbonation of three types of AAC

Infrared spectroscopy was employed to determine quantitatively the amount of $CaCO_3$ in the carbonated AAC samples.

Calcium carbonate is indicated by the 1430 cm^{-1} absorbing peak and two sharp peaks at 874 cm^{-1} and 711 cm^{-1} (Fig.3). In the quantitative IR analysis of cement raw meal 874 cm^{-1} peak is often used as the spectrum band for $CaCO_3$ analysis. However, in the carbonation of AAC, the formation of $CaCO_3$ is accompanied by the dissociation of calcium silicate hydrate whose 965 cm^{-1} peak fades away correspondingly (see also Fig.1). Moreover, the difference in the crystallinity of different types of AAC will give rise to a great difference in the shape of this peak. The 965 cm^{-1} peak and the 874 cm^{-1} peak are so near to each other that the use of the latter for quantitative determination of $CaCO_3$ leads to erratic results.

In our experiment 1430 cm^{-1} was used for this purpose

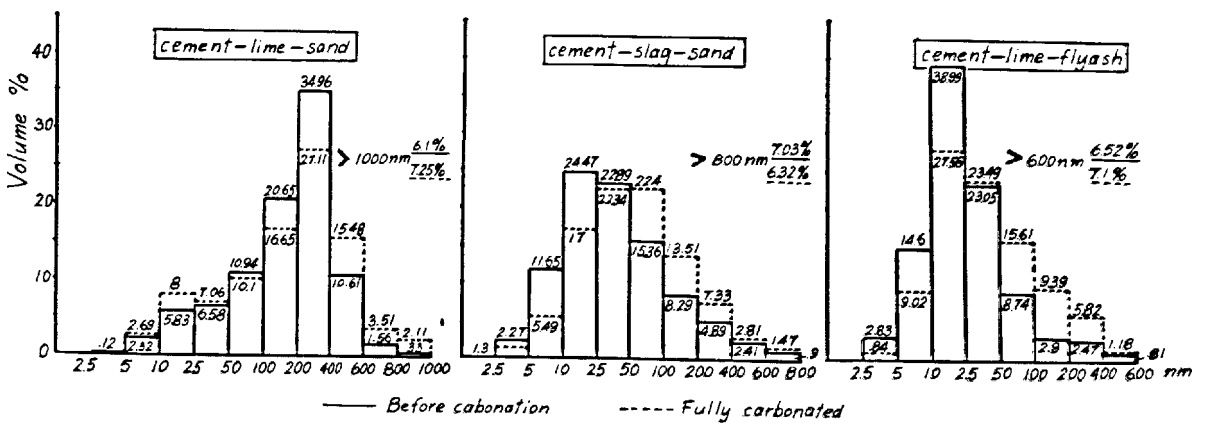

Fig.2 The histogram of the pore size distribution of AAC before and after carbonation (fractions of the large pores not included)

ZHAO YUPING, LI DEDONG AND SUN GUOKUANG
Research Institute of Building Materials, Beijing, People's Republic of China

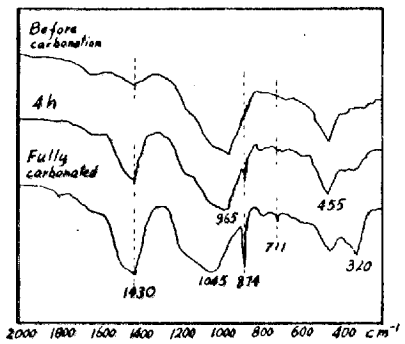

Fig.3 IR curves of AAC showing variation of $CaCO_3$ and concerned peaks

with satisfaction. Samples were homogenized with KBr in the weight ratio of 1:200. A calibration curve has been constructed.

The rate of carbonation of three types of AAC carbonated in artificial environment and in natural environment was determined. AAC samples were crushed to 3-6 mm across and placed in a tube. Air with R.H. 50%, CO_2 50% was conducted through the particle layer (Fig. 4). Samples were analyzed for $CaCO_3$ content (calculated as CO_2) after different time period. When fully carbonated, C-L-F AAC absorbed the smallest amount of CO_2. However, its rate of carbonation is the highest (Table 1).

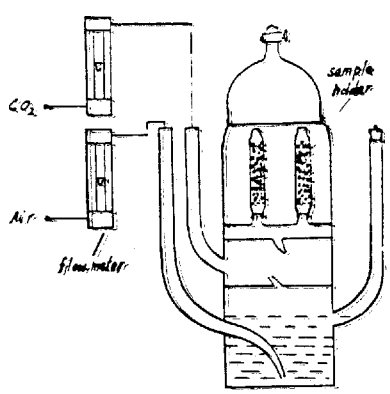

Fig.4 Sketch of a device for the carbonation of AAC particles in flowing air

Table 1 CO_2 absorbed (gm CO_2/100 gm sample) and degree of carbonation (%) in different ages

Type	Age(h)	2	4	12	24	Fully carbonated
C-L-S	CO_2 absorbed	3.0	3.5	3.7	5.3	14.9
	Degree of carbonation	20.1	23.7	25.11	35.6	100.0
C-S-S	CO_2 absorbed	2.3	4.4	5.0	8.6	15.7
	Degree of carbonation	14.6	28.1	32.0	54.8	100.0
C-L-F	CO_2 absorbed	4.8	5.4	6.5	9.4	11.2
	Degree of carbonation	43.3	48.0	58.3	83.9	100.0

The same order of rate of carbonation is found for samples carbonated in natural environment (Table 2).

Table 2 CO_2 abosrbed and degree of carbonation of AAC after two years of outdoor exposure

	gm CO_2 per 100 gm sample	Degree of carbonation %
Cement-lime-sand	1.8	12.0
Cement-slag-sand	2.8	18.8
Cement-lime-flyash	3.8	33.9

Calcium silicate hydrates that are related to autoclaved aerated concrete were synthesized under 10 atm for 24 hours /3/. They are tobermorites with and without Al substitution and ill-crystallized C-S-H. They were placed separately in disks in a sealed container which was filled with air containing 90% CO_2, R.H. being 100%. After 6 and 46 hours, samples were taken out for XRD analysis (Fig.5).

XRD analyses show that Al containing tobermorite is more apt to carbonate than tobermorite without Al. Ill-crystallised C-S-H synthesized from lime and amorphous SiO_2 is higher in the rate of carbonation than the well-crystallized tobermorites. This may explain why C-L-F AAC (its chief hydration product is ill-crystallized C-S-H) has a higher rate of carbonation than C-L-S (chiefly composed of well-crystallized tobermorite).

ZHAO YUPING, LI DEDONG AND SUN GUOKUANG
Research Institute of Building Materials, Beijing, People's Republic of China

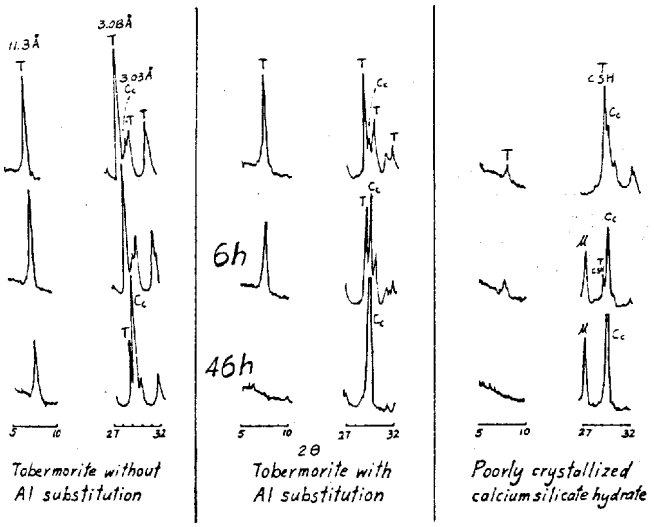

Fig.5 XRD diagram of three synthetic compounds in the course of carbonation

The carbonation of hydrogarnet also shows that crystallinity has much bearing one its rate. While pure hydrogarnet synthesized in autoclaving (the particles may be as large as 15 μm across /3/) has hardly any sign of carbonation in 46 hours under the condition given above, the hydrogarnet in autoclaved aerated concrete owing to its low crystallinity is not less liable to CO_2 attack than calcium silicate hydrates.

3.3 The effect of artificial and natural carbonation on the strength of AAC

Three types of AAC cut into 10 cm cubes were put into an artificial carbonation chamber until fully carbonated (no more indication of tobermorite and C-S-H in XRD analysis). Two sets of experiment (R.H. 90%, CO_2 65-90% and R.H. 50%, CO_2 50%) were performed. The strength tests before and after carbonation indicate a loss of strength for all the samples. The drop in strength for each type of AAC is similar in the two conditions, which is 5-10%, ≈20% and ≈25%, respectively for C-L-S, C-S-S and C-L-F.

The strength of AAC after one year exposure in natural surroundings is another story. Taking into account the effect of humidity of the samples on strength, the strengths of C-L-S and C-S-S are increased while that of C-L-F drops to a certain extent. It is interesting to note that the strengths of all the three types of AAC after two years exposure are nearly the same as or higher than the values of one year (Table 3).

Table 3 Comp. strength (MPa) and H_2O content (%) of AAC after exposure in natural surroundings

	Before carbonation		1 year				2 years Outdoor	
			Indoor		Outdoor			
	H_2O	Comp. str.	H_2O	Comp. str.	H_2O	Comp. str.	H_2O	Comp. str.
C-L-S	3.7	2.73	2.6	3.14	4.8	3.09	4.0	3.29
C-S-S	8.1	4.14	3.1	5.28	5.3	5.26	4.7	5.14
C-L-F	12.5	3.85	3.5	2.92	5.4	3.27	4.6	3.77

The change in strength in the course of carbonation has been reported /4/ to be related to the rate of carbonation and high rate of carbonation is believed liable to cause microcracks which leads to greater loss in strength.

3.4 The difference in the mechanism of natural carbonation and artificial carbonation

AAC carbonates rapidly in artificial carbonation where R.H. and CO_2 concentration are high. SEM shows all the air pores of the AAC carbonated in these surroundings are covered with a thick layer of calcite (Fig.6). According to EDAX analysis, the acicular particles underneath are SiO_2 gel.

The build up of a great quantity of calcite in the air pores and its interspersion in the network structure just underneath the air pore surface indicate the reaction between CO_2 and Ca ions begins at the pore surface. As carbonation proceeds, Ca^{++} concentation in the liquid phase in the structure is lowered. This enables the Ca ions in the calcium silicate hydrates to transfer further into the liquid phase and migrate to the surface to react with CO_2 there. As the reaction proceeds through solution, it does rapidly.

The SEM observation on samples carbonated in natural environment gives a different picture. The degree of carbonation of C-L-F sample carbonated for two years in outdoor exposure attains 30%, but there is no sign of serious $CaCO_3$ aggregation in the air pores.

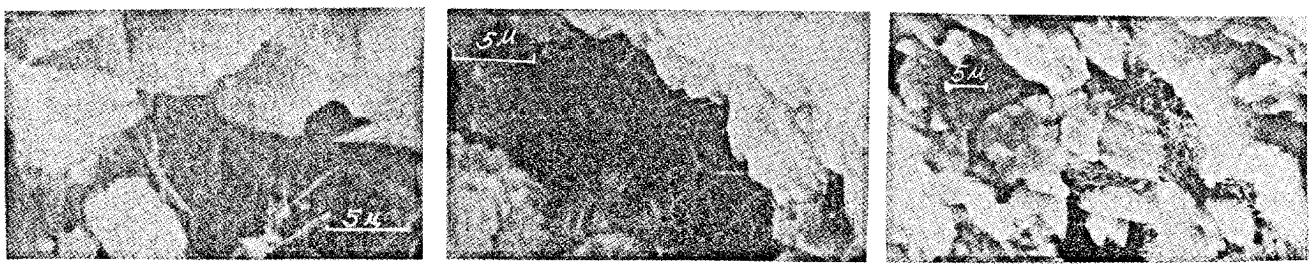

cement-lime-sand (3000 X)

cement-slag-sand (3000 X)

cement-lime-flyash (1500 X)

Fig.6 SEM micrographs of AAC fully carbonated in an artificial environment (R.H. 90%, CO_2 65-90%)

In addition, EDAX has not found particles in the network structure that are very low in Ca content. It sounds reasonable to assume that SiO_2 gel and $CaCO_3$ are so close together that EDAX has difficulty in locating them separately. Probably, in surroundings low in R.H. and CO_2, CO_2 may have a chance to penetrate into the network structure to react in situ with calcium silicate hydrate. This will not have much adverse effect on the strength of the structure.

4. CONCLUSIONS

Infrared spectroscopy is an effective means for monitoring the phase change of AAC from calcium silicate hydrate to silica gel in the course of carbonation. It can also be used to determine quantitatively the $CaCO_3$ content in the carbonated AAC. For this purpose, 1430 cm^{-1} and not 874 cm^{-1} should be used as the absorbing band for analysis.

Mearcury intrusion porosimetry employed to determine the pore size distribution of AAC shows carbonation leads to a drop in the percentage of small pores and an increase in larger ones.

Rate of carbonation tests reveals C-L-F AAC has a higher rate of carbonation as compared with C-L-S and C-S-S. This is in agreement with the data obtained for AAC after two years outdoor exposure. The higher rate of carbonation of C-L-F is ascribed to its higher content of ill-crystallized C-S-H which is more liable to CO_2 attack than tobermorite as evidenced by an experiment made previously.

Strength tests show retrogression of strength ensues for all the three types of AAC cubes carbonated in artificial environments. However, there is an increase in the strength of C-L-S and C-S-S after one year exposure in natural environment and the strength remains unchanged at least till two years.

SEM shows there is serious build up of calcite in the air pores of AAC carbonated in surroundings high in R.H. and CO_2 content. There is no such build up of calcite in the air pores of AAC carbonated in natural environment where R.H. and CO_2 are both low. The carbonation mechanism involved in these two conditions is likely to be different.

5. REFERENCES

1. SUN GUOKUANG, TAND DI and ZHAO YUPING, The carbonation of autoclaved aerated concrete and its hydration products, Journal of the Chinese Silicate Society, 1985, No.4, p414
2. SAUMAN Z., Carbonation of porous concrete and its main binding components, Cem. Concr. Res., 1971 No.1, p645
3. SUN GUOKUANG and ZHAO YUPING, Study of hydrates in the $CaO-SiO_2-Al_2O_3-H_2O$ system under autoclave condition, Journal of the Chinese Silicate Society, 1983, No.2, p149
4. RESEARCH INSTITUTE OF BUILDING SCIENCES OF SHANGHAI and RESEARCH INSTITUTE OF BUILDING SCIENCES OF SHAANXI, Hydration of autoclaved concrete, Symposium on the comprehensive utilization of flyash, Hangzhou, 1981

A. Bajza, I. Rousekova and O. Vrana, Slovak Technical University, Bratislava, Czechoslovakia

CORROSION OF HARDENED CEMENT PASTES BY NH_4NO_3 SOLUTIONS

SUMMARY: The influence of solutions on the physical and mechanical properties, structure and phase composition of cement paste made from portland cement and cements with 20 and 40% blast furnace slag was investigated. The progress of corrosion was evaluated on the basis of appearance and weight changes, changes of compressive strength, total porosity, pore volume and pore size distribution. The degree of deterioration increased with increasing water-to-cement ratio, solution concentration and time. Visible corrosion of the pastes treated in 0.5% NH_4NO_3 solution was not detectable until one year of treatment.

Foi investigada a influência de soluções sobre as propriedades físicas e mecânicas, estrutura e composição de fase de pasta de cimento feita com cimento portland e cimentos com 20 e 40% de escória de alto forno. O progresso da corrosão foi avaliado com base nas mudanças de aparência e de peso, alterações da resistência à compressão, porosidade total, volume de poro e distribuição de tamanho de poro. O grau de deterioração aumentou com o aumento da relação água/cimento, concentração da solução e tempo. Não foi detectada corrosão visível de pastas tratadas com solução de 0,5% de NH_4NO_3 até um ano de tratamento.

1. INTRODUCTION

Literature data on the negative effects of NH_4NO_3 on the durability of concrete are scarce (refs. 1-3), although such deterioration of concrete in agricultural conditions in common. According to Soboličová (4), bending and compressive strengths of a slag portland cement concrete, exposed for 6 months to NH_4NO_3 + $CO(NH_2)_2$ solution, were only 32 and 42 percent, respectively, of the control sample.

According to Biczók (5) the corrosion occurs in two steps. In the first step:

$$2NH_4NO_3+Ca(OH)_2 \longrightarrow Ca(NO_3)_2) + 2NH_4OH \quad (1)$$

NH_4OH decomposes to give NH_3 which leads to increased porosity (Type II corrosion of Moskvin(6)). The formed $Ca(NO_3)_2$ reacts to form $C_3A{\cdot}Ca(NO_3)_2{\cdot}10H_2O$; this causes expansion and degradation of the paste (7) (Type II corrosion).

2. EXPERIMENTAL

A commercial portland cement, having a calculated compound composition of 64.7% C_3S, 9.6% C_2S, 7.5% C_3A, 10.1% C_4AF and 2.6% $CaSO_4$, has been used, with or without additions of 20 and 40% blast furnace slag. After 28-days of water curing, the d = 30 mm cylindrical paste samples (w/c = 0.1, 0.3 and 0.4) were placed into 0.5, 3 and 5% solutions of NH_4NO_3 for 1, 28 (29), 35, 56, 119 and 393 days. The w/c = 0.1 samples were made by compaction; those with w/c = 0.3 and 0.4 were densified by vibration.

The samples were evaluated visually, for changes in density, porosity, strength, composition of hydrates and morphology.

3. DISCUSSION OF RESULTS

When examined visually, the appearance of the samples did not change for about 90 days. After 365 days, this was true only for samples cured in 0.5% NH_4NO_3 solutions. The degree of degradation, including decrease in density, increased with w/c, solution concentration and time. Slag portland cement pastes did not exhibit increased durability.

Fig. 1 shows the strength development vs. time for portland cement pastes. Already after 1 day of curing in NH_4NO_3 solutions (following 28-days in water), the compressive strength decreased: at w/c = 0.3, this decrease was 27.8%! After 7 days (a total of 35 days), the strength increased somewhat, but this was followed by another decrease. At 365 days in NH_4NO_3 solution, the strengths were only about 26-71% of the control strength. Similar results were found for the slag portland cement samples (a decrease of 76%).

As expected, the porosity of the samples was found to be inversely related to strength data (Fig. 2). The relationship between strength and porosity is shown in Fig. 3. The decrease of strength after 1 day of curing in NH_4NO_3 solution is believed to be related to reaction (1). The following decrease in porosity and strength increase relate to formation in the paste pores of $C_3A{\cdot}Ca(NO_3)_2{\cdot}10H_2O$ in the absence of expansive pressures. The final degradation of properties is a consequence of both types of corrosion reactions.

Formation of $C_3A{\cdot}Ca(NO_3)_2{\cdot}10H_2O$ has been detected by XRD in pastes stored in 0.5, 3 and 5% NH_4NO_3 solutions after 28, 7 and 1 day, respectively. X-ray data showed a stabilization of ettringite prior to its conversion to calcium monosulfoaluminate; at increased NH_4NO_3 concentrations the amount of ettringite and $C_3A{\cdot}Ca(NO_3)_2{\cdot}10H_2O$ increased, whereas only minute amounts of monosulfoaluminate were detected.

DTA and TG data confirmed the above findings. The endothermic peak at 285-305°C, believed to represent decomposition of $C_3A{\cdot}Ca(NO_3)_2{\cdot}10H_2O$, increased with increased concentration of NH_4NO_3 solution. For 0.5, 3 and 5% NH_4NO_3 solutions, this endotherm appeared at 91, 7 and 7 days of NH_4NO_3 solution curing. The endotherm at 480-540°C exhibited a doublet ascribed to the decomposition of $Ca(OH)_2$ and $Ca(NO_3)_2$; the latter compound formed during the previous decomposition of $C_3A{\cdot}Ca(NO_3)_2{\cdot}10H_2O$.

When compared to those cured in water, an increase in nonevaporable water (W_n) content for samples cured in NH_4NO_3 solutions was found. W_n increased with w/c, time and concentration of the solution. N.b.: no corrections were made for carbonation of samples.

As can be seen in Table I, the porosities of pastes (obtained by Hg porosimetry) stored in water vs. NH_4NO_3 solutions differ: Whereas the porosities decrease in water-cured samples, those cured in NH_4NO_3 solutions, especially at higher concentrations, show an increase(!) in porosity. In line with other data, porosimetry data show a more severe degradation of samples made from slag portland cement (SPC, 40% slag) than those made from ordinary portland cement (PC). Note the continuous decrease in the percentage of pores larger than 100 nm and the decrease in those smaller than 100 nm for samples stores in NH_4NO_3 solutions.

SEM data show that the main hydration products formed after 1 year in 0.5% NH_4NO_3 solutions are Type I and III C-S-H (10). Additionally, hexagonal plates of $Ca(OH)_2$ and irregular crystallites of $C_3A{\cdot}Ca(NO_3)_2{\cdot}10\ H_2O$ or calcium monosulfate

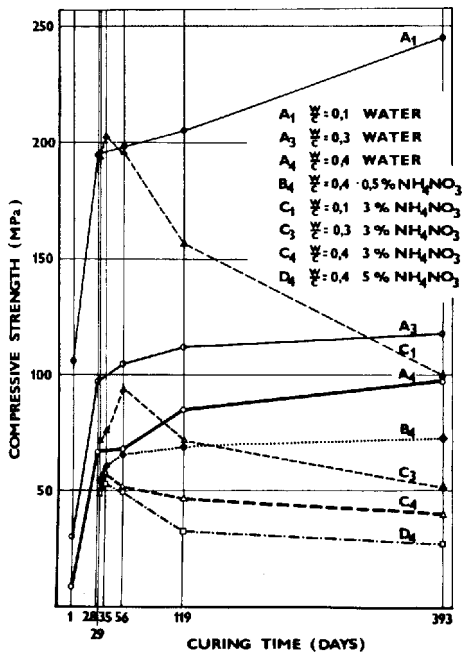

Fig. 1 - Strength development of portland cement pastes vs. curing time, w/c and concentration of curing solutions.

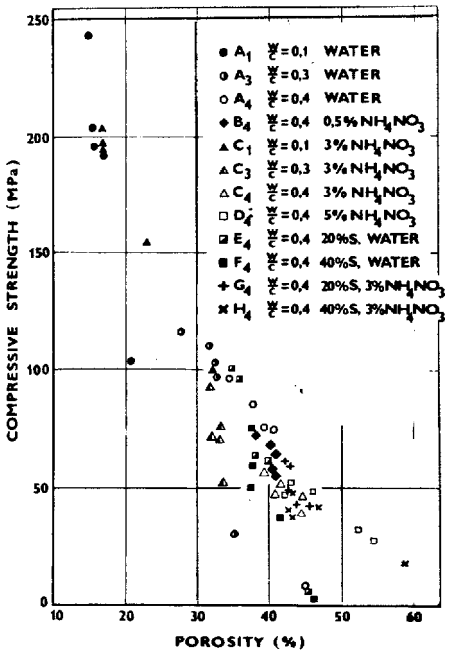

Fig. 3 - Compressive strength of portland and slag portland cement pastes vs. porosity, w/c and concentration of curing solutions.

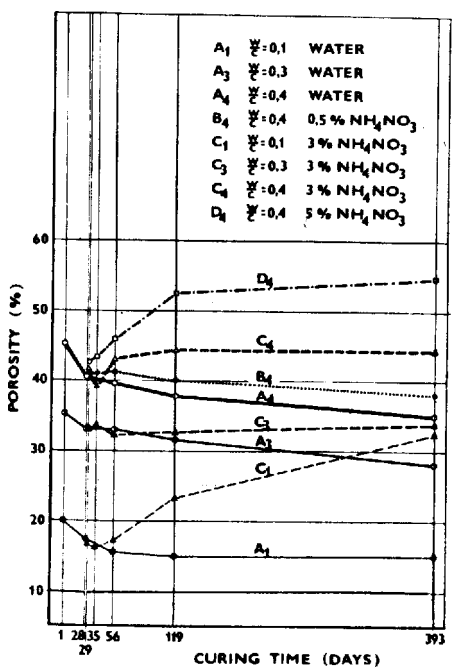

Fig. 2 - Porosity of portland cement pastes vs. curing time, w/c and curing solutions.

were detected. In samples stored in 5% NH_4NO_3 solutions, the microstructure was found to be coarser, C-S-H appeared to be Type III, and both needle-like ettringite and hexagonal $C_3A \cdot Ca(NO_3)_2 \cdot 10H_2O$ or monosulfate were detected in the pores (Fig.4).

The one-year slag portland cement samples stored in 3% NH_4NO_3 solutions showed Type III C-S-H to be the main product of hydration. Large amounts of microcracks, stacks of $Ca(OH)_2$ crystals, and irregular hexagonal plates of $C_3A \cdot Ca(NO_3)_2 \cdot 10H_2O$ or monosulfoaluminate were clearly visible. An example of the slag portland cement morphology is shown in Figure 5.

4. CONCLUSIONS

NH_4NO_3 solutions severely corrode hardened pastes made from both portland and slag cements. For short-term exposure, slag cements demonstrated somewhat better resistance. Due to lesser amounts of $Ca(OH)_2$ present, formation of $Ca(NO_3)_2$, needed for the formation of $C_3A \cdot Ca(NO_3)_2 \cdot 10H_2O$, causing the expansion, is diminished.

The corrosion effectiveness of NH_4NO_3 increases with its concentration and time of exposure. It causes decreases in paste density and strength, and increases in nonevaporable water content, porosity, and structural defects.

The hydration products formed in the presence of NH_4NO_3 are the same as those formed by water curing plus $C_3A \cdot Ca(NO_3)_2 \cdot 10H_2O$. The latter compound stabilizes ettfingite prior to its recrystallization to monosulfoaluminate.

5. REFERENCES

1. ACI Committee 515: Guide for the Protection of Concrete Against Chemical Attack by Means of Coatings and Other Corrosion-Resistant Materials. ACI Journal, Proc. V, 63, No. 12, pp 1305-1391 (1966).

2. ACI Committee 201: Guide to Durable Concrete, ACI Journal, Proc. V. 74, No. 12, pp 573-609 (1977).

3. Lea, F. M., The Action of Ammonium Salts on Concrete. Magazine of Concrete Research, V. 17, No. 52, pp 115-116 (1965).

4. Soboličová, R., Spôsoby ochrany betónu proti korózii vyvolanej priemyselným hnojivom DAM-390. Stavební výzkum, č. 1, s. 22-27 (1984).

5. Biczók, I., Betonkorrosion, Betonschutz. Budapest. Verlag der Ungarischen Akademie der Wissenschaften (1960).

6. Moskvin, V. M., Ivanov, F. M., Alexejev, S.N., Gusejev, E.A., Korrozija betona i železobetona, metody ich zaščity, Moskva. Strojizdat (1980).

7. Živica, V., Korózia zatvrdnutých cementových kaší roztokmi dusičňanu vápenatého. Stavebnícky časopis SAV, XVIII, č. 4, s 323-342 (1970).

8. Bajza, A., On the Factors Influencing the Strength of Cement Compacts, Cement and Concrete Research, V. 2, No. 1, pp 67-78 (1972).

9. Diamond, S., Cement Paste Microstructure - An Overview of Several Levels. Hydraulic Cement Pastes: Their Structure and Properties, Proc. Conf. University of Sheffield, pp 2-30, London Cement and Concrete Association (1976).

TABLE 1: Pore Size and Distribution of Cement Pastes

Cement	w/c	Solution	Age (days)	Density ($g.cm^{-3}$)	Porosity (%)	$V_{3}mp_{-1}$ ($cm^{3}.g^{-1}$)	Pore Size Distribution 3.75-10nm (%)	$10-10^{2}$nm (%)	$10^{2}-10^{3}$nm (%)	10^{3} 7.5x10^{3}nm (%)	r' (nm)
PC	0.4	Water	1	1.568	45.22	0.2358	6.66	28.68	52.66	12.00	250
			28	1.627	40.35	0.1394	11.33	74.68	13.33	0.66	35
			56	1.644	39.63	0.1226	11.33	73.34	14.00	1.33	48
			393	1.705	34.80	0.0942	20.00	69.34	7.33	3.33	26
PC	0.4	0.5% NH_4NO_3	29/1	1.629	40.99	0.1472	12.66	62.68	24.00	0.66	55
			56/28	1.732	40.93	0.1305	11.33	70.01	16.66	2.00	41
			393/365	1.654	38.21	0.0971	18.33	74.01	6.00	0.66	25
PC	0.4	3% NH_4NO_3	56/28	1.594	42.89	0.1491	17.33	68.01	12.66	2.00	32
			393/365	1.503	44.20	0.1748	26.00	65.34	7.33	1.53	19
PC	0.4	5% NH_4NO_3	29/1	1.524	42.27	0.1497	10.66	68.01	19.33	2.00	44
			56/28	1.526	45.81	0.1388	18.66	65.34	12.00	4.00	32
			393/365	1.249	54.76	0.3202	25.33	56.68	15.33	2.66	27
SPC	0.4	Water	28	1.609	42.22	0.1459	16.00	56.68	26.66	0.66	50
			393	1.663	38.06	0.0799	35.33	57.34	5.33	2.00	17
SPC	0.4	3% NH_4NO_3	56/28	1.561	43.31	0.1511	13.33	59.35	24.66	2.66	58
			393/365	1.185	59.24	0.2722	27.33	54.00	16.67	2.00	25

V_{mp} = volume of micropores (3.75-7,500 nm)
r' = radius of micropores at 50% of total volume of micropores ("median micropore radius").

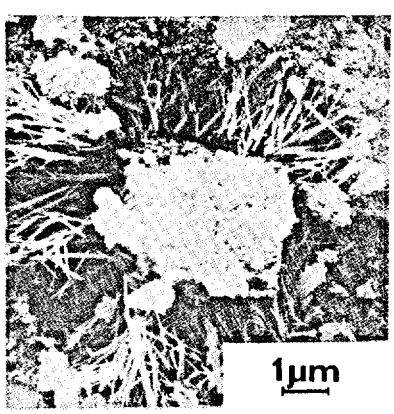

Fig. 4 - Micrograph of portland cement paste (w/c = 0.4) after 28-day water curing and 365-day curing in 5% NH_4NO_3.

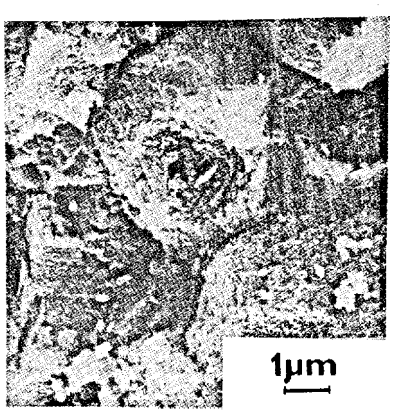

Fig. 5 - Micrograph of slag (40%) portland cement paste (w/c = 0.4) after 28-day water curing followed by 365-day curing in 3% NH_4NO_3.

H.Y. GHORAB AND E.A. KISHAR, Cement Chemistry Laboratory, University College for Girls, Ain Shams University, Heliopolis, Cairo, Egypt. 1

THE STABILITY OF THE CALCIUM SULFOALUMINATE HYDRATES IN AQUEOUS SOLUTIONS.

STABILITE DU SULFOALUMINATE HYDRATE DANS DES SOLUTIONS AQUEUSES. 4.2

Summary

The stability of the calcium sulfoaluminate hydrates in pure water and in different concentrations of sodium hydroxide solutions has been studied at normal pressure and temperatures up to 100°. The amount of the dissolved sulfate and aluminium has been measured in solution and related to the behaviour of the solid phases.

Under normal conditions the ettringite resists alkaline solutions of concentrations equal to or less than 0.2M. Its decomposition is accelerated by temperature and alkali. It forms as a result of the decomposition of the monosulfate hydrate in water at temperatures $\leqslant 60°$.

Alkali causes the dissolution of the sulfate species but temperature is needed for the splitting of the aluminate. The low sulfate form persists 1M NaOH at 30° and decomposes to portlandite on boiling in 0.2M NaOH.

Foi estudada a estabilidade dos hidratos de sulfoaluminato de cálcio em água pura e em diferentes concentrações de solução de hidróxido de sódio, sob pressão normal e temperaturas de até 100°C. A quantidade de sulfato e de alumínio dissolvida foi medida na solução e relacionada com o comportamento das fases sólidas.

Sob condições normais a etringita resiste às soluções alcalinas com concentrações iguais ou menores que 0,2M. Sua decomposição é acelerada pela temperatura e pelo álcali. Ela se forma como resultado da decomposição de hidrato monossulfato em água à temperatura $\leq 60°C$.

O álcali causa a dissolução das espécies de sulfato, mas a temperatura é necessária para a divisão do aluminato. A forma de baixo sulfato persiste em 1M de NaOH a 30°C e se decompõe em portlandita sob fervura em 0,2 M de NaOH.

H.Y. GHORAB AND E.A. KISHAR, Cement Chemistry Laboratory, University College for Girls, Ain Shams University, Heliopolis, Cairo, Egypt.

Introduction

The behaviour of the calcium sulfoaluminate hydrates in aqueous solutions is of a special interest to the cement chemists, the problem of their stability being directly related to the physical and mechanical properties of Portland cements as well as corresponding mortars and concrete. These phases are the first responsible for the setting behaviour of the cement and affect the hardening process at later stages of hydration.

The crystallographic nature of these phases are well known and a relatively more concern has been forwarded to the stability of the ettringite than that of the monosulfate hydrate. The existing gap in the literature is the correlation between the stability of these phases in aqueous solutions and the solution composition under the different conditions of temperature and pH value which subject has been the purpose of the present work.

Experimental

The ettringite used was prepared by stirring anhydrous tricalcium aluminate with gypsum (mole ratio = 1:3) in an excess amount of water at room temperature. The monosulfate hydrate was prepared according to the method of Lerch et al (1). The solubility measurements were carried out in pure water two weeks long, also in different concentrations of sodium hydroxide solutions (0.08, 0.2 and 1M) for one hour and one day. The detailed procedure can be described as follows: A known weight of the sample (0.5 g ettringite and 0.2 g of the monosulfate hydrate) was stirred in 100 ml redistilled water in well stoppered glass flasks immersed in a thermostated water bath adjusted at 30°, 60° or boiled with a water condenser. Filtration of the solutions were performed in a double walled funnel in which thermostated water was circulated at the desired temperature. The precipitates were dried in a drying oven at 50° for one day then analysed by means of a Philips type 1390 X-ray diffractometer. In the clear filtered solution the aluminium was determined colourimetrically (2) then the solution was slightly acidified with HCl and the sulfate content was measured spectrophotometrically according to the turbidity method (3).

Results

The variation in the solution composition of the calcium sulfoaluminate hydrates in water with time, also the change in the pH value are illustrated in figure 1 for the three studied temperatures. For purpose of a better comparison the behaviour of the dissolved species in the solutions of the high and low sulfate forms are plotted parallel to each other, the maximum scale of the sulfate content being three moles for the ettringite and one mole for the monosulfate hydrate.
Figure 4 illustrate further the sulfate and aluminium content of the different alkaline solutions of the phases studied after one day treatment, the values plotted on the abssicae representing the solubility values in pure water.

The X-ray diffraction patterns of some chosen solid phases obtained from treating the ettringite and the monosulfate hydrates with water and with different concentrations of alkaline solutions at temperatures up to 100°C are shown in figures 2,3 and 5.

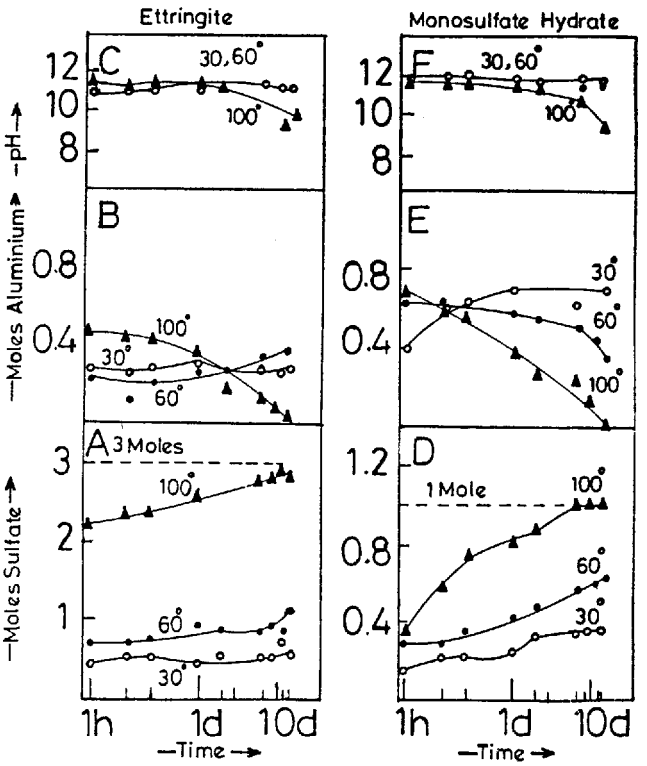

Fig. 1 The solution composition of the calcium sulfoaluminate hydrates in water at different time at 30°, 60° & 100°C. Also the variation of pH value with time is shown.

In pure water

The ettringite phase is found to be stable in water at 30 and 60°, the resulting solution having a pH value of 11.2. The solution composition tends to equilibrium values of 0.5 mole sulfate and ~ 0.26 mole aluminium over two weeks stirring at 30°. At 60° the X-ray diffraction analysis shows broadening of some weak diffraction lines after 14 days, also the slow rise of the sulfate ion concentration of figure 1A predicts a very slow decomposition process.
At 100° 2.25 moles sulfate are quickly splitted from the ettringite crystals and the monosulfate hydrate forms during the first hour. The low sulfate form decomposes to gypsum after 11 days boiling in a solution containing three moles sulfates and having a pH value of 9.0. Under these conditions the aluminium is totally depressed from the solution (Fig. 1B) and is probably present as amorphous gel in the solid. Further details are published elsewhere (4).

On the other hand the monosulfate hydrate is unstable in water at 30° and decomposes partially to the high sulfate form after 6 hours. Both phases remain in an apparent equilibrium in contact with a solution containing 0.36 moles sulfate and 0.7 moles aluminium (Fig. 1D & E). Figure 5 illustrate the presence of both phases in the one day stirred sample.

At 60° the monosulfate hydrate enters into a solid

H.Y. GHORAB AND E.A. KISHAR, Cement Chemistry Laboratory, University College for Girls, Ain Shams University, Heliopolis, Cairo, Egypt.

solution with the tetracalcium aluminate hydrate during the first six hours which decomposes to the ettringite after a day. On prolonged exposure the aluminium concentration decreases from the solution and a silicate bearing-calcium aluminate hydrate (gehlenite hydrate) forms which appears better on boiling the low sulfate form in water for five days (Fig. 2). This phase precipitates from an aluminium-free (or poor) solution containing a whole mole of sulfate corresponding to the weighed sample, and having a pH value of 9.

In alkaline solution

Dilute alkaline solution of 0.08 M does not affect the stability of the ettringite at 30°C, the sulfate and aluminium concentrations remaining quite similar to those of pure water except for a relatively higher curve of the aluminium (5). In 0.08 M NaOH the decomposition process of the ettringite to the low sulfate form takes place already at 60° and both phases are maintained for long exposure time. On boiling a sulfate free-hexagonal monophase forms after one hour (d-value 8.2 Å) and converts to the more stable cubic hydrogarnet phase after a day (Fig. 3).

The high sulfate form ressists further the attack of 0.2M NaOH one day long at 30° but converts totally to the tetracalcium aluminate hydrate which carbonate quickly and appears as the monocarbo-aluminate hydrate (d-value = 7.6Å) at 60°C. The total release of the sulfate and aluminium content takes place at boiling temperature. Under these conditions the only remaining solid is the portlandite.

One molar sodium hydroxide solution succeeds to split the total sulfate content of the ettringite in an hour time at 30°. The splitting of the aluminium needs however temperature. Therefore at 60°C 0.7 mole Al is given off to the solution and a whole mole at 100° (Fig. 4 A,B). The calcium hydroxide precipitated from an aluminium and sulfate rich-solution reacts with the glass container and form an aluminium-free calcium silicate hydrate having diffraction lines similar to those of the tobermorite like structure (Fig. 3). It is noticed that the rate of the decomposition is time dependent. Samples ltreated with alkali and temperature for one day lead to a splitting of the sulfate, the formation of the hexagonal phase, the conversion to cubic hydrogarnet, the consequent precipitation of the portlandite and the corresponding attack to the glass container in a rate faster than those treated for one hour.

Furthermore the stability of the monosulfate hydrate is raised in alkaline solution where the conversion process to the ettringite does not take place(Fig.5) Sodium hydroxide solutions favour the splitting of the tetracalcium aluminate hydrate which shows up increasingly in its carbonated form at 30° and 60°C and the concentration of the dissolved sulfate rises markedly with alkali and temperature (Fig. 4 C & D). Boiling the monosulfate hydrate in 0.08M NaOH leads however to the formation of the cubic hydrogarnet and not the hexagonal monophases. At 100°C the portlandite phase predominates in 0.2M NaOH and in 1M it becomes the only hydrate present in the solid where it reacts with the glass container forming calcium silicate hydrate.

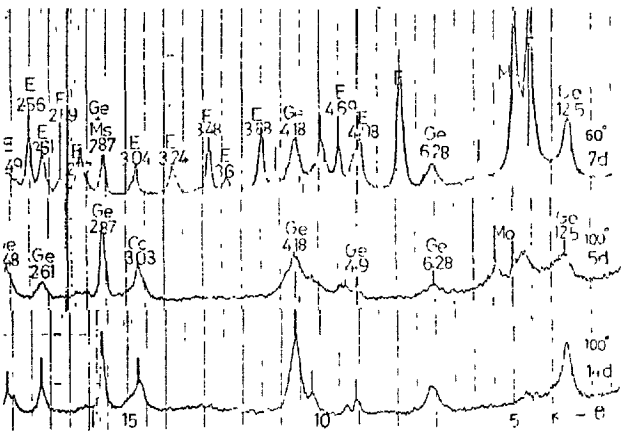

Fig. 2 The X-ray diffraction patterns of the solids obtained from treating the monosulfate hydrate with water at 60° and 100°C.

Discussion

On discussing the stability of the calcium sulfoaluminate hydrate phases usually both types of hydrates are considered because of the expected transformation of one type to the other under the different conditions.

The extensive work found in the literature on the behaviour of these phases have confirmed the stability of the ettringite at normal temperature and pressure (6-8), The maximum stability temperature of the ettringite in water has been variably reported between 90 and 100° (9-11), its conversion temperature lying in the range of 80° to 148° (12-13), also in a saturated steam pressure.

According to the present work, states of equilibrium are found at 30°, for the ettringite in water and in 0.08M NaOH also apparently for the monosulfate hydrate in water. The equilibrium concentration of the ions present in contact with the ettringite in water lie relatively close to those obtained by Lea (14) where the incongruent solubility is proved. In more concentrated sodium hydroxide solutions and higher temperatures the solution concentration does not attain a state of equilibrium.

The gypsum phase appears as a decomposition product of the ettringite in boiling water after the release of three moles sulfates to the solution i.e. 1.136g sulfate per liter which is the total sulfate present in 0.5g ettringite. This value is very close to the saturation value of gypsum at 100° found to be 1.18g(15) and 1.12g (16) per liter of the solution. The gypsum phase does not however show up during the decomposition of the monosulfate hydrate under severe attack of alkali and temperature which may be attributed to the low sulfate content in the monosulfate hydrate used (0.2 g).

H.Y. GHORAB AND E.A. KISHAR, Cement Chemistry Laboratory, University College for Girls, Ain Shams University, Heliopolis, Cairo, Egypt.

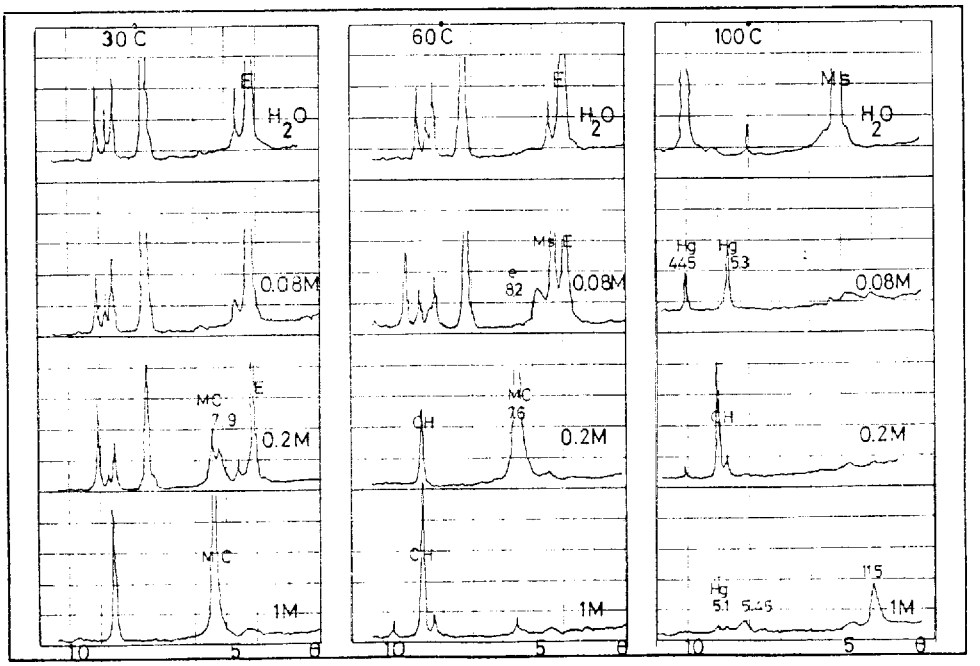

Fig. 3 The X-ray diffraction patterns of the solids obtained from treating the ettringite with water and sodium hydroxide solutions for one day at 30°, 60° and 100°C.

A simultaneous appearance of both types of the calcium sulfoaluminate hydrates takes place during the decomposition of the monosulfate hydrate in water at 30° and 60° and as a result of the decomposition of the high sulfate form in 0.08M NaOH at 60°C. The concentration range of the solution varying from 0.2 to ~ 2 moles sulfate and 0.2 to 0.6 mole aluminium, and consequently that of the solid from 0.8 to 1 mole sulfate and 0.8 to 0.4 mole aluminium which indicate the formation of these phases in highly unstoichiometric solids.

Jones (10) reported the stability of the ettringite phase in presence of 1% NaOH (0.25M) which corresponds to the content of alkali present in the liquid phase in a setting cement. This agrees with the present work at temperature condition of 30°C where the high sulfate form resists alkaline solutions of concentrations up to 0.2M.

Other work however (17-20) have established the stability of the low sulfate form in a solution containing 1% or more alkali which is in accordance with the results obtained in this work at temperature of 60°C for alkaline solutions ≥ 0.2M. At more severe conditions the cubic hydrogarnet and portlandite form.

It is worth to note that in alkaline solution a whole range of monophases containing sulfate, hydroxyl and the indispensible carbonate ions form, the concentration of which depending largely on the alkali concentration and temperature. The insertion of the carbonate ion in an amount less than one mole seems to occur in a way more or less parallel to the amount of sulfate released from the solid and is favoured in alkaline solutions. This observation needs further work before being finally argued.

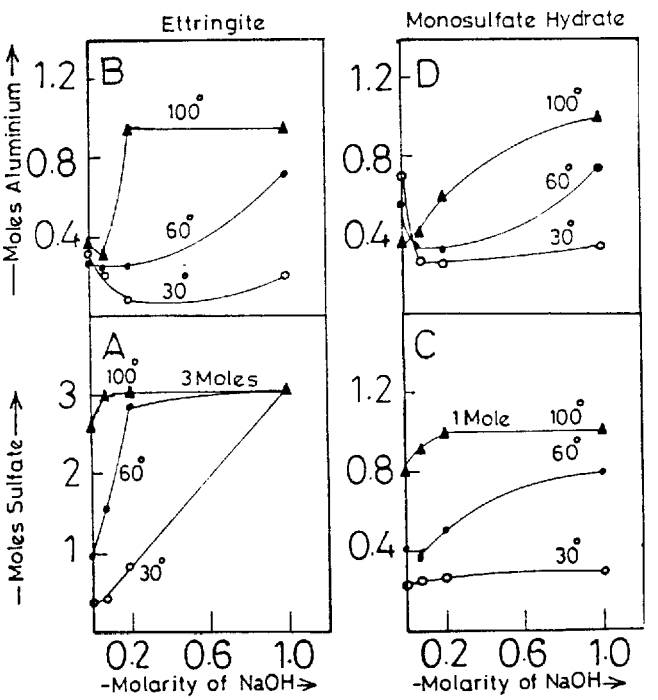

Fig.4 The solution concentration of the calcium sulfoaluminate hydrates in water and in sodium hydroxide solutions after one day treatment at temperatures 30°, 60°, 100°C.

H.Y. GHORAB AND E.A. KISHAR, Cement Chemistry Laboratory, University College for Girls, Ain Shams University, Heliopolis, Cairo, Egypt.

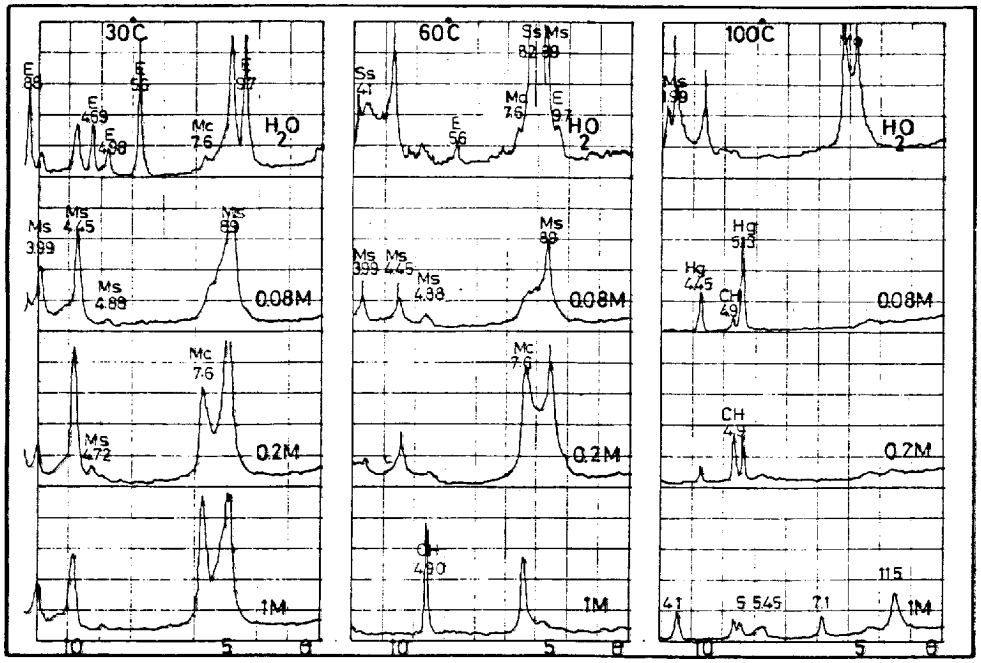

Fig. 5 The X-ray diffraction patterns of the solids obtained from treating the monosulfate hydrate with water and sodium hydroxide solutions for one day at 30°, 60° and 100°C.

Summary

1. The ettringite phase is stable in water at 30° and 60°. It forms as a result of the decomposition of the low sulfate form in water at these two temperatures.
   It persists alkaline solutions of concentrations up to 0.2M at 30°.
   It converts to the monosulfate hydrate in water at 100° and in 0.08M NaOH at 60°.
   It converts to the sulfate free monophases in 1M NaOH at 30° and in 0.2M NaOH at 60°.
2. The stability of the monosulfate hydrate is greatly enhanced in alkaline solutions where splitting of the sulfate free monophase is favoured.
3. Under boiling conditions the high and low sulfate forms decompose to the hydrogarnet in dilute alkaline solutions and to portlandite in concentrated sodium hydroxide solutions.
4. The gehlenite hydrate forms as a result of the interaction of the precipitated calcium hydroxide with the glass container in an sulfate rich, aluminium poor solutions of low pH value. The calcium silicate hydrate forms in a sulfate rich, aluminium rich solution of high pH value.

References

1. W. Lerch, F.W. Ashton and R.H. Bogue, J. Res. Natn. Bur. Stand. 2, 715 (1929).
2. V.I. Vogel, Quantitative Inorganic Analysis. Longmans, Green & Co. Ltd. 792 (1961).
3. A.E. Greengerg, APHA, J. Connors, AWWA, D. Jenkins, WPCF. Standard Methods for the Examination of Water and Waste Water. American Public Health Association. Washington, 439 (1980).
4. H.Y. Ghorab and E.A. Kishar. Cem. and Concr. Res. 15, 93-99 (1985).
5. E.A. Kishar, Kinetic Studies on the Stability of Some Calcium Aluminate Hydrates. Master Thesis 1986. Cement Chemistry Laboratory. Ain Shams University.
6. F.E. Jones, J. Phys. Chem. 48, 311-356 (1944).
7. J. D'Ans and H. Eick, Z.K.G. 6, 302-311 (1953).
8. H.Y. Ghorab, D. Heinz, U. Ludwig, T. Meskendahl, and A. Wolter, 7th International Congress on the chemistry of cement, Vol. 4, 49, 496-503, Paris (1980).
9. W. Lieber, Z.K.G. 16, 364 (1963).
10. F.E. Jones, Proceeding of the Sym. on the Chemistry, Cements, Stockholm, 231 (1938).
11. M. Butt Yu. A.A. Marie, B.G. Varshal, Dokl. Akad. Nauk. SSSR. 136, 398 (1961).
12. P.K. Mehta, J. Amer. Ceram. Soc. 55-56 (1972).
13. H. Kollmann, G. Struble and F. Trost, Tonind. Ztg. 101 Nr 3, 63-70 (1977).

14. F.M. Lea and C.H. Desch, The Chemistry of Cement and Concrete, Edward Arnold Ltd., London (1956).

15. F.M. Lea, The Chemistry of Cement and Concrete, Edward Arnold Ltd., London, 186 (1970).

16. H.Y. Ghorab, M. Wassef and S.H. Abou El Fetouh, J. Chem. Tech - Biotechnol. 34 A, 464-467 (1984).

17. G.L. Kalousek, The Sulfoaluminates of Calcium as Stable and Metastable Phases and a Study of a Portion of the Five Component System CaO - Al_2O_3-Na_2O-H_2O-SO_3 Thesis, Univ. of Maryland (1941).

18. I. Mituzas, A. Mituzas, Vses - Naucho - Issled. Inst. Teploizol., Akmyany, USSR, (1975).

19. D. Knofel, Silikate Technik 22, 8, 262-265 (1971).

20. J. Otteman, Silikattechnik 2, 143 (1951).

OBERSTE - PADTBERG R. ETUDES ET FABRICATIONS DOWELL SCHLUMBERGER SAINT ETIENNE (FRANCE)

4.2

DEGRADATION OF HYDRATED CEMENTS BY CHLORIDE BRINES

DEGRADATION DES CIMENTS HYDRATES PAR DES SAUMURES HYDRATEES

ABSTRACT:
The interaction between alkali and alkaline earth saturated brines and hydrated high sulfate resistant cements, mixed with both, fresh and 30% NaCL containing water, are presented.

The reasons for the resulting cement degradation were studied by XRD, optical and scanning electron microscopy of the attacked cement samples as well as by chemical analysis of the different brines after reaction with the cement.

KCl brine only attacked the fresh water cement at the direct cement-brine interface, whereas the salt water cement was hardly modified.

Both $MgCL_2$ and $CaCL_2$ attack on fresh and salt water cements were severe. The degrading mechanism is explained by the formation of alkali hydroxides and silicates, and the related pH decrease that leads to C-S-H instability. Furthermore the formation of chloroaluminates, gypsum, and an unrecognized Ca containing phase is presented.

Apresenta-se a interação entre álcali e salmouras saturadas de terra alcalina e cimentos de alta resistência a sulfato hidratados, misturados seja com água pura, seja com água contendo 30% de NaCL.

As razões da degradação do cimento foram estudadas por XRD, microscopia ótica e eletrônica de varredura nas amostras de cimento atacadas, bem como por análise química das diversas salmouras após a reação com o cimento.

A salmoura de KCl somente atacou o cimento de água pura na interface direta de cimento-salmoura, enquanto o cimento de água salgada foi pouco modificado.

Tanto o ataque de $MgCl_2$ como $CaCl_2$ aos cimentos de água pura e de água salgada foi severo. O mecanismo de degradação é explicado pela formação de hidróxidos e silicatos alcalinos, e a relativa diminuição do pH, que leva à instabilidade de C-S-H. Além disso se apresenta a formação de cloroaluminatos, gesso, e de uma fase não conhecida contendo Ca.

INTRODUCTION:

Hydrated Portland cements are occasionally exposed to highly degrading environments : sulfates, low pH, and chlorides alter hydrated cements.

The most common agents are the chloride salts of sodium, potassium, calcium, and magnesium. The degrading action of these salts occurs when deicing salts remain on pavements or car parking areas, and when cemented oil-, gas-, or geothermal wells pass natural complex salt zones or pressurized brine containing formations.

The aim of the present study is to describe the mechanism of the reactions between cement low in C_3A (high sulfate resistant oilwell class G), mixed either with fresh or 30% NaCL containing water (as commonly applied in the field of oil well cementing) and saturated alkali- and earth alkali chloride brines.

LITERATURE REVIEW

Most of the previous investigations on cement to salt water interactions were focussed on sea water attack (see [1] and references). Data on the reaction between saturated salt solutions and hydrated portland cements are less frequent.

The interaction between hydrated Portland cements and saturated chloride brines is very complex: on one hand, a diffusion controlled penetration occurs (see [2]), on the other hand, complex combinations of dissolution and mineral replacement as well as precipitation of newly formed minerals can be observed. These reactions will favour the accessibility of the respective brines to inner parts of the cement (see [2] and [3]). The importance of the chemically and mechanically formed fissures will be increased under field conditions such as freeze-thaw cycles for surface environments and by high temperature and pressure conditions for borehole conditions.

The data on the chemistry of cement - chloride brine interaction are contradictory : Midgley [2] stated that the quantity of portlandite within a cement sample hardly varied with NaCL penetration, whereas Kawadkar [4] found that the solubility of portlandite can be increased by up to 40 % in the presence of both, Na and Ca chlorides.
Chatterji [5] explains the disappearance of $Ca(OH)_2$ by the formation of a complex salt containing both, $CaCl_2$ and portlandite, as soon as brines rich in calcium chloride come into contact with calcium hydroxide.
The action of $MgCl_2$ rich solutions on hydrated cements too, has been the matter of the most controversial discussions: Lea [6] stated that "solutions of $MgCl_2$. produce a gradual diminution in the strength of portland cements, portland blast furnace, and pozzolanic cements", wheras Heppner et al [7] report high Mg resistance of cement-pozzolan blends. Oberste-Padtberg [3] showed that blast furnace slag cements were attacked in the same way as ordinary portland cements.

EXPERIMENTAL WORK

Class G oilwell cement (oxide analysis : see table 1) was mixed with fresh water and also with 30 % NaCL containing water to a specific gravity of 1.98 and water cured (fresh and salt water) for 48 hours at 45°C and atmospheric pressure. After this, disks of the respective cement sample (h = 20mm ; d = 40 mm) were introduced into deionized water as well as supersaturated brines of KCl, $CaCl_2$ and $MgCl_2$. The brine/hydrated sample ratio at the beginning of the test was 6.7.

CaO	SiO_2	Fe_2O_3	Al_2O_3	MgO	Na_2O	K_2O	SO_3
64.7	21.6	5.9	3.6	0.75	0.11	0.6	2.3

Table 1 : Oxide composition of cement (in wt %)

After a reaction period of 3 months at 55°C, the reacted brines were analysed by ICP for major cations (see table 2),and the altered cement samples were examined by XRD,SEM/EDAX,TGA, and optical microscopy.

RESULTS

1. Reaction with deionized water

Only the salt cement was degraded by deionized water. The reason for this was mainly the NaCl dissolution out of the hydrated cement sample. In fig.1, we can see halite crystals that have been formed during the hydration of a cement mixed with a 30 % NaCl containing brine. Water with a salt dissolving capacity will leach NaCl out of the hydrated cement, thus leaving a porous cement/water contact rim. After three months at 55°C this rim has a thickness of 2 to 3 mm. The pores, observed in this sample still trace in many cases the cubic form of the NaCl crystals (center of fig.2).

2. Attack by $MgCl_2$ brines

Both, salt and fresh water based cements were highly degraded by a concentrated $MgCl_2$ brine. The degrading mechanism proved to be mainly based on the formation of brucite (up to 23 wt % $Mg(OH)_2$ of the attacked sample). This magnesium hydroxide formation is related to a pH decrease.
A combination of mechanical fissuring due to $Mg(OH)_2$ precipitation and C-S-H- decay due to changed pH conditions will render the cement stone brittle.
It could be shown that the brucite within the Mg attacked sample can be of different generations (for details see [3]).

3. Attack by KCl brines

The effect of a KCl saturated brine on both, salt and fresh water based cement stone was minor : after three months, a slightly altered rim of about 2-3 mm thickness has been formed at the cement - brine interface (see fig.3). Throughout all the KCl stored samples, more or less constant amounts in portlandite (about 5 wt % of the brine stored sample) were determined. At the reaction interface all initially existing C_3A and calcium sulfoaluminate was converted to $C_3A.CaCl_2.10H_2O$. Neither ettringite nor syngenite could be detected within the aged samples. A new mineral phase with a broad XRD peak at d = 6.2 was formed at the direct brine-cement contact. It was found by optical microscopy that it is the reaction product between anhydrous calcium silicates and the brine (see fig.4); this alteration product always occurs in the form of very fine grained crystals.

The pH at the brine-cement interface is hardly affected by KCl contamination; the dissolution of Si, Fe and Al out of the cement by a KCl rich solution is also negligible (see tab.2).

4. Attack by $CaCl_2$ brines

Like $MgCl_2$ saturated brines, $CaCl_2$ saturated ones have a most detrimental effect on hydrated portland cements. Both, salt and fresh water mixed samples were highly fissured.
The calcium chloride brine has drastically decreased the pH at the cement-brine interface and dissolved considerable amounts in Al, Fe and Si out of salt- and fresh water mixed cement stones (see tab.2).

A common reaction product of the brine with both, fresh- and salt water mixed cement samples is C_2SH_{2-4} (see JCPDS file n° 11-211), which occured throughout the sample in the pores and on fissures. By transmitted light microscopy this mineral was identified as colourless and biaxial negative with a relatively low birefrigence. Its dominant cleavage plane is parallel to the Z axis. SEM observations revealed on fractures within the altered cement samples their idiomorphic appearance and their gypsum like twinning (fig.5).

Only in the 30 % NaCl containing water mixed sample, a further mineral species occured: its main XRD peaks occured at d = 9.56 and 5.46 (see [5]). In transmitted light, this constituent could be identified on pores, probably replacing primary hydrates such as C-S-H and CH phases, as a biaxal (negative) mineral of relatively high birefrigence (about0.020-0.025) that occured as a monocrystalline fracture filling (fig.6).

Both, salt water and fresh water mixed $CaCl_2$ aged cement samples contained less than 3 wt % portlandite (detected by TGA).

SAMPLE	A + $MgCl_2$ brine	B + $MgCl_2$ brine	A + KCl brine	B + KCl brine	A + $CaCl_2$ brine	B + $CaCl_2$ brine
Fe	5.0	4.9	0.3	0.3	113	98
Al	22.0	19.5	0.0	0.4	26	34.3
Si	0.0	0.0	0.0	0.0	198	171
pH	7.2	7.4	12.3	12.2	8.1	7.6

Tab.2 : pH values and ionic concentrations in ppm, after 3 months reactions of 300 ml saturated chloride brine with 45 g hydrated cement at 55 C.

A = fresh water cement ; B = salt water cement

DISCUSSION

A salt free or poor aqueous solution can deteriorate hydrated salt water based cements. This attack is mainly due to salt dissolution out of the hydrated cement, creating propagating pores at the cement water interface.

The interaction of hydrated and hydrating cements with all alkali and alkaline earth chlorides yields $C_3A.CaCl_2.10H_2O$; gypsum was the only sulfate carrier detected in all the altered cements.

The mechanism and severity of different chloride attacks on hydrated cements are different: the replacement of calcium silicates by a fine grained mineral phase after long KCl exposure has only very low influence on the integrity of a hydrated cement sample. Furthermore, the pH of the pore water is hardly affected by KCl brines; consequently, the originally formed C-S-H phases remain - apart from Cl-incorporation - stable [9] .

The common effect of both, calcium and magnesium chlorides is a drastic decrease in the pH at the brine- cement interface. This leads to a CSH decay and, consequently, to the cement degradation. Differently to the $CaCl_2$ attacked cement, where high amounts of the Si from the CSH phase within a, under all pH conditions, stable chrysotile like magnesium silicate which has no bonding properties (see [3]).

For $MgCl_2$ attack, the degree of degradation will still be increased by the precipitation of different generations of brucite, leading to a further fissuring of the cement.

The interaction between a $CaCl_2$ brine and hydrated NaCl containing and NaCl free cements yielded the formation of two mineral phases : C_2SH_{2-4} and an unknown phase with XRD peaks at d = 9.56 and 5.46 A (in salt cement only). As after the reaction of calcium chloride with hydrated cement no portlandite could be detected, this unidentified phase has been attributed by Chatterji [5] to the reaction product between water, portlandite, and $CaCl_2$.
A synthesis of this phase from $CaCl_2$- $Ca(OH)_2$-H_2O (-NaCl) at different concentrations did not succeed.

Beside the formation of these mineral phases with probably no binding properties at the expense of the originally present CSH, and beside the CSH decay due to pH drop, the dissolution of cementitious compounds (see table 2) will lead to a drastic cement degradation as soon as $CaCl_2$ rich brines come into contact with hydrated portland cements.

A possibility of rendering the hydrated cement stones less sensitive to chloride brine attack appears to be the addition of sodium chloride to the cement mix water. According to equilibrium data by [8] the solubility of NaCl in the system NaCl-KCl-$MgCl_2$-$CaCl_2$-H_2O can be drastically decreased by addition of alkaline earth chlorides. Consequently, the halite crystals formed within the cement during hydration cannot be entirely dissolved, and thus form a protective layer within the cement, being in contact with a (K,Mg, Ca)Cl_2 brine. In fact, this protecting halite is only stable as long as the above mentioned water-chloride system is in equilibrium; i.e. as long as the amount of attacking brine is low in comparison to the attacked cement.

LITERATURE

[1] Massazza, F. : Concrete Resistance to Sea Water and Marine Environment ; Il Cemento, V.1, pp 3-26 (1985)

[2] Midgley, H.G.; Illston, J.M. : The Penetration of Chlorides into Hardened Cement Pastes; Cement and Concrete Research, V.14,pp 546-558 (1984)

[3] Oberste-Padtberg, R. : Degradation of Cements by Magnesium Brines - a Microscopic Study; 7th International Conference on Cement Microscopy, pp 24-36 (1985)

[4] Kawadkar, K.G. : Behavior of Cement Concrete Under Common Salt Solutions Both Under Hydrostatic and Atmospheric Pressure; Cement and Concrete Research, V.11, pp 103-113 (1981)

[5] Chatterji, S. : Mechanisms of $CaCl_2$ Attack on Portland Cement Concrete; Cement and Concrete Research, V.8, pp 461-468 (1978)

[6] Lea, F.M. : The Chemistry of Portland Cement and Concrete, 3rd edition; pp 202, 301, 347 (1971)

[7] Heppner, J. ; Peter S.; Weickhardt,O. : Zur Bestaendigkeit von Tiefbohrzementen gegenueber Formationswaessern mit hohen Gehalten an Magnesium-salzen; Erdoel-Erdgas Zeitschrift, V.84, pp 371-375 (1968)

[8] Borchert, H. : Die Salzlagerstaetten des deutschen Zechsteins; Reichsstelle fuer Bodenforschung, pp 13-23 (1940)

[9] Regourd, M.; Hornain, H.; Montureux, B.: Microstructure of Concrete in Agressive Environment; 1st Intern. Conf. on Durability of Building Materials and Components Nat. Res. Counc. Canada, Ottawa (1978)

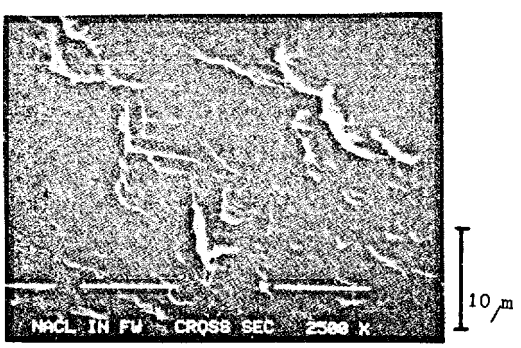

Fig. 1: SEM photo of NaCl crystals in hydrated 30% NaCl brine mixed cement.



Fig. 2: SEM photo showing the effect of fresh water attack on 30% NaCl brine mixed cement. Note : hole in the center of the fig. traces the cubic habit of NaCl

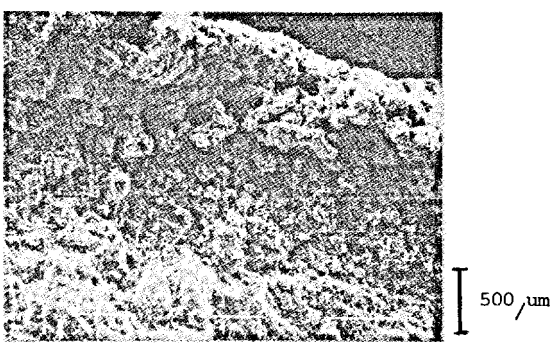

Fig. 3: KCl brine attacked fresh water mixed cement (contact brine-cement)

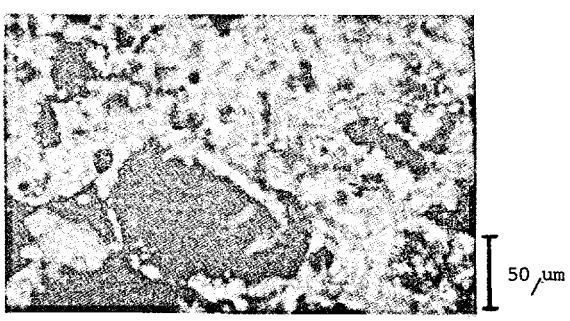

Fig. 4: Belite crystal, marginally replaced by an unknown mineral phase (see text). Fresh water cement in KCl brine after 3 months (optical microphoto, trasnmitted light, crossed Niccols)

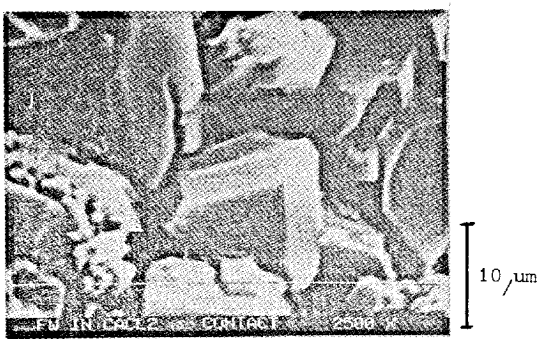

Fig. 5: SEM photo of C_2SH_{4-10} twins on a facture within the fresh water cement stored in a $CaCl_2$ brine.

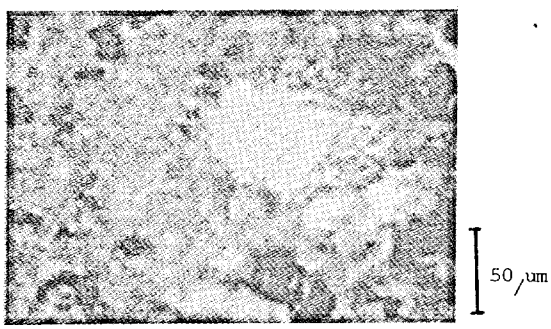

Fig.6 : Unknown mineral phase formed within a pore of a 30% NaCl brine mixed cement (optical microphoto, transmitted light, crossed Nicols + gypsum).

R. DRON, F. BRIVOT - LABORATOIRE CENTRAL DES PONTS ET CHAUSSEES
58, Bd Lefebvre - 75015 PARIS - FRANCE

CONTRIBUTION A L'ETUDE DU GONFLEMENT ETTRINGITIQUE

4.2

A CONTRIBUTION TO THE STUDY OF ETTRINGITE CAUSED EXPANSION

RESUME : L'ettringite synthétique calcinée à 1000 °C constitue un bon matériau modèle pour l'étude du gonflement lié à la formation d'ettringite, la réhydratation en pâte pure étant complète en 2 heures environ et s'accompagnant d'une expansion linéaire totale de l'ordre de 10 % en l'absence de contraintes.

On montre que la variation de l'expansion finale en fonction du rapport solide/eau est conforme au modèle en sphérolithes croissant radialement. En absence de toute contrainte latérale, l'application d'une contrainte uniaxiale, au delà d'un certain seuil de l'ordre de 0,1 MPA, annule totalement l'expansion dans la direction correspondante.

Le mécanisme de l'expansion est discuté, sur la base d'une expérimentation sur des compacts d'ettringite ultra fine s'imprégnant d'eau par capillarité, qui met en évidence l'absence de tout gonflement colloïdal de l'ettringite elle-même. On a pu chiffrer le degré de sursaturation de la solution mère des cristaux d'ettringite et en déduire la pression de cristallisation. L'expansion doit être attribuée à l'effet de cette pression à l'extrémité des aiguilles situées en périphérie des sphérolithes et non à leur base, l'ettringite se formant par un mécanisme de dissolution cristallisation si l'on part du produit calciné à 1000 °C.

Le produit amorphe à 4 H_2O résultant de la calcination à 250 °C se réhydrate instantanément par un processus topochimique qui ne s'accompagne d'aucun gonflement.

A etringita sintética calcinada a 1.000°C constitui um bom material modelo para o estudo da inchação ligada à formação de etringita, estando completa a reidratação da pasta pura em cerca de 2 horas e sendo acompanhada duma expansão linear total da ordem de 10% com ausência de tensões.

Mostra-se que a variação da expansão final em função da relação sólido/água está de acordo com o modelo de esferólitos radialmente crescente. Na ausência de qualquer confinamento lateral, a aplicação de uma tensão axial, acima de um piso determinado da ordem de 0,1 MPa, anula totalmente a expansão na direção correspondente.

Discute-se o mecanismo de expansão com uma experiência com etringita ultra-fina compactada impregnada de água por capilaridade, que evidencia a ausência de qualquer inchação coloidal da etringita propriamente dita. Pôde-se quantificar o grau de super-saturação da solução pura de cristais de etringita e deduzir-se a pressão de cristalização. A expansão deve ser atribuída ao efeito desta pressão na extremidade das agulhas situadas na periferia dos esferólitos e não na sua base, formando-se a etringita por um mecanismo de dissolução cristalização se se parte do produto calcinado a 1.000°C.

O produto amorfo com 4 H_2O resultante da calcinação a 250°C se reidrata instantaneamente por um processo topoquímico que não é acompnhado de qualquer inchação.

INTRODUCTION

Etant donné son importance dans la technique des bétons expansifs et son intervention dans le processus d'attaque sulfatique des ciments, le gonflement ettringitique a donné lieu à de nombreuses recherches et publications |1 à 10|. Dans une étude récente, Cohen |8| distingue en matière d'explication du phénomène deux "écoles de pensée". Ce point de vue, contesté par Mathers |9| nous parait reflèter assez correctement la littérature de ces dernières années et nous l'adopterons pour la clarté de l'exposé.

Selon la première de ces écoles, l'expansion est liée aux propriétés colloïdales de l'ettringite, lesquelles seraient dues à l'extrême petitesse des cristallites, dont la taille est de l'ordre du µm et d'autre part à leur caractère hautement hydrophile. Le système formé par les microcristaux et l'eau constitue selon Mehta |2| un "gel" qui gonfle par absorption d'eau.

Selon l'autre école, l'expansion est provoquée par la croissance des aiguilles d'ettringite. Les modèles proposés mettent en avant la morphologie aciculaire des cristaux élémentaires et leur disposition rayonnante qui confère aux sphérolithes familiers à tous les observateurs l'aspect d'un hérisson ou d'une bogue de châtaigne. Cette comparaison naturaliste nous permet d'illustrer une première question irrésolue: les aiguilles s'allongent-elles par leur racine, à la façon des cheveux ou des piquants du hérisson (mode animal), ou par leur apex, comme croissent les tiges des plantes et les épines de la châtaigne (mode végétal) ? Curieusement, c'est la première hypothèse qui est le plus généralement postulée, bien que la réalité du mécanisme de formation par l'intermédiaire de la solution ait été démontrée |10|.

L'autre question irrésolue, et bien posée par Mathers, concerne l'origine ultime de la force qui s'exerce sur la matrice et qui prend naissance sur l'ettringite déjà formée (1ère école) ou sur l'ettringite en cours de formation (2ème école), étant entendu que le phénomène ne saurait être expliqué par la variation volumique de réaction de formation à partir des constituants solides et de l'eau, cette variation étant négative.

CONDITIONS DE FORMATION DE L'ETTRINGITE

Les conditions de stabilité, et donc de formation de l'ettringite, sont précisées par la connaissance du diagramme d'équilibre du système $CaO-Al_2O_3-CaSO_4-H_2O$ qui fut étudié par d'Ans et Eick |11|. Ces auteurs ont montré que deux variantes doivent être envisagées, selon qu'on s'intéresse aux espèces stables thermodynamiquement ou aux espèces métastables qui se forment naturellement dans les conditions usuelles. La représentation qu'ils ont adoptée utilise l'échelle linéaire des concentrations des oxydes en solution, exprimées en mg/l, ce qui conduit à l'élargissement démesuré de certains domaines, tandis que d'autres sont fortement réduits. Il en résulte un manque de lisibilité de la figure à trois dimensions qui rend son utilisation très incommode.

Nous proposons une représentation plus parlante, basée sur l'échelle des potentiels chimiques ou, ce qui revient au même, sur l'échelle logarithmique des produits ioniques.

On pose

$$C = |Ca^{2+}|.|OH^-|^2 \qquad \text{et} \quad x = \log C$$

$$A = |AlO_4H_4^-|^2/|OH^-|^2 \qquad y = \log A$$

$$C\bar{S} = |Ca^{2+}|.|SO_4^{2-}| \qquad z = \log C\bar{S}$$

On montre facilement que les surfaces de solubilité sont alors des plans dont les équations sont obtenues à partir du produit de solubilité des différents hydrates. On peut voir que le formalisme de l'écriture du produit de solubilité est calqué sur celui de la formule conventionnelle en oxydes, abstraction faite des molécules d'eau. Par exemple, pour l'ettringite, le produit de solubilité a pour expression

$$P_{C_6A\bar{S}_3H_{32}} = C^6A\bar{S}^3$$

Compte tenu des données de la littérature, on aboutit pour le système métastable à la figure 1 a dans laquelle les surfaces de solubilité sont des plans et les lignes monovariantes des droites dont les paramètres directeurs sont entiers et égaux aux coefficients stoechiométriques.

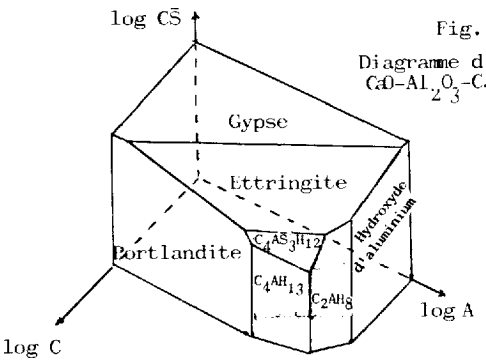

Fig. 1 a
Diagramme d'équilibre $CaO-Al_2O_3-CaSO_4-H_2O$

Le solide de solubilité se projette sur le plan x, z suivant la figure 1 b, qui résume clairement les conditions de formation et de coexistence des différents hydrates usuels et de l'ettringite en particulier.

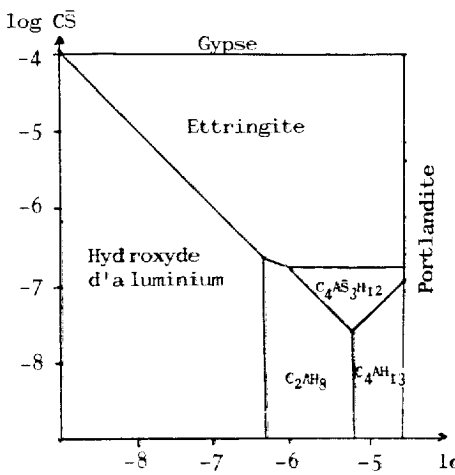

Fig. 1 b
Représentation plane du diagramme d'équilibre

PROPOSITION D'UN MODELE POUR L'ETUDE DU GONFLEMENT

L'étude de l'expansion liée à l'ettringite a été abordée par la plupart des chercheurs en prenant comme support expérimental un mélange en proportions stoechiométriques de réactifs anhydres tels que le produit unique de la réaction soit l'ettringite. Le sulfo-aluminate de calcium $C_4A_3\bar{S}$, qui constitue l'élément actif des ciments expansifs de type K a le plus souvent servi de base à ces mélanges, qui contiennent par ailleurs la chaux et le sulfate de calcium nécessaires à la réaction :

$$C_4A_3\bar{S} + 6\ C + 8\ C\bar{S} + 96\ H \longrightarrow 3\ C_6A\bar{S}_3H_{32}$$

Ce mélange est en général obtenu à partir de ses constituants, préparés séparément. Nous proposons de l'obtenir plus simplement par calcination à 1000 °C d'une ettringite commerciale préparée par voie humide à partir du mélange stoechiométrique de sulfate d'aluminium et de chaux éteinte pure. L'examen aux rayons X du produit calciné montre que la réaction inverse de la précédente a lieu et qu'elle est complète en 1 heure environ. Nous avons prolongé en fait la cuisson à 5 heures, de façon à faire grossir les grains de $C_4A_3\bar{S}$ aux environs de 5 µm, ce qui modère la cinétique de la réaction de réhydratation.

Si on limite la température de cuisson à 250 °C, on obtient un produit amorphe contenant 4 H_2O par mole d'alumine, qui se réhydrate instantanément par addition d'eau. Cette réhydratation a lieu également par simple exposition de la poudre à une atmosphère saturée en vapeur d'eau à 40 °C, ce qui tend à prouver que le composé amorphe $C_6A\bar{S}_3H_4$ est une ettringite "effondrée" qui redonne l'ettringite normale par fixation topochimique des molécules d'eau qui reprennent simplement leur place.

On est amené à penser qu'en revanche, la réhydratation du produit cristallisé obtenu par calcination de l'ettringite à 1000 °C est un processus trans-solution puisque les phases réactives sont séparées et que le transfert de matière aboutissant à la reconstitution de l'ettringite nécessite la présence d'une phase liquide. En effet, l'exposition de ce produit à la vapeur saturante conduit simplement à l'extinction de la chaux vive, tandis que l'anhydrite et le sulfo-aluminate de calcium anhydre ne sont pas affectés.

ETUDE CINETIQUE DE LA REACTION D'HYDRATATION DE L'ETTRINGITE CALCINEE

Dans la mesure où la transformation de l'ettringite calcinée en ettringite à 32 H_2O est un processus direct (en fait, cette réaction est précédée par l'extinction de la chaux vive) son degré d'avancement varie proportionnellement à la chaleur dégagée de l'instant t_0 à l'instant t. La microcalorimétrie constitue donc un bon outil d'étude de la cinétique de la réaction.

L'expérimentation a été conduite sur un microcalorimètre type Calvet, sur une prise d'essai de 0,6 g de matière.

Les courbes de chaleur cumulée en fonction du temps ont l'allure donnée Fig. 2 et peuvent être caractérisées par un temps de latence τ, un temps de demi réaction $t_{1/2}$ et le niveau Q_∞ de l'asymptote.

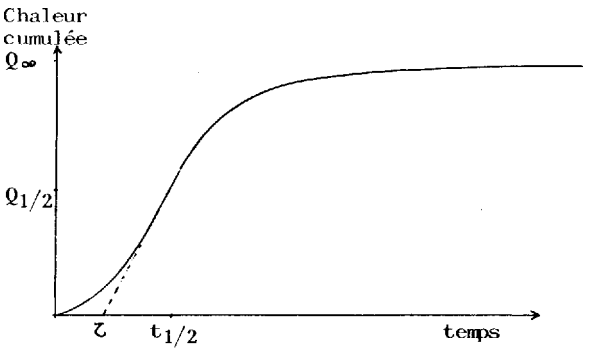

Fig. 2 : Allure des courbes calorimétriques

Au delà du temps de demi-réaction, la cinétique obéit assez bien à une loi d'ordre 2, c'est à dire que le flux de chaleur varie comme le carré du complément à 1 du degré d'avancement de la réaction :

$$\frac{dQ}{dt} = K\ (Q_\infty - Q)^2$$

ou encore

$$\frac{d\alpha}{dt} = K'(1-\alpha)^2$$

ce qui correspond à une variation hyperbolique de α en fonction du temps.

La chaleur totale d'hydratation est indépendante des conditions opératoires et est égale à 160 ± 5 calories par gramme d'ettringite calcinée soit 110 ± 4 KCal/mole

Le temps de latence est de l'ordre de 4 minutes et est indépendant du rapport eau/solide et du temps de cuisson en l'absence de retardateur.

Le temps de demi-réaction est de 20 minutes pour un produit calciné 1 heure, quel que soit le rapport e/c et de 40 minutes pour 5 heures de cuisson ou pour une addition de 18 g/l de lignosulfonate de sodium à l'eau de gâchage.
La réaction est pratiquement complète en 2 heures environ dans tous les cas, ce qui permet d'utiliser très commodément ce système modèle pour l'étude de l'expansion.

L'évolution de la phase aqueuse en cours d'hydratation peut être suivie par enregistrement de la conductivité électrique qui dépend de la concentration des ions en solution. Pour que la mesure soit une image correcte de l'évolution des concentrations, il faut que le volume des phases solides soit faible par rapport à celui de la phase aqueuse, ce qui nous a conduit à faire l'étude sur une suspension de rapport e/c = 20, à la température ambiante. L'enregistrement conductimétrique obtenu sur une suspension de 2 g d'ettringite calcinée dans 40 ml d'eau est reproduit Fig. 3.

Il comporte un pic initial qui est suivi d'un premier palier s'étendant sur 60 minutes, puis d'une chute vers un second palier qui se prolonge indéfiniment. La comparaison avec la conductivité de suspensions de même rapport e/c du mélange gypse-chaux éteinte d'une part et de gypse seul d'autre part montre que ces deux paliers correspondent respectivement à la saturation en gypse-chaux et en gypse, ce que confirme l'analyse chimique des solutions, après filtration.

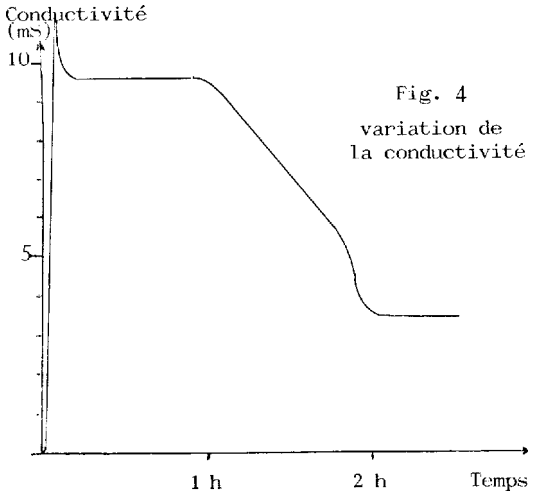

Fig. 4

variation de
la conductivité

sur le premier palier la solution contient également des ions $AlO_4H_4^-$, à la concentration de 0,042 millimoles par litre, soit 2,14 mg/l d'Al_2O_3, déterminée par TCP.

Le pic initial correspond probablement à l'extinction de la chaux vive et à la solubilisation d'anhydrite, suivies d'un retour à l'équilibre par précipitation de gypse.

La présence d'alumine dans la solution prouve que la phase $C_4A_3\bar{S}$ passe également en solution, sans qu'on puisse affirmer que l'équilibre de dissolution est atteint, ce qui sera discuté en fin de communication. Une expérience complémentaire permet de confirmer que $C_4A_3\bar{S}$ se dissout : Si l'on fait passer très rapidement 10 ml d'eau distillée sur 1 g d'ettringite calcinée placée sur un filtre millipore, on constate qu'au premier passage la solution contient 10 mg/l d'Al_2O_3, soit 0,2 mmole/l d'ions aluminate, avec 30,2 mmole/l d'ions OH^-, 2,7 mmole/l de SO_4^{2-} et 17,9 mmole/l d'ions Ca^{2+}. Si la solution filtrée n'est pas immédiatement acidifiée, il apparait rapidement un louche dû à la précipitation de l'ettringite. Si on prolonge la percolation par fractions de 10 ml, on arrive à la cinquième fraction à 1 mmole/l de OH^-, 1,6 mmole/l de SO_4^{2-}, 4,8 mmole/l de Ca^{2+} et 5,4 mmole/l d'$AlO_4H_4^-$ et la solution reste limpide.

DISPOSITIF D'ETUDE DU GONFLEMENT

Le montage de la Fig.4 nous a permis d'étudier l'expansion libre d'une pâte obtenue par mélange d'ettringite calcinée et d'eau.

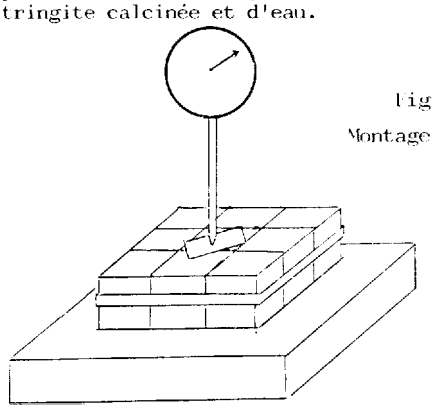

Fig. 4

Montage utilisé

La variation dimensionnelle d'un cube de pâte de 1 cm d'arête recouvert d'une plaquette de verre est mesurée à intervalles réguliers au moyen d'un comparateur mécanique sensible au µm, qu'on relève entre les mesures. Les cubes métalliques qui forment le moule sont graissés pour éviter les frottements, de même que la glace qui les supporte. Ils sont maintenus par un élastique faiblement tendu, de sorte que l'expansion peut être considérée comme libre dans les trois directions.

Les courbes de gonflement sont obtenues en portant la variation dimensionnelle en fonction du temps. Leur allure est semblable à celle des courbes de chaleur cumulée mais lorsqu'on effectue la normalisation en % de la valeur asymptotique, elles ne sont pas superposables. L'élimination de la variable temps entre la courbe de gonflement et la courbe de chaleur cumulée correspondant au même mélange donne une relation linéaire dans la seconde partie du domaine, ce qui signifie que l'expansion ne débute qu'à partir d'un certain degré d'avancement et qu'elle est ensuite proportionnelle à l'avancement de la réaction.

INFLUENCE DU RAPPORT EAU/SOLIDE SUR LE GONFLEMENT

On a fait varier le rapport eau/solide de la valeur 1 proche du minimum théorique de 0,85 nécessaire à l'hydratation complète, jusqu'à la valeur 2, au delà de laquelle il y a ressuage de la pâte.

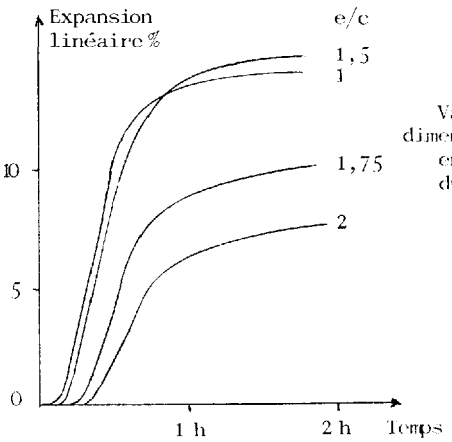

Fig. 5

Variations
dimensionnelles
en fonction
du temps

Les courbes de gonflement sont données Fig. 5. Leurs paramètres caractéristiques sont les suivants :

e/c	temps de latence (min)	temps de demi-expansion (min)	expansion linéaire limite (%)
1	9	20	13,5
1,25	10	24	14,35
1,5	11	22	14,25
1,75	16	32	9,8
2	19	37	7,45

On remarque que l'expansion finale est maximale aux environs de e/c = 1,25 et qu'elle décroit ensuite de façon régulière.

Les bilans volumiques des matières présentes dans la pâte fraiche et dans la pâte durcie permettent d'interpréter cette décroissance.

Pour faire le calcul, nous avons utilisé les données de Mathers |9| relatives à la réaction

$$C_4A_3\bar{S} + 8\ C\bar{S} + 6\ C + 96\ H \longrightarrow 3\ C_6A\bar{S}_3H_{32}$$

masses	610	1088	336	1728	3762
densités	2,6	2,96	3,32	1	1,73
volumes	235	368	101	1728	2175

La densité du mélange $C_4A_3\bar{S}$, 8 CS, 6 C est la suivante

$$d = \frac{610 + 1088 + 336}{235 + 368 + 101} = 2,89$$

Sa fraction volumique dans la pâte fraîche est $\frac{c}{c + ed}$

Δ étant l'expansion linéaire, le volume initial est 1 et le volume final $(1 + \Delta)^3$.

On en déduit les fractions volumiques des différentes phases, exprimées en % du volume total.

e/c	1	1,25	1,5	1,75	2
c/(c + ed)	0,257	0,216	0,187	0,165	0,1475
$(1 + \Delta)^3$	1,462	1,495	1,491	1,324	1,240
ettringite %	54,3	44,8	38,8	38,5	36,5
eau résiduelle	6,1	16,8	23,6	32,5	39,5
air % vol.	39,6	38,4	37,6	29,0	23,2

On constate qu'à partir de e/c = 1,5 la fraction volumique de l'ettringite est pratiquement constante et voisine de 3/8., ou ce qui revient au même, que le volume final $(1 + \Delta)^3$ est proportionnel au volume c/(c+ed) de matière anhydre présente dans la pâte fraîche, le coefficient de proportionnalité étant proche de 8.

L'eau résiduelle n'est pas suffisante pour compléter le volume final à 100 % et l'on est forcé d'admettre que les interstices sont particllement remplis d'air. Il est donc vraisemblable, étant donné la disposition radiale des aiguilles, que la phase aqueuse tend à se concentrer à leur base par capillarité aux faibles rapports e/c, et sur toute la longueur des aiguilles quand le volume de liquide devient suffisant.

L'hypothèse d'un développement des cristaux d'ettringite par un mécanisme trans-solution rend compte de la variation observée de la porosité finale en fonction du rapport e/c :
- Aux fortes valeurs du rapport e/c, le volume de liquide résiduel étant de l'ordre de celui de l'ettringite formée, les aiguilles restent enveloppées d'une couche liquide qui assure le transport de la matière dissoute, et peuvent croître par leur extrémité. La morphologie des sphérolithes est alors invariable et leur volume est proportionnel à la quantité de matière anhydre initialement présente.
- Aux faibles valeurs du rapport e/c, le confinement de la phase aqueuse à la base des aiguilles entraine une densification du coeur des sphérolithes et donc une extension moindre de leur surface enveloppe. La croissance suivant le mode "animal" se traduirait par une morphologie invariable, même à faible rapport e/c et par une expansion maximale à la stoechiométrie (e/c = 0,85).

INFLUENCE D'UNE CONTRAINTE UNIAXIALE SUR LE GONFLEMENT

Le dispositif expérimental utilisé pour l'étude du gonflement libre a été aménagé afin de permettre la détermination de l'influence d'une contrainte de pression simple.

On constate que lorsque la charge augmente, le gonflement décroit d'abord rapidement, puis de façon plus modérée jusqu'au voisinage de 1 Kg. Au delà, l'expansion diminue à nouveau très rapidement et s'annule pour une charge bien définie voisine de 1150 g/cm^2.

MISE EN EVIDENCE DU CARACTERE NON GONFLANT DE L'ETTRINGITE

Pour prendre parti entre les deux **"écoles de pensée"** expansion colloïdale ou liée à la cristallisation, il convient de savoir si le phénomène est lié à la simple présence ou à sa formation in situ. Dans la première hypothèse, l'expansion doit pouvoir être mise en évidence sur de l'ettringite existant préalablement à l'expérimentation.

L'expérience suivante tend à prouver qu'elle ne se manifeste pas dans ces conditions:

On part d'ettringite pure obtenue par réhydratation en pâte d'ettringite calcinée. La masse durcie est broyée au mortier et séchée à poids constant à 40 °C On réalise au moyen d'une presse, sous une pression de l'ordre de 50 MPa une pastille de 2,54 cm de diamètre et de 0,54 cm de hauteur. La porosité calculée est de 17 %. Cette pastille, très compacte, a une excellente cohésion. Elle est placée dans une boîte de Pétri dans laquelle on verse de l'eau jusqu'à affleurement de la face supérieure. Elle conserve son intégrité tandis que l'eau pénètre par capillarité et que l'auréole due à l'imprégnation par l'eau se resserre progressivement, avec un front circulaire qui s'amenuise jusqu'à disparaître en deux minutes environ. On mesure alors à nouveau le diamètre et on constate qu'il n'a pratiquement pas varié. On replace la pastille dans la boîte de Pétri et l'on constate que ses dimensions restent stables indéfiniment.

La variation dimensionnelle étant au maximum de 0,1 mm, soit 0,4%, on voit que le phénomène est sans commune mesure avec ce que l'on observe lors de la formation in situ de l'ettringite. La même expérience, faite sur une pastille semblable d'ettringite calcinée, conduit à une expansion diamétrale de 40 %, accompagnée d'une désagrégation.

DETERMINATION DE L'ORDRE DE GRANDEUR DE LA PRESSION DE CRISTALLISATION

Il apparait nettement que le phénomène d'expansion ne se manifeste que pendant que l'ettringite se forme et qu'il est lié à l'existence de forces qui agissent en cours de croissance cristalline. Le travail de ces forces doit être rattaché à l'énergie libre de la réaction de formation de l'ettringite par recombinaison des constituants de l'ettringite calcinée et de l'eau :

$$C_4A_3\bar{S} + 6\ C + 8\ C\bar{S} + 96\ H \longrightarrow 3\ C_6A\bar{S}_3H_{32}$$

En fait, l'hydratation de la chaux vive et de l'anhydrite étant rapide, on doit considérer la réaction

$$C_4A_3\bar{S} + 6\ CH + 8\ C\bar{S}H_2 + 74\ H \longrightarrow 3\ C_6A\bar{S}_3H_{32} \quad (2)$$

L'énergie libre de la réaction (2) a pour expression

$$\Delta G° = 2,3\ RT \log \frac{S_B}{S_A} \text{ pour 3 moles d'ettringite}$$

dans laquelle S_A et S_B sont respectivement les produits de solubilité du premier et du second membre de la réaction, étendus à l'ensemble des composés de chaque membre, c'est à dire :

$$S_A = S_{C_4A_3\bar{S}} \cdot S^6_{CH} \cdot S^8_{C\bar{S}H_2}$$

et $$S_B = S^3_{C_6A\bar{S}_3H_{32}}$$

En prenant les logarithmes $pS_i = -\log S_i$, l'énergie libre de la réaction s'écrit :

$$\Delta G° = -2,3\ RT\ (3pS_{C_6A\bar{S}H_{32}} - pS_{C_4A_3\bar{S}} - 6\ pS_{CH} - 8pS_{C\bar{S}H_2}$$

$$= -2,3\ RT\ (3.39 - pS_{C_4A_3\bar{S}} - 6.4,5 - 8.4)$$

$$= -2,3\ RT\ (\ 58 - pS_{C_4A_3\bar{S}}\ )$$

$\Delta G°$ est donc négatif si le produit de solubilité de $C_4A_3\bar{S}$ est supérieur à 10^{-58}.

La prise en compte des données de concentration déterminées dans l'expérience de conductivité (C_1) et de percolation rapide (P_1 et P_2) permet de donner une valeur seuil du produit de solubilité de $C_4A_3\bar{S}$. Les résultats sont donnés avec les symboles définis en début de communication.

$$C = Ca^{2+}.(OH^-)^2 \quad C\bar{S} = Ca^{2+}.SO_4^{2-} \quad A = (AlO_4H_4^-)^2/(OH^-)^2$$

	-log C	-log CS̄	-log A	$-\log C^6A\bar{S}^3$	$-\log C^4A^3\bar{S}$
C_1	4,21	3,65	6,06	29,64	34,46
P_1	4,79	4,31	4,36	31,66	31,79
P_5	8,32	5,11	-1,46	38,83	25,69

On voit que dans les expériences C_1 et P_1, le produit de solubilité de l'ettringite, qui vaut 10^{-39}, est dépassé de 8 à 9 ordres de grandeurs. L'ordre de grandeur du produit de solubilité de $C_4A_3\bar{S}$ ne peut être déterminé avec précision puisqu'entre les trois déterminations, on peut hésiter entre -25 et -32. En tout état de cause, il est à un niveau supérieur d'environ 27 puissances de 10 à la valeur seuil de 10^{-58}.

L'énergie libre de formation de 3 moles d'ettringite est donc au moins :

$$\Delta G° = -2,3.27.RT$$

soit pour 1 mole d'ettringite :

$$\Delta G° = -2,3.9.8,32.298$$
$$= -51380 \text{ joules/mole}$$

Compte tenu du volume molaire de l'ettringite (725 cm^3) ce travail, rapporté au cm^3 de cristal en cours de croissance, est de 71 joules/cm^3. Si nous considérons une surface de croissance de 1 cm^2, ce travail est dû au déplacement de 1 cm du point d'application d'une force de pression P_c s'exerçant à la surface du cristal et qui n'est autre que la pression de cristallisation (loi de Riecke [12]). Elle vaut 71 10^7 dynes/cm^2 dans le système CGS et 71 MPa dans le système d'unités international.

CONCLUSION

La cristallisation de l'ettringite à partir d'une phase aqueuse très fortement sursaturée alimentée par la dissolution du gypse, de la chaux et du sulfo-aluminate de calcium anhydre fait apparaître sur les faces de croissance une pression très élevée de plusieurs dizaines de MPa qui explique largement l'expansion qui accompagne cette cristallisation.

La morphologie aciculaire des cristallites et leur disposition rayonnante font que le travail des forces de pression s'exerce sur les faces de croissance préférentielles situées en extrémité d'aiguille et à la périphérie des sphérolithes, lorsqu'une de ces faces vient à buter sur un cristal d'un sphérolithe voisin, donc pendant le bref intervalle de temps qui sépare l'approche à l'échelle moléculaire du contact franc par soudure.

Ce faible rendement du travail de cristallisation explique que la pression de gonflement, estimée par la contrainte d'inhibition, ne représente qu'une fraction infime de la pression de cristallisation déduite du facteur de sursaturation.

REFERENCES

1 - G.L. KALOUSEK et E.J. BENTON, ACI Journal, n°G7-9, fév. 1970, 187.

2 - P.K. MEHTA, Cem. Concr. Res. vol. 3, 1973, 1.

3 - M. ISH - SHALOM et A. BENTUR, Cem. Concr. Res., vol. 4, 1974, p. 519, vol. 4, 1974, 709.

4 - C.W. RICHARDS et R.A. HELMUTH, T R-191, Dept. of Civil Engineering, Stanford University, janv.1977.

5 - K. OGAWA et D.M. ROY, Cem. Concr. Res., vol. 11, 1981, 741, vol. 12, 1982, 101 et vol.12, 1982, 247.

6 - V. ALUNNO ROSSETTI, G. CHIOCCHIO et A.E. PAOLINI, Cem. Concr. Res., vol. 12, 577, 1982, vol.12, 667 et vol. 13, 1983, 23.

7 - M.D. COHEN, Cem. Concr. Res., vol. 13, 1983, 519.

8 - M.D. COHEN, Cem. Concr. Res., vol. 13, 1983, 809.

9 - MATHERS, Cem. Conc. Res., vol. 14, 1984, 603.

10 - P.M. MONTEIRO et P.K. MEHTA, Cem. Concr. Res., vol. 15, 1985, 378.

11 - J. d'ANS et H. EICK, Zement-Kalk-Gips, déc. 1954, 449.

12 - E. RIECKE, Annal. Physik, 54, 1895, 731.

C. VERNET, Société des CIMENTS FRANCAIS - C.E.R.E.G. (FRANCE)

EVOLUTION DE LA MICROSTRUCTURE DES BETONS AU COURS DU TEST ASTM DE GEL-DEGEL. INTERVENTION DE PROCESSUS REPARATEURS.

EVOLUTION OF THE MICROSTRUCTURE OF CONCRETE DURING THE ASTM TEST FOR FREEZING AND THAWING.

RESUME

L'observation au M.E.B. de la microstructure de 25 bétons, durant le test ASTM de gel/dégel C 666-80-B, montre l'intervention de processus antagonistes.

- *Processus destructeurs* : le gel produit des microfissures, qui progressent rapidement jusqu'au coeur des éprouvettes, en passant de préférence par les gros pores capillaires, l'auréole de transition des granulats et les gros cristaux de portlandite. Lorsque les fissures s'agrandissent, des processus chimiques de redissolution des hydrates accélèrent la destruction. L'orientation des hydrates indique qu'au cours des cycles, le béton se comporte comme une pompe. Ceci rend le dégel dans l'eau plus destructeur que dans l'air et rend ce test ASTM sensible à la ventilation des enceintes.
- *Processus réparateurs* : le ciment dépense son énergie chimique pendant la période de maturation et au cours du test, en fournissant des hydrates, qui colmatent les fissures et remplissent les pores. Les résistances mécaniques des bétons de durabilité correcte augmentent au cours du test. Le gel fait pénétrer du liquide dans les bulles d'air et ce dernier laisse déposer des hydrates dans la partie remplie.
- *Interprétation* : nous analysons à l'échelon microscopique les possibilités de compensation de l'augmentation de volume des cristaux de glace des gros pores, en faisant intervenir le retrait de la pâte par cryodessiccation des CSH. La compensation n'est plus possible au voisinage des granulats, des gros cristaux de glace ou de portlandite, d'où la microfissuration. Le voisinage d'une bulle permet d'amortir les différences de pression locales, ce qui justifie le concept d'espacement critique. Ce concept pourrait être utilisé avec profit pour évaluer le risque présenté par les gros pores aqueux, qui sont la source des contraintes.

A observação com M.E.B. da microestrutura de 25 concretos, durante o teste de gelo-degelo conforme ASTM C 666-80-B, mostra a intervenção de processos antagônicos.

- Processos destrutivos: o gelo produz microfissuras, que progridem rapidamente ao coração dos corpos de prova, passando preferencialmente pelos grandes poros capilares, a auréola de transição dos granulados e os grandes cristais de portlandita. Quando as fissuras crescem, processos químicos de redissolução dos hidratos aceleram a destruição. A orientação dos hidratos indica que no decorrer dos ciclos o concreto se comporta como uma bomba. Isto torna o degelo na água mais destrutivo que ao ar, e torna o teste ASTM sensível à ventilação dos recintos.
- Processos reparadores: o cimento desenvolve sua energia química durante o período de maturação e no decorrer do teste, fornecendo hidratos, que colmatam as fissuras e enchem os poros. As resistências mecânicas dos concretos de durabilidade correta aumentam durante o teste. O gelo faz com que líquido penetre nas bolhas de ar e este último deixa que hidratos se depositem na parte preenchida.
- Interpretação: analisamos em escala microscópica as possibilidades de compensação do aumento de volume dos cristais de gelo dos poros grandes, provocando a retração da pasta por criodessecação do CSH. A compensação não é possível na vizinhança dos agregados, dos grandes cristais de gelo ou de portlandita, donde a microfissuração. A proximidade de uma bolha permite amortecer as diferenças de pressão locais, o que justifica o conceito de espaçamento crítico. Este conceito poderia ser utilizado vantajosamente para se avaliar o risco apresentado por grandes poros aquosos, que são a fonte de tensões.

1 - INTRODUCTION

Aucune des théories qui se sont succédées pour expliquer le comportement du béton au gel ne s'est montrée vraiment satisfaisante. Le problème est en effet très complexe, car aux difficultés d'ordre thermodynamique qu'il faut vaincre pour décrire la congélation de l'eau dans un système poreux, s'ajoute la nécessité de prendre en compte l'hétérogénéité microscopique du matériau, ainsi que son évolution dans le temps. On ne peut assimiler une éprouvette de béton à une simple brique poreuse. Pour en avoir la preuve, il suffit d'observer l'évolution de la résistance mécanique après un grand nombre de cycles de gel-dégel. Pour les bétons de durabilité correcte on constate une augmentation significative. C'est pourquoi nous avons tenté d'approfondir notre connaissance des mécanismes de la destruction par le gel par un grand nombre d'observations, qui seront utiles pour donner des bases plus solides à un modèle éventuel.

2 - PLAN D'EXPERIENCES

Nous avons observé au MEB, 25 bétons préparés avec divers types de ciments portland, contenant ou non des fillers. Le slump et la teneur en air occlus ont été maintenus dans une fourchette étroite. Nous n'avons pas utilisé d'entraineur d'air. Pour chaque béton, nous avons observé une éprouvette témoin, conservée dans l'eau à 20°C et une série de tranches découpées dans une éprouvette soumise au test ASTM C 666-80-B, afin de mettre en évidence l'évolution de la microfissuration et de la microstructure, en fonction du nombre de cycles. Chaque tranche a été concassée à la main. Des morceaux situés à des profondeurs différentes dans l'éprouvette ont été sélectionnés, puis séchés par cryosublimation, à l'aide d'un système spécialement mis au point au CEREG, pour diminuer la microfissuration parasite, due au retrait de séchage du gel de CSH. Les mesures classiques de durabilité au gel, gonflement, vitesse du son, module d'élasticité, variation de poids, résistances mécaniques, ont été pratiquées pour chaque échantillon, sur 3 éprouvettes identiques, préparées avec le même granulat standard silico-calcaire, dans les mêmes conditions opératoires, et placées dans la même enceinte.

3 - RESULTATS

De l'ensemble de nos observations, nous retiendrons les points essentiels suivants :

3.1 - ECHANTILLONS AYANT BIEN RESISTE AU TEST

Les dégradations sont difficilement observables et en général minimes (*Planche 1*).

- La presque totalité des fissures visibles sont larges et anguleuses, sans hydrates internes. Ce type de fissures est dû au retrait de la pâte de ciment pendant la cryosublimation, comme le montrent les échantillons témoins, non soumis au gel (fissures de préparation). La fracture est souvent transgranulaire.

- Dans quelques cas isolés, le gel a produit un début de décollement des auréoles de transition des granulats, montrant des cristallisations d'hydrates dans la fissure (*Photo.1*) et on peut trouver quelques microfissures partiellement ou totalement cicatrisées par des hydrates (*Photo. 2*).

- Les bulles d'air présentent un aspect caractéristique : elles sont entourées d'une épaisse "coquille" d'hydrates compacts (*Photo. 3*), où les cristaux de portlandite sont orientés en feuillets disposés radialement. Dans certains cas, le gel y a produit des fractures et la croissance de gros cristaux occupant une seule partie du volume interne, indique une pénétration de la solution interstitielle dans les bulles (*Photo. 4*). Ce phénomène n'est pas observé dans les bétons témoins.

- Les bétons présentant un comportement rhéologique défavorable, avec une demande en eau plus élevée à slump constant, montrent une plus grande densité de micropores capillaires. Ces pores se remplissent d'hydrates au cours du test et la porosité est donc plus faible après 300 cycles, qu'au début du test.

- La pâte des ciments avec filler calcaire est en général compacte. Les grains de filler, parfois reconnaissables d'après leur origine fossile, sont liés par des fibres de CSH et de la portlandite, les carboaluminates sont localisés principalement à la surface du C_3A (*Photo. 5*).

3.2 - ECHANTILLONS N'AYANT PAS RESISTE AU TEST

Ont été considérés comme tels, les échantillons présentant une chute de vitesse du son supérieure à 20 %, avant 300 cycles. A quelques exceptions près, ces bétons dégradés contenaient tous des cendres volantes. Cet ajout présente les inconvénients suivants vis à vis de la durabilité :

- Augmentation de la densité des pores aqueux (pores capillaires) de dimension supérieure à 5 microns.

- Elaboration trop lente de l'auréole de transition cendre-pâte de ciment. Cette liaison est particulièrement faible lorsque le ciment contient peu d'alcalins, qui accélèrent les réactions pouzzolaniques (*Photo. 6*). Pour ces ciments, une période de maturation de 28 jours avant exposition au gel est donc insuffisante.

Les dégradations ne deviennent franchement visibles qu'à partir de la chute de vitesse du son (*Planche 2*) :

- Le déchaussement des granulats est très fréquent. La destruction de l'auréole de transition s'accentue avec le temps. Des cristallisations secondaires se forment dans les fissures de décollement des granulats par le gel.

- Les zones riches en filler ou cendres, observables au voisinage des parois et des gros granulats (microségragation par ressuage interne), présentent des cristallisations d'ettringite secondaire de grande dimension. Les cristaux s'allongent au cours du test, aux dépens des aiguilles initiales très fines et courtes.

- Lorsque l'on pousse l'expérience au-delà des 20 % de chute de la vitesse du son, les dégradations deviennent très importantes et prennent un caractère chimique. On observe la dissolution progressive de la portlandite et la croissance d'hydrates secondaires en longues fibres, ainsi que l'augmentation de la porosité capillaire. Ces phénomènes sont liés à la technique du test, qui implique la pénétration d'eau dans l'éprouvette au cours du dégel, d'autant plus profondément que les dégradations et la microfissuration s'accentuent.

3.3 - EVOLUTION DE LA MICROSTRUCTURE AU COURS DE LA DEGRADATION D'UN BETON PAR LE GEL

Pour illustrer les propos précédents, nous décrivons maintenant l'évolution d'un béton, dont la ***figure 1*** montre la courbe de vitesse du son en fonction du nombre de cycles.

FIG 1. CPJ C1.
Découpage des tranches au cours de la dégradation d'un béton.
TEST ASTM GEL-DEGEL

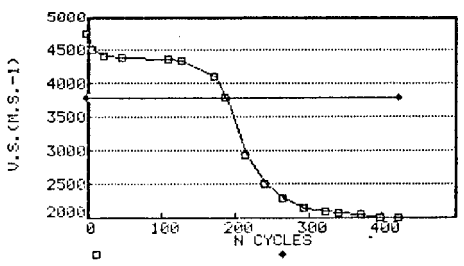

Trois tranches ont été observées au cours des 200 premiers cycles, où la chute de vitesse du son était inférieure à 20 %, puis 9 tranches au cours de la dégradation, jusqu'à 425 cycles (***Planches 2 et 3***).

- Dans la première période, de faible décroissance de la vitesse du son, on constate une évolution faible de la microstructure et de la microfissuration.
Au bout de 113 cycles, le béton a pratiquement conservé sa microstructure initiale. De très nombreuses microfissures ont été partiellement ou totalement colmatées par des hydrates fibreux. Elles se distinguent très bien des larges fissures dues à la préparation de l'échantillon, ces dernières présentant des bords nets et exempts d'hydrates (*Photo.7*). Les microfissures produitent par le gel aboutissent en général à des pores capillaires. Ces derniers se remplissent d'hydrates au cours du test.

- Dans la deuxième période, pendant la chute rapide de la vitesse du son, et par la suite, si l'on poursuit le traitement, l'évolution de la microstructure s'accélère. A 217 cycles, la pâte de ciment est devenue spongieuse (*Photo.8*). La taille des cristaux d'ettringite est de l'ordre de 5 à 7 microns, alors qu'à 113 cycles, elle était d'environ 1 micron. De longues fibres de CSH se développent dans un environnement plus poreux. La portlandite commence à se dissoudre, dans les fissures produites par le décollement des granulats, sous l'influence du gel. Cet effet est plus intense sur la face d'arasage des éprouvettes.

La *Photo. 9* montre un très gros cristal de portlandite en voie de dissolution dans la fissure de décollement d'un granulat, au bout de 243 cycles. La *Photo. 10* montre des plaques de portlandite fortement dégradées à 345 cycles. La *Photo. 11* montre la microstructure de l'auréole de transition d'un granulat décollé par le gel : à 425 cycles, les cristaux de portlandite ont pratiquement disparu. La pâte de ciment et uniquement constituée de fibres et de grains à peine liés. L'ensemble se désagrège sous le moindre choc mécanique.

4 - INTERPRETATION

Les observations précédentes semblent indiquer que l'évolution des bétons soumis à de nombreux cycles de gel-dégel résulte de phénomènes physiques et chimiques.

4.1 - PROCESSUS PHYSIQUES

4.1.1 - Approche du problème

Dans les années 1940-1960, la plupart des auteurs tentaient de calculer des forces de cisaillement issues de différences de coefficients de dilatation entre pâte de ciment et granulats, et des forces de pression liées à l'augmentation de volume lors de la transition eau-glace /1/ /2/ /3/ /4/. Depuis lors, l'approche thermodynamique de la congélation des solides poreux s'est affinée, avec le support d'expérimentations nouvelles, et on considère aujourd'hui que l'augmentation de volume de 9 % associée à la congélation de l'eau, ne peut suffire à expliquer les dégats produits. Les mêmes dommages se produisent en effet dans les solides poreux imbibés de solvants organiques qui contrai- rement à l'eau, se contractent au gel /6/ /17/. L'étude du diagramme d'équilibre eau-glace montre que la pression de vapeur de la glace est toujours inférieure à celle de l'eau métastable surfondue. Or celle-ci représente 60 à 70 % de l'humidité du béton. Elle est partiellement liée par des forces de capillarité dans les pores du gel de CSH, ce qui abaisse notablement son point de congélation, bien en-dessous de la température minimum atteinte au cours du test ASTM.
Dans notre interprétation, il en résulte les conséquences suivantes :

4.1.2 - Sites saturés et non saturés, phénomènes de transport

Au cours du refroidissement, les premiers cristaux de glace se forment dans les plus gros pores capillaires, où la probabilité de germination est maximum, et le point de congélation proche de 0°C. Suite à la différence des tensions de vapeur entre la surface de ces cristaux et l'eau non encore gelée des micropores, le degré de saturation de la vapeur d'eau diminue progressivement dans ces derniers, qui subissent une dessiccation. Cette cryodessiccation s'accompagne, d'une part, d'un transport de vapeur vers les cristaux de glace, ce qui entretient leur croissance, et d'autre part, d'une contraction du gel de CSH, analogue au retrait de dessiccation habituel /14/.
Dans ce système hors de l'équilibre, la solution interstitielle des bétons se répartit alors entre deux types de sites. Des sites en dépression, non saturés, dans les pores du CSH et des sites en surpression, saturés, dans les pores capillaires contenant de la glace.

Dans cette hypothèse, des phénomènes de transport d'eau peuvent se produire dans les sites saturés, entre pores capillaires gelés et non gelés, si la perméabilité de l'échantillon le permet, et sous l'influence de forces motrices, liées à des gradients : gradient de concentration en sels dissous, produisant des forces de pression osmotique, gradient de température, produisant le phénomène de cryosuccion /9/ /24/. Ce transport d'eau s'apparente à un ressuage d'eau et de glace ("cryoressuage"). Il serait localisé, soit à la surface, d'où l'écaillage, soit à l'environnement immédiat des cristaux de glace des gros pores communiquant par des fissures avec leur voisinage.
Le système ne peut revenir à l'équilibre qu'avec l'arrêt des transports de matière. Il faudrait pour cela atteindre une configuration dans laquelle la perméabilité deviendrait nulle, par congélation totale des pores capillaires saturés, et où l'égalité des potentiels thermodynamiques serait atteinte entre les deux types de sites : la dessiccation du CSH produit en effet un abaissement de l'enthalpie libre de l'eau résiduelle, les forces capillaires étant de plus en plus intenses avec la diminution du diamètre des pores /17/.

4.1.3 - Mécanisme de production des contraintes mécaniques par congélation de l'eau des pores capillaires

Sur le plan mécanique, les micro-contraintes qui vont s'exercer au voisinage d'un pore gelé vont résulter de la différence de volume résiduelle créée par les variations locales des volumes, à savoir l'augmentation associée à la croissance de la glace, d'une part, et la contraction de la pâte environnante, d'autre part. La différence pourra être négative, nulle ou positive, selon les volumes occupés par les zones mises en jeu, et leur arrangement spatial. Dans le cas où la vitesse de refroidissement ne laisserait pas au matériau le temps de relaxer ces contraintes, la compensation des variations locales de volume ne pourrait pas s'effectuer, d'où une hystérésis plus importante. Au voisinage d'une paroi, d'un granulat, ou d'un gros cristal, le volume de pâte entourant un pore est réduit de moitié, l'autre moitié étant occupée par l'objet adjacent, ce qui diminue également les possibilités de compensation. Il en est de même lorsque la dimension des pores, et donc des cristaux de glace qui s'y forment, devient grande par rapport à celle des zones de pâte compacte. Pour ces raisons, la variation résultante est en général un gonflement irréversible, accompagné de microfissuration, bien que la contraction du CSH soit globalement supérieure à l'augmentation de volume due à la transition eau-glace.

4.1.4 - Rôle de l'air occlus

Dans le schéma ci-dessus, la présence d'une bulle d'air au voisinage d'un pore permet d'amortir les fluctuations locales du volume, en accueillant une partie du liquide mis en pression autour de la glace au cours de sa croissance, d'où l'importance de la notion d'espacement critique.

4.2 PROCESSUS CHIMIQUES

4.2.1 - Pompage de l'eau

Pendant les périodes de gel, le béton a tendance à refouler vers l'extérieur son eau excédentaire par rapport à l'équilibre, les mécanismes précédents agissant avec une intensité plus grande pour les échantillons de plus grande perméabilité. Pendant les périodes de dégel, lorsque ce dernier a lieu dans l'eau, les flux d'eau sont inversés, le gel de CSH a tendance à se réhydrater et l'eau servant au dégel est aspirée par toutes les fissures apparues dans la période de gel. Les courbes déformation-température (*Fig. 2*) /4/ /6/ /7/ /10/ /12/ /13/ /15/ /16/ /17/, montrent bien qu'au cours d'un cycle, le béton se comporte comme une pompe aspirante et foulante. L'orientation particulière des cristaux dans les fissures de décollement des granulats en est une preuve directe (*Photo.12*). Ceci implique des conséquences sur le plan chimique.

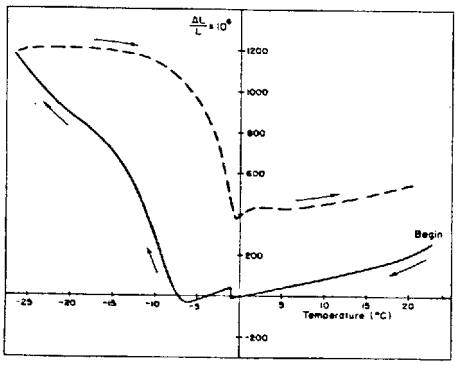

Fig. 2 - CYCLE DE GEL-DEGEL A LA VITESSE DE 0,25°C/mn (D'APRES /4/)

4.2.2 - Phénomènes réparateurs

La diminution du pH de la solution interstitielle accélère les réactions d'hydratation. Dans un premier temps, le ciment puise dans sa réserve d'énergie et fournit des hydrates qui vont colmater les fissures et s'opposer à l'extension des dommages de nature physique. Ceci permet d'interpréter la forme de la courbe de vitesse du son durant les 10 à 20 premiers cycles de gel-dégel : après une chute initiale rapide, on observe systématiquement un palier ou une période de variation lente (*Fig. 2*). Les dommages physiques étant cumulatifs et se développant exponentiellement, nous avons nécessairement affaire ici à un mécanisme réparateur induit par le processus initial.

4.2.3 - Processus destructeur

Au-dessous d'une certaine valeur du pH, le système parvient dans le domaine sous-saturé des hydrates, en commençant par les plus solubles et les plus basiques. Il se produit alors une dissolution, accompagnée des modifications de morphologie des hydrates que nous avons montré plus haut. Le processus réparateur est transformé en processus destructeur et l'énergie du liant ne peut plus compenser l'action des processus physiques. La chute de vitesse du son devient exponentielle. La porosité et la perméabilité de l'échantillon augmentent très rapidement, le volume d'eau pompé à chaque cycle devient de plus en plus grand, et les dégradations s'amplifient jusqu'à la destruction complète. Les zones les plus rapidement dégradées sont celles que nous avons citées au § 4.1.3, où les contraintes sont les plus intenses.

5 - CONCLUSIONS

PARAMETRES PRINCIPAUX DE LA DURABILITE AU GEL

Nous ne considérons l'interprétation du chapitre précédent que comme une première approche, essentiellement qualitative. En effet, pour quantifier les variations de volume dans les deux types de sites, saturés ou non saturés, et leurs conséquences, les connaissances théoriques doivent progresser. D'une part, nous ne disposons pas à l'heure actuelle d'un modèle satisfaisant du retrait de dessiccation /14/ /21/. D'autre part, bien que de récents progrès aient été faits récemment dans l'étude du gel et des phénomènes de transport dans les milieux saturés /22/ /23/, on ne peut aujourd'hui quantifier les contraintes mises en jeu par le gel, ni, à plus forte raison, leurs conséquences sur les déformations et le schéma de fissuration. A ce titre, le comportement du béton soumis à des cycles de gel-dégel présente des analogies frappantes avec celui du fluage, qui fait appel lui aussi à des mécanismes réparateurs chimiques /11/, et physiques, comme le montrent quelques études de fatigue sous contrainte cyclique /18/ /19/ /20/. De cette étude, nous tirerons les conclusions pratiques suivantes, qui nous paraissent fondamentales.

- La durabilité au gel du béton est conditionnée par son état initial, c'est-à-dire sa microstructure au moment de la congélation. Dans celle-ci, il faut prendre en compte la répartition de trois types de pores : pores aériens (bulles), pores capillaires et pores du "gel" de CSH. La répartition dimensionnelle de ces pores est au moins aussi importante que leur quantité globale. Les pores capillaires semblent jouer un rôle exactement inverse de celui des bulles, ce qui oblige à prendre en compte les deux paramètres simultanément. Ceci n'est pas le cas des méthodes d'évaluation indirecte actuelles. Il serait donc souhaitable d'appliquer la notion d'espacement critique aux pores capillaires. Mais ceci rendrait le test indirect très fastidieux, sans donner les garanties présentées par les méthodes directes.
- La mise en oeuvre du béton, le bon choix du dosage et la répartition granulaire de tous les composants jouent un rôle plus important que la nature du ciment. Celle-ci n'intervient de manière significative que dans des cas très particuliers, par exemple lorsqu'il contient un filler qui n'a pas encore atteint un taux de réaction suffisant lors de l'exposition au gel, ou dont la vitesse de réaction est trop faible pour qu'il participe de manière efficace aux mécanismes réparateurs (cendres volantes). Dans ce cas, une période de maturation plus longue résoud le problème.
- Il ne faut pas négliger la protection du béton après sa mise en oeuvre. La déshydratation est un facteur aggravant dans le cas du dégel dans l'eau, qui pénètre alors très rapidement dans les fissures de retrait, accentuant l'effet de pompe destructeur.

BIBLIOGRAPHIE

/1/ JONES F.E. "The physical structure of cement products and its effect on durability" IIIrd I.S.C.C. London, 1952, 12, pp 368-435.

/2/ NERENST P. "Frost action in concrete". VIth I.S.C.C., Washington, 1960, Paper VI-2, pp 807-828.

/3/ HELMUT R.A. (ibid.) Discussion, pp 829-833

/4/ HELMUT R.A. "Capillary size restrictions on ice formation in hardened portland cement pastes" (ibid.), Paper VI-S2, pp 855-869.

/5/ WITTMANN F. "Surface tension shrinkage and strength of hardened cement paste" (Ibid.), pp 547-552.

/6/ LITVAN G. "Further comments on the mechanism of frost action in cement paste". RILEM SCAV SYMPOSIA Colloque International sur la durabilité des bétons, 1969, B 139 à B 142, Thème I, Gen. Rep.

/7/ VUORINEN J. "On the freezable water in concrete" (Ibid.), pp 115-122.

/8/ FAGERLUND G. "Degré critique de saturation, un outil pour l'estimation de la résistance au gel des matériaux de construction". RILEM Mat. & Constr., Vol. 4, N° 23, 1971, pp 271-285.

/9/ AGUIRRE-PUENTE J. ; DUPAS A. "Vitesse critique du front de congélation dans les milieux poreux fins". Bull. Liaison L.C.P.C., 61, 1972, Réf. 1240, pp 145-154.

/10/ LITVAN G.G. "Frost action in cement paste". RILEM Mat. & Constr., Vol 6, N° 34, 1973, pp 293-298.

/11/ SOUSA-COUTINHO A. "A contribution to the mechanism of concrete creep" (Ibid.), Vol.10, N° 55, pp 3-16.

/12/ ROSTASY F.S. et coll. "Behaviour of mortar and concrete at extremely low temperatures". C.C.R., 1979, Vol. 9, pp 365-376.

/13/ STOCKHAUSEN N. et coll. "Untersuchung von gefriervorgangen in zementstein mit hilf der D.T.A.". C.C.R., Vol. 9, 1979, pp 783-794.

/14/ BUIL M. "Contribution à l'étude du retrait de la pâte de ciment durcissante". Rapport de recherche LCPC N°92, Déc. 1979, pp 1-72.

/15/ GRUBL P. ; SOTKIN A. "Rapid ice formation in hardened cement paste, mortar and concrete due to supercooling"- C.C.R., Vol. 10, 1980, pp 333-345.

/16/ ROSTASY F.S. ; WIEDEMANN G. "Stress-strain behaviour of concrete at extremely low temperatures". C.C.R., Vol. 10, 1980, pp 565-572.

/17/ LITVAN G.G. "Frost action in porous systems". Séminaire "Altération et durabilité des pierres", 1981, 11, pp 17-19.

/18/ PONS G. . MASO J.C. "Influence de chargements cycliques de faible fréquence sur le comportement mécanique d'éprouvettes d mortier" (Ibid.), Vol. 15, 1982, N°89, pp 461-467.

/19/ PONS G. ; MASO J.C. "Comportement mécanique d'éprouvettes de mortier soumises à des chargements cycliques de faible fréquence" (Ibid.), N°90, pp 539-547.

/20/ MASO J.C. "L'étude expérimentale du comportement du béton sous sollicitations monoaxiales et pluriaxiales"-"Le béton hydraulique", Presses de l'ENCP, Paris, 1982, pp 275-293.

/21/ BARON J. "Les retraits de la pâte de ciment" (Ibid.) pp 485-501.

/22/ MIKAEL P. ; OLSEN J. "Mathematical modeling of the freezing process of concrete and aggregates" C.C.R., Vol. 14, 1984, pp 113-122.

/23/ HUMBERT P. "Application de la méthode des éléments finis aux écoulements en milieu poreux". Bull. Liaison LCPC, 132, 1984, pp 21-37.

/24/ BOUTONNET M. ; LIVET J. "Influence du traitement des limons sur leur comportement au gel (Ibid.), 133, pp 83-90.

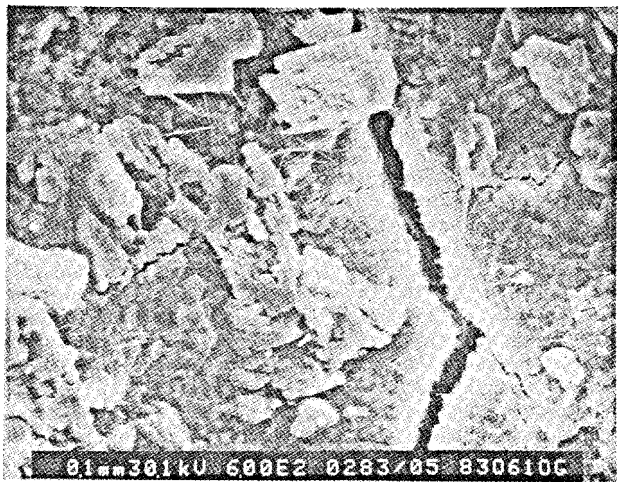

Photo 1 - Empreinte d'un granulat déchaussé par le gel

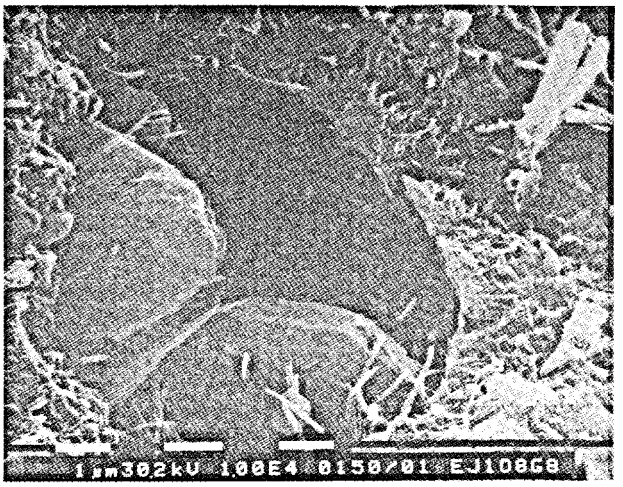

Photo 4 - Cristallisation de portlandite dans une bulle fracturée

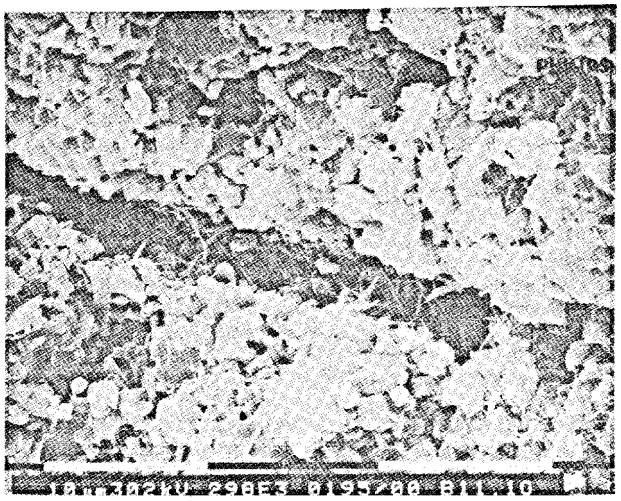

Photo 2 - Fissure partiellement cicatrisée

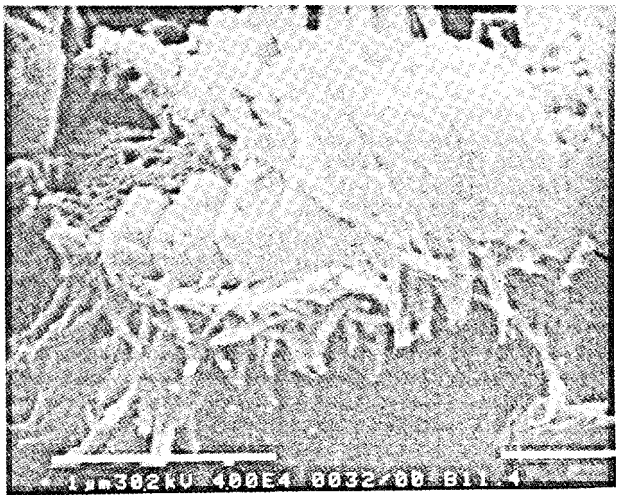

Photo 5 - Cocolite d'un filler calcaire lié par des CSH

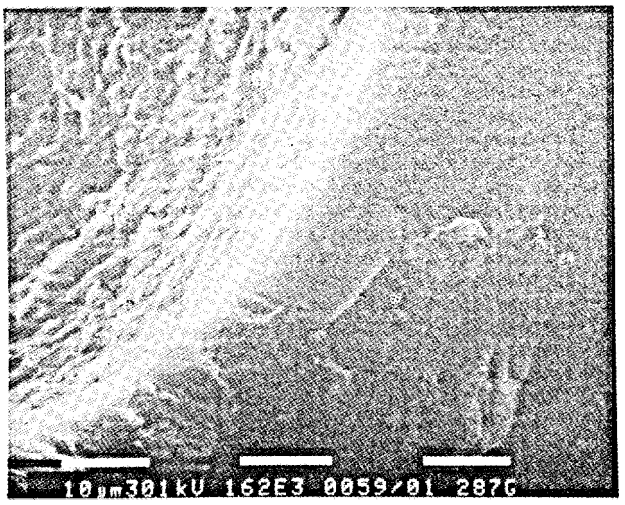

Photo 3 - Coquille d'hydrates autour d'une bulle d'air

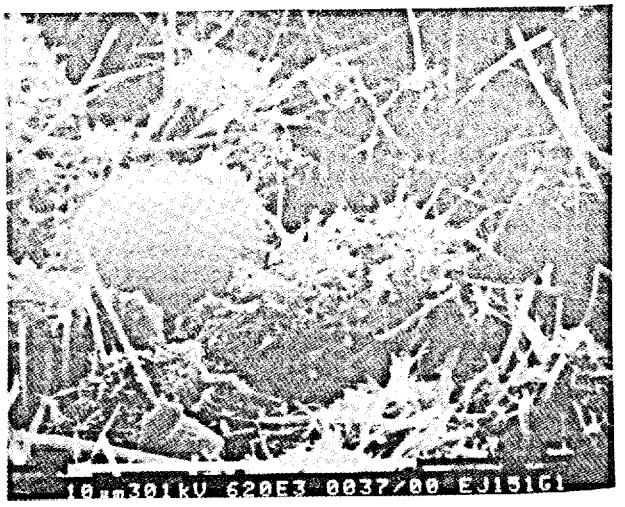

Photo 6 - Béton avec cendres volantes - Pâte poreuse



Photo 7 - CPJ C1 113 cycles



Photo 8 - CPJ C1 217 cycles

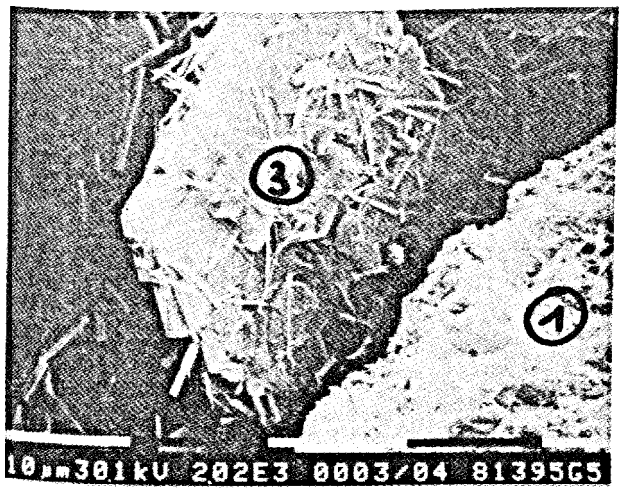

Photo 9 - CPJ C1 243 cycles
① CSH ② Granulat ③ CH

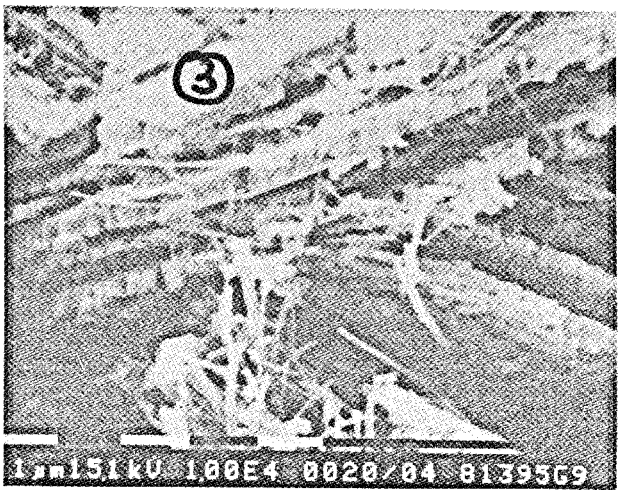

Photo 10 - CPJ C1 345 cycles
③ CH en cours de dissolution

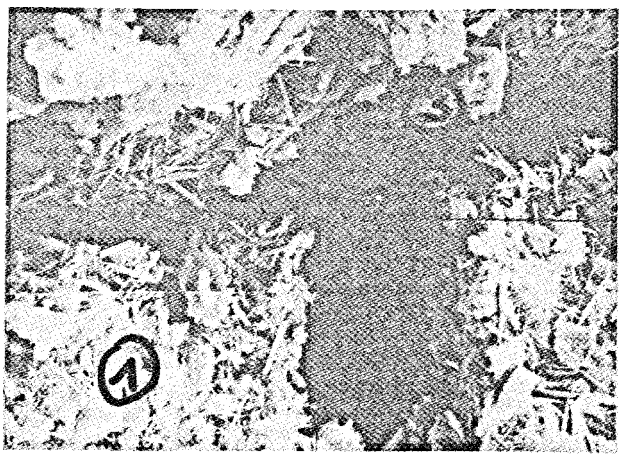

Photo 11 - CPJ C1 425 cycles
Destruction de l'auréole de transition

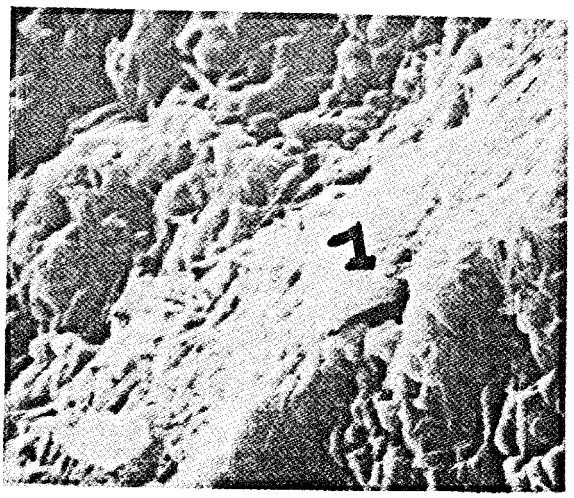

Photo 12 - Cristaux d'ettringite ① orientés dans une fissure de décollement

J. VOLANT et H. HORNAIN C.E.R.I.L.H. PARIS FRANCE

EVOLUTION OF STRENGTHS AND MICROSTRUCTURE OF CONCRETES HEATED UP TO 1100°C.

EVOLUTION DES RESISTANCES MECANIQUES ET DE LA MICROSTRUCTURE DE BETONS TRAITES JUSQU'A 1100°C.

RESUME

Le comportement de prismes de béton chauffés au four électrique jusqu'à 1100°C est étudié sous l'angle de l'évolution des caractéristiques mécaniques et des modifications de microstructures, en relation avec le type de ciment (CPA, CHF, CPJ), la nature minéralogique des granulats et le mode de conservation. Les observations effectuées par ATG, MEB, DRX et porosimétrie mettent en évidence les transformations du liant hydraté et des granulats; elles montrent l'effet néfaste de traitements répétés aux températures supérieures à 300°C où apparaissent des décohésions et des fissurations importantes.

Aux températures inférieures à 300°C, la compacité varie d'un béton à l'autre mais la microstructure, en particulier celle des C-S-H subit peu de changements.

Les bétons à base de ciments pauvres en chaux (CPJ aux cendres ou au laitier, CHF) montrent une meilleure résistance au feu qui se traduit par une fissuration faible après traitement à 390 ou même 550°C.

O comportamento de prismas de concreto aquecidos em forno elétrico até à temperatura de 1.100°C foi estudado sob o ângulo de evolução das características mecânicas e das modificações de microestruturas, em relação com o tipo de cimento (CPA, CHF, CPJ), a natureza mineralógica dos agregados e o modo de conservação. As observações feitas por ATG, MEB, DRX e porosimetria evidenciam as transformações do ligante hidratado e dos agregados; elas mostram o efeito nocivo de tratamentos repetidos sob temperaturas superiores a 300°C, onde aparecem separações e fissurações importantes.

Sob temperaturas inferiores a 300°C, a compacidade varia de um concreto para outro, mas a microestrutura, particularmente a dos C-S-H, sofre poucas mudanças.

Os concretos à base de cimentos pobres em cal (CPJ de cinzas ou de escória, CHF) apresentam melhor resistência ao fogo, que se manifesta por uma fissuração baixa após tratamento a 390 ou mesmo a 550°C.

1. INTRODUCTION

L'étude de l'évolution des principales propriétés mécaniques et thermiques du béton en fonction de la température a fait l'objet de très nombreux travaux. Ces travaux concernent : l'altération des caractéristiques mécaniques (module d'Young, résistances, ...), les variations des propriétés thermiques (chaleur massique, conductivité, dilatation, ...), la décomposition thermique des hydrates, la transformation des phases, les répartitions dimensionnelles des pores, l'apparition de fissures et d'écaillements, la perte de dureté superficielle, les changements de couleur (1 à 12).

Cependant, les causes exactes et le processus de l'éclatement du béton lors d'un incendie ne sont pas encore bien connus. Nous nous sommes donc proposé de suivre l'évolution du béton en fonction de la température, en mettant l'accent plus particulièrement sur les transformations de la microstructure, susceptibles d'apporter des éléments à la compréhension de l'éclatement du béton.

2. MATERIAUX TESTES

2.1. Composition des bétons.

Trois séries de bétons, notées A, B et C ont été étudiées. Les séries A et B, de six bétons chacune, ont été préparées avec deux CPA 55 dosés à 350 kg/m^3 et des granulats (0-15 mm) de nature minéralogique différente = silico-calcaires roulés, siliceux concassés ou roulés et calcaires roulés. Les rapports E/C s'échelonnent de 0,48 pour le béton silico-calcaire de la série A à 0,79 pour le béton calcaire de la série B ; les masses volumiques de ces bétons varient entre 2350 et 2435 kg/m^3. La série C, composée de huit bétons, a été préparée avec des granulats silico-calcaires roulés (0-20mm) et différents ciments : CPA 55, CHF (65 % de laitier), CPJ avec 25 % de cendres et 5 % de laitier ou avec des fillers calcaires (9 et 25 %). Le dosage en ciment est le même que dans les séries A et B, les rapports E/C varient de 0,55 à 0,60 et les masses volumiques des bétons varient de 2380 à 2400 kg/m^3. Certains bétons ont été carbonatés artificiellement (bétons de CPA et de CPJ aux cendres et laitier), d'autres contiennent de l'air entraîné (béton de CPA à 6 % d'air occlus).

2.2 Confection des éprouvettes.

Les bétons ont été confectionnés dans un malaxeur Ziklos à axe vertical de 75 litres. La mise en place des prismes 7 x 7 x 28 cm a été réalisée sur table vibrante pendant 2 minutes. Après 24 h de séjour en armoire humide, les éprouvettes démoulées ont été conservées, soit dans l'air à une température de 20°C et une hygrométrie relative de 50 %, soit dans l'eau à 20°C.

Les rapports E/C retenus correspondent à deux types d'affaissement au cône d'Abrams : sec (2 à 4 cm) et fluide (15 à 17 cm), pour les bétons des séries A et B et à un affaissement d'environ 5 cm pour les bétons de la série C.

3. TECHNIQUES MISES EN OEUVRE

Les techniques suivantes ont été utilisées : mesures du module d'Young par une méthode sonique (Grindo-Sonic MK3), mesures des résistances en traction par flexion et compression, fractographie au microscope électronique à balayage (M.E.B.) équipé d'un système d'analyse X par dispersion d'énergie, diffraction des Rayons X (DRX), porosimétrie à mercure haute pression et thermogravimétrie, pour laquelle un montage spécial a été mis au point pour suivre les variations de poids des éprouvettes de béton. Il se compose d'un four électrique d'une puissance de 22 KW montant à 1200°C et d'une balance électronique de précision Sartorius équipée d'un convertisseur numérique-analogique et d'une imprimante ; le programme de chauffage choisi correspond à une montée en température de 30°C/h.

4. RESULTATS EXPERIMENTAUX

4.1. Caractéristiques mécaniques et physico-chimiques du béton aux hautes températures.

4.1.1 Mesures du module d'élasticité et des résistances mécaniques à différentes températures.

Les mesures du module d'Young et des résistances mécaniques ont été réalisées sur des éprouvettes de béton silico-calcaire de la série B, âgées de 6 à 7 mois et maintenues une vingtaine d'heures en régime isotherme à différentes températures : 105, 160, 300, 390, 550 et 650°C.

A partir de 300°C, les valeurs du module diffèrent suivant que les mesures ont été effectuées sur une même éprouvette subissant l'ensemble des cycles thermiques ou sur des éprouvettes différentes ne subissant qu'un seul cycle à une température donnée : les éprouvettes soumises à l'ensemble des cycles de chauffage ont tendance à se détériorer davantage. Par ailleurs, le module décroît régulièrement en fonction de l'élévation de la température. La réduction est de l'ordre de 50 % à 300°C et de plus de 90 % à 550°C.

Les résistances en traction par flexion décroissent régulièrement lorsque la température croît, avec un palier plus ou moins net entre 160 et 300°C. A 550°C, la résistance est de l'ordre du dixième de la résistance initiale. Les résistances en compression sont, jusqu'à 300°C, comparables à celles du témoin à 20°C, puis elles décroissent régulièrement jusqu'à 550°C, avec une chute de l'ordre de 50 %. Ces résultats confirment les valeurs mentionnées par différents auteurs (1 à 8, 10 à 12).

Les résistances de l'ensemble des bétons chauffés à 1100°C sont très faibles : les résistances en traction par flexion sont pratiquement nulles alors que les résistances en compression s'échelonnent de 1 à 2 MPa, exceptionnellement 3,5 MPa.

4.1.2 Mesures thermogravimétriques.

Les premières mesures thermogravimétriques effectuées sur les bétons de la série B âgés d'au moins 4 mois (120 à 136 jours) traduisent nettement les modifications de la pâte de ciment et des granulats. Elles montrent que les pertes au feu totales à 1100°C sont différentes selon la nature du béton : de l'ordre de 6 % pour le béton siliceux, de 21 % pour le béton silico-calcaire et 37 % pour le béton calcaire. Mis à part le béton siliceux, cette perte correspond en majeure partie à la décarbonatation des granulats calcaires. La perte avant décarbonatation se chiffre à environ 5 % pour tous les bétons.

Le thermogramme isolé des granulats silico-calcaires 0/15 mm qui ont servi à la confection des bétons, indique une perte au feu de l'ordre de 2 % vers 800°C et de 15 % à 1100°C. Par différence, on peut ainsi évaluer la perte au feu correspondant à la seule pâte de ciment de ces bétons : elle est de l'ordre de 3 % vers 800°C et de 6 % vers 1100°C.

Les observations précédentes restent valables pour les bétons de la série A âgés de plus de 4 ans (52 à 55 mois). Si les thermogrammes montrent de grandes similitudes avec ceux de la série B, la perte au feu est cependant légèrement inférieure entre 100 et 800°C.

L'influence du mode de conservation étudiée dans le cas de bétons silico-calcaires de la série A âgés de 55 mois, se traduit par une perte au feu entre 150 et 250°C, trois à quatre fois plus importante pour la conservation dans l'eau comparée à la conservation dans l'air. Cette perte au feu augmente également avec le rapport E/C. Elle est de 25 à 27 % à 1100°C contre 21 à 22 % après conservation à l'air.

En ce qui concerne les bétons de la série C confectionnés avec différents ciments, les thermogrammes ont tous la même allure générale mais ils indiquent des pertes de poids différentes qui dépendent de la nature du ciment, du type et du pourcentage d'ajout, de la carbonatation. Les pertes jusqu'à 700°C sont d'autant plus élevées que le ciment est riche en chaux. A 1100°C, les pertes au feu sont comprises entre 16,3 (béton de CPJ avec 9 % de filler) et 23,7 % (béton de CPA carbonaté).

4.2 Etude de la microstructure de bétons traités à haute température.

L'évolution du comportement mécanique des bétons en fonction de la température se traduit par des modifications de la microstructure du liant hydraté et des granulats.

Des examens fractographiques ont été effectués au M.E.B sur trois catégories d'échantillons :

1) deux dalles de béton de 12 cm d'épaisseur, l'une protégée par une couche de vermiculite, l'autre constituée par un béton de granulats siliceux concassés (E/C = 0,7), toutes deux soumises à un essai normalisé de comportement au feu (4).

2) dallettes de différents bétons ayant subi un essai d'écaillage.

3) prismes de béton chauffés 20 h en régime isotherme.

4.2.1 Examen des dalles de béton.

Les observations au M.E.B. montre que dans le béton protégé la vermiculite ne semble pas avoir subi de transformations importantes au cours du traitement. Par contre, la pâte de ciment durcie sous la couche protectrice a subi des modifications notables dues à la déshydratation partielle de $Ca(OH)_2$ et des C-S-H et à la formation de CaO. La pâte de ciment au coeur de la dalle est peu transformée et les hydrates habituels des ciments C-S-H et Ca(OH) sont observés. Les granulats, principalement siliceux, apparaissent légèrement fissurés.

Dans le béton non protégé, la microporosité du liant hydraté est importante et des changements notables de microstructure et de composition sont mis en évidence : déshydratation de $Ca(OH)_2$ et des C-S-H, formation de CaO, fissuration et transformation superficielle des granulats.

4.2.2 Examen des bétons soumis à l'écaillage.

Des éclats de bétons provenant d'un essai d'écaillage à l'aide d'un chalumeau dont la flamme atteint environ 2500°C, ont été examinés au M.E.B. La surface "externe", fondue sous l'action du chalumeau, présente une fissuration importante ; elle est constituée par un mélange de phases non reconnaissables au M.E.B, résultant de la recombinaison des éléments des phases hydratées initiales et des granulats (formation de silicates de calcium, aluminates, ferrites, ...). La face "interne" opposée, qui a été portée à moins haute température, est également plus ou moins fissurée mais n'a pas subi de transformations minéralogiques notables. La pâte de ciment, assez compacte, renferme les constituants habituels des ciments hydratés : C-S-H, $Ca(OH)_2$, ettringite, monosulfoaluminates.

4.2.3 Examen des prismes de béton.

4.2.3.1 Le béton silico-calcaire de la série B (E/C = 0,64), âgé de 5 mois, soumis à un cycle d'isothermes différentes (105, 160, 390, 550 et 1085°C) présente à 20°C une microporosité de la pâte de ciment assez importante qui peut être reliée au mode de conservation de l'éprouvette en salle à 50 % H.R. La pâte de ciment (figure 1) est constituée essentiellement de C-S-H de texture fibreuse, d'ettringite abondante cristallisée en fines aiguilles, d'hydroxyde de calcium $Ca(OH)_2$ en amas plus ou moins massifs de plaquettes empilées, de grains de clinker en voie d'hydratation (essentiellement C_2S). Le granulat silico-calcaire est formé de grains de quartz et de calcaire et de quelques feldspaths. De gros cristaux de chaux et des C-S-H sont observés à l'interface pâte-granulat et une fine couche d'hydrate reste souvent attachée au granulat après rupture. Dans le cas des grains calcaires, la fracture est principalement transgranulaire. Elle est intergranulaire dans le cas des grains siliceux.

Après le chauffage à 105°C, la structure n'est pas différente (figure 2). L'ettringite, encore très abondante, se transforme partiellement en monosulfoaluminates de calcium. Les gros cristaux de chaux sont intacts.

A 160°C, les C-S-H n'ont plus la même texture, les fibres se sont ramassées en amas moins structurés. Les monosulfoaluminates sont présents sous forme de plaquettes, la quantité d'ettringite a beaucoup diminué (figure 3). Au contact pâte-granulat, on observe quelques décollements.

A 390°C, la structure devient très poreuse (figure 4). Les monosulfoaluminates sont encore présents. La chaux est inaltérée. La texture des C-S-H déshydratés devient microgrenue. Des cristaux en aiguilles plus ou moins enchevêtrés non identifiés, de morphologie voisine de celle de l'ettringite sont observés. Des décohésions importantes se traduisant par une forte fissuration et des défauts d'adhérence de la pâte hydratée sur le granulat, dus à la transformation des C-S-H, sont observés.

A 550°C, $Ca(OH)_2$ est fortement déshydraté, la chaux se présente essentiellement sous forme CaO (figure 5). Les cristaux massifs de $Ca(OH)_2$, en voie de déshydratation, sont eux-mêmes très fortement fissurés ; cette fissuration est une cause importante de la décohésion du matériau. A la surface des granulats, on observe des dépôts de silicates de calcium déshydratés ; la cohésion générale est faible

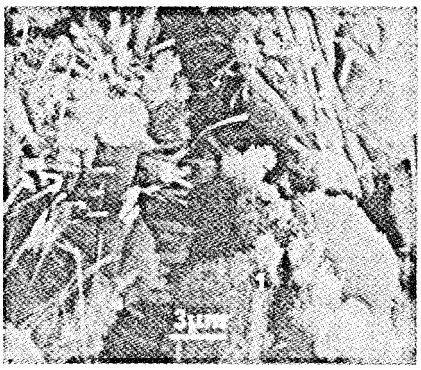

Figure 1 : 20°C

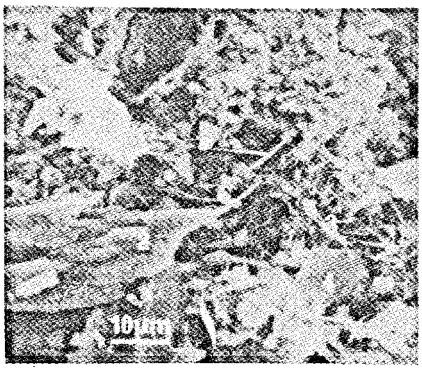

Figure 2 : 105°C



Figure 3 : 160°C

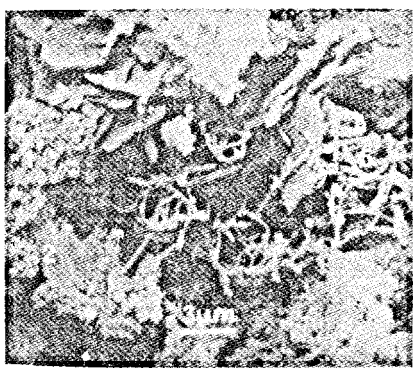

Figure 4 : 390°C

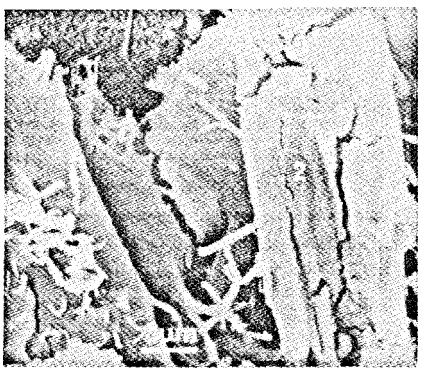

Figure 5 : 550°C

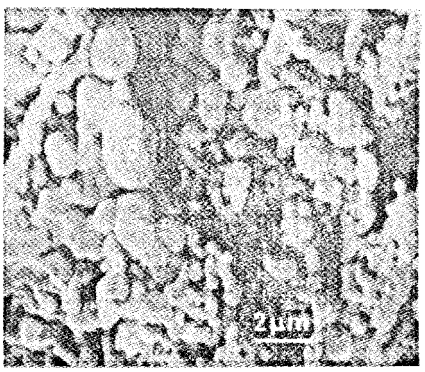

Figure 6 : 1085°C

Béton silico-calcaire soumis à un cycle d'isothermes

1 : C-S-H 2 : $Ca(OH)_2$ 3 : Ettringite

4 : Monosulfoaluminate 5 : Fibres non identifiées 6 : CaO

et les fissures abondantes. On note toujours la présence des cristaux fibreux qui pourraient être des fibres de $CaCO_3$ (vatérite) formées après le traitement thermique lors de la mise en contact des échantillons avec l'air ambiant.

A 1085°C, la décohésion du matériau est très nette. Les cristaux de $Ca(OH)_2$ se sont transformés in situ en conservant leur forme initiale mais ils sont maintenant constitués de petits grains de CaO et ont une texture microporeuse (figure 6). Les granulats calcaires et siliceux sont fissurés.

4.2.3.2 Tous les bétons de la série C ont été examinés au M.E.B après avoir été soumis aux mêmes cycles d'isothermes. A 20°C, dans tous les bétons témoins la pâte de ciment est constituée essentiellement de C-S-H, d'aiguilles d'ettringite et de plaquettes de monosulfoaluminate plus ou moins visibles, d'hydroxyde de calcium $Ca(OH)_2$ principalement en amas de plaquettes massives. Dans le cas des CPJ avec fillers calcaires on observe aussi des carboaluminates. Les bétons comportent des microfissures dont une partie peut être due aux contraintes subies par l'échantillon au cours de sa préparation (prélèvement, dessiccation). Lorsque l'échantillon est carbonaté (CPA), la structure est plus compacte du fait du bouchage partiel de certaines catégories de capillaires existant initialement entre les particules de C-S-H, par formation de microcristaux de $CaCO_3$ et de silicates de calcium hydratés carbonatés. Dans le cas du CPA à 6 % d'air occlus, la compacité est inférieure à celle des témoins carbonaté ou non carbonaté et de nombreuses bulles d'air entraîné de dimensions allant de 50 à 500 μm sont observées. La compacité du béton fabriqué avec le CHF 45 est bonne.

A 105 et 160°C, l'ettringite se transforme partiellement en plaquettes de monosulfoaluminate mais les C-S-H gardent le même faciès.

A 390°C, des décohésions notables se

4.2.

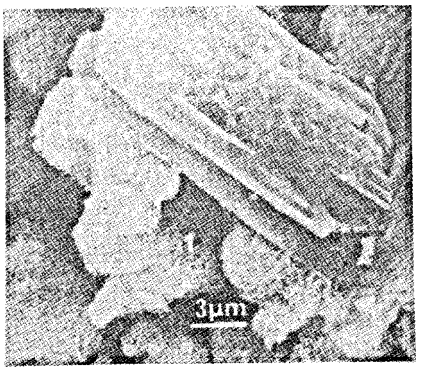

Figure 7 : 20°C

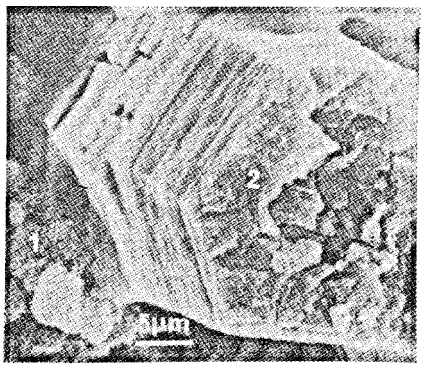

Figure 8 : 390°C

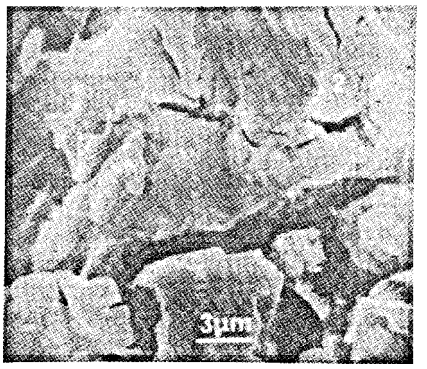

Figure 9 : 550°C

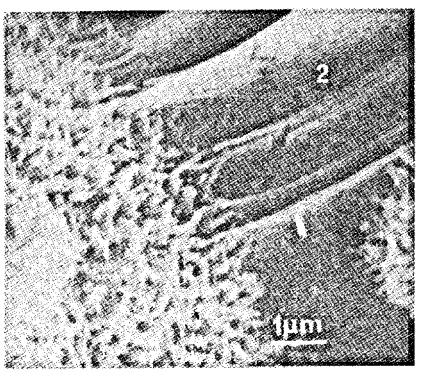

Figure 10 : 20°C

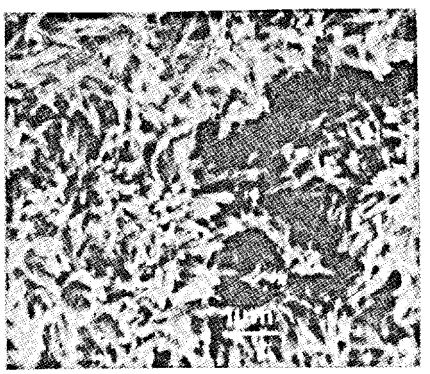

Figure 11 : 550°C

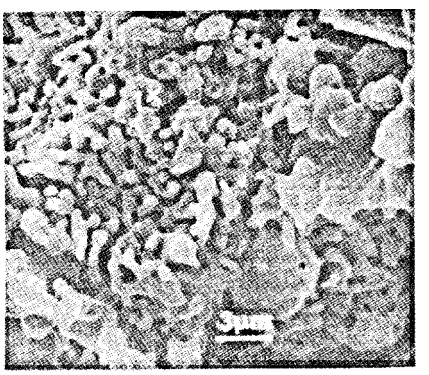

Figure 12 : 1080°C

Evolution de $Ca(OH)_2$ et des C-S-H en fonction de la température.

- 1 : C-S-H
- 1^x : C-S-H décomposés
- 2 : $Ca(OH)_2$

traduisent par une fissuration importante et des défauts d'adhérence de la pâte hydratée sur le granulat. Des cristaux en aiguilles qui peuvent être des sulfoaluminates anhydres sont mis en évidence. $Ca(OH)_2$ est généralement inaltéré mais les cristaux montrent un début de fissuration. Les C-S-H conservent leur faciès normal.

A 550°C, la structure de la pâte est très modifiée mais la morphologie des C-S-H est toujours inchangée dans les bétons de CPA et CHF 45. Les monosulfoaluminates, ainsi que les carboaluminates sont encore présents dans les bétons de CPJ avec fillers calcaires. On note la présence de fibres, vraisemblablement de l'ettringite déshydratée. La cohésion générale est faible et la fissuration importante. La fissuration de la chaux provoquée par la déshydratation est une cause importante de la décohésion du matériau. Les granulats se déchaussent.

A 1080°C, la décohésion du matériau est très nette et la fissuration très importante. Les cristaux de chaux $Ca(OH)_2$ initiaux se sont transformés en petits grains de chaux CaO (pseudomorphose) à la texture microporeuse et les C-S-H sont en majeure partie transformés en C_2S (8,9).

4.2.4 Examen fractographique des granulats portés à haute température.

Les granulats silico-calcaires qui ont servi à la confection des bétons de la série B ont été observés après avoir été chauffés à 1080°C. Les granulats calcaires sont fortement fissurés. Ils présentent une structure très poreuse constituée essentiellement de chaux. Leur cohésion est devenue très faible. Ils ont tendance à se pulvériser. Les granulats siliceux sont également fissurés. De larges fissures séparent les grains en fragments élémentaires.

4.2.5 Examen fractographique de systèmes simples.

Afin de préciser le comportement des différents constituants hydratés du ciment dans le béton, des systèmes simples : pâte de C_3S synthétique

et de mélange (C_3S + C_3A + gypse) ont été traités aux mêmes températures que les bétons. Des mini-éprouvettes de pâtes pures de C_3S (série I = 3000 $cm^2.g^{-1}$, E/C = 0,40 ; série II : fraction granulométrique 63-90 μm, E/C = 0,50) et du mélange 85 C_3S + 15 C_3A (fraction granulométrique 25 - 40 μm) gypsé à 5 % (E/C = 0,40) ont été conservées 50 jours dans une hygrométrie de 100 %.

4.2.5.1 Pâtes de C_3S hydraté

L'examen de la série I montre, pour le témoin à 20°C, de gros cristaux de $Ca(OH)_2$ massifs plus ou moins clivés. Dans la série II, la quantité de chaux est moins importante en raison du taux d'hydratation de C_3S plus faible. Les cristaux sont moins massifs, ils se présentent en lamelles assez minces. Les C-S-H sont, dans les deux cas, sous forme de fibres déposées sur les grains de C_3S qui ont l'aspect d'oursins. Les fibres sont un peu plus longues dans la série II où les espaces intergranulaires sont plus grands (fig. 7 & 10).

A 160°C, dans le cas de la série I, la cristallisation de $Ca(OH)_2$ ne change pas et les fibres de C-S-H sont moins bien individualisées. Par contre, aucune transformation n'est observée dans la série II.

A 390°C, les C-S-H montrent le même aspect fibreux qu'à 160°C pour la série I. Les cristaux de chaux subissent des contraintes dues à l'évaporation de l'eau et éventuellement au choc thermique. Ils sont fissurés (figure 8). Cette légère décohésion est moins visible dans la série I où les C-S-H se présentent en fibres un peu plus courtes et où les amorces de fissuration ne sont visibles que sur certains grains.

A 550°C, la série I montre une certaine décohésion et des fissures. La chaux est partiellement déshydratée. Dans la série II, la fissuration est moindre et les C-S-H ne sont pas encore modifiés (figure 11).

A 1080°C, les C-S-H sont totalement amorphisés dans les deux séries. La décohésion est très marquée, les grains ne sont plus liés les uns aux autres et le produit est très friable. La silice et la chaux se recombinent partiellement sous forme de C_2S.

4.2.5.2 Pâtes de $C_3S_{(85)}$ + $C_3A_{(15)}$ + $Gypse_{(5)}$

A 20°C, les mélanges hydratés âgés de 50 jours sont constitués de C-S-H fibreux, de $Ca(OH)_2$ en cristaux généralement massifs associés à une faible quantité de petits cristaux de monosulfoaluminate.

A 160°C et 390°C, les faciès cristallins restent inchangés pour toutes les phases.

A 550°C, les cristaux de $Ca(OH)_2$ sont très fissurés (figure 9). Les monosulfoaluminates sont encore visibles.

A 1080°C, on observe l'amorphisation des C-S-H ainsi que celle des aluminates qui se transforment en un produit de texture très poreuse (figure 12)

L'analyse par DRX de pâtes des 3 échantillons du mélange (C_3S + C_3A)gypsé, traitées respectivement à 20, 550 et 1080°C donne pour le témoin à 20°C les constituants hydratés habituels.

A 550°C, commencent à apparaître les signes de l'amorphisation des constituants hydratés : disparition des raies des aluminates hydratés et de $Ca(OH)_2$, formation de CaO libre encore peu abondante et mal cristallisée, amorphisation du C-S-H qui se traduit par un anneau d'amorphe aux environs de 3 Å, beaucoup plus étendu qu'à 20°C.

Enfin à 1080°C, on observe la cristallisation des constituants suivants : β C_2S principalement, aluminate anhydre du type $Ca_4Al_6O_{12}SO_4$ (sulfoaluminate anhydre), CaO libre bien cristallisée, C_3S. On note l'absence totale d'anneau d'amorphe : la transformation des hydrates en produits cristallisés anhydres est totale.

4.2.5.3 Ettringite synthétique.

Un essai complémentaire sur des pastilles compactées d'ettringite synthétique a été effectué dans le but de préciser le comportement de ce composé. On a pu observer qu'entre 105 et 550°C son faciès apparent était peu modifié.

4.2.6 Examen de la porosité du béton et de pâtes pures.

4.2.6.1 Le béton silico-calcaire de la série B (E/C = 0,64), a été examiné à 20°C et après chauffage, à 550°C. Après avoir vérifié que la porosité du granulat était faible par rapport à celle du béton, les plus gros granulats ont été éliminés afin d'assurer une représentativité convenable du liant dans les deux échantillons. La porosité du témoin est assez élevée et sans doute liée au mode de conservation du béton. La contribution des pores de diamètre supérieur à 1000 Å paraît assez importante. Le traitement thermique n'a pas modifié de manière significative les porogrammes. Des examens complémentaires sur une pâte pure âgée d'un an (ciment blanc) avant et après traitement thermique à 570°C montrent une modification très nette de la porosité sous l'effet du traitement thermique, résultant essentiellement de la formation de pores d'ouvertures voisines de 500 Å liée à la déshydratation de la pâte. Dans ces conditions, il peut paraître surprenant que cet effet n'ait pas été décelé dans le cas du béton étudié.

4.2.6.2. Des essais complémentaires sur pâtes pures soumises à des traitements thermiques diversifiés s'avérant très intéressants, l'examen de la porosité de pâtes pures (E/C = 0,35) des mêmes ciments qui ont servi à la confection des bétons de la série C, conservées plus de 3 mois dans l'eau à 20°C ou en armoire de carbonatation (CPA) montre que le volume total des pores est dans tous les cas de l'ordre de 2,5 fois plus élevé que celui du CPA. Les différences de répartition de pores s'observent dans le domaine d'ouvertures inférieures à 200 Å. On observe le phénomène classique de déplacement de la distribution vers les plus petits pores en présence de laitier. L'examen de l'effet de la carbonatation sur une pâte de CPA (5mois) révèle un léger accroissement du volume poreux (pores inférieurs à 10 Å) et un déplacement de la distribution des pores de 10^2 à 10^3 Å.

5. CONCLUSION

Les différentes techniques utilisées dans l'étude des bétons portés jusqu'à 1100°C ont permis de suivre l'évolution du matériau en fonction de la température :

1. Les mesures du module d'Young du béton silico-calcaire montrent qu'il décroît régulièrement

en fonction de la température.

2. Les mesures de résistance en fonction de la température ont confirmé les données généralement admises : décroissance des résistances en traction par flexion, maintien des résistances en compression jusqu'à 300°C, suivie d'une décroissance régulière.

3. Les mesures thermogravimétriques ont mis nettement en évidence l'évolution de la pâte de ciment et des granulats et ont précisé les pertes au feu à différentes températures. Ces pertes qui sont, avant décarbonatation, de l'ordre de 5 % pour tous les bétons, dépendent ensuite de la nature du granulat.

4. La microscopie électronique à balayage a montré que les faciès cristallins des C-S-H, $Ca(OH)_2$ et sulfoaluminates subissent peu de modifications jusqu'à 300°C. Ceci expliquerait le maintien des résistances en compression jusqu'à cette température. Les modifications de microstructure à ces mêmes températures se traduisent uniquement par des fissurations et des altérations de la liaison aux interfaces pâte-granulats qui se manifestent par des chutes de résistance en traction par flexion et du module d'Young. A partir de 550°C, les transformations structurales sont visibles en DRX mais elles ne correspondent pas encore à des changements très importants des faciès cristallins. Toutefois, la déshydratation de $Ca(OH)_2$ pseudomorphosé plus ou moins complètement par CaO réduit la participation de la portlandite aux résistances mécaniques par disparition des points d'ancrage des ponts cristallins qu'elle constituait initialement : les résistances en compression diminuent en effet d'environ 50 %. Aux températures très élevées, la transformation des hydrates est totale et parallèlement, les résistances en traction par flexion sont pratiquement nulles et les résistances en compression sont très faibles.

D'une façon générale, les bétons de ciments dont l'hydratation donne naissance à peu d'hydroxyde de calcium (CPJ aux cendres et laitier,CHF 45) auront une meilleure résistance au feu, ce que confirme la faible fissuration de ces bétons chauffés à 390°C, voire 550°C.

5. La porosimétrie au mercure apparaît capable de rendre compte des modifications de la structure poreuse du liant du béton, consécutive à l'élévation de température.

*
* *
*

Les mesures de porosimétrie et de DRX ont été effectuées par Messieurs THURET et MORTUREUX que nous remercions bien vivement.

REFERENCES

1 COLLET Y., TAVERNIER E., (1977), Etude des propriétés du béton soumis à des températures élevées, Centre National de Recherches Scientifiques et techniques pour l'Industrie Cimentière, Bruxelles, RR CRIC 45-f-1977, 32 p.

2 DELFIN F.A., GOMEZ E.G., TORRES O.S., (1983), Les effets du feu sur les structures en béton, Revista del IDIEM, 22, 2, 71-100.

3 DIEDERICHS U., SCHNEIDER U., WEISS R., (1980), Origines et effets de la désagrégation du béton aux hautes températures, Bauphysik, 2, 3, 104-9.

4 DTU, (1980),Méthode de prévision par le calcul du comportement au feu des structures en béton, cahiers du CSTB, n° 1642, livraison 208, 56 p.

5 LACHAUD R., (1968), Le comportement du ciment à la chaleur. Etude de l'évolution d'une alite hydratée dans la gamme de température 20-400°C, Matér. Constr. RILEM, 1, 4, 365-78.

6 LEHMANN H., MÄLZIG G., (1965), Le comportement aux hautes températures de mortiers confectionnés avec différents types de ciment, Tonind. Ztg. 89, 19-20, 437-51.

7 MARECHAL J.C., (1970), Variations in the modulus of elasticity and Poisson's ratio with temperature, Int. Seminar on Concrete for Nuclear Reactors, Berlin, 5-9 oct., A.C.I. special publication SP-34, vol 1, 495-503.

8 ODLER I., ABDUL-MAULAS, (1982), Thermal decomposition of hydrates formed in the hydration of Portland-Blast furnace slag cements, Silicates Ind., 47, 3, 73-6.

9 SCHNEIDER U., DIEDERICHS U., (1981), Physical properties of concrete from 20°C up to melting, Betonwerk + Fertigteil-Technik, 47, 3 et 4, 141-9 et 223 - 30.

10 THELANDERSSON S., (1972), Effect of high temperatures on tensile strength of concrete, Nordisk Betong, 16, 2, 91-118.

11 VOLZHENSKIJ A.V., CHAUS K.V., (1977), Bétons résistant au feu, Béton Zelezobeton, 10, 20-1.

12 WIERIG H.J., (1965), La résistance au feu des bétons, Zement Taschenbuck 1966/67, 269-304.

M. SHIZAWA, Y. JOE and H. KOTANI

Influence of Ionic Species on Alkali-aggregate Reaction

The influence of alkali-ionic species and co-existing anionic species on alkali-aggregate reaction was firstly investigated in this paper by mortar-bar method (ASTMC227), using pyrex glass as aggregate. Alkali content was adjusted by adding alkali compounds, such as chloride, sulfate, hydroxide and carbonate of sodium, potassium and litjium respectively to controlled ordinary portland cement with 0.75% total alkali content as equivalent percent Na_2O. Secondarily , 80PC and 3SRC were examined in order to confirm the correlation between alkali content and expansion.

Experimental results were summarized as follows.

(1) The expansion was accelerated by sodium and potassium ion but not by lithium ion. Lithium ion rather tends to reduce expansion.

(2) Even though equivalent Na_2O content were the same, expansion varied dependent on the type of alkali ion. Sodium ion has larger effect than potassium ion at same content of total alkali and with same anionic species.

(3) The expansion varied with the type of anionic species even if at same alkali content. The degree of influence was chloride > sulfate > hydroxide > carbonate.

(4) Alkali content is now estimated as equivalent percent Na_2O by the equation of $Na_2O + 0.658K_2O$, however, from our experimental results it can be considered that the effect of potassium ion upon expansion should be underestimated, but the factor must be determined by a number of experiments.

(5) Additional alkali compounds in every cases seemed to make structure of hardened mortar tight, however the mechanism how the expansion due to alkali-aggregate reaction changed with type of alkali ions and co-existing anionic ions can not be so clarified.

A influência de espécies iônicas alcalinas e de espécies aniônicas coexistentes na reação álcali-agregado foi investigada primordialmente neste trabalho pelo método de barra de argamassa (ASTM C 227), com emprego de vidro pirex como agregado. O teor de álcali foi regulado pela adição de compostos alcalinos, tais como cloreto, sulfato, hidróxido e carbonato de sódio, potássio e lítio respectivamente ao cimento portland comum controlado, com 0,75% de teor alcalino total como percentual equivalente de Na_2O. Depois foram examinados 8 cimentos portland comuns e 3 SRC para confirmação da correlação entre teor de álcali e expansão.

Os resultados experimentais podem ser resumidos como abaixo:

1 - A expansão foi acelerada por íon de sódio e potássio, mas não por íon de lítio. O íon de lítio apresenta mais tendência para reduzir a expansão.

2 - Ainda sendo o mesmo o teor equivalente de Na_2O, a expansão variou dependendo do tipo de íon alcalino. O íon de sódio tem efeito maior que o de potássio com o mesmo teor de álcali total e com as mesmas espécies aniônicas.

3 - A expansão variou com o tipo de espécie aniônica mesmo com igual teor alcalino. O grau de influência foi cloreto > sulfato > hidróxido > carbonato.

4 - O teor de álcali agora é estimado como percentual equivalente de Na_2O pela equação de $Na_2O + 0{,}658K_2O$, contudo, a partir de resultados experimentais, pode-se considerar que o efeito do íon de potássio sôbre a expansão poderia ser subestimado, mas o fator deve ser determinado por uma séria de experiências.

5 - Em todos os casos, pareceu que compostos adicionais de álcali tornam compacta a estrutura da argamassa endurecida, contudo não se pode esclarecer desta forma o mecanismo pelo qual a expansão devida à reação álcali-agregado se modificou com o tipo de íons de álcali e íons aniônicos coexistentes.

- Introduction -

Durability is one of the most impotant properties of concrete as construction materials.
Among lots of factors which control those durabilities, alkali-aggregate reaction is the most impottant one from old times.
In 1940, Stanton T.E. (1) published his views concerning to the occurrence of cracking due to expansion caused by alkali-aggregate reactions. Since then, many investigations and observations were carried out about alkali-aggregate reactions and they are classified into the following three groups: (A) Alkali-Silica Reaction (2)-(5), (B) Alkali-Carbonate Reaction (6)(7), (C) Alkali-Silicate Reaction

Alkali-aggregate reactions are occurred under the following conditions: (A) presence of alkalies (B) presence of reactive aggregate and (C) presence of water, however, it is also confirmed that they are controlled by many other environmental conditions.

In recent years, in Japan, those alkali-aggregate reactions are widely interested in by many investigators and from every point of view in every field, investigations were carried out and then standardization of low alkali cement will be published in near future. Sodium and potassium ion are the typical alkalies in cement, in low alkali cement their content as Na_2O equivalent are limitted under 0.6%.

However investigations were carried out concerning to the difference between the effect of sodium and potassium ion upon the expansion due to alkali-aggregate reactions and tentative results were obtained, they are by no means sufficient. (10)-(14)

The authors, on the standpoint of making truly durable concrete constructions, made some experiments for the purpose of making the difference clear between the effect of sodium and potassium ion upon the expansion due to alkali-aggregate reactions and then some interesting results were obtained and reported as follows.

- Experimental Procedures -

Series-1: Experiments were carried out following the methed of ASTM C227 in order to investigate the effect of alkali ionic species and coexisting anionic species upon the expansion due to alkali-aggregate reactions.

Controlled mortar bars were prepared by mixing ordinary portland cement with 0.75% Na_2O equivalent alkali content, pyrex glass as reactive aggregate and water.

Alkali content of test specimens were adjusted by adding 0.25%, 0.50% and 0.75% following alkali compounds as Na_2O equivalent, respectively, to the controlled ordinary portland cement; NaOH, NaCl, Na_2CO_3, Na_2SO_4, KOH, KCl, K_2CO_3, K_2SO_4, $LiOH-H_2O$, LiCl, Li_2CO_3 and $Li_2SO_4 \cdot H_2O$.

Test specimens were cured in the container of which temperature is 38C and R.H. is 100% until fixed period. Expansions were measured at 2, 4, 6, 8, 10, 12, 16, 20, 24 and 36 weeks.

Chemical compositions of controlled portland cement and pyrex glass were shown in Tab.1.

Tab.1. Chemical composition of materials

	OPC	Pyrex glass
SiO_2	22.12	80.9
Al_2O_3	5.95	2.3
Fe_2O_3	2.84	0.03
B_2O_3	——	12.7
CaO	63.97	——
MgO	1.53	——
SO_3	2.11	——
Na_2O	0.30	4.0
K_2O	0.68	0.04
R_2O	0.75	4.03

Series-2: Relation between alkali content and expansion were investigated using mortar bars which were prepared with 8 types of ordinary portland cement and 3 types of sulfate resisting cement with different alkali content and also pyrex glass as reactive aggregate.

Storage of mortar bars and measuring of expansions were carried out following the method of series-1.
Alkali content of cement, water cement ratio and flow when mortar were prepared were shown in Tab. 2.

Tab.2. Alkali contents of cement and preparing condition of mortar

	Na_2O	K_2O	R_2O	W/C	Flow
OPC-1	0.47	0.57	0.85	53.8	110
OPC-2	0.30	0.68	0.75	52.5	103
OPC-3	0.27	0.71	0.74	52.5	110
OPC-4	0.35	0.54	0.71	53.8	112
OPC-5	0.28	0.57	0.66	53.8	112
OPC-6	0.23	0.64	0.65	53.8	110
OPC-7	0.33	0.36	0.57	52.5	104
OPC-8	0.22	0.24	0.38	52.5	105
SRC-1	0.19	0.50	0.52	51.9	107
SRC-2	0.21	0.46	0.51	52.5	111
SRC-3	0.16	0.39	0.42	51.9	106

Series-3: The textural changes of mortars due to alakli-aggregate reaction were observed by means of Scanning Electron Microscopy and Porosimeter.

Test specimens were prepared by mixing 1 part of ordinary portland cement, 2.25 part of pyres glass which were crushed to powders passing 0.5mm sieve by 100% and 1 part of water and cured for 12 weeks.

Alkali contents of test specimens were adjusted by adding NaOH, NaCl, KOH, KCl, $LiOH.H_2O$ and LiCl respectively to the controlled mortar.

- Experimental Results and Discussion -

(1) Relation between Curing Period and Expansion

Relation between curing period and expansion at 0.75% Na_2O equivalent of the additional alkali compounds were shown in Fig.1.

In every compound of sodium and potassium, expansion largely increased until 12 weeks and at that period, about 90% expansion ofthose observed at 36 weeks were reached. On the other hand, in the case of lithium compounds, mortar showed shrinkage at relatively early stage, but after about 24 weeks they become to show expansion. Similar tendency as above was observed also in the case of additional lower alkali contents such as 0.25%,0.50%.

(2) Relation between Alkali Content and Expansion

Relations between alkali content and expansion at the curing period of 24 weeks were shown in Fig.2.

In the case of sodium compounds, every mortar spesimens showed the increasing expansion with increasing alkali content. However, in the case of potassium, maximum expansions were observed at 0.5% Na_2O equivalent of additional alkali content. The amount of pyrex glass as reactive aggregate seens to equal pessimum just at that alkali content. On the other hand, in the case of lithium compounds, shrinkage was observed in proportion to the alkali content at this curing period.

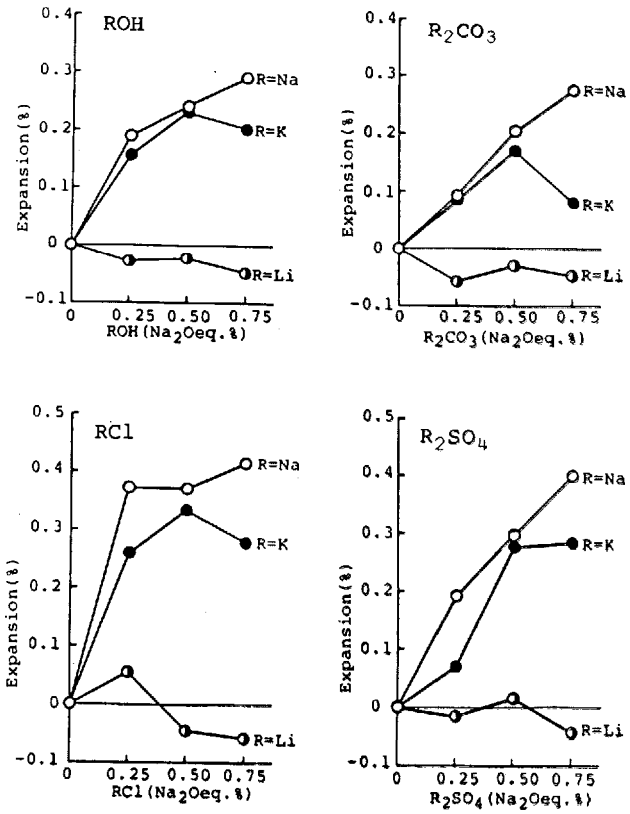

Fig.2. Relation between alkali contents and expansion (24 weeks)

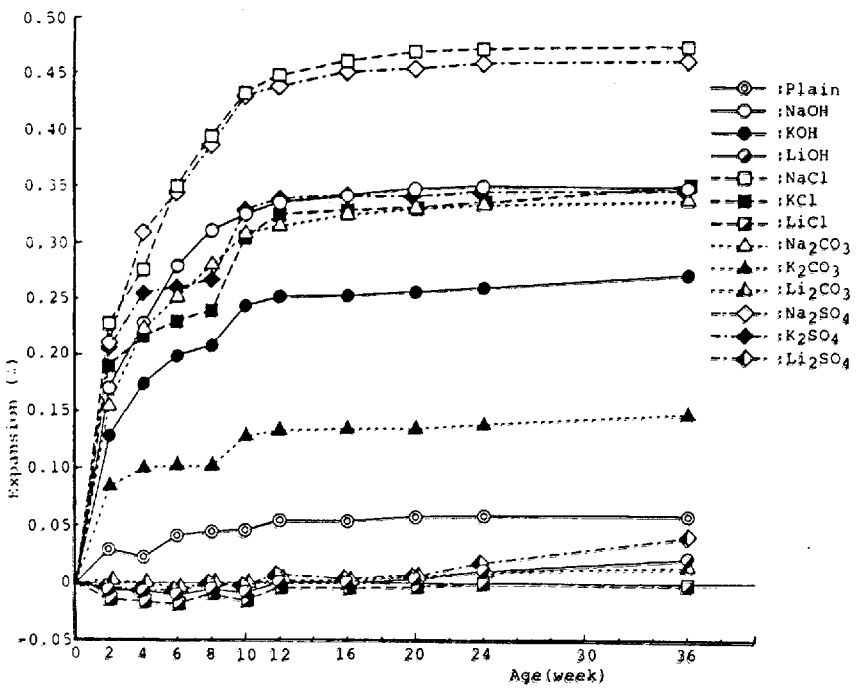

Fig.1. Change of expansion with curing time

(3) Effect of Type of Alikali Ion and Co-existing Anionic Ion upon Expansion

As apparently in Fig.1 and Fig.2, even if same amount of alkalies were added, expansion behavior was largely different with type of alkali ion. Namely, sodium and potassium promotes the mortar expansion, but in opposition, lithium suppress the expansion of mortar .

Furthermore, it is easily expected that even in the case of soduim and potassium which occurred expansion similarly their degree of effect upon expansion differs with type of qggregqte, therefore, sufficient considerations must be required concerning to the method of controlling the alkali content in order to reduce expansion due to alkali-aggregate reaction.

Differences of expansion due to type of anionic ion were shown in Fig.3a, and Fig.3b.

Fig.3a shows the case of sodium compounds and Fig. 3b shows the case of potassium compounds.

It was observed that even at same content of alkali compounds Na_2O equiv., mortar expansion was largely changed with the type of anionic ion and in the range of this experiments their effects upon expansion decreased in the order of Cl^-, SO_4^{2-}, OH^-, CO_3^{2-}.

The differences of the effect of alkalies with different anionic ions upon expansion have been investigated by Diamond(9), Chatterji(10), Pettifer(7) at al, however, the reason why the influence is different was by no means clear.

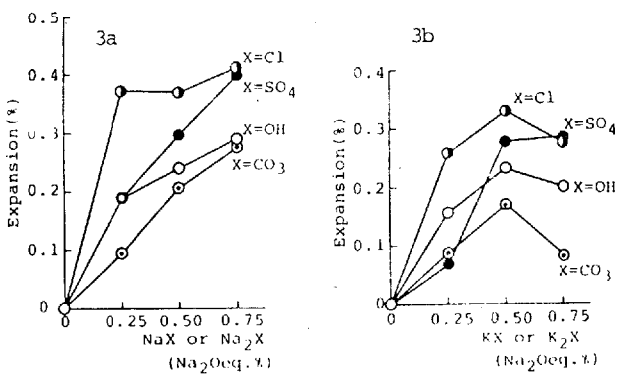

Fig.3. Effect of anionic ions upon expansion

Textural investigations were carried out on the mortar specimens prepared following the experinental procedures series-3.

Pore size distribution of hardened mortars with 0.75% Na_2O equiv. of alkali compounds and 12 weeks curing were shown in Fig.4 and photograph of mortar section by SEM in Photo. 1.

When alkali compounds were added to the mortar, even if they were chloride or hydroxide of sodium or potassium which promotes expansion as well as lithium compounds which suppress expansion, pore size distribution of each mortars was shifted towards smaller size, compared with controlled wortar.

It suggested that reaction products due to alkali-aggregate reaction made structure tight, regardless their effect upon expansion.

As dhown in Photo.1, in the case of controlled mortar, rough structure with lots of pore were observed, in the case of mortars with additional alkali compounds, every mortars showed the presence of gel products and tight structure, what were corresponded to the result of measurements of pore size distribution.

However, it's difficult to correspond the results of pore size distribution or SEM observation to the difference of expansion between sodium compounds and potassium compounds as shown above.

It must be required to investigate some problems relating to mechanism such as how the movement of alkali ion in pore solution varied because of coexisting anionic ion.

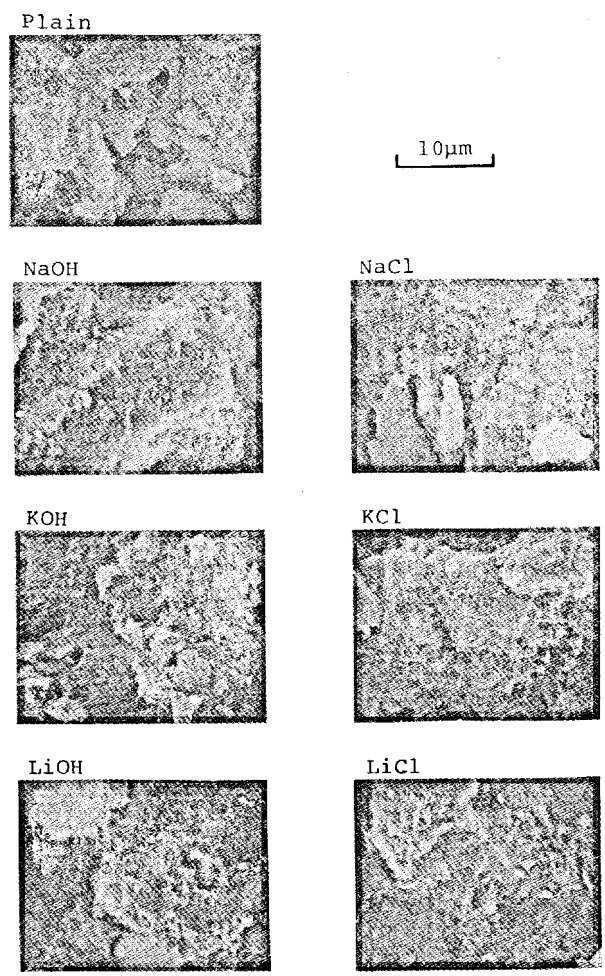

Photo.1. SEM photographs of hardened mortar section

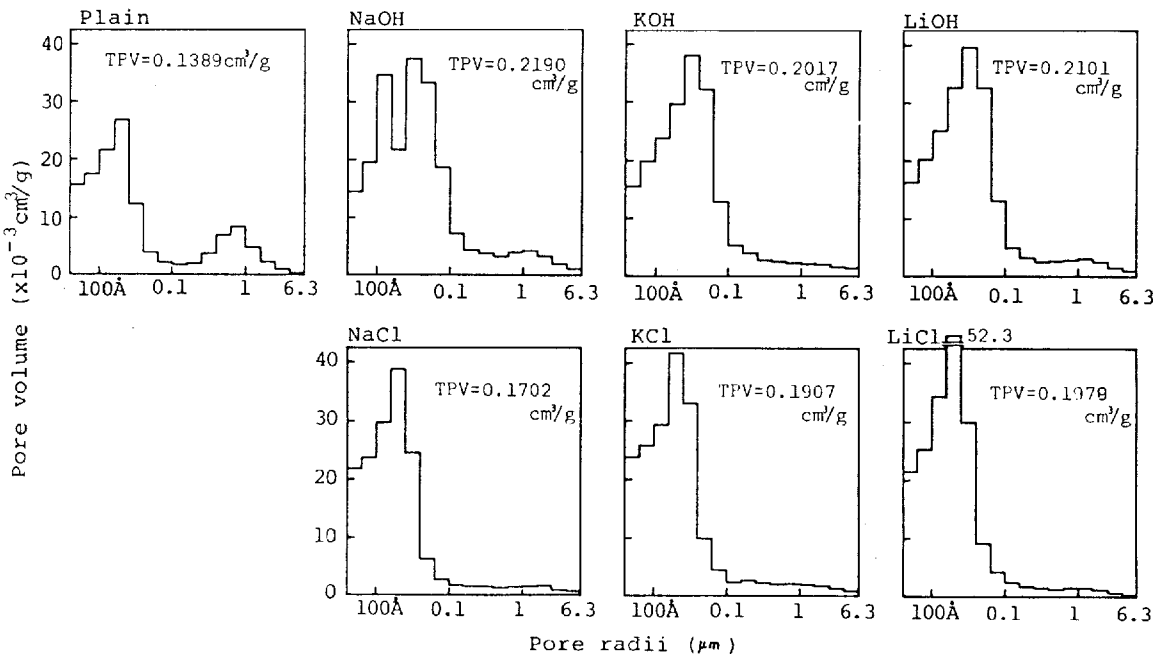

Fig.4. Pore size distribution of hardened mortar

(5) Estimation of Alkalies in Commercial Cement

The results of expansion measurements on commercial cement were shown in Fig. 5 at 6 weeks curing and in Fig.6 at 24 weeks curing, where, white circles showed ordinary portland cement and black circles showed suefate resisting cement.

Expansion were plotted against Na_2O equiv. alkali content in Fig.5a and Fig.6a and against modified alkali content calculated by changing coefficient of patassuim so as to obtaion the best linerity in Fig.5b and Fig.6b.

At 6 weeks curing relatively good linerity was obtained between Na_2O equiv. alkali content and expansion, however, at 24 weeks linerity became worse.

It shows that the effect of potassium upon expansion decreased with curing period, what were shown quantitatively in Tab. 3 as the change of coefficient of correlation between expansion and tatal alkali content.

As mentioned above, if we discuss the effect of alkalies upon expansion due to alkali-aggregate reaction, we can estimate the effect of alkali content more exactly by modified alkali content calculated by a small coefficient of potassium than by popular alkali content calculated by $Na_2O + 0.658 K_2O$.

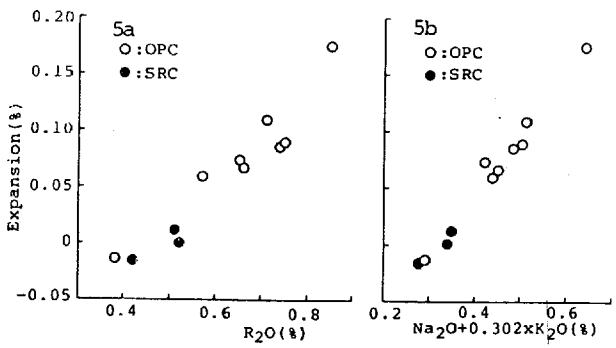

Fig.5. Expansion plotted against total alkali contents at 6 W curing

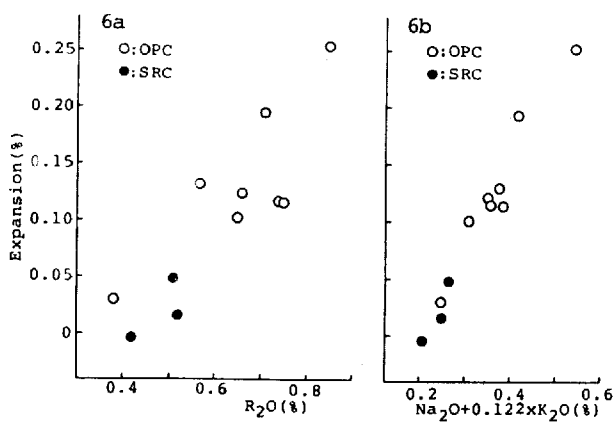

Fig.6. Expansion plotted against total alkali contents at 24 W curing

Tab.3. Correlation between total alkali content and expansion

Age (week)	Coefficient of correlation between Na_2O eq. alkali content and expansion	Coefficient of K_2O	Coefficient of correlation between modified alkali content and expansion
2	0.953	0.292	0.989
4	0.930	0.224	0.992
6	0.955	0.302	0.990
8	0.950	0.292	0.987
10	0.928	0.235	0.984
12	0.899	0.207	0.963
16	0.852	0.121	0.960
20	0.868	0.124	0.977
24	0.868	0.122	0.979
36	0.837	0.086	0.970

- Summary -

Following results were obtained from some experiments using ordinary portland cement with 0.75% Na_2O equivalent alkalies, pyrex glass as reactive aggregate and different type and quantity of alkali compounds in order to clarify the effect of alkali ions and coexisting anionic ions on expansion due to alkali-aggregate reaction.

(1) Sodium and potassium compounds promoted the expansion with curing period but lithium compounds suppressed the expansion at relatively early stage and after about 24 weeks also accelerated expansion.

(2) Expansion became larger with alkali contents in the case of soduim compounds but in the case of potassium compounds, maximum expansion was observed at 0.5% additional Na_2O equiv. content. On the other hand, mortar specimens with additional lithium compound showed shrinkage in proportin to contents until 24 weeks curing.

(3) Expansion changed due to coexisting anionic ions even at same kind of alkali ions and the degree of their effect decreased in the order of Cl^- , SO_4^{2-} , OH^- , CO_3^{2-}.

(4) From the investigation of the relation between alkali content and expansion on commercial cement, it was shown that the effect of potassium upon expansion decreased with curing period so that popular total alkali content calculated by $Na_2O + 0.658K_2O$ overestimated the effect of potassium.

(5) Additional alkali compound in every cases seemed to make structure of hardened mortar tight, however the mechanism how the expansion due to alkali-aggregate reaction changed with type of alkali ions and coexisting anionic ions can not be so clarified.

- Bibliography -

(1) Stanton, T. E., Proc. ASCE, 66, 1781 (1940)

(2) Bredsdorff, P., Idorn, G. M., Kjaer, A., Plum, N. M., Poulaen, P., Proc. 4th Int. Symp. Chem. Cement, 4, 749 (1960)

(3) Kondo, Y., Cement & Concrete, 49, 15 (1951) (in Japanese).

(4) Kondo, Y., Kitazawa, K., Semento Gijustsu Nempo, 5, 379 (1951) (in Japanese).

(5) Fukushima, M., Nimura, S., Cement & Concrete, 438, 8 (1983).

(6) Swenson, E. G., ASTM Bull., [226] 48 (Dec. 1957).

(7) Pagano, M. A., Cady, P. D., Cement and Concrete Research, 12, 1 (1982).

(8) Gillot, J. E., Symp. Alkali-Aggregate Reaction Measure, 213, Reykjavic, Iceland (1975)

(9) Gillot, J. E., Duncan, M. A., Swenson, E. G., Cement and Concrete Researvh, 3, 521 (1973).

(10) McCoy, W. J., Caldwell, A. G., ACI Journal, Proc. 47, 693 (1951)

(11) Davis, C. E. S., Aust. J. Appl. Sci., 9, 52 (1958).

(12) Figg. J., Concrete, 18, (Aug. 1981)

(13) Chatterji, S., Cement and Concrete Research, 8, 647 (1978).

(14) Woods, H., ACI Monograph, 4 (1968)

(15) Diamond, S., Symp. Alkali-Aggregate Reaction, Presentive Measures, 165-179, Reykjavic (1975).

(16) Chatterji, S., Cement and Concrete Research, 9, 185-188 (1979).

(17) Pettifer, K., Nixon, P. J., Cement and Concrete Research, 10, 173-181 (1980).

N.B. Milestone, D.A. St. John, J.H. Abbott and L.P. Aldridge, Chemistry Division, Department of Scientific and Industrial Research, Private Bag, Petone, New Zealand.

CO_2 Corrosion of Geothermal Cement Grouts

La corrosion geothermal du mortier de ciment par CO_2

SUMMARY: Recent failures of well casings and grout in New Zealand's Broadlands Geothermal Development have been attributed to corrosion by CO_2-rich, acidic fluids at 160°C. Although the alkaline fluids in the deep reservoir are not as agressive, they have production temperatures of up to 260°C raising questions about the long term stability of portland cement grout systems.

In-situ tests on typical grout formulations showed that CO_2-rich, acidic fluids at 160°C attack so rapidly that it is doubtful whether any portland cement system could withstand these conditions. At 260°C alkaline fluids containing CO_2 are rapidly carbonating the xonotlite which is formed when silica is added. Where silica is not added to the grout formulations the grouts have increased durability. It is hypothesised this is because the carbonates formed have a greater molar volume than the CH and hydrated products from which they are formed and hence reduce porosity. The reverse situation applies where silica is added to the grouts; the hydrated products in this case have a greater molar volume than the carbonates resulting in increased porosity.

Recentes falhas em revestimentos e argamassa de poço na New Zealand's Broadlands Geothermal Development foram atribuídas à corrosão por fluidos ácidos, ricos em CO_2, a 160°C. Apesar de os fluidos alcalinos no reservatório profundo não serem tão agressivos, eles têm temperaturas de produção de até 260°C, do que resultam perguntas sobre a estabilidade a longo prazo dos sistemas de argamassa de cimento portland.

Testes "in situ" com formulações de argamassa típica mostraram que fluidos ácidos, ricos em CO_2, a 160°C, atacam tão rapidamente que é duvidoso até que ponto qualquer sistema de cimento portland poderia suportar estas condições. A 260°C os fluidos alcalinos contendo CO_2 carbonatam rapidamente a xonotlita que se forma quando é adicionada sílica. Quando não houve adição de sílica às argamassas, estas tiveram sua durabilidade aumentada. Formulou-se a hipótese de que isto se deve ao fato de os carbonatos formados terem volume molar maior do que o CH e do que os produtos hidratados de que eles são formados, do que resulta redução da porosidade. Aplica-se a situação inversa quando se adiciona sílica às argamassas; neste caso os produtos hidratados têm volume molar maior do que os carbonatos, resultando em aumento da porosidade.

INTRODUCTION

The effect of CO_2, and CO_2-containing fluids on calcium silicate hydrates found in geothermal well grouts have not been extensively studied. Geothermal wells are normally grouted with a portland cement/ water slurry with added silica to prevent strength regression due to the formation of αC_2SH[1]. With added silica the binders normally formed are tobermorite or xonotlite, with the rarer formation of truscottite. In the long term testing conducted by the API Task Force[2] the only grouts to satisfy performance criteria were those containing added silica. The grouts require sufficient strength to anchor and support the casing and to prevent blowouts as well as providing the alkaline environment to prevent corrosion of the steel casing.

At the Broadlands development in the North Island of New Zealand, an upper aquifer lying between the production zone and the surface, has caused corrosion of both grout and steel casing in two wells. This aquifer has high CO_2 levels at 160°C. Because wells at the neighbouring Wairakei development have been successfully grouted for up to thirty years with cement slurries containing 3% bentonite, without added silica, this practice was continued at Broadlands. However, conditions at Broadlands are more severe with both higher temperatures and gas contents in the fluids. This study attempts to assess the effects of these fluids on typical grout formulations used at Broadlands and some others suggested as being more suitable.

EXPERIMENTAL

The two wells chosen for these exposure studies were believed to provide conditions typical of the upper aquifer and the deep reservoir. BR23 with a temperature of 160°C represents the corrosive upper aquifer while BR17 with an operating temperature of 260°C represents the deep reservoir, although it should be noted that each well has its own unique chemistry[3]. A series of 100 x 50 mm cylinders were prepared, Table I, and lowered to 563m depth in BR17 and 422m in BR23. After three months exposure the cylinders were reclaimed and then cut into halves along their lengths and dried at 60°C. One half was used for X-ray diffraction (XRD) and the other half was large-area thin-sectioned for petrographic examination[4].

RESULTS AND DISCUSSIONS

When the XRD analyses, Table II, are combined with the microscopic examinations, Table III, they give a detailed picture of the textures of the samples and the products formed in the zones (see fig.1). In BR23 (160°C), with high CO_2 levels and acid conditions,

Table I - Grout Formulations

Sample No.	Cement (g)	Bentonite (g)	Silica (g)	Water (ml)	w/c
		Bore 23			
1	500	15	-	280	0.56
2	500	15	-	320	0.64
3	350	-	140	217	0.62
4	350	-	140	280	0.80
		Bore 17			
5	620	19	-	310	0.50
6	620	19	-	347	0.56
7	393	-	236	283	0.72
8	393	-	236	305	0.78

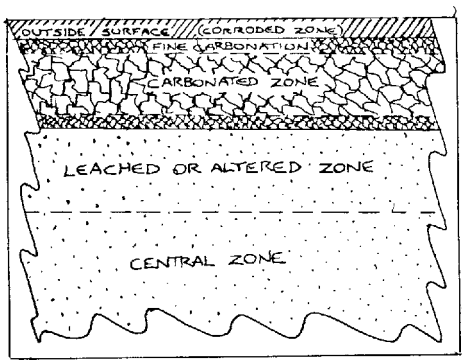

Fig. 1 Diagramatic representation of zones formed by attack on cement grouts

corrosion is severe on all samples with attack increasing from samples 1 through to samples 4. Thus both W/C ratio and the products formed appear to be important in determining degree of attack. In BR17 (260°C), with lower CO_2 levels and alkaline conditions, corrosion is minimal and attack is limited to carbonation which increases in severity from samples 5 to 8. Once again the same pattern as that found in BR23 is repeated.

Samples exposed in BR23 are exhibiting classical corrosive attack from CO_2-rich, acidic waters[5]. The corroded, carbonated and leached zones, (see fig.1), are merely the components of a moving front attacking

Table II - Results of XRD Analyses

Sample	Carbonated zone	Central Zone
	Bore 23 (160°C)	
1 & 2	Calcite, αC_2SH(tr), aragonite (tr)	αC_2SH, CH
3 & 4	Calcite Aragonite, qtz	Tobermorite, qtz(m)
	Bore 17 (260°C)	
5 $ 6	Calcite	Calcio-chondrodite, tri-calcium silicate hydrate, CH
7 & 8	Calcite, qtz(tr)	Xonotlite, qtz(tr), calcite (50-20%)

Table III - Results of Microscopic Examination

Sample	Corroded zone	Carbonated	Leached or altered zone	Central zone	Pores
			Bore 23 (160°C)		
1 & 2	Isotr. lattice, $C\bar{C}$(tr)	$C\bar{C}$	leached matrix	αC_2SH, CH,	CH
3 & 4	Isotr. lattice, qtz, $C\bar{C}$(tr)	$C\bar{C}$, qtz	altered matrix needles(m), qtz	Dark matrix, qtz, CH or $C\bar{C}$(tr)?	ettr.
			Bore 17 (260°C)		
5 & 6	Absent	$C\bar{C}$	leached matrix, $C\bar{C}$(tr)	Dark matrix, CH	CH
7 & 8	Absent	$C\bar{C}$, qtz(m)	Absent	Dark matrix, long fine needles, qtz(tr) $C\bar{C}$ (100-25%)	$C\bar{C}$

the samples. The total width of the front will be determined by its overall porosity. The driving forces are firstly, carbonation that draws out material via the leached or altered zone and secondly, the acidic conditions which corrode the carbonated zone and drives the front forward. The corroded zone is largely missing especially in samples 3 and 4. It is all that remains after everything but the silica and alumina has been removed from the cement, and rarely exceeds a few mm in depth in these samples because it is fragile, porous and easily lost. It will be obvious that it is easier for the front to move forward in the more porous samples. In contrast, attack in BR17 is limited to carbonation. The driving force of corrosion of the carbonated zone is absent. Thus the depth of attack will be controlled initially by the permeability of the hydration products but ultimately by the permeability of the carbonated zone.

The addition of silica in samples 3 and 4 has suppressed the formation of αC_2SH in favour of 11Å tobermorite and reacted with the CH. A surprising amount of the silica flour is unreacted, even down to 5μm particles, considering the time of exposure. XRD detected aragonite in the carbonated zone adjacent to the altered zone in samples 3 and 4. This has formed from carbonation of the tobermorite and altered to calcite in the outer portions of the carbonated zone.

From XRD analyses, a complex mixture of calcio-chondrodite (C_6S_5H), tri-calcium silicate hydrate ($C_6S_3H_3$) and CH was detected in the centres of samples 5 and 6 exposed in BR17. In samples 7 and 8 the main phase detected was xonotlite with calcite and a trace of quartz. It would

appear that as the temperature of exposure is increased, from 160° to 260°C the tobermorite alters to xonotlite.

Microscopy showed a complete absence of the corroded zone in samples exposed in BR17 which is to be expected because of the alkaline fluids present. Rather there were signs of calcite crystals and fine, dark, opaque grains which may be some form of sulphide, having been deposited on the outside surfaces. In samples 5 and 6, the remaining three zones (carbonation, leached and central) are clearly visible. The central zone consists of a rather feature-less, dark matrix containing well crystallised-CH. Under the microscope the texture of samples 7 and 8 is different from all the other samples examined but it is to be noted that attack may be sufficiently severe to have destroyed zones originally present. The central zone consists of a dark matrix in which are embedded long fine needles with similar optical properties to those of xonotlite. Scattered through this matrix are clumps of fine crystals of $CaCO_3$ which form nearly 100% of the texture adjacent to the carbonation zone and reduce to about 25% in the centre. All the interior pores contain large carbonate crystals which appear to be aragonite. Throughout samples 7 and 8 only the larger quartz grains remain in which reaction rims are clearly visible.

MECHANISM OF ATTACK

This study and previous work by L.M. Smith (private communication) clearly shows that grouts without added silica are more durable than those with added silica when exposed to the fluids in BR23. When grouts without added silica are exposed to these CO_2-rich, acidic fluids, the HCO_3- reacts with the CH to produce calcite. The calcite has a larger molar volume than CH (37 cc/mole Ca compared to 32 cc/mole Ca) and this blocks the pores of the grout reducing permeability and the rate of attack.

Where samples containing added silica are exposed to HCO_3-, attack must be directly on the hydrated calcium silicate binders giving aragonite. The molar volumes of tobermorite and xonotlite are 57 and 44 cc/mole Ca respectively so that the formation of either aragonite or calcite leads to an increase in porosity. In BR23 (samples 3 and 4) this increase in porosity increases the rate of attack so that the carbonated layer is not only wider but more porous than samples 1 and 2, and thus is corroded more rapidly by HCO_3-. In BR17 the attack by HCO_3-, although operating under alkaline conditions, is driven by high temperatures, so that no part of the samples 7 and 8 are unaffected by carbonation after the three months exposure. The carbonation of the xonotlite has produced sufficient porosity to give this rapid rate of attack and it must be concluded that xonotlite is not stable under these conditions.

CONCLUSIONS

Investigation of some typical geothermal well grout formulations, exposed in BR23 and BR17 at the Broadlands Geothermal Development to CO_2-rich, acidic fluids at 160°C and alkaline fluids at 260°C allows the following conclusions to be drawn.

1. At 160°C grouts exposed to CO_2-rich acidic fluids are undergoing rapid carbonation and corrosion from HCO_3-. It is doubtful if any portland cement system could withstand these conditions for the expected twenty year life required of the wells.

2. At 260°C grouts exposed to alkaline fluids containing CO_2 are carbonating only. If the binder is xonotlite the carbonation is rapid under these conditions and the phase cannot be considered to be stable.

3. Where silica is added to the formulations the grouts are less durable and rates of attack are increased. At 160°C the 11Å tobermorite is more corroded and carbonated than the αC_2SH. Similarly at 260°C the carbonation of the xonotlite is extremely rapid when compared with that of calcio-chondrodite, tri-calcium silicate hydrate and calcium hydroxide mixture.

4. It is hypothesised that the increased durability of the grouts without added silica is because the carbonates formed have a greater molar volume than the CH and hydrated phases from which they are formed and hence reduce porosity. The reverse situation applies to the hydrated products 11Å tobermorite and xonotlite formed when silica is added to the grouts.

REFERENCES

1.- E.B. Nelson (1980), Proc. Annu. Southwest. Pet. Short Course, 11-19.

2.- API Task Group, Oil and Gas Journal, Feb. 11, 1985, 93-97.

3.- J.W. Hedenquist and M.K. Stewart, International Symp. Geothermal Energy, Aug. 1985.

4.- D.A. St John and J.H. Abbott (1983) Industrial Diamond Review, Vol. 43, No. 494, 13-15.

5.- D.A. St John and H.R. Penhale (1978) "Durability of Building Materials & Compounds" ASTM STP 691, 1980, 377-387.

Demétrio Gaspar-Tébar*, José Luis Sagrera-Moreno* et Victoriano González-Vila**
*Instituto de la Construcción y del Cemento "Eduardo Torroja" - P.O. Box 19002 Madrid - Spain

CONTRIBUTION A L'ETUDE DE LA RESISTANCE CHIMIQUE DES CIMENTS. COMPORTEMENT MECANIQUE-RESISTANT D'UN CIMENT PORTLAND INDUSTRIEL RESISTANT AUX SULFATES AUX DIVERS SOLUTIONS AGRESSIVES.

CONTRIBUTION TO THE STUDY OF THE CHEMICAL RESISTANCE OF CEMENTS. BEHAVIOUR MECHANICAL-RESISTANCE OF A SULPHO-RESISTANCE PORTLAND CEMENT APPOSITE TO DIVERSE AGRESSIVE SOLUTIONS.

R É S U M É

Dans ce travail, qui fait partie d'un Projet de Recherche de l'IETcc à long terme, on étudie la variation des résistances mécaniques des éprouvettes de mortier (1:3) [de 1 x 1 x 6 cm, en flexotraction, de 4 x 4 x 16 cm, en flexotraction et compression, de 7 x 7 x 28 cm, en traction-centrifuge] et de béton [de 10 x 10 x 40 cm, en flexotraction et compression] fabriquées avec un ciment portland résistant aux sulfates (ciment 2; un des ciments faisant l'objet d'autres travaux présentés à ce Congres) sont soumises, après la période de conservation (1 jour en chambre humide et 21 jours pour les éprouvettes de 1 x 1 x 6 cm et 30 jours pour les éprouvettes restantes sous eau douce), à l'action de différentes solutions agressives pendant 56 - 90 - 180 - 360 - 540 - 720 - 900 et 1080 jours les éprouvettes de mortier de 1 x 1 x 6 cm et pendant 6 - 12 - 18 - 24 - 30 - 36 - 42 - 48 - 54 et 60 mois les éprouvettes de mortier (4 x 4 x 16 cm et 7 x 7 x 28 cm) et de béton (de 10 x 10 x 40 cm).

Les solutions agressives étudiées ont été: sat. de $CaSO_4.2H_2O$; Na_2SO_4 (2,1 g/l); Mg $SO_4.7H_2O$ (3,2 g/l); Mg $SO_4.7H_2O$ (32,2 g/l); sat. de $CaSO_4.2H_2O$ + Mg $SO_4.7H_2O$ (3,2 g/l); sat. de $CaSO_4.2H_2O$ + Mg $SO_4.7H_2O$ (32,2 g/l); Na_2SO_4 (3,5 g/l) + NaCl (20,0 g/l) et de l'eau de mer artificielle (ASTM D 1141-75), et d'un autre côté de l'eau douce; la concentration minimale de SO_4 (II) a été toujours, pendant le temps d'essai, de 500 mg/l. Les travaux ont permis d'établir une qualification de majeure à mineur, en accord avec le comportement mécanique-résistant des éprouvettes où ont été immergées.

Neste trabalho, que faz parte de um Projeto de Pesquisa do IETcc, a longo prazo, estuda-se a variação das resistências mecânicas de corpos de prova de argamassa (1:3) (de 1 x 1 x 6 cm, sob flexotração; de 4 x 4 x 16 cm, sob flexotração e compressão; de 7 x 7 x 28 cm, sob tração centrífuga), e de concreto (de 10 x 10 x 40 cm, sob flexotração e compressão), fabricados com um cimento portland resistente aos sulfatos (cimento 2; um dos cimentos é objeto de outros trabalhos apresentados neste Congresso). Após o período de conservação (1 dia em câmara úmida e 21 dias no caso dos corpos de prova de 1 x 1 x 6 cm, e 30 dias para os restantes em água doce), são submetidos à ação de diferentes soluções agressivas: durante 56 - 90 - 180 - 360 - 540 - 720 - 900 e 1.080 dias para os corpos de prova de argamassa de 1 x 1 x 6 cm, e durante 6 - 12 - 18 - 24 - 30 - 36 - 42 - 48-54e60 meses para os corpos de prova de argamassa (4 x 4 x 16 cm e 7 x 7 x 28 cm), e de concreto (de 10 x 10 x 40 cm).

As soluções agressivas foram: saturação de $CaSO_4.2H_2O$; Na_2SO_4 (2,1 g/l); $MgSO_4.7H_2O$ (3,2 g/l); $MgSO_4.7H_2O$ (32,2 g/l); saturação de $CaSO_4.2H_2O$ + $MgSO_4.7H_2O$ (3,2 g/l); saturação de $CaSO_4.2H_2O$ + $MgSO_4.7H_2O$ (33,2 g/l); Na_2SO_4 (3,5 g/l) + NaCl (20,0 g/l) e água marinha artificial (ASTM D 1141-75), e de outro lado, água doce; durante o tempo de ensaio a concentração mínima de SO_4 (II) foi sempre de 500 mg/l).

Os trabalhos permitiram estabelecer-se uma qualificação de maior a menor, de acordo com o comportamento de resistência mecânica dos corpos de prova no meio em que foram imersos.

1. Introduction

Dans d'autres travaux présentés dans ce Congrès nous étudions le comportement de différents ciments portland industriels hydratés (l'un d'eux, ciment 2 , est analogue à celui qui fait l'objet de ce travail) et des ses mélanges avec le laitier lorsqu'ils sont soumis à l'action de différentes solutions agréssives, pendant des périodes de temps diverses, déterminant la composition structurelle des nouvelles phases solides formées dans l'eau de mer artificielle où les éprouvettes de mortier ont été immergées, ainsi que les modifications des caractéristiques structurelles de la fraction enrichie (ciment hydraté et ciment hydraté-attaqué) extraite des éprouvettes de mortier (1); la variation de la concentration ionique de l'eau de mer artificielle où les éprouvettes de mortier mentionnées ont été immergées (2) et d'autres solutions agréssives qui ont traversé les lits élaborés avec ce ciment hydraté, ainsi que la composition chimique et structurelle des ciments hydratés-attaqués des lists mentionnés et de la nouvelle phase solide formée(3).

Ces travaux font partie d'un Projet de Recherche à développer à long terme, aussi bien à échelle de laboratoire qu'à échelle réele.

2. Partie expérimentale

Dans ce travail nous étudions le comportement chimique -résistant d'un ciment portland résistant aux sulfates, de fabrication espagnole, lorsque les éprouvettes de mortier ou de béton, élaborées avec ce ciment, et après la période de conservation, sont soumises à l'action des solutions agréssives (1-3-4-5-6 et 8, une partie des premières éprouvettes, et 1-2-3-7 et 8 les restantes) que nous présentons dans le Tableau 2, déterminant l'évolution des résistances mécaniques en la flexotraction des éprouvettes de mortier (1:3) de 1 x 1 x 6 cm, en flexotraction et compression d'éprouvettes de mortier (1:3) de 4 x 4 x 16 cm, en traction centrifuge d'éprouvettes de mortier (1:3) de 7 x 7 x 28 cm et en flexotraction et compression des éprouvettes de béton de 10x10x40cm.

2.1.- Matériaux utilisés

2.1.1.- Ciment: nous avons employé un ciment portland industriel résistant aux sulfates, de fabrication espagnole, qui répond aux caractéristiques chimiques, physiques et mécaniques du Tableau 1. Il a une teneur calculée (Bogue) en C_3A = 0%, en C_4AF = 10,8% et en C_3S (75,6%) + C_2S (6,1%) = 81,7%. Les DRX des phases cristallines correspondantes aux aluminates du ciment anhydride et du résidu de l'attaque de ce ciment par l'acide salicylique-méthanol sont représentées dans la fig. 1, où un pic du C_3A à 2θ = 33,15° et un autre du C_4AF à 2θ = 33,8° (34° théoriques) ont été détectés; il a été mis en évidence aussi, l'existence d'un pic à 2θ = 32,9°.

2.1.2.- Le sable employé pour la fabrications des éprouvettes de mortier de 4 x 4 x 16 cm et de 7 x x 7 x 28 cm a été spécifié dans le "Pliego español para la recepción de cementos (RC-75)"; pour les éprouvettes de 1 x 1 x 6 cm on a employé la fraction de sable comprise entre 1 et 1,5 mm.

2.1.3.- Les granulats employés pour préparer les éprouvettes de béton ont été roulés (siliciques) et lavés; ils répondent à la courbe granulométrique de Bolomey.

2.1.4.- Les solutions agressives utilisées sont celles du Tableau 2.

2.1.5.- Préparation et conservation d'éprouvettes de mortier et de béton.

a. les éprouvettes de mortier (1:3) de 1 x 1 x 6 cm ont été préparées comme signalé en (4); elles ont été conservées 1 jour en chambre humide, à 20 ± 1° C, avec une humidité relative supérieure à 95% et, par la suite, nous avons immergé 12 éprouvettes/1série/ /800 ml en eau potable filtrée et de chacune des solutions 1, 3, 4, 5, 6 et 8/par âge, où elles sont restées jusqu'au moment de la détermination des résistances mécaniques (56, 90, 180, 360, 540, 900 et 1080 jours). Nous avons préparé 56 séries d'éprouvettes (12 éprouvettes/série), une par âge et par solution, et elles ont été conservées dans les récipients correspondants situés dans le laboratoire.

b. les séries d'éprouvettes de mortier (1:3) de 4 x 4 x 16 cm et de 7 x 7 x 28 cm (10 éprouvettes par série, par âge et par solution) ont été préparées en accord avec le procédé opératoire décrit dans le "Pliego español para la recepción de cementos (RC-75)", elles ont été conservées 1 jour en chambre humide, comme les éprouvettes précédentes, et par la suite, sous eau potable pendant 30 jours. En suite, elles ont été immergées jusqu'au moment de la détermination des résistances mécaniques (1 série par âge : 6, 12, 18, 24, 30, 36, 42, 48, 54 et 60 mois) dans l'eau potable et dans les solutions agressives 1, 2, 3, 7 et 8 contenues dans des réservoirs d'asbeste-ciment protégés par un mortier epoxi. Les éprouvettes ont été placées en position verticale, séparées entre elles par une couche de solution d'au moins 5 cm; les réservoirs mentionnés ont été placés dans l'enceinte extérieure de l'Institut, sous conditions ambiantes.

Les solutions agressives ont été renouvelées lorsque la concentration d'ions sulfate était inférieure à 500 mg/l.

c. Les séries d'éprouvettes de béton de 10 x 10 x 40cm (10 éprouvettes par série, par âge et par solution) ont été préparées avec des granulats siliciques lavés, répondant à la courbe granulométrique de Bolomey; nous avons employé 400 Kg de ciment/ 1 m^3 de béton, une relation eau/ciment = 0,45 et elles ont été mises en vibration par groupes de quatre. Les séries d'éprouvettes conservées pendant les premières 24 heures atmosphère du laboratoire et, par la suite, sous eau potable pendant 30 jours dans des réservoirs construits dans l'enceinte extérieure de l'Institut (fig. 2); plus tard elles ont été placées sous eau potable et solutions agressives 1, 2, 3, 7 et 8 contenues dans des réservoirs analoaux précédents protégés par un mortier epoxi, où elles ont été placées en position verticale, séparées entre elles par, environ, 5 cm. Chaque réservoir contient 2000 l de chacune des solutions mentionnés, qui ont été renouvelées lorsque la concentration des ions de sufate était inférieure à 500 mg/l.

3.- Résultats obtenus

3.1.- Résistance chimique.

3.1.1.- Méthode Chatelier-Anstett: la variation expérimentée par le diamètre des éprouvettes (deux), ciment hydraté plus gypse, a été de 0,12% à 14 jours; valeur maintenue tout au long du temps d'étude (1 an). Dans ces érpuvettes ni fissures ni deformations ont été observées.

3.1.2.- Méthode ASTM C 452-73: l'augmentation en

longueur que les deux séries d'éprouvettes de mortier ont expérimenté, a été de 0,004% après 14 jours; cette augmentation, tout au long du temps étudié (1 an), a été inférieur à 0,009%.

3.1.3.- Méthode Koch-Steinegger: les valeurs des coefficients de corrosion Kock-Steinegger (Rt/R't) des differentes séries d'éprouvettes de mortier immergées dans les solutions agressives mentionnées dans le point 2.1.5, pendant 56, 90, 180, 360, 540, 720, 900 et 1080 jours, après la période de conservation (1 + 21 jours) ont été, dans tous les cas, supérieures à la valeur indice (0,70 pour t = 22 + 56 jours), comme nous pouvons l'apprécier dans la fig. 3.

De même, cette valeur est aussi supérieure à 0,70 dans le cas des éprouvettes immergées dans les solutions de Na_2SO_4(2,1 g/l) et de Na_2SO_4 (3,5 g/l), plus Na Cl (20,0 g/l), dans tous les âges étudiés.

En accord avec les valeurs obtenues on peut établir l'ordre de résistance chimique suivante:

Sol.6 > sol.4 > sol.1 ≃ et > sol.3 > sol.5 > sol.8

3.2.- Evolution des résistances mécaniques.

3.2.1.- éprouvettes de mortier de 1 x 1 x 6 cm

Dans la fig. 4 nous représentons l'évolution des résistances mécaniques en flexotraction (Kp/cm^2) des séries d'éprouvettes de mortier de 1 x 1 x 6 cm (valeurs moyennes de 12 éprouvettes par série et par âge) en fonction du temps d'immersion (jusqu'à 3 ans), où l'on peut apprécier que, en relation avec les résistances des éprouvettes de mortier conservées sous eau potable (sol.0), celles qui correspondent aux séries immergées dans les solutions 6, 4 et 1 sont supérieures, dans les solutions 5 et 3 elles sont du même ordre, présentant de légères modifications, et toutes plus grandes que les séries immergées dans l'eau de mer artificielle ASTM. Tout ceci permet d'établir l'échelle suivante:

sol.6 > sol.4 > sol.1 > eau potable ≃ et ≳ sol.5 ≃ sol.3 > eau de mer artificielle.

3.2.2. éprouvettes de mortier de 4 x 4 x 16 cm
Dans les figures 5 et 6 nous avons représenté l'evolution des résistances mécaniques en flexotraction (valeurs moyennes de 10 éprouvettes par série) et en compression (valeurs moyennes des 20 demi-prismes de chaque 10 éprouvettes), en Kp/cm^2, ainsi que les valeurs maximales et minimales de chaque série en fonction du temps d'immersion (jusqu'à 5 ans).
Dans la figure 5 on peut apprécier les résistances mécaniques en flexotraction des éprouvettes immergées dans les solutions 1 (sat. de Ca SO_4. 2 H_2O), 3($MgSO_4$. 7 H_2O; 3,22 g/l), 2 (Na_2SO_4; 2,1 g/l) et 7 (Na_2SO_4; 3,5 g/l +Na Cl; 20,0 g/l) sont supérieures à celles correspondant aux séries d'éprouvettes conservées sous eau potable. (sol. 0) et celles-ci, à leur tour, plus grandes que les séries immergées en eau de mer artificielle, faits inscrits dans la figure 7, où l'on peut apprécier que les coefficients Rt/R't (Rt = Résistances des éprouvettes immergées dans les solutions, pour une période t et R't = Id immergées sous eau potable pour une période t) sont plus grandes que l'unité dans le cas des éprouvettes immergées dans les quatre solutions agressives et plus petites que l'unité et plus grandes que 0,70 dans l'eau de mer artificielle.

Les résistances mécaniques en compression (fig.6) des séries d'éprouvettes de mortier conservées sous eau potable, sont du même ordre que celles qui correspondent aux séries immergées dans la solution de Na_2SO_4(3,5 g/l) + Na Cl (20,0 g/l), plus petites que celles des séries immergées dans la solution saturée de gypse, de Na_2SO_4(2,1 g/l) et plus grandes que celles des éprouvettes immergées dans l'eau artificielle.

L'aspect des éprouvettes soumises à l'action des différentes solutions, pour tous les âges, était normale, n'ayant pas observé d'altérations (analogue à celui de la fig. 11). Les éprouvettes soumises à l'action de l'eau de mer apparaissent recouvertes, partiellement, d'une pellicule de Mg $(OH)_2$.

3.2.3.- éprouvettes de mortier de 7 x 7 x 28 cm.

L'évolution des résistances mécaniques, en traction centrifuge, des séries d'éprouvettes de mortier de 7 x 7 x 28 cm (valeurs moyennes de 10 éprouvettes), en Kp/cm^2, immergées dans les solutions 1 (sat. de Ca SO_4. 2 H_2O), 2 (sol. Na_2SO_4; 2,1 g/l), 3 (sol. Mg SO_4. 7 H_2O; 3,22 g/l), 7 (Na_2SO_4; 3,5 g/l + Na Cl; 20,0 g/l) et 8 (eau de mer artificielle) se conduit d'une façon analogue à celle des éprouvettes de mortier conservées sous eau potable (sol. 0) (fig. 8). Les valeurs supérieures et inférieures plus fréquentes correspondent aux séries d'éprouvettes immergées dans la solution de Na_2SO_4 (2,1 g/l) et en eau de mer artificielle, respectivemente.

L'aspect des éprouvettes soumises à l'action des diverses solutions agressives, pour tous les âges, était normale; on n'a pas observé d'altérations. Les éprouvettes soumises à l'action de l'eau de mer apparaissent partiellement recouvertes d'une pellicule de Mg $(OH)_2$.

3.2.4.- éprouvettes de béton de 10 x 10 x 40 cm.
Dans les figures 9 et 10 nous avons représenté les résistances mécaniques en flexotraction (valeurs moyennes de 10 éprouvettes par série) et en compression (valeurs moyennes des 20 demi-prismes de chaque 10 éprouvettes), en Kp/cm^2, ainsi que les valeurs maximales et minimales de chaque série en fonction du temps d'immersion (jusqu'à 5 ans).
Dans la figure 9 on peut apprécier que les résistances mécaniques en flexotraction des differentes séries d'éprouvettes en béton immergées dans les solutions agressives 1 (sat. de Ca SO_4 . 2 H_2O), 2 (sol. Na_2SO_4; 2,1 g/l), 3 (sol. Mg SO_4 . 7 H_2O; 3,22 g/l) et 7 (Na_2SO_4; 3,5 g/l + Na Cl; 20,0 g/l) sont en règle générale, inférieures à celles qui correspondent aux éprouvettes conservées sous eau potable (sol.0) et toutes sont plus grandes que celles immergées dans l'eau de mer artificielle.

Dans la figure 10 on observe que les résistances mécaniques en compression des éprouvettes de béton immergées sous les différentes solutions agressives et sous eau potable, maintiennent une évolution semblable tout au long de 5 ans, formant un faisceau où s'entrecroisent ces valeurs.

L'aspect des éprouvettes soumises à l'action de l'eau potable et des solutions agréssives, était normal, à tous les âges, comme on peut l'apprécier dans la figure 11, où nous reproduisons la photo d'une éprouvette d'une des différentes séries soumises pendant 5 ans à l'action de ces solutions. Les éprouvettes immergées en eau de mer artificielle apparaissent recouvertes d'une pellicule de Mg $(OH)_2$.

D'après l'étude au moyen de DRX de la fraction enrichie (pâte de ciment) extraite de chacun des morceaux

des éprouvettes en béton (superieur et inférieur) immergées pendant 360 jours dans les différentes solutions agressives et tenant compte de l'intensité des pics (comptes) des composants cristallins ettringite, portlandite et calcite (pour 2θ = 8,9° - 18,0° et 29,5°, respectivement), intensité qui se réfère à celle du pic α - Si O_2(2θ = 26,7°) de l'échantillon extrait de l'éprouvette immergée en eau potable pendant 360 jours, on observe (Tableau 3):

a. que l'intensité des pics de l'ettringite (2θ=8,9°) est de la même magnitude dans les DRX des deux zones de chaque éprouvette, excepté dans celles immergées dans l'eau de mer artificielle (I zone supérieure > I zone inférieure); ainsi, cette intensité est de la même magnitude dans les DRX correspondents aux différentes séries d'éprouvettes, excepté pour les DRX de la zone supérieure des éprouvettes immergées dans la sol. de Na_2 SO_4 (elle est plus petite) et dans l'eau de mer artificielle (elle est plus grande).

b. que l'intensité de pic de la portlandite (2θ=18,0°) est différente selon qu'il s'agisse des DRX de la zone supérieure (elle est plus petite) ou inférieure (elle est plus grande) des éprouvettes et que cette intensité des DRX de la zone inférieure suit la graduation: sol. sat. de Ca SO_4 . 2 H_2O > sol. de Mg SO_4 . 7 H_2O, > eau potable > eau de mer artificiel > sol. Na_2 SO_4 + Na Cl > sol. Na_2 SO_4; cependant dans les DRX de la zone supérieure, la graduation est la suivante: sol. Mg SO_4 . 7 H_2O > eau potable > > sol. sat. Ca SO_4 . 2 H_2O > eau de mer artificielle > sol. Na_2 SO_4 > sol. Na_2 SO_4 + Na Cl.

c. que l'intensité des pics de la calcite est differente selon qu'il s'agisse des DRX de la zone supérieure (elle est plus petite) ou de la zone inférieure (elle est plus grande); la plus petite intensité, pour les deux diagrammes correspond à ceux de l'éprouvette immergée dans l'eau de mer artificielle et dans la dis. de Mg SO_4 . 7 H_2O. Phénomènes qui influent tous sur le comportement mécanique-chimique-résistant.

4.- Conclusions

Première:
L'évolution des résistances mécaniques des différentes séries d'éprouvettes de mortier immergées, après la période de conservation, sous eau potable ou sous eau potable filtrée et dans les différentes solutions agréssives (Tableau 2) pendant 3 à 5 ans, est fonction de la composition chimique de ces solutions.

Deuxième:
Les valeurs des résistances mécaniques permettent d'établir des classifications déterminées qui dépendent de la solution où elles ont été immergées et du procédé employé pour déterminer ces résistances.

5.- Bibliographie

(1) GASPAR-TEBAR, D. et SAGRERA-MORENO, J.L.; (1986).- L'action de l'eau de mer sur un ciment portland de haute resistance initielle, sur un ciment portland resistant aux sulfates et sur un ciment portland ordinaire: influence de l'addition de laitier. Etude par DRX.
Communication presentée à ce Congrès.

(2) GASPAR-TEBAR, D. et SAGRERA-MORENO, J.L.; (1968).- L'action de l'eau de mer sur un ciment portland de haute resistance initielle et sur un ciment portland resistant aux sulfates: influence de l'addition de laitier. Etude de la concentration ionique.
Communication presentée à ce Congrès.

(3) BERMEJO-MUÑOZ, F.; SAGRERA-MORENO, J.L. et GASPAR-TEBAR, D.; (1986).-Comportement d'un ciment portland resistant aux sulfates front a l'eau deionisée et les solutions de sulfate de sodium et de sulfate de magnesium.
Communication presentée à ce Congrès.

(4) GARCIA DE PAREDES, P.; (1967).- Inalterabilidad de los conglomerantes al ataque de los sulfatos. Comparación de métodos para apreciarla.- Cuadernos de Investigación del IETcc (Madrid); pp 11-14.

Remercíements

Nous voudrons experimer nôtre plus vive reconnaisance aux membres de l'EI "Durabilidad" del IETcc: Amalia Rodríguez, Lucila López, MªSol. Cid, Felipe Cantero et Manuel Cantero pour l'aide prêtée dans les réalisation de ce travail.

Tableau 1

Analise chimique;%, e. p.	
P.F.	1,1
R.I.	0,2
SiO_2	22,0
Fe_2O_3	4,1
Al_2O_3	1,8
CaO	67,9
MgO	0,5
SO_3	2,3
CaO libre	1,8
Composition potential (Bogue)	
C_3S	75,6
C_2S	6,1
C_3A	0,0
C_4AF	10,8

Essais physiques et mécaniques	
Masse volumique	3,12 g/cm^3
Surface specifique	3.553 cm^2/g
Stabilité volumen (autoclave)	0,0 %
Prise, debut	0 h 45 min
Prise, fin	3 h 15 min

Resistances mécaniques (Kp/cm)

Jours	Flexotraction	Compression
3	52	285
7	73	473
28	83	542

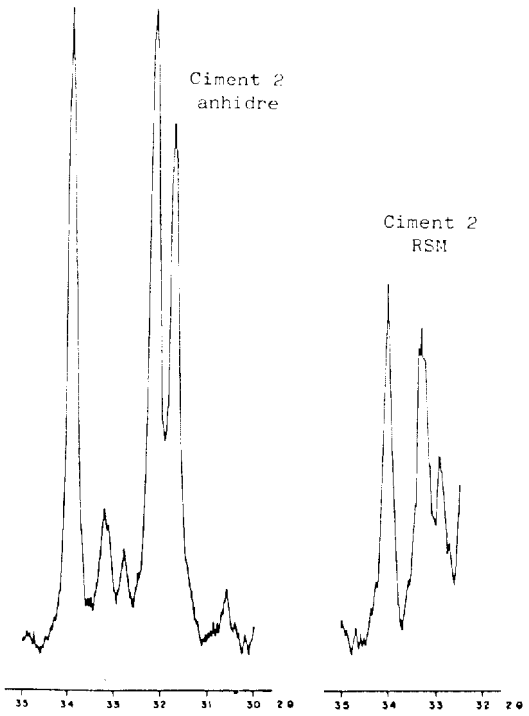

FIGURE 1

Ciment 2: anhidre et RSM. DRX.

Tableau 2

Solutions agressives

Solutions		Concentration, g/l			
nº	Agressives	SO_4(II)	Cl (I)	Ca (II)	Mg(II)
1	Sat. de $CaSO_4 . 2H_2O$	1,010	-	0,420	-
2	Na_2SO_4 (2,1 g/l)	1,210	-	-	-
3	$MgSO_4 . 7H_2O$ (3,22 g/l)	1,263	-	-	0,318
4	$MgSO_4 . 7H_2O$ (32,2 g/l)	12,630	-	-	3,180
5	Sat. de $CaSO_4 . 2H_2O$ + $MgSO_4 . 7H_2O$ (3,22 g/l)	2,273	-	0,420	0,318
6	Sat. de $CaSO_4 . 2H_2O$ + $MgSO_4 . 7H_2O$ (32,2 g/l)	13,280	-	0,420	3,180
7	Na_2SO_4 (3,5 g/l) + NaCl (20,0 g/l)	2,494	12,132	-	-
8	eau de mer artificielle	2,928	19,585	0,521	1,347
0	eau douce	0,003	0,007	0,005	0,0016

Tableau 3

Eprouvettes de béton. DRX.

Intensitées relatives de les pics d'ettringite (2 θ = 8,9°), portlandite (2 θ = 18,0°) et calcite (2 θ = 29,5°)

Compossant	Eau douce		Sol. saturée de $CaSO_4 . 2H_2O$		Sol. de Na_2SO_4		Sol. de $MgSO_4 . 7H_2O$		Sol. de $NaSO_4$ + NaCl		Eau de mer artificielle	
	Inf.	Sup.	Inf.	Sup.	Inf.	Sup.	Inf.	Sup.	Inf.	Sup.	Inf.	Sup.
Ettringite	217	243	223	242	194	173	223	231	219	194	215	304
Portlandite	1.080	918	1.403	698	682	549	1.242	969	818	396	1.056	693
Calcite	519	462	517	433	545	508	339	647	957	731	159	427

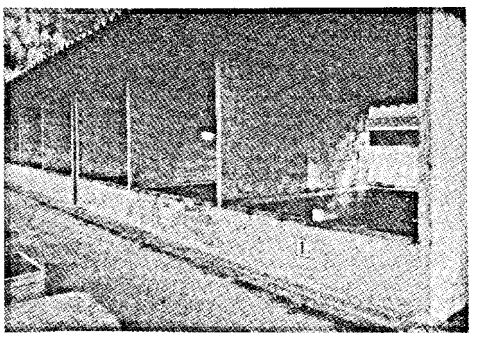

FIGURE 2

Vue des réservoirs des éprouvettes.

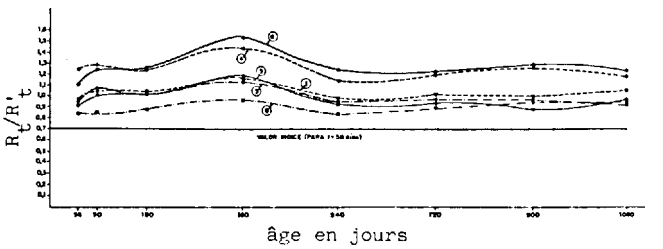

FIGURE 3

Evolution des coefficientes de corrosion Koch-Steinneger.

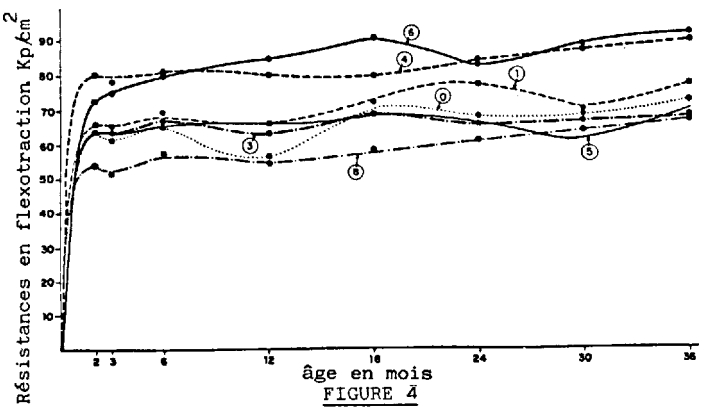

FIGURE 4

Evolution des résistances mecániques, en flexotraction, des éprouvettes de mortier de 1 x 1 x 6 cm.

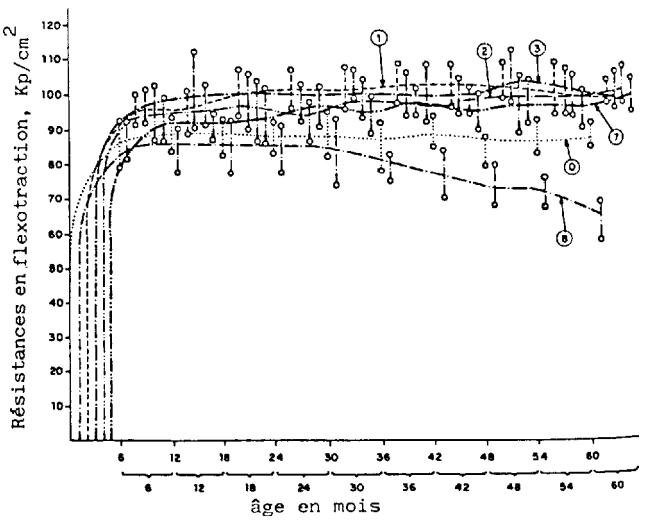

FIGURE 5

Evolution des résistances mécaniques en flexotraction, des éprouvettes de mortier de 4 x 4 x 16 cm.

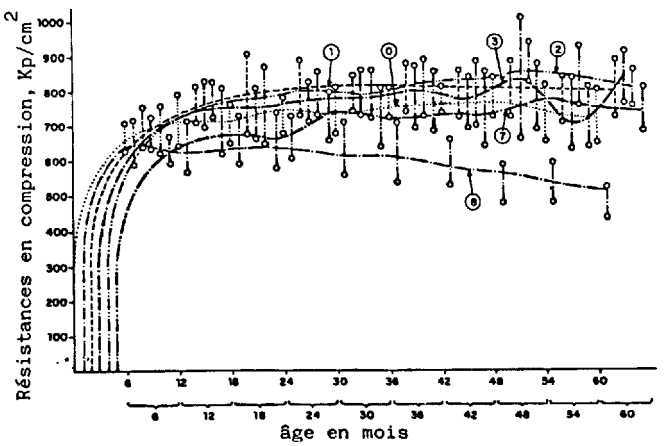

FIGURE 6

Evolution des résistances mécaniques,en compressión, des éprouvettes de mortier de 4 x 4 x 16 cm.

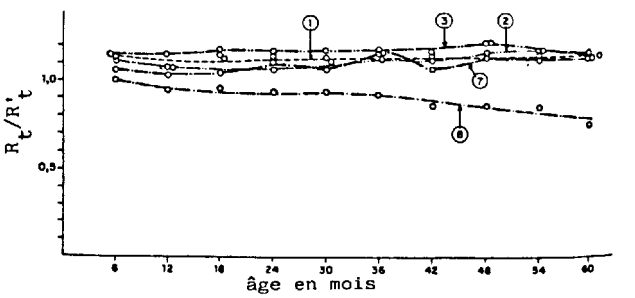

FIGURE 7

Evolution des coefficientes R_t/R'_t

R_t = Résistances en flexotraction (sol. agressive)

R'_t = Résistances en flexotraction (eau potable).

Rafael Talero Morales
Instituto de la Construcción y del Cemento "Eduardo Torroja". P.O. Box 19002 - Madrid - Spain

THE SULPHATE RESISTANT PORTLAND CEMENT, ARE NOT ULTIMATE ANSWER TO THE PROBLEM OF SULPHATE ATTACK.

LES CIMENTS PORTLAND RESISTANTS AU SALFATES NE SONT PAS L'ULTIME REPLIQUE A L'ATTAQUE D'EAUX SELENITEUSES.

SUMMARY: This work confirms the certainty of the predictions of useful service given by Kalousek and al. for the sulphate resistant portland cements (type V, USA), subject to severe selenitic attack.

Two sulphate resistant portland cements, were tested by means of the Le Chatelier - Anstett method. The tarts were destroyed at ages of three years, having detected in them the presence of thaumasite by XRD.

Even so, the impossibility and possibility thaumasite formation was confirmed in pozzolanic cements tarts, which either had or did not have adequate amount of pozzolana (diatomite) for such purpose.

Este trabalho confirma a certeza das predições de vida útil, feitas por Kalousek e outros, para os cimentos portland resistentes ao sulfato (tipo V, USA), sujeitos a severos ataques selenítiços.

Dois cimentos portland resistentes a sulfato foram testados pelo método de Le Chatelier-Anstett. Os corpos de prova foram destruídos à idade de 3 anos, tendo sido detectada neles, por XRD, a presença de taumasita.

Assim, confirmou-se a impossibilidade e a possibilidade de formação de taumasita em corpos de prova de cimentos pozolânicos, que tenham ou não a quantidade adequada de pozolana (diatomita) para tal fim.

Rafael Talero Morales
Instituto de la Construcción y del Cemento "Eduardo Torroja" P.O. BOX 19002.-MADRID Spain

Free Comunication

THE SULPHATE RESISTANT PORTLAND CEMENT, ARE NOT THE ULTIMATE ANSWER TO THE PROBLEM OF SULPHATE ATTACK.

4.2

LES CIMENTS PORTLAND RESISTANTS AU SULFATES NE SONT PAS LE ULTIMATE REPLIQUE AU ATTAQUE DE EAUX SELENITEUX.

I.- INTRODUCTION

Durability of concret structures is of the utmost importance and sulphate attack is one most well forms of concrete deterioration. As it is known, it is verified preferably through the C_3A portland cement concrete to forms expansive ettringite,

$$C_3A + 3CaSO_4.2H_2O + 25H_2O \rightarrow C_3A.3CaSO_4.31H_2O \quad (1)$$

Such nocive effect was treated to elude that by means of creation sulphate resistant portland cements, as are the cements C_3A small content and generally less 5%. For that reason, although the bibliography that is written at present about sulphate attack at the C_3A, is very abundant, it is noy the same for the sulphate attack C_4AF and deterioration possible of the concretes of sulphate resistant portland cement, because it only is a generally form:

1. The C_4AF also can be attacked for sulphates, however more slowly that the C_3A(2),

$$C_4AF + 3CaSO_4.2H_2O + 29H_2O \rightarrow C_3A.3CaSO_4.31H_2O + CH + FH_3$$

2. H.Kühl clasified the complex salts of Fe^{3+} ion in two types, in the same forms of Al^{3+} ion: $C_3F.3CaSO_4.31H_2O$ and $C_3F.CaSO_4.12H_2O$ (SFCH) (3)

All that connected,
-with serios problem of gypsipherous terrains that have much mediterranean regions, and
-the publication of Kalousek et al.(4), where they confirms that concretes made with Type V and II portland cements showed life expectancies of less than 50 years and that limitations on C_3A and C_4AF contents are not the ultimate answer to the problem of sulphate attack; and that by means of severe attack with Na_2SO_4, 2,1%, didn't give the intrinsic cause of their damage,
that has justified the realization of this work, with this purpose:
-to reproduce, in their foundation, the acts preconized by Kalousek et al.,
-to demostrate thet the same facts could be origined by means of cement paste of these concretes, and more concretely, by means of C_4AF,
-to investigate the certains causes of the nocivity of that attack, or crystalline compounds resulting of this attack, and
-ti treat to remedy that.

II.- EXPERIMENTAL PROCEDURE

Taking into consideration the fact Le Chatelier-Anstett, L-A, test(5), is practically tha more severe of all there are to mesure the grade of sulphatic resistance of cement, it was employed that same,
-by it condition of acelerated,
-because in determinated occasions can be reproduced in the reality the very rigorous conditions of selenitic hydration, for instance in the tunnels to overflow of water or subterranous or aerial conductions of water, both in gypsipherous terrains and
-to try to verify the fact which the deterioration of sulphate resistant portland cement concretes can proceed of the selenitic attack at the cement paste.

Therefore were tested by means of L-A method, two portland cements Type V, PY-4 and PY-6, and four mixture cements with pozzolana D (diatomite), PY-4/D 80/20 (80% in wt. PY-4, 20% in wt. Pozzolana D), PY-6/D 80/20 and PY-6/D 70/30, Table 1.

Nevertheless, before make the test of them by means of L-A method, was tried to see if the PY-6 (79,43% C_3S)cement and the pozzolana D, mixeds and not mixeds, was wides to origine ettringite and/or thaumasite and/or SSCH and/or SFCH, in a apropiate portlanditic and selenitic medium, in the same manner the possibility of it respective permanency in such medium until age 730 days old and their respective semi-quantitative study of the X-ray diffraction analyses. For that they were tested by means of Fratini test, although with a notable excess of gypsum or "Gypsipferous Fratini". The dosification of respective materials were the following, Table 2

TABLE 1 : Chemical and Potential Mineral Composition

Materials	Chemical Composition, WT %											Potential Mineral Composition in % (Bogue)			
	Ign. Loss	Insol. Res.	SiO_2	Al_2O_3	Fe_2O_3	CaO	MgO	Na_2O	K_2O	SO_3	C_3S	C_2S	C_3A	C_4AF
Cement PY-4	1,64	0,43	22,10	5,98	4,46	65,59	0,83	0,15	0,05	2,78	58,79	9,46	—	13,75
Cement PY-6	1,11	0,15	21,70	3,52	4,11	67,97	0,42	0,43	0,20	2,34	79,43	2,29	—	10,74
Pozzolana D (diatomite)	0,23	0,42	91,81	1,91	2,39	1,23	0,38	1,50	0,12	—				
Gypsum		0,26	0,04	—	—	32,54	0,36	0,02	0,01	45,84				

TABLE 2 : Materials Dosification "Gypsiferous Fratini"

	PY-6		PY-6/D 70/30		PUZ D	
	SO_3 Conglomerant - Mixture					
	7,0%	21,0%	7,0%	21,0%	7,0%	21,0%
Cement(g)	17,86	11,43	14,08	9,01	—	—
Pozzolana D(g)	—	—	3,52	2,25	4,78	3,09
Gypsum (g) $CaSO_4.2H_2O$	2,14	8,57	2,40	8,74	3,01	9,03
$Ca(OH)_2$ R.A (g)	—	—	—	—	12,21	7,88
TOTAL(g)	20,00	20,00	20,00	20,00	20,00	20,00
H_2O d.(cc)	100	100	100	100	100	100

TABLE 3 : Fratini Test

Liquid Phase Contents (mM/l)	Age (days)	Cements			
		PY-4/D		PY-6/D	
		80/20	70/30	80/20	70/30
$[OH^-]$	7	49,37	44,61	47,41	45,01
	28	16,74	6,00	27,14	11,88
$[CaO]$	7	17,50	16,50	16,25	14,87
	28	1,55	1,43	2,25	1,80

TABLE 4 : Le Chatelier-Anstett Test

Age (days)	Expansion, $\Delta\emptyset$ (%)					
	PY-4	PY-6	PY-4/D		PY-6/D	
			80/20	70/30	80/20	70/30
28	0,13	0,75	0,25	0,25	0,37	0,25
90	0,25	1,20	0,25	0,25	0,44	0,25
365	1,00	3,49	0,50	0,25	0,62	0,37
1095	10,43	22,88	0,80	0,55	11,22	0,63

Rafael Talero Morales
Instituto de la Construcción y del Cemento "Eduardo Torroja". P.O. Box 19002.-MADRID Spain

Free Comunication

THE SULPHATE RESISTANT PORTLAND CEMENT, ARE NOT THE ULTIMATE ANSWER TO THE PROBLEM OF SULPHATE ATTACK. 4.2

LES CIMENTS PORTLAND RESISTANTS AU SULFATES NE SONT PAS LE ULTIMATE REPLIQUE AU ATTAQUE DE EAUX SELENITEUX

At the ages of 1,7,14,21,28,60,90,270 and 730 days, were seized sample of solid phase of each of the conglomerant-mixtures of the Table 2, and it was proceded at their examination by XRD.

As it is known, the content $CaSu_4.2H_2O$ of a tart of L-A method is 33,33% in wt., or 15,50%SO_3, for this reason in the ultimate previous tests was pitchforked that content by means of the contens of 7,0% and 21.0% SO_3, respectively, because all that occurres at each tart it will have be necessarily formed in the conglomerant-mixtures inter 7,0% and 21,0% Su_3 correspondents, in this previous test.

Equally for the damaged L-A tarts was realized a examination by XRD with the same objetive.

To realize the analysis by XRD it has been employed a automatic equip with an analytic Solfware with small-orderer DIGITAL PDP 11/24.

III.- RESULTS AND DISCUSSION

The experimental results obtained are in the Tables 3 and 4, Figs.1 a) and b), Phots.1 and 2 and in the Graphics 1,2 and 3.

III.1.-"Gypsipherous Fratini"

The Figs. 1 a) and b), confirm thet in the "Gypsipherousfratini", practically without CO_2 during 730 days, ettringite is formed only, in all cases, it is supported during all test, in the 7,0% SO_3 case and in the 21,0 Su_3 case, since it has had quantity of gypsum and $Ca(OH)_2$ synt., or A.R., neccessary and sufficient for it maintenance. It is demostrated that with those portland cements that by means of Bogue calculation have not C_3A, practically have of 0% at 2% C_3A, in the case most unfavourable 2% C_3A, would neccessitate by calculations 1,84% SO_3 to pass at ettringite, for this in both cases of 7,0% and 21,0% Su_3, have sufficient gypsum for tha formation and permanency the same of the origined strong during all test and yet at advance ages, since the hermetic of the recipient of gypsipherous Fratini (avoiding the permanent carbonatation of the synthetical or A.R. $Ca(OH_2)$), permitted it. For this cause must not estrange the formation of ettringite of different origins and etiologies, that must come:

- in the case of cement PY-6,
  - . or well of it small possible of C_3A 1,0%, cause improbable enough,
  - . orwell of Al ion of the C_4AF, Graphics 1 and 2,
  - . or well of both a same or different age,
- in the case of the pozzolana D, of it small content of Al_2O_3, more in form of reactive alumine, and
- in the case of cement PY-6/D 70/30, of the respective fractions of PY-6 and D.

On the other hand the synousidal and ascendent form curve of PY-6 with 7,0% SO_3, is deduced that in spite of having been formed the greatest part of ettringite at the age of 21 days which still has not must be obtained the totality it seems that this is lograted something more slowly according to progress the test it can not be precised if is of residual C_3A origin (improbable fact) or origin C_4AF (more probable fact). The same can be said, still with more reason in the case of 21,0%SO_3 where the ascension is clear. For this reason it can be said with foundation and tha a forme approximate, that the amount of ettringite have been duplied from start, 1 day, to end, 730 days, more yet and potentially in the case 21,0% SO_3 that in the case 7,0% Su_3, then in the theoric supposition that the C_3A content of PY-6 cement was 1.0%, by calculations the cuantity of ettringite that would be formed by 1 g. C_3A would be 4,55 g., in the case 7,0% Su_3, and 4,54 g. in the case 21,0% Su_3, for this reason the small difference of intensity pick of the respective ettringite at the time of 730 days, in both cases, 7,0% and 21,0% Su_3, Figs. 1 a) and b).

On the contrary and in case of the pozzolana D the delay of 7 days showed in the appearance of the firts maximun of ettringite in the case 7,0% Su_3, in relation with the of 21,0% Su_3, it can be for the fact that so the greatest presence of pozzolana D as the best conditions of pH of medium (the pH of one satured $CaSO_4$ solution, 0,12% Su_3, is 6,3, and must be performed by more time with 21,0% Su_3 that with 7,0% Su_3) must facilite that the new-formation and origin pozzolana D tobermoritic gels (not detected by XRD or X-ray diffraction analy - ses, Graphic 2) (8), can be formed, perhaps, before in the firts case, 7,0% Su_3, that in the second case, 21,0% Su_3, difficulting so before the ionic overset, and setting back of this manner the formation of the respective ettringite total wich of this pozolana D is original. Furthermore, to have been repeated this fact in the case of the cement PY-6/D 70/30 with 7,0% and 21.0% SO_3 ,respectivally amplifies,perhaps, the possibility indicated of the specific actuation probable of each type of tobermoritic gel of the pozzolana D, in each case; therefore although in such related cases, cement PY-6/D 70/30 with 7,0% Su_3 and 21,0% Su_3,such tobermoritic gels respevtives were accurantly equals when the pozzolana D was only, which was not equal is the total cuantity of formed ettringite correspondent, that would be logically greatest, respectivelry in both when the pozzolana D was only, therefore the ettringite of origin fration matrix cement PY-6, although small as of the pozzolana D, also has be considered, and in from of news small cuantities of total ettringite formed in each case, but gretest respective-ly, that when the pozzolana D was only, perhaps the referied tobermoritic gels are yet the adecuates to difficult the ionic overset nessary to difficult the formation of that in each case until the age 21 days, and not when tha pozzolana D was only with 21,0% SO_3, how has happened in this work. So all that indicates the idea which as it seems, each total cuantity of ettringite to form in each case, needs a type gel tobermoritic determinated in precise and adequated quality, C/S, and quantity g.Et./g.CSH gel, to difficult notably the formation of that.

On the other hand, the fact which in all cases is maintained and inclosed the small quantity of ettringite formed in origin in spite of the presence of pozzolana D in them, point out yhe idea that the velocity of formation of tobermoritic gels of roigin pozzolana D, must be apreciably less than the velocity formation of the ettringite of any origin at the initial ages of test, since in in the contrary case this would must not appear since the origin.

Also and who will have it could be observed, before has been spoken of tobermoritic gels, and has not been spoken of crystalline tobermoritic I or II Taylor, therefore the Graphic 2 , do not confirms the presence of that, which have been in the medium in reason of the obtained results in the correspondent L-A test, Phots. 1 and 2. At same time,have been not detected SSCH similars at the ettringite, nor SFCH, Graphic 2.

III.2.- Le Chatelier-Anstett, L-A, Test

Making now the analysis and study of the obtained results in the L-A test, is observed how according to the correspondent specification the six

Free Comunication

THE SULPHATE RESISTANT PORTLAND CEMENTS ,ARE NOT THE ULTIMATE ANSWER TO THE PROBLEM OF SULPHATE ATTACK.

LES CIMENTS PORTLAND RESISTANTS AU SULPHATES NE SONT PAS LE ULTIMATE REPLIQUE AU ATTAQUE DE EAUX SELENITEUX.

4.2

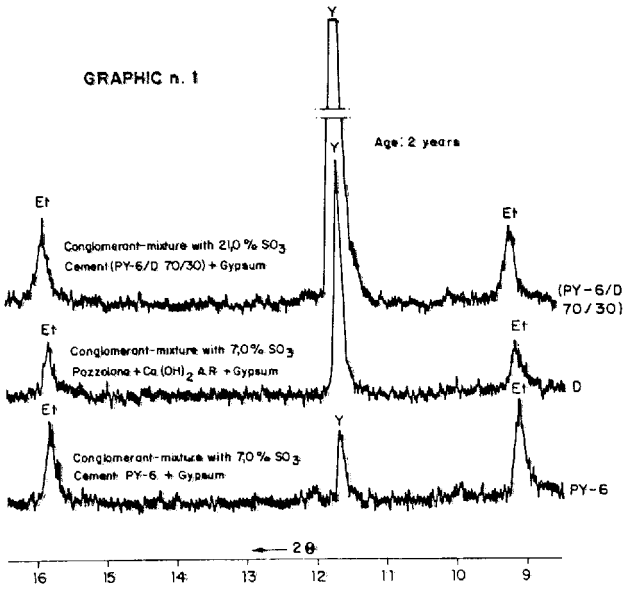

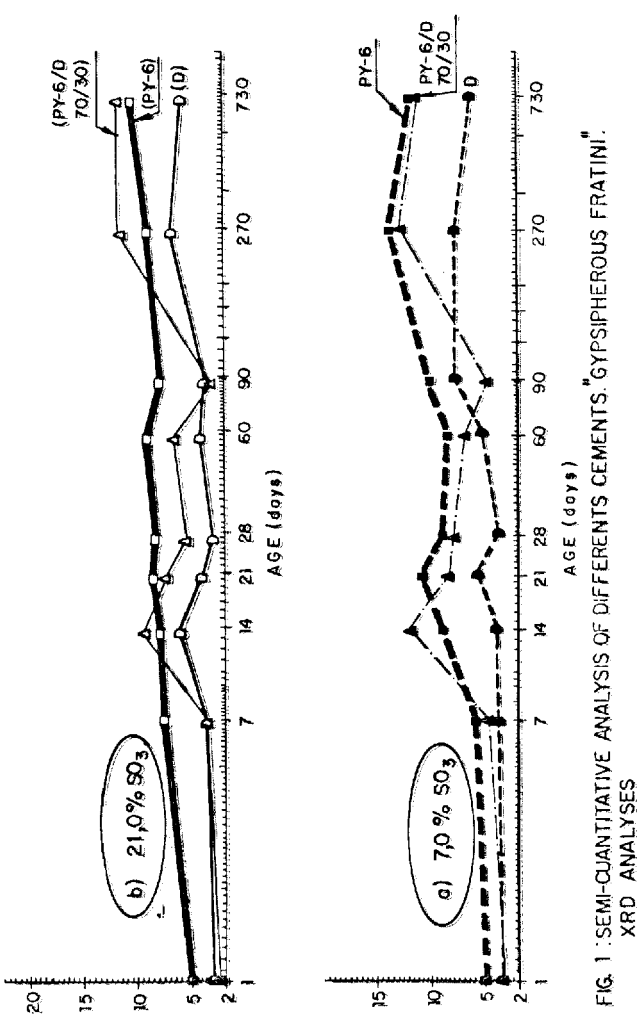

FIG. 1 : SEMI-QUANTITATIVE ANALYSIS OF DIFFERENTS CEMENTS. "GYPSIFEROUS FRATINI". XRD ANALYSES

cements tested are can calificated of high sulphatic resistance, since the value of the $\Delta\phi$ (%) at the time of the 28 days is less that 1,25% of the initial diameter, ϕ_o, proposed by Blondiau. In spite of that, it is eminent that it is not corresponded at the age 3 years only by the mixture cements PY-6/D 70/30, PY-4/D 80/20 and PY-4/D 70/30, and no by the cements PY-4, PY-6 and PY-6/D 80/20, Phots. 1 and 2, how it would be desidered. Nevertheless the fact of that Blondiau limited the space of time maximun permitted for the calification of the cement which forms until the age of 90 days of each tart, which implicated that cited author received reasonably that in this space of time it is must have verified almost the totality of the expansive reactions derivate of the ettrihgite of C_3A origin of cement constituient tart, and already that is occurred after the age of 90 days, would must not be accused at ettringite of such origin. Therefore the selenitic autodestruction of these tars of cements PY-4, PY-6 and PY-6/D 80/20 at the time of 3 years old (and notoin echange of the cements PY-6/D 80/20, PY-4/D 80/20 and PY-4/D 70/30) has be must necessarily at ettringite of other origin, in this case of Al^{3+} ion of C_4AF, which it is the only originating cause of these, which would be could forme at age old always and when are at that time, age 3 years, necessarily and sufficient portlanditic, pH and selenitic conditions for these, that will be could follow better with cements type V that with type I or II, and in the first if its content of C_3S is greater 56%, aacording to results obtained of this work. From here that the mixture-cements of this work, which tarts have not been cracked by selenitic attack at the time 3 years, have to possess a content of C_3S smaller 56% the PY-4/D 80/20 46,55% C_3S (58,19x0,8), the PY-4/D 70/30, 40,73% C_3S (58,19x0,7) and the PY-6/D 70/30, 55,60% (79,43%x0,7).

All these is confirmed likewise:

a) By the correspondent values of Fratini test, Table 3, specially that of [CaO] of respective li-quid phase, that in equality of age and mixture cement always have been greatest, in the case of matrix portland cement PY-6 and not PY-4, for the greatest content of C_3S of first on second, Table 1, it must be logically to support these differences of [CaO] , with more reason, aacording to progress of the test.

b) By the proper content of C_4AF of both cements PY-4 and PY-6, that
- which are so nearest, Table 1, invalid that the remarkable differences of $\Delta\phi$ (%) showed by tarts respectiv at the time 3 years, 18,58%, are imputed at the differences of C_4AF of sign contrary, 1,56%, that is in they, and forthermore
- if the main cause were the great content of C_4AF, as occurs usually for the case of C_3A, would have be the tart of cement PY-4 the greatest expansion at the time 3 years, and more thaumasite had be formed, and not tha tart of PY-6, as has occurred in the reality.

c) By the detection of tahumasite by means of XRD in each tart cracked, Graphic 3, and not in change of SSCH, equal of Lukas(8) (that detected this in tunnel concrete damaged by sulphatic attack), and as it is knowed it is formed by ettringite of origin C_3A in a rich medium in CaO and SiO_2, which must proceed necessarily of the that quantity of C_4AF which possess bater conditions of medium to origin it, in which have must be necessarily these of the PY-6 cement, as is

Rafael Talero Morales
Instituto de la Construcción y del Cemento "Eduardo Torroja" P.O. BOX 19002.-MADRID Spain

Free Comunication

THE SULPHATE RESISTANT PORTLAND CEMENTS, ARE NOT THE ULTIMATE ANSWER TO THE PROBLEM OF SULPHATE ATTACK.

LES CIMENTS PORTLAND RESISTANTS AU SULFATES NE SONT PAS LE ULTIMATE REPLIQUE AU ATTAQUE DE EAUX SELENITEUX.

GRAPHIC n. 2

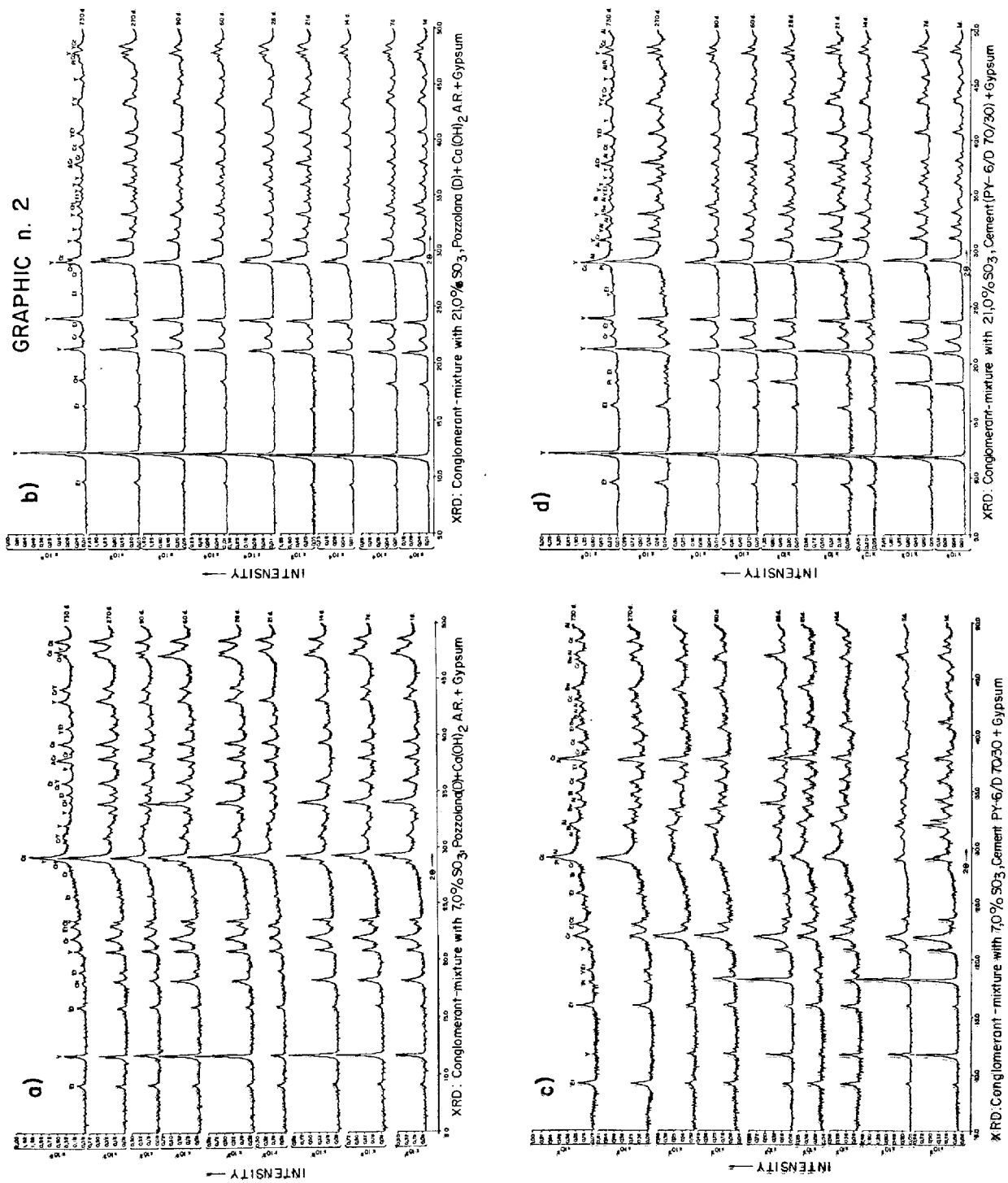

Rafael Talero Morales
Instituto de la Construcción y del Cemento "Eduardo Torroja" P.O. BOX 19002.-MADRID Spain

Free Comunication

THE SULPHATE RESISTANT PORTLAND CEMENTS, ARE NOT THE ULTIMATE ANSWER TO THE PROBLEM OF SULPHATE ATTACK.

LES CIMENTS PRTLAND RESISTANTS AU SULFATES NE SONT PAS LE ULTIMATE REPLIQUE AU ATTAQUE DE EAUX SELENITEUX.

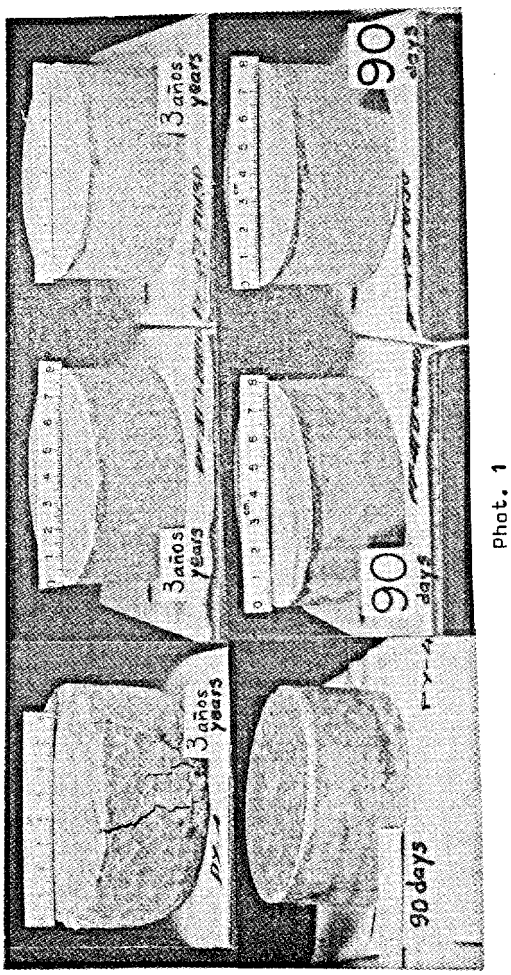

Phot. 1

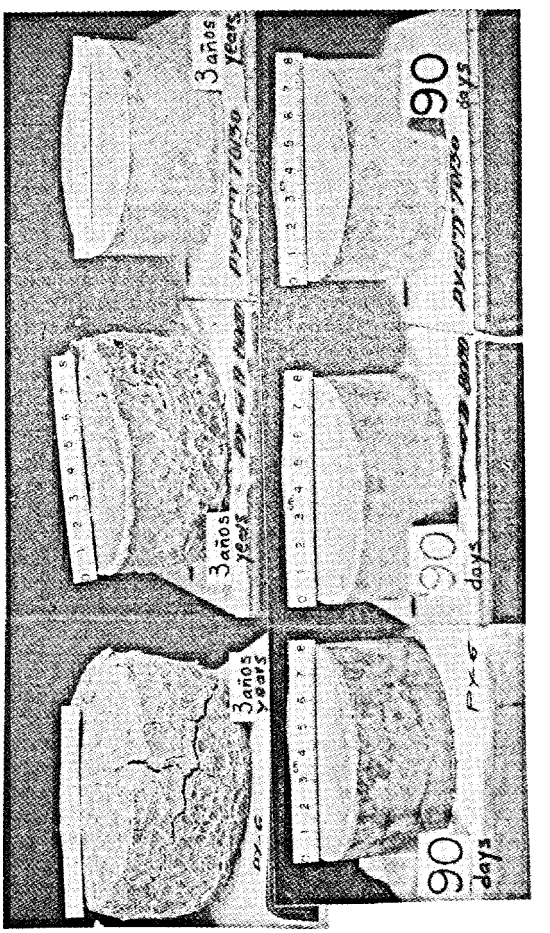

Phot. 2

Rafael Talero Morales
Instituto de la Construcción y del Cemento "Eduardo Torroja"

Free Comunication
THE SULPHATE RESISTANT PORTLAND CEMENTS, ARE NOT THE ULTIMATE ANSWER TO THE PROBLEM OF SULPHATE ATTACK.
LES CIMENTS PORTLAND RESISTANTS AU SULFATES NE SONT PAS LE ULTIMATE REPLIQUE AU ATTAQUE DE EAUX SELENITEUX.

4.2

confirmed again,

d) By means of the quantities of thaumasite origined in the tarts cracked, Phots. 1 and 2, and Graphic 3, which have resulted to be proportionals at the contents C_3S of it fraction portland respective, PY-6, 79,43%C_3S, PY-6/D 80/20, 63,54%C_3S and PY-4 58,19%C_3S, and not for the contrary and as it would be by calculations, at the contens of C_4AF of each them, according to that, these quantity of thaumasite of PY-6/D 80/20, was must be the less exceed by of PY-6 and PY-4, by this order, and not the contrary, as it has accurred in this work.

On the other hand of the last demostrative reasons c) and d), has be deduced also that if the thaumasite is origined in a CaO and SiO_2 rich medium, such medium would be obtained better in the case of the tart PY-6/D 80/20, that to be formed by diatomite pozzolana,D, with large content of opaline silica and by a large content of C_3S, 63,54%, would be congregate the better conditions for that. In this reason the quantity of thaumasite origined in the tart PY-6/D 80/20 will ave been in exclusive, or at least more greater of PY-6,and not on the contrary, as has accounted in this work; that united at the last reason d), confirms that opaline silica at the time 3 years must not be as reactive silica if not as CSH gel of different C/S relation (inadequate in this case of tart PY-6/D 80/20 and adequated in these case of tarts PY-6/D 70/30, PY-4/D 80/20 and PY-4/D 70/30), for this cause the principal fountain arrived of the necessary quantities of CaO and SiO_2 to be formed the thaumasite has to be the $C_3S^2$of portland cement fraction PY-6 in it hydration process, which first phase will be necessrily the separation of the Ca^{2+} and Si^{4+} ions of the crystalline net of C_3S before to forme portlandite syntetic and calcium silicates hydrated, which with constant presence although differents in the time will must be who will make that present ettringitepass at thaumasite, and as aditional proof of it is that the PY-4 have also thaumasite although logically in less quantity by last reason at the time 3 years.

And at latest and as aditional proof of that is the quantity of C_3S of each cement who is implicating indirectly in a case- crack tart- and the other - stable tart- is the fact happened at the -tarts PY-4/D 80/20 and PY-4/D 70/30 which have the content C_3S less 56% - and less 58,19% of the PY-4 alone, such contens are 46,55% and 40,73%, respectivelly- with the correspondent consecuences,
- C/S of the CSH gel, more adequate,
- Ettringite total/CSH total, more adequate , and
- CaO liquid phase, less adequate ,
which those of the tart PY-4, will must already elude the formation of ettringite or better thaumasite and this manner the cracking of the suitable tarts. And if content C_3S of the common constituve matrix portland cement of the mixture-cement 80/20 and 70/30 a quantity larger 58,19%C_3S (PY-4), case of PY-6, will be must attain the stable tart with additions greater 20% pf pozzolana D, as this manner has occurred with tart PY-6/D 70/30 and not with the tart PY-6/D 80/20.

GRAPHIC n. 3
XRD tarts L-A of different cements; Age : 3 years

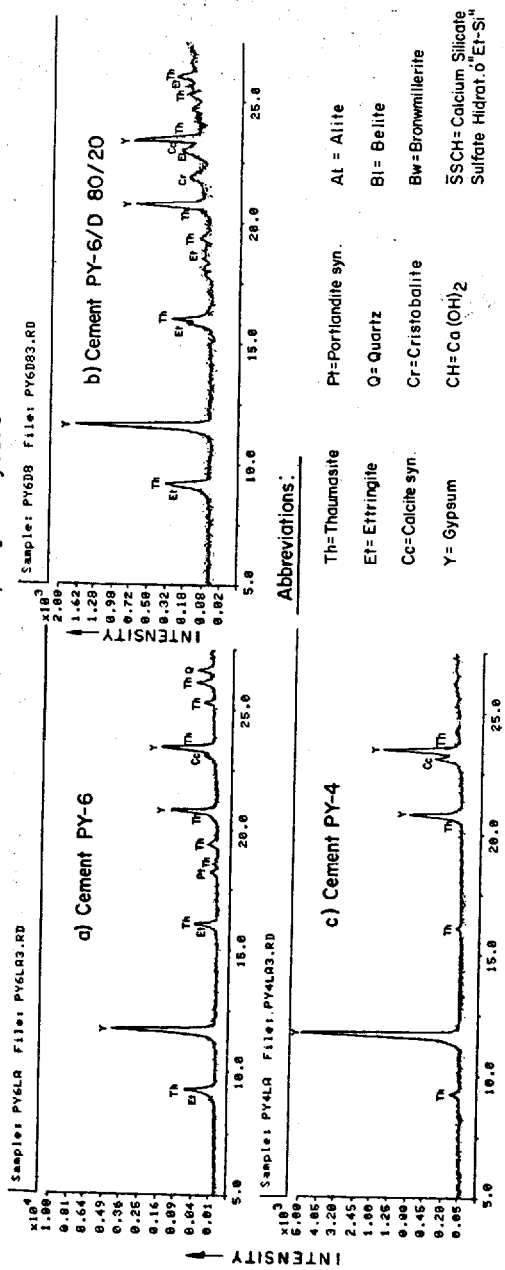

IV.- CONCLUSIONS

1. It is not impossible the sulphate attack at the sulphate resistant portland cement.
2. The employment of a pozzolana type diatomite or similar with the sulphate resistant portland cement, can elude a rigorous sulphate attack.
3. The quantity additionated of pozzolana type diatomite or similar to elude it, is function of C_3S (%) content of the sulphate resistant portland cement, at the same has must be function of the quality (C/S) and quantity (Ettringite total to form/Tobermoritic gels to form) of the tobermoritic gels, in each case.
4. The velocity formation of the ettringite of any origin must be greater than the velocity of formation of the tobermoritic gels of pozzolana D at the initial ages of the test.

V.- REFERENCES

(1) P.K. Mehta:"Effect of the Lima on Hydration of Pastes Containing Gypsum and Calcium Aluminates or Calcium Sulfoaluminates.J.Am.Cer.S,56(6)197

Rafael Talero Morales
Instituto de la Construcción y del Cemento "Eduardo Torroja" P.O. BOX 19002.- MADRID Spain
Free Comunication
THE SULPHATE RESISTANT PORTLAND CEMENTS, ARE NOT THE ULTIMATE ANSWER TO THE PROBLEM OF SULPHATE ATTACK. 4.2
LES CIMENTS PURTLAND REISITANTS AU SULFATES NE SUNT PAS LE ULTIMATE REPLIQUE AU ATTAQUE DE EAUX SELENITEUX.

(2)) M.Collepardi, S.Morosi, G.Moriconi and M.Corradi:"Tetracalcium Aluminoferrite Hydration in the Presence of Lime and Gypsum".- Cement and Concrete Research, 9, 431-37, 1979 .
(3)) H.Kühl: Zement Chemie,T III,118-130,3ª ed, 1961
(4)) G.L.Kalousek, L.C. Porter and E.J.Benton:"Concrete for Long-Time Service in Sulphate Environment".-Cement and Concrete Research, Vol.2,No1, 79-89, 1972.
(5)) L.Blondiau:"Considerations diverses relatives a l'essai de resistanza chimique au sulfate de calcium suivant le processus L'e Chatelier-Anstett.-Rev.Mat.Constr.Trav.Pub.,III,No.524,1961
(6)) Pliego de Prescriciones Técnicas Generales para la Recepción de Cementos,RC-75.-
(7)) P.Lapoujade and P.Vogein: Bull.Soc.Fran.Ceram. (28),3-12,1955
(8)) W.Lukas:"Betonzerstörung durch SO_4-Angriff unter Bildung von Thaumasit und Woodfordit".- Cement and Concrete Research,Vol.5,No.5,503-18 1975.

Emil Koelliker, Dr. ing.
Institute for Technical Research and Advice of the Swiss Cement Industry (TFB),
CH-5103 Wildegg, Switzerland

4.2

Skins of Calciumcarbonate and their Significance for the Corrosion of Concrete

Summary

Recent research is stressing the importance of superficial skins on the corrosion of concrete. This study is concerned with the layer which is most widespread, i.e. the calciumcarbonate.

Some observations of skins forming on concentrated solutions of calciumhydroxide are described. They retard - but do not prevent - evaporation of water and they prevent efficiently carbonization of the solution. The formation of such skins explains the characteristic structure of stalactites occurring on concrete through which water is penetrating.

SEM-observations show that on concrete layers of calciumcarbonate develop the structure of which depends on the conditions. In drinking water calcite crystals of varying size will develop whilst in air the structure is much finer and of poor crystallinity. It is characteristic that the state of the layer is not much changed by age. In water the thickness remains at about 50 microns and less on good concrete. The permeability (measured as rate of hydrolysis of the paste by pH-stat titrations) decreases in the course of exposure.

The results of the hydrolysis test suggest different action of water which does not allow formation of calciumcarbonate and of normal drinking water. It furthermore is possible to put forward a hypothesis on the leaching mechanism of concrete by "non-aggressive" water met in practical civil engineering.

Pesquisa recente destaca a importância das películas superficiais sobre a corrosão do concreto. Este estudo está relacionado com a camada que é mais dispersa, isto é, o carbonato de cálcio.

Descrevem-se algumas observações sobre películas que se formam sobre soluções concentradas de hidróxido de cálcio. Elas retardam mas não impedem a evaporação de água e previnem eficientemente a carbonização da solução. A formação de tais películas explica a estrutura característica de estalactites que acontecem no concreto no qual há penetração de água.

Observações de SEM mostram que no concreto se desenvolvem camadas de carbonato de cálcio cuja estrutura depende das condições. Em água potável, cristais de calcita de tamanho variável se desenvolvem, enquanto ao ar a estrutura é muito mais fina e de cristalinidade mais pobre. É característico o fato de que o estado da camada não é muito alterado pela idade. Em água a espessura permanece em cerca de 50 mícrons e menos em concreto bom. A permeabilidade (medida como índice de hidrólise da pasta por titulações de pH-stat diminui no decorrer da exposição.

Os resultados do teste de hidrólise sugerem ação diferente da água, que não permite a formação de carbonato de cálcio e de água potável. Adicionalmente, é possível formular uma hipótese sobre o mecanismo de lixiviação do concreto por água "não agressiva", encontrada na engenharia civil prática.

Emil Koelliker, Dr. ing.
Institute for Technical Research and Advice of the Swiss Cement Industry (TFB),
CH-5103 Wildegg, Switzerland

Skins of Calciumcarbonate and their Significance for the Corrosion of Concrete

1. Introduction

In a recent investigation [1] it was shown that cement paste and hence mortar and concrete will hydrolize in pure water at remarkable rates at pH 3 to 11 (and also at lower and higher pH values). As these rates are by far higher than suggested by all the evidence it is highly probable that protective mechanisms slow down the corrosion so much that concrete normally can be taken as resistant to water. The object of the present study is to test the effect and the behaviour of a skin of calcium carbonate which develops on the surface of concrete.

Calciumcarbonate ($C\bar{C}$) is precipitated by the following reactions:

(1) $C\,S\,H + H \rightleftarrows CH + SH_2$ (hydrolysis of cement paste)

(2) $\underbrace{CH + C\bar{C}_2H}_{\text{dissolved}} \rightarrow \underbrace{2\,C\bar{C} + 2H}_{\text{solid}}$

(3) $C\bar{C} + \bar{C} + H \rightleftarrows C\bar{C}_2H$

Most natural waters contain calcium dicarbonate ($C\bar{C}_2H$ = hardness) and dissolved carbon dioxide ($\bar{C}$) necessary to keep the former in solution. The quantity of dissolved $\bar{C}$ is related to equilibrium (3) by the "saturation index" (SI) which is zero at equilibrium, negative with $\bar{C}$ in excess (dissolving $C\bar{C}$) and positive with insufficient $\bar{C}$ (predipitating $C\bar{C}$).

Very soft waters have by definition no hardness. Nevertheless they contain dissolved $\bar{C}$ as in pure air $\bar{C}$ is present to the extent of 0.03 % by volume. Thus water will take up $\bar{C}$ by any contact with air.

The chance of formation of $C\bar{C}$ skins on concrete on contact with water is given as soon as the saturation index is zero or positive. In fact an earlier investigation [2] indicated the condition of "no corrosion" to be $SI \geq -0.3$.

2. Earlier observations

It has been observed [3] that on concentrated solutions of CH as well as on "cement extracts" (Portland cement stirred in water and filtered off) a skin of $C\bar{C}$ will develop on contact with air. If these solutions are diluted with water no skin will develop the $C\bar{C}$ being precipitated.

This skin of $C\bar{C}$ influences the behaviour of the solution remarkably on contact with air:

Evaporation of water: Reduced by 10 - 40 % depending on the thickness of the layer.

Carbonation / Neutralization: The solution underneath the skin practically does not carbonize, but after evaporation of the liquid all the material is neutralized.

Structure of stalaktites: If water penetrates concrete and is dripping off into the air (e.g. in a tunnel) stalaktites will develop on the concrete and stalagmites on the floor. Similar formations of $C\bar{C}$ may be observed in natural caverns in limestone. However a section through a stalaktite reveals that a natural one is solid and one grown on concrete is hollow with a typical structure of various skins (see fig. 1). Evidently the latter is caused by formation of skins of $C\bar{C}$ on the concentrated solution of CH resulting from hydrolysis of cement paste. Further evidence of this mechanism is given by the high alkalinity of the water dripping through this stalaktite.



Fig. 1 Section through a stalaktite from concrete showing skins of calcium carbonate.

3. SEM-observations on superficial skins

In order to test which structures will develop on the surface of concrete the following test series was made:

3.1 Experimental

Mortar prisms 40 x 40 x 160 mm using Portland cement prepared according ISO-R 679 i.e. with sand : cement : water = 3 : 1 : 0.5 and prisms of the same dimensions but with a mix 6 : 1 : 1 were cured for three days in the mould in a moist cabinet. After demoulding they were exposed to the following conditions:

Emil Koelliker, Dr. ing.
Institute for Technical Research and Advice of the Swiss Cement Industry (TFB),
CH-5103 Wildegg, Switzerland

Skins of Calciumcarbonate and their Significance for the Corrosion of Concrete

- Tap water (analysis see table), flowing gently
- Moist air of 90 - 100 % r.h. and 20 °C
- Air of 70 % r.h. and 20 °C

After 11 and 91 days fragments of these test pieces were subjected to the scanning electron microscopy (SEM).

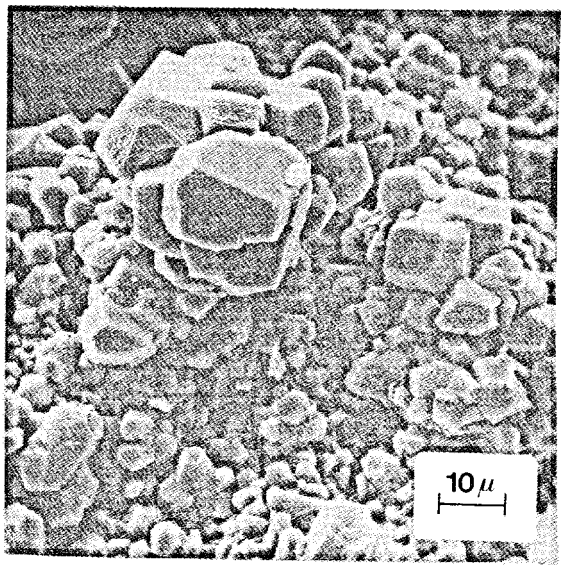

Fig. 2 SEM photograph of mortar surface after 11 days in drinking water.

3.2 Results

Water curing: Crystals of calcite with mostly well developed faces and varying in size from 1 - 10 μ diameter cover the surface after 11 days as well as after 91 days. The appearance is so similar that it is hard to discover differences. There is neither a clear difference between mixes 3 : 1 : 0.5 and 6 : 1 : 1 though on the latter some spots with remarkably different sizes of crystals were observed (1 to about 50 μ. The big crystals might develop across a pore (see fig. 2).

Curing in moist air: As compared to the above preparations the structure is evidently finer and the grains are not well crystallized. Their size is estimated to about 0.5 μ. After 91 days the grains seem to grow together leaving pores in between. No remarkable difference between mixes 3 : 1 : 0.5 and 6 : 1 : 1 could bo noticed.

Curing at 70 %: After 11 days a still finer structure was observed with forms reminding worms sticking out form the surface. Their size was about 1.5 μ in length and 0.25 μ in diameter. After 91 days this appearance was more indistinct the "individuals" having grown more and more together. Pores of a few microns diameter were distributed irregularly on the surface (see fig. 3). As in the tests described above there was no distinct difference observed between the mixes 3 : 1 : 0.5 and 6 : 1 : 1.

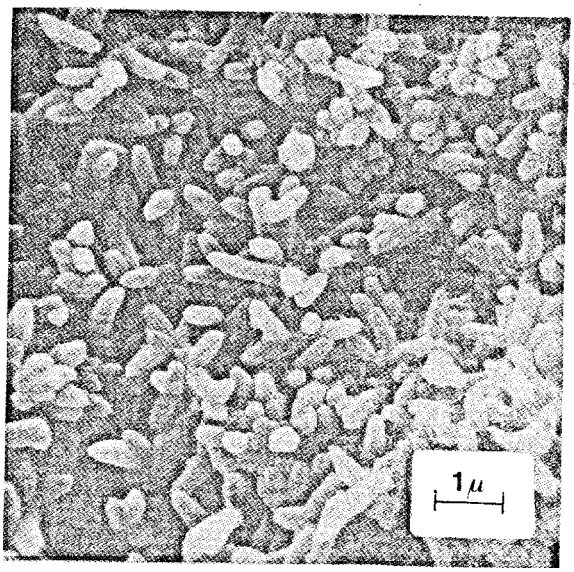

Fig. 3 SEM photograph of mortar surface after 11 days in air of 20 °C / 70 % r.h..

4. Thin section microscopy

Some observations on test pieces cured in water have been communicated in [4]. In the meantime they were confirmed and extended. In particular it was found that the carbonate skin is able to bridge over pores and that carbonate is deposited in pores and cracks as well as on aggregate which is not covered by paste (see fig. 4). However the skin essentially does not grow in thickness and even after prolonged immersion in flowing water no sign of leaching could be detected. As another test programme is being evaluated more detailed information will be given in a later communication [5].

5. The influence of the carbonate skin on the hydrolysis of mortar

5.1 General

In the investigation [1] a method has been described to test the rate of hydrolysis. It consists essentially in suspending the test piece in water and keeping the pH constant by automatically adding hydrochloric acid (pH-stat method). The conditions are selected such that no skin of carbonate can develop.

This method has been considered to be suitable also to test the influence of the CC-skin on the rate of hydrolysis.

The tests were carried out in the following way.

Emil Koelliker, Dr. ing.
Institute for Technical Research and Advice of the Swiss Cement Industry (TFB),
CH-5103 Wildegg, Switzerland

Skins of Calciumcarbonate and their Significance for the Corrosion of Concrete

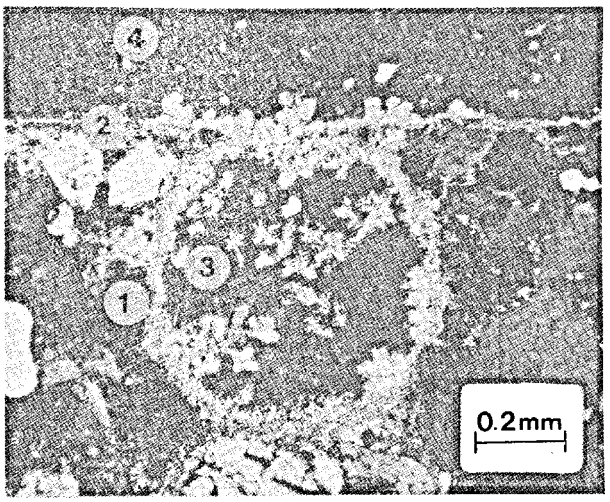

Fig. 4 Thin section through mortar surface after storage in drinking water shows 1 - mortar - 2 skin of calcium carbonate bridging over pore 3 - pore with carbonate precipitations 4 - embedding

5.2 Test pieces

Mortar prisms as in 3.1 were cured in water until use in test (about 3 months). From these prisms the test pieces were cut to get an exposed area of about 40 x 40 mm. Immediately before test the pieces were ground and etched as described in [1]. Now the samples were suspended in the tap water (see below) for the required time. When this had elapsed the areas which were not used were shielded with PE-sheet and then the titration was performed (see 5.4).

Water: The water in which the test pieces were immersed is described by the table. The flow was kept constant at about 40 mm/min. The development of a skin was visible by the white shade of the mortar.

5.3 Apparatus for hydrolysis

The same equipment as in [1] was used for the pH-stat titration. The titration vessel was filled with deionized water and flushed with nitrogen during the test.

5.4 Procedure

As described in [1] with the exception that the acid treatement was followed by water exposure and then shielding as indicated above. The pH-stat titration with 0.05 n HCl was carried out at pH 10 which corresponds to the equilibrium of $C\bar{C}$ in water. The acid consumption during 120 min was regarded as test result. Each test was done twice and the average of the two results (converted into

Table Analysis of water

Temperature		17.8 °C
pH		7.12
Saturation index	±	0.0
Ca^{++}		2.68 mmol/l
Mg^{++}		0.66 mmol/l
Na^{+}		0.22 mmol/l
K^{+}		0.04 mmol/l
SO_4^{--}		0.37 mmol/l
Cl^{-}		0.49 mmol/l
NO_3^{-}	ca.	0.48 mmol/l
SiO_2	ca.	0.25 mmol/l
Acid consumption to pH 4.3		6.34 mmol/l
Base consumption to pH 8.2		1.03 mmol/l

corrosion rate $\frac{mm}{d}$) was entered in fig. 5. In one test (after 100 min exposure to water) the period of titration was extended to 17 hours in order to determine the time function of the rate of hydrolysis. The temperature in all the tests was 25 ± 0.01 °C.

5.5 Results

The evaluation of the test results followed closely that given in [1]. In fig. 5 they are shown as corrosion rates ($\frac{mm}{d}$) in a log-log diagram. From this it follows that the function is linear with good approximation.

The evaluation of the 17 hours hydrolytic test yields that the rate of hydrolysis decreases with time according:

$$\frac{mm}{d} = 4.325 \cdot 10^{-3} \cdot t\,(min)^{-0.2595}$$

The coefficient of regression is

$$r = -0.9909$$

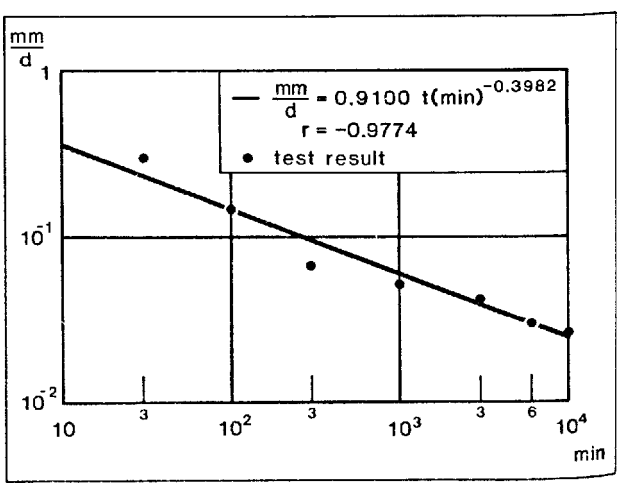

Fig. 5 Corrosion rates in $\frac{mm}{d}$ vs time of exposure to water

Emil Koelliker, Dr. ing.
Institute for Technical Research and Advice of the Swiss Cement Industry (TFB),
CH-5103 Wildegg, Switzerland

6. Discussion

6.1 Summary of observations

6.1.1 Skins of calciumcarbonate which develop on the surface of sulutions of calciumhydroxide or extracts of Portland cement and on mortar or concrete in air and in water slow down the exchange of matter appreciably though not completely.

6.1.2 This effect is dependant on the time of reaction.

6.1.3 The structure of the skin is different in water and in air. In water calcite crystals of 1 - 50 µ are observed, in air however the structure is finer and poorly crystallized.

6.1.4 The behaviour of the skin in the course of time varies with the conditions:

- In air the skin on solutions will grow in thickness but on mortar exposed to water it essentially does not grow (this study is not concerned with carbonation of mortar in air).
- In water a densification takes place which is not connected to a growth in thickness. This process leads to a remarkable retardation of the rate of hydrolysis.

6.2 Influence on the rate of hydrolysis

The tests to determine the influence of exposure to water give rise to some consideration. On one hand the drop of the rate of hydrolysis to less than 1/10 after 7 days immersion in tap water is remarkable. On the other hand it reflects the experience that water which is in contact with mortar does get alcaline if it is not continuously replaced. The "corrosion rate" given in fig. 5 is however not negligeable even after 7 days immersion. Evidently the carbonate skin acts as a diffusion barrier in the hydrolysis test, the highly alcaline liquid phase of the mortar diffusing through it. One has to be aware that in this hydrolysis test the conditions exclude the formation of calcium carbonate and its dissolution. Therefore one can assume that hydrolysis of the paste takes place just unterneath the skin. The residues of hydrolysis are however so soft that such a mechanism would finally lead to the underwashing of the skin and its eventual removal. Some indications [5] seem to support this conclusion as a possibility.

6.3 The action of normal water

Usually the skin is firmly attached to the mortar and no sign of leaching can be detected [4]. This fact suggests a different mechanism of action of water than described in section 6.2. As pointed out earlier normal water contains dissolved carbonic acid and calcium hardness (i.e. dicarbonate of calcium) which will react with the pore liquid according equation 2. We may recall the observation that the skin does not grow in thickness and that calcium carbonate may deposit in porous sites of the mortar even if there is no pressure gradient. This suggests that the diffusion of the di-carbonate ion into the mortar is faster than the diffusion of the products of hydrolysis out of the mortar.

If this holds true it might explain the probable fact that the "corrosion rate" of mortar and concrete in normal water is even much smaller than suggested by fig. 5 because a sealing effect will develop. Then the concrete may be regarded as "resistent" to water.

6.4 Mechanism of leaching

The information given in [1] and in this investigation lead to a better understanding of the mechanism of leaching of mortar and concrete.

In section 6.3 it is explained that mortar is sealed by precipitation of calciumcarbonate wherever water from outside has access. If the mortar is permeable and moreover if there is a flow of water the following steps of reactions will occur in the order given:

a) Water is penetrating the skin.

b) The hardness of water is precipitated in the pores of the mortar according equation (2). This is accompanied by an increase in pH and a loss in Ca^{++}-content water as indicated in fig. 6.

c) At pH 10 the Ca^{++}-concentration has reached the minimum. This water can no longer form a skin on the paste or seal the pores.

d) Paste without a skin will be hydrolized (i.e. leached) and the pH of the water and its Ca^{++}-concentration will rise until equilibrium is reached at pH about 12.5.

e) Now the aqueous solution is no more changed and it has no longer a leaching action on its way through the mortar, but when leaving to the air it will develop stalactites, when leaving to water it will precipitate calcium carbonate as described above.

f) Precipitates of calcium carbonate may build up and block drainage systems.

Emil Koelliker, Dr. ing.
Institute for Technical Research and Advice of the Swiss Cement Industry (TFB),
CH-5103 Wildegg, Switzerland

Skins of Calciumcarbonate and their Significance for the Corrosion of Concrete

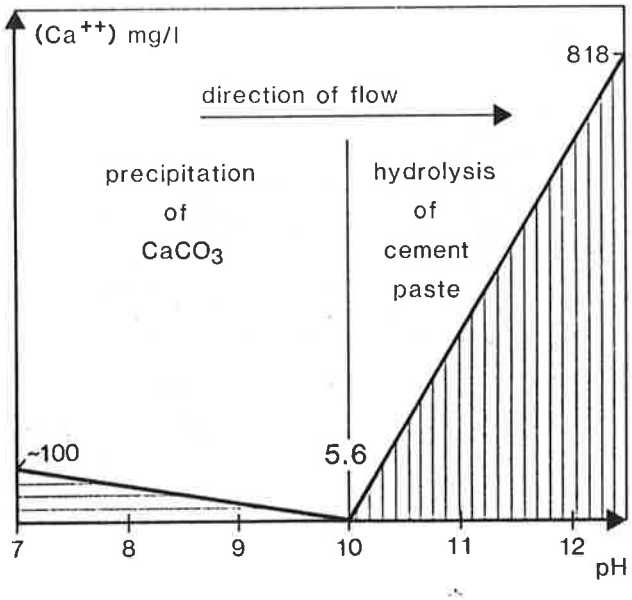

Fig. 6 Change of Ca^{++}-concentration in water penetrating mortar (schematic)

7. Conclusion

The effects of normal, "non-aggressive" water on mortar and concrete can be understood by the formation of a layer of calciumcarbonate which prevents the rapid hydrolysis of the paste.

The leaching effect of such water can be explained by the change of pH on the way through the mortar and the accompaning changes of the calcium saturation concentration.

Literature

[1] Koelliker E., On the hydrolytic decomposition of cement paste and the behaviour of calcarous aggregates during the corrosion of concrete by water, to be published in Betonwerk + Fertigteil-Technik März 1986

[2] Pro Rheno AG, Betonkorrosion, Basel August 1981

[3] Koelliker E., communication to RILEM International Symposium on Carbonation of concrete, Fulmer Grange 1976 (not printed)

[4] Koelliker E., On the effect of water and aqueous carbonic acid on concrete (in German), Proc. Int. Kolloquium Werkstoffwissenschaften und Bausanierung, 1983, Esslingen (F.R.G.)

[5] Test series in evaluation

Z. TSILOSSANI,
I. PANTSKHAVA,
K. KVARTSKHAVA, Institut de matériaux de construction Zavriev de l'Académie des sciences de la RSS de Géorgie, Tbilissi, URSS

CONTRAINTES INTERNES DANS LE BETON ET SA DURABILITE

Les auteurs ont mesuré directement, avec recours à des capteurs spécialement conçus, les contraintes internes qui se développent au sein du béton en cas d'action cyclique de la température et de l'humidité du milieu. On a mis en évidence l'influence qu'exerce sur ces contraintes la nature du ciment et les additions chimiques.

Les auteurs ont mis en évidence la relation entre la valeur des contrintes internes apparues et l'endurance du béton en cas d'alternance de gel et de dégel ou de chauffage (séchage) et de refroidissement (saturation) dans l'eau. Les auteurs proposent un modèle rhéologique qui simule le mécanisme de naissance et de développement des contraintes internes au sein du béton sous l'effet de ces facteurs.

Les auteurs ont émis une idée sur l'utilisation du modèle proposé pour formuler des prévisions sur la longévité du béton en cas de développement en son sein de phénomènes physiques intervenant sous l'effet de la température et de l'humidité.

Os autores mediram diretamente, por intermédio de captores especiais, as tensões internas que se desenvolvem dentro do concreto em caso de ação cíclica da temperatura e da umidade do meio ambiente. Colocou-se em evidência a influência que a natureza do cimento e as adições químicas exercem sobre estas tensões.

Os autores esclarecem a relação entre o valor das tensões internas surgidas e a duração do concreto em caso de alternância de gelo e degelo ou de aquecimento (secagem) e resfriamento (saturação) em água. Os autores propõem um modelo reológico que simula o mecanismo de nascimento e desenvolvimento das tensões internas dentro do concreto sob o efeito destes fatores.

Os autores expõem uma idéia sobre a utilização do modelo proposto para formulação de previsões sobre a longevidade do concreto em caso de desenvolvimento, dentro dele, de fenômenos físicos que atuem sob efeito da temperatura e da umidade.

Z. TSILOSSANI,
I. PANTSKHAVA,
K. KVARTSKHAVA

L'étude de l'influence des effets thermiques ainsi que des humidifications et séchages périodiques sur la durabilité des constructions en béton et en béton armé est l'objet d'une grande attention. Les expériments réalisés ont porté sur les principaux paramètres dont la mesure aurait permis de juger de l'intensité des processus se déroulant dans le béton et le béton armé. Ces paramètres étaient la résistance, les variations de volume et les caractéristiques de déformabilité. En ce qui concerne les efforts internes apparaissant sous l'effet des températures et de la teneur en humidité variables, ils n'ont pas été jusqu'à présent soumis pratiquement à des mesures directes (1, 2). Cependant, leurs valeurs évaluées d'après les effets qu'ils produisent: les variations de résistance, de volume et de déformabilité des échantillons soumis aux essais, ne sont pas toujours véridiques. Dans le présent travail sont présentés les résultats de mesures directes des efforts apparaissant dans le mortier de béton contenant des agrégats pleins et soumis périodiquement au chauffage, au refroidissement et à la saturation d'eau.

La mesure des efforts internes a été faite à l'aide de capteurs magnéto-élastiques "ДНБ-3" du système "GrouzNIIMGS" (3) noyés au milieu de prismes en béton de 7x7x21 cm. La composition de base du béton était de 1:1,4:3 en masse, la grosseur maximale des agrégats étant de 20 mm. On a utilisé du ciment Portland composé de: C_3S - 51 %, C_2S - 19 %, C_3A - 10 % et C_4A - 14 %, du sable quartzeux de grosseur ordinaire et du basalte concassé.

Les capteurs ont été placés au milieu des échantillons pendant la fabrication de ces derniers et ont été orientés de façon à enregistrer les efforts développés le long de l'axe longitudinal des prismes. Pour étudier l'influence des additifs sur les valeurs des efforts internes en développement on a utilisé de la bouillie alcool-levure (СДБ) (0,2 %) en combinaison avec un autre plastificateur (СНВ) (0,01 %) ainsi que С-3 (0,5 %) (С-3 est une dénomination d'un superplastificateur).

On a commencé à mesurer les efforts 24 heures après le traitement des échantillons par chaleur humide. En même temps, on enregistrait les déformations thermiques ainsi que celles de retrait et de gonflement des prismes. Ensuite, on soumettait les échantillons à un chauffage dans un thermostat "ТВЭ-25" à la température de 60 °C. Pour refroidir les échantillons, on mettait les thermostats hors tension. La saturation était obtenue en plongeant les prismes dans l'eau à température ambiante du local. Les mesures ont donné les résultats suivants.

Mis dans de la sciure humide, les échantillons jumeaux ne se sont pratiquement pas déformés. Les efforts internes ont été à peine visibles. Ils n'ont constitué que 0,4 MPa le 35-e jour d'essai. En revanche, les échantillons ont fortement réagi sur les effets thermiques. En se dilatant intensivement au début du chauffage, ils commençaient ensuite à se rétrécir progressivement à une température constante par suite du développement de la déformation de retrait. La réduction des dimensions progressait au cours du refroidissement. Pendant la saturation dans l'eau les échantillons se gonflaient intensivement.

La nature des efforts qui se développent pendant l'essai (fig. 1) éveille un intérêt du fait, notamment, que l'allure de déformation de l'échantillon de béton ne correspond pas à l'effort se développant dans le mortier. Au cours du chauffage, les prismes augmentaient de volume tandis que dans le mortier on a vue se développer des efforts de compression. A partir du moment où commençaient à prévaloir les déformations de retrait, le volume des prismes diminuait. Les efforts de compression diminuaient, eux aussi, bien que l'on ait pu attendre qu'à cause du retrait le mortier aurait subi une compression plus importante. Les efforts de compression diminuaient aussi pendant le refroidissement des prismes accompagné éga-

lement d'un rétrécissement du volume.

Une autre image se présentait pendant la saturation du béton d'eau bien que le signe des déformations ait été le même que lors du chauffage. L'augmentation du volume des prismes s'accompagnait dans le cas donné d'une réduction des efforts de compression qui s'y sont développés au cours du chauffage précédent. De cette manière, à une déformation libre de même signe des prismes, par exemple, à l'augmentation du volume (par suite d'un chauffage ou d'un gonflement) correspondait tantôt le développement des efforts de compression tantôt leur réduction jusqu'à la disparition totale. La même situation a été enregistré également lorsqu'on renouvelait à plusieurs reprises les cycles de chauffage, de refroidissement et de saturation d'eau. La loi générale de développement des efforts se conservait aussi en cas d'introduction d'additifs chimiques.

On doit chercher la cause du rapport ambigu enregistré entre la déformation des prismes et les efforts qui s'y développaient sous les effets de température et d'humidité dans les particularités de constitution du béton lourd composé de grains des roches pleines et du ciment durci poreux. Pour argumenter la thèse ci-dessus, référons-nous au modèle rhéologique du béton que nous nous représentons sous l'aspect suivant (fig. 2).

Les éléments I, II, III, ... représentent des couches distinctes de l'échantillon de béton et l'interaction des couches est modelée par l'élément 5 constitué d'un ressort et d'un élément frottant reliés l'un à l'autre. Les grains d'agrégats sont représentés dans le modèle par l'élément élastique 1. L'élément appelé à modeler le ciment durci est plus compliqué. Il est constitué des éléments élastiques 2, 3 et de l'élément 4 emprunté chez Powers (4). Ce dernier élément est destiné à modeler la saturation et l'évaporation de l'humidité du ciment durci. A l'absorption de l'humidité, les hémisphères de l'élément s'écartent en provoquant une dilatation du ciment durci tandis qu'à l'évaporation de l'humidité les hémisphères se rapprochent en faisant le béton se retirer. Dans ces conditions, étant donné que la plus grande partie d'une unité de volume est remplie de grains d'agrégats, l'accroissement du volume de ces derniers prévaut en grande partie contre celui du volume du ciment durci, c'est-à-dire, l'élément I du modèle représentant les grains d'un agrégat grossier et ceux de sable s'allonge plus que les éléments 2 et 3 représentant une fraction fine de sable et de ciment durci. Si l'on ajoute à cela que la déformation des éléments 1 et 2 est gênée par l'élément 5 appelé à modeler l'interaction des couches de surface et de celles de profondeur dont la déformation se développe avec un retard dans le temps, on comprendra le mécanisme de compression de l'élément 2. En ce qui concerne l'élément 4, il ne se déforme pas à la période initiale correspondant à l'évaporation de l'humidité des macropores et des capillaires.

Dès que l'humidité commence à s'évaporer des micropores et des microcapillaires, les hémisphères tendent à se rapprocher et à comprimer l'élément 3. Ainsi, sous l'effet de chauffage le ciment durci devient comprimé bien que l'échantillon de béton, tout entier, se dilate. C'est justement ce phénomène qui a été enregistré dans nos expériments. Le modèle explique également un affaiblissement avec le temps des efforts de compression dans le mortier du béton chauffé. Le rapprochement des hémisphères grâce à l'évaporation de l'humidité qui continue entre elles, conduit à une compression ultérieure de de l'élément 3 mais élimine celle des éléments 2. Ceux-ci s'allongent et suppriment la contrainte. Cette dernière prévaut contre la compression de l'élément 3 et l'effort de compression diminue en entier dans le mortier. Cet effort faiblit également par suite du refroidissement de l'échantillon à quoi correspond dans le modèle une contraction des éléments 1 et 2

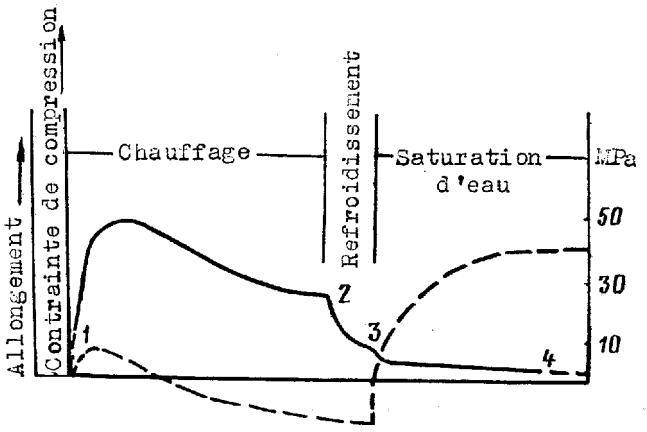

Fig. 1. Courbe caractéristique de variation des efforts dans le mortier de l'échantillon de béton soumis au chauffage (1, 2), au refroidissement (2, 3) et à la saturation dans l'eau (3, 4).
La ligne en pointillé représente la courbe de déformation

due à la température et, par conséquent, le déchargement de ces derniers.

Le volume des grains de l'agrégat plein ne varie pratiquement pas sous l'effet de la saturation d'eau. Aussi, l'élément 1 du modèle reste-t-il inerte. En ce qui concerne l'élément 4, il se dilate (le ciment durci se gonfle) en tendant l'élément 3. Il en résulte que les contraintes de compression restées dans ce dernier après la disparition de l'effet de température, diminue.

En l'absence d'interaction des couches (absence de l'élément 5), aucun effort n'apparaît dans les éléments 1 et 2. Mais de telles interactions existent en engendrant des efforts de compression. Ces derniers ne sont pas, cependant, grands à cause d'un important accroissement de la déformabilité du béton saturé d'eau (ceci est confirmé en comparant les valeurs des déformations de retrait et de température ainsi que de celles de gonflement dues à la saturation). Grâce à tout cela, au cours de la saturation de l'élément d'eau l'effet total se réduit à un affaiblissement des contraintes de compression dans le mortier.

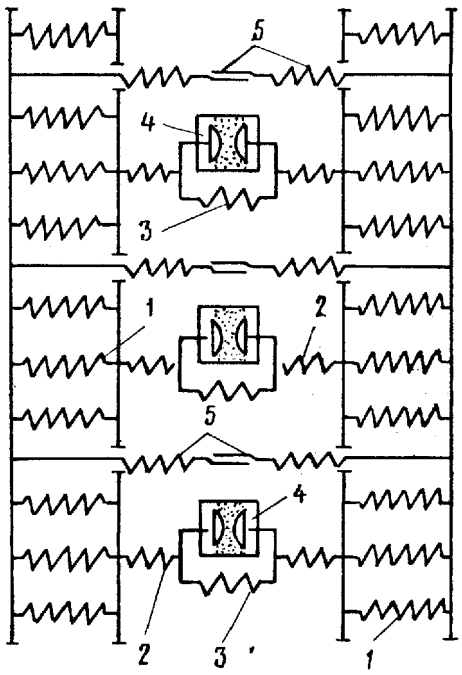

Fig. 2. Modèle rhéologique du béton

Ainsi, le modèle proposé ci-dessus reflète bien le comportement du béton additionné d'agrégats pleins sous l'effet des températures positives et de la saturation d'eau.

Notons, pour conclure, que l'étude du mécanisme d'apparition des efforts dans les composants du béton sous divers effets contribuera à l'élaboration des recommandations visant à réduire ces efforts et, par conséquent, à accroître la durabilité du béton. D'autre part, la mesure des efforts internes qui se développent dans le béton sous divers effets du milieu peut devenir utile à l'élaboration d'un procédé accéléré de l'appréciation comparative de sa stabilité. Ainsi, nous avons indiqué plus haut que la loi de développement des efforts internes sous l'action de la chaleur humide sur le béton n'a pas changé lorsque le mélange de béton a été additionné d'adjuvants chimiques. Cependant, les efforts se développant dans le béton avec adjuvants et sans adjuvants ont eu des valeurs différentes. Par exemple, les mesures ont montré que grâce à une introduction dans le mélange de béton des adjuvants

СДБ+СНВ les contraintes apparaissant dans le béton sous l'action de la chaleur humide étaient les plus petites: 5,45 MPa. Dans le béton sans adjuvants elles étaient de 6,30 MPa et dans celui additionné de C-3, de 5,95 MPa.

Les résultats des essais de la stabilité thermique des bétons ont montré que le béton le plus stable était celui additionné de СДБ+СНВ et le béton le moins stable était celui sans adjuvants. Les bétons indiqués se sont également rangés dans le même ordre au cours de l'essai de congélation et de décongélation alternées à l'état saturé d'eau. Notamment, le béton additionné de СДБ+СНВ, c'est-à-dire, le béton où les efforts dus à la congélation et à la décongélation ont été les plus faibles, avait le meilleur coefficient de résistance au gel.

REFERENCES

1. Л.П. Ориентлихер, В.М. Косарев, И.П. Новиков, И.Н. Гольфер. Сб. МИСИ им. В.В. Куйбышева, № 141, М., 1977.
2. В.Ю. Гашка. Автореферат канд. дисс. М., 1982.
3. К.К. Кварцхава. Бетон и железобетон, № 8, 1981.
4. T.C. Powers. RILEM Bulletin, No. 33, Dec. 1966.

F.F. ALKSNIS,
V.I. ALKSNE, Latholkhozproekt, Riga, URSS

SUR LE ROLE DE LA PHASE SILICEUSE DANS LES PROCESSUS DE DESTRUCTION DE LA PIERRE DE CIMENT DANS LES MILIEUX DE SULFATE

En se basant sur les résultats des études, on a montré que si les ingrédients contenant les anions SO_4^{2-} et CO_3^{2-} se présentent dans la pierre de ciment ou bien dans son ambiance, on observe les transformations non seulement de la phase alumineuse menant à la formation des quantités supplémentaires d'ettringite, mais, comme on a établi, dans ces conditions il peut se produire également la transformation de la phase siliceuse de la pierre de ciment conduisant à la formation de la phase sulfocarbosiliceuse - thaumasite. Avec cela, le rôle de ces transformations dans les processus de destruction de la pierre est contrôlé par la température du milieu ambiant. Par exemple, à la température plus de +20°C, la formation d'ettringuite a un rôle décisif, tandis qu' à la température inférieure à +10°C, c'est la formation de thaumasite qui joue le rôle déterminant. Dans les autres conditions égales, l'intensité de destruction de la pierre déterminée par le temps de sa destruction, en cas de formation de taumacite, est supérieure à un demi-ordre de grandeur qu'en cas de formation des quantités supplémentaires d'ettringite. De ce fait, au cours de détermination de la résistance aux sulfates de la pierre de ciment, le contrôle des transformations dans sa phase alumineuse est une condition nécessaire mais insuffisante. Le contrôle des transformations ayant lieu dans la phase siliceuse est également une exigence obligatoire supplémentaire.

Com base em resultados de estudos, mostra-se que, se houver presença de ingredientes contendo íons SO_4^{2-} e CO_3^{2-} no concreto ou em seu ambiente, observam-se transformações não somente da fase aluminosa, levando à formação de quantidades suplementares de etringita, mas também, como se verificou, em certas condições se pode igualmente produzir a transformação da fase silicosa do concreto, levando à formação da fase sulfocarbosilicosa - taumasita. Com isso, o papel destas transformações nos processos de destruição do concreto é controlado pela temperatura do meio ambiente. Por exemplo, a temperaturas superiores a 20°C, a formação de etringita tem um papel decisivo, enquanto a temperaturas inferiores a 10°C, é a formação de taumasita que exerce o papel determinante. Em igualdade de condições, a intensidade de destruição do concreto determinada pelo tempo de sua destruição, em caso de formação de taumasita, é superior em meia ordem de grandeza à do caso de formação de quantidades suplementares de etringita. Em conseqüência, no decorrer da determinação da resistência do concreto aos sulfatos, o controle das transformações na sua fase aluminosa é uma condição necessária, mas insuficiente. O controle das transformações que ocorrem na fase silicosa é igualmente uma exigência obrigatória suplementar.

La lutte contre la corrosion de sulfate de la pierre de ciment est un des problèmes actuels dans la pratique mondiale concernant l'utilisation du béton.

Jusqu'à présent, la corrosion de la pierre de ciment dans les milieux de sulfate s'expliquait principalement par des transformations se déroulant dans la partie alumineuse de la pierre de ciment qui ménent à la formation d'un "bacille de ciment" - ettringite. C'est pourquoi, pour augmenter la résistance aux sulfates du ciment Portland, on limite strictement la teneur en tels constituants qui sont responsables de la formation de l'ettringite.

En même temps, à partir des années 70, des recherches apparaissent /1-5/ montrant que dans les produits de corrosion de la pierre de ciment, outre l'ettringite, il y a également une thaumasite - hydrosulfocarbosilicate de calcium. Ce sel triple de calcium se forme sur la base du constituant principal - constituant siliceux de la pierre de ciment lors de l'action sur cette dernière des anions SO_4^{2-} et CO_3^{2-}.

Dependant, le degré d'influence de la thaumasite sur les processus de corrosion de la pierre de ciment n'a pas été apprécié dans les publications scientifiques.

A l'occasion de ci-dessus, les auteurs ont analysé le comportement de la pierre de ciment dans les milieux contenant les anions SO_4^{2-} et CO_3^{2-} (6, 7, 8). En effectuant les essais, on a tenu compte du fait que la synthèse de l'ettringite doit être faite de préférence à des températures élevées (jusqu'à 60°C) et que pour la synthèse de la thaumasite, la température de 2-4°C est considérée comme optimum. Avec cela, la formation de ce minéral n'est pas constatée à des températures supérieures à 25°C /2/.

En qualité du modèle on a utilisé dans les expériments une pierre de ciment se caractérisant par une teneur élevée en sulfate de calcium. On a assuré de cette façon une intensité donnée de l'interaction du sulfate de calcium avec les autres phases non compliquée par les processus de transfert de masse ainsi qu'une formation de la structure bien cristallisée de la pierre réagissant sensiblement aux déformations de volume causées par des transformations de phase. On a utilisé en qualité d'un étalon de comparaison une pierre sulfosiliceuse (ne contenant pas d'une phase alumineuse) à rapport molaire $SO_3/C_3S = 4,2$ dans le mélange de base. Dans les autres cas, lors de l'obtention de la pierre, on utilisait le clinker de la composition suivante (%) : C_3S - 59; β - C_2S - 16;

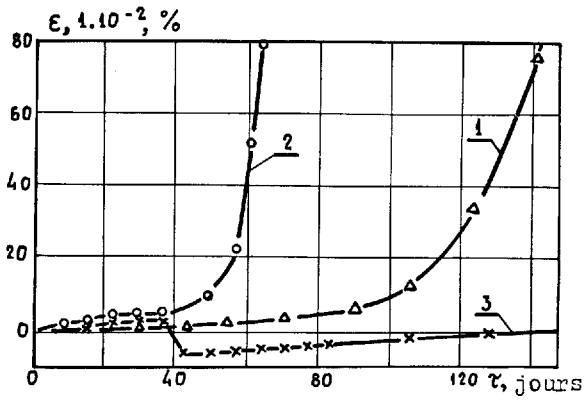

Fig. 1. Cinétique de l'expansion linéaire de la pierre sulfosiliceuse (I) et de la pierre de ciment (2; 3) dans l'eau à + 8°C (1; 2) et dans la solution gypsocalcaire saturée à + 60°C (3)

C_3A - 6; C_4AF - 14 dans le mélange avec le semi-hydrate de sulfate de calcium contenant 86,1 % de matière de base.

Les échantillons 40 x 40 x 160 mm ont été formés à partir du mélange 1 : 3 (par masse) sur un sable standard et ont durci (avant les essais de résistance aux sulfates) pendant 28 jours à la température de + 20°C et à l'humidité relative de l'air de 100 %. Les échantillons mentionnés ont subi l'action de l'eau suivant deux régimes:

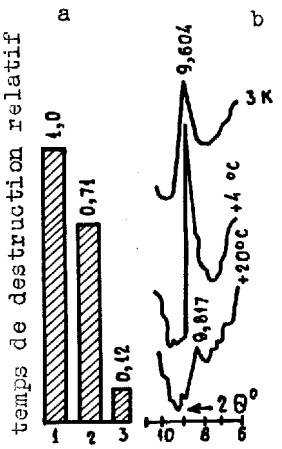

Fig. 2. Temps de destruction relatif (a) et radiogrammes (b) de la pierre à la température de + 20°C (2) et de + 4°C (3) dans le milieu air-humide (I) et dans le milieu aqueux (2; 3) (3k - échantillon détruit après 7 mois de conservation à + 20°C et à l'humidité relative de 70 % avec l'accès du CO_2)

- régime I - stimulant la formation de l'ettringite: action durable de la solution gypsocalcaire saturée à la température de + 60°C;

- régime 2 - stimulant la formation de la thaumasite: traitement des échantillons par l'eau à + 8°C renouvellée tous les 7 jours.

Les résultats des essais montrent (fig. 1) qu'en cas du régime 1, pas une seule composition étudiée n'a été détruite. Ainsi, une quantité supplémentaire d'ettringite n'a exercé qu'une faible influence sur la résistance des échantillons. En même temps, en régime 2, dans les échantillons des compositions étudiées on a vu apparaître des déformations d'expansion menant à la destruction complète des échantillons mentionnés. Sur l'exemple de l'échantillon sulfosiliceux la formation de la thaumasite dans ces conditions a été confirmée (6).

La présence de la phase alumineuse dans le ciment ne fait que accélérer ce processus (fig. 1, courbe 2). Cela confirme l'influence catalytique de l'ettringite sur la synthèse de la thaumasite (2). Il est nécessaire de prêter attention au fait que lors de la création des conditions optima pour la formation de la thaumasite, la destruction de la pierre se passe beaucoup plus vite et intensivement (fig. 2). Cela s'explique par la possibilité de former une grande quantité de formations nouvelles grâce à la diminution de la teneur en liant principal - hydrosilicates de calcium. C'est pourquoi dans ce cas le temps minimum de destruction correspond au pic maximum d = 9,61 Å sur le radiogramme de l'échantillon maintenu à 4°C par rapport à l'échantillon du même lot maintenu à la température ambiante (20°C). La comparaison des variations des vôlumes molaires lors de la formation d'ettringite et de thaumasite (voir tableau) confirme que la formation de la thaumasite n'est pas moins dangereuse que la formation du "bacille de ciment" universellement admis, dit ettringite. Dans ce cas, les ressources en matières de base dans le ciment qui limitent la quantité de l'ettringite en formation sont de 1,5 - 2 fois inférieures aux ressources limitant la quantité possible de la thaumasite en formation. La figure 3 montre la présence de quantités considérables de thaumasite dans les échantillons détruits de la pierre sulfosiliceuse et de la pierre de ciment contenant des quantités élevées de sulfate de calcium.

Un intérêt particulier consiste dans le comportement de l'ettringite lors de l'action du gaz carbonique sur la pierre de ciment. En particulier, nous avons établi que dans l'échantillon d'une composition $(CaO)_3 \cdot Al_2O_3 : CaSO_4 \cdot 0,5H_2O : CaCO_3 = 1 : 4,7 : 3$ (parties molaires) on observait une disparition complète de l'ettringite 6 mois après l'action du CO_2 du milieu ambiant. Avec cela on n'observe pas une formation réitérative de l'ettringite après le maintien de cet échantillon pendant 10 mois

à l'humidité de 100 % (fig. 4), et l'échantillon lui-même tend à se rétrécir. En même temps, l'action du CO_2 dans des conditions analogues ne mène pas à la décomposition de la thaumasite formée (fig. 2).

Il est à noter que pour augmenter la résistance aux sulfates il existe des procédés technologiques agissant sur la phase alumineuse tels que le broyage en commun du gypse et du clinker, l'introduction de l'addition pouzzolanique, la diminution de la teneur en phase alumineuse du ciment et d'autres. Quant à la thaumasite, le mécanisme de sa synthèse dans la pierre n'est pas encore suffisamment clair, et par conséquent, il n'est pas possible d'exercer une influence orientée sur ce processus.

Tableau

Variation des volume molaires lors de la formation de l'ettringite et de la thaumasite

Constituant de base		Phase solide lors de la formation de l'ettringite		Phase solide lors de la formation de la thaumasite	
Formule	Volume molaire, cm^3	Volume molaire, cm^3	Rapport des volumes	Volume molaire, cm^3	Rapport des volumes
C_3A	89,47	713,13	7,97	-	-
C_3AH_6	150,12	713,13	4,75	-	-
C_3S	71,58	-	-	404,87	5,66
Tobermorite 9 Å	255,46	-		1677,73	6,57
SiO_2	22,68	-		331,01	14,60

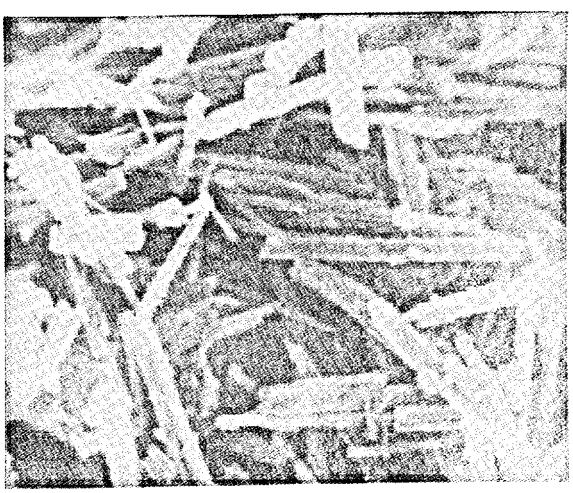

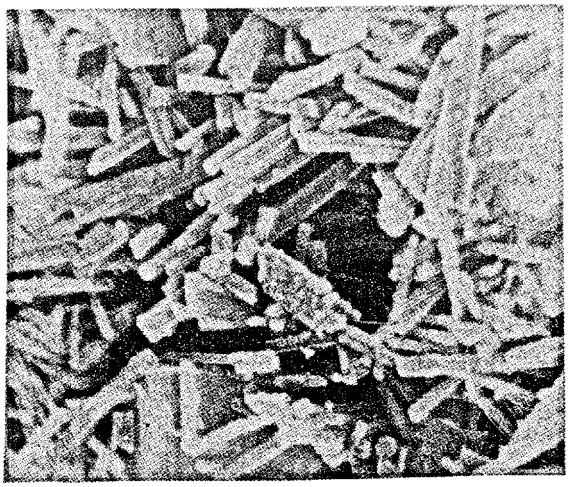

Fig. 3. Microscopie électronique (15000 x) de la pierre sulfosiliceuse détruite (a) et de la pierre de ciment (b)

En tenant compte de ci-dessus, on peut conclure qu'en cas de la présence dans la pierre de ciment ou dans le milieu agissant

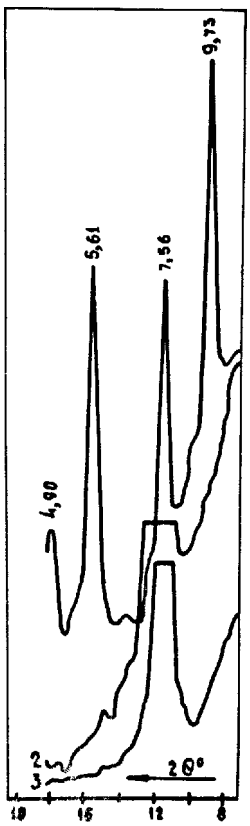

Fig. 4. Radiogrammes de la pierre sulfoalumineuse durcissant sans accès du CO_2 pendant 30 jours à + 20°C et à l'humidité relative de 100 % (I) carbonisée supplémentairement à l'air pendant 6 mois à + 20°C (2) et avec un maintien ultérieur de la pierre carbonisée à l'humidité relative de 100 % sans accès du CO_2 pendant 10 mois (3)

sur cette dernière des ingrédients contenant les anions SO_4^{2-} et CO_3^{-2}, la formation est possible, à des températures abaissées, non seulement de l'ettringite mais de la thaumasite.

Une telle constatation mène à ce que la considération des transformations se déroulant seulement dans la phase alumineuse de la pierre de ciment lors de la détermination de sa résistance aux sulfates est une condition nécessaire mais insuffisante. La considération des transformations se déroulant également dans la phase siliceuse de la pierre de ciment est une condition obligatoire supplémentaire.

De plus, le contrôle du comportement de la matière à des basses températures lors de la détermination de la résistance aux sulfates de la pierre de ciment (fait qu'on neglige jusqu'à présent) doit être considéré comme une exigence obligatoire.

REFERENCES

1. Грешухна Р. Кристаллы цементного теста в сульфатных и кислых растворах. В кн.: Труды VI Международного конгресса по химии цемента, т. 2,кн.I, М.,Стройиздат, I976, 337-339.
2. Kollman H., Strübel G., Frost F. Mineralsynthetische Untersuchungen zu Treibursuchen durch Ca-Al-Sulfat-Hydrat und Ca-Si-Carbonat-Sulfat-Hydrat. Tonind.-ztg, 1977, 101, No. 3, 63-70.
3. Gouda G.R., Roy D.M., Sarkar A. "Thaumasite in Deteriorated Soil-Cement. Cement and Concrete Research., 1975, vol. 5, 519-22.
4. Bensted J. Problems arising in the identification of Thaumasite. Cemento, 1977, No. 3, 81-90.
5. Regourd M., Hornain H., Levy P., Mortureux B. Resistance of concrete to physicochemical attacks. - (C.E.R.I.L.H., Fr.) Int. Congr. Chem. Cem. /Proc./ 7th 1980, 3, VII/104-VII/109 (fr.), Septima: Paris, Fr.
6. Алкснис Ф.Ф. Природные процессы, изменяющие состав силикатной фазы цементного камня в присутствии сульфата кальция. Тр. ВНИИ цементной промышленности, I983, № 7, I96-200.
7. Алкснис Ф.Ф., Алксне В.И. Гипсоцементные материалы для наружных стен зданий. - (опыт Латвийской ССР). Обзор. - Рига: ЛатНИИНТИ, I984, 57 с.
8. Алкснис Ф.Ф., Алксне В.И. Влияние силикатной фазы на процессы деструкции цементного камня в сульфатсодержащих средах. "Цемент", I984, № 9, I3-I5.

A. Zürz, I. Odler, S. Abdul-Maula. Technical University Clausthal, D-3392 Clausthal-Zellerfeld, Federal Republic of Germany.

Thermal decomposition of hydrated cement pastes.

4.2

Decomposition thermale des ciments hydratées.

SUMMARY: The thermal decomposition of fully hydrated pastes made from 12 different kinds of cement was studied. In all systems the combined water content declined and the porosity increased slightly at lower temperature and contracted only as the temperature increased even further. The newly formed phases were different in different cements. In most cements the compressive strength increased first upon heating and started to decline only after a critical temperature was exceeded.

Estudou-se a decomposição térmica de pastas totalmente hidratadas feitas com 12 tipos diferentes de cimento. Em todos os sistemas o teor de água combinada diminuiu e a porosidade aumentou ligeiramente à temperatura mais baixa, e se contraiu apenas quando a temperatura aumentou ainda mais. As fases recém-formadas foram diferentes nos diversos cimentos. Na maior parte dos cimentos a resistência à compressão primeiro aumentou com o aquecimento, e começou a diminuir somente depois que foi ultrapassada uma temperatura crítica.

A. Zürz, I. Odler, S. Abdul-Maula. Technical University Clausthal, D-3392 Clausthal-Zellerfeld, Federal Republic of Germany.

Thermal decomposition of hydrated cement pastes.

Hydrated cement pastes decompose chemically at high temperatures. This, in turn, may result in strength loss and volume changes of the material. These phenomena may be of importance when concrete constructions are used at elevated temperatures, or are exposed to fire. Very little has been published about the chemical and mineralogical aspects of the thermal decomposition of hydrated cements so far. As yet, we merely know, that hydrated portland cement continually loses chemically bound water as the temperature increases. At sufficiently high temperatures the present calcium hydroxide decomposes and calcium oxide and dicalcium silicate are formed as final products (1,2,3,4).

Materials

The cements used in this study were prepared by grinding industrial clinkers and raw materials with amounts of gypsum corresponding to 3% SO_3 in a laboratory ball mill to a specific surface area of 3000 cm^2/g (Blaine). The following cements were prepared and studied:

1. Ordinary portland cement
2. White portland cement (WPC) made from a clinker with 1% Fe_2O_3
3. Sulfate resistant portland cement (SRPC) made from a clinker with high iron oxide content
4. Pure tricalcium silicate (Ca_3SiO_5) - as reference material (with no gypsum added)

The blended cements studied were made from the above OPC-clinker by intergrinding it with the following additives, in addition to gypsum:

5.-7. Portland-blast furnace slag cements with clinker-slag ratios 75:25, 50:50 and 25:75
8. Portland-puzzolana cement with 25% of a natural puzzolana (trass)
9.-11. Portland-flyash cements with 25% of flyashes 1, 2 or 3
12. Portland cement with an addition of 25% silica fume

The composition of the clinkers and starting materials employed is shown in Tab. I.

	OPC	WHITE	ANTISULFATE	SLAG	TRASS	PFA 1	PFA 2	PFA 3	SI-FUME
CaO	64.60	67.50	65.10	41.50	11.90	3.18	5.90	14.60	0.05
SiO_2	23.00	24.90	22.70	32.40	61.50	38.50	42.80	61.20	98.40
Al_2O_3	5.34	4.45	3.38	13.10	14.20	31.20	23.70	8.53	0.22
Fe_2O_3	2.55	0.28	6.22	0.50	4.38	15.60	10.00	5.79	0.03
MgO	2.59	0.79	1.11	8.55	2.36	2.32	2.05	3.77	0.36
K_2O	1.14	0.98	0.85	0.66	2.76	4.37	1.00	0.94	0.64
Na_2O	0.13	0.10	0.05	0.46	1.65	1.56	1.86	1.06	0.16
SO_3	0.68	1.02	0.73	0.04	0.05	1.19	0.64	3.10	0.14
P_2O_5	n.a.	n.a.	n.a.	n.a.	n.a.	0.61	0.34	0.02	n.a.
MnO	n.a.	n.a.	n.a.	0.52	0.17	0.15	0.15	0.10	n.a.
TiO_2	n.a.	n.a.	n.a.	0.80	0.78	1.18	5.61	0.78	0.00

Tab. I: Oxidic composition of the clinkers and additives employed

Experimental

Specimens 10 x 10 x 60 mm were made from pure cement pastes prepared from the above cements with water-solid ratios between 0.26 and 0.30. The water-solid ratios were selected to obtain pastes of equal plastic consistency. The specimens were unmolded after one day and allowed to hydrate for at least one year at 20 °C in a saturated water vapor atmosphere. The hydration reaction was stopped and the free water removed by drying the specimens at 40 °C to a constant weight.

Sets of specimens were heated up in an electric furnace to temperatures between 100 and 1000 °C in steps of 100 °C with a rate of 1°C/min, kept at the maximum temperature for 12 hours and cooled down with a rate of 1 °C/min. This very gentle heating regime was employed to avoid formation of "thermal" cracks in the material. The specimens obtained in this way were used for flexural and compressive strength determination. The same material was also employed for ignition loss, free lime estimation and determination of phase composition, porosity and pore size distribution. Here, the total porosity was calculated from the bulk and wet densities of the material studied; the pore size determination was made by mercury porosimetry. On separate test specimens the longitudinal changes during the heating of the material were studied. The non-heated material was also used for DTA and DTG studies.

Results

The phase compositions of different cement pastes heated to different temperatures, as determined by x-ray diffraction, are summarized in Tab. II. In the pure tricalcium silicate and in non-blended cements free CaO and β-dicalcium silicate were formed as final

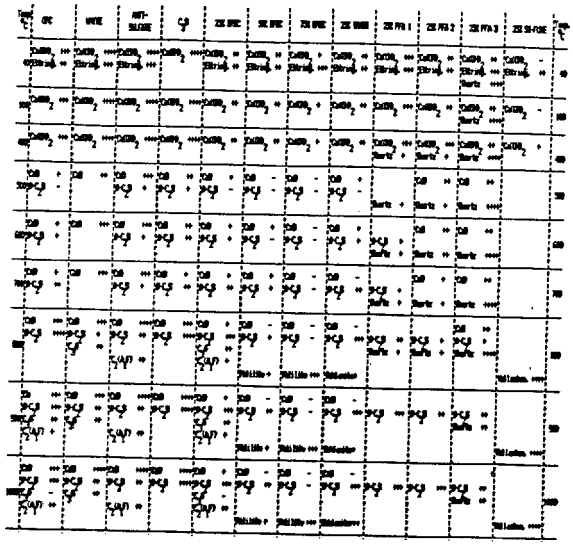

Tab.II: Phase composition of cement pastes heated to different temperatures

decomposition products. In addition, the phase $C_2(A,F)$ was formed in the OPC and antisulfate cements and the phase C_3A in the white cement. In blast furnace slag cement pastes melilite was formed with increasing slag content at the expense of β-dicalcium silicate. In flyash-portland cement pastes only β-dicalcium silicate was formed however no free lime was detected after exposure to high temperatures. In addition to that quartz was also detectable in one

cement with distinct amounts of this phase in the original flyash. Unlike in flyash cements, gehlenite was formed in the puzzolana-portland cement paste, in addition to ß-dicalcium silicate. Finally, wollastonite was the only final decomposition product if silica fume was added to the system.

Fig. 1 shows the obtained DTA and DTG curves of the cement pastes studied. The results are in line with those found by x-ray diffraction. In addition to an endothermic region between 100 and 300 °C belonging mainly to the CSH-phase, and an endothermic $Ca(OH)_2$-peak at 550 °C, exothermic peaks belonging to slag crystallization, ß- to α-quartz conversion and to wollastonite formation were also present. The small endothermic peak at 750 °C results from further CSH-phase decomposition and/or from the decomposition of small amounts of $CaCO_3$ present due to carbonation from CO_2 of the air.

The bound water content of the samples as function of decomposition temperature is shown in Fig. 2. The starting bound water content was different in different cements. The loss of water due to thermal decomposition was not a linear one and was greater at lower than at higher temperatures.

Fig. 3 shows the free lime content of the pastes after heating them to different temperatures. The obtained data determined by the Franke extraction method are in line with those found by x-ray diffraction and shown in Tab. II.

The total porosity and the volume of pores of different sizes as function of temperature is shown in Fig. 4 for selected cements. Expectedly, the total porosity increased significantly with increasing composition temperature, as the consequence of the bound water loss. Its slight decrease at very high temperatures in some cements was due to the shrinkage of the sample due to melt formation. Up to about 700-800 °C the formed new pore volume was located predominantly in the r = 10-100 nm pore size range. At even higher temperatures the volume of this pore fraction declined at the expense of even larger pores.

The longitudinal changes of different cements in the course of heating are shown in Fig. 5. Initially, all pastes exhibited a small thermal expansion followed by a significant shrinkage. The latter one occurred as the consequence of the chemical decomposition of the sample. A renewed expansion in some samples at even higher temperatures may be the consequence of the formation of new phases.

Finally in Fig. 6 the compressive strength of the test specimens after heating to different temperatures is shown. The initial strength of cement pastes was different for different cements and varied between 115 and 200 MPa. In most cements the obtained strength value increased initially (by up to 35 MPa) and reached values lower than those present initially, only after exceeding a critical decomposition temperature. The latter one varied in different cements between 40 and 600 °C. A slight strength increase in some cements exposed to very high temperatures was apparently due to melt formation in the material in this temperature range.

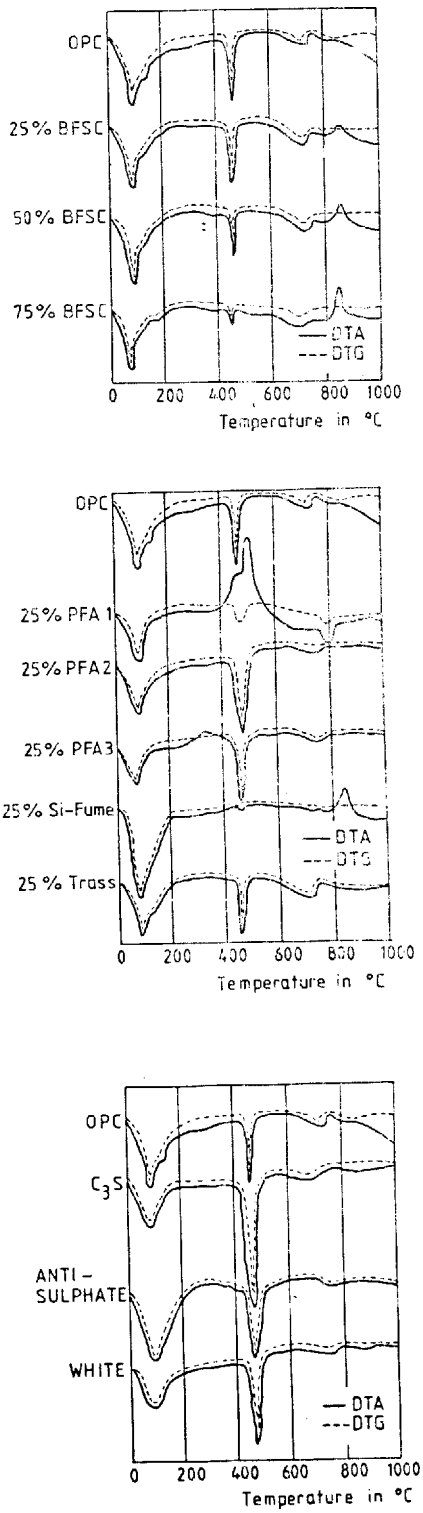

Fig. 1: DTA and DTG curves of the cement pastes studied

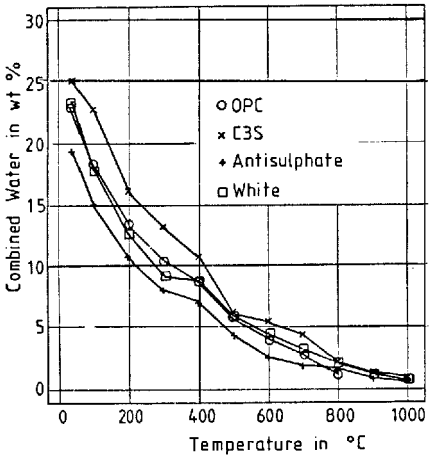

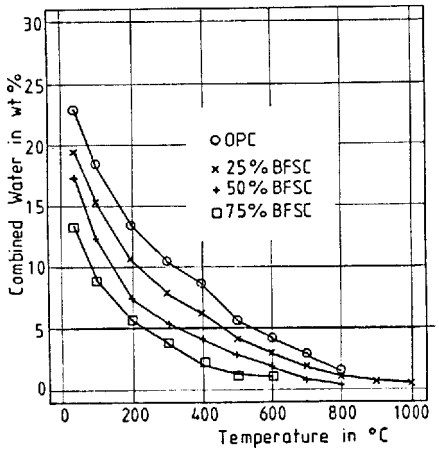

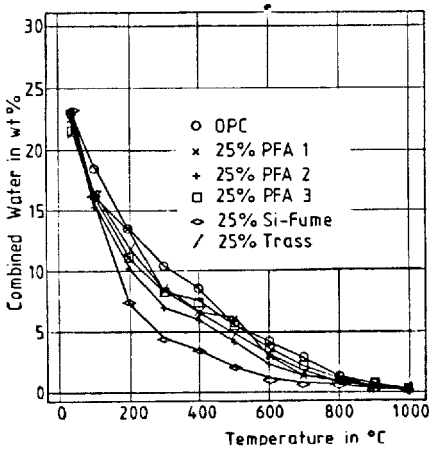

Fig. 2: Bound water content as function of decomposition temperature

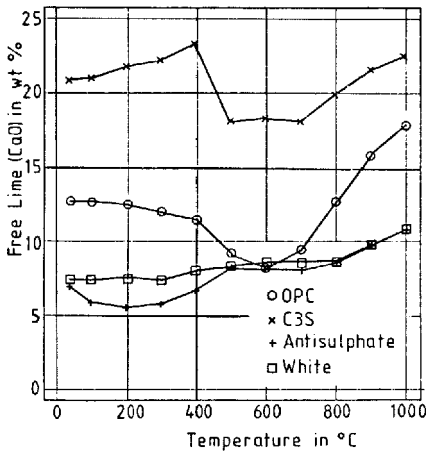

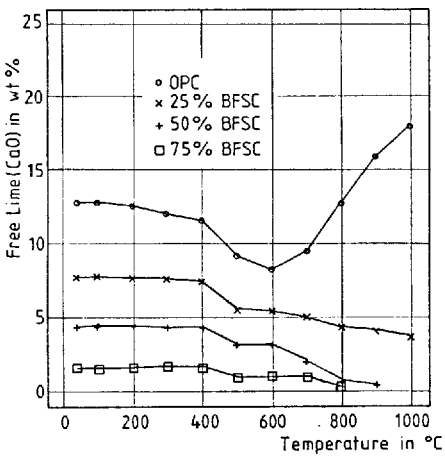

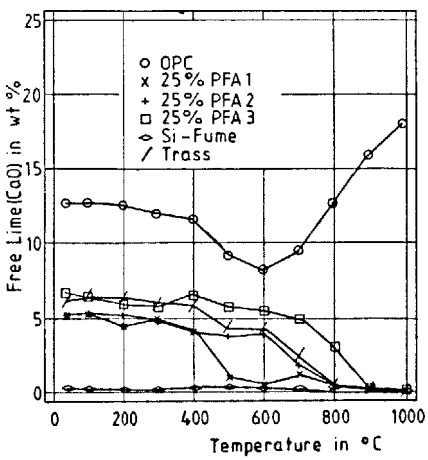

Fig. 3: Free lime content as function of decomposition temperature

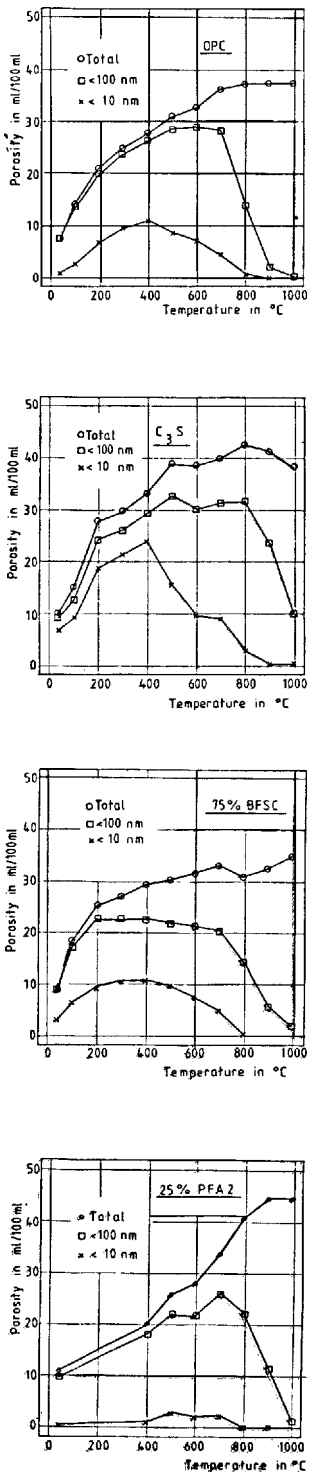

Fig. 4: Total porosity and pore size distribution of selected cement pastes as function of decomposition temperature

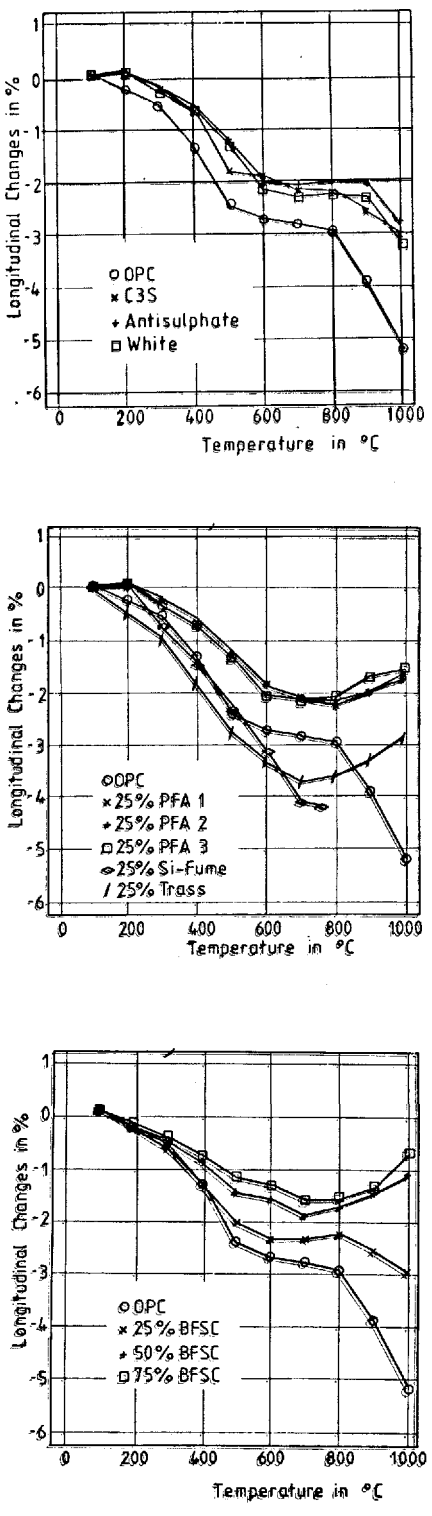

Fig. 5: Longitudinal changes of the studied cements as function of temperature

A. Zürz, I. Odler, S. Abdul-Maula. Technical University Clausthal, D-3392 Clausthal-Zellerfeld, Federal Republic of Germany

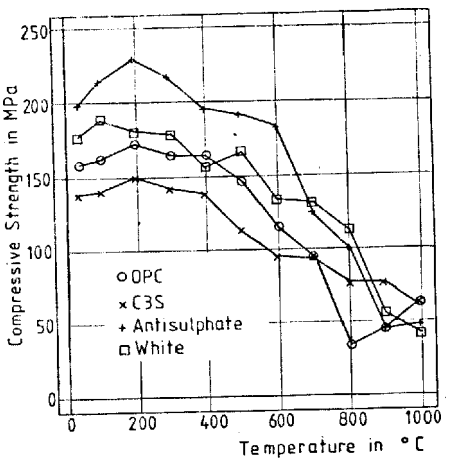

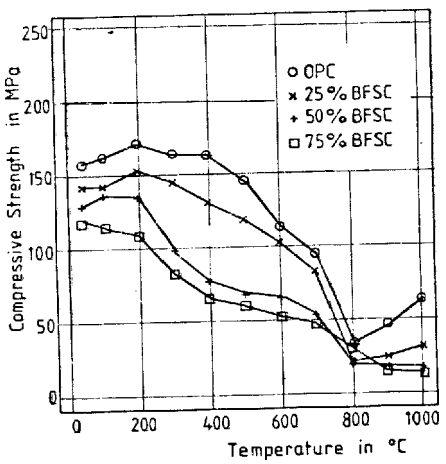

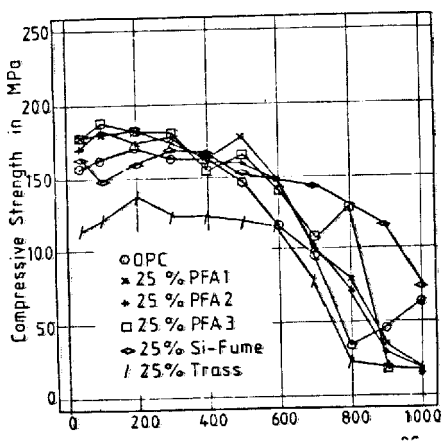

Fig. 6: Compressive strength as function of temperature

Discussion and Conclusions

The obtained data revealed both similarities as well as differences in the decomposition behavior of hydrated cement pastes made from different cements. In all systems studied a thermal decomposition of the hydrate phases, connected with an increase of porosity and average pore size, took place as the temperature increased. The new phases formed were, however, different in different cements, as, in addition to thermal decomposition, solid state reactions and even melt formation took place in the heating process. The observed loss of strength at increasing temperatures may be only partially related to the observed loss of bound water and increased porosity. At lower temperatures, namely, a significant loss of bound water content and an increase of porosity did result only in a moderate strength loss or even a strength increase. On the other hand significant strength losses at high temperatures were accompanied by only small additional increases of porosity. Thus it appears, that the gradual coarsening of the pore structure was an additional factor contributing to the strength loss at higher temperatures. On the other hand, differences in phase composition seem to be of less significance for compressive strength variations.

For the use in concrete exposed to elevated temperatures it is of importance that some of the cements studied did not losestrength up to relatively high temperatures despite a significant decomposition of the hydrates present. Thus by the selection of a right kind of cement the temperature range at which portland-type cements may be used can be widened significantly.

For the performance of concrete under fire condition the amount of free lime present after thermal decomposition may also be of significance, as a subsequent rehydration of the present calcium oxide may result in a further damage of the construction. From this standpoint it is of significance that only negligable amounts of calcium oxide are formed in some types of cement pastes which thus may be more resistant to fire exposure.

References

1. U. Schneider: On the thermal degradation of cement-bound concretes and its effect on mechanical and technological properties (in German). TIZ-Fachberichte, 404-407 (1977).
2. H. Tanaka, Y. Totany and Y. Saito: Properties of hardened cement paste after heating and their rehydration. Rev.Gen. Meeting Cem. Assoc. Jap. 36, 34-35 (1982).
3. J. Piasta, Z. Sawicz and L. Rudzinski: Changes in the structure of hardened cement paste due to high temperature. Mat. Construct. 17 (100), 291-296 (1984).
4. J. Piasta: Heat deformations of cement paste phases and the microstructure of cement paste. Mat. Construct. 17 (102), 415-420 (1984).

U. Ludwig and S. Mehr, Institut für Gesteinshüttenkunde , RWTH Aachen, West-Germany

Destruction of Historical Buildings by the Formation of Ettringite or Thaumasite

Summary Within mineralogical examination of building damages there have frequently been indentified the well known expansion causing ettringite ($C_3A \cdot Cs_3 \cdot H_{32}$) and thaumasite ($Cc \cdot Cs \cdot CS \cdot H_{14,5}$), or even thaumasite only within the destroyed area. This has also been the very result of investigations at deteriorated masonry of historical buildings. - The general incompatibility of high alkaline aluminate containing binders with gypsum or lime-gypsum mortars has to be considered as a main reason for this kind of damage formation. The potential endangering to masonry by a damage reaction can easily be shown at drill cores when measuring the expansion at storage in moest environment.

The technical and mineralogical investigations carried out for the examination of the determining parameters showed the following results:
Motars with OPC and such with cements of higher sulfate resistance become increasingly unstable when being mixed with calciumsulfate and calciumcarbonate at water storage with decreasing storage temperature. This effect is due to the primary formation of expansion causing ettringite. Only after longer storage periods at temperatures $\leq 20^{\circ}C$ thaumasite occured.
Mortars with C_2S or C_3S that are free from aluminate and ferrite form thaumasite when being mixed with calciumsulfate and calciumcarbonate and stored at $2^{\circ}C$ under water. The formation starts from the surface of the sample. Herewith the originally formed CSH-phase is destructed and the structure is strongly weakened.

The formation of a complete series of mixed crystals between thaumasite and ettringite can't be confirmed according to the present results.

Através de exame mineralógico de estragos em construções, freqüentemente se tem identificado as bem conhecidas etringita ($C_3A.Cs_3.H_{32}$) e taumasita ($Cc.Cs.CS.H_{14,5}$) causadoras de expansão, ou mesmo taumasita apenas na área destruída. Este também tem sido o resultado de investigações na alvenaria deteriorada de edifícios históricos. A incompatibilidade geral dos ligantes contendo aluminato altamente alcalino com gesso ou com argamassas de cal-gesso deve ser considerada como a razão principal para este tipo de estrago. O risco potencial para a alvenaria pela reação do estrago pode ser facilmente mostrada por amostras obtidas por perfuração quando da medição da expansão em cura em ambiente úmido.

As investigações técnicas e mineralógicas levadas a efeito para exame dos parâmetros determinantes apresentaram os seguintes resultados:

Argamassas com cimento portland comum e com cimento com resistência mais alta a sulfato tornam-se grandemente instáveis quando misturados com sulfato de cálcio e carbonato de cálcio em cura em água com diminuição da temperatura de armazenagem. Este efeito se deve à formação primária de etringita causadora de expansão. A taumasita ocorreu somente após períodos mais longos de cura a temperaturas $\leq 20^{\circ}C$.

Argamassas com C_2S ou C_3S, que estejam isentas de aluminato e ferrita, formam taumasita quando misturados com sulfato de cálcio e carbonato de cálcio e guardados sob água a $2^{\circ}C$. A formação começa a partir da superfície da amostra. Simultaneamente a fase de C-S-H, formada originalmente, é destruída e a estrutura é grandemente enfraquecida.

Não se pode confirmar a formação de uma série completa de cristais mistos entre taumasita e etringita, de acordo com os resultados atuais.

U. Ludwig and S. Mehr, Institut für Gesteinshüttenkunde , RWTH Aachen, West-Germany

Introduction

Since about 10 to 15 years in the northern part of Germany special severe damages are occuring on historical buildings. The picture of the damages partly are very broad, preferably cracks the outward brick shell of the building. The cause of these damages are the counter action of jointly incompatible mortars in the presence of water or humidity. Such incompatibility is p.e. given if highly alkaline and aluminate containing cement mortars are coming into contact with gypsum mortar (1,2).

It could be established in the examined cases that there are existing contacts between mortars of plain OPC or Portland cements low in C_3A with gypsum containing mortars. The gypsum mortars were used for the original construction or for the later repair of the buildings. Cement containing mortars are nearly exclusively used for the reconstruction of the outer shell of the masonry or in order to stabilize the inner core of the partly up to 2 m thick walls by cement injections. Besides in the case of church towers concrete stiffeners partly are contacting the gypsum containing mortar. These stiffeners and the reconstruction of the outer brickwork are giving contacts with the gypsum containing masonry only to a smaller extend.

The cement injections, however partly penatrate the masonry as fissure fillings looking like venes in the drilled core. The thickness of these fissures amounts from about 1 mm to 10 cm. In the case of the use of plain lime as binding material the cement injection provides a stabilization of the masonry, in the case of gypsum as binding material the cement injection leads to the detoriation of the masonry. This could be shown at humid cured drill cores. Lime containing masonry together with cement injection remained stable since several years whereas the gypsum containing specimen showed a strong expansion from up to 9 mm/m and besides a crack formation and deterioration. In comparison the plain expansion of hardend plaster of Paris at higher humidities amounts to <5 mm/m (3). The above mentioned method is suitable to measure the potential endangering of a masonry (1).
The mineralogical examination by x-ray and x-ray micro analysis showed ettringite and/or thaumasite as possible damaging hydrates. The damaging effect of an ettringite formation in hardened pastes, mortars and concretes is well known and needs no further discussion. The other two questions are

1. Do exist a complete solid solution series between ettringites and thaumasite?

2. How thaumasite or the mixed crystals with ettringite contributes to a damage reaction?

Some authors are of the opinion that a solid solution series is existing (4,5,6). Others found greater differences in the structure of ettringite and thaumasite (7). therefore they exclude the formation of mixed cristals. - At the examination of damages in some cases thaumasite besides ettringite were detected as the damage causing agents (8,9,10) in mortars, coatings and soil cements. Some authors derive from their experimental work on deteriorated concretes that the main influence was given by the ettringite formation. The thaumasite formed in a later stage is only of lower importance for the destruction.

Experimental

The formation of ettringite and/or thaumasite was checked with PZ 45 F and PZ 45 F-HS according to German standards. According to Bogues phase calculation the PZ 45 F-HS is free in C_3A. - In order to prevent any ettringite formation and to favour the development of thaumasite only, in two series alite and belite were used as starting materials. The alite contained 1 wt.-% of Fe_2O_3 and MgO at a time. The belite was stabilized by an excess of lime. - These starting materials were mixed with excess powdered gypsum and calcite. The calculated additions of gypsum and calcite were adjusted in such a way to get a final molar ratio of SiO_2 (from the binding material): $CaSO_4 : CaCO_3 = 1$. The admixture of gypsum and calcite were related to the SiO_2 contents of the binding materials. The proportions are given in table 1.

binding material	calcite wt.-%	gypsum wt.-%	w/b
PZ 45 F	35,5	61,0	0,71
PZ 45 F-HS	33,0	56,2	0,73
alite	75,4	43,9	0,71
belite	99,9	58,1	0,72

Table 1 Proportioning of the calcite and gypsum admixtures and of the water/binder ratio

More detailed analytical and physical data of the starting materials are given in (11).

From the mixtures mortars and specimen according to DIN 1164 were prepared. In exception to the rules calcite and gypsum was added instead of the fine and/or middle fraction of the standard sand and the specimen were provided with measuring points made of stainless steel. The water/binder ratio was about 0,70.

The storage of the specimen were carried out for 1 day at moist conditions and 20°C. Exceptionally the belite containing mortar was left under these conditions for 14 days to get a sufficient hardening before demolding.
- Afterwards the demolded specimen were stored under water at 2, 10, 20 and 40°C. At 2°C the specimen partly were stored diped into water in part. After deterioration rest pieces of the specimen were preserved in sealed plastic flasks. The weight and length change of the specimens were measured and related to the initial value. At the same time the resonance frequency was determined. It characterizes the course of the strengths.

The change of the phase composition was investigated by x-ray of the material 40 um. For this purpose the hydration of the wet mortar firstly was stopped by isopropyl alcohol, dried and pulverized carefully. Than the hydrated material was concentrated by sieving. The x-ray investigation was done with Philips P.W. 1130/00 with Cu-K -radiation.

The scanning electron microscopy (SEM) inspection and the x-ray micro analysis (RMA) was done with a Cambridge 250 MK 2. The samples were lumpy or dispersed powders.

RESULTS AND DISCUSSION

Investigations with PZ 45 F

The changes of the weight, the length and the resonance frequency of the mortars with PZ 45 F stored at different temperatures in function of the storage period are shown in fig. 1. From the figure it is clearly to seen that the PZ 45 F is instable against additional gypsum at all temperatures of storage. The weights and the lengths only increases. After 120 days the specimen stored at 2°C are destroyed. There is no difference in the storage conditions: totally or half diped under water. - The measure of the resonance frequency firstly showed an increase of the values up to about 14 days.

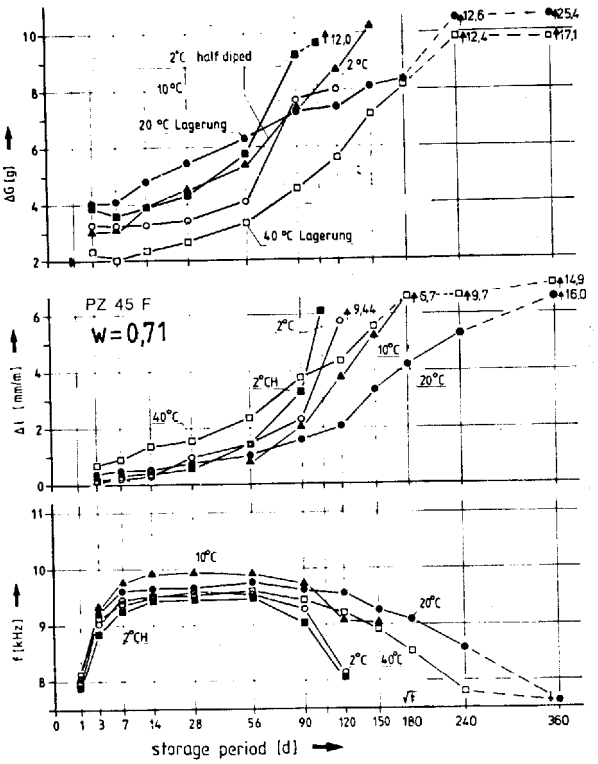

Fig. 1 Weight, length and resonance frequency of mortars with PZ 45 F calcite and gypsum stored at different temperatures

Up to about 56 days no change of the values is visible. At further storage a more or less sharp decreasetakes place place, starting with the specimen stored at 2°C.

The x-ray examination of the enriched hydrated material up to 56 days storage at 2°C showed the interferences of ettringite only. At 90 days and at further storage thaumasite is formed increasingly. After 450 days thaumasite is the main hydrated phase and the gypsum is consumed completely (fig. 2).

At 20°C storage the x-ray diagrams preferably showed the interferences of ettringite. After 600 days of hydration some thaumasite and a rest of gypsum is recognizible. - At 40°C reaction temperature up to 600 days of reaction ettringite was detected only. Besides a greater amount of unreacted gypsum is left.

U. Ludwig and S. Mehr, Institut für Gesteinshüttenkunde , RWTH Aachen, West-Germany

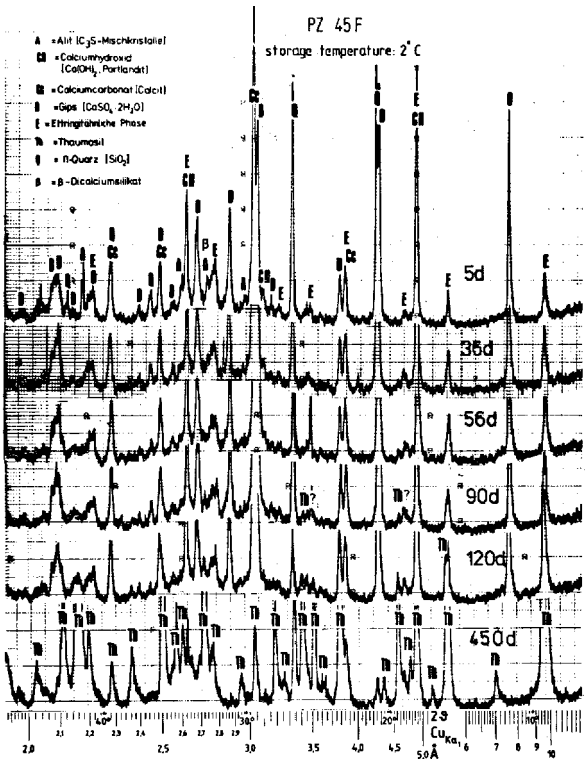

Fig. 2 x-ray diagrams of enriched mortars with PZ 45 F, calcite and gypsum stored under water at 2°C

The SEM investigations only show needle like crystals of about up to 0,5 µm diameter and up to 4 µm length. The RMA of the crystals shown in fig. 3 B mainly indicates the elementes Ca, Si and S. Al only occurs in traces.

From the results corresponding to the expectation the conclusion can be drawn that the PZ 45 F at storage temperatures from 2 to 40°C is instable against excess gypsum and calcite. The instability increases with decreasing temperatures and is caused by an ettringite formation. - At temperatures ≤ 20°C at later stages of the reaction thaumasite is formed with decomposition of the firstly formed ettringite and combining the unreacted gypsum and calcite.



Fig. 3 A-C SEM and RMA image from dispersed mortar with PZ 45 F, calcite and gypsum after 450 days reaction at 2°C

Investigations with PZ 45 F-HS

The mortars with PZ 45 F-HS showed a higher resistivity against direct admixture of gypsum than the mortars with plain OPC (fig. 4). The figure clearly indicates that mainly storage temperatures of 2 and 10°C are leading to a dramatic increase of the weights and expansions accompanied by an early drop

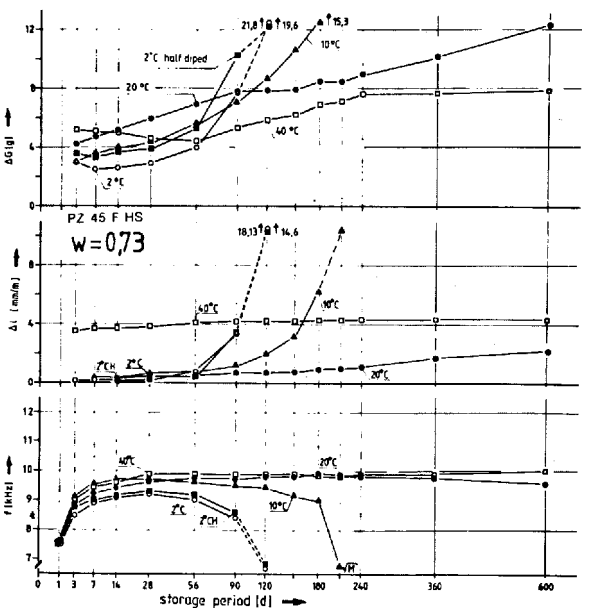

Fig.4 Weight, length and resonance frequency of mortars with PZ 45 F-HS, calcite and gypsum at different temperatures

in strengths. At 2°C again after 120 days the specimen are destroyed. At 10°C the time needed amounts to 210 days. 20°C storage temperature leads to a comparible low increase of the expansion and decrease of the resonance frequency. 40°C storage produces an early increase in weight and expansion and afterwards stability up to 600 days of water storage. - The x-ray diagram in fig. 5 showes that the storage at 2°C leads to an early formation of ettringite only. After 90 days firstly thaumasite appeared. Further wet storage of the mortar causes increased intensities of the thaumasite. After 450 days reaction period of ettringite nearly completely is converted into thaumasite. Parallel the calcite predominantly and the gypsum fully are reacted. Again, the formation of thaumasite gets distinguishable by splitting of the d-value at about 5,6 Å. Afterwards additional interferences appear in the diagram. - At 20 and 40°C up to 600 days storage no thaumasite could be detected. In this case, ettringite is the stable phase. Besides larger amounts of unreacted calcite and gypsum are still in the mortar.

From the results the conclusion can be drawn that the PZ 45 F-HS is instable at temperatures below 40°C in the presence of excess gypsum, calcite and humidity. As already shown at the attack of sulfate solutions (12) the instability increases with decreasing temperatures. The first expansion is accompanied by an ettringite formation. At lower temperatures < 20°C after about 56 days storage thaumasite occurs as a new phase decomposing the firstly formed ettringite and

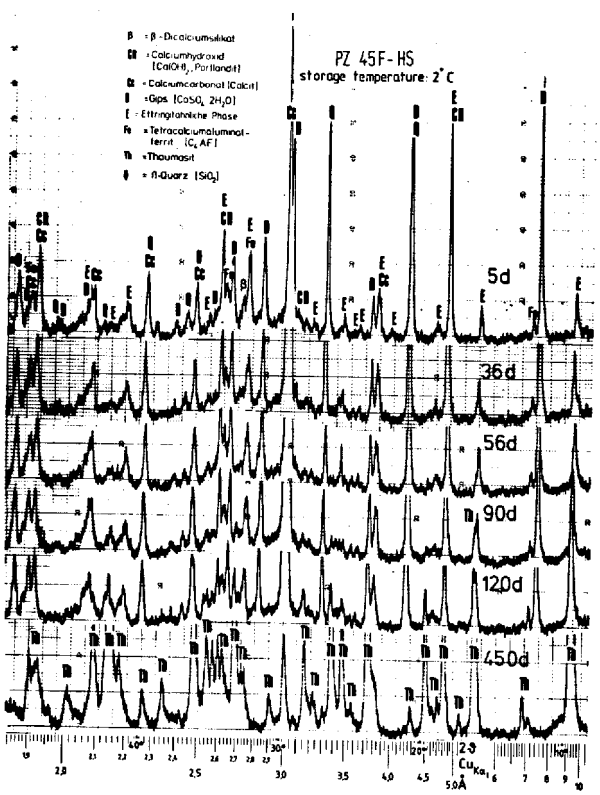

Fig. 5 x-ray diagrams of enriched mortars with PZ 45 F-HS, calcite and gypsum stored under water at 2°C

combining the still unreacted calcite and gypsum.

The SEM and RMA analysis again showed needle like crystals with only traces of alumina.

Investigations with FM-alite

For the only formation of thaumasite the alite was taken as starting material. This investigations should give an answer to the question how thaumasite contributes to the damage of mortars.

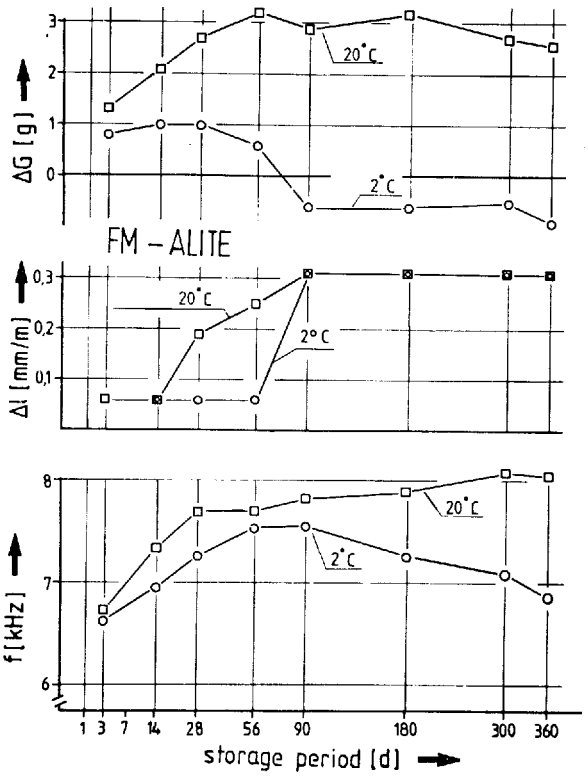

Fig. 6 Weight, length and resonance frequency of mortars with FM-alite, calcite and gypsum stored at different temperatures

In figure 6 the changes of the weight, the length and the resonance frequency of the mortars with FM-alite stored under water at 2 and 20°C are shown. At 20°C only a slight increase of the weight and the length is visible. At the early hydration up to 28 days the resonance frequency showed a distinct and in the later stage a smaller increase. The specimen show no sign of an attack.

At 2°C storage under water the specimen also show but a slight expansion of 0,3 mm/m and remain stable for the period of one year now. But besides a small decrease in weight and a significant drop in the resonance frequency is recognizeable. At the surface of this specimen a disintegration starts after about 200 days storage period. This dissolution of the structure explains the loss in weigth and in resonance frequency. The core of the specimen remained stable. Tis is proved by the low rate of expansion.

Furthermore, the enriched mortars were put to x-ray examination again. In this special case analyses were made from material of the average, the inner core and the outer surface. Figure 7 showes the results.

After 3 and 90 days storage period the average samples preferably show the interferences of gypsum, calcite, quarz, portlandite and unreacted alite. Thaumasite can be detected in traces only if present at all. This, too, is correct for the sample from the inner core of

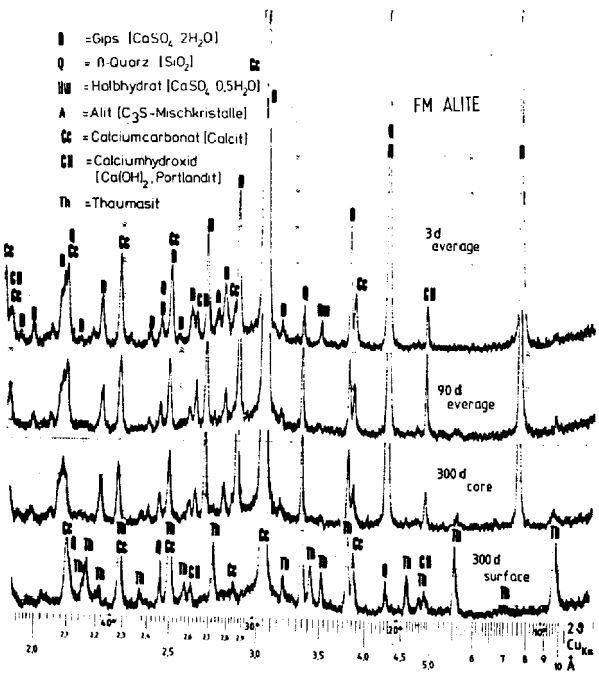

Fig. 7 x-ray diagrams of enriched mortars with FM-alite, calcite and gypsum stored under water at 2°C

specimen after 300 days storage period. In contrast the sample from the surface of the mortar prism shows the strong interferences of thaumasite.

Figure 8 demonstrates the transition zone from the corroded surface to the stable core of the specimen by means of a SEM image. The outer zone shows the well known needle like crystalls. The structure of the material from the core is more dense and compact.

From the above described results the conclusion can be derived that the formation of thaumasite causes no expansion but destroyes the mortar or concrete by loosening the structure. The dense structure of the hardened calcium silicate hydrates is converted into a loosened one of the new formed thaumasite.

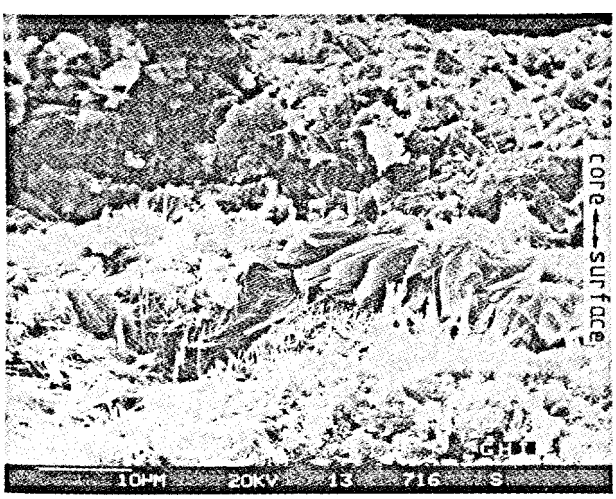

Fig. 8 SEM image from the transition zone of the mortar specimen with FM-alite, calcite and gypsum stored under water at 2°C for 200 days

Investigation with belite

The corresponding mortar specimen with belite are now stored under water at 2 and 20°C for a period of one year. At both curing conditions the results only show a very slight increase of the weight and the length. The resonance frequencies are increasing in both cases. So far no destruction could be observed.

Conclusions

The technological and mineralogical investigations on the influence of excess additions of gypsum and calcite on the hardening and durability of PZ 45 F, PZ 45 F-HS, alite and belite lead to the following conclusions:

1. Correspondingly to the expectation the PZ 45 F is instable at storage temperatures from 2 to 40°C. The instability increases with decreasing temperatures and is caused by an ettringite formation. - At later stages and temperatures ≤ 20°C the firstly formed ettringite is decomposed in favor of thaumasite. The still unreacted calcite and gypsum takes part in this reaction.

2. The PZ 45 F-HS is instable at temperatures below 40°C in the presence of excess gypsum, calcite and humidity. Accompanied by an ettringite formation the rate of damaging expansion increased again with decreasing temperatures. The further reaction corresponds to that of PZ 45 F.

3. No indication of an expansion caused by thaumasite formation is given by the results with alite or belite containing mortars. But the dense structure of the hardened calcium silicate hydrates can be converted in a loosened one of thaumasite.

4. The described results upon the formation of thaumasite in the presence of ettringite do not indicate a solid solution series but a mixture of this two hydrates.

Acknowledgement:
The authors are grateful to the Stiftung Volkswagenwerk for financing this investigation.

Literature

1. Ludwig, U.: "Ursachen und Schäden an historischen Bauwerken", Vortrag anlässlich einer Arbeitssitzung des Amtes für Bau- und Kunstpflege der Ev.-Luth. Landeskirche, Hannover, Oktober 1982
mit Mehr, S., Moldan, D.: Baumaschine und Bautechnik 10 (1984), S. 396-404

2. Werner, A.: "Bauschäden an historischen Gebäuden mit gipshaltigem Mauerwerk", Ber. zur Denkmalpflege in Niedersachsen, 5 (1985), S. 48-52

3. Kuhlmann, J.: "Beitrag zur Untersuchung der Raumbeständigkeit anhydrithaltiger Mischgipse", Diss. RWTH Aachen 1977
mit Ludwig, U., ZKG 30 (1977), S. 214-218

4. Kollmann, H., Strübel, G.: "Ettringit und Thaumasit-Mischkristalle von Brenk, Eifel", Chem. Erde 40 (1981), S. 110-126

5. Carpenter, A.B.: "Oriented Overgrowth of Thaumasite on Ettringite", The American Mineralogist 48 (1963), S. 1394-1396

6. Lukas, W.: "Betonzerstörung durch SO_3-Angriff unter Bildung von Thaumasit und Woodfordit", CCR 5 (1975), S. 503-518

7. Bensted, J., Prakash Varma, S.: "Studies of Thaumasite, Part II", Silicates Industriels 1 (1974), S. 11-19

8. Leifeld, G., Münchberg, W., Stegmaier, W.: "Ettringit und Thaumasit als Ursache in Kalk-Gips-Putzen", ZKG 4 (1970), S. 174-177

9. Gouda, G.R., Roy, D.M., Sarkar, A.: "Thaumasite in Deteriorated Soil-Cements", CCR 5 (1975), S. 519-552

10. Kollmann, H., Strübel, G., Trost, F.: "Reaktionsmechanismen zur Bildung von Treibkernen in Kalk-Gips-Putzen durch Ettringit und Thaumasit", ZKG (1977), S. 224-228

11. Mehr, S.: "Entwicklung von sulfatbeständigen Mörteln auf Zement-Hüttensand-Puzzolan-Basis", Diss. RWTH Aachen 1986

12. Därr, G.-M.: "Über die Sulfatbeständigkeit von Zementmörtel", Diss. RWTH Aachen 1977
mit Ludwig, U.: Forschungsbericht des Landes NRW Nr. 2636, Westdeutscher Verlag Köln-Opladen 1976

D. Heinz and U. Ludwig, Institut für Gesteinshüttenkunde, RWTH Aachen, West-Germany

Mechanism of Subsequent Ettringite Formation in Mortars and Concretes after Heat Treatment

Summary In the last years precast units made of high strength concrete, and having been heat treated during production, have partly shown damages of structure connected with loss of strength. These damages always occurred at those building components which, for several years, had been subjected to open-air weathering and thereby to frequent moisture saturating, as e.g. front panels and sleepers.

The kind of damage caused has often been characterized by a crack formation emerging from the edges of the building components, as well as by a laxation of the bond between the cement paste and the coarse aggregates. In order to clarify these damages, there have been examined a series of parameters within their influence on the durability of heat treated concretes. The findings, which will be discussed, are to give proof of the fact that those damages arisen in practise can be caused by a late formation of ettringite. The mechanism of the reaction is going to be explained.

When applying heat treatment to cement mortars and concretes made with PZ 55, increasing temperatures result in a more and more decreasing formation of defined calcium aluminate sulphate hydrate phases. Aluminate and sulphate ions get bound within the CSH-gel and in the subsequent storage under water are available as reaction partners for an Aft-phase formation. The interface between aggregate and cement stone represents the reaction point of this formation. The consequences of this very new formation consist in an expansion linked with a diminution of strength.

Nos últimos anos unidades premoldadas feitas de concreto de alta resistência, e tratados termicamente durante a produção, em parte apresentaram estragos da estrutura, relacionados com perda de resistência. Estes danos sempre aconteceram naqueles componentes de construção que, por muitos anos, estiveram ao ar livre expostos ao tempo e conseqüentemente à saturação freqüente de umidade, como por exemplo painéis e dormentes.

O tipo de estrago causado freqüentemente se caracterizou por formação de trinca com início nas bordas dos componentes de construção, bem como por um enfraquecimento da ligação entre a pasta de cimento e os agregados grossos. Com o fim de esclarecer estes danos, examinou-se uma série de parâmetros tendo em vista sua influência sobre a durabilidade de concretos tratados termicamente. Os resultados, que serão discutidos, pretendem provar o fato de que aqueles estragos ocorridos na prática podem ser causados por formação retardada de etringita. O mecanismo da reação é explicado a seguir.

Quando se aplica tratamento térmico a argamassas e concretos feitos com PZ 55, os aumentos de temperatura têm como resultado uma formação cada vez mais reduzida de fases de hidrato de sulfoaluminato de cálcio. Íons de aluminato e sulfato ficam bloqueados dentro do gel C-S-H e, na cura posterior sob água, ficam em disponibilidade como parceiros de reação para uma formação da fase de AFT. A interface entre agregado e pasta de cimento representa o ponto de reação desta formação. As conseqüências desta formação muito nova consistem numa expansão interligada com uma diminuição de resistência.

D. Heinz and U. Ludwig, Institut für Gesteinshüttenkunde, RWTH Aachen, West-Germany

INTRODUCTION

In the last years precast units made of high strength concrete, and having been heat treated during production, have partly shown damages of structure connected with loss of strength. These damages always occurred at those building components which, for several years, had been subjected to open-air weathering and thereby to frequent moisture saturating, as e.g. front panels and sleepers. The kind of damage caused has often been characterized by a crack formation emerging from the edges of the building components, as well as by a laxation of the bond between the cement paste and the coarse aggregates.

In order to clarify these damages, there has been examined a series of parameters within their influence on the durability of heat treated concretes. Thus, it has been possible on the one hand, to find out those conditions leading to the occurrence of a degradation in the heat treated concrete, and on the other hand, to show the favourable influence of portland cement without C_3A, or of puzzolanas, or granulated blast furnace slag added to portland cement on the durability (1). Furthermore, there have been subjects of investigation the W/C ratio and the humidity and temperature of storage as well as the grain size of aggregates, and the influence of freeze thaw cycles (2).

The findings, which will be discussed in the following, are to give proof of the fact that those damages arisen in practice can be caused by a late formation of ettringite. The mechanism of reaction, too, is going to be explained.

Ettringite, or the tricalcium aluminate trisulphate hydrate, or for short the Aft-phase, is the hydration product of the aluminate and ferrite phase of the cement clinker, water, and of the calcium sulphates added to the cement for the regulation of the setting. Moreover, there is tricalcium aluminate monosulphate hydrate, or for short called Afm-phase, occurring in OPC which, according to thermodynamical deliberations, has to be regarded as metastable below 70°C (3).

It is the early formation of ettringite that marks the beginning of the standard setting according to DIN 1164. On the contrary, formations of ettringite in the hardened cement stone have already for long been considered as a reason for expansion or diminution of strength.

EXPERIMENTAL PROCEDURES

To determine the above mentioned cases of damage, there have been carried out model experiments with mortar prisms according to DIN 1164. The first series of experiments were done to prove the influence of the treatment temperature. By means of a PZ 55 with a theoretical amount of C_3A at about 12 wt.-%, and an amount of SO_3 at 3.8 wt.-% mortar bars were produced and heat treated in their moulds after having been prestored for two hours. The temperatures of treatment ranged between 20 and 100°C. The duration of the various temperatures were fixed with the help of an empirical relation according to the well known Saul's equation in the way that all samples were to reach a hardening progress equivalent to a 72-hour hardening at 20°C. The heat treatments were effected in contrast to the generally applied steam curing in a thermostatical water bath without having to expect herewith a shift within the reaction mechanism. After cooling a storage in water was done at 20°C. There were then periodically taken the length and the weight, as well as the resonance frequency, in order to be able to control the development of strength.

In order to investigate the influence of the molar ratio of sulphate and aluminate within the cement there have been done a second series of experiments. There have been produced mortars with PZ 55, and by adding of finely ground clinker, it has been achieved to lower the amount of SO_3 and by adding of anhydrite, to increase the amount of SO_3 therein. Thereby, the SO_3 contents of the cements ranged from 2 to 8.6 wt.-%. The samples then got exposed to a heat treatment of 90°C which, as to the applied PZ 55, results in a damage reaction (figure 1).

RESULTS AND DISCUSSION

To start with, there will have to be discussed the influence of the treatment temperature. The visualization of weights, change of lengths, and resonance frequencies depending on the duration of a storage under water cover at 20°C after an early heat treatment, make us recognize the following correspondences (figure 1).

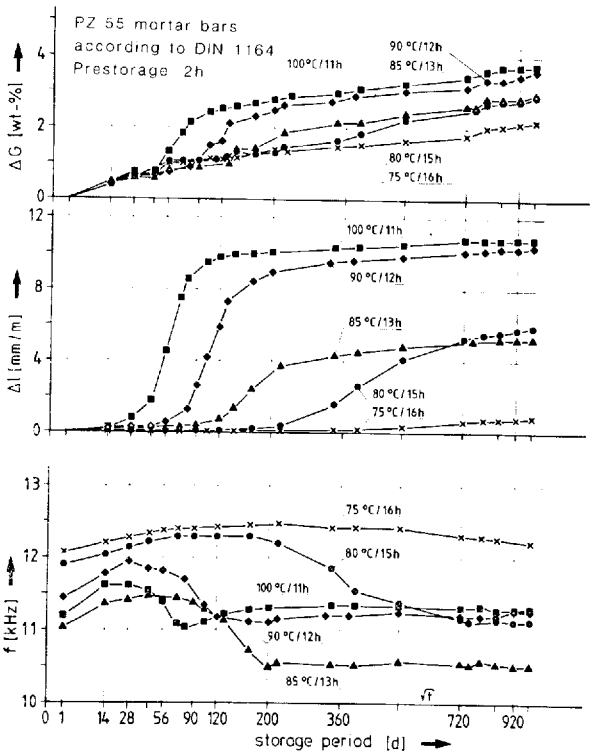

Figure 1
Influence of the treatment temperature on weight, length, and resonance frequency of mortars with PZ 55

Temperatures above or equal to 75°C lead to an expansion linked with a decrease of strength shown by the diminution of resonance frequencies and a partly over-proportional increase of weights. Increasing temperatures lead to an anticipation of the damage reaction. Temperatures below 75°C - not shown in the diagram - do not bring about the damage reaction.

As freeze-thaw-cycles or access of foreign ions can be excluded as reasons for the damage reaction during the storage of the samples, the very fact causing the expansion, and the decrease of strength is to be considered as due to a formation of a new phase in the cement stone of the mortars on account of a shift within the phase content brought about by the heat treatment.

The x-ray phase analysis of the enriched cement of the treated mortars, effected directly after the heat treatment, and after an almost 3-yeat water storage, provides full information concerning these correspondences.

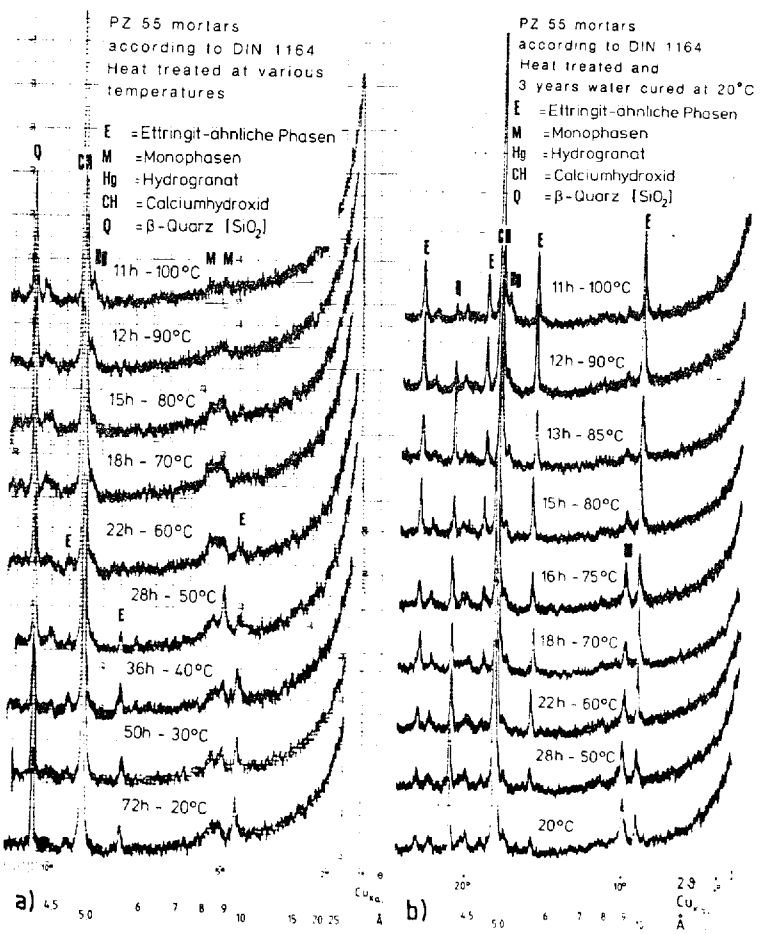

Figure 2a and 2b
X-ray phase analysis of heat treated mortars with PZ 55 effected directly after heat treatment (a) and after an almost 3-year water storage (b)

First of all the phase analysis taken directly after the heat treatment (fig. 2a). To begin with, increasing temperatures result in a decreasing amount of ettringite that is to be seen in the basal interference of 9.7 A. The mixed crystals of the Afm-phase, characterized by the interference of 8.2 and 8.9 A, start occurring at a temperature of 70°C as the only calcium aluminate sulphate hydrate phase. On the whole, the share of these phases is increasingly diminishing, and at a temperature of 100°C the amount of Afm-phase practically reaches the boundaries of detection as to the x-ray phase analysis. Furthermore, there is to be observed an occurrence of hydrogarnet, namely the mixed crystals of the tricalcium aluminate hexahydrate.

The result of this phase analysis can be summed up in such a way that with increasing temperatures aluminate and sulphate form defined hydrate phases to a lower degree, and that one has to be aware of increased application of these ions to the calcium silicate hydrate gel. This is in keeping with those results found by (4) and (5).

It can be derived from the diagrams showing the x-ray analysis of the mortars having been water-stored for 3 years after heat treatment that under certain conditions the sulphate ions at least are available for the formation of new phases (fig.2b). Those mortars having undergone an obvious expansion reaction and loss of strength, that means above all those samples treated at a temperature of 80 - 100°C, practically contain nothing but ettringite as calcium aluminate sulphate hydrate phase. To be compared with the sample permanently stored at 20°C, here we have a presence of Aft- and Afm-phases as at the beginning of the hydration.

In correspondence with the reaction partners participation in the formation of phases, the molar ratio of sulphate and aluminate within the cement assume a particular importance.

Figure 3 shows the development of weights, lengths and resonance frequencies of the heat treated mortars with SO_3 contents of 2 to 8.6 wt.-% in the cement. The curves in the diagrams are marked by the molar ratio of SO_3 and Al_2O_3.

The investigations proved that with a decrease of the molar ratio to 0.55 and with a respective amount of SO_3 of 2.5 wt.-% in the cement there is a chance to suppress the damage reaction.

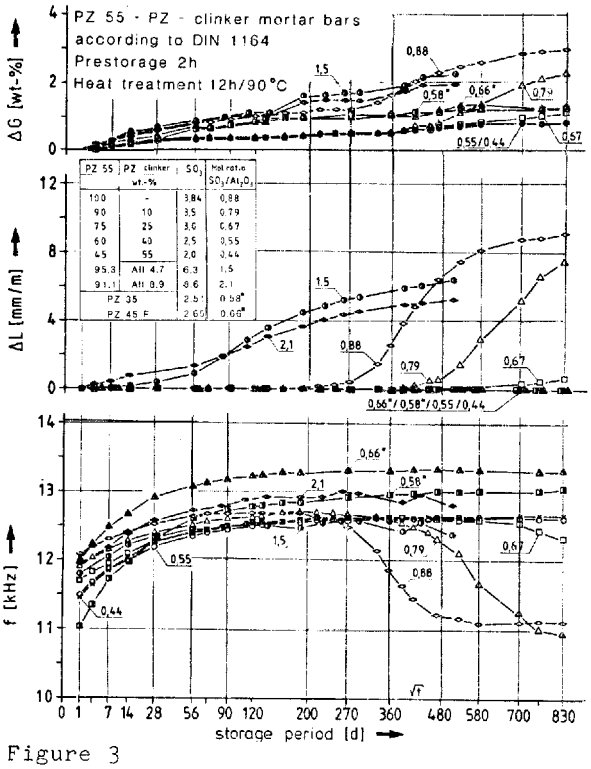

Figure 3
Influence of the molar ratio of SO_3 and Al_2O_3 within the cement on weight, length and resonance frequency of heat treated mortars

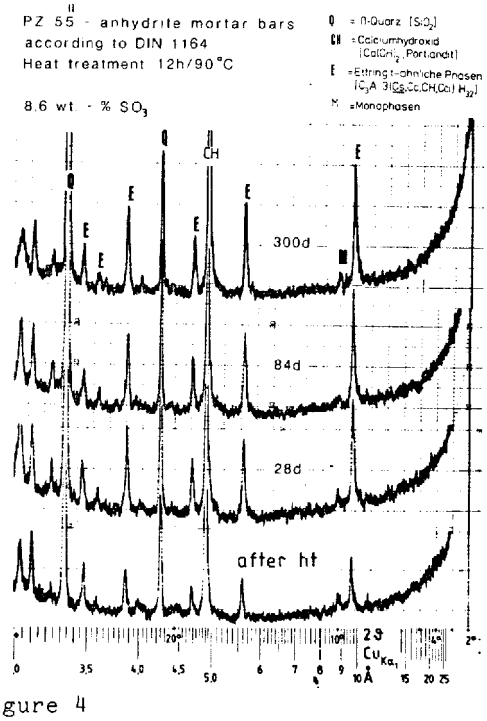

Figure 4
X-ray phase analysis of heat treated mortars with PZ 55 and a SO_3 content of 8.6 wt.-%

The behaviour of the mortar with PZ 55 containing 8.6 wt.-% SO_3 (molar ratio 2.1) is of special interest. Figure 4 visualizes the corresponding x-ray phase analysis. Ettringite is present even directly after heat treatment. Thereby it is obvious, that the otherwise observed decomposition of ettringite during a 90°C heat treatment (fig.2a) is not caused by thermal instability.

Instead of this, initially formed ettringite reacts with free aluminate to build monophases. Parallel sulphate and aluminate ions get increasingly bound to the CSH-gel. Evidently, the increased SO_3 content exceeds the capacity of the gel and a further ettringite formation becomes possible.

A swelling reaction connected with raising amounts of ettringite (fig.4) started within those samples directly after the heat treatment. That means that further sulphate is present in the pore solution at that time.

By means of scanning-electron microscopy it has been proved that the place of reaction where the formation of the new phases is performed, and herewith the origin of the degradation, is the very contact zone between the cement stone and the aggregates.

The photos were taken of samples consisting of PZ 55 mortar prisms after being treated at 90°C; their phase analysis has already been mentioned above. The first picture (fig.5) reflects the stadium directly after the heat treatment. On the right third of the photo, there is to be seen an aggregate-paste interface , which has been deprived of the aggregate. The relatively plain interface is a precise projection of the shape of the formerly attached grain. What we are confronted with according to findings in literature (8), is a layer of finest $Ca(OH)_2$ crystallites of 2 - 3 microns thickness which had grown onto the grain in a quite oriented way. The area in the middle of the photo allows a free view on the so-called intermediate layer beneath the interface, which possesses a thickness of 5 - 10 microns, consists of coarse $Ca(OH)_2$ crystals and CSH phases, and provides a hightened microporosity. The left part of the picture shows the surface of an aggregate grain.

The next photo (fig.6) shows that between the interface and the aggregate, there occurs a new formation which separates the aggregate from the cement stone. The strength of the layer amounts to about 4 - 8 microns.

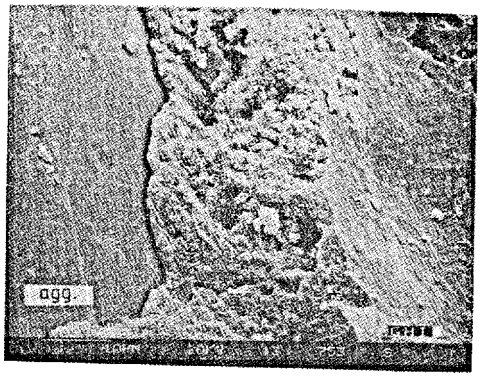

Figure 5
SEM micrograph of 12 h/90°C heat treated PZ 55 mortar 1 day after treatment

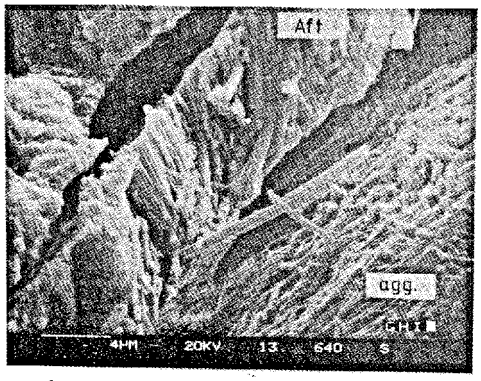

Figure 6
SEM micrograph of 12 h /90°C heat treated PZ 55 mortar after 3-year water storage at 20°C

The layer is constructed by parallel crystalls standing vertically with their longitudinal axis upon the surface of the aggregate.

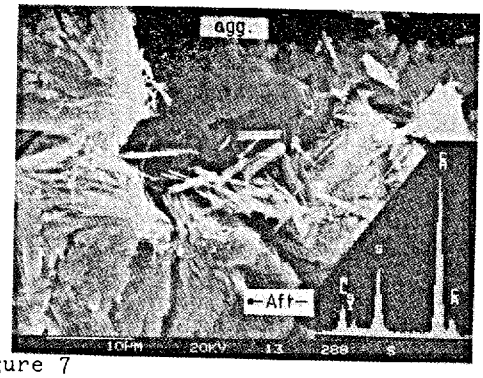

Figure 7
SEM micrograph of 12 h/90°C heat treated PZ 55 mortar after 3-year water storage at 20°C

Through electronprobe microanalysis these new formations have undoubtedly proved to represent an Aft-phase (fig. 7).

The following photo of a polished section (fig.8) once again visualizes the proportions showing to what degree the new formations carry with them a formation of cracks (lower right, fig.8).

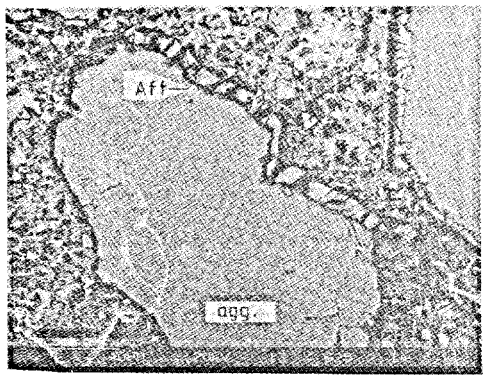

Figure 8
SEM micrograph of 12 h/90°C heat treated PZ 55 mortar after 3-year water storage at 20°C, polished section

The distribution of elements concerning the polished section - not represented in a picture - again makes clear that the new formations in their respective composition lead to an expressive enrichment of sulfur and a slight one of aluminium on the aggregate.

The details having been discussed here verify that the Aft-phase formation occurs by a through-solution mechanism.

The very reason for the formation of phases together with load and expansion at the aggregate grains is possibly to be laid down to the coexistence of the interface, which works as a semi-permeable membrane (9), as well as to a hightened microporosity in the neighbouring intermediate layer to the rest of the bulk cement stone. Both facts are suppositions for a phase formation where the solid phase grows under load whereas the feeding solution remains at atmospheric pressure. Besides this the adhesion cement stone-aggregate is the weakest part of the mortar structure.

CONCLUSION

When applying heat treatment to cement mortars and concretes, increasing temperatures result in a more and more decreasing formation of defined calcium aluminate sulphate hydrate phases. Aluminate and sulphate ions get bound within the CSH-gel and in the subsequent storage under water are available as reaction partners for an Aft-phase formation. The interface between aggregate and cement stone represents the reaction point of this formation. The consequences of this very new formation consist in an expansion linked with a diminution of strength. On the whole, the investigations that have been undertaken up to now put emphasis on the importance of keeping to the limit temperatures whenever producing precast concrete units being directly exposed to weathering.

ACKNOWLEDGEMENT

We are grateful to the Deutsche Forschungsgemeinschaft in Bonn for the financial support.

REFERENCES

(1) Ghorab H.Y., Heinz D., Ludwig U., Meskendahl T., and Wolter A.: On the stability of calcium aluminate sulphate hydrates in pure systems and in cements, 7th Int. Congr. Chem. Cem., Vol. IV, Paris 1980, p. 496-503

(2) Ludwig U., and Heinz D.: Einflüsse auf die Schadreaktion in wärmebehandelten Betonen, in: Baustoffe '85, edit. Inst. f. Bauforschung, RWTH Aachen, Wiesbaden/Berlin 1985, p. 105-110

(3) Mchedlov-Petrossyan O.P., et al: Thermodynamics of Silicates, Berlin/Heidelberg/New York/Tokyo 1985, Transl. of 4th edit., p. 309-310

(4) Kalousek G.L.: The reactions of cement hydration at elevated temperatures, Proc. 3rd Int. Symp. Chem. Cem. London 1952, Cement and Concrete Assoc., London, p. 334-355

(5) Aitken A. and Taylor H.F.W.: Steam curing of cement and cement-quartz pastes, Proc. 4th Int. Symp. Chem. Cem. Washington 1960, III-S.6, p. 285-290

(6) Copeland L.E., Bodor E., Chang T.N. and Weise C.H.: Reactions of tobermorite gel with aluminates, ferrites and sulfates, J. Res. Dev. Lab., Portland Cem. Assoc. 9 (1967) 1, p. 61-74, PCA Res. Bull. 211

(7) Odler I.:Interaction between gypsum and the CSH-phase formed in C_3S hydration, 7th Int. Congr. Chem. Cem. Paris 1980, Vol. IV, p.493-495

(8) Rehm G., and Zimbelmann R.: Untersuchung der für die Haftung zwischen Zuschlag und Zementmatrix massgebenden Faktoren, Dt. Ausschuss für Stahlbeton H. 283 (1977) p. 5-37

(9) Hoke E.: Die Charakterisierung des Korrosionsfortschritts im Beton durch Mikroanalyse von Grenzflächen, Berichtsband d. Int. Kolloq. "Werkstoffwissenschaften und Bausanierung", Techn. Akad. Esslingen, p. 187-194

4.2

THE INFLUENCE OF ALITE CONTENT ON THE SULFATE RESISTANCE OF PORTLAND CEMENT

THE INFLUENCE OF ALITE CONTENT ON THE SULFATE RESISTANCE OF PORTLAND CEMENT

Damijana Dimic and Stane Droljc, Institute for Testing and Research in Materials and Structures Ljubljana, Yugoslavia

SUMMARY

Six commercial Sulfate-resisting Portland cements with different mineralogical composition and one Ordinary Portland cement were investigated with regard to their sulfate resistance by the Koch-Steinegger method. It was found that C_3A and C_3S content in the cement are both of great importance for better resistance against sulfate attack, so that standard specifications for this type of cement should take into account the limit for the maximum C_3A content and the limit for the maximum C_3S content. It was suggested that our Standards Committee undertake the revision of the JUS B.C1.o14 standard.

Foram investigados seis cimentos portland comerciais resistentes ao sulfato, com composição mineralógica diferente e um cimento portland comum, utilizando-se o método de Koch-Steinegger com relação à sua resistência ao sulfato. Verificou-se que os teores de C_3A e C_3S são ambos grandemente importantes para melhor resistência ao ataque sulfático, de modo que as especificações padronizadas para este tipo de cimento devem levar em consideração o limite para teor máximo de C_3A e o limite para o teor máximo de C_3S. Sugeriu-se que nosso Comitê de Normas-Padrão faça a revisão da norma JUS B.C1.014.

INTRODUCTION

Durability of concrete structures is of a great importance and sulfate attack is one of the most well known forms of concrete deterioration. Therefore the choice of the corresponding materials plays an important role in preventing or at least minimising sulfate attack to ensure that concrete structures have an acceptably long durability.

Sulfate attack can be defined as a chemical or physical reaction, or both, between sulfates and cement paste matrix constituents.

Two basic chemical reactions between the cement and sulfate salt should be considered:

1) Formation of gypsum
2) Formation of ettringite

Both of these reactions results in an increase in solid volume.

Different types of cements have been developed with improved resistance against sulfate attack, such as portland cement with low C_3A content, portland cements blended with mineral admixtures like slag, pozzolana, silica fume, fly ash etc.

One of the very wide used cements for concretes with better resistance against sulfate attack is Sulfate-resisting Portland cement. Its main characteristic is a lower C_3A content; the limit is specified by standards and differs in different countries from a max. of 3,o % to 5,o % (1-4). Usually cements containing less than 3,o % to 5,o % of C_3A comply with the standard requirements and could be specified as *sulfate resistant*.

On the other hand, we have noticed that in practical situatíons some of our Portland cements that meet the C_3A requirement, and even the requirement for the sum of $C_4AF + 2C_3A$ (2) for Sulfate-resisting Portland cement, have showed very poor resistance to sulfate attack.

To throw some additional light on problems concerning the factors influencing sulfate resistance of Portland cement, the influence of alite content in Portland cement was studied.

MATERIALS

Six different commercial Sulfate-resisting Portland cements and one Ordinary Portland cement were tested.

The potential mineralogical composition calculated by Bogue is given in Table 1.

Table 1.: Chemical and Mineralogical Composition (calculated by Bogue) of the Cements (Percentage by Weight)

	Sulfate resisting Portland Cement						Ordinary Portland Cement
	A1	A2	A3	FI	GT	SI	PC
SiO_2	22.14	21.75	21.65	20.78	21.77	21.93	20.93
Al_2O_3	3,49	3.53	4.08	4.69	4.06	4.86	5.63
Fe_2O_3	3.56	3.52	4.31	5.10	5.32	5.14	2.72
CaO	66.82	65.34	64.58	62.53	63.93	61.20	63.97
MgO	1.45	1.52	1.54	2.89	1.24	2.31	1.81
SO_3	1.72	1.91	1.82	1.96	1.85	2.24	2.08
Insol.Res.	0.26	0.48	0.38	0.53	0.16	0.37	1.52
Loss on Ign.	0.58	0.72	0.73	0.68	0.86	0.82	0.94
Na_2O+undet.	0.98	1.23	0.91	0.84	0.81	1.13	0.94
Free CaO	1.21	0.62	0.53	0.60	1.15	0.72	0.72
$CaCO_3$	0.00	0.00	0.00	0.00	0.00	0.00	0.00
LSF	1.00	0.95	0.93	0.91	0.92	0.84	0.95
C_3S	77.0	66.5	59.6	52.2	54.6	36.1	57.8
C_2S	3.0	12.2	17.1	20.2	21.2	35.6	14.9
C_3A	3.7	3.4	3.5	3.8	1.8	4.2	10.3
C_4AF	10.8	10.7	13.1	15.5	16.2	15.6	8.3
$2C_3A + C_4AF$	17.7	17.5	24.1	23.1	19.8	24.0	28.9

According to some standard specifications, these cements could be classified as sulfate-resistant, as is shown in Table 2.

Table 2: Check on Compliance With Different Standard Requirements

Cement	Meats the standard specification requirements			
	JUS B.C1.014	ASTM: C150 Type V.	BS: 4027	DIN 1164
A1	yes	yes	yes	no
A2	yes	yes	yes	no
A3	yes	no	yes	no
FI	no	no	no	no
GT	yes	yes	yes	yes
SI	no	no	no	no

TEST METHOD

Sulfate resistance of cements was tested by the Koch-Steinegger method (5).

In this method the relative sulfate resistance of cements was assessed on 10 x x 10 x 60 mm mortar prisms, cured in water at 20° C for 21 days before exposure to 10 % w/v solution of $Na_2SO_4.10H_2O$ for 56 days. Sufficient prisms were prepared from each cement to allow ten prisms to be tested at the various ages after immersion. The cement mortar mix was made in the proportion of cement to sand (0.08 - - 0.5 mm) of 1 : 3, with a water to cement ratio of 0.6. The pH of the test solution was daily controlled by titration with 2N H_2SO_4 to the phenolphthalein endpoint, which at the same time gave data on the sulfate loss by the solution.These values represent the reactivity of cement with sulfate ions in the immersion solution, and could be used as one of the criteria for judging the relative sulfate resistance. The flexural and compressive strength of the test specimens were determined at the ages of 35, 49 and 77 days, and compared with water-stored controls.

RESULTS AND DISCUSSION

The results of strength are expressed as the percentage of flexural or compressive strength of the mortar prisms stored in the sulfate solution to those stored in water for the same period and are given in Table 3 and Figs. 1 and 2.

Table 3: Strength Expressed as Percentage of the Corresponding Strength After Storage in Water

Cement	Strength in % after storage in sulfate solution					
	Flexural			Compressive		
	14 d.	28 d.	56 d.	14 d.	28 d.	56 d.
A1	97	67	58	90	77	69
A2	98	70	63	96	80	70
A3	100	104	112	104	106	108
FI	145	103	103	117	118	127
TG	120	100	100	101	101	97
SI	137	105	98	122	118	112
PC	81	37	17	90	51	30

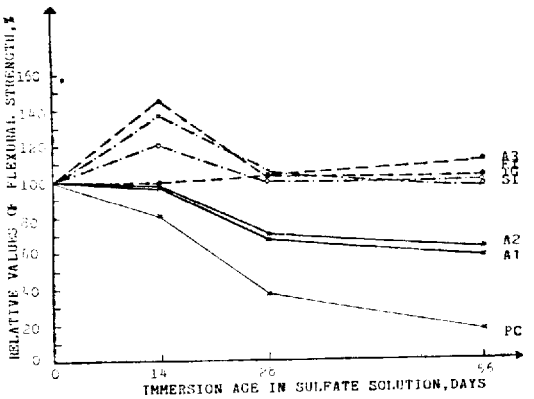

Fig.1 - Flexural strength of the prisms immersed in sulfate solution expressed as a percentage of water-stored prisms

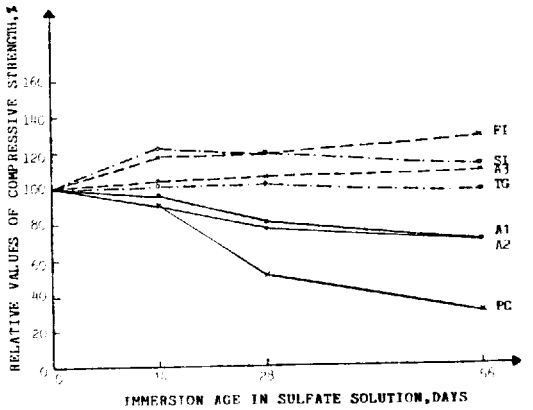

Fig.2-Compressive strength of the prisms immersed in sulfate solution expressed as a percentage of water-stored prisms

The consumption of sulfate ions from the test solution obtained by titration of the sulfate solution is given in Table 4 and Fig.3.

Table 4: Sulfate Consumption in ml 2N H_2SO_4 per one Prism Stored in Sulfate Solution

Cement	Consumption of 2N H_2SO_4 in ml/prism stored in sulfate solution for days					
	7	14	21	28	42	56
A1	1,40	2,21	2,80	3,30	3,98	4,58
A2	1,27	2,08	2,67	2,99	3,57	4,11
A3	1,03	1,69	2,19	2,50	3,09	3,48
FI	1,16	1,85	2,33	2,74	3,34	3,71
TG	1,09	1,34	1,52	1,77	2,15	2,48
SI	1,66	2,08	2,58	2,97	3,55	3,94
PC	1,43	2,34	3,08	3,79	5,26	6,30

In spite of the fact that the commonly known small-scale accelerated laboratory test methods do not give a good correlation with field experience, the results obtained allow us to evaluate the relative sulfate resistance of Portland cements with different C_3S contents.

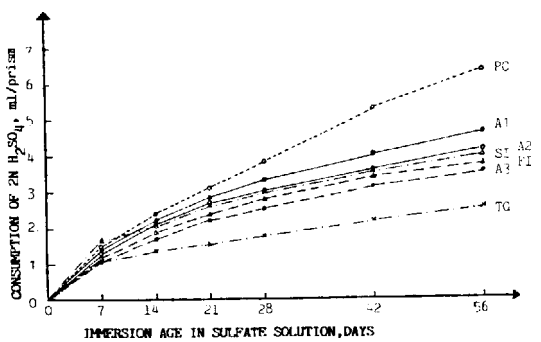

Fig.3-The reactivity of cements with sulfate ions expressed as a consumption of sulfuric acid by the titration of test solution

The results show that mortar prepared from Ordinary Portland cement with a high content of C_3A, as expected, significantly deteriorated in the sulfate solution. The flexural strength had fallen to 17 percent and the compressive strength to 3o percent of the water-stored prism strength, and also the sulfate consumption from the test solution was the highest. The effect of lower C_3A content is clearly seen in the comparative behaviour of the cements tested. Comparision of the results of six Sulfate-resisting Portland cements shows that the cements with relatively low C_3A content and with a C_3S content lower than 6o percent, could be declared as sulfate resistant only, while cements with a higher content of C_3S and at the same time a low C_3A content reacted more strongly with sulfate ions and showed a higher loss in strength. Both cements with a high content of C_3S strongly react with sulfate ions forming ettringite and gypsum, in contrast to the cements with lower C_3S, which contain significantly less gypsum at the end of the test. These data were obtained by X-ray analysis. The formation of these two reaction products in high quantities resulted in higher loss of strength. At the end of the test both Sulfate-resisting Portland cements with high C_3S content already showed small cracks at the surface of the prisms, Ordinary Portland cement was very badly cracked, whereas prisms made from cements with lower C_3S and low C_3A content were in sound condition.

CONCLUSION

On the basis of the test results and field experience, we could conclude that for better sulfate resistance of a Portland cement, the C_3S content is also an important factor, besides the C_3A content. Therefore we proposed that our Standards Committee revise the current Yugoslav standard for Sulfate-resisting Portland cement (4), JUS B.C1.o14, so that besides a maximum content of 3.5 % of C_3A, the maximum content of C_3S should also be limited.

Such cements will be better able to resist sulfate attack, especially the acidic type of sulfate attack, when a pure cement without pozzolanic materials will be used.

References

1. British Standard Specification for Sulfate-resisting Portland cement BS 4027-1980
2. American Society for Testing and Materials Standard Specification for Portland cement ASTM:C 150-81
3. Deutsches Institut für Normung DIN 1164-1978 Portland, Eisenportland, Hochofen- und Trass zement
4. Yugoslav standard JUS B.C1.014-82: Sulfate resisting Portland- and Portland blast furnace cement
5. A.Koch, H.Steinegger: A Rapid Method for Testing the Resistance of Cements to Sulphate Attack, ZKG 1960, Vol.13, No.7, pp 317-324

SUB-THEME/SOUS-THÈME 4.3

Compatibility of cement paste with aggregate and reinforcements, including electrochemical corrosion.

Compatibilité de la pâte de ciment avec les granulats et les armatures, y compris la corrosion électrochimique.

Chairman/Président:

R. Cigna
Facoltà di Ingegneria
Università di Roma
Roma, Italy

Principal Reporter/Rapporteur Principal:

R. Turriziani
Facoltà di Ingegneria
Università di Roma
Roma, Italy

Vl. Kadleček ; S. Modrý ; Building Research Institute, Prague, Czechoslovakia 1

Effect of degree of compatibility of cement and aggregates on concrete durability under conditions of higher temperatures action

Effet du degré de compatibilité du ciment et des granulats dans les bétons sur leur durabilité sous l'action de hautes températures. 4.3

SUMMARY: A model testing of the surface deterioration of concrete exposed to the repeated temperature action has been realized. For this purpose the concrete specimens prepared with two different types of aggregate - quartz and limestone and at the different moisture content have been examined.

For the evaluation of the extent of surface deterioration of cycled concrete specimens (temperature difference was. approx. 125 or 140°C resp. and the total number of temperature cycles 15) some test methods have been used. Changing of properties of concrete has been assessed by tensile splitting strength test, absorption and penetration of indication solution of sodium chloride on cubes and length changes (dilatation), ultrasonic velocity and pull-off strength on deteriorated surface of prisms.

Results obtained have shown pronounced structure deterioration of concrete in the surface layers after first several temperature loading cycles. Developement of deterioration was more intensive in the case of concrete with limestone aggregate and also was more pronounced in the case of partially humid concrete in comparison with fully saturated one. From the results was also evident that properties of quartz aggregates are more compatible on the contrary with limestone aggregates.

SUMÁRIO

Um modelo de ensaio da deterioração da superfície de concreto exposto à ação de repetidas temperaturas foi realizado. Para esse fim as amostras de concreto preparado com dois tipos de agregado quartzo e calcário e com diferentes unidades foram examinadas.

Para a avaliação da extensão da deterioração da superfície das amostras de concreto submetidos aos ciclos (a diferença de temperatura era aproximadamente de 125 ou 140°C e o número total de ciclos de temperatura 15) alguns métodos de ensaios foram usados. A mudança das propriedades do concreto foi avaliada em ensaio de tensão por compressão diametral, absorção e penetração de soluções indicadas de cloreto de sódio em cubos e variações de comprimento (dilatação), velocidade ultrasônica e resistência ao arrancamento na superfície deteriorada de prismas.

Os resultados obtidos mostraram uma pronunciada deterioração da estrutura do concreto nas camadas superficiais após os primeiros ciclos de várias temperaturas. O desenvolvimento da deterioração era mais intenso no caso de concreto com agregado calcário e também era mais pronunciado no caso de concreto parcialmente úmido em comparação com os completamente saturados. Pelos resultados foi também evidente que as propriedades do agregado de quartzo são mais compatíveis e ao contrário com agregado calcário.

1. INTRODUCTION

Rate of the surface deterioration of concrete in natural exposure under normal temperature and moisture conditions is usually very slow. That is reason for which it is useful to study the deterioration phenomen under more severe model conditions in laboratory. Results of such laboratory experimental project, which was realized a time ago are presented in this paper.

2. EXPERIMENTAL

The aim of the experimental programme was to determine the extent of surface deterioration, and, besides it, to compare the resistance of concretes with aggregates of different thermal expansion to the repeated action of high temperatures. For this purpose limestone and quartz were chosen as main representatives.

In all mixes of both investigated concretes the same aggregates grain size (36% of river sand 0-4 mm and 64% of granulated aggregate 4-16 mm) and the Portland cement PC 350 in the quantity 380kg/m^3 were used. Each part of mix was dosed according to its weight; at the same time the sand and granulated aggregate were precisely classified in the whole range of used grading. Details referring to the tested concrete mixes are given in Table 1.

TABLE 1

Composition and workability of concrete mixes

Mix	with limestone			with quartz		
W/C	D	A/C	Vebe	D	A/C	Vebe
0.38	La	5.06	45	Qa	5.01	41
0.43	Lb	4.92	14.5	Qb	4.88	14.1
0.48	Lc	4.79	7.2	Qc	4.75	7.1

W/C...water/cement ratio A/C...aggregate/cement ratio
D ...designation Vebe..workability in s

Tested specimens were cubes and prisms of sizes 100x100x100 mm or 100x100x300 mm respectively. Specimens were casted in steel moulds and compacted on the vibrating table. Up to the age of 28 days all specimens were cured in the water at the temperature 20°C and during following 21 days in the air with 65% RH. Then they were immersed in the water and kept there until the testing time; one of the prisms was kept permanently in the air with 65% RH. All tests were realized at the mean age of concrete - 60 days.

The influence of repeated high temperatures was modelled by heating of specimens in the muffle furnace followed by their instantaneous cooling. The individual cycles, repeated each hour, comprised the following steps, accordingly to the specimens curing:

cured in water

5 min furnace 550°C
30 min water 15
25 min air 20

cured in air

5 min furnace 550°C
5 min water 15
50 min air 20

Temperature gradient in concrete was indicated by thermocouples inserted in special cubes at five levels under the casted surface as follows: 0, 5, 10, 30 and 50 mm. The mean temperature differences at the cube surfaces reached in the course of cycles were: 125°C approx. in the case of water cured speciemens and 140°C approx. at the air cured ones.

Cubes were exposed to the action of 5, or 15 cycles. Then they were dried at the temperature of 105°C. The weighing and splitting strength testing was preceeded by their 30 min. immersing in the indication solution. After the splitting test the penetration of the indication solution into the deteriorated structure of cycled concretes was colorimetricaly determined. Results of all tests are graphicaly presented on the Fig. 1 - 4.

Prisms cured under different conditions were exposed to the action of 15 cycles. During the model experiments the surface dilatation changes were optically measured with the aid of catethometer. From the values measured the coefficient of thermal expansion was calculated (see Table 2).

In addition to the surface length changes pulse velocity was investigated in the direction of the longitudinal axis of prisms; these measurements were realized after 5, 10 and 15 cycles (in the center of cross section and in all its corners).

The extent of deterioration of exposed surfaces of cycled prisms was also assessed by pull-off test after non-destructive testing. At the top surface of prisms cores were partially bored (with diameter 50 mm and height 20 mm) on five places. These cores were than pulled-off from the surface layer with special equipment.

TABLE 2

Length changes and coefficients of thermal expansion on the prisms surface (mean values at final cycles)

W/C	Designation	Length changes x10^3 in mm/m		Coeff. of thermal expansion x10^6/°C	
		water	air	water	air
0.38	La	1.23	1.30	9.6	9.2
0.43	Lb	1.18	1.27	9.7	9.0
0.48	Lc	1.14	1.26	9.5	9.2
0.38	Qa	2.02	2.13	15.9	14.8
0.43	Qb	1.74	1.86	14.5	13.6
0.48	Qc	1.90	2.01	15.9	14.8

Determined values of pull-off strength influneced by concrete structure deterioration of exposed surface during the temperature shocks, were compared with pull-off strength of prisms, which were not cycled are given in the Table 3.

3. DISCUSSION OF RESULTS

Comparison of the obtained results shows great differencies in the sensitivity of the methods used for the investigation of gradual deterioration of structure of concrete surface exposed to the repeated temperature loading. By all tests methods an evident decrease of measured values after first cycles was proved.

The results reached from c u b e s testing verify the gradual changes (i.e. after 5 and 15 cycles of temperature loading) of investigated concrete properties; each value represents a mean value from the tests of 3 specimens.

Splitting strength (see Fig. 1) shows a steep decrease until the 5th cycle; then the decrease is comparatively easy. After 15 cylces the absolute values of the strength are practically same for both types of concrete. The strength decrease is more markedly pronounced for the concrete with limestone aggregates if expressed in percents.

Absorption (see Fig. 2) was assessed by weighing of cycled and dried cubes (for comparison a set of noncycled specimens was dired similarly) after their immersing in the indication solution for 30 min. The absorption increase indicates more obvious structure deterioration for the concrete with limestone aggregates if the weight differencies are expressed in percents.

Penetration of indication solution (see Fig. 3 and 4) into the deteriorated structure of temperature loaded concretes was determined by measurement of area colored with the aid of indication solution on the fresh fracture surfaces (after tensile splitting strength test). Similarly, as results of absorption values penetration data show more intensive deterioration of structure of concretes prepared with limestone aggregates.

The tested p r i s m s were exposed to the action of temperature loading similarly as cubes. Their foregoing different curing (for each type of concrete one prism was kept in water and another in air), made possible to evaluate also the effect of different moisture content on the deterioration of investigated concretes.

Length changes (see Table 2) measured on the surface of cycled prisms show more negative effect of lower moisture content in concrete on their magnitude.

Ultrasonic pulse velocity /1/ allows a continuous investigation of concrete deterioration on the same specimens. Also, in this case an evident decrease of measured values after early cycles appeared. The concretes with quartz show a greater relative decrease of pulse velocity values, nevertheless, the deterioration of surface layer of concretes with limestone aggregates is more pronounced in the case of the air curing.

TABLE 3

Test results of tensile splitting - 0_{bs}, direct tensile - 0_{br} and pull-off - 0_{bp} strength

Strength values N/mm^2	Designation of tested concretes					
	La	Lb	Lc	Qa	Qb	Qc
0_{bs} (100x100x100 mm)	6.20	6.16	5.53	5.11	4.93	4.22
0_{br} (100x100x400 mm)	4.01	3.64	3.37	3.22	3.01	2.91
0_{bp} (ø 50 mm, h=20 mm)						
noncycled	3.85	3.70	3.45	3.14	3.02	2.94
15 cycles-water	1.46	1.62	1.47	1.28	1.31	1.21
15 cycles-air	1.48	1.55	1.62	1.48	1.40	1.48

The values of pull-off strength of prisms (see Table 3) assessed after the end of temperature loading indicate the great decrease in comparison with strength values of noncycled sepcimens. This test method itself is evidently lesser sensitive to the different state of deterioration of exposed surface and different curing conditions of investigated prisms.

4. CONCLUSIONS

From the results of realized model testing of both concrete types exposed to temperature loading follows better performance of concrete with quartz aggregate (i.e. aggregate with higher thermal expansion) and, as well as, in fully saturated state. Finaly, the used test methods show different sensitivity for evaluation of the extent of deteriorated structure of exposed concrete surface.

BIBLIOGRAPHICAL REFERENCE

Kadleček, Vl., Modrý, S., (1974), IInd RILEM Intern. Symposium New Developments in Non-Destructive Testing of Non-Metallic Materials (Constanta), INCERC Bucuresti, Concrete Deterioration Under Action of High Repeated Temperature. Vol. II, pp. 223-228. English.

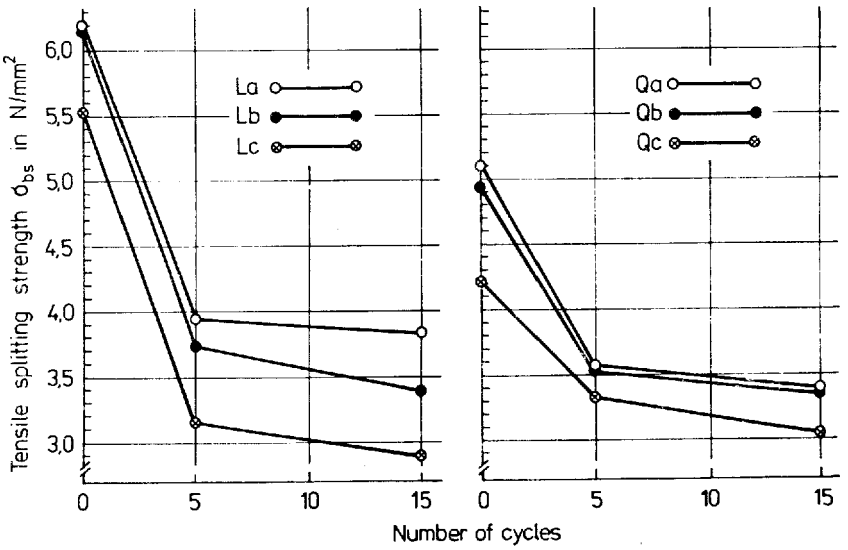

Fig.1. Relationship between tensile splitting strength of temperature loaded cubes and number of cycles

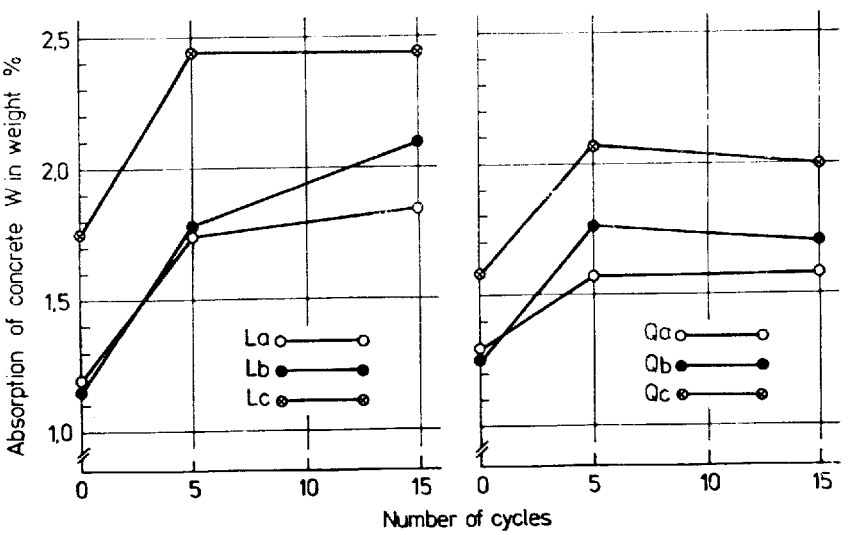

Fig.2. Relationship between absorption of indication solution into the deteriorated surface of temperature loaded cubes and number of cycles

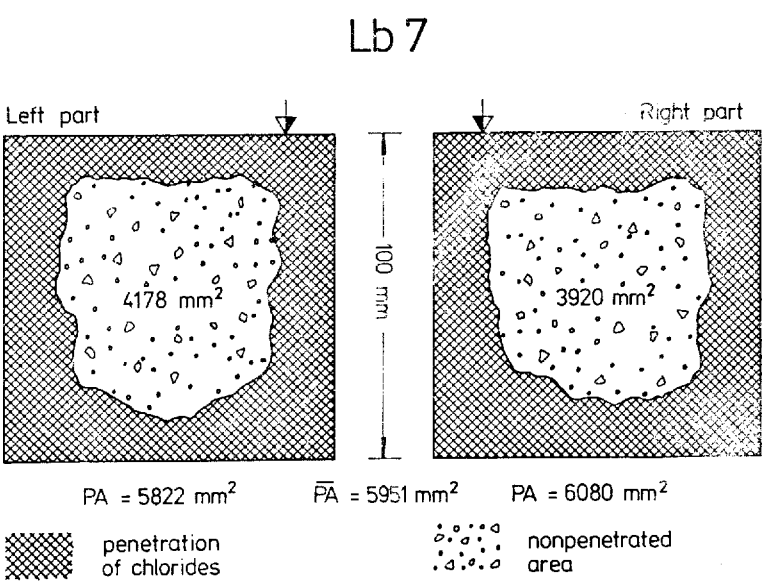

Fig.3. Evaluation of penetration area of indication solution into the deteriorated surface of temperature loaded cubes

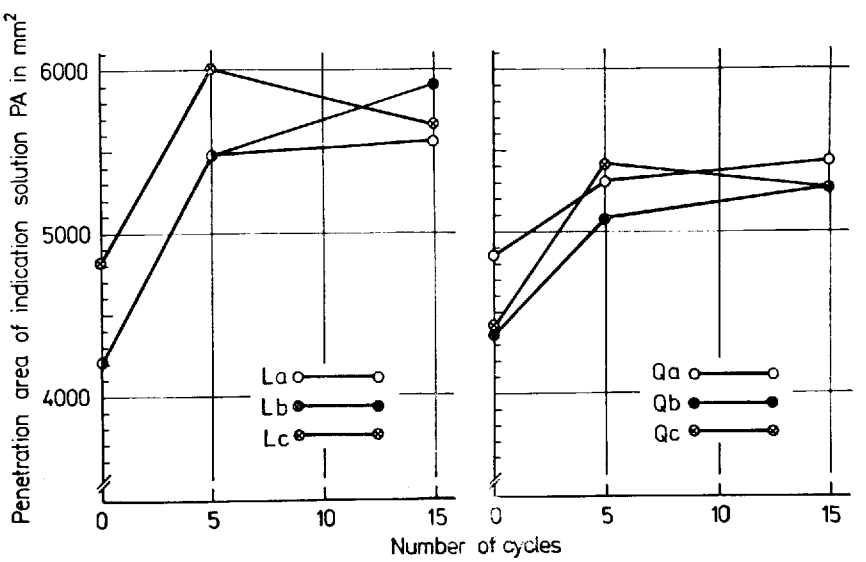

Fig.4. Relationship between penetration area of indication solution into the deteriorated surface of temperature loaded cubes and number of cycles

H.C. Visvesvaraya, A.K. Mullick, George Samuel, S.K. Sinha, R.C. Wason
National Council for Cement and Building Materials,
M-10, N.D.S.E. Part - II, New Delhi - 110 049, India.

Alkali Reactivity of Granitic Rock Aggregates

4.3

ALCALI-VARIATION AVEC GRANULATS GRANITIQUES.

SUMMARY: Compatibility of siliceous aggregates with the alkalies in cement has been an important factor in durability of concrete. In addition to conventional reactants like opal, chert, chalcedony or volcanic glasses, it is now held that presence of "strained" quartz in siliceous aggregates could also cause alkali silica reaction (ASR). This paper presents the results of an investigation of ASR in concrete containing granitic aggregates, possible mechanisms of deleterious reaction and its impact on cement specifications.

Granite aggregates in a 25 year old concrete gravity dam contained mainly quartz and alkali feldspars, with varying quantities of biotite and muscovite, 50-80% of quartz showed strain effect with undulatory extinction angle of 25-30°. Alkali feldspars included orthoclase, plagioclase, microline and microline - perthite.

The dam manifested typical external signs of distress associated with ASR. SEM and EDAX studies revealed the predominant presence of alkalies in the reaction rims on aggregates altering their borders, which consisted of fluffy, amorphous gel formation. Occasionally the reaction products were crystalline. The presence of typical white gel deposits in the concrete was less frequent.

In addition to the presence of strained quartz, the role of alkali feldspars were investigated. Microscopic studies indicated the alteration of alkali feldspars to clay minerals and sericite. XRD studies confirmed changes in the crystal structure and mineral composition.

These results tend to support the hypothesis that alkali feldspars can themselves release alkalies in the presence of calcium hydroxide to participate in ASR. Should that be the case, merely stipulating a low alkali level in the cement may not be adequate anddepletion of calcium hydroxide would assume importance. The role of modified cement compositions in alleviating ASR, which release little or low calcium hydroxide on hydration, is discussed in the paper.

Simário

A compatibilidade dos agregados silicosos com os alcalis do cimento têm sido um importante fator na durabilidade do concreto. Alem dos reagentes convencionais como a opala, calcedonia ou vidros vulcânicos, é agora considerado que a presença do quartzo "deformado" nos agregados silicosos pode também causar reação alcali silica (ASR). Este trabalho apresenta os resultados de uma investigação de ASR em concreto contendo agregado granítico, a possível mecanismo de reação deletéria e seu impacto nas especificações de cimento.

Agregado granítico de um antigo concreto com 25 anos de idade de uma barragem de gravidade continha principalmente quartzo e feldspatos alcalinos, com quantidades variáveis de biotita e muscovita. 50-80% do quartzo apresentou efeito de deformação com ângulo de 25-30° de extinção ondulatória. Os feldspatos alcalinos incluem ortoclave, plagioclase, microclina' e pertita-microclina e pertita-microclina.

A barragem manifestou sinais típicos externos de alterações associadas a ASR. Estudos com SEM e EDAX revelou a presença predominante de alkalis na reação nos bordos dos agregados alterando seu contorno, que consistiu sua formação de um gel amorfo. Ocasionalmente os produtos da reação eram cristalinos. A presença do depósito típico do gel branco no concreto foi menos freqüente.

Além da presença de quartzo distendido, foi investigado o papel dos feldspatos alcalinos. Estudos microscópicos indicaram a alteração do feldspato em argilo minerais e sericita. Estudos por XRD confirmaram as mudanças na estrutura do cristal e na composição mineral.

Esses resultados tendem a apoiar a hipótese que os feldspatos alcalinos podem eles mesmo liberar alcalis em presença do hidróxido de cálcio para participar na ASR. Se esse for o caso, a fixação meramente de baixo nível de alcali no cimento não pode ser adequada e a redução do hidróxido de cálcio assumiria importância. O papel da composição modificada do cimento, em reduzir a ASR, que libera pouco ou baixo hidróxido de cálcio na hidratação, é discutido neste trabalho.

INTRODUCTION

The deleterious reaction of silica bearing aggregates with the alkalies, mainly derived from cements have been known to be a matter of concern for the durability of concrete structures exposed to moisture. The primary cause of alkali silica reaction (ASR) due to the presence of secondary silica minerals like opal, chert, chalcedony or volcanic glasses in certain siliceous aggregates have been known for nearly four decades (1). Of more recent concern are the instances where aggregates exhibited ASR due to the presence of "strained" quartz (2, 3, 4). Because of the processes of geological formations, presence of some amount of strain effect in the quartz lattice will be inevitable, specially in metamorphic rocks and efforts have been made to set the limits of quartz in the rocks showing such strain effects and the magnitude thereof, expressed in terms of undulose extinction (UE) angle (2, 5).

Granitic rocks were generally believed to be more stable and sound where the proportions of quartz are also lesser than in, say, quartzite. However, recent instances of distress to concrete structures due to ASR containing granite, granodiorite or granitegneiss rock aggregates have, on the one hand, blown this myth and on the other, led to speculations whether in addition to strained quartz the presence of alkali feldspars could have also been responsible for ASR. This paper presents results of investigations relating to occurence of ASR in concrete containing such granitic rock aggregates, possible role of alkali feldspars and some suggestions for appropriate cement compositions to combat ASR.

CASE STUDY

A concrete gravity dam and the adjacent power house structure of a hydroelectric project have shown extensive distress within 25 years of construction, which have been ascribed to ASR. External manifestations included cracking of concrete, misalignment of machineries and difficulties in operation of gates, cranes and passenger lifts as a sequel to movements in concrete.

On visual examinations the crushed surface of concrete core samples showed presence of dark reaction rims altering the borders of aggregates, often with internal cracking (Fig. 1). Typical off-white, transluscent to opaque gels were present in voids or on aggregates, but their presence was less frequent than conventionally reported (6). Examinations under scanning electron microscope (SEM) with the energy dispersive analysis of X-rays (EDAX) revealed the reaction rims on aggregates altering their borders consisting of fluffy amorphous gel formation and containing significant amount of alkalies (Fig. 2). Occasionally the reaction products were found to be crystalline in nature (Fig. 3), but the EDAX spectra were similar.

Petrographic examination of aggregates extracted from concrete samples indicated these to be mainly biotite granite, muscovite granite and mica granite. In each of these rocks, quartz varied from 32 to 45 percent and alkali (sodium-potassium or sodium-calcium) feldspars like orthoclase, microcline and plagioclase from 35 to 45 percent with varying amounts of biotite and muscovite and other accessories including iron ore, chlorite, apatite, etc.

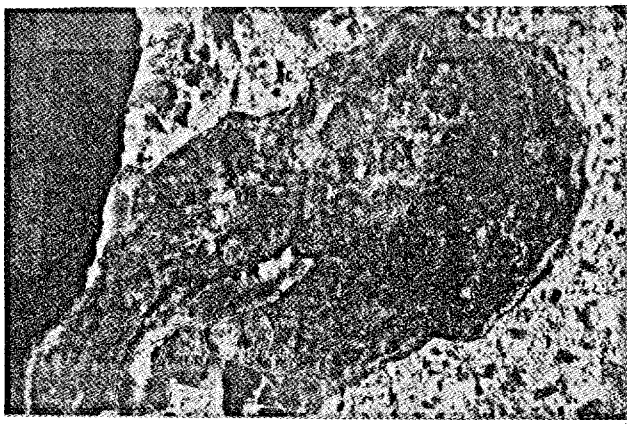

Fig. 1 : Dark reaction rim and internal fracture in the aggregate.

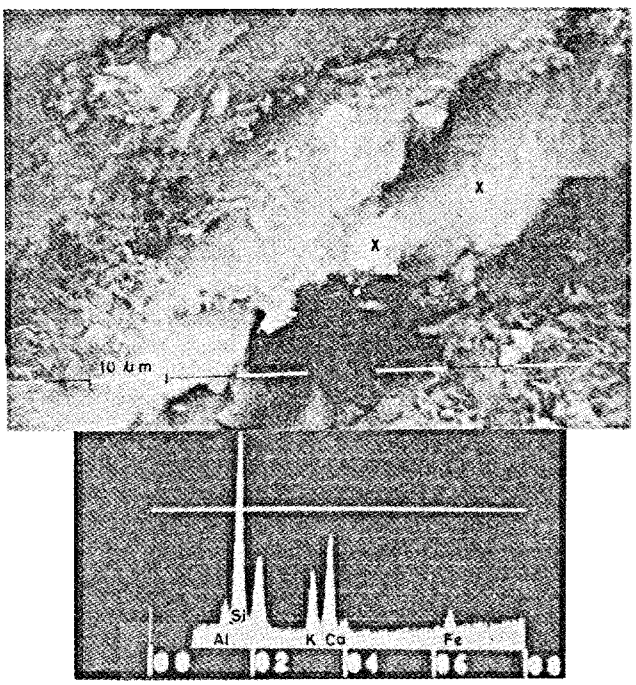

Fig. 2 : SEM of fluffy gel formation in the reaction zone and EDAX spectrum from the point marked X

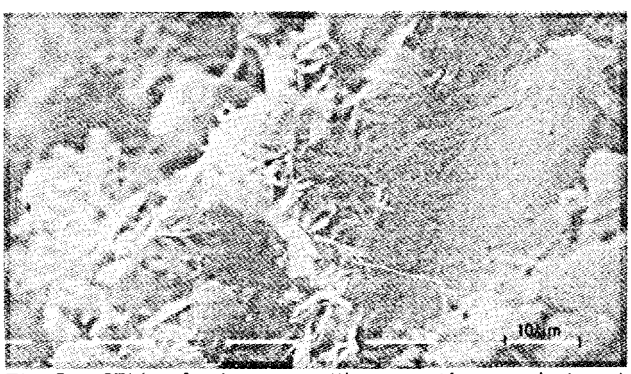

Fig. 3 : SEM of the crystalline reaction products at the edge of an aggregate.

The average grain size of quartz varied from 0.10 to 0.20 mm, with small grains upto 0.03mm in some cases and large grains upto 0.45mm in others. Nearly 50-80 percent quartz exhibited strain effect with UE angle varying from 25 to 30° (Fig. 4).

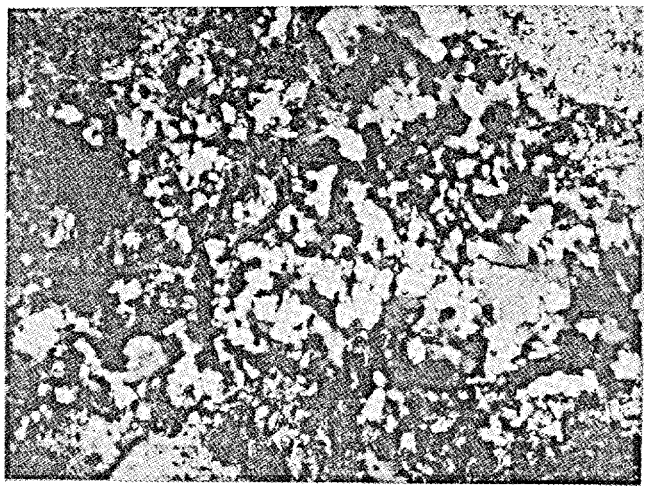

Fig. 4 : Quartz grains showing undulatory extinction.

Potash feldspar in most of the cases was orthoclase which was found to have altered to sericite (Fig. 5).

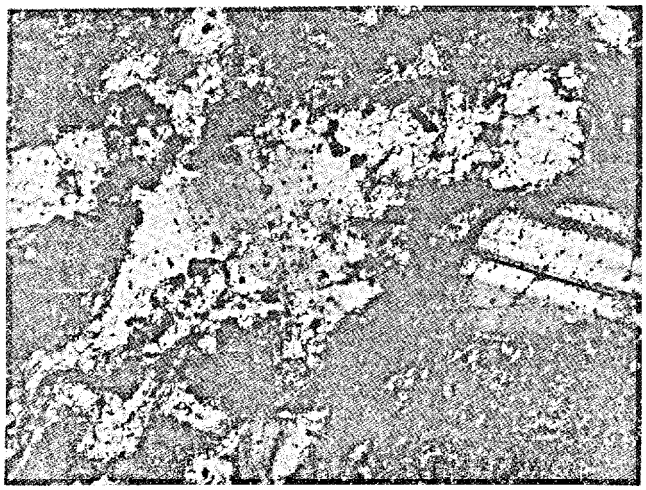

Fig. 5 : Alteration of feldspar to sericite

Plagioclase feldspars were found to have altered to clay minerals (Fig. 6). Biotite occured in the form of laths

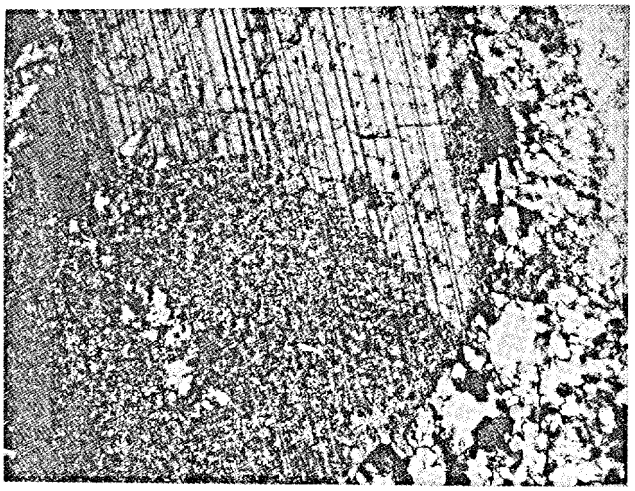

Fig. 6 : Alteration of feldspar to clay minerals.

and sometimes with sheath-like structures. These and muscovite showed bending effect. The normal granitic texture of the aggregate was highly disrupted due to high degree of alteration of minerals.

INVESTIGATIONS ON THE ROLE OF FELDSPARS

In the context of ASR the alkalies from cement are mostly talked of. However, for the reactions to proceed alkalies can similarly be derived from the environment or even the aggregates themselves (7). Alkali feldspars are known to be very apt to undergo alteration from the action of hydrothermal solutions and from the normal processes of weathering. Decomposition products commonly include kaolinite, halloysite, sericite, quartz or gibbsite (8). Comprehensive laboratory experiments by Van Aardt and Visser had postulated that alkali feldspars can release alkalies in presence of CH and water (9, 10, 11). The feldspars in the aggregates extracted from concrete did show alteration to sericite and clay minerals; however, how much of such alterations had indeed taken place in the presence of CH liberated in the concrete was difficult to establish.

Since samples of aggregates used at the time of construction were not available, representative samples from one of the quarries at the dam site were obtained. Petrographic examination revealed the granite aggregate showing inequigranular texture. The main constituents of the rock were quartz (39 percent), alkali feldspars (44 percent) and biotite (7 percent). Accessories included muscovite and iron ore. The potash feldspars were perthitic showing alteration to kaolinite (Fig. 7). However, the degree of alteration on an integral point count was less than in aggregates extracted from concrete.



Fig. 7 : Potash feldspar - Perthite showing alterations; quarry sample.

A typical X-ray diffractogram (Cu K-α radiation) of the quarry sample is shown in Fig. 8 (a); showing the presence of quartz, albite, muscovite and traces of chlorite, in that order of abundance. Contrasted to that, a typical X-ray diffractogram of the aggregates extracted from the concrete (Fig. 8 (b)) showed additional presence of anorthoclase as well as other peaks at 3.47, 3.87, 4.96 A° etc., corresponding to sodium silicate ($Na_2Si_3O_7$) (12). Chemical analysis showing the alkali content in the rock is presented in Table 1. Although the trend was somewhat erratic, alkalies as Na_2O in the aggregates extracted from concrete were in general lower than those of quarry rocks; the trend was reversed in the case of K_2O.

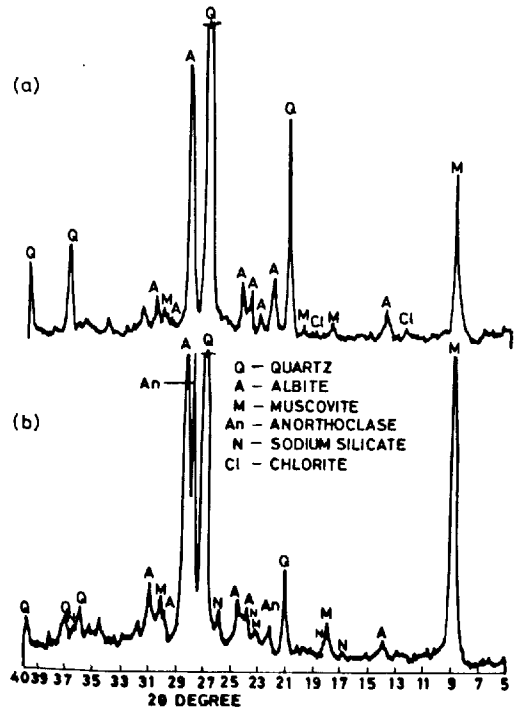

Fig. 8 : X-ray diffractograms of (a) quarry, sample and (b) aggregate extracted from concrete.

TABLE - 1

ALKALI CONTENT IN ROCKS

Source	Sample No.	Na_2O	K_2O
Quarry	1	2.92	2.21
	2	2.41	1.47
Concrete Cores	1	0.58	3.51
	2	2.86	4.37
	3	1.76	1.74
	4	2.48	4.50
	5	1.43	6.62
	6	1.21	3.85

DISCUSSIONS

The reactivity of alkali feldspars to CH in presence of water have been established (9, 10, 11, 13). In the present investigations, although the release of alkalies from feldspars under situations in mass concrete could not be firmly established, the general reactivity of alkali feldspars in the presence of cement and water were fairly conspicuous, both from petrographic and X-ray diffraction studies. Perhaps the situation can be summed up by the SEM of the concrete aggregate sample shown in Fig. 9 (a), which, in the continuum of silica-bearing crystalline phase (Fig. 9 (b)) shows subsequent formation of alkali-rich amorphous phases (Fig. 9 (c)). In view of the above, in addition to limit of alkali content in cement, the role of CH liberated by the hydration of cements would assume importance in the context of granitic rocks containing alkali feldspars.

The role of active siliceous pozzolan and hydraulic slags have been advocated for alleviating ASR. In addition to lowering the total soluble alkali content in the concrete to the extent cement is replaced by these additives, they also combine with the CH liberated during the hydration of cement. It has been reported that if the CH liberated can be fully consumed by large proportions of slags, ASR would not take place (14).

In the context of above, modified cement compositions having no C_3S phase (15) or lower amount of C_3S phase (16) merit consideration. In these cement systems, the amounts of CH liberated upon hydration are considerably lower (Fig. 10). Use of such cements with known reactive aggregates are presently under investigation and the results will be reported subsequently.



b

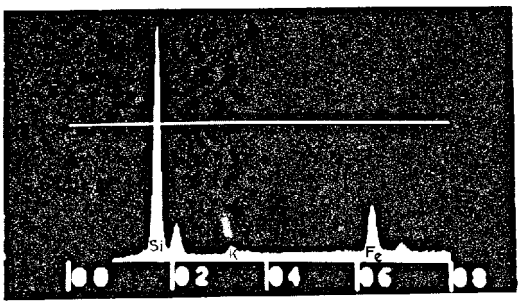

c

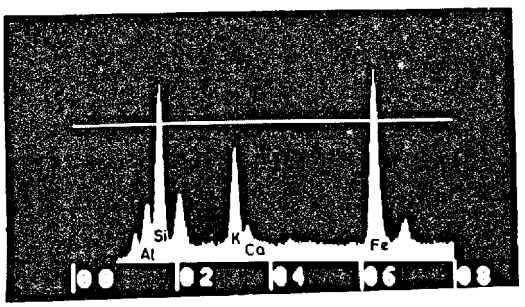

c

Fig. 9 :
Alteration of granitic aggregate (a) Typical Scanning Electron Micrograph, (b) EDAX of point marked X and (c) EDAX of point marked o.

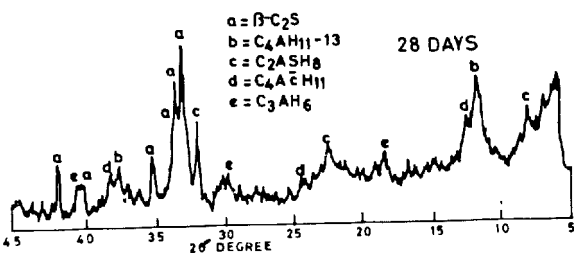

Fig. 10 : X-ray diffraction pattern of hydrated pastes of Porsal cement.

CONCLUSIONS

Alkali-reactivity of granitic rock aggregates containing alkali-feldspars and quartz showing strain effects was found responsible for widespread distress to a concrete dam. Investigations with opitical microscopy, XRD and SEM indicated considerable alteration of feldspars and microstructural modifications, possibly brought about in the presence of calcium hydroxide. Use of modified cement compositions which release little or no CH on hydration, are discussed.

ACKNOWLEDGEMENTS

This paper is based on the R&D work carried out at the National Council for Cement and Building Mateials. The authors have freely drawn upon the unpublished reports and results available with the Council. The paper is published with the permission of Chairman and Director General NCB.

REFERENCES

1.- L.H. TUTHILL (1982), "Alkali silica reaction - 40 years later", Concrete International, Design and Construction, 4, 32-36.

2.- L. DOLAR-MANTUANI (1983), "Handbook of Concrete aggregates, A petrographic and technological evaluation", Noyes Publication, NJ USA, 79-125.

3.- GEORGE SAMUEL, A.K. MULLICK, S.P. GHOSH and R.C. WASON (1984), "Alkali silica reaction in concrete - SEM and EDAX analyses", Proc. VI International Conf. on Cement Microscopy, Albuquerque, New Mexico, USA, 276-291.

4.- A.K. MULLICK, GEORGE SAMUEL and S.N. GHOSH (1985), "Indentification of reactive concrete aggregates containing strained quartz by SEM and IR", VII International Conf. on Cement Microscopy, Fort Worth, Texas, USA.

5.- A.D. BUCK (1983), "Alkali reactivity of strained quartz as a constituent of concrete aggregate", Cement, Concrete and Aggregates (ASTM), 5(2), 131-133.

6.- B. MATHER (1975), "New concern over alkali aggregate reaction", NRMCA Publication No. 149.

7.- H.E. VIVIAN (1975), "Alkali aggregate reaction", Symposium on Alkali-Aggregate Reaction, Preventive Measures, Reykjavik, 21-34.

8.- W.A. DEER, R.A. HOWIE and J. ZUSSMAN (1967), "Rock-forming minerals, Longmans, Green and Co. Ltd., 4, 54-55.

9.- J. H.P. VAN AARDT and S. VISSER (1977), "Formation of hydrogarnets : Calcium hydroxide attack on clays and feldspars", Cem. Concr. Res., 7, 39-44.

10.- J.H.P. VAN AARDT and S. VISSER (1977), "Calcium hydroxide attack on feldspars and clays : Possible relevance to Cement-aggregate reactions", Cem. Concr. Res., 7, 643-648.

11.- J.H.P. VAN AARDT and S. VISSER (1978), "Reaction of $Ca(OH)_2$ and of $Ca(OH)_2$ + $CaSO_4$.$2H_2O$ at various temperatures with feldspars in aggregates used for concrete making", Cem. Concr. Res., 8, 677-682.

12.- Joint Committee on Powder Diffraction Standards (1974), Powder Diffraction File No. 18-1240.

13.- S.J. WAY and W.F. COLE (1982), "Calcium hydroxide attack on rocks", Cem. Concr. Res., 12, 611-617.

14.- S. CHATTERJI and N.F. CLAUSSON - KAAS (1984), "Prevention of alkali-silica expansion by using slag-portland cement", Cem. Concr. Res., 14, 816-818.

15.- CEMENT RESEARCH INSTITUTE OF INDIA (1979), "Exploratory investigations on 'Porsal' a new cement", Research Bulletin, RB-11-79.

16.- S.N. GHOSH (1985), "Hydration of Polymorphs of dicalcium silicate", Il Cemento, 3, 139-146.

M.ARPAIA, Dept. of Materials and Production Eng., Univ. Naples, Italy
R.CIGNA, R.TURRIZIANI, Dept. ICMMPM, Univ. Rome 'La Sapienza', Italy

4.3 Corrosion Behaviour of TAD, Diffused Reinforcement Concrete Tubes

Summary: Several tests were carried out, under severe conditions, with samples taken by a one diameter concrete tube with diffused reinforcement, in order to evaluate the corrosion behaviour of the embedded steel.
The tests environments were tap water, magnesium chloride and sodium chloride solutions, sand containing NaCl solution, clay and sand.
The corrosion determination methods were the corrosion potential measurement, the polarization resistance or corrosion rate CR determination, and visual observations.
The results of experiments of over approximately two years showed that with the "as received" specimens, even with a rather small concrete cover (0.5 cm), no corrosion phenomena were observed at all, probably due to the low porosity of the artifact; in presence of scratches artificially made over the external surface in order to simulate an erroneous handling of the pipe, it was observed that the corrosive attack remained strictly localized in the part of the wires directly in contact with the aggressive environment, and did not propagate into the concrete.
Moreover, in presence of soils with different permeability (sand and clay) the results of the tests showed again the good corrosion behaviour of the reinforcement.

Sumário

Vários ensaios foram realizados, sob severas condições, com amostras tiradas de tubos de concreto de 1m. de diâmetro com armadura distribuída, de modo a avaliar o comportamento da corrosão do aço embutido. Os elementos dos ensaios foram água, soluções de cloreto de magnésio e cloreto de sódio, areia contendo NaCl em solução, argila e areia.

Os métodos de determinação da corrosão foram de medida da corrosão potencial, da resistência de polarização ou determinação da taxa de corrosão CR e observação visual.

Os resultados dos ensaios após aproximadamente dois anos mostraram que as amostras "como recebidas", mesmo com um pouco pequeno recobrimento (0,5 cm), nenhum fenômeno de corrosão foi observado, provavelmente devido à baixa porosidade do artefato; em presença de ranhuras feitas aritificialmente sobre a superfície externa de modo a simular um manejamento errôneo do tubo foi observado que o ataque corrosivo permaneceu estritamente localizado nas partes em que vergalhões estavam diretamente em contato com o ambiente agressivo e não se propagou ao concreto.

Além do mais, em presença de solos com diferentes permeabilidades (areia e argila) os resultados dos ensaios mostraram novamente, o bom comportamento à corrosão das armaduras.

Introduction

The corrosion behaviour of steel embedded in concrete is alleged to be very good, due to the passivity given to it by the alkaline environment which forms after the clinker components hydration processes (1,2).

Therefore reinforced concrete pipelines, like the other structures in civil engineering, should be, and usually are, sufficiently safe, from the point of view of the corrosion phenomena concerning the reinforcement.

Unfortunately many failures have recently occurred, either because of incorrect design and manufacturing, or because ot the strong aggressivity of the environment, with consequent relevant costs, whose magnitude has been adequately underlined (3,4); several preventive countermeasures may therefore be suggested whenever the possibility of steel depassivation is forecast (3,5-8). The main factors which may influence the iron passivation in concrete are carbonation, due to carbon dioxide penetration, and chlorides action. In both cases it has been strongly recommended that a suitable workmanship of the mix should be performed, in particular as far as its porosity and its permeability are concerned (9).

The TAD, diffused reinforcement concrete tubes, are fabricated in such a way as very dense concrete is obtained, usually with a rather thin cover (10). Maximum aggregate dimension is 3mm, cement content is 650 kg/m^3, water/cement ratio is 0.3; the cover of the pipe used in this experimentation is 0.5 cm. The use of such pipes for water transportation is spreading rapidly, even if their reinforcement corrosion behaviour has not yet been studied in depth.

TAD is a "new material" as far as the corrosion behaviour is concerned: it was therefore believed necessary to conduct an in-depth investigation in various experimental conditions. The experimentations started about two years ago and are still continuing.

Experimental

Several specimens (15 cm diameter; 5.5 cm thickness) were obtained by coring from a TAD tube 1m diameter and 5.5 cm thickness.

The specimens were utilized for the following experimentations:

- A - exposure of "as received" specimens to various environments, for a long period of time;
- B - exposure to various environments of specimens with artificial scratches on the external cover, made in order to leave bare some superficial wires;
- C - exposure to soils of scratched specimens prepared in order to measure the current of the corrosion couple generated between bare wires and concrete covered wires.

Fig. 1 shows the typical configuration of the specimen arrangement. A few wires, disposed on three parallel layers along the specimen thickness, were partly liberated from concrete in order to allow electrical measurements on superficial wires (S), medium wires (M) and deeper wires (D).

Type A investigation was carried out through a period of six months with the adoption of both traditional measuring techniques (spontaneous corrosion potential measurement, visual examination), and electrochemical techniques (polarization resistance, or CR, and polarization curve determination).

The selected environments were the following:

1. Tap water
2. 35 g/l sodium chloride solution
3. 10% magnesium chloride solution
4. River sand humidified with sodium chloride solution

12 specimens were used for each environment: i.e. 3 for each type of measurement. Measurements of spontaneous potentials (E_{corr}) and corrosion rate (CR) were made on S, M, D wires.

E_{corr} was measured utilizing a Digital Voltmeter (Schlumberger, type 1240 20 Mohm) and a saturated calomel electrode (SCE) immersed in the env nment for 1 cm. CR was measured with Atel corrosion meter

(Type AP 101) that utilizes galvanostatically measured linear polarization resistance.
Polarization curves were obtained with an Amel potentiostat Mod. 550. All reported results are the mean of three determinations.
At the end of the testseveral specimens were crushed to permit visual inspection of wire surface.
Type B investigation was carried out to simulate damages caused by transport and lay-down.
Scratches were made on concrete surface of some specimensin such a way that they left bare some superficial wires. These specimenshave been exposed to the aforesaid environments in order to verify whether corrosion of bare superficial wires can, in some way, influence deeper wires and whether the expansive nature of corrosion products at extremities of bare wires can far exceed the tensile strenght of concrete, thus causing further cracking of cover and further attack of wires.
The measurements techniques adopted in this case are the same as in the A type.
Type C investigation was carried out to study the corrosion couples that scratches generate in soils.
The bare surface of wires exposed the soils is affected by both the corrosive action due to intrinsic physical and chemical parameters of the soil (absolute corrosivity) (11) and that due to the couple generated between the bare surface of wires directly exposed to the environment and that of the same wires covered with concrete.
Specimens assembly is showed in fig. 2. In the A portion of the specimen one scratch left bare a small lenght of one wire (2 cm) whilst the concrete cover was sealed with waterproof silicon layer.
The insulating separator T allowed to measure short circuit current couple, with a null ammeter coupled with the superficial wires of A and C parts of specimen. Experimentation was carried out at air controlled relative humidity (95%) and temperature (20°C). Mixed potentials of the couple were measured with the aforesaid technique.

Results and discussion

Influence of the environment (Type A investigation)
Wires of specimens exposed at various environments exhibit throughout the exposure time (6 months) spontaneous potentials E_{corr} in a range of -0,16 - -0,030 volt (SCE).
Fig. 3 shows the diagram of E_{corr} of wires vs. time; Table 1 reports E_{corr} and CR values at 180 days of exposure. Experimental evidence indicates that, for each specimen, wires at higher position exhibit E_{corr} values slightly more negative than those of wires at medium and lower positions; for sake of simplicity fig. 3 reports only the potentials of superficial and deeper wires.
For steel in concrete (pH > 12), passivity is reached at potentials more positive than -0,14 V SCE (- 0,38 V SCE) (12,13). In all environments tested E_{corr} values are always more positive than - 0,38 V SCE, which means that wires surface is in any case passivated.
The low values of CR confirm this conclusion, corrosion rates being typical of passivated steel.
Fig. 4 shows a typical polarization curve that presents the plateau on anodic side.
Visual inspection of wires after the crush of specimens showed that in any case S, M and D wires were unattacked.
The behaviour of wires is scarcely influenced by the environments containing chlorides. That means that the concrete cover, in spite of its low thickness, insures,at least for the experimentation time, in those environments, for the top wires too, a chloride/ /hydroxyl ion molar activity ratio at steel concrete interface lower than 0,6, value recognized as a threshold for destroying the passivity of steel in presence of chlorides at the steel/concrete interface (14). The experimentation is still continuing to confirm in longer time exposure these results.
Influence of concrete cover scratches (type B investigation)
Table 2 summarizes the results of E_{corr} and CR

measured throughout 90 days. Bare wires exhibit typical potentials and corrosion rates of active steel, whilst those of M and D wires are typical of passive state. The steady state value of CR for bare wires is reached after 60 days.

Visual ispection has shown that corrosion attack was strictly localized on the bare surface ot the wires, whilst the surface still protected by the concrete cover was unattacked.

This behaviour is to ascribe to the concrete compactness and its high resistance to diffusion of aggressive ions assured by high cement content and low w/c ratio (15).

Couples generated by scratches (Type C investigation)

The corrosion rate due to specific soil corrosivity is negligible compared to that due to the couple. It has therefore been considered to be only the action of couple.

Fig. 5 shows corrosion current (I_c) of the couple for both specimens (type C, fig. 2) exposed to clay and sand. The rate of attack is markedly reduced after 42 days at 20% of the initial value. The anodic steady state currents density are: for specimens exposed to sand 8 $\mu A/cm^2$ (mean corrosion penetration rate of 0.08 mm/years); for those exposed to clay 4 $\mu A/cm^2$ (0.04 mm/y).

In few years the bare wires should be destroyed, but the corrosion attack being, in this case too, restricted to the bare area, whilst that one covered results unattacked, the corrosion process does not further propagate, as confirmed unequivocally by wires visual inspection of specimens crasched after exposure.

For both clay and sand specimens, mixed potential of the couple E_c (Table 3) becomes less negative as I_c decreases; that means that the stifling of corrosion attack is due to the protective effects of corrosion products in anodic area.

It is interesting to note that I_c is, in any case, lower in the clay than in the sand. Being corrosion in the sand under mixed control (both I_c and E_c decrease with time) the diffusion to cathodic areas is probably much more controlled by the sand than by the concrete cover. This hypothesis, supported by the low concrete cover thickness, should be confirmed by further studies.

Conclusions

Several points emerge from the results of about 2 years investigation on corrosion behaviour of specimens cut from TAD tubes, exposed to several corrosive environments (tap water, 3,5% NaCl solution, 10% MgCl solution, sand humidified with NaCl solution, clay, sand).

1) results of 6 months esperiments on "as received" specimens, exposed to all corrosive environments tested, show that there was no corrosion of reinforcing wires. The spontaneous potentials of wires lay in the range of steel passivity state;

2) in presence of artificial scratches on the external concrete cover (scratches made to leave bare superficial wires in order to simulate an erroneous handling of the tubes) it was observed that the corrosive attack remained strictly localized on the wires surface directly in contact with the aggressive environment, while there was no corrosion propagation on adjacent wires surface embedded in concrete;

3) for scratched specimens exposed to different soils (clay and sand), corrosion couple, generated between the bare surface of wires directly exposed to the soil and the surface of the wires covered with concrete, gives rise to mean corrosion penetration rates of 0.04 mm/y for bare wires exposed to clay and of 0.08 mm/y for those exposed to sand. In this case too, attack was strictly restricted to the bare area. Stifling during the corrosion attack is due to protective effects of corrosion products in anodic areas.

4) investigations are still continuing to verify the long time behaviour of TAD tube reinforcement.

REFERENCES

1. C.L.PAGE, K.W.J.TREADWAY"Aspects of the Electrochemistry of Steel in Concrete", Nature 297,109 (1982)

2. C.M.HANSSON "Comments on Electrochemical Measurements of the Rate of Corrosion of Steel in Concrete", Cement Concr. Res. 14(4),574 (1984)

3. J.E.SLATER "Corrosion of Metals in Association with Concrete", ASTM STP 818, Philadelphia (1983)

4. C.J.F.P. JONES "Maintenance Problems and Economics", Proc. Seminar Corrosion and Degradation of Building Materials and System Building, London, ed. Oyez (1985)

5. K.C.CLEAR "Solving Rebar Corrosion Problems in Concrete Research Update: Method and Materials", Proc. Seminar Solving Rebar Corrosion Problems in Concrete, NACE, Chicago, Paper n. 4, Sept. 1982

6. R.F. STRATFULL "Solving Rebar Corrosion Problems in Concrete-Past, Present and Future", ibidem Paper n. 16

7. K.KATAWAKI, M.OTA, T.YANAGIDA, K.KOKUBU "Corrosion and Protection Technologies for Concrete Structures in Marine Atmosphere", Proc. 4th Asian--Pacific Corrosion Control Conf., Tokyo, p. 531, May 1985

8. H.ROPER "State of the Art of Practical Prevention and Control of Corrosion in Concrete Structures", ibidem p. 716

9. M.ARPAIA "Conduites en Béton Precontraint et Phénomènes de Corrosion", Tribune du Cebedeau, n. 250-251, Août 1967

10. R.CIGNA, M.MARIANI, R.TURRIZIANI "Tubi in calcestruzzo ad armatura diffusa: metodologie di fabbricazione, caratteristiche e comportamento nei riguardi della corrosione", Proc. Conv. ASMI, p. 459, ed. Pitagora Bologna (1983)

11. M.ARPAIA "Soil Corrosivity", Proc. CEOCOR Int. Conf. on Corrosion, Louxembourg, May 1985

12. R.J.VETTER "Electrochemical Kinetics" Academic Press, New York, p. 750 (1967)

13. M.ARPAIA "Corrosione delle armature in acciaio dei manufatti in calcestruzzo" Rend. 8° Congr. Intern. Manufatto in Cemento, Stresa, May 1975

14. G.J.VERBECK "Mechanism of Corrosion of Steel in Concrete" ACI SP 49, p. 21, Detroit (1975)

15. CEB, Comité Eurointernational du Béton, Bulletin d'Information n. 166 "Guide to Durable Concrete Structures", Lausanne (1985)

Table 1 - Mean values of spontaneous potential E_{corr} and corrosion rate CR at the end of the test.

ENVIRONMENT	TAP WATER		NaCl 35g/l		$MgCl_2$ 10%		SAND HUMIDIFIED WITH NaCl	
WIRES	CR µm/y	E_{corr} mv	CR µm/y	E_{corr} mV	CR µm/y	E_{corr} mV	CR µm/y	E_{corr} mV
SUPERFICIAL	3.0	-122	3.0	-73	3.3	-87	2.8	-80
MEDIUM	3.4	-105	3.3	-65	3.2	-65	3.5	-63
DEEPER	2.0	-100	3.9	-62	3.1	-60	2.1	-60

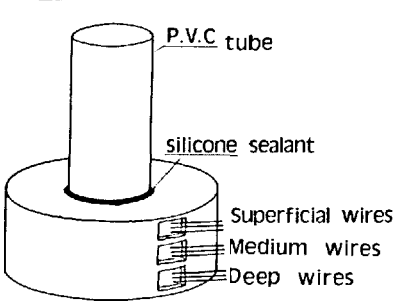

Fig. 1 Specimens used in experimentations A and B

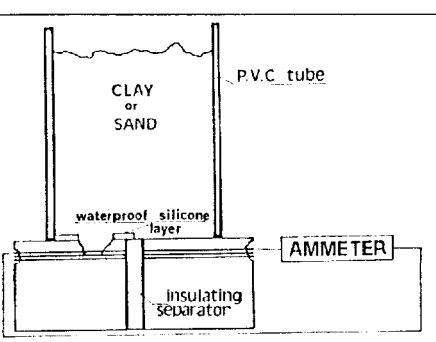

Fig. 2 Specimens used in experimentation C

Table 2 - Values of corrosion potential E_{corr} and corrosion rate CR vs. time for samples with scratched concrete cover.

	TIME	SAND HUMIDIFIED WITH NaCl SOLUTION			TAP WATER		
		WIRES			WIRES		
	(days)	SUPERFICIAL	MEDIUM	DEEPER	SUPERFICIAL	MEDIUM	DEEPER
E_{corr}	7	-0.25	-0.07	-0.05	-0.07	-0.05	-0.07
	12	-0.60	-0.20	-0.20	-0.06	-0.05	-0.04
	18	-0.61	-0.19	-0.19	-0.63	-0.10	-0.11
(VOLT)	60	-0.60	-0.11	-0.12	-0.62	-0.03	-0.02
	90	-0.61	-0.16	-0.14	-0.60	-0.04	-0.02
	7	30.0	4.0	3.0	33.0	3.0	3.0
CR	15	27.0	3.0	2.0	28.0	4.0	3.0
	60	40.0	3.0	4.0	40.0	5.0	3.0
μm/y	90	40.0	4.0	2.0	38.0	4.0	3.0

Table 3 - Values of mixed potentials E_c vs. time for samples used in type investigation.

CLAY	SAND	TIME (days)
-310	-420	20
-270	-400	30
-180	-200	45
-120	-150	55
-100	-130	62

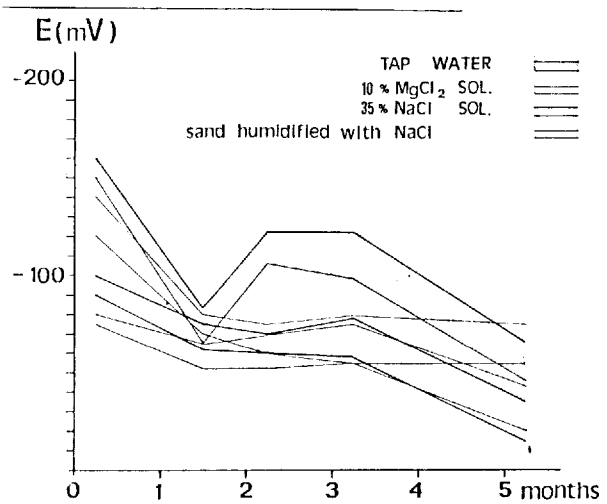

Fig. 3 Spontaneous potentials vs. time measured in investigation A

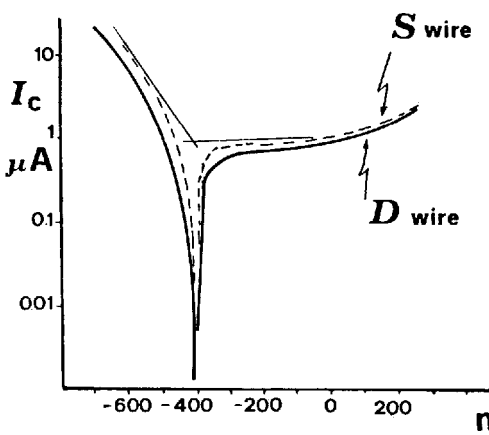

Fig. 4 Typical polarization curve in investigation A

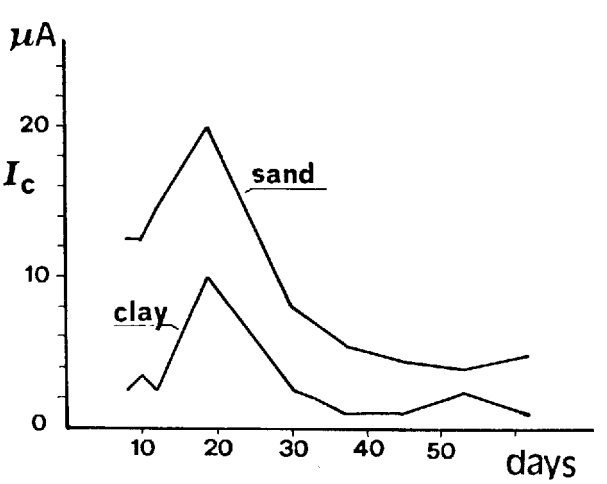

Fig. 5 Current intensity I_c of couples in investigation C

C.P. TOGNON, Chem. Eng., Italcementi, Laboratorio Chimico Centrale, Bergamo, Italy
S. CANGIANO, Chem. Eng., Italcementi, Laboratorio Chimico Centrale, Bergamo, Italy
G. COPPETTI, Chem. Eng., Italcementi, Laboratorio Chimico Centrale, Bergamo, Italy

THERMOMECHANICAL COMPATIBILITY OF AGGREGATES IN AUTOCLAVED VERY HIGH STRENGTH CONCRETES
COMPATIBILITE THERMOMECANIQUE DES GRANULATS EN BETON A TRES HAUTE RESISTANCE AUTOCLAVES

SUMMARY

The trends of compressive strengths and moduli of elasticity versus the aggregate $\emptyset_{max}$ were observed in autoclaved concretes made with aggregate consisting of limestone, quartz and a 50% mix of the two. The investigation was extended to concretes with aggregate ($\emptyset_{max}$ up to 20 mm) formed of basalt, jasper, granite and porphyry as well as 50% binary mixes of these aggregates, besides of limestone and quartz mixes with the above materials.

It could be noticed that the moduli of elasticity of concretes where the aggregate consists of 50% binary mix of the two materials depend on the moduli of elasticity of the mix constituents and their thermal compatibility related to the respective coefficient α.

The most interesting phenomena appear when limestone is present in the mix aggregates. Depending on the ratio of the modulus of elasticity of limestone to the aggregate with which it is mixed and as a function of the difference between the thermal expansion coefficient α of limestone and that of the aggregate, more or less marked deviations of the modulus of elasticity from the theoretical value are noticed.

In rather wide temperature ranges such as those related to the concrete autoclaving, in case an aggregate mix is used, a study on the thermal and elastic compatibility between them and the cement matrix seems necessary to foresee safely the mechanical and elastic properties of the relative concretes.

SUMÁRIO

As tendências das resistências à compressão e do módulo de elasticidade versus agregado $\emptyset_{max}$ foram observadas em concreto autoclavado com agregados de calcário, quartzo e 50% de mistura dos dois. A investigação foi ampliada a concretos com agregados ($\emptyset_{max}$ até 20 mm) formados por basalto, granito e porfiro assim como de misturas binárias desses agregados ao lado das misturas calcário e quartzo com os materiais acima.

Pode ser anunciado que os módulos de elasticidade dos concretos, onde o agregado consiste em mistura de 50% de dois materiais, depende do módulo de elasticidade dos constituintes da mistura e sua compatibilidade térmica relacionada com o respectivo coeficiente α.

O fenômeno mais interessante aparece quando o calcário está presente nas misturas de agregados. Dependendo da relação do módulo de elasticidade do calcário com o do agregado com o qual foi misturado e como uma função da diferença entre o coeficiente de expansão térmico α do calcário e do agregado, são notados desvios mais ou menos acentuados do módulo de elasticidade e do seu valor teórico.

Em variações de temperaturas bastante grandes como as relacionadas com o concreto autoclavado, no caso de uso de misturas de agregados, o estudo da compatibilidade térmica e elástica entre eles e a matrix do cimento parece necessário para prever com segurança as propriedades mecânicas e elásticas do concreto correspondente.

THERMOMECHANICAL COMPATIBILITY OF AGGREGATES IN AUTOCLAVED VERY HIGH STRENGTH CONCRETES

4.3

INTRODUCTION

The mechanical properties of autoclaved very high strength concretes made with quartz aggregate (1, 2) and aggregates differently interacting with the cement matrix (3) were studied in previous works.

In this work the effect of the thermal and elastic compatibility of binary mixes of different types of aggregates on the properties of autoclaved very high strength concretes was studied.

EXPERIMENTAL

Materials

- Aggregates - The following materials were used: basalt, limestone, jasper, granite, porphyry and quartz. they were chosen for their marked differences in chemical-mineralogical and physical-mechanical properties.
The study was focused on the properties of concretes containing quartz and limestone, for which continuous particle size distribution curves (Fuller) with maximum diameters ranging between 3 and 30 mm were adopted. The other aggregates were used in complementary tests and continuous particle size distribution curves (Fuller) with 20 mm maximum diameter were chosen.

- Binder - A mix of class 525 portland cement and silica ground to a fineness like that of cement was used. The cement/silica ratio was 1.8.

- Admixture - A naphthalene sulphonate superplasticizer in 25% acqueous solution was utilized.

- Concretes - The composition of the concrete mixes is given in table 1.

Table n° 1 - Composition of the concrete mixes

Component	aggregate $\emptyset_{max}$ (mm)					
	3	6	10	15	20	30
Binder (cement + silica)* (kg/m^3)	530	530	530	530	530	530
Aggregate (depending on type) (kg/m^3)	1500÷1600	1550÷1650	1650÷1700	1650÷1700	1650÷1700	1700
Water/binder ratio	0.42÷0.47	0.38÷0.43	0.36÷0.40	0.33÷0.38	0.32÷0.35	0.31÷0.32
Superplasticizer (25% solution) (% on binder)	4	4	4	4	4	4

(*) Cement/silica ratio = 1.8

The water/binder ratio, minimized by the superplasticizer, was changed depending on the type and maximum diameter of the used aggregate, to keep the mix workability nearly constant (slump = about 50 mm).

Cylinder specimens 250 mm high and with 100 mm diameter were made from each mix.

Curing

The autoclaved concretes underwent the following hydrothermal cycle (1):

- presteaming: 14 ÷ 20 hr at 20°C
- low pressure steam curing: 8 hr at 60°C
- high pressure steam curing: 24 hr at 190°C
- rate of temperature rise: 0,7 °C/min

Tests

The aggregate thermal expansion coefficient α was determined by the strain gauge method described by (4) in the 20-200°C temperature range.

The concrete thermal expansion coefficient was determined by measuring the deformation of the cylinder specimens (Ø 100 x 250 mm) during the whole hydrothermal cycle (low and high pressure) in an especially designed and built autoclave.

The static modulus of elasticity E was determined according to UNI Standards (5).

RESULTS

Thermal expansion

Table 2 gives the mean values of the thermal expansion coefficient α for aggregates, cement paste and concretes containing quartz, limestone and a 1:1 mix of the two aggregates.

This table also shows the values (at 20 C) of the modulus of elasticity relevant to the aggregates and these concretes.

The coefficient-α values for aggregates and paste are in agreement with those given in the literature (6, 7).

It can be noticed that coefficient α for the concrete containing the limestone-quartz mix nearly corresponds to the mean of α-values for the concretes containing only one of the two aggregates.

Table n° 2 - Thermal expansion coefficient α and moduli of elasticity E of aggregates, cement paste and concretes

Material	$\alpha(10^{-6}/°C)$	$E(N/mm^2)$
Jasper	13.5	76.500
Quartz	12.0	72.150
Granite	8.5	33.600
Basalt	5.5	100.350
Porphyry	5.0	42.300
Limestone	4.5	58.500
Autoclaved cement paste	7.6	26.000
Concrete with quartz	8.0	47.400
Concrete with limestone	3.0	42.300
Concrete with 50% quartz 50% limestone	6.0	31.000

Mechanical strength

Figure 1 shows compressive strength versus maximum aggregate diameter of autoclaved concretes made with quartz, limestone and a 1:1 mix of the two materials.

Strength of quartz-aggregate concretes increases as far as 20 mm maximum diameter and reaches the value of 160 N/mm^2. However, it tends to decrease beyond 20 mm.

Also the limestone-aggregate concretes initially show increasing strengths, but only as far as 10 mm maximum diameter (75 N/mm^2). Afterwards the strength values decrease to 65 N/mm^2.

Compressive strength of concretes made with a 1:1 mix of the two aggregates attains the highest value (135 N/mm^2) with a $\emptyset_{max}$ = 10 mm. Then it reduces appreciably to a value of 95 N/mm^2 with a $\emptyset_{max}$ = 30 mm.

The strength of these concretes does not correspond to the dotted lines in fig. 1, obtained by averaging the strength of the concretes containing only one type of aggregate. As far as $\emptyset_{max}$ = about 15 mm strengths are closer to those of quartz concretes. Beyond this value, they more and more approach those of limestone concretes.

Static modulus of elasticity

Figure 2 shows the modulus of elasticity relevant to autoclaved concretes (with limestone, quartz and a 1:1 mix of the two materials), always expressed versus the maximum aggregate diameter.

The quartz concrete modulus of elasticity constantly rises as the maximum aggregate diameter increases, and it attains 49000 N/mm^2 for $\emptyset_{max}$ = 30 mm.

The limestone concrete modulus of elasticity increases significantly up to a $\emptyset_{max}$ = 10 mm and then it remains nearly constant (about 42000 N/mm^2) as far as a $\emptyset_{max}$ = 30 mm.

The concretes made with a mix of the two aggregates show the highest value of the modulus of elasticity for a $\emptyset_{max} \simeq 10$ mm (34500 N/mm^2). As the maximum diameter increases, the modulus of elasticity reduces to a value of 31000 N/mm^2 which becomes constant for a $\emptyset_{max} \geq 20$ mm.

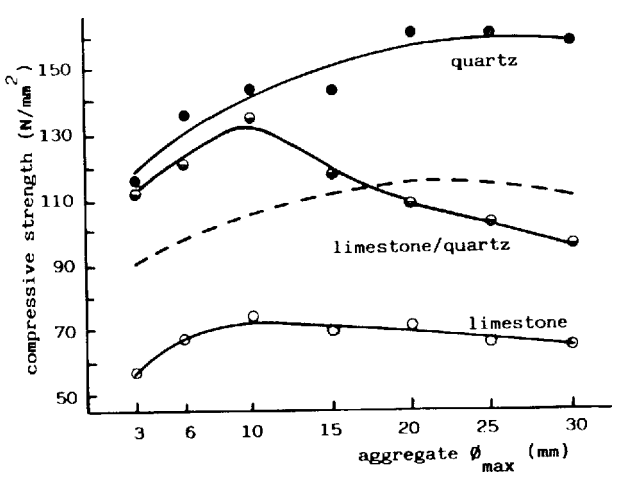

Fig. 1 - Compressive strength of autoclaved concretes versus maximum diameter of aggregate

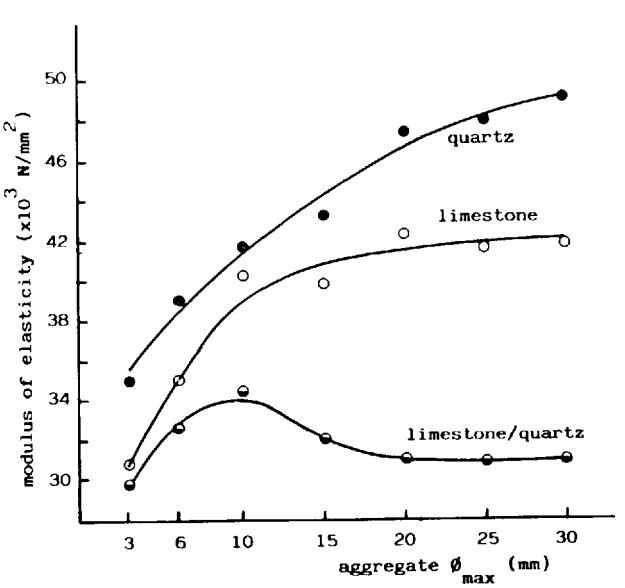

Fig. 2 - Moduli of elasticity of autoclaved concretes versus maximum diameter of aggregate

As can be observed, the modululs of elasticity of the concretes made with the limestone-quartz mix is always lower than that of concretes containing only one type of aggregate. Moreover it is lower by 10÷30% with respect to the curve obtained by averaging the values relevant to the concretes containing only one type of aggregate.

More precisely, as shown in fig. 3, the per cent deviation, limited for the small aggregate concretes, increases gradually and stabilizes on a 30% value for $\emptyset_{max}$ > 20 mm.

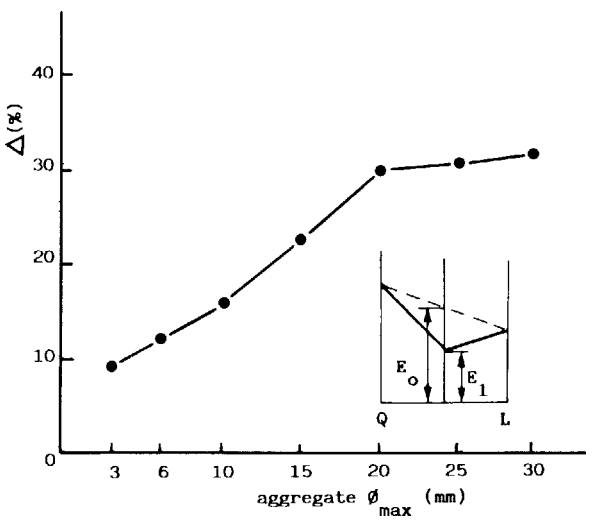

Fig. 3 - Per cent deviation from linearity of the modulus of elasticity of concretes made with limestone/quartz mix versus maximum diameter of aggregate

$$(\Delta = \frac{E_0 - E_1}{E_0} \cdot 100)$$

The fact that the modulus of elasticity of the concretes made with 1:1 limestone-quartz mix was, for any maximum aggregate diameter, appreciably lower than that of the concretes made completely with one or the other of the two aggregates appeared to be a phenomenon deserving additional study.

Therefore the investigation to check whether the phenomenon was related to the particular materials in question or it was in common with other materials was extended.

Figure 4 shows the moduli of elasticity of the concretes made with different aggregates, besides with their 50% binary mix, versus the aggregate percentage.

The left-hand area of the figure points out that the concretes made with a binary mix of quartz and other materials (except for limestone) have more or less marked deviation in absolute value, and in some cases (jasper, basalt) also of opposite sign, from the mean value calculated by the mix rule (8).

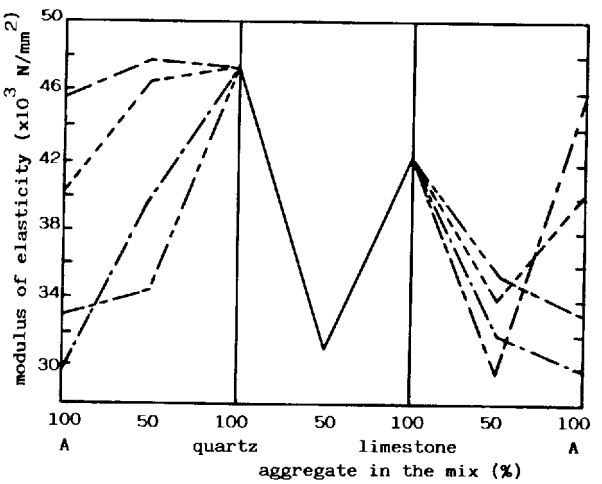

A: ------- basalt
— — — jasper
—·—·— granite
—··—·· porphyry

Fig. 4 - Moduli of elasticity of concretes made with different aggregates and mixes of these versus the aggregate percentage ($\emptyset_{max}$ = 20 mm)

In the central area of the figure, having as extremes the moduli of elasticity of the concretes made with only quartz and only limestone ($\emptyset_{max}$ = 20 mm), the relative curve deviates from the theoretical one and forms a sharp minimum at the modulus of elasticity of the concrete with 1:1 mix of the two materials. The position of the minimum is confirmed by experiences with the results of which fig. 5 curve was plotted.

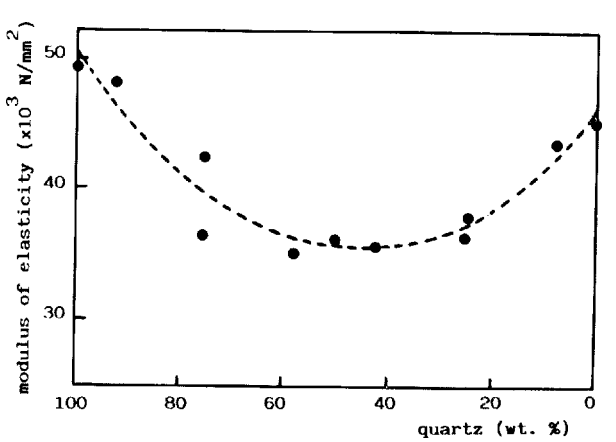

Fig. 5 - Modulus of elasticity of concretes made with quartz/limestone binary mixes versus the quartz percentage in the mix

Finally, the right-hand area of figure 4 shows that the calcareous aggregate causes the formation of minima in the modulus of elasticity of the relative concretes only when it is present with jasper and basalt in 50% binary mix. By contrast, with granite and prophyry, there are deviations from the mean value, without formation of minimum.

REMARKS

The autoclaved concretes containing only quartz are much more resistant than those with only limestone, owing to the formation of a stronger matrix/aggregate interface bond (9).

As regards the concretes made with 1:1 limestone/quartz mix, for maximum diameters over 10 mm, strength are appreciably affected by the different α and E of the two materials, the more the larger the maximum diameter of the aggregate. Strengths reduce by about 30% by passing from $\emptyset_{max}$ = 10 mm to $\emptyset_{max}$ = 30 mm. The modulus of elasticity of ordinarily cured concretes changes linearly versus the substitution percentage of an aggregate for another (10) and increases as the maximum aggregate diameter increases (11).

Autoclaved concretes have the same behaviour when the aggregate consists of only one material. Deviations from linearity generally occur in the concretes made with 50% binary mixes of the different aggregates.

A positive deviation can be observed in concretes containing jasper/quartz and basalt/quartz mixes. A negative deviation is found in concretes with porphyry/quartz mix. As regards the concretes made with granite/quartz mix the trend is practically linear.

However, when one of the two components is limestone, there is:

- negative deviation with minimum, when the remaining 50% of the aggregate consists of:
  - quartz, jasper } with higher α and E than those of limestone
  - basalt with α like that of limestone, but E almost double.
- negative deviation without minimum, when the remaining 50% of the aggregate consists of:
  - porphyry with α like that of limestone and lower E
  - granite with higher α than that of limestone and much lower E.

Figure 6 shows that the per cent deviation from linearity is related to the ratio between the moduli of elasticity of limestone and the second aggregate in the mix.

Two areas are pointed out: the former with a modulus of elasticity ratio relevant to aggregates below 1, where the relative concretes show the minimum in the modulus of elasticity trend, and the latter with a modulus of elasticity ratio for aggregates above 1, where the relative concretes display a negative deviation from linearity, but without minimum.

The figure also points out that, at the same modulus of elasticity ratios, the deviation from linearity is the more marked the more the α of the added material deviates from that of limestone.

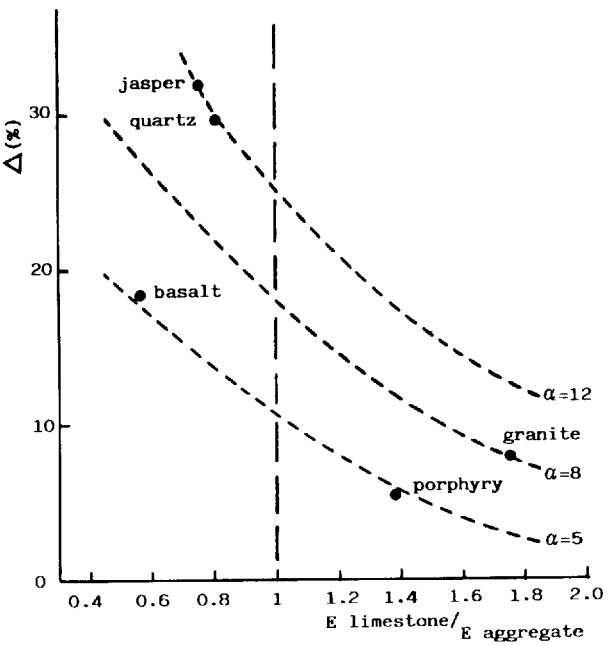

Fig. 6 - Per cent deviation from linearity of the modulus of elasticity of concretes made with limestone-another aggregate mixes versus the ratios of the moduli of elasticity of limestone to the other aggregate and versus the thermal expansion coefficient α

CONCLUSIONS

In case of concrete autoclaving, it can be useful to use only one type of aggregate rather than choose a mix of materials having different thermomechanical properties. In fact in rather large temperature ranges, such as those found in the hydrothermal treatment, the difference in the moduli of elasticity and thermal expansion coefficients relevant to aggregates affects strengths and, above all, the modulus of elasticity of the relative concretes.

The use of aggregate mixes containing limestone can involve a drop in the modululs of elasticity, however not expectable from the compressive strength values that follow an intermediate trend between those of concretes with aggregate consisting of only one component.

REFERENCES

1. G.P. TOGNON, G. COPPETTI, P. URSELLA, 9. Internationaler Kongress der Beton- und Fertigteilindustrie (Wien, 8-13 Oktober 1978), 39-46

2. G.P. TOGNON, P. URSELLA, G. COPPETTI, J. Am. Concr. Inst., 1980, 77 (3), 171-178

3. G.P. TOGNON, P. URSELLA, G. COPPETTI, 7th Int. Congress Chem. Cem. (Paris, 30 juin - 5 juillet 1980), VII-75-80

4. P. CAPPA, Ingegneria, 1984 (5/6), 145-148

5. UNI 6556, Prove sui calcestruzzi - Determinazione del modulo elastico secante a compressione, 1976, 3 pp.

6. Y.S. TOULOUKIAN, C.Y. HO, Data Series on Material Properties vol. II-2: Physical Properties of Rock and Minerals, McGraw-Hill Book Co., New York, 1981, 548 pp.

7. H. DETTLING, Bulletin n° 164, Deutscher Ausschuss für Stahlbeton, Berlin 1964, 1-64 (Translation n° 458 PCA Technical Information Dpt.)

8. T.C. HANSEN, J. Am. Concr. Inst., 1965, 62 (2), 193-216

9. G.P. TOGNON, L'Ingegnere Libero Professionista, 1977 (11), 889-901

10. F.R. SCHÜTZ, Der Einfluss der Zuschlagelastizität auf die Betondruckfestigkeit, Fakultät für Bauwesen der Rheinisch-Westfälischen Technischen Hochschule, Aachen (Dissertation), 1970, 145 pp.

11. W. MANNS, Beton, 1970 (9), 401-405; (10), 455-460

C.Tashiro, Faculty of Engineering, Yamaguchi University, Japan and Y.Fukushima, Faculty of Engineering. Yamaguchi University, Japan.

Effect of Zinc Oxide Admixture on Corrosion Inhibition of Iron in Cement Mortar Containing Sea Water.

"L'Effet de l'adjuvant de zinc oxide sur la corrosion-contrainte du fer au ciment mortier comprenant de l'eau de la mer".

SUMMARY: Iron plate was embedded in ordinary Portland cement mortar containing a small amount of zinc oxide powder. Sweet water and sea water were used as mixing water and steam curing was used for acceleration of corrosion for 90 days. Iron corrosion, spontaneous potential and microstructure of specimens were investigated.

When the cement mortar was mixed with sea water, the iron plate was found to be vigorously corroded, and the spontaneous potential showed about -400 mv. Also, large plate-crystals of calcium hydroxide were formed in the interfacial region between the iron plate and the cement mortar. On the other hand, with the mortar containing the zinc oxide admixture, corrosion of the iron plate did not occur.

It is concluded that the use of zinc oxide as an admixture is very effective for inhibition the corrosion of iron.

Sumário

Uma chapa de aço foi colocada dentro de uma argamassa de cimento Portland comum contendo pequena quantidade de pó de óxido de zinco. Água doce e água do mar foram usadas como água de mistura e cura à vapor foi usada para acelerar a corrosão por 90 dias. Corrosão do aço, potencial espontâneo e microestrutura de amostras foram investigadas.

Quando a argamassa de cimento foi misturada com água do mar, a chapa de aço foi encontrada vigorosamente corroída e o potencial espontâneo foi de cerca de -400 mv. Também, grandes placas de hidróxido de cálcio cristalizado formaram-se na região interfacial entre a chapa de aço e a argamassa de cimento. Por outro lado, com a argamassa contendo óxido de zinco, não ocorreu corrosão na chapa de aço.

Conclui-se que o uso de óxido de zinco como uma adição é muito efetiva para a inibição da corrosão do aço.

C.Tashiro, Faculty of Engineering, Yamaguchi University, Japan and Y.Fukushima, Faculty of Engineering, Yamaguchi University, Japan.

Introduction

The authers have made various investigation aimed at the effects of metal oxides on hydration of cement, and microstructure and properties of hardened cement paste (1-3). From these investigation, it was found that some of the heavy metals dissolve easily in cement and effect the characteristics and properties of hardened cement paste. On the other hand, many studies are known on the corrosion of iron or steel in concrete(4-6), but several points on the corrosion inhibition still remained unsolved.

This experimental study deals with the inhibition of corrosion of iron, and clarification of the relationship between the corrosion of iron and microstructure of hardened cement mortar.

Experimental method

A high-purity iron plate, 20 by 20 by 1 mm ,was embedded in a 40 by 40 by 10 mm cement mortar as shown in Fig.1. The iron plate was cleaned by ethylalcohol in an ultravibrator after it was polished by a #1000 sand paper. A commercially available ordinary Portland cement was used. The zinc oxide used was of commercial"First Grade" quality. Standard sand from Toyoura in Yamaguchi Prefecture in Japan was employed for making the mortar.

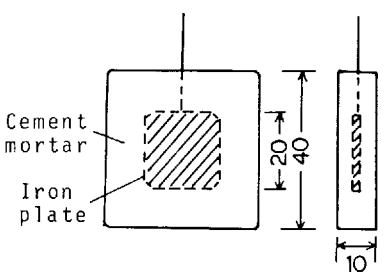

Fig.1. Schematic diagram of specimen.

The cement mortar was made with cement to sand ratio of 1:3, and water to cement ratio of 0.8. The amount of the zinc oxide used was 0.2 wt% of cement. The reference specimens mixed with sweet water or sea water were designated as C-W and C-S,respectively. The mortars containing zinc oxide and sweet water or sea water were designated as Z-W and Z-S respectively. Steam curing at 65 °C for 90 days, after pre-curing at 20 °C for 4 hours, was used for accelerating the corrosion process.

The spontaneous electromotive potential of specimens was measured by the use of milli voltmeter, saturated potassium chloride solution and silver chloride electrode as a reference electrode, as shown in Fig.2. The measurement was carried out in a sealed case every three days after holding at 20 °C for 0.5 hours.

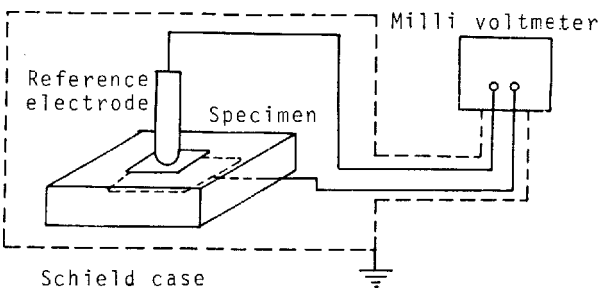

Fig.2. Schematic representation of experimental apparatus.

The rust area was measured on the iron plate after crushing the specimens. The measurements were made at 7,14,28,56 and 90 days.

The cement hydration products in contact with the iron plate were investigated using a scanning electron microscope. The pore size distribution of the cement mortars were measured by means of mercury penetration porosimeteric analysis.

Results and discussion

Table 1 shows the data on the amount of rust area at the iron surface. When sweet water was used corrosion was not observed in all the specimen. It seems that the amount of corrosion was not appreciable under the conditions of water/cement ratio, thickness of mortar cover, and the accelerated curing used in this study. On the other hand, when sea water was used, the corrosion was observed in the control specimen (without zinc oxide). Namely, the rusted area of the control specimen was over 80% at 90 days. However, when zinc oxide was

C.Tashiro, Faculty of Engineering, Yamaguchi University, Japan and Y.Fukushima, Faculty of Engineering, Yamaguchi University, Japan.

used, no corrosion was observed.

Table 1. Amounts of rust area at the iron plate surface.

(%)

Curing time, days / Specimens	7	14	28	56	90
C - W	0	0	0	0	0
C - S	0	0	12	69	80
Z - W	0	0	0	0	0
Z - S	0	0	0	0	0

The data on spontaneous potential of specimens is shown in Fig.3. When the specimens were mixed with sweet water (C-W or Z-W), the spontaneous potential was about -100 mv. On the other hand, when the specimens contained sea water (C-S or Z-S), the spontaneous potential was about -300 mv at early stage after mixing. In the former case the potential was negatively larger with curing time, but in the latter case it became negatively smaller with curing time . It remained at about -150 mv after curing for 30 to 35 days.

Fig.4 shows the scanning electron micrographs of the hydration products on the iron plate in 28 days old specimens. These micrographs may be grouped into two types. The hydration products in C-W ,Z-W and Zn-S consisted mainly of CSH and calcium hydroxide, and the texture was compact. On the other hand, the hydration products in control specimen mixed with sea water, consisted mainly of hexagonal plate-calcium hydroxide which was arranged in C-direction parallel to the iron plate, and the texture was porous. In the case of zinc oxide addition, probably this compound $Ca(Zn(OH)_3.H_2O)_2$ may have formed(7).

Fig. 5 shows the total pore volume and pore size distribution of 28-day specimens. In spite of differences in the type of mixing water, the total pore volume of specimens containing the zinc oxide admixture, were slightly smaller than that the control. The zinc oxide admixture effected the microstructure of the cement mortar in a beneficial manner which is related to prevention of diffusion of oxygen and other harmful constituents. In another study(6)

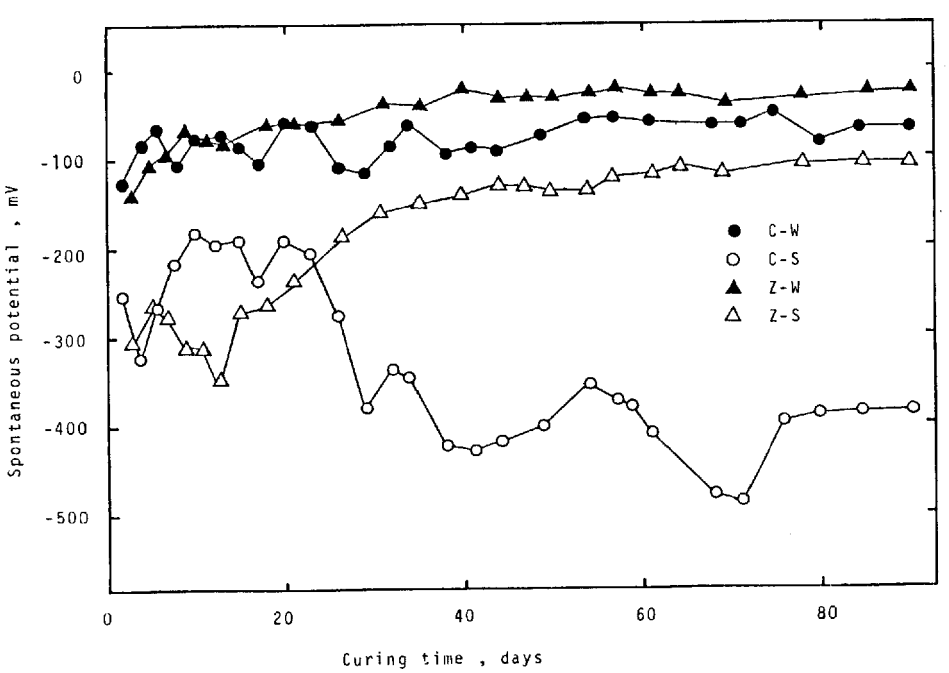

Fig.3. Spontaneous potential versus curing time.

C.Tashiro, Faculty of Engineering, Yamaguchi University, Japan and Y.Fukushima, Faculty of Engineering, Yamaguchi University, Japan.

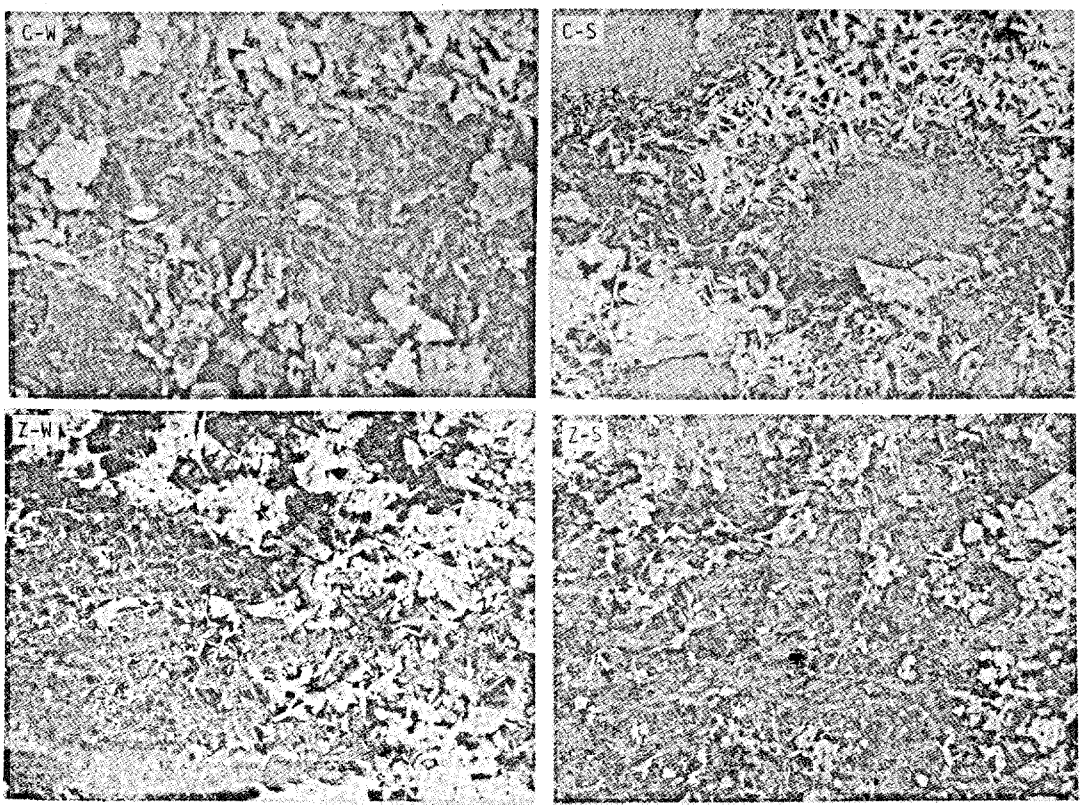

Fig.4. Scanning electron micrographs of cement hydrates on the iron plates of 28 days specimens.

it was found that cement mortars having a porevolume less than 0.06 cm3/g had a high corrosion resistance.

Another reason of influence of zinc oxide admixture on the iron corrosion is not always clear,but it seems as follows. When zinc oxide is added, it is dissolved as zinc ion or calcium-zinc compound ion which migrates electrophoretically to cathode and the cathode is coverd with inhibition film. On the other hand, the oxygen ion from the zinc oxide passivates the anode. Namely, the mechanism may involve cathodic protection and anodic protection(8). In addition, calcium hydroxide and calcium silicate may also be useful as corrosion inhibiters. Further study on zinc oxide admixture is being continued to clarify the mechanism of corrosion inhibi-

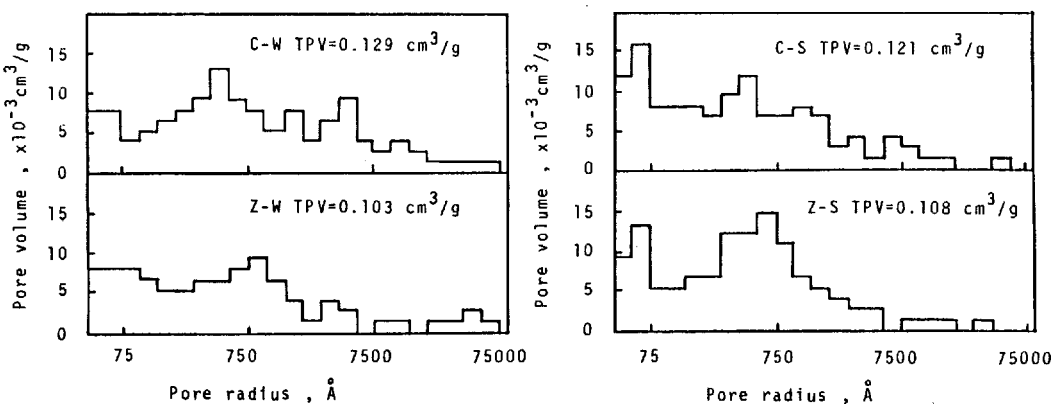

Fig.5. Total pore volume and pore size distribution of 28 days specimens.

tion.

Conclusion

Iron plates were embedded in cement mortars both with and without the addition of zinc oxide admixture. Sweet water or sea water was used as the mixing water. The iron corrosion, the spontaneous potential and the microstructure of the specimens were investigated.

It was found that when the cement mortar was mixed with sweet water,the iron plate was not corroded, and the spontaneous potential was maintained at about -100 mv immediately after the accelerated curing. On the other hand, when the mortar was mixed with sea water,the iron plate in the control specimen (without zinc oxide) was badly corroded and the spontaneous potential became negatively larger with the curing time, and was about -400 mv at 90 days. In the latter case large hexagonal crystals of calcium hydroxide were formed in the interfacial region between the iron plate and the cement mortar. However, the specimen containing sea water and zinc oxide was not corroded, and its spontaneous potential remained at about -150 mv after the accelerated curing for 30 to 35 days.

It was concluded that the zinc oxide admixture was very effective as a corrosion inhibiter for iron in cement mortar containing sea water.

Acknowledgments

The authors appreciate the technical assistance of Dr K.Ueoka and S. Tachibana.

References

1) C.Tashiro et al.,(1977), Hardening property of cement mortar adding heavy metal compound and solubility of heavy metal from hardened mortar, Cement and Concrete Research, Vol 7, pp545-552.

2) C.Tashiro,(1980), The effects of several Heavy metal oxides on the hydration and the microstructure of hardened mortar of C_3S, Proc. 7th Inter. Cong. Chemistry of Cement, Paris, II, PP37-42.

3) C.Tashiro and J.Oba,(1980), The effects of $Cu(OH)_2$ on the hydration of C_3A, Proc. 7th Inter. Cong. Chemistry of Cement, Paris, II, pp58-63.

4) H.Berman,(1975), Sodium chloride corrosion of reinforcing steel and pH of calcium hydroxide solution, Jour.of ACI, Vol.72, PP150-157.

5) K.Okada et al.,(1980), Detection techniques for chloride corrosion of reinforcing steel, JCI 2nd Conference, PP5-8.

6) C.Tashiro ,K.Ueoka and N.Iizuka,(1982), Spontaneous potential and micropore on chloride corrosion of reinforcing steel in concrete, JCI 4th Conference, pp65-68.

7) W.Lieber,(1968), The influence of lead and zinc compounds on the hydration of portland cement, Inter.-Cong. chemistry of cement, Tokyo, pp444-453.

8) G.Wranglen,(1972), An introduction to corrosion and protection of metals,(in Japanease), pp151-157.

W. Kobayashi, Ube Industries Co, Ltd, Japan; N. Kataoka, Ube Industries Co, Ltd, Japan and Y. Tsutsumi, Ube Industries Co, Ltd, Japan

On the Behaviour of Alkali in Alkali-Aggregate Reaction

Sur le Comportement de l'Alkali en Alkali-Réaction des Agrégats

SUMMARY: In the case siliceous aggregate is immersed in sodium hydroxide solution, the following reactions may occur; (1)adsorption of NaOH to silanol groups of aggregate, (2)rupture of surface siloxane bridge of aggregate by attack of NaOH and dissolution of SiO_2 , (3)rupture of inside siloxane bridge of aggregate and loosing of the structure of it, (4)adsorption of NaOH to inside silanol groups made by reaction(3).
The quantity of reaction(4) in mortar bar was estimated and the relation of it to the expansion of mortar bar was investigated.
The more reaction(4)/unit reactive aggregate is, the more the expansion is. Reaction(4)/unit reactive aggregate shows a peak at the pessimum proportion. From these results and the fact that reaction(4) is closely related to reaction(3), reaction(3) seems to be a cause of the expansion by alkali-aggregate reaction. To estimate the reactivity of siliceous aggregate, it may be sensible to measure the quantity of ruptured inside siloxane bridge of aggregate immersed in sodium hydroxide solution.

Sumário

No caso de agregado silicoso imersão em solução de hidróxido de sódio, as seguintes reações podem ocorrer: (1) - adsorção do NaOH por grupos silanol do agregado, (2) rutura da superfície da ligação siloxano do agregado pelo ataque do NaOH e dissolução do SiO_2, (3) ruptura interna da ligação siloxano do agregado e perda de sua estrutura, (4) adsorção do NaOH no interior do grupo silanol devido à reação (3).

A quantidade da reação (4) em barras de argamassa foi estimada e entre isso e a expansão de barras de argamassa foi investigada.

Quanto maior a relação reação (4)/unidade de agregado reativo maior é a expansão. Reação (4)/unidade de agregado reativo apresenta um pico na proporção pessimum. Por esses resultados e pelo fato que a reação (4) é intimamente ligada à reação (3), a reação (3) parece ser a causa da expansão por reação álcali-agregado. Para avaliar a reatividade de agregado silicoso, pode ser sensível à medida da quantidade rompida, no interior da ligação siloxano do agregado imerso em solução de hidróxido de sódio.

W. Kobayashi, Ube Industries Co, Ltd, Japan; N. Kataoka, Ube Industries Co, Ltd, Japan
and Y. Tsutsumi, Ube Industries Co, Ltd, Japan

Introduction

One of authers studied on the chemistry of alkali-aggregate reaction by using silica gel–sodium hydroxide model[1,2].
In the case siliceous aggregate is immersed in NaOH solution, the following reactions occur.

(1) adsorption of NaOH to silanol groups of aggregate
(2) rupture of surface siloxane bridge of aggregate by attack of NaOH and dissolution of SiO_2
(3) rupture of inside siloxane bridge of aggregate and loosing of the structure of it
(4) adsorption of NaOH to inside silanol groups made by reaction(3)

If the siliceous aggregate is well-crystallised form, the attack of NaOH takes place mainly at the surface and only reaction(1) and (2) occur.
On the other hand, in the case of poorly crystallised silica, NaOH penetrates into the interior of it and reaction(3) and (4) occur too. Reaction(3) loosens the network of silica and produced a cross-linked polyelectrolyte containing Na^+. This type of structure, in contact with water, set up an imbibition pressure and because the silicon-oxgen framework is partly disruptured the material swells.
In this paper, the behaviour of alkali in mortar bar which expands caused by alkali-aggregate reaction is discussed based on the above hypothesis.

Experimental

1) Materials

① Aggregate

Pyrex glass and four kinds of natural rock were used as reactive aggregate and a kind of natural rock,(No.5) was used as unreactive aggregate.
The chemical compositions of these aggregates are shown in Table 1.

Table 1 – Chemical compositions of aggregates (%)

aggregate	ig.loss	SiO_2	Al_2O_3	Fe_2O_3	CaO	MgO	Na_2O	K_2O
pyrex glass	0.2	81.2	2.3	0.3	0.1	0.0	3.50	0.06
rock No.1	0.9	57.1	18.2	5.9	8.4	5.3	2.92	1.47
rock No.2	1.3	60.1	21.1	4.5	6.8	1.8	3.53	1.15
rock No.3	0.1	60.4	21.0	4.5	7.4	2.0	3.68	1.13
rock No.4	1.5	90.0	3.9	2.3	0.6	0.5	0.30	0.80
rock No.5	2.5	66.0	15.0	4.8	4.7	1.7	3.34	2.25

The type and main rock-forming minerals of natural rock aggregates are shown in Table 2.

Table 2 – Type and main rock-forming minerals of natural rock aggregates

aggregate	type of rock	rock-forming minerals[1]				
		quartz	feldspar	pyroxene	mica	iron minerals
rock No. 1	andesite		◎	○		△
rock No. 2	andesite		◎	○		
rock No. 3	andesite		◎	○		
rock No. 4	chert	◎			△	△
rock No. 5	sandstone	◎	○		△	

Note: 1) ◎—much, ○—relatively much, △—a little

Potential reactivity of these aggregates was tested according to ASTM C289(Standard Test Method for potential Reactivity of Aggregates, CHEMICAL METHOD). The result is shown in Fig.1.

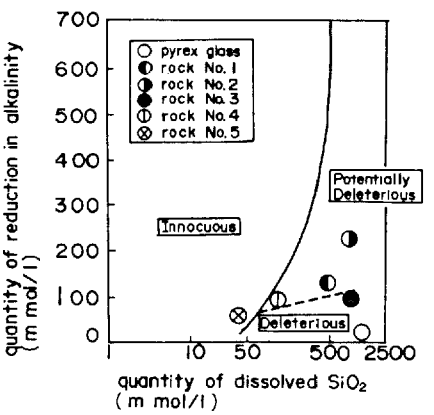

Fig.1 – Potential reactivity of aggregate by CHEMICAL METHOD

② Cement

Commercial ordinary portland cement containing relatively high alkali was used in this study. The chemical composition of the cement is shown in Table 3.

Table 3 – Chemical composition of cement (%)

ig.loss	insol	SiO_2	Al_2O_3	Fe_2O_3	CaO	MgO	SO_3	Na_2O	K_2O	TiO_2	P_2O_5	R_2O
0.3	0.1	22.5	5.3	3.2	63.6	1.7	1.8	0.56	0.57	0.41	0.05	0.94

Notes: 1) $R_2O = 0.656K_2O + Na_2O$
2) Blaine surface area: 3,050 cm^2/g

2) Test method

① Immersion test

Aggregates were immersed in NaOH solution according to ASTM C289. Immersed time was varied from 1 hour to 366 hours.
The concentration of OH^- in filtrate was measured by using pH meter and the concentrations of Na^+ and SiO_2 in it were measured by using atomic absorption spectrophotometer.
The quantity of silanol group in residual aggregate was measured by the following method; the residual aggregate separated by filtration is put into 200 ml of deionized water and pH of it is adjusted to 2 by adding HCl(1+1). Then the aggregate is separated by filtration and the weight loss of it from 378 to 1223 °K is measured. The quantity of silanol group is calculated from the weight loss supposing that a molecular water is released from two silanol groups.
The weight loss may contain the water in micropore not dried at 378 °K. In this paper, therefore, only the change of quantity of silanol group is discussed.

② Mortar bar test

Mortar bar test was carried out according to ASTM

W. Kobayashi, Ube Industries Co, Ltd, Japan; N. Kataoka, Ube Industries Co, Ltd, Japan
and Y. Tsutsumi, Ube Industries Co, Ltd, Japan

C227(Standard Test Method for Potential Alkali Reactivity of Cement-Aggregate Combinations).
The mixing ratio of each reactive aggregate and unreactive aggregate was varied to investigate the pessimum proportion.

③ Analysis of pore solution

Mortar bar cured for various period was crushed in the range of 1 – 2.5mm with particle size. 100g of crushed specimen was molded in the expression device[3] and pore solution in the specimen was extracted by operating at the pressure of 392 MPa. The concentrations of OH^-, Na^+, K^+, Ca^{2+} and SiO_2 were measured by using pH meter and atomic absorption spectrophotometer.

Result

1) Immersion test

The change of the concentration of SiO_2 and Na in NaOH solution and the increase of silanol group in residual aggregate are shown in Fig.2. To compare with Fig.1, the concentration of SiO_2 is indicated as the quantity of dissolved SiO_2 and the concentration of Na^+ is indicated as the quantity of reduction of Na^+.

The dissolution rate of SiO_2 varies depending on the kind of aggregate. The dissolution rate decreases with immersion time and at the long immersion time the quantity of dissolved SiO_2 of some aggregates whose dissolution rate is high decreases, because when the concentration of SiO_2 approaches the saturation curve of SiO_2 the dissolution rate slows down and once the concentration of SiO_2 passes over the saturation curve the excess SiO_2 precipitate[2].

The quantity of reduction of Na^+ increase up to certain level at the immersion time of 1 hour and then increases gradually. It is considered that the reduction of Na^+ at the immersion time of 1 hour is mainly caused by reaction(1) and the reduction of Na^+ after 1 hour is mainly caused by reaction(4). In the

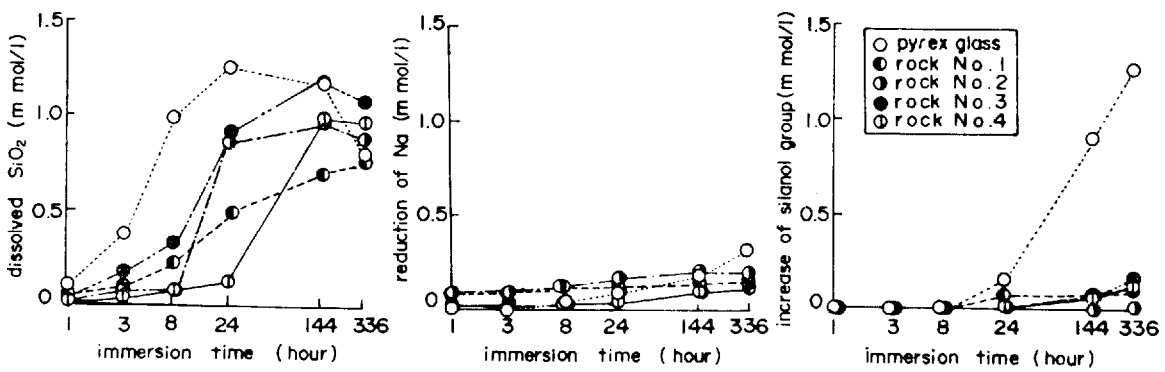

Fig.2 – Quantities of dissolved SiO_2 and Na^+ in NaOH solution and increase of silanol group in aggregate

Note : 1)increase of silanol group : the increase of silanol group in aggregate from 0 to various immersion time

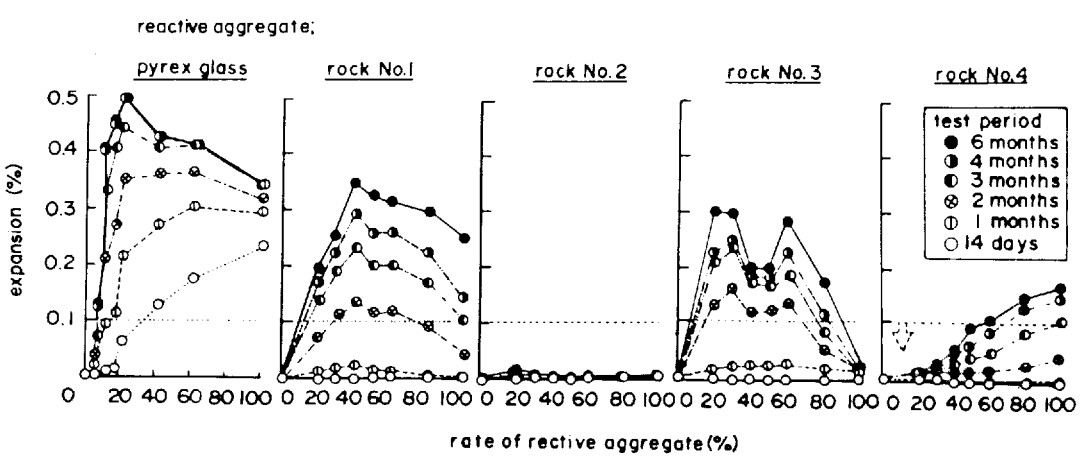

Fig.3 – Result of mortar bar test

Note : dot line indicates the permitted level of alkali specified according to ASTM C227

case of pyrex glass, the quantity of reduction of Na^+ is very small at the immersion time of 1 hour but after 1 hour it is much larger than in the case of the other aggregates. The quantity of silanol group generally increases with immersion time and that of pyrex glass increases significantly.

2) Mortar bar test

The result of mortar bar test is shown in Fig.3. The degree of expansion and pessimum proportion vary depending on the kind of reactive aggregate. The pessimum proportion of pyrex glass varies with the test period. Dot line in Fig.3 indicates permitted expansion at 6months specified in ASTM C227 and all the aggregates except rock No.2 are considered of harmful reactivity.

3) Analysis of pore solution

On the mortar bars prepared by using pyrex glass and rock No.3 as reactive aggregate, the concentrations of Na^+, K^+, Ca^{2+}, OH^- and SiO_2 in extracted pore solution were measured. The concentrations of Na^+, K^+, OH^- and SiO_2 are shown in Fig.4. The concentrations of Na^+, K^+ and OH^- generally decrease with test period. That of SiO_2 increases very slightly with test period but it is very low compared with other ions. The concentration of Ca^{2+} decreases at early age and becomes almost constant but it is very low (0.10 – 1.85 m mol/l) and is not shown in Fig.4. It is considered that the concentrations of ions other than Na^+, K^+ and OH^- are low and the quantity of OH^- almost balances to the quantity of $Na^+ + K^+$.

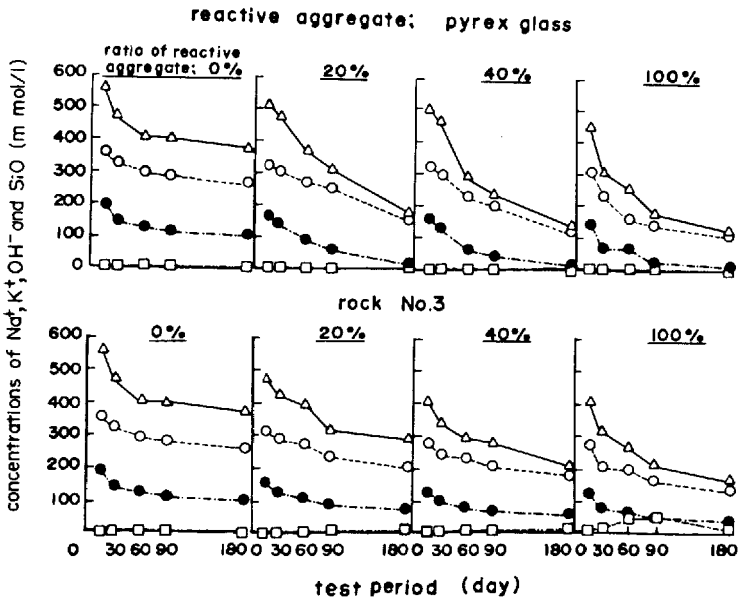

Fig.4 – Concentrations of Na^+, K^+, OH^- and SiO_2 of pore solution in mortar bar

Discussion

1) Relation between reaction(3) and reaction(4) in aggregate immersed in NaOH solution

Reaction(3) (the rupture of inside siloxane bridge) is considered to be a cause of expansion as described above and it is desirable to investigate the relation between the expansion and reaction(3) in mortar bar. It is, however, very difficult to quantify reaction(3) of aggregate in mortar bar. On the other hand, it is possible to estimate the quantity of reaction(4) (adsorption of NaOH to ruptured inside siloxane bridge) in mortar bar. Using the results of immersion test, therefore, the relation between reaction(3) and reaction(4) is investigated.

The relation is shown in Fig.5, supposing that the increase of silanol group is caused by reaction(3) and that the reduction of Na^+ fron 1 hour immersion to varied immersion time is caused by reaction(4). It is considered that there is close relation between reaction(3) and reaction(4), though concerning to aggregate immersed in NaOH solution. In Fig.5 the increase of silanol group by reaction(3) is not equivalent to the reduction of Na^+ by reaction (4), because alkali does not adsorb to all of silanol groups[4].

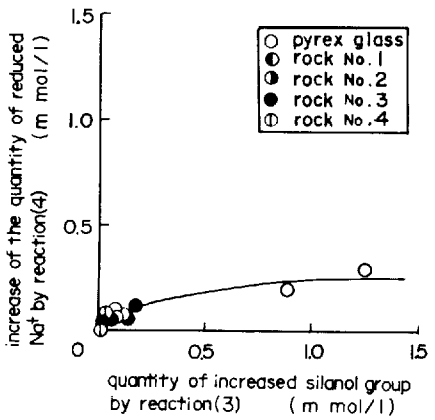

Fig.5 – Relation between the increase of silanol group and the reduction of Na^+

2) Estimation of the quantity of reaction(4) in mortar bar

As the quantity of reaction(3) is tightly related to that of reaction(4), the quantity of alkali adsorbed by reaction(4) in mortar bar is estimated by assuming the follows;

i) alkali in cement dissloves completely into pore solution

ii) the quantity of pore solution is the same as that of mixing water used to prepare mortar bar

iii) the quantity of adsorbed alkali by reaction(1) is equivalent to the quantity of reduction of alkali at 1 hour in immersion test

iv) the quantity of adsorbed alkali by reaction(3) is estimated by the following equation;

$$T - P = A$$
$$A - [Iu + Ir] = IV$$

T :total alkali dissolved from clinker
P :alkali in pore solution
A :the quantity of adsorbed alkali
Iu:alkali adsorbed to unreactive aggregate by reaction(1)
Ir:alkali adsorbed to reactive aggregate by reaction(1)
IV:alkali adsorbed by reaction(4)

Fig.6 shows the quantity of adsorbed alkali by reaction(4), IV, estimated by using above equations.

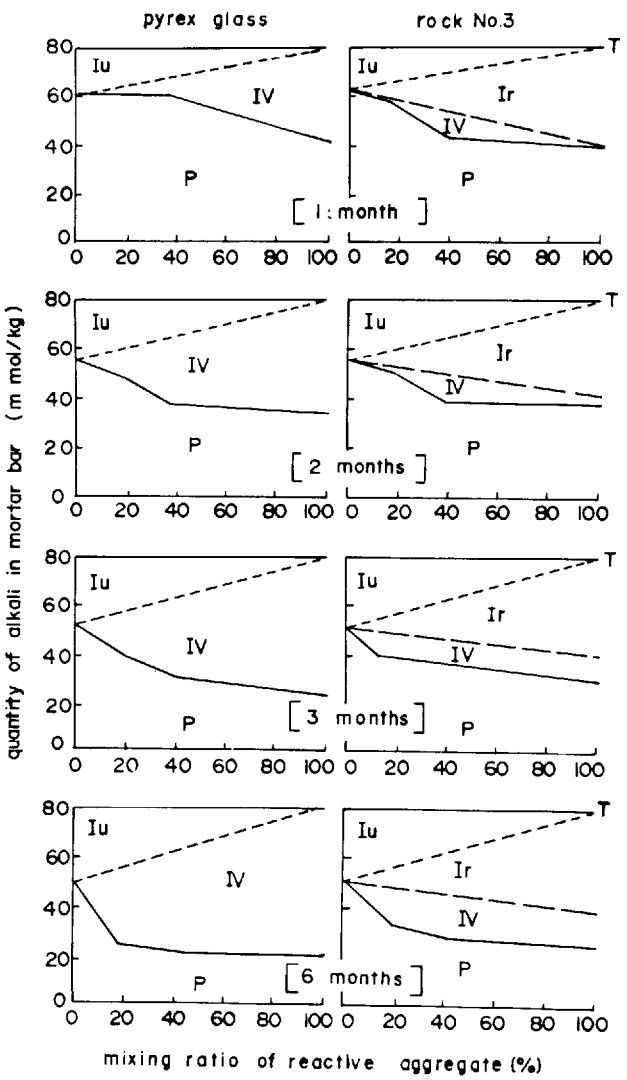

Fig.6 –Quantity of alkali adsorbed by reaction(4), IV

(T) is constant and (Iu) and (Ir) at certain mixing ratio of reactive aggregate are constant at any test period according to the assumptions. (IV) of pyrex glass is larger than that of rock No.3. In the case of pyrex glass, (IV) is the largest at 100% of mixing ratio of reactive aggregate initially and the increase of (IV) is more at less mixing ratio of reactive aggregate. On the other hand, in the case of rock No.3, (IV) is the largest at 40% of mixing ratio of reactive aggregate and the increase of (IV) is almost even at any mixing ratio of reactive aggregate.

3) Relation between reaction(4) and expansion

(IV) estimated in Fig.6 was converted to (IV)/unit reactive aggregate, (IVu).
(IVu) and expansion of mortar bar are shown in Fig.7.

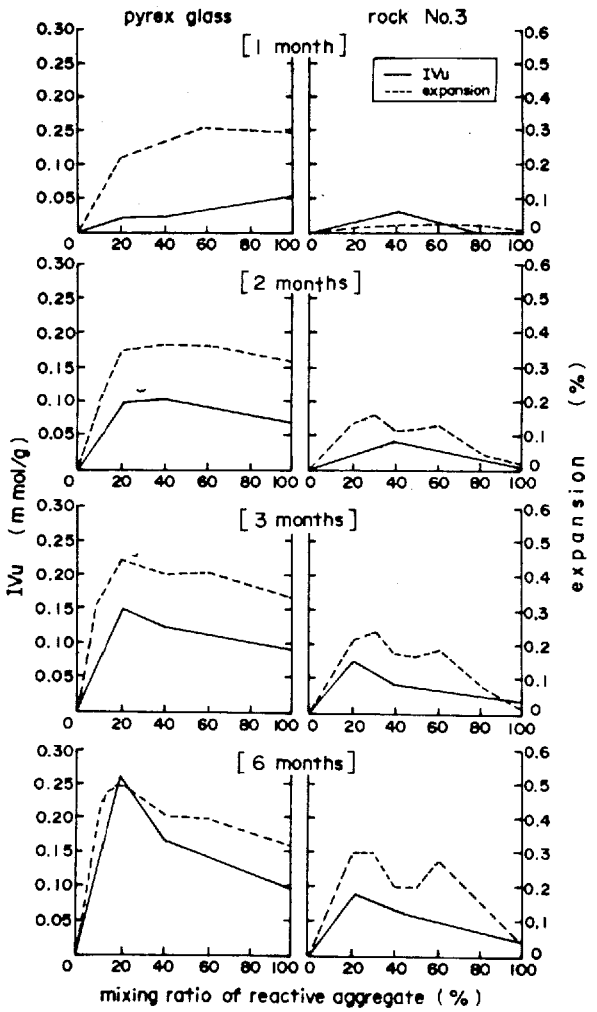

Fig.7 – Quantity of alkali adsorbed by reaction(4)/ unit reactive aggregate, (IVu), and expansion of mortar bar

The tendency of (IVu) coincides with that of expansion of mortar bar. (IVu) has a peak almost at the pessimum proportion.
The relation between (IVu) and expansion is shown in Fig.8.
(IVu) is tightly related to expansion of mortar bar and expansion becomes larger with the increase of (IVu). The quantity of alkali adsorbed by reaction(4) is considered to represent the rupture of inside siloxane bridge(reaction(3)) indirectly as shown in Fig.5. Thus, though the above results have been led using many assumptions, the hypothesis of expansion mechanism that the expansion is caused by rupture of siloxane bridge is considered to be possible.
There is difference in the relation curve of (IVu) to expansion between pyrex glass and rock No.3.
Each aggregate has different structure and the required quantity of rupture of siloxane bridge to expand may vary depending on the structure.

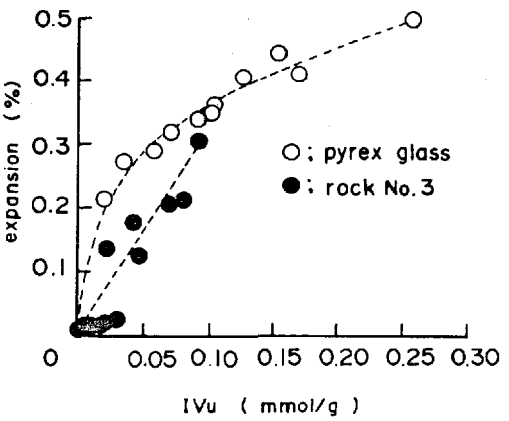

Fig.8 – Relation between IVu and expansion

In CHEMICAL METHOD according to ASTM C289, reduction in alkalinity(reaction(1) + reaction(4)) and dissolved SiO (reaction(2)) are measured and potential reactivity of aggregate is judged. To estimate the potential reactivity of aggregate, however, it may be more sensible to measure the quantity of ruptured inside siloxane bridge of residual aggregate immersed in NaOH solution (reaction(3)).

Conclusion

On the aggregate immersed in NaOH solution, there is close relation between the quantity of ruptured inside siloxane bridge and the quantity of alkali adsorbed to ruptured inside siloxane bridge.
On the mortar bar, the quantity of alkali adsorbed to ruptured inside siloxane bridge/unit reactive aggregate is tightly related to expansion.
From these results, the rupture of inside siloxane bridge by the attack of alkali seems to be a cause of the expansion by alkali-aggregate reaction.

References

1. L.S.D.Glasser and N.Kataoka (1981),"THE CHEMISTRY OF ALKALI-AGGREGATE REACTION", 5th.Int.Conf.Alkali-Aggregate Reaction in Concrete, S252/22
2. L.S.D.Glasser and N.Kataoka (1981),"THE CHEMISTRY OF ALKALI-AGGREGATE REACTION", Cem.Concr.Res,11, 1 – 9
3. R.S.Barneyback Jr. and S.Diamond (1981),"EXPRESSION AND ANALYSIS OF PORE FLUID FROM HARDENED CEMENT PASTES AND MORTAR", Cem.Concr.Res,11, 279 – 285
4. R.K.Iler (1979),"THE CHEMISTRY OF SILICA", (Wiley-Interscience), pp.182 – 185

Kin-ichi NAKANO, Shigehiro KOBAYASHI and Seiichi NAGAOKA

Influence of Reactive Aggregate and Alkali Compounds on Expansion of Alkali-Silica Reaction

SUMMARY: Deleterious cracks in concrete structures considered to be caused by alkali-silica reaction are being often found in Japan from about 1975.

In this study, investigation was carried on the factors affecting expansion of mortar bar, that is, types of reactive aggregate, alkali contents of portland cement, types of alkali compounds as several source of alkali, amount of alkalis and types of chemical admixtures.

Results show that even though the total alkali content is same amount, the expansion increases with increase of afterward additional alkali.

It is technologically importance that alkali introduced afterward shows remarkable influence for mortar bar expansion comparing with intrinsic alkali in cement.

Sumário

Fissuras deletérias em estruturas de concreto consideradas como causadas por reação alcali-agregados estão sendo encontradas com freqüência no Japão desde 1975.

Neste estudo, foram efetuadas investigações sobre os fatores que afetam a expansão em barras de argamassa, ou seja, tipos de agregados reativos, conteúdo de álcalis no cimento portland, tipos de compostos de álcalis como várias fontes de álcali, quantidade de álcalis, e tipos de aditivos químicos.

Resultados mostram que, embora seja o mesmo o conteúdo total de álcalis, a expansão aumenta com o aumento de álcalis adicional.

É tecnologicamente importante que o álkali introduzido depois apresenta notável influência na expansão da barra de argamassa comparada com o álcali intrínseco do cimento.

1. Introduction

Deleterious cracks in concrete structures considered to be caused by alkali-silica reaction are being often found in Japan from about 1975.

Deleterious expansion due to alkali silica reaction is known as following processes.

Silica of thermo-dynamically unstable phase react with alkali introduced from cement, seadraged sand and chemical admixtures, etc., at high alkalinity condition, and forms alkali silica gel. And this alkali silica gel gradually swells with absorbing water. Damage of concrete structure due to deleterious expansion of alkali-silica reaction is particularly caused with about pessimum condition under co-existing of alkali, silica and water, in concrete.

In this study, investigation was carried out on the factors affecting expansion of mortar bar, that is, types of reactive aggregate, alkali contents of portland cement, kinds of alkali compound as several source of alkali, amount of alkalis and types of chemical admixture.

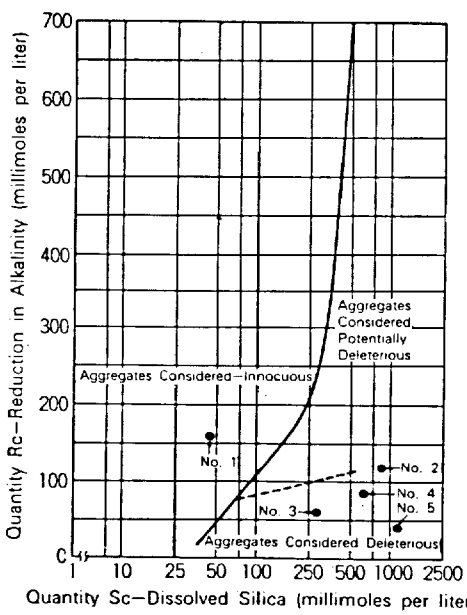

Fig.-1 Results of ASTM C-289 Test

2. Material

The following materials were used for preparing mortar bars.

1) Cement: 9 kinds of normal portland cement were used. Alkali contents of these cements were shown in Table-1. These figures range from minimum 0.56% up to 0.90%, expressed as equivalent sodium oxide. (Na_2O equ.)

2) Aggregate: Types of aggregate and those typical properties and characters are shown in Table-2 and Fig.-1. Aggregate No.2, 3and 4 were reactive natural aggregates containing α-cristbalite.

3) Alkali compound: Kinds of alkali compound used were NaCl, $NaNO_2$, NaOH, Na_2SO_4, Na_2CO_3, KCl, KOH and K_2SO_4 of reagent grade.

4) Chemical admixture: Air entraining agent, Air Entraining-water reducing agent(AE water reducing agent), water reducing agent and high-range water-reducing agent were used.

Table-1 Alkali contents of Cements

Cement	Alkali(% by weight)		
	Na_2O	K_2O	equiv.Na_2O
1	0.22	0.58	0.60
2	0.40	0.57	0.78
3	0.23	0.67	0.67
4	0.31	0.89	0.90
5	0.46	0.49	0.78
6	0.53	0.56	0.90
7	0.30	0.40	0.56
8	0.26	0.65	0.69
9	0.30	0.61	0.70

Table-2 Properties of Aggregates

No.	Types of Rock	Results of ASTM C289 Test		Specific gravity	Absorption (%)
		Sc	Rc		
1*	Sand Stone	43	152	2.70	0.67
2	Bronzite Andesite	807	119	2.54	1.25
3	Two Pyroxene Andesite	259	62	2.69	1.58
4	Rhombic Pyroxene Andesite	684	83	2.56	2.28
5	Pyrex Glass	1085	35	2.22	----

* Innocuous aggregate used for control.

3. Test Method

The test method employed was ASTM C-227 "Alkali Reactivity,Potential,of Cement-Aggregate Combinations(Motar Bar Method)".

4. Results

1) Types of reactive aggregate

The types of reactive aggregate as factor influencing expansion were examined. Aggregate No.2,3,4 and 5 shown in Table-2 were tested at prescribed total alkali content of 0.60,1.20 and 2.00% by adding NaCl to No.1 portland cement(Na_2O equ.=0.60 %). The mortar expansion of these aggregates at various alkali content were shown in Fig.-2.

Mortar expansion due to ASR was effected by types of aggregate and alkali content,that is, at 0.60% alkali content,no expansion was detected up to 20 weeks expect in case of Aggregate No.5(Pyrex glass),but thereafter Aggregate No.3(Two Pyroxen Andesite) showed gradual increase of expansion and reached in near value of Aggregate No.5 at 52 weeks.

Expansion of Aggregate No.2,3,4and 5 increased with increasing alkali content.

Expansion of Mortar Bar made with the cement contained 1.20% and 2.00% alkali as Na_2O equ. was saturated at age of 20 weeks.

2) Influence of alkali content in portland cement

To investigate the influence of alkali content in portland cement on expansion, 8 portland cements of varied alkali content (No.2-9: shown in Table-1)were prepared. Their alkali contents ranged from minimum 0.56% up to 0.90% as Na_2O equ. Aggregate No.2 were used as reactive aggregate. Obtained results of varied alkali contents were shown in Fig.-3,4and 5. Increase of mortar expansion with increasing alkali was summerized in Fig.-6 at age of 26 weeks. From Fig.-3,it is known that o.90% or less alkali originally contained in portland cement results in harmless or no expansion, the amount of which is only 260×10^{-6} at 26 weeks. These values were considerably smaller than the criteria of 1000×10^{-6} in ASTM C-227.

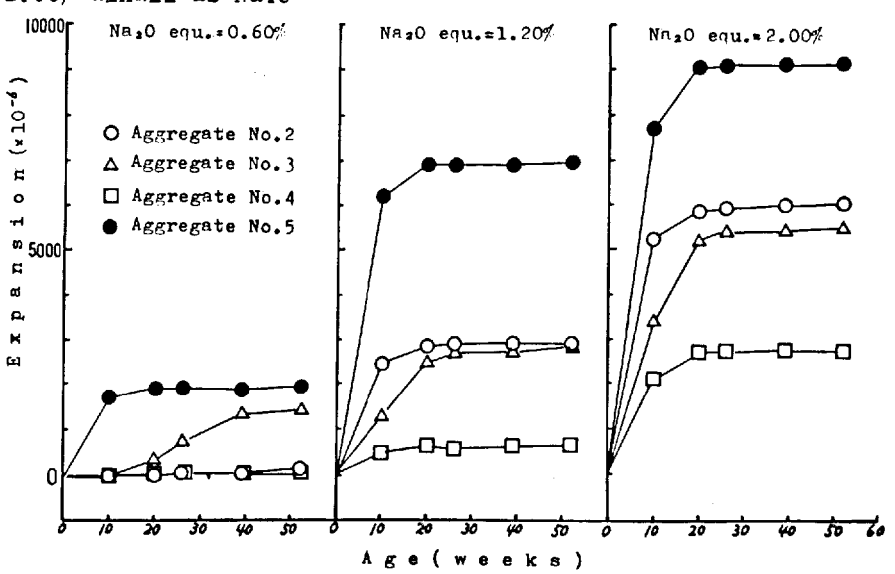

Fig.-2 Influence of types of Aggregate on Expansion of Mortar Bar at Various alkali content.

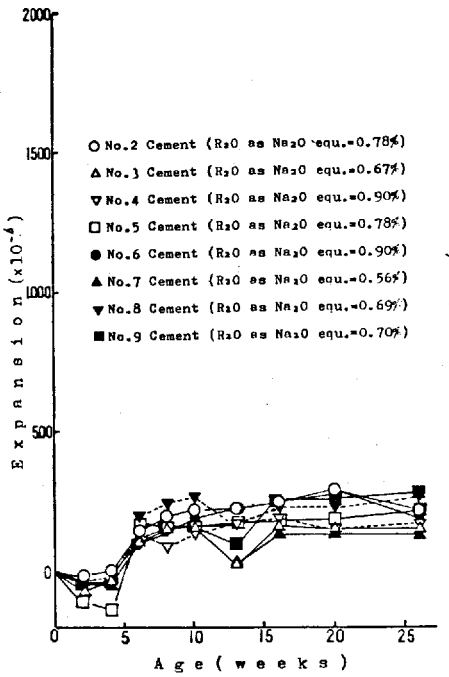

Fig.-3 Influence of Alkali originally contained in Cement on Expansion of Mortar Bar.

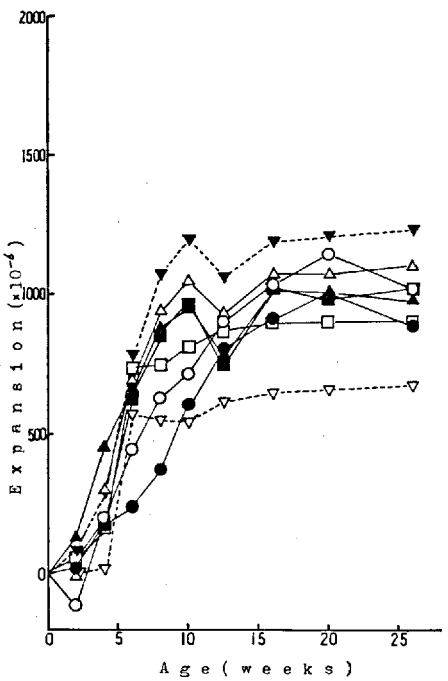

Fig.-4 Influence of additional Alkali(Na_2SO_4,K_2SO_4) on Expansion of Mortar Bar, total Alkali content controlled to 1.20%, difference between intrinsic Alkali in Cement and controlled alkali 1.20% was adjusted by Na_2SO_4 and K_2SO_4.

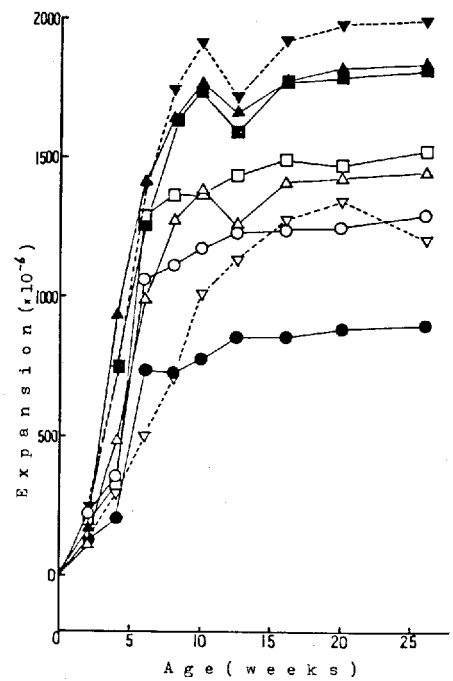

Fig.-5 Influence of additional Alkali(NaCl) on Expansion of Mortar Bar, total alkali content controlled to 1.20%, difference between intrinsic Alkali in Cement and controlled alkali 1.20% was adjusted by NaCl.

3) Influence of additional alkali

Fig.-4,5 and 6 also showed the influence of additional alkali.

Total alkali content against to cement was adjusted to 1.20% Na_2O equ.

The difference of 1.20% and intrinsic alkali content in cement was added alkali salts.

In the case of Na_2SO_4 and K_2SO_4, the ratio of Na_2SO_4 to K_2SO_4 was adjusted to its intrinsic ratio of Na_2O to K_2O in cement(Fig.-4).

It is known that low alkali cement with large amount of adding alkali shows much expansion than that of high alkali cement with small amount alkali addition if their total Na_2O equ. is same. Furthermore these tendency was more pronounced in the case of NaCl addition.

These phenomena suggested that expansion of mortar bar were largely influenced by water soluble alkali content.

4) Influence of the types of alkali compound

Influence of the types of alkali compound were examined using low alkali cement(No.1 cement:Na_2O equ.=0.60%) and Aggregate No.2. The total Na_2O equ. was adjusted to 2.00% by addition of some kinds of alkali compounds.

The expansion of mortar bars up to 52 weeks were shown in Fig.-7. Addition of alkali compounds affected large influence on expansion.

NaCl intensified the most,and $NaNO_2$ was next.

These results indicated that even though equivalent Na_2O contents were the same, extent of expansion varied widely dependent upon the kinds of alkali ions.

Furthermore sodium compounds affected more

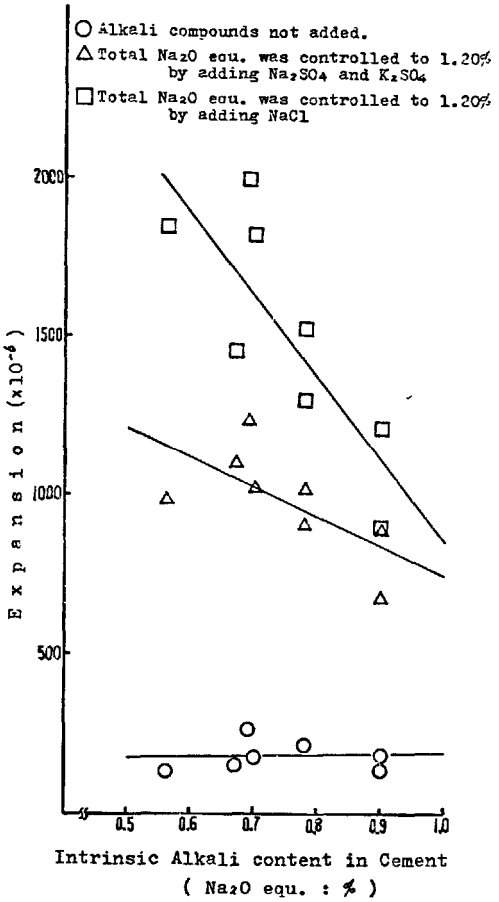

Fig.-6 Influence of additional Alkali on Expansion of Mortar Bar at the age of 26 weeks ,total Alkali cotent controlled to 1.20% by addition of Alkali compounds.

than potassium compounds, shown in Fig.-7.

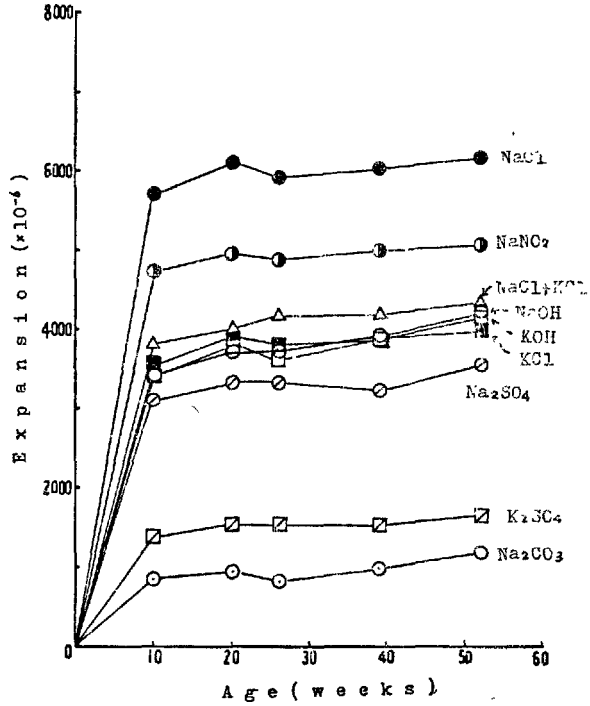

Fig.-7 Influence of types of Alkali compounds on Expansion of Mortar Bar,total Alkali content controlled to 2.00%.

5) Influence of chemical admixtures

The influence of chemical admixtures on expansion was examined using low alkali cement(No.1 cement: Na_2O equ.=0.60%) and Aggregate No.2.

The total alkali as Na_2O equ. was adjusted to 0.60,1.20 and 2.00% by adding NaCl to low alkali cement.

Chemical admixtures used were Air entraining agent, AE water reducing agent,water reducing agent for high strength concrete and high-range water-reducing agent,these admixtures were added complying with the standard quantity fixed by manufacturer. Dosage of admixtures were as follows.

Kin-ichi NAKANO, Shigehiro KOBAYASHI and Seiichi NAGAOKA

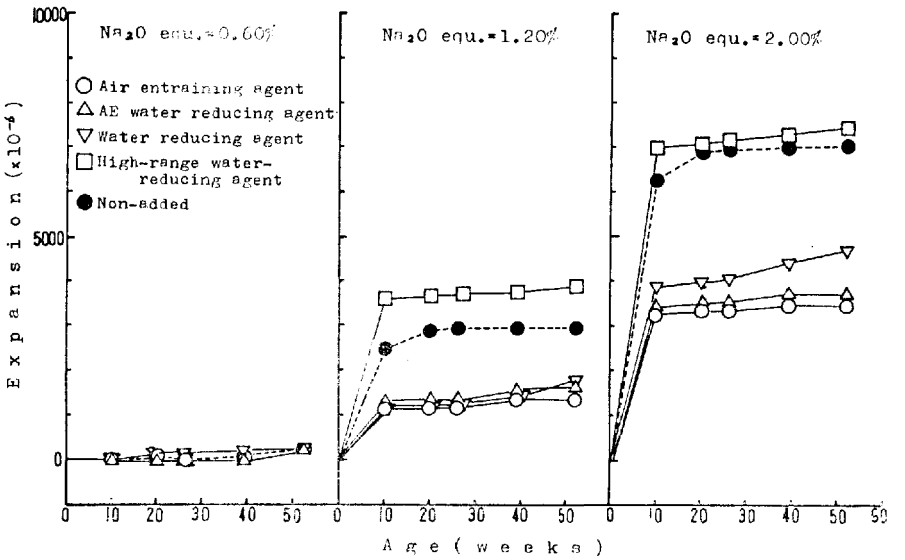

Fig.-8
Influence of chemical admixtures on expansion of mortar bar at varied alkali content.

Air entraining agent C×0.04%
AE water reducing agent C×0.25%
Water reducing agent C×1.50%
High-range water-reducing agent 2000cc/100kg-C

The expansion of mortar bars up to 52 weeks obtained were shown in Fig.-8. Mortar bars made with adding chemical admixtures did not expanded at all at alkali content of 0.60%, but at 1.20% and 2.00% content, mortar expansion increased considerably with increasing total alkali and its value exceeded 1000×10^{-6} at 10 weeks. Addition of high-range water-reducing agent showed especially largest expansion as same as that of non-added, and other admixtures reduced expansion about half comparing with non-added.

These results suggested that reduction of expansion was closely related to air content of each mortars. For example, high-range water-reducing agent entrained little air but dispersed cement particles. But to clarify these phenomena, further investigation is necessary.

5. Conclusion

Even though the total alkali content is same amount, the expansion increased with increase of afterward adding alkali. It is technologically importance that alkali introduced afterward shows remarkable influence for mortar bar expansion comparing with intrinsic alkali in cement.

"REFERENCES"

1) Nakano,K. Kobayashi,S. Nagaoka,S and Arimoto,Y. "Influence of Alkali Compounds on Expansion of Reactive Aggregate" Cement & Concrete,No.446 1984

2) S,Chatterji."An accelerated Method for the Detection of Alkali-Aggregate Reactivities of Aggregates" Cement and Concrete Reserch vol.8 No.5 1978

J.Wiśniewski,École Polytechnique de Kielce;J.Karyś,École Polytechnique de Wrocław;J.Czaja,École Polytechnique de Wrocław,Pologne.

Protection chimico-potentiostatique de l'armature dans le béton

Chemical-potentiostatic protection of reinforcing steel in concrete

RESUME:Les méthodes de protection de l'armature,utilisées jusqu'à présent,sont les suivantes:
- utilisation du béton compact avec les adjuvants,
- réalisation d'une couche de polymère,
- aluminiage et galvanisation,
- réalisation d'une couche protégeante sur surface extérieure des éléments,
- protection cathodique et anodique.

La protection chimico-potentiostatique consiste dans l'introduction à la composition du béton d'un mélange des acides adipiques et abiétiques.Ensuite,après avoir installé l'armature il faut mettre en circuit le courant électrique de potentiel constant en changeant sa densité pendant 72 heures.La valeur pH du béton doit dépasser 12,0.

Dans ces conditions,l'armature se couvre par une couche d'oxyde ferrique qui a les propriétés protégeantes.La couche protégeante est compacte et possède la même épaisseur.

On a utilisé cette solution dans l'industrie en protégeant l'armature des éléments de béton armé dans les colecteurs municipaux.

Sumário

Os métodos de proteção da armadura, utilizados até o presente, são os seguintes:

- utilização de concreto compacto com aditivos;
- realização de uma camada de polímero;
- aluminagem e galvanização;
- realização de uma camada protetora sobre a superfície externa dos elementos;
- proteção catódica e anódica.

A proteção químico-potenciostática consiste na introdução na composição do concreto de uma mistura de ácidos adípicos e abiéticos. Em seguida, depois de ter instalado a armadura, é preciso colocar em circuito a corrente elétrica de potencial constante mudando sua densidade durante 72 horas. O valor do pH do concreto deve ultrapassar 12,0.

Nessas condições, a armadura se cobre por uma camada de óxido férrico que possui as propriedades protetoras. A camada protetora é compacta e possui a mesma espessura.

Utilizou-se essa solução na indústria, protegendo a armadura das peças de concreto armado dos coletores municipais.

T.Wiśniewski,École Polytechnique de Kielce;J.Karyś,École Polytechnique de Wrocław;J.Orda,École Polytechnique de Wrocław,Pologne.

1.INTRODUCTION

La capacité du béton à absorber de l'eau et des substances qui se trouvent dans l'eau,ainsi que des gaz par exemple O_2,CO_2, SO_2,HCl,NO peut rendre les propriétés protectrices du béton insuffisantes pour l'acier. Cette situation nécessite une protection complémentaire.

La méthode de protection la plus universelle est la réalisation d'un gros revêtement en béton compact,d'une résistance chimique correcte et d'une structure poreuse très spécifique.On peut améliorer les propriétés anticorrosives du béton à l'aide d'un inhibiteur de corrosion.

D'autres méthodes ce sont:

- la protection de la surface extérieure du béton à l'aide des résines organiques,des produits de vernis,ou au moyen du collage d'une feuille synthétique,
- l'enrobage de l'armature avec une couche de protection de résines synthétiques,de la suspension aqueuse de bitumes,du nitrate de sodium,du bitume dans du toluène,du polystyrène dans du xylène et des compositions différentes sans solvants;on utilise également une couche métallique de Cd,Zn,Al,Sn,Pb,Cr,Co,Ni,
- la protection cathodique unique ou avec les inhibiteurs de corrosion dans le revêtement en béton.

L'interaction simultanée de la protection d'inhibiteur dans le béton et de la couche sur l'acier semble la méthode la plus complexe pour protéger l'armature dans le béton. Cette méthode est efficace même dans le cas où un de ces éléments subit un affaiblissement avec le temps.

L'efficacité d'une protection augmente relativement,par rapport aux autres solutions, quand l'agressivité du milieu augmente également.Mais,la protection cathodique diminue l'adhésion entre le béton et l'armature.

Il est difficile également de prévoir la dispersion des potentiels dans les joints d'acier de diamètres différents.Cela forme des piles de concentration après interruption de la protection cathodique.C'est pourquoi on a décidé de procéder à la passivation de l'armature à l'aide de la polarisation anodique au moyen du courant de densité exactement déterminée.La nouveauté de cette méthode est l'utilisation des inhibiteurs organiques sous forme de mélange de l'acide abiétique et adipique et la détermination de l'étendue optimum de la densité du courant après la formation de la couche passive.

Un des éléments nouveaux c'est le système électrique qui réalise la couche passive et les électrodes pour mesurer les paramètres d'estimation de la passivation.

2.FORMATION POTENTIOSTATIQUE DE LA COUCHE PASSIVE AVEC LA PROTECTION D'INHIBITEUR SIMULTANÉE

Pour éclaircir le mécanisme de la passivation on considère le plus souvent deux théories.La première c'est la théorie de la couche d'oxyde,la deuxième c'est la théorie d'absorption de la passivation.

En utilisant les éléments de ces théories, on a essayé de déterminer les propriétés de la couche passive formée sur la surface de l'armature dans la pâte de ciment et dans le mortier de ciment Portland.

Pour cela,on a mis au point le système de mesure qui permet de former et estimer les propriétés de la couche passive sur la surface de l'armature (Fig.1) .

Pendant la première phase des essais,on a déterminé la relation des changements de la résistivité active et du potentiel de l'armature,au cours de la prise de la pâte de ciment et du mortier du rapport e/c=0,5; 0,6;0,7,en fonction du temps (le rapport sable/ciment égal à 3:1) .

On a opéré des mesures identiques pour les pâtes de ciment et pour les mortiers avec addition de 4% de mélange des acides abiétiques ($C_{20}H_{30}O_2$) et adipiques ($C_4H_8(COOH)_2$). Ensuite,on a déterminé l'étendue de la densité du courant de passivation.

La mesure du changement de la résistivité active s'est faite à l'aide du conductivi-

J.Wiśniewski,École Polytechnique de Kielce;J.Karyś,École Polytechnique de Wrocław;J.Czaja,École Polytechnique de Wrocław,Pologne.

-mètre en utilisant le courant de fréquence de 10000 Hz et de tension de 4 V.

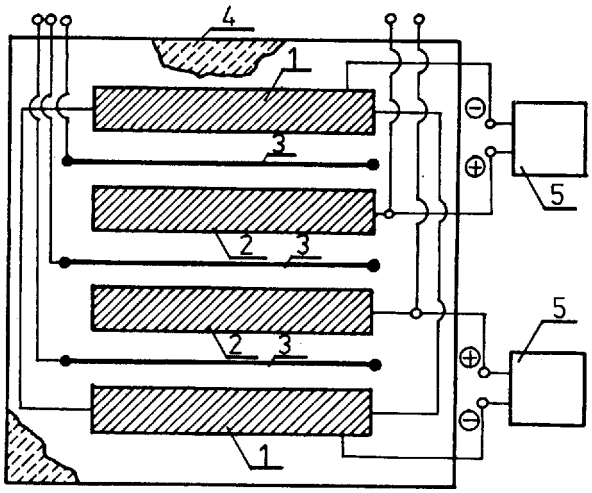

Fig.1.Schéma du système électrique pour former la couche passive et pour mesurer le degré de passivation anodique de l'armature
1-les électrodes en acier résistant aux acides;2-les électrodes en armature (C=0,20%,Mn=0,58%,Si=0,07%, P=0,05%,S=0,055%,Cr+Ni+Cu=0,66%) ; 3-les électrodes d'argent;4-le revêtement de composite;5-le potentiostat

On a mesuré le changement de pH au moyen de l'électrode à antimoine préparée spécialement.Le changement du potentiel électrique était établi à l'aide de l'électrode au calomel préparée,elle-aussi,spécialement.
Pour éliminer l'influence de la température,on a utilisé un compensateur de température.

La composition chimique des ciments utilisés pendant les essais est presentée au tableau 1.
Les propriétés physiques des ciments A,B,C sont pareilles:densité de 3030 à 3160 kg/m^3, surface spécifique de 2931 à 3400 cm^2/g, temps de prise - début:de 3h20'à 5h30' - fin:de 5h10' à 7h15'.

À la fig.2,on présente la relation de la résistivité active (R_a) ,des pâtes de ciment et des mortiers de ciment A de e/c=0,5,sans ou avec addition du mélange de l'acide abiétique et adipique (4% par rapport à la masse du ciment) ,en fonction du temps.
Les changements de la résistivité active pour le revêtement de ciment B,C et de e/c= 0,6 et 0,7 ont la même tendence.

Les valeurs obtenues pour les pâtes de ciment et les mortiers avec addition sont supérieures à celles des composites sans addition.

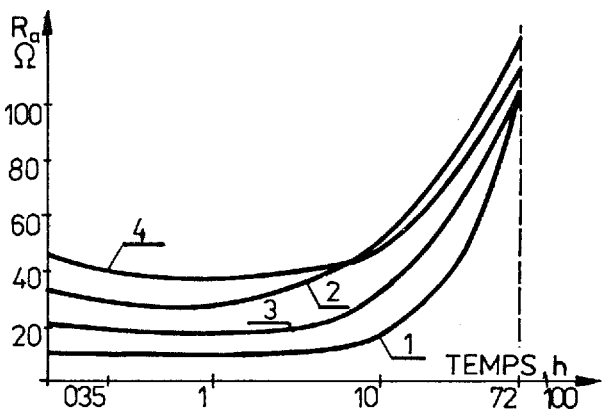

Fig.2.Relation de la résistivité active (R_a) des pâtes de ciment et des mortiers de ciment A,pendant 72 heures de prise en fonction du temps
1-la pâte sans addition,2-le mortier sans addition,3-la pâte avec addition, 4-le mortier avec addition

Tableau 1

Les propriétés chimiques des ciments

Constituants du ciment	Teneur en %		
	A	B	C
SiO_2	20,9	19,7	18,6
Al_2O_3	4,9	4,3	5,0
Fe_2O_3	3,0	2,8	3,8
CaO	63,3	56,3	56,7
MgO	1,5	1,7	1,5
SO_3	2,2	2,1	2,5
Perte de calcination	3,7	1,8	3,9
Teneur en éléments insolubles dans HCl	0,5	11,3	8,0
C_3A	7,7	6,8	6,9

Cette influence est liée avec la précipitation des sels calciques des acides qui font partie de cette addition.Ce sont les adipate et abiétate de calcium.Les sels soumis à l'hydrolise ont les propriétés des solutions-tampons.
Le changement du potentiel de l'armature (E_{cal}) par rapport à l'électrode au calomel

J.Wiśniewski,École Polytechnique de Kielce;J.Karyś,École Polytechnique de Wrocław;J.Czaja,École Polytechnique de Wrocław,Pologne.

est présenté à la fig.3.

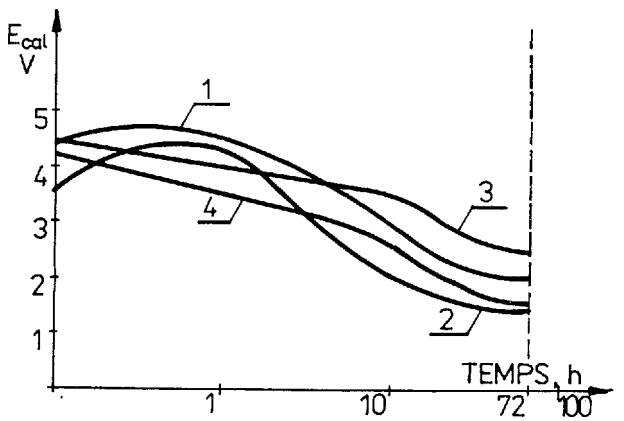

Fig.3.Changement du potentiel de l'armature en fonction du temps de prise des pâtes de ciment A et des mortiers pendant 72 heures
1-la pâte de ciment sans addition,
2-le mortier sans addition,
3-la pâte de ciment avec addition,
4-le mortier avec addition

En tenant compte des resultats de ces essais on a pu calculer le changement théorique de la densité du courant (i) qu'il faut appliquer pendant la prise des pâtes de ciment et des mortiers pour obtenir la passivation de l'armature,parce que:

$E_o = f(R_a, E_{cal})$,donc $i = f(E_o, k, l)$,

où: E_o - la chute de potentiel de l'électrolyte,V,

k - la conductivité du revêtement,$1/\Omega \cdot cm$,

l - l'épaisseur de la couche de l'électrolyte (du revêtement des composites), cm.

Ce calcul a permis de déterminer la densité minimum du courant égale à 5 $\mu A/cm^2$ et celle maximum égale à 200 $\mu A/cm^2$,ainsi que l'étendue de temps (Δt) égale de 8 à 48 heures (fig.4).

En utilisant cette étendue on a opéré une passivation anodique pratique de l'armature à l'aide du système électrique présenté à la fig.1.

Le revêtement a été réalisé en pâtes de ciment et en mortiers de ciments A,B,C pour le rapport e/c=0,5;0,6;0,7 avec ou sans addition du mélange d'acide abiétique et adipique.La caractéristique de la porosité et la résistance à la corrosion des pâtes de ciment et des mortiers est présentée aux tableaux 2,3.

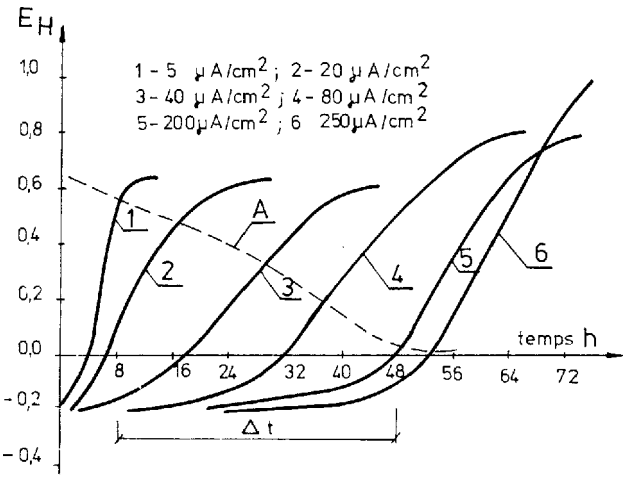

Fig.4.Changement du potentiel de l'armature par rapport à l'électrode à hydrogène en fonction du temps de prise du mortier de ciment C
A-la courbe de potentiel

Tableau 2

La porosité et la résistance à la corrosion des pâtes de ciment avec addition et sans addition

Propriétés des composites	Ciment	Valeurs pour e/c égal à		
		0,5	0,6	0,7
Porosité absolue,% (composites sans addition)	A	23,4	25,4	27,6
	B	35,1	38,1	39,6
	C	27,3	29,4	31,0
Porosité absolue,% (composites avec addition)	A	21,6	23,1	25,0
	B	32,3	33,8	35,7
	C	25,4	26,9	28,9
Degré de saturation(composites sans addition)	A	0,81	0,88	0,90
	B	0,86	0,89	0,93
	C	0,86	0,87	0,87
Degré de saturation (composites avec addition)	A	0,83	0,84	0,86
	B	0,85	0,87	0,87
	C	0,84	0,84	0,86
Coefficient de la résistance à la corrosion (composites sans addition)	A	0,61	0,60	0,40
	B	0,65	0,61	0,46
	C	0,68	0,59	0,49
Coefficient de la résistance à la corrosion (composites avec addition)	A	0,67	0,67	0,57
	B	0,72	0,70	0,60
	C	0,73	0,70	0,59

Après le processus de la passivation anodique les éprouvettes ont été curées pendant 28 jours dans des conditions humides

J.Wiśniewski,École Polytechnique de Kielce;J.Karyś,École Polytechnique de Wrocław;J.Czaja,École Polytechnique de Wrocław,Pologne.

(l'humidité relative égale à 95%).
Ensuite ces éprouvettes ont été immergées dans la solution de HCl ($0,274$ mol/dm^3) de façon à ce que le facteur agressif pénétre dans l'éprouvette seulement à la surface supérieure et inférieure (voir la fig.1).

Tableau 3

La porosité et la résistance à la corrosion des mortiers avec et sans addition

Propriétés des composites	Ciment	Valeurs pour e/c égal à		
		0,5	0,6	0,7
Porosité absolue,% (composites sans addition)	A	20,6	22,3	23,8
	B	33,1	33,3	35,1
	C	24,5	26,1	28,6
Porosité absolue,% (composites avec addition)	A	19,8	20,0	22,3
	B	31,2	32,3	33,6
	C	22,8	24,1	25,7
Degré de saturation (composites sans addition)	A	0,83	0,86	0,86
	B	0,85	0,87	0,86
	C	0,83	0,85	0,87
Degré de saturation (composites avec addition)	A	0,84	0,87	0,89
	B	0,85	0,88	0,88
	C	0,86	0,87	0,88
Coefficient de la résistance à la corrosion (composites sans addition)	A	0,73	0,63	0,52
	B	0,75	0,68	0,54
	C	0,79	0,70	0,52
Coefficient de la résistance à la corrosion (composites avec addition)	A	0,79	0,73	0,63
	B	0,77	0,71	0,65
	C	0,83	0,76	0,63

On a choisi comme paramètre déterminant les résultats de la passivation - le temps après lequel le milieu agressif avait gagné la surface de l'armature (t_e).
Ce moment a été déterminé au moyen de la résistivité active du revêtement et du potentiel électrique de l'armature.
Les résultats des essais sont présentés à la fig.5.

3.ANALYSE DES ESSAIS

Les ciments utilisés dans les essais possèdent les compositions chimiques approchées.La teneur en CaO,un peu plus élevée dans le ciment A,n'influe pas de façon importante sur la résistance chimique des composites (des pâtes de ciment et des mortiers) dans un milieu acide.C'est pourquoi les résultats des essais de la résistance à la corrosion du revêtement dépendaient d'abord de l'addition du mélange de l'acide abiétique et adipique.

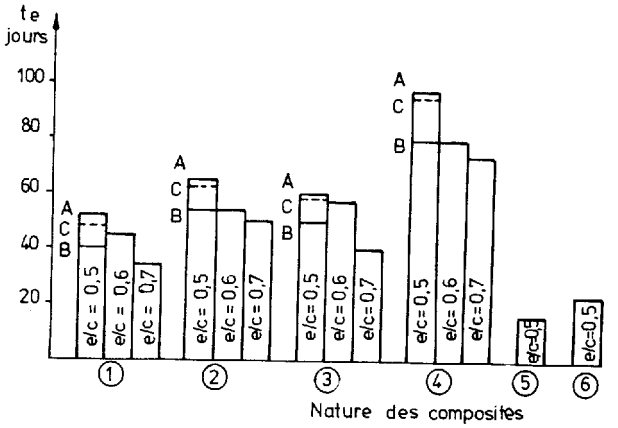

Fig.5.Temps après lequel le milieu agressif a gagné la surface de l'armature pour les revêtements différents
1- la pâte de ciment sans addition,
2- le mortier sans addition,
3- la pâte de ciment avec addition,
4- le mortier avec addition,
5- la pâte de ciment sans addition et sans passivation de l'armature,
6- le mortier sans addition et sans passivation de l'armature

Les valeurs de la résistivité active et du potentiel de l'armature agissent sur l'équilibre de résistivité active entre le revêtement et la couche passive après au moins 10 heures de passivation.Après 72 heures la couche passive est formée.Le changement concerne seulement la structure de cette couche.
L'addition du mélange de l'acide abiétique et adipique provoque une action physico-chimique surtout dans le revêtement de composite (fig.3,tab.2 et 3).
La structure de la porosité et l'utilisation de l'inhibiteur influent sur les propriétés du revêtement de la même façon (tab.2 et 3).
La vitesse de pénétration du milieu agressif augmente en proportion directe avec l'augmentation de la porosité absolue,du rapport e/c et du degré de saturation.Cette vitesse augmente également avec diminution du coefficient de résistance à la corrosion.
Le mortier offre de meilleures conditions

J.Wiśniewski,École Polytechnique de Kielce;J.Karyś,École Polytechnique de Wrocław;J.Czaja,École Polytechnique de Wrocław,Pologne.

pour la protection contre la corrosion que la pâte de ciment.
Les systèmes électriques utilisés pour produire et évaluer la passivation ont fait leurs preuves en permettant de déterminer la densité minimum et maximum du courant et l'étendue de temps pour la formation de la couche passive sur l'armature.

4.CONCLUSIONS

1. L'application de la protection d'inhibiteur dans le revêtement de composite sous la forme du mélange de l'acide abiétique et adipique ainsi que l'application de la couche passive constituée potentiométriquement créent de bonnes conditions pour le travail des constructions de béton armé en milieu aggressif.
2. Les conditions elaborées pour la constitution de la couche passive et le système électrique lui-même permettent d'appliquer de façon rapide et facile cette méthode de protection.

LITTERATURE

[1] Carpentier L.,Soretz M.S.:Contribution à l'étude de la corrosion des armatures dans le béton armé,Annales de l'ITBTP, n°223,224/1966.
[2] Cubaut J.C.,Murat M.,Eyraud C.:Comportement électrochimique des aciers pour le béton armé dans du ciment Portland artificiel en cours d'hydratation, Rev.des Mat.de Constr.n°603/1965.
[3] Dumas M.E.:Sur une méthode de protection des aciers contre la corrosion,Annales de l'ITBTP,n°23/1964.
[4] Longuet P.,Péguin P.,Rubaud M.,Zelwer A.: Bases expérimentales de l'étude électrochimique du comportement de métaux en présence du béton,Corrosion,Traitement,Protection,Finition,n°3/1973.
[5] Monfore G.E.:The Electrical Resistivity of Concrete,Journal of The PCA Research and Development Laboratories,1968.
[6] Petrocokino M.D.:Les divers aspects de la corrosion des armatures dans les ouvrages en béton armé et précontraint, Annales de l'ITBTP,n°153/1960.
[7] Ściślewski Z.:Korozja i ochrona zbrojenia,Arkady,Warszawa 1981.
[8] Wieczorek G.:Wpływ inhibitorów korozji na trwałość zbrojenia w betonie,ITB, Warszawa 1977.
[9] Le brevet polonais n°127736 du 20.12.84, les auteurs:J.Czaja,J.Karyś,J.Wiśniewski.

G Davies, Chief Research Officer and R E Oberholster, Senior Specialist Researcher both of the National Building Research Institute, CSIR, Pretoria, South Africa.

CHEMICAL AND SWELL PROPERTIES OF THE ALKALI-SILICA REACTION PRODUCT

SUMMARY: The alkali-silica reaction product found in deteriorated concrete consists of two amorphous phases and a number of morphologically distinct crystalline phases, three of which (the rod-like, blade-like and rosette-like crystals) are very widely distributed. The massive gel and the crystalline phases are characterised by the presence of Si, K and Ca. The massive gel generally has a much higher Ca and lower K content than the crystalline phases. Na is consistently present in the rod-like crystals only. Close to the contact with the aggregate, the alkali-silica reaction product found in voids alongside the aggregate is highest in Si. There appears to be a depletion of Ca in the cement paste at the boundary with the reaction product.

Reaction products removed from deteriorated concrete affected by alkali-silica reaction do not produce measurable swell pressures on absorption of water.

Sumário

Os produtos da reação alcali-silica encontrados em concretos deteriorados consistem em duas fases amorfas e um número morfologicamente distinto de fases cristalinas, três das quais (de cristais como barra, como lâmina ou como rosetas) são amplamente distribuídas. O gel compacto e as fases cristalinas são caracterizadas pela presença de Si, K e Ca.O gel compacto geralmente tem um conteúdo maior de Ca e menor de K que as fases as fases cristalinas. Na está consistentemente presente nos cristais semelhantes a barras. Junto com o contato com o agregado, os produtos da reação alcali-silica encontrados nos vazios ao longo do agregado é o mais alto em Si. Parece que há um esgotamento do Ca na pasta de cimento em seu bordo com o produto da reação.

Produtos de reação removidos de concreto deteriorado afetado pela reação alcali-silica não produzem pressões expansivas pela absorção da água.

INTRODUCTION

Identification of the alkali-silica reaction product (asrp) in deteriorated concrete is probably the most positive way of diagnosing alkali-silica reaction (asr). Confirmation of asr is usually obtained by performing scanning electron microscopy combined with EDX analysis, or X-ray diffraction analysis, or both on reaction product. However, characterisation of the asrp mineralogically and morphologically as well as chemically and physically, can assist in elucidating the mechanism of the reaction and thereby contribute to the prevention of the problem.

The possibility also exists that the asrp observed in concrete and characterised in the laboratory is a harmless end product and is in itself not deleterious in that it cannot exert swell pressure (1).

Recently Davies and Oberholster (2) presented extensive XRD and SEM-EDX data on the asrp. They described two amorphous phases, and a number of morphologically distinct crystalline phases, three of which are very widely distributed.

X-ray diffraction data on reaction products (2,3,4) have revealed at least two crystalline phases, one with a characteristic peak at 12 Å and the other with one at 8 Å. A third phase with a characteristic peak at 2.90 Å has also been suggested (2) (see Table I). A characteristic of the 12 Å phase is that the 12 Å peak shifts progressively down to 8.26 Å when heated to between 40 and 110°C. This shift is reversible.

CHEMISTRY

The asrp is a multicomponent system. Included with the different crystalline and amorphous phases are contaminants such as quartz and various forms of calcium carbonate. Although whole sample analyses naturally give the combined composition of all the different phases plus contaminants, the advantage of this type of analysis is that the amount of water and CO_2 in the reaction product can be determined.

A semi-quantitive EDX analysis can be obtained from a non-polished surface and is very useful to

TABLE I

XRD Peaks of the three crystalline phases which are part of the alkali-silica reaction product (2)

12 Å phase		8 Å phase		2.90 Å phase	
d	I	d	I	d	I
12.16	100	8.70	69	2.90	100
6.12	11	6.60	24	1.75	23
4.46	8	5.01	31		
3.04	29	3.89	13		
2.82	4	3.56	100		
2.44	9	3.10	18		
2.31	13	2.98	31		
2.04	7	2.84	29		
1.91	7	2.63	20		
1.89	8	2.22	11		
1.82	12	2.13	29		
1.71	6	1.87	27		
1.66	7				
1.47	11				

TABLE II

Published results of whole sample analysis of reaction product

Property	Percentage obtained					
	USA structures (5)			Australian dam (4)		
	1	2	3	4	5	6
SiO_2	49.82	61.73	50.70	66.00	85.91	59.90
Al_2O_3	1.15	2.17	n.a.	1.88	n.a.	3.78
Fe_2O_3	0.81	0.47	n.a.	n.a.	n.a.	n.a.
CaO	21.11	12.28	4.76	11.54	1,25	18.47
SO_3	0.16	0.00	n.a.	n.a.	n.a.	n.a.
Cl	n.a.	n.a.	n.a.	0.39	n.a.	n.a.
Na_2O	n.a.	n.a.	6.75	1.30	2,41	0.94
K_2O	n.a.	n.a.	6.68	19.00	0,60	4.66
H_2O*	34.6	9.81	24.80	17.23	8,31	n.a.
LOI	n.a.	14.84	n.a.	n.a.	n.a.	n.a.
Total	107.65	109.40	93.69	117.34	98.48	87.75

* Moisture loss at 450°C
n.a. Not analysed for
Column 6 Pure 8 Å phase

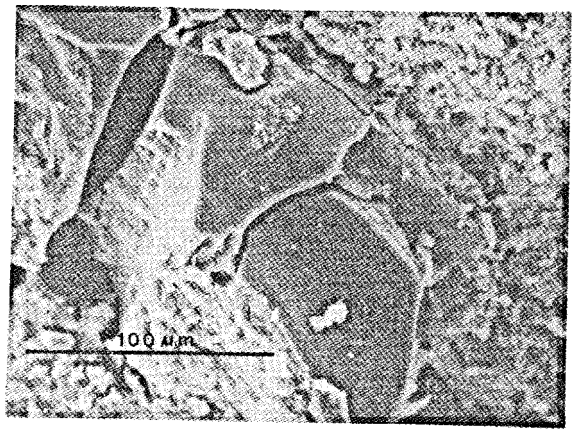

1a. Massive gel

	1%	2%	3%
SiO_2	40.16	60.69	61.60
Al_2O_3	-	-	-
CaO	51.59	33.08	23.35
Na_2O	-	-	-
K_2O	2.25	6.23	15.35

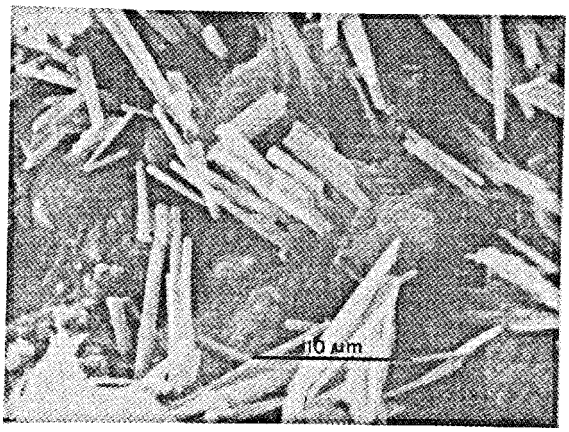

1b. Rod-like crystals

	1%	2%
SiO_2	63.70	60.30
Al_2O_3	-	-
CaO	8.87	13.15
Na_2O	13.09	8.37
K_2O	14.34	18.18

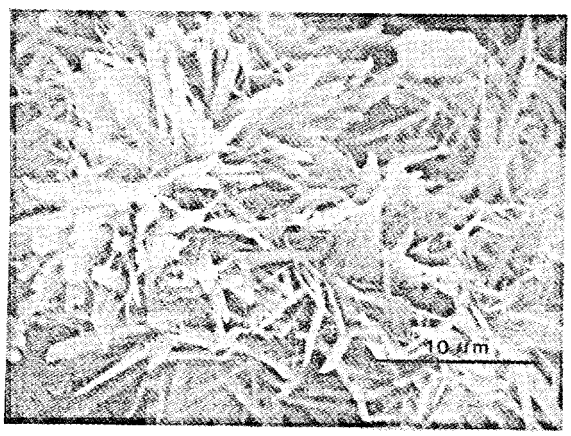

1c. Blade-like crystals

	1%
SiO_2	71.18
Al_2O_3	-
CaO	11.61
Na_2O	-
K_2O	17.21

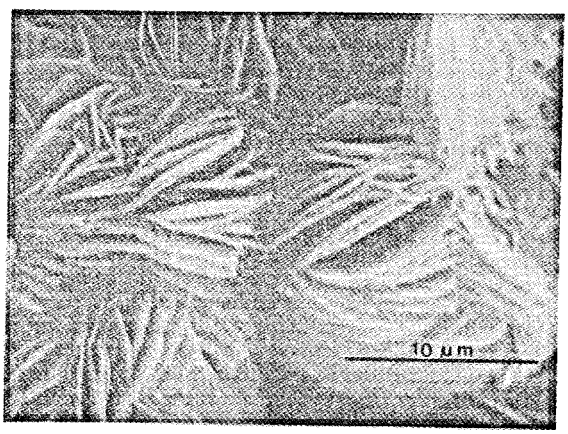

1d. Rosette-like crystals

	1%	2%	3%
SiO_2	68.59	71.12	76.96
Al_2O_3	-	-	4.62
CaO	18.19	17.79	9.38
Na_2O	-	-	-
K_2O	13.21	11.79	9.05

Fig. 1 - SEM photographs and normalised semi-quantitative EDX analyses for common phases of the asrp removed from various concrete structures

\- not detected in the spectrum

characterise the different phases. However, X-ray scattering and absorption severely hamper the reliability and reproducibility of the analyses.

Quantitative microprobe analyses are the most suitable for obtaining the composition of the different phases in the asrp. However, the fact that a flat, well polished surface is required means that the morphology, whereby the phase is characterised, is largely destroyed. Consequently, it is often difficult to distinguish between amorphous gels and crystalline phases and impossible to recognise different morphologies. In addition, water and usually carbon are not determined by microprobe analyses.

Whole sample analysis

In Table II, whole sample analyses from the literature (4,5) are given. As can be seen from the totals, which vary from 87.75 to 117.34 per cent, the quality of the analyses is poor.

TABLE III

Average normalised analysis of asrp from seven structures

Oxide	Percentage composition of asrp							
	Five bridges* (E Cape) Quartzite aggregate		Paul Sauer Dam** (E Cape) Quartzite aggregate				Lansdowne bridge* (S W Cape) Greywacke/ hornfels aggregate	
			Crystalline		Amorphous			
	Mean (13)+	Std dev	Mean (4)+	Std dev	Mean (8)+	Std dev	Mean (4)+	Std dev
SiO_2	72.77	2.43	72.12	1.02	69.04	0.65	71.99	1.31
Al_2O_3	0.32	0.10	-	-	-	-	0.29	0.06
CaO	14.57	1.71	15.53	0.67	18.26	0.43	15.96	1.98
Na_2O	1.77	0.75	-	-	-	-	1.92	0.65
K_2O	9.56	1.56	12.34	0.52	12.57	0.67	8.98	1.59
EPMA total	70.31	9.78	62.82	5.82	79.82	2.96	75.14	8.14

EPMA Electron probe micro-analysis
* Using wavelength spectrometer
** Using energy dispersive system
\+ Number of analyses used per structure given in brackets

SEM-EDX analysis

Davies and Oberholster (2) observed that the more common phases of the asrp in concrete from affected structures are a massive, amorphous gel and three distinct crystalline phases, namely rod-like, blade-like and rosette-like crystals. These phases are presented in Figure 1 together with their normalised semi-quantitative EDX analyses. Although the quality and reproducibility of standardless EDX analyses are poor, a good indication of the chemical composition of the various phases can be obtained.

The massive gel is very often associated with the rosette-like crystals. It has a much higher Ca and lower K content than the crystalline phases. The composition of the crystalline phases is much less variable than that of the amorphous gel. All three crystalline phases are characterised by the presence of Si, K and Ca. Small amounts of Na can be found in the blade-like and rosette-like crystals but this element is consistently present only in the rod-like crystals. Other elements that may be present in minor amounts are Al, Fe and, very occasionally, Mg. The rosette-like crystals are not only the most common crystalline phase observed in affected concrete but are generally chemically the most consistent and have the highest CaO content of the three.

Microprobe analysis

Average normalised microprobe analyses of asrp from different structures from the South Western and Eastern Cape affected by asr are presented in Table III.

The analyses using a wavelength spectrometer are very similar to analyses using an energy dispersive system. Even though no attempt to distinguish between crystalline and amorphous reaction product was made in the study where a wavelength spectrometer was used, the mean values for the material from the bridges are very similar to those for the crystalline material from the Paul Sauer Dam which were analysed using an EDS. The amorphous gel from the Paul Sauer Dam has a very similar K_2O content to that of its crystalline material, but a lower SiO_2 and higher CaO content. The dam samples had no Na_2O and Al_2O_3, and a higher K_2O content than the samples from the bridges. The asrp is similar, irrespective of whether quartzite or greywacke/hornfels aggregate has been used.

A detailed microprobe study across an air void filled with reaction product was undertaken to investigate the chemical zoning within the reaction product and the elemental distribution at the interface of the reaction product with the aggregate and the cement.

A backscattered electron image of the polished sample is shown in Figure 2. The two phases can be distinguished in the filled void, an outer envelope of clear gel which surrounds white powdery material. The boundary between the two phases is clearly cuspate and cracks running through both phases and the cement paste are also evident. The clear gel only intervenes between the powdery material and the cement paste, while the white powdery material is directly juxtaposed to the aggregate.

Analyses were undertaken at the points numbered 1-27

TABLE IV

Normalised microprobe analyses across an air void filled with reaction product, in a sample of concrete from the Paul Sauer dam

Analysis position (Fig. 2)	Percentage				Normalisation factor	Ratios		
	SiO_2	Al_2O_3	CaO	K_2O		CaO/SiO_2	K_2O/SiO_2	CaO/K_2O
Traverse 1								
24	100.00	-	-	-	1.018	-	-	-
25	59.13	2.53	28.66	9.68	0.751	0.485	0.164	2.961
26	68.43	-	17.83	13.74	0.843	0.261	0.201	1.298
27	68.53	-	18.03	13.44	0.811	0.263	0.196	1.331
Traverse 2								
1	100.00	-	-	-	0.987	-	-	-
2	100.00	-	-	-	0.992	-	-	-
3	100.00	-	-	-	0.989	-	-	-
4	100.00	-	-	-	1.007	-	-	-
5	73.15	-	15.16	11.68	0.615	0.207	0.160	1.298
6	72.76	-	15.00	12.23	0.619	0.206	0.168	1.226
7	71.63	-	15.46	12.90	0.570	0.216	0.180	1.198
8	70.93	-	16.51	12.56	0.709	0.233	0.177	1.315
9	69.02	-	17.97	13.01	0.750	0.260	0.188	1.381
10	68.66	-	18.25	13.09	0.768	0.266	0.191	1.394
11	69.87	-	18.25	11.88	0.787	0.261	0.170	1.537
12	63.96	-	27.37	8.67	0.781	0.455	0.144	3.156
13	49.75	3.49	43.52	3.24	0.751	0.875	0.065	13.45
14	57.85	3.69	37.04	1.41	0.878	0.640	0.024	26.23
15	43.09	1.84	53.94	1.12	0.721	1.252	0.026	48.04
16	41.26	1.85	52.94	3.95	0.567	1.283	0.096	13.40
Traverse 3								
17	100.00	-	-	-	0.991	-	-	-
18	100.00	-	-	-	0.992	-	-	-
19	69.01	-	18.52	12.47	0.803	0.268	0.181	1.485
20	68.66	-	19.18	12.16	0.802	0.279	0.177	1.576
21	70.20	-	18.05	11.75	0.822	0.257	0.167	1.536
22	100.00	-	-	-	1.020	-	-	-
23	100.00	-	-	-	1.016	-	-	-

- not detected

(Fig. 2), along three traverses, all of which started in the aggregate and proceeded into the reaction product. Only traverse 2 proceeded through the reaction product and into the cement paste. The normalised analyses for each point, as well as the oxide ratios, are presented in Table 4. Plots of the CaO/SiO_2, CaO/K_2O and SiO_2/K_2O ratios along each traverse are presented in Figures 3a, b and c. The contact between the powdery crystalline reaction product (PRP) and the aggregate is sharp with no gradation. The powdery reaction product has a slightly lower CaO/SiO_2 than the clear amorphous reaction product (CRP).

The contact between the cement paste (CP) and the clear reaction product (CRP) is gradational. There appears to be a SiO_2 gradient across the reaction product. Analyses taken close to the siliceous aggregate are higher in SiO_2 and the CaO/SiO_2 ratio increases in a systematic manner towards the cement paste. The K_2O content increases fairly sharply from the cement paste into the clear reaction product and decreases slightly in the powdery reaction product.

SWELL TESTING

Concrete will crack if the tensile strength of the cement paste is exceeded. Values quoted for the tensile strength of cement paste range from as low as 3 MPa (6) to 6 MPa (7) to 10 MPa (8).

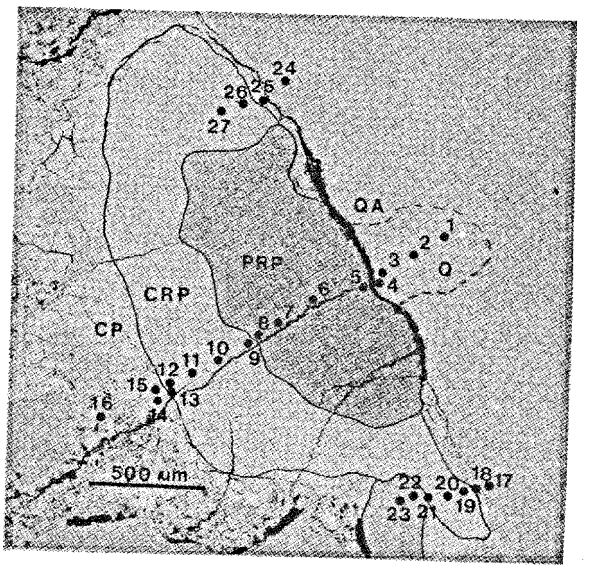

Fig. 2 - (Left) Backscattered electron image of air void filled with asrp. The positions of the microprobe analyses and boundaries between the different phases are indicated. CP = cement paste; CRP = clear reaction product; PRP = powdery reaction product; QA = quartzite aggregate; Q = quartz.

Pike (9) obtained a pressure of 14 MPa when he allowed mortar made with opal-containing aggregate to react in a sealed pressure-cell. McConnell et al (10) measured a pressure of 3.8 MPa when waterglass was allowed to absorb water through a cement-mortar membrane. Verbeck and Gramlich (11) reported a maximum pressure of 0.7 MPa when opal was allowed to react with NaOH through a cement-paste membrane. Struble (12) found that when synthetic sodium silica and calcium sodium silica gels were allowed to absorb water, a free swell developed that varied from 0.5 to 18.6 per cent, by volume, while at the same time the swell pressure ranged from 0.08 to

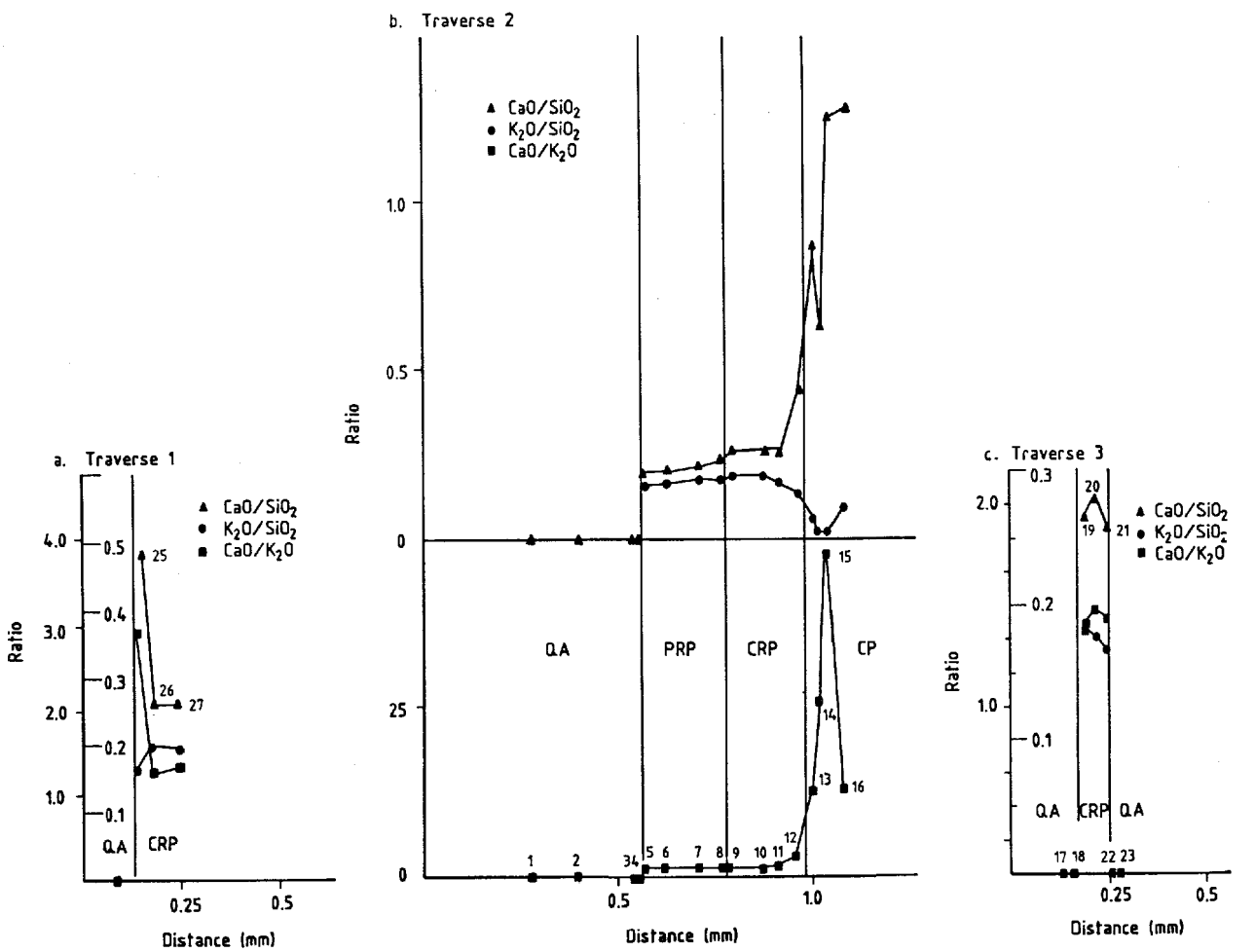

Fig. 3 - Variation in oxide ratios along three traverses at the numbered points shown in Figure 2. In traverses 1 and 3 the values on the left-hand side of the vertical axis are CaO/K_2O ratios while those on the right hand side are CaO/SiO_2 and K_2O/SiO_2 ratios. CP = cement paste; CRP = clear reaction product; PRP = powdery reaction product; QA = quartzite aggregate.

10.89 MPa. The highest swell pressure found was for a sodium silica gel with a Na_2O/SiO_2 ratio of about 0.35.

Swell tests were done, on asrp separated from affected concrete structures, using a sample container based on the design of Struble (12). An 'Interface' load cell (type 1210 AF) with a maximum measuring capacity of 9 kN was used. The load cell was calibrated using an 'Instron' strain data unit. The area of the piston (diameter of 13 mm) on which the sample exerted pressure is 132.73 mm^2. Initial tests with the apparatus were carried out using a montmorillonite clay.

Reaction product from two structures, both showing only peaks of the 12 Å phase, were heated at 40°C for one hour and XRD analysis used to confirm that the 12 Å peak had shifted to about 8 Å. The samples were weighed, compacted at 1 MPa pressure for 10 minutes, the load removed and the sample allowed to recover; pressures of 0.34 MPa and 0.28 MPa were then applied to the two different samples, respectively, and water added. Neither of the samples expanded and, in fact, in both the pressure started to decrease after an hour or more.

A sample of the 8 Å phase was also heated to 40°C for one hour. XRD analysis indicated no shift of the 8 Å peak. The procedure described above was followed, using a confining pressure of 0.28 MPa. No expansion was measured.

CONCLUSIONS

(i) The more usual phases of the asrp found in deteriorated concrete structures are an amorphous massive gel and three morphologically distinct crystalline phases, namely rod-like, blade-like and rosette-like crystals.

(ii) The massive gel has a higher Ca and a lower K content than the crystalline phases.

(iii) The rosette-like crystals are the most common, are chemically the most consistent and have the highest Ca content of the three crystalline phases.

(iv) The reaction products from structures containing widely different quartz-bearing aggregates and geographically far apart, are similar.

(v) Both the crystalline and amorphous reaction products are calcium alkali silicates.

(vi) Close to the contact with the aggregate the asrp is highest in Si. There is a decrease in Si content on moving into the reaction product.

(vii) There appears to be a depletion of Ca in the cement paste at the boundary with the reaction product.

(viii) No measurable swell pressures were produced by either the 12 Å phase converted to a lower d-spacing at about 8.26 Å by heating and the 8 Å phase separated from concrete of deteriorated structures.

REFERENCES

1. R.E. OBERHOLSTER (1983), "Alkali reactivity of siliceous rock aggregates: diagnosis of the reaction, testing of cement and aggregate and prescription of preventive measures", Proceedings 6th International Conference on Alkalis in Concrete, Copenhagen, pp 419-433.

2. G. DAVIES and R.E. OBERHOLSTER (1986), "The alkali-silica reaction product: A mineralogical and an electron microscopic study", Submitted to the Eighth International Conference on Cement Microscopy, Orlando, Florida.

3. W.F. COLE, C.J. LANCUCKI and M.J. SANDY (1981), "Products formed in aged concrete", Cement Concrete Research, 11, pp 443-454.

4. W.F. COLE and C.J. LANCUCKI (1983), "Products formed in aged concrete - the occurrence of okenite", Cement Concrete Research, 1, 611-618.

5. A.D. BUCK and K. MATHER (1978), "Alkali-silica reaction products from several concretes: optical, chemical and X-ray diffraction data", Proceedings 4th International Conference on the effects of alkalis in cement and concrete, Purdue University, USA, pp 73-85.

6. R.N. SWAMY (1979), "Polymer reinforcement of cement system", J Mater Sci, 14, pp 1521-1553.

7. W.A. GUTIERIDGE and C.D. POMEROY (1983), "Cement in its conventional uses: problems and possibilities", Phil Trans R Soc London, A310, pp 7-15.

8. D.N. WINSLOW and W.L. DOLCH (1976), "Cement plaster hydrated in $Sr(OH)_2$", Cement Concrete Research, 6, pp 309-320.

9. R.G. PIKE (1958), "Pressure developed in cement pastes and mortars by alkali-aggregate reaction", Nat Res Council Highway Res Board Bull, 177, pp 34-36.

10. D. McCONNELL, R.C. MIELENZ, W.Y. HOLLAND and K.T. GREENE (1947), "Cement- aggregate reaction in concrete", J Amer Soc Testing Mater, 44, pp 93-128.

11. G.J. VERBECK and C. GRAMLICH (1956), "Osmotic studies and hypothesis concerning alkali-aggregate reaction", Proc Amer Soc Testing Mater, 55, pp 1110-1128.

12. L.J. STRUBLE (1979), "Swell and other properties of synthetic alkali-silica gels", Unpublished MSc Thesis, Purdue University, USA, 150 p.

C. Andrade, C. Alonso, P. Santos and A. Macías. Instituto de la Construcción y del Cemento "Eduardo Torroja" - Consejo Superior de Investigaciones Científicas - Spain.

Corrosion behaviour of steel during accelerated carbonation of solutions which simulate the pore concrete solution

Corrosion des armatures pendant la carbonatation accelerée des solutions qui simulent la phase aqueuse renfermée dans les pores du béton.

In spite of the numerous studies carried out on carbonation of the concrete, very few data have been published on the mechanism of steel depassivation and the corrosion rates involved in this type of phenomenon. Also some uncertainties remain as to the chemical composition of the pore solution of a carbonated concrete.

Random behaviours related with the changes in the corrosion rate of steel during accelerated carbonation of cement mortars have suggested the need to study the process in a more simple medium which allows the isolation of the different parameters. Thus, saturated Ca $(OH)_2$ - base solutions with different additions of KOH and NaOH have been used to simulate the real pore concrete solution.

In the present work, simultaneous changes in the pH value, corrosion potential and corrosion rate (measured by means of the determination of the Polarization Resistance) of steel roads have been monitored during accelerated carbonation produced by a constant flux through the solution of CO_2 gas and/or air.

Some clear differences in these variables have been established between solutions with and without Na^+ and K^+ ions, which may clarify the different corrosion behaviours observed in mortar made with different types of cements. Because CO_3 Ca is insoluble, the solution not containing alkalies are carbonated more quickly than those containing them. Final pH values in the case of a sat. Ca $(OH)_2$ alkali-free solution are always near neutrality (pH-6-7), but solutions containing alkalies may have a final pH value of about 10,4 where a buffer of $CO_3^=/HC_3^-$ is established. Only when an excess of CO_2 gas is passed through the solution, are all sodium and potasium carbonates transformed into bicarbonates and the final pH value is about neutrality.

These results lead to an apparent contradiction between the final pH values of real carbonated concretes an those carbonated in an accelerated form.

Concerning the corrosion behaviour, the previous hypothesis is confirmed using air as the carbonating agent. The corrosion potential of steel rises simultaneously with the decrease in pH value is until a limit is reached and depassivation occurs. After this moment corrosion starts and the corrosion rate is dependent on the final pH value of the solution and, therefore, its bicarbonate content.

Sumário

Apesar dos numerosos estudos levados a efeito sobre a carbonatação do concreto, poucos dados foram publicados sobre o mecanismo da despassivação do aço e as taxas de corrosão envolvidas nesse tipo de fenômeno. Também algumas incertezas permanecem como a composição química da solução no poro de um concreto carbonatado.

O comportamento aleatório relacionado com as mudanças nas taxas de corrosão do aço durante a carbonatação acelerada de argamassas de cimento sugeriu a necessidade de estudo do processo em um meio mais simples que permita o isolamento dos diferentes parâmetros. Então, soluções de base saturadas de $Ca(OH)_2$, com diferentes adições de KOH e NaOH foram usadas para simular a solução real nos poros do concreto.

No presente trabalho, mudanças simultâneas do valor do pH, do potencial de corrosão e taxa de corrosão (medida por meio da determinação da Resistência de Polarização) de barras de aço foram acompanhadas durante carbonatação acelerada produzida por um fluxo constante, através da solução, de gás CO_2 e/ou ar.

Algumas claras diferenças nessas variáveis foram estabelecidas entre soluções com e sem íons Na^+ e K^+, que pode esclarecer os diferentes comportamentos de corrosão observados em argamassas feitas com diferentes tipos de cimento. Devido ao $CaCO_3$ ser insolúvel, a solução não contendo álcalis é carbonatada mais rapidamente do que aquelas que contêm. Valores finais do pH no caso de solução saturada de $Ca(OH)_2$ livre de álcalis estão sempre próximos da neutralidade (pH 6-7), mas soluções contendo álcalis podem ter um valor final de pH cerca de 10,4 onde um estado de $CO_3^=/HC_3^-$ fica estabelecido. Somente quando um excesso de CO_2 passa através da solução, todos os bicarbonatos de sódio e potássio transformam-se em bicarbonato e o valor final do pH é próximo da neutralidade.

Esses resultados levam a uma aparente contradição entre os valores finais do pH do concreto realmente carbonatado e aqueles carbonatados de forma acelerada.

Em relação ao comportamento de corrosão, a hipótese prévia é confirmada usando ar como agente de carbonatação. O potencial de corrosão do aço sobe simultaneamente com o decréscimo do valor do pH até alcançar um limite e a despassivação ocorre. Após esse momento a corrosão começa e a taxa de corrosão é dependente do valor final do pH da solução e, portanto, do seu conteúdo de bicarbonato.

The carbonation of concrete is a matter of increasing concern in Europe, where many structures have their concrete surface directly exposed to the action of the atmosphere and the tandard allow relatively little depth of cover of reinforcements.

As is already well known "carbonation" means the reaction between the atmospheric CO_2 with the pore concrete solution and with the solid phases of the cement paste. As different authors have stated (1) (2) the final state of this process consists of amorphous SiO_2, $Al(OH)_3$, SO_4Ca^{-2} H_2O, CO_3Ca in different polymorphic varieties and H_2O. Thus, the initial alkaline pH in the pore concrete solution is neutralized. This neutralization allows the corrosion of reinforcements if a minimum of moisture and oxygen are present (3).

But in spite of numerous studies (4) (5) on the carbonation of concrete, very few of them have addressed the question of how and to what extent the corrosion of reinforcements occurs during carbonation. The ascertaining of the corrosion rates of the steel would permit the calculation of the residual service life of the structure.

The only common statement in carbonated concrete is that pH value decreases and the reinforcements corrode. Only authors who have studied the effect of cracks and have measured the decrease in diameter of the bars due to carbonation in the region of cracks (6) give an approximate and medium value of the corrosion rate at these points.

Some years ago a research project was initiated in our Institute to study this gap in knowledge and some results have already been published (3) (7). The experimental work mainly dealt with the study of the corrosion parameters of reinforcements embedded in hardened carbonated mortar or concrete and immersed in carbonated solutions that reproduce the composition of the pore concrete solution.

But the system used for carbonating in these experiments was one accelerated by pure CO_2 gas. This method produces a saturation of CO_2 in the solution or in the carbonation chamber and may lead to different phenomena from those which occurs when carbonation is produced naturally (the proportion of CO_2 in the atmosphere is about 0,03 %). This point is analyzed in the present paper and is taken into account in the future experimental work.

This paper sets out changes in the chemical composition of like-pore concrete solutions during accelerated and natural carbonation (by air) and also the results of simultaneous changes of corrosion potentials and corrosion rates of reinforcements. The results confirm the previously published hypothesis (3) (7) giving a new insight into the phenomenon.

EXPERIMENTAL

Materials and solutions

Corrugated steel bars 6 mm in diameter and 8 cm in length were used. The air/solution interphase and the lower end of the steel were covered with an adhesive tape. The surface exposed to attack was about 5 cm2.



Fig. 1.- Corrosion cell of polyethylene.

The corrosion cell is a polythylene bottle shown in figure 1.

The following solutions were tested. They were prepared with reagents in analytical grade:

Solution A - Saturated solution of $Ca(OH)_2$ (8g/l) - pH = 12,6

Solution B - Saturated solution of $Ca(OH)_2$+0,1 M NaOH+0,1 M KOH - pH = 13,2

Solution C - Saturated solution of $Ca(OH)_2$+0,5 M NaOH - pH = 13,5

Solution D - Saturated solution of $Ca(OH)_2$+0,1 M $NaNO_2$ - pH = 12,8

Solution E - Saturated solution of $Ca(OH)_2$+0,1 M Na OH+0,1 M KOH+ +0,1 M $NaNO_2$ - pH = 13,3

After the completion of the carbonation period the proportion of $CO_3^=$ and HCO_3^- were analyzed in some solutions by the traditional method of titration by HCl.

Experiments

The carbonation was produced by slowly bubbling either pure CO_2 gas or air through the solution. During the flux of the gases the pH--value was continously recorded with a pH-meter and a combined electrode of the pH range 0 - - 14. The electrode was calibrated from time to time with two buffers of pH = 7,12 and pH = 13.

The concentration of O_2 in the solutions was measured by a special ORION electrode of oxygen. It was also monitored constinously.

The flux of gases lasts up to 24h, after which time the cell is held at room temperature (21± 1°C) for a further 5-8 days.

The corrosion potential, E_{corr}, was also simultaneously and continously monitored through a potentiostat. However, given the abrupt changes during the flux of gases the corrosion rate was only measured just prior to and on completion of the test. It was also measured every day after the solution had been carbonated.

The corrosion rate is calculated from the Polarization Resistance, Rp, determinations by the Stern's et al method (8) through the formula:

$$I_{corr} = B \frac{\Delta I}{\Delta E} = \frac{B}{Rp}$$

The $Rp = (\Delta E/\Delta I)\Delta E \rightarrow \emptyset$ measurements were taken with a potentiostat. Values of the constant B of 26 and 52 mV were used for steel in the active and passive states respectively, as it has been described (3).

RESULTS

The results of the variations of pH-values, corrosion potential and corrosion intensity during and after accelerated carbonation by pure CO_2 gas of the solution A (satured solution of Ca $(OH)_2$) and B (saturated solution of $Ca(OH)_2$ -- + 0,1 M NaOH + 0,1 M KOH) were published in a previous paper (7). For the purpose of comparison the results are reproduced in figures 2 and 3.

One of the points to be clarified in these tests concerns the dramatic changes measured in the E_{corr} and I_{corr} values during the accelerated carbonation These changes were attributed to the lowering of the pH and therefore to the depassivation of the steel, but they may also be due to the deareation of the solution provoked by the flux of the pure CO_2 gas.

Therefore a previous experiment was carried out consisting of measuring the concentration of oxygen during the carbonation experiment compared with a simple deareation by flux of N_2. The results of the decrease in O_2 concentration during the pass either of CO_2 flux or of N_2 flux through a type A solution are shown in figure 4. The deareation due to the flux of CO_2 is deeper than with N_2.

The test of carbonation of the type A solution (saturated solution of Ca $(OH)_2$ only) was subsequently repeated but using a flux of air (using a small air pump) to produce carbonation and avoid deareation. The evolution of the pH value, E_{corr}, I_{corr} and O_2 concentration is presented in figure 5. The abrupt changes are now produced about 24h after the beginning of the test and not after few minutes (as with pure CO_2), but the trend of the changes is identical to those shown in figures 2 and 3. The deareation provoked by the pure CO_2 only influences the final value of the corrosion potential and the absolute value of the corrosion intensity. Therefore, this confirms the previous hypothesis (3) (7) attributing the dramatic change to the

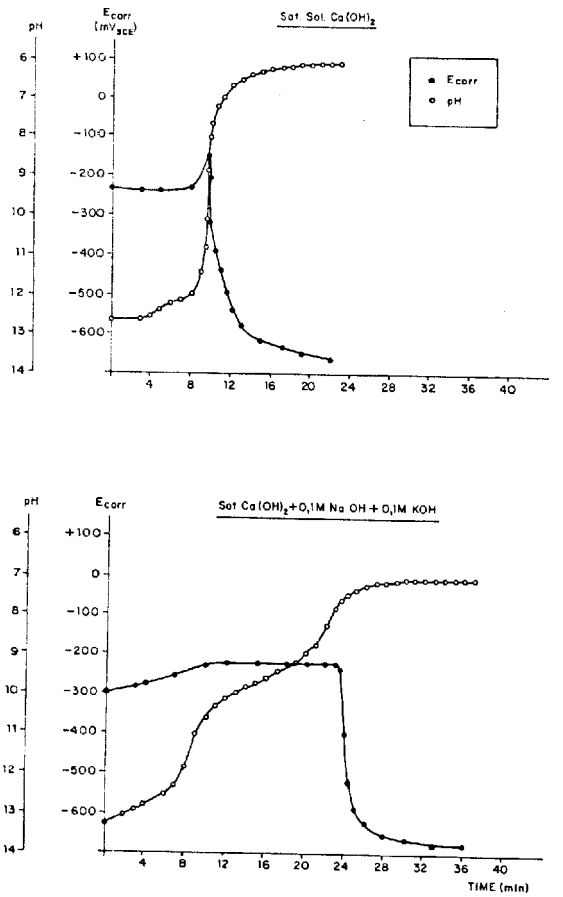

Fig. 2.- Evolution of E_{corr} and pH during carbonation of Sat. Sol. of Ca $(OH)_2$ with and without Na^+ and K^+ ions (7).

lowering of the pH value and the depassivation of the steel.

A solution with a higher concentration of alkali was also tested (after some days the pH of the pure concrete solution is usully above 13.5). Figure 6 shows the evolution of pH value, E_{corr}, I_{corr} and O_2 concentration of type C solution (saturated solution of Ca $(OH)_2$ + 0,5 M NaOH) carbonated now by a flux of pure CO_2. The trend of the changes in every variable is identical to that of solutions with a lower alkaline concentration and different the solution containing only Ca^{+2}. Again a similar buffer effect is produced of about pH ≃ 10,5 and the changes are less abrupt than when Na^+ and K^+ are absent. The final pH values are more alkaline.

Finally, figure 7 and 8 also present the evolution of the same variables but when $NaNO_2$ is added as a corrosion inhibitor admixture. In this case it must be pointed out that the corrosion potential does not dramatically change and the corrosion intensity increase very little, because of the inhibitor (oxydant and anodic in this case) effect of NO_2^-. Also the i_{corr}

increases less and the final values are smaller than when Na NO_2 is absent.

DISCUSSION

Before continuing, it must be pointed out that solutions do not reproduce the real situation of the bars embedded in concrete because of the differences in the physical parameters (electrical resistivity, the solid layer of Ca $(OH)_2$ precipitated on the surface of the steel, pore geometry, etc.) and the constant evolution of the pore concrete solution. However, they occasionally constitute the only method by which to make an approach and to study isolated variables. In the present experiments the work in solution has clarified many points related with steel corrosion in carbonated concrete, but a simple and direct extrapolation is not recomended without a careful review of all the errors that this extrapolation may introduce and without a comparison with parallel experiments in hardened concrete (7).

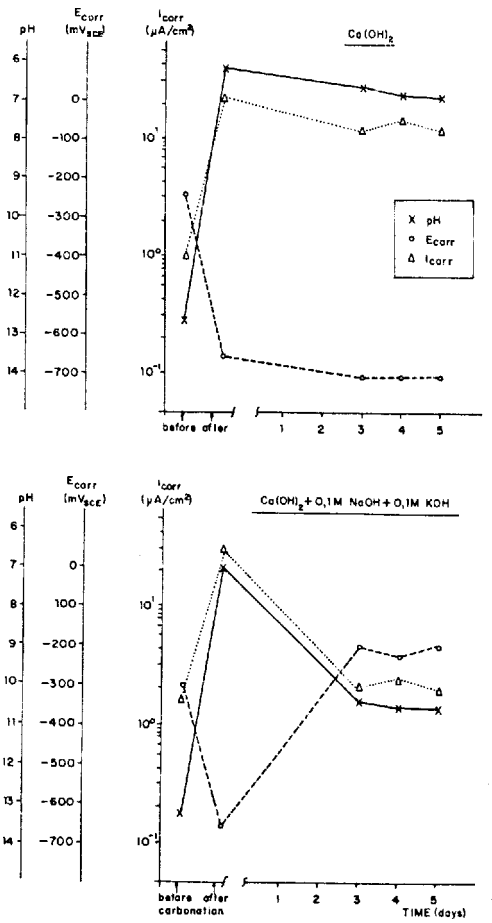

Fig. 3.- Values i_{corr} until 5 days after carbonation of the same solution of previous figure (7).

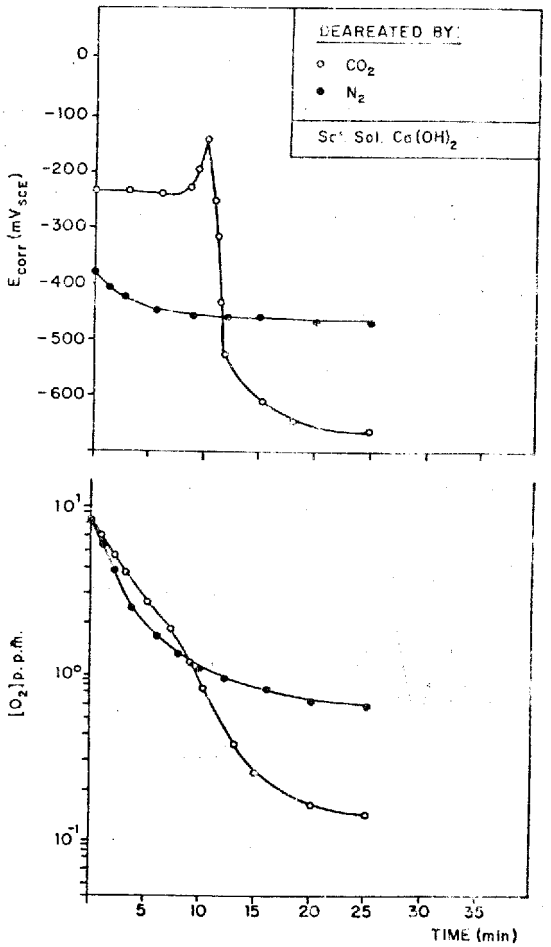

Fig. 4.- Decrease in O_2 concentration in a saturated solution of Ca $(OH)_2$ deareated by flux of CO_2 and of N_2.

Carbonation of the solutions

When pure CO_2 or air or the two gases together are bubbled into a saturated solution of Ca CO_3, which precipitates owing to its extremely low solubility, and water are formed. The final pH value would depend on the partial pressure of the CO_2 in the atmosphere, when the flux of the gases is stopped. Dissolved CO_2 and Ca $(HCO_3)_2$ are the substances present just after stopping bubbling because, due to the high concentration of CO_2, carbonates are redisolved as bicarbonates:

$$Ca\ CO_3 + CO_2 + H_2O \rightarrow Ca\ (HCO_3)_2$$

But the solution containing Na^+ and K^+ ions behaves differently because Na_2CO_3 and K_2CO_3 are soluble and may remain as ionic species in solution. In this case, the carbonation produces a less abrupt pH change and, although the final pH value just when the flux of CO_2 stops in again around neutrality (only bicarbonates

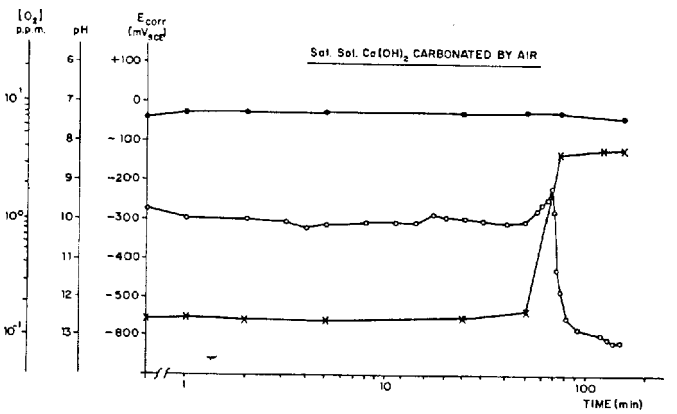

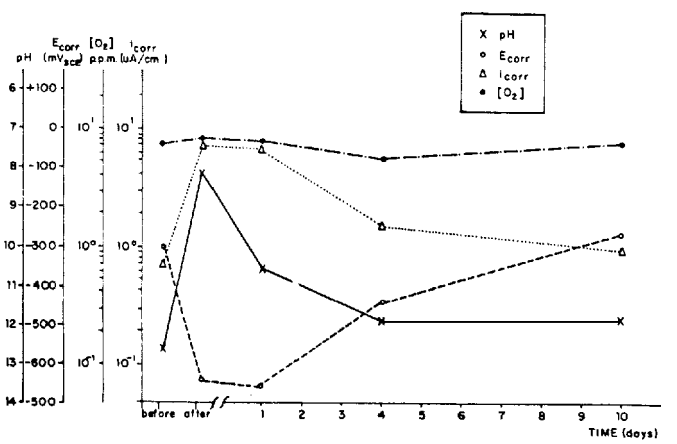

Fig. 5.- Evolution of the pH values, E_{corr}, i_{corr} and O_2 concentration of a saturated solution of Ca $(OH)_2$ carbonated by air during the carbonation process and for a further 10 days.

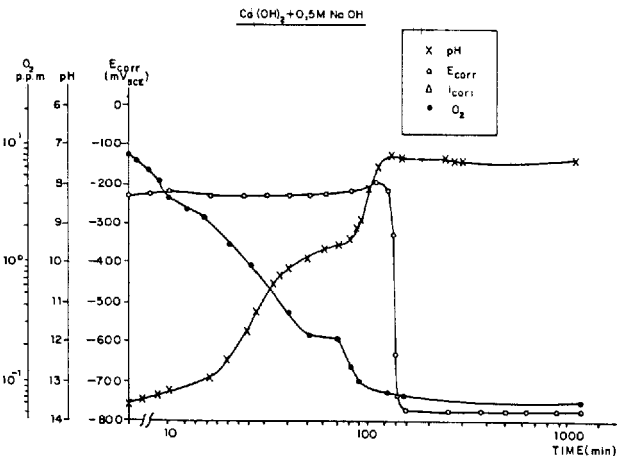

Fig. 6.- Evolution of the pH value, E_{corr} and O_2 proportion of a sat. sol. of Ca $(OH)_2$ plus 0,5 M NaOH during carbonation.

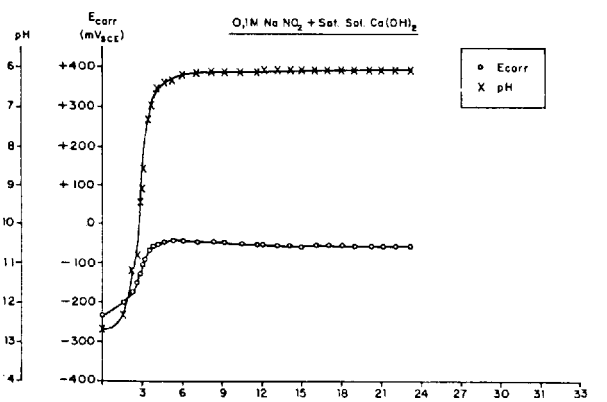

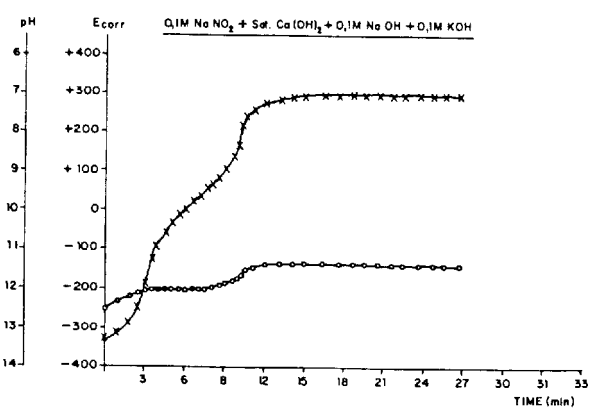

Fig. 7.- Evolution of the some variables and solutions presented in figure 2 but with the addition of 0,1 M $NaNO_2$.

and dissolved CO_2, are present), because of the well known equilibrium shown in figure 9, the pH spontaneously evolves to a value of around 10,4, that of the buffer carbonate - bicarbonate (9).

A simple extrapolation of these results to the real behaviour would conclude that an alkaline solution containing Na^+ and K^+ ions and completelly carbonated may have pH values of around 10,4 where the phenolphtalein indicator would have a clear red-purple colour. But all cements have alkalies in a higher or lower proportion and it has been observed in all carbonated concretes that the phenolphtalein indicator (colour variation from pH = 8 to 9,5) is colourless, thus pH is below 8. Therefore, either Na^+ and K^+ remain always as bicarbonates -which is not possible at the usual CO_2

partial presures in the atmosphere- or these ions "disappear" from the solution. One hypothesis is that they (Na^+ and K^+ ions) are consumed by the amorphous silica (pozzolanic reaction) (10) produced by the action of the CO_2 on the silicates (2) and, thus, only H_2O with dissolved CO_2 would be the final composition of the pore solution. Bicarbonates would be present only if the CO_2 partial pressure were high enough

The interpretation given here as to accelerated carbonation and the equilibrium of $CO_3^=/HC_3^-$ and the pH values involved is well known concerning natural and tap waters as is even the corrosive effect of these waters on the concrete itself. However the authors have never found it in the literature reviewed except (11) (12) and the "surprise" reported by Verbek (13) when he considers "the effect of alkaly hydroxide concentration on the equilibrium pH values at different CO_2 pressures. The calculation shows that for a liquid phase containing 1 N KOH the equilibrium at CO_2 pressure of the natural air should be about 10,5. This presents a paradoxical situation where such a concrete remain alkaline to phenolphtalein whilst being as carbonated as the partial pressure of CO_2 in air will allow. Some leaching must occur before the phenolphtalein will indicates a carbonation edge".

When natural carbonation is produced, the mechanism is the same but only negligible amounts of bicarbonates are produced. Higher amounts may be found in industrial or contaminated atmospheres.

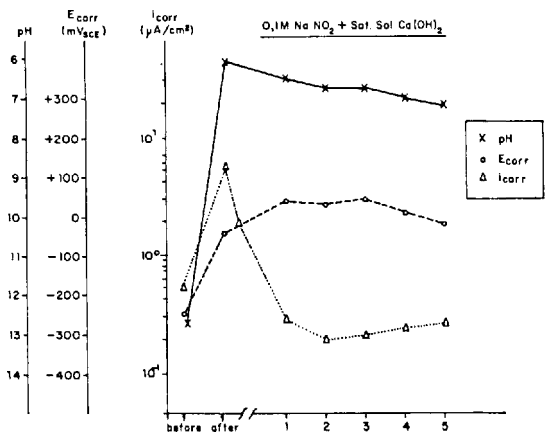

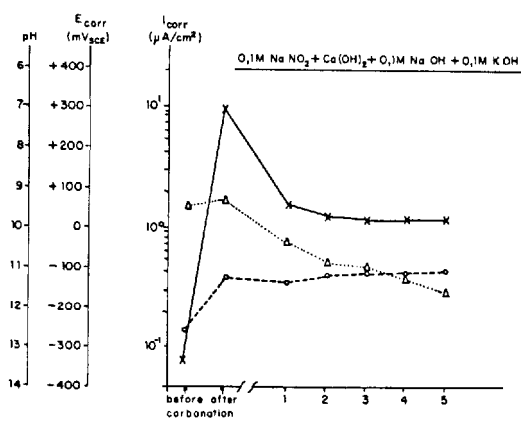

Fig. 8.- Evolution of the same variable and solutions presented in figure 3 but with the addition of 0,1 M $NaNO_2$.

Corrosion of steel

Studies (14) were carried out in solution in an attempt to stablish the threshold at which steel is depassivated when its pH is lower that of the saturated solution of Ca $(OH)_2$. No agreement was reached and many pH values have been published as the limit. One possible explanation of this disgreement is the variety of methods used to decrease the pH from 12,6.

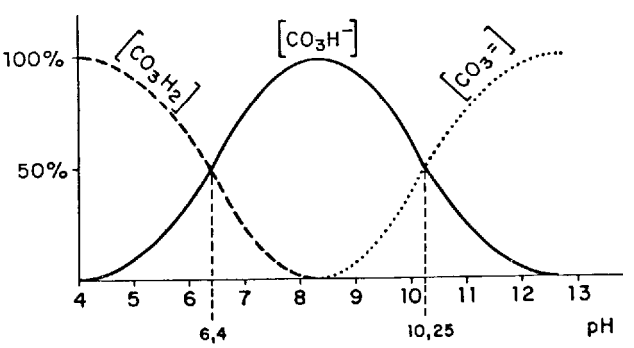

Fig. 9.- Variation with the pH of the relative concentrations of $CO_3^=$ H CO_3^- and H_2CO_3.

Concerning corrosion and carbonation a previous hypothesis (7) was stated (see figure 10 already published) to the effect that depassivation occurs at pH $\simeq$ 8 as Pourbaix has described many years ago (9). However some doubts remained over deareation using pure CO_2 for carbonation. The present results using simply air for carbonating confirm this previous explanation. They also support Pourbaix's results which show that the passive layers remains in spite of the lovering of the pH value, when Na NO_2 (oxydant inhibitor) is present. Changes in the corrosion potential are due mainly to Nersnt's law and corrosion intensity depends on the pH value, as previously reported (3).

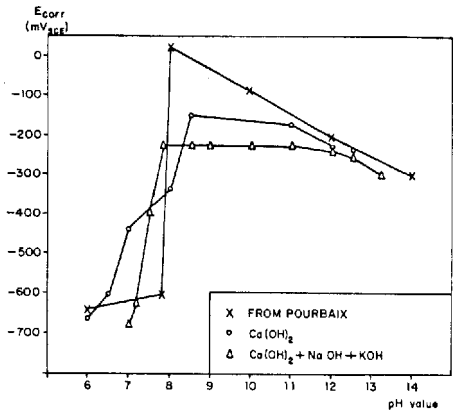

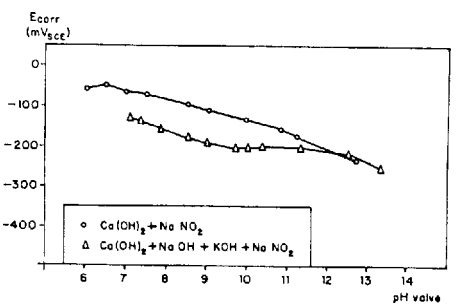

Fig. 10.- Dependence of the E_{corr} on the pH values for the solutions whose evolution during carbonation was presented in figures 2 and 7.

CONCLUSIONS

1ª) Acelerated carbonation (high partial pressure of CO_2) induces a deareation of the solution, but this deareation only influences the corrosion rate and not the mechanism of depassivation.

2ª) Accelerated carbonation during the flux of CO_2 gas produces high amounts of bicarbonates which modify the pH values. Spontaneous carbonation should produces negligible amount of bicarbonates.

3ª) When Na^+ and K^+ are present the final pH value of a completely carbonated solution simulating the pore concrete solution is around pH = 10,4, under test conditions.

4ª) The passive layer disappears from steel at pH $\simeq$ 8, as Pourbaix has stated many years ago. When Na NO_2 is present, the passive layer remains in spite of the lowering of the pH value.

REFERENCES

1 N. HAMADA - Proceedings of the 5th Int. Symposium on the Chemistry of Cement. Tokyo (1968) - vol III, 343.

2 D. GASPAR, M. MUÑOZ, T.VAZQUEZ - Materiales de Construcción, núm. 168 (1977).

3 J.A. GONZALEZ, S. ALGABA, C. ANDRADE - British Corrosion Journal (1980), 15, 3, 135.

4 M. VENUAT - Materiaux et Construction (1978) 11, 142.

5 H.G. SMOLCZYK - Rilem Symposium on Carbonation of Concrete. C.C. As. April (1976) - Wexham Springs. Theme 3.2.

6 P. SCHIESSL - Betonwerk + Fertigteil Technik (1975), 12, 594.

7 J.A. GONZALEZ, C. ALONSO, C. ANDRADE - "Corrosion of reinforcements in concrete construction" - Chapter 11 - The Society of Chemical Industry - Ellis Horwood Ltd - (1983), 159.

8 M. STERN, A.L. GEARY, J. Electrochem. Soc. (1957) 104, 56.

9 M. POURBAIX - "Lectures on Electrochemical Corrosion" - Plenum Press, New York and London, (1973).

10 C.L. PAGE, Ø VENNESLAND - Materiaux et Construction (1983) 16, 19.

11 N. ASCHAN - Nordisk Betong (1963) 3, 275.

12 D. BONNET, M. RUBAUD - Cahiers nº 1371 du CSTB nº 168 (1976).

13 G.J. VERBECK - Bulletin P.C.A. nº 87 - February (1958).

14 V.K. GOUDA - British Corrosion Journal (1970) 5, 198.

R.I.A. Malek, P.H. Licastro, and D.M. Roy*, Materials Research Laboratory, *Also, Dept. of Materials Science and Engineering, The Pennsylvania State University, University Park, PA 16802, USA

THE COMPATIBILITY BETWEEN AS EXPANSIVE GROUT AND ITS RESTRAINING ENVIRONMENT

4.3

SUMMARY: Cementitious materials are used to seal shafts and boreholes in many underground systems where their primary function is to provide a tight seal at the interface with the host environment. This is achieved by developing and maintaining a positive normal stress across the interface. Successful performance, in this respect, is partially dependent on the expansivity (or non-shrinking property) of the plug or seal relative to the restraining force of the surrounding host media. In expansive cementitious formulations, the degree of restraint offered by the surrounding mass is of importance to the development of interfacial stress. Information exists on unrestrained and standard restrained expansion of mortars and concrete, however, most do not permit calculation of actual interface stresses under the existing restraining forces of actual seal geometry. Such information is vital to the long-term durability.

A system was developed to determine the radial stresses imposed by a grout under confinement. It consists of a strain gage instrumented cell and its associated signal conditioner/amplifier. The test cell used in the system is unique in that it provides for direct calibration of the complete system. The system is versatile in that the cell material and dimensions can be selected to simulate restraint of a given host material under a geostatic load reflecting depth. Samples can be run under a range of temperature and pressure conditions, with the latter simulating either injection pressure or hydrostatic load conditions.

Different expansive cementitious formulations were evaluated. Those are based on type K shrinkage-compensating cement, Class-H oil well cement plus calcium sulfate hemihydrate and salt (NaCl)-containing formulations. Three distinct phases of expansion were found: the first is a thermal phase occurring with early heat liberation, the second occurs after the cement reaches its thermal maximum when simultaneous cooling and crystallization of expansive components takes place, and the third phase occurs after total relief of thermal stresses. The impact on seal system performance and longevity is discussed.

Sumário:

Materiais cementários são usados para selar falhas e buracos em muitos sistemas de sub-solo onde a sua principal função é de assegurar uma selagem na interface com o ambiente que o recebe. Isto é conseguido pelo desenvolvimento e manutenção de tensão positiva normal através da interface. Resultado com sucesso, a esse respeito, é parcialmente dependente da expansibilidade (ou propriedades de não-retração) do plug ou selo em relação às forças de impedimento do meio circundante. Em formulações cimentícias expansivas, o grau de impedimento oferecido pela massa circundante é de importância para o desenvolvimento de tensões na interface. Existem informações sobre a expansão de argamassas e concreto não encurtáveis ou com encurtamento padrão, entretanto, muitas não permitem o cálculo da tensão real na interface sob forças existentes de impedimento da geometria real do selo. Essa informação é vital à durabilidade à longo prazo.

Um sistema foi desenvolvido para determinar a tensão radial imposta por um grante sob confinamento. Consiste de uma célula instrumentada com "strain gage" e seu sinal associado condicionador/amplificador. A célula de ensaio usada no sistema é única no sentido que assegura a calibração direta do sistema completo. O sistema é versatil pois o material da célula e dimensões podem ser escolhidas para simular o impedimento do material circundante sob carga geoestática refletindo a profundidade. Amostras podem ser ensaiadas sob várias condições de temperatura e pressão, podendo simular ou pressão de injeção ou carga hidrostática.

Diferentes formulações cimentícias expansivas foram avaliadas. Foram baseadas no cimento tipo K de retração compensada, classe H de cimento para poços mais sulfato de cálcio hemihidrato e sal (NaCl) na formulação. Três fases distantas de expansão foram encontradas: a primeira é a fase térmica ocorrendo com a liberação inicial de calor, a segunda ocorre quando o cimento atinge seu máximo térmico quando simultaneamente ocorre o resfriamento e cristalização dos componentes expansivos, e a terceira fase ocorre após total liberação das tensões térmicas. O impacto na eficiência do sistema do selo e longevidade é discutida.

R.I.A. Malek, P.H. Licastro, and D.M. Roy*, Materials Research Laboratory, *Also, Dept. of Materials Science and Engineering, The Pennsylvania State University, University Park, PA 16802, USA

INTRODUCTION

Cement-based plugs/seals have been designed to seal access shafts and boreholes in many underground systems e.g. radioactive-waste repositories. Their primary function is to provide a tight seal at the interface with the host environment by developing and maintaining a positive normal stress across the interface. Successful performance, in this respect, could be dependent almost entirely on expansivity of the plug relative to the restraining forces of the surrounding host rock.

In cementitious formulations, whether ettringite or salt (NaCl) is the principal expansive component, the degree of restraint offered by the surrounding rock mass is of importance in the development of interfacial stress. Information exists on unrestrained and standard restrained expansion for mortars and concrete , however, most do not permit calculation of actual interface stresses under the existing restraining forces of actual borehole geometry.

A system to determine the radial stresses of the grout/concrete on the host environment which permits simulation of the surrounding rock mechanical properties was designed. A brief description of the system is presented together with typical data, and their implications on seal durability.

DESIGN

The apparatus used for expansive force determinations consists of a steel cylinder capped with base and top plates, as shown in Figure 1. Both bottom and top plates are provided with 'O' rings to ensure effective sealing of the steel cylinder during calibration. This design eliminates the effect of hydrostatic load in the vertical direction on the steel cylinder, i.e., any internal pressure on the top and bottom plates is transferred to the external clamping bolts. The physical and mechanical characteristics of the steel cylinder are shown in Table I.

Table I. Physical and Mechanical Characteristics of the Test Cell Used in Stress Measurement.

Modulus of elasticity, (10^6 psi):
tension: 26.0
compression: 26.0
torsion: 9.5
Poisson's ratio: 0.32
Coefficient of linear expansion (in/in/^{o}Fx10^{-6})
[at 70-200°F]: 7.7
Thermal conductivity (BTU/in/hr/sq.ft/^{o}F),
at 70°F; 151.0; at 200°F; 167.0
Specific heat (BTU/lb/^{o}F), at 70°F; 0.102;
at 200°F; 0.105
Physical dimensions:
length: 9.0 in.
internal diameter: 1.60 in.
external diameter: 1.84 in.

A 90° rossette strain gage is attached to the central part of the outer surface of the cylinder. The gage is connected to a signal conditioner and recorder. Both radial and longitudinal strains are recorded continuously. The physical characteristics of the strain gage are shown in Table II.

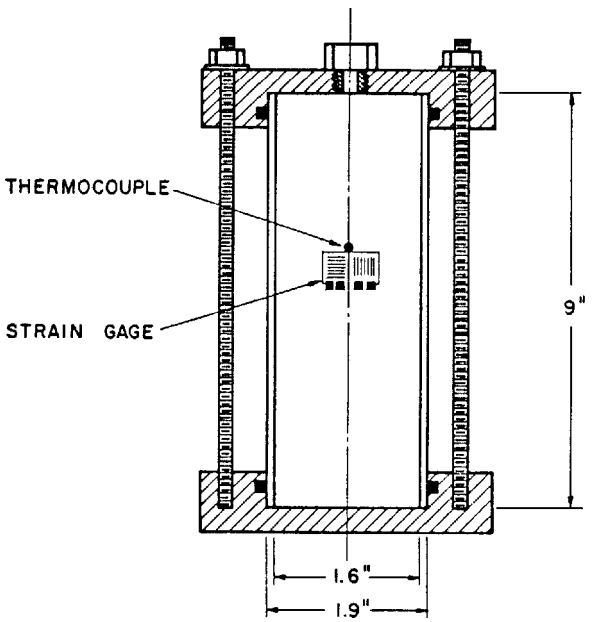

Figure 1. Test cell for determination of expansive force.

Table II. Physical Characteristics of the 90P Rossette Strain Gage.

Type: CEA-06-125UT-120
Micro-measurements Group, Raleigh, NC
Resistance (OHM): 120.00 $\pm$ 0.4%
Gage Factor (75°F): 2.025 $\pm$ 0.5%
Transverse sensitivity (X_t %)[a]: Radial + 1.4%; Longitudinal +0.6%

[a]The values of transverse sensitivities gave very minute correction factors to the recorded strains, which are considered the true values of strains in both directions.

A chromel-alumel thermocouple is attached to the outer surface of the cylinder, in close proximity to the strain gage, to record any temperature variations and supply the necessary corrective factors for the temperature-induced strains. The entire cell is placed in a chamber, adjusted to the desired experimental temperature. The chamber is surrounded by a heated water jacket to ensure constant temperature, and to minimize the effects of thermal pulses of the heating elements on the strain gage output. The temperature control accuracy is $\pm$0.5^{o}C, over extended periods of time.

The current design of the stress-measurement system permits using cells having different mechanical properties (different material or thicknesses) to simulate the in situ deformational characteristics of the surrounding rock. The following relationship was developed to calculate

R.I.A. Malek, P.H. Licastro, and D.M. Roy*, Materials Research Laboratory, *Also, Dept. of Materials Science and Engineering, The Pennsylvania State University, University Park, PA 16802, USA

the ratio of outside radius to the inside radius from the knowledge of the host rock mechanical properties [1]:

$$r_o/r_i = \left[\frac{1/2G_R + (1-\nu_s)E_S}{1/2G_R - 1/2G_S} \right]^{1/2} \quad (1)$$

where r_o = outer radius of the cylinder,
r_i = internal radius of the cylinder,
G_R = modulus of rigidity of the rock (GPa),
G_S = modulus of rigidity of the cylinder (GPa),
E_S = Young's modulus of the cylinder (GPa), and
ν_s = Poisson's ratio of the cylinder.

For a given material e.g., steel, it is possible to construct a plot representing variation of r_o/r_i versus modulus of rigidity of the rock (Figure 2).

Knowing the modulus of rigidity of the surrounding rock, and using either equation (1) or Figure 2, it is possible to determine the ratio of outer to internal radius of the cylinder as required to simulate the mechanical properties of the surrounding rock at a given depth. In the present investigation, a tuff was simulated. Its modulus of rigidity was found to be 16.5 GPa. This value corresponds to a steel cylinder of r_o/r_i = 1.2. The length of the cylinder was 9 inches, a sufficient length to reduce longitudinal end effects.

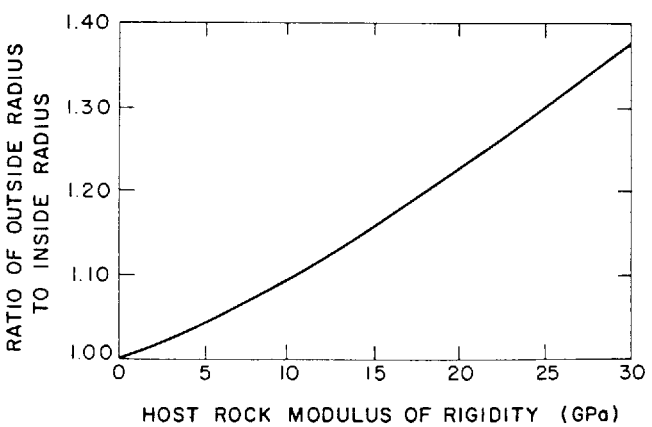

Figure 2. Ratio of outer to inner radii of test cell related to modulus of rigidity of host rock.

EXPERIMENTAL PROCEDURE

Calibration

Prior to each experiment, the steel cylinder-strain gage combination is calibrated. These procedures permit precise measurement of the actual stresses exerted by the grout inside the steel cylinder. They also allow applying corrective terms for different conditions to the recorded strains, in order to obtain the true stresses applied by the grout on the cylinder.

The cell is filled with water, the upper cap is placed and the four restraining bolts are tightened to a given torque. The upper cap is connected to a water pump that provides controlled pressurization of the cell. The entire assembly is placed inside the thermal chamber, adjusted to the temperature at which the stress is to be determined with the strain gage output and temperature of the surface of the restraining steel cylinder being recorded. When thermal equilibrium is obtained calibration is initiated by pressurizing the cell with water at successively increasing pressure increments and recording the corresponding outputs of the strain gage. Calibration curves were constructed as shown in Figures 3 and 4. The radial strain is recorded as positive output indicating tension, whereas the longitudinal strain is negative. The ratio of longitudinal strain to radial strain is equal to 0.327, which equals the Poisson's ratio of the steel material of the cylinder. The results of the calibration of several cylinder-strain gage combinations are shown in Table III.

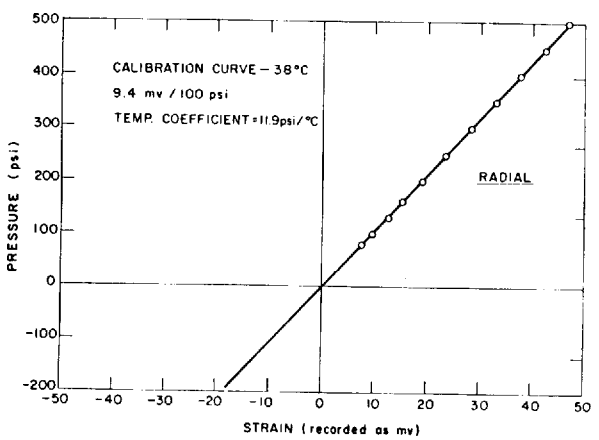

Figure 3. Sample calibration curve for radial expansion.

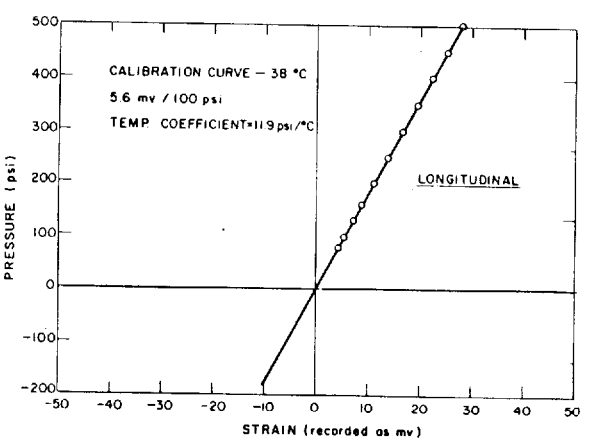

Figure 4. Sample calibration curve for longitudinal expansion.

To separate actual strains exerted by the grout from temperature-induced strains, the steel cylinder-strain gage combinations were also

R.I.A. Malek, P.H. Licastro, and D.M. Roy*, Materials Research Laboratory, *Also, Dept. of Materials Science and Engineering, The Pennsylvania State University, University Park, PA 16802, USA

calibrated for thermal effects. The steel cylinder is filled with water and a heating element is inserted. Heat is applied in successive increments with constant slow rate of heating. The output is recorded after a period of time adequate to ensure the attainment of thermal equilibrium. The resultant temperature coefficient of induced strain is calculated (Table III). Thus, it is possible to apply corrective terms for temperature-induced strains.

Table III. Results of Calibration for Steel Cell-Strain Gage Combinations.

	strain (mvolts/psix10^{-2})	coefficient of temperature induced strains (psi/°C)
Cell I: (38°C)		
Radial	+8.88	11.50
Longitudinal	-5.32	14.34
Cell II: (38°C)		
Radial	+9.40	11.90
Longitudinal	-5.60	11.90
Cell III: (38°C)		
Radial	+8.88	11.50
Longitudinal	-4.96	11.50

After calibration of the steel cylinder/strain gage combination for stress and temperature, the complete assembly is placed in the thermally controlled chamber until the cell is loaded with the material to be tested.

Formulations and Mixing Procedures

Two ettringite-based expansive formulations have been chosen for the present study. Formulation I (F-I) a mortar based on type K expansive cement and formulation II (F-II), a grout based on Class H cement with added calcium sulphate hemihydrate. A third, salt (NaCl)-based formulation (F-III) was also tested. This is a mortar containing much smaller hemihydrate than F-I and F-II and mixed with supersaturated NaCl solution. The compositions of these formulations are shown in Table IV. Standard ASTM procedures as applicable were used throughout the present study. The mixing water was preheated to 38°C prior to mixing. This procedure is adapted to avoid severe temperature fluctuations during the initial stages of hydration. The temperature of the mixes prior to placement in the steel cylinder was to be 34°C. The mix is quickly cast into the test cell, equilibrated to the experimental conditions, tamped and the test cell reassembled. The complete assembly loaded with cement grout is placed in the curing chamber adjusted to 38°C. The radial and longitudinal strains as well as the temperature of the steel cylinder are continuously monitored.

TEST RESULTS AND DISCUSSION

Ettringite-based Expansive Formulations

The two ettringite-based mixtures are contrasted in Figure 5, which shows much greater stress being generated by the F-II grout relative to the F-I mortar, in which the sand in the mixture may mitigate stress generation.

Table IV. Compositions of Cementitious Mixtures.

	Formulation I	Formulation II	Formulation III
Type K cement	33.8%	—	—
Class H cement	—	47.3%	20.1
Deionized water	15.9	20.3	8.2
Silica fume	7.3	4.8	—
Low-Ca fly ash	8.2	—	—
High-Ca fly ash	—	15.20	6.8
Silica flour	—	4.8	—
ASTM C109 sand	33.8	—	58.8
Hemihydrate	—	6.5	2.5
Sodium chloride	—	—	2.6
Dispersant	0.5	1.1	1.0
Defoamer	0.005	0.02	0.07
Total	99.51	100.02	100.07

All stress curves were corrected for temperature effects, and normalized to the experimental conditions. These curves reveal several stages of expansion, as anticipated for expansive cementitious mixtures. The initial stresses represent a thermal phase, occurring with early heat liberation. Although the curves were corrected for temperature variation, this correction was accomplished only for the apparatus (especially the strain gage). Thus variations in the grout itself still play a role in early stages of hydration.

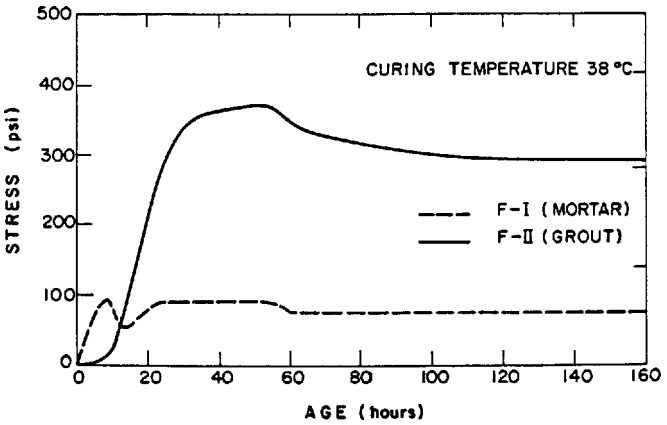

Figure 5. Comparison of radial stresses of the ettringite-based mixtures.

These initial thermal stresses are of short-term duration and have little effect on the ultimate strength of the cementitious material, because the latter is still in a plastic state. However, in scaling up to mass curing, heat dissipation may be much slower, and thermal stress may outlive the plastic state of the concrete or mortar.

The second phase of expansion occurs after the cement reaches its thermal maximum, and cooling is initiated. At least two simultaneous processes occur during this phase of hydration. The grout

begins to harden, fixing to a certain extent its physical integrity and porosity. Simultaneously, crystallization/formation of the expansive component takes place.

For mixtures in which initial porosity is low, chemical expansion can become quite large even before the thermal stresses are relieved. This can be seen on the curve for mixture F-II in Figure 5, wherein the initial thermal expansion is totally masked by expansion. It is difficult to compare the performances of the two mixtures based on the data in this figure, however, due to the fact that only one of them (F-I) contains sand.

A third phase in the expansion process is characterized by total relief of thermal stress. At this stage, controlled by the combination of cooling and of formation of the expansive component(s), the measured stress may show a slight decreases. This phase appears on Figure 5 at about 60 hours after initiation of the experiment.

Salt-based Expansive Formulations

In numerous field applications of expansive cements and seal material, it is necessary to attain chemical compatibility between the concrete formulation and the surrounding environment. In salt-host sites (largely in oil and gas industry as well as radioactive waste repositories) it was found that the use of saturated salt solution as a mixing fluid instead of water is necessary to prevent salt migration and subsequent adverse effects on seal durability. One salt-containing formulation (F-III) has been tested in the present investigation whose composition is included in Table IV. This formulation contains 2.6% hemihydrate in addition to salt (NaCl). The mixed expansive functions of sulphate and salt has an important significance in field applications in conjunction with temperature effects on stability of the seal material.

Although the restraining forces in a salt environment may differ from those of tuff rock (for ettringite-based formulations), the same restraining forces were applied to the salt-based formulation in order to establish a basis for comparison. A simple mathematical relationships can be applied to transform the resulting data into actual stresses in a salt environment. A cell having the same typical characteristics as cell I (Table III) was used in testing salt formulation (F-III). The normalized expansive stress curve (at 38°C) for this formulation (F-III) is shown in Figure 6. The curve reflects the general expansive characteristics explained in the previous section. The expansion is partly due to Friedel's salt and ettringite. However, crystallization of salt with curing (water consumption in hydration process) may be the primary cause of expansion. The micrograph shown in Figure 7 shows salt crystals growing inside pores of cement matrix. Crystallization starts at the walls and progress to the center exerting pressure on the pore walls.

SUMMARY AND CONCLUSIONS

A system was developed to determine the radial stresses imposed by a grout under confinement. The test cell used in the system is unique in that it provides for direct calibration of the complete system including signal conditioners and output recording. The system is versatile in that cell material and dimensions can be selected to simulate restraint of a given host material under a geostatic load reflecting depth. Samples can be run under a range of temperature and pressure conditions, with the later simulating either injection pressure or hydrostatic load conditions existing in a borehole.

Three cement-based formulations were evaluated, the first contained type K expansive cement with sand, the second contained Class H cement with hemihydrate, and the third contained Class H cement mixed with saturated salt solution (NaCl) and hemihydrate. The second formulation was found to give the highest stresses, whereas the third formulation gave the lowest stresses.

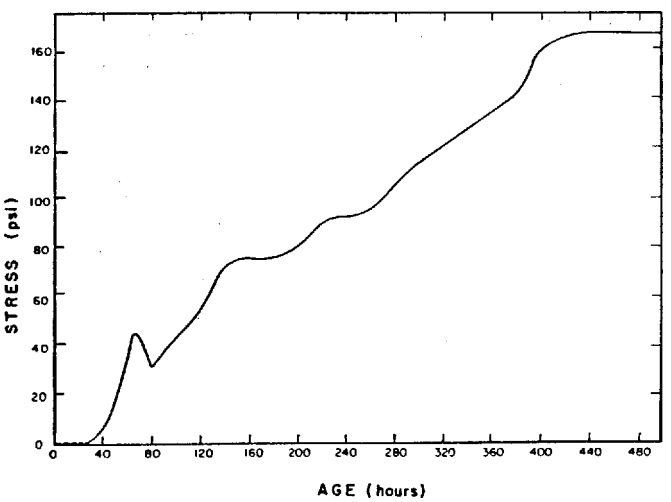

Figure 6. Radial stresses of the salt-based mixture.

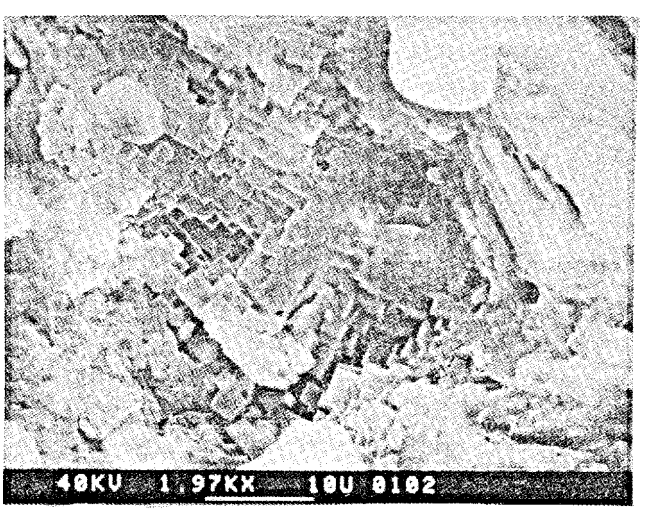

Figure 7. SEM image of F-III (salt-containing mixture). Horizontal line at bottom of the micrograph is 10μm long.

REFERENCES

1. S.K. TIMOSHENKO and J.N. GOODIER, Theory of Elasticity, McGraw Hill, New York (1970).

Z.M. LARIONOVA,
I.I. KOURBATOVA, NIIZhB, Gosstroy URSS

PREMIERE HYDRATATION DES CIMENTS ET FORMATION DE GEL AU CONTACT AVEC DES AGGREGATS

L'influence sur l'hydratation des ciments d'un nombre des facteurs ainsi que les traits, spécifiques à l'hydratation des nouveaux types des ciments, peuvent être mis en evidence par l'étude en cinétique des compositions des phase liquides. On a déterminé un nombre des régularités en se basant sur lesquelles a été mis en evidence le mécanisme de l'action des adjuvants organiques.

La composition des formations nouvelles et le caractère de la jonction epitaxique influence sur la force d'adhésion des couches de contact et sur les propriétés du béton. Les aggrégats différents adsorbent les formations nouvelles des hydrates d'une composition déterminée. Sous les actions défavorables exercées sur le béton (par example, une incendie), l'état des contacts s'empire. Pendant un durcissement ultérieur la zone de contact "se cicatrise"; les valeurs de microrésistance augmentent.

Sumário

A influência, sobre a hidratação dos cimentos, de um certo número de fatores bem como os aspectos específicos à hidratação dos novos tipos de cimento podem ser postos em evidência pelo estudo da cinética das composições das fases líquidas.

Determinou-se um certo número de regularidades e baseando nelas foi posto em evidência o mecanismo da ação dos aditivos orgânicos.

A composição das novas formações e o caráter da função epitáxica influencia as forças de adesão das camadas de contato e as propriedades do concreto. Agregados diferentes absorvem as novas formações de hidratos de uma composição determinada. Sob as ações desfavoráveis exercidas sobre o concreto (por exemplo, um incêndio), o estado dos contatos piora. Durante um endurecimento ulterior a zona de contato "se cicatriza": os valores das microresistências aumentam.

La formation de la structure dans les bétons est déterminée par l'ensemble des processus physico-chimiques qui ont lieu pendant le durcissement du liant et à son contact avec des aggrégats.

Les premiers stades du durcissement des liants représentent une période le plus importante conditionnant les caractéristiques de résistance, de déformation et d'autres caractéristiques des systèmes. L'influence sur l'hydratation des ciments d'un nombre des facteurs (température, régime de durcissement, introduction des adjuvants etc.) ainsi que les traits propres à l'hydratation des nouveaux types des ciments (ciment alinite, ciment contenant barium etc.), peuvent être mis en evidence par l'étude en cinétique des compositions des phases liquides /I/.

Pendant l'étude de l'influence sur la composition des phases liquides de la composition minéralogique de clinker, de la présence en clinker des alcalis et de sa dispersité ainsi que de température, de gypse et d'autres adjuvants a été mis en evidence un nombre des régularités. Il a été constaté que d'après l'allure des courbes cinétiques $C_{R^+}(t)$, $C_{Ca^{2+}}(t)$, $C_{SO_4^{2-}}(t)$ peut être evaluée l'influence de beaucoup de facteurs sur le processus de durcissement. Donc, la venue intense dans la phase liquide de R^+ temoigne l'accélération de la dissolution de clinker. Cette dépendance est distinctement observée pendant l'étude de l'influence de la température (5-80°C) sur la composition de la phase liquide du ciment hydratant (Fig. Ia).

D'après la modification dans la phase liquide de la concentration d'ions des métaux alcalins, on peut dans certains cas évaluer d'une façon quantitative le degrée d'hydratation /2/.

L'allure en pente douce de la courbe $C_{Ca^{2+}}(t)$, ainsi que le deplacement du maximum sur celle-ci à droite montre le ralentissement de la cristallisation des phases contenant le calcium. L'abaissement brusque de la concentration de calcium dans la phase liquide, le déplacement de maximum sur la courbe $C_{Ca^{2+}}(t)$ à gauche ainsi que la diminution (jusqu'à disparition entière) de la section parallèle à l'axe des abscisses montre l'accroissement de vitesse de la cristallisation des phases contenant le calcium sous la monte de la température (Fig. Ib).

Une abaissement brusque de la concentration des sulfates correspond au liage de la masse principale du gypse en ettringite, c'est que se confirme par les données de sa détermination quantitative par une méthode chimique. La vitesse de combinaison du gypse en ettringite dépend de la composition de minéral-phase du clinker et du contenu en alcalis: elle s'accélère avec l'augmentation du contenu en C_3A et avec la diminution de quantité de C_3S. La formation d'ettringite se ralentit en ciment avec un haut contenu en R_2O, c'est pourquoi la concentration de sulfates de ces ciments dans la phase liquide reste haute pendant 24 heures. Au contraire, en ciments alinites ou la cristallisation d'ettringite se réalise très vite, celle-ci s'abaisse brusquement en 2 heures (Fig. 2).

En se basant sur les études en cinétique des compositions des phases liquides on a précisé le mecanisme de l'action des adjuvants organiques, en particulier, de superplastifiant S-3, sur la base de resines naphtalene-formols sur le durcissement des ciments avec des compositions minéralogiques différentes.

L'introduction de S-3 change la composition de la phase liquide, la proportion des concentrations dans cette phase des constituants solubles et la cinétique de dégagement des formations nouvelles et abaisse pH. Par la méthode photocolorimétrique on a établi que l'intensité de sorption de S-3 dépend de la composition minéralogique du ciment et du contenu en alcalis dans ces ciments. Elle augmente avec l'accroissement du contenu en aluminates. Comme il se voit d'après l'allure des courbes $C_{R^+}(t)$ et

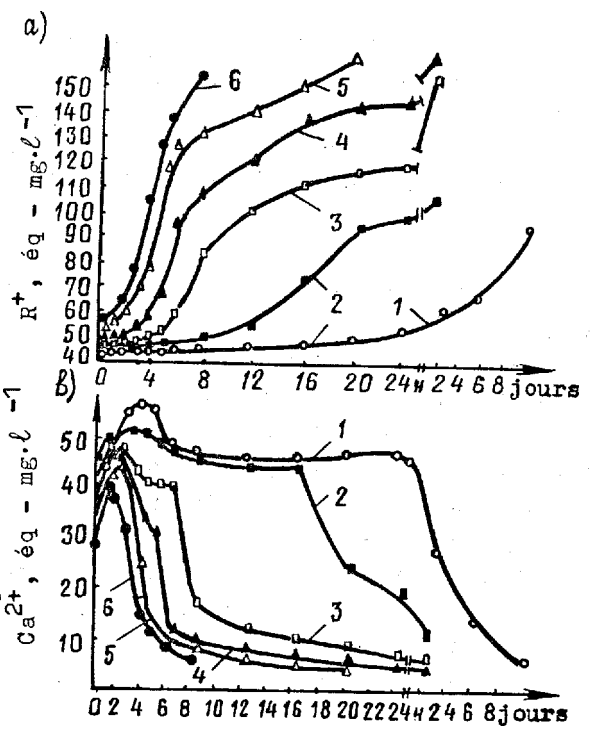

Fig. 1. La variation avec le temps de la concentration de R^+ et de Ca^{2+} dans la phase liquide pendant la hydratation du ciment portland sous la température: I - 5°C; 2 - 20°C; 3 - 35°C; 4 - 50°C; 5 - 65°C; 6 - 80°C

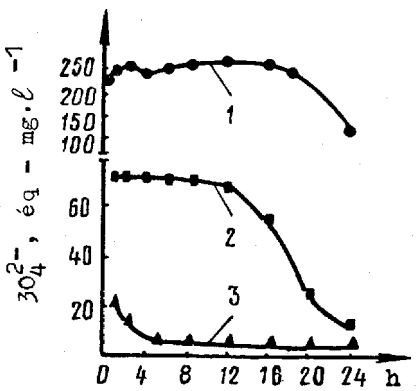

Fig. 2. La variation avec le temps de la concentration de SO_4^{2-} dans la phase liquide pendant la hydration des ciments: I - ciment portland; 2 - 2 - ciment portland avec une haute teneur en R_2O; 3 - alimithe

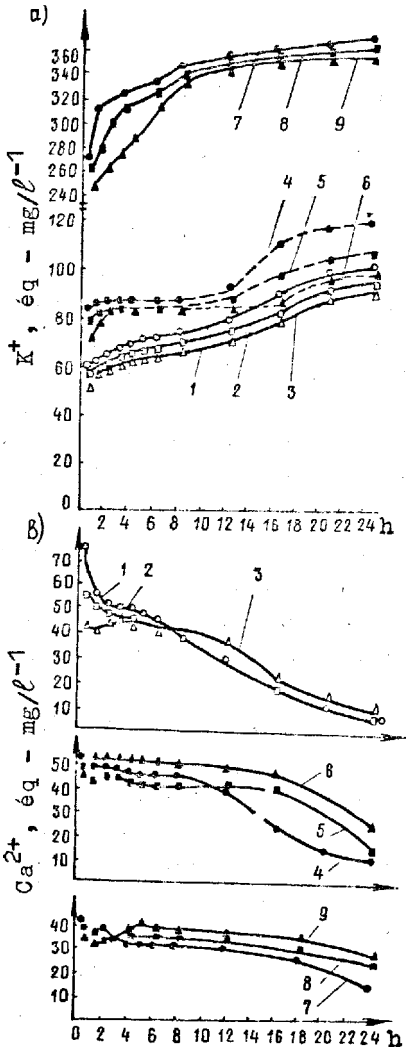

Fig. 3. La variation avec le temps de la concentration de K^+ et de Ca^{2+} dans la phase liquide pendant la hydratation des ciments: I - ciment avec une basse teneur en aluminate sans adjuvant; 2 - le même, avec l'adjuvant de 0,3% de C-3; 3 - le même avec 0,7% de C-3; 4 - ciment avec une moyenne teneur en aluminate sans adjuvant; 5 - le même avec l'adjuvant de 0,3% de C-3; 6 - le même avec 0,7% de C-3; 7 - ciment avec une moyenne teneur en aluminate et avec une haute teneur en alcali sans adjuvants; 8 - le même, avec l'adjuvant de 0,3% de C-3; 9 - le même avec 0,7% de C-3

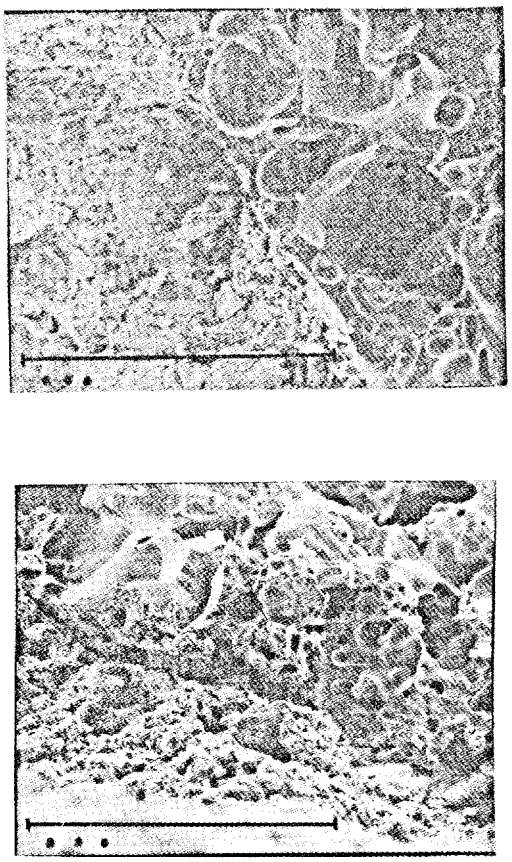

Fig. 4. Le contact de la pierre du ciment avec le grain de keramsite sous 20°C (a) et sous 600°C (b) MSE, x700

$C_{Ca}^{2+}(t)$ (Fig. 3), S - 3 ralentit en moment initial la dissolution du clinker et le dégagement des phases contenant le calcium. L'effet de ralentissement de la cristallisation se manifeste plus fort avec l'accroissement du contenu en C_3A dans le ciment et avec l'accroissement du dosage d'adjuvant.

S-3 augmente la force ionique de la phase liquide. Ce fait, ainsi que le changement de la composition et du degrée de la sursaturation de la phase liquide par rapport au hydrosilicates, doit influer sur leur morphologie et sur le dégrée de polymérisation ce qu'avec le changement de la résistance des contacts "polymère-phase solide", peut influer sur la résistance de la structure de durcissement. C'est pourquoi il est utile d'introduire S-3 en quantités minimales, suffisantes pour le but de plastification. En formant dans la période initial de l'hydratation sur la surface de la phase solide des films d'adsorption, S-3 assure l'abaissement du coefficient de frottement et l'augmentation de fluidité à cause de faible résistance des contacts "polymère-polymère", ce qui en fin de compte amène à l'obtention d'effet plastifiant.

La pierre de ciment au contact avec des aggrégats dans le béton, en règle, a un degré un peu élévé en comparaison avec le volume. La composition de minéral-phase des formations nouvelles et le caractère de maclage epitaxique des cristaux influent sur la force d'adhérence des couches de contact et sur les propriétés techniques du béton /2/.

Les aggrégats différents adsorbent sur leures surfaces les formations nouvelles des hydrates d'une composition déterminée. Au contact avec le quartz (SiO_2; d = 4,25; 3,35; 2,45; 1,82 Å), au microscope électronique, on peut voir les hydrosilicates de calcium très fins, les plaquettes hexagonales d'hydroxyde de calcium et les cristaux aciculaires d'ettringhite. La largeur de couche de contact de la pierre de ciment est renfermée dans les limites de 60-110 mcm, de couche de contact du quartz - pas plus de 20 mcm. Avec le temps dans la pierre du ciment au contact avec le quartz a lieu l'accroissement des valeurs de microrésistance (à 30%) en comparaison avec la pierre du ciment en volume. La ligne de contact paraît floue.

Au contact avec le feldspath (microclin KAl Si_3O_8, d = 4,03; 3,20; 3,14 Å) cristallise l'ettringite, est possible l'hydroaluminate de calcium et aussi il y a une masse di hydrosilicates. La largeur de couche de contact de la pierre du ciment est de 30-45 mcm, dans la couche de contact du feldspath il n'y a pas de variations importantes en microrésistance. Dans les éprouvettes d'un

durcissement de longue durée on peut observer l'accroissement des valeurs de microrésistance au contact à 15-20%. La ligne de contact est nette.

Au contact avec la calcite compact ($CaCO_3$, d = 3,04; 2,49; 2,28; 1,92 Å) on voit les cristaux de hydroxyde de calcium, les formations à grains fins de calcite secondaire, les aiguilles isolées d'ettringite. Il y a la masse de hydrosilicates, la présence de hydrocarboaluminate de calcium est possible. La largeur de couche de contact de la pierre de ciment, en dépendance de l'âge de l'éprouvette, varie de 40 à 120 mcm, la largeur de couche de contact du calcaire - de 20 20 à 45 mcm. Est rémarquée la diminution des valeurs de microrésistance (environs de 10 à 15%) au contact en comparaison avec la pierre du ciment en volume. La ligne de contact est nette, exempte de defauts. Les régularites constatées pour la formation des contacts avec les minéraux sont les mêmes pour les bétons sur la base de granit et de calcaire.

L'accroissement du dégré de rugosité de la surface d'aggrégat influe positivement sur l'état de la zone de contact. C'est pourquoi l'adhérence de la pierre du ciment avec la kéramsite est la plus forte. Au microscope on peut observer une pénétration profonde de la masse cementante dans le grain poreux d'aggrégat. Sur la fig. 4a, à gauche - la pierre de ciment, à droite - le grain de kéramsite (MSE, x700). La largeur de la zone de contact est égale à 50 mcm. La microrésistance de la pierre de ciment en volume est égale à 700-800 MPa; et celle de la couche de contact - à 900-100 MPa. La compaction de la pierre de ciment au contact avec de la kéramsite a lieu par suite de l'aspiration de la phase liquide et de la naissance des cristaux complémentaires di hydrosilicates du calcium.

Sous les actions défavorables sur les bétons (par exemple, une élévation brusque de température pendant l'incendie) l'état des contacts s'empire par suite d'une déhydratation partielle de la pierre de ciment /3/. Sous le chauffage jusqu'aux 400°C, les éprouvettes avec de la kéramsite gardent une structure rélativement compacte de la zone de contact. Puis, avec l'élévation de température les fissures et les espaces libres ayant la largeur jusqu'à 100 mcm apparaissent. La porosité de la pierre de ciment augmente, et les valeurs de microrésistance diminuent. Sur la fig. 4b, dans l'éprouvette avec de la kéramsite (600°C) on peut observer l'ecaillement de la pierre de ciment (à gauche) du grain d'aggrégat (à droite) (MSE, x700). Pendant un long durcissement ultérieur dans les conditions normales des éprouvettes cuites la zone de contact "se cicatrise" par les formations nouvelles secondaires. La structure des eprouvettes devient plus compacte, les valeurs de microrésistance augmentent.

BIBLIOGRAPHIE

I. Курбатова И.И. Химия гидратации портландцемента. М., 1977.
2. Структурообразование бетона и физико-химические методы его исследования. М., 1980.
3. Ларионова З.М., Никитина Л.В., Гарашин В.Р. Фазовый состав, микроструктура и прочность цементного камня и бетона. Стройиздат, М., 1977.



8.º Congresso Internacional de Química do Cimento

8th International Congress on the Chemistry of Cement

8e Congrès International de la Chimie des Ciments

General Reports — Posters — Seminars
Rapports Généraux — Posters — Séminaires

Volume VI

22-27 de setembro de 1986
Rio de Janeiro — Brasil

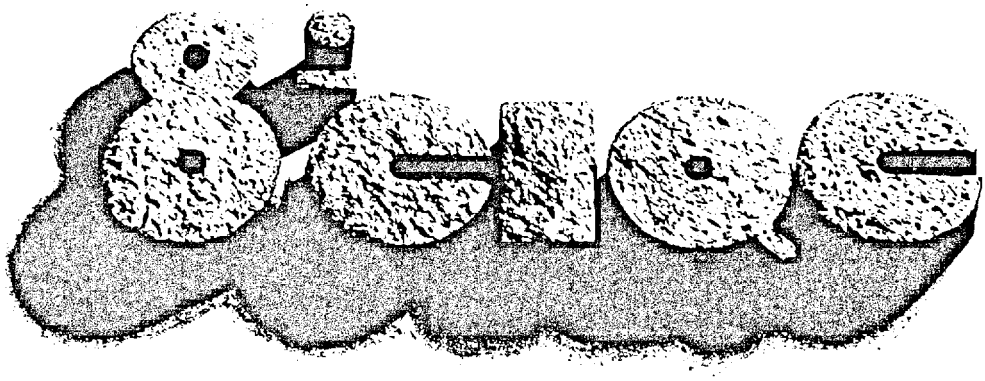

8.º Congresso Internacional de Química do Cimento

8th International Congress on the Chemistry of Cement

8e Congrès International de la Chimie des Ciments

General Reports — Posters — Seminars
Rapports Généraux — Posters — Séminaires

Volume VI

22-27 de setembro de 1986
Rio de Janeiro — Brasil

Não é permitida a reprodução dos Anais sem prévia autorização da Comissão Organizadora do Congresso.

The Proceedings are not to be reprinted without a previous permission of the Organizing Commission of the Congress.

La reproduction des Annales est interdite sans, au-devant, l'autorisation de la Commission d'Organisation du Congrès.

• • •

A substância e a forma de apresentação dos trabalhos que compõem os Anais do Congresso são de exclusiva responsabilidade de seus autores.

The substance and the form of presentation of the papers that compound the Proceedings of the Congress are exclusive responsability of their authors.

Le fond et la forme de publier les travaux qui composent les Annales du Congrès sont d'exclusive responsabilité de leur auteurs.

Secretaria Geral do 8º CIQC:
Rua da Assembléia, 10 - 40º and. - Gr. 4001
Tel.: 221-6562 – Telex: (021) 33191
20011 Rio de Janeiro – RJ – Brasil

Apoio financeiro da

finep FINANCIADORA DE ESTUDOS E PROJETOS

ORGANIZING COMMISION:

PRESIDENT:	JOSÉ ERMÍRIO DE MORAES FILHO	BRASIL
EXECUTIVE VICE-PRESIDENT:	PAULO MÁRIO FREIRE	BRASIL
TECHNICAL DIRECTOR:	FRANCISCO DE ASSIS BASÍLIO	BRASIL
ADMINISTRATIVE DIRECTOR:	JOÃO BATISTA MENESCAL FIUZA	BRASIL
DIRECTORS:	ALBERTO LUIZ GONÇALVES SOARES	BRASIL
	ENRIQUE GUNTHER DREWES	BRASIL
	EPAMINONDAS MELO DO AMARAL FILHO	BRASIL
	MARCÍLIO DE BRITO	BRASIL
	NEWTON GOULART	BRASIL

SCIENTIFIC COMMITTEES:

– SOUTH AMERICA:		
• PRESIDENT:	FRANCISCO DE ASSIS BASÍLIO	BRASIL
	ALVARO AUGUSTO ALVES PINTO	BRASIL
	DANTE E.J. VERONELLI	ARGENTINA
	FLEMING OEST	BRASIL
	HANS BUCHER	BRASIL
	JOÃO GASPAR DJANIKIAN	BRASIL
	LUIZ ROBERTO MARTINS DE MIRANDA	BRASIL
	MARIA DAS GRAÇAS JAQUÁ	BRASIL
	MARIA LUIZA MOREIRA DE MORAES	BRASIL
	NEY JOSÉ DE SOUZA E SILVA	BRASIL
	PABLO KITTL D.	CHILE
	PAULO RODRIGUES	BRASIL
	ROBERTO R. COELHO	BRASIL
	YASUKO TESUKA	BRASIL
	YUSHIRO KIHARA	BRASIL
– NORTH AND CENTRAL AMERICA, AND FAR EAST:		
• PRESIDENT:	JAN P. SKALNY	U.S.A.
MEMBERS:	DELLA M. ROY	U.S.A.
	GEOFFREY FROHNSDORFF	U.S.A.
	GERARD G. LITVAN	CANADA
	HIROSHI UCHIKAWA	JAPAN
	J. FRANCIS YOUNG	U.S.A
	JORGE MARIO VILLASENOR	MEXICO
	R.E. OBERHOLSTER	SOUTH AFRICA
	SIDNEY DIAMOND	U.S.A.
	S.W. TRESOUTHICK	U.S.A.
	WU ZHONG-WEI	CHINA
– EUROPE, ASIA AND AFRICA:		
• PRESIDENT:	JEAN PAUL MERIC	FRANCE
MEMBERS:	C. CHARRETON	FRANCE
	FRANCO MASSAZZA	ITALY
	FRANÇOIS LE BEL	FRANCE
	FRIEDRICH W. LOCHER	WEST GERMANY
	F. YAGIZ	TURKEY
	H.W.W. POLLITT	ENGLAND, U.K.
	JOSE CALLEJA	SPAIN
	J. TALLABER	HUNGARY
	LABO KADA ABOUBACAR	NIGERIA
	O.P. MTCHEDLOV-PETROSSIAN	U.S.S.R.
	P. DUTRON	FRANCE
	RENATO BUCCHI	ITALY
	S.K. CHOPRA	INDIA
	T.V. KOUZNETSOVA	U.S.S.R.
	WIESLAW KURDOWSKI	POLAND

PRINCIPAL REPORT OF THE SUB-THEME 1.1

Pages

15 F.P. Glasser (Scotland, U.K.) – Kinetics of cement-making reactions.

GENERAL REPORTS OF SUB-THEMES' COMMUNICATIONS:

33	M.S. Marinho	(Brasil)	Sub-theme 1.1
38	Y. Kihara	(Brasil)	Sub-theme 1.2
46	P. Rodrigues	(Brasil)	Sub-theme 1.3
50	Y. Tezuka	(Brasil)	Sub-theme 2.1-a
56	A. Ferreira	(Brasil)	Sub-theme 2.1-b
62	F.A. Basílio	(Brasil)	Sous-thème 2.1-c/d
67	P. Kittl	(Chile)	Sub-theme 2.2
76	P.J.M. Monteiro	(Brasil)	Sub-theme 2.3
80	A.F. Battagin	(Brasil)	Sub-theme 3.1
89	Y. Tezuka	(Brasil)	Sub-theme 3.2
96	H.R.E. Bucher	(Brasil)	Sub-theme 3.3
104	S. Priszkulnik	(Brasil)	Sub-theme 4.1
123	J.G. Djanikian	(Brasil)	Sub-theme 4.2
128	H.V. Armandola	(Argentina)	Sub-theme 4.3

SEMINARS/SÉMINAIRES

SEMINAR/SÉMINAIRE 1
Magnesium Oxide in Portland Cement and Concrete
Oxyde de Magnésium dans le Ciment Portland et dans le Béton
Chairman/Président: Y. NIKIFOROV (U.S.S.R.)

Pages		
143	N.F. Ananenko (U.S.S.R.)	General Report
		Communications:
149	A. Palomo, J. Vazquez, M.T. Blanco-Varela (Spain)	Influence of MgO on the crystalline microstructure of the liquid phase of portland cement.
154	J. Gebauer (Switzerland)	Effect of high MgO content in cement upon-turn properties of concrete.
158	V.K. Kozlova (U.S.S.R.)	Sur la formation des phases nouvelles dans le clinker lors de la cuisson des mélanges crus à base des produits sécondaires.
164	I.G. Louginina, V.M. Konovalov, L.D. Chaklova, V.A. Beletskai (U.S.S.R.)	Durcissement du ciment portland à teneur elevée en oxyde de magnésium et en autres compositions magnésiennes.

SEMINAR/SÉMINAIRE 2
Cements with Mineral Additions/Ciments Contenant des Additions Minérales
Chairman/Président: M. VON EUW (France)

170	M. Von Euw (France)	Rapport Général
		Communications:
178	V.S. Ramachandran (Canada), Z. Chun-mei (China)	Cement with calcium carbonate additions.
183	J. Almeborg, J.T. Christensen (Denmark)	Danish portland-fly ash cement.
189	J.P. Ollivier (France)	Rôle des additions minérales sur la formation de l'auréole de transition entre gros granulat et mortier.
198	R. Guyot, R. Ranc, B. Cariou (France)	Utilisation de la potentialité hidraulique du clinker dans les ciments portland avec ajout de fillers calcaires.
204	K. Takemoto (Japan)	The variation of activity index of slag.
207	T.V. Kuznetsova, S.D. Makachev, Z.B. Entin (U.S.S.R.)	Cements with mineral admixtures: state of the art and prospects.
211	Gerd Wischers (West Germany)	Optimization of cements with mineral addictions.

SEMINAR/SÉMINAIRE 3

Effect of the Chemical and the Physico-chemical Properties of Cement Paste and Aggregate Characteristics on the Rheological Behaviour of Mortar and Concrete.

Influence des Propriétés Chimiques et Physico-chimiques de la Pâte et des Caractéristiques des Granulats sur le Comportement Rhéologique des Mortiers et des Bétons.

Chairman/Président: J.P. BOMBLED (France)

217	S. Feneuille, J.P. Bombled (France)	Rapport Général Communications:
223	P.F.G. Banfill, S.M. Gill (England, U.K.)	The rheology of aluminous cement pastes.
228	G.H. Tattersall (England, U.K.)	Components of workability and rheological measurements on mortars and fresh concrete.
239	M. Michaux, R. Oberste-Padtberg (France)	The effect of mix water salinity on cement slurries containing polynaphtalene sulphonate dispersants.
243	J. Orban, P. Parcevaux, D. Guillot (France)	Influence of shear history on the rheological properties of oil well cement slurries.
248	U. Costa, F. Massazza (Italy)	Structure and properties of cement suspensions.
260	F. Basile, S. Biagini, G. Ferrari, M. Collepardi (Italy)	Effect of condensation degree of polymers based on naphthalene on fluidities of cement pastes.
264	F. Basile, S. Biagini, G. Ferrari, M. Collepardi (Italy)	Properties of cement mixes containing naphthalene sulfonated polymers of different molecular weight.
269	S. Grzeszczyk, L. Kucharska (Poland)	The influence of alkallies upon the water demand of early hydration stage cement pastes in the light of rheological studies.
274	J. Mierzwa (Poland)	Thixotropic-plastic-viscous rheological model of cement paste as the result of physical and mineralogical cement properties.
279	S. Sprung (West Germany)	Influence of the composition of clinker and cement on the rheological behaviour of fresh concrete.
284	H.J. Wierig (West Germany)	Influences of cement and temperature on the consistency of fresh concrete.

SEMINAR/SÉMINAIRE 4:

Cement Specifications and Development of Testing Procedure. / Bases Scientifiques des Spécifications pour le Ciment et le Développement des Méthodes d'Essais.

Chairman/Président: P. Dutron (France)

288	P. Dutron (France)	Rapport Général
		Communications:
296	T. Sanduo (China)	Some views on cement specification.
300	P. Terrier (France)	Gestion et assurance de la qualité des essais.
308	A.K. Mullick, K.H. Babu, P. Bhaskara Rao (india)	Evaluation of pozzolanic activity and its impact on specification of blended cements.
312	O. Kato (japan)	Trend of the specification and the method on alkali-silica reaction in Japan.
316	G. Frohnsdorff, P.W. Brown, J.H. Pierlet (U.S.A)	Standard specifications for cements and the role in their development of quality assurance systems for laboratories.
321	E.B. Entin, L.S. Klyueva (U.S.S.R.)	Cement quality: key measures and evaluation techniques.
328	I. Odler, S. Abdul-Maula, U. Hennicke (West Germany)	A new method for determination of cement setting time.

POSTERS

Pages	Authors (Countries)/Auteurs (Pays)	Titles of Papers/Titres de Travaux
331	G. Giaccio, R. Zerbino (Argentina)	Factors affecting cement paste-aggregate bond.
334	J.K. Shukuzawa, H.C. Rodrigues Filho, V.A. Zampieri (Brasil)	Relationship between alite microscopic reactivity and clinker hydraulicity.
337	G. Babachev, K. Kolev (Bulgaria)	The influence of the cement type on the values for light constructive – thermal insulating concrete.
340	T. Ming-shu, X. Zhong-zi, H. Su-fen (China)	Alkali reactivity of glass aggregate.
344	L. Zonghan X. Xianyu, H. Ren, Ch. Yimin (China)	Calcium silico-fluoride phase A and its effects on formation of C_3S.
349	J.A. Forrester, S.A. Jefferis (England, U.K.)	Effects of high shear mixing on hydration behaviour of cement paste and rheological interpretations.
351	M.J. Coole, A.M. Harrisson (England, U.K.)	The effect of simulated large pour curing conditions on the temperature rise and strength growth of PFA containing concrete.
356	C. Vernet (France)	Réactions periodiques lors de l'attaque des ciments par des réactifs chimiques.
358	C. Vernet (France)	Évolution de la microstructure des hydrates des ciments – Aspects théoriques.
361	C. Vernet (France)	Un nouvel instrument pour l'étude des réactions d'hydratation: le GECS (générateur électrochimique de chaux sursaturée).
364	J. Ambroise, J. Péra, M. Murat (France)	Interêt de l'addition de métakaolin au ciment portland pour l'élaboration de matériaux composites renforcés par des fibres de verre.
371	R. Kovács (Hungary)	Rapid method for cement strength prediction.
374	F.D. Tamás, E. Farkas, M. Vörös, (Hungary) D.M. Roy (U.S.A.)	Low-frequency electrical conductivity of cement, clinker and clinker mineral pastes.
381	G. Scarinci, D. Festa, G. Sorarù, G. Grassi, L. Stafferi, C. Badini (Italy)	Portland cement renforced with new alkali-resistant glass fibers.
384	G. Mascolo, P. Pernice, O. Marino (Italy)	Ionic conductivity of lamellar calcium aluminate hydrates.
386	R. Sersale, R. Aiello, G. Frigione (Italy)	Natural zeolites as active additions to the portland clinker.
389	K. Ikeda (Japan)	A new type of pozzolanic cement utilizing red mud and fly ash.
395	K. Isozaki, S. Iwamoto, K. Nakagawa (Japan)	Some properties of alkali activated slag cement.

400	N. Tsuyuki, N. Hirota, K. Miyakawa, J. Kasai (Japan)	The physical properties and the hydration mechanism of C_3A in the presence of $CaSO_4.2H_2O$ and $Ca(OH)_2$.
405	S. Goto, M. Daimon (Japan)	Ion diffusion in cement paste.
410	S. Grzeszczyk (Poland)	C_3A-Na_2O solid solutions in pseudo-two-component system NC_8A_3-C_3A.
413	W. Brylicki (Poland)	Phase composition and morphology of autoclaved γ Ca_2SiO_4 containing pastes.
418	I. Cotea, D. Puscasu, D. Nicolau (Romania)	Contributions to the clinker grindability physics.
422	I. Cotea, N. Butucescu, L. Bucea, V. Mihai (Romania)	Study of thermal effects obtained in the clinkerization process by thermodifferential analysis.
427	I. Cotea, A. Romanescu, C. Dumitrescu (Romania)	Researches concerning the harmful components elimination from phosphogypsum for using it as cement setting time regulator.
434	C. Dumitrescu, G. Nistor (Romania)	Binders of base-acid type setting used in dental technique.
439	C. Popescu, A. Antonescu (Romania)	Clinker manufacturing with alkali, chlorine and sulphur compound controlled contend by gas deviation in stages clinkerization equipment.
445	A. Romanescu, C. Dumitrescu (Romania)	Considerations concerning the hardening mechanism of the controlled expansion cements.
450	A. Romanescu, L. Bucea, F. Amzica (Romania)	Clinker compositional field modification for lowring its formation temperature.
454	M. Enculescu (Romania)	Contributions to clinker forming kinetics.
460	D. Gaspar-Tébar, J.L. Sagrera-Moreno (Spain)	L'àction de l'eau de mer sur un ciment portland de haute résistance initielle et sur un ciment portland résistance aux sulfates: influence de l'addition de laitier, étude de la concentration tonique.
463	F. Bermejo-Muñoz, J.L. Sagrera-Moreno, D. Gaspar-Tébar (Spain)	Comportement d'un ciment portland résistant aux sulfates face à l'eau deionisée et les solutions de sulfate de sodium et de sulfate de magnésium.
468	M.P. de Luxan, M.I. Sanchez de Rojas, M.T. Martin Patino, J. Saavedra (Spain)	Characterization and pozzolanic properties of sedimentary opaline rocks.
470	G. Peter, Q. Yang, A. Rosli (Switzerland)	Infiltration of chloride under capillary action.
471	Sandor Popovics (U.S.A.)	Modeling mathematically the effect of curing temperature on the strength development of cements.
476	M.D. Cohen, B. Mobasher (U.S.A.)	Physico-chemical, microstructural, and micromechanical investigations of sulfoaluminate-type expansive cements.
481	V. Klassen (U.S.S.R.)	Interactions in $CaCO_3$ – $SiO_2R_2CO_3$ (R_2 SO_4) mixtures.
483	K. Karibaev, N. Bajirov, A. Patcenko, N. Panina (U.S.S.R.)	Modification de la structure des scories de la déphosphoration thérmique électrique.
485	V.M. Kolbassov (U.S.S.R.)	Modification de la structure hydratée des ciments.
489	A.M. Ilyinets, V.I. Simonov, M. Ya. Bikbau (U.S.S.R.)	New-data concerning atomic structures of portland cement silicates.
492	L.S. Klueva, A.I. Markov (U.S.S.R.)	Modification of cement contraction due to false setting.
494	N. Komarova, V. Riasine, G. Tchistiakov, A. Korenga (U.S.S.R.)	Stabilisation orientée d'une composition de phases desequilibrés du clinker blanc.

500	Z.M. Larionova, I.I. Kourbatova, N.S. Zhelvakova, L.P. Moiséeva (U.S.S.R.)	Influence des additions organiques sur la formation de la structure de la pierre de ciment.
503	L.I. Levin, G.M. Tarnarutski (U.S.S.R.)	Modified lignin-base sulphonates in the materials on cement base.
506	A.J. Mituzas, V.V. Montvilla, L.V. Petravichys, O.M. Stanylenis (U.S.S.R.)	Technology of production of high alite portland cement clinkers.
508	I.L. Luginina, M.A. Putrenko (U.S.S.R.)	Particularities of cement hydration in suspensions with alcali additions.
510	I.L. Luginina, R.G. Nigmadilova (U.S.S.R.)	Kinetics of assimilation of calcium oxide in presence of titanium compounds.
511	B. Noudelman, A. Clutchariov, G. Galimova, A. Bessmertnykh (U.S.S.R.)	Particularités thermochimiques du processus de cuisson du clinker alinitique.
513	A.A. Pachtchenko, E.A. Miasnikova, V.V. Tokartchouk, V.A. Chevtchenko (U.S.S.R.)	Particularités de la clinkerisation des crus à composants aluminosilicieux à haute réactivité.
517	V.P. Rjazin, Z.B. Entin, N.I. Komarova, N.A. Shebanov (U.S.S.R.)	Some features of mineral formation on the sample surface.
520	U. Ludwig, C. Urrutia (West Germany)	Influence of sucrose on the setting of portland cement.

FREE COMMUNICATIONS / COMMUNICATIONS LIVRES

Pages	Authors (Countries/Auteurs (Pays)	Titles of Papers/Titres de Travaux
523	E. Marciano Jr., (Brasil) P. Bartha (West Germany)	Contribution to the knowledge of the phase composition of different magnesia – chrome bricks after the attack by cement clinker.
529	C. MacInnis, P.P. Hudec, M. Moukwa (Canada)	Effect of microclimate on concrete deterioration.
534	J. Baron, R. Guyot (France)	Um modele phenomenologique de l'evolution de la resistance en compression parametrant l'influence du clinker et celle des granulats.
539	C. Bertrand, C. Bonet, P. Garde (France)	Movel combustion and volatilization deagnostic techniques in cement kilns.
544	J. Chappuis (France)	Physical elementary mechanisms of fluidification by superplasticizers or water-reducing agents.
550	C. Vernet (France)	Modelisation des diagrammes d'equilibre de solubilites des hidrates-interactions ioniques.
556	F. Indelicato, L. Cussino (Italy)	Comportement viscoélastique à long terme des bétons de ciment alumineaux.
562	J.R.L. Dyczek, M. Petri (Poland)	Mechanical properties of autoclaved, monomineral materials from tobermorite, zonotlite and hillebrandite.
565	O.Z. Cebeci, W.H. Mirza, S.I.Al. Noury (Saudi Arabia)	Strength development of mortars in hot and dry environment.
569	K.S. Han, J. Rhee (South Korea)	Etudes sur la synthese de C_3A par le Procede sol-gel.
573	I.Y. Seo, S.H. Choi (South Korea)	The unstable state of alkali in cement clinker.
578	T. Vazquez, M.T. Blanco-Varela, A. Palomo-Sanchez (Spain)	Lumping of anhydrous portland cement: study through is spectroscopy.
582	L.J. Struble (U.S.A.)	Synthesis and characterization of ettringite and related phases.
589	A.C. Chou, H.C. Eaton, F.M. Cartledge, M.E. Tittlebaum (U.S.A.)	A tem study of the interactions between certain organic hazardous wastes and type in portland cement.
594	J.G. Griffin, K.E. Daugherty (U.S.A.)	The effect of glass content on hidration in the system $CaO-Al_2O_3-MgO-SiO_2$.
598	G. Frohnsdorff, J. Clifton, H. Jennings, P. Brown, L. Struble, J. Pommersheim (U.S.A.)	Implications of computer-based simulation models, expert systems, databases, and networks for cement research.
603	V.I. Akunov, S.D. Makashev, V.A. Dmitriyeva, N.V. Tsukanova, B.E. Yudovich (U.S.S.R.)	Mechanochemical activation of materials in cement manufacture.

607	Y.M. Bazhenov (U.S.S.R.)	Evaluation of reological characteristics of cement paste and concrete with help of computers.
611	L.S. Geidarova, M.A. Astakhova (U.S.S.R.)	Certains aspects de l'activation lors de l'obtention du liant saus clinker.
614	V.D. Gloukhovsky, P.V. Krivenko, R.F. Rounova (U.S.S.R.)	Particularites de la formation de structure dans le ciment durci contenant des alcalis.
617	A.V. Voljenskiy (U.S.S.R.)	Influence de la concentration des liants en melange avec l'eau sur la resistance et deformabilite de cemelange lors du durcissement.
621	W.Weisweiler (West Germany)	Quantification of thallium – and lead – cycles in cement plants.
625	W. Weisweiler, B. Schwarz, E. Mallon (West Germany)	Isolation of thallium – and lead – halides originating from electric separator dust of cement plants by vaporization analysis.

SPEECHES / ALLOCUTIONS
Organizing Commission / Commission d'Organization

Pages

629 Opening Session / Séance Inaugurale
Dr. José Ermírio de Moraes Filho (President/Président)

631 Closing Session / Séance de Clôture
Dr. Paulo Mário Freire (Executive Vice-President/Vice-Président Exécutif)

632 Dr. Francisco de Assis Basílio (Technical Director/Directeur Technique)

635 Participants List / Liste de Participants

F.P. Glasser - Department of Chemistry, University of Aberdeen,
Meston Walk, Old Aberdeen, AB9 2UE, Scotland, U.K.

KINETICS OF CEMENT-MAKING REACTIONS

1. INTRODUCTION

The kinetic aspects of cement clinkering have not been specifically addressed at previous International Cement Congresses, although its proceedings contain many valuable contributions on various aspects of kinetics. The reasons for this absence lie partly in the complexity of cement reactions: it is difficult to analize from the kinetic standpoint complex and ill-understood processes. But partly, the nature of kinetic studies is responsible. Kinetic studies may be contrasted with equilibrium thermodynamic studies; the latter have a coherent and well defined body of theory which serves as a unifying thread. Kinetic studies appear at first sight to lack this unification. The nature of the kinetic treatment has to be varied to suit the particular type of reaction, and a wide range of processes involving solid, liquid and vapour phases occur all of which appear to require special treatments. Moreover, while equilibrium conditions prevailing in the kiln can generally be defined in terms of accessible physiochemical parameters - temperature, composition, etc. - kinetic parameters often seem to be elusive and difficult to evaluate and apply in practice.

The general applicability of kinetic concepts to cement making cannot however be questioned: equilibrium may govern the ultimate nature of the products which can be obtained in a cement kiln, but kinetic factors determine the economics of achieving these ends. We thus recognize that kinetics and equilibrium studies are intertwined. Both aspects are important in determining the process parameters and economics of cement production. It is apparent that continued economic pressures on cement makers will intensify the need to make a more uniform product as well as increasing the performance parameters of concrete systems. It is unlikely that this can be achieved by application of empirical methods alone, hence the need to emphasize fundamental aspects, including process kinetics.

A full review of kinetic theory relevant to cements is beyond the scope of this contribution. However, a number of excellent monographs have appeared, notably those of Budnikova and Ginstling (1968), Kingery et al (1976), Young (1966) Schmalzried (1981) and Doremus (1985). These develop basic concepts, give mathematical treatments and illustrate their application to a wide range of solid state reactions. Cement scientists have perhaps lagged somewhat behind their colleagues engaged in the study of ceramic systems. Yet parallels undoubtedly exist, and are drawn in this review where deemed to be appropriate.

2. SURVEY OF THE KINETICS OF CEMENT MAKING

Cement making raw materials bear little similarity to the final clinker product in terms of phase composition, texture, microstructure, or in the crystal structures, compositions and reactivity towards water of the constituent phases. The alteration in bulk chemical composition is less marked, although substantial: many of the components of clinker batches are essentially involatile, e.g. CaO, $A\ell_2O_3$, SiO_2, and are thus preserved through the cycle, eventually appearing in the solid phases. Other phases are volatile but may condense in part at some stages of the process: examples include SO_x and alkalis. Yet others are sufficiently volatile to be essentially eliminated in the kiln; CO_2 and H_2O, arising both from fuel and raw materials, are examples.

During cement making, the raw materials undergo a thermal excursion in which they are heated comparatively slowly to $\sim 1450^{\circ}C$, maintained briefly for a matter of minutes at the high temperature and finally cooled, typically at a relatively fast rate. It is difficult to construct a typical profile because many modern plants depart from older practice and use a suspension preheaters to raise batch temperatures to $\sim 900^{\circ}C$, finishing the partially calcined batch in a short rotary kiln. However, it suffices for present purposes to recall the general features: a progressive heating to temperatures such that partial fusion occurs, followed by comparatively rapid cooling of the product, termed clinker.

The early stages of reaction are characterized by decomposition reactions, of which the most important is the decomposition of calcite, $CaCO_3$. Other important decompositions occur: much of the $A\ell_2O_3$ and Fe_2O_3 contents of the raw meal are present as clays and hydrous oxides, which loose water. At the same time, reaction begins. The vapour atmosphere in contact with the decomposing mass is comparatively rich in S, mainly SO_2, and in CO_2 and H_2O. Moreover, the raw meal contains at this stage large quantities of carbonate (CO_3^{2-}) ions; possibly also sulphate, etc. Secondary reactions occur leading to formation of intermediate phases such as sulphate apatites and silicocarbonates, e.g. spurrite. These intermediate phases may subsequently break down in the higher temperature zones of the kiln, but their role as intermediates to the synthesis of C_3S, C_2S etc. may be important, although not yet fully investigated. Moreover, the presence of low-melting sulphates may lead to transient liquid formation even at the comparatively low temperatures encountered in the decarbonation zones.

During the final stages of clinkering, a melt phase develops which has a vitally important role in the kinetics of the clinkering process. Microstructural evidence obtained on simulate clinker batches suggests that the melt phase is very fluid and strongly wets the solid phases. Development of this liquid phase occurs over a rather narrow temperature range, if transitory premelting phenomena are ignored. The main melting, which results in formation of 15-20% of an oxide melt, occurs at comparatively high temperatures. Lea and Parker (1934) who studied phase equilibrium in the $CaO-A\ell_2O_3-Fe_2O_3-SiO_2$ system determined that a eutectic occurred between C_3S, C_2S, C_3A, ferrite and melt at $1338^{\circ}C$; its melt composition was given as 54.8 CaO, 22.7 $A\ell_2O_3$, 16.5 Fe_2O_3 and 6.5 SiO_2 (wt %), The phase equilibrium data are not strictly applicable to clinker batches for two reasons. Firstly, the presence of additional components, e.g. MgO, Na_2O, K_2O, TiO_2, alter somewhat the position and temperature of melting; presumably the temperature is shifted to lower values. Secondly, when clinker batches commence melting, they are far from equilibrium and contain as yet much unreacted SiO_2, CaO, etc: C_3S will not yet be present in substantial quantities. Thus melting occurs under metastable conditions. In general, metastable solid phase assemblages commence melting at lower temperatures than would obtain if stable phases were present. Thus both factors work in the same direction, shifting the temperature at which extensive melting occurs to less than $1338^{\circ}C$. The quantitative extent of the

reduction in the temperature of initial fusion is not known, but is unlikely to be greated than 20-40°C. Thus extensive melting can be expected to occur at or just above 1300°C.

Correspondingly, the composition of the liquid may also be subject to change, both on account of the metastable nature of the melting which affects the solubilities of the major components, but also on account of the solubility of minor components. These minor components do not necessarily dissolve entirely in the melt (indeed, some are probably inaccessible, being locked into undissolved solids) and there are no grounds, based on present evidence, to suppose that the liquid composition differs substantially greatly from that of the equilibrium eutectic.

Once melt develops, with formation of a substantial quantity of oxide liquid, material transport is facilitated. The melt phase dissolves material from phases which are unstable in the new conditions e.g. SiO_2, CaO, and deposits transported species either on those phases which are stable, e.g. C_2S or nucleates stable phases not hitherto present, e.g. C_3S.

The inability of the clinker batch to develop much C_3S in the solid state arises because C_3S itself is only stable at temperatures above 1250° - 1275°C, and this lower limit below which C_3S is unstable, fortuitously lies so close to the partial fusion temperature that the two happenings are practically coincident, in terms of the thermal regime imposed on the batch in the course of its passage through the kiln.

The dissolution of metastable phases is of course of crucial importance. Clinkers which contain substantial quantities of undigested raw materials are apt to be unsatisfactory. The mechanisms of dissolution require to be examined. Fig. 1 shows three of the most important mechanisms involved in dissolution reactions. Fig. 1(a) shows a CaO grain dissolving in a clinker liquid which is undersaturated with respect to CaO but saturated with respect to C_3S. The CaO-melt interface has, however, served as a site for preferential nucleation of C_3S, which now forms a protective barrier around the CaO, thereby retarding further dissolution. Textures of this type are sometimes observed in clinker thin sections, where grains of CaO become isolated from contact with melt by inclusion in C_3S. The remaining two cases are uncomplicated by the appearance of additional solid phases: the kinetic barrier in 1(b) is the rate at which material can diffuse away from the interface. This mechanism operates in the case of SiO_2 grains; adjacent to the interface, the SiO_2 content of the melt rises locally, its viscosity increases and the grain becomes embedded in a sheath of melt having relatively poor transport properties. Thus transport through the liquid and removal of material from the dissolving grain becomes rate-determining. Fig. 1(c) illustrates another type of kinetic control which can operate. In this instance, the surface of the grain is kinetically inert, and becomes the barrier to dissolution. The dissolution of periclase, MgO, in clinker melts is an example. Although the melt phase is normally undersaturated in MgO, and the MgO grains may be quite small, their comparatively unreactive surfaces inhibits dissolution in the course of typical clinkering cycles. Much of the evidence concerning dissolution of reactants in clinkering is indirect, from mineralogical thin

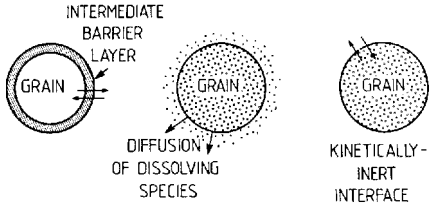

Fig. 1. Kinetic limitations to the dissolution of solid in melt, showing (left) solid barrier layer formation, (centre) sluggish diffusion in the melt and (right) surface control.

sections, and direct experimental verification is thus far lacking.

However, numerous empirical trials of clinker batches, as well as works experience, show that an upper limit of the grain size which can be digested can be established on a purely empirical basis, at least for CaO and SiO_2. These observations correlate well with theory.

Normal clinkering processes attain a sufficiently high temperature that the only phases coexisting stably with melt are C_3S and C_2S. The nucleation of C_3S appears not to be difficult, although clinker microstructures reveal a range of C_3S crystal sizes and habits. Well-burnt clinkers are characterized by relatively large C_3S crystals having well-developed euhedral morphology. However, as noted, this is not invariably the case, and it would be interesting to have better-established the relationship berween clinker microstructure and the nucleation and subsequent growth conditions of C_3S.

Since C_3A and ferrite are not present at peak clinkering temperatures, they originate by crystallization from the melt during clinker cooling. It is of course possible for the liquid phase present during high temperature processing to be preserved as a glass. Indeed, the eutectic composition in the C-A-F-S system can be prepared in laboratory furnaces on a 10g scale and readily preserved to ambient in glassy form by quenching the melt in water. Thus the formation of potential C_3A and ferrite could potentially be suppressed in clinkers in favour of glass. It is not conclusively proved that OPC clinkers do contain glass and since Bogue calculations of the potential compound content generally give reasonable agreement with the actual compound content, as determined by X-ray diffraction, glass must be absent or comparatively scarce. Nevertheless there are cases where Bogue calculations differ significantly from observed phase contents. In this context it is important to note that more rapid cooling, or the presence of more glass stabilizers, or both, could rapidly alter the compound content, by preserving glass mainly at the expense of C_3A and ferrite. Another important consequence of the cooling rate is that it must be sufficiently rapid to retard decomposition of C_3S which, below 1250° ± 25°C, tends to decompose to C_2S and free lime.

This brief survey highlights some of the kinetic aspects of cement making and serves as an introduction. These will be analized in more depth in

subsequent sections, but it is essential that aspects of the kinetics, although treated separately, should be seen to be part of a continuous, integrated process.

3. THE THERMAL ACTIVATION CONCEPT

A salient feature of the cement burning process is the relationship between temperature, thermodynamic state and reactivity. Reactions can occur, in theory, both during rising and falling temperatures. However, the clinker tends to reflect the high temperature state, many reactions occurring more sluggishly on the falling temperature cycle than on the rising temperature cycle. These and other phenomena find more quantitative explanation in terms of the activation energy concept. In order for a reaction to proceed, it must have a favourable driving force, usually defined in terms of the Gibbs free energy, ΔG, the criterion of an energitically feasible reaction being that it has a negative free energy. However, a reaction may not proceed directly, but may proceed through an activated state. Fig. 2 shows the concept applied to a comparatively simple case, in which atom migration results in a phase change. The atom which moves is shown in shading to distinguish it from other atoms which, in the example, remain essentially fixed. Atoms or ions must acquire sufficient energy to attain an activated state in which they can react, yielding a product having a lower free energy than the reactant. The exact nature of the activation barrier in atomistic terms is often not known, but we return to this point subsequently. One way in which the activation barrier may be overcome is by giving atoms, ions, etc. sufficient energy to overcome this barrier. At a fixed temperature, atoms or ions, even if all of the same kind, may vary in energy. This is the Boltzmann distribution, relating the energy spectrum of constituent particles to temperature. Given a system of N particles, in kinetics we are concerned by the number of such particles, N_i, having more than a specific energy, E_i. From the Boltzmann distribution

$$N_i = \frac{N}{Z} \exp\ (-E_i/kT)$$

where Z is the distribution function, k the Boltzmann constant and T the absolute temperature. If

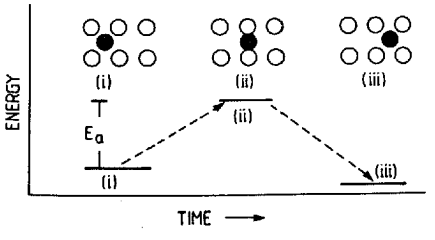

Fig. 2. Schematic view of activation energy showing it (top sequence) in terms of atom migration and (bottom sequence) in terms of energy changes. The overall difference between (i) and (ii) is the activation energy while the thermodynamic driving force is the difference between (i) and (iii)

the critical energy in question is taken to be E_a the activation energy, it can be seen from the shape of the normal distribution curve that the number of particles having greater than the critical energy increases rapidly with temperature.

Further development of the Boltzmann relationship assumes many forms - a result which often but unnecessarily leads to concern over which is the 'right' equation. All, however, contain a factor of the general form $\exp\ (-E_a/RT)$ where R is the gas constant. From this, a reaction rate constant, K, may be defined such that:

$$K = A \exp\ (-E_a/RT)$$

Most kinetic treatments use these equations, either in the form given here or in some derivative form. It is seen that the number of particles which acquire sufficient energy to become activated, and initiate a reaction, increases rapidly with temperature. Fig. 2 shows the activation for motion for a single ion or atom. This event might occur, for example, in a crystallographic phase transformation. Other events, such as transport to a surface and across an interface, clearly have a more complex activation energy which is the summation of a number of separate processes

$$E_a = \Sigma(E_{a_i} + E_{a_{ii}} + E_{a_{iii}} \ldots.)$$

Whilst it may not be possible to separate these terms, in practice one may be rate-limiting and hence determine the kinetics. If a reaction occurs at some equilibrium temperature, it may be necessary to achieve a substantial driving force in order for the reaction to proceed at a perceptible rate. Jøns (1980) has tabulated driving forces for the reaction:

$$Ca_2SiO_4 + CaO = Ca_3SiO_5$$

Fig. 3 shows schematically the situation. Below the equilibrium temperature, T_E, Ca_2SiO_4 and CaO are the more stable assemblage: above, Ca_3SiO_5 is the more stable. If, however, activation forces are examined at some increment ΔT above and below T_E, the proportion of thermally activated species will be greated at $T_E + \Delta T$ than at $T_E - \Delta T$, so the forward reaction, leading to C S formation, will tend to proceed more rapidly than the back reaction leading to its decomposition. The practical consequences are that reactions leading to C_3S formation occur rather more quickly at clinkering temperatures than in the reverse direction, so that C_3S is not significantly decomposed during clinker cooling. The reaction leading to C_3S formation does, however, have some other noteworthy features. The positive free energy of formation at low temperatures is low: $\Delta G = 0.32$ and 0.16 Kcal mol^{-1} at 1050°C and 1150°C respectively. However, even in its range of stability the driving force is small, only -0.16, -0.30 and -0.27 kcal mol^{-1} at 1350°, 1450° and 1550°C respectively. The rather small driving force for Ca_3S formation from C_2S and CaO is a noteworthy feature of clinkering chemistry. As will be shown, the presence of a liquid phase is important to facilitate material transport.

4. KINETIC ROLE OF DEFECTS AND IMPURITY IN CEMENT MAKING

It has been known for many decades that the migration of atoms in solids, and hence their reactivity, is greatly enhanced by the presence of

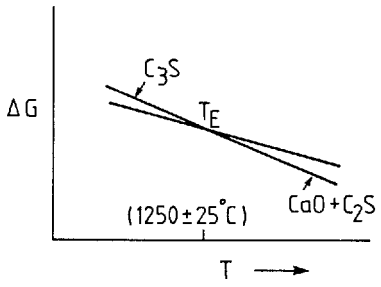

Fig. 3 Free energy changes for the reaction: $CaO + SiO_4 \rightleftharpoons Ca_3SiO_5$ close to the equilibrium temperature, T_E.

defects. Simple atomic defects are readily characterized: atom sites normally occupied may be left vacant (so-called Schottky disorder: in ionic substances, it may be necessary to have charge-equivalent numbers of cation and anion defects) and Frenkel defects, in which extra atoms or ions occupy interstial sites. In fact, these intrinsic defects are best observed in chemically very pure solids. Clinker minerals do not however fit this description, and most of the defects are chemically-induced: these and other related defects are termed 'extrinsic defects'. That is not to say that Schottky and Frenkel defects are absent: they occur, but in numbers which are effectively chemically controlled. An example of a chemically induced defect is in the substitution of Aℓ in C_3S; if the substitution occurs for Si, and in the absence of other charge-compensating mechanisms, it would be necessary to introduce $4A\ell^{3+}$ to balance $3Si^{4+}$. Of course in practice other compensatory mechanisms do also exist, so the actual substitutions observed are a complex mixture of isomorphous crystallo-chemical substitutions as well as vacancies and interstitials. The exact balances have not been quantitatively characterized, but it is apparent that the number of extrinsic defects in a typical clinker mineral vastly exceeds the number of intrinsic defects. Moreover, defects in the more general sense need not be confined to points i.e., individual lattice sites or paired vacancy interstitials. Real crystals of cement phases consist of a mosaic of slightly misoriented domains. Moreover, owing to the complex polymorphism of the C_3S and C_2S phases especially, they will have undergone a complete series of polymorphic transformations during cooling. This results in twinning, the creation of polytypes and the accumulation of lattice strain and misfit along domain boundaries arising in part from the progressive lowering of crystal symmetry and lattice misfit which accompanies these events. Groves and colleagues (1984) have recently contributed to crystallographic studies of the polytypism of real C_3S crystals. Although these studies disclose the finer details of the crystal structure, they do not enable the number and type of defects to be calculated nor can their effect on the thermodynamic properties be determined. However, another approach to defect characterization has been taken which allows the number of defects to be integrated over a bulk sample. This method utilizes the principle that the defect content is, in part, metastable at low temperature and can be discharged by low-temperature annealing.

In the course of discharging these defects, many of which serve as electron traps, both thermoluminescence and phosphorescence can be observed. C_3S, for example, has a thermoluminescence peak at -118°C and the rate law for the decay of the subsequent phosphorescence was determined. Theoretical interpretations have enabled the electron depths to be determined, giving insight into the nature at least of the photo-optically-active centres: Descamps (1974) and Firens and Tirlocq (1980). They correlate defect content with reactivity: Maycock, et al. (1974) have also given an account of the role of lattice defects in controlling reactivity.

It therefore appears that the existence of defects in clinker minerals has been established. Crystallographic defects appear to predominate, mainly extended defects and point defects controlled by chemical substitution. We are, however, some way from being able to quantify the absolute number of defects and to control this type and character.

5. DECOMPOSITION REACTIONS

Broadly, decomposition reactions in cement systems can be classified into one of several types. Table 1 shows classification. The early stages of clinkering are associated with events such as the decomposition of calcite and clay minerals, etc. These kinetics have been extensively investigated especially in connection with ceramic processes.

The decomposition of calcite, $CaCO_3$, is an important step in clinkering. In suspension pre-heaters, grains of calcite are essentially in contact with only a gas stream. Under these conditions, the physico-chemical conditions leading to calcite decomposition can be specified in terms of temperature and ambient CO_2 pressure, but the kinetics are still rather complex. Fig.4,5 shows in superposition the equilibrium P-T curve and observed rate data. As the CO_2 pressure rises the minimum temperature necessary to initiate dissociation increases. Once, however, this

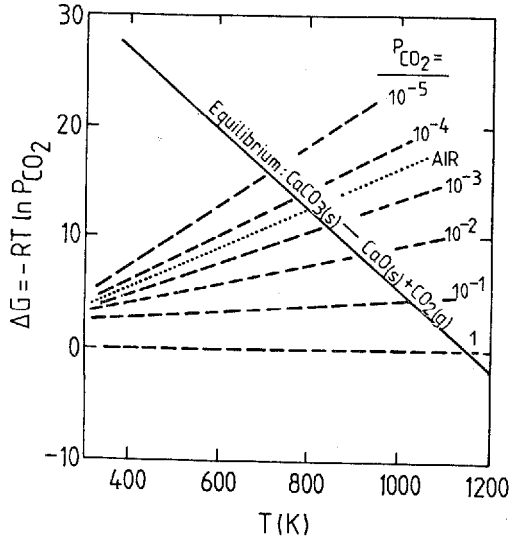

Fig. 4. Free energy changes in the system $CaO-CO_2$. The solid line gives ΔG values, while the corresponding dashed lines indicate equilibrium CO_2 pressures (dotted line, P_{CO_2} in free air) in atmospheres.

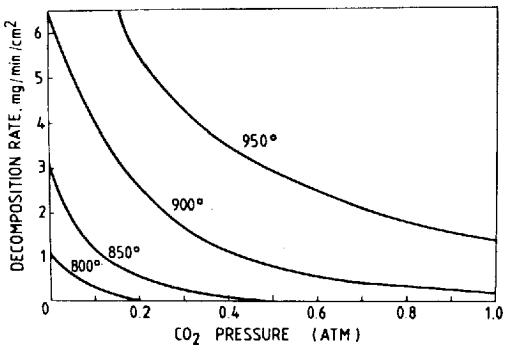

Fig. 5. The decomposition rate shown for successive isotherms. Decomposition can only occur within the limited range of pressure temperature conditions as defined in Fig. 4. However, within these favourable regimes, the rate is still dependent on many factors (see text). In the region for which data are shown, the reaction proceeds such that the kinetics are formally first-order.

decomposition threshold is exceeded it is necessary to consider three factors in order to analize the reaction kinetics. These factors are (i) processes leading to the initiation of reaction, generally termed 'nucleation', (ii) the reaction mechanism of the main (bulk) stage of decomposition and (iii) the energetics and geometry of reaction, including heat flow and mass balance as well as surface area and particle size. Fig. 6a shows the initial stage of reaction. Nucleation of the solid product of decomposition, CaO, is accomplished by loss of CO_2. Since this occurs at the surface, a product layer is quickly established; although nucleation may occur at selected sites, it spreads rapidly. Electron micrographs disclose that the product is adherent but, on account of the large density difference between solid product (CaO) and its substrate consisting of unreacted $CaCO_3$, the product layer is microporous. The kinetics now become controlled by other factors. Firstly, the decomposition is endothermic, so heat must be supplied to make the reaction proceed; ΔH_{298}^{o} is 44.3 kcal mol^{-1} and remains large at all temperatures, so energy input exerts an important control over kinetics. Secondly, reaction must occur through a thickening skin of product. Fig. 6b shows the situation. The material and thermal balance now affects the rate markedly: the CO_2 flux through the product layer experiences a pressure drop, while the thermal flux ensures also that a temperature gradient occurs. Kingery et al (1976) summarizes these balances. The net effect resulting from a thickening product layer is somewhat dependent on temperature: at low temperatures, the kinetics are strongly dependent on geometric surface area, and hence particle size and packing. Increasing surface area favoursdecomposition while dense powder packings inhibit decomposition by decreasing the effective surface area as well as impeding diffusion of CO_2. Suspension preheaters favour open packings, whereas kiln decomposition occurs partly in packed beds of material, partly in particles being tumbled through a vapour stream. But at

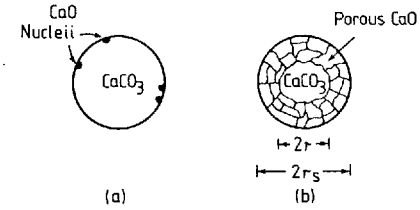

Fig. 6. Showing spatial arrangement of product on decomposing $CaCO_3$ particle at (left) the initial nucleation stage and (right) a shell of undecomposed $CaCO_3$ surrounded by CaO.

higher temperatures, such that the absolute rate of decomposition is more rapid, heat transfer tends to dominate. Not surprisingly, therefore, kinetics studies undertaken by various investigations, differ somewhat in their conclusions, depending on the range of conditions studied. However, experiments on loose powders usually show that the kinetics are first order, i.e., for cylindrical particles of initial radius r_o, α the fraction decomposed in some time t is given by a relation having the form

$$(1-\alpha)^{\frac{1}{2}} = 1-kt/r_o$$

where k is the activation energy: a graph of $1-\alpha$ vs time t produces a straight line relationship for a particular temperature. These conclusions have been verified and expanded for a range of cement-making raw materials. Among the more recent studies are those of Rudolph (1979) who examined process data for vibratory furnace decomposition of $CaCO_3$. The kinetics were also studied by Mueller, et al (1977) who obtained good agreement with previously published data. Parallel studies by Fredericks (1979) and Drozdetskaya and Gropyanov (1977) reached similar conclusions. The data were applied to large-scale reactors by Biernacki and Kowalski (1981). General analyses of the data relevant to clinkering have also been made by Mueller, et al (1979) and Rao and Cutler (1975). This latter study also included an analysis of the role of coal ash in promoting decomposition while Veruto, et al. (1984) examined the surface area of the product and the catalytic role of CO_2. The kinetics are of course influenced by the presence of impurity, and important studies in this area have been undertaken by Talaker, et al (1982) who examined the effect of Ca (as $Ca(NO_3)_2$), $A\ell_3(PO_4)_6$ and CaF_2; calcium nitrate was found to be a powerful accelerator while aluminium phosphate was a retarder. CaF_2, on the other hand, behaved as an accelerator at low temperatures, but retarded at high temperatures. Shearer, et al (1980) studied the effect of $NaC\ell$ on the decomposition. Even trace amounts of $NaC\ell$, insufficient to wet the grains significantly affected the decomposition. Moreover melt temperatures were depressed to as low as 690°C because $CaCO_3$ CaO and $NaC\ell$ have a significantly lower melting point than $NaC\ell$ alone (801°C). In the presence of 2 wt.% $NaC\ell$, sintering of CaO was accelerated and pore sizes grew to 1.5-3.0 μm, contrasted with 0.01-0.02μm in pure limestone (90-99% $CaCO_3$) batches also sintered for 1h at 850°C in a $N_2/O_2/CO_2$ atmosphere.

TABLE 1

DECOMPOSITION REACTIONS INVOLVING A VOLATILE PHASE

Reaction: Example	Features	Comments
$CaCO_3 \rightarrow CaO + CO_2$	One step reaction: solid 1 → solid 2 + gas. Decomposition initiated at surface.	Kinetics approximate to first order. Rate limiting factor varies with temperature and absolute rate of decomposition.
$CaSO_4 \cdot 2H_2O \rightarrow CaSO_4$	As above, but decomposition occurs in stages. Two intermediate products, α and β hemihydrate possible.	Kinetics approximate to 2nd order but complicated by retention of water in pore structure.
melt impurity $CaCO_3 \rightarrow CaO + CO_2$	Liquid phase film provides complex interface.	Apt significantly to affect rate of decomposition.
kaolin $Al_2Si_2O_5(OH)_4 \rightarrow$ "metakaolin" $+ H_2O$	Bulk diffusion of H species (H^+, OH^-) rate controlling: structure of metakaolin is topotactic after kaolin percursor.	Metastable but persistent intermediate phase obtained before final decomposition to mullite and silica.

The kinetics of other decomposition reactions have been studied on account of their technical importance, and are found to differ significantly from $CaCO_3$, whereas the $CaCO_3$ decomposition occurred in a single stage, other examples are known in which decomposition occurs with formation of intermediate solid products. For example, $CaSO_4 \cdot 2H_2O$ decomposes in stages, yielding the so called hemihydrate, ideally $CaSO_4 \cdot \frac{1}{2}H_2O$, before decomposing first to $CaSO_4$ and eventually to $CaO + SO_2 + O_2$. The hemihydrate intermediate occurs in two modifications, the so-called α and β forms. They have not always been accepted as distinct polymorphs, but do appear to differ sufficiently to warrant a distinction on kinetic grounds. The α and β hemihydrate inherit a pore structure which is conditioned in part by the crystal structure of the percursor gypsum, but the extent to which recrystallization occurs appears to depend partly on the rate of water removal, chemical purity of the parent, etc. For example, during subsequent removal of water, the α phase dehydrates sharply over a narrow range of temperatures where β loses the last $^1/_4$ of its water over a wide range of temperatures. Ball and Norwood (1977, 1978) attributed these differences to the smaller pores in β which, it was suggested, trapped liquid water. The retention of water to relatively high temperatures is not, however, believed to reflect on the stoichiometry of the material. The final stage of thermal decomposition, marked by the reaction of $CaSO_4 \rightarrow CaO + SO_2 + O_2$, has been studied recently by Hanic, et al (1985). They distinguished two kinetic conditions: one, which obtained below the $CaO + CaSO_4$ eutectic at 1638K, the other at higher temperatures such that partial melting occurred. Below 1638K, the decomposition was found to obey second-order kinetics of the type $G(\alpha) = 1/(1-\alpha) - 1$ where α = the fraction decomposed, whereas above the eutectic, the kinetics were controlled by a phase boundary reaction in which an interface moves at a constant velocity inward, with $G(\alpha) = 1-(1-\alpha)^{\frac{1}{2}}$. The distinction berween solid state and liquid-phase reactions is of considerable importance and has enabled the authors to show that E_a, the activation energy, decreased from 622 ±7kJ mol^{-1} in the solid state to only 373 ±4kJ mol^{-1} in the presence of liquid. A vast literature exists on the effect of impurities supposedly to catalize $CaSO_4$ decomposition. It is impossible to assess, in modern terms, the worth of these studies. Undoubtedly many of the reactions described occurred under conditions such that partial melting occurred while in others, decomposition occurred simultaneously with solid state reaction, as with SiO_2 to form C_2S.

The decompositions of clays, e.g. kaolin, have also been extensively studied. Kaolin is an interesting example of a special type of decomposition because the decomposition proceeds topotactically, i.e. with preservation of structure. Water is lost in the course of reaction but the oxygens and many of the cations present in kaolin remain on essentially the same positions throughout; this structural control has a profound influence on the kinetics and mechanism of the decomposition, as well as on the structure of the solid decomposition product. The kinetics are controlled essentially by diffusion of OH^- ions in the bulk rather than by surface reaction.

Decomposition reactions thus reveals a wide range of reaction types. Table 1 summarizes these with respect to reactions, all of which are characterized by evolution of a volatile phase. Even in the absence of complicating factors, e.g. reactions with other phases, the reactions are of sufficient complexity as to require application not only of formal kinetic treatments to the data, but also application of other structure sensitive techniques, e.g. X-ray and electron diffraction and microscopy. Given the complex nature of some of the decompositions, and the effect of impurity in clinker batches, it is easy to appreciate that the regime of steadily rising temperatures encountered by material in the kiln leads to a complex series of reactions. Moreover, with rising temperature, the minerals in the raw meal cease to behave as an isolated system of individual particles but instead begin to react with each other. Where reaction occurs with

elimination of a volatile (CO_2, SO_2, H_2O etc.) concomitant chemical reaction may not only be affected by the rate at which reactants are formed from percursors, but the very existence of the reaction may affect the decomposition rates.

6. CLINKER MINERAL FORMATION

6.1. The Industrial Perspective

The study of burning reactions in the cement kiln is largely qualitative on account of the great chemical complexity and physical inhomogeneity of the raw materials. However, more quantitative studies have been made on model systems - chemically simplified, but containing many of the components of real clinker batches. Much valuable information has been obtained from this type of study.

The general question of reactivity of industrial clinkers has been examined on account of its great importance to industrial practice. This aspect has been reviewed at previous Congresses, but subsequent to Paris, important reviews have been made. The calcination behaviour of batches has been studied by Kupper and Tiggeobacumber (1983) using a new laboratory apparatus. The evaluation of the reactivity and burnability has been advanced by Chromy (1985) and Ludwig and Ruchkensteiner (1973) (1976) who showed that increasing the rate of heating of the raw meal above the decomposition temperature required to achieve reaction at the maximum sintering temperature was reduced by as much as 40%. Other studies, notably those of Fundal (1979, 1981) have enabled mathematical expressions for the burnability to be formulated. The information required includes the lime saturation factor, silica modulus and the fractions of acid insoluble quartz > 44 μm and of calcite > 125 μm. These grain sizes seem to correspond to the maximum grain size which can be effectively assimilated in the course of a typical clinkering cycle. Although the sizes were fixed largely on the basis of reaction in model systems, plant trials show that these limits are applicable to typical burning schedules. The continuing importance of grinding as an aid to enhancing batch reactivity was also quantified by Mosikas, et al (1981). The general concept of 'burnability' has also been addressed by Humpola (1981), Krachner (1985) and Teoreanu, et al (1985) and by Ludwig (1981). Special aspects of the burning process have also been investigated; Gouda (1979) examined the relationships between clinker composition and grindability, while the effect of fuel source on batch reactivity was addressed by Vogel (1983) and by Waechtler, et al (1984). Sulphate, present in fuel and raw materials, apparently influences greatly the rate of calcium silicate formation. This aspect was studied by Lim and Park (1983, 1984a, b). The microstructural aspects of clinkering have also been related to composition and burning history in a series of papers by Chatterjee (1979a, 1979b) Sarkar (1979) and Chatterjee, et al. (1980).

The kinetics of reaction have also been studied from a more theoretical standpoint by Mchedlov-Petrosyan et al (1978) and by Chatterjee et al (1980). The importance of minor components, and of low-temperature batch reactions leading to the development of phases intermediate between the starting materials and the high-temperature clinker minerals, are emphasized.

The formation of intermediate phases in cement kilns has long been known from a study of kiln coatings but many of the phases found occurring e.g. spurrite, a calcium silicate carbonate, have been assumed to be oddities. However, it appears that under some conditions they may represent an alternative pathway to the formation of clinker minerals. Spurrite, (to give one example) is actually somewhat more stable at high temperatures with respect to dissociation than is calcite. Mchedlov-Petrosyan et al (1975) has also emphasized the role of thermodynamic metastability and metastable reaction sequences in controlling overall batch reactivity. The effect of furnace atmosphere on reaction kinetics has also been analized by Sylla (1981); reductive burning lowers potential ferrite, but also increases the content and reactivity of C_3A. Mackenzie and Aldridge (1980) have also analized the effect of reducing atmospheres: the differences are partly kinetic and partly due to a shift in equilibrium. The distribution of reactants in clinker batches reflects the statistics of mixing in inhomogeneous particulate systems, and the influence of inhomogeneity on kinetics, as reflected by mix burnability and nodule formation, has been analized by Petersen, et al (1979).

6.2. Reactions between Selected Solid Components

Studies of the reactions between selected components of clinker batches have contributed to understanding the reaction kinetics. We first note that kinetic studies cannot be extended over too wide a range of temperatures without a fundamental change occurring in the nature of the reaction mechanism. For example, Delinge, et al (1977) studied reactions leading to C_3A formation from CaO-$A\ell_2O_3$ mixtures using pure reactants as ca 20 μm grains. The reactants were in a DTA apparatus. At 1300°C, some reaction forming CA and $C_{12}A_7$ occurred, but above 1355°C, metastable melting occurred resulting in rapid transfer of material through the melt and recrystallization of $C_{12}A_7$. This $C_{12}A_7$, persisted only up to 1375°C forming C_3A by reaction of the melt with CaO and $C_{12}A_7$. Formation of C_3A in the solid state has a relatively high activation energy, and is a comparatively slow process relative to $C_{12}A_7$ formation. The formation kinetics of C_3A have been studied by Mackenzie and Bonerjee (1978) and in the presence of SiO_2 as an additional component by Chow and Burnet (1981a, 1981b). The formational kinetics of the monocalcium aluminate have also been studied by Singh and Ali (1980). Tetracalciumalumino ferrite has also been synthesized by solid state reaction, and its formation kinetics have been determined by Mackenzie and Alasti (1978).

Reaction kinetics leading to the formation of C_2S and C_3S have extensively studied by Shrader and Kenhe (1973): calcium aluminates were included, by Ludwig and Wolter (1977) and Odler and Doerr (1977). In the latter study, fine grained chemically pure reactants were heated isothermally at temperatures in the range 1370°C and 1520°C. The velocity of formation was very slow at 1370°C but much more rapid, and relatively comparable at temperatures between 1420° and 1520°C. They tentatively concluded that the reaction rate could not be expressed in terms of a particular order of reaction, or that any simple interpretation could be placed on the kinetic data. They supposed that

the great enhancement of reactivity between 1370^{0} and 1420^{0}C arose from the greater reactivity between α Ca_2SiO_4, relative to $\alpha'Ca_2SiO_4$ which would be present at 1370^{0}C, and that the sharp retardation with increasing time arose from the formation at high temperatures of diffusional barriers, presumably of C_3S product. After reaction had slowed, the batch was reground and refired. This led to a fresh burst of reactivity, which arose as a consequence of disrupting the barrier layer.

The effect of atmosphere on the reaction has also been investigated by Svetik, et al (1982). Their investigation was in the range 700^{0}-1000^{0}C, so the product of reaction in $CaO-SiO_2$ mixtures was C_2S and to a lesser extent CS and C_3S_2. Reducing atmospheres, generated from mixed CO_2/H_2, accelerated the reaction. This was attributed to water vapour rather than the presence of reducing components, e.g. CO, H_2. Barrier layer formation occurred which retarded reaction rate. Water vapour is of course known to have an appreciable effect on formation of "$C_{12}A_7$". It is well established that at temperatures below 1050^{0}C, appreciable water can be accommodated. However, the status of $C_{12}A_7$ as an anhydrous compound in the $CaO-A\ell_2O_3$ system is questionable. There seems no doubt that the presence of water vapour acts as a powerful agent to promote its formation, even at 1300^{0}C. The role of the water, whether kinetic or structural both,is not known with certainty.

In an interesting study, Mackenzie and Hadipour (1978) determined the effect of DC voltages on reaction kinetics in the range 950^{0}-1150^{0}C. Electrolysis, particularly at higher applied potential, markedly affects the amount of phases formed. This was explained in terms of the thermal diffusivities and electrical mobility of the ions,the oxygen packing of the matrices through which diffusion occurs and the orientation relative to the applied field of the reactant grains.

6.3. Reactions in the Presence of a Liquid Phase

Studies performed on selected components of cement batches as well as on raw meals show that calcium aluminate- ferrites and to a lesser extent, silicates can form by solid state reaction. However formation of alite, while possible in the solid state, will be preceeded or accompanied by extensive melt formation in commercial kiln feeds. Thus one of the most important steps in the kiln process, development of C_3S (the term as used here embraces alite),is accomplished by sintering in the presence of a reactive liquid. The liquid phase is reactive in the sense that it wets grains, has good transport properties, is capable of dissolving in substantial amounts all major and minor components of clinker batches and, moreover, is present in sufficient quantities not only to bridge adjacent grains but also to facilitate material transport over longer distances. This ability to facilitate long-range transport also enables statistical fluctuation in the local composition of the clinker feed to be averaged out, with the result that the final clinkered product is texturally and mineralogically homogeneous.

During the clinkering process, grain growth also occurs, Initially, when the feed is essentially solid, grains grow by solid state diffusion. Generally, the driving force for recrystallization and hence the rate of grain growth, is inversely proportional to grain size such that if r_o is the radius at time zero, the growth at some time is given by

$$r-r_o = (2k)^{\frac{1}{2}}(t)^{\frac{1}{2}}$$

where k is a constant of the particular system. In relatively pure single-phase materials, when r is plotted *vs* log t, a straight line is obtained whose slope is 0.5. However, impure ceramic materials frequently exhibit phase formation at the surface, so that slopes less than 0.5, ranging as low as 0.1 are frequently obtained. Little work seems to have been done on cement clinkers, but it would appear that grain growth is minimized by fairly rapid heating, so that t is small, (ii) formation of intermediate phases, e.g. Ca_2SiO_4 barrier layer between CaO and SiO_2, which slows grain growth, (iii) premelting, which produces small amounts of liquid which inhibit solid-phase grain growth. Much energy is expended in grinding the raw materials, so grain growth especially of CaO is clearly an important but undesirable phenomenon

Grain growth can also occur by vapour-phase transport. But it would appear that the vapour pressure of clinker constituents is too low to make this an effective means of transporting silicate components. Matsumoto and Sata (1981) examined volatilization of C_3S in the range up to 1749^{0}C (in air) and 1900^{0}C (in vacuo). Although incongruent volatilization occurred, leaving Ca_2SiO_4, the rate at which it occurred was slight except at the highest temperatures, well above those normally encountered in clinkering.

The process of densification of the clinker also proceeds by sintering. It is commonly assumed that densification is associated with grain growth. Indeed, while the two processes often proceed simultaneously, there is not necessarily any connection. The first stages of densification of the clinker are probably aided by condensation of thin films of alkali sulphates, etc., on surfaces occurring at temperatures such that the condensate is liquid; this causes the the grains to stick and be drawn together by capillary forces. The hot consolidation of grains is also assisted by the mechanical compaction arising from the rotatory motion of the kiln. However, low temperature liquid formation may well be a transient phenomenon, the liquid disappearing by evaporation of some of its constituents.

Once a silicate liquid develops, wetting of grains can occur on a large scale. It is characteristic of clinker batches that this liquid content remains close to zero until some critical temperature is attained, following which the proportion of liquid increases rapidly as heat is added over a short temperature range, following which interval the amount of liquid remains relatively insensitive to changing temperature. The critical range of temperatures, over which much (ca 20%) liquid develops is probably in the range 1300-1340^{0}C. The wetting relationships are a complex relationship between competing reactions: grains of solid may react with each other, as well as with liquid. Although of considerable importance to the clinkering process, relatively little systematic study has been made. In general, the situation is as shown in Fig. 7. The microstructure can be quantified in terms of the dihedral angles ϕ, between melt and solid and between two

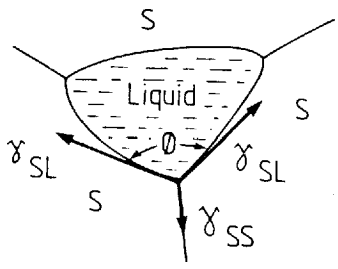

Fig. 7. Interfacial relationships between liquid-solid contacts in a two phase system: γ is the surface tension, S = solid, L = liquid.

solids. The numerical value of the ϕ is a function of the interfacial energy, γ, between two phases, γ_{SL} is the interfacial energy between a solid-liquid pair, such that

$$\cos\frac{\phi}{2} = \frac{1}{2}\frac{\gamma_{SS}}{\gamma_{SL}}$$

We can distinguish several cases, depending on the value of ϕ. In cement clinkering, the important cases are shown in Table 2.

TABLE 2

Wetting of Solids by Melt

γ_{SL}/γ_{SS}	Consequences
< 1.0	$\phi > 120^0$: second phase forms isolated pockets.
between 1. and $\sqrt{3}$	ϕ between 60^0 and 120^0: some liquid penetration along boundaries.
between $\sqrt{3}$ and 2	ϕ less than 60^0: extensive wetting.
> 2.0	$\phi = 0$: solid grains isolated

These wetting relationships are crucial to the ability of the liquid to transport material. In Fig. 7 the value of ϕ is fairly high, whereas in a real clinker it is lower. The consequences of this are shown in Fig. 8 which depicts an idealized clinker microstructure in which ϕ for C_3S-L pairs are sufficiently low that the C_3S grains are completely wetted by liquid but ϕ for C_2S-L pairs is much higher, ca 90^0, so incomplete wetting occurs at C_2S-L boundaries. Of course this stage is achieved only towards the end of the clinkering process when a textural equilibrium obtains. Nevertheless, a microstructure shown is generally favourable to densification and nearly maximizes the ability of the liquid to transport material. The physics of this densification may be treated as follows. If two particles are initially in contact, a negative pressure is developed at the small negative radius of curvature, ρ, compared with the free surface of the particles. This results in a spontaneous viscous flow of material into the neck regions. The initial rate of neck growth is given by Kingery (1976) as

$$\frac{x}{r} = \left(\frac{3\gamma}{2\eta\rho}\right)^{\frac{1}{2}} t^{\frac{1}{2}}$$

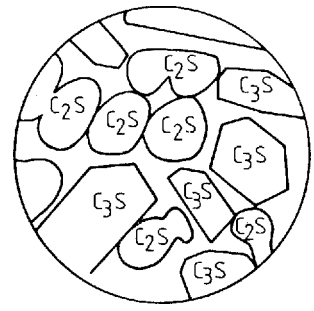

Fig. 8. Idealized clinker microstructure of C_3S and C_2S crystals in liquid.

where the various geometric parameters are designated in Fig. 9; γ is the surface tension, η the viscosity and ρ the negative radius of curvature. The increase of contact diameter is only proportional to $t^{\frac{1}{2}}$, which explains why the initial rate of densification is so much more rapid than the latter stages. Thus, given the comparatively brief sintering period employed in clinkering, many pores persist, especially in the large size range. The smaller pores are reshaped by surface tension and material transport, but the larger pores which depend mainly on viscous flow if they are to shrink, remain relatively unaffected. Indeed, it is fortunate that this should be the case, because their presence greatly facilitates subsequent grinding of the clinker: the larger pores act as flaws, fracture being preferentially initiated between adjacent large pores and propagated through the solid.

Fig. 8 shows schematically differing morphologies for C_3S and C_2S crystals. Cement clinkers vary widely in mean crystal size of the solid phases which are stable at clinkering temperatures, as well as in their morphologies. Nevertheless, microscopists will recognize that a characteristic texture occurs in well-proportioned and well-burnt clinkers. This texture is characterized by having relatively large and well-formed i.e., faceted, C_3S crystals and less well-formed, rounded crystals of C_2S. This texture arises from a variety of

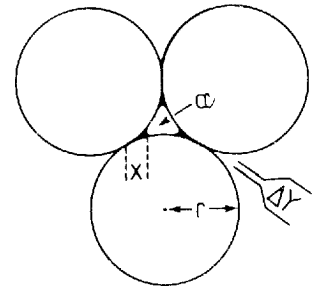

Fig. 9. Contraction of grains resulting from sintering. The grain overlap is ΔY, producing solid-solid contacts, which are available for material transport, along x. The grain radius is r: α is a pore, either empty or liquid-filled.

circumstances. First, sufficient liquid must be present, and the liquid have sufficient wetting power, to achieve this texture. Secondly, growth conditions must permit larger crystals to develop at the expense of smaller. But the development of faceted, rather than rounded morphologies, arises from the difference in energy between various faces of the crystals. These facets are planes which have rational Miller indices, but vary depending on spatial orientation in surface energy, γ. In practice, the function which the crystal strives to minimize is given by

$$\gamma = \Sigma_i A_i \gamma_i$$

where A_i and γ_i are the area and specific surface energy of a plane with indices (i). In practice, the energy driving transport of material from one face to another is comparatively small and the crystal shape is more apt to be determined by rates of growth of different crystal faces, rather than their specific surface energies. The fastest-growing faces tend to grow themselves out of existence leaving behind the slowest-growing faces which ultimately dominate the morphology. The C_2S crystals, with their characteristic rounded morphology, probably reflect growth occurring mainly in the solid state, where material transport is comparatively slow and the impingement of other grains impedes the development of an equilibrium morphology. Thus the texture of a cement clinker reflects the kinetic controls exerted during the firing process, C_2S crystals having typically grown by solid state reaction while the better faceted C_3S crystals reflect growth in the presence of a reactive liquid phase. Variants of the texture described can, of course, occur but while microscopists have frequently noted these, they have not generally been interpreted on a kinetic basis except for certain obvious features, such as the metastable persistence of CaO clusters in the vicinity of former large fragments of calcite, or of undissolved periclase (MgO) on the site of former dolomite grains.

The transport properties of the melt phase are of considerable importance, and have been studied by a number of workers. Diffusion profiles were determined, using a Pt marker to define the original interface, by Kondo and Choi (1968) and Heilmann (1960). Both workers were interested in determining the role of coal ash, and used crucibles fashioned from clinker to contain ash. At 1500°C the ash was fully molten, but the contact between clinker and melt was marked by consecutive zones rich in C_3S (closest to the clinker crucible) and in C_2S. These studies reveal essentially that diffusion proceeds as would be expected from the CaO-$A\ell_2O_3$-SiO_2 phase diagram; if the compositions of the two phases (ash and clinker) are superimposed on the appropriate isothermal section, and the disposition of the tie line connecting the two compositions with respect to the phase regions which it traverses, enables the phase zonation to be predicted. The phase diagram cannot of course predict the relative prominence of the zones, as judged by their thicknesses; this can only be determined by experiments of the type which have been undertaken, for example by Christensen and Simonsen (1970) who made use of an isothermal section technique. Fig. 10 shows a portion of this isotherm. The clinker composition lies at point Cl, while the ash composition lies at A2. The tie line

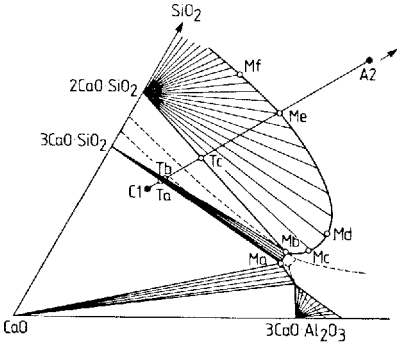

Fig. 10. Part of an isothermal section of the system CaO-$A\ell_2O_3$-SiO_2 at 1500°C. The dashed lines show liquidus phase equilibria. In the example, an ash whose composition lies at A2 is reacting with a clinker at Cl. A tie line is shown and the course of the reaction explained in the text.

connecting the two passes through successive zones of (i) C_3S, CaO and liquid the latter having the composition corresponding to M_a, (ii) C_3S and liquid the latter varying between M_a and M_b, (iii) C_3S, C_2S and liquid which composition lies at point M_b, (iv) C_2S and liquid, varying between M_b and M_e (M_c, M_d...mark successive tie lines) until at M_e the local composition is completely molten. Interestingly, as C_2S develops in region (1D) upon adding more SiO_2 as ash, and as the liquid composition changes progressively from M_b....M_d, partial freezing occurs: the added "fluxes" actually serve to decrease the amount of liquid present over this composition range. The phase diagram can thus be used to predict the zonation occurring in diffusion couples.

The interfaces between zones do not of course remain stationary but undergo spatial shifts as diffusion proceeds. It is therefore necessary to add to the diffusion equations in order to develop a dynamic model. Fick's equations, as well as a moving boundary condition and a 'tortuosity factor' to allow for the existence of lengthened diffusion paths around crystalline grains, it being assumed that diffusion rates through the crystals were negligible compared to those through the melt, have been incorporated. The necessary equations, while rather cumbersome, appear to give a good fit between experimental data and observation and represent the most comprehensive model developed especially for clinkering reactions.

Studies aimed at correlating kinetic and phase equilibria have also been developed by Christansen and Jepsen (1971) who made diffusion couples of 'sandwiches' composed of discs of selected reactants. These were heated isothermally at temperatures such that a liquid developed. The layer thickness of the intermediate, partially melted zone was found to increase linearly with $t^{\frac{1}{2}}$. An apparent diffusion coefficient, for the diffusion of the CaO component through the liquid, D, = $4.37 \times 10^{-7} cm^2 s^{-1}$ was calculated. This value is termed 'apparent'

because the liquid phase composition varies across the interface, hence D could only be a mean value.

One important measure of the kinetics of reaction is the rate at which CaO particles can be dissolved in melt. The liquid phase developed during firing is of course normally undersaturated with respect to the maximum solubility of CaO which can be obtained at saturation so a driving force should be available for its dissolution. The problem has been addressed by Johansen and Jepsen(1978) and Christensen (1981).

The rate of alite formation in clinker sandwiches was determined by Christensen, Jepsen and Johansen (1978). The sandwich construction imposed by the geometry ensured that transport occurred bidirectionally, across the interface. After a period of isothermal annealing, the sandwich was sectioned to determine the rate of alite growth. The width of the alite layer, x, was found to increase with reaction time according to the relation.

$$k^1 = k^1 t$$

The value of k^1 was fixed by the parameters of the reacting system; it was increased by increasing melt content, by increasing temperature, and by substitution of Fe_2O_3 for $A\ell_2O_3$. The effect of increasing temperature is two-fold; it increases somewhat the amount of melt and also lowers its viscosity and increases its wetting power. Substitution of Fe_2O_3 for $A\ell_2O_3$ presumably also contributes to lowering viscosity and surface tension. It has been suggested that small amounts of MgO are beneficial in clinkering, but substitution of MgO up to saturation did not have an appreciable effect on k. In these experiments, lime particles of known size were mixed with a pre-reacted synthetic clinker batch which had the composition 67CaO, $6A\ell_2O_3$ and $27SiO_2$ (wt.%). The mixture was pressed into cylinders and fired at 1500°C for different times: the amount of CaO added was such that the liquid was under-saturated. After annealing, the samples were quenched and analized for free CaO content. Its rate of disappearance in terms of x, the fraction reacted, as a function of time was found to be expressed in the equation:

$$(1+\beta_x)^{2/3} - {}^{2}/_{3}X = 1-[(2\alpha\beta D\Delta C)d_1]t/r_o^2$$

where D is the effective binary diffusion co-efficient of 'CaO' in the melt, ΔC the concentration difference of CaO across the reaction layer, α the volume fraction of liquid in the interfacial layer, d_1 the density of CaO, t the time and β a complex constant related to the composition and porosity of the material. The physical significance of the quantities is worth examining: the rate of disappearance of CaO is proportional to $1/r_o^2$ where r_o is the original radius of the particles: hence the importance of particle size reduction. The amount of liquid in clinker probably cannot be greatly increased in practice nor can the value of ΔC which, together with α is effectively fixed by the nature of the phase equilibria, as expressed by the phase diagram. Calculations made using representative values for α, β and ΔC gave a value for t/r_o^2 of $\sim$2600 min mm^{-2} which, for a burning time of 20 minutes, corresponds to a maximum size for dissolution of 90μm. CaO grains $\sim$90μm would be furnished by $CaCO_3$ grains $\sim$120μm, and this upper limit to the size of CaO grains which can be assimilated agrees with empirical observations. These concepts have continued to be developed in studies of the application of phase diagrams to industrial clinker formation by Johansen (1979) and Petersen (1983), who determined the course of isothermal sintering studies and interperted the kinetics of reaction, and by Odler and Abdul-Maula (1980a) as a prelude to determining the role of mineralizers. The importance of CaO clustering in the isothermal burning stage was also revealed in the kinetic clinkering studies of Chromy (1982) and Chromy and Hrabe (1982) and other kinetic considerations, as elucidated by Teoreny and Dulamescu (1981).

6.4. Role of Fluxes and Mineralizers.

Many of these studies just described were made on chemically simplified systems. Data have also been accumulated in the role of other components. These may be regarded as either fluxes of mineralizers, or both. Fluxes assist reaction without altering the basic stability of the calcium silicates, etc. whereas mineralizers enter into solid solution in the clinker phase thereby altering significantly the thermodynamic stability of the solids. Mineralizers may also act as fluxes by virtue of their partition between solid and liquid phases. Fluxes and mineralizers are reviewed elsewhere, so we confine ourselves to citing specifically studies in which the kinetic effects are included. Odler and Abdul-Maula (1980b) have analized the mode of action of mineralizers including CaF_2, ZnO, CuO and Cr_2O_3; Packter and Zaidi (1981) have examined the role of $CaC\ell_2$ in mineralized batches containing SiO_2 which reacted with dissolved CaO to form βCa_2SiO_4. Luginina, et al (1973) examined the role of naturally-occurring volatile additives; Draynea et al (1976) the role of iron salts in accelerating reactions to form calcium aluminates, while Johansen and Christensen (1979a, 1979b) analized the mineralizing effect of CaF_2. They found that 0.5% CaF_2 increased the rate of reaction by a factor of 2.4 at 1350°C and by 1.2 at 1500°C; a 1% addition was only slightly more effective, increasing the rate by 2.8 and 1.7 at 1350° and 1500°C respectively. The enhancement was interperted in terms of the width of the stability field of C_3S which is greater in the presence of CaF_2 than in the usual case, where only $A\ell_2O_3$ and Fe_2O_3 are present. This in turn increases the ΔC term in the equation above, and hence increases the driving force for the solution of CaO and its reprecipitation from the melt as C_3S. Whilst this explanation is undoubtedly valid, the real picture is perhaps more complex: the presence of F in the melt in place of O^{2-} substantially enhances the solvent and tranport properties of the melt, as well as its wetting power. Moreover, since F^- behaves partly as a mineralizer, inasmuch as it can be incorporated into the C_3S structure and thereby causing it to become the stable phase relative to CaO and C_2S at temperatures less than 1250°C, it may facilitate formation of C_3S in the solid phase even before much melting has occurred. CaF_2 appears to be the only common mineralizer which permits C_3S to be formed essentially by solid state reaction, its formation having been observed at temperatures as low as $\sim$1025°C by Shame and Glasser (1986).

Although the role of mineralizers is of very considerable theoretical interest, it is probably not practicable to incorporate them on an industrial scale. Even F^-, known to be a very effective flux and mineralizer, leads to problems on an industrial

scale on account of its partial volatility, therefore: parallel studies of the classical fluxes used -$A\ell_2O_3$, Fe_2O_3 and to a lesser extent alkalis and MgO, etc.- continue. Many of the advances made in recent years concerning the action of ordinary fluxes have been incorporated into a four-stage model of cement burning by Imlach (1976); valuable data have also been obtained on the mobility of Aℓ and Fe in clinker melts by Osokin, et al. (1973).

6.5. Additional Observations on C_3S Formation.

Many details of the kinetics of C_3S formation in clinker batches seem not to have been completely investigated. The first step in C_3S formation, its nucleation from melts, seems not to have been studied. In many silicate systems, nucleation, particularly of incongruently melting phases (of which C_3S in an example) has proved difficult. However, there is no evidence concerning C_3S; certainly solid surfaces frequently serve as sites for nucleation of silicates and the abundance of crystalline particulate matter present at all stages of the clinkering process could presumably provide potential sites for C_3S nucleation. Many clinkers typically contain comparatively coarse-grained C_3S. This could suggest that nucleation in fact occurs relatively infrequently but that once nucleated, crystal growth had occurred rapidly. On the other hand, this texture could be explained by assuming that nucleation occurred at numerous sites but subsequently unequal growth conditions and rapid material transport favoured assimilation of smaller nucleii by larger crystals. The mathematics of diffusion and transport relevant to these processes have been reviewed by Crank (1975) whose treatise will at least provide the necessary mathematical background to the diffusional aspects. Growth of crystals is, additionally, complicated in this case because it may be facilitated by convective transport as well as diffusion and it appears that a complete analytical solution is not available for cases such as this where both mechanisms operate. If, however, one or the other mechanism is found to dominate, the existing body of theory is adequate. Considering the rate at which C_3S crystals often grow in the high temperature zone - ca0.1-1mm hr - and the large compositional difference which exists between C_3S and the nutrient melt phase - it is tempting to conclude that both convection and diffusion transport work cooperatively to facilitate crystal growth. Goldstein, et al. (1976) have contrasted the differing growth morphologies of calcium silicates obtained from the melt with these obtained by solid state reaction. Space precludes a lengthier description of the background, but the particular problem of competitive growth of crystals, where one nucleus competes with another of the same phase, as well as with other phases having one or more components in common, has been extensively treated in other branches of materials science. Further analysis of the earlier stages of precipitation will be found in papers treatments by Kahlweit (1976) and in numerous texts on crystallization.

The presence at high temperatures of C_3S and C_2S with liquid also implies that C_3A and ferrite are not present. Indeed, this appears to be the case: the liquid phase may be regarded as forming by melting of the $A\ell_2O_3$ and Fe_2O_3 components together with appropriate amounts of CaO and SiO_2. Minor components, such as alkalis, are partitioned between melt and solid phases (C_3S, C_2S). It would not be correct to assume that the minor components are contained exclusively in the melt, nor is equilibrium necessarily attained with respect to their distribution. Clinker liquids are capable of dissolving substantial MgO, although in practice the inert surfaces of MgO grains inhibit solution. This inertness, as well as local clusters of MgO-rich regions and the reduction in solvent power as the melt approaches local saturation, all conspire to ensure that the maximum solvent power of the melt cannot in practice be attained.

6.6. Reactions Occurring During Clinker Cooling. Kinetics of events occurring during clinker cooling.

Many important events occur during clinker cooling. For example, most if not all the C_3A and ferrite develop during cooling. Other possibilities may, however, intervene to prevent these compounds from crystallizing: the melt may fail to crystallize and instead persist as glass. We may first analize the fate of the liquid phase in themodynamic terms, as shown in Fig. 11.

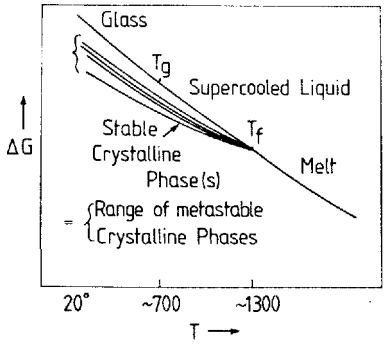

Fig. 11. Free energy - temperature diagrams showing the thermodynamic relationship of a melt and possible products occurring as a consequence of its cooling. T_f is its normal fusion point, T_g the glass transition temperature.

The example depicted strictly relates to precipitation of a single phase, but is in principle applicable to systems of greater complexity. Above ~1300°C, a fully fluid melt exists, It has a fusion point, in this instance close to 1300°C, below which crystalline material develops. In polycomponent systems, freezing occurs over a range of temperatures but is simplified in the diagram to show a definite point. Many oxide melts are distinguished by their tendency to persist as supercooled melts rather than crystallizing. Therefore a metastable prolongation of the free energy curve can be obtained below T_f where the melt still persists as a true liquid. If this melt continues to persist below T_f, with falling temperatures its viscosity increases steadily until eventually it achieves the mechanical properties associated with a rigid solid, below which temperature it is best described as a glass. This transformation temperature, T_g, or strictly range of temperatures, is therefore termed the glass transformation. It was initially defined in terms of viscosity, but in fact thermophysical studies disclose that a variety of

significant changes also occur at an accelerated rate at about this temperature: for example, the free volume available to the liquid suddenly decreases, as evidenced by the concommitant increase in density which occurs at an accelerated rate over a short range of temperatures. It is likely that atomic and ionic motions and structural relaxations occur relatively rapidly above T_g, whereas below T_g these motions are frozen in by quenching. Below T_g, the structural state can be altered only slightly by annealing or very slow cooling. Glasses thus have structural 'memories' for thermal histories below T_g. However, what is of primary concern to cement makers is the preservation or non-preservation of a glassy phase which, if present, must occur at the expense of C_3A and ferrite phases.

If the supercooled liquid is to crystallize, nucleation must occur with only small degrees of undercooling. Nucleation theory is itself in a semi-satisfactory state of development, but if it is assumed that the rate of nucleation I is the rate at which accreting molecules or ions strike the surface of a critical nucleus,

$$I = ZA^X N^X$$

where A^X is the surface area of the critical nucleus Z the collision frequency per unit area and N^X the number of nucleii per unit volume (the theory borrows from condensation of liquid droplets from vapour, where N^X is related to droplet density, the droplets being considered to be the critical nucleus). At small supercooling, critical nucleii form readily and the ionic mobility of species, i.e., Ca, Al and O in the case of a C_3A nucleus, remains high. However, with increasing undercooling the mobility of species in the melt decreases rapidly so while nucleation may still occur, growth rates decrease drastically. Critical undercoolings necessary effectively to suppress growth and hence preserve glass would appear to be in the order of a few hundred degrees, so that supercooled melts preserved to temperatures approaching T_g are unlikely to exhibit bulk crystallization. It would appear that the liquid phase in clinker is not a good potential glass former, but lies on the threshhold of glass formers, given the typical cooling cycles employed in cement production. Of course clinker cooling is far from uniform and the more rapidly cooled fraction, e.g., dusts, is more likely to preserve glass than large lumps of clinker, the interior of which inevitably experience slow cooling. Maki (1979) has specifically discussed the mechanism of glass formation with reference to melt composition and cooling history. He delineated areas of glass formation in the low-silica portions of cement-clinkering systems. Both SiO_2 and Al_2O_3 contribute to network formation, which is an essential prerequisite to the formation of a 'structured' liquid. The Al is, however, only partly a network former, so the presence of SiO_2 contributes more significantly to the glass-forming properties of the liquid. Maki measured T_g for a range of compositions and found little variation: T_g ranged between 675 and 704°C. He noted that the viscosity, ν, of the undercooled melt varied with temperature according to the usual relation, $\log \nu = A_\nu + E_\nu/RT$ where E_ν is an activation energy for viscous flow. If crystallization can be suppressed as by rapidly cooling its viscosity rises and the melt is increasingly liable to be retained as glass.

If some crystallization occurs, the principal products - C_3A and ferrite - reject SiO_2, which concentrates in the remaining amorphous phase, thereby also increasing its tendency to persist as glass. This mechanism, supercooling plus fractional crystallization, made it feasible to obtain at least some glass in commercial clinkers.

Once nucleation and growth occur, the nature of the crystalline phases produced may not be that which would be obtained at equilibrium. Two types of phenomena may occur: one is the development of totally new phases, different from those obtained at equilibrium while the other leads to formation of variants of the stable phases. The first seems not to occur in clinker batches, although common in other systems. However, the C_3A phase crystallizing from undercooled melts has been found to differ significantly from C_3A produced under equilibrium conditions. Its crystallization was studied by Han and Glasser (1980) and by Han et al (1980, 1981), with increasing cooling velocities, C_3A crystallized from simulated clinker melts containing CaO, MgO, Al_2O_3, Fe_2O_3 and SiO_2, together with incremental alkali additions, was found to differ progressively from ordinary C_3A, obtained by subsolidus isothermal reaction. The crystals became progressively more disordered, resulting in a decrease in intensity of X-ray reflections with $h + k + l \neq 4n$, but also, the range of solid solution $Tn\ \overline{C_3}\ \overline{A}$ was greatly enhanced, albeit metastably, to include Si, Mg, Fe, etc., in quantities much in excess of their equilibrium concentrations. This new variety of C_3A, formed proto-C_3A, arises as a consequence of cooling history. Although first isolated in laboratory preparations, it has been encountered in clinker. The consequences of these new types of compositional and structural variations are as yet unclear, but could affect markedly the reactivity of the aluminate phase. Equilibrium substitution of alkali, which lowers the symmetry of C_3A from cubic to orthorhombic or to tetragonal has very little influence on its reactivity with water. But the substitution of substantial quantities of Mg, Si, Al and Fe in proto C_3A could have a more significant effect. Moreover, by incorporating large quantities of these elements in the C_3A structure, the potential for forming other phases, e.g., C_2S and ferrite during clinker cooling is altered. The characterization of proto C_3A has been made by Han and Glasser.

Another potential consequence of the cooling history imposed on clinker is that C_3S, stable at high temperatures, tends to decompose upon cooling. The kinetics of its decomposition were studied systematically by Mohan and Glasser (1970a,b,c). Phase pure C_3S was annealed isothermally. Fig 12 shows a typical decomposition using initially pure C_3S. A prolonged induction period is required, during which nucleii of the decomposition products CaO and Ca_2SiO_4 develop. This gradually gives way to an acceleration in decomposition as nucleii begin to grow. Eventually, geometric impingement slows growth as nucleii coalesce and the reaction rate decreases. The importance of the induction period and its attribution to nucleation, was supported by showing that, if nucleii of the decomposition products were supplied, the time required for nucleation was greatly reduced: the nucleii acted as decompositional catalysts. Analysis of the decompositional reaction was made by the Avrami equation.

1.1

$\delta = 1-\exp(-kt^n)$

where k is a constant and the value of n is related to the mechanism of nucleation.

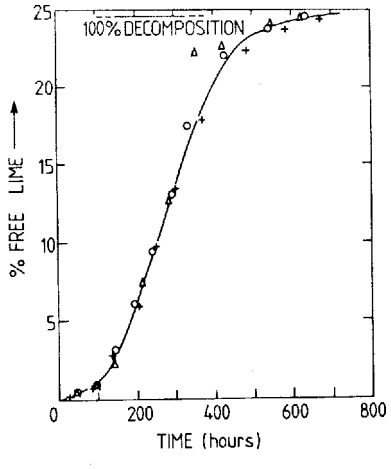

Fig. 12. Kinetics of the decomposition of C_3S at 1175°C, as determined by the rate of free lime production; 100% decompostion corresponds to 24.6% lime content.

For three-dimensional nucleation and growth, $3 \leq n \leq 4$, and for two dimensional nucleation and growth, $2 \leq n \leq 3$. The value of n was determined in this instance by plotting log [1/1-δ)] against log t: a straight line slope was obtained corresponding to n = 2.59. In this instance, microscopic observations supported the surface growth mechanism. However, some doubts have been expressed as to the validity of inferring mechanisms from the Avrami treatment. It would appear that in cases such as the present where the reactant and product(s) have well-defined stoichiometries the procedure is valid, but its application to other, less straightforward cases, e.g., hydration reactions, may require additional justification. The sensitivity of the surface condition was demonstrated by using water vapour, and it was shown that the rate of decomposition at constant temperature was a linear function of P_{H_2O}; Fig. 13 shows data. In general, if data from various temperatures were to be compared, it was found best to recalculate data in such a way as to plot a family of time-temperature-transformation curves.

The formation of ferrite during undercooling has been observed by Maultzsch and Scholze (1973). They found that during rapid growth, the inner zones of crystals failed to maintain equilibrium with subsequent zones and the crystals were compositionally inhomogeneous with respect to their A/F ratio.

Many events happening during cooling undoubtedly influence clinker properties. Indeed, it has long been believed that cooling rate influences clinker properties; for example, Sylla (1975) has determined the relation between clinker cooling and the

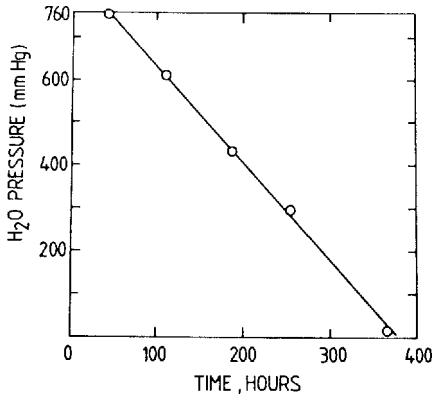

Fig. 13. Influence of H_2O vapour on the decomposition of C_3S at 1025°C. The time shown is that required to attain 50% decomposition.

set and strength gain of cement. However, many kinetically-controlled phenomena can occur during cooling in addition to those described here. There is suspicion that the polymorphism of C_3A is influenced by cooling rate. C_3S has numerous polymorphs; present evidence is that monoclinic and triclinic phases have about the same reactivity, but rhombhedral may be more active. The polymorphs of C_2S differ widely in reactivity, γ being especially inert but having two polymorphs, α' and β, both of which might be present at ambient. The connection between impurity content, cooling history and the preservation of reactive forms of C_2S, C_3A and C_3S is not at present well understood but remains an area fruitful for further work.

6.7. Summary of Clinker Formation.

A satisfactory qualitative account of the overall picture of clinkering kinetics can be given on the basis of the currently-available literature and many aspects can be treated more quantitatively. Nevertheless, it is difficult to fit the seperate quantitative approaches together to obtain an overall quantitative presentation. This is considered to arise because of the many overlapping reactions occurring in the process, which occur competitively. The following general features emerge as a key area of kinetic control.

(i) at temperatures above 600°-700°C decarbonation and dehydroxylation of the clinker feed occurs. Fine-grained, porous and chemically reacted solid decomposition products are formed. The gas phase contains reactive components, such as CO_2, and catalytic components, e.g. H_2O, which assist reaction.

(ii) at these low temperatures, intermediate phases, e.g. carbonate-silicates form. While these phases are subsequently decomposed in the high-temperature zone of the kiln, they may act as important precursors to the formation of C_2S, aluminates and ferrites, etc. Their role in the overall kinetics of formation is yet to be evaluated.

(iii) the high local concentrations of "volatiles" - e.g. chlorides, sulphur oxides, F - reached in modern fuel-efficient kilns may also play an important role in promoting reaction. In particular

high local concentrations of these components may exceed the dew point, resulting in formation of a transient low melting point salt-rich liquid.

(iv) reactions amongst the main components - CaO, $A\ell_2O_3$, Fe_2O_3 and SiO_2-proceed at unequal rates. Formation of calcium aluminates and ferrite seem to occur at lower temperatures, and at more rapid rates, than formation of calcium silicates during the early stages of batch reaction.

(v) the early stages of clinkering are also marked by formation of calcium aluminates, ferrites, silicates etc. which are thermodynamically metastable in terms of the overall batch composition. Examples include aluminates, e.g. $C_{12}A_7$ silicates, e.g. C_2AS (gehlenite), and ferrites e.g. CF. Their formation is conditioned partly by more favourable kinetics, but also by statistical distribution of the chemical components, which give rise to local areas which are enriched relative to the bulk in compounds of the exotic phases. Dicalcium silicate forms at much lower temperatures than tricalcium silicate. The C_2S phase can be developed in the solid state, whereas C_3S for all practical purposes forms only in the presence of a liquid phase.

(vi) Above 1300°C liquid develops and C_3S crystals. In well blended, well fired clinker batches a mineralogical and texture equilibrium is attained. The transport mechanisms via the liquid phase have been extensively studied in recent decades and it is possible to quantify the driving forces leading to C_3S formation, determine in general the role of minor components and mineralizers on the process kinetics.

SUMMARY.

The kinetics of cement making are reviewed. The early stages of calcining are dominated by decomposition reactions, by solid state diffusion leading to formation of calcium aluminates, Ca_2SiO_4 as well as by intermediate phases formed by partially-volatile constituents such as SO_4^{2-} and CO_3^{2-}. The main formation of C_3S occurs later, by sintering in the presence of a reactive liquid which also facilitates compaction of the mass. C_3A and ferrite arise mainly from crystallization of the high temperature liquid.

As a result of recent researches, the kinetics of many of these reaction have been analized in much more detail. Model studies on chemically simplified systems have explained and anticipated many of the kinetic phenomena occurring in chemically more complex batches as are used commercially. Kinetic treatments appropriate to the various stages of reaction are developed on a formal mathematical basis, but it is also essential to have a thorough understanding of the equilibria involved if the kinetic analyses are to be applicable to real problems.

REFERENCES

M.C. BALL and L.S. NORWOOD, (1977) "Surface area and porosity changes in the dehydration of calcium sulphate hydrate". J. Chem. Soc. Faraday Trans.(1) 73 [6] 932-941.

- ibid, (1978) J. Chem. Soc. Faraday Trans., (1) 74 [6] 1477-1487.

D. BERUTO, L. BARCO and A.W. SEARCY (1984) "CO_2 catalized surface area and porosity changes in high surface area CaO aggregates. J. Amer. Ceram. Soc., 67 [1] 512-515.

J. BIERNACKI and I. KOWALSKI (1981) "Calcination of limestones suspended in a gaseous phase." Cem. - Wapno- Gips. No. 6, 154-159.

P.P. BUDNIKOVA and A.M. GINSTLING (1968) "Principles of Solid State Chemistry" (translated by K. Shaw) Maclaren and Sons, London.

K.S. CHOU and G. BURNETT (1981) "Formation of calcium aluminates in the lime-sinter process" Cement Concr. Res. 11 (1) 57-64.

- ibid (1981) 11 (2) 167-174.

J. CRANK (1975) "Mathematics of Diffusion", Oxford University Press, London.

A.K. CHATTERJEE (1979) "Phase Composition Microstructure and Burning of Portland Cement Clinker" World Cem. Tech., 10 (4) 124-127.

T.K. CHATERJEE, A.K. CHATTERJEE and S.N. GOSH.(1980) "Clinkering reactions in Portland cement manufacture - a review of sequence and kinetics." Silicates Industriel. No. 4-5, 81-87.

N.H. CHRISTENSEN (1979) "Burnability of cement raw materials at 1400°C: I. The effect of chemical composition." Cement Concr. Res., 9 [1] 35-44(1979).

- ibid (1979) II "Effect of fineness" Cement Concr. Res., 9 [3] 285-293.

- ibid (1981) World Cement Tech., 12, 238.

N.H. CHRISTENSEN and O.L. JEPSEN, (1971) "Diffusion in three component cement clinkers". J. Amer. Ceram. Soc., 54 208-210.

N.H. CHRISTENSEN, O.L. JEPSEN and V. JOHANSEN (1978) "Role of a formation in clinker sandwiches" Cement Concr. Res., 8 [6] 693-702.

N.H. CHRISTENSEN and K.A. SIMONSEN (1970) "Diffusion in Portland cement clinkers" J. Amer. Ceram. Soc., 53 (1) 361-364.

CHROMY (1982) "Portland clinker formation processes I. Mechanisms. ZKG, Zem-Kalk-Gyps, Ed. A 35 (4) 204-210.

CHROMY, S. (1985) "Evaluation of the reactivity and of burning ability of industrial cement raw materials by a kinetic method" Stavivo 63 (5) 198-204.

DELIGNE, M. FIRENS, P., PICQUET P. et al. (1977) "Mechanism of dynamic synthesis of calcium aluminates." Silic. Ind., 42 (6) 261-266.

DESCAMPS, J., FIRENS, P. and VERHAGEN, J.P. (1974) "Application of thermoluminescence to the study of chemical defects in tricalcium silicate." Silic. Ind. 39 (7-8) (215-227.

DOREMUS, R.H. (1985) "Rates of Phase Transformations" Academic Press.

DRAYNEA, I., MUNTEAN, M. and TEOREANU, I. (1976) "Effect of $FeSO_4$ on burning oxidic mixtures in the system CaO ($CaCO_3$) -$A\ell_2O_3$. Silic. Ind. 41 (9) 357-362.

DROZDETSKAYA, G.V. and GROPYANOV, V.M. (1977) "Calculation of the kinetics of $CaCO_3$ decompostion under nonisothermal conditions. Zhur. Prikl. Khim, 50 (3) 496-499.

FIRENS, P. and TIROCQ, J. (1980) "Phosporescence and thermoluminescence of tricalcium silicate at low temperatures. Silic. Ind. 45 (4-5) 75-79.

FUNDAL, E. (1979) "Burnability of cement raw mixes" World Cem. Technol., 10 (6) 195-196.

FUNDAL, E. (1981). "Burnability of cement raw mixes". Cem.-Wapno-Gips. No.1, 16-21.

GOL'DSHTEIN, L. Ya., SMIRNOVA, L.V. and CHISTYAKOVA, A.A. (1976) "Characteristics of mineral formation during production of Portland cement clinker by melting". Zh. Prik. Khim. 49 (8) 1694-1698.

GOUDA, G.R. (1979) "Effect of clinker composition on grindability." Cem. Concr. Res., 9 (2) 209-218.

GROVES, G.W. and SINCLAIR, W. (1984) "The structure of alites" pp 93-100 in British Ceramic Proceedings No. 35, ed. F.P. Glasser, Stoke-on-Trent,England.

HAN, K.S. and GLASSER, F.P. (1980) "Crystallization of the liquid phase developed during clinkering." Cement Concr. Res. 10 483-489.

HAN, K.S. and GLASSER, F.P. and GARD, J.A., (1980) "Studies of the crystallization of the liquid phase in Portland cement clinker: effects of MgO and Na_2O." Cement Concr. Res. 10 443-448.

HAN,K.S., GARD, J.A. and GLASSER, F.P. (1981) "Composition of stable and metastable C_3A solid solutions crystallized from simulated clinker melts". Cement Concr. Res., 11 79-84.

HANIC, F., GALIKOVA, L., HAVILICA, J. et al. (1985) "Kinetics of thermal decomposition of $CaSO_4$ in air" Brit. Ceramic Trans. Jour. 84 (1) 22-25.

HEILMANN, T. (1960) in "Chemistry of Cement". Vol.1 (Proc. 4th Intl. Conf. on the Chemistry of Cement Washington, D.C.) p87.

HUMPOLA, H. (1981) "Optimization of the reactivity of cement raw material powder." Stavivo, 59 (1) 29-33.

IMLACH, J.A. (1976) "Non-isothermal investigation of the kinetics of reactions occurring during clinker formation" Cement Concr. Res. 6 (6) 747-755.

JOHANSEN, V. (1979) "Application of equilibrium phase diagrams to industrial clinker formation" Zem.-Kalk-Gips, 32 (4) 176-181.

JOHANSEN, V. and CHRISTENSEN (1979) "Role of formation of C_3S in the system CaO-SiO_2-$A\ell_2O_3$-Fe_2O_3-MgO with addition of CaF_2" Cement Concr. Res. 9 (1) 1-5.

JOHANSEN, V., JEPSEN, L., CHRISTENSEN, N.H. et al., (1979) "Ternary diffusion in cement clinker at 1500°C". Cement Concr. Res., 8 (3) 301-309.

JØNS, E.S. (1980) "Thermodynamic driving force for formation of tricalcium silicate

KAHLWEIT, M. (1976) "Kinetics of Crystallization". Ann. Rev. Phys. Chem., 27 59-63.

KINGERY, W.D., BOWEN, H.K. and UHLMANN, D.R. (1976) "Introduction to Ceramics" (2nd Ed.) Wiley Interscience, New York.

KONDO R. and S. CHOI, S. (1968) "Chemistry of Cement Clinker". Vol.1, Proc. 5th Intl. Symp. Chemistry of Cement (Tokyo) p 163.

KRACHNER, A., KEISER, J. and GATHEMANN, B. (1985) Mater. Constr. (Bucharest) 15 (2) 106-108; 111.

KUPPER, D. and TIGGESBAUCUMBER, P. (1983) "Calcination behaviour of cement raw meals". ZKG., Zem.-Kalk.-Gips. Ed. A. 36 (5) 275-280.

LEA, F.M. and PARKER, T.W. (1934) "Investigations of the quaternary system CaO-$A\ell_2O_3$-SiO_2-Fe_2O_3". Phil. Trans. Roy. Soc. (London). Sec. A. 234, 1-41.

LIM. E. -K. and PARK, B.-C. (1983) Jour. Korea Ceram. Soc. 20 (4) 295-304.

- ibid., (1984) 21 (2) 113-120.

- ibid., (1984) 21 (3) 221-230.

LUDWIG, U. (1981) "Influence on the sintering behaviour of cement raw meal", ZKG, Zem-Kalk-Gips. Ed.A. 34 (4) 175-186.

LUDWIG, U. and RUCHENSTEINER, G. (1973) "Firing of cement meals and quality of clinker". Tonind.-Ztg. Keram. Rundsch, 97 (1,2) 313-315.

LUDWIG, U. and WOLTER, A. (1979) "Formation and stability of tricalcium silicate and alites". Zem-Kalk-Gips. Ed. A. 32 (9) 455-459.

MACKENZIE, K.J.D. and ALASTI, H. (1978). "Formation kinetics of Portland cement clinker phases II. Tetracalcium aluminoferrite". Trans. Jour. Brit. Ceram. Soc. 77 (5) 162-167.

MACKENZIE, K.J.D. and ALDRIDGE, L.D. (1980)"Effect of reaction atmosphere on phase development in Portland cement clinker". Trans. Jour. Brit. Ceram. Soc. 79 (2) 29-36.

MACKENZIE, K.J.D. and BANERJEE (1978) "Formation kinetics of Portland cement clinker ". Trans. Jour. Brit. Ceram. Soc., 77 (3) 88-92.

MACKENZIE, K.J.D and HADIPOUR N. (1978) "Formation kinetics of Portland cement clinker, III. β dicalcium silicate and tricalcium silicate". Trans. Jour. Brit. Ceram. Soc. 77 (6) 168-172.

MAKI, I. (1979) "Mechanism of glass formation in Portland cement clinker". Cement Concr. Res. 9 (6) 757-763.

MATSUNOTO, K. and SATO, T. (1981) "Vaporization of tricalcium silicate at high temperatures". Nippon Kagaku Kaishi No. 10, 1676-1680.

MAULTZSCH, M. and SCHOLZE, H. (1973) "Formation of the ferrite clinker phase from the melt", Zem.-Kalk-Gips, 26 (12) 583-587.

MAYCOCK, J.N., SKALNY, J. and KALYONCU, R. (1974) "Crystal defects and hydration. I Influence of lattice defects" Cement Concr. Res. 4 (5) 835-847.

MCHEDLOV-PETROSYAN, O.P., SHCHETKINA T. Yu. and FATALIEV, S.A. (1975) "Role of metastable phases in formation processes of silicates." Silikattechnik 26 (8) 258-260.

MCHEDLOV-PETROSYAN, O.P., SHCHETKINA, T. Yu. and SAPOZHNIKOVA, N.J. (1978) "Development of solid-phase reaction theory and clinker mineral formation" Tsement No.9, 8-9.

MERAIKIB, M. and FRIEDRICHS, H.A. (1979) "Kinetics of limestone calcination". Arch. Eisenhuttenwes. 50, (8) 323-328.

MUELLER, A., DAHM, B. and STARK, J. (1977) "Decomposition kinetics of calcium carbonate" Silikattechnik, 28 (1) 4-7.

MUELLER, A., DAHM, B. and STARK, J. (1979) "Kinetics of calcium carbonate dissociation" Zem.-Kalk-Gips. 32 (2) 78-82.

MOHAN, K. and GLASSER, F.P.G. (1977) "The thermal decomposition of Ca_3SiO_5 at temperatures below 1250°C I. Pure C_3S and influence of excess CaO or Ca_2SiO_4" Cement Concr. Res. 7,1-8.

- ibid., II. The influence of Mg, Fe, Aℓ and Na oxides on the decomposition. 7,269-275.

- ibid., III. The influence of water and sulphate on the decomposition. 7, 379-383.

MOSIKAS, N., HAAG, E. HENIN, J.P., et al. (1981) "Burnability of cement raw materials as a function of their grinding fineness". Cir., Betons, Platres, Chaux. No. 729, 75-78.

ODLER, I. and DOERR, H. (1977) "Tricalcium silicate formation by solid state reactions". Amer. Ceram. Soc. Bull. 56 (12) 1086-1089.

ODLER, I. and ABDUL-MAULA, S. (1980) "Effects of mineralizers on the burning of Portland cement clinkers. I. Kinetics of the process." ZKG, Zem.-Kalk-Gips. Ed. A. 33 (3) 132-136.

- II. Mode of action of the mineralizers. 33 (6) 278-282.

OSOKIN, A.P., BUTT, Yu. M. and TIRNASHEV, V.V. (1973) "Mobility of Aℓ and Fe in clinker melts." Tr.Moscow. Khim-Technol. Inst., No. 72, 108-111,

PACKTER, A. and ZAIDI S.A. (1981) "Heterogeneous reactions of silica powders with calcium oxide solution in calcium chloride melts to form β dicalcium silicate - kinetics and mechanism." Silic. Ind. 46 (9) 173-177.

PETERSEN, I.F. (1983) "Isothermal sintering of Portland cement raw mixes." World Cem. 14 (6) 220-228.

PETERSEN, I.F. and JOHANSEN, V. (1979) "Burnability and clinker nodule formation from a statistical point of view". Cement Concr. Res., 9 (5) 631-639.

RAJA RAO, W. and CUTLER I.B. (1975) "Effects of calcining conditions on the dissociation rate of limestones and properties of lime." Bull. Centr. Glass Ceram. Inst. (Calcutta) 22 (2-3) 66-72.

RAUSCHENFELS, E. (1976) "Clinkerability of cement raw meal". Zem.-Kalk-Gips, 29 (2) 78-85.

RUDOLPH, R. (1979) "Output and process data characteristics for $CaCO_3$ decomposition in vibratory furnaces" Silikattechnik 30 (6) 169-171.

SARKAR, S.L. (1979) "Phase composition, microstructure, quality and burning of Portland cement clinkers" World Cem. Technol. 10 (9) 371. (see also 371-373).

SCHMALZREID, H. (1981) "Solid State Reactions" 2nd Ed. Monographs in Modern Chemistry, Verlag Chemie. (Weinheim).

SHEARER, J.A., JOHNSON, I. and TURNER, C.B. (1980) "Interaction of NaCℓ with limestones during calcination". Amer. Ceram. Soc. Bull., 59 (5) 521-524.

SHRADER, R. and KENKU, K. (1973) "Kinetics of reactions in the systems $CaO-SiO_2$ and $CaO-Aℓ_2O_3$". Tsement No. 2, 12-13.

SINGH, V.K. and ALI, M.M. (1980) "Formation kinetics of high alumina cement phases. I. Monocalcium aluminate". Trans. Jour. Brit. Ceram. Soc. 79 (5) 112-114.

SYLLA, H.-M. (1975) "Effects of clinker cooling on the setting and strength of cement". Zement-Kalk-Gips. 28 (9) 357-362.

SYLLA, H.-M. (1981) "Influence of reductive burning on the properties of cement clinker" ZKG Zem.-Kalk-Gips, Ed. A. 34 (12) 618-630.

SVETIK, S., JESENAK, V. and HARABE, Z. (1982) "Effect of atmosphere on the rate and mechanism of reactions in the system $CaCO_3-SiO_2$ at low temperatures". Silikaty, 26 (4) 289-298..

TALABER, J. SZNI, F., BERECJ, K. et al. (1982). "Effect of additives on the dissociation rate of calcium carbonate". Epitoanyag 34 (6) 201-206.

TEOREANU, I. and DULAMSCU, D. (1981) "Kinetic considerations concerning the clinkering behaviour of Portland cement raw mixes". Cemento 78 (4) 183-196.

TEOREANU, I., GEORGESCU, M., PURI, A. et al. (1985). "Clinkering potential of some mixes of raw materials" Mater. Constr. (Bucharest) 15 (1) 42-47.

VOGEL, E. (1983) "Reactions between solid fuel and the batch in cement rotary kilns" Baustoffindustrie 26 (1) 5-7.

1.1

WAECHTLER, H-.J., GAHRMANN, N., IGNER, R.I., et al. (1984) "Influence of the energy source on cement clinker quality" Silikattechnik 35 (9) 259-263.

YOUNG, D.A. (1966) "Decompositon of solids (Topic 21, in Vol. 1 of The International Encyclopedia of Physical Chemistry and Chemical Physics: Pergamon Press, Oxford).

M.S.MARINHO, ICI BRASIL S.A., SÃO PAULO, BRASIL

COMMUNICATION REPORT - SUB-THEME 1.1.

1- INTRODUCTION

Theme I of the congress (President Dr. C.D.Pomeroy - UK) is mainly concerned with studies on clinker formation and properties which are directly connected with the industrial process of cement manufacturing. From those studies in the past, that modern cement plants of today were idealized (short kilns, pre-calcining stages, low-alkali plants, etc.) and also new cements, generally utilizing less energy for its manufacturing than conventional O.P.C.

Sub-Theme 1.1 (President Prof.Mechedlov Petrossian - USSR) is devoted to the kinetic of clinker formation, a subject of considerable complexity, but of enormous importance to the development of clinker burning techniques. However, in the last decade, although many works have arisen on the subject, we are still far on the understanding of reaction kinetics during clinker formation. Mathematical modelling have been exaustively applied in this field to identify reaction mechanisms, but the limitations of such methods, like availability of reliable data and approximations from simpler systems, have led to a general disbelief on such models for the complex cement matrix. Works on pure cement phases especially C_3S have thrown some light to the problem and certainly will help further studies in the future.

At this congress, the communications presented in the sub-theme 1.1 have been divided into two groups: (1) kinetc studies done with industrial or laboratory prepared raw mixes and (2) studies done in pure or a mix of cement phase raw-materials.The author shall only be making a summary of relevant communications, highlighting important and new information, with exemption of any personnal opinion as it is the scope of a communication report.

2- KINETICS OF CLINKER REACTIONS

-Communications

1.0 - Prof. F.P.Glasser (UK)

"Principal report of Sub-theme 1.1"

1.1 - D.Gosch, S.A. Khadilkar, R.K. Agarwal, G.A. Mudhbhatkal and A.K. Chatterjee (India)
"Specific Surface as a parameter for raw mix burnability and its relation with volume change of fired raw mix pellets".

1.2 - F. Petersen (Denmark)
"The Ability of Clinker Nodule Formation".

1.3 - P. Burki and H. Braun (Switzerland)
"Investigations on influence of raw mix reactivity and rate of clinker formation".

1.4 - A. Wolter (West Germany)
"Phase composition of calcined raw meal".

1.5 - R.Costanet and F.P. Sorrentino (France)
"Study of clinkering reactions by high temperature calorimetry".

1.6 - S.J.Raina, P.Bhaskara Rao, S.K.Handoo and George Samuel (India)
"A new approach for estimation of heat requirement for clinkerization".

1.7 - A.Ossokin and E.Potapova (URSS)
"Mineral Formation in the Melt".

1.8 - W.Feng and S.Yu
"A study on the Kinetics of the burning of Portland Cement Clinker in different processes".

An attempt to improve the theoretical prediction of burnability (com.1.1) has been presented. It is a modification from previous theories of Jander (1) and Ginstling (2), which are based on the diffusion mechanism of monodisperse spherical particles, contrasting with the polidisperse nature of industrial mixes.
Firing samples with varying surface area, temperature of reaction and retention time, a equation (a) was derived by multiple regression technique.

$$\alpha = 0.7396+2.158\times10^{-3}\rho_1+6.209\times10^{-4}\rho_2+3.605\times10^{-5}\rho_3-0.013\rho_4 \quad (a)$$

Where α is the lime combinability ratio, ρ_1 the retention time in minutes, ρ_2 the temperature in ^{o}C, ρ_3 the surface area in cm^2/gm and ρ_4 percent total CaO in raw mix after burning.
The equation is valid within a temperature range of 1200-1500°C. This equation was tested with industrial raw mixes, where calculated values of lime combinability were compared with experimental. Calculated values were always lower and that was attributed to the influence of minor elements acting as mineralizers.
A better qualitative insight to the equation was done by expansion/shrinkage studies on the industrial raw mixes used on the experiments above. Those studies could give some information on lime combinability, solid-state reactions (intermediate phases forming), formation of liquid and compressive strenght of the pellet.
The equation can be used to predict free-lime of a clinker given the surface area of raw mix, temperature of burning and retention time. However, absolute values are far to be obtained and caution must be taken due to interference of minor elements. The shrinkage/expansion experiments are fundamental for better interpretation of results.

A study of nodule size that can survive in the burning zone of a rotatory kiln (com.1.2), had been done utilizing a computer program. A worst case model is assumed where two clinker nodules at a foot of a charge will be consolidated into a permanent contact or sheared apart. By fixing several kiln parameters and physical properties of the mix and varying the capillary pressure and viscosity, a graph of Fraction of contacts surving against nodule diameter was derived. The model seemed sensitive to changes in physical properties, but critical regarding size of nodules that can form permanent contacts.

Two raw meals, with substantial difference in reactivity (measured as % free lime at 1500°C) due to raw-material nature,were studied in view of accessing the influence of a slow and a rapid upheating (com.1.3). The influence on burnability and microstructure of the clinker were investigated. It has been shown that burnability is better in both raw meals, in the case of a rapid upheating. The suggestion that a gain in reactivity is due to the preservation of small and disordered intermediate minerals up to stage of alite formation (3, 4) has been confirmed by an increase of width and poor peak resolution of belite (XRD) on the reactive meal/rapid upheating sample.
Optical microscopy showed clear differences between the two clinkers formed concerning pore and clinker minerals size. The importance of microhomogeinity of the meal was stressed, being inherent to the raw components and it is not significantly affected at the grinding fineness, typical of industrial raw mills. The authors point out that further work is needed to a better understanding of process condition, influencing clinker microstructure.
Another work (com.1.4) studied calcined meals extracted from 20 Kiln inlets. Those were thoroughly examined by XRD to identify phases present. Those phases were classified within groups: (1) - non-reacted materials, (2) - new phases formed during calcination, (3) - condensed salts and (4) - dusts.
Interrelation between the formation of new phases and degree of calcination (DCAL) was one of the main aspects of the study. DCAL has been related to various aspects of raw meal composition and free-lime amount.
Attention was also devoted for the exothermal heat, which is liberated in the reaction between free lime and "hydraulic factors", especially SiO_2. The degree of belite formation DC_2S in relation to the heat release in the kiln and degree of calcination have been shown. Subject to complete calcining, the range of exothermic heat liberated in the rotatory kiln varies between a minimum of 30% (very homogeneous meal) and a maximum of 80% (extremely heterogeneous meal). The presence of clinker dust was concluded to be of importance in pre-calcining.

A portfolio of new applications for calcined meal was also suggested (ex.: substitute clinker in fly-ash and slag cement, acting as main component of hydraulic active binders, for solidifying waste material).

High Temperature Isothermal Calorimetry have been used to study the change of enthalphy of all stages of clinkering reaction (com. 1.5). Experimental values were compared with calculated based on several data published in the literature for the enthalphy of formation of different reaction stages.
Results compared well taking into account some factors not included in the studies where data was taken from. The calculations gave at the end, a difference of 77 cal/g. at the exothermic part of the curve (C_2S formation). This could not be explained as no new phase have been detected by XRD. The authors mentioned that studies are underway to investigate such phenomena.

The authors (com.1.6) have suggested a new method of experimental determination of theoretical heat requirement for clinkerization. Zur Straussen (5) formulas, which are widely used, are only suitable to special compositions of the raw meal (limestone rich in calcite, clay minerals made up of equal contributions from the principal clay minerals, etc.). The idea was to develop a method by which no mineralogical composition of the raw meal or the heats of formation of the complex minerals were needed. Five clinkers were submitted to the method based on DTA analysis. Three had the composition suited to Zur Straussen formula and the others scaped quite considerably.
The results between the two methods agreed well for the first three clinkers and as expected were different for the last two. The method seems to work well, but high precision thermal analyser is required.

The effect of several anions and cations in relation to melt formation speed was analysed (com.1.7). A study of the time taken for CaO to be transformed in C_3S against grain size for various additions was presented. An addition of F^-, decreased the time from 52 to 14 minutes for the same grain size. The presence of $CaF_2 + CaSO_4$ decrease the time even further. A formula was finally proposed to calculate the firing time needed for the transformation of CaO into C_3S, depending on the medium grain size of CaO.

A raw mix was submitted to two different burning processes (com.1.8). A rapid and a slow one. The rapid method consisted in placing a pellet into a furnace at a range of 1280° - 1320^oC, and the slow at a temperature rise of about 350^oC/hr, simulating an industrial kiln operation. The rapid method yielded a lower activation energy and a higher velocity rate constant.

3- REACTION KINETICS OF PURE OR COMBINED CLINKER PHASE

- Communications

1.1 - B.Cottin, A.Rovanet and M.Conjeaud (France)
"Mineralogical changes of lime-silica-alumina raw-materials at 830^oC".

1.2 - W.Weisweiler, E.Osen and M.Lemperle
"Effect of Fe_2O_3 and Al_2O_3 admixtures on the reaction kinetics between CaO-SiO_2 powder compacts".

1.3 - S.C.Ahluwalia and V.K.Mathur (India)
"Thermal studies on the effect of some transition metal oxides on the kinetics of formation and stabilization of β -Dicalcium Silicate".

1.4 - T.V.Kuznetsova, I.A.Brytov, N.A.Kozreva, B. Ivanov, I.I.Kiselyova and E.A.Tsukerman (USSR)
"Auger electron spectroscopic study of calcium silicates and aluminates".

1.5 - A.V.Bessmertnykh, V.K.Khokhlov and V.V. Sheludko (USSR)
"Thermodynamic study of Decarbonation kinetics".

1.6 - N.F.Fiodorov, A.P.Gavrilov, N.I.Ivanov and O.M.Khalina (USSR)
"Synthesis kinetics of calcium aluminates by the heat treatment in a cast-iron bath".

1.7 - A.Rovanet (France)
"Solid state reactions between lime and alumina".

1.8 - M.Dragicevic (Yugoslavia)
"Prognosis of the physical-mechanical characteristics of Portland Cement".

Four raw mixes with distinct variations on the amounts of C, S and A were studied (com.1.1), regarding decarbonation, degree of reaction ($CaO \rightarrow C_2S$) and phase formation occuring at a fixed temperature of 830°C. The morphology of the treated raw mixes was a varying parameter (simple mixing, compactation(pellets)and micronization in a high efficiency mill).
The influence of CO_2 and water vapour on the velocity of combination and the nature of phases formed has been analysed. The following aspects are interesting to be noted:

Decarbonation
- The sample which has been micronized, because of grain shape, had a remarkable speed of decarbonation.
- The resistance of CO_2 transfer is rather higher in the already decarbonated region of the lime grain, than in the porous region inter-grains.
- The water vapour helps the decarbonation rate through the layer of carbonated material around the grain (catalytic effect due to acceleration of diffusion of CO_2 in water vapour and a change on thermal conductivity of the gas).

Degree of Reaction
- Micronized sample had a superior speed of reaction, due to grain fineness (specific surface area).
- Pelletized sample did not yield a better speed of reaction compared with a simple mixture.
- Water vapour had a good catalytic effect on the samples, which were simply mixed.

Phase Formation (examined by XRD)
- Two equilibrium phases are formed (C_2S and $C_{12}A_7$) and also some non-equilibrium such as CS, C_3A, CA and C_2AS. Various tables in the text showed the results obtained.

Interface phase formation between CaO and SiO_2 in the presence of Al_2O_3 and Fe_2O_3 were studied by diffusion couple technique at high temperatures (com.1.2) and phase formation was analysed by Electron Probe Micro Analysis (EPMA) and optical microscopy. Layer thickness of undoped CaO - SiO_2 mixtures were compared to those with Fe_2O_3 or Al_2O_3 ($CaO\ (Fe_2O_3)/SiO_2$, $CaO/SiO_2\ (Fe_2O_3)$, $CaO\ (Al_2O_3)/SiO_2$ and $CaO/SiO_2\ (Al_2O_3)$).
Additions of Fe_2O_3 either to the CaO or SiO_2 showed a rather similar trend for the curves. Values in the region at 3% by weight Fe_2O_3 in SiO_2 and Fe_2O_3 in CaO, decreased the overall reaction rate. Values above that (especially at high temperatures >1350°C) increased the thickness of total reaction zone. At temperatures below 1450°C, the effect of Fe_2O_3 in SiO_2 beyond 3%, does not contribute for any increase in layer thickness. C_2S is the dominant phase between 1100 - 1400°C. Above 1400°C, CS or a glass phase "CS_2" are predominant.

Additions of Al_2O_3 in CaO gave similar results as above, sharp decrease up to 3% by weight Al_2O_3 and an increase in layer thickness for higher percentages (more pronounced at higher temperatures). In the case of Al_2O_3 in SiO_2, a continuous increase in total layer thickness was observed. Samples with 5-10% by weight Al_2O_3 fired at 1450°C for 15 minutes, complete reaction of the diffusion couple had taken place leaving mainly CS and "CS_2" phases. Explanations about the findings are given based on disorder and vacancies in CaO. Activation energies had also been calculated.

The effect of MnO_2, TiO_2 and Ci_2O_3 on the decomposition of $CaCO_3$ and formation of β-C_2S were studied (com.1.3). Decomposition temperature of $CaCO_3$ was lowered by the presence of three dopants within the range 0.1-1.0%. Formation temperature of β-C_2S is not significantly affected up to 1%, but has been reduced at 5% addition of TiO_2 and MnO_2.

The stabilization of α',β and γ C_2S in the presence of this dopants was also studied.

A mathematical treatment for the decarbonation kinetics of CO_2 and a solid ($CaCO_3$, for example), based on the linear thermodynamics of irreversible processes was given (com.1.5). A final equation for the degree of decarbonation is presented. The limits of validity of such equation is also given.

A report on the production of Alumina and High Alumina cements by immersion on a cast-iron melt was presented (com.1.6). It has been shown that the speed of formation of the phases of Alumina Cements are faster using this method than obtained using conventional rotatory Kiln methods. The quality of the product obtained is also very good. It is suggested that such methods could be used succesfully in industrial scale. Advantages such lack of pollution from combustion products and the elimination of dust from the system are among some of the described in the text.

A study on the kinetics of formation of Calcium Aluminates was done by two different experimental conditions (com.1.7).
In the first, Alumina was melted and cooled slowly to form a compact pellet, which was deeped into $CaCO_3$ powder. The maximum temperature of reaction examined was 1370°C. The interface between the powder and pellet was studied by electron and optical microscopy after etching and also XRD. XRD analysis on the surface of the compact layer showed the existence of $C_{12}A_7$. At more profound regions of the product CA, CA_2 and CA_6 were present. An investigation on the powdered region close to the Alumina block showed only the presence of C_3A.

Secondly, raw mixes of the two oxides in proportions of the existing Calcium-Aluminates were prepared and fired at the same temperatures as above. Several graphs on the kinetics of formation of the different phases are presented and discussed. A relation between time of saturation at each phase with the chemical potencial of the calcium is presented.

Auger Spectroscopy was used as a new technique to analyse cement clinker minerals (com.1.4) and a mathematical model has been described to foresee Potland Cement strenghts values after 3 and 28 days (com.1.8). Although results have a good agreement with experimental data, the author stresses, that due to accuracy of chemical and physical-mechanical investigations, the model gives a good qualitative guidance to work done at cement factories.

REFERENCES

1) W.Jander, Zement 20, 936-39, 951-53 (1931)

2) A.M.Ginstling and B.I.Braunstein, J.Applied Chemistry (USSR), 23, nº 12 (1950)

3) H.Bomas, V.Ludwig, A.Wolter, Tonind. Z tg. 105, 144 (1981)

4) A.Wolter, Zement - Kalk - Gips, 38, 612 (1985)

5) H.Zur Strassen, Zement Kalk Gips 10 (11, 1-12) (1957)

YUSHIRO KIHARA - Associação Brasileira de Cimento Portland

COMMUNICATION REPORT: RELATIONSHIP OF PROCESSING PARAMETERS TO CLINKER PROPERTIES; INFLUENCE OF MINOR COMPONENTS

1 INTRODUCTION

The sub-theme 1.2 *Relationship of processing parameters to clinker properties; influence of minor components* belongs to theme 1 *Clinker formation and properties.*

Dr. Iwao Maki (Japan) is responsible for the Principal Report of sub-theme 1.2, and Dra. A. Boikova (URSS) is in charge of the Special Report, which deals with the topics considered most relevant to deserve the researchers attention in the near future.

Thirty (30) Basic Communications from 16 countries were received in this sub-theme, distributed as following:

URSS	6
China	4
India	4
Italy	4
Brazil, Bulgaria, Czechoslovakia, Denmark, France, Germany, Japan, Poland, Romania, Spain, USA and Yugoslavia (each one)	1

Contributions from URSS, China, India and Italy make up 59% of the papers presented in this sub-theme.

The papers presented deal basically with:

1. the influence of processing parameters in the characterization and properties of clinker phases.

2. the crystal chemistry and influence of minor elements in the stabilization and activation of clinker phases.

A critical analysis of the communications allows to notice the general deep concern in presenting well founded data in experimental studies, supported by various analytical techniques (x-ray diffraction, optical microscopy, scanning electron microscopy, energy-dispersive analysis, electron microprobe analysis, differential thermal analysis, thermogravimetry, infrared absorption spectrophotometry, etc.) correlating them with industrial practice. The papers aim a major knowledge in the kinetics of clinkering reactions in the kilns, as well as in the crystal chemistry of phases actived and stabilized by minor elements.

The practical application of the scientific knowledge about the chemistry of cement from sub-theme 1.2 aims:

a) improvement in the quality of the industrial product;

b) energy saving in cement manufacturing processes;

c) activation techniques of clinker phases; and

d) development of new hydraulic binders.

The Basic Communications presented in this sub-theme are listed at the end of this Communication Report.

2 RELATIONSHIP OF PROCESSING PARAMETERS TO CLINKER PROPERTIES

2.1 Fuel and Raw Material

The use of high ash content (35-54%) mineral coal in cement industry has a strong influence over the behaviour of rotary kiln running, as well as modifies clinker characteristics, changing their composition and reactivity, which can extreme situations undermine the quality of the cement so produced. Irregularities in the coal burning and in the assimilation of the ashes by the clinker are shown by the segregate distribution of the C_2S, corrosion and excessive growth of the C_3S, digitation of the C_2S crystals, formation of $C_2S\gamma$ and exsolution in the C_3S crystals, appearence of reduced phases, and variation in the C_3S, C_2S and C_3A contents. This undesirable microstructural features affect the quality of the cement, influencing the setting time, the heat of hydration, the optimal gypsum content, the evolution of mechanical strength and the grindability of the clinker *(Y. KIHARA[1])*.

The use of certain solid fuels in cement kilns may conduct to accidental formation of reduced conditions. *VERNET[2]*, studying the burning influence at reduced conditions in the clinker phase stability and hydraulicity, observed that CaO reduction by carbon provoques an improvement in belite content, without free secondary CaO formation. Reduced conditions little affect alite crystal lattice, composition and reactivity, in spite of belite allotropic transformations being accelerated with important changes in their composition and reactivity. The reduction causes improvement in C_3A and C_2S contents and decrease in the C_3S amount, influencing the setting time and the early behaviour of the cement.

MASSAZZA and PEZZUOLI[3] studied the interactions between alkaline vapours and coal ashes. Coal ashes brought to high temperature can fix high amount of K_2O from atmospheres containing potassium carbonate or sulphate vapours. The alkali absorption in the coal ashes and in the coatings present in cement kiln is a complex process, which depends not only on the concentration of the alkaline elements but also on , the composition of the atmosphere on the material present in the kiln , and on the structure of the solid phase.

Variation in raw materials and coal can add alkali sulphate to the clinker. Coal contributes with a varying percentage of SO_3 and ash, which greatly affects the process and, accordingly, the cement quality. Alkali sulphates are incorporated in the crystal lattice of clinker minerals. Higher amounts of Na, K and S alter the structure of the clinker as the alkali sulphate (thenardite, arcanite, anydrite, aphthitalite and calcium langbeinite) are crystallized and precipitated over the calcium silicate grains as small crystallites and fine polysynthetical stripes. Belite crystals show higher concentration of K and it seems that the structure of C_2S changes to $KC_{23}S_{12}$. The presence of alkali sulphates changes the morphology of the crystals, which results in changed hydration properties, early setting and stiffening, slump loss, early increase and late decrease in strength. The most important parameters influencing strength are the soluble potassium oxide and the alteration of the Ca-silicate grains, especially C_2S *(C.R. GOUDA[4])*.

A new potassium - alumina phase ($K_2O.Al_2O_3$) and free K_2O in clinkers burned with an alkali-rich raw material are described by *FUNDAL[5]*. They have strong hygroscopic properties and can influence the setting behaviour, the storage and the strength properties of the cement. The so-called alkali aluminate forming in alkali-rich clinker by cooling doesn't crystallize by prolonged burning time at normal sintering

3 CRYSTAL CHEMISTRY OF CLINKER PHASES AND INFLUENCE OF MINOR COMPONENTS

3.1 Crystal Chemistry of Clinker Phases

Mg^{2+}, Na^{+} e S^{6+} ions in structures of clinker phases cause changes and distortions favouring the reactivity. They influence the stabilization of phases and crystal morphology of alites and belites. They modify aluminoferrite contents and the $A\ell_2O_3/Fe_2O_3$ ratio. Till the following limits: 2% MgO; 0,5% SO_3 and 1% Na_2O the clinker reactivity is increased, and surpassing these limits the clinker quality can be altered by the formation of independent phases of MgO, sulphates and alkalies and finally by the modification of the phase relations *(T.V. KOUNETSOVA*[15]*)*.

The modification of alite is influenced by the burning conditions and the MgO content in clinker. Monoclinic alite M_1 is always observed when clinker is burnt for short time or by slow burning. It converts into M_3 with prolonged burning at high temperature. High MgO contents favours the convertion from M_1 to M_3.M_3 alite hydrates more slowly than M_1 alite at early age. After 3 days, the hardened cement containing M_3 is denser than that containing M_1 and the former shows greater strength than the latter *(M.NAGASHIMA, E. ASAKURA, S.UDA and H. KAWABATA*[16]*)*.

The study of belite has received special attention from some researchers dealing with special cements of low energy consumption. The activation of belite by stabilizing more reactive phases (α') employing minor elements (P_2O_5, SO_3, MgO, alkalies,etc.) and by modifying process parameters (burning conditions and temperature) is the subject of *CHOUBINE and XHNYKINE, MATROVIC et alii, KRIVOBORODOV et alii, FENG XIU-JI et alii and SARASWAT et alii's* contributions.

The formation of a βC_2S phase in the $CaCO_3$-SiO_2 system increases with increasing percentage (0.1-1.0 as % Na_2O/K_2O) of Na_2CO_3 5% of dopant give most predominant βC_2S phase alongwith a little α'-C_2S, C_3S and alkali-silicate. Sodium carbonate is found to be most effective in turning down the temperature of formation of most desired α' and β phases than potassium carbonate *(I.P. SARASWAT, V.K. MATHUR and S.C. AHLUWALIA*[17]*)*.

In C_2S doped with phosphates it was observed that solid solution of the α' form develops strength much faster than those in β modification, due to faster hydration. The change of crystal modification and impurity types distributions modify only the rate of hydration *(B. MATKOVIC, V. CARIN, R. HALLE and J.F. YOUNG*[18]*)*.

The positron annihilation technique is used to study changes of microstructure defects in C_2S doped with Na_2O (1-2%) and P_2O_5 (0,5-1,5%). The Na^{+} replaces Ca^{2+} and P^{5+} replaces Si^{4+}, creating vacancies in the C_2S structure. The vacancy concentration and the rate of C_2S formation increases with doped Na^{+} and P^{5+} *(F.XIU-JI, M.S.LONG SHI-ZONG, DING QUING-JUN, HUANG CONG-YUN, S.DE-XUN, TENG MIN-KANG, YIN CHUAN-YUAN*[19]*)*.

White belite portland cements with various MgO (1-10%) and SO_3 (5%) contents and low Fe_2O_3 content were synthesized in laboratory. The positive influence on acceleration of the clinkerization processes is registered when the clinker contains 7% MgO and 5% SO_3. Both the whiteness of the clinkers and the mechanical strength (above 33-35 MPa in 28 days) of the resulting cement are good. Sulphate aluminate compound of the $(C, M)_4A_3\bar{S}$ type was formed and incorporated all MgO in the crystal lattice *(I. TEOREANU, M. MUNTEAN, M. BEDO and T. SUDRIGEAN*[20]*)*.

Modifications of the phases of clinkers with sulphoaluminate and sulpho-ferrites with the aid of admixtures and changes in the thermal regime permit to control the

formation and mechanical strength. The experimental results obtained do not seem to be in accordance with bibliographic data. In water quenched clinker trigonal alite with Aℓ and Mg in solid solution was characterized, less reactive than monoclinic alite obtained in air quenched clinkers. The mechanical strength was always lower than of those quenched by air, possibly due to trigonal alite. In air quenched clinker monoclinic alite (possibly a mixture of M_1 + M_3 forms) was obtained.

The increase of whiteness of bleached clinkers can be attained by burning at the highest possible temperature, by sharp quenching, and by decreasing time of burning which promotes the fine crystallization of the phases. Quenching by water increases the amount of alite, decreases the amount of aluminate and belite with high impurity contents, favours the glassy phase formation and changes the crystallization features of the minerals. The majority of Fe^{3+} is concentrated in the aluminate and glassy phases and the Fe_2O_3 contents in alite and belite does practically not change in bleached and unbleached clinkers *(A.I. BOIKOVA, O.I. FOMICHEVA and A.P. ZUBEKHIN*[12]*)*.

According to *BHASKARA RAO, HANDOO and SAMUEL*[13] the use of La^{140} with activity, as radiotracer, in a wet process cement rotary kiln shows that the assumptions made in the existing equations defining the material movement phenomenon in rotary kilns are valid only over a very limited length within which the material is in the form of a dry flowing powder without any appreciable physico chemical change. This zone is limited to the conventional preheating zone. The study revealed that the material movement in the transition and burning zone was much faster than that of the fine powdery material which is explained by the fact that nodulization takes place in this zone.

2.3 Prediction of Cement Strength

HARGRAVE, VENKATESWARAN, DESHMUKH and CHATTERJEE[14] proposed an approach for prediction of 28 days cement strength, based on microstructure parameters under reflected light microscopy. The parameters are:

- phase index (PHI)
- crystal size index of alite (CSI-A)
- crystal size index of belite (CSI-B)
- morphology index of alite (MOI-A)
- morphology index of belite (MOI-B)
- twinning index (TWI)
- cluster index (CLI)

By multiple linear regression analysis of microstructural parameters in relation to compressive strength of a large number of data *(Figure 1)* the following equation was obtained:

$$28D\ strength = 0.028 + 98.598(PHI) + 90.571(CSI\text{-}A) + 1.539(CSI\text{-}B) + 61.437(MOI\text{-}A) + 2.943(MOI\text{-}B) + 85.049(TWI) - 84.308(CLI)$$

The coefficient of multiple correlation (r) is 0.836 and the standard error of estimate is 52.794.

The method compared with *ONO*'s technique shows similarities, but it is considered more accurate and with greater potential to predict the 28 days cement strength in short time.

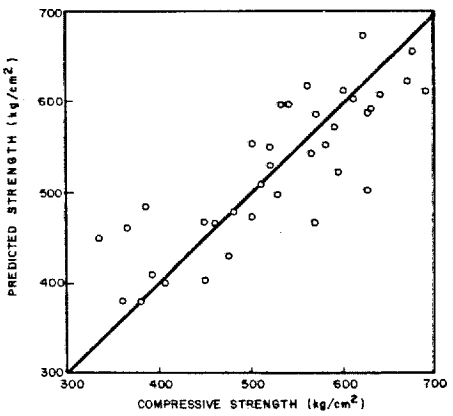

FIGURE 1- Correlation between 28D cement compressive strength with predicted strength by mycroscopic techniques.

3 CRYSTAL CHEMISTRY OF CLINKER PHASES AND INFLUENCE OF MINOR COMPONENTS

3.1 Crystal Chemistry of Clinker Phases

Mg^{2+}, Na^{+} e S^{6+} ions in structures of clinker phases cause changes and distortions favouring the reactivity. They influence the stabilization of phases and crystal morphology of alites and belites. They modify aluminoferrite contents and the Al_2O_3/Fe_2O_3 ratio. Till the following limits: 2% MgO; 0,5% SO_3 and 1% Na_2O the clinker reactivity is increased, and surpassing these limits the clinker quality can be altered by the formation of independent phases of MgO, sulphates and alkalies and finally by the modification of the phase relations (*T.Y. KOUZNETSOVA*[15]).

The modification of alite is influenced by the burning conditions and the MgO content in clinker. Monoclinic alite M_1 is always observed when clinker is burnt for short time or by slow burning. It converts into M_3 with prolonged burning at high temperature. High MgO contents favours the convertion from M_1 to M_3. M_3 alite hydrates more slowly than M_1 alite at early age. After 3 days, the hardened cement containing M_3 is denser than that containing M_1 and the former shows greater strength than the latter (*M.NAGASHIMA, E. ASAKURA, S.UDA and H. KAWABATA*[16]).

The study of belite has received special attention from some researchers dealing with special cements of low energy consumption. The activation of belite by stabilizing more reactive phases (α') employing minor elements (P_2O_5, SO_3, MgO, alkalies,etc.) and by modifying process parameters (burning conditions and temperature) is the subject of *CHOUBINE and XHNYKINE, MATROVIC et alii, KRIVOBORODOV et alii, FENG XIU-JI et alii and SARASWAT et alii's* contributions.

The formation of a βC_2S phase in the $CaCO_3$-SiO_2 system increases with increasing percentage (0.1-1.0 as % Na_2O/K_2O) of Na_2CO_3 5% of dopant give most predominant βC_2S phase alongwith a little α'-C_2S, C_3S and alkali-silicate. Sodium carbonate is found to be most effective in turning down the temperature of formation of most desired α' and β phases than potassium carbonate (*I.P. SARASWAT, V.K. MATHUR and S.C. AHLUWALIA*[17]).

In C_2S doped with phosphates it was observed that solid solution of the α'' form develops strength much faster than those in β modification, due to faster hydration. The change of crystal modification and impurity types distributions modify only the rate of hydration (*B. MATKOVIC, V. CARIN, R. HALLE and J.F. YOUNG*[18]).

The positron annihilation technique is used to study changes of microstructure defects in C_2S doped with Na_2O (1-2%) and P_2O_5 (0,5-1,5%). The Na^{+} replaces Ca^{2+} and P^{5+} replaces Si^{4+}, creating vacancies in the C_2S structure. The vacancy concentration and the rate of C_2S formation increases with doped Na^{+} and P^{5+} (*F.XIU-JI, M.S.ZONG SHI-ZONG, DING QUING-JUN, HUANG CONG-YUN, S.DE-XUN, TENG MIN-KANG, YIN CHUAN-YUAN*[19]).

White belite portland cements with various MgO (1-10%) and SO_3 (5%) contents and low Fe_2O_3 content were synthesized in laboratory. The positive influence on acceleration of the clinkerization processes is registered when the clinker contains 7% MgO and 5% SO_3. Both the whiteness of the clinkers and the mechanical strength (above 33-35 MPa in 28 days) of the resulting cement are good. Sulphate aluminate compound of the (C, M)$_4A_3\bar{S}$ type was formed and incorporated all MgO in the crystal lattice (*I. TEOREANU, M. MUNTEAN, M. BEDO and T. SUDRIGEAN*[20]).

Modifications of the phases of clinkers with sulphoaluminate and sulpho-ferrites with the aid of admixtures and changes in the thermal regime permit to control the

the hydraulic activity of the phases and the properties of the cement so obtained *(Y. KRIVOBORODOV, O. FOMITCHEVA and A. BOIKOVA*[21]*)*.

The synthesis are oriented towards the stabilization of the α' form with high cooling rates, to guarantee the stability of the high temperature modifications *(V.CHOUBINE and Y.KHNYKINE*[22]*)*.

The solid-state equilibrium relationship between C_3A, $C_{12}A_7$ and the solid solution of calcium aluminoferrite at 1200°C, in the most basic part of $CaO-Al_2O_3-Na_2O-Fe_2O_3$ system was studied by *GILIOLI et alii*[23]. There is no formation of quaternary compounds and sodium preferentially dissolves in calcium aluminates extending their stability inside the quaternary system.

3.2 Influence of Mineralisers

The use of mineralisers in clinker burning lowers the clinkering temperature, increasing the kiln production, and promotes energy saving. Four papers present the fluorine and sulphate influence on clinkering conditions and strength developments.

The use of CaF_2 and $CaSO_4$ in cement clinkering can depress the melting point of the eutectic mix T_2 and reduce the viscosity of the eutectic melt, favouring the clinker formation at lower temperatures (1300-1350°C). $2C_2SCaF_2$ and $3C_3SCaF_2$ can hardly form in the presence of SO_3. The $2C_2SCaSO_4$ occurs only in the mix with $F/SO_3 < 0.158$ and $3C_2S - 3CaSO_4.CaF_2$ forms easily owing to the melting of the eutectic mix *(D. TONG and Z. LIN*[24]*)*.

In clinker doped with CaF_2, the fluorine concentration is highest in the alite phase, lower in the belite phase, and lowest in the intersticial phase. The amount of fluorine dissolved in the silicate increases with the amount of fluorine in the clinker. The fluorine content in the clinker, with an appropriate amount of SO_3 (> 1.35%), prevents the formation of $Ca_{12}Si_4O_{19}F_2$ and favours the increase of alite content, the decrease of its crystal size and its complete crystallization, improving the strength development *(S. WEI and F. MINGFEN*[25]*)*.

The use of fluorite, fluorsilicate and sulphate compound as a mineraliser was studied by *PAGE*[26] et al. in four Indian Plants. The improvement in quality of clinker doped with mineraliser can be primarly attributed to the formation and development of C_3S phase, more than to the incorporation of mineralising ions in the structure of phases. The incorporation of fluorine in C_3S or other clinker phases, by itself, cannot insure better hydraulic potential for a clinker. Complex reactions involving F, SO_3 and P_2O_5 in the structure of C_3S thereby don't improve strength developments.

Addition of gypsum to Na_2O containing raw meals leads to a modification of the clinker structure towards a better developed alite and belite crystals. Reactivity of the raw mix is increased so that more C_3S can be formed and the C_3A phase tends to crystallize in the cubic form, improving the compressive strength of the cement. When more gypsum is added in the raw mix than the optimum content, the compressive strength of resultant cements decreases possibly due to reduction of the hydraulic reactivity of βC_2S *(R.J. SLOTA and A. LEWANDOWSKA - KANAS*[27]*)*.

3.3 Other Contributions

The formation of an intermediate compound containing magnesium has received much attention in the alinite cement process formation. A new compound, $Ca_8Mg(SiO_4)_4Cl_2$ was synthesized in the $CaO-MgO-SiO_2-CaCl_2$ system and the crystal structure study is presented by *Y. RUILUN, W.BOLIN and W. XINRONG*[28].

PEREZ - MENDEZ & FAYOS[29] studied the crystal structure of $K_3Ca_2(SO_4)_3$, a compound identified in coatings on heat recovery cyclones in portland cement kilns. It showed a very distorted structure analogue to apatite $M_5(YO_4)_3X$.

Fluorine compounds present in industrial gypsum - waste used as a cement setting regulator may cause as much as 3 days significative retardation in the growth of initial strengths of cement paste or mortar. Small quantities (1%) of silico fluorides in gypsum, mainly Na_2SiF_6, accelerate considerably the formation of ettringite and reduce the alite hydration degree. NaF exhibits lower retardation effects, whereas CaF_2 shows almost no influence on the initial strengths (*Z. SAUMAN*[30]).

REFERENCES

1 - *Influence of high ash content mineral coal in portland cement clinker characteristics.* Y. KIHARA - Brazil.

2 - *Cuissons reductrices - consequences relatives à la stabilite des phases du clinker.* C. VERNET - France.

3 - *Interactions between alkaline vapours and coal ashes.* F. MASSAZZA and M. PEZZUOLI - Italy.

4 - *Microstructure and properties of high-alkali clinker.* G. R. GOUDA - USA.

5 - *The description of a new potassium-alumina phase in ordinary portland cement.* E. FUNDAL - Denmark.

6 - *A study on the utilization of an italian steel slag.* R. SERSALE, V. AMICARELLI, G. FRIGIONE and P. UBBRIACO - Italy.

7 - *Investigation on the influence of the kiln system on clinker quality.* B. SCHEUBEL - Germany

8 - *Durée de cuisson du clinker et ses propriétés.* B.S. AL'BATS, M. A. VERDIAN, L.S. FILLIPPOVA and E.L. LEBEDEVA - URSS

9 - *The effect of burning conditions on the structure of portland clinker and the reactivity of the resultant cement.* I. ODLER, S.ABDUL-MAULA - Germany, and T.ANGELOVA - Bulgaria

10 - *Influence of the burning degree on the rheological and strength properties of clinkers.* U. COSTA and F. MASSAZZA - Italy.

11 - *Modifications clinker phase and mechanical strength in relation to type of quenching.* F. PUERTAS and F. TRIVIÑO - España

12 - *Chemical composition of phases and phase relations in unbleached and bleached clinkers.* A.I. BOIKOVA , O.I.FOMICHEVA and A.P.ZUBEKHIN - URSS

13 - *Radio tracer technique: a diagnostic method for evaluation of raw meal and clinker movement, in a cement rotary kiln.* P.BHASKARA RAO, S.K. HANDOO and SAMUEL - Inde

14 - *Quantification of OPC clinker microstructure - An approach for prediction of cement strength.* R.V. HARGAVE, D. VENKATESWARAN, V.V. DESHMUKH, and A.K. CHATTERJEE - Inde

15 - *Influence des facteurs differents sur la composition de phase et les propriétés du clinker.* T.V. KOUZNETSOVA - URSS

16 - *Characteristics of alite in portland cement clinker and C_3S solid solution.* M.NAGASHIMA, E.ASAKURA, S. UDA and H.KAWABATA - Japan

17 - *Thermal decomposition and phase transformation studies of $CaCO_3$-SiO_2 (2:1) system in presence of sodium and potassium carbonate.* I.P. SARASWAT, V.K. MATHUR and S.C.AHLUWALIA - Inde

18 - *Dicalcium silicate doped with phosphates.* B.MATKOVIC, V.CARIN, R. HALLE - Yugoslavia and J.F.YOUNG - USA

19 - *Investigation on doped β-C_2S with positron annihilation.* F.XIU-JI, M.S.LONG SHI-ZONG, DING QING-JUN HUANG CONG-YUN, SHEN DE-XUN, TENG MIN-KANG and YIN CHUAN-YUAN - China

20 - *Belitic portland cements with various content of MgO and SO_3.* I.TEOREANU, M.MUNTEAN, M.BEDO and T. SUDRIGEAN Romania

21 - *Composition des phases des clinkers contenant des sulfoaluminates et sulfoferrites.* Y. KRIVOBORODOV, O.FOMITCHEVA and A. BOIKOVA - URSS

22 - *Modification des clinkers de belite.* V.CHOUBINE and Y.KHNYKINE - URSS

23 - *Solid state relationships in the lime-richest part of the CaO-Al_2O_3-Na_2O - Fe_2O_3 system.* C. GILIOLI, F. MASSAZZA and M.PEZZUOLI - Italy

24 - *The role of CaF_2 and $CaSO_4$ in cement clinkering.* D. TONG and Z.LIN - China

25 - *A study of the effects of CaF_2 on clinker doped with compound mineralizer.* S,WEI and F. MINGFEN - China

26 - *Influence of mineralisers on the constitution and properties of industrial clinkers.* C.H. PAGE, D.GHOSH and A.K.CHATTERJEE - Inde

27 - *Modification of clinker phase composition and strength properties of a high - alkali cement clinker by gypsum addition.* R.J.SLOTA and A.LEWANDOWSKA-KANAS - Poland

28 - *The synthesis and crystal structure of a new compound $Ca_8Mg(SiO_4)_4Cl_2$.* Ye. RUILUN, Wu. BOLIN and Wang XINRONG - China

29 - *A very modified apatite-type structure: $K_3Ca_2(SO_4)_3F$.* M.PÉREZ-MÉNDEZ and J.FAYOS - Spain

30 - *Influence of fluorides and silico-fluorides on the hydration of cement.* Z.SAUMAN - Czechoslovakia.

PAULO RODRIGUES - Associação Brasileira de Cimento Portland

SUB-THEME 1.3 - LOW ENERGY CLINKER FORMATION

1 INTRODUCTION

The reduction in energy consumption on clinker manufacture has been taken into account in many aspects, such as changes in industrial process and modification or distortion in the microstructure.

In the papers received concerning the sub-theme 1.3, tendency in emphasizing clinker alinitic and belitic cements was verified.

Secondly, the reexamination of intermediate phases, influence of mineralizers, and modification in raw meals composition were the themes of major authors interest.

It was received 14 research works, being(2) from China, (6) from URSS, (2) from India, (1) from France and (3) from Germany.

The research works were classified in three groups.

Group 1: - Mineralizers utilization

Group 2: - Composition and raw meal modifications

Group 3: - Formation kinetics

2 GROUP 1: MINERALIZERS UTILIZATION

2.1 CHLORIDE SALTS AS REACTION MEDIUM FOR LOW TEMPERATURE CLINKERISATION - A PROBE INTO ALINITE TECHNOLOGY

R.K. Agarwal, S.V.Paralkar and A.K.Chatterjee

The authors compare the morphologic and microstructural characteristics of alinitic clinkers with ordinary portland clinkers.In order to analyse the reactions that occur at various temperatures from 150°C to 1400°C , experiments were made with additions of $CaCl_2$.

The authors tried additions of magnesium salts and non-calcium chloride salts in combination with $CaCl_2$.

It was observed that magnesium salts, irrespective of their froms, when mixed with $CaCl_2$ are more effective as a mineralizer than $CaCl_2$ alone.

It was also observed that $MgCO_3$ and $MgCl_2$ are equally effective in lowering the decarbonation temperature.

The authors concluded that clinkerisation is possible at temperatures lower than 1200°C with the utilization of chloride salts as a reaction medium. The formation temperature of alinite phase seems to be around 900°C under optimum conditions, the phase can be stable up to 1150°C and the clinkers are characterized by the presence of chloride in fixed and free forms.

Moreover the presence of chloride was observed in silicate and aluminate phases.

2.2 SYNTHESIS OF CALCIUM SILICATES AT LOW TEMPERATURES AND INFLUENCES ON THEIR REACTIVITY

D. Bürger and U. Ludwig

The paper shows some results obtained from C_3S and alite production at temperature range of 1150°C - 1350°C and measurements of hydration processes of these synthetics.

The authors obtained correlations among crystal symmetry, burning reactivity, microstructural development dependent on burning conditions and the hydraulic reactivity of the tricalcium silicates with and without additional agents.

The synthetics were obtained by burning pure chemical products and their characterization was realized in the following aspects:

- Microstructure and morphology by means of SEM
- Hydraulic reactivity by means of conduction calorimeter traces (heat liberation) and quantitative X-ray analysis to determine the unreacted C_3S residue.

Other properties were investigated, such as:

- Rheological properties
- Compressive strenght
- Studies of the hydrated phases

Studies on CaF_2 and ZnO influence demonstrated that the temperature decreasing on the formation of the synthetics is correlated with the increasing of the symmetrical properties.

The authors concluded that it is possible to reduce the burning temperature on the synthesis of the calcium silicates and at the same time, saving grinding energy, keeping the hydraulic

activity or even to increase it.

The use of mineralizers allows the synthesis of alites at 1150°C with CaF_2 and 1250°C with ZnO.

2.3 LOW TEMPERATURE SYNTHESIS OF BELITE REACTIVITY

C. Vernet

By activation with $Ca(NO_3)_2$ and $CaC\ell_2$, the author produced C_2S at low temperatures.

This research work shows the mechanisms that can conduct to a network distortion at low temperature and so obtain good reactivity.

The studies on the reactivity were performed with the products obtained from pure and impure raw meals.

The author concluded that the multiplicity of melted salts, enclose a very promising investigation field on the synthesis of hydraulic materials at low temperatures.

The study on belite allowed to delimit three temperature ranges where the characteristics of crystallinity and reactivity were differents.

2.4 RESEARCH ON AN EARLY STRENGTH CEMENT CONTAINING HIGH CONTENT OF IRON

Feng Xiuji
Zhu Yufeng

The authors discuss the characteristics of C_4AF, pointing out the possibility of attainning a cement with high early strength from clinker with high content of ferrite phase.

The clinker of such cement besides the high early strength is produced at lower temperatures.

3 GROUP 2: COMPOSITION AND RAW MEAL MODIFICATIONS

3.1 INVESTIGATIONS ON THE PRODUCTION OF LOW LIME PORTLAND CEMENTS

U. Ludwig and R. Pöhlmann

The paper is a review on clinker burning behaviour and clinker reactivity produced with natural raw mixes, with or without sintering admixtures, having their compositions in the range of k = 75 to k = 99.

The experiments were made with the use of the following sintering agents: MgO, SO_3, ZnO, CaF_2 and their combinations.

Based on the results, the authors discussed the theoretical concepts about the mineralizers effect on clinker formation and properties.

From burning investigations it can be detached:

- Favourable influences of CaF_2 and ZnO additions in raw mixes high and low lime standards.
- Porosity and densification of the clinker produced at lower temperatures and influency on grindability.
- Studies on burning temperatures as a function of lime standard and sintering agents.
- Favourable influence of liquid phase on formation of clinker using a higher content of MgO.

Tests made with clinker, produced in laboratory kiln, in order to verify the reactivity showed the following:

- Phase composition and its properties in relation to the lime standard.
- Grindability index of clinkers as a function of burning degree and lime standard.
- Compressive strength development as a function of lime standards.
- Compressive strength development as a function of fine-grinding and burning conditions.
- Compressive strength of portland cement mortars made from clinkers with different lime standards as a function of the burning degree and of a "mineralization".

3.2 CLINKERISATION WITH LOW ENERGY CONSUMPTION DURING THE BURNING OF RAW MIXES CONTAINING NOT GROUND SLAG

N.M. Javoronkov
O.P. Mtchedlov - Petrossian
N.P. Kogan
A.I. Zdorov
Y.G. Ientch

The paper relates a theoretical study on the amount of energy, necessary to attain the clinkerisation by the use of metallurgical slags, compared to the amount needed to produce clinkers having clay as raw meal.

To reach this objective the authors established new coefficients, so energetic estimative can be obtained when such metallurgical slags are used.

According to the authors, the calculations showed that the theoretical energy consumption on the clinker formation where metallurgic slags are used, can be fixed at 1061kj/kg.Cℓ.

3.3 STUDY ON LOW BASICITY CLINKERS

L.G. Soudakas
U.V. Nikiforov
M.V. Kougia
N.A. Sokolova

The paper deals with the reducing of energy consumption by decreasing clinker basicity.

Results on laboratory and semi-industrial researches with clinkers, with KS in the range of 0,76-0,90 and invariable silica and alumina modulus, showed to be possible to save about 8%-12% in the clinkerisation heat.

The authors have syntherized 39 raw mixes and the obtained clinkers were cooled by two ways: rapid and slow.

With the X-ray and microscopic analysis of the clinkers the authors concluded:

- The samples burnt in laboratory and cooled rapidly exhibited the belite in the α'form, while the samples cooled slowly showed the β form.
- In spite of the rapid cooling, in the clinkers obtained by semi-industrial experiments, several samples did not present the $\alpha'C_2S$, although they showed high hydraulic activity.

The clinkers obtained by semi-industrial experiments, having the same phase compostion, but differing on its microstructure, showed different chemical activity during interaction with water, causing differences in compressive strenghts at 28 days.

3.4 MICROSTRUCTURE AN SOLID SOLUTIONS OF LOW TEMPERATURE CLINKERS

S.N. Ghosh
V.K. Mathur
A.K. Parashar

The paper refers to the production of clinker in laboratory furnace and pilot plant using marginal grad plant raw materials, at temperatures lower than ordinary clinker.

With the electronic microscopy SEM-EDXA and tests on compressive strength performed on clinker, the authors concluded that reactive belite cement and low temperature alitic cement, prepared in the laboratory and in the pilot plants have irregular morphology leading to early development of strength.

4 GROUP 3: FORMATION KINETICS

4.1 PHYSICOCHEMICAL ASPECTS ON CHLOROSILICATES CRYSTALLIZATION DURING THE CLINKERISATION AT LOW TEMPERATURES IN SALINE MELT

B.I. Nouldelman
A.J. Gadaev

The research work explains the formation kinetic mechanisms of alinitic clinkers minerals.

The authors found out that the "gas-liquid-solid" interphases play an important role on the mineral formation processes.

Two mechanisms of chlorosilicates crystallization were pointed out. One is associated (to properties of the interphases), and the other with volumetric properties of liquid phase.

It was also verified the presence of two kinds of liquid phase, which are responsible for the formation of a thin superficial layer that activates the crystal formation of chlorinated minerals. This reveals the necessity of creating a well developed interphase in order to obtain high kinetic parameters on formation of alinitic clinker minerals.

4.2 FORMATION, CRYSTAL CHEMISTRY AND PROPERTIES OF ALINITE AND JASMUNDITE

M.Y. Bikbaou

The paper reports the studies on general mechanisms of mineral formation in chloride and sulphide clinker systems, more specifically the formation of high-basicity silicates, alinite and jasmundite.

Studying the crystallization mechanisms of this silicates prepared from pure products, the author concluded:

- The crystallization raté for alinite and jasmundite is 7-8 times greater than that of C_3S, in spite of lowering the synthesis temperature by 300k-400k.
- The activation energies of formation is 83kJ/mol for alinite and 114kJ/mol in the temperature range 1670k-1770k.
- Alinite does not crystallize is a saline melt of calcium chloride, as it was supposed before, but rather in a silicate melt containing some dissolved chloride.
- Jasmundite also crystallizes in a silicate melt containing sulphur as sulphide.

Analysing the F, Cℓ and S effects on the properties of silicate melts, the author concluded that there is a decrease in the formation temperature of the melt, a decrease in its viscosity and surface tension; another effect is an acceleration of the ion exchange processes in the melts, and a more intense solidification of minerals.

Finally, the author presents comparative studies among the hydration of alinite, C_3S and jasmundite, concluding that alinite presents higher hydration rate due to the presence of chloride on its crystal lattice, while the presence of sulphur in the crystal lattice of jasmundite causes a radical reduction in the hydration rate.

4.3 AN INVESTIGATION INTO CEMENT $CaO-SiO_2-A\ell_2O_3-Fe_2O_3-SO_3$ SYSTEM

Wang Yanmou
Deng Jun'An
Su Muzhen

Showing the production of ferroaluminate cement clinkers with $C_4A_3\bar{S}$, C_2S and C_4AF as their main components and the hydration of respective cements, the authors point out the low energy consumption and the higher cement properties.

To obtain the cement clinker ferroaluminate, experiments were made by using pure chemical products and natural raw meals.

Detailed studies on formation of intermediate phases in the C-A-F-$\bar{S}$, C-A-S-$\bar{S}$ and C-S-A-F-$\bar{S}$ systems are presented along with studies on burning phenomena.

With the XRD, DTA, high temperature XRD and SEM-EDAX techniques, the authors studied the phases characterization of clinkers burnt at different temperatures.

The performance tests made on the produced cements, showed that the ferroaluminate

cements exhibit the properties of high early strength, constant increase of strength in frost resistance and excellent impermeability.

The authors conclude that besides the higher properties, the ferroaluminate clinker cements, are produced with low energy consumption. The clinkerisation temperature is low (1250°C), the grindability is high and the content of limestone in its raw meal is much lower than that in the raw meal of ordinary portland cement.

4.4 ALITESULFOALUMINATE CLINKER: PRODUCTION AND PROPERTIES

V.B. Khlousov

The paper presents the simultaneous attainment of alite and sulphoaluminate by the creation of adequate conditions to earlier formation of liquid phase which high reactivity, assuring by this way, the alite formation at lower temperatures.

The sulphoaluminate formation is assured by adjusting raw meal composition wich must contain sufficient amount of $A\ell_2O_3$ and $CaSO_4$.

To obtain the alitesulphoaluminate clinkers, raw mixes were partially prepared from natural raw meals, and partially from industrial wastes rich in $A\ell_2O_3$ and containing fusing materials.

Studying phase formation kinetics, composition and properties of alitesulphoaluminate cements produced in industrial kiln, the author concluded:

- The clinker composition is: alite (C_3S), belite (βC_2S), calcium sulphoaluminate ($C_4A_3\bar{S}$) calcium aluminate |wich depends on raw mixes basicity ($C_{12}A_7$, C_3A)|, calcium ferroaluminate (C_4AF), calcium suphate ($C\bar{S}$) and gehlenite (C_2AS).
- By the intensification of clinkering process it is possible to lower the burning temperature to 1250-1350°C, reducing energy consumption in about 18% and increasing kiln capacity in 27%.
- Sulphoaluminate cements present quick hardening and high compressive strength.

4.5 CONDITIONS OF THE EXISTENCE OF HYDRAULICALLY ACTIVE BELITE CEMENT

J. Stark
A. Müller
R. Seydel
K. Jost

The paper relates the laboratory and pilot plant experiments with the active belite cements, evidencing the studies about the phase composition related do KS and the rate of cooling.

Through the laboratory tests and verifications the authors concluded:

- By thermal and chemical activation, the belite is high influenced so, because of its strength and other structural properties it becomes similar to an ordinary portland cement.
- The cooling is the most important factor for the hydraulic activity where under conditions of rapid cooling, about 727°C/min and cooling temperature range, from 1300°C to 900°C, an active belite clinker can be produced with sufficient early strength, and good strength after 28 days.

The active belite cement allows the production of ordinary portland cement with a specific heat consumption of 320kJ/kg.Cℓ.

4.6 TECHNOLOGICAL ASPECTS OF STRUCTURE REPLICATION IN SILICATES

G.I. Ovcharenko

The paper presents results on studies about structure replication in silicate reactions.

The author studied the interference of sintering agents (on production of binding materials) by melting and sintering.

A crystal chemical model and mechanisms for belit stabilization by lime are given.

YASUKO TEZUKA - Associação Brasileira de Cimento Portland

COMMUNICATION REPORT ON SUB-THEME 2.1 - *PHYSICAL CHEMISTRY OF HYDRATION PROCESS - INFLUENCE OF MINOR COMPONENTS AND ADMIXTURES.*
Group a

1 INTRODUCTION

The 52 basic reports on sub-theme 2.1 - *Physical chemistry of hydration process - Influence of minor components and admixtures* have been broken down into four groups.

a - Hydration of portland cement and individual clinker minerals with admixtures - 18 communications.

b - Hydration of portland cement - 17 communications

c - Hydration of individual clinker minerals - 13 communications

d - Hydration of cement-solid solutions - 4 communications.

2 HYDRATION OF PORTLAND CEMENT AND CLINKER MINERALS WITH ADMIXTURES

The contributions to this topic come from Italy (3), Poland (2), Czechoslovakia (2), China, Belgium Korea, Japan, U.S.A., France, U.R.R.S., Spain, Scotland, Rumania and India (one each).

There seems to be general agreement that, even small additions of inorganic or organic admixtures can change the course of the hydration reaction of portland cement and clinker minerals.

This subject was subdivided into the following three items:

- Inorganic admixtures
- Organic admixtures
- Experimental techniques.

3 INORGANIC ADMIXTURES

The six papers on the influence of the inorganic admixtures on the hydration of portland cement and minerals are as follows:

3.1 *Induction period in calcium silicate hydration in the light of some new experimental results.* W. Kurdowski, W.Nocun Wczelik, K. Miskiewicz, J. Szuba - Poland.

3.2 *-Ca_3SiO_4 hydration in the presence of electrolytes.* M. Gawlicki, W. Nocun Wczelik - Poland.

3.3 *Accelerating effect of chloride salts on the hydration of portland cement.* Guo Chengju - China.

3.4 *Mécanisme réactionnel et cinétique de l'hydratation du silicate tricalcique en présence de chlorure de calcium.* P.Fierens, Y. Kabuema, J. Orszagh, N. Tenoutasse , J. Terloco - Belgium.

3.5 *Extension of setting time by means of mineralized clinkers.* J. R. Baragano , G. Campos - Spain.

3.6 *Alliage d'hydrolicite des ciments* A.M. Dmitriev, A.K. Zapolszky, T.V. Kouznetzova, B.E. Yudovitch, I. D. Ponomarev - U.R.S.S.

Kurdowski and co-worker[3.1], using microcalorimetry, Q x RD and DTA, studied the early stages of the C_3S and $C_2S.CaCl_2$ hydration process in order to elucidate which of the following phenomena is the main factor responsible for the retardation of the process in the induction period

- calcium silicate hydrate nucleation;
- calcium hydroxide or basic calcium chloride nucleation;
- liquid phase supersaturation with Ca^{2+} or other ions in relation to hydration products.

They found that in the hydration process of C_3S and $C_2S.CaCl_2$ with some admixtures acting as Ca^{2+} binding agents, i.e. CH, C-S-H and SiO_2, the liquid phase plays a decisive role as a rate controlling factor acting either directly and indirectly.

This means that the nucleation process is not the decisive factor hindering the reaction in the induction period. The above mentioned admixtures can act as a nucleation barrier eliminating agent but in general they change the reaction in the liquid phase.

When a high amount of SiO_2 or a C-S-H phase is introduced into the hydrating C_3S-H_2O mixture, the complete disappearence of the induction period is observed.

The active silica is the best acceleration as it ensures relatively fast Ca^{2+} ion combination and considerable Ca^{2+} ion supersaturation decrease with a simultaneous C-S-H phase formation.

Jawlicki and Nocun-Wczelik[3.2] investigated the influence of the K_2SO_4, Na_2SO_4, K_2CO_3 and Na_2CO_3 on the hydration of β-C_2S at room temperature, in water, and water/solid ratio equal to 50.

They showed that the sodium salts act more strongly than potassium salts, especially at the beginning of the reaction and that the carbonates are better β-C_2S hydration accelerators than sulphates. 2% Na_2CO_3 additions rises the degree of β-C_2S hydration from about 40% to 80% after 24 hours.

The liquid phase analysis indicated that K_2SO_4 and Na_2SO_4 addition facilitates the calcium and silica leaching into the solutions. Therefore the liquid phase supersaturation occurs earlier than in a suspension without any admixture.

According to Guo Chengju[3.3], the dissolution, diffusion and crystallization of calcium hydroxide are markedly intensified by the calcium chloride, presumably because of the formation of calcium oxychloride.

When cement grains are introduced into the $CaCl_2$ solution, the CH dissolves more rapidly than in pure water, forming a complex solution, which contains less discrete CH than an ordinary saturated or supersaturated CH solution. The dissolved lime bearing substance, probable a basic calcium chloride diffuses far away from the reaction site and crystallize, both at intensified rates. The resulting solid may be either portlandite or calcium oxychloride, depending on the $CaCl_2$ concentration in the pore liquid.

The calcium oxychloride is a metastable phase, which can stand in equilibrium with a solution containing 15-30 parts of $CaCl_2$ in 100 parts of water. In a higher or lower $CaCl_2$ concentration, it decomposes.

Chengju concluded that the role of $CaCl_2$ in accelerating the hydration of portland cement is that of a catalyzer with the oxychloride produced acting as the intermediate product.

Fierens et al.[3.4] reported that the kinetics of C_3S hydration with $CaCl_2$ comply with the Avrami and Jander laws and that the effect

of $CaCl_2$ is expressed by the reduction of the induction period and acceleration of reaction rate.

In the communication[3.5] by Baragans and Campos it is shown that certain minor elements, as components of raw meals may influence the hydration processes and change the setting and hardening of cement pastes.

In the raw meals contained P_2O_5, the setting time become longer with percentages from 0.4% P_2O_5 and increased accordingly on that basis. With 1% P_2O_5, the free lime content decreases, setting times being maintained without any remarkable variation.

Mechanical strengths with 0.4% P_2O_5 increased after 3 days and are greater at 28 days, while with 1% P_2O_5 the strengths are lower up to 7 days, although at 28 days they exceed those of the initial clinker.

The raw meals containing fluorites expressed as F^- ranging from 0.12% to 0.62% showed that free lime decreases according to the greater F^- content, as the setting lengthens. It was observed that when F^- increases, not only the initial setting is lengthened, but also the interval between the initial and the final setting increases.

It was reported that while in the clinker without F^-, the C_3A is in the cubic form, the tetragonal form increasing according to the F^- percentage and the possible presence of $C_{11}A_7CaF_2$ also being detected, which would explain the lengthening of the setting time.

4 ORGANIC ADMIXTURES

There are nine communications on this item, as can see from the following list:

4.1 *Interpretation of the effects of retarding admixtures on pastes of C_3S, C_3A plus gypsum and portland cement.* H.M. Jennings, H. Taleb, G. Frohnsdorff and J. R. Clifton - U.S.A.

4.2 *Retardation of portland cement hydration by citric acid.* N.B. Singh, A.K. Singh and S.P. Singh - India.

4.3 *Effect of alkali content in clinker on the cement hydration with and without sodium gluconate.* G. Moriconi, S. Monosi, M.Pauri and M. Collepardi - Italy.

4.4 *Effect of retarding admixtures on the portland cement hydration.* S. Monosi, G. Moriconi, M. Pauri and M. Collepardi - Italy.

4.5 *Effect of calcium lignosulfonate on the early hydration process of portland cement.* J.Y. Moon, K. S. Han and S.H. Choi - Korea.

4.6 *Effect of triethanolamine on the tricalcium silicate hydration.* M. Pauri, S. Monosi, G. Moriconi and M. Collepardi - Italy.

4.7 *Hardening processes in some C_4AF - additives - water systems.* I. Teoreanu , A. Puri and M. Georgescu - Rumania.

4.8 *Adsorption of superplasticizers on C-S-H(I) and ettringite.* Y. Fukaya and K. Kato - Japan.

4.9 *Effects of molar parameters of sulphonated melamina and formaldehyde polycondensates on mortar properties.* T. Sebok - Czechoslovakia.

In the communication[4.1] by Jennings et al. it is reported that during the short initial period of rapid reaction and in the induction period, the cement paste is plastic, while after the induction period the reaction accelerates and the paste begins to stiffen.

The length of the induction period and the *time of set* is influenced by organic retarders. According to the authors, the reactions between cement and water which end the induction period could occur in any of three positions:

a - on the surface of the anhydrous material or of the hydration product;

b - in the aqueous phase; and

c - in the hydration product.

Although retarders are normally added to the aqueous phase, they could influence reactions in the other two positions by adsorption onto a surface or incorporation into a product.

Studing the effects of the retarders on pastes of C_3S and of C_3A - gypsum systems , they concluded that the two systems have different, possibly independent, influences on the concentrations of retarders in the aqueous phase of a portland cement paste.

In the case of C_3S, some of the retarder is incorporated into the layer of the product which forms around the grains during the early stages of reaction. It appears that a process which controls the induction period occurs within this C-S-H layer and that the incorporation of a retarder somehow slows the process.

The C_3A - gypsum - water system removes a large amount of retarder from the aqueous phase during the early stages of hydration, with the rate of removal falling with time.

It seems probable that, at least for some organic retarders, the effects on the portland cement reaction may be considered to be a combination of separate processes occuring in the C_3S - water and C_3A - gypsum - water systems.

Singh and co-workers[4.2] found that the hydration of both aluminate and alite in the presence of citric acid is retarded at all concentrations. The conversion of ettringite into monosulphate occurs before the hydration of alite. The amount of CH and its crystallinity and compactness is lowered by the addition of citric acid.

Sodium gluconate as a retarder was studied by Moriconi et al.[4.3] and Monosi et al.[4.4]

In communication (4.3) they reported that the addition of sodium gluconate significantly retarded both the ettringite production and the calcium silicates hydration for the three cements: an industrial clinker with 0.22% Na_2O and 0.54% K_2O, the same clinker heated in a laboratory in the presence of 1% Na_2CO_3 (Na_2 content became 0.56%) and the same clinker thermally treated in the absence of Na_2CO_3.

This retarding action was particularly effective in the case of the cement with the higher alkali content.

In the communication (4.4) the authors confirmed the retarding action of gluconate on portland cement.

The retarding effect was much more remarkable on ASTM type V portland cement with nil C_3A content. They also reported that the sodium lignosulfonate has negligible effects on the kinetics of cement hydration.

Moon and co-workers[4.5] also studied the influence of lignosulfonate salt on the early hydration of clinker minerals.

From the results of their experiments they suggested that the retardation in the hydration of clinker minerals when the calcium lignosulfonate is added is related to the amount of C_4AF and gypsum.

The hydration of C_3S in the C_3S-C_3A-C_4AF system varies considerably in accordance with the content of gypsum and lignosulfonate.

They found that the optimum content of SO_3 was 2.0% when 0.25% calcium lignosulfonate is added to portland cement while addition of 0.5% calcium lignosulfate requires 2.5% SO_3.

Pauri et al.[4.6] reported that triethanolamine (0.1%) slightly retarded the early hydration of C_3S paste during the first 6 hours. This retarding effect is almost eliminated when C_3S hydrates in the presence of C_3A or NC_3A and $C\bar{S}H_2$.

Addition of triethanolamine accelerates the early production of ettringite and its conversion into monosulfate. It seems that adsorption of triethanolamine by ettringite can remove them from the aqueous phase and reduce the retarding effect on the C_3S hydration.

Teoreanu et al.[4.7] showed that the addition of an industrial product containing mostly dimethylterephtalate into the C_4AF - $C\bar{S}H_2$ - water system roused moderate retarding effect but did not essentially affect the kinetics of the hydration, conversion processes and the relative amounts of phases formed. The presence of the admixture determined a finer grain size of the hydrated compounds associated with the formation of a compact microcrystalline hardening structure which determines the development of high mechanical strengths.

Fukaya and Kato[4.8] studied the adsorption behaviour of β-naphthalene sulfonate formaldehyde condensates (NSF) on ettringite and C-S-H by use of the acidity or basicity of the solid surface as an index of the surface characteristics of hydrates.

The adsorption of an admixture is considered to have a deep relationship with the crystalline structure or surface characteristics of the hydrate as well as the molecular structure of the admixture. From the relationship between the surface basicity of the hydrates and the amount of adsorption, they found that NSF is adsorbed on the surface of the hydrate in flat form. Also, the NSF is adsorbed on C-S-H (I) in a monolayer while ettringite forms multilayers.

As a result of the study of the effect of various ions coexisting with an admixture in liquid phase, they showed that Na^+ or K^+ ion does not adsorb on ettringite but on C-S-H (I).

The adsorption of these cations did not affect the amount of adsorption of the admixture. On the other hand, they found that Ca^{2+} ion adsorb on either C-S-H (I) or ettringite, and that Ca^{2+} ion has a direct effect on the adsorption mechanism of an admixture.

Sebok[4.9] reported that the efficiency of sulfonated melamine and formaldehyde polycondensates on the rheological properties of cement mortars as well as on the strength after 28 days depend on their molar parameters mainly on the molar weight (M_w) and polydispersity (R_p). He found that the sulfonated melamine and formaldehyde polycondensates slow down hydration of C_3A to a significant extent but their influence on the kinetics of C_3S and β-C_2S hydration is smaller.

5 EXPERIMENTAL TECHNIQUES

Three communications concerning the experimental methods that might provide additional insight into the physico-chemical processes occuring during early hydration of cement paste with admixtures are presented at this Congress.

5.1 *Monitoring the influence of admixtures and composition on the early hydration*

characteristics of cement paste using a.c. electrical response techniques. A.B. Afshar and W.J. McCarter - Scotland.

5.2 *Mécanisme d'action des fluidifiants étudié par RMN du proton.* M. Letellier, H. Van Damme, B. Mortureux, M. Regourd - France.

5.3 *Influence of temperature and admixtures on the C_3S and cement hydration investigated by radiometric emanation method.* V. Balek, J. Kriz, J. Dohnálek - Czechoslovakia.

Afshar and McCarter[5.1] reported that they have developed an a.c. electrical method for monitoring hydration processes by measuring the changes in electrical response during the initial 24 hours after gauging cement with water. In essence, the technique entails accurately monitoring the variation in electrical resistivity and dielectric constant value of the paste.

The initial stages of hydration are characterised by a relatively high dielectric constant value and a low resistivity value, caused by high ionic concentrations, particularly Ca^{2+} and OH^- ions leached from the cement grains. There is a small drop in dielectric value over the initial 30 minutes.

The induction period is terminated by a rapid rise in dielectric value. The sudden drop in dielectric value coincides with the rise in resistivity value and a general increase in rigidity of the mix due to the formation of CH and more stable C-S-H hydrates. The authors postulated that the dielectric constant value and resistivity curves are better indicators of the hydration characteristics during the early hydration of cement of various chemical compositions.

They also concluded that the influence of admixtures on the hydrolysis and hydration processes can be quantified and a required percentage of admixtures for a given setting time can be calculated.

Letellier et al.[5.2] showed that the nuclear magnetic resonance (NMR) is a suitable technique for studying the hidration of cement pastes.

They pointed out that in the hydration of C_3S, the proton relaxation spin-lattice T_1 variation was linear up tc about 10 hours and permitted the observation of hydrated surface development.

The interpretation of C_3A hydration seems difficult and is very dependent on the water/solid ratio. In the C_3S-C_3A system the proton relaxation times were essentially influenced by C_3A, and the introduction of the plasticizer into the system, for a same water/solid ratio did not change the average proton relaxation times but the initial reaction was lengthened as the C_3A was reduced.

Balek et al.[5.3] studying the hydration processes, especially those taking place during the early hydration stage, proved that the radiometric emanation method (REM) enabled the investigation of the kinetics of early hydration of C_3S and cement as influenced by temperatures and various admixtures.

The radiometric emanation method is based on the measurement of the radon released from samples, previously labelled by its parent isotopes (Th - 228 and Ra - 224).

They also reported that the experimental results of REM agree fairly well with the theoretical curves obtained by computer simulation on the basis of the theoretical model.

COMMUNICATION REPORT ON SUB-THEME 2.1 - PHYSICAL-CHEMISTRY OF HYDRATION PROCESS - INFLUENCE OF MINOR COMPONENTS AND ADMIXTURES
Group - b

2.1.b The following papers were received for comments:

b.1 Computation of solubility relationships for hydrating cement systems. E. GARTNER, J.P. SKALNY (U.S.A.).

b.2 Conduction calorimetry and hydration kinetics - A thermodynamical and analytical approach of the interactive bahaviour of cements. C. VERNET (France).

b.3 Monitoring chemic-physical changes and microestructure development in OPC during early hydration. W.J. McCARTER, A.B. AFSHAR (Scotland, U.K.).

b.4 Sequence and kinetics of hydration reactions of C_3A with gypsum, lime and calcareous fillers. C. VERNET (France).

b.5 Phénomènes électrochimiques intervenant aux premiers stades d'hydratation et de formation de la structures des pâtes de ciment. A. KOCHMAI, O. P. MITCHEDLOV - PETROSSIAN (U.S.S.R.).

b.6 Hydration study of pure phases of cement and synthetic mixtures by microware dielectric relaxation. F. HENRY, P. BAILLEUL, B. COURTAULT (France).

b.7 Cement hydratation control. M. M. SYCHEV (U.S.S.R.).

b.8 Étude de la cinétique de l'hydratation du ciment portland par la serie de méthodes nucleaires. E. I. FEDIN, T. V. KOUZNETSOVA, A. V. NEKHOROCHEV, M. A. SOROTSHKIN, A. L. BLUMENFEL'D, A. B. KOUDRIAVTSEV, G. AKIMOV (U.S.S.R.).

b.9 The role of kinetic parameters on the properties of hydrating cement paste. V. MLAKAR (Yugoslavia).

B.10 Rôle des processus de la polycondensation au cours du durcissement d'hydratation des liants siliceux. E. D. CHOUKIN, E. P. ANDREEVA, S. I. KONTOROVITSH, E. A. ALMELINA (U.S.S.R.).

b.11 Certaines nouvelles conceptions sur le mécanisme d'hydratation des liants. A. POLAK (U.S.S.R.).

b.12 Effect of carbonates on early stage of hydration of alite. H. USHIYAMA, Y. KAWANO, N. KAMEGAI (Japan).

b.13 Early hydration of alite at low water to powder ratio. I. MINO, F. FUSHII, E. SAKAI (Japan).

b.14 Vanadium pentoxide effect of cement hydration. L. CUSSINO, L. MONTANARO, A. NEGRO (Italy).

b.15 On the use of limestone to control cement setting. A. NEGRO, G. ABBIATI, L. CUSSINO (Italy).

b.16 Classification des processus de durcissement des liants. O. P. MITCHEDLOV - PETROSSIAN, A. V. OUCHEROY - MARCHARK (U.S.S.R.)

b.17 Cement hydration under partially saturated curing conditions. L.J. PAROTT, D. C. KILLOH, R. G. PATEL (England, U.K.).

i - Chemical reactivity could be handled considering two general aspects: velocity of reactions, (kinetic treatment) and extension of the reactions (thermodynamical treatment).

The velocity of a reaction is controled by the activation energy and by many factors such as temperature, pressure, concentration and catalyst which affect the activation energy therefore will change the velocity of the reaction.

On the other hand, the extension of a reaction is also controled by the system capacity of producing work that is the free energy.

Free energy describes the balance between energy change (entalpy) and entropy change (organization energy).

As a constant temperature, a system tends

to undergo a reaction so that in its final state it has lower energy and higher entropy than in its initial state.

ii - Most of the received communications have handled on hydration reaction concerning kinetics.

iii - GARTNER and Other (b.1) in their paper have written:

Because of limited experimental data, the approach taken in this paper deals only with a few selected aspects of the problem. We will come suggestions by others as to how to extend this approach and improve it.

The lack of comprehensive phase equilibrium data for the cement water system is noted, and further work in this area recommended.

We would like to propose that, in the coming years, a concentrated worldwide emphasis be put on phase equilibrium studies, and that the results of such studies be handled in a special session of the 9th International Symposium on the Chemistry of Cements.

iv - C. VERNET (b.2) in his paper said that:

The possibility of measuring the extension of the reaction of others phases led us into one of the most interesting observation. It seems that during the 3rd period of hydration, all reactions have increased its activities, particularly that of alite dissolution. The extension of oversatured lime is increased and this means that the released energy contributes the equilibrium displacement.

v - On the other hand, POLAK (b.11) in his paper pointed out:

The studies of the last years developped by many authors by means of electronic microscopy and X-rays analyses showed in a apparent manner that following the hydration of initial phases of the binders (PI) - x, there is the formation of one intermediary phase - primary hydrate (HP) - y and then one stable phase - secondary hydrate (HS) - z. Such developing formation process x → y → z needs that positive ratios of chemical potentials according Ostwald ($ux > uy > uz$) and the dissolved phases ($Cx^{\infty} > Cy^{\infty} > Cz^{\infty}$) respectively must be established.

vi - Concerning the several periods of the hydration reaction in general all authors agree. So that C. VERNET (b.2) in his paper points out four periods:

I - Initial period, with fast reaction and high thermic flux.

II - Dormant period, with very weak thermic flux, very slow reaction, during that the solution is saturated in lime.

III - Setting period, starting with the portlandite precipitation ($_2$) $Ca^{2+} + 2\overline{OH} \rightarrow Ca(OH)_2$, with the acceleration of the reaction (I) and the appearance of a second peak of thermic flux.

IV - Period of decreasing activity, concerning the C_3S consumption and the thickening of the hydrate layers.

vii - McCARTER and Other (b.3) in their paper only changed the name of the second period; then it was named induction period.

viii- A. KOCHMAI and Others (b.5) in their paper added one more period that is period of formation of the structure of hardened cement concerning further formation of CSH phases and to the initial process of its polycondensation.

ix - A. VERNET (b.4) in his paper have considered also four periods for the hydration of C_3A as it was for the cement hydration. The fourth period is described as follows:

As soon as the C_3A is finished, only the reaction number (6) continues and the end products being ettringite and carbo-alumina

te.

x - Concerning hydration mechanisms at early ages it shall be emphasized:

xi - McCARTER and Other (b.3) in their paper described how they could correlate changes in conductivity and dielectric constant with hydration mechanisms by using scanning electron microscopy techniques and by application of AC electrical field to cement paste, measuring dielectric constant and resistivity changes.

Thus the authors have described the initial changes in electrical parameters (0 - 50 minutes) as the initial period of chemical activity. At intermediate frequencies (200 Hz - 2kHz) the gradual increase in dielectric constant up to 170 minutes would indicate an increase in charge to grain surfaces, possibly due to dissolution of the grain by imbibition of water through the gelatinous C-S-H coating formed on initial hydration. These changes should be attributed to the dormant stage. The authors have attributed the peak in dielectric constant at ≅ 200 minutes to renewed chemical activity on C_3S phase which leads to a rapid gain in rigidity of the paste. The period 170 - 500 minutes could be visualised as stage 3 of hydration process. The authors also ascribe the period form 500 minutes onwards as stage 4 of hydration process.

xii - HENRY and Others (b.6) have made hydration studies of puere phases and synthetic mixtures by microwave dielectric relaxation.

The used method differs from that of McCARTER because HENRY and Others used much higher frequency up to gigahertz whereas McCARTER and Other used up to 200 kHz frequency.

HENRY and Others have examined three hydration cases: C_3S hydration, C_3A hydration and mixture of 90% C_3S + 10% C_3A. They have concluded that in presence of lime formed by the C_3S hydrolises, the hydration of C_3A produced C_4AH_{13}. The response curves of permitivity (ε'/m) and dielectric loss give us an information on the beginning of the paste after 8h30 minutes. Adding 5% of gypsum to the mixture this time drops to 6 hours.

xiii- KOCHMAI and Others (b.5) have studied the interaction between the hydration and crystallization process and the electrochemical phenomena by examining the electrochemical cell Ag, $AgC\ell$, $KC\ell m_1$/Cement Paste/ $KC\ell m_2$, $AgC\ell$, Ag where m_1 e m_2 are the concentrations of $KC\ell$ solutions.
They have measured σs (charge densities)
ρs (osmetic pressures)
ϕm (membrane potentials)
ϕtrm (transmembrane potentials)

through the hydration process and could conclude that the hydration process is running through five stages and the 5th one is the period of structure formation of the hardened cement associated to further formation and polycondensation process of CSH phases. This fact causes a reduction of CSH and starts the dropping of ρel and a reduction of ϕtrm.

xiv - VERNET and Others (b.2)

Studying the cement hydration they concluded:

a - the reactivity concept should be taken into account the interactions, that is, from one side the solid properties and from the other the environment conditions.

b - Each hydration period presents one phase with main reaction which is the fastest of the system. The other reactions do not have its initial development in a independent way; its activation energy changes and then its velocities increase as increasing the rate of the main reaction. This is the principal characteristic of the portland cement hydration; for this reason this subject shall be called: dynamic interactant environment.

c - Besides that, the kinetic behaviour of the cement depends on the interaction of its principal compounds, alite and C_3A.

We can say therefore that there is a real coupling between both phases.

xv - Concerning hydration mechanisms at late ages, the paper of MLAKAR (b.9), the paper of FEDIN et al. (b.8) and the paper of CHOUKIN and Others (b.10) shall be considered.

xvi - MLAKAR (b.9) has figured out the rate constants for the characteristic process of hydration: nucleation and growth of hydration products, phase-boundary interaction, and diffusion through growing hydration layer on a group of commercial cements and a synthetic one by adding alkali sulphates. The kinetic constants were obtained on the basis of kinetic study of alite hydration of these samples, using the method of kinetic parameter determination taking into account the α-t dependence and polydispersity of the examined systems.

xvii- FEDIN et al. (b.8) could determine the thickeness of the hydrated layers and the specific surface in the initial hydration stage. For that, they have used the time changes of spin-lattice relaxation as variation of the thin water layers.

By means of the magnetism it is possible to define the content of solid phase in water. After 24 hours, when the gel quantity is still low they discovered only traces of water in the solid phase; at the fourth day the water content independently of the water/solid ratios is 6.5 to 8% in weight; at 28th day the content increases to 8 - 9%.

For tobermorite gel quality parameter at all hardening ages the authors have taken the ratio between compression strength and hydration degree (R/γ). In presence of low values for the water/solid ratios the R/γ reachs its maximum value. This could be because the formation of the polyhydrated hydrosilicates at initial hydration stage as well as due to polymerization-recrystallization process ocurring intensively at older ages.

xviii - CHOUKIN and Others (b.10) have concluded:

During all period of silicates hydration in water and in calcium chloride solution, there is the formation of polycondensation process of siliceous ions. These processes are produced in such a manner that very soon there is the extration of the calcium hydrosilicates with low polycondensation degree ("n") corresponding n = 1 to 4. During the hydration process we observe an increase of the average value of "n" and of the fraction of high polymerization where the polycondensation degree is equal and higher than 6.5 ($Q_n \geqslant 6.5$) with a decrease of the low polymerization fraction.

xix - Concerning hydration Activation there are two important papers: M.M. SYCHEV's (b.7) and C. VERNET's (b.2).

xx - SYCHEV has pointed out:

Dissociative adsorption involved the following recombination processes

$$\overline{OH} + p^+ \rightarrow OH_{ad}$$
$$H_2O + e^- \rightarrow H_{ad} + OH^-$$
$$H_{ad} + OH_{ad} \rightleftarrows H_2O_{ad}$$

The latter is involved in the rupture of -Ca-O-Si$\equiv$ bonds, hydration surface of Ca^{++} ions, and release of these ions + into solution. Thus, the factors that increase the concentration of surface traps and free charge carriers will activate the process of cement setting. This statement is substantiated by correlation of free carrier concentration and length of induction period.

Electrolites can activate not only the surface of cement minerals, thus increasing the concentration of acceptor species, as for example in chromate ion absortion, but also the adhesive interactions of cementi-

tions phases with the structural materials.

By muclear gamma resonance studies of the behavior of oxidizing and reducing species added into the water of mixing SYCHEV could conclude that the activating effect of chromium ions is due to ionsorption, whereas that of manganese or tin compounds is due to oxidation-reduction properties. SYCHEV points out:

Thus, the presence of a solid, finely ground, acidic activator facilitates the appearance of nuclei of high-polymeric hydrosolicate phase-fibrous calcium silicate hydrates of morphological form which positively affects the kinetics of hydration and setting.

xxi - VERNET (b.2) in his paper has written:

The thermic activation is not only a phenomenon of mass heating, although it could be so, if the grains are close enough and therefore the heat transfer will be facilitated. In the case of pure pastes it will be possible to define a global activation energy for each hydration period where we have a process in the same chemical system.

The fineness of grinding is the predominant parameter for increasing the "coupling degree". It facilitates the thermic and ionic transfers. Since the hydration is a surface reaction, the dissolution ionic debits of the phases will be increased; in consequence it will result in higher extension of reactions and in higher velocity of reactions.

xxii - Concerning the hydrations and additives I have selected four papers:

xxiii - H. USHIYAMA and Others (b.12).

It shall be emphasized the conclusion of the authors:

(1) A small amount of carbonates or bicarbonates delays but a large amount accelerates the hydration.

(2) The difference of cation in carbonates or bicarbonates little causes the change of hydration rate.

(3) The degree of delay-effect addition of bicarbonates on hydration is larger than that of carbonates.

xxiv - I. MINO and Others (b.13)

The authors concluded:

The hydration ratio of cement was gradually decreased by the augmentation of packing fraction of particles. In DSP materials, cement particles act as strong internal filler and the source of $Ca(OH)_2$ supply. The total pore volumes of DSP are small and the pore sizes of DSP materials become small compared with conventional cement paste with the increase of packing fraction and the pozzolanic reaction of silica fume. Considering the reaction of cement and silica fume, the control of relation between the packing fraction and the hydrations of hydraulic materials appears to be very important in DSP materials.

xxv - CUSSINO and Others (b.14) have studied the influence of V_2O_5 on nine cements and have concluded:

1 - When V_2O_5 is dissolved into the clinker, mainly into belite, there was not significant changes either in setting or hardening of the cement.

2 - When V_2O_5 is simply added to the cement the settings change; for cement with additions up to 0.25% of V_2O_5 the setting increases as increasing the V_2O_5 content. For V_2O_5 bigger than 0.25% the setting decreases as increasing the V_2O_5 content.

The setting acceleration is due to the thickening of the paste without hydration advancing as it can be seen from calorimetric curves.

The setting delay is, probably due to the formation of calcium vanadate which covers

the cement grains and so hinders hydration.

xxvi - NEGRO and Others (b.15) have concluded:

It is possible to displace 50% of gypsum by limestone without compromissing the cement behaviour.

According to known data, there is a optimum gypsum/limestone ratio which determines the best performance of the cement.

Although the role of the limestone is sometimes limited as setting regulating device, always the limestone reacts with cement producing carbo-aluminate and so proceeding as an active compound of cement.

xxvii - Finally it shall be considered the paper of MITCHEDLOV and Others (b.16) concerning classification of the hardening process of the binders and that of PARROT and Others (b.17), cement hydration under partially saturated curing conditions.

xxviii - MITCHEDLOV and Others (b.16) have proposed to classify the hardening processes of the binders in three types:

a) The first type involves the rapid hardening processes of the most reactive binders: CaO, C_3A, C_4AF. These processes are running with the development of great amount of heat. The hydration induction period is lacking. The maximum hydration rate corresponds to the initial reaction ($\alpha \cong 0.05 - 0.1$).

b) The second type is characteristic for hardening of most of the binders. The accelerated and retarded induction periods are determined through the hydration. The duration of the changes which determine the amounts of heat liberation is not more than one day. The maximum value of hydration rate corresponds to $\alpha \cong 0.3 - 0.5$.

c) The extremely low rate of the reaction with considerable high duration (up to several months) is characteristic of binders like slags, glasses, ashes. In normal conditions the reactivity of those material is practily zero. The maximum reaction velocity and transformation extension correspond to a $\alpha \cong 0.6 - 0.8$.

xxix - PARROTT and Others (b.17) through their paper concluded:

- The results suggested that the rate of cement hydration was related to the amount of water in the layer capillaries rather than the amounts of water in the porous hydrate coatings that surround residual, unhydrated cement grains.
- The effects of relative humidity observed in this study are consistent with reported gradients of microstructure in drying, hydrated cement paste (1). Thus it may be concluded that the surface of prematurely dried concrete will have a low degree of reaction, a higher proportion of large diameter pores and will offer less protection to underlying concrete and any steel reinforcement.

RAPPORT DES COMMUNICATIONS DU SOUS-THÈME 2.1
GROUPE C - HYDRATATION DES CONSTITUANT DU CLINKER

RC
2.1

Les 13 Communications du groupe C ont les titres et auteurs suivants:

T. Mitsuda, S. Kobayakawa et H. Toraya
Caracterisation du C-S-H formé hydrothermiquement

- Il y a plusieurs façon d'obtenir le C-S-H au laboratoire. Les auteurs de la Communication C.1 font reagir l'acide silicique et la chaux aux temperatures superieures a 120°C jusqu'a 210°C. La relation Ca/Si a aussi variée de 0,4 a 3,0 (silicate tri-calcique). Les C-S-H formées se presentèrent sur differentes formes crystallines qui furent examinées en detail par TEM, DRX, IRS, DTA et TG et la superficié specifique par BET.

T. Hara, N. Inoue, H. Noma et T. Hosegawa
Formation et caracterization de la jennite

- Au moin, depuis 1966, d'après les auteurs, de la C.2 la formation de jennite ($Na_2O.8CaO.5SiO_2.11H_2O$) pendant l'hydratation des silicates, a interessé les scientistes. Dans cette Communications, les auteurs font une étude sur les conditions dans lesquelles se forme la jennite. Les auteurs ont montré que un melange de β-C_2S et fumée de silice, en certaines conditions, conduit à la formation de jennite après 91 jours de hydratation a 80°C.

D. Bertrandie et P. Barret
Etapes elementaires interfaciales de l'hydratation des aluminates de calcium, constituants des ciments.

- Malgré le titre de la C.3 en realité elle traite de l'hydration des aluminates et silicates de calcium aussi bien pour des ciments alumineux et ciments portland. Ils disent que "nous avons faite, dans le cas des silicates C_3S et C_2S, un exposé sur nos hypothèses, nos idées et leur rapport experimental et theorique en ce qui concerne les etapes elementaires de l'hydration des principaux aluminates de calcium utilisées dans le ciment". Ils acceptent un processus d'hydratation topochimique preliminaire suivi de la dissolution car "nous postulons l'existance d'une étape irreversible d'hydroxilation superficielle s'accompagnant d'un abaissement d'enthalpie libre susceptible d'expliquer la différence entre la solubilité theorique calculée et les valeurs limites des concentrations observées". Les detailles de l'hydration des silicates et aluminates sont presentées, suivant ses hypothèses, minutieusement.

P. Barret
Mecanisme de l'hydratation des silicates de calcium (C_3S, C_2S) constituant du ciment, vu à travers les concepts generaux de la reactivité des solides.

- La C.4 est bien relationé au travail com-

mentê anterieurement de D. Bertrandie et P. Barret. P. Barret dans ce travail présente encore plus de detailles, sur l'hydratation des silicates, et cherche à complementer et discuter celui que H.F.W. Taylor à presenté à la reunion du Commité 68 de la RILEM, sur formation d'une couche totalement protectrice du grain de ciment, admetant aussi l'existance d'un processus topochimique prealable.

P. W. Brown
Consequences de l'equilibre des phases dans l'hydratation du système C_3S-eau et C_3A-gypse-eau.

- L'auteur la C.5 examine en detail le mechanisme et la cinètique de l'hydratation du C_3S et du C_3A, en presence ou non du gypse, dans la periode de pre-induction de l'hydratation. En ce qui concerne l'hydratation du C_3S il trouve incertain son controle par la variation de la relation C/S. Avec l'aide du MEB il a observé le développement d'une couche de produits d'hydratation sans une forme definie, sur les cristaux de C_3S, pendant la periode de pre-induction. La periode d'induction commence quand la couche à terminé sa formation et finit quand la couche presente des transformations morphologiques avec l'apparition des cristaux en aigüilles de C-S-H. L'hydratation du C_3A est examiné en detail prenant attention à la solubilité du CaO et du Al_2O_3 à la periode de pre-induction, et avec le sulfate quand on etudie le systeme Al_2O_3-$CaSO_4$-H_2O. L'auteur examine les conditions pour la formation du gel AH_3 et a l'ettringite dans la periode de pre-induction.

K. Asaga, M. Daimon, S. Sibata, K. Kishi, K. Yano, P.R. Shrestha
Les effets de l'histoire thermique et des additifs sur l'hydratation du β-C_2S.

Les auteurs de la C.6 ont preparé le β-C_2S par melange de $CaCO_3$ et SiO_2 dans la proportion de 2 de CaO et 1 de SiO_2. En suite, le melange est porté a 1.500°C, dans un creuset de platine, pendant 1 a 1,5 heures et refroidi a l'air: on a obtenu la γ-C_2S. Les auteur ont examiné l'influence de l'addition de Fe_2O_3, de Fe_2O_3 + K_2O et de B_2O_3, sur l'inversion β-$C_2S \rightarrow \gamma$ C_2S. Les recherches des auteurs, sur l'hydratation du β-C_2S ont montré que son hydratation est largement affectée par l'histoire thermique de sa preparation (1.000°C ou 1.500°C, par exemple).

Y. Nanru, Z. Baigian et W. Zhanwen
Un β-C_2S actif - Preparation et hydratation

- Les auteurs de la C.7 présentent l'étude de l'hydratation, de ses proprietés de resistances à compression d'un type de β-C_2S preparé à basse temperature, inferieur a 1.123°K. Il s'agit d'une recherche de laboratoire dans le même sens d'autres recherches pour obtenir un β-C_2S actif.
C'est un minutieux travail de recherches utilisant les techniques modernes pour l'examen de l'evolution de l'hydratation, comme la trimetyl-sililation (TMS), DRX, IR, cromatografie, evolution thermique, et le microscope electronique à balayage.

N.J. Clayden, C.M. Dobson, C.W. Groves et S.A. Rodger
Application des methodes spectroscopique de la resonance magnetique nucleaire (RMN) dans l'état solide pour l'étude de l'hydratation du C_3S.

- Les auteurs de la C.8 ont utilisé l'essai par resonance magnetique necleaire pour l'étude des produits formé par l'hydratation d'un C_3S synthetic pendant les periodes de pre-induction, induction, post-induction accélerée et retardée. Dans la periode de pre-induction, l'indication, à la Fig. 1, du chaleur degagé est significativement petit a cause de l'additif. L'action des additifs comme le $CaCl_2$ et l'acide maleic "n'ont pas presenté aucun effet

significatif dans la composition chimique ou à la structure du C-S-H. Le seul effet semble être dans la cinetique de l'hydratation". En accompagnant l'hydratation des silicates par RMN, les auteurs ont arrivé à de resultats sur la polymerisation de la silice semblables a ceux obtenus par trimethyl sililation (TMS).

A.R. Ramachandran et M.W. Grutzeck
Hydratation du C_3S a un pH fixé.

- Les auteurs de la C.9 presentent le résultat de la recherche sur l'hydration du C_3S preparé au laboratoire avec un melange de $CaCO_3$ et de la silice colloidale. L'objectif etait de verifier l'influence de la variation du pH (de 8 a 11,5) sur l'hydratation de C_3S en suspension, et à trois temperatures 10°, 25° et 40°C. La variation de la concentration du calcium et de silice en fonction du pH de 8, 10, 11, 11,5 et 12 à 25°C a demontré l'importance de la recherche. Le titre de ce travail ne traduit pas l'importance de la recherche presentée dans la C.10 sur les premiers pas de l'hydratation du C_3S, soit dans la periode de pre-induction et d'induction. Les auteurs ont examiné en detail le mecanisme de la formation initial du gel de silice, en quantifiant la variation de la concentration de calcium en fonction du pH de la solution cette variation conduit à la precipitation du C-S-H avec le pH de 11,5 a 12. Pour arriver a ces conclusions les auteurs ont etudié et discuté en detail la methode de synthese du C-S-H qui conduit à une hydration semblable à l'hydratation reel du C_3S du ciment portland.

Francisa Hannawaya.
Proprietés du C_4AF après 8 années d'hydratation

- L'auteur de la C.11 presente une recherche sur l'hydration du C_4AF synthetic pur et avec l'adition de gypse depuis le periode initial jusqu'a 8 ans. Le melange du CaO (en partant du $CaCO_3$ avec 96 - 98% de pureté), de l'hydroxide d'aluminium (gibbsite) et oxyde ferrique est porté à la temperature de 1.320°C pendant 2 a 3 heures. Le C_4AF en presence d'eau, s'hydrate rapidement et termine la reaction à 28 jours. Les phases crystallines sont: $C_4(A,F)H_n$, $C_3(A,F)H_6$, solutions solides entre les phases precedentes, phase amorphe d'hydroxyde de fer ou d'aluminium et hydroxyde de calcium. Le C_4AF en presence du gypse, s'hydrate plus lentement et donne lieu à la formation d'ettringite qui evolue en monosulfate. Après 8 ans le monosulfate $C_4(A,F)\bar{S}H_{18}$ presente, aux DRX, une plus forte intensité que le $C_4(A,F)\bar{S}H_{12}$.

S. Menosi et M. Collepardi - Italie
Effet de fumée de silice sur les produits d'hydratation du systheme C_3A-$6\bar{S}$ H_2

- Les auteurs de la C.12 ont etudié l'hydratation du C_3A synthetic (CaO - de $CaCO_3$ - e Al_2O_3) en melange avec la fumée de silice, avec le gypse et un additif de sulphonate de naphtalene. Ils ont utilisé surtout l'analyse thermogravimetrique (ATG) et l'analyse thermo differentiel (ATD) pour accompagner la cinètique de l'hydratation des differents melanges. Une conclusion importante c'est que l'addition de la fumée de silice accelère la production de l'ettringite et sa conversion en monosulfate.

I.
A.J. Boikova, L.V. Grishchenko, et A.J. Domansky - URSS
Activité d'hydratation des phases contenant du chlore.

- Les auteurs de la C.13 ont étudié l'hydration d'un clinker contenant des phases comme le chloride-silicate de calcium(alunite) et le chlore-aluminate de calcium ($Ca_{11}Al_{14}O_{32}$, $CaCl_2$). Ce clinker contenait

55 - 65% d'alinite et 5 - 10% de chloro-aluminate de calcium. L'etude de la cinétique de l'hydration de l'alinite pure à montré qu'elle à court terme et à long terme, a une activité beaucoup plus grande que le C_3S. Les auteurs ont etudié, en detail, l'influence de composés mineurs sur l'hydratation.

Groupe D - HYDRATATION DU CIMENT CONTENANT DES SOLUTIONS SOLIDES

Les 4 Communications du groupe D ont les titres et auteurs suivants:

Polman Herbert
Solution solide du complexe d'aluminate de calcium hydraté contenant des anions Cl^-, $(OH)^-$ et CO_3^{2-}

- L'auteur de la C.14 presente une recherche faite sur l'hydratation du C_3A, contenant Cl^-, OH^- et CO_3^{2-}. En plus des aluminates hidratés, il a verifié la formation des hydrates du chlore aluminate de calcium, du carbo-aluminate de calcium, et de l'hydroxide de calcium. En fonction de la composition chimiques des hydrates il y a la formation des solutions solides, étudiées en detail par l'auteur.

R. Wenda et H. J. Kuzel
B^{3+} dans les aluminates de calcium hydratés

- Les auteurs de la C.15 ont fait de recherches sur les effets d'addition de borates sur l'hydratation d'un aluminate monocalcique (CA) synthetic avec l'addition de $H_3 B O_3$ ou de la colemanite ($Ca[B_3O_4(OH)_3].H_2O$ pendant l'hydratation à des temperatures variables de 5° a 60°C. Ils ont utilisé aussi un "Ciment Fondu" Secar 250. Ils ont detecté quelques nouveaux aluminates de calcium contenant du bore et ont arrivé à la conclusion que le $2CaO.B_2O_3.H_2O$ "est le responsable de la stabilisation des ciments alumineux contenant des borates". Les auteurs indiquent que "l'addition de 5% calemanite, conduit a limiter la formation de 50% des hydrates CAH_{10} et C_2AH_8 qui peuvent avoir de convertion en $C_4A.1/2\ B_2O_3.12H_2O$ et que la transformation de cette fraction en C_3AH_6 est bloquée".

V. Akimov, T. Kouznetsova, A. Koudriavtsev' et V. Paniouchkine - URSS
Defectuosités de structure et activité d'hydratation des mineraux entrant dans le clinker de ciment portland

- Les auteurs de la C.16 ont montrés certains details de l'influence des defectuosités de la structure crystalline des mineraux du clinker, dû à la presence de solutions solides, sur l'activité d'hydratation du ciment portland. Les auteurs ont confirmé que "l'hydratation n'interesse pas toute la surface des cristaux mais essentiellement les centres actifs" et en plus, les défauts superficiels, resultant d'un traitement thermique ou mecanique, des cristaux influent directement sur la durée de la periode d'induction lors de l'hydratation de C_3S". Les auteurs ont largement étudié le phenomène en detail, avec l'utilisation des essais par resonance magnetique nucléaire et d'autres.

T. Kouznetsova et V. Akimov - URSS
Silicate dicalcique et aluminates de calcium

- Les auteurs de la C.17 ont fait de recherches sur l'influence de solutions solides des silicates avec plusieurs substances comme K_2O, B_2O_3, Al_2O_3, Fe_2O_3, Mn_2O_3 et Cr_2O_3 dans l'activation de son hydratation. Les recherches ont été faites en des silicates et aluminates de calcium obtenus au laboratoire. La cinetique de l'hydratation des silicates et aluminates de calcium contenant des solutions solides à été suivi avec l'utilisation des essais par analise microcalorimetrique, analyse des phases par RX et par resonance magnetique nucleaire. En conclusion, les auteurs ont

montré que certaines defectuosites dans les mineraux des clinkers industriel et des phases sinthetiques ont une influence dans le degré d'hydratation et dans la cinetique de l'hydratation des silicates et aluminates de calcium.

P. Kittl, Researcher and Head of the Electron Microscopy Laboratory, Engineering and Material Science Department, IDIEM, Faculty of Physical and Mathematical Sciences, University of Chile, P.O. Box 1420, Santiago, Chile. RC 2.2

Theme 2.- HYDRATION OF THE CLINKER COMPONENTS AND OF THE CEMENTS

Sub-Theme 2.2 - MICROSTRUCTURE OF HARDENED CEMENT PASTE AND ITS EFFECTS ON ITS BEHAVIOUR

1. INTRODUCTION

It is worthwhile to emphasize that in this sub-theme there are a variety in the research, that comes from a work in pure kinetics in a pure phase to a work on fracture mechanics in a hardened hydraulic cement, passing through the morfologic features, So the participation of the different countries, with a maximum of three works to Czechoslovakia and United Kingdom followed by contributions of one work to Brazil, Canada, China, France, Italy, Japan, Poland, Saudi Arabia, U.S.A. and USSR, is also very varied.

In order to make a gradual report of all the works, it was intended an ordenation in the previously shown sense.

Works which deals principally with hydratation kinetics

1.- "Structure and kinetics of formation of the gel phase in hydrated tricalcium silicate".
D. R. VOLLET and A. F. CRAIEVICH - Brazil

2.- "On the hydration of ferrite phase in the presence of lime and gypsum".
A. NEGRO, L. MONTANARO and A. BACHIORRINI - Italy.

3.- "Hydration and porosity of cement paste cured in warm and dry environment".
O. Z. CEBECI - Saudi Arabia

4.- "Phenomenes cristallochimiques intervenant dans l'hydratation des mineraux du ciment".
L. CHPYNOVA, V. ILIOUKHINE, M. SANITSKY et S. MELNIK - U.S.S.R.

Works which deals principally with the morphology of the hydration products

5.- "A study of the microstructure of two old cement pastes".
K. L. SCRIVENER - United Kingdom

6.- "Structure and morphological aspects of calcium silicate hydrates". *1

7.- "Microstructure of hardened pastes of gypsum - free portland and slag cements".
F. SKVARA - Czechoslovakia

8.- "$Ca_3SiO_4Cl_2$ hydration under hydrothermal conditions".
W. KURDOWSKY and K. MISKIEWICZ - Poland

9.- "Behaviour of ettringite in high strength hardened cement paste".
K. ISOZAKI and K. NAKAGAWA - Japan

Works which deals principally with fracture and mechanical properties

10.- "The formation of $C_2SH(A)$ and C_3SH at the hydration of portland cement".
V. LACH - Czechoslovakia

11.- "Relationships between ettringite and chloroaluminate, strength, and expansion in paste mixtures".
A. D. BUCK - U.S.A.

12.- "Pore structure and strengths of hardened cement pastes".
J. JAMBOR - Czechoslovakia

13.- "A study of the intrinsic properties of hardened cement pastes (HCP)".
L. PING and H. YIUN-YUAN - China

14.- "Dependence of degree of silica polymerization and intrinsic mechanical properties of C-S-H on C/S ratio".
J. J. BEAUDOIN and R. F. FELDMAN - Canada and J. BARON and M. CONJEAUD - France

15.- "Crack tip processes and fracture mechanism in hardened hydraulic cements",
N. B. EDEN and J. E. BAILEY - United Kingdom

2. PARTICULAR DISCUSSION OF THE WORKS

2.1 Vollet and Craievich, which are the authors of the first work has been studying the hydration of tricalcium silicate with a small-angle X-ray scattering (SAXS) at different temperatures. The degree of the hydration was determined by quantitative X-ray diffraction analysis (QXDA). The kinetics of setting of the pastes is well described by the Johnson-Mehl equation with n=2

$$J_\infty - J_t = (J_\infty - J_0) \exp \{ - k^n \frac{t^n}{n} \} \qquad (1)$$

where J_t, J_0 and J_∞ are the scattering intensity values, respectively, at time t, extrapolated to t=0 and corresponding to the apparent upper asymtote. k is an empirical velocity constant and n a parameter that is a function of the phase transformation determinant mechanism. The

$\ln\ln \frac{J_\infty - J_0}{J_\infty - J_t}$ vs. lnt plot must be linear in this

range, with a slope n, which in the graph presented by Vollet and Craievich is quite nearly 2. The Arrhenius plot for the empirical hydration velocity $k \alpha \exp(-\Delta E/RT)$ give an empirical activation energy of ΔE = 37.2 KJ/mol. Analysed the SAXS data they can obtain the mean size parameters l_p and l_s respectively of the pores and the solid gel particles, $\bar{l}_p \simeq 0.80$ nm and $\bar{l}_s \simeq 2.05$ (nm), for the satured samples. In the dried samples l_p and l_s can become 2.5 nm and 6.4 nm respectively. This increases, indicating a clustering of the gel particles and pores, when the tricalcium silicate paste dried. His hydration kinetics studies suggest that the hydrated gel correspond to about one layer of tobermorite type, separated by one or two monolayers of water, on the average.

2.2 The second work by Negro, Montanaro and Bachiorrini, is about the hydration of ferrite phase in the presence of lime and gypsum. It is in general accepted that the ferrite phase is a solid solution of the type $C_2(A_nF_{n-1})$ where $0 < n < 0.7$. From the components of this solid solution C_6A_2F, C_4AF and C_6AF_2. With an addition of CH, $C\bar{S}H_2$, and the siliceous powder, they prepared the mortar where the relation water/solid = 0.3. They measure the expansions after 28 hydratation days of three mortars prepared as it is said before and they are compared with two reference mortar containing C_3A, CH and $C\bar{S}H_2$, for the first, and by C_3A with 5% of F, CH and $C\bar{S}H_2$ for the second. They observed that the expansion of this mortar made of ferrite phase is function of the content of A and they amount a minor quantity that of the mortar made with C_3A. For this C_3A mortar the expansion is lower, when the C_3A is replaced by the C_3A with additions. Differential thermal analysis is used for studying the hydration kinetics of this mortar by the evaluation of the amount of ettringite[*2] that they have. After this results is possible to say that the little quantity of ettringite and expansion shown by the ferrite in relation to C_3A, are doing not only to his mediocre reactivity, but to formation of amorphos ferritiques components which implies a lowered of hydratation. The plates showing scanning electron microscopy of the different stages of the phases are very useful.

2.3 The work of Cebeci, which is the third, is about the hydration and porosity of a cement paste cured in warm and dry environment. In order to accomplish this two differents temperatures 17°C and 37°C were maintained during mixing and in the three different curing media: in lime satured water, 75% and 33% relative humidity. The hydration was determined by ignition at 1050 ±50°C to measure the non evaporable water content. The ratio of this to the nonevaporable water content of the paste completely hydrated with excess water in a ball-mill, indicates the degree of hydration of the specimen. The figures shown by the author in which he describes the hydration kinetics, are quite different from the one of Vollet and Craievich, and it is necessary further studying in order to obtain a coherence between this two important experimental facts. Using their own words: "The degrees of hydration and mercury intrusion pore size distributions of the hardened pastes were determined at various ages from one to ninety days. The results indicated that the deficiency

in the relative humidity of the environment, rather than the increase in the hydration temperature, is the dominant factor affecting the parameters investigated in this study. The cement pastes hydrated at lower humidity attained lower ultimate degree of hydration and greater porosity, particularly in macropores, as compared to the pasted hydrated in water".

2.4 The fourth and last work of the first subdivission of this sub-theme is by Chpynova, Ilioukhine, Sanitsky and Melnik, and deals with the crystallographic fenomenous that participate in hydratation of the clinker phase. They show the influence which perfoms the anisotropy of chemical union in the structural polyedres and the nonsaturation of valence forces in the anions on the hydratation of the clinker minerals. They discuss, in the same way, the possibility of formation, when the C_3S hydratation is taking account, of a hydrosilicate with high basicnees nature, which are analogous to the calcium hidroxide structure. With the calcium silicate they obtain that the procesus which is determinant in the hydration are: the polycondensation of SiO_4 in the hydrosilicate, the lixiviation of CH and his crystallisation in the pores upon the form of portlandite; for the aluminates and the calcium aluminaferrite: the protonisation of all $O^{=}$ and the tranformation of Al^{+3} and Fe^{+3} to the IV in VI coordination with the total destruction of the crystalline structure of the original mineral. So, this authors describe a topochemical reaction where only the CH is dissolved and critalized.

2.5 In this work, the first which uses morphology principally and made by Scrivener, deals with the microstructure of two old cement pastes. They have been examined by backscattered electron (bse) imaging of flat polished section in the SEM. One paste has been hydrated under carefully controlled conditions for 23 years. A cement made by William Aspdin is the other and is mixed with water in 1848. The bse imaging technique allows, that the different phases and porosity in the pastes can be observed. The resolution is about 0.1 μ m. Many features of the original cement can be obtained from the microstructure of the pastes. Many relicts of the original cement grains can be distinguished, and the original particle size distribution can be obtained and the water cement ratio of the paste. As the author said "This study indicates that the net movement of most ionic species during hydration is very small and provides evidence for an in situ reaction mechanism during the latter stages of hydration". This in situ reaction must be correlated with the previously said solid state reaction or a reaction controlled by diffusion, in some previous discussed work.

2.6 The second work which deal principally with morphology is made by Henderson and Bailey and is about the structure and morphological aspects of calcium silicate hydrates. As the authors said the 70% calcium silicate hydrate (C-S-H) have a micro and molecular structure which remains practically uncertain. In order to elucidate this uncertainty of molecular and microstructural characteristics, they prepared various synthetic C-S-H with particular reference to possible structural relationships with the hydrates in portland cement paste. They studied C-S-H formed in a model two phase system, consisting of an aqueous CH solution and an organic layer of hexane containing $(C_2H_5O)_4Si$. The C-S-H prepared in various conditions which give different C/S ratios were observed in TEM. The principal results obtained by the technique are: "The presence of ~1 nm foils extending to 10^2-10^3 nm along the sheet have been directly observed in both amorphous and microcrystalline hydrates, with compositions in the range C/S = 0.9 to 1.75. The ~1 nm thick foils appear to represent the basic core structure of these hydrates, consisting of a CaO_x polyhedral sheet sandwiched between short chain silicate groups. The presence of double ~1 nm foils ~2 nm and less apart, extending over 10^2-10^3 nm are indicative of incipient short range ordering at right angles to the sheet. The non-interfacial C-S-H (C/S = 1.7) was thought to have a fibre-like microstructure when examined at low magnification. However, more detailed microscopy revealed the actual character of this hydrate at a micro and molecular level. Highly directionally orientated foils ~1 nm thick extending some 10^2-10^3 nm were observed. Instead of doublets, multilayered C-S-H foils between ~2 nm and 4 nm apart, consisting

of up to 6 layers, were also observed. In spite of the overall highly directionally orientated character of these foils, conventional electron diffraction contained but two diffuse bands typical of amorphous materials. The thickness of these ~1 nm foils, like similar but more highly curved interfacial C-S-H foils, is again consistent with a basic structural core, consisting of a CaO_x polyhedral sheet sandwiched between silicate groups. The difference in foil character, between the interfacial C-S-H, where they are high curved and the highly directionally orientated non-interfacial hydrate foils, is probably related to the great difference in preparative conditions, rather than to any basic change in their overall sheet-like molecular[*] level structure, containing CaO_x polyhedral sheets sandwiched between silicate groups of various types; independent of mode of formation, composition or degree of order, strongly suggests that the C-S-H in paste hydrated portland cement, could well, also contain this basic highly orientated layer-like molecular structure."

2.7 The following work, by Skvára, is about the microstructure of hardened pastes of gypsum-free portland and slag cements. They prepared a ground cement clinker of specific surface 300 to 700 m^2/kg, in which the common setting regulator, the gypsum, is replaced by lignine derivate (or sulphonated polyphenolate) plus alkali carbonate, with w = 0.20. This pastes GF, attain a compressive strenght of 1 to 9 MPA after 1 to 3 hours, and are composed of crystalline and amorphous patterns featuring the ratios C/S = 1 to 5, and C/A = 10 to 50. With SEM it is found that a dense structure is developed in the course of 12 to 24 hours the morphological character of which does not undergo any further changes through the paste strength increases (to 100 MPa and more after 28 days). It is very interesting that this dense structure was not found to contain the crystalline formation typical of hardened PC pastes (portlandite ettringite). A high-lime C-S-H phase (mean C/S ratio = 2.7 $\pm$ 0.1, EDAX analysis) intergrown with very fine CH and highly dispersed hydroaluminates (cubic and hexagonal). The gypsum-free slag cement (GFS) attain a compressive strength of 50 to 90 MPa after 28 days, and over 100 MPa after 180 days. SEM said that his hardened pastes present a dense microstructure composed of the C-S-H phase intergrown with highly dispersed hydroaluminates and hydroalumosilicates. They do not contain CH. The hydrosilicate phase of GF and GFS cements may be classified as C-S-H type III. The major constituent of bonding products in hardened GF cement pastes is mostly the hydrosilicates of the C-S-H II (Taylor) interspersed with very fine CH and highly dispersed hydroaluminates. The major mechanical strength of the hardened GF and GFS cements respect to the PC and SPC ones is the result of the greater bonking capacities of the new hydration products.

2.8 Kurdowsky and Miškiewicz studied the $C_2S \cdot Cl_2Ca$ hydration under hydrothermal conditions. X-ray examination, differential thermal analysis and SEM was used for this investigation. The calcium chlorosilicate which is formed at about 600°C in system C-S-$CaCl_2$, was synthesizes starting from a mixture of calcium carbonate, amorphous silica and calcium chloride with molar ratio 2:1:1, in a laboratory furnace. This calcium chlorosilicate was mixed with amorphous silica in molar proportion 0, 1, 2, which are the samples A, B, C, respectively. The behaviour of this samples in autoclaving is summarized as follows from figures of the authors.

Sample A:

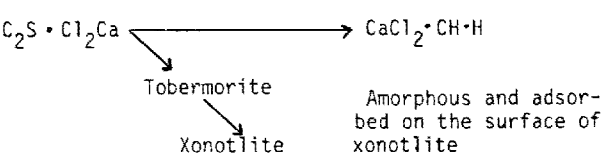

Sample B:

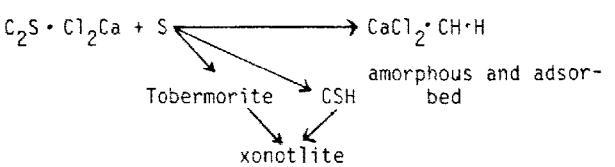

Sample C:

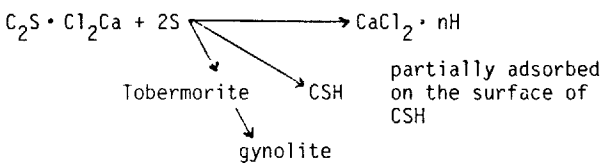

2.9 The last work of this group deals principally with morphology. It was made by Isozaki and Nakagawa and is the behaviour of ettringite in high strength hardened cement paste. They used SEM, mercury pressure porosimetry and powder X-ray diffractometry in order to study the morphology of ettringite and hydrate structure in high strength hardened cement pastes made with normal portland cement containing type II anhydrous calcium sulfate (anhydrite) at long term water curing. The amount of anhydrite added to the normal portland cement were varied from 0 to 20 wt%, $w \approx 0.3$, after precuring at 20°C, they were steam cured at 65°C for 4 hrs and inmersed in water at 20°C for forty months. The addition of anhydrite in the high strength hardened cement paste at forty months of age gives a stable ettringite and monosulfate hydrate was not detected. In the SEM figures shown in the work the average shape of ettringite was a needlelike form of 0.2 to 0.8 μm in diameter and 2 to 6 μm in length. Some ettringite crystals can concentrate in the small voids and some times sintered together, growing into a large crystal, this depends on the amount of unreacted anhydrite and the compactness of the matrix of cement paste.

2.10 The work of Lach about the formation of $C_2SH(A)$ and C_3SH at the hydration of portland cement, is the first of the works where the mechanical properties have a very important rol, which go to increase to the last work coomented here. Various methods as X-ray diffractometry, microporosimetry, SEM and, of course, mechanical tests, was used in this work . It is found that the phase composition of microstructure varies significantly with the temperature of autoclaving process (140, 165, 190 and 215°C). At 190 and 215°C temperatures, besides common phases CH and C-S-H gel, the basic hydration products $C_2SH(A)$ and C_3SH were formed according to the reaction:

$$m\ (\text{C-S-H gel}) + n\text{Ch} \longrightarrow x\text{C}_2\text{SH(A)} + y\text{C}_3\text{SH} \qquad (2)$$

In relation to the mechanical properties of hydrated paste, the higher is the crystallinity and basicity of calcium hydrosilicates at the expense of gel and less crystalline ones, the lower is the strength of autoclaved paste. The hydration is not completed even with high autoclaving temperature, and the specimens places in humed atmosphere after autoclaving increased their strength and reduced microporosity. The higher the degree of hydration, the higher the temperature of autoclaving.

2.11 In the work of Buck, the theme is a relationships between ettringite and chloroaluminate, strength, and expansion in paste mixture and this is a part of study of cementitious mixtures for underground sealing and isolation of nuclear wastes. The stability of these phases on such factors as strength and expansion was studies. In order to carry on this objective a serie of paste mixtures using a portland cement, plaster of paris, and two levels of water content with or without the presence of fly ash, ground granulated iron-blast furnace slag, silica fume, or natural pozzolan were made; four mixtures contained sodium chloride instead of plaster of paris were also made. Samples of these mixtures were treated at different temperature and at different age up to one year. The phase composition was studies by X-ray diffraction. Compressive strength and restrained expansion was studied, too. The most significant finding was in his own words: "that since loss of ettringite crystallinity at about 100°C, as determined by XRD, did not affect either compressive strength or expansion significantly, the thermal stability of ettringite in this temperature range do not need to be a concern for repository sealing use of cementitious mixtures. Other findings were: **a)** Some ettringite was destroyed at about 75°C while that in other mixtures persisted to about 100°C. The higher stability seemed to relate to impurity, but this could not be definitely proved by XRD. **b)** If a long-term source of alumina is available and other necessary ingredients are present, new ettringite may continue

to form for at least a year. **c)** Once ettringite had been destroyed by heat, it did not tend to reform under moist storage conditions at room temperature. **d)** When ettringite was destroyed by heat, tetracalcium aluminate monosulfate-12-hydrate (monosulfoaluminate) did not replace it. Instead there was sometimes formation of hydrogarnet after heating to 100°C. **e)** Conversion of ettringite to chloroaluminate in the mixtures containing salt ranged from none to complete at 23°C with some coexistence for a year. In no case did ettringite replace chloroaluminate".

2.12 The third work of the last subdivission is written by Jambor about pore structure and strength of hardened cement paste. Pore structure is an unseparable of the production processes of the cement paste, and in this sense that this work was made, and his principal objective is a connection between strength and porosity. The early works said that the strength decreases very rapidly with increasing porosity. When it is increasing w the unfavorable influence is expressed by the well known formulas of Feret, Abrams, and Bolomey. The influence of porosity in strength are given by the formulae of Powers, Schiller and Ryshkewitch. But because the greath variability of the cement respect to the total porosity and the pore structure which change with time and in dependence on their cure conditions. Porosity and pore structure and his relation to the strength is the aim of this work. A variade group of selected cement pastes with various water-cement ratios was prepared by the author with the effective method of compacting the pastes in various ways. The pore size distributions is analized in a high pressure mercury porosimeter, and presented by the value of his average pores radious. The specific surface of the tested pastes was determined by the BET method and nitrogen was uses as the sorption gas. The values of the bound water in the linding hydration products were determined by the complex thermal analysis and are identical with the ignition loss in the temperature range of 100 to 450°C. Two formulas (3) and (4) allow to predict the changes of the porosity of hardened cement pastes - in dependence of their curing time. Provided no microcracks and additionally created pores in the hardened cement composite are present, its total porosity P in every stage of its hardening way be expressed by formula

$$P = P_o - \Delta V_{hp} \tag{3}$$

where: P_o is the theoretical initial porosity the value of which is given by the sum of the volumes of mixing water (V_w) and air voids (V_v) in a volume unit of the composite inmediately after its compaction, i.e., $P_o = V_w + V_v$ and ΔV_{hp} is the difference between the volume of the developed hydration products (V_{hp}) and the volume share occupied by the hydrated cement in its original unhydrated state in the volume unit of the composite (V_{hc}), i.e., $\Delta V_{hp} = V_{hp} - V_{hc}$. This difference corresponds to the volume increase of the solid phases in the volume unit of the composite due to the hydration process. The results of a great number of hardened cement pastes made of portland cements with different w/c ratios and cured for different time period in water at 20°C showed, that the volume increase of the solid phases due to the cement hydration ΔV_{hp} in the volume unit of hardened cement pastes may be roughly expressed by

$$\Delta V_{hp} = A \cdot w/c \; - \frac{B}{\sqrt{T} + \frac{B}{A \cdot w/c}} \tag{4}$$

where A is a coefficient depending on the cement composition, the value of which in case of portland cements is approximately 68.4; the product A·w/c is then the maximum possible volume increase of the solid phases that may be achieved in the cement pastes with given w/c after their long term curing in water at 20°C; B is a coefficient depending mainly on the class and fineness of cement, its value for portland cement of class 400 is approximately 17.1; T is time period of curing in water at 20°C in days. Finally the porosity (P)- strength (S) relationship is given by formula (5)

$$S = K \frac{\sqrt{P_o - P}}{P \cdot w/c} \tag{5}$$

where P is the total porosity in the time of test, P_o is the initial porosity as it has been defined above, and K is coefficient, the value of which

depends on the type and activity of cement, on the curing conditions, on the dose of cement in a volume unit of the composite and also on the type of test specimens. The comparison of the experimental and calculated values of the compression strength of the tested cement pastes confirms a satisfactory accuracy of this formula.

2.13 The fourth work of this last subdivission and the thirteenth of the sub-theme is by Ping and Yiun-Yuan and deals with the intrinsic properties of hardened cement pastes (HCP). The fracture strength depends on porosity in a way that the fracture strenght at zero porosity is a parameter in such a well known expression as:

$$\sigma = \sigma_0 (1 - P)^A$$
$$\sigma = \sigma_0 e^{-BP} \qquad (6)$$

where P is the total porosity and σ_0 intrinsic strength at zero porosity, A, B are constant. Or the more recently

$$\sigma = \left(K_1 K_2^{K_3+K_4}\right)\left[K_2^{K_3(W-1)}(1-P)^{K_3 W+K_4}\right]\left(\frac{1-P}{1+2P}\right) \qquad (7)$$

where W is the factor of relative specific surface area of the pores, and $K_1 \sim K_4$ constants depending on intrinsic properties of hardened cement paste, furthermore $K_3+K_4 \approx 3$. Formulaes (6) comes from ceramics, formulae (7) comes from some Weibull statistics consideration, the three formulaes involved the intrinsic strength σ_0 at zero porosity. The objective of this study is to correlate the intrinsic strength σ_0 in hardened cement paste and its mechanical behaviour, σ_0 can be changed by altering the molecular weight distributions of silicate in C-S-H gel by addition of inorganic complex ions and/or organic silane coupling agents to hydrating cement pastes. Low porosity samples was prepared by compactation of a cement with a w/c $\approx$ 0.1 and them cured in water. Gel permeation chromatography, compressive strength, splitting tensile strength, amounts of non-evaporable water, pore size distributions by mercury porosimetry, fracture parameters as G_{IC} (fracture toughness), K_{IC} (critical stress intensity factor) and B (index of brittleness, defined by the irrecoverable dissipated energy of the specimen during the test up to maximum load), SEM and (EPMA) electron microprobe analysis, are the experimental technique used in this work. So it is obtained samples between 5.17 and 1.63 $cm^3/g \cdot 10^2$ total pore vol. The degree of silica polymerization (DSP) did not mean progress of hydration, but can change the intrinsic properties. The conclusions of the authors are: "(1) Both pore structure and intrinsic properties of HCP play an important role on its mechanical characteristics. This intrinsic properties can be modified by the DSP in the microstructure of HCP; (2) The DSP can be increased by addition of inorganic complex ions Fe^{++} and Cu^{++} and organic coupling agents VTES (CH_2=CH-Si (OC_2H_5)$_3$) and MDES ((CH_3)$_2$Si(OC_2H_2)$_2$) to cement during its hydrating. Mechanical strength develops with increasing the DSP. The lower the porosity of HCP is, the more sensitive is the influence of the changing of DSP on its mechanical strength; (3) The increase of DSP greating improves its index of brittleness. On this basis, they obtained a high strength and low brittleness HCP which is named by their polymerized silicate cement (PSC)."

2.14 The fourteenth work by Beaudoin, Feldman, Baron and Conjeaud is about the dependence of degree of silica polimerization and intrinsic mechanical properties of C-S-H on C/S ratio. Synthetic C-S-H compositions were produced in aqueous solutions containing variable proportions of sodium metasilicate and calcium oxide. The objective of this investigations was to determine in six C-S-H prepared compositions, the degree of polimerization, adsorption characteristcs and intrinsic mechanical properties on C/S ratios. Silica polymerization measurements was made with the method developed by Parrot and Taylor; weight and length change isotherms; porosity measurements, modulus of elasticity measurement, microhardness measurement, was made too. The conclusions obtained by authors are: "1. Degree of polymerization of C-S-H depends on C/S ratio. It decreases as C/S ratio increases. 2. Synthetic C-S-H materials prepared using sodium metasilicate solutions are generally layered systems. Irreversible length and weight change characteristics on exposure

to water vapor are due to intercalation processes and aging phenomena. 3. Zero porosity values of modulus of elasticity and microhardness for the C-S-H preparations studied appear to be independent of C/S ratio. As microhardness generally correlates with strength, values for intrinsic strength would appear to be independent of C/S ratio over the range studied. 4. Highest values of modulus of elasticity were obtained for the preparation (C/S = 1.26), which exhibited reversible sorption characteristics in the low pressure region of the water isotherm. Intercalation processes and their effects on the proximity of silicate sheets may have a greater effect on intrinsic mechanical properties than composition and/or degree of poymerization".

2.15 The last work of this sub-theme by Eden and Bailey is about the crack tip processes and fracture mechanism in hardened hydraulic cements. The problem in examining crack tip processes in hardened cement paste is solved utilizing the transluscence of cement pastes and the ability of fine cracks, about 0.1 μm wide to scatter transmitted light. By the use of this technique in conjunction with a straining stage, the following conclusions by the authors are obtained: "1. Stable cracking of portland cement materials is observed to proceed in a single, ralatively straight, path. 2. Fracture mechanics indicate that this stable crack growth is the formation of a process zone, which grows to a characteristic size before failure occurs. 3. The process zone can be described mathematically in terms of a "tied-crack" model. 4. The most direct interpretation of this is that fracture of portland cement materials occurs by the parting of two-dimensional hydrate particles, primarily by shear across their interfaces."

3. GENERAL DISCUSSION OF THE WORKS

General objective of science, in order to prove the truth of the models with which they describe a definite branche of phenomenology, is to obtain the same parameters, which describes the models, from independent paths. Here we can have some examples and if it is added the obtention of certain features with technical utility, progress in this branch of the science is secure. In this brief general discussion, we intend to give some examples from the works described and discussed individually before and taken now as a whole.

In the first work (1) by Vollet and Craievich it is suggest that hydration of C_3S paste is controlled by a diffussion mechanism. Another work where hydration kinetics is used is by Cebeci (3) where hydration is studied by the measure of the nonevaporable water content. The figures obtained by Cebeci means a diffussion mechanism with a great velocity in the first stages of production of the hydrated material, which is in contradiction with the model of Vollet and Craievich which means as zero velocity of hydration when at the begining of the reaction. Both facts are in contradiction and further investigation must be made in order to put in accord with some model the experimental facts which always remain. Chpynova, Ilioukhine, Sanitsky and Melnik (4) describe a model of hydratation which is a topochemical reaction governing by diffussion. In his study of the microstructure of a very old cement paste Scrivener (5) describe facts which are in accord with a topochemical reaction governed by diffussion. So we have four coincident opinions about that hydration is governed by a slow diffussion mechanism. This concepts about hydration corresponds to the main phase which is tobermorite, when it is speaking of ferrite phase as Negro, Montanaro and Bachiorrini (2) the model must be another. Because this reaction is very complexe it is necessary further investigations in order to make a quantitative model.

About the mmorphology of the C-S-H the dimensions give by Henderson and Bailey (6) are in accord with the data of Vollet and Craievich (1) and the method of investigations are quite different.

It is an accord that a gypsum-free cement, as it was detected by Skvára (7), have a hight strength, which can be found in the work of Isozaki and Nakagawa (9).

In this enumeration the work of Kurdowsky and Miškiewicz (8) is isolated, because any other deals with a silica calcium chloride. In the same sense the work of Lach (10) and Buck (11) can not be compared with other in this sub-theme.

Pore structure is treated by Jambor (12) with formulaes which comes from cement investigations, Ping and Yiun-Yuan (13) made an approach that coming from ceramic research, and is necessary further discussion to put in accord this different point of views.

In the work of Eden and Bailey (15) it is find that fracture occurs primarily by shear between the S-C-H particles, where bonding is weak, in consecuence, like Ping and Yiun-Yuan (13) made, strength must be increased by bonding these particles with a polysilicate.

More extense discussion of the very interesting work in this sub-theme must be avoided by a lack of space and time. Words, sentences and paragraphs of the original works must be used, because this lack of time; finally we acknowledge the colaboration of G. Díaz and our secretary M. E. Lillo, without them this discussion can not be written.

Errata: To add in the asterisks:

* 1.- E. HENDERSON and J. E. BAILEY - United Kingdom
* 2.- in function of time. They show that exists a relation between expansion of mortar and the amount of ettringite.
* 3.- structure. The retention of this foil-like molecular

Addenda

After this report was finished, two work arrived, one from Brazil-Japan and the other from Denmark. The two works are:

16.- "The dispersion model for hydration of portland cement.II. The influence of fineness".
T. KNUDSEN - Denmark.

17.- "Hydration characteristics and properties of mixture of cement and high content of calcium*
Y. TEZUKA and J. G. DJANIKIAN - Brazil and
H. UCHIKAWA and S. UCHIDA - Japan.

2.16 In the dispersion model for hydration of portland cement with special emphasis on the influence of fineness Knudsen obtains some interesting results. It is suppose that the hydration of a single grain with size r follow the equation:

$$\alpha(r\ ,\ t) = \exp\ (-r/kt) \qquad (8)$$

where k is the rate - constant corresponding to a linear kinetics reaction mechanism and t is the time, it is suppose too that the particles size distribution followed the Rosin-Rammler's equation

$$F(r) = 1 - \exp\ (\frac{-r}{r_o}) \qquad (9)$$

where r_o is the fineness constant. By integrating over all grain sizes

$$\alpha(t) = \int_o^\infty \alpha(r\ ,\ t)\ d\ F(r) = \frac{t}{t+r/R} \qquad (10)$$

The experimental results are in accord with this formula (10) but with an inicial time t_o

$$\alpha(t) = \frac{t - t_o}{t - t_o + r/R} \qquad (11)$$

t_o is the normal period, which is about 6 $\pm$ 2 hours for w/c= 0.5, k= 0.54 μm/h. This theory, which connect the particles size distribution with a kinetic reaction of a particle, can be put in accord with the others theories of kinetic hydratation discussed before.

2.17 In the work of Tezuka, Djanikian, Uchikawa and Uchida a cement with high content of calcium sulfate was studied, the hydration products detected by powder X-rays diffraction were ettringite monosulfate hydrate and calcium hydroxide. The calcium hydroxide increased with age. With natural gypsum : mixture, no monosulfate detected and ettringite increased with age. On β heminydrate mixture, the calcium sulfate dehydrate appeared before one day and increased little after this age. With anhydrite mixture, calcium sulfate dehydrate produced increased with age, but even at the age of 28 days, there remained anhydrite still not hydrated. The kinetics of the hydratation studying by the amount of combined water give figures similar to the obtained by Cebeci (3). Unfortunately the largest amount of calcium sulfate produced a fall in the strength, in some cases so much that they have practically non strength. Clear scanning electron micrographs illustrated the work. This work belong to the second group were morfology is the principal aim.

* sulfate".

Paulo J. M. Monteiro Companhia de Cimento Portland Paraíso Brasil

2.3

Communication Report Bond Paste - Aggregate, paste-reinforcement and paste-fibers

The importance of how well a cement paste would "bond" with an associated material has been realized by researchers and practical engineers for some time. However, its study proved to be very complex. It is interesting to note that this difficulty happens in most of the research levels. At the engineering level, the different thermal and elastic properties of the many phases in concrete, create stress concentrations precisely at the interfacial zone. At the microstructural level, the interface between the cement paste and associated materials creates a transition zone in the paste with unique properties.

The difficulty of this topic is again shown by the smaller number of communications than other sub-themes: it takes a long time to develop new methods of analyzing the bond in concrete.

In this section, the following communications were presented:

Distribution of Ca(OH)2 and of the CSH phase in the Oolithic marble/hydrated cement paste interfacial zone; by Chen Zhi-Yuan and Zhang Xio-Zhong.

A preliminary study of the microstructure of the cement/sand bond in mortars; by K.L. Scrivener and P.L. Pratt.

Improvement of paste-aggregate interface by adding silica fume; by Wang Jia, Liu Baoyuan, Xie Songshan and Wu Zhongwei

Improvement of the aggregate-cement paste transition zone by grain refinement of hydration products; by P.J.M. Monteiro and P.K. Mehta.

Effect of pretreatment of aggregate surface on the properties of concrete; by Wu Xuequan, Han Sufen, Bian Qinghan, Tang Mingshu.

Microcracking propagation in flexural loaded portland and high slag cement concretes; by G. Frigione, B. Marchese and R. Sersale.

Durabilite de la liason acier galvanise--pate de ciment portland; by G. Arliguie and J. Grandet.

Investigations on the Zinc/Hydrated cement paste interfacial zone; by Chen Zhi-Yuan and Zhang Xio-Zhong.

Bond in cements reinforced with bundles of fibres; by P. Bartos.

Compatibility of copper fibre with compacted cement and low thermal-shock fatigue thereof; by P. Kittl and G. Dias.

Next some of the main contributions presented by these authors will be highlighted:

Yan and Zhong used the differential scanning calorimetry and the gel chromotography to study the distribution of CH and CSH phase in the Oolithic marble--cement paste transition zone. It was shown that the larger quantities of the hydrate phases are located closer to the interface and the reason is the existence of a water film at the interface. These results seems to support the through--solution type of hydration.

Evidence that the marble reacts with the cement hydration products is given by scanning electron microscopy of the marble surface which is "corroded", indicating a dissolution of the calcite.- An interesting result is that the CH content in the vicinity of the marble surface decreases with longer curing time for pure portland cement paste. No explanation is given to this fact, however the writer would like to mention that this is expected according to Monteiro and Mehta's theory in which the CH reacts with the calcite, with time, in the transition zone.

Additions of silica fume increased the cleavage strength and it was shown that the CH content in the transition zone decreased when silica fume was added.

The data indicated a difference in the degree of the CSH within the transition zone and the bulk paste. In the former the CSH has a higher degree of polymerization than in the bulk paste.

Jia et al. studied the mean size and orientation index of CH and AFt in the transition zone. Also the fracture energy and microhardness at the interface were investigated for pure portland cement and with of silica fume.

The experimental results indicate that the mean size of AFt crystals decreases with increasing distances from the interface. Also the mean size and range of variation decrease with w/c ratio.

Additions of silica fume to the cement paste reduce the size of the CH crystals.- It is shown that with silica fume additions, the microhardness and effective fracture energy increases.

The authors propose that during early cement hydration, the fine particles of silica fume play the same part as nuclei on which CH germs attach. Over time, the silica fume reacts with the CH crystals producing CSH.

Scrivener and Pratt studied the microstructure of the cement paste/sand interface using secondary electrons to analyze the fracture surfaces and backscattered electron imaging to analyze flat polished surfaces. The results indicate that, at early ages, a layer of CSH forms on the

surface of the sand grains by a through-solution mechanism. This same mechanism of hydration is responsible for the precipitation of AFt around the sand grains. This study showed that a much higher concentration of AFt is observed in the interfacial region, in agreement with the published literature. The authors concluded that there is no evidence for the formation of an epitaxial layer of calcium hydroxide around the sand grains. They, also, suggested that the specimen configuration in which cement paste is cast against a large flat piece of aggregate may lead to localized bleeding along the interface, resulting in anomalous results.

Monteiro and Mehta discussed three cases where an improvement of the aggregate-cement paste transition zone was achieved by grain refinement of the hydration products. The main idea is that the strength and durability of concrete could be enhanced if the large grains of calcium hydroxide present in the transition zone are either eliminated or reduced in size.

The first case studied the grain refinement that occurs when condensed silica fume is used. It was shown that the thickness of the transition zone is remarkably decreased when condensed silica fume is used. Also, SEM studies showed the existence of a pozzolanic reaction between the CH film and the condensed silica fume particles.

The second case analyzed the transition zone with type K cement. It was shown that when type K cement is used, small CH crystals are precipitated with a random orientation on the top of a discontinuous CH film. Therefore, there is a CH grain refinement in the interfacial zone.

The third case studied the grain refinement which takes place when instead of silicious rock, carbonate aggregate is used. The authors proposed that the strengthing of concrete, when carbonate aggregate is used, is due to an interaction between CH and calcite, rather than due to the formation of carboaluminates hydrates.They also suggested that the transition zone improvement is due to the replacement of large CH crystals by small crystals of a basic calcium carbonate.

Xuequan et. al. studied the effect of pretreatment of aggregate surface on the properties of concrete. The authors studied the following solutions for aggregate pretreatment: dilute sulphuric acid, alum. solution, sulfuric acid and alum. solution, acidized sodium silicate solution, alum. and water glass solution, sulphuric acidized cement suspension. Silicious and calcareous rocks were used as aggregate.

The results indicate that the mechanical strength of mortars and concretes with pretreated aggreagates are higher than the ones with inert aggregates. This improvement is a result of a combination of physical, chemical and mechanical interlocking effects.

Frigione et al. presents interesting experimental results on the microcracking propagation in portland and high slag cement concretes. Their approach to correlate the mechanical properties of both reinforced and plain concrete to the existing microstructure is commendable and it should be encouraged.

It is shown that high slag cement concretes have a different cracking behavior when compared to pure portland cement concretes. The former has under increasing loads, progressively more cracks with a moderate width ; and the latter develops an approximately number of cracks swiftly growing with stress. It should be mentioned that steam curing decreases these differences.

This cracking behavior may be associated to the different transition zones when high amounts of slag are used. The reduction of the calcium hydroxide in the transition zone for the slag concrete may explain the higher adhesion paste-aggregate. Also, the unreacted slag particles can act as crack-arrestor, causing frequent interruption of the fracture process and preventing the widening of the cracks.

Zhi-Yan and Xio-Zhong studied the zinc/cement paste transition zone using XRD, SEM, EPM and DSC. The results showed that the calcium hydroxyzincate is found mainly in the region 0-10 um from the interface. When silica fume is used the intensity of the Ca-zincate peak declined probably because of a smaller supply of the CH for the formation of the Ca-zincate.

The study of the durability of the galvanized steel and portland cement paste transition zone was studied by Arliguie and Grandet. They showed that a plate of zinc with one extremity embedded in concrete and the other exposed to the atmosphere for six years had a very good bond between the metal and the concrete.

XRD analysis demonstrated that the calcium hydroxyzincate is very stable in an environment containing carbonic gas.- This is an important fact because the penetration of carbonic gas in concrete is one of the main factors of non-galvanized steel corrosion.

The calcium hydroxyzincate is also very stable to the action of chlorides.

TDA analysis of the calcium hydroxyzincate shows that it decomposes in the following sequence:

150-190 C: progressive elimination of the water of hydration

190-200 C: $Zn(OH)_2$ decomposition

480 C: decomposition of CH

Bartos analyzed the pullout modes of failure of glass strands, including aging effects. The experimental program included a comprehensive series of pullout tests for different combinations of matrices, glass fibers, curing conditions and age. The following modes of failure were identified-: (I) complete tensile fracture of the whole strand; (II) complete pullout of the whole strand; (III) intermediate failure mode. The last case could be divided into two different types: (a) combined pullout and tensile failure, (b) telescopic failure. The energy absorption of the fiber bundles failing in these modes was greater than the other failure modes.

It should be mentioned that acrylic polymer increased the bond to such a degree that only very short embedment lengths produced a pullout or a combined failure.- Also, wet curing increased the bond considerably.

The author suggests some criteria to design bundles of fibers to act as reinforcement which can improve both strength and thoughness of the matrix.

Kittl and Diaz studied the compatibility of copper fibers with compacted cement and its low thermal;-shock fatigue resistance. Copper fibers (4% by weight) were mixed with portland cement having a water/cement ratio of 0.04 and compacted by compression.

The authors suggest that the difference in the cement paste and copper thermal expansion coefficients can create microcracks that are able to modify the thermal fatigue behavior, once the can stop the fatigue crack propagation and modify the mean strength. The compacted copper fiber-cement composite withstood 3000 cycles of a thermal shock between 283 K and 373 K with no rupture but only a reduction in the mean strength.

No corrosion was observed in the 2 years old composite samples nor in the ones stored in water at 373 K for 50 hours.

Conclusions

In summary, after analyzing the work presented in this section we can conclude the following:

I) The microstructure of the transition zone created by the interface between the cement paste and a plane of discontinuity (simulating the aggregate) has been well characterized and understood. A summary of the transition zone characteristics for this particular configuration is presented in many review articles, and in this congress it can be found in the principal reports by Massazza and Diamond.

II) The addition of sand particles in the cement paste increases the degree of variables to define the transition zone, because now the interfaces between the cement paste and the rocks have variable radius of curvature and the transition zone around a sand particle may interfere with another transition zone of a neighbor sand particle. Also, because of the sand gradation, it is possible to have distinct localized bleeding around the sand particles, producing transition zones with potentially different microstructures. The understanding of the transition zone existing in mortar is not complete, however the work by Scrivener and Pratt is very promising and more research should be done in this area.

III) The knowledge of the transition zone in concrete is mainly based on the extrapolation of the microstructural knowledge gathered using simplified models. It is expected that some of the basic features already known should apply to the transition zone in concrete: a zone of lower density with a higher concentration of ettringite and calcium hydroxide (some of them with a preferred orientation). However, these hypothesis should be experimentally verified in a more complex system. Besides considering the effect of different sizes and types of aggregates, it is necessary to study the effect of admixtures such as silica fume, slag, fly-ash on the transition zone.

IV) Usually, the aggregate-cement paste interface microstructure tends to receive most of attention. This is somewhat unfair because concrete, in most of civil engineering applications, is used in association with other materials and these interfaces should be equally important. It should be noted, however, that the interface between galvanized steel and cement paste has been well described by the continuous work of the Toulouse research group.

The present writer feels that the study of the transition zone is at a turning point, and, therefore he would like to point out some research areas, where some intense work should be dedicated. Of course, the list is not complete and reflects some of the writer's personal research interests and bias.

I) The interface between the aggregate and the cement paste was studied using very simplified models. The writer feels that the researchers should now take a bold step and analyze the real microstructure existing in concrete. It would be very helpful to understand the kinetics of the transition zone between the paste and the aggregate in a real situation where there is the aggregate gradation, the effect of bleeding, the mutual effect between

aggregates, and air voids.

II) To study the effect of the existing microstructure of the transition zone on the properties of concrete. For instance, it has been taken for granted that the precipitation of CH with a preferential orientation in the transition zone has a deleterious effect on the mechanical properties of concrete because of the "easiness" to cleave along the basal plane; however there is no experimental measurement of this effect in real concrete. Also there is a lack of basic studies on the correlation between the microstructure of the transition zone and the durability of concrete.

III) Most of the work on the transition zone has been on the description of the existing microstructure.- There is a tremendous lack of mathematical modeling. These models are important to establish a scientific framework of study, which can provide sound predictions and guidelines for concrete improvements. The models should also correlate the existing microstructure with the mechanism of crack propagation.

IV) The transition zone with limestone aggregate should be continued to be studied in details, because of the practical applications and because the reaction between the calcite and the hydration products is not yet clear.

V) To study concrete (or mortar) as a complete composite material. The new research should model concrete as a porous-granular material, that is, consisted of discrete particles of rock dispersed in a porous medium. The attraction of this model is that some of the transition zone characteristics (specially a localized higher porosity) could be easily incorporated in the model. Also the inclusion of fibers could be naturally added as another phase, once the pertinent constitutive laws are given.

Finally, it should be understood that concrete is a complex system; one cannot recommend an improvement of a particular property without studying the influence on the other properties. In this sense, concrete improvement has to be dealt as an optimization problem with the adequate constrains. Suppose, for instance, that it is possible to improve the transition zone to such a degree that there is virtually no microcracking there: the concrete most likely will have a greater mechanical strength but the concrete may lose a important energy absorption mechanism and may became brittle. Another example would be the reduction of most of the CH crystals in the transition zone to improve the mechanical properties and creating potential problems of reinforcement corrosion due to the localized PH reduction.

This should not discourage the material scientists and engineers, but, on the contrary, they should unite forces to create a new "material engineering" for concrete.

COMMUNICATION REPORT OF SUB-THEME 3.1: CHARACTERISTICS AND ACTIVATION OF BLENDING COMPONENTS

RC 3.1

1 INTRODUCTION

The sub-theme 3.1 embraces 21 investigations carried out on different materials used as addition to the cement. This fact led us to classify the papers into four different groups according to the type of material. The classification was made only with the purpose of clarifying the comments on the communications.

First Group takes into account the communications about slags, Second Group about fly ashes, Third Group about silica fumes and Fourth Group, about miscellaneous materials. The latter embraces investigations of burnt clays, kiln dust, calcareous filler etc., or two or more types of the former materials.

2 FIRST GROUP: SLAGS

About 48% of the papers were included in this group that deals with investigations on activation of slags, structure and reactivity of slags and slag hydration. The following papers were listed:

- *Dissociation of Aluminium from Slag Glasses and Formation of Ettringite* by LOU ZONGHAN and collaborators, from China.
- *Alkali Activation of Indian Blast Furnace Slags* by P.S.PARAMESWARAN and A.K.CHATTERJEE, from India.
- *Activation of Synthetic Melilite Slags by Alkalies* by J. MALOLEPSZY, from Poland.
- *High Strength Slag-Alkaline Binders* by J.MALOLEPSZY and M.PETRI, from Poland.
- *Hydration of Blast Furnace Slag Particle* by K.SATO and collaborators, from Japan.
- *Some Features about the Slag Structure* by A.A.GOVOROV, from Soviet Union.
- *The Use of Microscopy for Estimating the Basicity of Slags in Slag Cements* by A.F. BATTAGIN, from Brazil.
- *Structure and Reactivity of Glassy Slags* by R. DRON, from France.
- *Physicochemical Principles of the Hydraulic Activity of Blast Furnace Slags* by Y.S. SHKOLNICK, from Soviet Union.
- *The Effect of Hydration Products in Steam Treated Steel Slag on the Hydration of Blended Cement* by WANG YUJI, from China.

2.1 Activation of Slags

LOU ZONGHAN and collaborators suggest that Al_2O_3 plays an important role on slag activity. As Aluminium dissociation and the formation of ettringite are closely related, they consider this fact an important parameter in the study of slag cement hydration mechanism. In a solution with different pH values, Aluminium will exist in the form of AlO_2^- or Al^{3+} or $Al(OH)_3.Al^{3+}$ ions in the slag glasses are four fold co-ordinated but after

the slag is attacked by alkalies, the co-ordination state of Al^{3+} changes to six fold co-ordination. Simultaneously, bridging Oxygen in glass network changes into non-bridging Oxygen. As a result, the network structure is broken. After the slag glass is attacked, the hydrate products, ettringite and C-S-H gel will form rapidly by the surface reaction between the slag glass and alkaline solution and this fact will promote the dissociation of slag glass. According to the authors, the change in the state of co-ordination of Aluminium is a result of alkaline activation. As only after this change of Aluminium co-ordination ettringite will form by the sulphate activation, the authors concluded that sulphate activation factually does not exist.

PARAMESWARAN and CHATTERJEE reported studies on alkali activated Indian slags with high alumina contents (20-24%) and low lime contents (30-35%). Experimental results showed that strength development patterns depend on the slag glass content, slag fineness and on optimisation of the activator dosage. They concluded from an exhaustive study that for the slags under consideration, an activator mix of 1% Na_2CO_3 + Na_2SO_4 + hydrated lime is practically as effective as the optimum dosage of the caustic NaOH, the former being easily handled and used.

Investigations of *MALOLEPSZY* revealed that compressive strength of hardened slag pastes depends first of all on the type of alkaline activator. Tests carried out on synthetic melilite slags with different compositions showed that Na_2CO_3 is especially suitable for activation of melilite slags rich in C_2MS_2 (akermanite) and NaOH for activation of melilite slags rich in C_2AS (gehlenite). It was also concluded that autoclaved pastes made from gehlenite slags attained the highest strengths.

In other communication, *MALOLEPSZY and PETRI* showed by means of X-Ray Analysis and Scanning Electron Microscopy (SEM) that reaction products of Na_2CO_3 activated slag are C-S-H, calcite and a zeolite-type mineral. Using a water glass as activator, the same products were obtained but the stage of slag reaction was higher. Consequently, the contents of C-S-H phase and zeolites were also higher. The more compact structure of C-S-H gel and smaller porosity assure the higher values of compressive and bending strength in the case of water-glass activation.

SATO and collaborators investigated the factors affecting the hydration of slag particles, as for example, the particle size, the surface area and the kind of activator. They pulverized a slag to a Blaine specific surface of 3720 cm^2/g and separated it into five samples. The thickness of the hydrated layer with respect to each sample was evaluated by means of the particle size distribution and the rate of hydration. The latter was obtained after the activation of the slags by NaOH, $Ca(OH)_2$ or OPC and the dissolution of the hydrated parts by a salicylic acide-acetone-methanol solution. They concluded that the thickness of the hydrated layer on slag particles does not depend on the particle size. The rate of hydration depends only on the total surface area. It was also suggested that the difference between NaOH and $Ca(OH)_2$ in activating capacity is not noticeable up to 3 days but the NaOH effectivity is greater after 7 days. On the other hand, OPC activating capacity is always greater, especially in the early stages.

2.2 Structure and Reactivity of Slags

GOVORCV reported experiences carried out on many slag samples that confirmed the important role of potential crystalline phases (related to the vitreous matrix) and its structure as factors that influence the slag hydraulic activity. Effectively, through the equilibrium diagram for the quaternary system $CaO-MgO-Al_2O_3-SiO_2$, the chemical

composition and the potential mineralogical composition, the author determined the S + A contents (percent by mol). Four different technological slag types were classified according to their S + A contents, that is, Martin process slags presented less than 40% S + A; blast furnace slags and slags produced in the manufacture of phosphorous, between 40% and 50% S + A; acid steel slags and slags from the smelting of copper and nickel with more than 50% S + A. By means of potential mineralogical composition determination and infrared analysis, *GOVOROV* found out that in slags with 40-50% S + A contents, the structural unit was the $Si_2O_7^{6-}$ (melilite, mainly), with 50-60% the structural unit was $Si_3O_9^{6-}$ (pseudowollastonite, mainly), with 60-65%, it was the anorthitic chain $Si_2Al_2O_8^{2-}$ or pyroxenitic SiO_3^{2-}. In slags with more than 65% S + A, the structural unit was the silica tetrahedron (tridymite). Therefore, the S + A contents are related not only to the different technological kinds of slags but also to their structural units. Different structural elements and different S + A contents influence the rate of silica dissolution under water action and the compressive strength.

BATTAGIN reported the existence of a close relationship between the chemical composition and the refractive index of granulated blast furnace slags. The determination of the latter may give information concerning the basicity of the slags, base of the most current methods of slag quality control. By means of the linear regression analysis, an attempt of correlating the refractive index of slags to the most usual chemical moduli resulted in correlation coefficients ranging from 0.96 to 0.99. Simultaneously, r values of 0.91, 0.86 and 0.87 were obtained correlating the refractive index of slags to the compressive strength of laboratory slag cements at 7, 28 and 90 days, respectively. In addition, the method proved to be advantageous due to the fact that it can be applied to slag cement samples, where chemical methods are limited, requiring previous and laborious slag separation.

DRON studied the slag structure by means of Raman Spectroscopy Analysis carried out on sinthetic glasses obtained after fusion at 1600°C and quenching of mixtures of pure oxides. He suggests that the glass structure is an instantaneous configuration image of the liquid after the quenching. The author proposes the concept of acid-base, that is, the characterization of the mean liquid by the parameter pO^{2-} that is similar to the pH of water solution. The pO^{2-} can be deduced from Raman Spectroscopy Analysis which originates bands that are typical of the structural elements SiO_2(X), $SiO_{2,5}$(Y), SiO_3^{2-} (E), $SiO_{3,5}^{3-}$(Z) and SiO_4^{4-}(S). The glassy slag structure is characterized by a silicatic anionic *sub-network* made of SiO_3^{2-} units between $SiO_{2,5}^{-}$ and $SiO_{3,5}^{3-}$. The bond between the silicium and bridging or non-bridging oxygen atoms is covalent. Calcium, Magnesium and Aluminium (AlO^{+}) form, in their turn, cationic *sub-networks*, without internal bonds. They are self connected by electrovalent bonds. The two *sub-networks* form together the vitreous network whose bond are made by the Silicium, Calcium, Magnesium and Aluminium atoms. These atoms are bound by means of Oxygen atoms. Thus, the type of bond can be covalent or electrovalent. The latter constitutes the weaker points of the network and plays an important role in the slag reactivity. The reactivity of the glassy slag is due to its solubility in basic solutions, generally higher than the solubility of the hydrated phase originated from the hydration itself. The reactivity can be measured by means of slag solubilization in an aqueous 0.04N Sodium Hydroxide solution. On the other hand, it can be also known through the index:

$$R' = \frac{Al_2O_3.CaO}{(Al_2O_3 + SiO_2)^2},$$

which presents a good correlation to both the slag solubility and the compressive

strength. A slag of satisfactory quality has a reactivity index higher than 0.18.

According to *SHKOLNICK*, in modern methods of producing granulated slags, water cooling is mainly used. As a result, the hydrolysis of Calcium Sulphide occurs, with losses that might be up to 20-30% of initial sulphur content in the melt. Experiments carried out by adding different amounts of S^{2-} into slag samples at constant $\frac{CaO}{SiO_2}$ ratio showed an influence on slag reactivity. This influence is advantageous up to 2 - 2,5% of S^{2-}, that is, its solubility range. A further increase in its content has no effect on hydration. *SHKOLNICK* explained in his communication that this fact might be attributed to S^{2-} entrance into glassy slag structure. Within its solubility range, S^{2-} forms Si-O-Ca-S groups in which the binding energy Si-O-Ca is reduced because of the most covalent character of Ca-S bond. He concludes *In view of this it seems desirable to use air or, still better, inert gases for cooling slag melts*. Due to the reduction of sulphur losses, this would improve both the slag quality and the environmental conditions.

2.3 Slag Hydration

WANG YUJI presented the results of an investigation carried out on steel slags and blended cements made from these slags. To prevent unsoundness due to free lime hydration, slags must be treated by steams or water. By means of *SEM*, the author found out that steel slags treated in steams under different pressures for different periods originate, in their turn, different amounts of $Ca(OH)_2$ and C-S-H with different morphologies. Irregular round particles of $Ca(OH)_2$ were found under lower pressures and shorter time. With the increase of pressure and time, $Ca(OH)_2$ crystals enlarge in size and gradually change from irregular into regular hexagonal shape. Calcium silicate hydrates are chiefly fibrous and needle-like.

When the treated steel slag is used for making blended cement, the hydrates formed during the steam treatment process will decrease the cement initial hydration rate. On the other hand, they will promote the hydration of unhydrated particles of blended cement in later stages. As a result, the compactness of the hardened cement paste will increase and, therefore, the strength at later stages also will increase. The optimum condition of steam treatment for steel slag is supposed to be 1-3 atm pressure of satured steam for a time below 3 hours. In such condition most of free lime will hydrate while the degree of hydration of slag silicates will be inexpressive.

3 SECOND GROUP: FLY ASHES

About 14% of the papers were included in this group that deals with investigations on fly ash reactivity, activation and hydration. The following papers were listed:

- *The Evaluation of Pozzolanic Reactivity of Fly Ashes* by H. SHIYUAN and C. JIPING, from China.
- *Effects of Fly Ash Grinding on the Hydration and Strength Development of Fly Ash Cements* by H. CHENG, from China and B. OSBAECK, from Denmark.
- *Reaction Process and Microstructure in Compacted Fly Ash and Fly Ash-Chemical Additive Mixtures* by M.KAWAMURA and collaborators, from Japan.

3.1 Fly Ash Reactivity

SHIYUAN and JIPING have investigated seven fly ash samples selected from various Chinese power stations. By dissolving mixtures of fly ash - CaO (ratio 4:1) and fly ash - cement (ratio 3:7) into 2N hydrochloric aqueous solution at different times, they calculated the fly ash reaction degree. The fly ash reaction degree, that is, the amount

of dissolved fly ash at a defined time, seems to possess a good correlation with the strength of fly ash - $Ca(OH)_2$ and fly ash - cement pastes. Although the fly ash reaction degree has a good correlation with the fly ash-cement paste strength, its determination demands a long time. Thus the method is not suitable for practical uses. However, the pH value of the liquid in fly ash suspension in deionized water was found to have some correlation with the fly ash reaction degree and in its turn, with the compressive strength. Measurements of pH values of fly ash suspensions might be taken as a simple and rapid method for comparative evaluation of the pozzolanic reactivity of fly ashes.

3.2 Fly Ash Activation and Hydration

CHENG and OSBAECK reported experiments carried out on a Danish coarse fly ash (specific surface of about $200m^2/kg$) that was ground to $450m^2/kg$ and $650m^2/kg$. The three materials were tested on fly ash - cement mixes with 10, 20 and 30% of fly ash replacement. When fly ash was ground, three major changes in its physical caracter were detected: its fineness was increased, there was an increase in the density due to the crushing of hollow particles and there was a change in particle shape, running away from the predominant spherical shape. These changes affected cement properties and characteristics like setting, water requirement, strength development, etc. With regard to the latter, it was shown that fly ash grinding can lead to an expressive increase of fly ash cement strength at all ages. This fact is probably due to an enhancement of the rapid aluminate reaction taking place just after the induction period, an increased pozzolanic reaction corresponding to the lime consumption, a decreased content of air entrained and a reduced intrinsic porosity of the fly ash.

KAWAMURA and collaborators investigated the microstructure of three fly ashes produced from the burning of pulverized bituminous coals. The investigations were made by means of *SEM*, X-Ray Diffraction Analysis, Differential Thermal Analysis and pore size distribution determined by Mercury Porosimeter. When usual bituminous fly ashes were compacted at an appropriate moisture condition, they exhibited a slow hardening property, the same occuring to fly ash - chemical additives mixtures. From the results obtained in their study, the authors concluded that the hardening property exhibited by compacted fly ashes was supposed to be derived from the free lime and anhydrite contained originally in the fly ash. The reaction for the formation of ettringite actively occurred in compacted fly ashes. The addition of hydrated lime and gypsum effectively promoted the formation of ettringite in compacted mixtures. The strength of compacted fly ash--hydrated lime and fly ash-hydrated lime--gypsum mixtures is closely related to the amount of ettringite and to the changes in pore size distribution. However, there was a poor correlation between strength and the amount of ettringite in compacted fly ash-portland cement mixtures. The needle-like crystals of ettringite produced on the surface of fly ash particles appear to contribute to the strength development of compacted fly ash mixtures due to the densification of their structure.

4 THIRD GROUP: SILICA FUMES

About 10% of the papers were included in this group that deals with investigations on silica fume characteristics and reactivity. The following papers were listed:

Influence of Elements (Si, Al, K, Na, Ca, Cl, C) in the Reactivity of Condensed Silica Fume by P.C.AITCIN, from Canada and A. CARLES - GIBERGUE, N. OUDJIT and A. VAQUIER, from France.

. *Blended and Special Cements Incorporating Condensed Silica Fume* by K. POPOVIC, from Yugoslavia.

4.1 Condensed Silica Fume (CSF) Characteristics and Reactivity

AITCIN and collaborators studied 18 silica fumes from different origins. The materials are by-products of manufacture of silicon, ferrosilicon and other silicon alloys and have different chemical composition (SiO_2 ranging from 96% to 23%). Physical properties are also variable, specific surface area ranging between 7500 and 24000 m^2/kg and bulk density between 125 and 600 kg/m^2. The authors concluded that both the CSF dissolution by pure water and the pozzolanic activity (amount of fixed lime in mortar) depend mainly on the glassy silica contents. The specific surface area influences very little the rate of pozzolanic reaction. Three samples did not exhibit typical pozzolanic behaviour. CSF-16 is an inert material due to its low glass contents. CSF-8 has a low pozzolanic degree due to the presence of carbon recovering the reactive silica glassy phase, this fact promoting the decrease of the reaction rate. The elimination of carbon by heating improved the pozzolanic activity. CSF-15, due to its low silica contents and low vitrification degree, showed a low capacity of fixing hydrated lime. On the other hand, it showed a typical behaviour of hydraulic binder due to the presence of hydrated lime and dicalcium silicate in its composition.

POPOVIC and collaborators carried out experiments to find out the influence of different forms of condensed silica fume on cement properties. By comparing test results of cement samples prepared by addition of original very fine silica dust to portland cement, ground pellets of CSF to portland cement, predensed dust to portland cement and laboratory and industrial interground PC clinker and CSF pellets, they concluded that the silica fume has a positive influence on cement properties. Although some previous experiments had showed that specific surface of predensed dust was approximately one half of the original fine dust surface (for ground pellets even one third of dust) and that the pozzolanic activities of these two forms were reduced in the same proportion, the increase in cement later strengths was still significant. In addition to this, the water requirement and drying shrinkage of such cements were not so high as those caused by very fine original silica dust. This material also presented problems of handling and transport due to its inconvenient physical characteristics. According to the authors the more acceptable properties of cements incorporating ground pellets or predensed dust can be explained by the particle agglomeration. This fact reduces the active surface of silica particles and therefore their water requirement. It seems, however, that the bonds among silica particles in agglomerated grains are not so strong to hinder the pozzolanic reaction which contributes to strength and durability of hydrated cement pastes.

5 FOURTH GROUP: MISCELLANY

About 29% of the papers were included in this group that deals with investigations on blended cement composition, particle size distribution of calcareous filler, clay mineral activation, properties of blended cements with kiln dust mixtures, etc. The following papers were listed:

. *Generalized Method for the Determination of the Composition of Portland Cement Mixtures with Additions* by F.GOMA, from Spain.

. *Particle Size Distribution in Blended Cements* by D.M. SORRENTINO, from France.

. *Particle Size Distribution and Specific Surface Measurements of Components of Co-ground Blended Cements: Application to Fillers and Slags* by J.P. BOMBLED and collaborators, from France.

. *Various Activation Means of Potentially Pozzolanic Materials: Application to Lime-Pozzolana Cements* by J.P. BOMBLED, from France.

. *The Different Activation Processes of Clay Minerals to Obtain Pozzolanic Binders with Optimal Strengths* by M. MURAT and collaborators, from France.

. *Properties of Blended Cements Made with Portland Cement, Cement Kiln Dust, Fly Ash and Slag* by M. BHATTY, from U.S.A.

5.1 Blended Cement Composition Determination

GOMA has proposed a method for the determination of the composition of portland cement with additions. His method is based on the dissolution of cement samples by means of an aqueous solution of 10% hydrochloric acid (cold). The composition of soluble fraction was determined (main oxides) and a triangular diagram (SiO_2-CaO-R_2O_3) was used. Portland cements without additions from different origins gave a narrow location area. This point is technically useful when the type of cement is unknown. Different types of addition (slags, pozzolans, fly ashes, basalt rock, calcareous) gave location areas on the diagram that were sufficiently isolated to be identified very easily. So, the type of cement can be recognized. In addition, when we have the materials which make up a binary mixture, it is possible to determine the proportion of addition.

5.2 Particle Size Distribution of Blended Cements

SORRENTINO, investigating the particle size distribution in blended cements developed a method based on sieving and sedimentation with Andreasen's pippetes. He dedicated special attention to the cements with calcareous filler, in the particular case where clinker and filler are industrially produced by co-grinding. In order to obtain the respective grain size distribution of the clinker and the calcareous filler, besides the granulometric analysis, a simultaneous $CaCO_3$ content determination in each fraction was addopted. At first, the method was tested with success on three laboratory cements, since the grain size distribution of each component was previously known before the blend was made. In the three industrial blended cements, the author concluded that calcareous filler contained a high amount of very small grains. The mean ranged between 2,7 and 7,5µm. On the other hand, in the three cements, clinker contained a large proportion of large size grains, that is, 20.1, 30.9 and 35.1% of particles above 45µm. *SORRENTINO* concludes: *These grains are not easily hydrated and do not take part in the development of early strength. Thus, co-grinding is not the most well adapted process in the case where the filler of the C.P.J. (French blended cement) is calcareous, since it partially counteracts the beneficial effects brought by the addition of limestone.*

BOMBLED and collaborators also applied an interaction of sedimentation by Andreasen's pippetes and X-Ray Diffraction Analysis to investigate the particle size distribution in blended cements. Phase analysis by X-ray diffraction was truely used to crystalline materials as, for example, calcareous filler. On the other hand, when the material blended to the clinker is amorphous (case of slags), the authors suggest the use of Atomic Absortion or Plasma Spectrometry Analysis, for the determination of a trace element, like for example, Manganese in slags. Table 3 of their communication shows a complete size distribution of calcareous filler and clinker in a blended cement with 25% of filler. As

an example of this distribution we can mention the case of granulometric fraction nº 7 (diameter below 7μm) that was enriched in calcareous filler, having a 50%/50% ratio clinker/calcareous filler. Another example, the fraction nº 11 of the same blended cement, with particle diameter below 1μm, has a 10%/90% ratio clinker/calcareous filler.

5.3 Activation of Pozzolanic Materials

BOMBLED showed in his communication, results of different means of activation of various potentially pozzolanic materials from different origins. Most tests were carried out on samples of laterite, kaolin, basalt, bauxite, silica fume, pozzolan from Volvic (France) etc. To increase the pozzolanic reaction rate of mixtures of lime/pozzolan (ratio 20:80), several activation means were addopted: thermal treatment, chemical additives to improve the burning, mechanical procedure (fine grinding), chemical activation and rheological means (decrease of water contents, compactation).

The thermal treatment increases the pozzolanic activity of materials mainly due to the dehydration of clay minerals, crystallographic changes and increase of surface area (microfissuration, porosity). There is always an *optimum* temperature which enables the material to obtain a *maximum* strength. Mortar strength increased for most samples, except for the basalt and the pozzolan from Volvic. The use of chemical additives to improve the burning, like sodium and calcium carbonates, calcium, sodium and potassium sulphates etc. modifies the kinetics of temperature activation and consequently increases the compressive strength of pozzolan-lime mortar. It is remarkable in the laterite the increase of strength with the use of sodium silicate in the raw material, followed by burning at 800°C. However, a larger increase of strength is reached, in both laterite and kaolin, when these materials are burnt at 800°C and then chemically activated by sodium hydroxide or sodium silicate.

MURAT and collaborators have also investigated the activation processes but related specifically to clay materials. The use of clay materials as pozzolanic binders requires previous activation processes that are classified into chemical, thermal and mechanical activation. The chemical activation takes into account the existence of OH^- and Ca^{2+} ions in solution as elements that are able to modify or to destroy the structure of a natural or burnt clay and consequently to originate hydration products. These hydration products are responsable for the hardening properties of the pozzolanic binders. When the chemical activator is calcium hydroxide, the main hydration product in the kaolinite is the C-S-H. In montmorillonite, hydrated calcium aluminate is more frequently observed.

The thermal activation is promoted by burning some clays at temperatures between 600 and 900°C. As a result, the clay crystalline structure is more or less destroyed. Under these conditions, the burnt clay is more active than the natural clay, but it also demands the use of chemical activator to produce a material with hardening properties. A typical case of thermal activation is the kaolinite dehydration at 700-800°C that originates the metakaolinite. The metakaolinite activated by calcium hydroxide originates the C-S-H, hydrogehlenite (C_2ASH_8) and lesser amounts of C_4AH_{13}. By comparing the activity of burnt clay mineral to the natural clay mineral, the authors found significative differences. The following growing order is supposed to occur in burnt material: kaolinite > montmorillonite > illite > crystallized mica, while in natural clay mineral it was found: montmorillonite > illite > kaolinite.

Mechanical activation of clay mineral is got by grinding the thermally activated clays.

The increase of the hardening rate of these materials is due to the formation of surface defects during the grinding that increase, in their turn, the material activity.

5.4 Blended Cements Properties

BHATTY showed in his communication, results of tests carried out on three cement kiln dusts with different chemical compositions, two fly ashes and one slag. By preparing blended cement with binary, ternary and quaternary mixes, he compared some properties of blended cements to those of portland cements. Some of his main conclusions were:

. *At addition levels of 10% and 20% in binary and ternary blends, fly ashes were much better inhibitors of sulphate expansion than slag but at higher addition levels both fly ashes and slag behaved similarly in reducing the expansion significantly compared to cement alone.*

. *All ternary blends made with cement, kiln dusts and slag or fly ash showed higher autoclave expansion than cement alone except the ternary blends made with cement, high sulphate dust and Class F fly ash.*

. *Most ternary blends made from cement, high sulphate or high chloride kiln dust and slag or Class F and Class C fly ash developed significantly higher strengths than cement alone at 1 day. One year strengths of most ternary blends were higher than cement.*

. *At later ages, ternary blends containing kiln dusts and slag produced higher strengths than ternary blends containing kiln dust and either Class F or Class C fly ash.*

. *Alkali-aggregate mortar bar expansions of binary cement-kiln dust, cement-slag and cement-Class F fly ash blends were comparable to cement alone. However, binary cement-Class C fly ash blends showed much higher expansions at one year when these blends contained 20% and 30% Class C fly ash.*

YASUKO TEZUKA, Associação Brasileira de Cimento Portland

COMMUNICATION REPORT ON SUB-THEME 3.2 - EFFECT OF BLENDING COMPONENTS ON HYDRATTION AND STRUCTURE FORMATION

1 INTRODUCTION

There are one principal report by H. Uchikawa, one special report by J. Calleja and 23 basic reports on sub-theme 3.2 - *Effect of blending components on hydration and structure formation.*

The 23 basic reports are coming from Japan(4), England(4), Italy(3), France(3), U.S.A.(3), China, Hungary, U.R.S.S., Poland, Yugoslavia and Argentine, (one each) as we can see in the following list:

1 - *Zeta potencial and rheológical behavior of slag cement pastes.*
R.I.A. Malek, M. Silsbee and D.M. Roy - U.S.A.

2 - *Rhéologie du béton frais.*
J. P. Bombled - France.

3 - *Influence of character of blending component on the diffusion of* Na^+ *and* Cl^- *ions in hardened blended cement.*
H. Uchikawa, S. Uchida, K. Ogawa - Japan.

4 - *Measurement of* OH^- *ion concentrations of pore fluids and expansion due to alkali-silica reaction in composite cement mortars.*
J.J. Kollek, S.P. Varma, C. Zaris - England.

5 - *Hydration of alite and* C_3A *and changes of some structural characteristics of cement pastes by addition of silica fume.*
D. Andrija - Yugoslavia.

6 - *Action d'un fluidifiant et d'une fumée de silice condensée réactive aux courtes échéances sur la liaison gros granulat-mortier.*
J.P. Ollivier, J. Grandet, B. Hanna - France.

7 - *Properties of very fine blast furnace slag prepared by classification.*
K.Sato, E.Konishi, K.Fukaya - Japan.

8 - *Effect of fine mineral admixtures on the properties of hardened cement pastes.*
C.Atzeni, A.Marcialis, L.Massidda, U.Sanna - Ttaly.

9 - *Texture et performance des ciments fillerises.*
P. Gegout, H. Hornain, B. Thuret, B. Mortureux, J. Voland, M. Regourd - France.

10 - *Activity of fly ashes used as a pozzolanic admixtures to cement.*
W. Roszczynialski, K. Gustaw - Poland.

11 - *Behavior of Italian fly ash in portland cement mortars.*
G. L. Valenti, R. Cioffi, R. Sersale - Italy.

12 - *Effect of cement composition on the strength contribution of fly ash.*
Z.Z.Gu, B.W. Zhou, M.L. Yue, T.F. Tang, W.J. Wang - China.

13 - *Effect of* $Ca(OH)_2$ *and* $CaSO_4.2H_2O$ *on the strength of fly ash cement pastes.*
S.B. Wang, R.L. Berger - U.S.A.

14 - *The effect of the curing temperature on the pozzolanic reaction in fly ash blended cement.*
Y. Halse, H.V. Jensen, P.L. Pratt - England.

15 - *Composition of pore fluids extruded from slag cement pastes.*
M. Silsbee, R.I.A. Malek, D.M. Roy - U.S.A.

16 - *Effect of the addition of blast-furnace slag on the physical and mechanical properties of mortars cured at high temperatures.*
A.I. Elola, A.S. Szteinberg, R. J. Torrent - Argentine.

17 - *Interfacial microstructural alterations of mature blast furnace cement pastes.*
B. Marchese - Italy.

18 - *Ciments multicomposants a base des laitiers de metallurgie des metaux non ferreux.*
P.I. Bojenov, B.A. Grigor'ev - URSS.

19 - *Research on making cements of improved sulfate resistance and watertightness.* L. Opoczky, I. Vincze - Szekely, L. Szatura - Hungary.

20 - *Effect of character of glass phase in blending components on their reactivity in calcium hydroxide mixture.* H. Uchikawa, S. Uchida, S. Hanehara - Japan.

21 - *An examination of some pure and composite portland cement pastes using scanning electron microscopy with X-ray analytical capability.* A.M. Harrison, N.B. Winter, H.F.W. Taylor - England.

22 - *Effect of polymer modifications on the mechanical properties of calcium silicate and calcium aluminate cements.* N.B. Eden, J.E. Bailey - England.

23 - *Influence of kind of calcium sulfate on hardening of cement paste mixed with humic acid.* Y. Takano, Y. Mizukami - Japan.

The basic reports on sub-theme 3.2 can be classified as follows:

a) Effect of fly ashes	5
b) Effect of blast furnace slag	6
c) Effect of silica fume	3
d) Effect of mineral fillers	3
e) Effect of polymer	1
f) Effect of calcium sulfate	1
g) Methods of investigation	2
h) Influence of blending component on the durability	2
	23

Many communications pointed out that the substitution of various kinds of blending components (fly ashes, blast furnace slags, silica fume, mineral fillers etc.) for part of portland cement is interesting not only because it can improve certain properties of cement, eg. lowering the heat of hydration, lessening alkali-aggregate reaction, improving sulphate and sea water resistance but also saves energy and resources and safeguard the environment.

The effect of the blending components on the hydration characteristics of the blending cements was examined by:

- physical and mechanical tests;
- scanning electron microscopy (SEM)
- electron probe microanalyser (EPMA)
- energy disperson X-ray spectrometry (EDXRA)
- X-ray diffractometer (XRD)
- thermogravimeter (DTA)
- mercury porosimeter
- Na_2 adsorption method
- pore fluid analysis
- conduction calorimeter
- trimethylsililation method
- molybdate method
- zeta meter
- viscosimeter.

2 FLY ASH

2.1 Pozzolanic Activity

The determination of the pozzolanic activity of fly ashes is important for deciding whether a given type of fly ashes can be applied as addition to cements.

However, the measure of the pozzolanic activity of fly ashes seems to be hard because very often the various methods for determining the pozzolanic activity do not characterize this activity unequivocally.

Four communications were presented about this subject.

Uchikawa, Uchida and Hanehara[20] suggest that the simple but effective method to evaluate the pozzolanic reactivity of fly ash is amount of acid soluble $SiO_2 + Al_2O_3$.

Since fly ashes with larger amount of glass phase and higher glass basicity has higher pozzolanic reactivity, date of soluble amount of glass phase, could be considered to reflect their character.

Weakly bonded SiO_2 and Al_2O_3 with comparatively high reactivity was easily dissolved by Na_2CO_3 solution after boiled in conc. HCl (acid soluble part).

Acid soluble part per specific surface area of blending component is considered to correspond to their basicity and condensation degree of silica ion.

Wang and Berger[13] observed that the fly ash with 8% monomer and about 90% dimer and polymer, exhibited very low reactivity, only 7-12% reaction degree at 60 days. This lower reactivity is probably associated with small amount at monomer in fly ash.

Roszczynialski and Gustaw[10] report that the most reliable method of pozzolanic activity of fly ashes consists in determining the content of SiO_2 and Al_2O_3 (ASTM C 593-69) and compressive strength (method proposed by Fratini and Lea); additional determination of carbon content in ashes can be usefull. They found that carbon content above 3% renders the fly ash unapplicable as addition to cement.

In the communication[11] by Valente, Cioffi and Sersale it is shown that particle size

distribution of fly ash and their calcium oxide content are the main factors that influence the performance of fly ash in portland cement.

2.2 Hydration

The hydration of cement containing fly ash was studied by the authors by means of heat of hydration and phase composition of cement pastes.

a) Heat of hydration

Roszczynialski and Gustaw[10] found that the fly ash addition to cement diminishes the heat evolution and retards the appearance of the maximal heat corresponding to the hydration of alite and C_3A.

Those results are confirmed by Halse, Jensen and Pratt[11]. They studied the influence of the temperature on the hydration of portland cement containing 30% fly ash.

Conduction calorimeter measurements show that increasing the temperature to 40°C advances and enhances the hydration substantially, while decreasing to 10°C extends the induction period, broadens the peaks and lowers the peak rate of heat output substantially. Despite the inicial retardation of hydration, clearly the fly ash has enhanced the amount of hydration in the first 2-3 days at all temperatures.

b) Phase composition

Halse, Jensen and Pratt[14] observed that in the initial wetting and induction period, short rods of AF_t are seen to form over the surface of both cement and fly ash particles. During the acceleratory period the surfaces of both cement and fly ashes become covered with small crystals of CH and type I C-S-H, engulfing the short rods of AF_t, and AF_m phase appear as a large hexagonal platelets.

Uchikawa, Uchida and Ogawa[3] report that the ordinary portland paste had dense C-S-H around alite and large layer agglomeration of CH while fly ash cement paste contained fine C-S-H around fly ash particles and locally produced CH and AF_m phase; this later phase was increaser in fly ash cement when compared with ordinary portland cement. The amount of CH in hardened fly ash cement was decreased with the increasing amount of fly ash.

In the communication[21], Harrisson, Winter and Taylor show that in the fly ash cement, additional C-S-H is formed not only in space occupied previously by fly ash or pore solution, but also in space previously occupied by CH.

The C-S-H forming as a result of CH reacting with fly ash has a higher Aℓ/Ca ratio than that formed as inner product of alite or belite.

Harrison et al.[21] and Uchikawa et al.[3] in their communications, report that the presence of fly ashs seems to affect not only the composition of C-S-H formed close it or as its own inner products, but also that of the C-S-H formed as inner product of alite or belite, but to a lesser extent.

Habe et al.[14] found for the ordinary portland cement the Ca/Si ratio of C-S-H between 1.89 and 2.00. The inner product of either alite or belite were substantially pure C-S-H. The outer product, somewhere also pure C-S-H, but others were mixtures of C-S-H with AF_m phase or CH.

In pastes with fly ash the Aℓ/Ca and Si/Ca ratios were higher and it is likely that etrantligite (C_2ASH_8) was formed.

Uchikawa et al.[3] also show that for ordinary portland cement paste the Ca/Si ratio of C-S-H was 1.90 and for cement with fly ash addition 1.32.

2.3 Compressive Strength

According to Gu, Zhow, Yue, Tand and Wang[12], cement composition influences significantly the strength contribution of fly ash.

They report that fly ash cements, with 17 typical clinker ground to the same specific surface area, gypsum content same as that in the factors and 30% fly ash, exhibited at 7 and 28 days decreased compressive strength and increased compressive strength at 90 days when compared with cements without fly ash addition.

For the suitable clinker the strength of fly ash cement was reduced only by 10% at 28 days and increased by 15% at 90 days.

Using the regressive analyses, the authors suggest that the K_2O, C_3S and KH of cement are directly proportional to the strength, while $CaSO_4$ and C_2S are inversely proportional to that.

The C_2S is desadvantageous to the strength contribution of fly ash because the hydration rate of C_2S is very slow at earlier ages. $CaSO_4$ was inversely proportional to the strength of fly ash cement at 28 and 90 days; it might result from that the $A\ell_2O_3$ in fly ash had speed up the transformation of AF_t to AF_m.

K_2O of cement accelerated the hydration of C_2S when fly ash was added and increased the solubility of acid oxides in fly ash.

Halse, Jensen and Pratt[14] studied the influence of the temperature on the strength

and found that the highest 28 days strenght for the fly ash cement was obtained at 40°C curing, but, by 180 days curing at 20°C gives higher strength than at 40°C. Curing at 8°C appears to slow down the strength.

Wang and Berger[13] report the effect of CH and $C\bar{S}H_2$ on the strength of fly ash cement pastes. The strength decreases with the addition of CH at early ages and the more CH addition, the lower the compressive strength.

It seems that only about 10% of CH added react with fly ash, 90% of CH added exists as fine aggregate.

$C\bar{S}H_2$ added to fly ash cement decreases the strength at early ages but increases the strength at later ages.

The contribution of $C\bar{S}H_2$ added to the strength lies in the reaction of $C\bar{S}H_2$ with C_3A or with $A\ell_2O_3$ from fly ash to form ettringite in the capillary and densification of the structure of the paste at later age by the pozzolanic reaction of fly ash with CH to form C-S-H gel.

Most of ettringite were formed before 14 days and was consumed up at 28 days indicating that the contribution of $C\bar{S}H_2$ to strength was limited within 28 days.

2.4 Durability

Kolleck, Varma and Zaris[4], using the techniques of pore fluid extraction from pastes and mortar bar expansion, studied the effect of fly ash upon the potential for alkali-silica reaction.

They concluded that if the pore fluid OH^- ion concentration of fly ash cement is less than 0.3M at 180 days, a deleterious expansion with opal is unlikely to occur.

In the communication[10], Roszczyniashi and Gustaw shown that fly ash addition increases the resistance of the fly ash cement to sulphate corrosion.

Uchikawa, Uchida and Ogawa[3] studied the effect of fly ash on the depression of concrete deterioration by alkali-aggregate reaction and by chloride attack to reinforcement.

They found that the diffusion coefficient of Na and Cℓ ion through ordinary portland cement was largest while fly ash cement was smaller.

The diffusion of Cℓ ion was about ten times as large as that of Na ion.

In the fly ash cement, the diffusion of ions appears to become difficult with increasing pore volume ratio of 5-50 nm in spite of its high total porosity.

Because of fly ash cement had larger total porosity and pore volume ratio of 5-50 nm than ordinary portland cement, it is considered that fly ash cement have resistance to the diffusion of alkali ion and Cℓ ion than ordinary portland cement paste.

3 BLAST FURNACE SLAG

3.1 Hydration

Uchikawa, Uchida and Hanehara[20] consider that the hydration of slag is based on the elution of the chain structure of SiO_4^{4-} and $A\ell O_4^{5-}$ in slag by the attack of OH^-.

They found that the hydration degree of slag with high crystalline phase (15-28%) was small and that of slags with less than 5% crystalline phase, was not related to glass phase content. The hydration degree of slag was related to the amount of SiO_2 eluted by 0.1N NaOH solution.

Slags with lower content of crystalline phase and higher ratio of monomer/dimer had higher reactivity.

In the communication[21], Harrison and Winter report that reactions rims around the larger slag grains were barely detectable at 28 days old slag cement paste, but the 180 days old paste showed well developed rims up to 10μm wide. Fully reacted relics of smaller grains were also abundant.

At 180 days old slag cement paste there was a matrix apparently of C-S-H closely mixed with AF_m phase, in which were embedded the partly and fully reacted slag grains, together with relies of clinker phases, regions of CH, occasional unreacted clinker phases, and aggregats of AF_m crystals up to 30μm in size.

The slag rims and relics contained substantial amount of MgO, $A\ell_2O_3$, SiO_2 and CaO.

Uchikawa, Uchida and Ogawa[3] also report that the blastfurnace slag cement had dense C-S-H complicated with AF_m.

3.2 Compressive Strength

According to Sato, Konishi, Fukaya, Koibuchi, Ishikawa and Iijima[7], the low early strength caused by addition of granulated blast furnace slag can be improved by making it finer.

The authors shown that the strength of cement with slag 7000 cm^2/g fineness was higher than that of pure cement and considerably higher than ordinary slag cement.

Elola, Szteinberg and Torrent[16] studied the effect of high temperature curing on the strength of blas furnace slag cements.

They report that no significant acceleration of the reaction was found between mortars cured at 40°C and 80° for the portland cement, while for the slag cement, some acceleration in strength development was observed in mortars cured at 80°C when compared with those cured at 40°C. The different strength behaviour of slag cement and portland cement when the curing temperature was raised from 40°C to 80°C can be explained by the change in pore structure.

For the slag cement, the high temperature leads to a strong refinement of the pore structures.

Bojenov and Grigor'ev[18] report the use of slag from the pyrometallurgic treatment of the coppernickel agglomeration as a blending component of cement. They showed that the strength at early ages was lower than pure cement but at late ages was similar to that.

3.3 Durability

Kollek, Varma and Zais[4] and Silsbee, Malek and Roy[15] used the method of pore fluid extraction from cement pastes to analyse the effect of slag addition to cement concerning about alkali-aggregate reactions and the passivation of steel in concrete.

Kolleck et al.[4] found that blastfurnace slag invariably contribute to the OH^- ion concentration of pore fluid. This contribution depends on the alkali content of the slag and on its reactivity.

The authors concluded that the damaging effect of alkali silica reaction can be effectively reduced at higher levels of cement substitution by slag. An ON^- ion concentration of 0.5M appears to be a threshold for damaging reaction at 180 days with blast furnace slag cements.

Also, according to Silsbee et al.[15], additions of slag always lowered the alkali levels substantially from that found in the pure cements.

Tests conducted by Silsbee et al.[15] show that in the slag cement, generally the calcium levels an somewhat lower than for the corresponding pure cement, because lower calcium content of the cement and increased consuption of the calcium by the relatively silica-rich slag cement.

The sulfate levels in the slag cement remained relatively constant, while in the portland cement tended to pass through a minimum and then increase. This behaviour suggests early ettringite formation (low SO_4^{2-} in solution) followed by release of sulfate to solution along with Ca and Al.

The authors also show that the reduction in pH values of the pore fluids extracted from the samples caused by additions of blast furnace slag is not likely to cause major deleterious effects. In all cases, the slag cements contained much lower chlorid levels in the pore solution than the pure cement.

Additionally, Silsbee et al.[15] report that the diffusion rates of ions through blast furnace slag cement paste are much lower than for portland cement pastes, diminishing the rate of penetration of harmful species from the environment.

Uchikawa, Uchida and Ogawa[3] also have concluded that the diffusion coefficient of Cl and Na ions through blastfurnace slag cement paste was smaller than for pure cement.

They observed that blastfurnace slag cement with 70% of slag tended to have larger total porosity and pore volume ratio less than 5nm whereas cement with 40% slag had smaller total porosity and larger pore volume ratio less than 5nm.

The diffusion coefficient of ions in the blastfurnace slag cement became smaller with increase in pore volume ratio less than 5nm.

Sato, Konishi, Fukaya, Koibuchi, Ishikawa and Iijima[7] confirm that the addition of granulated blastfurnace slag is effective in preventing the alkali-aggregate reaction and durability against sea water.

They report that the higher the slag content, the shallower the permeation depth of Cl^- ion.

Marchese[17] studied the microstructural modifications of reinforced slag cement past at crack surfaces and steel/cement pastes interfaces cured 6 months and then immersed for 3 years in natural sea water.

They found that the contact between static sea water and mature slag cement paste has not presented apparently alterations after long time.

The pre cracking patterns have not changed in the number and width of the cracks.

When cracks were formed in the mature paste, the sea water penetrated in them and arouse the latent chemical reactivity.

The second generation products observed were: honeycombe or reticulated C-S-H, leaf-shaped aragonite, granular Ca-rich form; flat fish shaped form, presumably of an organic nature; hexagonal lamallae of CH and fibres of ettringite type I, in pre-existing cavities.

The crack that forms at the interface paste/steel consists of two distinct surfaces. The paste surface shows a typical compact cristalline microstructure where Mg, Si,

Cℓ and Fe are present in notable quantities. Sensible larger grains of calcite are distributed in it. The steel surface shows compact areas beside extremely porous ones, both indicative of high degree of corrosion.

Malek, Silsbee and Roy[1] using the microelectrophoresis technique concluded that the zeta potential value of slag particles reflects its agglomeration tendency, the more negative its value the more dispersed the slag. Thus a negative zeta potential slag was found to exhibit favorable workability.

4 SILICA FUME

A number of investigations have reported that the silica fume a by product from the silica metal and ferro-silicon alloys production in electric arc furnaces has been mixed with portland cement from the view point of improving strengths, preventing alkali-aggregate expansion and chemical attack.

The silica fume or microsilica is a very active material with high amount of amorphous SiO_2, particles with submicron size and very high total specific surface area.

4.1 Hydration

Opczky, Vincze, Szekely and Szatura[19] verified in their investigations that silica fume reacts with CH formed at the hydration of cement. The formation of C-S-H is evident even after 3 days.

The hydration process of cement is accelerated by silica fume because even at the early stage of hardening Ca^{2+} ions are adsorbed by it and high specific surface area is ensured for the formation of hydrates. Due to the reaction between silica fume and CH, high amount of C-S-H is formed in some capillary pores thus compacting the pore structure of the cement paste.

During the hydration of cement with silica fume C-S-H phase is occuring first in form of islands of small equant grains at 3 days, then it exhibits at 7 and 28 days, elongated and fibrous morphology.

The heat of hydration for cement with silica fume is higher than that of the pure cement.

Uchikawa et al.[3] report that the cement with silica fume was rich in C-S-H, poor in Aℓ bearing hydrates; the amount of AF_m and CH was remarkably small than that in cement paste with ordinary fly ash.

According to Uchikawa et al.[20] reactivity of silica fume was dominantly controlled by specific surface area and glass phase content. The hydration degree could be evaluated by reacted $Ca(OH)_2$ and SiO_2.

Andrija[5] reports that in the cement paste containing silica fume the acceleration of alite was detected at entire 28 days period and the acceleration of hydration of the C_3A was relatively retarded at 3 days.

Because CH diminishing continue at 7 and 28 days hydration, the author suggests that the alite hydration acceleration takes place not predominantly by hydrolysis equilibrium shift due to pozzolanic lime consumption.

Olliver, Grandet and Hanna[6] studied the effect of silica fume on the interface mortar/coarse aggregate.

They found that the addition of silica fume modify the structure of the transition rims. It was not observed the preferencial orientation of the C-S-H near the coarse grains and the adhesion between the interface mortar/coarse aggregate was enhanced.

4.2 Compressive Strength

Opoczky, Vincze, Szekely and Szatura[19] report that the compressive strength of the cement increased 20-40% by addition of 15-25% silica fume.

Also, Andriga[5] report that the compressive strength of hardened cement with silica fume were increased in comparing with them of the pure cement.

4.3 Durability

Uchikawa et al.[3] showed that the cement with silica fume have smaller diffusion coefficient of alkali ions than the pure cement, and the total porosity and pore volume ratio less than 5nm increased compared with ordinary portland cement.

Opsczky et al.[19] report that the characteristic pore size in cement silica fume added is shifted from 100nm to 10 nm. They also shown that the cement with silica fume has an enhanced watertightness compared with that of pure cement and that the sulfate resistance increased 80-90% by 15-25% silica fume additions.

5 MISCELLANESUS

5.1 Filler

According to Bombled[2] the mineral fillers when added in the cement could play many roles: to replace the deficient fine grains in the size distribution curve, to fill the capillary pores, to modify the rheological properties and accidentaly to participate in hydration reactions of the cement pastes.

He reports the influence of the filler addition less than 25% to cement on the

rheology and water content was small compared with pure cement. If any influence exists, the plasticity and the cohesion was enhanced and somewhat pseudo-acceleration of the setting time observed.

Gegout, Hornain, Thuret, Mortureux, Voland and Regourd[9] report that the mechanical performance and porous texture of the hardened cement paste with up to 15% addition of limestone filler was similar to that of pure cement.

They found that the compressive strenght is proportional to the solid volume increased during the hydration of cement paste for one initial porosity.

Atzeni, Marcialis, Massidda and Sanna[8] in their experiments found that the strength properties depends not only on total pore volume but also on a new parameter related to pore distribution defined as mean distribution radius.

5.2 Polymers

Eden and Bailey[22] report the effect of polymer on the properties of calcium silicate and calcium aluminate cements.

They found that the polymers affect the hydration reaction to varying degrees, depending on their own reactivity and this may lead to a complex polymer/hydrate gel or even a chemically cross-linked polymer, rather than hydrate particle alone being the main binding agent.

The effect of reaction between the polymer and hydrates in the calcium silicate system may be limited by the presence of conventional hydrates, but in the calcium aluminates the formation of the conventional crystalline hydrates is strongly suppressed by the presence of large amount of polymer.

The mechanical properties and the durability of the polymer modified cements are influenced by the polymer content, water content, and the nature of any polymer/cement interation.

5.3 Calcium Sulfate

Takano and Mizukami[23] studied the influence of the type of calcium sulfate on the initial hydration of cement paste mixed with humic acid.

It seems that if the amount of dissolved humic acid is great with low $[Ca^{2+}] \cdot [SO_4^{2-}]$ saturation ratio in the liquid phase, as is seem when the 5% humic acid is added to cement with anhydrite, more humic acid is adsorbed on fine hydrate formed at the initial age. Thus the crystallization and conversion of initial hydrates are hampered. This retardation ends with the decrease in the dissolved amount of humic acid and the rise in $[Ca^{2+}] \cdot [SO_4^{2-}]$ saturation ratio.

At the initial age, the $[Ca^{2+}] \cdot [OH^-]^2$ saturation ratio depends on the kind of calcium sulfate added to cement and free lime of cement.

They found that the $[Ca^{2+}] \cdot [OH^-]^2$ saturation ratio decreses as the elution of Ca^{2+} from alite is hampered as a result of adsorption of humic acid thereon.

HANS ROMAN EDMUNDO BUCHER - Associação Brasileira de Cimento Portland

COMMUNICATIONS REPORT: SPECIAL CEMENTS, HIGH-ALUMINA CEMENT AND OTHER NON-SILICATIC CEMENTS

1 INTRODUCTION

The meaning and content of the chapter *Special Cements* has been always changing in the course of the last succeeding International Congresses on the Chemistry of Cements. Traditionally, only cements differing from straigth portland were considered *special* or *all others excluding portland*. Later on, any binder whose manufacture and/or use and application had a special intrinsic nature or a specific performance were considered *special*. Actually as the best-known *special cements* may be considered:

- High-alumina cement
- Expansive cement
- Oilwell cement
- Magnesium Oxychloride cement (Sorel)
- Decorative purposes cement (mainly white)
- Miscellaneous cements (phosphate, activated belitic, alunitic, anhydrite-based, etc.)

To the present Congress, 28 papers were submitted covering the following areas:

9 papers on high-alumina cement,
6 papers on expansive cement,
2 papers on oilwell cement,
2 papers on fast setting and hardening cement,
2 papers on decorative purposes cement,
1 paper on magnesium oxychloride cement, and
3 papers on unclassified subjects.

2 HIGH-ALUMINA CEMENT

The nine papers on high-alumina cement came from the following countries: Spain (1), France (2), United Kingdom (2), Hungary (1), Italy (2) and Poland (1), and have the following indicated titles and authors

(2.1) The Development of Microstructure in High-alumina Cement, by Halse, Y. and Pratt, P.L.;

(2.2) The Effect of Superplasticisers in the Hydration of Aluminous Cement, by Gill, S.M., Banfill, P.F.G. and El-Jazairi, B.;

(2.3) Hydration of Monocalcium Aluminate with Calcite, by Bachiorrini, A., Guilhot, B. Murat, M., Negro, A., Soustelle, M., and Fournier, A.A.;

(2.4) Stability of the Compond C_5A_3 in the System $CaO-Al_2O_3$, by Lucco, M.B.,and Brisi, C.;

(2.5) Aluminous Cement: How to Avoid Degrading of Mechanical Strength, by Trivino, F.;

(2.6) The Effect of Synthesis and Cooling Conditions on Phase Properties of the $C_{12}A_7$, by Grzymek, J. Derdacka-Grzymek, A., Konik, Z., Pyzalski, M., Stok, A., and Iwanciw, J.;

(2.7) A Summary of Experiences on Estimating the Expectable Changes of Strength of Concrete made with High Alumina Cement, by Revay, M.;

(2.8) The Setting and Hardening Characteristics of Calcium Aluminate Cements: Studies of the Systems $C_{12}A_7$ - C_3A and $C_{12}A_7$ - CA, by Menestrier-Sorrentino, D., George, C.M., and Sorrentino,F.P., and

(2.9) Alumina Cement Hydration in Pure Water and in Sulphate Solution in the Presence of Siliceous or Calcareous Aggregate, by Bachiorrini, A. and Cussino, L.

High-alumina cement has traditionally been a

point of concurrent interest in light of contributions sent to the last 3 International Congresses on the Chemistry of Cement: 15 papers were sent to Paris in 1980, 6 were sent to Moscow in 1974 and 9 to the 5th Congress in Tokyo in 1968. Besides these specific papers, a considerable amount of new scientific and technological knowledge has been widespread in the last decades on this subject in specialized publications. Recent advances in the field are resumed in the Principal Paper in a more comprehensive way.

Subdividing the main subject *High-alumina Cement* into the following three items:

a) formation, composition and structure;

b) hydration and hardening; and

c) properties and uses, the content of the supplementary papers received may be summarized as follows:

2.1 Formation, Composition and Structure

The authors of *Stability of the Compound C_5A_3 in the System $CaO-Al_2O_3$* (2,4) intend to prove that this compound, firstly described by Shepard, Rankin and Wright in 1909, is really a phase forming part of thermodynamical equilibrium of the $CaO-Al_2O_3$ system. They believe the compound that can be in fact considered as instable is $C_{12}A_7$ with which C_5A_3 used to be confounded in the past. Moreover, from their experimental work they conclude that pentacalcium trialuminate is far more stable at 1200°C than the mixture of C_3A plus CA. By this way of reasoning, C_5A_3 may not be just considered as transition product between these two compounds.

Another study (2.6) on the equilibrium of the $CaO-Al_2O_3$ system belongs to Grzymek and refers to the existence of two polimorphisms of dodecacalcium heptaluminate. These polimorphisms are in his opinion of isotropic and anisotropic optical nature an their transition temperature for changing from the γ to the α form can be established as 1673°K. According to his results, the researcher suggests that the *d* values, in Å, currently assigned to this compound and published in technical literature corresponds in reality to the property of a mixture of both α and γ polimorphs.

2.2 Hydration and Hardening

As could be expected in the case if high-alumina cement, this is the most interest awaking subject of all papers devoted to this kind of cement. In the last decades there has been an ever increasing attraction of the mechanism of hydration and hardening whose origin lies in the *Conversion* of hydration products and resulting in drop of mechanical strength.

The authors of paper (2.8) *The Setting and Hardening Characteristic of Calcium Aluminate Cements: Studies of the Systems $C_{12}A_7$ - C_3A and $C_{12}A_7$ - CA*, synthetized experimental high-alumina cements composed predominantly by calcium rich aluminates by fusion at 1450°C and slow cooling.

These mixtures covered a wide range of the $CaO-Al_2O_3$ interval which compound composition varied for $C_{12}A_7$ between 24 and 93% , for C_3A content was between 6 and 28% and, finally, monocalcium aluminate extended from 7,1 to 27%. Hydration of the most representative of these experimental cements revealed to the authors that reaction speed with water increases with $C_{12}A_7$ and C_3A. On the other hand, continous substitution of C_3A for CA results in predominant hydration products changing from C_2AH_8 to CAH_{10}. This constitutes a means for directing hydration compounds in a specific way.

High-alumina cements present the pecularity that the composition of their hydration products do not depend solely on the

initial anhydrous mineralogical composition, but also on water: cement ratio and temperature of the reacting media. In consequence, another way of directioning the hydration process is based on the selection of a water; cement ratio that is equal or less than the so-called *critical value*. Nevertheless it isn't always possible to fix such a value in practice by the fact that the fresh mixture has to fulfill at the same time a certain specificied workability. In accordance with this line of thought, the paper (2.2) by Gill, Banfill and El-Jazairi suggests the use of chemical additives to attain this condition in mortar and concrete with high-alumina cement. The authors used as water reducing additives high range superplasticizers jointly with water:cement ratios between 0,3 and 0,4 in the experimental temperature range from 5 to 40°C. The tendency of the additive in promoting the retarding of hydration was compensated by the researchers by adding a lithium salt. The mechanical strength of the specimens — measured indirectly by means of ultrasound pulse velocity — was considerably higher in the 5 to 20°C temperature range than in the 30 to 40°C. Unfortunately, the authors do not show results on the effect of both additives on the consistency of pastes and mortars used.

Paper (2.1) deals with the hydration process of high-alumina cement pastes during their first 12 hours cured at 8,23 and 40°C in a thermostatic bath. The authors compare pastes mixed with tap water and with sea water by means of S.E.M. complemented with X-ray diffraction and D.T.A. analysis. They also describe the evolution of the structure with time and especially accompanying alumina gel transformation besides hydration products responsible for mechanical strength. They conclude that hydration reaction speed rises with temperature but the onset of structure formation occurs first at 8 and 40°C then at 23°C. Sea water used as mixing water retarded high-alumina cement hydration.

Papers (2.3), (2.5), (2.7) an (2.9) covered specifically the *conversion* problem characterized by the transformation of the initially formed hexagonal hydrates into the cubic form with a corresponding loss in strength by the significant increase in porosity.

Révay (2.7), complementing a paper presented for the first time at the Moscow Congress in 1974, establishes equations by which he can estimate the relative strength evolution with time of concrete structures built in Hungary with high-alumina cement. By extensive sampling and testing the composition of site concretes in order tc determine the level of hydration, the extension of conversion and the degree of carbonation, he may estimate the relative stage of the strength evolution in any particular structure. In the authors opinion, these formulas should be useful in foresighting the time by which the maximum drop in strength will occur in any specific structure unde the Hungarian prevailing conditions.

In (2.3) under *Hydration of Monocalcium Aluminate with Calcite*, the authors studied the modifications accomplished by monocalcium aluminate hydration in the presence of calcite. An analysis of the thermodynamic stability of the different possible phases present during hydration of CA and the study of the formation kinetics of the hydration products, permits the authors to conclude about the mechanism of monocarboaluminate formation. The scheme idealized here accounts for sharp differences in ionic concentrations in the solution at the calcite interface. In this way, the precipitation of carboaluminate in the neighborhood of calcite surface implies an alteration in the proportions of the hydrates formed: CAH_{10} and C_2AH_8. The increase of calcite concentration and their fineness is responsible for higher or lower amounts of monocarbonate formation. On the other hand, agitation during hydration and higher

water:cement ratios is the main cause in diminishing monocarboaluminate precipitation. Consequently, fixing calcium aluminate as tabular $C_4A\bar{C}H_{11}$ during reaction of high--alumina cement with water contributes to significantly reduce the hexagonal hydrates and their conversion.

In more or less the same way, Bachiorrini and Cussino (2.9) follow the hydration of mortar and concrete specimens during 5 and 7 years. As the title suggests, the authors compare the performance of specimens molded with calcareous or siliceous fillers and aggregates and conclude on the fundamental importance of calcium carbonate in promoting carboaluminate formation and altering pore size distribution. Micropore promotion instead of macrosizes contributes to enhance dimen sional stability by reducing penetration of sulphate solution that may provoke expansion.

Finally, the contribution of paper (2.5) *Aluminous Cement: How to Avoid the Degrading of Mechanical Resistance* is the last on the conversion subject. The author focuses conversion counteraction in a multiple way in order to conclude about the more convenient remedy. The use of up to 20% calcium carbonate (fineness is not shown) in pastes and mortars in combination with different curing treatments (temperature, humidity and low pressure CO_2) is the way the researcher considers more appropriate to avoid the formation of cubic C_3AH_6 and promote AH_3, $C\bar{C}$ and $C_4A_3\bar{C}H$ instead. The only trouble of this procedure is that the more efficient curing conditions are cumbersome from the practical point of view: 15 to 72 hour duration under 70 to 105°C temperature.

3 EXPANSIVE CEMENT

Six papers were accepted from the following countries: Peoples Rep. of China (2) and one each of Bulgaria, Italy, Japan and U.S.S.R., whose titles and authors are:

(3.1) Effect of Alkali on the Expansive Properties of Sulfoaluminate Cement Pastes, by Shan-Ba, W., Shang-Xing, J., Yin-Jang, L. and Ke-Yong, H.;

(3.2) *Hydrogarnet and Calcium Hydrocarboalumi nate Based Cements*, by Korneer, V.I., Andreew, V.V. and Niliforow, U.V.;

(3.3) *Calcium Sulfoaluminate made from Phosphogypsum and its Hydration Properties*, by Santoro, L., Garofano, R., and Valenti, G.L.

(3.4) *Expansive Cement With Hydroxyde Expanding Phase on Admixture's Basis* by Djabarrow, N.B.

(3.5) *Mechanism of Expansive Pressure Develop ment with Hydration of CaO* by Yamazaki, Y. and Sakakibara, Y.

(3.6) *Study on High Self-Stressing Aluminate Cement* by Jungan, X., Xueli, T. Wenhao, Ch., Jizhi, X., Yaozhong, X. and Yiyu, Z.

Of these six papers, two refer to type K expansive cement based on sulphoaluminates: (3.1) and (3.3). One treats about tipe M expansive cement based on high-alumina plus calcium sulphate (3.6); another handles a kind of type S expansive cement (3.2); a fifth refers to an expansive agent based on calcium oxide (3.5), and the last describes an expansive addition based on an unidenti field metalic hydroxide (3.4).

Paper (3.1) is devoted to study the influence of alkali on the hydration of an expansive cement based on a mixture of high $C_4A_3\bar{S}$ clinker with gypsum. Using 0,06M up to 0,7M NaOH solution as the mixing water (w/c ratio = 0,36), the authors succeed in accelerating crystaline ettringite forma tion even at pH of 13,3. In this way, it is possible to reach higher expansions and

higher strength in a shorter period of time comparatively to speciments molded only with pure water. However, at later ages the mechanical strength of specimens molded with water is higher than those with the alkali solution.

The researchers of the University of Naples show in their paper (3.3) that the formation of $C_4A_3\bar{S}$ in expansive clinker by firing a mixture of calcium carbonate, alumina and gypsum is much eased when the calcium sulphate dihydrate is substituted by phosphogypsum containing fluor and phosphate. The burning temperature and the clinkering time are significantly reduced by the catalytic action of the minute impurities contained in the synthetic gypsum. According to the authors findings, there are no noticeable differences in the hydration of both clinkers.

The soviet writers of paper (3.2) describe the production of a binder based on the pyroprocessing of hydrogarnets and calcium hidrocarboaluminate rejects coming from alumina manufacture. The material can be added to cement in order to produce, among others, expansive cements.

In *Study of High Self-Stress Aluminate Cement* (3.6) the authors present the expansive characteristics of high-alumina cement combined with calcium sulfate and analyze its performance as a function of parameters like an alkalinity coefficient, SO_3 level and curing temperature. The hydration products of this cement are basically ettringite and alumina gel. The authors conclude that the hydrated cement has a high long time stability and a highly compact structure that makes this kind of cement especially suitable for concrete for hydraulic tubes or penstocks.

The use of CaO as an expansive agent is thoroughly studied in paper (3.5). The authors use a mixture of calcium oxide, ground quartz and a retarding additive for composing a product usually employed as demolition agent. The paper shows the evolution of pressure and volume increase with time of hydration and comment on the change of the crystalline structure of $Ca(OH)_2$.

4 OILWELL CEMENT

The two papers received were: one from Brazil and the other from United Kingdom and the summary of both follows.

(4.1) *The Effect of the Hemihydrated and Dihydrated Crystalline Forms of the Calcium Sulphate on the Thickening Time, Rheological Properties and Compressive Strength of the Oilwell Cement Slurries* by Silva, M.G.P., de Moraes, de Moraes, M.L.M. and Abdel--Rehim, H.A.A. the paper compares the influence of different amounts of gypsum and plaster of Paris on the specific properties of oilwell cement slurries made with three different portland clinkers for API type G oilwell cements. The authors conclude that in comparison to dihydrate, plaster of Paris raises the yield point and the apparent viscosity and may increase plastic viscosity of slurries made with the same clinker. At the same time, hemihydrate gives higher strength and delays slurry thickening up to a certain amount.

(4.2) The paper *Infrared Spectral Examination of Oilwell Cements* by Bensted, O. is centered on infrared identification of calcium sulphate forms and detection of aeration influences on type H and G oilwell cement waveband spectra in order to advance some indication of slurry performance alteration. According to the author ... *such an infrared spectroscopic examination is no substitute for the usual quality examination of oilwell cements.*

5 MAGNESIUM OXICHLORIDE CEMENT

(5.1) *Investigations on the System MgO - $MgCl_2$ - H_2O, and Hydration of Sorel Cement* by Menetrier - Sorrentino, D., Barret, P. and Saqout, S. Although Sorel cement is almost 120 years old, continously appear new works on this kind of binder, like basic research by present authors. The paper analyses kinetic behaviour of MgO + MCl reaction in aquous solution and the thermodynamic equilibrium of the four possible hydrates by which can be predicted outdoor exposure performance in any particular case.

6 DECORATIVE PURPOSE CEMENT

(6.1) *Pecularities of Mineral Formation and Hydration Phenomena of Decorative and High-Iron Content Cements* by Gaidjouvov, P. The author devoted his work to estabilish optimum condition for bleaching white cement clinker during pyroprocessing. By means of a (gas + plus wate vapor) mixture treatment for reduction of ferric oxides, decarbonation is enhanced, liquid formation is accelerated and whitening is favoured. On the other hand, the author gives some general outlines on a calcium-ferric clinker production for decorative application.

(6.2) *New Aspects of White Cement Physico-Chemistry* by Zoubekhin, A.P. This paper deals with the cristallochemical transformations of titanium, manganese and iron oxidizing which influence chromaticity and reflection coefficients of while cements. The author also discusses the weakening or strengthening of whiteness index by combination of these chromophoric oxides in reducing or oxyding burning atmosphere with slow cooling or quenching condition.

7 QUICK-SETTING AND HARDENING CEMENT

(7.1) *Shrinkage Problem of Quick-setting Cement* by Hosek, J., Kolar, K. and Novotny, J. The authors describe technical characteristics of quick--setting and rapid-hardening cements made in Checoslovaquia by high--fineness grinding of portland cement clinker with addition of ligninsulphonate as grinding-aid and sodium carbonate as set-retarding addition. The paper also details the way used to measure the true early shrinkage of low w/c paste, free from thermal expansion or mechanical restrain.

(7.2) *Development of a Fast Setting High Strength Cement Composite* by Lasmi , S., Mandal, P.K., Ghosh, R. and Subba RaO, V.V. The paper describes a cement which composition is based on a mixture (not indicated) of high strength portland cement, high-alumina cement, anhydrous calcium sulphate, fused calcium chloride and ground sand for special rapid setting and hardening applications (like plugging, anchoring or grouting). The material hardens in 15 minutes, attains around 10 MPa in one hour and approximately 75 MPa in one day. Heat of hydration, X-ray diffration curves, scanning electron micrographs at different hydration periods and strength development at various ages are given.

8 MISCELLANEOUS CEMENTS

Under this classification enter all binders who have in common only the word cement. A brief review of the three papers coming from India (1), U.S.S.R. (1) and U.S.A. (1) is given bellow.

(8.1) *Non-alitic Cement from Calcium Sulpho aluminate Clinker - Optimization for High-strength and Low-temperature*

Application, by Mudbhatkal, G.A., Parmeswaran, P.S., Heble, A.S., Pai, B.V.B., and Chatterjee, A.K.. These researchers optimized clinker with a mineralogical composition in the $C_4A_3\bar{S}$ - C_2S field as principal compounds and C_2AS, CA, CS, C_4AF, etc. as eventual accessory minerals. They covered in experimental trial batches firing the compositional interval of $3,6<A/S<4,0$ and $2,0<A/\bar{S}<3,0$ at L.S.F. (sulphoaluminate) equal to 1,0 at burning temperatures in the 1200 - 1300°C range. The composition with the best compromise between good mechanical strength and low clinkering temperature was later materialized in pilot plant scale in order to produce cement for field concrete evaluation. According to the authors conclusion, the non-alitic cement performed well up to 4 years exposure to site conditions showing good initial strength, no longtime reversion in mechanical resistance, good sulphate attack and corrosion performance, and excellent low-temperature behavoir during initial hydration.

(8.2) *Sulphate Resistant Alinite Cement*, by Poulatov, Z.P. and Noudelman, B.I. The paper makes a general description of composition and some properties of this kind of cement produced in the Soviet Union on industrial scale. Emphasis is given on the excellent properties against sulphate attack and data is presented on flexural strength and linear expansion of specimen. stored up to approximately 2 years.

(8.3) *Hydrogarnet - Gehlenite Hydrate Cements from $CaO - Al_2O_3 - SiO_2$ Glasses*, by Mac Dowell, J.F. The author presents the results of a comprehensive research about the hydration of $CaO - Al_2O_3 - SiO_2$ glasses, which composition hasn't been much studied yet. The main feature of this work is establishing that the hydration products of these *glassy-cements* are stable hydrogarnet und gehlenit-hydrate, presenting low porosity and high mechanical strength in a fast-hardening way. The potential practical value of this research lead the author to file a patent application.

9 MISCELLANEOUS SUBJECTS

Three papers handle different aspects which are not readily grouped in foregoning subjects and are listed followingly.

(9.1) *Cement of Thermally Activated Laterites. Role of Iron Oxydes on the Strength Development*, by Pera, J. Ambroise, M., Murat, M. and Silveira, M. This contribution belongs to the subject more properly covered by the pozzolanic materials. The authors submitted different laterites to heat treatment at 750°C in order to activate their kaolinitic minerals. Best pozzolanity was achieved with materials containing less than 50% quartz and whose kaolin has a minimum of 10% iron oxyde.

(9.2) *The Behavoir of Certain Compositions Belonging to the $3CaO.SiO_2 - 2CaO.SiO_2 - 2BaO.SiO_2$ System During Hardening*, by Teoreanu, I., and Andreonescu, E.. The authors have synthesized different mixtures containing CaO, BaO and SiO_2 with the aim of producing mineral compounds of the form indicated in the title of the paper. The experimental cements were tested in order to evaluate some of their physical properties in pastes at the initial hydration period and the evolution of hardening by means of compressive strength up to 21 days. According to the authors, the introduction of BaO contributes to stabilize C_2S ss in the α' form during pyro-

processing and to enhance the reactivity with water with a positive effect on hardening by raising mechanical strength.

(9.3) *The influence of Some Additions on the Hydration and Hardening of Tricalcium Aluminate*, by Teoreanu, I. Georgescu, M. and Puri, A.. The paper describes through XRD and DTA data the behavoir of C_3A during hydration in the presence of gypsum and dimethylterephtalate (DMTP).

S. PRISZKULNIK

RC
4.1

Le sous-thème 4.1 "STRUCTURE DES PORES, PERMÉABILITÉ ET DIFFUSION EN RAPPORT À LA DURABILITÉ"a été enrichi par la présentation des 12 travaux suivants:

1. "Microfissuration des bétons", par H.HORNAIN et M.REGOURD.

2. "Le rapport entre la microstructure et la durabilité des ciments avec ajouts", par N.TENOUTASSE et A.M.MARION.

3. "À l'égard de l'analyse de la structure poreuse du ciment durci", par G.BOZHINOV et N.BAROVSKI.

4. "Sur la distribution de chlorure dans la pâte de ciment durcie et sa solution poreuse", par G.BLUNK, P.GUNKEL et H.G.SMOLCZYK.

5. "Rôle de la porosité dans la durabilité des liants hydrauliques", par E.REVERTEGAT et F.BERNAUDAT.

6. "Relation entre la lixiviation d'éléments traces (Cs,Sr et Co) et la microstructure au cours du vieillissement d'un mortier à base de CPA", par J.M.LAMEILLE, R.CHIAPPINI, G.GOUTIÈRE, J.C.PETIT et M.REGOURD.

7. "Modélisation des phénomènes de transport dans les mécanismes d'altération d'une pâte de ciment", par F.BERNAUDAT et E.REVERTEGAT.

8. "Structure poreuse et diffusion ionique aux systèmes adjuvant-ciment Portland avec ajouts", par AMITABHA KUMAR et DELLA M.ROY.

9. "Influence des cendres volantes, ajoutées au ciment, sur les changements de la structure des pores dans les mortiers conservés dans des solutions de NaCl", par S.KRISHNAMOORTHY et N.K.JAIN.

10. "Résistance au gel des ciments aux fillers", par P.GEGOUT, H.HORNAIN, B.THURET et M.REGOURD.

11. "Influence des conditions de durcissement sur la durabilité de la pâte de ciment et du béton", par G.TEODORU.

12. "Le mesurage de la perméabilité", par C.D.LAWRENCE.

La quantification du réseau microfissural des bétons fait l'objet du travail nº 1.

Le travail nº 2 concerne l'évolution de l'hydratation des ciments Portland avec ajouts de cendre volante et inclut un modèle pour le mecanisme de la réaction pouzzolanique.

Le travail nº 3 présent un modèle physique pour l'analyse de la structure poreuse de la pâte de ciment.

Le travaux nº 4 à 9 présentent l'évolution de la diffusion ionique dans la structure poreuse des pâtes de ciments sans et avec ajouts minéraux, ayant en vue soit la résistance à la corrosion de l'acier soit l'interaction avec des déchets atomiques.

La rélation entre la résistance mécanique et la structure poreuse avec la tenue au gel fait l'objet des travaux nº 10 et 11.

Finalement, le travail nº 12 présente une cellule pour mésurer la perméabilité et la diffusion de gas et la perméabilité à l'eau des bétons.

La qualité et l'actualité des cex travaux exigent la présentation et la discussion de chacun d'eux. La restriction du temps a determiné ce resumé que, malheuresement, ne transmet pas avec fidelité leurs précieuses idées.

S. PRISZKULNIK

Dans l'étude intitulé" MICROFISSURATION DES BÉTONS", M.HORNAIN et M.REGOURD ont observé et quantifié le réseau microfissural de bétons.

Les techniques microscopiques et stéréologiques ont été appliquées à l'étude de deux bétons avant et après chargement: l'un de granulats silico-calcaries et l'autre de granulats légers.

Les observations ont été effectuées à 3 échelles (niveaux de structure I, II e III).

À l'échelle centimétrique (niveau de structure I), les exames ont été faits sur plaques polies de béton 10x10 cm, aux gradissement 4 à 40 à l'aide d'une loupe binoculaire qui permet l'observation des distributions et orientations préférentielles des granulats et des interfaces.

À l'échelle millimétrique (niveau de structure II), l'observation a été faite sur sections polies, lames minces ou de répliques, à l'aide du microscope optique ou au microscope électronique à balayage (M.E.B.) à des grandissements compris entre 300 et 1000 environ.

En plus, à l'échelle micrométrique (niveau de structure III), les auteurs ont utilisés le MEB sur fractures, aux grandissements 1000 à 10.000.

Les auteurs discutent les techniques de traitement préalable des échantillons, et le risque que ces opérations peuvent engendrer des contraintes mécaniques, donc des microfissures. Un certain nombre de précautions sont recommandées: échantillons suffisament épais, sciage ménagé, plissage progressif, et contrôle de la déshydration des échantillons destinés aux observations microscopiques.

Pour la visualisation et observation des microfissures, au niveau de structure I, les auteurs utilisent la coloration du béton à l'aide d'une solution alcoolique d'un colorant insoluble dans l'eau (rouge Irgacete par example).

La méthode par imprégnation de résine (epóxy, méthyl-métacrylate...) est surtout utilisée pour caractériser le niveau de structure II. La fractographie au MEB permet la caractérisation du faciès des hydrates et de leur mode de rupture, l'étude des interfaces pâtes de ciment-granulat; l'observation du mode de rupture des granulats et autres inclusions.

La technique des répliques a été aussi developpée et utilisée, permettant l'observation soit au microscope optique en transmisson ou en reflexion, et au MEB après métallisation à des grandissements ne dépassant pas 1000.

Pour la quantification du réseau microfissural, les auteurs ont utilisé la stéréologie, par laquelle ils ont mesuré le nombre d'intersections des microfissures avec un réseau de sécants aléatoires ou orientées.

L'application de ces méthodes a un béton de granulats silico-calcaires et aussi un de granulats légers de schiste expansé a permis d'extraire les conclusions suivantes:

a) avant chargement, au niveau de structure I, dans les deux bétons , des zones de moindre cohésion assimilables à des fissures se manifestant par la pénétration ou la diffusion du colorant, existent aux interfaces pâte de ciment durcie-granulats. Leur quantification montre que leur densité est plus faible dans le béton de granulats légers, la différence étant due à une meilleure liaison entre le liant hydraté et les granulats de schistes expansés.

b) après chargement, les observations faites a niveau de structure I, mettent en évidence

dans les deux bétons la formation d'une fissure principale sous forme d'une bande étroite microfissurée, de quelques centaines de microns de largeur, tortueuse souvent oblique par rapport à la direction de contrainte.

Sous chargement contrôlé, la fracture des deux bétons est essentiellement intergranulaire, sauf localement ou les granulats étaient préfissurés. Dans le béton silico-calcaire, la trace des différentes microfissures constituant la fissure principale est nette et bien dessinée; par contre, elle apparaît plus diffuse dans le béton de granulats légers, dont les propriétés mécaniques (module d'Young en particulier) sont plus proches de celles de la pâte. Cet aspect plus diffus paraît correspondre a un microendommagement de la pâte de ciment proprement dite sur le trajet de la fissure.

S. PRISZKULNIK

RC
4.1

Au travail de N.Tenoutasse et A.M.Marion, sous-titre "LE RAPPORT ENTRE LA MICROSTRUCTURE ET LA DURABILITE DE CIMENTS AVEC AJOUTS", il a été etudiée l'évolution de l'hydratation des ciments composés d'un ciment Portland et de cendre volante, aussi bien que discuté le mécanisme de la réaction pouzzolanique et son rapport avec l'inhibition de la réaction alcalis-granulats.

Les auteurs ont employé un ciment Portland du type I de l'ASTM et une cendre volante de la classe F de l'ASTM, avec lesquels ils ont préparés des ciments contenant de 0 a 80% de cendre, dont l'hydration a été examinée par microscopie électronique à balayage avec le spectre de diffraction des rayons X par énergie dispersive, dès l'âge de 3 jours jusqu'à 2 ans.

La solubilité des alcalis de la cendre a été analysée encore par spéctrométrie d'absorption atomique.

A propos de la solubilité des alcalis de la cendre dans l'eau et dans des solutions saturées de chaux, des essais ont été faits au ciment Portland et au ciment avec ajout de 25% de cendre, pour la détermination de la composition chimique de la solution poreuse dès 5 minutes jusqu'à 8 h.

Les résultats montrent la basse solubilité du K_2O de la cendre, sa libération étant plus facilité à partir du ciment. En relation au Na_2O, aucune altération significative a été observée par la présence de la cendre dans la composition du ciment, ce qui confirme la plus basse solubilité des alcalis de la cendre.

Les micrographies électroniques de l'hydratation des ciments avec ajouts montrent, déjà à l'âge de 14 jours, l'activité pouzzolanique de quelques particules de la cendre volante, à cause de l'occurrence des cristaux typiques de mullite sur ses surfaces. Cependant, la présence de chaux libre et le comportement mécanique de tels ciments composés ne permet la caractérisation d'une importante réaction pouzzolanique à cet âge.

Les auteurs signalent la persistance des particules des cendres intactes après 2 ans d'hydratation, même aux ciments composés avec 10% de cendre, ce qui révèle la profonde hétérogéneité de la réaction pouzzolanique, liée à l'histoire thermique de chaque grain de cendre.

La réaction évoluant, des macropores se font visibles à la surface des particules de cendre, pourtant ils sont invisibles sur les particules intactes.

Au dernier stage de la réaction, les particules se desintègrent.

La réaction pouzzolanique cause la formation massive de silicate de calcium hydraté. La diffraction des rayons X par énergie dispersive révèle la présence de teneurs pas méprisables d'aluminium au silicate, ce qui bien démontre la réaction pouzzolanique entre la phase vitreuse silico-alumineuse de la cendre et l'hydroxide de calcium.

Après des longues périodes de temps d'hydratation, la microscopie électronique ne montre dans la pâte de ciment aucun trait de cristaux de mullite, tandis que la diffraction des rayons X révèle un spectre typique de mullite. On obsèrve, aussi, le monosulfoaluminate de calcium (MSA), mieux cristallisé que dans la pâte pure.

Un aspect notable dans les micrographies concerne la présence des plaques bien cristallisées au ciment composé, avec une morphologie qui rappele celle du $Ca(OH)_2$ et/ou du MSA, mais la diffraction des rayons X par énergie dispersive présente des hautes teneurs de silice et d'alumine et un contenu apreciable de potassium. Le numéro des plaques paraît être proportionnel au contenu de cendre dans la pâte durcie.

S. PRISZKULNIK

La présence de potassium démontre que les alcalis de la cendre sont maintenus dans les produits hydratés qui résultent de la ráction pouzzolanique.

L'analyse des résultats a été, alors, étendue à la réaction alcalis-silice, attribuant l'action bénéfique de la cendre à la facilité de mobilisation du calcium dans les particules siliceuses reactives, ce qui amène à la formation du gel avec haute concéntration en calcium. De la réaction du complèxe alcalis-silice avec le $CA(OH)_2$ résulte le complèxe blanc et opaque d'hydroxide de calcium hydroxide alcalin-silice, non expansible.

Les observations effectuées ont permis, encore, la présentation d'un mécanisme originel pour expliquer la réaction pouzzolanique, incluant les 3 stages suivants:

- diffusion de la phase aqueuse à travers de la pâte de ciment et ou des macropores des particules de cendre aux locaux actives;

- précipitation de $Ca(OH)_2$ au local active (interne ou externement) pour former des masses circulaires de $Ca(OH)_2$;

- réaction entre les masses et la phase vitreuse silico-alumineuse des particules de cendre, amenant à la formation du gel de silicate de calcium-hydraté contenant de l'aluminium (et le potassium en quelques cas), et du silicoaluminate de calcium bien cristallisé contenant du potassium.

S. PRISZKULNIK

Dans le travail intitulé "À L'ÉGARD DE L'ANALYSE DE LA STRUCTURE POREUSE DU CIMENT DURCI", G.BOZHINOV et N.BAROVSKY proposent un modèle physique pour définir et illustrer les principaux caractéristiques de la pâte de ciment.

Les auteurs signalent les suivants facteurs qui intérviennent à l'origine des pores:

a) Immédiatement après le mélange du ciment avec l'eau, le volume absolu de la pâte resulte des parties des volumes du ciment, de l'eau de gâchage et éventuellement par des bulles d'air. Les parties de l'eau et les bulles composent ce qui est appelé volume libre de la pâte du ciment qui est premièrement disponible pour l'augmentation des produits d'hydratation dy ciment.

b) Pendant l'hydratation, ce volume libre augmente par conséquence de la réaction du ciment avec l'eau ayant une partie remplie en même temps avec les produits d'hydratation. Ainsi la quantité d'eau de la pâte est une des principales sources des pores et l'état de l'eau dans le système durci est très important.

c) Les produits d'hydratation présentent des formes et dimensions variées avec plus ou moins d'embriquement entre les particules dont la phase liquide présente des propriétés specifiques au système durci.

Le volume absolu des hydrates est plus grand que celui des grains anhydres, mais il est plus petit que le total des volumes absolus des grains anhydres et de l'eau d'hydratation. Comme, pendant l'hydratation, le facteur E/C en plus de celui strictement demandé par les réactions ne change pas le volume initial de la pâte, le résultat de cet équilibre cause les pores de contraction.

d) La structure complexe des hydrates, ayant des surfaces specifiques, des capacités d'absorption et adhérence extrêmement developpées, outre de la distribution reciproque et de la cohésion entre les particules, predéterminent les conditions à la formation d'une structure poreuse typique.

Dans ce contexte une partie de l'eau est combinée dans les produits d'hydratation, une partie est absorbée aux surface solides et une partie reste hors des champs de force des surfaces solides (eau capillaire). Ces espèces d'eau, présentent des densités diverses et, par conséquent, sont différents quant à leur volumes specifiques, à la force d'adhérence à la phase solide et la volabilité. Sont les espèces que Powers a appelé l'eau évaporable et non évaporable

Ainsi, l'éspace occupé par l'eau évaporable dans la pâte durcie du ciment corréspond au volume total des pores, lequel contient les pores du gel et les pores capillaires. Les pores du gel sont differenciés par Kando et Daiman en intercrystallite et intracrystallite.

On obtient alors que le volume total des pores peut-être presenté par la partie durcie à un certain âge et le volume absolu de la phase solide au même âge, pourvu que le contenu d'air ne soit pas consideré. Dans certains cas la porosité de contraction doit être specialement considerée et traitée comme une partie en separée du volume total des pores.

Pour quantifier les parties des volumes de pores du gel, pores de contraction et pores capillaires, les auteurs proposent, alors, un modèle physique pour la pâte de ciment.

Le concept basique du modèle est que l'origine et l'évolution dans le temps de la structure poreuse sont relacionnées à l'état initial de la pâte et suivent le procès d'hydratation du ciment. Il tient en compte que la contraction est due principalement au gel d'aluminates de calcium hydratés et occupe une partie de l'éspace intra-gel rempli par l'eau capillaire. Les pores du

gel sont relacionnées au gel des silicates de calcium hydratés.

La validité du modèle est limitée aux conditions suivantes:

- le clinker du ciment reçoit seulement l'addition de gypse;
- l'hydrataion a lieu dans un tube d'essai, à la température d'ambiance, de manière à éviter l'évaporation;
- l'hydratation des composés du clinker ne diffère pas de l'hydratation des minéraux purs, le principe de superposition d'effets étant valide;
- le gypse réagit completement avec le C_3A pour former l'ettringite pendant la période initiale d'hydratation;
- le mot gel se refère au gel de silicate de calcium hydraté;
- la teneur en air de la pâte de ciment n'est pas considerée.

Pour le calcul des différentes parties de volumes de pores, sont considerées la composition minéralogique du ciment et les équations chimiques correspondentes aux réactions d'hydratation.

Pour essayer le modèle proposé, les auteurs ont preparé des pâtes de ciment, avec des rapports E/C = 0,30-0,35-0,40-0,45 et 0,50, et ils les ont mises dans de tubes de verre, maintenus hermetiquement fermés à la température d'ambiance, pour les essayer aux âges de 1,3,7,28 et 180 jours.

La quantité d'eau combinée a éte mesurée par analyse thermique différentiel; le volume total des pores a été estimé sur la base de la masse volumique et du poids spécifique de la pâte durcie. La distribution des pores entre 5 et 10^4 nm a été mesurée par le porosimètre à mercure, pour évaluer les pores de contraction et capillaires. La capacité d'absorption a éte mesurée par la méthode d'absorption d'eau.

Les résultats ont confirmé la tendance générale du développement de la structure poreuse avec la réduction progressive du volume total des pores au cours du temps et la conséquente rédistribution des parties des volumes des pores, c'est à dire l'augmentation des volumes des pores du gel et de contraction et décroissement des volumes des pores capillaires et bulles d'air.

Comparant les valeurs estimées selon le modèle, les auteurs ont confirmé une bonne approximation avec le volume total des pores, tandis que la prévision des parties des volumes éxige une confirmation expérimental additionelle.

S. PRISZKULNIK

RC
4.1

Au travail intitulé "SUR LA DISTRIBUTION DE CHLORURE DANS LA PÂTE DE CIMENT DURCIE ET SA SOLUTION POREUSE", les auteurs G.Blunk, P. Gunkel et H.G. Smolczyk, ont appliqué de pressions jusqu'à 500 N/mm² (MPa) pour l'extraction de la solution contenue dans les pores des pâtes de ciments, aux phases de prise et de durcissement, ayant pour objet l'étude de l'évolution de la concentration des chlorures de sodium et de calcium.

Ils ont été utilisés plusieurs ciments Portland et de laitier, aussi bien que les minéraux purs du ciment C_3S et C_3A. Le C_3A a été mélangé avec le $CaSO_4$. H_2O et $Ca(OH)_2$ dans la rélation moléculaire 1:1:0,3.

Les pâtes des ciments et celle contenant le minéral C_3S ont été préparées avec un rapport E/C de 0,60, tandis que la pâte du minéral C_3A a été preparée avec E/C de 0,90.

Pour l'étude à la phase de prise, le chlorure a éte ajouté à l'eau de gâchage des pâtes en teneurs variables de 0,2 a 3,0% par rapport au poids du matériau sans perte au feu.

Pour l'étude à la phase du durcissement, ils ont broyé et tamisé des pâtes sans chlorures et ont conservé les grains compris entre 0,5 et 1 mm dans une solution de chlorure, pendant 28 jours, pour les essais de diffusion.

Les résultats ont montré que le mélange du C_3A fixe une grande partie des chlorures, aussi bien que du calcium et sodium.

Les essais avec C_3S ont montré que les chlorures sont fixés aux ciments non seulement chimiquement pour les aluminates, mais aussi pour les silicates hydratés. En effet, les ciments fixent des teneurs de chlorure compris entre ceux fixés par les minéraux C_3A et C_3S.

Le C_3S a une capacité de fixer les chlorures inférieure à celle du C_3A. Particulièrement, le chlorure de calcium est fixé en grande quantité par le C_3S, tandis que pour le chlorure de sodium elle est limitée, de manière que, au cas du chlorure de sodium, la teneur de chlorure restante en solution est plus grande, comparativement au chlorure de calcium. En même temps, selon les mesures effectuées dans la solution contenue aux pores, le pH accroît avec de chlorure de sodium et decroît avec celui de calcium, par rapport au pH de la solution sans chlorures.

Considérant, alors, la rélation d'ions Cl^-/OH^-, importante pour la corrosion de l'acier, les auteurs l'ont calculée à partir des valeurs mesurées dans des solutions contenues aux pores des pâtes dont l'eau de gâchage a reçu l'addition de 1% de chlorure.

Les résultats ont montré que le désavantage de la plus grande concentration de chlorure de sodium dans la solution est contrebalancé par l'alcalinité supérieure. Ainsi, le chlorure de calcium doit être également consideré ou, bien encore, moins favorable à la corrosion de l'acier par rapport à celui de sodium.

Pour complémenter, ils ont calculé la rélation d'ions Cl^-/OH^- pour des solutions contenues aux pores des pâtes dont l'eau de gâchage a reçu l'addition de chlorure de sodium et qui ont été préparées sans et avec l'addition de sulfates de calcium et de sodium et d'hydroxide de sodium, à la proportion de 0,10 mol par kg de ciment.

Par rapport à la solution sans addition, les résultats ont montré que l'addition de sulfate de calcium augmente un peu la teneur de chlorure soluble, tandis que l'addition d'une quantité equivalente d'hydroxide de sodium augmente d'un tiers la teneur de chlorure soluble et, finalement, l'addition de sulfate de sodium double cette teneur.

· Comme les deux additions, de NaOH et Na_2SO_4, augmentent la concentration de OH^- dans la même échelle, les auteurs montrent que, au cas du sulfate de sodium, les deux anions OH^- et SO_4^{--} diminuent la fixation de chlorure.

S. PRISZKULNIK

Le rapport presenté par E.Revertegat et F. Bernaudat sous-titre "ROLE DE LA POROSITÉ DANS LA DURABILITÉ DES LIANTS HYDRAULIQUES" fait part d'une étude de la prévision de la durabilité des liants hydrauliques utilisés dans les stockages des déchets radioactifs pour la fabrication de l'infrastructure des conteneurs et des matrices d'enrobage.

Pour justifier une durabilité sur 300 ans de ces liants, deux types d'essais sont menés en parallèle:

- mise en évidence des interactions chimiques entre les pâtes de ciment et diverses solutions aggressives(chlorure, sulfate, acides carboniques et humiques) qui peuvent être présents dans l'eau souterraine dans un site de stockage de déchets;

- détermination des paramètres régissant le transport des ions en solution dans la pâte de ciment et, en particulier, mesure des coefficients de diffusion.

Le travail présente les premiers résultats concernant les ciments CPA et CLC, agressés par des solutions de NaCl.

Les éprouvettes utilisées dans l'etude des mécanismes d'interactions chimiques sont des plaquettes rondes de 4 mm d'épaisseur et de 70mm de diamètre. Le rapport E/C des pâtes est de 0,37. Après conservation des plaques pendant 3 mois dans une eau saturée en chaux, elles sont immergées dans des bacs, dont la concentration em ions Cl^- est respectivement de 0- 0,2- 2et 20g/l. Pour chaque concentration, deux valeurs de pH sont étudiées: 11,5 et 13.

A chaque échéance (0-1-3-6 mois) les mesures et analyses suivantes ont éte réalisées: resistance mécanique en flexion; porosité au mercure et à l'eau; teneur en $Ca(OH)_2$par thermogravimétrie; analyse chimique des éléments par fluorescence X; profil de diffusion du chlore par microanalyse électronique; étude microstructurale par diffraction des rayons X et microscopie électronique à balayage.

L'étude de la diffusion est réalisée en cellule de diffusion sur des éprouvettes de 4mm et 1,5mm d'épaisseur . Le pH de la solution dans chaque compartiment est égal à 13. La concentration en ions Cl^-dans le compartiment "amont" présente les valeurs 0,2, 2 et 20g/l, et la teneur en ions chlorure qui diffusent dans le compartiment "aval" est analysée par chromatographie en phase liquide.

Les auteurs présentent les conclusions suivantes:

La principale dégradation observée dans une pâte de ciment CPA, soumise à l'agression d'une eau chlorée, ne sera pas due à l'apparition des chloroaluminates, mais à une augmentation de la porosité engendrée par la solubilisation de l'ettringite et essentiellment de la chaux. Ce phénomène de solubilisation et de lixiviation de $Ca(OH)_2$ est d'autant plus important que le pH de l'eau de contact est faible et que la concentration en ions Cl^- est élevée.

Pour une pâte de ciment CLC les differences essentielles de comportement avec la pâte de ciment CPA sont les suivantes:

- une distribuition de pores à l'origine plus fine et qui ne pourra que s'accentuer lors de l'hydratation progressive de produits siliceux. Par conséquence le ciment CLC possède un chemin diffusionnel, pour les ions agressifs ou radioactifs, plus fins que le ciment CPA;

- une quantité de $Ca(OH)_2$ a l'origine plus faible et qui ne peut que décroître lors de l'hydratation. Par conséquence un ciment soumis à l'action des chlorures étant

essentiellement affecté par la disparition de la chaux, le ciment CLC sera plus résistant qu'un ciment CPA;

- après attaque, l'augmentation de la porosité totale est nettement inférieure (+ 18% au lieu de 62% pour les ciments CPA à l'echéance de six mois dans une solution à 20 g/l de Cl^-). La quantité de chaux qui réagi avec les chlorures et qui s'est lixiviée est nettement moins importante que celle d'un ciment CPA;

- absence d'un domaine poreux entre 0,06 µm et 0,90 µm, observé sur les ciments CPA après attaque, et qui a été attribué à la lixiviation de la chaux;

- bien qu'un retard dans l'hydratation des produits siliceux a été observé à pH = 11,5 un début de cloisonnement de la fine porosité apparait pour les fortes concentration en chlorure. Ce phénomène est probablement dû à l'apparition abondante de chloroaluminate dans une structure peu lixiviée. Pour de ciment CPA il y a à la fois cloisonnement et augmentation de la fine porosité, sous la double action de l'appartition des chloroaluminates et de la lixiviation importante de la chaux et de l'ettringite.

Lorsque les ions Cl seront véhiculés dans une eau interstitielle de pH = 13 la modification de la matrice du ciment CLC sera pratiquement inexistante. Il n'existe donc pas une barrière "protectrice", comme dans le ciment CPA, qui pourrait freiner la lixiviation des radioéléments vers l'extérieur du béton. Reste à savoir comment évoluera cette "barrière" lorqu'elle sera atteinte par le front de dégradation.

S. PRISZKULNIK

RC
4.1

Le travail sous-titre "RELATION ENTRE LA LIXIVIATION D'ELEMENTS TRACES (Cs, Sr et Co) ET LA MICROSTRUCTURE AU COURS DU VIEILLISSEMENT D'UN MORTIER A BASE DE CPA", presenté par J-M.Lameille, R.Chiappini, G.Goutière, J-C.Petit et M.Regourd concerne les relations existentes entre les relâchements de certains radioéléments (60 Co, 90 Sr et 137 Cs) sous l'action du lessivage par l'eau et l'évolution des caractéristiques cristallochimiques et microstructurales de la matrice cimentée à base de ciment Portland artificiel (CPA) dans laquelle certains déchets radioactifs sont solidifiées, en vue de leur stockage.

L'étude a envisagé les 2 types possibles d'altération affectant le confinement des radioéléments, soit la déstruction directe de la matrice due aux différentes aggressions physiques et chimiques, et les modifications minéralogiques, structurales ou textures qui pourraient conduire à une augmentation excessive des relâchements de radioactivité.

Le mortier utilisé comme enrobé avait la composition suivante: 1000 kg de ciment, 750 kg de sable, 400 l de concentrât d'evaporateur, c'est à dire d'une solution contenant principalement des borates de sodium (~25.000 ppm de bore) et 60 kg de chaux, ce qui donne un rapport E/C de 0,4. La chaux introduite sert à stabiliser les borates sous forme calcique et donc à diminuer leur effet retardateur.

Ce mortier a été utilisé pour la confection des éprouvettes 2 x 2 x 16 cm, qui ont été placées sous une couverture de 2 cm d'argile, recouverte par 2 cm d'eau.

En plus d'une étude en "temps réel" à 10°C (température interne du site) qui sert de reférence, les auteurs ont choisi d'accélérer les cinétiques tout en évitant de dégrader trop brusquement et articiellement la matrice. Ceci a été réalisé en augmentant la température de conservation des éprouvettes jusqu'à 60°C. A chaque échéance, ils ont mesuré sur les différentes éprouvettes les paramètres physiques suivants: résistances mécaniques en compression, porosités, masses et gonflements. La microstructure a été étudiée au moyen d'un microscope électronique à balayage (MEB), d'une microsonde électronique et de la diffraction des rayons X.

Les éprouvettes dopées au césium 137 ou au cobalt 60 sont des orthocylindres carottés de 2 cm. Elles ont été ensuite stockées à 10°C, 40°C ou 60°C pendant un temps donné, puis lixiviées à 10°C dans de l'eau déminéralisée. Les lixiviations ont été menées en dynamique, c'est-à-dire avec renouvelement de l'eau: 3 fois la première journée, chaque jour la première semaine, chaque semaine le premier mois, chaque mois le premier semestre et enfin tous les semestres. Un enrobé n'ayant pas subi de vieillissement (lixivié immédiatement après la cure en atmosphère humide) sert de referénce. Les mesures de radioactivité dans les lixiviats on été effectuées au moyen d'un spectromètre muni d'un détecteur NaI ou GeLi.

Lors des expériences d'hydratation des composés simples, il a été étudié la rétention de chaque élement trace au cours des hydratations de C_3S, de C_3S + C_3A puis de C_3S + C_3A + gypse avec un rapport e/s ~10. La filtration a été effectuée sur filtre millipore de 0,45 µm et l'hydratation a été stoppée par trois lavages à l'éther et par cryosublimation. Le solide a été ensuite examiné au cours du temps au moyen de diverses techniques physiques d'analyse complémentaires (MEB, DRX, microsonde électronique et ionique etc...). La solution a été analysée soit par volumétrie et par absorption atomique.

La principale observation de cette étude est qu'il n'existe pas de lien directe entre les variations, au cours du vieillissement,

des caractéristiques macroscopiques de la matrice cimentée (résistances mécaniques, porosité, texture etc...) et les taux de lixiviation du césium et du cobalt. En fait, cette matrice se comporte comme un CPA classique du faite que le borate de sodium est stalibisé par de l'hydroxyde de calcium et que sa teneur dans la formulation est maintenue à une valeur suffisamment faible (<25.000 ppm dans la solution de gâchage). Compte tenu des concentrations en radioéléments introduites (Cs: ~$4,1.10^{-3}$ ppm; Co: ~$1,6.10^{-3}$ ppm), il est vraisemblable que les composés incorporant effectivement ces radioéléments représentent une très faible fraction de la masse totale de la matrice. Il est donc normal que la formation et/ou l'évolution au cours du temps de ces composés n'induisent pas de modifications des proprietés macroscopiques de la matrice.

Par contre, les caractéristiques de lixiviation de ces élements sont directement liées à la forme chimique sous laquelle ils sont présents. En particulier, les courbes de lixiviation suggèrent l'existence de deux étapes: dans un premier temps la fraction des radioéléments restée dans l'eau interstitielle (~30%) est relâchée par diffusion; cette fraction est déterminée par le coefficient de partage solide/liquide lors de la prise du ciment. Ceci se produit lorsque les conditions physico:chimiques sont peu agressives. La durée de cette première étape, qui est effectivement observée expérimentalement, diminue lorsque la température de vieillissement des échantillons augmente. Par exemple à une transformation des composés incorporant le radioélément soit à leur corrosion par la solution lorsque celle-ci est suffisament aggressive.

Les auteurs ont discuté les comportements spécifiques du Cs et du Co et ont presenté les conclusions suivantes:

- la température induit des variations microstructurales importantes de la matrice. Toutefois, les taux de lixiviation observés ne peuvent être directement corrélés à ces modifications physiques mais plutôt aux formes chimiques de rétention des radioéléments. La température influe également fortement sur la transformation au cours du temps de ces composés. Par exemple, la transformation des aluminates en leur forme stable induit le piégeage d'environ 10% de césium supplémentaire et, après 6 mois à 60°C, 80% du césium se trouve dans les aluminates. A long terme, seule leur transformation ou leur destruction sous l'action de l'environnement peut permettre la libération du césium. De même la fraction du cobalt piégé dès la prise est ~99,8%; la destruction de l'hydroxychlorure formé initialement entraîne l'incorporation de cet élément dans les CSH qui gouverneront donc son relâchement à long terme.

Toutefois, compte tenu des périodes de temps (300 ans) sur lesquelles une évaluation du relâchement des radioéléments doit être effectuée, il est nécessaire de poursuivre ce type d'étude sur des durées beaucoup plus longues (plusieurs années), au moins jusqu'à ce qu'un état stationnaire soit observé. L'identification des composés dans lesquels s'incorporent les divers radioéléments, ainsi que la connaissance de leurs propriétés thermodynamiques, est un élément clef d'une telle étude. Par conséquent, le confinement des déchets nucléaires dans des matrices à base de ciment est un problème auquel la chimie des ciments, et en particulier des éléments traces, doit apporter une contribution décisive.

RC 4.1

S. PRISZKULNIK

Au travail intitulé "MODELISATION DES PHENOMENES DE TRANSPORT DANS LES MECANISMES D'ALTERATION D'UNE PATE DE CIMENT", F. Bernaudat et E. Revertegat étudent une modélisation pour la prédiction du comportement d'un liant hydraulique en présence d'eau chargée d'ions dans le cadre d'un stockage de déchets radioactifs, dont la durée de vie est de 300 ans

L'approche expérimental entreprise a été décomposée en trois séries d'essais: des essais d'attaque de pâtes de ciment par des ions agressifs (ciments CPA et CLC, attaque par des ions chlorure et sulfate); des essais en cellule de diffusion permettant de mesurer le coefficient de diffusion d'ions agressifs. La troisième série d'essais a permis de mesurer les paramètres du transport des éléments radioactifs tels que le césium, et l'eau tritiée.

Dans un premier temps les auteurs ont cherché à interpréter les expériences de diffusion par un modèle simple faisant intervenir un transport par loi de Fick dans un milieu poreux. Dans les cas où un transfert a pu être détecté, ils ont montré qu'un phénomène d'adsorption-désorption quelquefois réversible se superpose à la diffusion, et cela même pour l'eau tritiée. De plus, le régime permanent qui est atteint au cors de ces essais n'est qu'apparent. Au bout d'un temps assez long après le passage en régime permanent, les points expérimentaux ne s'alignent plus sur la courbe théorique.

Dans d'autres cas, la seule loi de Fick, même avec adsorption réversible, ne permet pas d'expliquer les résultats. C'est ce qu'on obsèrve avec un ciment très poreux comme le CLC (porosité ~32%) lequel ne laisse pratiquement rien diffuser alors qu'un CPA (~25%) donne un résultat tout à fait interprétable.

Un autre modèle a donc été développé. Celui-ci fait intervenir à la fois des phénomes de transport par diffusion (avec ou sans adsorption) et des équilibres chimiques dans la solution interstitielle de la pâte de ciment. L'équation de diffusion a été modifiée de façon à tenir compte des variations de porosité dues à la formation ou à la disparition de précipités. Les équations "chimiques" sont résolues par une méthode de Newton-Raphson. L'ensemble permet d'interpréter aussi bien des essais de diffusion que des essais d'agression.

Le modèle résout simultanément et à chaque pas de temps:

. Une équation de diffusion, pour chaque espèce en solution dont on aura déterminé le coefficient de diffusion et le taux de retard,

. Un système d'équations que l'on peut diviser en deux types:

  - des équilibres chimiques

  - des équations de conservation.

RC
4.1

S. PRISZKULNIK

Le travail presenté par Amitabha Kumar et Della M. Roy, sous titre"STRUCTURE POREUSE ET DIFFUSION IONIQUE AUX SYSTÈME ADJUVANT-CIMENT PORTLAND AVEC AJOUTS", concerne l' invetigation sur matériaux cimentés durcis saturés de l'eau des mécanismes de diffusion d'éspèces ioniques et son rapport aux propriétés basiques des matériaux, ayant pour but reveler les effets de la porosité et de la distribution des dimensions des pores sur la diffusion ionique dans ces matériaux.

L'étude expérimentale s'est developpé en pâtes preparées avec du ciment Portland type I de l'ASTM sans et avec l'addition de laitier de haut fourneau, cendre de basse teneur en calcium, silice amorphe ulrafine et grains fins de quartz . Le rapport E/C de ces pâtes a varié de 0,30 a 0,40 et une partie d'elles a reçu l'addition d'un superfluidifiant, au dosage de 0,331% par rapport au poids des solides.

Des éprouvettes cylindriques de 3,5 cm de diamètre et 1,7 ou 3,2mm de hauteur ont été moulées et conservées pour le premier jour sous l'eau déminéralisée et, après démoulage, dans une solution saturée d'hydroxide de calcium, aux temperatures de 27°, 38° et 60° C.

La diffusion de chlorure de cesium a été étudiée après 7, 28, 90, 180 et 365 jours. 4 éprouvettes de chaque hauteur pour chacune pâte ont été essayées a chaque âge.

Les éprouvettes on été preparées un jour avant le début de l'essai. Elles ont été retirées des bacs de conservation, lavées sous l'eau déminéralisée et polies aux deux faces avec feuille de carbure de silicium, pour l'obtention de disques de 1,68± 0,05 ou 3,18± 0,05mm d'épaisseur. Ces disques se sont constitués en cellules de diffusion saturées de solution d'hydroxide de calcium.

A chaque semaine, un disque de chaque épaisseur a été retiré du bac pour la détermination des teneurs de Cs^+ et Cl^-présents dans la solution contenue dans la cellule.

L'analyse de Cs^+a été faite par absorption atomique, tandis que le Cl^-a été mesuré avec un électrode ionique spécifique.

Des disques semblables ont été soumis aux essays en porosimètre à mercure. Avant les essais, les éprouvettes ont été sechées a - 80°C et 2,67MPa. La porosité et la distribuition des dimensions de de pores entre 7,5 µm et 1,9 nm ont été mesurées par l'emploi de mercure sous pression jusqu'à 386 MPa et le calcul a été fait sur la base d'un angle de 140° pour le contact entre le mercure et la pâte sèche.

Les resultats obtenus montrent que la porosité des pâtes de ciment Portland decroît de 3 à 5% avec la réduction de 0,05 au rapport E/C. A mesure que l'âge avance, la porosité diminue, la différence étant supérieure à 27°C et inférieure à 60°C. La dimension moyenne des pores augmente avec l'âge pour les rapports E/C plus élevés et augmente toujours entre 6 mois et 1 an d'hydratation, la porosité diminuant quand même.

L'addition de laitier provoque une réduction à la porosité et aux dimensions des pores. Pour la silice amorphe finement broyée les pores ont des dimensions inférieures, tandis que la porosité est nominalement supérieure. La pâte avec du quartz finement broyé présente un comportement semblable à celle de réference a 27°C, tandis qu'à 60°C elle présente une porosité inférieure et des pores plus petits. La cendre volante produit des porosités supérieures à 7 et 28 jours, mais la distribution des dimensions de pores à 28 jours preuve qu'il y a eu une augmentation des pores plus fins.

L'accroissement des pores plus fins élève la tortuosité ou l'entreliaison des pores, aménant le délai de la diffusion ionique, ce qui a été confirmé pour les résultats d'essais.

L'essai de diffusion ionique des pâtes de ciments Portland a permit démontrer qu'une augmentation du rapport E/C accroît le coefficient effective de diffusion d'ions Cl^+et Cs^-.

Les résultats montrent encore que la diffusion du cation est en général rallenti par rapport à celle de

l'anion, ce qui permet de considérer la pâte de ciment Portland comme une mebrane électronegative.

En particulier, le laitier de haut founeau retarde effectivement la diffusion du Cl^-, tandis que la diffusion du Cs^+ est exceptionnellement basse quand la pâte est préparée avec de la silice amorphe finement broyée.

Ces résultats ont une application directe à la protection des aciers contre la corrosion et à l'enrobage des déchets nucléaires.

S. PRISZKULNIK

Le travail de S.Krishnamoorthy et N.K.Jain, intitulé "INFLUENCE DES CENDRES VOLANTES, AJOUTÉES AUX CIMENTS, SUR LES CHANGEMENTS DANS LA STRUCTURE DES PORES LES MORTIERS CONSERVÉS DANS DES SOLUTIONS DE NaCl", concerne l'étude de l'influence de l'addition de cendre volante à 2 ciments Portland, en vue de déterminer la nature des changements au grandeur des pores des pâtes durcies et son influence sur la durabilité des éprouvettes de mortiers preparés avec ces ciments.

A propos de la composition chimique pontentiel de Bogue, un des ciments présente 3,63% de C_3S et l'autre 33%. Deux autres ciments composés ont été préparés par l'addition de 25% de cendre volante à chacun de ces ciments Portland.

En utilisant un motier mélangé avec 1 partie de ciment, 3 de sable normal et 0,4 de l'eau distillée, des éprouvettes prismatiques de 40x40x160mm³ ont été moulées. Elles sont restées pendant 24 heures sous un tissus de jute mouilleé et, après, sous l'eau courante et dans de solutions à 3% et 6% de chlorure de sodium, pour des essais en 7, 28, 90, 180 et 365 jours.

Les éprouvettes prismatiques ont été soumises à la détermination de la résistance à la flexion et, ensuite, les respectives parties ont été essayées à la compression. Après la rupture, des pétits échantillons ont été retirés, traités avec acétone, sechés à 105°C et conservés dans un déssiccateur à vacuum pour arrêter l'hydratation.

Des mesures en porosimètre à mercure ont été faites aux échantillons ainsi traités, avec de pressions jusqu'à 407 MPa.

Par la fragmentation des échantillons, les grains passants par le tamis de 45 μm ont été separés en vue de l'obtention de difractogrammes de rayons X, en relation à l'étalon de platine.

Les résultats obtenus ont montré:

a) les mortiers de ciment curés dans des solutions de NaCl présentent une résistance mécanique inférieure que ceux maintenus sous l'eau courante, étant la chute de résistance plus accentuée au ciment avec moins de C_3S. L'addition de la cendre volante attenue cette chute;

b) l'attaque des mortiers de ciment Portland par le chlorure de sodium provoque une augmentation de la grandeur des pores, à cause de la dissolution de la pâte durcie, liée à la formation de chlorure de calcium et de chloroaluminate de calcium. L'addition de la cendre volante à ces ciments inhibe la formation de pores plus grands, au cas de la cure faite dans des solutions de NaCl;

c) les difractogrammes de rayons X indiquent la formation d'une grande quantité de $Ca(OH)_2$ aux mortiers préparés avec les deux ciments portland et curés à l'eau courante. Quand ces mortiers sont curés dans des solutions de NaCl, il est observé la formation de chloroaluminate de calcium, avec la reduction considérable de $Ca(OH)_2$.

Pour les épprouvettes préparées avec les ciments composés avec de la cendre volante des petits teneurs en $Ca(OH)_2$ sont observés. Pourvu que le $Ca(OH)_2$ a été consumé dans la réaction pouzzolanique avec la cendre volante et qu'une autre partie a reagi pour former le chloroaluminate de calcium, la possibilité de lixiviation de produits solubles est sensiblement diminuée.

S. PRISZKULNIK

Le rapport de P.Gegout, H.Hornain, B.Thuret et M.Regourd sous-titre "RESISTANCE AU GEL DES CIMENTS AUX FILLERS" a pour objet caractériser l'influence d'un filler calcaire sur la tenue au gél des mortiers de ciment Portland avec ajouts (CPJ).

Deux ciments, contenant respectivement 15% et 30% de filler calcaire, ont été préparés par mélange d'un CPA industriel et d'un calcaire (98% de $CaCO_3$) broyés séparément à 3.500 et 3.700 cm^2/g respectivement.

Des prismes de mortiers 4x4x16cm ont été gâchés avec différents rapports E/C dans le but de comparer leur comportement soit à E/C constant, soit à E/(CPA contenu dans le mélange) constant.

Des quantités variables d'entraîneur d'air ont été ajoutées à l'eau de gâchage afin d'obtenir des quantités d'air différentes et des bulles plus ou moins éspacées.

Les prismes ont été conservés dans l'eau à 20°C.

Après 7 jours, le module d'Young a été determiné à partir des mesures de résonance en flexion, sur les 9 prismes de chaque série. Le prisme présentant la valeur médiane a été sélectionné pour le compactage des bulles d'air et le calcul du facteur d'éspacement de ces bulles, par la technique des traversées linéaires. Les 8 autres prismes ont été conservés dans l'eau a 20°C jusqu'à 105 jours.

A 105 jours, 4 prismes sur 8, présentant le module d'Young le plus proche de la valeur médiane, ont été introduits dans l' enceinte de gel, et les 4 autres ont été soumis à la détermination de la résistance mécanique en compression.

Les prismes ont subi 300 cycles au total, restant chacun 3h à l'air à une temperature de -20°C et 1h dans l'eau à une temperature de +20°C, étant de l'ordre de 10°C/h la vitesse de refroidissement.

En plus, il a été calculé a l'espacement moyen critique des bulles d'air ($\bar{L}cr$), définie comme l'espacement au-delà duquel un matériau donné ne résiste pas aux conditions de gel imposés. Cette valeur a été déterminé après 100 cycles.

Les principaux résultats obtenus ont permis de mettre en évidence les points suivants:

Avant gel:

- A E/C égal, les résistances mécaniques diminuent quand la teneur en filler augmente.

- La diminution des résistances est due dans ce cas, à l'accroissement de la proportion d'eau disponible relativement à la quantité de CPA proprement dit dans le ciment fillérisé. Pour un rapport E/C constant, le rapport"E/CPA" augmente avec la teneur en filler.

- Une correction du rapport E/C tenant compte de l'excès de l'eau engendré par la présence de filler, permet d'obtenir des résistances comparables à celles des CPA.

Après gel:

- L'addition d'entraîneur d'air permet d'introduire dans les mortiers un réseau de bulles susceptibles d'améliorer leur comportement au gel.

- En fonction du rapport E/C et de la teneur en filler, il est possible de déterminer un espacement moyen critique des bulles d'air ($\bar{L}cr$), au-delà duquel le mortier devient gélif dans les conditions expérimentales choisies.

- Pour un même ciment, $\bar{L}cr$ diminue quand **E/C augmente.**

- Toutefois la correction du E/C tenant compte de l'excès de l'eau apporté par la présence de filler permet d'obtenir des $\bar{L}cr$, donc des résistantes au gel, comparables à celles des CPA.

- L'abaissement des résistances mécaniques dans le cas des fortes teneurs en air entreiné, ($\bar{L}$ faible), n'a pas d'incidence néfaste sur la tenue au gel des mortiers dont les $\bar{L}$ restent inférieurs aux $\bar{L}cr$.

RC
4.1

S. PRISZKULNIK

Le rapport de M.George Teodoru, intitulé "INFLUENCE DES CONDITIONS DE DURCISSEMENT SUR LA DURABILITÉ DE LA PÂTE DE CIMENT ET DU BÉTON", présente les recherches sur des composants minéralogiques purs du ciment Portland, sur des ciments et bétons, en vue d'expliquer qu'une haute résistance mécanique n'est pas un indice suffisant pour un béton durable, mas c'est surtout sa structure qui est déterminante.

Les recherches entreprises incluent d'abord des examens aux microscopes, optique et électroctronique, sur les silicates tricalcique (C_3S) et dicalcique (C_2S),l'aluminate tricalcique (C_3A), l'aluminoferrite tétracalcique (C_4AF) et sur suspensions de ciment, pour deux conditions d'hydratation: l'une à 20°C et l'autre par l'autoclavage.

La suspension de C_3S après autoclavage présente après 6h la formation de grands "éventails" vigoureux ayant comme point de départ les granules de C_3S. Le champ reste presque vide, ou peuplé par des petits fragments. Le développement des cristaux après traitement est réduit, le processus étant presque terminé à ce moment-là. On trouve dans les suspensions après autoclavage de moins nombreux cristaux de portlandite.

L'autoclavage augmente fortement la vitesse d'hydratation du C_2S, plus que dans le cas du C_3S. Cette constatation est confirmée aussi par l'action favorable de l'autoclavage sur les résistances en compression par rapport aux résistances à 28 jours de durcissement des pâtes de C_2S pur.

Pour le C_3A, le traitement à l'autoclave est le plus défavorable, parce qu'il freine l'hydratation, la résistance en compression après autoclavage étant presque nulle.

Sous le traitement en autoclave, le C_4AF s'hydrate plus intensément que dans le cas du durcissement à 20°C et donne de grandes quantités d'hydroxide de calcium et d'hydroxide de fer.

En général, les formations cristallines qui résultent de l'autoclavage possèdent des dimensions beaucoup plus petites que celles obtenues par les traitements hydrothérmiques sans pression et par conséquent un grand degré de dispersion, ce qui mène à un haut niveau d'énergie potentielle de surface.

L'auteur a utilisé aussi la vitesse de propagation longitudinale et l'atténuation des ultrasons ayant comme but l'obtention des informations plus globales sur un grand volume de béton caractérisé par une répartition aléatoire des phénomènes remarqués à microéchelle.

Les résultats laissent entrevoir l'existence des défauts sur la structure des bétons traités à l'autoclave. Malgré les très grandes résistances du béton autoclavé, les vitesses des ultrasons sont basses par rapport aux valeurs obtenus pour le béton durci dans de conditions normales.

La présence de ces défauts dans la structure des bétons autoclavés influence la durabilité, comme il a été verifié par l'auteur à travers des essais sur des prismes de béton 10x10x55cm³ après saturation à l'eau, en mesurant la variation de:
- module d'élasticité dynamique par l'excitation des oscillations longitudinales;
- décrément logarithmique des oscillations forcées de la courbe de résonance;
- décrément logarithmique des oscillations libres mesuré de la courbe de décroissance des amplitudes, suite à l'exposition aux cycles de gel-dégel.

Les résultats obtenus montrent pour le béton durci dans des conditions standard une résistance au gel-dégel beaucoup plus grande que pour celui autoclavé.

S. PRISZKULNIK

Le travail de C.D. Lawrence, sous le titre de "LE MESURAGE DE LA PERMEABILITÉ" décrit le projet et les essais entrepris pour la mise en service d'une cellule de perméabilité, en utilisant des éprouvettes de 150 mm de diamètre et 50 mm de hauteur.

Pratiquement, la même cellule permet la réalisation des essais de perméabilité et de diffusion au gas et de perméabilité à l'eau.

Au cours des essais de perméabilité au gas oxygène, l'auteur identifique la grande influence de l'humidité relative des échantillons, qui doit être soigneusement équilibrés avant l'essai, et propose un période de 4 semaines pour la conservation des éprouvettes en béton commun.

Ces essais ont permis, encore, montrer une correlation entre la perméabilité à l'oxygène et la résistance à la compression de bétons curés à 20°C sous l'eau, préparés avec du ciment Portland ou bien avec de remplacement partiel de laitiers granulés de haut fourneau ou de cendres volantes.

Pour le mesurage de la diffusion d'oxygène, la cellule exige une modification pour permettre l'entrée et la sortie du gas à travers des surfaces planes des éprouvettes. Une autre modification necéssaire est à respect de la ceinture d'etancheité, cas il a éte verifié que la ceinture de PVC a presenté une légère absorption de l'oxygène, alors elle a été substituée par du polyuréthane.

Pour la mesure de petites concentrations d'oxygène au courant de gas nitrogène il a été employée une cellule électrochimique contenant un diaphragme chauffé d'oxide de zirconium.

Les essais ont permis démontrer une correlation entre la perméabilité et la diffusion de l'oxygène, au cas des éprouvettes conservées à 55% d'humidité relative.

La mesure de la perméabilité à l'eau est faite avec une cellule semblable, mais la longue durée de l'essai a exigée des précautions aditionnelles incluant la ceinture d'étancheité en polyuréthane et l'enveloppement du tube interne avec un gros tissus de nylon pour libérer des très petites quantités de gas sous pression qui diffusent à travers des parois du tube interne, sous-peine d'intérferer à l'écoulement de l'eau par l'épprouvette.

COMMUNICATIONS REPORT ON SUB-THEME 4.2 -
MECANISMS OF CEMENT PASTE DEGRADATION DUE TO
CHEMICAL AND PHYSICAL PROCESSES

RC
4.2

I - INTRODUCTION

Eighteen communications received by the Congress were classified as relating to subtheme 4.2 and proceeded from France (4), West Germany (3), URSS (2), Spain (2), China, Switzerland, New Zealand, Japan, Yugoslavia, Czechoslovakia and Egypt (one from each country).

In a previous appreciation of described subjects, the works can be distributed as follows: sulfate attack (6), decomposition by heat treatment (3), CO_2 corrosion (3) and other studies (6).

1. Sulfate attack

1.1 - "The influence of alite content on the sulfate resistance of Portland cement."
D. DIMIC and S. DROLJC - Yugoslavia

1.2 - "Contribution to the study of the chemical resistance of cements. Behaviour mechanical - resistance of a Portland cement (with a content calculated of C_3A null) opposite to diverse aggressive solution".
D.G. TEBAR, J.L.S. MORENO, V.G. VILA
Spain.

1.3 - "A contribution to the study of ettringite caused expansion".
R.DRON, F. BRIVOT - France

1.4 - "Sur le role de la phase siliceuse dans les processus de destruction de la pierre de ciment dans les milieux de sulfate."
F.F. ALKSNIS, V.I. ALKSNE - URSS

1.5 - "Destruction of historical buildings by the formation of ettringite or thaumasite".
U. LUDWIG and S. MEHR - West Germany

1.6 - "The sulphate resistant Portland cement are not ultimate answer to the problem of sulphate attack"
R.T. MORALES - Spain

On the work 1.1, of DIMIC and DROLJC, the authors investigate six sulfate-resisting Portland cements and one ordinary Portland cement, with different mineralogical composition, in regard to their sulfate resistance by the Koch-Steinegger method. The results show that mortar prepared from ordinary Portland cement with a high content of C_3A (10,3%), as expected, deteriorated significantly in the 10% w/v solution of Na_2SO_4 . 10 H_2O.

Comparison of sulfate-resisting Portland cements shows that the cements with relatively low C_3A content and with a C_3S content lower than 60% could be declared as sulfate resistant, while cements with higher content of C_3S (77,0% and 66,5%) and at the same time lower C_3A(3,2% and 3,4%)

content reacted more strongly with sulfate ions, forming ettringite and gypsum, as showed by X-ray analysis.

On the basis of test results and field experience they conclude that for better sulfate resistance of a Portland cement, the C_3S content is also an important factor, besides the C_3A content, and propose a revision on Yugoslav Standard.

On the work 1.2, TEBAR et al. present the results of a long-therm laboratory study of submitting a industrial sulfate-resisting

Portland cement, of calculated Bogue potencial composition of C_3A null, C_4AF 10,8%, C_3S 75,6% and C_2S 6,1% to solutions of gypsum, sodium and magnesium sulfate during 1.800 days, in mortar samples of 1x1x6 cm, 4x4x16 cm, 7x7x28 cm and concrete samples of 10x10x40 cm.

The results show that the Koch-Steinegger coefficient is higher than 0,70 on all cases and the evolution of mechanical strength is function of the solution composition.

On the work 1.3, DRON and BRIVOT propose a model for studying the ettringite expansion by calcining at 1000°C a stechiometric mixture of aluminum sulfate and pure calcium hydroxide.

The hydration of this calcined ettringite, to the form with 32 H_2O, is accompained by a type Calvet microcalorimeter and the expansion mesured by an apparatus properly developed (p.4).

The rehydration of a pure paste is completed within 2 hours, having a linear expansion near of 10%, without restriction.

The greatest pressure is given by the cristallization forces; the application of a unilateral restriction, even near of 0,1 MPa neutralizes completely the expansion in the correspondent direction, pointing out that the expansion pressure is not significant, when compared to cristallization pressure.

On the work 1.4, of ALKSNIS and ALKSNE, the authors show that in environment conditions, in presence of SO_4^{2-} and CO_3^{2-}, besides the transformation of aluminous phase in ettringite, thaumasite formation will be expected, by transformation of siliceous phase; and more, the mechanism of this reaction depends on ambient temperature. Over 20°C ettringite is detected and bellow 10°C, thaumasite.

On sample with composition $(CaO)_3.Al_2O_3$: : $CaSO_4.0,5\ H_2O$: $CaCO_3$ = 1:4,7 : 3 (molar parts) was observed a complete desapearence of ettringite, 6 months after the action of CO_2 of environment.

Although this thaumasite formation mechanism is not sufficiently clear, the material behaviour control at low temperatures, besides sulfate resistance determination, would be considered as mandatory requirement.

On the work 1.5, of LUDWIG and MEHR, the formation of ettringite ($C_3A.Cs_3.H_{32}$) and thaumasite ($Cc.Cs.CS.H_{14,5}$) is identified through the mineralogical examination of damages on historical buildings, as due to incompatibility of high alkaline aluminate binders with gypsum or lime-gypsum mortars.

Mortars with higher sulfate resistant cement, in excess of gypsum and calcite, are instable at temperatures of 2 to 40°C, caused by ettringite formation.

At a later stage, on temperatures below 20°C, thaumasite is formed with decomposition of the initially formed ettringite, by combining the unreacted gypsum and calcite. After 120 days, the specimens stored at 2°C are destroyed.

On mortars with C_3S and C_2S as starting materials, and molar ratio SiO_2:$CaSO_4$ = 1, thaumasite was formed, without expansion, when stored at 2°C under water, but the original CSH-phase is destroyed and structure is strongly weakened.

On the work 1.6, MORALES presents a study

of two Portland cements type V, PY-4 and PY-6, and four mixture cements with pozzolan D (diatomite) by the Le Chatelier - Anstett Method.

By XRD investigation on cracked tarts, thaumasite was detected after 3 years, in mixtures where C_3S content are: 79,43% (PY-6) 63,54% (PY-6/D80/20) and 58,19% (PY-4).
On mixture with C_3S below 56% cracks have not occured.

2. Decomposition by heat treatment

2.1 - "Mechanism of subsequent ettringite formation in mortars and concretes after heat treatment".
D. HEINZ and U. LUDWIG - West Germany

2.2 - "Thermal decomposition of hydrated cement pastes"
A.ZÜRZ, I. ODLER, S. ABDUL-MAULA - West Germany.

2.3 - "Evolution of strength and structure of concretes heated up to 1.100°C"
J. VOLANT and H. HORNAIN - France

On the work 2.1, HEINZ and LUDWIG to justify damages occured in precast units, that had been heat treated during production and subjected for several years to open-air weathering, study the influence of heat treatment, ranging between 20% and 100°C, in mortars made with PZ55 cement (C_3A at about 12%) and SO_3 3,8%; parallelly study a finely ground clinker with adding anhydrite, to have the SO_3 amount ranged from 2 to 8,6%, to investigate the influence of molar ratio of sulfate and aluminate.

It is verified by X-ray analysis, that at increased temperatures, there is a decreasing formation of calcium aluminate hydrate and it is concluded that, aluminate and sulfate ions get bound within the CSH-gel, and, in the subsequent storage under water, are available as reaction partners for an Aft-phase formation, resulting in expansion and a diminution of strength.

On the work 2.2, ZÜRZ et al. present a study of prepared cements, grinding industrial clinkers and raw materials with amounts of gypsum corresponding to 3% SO_3, in a laboratory ball mill, to a specific surface area of 3.000 cm^2/g (Blaine). Specimens 10x10x60 cm of pure cement pastes, water/solids ratios between 0,26 and 0,30, hydrated for at least one year at 20°C in a satured water vapor atmosphere, were heat up in an eletric furnace to temperatures between 100 and 1.000°C.

By X-ray diffraction was determined that the phase composition after heating consisted of free CaO and β-dicalcium silicate, for pure tricalcium silicate and non-blended cements; C_2 (A,F) for the OPC and antisulfate cements; C_3A for the white cement; melilite for blast furnace cement; β-dicalcium silicate and no free lime for fly ash-Portland cement, gehlenite for the pozzolan-Portland cement and wollastonite for the silica fume system. In addition, an increase in porosity and average pore size was observed, with loss of strength, as the temperature increased, partially related to a loss of bound water.

On the work 2.3, VOLANT and HORNAIN show that concretes prisms of 7x7x28 cm made with cements CPA, CHF and CPJ, have had weight losses of 5%, when heated up to 1.100°C.

At 105°C, the ettringite is transformed into monosulfo-aluminate and at 390°C, the structure became porous with loss of strength. At 550°C, the Ca $(OH)_2$ is strongly dehydrated, being fissurated and causing separation of material. The cements poor in lime (CPJ with fly ash or slag, CHF) have better strength due to less fissuration.

3. CO_2 Corrosion

3.1 - "Skins of calciumcarbonate and their significance for the corrosion of concrete".
E. KOELLIKER - Switzerland

3.2 - "CO_2 corrosion of geothermal cement

grouts"
N.B. MILESTONE, D.A. ST. JOHN,
J.H. ABBOTT, L.P. ALDRIDGE -
New Zealand

3.3 - "Investigation into the carbonation of autoclaved aerated concrete (AAC)"
Z. YUPING, L. DEDONG and S. GUOKUANG - China

On the work 3.1, KOELLIKER submits mortars prism of 40x40x160 mm to the action of concentrated solutions of calcium hydroxide, moist air of 90 - 100% r.h. and air of 70% r.h., both to 20°C.

SEM investigation revealed that in water, crystals of calcite had well developed faces and sizes from 1-10 μ diameter. On the other hand, in the air was observed a finer structure and grains not well crystallized, estimated of about 0,5 μ.

On the work 3.2, MILESTONE et al. presents a study of cement grouts corrosion in wells casings, exposed to conditions of CO_2^- rich, acidic or alkaline fluids, respectivelly. On the first condition, rapid carbonation and corrosion from HCO_3^- put doubt if any Portland cement system could withstand it. On the second condition, grouts are carbonating only.

It was observed that when silica is added to the formulations, the grouts are less durable and rates of attack are increased. It is hypothesized that without added silica, the HCO_3^- reacts with the CH for producing calcite, that has a larger molar volume, reducing the porosity; on the contrary, with added silica, the HCO_3^- attack must be directly on the hydrated calcium silicate (tobermorite and xonotlite) giving aragonite, that leads to an increase in porosity.

On the work 3.3, YUPING et al. present the study of three types of autoclaved aereted concrete: cement-lime-sand, cement-slag-sand and cement-lime-fly ash submitted to natural and artificial carbonation.

Mercury intrusion porosimetry shows that carbonation leads to a drop in the percentage of small pores and an increase in larger ones.

Strength tests show retrogression for all three types in artificial environment, although in natural, C-L-S and C-S-S presented an increase after one year exposure.

Concrete of C-L-Γ has a higher rate of carbonation as compared with C-L-S and C-S-S.

SEM shows that carbonation mechanism in artificial and natural environment is different; in the former, there is a serious build up of calcite on air pores of all concretes, not seen in the last.

4 - Other studies

4.1 - "Evolution of the microstructure of concrete during the ASTM Test for freezing and thawing"
C. VERNET - France

4.2 - "Influence of ionic species on alkali-aggregate reaction"
M. SHIZAWA, Y. JOE and H.KOTANI - Japan

4.3 - "Degradation of hydrated cements by chloride brines"
R. OBERSTE - PADTBERG - France

4.4 - "The stability of the calcium sulfoaluminate hydrates in aqueous solutions"
H.Y. GHORAB and E.A. KISHAR - Egypt

4.5 - "Contraintes internes dans le beton et sa durabilité"
Z. TSILOSSANI, I. PANTSKHAVA, K. KVARTSKHAVA - URSS

4.6 - "Corrosion of hardened cement pastes by NH_4NO_3 solutions"
A. BAJZA, I. ROUSEKOVA and O. VRANA Czechoslovakia

On the work 4.1, VERNET study the freezing and thawing action by ASTM 666-80-B Method and observe that the microcraks developed to sample center, passing by big size cappilary pores, the transition aureola of aggregates and big portlandite crystals. The subsequent stage, when cracks reach a certain dimension, chemical process of redissolution of hydrates speed the destruction.

By SEM investigation of hydrates orientation, it is assumed that concrete acts like a pump, resulting that thawing action being more destructive in water than in air.

On the work 4.2, SHIZAWA et al. using ASTM C227 Method, in order to investigate the effect of alkali ionic species and coexisting anionic species, upon the expansion due to alkali-aggregate reactions, conclude that the expansion was accelerated by sodium and potassium, but not lithium.

In relation to coexisting anionic species, the degree of expansion was decreased in following order: chloride, sulfate, hydroxide and carbonate.

Sodium ion has larger effect than potassium ion, at same content of total alkali and with same anionic species.

On the work 4.3, OBERSTE-PADTBERG show the study on degradation of hydrated high sulfate resistant oilwell class G cement, introducing samples of disks pastes (h=20mm; d=40mm) in saturated brines of KCl, $CaCl_2$ and $MgCl_2$, for a reaction period of 3 months at 55°C. The pastes were prepared with fresh water and also with 30% NaCl containing water (as commonly applied in the field of oil well cementing).

SEM investigation shows that salt water cement paste is attacked for all brines severally. The degrading mechanism is explained by the formation of alkali hydroxides and silicates, and the related pH decrease that leads to C-S-H instability.

On the work 4.4, GHORAB and KISHAR, studying the stability of calcium sulfoaluminate hydrates in water and NaOH solutions, at temperatures up to 100°C, and by XRD patterns of solids obtained, show that ettringite is found to be stable in water at 30°C and 60°C, the resulting solution having a pH value of 11,2; it persists alkaline solutions of concentration up to 0,2M at 30°C; it converts to the monosulfate hydrate on water at 100°C and in 0,08M NaOH at 60°C. On the other hand, monosulfate hydrate is unstable on water at 30°C, but it stability is greatly enhanced in alkaline solutions.

On the work 4.5, TSILOSSANI et al. measuring the internal effort by means of magnetic - elastic catchings put into concrete prisms of 7x7x21 cm, suggest a model to make statements for prevision the longevity of concrete, under the effect of temperature and humidity.

On the work 4.6, BAJSA et. al on a study of deterioration of concrete in agricultural conditions, submitting cement pastes in cylindrical samples (d = 30mm), to 0,5, 3 and 5% NH_4NO_3 solutions, for period close to 1 year, show that the hydration products are the same as those formed by water curing plus $C_3A.Ca(NO_3)_2 . 10\ H_2O$, causing expansion, decrease in density and strength, and increase in porosity.

SUB - THEME 4.3

CEMENT PASTE COMPATIBILITY WITH AGGREGATES AND CONCRETE REINFORCEMENTS INCLUDING ELECTROCHEMICAL CORROSION

BY MRS. HAYDEE ARMANDOLA

INTRODUCTION:

The contents of the sub-theme we are going to tackle in this 8th. International Congress on the Chemistry of Cement, as well as those of sub-theme IV - 1 and sub-theme IV - 2, under a slightly different title, carry on with certain subjects already dealt with in the VII Theme of the 7th. Congress: "Interface reactions between cement and aggregate in concrete and mortar", "Durability" "Bond Strength". It is probably called differently due to the fact that the present title further focusses on this problem by aiming at an approach to the traditional essence of these Congresses, i.e. "The Chemistry of Cement".

But it is downright obvious that even if the contents of some of the communications only give an incomplete answer to the essence, we cannot disregard the complex problem of durability, so long as its crucial consequences in the fields of Technology and Economy, make it unavoidable; let alone when there is a well-founded opinion that the new advances in concrete durability must have cement chemistry research as the driving force.

Undoubtedly, technological aspects are predominant in most of the reports submitted dealing with this subject, but effects are analized without taking into account causes or mechanisms, and neither research is carried out nor is there any conclussion grounded on a scientific basis, thus in most cases Empirism prevails.

Mr. J. Calleja (1) has been working hard on this subject that undoubtedly springs from the inherent features of the theme already dealt with. The problems brought about by research work on durability make it highly complex and usually impossible to simplify. It includes certain interacting factors of a very different nature and sometimes the effects of those factors have no close links with their relevance.

In his Research Paper, Mr. J. Calleja has carried out a deep survey of different viewpoints on the theme of durability, but at the same time bearing in mind its own limits and keeping it within the fields of chemistry of cement and Plain Concrete.

The 8th. Congress brings in the question of corrosion-passivation in reinforcements in sub-theme IV - 3. What has been said about the durability of plain concrete holds good when it refers to the durability of stressed or prestressed metallic reinforcements embedded in concrete.

Thus all the factors are linked with the electrochemical degradation of metals embedded in concretes of different characteristics deriving from its components and its technology and those springing from the environment.

COMMUNICATIONS

The chairman of sub-theme IV - 3 has been sent twelve Communications from nine countries:

IV-3.1 ALKALI - REACTIVITY OF GRANITIC ROCK AGGREGATES. H.C. Visvesvaraya, A.K. Mullick, George Samuel, S.K. Sinha and R.C. Wason. INDIA.

IV-3.2 INFLUENCE OF REACTIVE AND ALKALI COMPOUNDS ON EXPANSION OF ALKALI-SILICA REACTION. Kin-ichi Nakano, Shigehiro Kobayashi and Seiichi Nagaoka. JAPAN.

IV-3.3 ON THE BEHAVIOUR OF ALKALI IN ALKALI-AGGREGATE REACTION. W. Kobayashi, N. Kataoka and Y. Tsutsumi. JAPAN.

IV-3.4 CHEMICAL AND SWELL. PROPERTIES OF THE ALKALI-SILICA REACTION PRODUCT. G. Davies and R.E. Oberholster. SOUTH AFRICA.

IV-3.5 FIRST STEPS OF CONCRETE HYDRATION AND GEL FORMATION IN SURFACE CONTACT WITH AGGREGATES. Z.M. Larionova and I.I. Kourbatova. U.S.S.R.

IV-3.6 EFFECT OF DEGREE OF COMPATIBILITY OF CEMENT AND AGGREGATES ON CONCRETE DURABILITY UNDER CONDITIONS OF HIGH TEMPERATURE ACTION. V.I. Kadlecek and S. Modry. CZECHOSLOVAKIA.

IV.3-7 THERMOMECHANICAL COMPATIBILITY OF AGGREGATES IN AUTOCLAVED VERY HIGH STRENGTH CONCRETES. G.P. Tognon, S. Cangiano and G. Coppetti. ITALY.

IV.3-8 THE COMPATIBILITY BETWEEN AN EXPANSIVE GROUT AND ITS RESTRAINING ENVIRONMENT. R.I.A. Malek, P.H. Licastro and O.M. Roy. U.S.A.

IV.3.9 CORROSION BEHAVIOUR OF STEEL DURING ACCELERATED CARBONATION OF SOLUTIONS WHICH SIMULATE THE PORE CONCRETE SOLUTION. C.Andrade, C. Alonso, P. Santos and A. Macías. SPAIN.

IV.3.10 CHEMICAL POTENTIOSTATIC PROTECTION OF REINFORCING STEEL IN CONCRETE. J. Wisniewski, J. Karys, J. Czaja. POLAND.

IV.3.11 EFFECT OF ZINC OXIDE ADMIXTURE ON CORROSION INHIBITION OF IRON IN CEMENT MORTAR CONTAINING SEA WATER. C. Tashiro and Y. Fukushima. JAPAN.

IV.3.12 CORROSION BEHAVIOUR OF TAD, DIFFUSED REINFORCEMENT CONCRETE TUBES. M. Arpaia, ... Cigna and R. Turrizia-ni. ITALY.

After surveying the different papers, it was deemed convenient to group them according to the themes developed in them.

1. Cement - aggregate reaction

It is well-known that the chemical reactions of aggregates with concrete can affect the performance of concrete. Some reactions may be beneficial but others result in serious damage to concrete by causing abnormal expansion, loss of strength and cracking. During the 7th. International Congress the main paper (1) and the General Report on Theme VII (2) showed a comprehensive and critical review of the complex problem and accumulated knowledge in this field.

Both papers are backed up by plenty of bibliography by referring to the different kinds of reactions, their ocurrence, materials involved, mechanisms developed, identification by laboratory tests and criteria for judging reactivity and recommended procedures to minimize the effects of the reaction. Contradictions found in some of the research works are also mentioned.

Summing up, we can state that degradation is caused by the simultaneous influence of factors such as:

* The alkali content in cement, but also the alkali liberated by some aggregates or any other concrete component.
* Type of cement (rate of transport).
* The content and type of unstable minerals in the natural aggregates: "pessimum content" and grain size.
* Reactivity of aggregate, which is based on the presence of amorphous or partly crystallized silica.
* The humidity of the surrounding environment.
* The wet and dry cycling.
* Exposure conditions (external amount of aggressive substance).
* The temperature.

The interface (cement-aggregates) begins to be created when thin films of wa-

ter are formed on aggregate surfaces during the mixing of concrete. Alkalies from the cement dissolve immediately in the liquid, and lime commences to be released by the hydration reactions. From this outset, with its concurrent creation of strong OH-concentrations, any of the following cement-aggregate reactions may proceed in the interface-zone, dependent upon the available constituents and the conditions for mass-transport and energy-conversion in the system: pore - liquid - interface - interior of aggregate particles. Thus, according to different cases, there are different reactions: siliceous-aggregate; silicate-aggregate; dolomithic-aggregate; calcium-carbonate aggregates.

The mechanism in each reaction has often been analysed by different researchers (2). It is not a priori possible to evaluate such reactions as converging towards increased performance quality and equilibrium, or as contributions to deterioration, and also the position of cracks, for instance in a zonal interface system, ought to be cautiously interpreted at the present stage of knowledge.

The communication IV-3.1 presents the results of an investigation of alkali silica reaction in concrete containing granitic aggregates, possible mechanisms of deleterious reaction and its impact on cement specifications. Compatibility of siliceous aggregates with the alkalies in cement has been an important factor in durability of concrete. In addition to conventional reactants like opal, chert, chalcedony or volcanic glasses, it is now held that presence of "stained" quartz in siliceous aggregates could also cause alkali silica reaction (ASR).

Granite aggregates in a 25 year old concrete gravity dam contained mainly quartz and alkali feldspars, with varying quantities of biotite and muscovite 50-80 % of quartz showed strain effect with undulatory extinction angle 25-30°. Alkali feldspars included orthoclase, plagioclase, microcline and microcline-perthite.

The dam manifested typical external signs of distress associated with alkali-silica reaction, scanning electron microscope (SEM) and energy dispersive analysis of X-rays (EDAX) studies revealed the predominant presence of alkalies in the reaction rims on aggregates altering their borders, which consisted of fluffy, amorphous gel formation. Occasionally the reaction products were crystalline. The presence of typical white gel deposits in the concrete was less frequent.

In addition to the presence of strained quartz, the role of alkali feld spars were investigated. Microscopic studies indicated the alteration of alkali feld spars to clay minerals and sericite. X-ray diffractogram (XRD) studies confirmed changes in the crystal structure and mineral composition.

These results tend to support the hypothesis that alkali feldspar can themselves release alkalies in the presence of calcium hydroxide to participate in ASR. Should that be the case, merely stipulating a low alkali level in the cement may not be adequate and depletion of calcium hydroxide would assume importance.

The role of active siliceous pezzolan and hydraulic slags have been advocated for alleviating ASR. In addition to lowering the total soluble alkali content in the concrete to the extent cement is replaced by these additives, they also combine with the calcium hydroxide (CH) liberated during the hydration of cement. It has been reported that if the CH liberated can be fully consumed by large proportions of slags, ASR would not take place.

In the context of above, modified cement compositions having no C_3S phase or lower amount of C_3S phase merit consideration. In these cement systems, the amounts of CH liberated upon hydration are considerably lower. Authors point out that the use of such cements with known reactive aggregates are presently under investigation and the results will be reported subsequently.

The communication IV-3.2 refers to deleterious cracks in concrete structures considered to be caused by alkali-silica reaction. These have been often found in Japan from about 1975.

In this study, investigation was carried on the factors affecting expansion of mortar bar, that is, types of reactive aggregate, alcali contents of portland cement, types of alkali compouds as several sources of alkali, amount of alkalis and types of chemical admixtures.

The present work includes studies with 9 kinds of normal portland cement and 5 aggregates. The tests were effected by using ASTM techniques (Petrographic Examination of Aggregates; Potential Reactivity by

Chemical Method; and Mortar Bar Method).

Results show that even though the total alkali content is the same amount, the expansion increases with increase of afterwards additional alkali.

Low alkali cement with large amount of adding alkali shows more expansion than that of high alkali cement with small amount alkali addition if their total Na_2O equ. is same. Furthermore these tendency was more pronounced in the case of NaCl addition.

These results assess that expansion of mortar bars was largely influenced by water soluble alkali content. These results indicated that even though equivalent Na_2O contents were the same, extent of expansion varied widely dependent upon the kind of alkali ions. Furthermore sodium compounds affected more than potassium compounds.

The influence of chemical admixtures on expansion was examined using low alkali cement.

The total alkali as Na_2O equ. was adjusted to 0.60, 1,20 and 2.00 % by adding NaCl to low alkali cement.

Even though the total alkali content is the same amount, the expansion increased with the increase of afterwards adding alkali. It is technologically important that alkali introduced afterwards shows remarkable influence for mortar bar expansion comparing with intrinsic alkali in cement.

The communication IV-3.3 sets out to carry on research works effected by one of the authors, who studied on the chemistry of alkali-aggregate reaction by using silica gel-sodium hydroxide model (3) (4).

In the case siliceous aggregate is immersed in NaOH solution, the following reactions occur:

(1) adsorption of NaOH to silanol groups of aggregate

(2) rupture of surface siloxane bridge of aggregate by attack of NaOH and dissolution of SiO_2.

(3) rupture of inside siloxane bridge of aggregate and loosing of its structure

(4) adsorption of NaOH to inside silanol groups made by reaction (3)

If the siliceous aggregate is well-crystallised, the attack of NaOH takes place mainly at the surface and only reaction (1) and (2) occur.

On the other hand, in the case of poorly crystallised silica, NaOH penetrates into it and reaction (3) and (4) occur too. Reaction (3) looses the network of silica and produces a cross-linked polyelectrolyte containing Na^+. This type of structure, in contact with water, sets up an inhibition pressure and because the silicon-oxigen framework is partly disrupted the material swells.

In this paper, the behaviour of alkali in mortar bar which expands caused by alkali - aggregate reaction is discussed based on the above hypothesis.

In the research works carried out Perex glass, four reactive aggregates and a non-reactive aggregate were used. High alkali Portland cement was used. Experiments included immersion test in NaOH, mortar bar structure formation and analysis of pore solution obtained from cured and crushed-out mortar bars.

The immersion tests were effected in NaOH solution according to ASTM-C-289. The quantity of silanol group in residual aggregate was measured. The method followed is stated in the work. Mortar bar test was carried out according to ASTM-C-227.

Test and analysis results are stated and drawn up in charts. After discussion of those, the following conclusions were agreed upon.

On the aggregate immersed in NaOH solution, there is close relation between the quantity of alkali adsorbed to ruptured inside siloxane bridges. On the mortar bar, the quantity of alkali adsorbed to ruptured inside siloxane bridge/unit reactive aggregate is tightly related to expansion.

From these results, the rupture of inside siloxane bridge by the attack of alkali seems to be a cause of the expansion by alkaly-aggregate reaction.

The communication IV-3.4 deals with the identification of the alkali-silica reaction product (ASRP) in deteriorated concrete, considering it as a positive way of diagnosing alkali-silica reaction (ASR). Confirmation of ASR is usually obtained by performing scanning election microscopy (SEM) combined with electronic diffraction x-ray analysis (EDAX), or x-ray diffraction analysis (XRD), or both, on reaction product. However, characterisation of the ASRP mineralogically and morphologically as well as chemically and physically , can assist in elucidating the mechanism of the reaction and thereby contribute to the

prevention of the problem.

The possibility also exists that the ASRP observed in concrete and characterised in the laboratory is a harmless end product and is in itself not deleterious that it cannot exert swell pressure.

The present work includes a complete bibliography on this theme and a thorough series of charts to illustrate what has been stated.

Recently the authors of the present work have submitted extensive XRD and SEM-EDAX data on the ASRP. They described two amorphous phases, and a number of morphologically distinct crystalline phases, three of which are very widely distributed.

X-ray diffraction data on reaction products have revealed at least two crystalline phases, one with a characteristic peak at 12 Å and the other with one at 8 Å. A third phase with a characteristic peak at 2.90 Å has also been suggested. A characteristic of the 12 Å phase is that the 12 Å peak shifts progressively down to 8.26 Å when heated to between 40 and 110° C. This shift is reversible.

The ARSP is a multicomponent system. Included with the different crystalline and amorphous phases are contaminants such as quartz and various forms of calcium carbonate. Although whole sample analysis naturally give the combined composition of all the different phases plus contaminants, the advantage of this type of analysis is that the amount of water and CO_2 in the reaction product can be determined.

A semi-quantitative EDX analysis can be obtained from a non-polished surface and is very useful to characterise the different phases. However, x-ray scattering and absorption severely hamper the reliability and reproductibility of the analysis.

Quantitative microprobe analysis are the most suitable for obtaining the composition of the different phases in the ARSP. However, the fact that a flat well-polished surface is required means that the morphology, whereby the phase is characterised, is largely destroyed. Consequently, it is often difficult to distinguish between amorphous gels and crystalline phases and impossible to recognise different morphologies. In addition, water and usually carbon are not determined by microprobe analysis.

The more common phases on the ASRP in concrete from affected structures are a massive, amorphous gel and three distinct crystalline phases, namely rod-like, blade-like and rosette-like crystals. Although the quality and reproductibility of standardless EDX analysis are poor, a good indication of the chemical composition of the various phases can be obtained.

The massive gel is very often associated with rosette-like crystals. It has a much higher Ca and lower K content than the crystalline phases. The composition of the crystalline phases is much less variable than that of the amorphous gel. All three crystalline phases are characterised by the presence of Si, K and Ca. Small amounts of Na can be found in the blade-like and rosette-like crystals but this element is consistently present only in the rod-like crystals. Other elements that may be present in minor amounts are Al, Fe, and very occasionally, Mg. The rosette-like crystals are not only the most common crystalline phase observed in affected concrete but are generally chemically the most consistent and have the highest CaO content of the three.

Close to the contact with the aggregate, the alkali-silica reaction product found in voids alongside with the aggregate is highest in Si. These appears to be a depletion of Ca in the cement paste at the boundary with the reaction product.

No measurable swell pressures were produced by either the 12 Å phase and the 8 Å phase separated from concrete of deteriorated structures.

The communication IV-3.5 refers to the fact that a concrete structure is determined by a set of physicochemical processes taking place during binder-hardening and its possible reactions when they come into contact with aggregates. The first steps in binder-hardening constitute the period which conditions the resistance; deformation and other characteristics in the executed concrete.

The present work states that by means of studying variables according to the time of liquid-phase formation in concretes, we can assess the influence of different factors (such as temperature, additives, etc.) on cement hydration.

It also points out the influence on the liquid-phase composition by the clinker mine

ralogical structure, its alkali content, plaster included and admixtures added. Special reference is made as regards a superplastifying formed by naftalen-formol resins.

It is also stated that different aggregates adsorb hydrogels of a certain composition. This has been checked by using an electronic microscope. Different observations and verifications on this theme are given in detail.

2. Surface deterioration of concrete.

The communication IV-3.6 deals with this complex problem. Rate of the surface deterioration of concrete in natural exposure under normal temperature and moisture conditions is usually very slow. That is the reason why it is useful to study the deterioration phenomenon under more severe model conditions in laboratory. Results of such laboratory experimental project, which was realized a time ago are presented in this paper.

The aim of the experimental programme was to determine the extent of surface deterioration and besides, to compare the resistance of concrete with aggregates of different thermal expansion to the repeated action of high temperatures. For this purpose limestone and quartz were chosen as main representatives.

The work includes details related to materials used; their grain size; the way in which test probes have been used, steps making up the cycles to which they are submitted; studies of temperature gradient in and on the surface of test probes, and so on.

For the evaluation of the extent of surface deterioration of cycled concrete specimens (temperature difference was approx. 125 or 140°C respectively and the total number of temperature cycles was fifteen) some test methods have been used. Changing of properties of concrete has been assessed by tensile splitting strength test, adsorption and penetration of indication solution of sodium chloride on cubes and length changes (dilation), ultrasonic speed and pull-off strength on deteriorated surface of prisms.

The experimental programme constitutes an interesting example carried out in a laboratory since it takes into account both traditional and modern techniques to evaluate the behaviour of concretes of a specific composition.

Results obtained have shown pronounced structure deterioration of concrete in the surface layers after first several temperature loading cycles. Development of deterioration was more intensive in the case of concrete with limestone aggregate and also was more pronounced in the case of partially humid concrete in comparison with a fully saturated one. From the results it was evident that properties of quartz aggregates are more compatible with limestone aggregates.

Finally, the used test methods show different sensitivity for evaluation of the extent of deteriorated structure of exposed concrete surface.

It is obvious that as it usually happens with most models including cycles with temperature conditions more demanding than the normal ones, quantitative conclusions gathered from those prompt experiments can only be applied to similar situations to those simulated. So that we should be aware of rushing to conclusions. On the whole it would be highly interesting to research not only the effects but also physicochemical as well as chemical changes taking place during the experiment.

3. Compatibility of mixes of different aggregates

The communication IV-3.7 analyses the effect of the thermal and elastic compatibility of binary mixes of different types of aggregates on the properties of autoclaved very-high-strength-concretes.

The mechanical properties of autoclaved very-high-strength-concretes made with quartz aggretate and aggregates differently interacting with the cement matrix, were studied in previous works (5) (6) (7).

The trends of compresive strengths and moduli of elasticity versus the aggregate of maximum diameter were observed in autoclaved concretes made with aggregate consisting of limestone, quartz and a 50 % mix of the two. The investigation was extended to concretes with aggregate of maximum diameter up to 20 mm formed of basalt, jasper, granite and perphyry as well as 50 % binary mixes of these aggregates, besides of limestone and quartz mixes with the above materials.

The work assesses the characteristics of materials used in concrete mixes; the composition of the concrete mixes; the hydrother-

mal cycles applied to the autoclaved concretes; the tests made and results obtained.

It could be noticed that the moduli of elasticity of concretes where the aggregate consists of 50 % binary mix of the two materials depend on the moduli of elasticity of the mix constituents and their thermal compatibility related to the respective coefficient α .

The most interesting phenomena appear when limestone is present in the mix aggregates. Depending on the ratio of the modulus of elasticity of limestone to the aggregate with which it is mixed and as a function of the difference between the thermal expansion coefficient α of limestone and that of the aggregate, more or less marked deviations of the modulus of elasticity from the theoretical value are noticed.

In the case of concrete autoclaving, it can be useful to use only one type of aggregate rather than choose a mix of materials having different thermomechanical properties. In fact in rather large temperature ranges, such as those found in the hydrothermal treatment, the difference in the moduli of elasticity and thermal expansion coefficients relevant to aggregates affects strengths and, above all, the modulus of elasticity of the relative concretes.

The use of aggregate mixes containing limestone can involve a drop in the modulus of elasticity. However it is expected from the compressive strength values that follow an intermediate trend beween those of concretes with aggregate consisting of only one component.

In rather wide temperature ranges such as those related to the concrete autoclaving, in the case an aggregate mix is used, a study on the thermal and elastic compatibility between them and the cement matrix seems necessary to foresee the mechanical and elastic properties of the relative concretes.

4. Mechanical properties and durability of cement-based plug-seals

The communication IV-3.8 deals with this subject. Cementitious materials are used to seal access shafts and boreholes in many underground systems e.g. radioactive-waste repositories. Their primary function is to provide a tight seal at the interface.

Successful performance in this respect could be dependent almost entirely on expansivity of the plug relative to the restraining forces of the surrounding host rock.

In cementitious formulations, whether ettringite or salt (ClNa) is the principal expansive component the degree of restraint offered by the surrounding rock mass is of importance in the development of interfacial stress. Information exists on unrestrained and standard restrained expansion for mortars and concrete, however, most do not permit calculation of actual interface stresses under the existing restraining forces of actual borehole geometry.

A system to determine the radial stresses of the grout/concrete on the host enviroment, which permits stimulation of the surrounding rock mechanical properties was designed. A brief description of the system is presented together with typical data, and their implications on seal durability.

It consists of a strain gage instrumented cell and its associated signal conditioner/amplifier. The test cell used in the system is unique in that it provides for direct calibration of the complete system. It is versatile in that the cell material and dimensions can be selected to stimulate restraint of a given host material under a geostatic load reflecting depth.

Samples can be run under a range of temperature and pressure conditions, with the latter simulating either inyection pressure or hydrostatic load conditions. Details of the design and grading of the apparatus employed are pinted out in the paper.

Two ettringite-based expansive formulations have been chosen for the present study. Formulation I (F-I) a mortar based on type K expansive cement and formulation II (F-II), a grout based on class H cement with added calcium sulphate hemihydrate. A third, salt (NaCl)-based formulation (F-III) was also tested. This is a mortar containing much smaller hemihydrate than F-I and F-II and mixed with supersaturated NaCl solution. F-II was found to give the highest stresses, whereas F-III gave the lowest stresses.

Three distinct phases of expansion were found: the first is a thermal phase occuring with early heat liberation, the second occurs after the cement reaches its thermal maximum when simultaneous cooling and crystallisation of expansive componets takes place, and the

third phase occurs after total relief of thermal stresses.

In numerous field applications of expansive cements and seal materials, it is neccesary to attain chemical compatibility between the concrete formulation and the surrounding enviroment. In salt-host sites (largely in oil and gas industry as well as radioactive waste repositories) it was found that the use of saturated salt solution as a mixing fluid instead of water is necessary to prevent salt migration and subsequent adverse effects on seal durability. One salt-containing formulation (F-III) has been tested in the present investigation. This formulation contains 2.6 % hemihydrate in addition to salt (NaCl). The mixed expansive functions of sulphate and salt has an important significance in field applications in conjuntion with tempeature effects on stability of the seal material.

Although the restraining forces in a salt environment may differ from those of tuff rock (for ettringite-based formulations), the same restraining forces were applied to the salt-based formulation in order to establish a basis for comparison. A simple mathematical relationship can be applied to transform the resulting data into actual stresses in a salt environment.

The normalized expansive stress curve (at 38°C) for this formulation (F-III) reflects the general expansive characteristics explained. The expansion is partly due to Friedel's salt and ettringite. However, crystallization of salt with curing (water consumption in hydration process) may be the primary cause of expansion. The micrograph salt crystals growing inside pores of cement matrix. Crystallization starts at the walls and progresses to the center exerting pressure on the pore walls.

5. Corrosion-passivation in reinforcements

Metallic corrosion is always a heterogeneous reaction taking place in an interface metal-environment. Metallic corrosion arises due to the trend in metals to return to their original state i.e. as compounds which are more stable and have minimum potential energy.

The mechanism in a corrosive process consists of a spreading oxidation i.e. a loss of electrons on the part of the corroding metal.

Most of the corrosive processes fall within the electrochemical type, which implies the generation of an electric current or the flow of electrons from one part of the metal to the other. There is micro or macrocell formation, thus resulting in metal dissolution which always takes place in the anode. That trend to lose electrons varies according to the respective metal and it is influenced by the harmful environment or the electrolyte where the reaction of the corroding metal takes place.

When a metal comes into contact with a dissolution of its own cations, apart from the trend to bring about ion-production by the respective metal which becomes negatively charged (electrolytical dissolution), there is a driving force that leads cations to discharge on the metal, thus turning into neutral atoms and charging the metal positively. This driving force is measured by the osmotic pressure of dissolving cations.

A metal coming into contact with its own ion-dissolution becomes a voltaic hemi-cell electrode. Its own potential value should be measured by referring to another reference electrode. Thus, isolated potentials are relative, not absolute, and they are expressed according to an hemi-cell which is assigned a zero potential value by agreement. By that we mean, for eg. the hydrogen electrode and the choice of which to use depends on the electrolyte where the reaction (for eg. a corrosive reaction) takes place. Metallic potential (for eg. that of a corroding metal) should be expressed according to a reference electrode.

Usually bare steel exposed to the air or in contact with soils, water or any other aggresive environment, is prone to corrosion.

Simplified, the corrosion process can be separated into two single processes, the cathodic and the anodic process. The anodic process is the real dissolution of iron. Positively charged iron ions pass into solution:

$$Fe \longrightarrow Fe^{++} + 2e^{-}$$

The surplus electrons in the steel will combine at the cathode with water and oxigen to form hydroxil ions:

$$2e^{-} + \frac{1}{2}O_2 + H_2O \longrightarrow 2OH^{-}$$

After some intermediate stages, the ion and hydroxide ion will combine to form rust which at least theoretically, can be written as Fe_2O_3.

Under practical conditions, rust product are more or less water-containing compounds. This means, that only oxigen is consumed to form rust product. This oxigen must normally diffuse towards the metal. Water is only necessary to enable the electrolytic process to take place. On the contrary, steel in concrete is protected against corrosion by passivation.

The reason for this passivation is the alkalinity of concrete (the pH-value of the pore-water runs up to pH $>$ 12,5) and relatively high electrical resistivity in atmospheric exposure.

In the case of such high pH values, a microscopic oxide layer is formed on the steel surface, the so-colled passive film, which prevents the anodic dissolution of iron. Thus, corrosion of reinforcement is impossible, even if all other preconditions for corrosion are fulfilled (mainly the presence of mositure and oxygen).

If this pH value drops below pH=9 due to carbonation, or the chloride content exceeds a certain critical value, the passivated coating and, consequently, the corrosion protection will be lost locally or in even grater surface areas.

Corrosion of the reinforcement will only be possible after carbonatation or a harmful amount of aggressive substances has reached the surface of the reinforcement or when said substances belong to the concrete mass surrounding the reinforcement. That is the case of chlorides being added to the concrete mix.

Varied and multiple causes may bring about corrosion in reinforcements. Among them we can mention the carbonation of concrete, this being a matter of permanent concern, because many structures have their concrete surface directly exposed to the action of the atmosphere and the standard allow relatively little depth of cover of reinforcements.

As is already well known "carbonation" means the reaction between the atmospheric CO_2 with the solid phases of the cement paste.

The $Ca(OH)_2$, Na (OH) and K(OH) dissolved in the pore water of the concrete and, possibly, the soluble alkali of the aggregates provide the pore water with a pH between 12,5 and 13.5.

As different authors have stated the final state of this process consists of amorphous SiO_2,$Al(OH)_3$, $SO_4Ca.2H_2O$, CO_3Ca in different polymorphic varieties and H_2O. Thus, the initial alkaline pH in the pore concrete solution is neutralized. This neutralization allows the corrosion of reinforcements if a minimum of moisture and oxygen are present.

This reaction requires small amounts of water, as dry concrete will not carbonate. The highest rate of carbonation will'be found in air with a relative humidity of 50-60 %. Under conditions of higher atmospheric humidity, diffusion of the CO_2 will be inhibited by the water that has accumulated in the pore cavities.

After all the Na(OH), K(OH) and $Ca(OH)_2$ in the pore cavities has been re-dissolved and carbonated, the pH will commence to decrease. At the same time the calcium silicates will partly pass into solution and also react with the CO_2 of the air. As soon as the hardened cement has been completely carbonated, a pH of about 8.3 will develop under normal partial pressure of the CO_2.

The chemical reaction, illustrated in simplified terms, will at a certain moment take place not in a specific depth, but rather in a certain range of depth.

The alkalinity interface does not run exactly parallel to the concrete surface but will vary more or less in relation to the inhomogeneities of the conrete.

Carbonation of the concrete may, besides other methods, be rendered visible by simply spraying colour indicators onto the fresh concrete surfaces. The essence of this procedure is that such colour indicators show different colours in different pH regions. For investigations on the carbonation of concrete phenolphtalein, among others, proved useful as it appears colourless with a pH below 9, but shows an intensive red with a pH above 9.

The carbonation rate of the concrete and/or the rate at which the alkalinity interface, which is of major importance with respect to corrosion protection, will enter the interior of the concrete, depends on the following factors:

- partial pressure of the CO_2 (normal CO_2 content of the air, 0.03%)
- concrete permeability (w/c-ratio, curing, concrete humidity, cement content, grain size distribution curve)
- amount of substance capable of reacting with CO_2 (cement content, type of cement applied).

As this is a diffusion process, calculations in very simplified terms first exhibit a so-called $\sqrt{t}$ dependence, i.e. the alkalinity interface penetrates into the interior of the concrete almost linearly with the square root of the concrete age.

This holds true for relatively low environmental humidity, e.g. indoor conditions. However, for out_door constructions more precise bases of calculation reveal that due to subsequent hardening of the concrete, $Ca(OH)_2$ diffusion from the interior of the concrete, changing humidity near the surface and some other influences, the alkalinity interface will penetrate into the interior of the concrete at an increasingly slower rate than a $\sqrt{t}$ function would suggest, approaching an ultimate value over a very extended period of time.

In the region of cracks in concrete, the penetration rate of carbonation down a crack into the interior of the concrete is considerably higher than in uncracked concrete. Influencing factors of major importance are:

- crack widths
- permeability of concrete
- humidity of concrete

If the passivation on the steel surface is destroyed within a strictly confined area, i.g. within the region of cracks in concrete or peaks of carbonation that reach to the surface of the reinforcement, then the situation and distribution of anodically and cathodically acting bar regions will become an important factor with regard to the rate of corrosion.

In the region of cracks in concrete it should further be considered that owing to the slip existing between steel and concrete, the active steel surface will not be confined to the actual cross-section of the crack.

Depending on the specific environmental and concrete conditions, the maximum corrosion rate can be assumed in the range between 60 and 200 μ/year. (9) (10).

The minimum values of uncracked concrete cover as indicated in the CEB-FIP Model Code 1978 are sufficient to assure that the carbontion of concrete exposed to the open air, even during a very long period of time, will not reach the surface of the reinforcement in uncracked regions. However, this applies only to concrete which has been properly composed, compacted and cured. Only in very dry environmental conditions carbonation may penetrate deeper, exceeding the concrete cover. In such cases, however, the moisture content will, as a rule, not be high enough to produce any significant corrosion. The concrete covers given by the Model Code thus guarantee sufficient durability of the steel in uncracked concrete of structures exposed to the open air.

Within the region of cracks carbonation can penetrate to the reinforcement at a substancially higher rate than in uncracked concrete. In reinforced concrete construction the width of cracks cannot be limited to such an extent that corrosion during the whole service life of the structure could be completely ruled out. Yet, the width of cracks is no longer to be regarded as a major factor in corrosion protection of the reinforcement. Carbonation in the region of smaller cracks, will reach the reinforcement only at a later time than in that of wider cracks. From this point, however, the rate of corrosion is almost independent of the crack width, as the diffusion of oxygen is in general not influenced by the width of cracks. Corrosion normally tends to cause only a small reduction of the bar diameter so that a sufficiently long service life is to be expected, provided that the bars applied are not too thin. (11)(12).

The thickness of concrete cover is of major importance due to the fact that with increasing thickness of cover the risk of concrete being spalled off by corrosion products will be substantially reduced.

The state of knowledge with respect to cracks transverse to the reinforcement is illustrated diagrammatically.

There are not very reliable findings available as regards the situation in the region of longitudinal cracks (stirrups in webs,

two-ways slabs, etc.). But here, too, it is obvious that an increased concrete cover may substantially reduce the risk of spalling. In view of the considerable importance of this problem, investigations in this field are felt to be urgently required.

The communication IV-3.9 lets us know about results obtained from works carried out by the authors as part of a research project initiated some years ago adressed to the question of how and up to what extent the corrosion of reinforcement occurs during carbonation. The ascertaining of the corrosion rates of the steel would permit the calculation of the residual service life of the structure.

The only common statement in carbonated concrete is that pH value decreases and the reinforcements corrode. Only authors who have studied the effect of cracks and have measured the decrease in diameter of the bars due to carbonation in the region of cracks give an approximate to a medium value of the corrosion rate at these points.

Some years ago a research project was initiated in our Institute to study this gap in knowledge and some results have already been published. The experimental work mainly dealt with the study of the corrosion parameters of reinforcements embedded in hardened carbonated mortar of concrete and immersed in carbonated solutions that reproduce the composition of the pore concrete solution.

But the system used for carbonating in these experiments was one accelerated by pure CO_2 gas. This method produces a saturation of CO_2 in the solution or in the carbonation chamber and may lead to different phenomena from those which occurs when carbonation is produced naturally (the proportion of CO_2 in the atmosphere is about 0.03 %). This point is analyzed in the present paper and is taken into account in the future experimental work.

This paper sets out changes in the chemical composition of like-pore concrete solutions during accelerated and natural carbonation (by air) and also the results of simultaneous changes of corrosion potentials and corrosion rates of reinforcements. The results confirm the previously published hypothesis giving a new insight into the phenomenon.

Random behaviours related with the changes in the corrosion rate of steel during accelerated carbonation of cement mortars have suggested the need to study the process in a more simple medium which allows the isolation of the different parameters. Thus, saturated $Ca(OH)_2$-base solutions with different additions of KOH and NaOH have been used to simulate the real pore concrete solution.

In the present work, simultaneous changes in the pH value, corrosion potential and corrosion rate (measured by means of the determination of the Polarization Resistance) of steel roads have been monitored during accelerated carbonation produced by a constant flux through the solution of CO_2 gas and/or air.

Some clear differences in these variables have been established beween solutions with and without Na^+ and K^+ ions, which may clarify the different corrosion behaviours observed in mortar made with different types of cements. Because CO_3Ca is insoluble, the solution not containing alkalies are carbonated more quickly than those containing them. Final pH values in the case of a saturated $Ca(OH)_2$ alkali-free solution are always near neutrality (pH 6-7), but solutions containing alkalies may have a final pH value of about 10,4 where a buffer of $CO_3^=/HOC_3^-$ is established. Only when an excess of CO_2 gas is passed through the solution are all sodium and potasium carbonates transformed into bicarbonates and the final pH value is about neutrality.

These results lead to an apparent contradiction between the final pH values of real carbonated concretes and those carbonated in an accelerated form.

Concerning the corrosion behaviour, the previous hypothesis is confirmed using air as the carbonating agent. The corrosion potential of steel rises simultaneously with the decrease in pH value is until a limit is reached and depassivation occurs. After this moment corrosion starts and the corrosion rate is dependent on the final pH value of the solution and, therefore, its bicarbonate content.

The passive layer disappears from steel at pH - 8, as Pourbaix has stated many years ago. When $NaNO_2$ is present, the passive layer remains in spite of the lowering of the pH value.

The communication IV-3.10 describes experiments carried out to complete the natural passivation that concrete produces to embedded reinforcements.

Although high quality portland cement concrete offers an adequate protection to embedded reinforcements, sometimes the access to metallic reinforcements of aggressive substances and gases determines that the measures taken may not be sufficient to ensure appropriate durability.

Especially in the case of severe attack it is frequent to try and improve protection of reinforcements by applying supplimentary measures. Among them we can mention:

* outer surface protection of concrete with different coatings
* recoating reinforcements with synthetic resin, bitumen or others
* anodic or cathodic protection
* addition of inhibitors to mortar
* galvanic reinforcement

The present communication describes the experiments carried out to obtain passivation of reinforcements with the aid of anodic polarization through a cement of a specific density together with organic inhibitors consisting of an abietic and adepic acid mix.

We have aimed at determining the propierties of the passive film resulting on the surface of the reinforcement embedded in cement paste and portland cement mortar. We have determined the relationship between changes in active resistivity and reinforcement potential during cement paste hardening. Test probes which had 4 % of the abietic and adepic acid mix were measured similarly. The equipment employed in this experimental project was especially devised by the authors.

The influence of concrete composition was studied by using different qualities as well as different values in concrete-water relationship. Porosity and resistance to corrosion by cement paste and mortars were measured. We chose as an indicating parameter of passivation the time after which the aggressive environment (ClH) reaches the surface of the reinforcement, at that time determining an active resistance of the coat and the electric potential of the reinforcement.

The conclusions we gather are that by applying inhibitors to reinforcement coatings as an abietic and adepic acid mix together with the creation of a passive film devised constitute good protection to concrete reinforcements exposed to aggressive environmets. Condictions stated for the creation of a passive film and the electric system devised allow a prompt and easy protective method.

Among other procedures tested to improve on passivation and corrosion resistance to steel embedded in cement paste, reinforcement galvanization stands out. As zinc dust, zinc chloride or zinc oxide, this metal has been used with this aim. In a work presented in the 7th. Congress (8), the adherence between the cement paste in concrete and reinforcement bars was discussed with zinc and cement paste as special experimental materials. Implicitly referring to the possible passivating role of zinc-coating on steel reinforcement bars. The development of calcium hydroxyzincate is found as the interface reaction product in lime-solutions, whereas the presence of alkalis promote the formation of zinc-oxides and soluble zincates are formed in pure alkaline solutions.

The communication IV-3.11 describes the experiments carried out to complete with addition of zinc oxide the natural passivation that concrete produces to embedded reinforcements.

The passivation or corrosion of iron plates embedded in ordinary portland cement mortar containing a small amount (0.2%) of zinc oxide powder. The cement mortar was made with cement to sand ratio of 1:3, and water to cement ratio of 0.8. Sweet water and sea water were used as mixing water and steam curing was used for acceleration of corrosion for 90 days.

The spontaneous potential of specimens was measured, using silver chloride electrode as a reference electrode.

The rust area was measured on the iron plate after crushing the specimens. The measurements were made at 7, 14, 28, 56 and 90 days.

The cement hydration products in contact with the iron plate were investigated using a scanning electron microscope. The pore size distribution of the cement mortars were measured by means of mercury penetration poro-

simeter analysis. When sweet water was used, corrosion was not observed in any of the specimens. It seems that the amount of corrosion was not appreciable under the conditions of water/cement ratio, thickness of mortar cover and the accelerated curing used in this study. On the other hand, when sea water was used, the corrosion was observed in the control specimen (without zinc oxide).

Namely the rusted area of the control specimen was over 80% at 90 days. However, when zinc oxide was used no corrosion was observed.

When the specimens were mixed with sweet water (specimens with or without zinc oxide) the spontaneous potential was about -100 mv. When the specimens contained sea water (specimens with or without zinc oxide), the spontaneous potential was about -300 mv at early stage after mixing. In the former case the potential was negatively larger with curing time (-400 mv), but in the latter case it became negatively smaller with curing time. It remained at about -150 mv after curing for 30 to 35 days.

The scanning electron micrographs of the hydration products on the iron plate in 28 days old specimens, may be grouped into two types. The hydration products in plate with zinc and sweet water, zinc and sea water and cement and sweet water consisted of CSH and calcium hydroxide, and the texture was compact. On the other hand, the hydratation products in control specimen mixed with sea water, consisted mainly of large hexagonal crystal of calcium hydroxide formed in the interfacial region between the iron plate and the cement mortar. The texture in this case was porous.

In the case of zinc oxide addition, probably this compound $Ca(Zn(OH)_3.H_2O)_2$ may have formed.

In spite of differences in the type of mixing water, the total pore volumen of specimens containing the zinc oxide admixture, were slightly smaller than the control. The zinc oxide admixture affected the microstructure of the cement mor tar in a beneficial manner which is related to prevention of diffusion of oxigen and other harmful constituents.

It was concluded that the zinc oxide admixture was very effective as a corrosion inhibitor for iron in cement mortar containing sea water.

It should be pointed out that the conclusion is valid as to test conditions. Now, one should be careful in trying to extend it to other situations. It is also important to bear in mind that the addition of zinc to mortar and concrete above certain concentrations may change the hardening process. Consequently, besides research as regards its effect on embedded reinforcement passivation in an all-round work on the theme, said effects should be mentioned and enlarged upon.

The communication IV-3.12 sets out to study the corrosive process in a special type of reinforced concrete tubes.

The corrosion behaviour of steel embedded in concrete is alleged to be very good, due to the passivity given to it by the alkaline environment which forms after the clinker components hydration processes.

Therefore reinforced concrete pipelines, like the other structures in civil engineering, should be and usually are sufficiently safe, from the point of view of the corrosion phenomena concerning the reinforcement.

Unfortunately many failures have recently occurred, either because of incorrect design and manufacturing, or because of the strong aggressivity of the environment, with consequent relevant costs, whose magnitude have been adequately underlined. Several preventive countermeasures may therefore be suggested whenever the possibility of steel depassivation is forecasted.

The reinforced concrete tubes, which constitutes the object of study in the present communication, are manufactured in such a way that very dense concrete is obtained, usually with a rather thin cover.

Maximum aggregate dimension is 3 mm, cement content is 650 kg/m3, water/cement ratio is 0.3; the cover of the pipe used in this experiment is 0.5 cm. The use of such pipes for water transportation is

spreading rapidly, even if their reinforcement corrosion behaviour has not yet been studied in depth.

The tubes tested were "new material" as far as corrosion behaviour is concerned: it was therefore believed necessary to conduct an in-depth investigation in various experimental conditions. The experiments started about two years ago and are still continuing.

The corrosion determination methods were the corrosion potential measurement, the polarization resistance or corrosion rate CR determination, and visual observations.

The specimens obtained from a tube were used for the following experimentations:

A - exposure of specimens to various environments. The tested environments were tap water, magnesium chloride and sodium chloride solutions, sand containing NaCl solution, clay and sand;

B - exposure to various environments of specimens with artificial scratches on the external cover, made in order to leave bare some superficial wires;

C - exposure to soils of scratched specimens prepared in order to measure the current of the corrosion couple generated between bare wires and concrete covered wires.

A few wires, disposed on three paralld layers along the specimen thickness, were partly liberated from concrete in order to allow electrical measurements on superficial wires, medium wires and deep wires.

The investigation was carried out with the adoption of both traditional measuring techniques (spontaneous corrosion potential measurement, visual examination) and electrochemical techniques (polarization resistance or CR and polarization curve determination).

The results of experiments of over approximately two years showed that with the specimens, even with a rather small concrete cover (0.5 cm) no corrosion phenomena were observed at all, probably due to the low porosity of the tube, in the presence of scratches artificially made over the outer surface in order to simulate an erroneous handling of the pipe; it was observed that the corrosive attack remained strictly localized in the part of the wires directly in contact with the aggressive environment, and did not spread into the concrete.

Moreover, in the presence of soils with different permeability (sand and clay) the results of the tests showed again the good corrosion behaviour of the reinforcement.

Several points emerge from the results of about two years investigation on corrosion behaviour of specimens cut from tubes, exposed to several corrosive environments (tap water, 3,5 % NaCl solution, sand humidified with NaCl solution, clay, sand).

(1) Results of six month-experiments on specimens exposed to all corrosive environments tested, show that there was no corrosion of reinforcing wires. The spontaneous potentials of wires lay in the range of steel passivity state;

(2) In the presence of artificial scratches on the outer concrete cover (scratches made to leave bare surface wires in order to simulate an erroneous handling of the tubes); it was observed that the corrosive attack remained strictly localized on the wire surface directly in contact with the aggressive environment, while there was no corrosion propagation on adjacent wire surface embedded in concrete;

(3) for scratched specimens exposed to different soils (clay and sand); corrosion couple, generated between the bare surface of wires directly exposed to the soil and the surface of the wires covered with concrete, gives rise to mean corrosion penetration rates of 0.04 mm/y for bare wires exposed to clay and of 0.08 mm/y for those exposed to sand. In this case too, attack was strictly restricted to the bare area. Stifling during the corrosion attack is due to protective effects of corro-

sion products in anodic areas.

(4) Investigations are still continuing to verify the long-time behaviour of tube reinforcement.

The communication presented explains a complete methodology as to how a new product should be studied, in this case a concrete reinforced tube, in order to evaluate the corrosion behaviour of the embedded steel.

--- 0 ---

REFERENCES

1.- CALLEJA, J., "Durability". Principal paper. Theme VII, sub-theme 2. 7th. International Congress on the Chemistry of Cement, 1980.

2.- IDORN, G.H., "Interface reactions between cement and aggregate in concrete and mortar". General report. Theme VII. 7th. International Congress on the Chemistry of Cement, 1980.

3.- GLASSER, L.S.D., and KATAOKA, N., (1981), "The Chemistry of Alkali-aggregate reaction". 5th. Int. Conf. Alkali-Aggregate Reaction in Concrete, 5252/22.

4.- GLASSER,L.S.D. and KATAOKA, N., (1981). "The Chemistry of Alkali-aggregate reaction", Com. Concr. Res. 11, 1-9.

5.- TOGNON, G.P., COPETTI, G., URSELLA, P., 9 Internationaler Kongress der Beton- und Fertigteilindustrie (Wien, 8 - 13 Oktober 1978), 39-46.

6.- TOGNON, G.P., URSELLA, P., COPPETTI, G., J.Am. Concr. Inst., 1980, 77 (3), 171-178.

7.- TOGNON, G.P., URSELLA, P., COPPETTI, G. 7th. Int. Congress Chem. Cem (Paris, 30 juin - 5 juillet, 1980), VII - 75-80.

8.- ARLIGUIE, G., GRANDET, J., and DURAL, R., "Study of the contact zone between zinc and Portland cement paste". 7th. International Congress on the Chemistry of Cement, 1980.

9.- SCHIESSL, P., Zur Frage der Zulassigen RiBbreite und der erforderlichen Betondeckung im Stahlbetonbau unter besonderer beruckrichtigung der Karbonatisierung der Betons. Deutscher Ausschub fur Stahlbeton, Heft 255, Berlin 1976.

10.- TUUTTI, K., Corrosion of Steel in Concrete. CBI forskning 4/82. Cement-och Betonginstitutet, Stockholm.

11.- BEEBY, A.W., Concrete in the Oceans. Cracking and Corrosion. Technical Report Nro.1 CIRIA/VEG, Cement and Concrete Association, Department of Energy, 1978.

12.- TUUTTI, K., Craks and Corrosion. Cement-och Betonginstitutet, Fo 6:78, Stockholm 1978.

--- 0 ---

N.F. ANANENKO, Guiprocement, Leningrad, USSR

MAGNESIUM OXIDE IN PORTLAND CEMENT

The problem on the maximum permissible MgO content in Portland cement clinker is up to now one of important matters of concern in cement chemistry and technology.

For the first time commercial production of magnesia clinker with clinker burning in rotary kilns was organized by V.V. Serov (1). On the basis of extensive experiments V.V. Serov established appropriate requirements for the chemical and mineralogical composition of magnesia clinker and developed specifications for cement soundness tests. With magnesia clinker as the basis there was organized manufacturing of magnesia slag portland cement specifications for which were also standardized. The mentioned above types of cement were manufactured for a long time at one of cement plants in the USSR (2).

The investigations of V.V. Serov were further continued and developed by P.P. Bydnikov (3), N.A. Toropov (4), S.M. Royak (5-6), L.Yu. Astansky (7) and by other Soviet scientists.

The publications on problems in researching and obtaining cements with elevated and high MgO content within the period from the VII-th International Congress on the Chemistry of Cement (Paris, 1980) were concerned mainly with magnesium oxide effect of clinker structure, alite polymorphism, mineral formation processes at various temperatures (8-10).

In the recent years there have been published a number of works aimed at further investigation of constructional and engineering properties of cements with various MgO contents to ensure soudness of cement (11-12).

Certain countries have introduced alterations into their standards as regards the permissible MgO content increasing it to 6% (USA, India) (13). Table 1 gives values for MgO content and methods of test for cement soundness in international standards.

The amount of magnesium oxide acceptable in clinker is in the range from 3 to 6.5%. The minimum MgO content in cement can be ascribed to absence of the necessity to revise the traditions.

The requirement for cement soundness is envisaged in standards of all the countries (13), but the methods used for testing are various: boiling test or cold water pat test, expansion measuring on cement paste samples in boiling or wet stored (Le Chatelier test), autoclave test under 2 MPa to detect sample expansion.

The Le Chatelier test is most extensively employed as it permits to give a quantitative estimation of the cement expansion value. But this method doesn't allow to detect unsoundness due to periclase hydration and hence it can be only used with cements of low MgO contents.

The autoclave test has been standardized in 9 countries inclusive of USA, Canada, Belgium, Finland. The acceptable linear expansion being from 0.5 (Venezuela) to 1.3 (Argentina, Belgium).

In the USSR practice when carrying out scientific and research works (14) for quality assessment of cement featuring elevated MgO content, the linear deformation of bar specimens is determined through autoclave tests after previous 4-hour boiling. In our opinion, such a method of expansion assessement makes it possible to reveal the effect of both magnesium oxide and calcium oxide on this particular characteristic.

Special investigations of prof. I.G. Luginina on magnesia cement stone expansion in autoclave tests disclosed that volume deformation manifests itself during isothermal curing.

The alterations in the steaming conditions consist in lowering the maximum pressure, on achieving it, within the time interval of 1-1.5 hour, down to 0.6-0.7 MPa and then raising it again to the maximum one and retaining it constant during 3-4 hours. Within the initial stage intensive hydration of clinker minerals and crystallization of the hydration products take place, that strengthen the cement stone

Table 1

Magnesium Oxide Contents and Methods for Cement Soundness Tests in Different National Standards

Country	MgO content limit in clinkers, %	Soundness, h	
		Method	Permissible expansion
Austria	5.0		
Great Britain	4.0	Le Chatelier test	10 mm
Brazil	6.5	Le Chatelier test	5 mm
Denmark	3.0	Le Chatelier test	10 mm
India	6.0	Le Chatelier test autoclave test (at MgO 3%)	10 mm 0.8%
Italy	4.0	Le Chatelier test	10 mm
Canada	5.0	Autoclave test	1%
France	5.0	Le Chatelier test or 7 days water storage	10 mm
FRG	5.0	Boiling test	
Czechoslovakia	6.0 4.0	Boiling test	
Rumania	2.5-5.0	Le Chatelier test	10 mm
USA	6.0	Autoclave test	0.8%
USSR	5.0	Boiling test	no cracks
Japan	5.0	Boiling test	no cracks

structure prior to periclase hydration. The subsequent curing under 2 MPa pressure has practically no effect on the value of the linear deformation of the cement specimens. The proposed conditions simulate cement hardening more exactly.

The question on the method for soundness tests and the criterion for its assessment with cements featuring an elevated and high MgO content deserve special study and discussion.

When working out chemical and technological technique which would assist in obtaining cement withstanding autoclave tests at elevated MgO contents, some investigators aimed at binding magnesium oxide into chemical compounds and thus to neutralize its detrimental effect on hydration. In doing this various additives were introduced into the raw mixture, burning temperature was changed. The results obtained were rather contradictive and therefore couldn't be used in production.

To clear out the possibilities in formation of magnesium-containing compounds in the field of Portland cement clinker compositions, special investigations were carried out to study products of clinker formation within the temperature interval from 700°C to 1300°C (15).

The raw mixtures contained magnesium oxide (on clinker basis) in amounts of 1-10%. The control raw mixture containing no magnesian component was also investigated. The burning products underwent X-ray phase analysis in a DRON-1 apparatus. For identification of X-ray photographs use was made of the data from the ASTM roentgenometry file.

No interference lines which would indicate the presence of magnesium silicates or spinel in the burning products were found on any of the diffractograms in the whole of the temperature interval investigated, free magnesium oxide was identified in the burning products of raw mixtures containing MgO. No other magnesium containing compounds were found. Thus it was proved once and again that MgO is present mainly in a free form from the moment of magnesium carbonate decomposition till completion of clinker formation.

The research in magnesium oxide effect on clinker phase composition and its microstructure under various burning conditions 16 have disclosed that the nature of MgO effect on clinker microstructure is closely connected with the gaseous atmosphere during burning. At clinker burning in a neutral atmosphere presence of magnesium oxide in amounts of 3% and above noticeably affects the microcrystalline structure - the alite and belite crystals acquire an indefinite form.

Clinker burning in a reducing medium impairs its microstructure, as compared to the control clinker containing no magnesium oxide, only when MgO content reaches 5% and above. The alite and belite crystals of clinkers with 2-3% of magnesium oxide present had in contrast a more regular form.

Both the phase composition of clinkers and their microcrystalline structure change under the effect of magnesium oxide depending on the burning conditions. It has been found out that with an increase in magnesium oxide content in clinkers of neutral atmosphere burning the proportion between the aluminate and aluminoferrite phases changes so that the portion of C_3A reduces while the portion of $C_2A_xF_{1-x}$ increases. This change has no monotonous character but reaches a maximum when magnesium oxide content is about 3%. With a further increase in MgO content the amount of C_3A again begins to grow.

In clinkers obtained in a reducing atmosphere this regularity has somewhat another character: - the shift maximum is observed at MgO content of about 2%, and the relative value of the phase shift decreases.

The investigations on assessement of the effect of simultaneous presence in the raw mixture of a mineralizing (CaF_2) and alloying (MgO) components have shown that the latters produce a noticeable influence on clinker phase composition causing an elevated alite and intermediate phase contents (17, 18). An increase in magnesium oxide content above 3.0% results in a decrease in the amount of high-basic calcium silicate.

Incorporation of magnesium oxide in amounts up to 3.0% in fluor-containing clinkers favourably effects crystallization of alite forming mainly a high symmetrical modification.

The investigations on admixture distribution among the basic clinker phases, carried out in the "Camebaks" plant, have demonstrated, that magnesium oxide is concentrated mainly in the aluminate and aluminoferrite constituents.

One of technological methods making it possible to reduce the adverse effect of an elevated magnesium oxide content on cement quality as regards its soundness is introduction of active mineral additives into the binder composition.

The favourable effect of active mineral additives on the results of autoclave tests of cements featuring an elevated MgO content is accounted by the fact that silica present in the additive partially binds periclase into magnesium hydrosilicates. Besides, during hydrothermal treatment of cement in presence of ash one can notice a retardation in periclase hydration due to an elevated density of the cement stone.

The technological method of introduction of active additives into cement with elevated MgO content has been studied and examined by a number of authors (19-20). Since autoclave treatment doesn't simulate cement hardening under normal conditions, the data on hardening high magnesian cements obtained for many years are of great interest for revealing possible consequences due to retarded hydration of periclase.

Table 2 represents the results of determining linear deformations of cements with 6-6.5% magnesium oxide contents which were water-stored during 20 years (19). The linear deformations of the cements no matter whether they contain or not a mineral additive are rather insignificant. Thus, expansion of plain cement on the basis of clinker with 6.03% MgO content after 20 years of storage in water was only 0.29%, the linear expansion for the last five years increased in this case only by 0.01%. Cement obtained from clinker having a 6.5% MgO content without active mineral additives in 10 years of hardening showed linear expansion as high as 0.30% and in 15 years - 0.31%. It should be noted that this cement failed autoclave tests on soundness (expansion being 12.2%).

Introduction of a 15% mineral additives

Table 2

Cement Soundness and Linear Deformation under Normal Hardening Conditions

Description of Cement Additive	Linear Expansion, %						
	Autoclave test at 2 MPa	Hardening Duration, years					
		1	3	5	10	15	20
	Clinker of pilot plant burning at MgO = 6.54%						
Plain cement	12.2	0.13	0.22	0.25	0.30	0.31	0.32
Tripoli earth	0.33	0.06	0.09	0.10	0.13	0.14	0.15
Fly ash	0.43	0.08	0.13	0.14	0.15	0.15	0.17
Tuf	0.16	0.10	0.15	0.16	0.18	0.18	0.20
	Commercial clinker MgO = 6.03%						
Plain cement	11.3	0.10	0.16	0.19	0.25	0.28	0.29
Tripoli earth	0.11	0.07	0.11	0.14	0.17	0.20	0.20
Fly ash	0.07	0.06	0.11	0.13	0.16	0.17	0.18
	Commercial clinker MgO = 5.22%						
Plain cement	5.28	0.13	0.20	0.24	0.29	0.33	0.34
Tripoli earth	0.15	0.06	0.10	0.15	0.19	0.20	0.21
Fly ash	0.16	0.07	0.12	0.14	0.17	0.17	0.17
	Commercial clinker MgO = 1.13						
Plain cement	0.02	0.07	0.09	0.09	0.12	0.13	0.13

(Tripoli earth, tuf, fly ash) into cements as seen from Table 2 noticeably diminished linear deformation of cements both under water hardening and in autoclave treatment.

For example, expansion of plain cement obtained of clinker with a 5.22% MgO content after 20 years amounted to 0.29%, and with Tripoli earth and fly ash introduction the same 0.20 and 0.18%, respectively.

The 20-year storage specimens of cements produced on the basis of clinker with 6.03% magnesium oxide content were studied using roentgenographic and derivatographic methods of analysis. The data obtained point to the presence of unhydrated periclase (reflection 2.09-2.10 Å) in the hardening products along with magnesium hydroxide (reflection values 2.35-2.36; 1.570-1.574 Å). By application of calibration mixtures featuring various magnesium oxide contents the amount of residual periclase in the cement stone of plain cement and cement with a 15% Tripoli earth additive was determined. It comprised 1.64 (±0.1%). The degree of periclase hydration in 20 years of cement hardening constituted 72% in the first case and 68% in the second case.

The X-ray photographs show no interferentional lines which could be attributed to magnesium hydrosilicates. The possibility of formation of the latters (chrysotile-type) in hardening under normal conditions cements with addition of the ash, Tripoli earth, trass and other siliceous materials has been marked in publication (22).

No magnesium hydrosilicates were either found in specimens of cement stone by a derivatographic analysis. The whole of the thermograms irrespective of additives present in cement show endothermal effects at 150°C (calcium hydrosilicates), 420-430°C (magnesium hydroxide), 545-550°C (portlándit) and at 820°C (hydrosilicates and cal-

cium corbonate). With the help of infrared spectroscopy calcium carbonate was detected in hardening products (lines at 713, 875 and 1430 cm^{-1}).

Electron-microscope investigations on specimens at 20 years storage in water in a scanning microscope provided no means to reveal the variations in cement stone structure depending on active mineral additives present in the cement.

The cement stone on the basis of the control cement (plain) only features more pores which are larger than those in specimens of cements with fly ash and Tripoli earth additives. The whole of cement stone specimens are characterized by a dense mass and pores partially or completely filled with hydration products in a form of plates and needle-like crystals.

Investigations carried out by Dr. S.S. Rehsi have made it possible to look into the composition, soundness, strength of high-magnesis cement (up to 15% MgO) with a fly ash additive (20-40%) (20, 21) at 14 years hardening.

It has been ascertained that incorporation of fly ash in high-magnesia cement has an efficient stabilizing influence on technical characteristics of such a binder. The compressive strength as well as the tensile strength of high-magnesia cement without fly ash appreciably falls even after 90 days of storage in water at 27±2°C, while introduction of 30% fly ash ensures a steady strength development during the first five years whereupon it remains constant. The expansion of high-magnesia cements containing fly ash and without it at 14 years storage in water was 0.239 and 1.833%, respectively. Incorporation of fly ash brings about no changes in the composition of the hydration products of high-magnesia cements, so in specimens of 14 years storage in water CSH, ettringite, $Mg(OH)_2$, $Ca(OH)_2$, $CaCO_3$ and residual inhydrated MgO were indentified.

Practically the whole of investigations on the effect of hydraulic additives on magnesian cements properties points to their favourable action. This technological method would assure obtaining of high-quality magnesian cements and application of dolomite limestones.

The production practice has proved that magnesium oxide impedes obtaining of high-quality cement. In view of this technological methods aimed at raising the product quality are under development at cement plants. Significant works in this field have been carried out by M.A. Teixeira de Castro (23).

As mentioned above, according to the Brazil standards the permissible magnesium oxide content in cement is up to 6.5%. Therefore the problem on provision of manufacturing high-quality magnesian cement is of great urgency.

The major recommendations on improvement of the quality of high-magnesia cements are as follows:

- fine grinding of raw mixture;
- thorough mixing of raw mixture;
- sharp burning of clinker in oxidizing atmosphere;
- fine (possibly repeated) cement grinding;
- clinker should feature:
  a) as high tricalcium silicate content as possible;
  b) elevated iron content

For each plant and its raw base the mentioned conditions should naturally be refined, but they are obligatory to a certain degree. Unfortunately the work under consideration doesn't touch upon the subject of cement soundness provision by autoclave tests, but adduces data obtained in Le Chatelier tests.

Currently the problems on the phase composition of clinkers featuring various magnesium oxide contents as well as the effect of chemical and technological factors (chemical composition and fineness of raw mixtures, cement fineness etc.) on the properties of magnesian cements have been studied fully enough (24, 25).

However there are no data on organization of commercial magnesian cement manufacture. Different standards for assessment of cement soundness not always allow to compare characteristics of cements obtained and investigated. Moreover, there is no unified opinion on suitability of autoclave cement test since, as it has been found, its results are influenced by some other factors.

The results of physicomechanical tests and linear expansion values obtained on long-term hardening under normal conditions have evidently a great importance in solving the problems under consideration. These data for 25-30 years of cement hardening would allow to evaluate cement characteristics and methods for cement testing.

REFERENCES

1. Serov V.V. Tsement No. 1, 1934; No. 7, 1935.
2. Getchert I.E., Zhukov M.P. Trudy Giprotsementa, vyp. 16, Promstroiizdat, 1963.
3. Budnikov P.P., Vorobev H.S. Tsement No. 1, 1960.
4. Toropov N.A., Merkov L.D., Shishakov N.A. Tsement No. 1, 1937.
5. Royak S.M., Myshlyaeva V.V., Trudy NIITsementa, vyp. 7, Promstroiizdat, 1953.
6. Royak S.M., Myshlyaeva V.V. Vliyanie povyshennogo soderzhaniya okisi magnia na svoistva tsementov. Promstroiizdat, 1956 (MPSM SSSR, TsBTI Tekhnicheskoe Upravlenie, Informatsionnoe soobshchenie).
7. Astanskii L.Yu. Issledovanie rezhima okhlazhdenia tsementnogo klinkera. Ufa, 1959.
8. Y.V. Nikiforov, R.A. Zozoulia. 7-th International Congress on the Chemistry of Cement. V. II, Paris, 1980, p. 1-34.
9. R. Bucchi. 7-th International Congress on the Chemistry of Cement. V. I, Paris, 1980, p. 1-1/3.
10. V.V. Timashev. 7-th International Congress on the Chemistry of Cement. V. I, Paris, 1980, p. 1-3/1.
11. G. Goswami, S.K. Mohanty, J.D. Panda. Cement and Concrete Research. Vol. 14, p.p. 407-412, 1984.
12. Mangelnde Raumbeständigkeit im Autoklaven von Klinkern mit niedrigen MgO-Gehalten. Reports. Zement-Kalk-Gips, 1982, Nr. 9, S. 508.
13. Cement Standards of the World. Cembureau. The European Cement Association.
14. Kogan L.S., Nikiforov Y.V. Trudy instituta Giprocement, vyp. 24, 1962, L.
15. Nikiforov Y.V., Zozoulia R.A. Trudy Instituta NIITsement, vyp. 63, M., 1982, S. 123-132.
16. Kuznetsova T.V., Soboleva K.L. Tsement, 1979, No. 12, S. 12-13.
17. Nikiforov Y.V., Svatovskaia M.B. Tsement, 1983, No. 1, S. 14-16.
18. Nikiforov Y.V., Svatovskaia M.B., Tsintsiper M.S., Milovanov Y.A. Tsement, No. 8, 1983.
19. Nikiforov Y.V., Zozoulia R.A. Trudy instituta NIITsement, No. 77, M., 1983, S. 64-70.
20. S.S. Rehsi. Magnesium Oxide in Portland Cement. Adv. Cem. Technol., Crit. Rev. and Stud. Manuf. Qual. Contr., Optimizat. and Use, Oxford e.a. 1983, p. 467-483.
21. S.S. Rehsi, Garg S.K. "Durabil. Build. Mater.", 1985, 2, No. 3, 265-273.
22. Rosa J. Stavivo, 1961, No. 12.
23. M.A. Teixierde de Castro. Tecnica, 1981, 41, No. 458, 263-273.
24. Dreizler J., Knöfel D. Zement-Kalk-Gips, 1982, Nr. 10, S. 537-550.
25. Chr. Rott., D. Knöfel, J. Dreizler. Zement-Kalk-Gips, 1984, Nr. 4, S. 195-199.

PALOMO, A.; VAZQUEZ, T. and BLANCO-VARELA, M.T. 1

Instituto Eduardo Torroja de la Construcción y del Cemento (C.S.I.C.) Madrid (España)

INFLUENCE OF MgO ON THE CRYSTALLINE MICROSTRUCTURE OF THE LIQUID PHASE OF PORTLAND CEMENT S1

INFLUENCE DE MgO SUR LA MICROSTRUCTURE CRISTALLINE DE LA PHASE LIQUIDE DU CEMENT DE PORTLAND

Introduction

Due to the pernicious effect that the magnesium oxide effectuates on the stability of the concrete's volume, generally the contents of Mg in Portland cement are restrained in the legislation of the countries of the world. Although, the presence of Mg in raws mixes can also generate important benefits. The MgO, for example, is a well known fluxing agent, and it improves the burnability of raws; and it also accelerates the rate of combiantion of lime. Besides this, if the formation of periclase in the clinker could be diminished or delayed, there would be the important chance of using in the elaboration of the cement big calcareous beds useless nowadays by problems of dolomitization; and many times with important increases of costs due to the provision of lime stone with less contents in magnesium oxide, worked out in more grievous conditions.

In the present work a special emphasis has been put in the study of the modifications that the compo - nents of the liquid phase of the clinker (aluminates and ferrites) undergo, and the micro-structures that are generated by the presence of a certain quantity of MgO.

Bibliography about this subject isn't abundant. Nevertheless, we can consider the studies of Müller-Hesse and Shwiete (1), Midgley (2), Woermann et al. (3), Locher (4), and Miyazawa and Tomita (5) about the capacity of aluminates and ferrites to incorporate MgO in their crystalline lattices, and the studies of Dreizler et al. (6), Christensen (7), Bucchi (8), Budnikow and Worobjew (9), Guyo (10), Ramachandrán (11), and Nikiforov et al. (12) about different aspects of the role of MgO in Portland cement.

Experimental Procedure

The materials used in the realization of this work have been laboratory reactives of a high degree of purity (99%): $CaCO_3$, Al_2O_3, Fe_2O_3 and MgO. The procedure to whom these compounds were submitted is described in the following way:

- Five mixtures in correspondence with five compositions of the ternary system C-A-F (see Table 1) were prepared.
- A study by Differential Thermal Analysis of each compositions was made.
- Pellets, of about 0.4 gr. belonging to each composition, were made using for it a 7 mm - internal diameter cylindric mould and an hydraulic press that was activated to a pressure of 4 free tons.
- The tablets, introduced in tiny platinum crucibles were submitted to a thermic programmed treatment (similar to the DTA) in a vertical laboratory furnace with an attached programmer controller of temperature. This thermic treatment (identical for all the compositions except in the final temperature that was reached) consisted in the preservation of the sample up to 1100ºC during 25 minutes, heat it immediatelly up to 1500ºC (at a velocity of 40ºC/min.), preserve it 10 minutes at that temperature and finally cool it at a velocity of 8ºC/min. until it reached the required temperatures. These temperatures were different for each composition and they depended on the results obtained before by DTA. Table 2 shows the list of temperatures selected in each case.

Table 1

	CaO (wt%)	Al_2O_3 (wt%)	Fe_2O_3 (wt%)
composition 1	42,1	23,7	34,2
composition 2	53,1	28,2	18,7
composition 3	49,5	35,6	15,5
composition 4	41,8	34,9	23,3
composition 5	44,9	45,3	9,8

Table 2

compositions	temperatures of treatment (ºC)
1 and 1+ MgO	1390 - 1260 - 1050
2 and 2+ MgO	1355 - 1285 - 1210
3 and 3+ MgO	1325 - 1185
4 and 4+ MgO	1370 - 1290 1242 - 1145
5 and 5+ MgO	1280 - 1190 - 1130

Once the required temperature was reached, the sample was kept during an hour at that same temperature and immediatelly after it was taken out of the furnace and quenched in an air current.

- The quenched samples were analysed by infra-red spectroscopy and by X-ray diffraction (Table 3 resumes the data obtained with these methods). They also were prepared for its observation through reflected light optical microscopy.
- All the stages described up to here, were repeated one by one with the same compositions given in Table 1, but all of them doped with 6.5% of MgO.

Results and Discussion

In figures 1 and 2 the results obtained in the study by DTA about the thermic behaviour of the five chosen compositions are shown.

In the DTA curves (in the section corresponding to the heating), compositions 1, 2 and 3 show a double peak that indicates consecutives meltings. The first of these peaks presents its maximum at about 1315ºC and the second one presents it in a range of temperature that goes from 1340ºC to 1375ºC.

Compositions 4 and 5 present an only peak assignable to the melt with the maximum over 1320ºC.

Concerning with the cooling, all the compositions, except number 3, show two peaks corresponding to consecutive solidifications. The first one in a range

PALOMO, A.; VAZQUEZ, T. and BLANCO-VARELA, M.T.

INFLUENCE OF MgO ON THE CRYSTALLINE MICROSTRUCTURE OF THE LIQUID PHASE OF PORTLAND CEMENT S1

INFLUENCE DE MgO SUR LA MICROSTRUCTURE CRISTALLINE DE LA PHASE LIQUIDE DU CEMENT DE PORTLAND

of temperatures between 1321 and 1239ºC and the second one between 1225ºC and 1132ºC. Composition No 3 presents an only peak of solidification with a minimum at 1282ºC.

With the base of these data it is described and explained the results obtained for each composition:

Composition No.1

From micrographs 1 and 2 and from Table 3 it is infered the evolution of this composition when the temperature falls: First the ferritic phase crystalizes in needles shapes, and among the needles a poorly crystalized material, rich in Al, solidifies. As the essay temperature decreases, the kind of texture doesn't change, but the material that initially was nearly vitreous, has been transformed into a heap of tiny crystals of CA that rest upon a whitish base of ferritic nature though clearly different from the already mentioned ferritic needles. This reveals that two ferritic phases with different contents in Fe and in Al have been formed; this is logic if it is considered that when CA crystallizes from a rich in Al melted phase, segregations are produced; this helps to form a second ferritic phase poorer in Al than the primary needles. The IR spectroscopy sustain these deductions, because the bands of absorption in the 650-730 cm^{-1} zone (characteristic of vibrations FeO_4) wouldn't be observed as continuous if it existed one only phase; an only ferritic phase would produce definite bands in determinate frequencies. The same thing can be said about the band in 570 cm^{-1}, attributed to Al-O vibrations of ferritic phase that do not appear single and clear and this because surely existes an overlapping of Al-O bands due to more than one ferritic phase.

The IR spectroscopy is also in agree with the existence, at a high temperature of aluminates that aren't crystallized because in 780-800 cm^{-1} zone (characteristic of AlO_4 vibr.), it is observed a difusse absortion. By XRD the presence of a little amount of crystallized CA is detected, it really corresponds to some crystalline nucleus of the monoaluminate.

Table 3
IR and X-ray examination

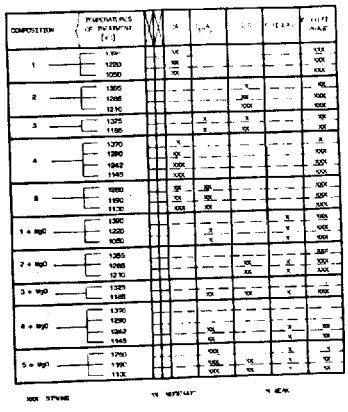

The composition No. 1 lies down upon the primary field of crystallization of C_2Fss and upon the area of compatibility CA-C_2Fss; this corroborates that the crystallization sequence described for this composition is in agree with the equilibrium established in the ternary diagram C-A-F.

Fig. 1

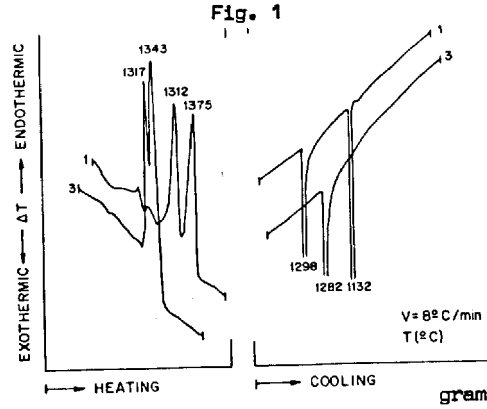

Fig. 2

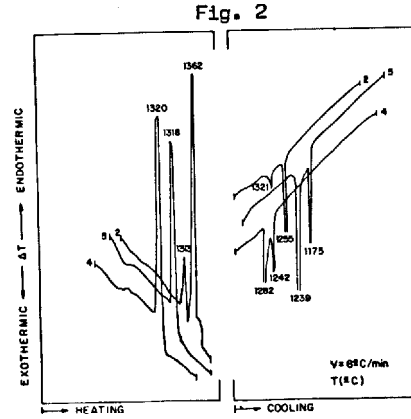

Composition No.2

Composition 2 lies upon the primary crystallization field of the CaO and upon the triangle of compatibility C-C_3A-C_2Fss. This composition presents at the highest temperature of treatment a vitreous solidification that on the microscope is seen as an uniform and grayish mass. Although not only the IR spectroscopy but also the XRD (see Table 3) discovers the presence of C_3A traces and a little of ferritic phase (type C_6A_2F). When the treatment temperature diminishes, a texture like the one of micrograph 3 is found. In this microstructure, that doesn't have posterior changes, it is observed a great number of dark and long crystals of C_3A that are homogeneously distributed upon a surface of clear colour and of ferritic nature. Decreasing the treatment temperature a little bit more, it is observed that the degree of crystallization of the phases improves. The ferritic phase gets on being rich in Al.

Composition No. 3

This composition presents a microstructure as the ones of micrographs 4 and 5. Apparently, two only phases appear but the presence of 3 phases is deduced through XRD and IR spectroscopy $C_{12}A_7$, C_3A and ferritic phase. Ferritic phase (the clearest one) is rich in Al and crystallizes in shape of small needles that are partially cut by aluminates (tinier crystalls but longer). Composition 3 shows us a case where the proximity of the succesive temperatures of crystallization, don't allow the observation of intermediate stages. This composition lies upon the primary field of crystallization of the C_3A, near the boundary that separates this field with that of C_2Fss and also near the ternary eutectic C_3A - C_2Fss - $C_{12}A_7$. This justifies the similitude between the texture

INFLUENCE OF MgO ON THE CRYSTALLINE MICROSTRUCTURE OF THE LIQUID PHASE OF PORTLAND CEMENT S1

INFLUENCE DE MgO SUR LA MICROSTRUCTURE CRISTALLINE DE LA PHASE LIQUIDE DU CEMENT DE PORTLAND

MIC. 1 comp. 1 (1390ºC)

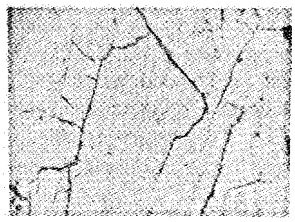

MIC. 2 comp. 1 (1050ºC)

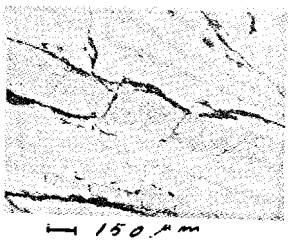

MIC. 3 comp. 2 (1285ºC)

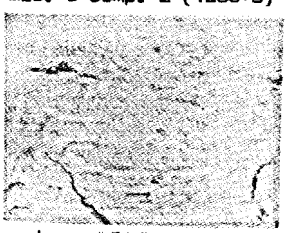

MIC. 4 comp. 3 (1185ºC)

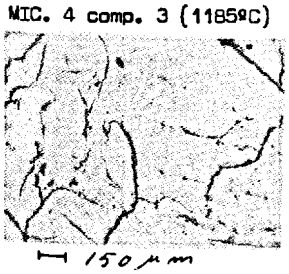

MIC. 5 comp. 3 (1185ºC)

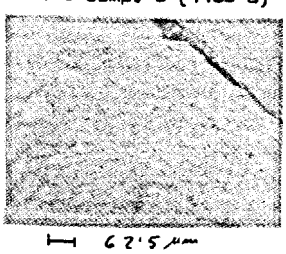

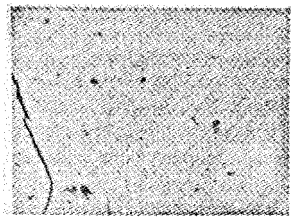

MIC. 6 comp. 4 (1370ºC)

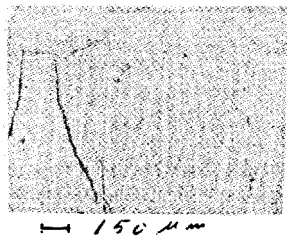

MIC. 7 comp. 4 (1290ºC)

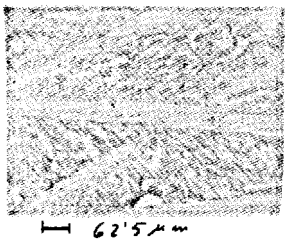

MIC. 8 comp. 4 (1145ºC)

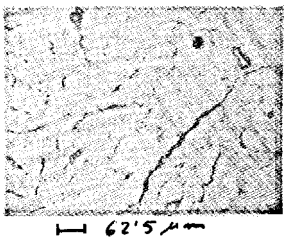

MIC. 9 comp. 5 (1280ºC)

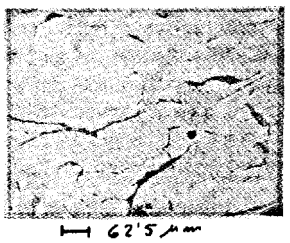

MIC.10 comp. 5 (1130ºC)

found in this composition and the typical texture of the compositions that lie upon the primary crystallization field of C_2Fss, because the early crystallization of the C_2Fss, when the amount of crystallized C_3A isn't big yet, enables the formation of this kind of texture.

Composition No. 4

Microscopy (micrographs 6,7 and 8),XRD and,IR spectroscopy give the following data about the development of this composition with the temperature.In a first stage, ferritic crystals with needle shape solidity and among them, an amorphous material rich in Al. In an ulterior stage,the vitreous material crystallizes in the shape of tiny crystals of CA at the same time that the ferritic needles grow slighty. Finally, all the crystals (ferrites and aluminates) grow and increase their degree of crystallinity considerably, locating the CA crystals upon a base of ferritic origin that on the micriscope presents a lighter colour than the one of the ferritic needles; so that two ferritic phases with different proportions of Fe and Al are formed.

This composition shows a great similitude with composition 1 and this is logica because composition 4 is also localetd upon the primary crysta

MIC. 11 comp 1 M (1390ºC)

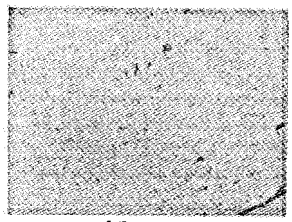

MIC. 12 comp 1 M (1050ºC)

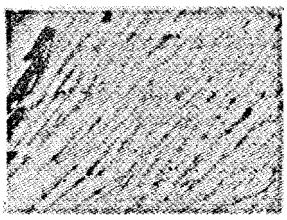

MIC. 13 comp 4 M (1145ºC)

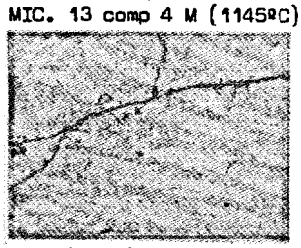

MIC. 14 comp 2 M (1285ºC)

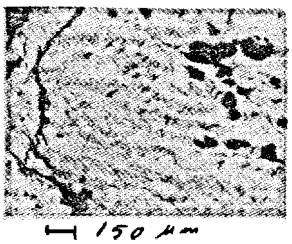

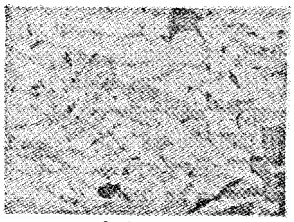

MIC. 15 comp 2 M (1285ºC)

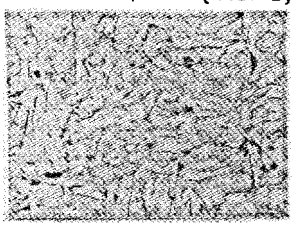

MIC. 16 comp 3 M (1185ºC)

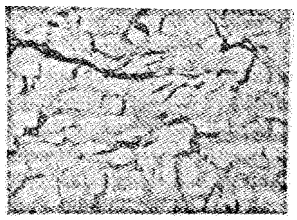

MIC. 17 comp 3 M (1185ºC)

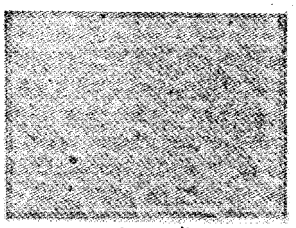

MIC. 18 comp 5 M (1280ºC)

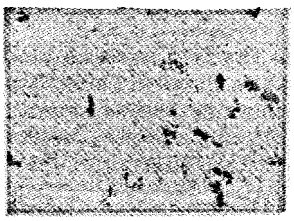

MIC. 19 comp 5 M (1190ºC)

INFLUENCE OF MgO ON THE CRYSTALLINE MICROSTRUCTURE OF THE LIQUID PHASE OF PORTLAND CEMENT S1

INFLUENCE DE MgO SUR LA MICROSTRUCTURE CRISTALLINE DE LA PHASE LIQUIDE DU CEMENT DE PORTLAND

llization field of the C_2Fss and upon the compatibility area CA - C_2Fss. The only difference between both compositions is that composition 4 is richer in Al and it is nearer to the boundary CA - C_2Fss; this makes that this composition will have a bigger proportion of CA and a less proportion of ferritic primary phase . The rest of the resultants are interpreted exactly the same as in composition 1.

Composition No.5

The solidification of this composition can be described in the following way: First dendritic crystals of $C_{12}A_7$ begin to nucleate and grow (this crystals that lie upon a slightly devitrified and rich in Al bass can be seen in micrograph 9); afterwards and due to the annealing it can be observed an increasing in the dendrites size together with an eutectic crystallization where $C_{12}A_7$, CA and a ferritic phase rich in Fe solidify simultaneously (see micrograph 10). The facts described for composition 5, are in good agree with the situation of this composition in the equilibrium diagram. Composition 5 lies upon the primary field of crystallization of the $C_{12}A_7$ and upon the triangle of compatibility $C_{12}A_7$ - C_2Fss -CA.

Effects of the MgO

The addition of a 6.5% of MgO to each one of these compositions produces a group of effects that can be described in the following way:

In composition 1, the MgO acts upon the nature of the phases and upon the evolution of microstructure (see Table 3 and micrographs 11 and 12). Concerning with the nature of the phases, MgO helps to form $C_{12}A_7$ in detriment of monocalcic aluminate and favours the formation of an only ferritic phase; concerning to the evolution of the microstructure, MgO alters the temperatures when the phases begin to crystallize.

When it is added to composition 1, 6.5% of MgO, it is observed that at a high temperature ferritic phase with a little of periclase crystallizes (crystalline aluminates aren't detected). When the temperature diminishes, together with the ferrites, it crystallizes a tiny amount of $C_{12}A_7$. The final texture found is similar as the one of composition 1 without MgO, although the stages of crystallization are produced in lower temperatures, this gives us an idea of the fluxing action of MgO.

The presence of $C_{12}A_7$ instead of CA, gives also an idea of the power of Mg to replace the Ca atoms in the lattice of $C_{12}A_7$, producing $(C_{1-x}M_x)_{12}A_7$.

The ferritic phase is also affected by the presence of MgO, because it appears an only ferritic phase, rich in Fe (richer than C_4AF). This is infered by IR spectroscopy, because of the situation of the band that appears in 705 cm^{-1}.

As it was mentioned before, composition 4 has many things in common with composition 1: its final microstructure scarcely changes with the presence of MgO (see micrograph 13); what logicallychanges, are the temperatures of the stages of crystallization.

Also, and the same as it happened with composition 1, in presence of MgO, the only aluminate that crystallizes in composition 4 is the $C_{12}A_7$. Also there is an only one feritic phase.

The differences between compositions 1 and 4 with addition of MgO, are due to the positions of each of these compositions in the diagram C-A-F.

Being composition 4 richar in Al we found more amount of aluminate and also a ferritic phase richer in Al (type C_6A_2F), hipothesis based on the position of a band found in the IR spectra near to 720 cm^{-1}.

Besides this, with respect to the effect of MgO on composition 4, there is an important detail in relationship with the fluxing power of the compound and is the vitreous solidification of the sample quenched at the highest temperature. Composition 2 doesn't change appreciably by the presence of MgO in relation to the nature of the phases that are formed in the different tested stages, but at 1350ºC the fluxing effect of the MgO and the primary crystallization of ferrite are observed.

From the microstructural point of view there are changes that deserve being mentioned (see micrographs 14 and 15); in composition 2 predominates an eutectic crystallization, but in presence of MgO a very clear separation between ferrites and aluminates is observed (aluminates have a considerable size); besides due to the aspect of aluminates (it is observed a union of tiny crystals) it can be said that an eutectic crystallization happened though not in the magnitude when MgO wasn't present. About the ferritic phase it can be said that is a rich in Al one.

Micrographs 16 and 17 show the microstructural evolution of composition 3 in presence of MgO. Textures are similar when MgO wasn't present; nevertheless the presence of this oxide makes crystals have a grater size. What before were ferritic needles, very well formed, now they are crystals withan indefinite shape. Aluminates conserved its lengthened shape. It is also observed with a great clearness aggroupments of tiny crystals separated by ferritic phase.

It is important to express again the fluxing power of the MgO (the sample of high temperature with MgO is amorphous).

Finally, and concerning to composition No.5, we have to say that MgO effectuates a quite perceptible action principally from the point of view of the nature of the phases.

In presence of MgO isn't detected anything of CA but although it is found much $C_{12}A_7$ and also some C_3A. Logically this has a repercussion over the studied microstructures. The kind of texture is similar but when the nature of the aluminates is changed, diffe

rences are detected (see micrographs 18 and 19), such as the exposure that the crystalline mass presents, fact that is surely connected with the data that the IR spectroscopy adduces about the $C_{12}A_7$ found in the sample of 1280ºC, that has a big symmetry.

To finish this study it is suitable to appoint that the amount of periclase found in almost the total cases, has never passed the traces.

Conclusions

- If it is added 6.5% wt of MgO to the compositions of the system C-A-F studied in this work, the MgO comes into the lattice of the aluminates in substitution of calcium, generating $(C_{1-x}M_x)_{12}A_7$ in the compositions that being absent Mg produce CA and $(C_{1-x}M_x)_3A$ in those where it is formed $C_{12}A_7$. And also the Mg gets into the lattice of the ferritic phase.
- The modifications observed in the microstructures by the effect of adding MgO is generally justifiable by the fluxing action of this compound and/or by the modifications that magnesium oxide introduces in the equilibrium of the phases.
- The Mg incorporated to the primary $C_{12}A_7$, lattice improves notably its structural order.

References

1.- Müller-Hesse, H. and Schwiete, H.E. - Zement-Kalk - Gips nº 9, p. 386 (1956)
2.- Midgley, H. - Proc. 5th Intern. Symp. on Chem. of Cement. Paper nº 1-12, S-230. Tokyo (1968)
3.- Woerman, E. Hahn, Th. and Eysel, W. - Zement Kalk - Gips nº 16 p. 370 (1963); nº 20, p. 385 (1967); nº 21 p. 241 (1968); nº 22 y 235 (1969)
4.- Locher, F.W. - Proc. 4th Intern. Symp. on Chem. of Cement. Paper II - S5. Washington (1960)
5.- Miyazawa, K. and Tomita, K. - Zement-Kalk-Gips nº 19, p. 82 (1966)
6.- Dreizler, I. and Knöfel, D. - Zement-Kalk-Gips nº 10 p. 237 (1982)
7.- Christenssen, N.H. - World Cement Technology p. 223 October (1978)
8.- Bucchi, R. - World Cement Technology p. 210 June (1981); p. 258 July/August (1981)
9.- Budnikow, P.P. and Worobjew, Ch. S. - Silikattechnik nº 4 p. 158 (1958)
10.- Guye, F. Revue des Materiaux de Construction nº 567 p. 333 (1962)
11.- Ramachandran, V.S. - Il Cemento nº 3 p. 159 (1980)
12.- Nikiforow, IU. V. - Proc. 6th Intern. Symp. on Chem. of Cement, S - 110 Moscow (1974)

J. Gebauer, "Holderbank" Management and Consulting Ltd., Switzerland

EFFECT OF HIGH MgO CONTENT IN CEMENT UPON-TERM PROPERTIES OF CONCRETE

1. Introduction

The various national cement standards, prescribing the permissible limits for magnesia in cement, list maximum values from 3.0 up to 6.5 %. This limitation of the MgO content is due to the potential negative effect of uncombined magnesia (periclase) on concrete durability.

Any increase of the permitted magnesia content in cement would be of great practical importance, offering a considerably increased choice of raw materials for cement manufacture.

Up to date, there is no firm evidence that cements with 7 - 8 % MgO in clinker cause any deterioration of concrete specimens either in laboratory tests or in practice. Most of the investigations on MgO expansion are carried out on neat cement paste or mortar specimens and only very limited data exist on either concrete specimens or concrete constructions. To our knowledge, the only long-term tests in concrete were carried out by Gonnermann et al (2) and showed no strength loss for concrete cylinders made with autoclave- unsound cements with 7 - 10 % MgO even after 15 years of water storage.

A quick and reliable performance test would make the stringent MgO limitatations superfluous. The only standardized performance test available and used in practice, the ASTM autoclave test, has been subjected to serious criticism. The main objections against this autoclave test have been summarized by Mehta (1):

> The autoclave test conditions force the crystalline MgO to hydrate and expand whereas in normally cured concrete, the MgO hydrates at a rate too slow to be of any consequence
>
> The magnitude of the expansion in neat cement bars caused by hydration of free MgO or CaO may be high, but in corresponding concretes it is not even high enough to cause cracking
>
> No correlation has ever been shown between the autoclave test specification limits and the soundness of concrete.

In 1981 a research program was initiated at the Technical Center of "Holderbank" Management and Consulting Ltd. on the long-term properties of concrete produced with cements containing an elevated amount of MgO to classify the relevance of the autoclave test from the viewpoint of concrete as well as the justification of the low limiation of the MgO content in cement. Besides Portland cement, blended Portland cements - a cement type which has recently been gaining in importance - were also included in the investigation. In the following, the presently available results of our long-term research program are presented and discussed.

2. Experimental work

2.1. Materials used

An industrially produced ordinary Portland cement and three blended cements, prepared from ordinary Portland cement and various hydraulically active additives, were used for the investigations.

The ordinary Portland cement's clinker, containing 7.5 % MgO, was produced in a wet process kiln under normal operating conditions in order to achieve the maximum autoclave unsoundness for the given MgO content. As microscopical observations showed, the clinker contained a large amount of coarse, crystalline periclase as well as large clusters of periclase.

The blended cements were produced by blending ordinary Portland cement with 20 % additives, namely preground blast furnace slag, natural pozzolan and fly ash.

The chemical composition and fineness of the ordinary Portland cement and of the hydraulically active additives are shown in table 1.

The Bogue mineralogical composition of the ordinary Portland cement, the free lime content and the periclase content are shown in table 2. The periclase content was determined by means of the X-ray diffraction method using the principal reflection at d = 2'106 A.

Table 1: Chemical composition of cement and additives

	Portland Cement	Fly ash	Slag	Pozzolan
L.o.i. (%)	0.87	3.2	1.0	4.4
SiO_2	18.4	50.8	34.3	70.7
Al_2O_3	5.8	25.2	9.0	13.1
Fe_2O_3	3.3	7.8	0.92	1.5
CaO	59.7	3.2	43.7	1.8
MgO	7.1*)	2.1	5.6	0.31
SO_3	1.92	1.8	3.5	0.05
K_2O	1.3	3.9	0.66	3.4
Na_2O	0.14	0.53	0.51	3.9
TiO_2	0.31	0.86	0.45	0.19
Mn_2O_3	0.10	0.10	0.39	0.05
P_2O_5	0.23	0.19	0.03	0.09
Cl	0.01	0.01	0.02	0.06
Blaine (cm^2/g)	3210	4060	3240	4950

*) MgO content in clinker = 7.5 %

Table 2: Mineralogical composition of Portland cement

C_3S	54.1 %
C_2S	12.0 %
C_3A	9.8 %
C_4AF	10.1 %
Periclase (XRDA)	5.8 % (in clinker 6.1 %)
Free lime (acc to ASTM)	1.9 % (in clinker 2.0 %)

2.2. Preparation and testing

The cements included in the long-term program were tested on concrete slabs. The slabs, 100 x 50 x 7 cm in size, were prepared from concrete mixes containing a constant 300 kg cement per m^3 of concrete and natural aggregate of 32 mm maximum grain size. The water content of the concrete was as required to reach a concrete consistency of 7.5 ± 1 cm slump. The concrete slabs were cured for up to 7 days in a curing room at 20°C and 95 % relative humidity. Thereafter, one slab of each concrete mix was deposited at the outdoor testing facilities in Holderbank, Switzerland, while the other one was kept in the curing room. The outdoor storage of slabs is shown in Fig. 1.

The slabs were tested after 28 days, 0.5, 1, 2, 3 and 4 years. Further tests are foreseen after 5, 10 and 20 years. In addition, concrete cores from the 4 year old slabs were exposed to autoclave treatment according to the ASTM procedure and tested thereafter.

On the concrete slabs, the following tests were carried out:

Compressive strength tests on cores (dia. 50 mm and h = 5.6 mm) drilled from the slabs; each strength test result quoted represents the average of 6 cores.

Ultrasonic pulse velocity measurements with the aid of a Pundit apparatus.

Periclase and microstructure investigation by means of light microscopy on polished cross-sections of cores.

Determination of the periclase content by means of X-ray diffraction, using the mortar fraction of the cores. The content of periclase was recalculated as a percentage of the total concrete mix, including ccarse aggregate and assuming no hydration of periclase in the reference 1-day old concrete.

The cements were also tested on standard soundness tests according to the Le Chatelier and ASTM autoclave method.

3. Discussion of the results

The autoclave expansion of the cements is - with the exception of pozzolanic cement - excessive and higher than that specified in ASTM. The high autoclave expansion is due to the high periclase content and the elevated amount of free lime in the cement (table 3).

The concrete, however, shows after four years no signs of deterioration, and a continuous strength gain can be observed over the entire 4 year testing period in all concrete slabs stored indoor (Fig. 2). The ultrasonic pulse velocity measurement confirms these findings. At the outdoor facilities, some degradation of the concrete due to freezing/thawing cycles is observed as the concrete had not been air-entrained and thus is not sufficiently frost resistant.

Table 3: Physical properties of cements and concrete slabs

Cement	PC		PC/FA		PC/SL		PC/POZZ	
Proportioning	100		80/20		80/20		80/20	
Blaine (cm^2/g)	3210		3380		3180		3580	
ASTM autocl.(%)	7.14		8.00		6.39		0.45	
Le Chatelier(mm)	1.75		0.75		1.00		2.25	
Concrete slab								
W/C ratio	0.56		0.56		0.56		0.58	
Strength(N/mm^2)	I	0	I	0	I	0	I	0
28 days	35.9	35,0	34,7	32.4	36.5	36.5	33.8	29.8
0.5 year	51.1	46.4	45.5	42.8	49.9	46.0	43.2	39.3
1 year	53.6	44.8	45.9	44.2	52.4	48.8	44.0	38.2
2 years	56.2	51.4	48.1	45.7	54.8	53.5	45.5	43.4
3 years	58.7	55.0	50.2	46.0	58.2	55.2	46.0	44.0
4 years	60.7	57.6	52.5	46.6	60.8	55.0	46.9	42.9
4 years and autoclave	65.1		55.9		69.3		56.8	
UPV (m/sec)								
28 days	4700	4645	4667	4560	4711	4560	4571	4435
0.5 year	4837	4733	4861	4768	4849	4678	4756	4613
1 year	4849	4814	4397	4837	4849	4802	4745	4711
2 years	4875	4802	4897	4849	4873	4825	4768	4733
3 years	4921	4802	4945	4791	4873	4791	4837	4685
4 years	4958	4766	4929	4745	4890	4779	4795	4633

I = Indoors (curing room)
0 = Outdoor facilities
UPV = Ultrasonic pulse velocity

Table 4: Periclase in Portland cement concrete (XRD analysis)

Age of concrete	% of reference	periclase content in concrete (%)
1 day (reference)	100	0.73
4 years	70	0.51
4 years and autoclave	40	0.29

The microscopical investigation and X-ray diffraction analysis of the concrete shows that part of the periclase has hydrated within the four years without any harmful expansion. The microphotograph of the 4-year old concrete shows the position of a periclase containing clinker particle which has partially hydrated. Periclase crystals can be seen also in the hydrated zone of the clinker particle (Fig. 3).

During the autoclave treatment, periclase is further hydrated, again without any negative effect on concrete properties. On the contrary, the concrete experienced a substantial strength gain. Part of the periclase remains unreacted, even after the severe autoclave treatment as shown in the microphotograph (Fig. 4) and confirmed by X-ray diffraction analysis. The results of the X-ray diffraction analysis of concrete made with the Portland cement are shown in table 4 and figure 5, indicating the reduction of periclase content in concrete during

the 4 years of normal curing and autoclave treatment.

These findings suggest that the periclase is hydrating very slowly at normal curing conditions in concrete and without impairing the concrete properties.

The main reasons for the absence of any detrimental effect of periclase in concrete in contrast to the ASTM autoclave test are the lower percentage of periclase in concrete compared to neat cement paste and the slower rate of periclase hydration in concrete under normal curing conditions compared to the autoclave curing. The stresses developed by slow hydration of the smaller amount of periclase begins to act after the mature concrete has gained sufficient strenth. On the contrary, in the autoclave test the sudden development of expansive forces due to periclase hydration easily surpasses the cohesive forces of the relatively immature and weak cement paste. The autoclave test has therefore no practical significance for the performance of concrete in practice.

4. Conclusions

Both Portland cement and blended Portland cements produced with a clinker of 7.5 % MgO content show satisfactory properties in 4-year old concrete, even when the major part of the MgO is present as coarse crystalline periclase. It can thus be concluded that the current cement standard specifications regarding the permissible MgO content in cement are not adequate and even hinder the economical use of cement raw material resources. The investigations confirm the irrelevance of the ASTM autoclave test for the performance of concrete in practice, already stated already by other investigations.

Literature

(1) P.K. Mehta: History and status of performance tests for evaluathion of soundness of cements ASTM Publication, STP 663, 1953, pp 35 - 55

(2) H.F. Gonnermann, W. Lerch and W.M. Whiteside: PCA, Research Laboratory Bulletin No. 45, 1953, pp 1 - 168

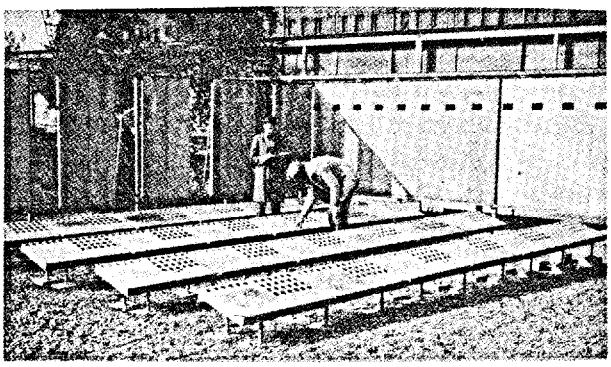

Fig. 1: Outdoor stored slabs at the testing station in Holderbank, Switzerland



Fig. 3: 4 year old Portland cement concrete, arrows indicate periclase crystals

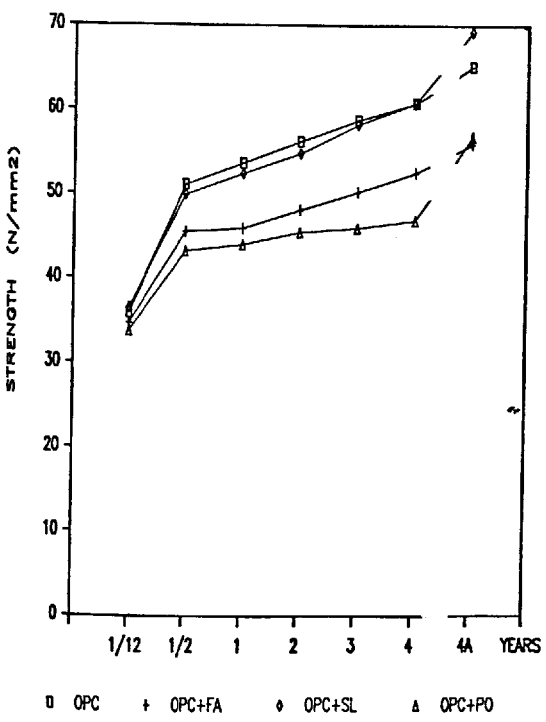

Fig. 2: Strength development of concrete

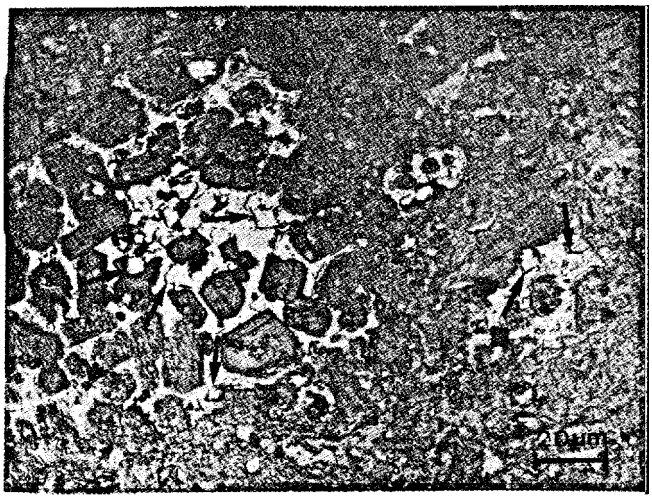

Fig. 4: 4 year old concrete, autoclaved, arrows indicate periclase crystals

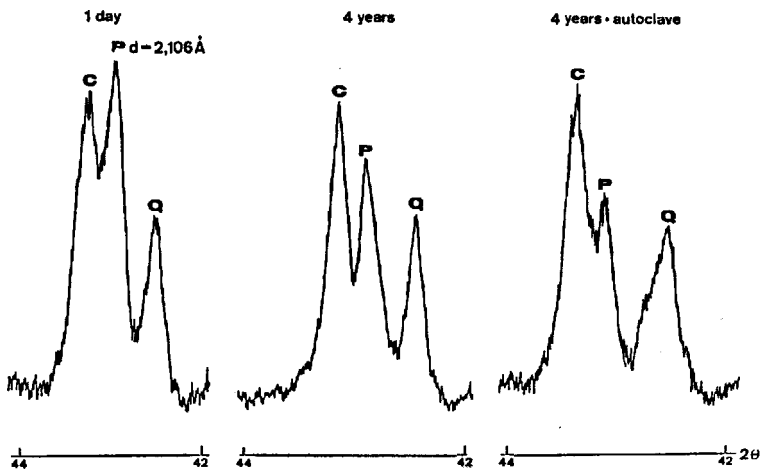

Fig. 5: X-ray diffraction analysis of concrete (C = calcite, P = periclase, Q = quartz)

V.K. KOZLOVA - Institut Polytechnique Altaique I.I. Polzounov, U.R.S.S.

SUR LA FORMATION DES PHASES NOUVELLES DANS LE CLINKER LORS DE LA CUISSON DES MELANGES CRUS A BASE DES PRODUITS SECONDAIRES

Lors de la planification du développement ultérieur de la cimenterie, une attention toujours croissante est faite à l'utilisation des produits secondaires et des déchets des autres industries.

A présent, les particularités des propriétés des mélanges crus et celles des processus de formation du clinker, en cas de l'utilisation des laitiers et des cendres d'une nature différente en qualité du constitant alumosilicate ou de l'addition de correction, sont étudiées en détail.

La plupart des laitiers, des cendres et des autres produits secondaires se distinguent du constituant argileux utilisé dans la production du ciment par une teneur élevée en sesquioxydes, en particulier, en oxyde d'aluminium. Les particularités des processus de formation des minéraux lors de la cuisson des mélanges crus basés sur les produits secondaires sont déterminées justement par cette distinction.

Les recherches des dernières années montrent que lors de la cuisson des charges de ciment crues dans lesquelles le constituant argileux se trouve remplacé par le laitier ou les cendres, il est utile d'obtenir les clinkers en vue de la production du ciment Portland particulier: ciment à haute teneur en alumine, ciment ferreux, ciment à durcissement rapide sur la base des sulfoaluminates ou des fluroaluminates (en cas de la présence d'une quantité nécessaire de sulfates ou de fluorures).

Les systèmes de sulfates et de fluorures jouent un rôle toujours croissant en vue de produire les ciments contenant les minéraux dans la composition desquels entrent les sulfates et les fluorures, en particulier, les minéraux se formant sur la base des sesquoxydes (plus souvent de l'oxyde d'aluminium) et sur la base des composés mentionnés.

Il est naturel que la particularité de la production des ciments de ce type consiste dans l'utilisation du cru riche en sesquioxydes ce qui est typique pour une série des produits secondaires les plus employés.

Au cours de l'étude des propriétés d'un grand nombre de clinkers et de ciments obtenus à partir des charges crues dans lesquelles on a utilisé, en qualité du constituant alumosilicate, les cendres provenant du charbon minéral avec une introduction simultanée des adjuvants de modification en sulfates ou en fluorures, nous avons établi la possibilité d'obtenir les ciments répondant aux exigences du "ГОСТ" (norme d'Etat) à une augmentation considérable de la teneur en oxyde de magnésium dans le constituant carbonate.

Les normes de tous les pays concernant les ciments ont une exigence nécessaire pour la quantité maximum admissible de MgO dans le clinker de ciment Portland. Cette teneur limite en MgO correspond à 3-5 %. La cause principale de ces limitations est un danger de l'expansion tardive du ciment lors de l'hydratation du MgO est une parte de résistance qui y est directement liée. Les limitations de la teneur en MgO dans la composition du clinker rétrécissent considérablement les ressources de matières premières de la cimenterie et compliquent l'exploitation des gisements isolés, puisque l'oxyde de magnésium entre en grandes quantités dans la composition des roches carbonatées des plusieurs gisements sous forme des inclusions des calcaires magnésiens et dolomitiques.

Les recherches des procédés en vue l'obtenir les ciments de haute qualité avec une teneur élevée en oxydes de magnésium dans la composition du clinker ont une grande importance pratique. A présent, on considère comme le fait établi avec une précision assez suffisante que l'oxyde de magnésium est représenté dans la composition du clinker de ciment Portland essentiellement sous forme de la périclase. Certaine sa quantité se trouve en état de dissolution dans le constituant vitreux du clinker. Une part déterminée de MgO, grâce aux substitutions isomorphes, entre dans la composition des minéraux principaux du clinker. Par exemple,

jusqu'à 1,5 % de MgO se trouve dans l'alite, 1-3 % - dans les alumoferrites de calcium, jusqu'à 2,5 % - dans l'aluminate tricalcique et 6 % - dans la phase vitreuse.

Une série d'essais montre que lors du refroidissement rapide du clinker la quantité d'oxyde de magnésium dans la composition de la phase vitreuse augmente. Par conséquent, sa quantité plus faible reste sous la forme de la périclase et les grains de cette dernière ont des dimensions plus petites par rapport au régime normal de refroidissement (1, 2). La périclase sous forme finement dispersée est capable de s'hydrater simultanément avec les autres minéraux de clinker et ne cause pas de grandes contraintes locales lors du processus de durcissement. Les garanties d'une cristallisation plus fine de la périclase et sa distribution plus homogène dans le clinker peuvent être considérées comme des mesures permettant d'augmenter la quantité admissible du MgO dans le ciment. Selon les données des auteurs de l'étude (3), l'utilisation d'un minéralisateur fluoritique lors de la cuisson favorise la formation des cristaux plus fins de la périclase et leur distribution homogène dans la masse de clinker.

La possibilité d'augmenter la teneur en oxyde de magnésium dans la composition du mélange cru a été observée lors de la caractéristique des particularités portant sur la composition et les propriétés des clinkers obtenus à l'aide des cendres utilisées en qualité du constituant alumosilicate de la charge (4). En cas de la teneur en MgO du mélange cru allant jusqu'à 6 %, l'expansion d'autoclave du ciment préparé sur la base du clinker de cendre constitue 0,8 %. En cas de l'utilisation de l'argile, le clinker ayant les mêmes valeurs du coefficient de saturation (CS) et le même module alumine est caractérisé par une expansion de 6,5 %, déjà à la teneur en MgO égale à 5,5 %.

Pour résoudre les problèmes d'obtention du ciment Portland standard avec une teneur élevée en oxyde de magnésium, beaucoup de chercheurs ont été orientés vers le choix de la composition minéralogique optimum du clinker et vers l'introduction des certains adjuvants.

Les résultats des essais (5) montrent qu'aux autres conditions égales et à la quantité équivalente de MgO dans les clinkers, l'expansion d'autoclave des ciments diminue considérablement à mesure de l'augmentation de la teneur en SO_3 dans le clinker. Selon l'opinion de l'auteur, l'introduction des sulfates peut neutraliser l'effet négatif sur les propriétés des clinkers dû à une teneur élevée en MgO. En cas de la présence des sulfates, on peut obtenir un ciment se caractérisant par une stabilité de volume si le clinker contient jusqu'à 6 % de MgO. Pour calculer la quantité nécessaire du SO_3 dans la composition de clinker, on propose la formule suivante:

$$\% SO_3 = 0,67 (\% MgO - 2)$$

En cas de la teneur en MgO jusqu'à 2 %, son influence négative se neutralise par le fait qu'il entre dans la composition des phases de clinker. Pusque l'utilisation des cendres en qualité du constituant cru rend utile l'obtention des ciments à partir des ciments à haute teneur en alumine jusqu'aux ciments ferritiques ainsi que des ciments à base des clinkers contenant les adjuvants des sulfates et des fluorures, nous avons étudié la possibilité de fabrication des ciments mentionnés avec une teneur élevée en MgO dans la composition du cru. A cette fin, on a préparé quatre types des clinkers ayant une haute teneur en MgO. Les mélanges crus n°n° 1, 2, 3 (tableau I) s'approchent, d'après leurs compositions, du mélange cru destiné à la fabrication du ciment Portlant normal. Dans ce mélange cru, le constituant argileux a été complètement remplacé par la cendre. Les compositions des mélanges crus n°n° 4, 5, 6 correspondent à la composition du mélange cru destiné à la fabrication du clinker ferritique. Les mé-

langes crus pour les clinkers n° 7, 8, 9 contiennent 3,5 % de gypse. Les mélanges crus destinés aux clinkers n°n° 10, 11, 12 ont eu 1,5 % de CaF_2. Lors de la fabrication de tous les clinkers, on a utilisé en qualité du constituant alumosilicate les cendres prevenant des charbons minéraux. La composition chimique des cendres est la suivante: SiO_2 - 52,46%, Al_2O_3 - 28,54%; Fe_2O_3 - 9,96%; CaO - 6,24%. Pour augmenter la teneur en MgO, on a introduit dans tous les mélanges crus une quantité différente de magnésite. La température de cuisson des clinkers a été de 1350-1380°C. La cuisson a été faite selon un régime lent, et le refroidissement a été effectué dans l'air.

Les analyses pétrographiques montrent que tous les clinkers se caractérisent par une distribution homogène de la périclase par la masse des grains. Dans les clinkers n° 1-6, la masse principale des grains de périclase a des dimensions de 3 à 17μ . Dans les clinkers obtenus avec les adjuvants de gypse ou de fluorure de calcium, les dimensions moyennes des grains de périclase sont de I - 10μ. La quantità de périclase dans ces clinkers est un peu plus petite que dans les autres clinkers. La teneur en oxyde de magnésium non lié a été déterminé selon la méthodologie de l'Institut "Giprocement" (6).

La détermination de la composition minéralogique des clinkers obtenus par la méthode d'analyse chimique rationnelle n'a pas permis de fixer une variation qulques peu considérable en quantité des minéraux isolés, à l'exception d'une certaine augmentation de la teneur en CaO libre. Sur la base des clinkers obtenus, é l'aide du broyage en commun avec l'adjuvant de gypse (3-5%), on a fabriqué les ciments pour lesquels on a déterminé l'expansion linéaire après le traitement d'autoclave à 2,1 MPa et la limite de compression (tableau 2). Lors de la fabrication des ciments à base dés clinkers contenant du SO_3, l'addition de gypse a constitué 3 %, tandis que pour tous les autres ciments cette dernière a été de 5 %. La surface spécifique des ciments a été de 2900 - 3100 cm^2/g. Les ciments préparés avec l'utilisation des cendres en qualité du constituant alumosilicate ont une stabilité de volume à la teneur en MgO jusqu'à 6,0 - 8,0 %. En cas de la fabrication du clinker de ciment Portland normal sur la base des mélanges crus dans lesquels on a utilisé la cendre en qualité du constituant alumosilicate, il est possible d'augmenter la teneur en MgO jusqu'à 6 %. Si on introduit dans la composition des mélanges crus préparés avec l'utilisation des cendres, des adjuvants supplémentaires de correction ou de modification, en vue d'obtenir des ciments Portland particuliers, on peut augmenter la quantité de MgO admissible jusqu'à 8 % et plus. Le clinker de ciment Portland ordinaire obtenu avec l'utilisation des cendres provenant des charbons minéraux se distingue par une quantité élevé de la phase vitreuse alumoferritique (25-28 %). La quantité de cette phase augmente de plus dans les clinkers du type ferritique (jusqu'à 40 %). C'est pourquoi, l'augmentation de la teneur admissible en MgO de ces clinkers peut être expliquée par la présence d'une plus grande quantité de cet oxyde sous forme des solutions solides dans la composition de la phase vitreuse alumoferritique.

La cause de l'influence favorable des additions de fluorures et de sulfates sur les propriétés des clinkers avec une teneur élevée en MgO n'est pas suffisamment claire à présent. A première vue, une influence positive des additions des sulfates, en cas de l'obtention des ciments avec une teneur élevée en MgO, pourrait être expliquée par une formation, due aux réactions d'échanges, du $MgSO_4$ dont la température de la dissociation est de 1135°C. Donc, lors de la cuisson jusqu'à la température mentionnée, une partie de MgO peut se trouver dans la composition du sulfate de magnésium ce qui favoriserait l'inhibition du processus de recristallisation accumulative de la périclase. Cependant, un tel mécanisme chimique

Tableau 1

Clinker, numéro	n	p	CS	Teneur totale en MgO, %	Quantité de MgO libre, %
1	0,99	1,15	0,89	4,5	2,27
2	0,99	1,15	0,89	5,5	3,18
3	0,99	1,15	0,89	6,0	3,98
4	0,73	0,63	0,89	6,0	2,85
5	0,73	0,63	0,89	7,0	3,65
6	0,73	0,63	0,89	8,0	4,43
7	1,76	2,50	0,82	6,0	2,35
8	1,76	2,50	0,82	7,0	3,15
9	1,76	2,50	0,82	8,0	3,53
10	1,29	2,53	0,77	6,0	2,57
11	1,29	2,53	0,77	7,0	3,45
12	1,29	2,53	0,77	8,0	3,90

Tableau 2

Ciment, numéro	Teneur en MgO, %	Expansion linéaire des échantillons-poutrelles, %	Limite de résistance à la compression, MPa		
			3 jours	7 jours	28 jours
1	4,5	0,26	17,5	32,1	40,6
2	5,5	0,37	16,3	31,0	39,1
3	6,0	0,52	15,8	29,7	38,4
4	6,0	0,19	17,4	24,3	42,5
5	7,0	0,28	16,0	20,8	39,5
6	8,0	0,45	14,7	21,9	40,5
7	6,0	0,13	23,1	31,1	40,7
8	7,0	0,21	21,9	29,8	39,4
9	8,0	0,30	22,2	29,3	38,6
10	6,0	0,17	34,1	42,9	49,3
11	7,0	0,26	31,7	41,1	48,1
12	8,0	0,29	30,3	39,7	47,5

de l'influence des sulfates exigerait leur quantité considérable pour former $MgSO_4$. L'action des sulfates pourrait être expliquée également par une formation en leur présence du composé $3Ca{\cdot}MgSO_4$ dans la composition duquel une partie de MgO est fixée sous forme du $MgSO_4$. Dans le travail (7) on parle de la possibilité de formation d'un tel composé lors de la cuisson des mélanges $C_3A + MgSO_4$. Pourtant, il est nécessaire d'avoir dans ce cas dans la composition du clinker une quantité élevée de SO_3 et de Al_2O_3 pour neutraliser l'influence négative du MgO. Les données expérimentales disponibles (5) montrent que la quantité nécessaire de SO_3 est beaucoup plus petite par rapport à celle dont on a besoin pour former $MgSO_4$. Apparemment, en présence des adjuvants des sulfates lors de la cuisson des clinkers avec une teneur élevée en MgO, des composés se forment se caractérisant par une grande valeur du rapport MgO/SO_3. C'est pourquoi, nous avons effectué des recherches supplémentaires ayant pour but une étude de l'interaction dans les systèmes $MgO - Al_2O_3 - MgSO_4$ et $MgO - SiO_2 - MgSO_4$. Selon nos données, on n'a pas effectué des recherches sur des systèmes semblables ainsi qu'on n'a pas mentionné une formation des composés quelconques relatifs aux systèmes ci-dessus en cas de la cuisson du clinker de ciment Portland à une teneur élevée en MgO.

La formation du sulfoaluminate de calcium ($3Ca{\cdot}CaSO_4$) dans le système $CaO-Al_2O_3-CaSO_4$ (7, 8, 9) et du sulfoaluminate de baryum ($4BaO{\cdot}Al_2O_3{\cdot}BaSO_4$) dans le système $BaO-Al_2O_3-BaSO_4$ (10) permet de supposer la formation du sulfoaluminate de magnésium dans le système $MgO-Al_2O_3-MgSO_4$. L'analyse chimique et à rayons X des produits de la cuisson à double reprise des mélanges $MgCO_3$, Al_2O_3 et $MgSO_4$ (cuisson effectuée dans les fours électriques à la température de 1000-1300°C et avec le maintien de 2 heures) témoigne de la présence de l'interaction chimique avec une formation d'une phase nouvelle qui se décompose progressivement en cas de l'augmentation de température ultérieure. La composition de la combinaison qui se forme s'approche de $3(MgO{\cdot}Al_2O_3){\cdot}MgSO_4$. Il est à noter que la formation de la combinaison nouvelle s'effectue plus complètement en cas de la cuisson des mélanges se composant du $MgCO_3$, Al_2O_3, $MgSO_4$ par rapport à la cuisson des mélanges $MgSO_4$, $MgO{\cdot}Al_2O_3$ synthétisé préalab-

lement. Selon les données préliminaires, le sulfoaluminate de magnésium qui se forme n'a pas de propriétés liantes. Lors de la formation du composé mentionné, 1 % de SO_3 fixe environ 2 % de MgO et 1,3 % de Al_2O_3.

Nous n'avons pas examiné l'interaction dans le système $MgO-Al_2O_3-MgF_2$, mais par analogie avec le même système contenant CaO, on peut supposer la probabilité de la formation du fluoraluminate de magnésium en présence des fluorures. La possibilité de formation du sulfoaluminate de magnésium lors de la cuisson des clinkers avec une haute teneur en MgO (pour le compte du SO_3 se trouvant dans la composition du clinker) est en bonne concordance avec les publications concernant l'influence du MgO sur la composition minéralogique du ciment (II) qui montrent qu'en cas de l'augmentation de la teneur en MgO, la quantité du C_3A dans le clinker diminue tandis que la quantité d'alite s'accroît. La quantité de C_3A peut diminuer grâce à la fixation du Al_2O_3 en sulfo aluminate de magnésium. A la diminution de la quantité de C_3A, une quantité supplémentaire de CaO se dégage pour former C_3S.

Selon les données des auteurs de la recherche (II), les silicates de magnésium et les spinelles ne se forment pas lors de la cuisson des charges crues contenant une quantité élevée de MgO. La quantité principale de MgO se trouve dans le clinker sous forme de la périclase. En cas de l'introduction du fluorure calcique dans la charge, on ne fixe pas également une formation des composés quelquonques. On n'observe qu'une variation du caractère de cristallisation de la périclase disponible. En même temps, G.D. Ouryvaéva montre dans ses recherches (12) la présence d'une certaine quantité des silicates de magnésium: montitshellite ($CaO \cdot MgO \cdot SiO_2$), okermanite ($2CaO \cdot MgO \cdot SiO_2$), mervinite ($3CaO \cdot MgO \cdot 2SiO_2$) dans les clinkers à une quantité élevée de MgO cuits à des températures de 1200-1300°C. Si la température de cuisson est portée jusqu'à 1400-1500°C, la quantité des silicates de magnésium diminue, et la teneur en périclase augmente. Apparemment, la cause des divergences des données disponibles consiste dans la détermination de la composition minéralogique aux différents stades de cuisson. Il est possible que les silicates de magnésium ci-dessus représentent des composés intermédiaires qui se forment lors de la cuisson du clinker de ciment Portland ayant une telle composition.

Nous avons supposé que la formation des silicates de magnésium mentionnés est la conséquence de l'existence, à des températures plus basses, des autres composés intermédiaires sur la base desquels, en cas de l'augmentation de température de cuisson et de la présence du CaO, l'apparition des montitshellites, des okermanites et des mervinites est possible. En présence des adjuvants de sulfates et de fluorures lors de la cuisson du clinker de ciment Portland ayant une quantité élevée de MgO à des températures de 800-1200°C, des sulfosilicates ou des fluosilicates de magnésium peuvent se former en qualité des combinaisons intermédiaires dont la composition chimique hypothétique, par analogie avec les sulfosilicates et les fluosilicates de calcium peut être écrite comme la suivante: $2(MgO \cdot SiO_2)MgSO_4$ et $2(MgO \cdot SiO_2)MgF_2$.

L'analyse des mélanges $MgCO_3 + SiO_2 + CaSO_4$ et des mélanges $MgCO_3 + SiO_2 + MgSO_4$ cuits à des températures de 800-1300°C confirme l'existence de l'interaction qui peut être appréciée d'après la dynamique de la fixation et du dégagement du groupe de sulfate. Les combinaisons qui se forment commencent à se décomposer même à des températures dépassant 1100°C.

En tenant compte des faits mentionnés, on peut représenter le schéma de formation d'une partie de la périclase qu'on peut détecter dans les clinkers cuits de la façon suivante:

$$2(MgO \cdot SiO_2) \cdot MgSO_4 \xrightarrow{\text{environ } 1100^\circ C} 2(MgO \cdot SiO_2) + MgSO_4$$

$$MgSO_4 \xrightarrow{1155^\circ C} MgO + SO_3$$

$2(MgO \cdot SiO_2)+2CaO \longrightarrow 2(CaO \cdot MgO \cdot SiO_2)$ ou

$2(MgO \cdot SiO_2)+2CaO \rightarrow 2CaO \cdot MgO \cdot 2SiO_2+MgO$ ou

$2(MgO \cdot SiO_2)+3CaO \rightarrow 3CaO \cdot MgO \cdot 2SiO_2+MgO$

Si la température de cuisson augmente, il se produit une substitution ultérieure du MgO par CaO dans la composition des silicates de magnésium:

$$CaO \cdot MgO \cdot SiO_2+CaO \xrightarrow{1300-1400^\circ C} 2CaO \cdot SiO_2+MgO \text{ ou}$$

$2CaO \cdot MgO \cdot 2SiO_2+2CaO \longrightarrow 2(2CaO \cdot SiO_2)+MgO$ ou

$3CaO \cdot MgO \cdot 2SiO_2+CaO \longrightarrow 2(2CaO \cdot SiO_2)+MgO$

D'une façon analogue doivent se dérouler les réactions de formation des silicates de magnésium et de leurs transformations en silicates de calcium avec le dégagement du MgO si le composé intermédiaire initial est un fluosilicate de magnésium.

Selon le schéma proposé sur le déroulement des réactions, on peut voir qu'en présence des adjuvants des fluorures ou des sulfates dans le cru, la composition minéralogique des matières cuites à une large gamme de températures (de 800 à 1400°C) se caractérise par une teneur considérable en oxyde de magnésium dans la composition des combinaisons intermédiaires. La formation de la périclase s'effectue progressivement, à mesure de la décomposition de ces combinaisons. La formation de la périclase suivant ce schéma peut expliquer sa distribution homogène et la cristallisation sous forme des grains fins en cas de la présence des adjuvants de gypse et de fluorine dans le cru. Ce fait est illustré dans la recherche (II) et est confirme par nos propres données.

Pour résoudre la question sur la possibilité de la conservation partielle des combinaisons intermédiaires mentionnées dans la composition du clinker cuit, des essais supplémentaires sont nécessaires.

REFERENCES

1. Астреева О.М., Лопатникова Л.Я. О растворимости трехкальциевого алюмината в алюмоферритах кальция. Труды НИИЦемента, 1952, вып. 5.
2. Рояк С.М. Определение фазового состава портландцементного клинкера и глиноземистого цемента химическим методом. Научные сообщения НИИЦемента, 1958, № 2(33).
3. Коган С.Л., Никифоров Ю.В., Окороков С.Д. Труды Гипроцемента, 1963, вып.XXIX.
4. Рехси С.С., Гарт С.К. Производство клинкера с использованием золы-уноса. Шестой Международный конгресс по химии цемента. Стройиздат, М., 1976.
5. Шмидт-Хенко К. Содержание оксида магния в клинкере, автоклавные испытания и прочность. Шестой Международный конгресс по химии цемента. Стройиздат, М., 1976, т. I.
6. Богданова И.В., Ситчикова В.А. Химический метод количественного определения оксида магния в различных фазах цементного клинкера и доменного шлака. Труды Гипроцемента, 1969, вып. 34.
7. Окороков С.Д., Голынко-Вольфсон С.Л., Саталкина М.А. О взаимодействии алюминатов кальция с сульфатами элементов II группы периодической системы Д.И. Менделеева при их спекании. ЖПХ, т. 36, вып. 10, 1963.
8. Рагозина Т.А. Взаимодействие сульфата кальция с алюминатами при 1200 °С. ЖПХ, т. 30, вып. II, 1957.
9. Рагозина Т.А. Влияние $CaSO_4$ на фазовый состав силикатов и алюминатов кальция при обжиге. Узбекский химический журнал, 1952, № 2.
10. Волков В.В., Вербенова Х.И., Сычев М.М., Касьянова Г.Н. Образование сульфоалюмината бария при получении бариевых цементов. Цемент, 1972, № 5.
11. Никифоров Ю.В. Влияние оксида магния на свойства и качество клинкера и цемента. Цемент, 1975, № 6.
12. Урываева Г.Д. Цементы из шламов. Издательство "Наука", Новосибирск, 1970, стр. 82.

I.G. LOUGININA,
V.M. KONOVALOV,
L.D. CHAKHOVA,
V.A. BELETSKAIA, Institut technologique des matériaux de construction, Belgorod, U.R.S.S.

DURCISSEMENT DU CIMENT PORTLAND A TENEUR ELEVEE EN OXYDE DE MAGNESIUM ET EN AUTRES COMPOSITIONS MAGNESIENNES

L'Institut technologique de Belgorod présente une étude concernant les compositions à haute teneur magnésienne qui sont proches des compositions de ciment Portland et des compositions liantes, pareilles au ciment Sorel. Le but de cette recherche est d'utiliser les calcaires dolomitiques à haute teneur magnésienne dans la technologie du ciment Portland et d'emplouer plus largement les compositions liantes à haute teneur magnésienne en conférant à ces dernières des propriétés différentes.

Tout d'abord, nous avons tâché d'obtenir le ciment de bonne qualité à partir du calcaire dolomitique en cas de la concentration de l'oxyde de magnésium dans le clinker plus de 5 % en masse et d'étudier l'influence des régimes différents et des conditions de durcissement sur la régularité du changement de volume lors du durcissement.

Nous avons étudié les mélanges crus d'une large gamme de compositions avec des coefficients de saturation de 0,85 à 0,93 à module alumine - 1,3 - 2,2 et à module silicique 2,1 - 2,2. Ces mélanges crus contenaient dans le clinker 5-10 % en masse d'oxyde de magnésium, des impuretés des composés des alcalis, du fluor, du phosphore et du soufre. Les adjuvants minéralisants accélèrent les processus de formation des silicates à des températures de 1100 à 1350°C, stabilisent les solutions solides du silicate dicalcique, type α et α' et diminuent la température de l'apparition du clinker fondu de 30-70°C. Si la température de cuisson est de 1100 - 1300°C, des solutions solides se forment s'échelonnant entre le mervinite et le silicate dicalcique et ayant la structure α' - C_2S. Aux températures mentionnées, il est possible la formation dans ces charges des Ca_2MgSiO_8, $Ca_3MgAl_4O_4$, $MgFe_2O_4$. La décomposition des phases contenant du magnésium s'effectue à des températures supérieures à 1350°C. La diminution de l'intensité de réflexion du périclase a été observéée lors de l'introduction des adjuvants complexes qui favorisaient simultanément la cristallisation de gros cristaux d'alite (jusqu'à 100 μ). On observe l'augmentation de la teneur en minéraux (par rapport à la teneur calculée), en particulier, de la teneur en aluminoferrite de calcium. Les paramètres de résistance des ciments (1:0 tableau I) obtenus à partir des clinkers avec les minéralisateurs complexes témoignent de leur haute qualité. Pour tous les délais de durcissement, le ciment magnésien avec les adjuvants complexes a montré une résistance plus haute et un accroissement relativement plus actif de cette résistance.

Tableau 1

Résistance des ciments durcissant dans l'eau, 20°C

n° du ciment	Teneur en oxyde de magnésium	Addition du minéralisateur	Résistance à la compression, MPa, à l'âge de			
			3 jours	7 jours	28 jours	1100 jours
1	0	0	34	46	74	82
2	10	0	26	53	62	77
3	10	1	38	54	63	110
4	10	2	42	66	106	136

Le vaporisage dans l'autoclave des échantillons de ciment avec une haute teneur en oxyde de magnésium est inséré dans les normes de la majorité des pays. Cependant, le traitement d'autoclave ne simule pas le durcissement des ciments dans les conditions normales correspondant au service du béton. C'est pourquoi, nous avons observé pendant quelques années le durcissement des ciments magnésiens en vue de déterminer les conséquences possibles dues à l'hydratation tardive du périclase.

Les déformations linéaires des échantillons prismatiques faits de la pâte de ciment (10x10x60 mm) qui ont durci dans l'eau pendant 6 années sont montrées sur la figure 1. L'examen de ces échantillons ne détecte pas de défauts sous forme des fissures, des incurvations des prismes, de l'écaillage de surface. Vers six ans de

I.G. LOUGININA,
V.M. KONOVALOV,
I.D. CHAKHOVA,
V.A. BELETSKAIA

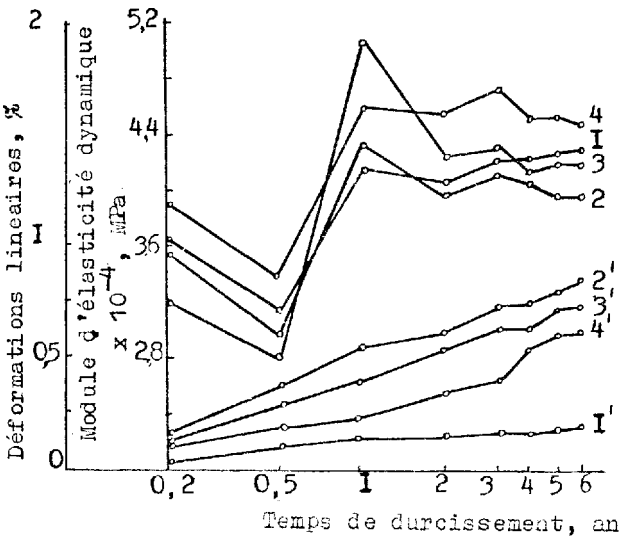

Fig. 1. Changement de module d'élasticité (1-4) et de déformations linéaires (1'-4') de la pierre de ciment durcissant dans l'eau à 20°C. Pour les désignations, voir Tableau 1

cissement, les déformations linéaires du ciment n°2 atteignent 0,98 %. L'allongement maximum est observé chez le ciment fait à partir du clinker obtenu sans minéralisateur. Le degré d'hydratation du périclase dans le ciment calculé selon les données de l'analyse thermogravimétrique atteint vers 6 ans de durcissement 12,6 - 13,4 %.

Les essais d'autoclave ont été effectués selon la norme de magnésium. Tous les ciments contenant MgO jusqu'à 10 % ont montré un changement de volume irrégulier. La valeur d'expansion des échantillons prismatiques du ciment variait de 10,65 à 31,00 %. Cependant, le degré d'hydratation du périclase après le vaporisage dans l'autoclave a été de 87 - 96 %.

Nous avons établi que la déformation des ciments magnésiens dépendait de la durée et des conditions de leur durcissement. Un durcissement suffisant de la structure de la pierre de ciment avant le traitement hydrothermal favorise la diminution de l'expansion magnésienne.

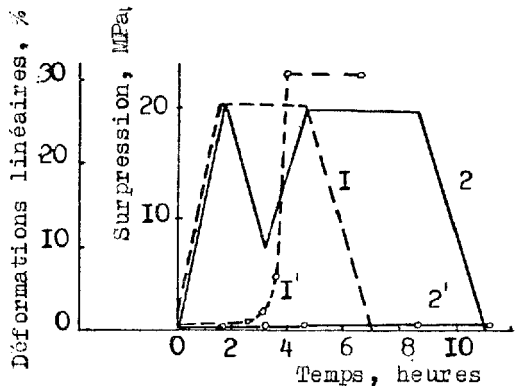

Fig. 2. Régime comun (I) et régime proposé (2) du traitement d'autoclave. Déformations linéaires des échantillons de ciment vaporisés selon les régimes 1(1') et 2(2')

Il est connu que les produits d'hydratation aux périodes initiales de durcissement ne sont pas stables. Cela est confirmé par les variations en temps des propriétés élastiques et de déformation de la pierre de ciment (figure 1). La cristallisation des hydrosilicates dans la pierre de ciment durcissante est accompagnée d'une chute de résistance. Cependant, dans deux ans de durcissement, si en juger d'après les variations peu considérables du module d'élasticité dynamique, l'équilibre s'établit, et à l'avenir, la pierre gagne des propriétés stables.

Les ciments qui ont montré un changement de volume irrégulier un jour après le gâchage (expansion 6-10 % en cas de la teneur en oxyde de magnésium de 6,5 - 7 % en masse) ont subi les essais d'autoclave à l'âge de 2 ans de durcissement dans l'eau. Dans ce cas, les ciments sur la base des clinkers avec les minéralisateurs complexes possédaient une plus haute résistance (3 à 5 fois).

On estime que l'essai des ciments magnésiens par le vaporisage (2 MPa, 3 heures) assure l'hydratation complète du périclase. En déterminant le degré d'hydratation du périclase pour les ciments fabriqués à l'usine (teneur en MgO - 4,5 - 5,0 % en masse) et pour les ciments de laboratoire (teneur en MgO - 5 - 6 % en masse) qui ont subi les essais normalisés, on a constaté que la

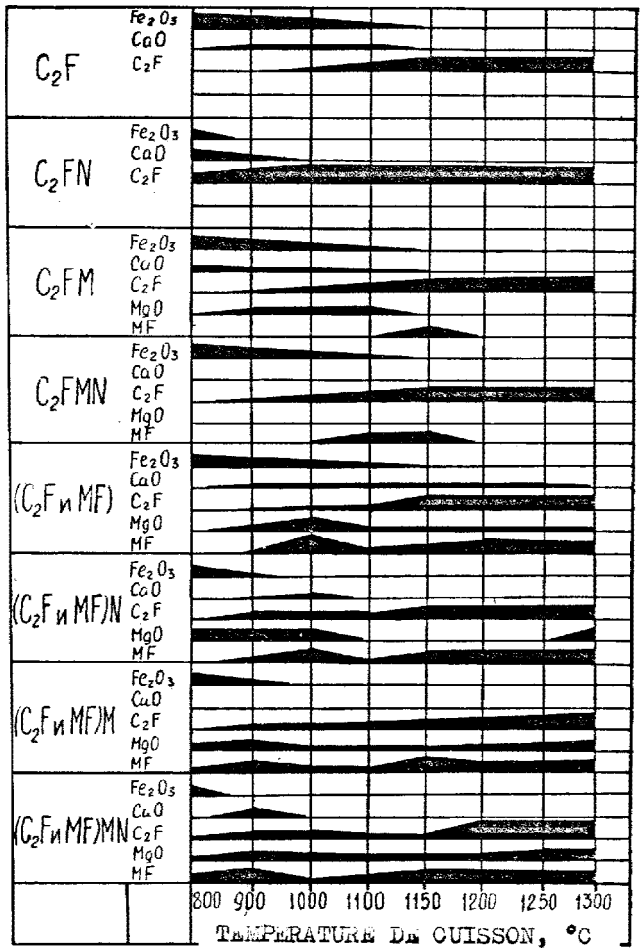

Fig. 3. Variation de l'intensité des pics de diffraction des minéraux sur les diffractogrammes des charges en fonction de la température et des additions. C_2F - charge comptée sur la formation du $2CaO \cdot Fe_2O_3$; N et M - - additions sous forme des carbonates Na_2CO_3 et $MgCO_3$; C_2F et MF - - charge comptée sur la formation du $2CaO \cdot Fe_2O_3$ et $MgFe_2O_4$ à rapport 1:1

quantité de l'oxyde de magnésium passé en brucite était limité de 30-45 %.

Une étude spéciale sur l'expansion magnésienne de la pierre de ciment dans l'autoclave montre que les déformations de volume se manifestent à la période du maintien isothermique (fig. 2). Le régime modifié du vaporisage consiste dans le fait qu'après l'obtention de la pression maximale, on la diminue pendant 1 - 1,5 heures jusqu'à 0,6 - 0,7 MPa, après quoi, elle est reportée à la valeur maximale et est maintenue constante pendant 3 - 4 heures. Dans ce cas, à la période initiale, il y a une hydratation intense des minéraux de clinker et une cristallisation des produits d'hydratation qui mènent au durcissement de la structure de la pierre de ciment avant le début d'hydratation du périclase. Le maintien ultérieur à 2 MPa n'influe pas pratiquement sur les valeurs des déformations linéaires des échantillons de ciment. Le régime proposé simule plus précisément les processus de durcissement du ciment dans les conditions normales et il est recommandé, au lieu du régime existant, pour les essais des ciments contenant du magnésium en vue de déterminer la régularité du changement de volume.

Par conséquent, si on assure un degré d'hydratation assez haut à l'aide de la structure solide de la pierre de ciment qui rend plus difficile l'accès de l'eau au périclase et qui est capable de résister à l'expansion magnésienne, on peut garantir un changement de volume régulier à des concentrations plus hautes en oxyde de magnésium par rapport à celles prévues par les normes.

Dans la deuxième partie de notre recherche, nous avons tâché d'utiliser la dolomite en qualité du constituant cru obligatoire. L'utilisation des roches carbonatées à haute teneur magnésienne en qualité du constituant de départ lors de la production des ciments spéciaux augmente les ressources de matières premières.

Actuellement, on travaille activement dans le domaine de la création du liant efficace pour l'agglomération des concentrés de minerai de fer finement dispersés. Des liants obtenus à partir des concentrés de minerais de fer et du constituant du flux contenant de l'oxyde de magnésium peuvent être les plus perspectifs. Dans la métallurgie, on utilise largement la dolomite en

I.G. LOUGININA,
V.M. KONOVALOV,
L.D. CHAKHOVA,
V.A. BELETSKAIA

qualité du flux.

Le but de cette recherche est d'obtenir le liant susceptible d'augmenter la fluidité et le pouvoir de désulfuration du laitier de haut fourneau ce qui est assuré à l'aide de l'oxyde de magnésium contenant dans les flux. Cependant, les normes de tous les pays limitent la teneur en oxyde de magnésium dans le ciment Portland.

Nous avons réussi à synthétiser le liant ferreux contenant de l'oxyde de magnésium jusqu'à 18 % en masse. Dans le système la série $CaO-SiO_2-Al_2O_3-Fe_2O_3-MgO$ on a choisi à cinq constituants la série des minéraux suivants: $C_2F-C_2S-C_4AF-MF-MgO$. La quantité d'oxydes acides de silicium et d'aluminium est limitée dans le système ce qui est une condition nécessaire de la composition optimum.

Les charges crues ont été obtenues sur la base des calcaires à différente teneur en oxyde de magnésium, de la dolomite et du concentré de minerai de fer. Le silicate dicalcique (forme β), les aluminoferrites et la solution solide du fer magnésifère dans le périclase constituaient les minéraux principaux des compositions synthétisées. Dans les agglomérés ferreux on a trouvé de nouvelles ferrites calciques-magnésiques - $Ca_mMg_n(Fe_2O_6)$. La composition des formations nouvelles dépend des conditions de cuisson et du rapport des agents. Le liant nouveau durcit à l'air. L'activité d'hydratation dépend de la composition minéralogique où une influence décisive est exercée par la ferrite calcique-magnésique et les fers magnésifères.

Les mélanges comptés sur la formation des ferrites calciques et magnésiques à rapport $C_2F:MF = I$ ont été analysés par la méthode de phase à rayons X. On a établi la suite de formation de la ferrite dicalcique en cas de l'introduction des additions catalytiques, de l'oxyde de magnésium à des températures de 800 à 1300°C. La variation de l'intensité des réfexions principales est montrée sur le diagramme (fig. 3).

L'introduction des combinaisons alcalines mène à la formation des carbonates magnésiques et calciques doubles qui conditionnent l'apparition des matières fondues eutectiques perturbant la topochimie de formation des minéraux.

L'oxyde de magnésium de la dolomite comptée sur la formation de la ferrite dicalcique favorise l'apparition du fer magnésifère qui passe ensuite en bain fondu. La ferrite calcique-magnésique $Ca_2Mg(Fe_2O_6)$ apparaît dans le bain fondu.

En cas d'une teneur considérable en oxyde de fer dans le bain fondu, la formation des ferrites calciques-magnésiques est ralentie à cause de la diminution de solubilité de l'oxyde de calcium. Les combinaisons alcalines diminuent la viscosité des matières ferreuses-magnésiques en fusion ce qui favorise la formation des minéraux et diminue l'intervalle de température de la cristallisation. En présence des minéralisateurs, l'assimilation de l'oxyde de fer s'achève presque dans toutes les charges à une températures diminuée de 100-200°C. Apparemment, cela est conditionné par la formation des ferrites alcalines.

Il résulte de la figure 3 que le minéralisateur se trouvant dans la charge comptée sur la synthèse des ferrites dicalciques et magnésiques fait varier les conditions de formation des minéraux, de solubilité de la ferrite de magnésium et celles de cristallisation de la ferrite calcique-magnésique à partir du bain fondu. En présence du minéralisateur, à la température de 1100°C, les oxydes de magnésium, de calcium et de fer passent complètement dans le bain, et le fer magnésifère y passe partiellement. La cristallisation simultanée des ferrites calciques et magnésiques est accompagnée à la température de 1300°C par un dégagement d'une grande quantité de périclase.

Dans la charge $(C_2F + MF)M$, le fer magnésifère se forme à la température de 800°C, la quantité maximale est observée à la température de 900°C, la matière fondue apparaît à une température diminuée de

I.G. LOUGININA,
V.M. KONOVALOV,
L.D. CHAKHOVA,
V.A. BELETSKAIA

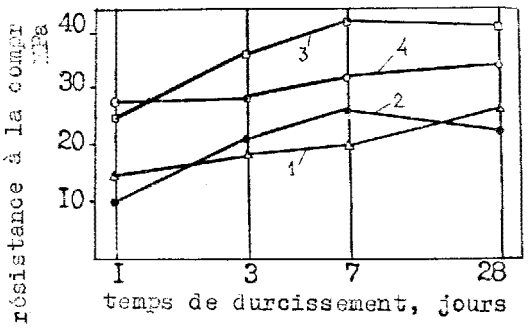

Fig. 4. Influence des compositions des ferrites calciques sur la résistance des échantillons hydratés.
1 - C_2F; 2 - C_2FN
3 - C_2FM; 4 - C_2FMN

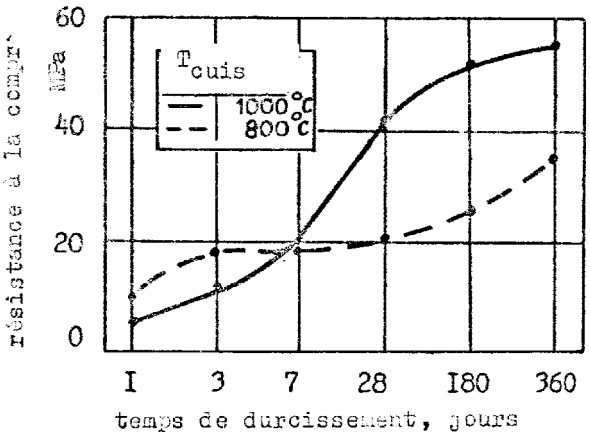

Fig. 5. Cinétique de durcissement de l'oxyde de magnésium gâché par la solution de l'aluminate de sodium

100°C et a une plus large intervalle de température en ce qui concerne la stabilité. Le fer magnésifère se cristallise le premier, ensuite c'est la ferrite calcique-magnésique qui se dégage. L'introduction du minéralisateur dans la charge mène à une assimilation précoce de l'oxyde de fer, à l'apparition du bain fondu et à une formation relativement à des basses températures de la ferrite dicalcique. La quantité de ferrite dicalcique reste à un même niveau à des températures de 1000-1150°C. A la température de 1200°C, un dégagement rapide et complet de la ferrite calcique-magnésique est observé.

L'accroissement de résistance des compositions synthétisées avec le temps est montré sur la figure 4. On a essayé les echantillons préparés de la pâte à rapport E/S = 0,26. La ferrite calcique-magnésique se distingue de la ferrite dicalcique par une plus haute activité d'hydratation. La diminution de résistance des compositions C_2FN et C_2FMN s'explique par une hydratation ralentie des minéraux en cas d'addition des minéralisateurs.

A l'aide de la spectroscopie à résonance γ-nucléaire, on a déterminé la distribution des ions selon les positions cristallographiques. Les valeurs calculées des rapports des ions de fer se trouvant dans les positions octaédriques et tétraédriques sont en bonne corrélation avec les données sur la résistance à l'âge d'un mois.

Les recherches effectuées ont permis d'élaborer les paramètres technologiques en vue d'obtenir un ciment ferreux spécial avec une teneur en oxyde de magnésium jusqu'à 18 % en masse sur la base des roches à haute teneur magnésienne.

On a étudié également les propriétés liantes de l'oxyde de magnésium gâché par la solution d'aluminate de sodium contenant de l'alcali. La matière de gâchage est constituée de résidus industriels.

Les matières de départ pour synthétiser le liant ont été représentées par l'oxyde de magnésium cuit aux températures de 800 et 1000°C et par la solution d'aluminate de sodium d'une densité élevée. La détermination de la résistance des échantillons s'effectuait à l'aide des essais des poutrelles 10x10x60 mm, I:0 lors du durcissement à l'air et après le traitement thermique à des températures de 100 - 140°C.

L'oxyde de magnésium gâché par la solution de l'aluminate de sodium forme une pâte plastique. La cinétique du durcissement de l'oxyde de magnésium gâché par l'aluminate de sodium est montrée sur la figure 5.

I.G. LOUGININA,
V.M. KONOVALOV,
L.D. CHAKHOVA,
V.A. BELETSKAIA

En faisant varier la concentration de la solution de gâchage, on peut régler le processus de durcissement du liant obtenu. Si on augmente la densité de la solution d'aluminate de sodium, l'hydratation et la cristallisation de l'hydroxyde de magnésium sont accélérées.

La vitesse de cristallisation et de durcissement de l'hydroxyde de magnésium gélatinisé peut être augmentée par le traitement thermique à des température de 110-120°C. A l'âge de deux heures, la résistance augmente jusqu'à 39,5 MPa et devient commensurable avec la résistance à l'âge de 28 jours de durcissement à l'air. Le traitement thermique permet d'atteindre la résistance du liant magnésien jusqu'à 80 - 100 MPa. Sur les radiogrammes du liant durcissant lors du chauffage, outre les lignes analytiques de l'hydroxyde de magnésium, on voit apparaître les pics de diffraction supplémentaires appartenant à $NaAlCO_3(OH)_2$.

La microscopie électronique du liant durci a montré que les cristaux de l'hydrocarbonate aluminosodique avaient une forme aciculaire et sé trouvaient à la surface des gros grains de l'hydroxyde de magnésium.

Par conséquent, lors du gâchage de la magnésite caustique par la solution de l'aluminate de sodium on a reçu un nouveau liant magnésien durcissant à l'air même à la température de 110 - 120°C. La formation de structure du durcissement est accompagnée par le dégagement et la cristallisation de l'hydroxyde de magnésium et de l'hydroxycarbonate aluminosodique. Le degré de radoucissement du liant obtenu à la température de 500 - 900°C est beaucoup plus petit par rapport au ciment d'oxychlorure magnésien qu'on utilise jusqu'à présent. Lors de la cuisson à des températures supérieures à 1200°C, le liant atteint une résistance considérable (100 - 150 MPa). Le liant magnésien proposé peut être utilisé en qualité d'un réfractaire.

M. VON EUW Societé des Ciments Français - Paris, France

CIMENTS CONTENANT DES ADDITIONS MINERALES

1. INTRODUCTION

Le ciment portland artificiel est unanimement classé en tête de liste des liants hydrauliques. Cela ne veut cependant pas dire qu'il est apte à résoudre tous les problèmes de formulation des bétons, que ce soit dans le domaine du batiment ou dans celui des travaux publics.

Les caractéristiques des bétons prises en compte selon les emplois concernés se regroupent essentiellement dans les thèmes suivants :

- rhéologie des bétons frais
- évolution des résistances en fonction du temps
- évolution du dégagement de chaleur pendant le durcissement
- résistances aux divers types de corrosion des bétons durcis.

Pour parvenir à satisfaire les exigences à l'emploi, on demande souvent aux ciments d'avoir des propriétés contradictoires, ce qui conduit le fabricant à proposer une palette plus ou moins large de produits.

Dans le cas le plus simple il fabrique un seul clinker et le broie à diverses finesses; mais s'il se rend maître des résistances mécaniques, il risque de faire apparaître des différences rhéologiques et il ne résoud pas simultanément les problèmes liés à la corrosion chimique.

Cela veut dire que les cimenteries ne produisant que du ciment portland sont très souvent obligées de fabriquer deux clinkers :

- un clinker à saturation élevée pour ciment à hautes résistances mécaniques et fort dégagement de chaleur, mais à faible résistance chimique,

- un clinker peu saturé pour ciment à forte résistance à la corrosion chimique et faible dégagement de chaleur, mais à résistances mécaniques limitées.

La cimenterie moderne est conçue de préférence en une seule ligne de fabrication de clinker pour optimiser les investissements et les frais d'exploitation.
Par ailleurs, dans l'intérêt général aussi bien que dans la recherche du meilleur prix de revient, les cimentiers sont incités à économiser l'énergie et à consommer des sous-produits.

Pour ces deux raisons, on observe une tendance à ne fabriquer qu'un seul clinker, potentiellement très performant, et à le broyer avec des additions minérales de provenances diverses. En choisissant convenablement ces constituants secondaires, on peut résoudre les deux problèmes essentiels que sont la classe de résistance mecanique et l aptitude à résister aux attaques chimiques des bétons.

Les matériaux utilisés varient en premier lieu selon les ressources naturelles et le développement industriel régional, c'est-à-dire la mise à disposition de sous-produits.

L'industrie cimentière est ainsi amenée à consommer couramment des laitiers de haut-fourneau, des cendres de charbon, des pouzzolanes naturelles ou des matières douées d'activité pouzzolanique. Dans certains pays on utilise également des roches calcaires comme addition minérale.

En consultant les recueils de norme, on dénombre :

35 pays prévoyant des ciments au laitier
14 pays prévoyant des ciments aux cendres
31 pays prévoyant des ciments à la pouzzolane
15 pays prévoyant des ciments au filler calcaire.

En Europe 19 pays utilisent ces additions dans des ciments binaires ou composés avec plusieurs constituants. La France a innové dans ce domaine en développement fortement la consommation de filler calcaire en co-broyage à la cimenterie avec le clinker, seul ou avec le laitier ou les cendres de charbon.
En 1984, les quantités absorbées par les cimenteries françaises s'élevaient à :

2 086 000 tonnes de laitier granulé
719 000 tonnes de cendres volantes
93 000 tonnes de pouzzolanes
855 000 tonnes de fillers.

C'est en raison de la longue expérience française dans ce domaine que le Comité d'Organisation du 8 ème Congrès International de la Chimie du Ciment m'a confié la présidence de ce Séminaire. Je le remercie de sa confiance, et j'ai maintenant l'honneur de vous présenter les personnalités qui vont animer notre réunion par l'apport de leurs connaissances et la participation aux discussions qui suivront la présentation de leurs rapports :

Dr. Baron, de Lafarge Coppée - France
Dr. Christensen, de Aalborg Cement - Danemark
Dr. Ghosh, de Cement Research Institut - Inde
Pr. Ollivier, de l'Institut National des Sciences Appliquées - France
Dr. Ramachandran, du Conseil National de la Recherche - Canada.
Dr. Takemoto, de Onoda Cement - Japon
Pr. Wishers, du V.D.Z. - République Féd. Allemande.

Le précédent Congrès tenu à Paris en 1980 avait consacré un thème entier aux ciments avec laitiers et un autre aux ciments avec pouzzolanes. Les fillers calcaires n'avaient pas été pris en considération. Le programme de l'actuel Congrès comprend dans son thème 2 l'influence des matières d'addition sur le processus d'hydratation, et dans son thème 3 les effets de leurs composants sur l'hydratation et la structure.

Pour éviter trop de répétitions, il m'a donc semblé opportun d'orienter nos travaux vers les aspects techniques dérivant des connaissances scientifiques. Dans ce but, nous essaierons de faire une synthèse basée sur les propriétés d'usage des ciments. Une telle synthèse doit faire apparaître les comportements et les phénomènes particuliers liés à la présence des laitiers, des matériaux pouzzolaniques et des fillers calcaires. Les deux premiers ont donné lieu depuis longtemps à de nombreuses recherches, en revanche les fillers calcaires, en raison de leur utilisation plus récente, occupent une place nouvelle et encore peu développée dans les programmes de recherches.

Comme c'est souvent le cas, les résultats de certains essais paraitront contradictoires. Il en est ainsi par exemple de la comparaison des résistances mécaniques en essais normalisés des ciments portland additionnés de diverses poudres minérales, et de celles obtenues par broyage du mélange de l'ensemble des constituants.

Je souhaiterais être clair à ce sujet:

Quelle que soit la propriété d'usage que l'on veuille examiner, la comparaison ne peut valablement être faite qu'entre des ciments de même classe de résistance. Cette notion est d'ailleurs d'autant plus facile à appliquer que les normes nationales définissent les classes de résistance entre des limites inférieures et supérieures : c'est le cas par exemple pour l'Allemagne Fédérale et pour la France depuis plusieurs années et ce le sera à l'avenir pour l'ensemble des pays européens qui établissent actuellement un projet de normes communes.

Un autre point essentiel sur lequel je dois attirer l'attention est celui du choix de l'addition minérale. Là encore il peut y avoir contradiction entre les résultats de certains chercheurs et ceux de l'industrie cimentière; il y a en effet une grande différence de conception entre la revue systématique d'un ensemble de minéraux et la sélection faite par les industriels à l'aide de critères engageant leur responsabilité. On peut par exemple trouver dans une étude de laboratoire des fillers qui diminuent la maniabilité ou la résistance au gel mais ce sont précisément de tels minéraux qui sont rejetés pour un emploi industriel.

Ces deux réserves étant faites, les caractéristiques essentielles retenues pour la commercialisation des ciments doivent à la fois être conformes aux normes et satisfaire les exigences des emplois.

2. NORMES

D'une manière générale, les normes nationales donnent une définition plus ou moins précise des constituants, suivie d'un classement des liants en fonction des proportions admises pour chaque constituant. Un autre classement est ensuite ouvert à ces divers types de ciments en fonction de leur classe de résistance, puis des spécifications particulières, principalement d'ordre chimique, sont imposées à certaines catégories.

Cette conception des normes peut faire l'objet de certains commentaires :

2.1. DEFINITION DES CONSTITUANTS

Doit-on normaliser les constituants, c'est-à-dire leur donner une définition précise assortie de tests de qualité et de spécifications chiffrées ? Cette question est très controversée. Pour certains, des normes de sous-produits tels que les laitiers et les cendres, ou de produits pouzzolaniques ou calcaires, n'auraient pas de sens puisque ce ne sont pas des produits élaborés. Pour d'autres, la normalisation serait sécurisante; c'est ainsi que plusieurs pays étudient un projet de normes pour les cendres volantes. A mon avis, ce projet ne peut intéresser que les bétonniers, qui ne disposent pas des moyens d'optimisation qu'ont les cimentiers.

2.2. COMPOSITION DES CIMENTS

Je voudrais citer l'exemple des normes françaises devant le projet de normalisation européenne (CEN). L'Institut Français de Normalisation a mis en application en 1979 ses normes P 15 300 et P 15 301 en créant une catégorie de ciments composés appelés CPj pouvant contenir jusqu'à 35 % d'additions minérales, prises individuellement ou par mélange de plusieurs constituants, sans imposer à ces produits de spécifications chiffrées. Evidemment les additions choisies par le cimentier sous sa responsabilité ne doivent pas perturber les caractéristiques des bétons.

En 1980, ces normes ont été complétées par l'introduction d'un ciment CLC pouvant contenir entre 40 et 75 % d'un mélange de laitier et de cendres et constituant un produit intermédiaire entre les CHF ayant des proportions semblables de laitier seul et les CLK renfermant au minimum 80 % de laitier.

Alors que les CPJ sont destinés à réaliser sans difficultés et en économisant l'énergie, des ciments qui répondent aux besoins les plus courants, les CLC, les CHF et les CLK sont fabriqués pour résister aux corrosions d'origine chimique, telle que l'eau de mer et les terrains gypseux.

Dans ces conditions, les éléments composés occupent dans le marché français des liants hydrauliques une place prépondérante ainsi que le montre la répartition suivante pour l'année 1984:

CPA = 23,8 %
CPJ = 63,2 %
CHF, CLK, CLC = 5,9 %
Autres liants = 7,1

La proposition faite par la France d'introduire dans le projet de normes européennes les ciments du type CPj, s'est d'abord heurtée à une opposition basée sur le manque d'informations concernant la durabilité des bétons de CPj, mais il faut savoir qu'en réalité les difficultés rencontrées sont de divers ordres :

- Les approvisionnements en additions minérales sont à caractère régional,
- les règlements de sécurité concernant les constructions sont nationaux,
- les procédures de certification de conformité sont nationales,
- la reconnaissance mutuelle des contrôles n'est pas acquise.

Malgré ces difficultés et devant l'intérêt, si ce n'est l'obligation, de supprimer les entraves techniques à la libre circulation des marchandises entre les pays du Marché Commun Européen, des études ont été effectuées pour aboutir à une caractérisation satisfaisante des constituants, notamment des fillers calcaires. La durabilité des bétons de ciments fillérisés a ainsi été vérifiée par des essais en commun. Le Pr. WISCHERS, responsable de ces questions au sein du Comité Européen de Normalisation fera le point de l'optimisation des additions minérales dans les ciments (1).

Je voudrais simplement préciser que les cimentiers disposent de moyens importants et efficaces pour sélectionner leurs approvisionnements, les homogénéiser, les contrôler :

- les pouzzolanes sont choisies en tenant compte des possibilités d'obtenir une efficacité régulière avec le clinker auquel elles sont ajoutées.
- les cendres volantes subissent en particulier un contrôle de régularité de leur teneur en carbone imbrulé(2).
- les laitiers sont souvent homogénéisés, par exemple, sur parc après avoir subi un contrôle d'hydraulicité avec le clinker.

- les fillers calcaires sont choisis à partir de tests de composition basés notamment sur une faible teneur en argile et en matières organiques. Leur sélection est complètée par une étude du comportement rhéologique et de la durabilité des ciments auxquels ils sont incorporés.

De toute façon, après avoir optimisé la composition de ses ciments, le cimentier s'assure de la régularité des performances et il a les meilleurs moyens d'y parvenir par un pilotage bien contrôlé des doseurs et des broyeurs.

3. SATISFACTION A L'EMPLOI

Les ciments sont livrés à la clintèle par classes de résistance en fonction de l'échéance de durcissement en milieu humide; mais un premier écueil auquel on se heurte selon que l'on se réfère au respect des normes ou à la satisfaction de l'utilisateur est lié au rapport eau/ciment : en effet, les essais normalisés sont faits en mortier ISO à E/C = 0,5 alors que les bétons de chantiers sont généralement confectionnés à maniabilité définie, ce qui revient à ajuster le rapport E/C pour tenir compte des caractéristiques rhéologiques.

Un second écueil est celui de l'évolution des résistances en fonction du temps, laquelle dépend à la fois de la nature des constituants et de leur finesse.

L'optimisation d'un ciment renfermant une ou plusieurs additions minérales conduit donc le fabricant à une étude complexe portant sur le choix des constituants, leur mode de broyage, la granularité du ciment et son taux de gypsage.

3.1. RHEOLOGIE

La maniabilité des bétons frais conditionne la mise en place, c'est-à-dire les moyens, l'économie des procédés et en définitive la qualité des bétons; c'est pourquoi elle constitue en particulier pour le choix des fillers un critère des plus sévères. Les laboratoires attachent donc un grand intérêt aux contrôles rhéologiques en vue d'obtenir l'ouvrabilité optimale avec la régularité maximale. J.P. BOMBLED rappelle quels sont les facteurs intervenant sur la maniabilité et rend compte de l'influence des fillers notamment dans la pâte interstitielle (3).

Il faut tout de suite préciser que les appareils de mesure sont fort différents selon que l'on fait des études sur pâtes de ciment, sur mortiers ou sur bétons. Dans les deux premiers cas, on utilise des viscosimètres à cylindres coaxiaux ou des pénétromètres à aiguille ou à sonde, alors que les contrôles sur bétons sont effectués avec des méthodes adaptées au type de béton. Il faut savoir que la maniabilité du béton est dépendante de toute l'étendue granulaire; c'est pourquoi on n'observe pas systématiquement de concordance entre les essais sur pâte de ciment et ceux sur béton. Par ailleurs, les appareils de contrôle rhéologique des bétons diffèrent selon la consistance:

- flow test pour les bétons fluidifiés,
- slump test (ASTM) et maniabilimètre LESAGE-LCPC pour les bétons à consistance molle,
- coefficient de serrage de WALZ (DIN) pour les bétons de consistance sèche.

Ces déterminations sont indispensables pour mettre au point la fabrication d'un nouveau ciment car l'utilisateur n'admet pas les changements d'ouvrabilité dûs à des variations de qualité du ciment. De plus, il ne faut pas se contenter de rechercher une demande en eau acceptable au malaxage mais il faut s'assurer que la variation de la rhéologie dans le temps ne conduit pas à remalaxer le béton de centrale avec une addition d'eau à l'arrivée sur chantier, ce qui se ferait au détriment de la résistance.

L'expérience a montré des comportements sensiblement différents selon l'origine des cendres de centrales thermiques ou celle des fillers calcaires.

La nature du régulateur de prise(gypse, plâtre, anhydrite, gypse chimique) influence la maniabilité et il faut savoir que des comportements anormaux peuvent être observés en présence de fluidifiants : des difficultés sérieuses ont été rencontrées sur des chantiers importants, par exemple avec des ciments au laitier.

L'introduction des fillers calcaires dans les ciments CPj fabriqués en France a succédé à de nombreuses études dans lesquelles la demande en eau et la maniabilité des bétons ont eu une place importante. La synthèse des résultats obtenus par les laboratoires cimentiers permet de conclure que le comportement rhéologique des bétons, à classe de résistance égale, n'est pas affecté par l'emploi de ciments renfermant moins de 30 % de filler calcaire, si la pureté du filler répond au test d'absorption du bleu de méthylène qui caractérise la teneur limite acceptable en argile.

Contrairement à certaines idées reçues, ces mêmes études ont montré que les variations de finesse des constituants de ces CPj au calcaire n'ont pratiquement pas d'influence sur la demande en eau.

L'ouvrabilité et son évolution ne sont pas les seules caractéristiques à prendre en compte; le ressuage et le retrait, responsables de la microfissuration, ont des conséquences que nous examinerons dans le cadre de la durabilité.

3.2. CINETIQUE DE L'HYDRATATION ET DEVELOPPEMENT DES RESISTANCES

Toutes les études à caractère scientifique, aussi bien que les essais visant à comparer les résistances en fonction de l'addition minérale, montrent une participation aux réactions physico-chimiques d'hydratation, plus ou moins rapide pour les laitiers et les pouzzolanes, mais non négligeable pour les fillers calcaires.

La finesse des constituants en présence joue un rôle essentiel dans la vitesse des réactions. Selon les aptitudes comparées au broyage on obtient des ciments dans lesquels les surfaces spécifiques des constituants peuvent être extrêmement différentes. L'étendue des plages granulaires a des conséquences multiples sur le déroulement des phénomènes physico-chimiques du durcissement.

3.2.1. Laitiers

Les phénomènes de durcissement des ciments au laitier sont maintenant assez bien connus. Nous avions à ce sujet retenu du Congrès de Paris, d'abord le rôle de la structure du verre de laitier, structure non pas désordonnée, mais organisée à très courte distance. Nous savons

aussi que pour obtenir cette structure où le silicium forme des tétraèdres SiO_4^{4-} plus ou moins polymérisés, les cavités laissées libres dans le réseau sont occupées par les cations Ca, K, Na. Plus la part de ces cations est importante, plus les tétraèdres SiO_4^{4-} sont isolés et plus le verre est instable donc chimiquement actif. C'est là l'explication de l'utilisation en cimenterie des seuls laitiers vitreux de composition chimique basique.

Les études récentes du mécanisme de l'hydratation, en particulier celles de VERNET , en on mis en évidence les différentes phases par le suivi de l'évolution des concentrations ioniques de la solution interstitielle et la simultanéité des pics de flux thermique (4).

Il a été démontré que dans le système clinker-laitier-gypse-eau les réactions s'influencent par différents couplages. Ces réactions débutent par la chimisorption de l'eau, suivie de la rupture des liaisons à la surface des grains, puis de la solvatation; elles aboutissent à la précipitation de l'éttringite, du CHS et de la portlandite. Après épuisement du gypse l'éttringite se transforme en monosulfoaluminate puis l'excès d'aluminates précipite sous forme de C_4AH_{13}.

Le laitier joue un rôle actif dès les premiers instants du contact avec l'eau, ce qui a été facilement démontré par Mme REGOURD, mais ce n'est qu'après la période dormante et l'épuisement du gypse que s'accélère l'hydratation du laitier(5).

Les travaux de VERNET expliquent que les courbes de croissance des résistances des ciments au laitier varient non seulement avec le laitier mais avec le clinker utilisé. Cette particularité avait été mise en évidence par HAWTHORN. Elle fait l'objet du rapport du Dr. TAKEMOTO et plaide en faveur de l'emploi du laitier. à la cimenterie (6) (7).

3.2.2. Pouzzolanes et cendres

Alors que les laitiers doivent leur hydraulicité précoce à leur teneur relativement élevée en ions Ca dans leur propre structure, les pouzzolanes ne peuvent participer au durcissement des ciments que très lentement en réagissant avec la chaux du milieu aqueux auquel elles sont incorporées.

La pouzzolanicité est une qualité difficile à quantifier; initialement attachée à des roches éruptives de structure vitreuse finement divisées, elle a été étendue à des matériaux siliceux sédimentaires ou encore d'origine organogène, ainsi qu'à des produits artificiels tels que les argiles cuites et à des sous-produits comme les cendres de houille et les fumées de silice.

Le taux et la vitesse de fixation de la chaux par le matériau pouzzolanique sont fonction de sa composition chimique acide (SiO_2 + Al_2O_3 + Fe_2O_3 > 75 %), de sa structure vitreuse ou amorphe, de sa surface spécifique et de sa porosité, ainsi que de la quantité de chaux et de sulfate disponibles dans le milieu; l'élévation de température permet d'accélérer les réactions, très lentes à la température ordinaire.

On a essayé de définir l'activité pouzzolanique par diverses méthodes, principalement chimiques, basées sur le taux de fixation de chaux ou la solubilité de la silice et de l'alumine dans la soude ou la potasse.

La fixation de la chaux, si elle est indispensable, n'est malheureusement pas suffisante pour développer des résistances mécaniques; les zéolithes, par exemple, ne doivent pas être confondues avec les pouzzolanes.

Le cimentier n'a donc pas d'autres moyens pratiques que de procéder à deux types d'essais complémentaires pour choisir un matériau à usage pouzzolanique. Le premier, très rapide consiste à chiffrer l'aptitude à fixer la chaux pour éliminer les matériaux non réactifs, le second est destiné à suivre les résistances mécaniques de mortiers expérimentaux en fonction du temps par comparaison à des mortiers de référence.

La structure vitreuse ou tout au moins amorphe de la pouzzolane donne lieu à des phénomènes physico-chimiques en présence d'eau, de chaux et de sulfates, comparables à ceux observés avec les laitiers, à savoir : chimisorption, hydrolyse, lixiviation lente de la masse, solvatation des ions libérés, puis précipitation et cristallisation des espèces hydratées en sursaturation dans la solution interstitielle.

Comme dans le cas, des laitiers, la présence de germes cristallins dans la structure favorise la précipitation des hydrates sous forme de fibrilles, aiguilles et plaquettes enchevêtrées, indispensables à une bonne cohésion et à de grandes résistances.

Ces hydrates sont pratiquement les mêmes que ceux observés avec les ciments de laitier, mais ils se forment très lentement à partir de la pouzzolane car les tétraèdres SiO_4^{4-} de la masse anhydre y sont moins indépendants.

Les résistances à court et moyen termes, contrairement aux ciments de laitier, ne sont dues qu'à l'hydratation du clinker dans les ciments et la pouzzolane; la pouzzolanicité n'intervient qu'au-delà de 90 jours et se poursuit très longtemps à la condition de rester en milieu humide.

Le type d'ouvrage et le milieu de conservation sont donc déterminants dans l'utilisation des ciments à la pouzzolane.

Le Docteur GHOSH fera un exposé sur les recherches expliquant la faveur croissante des utilisateurs pour les ciments avec additions de laitiers et de pouzzolanes (8). Puis MM. CHRISTENSEM et ALMEBORG feront part des résultats de leurs recherches pour valoriser les ciments aux cendres volantes au Danemark (9).

3.2.3. Fillers calcaires

La pratique courante depuis une dizaine d'années, de l'addition de fillers calcaires à la fabrication de ciments normalisés, est considérée en Europe comme une initiative française, bien que quelques autres pays dans le monde l'aient adoptée par exemples le Canada, le Chili; la Chine, l'Espagne la Finlande.

La fabrication de ces ciments est généralement faite par co-broyage des constituants, mais ils peuvent également être produits par broyage séparé et homogénéisation.

Le cobroyage d'éléments de dureté très différente comme les clinkers et certains calcaires conduit à des ciments dont l'étendue et

la répartition granulaires diffèrent évidemment de celles de chaque constituant.

BOMBLED et al consacrent une communication à ces mesures sélectives de finesse et montrent que l'on atteint des différences très significatives qui conditionnent les performances (10).

Je voudrais faire remarquer que cela constitue un degré de liberté dont use le cimentier pour ajuster la qualité de son produit.

R. GUYOT et al présen ent d'ailleurs à ce sujet une communication qui met bien en valeur la possibilité d'utiliser la potentialité hydraulique du clinker dans les ciments fillérisés au calcaire. Ils montrent que pour une même classe de résistance définie à 28 jours, le clinker du ciment fillérisé est broyé plus fin que dans un ciment pur et, de ce fait, développe aux courtes échéances une quantité d'hydrates plus importante. Ils expliquent ainsi que l'on trouve toujours des résistances plus élevées pendant les premiers jours pour des résistances identiques à 28 jours. Nous verrons cependant que le calcaire participe lui aussi à ces résistances précoces (11).

Pour comprendre les réactions d'hydratation des ciments fillérisés au calcaire nous disposons de quelques études récentes à caractère scientifique :

- le Pr OLLIVIER montre le rôle des fines particules d'additions minérales dans la formation de l'auréole de transition entre les grains fins de la pâte et les granulats du béton. Il rappelle que cette auréole qui constitue la zone de liaison pâte-granulats est le point faible des bétons en raison de l'orientation préférentielle des cristaux et de la forte porosité qui favorise le passage des agents de corrosion (12).

Les additions minérales, et particulièrement les calcaires, peuvent modifier favorablement les paramètres de l'auréole de transition et améliorer ainsi les caractéristiques du béton.

Les fillers calcaires se distinguent des autres additions minérales par leur réaction avec les aluminates de calcium pour former du carboaluminate, concurremment à la réaction de formation du sulfo-aluminate à partir du gypse.

- Cette activité chimique des fillers calcaires a été montrée par M. REGOURD et al (13). Elle fait l'objet du rapport du Dr. RAMACHANDRAN (14) qui a étudié séparément les trois systèmes :

- silicate tricalcique-carbonate de calcium-eau
- aluminate tricalcique-gypse-carbonate de calcium -eau
- ciment portland-carbonate de calcium-eau.

Le Dr. RAMACHANDRAN exposera son important travail dans un instant, mais je retiendrai dès maintenant que ses résultats permettent de réfuter le classement des fillers calcaires dans la catégorie des additions inertes. En mettant en évidence leur participation aux réactions chimiques d'hydratation des aluminate et silicate tricalciques, le Dr. RAMACHANDRAN fait des fillers calcaires des constituants actifs des ciments, qui en accélèrent le durcissement.

- Le travail du Dr. RAMACHANDRAN trouve un complément particulièrement constructif dans la communication de C. VERNET consacrée à la cinétique de l'hydratation de l'aluminate tricalcique en présence de gypse, chaux et filler calcaire. C. VERNET applique sa méthode de suivi des concentrations ioniques et de mesure des flux thermiques pour comparer les séquences de l'hydratation sans $CaCO_3$ et avec diverses proportions $CaCO_3$/gypse. Il montre ainsi comment se succèdent les phases ettringite carbo-aluminate. Ses observations au MEB et ses mesures par DRX lui permettent de situer la formation du carboaluminate au voisinage des grains de C_3A et de différencier la réactivité des fillers en fonction de la consommation des ions carbonates pour donner du carboaluminate (15).

La conséquence pratique que l'on peut déduire de telles études est essentiellement le rôle de régulateur de prise joué par la calcite. En optimisant le gypsage en présence de filler calcaire, le cimentier dispose d'un moyen subtil pour moduler la vitesse de dégagement de chaleur et la progression des résistances.

3.3. DURABILITE

La durabilité d'un matériau est son aptitude à résister pendant longtemps à des agressions d'ordre mécanique et chimique. C'est certainement la qualité faisant l'objet à la fois des plus grandes exigences et des spécifications les moins significatives. La raison en est simple: elle fait avant tout intervenir le temps et cette donnée n'est pas rigoureusement remplaçable par des essais accélérés.

Quels sont les paramètres qui interviennent dans la capacité d'un béton de ciment à résister à la corrosion ? J'aurais tendance à répondre qu'il n'y en a qu'un seul : la compacité; malheureusement il n'y a pas de béton réellement compact et si l'on veut le protéger efficacement il faut lui donner, avant l'application des forces de destruction, une résistance mécanique élevée et une composition chimique adaptée.

Si l'on voulait approfondir la connaissance des phénomènes de dégradation il faudrait examiner en détails deux groupes de paramètres, ceux qui caractérisent le béton et ceux qui définissent l'agent agressif:

béton		agent agressif	
	composition		nature ou composition
	âge		intensité ou concentration
	taux d'hydratation		instant d'application
	compacité		

Je ne pourrai bien entendu m'arrêter au cours de mon exposé qu'aux observations essentielles permettant de situer le comportement des additions minérales dans ce vaste contexte.

Au double point de vue de la composition du béton et de la nature de l'agent agressif il suffit de rappeler que les clinkers à la fois les moins saturés en chaux et les plus pauvres en aluminate sont les plus résistants chimiquement et les moins résistants mécaniquement. Dans chaque pays il existe des normes et des règlements pour cette catégorie de ciments à base de clinker spéciaux.

Ce qui nous intéresse plus ici c'est l'usage en cimenterie des laitiers, pouzzolanes et fillers en regard de la durabilité. Deux groupes de ciments devraient être examinés séparément :

- les ciments spéciaux à fortes proportions d'additions, tels que les ciments pouzzolaniques,

pouzzolano-métallurtiques, de haut-fourneau et à très fortes teneurs en laitier.

- les ciments portland composés, à teneurs limitées en additions, dont les CPJ fabriqués en France constituent un des groupes les plus importants.

Les additions à activité pouzzolanique et les laitiers offrent l'intérêt de réaliser des bétons moins basiques que les portlands, donc de s'opposer à la corrosion d'origine chimique. Nous ne pouvons nous étendre sur cet aspect du problème qui est traité dans d'autres thèmes du Congrès.

La compacité étant l'impératif essentiel, je trouve opportun de réfléchir sur les défauts de compacité, à savoir la porosité et la microfisssuration.

3.3.1. Porosité initiale et évolution

La porosité initiale dépend de la granularité des constituants, du dosage en eau du béton et de l'air entraîné. Le ciment complète la courbe granulaire en tant que filler, ce qui nécessite un dosage optimal. Les micropores aqueux sont d'autant plus nombreux que la courbe est discontinue dans le domaine des fins et ultrafins et que la demande en eau est élevée. Les fines particules d'additions minérales permettent d'étendre et de compléter cette courbe, d'où une diminution du volume des pores à colmater par les hydrates, ce qui donne un avantage aux ciments composés.

L'évolution de la porosité en l'absence d'agression dépend de la rapidité de formation des hydrates et de la quantité de ces hydrates. Dans ce cas GUYOT et al ont fait des mesures comparatives de porosité avec des ciments portland et des ciments fillérisés au calcaire, de même classe de résistance à 28 jours. Ils ont accompagné ces mesures d'un suivi de l'eau liée au cours de l'hydratation et de la dimension des pores de la pâte.

La conclusion de l'étude remarquable de GUYOT est que les deux types de ciment, malgré leur différence de teneur en clinker, mais grâce à leur différence de finesse produisent les mêmes quantités d'hydrates pour aboutir à la même résistance et à la même compacité (11).

En ce qui concerne les autres additions minérales, on retiendra que les laitiers ont les taux de réaction les plus élevés ; l'hydratation précoce des laitiers contribue donc à donner un matériau compact au jeune âge. En revanche, dans le cas des cendres volantes et des pouzzolanes naturelles, la porosité diminue moins vite, mais de façon continue pour arriver tardivement à la même valeur à résistance égale.

Ce processus se déroule régulièrement tant que le béton est maintenu en milieu humide et en l'absence d'agressions.

Comme les micropores et les microfissures, l'auréole de transition faisant l'objet du rapport du Pr. OLLIVIER constitue une zone de fragilité où s'accumulent des contraintes mécaniques qui s'ajoutent aux sollicitations d'ordre chimique. Les additions consommatrices de chaux -laitiers et pouzzolanes- contribuent à diminuer cette fragilité en agissant favorablement sur l'orientation de la portlandite et en emplissant progressivement les pores.

3.3.2. Microfissuration

La microfissuration résulte des tensions créées au cours du premier et du second retraits, c'est-à-dire avant et pendant la prise.

Les microfissures qui apparaissent les premières sont liées au ressuage ; les suivantes sont dépendantes de la contraction chimique ou LE CHATELIER, et au phénomène d'échauffement suivi de refroidissement.

Comment interviennent les additions minérales dans ce processus ?

Il est connu que le laitier à cause de sa structure a une tendance à augmenter le ressuage donc les risques de microfissuration avant prise, alors que les pouzzolanes et les fillers calcaires ont un effet plutôt bénéfique.

Les additions minérales les moins réactives pendant la prériode de prise sont les matières pouzzolaniques ; ce sont celles qui sont conseillées pour les ouvrages où les phénomènes d'origine thermique sont les plus gênants.

Les ciments composés au filler calcaire ont un comportement intermédaire entre ceux aux pouzzolanes et ceux au laitiers.

Dans tous les cas, les risques de microfissuration sont plus faibles qu'avec les portlands ordinaires, étant données les différences de flux thermique pour des ciments de même classe de résistance.

3.3.3. Résistances à la corrosion

Quelle que soit l'origine des forces de destruction - lixiviation - développement de cristaux expansifs d'origine chimique - gel, dégel de la solution interstitielle - on assiste toujours à une compétition entre l'action de destruction et une action réparatrice se manifestant par la cicatrisation des microfissures tant que le milieu humide permet la croissance des hydrates.

Les ciments fillérisés au calcaire ne font pas exception et se comportent aussi bien que leurs homologues au laitier ou aux pouzzolanes.

J. BARON rend compte à ce sujet d'essais comparatifs de durabilité à l'eau de mer entre des CPJ à 10 et 20 % de calcaire et des CPA, tous les ciments étant faits avec du clinker de composition chimique résistant à la mer. Pour la même classe de résistance, il n'observe pas de différence de comportement (16).

Les cimentiers européens se sont particulièrement penchés sur les épreuves de résistance au gel-dégel des ciments au filler calcaire. Après avoir confronté avec beaucoup de difficultés les résultats d'essais effectués dans des conditions pas toujours comparables, ils sont arrivés à la conclusion que les ciments commercialisés avec addition de calcaire avaient une tenue au gel-dégel satisfaisante. De très nombreux clichés au M.E.B. ont d'ailleurs bien

illustré le comportement de ces ciments.

Dans sa communication intitulée "Evolution de la microstructure des bétons au cours du test ASTM de gel-dégel", C. VERNET rend compte de ses observations résultant d'un plan d'expérience basé sur l'examen au M.E.B. de 25 bétons de ciments Portland et de ciments fillérisés. Il met particulièrement bien en évidence les processus destructeurs et réparateurs et montre le bon comportement des ciments aux fillers calcaires, alors que les cendres volantes sont génératrices de dégradations (17).

Nous avons vu que les calcaires étaient sélectionnés pour garantir une bonne compacité initiale des bétons et que la formation relativement rapide de carboaluminate venait s'ajouter au CSH et à la portlandite pour renforcer les liaisons entre les grains ; il est donc logique que les bétons correspondant aient une bonne durabilité. En revanche, C. VERNET a montré que les cendres volantes ne développent leurs liaisons que très tardivement et qu'elles introduisent une porosité de dimension élevée, d'où leur comportement médiocre.

Le rôle des bulles d'air dans le mécanisme de dégradation au gel-dégel a d'abord été étudié par T.C. POWERS qui a émis la notion de "facteur d'espace critique" ; puis Monsieur PIGEON a montré que ce facteur critique d'espacement des bulles d'air varie en fonction de la vitesse de refroidissement.

M. REGOURD et al ont étudié les conséquences favorables de l'addition d'un entraîneur d'air qui ramène l'espacement moyen des bulles d'air à moins de 100 microns pour tous les ciments, c'est-à-dire, largement au-dessous de la valeur critique. Ceci veut dire que le choix du ciment pour la tenue des bétons au gel-dégel ne constitue pas un réel problème, et que l'emploi d'un entraîneur d'air résoud à coup sûr les cas litigieux (18).

3.3.4. Protection des armatures

Je ne voudrais pas omettre d'évoquer, au titre de la durabilité, le problème de la protection des armatures.

Il est bien connu que la pâte de ciment protège les armatures de la corrosion électrochimique grâce à sa forte basicité. En présence de l'excès de chaux libérée par l'hydratation du clinker, le pH de la solution interstitielle est d'environ 12,5 , cette valeur est vérifiée pour tous les ciments, sauf pour ceux qui sont très riches en laitier. Si le pH descend au-dessous de 10, la protection n'est plus assurée ; cette situaation peut résulter d'une pénétration du CO_2 atmosphérique par les pores ouverts et les microfissures.

Les risques de carbonatation sont donc essentiellement dépendants de la compacité du béton ; ceci nous ramène donc aux résultats de C. GUYOT, à savoir qu'à résistance égale, au même âge, la compacité est pratiquement la même pour les ciments fillérisés que pour les ciments purs. J. BARON en a vérifié les conséquences favorables en mesurant les profondeurs de pénétration de la carbonatation sur des mortiers standards après un an de conservation : que ce soit en Portland pur ou avec 15 et 30 % de filler calcaire, les résultats étaient les mêmes, et bien meilleures qu'avec le laitier (16).

4. CONCLUSION

Les pouzzolanes et les laitiers de haut-fourneau sont bien connus pour les propriétés qu'ils confèrent à certaines catégories de ciments à haute résistance chimique. Leur utilisation en proportions modérées comme additif au clinker permet en outre de moduler facilement la palette des ciments par classe de résistances mécaniques.

Les fillers calcaires peuvent, sans inconvénients, être utilisés pour ce même usage visant à économiser le clinker.

La participation de ces diverses additions minérales au processus de durcissement n'est évidemment pas la même, mais chacune d'entre elles fait preuve d'une activité chimique que le cimentier est à même de contrôler pour produire des ciments de qualité régulière.

Les aspects scientifiques des différents processus intervenant dans la confection et la mise en place des bétons, puis dans leur durcissement et leur aptitude à résister aux divers types de corrosion, ont été abordés dans le but d'être discutés par les spécialistes réunis dans notre séminaire.

5. BIBLIOGRAPHIE

1. G. WISCHERS – VDZ : Optimisation of cements with mineral admixtures (ce congrès).

2. M. VON EUW – Société des Ciments Français: L'utilisation des Cendres Volantes en cimenterie. VII Congrès ERMCO – LONDRES, mai 1983.

3. JP. BOMBLED – CERILH – Rhéologie du béton frais. Influence de l'ajout de fillers aux ciments (ce congrès).

4. C. VERNET. Société des Ciments Français : Etude de la cinétique des réactions d'hydratation des ciments artificiels. Thèse CNAM, chap. 2.2, Octovre 1982.

5. M. REGOURD, JH THOMASSIN, P. BAILLIF and JC. TOURAY : Blast Furnace Slag Hydration Surface Analysis. Cement Concrete Research, 13, 549-556 (1983).

6. F. HAWTHORN, E. DEMOULIAN, P. GOURDIN, C. VERNET. Société des Ciments Français : Laitiers et Clinkers – Influences réciproques. Paris 1980, thème III-145.

7. K. TAKEMOTO – ONODA Cement. Japon : Variation of Activity Index of Slag (ce congrès).

8. S.N. GHOSH. Nat. Council for Cement and Building Materials. Indian : Chemical Composition vis-à-vis Optimal Addition of Minerals to Cement (ce congrès).

9. J. ALMEBORG and JT. CHRISTENSEN – Aalborg Portland Denmark : Danish Portland. Fly Ash Cement (ce congrès).

10. JP. BOMBLED, G. BELLINA et B. MORTUREUX –

CERILH - : Détermination des courbes granulométriques et des aires massiques des constituants de mélanges cobroyés - applications aux fillers et aux laitiers. (ce congrès).

11. R. GUYOT, R. RANC, B. CARIOU - Lafarge Coppée : Utilisation de la potentialité hydraulique du clinker dans les ciments portland avec ajout de filler calcaire (ce congrès).

12. JP. OLLIVIER - I.N.S.A. - UPS - Toulouse, France : Rôle des additions minérales sur la formation de l'auréole de transition entre gros granulats et mortier (ce congrès).

13. M. REGOURD, B. MORTUREUX, H. HORNAIN - CERILH. Liaison pâte de ciment filler dans les ciments composés. Colloque International Toulouse. France nov. 1982. A. 64-A-72.

14. V.S. RAMACHANDRAN and ZHANG CHUN-MEI - Nat. Research Council Canada : Cement with calcium carbonate additions (ce congrès).

15. C. VERNET. Société des Ciments Français : Séquence et cinétique des réactions d'hydratation de l'aluminate tricalcique en présence de gypse, de chaux et de fillers calcaires. (ce congrès).

16. J. BARON - Lafarge Coppée Recherche - France : The Durability of Limestone Composite Cements in the Context of the French Specifications. Communication to International Seminar on some Aspects of Admixtures and Industrial by-products on the Durability of Concrete (avril 1986 Chalmers University of Technology Sweden).

17. C. VERNET. Société des Ciments Français : Evolution de la Microstructure des Bétons au cours du Test ASTM de gél-dégel (ce congrès).

18. P. GEGOUT, H. HORNAIN, B. THURET, M. REGOURD-CERILH- Résistance au gel des ciments aux fillers calcaires.

V.S. Ramachandran, Division of Building Research, National Research Council Canada;
Zhang Chun-mei, Nanjing Institute of Technology, Nanjing, The People's Republic of China

CEMENT WITH CALCIUM GARBONATE ADDITIONS

INTRODUCTION

Limestone is used for various purposes in concrete technology, viz, as raw material for clinker production, partial replacement of gypsum, and as coarse or fine aggregate. Limestone dust produced in quarrying operations poses disposal and environmental problems and has been suggested for use as an additive to portland cement. Some standards do allow the use of calcium carbonate as an additive in cement provided the properties of concrete made with such a cement are not adversely affected. Work carried out on its effect on hydrating cement shows that the physical and mechanical characteristics are influenced to different extents.

Some work has been carried out on the effect of $CaCO_3$ on cement paste, but there is no general agreement on the relative effects of different amounts of it on the cement paste properties (1-9). This may be mainly due to differences in the characteristics of the materials and the methods used. The objective of the present work is to assess the effect of various amounts of $CaCO_3$ on the hydration of C_3S and C_3A in order to explain the physico-chemical changes occurring during hydration of portland cement.

EXPERIMENTAL

Type 1 portland cement containing C_3A 12.8%, C_4AF 6.6%, C_3S 51.5%, C_2S 19.8%, and $CaSO_4$ 5.1% was used. C_3A and C_3S were supplied by the Tetratech Co. and Portland Cement Association, respectively. The C_3S had a Blaine surface area of 3600 cm^2/g. Gypsum and calcium carbonate (N_2 surface area 6.5 m^2/g), both of reagent quality, were supplied by Fisher Scientific Co. and Anachemia Chemical Co., respectively.

Conduction calorimetry, differential scanning calorimetry (DSC), thermogravimetry (TGA), differential thermal analysis (DTA), X-ray diffraction (XRD), scanning electron microscopy (SEM), and high-pressure Hg porosimetry were used in this work and have been described elsewhere (10-13).

Cement pastes containing various amounts of $CaCO_3$ were subjected to compressive strength measurements using 2-cm cubes. The setting times were determined according to ASTM C191-82. Samples were prepared as follows:

1. C_3S was mixed with 0, 5, 10, 15 and 50% $CaCO_3$ (with respect to the total weight of C_3S + $CaCO_3$) at a water/solid ratio of 0.4 or 0.7. The pastes were hydrated in capped polyethylene vials for specified intervals of time, then subjected to drying under vacuum for one day before being examined.
2. C_3A and 0, 12.5 and 25% gypsum/$CaCO_3$ or 12.5% gypsum + 12.5% $CaCO_3$ or 25% gypsum + 12.5% $CaCO_3$ (based on the weight of C_3A) were mixed with water at a water/C_3A ratio of 4. All were hydrated in closed containers for specified intervals of time; cold methanol was used to terminate hydration. The pastes formed from C_3A + gypsum or C_3A + gypsum + $CaCO_3$ were dried at room temperature under vacuum and others at 50°C under vacuum.
3. Samples of cement containing 0, 5, 10, 15 and 50% $CaCO_3$ with respect to the total weight of cement + $CaCO_3$ were mixed with water at a water/solid ratio of 0.4 or 1.0. Those for TGA were prepared from cubes tested for compressive strength; some of the broken pieces were ground and dried for one day under vacuum.

RESULTS AND DISCUSSION

Hydration characteristics of C_3S

Tricalcium silicate was hydrated in the presence of 0, 5, 10, 15 and 50% $CaCO_3$ at a water/solid ratio of 0.4 or 0.7. The resulting products were examined by TGA, DTA, SEM and conduction calorimetry. Strength and shrinkage data were also obtained. The $Ca(OH)_2$ formed at different times is shown in Figure 1. The results are calculated on the basis of C_3S to avoid dilution effect. The amount of lime formed at 0% $CaCO_3$ increases from 8.9% at 1 day to 23.2% at 28 days. Addition of $CaCO_3$ increases the amount of $Ca(OH)_2$ at all times of hydration, indicating that $CaCO_3$ increases the rate of hydration of C_3S. At 28 days addition of 0, 5 and 15% $CaCO_3$ yields 23.2, 24.0 and 25.5% $Ca(OH)_2$, respectively. The results also indicate that 15% $CaCO_3$ shows a greater accelerating effect than 5% $CaCO_3$.

The conduction calorimetric curves showing the rate of heat development of C_3S during hydration up to 24 h are given in Fig. 2. The onset of the accelerating period representing the hydration of C_3S does not seem to be affected, but the intensity of the peak increases as the amount of added $CaCO_3$ is increased. The total heat developed at 24 h decreases in the following manner: C_3S - 15% $CaCO_3$ > C_3S - 10% $CaCO_3$ > C_3S - 5% $CaCO_3$ > C_3S - 0% $CaCO_3$. The conduction calorimetric curves also show the accelerating effect of $CaCO_3$.

Results were also obtained for the non-evaporable water and C_3S contents for C_3S pastes hydrated to different times. At any time of hydration the non-evaporable water content was higher and the unhydrated C_3S lower in pastes containing $CaCO_3$, confirming that hydration rate is increased in the presence of $CaCO_3$.

Thermogravimetric analysis of the C_3S + $CaCO_3$ + H_2O system revealed that as hydration proceeded the peak due to $CaCO_3$ decomposition at about 750°C diminished. This indicated that some $CaCO_3$ was consumed during the reaction. Figure 3 shows the amount of free $CaCO_3$ remaining at different times of hydration. In the C_3S - $CaCO_3$ mixture containing 15% and 5% $CaCO_3$ the amount of $CaCO_3$ that was combined or incorporated into the hydrating C_3S was 2.4 and 1.3 percentage points, respectively.

The SEM photograph of C_3S paste hydrated for 1 day in the presence of 50% $CaCO_3$ is shown in Fig. 4. Fibrous particles of C-S-H grow on both the C_3S (marked by C) and $CaCO_3$ (marked by L) particles. It is possible that $CaCO_3$ acts as a nucleating agent. Another possibility is that C-S-H containing $CaCO_3$ forms on the C_3S particles having higher

permeability than that occurring with 0% $CaCO_3$; this would result in an increase in the rate of reaction.

Other effects of $CaCO_3$ on C_3S pastes included increase in modulus of elasticity, microhardness, C/S ratio of the C-S-H phase, rate of shrinkage, and development of smaller diameter pores up to 7 days of hydration.

Hydration of C_3A

The hydration of C_3A alone and of that containing 12.5 or 25% $CaCO_3$, 12.5 or 25% gypsum, and a mixture of $CaCO_3$ and gypsum hydrated to different times was followed by DSC. The C_3A samples formed hexagonal aluminate hydrates at earlier times, identified by endothermal peaks at about 150 and 250°C. Both peaks increased in intensity up to 4 h, then decreased until at 1 day there was only an intense peak at 314°C, indicating formation of cubic C_3AH_6. It is difficult to conclude from DSC just when the formation of C_3AH_6 was initiated; thermograms indicate, however, that almost all of the hexagonal phase was converted to the cubic phase within 7 h. SEM examination revealed the formation of cubic aluminate at 4 h and X-ray indicated C_3AH_6 even after 1 h of hydration.

By adding $CaCO_3$ to C_3A the endothermal peak at 160-165°C and another at 235-250°C developed even at 5 min. They increased in intensity with time and are ascribed to the carboaluminate hydrate, mixed perhaps with hexagonal aluminate hydrates. The formation of the cubic phase was suppressed for up to 2 days.

Unhydrated C_3A + $C\bar{S}H_2$ mixtures containing 25% $C\bar{S}H_2$ indicated an endothermic effect at 135°C (due to $C\bar{S}H_2$). This peak decreased with hydration. One representing the formation of ettringite was observed at about 100°C after as little as 5 min. Most gypsum was consumed in the first hour. At 2 h the formation of monosulfoaluminate was evidenced by an endothermal peak at 165°C.

By the addition of 12.5% $CaCO_3$ to the C_3A + 25% $C\bar{S}H_2$ mixture the rate of consumption of $C\bar{S}H_2$ increased. Practically no $C\bar{S}H_2$ remained even at 30 min. Consequently, the rate of ettringite formation is increased, as is also the rate of conversion of ettringite to monosulfoaluminate.

Conduction calorimetric curves of C_3A + 12.5% $C\bar{S}H_2$ and C_3A + 12.5% $C\bar{S}H_2$ + 12.5% $CaCO_3$ are shown in Fig. 5. The C_3A + 12.5% $C\bar{S}H_2$ mixture developed heat as soon as it came into contact with water. A peak at about 3 min represents the maximum rate of formation of ettringite. In the presence of $CaCO_3$ the earlier peak becomes more intense and occurs at about 5 min. Simultaneous formation of carboaluminate and ettringite results in a more intense peak than that for ettringite alone formed by the C_3A + 12.5% $C\bar{S}H_2$ mixture. DSC curves show that at 5 min both ettringite and carboaluminate (peak at about 160-170°C) are formed. There was also indication that more ettringite was formed in the C_3A + 12.5% $C\bar{S}H_2$ + 12.5% $CaCO_3$ mixture than in the C_3A + 12.5% $C\bar{S}H_2$ mixture. After 20 min there was an additional peak at about 180°C, indicating the presence of monosulfoaluminate. Comparison of thermograms for different times showed that formation of ettringite and its conversion to monosulfoaluminate is accelerated in the presence of $CaCO_3$. Such results suggest that $CaCO_3$ existing as a complex layer on the surface of hydrating C_3A is more permeable than that formed by gypsum and accelerates formation of ettringite and monosulfoaluminate.

Hydration of cement

Figure 6 compares the amounts of $Ca(OH)_2$ formed at different times in cement pastes hydrated with 0, 5, 10 and 15% $CaCO_3$. Results are reported on the basis of cement content to avoid dilution effect by $CaCO_3$. At all periods from 3 h to 28 days there is evidence that $CaCO_3$ promotes formation of $Ca(OH)_2$. The amount of CH formed is increased in cements containing larger amounts of $CaCO_3$. This is particularly significant at earlier times. Calcium hydroxide is derived from the hydration of C_3S and C_2S, and the results indicate that C_3S and C_2S phases in cement may be accelerated by $CaCO_3$. Hydration of pure C_3S is accelerated by $CaCO_3$, as shown in Fig. 1.

The rate of heat development in cement containing 0, 5, 10, 15 and 50% $CaCO_3$ is shown in Fig. 7. Although the time for the onset of heat evolution is not changed significantly in the samples containing different amounts of $CaCO_3$, heat evolution is accelerated. At 50% $CaCO_3$ the amplitude of the peak occurs 3½ h earlier than in that hydrated without $CaCO_3$. Figure 8 shows the total heat developed in these pastes for up to 24 h. The curves demonstrate that at all dosages of $CaCO_3$ more heat is developed, signifying the accelerating effect of $CaCO_3$. In pure C_3S pastes there is a similar accelerating effect (Fig. 2). The total heat developed in cement containing 15% $CaCO_3$ is 8 and 28 cal/g at 4 and 8 h, respectively; the corresponding values for C_3S containing 15% $CaCO_3$ are 6 and 22 cal/g. If this heat is derived mainly from the C_3S portion of cement (52% C_3S), the heat evolution in cement should be far lower than the values determined. The higher values signify that either the accelerating influence of $CaCO_3$ on C_3S is more significant in cement or that part of the heat should be attributed to the hydration of the C_3A or C_4AF phases.

It has been shown that in the C_3S-$CaCO_3$-H_2O system some $CaCO_3$ is incorporated into the C-S-H phase (Fig. 3). In portland cement C_3A reacts with $CaCO_3$ to form carboaluminate, and some $CaCO_3$ is incorporated also into the hydrated C_3S phase. Figure 3 compares the relative amounts of free, unreacted $CaCO_3$ with hydrating portland cement or C_3S initially containing 5 or 15% $CaCO_3$. Generally more $CaCO_3$ seems to be incorporated into cement paste than into C_3S paste. This can be explained by consumption of some $CaCO_3$ by the C_3A phase in cement. It would be expected that part of C_3A reacts with the $C\bar{S}H_2$ and part with the $CaCO_3$.

Because of the accelerating influence of $CaCO_3$ on the hydration sequence of C_3A and C_3S it would be expected that $CaCO_3$ would influence the setting property of cement. Figure 9 gives the initial and final setting times of cement prepared at a w/s = 0.4, or at the same consistency. Setting time decreases as the amount of added $CaCO_3$ is increased. The acceleration of setting time at 15% $CaCO_3$ varies

between 0.8 and 1.5 h. Setting times, even at 15% $CaCO_3$, exceed the minimum limit requirements of the Canadian standard (14). Comparison of setting time with calorimetric and TGA results (Figs. 5, 6 and 7) suggests that at time of setting C_3A and C_3S have hydrated to different extents. The accelerated setting can therefore be explained by the acceleration of hydration of C_3A to form sulfoaluminate and of C_3S to form C-S-H and CH in cement.

The rates of strength development in cement pastes containing 0, 5, 10 and 15% $CaCO_3$ are given in Fig. 10. Up to 1 day the strength seems to be higher in pastes containing $CaCO_3$. Later strengths at 7 and 28 d indicate lower strengths in paste containing 10-15% $CaCO_3$. At 28 days they are as follows: cement - 5% $CaCO_3$ > cement - 0% $CaCO_3$ > cement - 10% $CaCO_3$ > cement - 15% $CaCO_3$. The decrease in strength at dosages of 10-15% $CaCO_3$ at 28 days may be due partly to lower degree of hydration (based on the weight of cement paste containing $CaCO_3$); the amount of CH in cement pastes with 0, 5, 10 and 15% $CaCO_3$ is, respectively, 12.9, 12.6, 11.9 and 11.5 at 28 days. The porosity values show that total porosity of paste with 15% $CaCO_3$ is higher than that containing 0% $CaCO_3$ at 28 days, the values being 30.9 and 25.5%, respectively (Fig. 11). Higher porosity in pastes containing 15% $CaCO_3$ may be responsible for the decrease. A part of $CaCO_3$ that remains unreacted may act as a diluent. That not all added $CaCO_3$ acts as a diluent is evident from the results for mortars. If strengths of mortars containing cement + quartz and cement + $CaCO_3$ are compared, higher strengths are obtained with $CaCO_3$, indicating that it participates in forming bonds in the paste (3). Microstructural studies indicate this possibility (Fig. 4). At 90 days cements with 0, 5 and 10% $CaCO_3$ have about the same strength. Further long-term strength development studies in pastes containing 15% $CaCO_3$ will have to be carried out to examine whether, at this dosage, strength will eventually reach the same value as that for the paste containing 0% $CaCO_3$.

CONCLUSIONS

Hydration of $C_3A + C\bar{S}H_2$ in the presence of $CaCO_3$ results in accelerated formation of ettringite and its conversion to monosulfoaluminate hydrate. This is probably due to the formation of highly permeable carboaluminate on the hydrating surface of C_3A.

Calcium carbonate accelerates the hydration of C_3S and is partially incorporated into the C-S-H phase. The modified surface of the hydrating C_3S and nucleation on the $CaCO_3$ particles are two mechanisms that could produce this effect.

Hydration of cement is also accelerated by $CaCO_3$. In the paste, $CaCO_3$ is incorporated into the hydrating C_3A and C_3S phases. Setting times are reduced owing to accelerated formation of ettringite and C-S-H. Earlier strengths of cement pastes are increased by the addition of $CaCO_3$, but at 28 days strengths decrease in the presence of 10 and 15% $CaCO_3$. At 90 days the strength for 15% $CaCO_3$ is lower than that of the other mixes. There is evidence that all added $CaCO_3$ does not act as an inert additive in terms of chemical reaction and strength development.

ACKNOWLEDGEMENTS

The authors are very grateful to J. Clark and G.M. Polomark for experimental assistance. The paper is a contribution from the Division of Building Research, National Research Council of Canada.

REFERENCES

1. Soroka, I., Stern, N.: "Calcareous fillers and the compressive strength of portland cement", Cem. Concr. Res., 6, No. 3, 367-376 (1976).

2. Soroka, I., Setter, N.: "The effect of fillers on strength of cement mortars", Cem. Concr. Res., 7, No. 4, 449-456 (1977).

3. Mortureux, B., Hornain, H., Regourd, M.: "Cement paste-fillers bond in blended cements", presented at Conference of CERILH, 1-9 (1982).

4. Bensted, J.: "Some hydration investigations involving portland cement - effect of calcium carbonate substitution of gypsum", World Cement Technology, 11, No. 8, 395-406 (1980).

5. Bensted, J.: "Further hydration investigations involving portland cement and the substitution of limestone for gypsum", World Cement Technology, 14, No. 10, 383-392 (1983).

6. Timashev, V.V., Kolbasov, V.M.: "Properties of cements with carbonate additives", (Rus.). C.R., URSS, No. 10, 10-12 (1981).

7. Lyubimova, T. Yu., Nismevich, M.L., Levkova, N.S., Mikhailov, N.V.: "Structure formation kinetics during hardening of cements in the presence of carbonate fillers", Kolloidnyi Zhurnal, 34, No. 6, 868-877 (1972).

8. Spohn, E., Lieber, W.: "Reactions between calcium carbonate and portland cement, Contributions to the systems C_3A-$CaCO_3$-H_2O and C_4AF-$CaCO_3$-H_2O", Zement-Kalk-Gips, 18, No. 9, 483-485 (1965).

9. Tong, S.D., Fang, D.R.: "Blended cement using zeolite and limestone as fine fillers", Silicates Industriels, 48, No. 6, 127-132 (1983).

10. Ramachandran, V.S., Polomark, G.M.: "Extraction of $Ca(OH)_2$ from portland cement and $3CaO.SiO_2$ pastes", J. Chem. Tech. Biotechnol., 32, No. 10, 946-952 (1982).

11. Traetteberg, A., Ramachandran, V.S., Grattan-Bellew, P.E.: "A study of the microstructure and hydration characteristics of tricalcium silicate in the presence of calcium chloride", Cem. Concr. Res., 4, No. 2, 203-221 (1974).

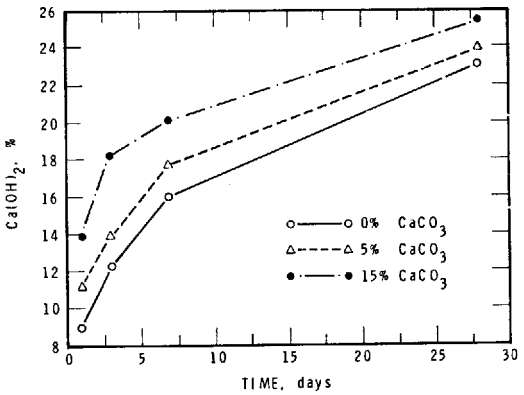

Figure 1. Formation of $Ca(OH)_2$ in C_3S pastes containing different amounts of $CaCO_3$ (C_3S basis)

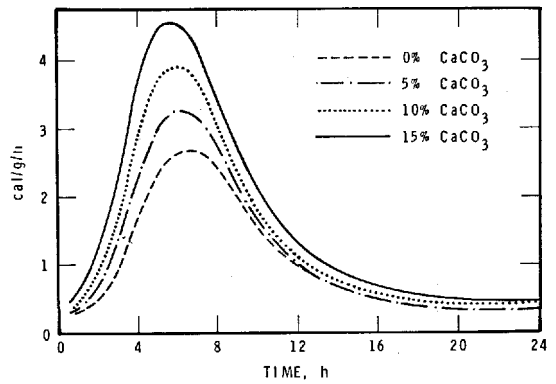

Figure 2. Conduction calorimetric curves of C_3S hydrated with different amounts of $CaCO_3$ (C_3S basis)

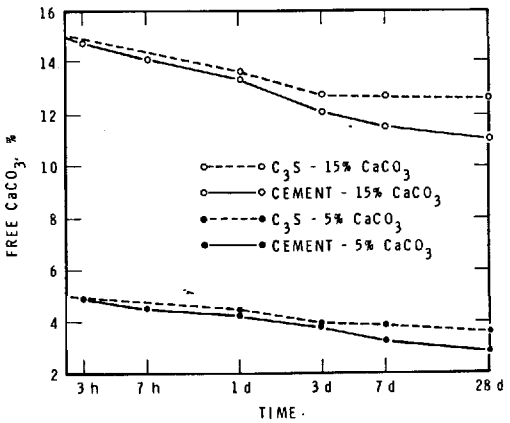

Figure 3. Free $CaCO_3$ remaining in the C_3S and cement pastes at different times of hydration (based on C_3S + $CaCO_3$ or cement + $CaCO_3$)

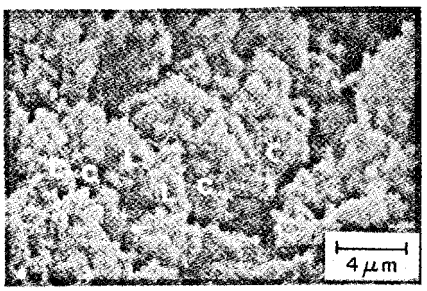

Figure 4. Micrograph of C_3S paste containing 50% $CaCO_3$ hydrated for 1 day (w/s = 0.7) C: growth on C_3S; L: growth on $CaCO_3$

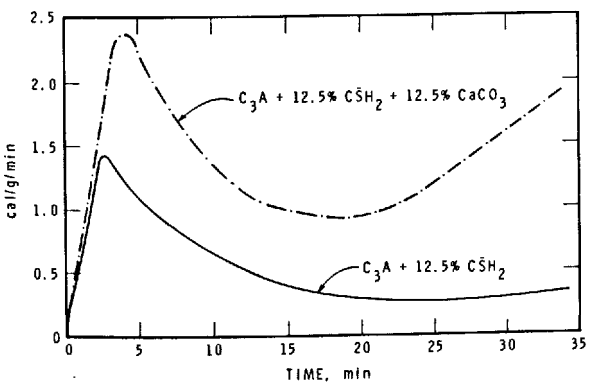

Figure 5. Conduction calorimetric curves of C_3A hydrated with $C\bar{S}H_2$ and $CaCO_3$

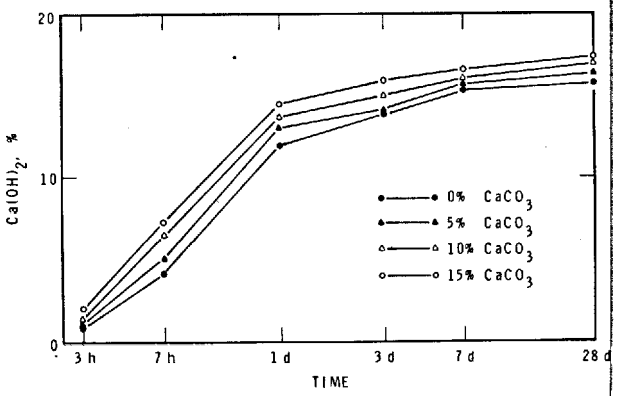

Figure 6. Formation of $Ca(OH)_2$ in cement pastes containing different amounts of $CaCO_3$ (cement basis)

12. Ramachandran, V.S., Beaudoin, J.J.: "Significance of water:solid ratio and temperature on the physico-mechanical characteristics of hydrating $4CaO.Al_2O_3.Fe_2O_3$", J. Mater. Scie., 11, 1893-1910 (1976).

13. Ramachandran, V.S.: "Estimation of tricalcium silicate through polymorphic transformation", J. Thermal Analysis, 3, 181-190 (1971).

14. Canadian Standards Associates: "Portland Cements", CAN3-AS-M83 (1983).

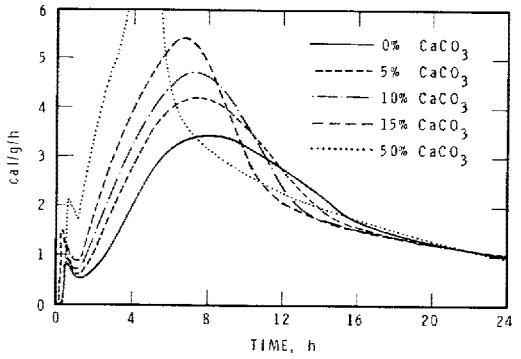

Figure 7. Conduction calorimetric curves of cement hydrated with different amounts of $CaCO_3$ (cement basis)

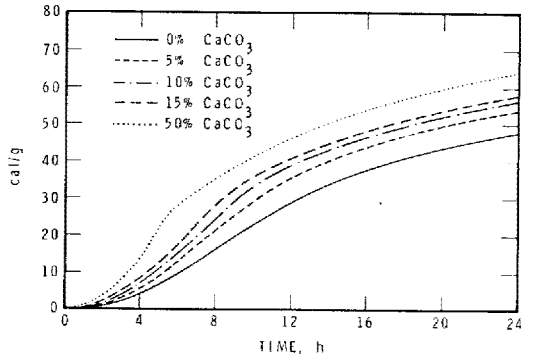

Figure 8. Heat developed in the hydration of cement containing different amounts of $CaCO_3$ (cement basis)

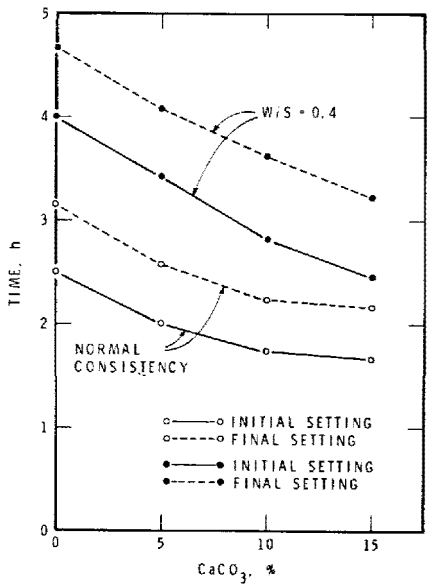

Figure 9. Setting times of cement pastes with different amounts of $CaCO_3$

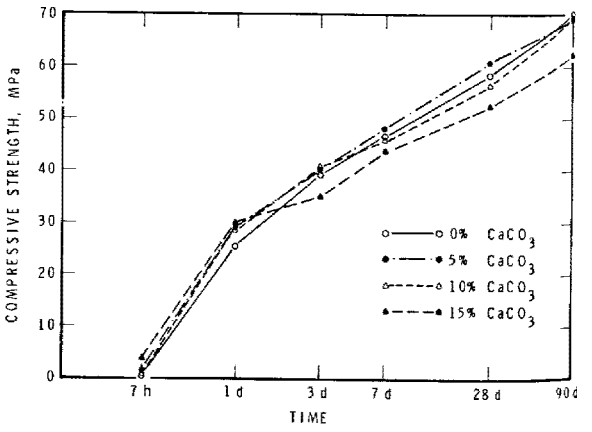

Figure 10. Compressive strength of cement pastes containing different amounts of $CaCO_3$

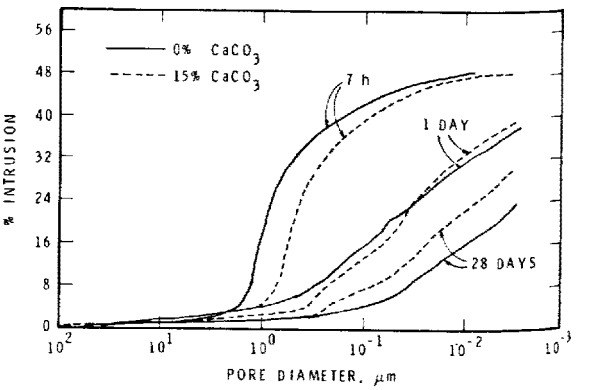

Figure 11. Pore size distribution curves of cement pastes containing 0 and 15% $CaCO_3$

J. Almeborg and J. T. Christensen, Aalborg Portland, Denmark

Danish Portland-Fly Ash Cement

Introduction

Before the oil crisis in 1973/74, only 25% of the electric power used in Denmark came from coal fired power plants and the production of fly ash was less than 0.3 million tonnes per year.

By 1980 the use of coal had increased to 75% of the total fuel consumption and the fly ash production had reached 1.0 million tonnes per year.

Part of this fly ash is used by Aalborg Portland - the only cement manufacturer in Denmark - in three different ways:

- As a substitute for clay in the raw mix. The fly ash is insufflated into the burning zone of the cement kilns at a rate of up to 12% of clinker output.
- For manufacture of rapid hardening portland cement containing up to 5% of fly ash.
- For manufacture of portland-fly ash cement containing about 24% of fly ash.

Production of portland-fly ash cement

The portland-fly ash cement was designed to fulfil the requirements of the Danish cement standard, DS 427, and the future European standard for cement, EN 197. Furthermore, it was decided that the new cement should have a compressive strength at any age not lower than for Danish ordinary portland cement. Laboratory investigations and grinding tests in the plant revealed that these requirements would be met by a cement containing about 24% fly ash and having a specific surface of 450 m^2/kg.

Production of portland-fly ash cement takes place on mill installations as shown in Figure 1.

The 24% of fly ash for portland-fly ash cement is extracted directly from the storage silo to weight feeders. The feed control to the cement mills is based on the loss in weight principle. The shape of the feed bin and its mechanical stirrers were important design features for maintaining steady flow of fly ash to the cement mill.

As a further control fly ash, material from the primary grinder, and material from the secondary grinder are analyzed by XRF every 4 hours and the amount of fly ash in the portland-fly ash cement is calculated.

The fly ash used comes from different power plants and from coal of different origin but the fly ash always complies with the requirements set out in Table 8.

The portland-fly ash cement produced has average properties as shown in Table 1.

As illustrated by Table 2 it was possible to discontinue production af ordinary portland cement shortly after the introduction of the portland-fly ash cement. This does, however, not mean that ordinary portland cement has simply been substituted by portland-fly ash cement. For example has the portland-fly ash cement substituted some of the use of rapid hardening portland cement for certain purposes, especially in concrete products (slabs, pipes). In this connection it should also be mentioned that some ordinary portland cement has been replaced by a combination of rapid hardening portland cement and fly ash mixed at the concrete plants.

Research projects

At the design stage several research projects were initiated, all aiming at providing information on important subjects related to the use of portland-fly ash cement. Summaries of results of the projects are given below.

Water penetration

Water penetration was measured in accordance with ISO 7031 on concretes differing in the type of cement used and the cement content. All concretes were air-entrained (air content 4-7%) [1,2]. The samples were cured 28 days in water (20°C), 14 days in air (20°C, >65%RH) and finally 14 days in water (20°C) before testing. The results are given in Table 3.

The results, although not unambiguous, indicate that at this testing age the two types of cement will yield the same level of resistance to water penetration provided that the concretes are cured properly.

Alkali-silica reactivity

The effect of substituting 30% by weight of ordinary portland cement containing either 0.68 or 1.14% Na_2O eq. with two Danish fly ashes (Composition as shown in Table 4) on alkali-silica reactivity was tested according to ASTM C 441 (expansion of mortar bars at 37.8°C).

The result shown in Figure 2 clearly demonstrates the beneficial effect of fly ash 0029 on expansion caused by alkali-silica reaction. Similar results were obtained with fly ash 0038. Similar results were also obtained with both fly ashes when tested according to the modified methods described by Brotschi and Mehta [3].

Diffusion of chloride

The effect of cement type, w/c ratio, temperature and curing time on the diffusion of chloride through cement paste has been studied at The Danish Corrosion Centre [4]. The technique used for diffusion measurements is outlined in Figure 3.

From the results of Table 5 the superior behaviour of portland-fly ash cement compared with the behaviour of rapid hardening and sulfate resistant portland cement is noted.

Carbonation

Based on a literature survey, Justesen and Nepper-Christensen [5] have expressed the following opinion concerning carbonation of concrete containing portland-fly ash cement:

- The carbonation proceeds faster in an initial period which may be of a duration of about one year. The rate of carbonation depends to a high degree on the curing conditions, particularly on the protection of the concrete against drying-out at the very early stage of hardening.
- At later ages the difference in carbonation depth seems to be rather independent of the type of cement used.

The results from a long term durability project (25 years) commenced in 1983 in order to evaluate the durability of concrete with mineral admixtures (fly ash, microsilica) support the first of these conclusions. The concrete structures included in the testing project are still too young to give evidence for the second conclusion, see Table 6 [6].

Freeze/thaw resistance

The long term project [6] referred to above also includes testing the concretes for freeze/thaw resistance according to ISO 4846. 28 days old slabs and 2 year old drilled cores were tested with the result (Table 7) that good freeze/thaw resistance (scaling less than 0.5 kg/m^2) was obtained for all concretes, irrespective of cement type, which were designed to provide frost resistance (marked with * in Table 7).

Since 1976 many thousands of square metres of concrete pavement were made with concrete containing fly ash or from portland-fly ash cement in Denmark and they have been exposed to severe freeze/thaw conditions during the winters. The experience gained is that air-entrained concrete (4-6% air) produced with a strength (>30 MPa) and a w/c ratio (<0.5) corresponding to the specifications for concrete in aggressive environment in Dansk Ingeniørforenings Code of Practice [7] will have excellent freeze/thaw resistance.

Wear resistance

Following some cases of unsatisfactory wear resistance of concrete floors (laid in pigsties) made with portland-fly ash cement an investigation of the influence of cement type and the use/non-use of a curing membrane on this property was taken up. The wear resistance was measured by sand blasting the concrete surface with a sand-water slurry according to a method developed by The Danish Agricultural Engineering Institute [8].

Only minor differences in wear resistance could be attributed to the cement type whereas both the use/non-use of curing membrane and the compressive strength were found to be important parameters, see Figure 4 [9].

Quality of fly ash

As part of the quality control of fly ash used by the cement and concrete industry in Denmark the chemical and physical properties are tested on monthly average samples from 8 major power plants. The control also comprises preparation of a blended cement (70w% Rapid hardening portland cement + 30w% fly ash) which is tested for compressive strength, setting time and soundness.

The quality control requirements for fly ash, the average test results and standard deviations for the years 1983-85 are shown in Table 8.

Taking into account that the data of Table 8 represent fly ashes produced at different power plants from coal of different origin the resulting strengths of the blended samples show remarkable uniformity.

The standard deviations shown in Table 1 for portland-fly ash cement also confirm that it is possible to manufacture uniform cement from fly ashes from different power plants and from different coals.

Thus it has not been found necessary to introduce further requirements for fly ash used for manufacturing portland-fly ash cement in Denmark.

Conclusion

Portland-fly ash cement has been marketed in Denmark for 5 years and covers a market share of 35-40% of the total cement consumption.

Danish research projects concerning water permeability, alkali-silica reactivity, chloride diffusion, carbonation, freeze/thaw resistance and wear resistance confirm that portland-fly ash cement has similar or better properties in those respects than ordinary portland cement.

J. Almeborg and J. T. Christensen, Aalborg Portland, Denmark

Danish Portland-Fly Ash Cement

References

1. Geiker, M.: Standardbetons frostbestandighed og vandtæthed, Aalborg Portland, Internal Report, December 1984

2. Bækmark, K.: Betons vandtrykpermeabilitet efter ISO 7031, Aalborg Portland, Internal Report, September 1984

3. Brotschi, J. & Mehta, P. K.: Test methods for determining potential alkali-silica reactivity in cements, Cement and Concrete Research, Vol. 8, pp. 191-200, 1978.

4. Hansson, C. M., Strunge, H., Markussen, J. B. & Frølund, T.: The effect of cement type on the diffusion of chloride, Nordic Concrete Research, Publication no. 4, pp. 70-80, Oslo 1985.

5. Justesen, C. F. & Nepper-Christensen, P.: Portlandflyveaskecement, Aalborg Portland, Internal Report, August 1985.

6. Rasmussen, T. H.: Langtidsforsøg vedrørende holdbarheden af beton med flyveaske og mikrosilica, Aalborg Portland, Internal report, November 1984.

7. Dansk Ingeniørforenings Code of Practice for the Structural Use of Concrete, DS 411, 3. edition, March 1984.

8. Pedersen, S.: Metode til karakterisering af staldgulve, Danish Agricultural Engineering Institute, Orientering nr. 8, 1981.

9. Pedersen, S. & Johansen, P.: Undersøgelse over forskellige betontyper til svinestalde, Danish Agricultural Engineering Institute, Orientering nr. 32, 1985.

Tables

Chemical properties	
M	1.3 +/- 0.3 %
$\bar{S}$	2.6 +/- 0.2 %
Loss on ignition	2.5 +/- 0.2 %
Fly ash	24 +/- 1.5 %
Physical properties	
Setting time	
Initial	130 +/- 16 minutes
Final	165 +/- 18 minutes
Soundness	0 +/- 0 mm
Compressive strength	
1 day	14 +/- 1.8 MPa
2 days	24 +/- 1.8 MPa
7 days	37 +/- 2.0 MPa
28 days	49 +/- 2.2 MPa

Table 1. Average properties and standard deviations of Danish portland-fly ash cement. Testing performed according to the methods of Danish Standard 427 which closely resemble the methods of ISO R 679 and R 680.

Type of cement	1980	1981	1982	1983	1984	1985
Ordinary portland cement	40	36	24	14	0	0
Portland-fly ash cement	0	6	23	31	40	35
Rapid hardening portland cement	56	52	46	49	52	60
Special cements	4	6	7	6	8	5

Table 2. Use of different cement types (%) in Denmark.

Type of cement	Cement content kg/m³	w/c ratio	Compressive strength MPa	Water penetration min - max mm	Water penetration average mm	Test series no.
Rapid hardening portland cement	288	0.49	25	0 - 13	3	1
	300	0.46	33		16	2
	348	0.41	35	0 - 23	4	1
Portland-fly ash cement	289	0.48	30	0 - 10	1	1
	325	0.43	32		8	2
	348	0.42	32	0 - 15	3	1
	350	0.44	35		4	2

Table 3. Water penetration for concretes differing in cement type and cement content. Compressive strength results refer to 28 days curing. Averages refer to 6 samples in series 1 and 3 in series 2.

Oxides		Danish ordinary portland cement	High alkali portland cement	Fly ash 0038	Fly ash 0029
S	%	21.2	20.3	49.5	50.7
A	%	4.7	4.5	22.4	24.9
F	%	2.8	2.9	10.1	7.7
C	%	64.2	63.4	6.3	5.4
M	%	1.2	2.3	3.6	2.5
$\bar{S}$	%	2.6	3.2	0.7	0.7
LOI	%	1.3	0.9	3.2	3.9
Na_2O	%	0.33	0.40	0.59	0.93
K_2O	%	0.53	1.13	2.64	3.80
Na_2O eq	%	0.68	1.14	2.33	3.43

Table 4. Composition of cements and fly ashes used in alkali-silica reactivity tests.

Cement type	Temperature °C	Curing time 28 days w/c ratio 0.40	0.50	0.60	90 days w/c ratio 0.40	0.50	0.60
Rapid hardening portland cement	20	-	122	-	-	100	-
	30	67	132	263	45	125	257
	50	-	289	-	-	284	-
Low alkali sulfate resistant portland cement	20	-	151	-	-	140	-
	30	106	193	279	83	171	160
	50	-	370	-	-	388	-
Portland-fly ash	20	-	92	-	-	29	-
	30	41	116	139	5.8	37	88

Table 5. Effective diffusion coefficients for cement pastes, 10^{-13} m^2/s.

Type of cement	Cement content kg/m^3	w/c ratio	Compressive strength MPa (28 days)	Depth of carbonation mm average	mm std.dev.	Age years
Rapid hardening portland cement	260	0.54	22	2.1	1.0	2.0
	340	0.43	37	1.3	0.5	1.8
Low alkali sulfate resistant portland cement	260	0.52	29	3.0	1.2	2.0
	340	0.42	36	<0.5	-	1.8
	390	0.36	51	0.8	0.4	1.8
Portland-fly ash cement	260	0.54	29	2.7	1.4	1.7
	340	0.44	30	2.8	0.8	2.0
	390	0.42	35	1.8	0.7	1.8

Table 6. Depth of carbonation for concretes with different cement types.

Cement type		Cement content kg/m^3	w/c ratio	Air content %	Compressive strength 28 days MPa	Scaling, 25 cycles Slabs 28 days kg/m^2	Drilled cores 2 years kg/m^2
Rapid hardening portland cement		261	0.54	5.5	28	0.11	0.00
		255	0.53	6.0	32	0.03	
	*	334	0.43	5.0	38	0.15	0.00
Low alkali sulfate resistant portland cement		264	0.52	5.0	25	2.60	0.03
		262	0.51	5.5	32	0.33	
	*	340	0.42	6.0	40	0.06	0.01
	*	390	0.36	5.0	48	0.07	0.00
Portland-fly ash cement		257	0.52	4.5	28	0.68	
		261	0.54	5.5	27	0.31	0.32
	*	333	0.44	5.0	32	0.09	0.00
	*	341	0.45	5.0	33	0.15	
	*	397	0.42	3.0	38	0.11	0.02

Table 7. Freeze/thaw resistance according to ISO 4846 of concretes with different cement types.

J. Almeborg and J. T. Christensen, Aalborg Portland, Denmark

Danish Portland-Fly Ash Cement

		Requirements	Power plant no. 1	2	3	4	5	6	7	8	All
S	%	>40.0	53.2 3.3	54.5 2.9	54.0 8.0	51.0 2.9	56.3 3.9	51.8 2.3	52.3 2.4	53.2 3.7	53.3 4.5
A	%		25.1 1.9	29.7 2.1	32.0 4.6	30.7 3.6	28.3 3.2	30.6 3.3	32.2 0.7	32.4 3.5	29.7 4.0
F	%		9.3 1.5	6.7 1.2	4.9 1.4	7.2 1.8	6.3 1.4	6.6 1.8	5.2 0.8	6.0 2.6	6.7 2.1
C	%	<12.0	5.2 0.9	4.8 1.3	6.5 2.5	6.1 1.4	4.6 2.8	6.3 1.1	7.3 1.3	5.1 1.9	5.7 1.9
M	%	<5.0	3.2 0.6	1.9 0.5	1.4 0.5	2.2 1.1	1.6 0.5	2.3 1.1	1.8 0.5	1.4 0.8	2.0 1.0
$\bar{S}$	%	<3.0	1.0 0.3	0.6 0.2	0.5 0.2	0.8 0.3	0.6 0.2	0.6 0.2	0.6 0.2	0.5 0.2	0.7 0.3
LOI	%	<5.0	3.0 0.6	1.3 0.3	3.2 0.7	2.6 0.5	2.7 0.7	3.2 0.6	3.1 0.6	2.5 0.4	2.7 0.8
Avail. Na_2O eq.	%	<1.5	0.8 0.1	0.4 0.1	0.2 0.1	0.5 0.2	0.5 0.1	0.4 0.2	0.3 0.1	0.4 0.2	0.5 0.2
Residue on 45µm	%	<40.0	26.3 3.7	23.6 3.6	30.7 4.3	25.5 3.7	20.7 5.8	20.8 2.4	26.6 2.1	22.8 2.8	24.7 5.0
Compr. strength DS 427 MPa 1 day			10.3 0.9	10.0 0.9	9.3 1.1	9.8 1.0	10.7 1.1	9.6 0.9	9.6 1.0	10.4 0.8	10.0 1.1
7 days			30.9 1.8	30.9 1.6	29.8 2.0	30.5 2.3	30.9 1.9	30.2 2.0	29.2 2.4	32.3 0.8	30.6 2.0
28 days			41.8 2.2	42.1 1.5	40.3 2.6	41.3 2.9	42.5 2.3	40.9 2.3	40.2 1.9	43.3 1.5	41.6 2.4
56 days			52.1 2.7	51.3 1.9	48.8 3.0	50.6 3.3	53.0 3.3	50.7 3.1	49.5 2.1	53.4 1.4	51.2 3.2
Setting time min. Initial			180 20	188 20	203 33	202 28	178 16	201 21	209 37	190 24	193 27
Final			213 22	222 25	236 38	239 33	208 19	234 23	241 39	224 27	226 30
Number of samples			31	18	26	30	27	23	11	16	182

Table 8. Average(first line) and standard deviation(second line) for chemical and physical data for samples from 8 Danish power plants. Compressive strengths and setting times are measured on a mix of 70% rapid hardening portland cement and 30% fly ash. Soundness of all mixes was 0 mm. Requirements not shown in the table: Moisture <1.5%, S+A+F >70%, Cl^- <0.1%.

J. Almeborg and J. T. Christensen, Aalborg Portland, Denmark

Danish Portland-Fly Ash Cement

Figures

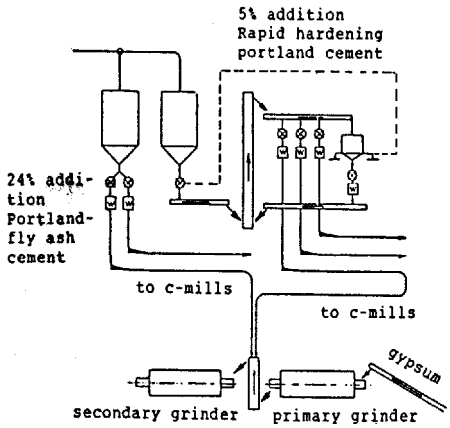

Figure 1. Diagram of mill installations for production of portland-fly ash cement

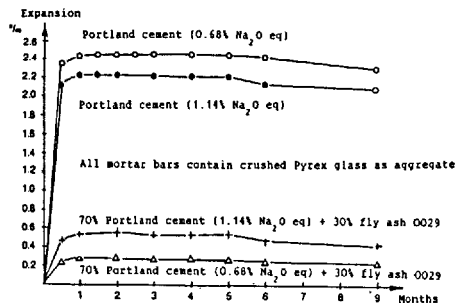

Figure 2. Time-expansion curves for mortar bars (ASTM C 441)

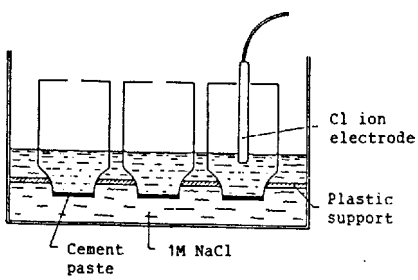

Figure 3. Schematic drawing of experimental arrangement for diffusion measurements

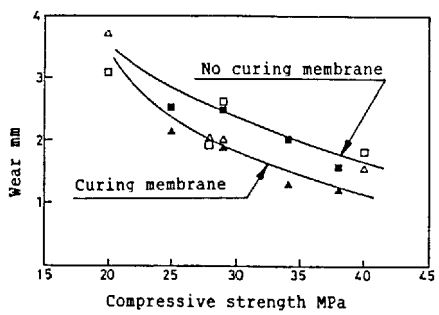

Figure 4. Effect of curing membrane and compressive strength on wear resistance

- △ Portland-fly ash cement, curing membrane
- □ Portland-fly ash cement, no curing membrane
- ▲ Rapid hardening portland cement, curing membrane
- ■ Rapid hardening portland cement, no curing membrane

J.P. OLLIVIER - Laboratoire de Génie Civil - I.N.S.A-U.P.S.-Toulouse - France

RÔLE DES ADDITIONS MINÉRALES SUR LA FORMATION DE L'AUREOLE DE TRANSATION ENTRE GROS GRANULAT ET MORTIER

La structuration de l'auréole de transition, zone de liaison entre la pâte de ciment et les granulats, a fait l'objet de nombreuses études dans le cas des ciments portland. C'est en effet le point faible des bétons puisqu'elle présente une forte porosité et une morphologie cristalline qui lui confèrent de mauvaises caractéristiques mécaniques et en font un chemin privilégié pour la migration des agents aggressifs.

Les additions minérales utilisées dans les ciments agissent sur certains paramètres qui commandent la formation de l'auréole de transition : l'arrangement granulaire au voisinage de l'interface avec les granulats, la vitesse d'hydratation, la fluidité de la pâte et le contrôle de l'hydratation du C_3A. Nous avons donc axé notre contribution sur les modifications de la zone de liaison apportées par diverses additions minérales.

Une première partie est consacrée à des additions dont la granularité est voisine de celle des grains de clinker et qui peuvent être utilisées comme filler sans fluidifiant (cendres volantes, laitier, calcaire).

Dans une seconde partie nous présentons l'action de la fumée de silice de granularité très inférieure à celle du clinker dont l'emploi comme ajout nécessite l'usage d'un fluidifiant. Nous étudions en particulier le rôle de la nature de la silice sur la structuration de l'auréole de transition.

I - METHODE EXPERIMENTALE

L'auréole de transition formée au voisinage des gros granulats d'un béton est étudiée au moyen d'une éprouvette mixte constituée d'un bloc de marbre plan poli contre lequel est coulé un mortier ou une pâte pure de ciment. Après rupture au voisinage immédiat de l'interface, les deux demi-éprouvettes sont observées au microscope électronique à balayage (MEB). La structuration de la phase liante (pâte ou mortier) est analysée par diffraction de rayons X (DRX) selon la méthode d'abrasion progressive (1). Cette méthode permet :

- de caractériser l'orientation préférentielle des cristaux de portlandite qui se développent avec leur axe c perpendiculaire au gros granulat. On défini à cet effet un indice I d'orientation dont on étudie la variation avec la distance δ à l'interface ;

- de connaître la répartition des phases anhydres ou hydratées cristallisées depuis la surface de rupture jusqu'au coeur de l'éprouvette.

II - RAPPEL SUR LA STRUCTURATION DE LA PATE DE CIMENT PORTLAND NON FILLERISEE AU VOISINAGE D'UN GROS GRANULAT

La variation de l'indice d'orientation des cristaux de CH varie typiquement en fonction de la distance à l'interface selon la courbe de la figure 1.

On rappelle que :

$$I = \frac{\text{intensité raie (00.1)}/\text{intensité raie (10.1)}}{0,74}$$

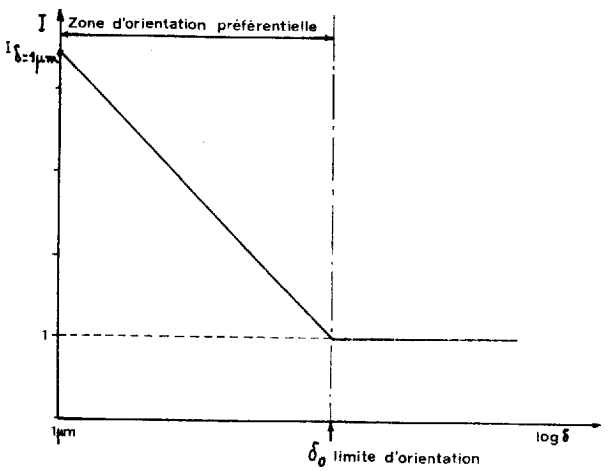

Figure 1 - Schéma caractéristique de l'orientation des cristaux de CH au voisinage d'un gros granulat.

L'orientation préférentielle de la portlandite et l'hydratation particulière de la pâte sont interprêtées par l'existence d'un gradient de teneur en eau dû à un effet de paroi entre le gros granulat et les grains de ciment (2). L'amplitude de l'orientation des premiers cristaux voisins de l'interface est déterminée par les conditions d'hydratation du C_3A et du C_3S selon le schéma de la figure 2 dans le cas d'un granulat inerte.

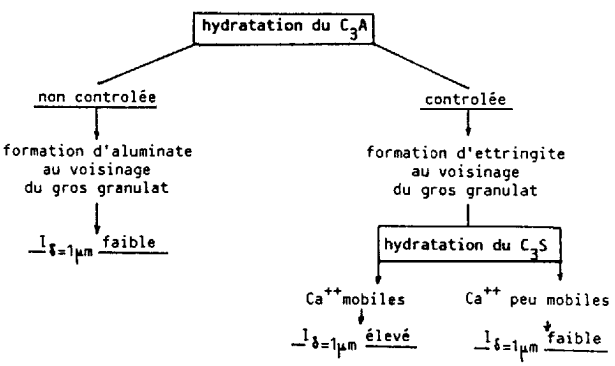

Figure 2 - Analyse schématique de la croissance des cristaux de portlandite dans l'auréole de transition

Dans le cas d'un gros granulat calcaire, l'orientation des premiers cristaux de CH est notablement diminuée si la calcite réagit précocement avec les aluminates de calcium hydratés c'est-à-dire si la réaction du C_3A n'est pas efficacement contrôlée par les sulfates.

La limite d'orientation δ_0 augmente avec les possibilités de migration des ions Ca^{++} dans la pâte de ciment. Dans le cas des pâtes pures δ_0 est ainsi une fonction croissante de la teneur en eau de gâchage et du temps de début de prise.

III - INFLUENCE D'ADDITIONS MINERALES DE DE GRANULARITE VOISINE DE CELLE DU CIMENT SUR LA FORMATION DE L'AUREOLE DE TRANSITION

Les additions minérales jouent un rôle physique sur le comportement rhéologique de la pâte fraîche de ciment et chimique sur son hydratation. Leur présence peut donc agir sur la formation de l'auréole de transition. Ceci a été vérifié avec des cendres et des laitiers par CARLES et al (3, 4) dont nous résumons tout d'abord les principaux résultats. Nous présenterons par la suite d'autres résultats plus partiels obtenus avec des fillers calcaires (5).

Les études avec cendres et laitiers ont été conduites au moyen d'éprouvettes mixtes confectionnées avec des pâtes à base d'un ciment CPA 55 R gachées à une concentration volumique $\gamma = \frac{c}{c+e} = 0,527$ sur un marbre de carrare (teneur en $CaCO_3 > 99$ %). Trois ajouts ont été utilisés au taux unique de substitution de 30 %. Il s'agit :

- d'une cendre volante de houille n°1 (395 $m^2 kg^{-1}$ Blaine) ;
- d'une cendre volante de lignite n°2 (210 $m^2 kg^{-1}$ Blaine) ;
- d'un laitier de fonte Thomas granulé broyé à 350 $m^2 kg^{-1}$ Blaine.

La composition chimique du ciment (320 $m^2 kg^{-1}$ Blaine) et des additions est indiquée au tableau 1

	SiO_2	Al_2O_3	Fe_2O_3	CaO	MgO	Na_2O	K_2O	SO_3	Perte au feu
ciment	21,4	5,3	2,3	64,0	1,4	0,04	0,49	2,98	1,02
cendre n°1	54,8	27,1	8,8	3,3	2,1	0,3	2,6	0,9	3,6
cendre n°2	24,8	14,9	10,1	50,7*	3,7	0,8	1,0	9,1	0,4
laitier	33,1	11,4	FeO = 1,90	42,4	8,3	0,6			

* dont 28 % de chaux libre

TABLEAU 1

Composition chimique du ciment, des cendres et du laitier

La croissance des cristaux de CH aux premiers ages peut être analysée au moyen des courbes de la figure 3.

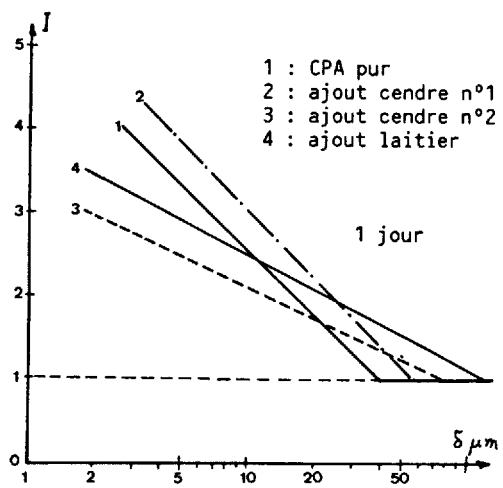

Figure 3 - Croissance préférentielle des cristaux de portlandite dans des ciments fillérisés au voisinage d'un gros granulat.

La limite d'orientation δ_o est d'autant plus grande que la ressuée est importante après la mise en place. Celle-ci augmente si le pourcentage de grains irréguliers, la porosité ouverte ou la surface spécifique des grains de l'ajout diminuent. La valeur de δ_o et l'orientation préférentielle des cristaux de CH formés au voisinage immédiat de l'interface, caractérisée par $I_{\delta=1\mu m}$, peuvent être analysées comme suit d'après les indications de la figure 2.

* cendre de houille n°1 :

La grande porosité (7%) explique que cet ajout n'ait qu'un faible rôle fluidifiant. La valeur de δ_o est donc peu accrue par rapport à celle de la pâte pure (65 µm au lieu de 40 µm). Cette cendre apporte des sulfates rapidement solubles qui contribuent à la formation d'ettringite autour des grains de C_3A. Il n'apparaît donc pas d'aluminate hydraté et la surface du gros granulat de marbre demeurant inattaquée et plane, les cristaux de portlandite ont un indice d'orientation élevé.

* cendre de lignite n°2 :

La faible surface spécifique, ajoutée à la forme sphérique de nombreux grains et à l'inexistence d'une porosité ouverte notable font que cette cendre est un excellent fluidifiant. La limite d'orientation δ_o est donc notablement accrue (de 40 μm à 90 μm).

La composition chimique de cette cendre est remarquable par ses hautes teneurs en sulfate et en chaux avec une fraction importante de cette dernière sous forme de CaO libre. La désorientation des cristaux de portlandite au voisinage du gros granulat s'explique ici par l'existence de germes de cristallisation homogène formés autour des grains de cendre par l'extinction de la chaux vive qu'ils contiennent. Un résultat analogue a été obtenu par l'utilisation de germes de CaO ou de $Ca(OH)_2$ mélangés au ciment : cette activation cristallochimique conduit à une forte désorientation des cristaux de portlandite dans l'auréole de transition (6).

* laitier de fonte :

Le laitier granulé a une action fluidifiante sur la pâte de ciment ce qui se traduit par une augmentation de la valeur de δ_o. Dans l'auréole de transition le rapport eau/clinker est accru par rapport au cas des CPA purs. Les seuls sulfates présents provenant de la dissolution du gypse, le contrôle de l'hydratation du C_3A est alors insuffisant pour éviter la formation d'aluminates de calcium hydratés au voisinage du gros granulat. Les cristaux de portlandite formés sont alors plus faiblement orientés, la modification étant encore plus importante au voisinage des granulats calcaires qui sont corrodés avec la formation de carboaluminate.

Le laitier et les cendres utilisés dans ces essais ne sont pas des additions inertes ; leur réaction contribue donc au remplissage progressif de la porosité de l'auréole de transition comme de celle de la masse de la pâte. Au fur et à mesure du temps l'évolution de l'orientation préférentielle des cristaux de portlandite près de l'interface est très faible : légèrement croissante avec le laitier et décroissante avec les cendres. Enfin la faible pouzzolanicité des cendres utilisées n'a pas permis de mettre en évidence la consommation de la portlandite par DRX avant 6 mois ni dans la pâte, ni dans l'auréole de transition.

* Fillers calcaires:

Comme les additions précédentes les fillers calcaires utilisés comme ajout ont une surface spécifique de l'ordre de celle du clinker qu'ils remplacent. Par conséquent l'effet de paroi entre grains de ciment et gros granulat ne devrait pas être notablement modifié. On constate effectivement que l'orientation des cristaux de portlandite est peu affectée par l'ajout de filler calcaire (5).

Des études morphologiques de faciès de rupture d'éprouvettes mixtes ont montré l'existence d'un film dense d'hydrates, essentiellement constitué de portlandite, déposé sur le granulat (7). Ce film est analogue à celui observé avec des ciments portland non fillérisés ou contenant des ajouts de cendre volante ou de laitier. Avec un filler silico-calcaire cette morphologie est modifiée : il se forme alors davantage d'ettringite bien cristallisée au voisinage de l'interface.

Les fillers calcaires se distinguent des cendres et laitiers par leur réaction avec les aluminates de calcium qui conduit à la formation du carboaluminate $C_3A.CaCO_3.11H_2O$ (8). Dans l'auréole de transition comme dans le coeur de la pâte cette réaction de la calcite se fait concurremment avec celle du gypse (7). Ainsi, près de l'interface, la forte teneur locale en eau due à l'effet de paroi entraîne un développement plus abondant des aluminates hydratés (9) qui réagissent avec le filler calcaire pour former davantage de carboaluminate (5). Cette activité chimique des fillers calcaires a des conséquences favorables sur la résistance mécanique et la porosité des pâtes de ciment ou des mélanges C_3A + $CaCO_3$ (10). Puisqu'elle y est plus intense qu'à coeur on peut penser que ses conséquences sont encore plus importantes dans l'auréole de transition.

IV - INFLUENCE DE LA FUMEE DE SILICE CONDENSEE SUR LA FORMATION DE L'AUREOLE DE TRANSITION

La fumée de silice se distingue des additions précédentes par sa grande surface spécifique (de l'ordre de 20 000 m^2kg^{-1}) et sa réaction pouzzolanique rapide. Comme l'ont noté récemment Carles-Gibergues et al. (11) et Oudjit (12) il y a lieu de considérer que la fumée de silice ne présente pas la même réactivité quelle que soit sa provenance et qu'en particulier sa teneur en impuretés, notamment en carbone, joue un très grand rôle.

Nous avons indiqué par ailleurs (13) le rôle d'une fumée de silice sur la formation de l'auréole de transition ; nous présentons ici l'influence de la nature de la fumée de silice sur cette zone de contact dans la continuité des travaux de Carles-Gibergues.

Les études ont été effectuées au moyen d'éprouvettes mixtes associant un gros granulat de marbre de carrare et un mortier préparé avec un rapport liant/sable calcaire = 1,5. Ce rapport est choisi conformément au dosage du mortier retenu dans les bétons de haute résistance préparés avec 700 kg de ciment par m^3. Nous présentons tout d'abord les résultats obtenus en l'absence de fluidifiant comme dans le chapitre précédent. Dans l'optique d'une application à l'analyse du comportement des bétons de haute résistance nous présenterons ensuite l'influence de la nature de la fumée de silice en présence de naphtalène sulfonate.

Les caractéristiques des silices choisies sont reportées au tableau 2. Nous avons choisi une silice réactive (n°1) et une autre contenant un pourcentage élevé de carbone qui la rend moins réactive aux jeunes âges (n°2). Nous avons également utilisé la silice n° 2 chauffée à 550°C de façon à brûler son carbone résiduel : après traitement, elle est repérée silice n°3 dans nos résultats.

	SiO_2	Na_2O	MgO	Al_2O_3	CaO	MnO	K_2O	Fe_2O_3	SO_3	Cl^-	C 500°C	Perte au feu
Silice n°1	93,4	0,4	1,9	0,8	0,3	'	1,3	0,9	0,7	0,2	0,1	3,9
Silice n°2	81	0,5	2,5	0,8	0,1	0,1	3	1,5	0,4		5	10,2

Silice n°1 S_s BET = 19 000 $m^2 kg^{-1}$
Silice N°2 S_s BET = 23 000 $m^2 kg^{-1}$

TABLEAU 2

Caractéristiques des fumées de silice

IV - 1- Influence de la nature de la fumée de silice en l'absence de fluidifiant

Les différents mortiers sont préparés avec une teneur pondérale en eau (eau/ciment + silice) = 0,40

Les courbes de la figure 4 illustrent la croissance préférentielle des cristaux de portlandite dans le mortier au voisinage du gros granulat. Les deux silices dosées à 10 % en poids de liant conduisent à une réduction notable de l'indice d'orientation. Ceci peut s'expliquer par la diminution de la porosité près de l'interface due au remplissage des vides intergranulaires par les grains de fumée de silice qui jouent également le rôle de germe de cristallisation pour la portlandite. En outre il y a lieu de noter que la silice n°1 accélère l'hydratation du ciment et diminue la fluidité ce qui contrarie le libre développement des cristaux de portlandite. La silice n°2 entraîne au contraire un retard aux jeunes âges mais il se forme une plus grande quantité d'aluminates hydratés dans l'auréole de transition.

Comme dans le cas des échantillons préparés avec du ciment pur, on peut enfin remarquer que l'ettringite se forme en plus grande quantité au voisinage du gros granulat avec la silice comme l'indiquent les courbes de la figure 5. Ceci s'explique par la diffusion des ions SO_4^{--} vers l'interface due à l'existance d'un gradient de teneur en eau. En outre, dans le cas de la silice n°2 la quantité d'ettringite est plus importante que pour les autres échantillons. Il semble donc que le C_3A s'hydrate plus rapidement avec cet ajout puisque nous avons mentionné précédemment que la quantité d'aluminate hydraté était elle aussi plus importante.

L'examen du MEB indique que la morphologie des faces de rupture des éprouvettes mixtes n'est pas affectée par l'addition de silice aux jeunes âges. On retrouve, côté granulat (figure 6), des dépots de portlandite analogues à ceux présentés dans le cas des éprouvettes mixtes préparées sans silice (figure 7).

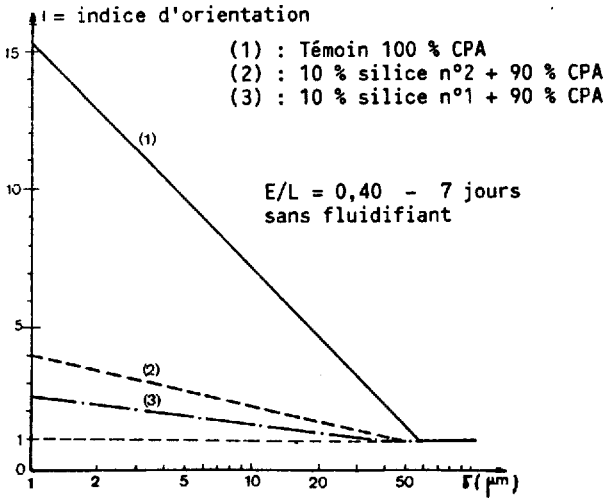

Figure 4 - Orientation des cristaux de portlandite dans les mortiers au voisinage d'un gros granulat : influence de la nature de la silice en l'absence de fluidifiant.

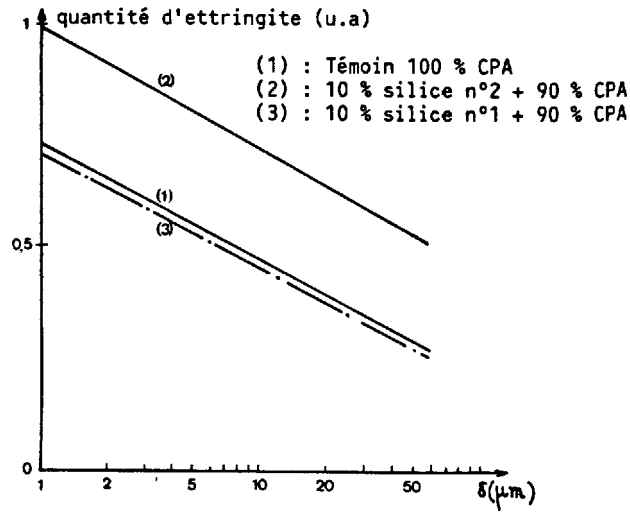

Figure 5 - Formation de l'ettringite au voisinage d'un gros granulat dans des mortiers préparés sans fluidifiant (E/L = 0,40 - 7 jours)

La figure 8 illustre le faciès de rupture côté mortier d'une éprouvette préparée avec de la silice n°2 âgée de 7 jours. Sous le film dense de portlandite l'ettringite finement cristallisée s'est développée de façon plus abondante que dans les autres éprouvettes ce qui confirme les analyses par DRX.

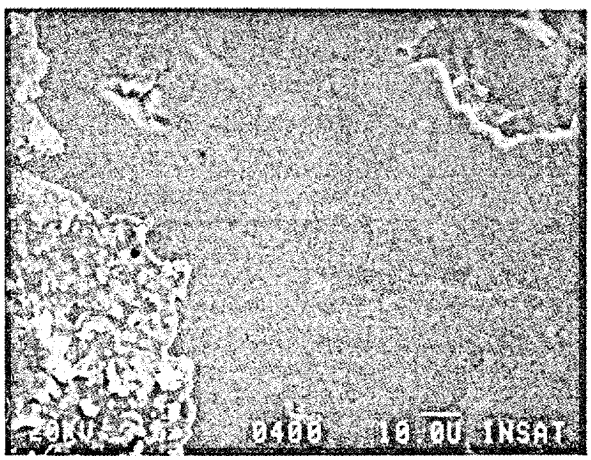

Figure 6 - Face de rupture côté granulat d'une éprouvette mixte préparée avec un mortier contenant de la silice n°2 (10% du liant) sans fluidifiant (E/L = 0,40 - 7 jours)

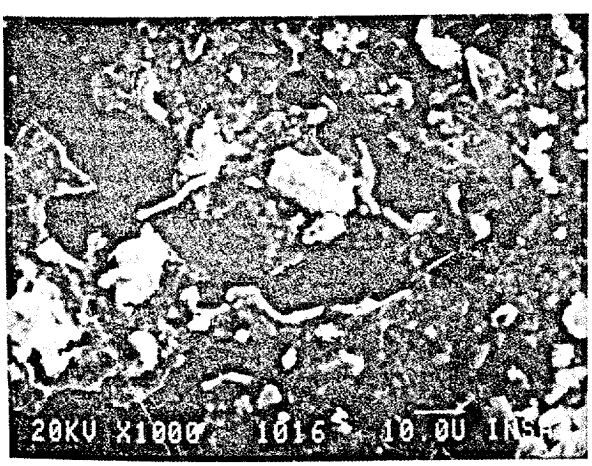

Figure 7 - Face de rupture côté granulat d'une éprouvette mixte préparée avec un mortier sans silice et sans fluidifiant (E/L = 0,40 - 7 jours)

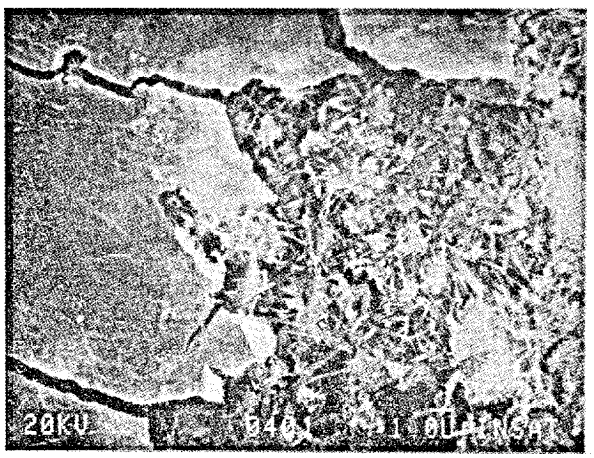

Figure 8 - Eprouvette analogue à celle de la figure 7 face de rupture côté mortier

IV -2- Influence de la nature de la fumée de silice en présence de fluidifiant

IV -21- Hydratation des mortiers en présence de fluidifiant

La cinétique d'hydratation a été analysée par calorimétrie adiabatique sur des mortiers 1/3. Les courbes de la figure 9 indiquent la variation des instants d'apparition du maximum du flux thermique en fonction du dosage en fluidifiant.

Avec la silice n°1 l'hydratation aux jeunes âges est toujours accélérée par rapport au témoin ne contenant pas de silice pour un dosage en fluidifiant inférieur à 4 %. Ce résultat n'est pas vérifié quelque soit le dosage en fluidifiant ; nous avons en effet pu vérifier que pour une valeur de 10 % il y avait au contraire un retard par rapport au témoin.

Avec la silice n°2 le changement de comportement se produit à un dosage beaucoup plus faible en fluidifiant (de l'ordre de 4%) qui correspond à une valeur extrême utilisée dans la fabrication des bétons de haute résistance. Buil |14| a déjà mentionné que la silice pouvait avoir ce rôle retardateur aux forts dosages en fluidifiant. Nous indiquons ici que toutes les silices ne se comportent pas de la même manière et nous pensons que ceci peut être attribué aux impuretés présentes. En effet avec la silice n°3 (silice n°2 réchauffée à 550°C) et 4% de fluidifiant, le maximum de flux thermique apparaît au bout de 10 heures comme dans le cas de la silice n°1 au lieu de 14,5 heures avant le réchauffage.

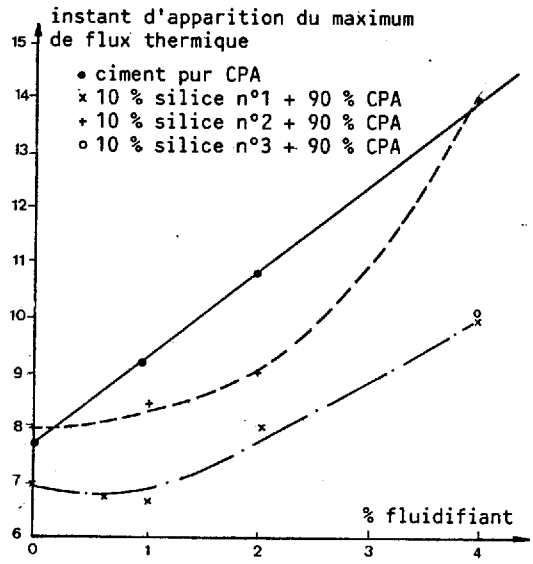

Figure 9 - Influence de la nature de la fumée de silice et du dosage en naphtalène sulfonate sur l'hydratation des mortiers.

IV -22- Formation de l'auréole de transition

Les courbes des figures 10, 11 et 12 représentent l'orientation préférentielle des cristaux de portlandite au voisinage d'un gros granulat dans des mortiers préparés respectivement avec 1% de fluidifiant et diverses silices dosées à 10%, 4% de fluidifiant et diverses silices dosées à 10%, 4% de fluidifiant et divers dosages de la silice n°1.

En l'absence de silice et comme nous l'avons indiqué par ailleurs |13| les cristaux de portlandite restent bien orientés au voisinage du gros granulat.

Au contraire, la présence de fumée de silice conduit à une désorientation des cristaux de portlandite dans la zone interfaciale quelque soit le dosage en fluidifiant. Les courbes de la figure 13 permettent de vérifier l'une des hypothèses formulées précédemment pour expliquer ceci : le rôle de remplissage des grains de silice. Lorsque le dosage en silice augmente (à teneur en eau constante) on observe une désorientation progressive des cristaux de portlandite dans l'auréole de transition. Par ailleurs la répartition des cristaux d'ettringite dans cette zone est modifiée à cause de la diminution du gradient de teneur en eau (figure 13). Les vides intergranulaires sont progressivement comblés par les quantités croissantes de silice bien dispersée au voisinage du gros granulat. De même que pour les ions SO_4^{--}, la migration des ions Ca^{++} vers l'interface est alors plus faible et les cristaux de portlandite sont faiblement orientés malgré la bonne fluidité des mortiers

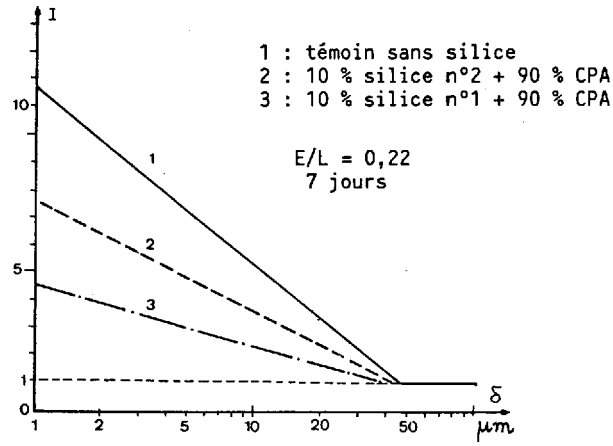

Figure 10 - Orientation des cristaux de portlandite dans les mortiers au voisinage d'un gros granulat : influence de la nature de la silice en présence de fluidifiant (1% en poids de ciment)

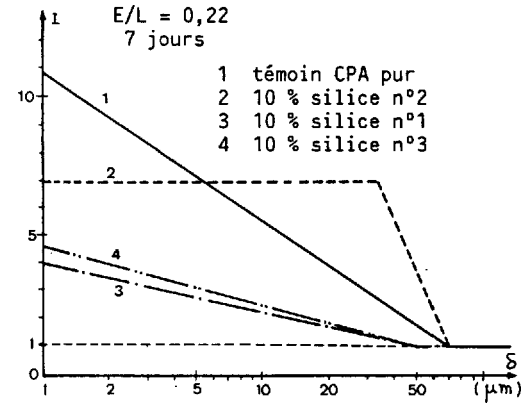

Figure 11 - Orientation des cristaux de portlandite dans les mortiers au voisinage d'un gros granulat : influence de la nature de la silice en présence de fluidifiant (4%)

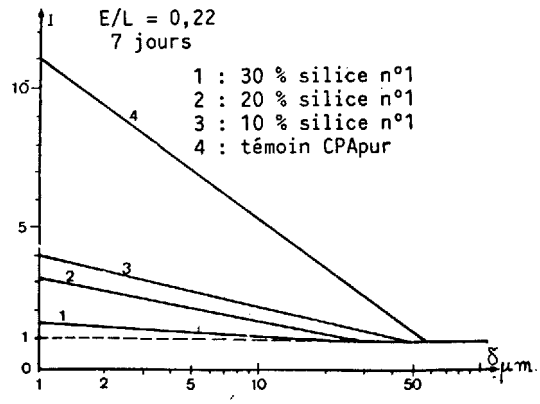

Figure 12 - Orientation des cristaux de portlandite dans les mortiers au voisinage d'un gros granulat : influence de la teneur en silice en présence de 4% de fluidifiant

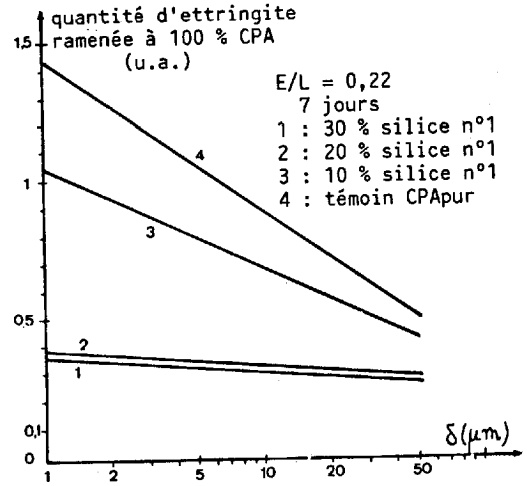

Figure 13 - Quantité d'ettringite formée dans les mortiers au voisinage d'un gros granulat : influence de la quantité de silice en présence de fluidifiant

Les figures 10 et 11 confirment l'influence relative des deux fumées de silice sur le développement des cristaux de portlandite au voisinage d'un gros granulat. Comme en l'absence de fluidifiant, la silice n°1 modifie davantage l'orientation préférentielle que la silice n°2. Ceci est probablement dû, comme l'indique la figure 9, à une accélération plus importante de l'hydratation.

Avec un dosage de 4% en fluidifiant la courbe de la figure 11 relative à la silice n°1 présente un palier. Nous avons déjà noté une telle forme de courbe dans le cas des pâtes pures de ciment portland gâchées avec de fortes teneurs en eau |15|. On constate également un développement des cristaux de portlandite avec orientation constante dans une zone de 10 à 20 μm voisine de l'interface avec de très forts dosages en fluidifiant (10%) et avec ou sans la fumée de silice n°1. L'existence de ce palier n'est donc pas causée par la seule présence de fumée de silice bien que l'ajout d'une silice qui, par sa teneur en impuretés, retarde l'hydratation puisse permettre une telle croissance de la portlandite à de plus faibles dosages en fluidifiant. La teneur en impureté, notamment en carbone, peut effectivement être mise en cause car si on remplace la silice n°2 par la silice n°3 la courbe calorimétrique (cf. figure 9) et le développement des cristaux de CH (cf. la figure 10) sont pratiquement analogues à ceux obtenus avec la silice n°1.

L'examen au MEB des faciès de rupture des éprouvettes mixtes permet de compléter l'analyse de l'influence des silices.

Pour un dosage de 4% en fluidifiant les figures 14a et 14b représentent respectivement la face granulat et la face mortier d'une éprouvette âgée de 7 jours. Au voisinage immédiat du granulat la portlandite se développe sous forme de gros cristaux selon la face (00.1) parallèle à l'interface . La figure 14b montre que de petits cristaux de CH, bien formés mais plus petits, se développent à distance de l'interface de façon plus désordonnée.

Avec le même dosage en fluidifiant et 10% de la fumée de silice n°2 les figures 15a et 15b présentent des faces de rupture côté mortier également après 7 jours de conservation. De gros cristaux de portlandite se développent encore au voisinage de l'interface mais leur faciès est tout à fait différent : la croissance est beaucoup moins orientée qu'en l'absence de silice.

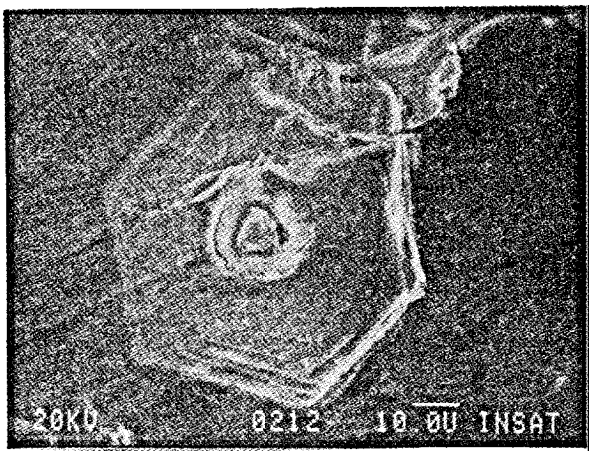

a - face granulat

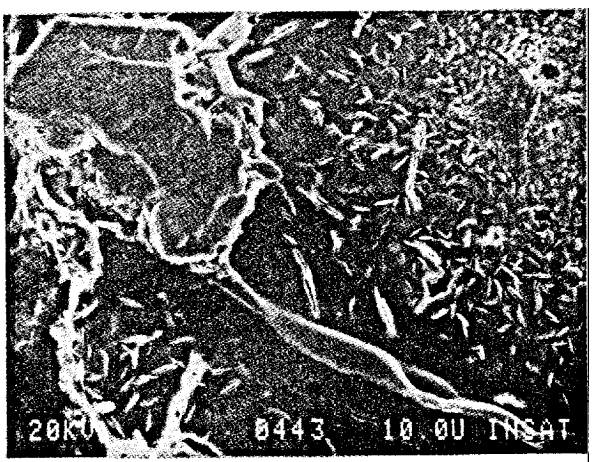

b - face mortier

Figure 14 - Faciès de rupture d'une éprouvette mixte le mortier est préparé avec 4% de fluidifiant sans silice (E/liant = 0,22 - 7 jours)

Enfin avec la silice n°1 les figures 16 a et b illustrent un troisième mode de croissance à faible orientation préférentielle (faces de rupture côté mortier).

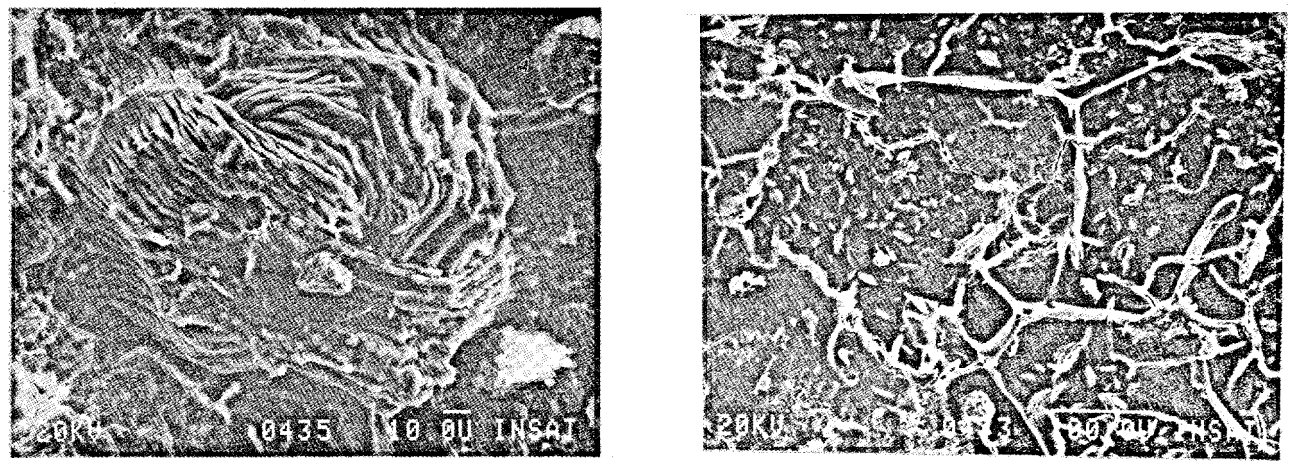

Figure 15 - Faciès de rupture d'une éprouvette mixte côté mortier : 4% fluidifiant, 10% silice n°2, E/liant = 0,22 = 7 jours

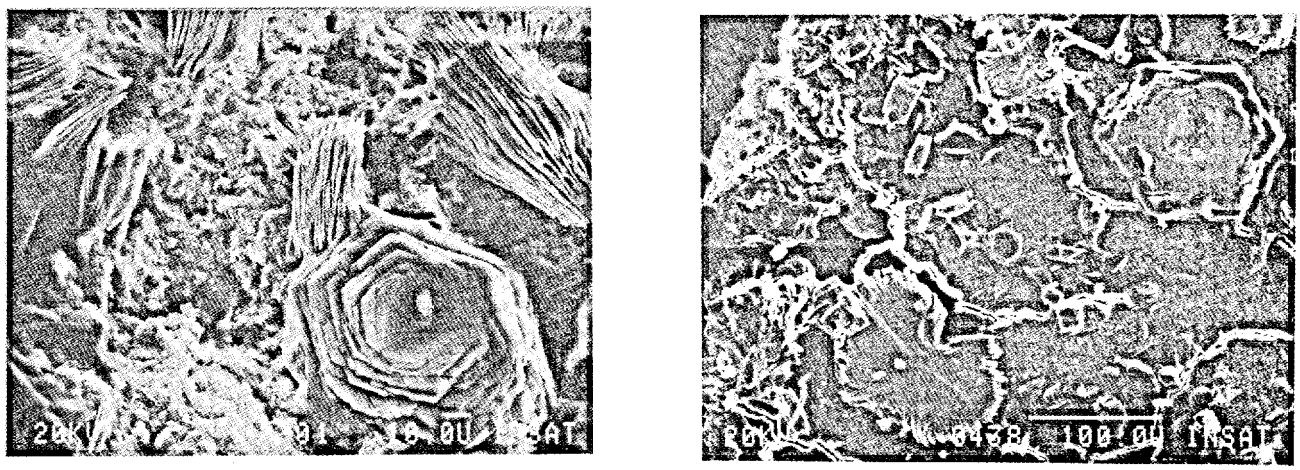

Figure 16 - Faciès de rupture d'une éprouvette mixte coté mortier : 4% de fluidifiant, 10% de silice n°1, eau/liant = 0,22, 7 jours

Ces clichés montrent que l'addition de fumée de silice modifie le développement de la portlandite vraisemblablement parce que ses grains constituent des germes de cristallisation. L'orientation préférentielle est alors logiquement plus faible mais il y a lieu de noter que la taille des cristaux formés au voisinage de l'interface n'est pas réduite. Nous pouvons enfin remarquer des structures filamenteuses sur les faces de rupture : nous pensons qu'elles sont dues à la condensation des molécules de naphtalène sulfonate qui, en migrant vers le granulat, ont saturé la zone de contact.

La microstructure de l'auréole de transition évolue considérablement entre 7 jours et 28 jours du fait de la réactions pouzzolanique. Celle-ci se manifeste par une diminution de l'intensité des pics de diffraction et par une modification du faciès des hydrates : les gros cristaux formés à l'interface se transforment en un gel de texture plus dense (figure 17).

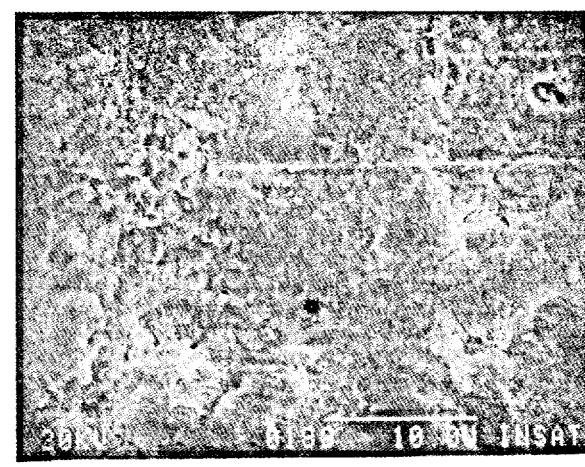

Figure 17 - face de rupture d'une éprouvette mixte côté granulat - mortier âgé de 28 jours 10% silice n°1

V - CONCLUSIONS

Les additions minérales agissent sur la formation de l'auréole de transition par leur présence physique et leur activité chimique.

Lorsque la granularité de l'ajout est voisine de celle des grains de clinker l'effet de paroi n'est pas notablement affecté. Cependant l'épaisseur de l'auréole de transition augmente si les additions minérales accroissent la fluidité de la pâte.
Lorsque la granularité de l'ajout est beaucoup plus faible que celle du clinker, la compacité au voisinage des interfaces avec les granulats augmente comme dans le reste de la phase liante. Un dosage suffisant en particules fines peut annihiler les caractéristiques néfastes de l'auréole de transition : gradient de teneur en eau et orientation préférentielle des cristaux de portlandite.

Les réactions chimiques des ajouts peuvent avoir des conséquences à la fois sur la formation de l'auréole de transition puis sur son évolution dans le temps.

Leur influence aux jeunes âges est essentiellement liée à la cristallogénèse des hydrates : ils peuvent constituer des germes de cristallisation (cas de la silice et des cendres contenant de la chaux vive) ou modifier la cinétique d'hydratation du clinker. A ce propos, il y a lieu de noter l'importance de leur action sur le contrôle de l'hydration du C_3A.

L'influence des additions minérales dans l'auréole de transition aux plus longues échéances n'est pas notablement différente de ce qu'elle est dans la masse du liant sauf lorsque l'environnement particulier favorise leur réaction. C'est le cas du filler calcaire avec les grandes quantités d'aluminates hydratés formés dans leur voisinage, près des interfaces. C'est aussi celui des fumées de silice qui peuvent réagir plus rapidement près de l'interface où la teneur en eau est localement plus élevée.

En conclusion lors du choix de la nature et des caractéristiques d'une addition minérale il est opportun de considérer son rôle spécifique dans l'auréole de transition. En effet si certaines additions contribuent à diminuer les performances du ciment, leur action bénéfique sur la zone de liaison pâte - granulat peut se traduire par une altération moins significative des qualités du béton. Les études aux interfaces et sur bétons doivent de ce fait constituer l'un des éléments d'analyse pour l'optimisation des additions minérales.

Remerciements :

Le document présenté ici constitue une synthèse de travaux dont la plupart ont été effectués au laboratoire de Génie Civil I.N.S.A.-U.P.S. de Toulouse. En plus des chercheurs cités dans ce texte je souhaite remercier M. HANNA pour la part prise dans l'étude des fumées de silice.

BIBLIOGRAPHIE

(1) J. GRANDET, J.P. OLLIVIER. Nouvelle méthode d'étude des interfaces ciment-granulat. 7ème Congrés Int. de la Chimie des Ciments. VII.85. Paris 1980.

(2) J.P. OLLIVIER, J. GRANDET. Processus de formation de l'auréole de transition. Liaisons pâtes de ciment - matériaux associés. Colloque Int. Toulouse 17-19 novembre 1982.

(3) A. CARLES-GIBERGUES, J. GRANDET, J.P. OLLIVIER. Modification of the ciment paste-aggregate interfacial region due to addition of fly ash or silica fume in mortars of portland cement. MRS Meeting Boston, novembre 1981.

(4) A. CARLES-GIBERGUES, J. GRANDET, J.P. OLLIVIER. Evolution dans le temps de l'auréole de transition de pâte contenant des ajouts. Ib (2).

(5) ESCADEILLAS. communication personnelle.

(6) J.P. OLLIVIER, J. GRANDET. Désorientation des cristaux de portlandite dans l'auréole de transition. Ib (2).

(7) B. MORTUREUX, H. HORNAIN, M. REGOURD. Liaison pâte de ciment - filler dans les ciments composés. Ib (2).

(8) J. FARRAN. Contribution minéralogique à l'étude de l'adhérence entre les constituants hydratés du ciment et les matériaux enrobés. Revue des matériaux de construction. n°s 490 - 491 - 492, 1956.

(9) J. GRANDET, J.P. OLLIVIER. Etude de la formation du monocarboaluminate de calcium hydraté au contact d'un granulat calcaire dans une pâte de ciment portland. Cem. concr. Res. vol. 10, pp. 759 - 770, 1980.

(10) J. JAMBOR. Binding capacity of calcium aluminate hydrates containing other ions. Ib (2).

(11) P.C. AITCIN, A. CARLES-GIBERGUES, N. OUDJIT, A. VAQUIER. Influence des éléments autres que Si sur la réactivité des fumées de silice. Congr. Int. Ch. des Ciments Rio 1986.

(12) M. N. OUDJIT. Réactivité des fumées de silice condensées en présence de chaux ou de ciment portland. Thèse D.I. I.N.S.A. de Toulouse 1986.

(13) J.P. OLLIVIER, B. HANNA. Action d'un fluidifiant et d'une fumée de silice condensée réactive sur la formation de la liaison gros granulat-mortier Congr. Int. Chimie des Ciments Rio 1986.

(14) M. BUIL, A.M. PAILLERE, B. ROUSSEL. High strength mortars containing condensed silica fume. Cem. and Concr. Res. Vol. 14. pp.693 704 , 1984.

(15) J.P. OLLIVIER. Contribution à l'étude de l'hydratation de la pâte de ciment portland au voisinage des granulats. Thèse d'Etat. Toulouse 1981.

(16) Ph. PINSONNEAULT. Influence des fumées de silice sur les propriétés physiques et chimiques des bétons et des mortiers. Université de Sherbrooke 1983.

R.GUYOT, R.RANC, B.CARIOU
LAFARGE COPPEE RECHERCHE, FRANCE

UTILISATION DE LA POTENTIALITE HIDRAULIQUE DU CLINKER DANS LES CIMENTS PORTLAND AVEC AJOUT DE FILLERS CALCAIRES

1 - INTRODUCTION

Les ciments avec ajout calcaire se sont développés en France depuis 1979, date à partir de laquelle la Normalisation Française a autorisé leur fabrication et leur commercialisation en même temps qu'elle établissait des exigences très strictes au niveau des performances et de la régularité.

Le respect des exigences de performances imposées par la Règlementation et l'adéquation du produit aux besoins réels du marché ont conduit à des ciments dont le taux d'ajout calcaire se situe actuellement entre 10 et 25 % suivant les classes de résistances, mais plus généralement autour d'un taux de 20 % d'ajout calcaire.

En 1983, sur vingt-trois millions de tonnes de ciment consommées en France, il y en a 16,5 millions de tonnes ayant un taux d'ajout compris entre 5 et 35 % qui se distribuent ainsi : 7,7 millions de tonnes de ciment, où rentrent des ajouts de filler calcaire, soit seuls, soit en association avec du laitier, des cendres ou des pouzzolanes ; 4,8 millions de tonnes de ciment avec ajout de laitier seul ; 2,8 millions de tonnes de ciment avec ajout de cendres ou pouzzolanes seules et 1,2 millions de tonnes de ciment avec ajout mixte laitier-cendres. Ceci montre la part importante des ciments avec ajout et en particulier de ceux qui ont comme constituants des fillers calcaires.

Pour que ces ciments à taux d'ajout calcaire relativement élevé puissent se développer commercialement et avoir la part de marché qu'ils occupent actuellement, il était nécessaire de bien montrer qu'un ciment Portland avec ajout de filler calcaire (CPJ) possède les mêmes propriétés que le ciment Portland pur sans ajout (CPA) issu du même clinker et appartenant à la même classe de résistance en compression à vingt-huit jours.

Il arrive en effet que ce point soit contesté en tenant le raisonnement spécieux suivant : "Lorsqu'un ciment Portland pur (CPA) et un ciment Portland avec ajout de filler calcaire (CPJ) appartenant à la même classe de résistance à vingt-huit jours sont gâchés au même rapport eau sur ciment, le rapport eau sur clinker du CPJ étant plus élevé que celui du CPA, il en résulte une porosité plus grande de la pâte hydratée du CPJ avec tous les risques qu'entraînerait cette conséquence".

S'il est vrai, par définition même, qu'il y a moins de clinker dans un ciment avec ajout calcaire que dans un ciment Portland pur, il est tout aussi évident que dans chacun des cas ce clinker ne pourra agir et développer ses résistances que s'il est suffisamment broyé. Ce qui importe donc, ce n'est pas tant la quantité de clinker présente que l'activité hydraulique de ce clinker. Celle-ci se développe grâce au broyage et se traduit, après gâchage, par la formation d'hydrates qui donneront les résistances et la réduction progressive de la porosité du matériau.

2 - VALORISATION du POTENTIEL HYDRAULIQUE du CLINKER par AJOUT de FILLER INERTE

En France, comme dans de nombreux pays, les classes de ciments sont définies par le niveau des résistances mécaniques à vingt-huit jours en mortier ISO à 20°C. La classe de résistance la plus demandée est la classe 45 c'est-à-dire celle pour laquelle les ciments doivent avoir en moyenne une résistance à 28 jours en mortier ISO proche de 45 MPa ; elle représente près de 65 % des demandes des utilisateurs.

La finesse de broyage nécessaire pour obtenir 45 MPa de résistance en compression à vingt-huit jours varie suivant les clinkers. Une expérience faite sur une population de quatorze clinkers industriels de provenances différentes et donnant les résistances à vingt-huit jours en mortier AFNOR en fonction de la finesse Blaine de broyage (figure 1) montre que :

- La finesse de broyage nécessaire pour obtenir 45 MPa à vingt-huit jours est toujours inférieure à 2700 $cm^2\ g^{-1}$.
- Pour près de la moitié des clinkers, la finesse de broyage pour obtenir 45 MPa est même inférieure à 2000 cm^2/g^{-1}.

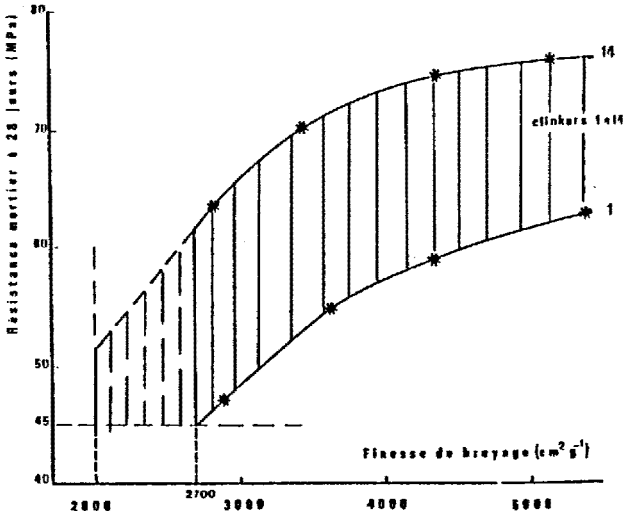

Figure 1 : Résistances à vingt-huit jours obtenues en mortier AFNOR à partir de quatorze clinkers en fonction de leur finesse de broyage (la partie hachurée entre les courbes enveloppes (1) et (14) est la zone où se situe l'ensemble des courbes résistances-finesse des quatorze ciments.

On voit donc que pour obtenir la classe de résistance 45 la plus couramment demandée, le clinker ne devra être que grossièrement broyé si on veut un ciment Portland pur sans ajout. La fraction granulaire la plus grossière du ciment obtenu est alors constituée de grains de clinker qui ne s'hydratent pas et qui sont donc, en grande partie, inutiles pour le développement des propriétés hydrauliques.

On conçoit donc bien que la seule façon de valoriser le potentiel hydraulique du clinker est de le broyer plus finement tout en ajoutant un filler inerte pour maintenir la résistance à vingt-huit jours du ciment à la valeur nominale de la classe de résistance demandée.

3 - EXPERIMENTATION et CARACTERISTIQUES des CIMENTS

Pour montrer que dans un ciment Portland avec ajout calcaire le résultat de l'activité hydraulique du

R.GUYOT, R.RANC, B.CARIOU
LAFARGE COPPEE RECHERCHE, FRANCE

clinker est au moins égal à celui du CPA de même classe, malgré un taux de clinker moins important mais grâce à une finesse de broyage plus poussée, nous avons suivi le développement des hydrates et l'évolution de la porosité de quatre ciments issus d'un même clinker :

. CPA 55 : ciment Portland sans ajout ayant une résistance à vingt-huit jours de 58,3 MPa.

. CPJ 55 : ciment Portland avec 15 % d'ajout calcaire ayant une résistance à vingt-huit jours de 57,3 MPa à peu près identique au précédent.

Ces deux ciments, avec et sans ajout, appartiennent tous deux à la classe de résistance 55.

. CPA 45 : ciment Portland sans ajout ayant une résistance à vingt-huit jours de 49,9 MPa.

. CPJ 45 : ciment Portland avec 27 % d'ajout calcaire ayant une résistance à vingt-huit jours de 48,7 MPa, donc très proche de celle du CPA 45 précédent.

Ces deux ciments, avec et sans ajout, appartiennent tous deux à la classe de résistance 45.

Les ciments CPA 55 et CPA 45 ont été obtenus en broyant le clinker d'origine aux finesses Blaine respectives de 3340 cm^2g^{-1} et 2250 cm^2g^{-1}.

Les ciments CPJ 55 et CPJ 45 ont été obtenus en ajoutant respectivement 15 et 27 % d'un même filler calcaire à un CPA du même clinker broyé à une finesse Blaine de 3970 cm^2g^{-1}. Il est à remarquer que la finesse de broyage du clinker dans le CPJ 45 est plus élevée que celle du CPA 55.

Les caractéristiques de ces quatre ciments figurent au tableau 1.

	Finesse Blaine du ciment (cm^2g^{-1})	Finesse Blaine clinker seul (cm^2g^{-1})	Finesse Blaine du calcaire (cm^2g^{-1})	Taux d'ajout calcaire (%)
CPA 55	3340	3340	-	0
CPJ 55	4180	3970	5400	15
CPA 45	2550	2550	-	0
CPJ 45	4360	3970	5400	27
	Résistance compression mortier AFNOR (MPa)			
	1 j	2 j	7 j	28 j
CPA 55	15,1	25,5	43,8	58,3
CPJ 55	18,4	27,9	45,0	57,3
CPA 45	11,2	19,8	35,4	49,9
CPJ 45	14,9	23,3	37,3	48,7

Tableau 1 : Caractéristiques des quatre ciments étudiés.

On peut noter que dans chaque classe de ciment, pour des résistances à vingt-huit jours équivalentes en CPA et CPJ, les résistances initiales à un et deux jours des deux CPJ sont supérieures à celles des CPA correspondants. On retrouve là un caractère général qui est la supériorité des résistances initiales du CPJ par rapport à celles du CPA de même classe.

Cela s'explique si l'on sait que l'effet de la finesse de broyage du clinker se fait beaucoup plus sentir sur les résistances initiales que sur les résistances à vingt-huit jours alors que l'effet de l'ajout se fait sentir d'une façon égale sur les résistances initiales et sur les résistances à vingt-huit jours.

4 - SUIVI de l'EAU LIEE au COURS de l'HYDRATATION

L'eau liée déterminée sur les pâtes pures hydratées à E/C 0,5 et 0,28 de chacun des quatre ciments à différentes échéances après stoppage d'hydratation à l'acétone éther, permet de suivre l'évolution des taux d'hydratation de huit heures à quatre-vingt dix jours (tableau 2).

Malgré une certaine dispersion des résultats obtenus, on voit très nettement que le clinker des CPJ s'hydrate plus rapidement que celui des CPA car :

- à huit heures, l'eau liée des CPJ est toujours plus élevée que celle des CPA correspondants de même classe ;
- à un, deux, sept et vingt-huit jours, les valeurs de l'eau liée sont très voisines entre le CPJ et le CPA de même classe ;
- à quatre-vingt dix jours, la quantité d'eau liée des CPJ a tendance, trois cas sur quatre, à être sensiblement inférieure à celle des CPA correspondants.

	E/C = 0,50			
	CPA 55	CPJ 55	CPA 45	CPJ 45
8 h	4,5	7,0	4,6	6,4
1 j	15,2	15,3	14,0	13,8
2 j	18,8	17,2	16,2	15,5
7 j	22,0	22,0	19,8	19,5
28 j	24,6	23,6	24,4	22,5
90 j	27,0	24,6	26,2	23,1
	E/C = 0,28			
8 h	7,4	8,4	5,9	7,0
1 j	15,1	14,2	13,2	13,0
2 j	16,8	15,8	15,5	15,0
7 j	18,9	18,2	17,2	17,5
28 j	20,6	19,5	18,9	19,6
90 j	20,6	19,5	18,9	19,6

Tableau 2 : Pourcentage d'eau liée à différentes échéances de chacun des quatre ciments hydratés en pâte pure à E/C = 0,5 et à E/C = 0,28.

Ainsi les CPJ, bien que contenant moins de clinker que les CPA de même classe, ont grâce à la plus grande fi-

nesse du clinker un taux d'hydratation d'abord plus élevé aux très courtes échéances, puis identique à celui des CPA jusqu'à vingt-huit jours et légèrement inférieur de vingt-huit à quatre-vingt dix jours, période pendant laquelle l'évolution du taux d'hydratation s'est aussi stabilisée.

Il est à remarquer par ailleurs que cette stabilité est plus vite acquise tant pour les CPJ que pour les CPA, au E/C de 0,28 qu'au E/C de 0,5. Nous pouvons expliquer cela par le fait qu'à un rapport E/C de 0,28 les quantités d'eau disponibles pour l'hydratation deviennent rapidement plus faibles et la vitesse d'hydratation se ralentit.

5 - EVOLUTION de la POROSITE

La porosité des pâtes pures hydratées à E/C de 0,5 et de 0,28 pour chacun des quatre ciments entre un et quatre-vingt dix jours a été mesurée au moyen d'un porosimètre à mercure. Celui-ci permet d'obtenir (tableau 3) la porosité comprise entre 0,0075 micromètres (75 Å) et 120 micromètres.

	E/C = 0,50			
	CPA 55	CPJ 55	CPA 45	CPJ 45
1 j	41	40	44	42
2 j	38	38	40	40
7 j	32	32	34	34
28 j	26	26	27	30
90 j	21	23	23	26
	E/C = 0,28			
1 j	22	21	23	25
2 j	16	18	17	19
7 j	13	13	14	15
28 j	9	10	10	12
90 j	7	7	9	9

Tableau 3 : Mesure de la porosité (exprimée en pourcentage de volume) à différentes échéances de chacun des quatre ciments hydratés en pâte pure à E/C = 0,5 et à E/C = 0,28.

Avant chaque mesure, l'échantillon de pâte hydratée a été :

- concassé à une dimension de 5 à 10 mm ;
- mis sous vide pendant cinq minutes ;
- soumis pendant six heures à un échange eau-méthanol ;
- séché à l'air pendant une demi-heure, puis à l'étuve à 40° pendant douze heures.

D'une façon tout à fait analogue à ce que nous avons remarqué précédemment pour la teneur comparée en eau liée des CPA et CPJ de même classe, on voit que :

- à un jour, la porosité des CPJ a tendance (trois cas sur quatre) à être moins élevée que celle des CPA de même classe ;
- à deux, sept et vingt-huit jours, les valeurs des porosités sont très voisines entre le CPJ et le CPA correspondant de même classe ;
- à quatre-vingt dix jours, la porosité des CPJ a tendance (uniquement pour les pâtes hydratées à un rapport E/C de 0,5) à être sensiblement plus élevée que celle des CPA de même classe.

L'évolution de la porosité se stabilise également au cours de cette période et plus particulièrement en pâtes hydratées au E/C = 0,28.

En résumé, on constate donc qu'entre CPA et CPJ de même classe, les porosités sont très voisines avec toutefois une tendance pour les CPJ à avoir une porosité légèrement plus faible à un jour et un peu plus élevée après vingt-huit jours.

L'examen des spectres de porosité de chacun de ces quatre ciments hydratés en pâte pure à E/C = 0,5 montre, de la même manière, que la répartition des pores en fonction de leur dimension est la même pour les ciments purs que pour les ciments avec ajout de filler calcaire (figures 2 a,b,c).

La dimension des pores de la pâte hydratée est essentiellement fonction de l'avancement de l'hydratation ; c'est pourquoi à vingt-huit et quatre-vingt dix jours, les pores se situent respectivement à partir de 0,1 micromètres et 0,05 micromètres quel que soit le ciment alors qu'à deux jours la dimension des pores est un peu plus élevée pour le CPA 45 que pour le CPA 55 et les deux CPJ, ce qui traduit bien l'avancement plus poussé de l'hydratation des deux CPJ aux jeunes âges.

6 - POROSITE - RESISTANCE

Les corrélations entre les résistances en mortier AFNOR et les porosités en pâte pure à E/C = 0,5 sont excellentes (tableau 4).

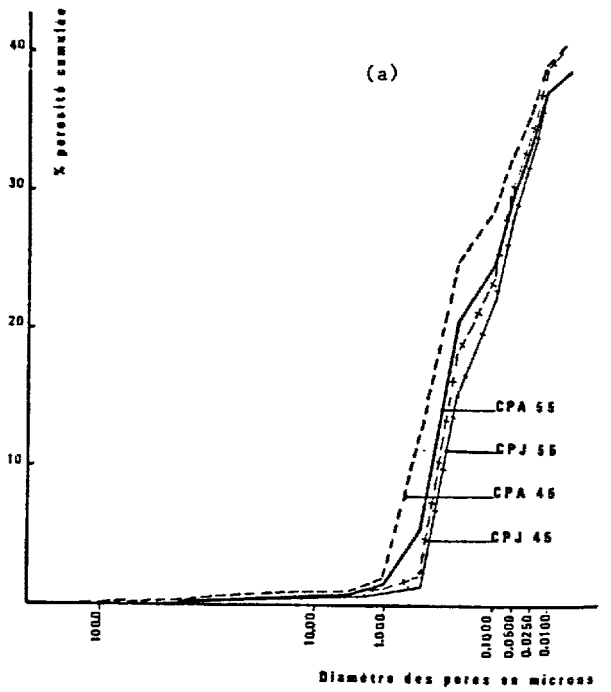

R.GUYOT, R.RANC, B.CARIOU
LAFARGE COPPEE RECHERCHE, FRANCE

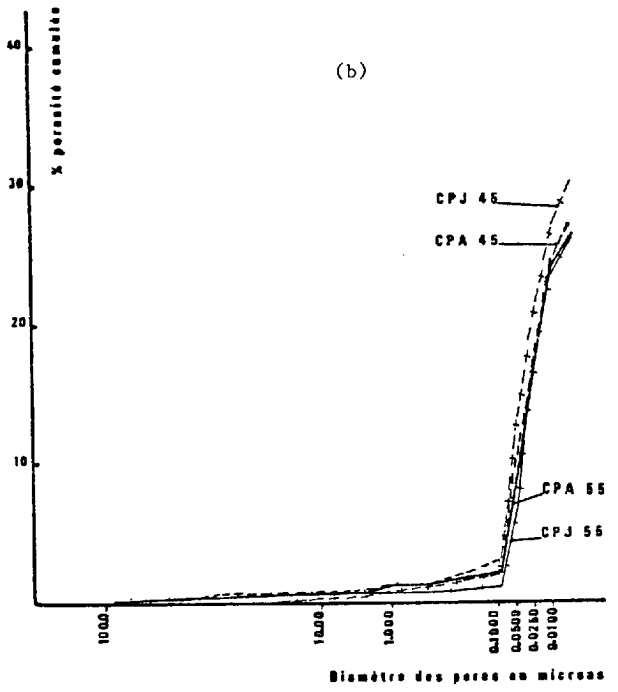

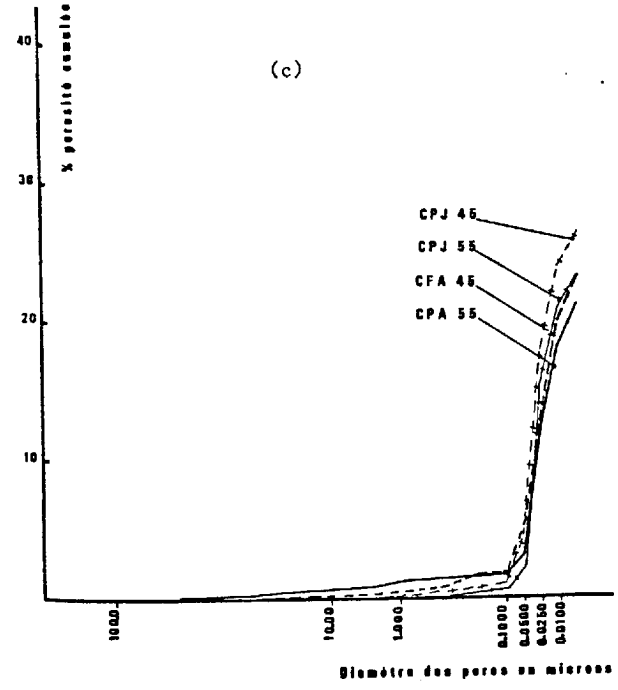

Figure 2(a) (b) (c) : Répartition de la porosité en pâte pure à E/C = 0,5 aux échéances de : (a) 2 jours ; (b) 28 jours ; (c) 90 jours.

Pour les huit valeurs de CPA (deux CPA, quatre échéances), le coefficient ρ de corrélation simple résistance-porosité est égal à -0,991 (il est même égal à 0,996 si on écarte l'échéance à vingt-huit jours du CPA 45).

Pour les huit valeurs de CPJ (deux CPJ, quatre échéances), le coefficient ρ de corrélation simple résistance-porosité est égal à -0,993.

Lorsqu'on groupe les huit valeurs de CPJ et les sept valeurs de CPA, cette corrélation reste excellente et le coefficient de corrélation reste inchangé ρ = -0,994 (figure 3).

Echéance	1 jour		2 jours		7 jours		28 jours	
	P	R	P	R	P	R	P	R
CPA 55	41	15,1	38	25,5	32	43,8	26	58,3
CPA 45	41	11,2	40	19,8	34	35,4	(27	49,9)
CPJ 55	40	18,4	38	27,9	32	45,0	26	57,3
CPJ 45	42	14,9	40	23,3	34	37,3	30	48,7

	Coefficient de corrélation multiple	
CPA 55	Pour les 8 couples de valeurs ρ = -0,991	Pour les 15 couples de valeurs ρ = -0,994
CPA 45	Pour les 7 couples de valeurs (1) ρ = -0,996	
CPJ 55	Pour les 8 couples de valeurs ρ = -0,993	
CPJ 45		

P = % porosité pâte pure E/C = 0,5
R = résistance mortier AFNOR en MPa

(1) en ne prenant pas en compte l'échéance à vingt-huit jours du CPA 45.

Tableau 4 : Corrélation Résistance mortier AFNOR/ Porosité pâte pure à E/C = 0,5.

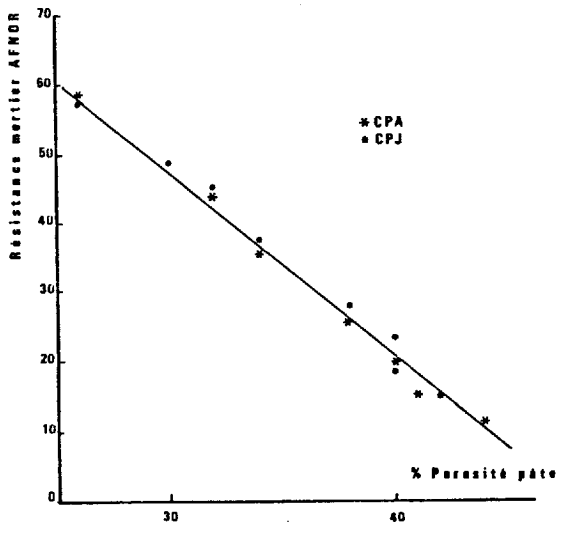

Figure 3 : Corrélation Résistance mortier AFNOR et porosité pâte pure à E/C = 0,5.

Ce qui indique bien qu'un CPJ présente la même porosité qu'un CPA pour une même résistance mortier.

R.GUYOT, R.RANC, B.CARIOU
LAFARGE COPPEE RECHERCHE, FRANCE

7 - SUIVI du TAUX de PORTLANDITE en COURS d'HYDRATATION

Le taux de Portlandite $Ca(OH)_2$ déterminé par analyse thermo-pondérale (ATP) sur pâte pure à E/C = 0,5 (tableau 5) est également un moyen de suivre le taux d'hydratation comme nous l'avons fait précédemment avec le taux d'eau liée. Il est intéressant de noter tout d'abord qu'il y a effectivement une très bonne cohérence entre le taux d'eau liée et le taux de Portlandite aussi bien pour les CPA que pour les CPJ avec ajout calcaire (tableau 6). Le rapport % eau liée/% Portlandite est le même pour le CPJ que pour le CPA.

Les conclusions que l'on peut tirer du suivi des taux de la Portlandite sont donc les mêmes que celles établies avec l'eau liée : teneurs en $Ca(OH)_2$ très voisines entre CPA et CPJ de même classe, donc même taux d'hydratation jusqu'à vingt-huit jours.

Echéances	CPA 55	CPJ 55	CPA 45	CPJ 45
7 j	12	12	13	12
28 j	14	14	15	13
90 j	16	15	16	14

Tableau 5 : Taux de Portlandite mesuré par ATD sur pâte pure à E/C = 0,5 à différentes échéances.

Echéances	CPA 55	CPJ 55	CPA 45	CPJ 45
7 j	1,8	1,8	1,5	1,6
28 j	1,8	1,7	1,6	1,7
90 j	1,7	1,6	1,6	1,7

Tableau 6 : Valeurs du rapport % eau liée/% Portlandite à différentes échéances pour les quatre ciments.

8 - EVOLUTION de la DECROISSANCE du C_3S par DIFFRACTION X

Les mesures de diffraction ont été faites pour suivre la disparition des anhydres : C_3S (raie à 1.77 Angström) au cours de l'hydratation en pâte pure à E/C = 0,5 et à E/C = 0,28 de chacun des quatre ciments (tableau 7).

De même que nous avions observé un développement plus rapide des hydrates en CPJ qu'en CPA, nous retrouvons une diminution plus rapide du C_3S dans le CPJ comparativement au CPA de même classe.

Cette diminution plus rapide du C_3S dans les CPJ est particulièrement nette avec les ciments de classe 45 où la différence de finesse du clinker entre CPA et CPJ est la plus grande.

Il est à noter que dans les deux CPA hydratés en pâte pure à E/C = 0,5, il reste après vingt-huit jours encore près de 10 % du C_3S initial non combiné alors que dans le CPJ le C_3S s'est entièrement hydraté.

Au-delà de vingt-huit jours, le C_3S des CPA continue de s'hydrater en partie mais il en reste d'une façon visible à quatre-vingt dix jours et vraisemblablement au-delà sans peut-être ne jamais se combiner, ni donner de résistance car insuffisamment broyé.

Echéances	E/C = 0,50			
	CPA 55	CPJ 55	CPA 45	CPJ 45
Anhydre	62	56	60	49
8 h	-	50	50	36
1 j	30	28	30	15
2 j	27	23	24	11
7 j	13	6	14	3
28 j	5	traces	6	traces
90 j	2	traces	traces	traces
	E/C = 0,28			
Anhydre	62	56	60	49
8 h	57	46	57	33
1 j	32	25	30	19
2 j	22	20	23	13
7 j	20	13	23	6
28 j	17	10	17	4
90 j	12	10	15	4

Tableau 7 : Evolution des hauteurs de pics (raie à 1,77 Å) du C_3S dans les pâtes hydratées à E/C = 0,5 et E/C = 0,28 des quatre ciments.

Le comportement est analogue à E/C = 0,28 mais, à partir de sept jours, la diminution du C_3S se ralentit encore plus fortement et à quatre-vingt dix jours la quantité de C_3S initial demeure encore relativement importante.

9 - ALUMINATE TRICALCIQUE et FORMATION de MONOCARBOALUMINATE

Les mesures de diffraction X ont permis également de suivre la disparition du C_3A (raie à 2,7 Angström) au cours de l'hydratation en pâte pure à E/C = 0,5 et à E/C = 0,28 (tableau 8).

	E/C = 0,50			
	CPA 55	CPJ 55	CPA 45	CPJ 45
Anhydre	32	39	32	33
8 h	33	35	32	27
1 j	26	27	22	20
2 j	15	22	14	16
7 j	5	5	9	4
28 j	traces	traces	2	traces
90 j	traces	traces	traces	traces
	E/C = 0,28			
Anhydre	32	39	32	33
8 h	29	31	28	25
1 j	23	23	23	20
2 j	16	18	18	14
7 j	13	12	13	5
28 j	9	8	9	4
90 j	7	8	9	4

Tableau 8 : Evolution des hauteurs de pics (raie à 2,7 Å) du C_3A dans les pâtes hydratées à E/C = 0,5 et E/C = 0,28 des quatre ciments.

Le pic du C_3A étant moins important, il est plus difficile d'observer une différence significative entre CPA et CPJ.

Cette différence cependant apparaît encore assez nettement avec la classe 45 où l'on retrouve la diminution plus rapide du C_3A dans le CPJ.

A E/C = 0,28, la diminution du taux d'aluminate tricalcique se ralentit fortement à partir de sept jours comme pour le C_3S ; à quatre-vingt dix jours la quantité de C_3A initial demeure encore relativement importante.

Les mesures de diffraction X montrent à l'échéance de sept jours l'apparition de monocarboaluminate de chaux : C_3A, $CO_3Ca.11H_2O$ (raie à 7,63 Å) dans chacun des deux CPJ (tableau 9). Il est difficile de donner une estimation en pourcentage des quantités formées mais elles paraissent sensiblement identiques dans chacun des deux CPJ qui, rappelons-le, sont constitués du même clinker broyé à la même finesse et ne diffèrent que par la quantité de l'ajout calcaire plus élevé dans le CPJ 55 que le CPJ 45.

Le filler calcaire n'est donc pas véritablement un inerte puisqu'il réagit avec l'aluminate tricalcique pour donner du carboaluminate comme cela a déjà été montré par d'autres chercheurs(1). Malgré l'intérêt que présente cette réactivité du filler, nous ne pensons pas qu'elle soit déterminante dans les propriétés du CPJ et, compte tenu de ce que nous avons vu précédemment, ce sont avant tout les hydrates développés par la finesse de broyage du clinker qui sont les éléments déterminants de la qualité et des performances des ciments avec ajout calcaire.

	E/C = 0,50			
	CPA 55	CPJ 55	CPA 45	CPJ 45
8 h	0	0	0	0
1 j	0	0	0	0
2 j	0	0	0	0
7 j	0	11	0	11
28 j	0	19	0	28
90 j	0	38	0	39
	E/C = 0,28			
8 h	0	0	0	0
1 j	0	0	0	0
2 j	0	0	0	0
7 j	0	3	0	5
28 j	0	7	0	10
90 j	0	6	0	12

Tableau 9 : Evolution des hauteurs de pics par diffraction X (raie à 7.63 Å) du monocarboaluminate de chaux dans les pâtes hydratées à E/C = 0,5 et E/C = 0,28 des quatre ciments.

CONCLUSION

Nous avons ainsi montré que lorsqu'un ciment Portland pur (CPA) et un ciment Portland avec ajout de fillers calcaires (CPJ) appartenant tous deux à la même classe de résistance à vingt-huit jours sont gâchés au même rapport eau sur ciment (eau/CPA = eau/CPJ), on obtient des pâtes hydratées de même porosité ; les propriétés en mortiers et bétons qui en découlent seront donc identiques pour chacun des deux ciments.

Ce résultat est obtenu par un broyage plus poussé du clinker dans le CPJ que dans le CPA, ce qui permet d'obtenir avec le CPJ des quantités d'hydrates identiques à celles du CPA bien qu'il y ait moins de clinker dans le ciment CPJ avec ajout que dans le ciment pur CPA.

L'intérêt de l'incorporation d'un filler calcaire dans un ciment apparaît ainsi très clairement : en utilisant moins de clinker mais en développant mieux le potentiel hydraulique de ce clinker par un broyage approprié, on obtient un ciment avec ajout qui aura en tout point les mêmes propriétés que celles d'un ciment Portland pur habituel. Il pourra répondre aux mêmes exigences car la composition et la structure de la pâte liante obtenue après hydratation sont identiques.

En corollaire, il faut souligner toute l'importance qu'il y a à contrôler et à maîtriser la finesse réelle de broyage du clinker dans le ciment avec ajout car c'est la finesse de broyage du clinker qui est l'élément déterminant de la qualité du CPJ au filler calcaire.

REFERENCES

(1) Liaison pâte de ciment-filler dans les ciments composés. B.MORTUREUX - H.HORNAIN - M.REGOURD - Colloque International Liaison Pâte de Ciment - Matériaux Associés - TOULOUSE - Novembre 1982.

K. TAKEMOTO Onoda Cement Co, Ltd, - Japan

THE VARIATION OF ACTIVITY INDEX OF SLAG

1. Introduction

The sum of blast furnace slag produced in Japan was 24.8 × 10^6 ton in 1984. The share of water-quenched granulated slag was 46.6%. The gradually-cooled slag was used mainly for subbase of road, and the use of granulated slag was mainly for slag cement. The production of slag cement was 8.6 × 10^6 ton, which holds 12.3% of total production of all cements, and is estimated to hold 20% in near future.

The method of manufacture of slag cement is mostly separate-grinding of slag with gypsum, and then mixing with ordinary portland cement (OPC) at cement plant. The blending ratio is around 50 : 50.

The slag activity index is one of the method of evaluation for the latent hyraulicity of slag. But, the author shows that the slag activity index varies not only with slag, also with OPC used.

2. Slag Activity Index

The slag activity index (A.I)(1) is calculated as follows;

$$A.I = S_1/S_0 \times 100 \qquad --1)$$

where S_1 and S_0 is strength of blended cement and OPC, respectively.

On the other hand, the basicity (2) of slag is also used for evaluating the hydraulicity of slag.

$$Basicity = (A+C+M)/S \qquad --2)$$

where A, C, M and S is Al_2O_3, CaO, MgO and SiO_2, respectively.

Fig. 1 shows the relation between A.I. and basicity. The slags were 13 kinds, which came from 13 different iron works, and mixed with one of OPC in laboratiry mixer. The mixing ratio was 50 : 50. The strength test was done by JISR5201, which uses 1 : 2 mortar and water-cement ratio of 65%. The specimen was cured up to 28 days in water at 293°K. Then, compressive strength was tested. The relation is better with considering the fineness of slag.

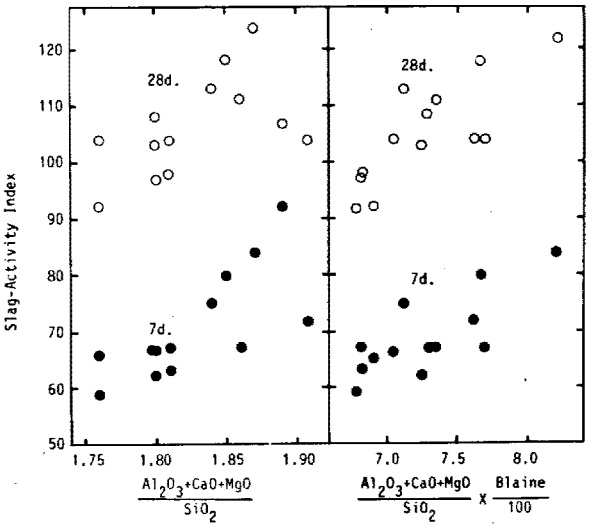

Fig. 1 Activity Index and Basicity of Slag

Table 1 Chemical composition of slag ground with Gypsum

slag	chemical analysis (%)								basicity	glass content(%)	Blaine (cm^2/g)
	SiO_2	Al_2O_3	Fe_2O_3	CaO	MgO	SO_3	Na_2O	K_2O			
A	31.7	14.2	0.5	41.1	6.2	2.8	0.22	0.33	1.88	100	3,580
B	32.1	13.4	0.5	40.9	6.0	3.4	0.15	0.27	1.80	100	3,840
C	31.9	13.1	0.8	39.1	7.1	3.3	0.22	0.37	1.79	100	3,950
D	31.6	11.9	0.4	41.7	8.5	3.1	0.15	0.24	1.90	98	4,090
E	31.8	12.2	0.4	41.1	5.4	3.1	0.20	0.34	1.78	99	4,230

Table 2 Chemical composition of ordinary portland cement

OPC No.	chemical analysis (%)										Blaine (cm^2/g)
	Loss	Insol	SiO2	Al_2O_3	Fe_2O_3	CaO	MgO	SO_3	Na_2O	K_2O	
1	0.6	0.1	22.1	5.3	3.0	63.6	1.8	2.0	0.39	0.56	3,520
2	1.0	0.1	21.9	5.4	2.8	63.9	1.5	2.0	0.33	0.71	3,170
3	0.5	0.1	21.4	5.5	3.6	64.5	1.1	1.9	0.28	0.54	3,030
4	0.8	0.1	22.0	5.8	3.0	63.8	1.7	2.0	0.29	0.51	3,300
5	0.7	0.2	21.6	5.5	3.0	64.0	1.2	2.1	0.40	0.51	3,480
6	0.5	0.1	22.2	5.5	2.8	63.7	1.6	2.1	0.26	0.64	3,230
7	1.1	0.4	21.7	5.1	3.0	63.5	1.6	2.0	0.49	0.45	3,200
8	0.8	0.1	22.3	5.9	2.7	63.2	1.7	2.0	0.26	0.26	3,120
9	0.7	0.1	22.4	5.0	3.1	64.2	0.9	2.1	0.31	0.56	3,270

3. Strength of Slag Cement

To evaluate the A.I., mortar strength of blended cements, which are the mixtures of 5 kinds of slag and 9 kinds of OPC., were tested. All of them came from different iron works and cement plants. The chemical compositions and fineness were shown in **Table 1 and 2.** The mixing ratio of slag to OPC was 50 : 50.

Fig. 2 is the results of strength tests. The 7 days-strength of slag cement depends mainely on the strength of OPC. The 28 days-strength is not parallel to that of OPC. This means that slag contributes to the later-age strength of slag cement. Here, the author emphasizes that the 28 days-strength of a slag cement is influenced by the OPC used. For example, the slag cements made with OPC NO.1 and 3 show the better strength development. On the other hand, the slag cements made with OPC NO.6 and 8 show the worse strength development. This means that the capability of OPC as activator to the hydraulicity of slag differs between OPCs. The specification (1) informs such phenomena in its Appendix. F.Schroeder and R.Vinkeloe (3) mentioned two examples which clinkers having high lime contents gave good influence to the strength of slag cements. R. Kondo (4) found early that the strength distribution of synthetic slags differs by the kind of activator, such as $Ca(OH)_2$ and $CaSO_4$.

The author tried to find the factors to dominate the activation capability of OPC, but could not succeed.

4. Variation of Slag Activity Index

The above mentioned results bring on the fear that the slag activity index varies with slag, also with OPC used. **Table 3** shows the slag activity index calculated from **Fig. 2.** The coefficient of variation of A.I. between slags is Cs = 8.4% in average, and that between OPC is Cp = 4.4%. Namely, the slag-activity index is influenced considerably with OPC used. This fact was confirmed statistically in **Table 4** of analysis of variance, which shows that OPC is highly significant to A.I., just as slag is so.

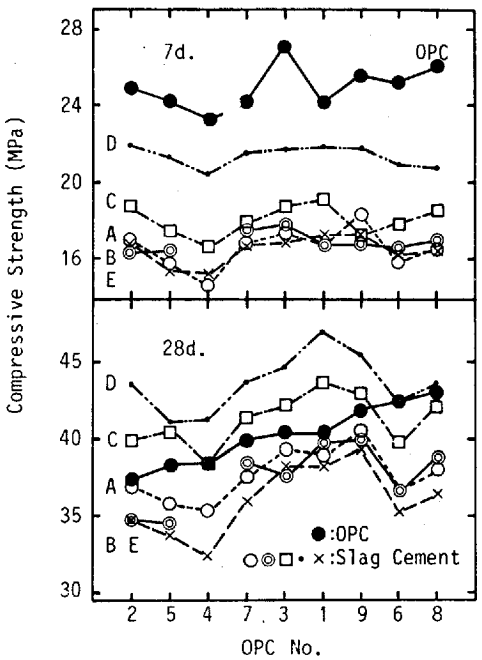

Fig. 2 Mortar Strength of OPC and Slag Cement (Slag /OPC=50/50)

Table 4 Analysis of variance for activity index

factor	sum of squares	degrees of freedom	variance	variances ratio
slag	2004.42	4	501.10	40.61**
OPC	672.02	8	84.00	6.81**
residual	394.89	32	12.34	
total	3071.33	44		

Table 3 Slag activity index and its variation (28d.)

slag	OPC 1	2	3	4	5	6	7	8	9	statistics $\bar{x}_p$	σ_p	C(%)
A	95.4	98.9	97.1	92.1	93.6	86.5	94.5	88.8	96.7	93.7	3.37	4.0
B	95.1	93.1	94.7	84.6	88.7	83.4	90.3	84.9	94.8	90.0	4.49	5.0
C	107.8	107.1	104.4	99.7	105.9	93.7	104.0	98.2	102.6	102.6	4.35	4.2
D	115.5	116.4	110.2	106.9	107.2	99.8	110.0	101.4	108.7	108.5	5.28	4.9
E	98.5	94.2	92.7	-	90.5	86.7	96.3	90.6	95.5	93.3	3.59	3.8
$\bar{x}_s$	102.5	101.9	99.8	95.8	97.2	90.0	99.0	92.8	99.7	$\bar{\bar{x}}$	$\bar{\sigma}_p$	$\bar{c}_p$
σ_s	8.76	10.00	7.51	10.83	7.94	7.04	8.45	7.08	5.97	97.6	4.22	4.4
C_s(%)	8.5	9.8	7.5	11.3	8.2	7.8	8.5	7.6	6.0			
$\bar{C}_s$(%)	8.4											

$\bar{x}$: mean
σ : standard deviation
c : coefficient of variation

5. Quality control of Slag Cement

The fact above mentioned means that the slag activity index is not useful to control the strength development of slag cement. Actually, the control at cement plant depends on the basicity and fineness of slag, and clinker quality and fineness of OPC, and also mixing ratio. They can control the quality of slag cement at real time.

In U.K., some of the ready-mixed concrete plant mix the ground slag in replacement of OPC (5)(6). But, they have not so many factors at ready mixed-concrete plant site, as at cement plant site, to control the quality of slag cement. The author claims such ready-mixed slag concrete should not be applied in general use.

6. Conclusion

The slag activity index varies not only with slag, but also with OPC. The activation capability of OPC to the hydraulicity of slag differs between OPCs. The author feels the difficulty in controling the quality of slag-replacement ready-mixed concrete.

Acknowledgement

The author appreciates the Laboratory of Cement Association of Japan permited him to use the test results on slag cement.

Literature

(1) ASTM C989-85

(2) JIS R5211-1964

(3) Schroeder, F and Vinkeloe, R., (1968) Proc. of Vth international Symposium on the Chemistry of Cement, part IV, p.177, Tokyo.

(4) Kondo, R., (1952) Semento-Gijutsu-Nenpo, VI, pp.180-186.

(5) Reeves, C.M., (1982) The Use of Ground Granulated Blastfurnace Slag for within-mixer Production of Portland-Blastfurnace Cement Concrete:Background and Development of the System in the U.K., Silicates Industriels, pp. 109-113.

(6) Jones, P.R., Reeves, C.M. and Dewae, J.D., (1982 Progress in the Use of Ground Granulated Blastfurnace Slag by the U.K. Ready Mixed Concrete Industry, Silicate Industriels, pp.253 -258.

T.V. KUZNETSOVA, S.D. MAKACHEV,
Z.B. ENTIN, Cement Research Institute, Moscow, USSR

CEMENTS WITH MINERAL ADMIXTURES: STATE OF THE ART AND PROSPECTS

Although the manufacturing and use of cements with mineral admixtures had been known from the beginning of this century it were only the last one or two decades that saw an increasing interest to this cements in all industrial countries aroused in connection with multipled fuel costs. The report by Dutron /1/ predicts that the average content of admixtures in cement will increase by 1990 to as much as 23% in Western Europe, to 12% in the United States, and to 10% in Japan. By 2000, the proportion of admixtures in cement will increase, on the average, 1.5 or 2 times above this level.

1. Classification of admixtures. Standards concerning classification of admixtures used in cement manufacture and/or specifications for such admixtures have been developed in many countries, including, for example, the USA, West Germany, Romania, and East Germany. One of the more complete classifications may be found in the Soviet standard GOST 24640-81 /2/. It categorizes the admixtures into active mineral, fillers, technological, and those controlling the main and special properties of cement.

This report will survey the experience which has been accumulated in using cements with mineral admixtures.

2. Specifications and estimation of effectiveness of mineral admixtures. Despite the vast literature on the chemistry and properties of cements with admixtures /3-5/ there has not been elaborated so far a suitable method of direct quantitative estimation of activity of admixtures which could substitute for the existing empirical techniques. Indeed, the data on chemical and mineralogical composition of an admixture, degree of crystallization, content of vitreous phase, etc., enable one to characterize the material as an active mineral admixture only with some probability, but to issue an accurate conclusion direct testing is needed.

According to the Soviet standard, an admixture is categorized as active provided it meets the requirements as follows:

- for a cement paste of normal consistency prepared of the mix of the finely ground material with hydrated lime in the 4:1 proportion with a small addition of gypsum, the final set is not later than 7 days after mixing with water;
- the specimen immersed in water after the final set is not washed out and retains clear cut edges for at least 3 days;
- for blended portland cement containing 30% or 40% of the characterized material (depending on the type of admixture), the setting concentration of calcium hydroxide in the liquid phase should be at least 0.5 mmol/l below the saturation isoterm.

For artificial admixtures, the latter test is replaced by the strength tests for rod specimens prepared from a mix of the material being defined with hydrated lime and gypsum and steam cured to some specified procedure. The bending strength of these specimens should be at least 1 MPa, and the compressive strength at least 3 MPa.

A simple and convenient criterion to estimate the effectiveness of an admixture is the coefficient of relative clinker requirement for a concrete defined as the ratio

$$K_{cl} = \frac{BC\ (100 - A)}{100\ PC}$$

where BC stands for blended cement (with admixture) requirement in kg/m^3; A for the percentage of admixture; and PC for plain cement requirement in kg/m^3.

An admixture is claimed efficient if $K_{cl} \leqslant 0.95$.

3. Nomenclature of active mineral admixtures. In the USSR 28 to 30 million tons of various materials, mainly industrial wastes, is annually used as admixtures in cements. These materials include metallurgical slags (blast-furnace and thermophosphorous), bergmeal, metallurgical molding sand, diatomite, belite slurry, flyash and cinder. The list of admixtures in use is being expanded but the main proportion falls to blast furnace granulated slags which are completely uti-

lized in this country.

The quality of slags is assessed mainly by their chemical analysis. The reactive components of slag are CaO and Al_2O_3 added by MgO given its content not exceeds 10 wt %. The passive components include SiO_2, TiO_2, MnO and a proportion of MgO in excess of 10%.

When the MgO content of slag exceeds 14-15%, there is a risk of magnesial expansion and the quality of slag is markedly lower. Therefore, the Soviet standard GOST 3476-74 puts the upper limit on MgO content at 15%. It allows, however, a higher contents of MgO up to the highest level met in industrial slags (16-17%) provided the material simultaneously contains exceedingly high percentage of Al_2O_3, up to 12-15%. A high MgO content increases the activity of Al^{3+} ions and facilitates their transition into an octahedral coordination with oxygen. As a result the mobility of the Al-O bond increases and this compensates to a large degree of decrease of CaO in the slag. Higher proportions of Al_2O_3, an oxide of intermediate basicity, leads also to a narrow field of primary crystallisation of MgO and increases its solubility in slags glass. This prevents magnesial expansion of the cement.

Thermophosphorous slags of electric steelmaking primarily contain glass of vollastonite composition. The activity of O^{2-} in these slags is lower than in blast furnace slags, and the degre of polymerisation of the anionic sceleton is higher in accordance with the lower ratio O^{2-}/S^{4+}. Accordingly, equal strength cements with thermophosphorous slags contains 10% to 15% smaller proportions of admixture than blast-furnace slag cements.

An advantage of thermophosphorous slag cements is due to their enhanced sulphate resistance, which results from almost complete absence of Al_2O_3 in the slag. This quality have led to an industrial technology which uses these slags and ordinary clinker to yield high quality, sulfate-resistant, slag portland cement which excels in quality the sulfate-resistant portland cement and is much cheaper to produce and with lesser energy requirements.

The slags of nonferrous metallurgy contain large proportions of ferrous oxides in the form of Fe_2O_3 and FeO. Granulation virtually does not improve their activity, but has a bearing on their hardness and grindability. When these slags are hydrated in an alkali medium, FeO is gradually oxidized by air oxygen into Fe_2O_3 so that the initial ratio of FeO/Fe_2O_3 almost does not affect the slag activity. By their effect on the cement strength, the ferrous slags are inferior to blast furnace and thermophosphorous slags, and are about equivalent to pozzolans. No loss of strength was noted in a prolonged hydration of cement containing portland cement clinker, gypsum, and ferriferous slag from copper-melting manufacture in a proportion of 30 wt %. After one year of setting the cement stone exhibited low basicity hydrosilicates, hydroferrites, and iron hydroxide. There was no evidence of ferrous compounds similar to calcium sulfoaluminate hydrates.

A remarkable property of nonferrous slag cements is due to the high degree of protection they offer to steel reinforcement elements. They consume oxygen which penetrates into the cement stone by oxidizing FeO to Fe_2O_3. This property of the slags to inhibit oxygen agressive action is even higher than that of the known inhibitor - sodium nitrite-nitrate.

Coal slags containing CaO in proportions of 25-40% approach in their basicity to electric thermophosphorous slags, but differ from the latter by a greater activity of the glass which they contain in lesser proportions. With 30 to 40% coal slags interground with clinker, the resultant cement exhibits a 28-day compressive strength of up to 35-40 MPa.

The quality of belite slime is governed by the residual content of alkali oxides, basically Na_2O. Given the residual content

of R_2O in slag not exceeds 1.0-1.2% (expressed as the Na_2O equivalent of the total alkalies), the belite slime is a valuable component for portland cement clinker and an effective admixture to cement. The 28-day compressive strength of cements with up to 15-20% of belite slime amounts to 40-50 MPa. Where the slag contains a higher proportions of R_2O, special precautions should be considered to protect the concrete from cement bleeding and alkali corrosion.

Acid flyash as admixture has received a rather thorough treatment and is widdly utilized in many contries, including Hungary, France, Poland, and the Soviet Union.

A considerable interest is attracted to basic flyash containing higher proportions of free CaO. In the USSR, such flyash has been utilized to produce a self-stressing cement with a self-stress energy is excess of 2.0 MPa, a non-shrinking cement, and a cement with controlled linear expansion.

Scanning electron microscopy has revealed that the expansive properties of a cement are conditioned by the shape of ettringite formations that occur in hydration of the flyash cement. If the cement stone exhibits formless star-like clusters of subfine-crystalline fibres of ettringite, it will possess excessive expansion and the flyash cement will not pass a soundness test. Where ettringite forms into long prismatic crystals, these reinforce the setting cement paste and give it an increased strength and density. Such cements exhibit linear expansion within 0.5-2%, pass soundness tests, and demonstrate a 28-day compressive strength of 40-50 MPa at a self stressing of 2.0-3.0 MPa. Prolonged tests of complex reinforced concrete structures made with these cements have confirmed their high durability.

The most general and definitive property of all active mineral admixtures is in their lower basicity as compared with portland cement clinker. Therefore, admixtures enter acid-basic interactions with minerals of clinker and facilitate more full utilization of its chemical energy. The intensity of the interaction defines the activity of the admixture, being controlled by many factors such as chemical composition, the degree of vitreous phase, fineness, surface morphology of grains, and such.

In hydration of admixtures a significant role is played by alkali oxides entering into the liquid phase from the admixture proper and from portland cement clinker. At the initial stage, movable alkali ions accumulate near the surface of the particle and diffuse along the microcracks and phase interfaces. These ions interact with the admixture, demolish the surface layer of the glass and yield soluable but immobile alkali silicates and aluminates. This in turn increases the osmotic pressure in the reaction zone causing an influx of water so that the particle of admixture finds itself surrounded by a liquid envelope separating it from the rest cement paste at the initial setting stage.

The aforementioned process can be readily observed in electron micrographs recorded in the hydration of flyash cements owing to a right spherical shape of flyash particles. In further stages of setting, the substitution of alkali ions with calcium ions leads to the formation of hydrosilicates, hydroaluminates, and hydroferrites of calcium, dense integration of the particle into the cement stone and consolidation of the stone.

The outlined mechanism satisfactorily explains the principle engineering properties of cement with mineral admixtures, namely, a decreased early strength, ability of prolonged strength development, lower frost resistance, increased sulfate resistance, increased shrinkage deformations in setting on air, and such. This mechanism also defines the directions for further improvements of additive cement qualities. The principal direction concerns with the acceleration of the rate of setting to enhance the strength of these cements to the

level of plain cements, retaining all the specific engineering properties of these cements and their low power requirements in manufacture. One of the important trends to produce the most effective cements of this kind, as it was shown by the special researches, is the utilization of clinker with rational chemico-mineralogical composition, which fully corresponds to physico-chemical properties and composition of the admixtures to be used.

REFERENCES

1. Дютрон "Настоящее и будущее цементов, предназначенных для бутона заводского производства". П-й Международный конгресс по бетону заводского производства, Лондон, сентябрь 1984.
2. В.И. Сатарин "Шлакопортландцемент". УІ Международный конгресс по химии цемента, т. 3, 45-56, Москва, 1976.
3. M. Daimon "Mechanism and kinetics of slag cement hydration" VII Intern. Congress on the Cem. of Cem., v. 1, Theme III - 2/1, Paris, 1980.
4. R. Sersale "Structure and characterization of pozzolanas and of fly ashes" VII Intern. Congress on the Cem. of Cem., v. 1, Theme IV - 1/3, Paris, 1980.
5. K. Takemoto, H. Uchikawa "Hydration of pozzolanic cement". VII Intern. Congress on the Cem. of Cem., v. I, Theme IV - 2/1, Paris, 1980.

Gerd Wischers - Research Institute of the German Cement Industry, Dusseldorf, West Germany

OPTIMIZATION OF CEMENTS WITH MINERAL ADDICTIONS

In general the optimization of an industrial product denotes the attainment of a particularly favourable ratio between its performance and its cost of manufacture. An improvement in the performance/cost ratio can be achieved by, for example, raising the quality while keeping the cost unchanged or by lowering the manufacturing cost while keeping the quality unchanged. However, an improvement may also be obtained when, in conjunction with a slight lowering of quality, the cost is substantially reduced.

The quality of a product is judged by the properties which are of decisive importance with regard to its utilization. In the case of cement its quality must therefore be judged by its performance in concrete. Optimization moreover always presupposes a standard of comparison to which both the performance and the price can be referred. In the case of the optimization of cements with mineral additions it is obviously meaningful to judge them with reference to the cement which is most extensively manufactured and used worldwide and with which therefore most experience has been gained, namely, portland cement.

1. Functions of cement in concrete

Cement always has a number of functions to perform in concrete, some of which are essential in all cases, e.g., attainment of a sufficiently high strength, and some that are required only for special purposes, e.g., adequate resistance to sea-water. The functions that cement in concrete always has to perform include:

- satisfactory rheological properties for good workability;
- satisfactory strength development and sufficiently high 28-day strength;
- satisfactory durability of the concrete under usual environmental conditions;
- lasting corrosion protection of the reinforcing steel.

In addition to these basic requirements there may be other requirements which, though not applicable worldwide, have the character of basic requirements in some countries. These include, for example, adequate freeze-thaw resistance in countries where all external structural components are frequently exposed to frost action in the normal course of things. Besides for special purposes cements with pronounced special properties can give better service and higher performance, which justify higher cost and higher prices. These include, for example, particular rheological properties of grout, particularly rapid hardening for prestressed precast concrete units, or a particular chemico-mineralogical composition to withstand chemical attack. To keep within the allotted time, the following treatment of the subject will confine itself to the above-mentioned basic requirements and, in addition, to freeze-thaw resistance.

2. Mineral additions

The principal constituents of cement can, with regard to their properties, be divided into four groups, namely, hydraulic constituents, latently hydraulic constituents, pozzolanic constituents, and fillers. Furthermore, cement always contains additions of calcium sulphate as a setting time controlling agent and sometimes additives such as grinding aids, for example.

2.1 Hydraulic constituents

Hydraulic constituents, e.g., portland cement clinker, consist predominantly of calcium silicates with a lime/silica ratio distinctly higher than 2.0. In finely ground form they react relatively rapidly with the mix water, i.e., they set and harden rapidly. The hydration products - in the case of complete hydration - occupy about twice as large a volume as the original clinker particles, and in this way they have both a strength-developing and a pore-filling action.

2.2 Latently hydraulic constituents

Latently hydraulic constituents such as, for example, granulated blastfurnace slag likewise consist predominantly of calcium silicates, but their lime/silica ratio is much lower, usually between only 1.0 and 1.5. Therefore they react only at a slow rate with the mix water and require activation - e.g., by alkalies, calcium hydroxide or sulphates - in order to harden more rapidly. In so far as they achieve complete hydration, which requires moist curing for a relatively long time, their hydration products also occupy about twice as large a volume as the original particles of granulated blastfurnace slag.

2.3 Pozzolanic constituents

Pozzolanic constituents such as, for example, natural pozzolanas or certain fly-ashes from coal-fired power stations consist in part of reactive silica or reactive aluminates, the remainder usually being inert matter. In contrast to hydraulic and latently hydraulic constituents, they cannot harden on their own, but need for this the presence of calcium hydroxide in solution, e.g., calcium hydroxide which is split off in the hydration process of portland cement clinker. The chemico-mineralogical reaction of pozzolanas with calcium hydroxide proceeds at a distinctly slower rate than the hydration of hydraulic and latently hydraulic constituents. Because of the content of inert matter the reaction products moreover occupy less than twice as large a volume as the original pozzolana or fly-ash particles.

2.4 Fillers

Fillers are finely divided mineral substances which do not react, or react only very slightly, with the mix water or with other constituents of the cement. If they are of suitable fineness, they can so complement the particle size distribution of the cement that the rheological properties (water demand, workability) are distinctly improved and a space-filling and stabilizing effect is achieved within the structure of the cement paste. Because fillers have no, or only very little, chemico-mineralogical reaction, they yield no reaction products which reduce the porosity existing after the concrete has been mixed and compacted. Limestone with a high content of calcium carbonate is particularly suitable as filler. The proportion of clayey constituents in the filler must be limited, otherwise the water demand of the cement will be greatly increased and the resistance to freeze-thaw cycles drastically diminished.

3. Cement-technological measures

In principle, all the above-mentioned initial materials are suitable for making cements with approximately equal properties. However, they require the application of cement-technological measures duly suited to the individual constituents. It is up to the cement manufacturer so to choose these measures that with the use of mineral additions an optimum is attained with regard to the ratio of performance to manufacturing cost. The first condition for such optimization is not of a technical but of an economic nature, namely, that the mineral additions in question supplied "free to cement plant", i.e., inclusive of the frequently very high freight charges for transporting them from their source, should be distinctly cheaper than the cement clinker produced in the cement plant. They should be cheaper because the technological operations for making cement with mineral additions are often more expensive than those for making portland cement. If such mineral substances are cheaply available, it will then be necessary to check their performance, e.g., as regards workability and strength, and to investigate whether they contain harmful matter which may, for example, accelerate carbonation or impair frost resistance. For cement manufacture there are then essentially three technological

measures available, which will be described below.

3.1 Composition of the cement

All cements made with mineral additions contain portland cement clinker. In comparison with portland cement containing - along with calcium sulphate and admixtures - 100 % clinker a portland cement with up to, say, 5 % mineral additions may have distinctly better properties with regard to constructional technology, e.g., workability, bleeding, or uniformity of colour. As to the proportion of the various mineral additions a distinction should be drawn between the highest possible and the optimum proportion. Purely scientific publications often give information on the highest possible proportion of mineral additions. Although it is possible largely or entirely to compensate for their effect on the properties by means of other cement-technological measures, e.g., higher fineness of grinding, there are technical and economic limits to such compensation. For optimizing the ratio of performance to manufacturing cost it must therefore be considered what change in the cement properties as compared with portland cement is brought about by mineral additions, what degree of change the makers of concrete - i.e., the cement manufacturer's customers - can accept, by what cement-technological measures the influence of the mineral additions upon the cement properties can be wholly or partly compensated, and what extra burden this will place upon the cost of manufacture. The result of such considerations will very probably vary from one cement plant to another, from one country to another and most notably from one continent to another. In this context the prices of fuel for clinker production and the rates charged by electricity suppliers, as well as the availability and prices of the mineral additions, play a major part. In the last 15 years, which have been characterized by a drastic rise in fuel and electricity costs, an optimum with regard to the composition of cement with mineral additions has emerged in Western Europe, as represented in Table 1.

Table 1: Optimum proportions of mineral additions

Mineral addition	Optimum proportion of addition in % by weight	Significant changes in properties as compared with portland cement
Limestone filler	15 ± 5	-
Natural pozzolana	25 ± 10	Slower hardening longer curing
Coal fly-ash	25 ± 10	Slower hardening longer curing
Granulated blastfurnace slag	25 ± 10	-
	60 ± 15	Slower hardening longer curing

3.2 Chemical optimization

Various substances can accelerate the rates of hydraulic and pozzolanic reactions. Because the mineral additions either do not react at all (fillers) or react much more slowly than cement clinker, there is good reason to activate the reactivity of latently hydraulic and pozzolanic added substances. Particularly reactive clinkers with relatively high alkali and tricalcium aluminate content can stimulate granulated blastfurnace slag, pozzolana and fly-ash to react notable more rapidly. It has been found suitable to relieve the clinker of too high a content of alkalies by appropriate measures applied in the burning process and to add the alkali-enriched substances thus obtained to the cement with slowly reacting mineral additions. A procedure of this kind is in accordance with the cement standards of several Western European countries and is to be included also in the future European cement standard. Calcium chloride is likewise able effectively to activate slowly reacting mineral additions, but in many countries the addition of substances containing chloride is banned be-

cause of their corrosion-promoting effect on reinforcing steel.

3.3 Fineness and particle size distribution

Besides the composition of the cement and its chemical optimization, its fineness of grinding and particle size distribution are of major influence on the properties of the cement, namely, the rheological properties as well as hardening and imperviousness. The specific surface area measured by the Blaine method is often used as the measure of fineness. This characteristic value is relatively simple to determine and can suitably be used for cement production monitoring. The Blaine value is, however, an integral value with only very limited informative usefulness as to the cement properties. More information is provided by the particle size distribution such as can now be determined fairly simply with a laser granulometer and which is represented as the cumulative line for the particle sizes in a special granulometric diagram called the Rosin-Rammler-Sperling-Bennet or RRSB diagram. For cement the particle size cumulative line generally appears as a straight line. As an example, Fig. 1 shows the cumulative line for a normal portland cement plotted in the RRSB diagram.

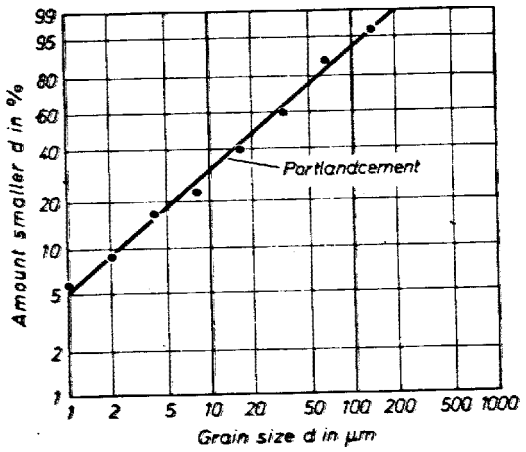

Fig. 1: Example of a grain size distribution diagram

If cement of the same composition is ground to a somewhat greater or less fineness in the same grinding plant, the straight lines in the RRSB diagram undergo an approximately parallel shift, as shown schematically in Fig. 2. Only if the cement is ground very fine does the slope of the lines change.

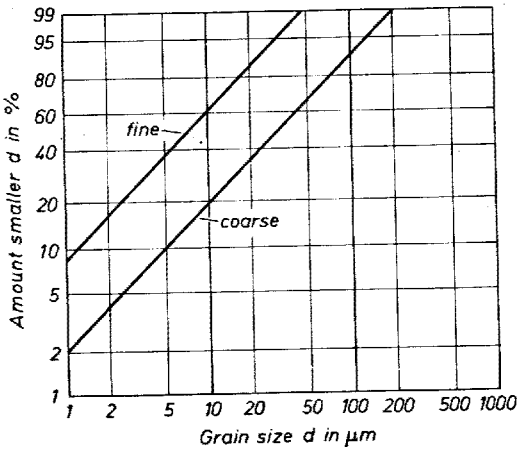

Fig. 2: Grain size distribution curves of fine and coarse cement

The slope of the lines (gradient) can be varied within certain limits by modifications to the grinding plant, e.g., by changing over to a differently composed ball charge in the mill or by altering the circulating load in a closed-circuit plant. The nature and quantity of the mineral additions also affect the slope of the lines: such added substances which are more easily grindable than cement clinker - limestone fillers, for example - cause them to slope less steeply, whereas substances which are more difficult to grind - granulated blast-furnace slag, for example - cause them to slope more steeply. Fig. 3 schematically represents two cements with approximately equal specific surface areas but with different slopes of their respective particle size cumulative lines.

The position and slope of the particle size cumulative lines are manifested in the properties of the ciment and in the cost of

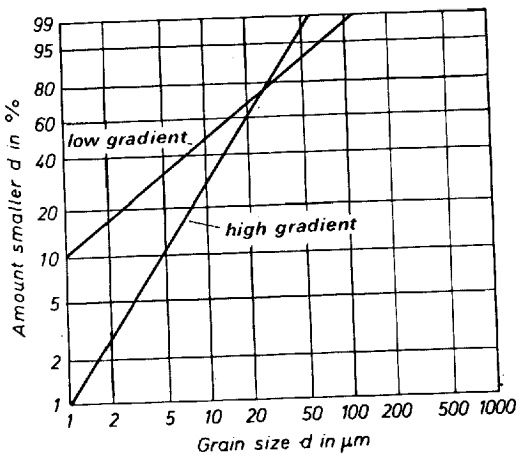

Fig. 3: Grain size distribution diagrams with different slopes

grinding. If cement of a given composition is merely ground to a greater fineness (straight line in Fig. 2 shifts to the left), the strenght increases in consequence, the water demand usually increases a little, but overall there is little change in workability. Greater fineness involves higher grinding cost, however. Since the contribution of the mineral additions to strength is in general distinctly less than that of portland cement clinker, cements made with such added substances always have to be more finely ground. For example, as against a Blaine value of 3000 cm^2/g for portland cement, a blastfurnace cement with a slag content of 60 % will have to be ground to approximately 4000 cm^2/g.

The slope of the particle size cumulative lines has opposite effects on the rheological properties and on the strength. The steeper the slope, the higher is the strength attained for equal specific surface area. The less steep the slope, the lower is the water demand and the better the workability. An addition of 10 - 15 % of limestone filler will make the cumulative line become less steep when grinding is performed in the same plant. Because the filler makes little contribution to the 28-day strength, such cement must be ground more finely in order to attain the same strength as it would attain without the filler. At the same time, however, the reduced steepness of the cumulative line results in lower demand and better workability despite the greater fineness of grinding.

4. Uniformity

For the concrete maker it is very important that the cement properties should vary as little as possible. That is why this problem receives the cement manufacturer's particular attention. Now cement clinker and, even more so, the mineral additions always show a certain amount of variation, which is sometimes very considerable and which must be smoothed as much as possible in the process of cement manufacture, as is schematically represented in Fig. 4.

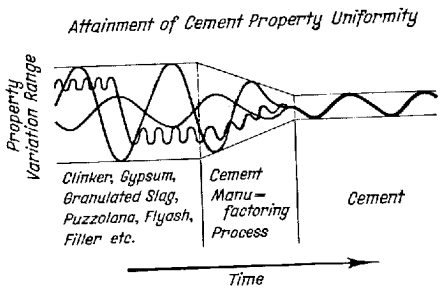

Fig. 4: Homogenization of cement properties

If, as is sometimes required by cement consumers, in the manufacture of cement with mineral additions the composition and fineness thereof are kept constant, the variations in the properties of the cement will fully manifest themselves. Therefore the properties of the cement constituents must be permanently monitored. With the aid of suitable control technology it can be ensured that there is the least possible variation in the cement properties overall. Such control, however, presupposes that - within certain limits - the composition of

the cement made with mineral additions, its chemical optimization, its fineness and, if necessary, also its particle size distribution are allowed to be changed. Most national cement standards allow scope for such control, and it is also to be incorporated in the future European cement standard.

J.P. BOMBLED - Centre d'Etudes et de Recherches de l'Industrie des Liants Hydrauliques, Paris - France
S. Feneuille - Lafarge Coppée - Paris, France

INFLUENCE DES PROPRIÉTÉS CHIMIQUES ET PHYSICO-CHIMIQUES DE LA PÂTE ET DES CARACTÉRISTIQUES DES GRANULATS SUR LE COMPORTEMENT RHÉOLOGIQUE DES MORTIERS ET DES BÉTONS.

S3

1. INTRODUCTION

Le sujet de ce séminaire n'est certes pas nouveau puisque, sous une forme ou sous une autre, il figurait déjà dans le programme des précédents congrès internationaux de la chimie des ciments. En outre, les phénomènes physico-chimiques de base qui gouvernent la rhéologie des mortiers et des bétons ont été depuis longtemps reconnus (voir par exemple les références 1) et ils ort été eux-mêmes très largement étudiés sur des systèmes modèles permettant d'isoler l'effet de tel ou tel d'entre-eux.

Pourquoi alors éprouver le besoin de refaire le point sur ce sujet?. La réponse à cette question doit être vraisemblablement recherchée dans l'impossibilité qui subsiste encore aujourd'hui de modéliser ces matériaux très complexes que sont les bétons, les mortiers et même les pâtes pures de ciment, qu'ils soient à base de ciments Portland ou de ciments alumineux .

Certes, l'on sait maintenant expliquer *a priori* le comportement rhéologique de tel ou tel mélange contenant un liant hydraulique en cours d'hydratation mais l'on ne sait pas prévoir quantitativement les propriétés de mise en place d'un mortier ou d'un béton à partir des paramètres physico-chimiques qui permettent de caractériser ses différents constituants . Peut-être d'ailleurs parce que l'on ne sait pas définir précisément ce que sont ces propriétés de mise en place. En outre, la simple caractérisation du comportement rhéologique intrinsèque du matériau reste encore aujourd'hui un sujet de controverse puisque les résultats obtenus dépendent en général de la méthode et même des instruments de mesure utilisés.

Et pourtant, l'on ne saurait se satisfaire de cette situation car les professionnels du béton sont journellement confrontés à des problèmes qui trouvent leur origine dans les propriétés rhéologiques du matériau. Ainsi, pour tenter de résoudre ces problèmes, se sont développées dans les laboratoires de recherche industrielle de nombreuses études purement empiriques . Leur objectif se réduit dans la plupart des cas à mettre en évidence des corrélations entre deux paramètres et, comme il arrive souvent dans ce type d'approche, les résultats obtenus sont peu significatifs, parfois même contradictoires. Ils ne permettent pas de construire les connaissances solides qui seraient nécessaires pour résoudre, autrement que par des palliatifs, les problèmes pratiques rencontrés .

Est-ce à dire que rien ne se passe dans ce domaine et que les choses n'y progressent que très lentement. Une façon de répondre à cette question est de commencer par rappeler quelle était la situation au terme du précédent congrès international de la chimie des ciments qui s'est tenu à Paris en 1980. Ensuite, nous tenterons de dégager les faits importants ou les tendances qui ont caractérisé l'apport au sujet de ces cinq dernières années. Enfin, nous donnerons un bref résumé des contributions présentées à ce séminaire et nous indiquerons quelques voies qui, peut-être, mériteraient d'être explorées à l'avenir .

2. RAPPEL DE LA SITUATION DU SUJET EN 1980.

Le sujet de ce séminaire n'était pas explicité sous la même forme dans le programme du dernier congrès international de la chimie des ciments. Toutefois, le thème VI présidé par S. Diamond[2] et intitulé : "Les pâtes de ciment : rhéologie, évolution des propriétés et des structures" présentait de larges plages de recouvrement et nombre de communications ont concerné directement ce sujet .

En 1980, les questions fondamentales restaient les suivantes :

- comment caractériser de façon appropriée le comportement rhéologique d'une pâte de ciment donnée?,

- quelles sont les modifications apportées dans ce comportement par un changement des caractéristiques du ciment ou par l'incorporation d'ajouts minéraux ou d'adjuvants chimiques, de superplastifiants en particulier?.

En effet, les méthodes de mesure des caractéristiques rhéologiques, et plus précisément de la relation déformation/effort de cisaillement, s'étaient progressivement sophistiquées au cours des années 70 mais, pour la plupart, elles modifiaient les paramètres qu'elles étaient censées mesurer et, en conséquence, les résultats correspondants étaient souvent incohérents sinon contradictoires .

Ces difficultés méthodologiques n'avaient pas empêché cependant de répondre, au moins partiellement, à la seconde des deux questions précédentes. Depuis longtemps déjà, en particulier, les principaux facteurs gouvernant la rhéologie des pâtes de ciment avaient été identifiés : géométrie et granulométrie des grains de ciment, constitution chimique et minéralogique des clinkers, éléments mineurs, teneur en eau, nature des ajouts, etc...

En outre, les phénomènes physico-chimiques correspondants avaient été également reconnus et avaient déjà donné lieu à des investigations parfois très poussées. C'est ainsi que l'origine (rupture des liaisons chimiques lors du broyage, différence de taille entre les anions et les cathions solubilisés) et les conséquences (floculation, thixotropie) de l'existence de charges électriques sur les particules solides étaient déjà bien comprises, en présence d'adjuvants notamment ; il en était de même de l'enchevêtrement des grains et de la dilatance ou encore de la tension superficielle et de la composition de l'eau interstitielle.

Les apports du congrès de 1980 ont avant tout :

- confirmé le comportement approximativement binghamien des pâtes de ciment;

- proposé quelques relations fonctionnelles permettant de déterminer le seuil de cisaillement ou la viscoplasticité apparente à partir des deux caractéristiques essentielles de la pâte : finesse ou surface spécifique du ciment , rapport eau/ciment[3] ;

- établi le rôle déterminant des sulfates[4] et celui, plus limité, de la teneur en aluminate tricalcique.

Comme l'indiquait le titre du thème VI, ces contributions ne concernaient pratiquement que les pâtes de ciment pures ou les mortiers . Certes le thème VII était intitulé :"Réaction aux interfaces entre ciment et granulat dans les bétons et les mortiers" mais aucune contribution à ce thème n'eut à voir vraiment avec les propriétés rhéologiques .

Toutefois, on savait bien déjà qu'il est impossible de décrire le béton frais comme un milieu homogène, et que les plus simples des modèles rhéologiques doivent faire intervenir au moins deux phases (pâte et granulat par exemple, ou dans d'autres conditions, phase liquide et particules solides) de comportement rhéologique différent, interagissant d'une façon inhomogène et évolutive dans le temps . En conséquence, la possibilité de relier scientifiquement des lois d'écoulement aux tests de maniabilité utilisés pour caractériser l'aptitude d'un béton à être mis en oeuvre était considérée de toute façon comme hors d'atteinte. Dans ces conditions, la tendance était de réserver les études "scientifiques" aux pâtes pures pour n'aborder le béton qu'au travers d'études purement empiriques orientées vers le pragmatisme des chantiers[5].

3. LES PRINCIPALES CONTRIBUTIONS DE 1980 A 1986

Dans le domaine considéré, les cinq dernières années ont été principalement marquées par deux événements. Tout d'abord en 1982, à Boston, la Materials Research Society a organisé un colloque sur l'effet des phénomènes de surface et des phénomènes colloïdaux sur les propriétés du béton frais; les comptes rendus de ce colloque ont été édités par Skalny[6]. Ensuite, en 1983, a paru le livre de Tattersall et Banfill intitulé : "The Rheology of Fresh Concrete"[7].

On pourrait également noter la parution de l'ouvrage sur "Le Béton Hydraulique" publié sous la direction de Baron et Sauterey[8], ainsi que les comptes rendus, publiés dans "il cemento", d'une journée de travail de l'A.I.T.E.C. sur la rhéologie des pâtes de ciment, des mortiers et des bétons[9,10,18,22] .

Les principales contributions que l'on peut trouver dans ces différents ouvrages indiquent bien les tendances qui caractérisent les recherches menées dans ce domaine durant la période considérée :

- effets des conditions expérimentales sur les propriétés rhéologiques mesurées ;

- influences respectives des propriétés rhéologiques du fluide interstitiel et de la friction entre aggrégats ;

- mécanisme d'action des adjuvants et effets des ajouts minéraux .

Concernant le premier point, un grand nombre d'études a encore concerné les conditions de validité et de fiabilité des mesures effectuées sur les viscosimètres à cylindres coaxiaux[10,11,12]. Si l'on excepte le cas favorable des pâtes pures soumises à des contraintes suffisamment faibles pour éviter tout glissement, les résultats correspondants ont été souvent décevants. Dans le cas des bétons en vérité, il semble bien que seul le recours à des méthodes anciennes plus ou moins empiriques puisse conduire à des mesures significatives. A cet égard, on peut citer notamment celles qui sont basées sur la puissance requise pour mélanger un béton frais. Leur utilisation ne devient simple cependant qu'à condition d'admettre un comportement de Bingham pouvant être décrit au moyen de deux paramètres seulement[7] . La nécessité de définir des procédés de mélanges standardisés est en tout cas soulignée par plusieurs auteurs. D'autres tests de propriétés rhéologiques ont été également discutés [13,14].

Le second point a été examiné notamment dans trois articles dont la synthèse permet, presqu'à elle seule, d'apprécier l'état actuel des connaissances dans ce domaine . Ainsi, Lawrence et Singh[15] ont analysé en grand détail l'apparition dans le temps des divers phénomènes physico-chimiques qui permettent de décrire qualitativement les propriétés rhéologiques des bétons frais .

Massazza et Costa[9] ont analysé l'influence des trois principaux facteurs qui conditionnent les propriétés rhéologiques des pâtes de ciment, des mortiers et des bétons : la cohésion, la friction entre particules solides et la viscosité de la phase interstitielle . Ils se sont intéressés en particulier aux effets de la répartition granulométrique des différentes particules solides et à ceux de l'hydratation .

Enfin, Hattori et Izumi[16] ont modifié la définition newtonnienne de la viscosité en utilisant le concept de friction intermoléculaire et après avoir obtenu la relation entre viscosité et nombre de points de friction, ils ont déduit de la théorie du taux de coagulation de Verwey et Overbeek[17] les équations de la viscosité dépendant du temps. Les applications de cette théorie restent pour l'instant assez limitées mais l'apport conceptuel est sans doute important .

Le dernier point a donné lieu durant ces cinq dernières années à une abondante littérature et à plusieurs articles de revue concernant les effets, tant des adjuvants chimiques[18,19], que des ajouts minéraux[20] cendres volantes notamment. Dans la plupart des cas, ces ajouts minéraux ont des effets bénéfiques sur la rhéologie du béton frais, en particulier lorsqu'ils sont utilisés en conjonction avec des superplastifiants . Au niveau des phénomènes physico-chimiques qui sont à l'origine des effets observés, une grande attention a continué d'être portée aux forces d'interaction électrique entre particules, notamment dans les suspensions denses[21], et à l'adsorption des fluidifiants sur les différents composés chimiques (silicates et aluminates) du ciment[22]. Enfin, les effets des adjuvants sur les propriétés rhéologiques de pâtes de clinker finement broyé mais non gypsé ont donné lieu à quelques études essentiellement empiriques[23].

4. LES COMMUNICATIONS PRESENTEES A CE CONGRES.

Pour la plupart, les différents points évoqués précédemment apparaissent d'une manière ou d'une autre dans l'ensemble des rapports et communications présentés à ce congrès .

C'est ainsi que Costa et Massazza[24] rappellent que le comportement et les propriétés rhéologiques des suspensions concentrées résultent d'un état d'équilibre entre, d'une part, des interactions ioniques et électriques (entre les grains eux-mêmes ou entre ceux-ci et les ions présents dans le liquide interstitiel) et, d'autre part, des actions purement mécaniques (forces capillaires, frottements internes, etc...).

Les interactions électrocinétiques expliquent en grande partie le fait, observé par tous, que l'état floculé est l'état habituel, en l'absence naturellement d'adjuvants défloculants, d'un ciment dans l'eau. On comprend également ainsi que l'architecture correspondante contribue à l'existence de la cohésion, du seuil de cisaillement et du comportement thixotrope des pâtes de ciment. L'action de nombreux fluidifiants s'interprète à partir des mêmes concepts[25].

Beaucoup de chercheurs continuent d'ailleurs d'aborder l'étude des propriétés rhéologiques par celle des phénomènes électrocinétiques au travers notamment de la zêtamétrie . Cette approche connaît un succès certain pour des suspensions de grains quasi inertes comme celles d'alumine par exemple[25], mais le problème s'est révélé très difficile pour un matériau évolutif toujours loin de l'équilibre comme le sont les suspensions de ciment dans l'eau[26]. Il semble que l'on ait eu quelques déceptions dans ce domaine et que beaucoup d'efforts devront y être encore consacrés si l'on veut progresser significativement .

La maniabilité des bétons et ses diverses composantes, cohésion, viscosité de la pâte interstitielle et frottement interne des granulats ne semblent pas donner lieu à des divergences d'interprétation[27]. Toutefois, on peut regretter qu'aucune étude ne soit présentée sur l'action "lubrifiante" de la pâte interstitielle qui est fournie par l'eau et les particules solides les plus fines . Il nous semble y avoir là un domaine qui mériterait un complément d'investigation . L'on sait en tous cas que la présence ou l'absence d'interface eau/air dans l'espace intergranulaire induit des comportements rhéologiques très différents qui ne peuvent être approchés de la même façon, notamment au niveau des mesures[28] .

Le comportement pratiquement binghamien du béton, au repos ou sous de faibles vitesses de cisaillement, est à nouveau confirmé par plusieurs auteurs[24,27] de même que le comportement quasi newtonien dans certaines conditions (vibration énergique, défloculation poussée, addition de résines) . Néanmoins, ce comportement est très souvent affecté par des transformations réversibles (thixotropie) ou irréversibles (sédimentation, hydratation) voire, dans certaines conditions par l'apparition de dilatance .

Concernant la mesure des coefficients rhéologiques des pâtes de ciment, différents travaux semblent montrer que finalement l'appareil le mieux adapté est le viscosimètre à cylindres coaxiaux à condition naturellement que n'apparaisse aucun phénomène de glissement, mais il faut noter que subsistent des variantes de réalisation ou d'exploitation des résultats[27]. Pour les bétons, les méthodes utilisées restent trop différentes dans leur principe et dans leur réalisation pour tenter de chercher de bonnes corrélations entre les différents résultats obtenus . Il reste difficile de passer de la pâte au béton[29] même si l'on peut signaler d'intéressantes tentatives tenant compte de plusieurs paramètres[24,30]. Au niveau des mesures, on peut noter une tentative, à la suite de nombreux travaux déjà existants, de suivre par ultra-sons l'évolution du seuil de cisaillement et la vitesse de prise[31].

Comme cela a déjà été souligné ci-dessus, l'on sait depuis longtemps que les caractéristiques rhéologiques des pâtes, des mortiers et des bétons frais dépendent non seulement de la composition du ciment (clinker, gypse et ajouts) mais aussi de facteurs liés à la préparation du béton (rapport eau/ciment, énergie de malaxage, température, etc...) et aux adjuvants éventuels. Comme il s'agit des premières minutes de la vie du matériau, ce sont évidemment les constituants les plus rapidement solubles (aluminate tricalcique, sulfates et alcalins) qui ont la plus grande influence. Ce point est confirmé dans plusieurs communications[29,32,33,34].

L'influence déterminante des sulfates de calcium incorporés au ciment sur le comportement rhéologique du béton frais est rappelée dans plusieurs communications[29,32]. Cette influence dépend bien sûr de la vitesse de dissolution de ces sulfates qui est liée à leur nature et qui permet de brider plus ou moins rapidement les premières liaisons qui pourraient se développer pendant la période de mise en oeuvre. A noter que, dans certaines conditions, le calcaire peut être substitué aux sulfates comme régulateur de prise[35].

Les ajouts (laitiers, cendres, pouzzolanes, etc...) ont en général une influence favorable sur la rhéologie; les facteurs importants étant l'écart de broyabilité avec le clinker ainsi que la géométrie des grains. Le cas des fillers calcaires, beaucoup moins étudié que les précédents, est discuté par Bombled[28].

L'on sait également que les facteurs granulométriques du ciment et des granulats (forme, état de surface et répartition de taille des grains), par le fait même qu'ils conditionnent le nombre de points de contact intergranulaires où s'exercent des forces de liaison, jouent eux aussi un rôle essentiel. Il est donc normal que l'étude de ces facteurs apparaisse dans plusieurs contributions. Ainsi, l'influence de la finesse du ciment est abordée par Costa et Massazza[24] ; celle des conditions de broyage dans le cas de ciments aux ajouts (broyage séparé ou cobroyage) et des différences de broyabilité des divers composants du ciment sont aussi discutées[28,29].

Parmi les conditions de préparation du béton, la température joue également un rôle; celui-ci est discuté par Wierig[32].

Enfin, un des points de grande importance actuelle est l'action de défloculants fluidifiants et l'évolution dans le temps de leur efficacité, ces fluidifiants étant d'ailleurs souvent utilisés comme réducteurs d'eau. Les recherches sur les mécanismes d'actions de ces adjuvants, l'influence de leur structure (et en particulier, de leur degré de polymérisation) et de leur composition ainsi que celle du ciment (présence d'éléments rapidement solubles, sulfates notamment) continuent d'être très actives[25,36,37] mais manifestement beaucoup reste encore à faire. Les effets de la salinité de l'eau interstitielle sont également un sujet d'intérêt[38].

Pour terminer l'examen des communications, il faut noter que les liants spéciaux, liants alumineux[39,40] et ciments pour forage pétrolier[38,41] n'ont pas été oubliés.

En conclusion, ce rapide survol semble montrer que les travaux conduits actuellement dans le domaine couvert par ce séminaire ont pour but avant tout de confirmer et d'approfondir des connaissances déjà acquises antérieurement plutôt que d'apporter des éclairages radicalement nouveaux. La progression est lente, ce qui confirme la difficulté du sujet.

5. QUELQUES PISTES POUR L'AVENIR

Il semble à présent que tous les phénomènes pouvant affecter la rhéologie des pâtes, des mortiers et des bétons sont assez bien compris individuellement. Peu d'entre eux cependant ont été analysés de manière quantitative et il reste vraisemblablement beaucoup de travail à faire dans ce domaine. Cette analyse quantitative supposera dans certains cas l'utilisation de nouvelles connaissances de base et, plus que jamais, seules les démarches pluridisciplinaires auront quelque chance de conduire au succès.

Ainsi, le concept d'objet fractal[42] a permis récemment de renouveler l'approche d'un grand nombre de phénomènes dans l'ensemble des sciences de la matière et il a été récemment appliqué à la structure des gels de ciment[43] ; on peut à juste titre se poser la question de savoir par exemple si l'introduction d'une dimension fractale pour caractériser la "rugosité" des granulats ne permettrait pas de quantifier plus aisément leur enchevêtrement.

Par ailleurs, de nombreuses équipes de recherches de base ont récemment reconsidéré la rhéologie des suspensions concentrées (voir par exemple la référence[44]) en utilisant des systèmes modèles, des simulations sur ordinateur[45] et les théories de la mécanique statistique comme la percolation[46,47] par exemple. Les phénomènes d'aggrégation dans les suspensions concentrées ont été également étudiées d'un point de vue géométrique en utilisant la notion de dimension fractale[48]. Ici aussi, sans doute serait-il utile de rechercher l'impact que pourraient avoir les résultats obtenus sur les questions abordées dans ce séminaire. Dans la même perspective, on peut se poser la question de savoir s'il ne serait pas intéressant de chercher à relier les propriétés rhéologiques[49] des solutions concentrées au problème du remplissage de l'espace par des grains de tailles diverses, problème dont les solutions ont récemment progressé, au moins sur des systèmes modèles[50,51,52].

Enfin, et de façon plus générale, on peut se demander si les méthodes de simulation qui ont été mises au point par et pour le génie chimique ne pourraient pas résoudre ce problème très délicat du caractère non additif des très nombreux phénomènes qui sont à prendre en considération si l'on veut élaborer un modèle rhéologique prédictif d'une pâte pure de ciment ou d'un béton adjuvanté. Bien entendu, cela ne veut dire en aucune manière que les phénomènes purement chimiques n'auront pas à être pris en compte ; cela signifie au contraire qu'ils auront à être intégrés dans une approche plus générale qui ne devra retenir que l'essentiel si elle veut être réellement efficace.

BIBLIOGRAPHIE

[1]J.-P. Bombled, "Rhéologie des mortiers et des bétons frais", Mater. Constr. (Paris), 688, 137-55, 1974 ; C. Legrand, "Contribution à l'étude de la rhéologie du béton frais", Mater. et Constr. (RILEM) 5, 275-95, 379-93.

[2]S. Diamond, "Cement pastes:rheology and evolution of properties and structures", 7ème Congrès International de la Chimie des Ciments (Paris), Vol. I, 113-23, 1980.

[3]R.A. Helmuth, "Structure and rheology of fresh cement paste", 7ème Congrès International de la Chimie des Ciments (Paris), Vol. III, VI-0/1-30, 1980.

[4]J.-P. Bombled, "Influence des sulfates sur les comportements rhéologiques des pâtes de ciment et sur leur évolution", 7ème Congrès International de la Chimie des Ciments (Paris), Vol. III, VI-164-69, 1980.

[5]M. Maultzsch et U. Meinhold, "Testing methods for the set of pastes and mortars", 7ème Congrès International de la Chimie des Ciments (Paris), Vol. III, VI-158-63, 1980.

[6]J. Skalny (ed.), "Concrete Rheology", Proc. Symp. M, Mater. Res. Soc. Ann. Mtg, Boston, MA, Nov. 1982, Mat. Res. Soc., (Pittsburgh, PA 15237), 233pp, 1982.

[7]G.H. Tattersall et P.F.G. Banfill, "The Rheology of Fresh Concrete", Pitman Books Limited (Londres), 356 pp, 1983.

[8]J. Baron et R. Sauterey (eds.), "Le Béton Hydraulique", Presses de l'Ecole Nationale des Ponts et Chaussées (Paris), 560pp, 1982.

[9]F. Massazza et U. Costa, "Rheological problems related to the use of cement", Il Cemento, 79 (4), 217-42, 1982.

[10]R. Lapasin, "Rheology of cement pastes", Il Cemento, 79 (4), 243-60, 1982.

[11]D.M. Roy, "Predicting fresh cement paste properties", in "Characterization and Performance Prediction of Cement and Concrete", J.F. Young (ed.), Engineering Foundation, New York, 219 pp, 151-4, 1983.

[12]R. Lapasin, A. Papo et S. Rajgelj, "Flow behaviour of fresh cement pastes. A comparaison of different rheological instruments and techniques", Cem. Concr. Res. 13(3), 349-56, 1983.

[13]C. Dulieu, "Rheology of fresh cement pastes and their variation with time testing methods", Cim., Bétons, Plâtres, Chaux (737), 230-5, 1982.

[14]J. Murata, "Flow and deformation of fresh concrete", Mater. Constr. (Paris), 17(98), 117-29, 1984.

[15]C.D. Lawrence et K.S.W. Sing, "The development of microstructure in fresh concrete", in ref.6, 2-13.

[16]K. Hattori et K. Izumi, "New rheological theory of concentrated suspensions", in ref. 6, 14-28.

[17]E.J.W. Verwey et J.Th.G. Overbeek, "Theory of the Stability of Lyophobic Colloids", Elsvier Publishing Co. Ltd, p 139-69, 1948.

[18]M. Collepardi, "Influence of admixtures on rheological properties of concrete", Il Cemento 79(4), 289-316, 1982.

[19]J.F. Young, "Effects of chemical admixtures on the rheological properties of fresh concrete", in ref. 6, 120-38.

[20]D.M. Roy, J. Skalny et S. Diamond, "Effects of blending materials on the rheology of cement pastes and concrete", in ref. 6, 152-73.

[21]J. Chappuis, "Relation of the rheological properties of dense suspensions to interparticle forces", in ref. 6, 38-45.

[22]U. Costa, F. Massazza et A. Barrila, "Adsorption of superplasticizers on C_3S. Changes in Zeta potential and rheology of pastes", Il Cemento 79(4), 323-6, 1982.

[23]F. Skvara et M. Rybinova, "The systems ground clinker-polyphenol sulphonate-alkali metal salts", Cem. Concr. Res. 15, 1013-21, 1985.

[24]U. Costa et F. Massazza, "Structure and properties of cement suspensions", ce congrès.

[25]J. Chappuis "Physical elementary mechanisms of fluidification by superplasticizers or mater-reducing agents", ce congrès.

[26]A. Zelver, "Interférences entre particules solides en suspension diluée", ce congrès(poster).

[27]G.H. Tattersall, "Components of workability and rheological measurements on mortars and fresh concrete", ce congrès.

[28]J.-P. Bombled, "Rhéologie du béton frais : l'influence de l'ajout de filler aux ciments", ce congrès.

[29]S. Sprung, "Influence des conditions de mise en place sur la rhéologie du béton frais", ce congrès.

[30]Y.M. Bazhenov, "Evaluation of rheological characteristics of cement paste and concrete with help of computers".

[31]I. Odler, S. Abdul-Maula et U. Hennicke, "A new method for determination of cement setting time", ce congrès.

[32]H.-J. Wierig, "Influence of cement and temperature on the consistency of fresh concrete", ce congrès.

[33]S. Grzeszczyk et L. Kucharska, "The influence of alkalies upon the water demand of early hydratation stage cement pastes in the light of rheological studies", ce congrès.

[34]J. Mierzwa, "Thixotropic-plastic-viscous rheological model of cement paste as the result of physical and mineralogical cement properties", ce congrès.

[35]A. Negro, G. Abbiati et L. Cussino, "Sur l'emploi du calcaire comme régulateur de prise du ciment", ce congrès.

[36]T. Sebök, "Effects of the molar parameters of sulphonated melamine and formaldehyde polycondensates on mortar properties", ce congrès.

[37]F. Basile, S. Biagini, G. Ferrari et M. Collepardi, "Properties of cement mixes containing naphtalene sulfonated polymers of different molecular weight" ; "Effect of condensation degree of polymers based on naphtalene sulfonate on fluidities of cement pastes" ; "Effect of the gypsum state in industrial cements on the action of superplasticizers", ce congrès.

[38]M. Michaux et R. Oberste-Padtberg, "The effect of mix water salinity on cement slurries containing polynaphtalene dispersants", ce congrès.

[39]P.F.G. Banfill et S.M. Gill, "The rheology of aluminous cement pastes", ce congrès.

[40]S.M. Gill, P.F.G. Banfill et B. El-Jazairi, "The effect of superplasticizers on the hydratation of aluminous cement", ce congrès.

[41]J. Orban, P. Parcevaux et D. Guillot, "Influence of shear history on the rheological properties of oil well cement slurries", ce congrès.

[42]B. Mandelbrot, "Les Objets Fractals", Flammarion (Paris), 203 pp, 1984.

[43]A.J. Allen et P. Schofield, "Possible fractal structure of cement gels", NATO ASI on "Scaling Phenomenon in Disordered Systems", Geilo, Norvège avril 1985, à publier par Plenum Publishing Company Ltd.

[44]R. Blanc, "Rheology of concentrated dispersions", à paraître dans le Journal de Physique (Paris), colloque Science of Ceramics 13, 1986.

[45]J.F. Brady et Bossis G., "The rheology of concentrated suspensions of spheres in simple shear of flow by numerical simulations", J. Fluid Mech. 155, 105-29, 1985.

[46]P.-G. de Gennes, "Conjonctures on transition from Poiseuille to plug flow in suspensions", J. Physique (Paris) 40, 783-7, 1979.

[47]P.G. de Gennes, "Dynamics of concentrated dispersions", Phys. Chem. Hydr. II, 1, 31-44, 1981.

[48]P. Meakin, "Diffusion-controlled cluster formation in 2-6 dimensional space", Phys. Rev. A 27, 1495-507, 1983.

[49]P.K. Haff, "Grain flow as a fluid-mechanical phenomenon", J. Fluid. Mech. 134, 404-30, 1983.

[50]R. Omnès, "Sur l'empilement aléatoire d'un système de sphères de rayons différents", J. Physique (Paris) 46, 139-45, 1985.

[51]M. Suzuki et T. Oshima, "Coordination number of a multicomponent randomly packed bed of spheres with size distribution", Powder Technology 44, 213-8, 1985.

[52]T. Stovall, F. de Larrard et M. Buil, "Linear packing density model of grain mixtures", à paraître dans Powder Technology.

P.F.G. BANFILL, S.M. GILL
School of Architecture and Building Engineering - The University of Liverpool
England, U.K.

THE RHEOLOGY OF ALUMINOUS CEMENT PASTES

INTRODUCTION

The rheology of cement pastes has been studied over several decades, but work has concentrated almost entirely on Portland cement (1), and no information seems to be available on aluminous cement pastes. In view of the industrial importance of Ciment Fondu grouts, particularly in marine applications where their superior durability and rapid strength gain are advantageous, it is useful to compare the rheology of Ciment Fondu pastes with that of ordinary Portland cement. This paper reports work carried out with a typical Ciment Fondu to provide this information.

RHEOLOGY OF CEMENT PASTES

The principal features of the rheology of cement pastes have been described in detail elsewhere (1), but may be briefly summarised as follows:

1. The flow curve of cement paste has been described in terms of various models:

Bingham	$\tau = \tau_o + \mu\dot{\gamma}$
Hershel-Bulkely	$\tau = \tau_o + A\dot{\gamma}^B$
Robertson-Stiff	$\tau = A(\dot{\gamma}+C)^B$
Ostwald-De Waele	$\dot{\gamma} = B\sinh(\tau-\tau_o)/A$

with associated observations in each case of shear thinning behaviour at high shear rates (τ shear stress, $\dot{\gamma}$ shear rate).

2. The existence of a yield value indicates that structure exists in the paste, due to the interactions between cement particles in the suspension. This structure breaks down on shearing because the energy input to the links between particles is sufficient to break the bonds. This structural breakdown manifests itself in two ways. Firstly, the yield value and plastic viscosity of the paste decrease with prolonged mixing, so that the method of preparing the paste affects the measured rheological parameters. Secondly, the torque, T, exerted by the paste on a continuously rotating cylinder or cone in a rotational viscometer decreases with time, t, according to an exponential relationship of the form

$$T - T_e = ke^{-bt}$$

where Te is the torque reached at equilibrium and k and b constants. The latter effect was treated theoretically by Tattersall (2) in terms of the number of links between particles in the paste.

3. The structural breakdown can also account for the variation in the reported flow curve shapes. Banfill and Saunders (3) found that when the time taken to complete an up and down cycle in a coaxial cylinders viscometer was short the flow curve showed a hysteresis loop with the downcurve falling to lower shear stresses than the upcurve (structural breakdown), whereas when the cycle time was long the loop was reversed. At intermediate cycle times flow curves with more than one loop were obtained. Furthermore the cycle times producing these types of curve varied from cement to cement. Only at cycle times of two minutes or less were the loop shapes consistent. They explained this in terms of the competition between shear-induced structural breakdown and the buildup of structure due to continuing hydration reactions. In addition, prolonged mixing results in reversible flow curves (up- and downcurves superimposable).

4. Variations in yield value over a 20-fold range and in plastic viscosity over a 50-fold range have been reported by different workers and can be explained by differences in experimental technique (4). In addition to the effect of mixing on the structural breakdown, cement pastes slip at the walls of the viscometer. This is assumed to be overcome by profiling or serrating the surfaces but no-one has shown conclusively that this is so. Nevertheless, Mannheimer showed that slippage could result in a sixfold reduction in the measured yield value of a cement paste (5).

5. Because of the variation of shear stress across the gap of a coaxial cylinders viscometer fluids with a yield value exhibit plug flow at low shear rates where the stress does not exceed the yield value at all points in the fluid, as shown by the Reiner-Rivlin equation:

$$\Omega = \frac{T}{4\pi\mu h}\left(\frac{1}{R_b^2} - \frac{1}{R_c^2}\right) - \frac{\tau_o}{\mu}\ln\frac{R_b}{R_c}$$

only when $T/2\pi R_c^2 h \geq \tau_o$ does all the fluid flow. This may be taken account of in the evaluation of data, but Tattersall and Dimond found that plug flow also occurred at much higher shear rates and stresses in conditions of steady continuous shear (6). They observed discontinuities in the exponential decay of torque with time which on visual examination of the paste were found to coincide with the times at which a solid plug of material broke up. When the observed width of the sheared zone was used in calculations instead of the instrument gap width, previously irreconcilable data on the effect of shear rate on the structural breakdown kinetics could be understood.

This complex behaviour of Portland cement pastes forms the background against which the rheology of Ciment Fondu pastes must be compared.

EXPERIMENTAL DETAILS

All experiments were carried out using a typical Ciment Fondu with the composition and other properties given in Table 1. The viscometer used in this work was a Haake Rotovisco RV2 with PG142 external speed programmer. Two coaxial cylinders geometries were used: (i) the Haake system MVIIP with inner cylinder radius 18.4mm, outer cylinder radius 21mm, height 60mm, both cylinders profiled with vertical ribs of 0.1mm square section, spaced 2mm apart round the circumference; (ii) the system S13/15 used by Tattersall and Dimond with inner cylinder radius 13mm, outer cylinder radius 15mm, height 50mm, both cylinders profiled with vertical serrations of 0.5mm square section, spaced 0.5mm apart round the circumference.

Pastes were prepared in batches of not more than 250g measured by weight and blended either by hand mixing with a spatula in a beaker for one minute or in a propellor type laboratory mixer at a speed of 1000 rpm for a predetermined time. Time and temperature were carefully controlled; all mixes were prepared and tested at 20 C.

The experimental programme studied the following: the effect of cycle time on flow curve shape; the effects of mixing time, concentration in water and age after mixing; and the behaviour under continuous shear.

Table 1 Properties of the Ciment Fondu

Setting time (BS 915): Initial						280 min			
Final						293 min			
90 μm residue (%)						3.8			
Surface Area (Blaine) (m^2/kg)						276			
Chemical Composition (%):									
SiO_2	Al_2O_3	Fe_2O_3	FeO	TiO_2	CaO	Na_2O	K_2O	SO_3	CO_2
4.14	28.67	10.43	5.63	1.98	38.5	0.06	0.04	0.19	0.42

RESULTS

EFFECT OF CYCLE TIME ON FLOW CURVE SHAPE

Pastes of 0.325 w/c were hand mixed and tested in the MVIIP geometry with shear starting 2.5 minutes after the first contact of cement and water. The total cycle time was varied from one minute to one hour and the maximum speed of rotation was 500 rpm. Figure 1 shows the three types of flow curve obtained, classified according to Banfill and Saunders, and Table 2 gives the cycle times at which these occurred. The relationship between speed and torque shown by the section XX in Figure 1, whether downcurve or upcurve, was independent of cycle time and conformed to the Reiner-Rivlin equation for a Bingham fluid. In view of these results the cycle time in all subsequent experiments was kept short to produce Type 1 flow curves, from the downcurve of which the yield value and plastic viscosity were calculated using that equation.

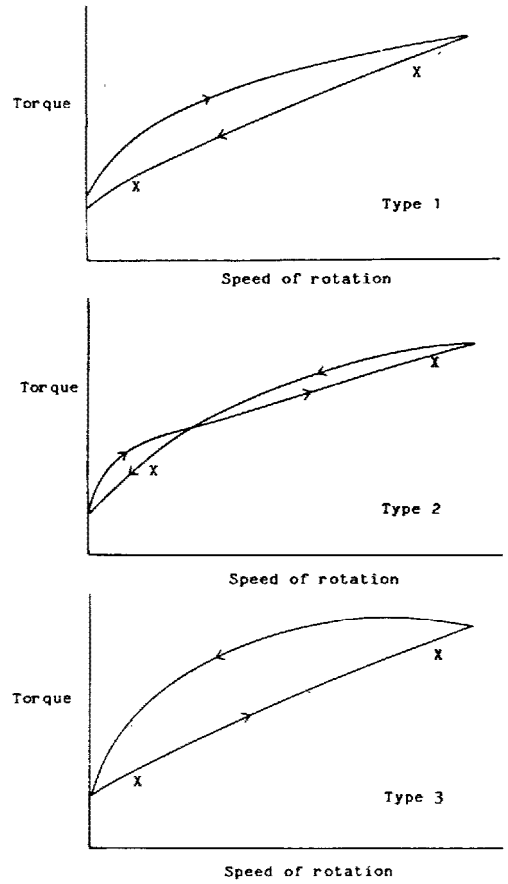

FIGURE 1 - Classification of flow curve types.

Table 2 Variation in flow curve with cycle time

Cycle time (min)	1	2	5	9.8	12	24	36	48	60
Flow curve type	1	1	1	1	2	3	3	3	3

EFFECT OF MIXING TIME

Pastes of 0.3 and 0.4 w/c were mechanically stirred for up to 10 minutes and tested in the MVIIP geometry with shear starting one minute after the end of stirring (i.e. up to 11 minutes from first contact of cement and water). The maximum speed was 500 rpm and the cycle time one minute. Figure 2 shows the effect of mixing time on the yield value and plastic viscosity.

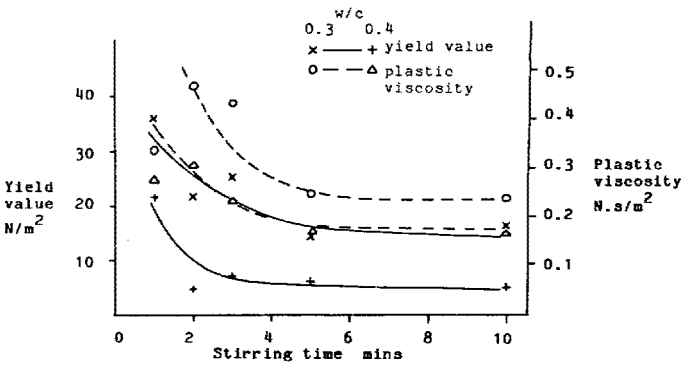

FIGURE 2 - Effect of mixing time on the rheology of Ciment Fondu pastes.

EFFECT OF CONCENTRATION OF PASTE

Pastes of different w/c ratios were mechanicaliy mixed for 5 minutes then tested in the MVIIP geometry to a maximum speed of 999 rpm and in the S13/15 geometry to 500 rpm, in both cases with a one minute cycle time. This mixing time was chosen in the light of the results in Figure 2. Separate paste samples were prepared for each test in both geometries. Figure 3 shows the variation in yield value and plastic viscosity with w/c ratio with comparative information on Portland cements drawn from Tattersall and Banfill's survey of the literature (1).

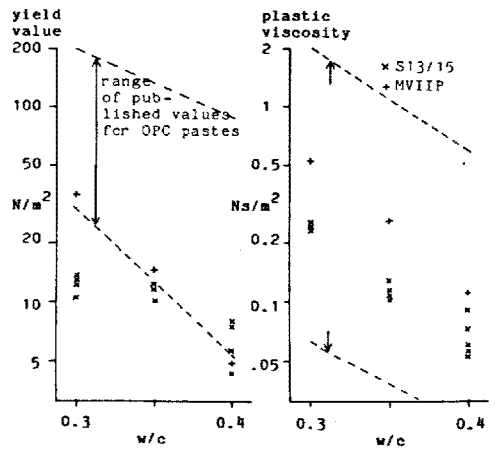

FIGURE 3 - Effect of w/c ratio on the rheology of Ciment Fondu and Portland cement pastes.

EFFECT OF AGE

Separate samples of paste at 0.3 w/c ratio were mechanically mixed for 5 minutes then left to stand for up to 90 minutes before testing in the S13/15 geometry to a maximum speed of 999 rpm or in the MVIIP geometry to 500 rpm with a one minute cycle time. Figure 4 shows the variation with age in yield value and plastic viscosity calculated as before.

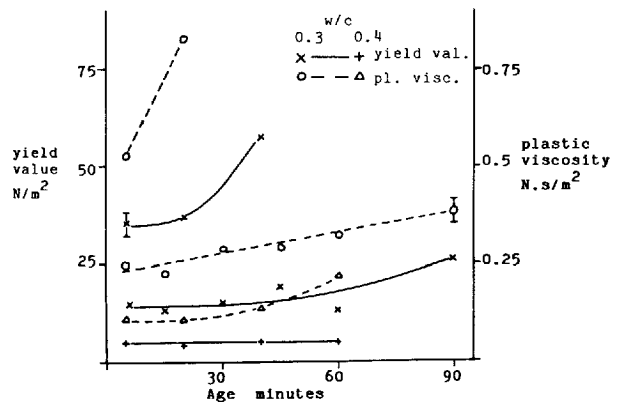

FIGURE 4 - Variation of yield value and plastic viscosity of Ciment Fondu pastes with standing time.

STRUCTURAL BREAKDOWN IN STEADY SHEAR

Hand mixed and mechanically mixed pastes of 0.3 and 0.4 w/c ratio were sheared in both geometries at several speeds of rotation. Typical torque-time behaviour observed in both geometries, as recorded on a continuous chart trace, is shown in Figure 5. However, plug flow taking the form of a stationary zone of paste up to 1mm thick adjacent to the stationary outer cylinder was observed in the MVIIP geometry but never in the S13/15 geometry. It occurred only in the pastes of 0.3 w/c, which suggests that it may be related to the stiffness of the paste. Because of the quantitative uncertainties introduced by this plug flow, only those results obtained in the S13/15 system will be reported here, but it must be borne in mind that the results from the two systems show close qualitative agreement. Table 3 summarises the results.

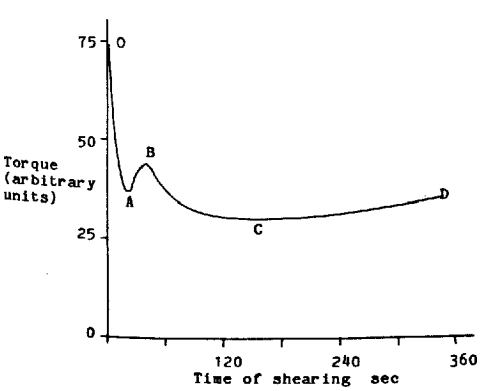

FIGURE 5 - Variation in torque with time during continuous steady shearing of Ciment Fondu paste.

DISCUSSION

Most of the features of the rheology of Portland cement pastes described earlier have been observed in these experiments on Ciment Fondu pastes, but some novel features are also present.

FLOW CURVES

Ciment Fondu pastes may be described by the Bingham model provided it is also realised that structural breakdown occurs on shearing which may distort the flow curve and give apparent shear thinning behaviour. Structural breakdown results in the greater effect on the yield value than on the plastic viscosity (Figure 2), exactly as is observed in Portland cements (7).

The changing flow curve/hysteresis loop pattern shown in Figure 1 follows the same sequence as for Portland cements. Loops indicative of structural breakdown are obtained at short cycle times, while the sense of the loop is reversed at long cycle times. At intermediate times of 10-20 minutes curves with more than one loop are observed. While Banfill and Saunders (3) attribute this to the competition in Portland cement between shear induced breakdown and hydration causing buildup, this cannot apply to Ciment Fondu because of the different chemistry involved. The hydration of Ciment Fondu proceeds via a "through solution" mechanism with dissolution of calcium aluminates. Structure development is delayed until their subsequent precipitation when the saturation level is exceeded (8). In contrast, in Portland cement the growth and interlocking of hydration products takes place from the first contact of cement and water (9). Therefore the observed changes in flow curve/hysteresis loop shape in both types of cement are probably due to physical effects arising from flocculation and deflocculation processes. Hattori and Izumi have explained the hysteresis loops by a theoretical model based on these considerations (10).

EFFECT OF CONCENTRATION AND AGE

Figure 3 shows that the yield value and plastic viscosity of Ciment Fondu pastes are related to w/c ratio in a similar way to Portland cement pastes but that the values determined are somewhat lower. Consequently a Ciment Fondu grout will be easier to pump but may show a slightly greater tendency to bleed. It also accounts for the well known harshness of Ciment Fondu concretes (11).

Because of the low rate of reaction between Ciment Fondu and water during the induction period, the relatively slow increase in yield value and plastic viscosity of undisturbed paste with time (Figure 4) is not surprising. There is a marked difference between results obtained in the two geometries which may be explained by the occurrence of plug flow in the MVIIP system as noted above. This would increase the effective shear rate in the paste and cause the apparently higher yield value and plastic viscosity which have been calculated from the instrument dimensions for Figure 4. In view of the observation of plug flow during continuous shear experiments this must be considered a plausible explanation.

STRUCTURAL BREAKDOWN AND BUILDUP

In general the structural breakdown behaviour of Ciment Fondu pastes is similar to that of Portland cement pastes, but this is the first time that observations of a double minimum in the torque-time behaviour have been reported.

Table 3 Structural breakdown under steady shear (S13/15 geometry)

Experimental Conditions					Torque (Nmm) at				Time (sec) from 0 to			Slope of semi-log plot (sec^{-1})	
W/C	Mixing method	Time (min)	Shearing speed (rpm)		0	A	B	C	A	B	C	OA	BC
0.3	Hand	1	200	)mean	35.7	16.9	19.3	12.9	22	41	175	10.3	1.84
	(4 replicates)			)s.d.	1.9	0.8	0.5	1.5	2.3	2	33	1.7	0.23
0.3	Hand	1	400		>46	19.7	21.2	18.6	45	72	160	3.7	0.73
0.3	Hand	1	500		>46	20.6	21.6	20.3	40	55	120	5.7	0.70
0.3	Machine	5	500		35.4	-	-	17.7	-	-	135	-	1.37
0.3	Machine	10	500		34.5	-	-	16.7	-	-	160	-	1.18
0.4	Hand	1	200		16.9	4.6	6.0	5.5	40	72	140	4.3	*
0.4	Hand	1	400		25.6	6.4	-	-	40	-	-	4.8	-
0.4	Hand	1	500		23.0	6.1	7.4	6.7	20	45	100	3.9	*
0.4	Machine	5	500		28.1	7.1	-	-	65	-	-	7.6	-
0.4	Machine	10	500		26.2	6.9	-	-	60	-	-	4.6	-

* The differences between the torques at points B and C are too small to allow accurate calculation of the slope of the semi-logarithmic graph.

The general form of the torque-time relationship under conditions of steady continuous shear is shown in Figure 5. The main features are the rapid initial decrease to a minimum at point A followed by a small peak B and another minimum C, after which torque steadily rises (D). When the torque reading, T, taken from the chart record is plotted in the form log(T-TeA) or log(T-TeC) against time, where TeA and TeC are the torques at the two minima A and C respectively, both portions fit a straight line relationship (Figure 6). The peak after the initial rapid fall in torque is generally well defined and two minima are clearly evident. However, in some experiments, particularly in mechanically mixed and less concentrated pastes the double minimum tends to merge into a single shallow one (Table 3). In the S13/15 geometry the second minimum is always below the first, but in the MVIIP geometry it is normally at the same torque or slightly above. This could be due to differences in the relative rates of breakdown and buildup at the higher shear rates prevailing in the MVIIP geometry when plug flow is taking place.

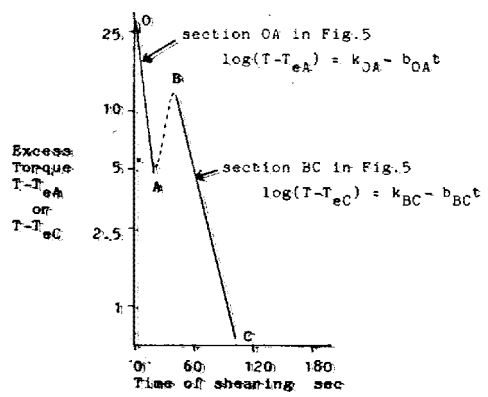

FIGURE 6 - Exponential form of the relationship between torque and time in continuous steady shear.

The linear relationship between log(T-TeA) and time is exactly as first reported by Tattersall for Portland cement pastes (2). However the slopes of the semilogarithmic plots shown in Figure 6 are different for the two portions of the torque-time curve. For the initial breakdown OA (Figure 5) the slope is 5-10 times that of the portion BC. There are insufficient data to confirm Tattersall's observations that the slope of the semilogarithmic plot is steeper at higher shear rates. The slope of the portion OA is not significantly affected by w/c ratio. No conclusion can be drawn about section BC because at 0.4 w/c the second minimum is either not present or so shallow that it is not possible to produce a semilogarithmic plot of the data.

Increasing the w/c ratio moves the whole curve to lower torques but has no significant effect on the times to any of points A, B or C. Mechanical mixing has the same effect but results in a single minimum, the position of which depends on w/c ratio (Table 3). At 0.3 w/c ratio the overall shape of the single minimum is shallow with the lowest torque occurring at times corresponding to point C of the curves with double minima, whereas at 0.4 w/c the minimum is sharply defined with the lowest torque corresponding in time to point A.

These observations tend to support the hysteresis loop behaviour. If the buildup of structure were of chemical origin the time after initial contact of water and cement would be critical whereas mechanical mixing for 10 minutes leaves the shape of the torque-time relationship unchanged. Thus the critical time is that from the start of shearing in the viscometer and the explanation of structural buildup must be sought in physical, flocculation changes.

STRUCTURAL MODEL

Tattersall's model for the structural breakdown of Portland cement pastse was proposed on the basis of the work done in a rotational viscometer (1) in overcoming normal viscous forces, (ii) in breaking linkages and (iii) in keeping them broken (2). Since he observed no rebuilding of structure, item (iii) was not considered. His model correctly predicts the exponential form of the experimental relationship between the excess torque (T-Te) and

time and gives the breakdown constant as

$$b = \frac{2\pi K}{n_0 \psi} w(w - w_1)$$

where w is the shear rate, n_0 and ψ are structural parameters - the initial number of linkages present and their strength repectively, and K, w_1 constants. Hattori and Izumi's structural model (10) explicitly allowed structural rebuilding or reflocculation and, as already noted, this accounted for the observed flow curve/hysteresis loop shapes.

If it is considered that the new structure which forms has different structural parameters then it too will undergo structural breakdown but at the same shear rate the value of the breakdown constant, b, will be different. For example, stronger linkages or more of them, perhaps arising from a different geometrical arrangement in the new structure, will result in a smaller constant b.

The existence of different types of flocculation structure in clay suspensions is well known and documented (12). The flat particles may associate through edge-edge, face-face or edge-face linkages and these types of linkage have different strengths arising from the different arrangements of atoms in the surface layers in these parts of the particles. These structural variations produce different rheological properties. Bombled (13) and Legrand (14) consider that the charge distribution on a grain of cement is not uniform. Ridges and other points where there are abrupt changes in direction of the surface are thought to be charged differently from flat faces. Consequently there is the possibility of face-ridge association relying on electrostatic charges. Because of the heterogeneity of cement particles the strength of this association may well depend on the relative orientation of the particle contacts.

The following model is therefore a plausible suggestion to account for the observed rheological behaviour of Ciment Fondu pastes. Particles are in contact when they are first mixed with water and remain together in the form of flocs, where the interparticle attraction is the resultant of attractive Van der Waals forces and the mutual repulsion of the electrical double layers around each charged particle in water. The particles in a floc are arranged randomly with some strong and some weak linkages. Shear breaks these flocs down, reduces the apparent viscosity of the suspension and individual particles can flow past one another and reorientate themselves. Particles collide but because of their freedom of movement are able to take up relative positions such that only the strongest linkages are formed. This results in a net increase in the strength of the structure, which is then followed by further breakdown, but at a lower rate because of the stronger linkages.

The model is somewhat speculative at this stage but further experimental evidence in support is provided by the effect of superplasticisers, to be described in a later publication. These admixtures remove the second minimum in the torque-time relationship, as would be expected for materials which adsorb all over the particle surfaces thereby obliterating any differences in the charge distributions. Consequently a single type of structure only is involved.

CONCLUSIONS

The rheology of Ciment Fondu pastes is broadly similar to that of Portland cement pastes. They show Bingham type behaviour with slightly lower yield value and plastic viscosity. They exhibit structural breakdown in the form of a dependence on the time of mixing. The flow curves show similar hysteresis loop behaviour to that shown by Portland cement pastes and which can be explained by the competition between structural breakdown and buildup due to flocculation.

In continuous steady shear experiments the behaviour shows novel features in the form of a double minimum in the torque-time curve. This behaviour can also be explained by a change in the flocculation structure upon shearing.

ACKNOWLEDGEMENTS

We gratefully ackowledge the financial support of the Science and Engineering Research Council and FEB (Great Britain) Ltd; provision of materials by Lafarge Aluminous Cement Co Ltd; and the experimental assistance of Miss P. Hooper.

REFERENCES

1. G.H. TATTERSALL, P.F.G. BANFILL (1983), The Rheology of Fresh Concrete, London, Pitman.
2. G.H. TATTERSALL (1955), Brit. J. Appl. Phys. 6 (5), 165-7.
3. P.F.G. BANFILL, D.C. SAUNDERS (1981), Cem. Concr. Res. 11, 363-70.
4. P.F.G. BANFILL (1985), 4th Nat. Conf. on Mechanics and Technology of Composite Materials, Varna, Bulgaria, 423-6.
5. R.J. MANNHEIMER (1983), Oil and Gas J. Dec 5, 144-7.
6. G.H. TATTERSALL, C.R. DIMOND (1976), Hydraulic Cement Pastes, Publicn. 15.121, Slogh, Cement and Concrete Association, 118-33.
7. P.F.G. BANFILL (1981), Mag. Concr. Res. 33 (114), 37-47.
8. F.M. LEA (1970), Chemistry of Cement and Concrete, London, Arnold.
9. D.D. DOUBLE, S.J. PERRY, A. HELLAWELL (1978), Proc. Roy. Soc. Lond. A 359,435-51.
10. K. HATTORI, K.IZUMI (1982), J. Dispersion Sci. Tech. 3 (2), 129-45; 147-67; 169-93.
11. T.D. ROBSON (1962), High Alumina Cements and Concretes, London, Contractors Record Ltd.
12. H. VAN OLPHEN (1977), An Introduction to Clay Colloid Chemistry, New York, Wiley.
13. J.P. BOMBLED (1974), Revue des Materiaux de Construction (688), 137-55.
14. C. LEGRAND (1981), Cahiers de la Groupe Francaise de Rheologie, (Special Number) October, 129-36.

G. H. TATTERSALL - University of Sheffield - England, U.K.

COMPONENTS OF WORKABILITY AND RHEOLOGICAL MEASUREMENTS ON MORTARS AND FRESH CONCRETE
COMPOSANTES DE LA MANIABILITE ET MESURES RHEOLOGIQUES SUR MORTIERS ET BETONS FRAIS

Introduction

The fact that the number of proposed methods for the measurement of workability is well into three figures (1) illustrates the importance attached to the subject, but it also demonstrates that except in the tautological, and therefore not very helpful, sense that the workability of concrete is its ability to be worked, there is not even a universally accepted definition of the term, as pointed out by Neville (2) in his summary of the differing views expressed at a conference in 1973. The situation has improved a little since then, but not much.

Workability seems to be a very complex property because it embraces a number of what might be called constituent properties, as follows.

(i) ability to undergo satisfactory mixing, to produce a homogeneous product.

(ii) ability to flow to fill a mould or formwork, which might be of a difficult shape and might contain congested reinforcement.

(iii) ability to be compacted to remove air so that the hardened concrete may achieve its maximum potential strength.

(iv) ability to resist segregation and excessive bleeding.

(v) ability to provide a satisfactory surface finish, either direct from the mould or as a result of some mechanical processing of a free surface.

(vi) ability to be transported by any one or more of a variety of methods including dumper truck, conveyor belt, pumping, tremieing, etc.

(vii) behaviour in response to various mechanical processes such as application of pressure or vibration.

The situation is further complicated by the necessity to deal with a very wide range of workabilities, from the very high workability of the flowing and almost self levelling concretes at one end of the scale, to the extremely low workabilities of the semi-dry mixes such as are used, for example, for extrusion processes, at the other end.

The workability of a concrete mix is affected by

(i) mix proportions (i.e. of cement, cement replacements, aggregates, and water)

(ii) chemical and physical properties of the cement

(iii) physical properties of the aggregates (particularly shape, particle size distribution and water absorption, and, to a lesser extent, surface texture)

(iv) presence and quantity of any admixtures

(v) age

and there are interactions between these variables. It might also be remarked that there are considerable difficulties in imposing on these variables a control that is adequate for the obtaining of good reproducibility of nominally identical mixes, even in the laboratory.

In terms of sophistication, though certainly not chronologically, the history of the development of tests for the measurement of workability can be considered as having taken place in a series of stages. The earliest stage is that of the very simple tests that were purely empirical and made no pretence of being otherwise, some of which have survived to the present day because of their simplicity rather than because of their usefulness. They include the best known of all, the slump test, and also a whole variety of penetration tests, drop tests and deforming tests. That this approach has still not been abandoned is demonstrated by the recent inclusion, in the latest edition of British Standard 1881, of the flow table test for high workability concretes.

A later stage of development is represented by tests that are based on the idea of isolating one of the constituent properties of workability listed above, and attempting to assess it separately. The compacting factor test of Glanville, Collins and Matthews (3) is an example of this class, and it has probably not been sufficiently appreciated that the authors themselves did not consider it to be an adequate measure of workability in general. A more recent example in this class is the 'efflux rheometer' of Bartos (4) which has been commented on elsewhere (5, 6). Other tests that were intended to imitate practical placing processes, such as that described by Baron (7) and the similar one proposed by Angles (8) some years later, may also be regarded as coming in this category.

These empirical tests have been listed and discussed elsewhere (1); serious criticisms may be made of each one individually but the defect they possess as a group is that any one of them may classify as identical in workability two concretes that are subsequently found to behave very differently on the job. Progress beyond this point became possible only when consideration was given to the question of the behaviour of fresh concrete under defined conditions of stress and/or strain. Early attempts to do this include the experiments of L'Hermite (9) with his annular shear box, and of Berthier (10) with his deforming cubical mould, but most of the work is more recent and includes that to be discussed below.

Tassios (11) has discussed the qualitative relationships between the constituent properties of workability and fundamental properties of the concrete which can, at least in principle, be measured, such as yield stress, yield strain, plastic viscosity and cohesion.

In spite of their obvious, and not so obvious defects, the various empirical tests have contributed to the development of mix design techniques, and in other ways. Nevertheless, any critical review of the field of workability measurement forces the conclusion that a great deal of time and effort has been wasted by some workers who quite clearly have not taken the trouble to study previous work, as is shown, for example, by the several instances that could be quoted of proposals for what purports to be a new test that is in fact similar in all essentials to one that was proposed perhaps 20 or 30 years earlier. In addition, considerable confusion has been caused by the careless and slipshod use of terminology so that, for example, words such as viscosity, mobility and fluidity, to which are properly attached rigorous definitions in terms of fundamental quantities (12), have been used to describe the results of measurements made with quite arbitrary apparatus.

Definition of workability

Attention has already been drawn to the existence of a wide range of opinions on the matter of the definition of the term workability, and these have included proposals for considering it not as a property of the fresh concrete alone but as one that necessitates a consideration of the placing process concerned, or the development of properties measured on the hardened concrete. For example Baron and Lesage (13) suggested a definition based on assessment of the porosity of concrete that had been laid in a given way.

It is clear that general development will be difficult, if not impossible, until there is a generally agreed acceptance of at least the approach to a definition. There seems to be no valid reason why that approach should not be the same as that used successfully for any other physical property, and that means (14, 15)

(i) workability is a property of the fresh concrete, and of the fresh concrete alone

(ii) workability can be defined as being measured by a set of constants W_i and, together, the constants in this set must provide a unique description. The number of constants required to achieve this, that is, the number of constants in the set W_i, is not known a priori.

(iii) the numerical value of each of the constants in the set should be independent of the method by which it is measured, that is, it should be expressible in fundamental units.

It seems reasonable to suggest that the validity of any proposed method of measurement should be judged in terms of how well these criteria are met. Every one of the methods incorporated in the various national standards, as well as every one of the many other methods proposed, fails conspicuously when judged in this way. In violation of condition (iii), results depend markedly on details of the apparatus used and in many cases depend also on details of just how it is used, i.e. they are operator sensitive.

More importantly, from the practising engineer's point of view, any one of the tests may classify as being identical in workability two concretes which are subsequently found to behave very differently in practice. For example, it is well known that two concretes of the same slump may exhibit quite different workabilities as assessed in terms of the job to be done, and this defect in the test has been responsible for some very expensive mistakes.

The detailed definition and determination of the constants W_i involves an investigation of a rheological nature, since rheology is defined as 'the science of the deformation and flow of matter' (12), and that means a consideration of the relationships between stress, strain, strain rate, and time, and perhaps the whole strain history of the material. The end result should be a rheological model, described in mathmatical terms, and obtained either experimentally or obtained theoretically with subsequent experimental verification.

Acceptance of the statement made above, that workability is a property of the fresh concrete alone, does not, of course, mean that the properties of the hardened concrete should be ignored. It has been pointed out previously that the former is important only in relation to the latter. Bombled (16) has commented 'one must never forget that the search for optimal rheological properties (of the fresh concrete) is not an end in itself and it would be disastrous if obtaining them were to be to the detriment of the ultimate properties of the hardened concrete'.

Rheology of cement pastes

Since concrete consists of aggregates, cement and water, it may be regarded as either a suspension of inert particles in a matrix of cement paste, or as inert particles coated with cement paste, and it is reasonable to suppose that a thorough understanding of the rheology of the paste must be obtained before satisfactory progress can be made in the study of the concrete of which it is a constituent. Such an argument was put forward some 30 years ago (17). More recently, Bombled (16) has argued that 'the cement has a predominant role to play in the rheology of the fresh concrete'.

In fact, limited work carried out later on the effect of cement properties on fresh concrete properties, by Dimond (18) and An-Keat Yeoh (19) indicates that this statement needs some qualification, but there is no denying the obvious importance of the cement paste.

Experiments with a coaxial cylinders viscometer, reported in 1954, (17, 20) showed

(i) at low shear rates cement pastes behaved according to the Bingham model

(ii) at low shear rate both the yield value and the plastic viscosity were related approximately exponentially to the water content of the paste

(iii) under higher shear rates plastic viscosity decreased with time while yield value appeared to remain approximately constant

(iv) there was little or no tendency for a rebuilding of structure to take place, at least in times considerably greater than those required for an experiment, so the change could not be classified as thixotropic

(v) at constant rate of shear, the structural breakdown as measured by decrease in torque could be well represented by a simple exponential equation.

A simple theory of breakdown was presented which explained quantitatively the main results.

These findings, which can be explained qualitatively (14) on the basis of Double's membrane theory of hydration (21), have on the whole been confirmed by the considerable amount of work that has been published subsequently, but several difficulties have become apparent. The main ones may by summarised as

(i) results obtained by various workers differ by orders of magnitude

(ii) many different types of hysteresis loop have been found, including positive and negative hysteresis and even figure of eight loops (22)

(iii) decay of torque at constant shear rate cannot always be described by a simple exponential law (23, 24). There may be a discontinuity which has been explained (25) by the presence of a plug whose existence is not predicted from normal plug flow considerations.

These matters have been dealt with fully elsewhere (14) and further discussion is outside the scope of the present paper as are also studies, such as those by Bombled (26) or by Hannant (27) which are intended to aid in the elucidation of hydration mechanisms. It is sufficient to make two observations about the use of the coaxial cylinders viscometer for experiments in cement past rheology, which, it is suggested, should be taken into account in future work.

(i) the finding of a plug, whose existence is so far unexplained, is sufficient to call into question all the results reported from coaxial cylinders viscometer measurements. Observations should be made of the nature of the flow pattern and experiments should be carried out with more than one experimental set-up.

(ii) as was pointed out over 30 years ago (17), the obtaining of hysteresis loops is useful in preliminary work but is not a satisfactory approach for quantitative considerations, because the results depend so markedly on details of experimental procedure. (Of course, it follows that the reporting of hysteresis loops is quite useless if experimental details are not reported at all, or inadequately.) Cheng and Evans have pointed out (28) that it is not possible to deduce the form of a rheological model from experiments carried out at varying shear rates, and Worrall and Tuliani (29) have shown experimentally that two suspensions of quite different thixotropic properties can give similar hysteresis loops.

Another, perhaps cynical, comment may be made and that is that while it can be useful to carry out measurements on fully broken down pastes, that should not be done simply because it is easier.

However, the main conclusion to be drawn, so far as a study of concrete rheology is concerned, is that the whole field of cement paste rheology is in such a state of confusion and uncertainty that to wait for it to be resolved before proceeding with work on the very practical problems relating to concrete, would be to impose a quite unacceptable delay.

Preliminary considerations for concrete

The fact that cement paste rheology is so little understood therefore implies that it is worthwhile carrying out investigations on concrete itself, but there are also some other implications. The first of these is that the approach should be an experimental one, because it is clear that any theoretical treatment would necessarily be based on inadequate information and is therefore unlikely to be successful. The only recent attempt (30) at a theoretical treatment resulted in a prediction of the effect of aggregate grading on workability in the opposite sense to the data given in Road Note 4, which was firmly established on practical experience and experiment. The theory itself was severely criticised (31) but this outstanding disagreement with practice is alone sufficient to condemn it.

The second implication, taking into account also the history of attempts to measure workability, is that a simple empirical approach is not likely to yield any further useful information, and the experiments to be carried out must involve studies of concrete behaviour under reasonably well known conditions of stress and strain or strain rate.

This suggests two possibilities; the first is by using the methods of soil mechanics and the second is by using techniques that have been established for investigating the rheological properties of suspensions. Several workers, including L'Hermite (9), Tassios (11), Ritchie (32), Uzomaka (33) and Mamillan (34) have adopted the first approach and this work has been reviewed elsewhere (1). More recently, Ukraincik (35) has carried out measurements with a type of shear box in investigations which also involved the use of rheological methods. However, the object in all this work was not the development of a practical workability test, because the methods are too cumbersome and time consuming for there to be much hope of their being sufficiently modified for use on site or even for control in a laboratory. A more promising approach seems to be to attempt to apply established rheological methods because they do offer the possibility of being so modified and also, some of them have the advantage of applying continuous shear which seems appropriate in relation to the practical use of fresh concrete.

Ordinary casual observation shows immediately that there is some limiting stress below which a given fresh concrete does not flow, as indicated for example by the mere fact that it is possible to measure a slump value, and this means that the material possesses a yield value. The nature and meaning of yield value have been the subject of some discussion (14, 36) but there is no doubt that from the practical engineering point of view it does exist.

It follows that the flow properties of concrete must be described by an equation of the type

$$\tau = \tau_o + f(\gamma, \dot{\gamma}, t) \qquad (1)$$

where τ is the shear stress at shear strain γ and time t, and τ_o is the yield stress. The simplest possible form of this equation is

$$\tau = \tau_o + \mu\dot{\gamma} \qquad (2)$$

where μ is the plastic viscosity, which is the equation of the Bingham model. It follows immediately that, in order to determine the two constants needed for a full description, measurements must be made at not fewer than two different shear rates. Any test in which only one measurement is made cannot in principle provide sufficient information, no matter how complicated the test procedure or how sophisticated the treatment of the results. This criticism applies to all the standard tests and explains why each of them suffers from the defect that it can classify as identical two concretes that are subsequently found to behave quite differently.

Bombled (37) has proposed that, in accordance with Coulomb's Law as applied in the treatment of results from the soil mechanics shear box, the yield value may be written as

$$\tau_o = c + k.\tan \phi \qquad (3)$$

where c is the cohesion and ϕ is the angle of friction; he considers that the former is provided essentially by the interstitial paste, and the friction by interference between large particles of aggregate.

The coaxial cylinders viscometer is an obvious possible apparatus for a rheological investigation and has been used on high workability concretes by Uzomaka (38), Murata and Kikukawa (39), and Sakuta, Yamane, Kasami and Sakamoto (40). In each case, the results indicated that the flow properties of fresh concrete fit the Bingham model, but the values of yield value and plastic viscosity obtained differed by orders of magnitude. Bloomer (41) has discussed in detail the requirements for the design of a viscometer suitable for measurements on concrete and has pointed out that

(i) the annular gap, $R_c - R_b$ should be not less than 10 times the maximum aggregate size d

(ii) the ratio of the radius of the outer cylinder R_c, to that of the inner cylinder R_b, should be not greater than 1.2 in order to reduce the variation in shear rate across the gap and to reduce the range of speeds in which plug flow occurs.

(iii) the ratio of the height of the inner cylinder, h_b, to the radius, should be not less than unity, in order to reduce end effects.

(iv) to avoid slippage, asperities should be provided on the surfaces of both cylinders and the depth of these asperities, a, should be not less than the maximum aggregate size, d.

Table I shows that all the viscometers fail in respect of gap size and some of them fail in other ways too.

Table I Dimensions of coaxial cylinders viscometers

Quantity	Value Desired	Value in apparatus of U	M&K	S et al
$(R_b - R_c)/d$	$\geq$ 10	1.6	2.25	3
R_c/R_b	$\leq$ 1.2	1.3	1.6	2.5
h_b/R_b	$\geq$ 1	0.8	3.4	2.5
a/d	$\geq$ 1	0.9 1.3	0	0

The only way of reconciling the conflicting requirements listed by Bloomer is to build a large apparatus; he estimates that a satisfactory one would have a sample volume of $2\frac{1}{2}m^3$ and would require a 4 h.p. motor to drive it. This is clearly impractical; an alternative possibility is to consider a mixer method.

Measurements using a mixer

Quite apart from any theoretical considerations, the attractions of attempting to use a mixer for measurements on a material such as concrete are obvious, and several workers have done so certainly as early as 1928. However, in all but two cases measurements were made at only one speed, and in the two cases (42, 43) in which a range of speeds was used, no attempt was made to plot a flow curve. This was first done in 1970 (44) from experiments with a food mixer, in which power consumption was measured at each of the three speeds of which the mixer was capable, and torque was calculated as net power divided by speed. It was found that when plotted as torque against speed, the three points fell close to a straight line which had an intercept on the torque axis, thus indicating that the flow properties of fresh concrete approximated to the Bingham model.

The equation to the line may be written as

$$T = g + hN \qquad (4)$$

where T is the torque at speed N, g is the intercept on the torque axis, and h is the reciprocal of the slope of the line. This equation is obviously analogous to the equation for the Bingham model and it seems apparent that the constant g is a measure of yield value while the constant h is a measure of plastic viscosity. Theoretical justification for this conclusion will be summarised later.

This result which was obtained before the coaxial cylinders work referred to above was published, was a very surprising one, in view of the known complexity of cement paste behaviour. Of course, an experimental result based on only three points is somewhat questionable but it has been amply confirmed since by a very large volume of work. It is now thought that the explanation of this simple behaviour is that the shear rates in the mixing process are substantially higher than those used in the test and the cement paste has already been subjected to structural breakdown so that the paste itself exhibits Bingham properties. It can now be regarded as firmly established that, over a range of shear rates that are important in practice, the flow

properties of fresh concrete are described by the simple Bingham model, and therefore can be characterised in terms of the two constants yield value and plastic viscosity. Whether this is the whole story will be discussed later.

Scullion (45) improved the original apparatus and used it in investigations on the effect on workability of the properties and proportions of mix constituents but further intensive investigations showed that its disadvantages were such that it should be abandoned in favour of a new apparatus that was developed.

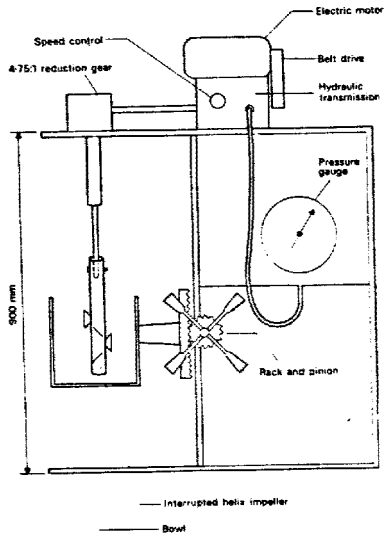

Figure 1 The two-point workability apparatus

The new apparatus, the development and construction of which have been described in detail elsewhere (46, 14), is shown diagrammatically in Figure 1. A suitable impeller is immersed in the concrete under test which is contained in a cylindrical bowl, and is rotated about its own axis by means of an electric motor driving through an infinitely variable hydraulic transmission. The torque required at each of a range of speeds is measured by monitoring the pressure of the oil in the hydraulic transmission. When net torque (that is, the difference between the torques when the bowl contains concrete and when it is empty) is plotted against rotational speed, the points are found to fit to the linear Bingham relationship with a correlation coefficient usually in excess of 0.99.

The apparatus in this form was developed specifically for high workability concretes and has been found to be suitable for a range from about 75mm slump to flowing concrete. For low workabilities it is unsuitable, because the concrete is found to move to the sides of the bowl and fail to fall back, so that the impeller then rotates in the hole it has made. For such concretes an alternative form was developed in which an impeller of a different shape is caused to rotate in planetary motion, and in this form it can be used for low workability concretes down to about 25mm slump. The apparatus can readily be changed from one form to the other; together, therefore, they can cover almost the whole range of practical workabilities, with the exception of extremely low workabilities.

The apparatus has been called the two-point workability apparatus because it satisfies the condition of providing measurements at the required minimum number of two different shear rates. In practice, more speeds are used in order to reduce experimental error.

Practical use of the apparatus

Two practical problems may arise in the use of the apparatus and were considered during the development work.

The first is that, because of trapping of coarse aggregate, the torque reading is not steady. Typically, the torque oscillates about a mean value by a few percent but on this oscillation are imposed larger 'kicks' which are due to aggregate trapping and should be ignored. The extent of the oscillation is reduced by introducing damping into the measuring system but not to such an extent that the response is sluggish. In practice, it is a relatively easy matter to adjust the damping to the right level and to 'learn' to ignore the kicks so that the mean of the small oscillations can be read. A previously inexperienced operator can be taught, or can teach himself, in about quarter of an hour. Of course, the process can be made even easier by automatic recording of torque as a function of time (at a given speed) when a trace of the form shown in Figure 2 is obtained, provided the chart speed is appropriate. The simple insertion of a pressure transducer in the hydraulic line permits this method to be used, and this was done by Gjorv and co-workers (47). An alternative approach, which was considered during the early stages of development of the apparatus, is to take signals from strain gauges fixed on the drive shaft and such a development has been reported recently by Cabrera and Hopkins (48). The disadvantages are that it is considerably more expensive and requires the provision of slip rings whose performance might be affected by even small amounts of dirt. Cabrera reports (49) that no such problem has been experienced but it may still be thought that the system is too vulnerable to be used on an apparatus that has been designed for operation under site and plant conditions.

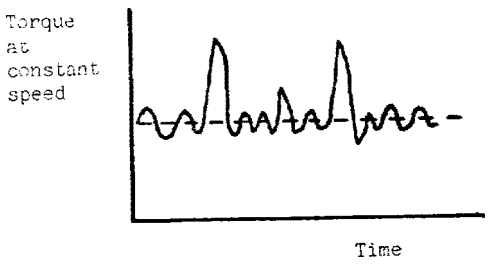

Figure 2 Oscillation of torque

The second problem is that of the possible occurrence of segregation during the test, and much effort was devoted to trials of impellers of various shapes (41, 50) to reduce this problem to a minimum. The result is that for a wide range of mixes it is clear from ordinary visual observation that the difficulty does not arise, but for some mixes there may be a separation of coarse particles on top of the concrete, or the development of a compacted layer at the bottom of the bowl. However, Wallevik and Banfill (51) have shown that even in such cases during a single test, taking a few minutes, 'the aggregate grading in the zone sheared by the impeller is unchanged'. This has been confirmed by other unreported experiments.

In practice therefore the concrete should be agitated only during loading (at low speed) and the actual carrying out of the test. Under these conditions segregation sufficient to affect the results should not occur; if it does, it is suggested that questions should be raised about the suitability of the mix in general and whether it is likely to segregate in the practical use for which it is intended.

The time needed for a test is under 3 minutes if 7 points are obtained, or under 2 minutes for the 4 points that are usually sufficient for site work. Sugden (52) who used the apparatus on site in both the uniaxial and the planetary form, reported that the time for a test, including loading, was 5 minutes, which he compared with the 3 minutes needed for a slump test.

A much more fundamental difficulty was raised by Ukraincik, (35) who questioned the validity of the straight line relationship for normal concretes and claimed to have obtained three different types of torque/speed curve. However, a plot of the numerical results he gave suggested that his curves had been much over-idealised and the only reasonable conclusion to be drawn was the restricted one that he had observed a curvature towards the origin (53). Even so, this does, as he points out, raise questions about the determination of yield value from linear extrapolation. The apparatus he used was of the food mixer type and one of the reasons that this apparatus has been abandoned, and is now regarded as obsolescent, is that Bloomer showed that the relationship between speed and average shear rate is not constant over the range of speeds used, so that a material whose shear stress/shear rate relationship is linear may well give a torque/speed line that is curved. Unfortunately, Ukraincik does not give any other information about his apparatus so a proper comparison of his results with those of others cannot be carried out, but measurements with the planetary form of the apparatus described above over a greater range than is normally used, showed that a lowest speed comparable with that used by Ukraincik there was no evidence of a curvature towards the origin. In no case has such behaviour been reported by any other worker, except when the concrete in the bowl was vibrated.

It may also be pointed out the criticisms concerning inadequate gap size, that were emphasised in the discussion of coaxial cylinders viscometers, may, with some modification, be levelled at both forms of the apparatus described here. It is necessary to attempt to reconcile what is theoretically desirable with what is practicable, and so to restrict sample size to a reasonable amount. The extent to which the compromise is acceptable must be judged on whether

(a) the method works in practice and yields results that are more useful than those from previous methods and

(b) the results of measurements comply with the theoretical treatment.

It has been shown that the evidence is very encouraging.

Accuracy and sensitivity

Banfill (54) has pointed out that in dealing with a material as variable as concrete, valid estimates of experimental error can be obtained only from properly designed experiments whose results can be processed statistically. For the usual empirical single point tests this involves very lengthy investigations and then the result, when obtained, applies only to the test in general and not specifically to a particular set of measurements. From factorial experiments by Orr (77), in which compacting factor was measured, and similar experiments by himself for slump and vebe, Banfill quotes standard deviations for slump as 11mm, compacting factor as 0.024, and for vebe time as 0.25 times the reading. The practical error figure taken for the slump test is $\pm$ 25mm.

In contrast, the experimental error in the two-point method can be readily calculated for each individual test by considering the variance about the line $T = g + hN$. Bloomer (41) has shown that the standard error in h is given by

$$\frac{\alpha_h}{h} = \sqrt{\left[\left(\frac{1-r^2}{r^2}\right)\cdot\left(\frac{1}{n-2}\right)\right]} \qquad (5)$$

where r is the correlation coefficient and n is the number of experimental points, and the standard error for g is given by

$$\frac{\alpha_g}{g} = 0.95\,\frac{h}{g}\left(\frac{\alpha_h}{h}\right) \qquad (6)$$

where the numerical factor (in this case 0.95) is fixed by the particular choice of speeds used in the test. The error at any chosen level of significance can be found by multiplying these values by the appropriate value of Student's t. The error on h is read off a graph (14) and that on g easily calculated. Typical errors on g and h are of the order of 10% at the 90% confidence level.

The fact that errors can be calculated for each individual test and that the error is usually around only 10%, has the consequence that small effects that would be undetected by other tests can be observed. For example, Bloomer (41) found effects of the variation of fines content that would have remained undetected by the slump test, and Saeed (50) demonstrated the variability caused by variations in water content of a moist aggregate. Recently, Ellis (56), in work on concretes containing ground granulated blast furnace slag, showed that the test was better at detecting significant changes in workability of GGBRS/OPC concretes relative to their OPC controls than any of the British Standard test methods. Waddicor (57) stated that he had been able to assess the performance of plasticising admixtures

more critically than previously. Crossley (58), who used the apparatus for evaluating cements, reported that correlation coefficients were always very high and that repeatability between nominally identical concrete mixes was such that the flow curves lay within bounds that were equivalent to a change in water/cement ratio of about 0.01.

Theoretical considerations

It has been stated earlier that the constants g and h are measures respectively of the yield value and plastic viscosity of the concrete, but the only justification offered so far is that of analogy between the equation of the flow curve and that of the Bingham model. Theoretical support can be provided by considering behaviour in the mixing process and it can also be shown how, following suitable calibration of the apparatus, the constants g and h can be converted to measures of yield value and plastic viscosity in fundamental units. This has been discussed in detail elsewhere (14, 59) and will only be summarised here.

It is first of all necessary to show that the apparatus is operating in the region of laminar flow. This was done by Bloomer using heavy oils (41) and by Saeed (50) using Newtonian polybutene solutions, who each demonstrated close adherence to the relationship

$$N_p = B.Re^{-1} \qquad (7)$$

up to a Reynolds number of 10, where N_p is the power number and Re is the Reynolds number. Then, on the basis of the postulate by Metzner and Otto (60) that the average shear rate in a mixer may be regarded as being simply proportional to the speed, it can be shown that the equation for a Bingham material is

$$T = (G/K)\tau_o + GN \qquad (8)$$

where G is a constant obtained by calibration with Newtonian liquids, and K is a constant obtained by calibration with non-Newtonian liquids whose apparent viscosities vary with shear rate in a known way, determined by separate experiments using a conventional viscometer.

By comparison of equations (4) and (8) it is apparent that

$$\tau_o = (K/G).g \qquad (9)$$

$$\mu = (1/G).h \qquad (10)$$

and hence both yield value and plastic viscosity can readily be expressed in fundamental units (14, 46). The calibration process is somewhat tedious and in practice it is quite satisfactory to express results simply in terms of g and h, which are simply proportional to τ_o and μ respectively.

For two nominally identical apparatuses, A and B, the constants K and G should of course be the same, but, if they are not, corrections may be made by writing

$$g_A = g_B \cdot \frac{G_A K_B}{G_B K_A} \text{ and } h_A = h_B \cdot \frac{G_A}{G_B} \qquad (11)$$

Figures have been published (46) to show that what was already good agreement between results from two nominally identical apparatuses could be improved further in this way; Banfill (61) has only recently applied the method again.

More importantly, it is possible to use the equations for comparison of results from different forms of apparatus, and in particular, from the uniaxial and planetary forms, with a view to establishing a single scale to cover almost the whole range of workabilities. Such a study was made by Bloomer (41) and later extended by Dimond (62) who used the same apparatuses but a greater number of mixes. Dimond found the agreement between experiment and theory to be very promising but to depend to some extent on a somewhat arbitrary choice from equally plausible assumptions about the nature of the calibration curves. The difficulty arises from the results obtained on the non-Newtonian liquids used in the determination of the constant K.

It would be very desirable to use a material whose properties are similar to those of the materials for which the apparatus is to be used, that is, one that conforms to the Bingham model. Unfortunately it has not been possible to find a suitable material, even after publication of an appeal (63); several that have been described by other workers as Binghams were tried but all were found to suffer from structural breakdown under shear. It was therefore necessary to use aqueous carboxymethyl cellulose solutions which are pseudo-plastics of the power law type and whose flow curve may therefore be described as

$$\tau = r\dot{\gamma}^s \qquad (12)$$

Unfortunately, detailed work has shown that, for the solutions used, the constant s is in fact dependent on shear rate to an extent that introduces uncertainties into the interpretation. Saeed (50) has made a thorough study of this problem but further work is needed before it is completely resolved.

Factors affecting workability

The two-point workability apparatus has been used by a number of workers in investigations of the effects of various factors on workability, as follows:-

Mix proportions and aggregate type - Scullion (45), Bloomer (41) and Saeed (50)

Cement properties - Dimond (62) and An-Keat Yeoh (64)

Plasticisers - Scullion (45), Waddicor (65), Banfill (66), Rixom and Waddicor (67), Bloomer (41), Edmeades and Hewlett (68) and Carlisle (69)

Air entrainment - Banfill (14)

Fly ash - Ellis (70)

Blast furnace slag - Arnold (71), Crowter (72), and Ellis (56)

Steel fibres - Urbanowicz and Dimond (73)

Fine dredged sand - Carr and Banfill (74)

A full discussion of this work is beyond the scope of the present paper but the main general results may be summarised as follows.

(i) There is in general no correlation between the values of g and h so it is necessary to measure both of them, and suggestions such as that of Hobbs (30), in support of single point tests are shown to be invalid (31).

(ii) There is strong interaction between the effects of the variables. For example the effect of a change in fines content depends very much on the values of other parameters such as water/cement ratio and aggregate/cement ratio.

(iii) For some factors interactions are less strong and generalisations may be made. For example, an increase in water content always reduces both g and h, an increase in plasticiser content decreases g but has very little effect on h, while an increase in air entraining agent content decreases h with little effect on g. Replacement of cement by ground granulated blast furnace slag has little effect on either g or h.

These results lead to two very important conclusions. The first is that measurement of the two quantities g and h readily provides a means of differentiating between concretes that are wrongly judged to be similar by other tests. The second conclusion is that because changes that affect workability affect g and h in different ways according to the causative agent, the two-point test presents possibilities for a control method that have not been available previously. It can not only detect that workability has changed, but can give strong indicators as to the cause of the change. This possibility has been discussed in detail elsewhere (75, 76).

Banfill (77) has produced the diagram shown in Figure 3 as a simplified guide to show in general terms the effect of increases in concentration of various components, on g and h. Of course, for control purposes, much more specific diagrams are needed but they can be readily constructed.

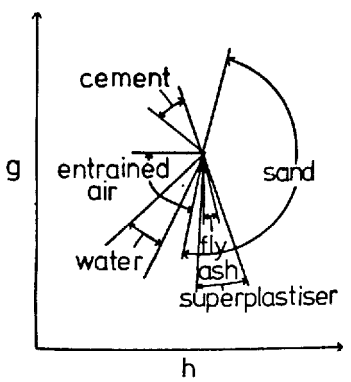

Figure 3 Effect of increase in quantity of various mix constituents

Effect of vibration on workability

The use of vibrators for the placing and compaction of concrete is a long established practice, yet the design of the equipment is still on a very much ad hoc basis. Early work on the effect of vibration was based mainly on assessments of the properties of the hardened concrete except for some empirical flow tests and some shear box experiments by L'Hermite (9) on fresh concrete. Clearly, it is the effect on flow properties of fresh concrete that is of major interest.

Just as ordinary casual observation shows that fresh concrete possesses a yield value, as mentioned earlier, so it is also obvious that when vibration is applied to concrete, the effective yield value is at least very much reduced, perhaps even to zero. This is indicated by the fact that the concrete flows easily under its own weight.

Reduction in yield value was studied in an interesting series of experiments by Lasalle and Legrand (78) in which they measured the minimum torque required to turn a paddle located at various distances from a vibrating source. They state that when a critical amplitude is exceeded the yield value is reduced to zero but the radius of effectiveness of a vibrator decreases as frequency increases, because of increased damping. They describe the existence of three zones, in relation to an internal vibrator:

Zone 1 near the source, where turbulence occurs and operates against satisfactory compaction

Zone 2 further away, where yield value is practically destroyed and compaction takes place satisfactorily

Zone 3 further still, where the vibration is damped to an extent that yield value is not sufficiently decreased, and satisfactory compaction does not occur.

The positions of the boundaries between these zones are conditioned by the amplitude and frequency of the vibration but in Zone 2 the parameters of vibration have little influence on rheological characteristics. It should be noted that they measured only yield value and, more importantly, that to avoid difficulties of change with time they used calcite pastes. This does raise a question about the validity of the application of the results to cement pastes and (even further removed) to concretes.

Because it is easy to mount the bowl of the two-point test apparatus on a vibrating table, it becomes possible to obtain the flow curve for a material when it is not being vibrated and of the same material when it is being vibrated. Preliminary experiments on these lines, using a concrete in which all the cement had been replaced by pulverised fuel ash, and a table vibrator actuated by a commercial shutter vibrator, have already been reported (14). Little was expected from these experiments because of the complex waveform of the vibrator, except an indication as to whether experiments with more expensive apparatus would be worthwhile, and these experiments have now been carried out (79).

The bowl of the workability apparatus was mounted on an electromagnetic vibrator whose amplitude and frequency could be controlled

independently, and which was capable of 70 kN peak thrust. A flow curve for unvibrated concrete was obtained in the normal way, then the impeller was run at its top speed and the vibrator was switched on at the chosen amplitude and frequency, resulting in a very rapid drop in torque followed by a slower rise, which was attributed to the occurrence of compaction. The minimum torque observed was taken as a measure of the effect on workability, and gave one point on the flow curve of the concrete under vibration. The concrete was then remixed, replaced in the bowl, and measurements repeated at a lower speed setting to give another point. In this way four points were obtained and the vibrated flow curve was constructed. Experiments of this type were carried out on two different mixes of 75mm slump at six frequencies from 15 to 100 Hz and four accelerations from 2½ to 10g.

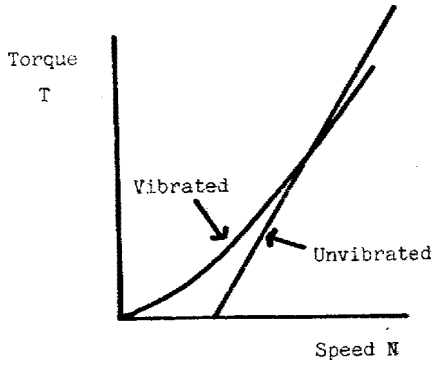

Figure 4 Effect of vibration on flow curve

The results were of the form shown in Figure 4. The flow curve for the vibrated concrete appeared to start from the origin and could be well represented by a power law equation of the type

$$T = A_v N^{B_v} \qquad (13)$$

This means that yield value has been reduced to zero but the flow curve has been changed from a straight line to a curve which crosses the original unvibrated line, so that at the higher shear rates the application of vibration actually reduces the workability of the concrete. Experimental points to confirm this were obtained, but whether any practical process operates in a shear rate range where the effect is important is not known. It can be shown that the straight line $T = g + hN$ for the unvibrated concrete can also be approximated very closely over the shear rate range covered in the test, by a power law relationship, so the effect of applying vibration may be presented in the form

$$(T_v/T) = (A_v/A).N^{B_v-B} \qquad (14)$$

There was some evidence that (A_v/A) was an exponential function of acceleration, and (B_v-B) an exponential function of velocity.

The indication that the curve pases through the origin means that at low shear rates, such as those produced by flow under self weight, concrete under vibration can be regarded as a Newtonian whose flow properties can be characterised by the viscosity η or its reciprocal, the fluidity ϕ, which may be found from the slope of the tangent from the origin. For both mixes studied it was found that the results fitted a relationship of the form

$$\phi = c_1(1 - \exp(c_2 A(f-F_c))) \qquad (15)$$

where A is amplitude, f is frequency and F_c is some small critical frequency that must be exceeded for there to be any effect at all. Note that, since velocity is proportional to the product of frequency and amplitude, this shows that the effect of vibration is to be measured in terms of the maximum velocity of the vibration.

The obtaining of the evidence that at low shear rates concrete under vibration behaves as a Newtonian prompts the carrying out of experiments that would have been unjustified in the absence of such evidence. Apparatus was set up to study the rate of fall of a column of concrete contained in a 100m dia. vertical pipe when vibration was applied at the bottom, where the concrete was allowed to flow out into a containing bowl. If the material behaves as a Newtonian the height H would be expected to decrease according to

$$dH/dt = -bH \qquad (16)$$

where b is proportional to the fluidity. The simplicity of this arrangement permits the carrying out of a large number of experiments and observations were made on six mixes at ten frequencies from 15 to 200 Hz and eight accelerations from 0.85 to 8.9 g. All the results were found to fit the relationship proposed and further, for each mix, to fit a relationship of the form

$$b = c_3.(A - A_o).\ln(1 - f/F) \qquad (17)$$

where A_o is a small critical amplitude and F is a large critical frequency in excess of 200 Hz. While the actual value of F is in some doubt, its existence is not, as was confirmed by subsidiary experiments at frequencies up to 1000 Hz. If the values of A and f are well away from the critical values, this expression again reduces to a simple function of velocity. Finally, a good correlation was found between ϕ from the two-point apparatus experiments and b from the quite different vertical pipe experiments.

The importance of velocity was also confirmed by experiments on cement pastes using a smaller scale version of the two-point apparatus, and this work has already been reported (80).

Other applications of the two-point apparatus

The two-point apparatus has been shown (81) to be satisfactory for measurements on grouts of the type used for filling prestressing ducts, provided the impeller is modified to produce greater values of net torque. It has also been used for mortars although in this case peculiar results have been obtained on several occasions, when the flow curve

has been found to have a negative slope. This is not yet explained, but in the case of mortars the requirements for gap width of a coaxial cylinders viscometer are obviously much less demanding than for concrete, so Banfill (61) has substituted a serrated cylinder for the normal impeller and has obtained satisfactory results.

The apparatus is also useful at a smaller scale (2/5) for investigations of cement pastes at low shear rates, but then the impeller and container are used in conjunction with a normal viscometer head and drive unit. This arrangement was used in the vibration experiments on cement paste, referred to above and has also been used by An-Keat Yeoh (64) in his investigation of the effect of cement properties. Yeoh found that for pastes made from a given cement with varying water contents, the ratio g/h was a constant and could be useful in looking for correlations between rheological properties and factors in the composition of the paste. It is interesting that Bombled has independently suggested the use of this ratio of yield value to plastic viscosity to characterise pastes, although his suggested term 'intrinsic plasticity' might be criticised.

A difficulty in using coaxial cylinders for cement pastes is that at the water/cement ratios normal in concrete heavy sedimentation occurs in the paste. Bhatty and Banfill (82) showed that using the helical geometry of the scaled down two-point apparatus, sedimentation, as measured by their sedimentation index, was only about 6% of that for coaxial cylinders, and even at a water/ cement ratio of 1.0, the difference in solids concentration from top to bottom of the sample was only 5%.

Conclusions

It can now be taken as established that, at the low rates of shear important in practice, the flow properties of concrete in the low to very high workability range, conform to the Bingham model, and can therefore be assessed in terms of yield value and plastic viscosity. This is not an assumption, as some authors seem to think; it is a statement well attested by a large volume of experimental results obtained by a large number of independent workers.

The two-point test apparatus is capable of measuring the two parameters and of ascribing an estimated experimental error to each determination. As a result, it can differentiate between concretes wrongly judged by other tests to be similar and it can form the basis of a production control system.

The knowledge now available leads to a greater understanding of the existing standard tests (83, 50, 14), and of processes such as pumping (14) and the application of vibration. Of course, there are still large gaps; the test itself might be improved by development of new impellers and further study is needed on the calibration with non-Newtonians, and certainly much more work is needed on the effects of various factors on g and h.

The test is not capable of dealing with extremely low workability concretes, which cannot even be regarded as a continuum so the approach must be different, and it cannot give information at stresses below the shear stress.

However, it can be claimed that it has already served in elucidating previously intractable problems and can do much more. Finally, it was never intended to be only a laboratory tool and it is believed that its use on site, or at the ready mixed concrete plant, would lead to substantial savings by avoiding disputes and lost production and by preventing expensive mistakes.

References

1. Tattersall, G.H. The Workability of Concrete, C&CA 1976.
2. Neville, A.A. RILEM, Chairman's Summary.
3. Glanville, W.H., Collins, A.R. and Matthews, D.D., Road Research Technical Paper No. 5, HMSO, 1947.
4. Bartos, P. Concrete, 12, (10), 28-30, 1978.
5. Tattersall, G.H., Concrete, 12,(12),15, 1978.
6. Banfill, P.F.G., Concrete 13 (1), 16, 1979.
7. Baron, J., RILEM, Vol. 1, 2D1-1.
8. Angles, J.G., Concrete 8 (12), 26, 1974.
9. L'Hermite, R., CERILH Pub. Tech. No. 1, 1948.
10. Berthier, R.M., Rev. des Mater. de Constr. et de Trav. Pub. (417), 187-9, 1950.
11. Tassios, T.P., RILEM Vol. 1, 1.3-1 to 1.3-36.
12. British Standard BS5168; 1975.
13. Baron, J. & Lesage, R., RILEM, 1.1-1 to 1.1-27.
14. Tattersall, G.H. & Banfill, P.F.G., The Rheology of Fresh Concrete, Pitman, London, 1983.
15. Tattersall, G.H., Proc. Symp. M. Annual Meeting Mater. Res. Soc., 1982, 78-97.
16. Bombled, J.P., Rev. des Mater. de Constr.(688), 137-155, 1974.
17. Tatersall, G.H., M.Sc., Thesis, University of London, 1954.
18. Dimond, C.R., Unpublished Report, University of Sheffield, Reported in Ref. 14.
19. Yeoh, An-Keat, M.A. Thesis, University of Sheffield, 1982.
20. Tattersall, G.H., Brit. J. Appl. Phys., 6, (5) 165-7, 1955.
21. Double, D.D., Perry, S.J. and Hellawell, A., Proc. Roy. Soc. A., 359, 435-451.
22. Banfill, P.F.G. and Saunders, D.C., C&CR, 11, 363-370, 1981.
23. Tirona, E.E., M. Eng. Thesis, SEATO Graduate School Engng, 1964.
24. Nessim, A.A. and Wajda, R.L., MCR, 17 (51), 59-68, 1965.
25. Tattersall, G.H. and Dimond, C.R., Proc. Conf. Hydraulic Cement Pastes, 118-133, C&CA, 1976.
26. Bombled, J.P., CERILH Pub. No. 213 & Rev.des Mater.de Constr. 1971.
27. Hannant, D.J. & Keating,J., C&CR, 15, 605-612, 1985.
28. Cheng, D.C. & Evans, F., Brit. J. Appl. Phys., 16, (11), 1599-1617, 1965.
29. Worrall, W.E. & Tuliani S., Trans. Brit. Ceram. Soc., 63 (4), 167-186, 1964.
30. Hobbs, D.W., MCR 28 (97), 191-202, 1976.
31. Tattersall, G.H. & Dimond, C.R., MCR 29 (101), 225-7, 1977.
32. Ritchie, A.G.B., MCR 14 (40), 37-42, 1962.
33. Uzomaka, O.J., MCR 23 (75-76), 111-8, 1971.
34. Mamillan, M., Suppl. Ann. de. L'inst. Bat. et Trav.Pub. (201), 912-952, 1964.
35. Ukraincik, V., C&CR 10, 203-212, 1980.
36. Cheng, D.C.H., Bull. Brit. Soc. Rheol., 21 (4), 60-5, 1978.

37. Bombled, J.P., Rheologie du Beton Frais et influence des Fillers; Synthese des Etudes 1982/4. CERILH.
38. Ujomaka, O.J., Rheol. Acta 13, 12-21, 1974.
39. Murata, J. & Kikukawa, H., RILEM Vol. 1, 1.2-1 to 1.2-33.
40. Sakuta, M., Yamane, S., Kasami, H. & Sakamoto, A., Proc. Conf. Quality Control Concrete, Vol. 2, 125-132, 1979, Stockholm.
41. Bloomer, S.J., Ph.D. Thesis, University of Sheffield, 1979.
42. Purrington, W. & Loring, H.C., Proc. ASTM 30 Pt. II, 654-673, 1930.
43. Harrison, O.J., Tech.Rep.27, Ready Mixed Concrete (UK) Ltd.
44. Tattersall, G.H., Paper to Conf. E. Midlands Region Concrete Soc., Nottingham, 1971.
45. Scullion, T., M.A. Thesis University of Sheffield, 1975.
46. Tattersall, G.H. & Bloomer, S.J., MCR 31 (109), 202-210, 1979.
47. Gjorv, O.E., Private Communication Jan. 1983.
48. Cabrera, J.G. & Hopkins, C.J., MCR 36 (129), 237-240, 1984.
49. Cabrera, J.G., Private Communication.
50. Saeed Ahmad, Ph.D. Thesis, University of Sheffield, 1982.
51. Wallevik, O. & Banfill, P.F.G., Internal Rep. University of Liverpool, 1983.
52. Sugden, A., Unpublished Report, 1981. Reported in Ref. 14.
53. Tattersall, G.H. C&CR 11, 485-7, 1981.
54. Banfill, P.F.G., MCR 29 (100), 156-7, 1977.
55. Orr, D.M.F., J.A.C.I. Proc. 69, (10), 619-624, 1972.
56. Ellis, C. Paper presented at Workshop on blast furnace slag cements and concretes, York, Oct. 1985.
57. Waddicor, M.J., MCR 32 (113), 244, 1980.
58. Crossley, A.N., Reported in Report BS74, University of Sheffield.
59. Cheng, D.C.H., Bull. Brit. Soc. Rheol. 21 (4), 60-5, 1978.
60. Metzner, A.B. & Otto, R.E., J. Amer. Inst. Chem. Engs. 3, 3-10, 1957.
61. Banfill, P.F.G., Private communication.
62. Dimond, C.R., Unpublished report. Reported in Ref.14.
63. Anon. Technical enquiry. Bull. Brit. Soc. Rheol. 21, 23, 1978.
64. Yeoh, An-Keat, M.A. Thesis, University of Sheffield, 1982.
65. Waddicor, M.J., Private communication to P.F.G. Banfill, Nov. 1980.
66. Banfill, P.F.G., MCR 32 (110), 17-27, 1980.
67. Rixom, M.R. & Waddicor, M.J., in Developments in the use of superplasticisers, Pub. SP-68, ACI 1981, pp. 359-380.
68. Edmeades, R.M. & Hewlett, P.C., Proc. Admixtures Cong. CI80 49-72, 1980.
69. Carlisle, J.S., B.Sc. Project, Sheffield City Polytech. 1981.
70. Ellis, C., MCR 33 (117), 233-5, 1981.
71. Arnold, S.R., Private communication to P.F.G. Banfill, Aug. 1981.
72. Crowter, G., B.Sc. Project, University of Sheffield. Reported in Ref. 14.
73. Urbanowicz, C., M.A. Thesis, University of Sheffield 1973.
74. Carr, M.P. & Banfill, P.F.G., Research Report, University of Liverpool, 1985.
75. Tattersall, G.H., Concrete 16 (3), 21-4, 1982.
76. Tattersall, G.H., Proc. Symp. M. Annual Meeting Mater. Res. Soc., 1982, 78-97.
77. Banfill, P.F.G., Proc. Conf. Mech. & Techny. of Composite Materials Varna, Bulgaria, 1985. pp. 443-6.
78. Lassalle, A. & Legrand, C., Mater. et Constr. (76), 315-322.
79. Tattersall, G.H. & Baker P.H., To be published.
80. Tattersall, G.H., Proc. Conf. Mech. & Techny of Composite Materials Varna, Bulgaria, 1985, pp. 419-422.
81. Tattersall, G.H., Unpublished report, Nov. 1984.
82. Bhatty, J.I. & Banfill, P.F.G., C&CR 13, 69-78, 1982.
83. Tattersall, G.H., MCR 28 (96), 143-7, 1976.

Abbreviations

MCR	Magazine of Concrete Research
C&CR	Cement and Concrete Research
RILEM	Proc. RILEM Seminar on Fresh Concrete : Important Properties and the measurement. Leeds 1973.

MICHAUX M.
OBERSTE - PADTBERG R. - Etudes et Fabrications Deowell Schlumberger - Saint Etienne - France

THE EFFECT OF MIX WATER SALINITY ON CEMENT SLURRIES CONTAINING POLYNAPHTALENE SULPHONATE.

S3

INTRODUCTION

Wherever cement slurries or concrete grouts are pumped, their rheological properties are of interest. In order to adjust a slurry at a given water to cement (W/C) ratio for pumpability, dispersants, also called superplasticizers, are added. The most frequently applied dispersants are of the naphtalene sulfonate formaldehyde condensate (NSFC) type. In the oil well cementing industry, they are exclusively applied in fresh water and low salinity water. For salt rich cementing slurries, as frequently designed for salt zone cementing, NSFC is reported to be of no use, and even to deteriorate the rheological behavior of the slurries.

In the present study the effect of both, mix water salinity and dispersant content on slurry rheology and NSFC adsorption on cement particles is reported. A model for salt - NSFC interactions in a Portland cement slurry is developed.

LITERATURE REVIEW

Many articles in the literature deal with the adsorption of NSFC on cement surfaces in fresh water based slurries. The cement to NSFC interactions in salt water based systems have not yet been studied. Usually, pseudo adsorption isotherms are determined for a particular cement and correlated with properties such as sedimentation velocity [1], zeta potential [2-6], or different kinds of rheology [3], [7]. Here, we should also refer to comprehensive studies by Tattershall and Banfill [8]. Michaux et al [9] studied the interaction between NSFC and fresh water mixed oil well cement slurry by zeta potential and adsorption measurements and correlated these results to the rheological slurry properties.

EXPERIMENTAL

1. Slurry preparation

All slurries were prepared according to the API specification N° 10 [10] at 25°C and agitated subsequently for 20 mn in an atmospheric consistometer before carrying out the measurements. For all tests a (water + NSFC)/cement ratio of 0.44 was maintained.

2. Chemicals

One single batch of cement and one single batch of dispersant solution (solid content = 40%) were used. The free Na_2SO_4 content of the NSFC, determined as described in [9] was less than 1% by weight of liquid (bwol).

3. Measurements

The determination of the adsorbed NSFC was done by UV absorption as described in [9]. Rheology tests were done according to [9] and [10].
Conductimetric measurements were also done on salt water solutions containing different concentrations in NSFC.
For turbidimetric tests, different amounts in NSFC were added to 10 cc of a cement slurry's interstitial water, filtrated 20 mn after mixing. This solution was left under static conditions for 48 h and subsequently tested for absorbance at 650 nm before and after filtration.

RESULTS

Fig.1 shows the evolution of the yield value (YV) of cement slurries with various low amounts in NSFC as a function of their mix water (NaCl)salinity. For the 1 and 2% by weight of cement (bwoc) NSFC containing cement slurries, salt has a highly viscosifying effect.

In Fig.2, we see the YV evolution as a function of NSFC concentration for three different salinities. For all three cases, we can see that a NSFC addition effects a slurry viscosification that, after a maximum YV, will result in a well dispersed slurry. These maxima occur at different NSFC concentrations, depending on the mix water salinity, and are of differing importance; compared to a NSFC free system the YV in the fresh water system increases only by about 20%, whereas for the 30% NaCl slurry by more than 500%. The high salinity cement goes between 7.2 and 7.8% bwol NSFC through a minimum (overdispersed).

Parallel to the increased NSFC demand for a well dispersed cement slurry with increasing salinity, we also experienced an increasing NSFC adsorption on both, cement particles after 20 mn hydration and synthesized calcium silicate hydrates (CSH) with higher slurry mix water salinity (see fig.3 and 4).

In order to determine the effect of both, cations and anions on the NSFC-cement interaction, we measured the dispersant adsorption in the presence of two other soluble salts, having a common ion with NaCl : KCl and $NaNO_3$ (see fig.5) in the presence of 2% bwoc NSFC. Both alkali chlorides influenced the NSFC adsorption in the same way: the dispersant adsorption increased drastically with increasing salinities (up to 95% adsorption). The $NaNO_3$ showed hardly any effect on the NSFC to cement interaction.

Conductimetric tests showed that at increasing water salinities NSFC additions had decreasing effects on the conductance of the resulting solution (see fig.6).

DISCUSSION

In the scope of the present tests, it was experienced for the first time that NSFC can be applied as salt cement slurry dispersant. It was shown that increasing mix water salinity increases the NSFC demand for a well dispersed slurry.
Adsorption tests revealed that the increase in dispersant demand for a well dispersed cement slurry is related to an increase in NSFC adsorption as soon as cement slurries are mixed with NaCl or KCl rich water.

This can be, partly, attributed to the formation of different initial hydration products (chloroaluminates, Na^+, K^+, and Cl^- containing CSH) with an increased specific surface in a NaCl rich system compared to a fresh water one. It was shown, however, that sodium chloride effects the NSFC adsorption on pure CSH phases in the same way. This means, that a specific surface modification of a cement during initial cement - water contact due to salinity variations cannot be exclusively responsible for the observed phenomenon.

A deactivation of the NSFC, leading to a higher dispersant demand, can be explained by the formation of ion pairs: the negatively charged sulfonate group of

the NSFC will interact with positively charged ions according to :

$$R - SO_3^- + Na^+ \rightleftharpoons [R - SO_3^- \ldots {}^+Na]^0$$

with R being the naphtalenic group.

This unity has no external electrical charge and its formation will be promoted if, for a given alkali activity, the NSFC concentration increases.

If this were the main mechanism responsible for the increased NSFC demand for constant slurry dispersion, the effect of NaCl replacement by $NaNO_3$ should have the same effect on polymer adsorption. This is not the case (see fig.5).

A possible mechanism for the increased NSFC adsorption on cement grains with increasing alkali chloride concentrations can also be due to a compaction of the NSFC unities as an effect of an increased electrolyte activity. Thus, the single dispersant molecules could have been agglomerated in the form of micelles (see fig.7). The quantity, size, and form of the micelles is reported to depend on the nature and concentration of electrolytes [11] . This could explain the differences in NSFC adsorption at different alkali salts.

The agglomeration of a certain number of micelles may finally lead to a precipitate. In fact, in the scope of additional tests, it was observed that, if NSFC was added up to a certain concentration into an interstitial salt cement slurry water (mix water salinity : 30% NaCl), a precipitate was formed. This precipitate disappeared when NSFC was added in excess (shown in fig.8).
Interstitial waters from cement slurries of lower mix water salinity ($\lesssim$26% NaCl) did not produce this precipitate.

The initial increase in YV for salt free as well as salt rich cement slurries, at low NSFC concentrations (see fig.2) can be explained by the patch model as described by Michaux et al. [9] .
The positive charge observed on cement particles without dispersants is a global charge. The actual charge is probably composed of positive patches separated by neutral or even negative regions. Therefore particles will tend to orientate themselves to align positive and neutral or negative patches. This will result in attractive forces creating a tridimensional structure. This strength is measured macroscopically by YV determination and is somehow proportional to the product of the average number of positive (n^+) and negative (n^-) patches on the particles.

For the neat formulation, $n_0^+ \gg n_0^-$. As we now increase the dispersant concentration, n^- increases and n^+ decreases.
Only a fraction of the sulfonate groups of the dispersant chains neutralizes the positive site. The rest brings an excess k of negative charges. Therefore we obtain :

$$n^- n^+ = (n_0^+ - km)\,[n_0^- + (\alpha - k)m]$$

where :

m is the average number of adsorbed dispersant molecules per cement particle surface unit.

α is the average number of sulfonate groups per dispersant molecule.

This product must go with increasing NSFC concentrations through a maximum and so must the YV.

This patch model is supposed to be responsible for the slight YV increases as soon as initial NSFC amounts are added to the 0 and 18% NaCl cement slurries. The main factor for the drastic YV increase and subsequent decrease in the high salinity cement slurry at NSFC concentrations between 0 and 7% bwol is supposed to be the formation and subsequent disappearance (see fig.8) or the dispersion of the precipitate observed with increasing NSFC amounts added to a high salinity interstitial water. However, within a cement slurry, we cannot differentiate between adsorbed and flocculated NSFC.

CONCLUSIONS

In order to disperse a cement slurry by NSFC, its molecules have to adsorb on cement surfaces. This will decrease attractive interparticle forces.

Salt water cement slurries of a W/C ratio of about 0.44 need for a YV close to zero by far more dispersant than fresh water mixed ones. The reason is that with increasing water salinities an increased NSFC amount is adsorbed on both, cement particles and pure CSH phases.
The mechanism for this can be explained by a deactivation of the NSFC at high electrolyte activities due to the formation of ion pairs. The compaction of NSFC layers, being adsorbed on the cement particles, may lead to the adsorption of additional NSFC.

Micellation is postulated, and agglomeration due to both, mix water salinity and NSFC addition could be observed. The appearance and subsequent disappearance or dispersion of a precipitate in slurry's interstitial water, prepared with 30% NaCl mix water, can explain the pronounced YV increase for a salt water slurry with increasing NSFC amounts.

LITERATURE

[1] Kondo,R. ; Daimon,M. ; Sakai,E. ; Il Cemento, V.3, pp 225-230 (1978)

[2] Daimon,M. ; Roy,D. ; J. Cem. Conc. Res., V.8, pp 753-764 (1978)

[3] Daimon, M. ; Roy,D. ; J. Cem. Conc. Res. V.9, pp 103-109 (1979)

[4] Suzuki, K. ; Nichikawa,T. , Kato,K. ; Hayashi,H; Ibo,S. ; J. Cem. Conc. Res. V.11, pp 759-764 (1981)

[5] Collepardi, M. : Il Cemento, V.4, p 298 (1983)

[6] Pauri, M. ; Ferrari,G. ; Collepardi, M.; J. Cem. Conc. Res., V.13, pp 61-68 (1983)

[7] Kishitani,K. ; Tomosana,F. ; Oka, S. ; ACI Publ. Sp 68-24, pp 423-439 (1979)

[8] Tattershall, G. ; Banfill, P/F/G. ;The Rheology of Fresh Concrete ; Pitman Publishing, London (1983)

[9] Michaux,M. ; Defosse, C. ; J. Cem. Conc. Res. V.16 (1986)

[10] API Specification for Materials and Testing for Well Cements, Spec. 10 ; American Petroleum Institute, Washington DC (1984)

[11] Hall, D.G. ; Tiddy, G.J.T. ; Anionic Surfactants - Physical Chemistry of Surfactant Action ; Lucassen & Reynders (Editors), pp 55-108 (1981)

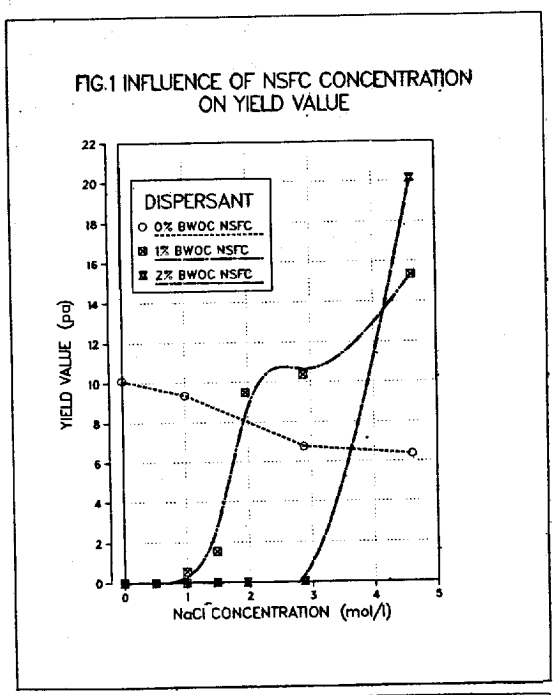

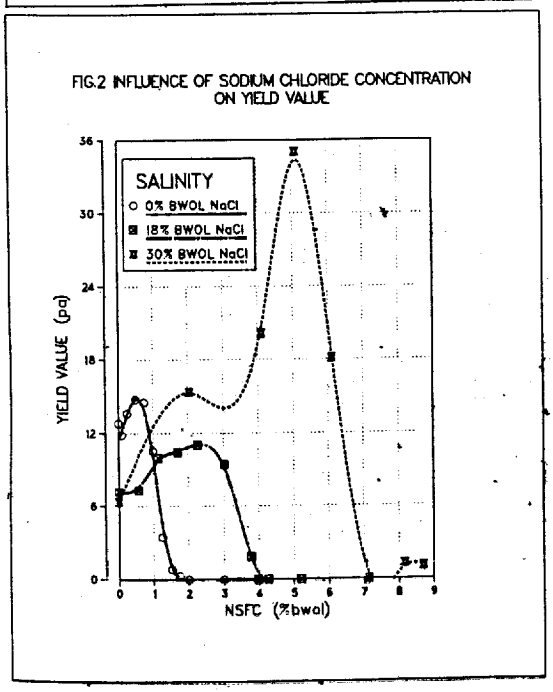

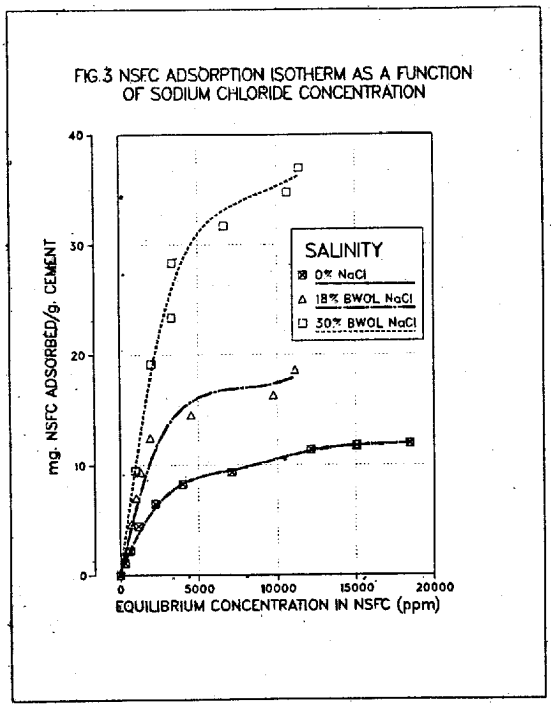

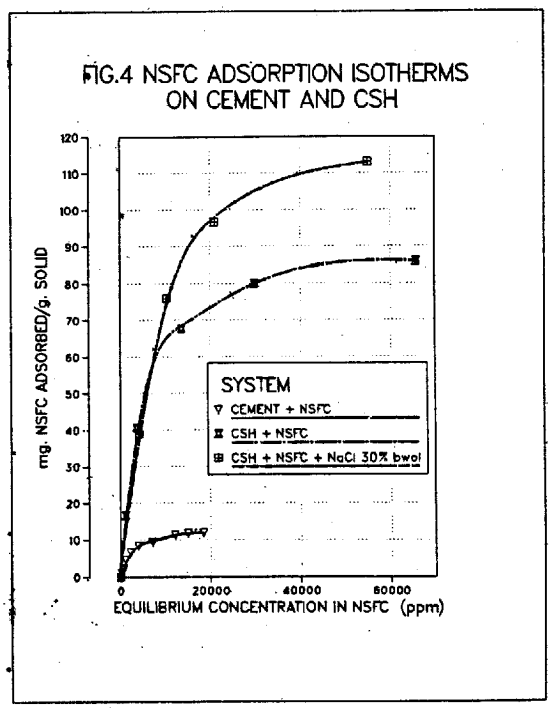

MICHAUX M.
OBERSTE - PADTBERG R.

S3

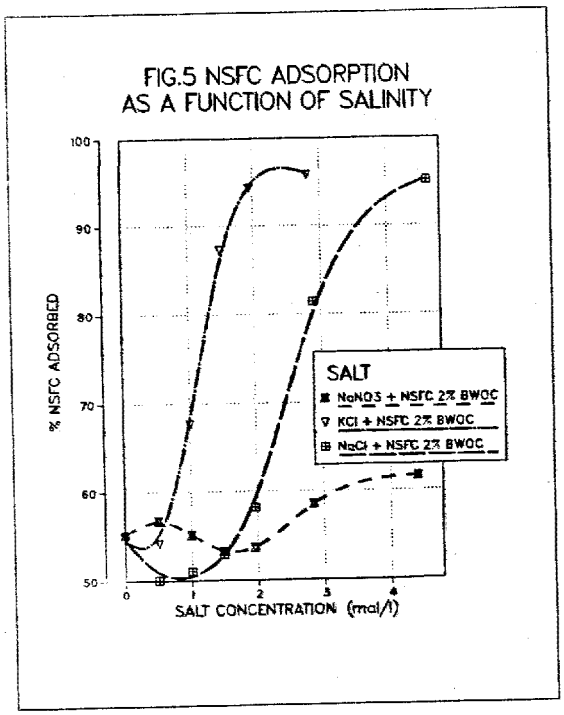

Fig. 7 : The Hartley spherical micelle showing surfactant ion of dubious status. (The representation of surfactant chains as rods is highly idealized.)

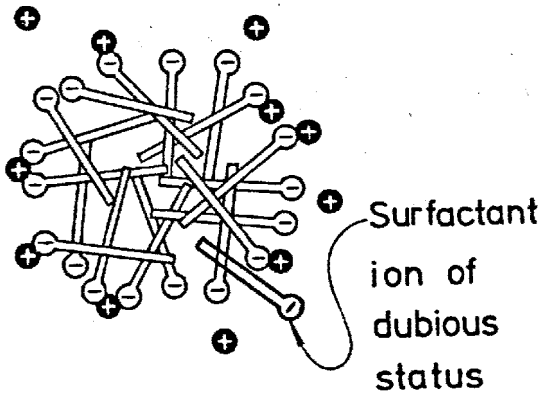

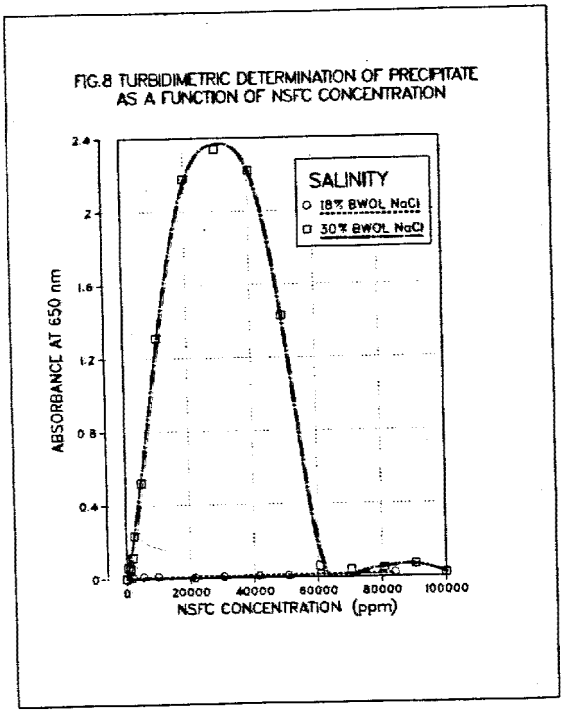

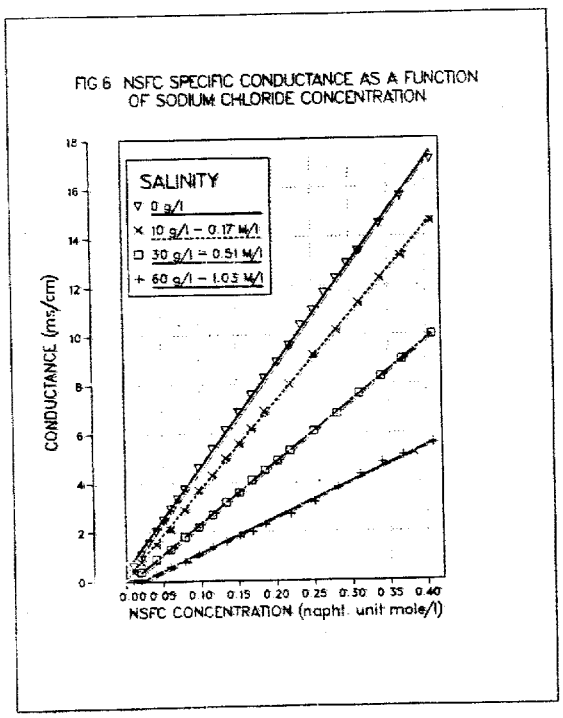

ORBAN, J.
PARCEVAUX, P.
GUILLOT, D.
Etudes et Fabrications Dowell Schlumberger - Saint Etienne - France

INFLUENCE OF SHEAR HISTORY ON THE RHEOLOGICAL PROPERTIES OF OIL WELL CEMENT SLURRIES

INTRODUCTION

Cement slurries are commonly considered to exhibit a shear dependent behavior. This is particularly true from a rheological point of view. In the construction industry and in civil engineering, Tattersall and Banfill [1] , and Lapasin and al. [2] , have analyzed this shear dependence. Lapasin proposed a thixotropic model to characterize slurry rheology. Banfill analyzed the influence of mixing conditions on the rheological behavior. He suggested the use of a Bingham Plastic model to characterize the equilibrium flow condition in most common situations.

In oil well cementing, cement slurry rheology plays an important role on the effectiveness of a cement job. A major problem is that job design is done from laboratory tests performed on slurry samples mixed in conditions, as per the API specification 10 [3] , that do not systematically simulate those of field mixing.

The influence of shearing not only should account for mixing, but also for pumping the cement slurry into the casing and displacing it into the casing to formation annulus. Here as well, the similarity between laboratory agitation in a consistometer [3], and field pumping is of utmost importance.

Finally, following to mixing and stirring, the cement slurry is rheologically characterized using a viscometer. A thixotropic model was proposed in [2], which mainly accounts for API Class A or ASTM type 1 cements which produce reasonably high levels of ettringite very soon after mixing. In fact, most API Class G or H cements show lower levels of thixotropy. However, the rheological test itself should not perturbate the fluid sample. This problem was analyzed by Batty and Banfill in [4] . It was concluded that rotational viscometers with coaxial cylinders are suitable to measure the rheology of a slurry the water to cement ratio of which is higher than 0.35, as sedimentation occurs during the test.

Up to now, the shear dependency of cement slurries has then been described as a function of several interdependent parameters, like time, shear rate, shear stress, flow regime, but no attempt has been made to combine all these factors into a single one that would biunivocally describe this shear dependency. The main objective of this work has consequently been to define such an independent parameter. Furthermore, as there is a large difference between laboratory and field or industrial mixing conditions, it has been attempted to compare both scales.

RHEOLOGICAL PROCEDURE AND CHARACTERIZATION

In this study two coaxial cylinder viscometers have been used :

the FANN 35 SA/SR12 with R1B1 geometry, a constant speed apparatus with a Couette fixture, standard in the oil industry [3] ,

the CARRI-MED CS100, a constant stress apparatus with a Searl fixture, with the CA 1809 geometry.

The Bingham Plastic model was used to characterize the rheological behavior of the slurries, as only equilibrium characteristics under shear were examined. Furthermore, wall slippage was not taken into account, although its influence is sometimes not negligeable for absolute measurements [5] . Wall slippage was here ignored because only comparison between results obtained with the same viscometer and the same geometry has been performed.

Preconditioning of the slurry was achieved with the standard API atmospheric consistometer [3] . The slurry consistency increase versus time is related to the appearance of a gel structure, most of the time related to cement hydration, in the slurry. It is commonly accepted that a fluid that generates a consistency of at least 40 Bc (arbitrary unit of torque on the consistometer) is unpumpable with oil field equipment.

SLURRY MIXING AND VOLUMETRIC SHEARING ENERGY

- Experimental -

The first part of this study was performed with the API standard laboratory mixer [3] . This mixer has an impeller that can rotate with a controlled speed up to 12000 RPM under load. Mixing conditions were varied by controlling the impeller speed and the mixing time.

The second part of the study was performed with a standard oil field mixer, also called jet mixer. This mixer works on the following principle : water is jetted at high speed, and cement powder falls by gravity into the high velocity zone. This permits the wetting of the cement powder by water, and some small shearing after wetting. Additional shearing was added into the slurry with different shearing devices or by pumping it through different orifices and at different pumping rates.

On all mixing devices, the shearing power could be determined through the measurement of torque and speed for a rotating system, or pressure and flow rate for orifices.

Cement slurries were composed of CEMOIL API Class G cement with 44% water by weight, with or without polynaphtalene sulfonate superplasticizer.

- Characterization of Mixing Conditions -

Bingham Plastic parameters were evaluated versus several factors that can characterize the mixing conditions, like the maximum shear rate, the shearing time, the typical Reynolds number if available, and the specific shearing energy.

This specific shearing energy Se, e.g. in fact the total mechanical energy given to a unit volume of slurry during the mixing process, can be expressed by :

$$Se = \frac{1}{V} \int_0^t P(t)dt \qquad (1)$$

where V is the slurry volume, P(t) the power and t the time.

ORBAN,J.
PARCEVAUX, P.
GUILLOT, D.

When a laboratory type mixer is used, Se is obtained using the following equation:

$$Se = \frac{1}{V.d} \int_o^t T(t).S(t)dt \qquad (2)$$

where T is the torque measured between the motor of the mixer and the mixing bowl, S is the rotational speed of the impeller, d the diameter of the impeller's blade, V the volume of the slurry, and dt the unit mixing time.

The torque due to the friction in the packing and the bearing of the mixing bowl was calibrated versus speed. It was then possible to determine the torque really applied on the impeller only to shear the slurry.

With a field type mixer, the total specific shearing power put in the slurry was evaluated through the measurement of the pressure drop and flow rate (Q) when the shearing is produced through small orifices, or torque (T) and speed (S) for rotating shearing devices, as per the following equations [6] :

orifice :
$$Se = \frac{\rho . Q^2}{2K^2A^2} \qquad (3)$$

rotating :
$$Se = \int_o^t \frac{T(t).S(t)}{Q(t)} dt \qquad (4)$$

where ρ is the slurry density, Q the flow rate, A the orifice area, and K the efficiency of the orifice

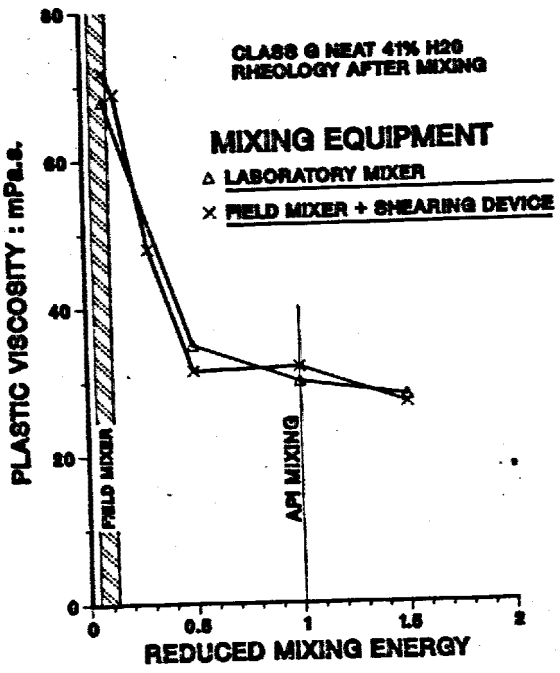

Pig.1: Comparison between field and laboratory mixer Plastic viscosity

In order to facilitate comparisons, the specific shearing energy was then adimensionalized by the energy level corresponding to the API laboratory mixing energy.

A clear dependence of the rheological behavior on the specific shearing energy during mixing is observed (see figures 1 and 2). The plastic viscosity regularly decreases when the specific shearing energy increases, while the yield stress first decreases at low energy levels, and then increases. The mixing technique, and the scale, laboratory or industrial, have only secondary effects on the slurry behavior. A similar type of dependency was already described in [1] , pages 268 to 271.

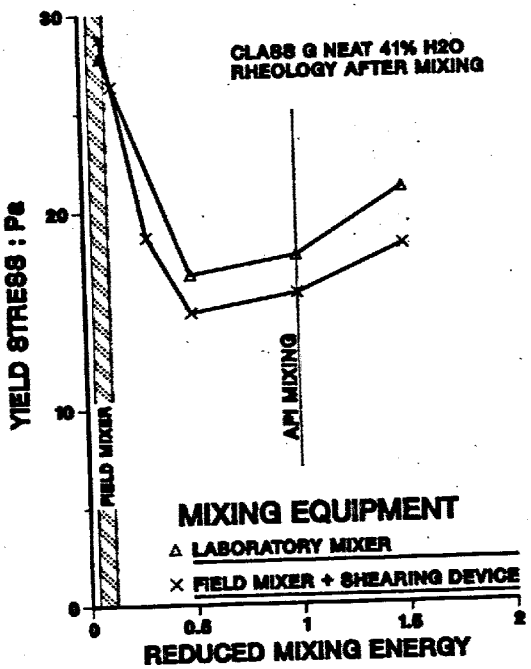

Fig.2 : Comparison between field and laboratory mixer' Yield stress

_ Discussion On Mixing -

This influence of shearing during mixing was also analyzed using cement slurries containing some organic superplasticizer (see fig. 3) of the polynaphtalene sulfonate condensate (PNS) family. Mixing was performed with a laboratory type mixer. The plastic viscosity shows the same dependence on the mixing energy as in the case of a neat slurry. Conversely, the yield stress stays close to a minimum value up to a critical specific energy. At this point, the yield stress increases quickly with the energy. Consequently, the efficiency of the superplasticizer is reduced by the mixing. This phenomenon was already observed by Vom Berg as described in [7] .

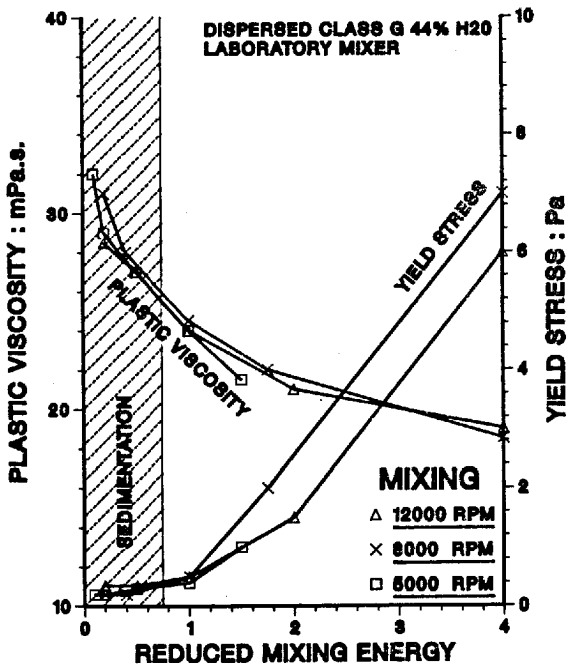

Fig.3: Influence of mixing energy on the rheology of dispersed cement slurry

The mechanism of action of polynaphtalene sulfonate dispersants has been described by Michaux and al. in [8] and [9] , through an adsorption model.

Furthermore, any cement powder being composed of agglomerates of cement particles linked through electrostatic forces, the action of the mixing process is, first, the deflocculation of these agglomerates and the wetting of residual particle flocs by the mixing water, and, second, the erosion of cement grains and possible generation of some colloidal particles.

A possible explanation for this influence of the specific shearing energy on cement slurry rheology is, then, that the average size of cement flocs and possibly of cement particles is reduced when the specific shearing energy increases, thereby promoting a better contact between water and cement, and increasing the cement specific surface area available to the dispersant, this artificially impairing the dispersant's efficiency.

A reduction in cement particle size is pretty well in line with the effect on rheology, as smaller particles in suspension are known to generate lower viscosities [7] , but will also promote higher yield stresses because of an increased surface activity. A secondary factor that tends to promote this mechanism is the reduction of bleeding with increasing specific shearing energy, as shown in table 1.

Table 1 : Influence of shearing energy on free water development, with a Class G Cemoil mixed with 1.8% PNS and 42% water by weight of cement.

Spec. Energy	0.15		1		3	
Temperature deg.C	20	85	20	85	20	85
Free water in mL/250mL	1	22	2	5	1	3

However no evidence to support this hypothesis could yet be found, neither through particle size determination, nor through microstructural investigations.

EVALUATION OF THE FLOW REGIME

After being mixed on surface, oilwell cement slurries are pumped with high pressure triplex displacement pumps, down a casing and up the casing to formation annulus. The exhibited flow regime can then range between fully developed turbulent flow and very low laminar, depending on flow geometry, slurry rheology and density, and pump rates.

Experimental

In the laboratory, the standard API atmospheric consistometer [3] used to simulate agitation produces a very good turbulent flow regime. At the other extreme, laminar flow conditions were simulated in the laboratory by the rotational viscometer.

The experimental study was then performed in the laboratory as follows: after standard API mixing at 20 deg.C, and a given agitation time in the consistometer (turbulent flow) at 80 deg.C, a rheological test was performed also at 80 deg.C. Laminar shearing was simulated by a given time at a given shear rate in the rotational viscometer.

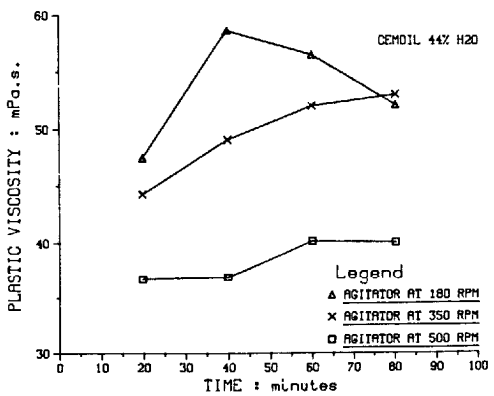

Fig.4 : Influence of turbulent stirring on cement rheology . Plastic viscosity

ORBAN, J.
PARCEVAUX, P.
GUILLOT, D.

Discussion

As can be observed on fig.4 and 5, the influence of time is not very relevant for turbulent agitation, while the level of energy or turbulence is a predominant factor affecting the plastic viscosity. It is important to notice that the yield stress is not very much affected by turbulent agitation.

In contrast, in a laminar flow regime (see fig.6 and 7), both plastic viscosity and yield stress increase drastically with time, while the influence of the level of energy or shear rate does not follow a definite trend. Slurries in totally static conditions exhibit similar behavior to those in the laminar dynamic state.

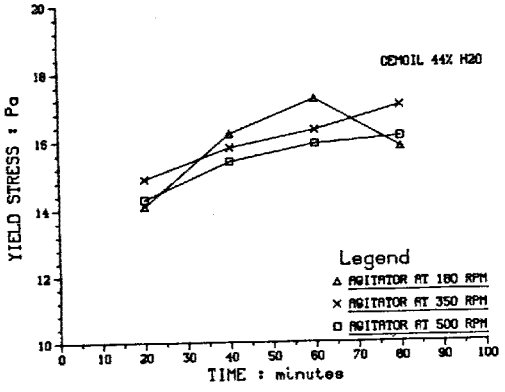

Fig. 5 : Influence of turbulent stirring on cement rheology. Yield stress

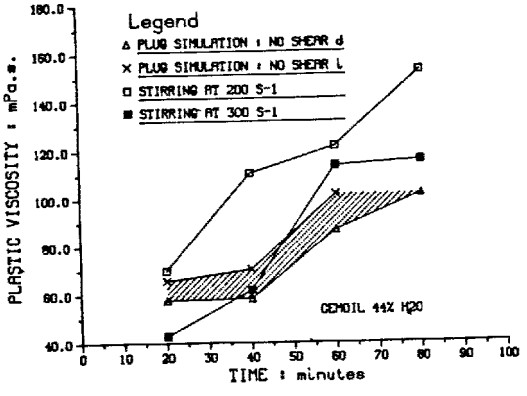

Fig. 6 : Influence of laminar stirring on cement rheology. Plastic viscosity

EVOLUTION OF SLURRY RHEOLOGY DURING THE RHEOLOGICAL TEST

Not only true or simulated pumping operations affect cement slurry rheological behavior, but the rheological test itself induces additional shearing in the slurry sample. This can modify the measurement, as any additional shearing energy would do. The specific shearing energy input by the viscometer can obviously be determined through equation (3).

Experimental

The influence of the test routine was then investigated, by varying either the time steps T at each shear rate, the number of steps, or the maximum rotational speed. Then the results were analyzed as a function of the shearing energy, or as a function of the maximum shear rate. For this study only neat Cemoil Class G slurry mixed with 44% fresh water by weight of cement was used. All experiments, from mixing the slurry till the end of the rheological test, were performed at a temperature of 20 deg.C.

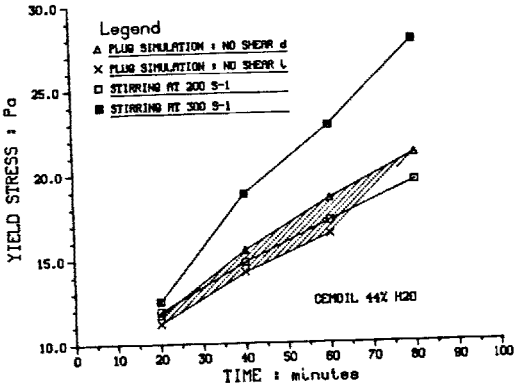

Fig. 7 : Influence of laminar stirring on cement rheology. Yield stress

Discussion

Test results presented in table 2 and in figure 8, show a strong dependence of cement slurry rheology on both the specific shearing energy and the maximum shear rate input during the rheological experiment.

Table 2: Influence of the test routine on slurry rheology

Specific energy M J/m^3	Plastic Viscosity m Pa.s.	Yield Stress Pa
0.03	61.7	12.1
0.28	47.2	13.4
0.68	40.5	13.9
1.20	40.0	15.0
2.00	39.0	19.0
4.00	39.0	19.0
6.80	38.0	19.0

When the test shearing energy increases, the plastic viscosity decreases while the yield stress increases. This is in agreement with the previous results. However, at very high levels of energy, both parameters

tend to reach a stable plateau. The same dependency is observed with increasing the maximum shear rate. Such a similar result is not surprising as the maximum shear rate accounts for a large part in the total specific energy.

The conclusion is that the test routine has a strong influence in the rheological measurements. As the test itself should disturb the sample as little as possible, it seems necessary to limit both the specific shearing energy and the maximum shear rate during the test.

The total shearing energy produced by the test should stay as small as possible in comparison with the shearing energy already put into the sample through mixing and preconditioning.

CONCLUSIONS

Cement slurry rheology dramatically depends on the shear history of the sample. Slurry mixing, dynamic conditioning, and the rheological test itself have a strong influence on the measured rheological parameters. This influence could be described by a single parameter, the specific shearing energy. The results obtained from laboratory and industrial conditions are then in good accordance.

Laboratory mixing procedure should be optimized to match the industrial specific mixing energy, and the laboratory dynamic conditioning should respect the flow regime expected in the field.

In order for the measured rheological parameters to be representative of the dynamic behavior of a given slurry sample, the rheological test itself should feature the minimum shearing energy possible, e.g. maximum shear rate, time step, and number of steps should be limited.

REFERENCES

[1] G.H TATTERSALL and P.F.G BANFILL "The rheology of fresh concrete", Pittman Advanced Publishing Program, 356 pages, 1983.

[2] R. LAPASSIN,A. PAPO,S. RAJGELJ, "The phenomenological description of the thixotropic behavior of fresh cement pastes", Rheologica Acta 22, pp. 410-416, 1983.

[3] API Specification 10 for Materials and testing for well cements, API production department, Second edition, June 15, 1984.

[4] J.I. BHATTY and P.F.G BANFILL " Sedimentation behavior in cement pastes subjected to continuous shear in rotational viscometers", Journal of Cement and Concrete Research Vol 12, pp. 69-78, 1982.

[5] R.J. MANNHEIMER "Effect of slip on the flow properties can flaw resistance calculations", Oil and Gas Journal, Dec.5,pp 144-147, 1983.

[6] R. BYRON, W.E. STEWARD and E.N. LIGHTFOOT "Transport phenomena", John Wiley & Sons Inc.

[7] R.W. WHORLOW "Rheological Techniques", Ellis Horwood Limited, 447 pages, 1980.

[8] M. MICHAUX and C. DEFOSSE "Oil well cement slurries. Microstructural approach of their rheology" Journal of Cement and Concrete Research, Vol 16, Jan. 1986.

[9] M. MICHAUX and R.O. PADTBERG "The effect of mix water salinity on polynaphtalene sulfonate containing cement slurries", to be presented at the 8th International Congress on the Chemistry of Cement, Rio de Janeiro, Sept. 1986.

[10] H. SCHLICHTING "Boundary Layer Theory", Mc Graw-Hill Book Company, 817 pages, 1979.

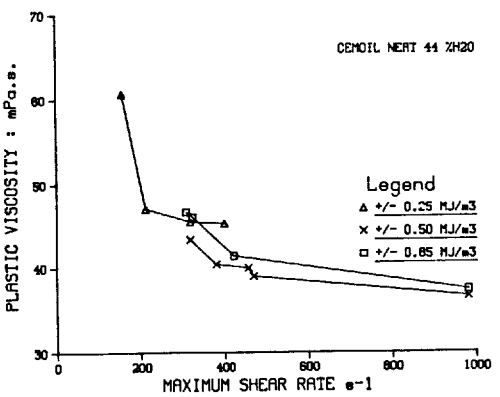

Fig. 8 : Influence of the maximum shear rate on cement rheology.

U. COSTA and F. MASSAZZA
Dr. of Chemistry and Prof. of Applied Chemistry (ITALCEMENTI- BERGAMO - ITALY)

S 3

STRUCTURE AND PROPERTIES OF CEMENT SUSPENSIONS
STRUCTURE ET PROPRIÉTÉS DES SUSPENSIONS DE CIMENT

1. INTRODUCTION

Fresh mortar and concrete can be considered as aggregate dispersions in a matrix formed of cement paste. According to this model the system deforms when it is submitted to stresses and the aggregate grains move in a deformable medium composed of the cement paste. Therefore the rheological behaviour of concrete could quite be explained if the rheological properties of paste and the interactions between these and aggregate were completely defined.
In the last few years many studies were devoted to the cement paste rheology but only few were carried out on the relationships between paste and concrete properties, owing to the difficulty of recognizing and evaluating all the parameters which characterize concrete. Difficulties were encountered also in defining the rheological state equations for concrete on account of the experimental difficulties related to the complexity of the material.
This report reviews the latest acquisitions on the cement dispersions and their influence on the interpretation of the behaviour of mortars and concretes.

2. RHEOLOGICAL MODELS

2.1 Methodological problems

The behaviour of fresh cement paste submitted to shear stresses can be classified into 3 fundamental types: Newtonian, viscoplastic (shear thinning) or dilatant (shear thickening) (1). These behaviours depend on the suspension structure on which concentration, specific surface, particle size distribution and solid shape act (2). As figure 1 shows, a mortar behaviour passes from shear thinning to Binghamian and shear thickening, as the solid concentration increases. In figure 2 the pseudoplastic behaviour of a mortar having angular grains changes to Newtonian when grains are spherical.
Under a constant shear rate the cement pastes show a rheological dependance on time, generally of thixotropic type (4)(5). The experimental preparation methodologies or the instrumental measuring techniques modify the paste structure so as they become preminent with respect to the factors involved in properties of the dispersed materials. This is a general problem concerning the rheological measurements carried out on thick suspensions whose macroscopic flowing properties are sensitive to the arrangement of the particles in the viscometer cell. Thick suspensions have viscosity or rheological flowing behaviours strictly dependent on the used measuring instrument and working conditions (6). In fact the results of the rheological tests largely depend on the geometry of the flow channel, the speed as well as the dimensional and shape properties of particles. Furthermore, the results can vary, even though the same instruments and working conditions are employed in repeated tests, since the paste does not take the same structure.

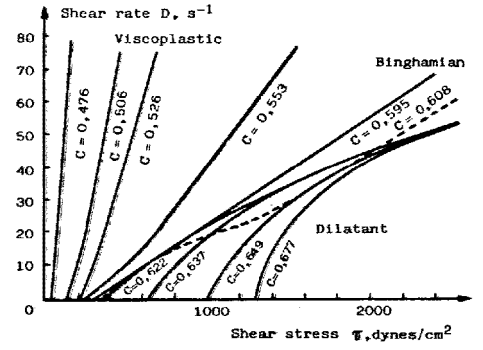

FIG. 1: Flow curves of mortars with different solid concentrations (c) (3)

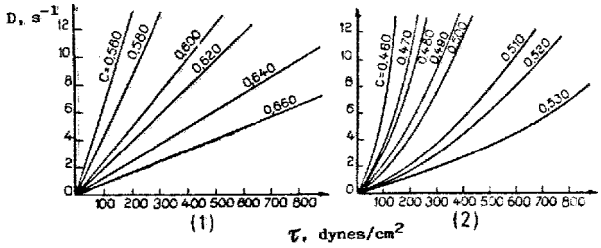

FIG. 2: Influence of the grain shape on the flow-curves of mortars (3): 1) spherical grains 2) angular grains

A complete description of the rheological behaviour would demand also observations of the cement paste under the microscope (for example by light scattering techniques) to point out the changes undergone by the particle movement, in connection with the shape and amplitude of the flowing channel, and to determine

the type of flow (laminar, elongational, a.s.o.) **(6)**. Therefore to obtain results expressing the real behaviour of the suspensions it is necessary to respect some design feature of the apparatus, and the experimental procedure. For example the annular section between the coaxial cylinders must be fixed with great attention. It must be limited to avoid settling phenomena and it must be wide enough with respect to the maximum particle size of the dispersed solid to obtain a laminar flow **(7)**.

The behaviour of similar pastes transforms from thixotropic into antithixotropic when the measurement cycle time varies (fig. 3). This fact is explained by the competition occurring between the breakdown and reconstruction processes, the latter due to the cement particle hydration **(8)**. The rotation speed of the rotor can affect the results in a different way. If the speed is slow, a slipping can occur between rotor surface and paste but, if it is fast, a centrifugation occurs **(9)**. Figure 4 shows that the flow curves change appreciably when the acceleration of the shear rate varies.

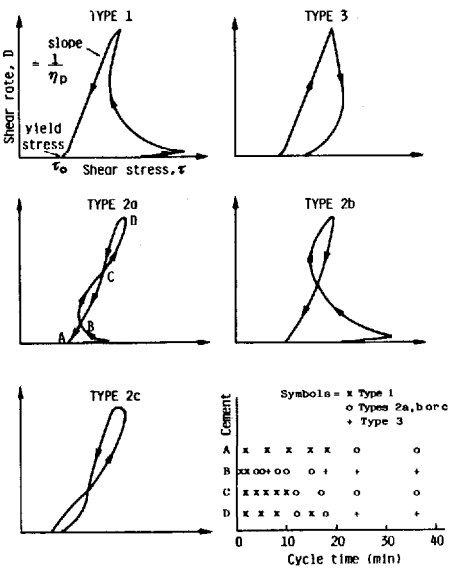

FIG. 3: Effect of the cycle time on the type of flow curves obtained on cement pastes **(8)**

The viscometric studies on cement pastes are generally carried out by using shear rates which are largely slower than the critical one for which Reynolds number exceeds the calculated value separating the laminar from the turbulent flow **(11)**. Nevertheless, conditions of turbulent flow were observed at shear rates, D, equal to 1800 s^{-1} and 1065 s^{-1}, by using rotors with smooth or grooved surface respectively **(10)**. This phenomenon takes place because the turbulence in suspension occurs for lower shear rates than those in pure dispersion medium **(12)**.

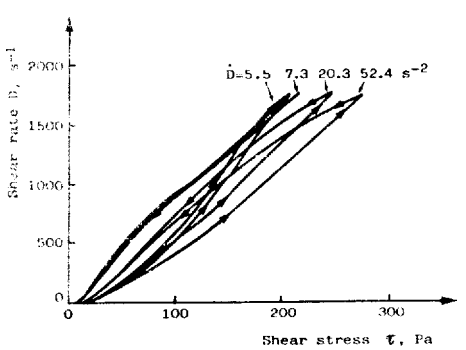

FIG. 4: Flow curves at different acceleration of shear rate D **(10)**

The most common procedures of the shear rate application to the paste are of 4 types: a) constant rate, b) step-increasing rate, c) step-decreasing rate, d) continuously varying rate. Procedure a) gives values corresponding to equilibrium conditions between applied stress and resistance to flow. The step-procedures have the advantage, compared with the previous one, that they allow measurements to be taken on a wider range of D values, by working on the same paste sample **(13)**. The last procedure is unable to characterize quantitatively the "shear-dependent" behaviour of the paste **(14)** and it often shows hysteresis loops. By working with pastes made with 0.6-0.7 w/c ratios, the settling phenomena in the viscometer can become very important if helicoidal rotors are not used **(15)**.

2.2 Rheological behaviours

The rheological characterization of a thick suspension demand two complementary descriptive elements. The former is the flow curve representing the equilibrium conditions between applied stress and shear rate (shear-dependent analysis). The latter is the structural strain curve versus time obtained by submitting the paste to a constant flow rate (time-dependent analysis). The formulation of the mathematical models interpreting the experimental curves allows the essential rheological parameters (viscosity, yield value, thixotropic breakdown energy, a.s.o.) related to the suspension structure, to be obtained.

2.2.1 "Shear-dependent" behaviour

Fresh cement pastes can comply with the linear models of simple fluids, such as Newton's or Bingham's, when the shear rate is limited and the structural demolition during mixing is complete. However, the relationship between shear rate D and shear stress τ is not generally linear and therefore the above models cannot be used in any case. Attempts to interpret mathematically the complex behaviours of the cement pastes date back to the end of the 70s and a great researching effort was made on this aspect of rheology.

Table 1 shows several proposed models, starting from Jones and Taylor's **(16)** who used two different equations (eq. 1 and 2). The former, composed of the combined Bingham and power law, derived directly from the classical Herschel-Bulkley's equation used for the first time to study benzene-rubber system **(17)**. The latter equation, based on the model proposed by Robertson and Stiff **(18)**, showed an excellent compliance with the experimental data. The results of these Authors pointed out that the cement paste was shear thickening at w/c ratios < 0.4, shear thinning

at w/c ratios > 0.4 and behaved in a Binghamian manner at w/c ratios = 0.40.
In a following work the linear term of Bingham equation was replaced by a hyperbolic function (eq. 3 of table 1). The model showed a good agreement with flow curves of paste in the rotational viscometer, up to D values of about 380 s^{-1} **(19)**. Functions of this type were proposed by Eyring to interpret the behaviour of fluids as gelatin and cellulose dispersions **(20)**.

TABLE 1: Rheological models proposed for the fresh cement pastes

MODEL			RHEOLOGICAL BEHAVIOUR
1) $\tau = \tau_0 + kD^n$	**(17)**	utilized by **(16)**	n>1 Dilatant n<1 Viscoplas.
2) $\tau = A(D+C)^B$	**(18)**		B>1 Dilatant B<1 Viscoplas.
3) $\tau = \tau_0 + B\sinh^{-1}(D/C)$	**(19)**		Viscoplastic
4) $D = \alpha\tau^2 + \beta\tau + \delta$	**(21)**		Viscoplastic
5) $D = k_1\tau + k_2\tau^n$	**(23)**	utilized by **(22)**	Pseudoplastic
6) $\tau^{\frac{1}{2}} = \tau_0^{\frac{1}{2}} + k_1 D^{\frac{1}{2}}$	**(24)**		Viscoplastic
7) $\tau = \sum_{i=1}^{n} A\sinh^{-1}(DB_i)$	**(20)**		Pseudoplastic
8) $\tau = \eta D$			Newtonian
9) $\tau = \tau_0 + \eta_{pl} D$			Binghamian

τ = shear stress; η = viscosity
τ_0 = yield stress; η_{pl} = plastic viscosity
D = shear rate
A, B, C, k, k_1, k_2, α, β, δ = constants

More recently the descending branch of the second isteresis loop was interpolated by a parabola equation (eq. 4 of table 1). This model allows two important rheological parameters to be obtained easily, that is yield value τ_0 and viscosity coefficient η_{pl} **(21)**.
The compliance of different models with the description of the viscometric flow of cement pastes, having w/c ratios between 0.30 and 0.45, was evaluated in a recent work **(22)**. For this analysis some other classical models applicable to the rheology of simple fluids and suspensions (given by equations 5, 6, 7 of table 1) were considered. By using statistical and iterative procedures it was possible to calculate the parameters of each equation giving the best agreement with the experimental flow curves. The compliance of the model was evaluated by the difference between the shear rate values calculated by the corresponding equation and the experimental ones. Good correlations resulted for Eyring's, Herschel-Bulkley's and parabolic models. The two last are constitutionally related, since Herschel-Bulkley equation becomes a parabola when exponent B is 2.
It is interesting to notice that the proposed equations generally show a constant term, which corresponds to the yield stress, and a second term of exponential type. In some cases also a linear term in D appears. The physical interpretation of this analytical formulation leads to assume, similarly to what found also for other rheological systems **(20)**, that the cement pastes consist of Newtonian and non-Newtonian units. The latter would identify with the flocculа formed from the aggregation of the particles that, during motion, undergo a structural breakdown. Therefore, as D increases, the motion resistance tends to decrease in an exponential manner.
An attempt to interpret the flow curves according to a more general model based on physical principles, considered different types of friction which determine the suspension viscosity **(25)**. In the interactions between components three types of friction liquid-liquid, liquid-particle, particle-particle were distinguished. Therefore viscosity was expressed on the basis of the number of molecular friction points per unit of shear plane according to

$$\eta = B_1 n_1^{2/3} + B_2 n_2^{2/3} + B_3 (n_3 u)^{2/3} \qquad 10)$$

where n_1, n_2, n_3 are number of friction points of the three species in question on the shear plane and **u** is dimentionless factor varying from 0 to 1.
Factor **u** expresses the ratio of the number of friction points to the initial number of non-agglomerated particles and it takes value 1 when agglomeration is complete. If **u** is constant as the shear rate varies, η is constant too and therefore the flow is Newtonian. Generalized flow curves can be derived by introducing the η expression in the Newton classic equation (eq. 8 in table 1).
Factor **u**, which determines the viscosity and therefore the material flow, was deduced by considering the competitive effects of coagulation and dissociation caused by the mechanical stresses acting during the flow. Unlike the previous models, this approach allows also the time factor to be introduced into the state equation. In this way it was possible to explain mathematically the changes in the shape of the curves shown in figure 3, depending on the variation of the test duration.

2.2.2 "Time-dependent" behaviour and thixotropy

When the shear rate is constant, the cement suspensions show shear stress-time transient characterized by 3 stages, as indicated in fig. 5. An initial stage, where τ reaches a maximum (τ_{max}) quickly, a period of stress decrease as far as a minimum value (τ_e), a third stage represented by a slight increase in τ. In some cases the appearance of an additional maximum was observed during the third stage **(13)**.
The trend of τ-t transient results from different phe

nomena having opposite actions. The demolition of the particle agglomeration caused by the shear stress **(4)**, and the grain orientation as a function of the lower hydrodynamic resistance during motion **(3)** cause a viscosity decrease with time. At the same time the hydration process of cement introduces new bonds among the dispersed particles, which increases the dispersion viscosity **(27)**. The paste viscosity depends on the inner structure resulting from the chemical-physical forces which act among particles. These forces react elastically at weak stresses, but if the stress becomes high enough, they fail and the structure degrades and flocs form which offer a lower resistance to flow. The change in the flocculation degree of the paste was considered to be the base of the thixotropic behaviour **(4)**.

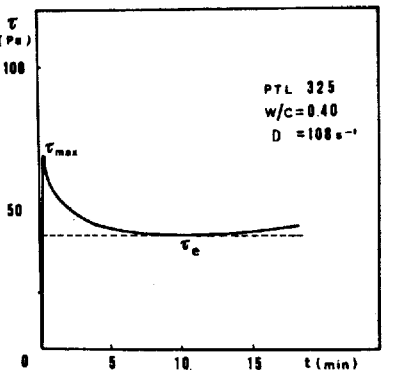

FIG. 5: A typical transient behaviour shear stress vs time at constant shear rate **(26)**

The quantitative measurement of thixotropy is not a simple question since a thixotropic material is sensitive to stress conditions and rheological hystory. The phenomenon is affected by rheological and experimental factors. The rheological ones include the rate constant and the order of the demolition process, in their turn related to the elastic energy and the relaxation time of the structure. The experimental variables concern temperature and shear rate.
It is practically impossible from a single τ-t curve to explain all these dependences, so thixotropy is generally measured by using empiric coefficients which express the aggregation degree of the dispersion. For instance, the coefficient of thixotropy is the ratio **(28)**

$$\lambda = \frac{\tau_{max} - \tau_e}{\tau_{max}} \qquad 11)$$

where τ_{max} is the peak stress corresponding to the initial degradation of the structure and τ_e is the stress required to keep the configuration in equilibrium. Thixotropy is also expressed by a similar coefficient given by the ratio

$$r = \frac{\tau_{max}}{\eta_e} \qquad 12)$$

where η_e is the equilibrium viscosity **(29)**.
The process of thixotropic demolition can be studied through the analysis of the $\tau = f(t)$ curves. A recent work **(30)** illustrated the mathematical method to derive the rheological state equation and to interpret the kinetics of the structural breakdown to obtain the rate constant and the process order. The rheological equation was expressed in the general form:

$$\tau = f_0(D) + \lambda' f_1(D) \qquad 13)$$

where D = shear rate

$$\lambda' = \frac{\tau - \tau_e}{\tau_{max} - \tau_e} \quad \text{structural parameter} \qquad 14)$$

Vom Berg's model (n° 3 of table 1) was used for the functions $f_0(D)$ and $f_1(D)$.
By means of a procedure of curve fitting, simultaneously applied to values τ_{max} and τ_e obtained with different shear rates, the parameters of equations $f_0(D)$ and $f_1(D)$ were calculated. The same data allowed the variation of parameter λ' with time to be analyzed and, therefore, the modification of the system thixotropy could be expressed through the deduction of the constant rate **k** and the order **n** of the breakdown process. The data obtained on cement pastes of different type are given in table 2 from which it results that **k** varies as the shear rate changes, according to a hyperbolic relation whose parameters considerably depend on the type of cement. On the contrary the changes in order **n** of the process with the type of cement are more limited.

TABLE 2: *Parameters of the breakdown rate equation:* $\frac{d\lambda'}{dt} = -k(D)\lambda'^n$ 15) **(30)**

CEMENT	w/c	n	a (s^{-1})	b
325 Ptl	0.40	1.36	678	26
425 Ptl	0.40	1.00	1356	62.4
425 Ptl	0.45	1.09	2634	27

λ' = structural parameter given by 14) equation
n = order of breakdown process
a,b = parameters of the equation: $k(D) = \frac{D}{a + b \cdot D}$ 16)
where D = shear rate

The influence of the shear rate on the kinetics of the demolition process was particularly examined in another study **(10)**. It was observed that, for $D < 1065 s^{-1}$, the τ-t curves are descending and can be described by an equation including two exponential terms. The need to introduce two terms instead of one, as in Tattersall equation **(4)**, is due to that the breakdown process can be subdivided into two stages: a primary which occurs very quickly and finishes in 5 seconds at the latest and a secondary which is much slower. The introduction of a third term into the equation became necessary to interpret the reascending of τ when shear rate D exceeds $1065 s^{-1}$. Tests performed by replacing the paste with water showed that a turbulent motion can be established with so high shear rates. Therefore this increase in τ and paste viscosity should not be interpreted as a rheopexy phenomenon and, hence, as a real change in the inner structure,

but as the consequence of the flow transition from laminar to turbulent.

2.2.3 Models and paste structure

The examination of the equations proposed to interpret the shear-dependent or time-dependent behaviours of cement suspensions showed that only some are based on physical hypotheses, whereas most of them derive from procedures of curve fitting applied to experimental data. This trend is rather common in rheological studies and can be attributed to three fundamental reasons (31). The first is to sum up the experimental data with a small number of parameters. In this way it is possible to establish quantitative relationships between the rheological parameters and the different chemical-physical factors affecting them: concentration, fineness, composition of cement, a.s.o. A second one is to extrapolate the experimental data outside the range of shear rate or solid concentration considered in the tests, especially to apply the results to the practice. Finally, the third reason it to correlate the rheological behaviour with the chemical-physical processes which occur, on a microscopic scale, among the suspension constituents. However, the factors and interactions determining the rheological behaviour of suspensions are many and complex and therefore it becomes difficult to consider all of them to establish models of general validity.

3. STRUCTURE OF PASTES

3.1 Structure factors

The structure, and therefore the suspension rheology, are affected by several chemical-physical factors concerning both the dispersed solid phase and the liquid.

3.1.1 Solid phase properties

Specific surface, particle size distribution and shape of grains are factors of primary importance since these parameters determine the number of the contact points between particles which result in frictions and agglomeration forces. Bombled (2) expressed the flow resistance (f) per surface unit of the suspension versus the grain number n_s, the number of contacts per grain λ^* and adherence A, which represents the sum of the intergrain forces (frictional, Coulomb's, Van der Wall's), by equation

$$f = n_s \lambda^* A \qquad 17)$$

Since the number of contacts per grain increases exponentially as the specific surface increases (32), equation 17) justifies the exponential-type relationships found experimentally between the paste viscosities or yield stress and the specific surface of cement (2)(33). It was also found that monogranular particles result in pastes having poor rheological properties (34). The improvement of these properties is chiefly related to the achievement of the particle size and shape favorable to the maximum filling of the empty space. Continuous particle size distributions represent the optimum about the matter (35). Also the particle shape plays an important role, as was pointed out by a study on hydrated lime suspensions (36). This property, together with the particle size distribution, appeared to affect the rheology of these suspensions more significantly than the electrokinetic potential of particles. The particle size distribution and the surface extension have also other indirect effects on the rheology of pastes.
In fact the particle size distribution determines the permeability of the granular whole, whereas the specific surface conditions the extent of the forces acting among the surface electric charges. As permeability decreases, the rheological behaviour can transform from shear thinning into thickening owing to the resistance that water finds when it flows inside the paste (2).
As the specific surface increases, the particle agglomeration caused by the electric charges induced by the clinker comminution process (37) and the cement hydration (38), increases.
These factors related to the physical state of the solid add to others of chemical nature. The mineralogical composition of clinker and the reactivity of phases affect the hydration process. Therefore, they can act on the paste rheology through the bonds forming between the hydrated products (39) and the changes in the solution ionic equilibria affecting the double-layer forces (40)(41). The mineralogical composition of clinker can affect the rheological behaviours also indirectly owing to the different grindabilities shown by the constituents (42).

3.1.2 Liquid phase properties

The mechanical properties of the liquid phase, that is surface tension and viscosity, and the chemical-physical properties such as affinity for surface and the dielectric constant, are other factors affecting rheology. In particular, the strong surface tension of water, together with the affinity for surface of the cement grains, cause intense capillary forces when the intergranular space is not quite saturated with water. Under these conditions air-liquid menisca form and a negative pressure P, given by the following Laplace formula, creates in the liquid:

$$P = -4 \frac{A}{r} \qquad 18)$$

where r = curvature radius of meniscus
and A = surface tension of water

This pressure is equilibrated by compressive forces acting in the grains. The paste cohesion reduces appreciably when the amount of water exceed that necessary for saturation, since the capillary forces cease(43). The dielectric constant affects the Coulomb and Van der Walls interactions acting between grains (44).

3.1.3 Solid-liquid interactions

The interactions occurring between the dispersed solid and the liquid can be subdivided into three categories:
- *hydrodynamic actions that cause a viscosity in -*

crease in the liquid;
- *attractions between particles that lead to the formation of floccula and aggregates and a continuous agglomerated structure;*
- *contacts between particles that create frictions during the motion.*

Cheng **(31)** tried to summarize, in a scheme given in fig. 6, the relationships between the categories of interactions and the factors conditioning them. The double-pointed arrows mean that the factor in question determines the appearance of the interaction but, in its turn, it is simultaneously affected by the interaction itself. Each of the fundamental interactions acquires a different importance depending on the solid concentration in the solution.

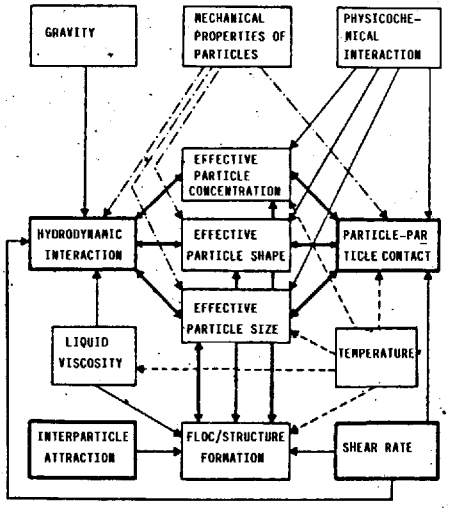

FIG. 6: Interplay of the three categories of interactions and factors affecting suspension viscosity **(31)**

For example, the contribution of the hydrodynamic factors increases at medium or low concentrations, the attractive forces predominate at medium-high concentrations and the friction between particles plays the main role at very high concentrations. In any case the predominant interaction determines the rheological behaviour of the suspension.

Figure 7 is a tentative to represent the rheological behaviours of the suspensions as a function of three fundamental types of interactions. A shift along axis **y** shows that, in the absence of attraction forces among the particles, the suspension behaviour varies from Newtonian to non-Newtonian as the solid concentration passes from low to medium values. Contacts predominate at a very high concentration, so the behaviour becomes at first dilatant as far as to transform into a more complex one (granulo-viscous).

If also the attraction forces among particles are considered, an increase in the suspension viscosity is observed in any case, since the dispersed solid tends to form floccula or aggregations. As the forces increase in dispersions having medium-low solid concentrations, the behaviours pass from pseudoplastic to viscoplastic and plastic. When the attraction forces are weak, floccula are broken easily but, as they become stronger, floccula become more resistant and can endure a certain stress without breaking. At this point the suspension shows a certain elasticity as far as a given threshold stress which represents the yield value and indicates the transition from pseudoplasticity to viscoplasticity.

This picture explains how it is difficult to interpret the macroscopic rheological behaviour of pastes in terms of structure. For example the same rheological response can be obtained by combining a low attraction force with a high solid concentration or a medium attraction with a low concentration. Therefore, to define the physical models of the structure of the concentrated cement suspensions, it becomes very important to examine the forces acting among particles and their variations as a function of the solid concentration.

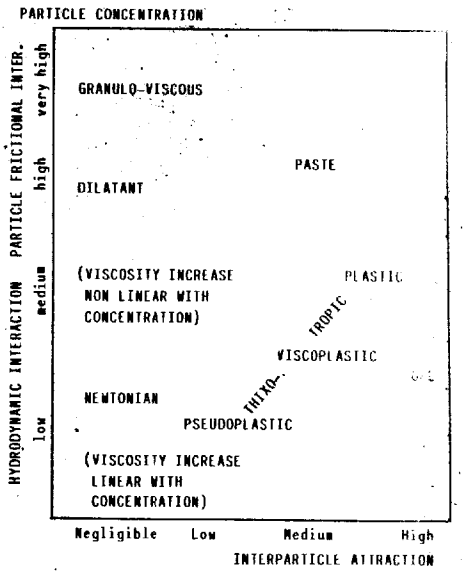

FIG. 7: Relation between different types of rheological behaviour and the three categories of interactions **(31)**

3.2 Forces among particles

3.2.1 Equilibria among particles

The main forces acting on a group of particles are Van der Wall's, generally attractive, and the electrostatic ones, generally repulsive. Moreover there are forces resulting from the presence of water films adsorbed on particles, referred to as "structural forces", which cause a repulsive effect known as "disjoining pressure" **(45)**. Finally, if systems containing particles with sizes above the colloidal ones are considered, also capillary forces can occur when air-water interfaces create in the system.

Table 3 summarizes the different types of acting forces and the dimensional range of the particles on which the action of each of them prevails.

TABLE 3: Forces acting between particles **(46)(62)**

TYPE OF FORCES	SIZE OF PARTICLES (mm)	EFFECT OF FORCES	ACTION DISTANCE (mm)
Capillary	1 - 0.1	Attraction	-
Van der Walls	0.1 -10^{-4}	Attraction	5-20·10^{-7}
Coulomb (double layer)	10^{-2} -10^{-6}	Repulsion	10-50·10^{-7}
Disjoining pressure	10^{-2} -10^{-6}	Repulsion	5-30·10^{-7}

The nature of the forces acting between particle was examined in several reviews **(43)**. Van der Walls forces result from electromagnetic interactions, between the atomic electron clouds, which give rise to orientation, dispersion and induction effects. These effects contribute to the cohesion of the materials.
The electrostatic forces derive from ionic double layers that, in water, surround the particles and can be quantitatively evaluated by the measurement of zeta potential. The structural forces, i.e. disjoining pressure, derive from the water adsorbed on the particles which has different chemical-physical properties from water in bulk. Water shows a certain degree of structural order and for this reason creates a physical and thermodinamyc barrier that hinders the contact between particles **(46)**.
According to DVLO classical theory **(40)(41)**, the stability of a colloidal suspension is determined by the balance between Van der Walls attraction forces (V_A) and the repulsive ones among the electrical double layers on the particles (V_R). The trend of V_A, V_R and the total potential energy $V_T = V_A + V_R$, expressed as a function of the distance between two particles, can be seen in figure 8.
The attraction and repulsion increase quickly starting from a certain distance, as the particles approach each other. The total energy curve passes through a maximum (V_{max}) that forms a barrier opposing the particle adhesion. The lower this barrier the higher the number of particles which agglomerate by taking the potential interaction energy corresponding to the primary minimum V_{1min}. V_{max} depends on the sizes of the particles and their surface charge. With relatively big particles the total potential energy curve can show a secondary minimum at a wider separation distance. If this secondary minimum is rather deep, 2-3 times the Brownian kinetic energy of the particle, it causes flocculation. The particle association due to flocculation is different from that occurring with the primary minimum since it is reversible and easily destroyed by shaking. Only if this secondary minimum were deeper than the primary one, a stable suspension could be obtained.

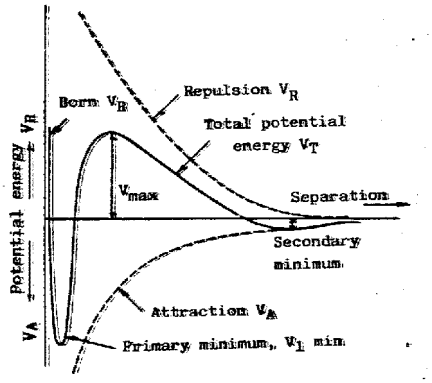

FIG. 8: Potential energy diagram for two particles **(47)**

These concepts have been taken from Powers who included in the balance among forces also those resulting from the disjoining pressure **(43)**. The relative energy of two quartz plates subject to Van der Walls forces (V_A) and the disjoining pressure (V_R) is shown in figure 9. The latter is calculated on the basis of thickness values of the water films adsorbed on hardened cement paste. It can be noticed that in this case the secondary minimum falls at about 25 Å. The floccula forming when the particles approach this distance remain isolated if the solid concentration is limited, but they can link by forming a continuous structure (flocculent state), when the particle compaction is as highest as possible. The system cohesion increases if the water is reduced. In this case the interstitial spaces are no longer completely filled with water. Air-water interfaces cause capillary forces between particles.

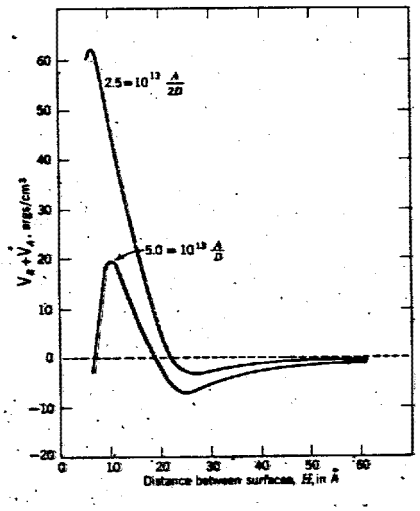

FIG. 9: Calculated potential energy of two parallel silica plates in water versus distance H. Curves refer to 2 values of parameter A/D of Van der Walls attraction force V_A **(43)**

The curves shown in figure 8 indicate two possibilities to prevent the particles from coagulating and, therefore, to obtain suspensions with good flowing properties. The former is to rise the height of the potential barrier V_{max} by intensifying the repulsion. The latter is to avoid the particles from approaching a lower distance than that corresponding to the secondary minimum of energy. Both effects can be attained by using plasticizers and superplasticizers that have a strong deflocculating action of the cement grains. They increase the absolute value of the surface charge (zeta potential) as well as they create a steric hindrance to the particle approach **(48)**. The possibility given by the theory to modify the flocculated structure of the suspension by acting on the double layer repulsion are applied in the concrete technology.

3.2.2 Zeta potential

The particles of inorganic oxydes are carriers of unequilibrated electrical charges from the non-compensation of positive and negative valencies of the surface atoms (accidental charges). Other charges can derive from isomorphic substitutions in the lattices between atoms of difference valence (inherent charges). Another contribution can come from the hydrolysis of the amphoteric hydroxyl groups **(49)** shown in figure 10. Therefore the surface has an electrical poten -

tial ψ_0 compared with that of bulk solution considered as zero.

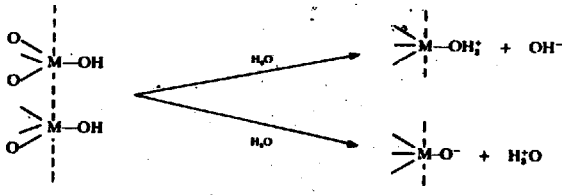

FIG. 10: Hydrolysis reactions of the surface hydroxyl groups **(49)**

The surface charges attract opposite-sign ions, present in the solution, which form a layer adjacent to the surface. This layer extends from the surface as far as a distance **d** (fig. 11). The trend of the electrical potential shows a linear reduction as far as distance **d**, which corresponds to the limit of the adsorbed ion layer (Stern's rigid layer). Beyond this limit, the decay is exponential in the so-called diffused ionic layer. Potential ψ_0, corresponding to the limit of the rigid layer, cannot be measured easily whereas a parameter strictly related to ψ_d, that is ζ potential, can be calculated. This is determined by microscopic observations of the electrophoretic mobility **u** of the suspended particles subject to an electric field. Mobility **u** is related to ζ by the expression

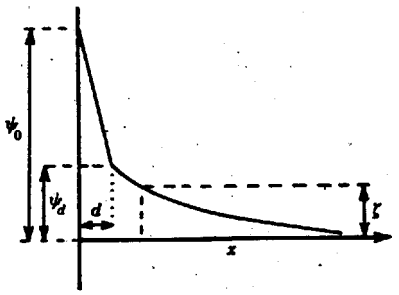

FIG. 11: Schematic illustration of the electrical double layer **(49)**

$$u = (\varepsilon_r \cdot \varepsilon_0 \cdot \zeta / \eta) \cdot f(ka, \zeta) \qquad 19)$$

where ε_r and ε_0 = permittivities of the solution phase and free space
η = viscosity of the medium
$f(ka, \zeta)$ = numerical factor

The oxide surface, by participating in the acid-base equilibria given in figure 10, show considerable changes in their surface charge and, therefore, in their zeta potential as a function of pH of the medium. Figure 12 exemplifies the electrophoretic mobilities obtained in alumina and silica suspensions as a function of pH **(49)**. It can be observed that silica particle charges become increasingly negative over a wide pH range. On the contrary alumina is charged positively as far as pH 9 and negatively above this value. The same figure shows that the increase in the ionic force of the medium reduces the potential owing to the compression of the double layer, but it does not modify its course.

These systems where it is possible to modify zeta potential, as a function of pH of the medium, are suitable to check the correlations provided by DVLO theory between the rheological properties of the suspension and zeta potential. When the surface potential is high, and therefore the repulsion forces prevail on Van der Walls attraction ones, a low viscosity must be expected. On the contrary, the aptitude for flow will be limited when the double layer interactions are poor and the cohesion between particles is high. These remarks have been confirmed experimentally in latest works **(50)**, always concerning alumina concentrated suspensions that showed the viscosity values versus pH given in fig. 13.

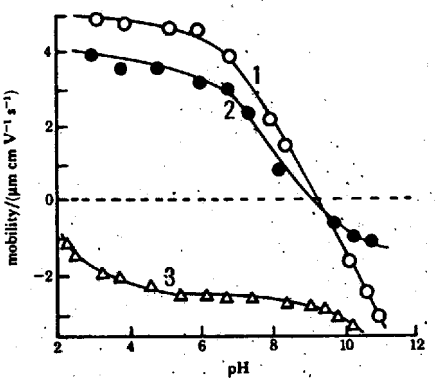

FIG. 12: Mobility against pH **(49)**
1) alumina in 10^{-3} mol/dm³ NaCl
2) alumina in 10^{-1} mol/dm³ NaCl
3) silica in 10^{-3} mol/dm³ NaCl

The comparison of figures 12 and 13 shows how the suspension viscosity attains a maximum value at the point of zero charge of the surfaces.

In these systems, where stable equilibria establish between the solution and the surface, the value of zeta potential has a well defined physical meaning. When the cement-water system is considered, the application of the classical model of the electric double layer becomes questionable since the interfaces in this case are not in thermodynamic equilibrium. When the cement surface come in contact with water, it reacts by producing ions and sur-

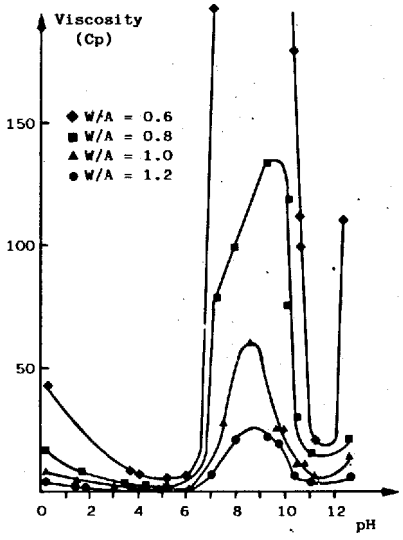

FIG. 13: Viscosities of alumina suspensions vs pH. The concentrations are expressed by W/A (mass of water/mass of alumina) **(50)**

charges in a large amount. These ions caused by hydration add to those already present in water and contribute to a large extent to the formation of the ionic envelope around the particles **(38)**. The ionic envelop differ from a normal double layer in that the inner part is being transformed continuously.
It was proposed to replace the classic concept of zeta potential with that of dynamic potential which evolves continuously with the hydration time and takes into account the ionic parameters of the contact solution **(51)**.
The evolutionary nature of zeta potential of the cement particles suspended in water is shown in fig.14. ζ potential decreases and then reaches a stable value after 25 minutes. pH reaches the value 10, as a result of the dissolution of calcium and alkaline hydroxides.

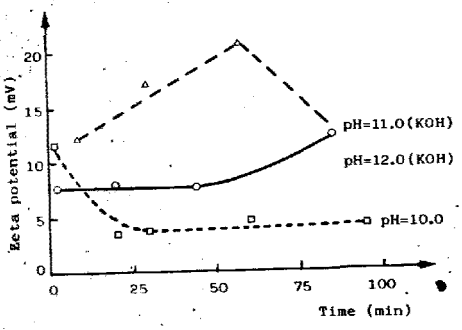

FIG. 14: Zeta-potential of portland cement as a function of time and initial pH-value **(38)**

When KOH is added to the cement suspension, the ζ potential shows increasing or decreasing trends according to the pH increase. However these behaviours have not found a rigorous explanation but, in any case, they testify a change in the surface composition with time. Nevertheless these composition changes, during the induction period or more advanced stages of the hydration process, have appeared as relatively slow. As a consequence, it is possible to detect a well defined zeta potential associated to a double layer that can be described by models derived from the classical Stern-Grahame's **(52)(53)**, as that given in figure 15. The correlation between zeta potential and rheological behaviour is complicated by that ζ measurements are carried out in diluted suspensions whereas viscosimetry utilizes pastes or concentrated suspensions. Moreover, in the rheological measurements the pastes are in a dynamic state that modifies the double layer structure and therefore the value of zeta potential, compared with that generally measured at the rest state **(63)**.

4. STRUCTURAL MODELS

At the present state-of-art the structural models proposed for fresh cement pastes are essentially qualitative. They are based on concepts of the colloid chemistry.
One of the first models for the flocculated state of the paste dates back to Powers **(43)** who imagined that fresh cement pastes made at the usual w/c ratio were composed of floccula. The mixing mechanical action produces hydraulic forces which tend to separate the individual particles and to create an uniform dispersion state. Only when the mixing action ceases, a continuous structure forms.
This is considered as a hypothetical single flocculus that involves the whole paste. The density of the floccula varies with the w/c ratio since the thixotropic structure forms very quickly when the mixing action has ceased, therefore the particles cannot reach the equilibrium position. Helmuth **(1)** resuming these concepts, represented the cement paste in the model of fig. 16, where the cement grains are considered as spherical in first approximation. This model points out the dispersing and stabilizing effect on the structure exerted by the disjoining pressure caused by the adsorbed water films. If the mixing action is strong enough, the thickness of the adsorbed water film tends to equalize as far as to take the value of the so-called hydraulic radius.

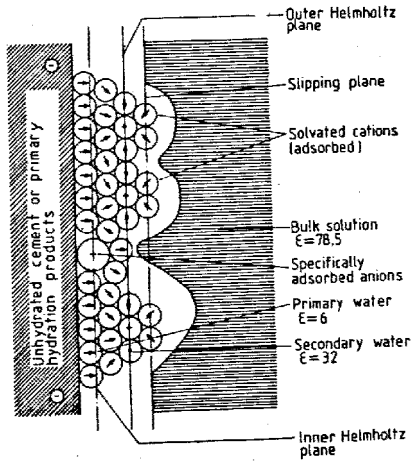

FIG. 15: Model of electrical double layer
ε = dielectric constant

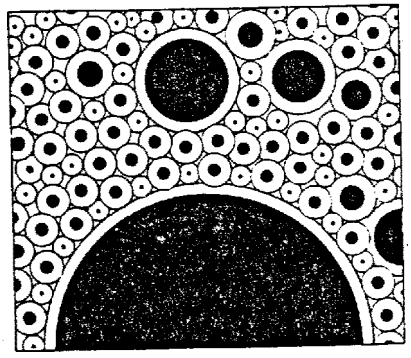

FIG. 16: Simplified model of spherical particles of fresh cement paste structure. a/c ratio = 0.5. Cement specific surface 430 m^2/kg **(1)**

The above-mentioned models are based on assumptions that simplify appreciably the real characteristics of the cement paste. First of all the shape of the cement grains is not spherical but angular and this morphologic feature can strongly affect the equilibria of the structure, as indicated in the model proposed by Legrand shown in fig. 17 **(55)**. In this model the formation of the continuous network of floccula in the cement paste becomes possible chiefly owing to the formation of direct tip-to-tip or tip-to-face coulomb

bonds between grains. These bonds, according to Bom - bled (2), are the result of the incomplete neutraliza tion from "counterions", in the aqueous medium, of the electric charges gathered in the tips and corners of the grains. These attraction forces, strengthened

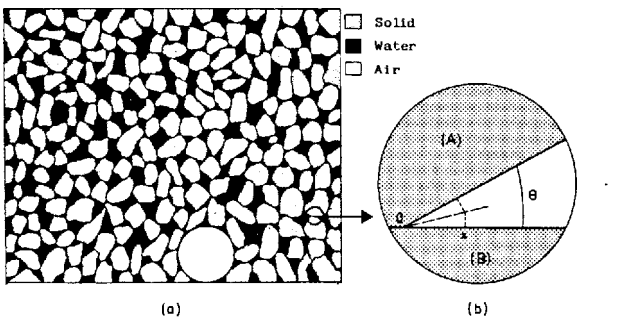

FIG. 17: Schematic model of fresh cement paste floc- culent state (55)

in the association point by Van der Walls forces, act on a limited surface. There fore it can be assumed that the contact area behaves as an articulated joint. On the surface of the grains adjacent to "articulated joint" the repulsion forces act. There are the disjoining pressure caused by the adsorbed water films and the interaction of the dou- ble ionic layers. These repulsion forces tend to en - large the contact angle Θ if the surrounding structure does not prevent it. The presence of unavoidable air bubbles entrained during mixing creates discontinui - ties in the structure and it gives rise to capillar y forces. Of course on the grains the gravity force acts. To conclude the structure is supported by local equi- libria between the repulsion and attraction forces.
This model allows the interpretation of some aspects of the rheological behaviour such as plasticity, thixotropy and viscosity, which affect considerably the workability of fresh cement paste. The grain displacement in the flocculated structure is possible only if the shear stress attains a suffi - cient value to break the intergrain bonds. In this ca se the paste behaviour is called plastic. Once attain ed the flowing threshold, it can happen that the mo - tion resistance of paste decreases with time: the known phenomenon of thixotropy takes place. Also this phenomenon is the result of the progressive breakdown of the bonds between grains. In any case,even though during the motion the primary bonds are broken, the grains still feel the so-called first, second- and third-type electroviscous effects caused by the ionic diffused layers (56). Moreover, also the interstitial liquid flowing between the grains will show a resi - stance depending on both its own viscosity and the permeability of the granular whole. Therefore all the se factors contribute to make viscosity higher than that belonging to a suspension of non-interacting ele ments.

5. RELATIONSHIPS BETWEEN PASTE AND CONCRETE

The previous paragraphs showed that fresh cement pastes, made at normal w/c ratios, have prevailingly viscopla stic behaviours and can be characterized by the two fundamental parameters τ_0 and η_{pl}.
Tests performed by means of rheometers with helicoi - dal rotor showed that the rheological behaviour of fresh concrete is of viscoplastic-Binghamian type (57). The refore also this system can be characterized by two rheological parameters (two point test), that is yield value and coefficient of viscosity. The analogy bet - ween the two systems is not casual but can be consi - dered as the result of the two essential roles that the interstitial paste plays in the concrete rheology, that is the cohesion and lubrication towards the ag - gregate. The former can be considered as directly de rived from the yield value, the latter from the paste viscosity.
The attempts made to establish quantitative relation- ships between the paste rheological properties and the mortar and concrete workability have not been nu merous so far. To establish a correlation between wor kability of fresh concrete and rheology of cement pa- ste, it is necessary to know the effective w/c ratio given by the formula

$$(w/c)_{eff} = \frac{w-(k_s \cdot s+k_g \cdot g)}{c} \qquad 20)$$

and the effective water content expressed by

$$p_{eff} = \frac{c}{1000}\left[\frac{1}{\varrho} - (w/c)_{eff}\right] \qquad 21)$$

where the coefficients k_s and k_g represent the increa se in the water content required to obtain the same workability when sand or coarse aggregate is added to the paste (58). The terms w, s, g and c represe n t the water, sand, coarse aggregate and cement contents (kg) of concrete and ϱ the cement density.
The values of slump and flowtable spread of mortars having different composition were correlated with a parameter X_η calculated by equation

$$X_\eta = \frac{\varrho \cdot g}{\eta \frac{(s/c)^2}{\psi}} \qquad 22)$$

where η is the viscosity coefficient of the paste mea sured by the rotational viscometer, s/c is the sand/ /cement ratio, ψ is the paste volume per surface u- nit of the sand, g the gravity and ϱ the mortar den sity (59). The empirical parameter X_η includes both the terms of the mortar composition and the rheologi- cal properties of the paste having the same w/c ra - tio. In the case of mortars with s/c ratios ranging between 2.1 and 3.9 it was found only a correlation curve bet ween the slump or flowtable values and the parameter X_η. When superplasticizers are present, the workabi- lity data, represented as a function of X_η, lie on different curves depending on the considered s/c ra- tios. To establish a more general correlation bet - ween paste and mortar properties, also valid in the presence of admixture, it would have been necessary

to introduce other parameters concerning the admixture-aggregate interaction, the entrained air a.s.o.
The model which consider fresh concrete in its whole as a dispersion, even though it includes a large dimensional range of grains, was the base of recent attempts aiming at characterizing the concrete behaviour in a rational manner.
The viscosity of mortars and concretes was calculated by an equation whose essential terms were the effective volume concentration of the solid phase and the maximum one permitted by particle size distribution and shape of the aggregate.
The obtained data were in good agreement with the experimental ones derived from rotoviscometric tests for a large range of mix composition (60).
Good results were obtained (61) by applying an equation deduced by Roscoe (12) for suspensions of stiff spheres. This equation includes fineness modulus, volumetric percentage related to the total solid content in concrete and volumetric concentration of the coarser part of the aggregate.

6. CONCLUSIONS

As a rule, the study of fresh cement paste rheology can give important information about the component interactions and the structure. Nevertheless the interpretation of the rheological behaviour is not simple because it depends not only on many factors concerning the chemical-physical properties of the cement or the liquid phase but also on the techniques and the experimental measuring instruments.
The development of the rheological studies on pastes allowed progress to be made in the rigorous interpretation of the flow curves by means of sophisticated mathematical calculations. These analysis methods allows a more accurate study of the influence of some chemical-physical factors. The possibility of establishing models of general validity is in conflict with the difficulty of expressing quantitatively the factors that show a very large variability, such as size, shape and mineralogical composition of the cement grains.
Another uncertainty reason lies in the imperfect knowledge of all the types of interactions solid-solid and liquid-solid.
Finally, the check of the assumptions by direct tridimensional observations of a suspension as the cement paste having high consistency and submitted to a chemical-physical evolution, presents great difficulties. Therefore at the present state-of-art it is possible to make only a schematic description of the structure based on simplified assumptions that can explain qualitatively the rheological properties of the material. The models proposed on the basis of the equilibria of the attraction and repulsion forces acting between particles can explain the existence of a yield value, a viscosity varying with the duration of the applied stress (thixotropy) and the admixture effect.
However the understanding of the phenomena concerning the paste rheology has not yet reached a sufficient level to interpret the most complex "suspension" formed of fresh concrete.

REFERENCES

(1) R.A. HELMUTH, *7th Int. Congr. on the Chem. of Cement (Paris, June 1980), vol. III, VI-0/16*

(2) J.P. BOMBLED, *Rev. Mat. Constr. 1974,(688), 137*

(3) C. LEGRAND, *Cem. Concr. Res. 1972, 2 (1), 17*

(4) G.H. TATTERSALL, *Nature 1955, 175, 166*

(5) R. LAPASIN, V. LONGO, S. RAJGELJ, *Cem.Concr.Res. 1979, 9 (3), 309*

(6) D.C.-H. CHENG, *Powder Technology 1984, 37, 255*

(7) R. LAPASIN, V. LONGO, S. RAJGELJ, *Il Cemento 1976, (2), 91*

(8) P.F.G. BANFILL, D.C. SAUNDERS, *Cem. Concr. Res. 1981, 11 (3), 363*

(9) K. WESCHE, H. FLATTEN, W. VOM BERG, *RILEM Seminar "Fresh Concrete: Important Properties and their Measurement" (Leeds, March 1973),vol.1, 2.10-1*

(10) W. VOM BERG, *VIII Int. Congr. on Rheology (Napoli, Sept. 1980), vol. 3, 665*

(11) E.L. WHITE, D.M. ROY, *Symp. M "Effect of Surface and Colloid Phenomena on Properties of Fresh Concrete" (Boston, Nov. 1982), 108*

(12) R. ROSCOE, *Brit. J. Appl. Phys. 1952, 3, 267*

(13) B. CAUFIN, A. PAPO, *Zement Kalk Gips 1984,(12),656*

(14) R. LAPASIN, *Il Cemento 1982, (4), 243*

(15) J.I.BHATTY, P.F.G. BANFILL, *Cem.Concr.Res. 1982, 12 (1), 69*

(16) T.E.R. JONES, S. TAYLOR, *Mag. Concr. Res. 1977, 29 (101), 207*

(17) W.H. HERSCHEL, R. BULKLEY, *ASTM Proc.1926,26, 621*

(18) R.E. ROBERTSON, H.A. STIFF Jr., *J. Soc. Petrol. Engin. 1976, 16, 31*

(19) W. VOM BERG, *Mag. Concr. Res. 1979, 31 (109),211*

(20) H. EYRING, *J. of Chem. Phys. 1936, 4, 283*

(21) C. ATZENI, L. MASSIDDA, U. SANNA, *Il Cemento 1983, (3), 141*

(22) C. ATZENI, L. MASSIDDA, U. SANNA, *Cem.Concr.Res. 1985, 15 (3), 511*

(23) S.B. ELLIS, *Thesis 1927, Lafayette College, Pa.*

(24) N. CASSON, *in Rheology of Disperse Systems 1959, Pergamon Press, 84*

(25) K. HATTORI, K. IZUMI, *Symp. M "Effect of Surface and Colloid Phenomena on Properties of Fresh Concrete" (Boston, Nov. 1982), 14*

(26) R. LAPASIN, A. PAPO, S. RAJGELJ, *Cem.Concr. Res. 1983, 13 (3), 349*

(27) Y. OTSUBO, S. MIYAI, K. UMEYA, *Cem. Concr. Res. 1980, 10 (5), 631*

(28) O.C.C. LIN, *Chemtech 1975, 5 (1), 51*

(29) C. LEGRAND, *7th Int. Congr. on the Chem. of Cement (Paris, June 1980), vol. IV, 124*

(30) R. LAPASIN, V. LONGO, S. RAJGELJ, *VIII Int.Congr. on Rheology (Napoli, Sept. 1980), vol. 3, 659*

(31) D.C.-H. CHENG, *Chemistry and Industry 1980, (10),403*

(32) C. LEGRAND, *Le Béton Hydraulique by J. Baron and R. Sauterey, Presses de l'Ecole Nationale des Ponts et Chaussées 1982, 115*

(33) K. RENDCHEN, *Beton 1976, (9), 321*

(34) V. SAINT-ETIENNE, *Ciment Betons Platres Chaux 1984, (747), 107*

(35) F. SKVARA, K. KOLAR, J. NOVOTNY, Z. ZADAK, *Cem. Concr. Res. 1981, 11 (2), 247*

(36) U. WITTNEBEN, *Zement Kalk Gips 1980, (10), 526*

(37) J. FRIPIAT, J. CHAUSSIDON, A. JELLI, *Chimie-Physique des Phenomènes de Surface, Masson et Cie Ed., Paris 1971*

(38) E. NAGELE, *Cem. Concr. Res. 1985, 15 (3), 453*

(39) Y. IVONOV, E. STANOEVA, *Silic. Ind. 1979, 14 (9), 199*

(40) B.V. DERJAGUIN, L. LANDAU, *Acta Physicochim. (USSR) 1941, 14, 633*

(41) E.J.W. VERWEY, J.TH. G. OVERBEEK, *Theory of the Stability of Lyophobic Colloids, Elsevier Publ. Co., Amsterdam 1948*

(42) M. REGOURD, *Le Béton Hydraulique by J. Baron and R. Sauterey, Presses de l'Ecole Nationale des Ponts et Chaussées, 1982, 193*

(43) T.C. POWERS, *The Properties of Fresh Concrete, J. Wiley & Sons, Inc., N.Y., 1968*

(44) J. TH. G. OVERBEEK, *Powder Technology 1984, 37, 195*

(45) W. DROST-HANSEN, *Ind. and Eng. Chem. 1969, 61 (11), 10*

(46) B.W. NINHAM, *The J. of Phys. Chem. 1980, 84 (12), 1423*

(47) T. SATO, R. RUCH, *Stabilization of Colloidal Dispersions by Polymer Adsorption, Marcel Dekker Inc., N.Y., 1980*

(48) F. MASSAZZA, *Advances in Cement Technology ed.by S.N. Ghosh, Pergamon Press, Oxford, 1983, 569*

(49) R.H. OTTEWILL, *Phil. Trans. R. Soc. Lond. 1983, A 310, 67*

(50) J. CHAPPUIS, *Symp. M "Effect of Surface and Colloid Phenomena on Properties of Fresh Concrete" (Boston, Nov. 1982), 38*

(51) A. ZELWER, *Ciments Bétons Plâtres Chaux 1984, (749), 213*

(52) O. STERN, *Z. Elektrochemie 1934, 30, pp. 508*

(53) D.C. GRAHAME, *ChemRev. 1947, 41, 44*

(54) J.O'.M. BOCKRIS et al., *Proc. Phys. Soc. 1963, London, 274, 55*

(55) C. LEGRAND, *Le Béton Hydraulique by J. Baron and R. Sauterey, Presses de l'Ecole Nationale des Ponts et Chaussées, 1982, 99*

(56) E.M. PETRIE, *Ind. Eng. Chem., Prod. Res. Dev. 1976, 15 (4), 242*

(57) G.H. TATTERSALL, P.F.G. BANFILL, *The Rheology of Fresh Concrete, Pitman Advanced Publ. Program, Boston 1983*

(58) YU. M. BAZHENOV, *7th Int. Congr. on the Chem. of Cement (Paris, June 1980), vol. IV, 125*

(59) C. ATZENI, L. MASSIDDA, U. SANNA, *AITEC 25°: Il Cemento ed il Calcestruzzo negli Anni'80 (Parma, October 1985), 217*

(60) S. KAKUTA, M. FUJII, T. AKASHI, *The Cem. Ass. of Japan - Review of the Thirty-Third Gen. Meet. (Tokyo, June 1979), 129*

(61) H. KIKUKAWA, *The Cem. Ass. of Japan - Review of the Thirty-Eighth Gen. Meet.(Tokyo, May 1984), 192*

(62) P.C. KREIJGER, *Concrete International 80 - Proc. of the Int. Congr. on Admix. (London, April 1980), 1*

(63) A. ZELWER, G. JUNGERS, *Internal Report of CERILH, Paris, pp. 91*

F. Basile, S. Biagini, G. Ferrari - MAC, R&D Laboratories, Treviso, Italy
M. Collepardi - Universitu of Ancona, Italy

EFFECT OF CONDENSATION DEGREE OF POLYMERS BASED ON NAPHTHALENE ON FLUIDITIES OF CEMENT PASTES.

Introduction

The modern technology makes extensive use of superplasticizers in order to improve the strength of hardened concrete by reducing the amount of water added to the fresh mix.

The phenomena associated with the fluidifying action of superplasticizers are quite complex and involve the adsorption of the macromolecules of the polymer onto the cement grains, the modification of the electrostatic charges on the surface of the cement particles and the modification of the kinetic of hydration of the various constituents of the cement.

It has been shown that, in the case of naphthalene sulfonate condensates, there is a relationship between the effectiveness as superplasticizer and the degree of polymerization, expressed by viscosity measurements (1).

Gel Permeation Chromatography (GPC) has been used by various authors to determine the molecular weight of superplasticizers based on condensates of naphthalene sulfonic acids with formaldehyde (2,3,4).

Recently, the influence of the molecular weight of naphthalene based polymers on the rheological properties of mixes made with different cements has been studied. It has been shown that the fluidity of the mixes increases up to a maximum value, which occurs at different values of the molecular weight of the polymer, depending on the cement used. Moreover, with polymers having extremely high values of molecular weight, a decrease in the fluidity of cement mixes has been observed (5).

In the present work, GPC and ultrafiltration have been used to study the effect of the degree of condensation of polymers based on naphthalene sulfonate on the fluidity of cement pastes, in a range for which an increase of the molecular weight of the condensate causes an increase in the fluidity of the cement mixes. In particular, the purpose of the present work is to examine whether the increase in the effectiveness of the superplasticizer with its degree of condensation is due either to the reduction in the low molecular weight fraction or to the change in the molecular weight distribution of the highly condensed polimeric fraction.

Experimental

Materials

Synthesis of naphthalene sulfonate based superplasticizer

Pure naphthalene (10.00 kg) was charged in a glass reactor and heated at 120°C. Then 8.36 kg of 98% H_2SO_4 ($H_2SO_4/C_{10}H_8$ molar ratio = 1.07) were added and the temperature was raised at 165 °C. This temperature was mantained for two hours to complete the sulfonation of naphthalene. The sulfonation mixture was diluted with 5.97 kg of water and then 7.81 kg of 36% formaldehyde solution ($HCHO/C_{10}H_8$ molar ratio = 1.20) were added. The condensation was carried out at 112°C for 14 hours and 7 samples of polymer were collected (one every 2 hours) having increasing degree of condensation. The samples, after neutralization with sodium hydroxide, had a total solids content of about 40% by weight.

Cement

Type I Portland cement with Blaine fineness of about 0.4 m^2/g has been used. The chemical composition of the cement is shown in Table 1.

Table 1 Chemical analysis of the cement used

CONSISTUENT	PERCENTAGE
SiO_2	21.56
Al_2O_3	4.88
Fe_2O_3	2.30
CaO	60.64
MgO	2.15
K_2O	0.66
Na_2O	0.39
SO_3	3.37
LOSS ON IGNITION	3.87

Techniques

Gel Permeation Chromatography

The samples of naphthalene sulfonic acid formaldehyde condensate to be analyzed were dissolved in 0.55 M KNO_3 aqueous solution to obtain concentrations of 3.0 g/100 ml.

The samples were analyzed using 0.55 M KNO_3 aqueous solution as eluant at a flow rate of 1 ml/min.

Shodex Ionpak S-803/S (exclusion limit 50,000 dalton) and Shodex Ionpak S-804/S (exclusion limit 500,000 dalton) coupled columns, made by semirigid crosslinked styrene-divinylbenzene sulfonate gel, were employed.

Columns were kept in a thermostatic oven at 68°C and all the samples were analyzed at this temperature.

Samples of monodisperse polystyrene sulfonate of different molecular weights (4,400-6,500-17,400-39,900-104,000), naphthalene 2-sulfonate and naphthalene 1,5-disulfonate were used as calibration standards for the columns.

Analyses were performed with a Perkin-Elmer liquid chromatograph equipped with pump mod. Series 4 and Perkin-Elmer ultraviolet detector mod. LC75 at a wavelength of 292 nm.

Chromatographic data were collected and processed by a Perkin-Elmer Data Station mod. 3600 equipped with Chromatographics 2 and GPC4 programs, both by Perkin-Elmer, used for data collection and data processing, respectively.

Ultrafiltration

Samples withdrawn after 4 and 14 hours of condensation were ultrafiltered in order to remove the monomer and the lower molecular weight products. Amicon stirred cell mod. 8200 and Amicon ultrafiltration membrane mod. YM2 having a nominal cut-off of 1,000 dalton, were employed.

Mini-slump test

The fluidity of fresh cement pastes (water/cement ratio = 0.35) in the presence of the condensates (0.4% of dry product by weight of cement) was evaluated by the mini-slump test, after five minutes of mixing. The results were expressed in cm^2 by measuring the area of the circular path described by the fresh cement paste, after having picked-up the cone (6).

Results and Discussion

In Fig. 1 the progressive development of the condensation reaction is shown, as it results from the GPC analyses at different condensation times.

According to the GPC theory, the higher molecular weight fractions elute at first, followed by the lower molecular weight fractions and the monomer (naphthalene 2-sulfonate). From Fig. 1 it is possible to recognize that, by increasing the condensation time, the monomer and the lower molecular weight fractions decrease and conversely the higher molecular weight fractions increase.

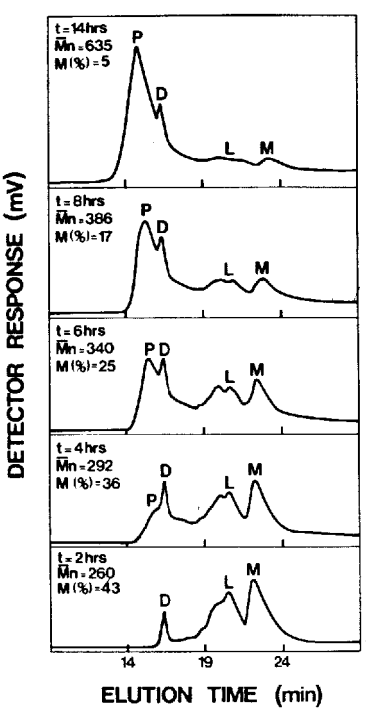

Fig.1 GPC chromatograms of some condensation products at different times (t) of reaction and different number average molecular weight ($\bar{M}n$). P = Polymer; M = Monomer; L = Low molecular weight fraction; D = Naphthalene disulfonate.

Fig. 2 shows the fluidity of fresh cement pastes as a function of the monomer content in the superplasticizer. It can be seen that there is a strong negative influence of the monomer content in the superplasticizer on the fluidity of cement pastes. This agrees with the results of authors who found that naphthalene 2-sulfonate does not exert any fluidifying effect (7).

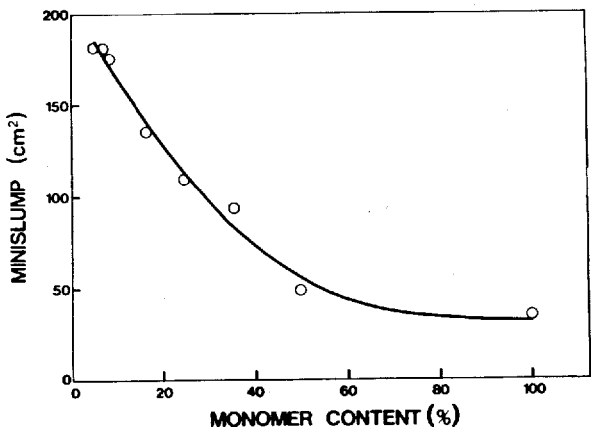

FIg.2 Effect of monomer content in the condensation product on the fluidity (mini-slump) of the cement pastes.

In Fig. 3 the mini-slump values are plotted versus the number average molecular weight ($\overline{Mn}$) of the condensate. This Figure shows that, with the cement used in the present work, the fluidity increases by increasing the $\overline{Mn}$ value up to about 600.

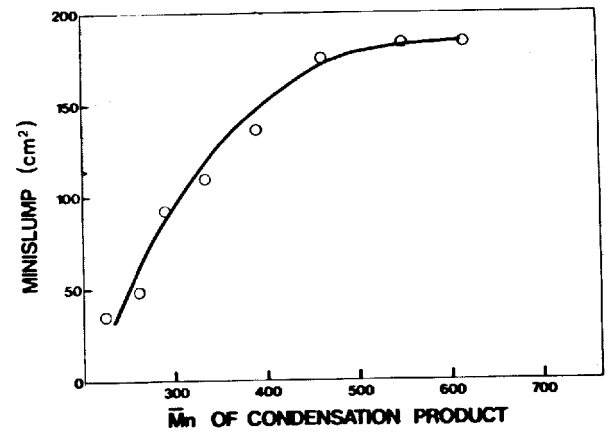

Fig.3 Effect of $\overline{Mn}$ of the condensation product on the fluidity (mini-slump) of the cement pastes.

By comparing the sample condensed for 4 hours ($\overline{Mn}$ = 292) with that condensed for 14 hours ($\overline{Mn}$ = 635), the latter appears to be much more effective as superplasticizer (Fig. 3). One cannot know whether the 14hr-condensate sample is better for the lower content in monomer and "L" fraction or for the higher molecular weight of the "P" fraction (Fig. 1). To clarify this point, both the samples were subjected to ultrafiltration process in order to remove the monomer and the "L" fraction. Figure 4 shows the GPC chromatograms of the two samples before and after ultrafiltration process. The mini-slump values of the cement pastes treated with condensation products before and after the ultrafiltration are shown in Table 2. The results show that, although the ultrafiltered products have different $\overline{Mn}$ values, their fluidifying effect is substantially the same. This demonstrates that, at least for the range of molecular weights considered in the present work, the "P" fraction content and not its molecular weight is determining the fluidifying effect of naphthalene based condensates.

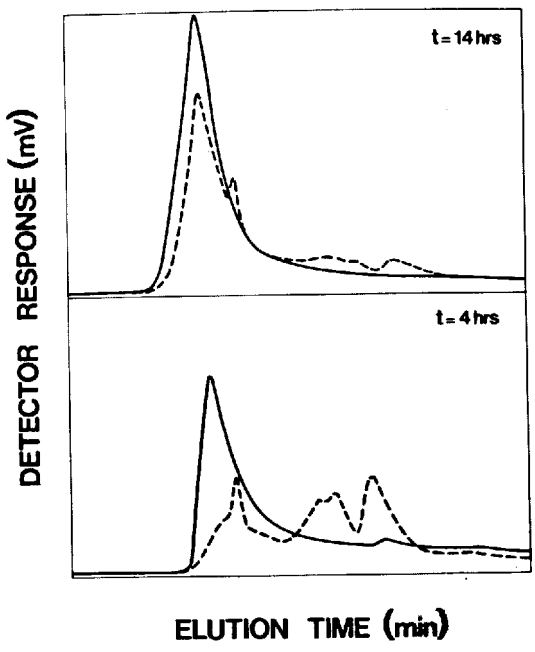

Fig. 4 GPC chromatograms of superplasticizer samples condensed for 4 hrs and 14 hrs before (dotted line) and after ultrafiltration.

Table 2 Effect of ultrafiltration on $\overline{Mn}$ and minislump.

	CONDENSATION TIME	$\overline{Mn}$	MINI-SLUMP (cm^2)
BEFORE ULTRAFILTRATION	4 HOURS	292	75
	14 HOURS	635	185
AFTER ULTRAFILTRATION	4 HOURS	435	185
	14 HOURS	735	185

Conclusions

It is possible to conclude that, for the range of $\overline{Mn}$ of the condensate examined in the present work, the effectiveness of naphthalene sulfonate polymer as superplasticizer is in relation to the content of the monomer and the lower molecular weight fraction, while the molecular weight value of the highly condensed polymeric fraction of the condensate is not determining the effectiveness of the superplasticizer. By using different cements, or by varying the range of $\overline{Mn}$ of the polymer examined, different results may be obtained, as previously reported (5).

References

(1) M. Collepardi, M. Corradi and M. Valente, "Developments in the use of Superplasticizers", pg 485, Publ. SP-68, Am. Concr. Inst., Detroit (1981).

(2) M.G. Garvey and T.F. Tadros, Kolloid-Z. u.Z. Polymere 250, 967 (1972).

(3) D.M. Roy, G. Varadi, F.D. Tamàs, G. Pàlyi and B. Bartha, Cem. Concr. Res., Vol. 14, 439 (1984).

(4) H. Edelstein, "Aqueous Gel Permeation Chromatography of Some Naphthalene Sulfonic Acid Formaldehyde Condensates", Mini-Symposium of the North Jersey Chromatography Group Subsection of the A.C.S., March 6, 1978, at Hoffman La Roche Auditorium, Clifton, New Jersey.

(5) G. Ferrari, F. Basile, A. Dal Bo', A. Mantoni, "The Influence of Molecular Weight of Beta-Naphthalene Based Polymers on the Rheological Properties of Cement Mixes", Symposium of the A.I.T.E.C., , October, 1985, Parma, Italy.

(6) L.M. Meyer, W.F. Perenchio, Concrete International, 36-43, January 1979.

(7) M. Collepardi, M. Corradi, G. Baldini, M. Pauri, 7th International Congress on the Chemistry of Cement, Vol. III, pg. VI- 20, Paris (1980).

F. Basile, S. Biagini, G. Ferrari - MAC, R&D Laboratories, Treviso, Italy
M. Collepardi - University of Ancona, Italy

PROPERTIES OF CEMENT MIXES CONTAINING NAPHTHALENE SULFONATED POLYMERS OF DIFFERENT MOLECULAR WEIGHT

Introduction

Sulfonated Naphthalene-formaldehyde polymers are the basic materials for the production of a class of superplasticizers, which are today extensively used to manufacture cement concretes and mortars. While a large amount of work has been devoted to examine the properties of fresh and hardened concretes containing superplasticizers (1,2), relatively few papers have been published to examine the effect of superplasticizers on the chemical characteristics of polymers and cement mixes (3-6).

This investigation was therefore carried out in order to correlate performances of cement mixes (including mortars), with the physico-chemical characteristics of cement pastes, manufactured with and without the addition of Naphtalene based superplasticizers.

In particular the work was carried out with a series of different superplasticizers based on sulfonated Naphthalene, in order to evaluate the effect of the polymer molecular weight on the hydration of cement and the performances of cement mixes.

Experimental

Materials

Four samples of sulfonated Naphthalene polymers of different molecular weight were obtained by a process described in an other work (7), where the final condensation step was maintained for 2, 4, 10 and 14 hrs respectively, at a temperature of 112°C.

The Number Average Molecular Weight ($\overline{Mn}$) of condensated superplasticizers was determined by use of Gel Permeation Chromatography (8) and specific values for each sample of polymer are given in Table 1.

Table 1 Number Average Molecular Weight ($\overline{Mn}$) of different samples of condensated Naphthalene sulfonate.

SAMPLE	CONDENSATION TIME (hrs)	$\overline{Mn}$
A	2	260
B	4	290
C	10	480
D	14	640

A type I ASTM Portland cement was used, and its chemical analysis is given in Table 2.

Table 2 Chemical analysis of Portland cement

	%w
L.O.I.	1.20
SiO_2	21.05
Al_2O_3	5.20
Fe_2O_3	3.12
CaO	63.70
MgO	0.75
Na_2O	0.20
K_2O	0.37
SO_3	1.90
Blaine fineness (m^2/gr)	0.380

Techniques

Polymer adsorption, zeta potential, minislump, heat evolution rate, differential thermogravimetry (DTG) were carried out on cement pastes (water/cement ratio = 0.40) hydrated at 20°C by following the techniques described in previous papers (5,6). Polymer adsorption, zeta potential and minislump were determined after 5 min of mixing. Moreover ASTM (with only 5 days) flow table, air-entrainment measurement and compressive strength on mortar mixes at 20°C (sand/cement ratio = 3) were carried out at a given water/cement ratio (0.45) or at a given flowability (flow cone = 70%).

The superplasticizer dosage was 0.4% of dry polymer by weight of cement.

Discussion of results

Fig.1 shows the polymer adsorbed on cement (by percentage of the original amount of polymer) as a function of its Number Molecular Weight ($\overline{Mn}$). By increasing $\overline{Mn}$ the polymer adsorption increases up to 70%. Beyond an $\overline{Mn}$ value of about 600 it seems that there is no significant increase in the polymer adsorption.

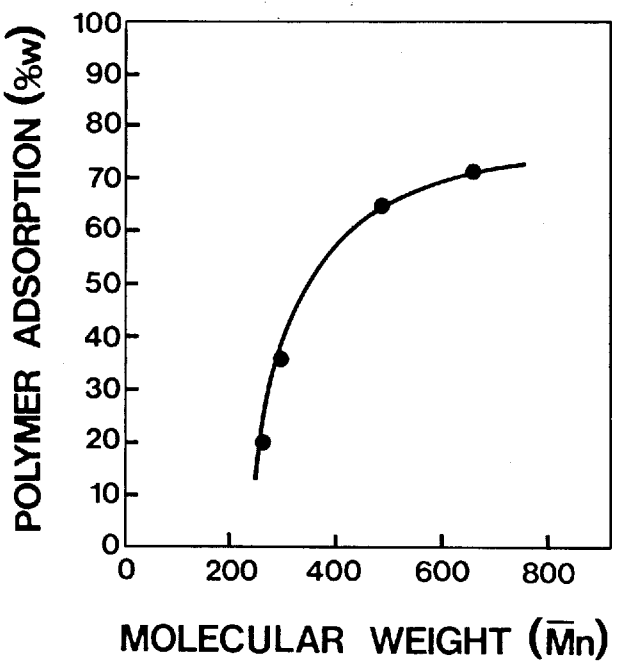

Fig.1 Adsorption of Naphthalene sulfonate polymers on cement paste as a function of the Number Molecular Weight ($\bar{M}n$) of polymers.

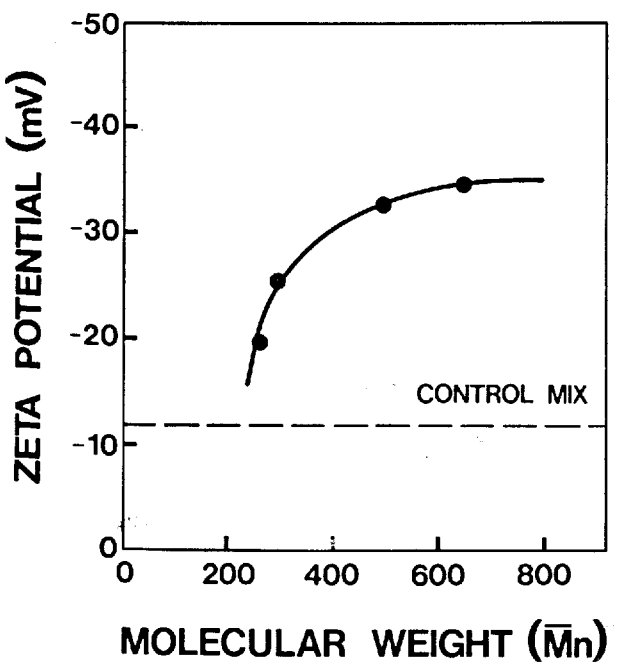

Fig.2 Zeta potential of cement pastes with and without Naphthalene polymers of different Molecular Weight ($\bar{M}n$).

A similar trend was recorded for the zeta potential vs $\bar{M}n$ curve (fig. 2). Also in this case it seems that there is no substantial increase in zeta potential for $\bar{M}n$ values higher than 600.

Figure 3 shows that the fluidifying effect of the polymer increases by increasing the polymer $\bar{M}w$ value. Also in this case it seems that the effect does not substantially change with polymers having $\bar{M}n$ value higher than about 600.

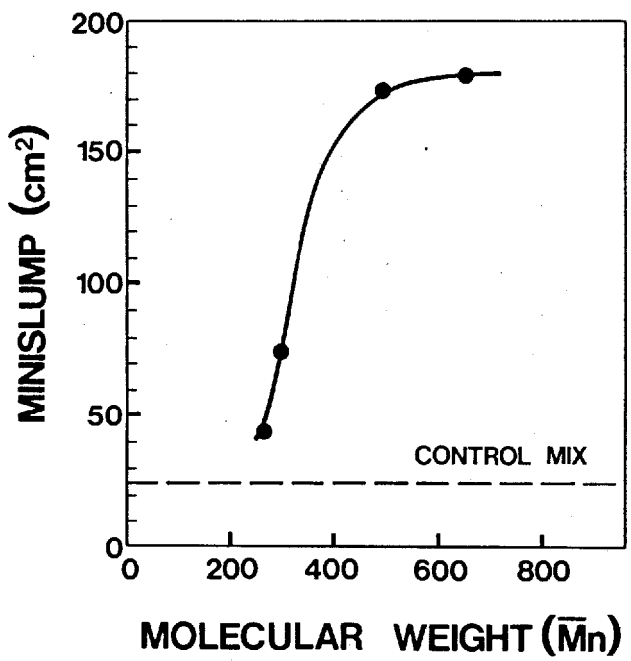

Fig.3 Minislump of cement pastes prepared with and without addition of Naphthalene polymers of different Molecular Weight ($\bar{M}n$).

Curves of heat evolution rate as a function of hydration time up to 24 hrs with and without superplasticizers are shown in Fig. 4. In the presence of those admixtures both the induction period and the time corresponding to the maximum in the heat evolution curve are increased with respect to the control mix without admixture. This indicates a retarding effect of the polymer on the early cement hydration. The higher the polymer $\bar{M}n$ value, the more effective the retarding action of the polymer.

In order to obtain more information about the effect of the polymer on the cement hydration, the percentage of $Ca(OH)_2$ produced from 8 hrs to 28 days was

determined by DTG (Table 3). At 8 hrs the percentage of $Ca(OH)_2$ decreases in the presence of polymers with respect of control mix. The higher the polymer $\overline{Mn}$ value, the more effective is the retarding action on the early cement hydration, thus confirming the results obtained by the calorimetry technique (Fig. 4). On the other hand, at longer ages, such as a 7 and 28 days, the polymer addition increases the cement hydration degree and the effect becomes more remarkable by increasing the molecular weight of the polymer.

Table 3 $Ca(OH)_2$ (% by weight of anhydrous cement) in pastes cured with and without Naphthalene polymers of different Molecular Weight ($\overline{Mn}$)

MOLECULAR WEIGHT OF POLYMER ($\overline{Mn}$)	$Ca(OH)_2$ (%w) after:			
	8 hrs	1day	7days	28days
CONTROL	2.0	7.3	9.0	10.5
260	1.8	6.6	9.5	10.7
290	1.7	6.5	10.5	11.2
480	1.6	6.7	11.0	12.1
640	1.5	6.8	12.0	15.2

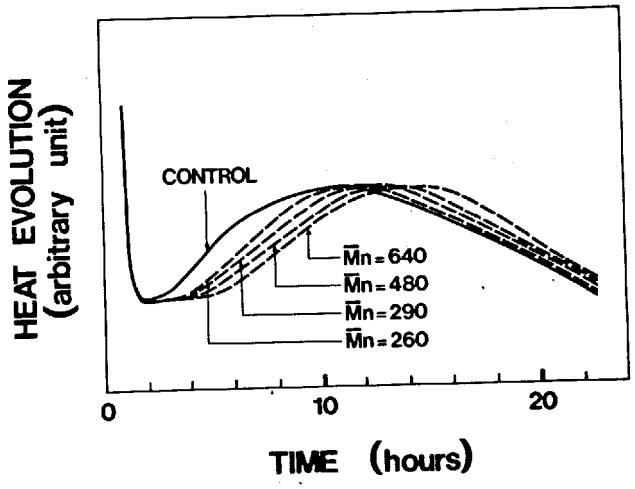

Fig.4 Heat evolution curves of cement pastes with and without addition of naphthalene sulfonate polymers of different Molecular Weight (Mn).

Table 4 and 5 show the results on mortars at a given w/c ratio and at a given flowability respectively. For the tests at a given w/c ratio, the superplasticizer addition causes an increase in the flow table of the mortar. The fluidifying effect increases by increasing the polymer $\overline{Mn}$ value. On the other hand the polymer addition causes an increase in the air-entrainment. This effect is greatest with the polymer having $\overline{Mn}$ value of 290. It would seem that the air-entrainment decreases with the molecular weight of the polymer and increase with the fluidity of the mortar, so that the highest increase in the air-entrainment is caused by the polymer with an intermediate $\overline{Mn}$ value such as 290 in the present work. Because of the high increase in the air-entrainment, the strengths of mortars with polymers having $\overline{Mn}$ values of 260 and 290 are lower than the strength of the plain mortar, in spite of a higher cement hydration degreee at 7 and 28 days of the superplasticized cement mixes with respect to the control mix (Table 3). For the polymers with $\overline{Mn}$ of 480 and 640 causing a lower increase in the air-entrainment, the strength of the superplasticized mortars at later ages (7 and 28 days) are slightly higher than the control mortar.

Table 4 Characteristics of mortars (water/cement = 0.45; sand/cement = 3) prepared with and without Naphthalene sulfonate polymers of different Molecular Weight ($\overline{Mn}$).

$\overline{Mn}$ OF POLYMER	FLOW *	ENTRAINED AIR %v	COMPRESSIVE STRENGTH (MPa) 1day	7days	28days
CONTROL	65	5.0	13.5	42.0	52.5
260	80	9.0	12.5	37.0	47.5
290	90	12.0	10.5	33.0	44.0
480	110	8.5	12.0	43.0	53.0
640	120	7.5	13.0	44.0	55.5

* ASTM C 109 - 5 drops only

The effect of the polymer $\overline{Mn}$ value on the air-entrainment in superplasticized mortars appears clearer in the tests at a given flowability (Table 5). In this case the increase in the air volume caused by the superplasticizer decreases by increasing the polymer $\overline{Mn}$ value from 280 to 640. The increase in strength is remarkable with the polymers having the highest $\overline{Mn}$ value (480 and 640) since there is the greatest reduction in the w/c ratio (Table 5), the highest increase in the cement hydration degree (Table 3) with a negligible or no increase at all in the air volume. For the polymers having lower $\overline{Mn}$ value (260 and 240), both the reduction in the w/c ratio (Table 5) and the increase in the cement hydration degree (Table 3) are much lower, so that the increase in the air volume with respect to the control mortar substantially reduces the above beneficial effects and no significant increase in strength is obtained in superplasticizerd mortars.

Table 5 Characteristics of mortars with a given flow prepared with and without Naphthalene sulfonate polymers of different Molecular Weight ($\overline{Mn}$).

Mn OF POLYMER	WATER/CEMENT RATIO	FLOW (*)	ENTRAINED AIR (%v)	COMPRESSIVE STRENGTH 1day	7days	28days
CONTROL	0.45	70	5.0	12.0	42.0	52.5
260	0.43	70	8.0	13.0	42.0	51.0
290	0.42	70	8.2	13.0	43.5	53.0
480	0.40	70	6.5	18.0	52.0	63.0
640	0.39	70	5.0	18.5	52.5	64.0

(*) ASTM C 109 - 5 drops only

Conclusions

By increasing the Molecular Weight of sulfonated Naphthalene polymer the fluidifying effect of the superplasticizer increases. This effect is accompanied with an increase in the zeta potential of cement pastes and in the amount of polymer adsorbed on hydrated cement. For the cement used in the present work no significant increase in fluididity, zeta potential and adsorption appears for Number Molecular Weight ($\overline{Mn}$) of the polymer higher than about 600.

By increasing the molecular weight of the polymer, the degree of cement hydration is reduced at earlier ages and increased at later ages. The retarding effect on the early cement hydration, which could be ascribed to the adsorption of polymer molecules on cement particles, seems to be advantageous to reduce slump loss in concrete mixes. The increase of the hydration degree at later ages could be ascribed to a better dispersion of cement particles, as a result of a higher zeta potential which increases by increasing the molecular weight of the polymer.

The molecular weight of the polymer significantly affects also the increase in the volume of entrained air in cement mixes. This volume decreses by increasing the molecular weight of the polymer. With $\overline{Mn}$ value higher than about 600 no substantial increase in the air volume is found with respect to the control mix. Consequently the increase in strength caused by polymers with $\overline{Mn}$ higher than a certain value (about 600 for the cement used in the present work) becomes very effective as the reduction in the w/c ratio and the increase in the degree of cement hydration are not counteracted by any increase in the volume of entrained air.

References

(1) Proceedings of International Symposium on "Superplasticizers in Concrete", ACI, SP-62, May 1978, Ottawa, Canada.

(2) Proceeding of International Conférence on "Development in the use of Superplasticizers", ACI,SP-68, (1981), Ottawa, Canada.

(3) R. Kondo, M. Daimon, E. Sakai "Interaction Between Cement and Organic Polyelectrolytes". Il Cemento, 75, 225-230, (1978).

(4) D.M. Roy et al., "Rheological Properties of Cement Mixes", Cem. Concr. Res. 8, 758-764, (1978); 9,

103-110, (1979); 9, 731-740, (1979); 10, 287-295, (1980).

(5) M. Collepardi, M. Corradi, G. Baldini, M. Pauri, "Influence of Sulfonated Naphtalene on Fluidity of Cement Pastes", Proc. 7th Int. Congress on the Chemistry of Cement, Vol. III, pg 20-25, Paris 1980.

(6) M. Collepardi, M. Corradi, M. Valente, "Influence of Polymerization of Sulfonated Naphtalene Condensate and its Interaction with Cement", in ref. (2)

(7) F. Basile, S. Biagini, G. Ferrari and M.Collepardi, "Effect of Condensation Degree of Polymers Based on Naphthalene Sulfonate on Fluidities of Cement Pastes", This Symposium.

(8) G. Ferrari, F. Basile, A. Dal Bo', A. Mantoni, "L'influenza del peso molecolare dei polimeri a base di beta-naftalensolfonato sulle proprietà reologiche degli impasti cementizi", in "Il Cemento ed il Calcestruzzo negli anni 80", pg 251-259, Parma, Italy, (1985).

Stefania Grzeszczyk, Dr., Institute of Cementing Building Materials, Opole, Poland
Leokadia Kucharska, Asst. Prof., D.Sc., Technical University of Wrocław, Poland

THE INFLUENCE OF ALKALIES UPON THE WATER DEMAND OF EARLY HYDRATION STAGE CEMENT PASTES IN THE LIGHT OF RHEOLOGICAL STUDIES

INTRODUCTION

The influence of cement paste alkalies upon mechanical quantities is considered to result from the changes in the liquid phase composition caused by sodium and potassium sulphates and from the changes in the hydraulic activity of clinker minerals due to the building-in of alkalies into the crystal lattice of minerals. The influence of alkalies upon the solution composition through the changes of clinker phase and gypsum solubility shows impact upon the water demand and the rheological qualities of cement pastes. According to Odler and others (1) the rheological qualities of cement pastes depend primarily on w/c, hydration time, mixing intensity and fine-graininess. The chemical and mineral composition is considered less important. The effects of Gebauer's and Schramla's (2) studies point to the significant influence of the following factors upon the water demand: C_3A content, the total content of alkalies and the content of 10 - 30 μm grains.

It has been proved that, of all parameters under investigation, the water demand of cements is linearly correlated with the water-demand of concretes made from these cements. Johansen's tests on cement pastes, as cited Jawed and Skalny (3), showed that the amount of water bound during the three minutes' hydration is negatively correlated with the twenty-eight days' strenght. This suggests that reactions occurring during very early contact of cement and water have a significant influence upon the forthcoming development of strenght. The practical consequence of early cement hydration reactions can be found in the rheological qualities of the paste.

The consistence of fresh cement pastes results from the overlapping of effects that flocculate and delay the early hydration of aluminates by means of gypsum. The impact of gypsum is modified by the presence of alkalies. According to Bombled (4), the sulphates of alkalies decrease the paste deformability, shorten considerably the time of setting, K > Na, and weaken the strenght. Ish-Shalom and Greenberg (5) have proved that alkalies, while having little influence upon the plastic viscosity of cement pastes, increase greatly the yield value, in proportion to the content of alkalies.

This paper presents the results of the research work into the influence of alkalies upon the rheological qualities of clinker and cement pastes during the first hour of hydration with regard to the kind and origin of alkalies.

EXPERIMENTAL

The tests were carried out with the aid of the RV-2 rotary viscometer-coaxial cylinders (made in the GDR), in which the geometry of both cylinder surfaces was modified to reduce sedimentation and slip.

The experiments were performed on industrial as well as laboratory-synthesized clinkers and cements. The clinkers for preparing the experimental cements were synthesized out of chemically pure ones containing Na_2O (0 - 1.3 %) or K_2O (0.8 %) and main clinker oxides. Various amounts of Na_2O or K_2O (in the form of carbonates) were being added to a standard raw meal.

The synthesis of clinker with no content of alkalies was repeated three times using the same composition and maintaining identical conditions. The chemical composition of synthesized and industrial clinkers is shown in Table 1.

Table 1.
The chemical composition of synthesized and industrial clinkers under investigation.

clinker	K_1	K_1'	K_1''	K_2	K_3	K_4	K_5	K_6	P_1	P_2	P_3
IgLoss	0.20	0.20	0.30	0.45	0.30	0.30	0.20	0.20	0.60	0.40	0.60
Insoluble	0.00	0.10	0.10	0.10	0.10	0.10	0.20	0.10	0.10	0.32	0.22
SiO_2	23.10	23.00	22.90	22.90	22.40	22.45	22.45	22.90	20.60	22.50	20.90
Fe_2O_3	3.85	3.85	3.75	3.75	4.00	4.15	4.15	4.15	4.40	2.60	2.45
Al_2O_3	7.90	7.80	7.80	7.85	7.60	7.70	7.50	7.60	6.00	5.80	7.40
CaO	63.70	63.60	63.70	63.30	63.35	63.30	63.65	63.30	64.80	65.20	65.10
MgO	1.40	1.30	1.30	1.30	1.20	1.20	1.10	1.20	1.30	1.80	1.00
SO_3	—	—	—	—	—	—	—	—	0.70	0.50	0.70
Na_2O	—	—	—	0.75	0.80	0.90	1.30	—	0.10	0.10	0.17
K_2O	—	—	—	—	—	—	—	0.80	0.70	1.20	1.20
Free CaO	0.40	0.60	0.75	0.95	0.80	1.00	0.80	0.80	0.97	1.72	1.95

The synthesized clinkers contained no SO_3 and alkalies were embodied in clinker phases. The identyfication (X-ray diffractometry and optical microscopy) of the synthesis products showed that sodium concentrates mainly in the C_3A phase and the increase in its amount in the clinker system produces a change in the symmetry of the Na_2O-in-C_3A solid solution, a regular one for a non-sodium clinker sample and a monoclinic one for the samples with 0.90 % and 1.30 % by weight of Na_2O.

Taking into account the content of SO_3 in the tested industrial clinkers, one may assume that some of their alkali contents are found in the form of sulphates and some, that are not bound into sulphates, remain built in the clinker phases. All the clinkers and cements used in the tests were ground to cover the identical area of 300± 20 m^2/kg in compliance with Blaine'a. The cements contained 5 % of gypsum ($CaSO_4 \cdot 2H_2O$). The way of preparing the samples for the rheological measurements was identical for all clinkers.

Test procedure:

The pastes were made by mixing the clinker or the cement with distilled water or with water containing 0.90 % of Na_2O or K_2O in the form of NaOH, Na_2SO_4 or K_2SO_4. The mixing was done by hand for 4 minutes, which was followed by a minute's mixing at 243 rpm. For clinker suspensions w/c was equal to 0.6, while cement pastes had the equivalent of 0.4. The flow curves were determined after 10 minutes from the moment of clinker or cement contact with water. The time of determining flow curve is 20 minutes. The stress in time at the constant shear rate of 46 s^{-1} was measured for the period of 60 minutes.

Stefania Grzeszczyk, Dr., Institute of Cementing Building Materials, Opole, Poland
Leokadia Kucharska, Asst. Prof., D.Sc., Technical University of Wrocław, Poland

RESULTS AND DISCUSSION

The flow curves of clinker pastes with no alkali content and with built-in alkalies are presented in Fig. 1, while Fig. 2 shows the flow curves of cement pastes with regard to the amount of built-in sodium.

The positions of the flow curves of non-alkali clinker pastes K_1, K_1', K_1'' point to varied reactivity of the said clinkers.

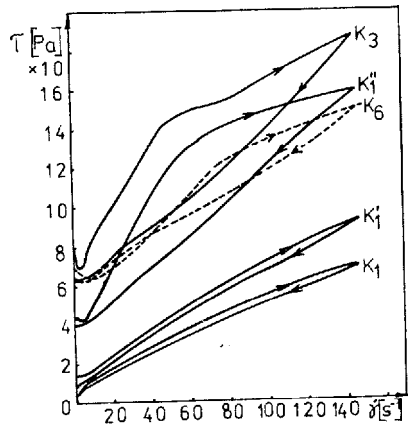

Fig. 1. The flow curves of clinker pastes with no alkali content (K_1, K_1', K_1'') and containing 0.8 % Na_2O (K_3) and 0.8 % K_2O (K_6).

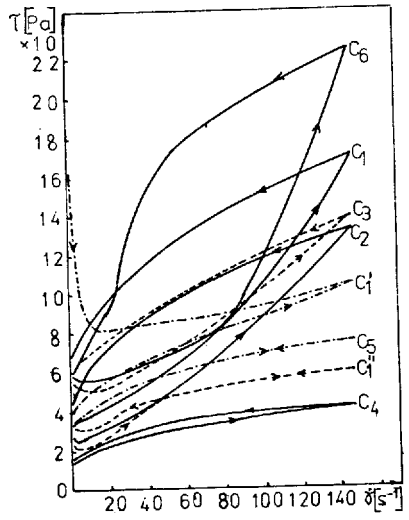

Fig. 2. The flow curves of cement pastes made from non-sodium clinkers C_1, C_1', C_1'' and from clinkers containing sodium (C_2 - 0.75, C_3 - 0.80, C_4 - 0.90, C_5 - 1.30 % Na_2O) and potassium (C_6 - 0.80 % K_2O).

The results show that increased activity of non-alkali clinker, reflected in the shift of the flow curves towards greater stresses, i.e.:

$$\underset{\text{consistence decrease}}{K_1'' > K_1' > K_1} \rightarrow ,$$

is related to greater consistence decrease of the cement pastes made from the said clinkers:

$$\underset{\text{consistence decrease}}{C_1 > C_1' > C_1''} \rightarrow .$$

The analysis of the built-in sodium impact upon the dynamic yield value and viscosity (Fig. 3), deducted from the setting curves of tested suspensions, suggests that built-in sodium brings about the decrease in yield value and viscosity when compared with non-alkali cement C_1.

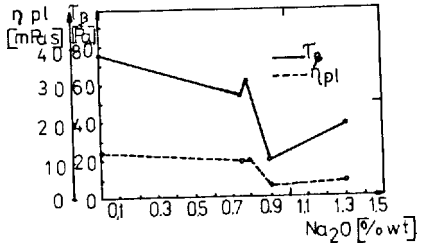

Fig. 3. The influence of built-in sodium upon the dynamic yield values (τ_β) and viscosity (η_{pl}) of cement pastes.

In the light of Hiroshi Uchikawa's and others' research results (6), the indicated differences in the reactivity of non-alkali cements may be connected with the differences in the reactivity of C_3S.

Taking into consideration the test results of non-alkali C_1' and C_1'' cement suspensions, which may also stand as a point of reference for the suspensions made from sodium-containing clinkers, it is possible to state that the influence of sodium built in clinker phases upon the water demand of the cement paste in the early hydration stage does not exceed the changes in the water demand linked to a varying degree of clinker phase crystallization if identical raw meal composition and synthesis conditions are preserved.

According to Shine and Glaser (7), sodium released during the hydration, decreases the content of Al^{+3} ions in the solutions and delays the hydration itself. This may justify the observed decrease in viscosity. Showing the lack of significant influence of built-in sodium upon the water-demand is consistent with the conclusions of several authors stating the lack or little positive impact of built-in sodium upon the cement strenght.

The position and course of the flow curve for the cement paste containing potassium suggests that some amount of potassium that is not bound with C_2S, due to the increased reactivity of the phases in which it occurs, has impact on the solubility of gypsum.

Stefania Grzeszczyk, Dr., Institute of Cementing Building Materials, Opole, Poland
Leokadia Kucharska, Asst. Prof., D.Sc. Technical University of Wrocław, Poland

As a result it affects the paste flow by showing an increased effect of the shear rate and clearlyvisible hysteresis anti - loop.

The effect of built - in alkalies reveals itself more clearly during the measurements of stresses in time. A considerable increase of stresses in time (Fig. 4) was observed both in clinker and in cement pastes, the growth being higher for the samples with sodium than the ones with potassium. The above research results are in keeping with the results obtained by other authors and suggest that sodium lessens clinker activity and thus weakens the efficiency of regulating the setting with gypsum. The great growth of stress in time for built-in sodium cement pastes may be justified by the greater reactivity of C_3A_{ss} if compared with C_2S_{ss}.

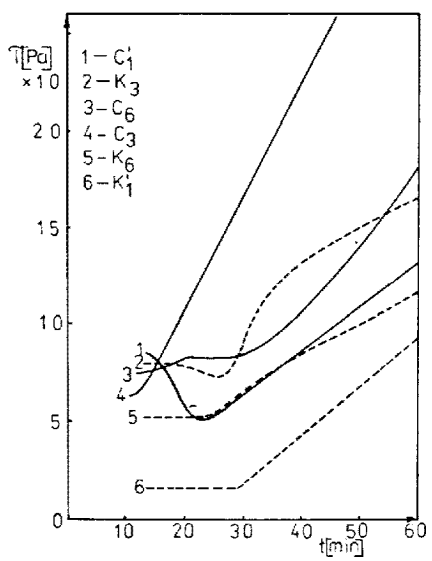

Fig. 4. The diagram of stress variation in time ($\dot{\gamma}$ = 46 s^{-1}) for the non-alkali clinker and cement pastes (K'_1, C'_1), the pastes containing 0.8% Na_2O (K_3, C_3) and the ones with 0.8% K_2O (K_6, C_6).

Bringing sodium as NaOH into the batch water (Fig. 5) causes an increased consistence of clinker pastes while the influence of NaOH upon cement pastes is dependent on clinker reactivity. The more reactive clinker is , the lesser impact of NaOH upon the cement paste consistence.

The effect of sodium added as NaOH is observed in the early stage of hydration (up till 30 minutes) as a change in the paste consistence. In the later stage (Fig. 6) this sodium does not affect changes of stresses in time streight lines in the stress - time system for samples without and with NaOH are parallel.

The constant concentration of NaOH in the solution reduces the amount of coagulating Al^{+3} ions- the precipitation of $Ca(OH)_2$ on the surface of C_3A grains at the initial stage and the reaction with the aluminium ions found in the solution contribute to the formation of C_4AH_6 mainly in non - gypsum suspensions. In accordance with Shine's and Glasser's research results the presence of gypsum reduces the amount of Al^{+3} ions in the solutions to 50 % of that in non - gypsum ones. The source of sodium does not affect the solution composition in the presence of gypsum. Reducing the number of ions coagulating in the solution does affect the paste consistence and its changes in time.

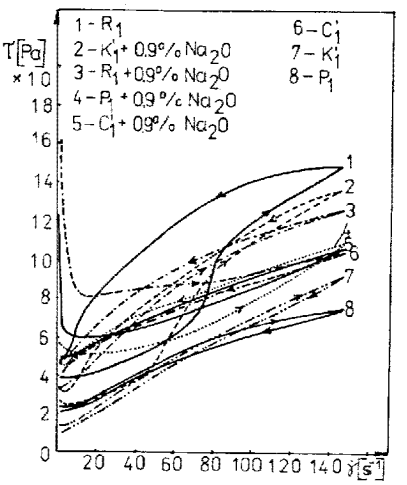

Fig. 5. Flow curves of clinker and cement pastes without and with 0.9 % Na_2O in the form of NaOH (K'_1, C'_1 - synthesized clinker and cement P_1 , R_1 - industrial clinker and cement).

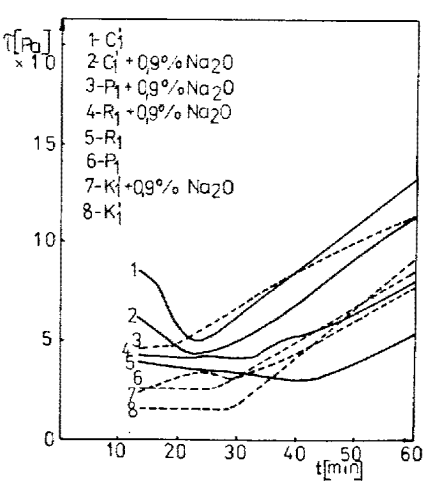

Fig. 6. The diagram of stress variation in time ($\dot{\gamma}$ = 46 s^{-1}) for clinker and cement pastes without and with sodium as NaOH .

Stefania Grzeszczyk, Dr., Institute of Cementing Building Materials, Opole, Poland
Leokadia Kucharska, Asst. Prof., D.Sc. Technical University of Wrocław, Poland

The results of rheological research work in the initial period (till 30 minutes) help reach the similar conclusion. In the presence of gypsum changes in both cases (i.e. cements with sodium embodied and introduced as NaOH) point to little influence of gypsum upon the paste consistence. However, changes in time for suspensions with sodium built-in and introduced as NaOH reveal diverse behaviour of C_3A_{ss} and C_3A in the presence of gypsum.

The research work into the impact of alkali sulphates (Na_2SO_4 , K_2SO_4) introduced into the batch water of clinker and cement pastes showed that, in both cases, sulphates increase consistence (Fig. 7).

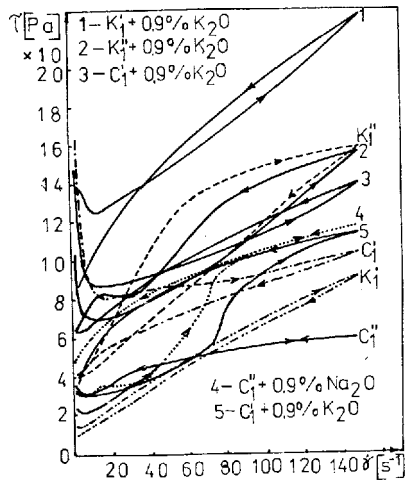

Fig. 7. Flow curves of non - alkali clinker and cement pastes (K'_1 , K''_1 , C'_1 , C''_1) whose batch water contained no or 0.9 % Na_2O or K_2O in the form of K_2SO_4 and Na_2SO_4 .

The quantity of changes is dependent upon clinker reactivity (compare K'_1 and K''_2 , Fig. 7) . The influence of sulphates is particulary clearly indicated at the initial stage of hydration.

Measuring stresses in time (Fig. 8) proved that sulphates in clinker pastes cause heavy coagulation, which means a significant growth of consistence during early hydration. In the later period of hydration, over 30 minutes, one observes a considerable decrease in the influence of alkali sulphates on the clinker consistence in particular.

Cement pastes containing K_2SO_4 or Na_2SO_4 show increased consistence and greater changes in time for K_2SO_4 . This is consistent with the research results (8) which attribute greater influence of K_2SO_4 to the formation of syngenite and calcium sulphate.

Rheological investigations of industrial cements confirmed the results obtained for synthesized ones (Fig. 9) .

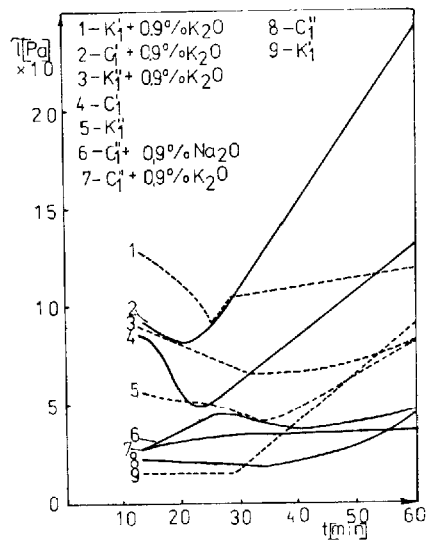

Fig. 8. The diagram of stress variation in time ($\dot{\gamma}$ = 46 s^{-1}) for clinker and cement pastes without or with Na_2SO_4 and K_2SO_4 to the amount of 0.9 % Na_2O or K_2O .

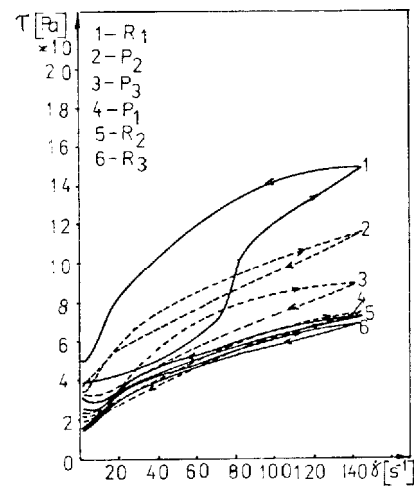

Fig. 9. Flow curves of industrial clinker and cement pastes.

The analysis of flow curves of clinker and cement pastes coupled with the analysis of the mineralogical composition of the said clinkers makes it possible to conclude that differences in the rheological behaviour of cement pastes at the early stage of hydration are related to clinker reactivity. In case of the weaker reactivity of P_1 clinker the efficiency of gypsum influence is smaller. The reverse is true for P_2 clinker , in which an efficient reaction of gypsum with C_3A is revealed by a decrease in the paste consistence.

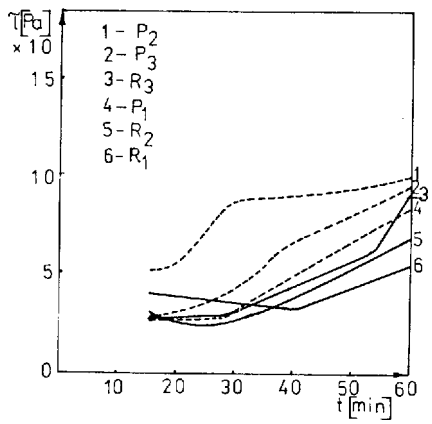

Fig. 10. Curves of stress variation in time ($\dot{\gamma}$ = 46 s^{-1}) for industrial clinker and cement pastes.

At the later stage of hydration (Fig. 10) the course of stress variation, though less intensive, is similar to that represented in Fig. 8 (the influence of potassium sulphate). The SO_3 and K_2O content in industrial clinkers suggests that part of potassium is found in the form of sulphate whose amount in P_1 clinker is greater. The cement paste made from the said clinker is characterized by more intensive growth of stresses in time.

CONCLUSIONS

1. The rheological method has been used to show that the more reactive clinker is the lesser water demand of the cement paste obtained from it.

2. It has been proved that the efficiency of gypsum influence as a setting regulator is dependent on the clinker reactivity. Increasing the clinker reactivity, even with the constant content C_3A , leads to decreasing the consistence of the cement paste.

3. Built in alkalies decrease the efficiency of regulating the paste setting by adding gypsum.

4. The more reactive clinker, the lesser impact of alkalies that are not built in clinker phases upon the consistence of cement pastes and the consistence changes in time.

5. The greatest changes of consistence in time occur in the cement pastes containing built - in sodium. On the other hand , potassium sulphate exerts the greatest influence upon the increase in consistence.

REFERENCES

1. I. Odler, T. Becker, B. Weiss : Rheological Properties of Cement Pastes. Il Cemento , No 3, 303-309 (1978) .

2. J. Gebauer, W. Schramli : Variations in Water Requirement of Industrially Produced Portland Cements. Bull. Am. Ceram. Soc., vol.52, No 2, 161-168 (1974) .

3. I. Jawed, J. Skalny : Alkalies in Cement : a Review II. Effects of Alkalies on Hydration and Performace of Portland Cement. Cem. Concr. Res., vol. 8, No 1, 37-52 (1978) .

4. J.P. Bombled : Influence of sulphates on the rheological behaviour of cement pastes and their evolution. Proc. of 7th International Congress on the Chemistry of Cements, vol. III , Paris, Editions Septima, VI 164-169 (1980)

5. M. Ish-Shalom, S.A. Greenberg : The Rheology of Fresh Portland Cement Pastes. Proc, 4th International Symposium on the Chemistry of Cements. Washington, vol. II, 731-748 (1960) .

6. Hiroshi Uchikawa, Kenji Ogawa, Shunichiro Uchida : Influence of Character of Clinker on the Early Hydration Process and Rheological Property of Cement Paste. Cem. Concr. Res., vol. 15, No 4, 561-572 (1985) .

7. G.Y. Shin, F.P. Glasser : Chemistry of Cement Pore Fluids. I . Suspension Reactions of $Ca_{3-x}Na_{2x}Al_2O_6$ Solid Solutions with and without Gypsum Additions. Cem. Concr. Res., vol. 13, No 3, 366-376 (1983) .

8. I. Odler, R. Wonnemann : Effect of Alkalies on Portland Cement Hydration. II. Alkalies Present in from of Sulphates. Cem. Concr. Res., vol. 13, No 6, 771-777 (1983) .

J. MIERZWA, Technical University of Cracow, Poland

Thixotropic - plastic - viscous rheological model of cement paste as the result of physical and mineralogical cement properties

1. INTRODUCTION

Development of industrial production and processing of concrete particularly intensive in the last period of twenty years sests larger and larger demands for scientific technology of concrete. One of these demands is a necessity of precise description of behaviour of fresh concrete during mixing, transportation and forming. That behaviour is a result of components properties as well as of kinematic-dynamic parameters of interactions of a certaing process of treatment.
To solve the problem the rheological methods obtained from the mechanics of continuous mediums have been applied.
Unfortunatelly, as the investigations which have been carried on till now have proved, fresh concrete have turned out to be anextremely complex real rheological body.

One of the ways which may lead to a solution is an attempt to describe rheological properties of cement paste which is a basic component of concrete. A wide interest connected with the rheological issue of concrete in the world is confirmed by large amount of publications. Their number, beginning from the first of Powers Wiler /in 1941/ includes now about 350 to 400 of items. More then half of them are works dedicated to the rheology of cement paste. On the one hand it ocknowleges the range of difficulties to encounter, on the other the essential significance of this issue for rheology of fresh concrete.

2. THE CURRENT STATT OF RESEARCH

The research works on rheology of cement pastes which have been carried on hitherto have proved the great complexity of the issue. Recapitulations of these works made in papers [1, 2, 3] have shown that the issue of cement paste rheology focuses on three topics:
a/ the influence of methodology of testing, measuring apparatus and physical state of sample in time of testing on the result of the test,
b/ the influence of physical, chemical and mineralogical characteristic of cement and solids concentration of paste on rheological characteristics,
c/ the influence of additions and admixtures on rheological characteristic of cement paste.

Publicated results of investigation diversify very seriously and thus their synthesis is practically impossible. This fact is caused by a paste characteristic. A fresh paste as an unstable body is continuously changing in time. So every act of shearing which has the aim of establishing τ-$\dot{\gamma}$ in relation to variable time "t" must destroy the current state of the structure. Therefore every established rheological value is a result of "history" of sample shearing in previous period. The method applied for testing and the way of initial preparation of sample influences therefore essentially the result of test. For instance, as the examinations have confirmed, a certain program of $\dot{\gamma}$-t in a sample enables to obtain a respectively optional shape, thereby, rheological nature of flow curve [4, 5].

On the present stage of development of research of cement paste and concrete rheology and of possibilities of practical applications one can assume that there is a vital need to create the system of comparable tests results of different research-centres all over the world [3]. So there is a need of standardization of rheological methodology of cement paste. It certainly doesn't exclude the possibility of carrying on other optional research programs according to certain needs.
At the Technical University in Cracov a wide program has been taken up on that issue at the beginning of this decade and the results obtained are going to be put forward in the following part of the paper.

3. "STANDARD" METHODOLOGY OF MEASUREMENT OF RHEOLOGICAL CEMENT PASTES PROPERTIES

Calculation of flow-curve /rheogram/ of rheostablie bodies resowes itself into determining their dependency in the system of variables τ-$\dot{\gamma}$/shear stress-shear rate/. In tests of cement paste which is treated as a rheologically unstable medium the test t is unsatisfactory because there is necessery to identify the function in relation to variable of time. There are two methods being put to this end: hysteresis loop method and the "equilibrium" curve method, suggested originaly by J.Pawlowski [6].

Keeping up the criticall opinion of D.C. Cheng, F.Evans and P.S.Worralland S.Tulliani on the hysteresis concept particularly in the light of tests results [4, 5], as the most adequate for rheological identification of paste the equilibrium curve method has been accepted. The method assumes realization of shear test with constant shear rate $\dot{\gamma}_i$ = constans, calculating values τ, as τ_{max} and τ_m as a minimal shear stress carried over by the structure.

A set of curves calculated on the same sample paste enables to calculate the general dependence τ-$\dot{\gamma}$-t. It has been found that the most advisable time for calculating τ-t

with $\dot{\gamma}_i$ = const. Ranges from 10 to 10^2 min. which is the period of reaction induction in portlnad cements after the water is added 7. Taking into account a particular significance of initial preparation of a sample the standardized program of mixing with the use of lab mixer /ISO/ has been applied the program consists of: t_1 = 60 s mixing with n_1 = = 140 rpm + t_2 = 30 s with n_2 = 285 rpm + 90 s pause + t_3 = 60 s with n_3 = 285+600 s pause + + t_4 = 15 s with n_4 = 140 + t_5 = 15s with n_5 = = 285 rpm /total 15 min./.
During the next 45-55 min a series of curves τ-t was performed with denotation τ_1/τ_{max}/ and τ_m /τ_{min}/ with different $\dot{\gamma}_i$ = const each. Tests have proved that for applied "standard" program of measurements the results dispersion does not exceed 12% when upper limit of time of testing does not exceed 0,65 of time of the initial setting period /Vicat/.

On the basis of testing over 680 curves τ-t which were obtained from testing of 20 different cements it may bestated that to establish a precise dependence τ-$\dot{\gamma}$-t it is enough to take 6 levels of constant shear rate $\dot{\gamma}_i$ from intervals $\dot{\gamma}_1$ = 0,5÷3 s^{-1}, $\dot{\gamma}_2$=6÷10s^{-1}, $\dot{\gamma}_3$=25÷30s^{-1}, $\dot{\gamma}_4$=70÷80s^{-1}, $\dot{\gamma}_5$=140÷160s^{-1}, $\dot{\gamma}_6$=400÷500s^{-1}.

The location of minimum of τ-t function on the time axis at the point t_m corresponding τ_{min} depends on concentration of paste solid phase c_v /and also w/c / and shear rate $\dot{\gamma}_i$. In lesser degree it depends on the surface area of cement and its mineralogical characteristic. For pastes with w/c= 0,37-0,75 values of t_m were on an average 6-8 min.
In Fig. 1 the exemplary series of curves τ-t for pastes with different w/c ratio and different shear rate $\dot{\gamma}_i$ = const. is shown.
The complex problem of establishing of the real value $\dot{\gamma}_i$ caused by heterogeneousnes of shear in the clearance of a viscometer /Bingham's flow/, according to the error analysis results /by Maron Krieger/ can be ignored /allowing an error up to 10%/ if the apparatus fulfius the condition $s = R_z/R_w < 1{,}05$ and the clearance $\Delta R = R_z - R_w > 1$ mm /for paste/.

4. EXPERIMENTS

Program of experiments included 20 clear - clinker cements with five different mineralogical compositions and appropriate amounts of gypsum /shown in Tab. 1/.

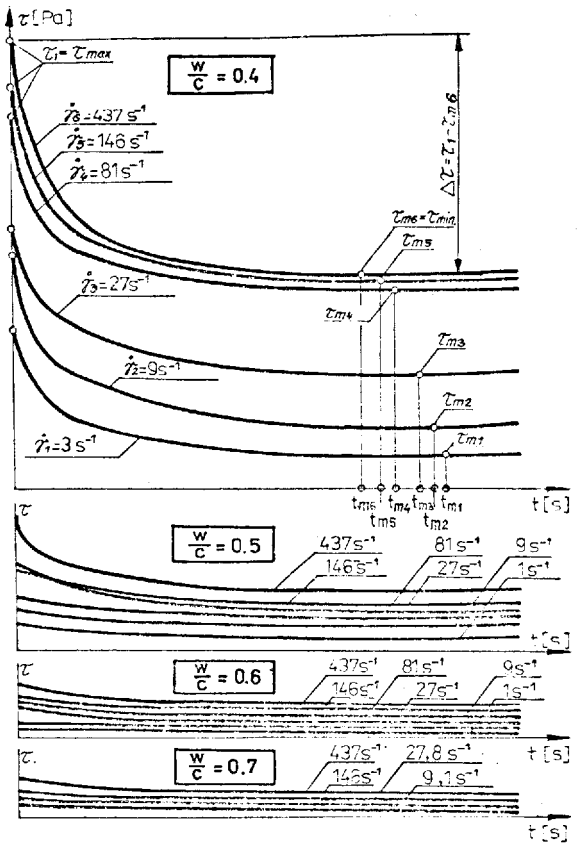

Fig.1. Series of "equilibrium" corves τ-t of flow for pastes with different w/c and constat shear ratio.

Table 1.

Cement series	Proportional amounts of certain mineralogical components Amount /%/				Gypsum %
	C_3S	C_2S	C_3A	C_4AF	
"G"	58	21	6	10	5,3
"P"	66	14	8	8	6,4
"C"	51	25	10	7	6,4
"Oz"	42	33	10	8	4,2
"Od"	50	20	16	9	6,0

Each of the cements with the same mineralogical composition was powdered up to four different levels of surface areas F_B= 300, 350, 400 and 450 m^2/kg. Every cement was used, according to "standard" program, to form cement pastes with w/c ratio = 0,4 0,5 0,6 and 0,7. Experiments were made on Rheotest RV2 type rotating coaxial cylinder with serrated surfaces /ΔR= 0,97 mm/. The full cycle of test included calculation of curves series

τ-t for each w/c and measurement of each following curve $\dot{\gamma}_i$ = const was preceded by repeated mixing for 10 s with n = 140 min^{-1}.

5. THE GENERAL RHEOLOGICAL MODEL OF CEMENT PASTE

Realization of such a vast program of investigations has given a basis to take up an attempt to establish the general rheological model of cement paste within the range of variation of its w/c ratio $0,4 < w/c < 0,70$, that is the most interestig from the technological point of view. Lack of rheostability of cement paste and manifested by it the thixotropical efect of flowing with simultaneous separated thixotropy from the efect of plastic-viscous flow /according to def. of Trapeznikow [8]/ imposes the necessity of approximation of rheological paste model in the three variables system $\tau - \dot{\gamma} - t$. The analysis of test results has demonstrated that as the most typical function in graphic formulation the plane layer for the exponential type function should be taken on /Fig. 2/.

of paste, connecting in its first part in form:

$$\tau_{HB} = \tau_o + \eta_{pn} \cdot \dot{\gamma}^n \qquad /2/$$

the Herschel-Bulkley's model with functional coefficient of thixotropy:

$$\Theta = t^A \cdot e^{B(t-1)} \qquad /3/$$

It is the five-parameter model where τ-shear stress [Pa], τ_o - liquid limit [Pa], η_{pn} - nonlinear plastic viscosity [$Pa \cdot s^n$], n - coefficient of flow speed [-], $\dot{\gamma}$ - shear rate [s^{-n}], t - value corresponding to shear time [-], A B - coefficients qualifying thixotropic predispositions of paste [-]. Qualification of the rheological parameters of the model is done by graduate analysis, where stationary state gained by paste in the proces of constant mixing with speed $\dot{\gamma}_i$ = const. after time $t = t_m$ is a starting point. For this moment coefficient of thixotropy $\Theta = 1,0$ and shear stress achieves its minimum $/\tau = \tau_m/$ for the structure is totally destroyed. Correlation analysis of rheological parameters of the equation /1/ resolves itself into analy-

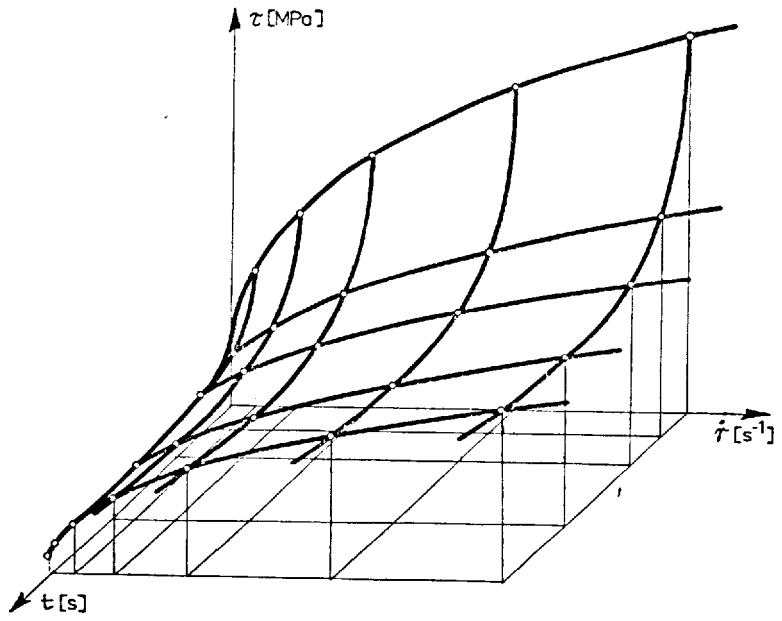

Fig. 2. Graphical image of function $\tau - \dot{\gamma} - t$ which models rheological properties of cement pastes according to equation /1/.

In a satisfactory precise manner it is described by the equation:

$$\tau = (\tau_o + \eta_{pn} \cdot \dot{\gamma}^n) \cdot t^A \cdot e^{B(t-1)} \qquad /1/$$

The structure of the equation /1/ underlines both the plastic-viscuous properties /Bingham's nonlinear/ and thixotropic properties

sis of equation /2/ or directly into linearized for technical application of Bingham's equation with parameters τ_o, η_p. They can be calculated either in three-parameter step-correlation assuming as an optimum the coefficient of the accuracy of correlation r or by the simple two-parameter method of least squares. Coefficients A, B of the functional

factor of thixotropy can be obtained by the method of succesive approximations on the ground of analysis of curves τ-t where value $t = t_m$ is known from experiments and extremum of the function θ is placed at the point:

$$\frac{d\theta}{dt} = 0 \longrightarrow t_m = -\frac{A}{B}$$

6. SOME PRACTICAL ASPECTS OF INFLUENCE OF PHYSICAL AND MINERALOGICAL CHARACTERISTICS ON THE RHEOLOGICAL PROPERTIES OF CEMENT PASTE

It is impossible to present fully the influence of mineralogical composition, surface area, grain composition of cement and additions on rheological parameters of pastes so interesting from the scientific point of view in the paper. The results of investigations on cement paste rheology has proved to be very useful in selcting composition od pastes for injections. When for certain technical mixing conditions of pastes for injections the thixotropical coefficient is calculated, the basic parameters of linearized /for technical applications/ of rheological equation /2/ is the liquid limit τ_o and viscous plasticity η_p. Experiments also shown that they are connected both with a cement surface area F_B and its mineralogical composition expressed by the coefficient M_α in the following equations:

$$\tau_o = (16.5 - 2M_\alpha) \cdot c_v^{(8+0.5F_B^2 \cdot 10^5)} \cdot 10^4 \ [Pa] \qquad /4/$$

$$\eta_p = 3.3 \cdot c_v^{(17+0.27M_\alpha)F_B^{-0.125}} \cdot 10^2 \ [Pa \cdot s] \qquad /5/$$

As an enough precise and useful measure of mineralogical predispositions of cement the factor resulting from a proportional composition of clinker can be assumed:

$$M_\alpha = \frac{C_3S + C_2S}{C_3A + C_4AF} \qquad /6/$$

Its value in ordinary portland cements oscillates in the range from 2,8 to about 5,6 and shows inconsiderable fluktuations in the years production of a certain cement plant and is in a way its characteristic value. The index of volume concentration of solids c_v is connected with the coefficient w/c or paste by the dependence:

$$c_v = \frac{1}{1 + \frac{w}{c} \cdot \rho_c} \qquad /7/$$

where ρ_c denotes specific density of cement.

Equations /4/ and /5/ similarly like the respective dependences of J.P.Bombled [1], G. Wischers, K.Rendchen [9], W. von Berg [10], H.P.Backes, W. von Berg [11] has confirmed also as a significant the influence of mineralogical composition and surface area of cement on paste rheology. Qualification of these dependencies and adequate equation of sedimentation makes easier the selection of composition of injecting pastes. As it results from Fig. 3 the influence of a quality of cement when its clinker mineralogical composition is taken into account /if the value of additions does not exceed 10-15%/ can play a significant role in optimal shaping of the parameters for injection in cable-canals of prestressed constructions.

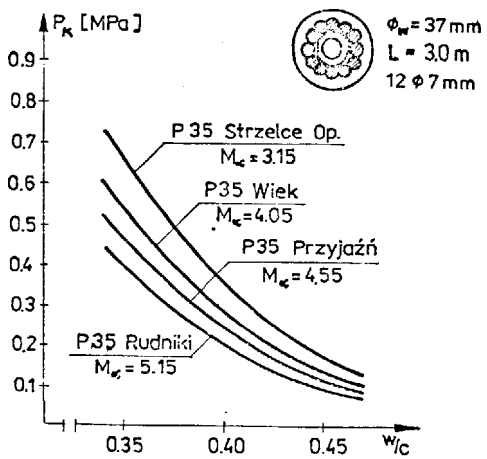

Fig. 3. Influence of mineralogical composition of cements from different cement plants /Rudniki, Przyjaźń, Wiek, Strzelce Opolskie/ on the parameters of the process of paste injection in cable-canals $\emptyset$ = 37 mm filling 12$\emptyset$7 mm, lenght 30 m [12].

7. CONCLUSION

In the paper an attempt of describing of the cynthetic rheological model of cement paste has been taken up. The research program was preceded by the selection of standardized methodology, apparatus and conditions of initial preparation of paste. Results of tests have demonstrated that in relation to properties in flow stage cement paste reveals characteristic of a thixotropic, nonlinear, plastic-viscouse body which is precisely qualified by five rheological parameters such as: τ_o, η_{pn}, n, A, B.
For technical applications this model /1/ can take on a simplified, linearized form. Values of rheological parameters in this model are under the influence of solids concen-

tration, of paste and mineralogical composition of cement with its surface area.

REFERENCES

[1] J.P.Bombled - RILEM Sem. Leeds 1973.

[2] G.H.Tattersall - The workability of concrete. Cem. Con. Assoc. 1976.

[3] R.A.Helmuth - 7-th Congr. Chem. Cem. Paris 1980. S.-T. VI-O.

[4] D.M.Roy, K.Asaga - Cem. Con. Res.9/1979.

[5] P.F.G.Banfil, D.C.Sannders - Cem. Con. Res. 11/1981.

[6] J.Pawlowski - Chem. Ing. Techn. 28/791/ 1956.

[7] R.Kondo, M.Daimon - 6-th Congr. Chem. Cem. Moscow 1976, V. II. B 1.

[8] A.A.Trapeznikow - VII-th Int. Congr. Rheology, Getheborg. 23-27.VIII.1976.

[9] G.Wischers, K.Rendchen - RILEM Semin. Leeds 1973.

[10] W. von Berg - Mag. Con. Res. Vol 31, Nr 109 Dec. 1979.

[11] H.P.Beckes, W. von Berg - IX Int. Congr. Rheology, Mexico 1984.

[12] J.Mierzwa - XXXI Konf. Nauk. KILiW PAN KN PZITB Krynica 1985.

[13] J.Mierzwa - II Konf. Nauk.-Techn. "Proj. i Realizacja Zbiorników", Kraków 1985.

S. Sprung - Research Institute of the German Cement Industry, Dusseldorf, West Germany

Influence of the composition of clinker and cement on the rheological behaviour of fresh concrete

1. Introduction

Ready-mixed concrete should in general remain workable for a longer time than concrete made on the construction site. The consistency of the fresh concrete and its change with time will, for given mix composition, grading curve and type of aggregate, depend to a great extent on the chemical and physical properties of the cement paste. Raised temperature of the fresh concrete accelerates hydration and hastens early stiffening in many cases. The evaporation of mix water, the increase in water demand due to absorption by the aggregate, the presence of fine particles due to aggregate abrasion or fine-grained additives, and the inexpert use of admixtures above all have an effect on the consistency of fresh concrete (1, 2, 3).

Hydration of the cement begins immediately after the mix water has been added. At first, tricalcium aluminate (C_3A) and readily water-soluble calcium sulphates are virtually the only substances that participate in the hydration reactions (4). The initial hydration reactions take place at the surfaces of the cement particles. At this stage their extent depends chiefly on the reactivity and the amount of the C_3A in the clinker, on the surface area and particle size distribution of the cement and on the temperature of the cement paste. Other cement clinker phases participate only to a minor degree in the initial hydration reactions. The first stage of hydration ends after a few minutes. Then follows the dormant period, lasting 2 - 6 hours. The resumption of hydration at the end of the dormant period results in hardening of the cement.

The extent of hydration up to the beginning of the dormant period as well as the amount and morphology of the hydration products which are formed up to that point of time determine the water demand for adjusting the initial consistency of the cement paste. During the dormant period the paste undergoes further stiffening. When the consistency has attained a certain condition, the cement begins to set, according to the standard definition. After the end of setting, the hardening phase of the cement paste commences (1).

Research in recent years has shown that the consistency of the fresh concrete changes in a manner similar to that of the cement paste (5, 6). In the first minutes after the mixing of the concrete its workability, measured for example in terms of spread in the DIN 1048 flow table test, decreases. The decline in workability depends largely on the amount and on the morphology of the hydration products formed in the cement paste. During the dormant period the consistency of the fresh concrete undergoes only little change if optimized cement is used for making the concrete and if the optimization of the cement achieved in the grinding process in the cement plant is not subsequently nullified by additives, admixtures and the working procedures applied in making the concrete. The relatively stable level of consistency is established after at most 10 minutes and has therefore proved useful in practice for characterizing the initial consistency of fresh concrete (a_{10}).

The consistency of cement paste and of fresh concrete depends on the water film thickness on the surface of the cement particles and on the thickness of the cement paste coating on the surface of the aggregate particles. Model calculations, which were confirmed by investigations on concretes as commonly used in practice, have revealed this (6). The thickness of the water film that forms on the individual cement particles depends at given surface area and voids between the particles primarily on the water/cement ratio. For constant water cement ratio the rheological effectiveness is influenced more particularly by the amount and morphology of the hydrate phases formed. Accordingly, the water film thickness is the governing factor for the initial consistency and for the change that the consistency of the cement paste undergoes with the passage of time. The importance of the composition, surface area and particle size distribution of the cement for the progressive change in the consistency of cement paste will be summarizingly discussed, on the basis of a large number of research results, in the following sections.

Similar relationships apply to the consistency of fresh concrete. For constant cement content, a stiffer consistency develops as time passes, but especially with decreasing water/cement ratio or if the cement has a marked tendency to early stiffening.

The consistency of fresh concrete depends furthermore also on the thickness of the cement paste coating on the aggregate particles. With diminishing thickness of the water film and correspondingly stiffer initial consistency of the cement paste, the desired consistency of the fresh concrete can be obtained by increasing the cement content and thus the amount of paste while leaving the water/cement ratio unchanged (6). That is the reason why the result of the consistency mearsurement performed on cement paste is not directly applicable to fresh concrete, despite similarity of behaviour in principle.

2. Composition

2.1 Clinker

The properties of cement clinker are to a great extent influenced by the composition of the raw mix and of the fuels, as well as by the burning and cooling conditions. Important with regard to the processes associated with early stiffening and with setting is the proportion of C_3A that undergoes hydration in the first minutes after the addition of the mix water and up to the beginning of the dormant period. It is referred to as C_3A conversion (ΔC_3A). Inves-

tigations have shown that the C_3A conversion of industrial cement clinkers of normal composition can amount to about 0.4 - 2.0 wt.-%. As a rule, the C_3A conversion is greater according as the clinker contains more C_3A and as more alkalies are combined in the clinker (7).

To diminish the influence of the C_3A conversion on stiffening and setting the C_3A content of the clinker can be reduced to a limited extent by a lowering of the alumina/iron ratio. The heightened reactivity of C_3A due to incorporation of alkalies can moreover be reduced. To achieve this, the alkalies must be bound in the form of alkali sulphate (sulphatization), e.g., as a result of the controlled use of inexpensive sulphur-rich fuels. With a fairly high total alkali content a degree of sulphatization of 40 - 70 %, and with a fairly low total alkali content a degree of sulphatization of up to 90 %, has been found to be advantageous for reasons of plant operation, emission and product quality (8, 9).

Besides the composition of the process materials, the kiln atmosphere and the rate of cooling of the clinker have a major effect on the C_3A content and on the reaction capability of the C_3A. The C_3A content and reactivity increase if the clinker is burned under reducing conditions and is cooled slowly from the clinkering temperature to around 1 300 °C (7). An increase in the C_3A content is also to be expected if, as a result of using coal with a very high ash content and of slow cooling of the clinker in the high-temperature zone of the kiln, the proportion of clinker melt is increased and its composition changed (9).

2.2 Cement

The C_3A content and the reaction capability of the C_3A determine the reactivity of the clinker. It can be gauged and monitored by measurement of the C_3A conversion. Closer monitoring in the context of industrial quality control would appear to be particularly appropriate if, during the manufacturing process, the clinker properties vary in consequence of using raw materials and fuels of varying composition, or because of irregular kiln operation or because the cooling rate is not properly adjusted to the composition of the kiln feed. In the cement grinding process the variations in the properties of the clinker can be taken into account by optimum adjustment of the added calcium sulfates to the C_3A conversion at any given time, in order to produce cement with uniform workability and strength development. In this connection the surface area and particle size distribution of the cement must moreover be taken into consideration.

An optimum dosage of calciumsulfates is achieved if the cement contains just so much readily water-soluble sulphate in the form of hemihydrate ($CaSO_4 \cdot 1/2H_2O$) or anhydrite III ($CaSO_4$ III) that the C_3A which undergoes hydration in the first few minutes can react with this sulphate to form fine-grained ettringite. The ettringite is deposited on the surfaces of the cement particles, as a result of which a structure is formed in which the hydration products do not yet bridge the water film between the cement particles. Fig. 1 is a scanning electron micrograph showing the stucture formed in the cement paste after 5 minutes hydration time.



Fig. 1: Scanning electron micrograph of cement paste after 5 minutes hydration (W/C ∿ 0,4).

The nature and quantity as well as the crystal shape and size of hydrate phases formed in the first minutes affect the consistency of the cement paste and the water demand. The relationships are represented schematically in Fig. 2, based on a model conceived by J. Krell (6). The left-hand diagram relates to cement paste made from an optimized, the right-hand diagram to paste made from a non-optimized portland cement. In both examples the paste is of standard consistency. The cements have been made from the same clinker, have equal surface area and particle size distribution and therefore equal C_3A conversion.

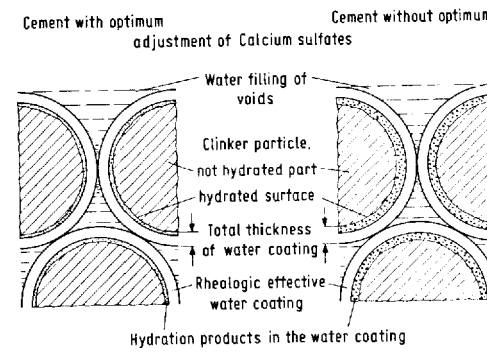

Fig. 2: Influence of optimization of the added calcium sulfates upon the water demand for obtaining the standard consistency.

Besides the proportion of the mix water which is chemically bound in the hydrate phases, the water serves primarily to fill the voids between the clinker particles and to form a water film on the surfaces of the incipiently hydrated clinker particles. The volume of these voids depends on the particle size distribution. The quantitative division of the mix water between what is needed for chemical binding in the hydration products and what is needed for rheological reasons is shown in Fig. 4 in Section 3. As model calculations indicate, the overall thickness of the water film on the surfaces of the clinker particles in a paste of standard consistency is of the order of less than 0.5 micron (6). The hydrate phases formed during the initial hydration grow more or less far into the enveloping water film. The remaining rheologically effective part of the film enables the clinker particles to slide along one another and is therefore of governing importance with regard to the consistency of the cement paste. For a particular thickness of the water film the paste possesses standard consistency.

With optimized cement the fine-grained ettringite which is formed as a result of the C_3A conversion is deposited on the surfaces of clinker particles and only slightly reduces the thickness of the water film (finely dotted area in left-hand diagram). If the water/cement ratio is not changed and there is a little C_3A conversion, only little stiffening of the cement paste occurs. With more C_3A conversion and correspondingly lager amounts of ettringite a stiffer consistency develops. In order to obtain a more plastic consistency, the amount of mix water and thus the effective water film thickness must be appropriately increased.

The recrystallization of the ettringite which begins during the dormant period will normally cause a slow stiffening of the cement paste. But if, with higher alkali content in the solution, the ettringite recrystallizes more rapidly and the lager crystals grow farther into the water film, this brings about early and rapid stiffening or manifests itself in an appreciably higher water demand for obtaining the standard consistency (8, 11,12).

If there is a deficiency of sulphate in the solution, coarsely tabular monosulphate is in part formed instead of ettringite. If there is an excess of sulphate, secondary gypsum and also syngenite are formed. Within a few minutes these hydrate phases build up a rigid interlocking structure of relatively large crystals which protrude far into the enveloping water film and which restrict the free mobility of the clinker particles (coarsely dotted area in right-hand diagram). In consequence of this the cement paste quickly stiffens if the water/cement ratio is left unchanged. To obtain the standard consistency, the rheologically effective water film thickness must therefore be increased to the requisite thickness for this purpose by the addition of substantially more mix water. The effect that deficient optimization of the calcium sulfates in the cement has upon the water demand is apparent from the experimental results represented in Fig. 3 (Section 3).

3. Surface area and particle size distribution

Besides the composition, the surface area and particle size distribution of the cement are particularly important with regard to the water demand and to the stiffening and the setting of cement paste (13, 14, 15). In Fig. 3 these relationships are represented for two cements which were ground from the same industrial clinker to mass related surface areas of 3 570 cm^2/g and 5 465 cm^2/g (Blaine) respectively. For equal slope n of the RRSB particle size distribution the two cements moreover differ in their position parameter x' (14, 15). In the lower diagram the C_3A conversion, and in the upper diagram the water demand of the cements measured in accordance with DIN 1164, are represented as functions of the proportion of the added calcium sulfates anhydrite II ($CaSO_4$ II) and hemihydrate ($CaSO_4 \cdot 1/2H_2O$). The total sulphate content is approximately 3.2 wt.-% of SO_3.

From the diagrams it appears, first, that the more coarsely ground cement displays less C_3A conversion (about 1.1 wt.-%) than the more finely ground cement does (1.6 wt.-%). The C_3A conversion is independent of the mix proportions of the calcium sulphates.

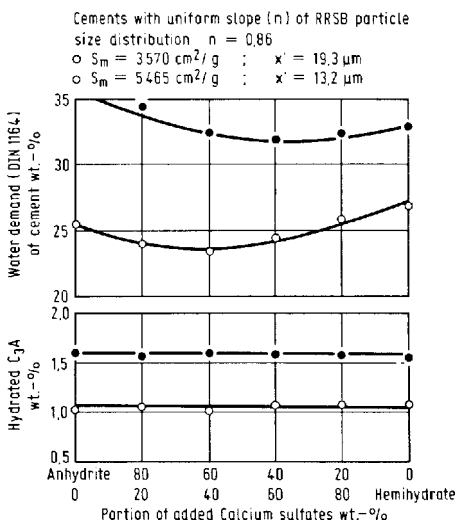

Fig. 3: C_3A conversion and water demand (Din 1164) of portland cements with different surface areas, as functions of the composition of the added calcium sulfates.

If the mixture of these substances is optimally adjusted to the C_3A conversion, a min-

imum water demand for obtaining the standard consistency is achieved for both cements. For this, however, the finer cement with the higher C_3A conversion requires a higher proportion of hemihydrate (about 80 %) than the coarser cement does (about 30 %). Besides, the water demand for standard consistency in conjunction with optimum dosage of calcium sulphates increases from about 23 wt.-% for the coarser to about 32 wt.-% for the finer cement. Investigations have shown that the surface area and the particle size distribution parameters affect the cement paste consistency more strongly according as the clinker contains more C_3A and/or the reaction capability of the C_3A is greater.

One of the causes of the higher water demand of the finer cement therefore is the greater amount of ettringite which, with optimum dosage of calcium sulphates, is formed as a result of the higher proportion of C_3A conversion that occurs (see also Section 2). In general, the water demand increases distinctly for non-optimized as compared with optimized cements. This is due to the fact that, for equal C_3A conversion, the water demand over and above the chemically combined portion depends very considerably on the morphological condition of the hydrate phases. The amount of water needed for wetting and for filling the voids between ettringite and monosulphate or ettringite and secondary gypsum is withdrawn from the rheologically effective water film and must therefore be replaced in order to give the cement paste the standard consistency.

As compared with the clinker and cement composition as factors affecting the water demand, however, the surface area as well as the position parameter x' and the slope n of the particle size distribution have the greater influence on the water demand of the cement (15). This emerged from investigations on cements which had been produced from one and the same industrially manufactured clinker. The nature and quantity of the added calcium sulfates were optimally adjusted to the different amounts of C_3A conversion associated with these cements. These relationships are shown schematically in Fig. 4 for cements with different values of the position parameter x' and constant slope n in the RRSB granulometric diagram.

It appears from this diagram that the water demand for obtaining the standard consistency increases with increasing proportion of fine particles or with decreasing value of the position parameter x'. The water demand is composed of three portions. The portion combined chemically in the hydrate phases before the beginning of the dormant period is the smallest (represented by the hatched area). In general, it increases with higher C_3A content of the clinker, higher reaction capability of the C_3A and, as shown in this diagram, with higher content of fine particles in the cement. This is also the case if the cement, for constant surface area, has a higher value of the slope of the particle

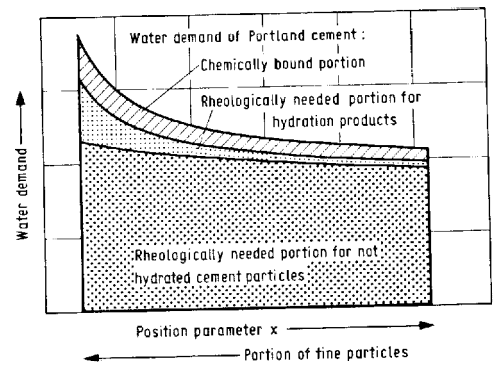

Fig. 4: Influence of the particle size distribution on the binding of water in portland cement at standard consistency.

size distribution. In all, however, at most only about 10 % of the total mix water amount is needed for chemical combining in the hydrate phases. This proportion decreases in the case of cements which contain dense and non-absorbent interground additions such as, for example, blastfurnace slag or limestone. These additions do not participate in the hydration reactions that occur before the dormant period begins. They behave like inert substances by which the clinker component of the cement is diluted. The C_3A conversion decreases roughly in proportion to the amount of interground additions contained in the cement (16).

The largest portion of the mix water (indicated by the dotted area) is necessary for rheological reasons to obtain the standard consistency. A smaller part of this water (finely dotted) serves to wet the hydration products and fill the voids between the hydrate phases. This portion increases more than proportionally according as more hydrate phases with increasingly high content of fine particles are formed in the cement. In the case of optimized cements this portion displays a minimum, as the research results represented in Fig. 3 show.

The major part of the water (coarsely dotted) serves to fill the voids between the clinker particles - just as it would with any inert finely divided material of equal surface area and particle size distribution - and to form the rheologically effective water film. In this case it corresponds roughly to a water cement ratio of 0.2. The rheologically necessary portion of the water demand increases drastically if the cement, for equal content of fine particles, has a steeper particle size distribution so that the volume of the voids between the clinker particles becomes larger.

When cements are interground with additions, the more easily grindable materials such as limestone or pozzolana may enrich in higher concentrations in the fine particle size

fraction. They are thus able to reduce the larger volume of voids of a clinker if the later has been ground in such a way as to have a steep particle size distribution. Because of this voids volume reduction and the dilution of the clinker component of the cement, the water demand for obtaining the standard consistency of the cement alltogether is reduced. On the other hand, if the volumetric proportion of the fine fraction derived from a more easily grindable addition because of overgrinding substantially exceeds the existing voids volume of the clinker, or if, in the event of poorer grindability, it has a very narrow particle size distribution so that the voids volume of the pulverized product as a whole is increased, the water demand becomes greater with increasing proportion of interground additions. It also becomes greater if the additive has a high inherent porosity of its own (16).

References

1. Wischers, G.: Ansteifen und Erstarren von Zement und Beton. Betontechn. Berichte 1980/81, pp. 145-167, Beton-Verlag GmbH, Düsseldorf, 1982.

2. Richartz, W.: Einfluß von Zusätzen auf das Erstarrungsverhalten von Zement. Betontechn. Berichte 1982/83, pp. 169-198, Beton-Verlag GmbH, Düsseldorf, 1984.

3. Krell, J.: Einfluß chemisch-mineralogischer Reaktionen des Zements auf das Ansteifen von Zementleim und Beton. beton 35 (1985), No. 12, pp. 465-472.

4. Locher, F.W., Richartz, W. und S. Sprung: Erstarren von Zement, Teil 1: Reaktion und Gefügebildung. Zement-Kalk-Gips 29 (1976), No. 10, pp. 435-442.

5. Rendchen, K.: Einfluß der Granulometrie von Zement auf die Eigenschaften des Frischbetons und auf das Festigkeits- und Verformungsverhalten des Festbetons. Schriftenreihe der Zementindustrie, No. 45, Beton-Verlag GmbH, Düsseldorf, 1985.

6. Krell, J.: Die Konsistenz von Zementleim, Mörtel und Beton und ihre zeitliche Veränderung. Schriftenreihe der Zementindustrie, No. 46, Beton-Verlag GmbH, Düsseldorf, 1985.

7. Locher, F.W., Richartz, W., Sprung, S. und H.-M. Sylla: Erstarren von Zement, Teil 3: Einfluß der Klinkerherstellung. Zement-Kalk-Gips 35 (1982), No. 12, pp. 669-676.

8. Locher, F.W., Richartz, W., Sprung, S. und W. Rechenberg: Erstarren von Zement, Teil 4: Einfluß der Lösungszusammensetzung. Zement-Kalk-Gips 36 (1983), No. 4, pp. 224-231.

9. Sprung, S.: Emissionsprognosen beim Einsatz von Abfallbrennstoffen. Zement-Kalk-Gips 37 (1984), No. 10, pp. 519-522.

10. Sprung, S.: Einflüsse der Verfahrenstechnik auf die Zementeigenschaften. Zement-Kalk-Gips 38 (1985), No. 10, pp. 577-585.

11. Mehta, P.K.: Effect of lime on hydration of pastes containing gypsum and calcium aluminates or calcium sulfoaluminates. J. Amer. Ceram. Soc. 56 (1973), No. 6, pp. 315-319.

12. Mehta, P.K.: Scanning electron micrographic studies of ettringite formation. Cem. Concr. Res. 6 (1976), No. 2, pp. 169-182.

13. Meric, J.P.: Influence of grinding and storage of clinker. Principal Report Sub-Theme I-4, 7. Intern. Congr. Chem. Cem., Paris, 1980, pp. I-4/1-4/16.

14. Kuhlmann, K., Ellerbrock, H.-G. und S. Sprung: Korngrößenverteilung und Eigenschaften von Zement, Teil 1: Festigkeit von Portlandzement. Zement-Kalk-Gips 38 (1985), No. 4, pp. 169-178.

15. Sprung, S., Kuhlmann, K. und H.-G. Ellerbrock: Korngrößenverteilung und Eigenschaften von Zement, Teil 2: Wasseranspruch von Portlandzement. Zement-Kalk-Gips 38 (1985), No. 9, pp. 528-534.

16. Ellerbrock, H.-G., Sprung, S. und K. Kuhlmann: Einfluß von Zumahlstoffen auf die Eigenschaften von Zement. Zement-Kalk-Gips 38 (1985), No. 10, pp. 586-588.

H.-J. Wierig - University of Hanover, West Germany

INFLUENCES OF CEMENT AND TEMPERATURE ON THE CONSISTENCY OF FRESH CONCRETE

As a result of the impetuous development of the ready mixed concrete industry in the past years, questions of fresh concrete technology have become increasingly important /1/. If we intend to keep a tight control on ready mixed concrete production, we need a qualitative and quantitative comprehension of the main factors effecting the quality of fresh concrete, especially the initial consistency and the temporal changes in consistency. This includes knowledge of the amount of water required by each single compound of the mix. To date considerations were often concentrated on the amount of water required by the aggregates, and the influence of cement and other compounds were in general neglected. Various research programmes, carried out at the Institut für Baustoffkunde und Materialprüfung der Universität Hannover were aimed at examining possiblities of grasping the influence of cement on the consistency of fresh concrete and stiffening under various temperatures.

Concretes with three different mixes, containing 16 various cements in normal commercial use, were tested at 3 temperatures. The concretes varied in their water/cement ratios (w/c = 0,75, 0,63 and 0,57) and in the grading of their aggregates. The cements were chosen along the lines of various sorts of cement, various compressive strengths and chemical composition. Detailed results of the examination will be published soon /2/. Fig. 1 shows an example to illustrate how the initial spreads according to the German flow table test of one of the concretes tested is set against temperature of fresh concrete. Each point stands for one concrete mix containing one cement. Fig. 2 shows the changes in consistency of the same concrete mixes in the first 45 minutes after production. Taking into consideration the varying scales of the ordinate the two figures show that the influence of the cement on the initial spread is, with its range of roughly 16 cm much stronger than on the changing spread with its range of only about 5 cm.

In order to grasp the influence of cement on consistency by material characteristics, various evaluation methods were employed. We came to the conclusion that it is not possible to describe this influence by way of one single characteristic, be it the amount of water required for standard consistency (Wa) according to DIN 1164, the specific surface (O), or the spread (a) of the standard mortar. But if we combine several of these cement properties to form one new characteristic, then relatively good relationships between the cement characteristic and the concrete spread values can be found, as seen in fig. 3. When evaluating the results shown in fig. 3 we have to consider that the deviation on repeating a flow table test is about ± 2 cm /3/.

The influence of temperature on spread becomes clear if we join the points of a concrete and its particular cement. For the sake of better understanding this is illustrated in fig. 4 with an example of 4 chosen concretes. In contrast to information such as in /4/ we found that fresh concretes containing various cements often showed widely varying "temperature characteristics" in the initial consistency.

In order to go into the influence of the initial consistency, the change in consistency and the temperature characteristic, additional tests were carried out using laboratory cements. These cements were ground in a laboratory mill from large-scale-produced portland cement clinker, slag and fly ash. Based on the investigations of Locher, Richartz and Sprung /6/, anhydrite and hemihydrate were added as sulphate-bearing agents, in various dosages. Setting, the amount of water necessary for standard consistency, the spread of standard mortar, the change in spread and other qualities were examined. The results of these examinations will too be appearing shortly in detail /5/. Figures 5 to 7 show some exemplary results. Firstly fig. 5 shows how, using laboratory cements from a single clinker, by way of varying the sulphate concentration from hemihydrate (HH) to

anhydrite (AH), the temperature characteristic of the mortar spread may be intentionally varied. As well as gradual lines, curves with distinct minima and maxima are formed.

Fig. 6a and 6b demonstrate that two cement characteristics (e.g. spread of standard mortar and water requirement for standard consistency) can independantly of each other be influenced by variation in the mixing proportion of the sulphate-bearing agents; this being carried out with laboratory cements, using two different clinkers. Fig. 7a and 7b also demonstrate that a change in dosage of calcium sulphate bearer must not necessarily have an affinitive effect on two cement properties; here, the initial setting and mortar spread. Thus it may be concluded that the "optimation" of a cement cannot be undertaken with an eye on only one characteristic (e.g. setting), but, rather by "system optimation" of several characteristics.

An explanation for the discovered phenomena is to be sought in the fact that the rheological behaviour of cement pastes, plastic cement mortars and concretes is similar to that of a Bingham model /7/, /8/, /9/. However, the rheogramm of a Bingham model shows two values which are independant of one another. Thus it is understandable that the influence on properties of fresh cement pastes, cement mortars and concretes can in general form only be described by two values in each case. These do not have to be physically exactly defined values. Any customary methods used for testing mortar and concrete are suitable, as long as their results do not correlate closely to one another; i. e. in as much as they describe different fields of rheological behaviour.

References

/1/ Wierig, H.-J., E. Scholz und H. Nelskamp: Zu offenen Fragen der Frischbetontechnologie, Betonwerk + Fertig- teil-Technik, Heft 11, 1984, S. 733-741

/2/ Wierig, H.-J. und B. Restorff: Ansteifen des Frischbetons (to appear shortly)

/3/ Wierig, H.-J. und H. Nelskamp: Meßstreuungen bei der Prüfung der Frischbetonkonsistenz, beton 33 (1983), S. 380-384

/4/ U.S. Bureau of Reclamation, Concrete Manual, 8th Ed. (Denver 1975)

/5/ Scholz, E.: Zum Einfluß von Temperatur und Calciumsulfat-Art im Zement auf die Ausgangskonsistenz und das Ansteifen von Normmörteln sowie andere Zementeigenschaften (to appear shortly)

/6/ Locher, F.W., W. Richartz, S. Sprung: Erstarren von Zement, Teil II: Einfluß des Calciumsulfatzusatzes, Zement-Kalk-Gips, Heft 6, 1980, S 271-277

/7/ Wesche, K. und W. vom Berg: Rheologische Eigenschaften von Zementleim und Frischbeton, Betontechnische Berichte 1973, S. 21-40, Beton-Verlag GmbH, Düsseldorf

/8/ Tattersall, G.H.: The workability of concrete, Cement & Concrete Association, Wexham Springs 1976, A Viewpoint Publication

/9/ Murata, J.: Flow and deformation of fresh concrete Matériaux et Constructions, Vol. 17 - No 98, 1984, S. 117-129

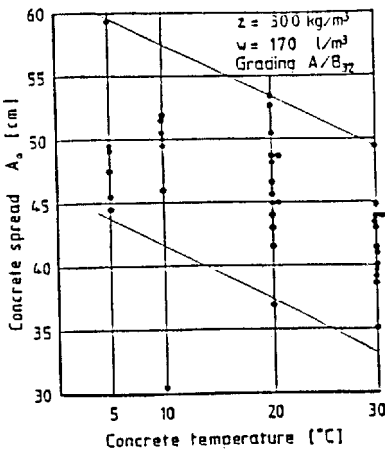

Fig. 1. Influence of cement and temperature on concrete spread A_o

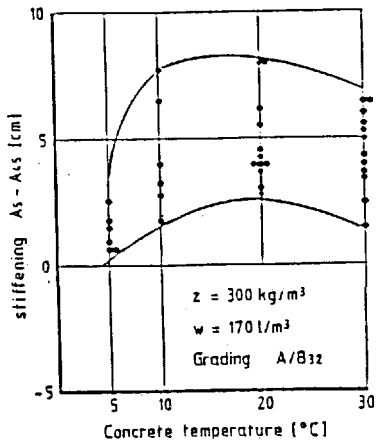

Fig. 2. Influence of cement and temperature on stiffening

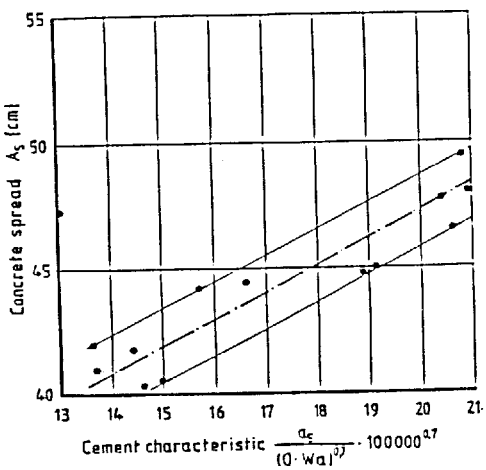

Fig. 3. Influence of cement on concrete spread
a_5 = spread of standard mortar
O^3 = specific surface of cement
Wa = water required

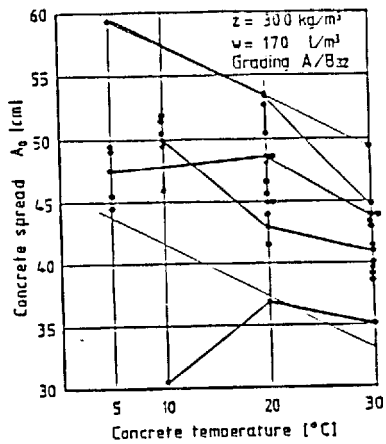

Fig. 4. Influence of cement and temperature on concrete spread A_o

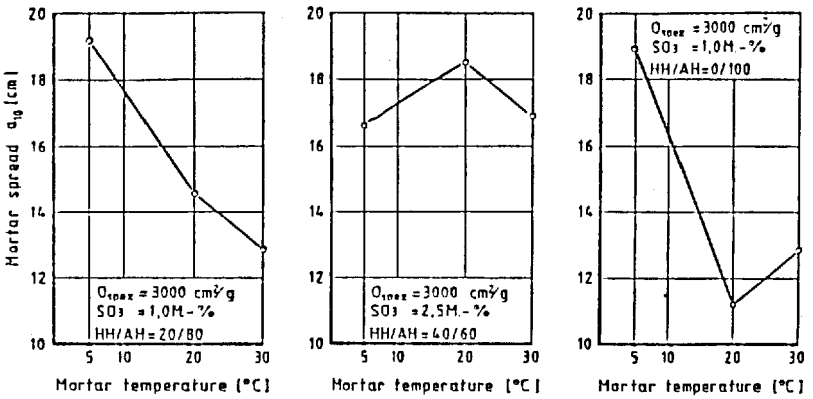

Fig. 5. Temperature characteristics of standard mortars made from clinker B (selected examples)

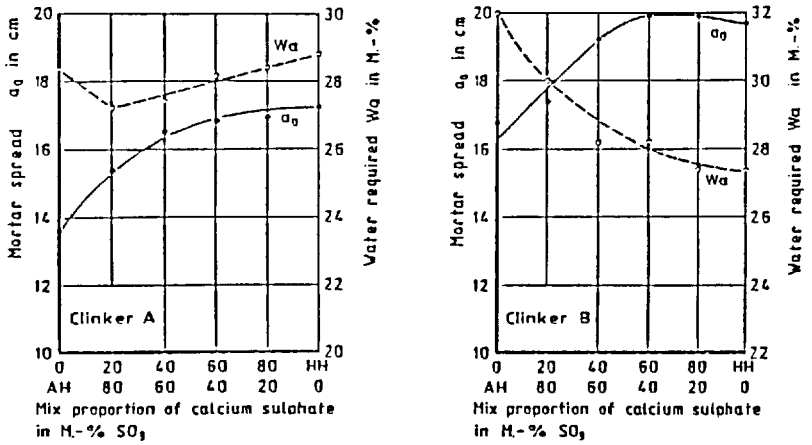

Fig. 6a. Fig. 6b.

Fig. 6. Influence of type of calcium sulfate on the amount of water required to reach standard consistency and the spread of the standard mortar

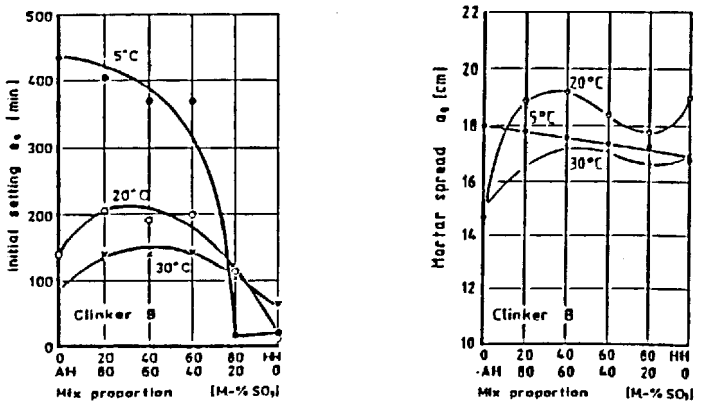

Fig. 7a. Fig. 7b.

Fig. 7. Influence of type of calcium sulfate on initial setting of cement pastes and spread of standard mortar

Pierre DUTRON, Cembureau

RAPPORT INTRODUCTIF AU 4ème SÉMINAIRE - BASES SCIENTIFIQUES DES SPÉCIFICATIONS POUR LE CIMENT ET LE DÉVELOPPEMENT DES MÉTHODES D'ESSAIS. S4

L'objet de ce rapport est de dresser un inventaire des principaux essais de caractérisation des ciments qui sont couramment utilisés et qui sont repris pour la plupart dans les normes nationales et internationales.

Nous établirons tout d'abord un classement de ces essais en les groupant en quatre catégories en fonction du type d'information recherchée. Nous verrons ensuite quelles sont, pour chacun de ces essais, la ou les méthodes utilisées et dans quelle mesure les résultats apportés par ces méthodes répondent aux besoins des producteurs et des utilisateurs.

Le rapport se terminera par quelques considérations en matière de vérification, voire de certification, de la conformité des ciments aux spécifications des normes.

1. Tentative de classification des essais du ciment

1.1 Vérification de la composition des ciments

On peut ranger dans cette catégorie :

- des mesures physiques indirectes telles que celle de la masse spécifique du ciment Portland ; cet essai tend toutefois à disparaître des normes ;
- des mesures chimiques parmi lesquelles la perte au feu et le résidu insoluble, destinées à déceler la présence dans le ciment Portland d'additions non autorisées ;
- des mesures chimiques, physiques ou physico-chimiques ayant pour but de déterminer la teneur en divers constituants (clinker, cendres volantes, pouzzolanes), dans les ciments composés ; ce type d'essai voit son importance croître avec le développement de ces ciments.

1.2 Appréciation des caractéristiques des ciments qui exercent une influence sur les propriétés des bétons frais

Il s'agit essentiellement de l'ouvrabilité et de son évolution qui peut être évaluée par la mesure

- de la demande en eau caractérisée par la détermination de la consistance normale ,
- du début et de la fin de prise.

Notons l'importance de ces caractéristiques pour la mise en oeuvre des bétons.

1.3 Appréciation des caractéristiques conférées par le ciment aux bétons au cours de leur durcissement

Ceci couvre :

- les résistances mécaniques, essentiellement à la compression, mesurées sur mortier normal ; c'est le maître-essai des ciments ;
- les variations de volume, d'origine hygrothermique, telles que le retrait ;
- certaines propriétés particulières telles que la chaleur d'hydratation.

1.4 Appréciation des caractéristiques des ciments qui exercent une influence sur les propriétés des bétons durcis

Il s'agit de s'assurer que le ciment est susceptible de garantir la durabilité du béton

- sous des conditions d'exposition normales au moyen d'essais physiques (Le Chatelier, autoclave, ...) et chimiques (MgO, SO_3, ...),

- sous des conditions plus sévères telles que des agressions de caractère chimique en fixant certaines caractéristiques de composition des ciments (teneur en C_3A, laitier, ...).

2. Examen critique des méthodes utilisées et en cours d'expérimentation

Remarques préliminaires

Inévitablement, le contenu d'une norme est le résultat d'un compromis équilibré entre les points de vue des diverses parties concernées.

En matière de méthodologie, ceci conduit à faire choix de méthodes de référence relativement simples, pas trop coûteuses, notamment au point de vue de l'équipement, et ceci explique que le plus souvent ce n'est pas le dernier cri de la technique qui est retenu dans les textes officiels. On a toutefois tenté de remédier à cette situation en autorisant dans les normes l'utilisation de méthodes plus modernes ou plus élaborées, le recours à la méthode de référence ne restant impératif qu'en cas de litige.

2.1 Vérification de la composition des ciments

Il est normal que l'organisme de certification, ou encore l'utilisateur, soit en mesure de vérifier si la composition d'une production ou d'une livraison de ciment correspond bien à la dénomination annoncée ou commandée.

Cette vérification revêt une importance croissante au cours de ces dernières années car, si l'on excepte le monde anglo-saxon, la part du ciment Portland pur est en diminution au profit des ciments Portland composés.

C'est donc un domaine où un effort particulier a été fait en matière de méthodes, notamment dans le cadre du CEN (Comité Européen de Normalisation), en définissant des essais basés soit sur un examen microscopique, soit sur une séparation des constituants en mettant à profit leurs différences de densité, ou encore leurs différences de dissolution dans certains solvants.

On peut dire que des résultats probants sont dès à présent obtenus pour les ciments binaires (mélanges de clinker et d'un autre constituant) mais que des études restent nécessaires pour les ciments ternaires, voire quaternaires.

Tout ceci constitue un progrès vis-à-vis des mesures plus rudimentaires telles que la masse spécifique, la perte au feu, ou le résidu insoluble, qui sont appelées à disparaître progressivement des normes.

2.2 Mesure des caractéristiques des mélanges frais

Il faut reconnaître l'importance capitale que représentent pour les utilisateurs du ciment la mesure et, de ce fait, la connaissance, voire même la préestimation de l'évolution rhéologique des bétons frais. Ce besoin d'information est devenu plus aigu par suite du développement remarquable du béton prêt à l'emploi.

Il faut tout autant reconnaître que les méthodes de mesure définies dans les normes ne répondent que très imparfaitement à ce besoin. L'appréciation de la demande en eau par la détermination de la consistance normale donne tout au plus une indication au temps t_0 sans qu'on puisse suivre l'évolution de cette demande dans le temps ; cette méthode d'essai n'est d'ailleurs plus guère prévue dans les normes et n'est accompagnée d'aucune exigence chiffrée.

L'essai de vitesse et de durée de prise (qu'il s'agisse de la méthode Vicat ou, plus rarement, de la méthode Gillmore) est certes respectable par son ancienneté mais il ne donne que des informations conventionnelles et ponctuelles, laissant de côté la période initiale de début de rigidification, si importante pour apprécier l'aptitude du béton à être compacté et moulé.

Cette lacune ne provient pas d'un manque d'études de caractère méthodologique ; la littérature scientifique fourmille de références sur des rapports de recherche touchant ce domaine. Des techniques de mesures continues faisant appel à la pénétrométrie ou encore à la viscosimétrie ont été mises au point et permettent de suivre avec plus de précision l'évolution dans le temps de ces phénomènes rhéologiques. Des tentatives ont également été faites en vue d'établir une corrélation entre cette évolution rhéologique et la variation de certaines propriétés physiques des pâtes de ciment telles que la vitesse de transmission des sons ou la conductivité électrique. Mais tous ces travaux n'ont pas encore abouti au point de permettre une évolution du contenu des normes. Les raisons en sont multiples :

Souvent ces nouvelles techniques font appel à des modes opératoires plus sophistiqués se prêtant mal à un emploi fréquent dans le cadre d'un contrôle de routine.

En général, ces méthodes d'essai sont applicables à des pâtes de ciment, rarement à des mortiers, et exceptionnellement à des bétons, car la présence d'un squelette pierreux dans le béton constitue un obstacle difficilement surmontable.

La corrélation entre l'évolution rhéologique de la pâte de ciment et celle du béton est loin d'être simple à apprécier, d'autant plus que les essais de laboratoire peuvent difficilement tenir compte des conditions de chantier : forme et compacité des granulats, teneur en ciment et en eau des bétons, température et durée de mise en oeuvre, ...

En conclusion, voilà certes un domaine où des progrès sont attendus.

2.3 Mesure des caractéristiques des ciments en voie de durcissement

On considérera ci-après essentiellement la mesure des résistances mécaniques qui constitue la caractéristique du ciment la plus importante, mesure qui est presque partout effectuée sur des éprouvettes de mortier, ce qui constitue un compromis technico-économique entre l'essai sur pâte et celui sur béton.

Sans vouloir faire preuve de chauvinisme européen, on croit pouvoir dire que la mise au point dans les années 60 de la méthode dite "RILEM-CEMBUREAU" qui a fait l'objet de la Recommandation ISO R 679 de 1967, puis tout récemment de la norme CEN 196-1, a constitué un progrès très important pour les raisons suivantes :

Elle est déjà reprise dans plus de 30 normes nationales, couvrant la majeure partie de l'Europe (Ouest et Est) et de l'Amérique du Sud et commence à s'implanter en Afrique et en Asie. De nombreux pays examinent l'opportunité d'y recourir de sorte que, sans être prophète, on peut escompter qu'elle deviendra d'ici la fin du siècle la méthode universellement reconnue avec comme conséquence que lorsqu'on citera des chiffres de résistance, tout le monde ou presque parlera le même langage.

La conception de son mode opératoire est telle qu'elle donne des résultats relativement peu dispersés qui supportent avantageusement la comparaison avec les autres méthodes les plus connues, comme cela fut déjà exposé au Congrès de Moscou en 1974.

La composition de son mortier, qui est presque un micro-béton, est telle que les valeurs obtenues donnent une indication assez proche des résistances que le ciment conférerait à des bétons de composition courante.

Tout ceci est-il de nature à donner entière satisfaction ? La réponse à cette question doit être négative en ce sens qu'il y a lieu d'être plus ambitieux et de sortir d'une certaine attitude routinière. En effet, la mesure directe de la résistance par des essais destructifs implique plusieurs sujétions dont il serait bon d'être dégagé :

- La préparation, la conservation et l'essai d'éprouvettes de mortier représentent un travail long et coûteux.

La réponse à la question posée, à savoir quelle sera la résistance du ciment (et conséquemment du béton) à divers âges , vient toujours trop tard, c'est-à-dire quand le béton est mis en oeuvre et qu'on ne peut plus guère réagir.

On a, bien entendu, essayé de trouver une solution à cet état de choses de deux manières. On a d'abord conservé le principe de l'essai direct sur éprouvettes, mais en accélérant par voie physique (température et quelquefois pression) le développement des résistances de manière à pouvoir estimer, après quelques heures, le niveau des résistances à 7 ou 28 jours d'âge. Il existe à cet égard une littérature abondante et cette technique a reçu certaines applications, surtout dans des cas privilégiés où la composition du béton et de chacun de ses constituants est tout-à-fait constante. Par contre, dans la pratique courante, l'essai de résistance accéléré ne s'est guère développé au cours des dernières années, d'autant plus que la multiplication des types de ciment à plusieurs constituants apporte un élément perturbateur ; en effet, certains de ces ciments peuvent présenter une même allure de développement des résistances sous une température normale, tout en réagissant différemment sous un régime thermique accélérant l'hydratation.

L'autre solution consiste à remplacer la mesure des résistances par une estimation indirecte de celles-ci en faisant appel à d'autres caractéristiques du ciment qui sont censées régir le développement de l'hydratation et du durcissement. On a songé, pour le ciment Portland tout au moins, à établir une relation entre résistance et composition minéralogique du clinker. On pourrait aussi avoir recours à la détermination de certaines caractéristiques physico-chimiques mesurées sur la pâte de ciment au cours de l'hydratation et établir sur cette base des modèles mathématiques permettant une préestimation de la résistance.

Même si l'on est encore loin de pouvoir abandonner dans les normes l'essai classique de compression, ce séminaire devrait permettre de faire le point des progrès réalisés dans ce domaine et des lacunes qui restent à combler.

Il y a d'autres caractéristiques du ciment qui intéressent l'utilisateur par l'effet qu'elles peuvent avoir sur les bétons au cours de leur durcissement. Retenons-en deux qui nous paraissent plus importantes, à

savoir le retrait et la chaleur d'hydratation.

Le retrait d'hydratation et surtout de dessiccation de la pâte de ciment constitue sans nul doute un point faible du ciment auquel on ne peut échapper, si l'on excepte le cas de quelques ciments spéciaux. La mesure de ce retrait effectuée sur pâte ou mortier de ciment ne se retrouve qu'exceptionnellement dans les normes nationales qui fixent, dans ce cas, une réduction maximale de longueur à un certain âge ; il faut dire que cet essai, assez conventionnel, est délicat et que les résultats présentent une dispersion non négligeable. Dans la mesure où l'on serait en droit d'associer la notion de retrait à celle de la finesse du ciment, on notera que les normes prévoient encore souvent l'essai de tamisage avec, toutefois, une prescription donnant une limite maximale plutôt que minimale au refus sur un tamis donné ; ce type d'essai a tendance à disparaître des normes car il n'apporte guère d'information utile, notamment parce que la majeure part des grains de ciment ont une dimension nettement inférieure aux mailles des tamis les plus fins. Tout au plus permet-il parfois de déceler l'absence ou la présence de certaines matières d'addition. Par contre, l'essai le plus courant est la mesure de la surface spécifique du ciment par perméabilimétrie qui donne une appréciation globale de la finesse ; encore une fois, on impose à cet égard plus souvent une valeur minimale que maximale. Il ne faut d'ailleurs pas demander à cet essai de fournir plus d'indications qu'il ne peut en donner. Disons qu'il permet surtout d'apprécier la régularité d'un ciment tant que sa composition ne subit aucune modification.

Un progrès substantiel, réalisé il y a plus d'une décennie, a consisté dans la mesure rapide et précise de la composition granulométrique, caractéristique qui conditionne bien des propriétés du ciment. Toutefois, la technique du granulomètre au laser reste essentiellement réservée aux recherches, voire pour l'auto-contrôle du producteur, mais elle n'est pas reprise dans les normes et l'on conçoit d'ailleurs qu'il serait pour le moins hasardeux de fixer une exigence, par exemple en définissant un fuseau granulométrique à respecter.

La mesure de la chaleur d'hydratation est d'application courante pour caractériser les ciments dits "à faible chaleur dégagée" destinés à la construction d'ouvrages massifs. C'est presque toujours la mesure par voie isotherme, issue de l'ASTM et utilisant le calorimètre à dissolution, qui est prévue dans les normes. On fait appel beaucoup plus rarement à la voie semi-adiabatique de la bouteille Thermos, ou encore à la méthode par conduction opérant en conditions isothermes, cette dernière convenant d'ailleurs mieux pour mesurer à court terme (quelques heures à 3 jours) le dégagement de chaleur de ciments à durcissement relativement rapide.

Si l'on peut ainsi estimer être bien armé pour les mesures sur ciment, par contre, on ne dispose pas encore de méthode satisfaisante pour apprécier le dégagement de chaleur ou plus simplement l'augmentation de température au sein d'une masse de béton en cours de durcissement, ce qui correspond au problème rencontré sur chantier. Voici encore un domaine pour lequel des études paraissent nécessaires.

2.4 Mesure des caractéristiques des ciments qui peuvent influencer le comportement à long terme des ouvrages en béton

Un certain nombre d'essais plus ou moins conventionnels sont prévus et normalisés dans le but de garantir aux utilisateurs que les

ouvrages en béton réalisés avec le ciment testé gardent dans le temps leurs qualités de stabilité dimensionnelle et de résistances mécaniques, ce dans des conditions d'exposition normales, c'est-à-dire non particulièrement agressives.

C'est le cas de certains essais physiques (Le Chatelier, autoclave, ...) et chimiques (MgO, SO_3, ...). Il ne semble pas qu'il y ait une grande évolution dans ce domaine, ni que cela donne lieu à des difficultés de la part des utilisateurs. Il faut toutefois être conscient que dans certains cas -nous songeons à l'essai à l'autoclave -, les informations obtenues par les mesures sont significatives s'il s'agit de ciments Portland pour lesquels ils avaient d'ailleurs été conçus mais qu'il n'en est pas nécessairement de même lorsque l'on se trouve en présence de ciments composés.

Par contre, si l'on aborde l'aspect de la durabilité des ouvrages en béton ayant à supporter des conditions d'exposition plus sévères, on peut se demander si l'on est aujourd'hui suffisamment pourvu en méthodes d'essai et en critères quantitatifs pour garantir au mieux le bon comportement de ces ouvrages dans le temps.

Nous nous limiterons à trois aspects qui se présentent plus ou moins fréquemment dans la pratique, à savoir le comportement au gel, la protection des armatures contre la corrosion et la résistance aux agressions chimiques. De quoi dispose-t-on tout d'abord pour s'assurer qu'un ciment donné est capable de fournir des bétons suffisamment résistants à l'action des cycles de gel-dégel ? On ne peut évidemment pas se baser sur la seule composition de ce ciment, et des essais de gel-dégel sur des pâtes ou des mortiers n'étant pas représentatifs, la seule possibilité retenue actuellement est de conduire ces essais sur bétons.

On est toutefois loin d'être au bout de ses peines puisque, suivant la composition du béton choisi (notamment sa teneur en ciment, en eau et en air) et le type de cycle retenu (notamment gel-dégel sous eau ou à l'air), on peut aux deux extrêmes obtenir des résultats satisfaisants ou désastreux avec n'importe quel ciment. On est donc conduit à choisir des conditions d'essai médianes et de comparer les résultats obtenus sur le ciment étudié avec ceux que donne le même béton contenant un ciment dit de référence, c'est-à-dire un ou plusieurs ciments pour lesquels on dispose d'une longue expérience attestant qu'ils permettent la réalisation de bétons durables.

Devons-nous nous satisfaire de cette façon de faire pragmatique et empirique, ou bien ne conviendrait-il pas de pousser plus avant les études pour aboutir à des solutions plus scientifiquement élaborées ?

Le problème de la protection des armatures est une question de toute première importance puisque on peut considérer que le phénomène de corrosion de ces armatures est le plus souvent à la base du mauvais comportement dans le temps des structures en béton.

A première vue, c'est évidemment aux spécifications relatives à la composition et à la mise en oeuvre du béton qu'il appartient de fixer les règles de bonne exécution dosage avec un rapport E/C relativement faible et une teneur minimale en ciment, épaisseur de recouvrement des aciers suffisante et bien contrôlée, protection adéquate de béton frais contre la dessiccation.

Si toutes ces règles sont respectées, il n'y a plus de problème de corrosion. Toutefois, l'expérience nous montre que, souvent, il

n'en est pas ainsi et ceci a conduit les experts en ciment à se pencher sur cette question.

Nous songeons par exemple aux mesures de l'évolution de la profondeur de carbonatation déterminées sur des éprouvettes de mortier de ciment. La relation entre corrosion et carbonatation est en effet bien connue et on sait également que la vitesse de carbonatation est liée à la rapidité de développement des résistances du ciment, cette rapidité pouvant à son tour dépendre de la composition et de la classe de résistance du ciment.

Si l'on en vient aux agressions chimiques, les spécifications qui figurent dans les normes concernent le plus souvent la résistance aux sulfates et fixent des exigences en matière de composition des ciments basées sur l'expérience des décennies précédentes. Pour le ciment Portland, il s'agit de fixer des limites pour les teneurs en C_3A, Al_2O_3, C_4AF, ..., tandis que pour les ciments composés, on exige une teneur minimale en certains constituants tels que le laitier. Pour les autres agressions chimiques, telles que, par exemple, les eaux pures, on se limite le plus souvent à des recommandations générales.

On a pourtant essayé maintes fois dans le passé de mettre au point des essais d'appréciation directe portant sur le comportement d'éprouvettes de pâtes, mortiers ou bétons, immergées totalement ou partiellement, de manière continue ou discontinue, dans des solutions contenant l'agent agressif à des concentrations plus ou moins fortes pour accélérer le processus de dégradation éventuelle.

Force est de constater qu'aucune de ces études n'a débouché sur la mise au point d'une méthode largement acceptée et permettant une appréciation directe des performances du ciment et qu'on en est donc resté aux exigences de caractère descriptif mentionnées plus haut.

Ceci est devenu d'autant plus nécessaire que, si certains essais bien connus de longue date, tel l'essai Le Chatelier-Anstett-Blondiau, étaient en mesure de donner des indications valables dans le cas de ciment Portland pur, ils risquent souvent d'induire en erreur lorsqu'ils sont utilisés sur des ciments composés.

3. Conformité des ciments aux spécifications des normes

Un certain nombre d'éléments nouveaux tels que les progrès en matière d'interprétation statistique des résultats, les possibilités offertes à l'égard du calcul des risques encourus par le producteur comme par l'utilisateur sont à la base d'une évolution marquée dans le domaine de la vérification de la conformité d'une production globale ou d'une livraison particulière de ciment vis-à-vis des exigences de la norme. Bien souvent, cette vérification donne droit en corrolaire à une certification, c'est-à-dire à l'attribution d'une marque de qualité certifiée par un organisme indépendant.

On constate de plus en plus que les méthodes de certification s'appuient, comme dans les industries les plus avancées, sur une vérification de la valeur de l'assurance qualité à l'intérieur des entreprises, en d'autres termes, de l'auto-contrôle industriel.

Cela implique un renforcement de la responsabilité des industriels, en l'occurrence des cimentiers, l'existence d'organismes indépendants et crédibles,

capables de vérifier la valeur de cette assurance qualité.

Conclusions

1. Il ne faut pas retenir de ce rapport introductif que tout va mal en matière d'essais et de spécifications pour les ciments. Les connaissances acquises et les réglementations en vigueur sont de nature à garantir à l'utilisateur que le ciment qu'il met en oeuvre lui permet de réaliser des bétons de qualité.

2. Ceci n'empêche pas que, pour chacun des domaines considérés plus haut, les progrès en équipement et techniques de mesures scientifiques sont tels qu'ils peuvent et doivent conduire à une évolution de la méthodologie appliquée aux ciments et aux bétons au plus grand bénéfice des producteurs et des utilisateurs.

3. Formons le voeu que ce séminaire, comme d'ailleurs le 8ème Congrès International de la Chimie des Ciments, nous permette d'avancer dans cette voie.

Tong Sanduo
Standardization Institute of Building Materials, Beijing, China

SOME VIEWS ON CEMENT SPECIFICATION

1. INTRODUCTION

For assuring cement and concrete quality chemical, physical and mechanical requirements as well as cement constituents are stipulated in all cement specifications. Most of stipulations are necessary, but some of them are so strict that the application of natural resources are restricted. In order to make good use of mineral resources it is reasonable to revise some of requirements under the prerequisite for ensuring cement performance and stability.

2. EXTEND THE MgO LIMIT

The main purpose of stipulating MgO limit in cement specifications is to avoid the unsoundness of hardened concrete in long term. The presence of excessive amounts of MgO in cement clinker may lead to expansion and crack development and cause the structure failure since the conversion of MgO to $Mg(OH)_2$ involves a volume expansion of 117% and it may take several years for its hydration. In order to prevent this harmful expansion the MgO content should not exceed a certain value, mostly 5.0%, in all specifications. As a result of this restriction some of limestones partially containing dolomite can not be well used thus the mineral resources are shortened. Our test results show that the MgO content could be extended to 6.0% or even more, e.g. 7.0%, the performance of the portland cement are unchanged and the cement pastes remain stable in long term. The long term strength of cement mortars with various MgO contents in clinker are shown in Table 1.

It has been proved that the MgO amount in clinker by chemical analysis cannot indicate the long term soundness of cement exactly, since MgO exists in clinker in the form of various morphology. Except for certain amount in the amorphous form and in the crystalline lattice of cement compounds, MgO exists predominantly in the form of periclase crystals with different sizes, and it is the periclase that cause harmful expansion. For clinker containing nearly same amount of MgO the autoclave expansion will be greater as the amount of periclase and free lime increase and the sizes of periclase become larger (Table 2).

Table 2 Autoclave expansion of the cement with different content of MgO

Plant	MgO %	fcao %	Periclase %	aver. diameter of periclase (μ)	autoclave expansion %
A	4.50	0.60	2.10	5.10	0.23
B	4.50	1.83	3.12	5.27	2.54
C	5.11	0.25	2.80	4.60	0.22
D	5.25	0.63	-	-	0.46
C	6.25	slight	3.30	4.80	0.30
E	6.08	0.39	-	-	failure

Appropriate measures have been taken in the process in plant C to control the free lime content and growing of periclase content as MgO increases, the cements remain sound under the autoclave test (Table 3). It can be concluded that the permissible MgO content might be extended to 7%.

Table 1 Strength development of cement with various MgO contents

Sample No.	MgO in clinker %	Compressive strength (MPa)					Tensile strength (MPa)				
		28days	6months	1year	3years	10years	28days	6months	1year	3years	10years
1	1.04	67.2	81.8	81.8	89.7	97.0	3.3	3.8	4.2	4.2	4.2
2	5.11	72.3	85.6	89.3	94.3	99.0	3.3	3.2	3.4	3.9	4.2
3	6.25	68.5	81.4	86.7	93.6	101.3	3.3	3.3	3.6	3.8	4.1
4	7.26	66.9	79.5	82.3	87.5	97.6	3.3	3.5	3.5	3.8	4.3
5	7.53	71.8	84.4	87.3	92.1	101.0	3.3	3.4	3.6	3.6	4.1

Tor.g Sanduo
Standardization Institute of Building Materials, Beijing, China

Table 3 Relation between MgO and periclase content for cement produced in same plant

MgO %	fcao %	Periclase %	Autoclave expansion %
5.11	0.25	2.80	0.22
6.25	slight	3.30	0.18
6.50	0.29	3.60	0.19
7.28	0.30	3.90	0.60
7.53	0.26	4.30	0.48

3. LIMESTONE CAN BE USED AS CEMENT ADDITION

Limestone used as mineral addition togather with blastfurnace slag and pozzolana in cement has good effect on the cement performance. In most of cement specifications limestone is defined as a filler and can only be added to cement within a few hundredths, except for French standard (AFNOR) in which more than 5% of limestones can be allowed in type CPJ cement. Our research shows that limestone can be used not only as a filler but a good secondary constituent in cement. Suitable amount of limestone blended with blastfurnace slag, pozzolana or fly ash in cement can improve the cement performance and get the energy saving effect. In the current standards in China 10% of limestones are permissible in blastfurnace slag portland cement and fine filler pozzolana (or fly ash) portland cement.

Limestone as a compound addition in cement has the following benefits:

(1) Reduce the water requirement and improve the workability (Fig.1).
(2) Shorten the setting time (Fig.2).
(3) Increase the early strength [Fig.3(a), 3(b)].
(4) Regulate the strength development (Fig.4).

The reason why limestone has above effects is that it gives good physical and chemical functions in cement hardening. It physically plays a role of a filler and has the water-reducing effect, besides there is chemical reaction between $CaCO_3$ and cement hydrates, $C_3A \cdot CaCO_3 \cdot 11H_2O$ can be formed after 3 days. Fig.5(a), 5(b), shows the XRD. Patterns of the pastes of the cement with limestone hydrated at 3 days.

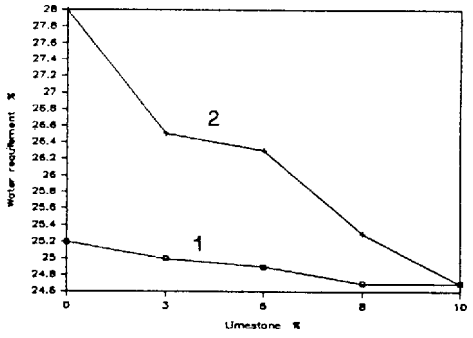

1. Protland slag cement
2. Portland pozzolana cement

Fig.1 Effect of limestone contents on the water requirement of cements

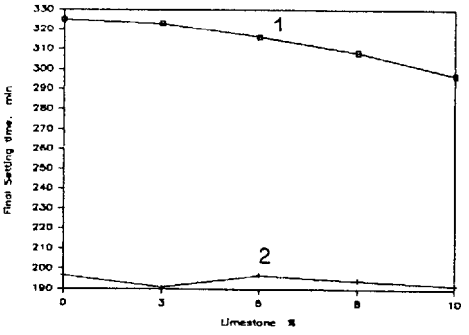

1. Portland slag cement
2. Portland pozzolana cement

Fig.2 Effect of limestone contents on the final setting time of cements

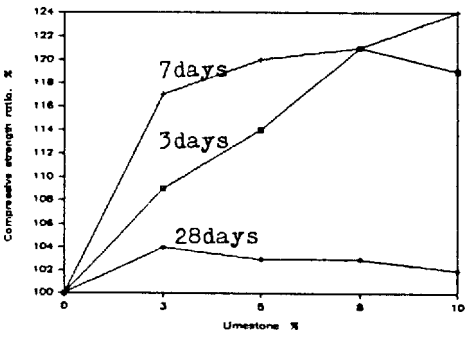

Fig.3 (a) Effect of limestone contents on the early strength of porltnad slag cement

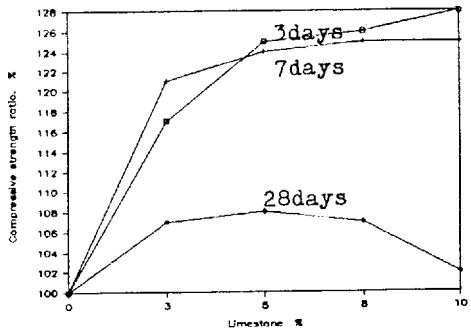

Fig.3 (b) Effect of limestone contents on the early strength of portland pozzolana cement

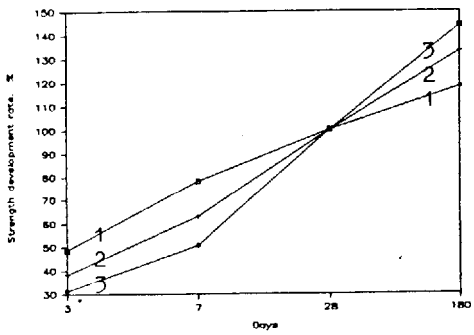

1. Ordinary portland cement
2. Portland slag cement with limestone
3. Portland Blastfurnace slag cement

Fig.4 The strength development rate of the portland slag cement

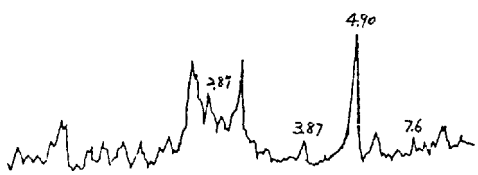

Fig.5 (a) XRD pattern of the paste of the portland slag cement with limestone hydrated at 3 days

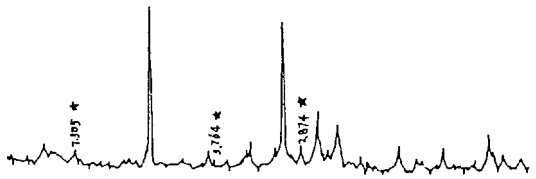

Fig.5 (b) XRD pattern of the paste of the portland pozzolana cement with limestone hydrated at 3 days

4. KILN DUST CAN BE USED AS A FILLER

Kiln dust as a waste was ejected into atmosphere or collected and dischanged. It pollutes surroundings. Our test results indicate that suitable amounts of kiln dust as an addition incorporated into cement are of no influance on the cement performance. In certain circumstances it can even improve the early strength, therefore using kiln dust as a filler in cement is in favor of saving amount of clinker thus saving energy. It is possible to define this stipulation in specification.

The constituents of kiln dust are changed apparently as the raw materials and fuel changes. It also varies with the kiln type and process. Table 4 shows the average chemical composition of kiln dust and its fluctuation ranges for 38 cement plants. But as to the same plant if the operation is stable the compositions of kiln dust are not changed so much.

From optic microscope observation and X-ray examination there are 16 types of mineral constituents in kiln dust, namely, calcium carbonate, dolomite, orthoclase, quartz, mica, slag residue (when slag used as raw materials), glass, Carbon, free lime, β-C_2S, C_2F, C_4AF, mullite, dehydrated clay, gypsum, alkali Sulphate. Those minerals come from decomposition and conbination of raw materials as well as fuel combustion. Among them some are inert materials, others belong to clinker minerals and pozzolanic materials. They are not harmful to cement performance, except that free lime should be noticed. As we know free lime in clinker might cause cement unsoundness, but free lime in kiln

Tong Sanduo
Standardization Institute of Building Materials, Beijing, China

Table 4 Chemical compositions of kiln dust (%)

	LOi	SiO_2	Ai_2O_3	Fe_2O_3	CaO	MgO	SO_3	K_2O	Na_2O	fCaO	TiO_2	S
Average	20.42	16.69	5.12	3.59	45.75	2.03	3.54	2.19	0.30	8.07	0.31	0.35
Range	5.72 ∫ 31.81	11.22 ∫ 24.55	2.83 ∫ 10.68	2.05 ∫ 7.29	37.65 ∫ 57.54	0.73 ∫ 5.86	0.18 ∫ 16.43	0.59 ∫ 7.71	0.12 ∫ 0.64	0.33 ∫ 21.73	0.16 ∫ 0.72	0 ∫ 2.83

dust stands in different condition. Most of them are finely dispersed and hardly appear as inclusion. They are not in a dead-burnt state, so free limes in kiln dust are not affected apparently on cement soundness as in clinker. Small amount of kiln dust incorporated in cement will not cause unsoundness.

Kiln dust presents certain reactivity during cement hardening process. By comparing cement with 30% kiln dust to the same cement with 30% quartz it shows that the compressive strength ratio at 3 months are greater than 100% (Table 5).

Table 5 Reactivity of kiln dust

Sample	Compressive strength at 3 months (MPa)	3M strength ratio %
Kiln dust A	46.6	113
Kiln dust B	51.7	125
Kiln dust C	42.4	102
Fly ash	48.8	117
Slag	46.3	112
Pozzolana	48.2	116
Quartz	41.5	100

Table 6 presents the compressive strength of ordinary portland cement and blast-furnace portland cement with 5% and 8% kiln dust respectively in comparison with corresponding cement without kiln dust addition. It proves that the strength of cements with kiln dust continously develop in long term. Other performance such as shrinkage, permeability and frozen resistance have been proved not to be changed as well, so it is considered that kiln dust can be used as a filler to incorporate into cement.

Table 6 Compressive strength of cements with kiln dust

Plant No.	Cement type	Kiln dust %	Compressive strength (MPa)					Relative value %				
			3days	7days	28days	6months	5years	3days	7days	28days	6months	5years
L	ordinary	0	17.4	28.4	42.1	68.0	78.0	100	100	100	100	100
	ordinary	5	19.1	31.2	45.3	69.4	83.6	110	110	108	102	107
	Blast-furnace slag	0	18.2	27.6	43.4	68.4	78.8	100	100	100	100	100
	Blast-furnace slag	8	17.9	28.4	45.3	72.0	85.4	98	103	104	105	108
G	ordinary	0	14.7	26.3	42.6	64.9	72.9	100	100	100	100	100
	ordinary	5	17.5	29.4	46.3	69.9	76.4	119	112	109	108	105
	Blast-furnace slag	0	15.4	25.7	45.1	68.8	80.8	100	100	100	100	100
	Blast-furnace slag	8	15.1	26.6	45.0	67.7	80.3	98	104	100	98	99

PIERRE TERRIER - C.E.R.I.L.H., France

GESTION ET ASSURANCE DE LA QUALITE DES ESSAIS.

La passation des marchés de fourniture, ou d'une façon plus simple la vente, a pour objet le transfert à l'utilisateur des produits ou composants aptes à satisfaire ses besoins. L'aptitude en question est mesurée par le moyen des essais, contemporains (essais de réception) ou préalables au contrat (marque de qualité) ; les essais sur des prélèvements conservatoires permettant éventuellement la vérification ultérieure de la qualité de la fourniture. Dans tous les cas, les essais associent à des échantillons représentatifs d'un produit, ici le ciment, des caractéristiques définies, mesurées sur l'échantillon lui-même ou sur des corps d'épreuve préparés spécialement, en mortier le plus souvent ; la mesure étant effectuée dans des conditions spécifiées, conformément à un document : la norme d'essai. (La norme de produit rattache, par ailleurs, la caractéristique mesurée lors de l'essai à la performance impliquée par l'application, c'est-à-dire le béton.

En milieu industriel, seule la pratique régulière des essais permet, en permanence, le pilotage des fabrications au voisinage de l'optimum économique. "Sans essais, pas de qualité" pourrait-on dire, cet aphorisme ne doit pas en cacher un autre : "pas d'essais sans qualité" qui est la cheville ouvrière de ma contribution.

La qualité est l'aptitude objective à satisfaire les besoins de l'utilisateur. Il faut distinguer la qualité de l'utilité, bien qu'elles soient quelquefois égales ; elles le sont quand nous offrons une chaise confortable à un homme fatigué mais remarquons que si nous offrons une deuxième chaise de même qualité, son utilité est à peu près nulle. La satisfaction n'est pas toujours proportionnelle à l'utilité (l'air est plus utile que l'or). En outre, sauf à vivre isolé, pour chaque individu, à la satisfaction de sa propre fonction d'utilité, peut s'ajouter (ou se retrancher) celle qu'il retire de la satisfaction de la fonction d'utilité d'autrui, c'est ce que PARETO a nommé l'ophélimité.

La qualité, qui seule retient notre attention, ne peut s'apprécier que par rapport à des critères objectifs.

Dans le domaine des essais où il y a peu de tris, pratiquement ni rebut ni retouche et pas d'après-vente, les défaillances ne sont généralement pas mesurables directement. La qualité ne peut être que constitutive et contemporaine de l'essai, elle n'est maitrisable que par la mise en place effective d'un système de gestion de la qualité recouvrant trois fonctions : définition, obtention et vérification de la qualité. L'assurance de la qualité apporte ensuite la preuve d'une bonne gestion et fait la démonstration que la qualité est obtenue. Pour cela, quelques actions sont nécessaires et suffisantes ; à l'occasion de son accréditation par le Réseau Nationale d'Essais, le C.E.R.I.L.H. les a mises en oeuvre ou développées.

Sur la base des dispositions du guide ISO/IEC25-1982 "Prescriptions générales concernant la compétence technique des laboratoires d'essais", une politique de gestion de la qualité est manifestée par l'existence d'un système dont les bases sont :

- un responsable, agissant par délégation de la Direction Générale doté du pouvoir et des moyens nécessaires pour que soient identifiés les problèmes liés à la qualité et pour provoquer et contrôler les actions correctives opportunes. Chargé du suivi de la qualité telle qu'elle est formalisée (manuel, plans qualité) et vécue (audits), il prépare le rapport annuel et l'échéancier Assurance qualité, propose les actions de formation et d'information et assure les relations avec les organismes d'accréditation et les partenaires extérieurs.

un Manuel Qualité. Document qui explicite les dispositions générales prises par le laboratoire pour obtenir et garantir la qualité des prestations d'essai ; rédigé dans un climat de participation des intervenants et révisable.

des Plans Qualité, spécifiques aux différents groupes d'essais : physiques et mécaniques, chimiques, calorimétriques. Ils indiquent les modes opératoires, les matériels d'essais ainsi que les précautions prises pour l'obtention effective de la qualité requise.

Responsable, Manuel, Plans sont les seules obligations de moyens, les autres obligations qui s'expriment en termes de résultat, sont résumées au tableau I et développées dans ce qui suit.

Tableau I . Le programme de gestion et d'assurance de la qualité.

ACTION	FONCTION	DOMAINE
1. Prévoir dans le détail toutes les modalités qui affectent la qualité, dégager les facteurs d'influence.	Définition de la qualité	Gestion de la qualité
2. Rédiger les dispositions prises en vue d'obtenir la qualité.	Obtention de la qualité	
3. Attribuer les rôles, désigner les responsables et obtenir des conduites conformes aux dispositions spécifiées.		
4. Organiser l'autocontrôle	Vérification de la qualité	
5. Analyser les défaillances, traiter les anomalies et les réclamations.	Démonstration de la qualité	Assurance de la qualité
6. Participer à des essais interlaboratoires.		
7. Déclencher des audits internes. Préparer et suivre un échéancier d'assurance qualité.		
8. Appartenir à un réseau d'accréditation et se soumettre aux audits externes.		

Pierre TERRIER
C.E.R.I.L.H.,FRANCE

S4

1. DEFINITION DE LA QUALITE.

La définition de la qualité passe par la prévision dans le détail de toutes les modalités qui affectent la qualité des essais comme cela se déduit de l'analyse des facteurs d'influence. Cette action est à la charge des commissions de normalisation, elle constitue un préalable à la rédaction de la norme. Elle a été pleinement assumée par le CEN TC 51 pour les normes d'essais, par exemple le projet EN 196 parti I "Détermination des résistances mécaniques" est un modèle du genre.

Dans ce domaine des essais mécaniques, FERET a proposé des 1892 l'éprouvette 4x4x16 cm Au Congrès International tenu en 1900 pendant l'exposition universelle, la FRANCE a préconisé le mortier plastique 1/3. En 1943, dans un article en forme de "suggestions au sujet des méthodes normales d'essai des liants hydrauliques", FERET a rappelé l'essentiel de ce qui lui paraissait recommandable :

- un mortier de composition granulométrique étendue,
- des prismes 4x4x16 cm,
- l'adoption d'une quantité fixe d'eau de gâchage,
- une température uniforme de 20° C dans les locaux,
- une mécanisation du gâchage.

Dans les années 50, un comité mixte RILEM -CEMBUREAU a rédigé, sur ces principes, une méthode d'essai en compression du mortier, présentée par M. DUTRON, adoptée par CEMBUREAU à HELSINKI en août 1956 et par la RILEM à la Convention Permanente de Munich de septembre 1956, cette méthode a été retenue par le Comité ISO/TC/71 dans sa recommandation ISO.R 679 de 1968 (révisée en 1982) avant d'être reprise, complétée et précisée par le CEN : projet EN 158 d'octobre 1980 devenu en août 1982 le projet EN 196 partie I.

2. DISPOSITIONS A PRENDRE.

Des dispositions sont prises pour que les locaux aient des caractéristiques en rapport avec les exigences des essais. Dans certaines salles ou enceintes, la température et l'humidité relative de l'air doivent être régulées et enregistrées. La vitesse de circulation de l'air peut être limitée (inférieure à 0,5 m/s pour les mesures calorimétriques selon la norme P 15 - 436).

Les instruments font l'objet lors de l'acquisition d'une évaluation de leurs performances, leurs qualités métrologiques sont qualifiées par comparaison avec les exigences des normes. Ils sont étalonnés périodiquement et les grandeurs sont rattachées aux étalons nationaux. Le Bureaux National de Métrologie (B.N.M.) ayant mis en place un système cohérent de dissémination des unités de mesure, les laboratoires d'essais pensent faire étalonner leurs instruments par des centres agréés B.N.M. qui garantissent le raccordement aux étalons nationaux (figure 2). Les réétalonnages sont réalisés selon un planning préétabli, consignés par écrit, matérialisés par des étiquettes qui peuvent comporter les constantes mesurées (figure 3).

Dans les mesures comparatives, un produit de référence est utilisé pour l'étalonnage: ciment étalon français, disponible au CERILH ou ciment étalon américain, disponible au NBS.

Suite à la résolution 76, prise à ROME en 1982, la constitution d'un stock de sable européen de référence est actuellement préparée par le CEN. Ce sable doit permettre d'étalonner les sables nationaux.

Les produits à essayer, les prélèvements faits, les éprouvettes préparées en vue des essais, les corps d'épreuve sont référencés et marqués de façon à se rattacher au lot d'origine. La gestion du système de référence permet de situer les en-cours géographiquement (salle de conservation dans l'eau, armoire humide) et par rapport au temps (temps légal et âge des essais). Cette traçabilité permet, notamment en cas d'anomalie, la mise en cause d'essais effectués dans un local identifié à une époque déterminée (coupure du courant par exemple).

L'obtention de la qualité commence donc par la rédaction des dispositons ci-dessus aptes à la mise en pratique des spécifications des normes. Dans cet esprit, un document de référence dont il conviendra de tenir compte pour les essais relatifs à la résistance mécanique est le guide rédigé sous l'égide de CEMBUREAU pour un groupe animé par le Docteur KOELIKER (Manual for Testing of strength of Cement draft 1981) pour l'application de la norme CEN.

3. ATTRIBUTION DES ROLES.

Les opérateurs doivent être formés à :

- conduire les essais conformément au Plan Qualité,
- rendre compte de toute anomalie,
- ne déroger aux dispositions du Plan Qualité qu'avec l'accord de l'encadrement,
- enregistrer les mesures et les identifications utiles de façon à formaliser le suivi des essais et permettre eventuellement le traitement des non conformités.

Les spécifications des modes opératoires impliquent la compétence de l'opérateur, les dispositions prises ne doivent pas être un obstacle à la confiance qui lui est faite ni le décharger de la responsabilité de la tâche qu'il accomplit.

Un des rôles du responsable qualité est précisemment d'animer l'ensemble des personnes impliquées par l'organisation de la qualité en vue d'obtenir l'adhésion complète à l'état d'esprit qualité ; mais l'adhésion n'est pas tout, l'entretien et l'acquisition des connaissances ne doivent pas être sous estimés non plus

Pierre TERRIER
C.E.R.I.L.H., FRANCE

que les moyens matériels mis à la disposition de chacun.

MATERIELS DE MESURE ET D'ESSAI

Ce tableau précise l'identification, la situation, les caractéristiques et le mode d'étalonnage ainsi que sa fréquence de chacun des appareils et instruments de mesure utilisés. Les responsables du matériel considéré sont aussi indiqués.

DESIGNATION	IDENTIFICATION	CARACTERISTIQUES SPECIFICATION D'ACHAT	MAINTENANCE	ETALONNAGE	RESPONSABLES
Balance analytique digitale.	SARTORIUS type 2474 Pièce 207	portée 160 g au 0,01 mg	Entretien annuel par fournisseur OSI	Vérification trimestrielle au moyen des poids étalonnés	Mme B. M. P.
Balance de précision digitale	SARTORIUS type 2257 pièce 207	portée 1600 g au 0,01 g	Entretien annuel par founisseur OSI	IDEM	Mme B. M. P.
Boite de poids RP1 étalonnés	PROLABO n°34924 pièce 209	masses 100 à 1 g et divisionnaires	Mise à disposition par Chef Section	Rattaché BNM Certificat LNE n° 408 211/1	Mme B. Mme B.
Four électrique réglable à ventilation naturelle	PIEZO CERAM type TH4 pièce 201	température maximum 1300°C 4000W	Intervention du fournisseur en cas de besoin	Vérification mensuelle de la température 1000±25°C et après chaque intervention	M. P.
Four électrique réglable à ventilation naturelle	PIEZO CERAM type TTSOP 33 P palier 2e étage	température maximum 1600°C 3500W	IDEM	IDEM 1200 ± 25° C	M. P.

TABLEAU II - EXTRAIT D'UN TABLEAU DE MAINTENANCE ET D'ÉTALONNAGE

RÉSEAU NATIONAL
D'ESSAIS



FIGURE 1. LE LOGO RNE

Pierre TERRIER
C.E.R.I.L.H., FRANCE

LABORATOIRE NATIONAL D'ESSAIS
Département
Métrologie et Instruments de Mesure

CENTRE D'ÉTALONNAGE MÉCANIQUE
1, rue Gaston-Boissier — 75015 PARIS
Tél.: (1) 532.29.89
Télex: LNE 202 319 F

Centre d'étalonnage agréé
par le
BUREAU NATIONAL DE MÉTROLOGIE
chaîne d'étalonnage unités mécaniques

FIGURE 2
En tête d'un certificat d'étalonnage émis par un centre d'étalonnage agrée BNM (arrêté du 11 mars 1977)



FIGURE 3
Modèle d'étiquette pour un calorimètre avec l'indication des constantes de l'appareil.

Pierre TERRIER
C.E.R.I.L.H., FRANCE

4. EXERCICE DE L'AUTOCONTROLE.

Dès lors que l'opérateur sait ce qu'on attend de lui, peut mesurer si ce qu'il fait correspond à ce qu'on attend de lui, peut agir sur le déroulement de l'essai l'autocontrôle est possible et peut-être organiser par :

- des essais à blanc pour tester l'appareillage.
- des essais de répétabilité,
- le recours à des échantillons types,
- la comparaison des méthodes, dans certains cas,
- la cohérence des résultats.

5. TRAITEMENT DES ANOMALIES.

Avec le traitement formalisé des anomalies commence l'assurance de la qualité.

Tout écart par rapport à une situation prévue, décelé au laboratoire, constitue une anomalie. Toute anomalie est traitée, en particulier l'anomalie de fonctionnement des matériels ou conditions d'essais fait remonter l'arbre des causes, provoque la remise en question des réglages, de l'entretien, de l'étalonnage avec mise hors service éventuelle jusqu'à conformité.

Il est utile de distinguer les modes de défaillances puis de classer leurs conséquences (mineure, significative, critique, catastrophique). L'analyse des risques doit être conduite dans l'esprit d'une prévention adaptée (maintenance des groupes de froid à l'entrée de la saison chaude).

6. ESSAIS INTERLABORATOIRES.

Les résultats d'une mesure sont entachés, par rapport à la valeur vraie, m, de la grandeur, d'erreurs provenant de deux sources : une erreur de répétition et une erreur de laboratoire. Le résultat d'une mesure peut être représenté de la façon suivante :

$$x_{i,k} = m + l_i + e_{i,k}$$

l_i est l'erreur entre les laboratoires,

$i = 1, 2, \ldots, p$

p est le nombre de laboratoires.

La valeur moyenne de cette erreur l_i est nulle mais sa variance n'est pas nulle. Celle-ci a pour expression $V(L)$ ou $\sigma^2(L)$. C'est la variance de laboratoire.

$e_{i,k}$ est l'erreur de répétition dans un même laboratoire d'indice i

$k = 1, 2, \ldots n$

n est le nombre de résultats ou d'essais dans le laboratoire.

La valeur moyenne de l'erreur $e_{i,k}$ est nulle mais sa variance n'est pas nulle. Elle a pour expression : $V(r)$ ou $\sigma^2(r)$. C'est la variance de répétabilité.

L'ensemble des np résultats est caractérisé par une moyenne $\bar{X}$ et une variance $V(R)$ ou $\sigma^2(R)$. Celle-ci est la variance de reproductibilité qui caractérise la distribution de l'ensemble des mesures.

On a : $V(R) = V(L) + V(r)$

que l'on peut écrire $\sigma^2(R) = \sigma^2(L) + \sigma^2(r)$

en général $\sigma(R)$ est beaucoup plus grand que $\sigma(r)$

La valeur vraie, m, est en général, sinon toujours, différente de la valeur moyenne $\bar{X}$. Toutefois, on peut estimer la valeur maximale de l'erreur $|m - \bar{X}|$. En effet si l'on se donne un petit nombre, α, appelé seuil des probabilités significatives ou niveau de signification, on peut trouver deux nombres λ_1 et λ_2 tels que la probabilité que l'on ait : $\lambda_1 \leqslant m \leqslant \lambda_2$ soit égale ou supérieure à $1 - \alpha$

L'intervalle entre les 2 nombres λ_1 et λ_2 est l'intervalle de confiance bilatérale. $1 - \alpha$ est appelé niveau de confiance, c'est la probabilité pour que l'intervalle calculé contienne la valeur vraie.

Selon le fascicule de documentation X 06-041 de la collection des normes françaises, l'intervalle de confiance bilatérale, au niveau de confiance $1 - \alpha = 0{,}95$ pour la valeur vraie m, est l'intervalle :

$$\bar{X} \pm 1{,}96\sqrt{\frac{\sigma^2(R)}{p} - \left(1 - \frac{1}{n}\right)\frac{\sigma^2(r)}{p}}$$

Lorsque l'on a pu déterminer par un essai interlaboratoires les caractéristiques des lois de reproductibilité, $\sigma(R)$, et de répétabilité, $\sigma(r)$, il est possible de connaître l'intervalle de confiance lié à une moyenne de résultats d'une autre mesure de même nature. Cette autre mesure peut être effectuée par un nombre de laboratoires inférieur au nombre p de l'essai interlaboratoires et chacun d'eux peut avoir obtenu un nombre de résultats différent de n.

De même, on peut, d'après $\sigma(R)$ et $\sigma(r)$, estimer l'écart maximal admissible entre les moyennes des mesures de deux laboratoires qui effectueraient un essai différent de l'essai interlaboratoires et dont l'un aurait obtenu n_1 et l'autre n_2 résultats.

En effet, d'après le fascicule X 06-041, au seuil de $\alpha = 5$ % ou $(1 - \alpha) = 0{,}95$, on doit avoir :

$$|\bar{X}_1 - \bar{X}_2| \leqslant 1{,}96\sqrt{2\left[\sigma^2(R) - \left(1 - \frac{1}{2n_1} - \frac{1}{2n_2}\right)\sigma^2(r)\right]}$$

si $n_2 = n_1 = 1$

$$|X_1 - X_2| \leqslant 1{,}96\sqrt{2\sigma^2(R)} = 2{,}77\sigma(R)$$

Ce mode d'utilisation ultérieure des caractéristiques de la dispersion d'une méthode d'essai, qui ont été déterminées au cours de l'essai interlaboratoires, est très utile (Tableau III).

Pierre TERRIER
C.E.R.I.L.H.,FRANCE

Ces essais en commun conduits par le C.E.R.I.L.H. depuis 1949 ont été étendus en 1960 à l'ensemble des essais courants du ciment. Ils regroupent maintenant environ cent cinquante participants. Ils permettent chaque année aux laboratoires de confronter leurs résultats à l'ensemble des mesures.

7. PRATIQUE DE L'AUDIT INTERNE.

Un audit interne est déclenchée dans chaque unité technique (chimie,calorimétrie,etc..) une fois par an par le Responsable Qualité avec la participation du responsable technique.

TABLEAU III. APPLICATION DES ESSAIS INTERLABORATOIRES AUX MESURES DE CHALEUR D'HYDRATATION.

A. Les résultats des mesures de chaleur d'hydratation sont fournis à diverses échéances jusqu'à cinq jours. A titre indicatif les échéances de 12h, 1j, 3j, 5j, peuvent être retenues.
Les écarts types de répétabilité (r) et de reproductibilité (R) déterminés selon le fascicule de documentation X06-041 "Fidélité d'une méthode d'essai. Guide pour les essais interlaboratoires", sont les suivants :

t	12 h	1 j	3 j	5 j
(r) ($J.g^{-1}$)	10	10	10	10
(R) ($J.g^{-1}$)	15	15	20	20
Valeurs moyennes ($J.g^{-1}$) obtenues lors des essais interlaboratoires (à titre indicatif).	150 à 250	285 à 360	350 à 400	360 à 410

B. Intervalles de confiance bilatéraux, en $J.g^{-1}$,rapportés à un résultat ou à la moyenne de deux ou quatre résultats.

Cas retenus		Vis-à-vis du laboratoire	Vis-à-vis de l'ensemble des laboratoires	
		12 h,1 j	12 h et 1 j	3 j et 5 j
1 résultat dans 1 laboratoire		± 20	± 30	± 40
2 résultats dans 1 laboratoire		± 14	± 26	± 37
Entre 2 laboratoires	1 résultat par laboratoire	± 20	± 21	± 28
	2 résultats par laboratoire	± 14	± 18	± 26

C. Ecarts admissibles entre les résultats de deux mesures ou de deux moyennes en $J.g^{-1}$

Cas retenus		12 h	1 j	3 j	5 j
2 résultats dans 1 laboratoires : $\|X_1-X_2\|$		28	28	28	28
ENTRE DEUX LABORATOIRES	1 résultat par laboratoire : $\|X_1-X_2\|$	42	42	55	55
	2 résultats par laboratoire : $\|X_1-X_2\|$	37	37	52	52

Pierre TERRIER
C.E.R.I.L.H.,FRANCE

L'audit a pour but de déceler les risques de non qualité dans le laboratoire. C'est un examen méthodique qui vise à caractériser principalement :

- l'efficacité des modes opératoires,
- l'efficacité des procédures,
- le respect des procédures et des modes opératoires.

L'audit doit être conduit en se plaçant autant qu'on peut sur le terrain (et non comme un scribe installé sur les gradins et qui critique les phases du combat dans l'arène !) Le but de l'audit est de supprimer les imperfections en décelant les points d'application des actions correctives et en identifiant les opportunités pour l'amélioration. A l'occasion de l'audit on vérifie que les actions préventives ou correctives prises antérieurement ont porté les effets escomptés.

8. ACCREDITATION.

Le réseau national d'essais RNE dispose d'une méthode d'investigation qui lui permet d'évaluer le degré de conformité de l'organisation interne du laboratoire avec les exigences du référentiel. L'audit lui permet, par l'information préalable (questionnaire), l'interview, la consultation de documents et la visite des installations de constater que pour les différentes activités élémentaires, l'action à mener est bien prise en compte, la procédure décrivant ce qu'il faut faire et par qui le faire existe et est complète et que son application est vérifiée.

L'accréditation par le réseau matérialisée par le droit d'usage d'un logo (figure 1) correspond pour le laboratoire à la reconnaissance de sa capacité technique à réaliser pour le compte de tiers les prestations d'essais pour lesquelles il est accrédité.

La création du Réseau National d'Essais permet la création d'un pôle de cohérence et de compétence en matière d'essais. Un réseau de laboratoire dont la crédibilité ne puisse être mise en doute, c'est aussi un moyen de répondre au besoin des utilisateurs qui exigent des assurances quant à la qualité des essais par lesquels ils orientent leurs décisions. En outre, l'accréditation est reçue avec fierté par chacun des intervenants du laboratoire ce qui contribue à développer l'esprit Qualité. La satisfaction du personnel résulte du double sentiment de bien faire et de faire quelque chose d'utile. A mesure que cette aptitude s'accroit et que des progrès sont réalisés, d'autres deviennent accessibles et sont souhaités. La recherche de la qualité est alors qualifiante pour l'individu. Les différents systèmes nationaux d'accréditation coordonnent leurs efforts au sein de l'ILAC. Dans le domaine des matériaux cette concertation s'effectue principalement par la RILEM laquelle participe depuis 1977 aux travaux de l'ILAC.

Le principe d'un nouveau Comité Technique sur les Procédures d'Evaluation pour les Laboratoires de référence du ciment et du béton au sein de la Rilem a été retenu à la réunion du Conseil Général à WASHINGTON, en septembre 1985 à l'initiative de M FROHNSDORFF (ETATS-UNIS) et du Dr. BASILIO (BRESIL). Dans un large domaine couvrant : l'harmonisation des méthodes d'essais, la reconnaissance mutuelle des contrôles, la mise en place des systèmes d'assurance de la qualité, les essais d'intercomparaison, l'audit et l'accréditation des laboratoires, ce comité peut entreprendre en 1986 Le recensement des procédures, la tenue d'un symposium pour la confrontation des expériences en 1987 et ultérieurement la préparation d'un guide de bonne pratique.

* * * *

Au terme de cette communication, il importe peut être de bien distinguer d'une part, la gestion de la qualité des produits attestée par la certification, et d'autre part, la gestion de la qualité des essais dont témoigne l'accrédition. Pourtant un certain parallélisme existe entre les deux démarches, comme cela apparaît au tableau IV.

La certification des produits met désormais en oeuvre trois niveaux de contrôles : contrôle de fabrication (niveau 1) autocontrôle (niveau 2) et contrôle par le service de vérification (niveau 3). L'attribution du droit d'usage de la marque NF-VP des ciments, laquelle est gérée par le Comité de la Marque, s'appuie sur les essais réalisés aux niveaux 2 et 3 aux conditions suivantes, relatives à la résistance, à la compression :

a) VERIFICATION DU BON ETALONNAGE.

Les prélèvements effectués au titre du contrôle NF-VP (12 par an au minimum) sont chacun divisés en deux parts égales, l'une étant essayée par le laboratoire du Service de Vérification (ville de Paris) donne un résultat x_i , l'autre essayée par le laboratoire du fabricant un résultat y_i.

On s'assure d'abord que les différences $d_i = y_i - x_i$ ne sont pas éxagérement dispersées. A cette fin, on vérifie que la valeur e_m définie par la formule ci-dessous est inférieure à un seuil $e_o = 1$ MP$_a$

$$e_m = 1/n \sqrt{\Sigma(y_i - x_i)^2 - 1/n\left[\Sigma(y_i - x_i)\right]^2} = \frac{\sigma_d}{\sqrt{n}}$$

n devant être au moins égal à 12.

b) VERIFICATION DE L'HOMOGENEITE DE L'AUTOCONTROLE.

La vérification ci-dessus étant faite, il convient de s'assurer que les essais d'étalonnage du fabricant (sur prélèvement Ville de Paris) appartiennent, avec une forte probabilité, à la même distribution statistique que l'ensemble des résultats de l'autocontrôle. A cette fin, on calcule :

$$u = \frac{|M - m| \sqrt{n}}{\sigma}$$

formule dans laquelle M est la moyenne de l'ensemble des résultats du fabricant et leur écart-type, m la moyenne de ses n essais d'étalonnage (12 en principe).

Pour $u > 2{,}58$ on serait conduit à conclure à la non identité de deux populations avec un

Pierre TERRIER
C.E.R.I.L.H, FRANCE

risque d'erreur de 1 %.

c) CORRECTION D'ETALONNAGE.

Dans le processus de vérification de la conformité aux normes par utilisation des résultats de l'autocontrôle ces derniers sont introduits dans les calculs après avoir effectué la correction d'étalonnage. En pratique le paramètre M (moyenne) de la distribution statistique de l'autocontrôle est remplacé par :

M + m' - m (où M est la moyenne de l'autocontrôle, m' la moyenne des essais NF-VP de l'étalonnage et m la moyenne des essais d'étalonnage du fabricant.

Ces vérifications et correction étant faites, la distribution des valeurs de l'autocontrôle doit satisfaire aux conditions fixées pour les limites nominales des classes de la norme NF.P.15-301 avec les probabilités suivantes :

- 90 % pour les valeurs minimales à 2 jours
- 99 % pour les valeurs minimales à 28 jours
- 90 % pour les valeurs maximales à 28 jours

Une certaine analogie apparait à cet égard entre les principaux systèmes européens de certification des produits permettant d'envisager entre les pays une reconnaissance mutuelle des procédures de certification (projet du sous-comité du CEN animé par M. VAN KLAVEREN).

L'accréditation s'applique déjà en FRANCE aux laboratoires qui interviennent au niveau 3 pour le béton et ses constituants (ciment, adjuvants, etc..) progressivement, elle peut concerner ceux du niveau 2. Elle qualifie, comme nous l'avons vu, une organisation et une aptitude à gérer la qualité des essais. Elle implique notamment le rattachement des grandeurs principales aux étalons nationaux. Elle correspond, elle aussi à trois niveaux de contrôle : l'autocontrôle, par l'unité technique (niveau I), l'audit interne et l'assurance de la qualité (niveau II) et l'audit externe (niveau III). Géré par le Réseau National d'Essais pour la FRANCE (par des Commissions sectorielles spécialisées : bâtiment Génie Civil etc...), la procédure s'inscrit dans une perspective de reconnaissance mutuelle de l'accréditation des laboratoires au sein de l'ILAC (International Laboratory Accreditation Conference).

CERTIFICATION DE QUALITE	ACCREDITATION
Niveau 1 contrôle de fabrication Niveau 2 autocontrôle du fabricant Niveau 3 contrôle du service de vérification	Niveau I autocontrôle par l'unité technique Niveau II audit interne et assurance de la qualité Niveau III audit externe par l'organisme accréditeur
Implique des conditions de prise en compte des résultats	Implique des conditions de réalisation des essais
Gérée par le Comité de Marque	Gérée par le Réseau National d'Essais
Evolution vers la reconnaissance mutuelle des certifications (CEN)	Evolution vers la reconnaissance mutuelle des accréditations (ILAC).

TABLEAU IV

A.K. MULLICK, K.H. BABU
P. BHASKARA RAO
National Council for Cement and Building Materials, New Delhi - India

EVALUATION OF POZZOLANIC ACTIVITY AND ITS IMPACT ON SPECIFICATION OF BLENDED CEMENTS.

INTRODUCTION

India has a long tradition in manufacture and use of blended cements, which presently comprise nearly three-fourth of the total cement production. Portland pozzolana cements (PPC), which comprise nearly half the total production, are made with flyashes and/or calcined clay pozzolana (CCP), mostly interground with cement clinker and gypsum.

Like in many other countries, cement specifications in India have some prescriptive and some performance requirements; characteristics and permissible proportion of pozzolana being such prescriptive requirements. In an effort to make the cement specifications as much performance-oriented as possible, the need of separate tests for pozzolanic materials in specifications of portland pozzolana cement (IS : 1489-1976) has been questioned. While the debate continues, it is held that, in order to ensure special properties of PPC claimed in standard specifications, viz better resistance to leaching, aggressive waters and alikali-reactive aggregates and reducing unsoundness due to free lime and magnesia hydration, some test to ensure its adequate reactivity to lime-systems is necessary. Such tests are also necessary to distinguish a pozzolana from a totally inert additive, for which performance requirements in terms of setting and compressive strength are not adequate. With this as a background, this paper reviews the characteristics of pozzolana and portland pozzolana cements in the country and makes recommendation for improvements in the cement specifications and methods of evaluation of pozzolanic materials.

CURRENT SPECIFICATIONS

IS: 1489-1976 permit addition of 10 to 25 percent pozzolana material in the manufacture of PPC. Being used as an all-purpose cement for plain and reinforced concrete interchangeably with ordinary portland cement, the specification requirements of compressive strength at 3, 7 and 28 days and setting times, in case of both types of cements, are identical. However, no tests for durability which may have a bearing on the long-term performance are prescribed. The pozzolanic materials are required to conform to requirements of IS: 3812 (Part I) - 1981 in case of flyashes and IS: 1344-1981 in case of CCP. As is common in many other countries (1,2), these requirements are in terms of chemical composition, fineness, drying shrinkage, lime-reactivity test (8 days at 50°C) as well as minimum 80 percent strength at 28 days in cement activity test with 20 percent replacement of cement by the pozzolanic material.

Out of these, pozzolanic activity has been found to have poor correlation with broad limits of chemical requirements specified, especially because the pozzolana used are essentially silica-and alumina-bearing, and pozzolana with sizeable calcium oxide content are seldom encountered. Fineness in terms of specific surface area (Blaine's) is important, but particle-size-distribution (fractions below 10 μm) is found to correlate better with pozzolanic activity (3). In order to evaluate the pozzolanic activity, one has, therefore, to fall back upon. the physical tests involving reactivity to lime, e.g. lime-reactivity and cement activity tests.

CHARACTERISTICS OF POZZOLANA AND CEMENTS

Large number of samples of pozzolana materials, clinkers and cements produced with these (both OPC and PPC) in different cement plants were evaluated periodically. A summary of results of lime-reartivity (LR) and cement activity tests of pozzolana are described in Fig. 1 & 2 respectively. It is seen that the pozzolana used in about 30 percent

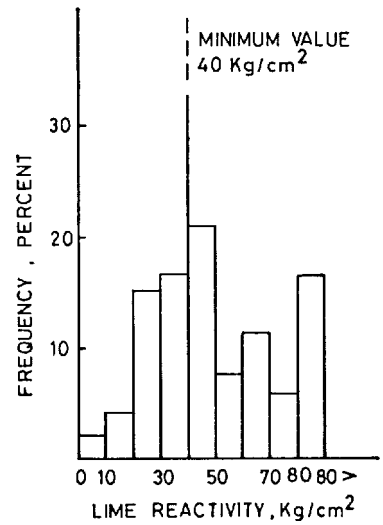

Fig. 1 : Histogram of lime-reactivity of pozzolana materials.

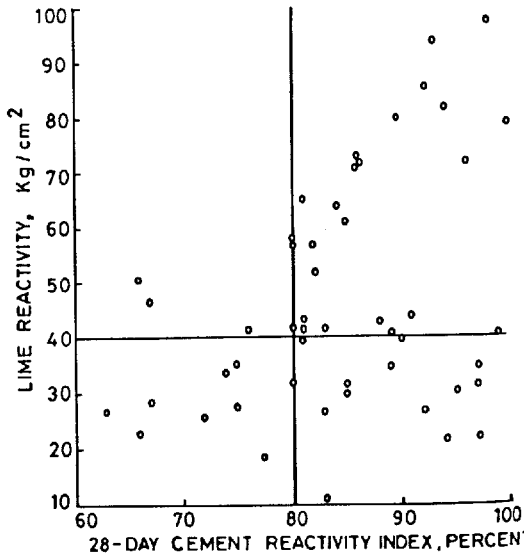

Fig. 2 : LR and Cement activity of pozzolana.

samples did not satisfy the requirement of minimum 40 kg/cm^2 lime-reactivity (Fig. 1). However, most of the samples satisfied the requirement of 80 percent cement activity and correlation with lime-reactivity was poor and the trend erratic (Fig. 2).

Reasons for this are not difficult to seek. Replacement of 20 percent cement amounts to a corresponding increase in the water-cement ratio and the resultant strength, in absence of any contribution from the pozzolana upto 28 days, could be of the order of 75 to 80 percent of the control (Fig. 3). Further modifications in the

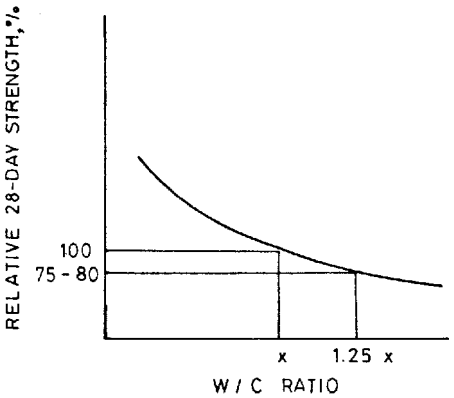

Fig. 3 : Effect of increasing w/c ratio by 20% on relative strength.

strength result due to the effect of granulometry of the pozzolana material in water requirement for the constant flow (105 percent). These are corroborated by the results in Table 1.

TABLE - 1

REACTIVITY OF INERT ADDITIVES WITH LIME AND CEMENT

Sl No *	Fineness cm^2/g	Lime reactivity kg/cm^2	Cement reactivity kg/cm^2	Increase (+) or decrease (-) in water requirement %
A_1	3085	1.5	80	- 0.7
A_2	3290	1.4	74	0
A_3	3590	1.2	70	+ 0.7
B_4	3010	1.5	60	+ 3.5
B_5	3350	1.8	55	+ 4.1
B_6	3475	2.3	52	+ 4.8

* A_1 to A_3 limestone, B_4 to B_6 sand

where 20 percent cement was replaced by inert additives like ground limestone and sand. It is seen that the resultant strength was of the order of 52-80 percent of the control, depending mainly on the modification of water demand. On the other hand, some pozzolana material having relatively high LR were found to have resulted in cement activity lower than 80 percent, because of increased water demand (Fig. 2).

The dosage of pozzolana material used in manufacture of PPC in India usually ranges between 10 to 15 percent. Data on strengths of PPC and OPC obtained from the clinker used in the manufacture, whenever ground to comparable finenesses, are given in Table 2.

TABLE - 2

STRENGTHS OF PPC AND OPC - PLANT DATA

Cement Plant	Fineness cm^2/g		Ratio of Strength PPC / OPC	
	OPC	PPC	7 days	28 days
1	3755	3800	0.65	0.74
	4090	4355	0.61	0.74
2	2755	3325	0.92	0.85
3	2965	3000	0.96	0.94
4	3086	3473	0.98	0.95
5	2855	3863	0.88	0.97
	2519	3293	0.89	0.87
	3074	3872	-	0.87
6	3474	3608	0.72	0.63
7	2871	3413	0.91	0.87
8	2941	3504	0.87	0.90
9	3546	3782	0.89	0.90
10	3453	3826	1.24	1.02
11	3726	3826	1.00	1.06
12	3050	3453	0.52	0.70
13	3293	3696	0.82	0.78
14	3826	3896	0.78	0.74
15	4659	4684	0.90	1.03
16	3765	3750	0.80	0.79
17	3300	3655	0.98	1.02
18	2822	3252	1.10	1.10
19	3395	3375	0.78	0.83
20	3020	3128	0.91	1.07
21	3113	3273	0.87	0.91

It would be seen that inspite of somewhat lower percentage of pozzolana in industrial production, the strength ratios were more or less similar to cement-activity indices and age of testing (7 or 28 days) did not make much difference. This would point to the fact that not much of pozzolanic reaction was taking place upto 28 days. This is corroborated by X-ray diffraction studies carried out in the manner suggested by Costa and Massazza (4). Typical results indictated that the reduction of CH upto 28 days in the presence of pozzolana was not high. Typical scanning electron micrographs upto 28 days' hydration (Fig. 4 & 5), showed substantial proportion of unreacted flyash or CCP-particles with some hydration products.

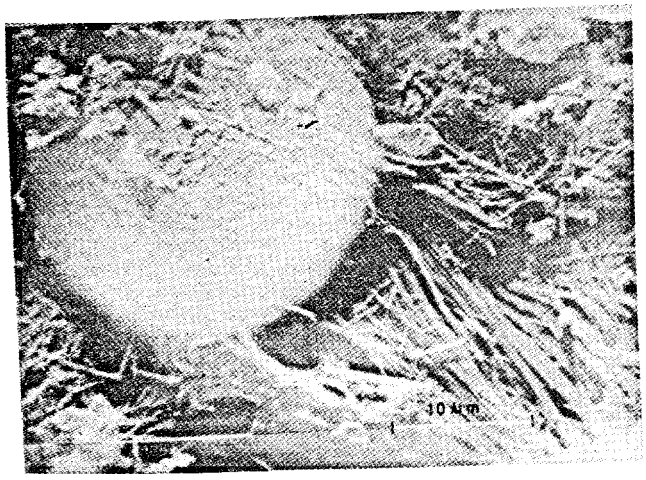

Fig. 4 : Electron micrograph showing unreacted fly ash particle.

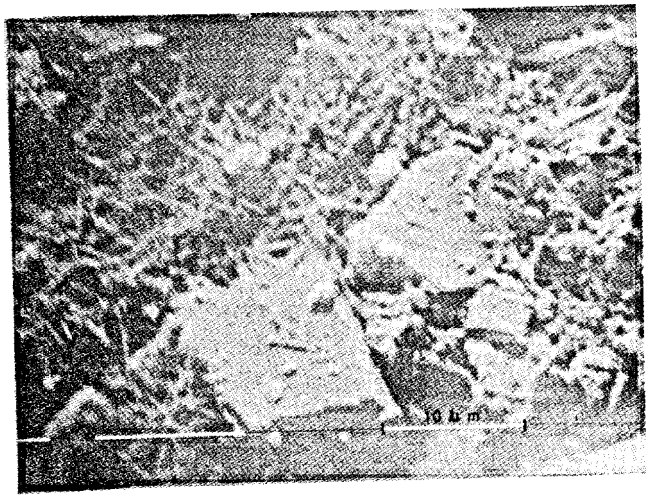

Fig. 5 : Electron micrograph showing unreacted CCP particle.

MODIFICATIONS IN CEMENT ACTIVITY TESTS

From the above it will be clear that the cement activity test does not serve the purpose of properly characterising a pozzolan or to distinguish it from an inert additive, mainly because the limit of 80 percent is not a stringent one, and secondly, not much of pozzolanic activity can be expected during 28 days hydration specially with pozzolana of marginal reactivities. On the other hand, variation in water content for constant flow introduces additional variability in results (5).

Lime reactivity test would seem to be preferable in that one of the reactants e.g. lime is constant and responses obtained with different pozzolana material help in evaluating and characterising them. Helmuth has discussed in detail the relevant reaction chemistry and the effects of amount of lime involved in evaluating pozzolana of both high and low reactivities (5). Although, the products of reaction in lime-pozzolana systems are essentially calcium silicate hydrates, there could be differences in the morphology and C/S molar ratio than what is expected in hydration with cements. It is for this reason that many tend to question the reliability of lime reactivity test under thermally activated regime in simulating the reaction of the same pozzolana with cements under normal conditions of curing.

Keeping these criticisms in view, attempts were made to assess the potential of strength contribution of a pozzolana to the cement under normal condition of curing in a more direct manner. For this, the standard cement sand mortar was tested for compressive strength at 28 days in the usual manner, except the water-cement ratio was kept constant at 0.5. Two other mixes were then tested; one with 20 percent extra cement (by weight) in the mix and the other with 20 percent pozzolana by weight in the mix with the water content same as in control. Since the water content was adequate to accommodate the increase in fines, no modification in the sand content was necessary. The contribution of the pozzolana to the strength development (PI), expressed as a proportion of an equal weight of cement was given by;

$$PI = \frac{C-A}{B-A}$$

where A is the cement strength in the control and B and C are the strength in mixes with additional cement and addition of pozzolan respectively.

Results of tests on different pozzolana samples are given in Fig. 6. Obviously the chemical composition

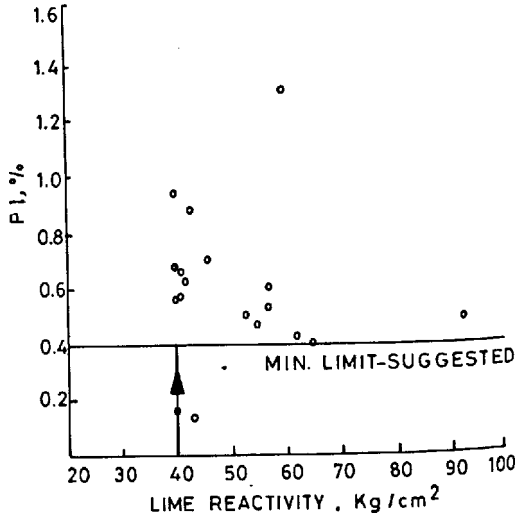

Fig. 6 : Relation between pozzolanacity index and lime reactivity.

and fineness of cement would be important parameters and a strict comparison would have called for a "standard" cement to be used in each case, similar to a standard "lime" being used in lime-reactivity test. However, from the standardisation point of view, it would require that such a standard cement be used in all the laboratories and cement plants in the country. The cement used in this exploratory tests were, therefore, purposely chosen at random. Although there was considerable scatter in the test results in Fig. 6, it would appear that a pozzolana activity index (PI) of around 40 percent and above corresponded the lime reactivity value of 40 kg/cm^2.

These results point to the possibility of improving the cement activity test and set a realistic strength limit. In absence of any strength contribution by the pozzolana, a 20 percent cement replacement can cause 20 percent lowering of strength due to increase in water-cement ratio, i.e. 80 percent relative strength. Complete pozzolanic reaction, on the other hand, would result in strength equal to that of control (i.e. 100 percent relative strength), may be at a later age. Between these two extremes, since pozzolana materials of satisfactory lime-reactivity were found to contribute about 40-50 percent strength as of cement of equal weight, a 20 percent replacement of cement should correspond to atleast 90 percent relative strength upto 28 days when tested in constant water content.

CONCLUSIONS

Based on these investigations, the following suggestions are made for incorporation in specifications of blended cements;

i) While attemptes to make cement specifications more performance-oriented should continue, characterisation of additives in blended cements is necessary.

ii) Lime-reactivity tests are better suited to characterise a pozzolana and distinguish it from inert additives.

iii) Cement-activity tests should be carried out at constant water content and a minimum 90 percent relative strength for 20 percent cement replacement would ensure satisfactory pozzolanic activity.

ACKNOWLEDGEMENTS

This paper is a contribution from the Centre for Standardisation, Calibration, Testing and Quality Control at the National Council for Cement and Building Materials and based on data available with the Centre. The paper is published with the permission of Chairman and Director General of the Council.

REFERENCES

1.- OSCAR E. MANZ (1983), "Review of international specifications for use of flyash in portland cement concrete", Flyash, Silica Fume, Slag and other Mineral By-Products in Concrete, Vol. I, Publication SP-79, ACI, pp 187-200.

2.- EDDIE ROSSOUW and JAPIE KRUGER (1983), "Review of specifications for use of flyash in portland cement concrete", Ibid, pp 201-220.

3.- P.K. MEHTA (1985), "Influence of flyash Characteristics on the Strength of portland-flyash mixtures", Cem. Concr. Res., 15(4), 669-674.

4.- U. COSTA and F. MASSAZZA (1983), "Some properties of pozzolanic cements containing fly ashes", Flyash, Silica Fume, Slag and other Mineral By-Products in Concrete, Vol. I, Publication SP-79, ACI, pp 235-254.

5.- RICHARD HELMUTH (1983), "Some questions concerning ASTM standards and methods of testing fly ash for use with portland cement", Cement, concrete and aggregates, 5(2), 103-110.

OSAMU KATO - THE CEMENT ASSOCIATION OF JAPAN - R&D LABORATORY OF THE CEMENT ASSOCIATION OF JAPAN

TREND OF THE SPECIFICATION AND THE METHOD ON ALKALI - SILICA REACTION IN JAPAN

Numbers of cracks were found in the concrete piers of highways in Osaka City in 1982. Core specimens were extracted from the concrete piers and tested. As a result, the cause of the cracks was determined to be alkali-silica reaction.
Committee of Research on alkali-aggregate reaction of Japan Concrete Institute conducted a nation-wide survey of concrete constructions in the later years, and the results revealed several deteriorated concrete structures, whose cause was suspected alakli-aggregate reaction.

In Japan the examples of alkali-aggregate reaction were hitherto unknown, thus, the specification and test method had not been formed. Since 1984 much has been discussed as to set the specification for low-alkali cement and test method to determine alkali reactivity of aggregate in a somewhat hasten manner.

Japanese Industrial Standard Specification (JIS) for low-alkali cement was issued on February 1, 1986. The specification defines the alkali content of low alkali Portland cement to be below 0.6%. In respect to the test method for concrete aggregate, there is no authorized test method in Japan.

1. Establishment of JIS Specification on Low-Alkali Portland Cement

The Cement Association of Japan prepared a draft proposal for evaluation of alkali content of low-alkali Portland cement in order to set the criteria. However, it was found difficult at that time to establish the standard value of alkali content which ascertained the ground and gained a strong consensus, because of the lack of sufficient data showing correlation between alkali content and concrete expansion of alkali-reactive aggregate. Therefore, the Cement Association of Japan decided to propose low-alkali Portland cement should contain less than 0.6% of alkali with the reference to ASTM C150 /1/ and other references /2, 3, & 4/. Agency of Industrial Science and Technology reviewed the proposal, and revised JIS R5210 /5/ to add specification for low-alkali Portland cement. The newly issued alkali content of low alkali Portland cement was defined as $Na_2O(\%) + 0.658K_2O(\%)$ to be below 0.6%, and it was published officially on February 1, 1986. (Note. 1)

Note. 1: Analysis for Na_2O and K_2O is defined by JIS R5202 /6/, and they are determined by atomic absorption spectrophotometry or flame spectrophotometry.

2. Study of the Test Methods for Potential Reactivity of Aggregate

There is no official test method in Japan that determines alkali reactivity of concrete aggregate at present. The Cement Association of Japan, Japan Concrete Institute, General Building Research Corporations, and Public Works Research Institute of Ministry of Construction are currently undertaking a research to formulate the test method. The outline of these test methods is summarized as follows:

1. The test method that determines alkali reactivity of aggregate with the use of chemical method.
2. The test method to determine expansion of mortar specimen or concrete specimen.
3. The test method to determine dynamic Young's modulus and ultrasonic pulse velocity of mortar specimen or concrete specimen.

It is envisaged that the test method with the application of chemical method (1), and one with

Osamu Kato
The Cement Association of Japan

the determination of expansion of mortar bar (2) shall be approved as the standard test method for alkali reactivity determination in the near future.

2.1 Chemical Method

ASTM C289 /7/ was partly modified to construct the test method with the application of chemical method. The flow chart of this method is shown in Fig. 1.

The difference of this method with ASTM C289 is:

1. Perchloric acid is used in the determination of dissolved silica.
2. Atomic absorption spectrophotometry is adopted, while ASTM C289 doesn't include the two devices.

The advantages of the test method are shortening of analysis period and minimization of analytical error.

It is considered the chart (Fig. 2) of ASTM C289, "Illustration of Division Between Innocuous and Deleterious Aggregates on Basis of Reduction in Alkalinity Test" can be applied to determining alkali reactivity of Japanese andesite. Chert, however, is subject to consideration as sufficient data are not available for this aggregate.

2.2 Mortar Bar Method

For mortar bar method, a prism specimen of 4 x 4 x 16 cm (see Fig.2) is recommended. The mix proportion for this test method is similar to the one defined by ASTM C227 /8/. The total alkali content (Na_2O eq.) must be controlled at 1.2% to form a mortar specimen.

This specimen is easy to handle, as it does not destroy its form when casted off the mold. Nor does it twist or deform while it is preserved in the container. In addition, our experience tells that the measurement precision is notable with this method.

Fig. 3. shows the comparison of expansion ratio of a 4 x 4 x 16 cm specimen with a Stanton's bar. The mix proportion of the two specimens is identical. The results are congenial at large.

3. Future Schedule

At present, several institutions are undertaking the research of alkali-aggregate reaction. Yet, the vital issue is where to locate the responsibility of such a test method and to standardize it. In short, determining the standard value of total alkali content of 1 m^3 concrete is indispensable. In such a case, alkali content of water reducing agent and other admixtures, and mixing water must be tested integrally.

References:

1. ASTM C150-85 Standard Specification for Portland Cement.
2. Report of a Working Party of the Cement and Concrete Association, Minimizing the Risk of Alkali-Silica Reaction, Guidance Notes. (1983)
3. Vorbeugende Massnahmen gegen schädigende Alkalireaktion im Beton, Vorläufige Richtlinie. (1974)
4. NBR 5732-1977 Portland comum cemento.
5. JIS R5210-1979 Portland Cement
6. JIS R5202-1981 Method for Chemical Analysis of Portland Cement
7. ASTM C289-81 Standard Test Method for Potential Reactivity of Aggregates (Chemical Method)
8. ASTM C227-81 Standard Test Method for Potential Alkali Reactivity of Cement-Aggregate Combinations (Mortar-Bar Method)

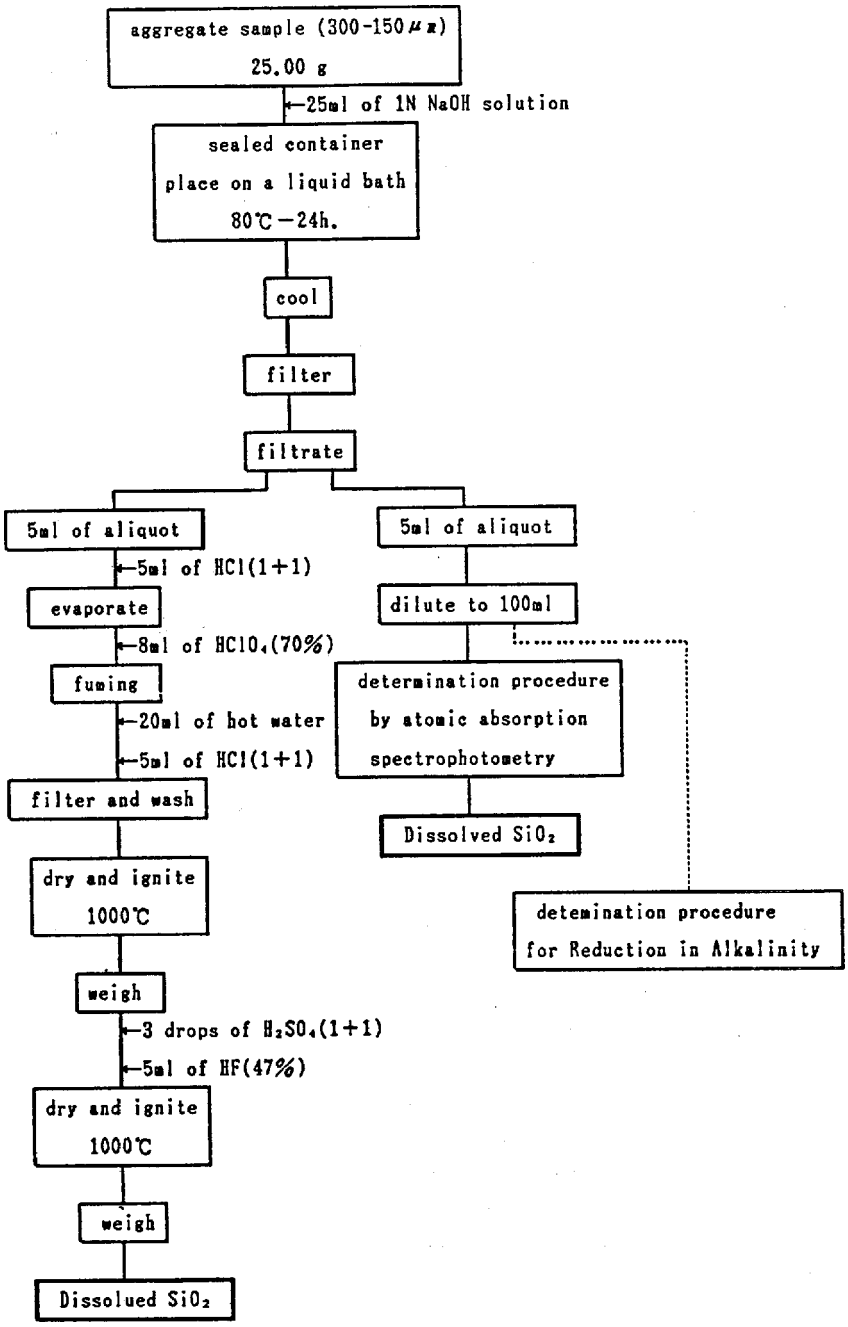

Fig.1 Flowchart of determination procedure of Dissolved Silica

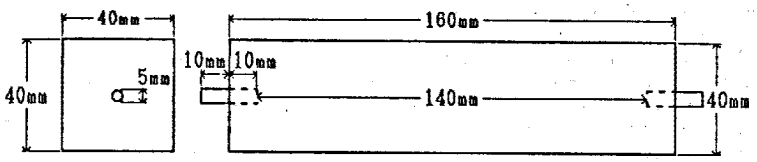

Fig.2 40×40×160mm Prism Specimen for Mortar bar test.

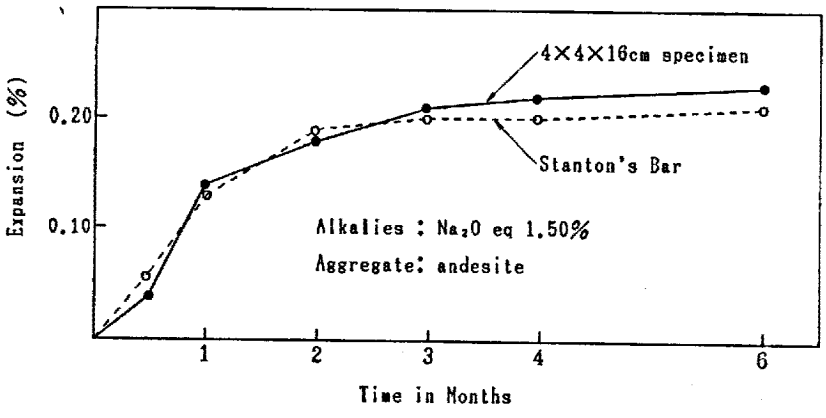

Fig. 3 A Example of Comparison of Expansion Ratio between the Stanton's Bar and 4×4×16cm Mortar Specimen

GEOFFREY FROHNSDORFF, PAUL W. BROWN AND JAMES H. PIELERT
CENTER FOR BUILDING TECHNOLOGY, U.S. NATIONAL BUREAU OF STANDARDS, GAITHERSBURG, MD 20899

STANDARD SPECIFICATIONS FOR CEMENTS AND THE ROLE IN THEIR DEVELOPMENT OF QUALITY ASSURANCE SYSTEMS FOR LABORATORIES.

1. INTRODUCTION

In recent years, there have been increasing pressures to broaden standard specifications for cements, particularly because of concern about conservation of fuels and other resources [1]. Concern is appropriate because, at least in the United States, cement manufacture is one of the largest industrial users of energy [2]. Whether or not changing cement specifications will have a significant effect on energy use, a number of important questions have been raised by the need to ensure that specifications do not unnecessarily hinder innovation in cement formulation. Unfortunately, these questions often end up as unresolved debates on the advantages and disadvantages of performance specifications, as opposed to prescriptive specifications.

In this paper, we discuss the purposes of standard specifications for cements, the types of specifications, the shortcomings of present specifications, the stimuli for changing the forms of cement specifications, the development of performance specifications for cements in ASTM, and the possibility of including optional prescriptive requirements in a performance specification. We also discuss the roles of quality assurance systems for cement testing laboratories and speculate about cement specifications of the future.

2. PURPOSES OF STANDARD SPECIFICATIONS FOR CEMENTS

The main purpose of a specification is to facilitate commercial transactions by defining a product in suitably precise terms acceptable to both the buyer and seller. In the case of a cement specification, it also facilitates the building design process by informing the designer and construction specifier about essential characteristics of the cement and helps protect public safety by defining materials which are likely to perform predictably and safely under normal conditions. Because most cements are commodities -- materials produced in large quantities which are sufficiently similar to each other for the products from different manufacturers to be interchangeable -- specifications must reflect their commodity nature. This requires specifications to address questions of quality, including aspects of performance and uniformity which affect interchangeability. In addition, specifications are usually expected to define minimum acceptable levels of performance, preferably through simple, short-term tests which have a strong, clearly-apparent, correlation with performance in common end uses. It is seldom considered essential for specifications to define maximum levels of performance, though maximum levels may be defined.

3. PRESCRIPTIVE AND PERFORMANCE SPECIFICATIONS FOR CEMENTS

Specifications are often discussed in terms of two extreme types -- prescriptive specifications and performance specifications [3]. A prescriptive specification defines a product in terms of its constituents and their relationships to each other, while a performance specification defines a product solely in terms of the functions it is to perform. Because it relies on measures of performance to assure the suitability of a product, a performance specification defines the product less narrowly, at least in terms of the constituents, than a prescriptive specification.

While it is useful to analyze specifications in terms of the extent to which they exhibit features of prescriptive and performance specifications, it often seems to be unrealistic to try to write specifications solely in either prescriptive or performance terms. On one hand, a purely prescriptive specification may require some knowledge which is not yet available, such as the relationship between composition and rate of strength development, or some analyses which are too sophisticated to be practical; on the other hand, a performance specification may require tests, such as tests for sulfate resistance, which are too complicated, time-consuming, and expensive for routine use. As a result, most product specifications have both prescriptive and performance requirements. Though such specifications are sometimes referred to as mixed specifications, they are still prescriptive.

In principle, a performance specification is less likely to inhibit development of new products since it gives a clear statement of the performance required and how a product's performance is to be evaluated. However, because of the frequent difficulty and slowness of performance testing, particularly where durability is concerned, compromises are often made. In view of the need to facilitate innovation, it is important to ensure that the elements in a specification, whether prescriptive or performance, are not unnecessarily restrictive.

Cement specifications differ greatly in the primary classification schemes used. For example, the main classification used in naming a cement may be in terms of strength (as in specifications in many European countries), of performance requirements other than strength (as in the ASTM C-150 Standard Specification for Portland Cements), or of the type and quantity of ingredients in the cement (as in the ASTM C-595 Standard Specification for Blended Hydraulic Cements).

4. SHORTCOMINGS OF PRESENT CEMENT SPECIFICATIONS

Cement specifications reflect the course of their evolution. Thus, a requirement in the current version of a specification may have been added long ago -- so long ago that the reason for the limit established, or even the precise reason for the requirement, may not be known by the active membership of the responsible committee. Such a requirement probably achieved its immediate purpose when first introduced though, possibly, at the expense of adding new restrictions on composition or performance which may now prove difficult to change. Also, prescriptive specifications are often vague, or completely silent, on the performance the products are intended to provide. In prescriptive specifications, the goal is usually to define the composition in unambiguous terms. For cements, this is not yet possible because of lack of adequate methods for determination of phase composition and particle size distribution.

Ideally, a specification should state explicitly what essential aspects of performance can be expected from the product. For example, a specification for a cement for use in reinforced concrete should indicate its ability to provide adequate corrosion protection for the reinforcing steel in general concrete construction. The specification should also state how compliance with necessary performance requirements can be demonstrated, whether by compositional analysis or by performance tests; in cases where performance tests for essential aspects of performance would take too long for routine use, or would be too expensive, provision should be made for alternative tests which will provide an equal or higher level of confidence that the required performance will be achieved. A list of performance characteristics which the authors recommend be considered in the preparation of a cement specification is given in Table 1.

Table 1. Performance Characteristics for Possible Inclusion in Performance Specifications for Cements

- o Strength at a given age
- o Dimensional stability
- o Flow properties (workability)
- o Setting time
- o Heat evolution
- o Sulfate resistance
- o Deleterious reactions with aggregates and reinforcement
- o Corrosion protection for steel
- o Response to air-entraining and other admixtures
- o Resistance to water
- o Uniformity of performance
- o Rate of strength gain at specified temperatures
- o Resistance to chemical attack
- o Color
- o Permeability to fluids
- o Electrical conductivity

Two of the most important characteristics in the list are often taken for granted, probably because they are always provided by portland cements. These are i) resistance to water, and ii) corrosion protection of steel. Although these characteristics are not specified in present cement specifications, they should be included in any performance specification for cements which are to be used in place of portland cements.

5. STIMULI FOR CHANGING THE FORMS AND CONTENTS OF SPECIFICATIONS

Cement specifications used in different countries have significant differences. This shows that there can be much flexibility in the formulation of cement specifications. It also suggests that few, if any, cement specifications are optimal. While cement specifications have been reasonably effective in meeting the normal, slowly-changing needs of most cement manufacturers and users, several new factors now suggest more urgent needs for changing the forms and contents of cement specifications. These include:

- o International agreements to encourage and support the use of international standards [4]
- o Governmental policies encouraging the development of performance specifications [5]
- o The need for conservation of the world's non renewable resources, e.g. fuels and industrial minerals used in cement manufacture
- o The need for minimizing detrimental effects on the environment of unused waste and by-product materials which are potentially useful as ingredients of cements, e.g. fly ash and by-product gypsum
- o Improvements which have been made in fundamental understanding of the factors affecting the performance of cements and concretes, e.g., factors affecting alkali-aggregate reactions [6]
- o Improvement which have been made in test methods and methods of materials characterization, e.g., X-ray diffraction
- o Possibilities for using knowledge-based expert systems to aid selection of concrete materials
- o Growing interest in providing comprehensive data bases to support the construction process and facilitate failure analyses.

These factors are stimulating critical reviews of cement specifications. As a result, changes are likely to be made and it is the responsibility of cement and concrete technologists to ensure the changes are rational.

6. INCLUSION OF OPTIONAL PRESCRIPTIVE REQUIREMENTS IN PERFORMANCE SPECIFICATIONS

It has already been mentioned that prescriptive specifications pose barriers to innovation because they put unnecessary limits on the range of permitted compositions. On the other hand, prescriptive specifications can reduce the risks which might arise from an unrestricted range of compositions, particularly when there is uncertainty about the adequacy of the available performance tests. Prescriptive specifications also, frequently, have the benefit of depending on analyses which can be carried out more rapidly than performance tests.

Performance specifications are usually believed to encourage innovation since they specify precisely what a product is intended to do and how its ability to perform satisfactorily may be assessed. They do not put unnecessary restrictions on factors such as composition or source of origin. Unfortunately, performance specifications may be inadequate in the choice of criteria intended to evaluate performance, and the performance tests, particularly ones relating to durability, may take a long time to carry out. This is a serious problem if the product cannot be used until a test is completed.

Because of the shortcomings of each of the extreme types of specification, practicality suggests that cement specifications should have both prescriptive and performance components, as is usually the case. However, to reduce the barriers to innovation, it is desirable that the specification include a complete performance specification, thereby establishing a logical basis for development of prescriptive criteria which may be needed as alternative, optional, criteria of compliance with the specification. A scheme of this type can be represented as in Figure 1.

In this scheme, the first four steps, 1 through 4, are the formulation of the performance specification; the next three, 5 through 7, are the conversion of some or all of the performance criteria into optional prescriptive criteria for acceptance testing; and the last two, 8 and 9, represent the generation and feedback of information on performance-in-use to the standards-writing body. At present, the feedback mechanism is usually too weak to have much effect on the standards-writing process, except when very severe problems are recognized. However, the scheme presented here can provide a model upon which to base the development of future performance specifications for cements. In essence, it describes the approach being taken in the development of a performance specification for blended cements in ASTM Committee C-1 on Cements.

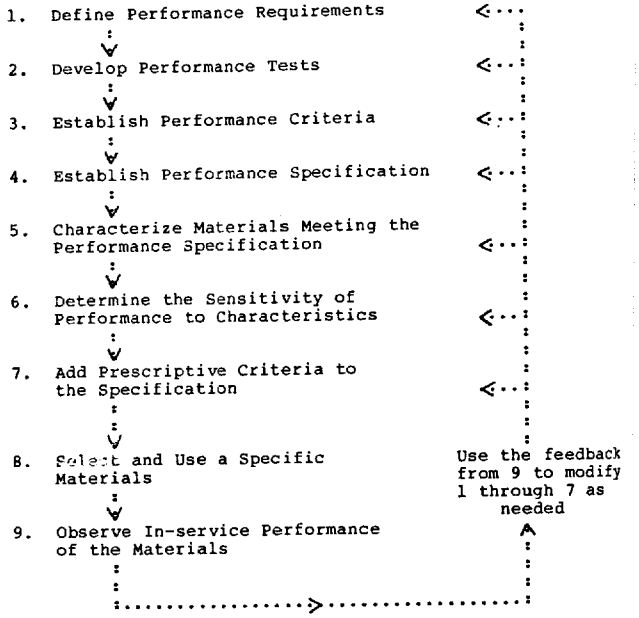

Figure 1. Scheme for Development of a Performance-Based Specification with Optional Prescriptive Criteria

7. THE ROLE OF A QUALITY ASSESSMENT SYSTEM IN THE EVOLUTIONARY DEVELOPMENT OF CEMENT STANDARDS

In many countries, a system for quality assessment of cement testing laboratories has been established. An example is the Cement and Concrete Reference Laboratory (CCRL) at the U.S. National Bureau of Standards (NBS). The CCRL is sponsored by ASTM Committees C-1 on Cements and C-9 on Concrete and Concrete Aggregates and managed for ASTM by NBS. Financial support for the CCRL is provided mostly by the fees charged for its services. The functions of the CCRL as related to cement [13], in decreasing order of importance, are:

i) Voluntary inspection of laboratories which use ASTM cement tests to identify, for the benefit of the laboratory managers, deviations from the correct procedures in the use of the standard tests;

ii) Provision of proficiency samples of cements for use by laboratories which wish to participate in an interlaboratory test program using ASTM cement tests; this gives laboratory managers a way of comparing their cement test results with those of other participants;

iii) Identification of problems with ASTM cement standards and bringing them to the attention of ASTM Committee C-1; and,

iv) Conduct of research needed for improvement of ASTM cement standards.

Quality assessment programs, such as the CCRL, can provide a powerful mechanism for improvement of cement standards through the feedback they provide on the effectiveness of the standards. For example, the databases they develop from interlaboratory cooperative test programs can be used for analysis of the variances in test results obtained using the standard tests; also, research on reasons for unexpectedly large variances can draw attention to problems with the standards. Because the quality assessment organization is constantly in touch with a large number of laboratories, it can develop an especially high sensitivity to the problems encountered; also if, as is the case with the CCRL, the organization is under the oversight of the standards committee, it can provide an effective means for feedback about the problems to the committee and its subcommittees. For these reasons concerning improvement of cement standards, it is strongly recommended that a high level of cooperation be maintained between quality assessment systems for cement testing laboratories and cement standards committees.

8. CEMENT STANDARDS OF THE FUTURE

In the future, increasing demands are likely to be placed on cement specifications. Because of the growing demands of some users for more information, there could be divergent needs for specifications between different types of users. Some users may only want the minimum assurance of quality while others may want precise data for use in predictive calculations and addition to databases. Further, depending on whether they are national or international, the specifications may have to meet the relatively narrow needs of individual countries, or the needs of groups of countries in different states of development. Nevertheless, it seems possible that a single specification could be prepared which could be used, in whole or in part, to meet the needs of different countries. Where the commodity nature of cements is emphasized, performance should be able to be defined in relatively precise terms, with lower and, possibly, upper limits being placed on acceptable performance for a given type of cement. In other cases, where there are many sophisticated users, emphasis might be placed on precise definition of the physical and chemical characteristics of a cement so that the user can apply his knowledge to predict how the cement will behave under diverse conditions.

It does not seem to be unrealistic to think in terms of prediction of the performance of a cement in concrete using computer-based mathematical models [7]. If and when this is achieved, the cement specification may require the manufacturer to transfer to the user data which is needed for predictive calculations.

Specifications sometimes show logical inconsistencies. To prevent this, the logic of each specification may, in the future, be subjected to computer analysis using techniques for standards analysis, synthesis, and expression [8, 9]. Also, recognizing the ever-present desire to use materials at close to their full potential, it is to be expected that computer-based systems to aid selection of the ingredients of concrete will be developed and standardized. An indication of this is that the American Concrete Institute (ACI) Committee 201 on Durability has established a subcommittee on knowledge-based expert systems. The National Bureau of Standards is working with the subcommittee in the development of a prototype expert system, DURCON [10], for selecting concretes for durability. The expert system is based on the ACI Guide to Durable Concrete [11]. Its development is proving valuable in drawing attention to gaps in the knowledge base available for selecting durable concrete. This should lead to more highly-focused research to improve our ability to make high quality decisions in the selection of cements and other building materials. It may provide a new incentive for specifications to include optional requirements for more information about cements to be transfered between manufacturer and user.

Overall, we must expect some cement specifications to develop as adjuncts to computer-integrated construction. This must include the establishment of integrated project information systems [12] whose lives will extend beyond those of the structures to which they apply. They must include the most relevant information about the materials used in the structures. In the case of concretes, it must be supposed that it will include information on the phase analysis and compositions of the cements and mineral admixtures used, together with the concrete mixture design. Thus, for reasons beyond those of performance specification, the future cement specification will probably require precise description of the cement in physical and chemical terms, whether or not explicit limits are set on physical and chemical properties.

9. CONCLUSIONS

As a result of a growing need of some users for more information, two distinct sets of needs seem to be developing for cement specifications. They are for specifications with which compliance can be shown by relatively simple tests based on, and logically traceable to, performance criteria; and specifications requiring the characterization of cements in the most precise chemical and physical terms so as to provide

the basis for prediction of performance using mathematical models. The growth in the power and availability of computers is likely to have several effects on specifications. For example, computers may be used for checking the logical consistency of specifications and for storing specified data about concrete materials used in individual construction projects. They may also employ specified data for predicting the performance of cements in concretes and mortars using mathematical models and for aiding decision-making on the selection of concrete materials using knowledge-based expert systems. Databases incorporating cement test results from quality assurance programs will aid the formulation of mathematical models and the development of expert systems. All of these foreseeable developments must be expected to cause further evolution of cement specifications.

10. REFERENCES

1. NMAB Report 361, The Status of Cement and Concrete R&D in the United States, National Materials Advisory Board, National Academy of Sciences, Washington DC, 1980, 105 pp.

2. Energy Consumption in Manufacturing, A Report to the Energy Policy Project of the Ford Foundation, Ballinger Publishing Co., Cambridge, MA, 1974, 610 pp.

3. B.E. Foster (ed.), Performance Concept in Buildings, Proceedings of the Joint RILEM-ASTM-CIB Symposium, NBS SP 361, 2 vol., National Bureau of Standards, Washington DC, 1972.

4. U.S. Trade Agreements Act of 1979, Statements of Administrative Action, Title IV - Technical Barriers to Trade (Standards), House Document No. 96-153, Part II, U.S. Government Printing Office, Washington, DC, 1979.

5. Circular A-119 (Revised), Federal Participation in the Development and Use of Voluntary Standards, Office of Management and Budget, Washington DC, October 26, 1982; see Federal Register, V. 47, No. 211, November 1, 1982, pp. 49497-49499.

6. G. Frohnsdorff, J.R. Clifton and P.W. Brown, History and Status of Standards Relating to Alkalies in Hydraulic Cements, in Cement Standards -- Evolution and Trends, ASTM STP 663, P.K. Mehta (ed.), American Society for Testing and Materials, Philadelphia, 1978, pp. 16-34.

7. G. Frohnsdorff and J.R. Clifton, A Review of Mathematical Modeling Applied to the Manufacture and Use of Cements, Cements Research Progress --1980, American Ceramic Society, 1981, pp. 279-298.

8. J.R. Harris and R.N. Wright, Organization of Building Standards: Systematic Techniques for Scope and Arrangement, Building Science Series Report BSS 136, National Bureau of Standards, Washington, DC, September 1981, 267 pp.

9. F.I. Stahl, R.N. Wright, S.J. Fenves and J.R. Harris, Expressing Standards for Computer-Aided Building Design, Computer Design, V. 15, 1983, pp. 329-334.

10. J.R. Clifton, B.C. Oltikar and S.K. Johnson, Development of DURCON, An Expert System for Durable Concrete; Part I, NBSIR 85-3186, National Bureau of Standards, Washington DC, July 1985, 18 pp.

11. Guide to Durable Concrete, J. American Concrete Institute, Detroit, 1977, pp. 573-609; also published as Section ACI 201.2R-77 in the Manual of Concrete Practice, Part 1, Materials and General Properties of Concrete.

12. R.N. Wright, Computers in Building -- A Strategy for Building Research, Building Research and Practice, V. 12, 1984, pp. 14-20.

13. J.H. Pielert, J.W. Haverfield, and P.A. Spellerberg, Application of CCRL Data in the Formulation of Precision Estimates for Selected Cement Standards, Cement, Concrete, and Aggregates, V. 7, Summer 1985, pp. 37-42.

E.B. ENTIN,
L.S. KLYUEVA, Cement Research Institute, Moscow, USSR

CEMENT QUALITY: KEY MEASURES AND EVALUATION TECHNIQUES

Specification of portland cement and its modifications is normally effected in conformity with the relevant ISO recommendations, national standards or SEV* standards (in the East European countries) as a set of widely agreed and practically significant performance measures, such as fineness of grinding, setting times, soundness, compressive strength and its development rate, and resistance to certain environments for special cements.

The most important figure of merit, from both engineering and cost-effectiveness viewpoints, is the 28-day compressive strength of a cement (specified in the USSR as the cement brand in kgf cm^{-2}) measured after 28 days of normal setting. However, this characteristic may vary for the same cement in wide range depending on the composition of standard test samples and the procedure of their preparation. Observing that cement is a semi-product, say, of concrete, it should be the principal, and more meaningful, requirement of cement testing techniques that there exist a strong correlation between the strength of cement and concrete.

The cement testing procedures, standardized in the industrial countries and widely used in the market and research practice, differ from each other by the sieve analysis of sand, composition and consistency of the mortar, and the size and consolidation of the test specimens.

A thorough review of the most widely used cement testing procedures has been reported by Dutron et al. /6/, another survey of relevant standards has been presented later by the World CEMBUREAU /7/. To date most countries have reconsidered their national standards for cement testing methods, but with no significant alterations. The Socialist countries have introduced a new standard SEV 3920-82: "Cement. Methods of testing for physical and mechanical properties" /8/.

In what follows we would like to examine certain general aspects of cement testing methodology.

Void content of sand and the composition of a standard cement mortar

Standard sands used in cement testing are normally natural quartz sands from a certain quarry for the country or a group of countries. Some national standards dictate the use of the so-called one-fraction sands with narrow sieve analyses of 0.15-0.60 mm in the USA, 0.50-0.90 mm in the USSR, 0.60-0.85 mm in Great Britain, and 0.10-0.30 mm in Japan. A common disadvantage of sands with narrow size distributions is an increased void content. For example, the void content of the one-fraction sand subject to the USSR cement testing standard amounts to 40-42% in a bulk state, 36-37% in a vibration consolidated state, and about 33% in a moist vibration consolidated state.

The structure of cement-sand mortars used in cement strength tests is consistent with a dense type in which the grains of sand are segregated by cement paste. The batch of cement paste naturally has to fill the intergrain voids and envelop sand grains thus separating them with a layer of paste.

Specimens of mortars prepared with the use of one-fraction sand are characterized by an increased macroporosity which depends not only on the void content of the sand but also on the composition of the standard mortar and, to a certain degree, on the consolidating means used. The standard mortar composition of the cement/sand ratio 1:3 should be recognized as unsatisfactory from the void-content spandpoint. Theoretical analysis of mortars conforming to the Soviet standard GOST 310.4-81 indicates that for a water/cement ratio of 0.40, the cement paste yield is hardly adequate to fill the voids

* SEV is the Russian acronium for the Council of Mutual Economic Assistance (CMEA or COMICON).

of the sand. For a collection of cements examined (compositionally different: straight and with admixtures of slag and flayash in proportions of 5, 12, and 20 wt. %), the coefficient showing excess of the cement paste varies predominantly between 1.11 and 1.13 growing as high as 1.14-1.16 for cements with an admixture of bergmeal and metallurgical sand. Accordingly, for cement test specimens by GOST 310.4-81, the macroporosity, defining the quality of the placement of the specimens, is about 4% /10/.

The unsatisfactory placement of specimens may degrade the normal profile of the strength versus W/C ratio dependence. At a constant W/C ratio, the strength of standard specimens can be increased by some technological means increasing the yield of cement paste. The increase in strength for such specimens will not be achieved in concretes made of these cements, that is, the correlation between the strength of cement in the mortar and concrete will be upset.

It is quite obvious, therefore, that a standard mortar should be prepared with such a ratio of cement and sand that would provide a warranted excess of the cement paste over the amount needed to fill the voids in the sand. For one-fraction sand mortars, the calculated macroporosity of specimens reduces in coming from 1:3 mortars to 1:2 mortars from 4-5% down to 1.5-2% (given isoplacticity of the mortars).

Comparison of variances for the ratio of concrete strength to cement strength, determined for isoplastic mortars with cement-sand proportions of 1:3, 1:2-3/4, 1:2-1/2, and 1:2 prepared at a constant cement consumption rate of 300 kg/m^3, indicates that the correlation of strength tests for cement and concrete improves for mortars of 1:2-1/2 and 1:2 proportionings (the level of significance for the variances being different is, respectively, 25, 25, 5, and 2.5%).

Thus, with one-fraction sand, one may achieve a considerable improvement of cement testing conditions by employing isoplastic mortars of 1:2-1/2 and 1:2 cement-sand ratios, which approach in their composition to the pastes of concrete mixes.

The recommendations of ISO and CMEA prescribe the use of sands with complex size distribution, the so-called three-fraction sands, of grain size measuring from 0.08 to 2.00 mm across. These sands exhibit a lower void content as compared with one-fraction sands (about 35% in a bulk state and 28% in a vibration consolidated state). The theoretical macroporosity of standard specimens in this case is small and amounts to about 0.7% for 1:3 composition mortars at a water/cement ratio of 0.50 /10/.

Comparison tests indicate, however, that the results may differ markedly if sands of a standard sieve analysis are from different sources. The respective tests with three-fraction sands of Polish and Czech origin, meeting the requirements of ISO and SEV recommendations, are summarized in Table 1. A perusal of the content of this table indicates that the 28-day strengths of specimens prepared with different-source sands and the same cement sample can differ from 4.0 to 11.7 MPa. It should be noted that these discrepances in compressive strength exceed both the laboratory and interlaboratory systematic errors resulted from using a standard sand of the same source.

Water/cement ratio and the consistency of standard mortars

Specification of cements as to the value of compressive strength is carried out by testing speciments of cement mortars prepared either with a constant water/cement ratio (ISO and CMEA recommendations, polyfractional sand procedure, national standards of Great Britain, Japan and some other countries) or with a constant consistency of the mortar (national standards of the USSR and the USA).

We have mentioned already that the qua-

Table 1

Effect of Three-Fraction Sands on Cement Strength Tests

Test place	No. of specim's	Sand source	Compressive strength, MPa for setting age (days) indicated			
			1	3	7	28
USSR	51	Poland	4.5	11.3	19.0	31.5
		CSSR	5.2	14.0	22.3	37.1
Hungary	26	Poland	6.0	13.0	21.0	39.0
		CSSR	9.0	19.0	28.0	43.0
Bulgaria	14	Poland	4.6	12.8	21.3	32.9
		CSSR	7.0	18.6	30.3	44.6

Table 2

Correlation Coefficients of 28-day Strength Tests by GOST 310.4-81 and SEV 3920-82

Test place	GOST vs SEV with three fraction sands from		Within SEV method on Polish and Czech. 3-fraction sands
	Poland	Czechoslovakia	
USSR	0.86	0.87	0.95
Hungary	0.78	0.83	
Bulgaria	0.88	0.80	

lity of a cement manifests itself in the final run by the cement behavior in concrete. Proceeding from this standpoint, two cements may be recognized as having identical quality if, given equal cement requirement and flowability of concrete mixes, they result in concretes of equal strength. Experience suggests, however, that these conditions of quality testing are impossible to meet if cement strength tests are carried out at a constant W/C ratio without taking account of mortar's flowability.

Constant W/C ratio tests are incapable of adequately revealing high engineering properties of cements with enhanced plasticity or decreased water requirements. These cements, however, are advantageous, if correctly specified, in that they open up the way for cement savings since a given placeability can be achieved at a lower W/C ratio than for cements of the same brand (28-day compressive strength) but unsatisfatory plasticity. From the viewpoint of cement quality testing, it is immaterial whether the difference in cement requirement occurred in manufacturing equally strong concretes of a given placeability has been caused by reduced activity or increased water requirement and unsatisfatory plasticity.

In cement specification, water requirements are estimated (simultaneously giving an indirect indication of rheological properties) with the normal consistency index of cement paste. Statistical processing of the data covering Soviet industrial cements suggests that there exists an approximately linear dependence between the normal consistency index and the W/C ratio of constant consistency mortars (Fig. 1), the correlation coefficient being 0.94. At an equal water requirement estimated with the normal consistency index, individual cements may, however, considerably differ in the W/C ratio of constant consistency mortar. Nonetheless, even with account of this remark, from the standpoint of cement behavior in concrete, the quality estimate is more objective in the case of tests with a constant mortar consistency rather than with a constant W/C ratio.

A constant consistency of mortar is not of that much significance in testing purely clinker cements which are characterized by close water requirements, but it is significant for cements with admixtures whose production is increasing by many cement producers.

Correlation of standard strength extimates from one- and three-fraction sand tests

Bulgaria, Hungary, and the Soviet Union carried out comparative tests of national cements by two methods as prescribed in the CMEA standard SEV 3920-82 and in the Soviet standard GOST 310.4-81. In the tests by GOST 310.4-81, all the countries used one-fraction sand in conformity with another

Table 3

Comparative Tests of Cements /11, 12/

Test place; method; cement	Participants (n) and reproducibility	Specific surface cm^2/g		Normal consistency,%		Initial set, min		Compressive strength, MPa for setting age (days) indicated											
								Laboratory (L)				Interlaboratory (IL)				International			
		L	IL	L	IL	L	IL	1	2	7	28	1	2	7	28	1	2	7	28
USSR;	n	10	19	10	19	10	19	10	10	10	10	19	19	19	19				
GOST	x	3428	3501	25,53	23,87	168	164	18,4	34,4*	45,6	57,8	14,7	29,2*	39,2	50,5				
310,4-81;	s	228	334	0,4	0,9	43,3	39,2	0,8	3,1	2,8	3,1	3,6	3,5	3,8	5,3				
portland	v, %	6,7	9,5	1,7	3,8	25,7	23,8	4,5	9,2	6,1	5,3	24,4	12,0	9,8	10,4				
cem,																			
France,	n		56		57		60	25	25	25	25	53	57	57	58	114	122	128	126
under	x		4253		30,2		150	18,1	28,2	40,0	53,2	18,1	28,2	40	53,4	18,1	28,2	39,9	52,9
CERILH	s		80		1,3		21	0,3	0,4	0,5	0,8	1,5	1,1	1,5	2,0	1,5	1,5	1,9	2,6
1982/83	v, %		1,87		4,33		14,0	1,85	1,35	1,21	1,43	8,03	3,96	3,71	3,66	8,3	5,32	4,71	4,86
ISO R 679,																			
C,P,A,																			
class 55-R																			

Note (*) 3-day compressive strength

Table 4

Physical Characteristics of Cements with Normal and False Sets

Portland cement producer	Setting type	NC, %	Setting test (hr-min)		W/C	Cone spread, mm	Compressive strength, MPa for setting age (days) indicated				
			beg.	end			normal setting				steam cure
							1	3	7	28	1
Brjansk cement plant	normal	24.00	2-35	4-30	0.36	113	10.8	22.7	36.5	48.0	26.2
	false type 1	27.25	2-30	4-35	0.38	112	11.5	25.7	37.8	51.4	26.2
Punane Kunda works	normal	25.25	2-50	4-50	0.37	113	17.0	31.4	39.7	50.0	34.5
	false type 2	26.50	2-45	4-40	0.40	113	12.5	25.0	35.4	47.1	29.7

Soviet standard GOST 6139-78. The tests by SEV 3920-82 were carried out with three-fraction sands from Poland and Czechoslovakia. These sands conformed to the standard but somewhat differed from one another by the surface morphology of the grains and the voids content (35% and 38% for Polish and Czech sands, respectively).

The correlation coefficients for the results of two testing methods are summarized in Table 2. As can be seen, the values of the coefficient are rather high (from 0.78 to 0.88 for international data), though somewhat lower than when one method of testing was employed on two different sands. However, the absolute value of the difference in the test results by two different methods does not exceed the test data difference in one method but with different sands. This allowed the following approximate relationship to be established between the classes of strength resulting from the two methods:

60, 55, 50, 40, and 30 MPa (GOST 310.4-81, 1-fraction sand)

55, 50, 45, 35, and 25 MPa (SEV 3920-82, 3-fraction sand)

Accordingly, the standard SEV 3920-82 "Cement. Methods of testing for physical and mechanical properties", superseding RS 138-73, allows for equal use of methods with one- and three-fraction sands. From January 1, 1985, Bulgaria, Hungary, Poland, and the Soviet Union have introduced this standard into commercial, industrial, and scientific spheres.

Assessing accuracy of cement testing methods

This purpose is served by systematically run comparison interlaboratory tests both within certain countris and on an international scale.

The comparative test data presented in Table 3 indicate that in general the physico-mechanical testing techniques are inaccurate, and the reason for this we see as follows. In the process of preparation and setting of specimens, a number of environmental and test parameters, such as setting temperature, stiffening amplitude, mass, etc, varies, although within the narrow limits specified by the standard, yet at random. Accordingly, the error of the test is in considerable degree due to the stochastic nature of the test procedure rather than to the properties of cement being evaluated.

False setting

False set relates to the properties of cement which affect the specification test results in a random way.

Abnomal phenomena at early setting age intervals may be broadly categorized into false sets of type 1 and 2 (respectively

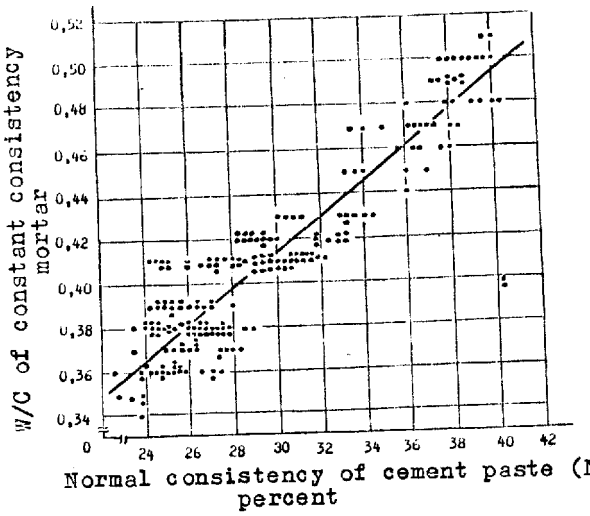

Fig. 1. Water/cement ratio of constant consistency mortar versus water requirement of cements. r = 0.94 for W/C = 0,008 (NC+21,6)

reflecting complete or partial premature loss of plasticity after mixing), and characterized by a trend to quick set and the quick set proper.

Transition from normal setting to false setting and from one false set type to the other is connected directly or indirectly with the change in the forms of gypsum in the cement. The trend to quick set, which manifests itself in degrading the initial set, and the quick set proper may be traced to both the lack of gypsum for setting control and a deep dehydration of gypsum in cement grinding. With the existing technology of cement manufacturing involving bihydrated gypsum as set retarder, the false set of 1 or 2 type and the trend to quick set are typical of industrial cements.

It is important to note that some cements exhibit both types of false set, whereas other cements give no evidence of type 1. Whether one or the other type of false set predominates depends primarily on the alkali content in the clinker /13/. With a moderate alkali content of a clinker (about up to 0.7% expressed as the Na_2O equivalent of the total alkalies), the cement having been heated in the mill to 100-150°C can exhibit both types of false set. With a higher alkali percentage of clinker than indicated, cements exhibit the false set of type 2 exclusively. An increase in temperature in the mill up to 170°C inescapably results in quick set properties.

The contact of cement with the environmental moisture in handling, shipment and storage may cause rehydration of the gypsum dehydrated in grinding, thereby eliminating the false set of type 1. The false set of type 2 is harder to eliminate.

Experience also exists on false set cases in shipment and storage of cements with initially normal setting properties. This is connected with the fact that the normal setting cements containing, as fresh from manufacturing, only bihydrate gypsum acquire in storage semihydrate gypsum whose content can vary both sides, increasing and decreasing. The appearance of semihydrate gypsum in storage in air may be attributed to surfase hydration in which both ambient moisture and gypsum crystal water take part.

The aforementioned variations of cement rheology that occur both in cement manufacturing and storage cast a shadow of randomness onto the specification of some cement performance measures, such as the normal consistency index, setting time, strength development rates, etc.

Choice of cements for steam curing

The methods of accelerated testing are well treated in /6/ devoted to the analysis of cement test methods. The lack of sufficient correlation between the strength test data at normal setting and various accelerated test methods bars the standartization of an accelerated test method. At the same time, a complete refusal of the common testing methods with 28-day compressive strength in favor of an accelerated test procedure would be undeserable due to a considerable proportion of cement being consumed in concretes not subjected to steam curing not to mention a need for rewriting the respective documentation involved in civil engineering procedures.

Summary

The consideration of cement testing methods in compliance with the Soviet State standard GOST 310.4-81 and the ISO and CMEA recommendations oriented to the use of sands which differ in sieve analysis indicates that all the methods are not free from shortcomings. The use of one-fraction sand inflicts a substantial shortcoming in the form of increased macroporosity of the specimens due to a shortage of cement paste which compounds the effect of random factors on the repeatability of the particular test method. With three-fraction sand, the reproducibility of the test method somewhat improves, but the test methods fail to take account of various water requirements of tested cements. Another shortcoming of the latter approach is its sensitivity to the sand, which is connected with the sand grain surface morphology and inconsistency of size distributions, in polyfractional sands.

An improvement of cement testing methods should be sought on the lines of using sands with a narrow sieve analysis and employing isoplastic mortars with a cement/sand ratio of about 1:2. The development of such a method and its promotion as a widely adopted approach is a challenge in the cement testing field. Achievement of this objective would considerably improve the correlation of strength test data from mortars and concretes.

REFERENCES

1. Organisation Internationale de Standartisation. Methode d'essais mechanique des ciments. Recommendation ISO R679, 1968.
2. Recommendation for standartization SEV RS 138-73 "Cements. Methods of physical and mechanical testing". Berlin, 1972.
3. The USSR State standard GOST 310.4-81 "Cements. Bending and compressive strength testing methods".
4. British Standard BS 4550: 1978 "Methods of Cement Testing".
5. ASTM C 109-80 "Cement hydraulic mortars". Methods of compressive strength testing with 2-in. specimens"
6. P. Dutron, K. Bang Peterson, S. Cral: Modern methods of mechanical tests for cement. In: The 4th International Congress on the Chemistry of Cement (Stroyizdat, Moscow 1976) in Russian.
7. Cement Standards of the World CEMBUREAU. The European Cement Association Library. Paris 1980.
8. Standard SEV 3920-82 "Cement. Methods of testing of physical and mechanical properties". The permanent CMEA committee on cooperation in standartization. Poland 1982.
9. USSR standard GOST 6139-78 "Normal sand for cement testing. Specification".
10. Z.B. Entin, L.S. Klyueva: in: The 4th International congress on the chemistry of cement (Stroyizdat, Moscow 1976) in Russian.
11. Z.B. Entin, Oleinikova, G.A. Rudneva, T.V. Kuznetsova: Estimation of accuracy for physico-mechanical cement tests. Tsement No. 5 (1978).
12. Centre d'Etudes at de Recherches de l'Industrie des Liants Hydrauliques. Essais Interlaboratores 1982/1983. Rapport General. Paris 1984.
13. Z.B. Entin, L.S. Klyueva: Liquid phase in anomalous setting of cements. Theses to 4th All-Union Conference on Cement Chemistry and Technology (Moscow 1982).

I. Odler, S. Abdul-Maula and U. Hennicke. Technical University Clausthal, D-3392 Clausthal-Zellerfeld, Federal Republic of Germany.

A NEW METHOD FOR DETERMINATION OF CEMENT SETTING TIME

For cement setting time determination the Vicat needle penetration method (1,2) and its numerous modifications (3) are most widely used. In addition to that the Gillmore method has been widely accepted in the USA (4). All these methods are arbitrary ones as the obtained results depend-in addition to the setting characteristics of the studied binder-also on the employed initial water-solid ratio, the diameter of the needle, the weight applied on the needle and other experimental factors.

In our work on acoustic properties of cementitious materials we observed consistently a very low initial acoustic conductivity of such systems right after mixing, which increased rather suddenly by several orders of magnitude after a period of time. We assumed, that this sudden increase in acoustic conductivity may be related to the setting of the system. To test this hypothesis we performed the tests reported.

EXPERIMENTAL

The set-up of the equipment employed is shown in Fig. 1. Electric impulses of preset frequency and intensity are produced in an impuls generator. They are converted into an acoustic signal of constant intensity using an ultrasonic generator equiped with piezoelectric transformers made from barium titanate. The fresh cement paste or mortar is placed between the generator and sensor. In the latter one the acoustic signal, which passed the paste or mortar, is converted again into an electric signal. The amplitude of the obtained signal, which indicates the fraction of acoustic energy not absorbed by the sample, is registered by the aid of an analog-digital-convertor. The data obtained this way are stored in a computer, and may be depicted graphically using a plotter.

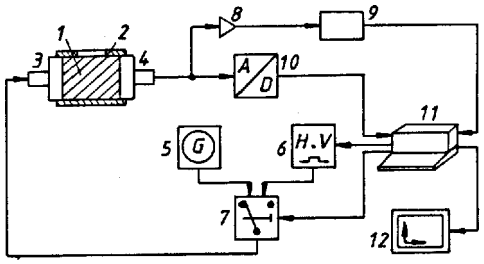

1. binder sample
2. sample holder
3. ultrasound generator
4. ultrasound sensor
5. frequency generator
6. impuls generator
7. switcher
8. amplyfier
9. digital chronometer
10. analog-digital-convertor
11. computer
12. plotter

FIG. 1: Set-up of the experimental equipment

RESULTS

To compare our acoustic data with results of other methods the setting time of a single portland cement paste (normal consistency ASTM C 187, DIN 1164 T 5) was determined using the following approaches:

1. Vicat method using a needle Ø = 1,13 mm and a load of 300 g (1,2)
2. Same - with a needle Ø = 2 mm
3. Same - with a needle Ø = 3 mm
4. Gillmore method (4)
5. Acoustic method using a frequency of 75 KHz. The gap width between generator and sensor was varied between 20 and 40 mm
6. Acoustic method using a frequenc of 160 KHz and a gap width of 20 mm

In Fig. 2a the distance from the bottom at which the needle became stuck in the paste is shown as function of time for all three needles employed. Expectedly, the time at which the needle ceased to penetrate to the bottom, just as the time at which it ceased to penetrate into the paste, shifted to shorter times with increasing diameter of the needle. The beginning and end of setting as determined by the Gillmore method is shown in the Figure with arrows designated G_b (beginning) and G_e (end).

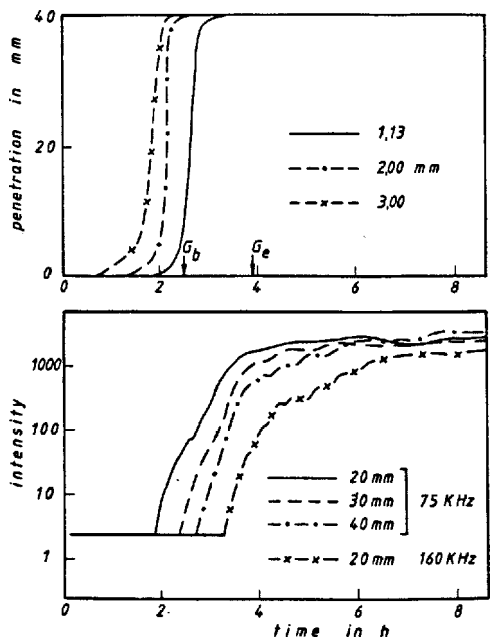

FIG 2: Setting data of an OPC obtained with
a) the Vicat and Gillmore methods and
b) the acoustic method

Fig. 2b shows the intensity of the measured acoustic signal as function of time. The time at which the signal became detectable increased with increasing

I. Odler, S. Abdul-Maula and U. Hennicke. Technical University Clausthal, D-3392 Clausthal-Zellerfeld, Federal Republic of Germany.

distance between the sonic generator and sensor and with its increasing frequency. It can be seen that the "setting time" determined acoustically lied within the range of setting time values determined by the classical methods, used for comparison. In subsequent experiments a constant frequency of 75 KHz and a gap between the generator and sensor of 20 mm were maintained. The data obtained this way were compared with those determined with the Vicat method using a 1,13 mm needle.

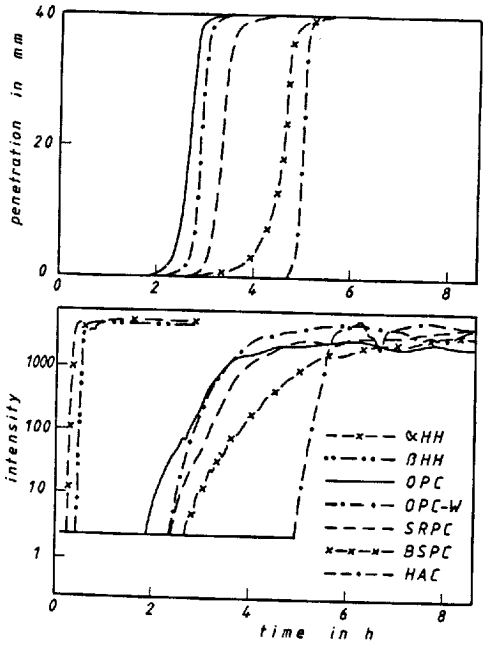

FIG. 3: Setting data for different kinds of inorganic binders a) Vicat method b) acoustic method

Fig. 3 shows data obtained on a series of various cements i. e. an ordinary portland cement (OPC), a "white" portland cement with no Fe_2O_3 (OPC - W), a "sulphate resistant" portland cement (ASTM type V) with increased Fe_2O_3 content (SRPC), a blast furnance slag portland cement (BSPC), a high alumina cement (HAC) and on two types of plaster of Paris (α HH and β HH). It can be seen that the orders in which the Vicat needle ceased to penetrate to the bottom and that in which the acoustic conductivity started to increase were identical.

Fig. 4 shows data obtained on our OPC cement with different chemical admixtures added. It appears that a setting acceleration brought about by an addition of $CaCl_2$ could be detected with both methods just as a retardation brought about by ZnO or sucrose.

Fig. 5 shows the effect of variations of the water-cement ratio on the obtained data. It appears, that the Vicat method is distinctly more sensitive to such variations than the acoustic one.

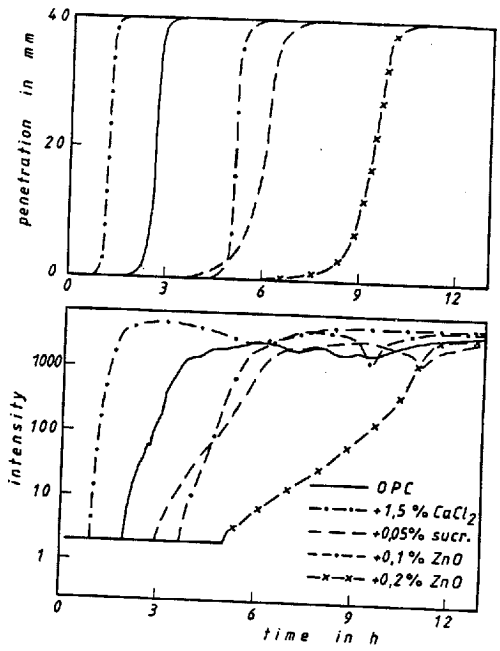

FIG. 4: Effect of chemical admixtures on setting a) Vicat method b) acoustic method

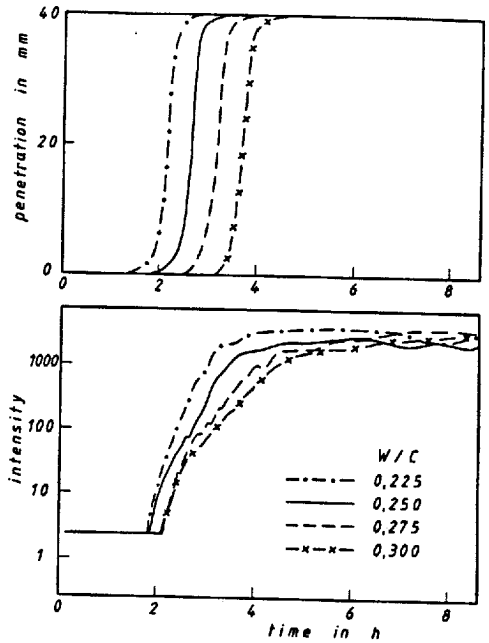

FIG. 5: Effect of water-solid ratio variation on setting a) Vicat method b) acoustic method

Finally, Fig. 6 demonstrates the possibility of the use of the acoustic method also in systems for which penetration methods are not suitable. It can be seen that the "setting time" of a pure cement paste was identical with that of a mortar with quartz sand made from the same cement with the same w/s (0.3). A mortar with a higher w/s(0.5)exhibited a retarded setting time; the measured setting time remained virtually unchanged if either quartz or expanded perlite were added as aggregate. An addition of glass fibers resulted in a retardation of setting whose origin is not obvious. Finally, a very significant retardation of setting was determined in a cement - pine wood chip blend, apparently due to the carbohydrate compounds present in the wood mass.

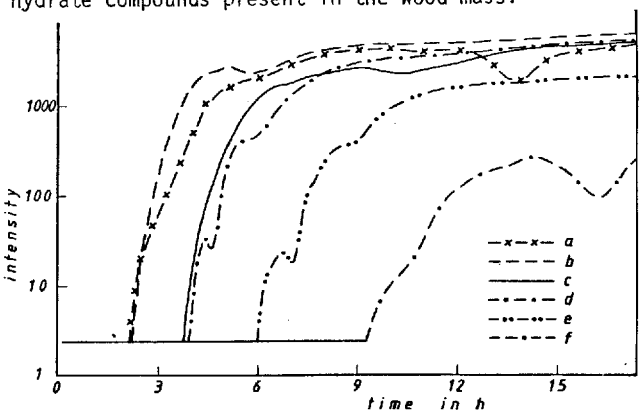

a. Paste OPC w/c 0,3 - d. Mortar OPC:Perlite 10:1 w/c 0,5
b. Mortar OPC:Sand 1:1 w/c 0,3 e. Mortar OPC:Glass Fibers10:1 w/c 0,5
c. Mortar OPC:Sand 1:3 w/c 0,5 f. Mortar OPC:Wood Chips10:1 w/c 0,5

FIG. 6: Setting characteristics of pastes and mortars made from same cement using different aggregates (acoustic method)

DISCUSSION

From the obtained data it becomes obvious, that the increase of acoustic conductivity observed in cementitious systems is due to the setting of the present binder. The phenomenon appears to be independent on the quality of the binder employed as an increase, of acoustic conductivity at the time of setting can be detected even if binders of different chemical nature are employed.

The origin of the increase of acoustic conductivity is not obvious at this time. We assume, that the solid framework formed in the paste at the time of setting causes - in addition to the ceasing of plastic deformability of the system - also its increased acoustic conductivity.

Just like in other methods, the exact setting time determined by our new method depends, to a certain degree, also on the conditions of testing. We assume that the obtained variations are due to different amounts of acoustic energy lost if signals of different frequency are employed or if the distance to be passed by the acoustic signal varies. It is of importance, however, that variations of setting time,such as those due to binder quality or to the effect of chemical additions, can be well detected acoustically if constant conditions of testing are employed. On the other hand the method is less sensitive to variations of the water-solid ratio which affect significantly the rheology of the cement paste and thus the outcome of measurements made with a penetrations method.

A special advantage of our new method is the possibility of its use in systems for which penetration methods are not, or only little suitable. Our experience shows that the acoustic method may be succesfully employed not only in ordinary cement pastes and mortars but even in glass or organic fibers or wood chips reinforced systems, not suitable for testing by any penetration method.

Our experiments were limited, so far, to systems that could be placed in a gap of maximum 40 mm, due to a limited output of our sonic generator. We believe, however, that the method may be employed even for concrete mixes, if the intensity of the entering acoustic signal will be increased appropriately.

CONCLUSIONS

A new method for setting time determination of cement pastes or mortars was developed in which the setting is determined on the basis of a sudden increase of acoustic conductivity of the system at the time of setting. The method is insensitive to the nature of the binder employed and little sensitive to variations in the rheology of the mix. The method may be employed also in mixes in which penetration methods cannot be employed due to the presence of foreign components, such as fibers, light weight aggregates, or wood chips.

REFERENCES

1. ASTM C 191-82
Test Method for Time of Setting of Hydraulic Cement by Vicat Needle.

2. DIN 1164 T 5
Test Method for Time of Setting of Hydraulic Cement by Vicat Needle (in German).

3. M. Maultzsch. Needle apparatus has existed for 100 years (in German). Zement-Kalk-Gips 36, 558-581 (1983).

4. ASTM C 266-77
Test Method for Time of Setting of Hydraulic Cement by Gillmore Needles.

G.GIACCIO (CIC-LEMIT) and R. ZERBINO (CONICET) - Argentina

FACTORS AFFECTING CEMENT PASTE-AGGREGATE BOND

P

1. INTRODUCTION

There is a general concense about the influence of cement paste-aggregate bond on the behaviour of concrete. It is recognized that the transition zone (interface) is the weakest link of the composite material and the one which directly affects mechanical properties and durability. In this way, the interest in factors that affect cement paste-aggregate bond, continuosly increases.

Adherence is partly due to mechanical interlocking produced by aggregate irregularities and to van der Waals forces which cause the adhesion between aggregates and cement hydration products. Besides there may be some slow chemical reactions that contribute to bond development.

This paper analyzes the influence of many factors on bond strength by mechanical tests. To do this, pastes with different water-cement ratios, chemical admixtures (a water reducing and two superplasticizers additives), expansive addition, and fly ash incorporation were used. Four types of rocks with different surface texture were included. Test age was also considered as a variable.

This study was complemented by SEM observations performed on fracture surfaces, for a qualitative analysis of interfaces and cement pastes.

2. EXPERIENCES

2.1 Test method:

The aggregate-hydrated cement paste bond strength was evaluated by flexure tests with mid-point loading system. Figure 1 shows a scheme of specimens.In every case, modulus of rupture of the corresponding cement paste were measured. Samples were cured in water until testing age.

A deformation-controlled testing machine was employed with a rate of 2 mm/minute.

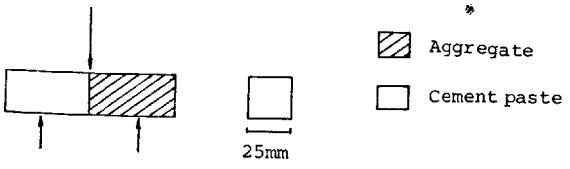

Figure 1: Cement paste-aggregate specimen and loading scheme.

2.2 Discussion of results:

Aggregate surface texture is one of the most important factors that affects bond strength, as it causes mechanical interlocking.

Meanwhile, fracture is preferentially produced at the interface in smooth surfaces, crack path can also develop through the paste and even sometimes, including aggregate grains in rough or broken surfaces.

Aggregates usually employed in concrete elaboration, present different surface texture, due to their porosity, grain size, cleavage plans, hardness, and also external factors as weathering.

Two textures for each aggregate were studied: natural fractured and swan surfaces. Table 1 shows the relationship Interface modulus of rupture (If_r) / Cement paste modulus of rupture (Pf_r). Bond strength is lower than paste strength, ranging from 20 to 62 %. It must be noted that fractured surfaces have always greater adherence than sawn surfaces.

Table 1. Influence of surface texture on aggregate-cement paste bond strength.(2)

Rock	Interface bond strength / Cement paste strength		sawn / fractured
	fractured surface	sawn surface	
SANDSTONE	0.40	0.32	0.80
MARBLE A	0.30	0.20	0.67
GRANITE B	0.46	0.20	0.43
BASALT	0.62	0.20	0.32

w/c ratio=0,40. Age;28 days.Paste strength= 12 MPa.

Although sawn surfaces are similar, when comparing many aggregates, their bond strength can be very different. In this case, the high bond developed by sand stone may be principally attributed to rock porosity. At the same time, variations produced by changes in surface texture for the same aggregate can be higher than those due to changes in aggregate type. Then, it becomes difficult to compare petrography influence as their effects are usually superposed.

To study other factors affecting bond strength, a unique surface texture was adopted. Marble or granitic aggregates were used with a grounded surface obtained by sanded.

Figure 2 shows the influence of water-cement ratio on bond strength. It appears that If_r variability is lightly lower than Pf_r; the relationship If_r/Pf_r trends to increase with high w/c ratios.

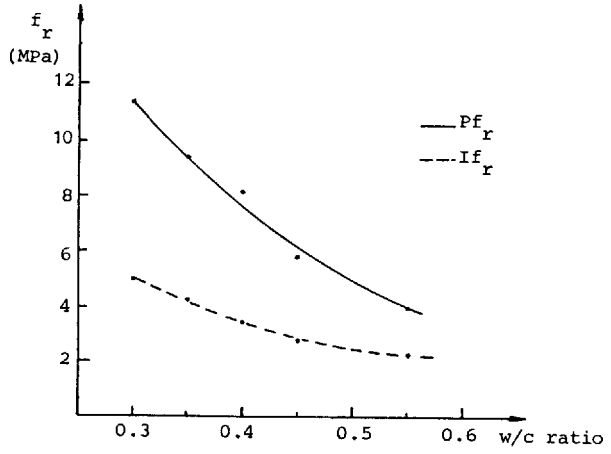

Figure 2: Influence of water-cement ratio on bond strength (If_r) and cement paste modulus of fupture(Pf_r)

If_r/Pf_r relationship is also modified by cement strength evolution rate. Generally strength gain takes place more slowly in interface than in cement paste. Table 2 shows the effect of age on bond and paste strength employing marble and granite, and a high early strength cement. It can be seen the significative differential evolution of interface and cement paste.

For normal cement or specially low heat cement the effect of age on If_r/Pf_r relationship is smaller.

If_r / Pf_r ratio prcbably changes because voids volume and size at the interface are larger than into the cement paste,(1) with time these voids are progressively filled, and, consequently, If_r / Pf_r ratio is modified.

Table 2. Effect of age on bond and paste strength.

Age (days)	Modulus of rupture (MPa) Interface: If_r Marble A	Granite A	Paste: Pf_r	If_r / Pf_r Marble A	Granite A
10	3.4	---	11.0	0.31	---
28	4.1	3.7	12.0	0.34	0.31
90	5.8	5.7	12.0	0.48	0.48
180	6.3	6.4	12.3	0.51	0.52

Grounded surfaces. w/c ratio = 0.40
Cement: C_3S:56%, C_2S:19%, C_3A:0.2%, C_4AF:15.8%.

To study influence of admixtures and additions series with w/c: 0.30 ahd 0.40 were made. Pastes included different types of superplasticizers (Naphtalene and Melamine basis, water reducing (lignosulfonate basis) expansive and fly ash addition.

Table 3 shows the obtained results of bond and paste modulus of rupture. As it can be seen some admixtures incorporate important air quantities as a secondary effect.

Air incorporation affects in different grade inter - faces and bulk paste behaviour. Pf_r decreases in a higher percentage than If_r by air presence, being the relationship If_r/Pf_r strongly increased.

Comparing NS with NSA (Table 3), air incorporation re duced paste strength in 41% and 26% at 7 and 60 days respectively; bond strength was only 10% lower at 7 days and it remains the same at 60 days.

All these experiences were made with vertical inter- faces, the effects of air bubbles could be different on horizontal interfaces.

Superplasticizers did not modify significatively If_r and Pf_r. Their principal effects appear by means of air incorporation. Naphtalene superplasticizer which did not entrained air gave almost the same If_r. Pf_r is higher at early ages probably due to the better dispersion of cement particles.

Melamine superplasticizer (MS) produced a small re- duction of strength at 7 days. However, it can be seen that at 60 days there is a little increment in bond strength for every superplasticizer.

Generally interfaces marble B-cement paste are slight ly weaker than granite's B.

The presence of this water reducing admixture, (which also incorporates air) produced higher If_r but smaller Pf_r. It appears again that interface is less sensi - tive than bulk paste, to air presence.

A modified behaviour was observed when fly ash was incorporated. Paste with 20% weight replacement of fly ash (Class F) finer than cement, was used. It may be seen that at 7 days paste strength decreased but bond strength wasn't affected. At 60 days If_r with fly ash is higher and Pf_r is still a bit small. Then If_r/Pf_r relationship is increased for fly ash blends, being the effect more evident at advanced ages.

Strength gain (7 to 60 days) is also more pronunciated at interfaces: while series $C_{0.4}$ increased bond and paste strength 50 and 37% respectively, this evolution for FA series was 100 and 61%. (Table 3).

It must be mentioned that there is a qualitative im- provement of interface, as fracture in 60 days FA bond tests was always through the paste nearly interface while for the corresponding control series($C_{0.4}$) only a small amount of paste remains adhered on the aggre- gate surface.

Fly ash reaction contributes to develop bond strength filling voids, that are originally larger at inter - face, and reducing large $Ca(OH)_2$ crystals concentra- tion. These crystals have lower adhesion capacity(van der Waals forces) and apport preferred cleavage plans.

SEM micrograph (Figure 3) shows a fly ash-cement paste -granite aggregate interface.Oriented $Ca(OH)_2$ crystals are clearly distinguished.Big crystals are often found close to interfaces probably due to a greater space for growth.

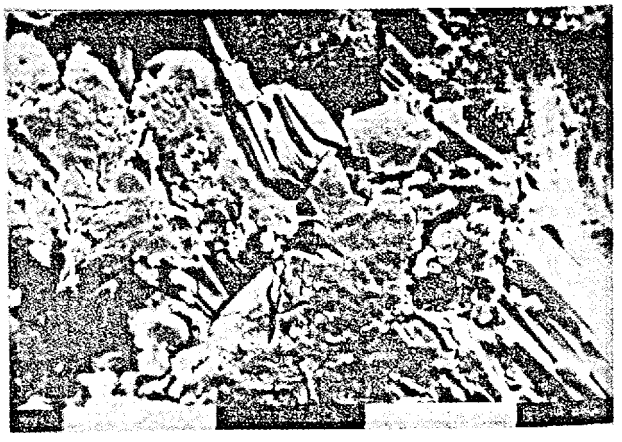

Figure 3: SEM micrograph of fly ash-cement paste-gran- ite B interface, view from aggregate(split along inter_ face). (Age: 60 days). Bar = 10 m. X 2700.

Table 3. Influence of additions or chemical admixtures on bond and cement paste strength.

Addition or chemical admixtures	Symbol	w/c	Air incorpo_ ration	Rock	Modulus of rupture (MPa) Interface: If_r 7 days	60 days	Paste: Pf_r 7 days	60 days	If_r / Pf_r 7 days	60 days
None	$C_{0.3}$	0.3	no	g	4.9	5.9	11.0	12.3	0.44	0.48
				m	4.6	5.4			0.42	0.44
Superplasticizer Naphtalene	NS		no	g	5.0	6.4	12.0	12.5	0.42	0.51
	NSA		yes	g	4.5	6.4	7.1	9.2	0.63	0.70
				m	3.8	6.5			0.54	0.71
Superplasticizer Melamine	MS		no	g	4.0	6.5	10.0	12.8	0.40	0.51
				m	4.0	6.0			0.40	0.47
None	$C_{0.4}$	0.4	no	g	3.6	5.4	8.4	11.5	0.43	0.47
Water reducing	WRA		yes	g	4.2	5.7	6.3	7.8	0.67	0.73
Fly ash(4200cm^2/g)	FA		no	g	3.4	6.8	6.7	10.8	0.51	0.63
Expansive	E		no	g	2.9	6.3	8.8	11.6	0.33	0.54

Rocks: Granite B(g), Marble B(m). Cement: 2860 cm^2/g. (C_3S:30%, C_2S:41%, C_3A:9.5%, C_4AF:10.9%).

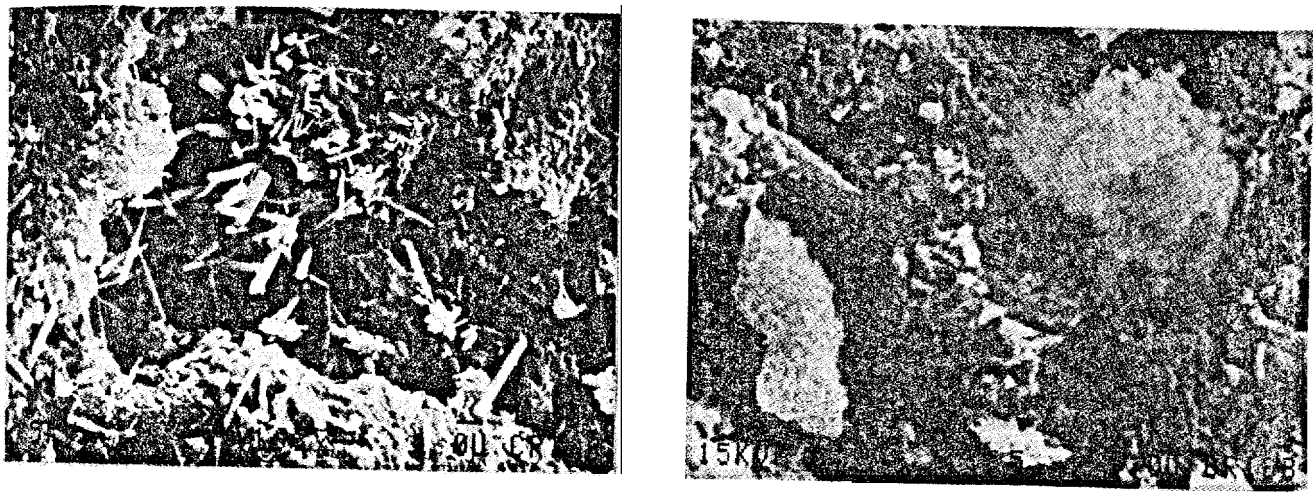

Figure 4: SEM micrographs of cement paste with expansive addition. (age: 100 days). a)(left):interface view from aggregate (split along interface). X4000. b)(right): bulk paste. X6000.

Paste incorporating 12% cement weight expansive addition was mixed. Expansion of bars inmersed continuosly in water were 44 /m/m and 54 /m/m at 7 and 60 days respectively. Pf_r was always similar to control paste ($C_{0.4}$). (Specimens had free expansion conditions)

Bond reduction at early ages and bond increment at advanced ages were found. Then If_r/Pf_r relationship had a strong evolution with time.

Figures 4.a and 4.b show respectively interface and interior paste characteristics of series including expansive addition. Bulk paste appears very compact, meanwhile bigger voids and crystals are observed at interface.

3. CONCLUSIONS

The principal conclusions extracted from these experiences can be summarized as follows:

- Surface texture is one of the most important factors affecting bond strength, and consequently If_r/Pf_r relationship. Rough surfaces had always higher bond than sawn surfaces. For practical purposes physical aspects, as mechanical interlocking, have more influence than petrographic aggregate characteristics.
- If_r/Pf_r ratio is modified by maturity. Interface bond develops more slowly than paste strength.Cement with high hydration rate showed clearly this phenomenon.
- It is confirmed that bond is less sensitive to w/c ratio than paste strength(mainly with high w/c ratio)
- Air presence affects in different magnitude interface and paste strength. While there is a substantial decrease in paste modulus of rupture (Pf_r), the effects on bond are very small.
- Fly ash incorporation modified If_r/Pf_r relationship. Fly ash reaction (60 days) produced an increase in bond (26%) while paste strength was still a bit lower than control (6%), and also a different crack path was observed.
- There weren't found important changes on cement paste-aggregate bond produced by the water reducing agent and the superplasticizers. Only melamine superplasticizer reduced stregth at 7 days. Nevertheless paste strength can be affected by air entrainment caused by these admixtures.
- Expansive addition, in this dosage, did not affect paste strength, however it modified bond development. It reduced bond at early ages and increased bond at advanced ages.

4. REFERENCES

(1). MASO,J.C.(1980) La liaison entre les granulats et la pate de ciment hydraté, VII Int.Cong.on the Chem.of cement.Vol 1. París.

(2). GIACCIO,G. ZERBINO,R. and GIOVAMBATTISTA,A.(1985) "Adherencia agregado-matriz".Colloquia 85.Vol 1. RILEM. Buenos Aires. Argentina.

J.K. Shukuzawa, H.C. Rodrigues Filho, V.A. Zampieri
Associação Brasileira de Cimento Portland

RELATIONSHIP BETWEEN ALITE MICROSCOPIC REACTIVITY AND CLINKER HYDRAULICITY

1 INTRODUCTION

The technique of etching polished section is an essential process for the reflected light microscopy studying of clinker. Because of the similar reflecting power of clinker minerals, it is only possible to observe of microscopic textures and structures through the etching of polished section by adequate chemical substances.

The thickness of coating of the reaction products formed in the crystal surface, determines the color observed by reflected light. The color is a result of light refraction and varies according to Newton's Series, while the thickness of coating grows[1]. So, as the color is closely related to the reaction rate of crystal with the etchant, it can be used as a crystal reactivity.

In order to check the relation between the alite crystals color and the clinker hydraulic activity, microscopic studies performed in industrial clinker samples are shown.

2 NH_4Cl ETCHING

The following aspects were obtained as a result of previous microscopic observations performed in clinkers from different plants, using NH_4Cl as etchant:

a) NH_4Cl must always be used in an aqueous solution, in concentrations about 0.1%, and when the room temperature is 22°C, the ideal etching time would be about 20 seconds.

b) with the increasing of the etching time, the alite crystals color changes progressively into the following degrees:

light brown
dark brown
dark blue
light green-blue
greenish-yellow
orange-yellow

↓ increasing of the etching time

c) the same color and tonality can be obtained, even after a new polishing and etching, because of the good repeatibility of the method.

d) with NH_4Cl the reaction rate is affected by the alite crystallographic orientation. With polished thin sections it was possible to see that the perpendicular section to crystallographic C-axis shows low reactivity, while parallel section shows a high one.
This etching anisotropy is closely related to the optical anisotropy. The optically less anisotropic alite sections are those that have minor reactivity.
The more anisotropic sections are the more reactives.
This reactivity increases with the growing of the optical anisotropy.

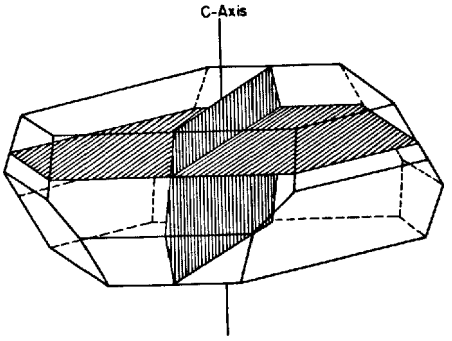

FIGURE 1- Sketch of a single cristal by Yamaguchi and Ono[2]

e) according to ONO[3], alite crystals of clinkers burned at high temperatures show greater birrefringence and are hydraulically more active. These alite crystals when submitted to reflected light microscopy show elongated forms and high reactivity to NH_4Cl.

f) small alite crystals are more reactive to NH_4Cl than the large crystals. In the same clinker nodule, it is observed that while the smaller crystals reach blue color, the large ones remain brown. These observations are in accordance with the results attained by other authors[3,4,5] that obtained a greater hydraulic activity for the small crystals in relation to the large crystals.

g) alite crystals with thin belite lamellae are usually observed in industrial clinkers burned in reducing environment. They occur in three different sets with strict crystallographic orientation with respect to the host[6]. This texture results from an oxidation of Fe^{2+}, which replaces part of Ca^{2+} in the alite crystal lattice. Less frequently, in some parts of the clinker alite crystals appear without fine lamellae and decomposition structure. Fe^{2+} is probably still in the lattice, since droplets of metallic iron and high frequency of C_3A can be observed in the nearness. Reactivities of alite crystal with lamellae and alite crystal without decomposition structure are very different. While the first one keeps the brown color, the second shows a light blue color. The behavior of these two types of alite after the NH_4Cl etching agrees with Woermann's observations. This author points out the incorporation of Fe^{2+} into alite crystal lattice to be responsible for the high crystal instability and thus for its reactivity.

h) alite idiomorphic crystals from quick cooling rate clinkers, are more reactive than irregular crystals from slower cooling clinkers. According to Dorn[1], cooling rate is supposed to be the most important factor in crystal color development.

3 ALITE REACTIVITY AND CLINKER HYDRAULICITY

By means of NH_4Cl etching of clinker polished sections an attempt was made with the purpose of correlating the alite microscopical reactivity to the clinker hydraulic activity. Three samples of industrial clinker from the same raw mix and burnt into the same rotary kiln (1,000 ton/day) were selected. Phase quantification by microscopy showed similar compositions, mainly with regard to the alite content. This fact lead us to conclude how insignificant is the influence of its content in the difference of hydraulic activity among the clinkers.

A method based on Dalziel's[7] proposition and adjusted by Ferreira[8] was used in order to evaluate the clinker hydraulic activity. This method consists in the determination of the compressive strength of 20mm diameter x 30mm high mini-cylinders. Powdered clinkers with a specific surface area (Blaine) of about 340 $m^2.kg^{-1}$ were dry pressed till a porosity of 35%. Then, the dry specimens were submitted to a vacuum lower than 0,60 mbar, during ten minutes inside a vacuum chamber. Under this condition the entering of water occurs without a significant alteration on the chamber interior negative pressure. After the vacuum application a sufficient amount of water was added, so that the specimens could be completely submerged; then the pressure was lightened in order to let the water enter. The submerged mini-cylinders were cured in a water temperature of 23°C, for 18 hours and 28 days, respectively, when finally tested. The final result of the test was obtained through arithmetic mean of four test specimens, with within coefficient of variation between 0,0 and 5,0%.

Due to the fact this method is not standarded and considering the comparative aim of this study, relative strengths were prefered.
Sample B with 36,4MPa at 18 hours and 147,0 MPa at 28 days was taken as reference (100%). According to *Figure 2*, the three samples were packed in the same polished section in order to make the etching acts in an uniform way. This procedure reduces differences during the etching time.
The polished surface was etched with NH_4Cl (0,1%) during 20 seconds just washed with water and dried.

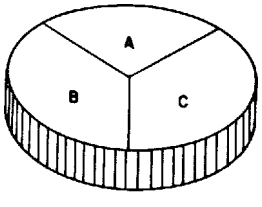

FIGURE 2 - Polished section with three samples of clinker

As it was discussed before, the alite reactivity depends on, among other factors, the crystallographic section. So, on the polished surface of a unique clinker fragment it is possible to recognize different alite sections, with a variety of colors. In addition varieties of crystal sizes and the heterogeneity of industrial clinker fragments, make it difficult to evaluate the color of alite in clinker as a whole.

In order to make this evaluation less subjective, the alite crystals were classified, according to color, in four types and the frequency of each one was determined by crystal microscopical counting, under a magnification of 250 times.

TABLE 1 - MICROSCOPICAL AND PHYSICAL CHARACTERISTICS OF CLINKERS

	COMPONENT		CLINKER A	CLINKER B	CLINKER C
PHASE COMPOSITION BY MICROSCOPY	ALITE (%)		61.6	65.4	65.5
	BELITE (%)		21.1	17.9	15.3
	C_3A (%)		4.2	2.0	2.3
	C_4AF (%)		12.0	13.4	15.8
	FREE LIME (%)		1.1	1.3	1.1
ALITE	SIZE (µm)		50-60	30-40	25-30
	BIRREFRINGENCE		0.0045-50	0.0045-50	0.0045-50
	FORM		subidio-morphic	idiomorphic	idiomorphic
	COLOR TYPE	I (%)	82	25	8
		II (%)	13	27	24
		III (%)	4	32	49
		IV (%)	1	16	19
BLAINE ($m^2.kg^{-1}$)			346	334	336
18 HOURS STRENGTH (%)			49	100*	122
28 DAYS STRENGTH (%)			92	100**	106

* 36,4 MPa
** 147,0 MPa

TYPE	COLOR
I	BROWN CRYSTALS
II	CRYSTALS OF BLUE COLOR IN THEIR CORE AND BROWN IN THEIR RIM (BROWN PREDOMINANCE)
III	CRYSTALS OF BLUE COLOR IN THEIR CORE AND BROWN IN THEIR RIM (BLUE PREDOMINANCE)
IV	BLUE CRYSTALS

Table 1 shows a good accordance between the alite color and the relative strength of clinkers. Differences among individual values of relative strength at 28 days decreased in relation to 18 hours values. However the same general tendency was kept. Clinker C not only showed the biggest strength but also the most content of types III and IV reactive alite crystals. On the other hand, in clinker A, with the lowest strength, most crystals are type I, in others words, the least reactivity.

In these three samples, the alite reactivity is mainly related to their size. In clinker A, besides of the alite biggest size, it seems that the alite irregular shape and the exsolution texture found in various crystals contributed to decrease its reactivity.

The birrefringence values of the alite crystals showed that the burning temperature was the same in the three clinkers. It means in this specific case that the reactivity was not influenced by this factor.

4 CONCLUSIONS

The alite crystal color after etching is a parameter that can be used to predict the reactivity. It can replace other parameters like crystal shape and size, birrefringence, incorporation of minor elements, cooling rate etc. that were known by their remarkable effect on clinker reactivity.

Although we haven't had yet enough data to correlate statistically the mini-cylinder strength to standarded method strength, results of research showed an inter dependence between alite microscopic reactivity and clinker hidraulicity.

We believe this kind of study and future advances like the belite reactivity evaluation will lead us to a better prediction of cement behaviour.

REFERENCES

1. DORN, J. *Theory of etch color development in portland cement*. In: BAYLES, J. ed. *Proceedings of the sixt International Conference on Cement Microscopy*, Albuquerque, 1984. p.421-26.

2. YAMAGUCHI, G. & ONO, Y. *Mikroskopische Untersuchungen am Alit des Portland zementklinkers*. *Zement-Kalk-Gips*, Wiesbaden, 20 (9):390-94, 1966.

3. ONO, Y. *Microscopical estimation of burning condition and quality of clinker*. In: *INTERNATIONAL Congress on the Chemistry of Cement*, 7th, Paris, 1980. v.2,

4. LONG, G.R. *Clinker quality characterisation by reflected light techniques*. In: GOUDA, R.G., ed. *Proceedings of the fourth International Conference on Cement Microscopy*, Las Vegas, 1982. p.92-109.

5. CAVENY, W.J. & WIGAND, W. & BAILEY, D.E. *Microscopic method helps assess cement performance*. *Oil & Gas Journal*, Tulsa, : 90-93, Sept. 26, 1983.

6. WOERMANN, E. *Decomposition of alite in technical portland cement clinker*. In: *INTERNATIONAL Congress on the Chemistry of Cement*, 4th, Washington, D.C., 1960. v.1, p.119-29.

7. DALZIEL, J.A. *A mini-cylinder test for the rapid determination of cement quality*. *Cement Technology*, London, 2(4): 105-12, July/aug. 1971.

8. FERREIRA Jr., S. *Um método de ensaio acelerado para determinar a resistência à compressão do cimento na temperatura normal*. In: ASSOCIAÇÃO BRASILEIRA DE CIMENTO PORTLAND (ABCP). *Reunião de Técnicos da Indústria do Cimento*, 34ª, São Paulo, 1983. (*paper avaiable only by contacting author*).

G. Babachev, K. Kolev - Sofia Bulgaria

THE INFLUENCE OF THE CEMENT TYPE ON THE VALUES FOR LIGHT CONSTRUCTIVE-THERMAL INSULATING CONCRETE.

The method for experiment planning and mathematic modelling (active experiment) is used to evaluate and to optimize the properties of the light concrete by varying factors on three levels according the type of the concrete - portland cement 20 PZ 350, fly-ash cement, shlake portland cement.

The following main receipt factors are selected to be investigated:

- Cement amount per 1 m^3 concrete (X_1), varying on three levels: 250, 300 and 350 kg/m^3. These limits are selected so that to be obtained a wider concrete range with properties and parameters, varying in a relatively wide range in order to meet the practice requirements;

- Water content per 1 m^3 concrete (X_2) varying on three levels: 190, 205 and 220 kg/m^3. The limits for the variation of the last factor are been so selected that to be obtained concrete mixes which are not hardly processed or startfying, considering also the necessary water content for the used additives.

- The ratio of the amounts for the coarse and fine additives (by volume) (X_3), varying on three levels: 0.7, 0.85 and 1.0. The reason to select the above limit values is based on the results of the preliminary research and investigations - in such manner the advisability of the above limit values has been proved.

On the basis of preliminary investigations and references about the possible kind of the mathematic relations, the type of the goal-function was selected as a full polynom of second degree, as follows:

$$Y = B_o + \sum_{i=1}^{3} B_i X_i + \sum_{i=1}^{3} B_{ii} X_i + \sum_{i<j} B_{ij} X_i X_j$$

where the symbol $\sum_{i<j}$ means a sum of all possible different $X_i X_j$ members.

In order to avoid difficulties in respect of the factors' dimensions, a coding procedure has been selected - as using non-dimensional values in limits of -1 to +1 according the following relation:

$$x_i = \frac{X_i - X_o}{0.5(X_{i\ max} - X_{i\ min})}$$

where:

$X_{i\ min}$ is the low limit for factor variation

$X_{i,o}$ is the middle (average) value of the factor in the investigated range

$X_{i\ max}$ is the top limit for factor variation.

To obtain maximum information from the mathematic model at lowest influence of the unknown or disturbing factors, an experiment plant is used - this plan of the experiment is near to D-optimal plan of type B_3, as shown in Table 1. for natural factor coordinates.

Table 1.

No.	Natural coordinates		
	X_1	X_2	X_3
I	350	190	0.7
II	250	220	0.7
III	250	190	1.0
IV	350	220	1.0
V	350	190	1.0
VI	250	220	1.0
VII	350	220	0.7
VIII	250	190	0.7
IX	350	205	0.85
X	250	205	0.85
XI	300	220	0.85
XII	300	190	0.85
XIII	300	205	1.0
XIV	300	205	0.7
XV	300	205	0.85

For goal-functions (Y) are selected: the consistency of the concrete mix, measured by technical viscosity meter; compressive strength after thermal traetment on the first day R_{H}ПП 1; tensile strength at bending on the first day R_{OI}ПП 1; compressive strength at normal setting or hardening conditions on the seventh day; voluminary density of the concrete after steam treatment $\rho_{o,w}$ПП.

The experiment was performed by portland cement 20 PZ 350 with 37.5 MPa activity. As a light additional material a shlake-ash mix was used - from the "Bobov Dol" thermal power station, with voluminal density of the grain equal to 1335 kg/m^3 . As a coarse additional material is used a ceramsyte gravel with 20mm maximal diameter of the grains and 860kg/m^3 voluminal density of grains. Part of the samples were thermally treated by steam at atmospheric pressure and T = 358 $\pm$ 5°K temperature of isothermal heating mode: 2.5 + 1.5 + 5 + 2 = 11 Hours

and the other part of the samples are at normal setting or hardening conditions.

Before introducing the test results in order to develop the relevant mathematic models a stochastical processing is necessary to determine mean arithmetic value, root-mean-square deviation, variation factor, to check for random errors with a significant deviation from the mean value, to determine the mean dispersion for the experimental cement bloc.

After the preliminary stohastical treatment/ processing the test results for every propery of the light concrete are introducing in the computer. By means of the relevant computer programmes are calculated and checked for valuability (weight) factors in the models, checked for adequatity according the Fisher criteria. The properties of the light constructive-thermal insulating concrete, experimentally determined, are show in Table 2. On the basis of the experimental results (Table 2) are calculated mathematical models with the following expressions (after the adequatity check for the relevant properties):

1/ Consistency (acc. the measurements by technical viscosity meter) - S

$$S = 8.3 + 0.6X_1 + 0.8X_3 - 2.7X_2 + 0.8X_1X_2 - 1.2X_2X_3 + 0.7X_2^2 - 2.5X_1^2 .$$

2/ Compressive strength after steam treatment- R_HII 1

$$R_H\text{II } 1 = 13.6 + 1.5X_1 - 0.8X_2 + 0.6X_3 - 1.6X_3^2 + 0.7X_1X_3$$

3/ Tensile strength at bending after steam treatment - R_{OI}II 1

$$R_{OI}\text{II } 1 = 1.45 - 0.12X_2 - 0.08X_3 - 0.19X_3^2 - 0.12X_2X_3$$

4/ Compressive strength after 7-day setting time R_H7:

$$R_H7 = 11.5 + 1.7X_1 - 0.5X_2 - 1.2X_1^2$$

5/ Voluminal density after steam treatment $\rho_{o,w}$II

$$\rho_{o,w}\text{II} = 1213 + 36X_1 + 12X_3 + 30X^2$$

Table 2.

No.	S sec.	R_oIII MPa	R_HIII MPa	R_H7 MPa	ρ_{o,w_3}II kg/m^3
I	9	1.45	13.6	12.7	1262
II	4	1.44	10.1	8.6	1183
III	3.5	1.44	11.0	9.1	1211
IV	9	1.16	14.2	11.2	1293
V	12	1.39	14.8	13.3	1302
VI	4	0.77	9.0	7.4	1194
VII	4.5	1.30	10.7	10.7	1244
VIII	6	1.27	11.0	9.1	1231
IX	4.5	1.31	15.0	12.3	1292
X	7	1.52	12.1	8.9	1211
XI	4	1.72	13.3	12.2	1227
XII	14	1.38	14.9	10.8	1193
XIII	10	1.17	13.6	13.0	1241
XIV	7	1.24	11.3	11.5	1198
XV	8	1.34	12.5	10.0	1204

All models meet the requirements of the criteria for adequatity of the description and can be used to analyse the properties of the light concrete.

A full polynom is obtained for the influence of the cement amount on the consistency, i.e. all investigated factors (members of the mix) has influence on the possibility of the concrete mix.

A prevailing factor is the bement amount. The influence of the last factor on the consistency of the concrete mix is non-linear and is realized by means of the other two investigated factors with relatively poor effects of mutual influence. The increasing of the cement amount up to certain limit causes increasing of the consistency i.e. in the investigated limits the optimal cement amount relating the consistency is 250 kg/m^3.

At selected thermal treatment mode the most important effect for the light concrete grades has the amount of the used cement - in order to increase the compressive strength after steam treatment. The maximal increasing of the compressive strength can be obtained at cement amount of 350 kg/m^3. The effect of the compressive strength increasing is more with higher shlake-ash mix: ceramsyte equal to 1.0. The mutual influence of these two factors is positive in respect of the compressive strength and can be used to produce light concrete with increased compressive strength values.

The influence of the concrete amount per 1 m^3 light constructive-thermal insulating concrete on the compressive strength is in the limits of the experiment's error and is not reported by means of the mathematic model. Possibly this mechanical factor is poor sensitive in respect of cement amount, as can be assured that the disturbance of the material is happened mainly from the light additional substances and the increasing of the cement amount is helpful to composite strengthening or consolidation.

The compressive strength of the light concrete after 7-day setting period at normal conditions is determined mainly by the cement amount. The increasing of the last factor in the limits of 250 to 350 kg/m^3 at the same other conditions causes compressive strength increasing by 5 MPa or at water content of 190 kg/m^3 is achieved maximal compressive strength of 12.7 MPa. At more cement amount the compressive strength is not increased.

References:

1/ Babachev, G.N. "Ash and Shlake - Valuable materials", Sofia, "Technika" 1984

2/ Voznesenskij V.A. "Statistical Methods for Experiment Planning in Technical-Economical Investigation". Moskow, "Finansi i Statistika"1981

Tang Ming-shu, Xu Zhong-zi and Han Su-fen
Nanjing Institute of Chemical Technology, China

ALKALI REACTIVITY OF GLASS AGGREGATE

Introduction

The properties of aggregate are vitally important to the performance of concrete, especially the durability. To date, the deterioration cases due to the alkali-aggregate reaction have been discovered in more than twenty countries. Due to the gradual lack of natural rock resources and the presence of enormous quantities of industrial solid wastes, the trend to use the solid wastes as aggregate will be increasing for the time to come. The blast furnace slag and coal cinder have been used as aggregates for many years. Besides, millions of tons of refuse glass are generated annually(1). The problem associated with the use of waste glass is the chemical composition of glass, which are responsible for the alkali-aggregate reaction. In volcanic glass, the relationship of their alkali reactivities to chemical compositions has also not yet been fully established. Until now, only R.G. Pike(2) and J.W.Figg(3) have investigated the alkali reactivities of glass aggregate, but the chemical compositions studied by Pike are only limited to binary systems. We made now nearly hundred samples of glass to study the relationship of chemical compositions to aggregate reactivities. The chemical compositions include in three ternary systems, N-A-S, N-C-S, C-A-S and a quaternary system N-C-A-S. The results obtained can be used to examine the alkali reactivities of volcanic glass and industrial glass waste.

Experimental Method

Glass samples were made from quartz sand, pure limestone, Al_2O_3 and Na_2CO_3. The raw materials were first ground to particles finer than 0.08 mm, then the mixes were melted in an electric furnace. Afterwards, the melts were allowed to flow into cool water for quenching. Some mixes which were difficult to melt were moulded into bars and then melted by oxygen-acetylene flame, the melts were also allowed to flow into cool water for quenching.

The alkali reactivities of glass aggregates were determined by rapid autoclave mortar bar test suggested by us(4): the size of aggregate: 0.15-0.75 mm, cement: aggregate = 10:1, w/c=0.30 and the alkali content of cement is 1.5% eqv. Na_2O. The mortar bars were removed from the molds after one-day curing in moist chamber, then precured in 100°C steam for 4 hours. After that, they were placed in a 10% KOH solution and autoclave-treated at 150°C for 6 hours. This method has been repeatedly proved to be effective to determine the alkali reactivity of aggregate of alkali-silica type.

Experimental Results

1. N-A-S System

18 glass samples of this system were made. The ranges of chemical compositions (in mol%) of these samples are: SiO_2 41.49-87.60, Al_2O_3 6.32-34.97, Na_2O 2.89-50.34. As the content of Na_2O was over 40 mol%, the products after melting and cooling was a xerogel, not a glass. Mortar bar test proved that the glass aggregates were non-reactive as the content of Al_2O_3 was over 24 mol%(Fig.1). The relations between the expansion values of mortar bars and the ratios A/(S+N)(mol) are shown in Fig.2. It shows that the values of expansion increase sharply as A/(S+N)=0.15, when the ratio A/(S+N) is higher than 0.3, the aggregates are non-reactive.

The experimental results proved that the value of expansion was almost maximum as the ratio N/S=0.5. On account of this result and the relationship of alkali reactivities to A/(S+N), the following formula was obtained by regression analysis. The coefficient of correlation of regression R=0.96.

$$\%e=0.025\,EXP(0.3416((A/(S+N))^{-1}-((N/S)-0.5)^2)) \qquad (1)$$

Where
%e—value of expansion of mortar bar
N,A,S—respective mol% of Na_2O, Al_2O_3, SiO_2 in glass-sample compositions

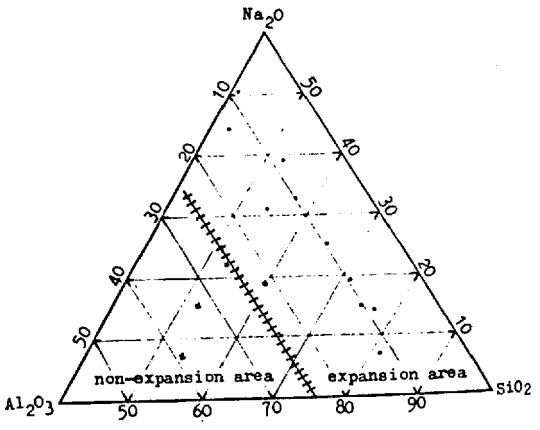

Fig.1 The expansion area and non-expansion area of glass aggregates in N-A-S system (mol %)

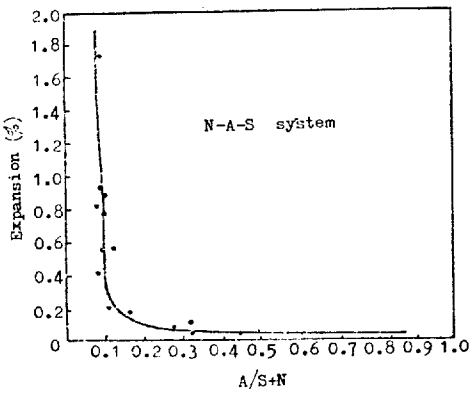

Fig.2 Relation between expansion and A/(S+N)(mol ratio)

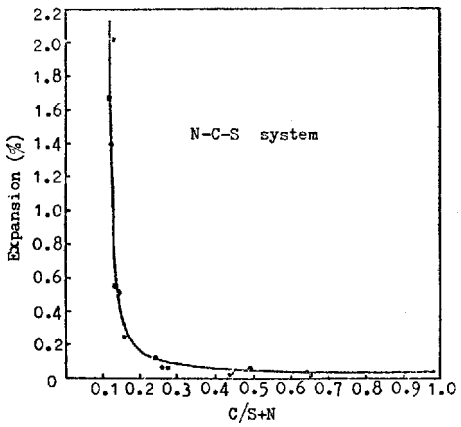

Fig.4 Relation between expansion and C/(S+N) (mol ratio)

2. N-C-S system

In this system, 15 glass samples were made by melting. The ranges of chemical compositions(mol%) of these glass samples are: SiO_2 39.19-71.62, CaO 6.60-44.60, Na_2O 8.97-40.68. In Fig.3, it shows that the aggregates are non-reactive when their CaO contents exceed 22 mol%. The expansion increases sharply as $C/(S+N) \leq 0.2$ and stops as $C/(S+N) \geq 0.3$(see Fig.4). Similarly, the following formula is obtained after regression analasis. The coefficient of correlations R=0.96.

$$\%e = 0.0251\ EXP(0.4912((C/(S+N))^{-1} - -((N/S)-0.5)^2)) \quad (2)$$

3. C-A-S system

For this system, 16 glass samples were made. The ranges of chemical compositions (mol%) of these samples are: SiO_2 42.51-100, CaO 0-35.53, Al_2O_3 0-35.60. It is proved that in this system the value of expansion increases with increase of SiO_2 content (see Fig.6). In Fig.5, it shows that the aggregates are non-reactive when the content (mol%) of silica is less than 66 mol%. The equation of regression which represents the relation of chemical composition to value of expansion is shown in formula(3), the coefficient of correlation R=0.99.

$$\%e = 0.0472 + 3.624 \times 10^{-4}(SiO_2 - 55)^2 \quad (3)$$

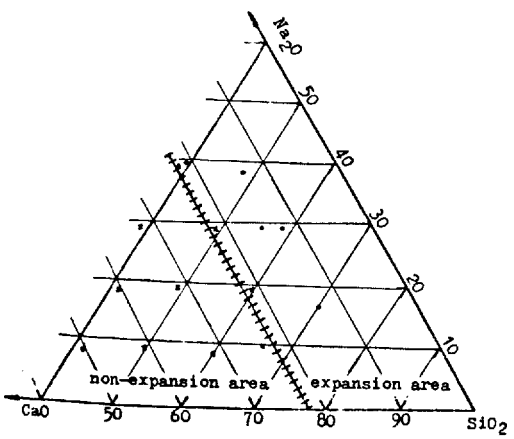

Fig.3 The expansion area and non-expansion area of glass aggregates in N-C-S System

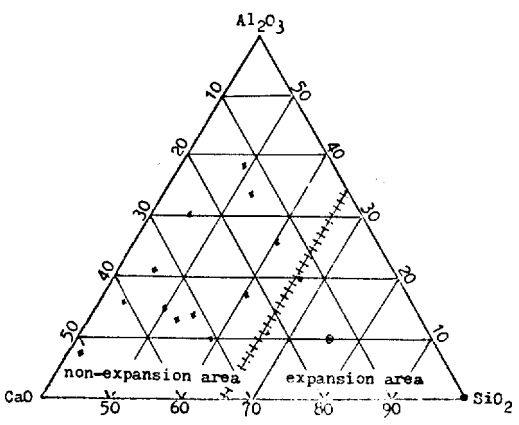

Fig.5 The expansion area and non-expansion area of glass aggregates in C-A-S system (in mol%)

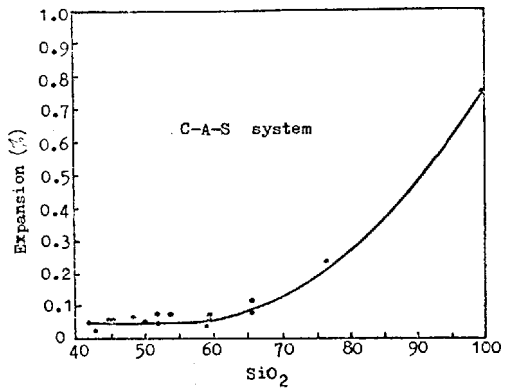

Fig.6 Relationship of expansion to S(in mol%)

4. N-C-A-S system

42 glass samples were made for this system. The ranges of chemical compositions (mol%) of these samples are: SiO_2 46.89-87.60, CaO 1.07-33.39, Al_2O_3 0.62-12.86, Na_2O 1.29-28.97. Similar to the above three systems, the value of expansion increases with the increase of S+N(mol%) contents, and decreases with the increase of C+A contents. In Fig.7, it shows that the region of expansion exists in the cone of the SiO_2 vertex. As shown in Fig.8, the value of expansion decreases with increase of ratio (C+A)/(S+N). The glass aggregates are reactive as this ratio is less than 0.2, and non-reactive as it is higher than 0.3. There is uncertainly in (C+A)/(S+N)=0.2-0.3. Formula(4) is the equation of regression, the coefficient of correlation R is 0.92.

$$\%e=0.0092\,EXP(0.5124((C+A)/(S+N))^{-1}-((N/S)-0.5)^2)) \qquad (4)$$

It is worth mentioning, When we put C=0 or A=0 in equation(4), the results seem to be not consistent with equation (1) or (2), maybe the reason is that there are influence from one another in the chemical compositions, it is not a simple additive relation between them.

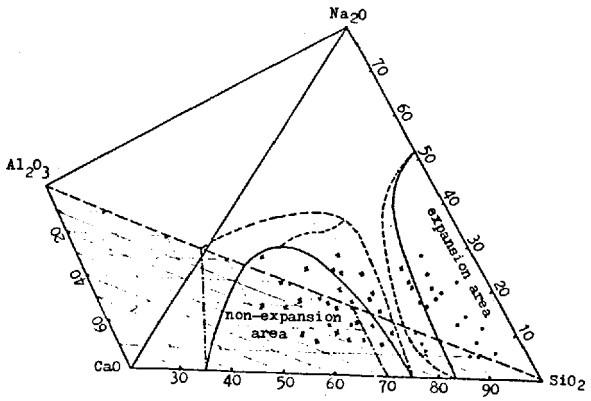

Fig.7 The expansion area and non-expansion area of glass aggregates in N-C-A-S system(mol%)

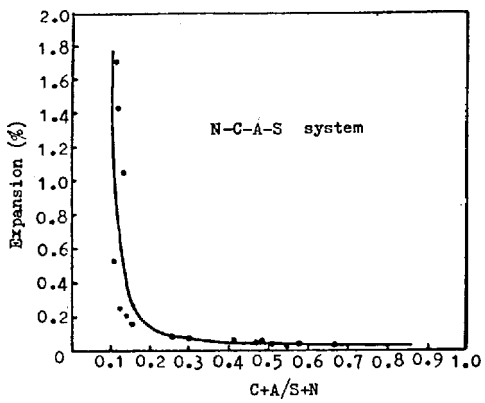

Fig.8 Relation of expansion to (C+A)/(S+N)(mol ratio)

Applications of the Reactive Index K

The alkali reactivities of some rocks of volcanic glass and industrial glass waste were determined by mortar bar test or chemical method. The comparison of these results to reactive index K((C+A)/(S+N)) is shown in Table I, it illustrates that all the rocks are reactive when K is less than 0.134. On the contrary, as K=0.471 or 1.390, the aggregates are expectedly not reactive. Therefor, we can use the reactivve index to predict the alkali reactivity of these kinds of rocks.

Table I Relationship of alkali reactivities of glass rocks to their reactivity index

Rocks	Chemical Compositions (in mol%)							Expansion %	K**	
	SiO_2	Al_2O_3	Fe_2O_3	CaO	MgO	K_2O	Na_2O			
perlite(1)	71.33	11.93	1.75	1.96		3.35	1.65	0.254	0.130	Reactive
perlite(2)	70.43	12.22	1.40	2.21		4.70	2.00	0.391	0.134	Reactive
perlite(3)	72.56	11.49	1.78	0.88		4.07	3.90	0.605	0.106	Reactive
perlite(4)	71.27	12.74	3.67	0.74	0.62	3.61	3.55	-*	0.132	Reactive
pichstone	72.70	11.29	1.78	0.81	0.10	3.30	3.15	0.383	0.107	Reactive
obsiden(1)	73.60	11.74	1.16	0.81		3.80	4.50	-*	0.102	Reactive
obsiden(2)	70.90	12.73	2.94	0.73	0.21	4.25	3.35	0.105	0.128	Reactive
cinder	55.73	23.42	14.14	5.16	1.41	0.97	0.50	0.034	0.471	Non-reactive
slag	34.73	9.88	1.05	37.85	4.96	3.97	1.80	*	1.390	Non-reactive

*Proved to be reactivity determined by ASTM C289 (chemical method)

**In calculation of K, CaO includes MgO, Al_2O_3 includes Fe_2O_3

Discussion

Three processes are present in alkali-silica reaction, they are: process of reaction, process of imbibition of water and process of swelling. It must be mentioned that all these glass aggregates made by us might react with the pore solution of cement paste, therefore, the difference in expansion of aggregates must be attributed to their different abilities of water imbibition and the swelling of their reaction products. The relationship of these abilities to chemical compositions of glass aggregates deserves to be studied further.

Conclusion

The alkali reactivities of glass aggregates depend on their chemical compositions. The reactivities increase with the increase of S+N contents, and correspondingly decrease with the increase of C+A contents. So far the alkali reactivities of glass aggregates can be predicted by reactive index K((C+A)/(S+N))(in mol%). The reactivity sharply increases as K is less than 0.1-0.2. On the contrary, they are not reactive as K is more than 0.3.

Acknowledgements

The authors gratefully acknowledge Professor Wang Zhong-jun and Dr. P.E. Grattan-Bellew for their valuable suggestions.

References

(1) S.N. Ghosh, Advances in cement technology, p.663(1982).
(2) R.G. Pick, Binary silicate glasses in the study of alkali silicate reaction, Highway Research Board Bulletin, No.275, pp39-44(1960).
(3) J.W. Figg, Reaction between cement and artificial glass in concrete, Proc. of 5th International Conference on Alkali-Aggregates Reaction in Concrete, Cape Town, 1981.
(4) Tang Ming-shu, Han Su-fen and Zhen Shihua, A rapid method for identification of alkali reactivity of aggregate, Cem. Conc. Res. Vol.13, No.3,417-422(1983).

LOU Zonghan, Professor, XU Xianyu, HAN Ren and CHENG Yimin, Lecturers
Zhejiang University, P. R. China

Calcium Silico-Fluoride Phase A and Its Effects on Formation of C_3S

For saving energy, the addition of CaF_2 or CaF_2 and $CaSO_4$ to the raw materials is often used in the burning of cement clinker in cement works. In this case, four transitional minerals may emerge in the burning process of cement clinker in kilns. They are calcium silico-fluoride phase A ($C_{19}S_7 \cdot 2CaF_2$), calcium silico-fluoride phase B ($2C_2S \cdot CaF_2$), calcium sulfo-silicate ($2C_2S \cdot CaSO_4$) and fluor-ellestadite ($3C_2S \cdot 3CaSO_4 \cdot CaF_2$). Many researches on these minerals have been done, but the research is far from over and some results of them are contradictious/1/,/2/,/3/,/4/,/5/,/6/. Calcium silico-fluoride phase A is the most important among the four transitional minerals. The present paper will describe its formation and decomposition, and its effects on the formation of C_3S.

1. The Formation of $C_{19}S_7 \cdot 2CaF_2$

Calcium silico-fluoride phase A was prepared by three methods with C_2S which was prepared beforehand, CaO, $CaCO_3$, SiO_2 and CaF_2 in c.p. grade, i.e., sample A with the mole ration of $CaO:SiO_2:CaF_2=19:7:2$; sample B with the mole ratio of $CaCO_3:SiO_2:CaF_2=19:7:2$; sample C with the mole ratio of $C_2S:SiO_2:CaF_2=7:5:2$.

Eight groups of sample A and sample C were burned at 1000°C for 15 min., then heated to 1080, 1090, 1100, 1110, 1140, 1160, 1170 and 1200°C respectively and at these temperatures for 15 min. The results of free CaO and XRD of them are shown in Fig. 1, Fig. 2, Fig. 3 and Fig. 4.

It can be found from these results that $C_{19}S_7 \cdot 2CaF_2$ exist at the temperature range of 1100-1170°C in sample A and of 1070-1170°C in sample C. In both sample free CaO decreases obviously and $C_{19}S_7 \cdot 2CaF_2$ increases obviously at 1110 C. That means the amount of $C_{19}S_7 \cdot 2CaF_2$ formed reaches maximum at this temperature.

From these results it can also be found that the formation rates of $C_{19}S_7 \cdot 2CaF_2$ are different in the two samples. C_2S which was prepared beforehand has a promo-

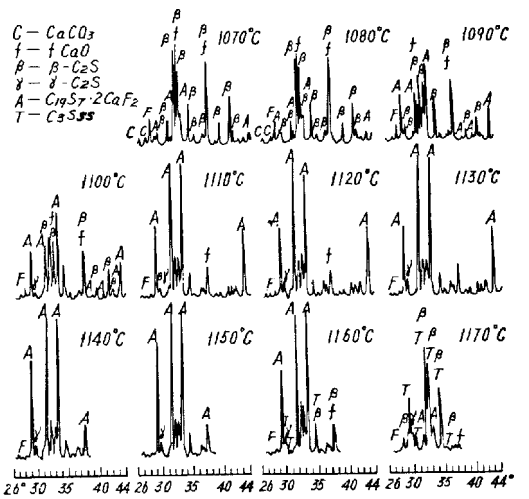

Fig. 2 XRD patterns of sample C at different temperature for 15 min.

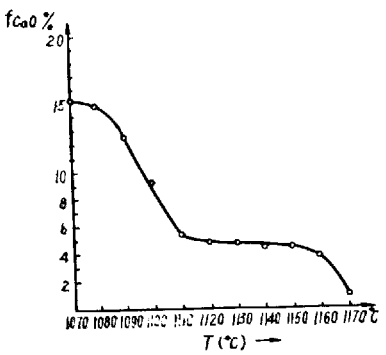

Fig. 1 Percentage of f·CaO of sample C at different temperature

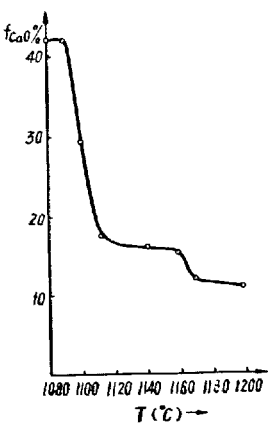

Fig. 3 Percentage of f·CaO of sample A at different temperature

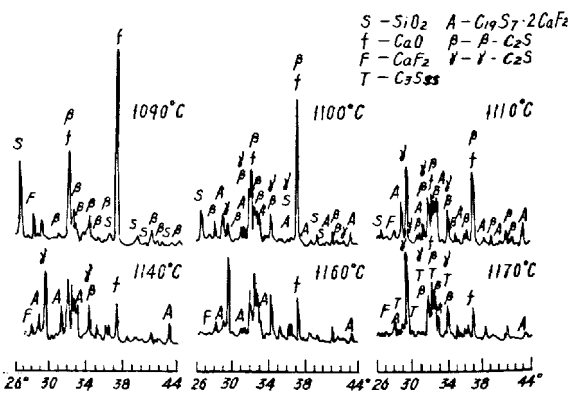

Fig. 4 XRD patterns of sample A at different temperature for 15 min.

tive effect on the formation of $C_{19}S_7 \cdot 2CaF_2$. W. Gutt has described that $C_{19}S_7 \cdot 2CaF_2$ is formed by C_2S, CaO and CaF_2/7/. The result of thermodynamic calculation also indicates this trend.

To investigate the formation rate of $C_{19}S_7 \cdot 2CaF_2$, five sample C's were burned at 1000°C for 15 min. and then heated to 1080, 1090, 1100, 1110 and 1120°C respectively and at these temperatures for 1, 5, 10, 15, 20, 30 and 60 min. respectively. The samples were cooled with liquid nitrogen, then free CaO of each sample was determined. The results are shown in Fig. 5.

In DTA curve of sample B shown in Fig. 7, the endothermic peak in 573°C represents the polymorphic transformation of quartz, in 843°C the decomposition of $CaCO_3$. The endothermic peak in 1179°C indicates that $C_{19}S_7 \cdot 2CaF_2$ melts incongruently at this temperature. According to the phase diagrams of the $CaO-C_2S-CaF_2$ system made by J. Mukerji/8/. W. Gutt/9/ and Mitsuo Tanaka/10/, in which there is a ternary eutectic at 1110°C, liquidoid should emerge at 1111°C. The exothermic peaks in 1101 and 1118°C represent the formation of $C_{19}S_7 \cdot 2CaF_2$. They should be a single peak, which is divided into two by the endothermic peak liquidoid emerged at 1111°C. The peak temperature of the exothermic peak of formation of $C_{19}S_7 \cdot 2CaF_2$ represents the temperature at which the formation rate of $C_{19}S_7 \cdot 2CaF_2$ is maximal.

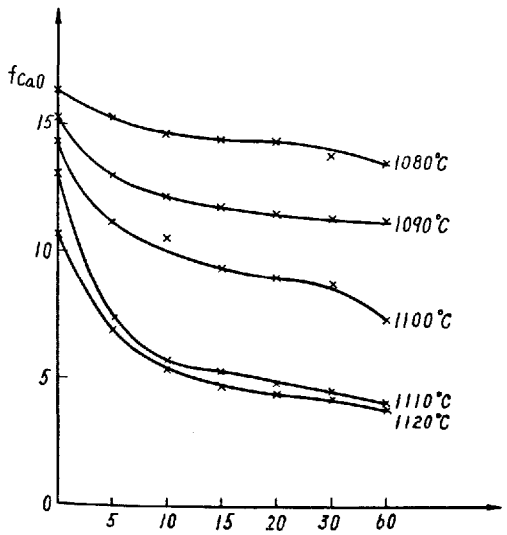

Fig. 5 Relationship between f·CaO of sample C and time at different temperature

The results shown in Fig. 5 were processed by Ginstring Equation, $f(G)=1-\frac{2}{3}(G)-(1-G)^{2/3}-Kt$. The relationship between f(G) and T is shown in Fig. 6. From Fig. 6 it can be shown that $C_{19}S_7 \cdot 2CaF_2$ formed through solid reaction below 1100°C, and through liquidoid above 1100°C, at which liquidoid emerges.

All the results obtained show that the amount of free CaO in sample C is maximal when the sample was burned at 1080°C, and reduces in order of 1090→1100→1110°C. But in the samples burned at 1110 and 1120°C the amount of free CaO is almost the same. So it can be inferred that both the amount and the formation rate of $C_{19}S_7 \cdot 2CaF_2$ formed at 1110°C are maximal.

2. Decomposition of $C_{19}S_7 \cdot 2CaF_2$

To examine whether calcium silico-fluoride phase A decomposes, sample B was burned at 1000°C for 15 min. making $CaCO_3$ decomposition, and at 1110°C for 30 min.

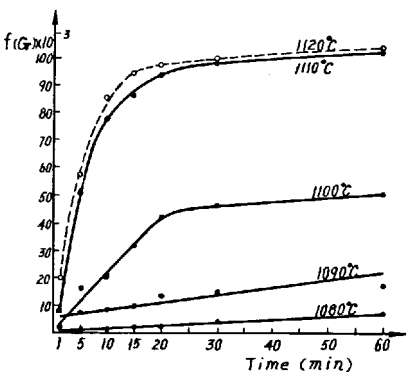

Fig. 6 Relationship between f(G) and time for sample C

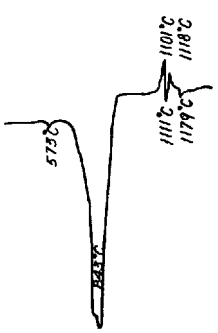

Fig. 7 DTA curve of sample B

making $C_{19}S_7 \cdot 2CaF_2$ formation, then heated to 1120, 1140, 1160, 1180 and 1200°C respectively and at these temperatures for 1, 5, 15, 30 and 60 min. respectively, then cooled with liquid nitrogen.

XRD semiquantitive analysis of these samples was carried out (Fig. 8). The peak intensity ratio of the characteristic peaks of $C_{19}S_7 \cdot 2CaF_2$ at d=2.087^0_A and $Al(OH)_3$ at d=4.85^0_A, which was added as a reference, is shown in Fig. 9. The determination result of free CaO of these samples is shown in Fig. 10.

From these results, it can be found that the amount of $C_{19}S_7 \cdot 2CaF_2$ decreases with the increase of temperature and burning time, and almost disappears at 1170°C, and

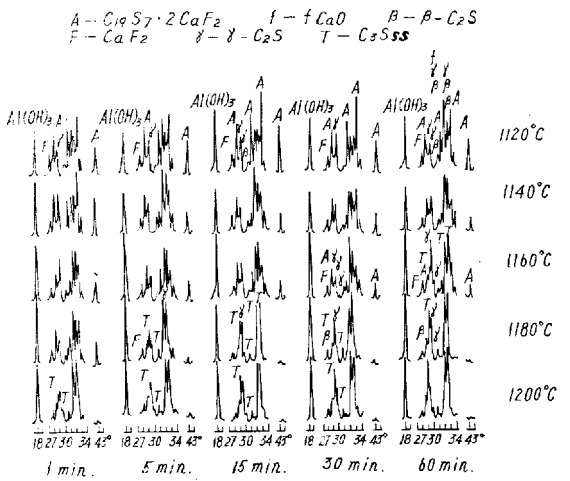

Fig. 8 Semiquantitive XRD patterns of $C_{19}S_7 \cdot 2CaF_2$

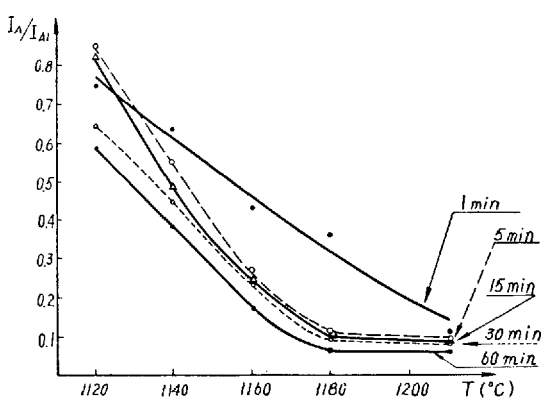

Fig. 9 Peak intensity ratio of $C_{19}S_7 \cdot 2CaF_2$ and $Al(OH)_3$ after the decomposition of $C_{19}S_7 \cdot 2CaF_2$

the amount of free CaO decreases at the same time and decreases rapidly at 1170°C. But in the samples burned at 1120°C, the amount of $C_{19}S_7 \cdot 2CaF_2$ increases for the time of 1 min. and 5 min. In the samples burned at 1120, 1140 or 1160°C, the amount of free CaO increases during the first 15 min. All these results indicate that $C_{19}S_7 \cdot 2CaF_2$ decomposes at these conditions.

The formation reaction of $C_{19}S_7 \cdot 2CaF_2$ is exothermic, so the increase of temperature is favorable to the decomposition of $C_{19}S_7 \cdot 2CaF_2$. Moreover, C_3S_{ss} can be found in the sample B burned at 1140°C for 18 hrs.

To sum up, the process of the formation and decomposition of $C_{19}S_7 \cdot 2CaF_2$ can be suggested as the following. In this process, there are two reactions. One is the formation of $C_{19}S_7 \cdot 2CaF_2$ by C_2S, CaO and CaF_2, the other is the decomposition of $C_{19}S_7 \cdot 2CaF_2$ to promote the formation of C_3S_{ss}. 1110°C is the eutectic in the C_2S-CaO-CaF_2 system and is the critical point of the formation reaction. 1170°C is the temperature at which $C_{19}S_7 \cdot 2CaF_2$ melts incongruently and is the critical point of decomposition reaction. Below 1110°C, $C_{19}S_7 \cdot 2CaF_2$ formed slowly through the solid reaction. in this case, formation reaction is the main reaction. Liquidoid emerges at 1110°C, and the amount and formation rate of $C_{19}S_7 \cdot 2CaF_2$ reach maximum. Above 1110°C, decomposition is dominant. At 1179°C, $C_{19}S_7 \cdot 2CaF_2$ disappears because it melts incongruently.

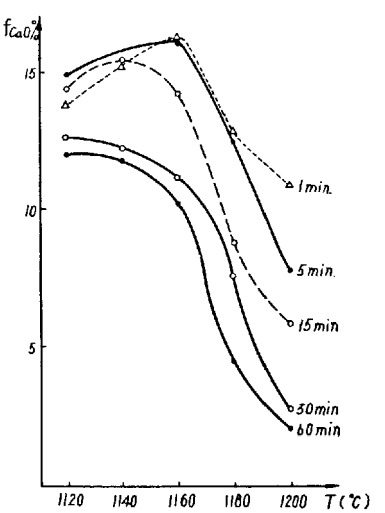

Fig. 10 Curve of f·CaO at different temperature after the formation of $C_{19}S_7 \cdot 2CaF_2$

3. The Effects of $C_{19}S_7 \cdot 2CaF_2$ on the Formation of C_3S_{ss}

To investigate the effects of $C_{19}S_7 \cdot 2CaF_2$ on the formation of C_3S_{ss}, a sample was prepared with $CaCO_3$ and SiO_2 according to the ratio of CaO/SiO_2=3:1. In addition, 3.68% CaF_2 was added into the sample. When all the CaF_2 was consumed, the percentage of $C_{19}S_7 \cdot 2CaF_2$ in the sample was 50%. The sample was burned at 1000°C for 15 min., and at 1110°C for 30 min., then heated to 1160, 1170, 1180, 1200, 1250, 1320 and 1350°C respectively and at these temperatures for 30 and 60 min. respectively. The results of determination of free CaO and XRD are shown in Fig. 11 and Fig. 12.

By means of XRD, C_3S_{ss} can be found in the sample burned at 1160°C. A large amount of C_3S_{ss} will emerge in the sample burned at 1180°C. In correspondence with that, at about 1170°C, the amount of free CaO decreases rapidly and $C_{19}S_7 \cdot 2CaF_2$ disappears finally. There is a lot of C_3S_{ss} "group" in $C_{19}S_7 \cdot 2CaF_2$/4/, so decomposition of $C_{19}S_7 \cdot 2CaF_2$ will promotes the formation of C_3S_{ss} by the nucleating and crystallizing process. This promoting effect will be more obvious when $C_{19}S_7 \cdot 2CaF_2$ incongruently melts at 1170°C.

As well known, through the solid reaction between $CaCO_3$ and SiO_2, only a little C_3S can form at such a high temperature as 1600°C. By the ordinary burning of clinker C_3S can not form until 1280°C. However, by the formation of transitional mineral, $C_{19}S_7 \cdot 2CaF_2$, a large amount of C_3S can form at 1170°C. The forming temperature of C_3S is 100°C below that in the clinker burned ordinarily and 400°C below that through the solid reaction. That indicates $C_{19}S_7 \cdot 2CaF_2$ has a obvious effect on promoting the formation of C_3S.

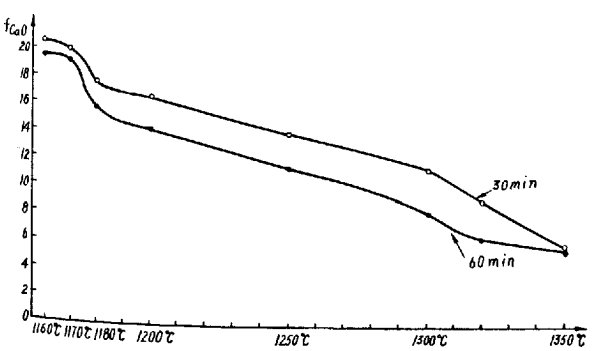

Fig. 11 Percentage of f·CaO of sample prepared with $3CaCO_3+SiO_2$+3.68 wt.% CaF_2

Calcium silico-fluoride phase B ($2C_2S \cdot CaF_2$) and calcium sulfo-silicate ($2C_2S \cdot CaSO_4$) are only related to the formation of C_2S/11/. The effect of fluor-ellestadite ($3C_2S \cdot 3CaSO_4 \cdot CaF_2$) is neccesary to be examined. $3C_2S \cdot 3CaSO_4 \cdot CaF_2$ and $C_{19}S_7 \cdot 2CaF_2$ can not coexist/3/. It is also proved by our experiments. Samples was prepared with $CaCO_3$ and SiO_2 according to the CaO/SiO_2 ratio=3:1, and 30% $3C_2S \cdot 3CaSO_4 \cdot CaF_2$ was added. They were burned at 1200, 1240, 1260, 1270, 1280, 1300 and 1350°C respectively for 30 or 60 min. The free CaO and XRD results of them are shown in Fig. 13 and Fig. 14.

From these results, it can be found that C_3S_{ss} doesn't emerge until 1250°C, and in correspondence with it, free CaO decreases rapidly and $3C_2S \cdot 3CaSO_4 \cdot CaF_2$ disappears at 1250°C. Compared with the results of the samples prepared with $3CaCO_3+SiO_2$+3.68% CaF_2, it can be found that the temperature at which C_3S emerges is 80°C higher. Obviously, it is the liquidoid, which emerges by the congruent melt of $3C_2S \cdot 3CaSO_4 \cdot CaF_2$ at 1250°C, that promotes the reaction of C_2S and CaO to form C_3S_{ss}. Actually, $3C_2S \cdot 3CaSO_4 \cdot CaF_2$ is a mineral with lower melt temperature, its effect mechanism on the formation of C_3S is different from that of $C_{19}S_7 \cdot 2CaF_2$.

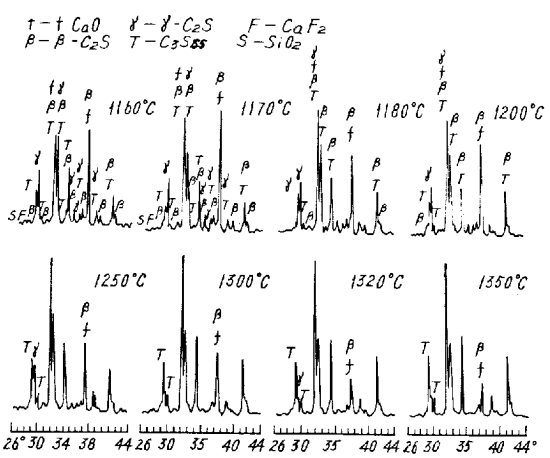

Fig. 12 XRD patterns of samples prepared with $3CaCO_3+SiO_2$+3.68 wt.% CaF_2 at different temperature for 60 min.

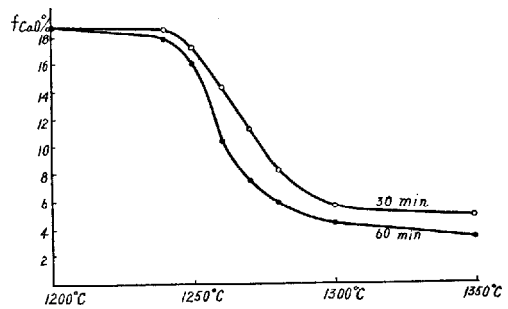

Fig. 13 Percentage of f·CaO of samples prepared with $3CaCO_3+SiO_2+30\%\ 3C_2S\cdot3CaSO_4\cdot CaF_2$ at different temperature

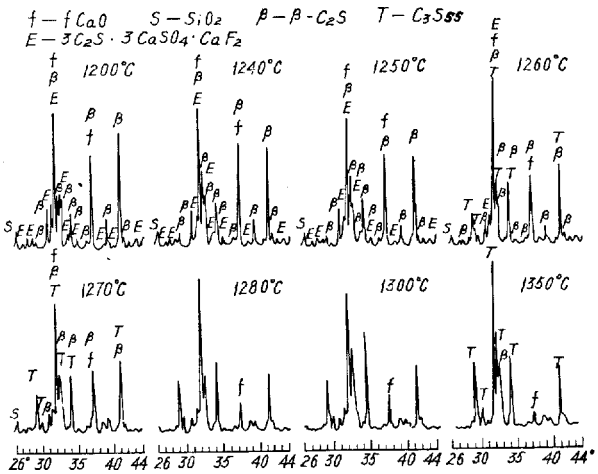

Fig. 14 XRD patterns of samples prepared with $3CaCO_3+SiO_2+30\%\ 3C_2S\cdot3CaSO_4\cdot CaF_2$ at different temperature for 60 min.

4. Conclusions

1). $C_{19}S_7\cdot2CaF_2$ forms at a temperature range of 1070-1160°C. At about 1110°C, the formation rate of $C_{19}S_7\cdot2CaF_2$ is maximal. The amount of $C_{19}S_7\cdot2CaF_2$ formed is almost maximal.

2). $C_{19}S_7\cdot2CaF_2$ is unstable at the temperature range at which it forms. Its formation and decomposition occur at the same time. Below 1110°C, the formation is the main trend, but above 1110°C, the decomposition is dominant. $C_{19}S_7\cdot2CaF_2$ disappears at 1170°C.

3). There is a lot of C_3S_{ss} "group" in $C_{19}S_7\cdot2CaF_2$. The decomposition of $C_{19}S_7\cdot2CaF_2$ promotes the formation of C_3S_{ss}. When $C_{19}S_7\cdot2CaF_2$ melts incongruently at 1170 °C, this promoting effect is more obvious. Its promoting mechanism is different from $3C_2S\cdot3CaSO_4\cdot CaF_2$, which is a mineral with a lower melt temperature and at 1250°C provides the liquidoid which is neccesary for the formation of C_3S.

REFERENCES:

1. PEIZHI FENG, DAMAO TONG, HONGFENG YI, "Study on the Promoting Effect of CaF_2 and $CaSO_4$ on the Formation of C_3S", 1984, (unpublished)
2. XIUJI FENG, BIN WU, "Study on the Reaction of Ferrari Cement Clinker with CaF_2 and $CaSO_4$, and the Forming Regularity of Their Main Phases", Cement, No. 8, 1983, pp. 7-16
3. C. GILIOLI, F. MASSAZZA, M. PEZZUOLI, "Study on Clinker Calcium silicates Bearing CaF_2 and $CaSO_4$", Cem. Concr. Res., 9(1), 1979, pp. 51-55
4. SHUZHEN YANG, "Study on the Composition and Character of Calcium Silico-Fluoride Phase A, and Phase Diagram of $CaO-C_2S-CaF_2$ System", M.Sc. Thesis, Wuhan Institute of Building Materials, 1982
5. BOLIN WU, "Formation Mechanism and Reaction Dynamics of Calcium Silico-Fluoride Phase A", M.Sc. Thesis, Wuhan Institute of Building Materials, 1982
6. RUILON YE, BOLIN WU, WEIDONG MA, "New Probe on the Mineralizing Mechanism of CaF_2", 1983, (unpublished)
7. W. GUTT, "Manufacture of Portland Cement from Phosphatic Raw Materials", Proc. 5th Int. Symp. Chem. Cem., Tokyo, 1968, Vol. I, pp. 93-105
8. J. MUKERJI, "Phase Equilibriam Diagram $CaO-CaF_2-C_2S$", J. of American Society, 48(4), 1965, p. 210
9. W. GUTT, G. J. OSBORNE, "The System C_2S-CaF_2", Trans. of the British Ceramic Society, 65(9), 1966
10. MITSUO TANAKA, GIICHI SODOH, SHIGEO AKAIWA, "New Compound $Ca_{12}Si_4O_{19}F_2$ in the System $CaO-SiO_2-CaF_2$ and the Role of CaF_2 in the burning of Cement Clinker", Proc. 5th Int. Symp. Chem. Cem., Tokyo, 1968, pp. 77-88
11. XIANGTAI REN, SHIFEN ZHOU, "Study on the Formation Mechanism of Calcium Silicate in $CaO-C_2S-CaF_2-CaSO_4$ System", Prof. Conf. Cem., 1983, pp. 185-194

P1

EFFECTS OF HIGH SHEAR MIXING ON HYDRATION BEHAVIOUR OF CEMENT PASTE AND RHEOLOGICAL INTERPRETATIONS

EFFETS DU MELANGE DE HAUTE TURBULENCE SUR L'HYDRATATION DE LA PATE DE CIMENT ET L'INTERPRETATION RHEOLOGIQUE

J.A. FORRESTER, Senior Research Fellow, King's College London
Formerly Chief Chemist, Cement & Concrete Association, U.K.

and

S.A. JEFFERIS, Lecturer in Civil Engineering
King's College London

The application of mechanical shear to a water cement mixture has a profound effect in the rate of hydration. The shear action also generates a product that modifies the rheological characteristic. These two functions add additional consideration to the chemistry of hydraulic cement hydration.

Mechanical shear can be considered as a slicing or grinding action on the surface of hydrating cement and can be said to exist in all concretes where shear action can arise from the impact of aggregate to aggregate contact. In special ways mechanical shear can be induced by purpose designed mixers. These usually incorporate rotor-stator geometries where a cement slurry will receive a strong shear action as it passes through the gap.

Cement hydration can be considered initially to be controlled by a through solution mechansim and later with deposits of hydrate products on cement surfaces the controlling action is by nucleation and diffusion control. The contribution to the mechanics of hydration introduced by mechanical shear is two fold. Firstly the removal of immediate colloidal hydrate products generates ideal nucleation sites for the deposit of through solution reaction products. Such sites act as alternatives to the cement particles themselves and hence deposition of retarding coatings is reduced. Secondly the physical removal of coatings allows access to fresh unhydrated cement surfaces.

The dispersion of colloidal particles of hydrated cement by shear action creates a liquid phase with unique properties that contribute to the rheological characteristics of cement water pastes or concrete.

The changes to the chemical kinetics are demonstrated by conduction calorimetry and rate of formation of hydration products. These are illustrated in the poster where it is shown that mechanical shear increases the rate and amount of silicate reaction and also shortens the time of reaction of aluminate with sulphate. The increase in amount of silicate reacted is confirmed by an increase in the rate of formation of calcium hydroxide. The effect on the sulphate reaction is similar to that induced by sulphate concentration. This similarity is to be expected as the rate has been shown to be a function of availability of reactants and shear can be expected to facilitate this availability.

The action of shear on rheological properties is demonstrated by the decrease in setting time and by the generation of thixotropic properties. An acceleration in the development of shearing threshold is demonstrated by measurements with a cone penetrometer and a Contraves viscometer. The latter indicates the creation of thixotropy. The generation of a gel like characteristic in the liquid phase increases cohesion and hence reduces tendency to bleed. This is a most desirable feature in grouting operations.

Examples of the practical applications of high shear mixing in grouting, waste disposal, self-draining concrete, cut-off wall construction, etc. are given in the poster.

Before rheological properties can be considered it is necessary to understand measurement procedures. In this note only two indicators of rheology/stiffening have been considered:
(i) rotational viscometry (ii) penetration testing. These techniques are not entirely separate but perhaps represent a continuum with rotational viscometry providing data at large strains possibly on an established failure surface and penetration testing providing data at generally much smaller strains and strain rates on a developing failure surface. However, as a result of the different processes involved the strength measured in a penetration test is quite distinct from the yield point determined by rotational viscometry. Considering first rotational viscometry:

If continuous rotation is employed then the rotation may establish a zone of preferred shear. Clearly such a zone cannot be produced in a pure liquid but in a particulate material it is quite normal and furthermore moisture migration to this zone is to be expected. Such moisture migration is well documented, for example in soil mechanics, and tends to reduce the shearing stresses. The migration is consistent with Le Chatelier's principle and may be regarded as a general phenomenon. Therefore, a simple rotational viscometry test is unlikely to measure the bulk properties of a paste but rather will measure the properties of an undefineable continuously sheared zone of water/cement ratio above the bulk value. A simple demonstration of this behaviour can be obtained using a viscometer with a stationary cup and rotating bob with torque measurement on the bob. The test requires a series of sleeves which can be inserted in the cup to reduce the bob to cup gap. With a Newtonian liquid reduction in the gap will increase the measured torque in a regular manner. However, for a series of cement pastes of water cement ratio 0.3 to 0.5 no effect was observed until the gap was reduced to less than 0.5mm at which point there was clearly audible grinding of the grains. Of course, insensitivity to the gap can be explained by a simple Bingham model. However, for the test situation equally simple calculations showed that this was not the case.

Thus in a rotational viscometry test one may have two distinct materials in the annular space between bob and cup: a fluid region of relatively high water/cement ratio adjacent to the moving surface and a stationary region of relatively lower water/cement ratio. These two materials will be rheologically distinct and it will not be possible to calculate the position of the interface between them from the rheological properties of the fluid region. The two materials will also show distinct development of properties with time and there may be further moisture migration.

A further demonstration of the complexity of water migration can be obtained by the use of serrated bobs. In a series of tests two bobs of identical overall diameter were used. One bob had a smooth stainless steel finish and the other had serrations 0.5mm deep. In general one might expect a serrated bob to tend to homogenise the mix and thus show higher shear stresses than a smooth bob. In practice the reverse was observed. Clearly the pumping action of the small serrations accentuated migration rather than reduced it. With deeper serrations homogenisation might be achieved. The fundamental point relating to rotational viscometry is that the system must be evaluated prior to the evaluation of results. External geometry seldom defines the internal behaviour except perhaps for very fluid mixes but for these settlement becomes a problem.

Considering now penetration testing:
Penetration tests can be operated at very low shear rates and continually expose new shear surface. At low shear rates viscous effects are negligible and the test thus measures solid type properties. As new surface is continually exposed the test tends to measure peak stresses rather than residual stresses. Whereas in rotational viscometry, even at very low strain rates, the actual magnitude of the strain will be large and hence the stress measured will be a post failure stress, that is residual stress. In a cementing material residual stresses must be expected to be significantly lower than the peak values.

As a detail of the test procedure consideration of the shape of the failure surface suggests that that data from cone penetration should be more straightforward to analyse than that from penetration of cylindrical rods and tests have shown this to be the case. In particular the relationship:

penetration load = ksh^2

where s is the shear strength of the paste,
h is the depth of penetration and
k is a constant related to the cone angle

has been demonstrated to be valid for cone penetration into cement pastes.

No satisfactory continuous function has been identified between the penetration resistance, s and h for penetration of rods except for narrow ranges of penetraton.

The introduction of controlled stress rheometers now means that stress build up prior to establishment of rotation can be studied. Hence both peak and residual stresses can be measured. Such results should be of great value in interpreting strength development results generally.

Having briefly considered the problems relating to rheological measurements it is now possible to discuss the effects of high shear mixing on rheology. High shear mixing changes the nature of a cement paste. A low shear mix is a two phase system of cement grains and water. High shear mixes tend towards a single phase material. The mixes contain sufficient colloid sized material to mask the effect of any remaining grains. As a simple analogy one may say that shearing converts a cement paste which would behave rather as a mix of very fine sand and water to the equivalent of a mix of clay and water with occasional fine sand grains. This change in paste structure is reflected in the development of cohesion and thixotropy of the mix and the suppression of settlement. Cohesion and thixotropy can be demonstrated by viscometric testing but great care must be paid to the selection of test geometries and shear rates. There is a vogue for the study of hysteresis loops for cement paste. Newcomers should be warned that even an empty viscometer will show an hysteresis loop due to the inertia of the system if rapid changes in shear rate are made.

M.J. COOLE and A.M. HARRISSON, Blue Circle Industries PLC, Research Division, Greenhithe, Kent.

THE EFFECT OF SIMULATED LARGE POUR CURING CONDITIONS ON THE TEMPERATURE RISE AND STRENGTH GROWTH OF PFA CONTAINING CONCRETE.

P

1. INTRODUCTION

The hydration of cement is an exothermic reaction which, in the case of large pours, can cause a considerable temperature rise in the concrete placed. When concrete is poured in a large quantity, it is necessary to be able to predict the temperature rise which may occur inside the mass because of the effect this may have on the ultimate properties of the hardened concrete. It is known that elevated temperatures may have a detrimental effect on the strength growth pattern of the concrete and that if the difference in temperature between the centre and surroundings of a pour exceeds 20 to 25°C cracking may occur[1,2,3]. Whether cracking occurs depends both on the magnitude of the temperature induced stress and the capacity of the concrete to accommodate the strain. The need to be able to predict these temperature rises is greater with composite cements, containing pfa or blast furnace slag, where the use of an extender introduces an additional uncertainty as to the effect of increased temperature on the development of strength with time. In the past, various methods have been employed to try to ascertain these effects, such as the adiabatic calorimeter and the vacuum flask calorimeter[4], but none of these methods is able to simulate the typical temperature-time profile of a large pour of concrete. In situ temperature measurement, using thermocouples placed at specific depths in the concrete, can be adopted and may be used to control an auxiliary cube curing bath thereby enabling internal strength values to be obtained[5&6]. This, of course is a retrospective method which can only give an indication of temperature profiles, and their effect on strength, in a structure when it is too late to undertake any corrective action.

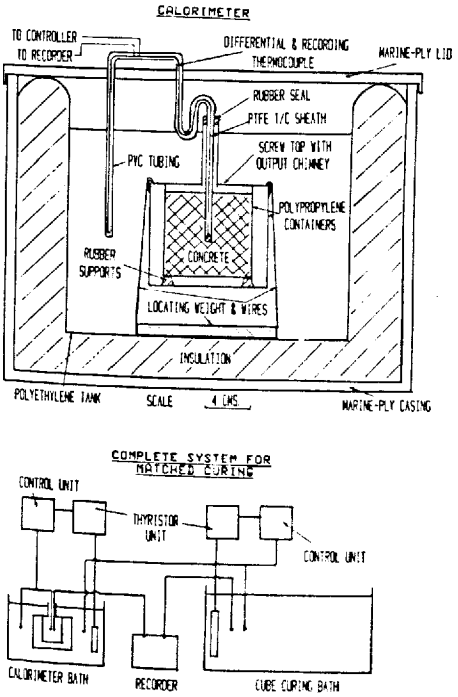

Fig. 1 Calorimeter and matched curing system

The calorimeter described in this paper (fully described by ref.7) is designed to simulate any size of pour of concrete, and to supply information on the associated temperature profile to a cube curing bath which follows the temperature of the main concrete sample by thermocouple control. Cubes from the curing bath can then be used to determine the development of strength in the simulated pour. This system (shown in Figure 1) only requires about 4 kg of cement to supply enough concrete for the control calorimeter and 12 (100mm) cubes. The equipment can therefore be used to explore the behaviour of a range of concrete mixes and composites, with regard to temperature rise and strength development, before undertaking a large pour on site.

2. EXPERIMENTAL

A pure Portland cement (OPC) and a Portland pfa cement (marketed in the UK as Phoenix), manufactured by intergrinding the same clinker with 25% pfa, were used to produce two 11 cube batches of concrete according to BS 4550. See Table 1 for chemical and physical characteristics. This provided enough concrete for the control calorimeter and for two 100mm cubes to be tested at ages of 1,3,7,28 and 91 days. The tests were carried out on both concretes with the control calorimeter set to give simulated pour sizes of 0.8,1.5 and 3 metres depth. Reference cubes were also cured at 20°C using the BS 4550 test procedure.

Small amounts of the Phoenix cement pastes were also stored with the cubes, in sealed plastic vials, so that the hydration could be stopped at the various curing ages in order to determine the amount of unreacted pfa, by a method of solution in diluted HCl (1:49). It was also thought useful to simulate the internal pressure experienced in a 3 metre pour, arising from the mass of concrete above, by mechanically loading the cubes. This was done by removing about 5mm of concrete from each cube mould and placing a steel plate (13mm thick), that was just able to slide within the 100mm mould, on top of the freshly mixed concrete. This plate was then loaded to 70 kPa uniaxially by placing a lead weight on top. On removal from underwater storage for testing, the cubes were also weighed and measured in order to determine the density of compaction. This was done after the saturated cubes had been surface dried.

After the strength tests were completed at the various stages of curing, the inside of each cube was sampled and hydration was stopped by dropping the sample into acetone. It was then prepared for examination by scanning electron microscopy. The sample was first dried under vacuum, then fractured, and the fracture surface was mounted on a stub and given a thin gold coating.

3. RESULTS

Figures 2,3 and 4 show the temperature rises obtained at the centre of simulated pours of 0.8, 1.5 and 3 metres deep respectively for both the OPC and the Phoenix mixes.

These show that as the pour size increased, although the Phoenix mix displayed a lower peak temperature than the OPC mix at all sizes, the time

P

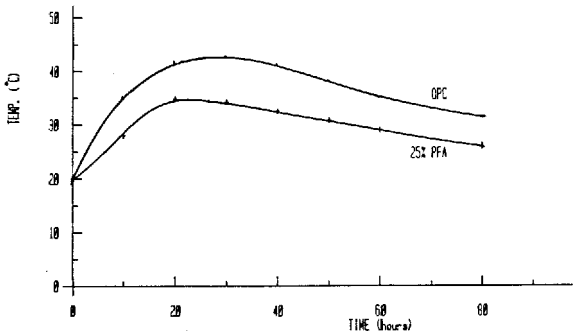

Fig.2 Temperature rise at centre of 0.8m pour

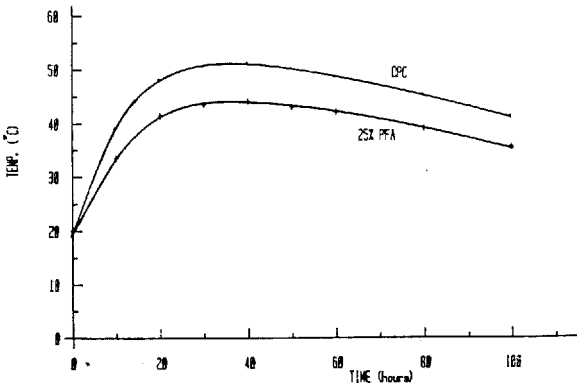

Fig.3 Temperature rise at centre of 1.5m pour

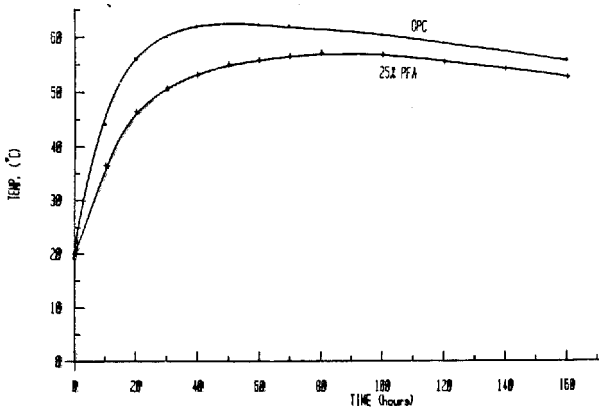

Fig.4 Temperature rise at centre of 3m pour

taken for the Phoenix mix to reach this maximum gradually increased, with respect to the OPC, until at 3 metres the time taken was nearly twice as long. It appears that once the higher temperatures of a 3 metre pour were reached, although the OPC hydration rate was accelerated as expected, the dilution effect of the pfa combined with increased reaction between the pfa and hydration products of the OPC, produced a lower early temperature rise but one which continued as the pfa reactivity increased to produce a much later peak temperature. This was also reflected in the strength growth of the concrete cured under the 3 metre simulated pour conditions (fig 5) as compared with concrete cured at standard 20°C conditions (fig 6).

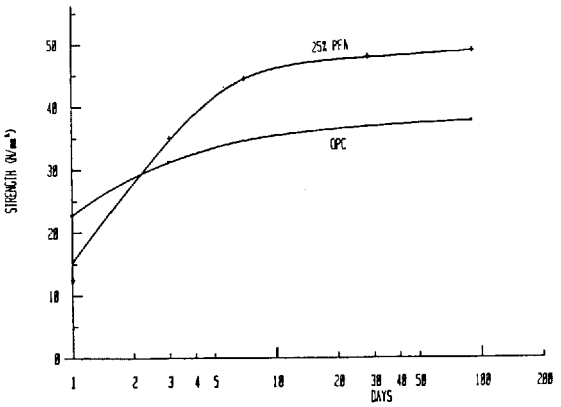

Fig.5 Strength at centre of 3m pour

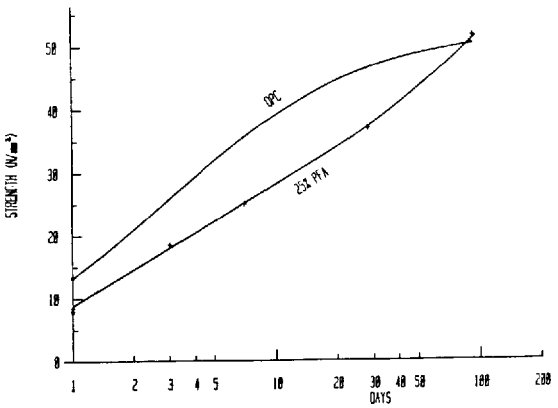

Fig.6 Strength cured at 20°C

With the OPC the rapid increase in temperature rise, and hence hydration rate, caused hydrates to grow in a rapid and perhaps disorganised manner, giving higher early strengths but eventually reduced later strengths. In contrast, the Phoenix concrete under these conditions produced a slower, more prolonged reaction which, together with reaction products between the pfa and OPC combined to give strength growth superior to that of the OPC concrete after 2½ days. Figures 7 and 8 show the strength growth in intermediate sized pours.

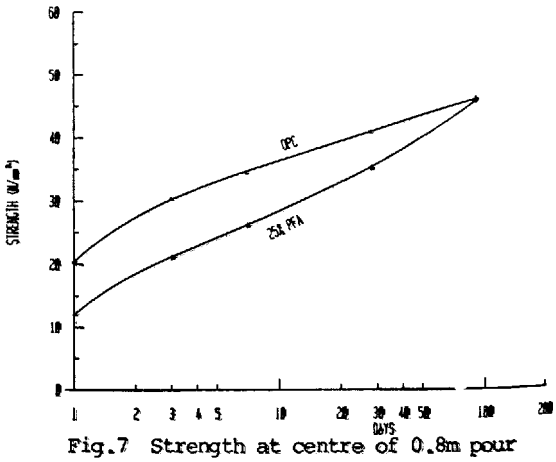

Fig.7 Strength at centre of 0.8m pour

P

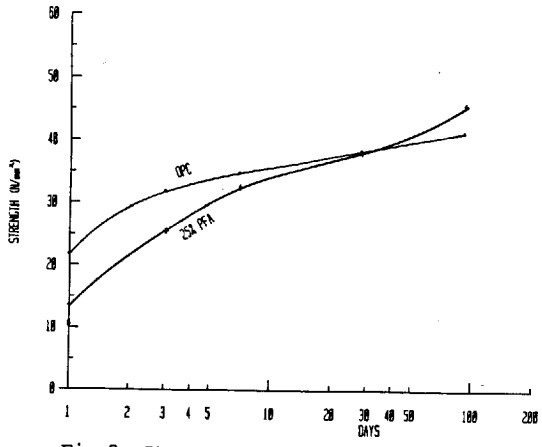

Fig.8 Strength at centre of 1.5m pour

The way in which the temperature has affected the strength growth of the Phoenix concrete, compared with the OPC concrete, is demonstrated in figures 9 and 10 where strength has been plotted against pour size at 1,3,7,28 and 91 days. This shows quite clearly the fall off in strength with increasing pour size for the OPC concrete after 7 days, whereas the Phoenix concrete was only slightly affected after 91 days.

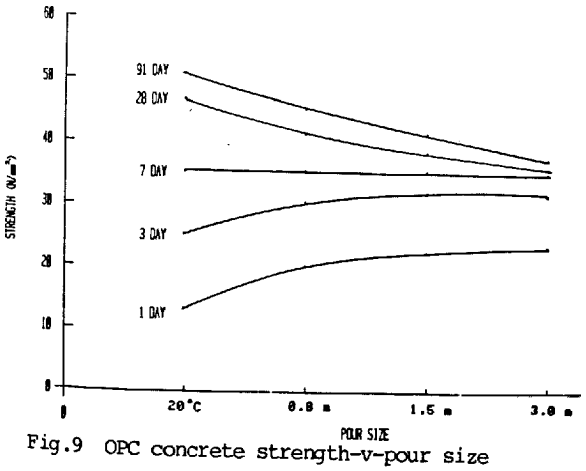

Fig.9 OPC concrete strength-v-pour size

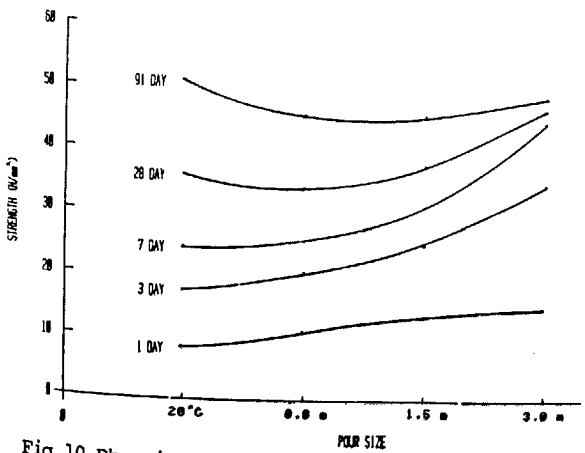

Fig.10 Phoenix concrete strength-v-pour size

The reaction rate of the pfa was determined at various ages, for each of the curing regimes mentioned, by arresting the hydration with acetone and measuring the amount of unreacted pfa by dissolving the ground sample in 1:49 hydrochloric acid (about 0.25N).

From these results (fig 11) it can be seen that the pfa reaction rate rapidly increases, in the larger pours, when a temperature of about 40°C or more is attained. This shows that in a 3 metre pour the amount of pfa reacted after 2-3 days can be expected to be similar to that reacted after 100 days curing at 20°C.

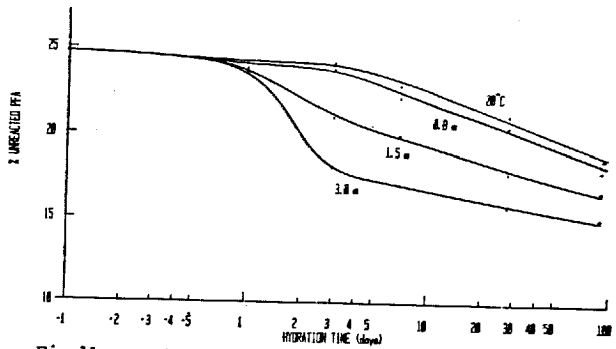

Fig.11 Reaction of pfa in hydrated Phoenix

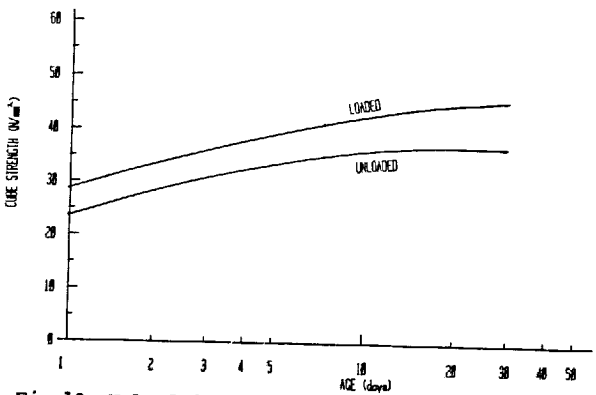

Fig.12 Unloaded and 70 kPa loaded cube strengths OPC concrete

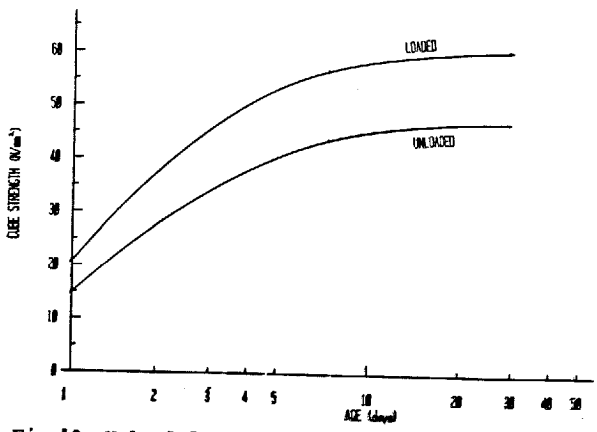

Fig.13 Unloaded and 70 kPa loaded cube strengths Phoenix concrete

The results of the tests in a simulated 3 metre pour with the 100mm cubes being loaded to 70 kPa are shown in figures 12 and 13. The strength results at 1,7 and 28 days show that loading the cubes improved the strengths for both OPC and Phoenix cement concrete. Fig 14 shows the predicted variation in 28 day strength with depth, through a 3 metre pour, as a consequence of both temperature and pressure effects.

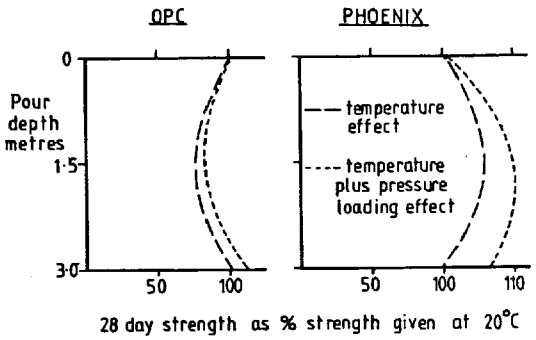

Fig.14 Predicted effect of temperature and pressure loading on 28 day strengths through a 3 metre pour.

Comparison between figures 12 and 13 shows that the concrete containing the Phoenix cement seemed to benefit most from this compaction. This could be a consequence of the better workability of the Phoenix concrete, resulting in a larger loss of expressed water, but may also be related to better hydrate morphology under load. Concrete w/c ratios could be adjusted to minimise any associated increase in bleeding.

In general, the results of the examination by scanning electron microscopy (SEM) reflect the concrete cube strength results. It is possible to relate the strength at a given age or in a given pour size to the observed degree of hydration of the pfa, and the maturity of the hydrate phases. The photographs shown as Figs 15-20 were selected as being representative of the degree of hydration in the concretes at 1,7 and 91 days. Figs 15,16 and 17 are from the 0.8m Phoenix concrete and Figs 18, 19 and 20 are from the 3.0m Phoenix concrete. At 1 day, the degree of reaction of the pfa spheres was limited to a similar extent in both size pours. The spheres was coated with calcium silicate hydrate (C-S-H) of an immature type but the sphere surfaces appeared uncorroded and the C-S-H resulted from precipitation of the outer product from the cement clinker phases.

By 7 days, the pfa in the 0.8m pour was still virtually unreacted, the smooth surface being visible through the now more mature C-S-H. In the 3.0m, concrete, the reaction of the pfa had proceeded to a considerably more advanced stage. Fig.19 shows the spherical shape of a pfa relief which has been almost all replaced by C-S-H, having a radial appearance characteristic of inner product from pfa spheres. The difference in compressive strengths of the two concretes directly reflects the differences seen in the photographs, the 0.8m concrete having a strength of 26.0 Nmm^{-2} and the 3.0m concrete, 42.1 Nmm^{-2}.

The two 91 day concretes show marked similarities and the two photographs given as Figs 17 and 20 show that spheres have reacted to a considerable extent in both concretes. The 0.8m pour has now caught up both in microscopic appearance and strength, the two values being 45.9 Nmm^{-2} for the 0.8m concrete, and 45.2 Nmm^{-2} for the 3.0m pour.

The white line displayed on all the photographs shown below represents 1 μm.



Fig.15 Phoenix, 1 day (0.8m)

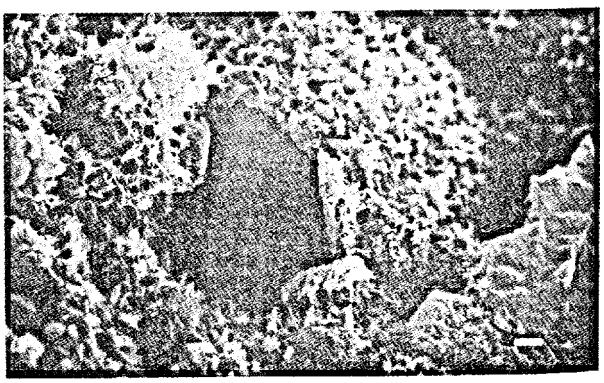

Fig.16 Phoenix, 7 day (0.8m)

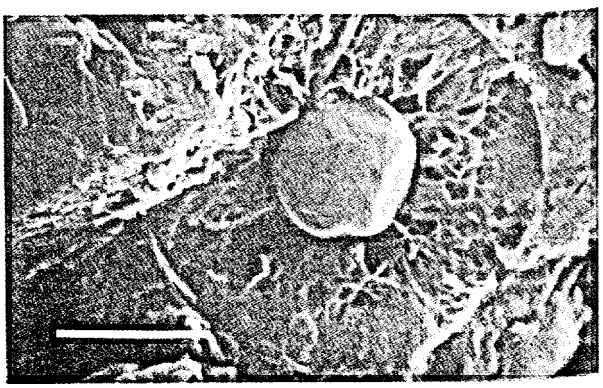

Fig.17 Phoenix, 91 days (0.8m)

P

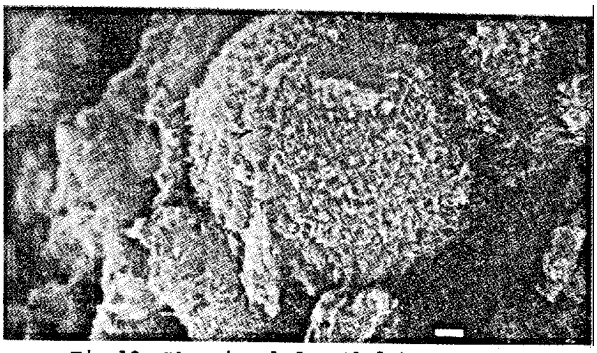

Fig.18 Phoenix, 1 day (3.0m)



Fig.19 Phoenix, 3 day (3.0m)

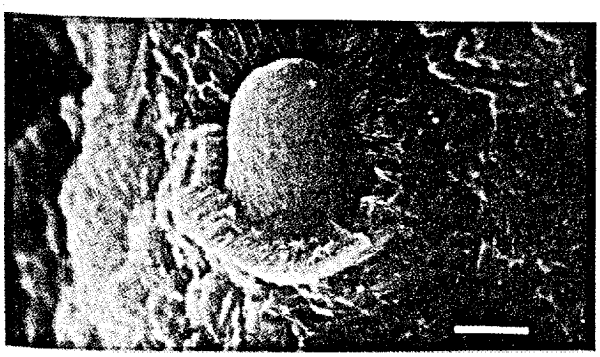

Fig.20 Phoenix, 91 day (3.0m)

Table 1 - Chemical and Physical Characteristics

	O.P.C.	Phoenix Cement	P.F.A
SiO_2	20.1	28.4	51.3
I.R.	0.57		
Al_2O_3	4.7	10.4	27.4
Fe_2O_3	2.5	4.2	9.2
Mn_2O_3	0.18	0.13	0.07
P_2O_5	0.12	0.15	0.23
TiO_2	0.22	0.41	0.97
CaO	64.4	48.6	1.2
MgO	2.1	2.0	1.6
SO_3	2.6	2.4	0.92
L.O.I.	1.4	1.3	2.0
K_2O	0.72	1.4	4.1
Na_2O	0.20	0.36	1.2
F	0.10	0.07	-
Free Lime	2.5	1.8	-
SSA	405	397	-
45 μ res.	9.3	5.3	8.4

4. CONCLUSIONS

1. The results show that Portland pfa cement can produce increased core strength in mass concrete pours where the temperature rise would normally reduce the strength of an OPC concrete to about 70% of its expected value.

2. From the temperature profiles of the simulated pours it can be seen that the interground pfa cement produced lower temperature rises, at later ages, than the OPC, so reducing the thermally induced stresses within a large pour.

3. Although the pfa was slow to react with OPC at standard curing conditions, once the curing temperature exceeded 40°C the reaction rate increased markedly. The extent of this acceleration is such that at the centre of a 3 metre pour, the amount of pfa reacted after 2-3 days can be expected to be similar to that reacted following 100 days curing at 20°C.

4. Simple mechanical loading of the sample cubes showed that, at 28 days, the pressure generated by the mass of concrete above can be expected to reduce the strength loss at the centre of the large OPC pours and further enhance the strength of Portland-pfa pours. Consequently, a full simulation of large pour conditions should include this loading factor.

5. ACKNOWLEDGEMENTS

The authors would like to thank both Dr.G.K. Moir and J.J. Kollek for their assistance and Blue Circle Industries PLC for permission to publish this work.

6. REFERENCES

1. DUNSTAN, M.R.H., MITCHELL, P.B. Results of a thermocouple study in mass concrete in the Upper Tamar Dam. Proc. Inst. Civ. Engrs. Part 1, 60, Feb, Feb.27-52, (1976).

2. FITZGIBBON, M.E. Joint free construction in rich concretes 20 or 2000 m^3. Appraisal decision and thermal control. Symposium (1973).

3. FITZGIBBON, M.E. Large pours 2. Heat generation and control. Current practice sheet 35, Concr. Mag. (1976).

4. ALEGRE, R. La Calorimetrie des ciments au C.E.R.I.L.H. Revue des Materiaux.

5. BLAKEY, H. Temperature matching curing bath - an aid to earlier formwork striking. Concrete (1976).

6. CANNON, R.P. Measurement of the in situ strength and temperature development of concretes containing Portland and Portland blastfurnace cements. Silicates Industriels (1982).

7. COOLE, M.J. Calorimetric Studies of the Hydration Behaviour of Extended Cements, British Ceramic Preceedings No.35 (1984).

REACTIONS PERIODIQUES LORS DE L'ATTAQUE DES CIMENTS PAR DES REACTIFS CHIMIQUES

C. VERNET - SOCIETE DES CIMENTS FRANCAIS C.E.R.E.G.

P

1 - INTRODUCTION

Ce travail se situe dans le cadre d'une recherche à long terme sur les mécanismes réactionnels à l'interface ciment-eau, ayant pour but d'en déterminer les différentes étapes élémentaires. Pour cela, on s'intéresse, non seulement au milieu aqueux, mais aussi aux milieux non aqueux, qui permettent de faire varier les propriétés du solvant ou l'activité de l'eau et peuvent déboucher sur des applications intéressantes dans le domaine du dosage des phases par dissolution sélective.

Au cours d'une étude sur l'attaque acide de l'alite en milieu méthanol, en circuit ouvert, (extension de la méthode de TAKASHIMA), nous avons remarqué des fluctuations des concentrations en espèces dissoutes. Nous précisons ici les conditions dans lesquelles apparaissent ces fluctuations périodiques, qui sont faciles à mettre en évidence à l'aide des moyens modernes de la chromatographie HPLC.

2 - MONTAGE EXPERIMENTAL - PRINCIPE

Le montage dérive d'un système de chromatographie HPLC avec programmateur de gradients, dans lequel on a remplacé la colonne par un filtre en ligne, contenant un disque de poudre compactée de l'échantillon à étudier. A travers ce disque, on peut donc faire circuler à l'aide des pompes haute pression, un réactif de composition déterminée par le programmateur de gradients (FIG. 1).

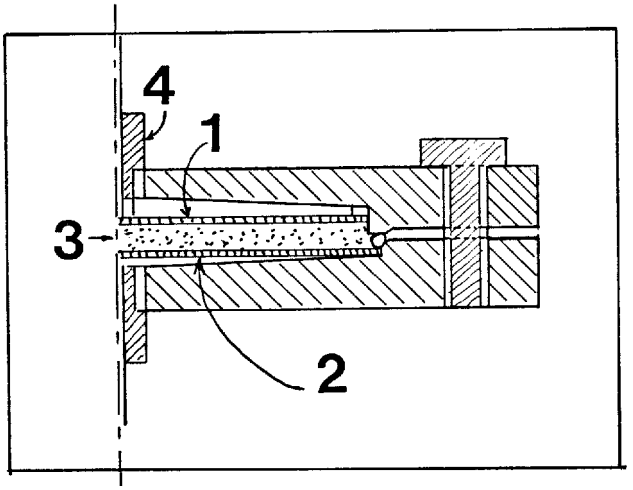

FIG. 1 - SCHEMA DU FILTRE EN LIGNE

1 Diffuseur
2 Grille support de filtre
3 Poudre compactée
4 Connecteur d'alimentation

Le passage en solution du composé étudié est détecté par une sonde conductimétrique à circulation, reliée à un système d'enregistrement.

La seule difficulté technique de la mesure réside dans la manière de réaliser le disque de poudre compactée, de façon à obtenir une répartition uniforme de la matière et éviter ainsi des passages préférentiels de réactif, qui pourraient s'accentuer jusqu'au percement du disque. Pour cela, il est bon de saupoudrer l'échantillon sur le filtre, en interposant un tamis de maille voisine de 160 microns.

3 - RESULTATS

Nous donnons ici quelques résultats obtenus pour les constituants des clinkers, soumis à une percolation par une solution d'acide acétique dans le méthanol, préparée par mélange automatique d'une solution mère à 1 Mol/l avec du méthanol pur. Le programmateur était réglé pour effectuer des paliers successifs de la proportion d'acide, entre 0 et 30 %, de façon à mesurer la période des fluctuations en fonction de la concentration en acide.

Cas de l'alite

On peut constater (Fig. 2), que le régime périodique se déclenche à partir d'un seuil situé vers 4 % de solution 1 M, pour une pastille de 47 mm de diamètre contenant 3 g d'alite broyée, de surface spécifique voisine de 3500 cm^2/g, traversée par un débit de réactif de 3 ml/mn. La fréquence et l'amplitude des fluctuations augmentent pour chacun des paliers de concentration en acide. La fréquence est proportionnelle à la concentration de l'acide acétique :

$$F = 3,8\ C$$

avec : F = Fréquence en mn - 1
C = Concentration molaire de l'acide acétique.

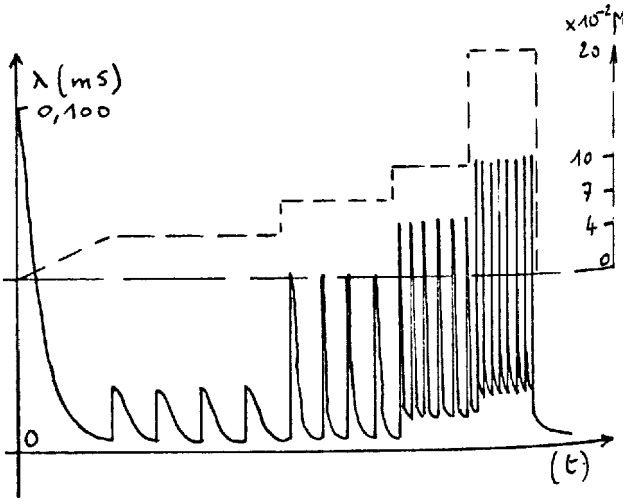

FIG. 2 - ALLURE DES FLUCTUATIONS PERIODIQUES

---- Gradient d'acide acétique
____ Signal conductimétrique

C. VERNET - SOCIETE DES CIMENTS FRANCAIS - C.E.R.E.G.

P

Les pics périodiques de conductivité ont une forme assymétrique. On observe une montée très rapide, correspondant à un passage en solution très rapide, puis une décroissance d'allure exponentielle.
La hauteur h des pics, traduisant la quantité d'ions libérés, montre une discontinuité en fonction de la concentration d'acide. Le graphe h = f(C) se présente comme une courbe de titrage conductimétrique, avec deux segments de droite de pentes différentes, le point d'intersection se situant vers c = 0,1 Mol/l (Fig. 3).

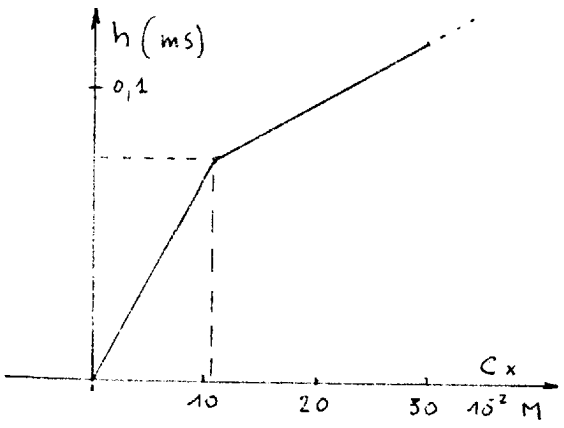

FIG. 3 - EVOLUTION DE LA HAUTEUR DES PICS

LE LONG DU GRADIENT

Autres constituants du clinker

Un comportement identique est constaté pour les autres constituants du clinker. La fréquence et l'amplitude des fluctuations sont beaucoup plus faibles pour les produits peu réactifs, comme la bélite et l'aluminoferrite, que pour le silicate et l'aluminate tricalcique.

4 - INTERPRETATION

Nous ne pouvons tenter ici une analyse détaillée de ces phénomènes périodiques, sur la base des premiers résultats expérimentaux. Leur interprétation nécessite des informations complémentaires, comme la composition chimique de la solution à la sortie du détecteur conductimétrique, ce dernier n'apportant qu'une information globale sur les concentrations en espèces dissoutes. La forme des pics et la discontinuité de l'évolution de la hauteur des pics semblent montrer que le mécanisme réactionnel comporte au moins deux étapes, dont la première est extrêmement rapide.

Dans l'interprétation du mécanisme, l'utilisation de la thermodynamique des processus irréversibles (T.P.I.) devrait se montrer intéressante. En effet, ce type de réactions périodiques n'est habituellement observé que dans des systèmes chimiques ouverts, appelés "structures dissipatives chimiques", où des couplages se manifestent entres diverses forces motrices (force chimique, force de diffusion, force électrocinétique) et les flux qui en résultent (taux de réaction, flux de diffusion, variation des charges électriques superficielles).

Les phénomènes observés ici présentent des analogies frappantes avec des réactions périodiques du type ZHABOTINSKI, de même qu'avec les réactions de précipitation dans des gradients de diffusion (anneaux de LIESEGANG), dont l'étude est du domaine de la T.P.I.

EVOLUTION DE LA MICROSTRUCTURE DES HYDRATES DES CIMENTS - ASPECTS THEORIQUES

C. VERNET - SOCIETE DES CIMENTS FRANCAIS C.E.R.E.G.

1 - INTRODUCTION

Depuis la thèse d'Henry LE CHATELIER, au début du siècle, de nombreuses études ont été publiées au sujet des mécanismes de l'hydratation des ciments. Il semble bien établi aujourd'hui que, au moins aux premiers âges, l'hydratation soit gouvernée par des processus de dissolution-précipitation, dont on cherche encore à décomposer les étapes élémentaires. Les lois qui régissent la croissance cristalline des hydrates seraient donc, d'une part, celles de la diffusion des espèces ioniques à partir des surfaces des grains, et d'autre part, les équations de vitesse des réactions de précipitation, traduisant les phénomènes de germination-croissance.

Si l'on cherche à donner un formalisme mathématique à ces mécanismes, dans le but de construire un modèle physique, on rencontre de grandes difficultés par exemple, devant le problème de la diffusion convective, qui est celui de pâtes de ciment immobiles. Dans le cas plus abordable de la diffusion régulière, où l'on peut faire entrer les suspensions agitées régulièrement, les solutions des systèmes différentiels issus de la combinaison des lois de FICK et des équations de vitesse des réactions, ne sont pas toujours stationnaires. La diffusion dans un gel peut par exemple produire des structures périodiques comme "les anneaux de LIESEGANG", découverts en 1896. En observant que la complexité de ces cas est liée surtout à celle du formalisme des équations de vitesse (par exemple lorsque le mécanisme comporte une étape autoctalytique), nous nous proposons d'étudier ici quelques modèles mathématiques très simplifiés, où nous envisagerons des équations de vitesse de forme simple, dans le cas de la diffusion plane unidimensionnelle. Bien que ces hypothèses de travail soient extrêmement réductrices de la réalité physique, quelques remarques peuvent en être tirées, concernant des particularités connues de la microstructure des hydrates.

2 - MISE EN EQUATIONS

Soit une réaction de précipitation de la forme :

$$A + nB \rightarrow AB_n \qquad (1)$$

Pour que cette réaction se poursuive, il faut que le taux de sursaturation, c'est-à-dire le rapport du produit ionique effectif au produit ionique à l'équilibre :

$$\tau_s = S_p / S^*_p = \frac{(A)(B)^n}{S^*_p}$$

soit supérieur à 1. L'enthalpie libre de la réaction (1) est alors négative :

$$\Delta G_p = - RT \, Ln \, \tau_s$$

La modification des gradients de diffusion des espèces A et B, que l'on suppose générées par la dissolution de grains anhydres va dépendre des vitesses relatives de diffusion et de précipitation.

Nous écrirons que le régime stationnaire auquel nous nous intéressons, est obtenu lorsque dans un intervalle de temps dt, la quantité des espèces apportées par diffusion, dQd, est égale à la quantité dQp consommée par la précipitation.

Pour chacune des espèces, dQd est tiré des lois de FICK :

$$dQd_i = - D_i S \, \partial C_i / \partial x \, . \, dt$$

où D est le coefficient de diffusion, S la surface de l'interface génératrice et C la concentration à la distance x de cette interface.

dQp est tirée de l'équation de vitesse de la réaction (1) :

$$dQp_i = A.V. \, f(C_i). \, dt$$

où f(Ci) est la fonction de vitesse, V le volume de solution et $A = A_o \, e^{-E/RT}$ est la constante de vitesse de la réaction (1).

Dans le cas de la diffusion plane unidimensionnelle, l'égalité de dQd et dQp s'écrit :

$$\frac{dC_i}{f(C_i)} = - \frac{AV}{D.S} \, . \, dx$$

C'est donc la forme de la fonction de vitesse f(Ci) qui va déterminer la forme des solutions. Deux cas particuliers simples peuvent être envisagés :

- Précipitation très rapide, limitée uniquement par la diffusion de l'ion de concentration C. On peut poser :

  $$f(C_i) \sim k(C_i - C_i^*)$$

  où C* est la concentration loin de l'interface.

- Précipitation lente, limitée par la cinétique de germination-croissance du précipité. On posera alors :

  $$f(C_i) = B. \, \tau_s$$

  où τ_s est le taux de sursaturation et B une constante.

3 - RESULTATS

Nous nous limiterons ici au cas où f(C) a une expression linéaire (précipitation rapide). Deux situations peuvent alors se présenter :

- les ions formant le précipité sont issus de la même interface (cas de l'alite donnant des CSH)

- les ions proviennent de la dissolution de 2 minéraux distincts (formation d'ettringite).

C. VERNET - SOCIETE DES CIMENTS FRANCAIS C.E.R.E.G.

1er cas. Ions de même origine

Les solutions sont de la forme :

$$(C - C^*) = (C_o - C^*) \exp\left(-\frac{V.A.}{D.S} . k.x\right)$$

où C^* est la concentration loin de l'interface et C_o la concentration à l'interface.

Il est pratique d'utiliser les paramètres habituels des ciments, surface spécifique s et rapport eau/solide r, au lieu du rapport V/S qui devient V/S = r/s.

Dans le cas ci-dessus, le taux de sursaturation est maximum à l'interface génératrice, qui sera donc un site privilégié de précipitation et l'on obtiendra des hydrates précipitant plus loin de l'interface lorsque les gradients seront plus faibles, c'est-à-dire lorsque s sera élevé, r faible et le rapport A/D des constantes de vitesse et de diffusion sera faible (Fig. 1).

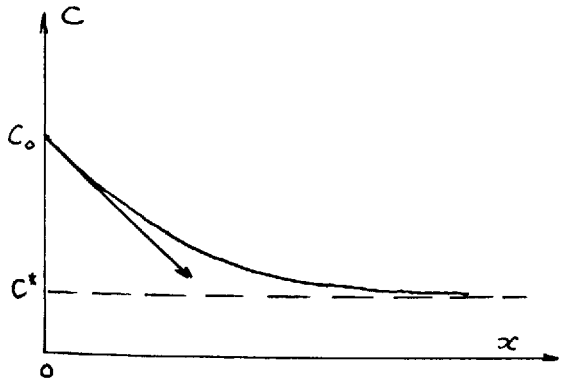

FIG. 1 -GRADIENT DE CONCENTRATION AVEC PRECIPITATION

L'interface génératrice est à l'abcisse x = 0

On constate que ce premier schéma très grossier est cohérent avec les données expérimentales sur l'évolution de la microstructure des silicates hydratés, en particulier l'obtention de fibres plus longues aux faibles E/S et les différences observées en fonction de la composition de la solution interstitielle.

2ème cas. Ions diffusant en sens inverse à partir de 2 interfaces génératrices (Fig. 2).

Les gradients des deux espèces ioniques s'écrivent à l'aide du formalisme précédent :

$$y = (C_1 - C_1^*) = (C_{o1} - C_1^*) \exp\left(-\frac{V.A_1}{S.D_1} . x\right)$$

$$z = (C_2 - C_{o2}) = (C_2^* - C_{o2}) \left[1 - \exp\left(-\frac{V.A_2}{S.D_2} .x\right)\right]$$

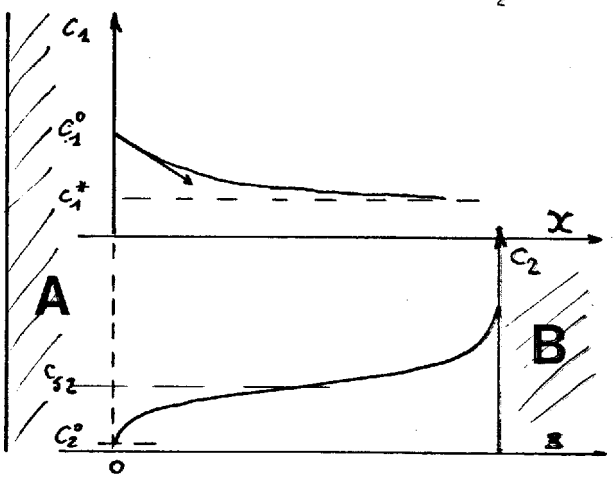

FIG. 2 - DIFFUSION INVERSE AVEC PRECIPITATION

La phase A génère l'ion de concentration C_1.
La phase B génère l'ion de concentration C_2.

On pose : $y = y_o \exp(-k_1 x)$

$$z = z_o . [1 - \exp(-k_2 . x)]$$

L'expression du taux de sursaturation sera la suivante :

$$\tau_s(x) = \frac{y.z^n}{S^*}$$

Posons $u(x) = S^*.\tau_s$

$$= \exp(-k_1 x) [1 - \exp(- k_2 . x)]^n .$$

La fonction du/dx s'annule pour :

$$x_m = \frac{1}{k_2} . l_n \left(n \frac{k_2}{k_1} + 1\right)$$

C. VERNET - SOCIETE DES CIMENTS FRANCAIS C.E.R.E.G.

Le taux de sursaturation passe donc par un maximum, à une distance xm de l'interface (Fig. 3). Cette distance est liée uniquement aux constantes thermodynamiques et cinétiques, dans l'hypothèse de travail qui avait été choisie, soit une expression linéaire des constantes de vitesse (Il n'en serait pas de même avec les expressions non linéaires).

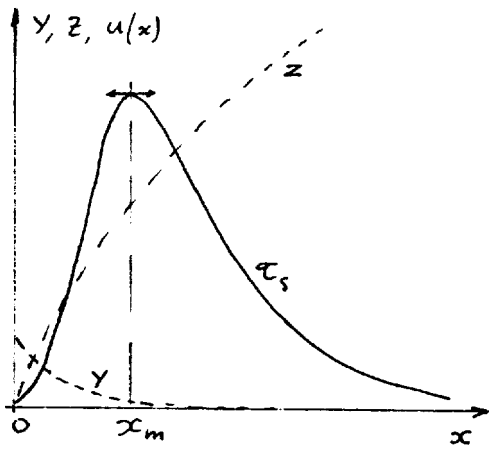

FIG. 3 - TAUX DE SURSATURATION DANS LE CAS DE LA DIFFUSION INVERSE

Ces résultats semblent également cohérents vis-à-vis des observations de la microstructure : l'existence de "coquilles d'ettringite" ou "grains de HADLEY" autour des cristaux de C_3A a été rapportée plusieurs fois.

4 - CONCLUSIONS

Ces quelques exemples simplifiés à l'extrême montrent tout l'intérêt de la modélisation des processus d'élaboration de la microstructure. Nous sommes encore très loin de pouvoir établir une relation formelle explicite entre l'évolution des taux de réaction et l'évolution des résistances mécaniques et notre démarche théorique donne la mesure des difficultés qu'il faudra vaincre pour y parvenir. Mais nous pouvons remarquer que la microstructure des hydrates ne s'établit pas totalement au hasard et qu'elle obéït aux lois habituelles des processus irréversibles. On peut donc espérer des progrès dans la compréhension de ces phénomènes, en comptant sur les moyens informatiques modernes, qui nous apportent une aide appréciable pour la résolution numérique des systèmes différentiels.

UN NOUVEL INSTRUMENT POUR L'ETUDE DES REACTIONS D'HYDRATATION : LE GECS (GENERATEUR ELECTROCHIMIQUE DE CHAUX SURSATUREE)

C.VERNET - SOCIETE DES CIMENTS FRANCAIS C.E.R.E.G.

1 - INTRODUCTION

Les réactions d'hydratation des ciments se déroulent en général dans le domaine sursaturé de la portlandite $Ca(OH)_2$. Ceci constitue un obstacle à la reconstitution en laboratoire des conditions réelles de la formation et de la croissance des hydrates, telles qu'elles se produisent dans les mortiers et bétons. En effet, l'instabilité des solutions sursaturées rend leur étude expérimentale difficile, et il n'existe pas de méthode fiable, permettant de créer un état de sursaturation déterminé, pendant un temps suffisamment long.

Le développement d'un appareillage répondant à cette question se justifie par exemple dans les applications suivantes :

- Etude de la période dormante, des phénomènes de germination-croissance de la portlandite et du CSH
- Etude des adjuvants des bétons et des modificateurs de la diffusion des ions à l'interface solide-liquide.
- Etude du mécanisme de l'hydratation de C_3S, grâce à la séparation des variables (flux de dissolution et de précipitation).
- Etude des diagrammes d'équilibre des hydrates dans le domaine sursaturé en chaux.
- Synthèse des hydrates en régime de sursaturation contrôlé.
- Mesure de la réactivité des matières pouzzolaniques et des ajouts minéraux.

Malgré ces applications nombreuses et importantes, seules quelques tentatives ont été faites dans ce domaine. La génération de solutions sursaturées en utilisant des résines échangeuses d'ions n'a pas permis de résoudre le problème, car cette technique présente l'inconvénient de libérer des impuretés anioniques et ne permet pas de maintenir un taux de sursaturation élevé pendant un temps suffisamment long, ni de faire varier ce taux en système fermé.
Nous avons donc tenté une nouvelle approche du problème en nous orientant vers les méthodes électrochimiques qui répondent bien aux impératifs techniques des mesures.

2 - IMPERATIFS TECHNIQUES DU SYSTEME

- La technique de sursaturation ne doit pas faire appel à la dissolution d'une phase solide, dont la surface réactive ou les propriétés évolueraient en fonction du temps.
- Le générateur doit être capable de fournir une solution très sursaturée en chaux, dont la concentration atteigne par exemple 40.10^{-3} $Mol.kg^{-1}$ avec une vitesse de sursaturation équivalente à celle de l'alite des ciments, soit 1 à 4.10^{-2} $Mol.kg^{-1}.h^{-1}$.
- La quantité de solution de travail soit être suffisante pour effectuer tous prélèvements et dosages, soit 100 à 500 ml.
- On s'orientera de préférence vers un système permettant de régler à volonté le débit de calcium fourni et, au besoin, de réaliser des asservissements à l'aide de capteurs, dans le but d'effectuer une régulation automatique du degré de sursaturation.

3 - PRINCIPE (Fig. 1)

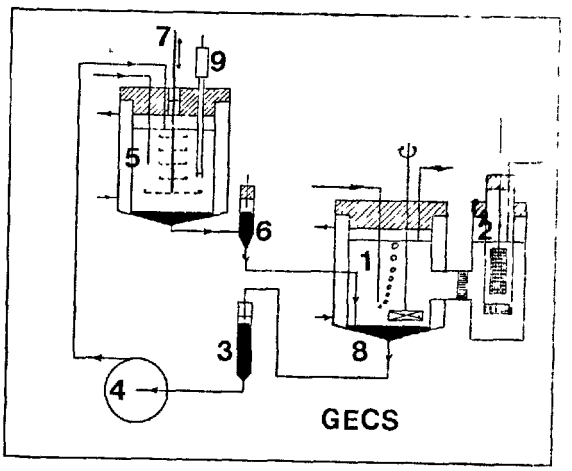

FIG. 1 - SCHEMA DE PRINCIPE DU G E C S

1 Cellule d'électrolyse Compartiment cathodique
2 Cellule d'électrolyse Compartiment anodique
3 Decanteur
4 Pompe
5 Cellule d'hydrolyse
6 Siphon
7 Tige du vibreur
8 Amalgame liquide de calcium
9 Sonde conductimétrique

Nous avons choisi un générateur de type coulométrique, constitué d'une cellule d'électrolyse, où l'on produit une solution de calcium métallique dans le mercure, selon l'équation :

$$Ca^{2+} + 2\ e^- + Hg \rightarrow Ca(Hg)$$

Cet amalgame liquide est introduit en continu dans une cellule d'hydrolyse, où le calcium est libéré au contact de l'eau, en produisant la solution de chaux, selon l'équation :

$$Ca(Hg) + 2\ H_2O \rightarrow Ca^{2+} + 2\ OH^- + H^2 + Hg$$

A la sortie de la cellule d'hydrolyse, le mercure est recyclé en continu vers la cellule d'électrolyse, où il se recharge en calcium.

4 - FONTIONNEMENT. ASPECTS TECHNIQUES

4.1 - CELLULE D'ELECTROLYSE (FIG. 1)

Le potentiel de décharge des ions calcium sur la nappe de mercure est inférieur au potentiel de réduction de l'eau. Ceci va limiter le rendement électrochimique du générateur. On peut faire reculer le "mur du solvant" en augmentant le pH de l'électrolyte, mais il ne faut pas dépasser le produit de solubilité de la portlandite, ce qui ferait chuter l'activité du calcium, qui doit rester la plus élevée possible, pour faciliter la diffusion. En pratique, l'électrolyte étant constitué d'une solution molaire d'acétate de calcium, le pH optimum se situe vers 11. Au cours de l'électrolyse, le pH a tendance à s'élever, à cause de la réduction cathodique de l'eau :

$$2\ H_2O + 2\ \rightarrow 2\ OH^- + H_2$$

Cette variation est éliminée en établissant une circulation d'électrolyte tamponné dans la cellule d'électrolyse. L'excès d'électrolyte est pompé au niveau du compartiment anodique, ce qui présente l'avantage d'éviter la rétrodiffusion de l'oxygène libéré à l'anode, vers le compartiment cathodique. Cette rétrodiffusion peut être également diminuée par l'utilisation d'une anode oxydable de grande surface (mercure, fer, carbone).

- A la sortie de la cellule, l'amalgame traverse un décanteur, qui sert à éliminer les traces d'électrolyte entraînées par capillarité, à réaliser l'isolation galvanique et à permettre des prélèvements d'amalgame à des fins analytiques.
- L'amalgame est ensuite pompé vers la cellule d'hydrolyse. La forte variation de la viscosité en fonction de la teneur en calcium du mercure oblige à utiliser un asservissement de débit.

En régime stationnaire, la concentration en calcium de l'amalgame à la sortie du décanteur peut s'écrire :

$C1 = C2 + rI/2d.F$ où

C2 est la concentration en calcium du mercure entrant dans la cellule (recyclage)
r est le rendement d'électrolyse,
I est le courant de génération,
d est le débit de mercure,
F est le Faraday

4.2 - CELLULE D'HYDROLYSE (FIG.1)

Cette cellule est thermostatée et équipée d'une sonde conductimétrique permettant de mesurer en continu la concentration en chaux de la solution.

Le rendement d'hydrolyse dépend de la concentration en chaux dans la cellule, de la surface d'échange amalgame-solution et du régime de diffusion du calcium à l'interface.

- Le premier de ces paramètres n'intervient que faiblement dans le domaine très sursaturé, au-delà de 25 mMol/kg. En effet, l'hydrolyse se produit hors de l'équilibre et la concentration en chaux dans la cellule agit principalement sur la valeur du gradient de diffusion à l'interface.
- Pour augmenter au maximum la surface d'échange, la cellule est équipée d'un système de plateaux perforés, sur lesquels ont fait arriver l'amalgame. Les plateaux horizontaux sont fixés sur une tige verticale, actionnée par un vibreur, ce qui permet de pulvériser l'amalgame en fines gouttelettes. Le fond de la cellule constitue un décanteur où se forme une large nappe de mercure, dont la surface vient s'ajouter à celles des gouttes. Le mercure est évacué en continu par un siphon et retourne vers la cellule d'électrolyse.
- Le régime de diffusion à l'interface mercure-solution est stationnaire tant que l'on ne dépasse pas un taux de sursaturation trop élevé. Dans ce cas, la vitesse d'hydrolyse reste constante et pour un courant de génération constant, la concentration en chaux de la solution augmente linéairement avec le temps. Pour une densité de courant d'électrolyse de 20 mA/cm^2, un débit de mercure de 200 g/mn, cette augmentation est de l'ordre de 20 mMol/kg.h, valeur satisfaisante comparativement à la vitesse de libération de chaux par l'alite.

Dans le domaine très sursaturé, la précipitation de la portlandite a tendance à s'amorcer dans un film de solution qui s'insère par capillarité entre le mercure et la paroi du récipient. Cet inconvénient est difficile à éviter. Un bon échange du calcium des gouttelettes et l'utilisation de parois hydrophobes sont donc indispensables.

5 - RESULTATS

Les courbes de conductivité obtenues pour des courants de génération constants sont très semblables à celles que l'on observe pour les suspensions d'alite (fig. 2).

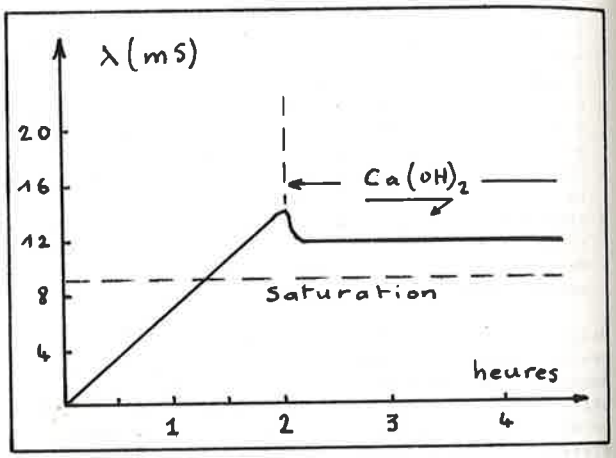

FIG. 2 - COURBE DE CONDUCTIVITE TYPIQUE, OBTENUE DANS LA CELLULE D'HYDROLYSE

- Après une montée pratiquement linéaire, la courbe s'infléchit, puis passe par un maximum pour lequel le taux de sursaturation semble dépendre uniquement de la température, indépendamment du courant de génération. Le facteur d'excès, c'est-à-dire le rapport entre concentration en chaux mesurée et concentration à l'équilibre, est de l'ordre de 1,6 à 1,7 lorsque l'on se trouve au maximum de conductivité. La précipitation de la portlandite produit alors une chute brutale de la concentration, suivie d'un palier traduisant l'établissement d'un régime stationnaire où la consommation de chaux par précipitation est égale à l'apport par le générateur. Ce palier stationnaire se trouve dans le domaine sursaturé de la portlandite. Le facteur d'excès est alors de l'ordre de 1,2 et varie en fonction du courant de génération.

6 - CONCLUSIONS

Ces tous premiers résultats obtenus avec le GECS suffisent à illustrer son utilité pour l'étude du domaine sursaturé de la portlandite et des mécanismes de l'hydratation. Nous avons montré ici que la réalisation d'un tel système est faisable, malgré les obstacles techniques liés à la génération électrochimique de l'amalgame de calcium et aux risques d'oxydation et de pollution de ce dernier par l'oxygène ou des éléments provenant du générateur lui-même. Ceci laisse entrevoir d'intéressantes perspectives pour les applications citées en introduction.

Par exemple, la grande similitude des courbes de conductance obtenues ici, avec celles des suspensions d'alite peut laisser à penser que l'allure de ces dernières n'est pas liée à des effets de barrière interfaciale, mais uniquement à l'existence d'un régime dynamique de dissolution-précipitation, qui est celui du GECS. Il reste à étudier le rôle que peut jouer la couche initiale de CSH sur le flux de dissolution et donc la durée de la période dormante, de même le rôle inverse que peut jouer la germination, de la portlandite sur la perméabilité de cette couche.

F. Ambroise, J. Péra et M. Murat.
Institut National des Sciences Appliquées de Lyon - France

INTERÊT DE L'ADDITION DE MÉTAKAOLIN AU CIMENT PORTLAND POUR L'ELABORATION DE MATÉRIAUX COMPOSITES RENFORCÉS PAR DES FIBRES DE VERRE.

I. INTRODUCTION.

Le renforcement des liants minéraux de type ciments et bétons par des fibres de verre a fait l'objet de très nombreux travaux (1-9) mais tous les problèmes relevant de cette technologie n'ont pas encore été résolus. Il en est ainsi du renforcement des ciments portlands artificiels par la fibre de verre E. En effet ce type de verre borosilicaté (7 à 9 % de B_2O_3) riche en silice (53 à 54 % de SiO_2) ne résiste pas dans un milieu basique tel que celui résultant de la réaction d'hydratation des silicates de calcium anhydres, réaction qui conduit à la formation d'un milieu riche en chaux amenant rapidement le pH à une valeur de l'ordre de 12,5.

La fibre de verre E est en effet attaquée en milieu basique avec destruction du réseau silicique et formation d'une couche superficielle perméable de silicate de calcium hydraté (1-4), couche poreuse permettant ainsi à l'attaque de se poursuivre jusqu'à dissolution complète du verre à long terme.

Ce phénomène est très préjudiciable au renforcement car il provoque très rapidement un abaissement notable des résistances mécaniques du composite.

Différents moyens ont été proposés pour remédier à cet état de fait (7) :

1. Modifier la composition de la fibre pour améliorer sa résistance chimique en milieu alcalin : fibres CEMFIL par exemple (1-3) mais dont le prix est très élevé par rapport à la fibre de verre E (30 F/kg au lieu de 9 F/kg).

2. Protéger la fibre par un dépôt organique ou minéral, procédé utilisant des technologies sophistiquées.

3. Diminuer l'humidité relative du milieu de conservation ou d'utilisation du composite.

4. Abaisser le pH du milieu cimentaire en cours de consolidation.

C'est cette quatrième solution que nous avons adoptée, conséquence d'une recherche plus générale sur la mise au point de liants pouzzolaniques de synthèse à partir de minéraux argileux thermiquement activés (10,11, 15-17).

II. PROCESSUS D'HYDRATATION COMPARES DU CIMENT PORTLAND ARTIFICIEL ET DES LIANTS POUZZOLANIQUES DE SYNTHESE.

Le phénomène d'hydratation et de consolidation des liants pouzzolaniques de synthèse à base de minéraux argileux thermiquement activés (cuisson de la matière première à 700-800°C pendant 5 heures dans un réacteur à lit fixe) nécessite l'addition d'un activateur chimique, en l'occurence l'hydroxyde de calcium $Ca(OH)_2$ qui apporte les ions calcium nécessaires pour former une solution sursaturée à partir de laquelle vont précipiter les différents hydrates responsables du développement des résistances mécaniques. Il est bien évident que l'activateur $Ca(OH)_2$ va être consommé au cours du temps, la vitesse de disparition étant fortement tributaire des conditions expérimentales.

En se fixant des conditions optimales de conservation des éprouvettes (10,11) on peut, par utilisation de l'analyse thermique différentielle (ATD), déterminer de façon semi-quantitative la nature et l'évolution des quantités d'hydrates formés au cours du durcissement, et détecter en particulier la présence ou l'absence de chaux résiduelle dans le matériau.

Dans le cas de l'hydratation de la métakaolinite par exemple (produit d'activation thermique de la kaolinite), les hydrates formés au cours de la consolidation sont essentiellement le silicate de calcium hydraté ou CSH_I de la classification de Taylor (12) et la gehlénite hydratée $2CaO.Al_2O_3.SiO_2.8H_2O$ (13-15). Ces deux hydrates sont caractérisés par les pics endothermiques notés respectivement C et G sur les courbes ATD (Fig. 1). La présence de chaux résiduelle est caractérisée par la présence du pic endothermique, noté CH, vers 550°C.

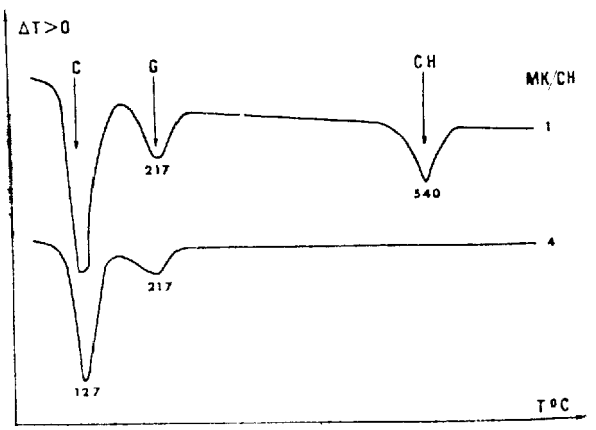

Figure 1. Exemple de courbes ATD des produits d'hydratation de métakaolinite en présence de chaux, à 28 jours, en fonction de la valeur du rapport "Métakaolinite/Hydroxyde de calcium" (MK/CH). Hydratation à E/S = 0,55.

Si on trace, à l'échéance de 28 jours, la hauteur des pics ATD (C, G, et CH) en fonction de la valeur du rapport massique initial Métakaolinite/Hydroxyde de calcium (rapport noté MK/CH), on constate que pour (MK/CH) > 2, il n'y a plus de chaux résiduelle dans le matériau (Fig. 2).

'. Ambroise, J. Péra et M. Murat.
Institut National des Sciences Appliquées de Lyon - France

INTERÊT DE L'ADDITION DE MÉTAKAOLIN AU CIMENT PORTLAND POUR L'ELABORATION DE MATÉRIAUX COMPOSITES RENFORCÉS PAR DES FIBRES DE VERRE.

I. INTRODUCTION.

Le renforcement des liants minéraux de type ciments et bétons par des fibres de verre a fait l'objet de très nombreux travaux (1-9) mais tous les problèmes relevant de cette technologie n'ont pas encore été résolus. Il en est ainsi du renforcement des ciments portlands artificiels par la fibre de verre E. En effet ce type de verre borosilicaté (7 à 9 % de B_2O_3) riche en silice (53 à 54 % de SiO_2) ne résiste pas dans un milieu basique tel que celui résultant de la réaction d'hydratation des silicates de calcium anhydres, réaction qui conduit à la formation d'un milieu riche en chaux amenant rapidement le pH à une valeur de l'ordre de 12,5.

La fibre de verre E est en effet attaquée en milieu basique avec destruction du réseau silicique et formation d'une couche superficielle perméable de silicate de calcium hydraté (1-4), couche poreuse permettant ainsi à l'attaque de se poursuivre jusqu'à dissolution complète du verre à long terme.

Ce phénomène est très préjudiciable au renforcement car il provoque très rapidement un abaissement notable des résistances mécaniques du composite.

Différents moyens ont été proposés pour remédier à cet état de fait (7) :

1. Modifier la composition de la fibre pour améliorer sa résistance chimique en milieu alcalin : fibres CEMFIL par exemple (1-3) mais dont le prix est très élevé par rapport à la fibre de verre E (30 F/kg au lieu de 9 F/kg).

2. Protéger la fibre par un dépôt organique ou minéral, procédé utilisant des technologies sophistiquées.

3. Diminuer l'humidité relative du milieu de conservation ou d'utilisation du composite.

4. Abaisser le pH du milieu cimentaire en cours de consolidation.

C'est cette quatrième solution que nous avons adoptée, conséquence d'une recherche plus générale sur la mise au point de liants pouzzolaniques de synthèse à partir de minéraux argileux thermiquement activés (10,11, 15-17).

II. PROCESSUS D'HYDRATATION COMPARES DU CIMENT PORTLAND ARTIFICIEL ET DES LIANTS POUZZOLANIQUES DE SYNTHESE.

Le phénomène d'hydratation et de consolidation des liants pouzzolaniques de synthèse à base de minéraux argileux thermiquement activés (cuisson de la matière première à 700-800°C pendant 5 heures dans un réacteur à lit fixe) nécessite l'addition d'un activateur chimique, en l'occurence l'hydroxyde de calcium $Ca(OH)_2$ qui apporte les ions calcium nécessaires pour former une solution sursaturée à partir de laquelle vont précipiter les différents hydrates responsables du développement des résistances mécaniques. Il est bien évident que l'activateur $Ca(OH)_2$ va être consommé au cours du temps, la vitesse de disparition étant fortement tributaire des conditions expérimentales.

En se fixant des conditions optimales de conservation des éprouvettes (10,11) on peut, par utilisation de l'analyse thermique différentielle (ATD), déterminer de façon semi-quantitative la nature et l'évolution des quantités d'hydrates formés au cours du durcissement, et détecter en particulier la présence ou l'absence de chaux résiduelle dans le matériau.

Dans le cas de l'hydratation de la métakaolinite par exemple (produit d'activation thermique de la kaolinite), les hydrates formés au cours de la consolidation sont essentiellement le silicate de calcium hydraté ou CSH_I de la classification de Taylor (12) et la géhlénite hydratée $2CaO.Al_2O_3.SiO_2.8H_2O$ (13-15). Ces deux hydrates sont caractérisés par les pics endothermiques notés respectivement C et G sur les courbes ATD (Fig. 1). La présence de chaux résiduelle est caractérisée par la présence du pic endothermique, noté CH, vers 550°C.

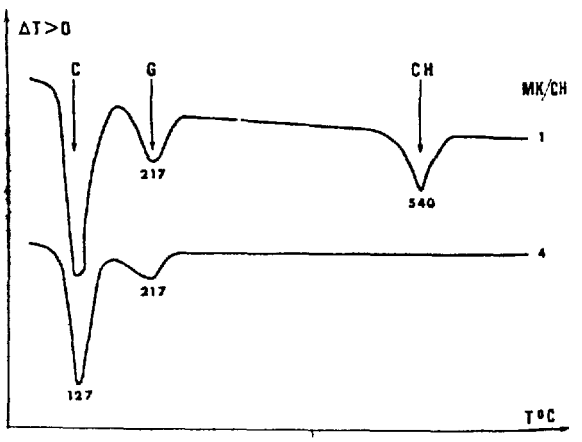

Figure 1. Exemple de courbes ATD des produits d'hydratation de métakaolinite en présence de chaux, à 28 jours, en fonction de la valeur du rapport "Métakaolinite/Hydroxyde de calcium" (MK/CH). Hydratation à E/S = 0,55.

Si on trace, à l'échéance de 28 jours, la hauteur des pics ATD (C, G, et CH) en fonction de la valeur du rapport massique initial Métakaolinite/Hydroxyde de calcium (rapport noté MK/CH), on constate que pour (MK/CH) > 2, il n'y a plus de chaux résiduelle dans le matériau (Fig. 2).

P

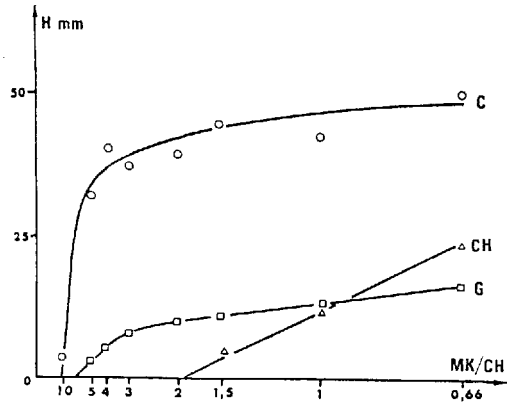

Figure 2. Variation de la hauteur des pics ATD de CSH_I(C), de géhlénite hydratée (G) et de l'hydroxyde de calcium (CH) à 28 jours en fonction de MK/CH.

De même, si on trace la hauteur de ces mêmes pics à différentes échéances d'hydratation, on constate que pour (MK/CH) = 1, la chaux n'est jamais totalement consommée, même à 90 jours (Fig. 3) bien que la formulation choisie corresponde aux conditions théoriques optimales de transformation stoéchiométrique de la métakaolinite en CSH_I et géhlénite hydratée.

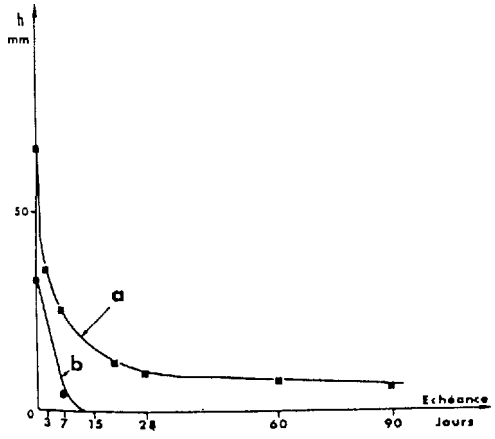

Figure 3. Variation de la hauteur du pic ATD caractéristique de l'hydroxyde de calcium (CH) en fonction de l'échéance d'hydratation pour deux compositions initiales de liants de métakaolinite + chaux : (MK/CH) = 1 (courbe a) et (MK/CH) = 3 (courbe b).

Par contre, pour (MK/CH) = 3, condition correspondant à l'obtention de résistances en compression optimales à 28 jours (de 25 à 35 MPa), la chaux a totalement disparu à l'échéance de 15 jours (Fig. 3).

Dans le cas de la consolidation du ciment portland artificiel, l'hydratation met en jeu les silicates de calcium anhydres (silicates bi- et tricalcique) et conduit à une formation quasi-continue de chaux selon des réactions du type :

$$3CaO.SiO_2 + H_2O \rightarrow CaO.SiO_2.xH_2O + 2\ Ca(OH)_2 \quad [1]$$

$$2CaO.SiO_2 + H_2O \rightarrow CaO.SiO_2.xH_2O + Ca(OH)_2 \quad [2]$$

La réaction [1] est beaucoup plus rapide que la réaction [2]. Par ailleurs le caractère nettement basique de la phase liquide intersticielle est renforcé par la solubilisation des alcalins présents initialement dans le ciment anhydre, phénomène qui conduit à la formation de bases libres (KOH, NaOH) (18) lesquelles sont également très agressives vis-à-vis des fibres de verre.

La différence flagrante entre les comportements respectifs à l'hydratation de ces deux types de liants, avec consommation rapide de la chaux pour les liants pouzzolaniques de synthèse, moyennant une valeur assez élevée du rapport pouzzolane/chaux, et apparition quasi-continue de chaux dans le ciment portland artificiel, nous a conduits tout naturellement à étudier le comportement de la fibre de verre E dans ces milieux cimentaires en cours de consolidation. L'emploi de liants pouzzolaniques de synthèse à base de minéraux argileux thermiquement activés et leur association au ciment portland artificiel, dans lesquels ils trouveront l'activateur chimique nécessaire sous forme de chaux naissante (Fig. 4) doivent permettre de réaliser un renforcement sans altération notable de la fibre de verre E, contrairement à ce qui se passe avec une pâte de CPA pur (19-21).

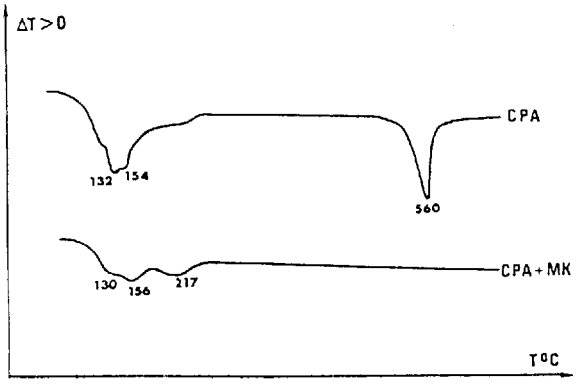

Figure 4. Courbes ATD du produit d'hydratation du ciment portland artificiel (CPA) pur et d'un mélange CPA/Métakaolinite (50/50 en masse) à 28 jours. Dans le cas du mélange CPA + MK on n'observe plus le pic caractéristique de la chaux vers 560°C

car la chaux naissante formée au cours de l'hydratation du CPA est consommée au fur et à mesure de sa formation pour réaliser l'hydratation de la métakaolinite.

On doit signaler cependant que l'idée d'ajouter au ciment portland un solide susceptible d'entrer en réaction avec la chaux au cours de la formation de celle-ci, n'est pas nouvelle : elle a été à la base de l'élaboration des ciments portlands aux pouzzolanes (anciennement CPAZ devenus CPJ ou "ciments aux ajouts" dans la nouvelle nomenclature). Mais les essais concernant le comportement de la fibre de verre E dans ce type de liant, les pouzzolanes ajoutées étant des cendres volantes, ont conduit à des résultats moins performants que ceux effectués avec les fibres à la zircone type CEMFIL (4). Par ailleurs, les résultats obtenus dans le cas du renforcement par les fibres CEMFIL sont très variables selon les caractéristiques chimiques et minéralogiques de la cendre volante utilée (22). L'addition de poussières de silice a également fait l'objet de travaux récents (23).

III. RESULTATS EXPERIMENTAUX ET INTERPRETATION.

La consommation de chaux dans le mélange CPA/MK a été suivie par diffraction des rayons X (Figure 5). Cette figure met clairement en évidence qu'à 28 jours, la chaux est totalement consommée pour le mélange 50/50 en masse.

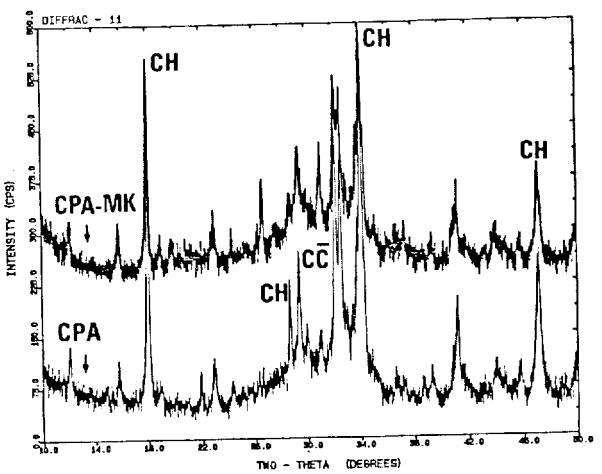

a

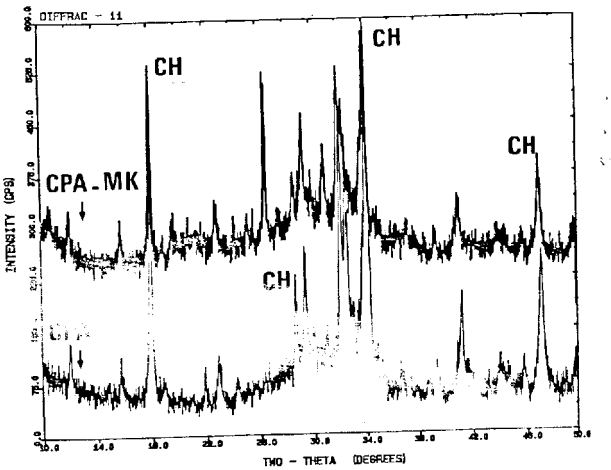

b

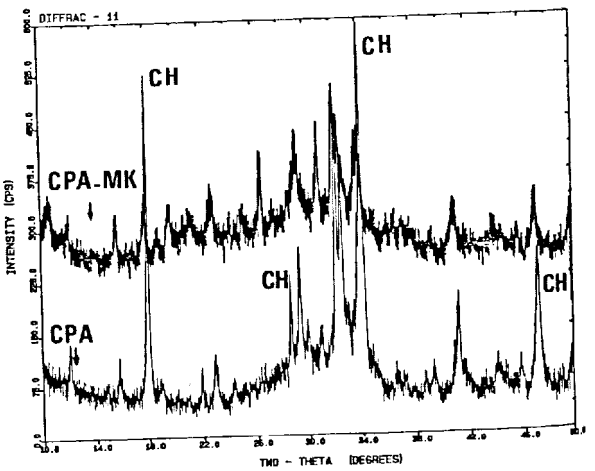

c

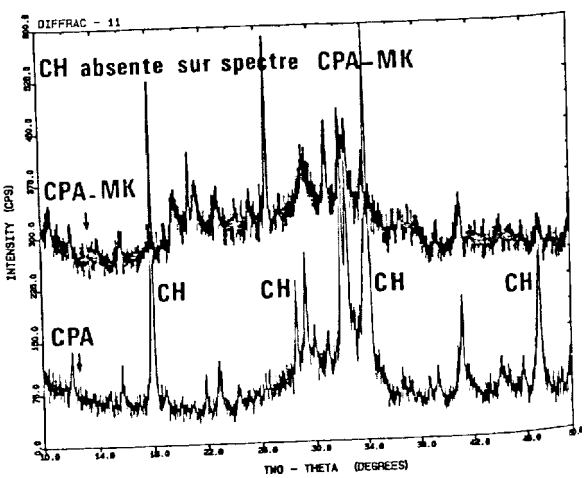

d

Figure 4. Etude de la consommation de chaux à 28 jours pour des mélanges CPA/MK en masse égaux à :

a. 80/20.
b. 70/30
c. 60/40
d. 50/50

Afin de suivre le comportement d'une fibre de verre E, des plaques de matériau composite, de dimensions 500x250x13 mm ont été réalisées à partir de trois types de liants :
- un ciment portland artificiel CPA 55 gâché avec un taux de gâchage E/S (rapport Eau/Solide) de 0,3,
- un liant pouzzolanique de synthèse, constitué de métakaolinite (MK), (obtenue par calcination d'une kaolinite pure pendant 5 heures à 750°C) additionnée d'hydroxyde de calcium pur (CH) dans un rapport massique (MK/CH) = 3. Le gâchage avec l'eau a été réalisé avec un rapport E/S = 0,6.
- un liant mixte "CPA 55 - Métakaolinite", en proportions massiques 50/50 gâché à E/S = 0,4.

Ces plaques, lors de leur élaboration, sont armées avec de la fibre de verre E à raison de 37,4 g de fibre par plaque, la fibre étant orientée dans le sens longitudinal de chaque plaque. Les composites ainsi obtenus sont conservés sous eau à 20°C jusqu'à l'échéance (J-1) jours, puis séchés 24 heures à 20°C dans une chambre de conservation à 60 % d'humidité relative avant de réaliser les essais mécaniques. Les plaques, après essais en flexion 3 points, sont ensuite conservées à la température ambiante pour observation des fibres par Meb à 160 jours et à 1 an.

Les essais en flexion centrée sont réalisés à l'échéance de 36 jours. Les lois de comportement jusqu'à rupture sont représentées sur la Figure 6. Le Tableau I fournit les résistances en compression (R_c) et en traction (R_m) pures des différents liants ainsi que les charges et les flèches ultimes des plaques renforcées par la fibre de verre.

de la plaque de liant de métakaolinite-chaux (colonne 2) n'est pas significatif (de l'ordre de 15 %) alors que les résistances respectives en traction de ces liants varient du simple au triple. La présence de pouzzolanes de synthèse dans les différents liants permet d'empêcher la rupture fragile des plaques comme le montrent les résultats obtenus dans le Tableau I et sur la Figure 6.

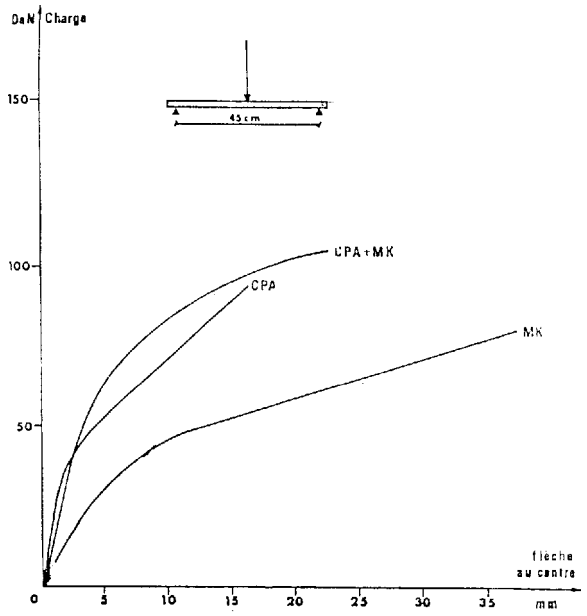

Figure 6. Courbes "charge-flèche" des plaques composites jusqu'à rupture.

TABLEAU I

Caractéristiques mécaniques des liants en pâte pure et des composites.

Propriétés mécaniques	Nature du liant		
	Pâte pure de CPA	MK + CH (3/1)	CPA + MK (1/1)
Pâte pure :			
. résistance en compression (MPa)	62	30	41
. résistance en traction (MPa)	6,9	2,3	3,7
Plaques composites :			
. résistance en traction par flexion (MPa)	15,2	12,8	16,8
. flèche ultime (mm)	16	37	25

Ce tableau met en évidence que, pour pour le liant mixte CPA+MK, la métakaolinite peut servir à consommer la chaux formée dans le ciment portland artificiel (colonne 3) et que l'écart observé entre les charges de rupture de la plaque de CPA pur et

Les fibres extraites des plaques après essais mécaniques à 36 jours ont été examinées en microscopie électronique à balayage (MeB) (utilisation d'un appareil CAMECA MeB 07) après avoir été recouvertes d'une mince couche d'or par métallisation sous

sous vide pour éviter les phénomènes de charge.

On constate très nettement, à l'échéance de 36 jours, que la fibre incorporée au ciment portland artificiel au cours de la consolidation en pâte pure présente un état de surface caractéristique d'une altération chimique et d'une dégradation très prononcée (Fig. 7). D'ailleurs la résistance mécanique propre de cette fibre a presque totalement disparu comme on peut le constater au simple toucher : les fibres émergentes du composite se désolidarisent très facilement de la plaque.

Par contre, les fibres incorporées au liant pouzzolanique de synthèse (métakaolite + chaux) ou au liant (CPA + MK), présentent une surface qui ne semble pas avoir été concernée par une altération chimique due à la chaux (Fig. 7). Les portions de fibre émergeant en bout de plaque sont très résistantes et ne se désolidarisent pas du composite.

L'observation des fibres à des échéances de 160 jours et de 1 an conduisent aux mêmes résultats (Fig. 8)

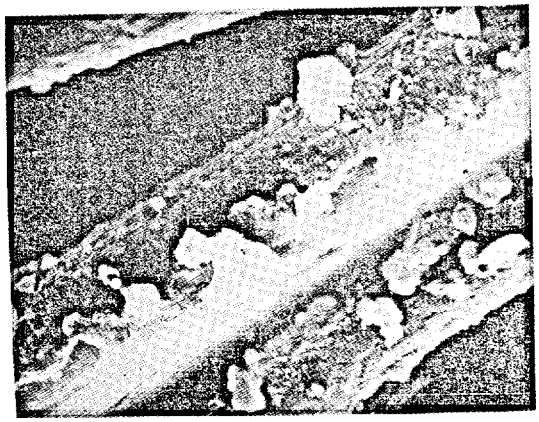

1

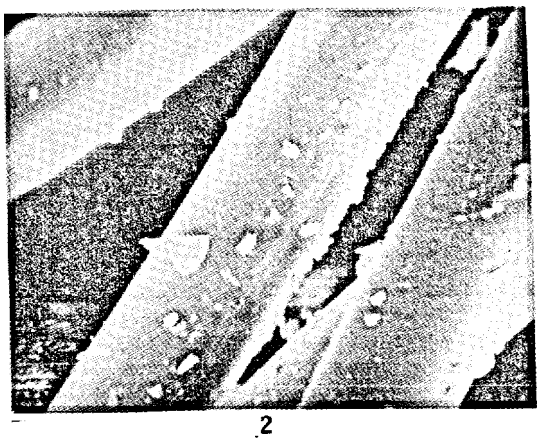

2



3

Figure 7. Comportement comparé de la fibre de verre E, à 36 jours, après incorporation dans les différents liants suivants (grossissement 2000) :
1) Ciment portland artificiel (CPA)
2) Métakaolin + chaux (MK + CH)
3) Ciment portland artificiel + métakaolin (CPA + MK).

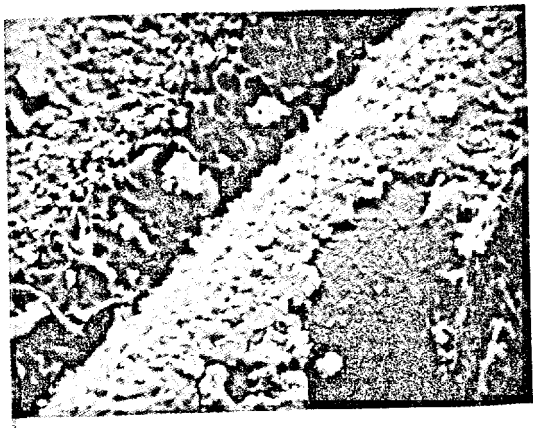

1



2

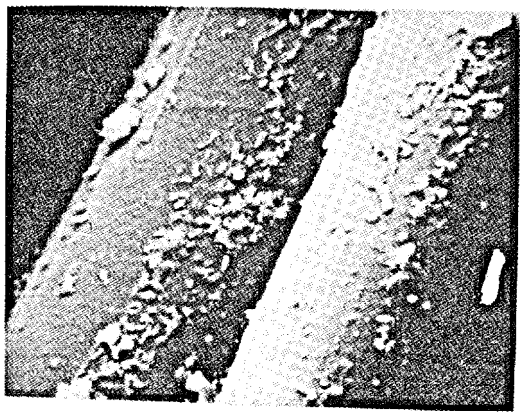

3

Figure 8. Comportement comparé de la fibre de verre E, à 365 jours, après incorporation dans les différents liants suivants (grossissement 4000) :
1) Ciment portland artificiel (CPA)
2) Métakaolin + Chaux (MK + CH)
3) Ciment portland artificiel + Métakaolin (CPA + MK).

IV. CONCLUSION.

Il apparaît donc qu'une solution relativement aisée pour réaliser des matériaux composites à base de liants minéraux renforcés par de la fibre de verre E consiste à utiliser une matrice dont la phase liquide intersticielle ne présente pas de caractère basique prononcé au cours du processus de consolidation. Les deux solutions proposées sont (19) :

- soit l'emploi de liants pouzzolaniques de synthèse (minéraux argileux thermiquement activés) dans des conditions telles que l'activateur chimique (chaux) soit consommé à des échéances raisonnables (une à deux semaines), le liant devant cependant développer des résistances mécaniques élevées à court terme (28 jours),

- soit l'association de ces liants pouzzolaniques de synthèse à du ciment portland artificiel, l'hydroxyde de calcium formé au cours de l'hydratation du second liant jouant le rôle d'activateur chimique pour le premier, donc étant consommé au fur et à mesure de sa formation.

Références.

(1) - MAJUMDAR A.J. and RYDER J.F., "Glass Reinforcement of Cement Products". Glass Technology, 9, (1968) p. 78-84

(2) - STEELE B.R., "Glass Fiber Reinforced Cement", Proc. Inter. Building Exhibition Conf. on Prospects for Fiber Reinforced Construction Materials, Building Research Etablishment, 1972, p. 29-39.

(3) - MAJUMDAR A.J. and TALLENTIRE, "Glass Fiber Reinforced Cement", Int. Symp. on Applications of Fiber Reinforced Concrete, Canada, 1973.

(4) - MAJUMDAR A.J., "The role of the Interface in Glass Fiber Reinforced Cement" Cem. Concr. Res., 4 (1974), p.247-266

(5) - NEVILLE A., (Editor), Proc.RILEM Symp. "Fiber Reinforced Cement and Concrete" The Construction Press, 1975

(6) - LARNER L.J., SPEAKMAN K. and MAJUMDAR A.J "Chemical Interactions between Glass Fibers and Cement", J. Non Crystalline Solids, 20, (1976)

(7) - SHIN Woo Seung,"Recent Development in Alkali-Resistant Fibers at the Battelle Institute", Proc. Inter. Congr.GRC in the 80s, V. BLAKE Ed., The glass Fiber Reinforced Cement Association, U.K., 1982, p. 351-374.

(8) - ROY D.M. MAJUMDAR A.J., SHAH S.P. and MANSON J.A. (Editors), "Advances in Cement-Matrix Composites". Materials Research Society, 1980.

(9) - ROTWELL K.P. and WARRIOR D.A., "Chemical Resistance of GRC", Proc. Intern. Congress GRC in the 80s, V. BLAKE Ed., The Glass Fiber Reinforced Cement Association, U.K., 1982, p. 100-112.

(10) - AMBROISE J., "Elaboration de liants pouzzolaniques à moyenne température et étude de leurs propriétés physico-chimiques et mécaniques". Thèse de Doctorat d'Etat, Lyon, Juillet 1984.

11) - AMBROISE J., MURAT M. and PERA J.,"HYdration and Hardening of calcined clays and related minerals. IV-Experimental conditions for strength improvment on metakaolinite minicylinders". Cem. Concr. Res., 15,(1985), p. 83-88.

(12) - TAYLOR H.F.W., "The Chemistry of Cement", Acad. Press, London and New-York, Vol. I, (1964), p. 167-232.

(13) - STRATLING W., "Die Reaktion zwischen gebranntem Kaolin und Kalk in wâseriger Lösung", Zement Verlag, Berlin,1938.

(14) - TURRIZIANI R. and SCHIPPA G., "Analisi termica differenziale dei productti di reazione del caolino disidrato con idrato di calcio", Ricer.Scientif. Ital. 24, (1954), 2, p. 366-374.

(15) - MURAT M., "Hydration and Hardening of calcined clays and related minerals. I. Preliminary investigations on metakaolinite". Cem. Concr. Res., 13, (1983), 2,p. 259-266

(16) - AMBROISE J., MURAT M. and PERA J., "Hydration and Hardening of calcined clays and related minerals. V- Extension of the research and general conclusions". Cem. Concr. Res., 15 (1985) p. 261-268.

(17) - AMBROISE J., BACOT J., MURAT M. et PERA J., "Valorisation de la latérite en tant que matériau de construction dans un habitat économique". Premier Congr. Intern. de Géomécanique des Sols Tropicaux et Saprolitiques, Brasilia (Brésil), 1985, Ed. ISSFME, Vol. II, (1985), p. 395-406.

(18) - LONGUET P., BURGLEN L. et ZELWER A., "La phase liquide du ciment hydraté". Rev. Mat. Constr., 678, (1973), 1, p. 35-41.

(19) - AMBROISE J., MURAT M. et PERA J., Brevet Anvar n° 85/00474 déposé le 10.01.1985.
(20) - AMBROISE J., MURAT M. and PERA J., "Durability of E-glass fiber in portland cement-metakaolinite matrix" Intern. Symp. Durability of GFRC, Chicago, Il, Nov. 1985.
(21) - AMBROISE J., MURAT M. et PERA J., "Durabilité des fibres de verre dans différents milieux cimentaires en cours de consolidation. Etude d'une fibre de verre E". VERRES ET REFRACTAIRES, N° 6, Nov. Déc. 1985.
(22) - LEONARD S. and BENTUR A., "Improvment of the Durability of Glass Fiber Reinforced Cement using Blended Cement Matrix". Cem. Concr. Res., 14, (1984), p. 717-728
(23) - BENTUR A., Communication à l'Intern., Symp. Durability of GFRC, Chicago, Nov. 1985.

Remerciements.

Les auteurs remercient la Société VETROTEX (France) qui a fourni les échantillons de verre E, ainsi que Mle BARDOT et Mme CHATELUT (E.R.A. CNRS n° 300, Université Claude Bernard Lyon I) pour les clichés de microscopie électronique à balayage.

R. Kovács
Central Research and Design Institute for Silicate Industry - Hungary

RAPID METHOD FOR CEMENT STRENGTH PREDICTION.

P

Elaboration of the method

Preliminary determination of cement strength has been dealt with for a long time. Forester and Keen /1960/, Leczner and Bernoff /1961/ recommended several methods the essence of lied in accelerating the process of hardening. Most of these methods apply steam curing at atmospheric pressure or above it. However, since the behaviour of various type cements under steam-curing is different, these methods cannot be equally applied to all the cements and don't supply directly comparable results. Besides in the course of steamcuring, especially that, carried out in autoclaves under enhanced pressure, the macro-and microstructure of hardened cement stone as well as the composition of arising hydration products changes considerably. According to methods proposed by Gaca/1963/ and Lawrence /1969/ specimens are prepared either from dry cement powder with the addition of some lubricant or from cement-paste or mortar by pressing The acceleration of hardening in this case is achieved by the closen arrangement of the hydrating cement particles. Yet, wider use of these methods was mindered by several factors. For instance the lubricant /alcohol, ethylene glycol/ applied affected the following hydration, while the preparation of specimens and ensurence of their homogeneity turned to be extremely difficult and connected with a significant subjective error because of the very low water:cement ratio /in the range of 0,1/. At the same time various water requirement of different cement types as well as the amount and composition of dissolved components leached out with the pressed-out water influencing further hydration is not taken into account at all. This is why as Nagy /1969/ had shown these methods have a rather wide variation in results.

Weighing out portions from the moist mixture before pressing is time-consuming and in exact, while drying up of the mixture during this operation also contributes to higher scatter of results. Dabriel /1971/ and lately Relis and Soroka /1974/ used vacuum, too, for the acceleration of hydration of the specimens but they did not suceed to eliminate all the abovementioned error-sources. To all this one can add that the known and widely used standard methods for cement-strength determination posess a lot of shortcomings/disadvantages/ explaining why, up to now no common agreement could be achieved in introducing a worldwide acceptable universal testing method, some of these disadvantages are as follows:

- -the sand or aggregate used for the preparation of specimens cannot be exactly defined,
- -the prescribed water cement factor leaves the factual water requirement of the cement out of consideration,
- -the conditions of preparing the specimens /weighing out portions of the moist mixture, filling them into the moulds, compaction, smoothing their surface etc/ give place to a number of subjective errors

As a consequence the permitted scatter of results for the majority of known standard methods amounts to $\pm$10 % with a poor reproducibility and reliability of results. Besides, the results determining the real quality of the product appear only after 28 days when the cement referred to had been already used up so that no correction is to be made as to its dosage /proportioning/. Outgoing from all above described in elaborating our new methods we paid special attention to the followings·

-utilization of the experience obtained by known standard and accelerated testing methods
-getting results in a short time with little materials- and labor requirement
-possible minimal scatter of results with possible maximal elimination of subjective factors and other error sources /like the use of sand or aggregates, variable w/c ratio etc/
-applicability for all cement types and possibility of the use of ordinary laboratory equipment,
-simlicity of operations with the possibility of succeeding automation,
-the hydration parameters and -products should not substantially differ from those obsrved in case of normal hardening

After years of investigation and continuous development a new rapid method /now patented under N°181334/ has been outlined the main featured of which are shown below

A rapid method for cement strength prediction

The essence of the method lies in weighing out portions of the dry cement sample to be tested each 25 g out of which cylinder shaped specimens of a determined porosity and are moulded by two-stage pressing These specimens undergo hydration by capillary moistening at ambient temperature in a water-vapour saturated room and are tested after 7-24 hours of hardening.
Under the given circumstances- because of the close dislocation of the cement particles - the hardening process takes place very intensively the compressive strength of the specimens achives in 4 hours about 1o MPa, in 8 hours about 2o MPa and in 24 hours about 6o-8o MPa depending on the cement quality. By this time the density of the specimens is in the range of 2,8-2,9 g/cm^3, the porosity between 2o-22%, the moisture and bound water content being 7-9 % and 5-7% respectively.

Usually 6 specimens are prepared for one testing and after a certain experience is gained by the personnel the coefficient of variation of the results is less than 5% ordinaly being even less than 3 % This can be explained by the almost complete elimination of the subjective factors.
The strength results obtained by the new method are in good correlation with the 3, 7, 28 days or any other age strengths of the cement sample as determined by standard methods.

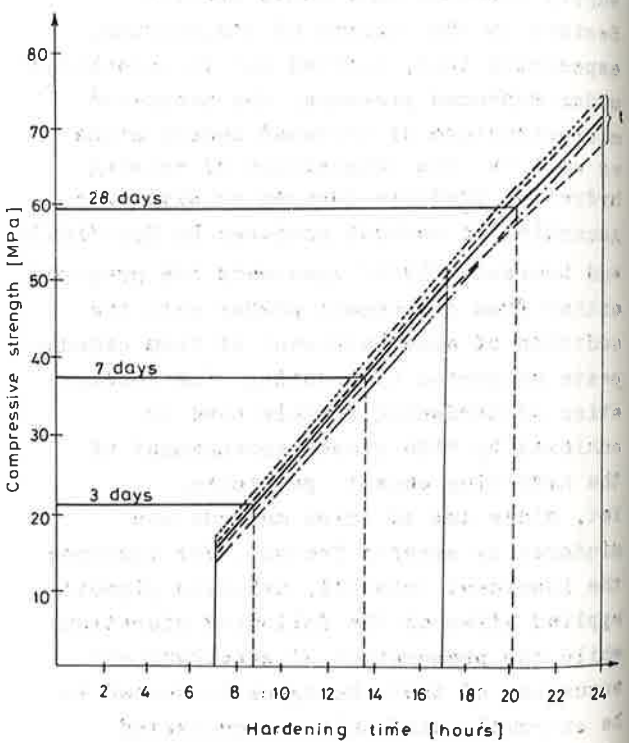

Figure 1
Calibration curve

Based upon these results a calibration curve is drown up /fig.1/ upon which the 3, 7,and 28 days strength values of the same cement samples /determined by standard methods / are marked. To the following it is sufficient to determine the strength of a given cement sample by the rapid method to be able to predict -using the calibration curve- the expect-

able standard strength at any age with a reliability meeting practical requirements /e g ±3 MPa/
The new method can be applied on one hand in plant laboratories for systematic quality control and on the other hand at cement consumers where - by quick determination of the expectable factual strength of cement - it makes possible the optimal proportioning of the latter at concrete mixing plants and thereby contributes to a cement economy of at least 5-1o % with a more uniform concrete quality at the same time.
The new method is regularly applied at one of the prefabricated concrete plants in Hungary since the beginning of 1986.
More detailed information can be obtained at the institute SZIKKTI, Budapest

References

Dabriel,J.A.: Cement Technology 2 N°4 1-8 1971.
Forrester, J.A.- Keen,R A. J.of Applied Chem N°9,358-365 196o.
Gaca,W.:Cement-Wapno-Gips 28 N°78,141-149. 1963.
Lawrence,C.D.: Th properties of cement paste under high pressure Res.Report. N°19, CCA, 1969, London,21.
Nagy,A : Építőanyag,21, N°12, 45o-458 1969
Leczner,F.J.-Barnoff, R.: J. of the Amer. Concr. Inst.Proc. 57, N°8, 973-975 1961
Relis, M.- Soroka,I : Materiaux et Construction 7 , N°38, 1o3-1o9. 1974.

F.D. Tamás, E. Farkas, M. Vörös (University of Veszprém - Hungary)
D.M. Roy (The Pennsylvania State University - U.S.A.)

LOW-FREQUENCY ELECTRICAL CONDUCTIVITY OF CEMENT, CLINKER AND CLINKER MINERAL PASTES.

INTRODUCTION

This paper deals with the time function of electrical conductance (or specific conductance = conductivity) of pastes made of portland cements, clinkers or clinker minerals. The effect of some variables (e.g. grinding fineness, temperature, measuring frequency, admixtures etc.) was studied. All tests reported here were made in the state of setting and early hardening and measured at relatively low A.C. frequencies (100 Hz - 10 kHz); this means that the changes in electrical conductance can be attributed to changes in the number or mobility (or both) of charge carrying ions. Other experimental circumstances (as e.g. high-frequency measurements, non-portland cements, suspensions rather than pastes) are excluded.

Regrettably almost no references exist in this narrow field, although the test is simple, yet informative. The first reported conductance measurements on cement pastes date back to 1936 /1/. More extensive research was made by Calleja /2,3,4/ and by Hammond and Robson /5/. Nikkanen /6/ examined the temperature- and moisture dependence of electrical conductance in cement paste and concrete specimens. Ana /7/ tried to utilise the conductivity method for the determination of setting time of oil-well cements. Monfore /8/ examined the change in electrical conductance of cement paste in the setting period and the same was done by Náray-Szabó and Szuk /9, 10, 11/ for normal and steam-cured concrete. Some data were published by Kolbasov et al. /12/, by Batalov and Klyusov /13/ and by Efimenko /14/. Reference is given to the D.C. electrical conductivity of fresh concrete in the booklet by Henning and Oelschläger /15/. Results of recent research by the authors were published in 1982 /16/ and presented at various scientific meetings /17, 18, 19/.

Most researchers agree that the electrical conductance of portland cement pastes increases shortly after mixing with water, followed by a continuous decrease. The increasing period can be interpreted as the liberation of various ions (mainly calcium-, hydroxide-, sulfate- and alkali-ions, etc.) due to hydrolysis; these ions are later immobilised in the lattice of new formations, thus decreasing their mobility and number, and, in turn, the conductance of the paste.

Some researchers found besides this general trend one or two additional, short-lived increases on the descending section of the conductance vs. time plot (to be cassed hereinafter: conductogram) (Fig. 1).

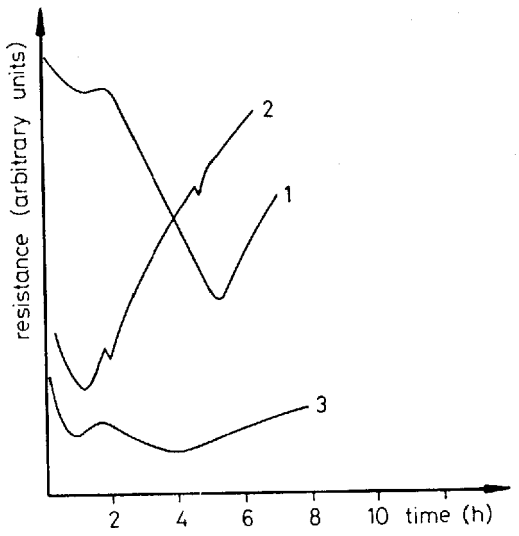

FIG. 1.
Sample conductograms published by Calleja /2/ (Curve 1), Szuk /11/ (Curve 2) and by Henning and Oelschläger /15/ (Curve 3)

In the recent work by Tamas /16/ it is shown that one, sharp, transient conductance maximum appears, the time of which depends on the temperature and w/c ratio of the paste. Retarders and accelerators affect the time and the intensity of this transient maximum, and it can be decreased, or fully eliminated by admixing gypsum to the cement. Later it was shown /17/ that not all cements behave in a similar way: clinker pastes and the majority of cement pastes exhibit no transient maximum on the conductogram, the descending section is usually smooth, with no maximum (although slight inflections or breakpoints max occur). However, by adding

a definite, critical amount of gypsum (for most clinkers approx. 2.5% $CaSO_4.2H_2O$, on the basis of dry cement mass) the transient maximum definitely appears. Adding slightly more or slightly less gypsum than this critical amount, the maximum would be converted into an inflection or breakpoint on the conductogram, while well over or under the critical gypsum content the descending section of the conductogram becomes smooth again /17, 18/.

EXPERIMENTAL

Most experiments were carried out at the Institute of Silicate Chemistry and -Technology of Veszprém University, Hungary. Some control tests, including the frequency variation method were made at the Materials Research Laboratory of the Pennsylvania State University, U.S.A.

Materials

Clinker minerals, clinkers and portland cements of different origin were used. The clinker minerals were prepared from pure reagents by multiple firing and regrinding. After final control (by chemical analysis and XRD) all substances were ground to the desired fineness (0.3 ± 0.005 m^2/g Blaine, unless otherwise stated). Some control tests were made with quartz sand ground to the same fineness.

Clinkers and cements were industrial products, their composition and moduli given elsewhere /17/. Gypsum was natural rock, its $CaSO_4.2H_2O$ content over 96%. Admixtures were CP grade reagents. De-ionised water was used in all experiments.

Method

The finely ground solids were weighed, transferred to a beaker, water added to give a paste of plastic consistency and thoroughly hand-mixed for one min. After this the paste was transferred to a conductance cell (Fig. 2.), carefully filled to assure a good contact between the paste and the electrodes.

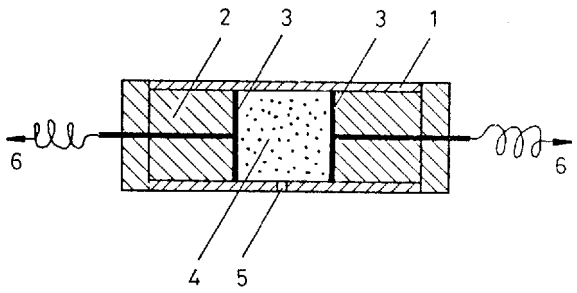

FIG. 2.

The conductance cell. 1 hard PE tube, 2 PTFE cylinder, 3 stainless steel electrodes, 4 cement paste, 5 opening for excess paste, 6 to conductometer and recorder

Excess paste protruded through opening 5. Electrodes were polished before each experiment. Measurement commenced exactly six minutes after the first contact with water; this is zero time on the conductograms. The temperature of the paste was kept constant at 32°C during the experiment with the aid of a flowthrough vessel of a conventional thermostat. Electrodes were hooked to a bridge-type electronic conductometer, the output of which was continuously recorded. In Veszprém a RADELKIS OK 102/1 conductometer (operating at 3 kHz frequency) and a RADELKIS OH 814/1 recorder was used. At MRL-PSU a HP 4274A LCR-meter (operating 0,1 - 100 kHz frequencies) was used, controlled by a HP 9825 computer. Measurements were made at one-minute intervals and recorded by a HP 9872A plotter. Conductances were measured in Siemens, the SI unit of conductance. Conductivity (i.e. specific conductance) values were calculated from the measured conductance by the known dimensions of the cell.

RESULTS AND DISCUSSION

In the following some sample conductograms are shown. The abscissa scale is time (in hours) while the ordinate is conductivity,

expressed in S/m and marked γ according to the rules of the International System.

If an inert material (quartz sand) is mixed with water or admixture solutions to make a paste, its conductogram is straight. A slight decrease of conductivity can be attributed to the adsorption of charge-carrying ions on the surface of the solid (Fig. 3.).

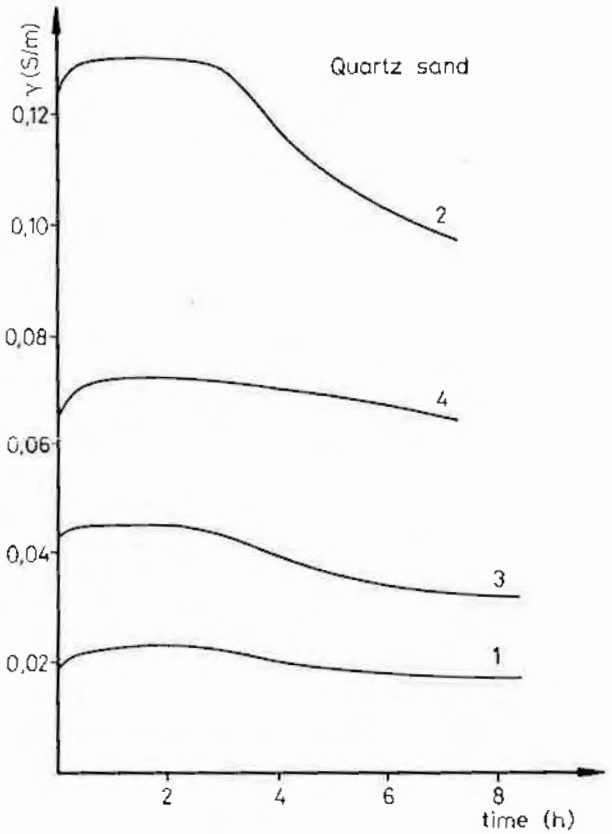

FIG. 3.

Conductograms of quartz sand. 1 no admixture, 2 0.1% Na-formate, 3 0.1% citric acid, 4 0.2% citric acid

All clinkers and the majority of cements investigated so far give only one conductivity maximum (Fig. 4.). Some cements however show a very characteristic second, transient maximum on the descending section of the conductogram, the intensity of which may reach, and (esp. at low measuring frequencies) even exceed that of the first maximum (Fig. 5.).

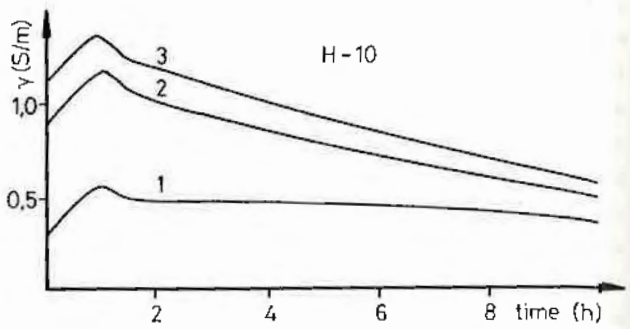

FIG. 4.

Conductograms of H-10 cement; the effect of measuring frequency. No transient maximum occurs. 1=100 Hz, 2=1 kHz, 3=3 kHz

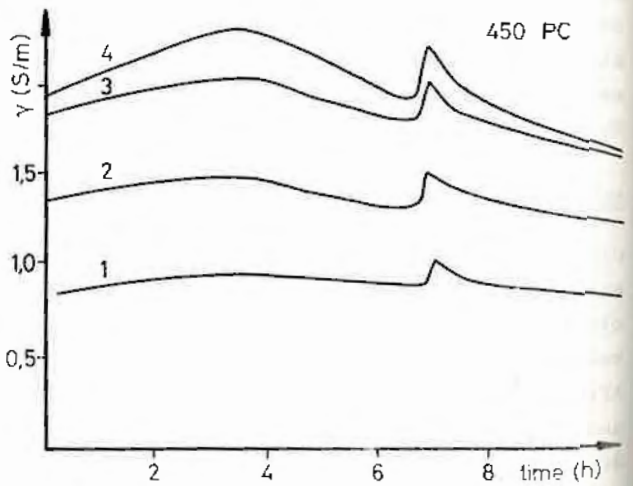

FIG. 5.

Conductograms of 450 cement; the effect of measuring frequency. A transient maximum can be observed. 1=100 Hz, 2=500 Hz, 3=1 kHz, 4=5 kHz

Both plots clearly show that conductivity increases with increasing measuring frequency, but the general "look" of the conductogram remains unchanged.

However, if gypsum is admixed to the clinker, a transient conductivity maximum appears in all clinkers investigated so far, if the amount corresponds to a "critical" value. If slightly higher or lower, the intensity of the transient maximum would diminish; still more or still less gypsum causes an inflexion or breakpoint on the descending branch of the conductogram rather than a

maximum. Well before or beyond the critical gypsum contents the conductogram becomes regular again, with no sign of maximum or inflection. In Figs. 6. and 7. two sample sets of conductograms are shown.

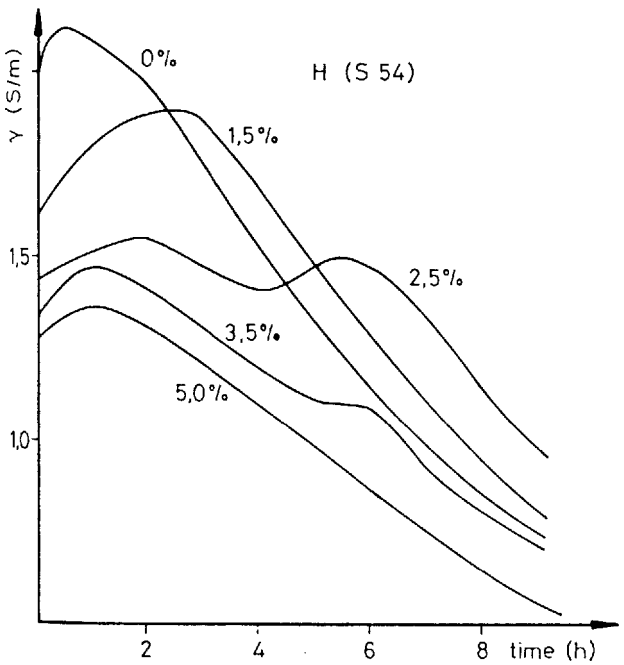

FIG. 6.

Conductograms of HS-54 clinker in the presence of various amounts of gypsum

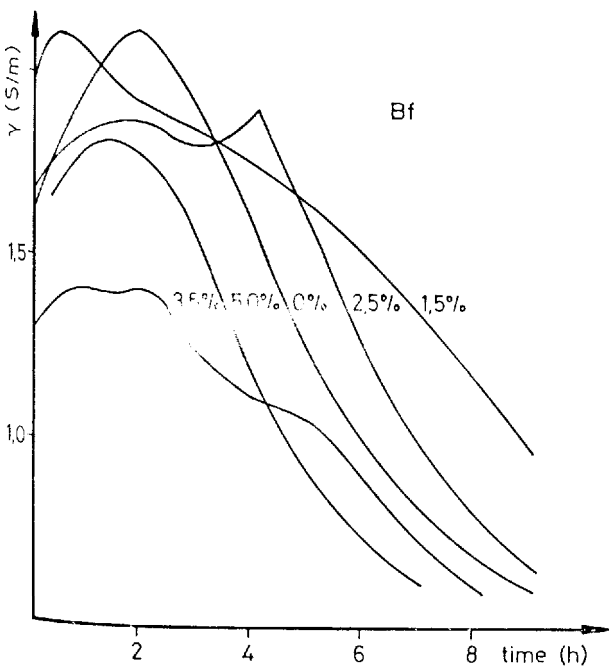

Conductograms of Bf clinker in the presence of various amounts of gypsum

Shape of the plot and values of conductivity of clinkers and cements depend highly on the composition of the particular material (although general trends can be found) and are influenced by several factors, as. e.g. temperature, grinding fineness (surface area), carbonation, and, most strikingly, by admixtures (accelerators, retarders, etc.).

Upon increasing temperature, the first conductivity maximum remains almost unchanged while the second, transient one appears earlier, at 8:10 hr. and 4:45 hr. from beginning, at 32°C and 50°C, respectively (Fig. 1. in /16/).

The effect of aftergrinding is shown in Fig. 8.

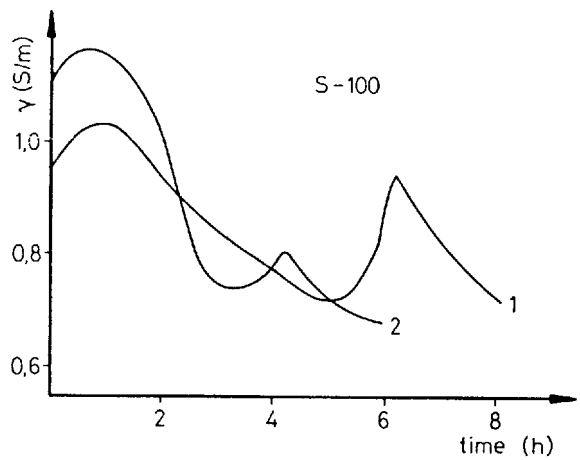

FIG. 8.

Conductograms of S-100 cement pastes - the effect of aftergrinding. Curve 1 surface area 0.337 m^2/g, curve 2 surface area 0.393 m^2/g

The intensity of the first maximum is increased, that of the transient one decreased by aftergrinding. This effect could obviously be attributed to the increase of surface area, but to a partial carbonation as well. To investigate this possibility in more detail the same sample which gave curve 1 in Fig. 8. was put to a desiccator filled with dry carbon dioxide. Results are plotted in Fig. 9. It is clearly visible that CO_2-treatment affects primarily the intensity of the first maximum.

P

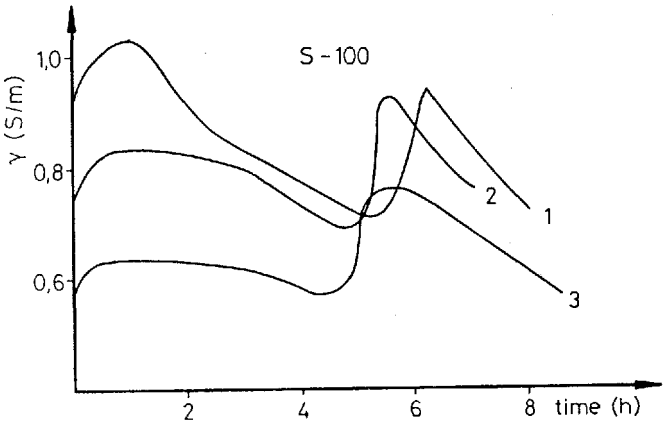

FIG. 9.
Conductograms of S-100 cement pastes - the effect of carbonation. Curve 1: no carbonation, curve 2: after 2 days of carbonation, curve 3: after 14 days of carbonation

The effect of accelerating and retarding admixtures has been described earlier /16/. Citric acid, a well-known retarder has given the most dramatic effects: the time of the first conductivity maximum remained practically unchanged, but its intensity decreased and its shape flattened. The transient maximum on the conductogram however appeared at much later times (in case of the original, no-admixture cement paste this occured at 8:45 hr., and was shifted to 12:00, 18:30 and 41:45 hr., upon adding 0.035%, 0.07% and 0.15% citric acid, resp. but ist shape remained almost unchanged as shown in Fig. 3. of /16/).

Clinker minerals

Conductograms of clinker mineral pastes without admixtures are shown in Fig. 10. It can be readily seen that all four clinker minerals show smooth curves with no transient changes in conductivity, although a slight inflection can be reproducibly observed on the conductogram of C_3S at the age of 1:25 hr. In case of C_4AF some irregularity were found at the beginning period. This phenomenon will be discussed later.

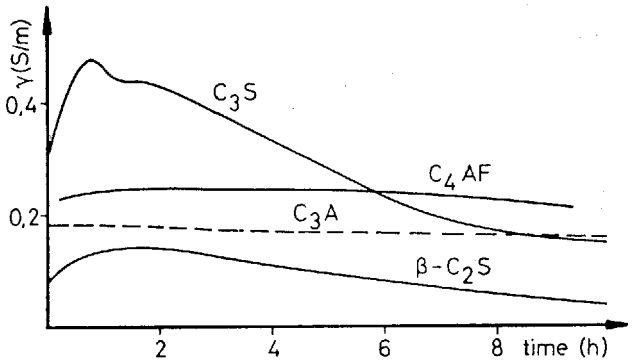

FIG. 10.
Conductograms of clinker mineral pastes

Conductivities of the two alumina-bearing phases change only slightly with time, while the ascending and descending branches are clearly visible on the conductograms of the silica-bearing minerals before and after the first maximum. Conductivity of C_3S pastes is obviously higher than that of the β-C_2S paste, which yields less ions than its more basic counterpart. (It should be mentioned that curves plotted here are not conform in every detail with earlier ones /16/, when other, less pure minerals were used).

The effect of accelerating and retarding admixtures on the conductance behavior is shown in the following figures. In Fig. 11. the conductograms of C_3S pastes are shown (here and subsequently curve 1 refers to the original, no-admixture paste the conductogram of which was already shown in Fig. 10). The addition of an accelerating agent, as sodium formate or calcium chloride increases the intensity of the first maximum (an that of the following inflection), but do not "accelerate" its development. Citric acid, on the other hand is a real retarder. The same can be seen in case of β-C_2S pastes in Fig. 12. (Here the scale of the vertical axis is changed to express phenomena in more detail. The intensity-increasing effect of sodium formate is evident. Calcium chloride has a similar effect, increasing the intensity of the first maximum to 0.8 S/m, without changing its time but this curve was omitted from the figure

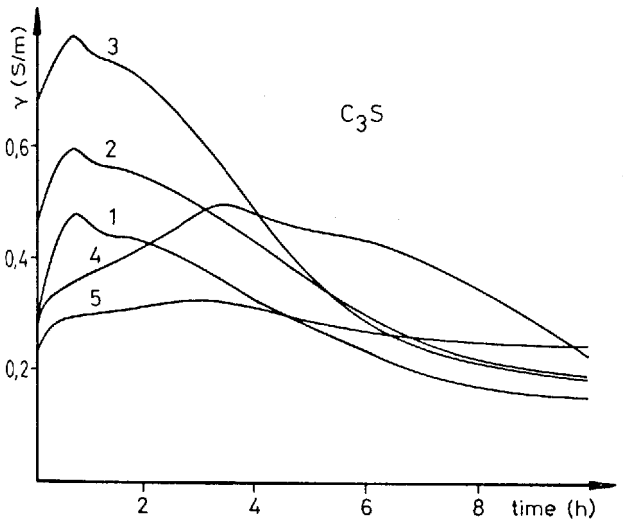

FIG. 11.

Conductograms of tricalcium silicate pastes - the effect of admixtures. Curve 1: no admixture, curve 2: 0.1% sodium formate, curve 3: 0.5% calcium chloride, curve 4: 0.05% citric acid, curve 5: 0.1% citric acid

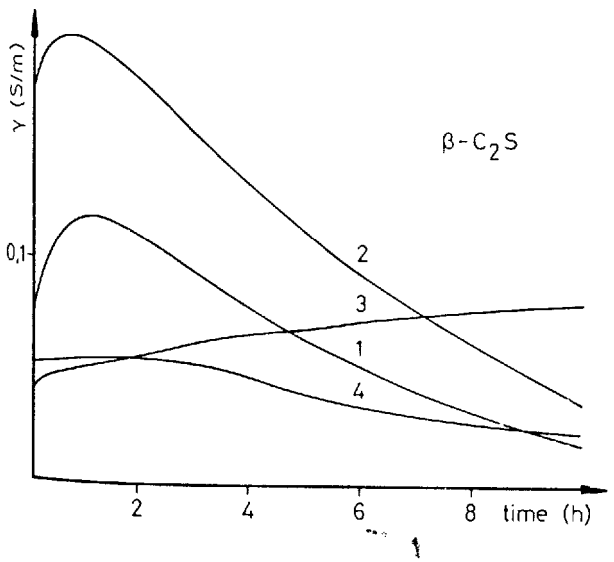

FIG. 12.

Conductograms of β-dicalcium silicate pastes - the effect of admixtures. Curve 1: no admixture, curve 2: 0.1% sodium formate, curve 3: 0.1% citric acid, curve 4: 0.2% citric acid

due to the lack of space. The retarding effect of citric acid is thus documented in the case of β-C_2S too.

The irregularities in the conductogram of C_4AF pastes have already been mentioned earlier. As the measurement of conductance prior to 6 minutes after first contact with water is impossible in our experimental setup, we tried to utilise the retarding effect of citric acid also in this case. Results are plotted in Fig. 13.

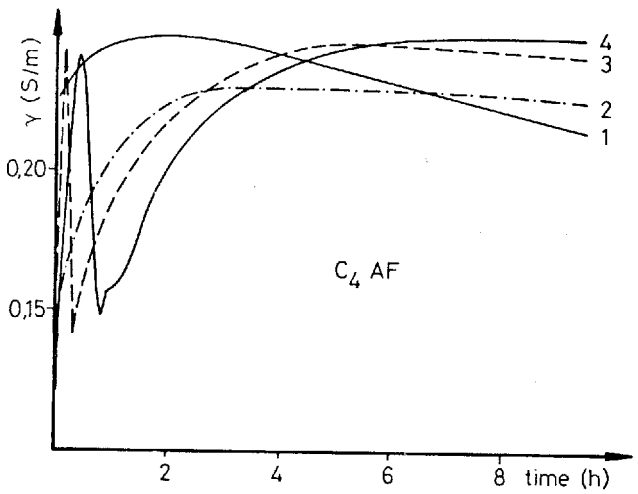

FIG. 13.

Conductograms of tetracalcium aluminate ferrite pastes - the effect of admixtures. Curve 1: no admixture, curve 2: 0.1% citric acid, curve 3: 0.2% citric acid, curve 4: 0.3% citric acid

It is seen on the curves that at the very beginning of hydration conductance is increased sharply, followed by a sudden decrease and a slow increase again. The presence of a short-lived maximum and minimum on the curves was observed reproducibly in each case as the retarding effect of citric acid has rendered these phenomena measurable.

Comments

In this paper only some representative examples were shown from the more than 800 individual tests carried out in the two laboratories. By repeated tests it can be stated that the reproducibility of the absolute conductance values is ± 20%, if the same

raw material batch is used and sample preparation (e.g. adjusting the w/c ratio, mixing, etc.) is done with care. The time of the transient conductivity peak can be reproduced within a few minutes. The general run, the "appearance" of the conductogram is fully reproducible.

It must, however, be borne in mind that - as shown in the paper and in earlier ones - several external factors may affect the conductance behavior of cement or clinker pastes. The evaluation of observations therefore requires great care and multiple parallel tests are recommended. The most frequent artifact, the loss of contact between the paste and the electrodes however is easily recognised by the sudden drop of conductance. (The newly designed cell, with steel clamps has already minimised this source of error).

The interpretation of results is not easy. The first conductivity maximum is undoubtably a consequence of hydrolysis, as stated earlier and the effect of carbonation can be explained by the immobilisation of calcium ions in the lattice of calcium carbonate.

The most interesting feature on conductograms, the appearance of the second, transient maximum on the descending section of the plot in case of near-critical gypsum-to-clinker ratios can only be tentatively explained by the ettringite → monosulfate transformation (no dramatic differences can be observed on XRD patterns of pastes cured to times shortly before and after the transient maximum, respectively). Alternately one could hypothesize protective layers around ettringite grains, which, when disrupted by osmotic pressure release sulfate and other ions into the environment is a transient way.

Experiments are continued to find better arguments for the role of gypsum in the appearance of the transient conductivity maximum in case of near-critical gypsum-to-clinker ratios; to collect correlations between critical gypsum content and the phase composition of clinker; for the utilisation of electrical phenomena in the interpretation of processes taking place during the setting and hardening of cements; and, last not least, the practical application of conductometry to replace empirical time-of-setting determinations.

ACKNOWLEDGEMENT

A part of this work was carried out under grant NSF-INT-80-11922. Some of the clinker minerals were donated by the Department of Binders, Mendeleev Institute of Technology, Moscow, USSR. The help of both organisations is gratefully acknowledged.

REFERENCES

/1/ Boast, W.B.: J. Amer. Concrete Inst. 33, 131 (1936)
/2/ Calleja, J.: J. Amer. Concrete Inst. 23, 525 (1952)
/3/ Calleja, D.: J. Amer. Concrete Inst. 24, 329 (1952)
/4/ Calleja, D.: J. Amer. Concrete Inst. 25, 249 (1953)
/5/ Hammond, E. - Robson, T.: The Engineer 1955 No. 4, 78
/6/ Nikkanen, P.: Valtion Teknillinen Tutkimuslaitos, Ser. 3, No. 60 (1962)
/7/ Ana, I.: Chem. Oil Gas Roman. 6 130 (1970)
/8/ Monfore, G.E.: PCA Res. Dev. Lab. 1968 35
/9/ Náray-Szabó, I. - Szuk, G.: Acta Geol. Acad. Sci. Hung. 3 105 (1955)
/10/ Szuk, G. - Náray-Szabó, I.: Acta Tech. Acad. Sci. Hung. 22, 83 (1958)
/11/ Szuk, G.: Acta Tech. Acad. Sci. Hung. 46 317 (1964)
/12/ Kolbasov, V.M. - Levshin, A.M. - Ptitsin, V.V.: Trudy Mosk. Khim.-Tekh. Inst. 92 138 (1976)
/13/ Batalov, D.M. - Klyusov, A.A.: Trudy Zapadno. Sibir. Nauchno-Issled. Geol. Neft. Inst. 86 (1975)
/14/ Efimenko, Yu. V.: Zh. Prikl. Khim. 48 1135 (1975)
/15/ Henning, O. - Oelschläger, A.: Bindebaustoff-Taschenbuch, Vol. 1, p. 305 (1984)
/16/ Tamás, F.D.: Cement Concr. Res. 12 115 (1982)
/17/ Tamás, F.D. - Salem, T.H. - Mikhail, R. Sh.: Paper presented at the 84th Annual Meeting of the Amer. Ceram. Soc., Cincinnati, Ohio, 1984
/18/ Tamás, F.D. - Farkas, E. - Roy, D.M.: British Ceram. Proc. No. 36, p. 237 (1984)
/19/ Farkas, E. - Tamás, F.D.: Tagungsbericht 9. IBAUSIL, Vol. 1, p. 163 (1985)

G.Scarinci*, D.Festa*, G.Sorarù*, G.Grassi°, L.Stafferi°, C.Badini°
* Istituto di Chimica Industriale, Facoltà di Ingegneria, Università di Padova
° Dipartimento di Scienza dei Materiali e Ingegneria Chimica, Politecnico di Torino

PORTLAND CEMENT RENFORCED WITH NEW ALKALI-RESISTANT GLASS FIBERS

1. Introduction

Glass fibers, to be used for cement reinforcement, should have good resistance toward alkaline attack (portland cement during hydration has a pH value of 12 to 13). Commercially available A and E glass fibers lose their strength rapidly in an alkaline enviroment because alkali attacks directly the silica network and completely dissolves the glass. The hydroxyl ion of the alkali breaks the Si-O-Si linkages according to equation:

$$-Si-O-Si- + OH^- \text{ ----- } Si-OH + Si-O^-$$

alkali resistant glass fibers, with high zirconia content (Cem-fil), developed as a reinforcement over the last few years, are expensive and difficult to fabricate because of their high melting and drawing temperature, thus cheaper compositions are required. This work relates the results obtained with glass fibers (about 15 μm in diameter) of different compositions from various systems obtained from a single nozzle drawing apparatus (table 1). For comparison purpose type E and Cem-fil glass fibers (N° 2 and 10 respectively) there also fabricated and tested.

2. Alkaline durability

Alkaline corrosion tests there carried out according to the following procedure. Five grams of fibers there introduced in a plastic bottle containing 200 ml of a satured solution of $Ca(OH)_2$, flushed with nitrogen to expell air and to avoid contamination of the liquor by CO_2. The bottle was immersed in a costant-temperature bath and mantained at 60 °C.
Tests were carried out for 8, 28, 60 and, sometimes, 90 days in triplicate and results averaged. The fibers there filtered through an alkali-resistant filter paper and washed with 50 ml of 2N-acetic acid and 200 ml of water and dried at 100 °C. The weight loss of fibers was expressed as a function of their exposed surface determined by measuring glass fibers density and diameter (tab 2).
The fibers behaviour in the $Ca(OH)_2$ is quite different, because for some compositions progressive degradation has been observed, whereas for others the corrosive process is gradually lessened (N°5) or stopped at a definite losses level (N°6,8,10). Such a different behaviour is certainly related to the different stability of the various oxides in the highly alkaline enviroment. The individual glass fibers components are not leached to the same extent nor do they all form alkali soluble species; microscopical examination by SEM has revealed the formation of a surface layer of corrosion products which can sometimes behave as a protective coating to limit further corrosion. The relative permeability of this coating to the diffusion of ionic species will be determining factor to promote or hinder the development of the corrosive attack.

3. Composite fabrication

On the ground of chemical durability tests, fibers N°6 and 8, and for comparison fibers N°2 (E glass type) and 10 (Cem-fil type), have been used for the manufacturing of composites. Prismatic samples (20 x 40 x 160 mm) have been made, by means of the pre-mix method, using glass fibers (30 mm long) and Portland cement (425). From preliminary tests the ratio w/c has been fixed at 0.35; this value allowed a good workability of cement slurry containing 3%wt glass fibers. All the operations of fabrication have been made at 20 °C and with a relative humidity not inferior at 75%. Storage has been made in water at 20 °C. After 7,28,60 and 90 days the samples have been broken in three point flexure by means of a LOSENHAUSENWERK apparatus. Obtained values (average of at least 8 tests) are plotted in Fig.1.

Components	Fiber N°									
	1	2	3	4	5	6	7	8	9	10
SiO_2	50.0	54,3	42.5	62.0	54.0	54.0	53.2	52.0	51.8	63.1
CaO	30.0	21.8	13.4	--	--	--	--	--	--	4.9
Al_2O_3	5.0	14.2	10.5	18.0	15.0	15.0	15.0	14.7	14.7	--
Na_2O	3.0	0.1	9.9	--	--	--	--	--	--	15.2
Li_2O	--	--	--	8.0	3.5	3.5	3.5	3.5	3.5	--
K_2O	2.0	0.3	1.3	2.0	2.0	2.0	2.0	2.0	2.0	--
ZnO	2.0	--	--	4.0	24.5	22.0	21.6	17.5	14.0	--
BaO	3.0	--	--	--	--	--	--	--	--	--
MgO	--	0.7	5.3	3.0	--	--	--	--	--	--
FeO	--	--	5.2	--	--	--	--	--	--	--
Fe_2O_3	--	0.2	3.3	--	--	--	2.4	6.8	6.8	--
MnO	--	--	--	--	--	--	1.3	2.5	6.2	--
TiO_2	1.0	0.1	5.8	--	--	2.5	--	--	--	--
ZrO_2	1.2	--	2.2	--	1.0	1.0	1.0	1.0	1.0	16.2
P_2O_5	2.8	--	0.6	--	--	--	--	--	--	--
B_2O_3	--	8.0	--	--	--	--	--	--	--	--
F	--	0.4	--	--	--	--	--	--	--	--
SrO	--	0.2	--	--	--	--	--	--	--	--

Table 1 : chemical composition of fibres, wt%

G.Scarinci*, D.Festa*, G.Sorarù*, G.Grassi°, L.Stafferi°, C.Badini°
* Istituto di Chimica Industriale, Facoltà di Ingegneria, Università di Padova
° Dipartimento di Scienza dei Materiali e Ingegneria Chimica, Politecnico di Torino

FIBER N°	FIBER CORROSION (weight loss in g cm^{-2} of fiber surface, X 10^6)			
	8 days	28 days	60 days	90 days
1	183.0	401.0	--	--
2	105.0	130.0	155.6	165.8
3	23.9	129.8	--	--
4	29.0	56.7	--	--
5	19.8	59.8	73.4	--
6	7.3	39.2	37.4	--
7	17.2	59.2	103.0	--
8	5.9	40.3	40.7	--
9	10.2	71.2	122.4	--
10	8.3	20.0	22.0	21.0

Table 2: fibers corrosion

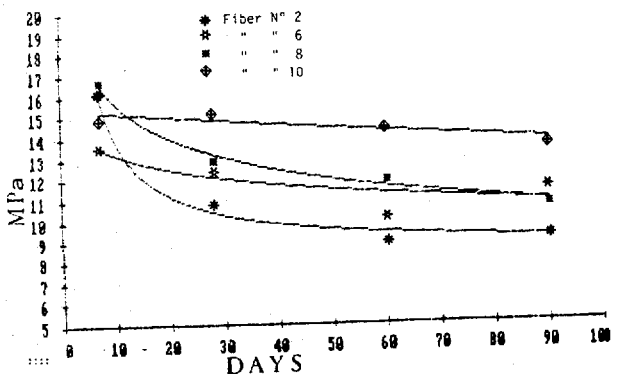

Fig.1 Bending strength vs hydration time for GRC

4. Porosity determination

Porosity of Portland cement paste and of glass fibers composites was determined after 7,28,60 and 90 days curing in water at 20°C.
1.5 g cubic samples were cutted from every specimen, dehydrated by ethil alcohol and ether and then cleaned by a 20' ultrasonic process in order to remove dust from pores. Porosity values were obtained by a Carlo Erba 200 mercury porosimeter which allows pores evaluation in the range from 75,000 to 35 A.
The data have been elaborated using an appropriate software, assuming cylindrical shaped pores, a 140° contact angle and a 480 dine/cm Hg surface tension.
The Hg cumulative volume corresponding to the total porosity of one gram of sample and the total surface area of the pores included in every gram of material are reported in Tab.3.
It is well known that porosity is the main factor governing the compressive strength of an hardened cement paste (1). Bending strength, on the contrary, can't be related to porosity, being only determined by the size of the greatest void in the material according to Griffith's theory (2).
Actually the results obtained for only cement pastes are quite spread for every curing time and follow unusual hardening trends. The addition of a few percent of glass fibers causes a remarkable change: bending strength values for every time interval are spread within a more narrowed range, they are much more reproducible and show a reasonable trend with the developing of hydration . This is due to the fact that fibers in a cement matrix reduce average cracks length by stress re-distribution in the matrix.
On examining the porosimeter data for a only-cement made paste, it may be seen that, according to other Authors (1,3),porosity diminishes with increasing hydration times (particularly during the first month) and the pores become smaller. For E glass fiber composites, on the contrary, porosity increases during the first month of hydration perhaps because these fibers are much more susceptible to chemical attack which give rise to new pores. For the other glass fiber composites porosity progressively decrease with hydration time: fibers are scarcely attacked and porosity gradually lowers owing to the increase of volume due to the cement hydration products.
From the strength vs hydration time plotsit may be noticed that the curves referring to the fibers N°6 and N°8 reach similar values at 90 days. Such values are well above the ones obtained with the fiber N° 2. It may therefore be stated that even if the fibers N° 6 and 8 don't give a reinforcement comparable to the one obtained with the zirconia fibers, anyhow they constitute a remarkable progress toward developing alkali resistant fibers.

G.Scarinci*, D.Festa*, G.Sorarù*, G.Grassi°, L.Stafferi°, C.Badini°
* Istituto di Chimica Industriale, Facoltà di Ingegneria, Università di Padova
° Dipartimento di Scienza dei Materiali e Ingegneria Chimica, Politecnico di Torino

Fiber N°	Time (days)	Average strength (MPa)	Cumulative volume ($cm^3/g\ 10^{-3}$)	Surface area (m^2/g)
2	7	15.67	58.61	6.76
2	28	10.82	67.07	8.47
2	60	8.80	51.91	6.04
2	90	9.01	37.46	5.99
6	7	13.50	59.62	6.82
6	28	12.37	53.53	7.05
6	60	10.20	56.79	6.24
6	90	11.45	36.91	6.57
8	7	16.68	68.89	7.65
8	28	12.85	64.30	8.65
8	60	11.86	45.51	5.36
8	90	10.66	37.08	5.16
10	7	14.81	51.86	5.74
10	28	15.11	45.45	5.36
10	60	14.42	39.10	4.42
10	90	13.54	35.72	5.56
Cement	7	---	55.39	5.57
Cement	28	---	28.38	6.81
Cement	60	---	34.67	6.56
Cement	90	---	26.72	6.71

Tab.3 : Average flexural strength and porosimeter data of composites studied

Bibliografy

1) Robbler,M. and Odler,I.
Cement and Concrete Research, 15, (1985), 320

2) Birkall,J.D.; Howard,A.J. and Kendall,K.
Nature, 289, (1981), 388

3) Winsolw,D.N. and Diamond,S.
A.S.T.M. Journal Materials, 5, (1970), 564

G. MASCOLO, P. PERNICE AND O. MARINO.
Dipartimento di Ingegneria dei Materiali e della Produzione, Universita' di Napoli, Italy

IONIC CONDUCTIVITY OF LAMELLAR CALCIUM ALUMINATE HYDRATES.

Introduction

It is well known that calcium aluminate hydrates of AFm type play a primary role in the hydration process of cement especially in relation to the additive employment.

The typical and lamellar structure of such compounds was widely described by Allmann (1), Kuzel (2) and Taylor (3). They are characterized by the general formula $[Ca_2Al(OH)_6][(1/n)X^{-n}(H_2O)_y]$ whose structure is made up by positively-charged layers $[Ca_2Al(OH)_6]^+$ balanced by a negatively-charged interlayer variable with the anion type X^{-n} and with the number of water molecules.

The AFm phases have an aptitude for anionic exchange with a rate, besides, depending on the selectivity of the anion (4).

Analogous structures of the type $[Zn_2Cr(OH)_6]X\cdot mH_2O$ have been studied in relation to their ionic conductivity. Their high values were explained considering the anionic interlayer as a concentrated semi-liquid or frozen solution (5,6).

The aim of the present work is that to extend such measures to the analogous phases of AFm type. The experiments were also carried out at different degree of relative humidity (RH) as it affects the hydration state of the AFm phases and in particular that of the prototype $[Ca_2Al(OH)_6][OH\cdot 3H_2O]$ whose basal spacing c', as we know, increases by increasing the degree of RH (7).

Experimental

The AFm type samples, characterized by interlayer anions such as OH^-, Cl^- and Br^-, were prepared with freshly ignited CaO, alumina gel, a Ca-salt of the corresponding anion and previously distilled and boiled water. The reaction suspension was shaken in a teflon container for ten days at room temperature. The reaction products were filtered under CO_2-free condition and dried by evacuation of the washing liquids which were acetone and ether.

The reaction products were characterized by: x-ray powder diffraction analysis using a Guinier de Wolff camera, TG and DTA analyses and density.

The powders, conditioned to 100% of RH under CO_2-free conditions, were pressed in a cilindrical die whose diameter was 18 mm at 16 MPa obtaining 5 mm in thickness disks. The compacts were analyzed in the relative density after drying on silica gel.

Electrical conductivity measures were carried out both on contact liquid of suspension containing the AFm phase and on the compacts conditioned for 7 days in a prefixed RH environment. The ionic conductivity was determined, keeping the compact under a prefixed RH, by the complex impedance measure employing a Solartron 1250 FRA and a Solartron 1286 Electrochemical interface, interfaced to a Hewlett-Packard 86 B desktop computer. Silver electrodes were painted onto the specimen faces. The signal applied across the sample was 30 mV.

Results and Discussion

Table 1 reports the results concerning the characterization of AFm phases as: basal spacing c', density, water molecules of the interlayer, the last one determined by TG with isoterm at 125 °C, and free $CaCO_3$ content. These results well match with the literature data (8,9).

Table 1 - Basal spacing c', interlayer H_2O molecules, density and free $CaCO_3$ content of AFm phases

Interlayer anion	c'(A)	$(H_2O)_y$	d (g/cc)	Free $CaCO_3$(%)
OH^-	7.95	3	2.04	-
Cl^-	7.80	2	1.90	4.5
Br^-	8.20	2	2.01	4.5

The electrical conductivity of the contact solution of AFm phases ranges between a minimum of $1.5\cdot10^{-3}\ \Omega^{-1}\cdot cm^{-1}$ for the bromide-form and a maximum of $2.7\cdot10^{-3}\ \Omega^{-1}\cdot cm^{-1}$ for the hydroxide-form. The relative density of the compacts ranges between 75 and 78%.
The a.c. conductivities of compacted samples were carried out taking into account that the complex impedance can be written as:

$$Z_{cell} = Z_{sample} + Z_F \qquad (a)$$

Z_{sample} is the impedance of the sample including also the contribute of geometrical capacitance (10), while Z_F is the impedance associated with electrode interface. According to Mayer (11) Z_{sample} may be represented by:

$$Z^{(\omega)}_{sample} = Z' + jZ'' = \frac{R_b}{1 + j\omega R_b C_g} \qquad (b)$$

with $\omega = 2\pi f$, f = frequency, R_b = bulk resistance and C_g = geometrical capacitance. Such an impedance, representable in the Nyquist diagram by a semi-circle, whose diameter R_b has $1/R_bC_g$ as maximum angular frequency, is responsable of the dispersion at the highest frequencies. So the electrical conduction has been obtained by measuring the complex impedance at 6 KHz frequency at which Z_F may be neglected.
From eq. (b) the bulk resistance has been obtained according to:

$$R_b = Z' \frac{(Z'/Z'')^2 + 1}{(Z'/Z'')^2}$$

Fig. 1 reports the conductivities of AFm phases as a function of the relative humidity. The hydroxide-form shows higher values of conductivity in all the range of the RH than those of the chloride and bromide-forms. This behaviour matches well with data of Lal and Howe (5) regarding the hydroxide-form of Zn-Cr salt . The presence, in fact, of disordered H_2O/OH^- pairs arranged in the interlayer (12) improves the proton mobility responsable of the semiconducting properties of such compounds. The conductivity variation results low in the 0 ÷ 80% of RH; this involves that the contribute to the conduction, related with intercrystalline regions, is to be considered negligible and that the bulk conduction is to be mainly attributable to the mobility of the interlayer species.

The remarkable increase of conductivity in the 80 ÷ 100% range of RH could be esplained, expecially for the hydroxide-form, by the further addition of water molecules in the interlayer that, as it is well known, involves an increase in the basal spacing c' (7). The conseguent major distance between the positively-charged layers $|Ca_2Al(OH)_6|^+$, acting on the interlayer anions, could increase the mobility of the interlayer species because of the minor intensity of the field of electrostatic forces.

The bromide-containing AFm phase shows a greater change in conductivity in the 0 ÷ 80% range of RH; this may be due to a conducting contribute of intercrystalline regions.

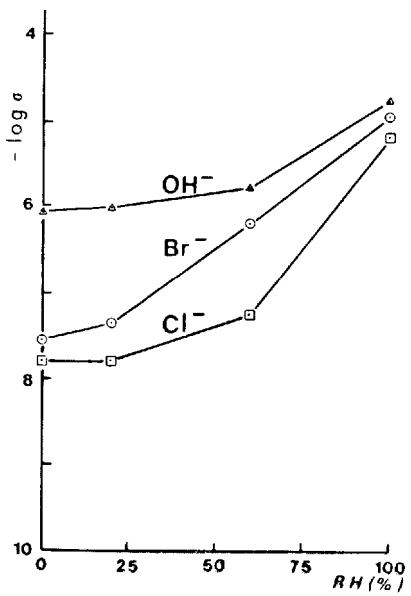

Fig. 1 Bulk conductivity of AFm phases, characterized by different interlayer anions, as a function of relative humidity.

The lower conductivities, observed for the AFm phases respect to those reported by Lal and Howe (5,6) for Zn, Cr samples, could be attributed both to the different methods in measuring the electrical conductivity and to the different composition of the samples and to their different degree of carbonatation. This effect, in fact, reduces the bulk conductivity (5).

Conclusions

The observed semiconduction of the AFm phases is mainly attributable to the mobility of the interlayer species. The hydroxide-form shows, in fact, the highest value of conductivity due to the high mobility of proton jumping from H_2O to OH^- of the interlayer.

The conductivities of the compacts are lower than those of the corresponding parent wash solutions.

The evaluating of an eventual anisotropy in the bulk conduction is not to be neglected because of the lamellar crystalline habitus of such compounds.

In the continuation of this study we intend to evaluate more deeply the impedance variations as a function of the frequency with the pourpose to find out both eventual distribution of relaxing constants and diffusional contributes to the impedance of the samples.

References

1. R. Allmann, Chimia (1970) 24, 99.
2. H. J. Kuzel, Proc. 5th Int. Symp. Chem. Cement, Tokyo, Vol. II, (1968) p. 92.
3. H. F. W. Taylor, Min. Mag. (1973) 39, 377.
4. G. Mascolo and M. Marroccoli, Cem. Concr. Res. 1986 (in press).
5. M. Lal and A. T. Howe, J. Chem. Soc. Chem. Comms. (1980) 737.
6. M. Lal and A. T. Howe, J. Solid State Chem. (1981) 39, 377. Ibidem (1981) 39, 368.
7. M. H. Roberts, Proc. 5th Int. Symp. Chem. Cement, Tokyo, Vol. II, (1968) p. 104.
8. H. J. Kuzel, N. Jb. Miner. mh. (1966) 193.
9. S. J. Ahmed, L. S. Dent Glasser and H. F. W. Taylor, Proc. 5th Int. Symp. Chem. Cement, Tokyo, Vol. II (1968) p. 118.
10. G. W. Jordan and M. F. Berard, J. Electrochemical Soc. (1985) 132, 464.
11. J. Maier, Z. für Phys. Chem. Neue Folge (1984) 140, 191.
12. S. J. Ahmed and H. F. W. Taylor, Nature (1967) 215, 622.

R. SERSALE , University of Naples, Italy
R. AIELLO , University of Calabria, Italy
G. FRIGIONE , University of Calabria, Italy

NATURAL ZEOLITES AS ACTIVE ADDITIONS TO THE PORTLAND CLINKER

INTRODUCTION

The problem of manufacturing blended cements represents since long a subject of very interesting researches, owing to the peculiar properties of such hydraulic binders (1).
Besides the interest of its manufacture with regards to the energy saving, chemical resistance, low heat of hydration , the property of minimizing the expansion following the reaction of the alkalies towards some reactive ingredients, sometimes present in the aggregates for concrete, suggest the use of this type of cement for many important works.
In the sphere of "pozzolanic" cements, several researches on samples manufactured with true pozzolanas, with the "trass" or with different products endowed with pozzolanic behaviour, as fly ashes for example (2), gave evidence of the peculiar characteristics of such binders.
This experimental investigation intends in turn to demonstrate the possibility and opportunity of utilizing also natural zeolites as active additions to the Portland clinker (3), with reference both to the opening of a new field of utilization of these interesting products, very abundant in the central-southern part of Italy, and to the advantages attainable in comparison to the equivalent binders manufactured with true pozzolanas.

EXPERIMENTAL

Neapolitan yellow tuff with a phillipsite content of about 80% has been employed as natural zeolitic product, whereas the true alkali-trachytic phlegraean pozzolana-representing the unzeolited counterpart of the above mentioned tuff - has been used as amorphous addition.
Both the active additions have been added to an industrial clinker in amount varying from 15 to 40%. The chemical compositions of all the product used are reported in Tab. 1

Tab. 1: Chemical composition of the products used for the manufacture of the "pozzolanic" cements.

	Neapolitan yellow tuff	Phlegraean Pozzolan	Clinker
SiO_2 %	54.68	57.00	21.31
$Al_2O_3+TiO_2+Mn_3O_4$	17.70	18.34	3.59
Fe_2O_3	3.82	2.20	4.50
FeO	0.29	2.14	-
CaO	3.66	3.15	65.31
MgO	0.95	0.97	1.04
Na_2O	3.43	4.18	0.70
K_2O	6.38	8.05	1.70
CO_2	-	-	-
SO_3	-	-	2.10
l.o.i.			0.11
Na_2O equiv.	-	-	1.80

The active additions in tab. 1, ground until a 10±2% residue remains on a 32 μm sieve have been added in the above mentioned ratios, to a sample of industrial clinker, typical of the current italian production, having a specific surface area Blaine of 370 m^2/kg. Before grinding the clinker , 5% natural gypsum, with a $CaSO_4 \cdot 2H_2O$ higher than 95%, has been added.

Stated by means of the pozzolanicity test (4) that all the samples, also for compositions poor in addition, can be classified as pozzolanic cements, its technical behaviour has been examined.

EXPERIMENTAL

Compressive strenght tests.

Have been performed on ISO-RILEM mortars (5) aged 3,7, 28, 90 days. Fig. 1 reports strenght progress as a function of addition content and age.

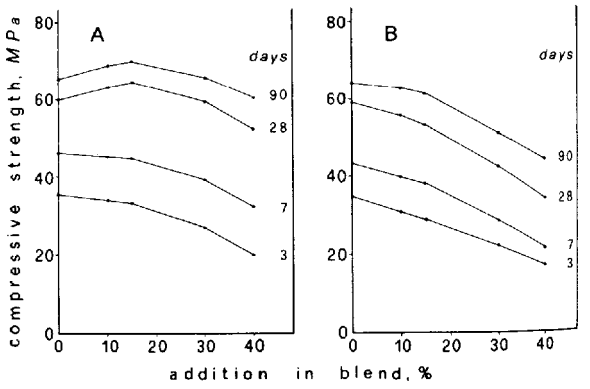

Fig. 1: Compressive strenght progress on mortars.
A = tuff - cement; B = pozzolana - cement.

It is to be seen that, at equal conditions, the zeolitic cements (A), particularly at long ages, show strength values generally higher than those of the typical pozzolanic cements (B).

Workability of the mixtures .

In order to define also the contribution of the zeolitic product to the workability of the mixtures, the flow test on ISO-RILEM mortars (6) with the same water cement ratio has been performed. It is in fact well known that the lower the water the higher the strength of the works.
Stated in advance that any kind of addition definitely decreases the workability of the single clinker, fig.2 reports per cent flow values as a function of the addition amount in the blend and shows that the workability decrease is lower for the vitreous pozzolanic addition (B) and a little bit higher for the zeolitic one (A), owing to its finer texture. The higher water requirement of the zeolitic cements however does not diminish the good results of compressive tests, so that

strenght progress remains at a higher level in comparison to that of the typical pozzolanic cements.

Potential alkali-reactivity.

Has been evaluated from the expansion, after suitable aging, of a series of mortar bars prepared with both the cements and using Pyrex glass as a siliceous reactive ingredient (7).

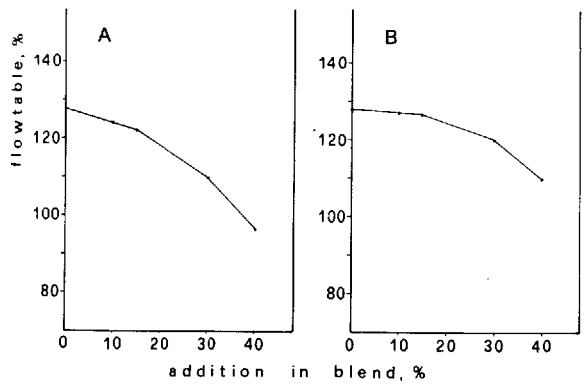

Fig. 2: Flow course of mortars.
A = tuff - cement; B = pozzolana - cement.

Fig. 3 reports the expansion values as a function of addition content and age (180 days) and emphasizes the specific role of the zeolitic addition (A) on the minimization of the expansion phenomenon.
A further improvement of this result can be reached after thermal activation treatment of the zeolitic product at temperature of about 500 °C.

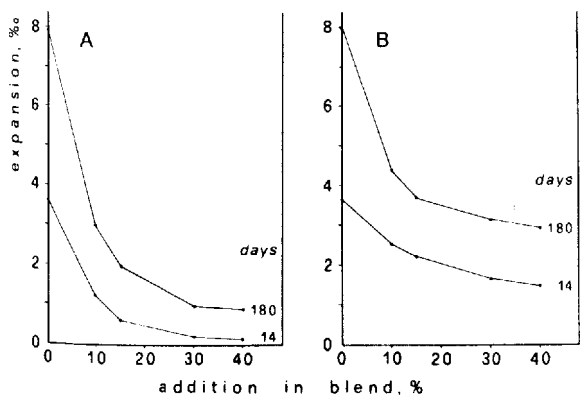

Fig. 3: Potential alkali reactivity tests on mortar bars.
A = tuff - cement; B = pozzolana - cement.

Fig. 4 shows X-ray diffraction diagrams of the untreated Neapolitan yellow tuff (a) and after thermal treatment at 600 °C (b) and Fig. 5 shows the expansion values course for mortar bars manufactured with cements containing as active addition the zeolitic tuff previously treated at 600 °C for one hour (A), and phillipsite pozzolan (B), respectively treated at the same temperature for the same time.

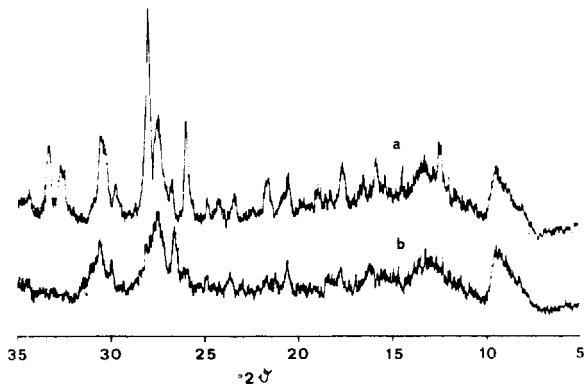

Fig. 4: X-ray diffraction diagrams.
a) untreated phillipsite tuff,
b) same sample treated at 600 °C.

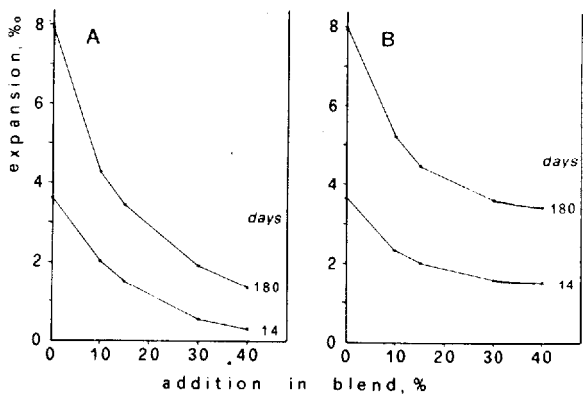

Fig. 5: Potential alkali reactivity tests on mortar bars.
A= blended cement with tuff treated at 600 °C.
B= blended cement with pozzolana treated at 600 °C.

It is to be seen that the use of the zeolitic product thermally activated, reduces by about 40% the expansion values measured, at equal conditions, on mortar bars manufactured with the typical pozzolanic cements.

DISCUSSION AND CONCLUSION.

The whole of the experimental results and of the deductions that can reasonably be drawn, strengthen the interest of the utilization of natural zeolitic product, after proper grinding, for the manufacture of blended cements endowed with special technical performances.
It has been emphasized in fact that mortars prepared with blended cements containing as active addition a powdered phillipsite tuff, show strength progress pretty higher than those of mortars manufactured with blended cements containing the unzeolitized counterpart (the phlegraean pozzolan) and that the zeolitic addition minimizes the more the expansion following alkali-aggregate reaction.
To this end the influence of a thermal treatment of the zeolitic addition as been emphasized and it has been demonstrated that the same thermal treatment does not influence the behaviour of a vitreous natural product when used as active addition to the clinker.
The behaviour of a zeolitic product when used as active addition to the Portland clinker, better than those of the unzeolitized counterpart, is to be brought back to a higher reactivity owing to the peculiar structure of the zeolitic minerals. The pores and channels running throughout the solid reasonably could in fact be responsible for a more rapid and complete attack under the action of the lime solution with a neo-formation as much rapid and complete of the hydration products.
To this higher reactivity is to be attributed the abatement of the expansion following alkali-aggregate reaction, too. A more rapid and complete neo-formation of poorly crystalline, low basicity hydrated calcium silicate, affordsin fact the possibility of incorporating large amounts of alkalies, which otherwise would be available for the deletereous reaction.
With reference to the further minimization of the expansion phenomenon due to thermal activation treatment of the zeolitic product, it is to be hypotesized that owing to the collapse of the structure of the fine-grained zeolitic mineral diffused in the cementing groundmass of the tuff, a quasi-amorphous solid, with specific surface area larger than that of the bubbly pozzolanic glass, owing to the pre-existing pores and channels, is formed, in this way favouring an easier breaking of the Si-O-Si bonds under the attack of the alkaline solution. Furthermore the evolution of the combined water following the thermal treatment promotes, in turn, the neo-formation of free surface bonds which share in the activation of the solid, even though such an activation, to a lesser extent, concerns the vitreous counterpart, too.

REFERENCES

1. SERSALE R. (1980), "Structure et caractérisation des pouzzolanes et des cendres volantes", 7th Int. Congr. on the Chem. of Cement, Paris I, pp IV-1/3-1/21.

- SERSALE R. (1983), "Aspects of the chemistry of additions". In "Advances in Cement Technology" Ed. Ghosh S.N., Pergamon Press, (Oxford) pp 537-567.

2. VALENTI G.L., CIOFFI R., SERSALE R., (1986), "Production and utilization of fly ash in Italy", Canmet/ACI Int. Conf. I, Ed. Malhotra V.M., American Concrete Inst., Detroit, pp 741-762.

3. SERSALE R., FRIGIONE G., (1985), "Natural zeolites as constituents of blended cements", Chimica e Industria, 67, 4, pp 177-180.

- SERSALE R., FRIGIONE G., (1985), "Blended cements manufactured with activated zeolitic additions", Chimica e Industria, 67, 10, pp 537-541.

4. FRATINI N., (1950), Ann. Chim., 40, 461.

5. ISO Recommendation R.679, March (1968).

6. ANSI/ASTM C 230-68.

7. ANSI/ASTM C 441-69.

Ko IKEDA, Department of Mining and Mineral Engineering, Yamaguchi University, 1
755 Ube, JAPAN.

A new type of pozzolanic cement utilizing red mud and fly ash.

Un nouveau type de ciment pozzolanique utilisant dé la boue rouge et de la cendre volante. P

SUMMARY: Bauxite from Australia contains boehmite which remains intact in the red mud after extraction of alumina. Therefore,this kind of red mud can be used as cement without clinkering process. Gypsum and/or portlandite were introduced to the red mud as activators. Two series of cement mixtures were prepared. One is blended with the activators for nearly stoichiometric compositions to produce ettringite and/or C_4AH_{13}. The other is blended with the activators of double amount for the stoichiometric compositions. These cement mixtures are called the red mud mixes and are hydraulic themselves. However,they are no use as cements due to the unstable hydration strength. To improve this defect fly ash was added to the red mud mixes to gether with 7 percent portlandite to the fly ash. Thus,moderately high strength cements were obtained, resulting compressive strength up to 9.7,16.4 and 20.1 MPa at 7,28 and 91-day age,respectively, when cured in water. However,deteriorations of strength were encountered in some specimens cured in air after 28-day water curing caused by the disintegration of ettringite,C_4AH_{13} and/or $C_4A\bar{C}H_{12}$.

1. INTRODUCTION

Alumina is usually manufactured from bauxite by the Bayer process,smelting with sodic solution in autoclaves. After extraction of alumina from the raw material,there remains huge amount of waste called "red mud",mainly composed of hematite. The annual production of this by-product reaches 2 million tons in Japan/1/,although full operation is now restricted due to international price competition.

Australian bauxite imported to Japan comprises some amount of boehmite,$Al_2O_3.H_2O$,in addition to gibbsite,$Al_2O_3.3H_2O$,as Al^{3+} bearing mineral due to weak metamorphism of ores. Accordingly,boehmite remains intact in the red mud because of the incapability of dissolving this mineral by the Bayer process completely. Therefore,pozzolanic type of cement can be produced from this kind of red mud by introducing some effective activators into the red mud to react with boehmite.

Since energy crisis of petroleum,construction of coal combustible power stations has been becoming popular in Japan and the production of by-product fly ash is estimated to become 12 million tons near the end of this century in Japan/2/. We should,therefore,pay attention to the effective use of the fly ash as well as the red mud.

The possibility of the production of this kind of pozzolanic cement utilizing red mud and fly ash has been already reported in the previous work in which stress was placed on the SEM observations/3/ and it was pointed out that this new type of pozzolanic cement is apt to deteriorate in long term,especially in air(partly unpublished). In this paper mixing range with more activators will be studied and the optimum conditions of mixing will be investigated.

2. EXPERIMENTAL

2.1 Red mud

The red mud used in this study is soda-reduced red mud commercially sold from Mitsui Alumina Company. They wash the soda-rich red mud with water,employing 7-stage anticurrent thickenners to reduce soda content down to 3 percent. It is generally said that the soda content of red mud is around 10 percent in alumina factories. According to XRD following minerals were identified in small amount

Table 1. Chemical compositions of the red mud and the fly ash.

	SiO_2	TiO_2	Al_2O_3	Fe_2O_3	MnO	CaO	MgO	Na_2O	K_2O	SO_3	Ig. loss
Red mud	9.14	8.55	19.88	48.86	-	2.47	-	3.02	-	-	8.51 %
Fly ash	58.00	1.10	21.40	5.22	0.04	2.84	2.64	1.40	2.29	0.18	4.40*

* Mainly carbon.

in addition to hematite and boehmite: sodalite, $2Na_2O.1.7Al_2O_3.3SiO_2.nH_2O$/4/, quartz, kaolinite, calcite and vaterite/3/. The latter two minerals are not essential ones, but are secondary precipitates during washing process, since the washing water dissolves some slaked lime as precipitating agent.

chemical composition of the soda-reduced red mud is given in Table 1. The amount of boehmite is estimated to be 13.7 percent in the red mud by calculation, neglecting the very small presence of quartz.

2.2 Fly ash

The fly ash used in this study is general one produced from domestic coal in Kyuden Sangyo Company. Chemical composition is given in Table 1. Small amount of quartz and mullite were found as crystalline phases in the glassy matrices of the fly ash by the X-ray diffractometry.

2.3 Activators

Chemical gypsum and portlandite (slaked lime) of JIS first grade were employed as activators. Physical characteristics are given in Table 2 as well as those of the other raw materials.

2.4 Red mud mixes

As shown in Fig. 1 two series and 10 mixtures were prepared by mixing red mud with gypsum and/or portlandite. These red mud mixes are hydraulic themselves. The series P is the same as investigated in the previous work/3/ and is represented here again for convenience. Mixing proportions of each series were determined on the basis of those for series P. First of all, mixes of two extremes, mix-100 and mix-0 were determined to give maximum formations of ettringite and C_4AH_{13} at 7-day age, respectively. The other mixes, 75, 50 and 25 were determined by simply dividing the amount of activators between the two extremes into proportions, 3 : 1 (75), 1 : 1 (50) and 1 : 3 (25). Gypsum and portlandite act reversely each other. detailed mixing proportions are given in Table 3.

Table 2. Physical characteristics of raw materials.

	Fineness, Blaine	S.G.
Red mud	8,600 cm^2/g	3.33
Gypsum	1,900	2.32
Portlandite	11,600	2.2
Fly ash	-	-

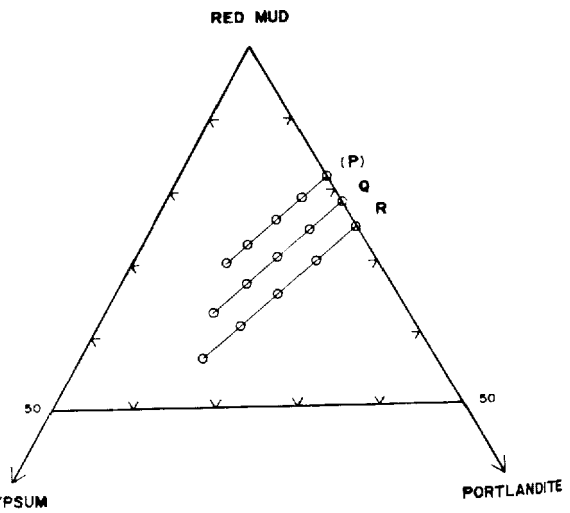

Fig. 1. Triangular representation of the mixing proportions of the red mud mixes.

Table 3. Mixing proportions of the red mud and the activators.

		Mix-100	Mix-75	Mix-50	Mix-25	Mix-0
Series (P)*	Red mud	70.0	73.0	76.0	78.9	81.9 %
	Gypsum	18.4	13.8	9.2	4.6	-
	Portlandite	11.6	13.2	14.8	16.5	18.1
Series Q	Red mud	63.3	67.1	70.9	74.6	78.3 %
	Gypsum	23.3	17.5	11.6	5.8	-
	Portlandite	13.4	15.4	17.5	19.6	21.7
Series R	Red mud	56.8	61.3	65.8	70.3	74.8 %
	Gypsum	28.1	21.1	14.0	7.0	-
	Portlandite	15.1	17.6	20.2	22.7	25.2

* Previous work/3/ and the base of mixing.

P

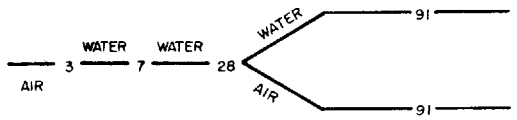

Fig. 2. Curing scheme of present cements.

2.5 Red mud mixes with fly ash

In order to improve long term strenght of the red mud mixes,fly ash blended with 7 percent portlandite was added to the red mud mixes in proportions of 1 : 1(1),2 : 1(2) and 3 : 1(3) in the increasing order of the fly ash. This portlandite acts as an extra activator in appearance. The contents of these mixtures are given in Table 4.

2.6 Curing and testing

Cements of the red mud mixes were tested on flexural and compressive strengths at 3, 7, 28 and 91-day age. Small scale test pieces were prepared in the molds of 1 x 1 x 4 cm dimension in the state of paste with W/C 0.40,i.e.,two pieces for flexural atrength and derived four for compressive strength. Demolding af er 3-day curing in humid air with R.H.90 percent,the test pieces were cured in water in semi-airtight plastic containers at ambient temperature. As illustrating in Fig. 2,the test pieces were divided into two groups at the age of 28-days. The water curing was continued for one group, whereas air curing was carried out in R.H. 90 percent condition for the other group. The air circulates spontenously and the object of this curing is to study the influence of carbon dioxide in air.

Table 5. Flexural and compressive strengths for the red mud mixes.

3	7	28	91	—days—	3	7	28	91
3.9	3.1	1.7	1.6	Q100-0*	8.3	8.1	8.6	6.4
			(1.5)					(6.8)
5.4	3.2	5.1	4.1	75-Q	10.1	10.4	13.9	16.4
			(1.7)					(13.6)
3.8	5.6	3.7	2.6	50-0	13.9	17.4	17.3	15.6
			(1.3)					(19.6)
2.6	3.2	2.5	2.3	25-0	7.7	8.8	9.3	8.9
			(0.5)					(6.0)
0.9	1.3	0.5	0.6	0-0	2.4	3.2	4.1	2.6
			(0.2)					(2.5)
3.1	2.6	2.1	2.3	R100-0*	8.2	6.9	5.8	5.1
			(2.1)					(7.4)
3.1	2.3	2.3	2.2	75-0	7.8	7.2	7.2	5.9
			(1.9)					(6.7)
4.7	4.2	3.8	3.8	50-0	10.4	12.2	11.6	12.3
			(-)					(6.8)
3.6	3.4	3.1	2.7	25-0	8.3	11.6	10.8	11.9
			(-)					(8.4)
1.1	1.0	0.2	1.0	0-0	1.8	2.5	2.7	3.4
			(0.4)					(2.6)

Mean values in MPa. () air curing. * 0 indicating no fly ash.

Table 4. Contents of the red mud mixes with fly ash

	1 : 1	2 : 1	3 : 1	
Red mud mix	50.0	33.3	25.0	%
Fly ash	46.8	62.3	70.1	
Portlandite ——extra	3.2	4.4	4.9	

2.7 Identification of hydrates

Test pieces after the strength test were preserved in acetone and served for the identification of hydrates by means of the X-ray diffractometry,using Mn-filtrated FeKα radiation at 30KV and 10mA.

3. RESULTS AND DISCUSSION

3.1 Strength for the red mud mixes

Results of the strength test are summarized in Table 5. For both of series Q and R decreasing of flexural strength is remarkable,especially in later age as noticed in series P in previous work/3/. This trend is also observed on compressive strength in some specimens. The mixes 0-0 of both series contain no gypsum and show low strength.

For series Q mixes 75-0 and 50-0 give rise generally good results. However,at 91-day age depression is noticed on these mixes cured in air and cured in water,respectively. Though the compressive strength is higher for 50-0 cured in air,the flexural strength becomes very low,i.e.,specimens become brittle. The mix 25-0 shows unstable strength with great deviation,when cured in air at 91 day age.

For series R mixes 50-0 and 25-0 show the saturation of strength,probably due to the exhaution of boehmite reacted with the sufficient amount of activators and depressions take place at 91-day age,when cured in air. Besides,cracking occurred on these specimens at 91-day age,when cured in air and the flexural strength was unable to determine.

3.2 Strength for the red mud mixes with fly ash

Results of the strength test are summarized in Table 6. For both of series Q and R decreasing of flexural strength is not marked but seen, especially in air curing and the strength is dependent on the content of fly ash,i.e.,more fly ash makes the strength decrease.

For series Q abrupt depression of flexural and compressive strengths are observed at 91-day age for the specimens of 75-1,75-2, 75-3 and 100-3 cured in air. For specimens of 0-2 depression is also noticed at 91-day age,when cured in water. On the whole mixes 50-1,50-2,25-1 and 25-2 are superior to the others and no depression of compressive strength was encountered.

For series R abrupt depression of flexural and compressive strengths are observed at 91-day age for the specimens of 100-1, 100-2 and 100-3,when cured in air. In this time no depression is noticed on the specimens 0-2 cured in air at 91-day age. On the whole, the mixes 50-1,50-2,50-3,25-1 and

Table 6. Flexural and compressive strengths for the red mud mixes with fly ash.

3	7	28	91	—days—	3	7	28	91
-	1.7	4.6	4.0 (2.3)	Q100-1*	-	3.5	10.1	15.1 (12.9)
-	4.3	5.0	2.9 (1.2)	75-1	-	9.4	13.2	18.5 (6.0)
-	4.1	4.3	3.1 (2.8)	50-1	-	8.1	12.2	16.8 (15.1)
-	2.6	2.7	3.7 (2.8)	25-1	-	7.2	15.2	16.6 (15.6)
-	1.6	2.8	3.2 (2.4)	0-1	-	6.9	12.0	14.0 (13.0)
-	0.8	3.8	3.3 (1.8)	Q100-2*	-	1.8	7.1	11.2 (10.3)
-	2.8	3.9	3.6 (0.3)	75-2	-	5.6	8.8	13.5 (2.4)
-	2.5	3.5	3.2 (2.1)	50-2	-	5.0	9.0	14.2 (11.3)
-	2.0	3.0	3.8 (2.6)	25-2	-	4.7	8.7	12.0 (11.8)
-	1.3	3.4	3.3 (2.1)	0-2	-	4.8	10.4	7.8 (10.8)
-	0.6	2.6	2.4 (0.6)	Q100-3*	-	1.2	4.8	8.1 (4.2)
-	1.9	2.7	2.7 (0.3)	75-3	-	4.2	7.1	11.3 (3.0)
-	1.5	2.5	2.3 (0.8)	50-3	-	3.2	5.6	9.6 (8.2)
-	0.8	2.4	3.2 (2.1)	25-3	-	2.9	7.3	9.4 (8.4)
-	1.4	2.4	2.7 (2.0)	0-3	-	3.4	8.3	9.2 (7.8)

3	7	28	91	—days—	3	7	28	91
-	1.6	3.2	5.7 (0.8)	R100-1*	-	3.3	5.2	15.2 (2.8)
-	1.8	4.5	3.7 (2.5)	75-1	-	4.0	10.1	14.9 (16.0)
-	4.6	4.4	3.8 (5.0)	50-1	-	9.7	16.4	20.1 (18.8)
-	4.1	4.4	4.6 (3.3)	25-1	-	9.2	13.0	17.7 (17.7)
-	3.1	3.1	3.3 (3.3)	0-1	-	6.5	12.1	14.6 (13.4)
-	0.8	3.4	3.8 (0.6)	R100-2*	-	1.7	7.0	13.9 (3.9)
-	0.9	3.3	2.6 (2.2)	75-2	-	1.9	6.4	13.6 (12.3)
-	2.8	3.6	3.8 (3.8)	50-2	-	6.0	11.3	14.6 (16.9)
-	3.0	3.0	3.6 (3.5)	25-2	-	5.1	9.4	11.4 (11.4)
-	2.9	3.1	3.3 (2.5)	0-2	-	4.3	9.0	11.4 (11.2)
-	0.5	3.6	3.6 (0.4)	R100-3*	-	1.2	6.5	10.7 (2.9)
-	0.8	2.3	2.6 (2.0)	75-3	-	1.8	5.5	11.2 (10.1)
-	1.7	2.7	2.9 (2.8)	50-3	-	4.1	9.2	12.0 (12.8)
-	1.8	2.4	2.8 (2.4)	25-3	-	3.3	6.3	10.5 (8.9)
-	1.9	2.3	3.0 (2.1)	0-3	-	3.3	8.0	10.5 (8.7)

Mean values in MPa. () air curing. * Numerals 1, 2 and 3 indicating the ratios 1 : 1, 2 : 1 and 3 : 1,respectively.

25-2 are superior. Although,the mix 0-2 is good in strength,it may be difficult to use in practice owing to low workability of the paste/3/.

3.3 Hydrates

3.3.1 For the red mud mixes

Hydrates encountered are summarized in Table 7 only limiting at 91-day age for saving space. When gypsum is present,formation of ettringite prevails as seen in the mixes 100-0 and 75-0. However,C_4AH_{13} begins to form gradually with increasing the content of portlandite as seen in the mixes 50-0,25-0 and 0-0 with occasional carbonation and finally no ettringite exists in the mix 0-0 containing no gypsum. It is curious that no C_4AH_{13} forms in the mixes 100-0 and 75-0 having some potential of C_4AH_{13}. This may be explained to consider the limited solid solution series of $C_6A\bar{S}_3H_{32}$–C_6AH_{32}/5,6/. Sometimes C_4AH_{13}(strictly this should be $C_4A\bar{C}_{0.5}H_{12}$/7/) converts to $C_4A\bar{C}H_{12}$ by carbonation, especially in later age. Disintegration of ettringite takes place in some specimens cured in air. This will be discussed later in detail. Calcite exists from the begining of curing,since the red mud contains some calcite and vaterite. However,most of the calcite would be derived from portlandite due to carbonation. Much calcite is detected in the specimens cured in air at 91-day age. Formation of Ca-monosulphate was scarcely observed. Presence of type II C-S-H was reported in the previous work/3/ by means of SEM. C-S-H probably formed after the reaction of quartz and other silicates contained in the red mud was not clearly identified. Judging from the amount of activators left in specimens cured in water at 91-day age, gypsum is wanting except 100-0,while portlandite is sufficient for reaction for series Q. For series R gypsum is also wanting except 100-0, while portlandite is in excess except 50-0. No distinct relations between hydrates and strength were found except the specimens of 75-0 and 25-0 in series R where disintegrations of ettringite,C_4AH_{13} and $C_4A\bar{C}H_{12}$ were seen.

3.3.2 For the red mud mixes with fly ash

Hydrates identified are summarized in Table 7 for mixes 1 : 1, 2 : 1 and 3 : 1,respectively. Hydrates are similar to those of the red mud mixes. When gypsum is present, ettringite forms preferencially. With increasing the content of portlandite, C_4AH_{13} as well as $C_4A\bar{C}H_{12}$ is observed. Since these mixes comprise fly ash blended with 7 percent portlandite,increasing of the content of portlandite takes place into two directions. One is the direction from mix 100 to mix 0 via mixes 75, 50 and 25. The other is the direction from mix 1 : 1 to mix 3 : 1 via mix 2 : 1. Therefore,formations of C_4AH_{13} and $C_4A\bar{C}H_{12}$ become common,when compared with

P

Table 7. Hydrates identified in present cements in relation to gypsum and portlandite. Listed only for 91-day age with relative amounts.

() air curing. E:ettringite,H13:C_4AH_{13},$\bar{C}H_{12}$:$C_4A\bar{C}H_{12}$,$C\bar{C}$:calcite,G:gypsum,P:portlandite. Peak height of X-ray, ++++:large,+++:medium, ++:small,+:detectable,-:undetectable.

	Q100-0	Q75-0	Q50-0	Q25-0	Q0-0
E	++++	++++	++++	++	-
	(++++)	(++++)	(++++)	(+++)	(-)
H13	-	-	-	++	++
	(-)	(-)	(-)	(-)	(+)
$\bar{C}H12$	-	-	++	++++	++++
	(-)	(-)	(-)	(-)	(++)
$C\bar{C}$	++	+	+	+	+
	(+++)	(++++)	(++++)	(++++)	(++++)
G	+	-	-	-	-
	(++)	(-)	(-)	(-)	(-)
P	+	+	+	+	-
	(+)	(+)	(+)	(-)	(-)

	R100-0	R75-0	R50-0	R25-0	R0-0
E	++++	++++	++++	+++	-
	(++++)	(++)	(++++)	(++)	(-)
H13	-	-	-	++	++
	(-)	(-)	(-)	(-)	(++)
$\bar{C}H12$	-	-	+	++	++++
	(-)	(-)	(-)	(-)	(+++)
$C\bar{C}$	+	+	+	+	+
	(++++)	(++)	(++++)	(++++)	(++++)
G	++++	-	-	-	-
	(++++)	(+)	(-)	(-)	(-)
P	++	++	+	++	++
	(+)	(+)	(-)	(+)	(-)

	Q100-1	Q75-1	Q50-1	Q25-1	Q0-1
E	++++	++++	+++	++	-
	(++++)	(+)	(+++)	(++)	(-)
H13	-	-	++	+++	++
	(-)	(-)	(+)	(+)	(+)
$\bar{C}H12$	-	-	-	+	++
	(-)	(-)	(-)	(+)	(+)
$C\bar{C}$	+	+	+	+	+
	(++)	(+++)	(+++)	(+++)	(+++)
G	-	-	-	-	-
	(-)	(++)	(-)	(-)	(-)
P	+	+	+	+	-
	(+)	(-)	(+)	(-)	(-)

	R100-1	R75-1	R50-1	R25-1	R0-1
E	++++	++++	+++	++	-
	(+)	(++++)	(+++)	(++)	(-)
H13	-	-	+	++	++
	(-)	(-)	(+)	(++)	(+)
$\bar{C}H12$	-	-	-	++	++
	(-)	(-)	(-)	(+)	(+)
$C\bar{C}$	+	+	+	+	+
	(+++)	(++)	(++++)	(++)	(++++)
G	-	-	-	-	-
	(++++)	(-)	(-)	(-)	(-)
P	+	-	-	-	-
	(-)	(-)	(+)	(-)	(-)

	Q100-2	Q75-2	Q50-2	Q25-2	Q0-2
E	+++	+++	++	+	-
	(+++)	(-)	(++)	(+)	(-)
H13	-	++	++	+++	++
	(-)	(-)	(-)	(++)	(+)
$\bar{C}H12$	-	-	-	+	++
	(-)	(-)	(-)	(+)	(+)
$C\bar{C}$	+	+	+	+	+
	(++)	(++++)	(++)	(+++)	(+++)
G	-	-	-	-	-
	(-)	(++)	(-)	(-)	(-)
P	-	+	+	+	-
	(+)	(-)	(-)	(-)	(-)

	R100-2	R75-2	R50-2	R25-2	R0-2
E	++++	+++	+++	+	-
	(-)	(+++)	(++)	(+)	(-)
H13	-	+	++	++	++
	(-)	(-)	(+)	(+)	(+)
$\bar{C}H12$	-	-	-	+	++
	(-)	(-)	(-)	(+)	(+)
$C\bar{C}$	+	+	+	+	+
	(++)	(++)	(++)	(++)	(+++)
G	-	-	-	-	-
	(+++)	(-)	(-)	(-)	(-)
P	+	+	-	-	+
	(-)	(-)	(-)	(-)	(-)

	Q100-3	Q75-3	Q50-3	Q25-3	Q0-3
E	+++	+++	++	+	-
	(++)	(+)	(++)	(+)	(-)
H13	+	+++	++	+++	+
	(-)	(+)	(+)	(++)	(+)
$\bar{C}H12$	-	-	-	+	+
	(-)	(-)	(-)	(+)	(+)
$C\bar{C}$	+	+	+	+	+
	(++)	(++++)	(++)	(++)	(++)
G	-	-	+	-	-
	(+)	(++)	(-)	(-)	(-)
P	+	+	-	-	+
	(-)	(-)	(-)	(-)	(-)

	R100-3	R75-3	R50-3	R25-3	R0-3
E	++++	+++	++	++	-
	(-)	(+++)	(++)	(+)	(-)
H13	-	+	++	++	++
	(-)	(-)	(+)	(+)	(+)
$\bar{C}H12$	-	-	-	+	++
	(-)	(-)	(+)	(+)	(+)
$\bar{C}C$	+	+	+	+	+
	(++)	(++)	(+++)	(++)	(+++)
G	-	-	-	-	-
	(+++)	(-)	(-)	(-)	(-)
P	-	-	-	-	-
	(-)	(+)	(+)	(-)	(-)

the hydration of the red mud mixes,especially in mixes 2 : 1 and 3 : 1. Formation of Ca-monosulphate is scarce and not distinct generally. Calcite exists from the beginning more or less and much formation of this mineral is seen in specimens cured in air at 91-day age. Disintegration of ettringite as well as C_4AH_{13} and $C_4A\bar{C}H_{12}$ is worthy to note and this phenomenon is closely related to the depression of strength at 91-day age, when cured in air as seen in the specimens 75-1,75-2,75-3 and 100-3 in series Q, and 100-1,100-2 and 100-3 in series R. The rate of consumption of gypsum is great and the amount is generally wanting,while that of portlandite is sluggish and is generally sufficient. Portlandite is apt to convert to calcite especially in air curing at 91-day age. C-S-H probably formed due to the hydration of the fly ash as well as quartz and other silicates included in the red mud was not clearly identified/8/. However,this may be present as reported previously by the observation of SEM/3/.

3.3.3 Disintegration of ettringite, C_4AH_{13} and $C_4A\bar{C}H_{12}$

As seen in Fig. 3 as well as Table 7, disintegration of these minerals occurs partly or completely in some specimens cured in air at 91-day age. Judging from the X-ray results, following reactions would take place in the course of curing.

For ettringite:

$$C_6A\bar{S}_3H_{32} + 3\bar{C} = 3C\bar{S}H_2 + AH_3 + 3C\bar{C} + 23H$$

Consequently,ettringite disintegrates into gypsum,gibbsite and calcite in addition to water and the gibbsite can be hardly detected due to the amorphous nature in the early stage of formation.

For C_4AH_{13} and $C_4A\bar{C}H_{12}$:

$$C_4AH_{13} + \bar{C} = C_4A\bar{C}H_{12} + H$$

$$C_4A\bar{C}H_{12} + 3\bar{C} = AH_3 + 4C\bar{C} + 9H$$

Consequently,the both minerals disintegrate into gibbsite and calcite in addition to water. If these reactions take place independently or simultanously,great depressions of strength are induced. However,it is quite curious that no depressions of strength were found in haüyne-belite cement cured in steam, in which ettringite and C-S-H are essential hydrates and disintegration of the ettringite occurs,when subjected to air after the steam curing. In this case the C-S-H derives from the hydration of C_2S and there may be fundamental difference of C-S-H between the haüyne-belite cement and the present red mud cement/9/.

4. SUMMARY AND CONCLUSION

Red mud cement can be made from soda-reduced red mud,when activated with gypsum and/or portlandite. Boehmite included in the red mud plays an important role in this kind of cement which is regarded as a type of pozzolanic cement,since boehmite cannot be a cement mineral by itself. Many kinds of cement are manufactured,varying the proportion of the red mud and the activators. However, these cements are generally unstable in

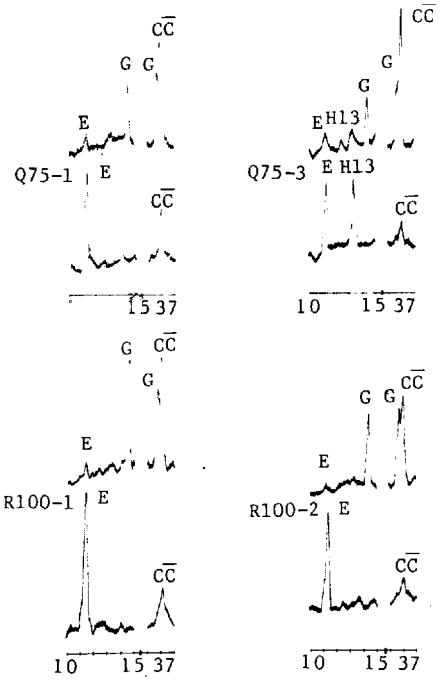

Fig. 3. Powder X-ray diagrams showing the disintegration of hydrates. Top,air curing,and bottom, water curing for each. Other notations, see Table 7. (FeKα).

strength. This defect is improved by introducing fly ash with 7 percent extra portlandite. Thus,hardened cement materials,for instance,having 9.7,16.4 and 20.1 MPa compressive strength at 7, 28 and 91-day age were obtained. However,some specimens show the deterioration of strength,when cured in air after 28-day water curing. This is caused by the disintegration of ettringite,C_4AH_{13} and/or $C_4A\bar{C}H_{12}$ which are the essential hydrates in present cement,probably in addition to C-S-H. Further investigation is necessary to make clear the disintegration of these minerals in various conditions of curing.

REFERENCES

1) The Asahi,No.37146,1984.
2) The Science News,No.1940,1082.
3) Ikeda, K.,Proc. Beijin Inter. Symp. Chem. Cem. Concr.,1985,(in Press).
4) Materials of Mitsui Alumina Co.,LTD.,1978.
5) Taylor, H.F.W.,The chemistry of cement, Academic Press,1,272,1965.
6) Midgley,H.G.,Rosaman,D.,Proc. 4th Inter. Symp. Chem. Cem.,Washington,1,259,1962.
7) Fischer, R.,Kuzel, H.-J.,Cem. Concr. Res., 12,517,1982.
8) Uchuikawa,R.,Uchida, S.,Proc. 7th Inter. Sym. Chem. Cem.,Paris.,3,IV-24,1980.
9) Ikeda, K.,Tashiro, C.,Techn. Repor. Yamaguchi University,2,522,1981.

K. Isozaki, S. Iwamoto and K. Nakagawa
Denki Kagaku Kogyo Co., Ltd, - Japan

SOME PROPERTIES OF ALKALI ACTIVATED SLAG CEMENT

I. INTRODUCTION

In recent years, alkali metal salt activated blast furnace slag cement containing no ordinary portland cement has attracted attention in regard to energy conservation and industrial by-product use as well as properties of high strength development, chemical resistance and heat resistance. However, some reports by other authors appear to fail to provide adequate data regarding the basic properties of this cement. (for example (1), (2)) In this paper, some properties of pastes made with blast furnace slag and NaOH were systematically studied.

II. EXPERIMENTAL

The chemical composition, basicity and glass content of blast furnace slag (BFS) used are shown in Table I.

TABLE I
Chemical composition, basicity and glass content of blast furnace slag (BFS)

Chemical composition (wt%)	
ig.loss	0.15
insol.	0.08
SiO_2	34.22
Al_2O_3	14.93
Fe_2O_3	0.03
CaO	41.76
MgO	7.7
SO_3	0.05
Na_2O	0.24
K_2O	0.44
Total	99.60

Specific gravity.... 2.90

Basicity... $\frac{CaO+MgO+Al_2O_3}{SiO_2} = 1.88$

Glass content... 90%
(determined by an optical microscope)

BFS was ground into blaine specific surface areas of 147, 220, 273, 407, 565 and 654 m^2/kg. The added amounts of NaOH to BFS were 0, 1.6, 3.3, 5.0, 7.5, 10.0, 20.0 and 30.0 wt%. The water to BFS ratios were 0.3, 0.4, 0.6 and 0.7.

The superplasticizers used were the sodium lignosulfonate (LS) and formalin condensates of β-naphthalene sodium sulfonate (NS). These admixtures were high commercial grade water reducing agents for cement. AS reference material, ordinary portland cement (OPC) was used. Table II shows its chemical composition.

TABLE II
Chemical composition of ordinary portland cement (OPC)

Chemical composition (wt%)	
ig.loss	0.7
insol.	0.4
SiO_2	22.1
Al_2O_3	5.0
Fe_2O_3	2.0
CaO	64.6
MgO	1.2
SO_3	2.0
Na_2O	0.41
K_2O	0.42
f-CaO	0.6
Total	99.43

Blaine specific surface area ... 305 (m^2/kg)

Each paste specimen (4x4x16 cm beam) was cured at 20°C, 80 %rh and subjected to a compressive strength test at a predetermined age. The crushed specimens were treated by D-dry method for 48 hrs and used as samples to be studied by a mercury pressure porosimeter, powder X-ray diffractometer, thermal analysis (DTA, TG) and SEM observation. The heat liberation curve of hydration was obtained using a conduction calorimeter. Rheological properties were measured with a coaxial cylinder viscosimeter. The pastes to be tested were prepared by mixing the cement with water or a NaOH solution in a beaker for 2 min by hand. Immediately following mixing, the pastes thus obtained were transferred into a measuring cell. During the experiment, the rotating bob speed increased in one minute from 0 to 350 rpm and in the next, resumed 0 rpm. This method was repeated at each age without interruption from the time each paste was placed in the cell untill completion of the test.

III. RESULTS AND DISCUSSION

III-1 STRENGTH DEVELOPMENT AND HEAT OF HYDRATION

The compressive strengths of the paste specimens increased in proportion to the fineness of BFS on adding 7.5 wt% NaOH. (Fig. 1) Fig.2 shows the relation between the added amount of NaOH and strength development in BFS having a 565 m^2/kg blaine specific surface area. The compressive strengths of the paste specimens increased with NaOH content being maximum at a 10 wt% addition.

OPC has a dormanant period at the early stage of hydration but is nonexistent in the hydration of NaOH activated BFS. (Fig. 3)

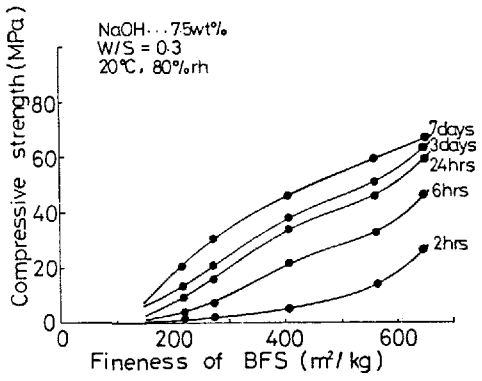

Fig. 1 Effect of fineness of BFS on strength development.

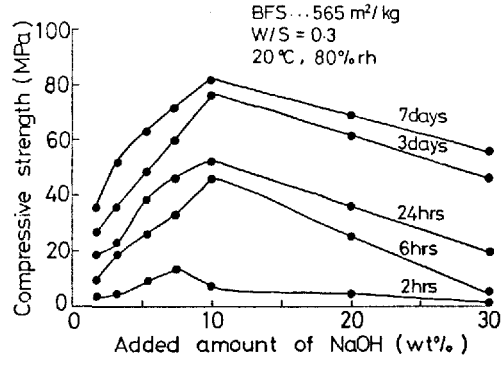

Fig. 2 Effect of added NaOH on strength development.

This should depend on the difference in their hydration mechanisms. The hydration of portland cement occurs mainly by a topochemical reaction and that of alkali activated BFS cement by a solution reaction. With increase in NaOH content and fineness of BFS, the rate of BFS dissolution was found to increase, resulting in enhancement of the hydration of BFS.

The compressive strength of each specific surface area of BFS is plotted as a function of the heat of hydration in Fig. 4. A nearly satisfactory linear plot was obtained for each amount of NaOH added. The 7.5 wt% and 10.0 wt% additions of NaOH to BFS seemed too much for effective strength development. The relation between compressive strength and heat of hydration for the 1.6 wt% addition of NaOH was similar to that of OPC.

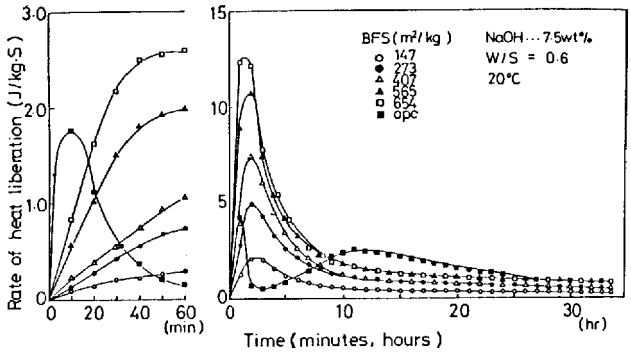

Fig. 3 Heat liberation curves of hydration as a function of time.

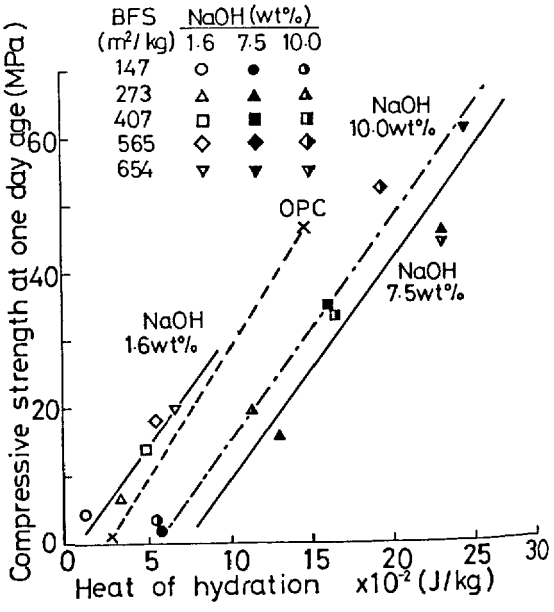

Fig. 4 Relation between heat of hydration and compressive strength for various surface areas of BFS.

Therefore, the optimum amount of NaOH addition is generally assumed to be a few wt%. (3)

III-2 HYDRATION PRODUCTS AND PASTE STRUCTURES

The X-ray diffraction pattern of BFS paste admixed with 7.5 wt% NaOH at 28 days of age is shown in Fig. 5. A broad peak with a maximum was found in the vicinity of 30° (Cu Kα, 2θ), and apparently C-S-H (I). (4)

The peaks at 11.7° and 30.4° were identified as $C_3A\ CaCO_3H_{11}$ and C_2ASH_8, respectively. (5)(6) No traces of $Ca(OH)_2$ dehydration in either the DTA or TG curves (Fig. 6) could be found. The endthermic peak at 170°C was regarded as the dehydration of C-S-H (I). (7)

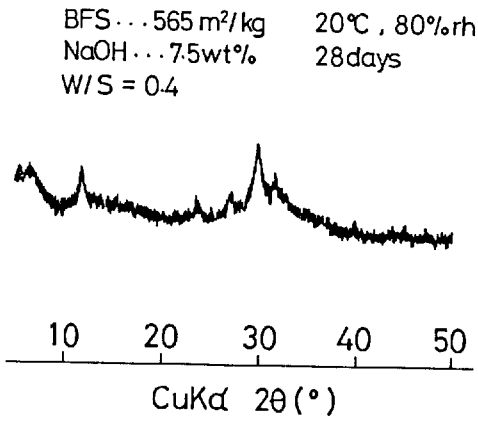

Fig. 5 Powder X-ray diffraction pattern of hardened paste.

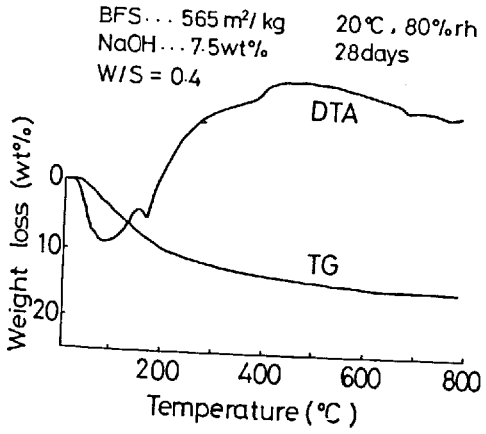

Fig. 6 Thermal analysis curves of hardened paste.

Fig. 7 shows the morphology of the hydrates as determined by SEM. The hydrate structures appeared to be homogeneous and dense compared with those of OPC. Correspondingly we can consider the result of mercury pressure porosimetry. Pore volumes of BFS paste ranging from 107 to 750 nm pore radii were extremely smaller than those of OPC paste. (Fig. 8)



(A) BFS paste —— 5 μm
(565 m^2/kg, NaOH... 7.5 wt%)

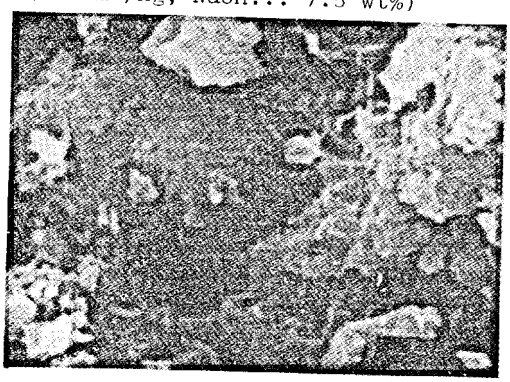

(B) OPC paste —— 5 μm

Fig. 7 SEM photograph of hardened pastes at 14 days of age.
(W/S = 0.4, 20°C, 80 %rh)

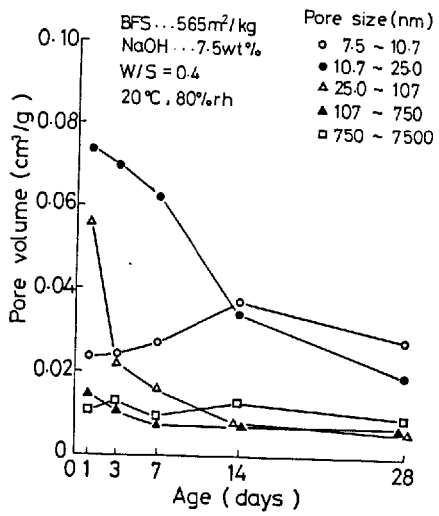

(A) BFS paste

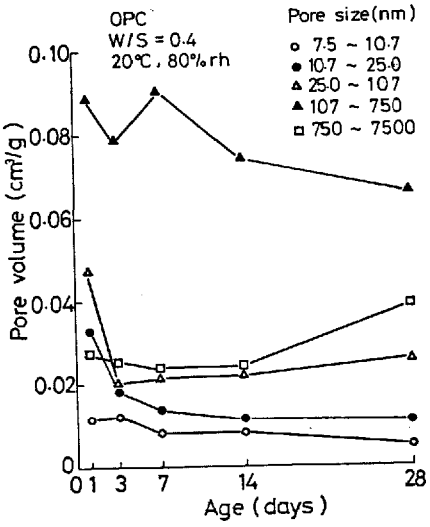

(B) OPC paste

Fig. 8 Pore size distribution of hardened paste as a function of time.

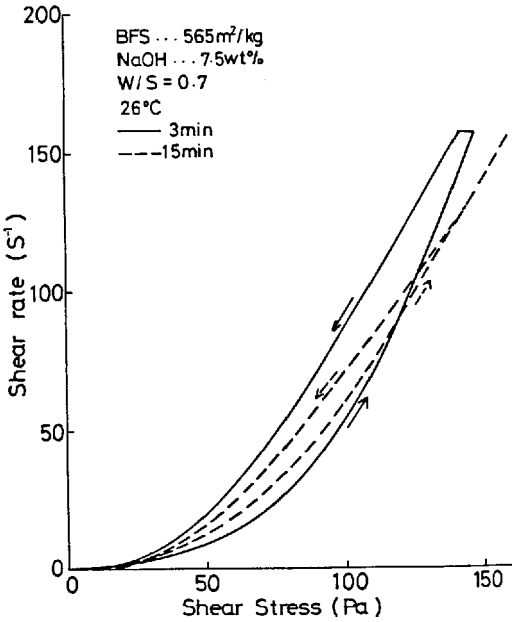

Fig. 9 Flow curves of fresh paste.

III-3 INFLUENCE OF SUPERPLASTCIZER ON RHEOLOGYCAL PROPERTIES

The flow curves obtained 3 and 15 min after the first cement-water contact are shown in Fig. 9 and are pseudoplastic type and thixotropically in reversible character. (8) (9)

A comparison of the effects of the superplasticizers (Fig. 10) indicated differences between LS and NS. LS exhibited strong plasticizing effects on the system of BFS only and the system of BFS admixed with NaOH. However, systems admixed with NS showed the same viscosity as those without superplasticizers since LS retards cement hydration but not NS. In Fig. 3, no dormanant period is present early in the hydration of BFS pastes, thus indicating that hydration strongly proceeds from the first contact of cement with water. Without a delay in hydration, NS is completely consumed at the start of hydration, as was confirmed by examination of the concentration of NS in the liquid phase. (10)

The yield values indicate the workability of fresh pastes. On adding NaOH and superplasticizers, paste behavior was noted to change considerably. (Fig. 11) This point warrants further investigation.

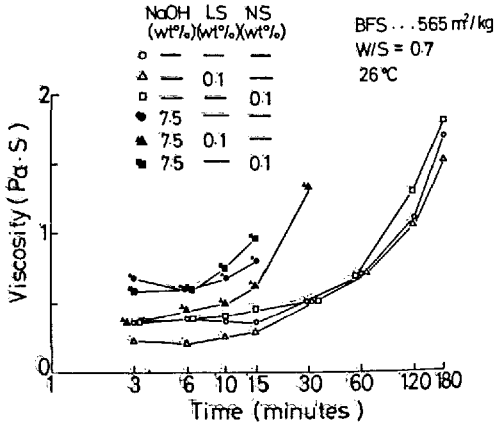

Fig. 10 Viscosity of fresh paste as a function of time.

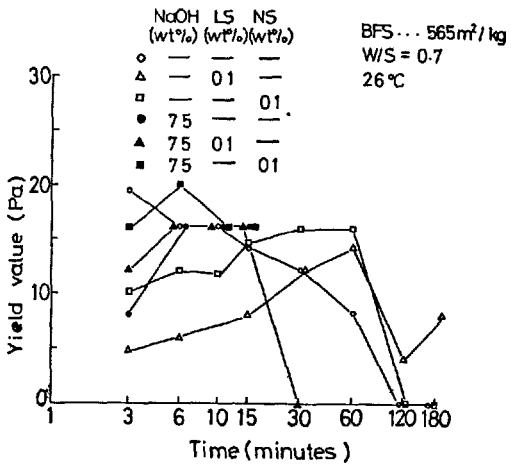

Fig. 11 Yield value of fresh paste as a function of time.

IV. CONCLUSIONS

(1) The optimum amount of NaOH to add to BFS is generally a few wt%. The compressive strengths of NaOH activated BFS paste specimens increases in proportion to the fineness of BFS.

(2) No formation of $Ca(OH)_2$ occurs in the hydration of BFS. The morphology of hydrates is relatively homogeneous and the paste structure is dense compared with that of ordinary portland cement.

(3) The flow curves of NaOH activated BFS pastes are of the pseudoplastic type and thixotropic in character. Sodium lignosulfonate is effective as a superplasticizer for NaOH activated BFS cement but not the formalin condensates of β-naphthalene sodium sulfonate.

REFERENCES

1.- T. Hakkinen and J. Ruohomaki (1985), "Alkali activated slag and blended cement research in Finland" Workshop on blastfurnace slag cements and concretes, York.

2.- V. Glukhovskij, Yy. Zaitsev and V. Pokhomov (1983), "Slag-alkaline cements and concretes-structure, properties, technological aspects of the use" Silicates Industriels, 4-5, 123-127.

3.- J. Metso and E. Kajaus (1983), "Activation of blast furnace slag by some inorganic materials", 1st Inter. Confer. on the use of fly ash, silica fume, slag and others mineral by-products in concrete, 2, 1059-1073.

4.- M. Daimon, C.T. Song, A. NISHITA, O. Yamaguchi and C.E. Kim (1982), "Change in the liquid concentration during the hydration of granulated blast furnace slag" Gypsum & Lime, 176, 3-8.

5.- M.H. Roberts (1969), "Calcium aluminate hydrates and related basic salt solid solutions" Proc. 5th Inter. Symp. Chem. Cement, Tokyo, SP II-29, 104-117.

6.- C.H. Schmidt (1960), Proc. 4th Inter. Symp. Chem. Cement, Washington, 2, 244.

7.- V.S. Ramachandran (1969), "Applications of differential thermal analysis in cement chemistry" Chemical publishing Company, INC. New York, 86.

8.- I. Odler, T. Becker and B. Weiss (1979), "Rheological properties of cement pastes " Il Cemento, 3, 303-310.

9.- R.A. Helmuth (1980), "Structure and rheology of fresh cement paste", 7th Inter. Symp. Chem. Cement, Paris, VI-0, 16-30.

10.- M. Daimon and D.M. Roy (1978), "Rheological properties of cement mixes; I. Method, preliminary experiments and adsorption studies", Cem. Concr. Res.,8, 753-764.

N. Tsuyuki, N. Hirota, T. Miyakawa and J. Kasai
Nikon University - Japan

THE PHYSICAL PROPERTIES AND THE HYDRATION MECHANISM OF C_3A IN THE PRESENCE OF $CaSO_4.2H_2O$ and $Ca(OH)_2$.

INTRODUCTION

On the retardation mechanism of C_3A in the presence of $C\bar{S}H_2$. Mehta[1] suggested that it was coated by gel-like form of ettringite. Corstanje et al. have deduced that the primary cause of C_3A retardation is not SO_4^{2-} but the precipitation of amorphous $Al(OH)_3$ on the surface of the C_3A grain. Tadros et al. suggested that the primary retardation of the dissolution was caused by the formation of an Al-rich layer. and that the induction period represented the process responsible for the removal of the Al-rich layer. The retardation was greatest when both $C\bar{S}H_2$ and CH were present.the authors have recently questioned the role of ettringite in the retardation of C_3A by SO_4^{2-} . The study aimed to clarify the physical properties of C_3A and the mechanism of the excessive retardation. When C_3A was dispersed in suspension of $C\bar{S}H_2$ and CH. the interaction between solid and liquid phases as a function of hydration time was investigated[2].

EXPERIMENTAL

(1) Two kinds of C_3A was synthesized to clarify the characterization. it was the pure C_3A, and other hand. the melt of C_3A composition ($G\text{-}C_3A$) which was synthesized by rapid quenching after fusion. The melt ($G\text{-}C_3A$)involved the slight presence of SiO_2 Various physical properties was measured.

(2) Pure solution and suspensions of $C\bar{S}H_2$ .C and mixing both $C\bar{S}H_2$ and CH were prepared. After the synthesized pure C_3A of 2.5 g was dispersed into 125 ml of various suspensions. these were fully shaken in incubater at 25℃ . A lot of poly-bottles containing suspension were prepared. these were filtrated by 17G-4 glass filter for each prescribed times. The concentration of Ca^{2+} .$Al(OH)_4^-$ and SO_4^{2-} which eluted from C_3A and pH in the filtrate were measured. On the other hand. after the each residue were stopped the hydration by CH_3OH and CH_3COCH_3 . it was dried in the desiccator. XRD and SEM of each specimens which correspond to hydration time were identified and observed.

RESULTS

(1) The physical properties of synthesized pure C_3A and the melt of C_3A composition ($G\text{-}C_3A$) were shown in Table 1. Surface binding energy[3] of C_3A and $G\text{-}C_3A$ by ESCA were shown in Fig.1.2. Fig.1 is wide scanning. and Fig.2 is narrow scanning about Ca.Al. From the results of measurements by Fig.2. the chemical shift of

Table 1. Physical properties of C_3A and the melt ($G\text{-}C_3A$).

	$G\text{-}C_3A$	C_3A
lattice const. (Å)	15.22	15.26
specific gravity	2.98	3.04
specific surface area (m^2 / g)	1.38	0.75
free CaO (wt %)	2.44	0.17

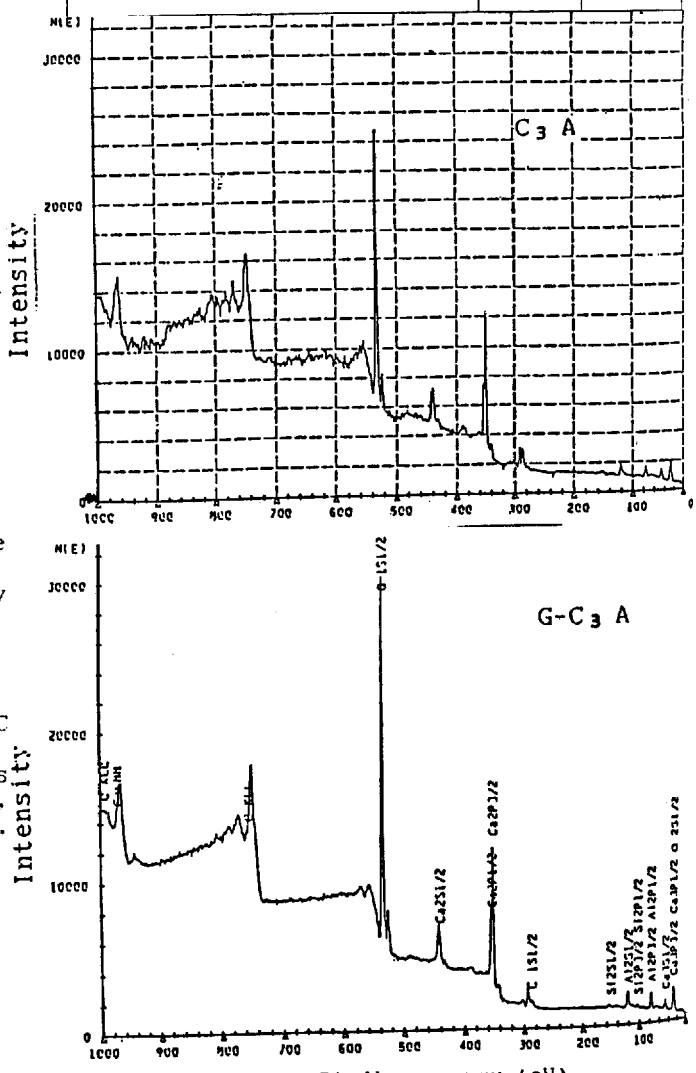

Fig.1. Binding energy of C_3A and the melt ($G\text{-}C_3A$) by XPS (ESCA).

binding energy were obtained about Ca-O. Al-O bond. The results are shown in Table 2.

(2) (i) Conduction calorimetric curves of C_3A and the melt ($G\text{-}C_3A$) which hydrated with pure water were shown in Fig. 3. W/solid ratio is 5. The appearance of the second peak was characterized in the melt ($G\text{-}C_3A$)-H system. Similarly. rate of heat liberation of C_3A which hydrated with various addtions of $C\bar{S}H_2$ and CH were shown in Fig. 4.

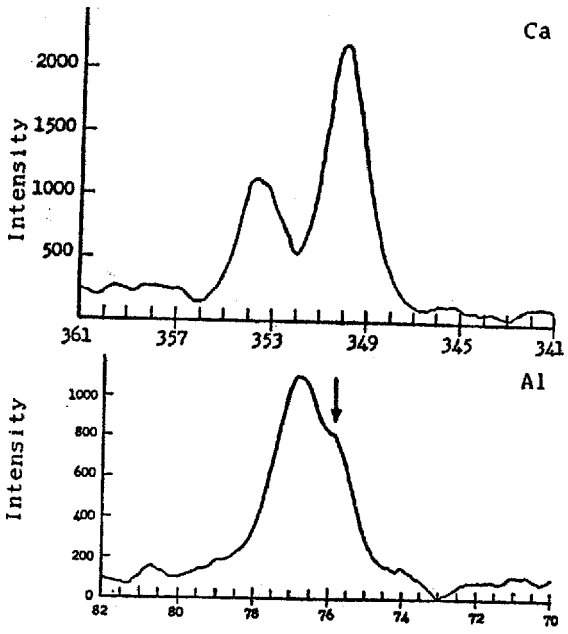

Fig.2. Binding energy of Ca-O, Al-O in C_3A by ESCA.

In case of higher ratio of CH to C_3A over 10%, rate of heat liberation were depressed, the appearance time of the second order peak was dependent on amount of $C\bar{S}H_2$.

(ii) When C_3A was dispersed into aqua solution, the concentration of Ca^{2+} and $Al(OH)_4^-$ which eluted from C_3A and pH in liquid phase were measured by ICP instrument. The result makes as CaO and Al_2O_3 is shown in Fig. 5. Similarly, when C_3A was dispersed into suspension of mixing both $C\bar{S}H_2$ and CH, the concentration of Ca^{2+}, $Al(OH)_4^-$, SO_4^{2-} and pH were obtained. The results are given in Fig. 6.

Although Ca^{2+} and $Al(OH)_4^-$ were immediately eluted after C_3A hydration, its C/A mole ratio in liquid phase was depend on hydration time. C/A=2 until 5min. C/A=4 until 3hr, C/A=1 after 3hr. pH is almost constant during this period. On C_3A-$C\bar{S}H_2$-CH system, the concentration of Ca^{2+} and SO_4^{2-} in the presence of $C\bar{S}H_2$ and CH and no C_3A is 1.80g CaO/l, 1.02g SO_3 /l, respectively, it isn't obeys to the common ion effect. The retention period at the highest concentration of SO_4^{2-} is depends on the amounts of $C\bar{S}H_2$ and CH.

(iii) XRD intensity of solid phase corresponds to hydration time was plotted for each hydrates. The results are indicated in Fig.7. Furthermore, SEM photographs are shown in Fig.8.

On C_3A-H system, XRD intensity of C_3A unhydrate rapidly fell, consequently, C_3AH_6 hydrate was growing with hydration progress. However, amorphous C_4AH_{13} hydrate was immediately confirmed by SEM as card-house

Table 2. Chemical shift of binding energy by ESCA.

atom	orbital	G-C_3A	C_3A	shift
Ca	2P	347.5 eV	346.7 eV	0.8 eV
Al	2P	74.1	73.4	0.7
Si	2P	101.7	——	——
O	1S	531.8	531.1	0.7

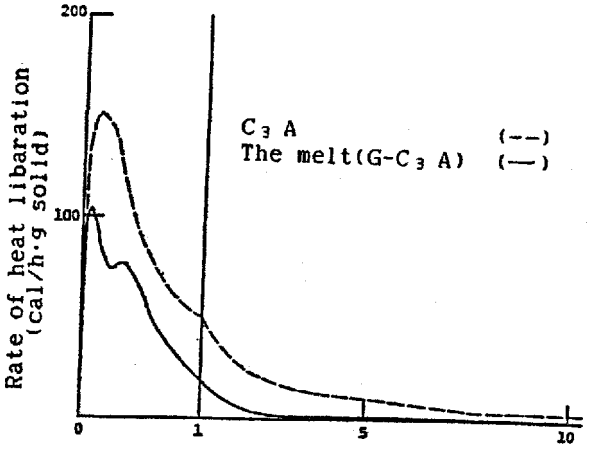

Fig.3. Conduction calorimetric curves of C_3A and the melt (G-C_3A) (W/solid=5).

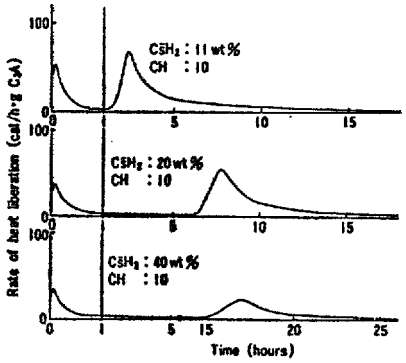

Fig.4. Conduction calorimetric curves of C_3A hydrated with various additions of $C\bar{S}H_2$ and CH (W/C_3A=5).

structure after contact with aqua solution. On C_3A-$C\bar{S}H_2$-CH-H system, it is difficult to confirm the formation of ettringite by XRD in spite of consumption of SO_4^{2-}. Monosulfate and C_4AH_{13} hydrate were remarkably growing with hydration progress.

DISCUSSION

(1) It is thought that the factor which controlled the hydration of C_3A is caused

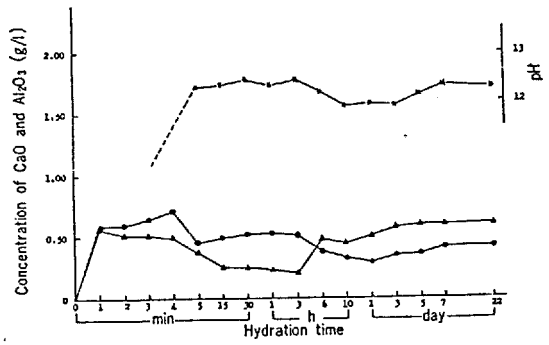

Fig.5. The concentration of CaO(●) Al_2O_3 (▲) and pH(✱) in liquid phase of C_3A-H system as a function of hydration time at 25℃ (W/solid=50).

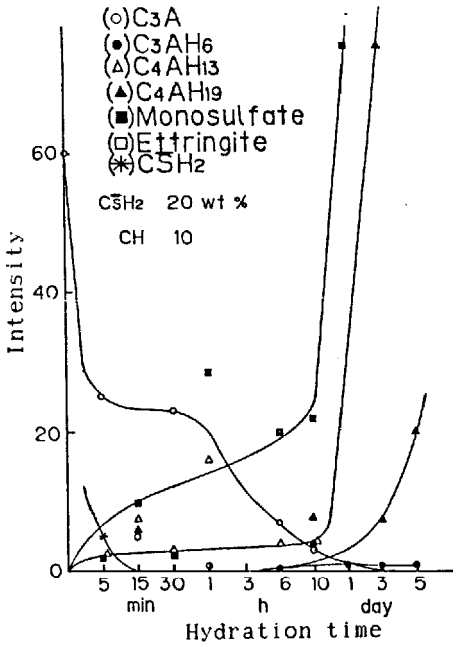

Fig.7. The changes in diffraction intensity of various hydrates as a function of hydration time at 25℃ (W/solid=50).

to binding energy of inner shell electron of Ca. Al and Si combined with O(oxygen). The satellite peak of Al shown in Fig.2 exhibits to become the shoulder by different binding distance of Al-O. The binding energy of C_3A which was synthesized by two different methods was clarified from Table 2. consequently. active C_3A on hydration is 0.7~0.8 eV lower than the melt (G-C_3A). Therefore. the hydration of C_3A is quicker than the melt (G-C_3A).

(2) CaO/Al_2O_3 mole ratio of Ca^{2+} .$Al(OH)_4$ which eluted from C_3A after contact with aqua solution isn't 3. it is 2 until 15 min. Because of unhydrate C_3A is attacked by the eluted Ca^{2+} .C_4AH_{13} is formed. resulting Ca^{2+} is consumed. unhydrate C_3A is coated by

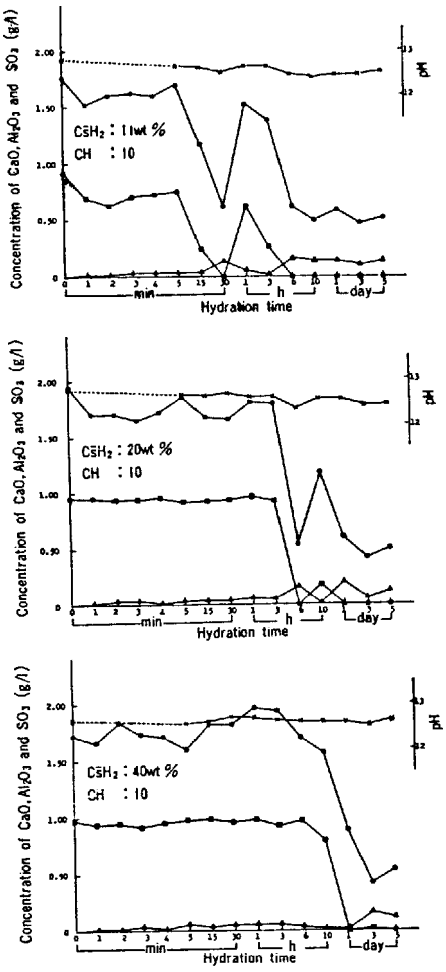

Fig.6. The concentration of CaO(●), Al_2O_3 (▲), SO_3 (■) and pH(✱) in liquid phase of C_3A-$C\bar{S}H_2$-CH-H system as a function of hydration time at 25℃ (W/solid=50).

hexagonal plate hydrate of C_4AH_{13}. C_4AH_{13} is instantly converted into C_3AH_6, while eluting Ca^{2+}. Particularly. C_3AH_6 is formed rapidly 5 minutes after the addition of water. At this time,the Ca^{2+} concentration in the liquid phase is increased and $Al(OH)_4^-$ is consumed for hydration. Accordingly. there may be such cases in which a C/A of 4 or above is obtained.

In the rapid hydration of C_3A, the above-mentioned reactions proceed continuously. liberating large quantities of heat from the start of hydration. Immediately after the addition of water. the surface of C_3A is covered with two layers: a layer of C_4AH_{13} and a stable layer of C_3AH_6. As a result,the elution of Ca^{2+} and $Al(OH)_4^-$ from C_3A is

remarkably reduced and the hydration is stopped. liberating only a small quantity of heat. In the liquid phase. Ca^{2+} and $Al(OH)_4^-$ are in equilibrium with C/A=1.

(3)In the solution of $C\bar{S}H_2$ and CH only. the concentration of SO_4^{2-} is about 1.02g SO_3 /l. regardless of the mixing ratio of $C\bar{S}H_2$ and CH and the presence or absence of CH. On the other hand. the concentration of Ca^{2+} does not follow the common ion effect but increases sharply to about 1.80g CaO/l. Now. let us study the concentration in a suspension produced by dispersing C_3A in the solution containing $C\bar{S}H_2$ and CH in excess of the saturation level. In this suspension. the total concentration of Ca^{2+} in the liquid phase is calculated by adding the amounts of Ca^{2+} eluted from $C_3A.C\bar{S}H_2$ and CH. Accordingly.

Total $CaO=CaO(C_3A)+CaO(C\bar{S}H_2)+CaO(CH)$ from Fig.6.

Total $CaO\fallingdotseq 1.70\sim 1.90$g CaO/l here.

$CaO(C\bar{S}H_2)+CaO(CH)\fallingdotseq 1.80$g CaO/l that is.

$CaO(C_3A)\fallingdotseq 0.0\sim \pm 0.10$g CaO/l

The amounts of Ca^{2+} and $Al(OH)_4^-$ eluted from C_3A are very small. In this case. the retention time at the highest concentration means the period of time in which the concentrations of 1.80g CaO/l and 1.02g SO_3 /l in the liquid phase are maintained so far as the suspension contains $C\bar{S}H_2$ and CH in excess of the saturation level.

Therefor, the added fully $C\bar{S}H_2$ and CH describes two roles as follows:

(A) $C\bar{S}H_2$ and CH are required to keep at the highest concentration of Ca^{2+} and SO_4^{2-} in liquid phase.
(B) The remained $C\bar{S}H_2$ and CH except for above (A) is present.

Since $C\bar{S}H_2$ and CH corresponding to above (B) is reacted with C_3A. AFt and AFm phases are immediately formed. the resulting C_3A surface is partly coated by these phases. However. C_3A is covered by the highest concentration of $C\bar{S}H_2$ and CH corresponding to above (A).

In this period. the reactions are stopped apparently and the hydration is remarkably retarded. After film formation. the elution of Ca^{2+} and $Al(OH)_4^-$ from C_3A is very small and hydrates are not formed. This finding agrees with the results reported by Mori et al[4]. At the end of the retention period at the highest concentration. $C\bar{S}H_2$ and CH described in (A). and C_3A coprecipitate. forming a thick film rapidly. This film is a solid solution of monosulfate-C_4AH_x system shown as 7.6~9.6Å phase. The retention period at the highest concentration is greatly affected by the mixing amount of $C\bar{S}H_2$ and CH. After the formation of a

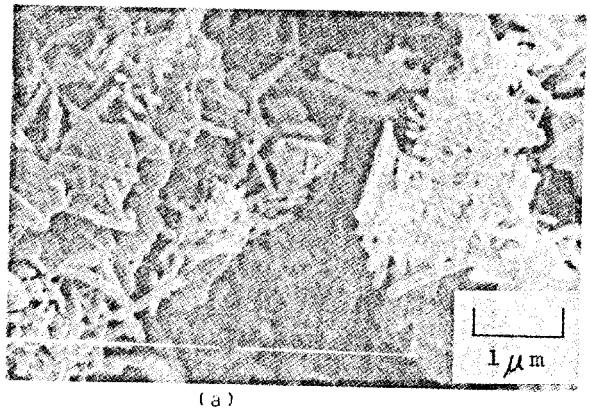

(a)

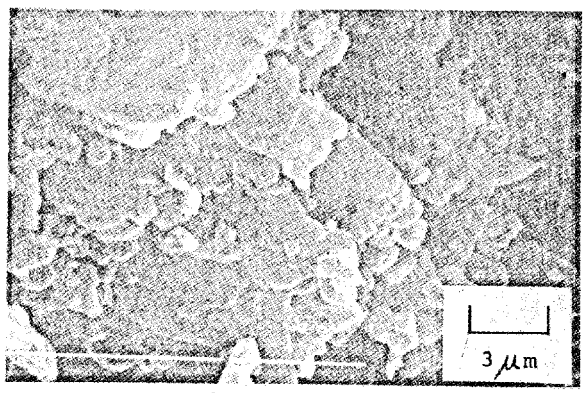

(b)

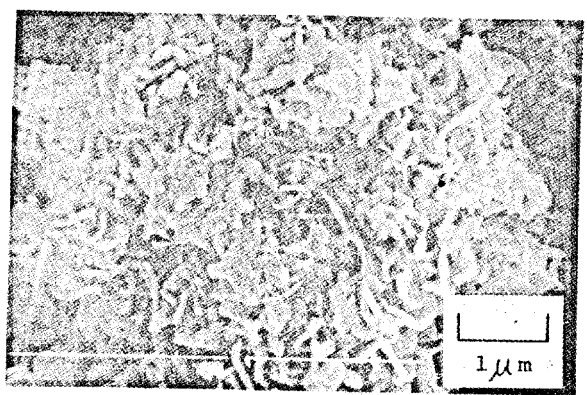

(c)

Fig.8. SEM of C_3A hydrated with addition of $C\bar{S}H_2$ .CH by various hydration time:(W/solid=50).

Mixing ratio against C_3A.	Time
(a) $C\bar{S}H_2$ 20wt%	15min
(b) $C\bar{S}H_2$ 20wt%	5d
(c) $C\bar{S}H_2$ 20wt%. CH 10wt%	30min

coprecipitate. the concentration of Ca^{2+} and SO_4^{2-} increase slightly again. It is. however.not clear whether this increase in concentration is attributable to the conversion of the ettringite formed immediately after the addition of water into monosulfate or to the formation of a solid solution.

Fig.8(a) and (b) show SEM of C_3A

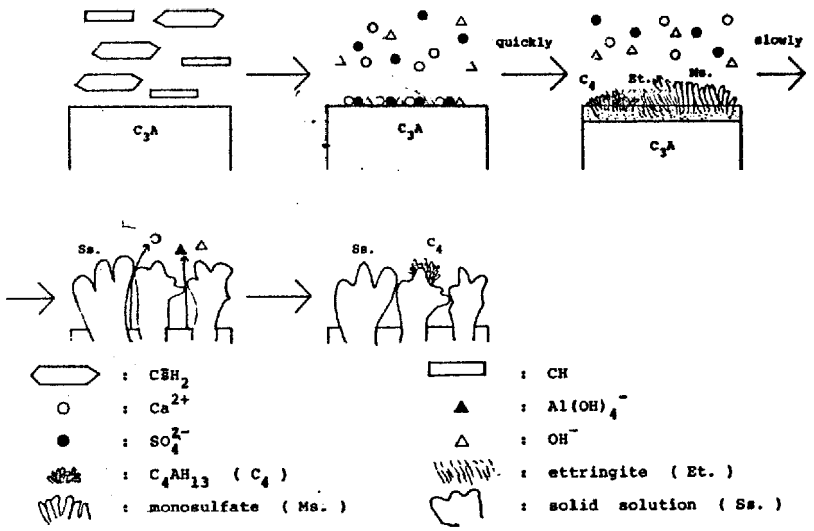

Fig.9. The illustration of C_3A-$C\bar{S}H_2$-CH system hydration process.

hydrated with $C\bar{S}H_2$ for 15 minutes and 5 days, respectively. Fig.8(c) is SEM of C_3A hydrated with $C\bar{S}H_2$ and CH for 30 minutes. Fig.8 shows that the properties of ettrigite and C_4AH_χ formed before the end of the retention period at the highest concentration may differ from those of ettringite and C_4AH_χ formed after the end of the retention time. Before the end of the retention time, ettringite and C_4AH_χ are observed as amorphous acicular ettringite and plate-state C_4AH_χ of card-house structure, respectively. After the end of the retention time, however, they are observed as thick plate-state crystals because of the formation of a solid solution.

The hydration process as described above is schematically shown in Fig.9. Based on this process, the authors would like to propose the following interpretation for the rate of heat liberation shown in Fig.4. Namely, the first peak of the curves corresponds to the start of the formation of ettringite, monosulfate and C_4AH_χ as described in (B) and the second peak corresponds to the start of the formation of a solid solution or the formation of C_3AH_6 in some cases by $C\bar{S}H_2$ and CH as described in (A), respectively.

CONCLUSIONS

The retardation was greatest when both $C\bar{S}H_2$ and CH were present, the authors have recently questioned the role of ettringite in the retardation of C_3A by SO_4^{2-}. Since $C\bar{S}H_2$ and CH is reacted with C_3A, AFt and AFm phases are immediatly formed, the resulting C_3A surface is partly coated by these phase. However, this cause was not essentially on the excessive retardation. Because C_3A is covered by the highest concentration of $C\bar{S}H_2$ and CH, consequently, during this period, the elution of Ca^{2+} and $Al(OH)_4^-$ from its surface has not been able to recognized. Therefore, it is concluded that the hydrates is not produced, and the hydration stops apparently.

REFERENCES

1) P.K.Mehta, J.Am.Ceram.Soc.,56,315-19 (1973).
2) N.Tsuyuki, N.Hirota, T.Miyakawa and J.Kasai, Yogyo-kyokai-shi, 92, 554-61 (1984).
3) N.Tsuyuki, H.Otake, T.Miyakawa and J.Kasai, Yogyo-kyokai-shi, 94, (1986).
4) H.Mori and K.Minegishi, Semento-Gijutsu-Nenpo, XXIX,89-94(1975).

Seishi Goto, Masaki Daimon
(Department of Inorganic Materials,
Tokyo Institute of Technology, Japan)

ION DIFFUSION IN CEMENT PASTE

1. Introduction

The diffusion of ion through hardened cement paste (HCP) takes an important role in the durability of concrete especially in marine construction. When ions penetrate into hardened cement body, the ions sometimes react with hydrates or reinforced steel and the deterioration of concrete will be resulted. A part of the penetrated ions react with hydrates, another part of that ion remains in pore to increase the concentration of pore solution and the rest diffuses into more inner part of HCP. The chemical composition of cement and pporosity of HCP have been discussed in many literatures as main factor which affects to the ion diffusivity in HCP.

The effect of chemical composition of cement on the durability of concrete had been well discussed[1-4]. It is thought that free lime and calcium aluminate hydrates are most undesiarable component for durability of concrete. It is resulted to develop sulfate resisting portland cement and acid resisting portland cement.

The apparent diffusion coefficient (Dap) is affected by the porosity and pore size distribution, because the ions diffuse in pore solution. The pore structure of HCP has been well examed[5-10] by mercury intrusion porosimeter, gas adsorption, permeability, small angle scattering X-ray diffraction and so on. But the discussion of the relationships between pore size distribution and the ion diffusivity is not sufficient[11-14]. Authors[13, 15-16] have shown that there are good co-relations between Dap and the amount of small pore with radius less than 2 nm, even when the hardened body was made from different type of cement or when it was made under different condition such as usual temperature curing or autoclaving. Hughes[14] also suggested that smaller pore may be more important in the consideration of permeability and ion diffusivity.

In this paper, measurement of Cl^- ion diffusivity are mentioned at first. The effects of many factors such as porosity, pore size distribution, chemical composition and ion species on the diffusion are discussed, in the second part. The states of Cl^- ion will also be discussed. We assume two states of Cl^- ion in HCP. One is the Cl^- ion that is in hydrates and the other is that in pore solution.

2. Methods to measure ion diffusivity

There are many mothods to determine the ion diffusivity in HCP ; to measure the depth where the pore solution has a particuler concentration of the diffusing ion[3, 17], to measure the distribution of total concentration of the ion[4, 17, 18], and to determine the amount of diffused ion through a plate of HCP[19, 12].

When HCP sample is immersed in some solution, it is better to seal all except one surface by something such as paraffine (Fig. 1a), because the result of one directional diffusion is easily analyzed mathmatically.

2-1 Colorimetric measurement of Cl^- ion penetrated depth: A sample immersed in a solution is cut parallel to the direction of ion diffusion. A groove is cut with 1-2mm in width on the surface with the same direction of diffusion (Fig. 1b). The groove is painted with aqueous solution of 1% fluorescein sodium salt and aqueous

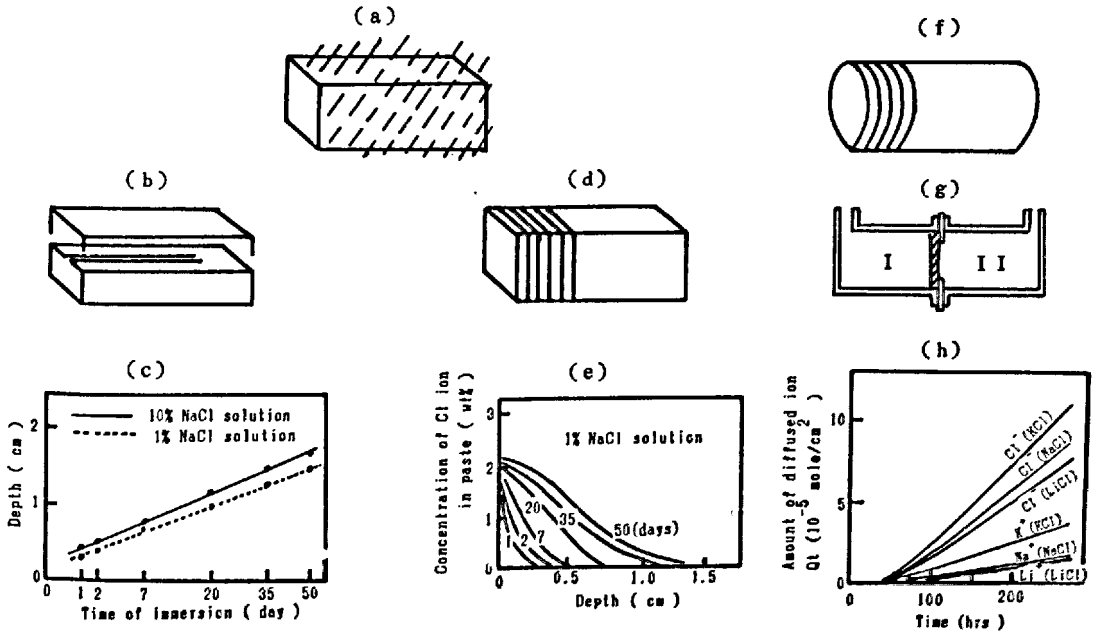

Fig.1 Measurement of ion diffusivity and typical results

Seishi Goto, Masaki Daimon
(Department of Inorganic Materials,
Tokyo Institute of Technology, Japan)

solution of 0. 1N AgNO3. Where the concentration of Cl^- ion is more than a certain value, white crystals of AgCl precipitate. When the concentration is lower than that value, the liquid presents a color of reddish brown. Point where the color changes shows that the pore solution has a concentration of Cl^- ion. The depth of this point from surface contacted with solution during immersion is measured as penetration depth. A typical result is shown in Fig. 1c[17]. We can get a straight line, but the line does not always cross original point, when diffusion proceeds with reaction.

2-2 Analysis with fluorescent X-ray spectroscopy :
A sample immersed in a solution for a period is cut at some distance (Fig. 1d) and make powder to analyse the contents of Cl^- ion by fluorescent X-ray spectroscopy. Total amount of Cl^- ion is measured by this mewthod. A typical result is shown in Fig. 1e[17]. The concentration distribution is almost same as that obeyed to the Fick's law, because the amounts of reacted Cl^- ion with hydrate are roughly proportional to the concentration of pore solution.

2-3 Measurement of the amount of Cl^- ion penetrated through a HCP plate : Fresh paste is degassed by rotary pump just after cement and water mixed, in order to aboid large voids. Cured sample are cut with diamond saw to make plates with 2-3mm in thickness (Fig. 1f). The plate is set in a diffusion cell which is divided to two rooms (Fig. 1g). Room I is filled with solution and room II is filled with distilled water. 25ml of solution is sampled from room II at required time and the same volume of distilled water put back into room II. When n-th sampling had been done at time t, the total amount of Cl^- ion (Qt) diffused thruogh a plate from room I to room II can be calculated as,

$$Qt=(Cn+dV/VII)\cdot\sum_{n=1}^{n-1}Cn\cdot VII$$

where VII is the volume of room II, dV is the volume of sampling at each time. Cn is the concentration of Cl^- ion in the sample. A typical result is shown in Fig. 1h[19]. In the early stage, Qt is not proportional to time, because of unsteady state. But in later stage, the relation betweem Qt and time shows almost strate line. Dap can be calculated from this slope.

3. Effects of ion species and co-exsisting ions[17, 19]

The rate of diffusion of ion in HCP varies with ion species, and is also affected with co-existing ion. Differences in the ion diffusivity of several ion species are shown in Fig. 2, as an example. This is a result obtained by measuring the amount of ion pass through a plate. The solution filled room I of diffusion cell was a mixed solution of LiCl, NaCl and KCl, where the concentration of Li^+, Na^+, $K^+$and Cl^-ion were 1/8-N, 1/8-N, 1/8-N and 1/2-N, respectively. The values of amount of diffused ion in Fig. 2 were calculated as the same concentration for that of bulk solution. There are differences in ion diffusivity in cations and it is clear that anion has larger diffusivity than cations. It is due to the positive charge of hydrates surface, and detailed discussion will be made later.

The rate of diffusion of Cl^- ion in HCP was affected by the co-existing ion, such as Li, Na, K and Mg ion. A result was shown in Fig. 3. This was also a result of the experiment using a plate of HCP and filled room I with each solution of LiCl, NaCl, KCl and MgCl2. The rate of difusion for cation decreases as $K^+>Na^+>Li^+$, but that of Cl^- ion increases as NaCl<KCl<LiCl<MgCL2. When Mg ion attacks HCP, it becomes porous because Mg(OH)2 is precipitates on the surface of HCP and free lime in HCP is desolved. Then the rate oif diffusion of Cl^- ion using MgCl2 solution was largest in these results.

The effect of SO_4^{2-} ion on the concentration distribution of Cl ion are shown in Fig. 4. This is a result of using a block immersed in solution and analysed the concentration distribution with fluorescent X-ray spectrometer. The concentration distribution of the sample immersed in 10% NaCl solution for 35 days and immersed in artificial sea water were similar in the inner parts and that of the samples immersed in 1% NaCl solution for 1 day and artificial sea water for 7 days were similar. But there are much differences in the concentration distribution at the part near the surface. When SO_4^{2-} ion coexisted, the concentration of Cl^- ion near the surface becomes lower with immersing time. It is due to that SO_4^{2-} ion

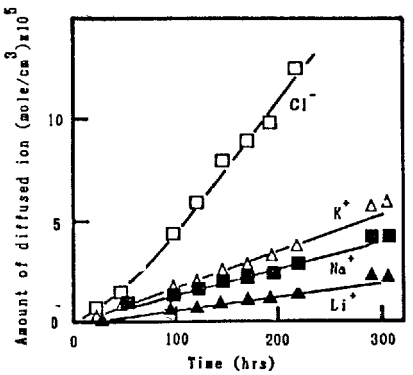

Fig.2 Effect of ion species.

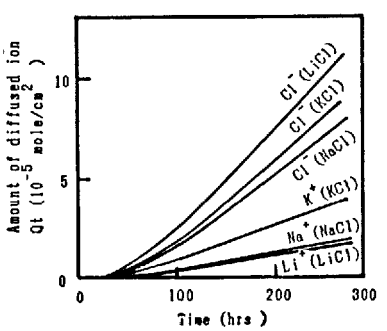

Fig.3 Effect of ion coexisting(1).

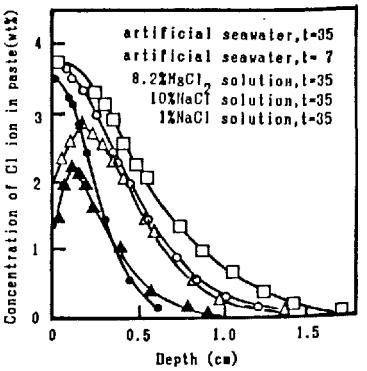

Fig.4 Effect of ion coexisting(2).

Seishi Goto, Masaki Daimon
(Department of Inorganic Materials,
Tokyo Institute of Technology, Japan)

has smaller diffusion coefficient and that calcium alumino sulfate hydrate has lower solbility than that of calcium alomino chloride hydrate.

4 Effect of pore size distribution

4-1. Pore size distribution of HCP[13]

Total porosity (Vt) and bulk density were calculated from the weight of water-saturated and dried sample and the weight in water. The pore volume between 7.5 μm and 7.5 nm measured by mercury intrusion porosimeter (VMIP), and the pore volume between 7.5 nm and 2 nm in radius was measured by N2 gas adsorption (VN2), calculated with Model-less method. Volume of pore with radius under 2 nm (Vs) was calculated from these pore volume.

Mercury intrusion porosimetric pore size distribution indicated that HCP had no pore with radius larger than 430 nm, since it was degassed by rotary pump before molded. Therefore Vs was able to be calculated by the equation of

$$Vs=Vt-(VMIP+VN2)$$

Pore size distribution of HCP are shown in Fig.5. Vt were mainly affected by water/cement ratio, and not by the kinds of cement Vs of PC, BF and SR decreased with the increase of water/cement ratio and with rising of curing temperature. But that of HCP autoclaved has very small volume of V2.

4-2. Relationships between Da and pore size distribution[13]

Dap were measured by the way as mentioned in 2-3. In Fig.6, Dap for ordinally portland cement were plotted with total pore volume. There are low corelationships between them.

Dap for Cl^- ion and Na ion are well correlated with Vs, as shown in Fig.7, even when cement and curing condition changed. Following equations were obtained by least square method.

For Cl^- ion ; log Da =- 6.3Vs - 5.84

For Na^+ ion ; log Da =-13.5Vs - 5.66

It was noticed that Da of Cl^- ion was larger than that of Na^+ ion, and that the gradient of the relation for Na ion was steeper than that of Cl^- ion. This is explained by electric double layer. Surface of the hydrates are positively charged by adsrption of Ca^{2+} ion. Then anion can diffuse in electric double layer but cation can not diffuse in that layer, as shown in Fig.8.

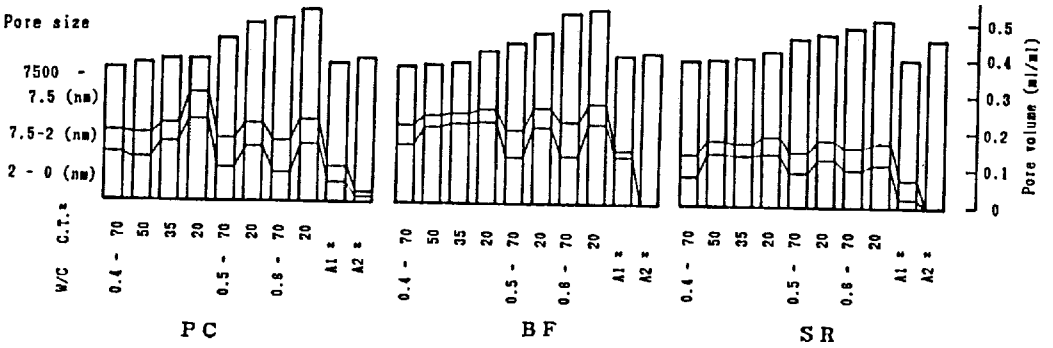

Fig.5 Pore size distribution of portland cement(PC), blastfurnace slag cement(BF) and sulfate resisting portland cement(SR). C.T. : curing temperature(℃), A1 : autoclaved at 180℃ for 3 h, A2 : autoclaved at 180 ℃ for 7 d.

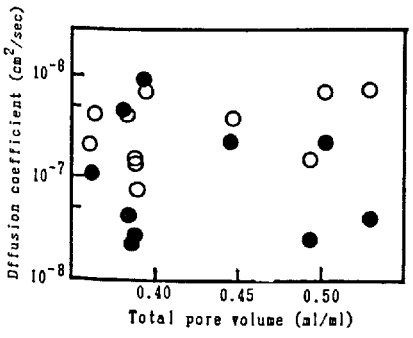

Fig.6 Relationships between total pore volume and apparent diffusion coefficient (Dap). ● Na^+ ○ Cl^-

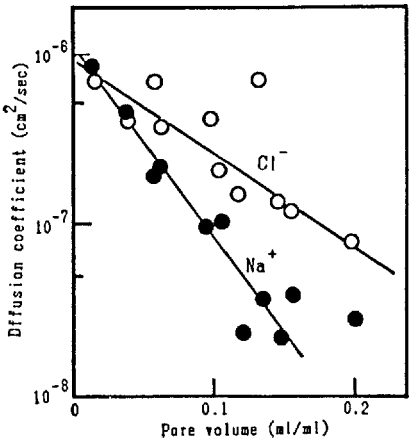

Fig.7 Relationships between pore volume with radius less than 2 nm and Dap.

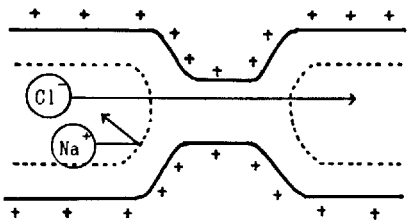

Fig.8 A model of ion diffusion in pore.

Seishi Goto, Masaki Daimon
(Department of Inorganic Materials,
Tokyo Institute of Technology, Japan)

5. Distribution coefficient and total amount of ion in HCP[15]

The amount of soluble ion in HCP and total amount of ion in HCP were measured by using samples which were immersed in the solution for 28 days. Time distribution coefficients between bulk solution and pore solution were calculated from Vt and the amount of soluble ion in HCP. Relationships between distribution coefficient and Vs are shown in Fig.9. The coefficients for Cl^- ion are larger than 1 and increase with Vs. Contrary, those of Na^+ ion are smaller than 1 and decrease with Vs. The surface of hydrates were positively charged because of adsorption of Ca^{2+} ion. And electric double layer could attract anion towards the surface. Then Cl^- ion can easily enter into the micro-pore. The effect of elecric double layer on ion diffusion is mainly due to the changes in distribution coefficient of solution in pore.

Total amounts of Cl^- ion are increased with the concentration in the pore solution as shown in Fig.10. But the total amount of ion has not so good correlation with Vs, because the Al2O3 content of cement is also important factor.

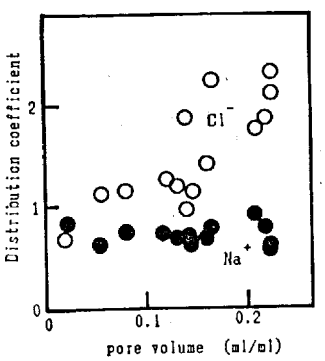

Fig.9 Relationships between distribution coefficient of Na^+ and Cl^- ion and pore volume with radius less than 2 nm.

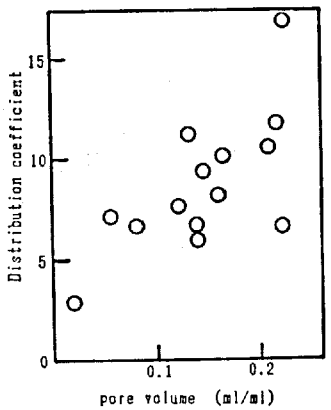

Fig.10 Relationships between distribution coefficient of Cl^- ion and pore volume with radius less than 2 nm.

6. Estimation of ion distribution in HCP[15]

Diffusion of reactive ion in semi infinit body are presented as following equation, which is derived from Fick's 2nd law.

$$Dd^2c/dx^2 = d(c+f(c,t))/dt$$

where f(c,t) is the amount of reacted ion and it is assumed that the reaction is very fast comparing with diffusion and that the amount of reacted ion is proportional to the concentration of solution. Then f(c,t) is presented as αc. Consequently, the ion concentration at position x and time t, CT(x,t), can be obtained as,

$$CT(x,t) = CoT\{1- erf(x/2(Dat/\epsilon kT)^{1/2}\}$$

where CoT is total amount of ion at surface and this is constant. Da is apparent diffusion coefficient. ϵ is total pore volume. kT is distribution coefficient for total amount of ion. In the steady state of diffusion through a plate, relationships among concentration of total ion, concentration of pore solution and concentration of bulk solution are schematically shown in Fig.11.

The ion distribution in HCP can be calculated, by assuming that HCP have been immersed in 1N NaCl solution for 10 years, assuming that HCP samples were

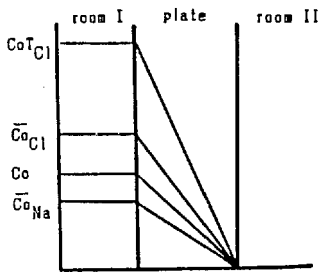

Fig.11 Distribution of ion concentration at steady state.
1: total chloride ion
2: ion in pore solution
3: apparent distribution
4: Na ion in pore solution

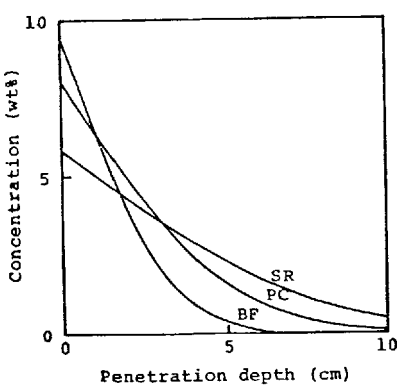

Fig.12 Calculated distribution of ion concentration for PC, BF and SR.

made of PC, BFand SR with water/cement ratio of 0.40, and cured at 35 ℃.

Results are shown in Fig.12. The total amount of Cl^- ion at the surface for BF is highest and that of SR is lowest. But that of BF at inner part is lowest and that of SR is highest. This means that the amount of reacted ion for BF is largest and Da for BF is smallest. This is due to the high content of Al2O3 and the large volume of Vs in BF paste. Contrary, Al2O3 content is lowest and Da is largest in SR paste. Properties of PC are between them. These results are well agreed with the results shown by Gjorv et al[4].

Seishi Goto, Masaki Daimon
(Department of Inorganic Materials,
Tokyo Institute of Technology, Japan)

7. Conclusions

Concerning with ion diffusion in hardened cement paste, many factors such as ion species, porosity, pore size distribution and distribution coefficient of ions were discussed. Ion diffusivity in HCP was measured by many method such as colorimetric method, fluorescent X-ray analysis and a method using thin plate. Pore size distribution was measured by means of mercury intrusion porosimeter and N2 gas adsorption. Pore structure were characterized with a volume of pore with radius less than 2 nm. Distribution coefficient of ion between bulk solution and pore solution and total amount of ion in HCP were also measured. Relationships between the distribution coefficient and pore structure were discussed. Following results are obtained.

1) Ion diffusivity changes with ion species. Anion have larger apparent diffusion coefficient (Dap) than cation. Ion diffusivity is also affected by the ion coexisting.

2) Dap of ions are well correlated to the pore volume with radius less than 2 nm, even when the hardened cement was made from different type of cement and also made under the different conditiuon such as room temperature curing and autoclaving.

3) Distribution coefficient of ion between bulk solution and pore solution is also well correlated to the pore volume with radius less than 2 nm.

4) Composition of cement affects mainly to the total amount of ion in hardened cement paste and the development of pore structure.

5) Finally, the distribution of ion concentration in pastes which had been immersed in NaCl solution for 10 years was calculated from the data of the relation between volume of pore with radius less than 2 nm and apparent diffusion coefficient, distribution coefficient and amount of reacted Cl^- ion. The calculated results has a good agreement with the distribution measured.

References

1)G.L.Kalousek and E.J.Benston, "Mechanism of seawater attack on cement paste", ACI Jour., 67(9),189-192(1970)

2)H.G.Smolczyk, "Chemical reactions of strong chloride-solutions with concrete", Proc.5th Int'l Symp. Chem. Cement, Tokyo 1968, Vol. III, 274-280

3)M.Collepardi, A.Marcialis and R.Turriziani,"The penetration of de-icing agents in cement pastes", Il Cemento, 3/1972, 143-150

4)O.E.Gjorv, O.Vennesland, "Diffusion of chloride ions from seawater into concrete", Cement and Concrete Res., 9, 229-238(1979)

5)R.F.Feldman and H.Cheng-yi, "Properties of portland cement-silica fume pastes. I. Porosity and surface properties", Cement and Concrete Res.,15,765- 774(1985)

6)T.C.Powers, "Physical properties of cement paste", Proc. 4th Int'l Symp. Chem. Cement, Washington,D.C.,1960, Vol.II, 577-613

7)P.K.Mehta and D.Monmohan, "Pore size distribution and permeability of hardened cement paste", Proc. 7th Int'l Cong. Chem. Cement, Paris 1980, Vol. III, VII-1-5

8)B.K.Nyame and J.M.Illston, "Capillary pore structure and permeability of hardened cement paste", Proc. 7th Int'l Cong. Chem. Cement, Paris 1980, Vol.III,VI-181-185

9)S.Goto and D.M.ROY, "The effect of W/C ratio and curing temperature on the permeability of hardened cement paste", Cement and Concrete Res., 11, 575-579(1981)

10)M.Daimon,S.A.Abo-El-Enein,G.Hosaka,S.Goto and R. Kondo, "Pore structure of calcium silicate hydrate in hydrated tricalcium siliate", J. Am. Cer. Soc.,60, 110-114(1977)

11)H.G.Midgley and J.M.Illston, "Effect of chloride penetration on the properties of hardened cement paste", Proc.7th Int'l Cong.Chem.Cement, Paris 1980,Vol.III, VII-101-103

12)C.L.Page,N.R.Short and A.El.Tarras, "Diffsion of chloride ion in hardened cement pastes", Cement and Concrete Res., 11, 395-406(1981)

13)S.Goto, K.Shigeru, T.Takagi and M.Daimon, "Effect of pore size distribution on diffusion of ion through hardened cement paste", Semento Gijutsu Nenpo,36 49-52 (1982)

14)D.C.Hughes, "Sulphate resistance of OPC, OPC/fly ash and SRPC pastes: Pore structure and permeability", Cement and Concrete Res., 15, 1003-1012(1985)

15)K.Shigeru, T.Takagi, S.Goto and M.Daimon, "Diffusion of ion through hardened paste of various cement", Semento Gijutsu Nenpo, 37, 112-116(1983)

16)T.Takagi, S.Goto and M.Daimon, "Diffusion of I ion through hardened cement paste", Semento Gijutsu Nenpo, 38, 78-81(1984)

17)S.Goto, M.Tsunetani, H.Yanagida and R.Kondo, "Diffusion of chloride ion in hardened cement paste", Yogyo-Kyokai -Shi, 87, 126-133(1979)

18)M.Collepardi, A.Marcialis and R.Turriziani,"Penetration of chloride ions into cement paste and concrete", J.Am.Cer.Soc., 55, 534-535(1972)

19)H.Ushiyama and S.Goto, "Diffusion of various ions in hardened portland cement paste", Proc. 6th Int'l Cong. Chem. Cement, Moscow 1974, Vol.II-1, 331-337

Stefania Grzeszczyk
Institute of Cementing Building Materials
45-641 Opole, Oświęcimska 21, Poland

C_3A-Na_2O solid solutions in pseudo-two-component system NC_8A_3-C_3A

P

SUMMARY: It was indicated in the paper that sdlid solutions are formed in the pseudo-two-cpmponent NC_8A_3-C_3A system, the symmetry of which is similar with the symmetry of Na_2O solid solutions in C_3A containing comparable quantities of sodium. It was confirmed that NC_8A_3 compound can not be synthesized out of reaction mixture whose composition corresponds to its stoichiometry. The value of η ratio between intensities of diffractions lines for which d= 1.889 Å and 1.916 Å found on X-ray diffractograms of solid solutions in pseudo-two-component system NC_8A_3-C_3A and solid solutions Na_2O in C_3A changes proportionally to the changes of sodium content in the structure of C_3A, and may constitute the criterion in distinguishing the polymorphic modifications of solid solution Na_2O in C_3A.

INTRODUCTION

According to currently assumed research results concerning C_3A-Na_2O solid solutions, the content of sodium equal to 5.7 % by wieght concentration of Na_2O constitutes the solubility limit of sodium in C_3A [1]. The presence of Si^{+4} ions increases the range of solubility of Na_2O in C_3A. In this case it is possible for the solid solution to form itself as NC_8A_3 [2] There were attempts aiming at synthesizing pure phase of NC_8A_3, but these produced no satisfactory results [3, 4]. The final product of the reaction usually contained small quantities of free CaO [4].

This paper presents results of the research on synthesizing NC_8A_3 phase as well as on solid solutions in pseudo-two-component system NC_8A_3-C_3A.

EXPERIMENTAL

The synthesis of NC_8A_3 compound was carried out in welded crucibles at 1400°C for 20 hrs, and at 1475°C for 5 hrs - similarly as in other works [4, 5]. Before, the reaction mixture corresponding to stoichiometric composition of NC_8A_3 phase containing an excess of Na_2O subjected to repeated thermal treatment at 1000°C until the moment the mixture contained 7.6 % by weight concentration of sodium. The synthesis product obtained at 1400°C contained 1.8 % by weight concentration of free CaO, whereas the one burnt at 1475°C contained considerable quantities of CaO and sodium aluminate NA.

For the experimental study of solid solutions in pseudo-two-component system NC_8A_3-C_3A, the NC_8A_3 phase was used and synthesized at 1400°C.

The synthesis of pseudo-two-component systems NC_8A_3 was carried out at 1300°C for 2 hrs. The following systems were subject of synthesis: NC_8A_3 and $0.5C_3A$, NC_8A_3 and C_3A, NC_8A_3 and $2C_3A$, NC_8A_3 and $3C_3A$ and NC_8A_3 and $4C_3A$. Additionally, the synthesis of sodium oxide solid solutions in tricalcium aluminate was performed. The synthesis consisted in roasting the tricalcium aluminate mixture together with appropriate additions of sodium carbonate at 1250°C The synthesized solid solutions contained the following quantities of sodium in C_3A: 1.8, 3.5, 4.2, 5.2, 5.7 % by weight concentration of Na_2O.

Stefania Grzeszczyk
Institute of Cementing Building Materials
45-641 Opole, Oświęcimska 21, Poland

C_3A-Na_2O solid solutions in pseudo-two-component system NC_8A_3-C_3A

RESULTS AND DISCUSSION

The identification research of synthesized compounds was performed by means of absorption infrared spectroscopy and X-ray diffraction. The infrared spectrum of synthesized NC_8A_3 phase is identical with the spectrum of C_3A-Na_2O solid solution sample containing 5.7 % by weight concentration of Na_2O. Fig.1 shows the infrared spectra of reaction mixtures samples of NC_8A_3 and C_3A compounds, Fig. 2 shows the spectra of synthesized systems of these compounds.

The analysis of infrared spectra of mixtures of NC_8A_3 and xC_3A compounds indicated that on synthesizing the mixtures of compounds where x equals 0.5, 1, 2 and 3 there is a monoclinic compound whose spectrum is identical with the spectrum of C_3A-Na_2O solid solution sample containing 5.7 % Na_2O in C_3A [6]. The spectra of these samples have their bands situated at 483, 513, 533, 720, 790, 867 and 923 cm^{-1}, with the increase of C_3A contet, however the intensity of these bands decreases.

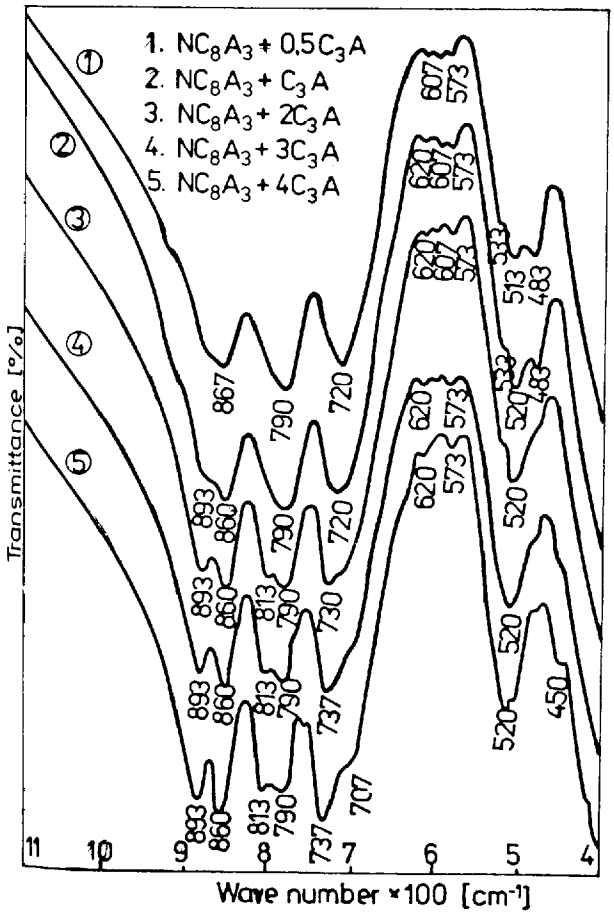

Fig. 1 Infrared spectra of mixture samples of NC_8A_3 and C_3A compounds.

The analysis of spectra of reaction mixtures samples of NC_8A_3 and xC_3A where x equals : 0.5, 1, 2, 3 and 4 indicated that proportionally to the increase of C_3A content in the mixtures, the spectra reveal the appearance and increase of intensity lines characteristic of this compound 520, 737, 813, 860 and 893 cm^{-1}. Alongside there is a decrease of intensity and disappearance of lines characteristic of synthesized phase NC_8A_3.

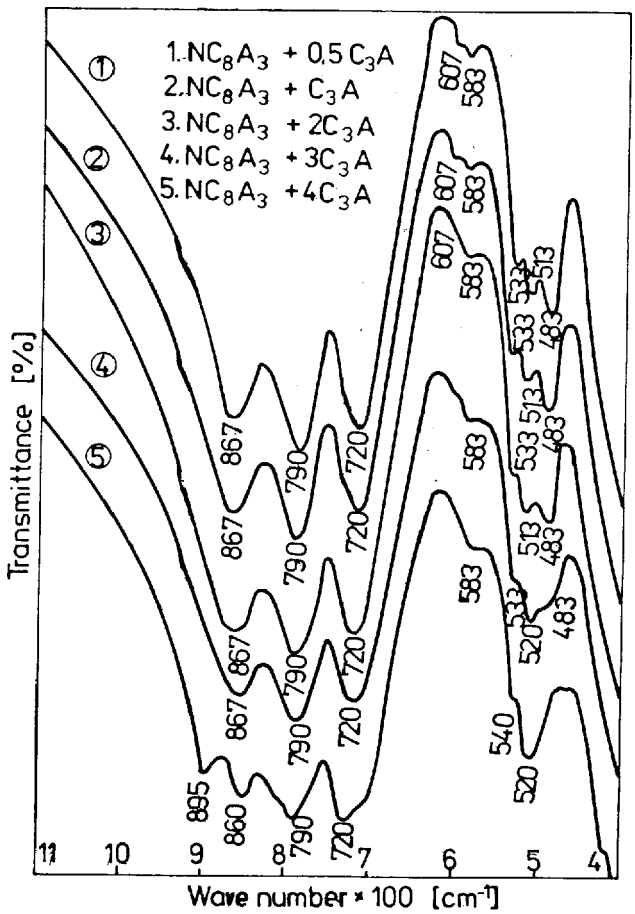

Fig. 2 Infrared spectra of samples of synthesized systems of NC_8A_3 and C_3A compounds.

The spectrum of NC_8A_3 and $4C_3A$ compounds mixture, apart from the bands characteristic of monoclinic modification of solid solution C_3A-Na_2O, also reveals characteristic bands of regular C_3A located at wave frequencies 520, 860 and 893 cm^{-1}.

The X-ray analysis of synthesized mixtures of NC_8A_3 and xC_3A compounds where x= 0.5, 1, 2, 3 and 4 indicated that X-ray diffractograms of the samples for which x= 0.5, 1, 2 and 3 are qualitatively similar to each other

Stefania Grzeszczyk
Institute of Cementing Building Materials
45-641 Opole, Oświęcimska 21, Poland

C_3A-Na_2O solid solutions in pseudo-two-component system NC_8A_3-C_3A

and reveal lines whose values are characteristic of the orthorhombic and monoclinic phase of solid solution C_3A-Na_2O [6].
It was also observed that as C_3A increases in the burnt compound mixture, i.e. when $x \longrightarrow 3$, the sample X-ray diffractograms reveal a decrease of intensity of lines whose value equals d= 1.889 Å in comparison with the intensity of the lines whose value equals d= 1.918 Å.

The values of η ratio between the intensities of diffraction lines for d= 1.889 Å and d= 1.916 Å for synthesized compounds are given in Table 1.

Table 1.

Values of η ratio between intensities of diffraction lines for d= 1.889 and d= 1.916 Å for NC_8A_3 and C_3A systems.

Stoichiometric composition of NC_8A_3 and C_3A compounds	Ratio values η	Sodium content [% wt]
$NC_8A_3+0.5C_3A=NC_{9.5}A_{3.5}$	0.57	6.5
$NC_8A_3+C_3A = NC_{11}A_4$	0.51	5.7
$NC_8A_3+2C_3A = NC_{14}A_5$	0.50	4.6
$NC_8A_3+3C_3A = NC_{17}A_6$	0.45	3.8
$NC_8A_3+4C_3A = NC_{20}A_7$	-	3.3

The research performed using infrared spectroscopy and X-ray diffraction indicated that following the reaction taking place in the pseudo-two-component system NC_8A_3 and xC_3A, there emerges a solid solution whose symmetry is similar to the symmetry typical of C_3A — Na_2O solid solution containing camparable quantities of sodium. It is worth noting that η ratio values are similar in the case of tested solid solutions Na_2O in C_3A and NC_8A_3 and C_3A compounds system, in which the percentage of Na_2O are similar.

Thus, for the tested pseudo-two-component system NC_8A_3 and C_3A containing 3.8 % Na_2O the value of η equals 0.45, whereas for the solid solution Na_2O in C_3A containing 3.5 % Na_2O η equals 0.41. For the systems NC_8A_3 and C_3A containing 5.7 % Na_2O the value of intensity of diffraction lines is 0.51, whereas for solid solution Na_2O in C_3A containing 5.2 % Na_2O the η value is 0.50.

Additionally to that, the research proved that is the tested system NC_8A_3 and $4C_3A$ apart from orthorhombic and monoclinic modification of C_3A-Na_2O solid solution, there is a presence of regular C_3A.

CONCLUSIONS

It was indicated in the paper that solid solutions are formed is the pseudo-two-component NC_8A_3-C_3A system, the symmetry of which is similar with the symmetry of Na_2O solid solutions in C_3A containing comparable quantities of sodium.

It was confirmed that NC_8A_3 compound can not be synthesized out of reactions mixture whose composition corresponds to its stoichiometry.

The value of η ratio between intensities of diffraction lines for which d= 1.889 Å and 1.916 Å found on X-ray diffractograms of solid solutions in pseudo-two-component system NC_8A_3-C_3A and solid solutions Na_2O in C_3A changes proportionally to the changes of sodium content in the structure of C_3A, and may constitute the criterion in distinguishing the polymorphic modifications of solid solution Na_2O in C_3A.

REFERENCES

1. M.Regourd, S.Chromy, L.Hjorth, B.Mortureux, E.A.Guinier : Polymorphysme des solides du Sodium dans L'Aluminate Tricalcique. Jornal of Applied Cryst., 6 , 355-364, 1973.

2. I.Maki : Nature of the prismatic darc interstitial material in portland cement clinker. Cem. Concr. Res., vol. 3, No 3, 295-313, 1973.

3. J.AConwicke, D.E.Day : Crystalline Solubility of Soda in Tricalcium Aluminate. J. Am. Ceramic Soc., 47 , No 12, 654-655, 1964.

4. A.I.Boikowa, W.A.Paramonowa, A.I.Domański: Sostaw i gidratacjonnaja aktywnost aljuminatnoj fazy klinkiera. Cement, 8 , 20-22, 1976.

5. Y.Suzukawa: Die Alkaliphasen im Portlandzement. Part I: Die Natriumphase. Zement-Kalk-Gips, 8 , 345-351, 1956.

6. S.Grzeszczyk: Influence of sodium on phase composition and hydratation activity of calcium aluminates and Portland cement clinker. /In Polish/, Raport PRE 6/83, 126, Technical University of Wrocław, Wrocław, 1983.

W. BRYLICKI, University of Mining and Metallurgy, Cracow, Poland

PHASE COMPOSITION AND MORPHOLOGY OF AUTOCLAVED γC_2S CONTAINING PASTES

1. INTRODUCTION

There is a commonly known opinion that under the normal conditions of hydration, γC_2S essentially does not reveal its binding properties /1/. Though the change of the isobaric-isothermal potential ΔG_{298} of hydration reaction γC_2S have a negative value /-2.91 kJ/mol according to /2/, /-5.82 kJ/mol according to /3/ /, kinetics of hydration is low and does not have an essential meaning for technology. However, the observed lack of binding properties of γC_2S under the normal conditions is caused only by kinetic factors. Changing the hydration conditions, e.g. increasing the temperature and pressure in the reaction medium causes the increasing of γC_2S hydration capacity /4, 5/. According to the prevalent opinion of many investigators, during the hydration of γC_2S under hydrothermal conditions the following compounds are created : hydrated calcium silicates with the structure derivative from γC_2S /kilchoanite, phase "P" and calcium chondrodite/ /6, 7, 8, 9/. The investigations on hydration of slurry containing γC_2S in autoclaved mixtures of C/S molar ratio less than 2 proved /6, 7, 10, 11, 12, 13, 14, 15/ that addition of SiO_2 to γC_2S under the appropriate conditions makes it possible to synthesize almost all hydrated calcium silicates existing in the CSH system. G.L. Kalousek /16/ synthesized hydrated calcium silicates from the mixtures γC_2S-SiO_2-H_2O of molar ratio C/S = 0.83 in the presence of 0 - 8% Al_2O_3 as hydrargillite and obtained the phase CSH_I and 11.3 Å tobermorite. The investigations carried out by Kurbus and Jelenic /17/, as well as Kalousek /16/ showed that in the presence of CO_2 in autoclaved mixtures γC_2S-SiO_2-H_2O of molar ratio C/S < 2, some amounts of scawtite were created very easily. During the production of alumina by the Grzymek sintering-selfdisintegrating method, after the extraction of calcium aluminates with 6% sodium carbonate the solid post-extraction residue containing mainly γC_2S is formed from the selfdisintegrating sinter /18/. Except for γC_2S and traces of βC_2S this residue called the postextraction slurry obtained under the industrial conditions contains also $CaCO_3$ - calcite, alkalies, residual aluminates and calcium aluminoferrite and other components. The paper presents the results of the investigations of γC_2S hydration, the model-synthetic post-extraction slurry and industrial slurry "Groszowice", from which the mixtures of different molar ratios were prepared.

2. DESCRIPTION OF EXPERIMENT.

2.1. The preparation of the initial substances.

γC_2S /sample A/ was synthesized from calcium carbonate /pure for analysis/ and silica gel /pure for analysis/. The right course of the synthesis was checked by the chemical, X-ray and infra-red spectroscopic analyses, as well as by the determination of the content of unbound CaO with the Frankie method /CaO_w = 0.108% by weight/. The fineness degree of γC_2S mesured by specific surface with the use of the Blaine device was 8200 cm^2/g. To obtain the synthetic-model post-extraction residues the following selfdisintegrating sinters were synthesized under the laboratory conditions : CaO-SiO_2-Al_2O_3 /calculated phase composition: C_2S - 70.86%, $C_{12}A_7$ - 29.14%/ - sample B and CaO-SiO_2-Al_2O_3-Fe_2O_3 /calculated phase composition : C_2S - 67.25 %, $C_{12}A_7$ - 26.67%, C_4AF - 6.08 %/ - sample C. The right course of the synthesis was checked by the methods of chemical, X-ray and microscopic analyses, using the scanning electron microscope. The sample of γC_2S and dust obtained during the disintegration of the selfdisintegrating sinters B and C were submitted to the 3-stage extraction with the use of soda aqueous solution ; concentration 60 g Na_2CO_3 per liter. The extraction were the same as the industrial ones. In this way, the synthetic post-extraction residues A', B' and C' were obtained, Moreover, the sample of the industrial post-extraction slurry "Groszowice" was taken and denoted as G. The phase chemical composition was determined by the RTG, DTA, DTG and TG methods, as well as morphology of the extraction products with the use of the scanning electron microscope. Table 1 presents the results of the chemical analysis of the initial samples.

On the basis of the phase composition analyses carried out by the above-mentioned methods and the accepted simplifying assumptions, the approximate quantitative phase composition of the initial substances was determined. The calculated phase composition is shown in Table 2.

The substances A, A', B', C and G were used to prepare the mixtures of different molar ratios C/S = 2.0 ; 1.0 ; 0.83; 0.60, where the ratio quantity C/S was corrected only on the basis of the calculated content of γC_2S. In the case of the samples A, A', B' and C', the ground quarz sand of high purity /99.6% SiO_2, specific surface according to Blaine - 5500 cm^2/g/ was used to correct the molar ratio quantity C/S, As far as the same correction is concerned in the post-extraction slurry "Groszowice" - sample G, the waste silica dust was used. It came from "Łaziska" plant and contained mainly β quarz, its specific surface determined by the BET method was 17.500 cm^2/g and chemical composition : SiO_2 - 93.20% ; Fe_2O_3 - 2.50% ; Al_2O_3 - 1.30% ; CaO - 1.75% ; MgO - 1.20%.

The prepared initial substances A, A', B', C' and G were dry mixed with the appropriate amounts of silica additives in the planetary agate mill /produced by Fritsch Co./ during 4 hours. The homogenized mixtures were wetted with 5% distilled water and after mixing pressed into pellets under the pressure 30 MPa. The samples of the powdered slurry were put in the laboratory autoclaves, then into the laboratory drier. The temperature in the autoclaves was increasing simultaneously with the temperature in the drier. The required temperature 200°C in the drier was reached within 2 hours. When the isothermal cycle of heating was over /8, 12, 24 and 36 hours, respectively/, the autoclaves were put out of

Table 1

Determined component	$\alpha'C_2S$ - sample A /%/	Extracted $\alpha'C_2S$ - sample A' /%/	Extracted dust, composition C-A-S -sample B' /%/	Extracted dust, composition C-A-S-F -sample C' /%/	Post-extraction slurry "Groszowice" - sample G /%/
CaO	66.80	59.60	57.90	55.40	53.59
SiO_2	33.20	26.40	23.30	21.50	21.00
Al_2O_3	-	-	2.2	1.90	5.76
Fe_2O_3	-	-	-	1.60	1.95
Na_2O	-	0.90	0.73	1.13	0.85
K_2O	-	-	-	-	0.24
MgO	-	-	-	-	0.81
SO_3	-	-	-	-	0.49
ignition loss	-	12.90	14.40	17.25	15.10
total	100.00	99.90	98.53	98.78	99.79

Table 2

Phase comp.	A /%/	A' /%/	B' /%/	C' /%/	G /%/
$\alpha'C_2S$	100	91	71	70	65
$CaCO_3$	-	6	22	23	12
$Na_2SiO_3 \cdot 6H_2O$	-	3	2	2	2.5
$C_{12}A_7$	-	-	4	4	4
$C_3A.0.4S.\ .^34.7H$	-	-	-	-	10
$C_3A.CaCO_3 \cdot 12H$	-	-	-	-	5
total /%/	100	100	99	99	98.5

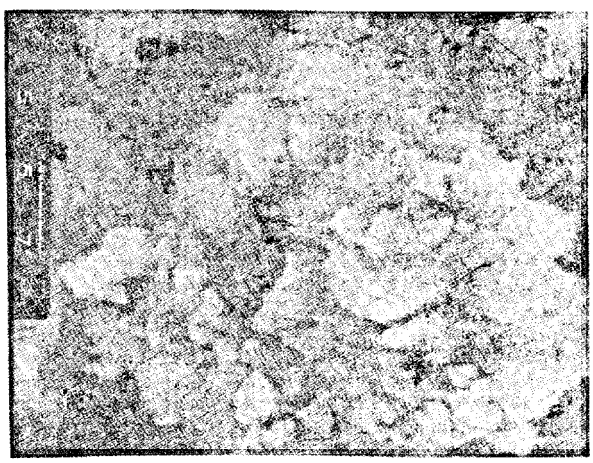

Fig. 1 - SEM. The post-extraction residue C' /enlarged 3000 X/.



Fig. 2 - SEM. The post-extraction slurry "Groszowice" G /enlarged 3000 X/.

the drier and cooled in the air. Then the samples of slurry were flooded with acetone what interrupted further hydration. The samples of slurry assigned for rentgenographic and thermal analyses were rubbed with acetone, while the samples for scanning electron microscope were in the shape of lumps. When hydration was stopped, the samples were treated with ether and dried in the vacuum drier at 65° C to the constant mass. The samples of hydrated slurry were kept in weighing vessels sealed up with stearin.

2.2. Testing equipment.

The diffractional determinations were accomplished by the Debay-Sherrer-Hull powder method by means of the diffractometer of the type TUR-61 /prod. People's Republic of Germany/ and Philips /The Netherlands/. In all measurements C_uK_α radiation and nickel filter were used. The thermal tests were

P

Table 3

C/S	2.0					1.0				
Time /h/	A	A'	B'	C'	G	A	A'	B'	C'	G
8	γC_2S P	γC_2S Ca,P Ch,Sk αC_2SH	γC_2S Ca,P Ch,T $C_{12}A_7$	γC_2S Ca,P Ch,T $C_{12}A_7$	γC_2S Ca,H $C_{12}A_7$ UKs	γC_2S K,Ks P	γC_2S K,Ca T,P Sk	K,Ca T,G Sk UKs	K,Ca T,G Sk UKs	γC_2S K,Ca H,T,G Sk
12	P Ch	γC_2S Ca,P Ch,Sk αC_2SH	γC_2S Ca,P Ch,T $C_{12}A_7$	γC_2S Ca,P Ch,T $C_{12}A_7$	γC_2S Ca,H $C_{12}A_7$ UKs	Ks,K Ch	Ca T,Sk FB UKs	K,Ca T,Sk UKs	K Ca T,Sk UKs	γC_2S K,Ca H,T Sk
24	P Ch	Ca P,Ch Sk αC_2SH	Ca P,Ch T $C_{12}A_7$	Ca P,Ch T $C_{12}A_7$	γC_2S Ca,H P,Ch UKs	Ks K Ch	Ca T,Sk UKs FB	Ca T,Sk UKs	K,Ca H,T Sk G	K,Ca H,T Sk G
36	P Ch	Ca P,Ch Sk αC_2SH	Ca P,Ch T,Sk $C_{12}A_7$	Ca P,Ch T,Sk $C_{12}A_7$	Ca H,P Ch Sk	Ks K Ch	Ca,T Sk UKs FB	Ca,T Sk UKs	Ca,T Sk UKs	Ca H T Sk

Table 4

C/S	0.83					0.60				
Time /h/	A	A'	B'	C'	G	A	A'	B'	C'	G
8	Ks K,T Sk	γC_2S K,Ca,T Sk,UKs	T,Sk K,Ca UKs	T,Sk K,Ca UKs	γC_2S K,Ca T,H	K,Sk Ks,G	γC_2S, K,Ca UKs	γC_2S K,Ca UKs	γC_2S K,Ca UKs	γC_2S K,T,H Ca,UKs
12	Ks,T Sk,K G	K,Ca T,Sk UKs	K,Ca T,Sk UKs	K,Ca T,Sk UKs	K,Ca,T G,Sk,H UKs	K,Ks G,Sk	K,G Ca,Sk UKs	γC_2S K,Ca T,UKs	γC_2S K,Ca T,UKs	K,Ca T,Sk H,UKs
24	Ks,T Sk,K	K,Ca T,Sk UKs	K,Ca T,Sk UKs	K,Ca T,Sk UKs	K,Ca T,Sk H,UKs	K,Ks G,Sk	K,G Ca,Sk UKs	K,Ca T,Sk UKs	K,Ca T,Sk UKs	K,Ca T,Sk UKs
36	Ks,T Sk,K	K,Ca T,Sk UKs	K,Ca T,Sk UKs	K,Ca T,Sk UKs	K,Ca T,Sk H,UKs	K,Ks G,Sk	K,G Ca,Sk UKs	K,Ca T,Sk G,UKs	K,Ca T,Sk G,UKs	K,Ca T,Sk H,UKs

Carried out with the use of "Derivatograph" type OD-102 of the Paulik-Erdey system, made in Hungary. The testing of the texture and morphology of hydration products was accomplished by the scanning electron microscope Jeol, type IXA-50A, Japanese production and British, type Cambridge. The observations were made with 1000 - 30.000 enlargement.

3. THE TESTING RESULTS AND DISCUSSION.

In Table 3 and 4 the results of the phase composition tests for slurry of different molar ratios, C/S were presented. The results were obtained by the diffractional and complex thermal methods. The Table comprises the following symbols : P - phase "P", Ch - - calcium chondrodite, Sk - scawtite, T - - tobermorite 11.3Å, UKs - hydrated sodium silicate, H - hydrogarnet, Ks - ksonotlite, K - quarz, FB - Bezjak "3, 15" phase, G - - gyrolite, Ca - $CaCO_3$.

Pure γC_2S, which is the component of the pastes of different molar ratios undergoes the total analysis after 12 hours resulting with the formation of the phase "P" and calcium chondrodite /C/S = 2/, ksonotlite /C/S = 1/, the mixture of ksonotlite and tobermorite 11.3Å /C/S = 0.83/, and the mixture of ksonotlite and gyrolite /C/S = 0.60/. The presence of Na^+ ions and particularly Al^{3+} ions in the substances A', B', C' and G independently of the C/S quantity strongly influences the stabilization of the tobermorite phase, which remains the main component of the examined pastes. In the presence of calcite in the pastes of C/S = 1.0 ; 0.83 and 0.60, a big amount of scawtite phase is formed. Simultaneously with the increase of shares of $CaCO_3$ and other components of the post-extraction slurry, e.g. hydrogarnets, the rate of hydrolysis and hydration of γC_2S decreases. It is particularly evident in case of the industrial slurry "Groszowice". The reason for the delayed hydration of γC_2S lies in the precipitation of the secondary calcite and other products of the extraction of calcium aluminates with the soda solution on γC_2S grains, which makes it difficult for water to reach them and decreases the reaction surface. It is visible particularly on the photographs 1 and 2. The carried out investigation revealed that the slurry "Groszowice" may be used to obtain insulating and insulating-constructional materials of the tobermorite and scawtite composition.



Fig. 3 - SEM. The pastes autoclaved for 12 hours, sample A, temp. 200°C, C/S = 2. Enl. 6000 X.



Fig. 4 - SEM. The pastes autoclaved for 12 hours, sample A, temp. 200°C, C/S = 1, Enl. 6000 X.



Fig. 5 - SEM. The pastes autoclaved for 8 hours, sample G, temp. 200°C, C/S = 1. Enl. 11 000 X.

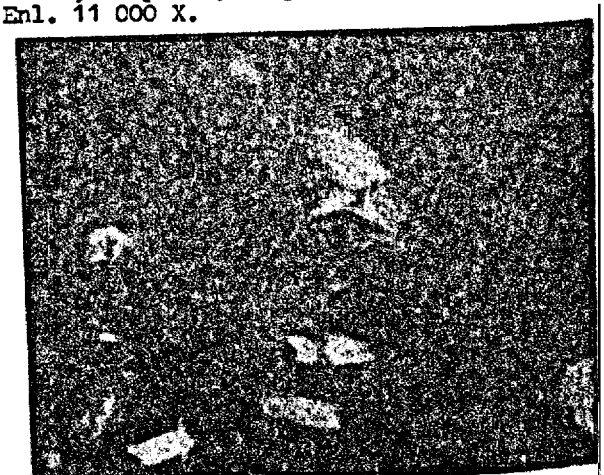

Fig. 6 - SEM. The pastes autoclaved for 12 hours, sample A, temp. 200°C, C/S = 0.83. Enl. 10 000 X.

P



Fig. 7 - SEM. The pastes autoclaved for 12 hours sample G, temp. 200°C, C/S = 0.83. Enl. 10 000 X.

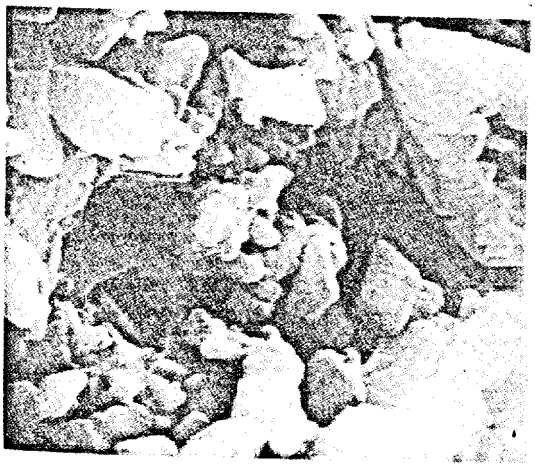

Fig. 8 - SEM. The pastes autoclaved for 12 hours sample A, temp. 200°C, C/S = 0.60. Enl. 5500 X.

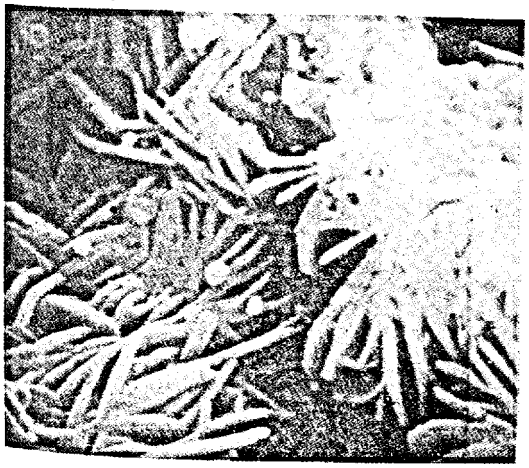

Fig. 9 - SEM. The pastes autoclaved for 12 hours, sample G, temp. 200°C, C/S = 0.60. Enl. 6400 X.

The observations of the pastes accomplished by means of electron scanning microscope revealed the essential differences in morphology of the products of γC_2S hydrolysis and hydration. In the pastes prepared from pure γC_2S /C/S = 2/ the presence of calcium chondrodite and phase "P" in plate forms was discovered. Their morphology confirms their close affinity with γC_2S. Ksonotlite obtained in the paste of molar ratio C/S = 1.0 crystallizes in the shape of long thin fibres /Fig. 4/, rather not typical and essentially different from ksonotlite crystals in the paste of C/S = 0.83 /Fig. 6/. In the paste of molar ratio C/S = 0.6 the typical plate crystals of gyrolite phase are visible /Fig.8/ Essentially different phase composition of the pastes A', B', C' and G causes that the tobermorite phase predominates on the photographs /Fig. 5, 7 and 9/. Apart from this phase, needle-shaped crystals covering tobermorite crystals are visible /Fig. 7/.

4. BIBLIOGRAPHY

1. H.F.W. TAYLOR, The chemistry of cements" Academic Press. London, New York 1964.
2. O.P. MCZEDŁOW-PETROSJAN and W.I.BABUSZKIN, 6th Int. Congr.on the Chem. of Cem. Part II/I 6-16, Moscow 1974.
3. J.M. BUTT and W.I. KAUSZANSKIJ, Nieorg. Mat. t. 10 nr 5/1974 p.947-948 /rus/.
4. M.M. SYCZEW, W.I. KORNIEJEW, E.N. KAZANSKAJA and J.N. MIEDWIEDIEWA, Journ.Prikł. Chim.3, 1973, p. 502-506 /rus/.
5. W.I. KAUSZANSKIJ, Journ. Prikł.Chim.8,1977 p. 1688-1692. /rus/.
6. T. MITSUDA and A. FUKUO, Min. Jour. Vol. 6 Nos 1/2 p. 17-35.
7. K. SPEAKMEN, H.F.W. TAYLOR, J.M. BENNETT and J.A. GARD, J.Chem.Soc. /A/, p. 1052--1060, 1967.
8. H.F.W. TAYLOR, 6th Int. Congr.on the Chem. of Cem. Moscow 1974, Part II/I p.192-207.
9. H.F.W. TAYLOR and D.M. ROY, 7th Int.Congr. on the Chem. of Cem., Paris 1980 s. II-2/2 - II 2/13.
10. J. JERNEJCIC and J. JELENIC, Int. Symp. Aut. Build. Mat. Utrecht 1973, Moscow, 1974, p. 135-146 /rus/.
11. J. JELENIC, J. JERNEJCIC and B. KORBUS, Vest. slov.kem.drustwa XVIII, nr 1-4, 1971 p. 43.
12. A. BEZJAK, Int.Symp.Aut.Build.Mat. Utrecht 1973, Moscow, 1974 p. 124-132.
13. A. BEZJAK, J. JELENIC and J. JERNEJCIC, Nature 248, 1974 Vol. 3 p. 581-582.
14. G.L. KALOUSEK and E.B. NELSON, Cem. Concr. Res. 8, 1978, p. 283-290.
15. K. LUKE, H.F.W. TAYLOR and G.L. KALOUSEK, Amer.Ceram.Soc.Bull. 59, 1979, p.334.
16. G.L. KALOUSEK, Cem. and Concr. Res. 6, 1976, p. 417-418.
17. B.KURBUS and J. JELENIC, Cement /Zagreb/ Br 2/1980-81, p.126-127.
18. J. GRZYMEK, Mat. Sci. Acad.Min. and Met. Cracow, Poland, Cer. Mat.nr 247-part.14, 1969, p. 191-211.

M.Dr.Eng. IOAN COTEA, Dr.Eng.D.PUSCASU, Dipl.Eng.D.NICOLAU

RESEARCH AND DESIGN INSTITUTE FOR BINDER AND ASBESTOS CEMENT INDUSTRY,ROMANIA

Contributions to the clinker grindability physics.

Les contributions à la physique de broyage du clinker.

1. Introduction

The problem of the clinker composition relationship has been studied by many researchers (1), (4), (5), (6), the results obtained being partly contradictory or non-comparable due to the criterion chosen as grindability measurement (work index, Zeisel method etc.)

In this paper, the authors present the results obtained at the trial of the clinker grains by quasistationary (slow) compression, a way of approach presented in previous papers as well (2), (3).

2. Experiments and work methods

Two sorts of clinker have been chosen; these two sorts have different chemical and mineralogical composition (table 1); they have been divided into granulometric classes. The grains, (of a shape almost spherical,) have been individually, subjected to a very slow (quasistatical) compression process.

Besides the chemical and mineralogical composition and the various relationships between the components, the study also involved the density, the liquid phase quantity, the void ratio.

The crushing force, the piston movement up to the crushing, the specific primary crushing energy have been measured and recorded.

The problem referring to the correlation between the crushing energy and the reduction ratio has been previously dealt with (2), (3).

3. The correlation between the specific crushing force and the diameter

The crushing force related to the grain mass, the mean quantity per colectivity (granulometric class) has been correlated with the mean diameter of the grains colectivity.

For both types of clinker, it has been noticed that the specific crushing force lessens with the mean diameter of the grain and that this variation on the d = 2 – 5 mm interval it is practically independent from the chemical and mineralogical composition, the liquid phase percentage and the void ratio (fig.1).

The processing of all the experimental methods by the smallest square method leads to the following:

$$(\mathcal{F} / M)_1 = 39{,}134.10^3 . e^{-0{,}572.d} \quad ; r = 0{,}975$$

$$(\mathcal{F} / M)_2 = 22{,}24.10^3 . e^{-0{,}372.d} \quad ; r = 0{,}979$$

The difference between the coefficients and the exponents of the two relations can be due to the different chemical compositions, according to (4).

4. The correlation between the adimensional ratio (1/d), the mean diameter and the void ratio.

The two types of clinkers have been chosen in such a way as mainly the $(\overline{1/d}) = f(d)$ correlation can be studied within one of them (type 2), free from the influence of the porosity (ε) – which, in this case, bars a confined variation whole, within the second one (type 1), the influence of the two factors can be studied.

M.Dr.Eng.IOAN COTEA, Dr.Eng.D.PUSCASU, Dipl.Eng.D.NICOLAU
RESEARCH AND DESIGN INSTITUTE FOR BINDER AND ASBESTOS CEMENT INDUSTRY ROMANIA

Contributions to the clinker grindability physics
Les contributions à la physique de broyage du clinker

4.1. The (1/ d) = f (d) correlation

Within it, (clinker 2), in which the porosity varies relatively in confined limits, the mechanism of the primary crushing is not structurally affected by this factor. The multiple regression analysis reveals in this case the (1/d) ratio lessens with the diameter and increases with the increase of the porosity, fig.2,3. The analytical relation is the following:

$$(1 / d) = o,6. e^{-o,28 d} . e^{4,842 \varepsilon} ; r = o,931$$

4.2. The (1 / d) = f (d, ε) correlation

Within it (type 1 clinker) the variation of the porosity is sensibly increased.

Besides the above mentioned influences, the effect of a higher variation of the porosity inducing structural modifications in the crushing mechanism is also added.

In this respect, according to the Griffith's theory, a more porous body is more friable than a less porous one.

The multiple regression analysis reveals a variation which is contrary to the type 2 clinker, as for as the (1 / d) ratio lessening with the porosity increasing is concerned.

The contradictory effect of the porosity is also shown in the lessening of the correlation coefficient. The analytical relation is the following:

$$(1/ d) = o.47. e^{-o,17 d} . e^{-3,36 \varepsilon} ; r = o,8$$

5. The w = f (d, ε) correlation

The primary crushing energy is connected with the values shown by the (2, 3) relation.

$$W = 1.4.1o^{-2} \left(\frac{F}{m_o}\right) .1$$

The relations ensured for the two types of clinkers are:

$$W_1 = 328,73. e^{-o,852 d} . d . e^{4,842 \varepsilon}$$
$$W_2 = 146,34. e^{-o,542 d} . d . e^{-3,36 \varepsilon}$$

If considering the mean porosity $\bar{\varepsilon} = o.142$, equal for the 2 types of clinker, the following relations one obtained:

$$W\, 1/_{\varepsilon=\bar{\varepsilon}} = 6.53,8 \cdot d . e^{-o,852 d}$$
$$W\, 2/_{\varepsilon=\bar{\varepsilon}} = 9o,81 \cdot d . e^{-o,542 d}$$

Which explain the variation form of the crushing energy with the diameter (fig.4).

6. Conclusions

For the 2 analysed clinkers, the variation of the specific primary crushing force mainly depends on the grain diameter, the analytical function being of the following type :

$$(F/M) = A. e^{-Bd.}$$

M.Dr.Eng.IOAN COTEA, Dr.Eng.D.PUSCASU, Dipl.Eng.D.NICOLAU

RESEARCH AND DESIGN INSTITUTE FOR BINDER AND ASBESTOS CEMENT INDUSTRY,ROMANIA

P

Contributions to the clinker grindability physics
Les contributions à la physique de broyage du clinker

the A, B coefficients being able to be in relationship with the chemical and mineralogical composition :

The (l/d) ratio decreases exponentially with the diameter increase and the porosity moulds it in a compley way.

The experiments carried out and the analytical relations established can be an explanatori for the contradictory results regarding the " grindability" and its correlation with the porosity, the liquid phase content the chemical and mineralogical composition.

7. Notations

F = crushing force (N)
M_1 = mass of the clinker grain before the crushing (g)
F/M_1 = specific crushing force (N/g)
d = mean diameter of the clinker grains (mm)
l - movement of the press punch up to the crushing (mm)
l/d - specific movement (mm/mm)
ε - porosity, void ratio/adimensionally
γ = correlation coefficient
W = crushing energy (kWhr/to)

Tabel no. 1

Granulometric fraction [mm]	clinker no. 1							clinker no.2					
	1-2	2-3	3-4	4-5	5-6	6-7	Cv[%]	1-2	2-3	3-4	4-5	5-6	Cv[%]
Loss ignition	0,63	0,83	0,6	0,7	0,83	0,65	14,1	1,01	0,97	0,74	0,67	0,68	20,1
SiO_2 + ins.	20,14	20,12	20,30	20,43	20,38	20,06	0,7	21,26	21,46	21,31	21,18	21,10	0,6
Al_2O_3	7,30	7,39	7,39	7,56	7,25	7,24	1,6	5,13	4,99	5,24	5,25	4,98	2,5
Fe_2O_3	3,62	3,82	3,51	3,67	3,52	3,60	2,9	5,99	5,99	5,76	5,76	5,70	2,3
CaO	65,22	64,80	65,9	65,60	65,50	65,60	0,54	63,20	63,23	63,65	64,21	64,65	1,0
MgO	1,27	1,27	0,81	0,71	0,92	1,35	23,00	1,56	1,56	1,40	1,25	1,20	12,1
SO_3	0,29	0,19	0,19	0,12	0,14	0,24	30,00	0,59	0,49	0,51	0,60	0,48	10,6
Na_2O	0,48	0,48	0,49	0,46	0,45	0,45	3,70	0,26	0,26	0,25	0,26	0,25	2,0
K_2O	0,79	0,85	0,85	0,89	0,87	0,96	6,0	0,79	0,75	0,73	0,71	0,71	4,5
TiO_2	0,24	0,23	0,32	0,35	0,36	0,19	24,0	0,18	0,21	0,24	0,20	0,21	10,4
Total	99,98	99,98	100,32	100,49	100,22	100,34	—	99,97	99,92	99,85	100,00	99,75	—
ins.	0,11	0,31	0,3	0,37	0,34	0,2	35,9	0,55	0,53	0,41	0,27	0,24	35,8
C_4AF	10,0	10,0	10,0	10,0	15,0	10,0	17,0	15÷20	15÷20	15÷20	15÷20	15÷20	0
C_3S	60÷65	60	65	60÷65	65	60÷65	3,6	50÷55	50÷55	50	55÷60	55÷60	5,7
C_2S	10	< 15	10	10	10	10	17	20÷55	15÷20	20÷25	≈ 15	15÷20	16,1
C_3A	15	15	15	15	15	15	0	≈5	≈5	≈5	≈5	≈5	0
P	3,044	2,985	3,125	3,03	2,955	2,764	5,4	2,985	2,8925	3,015	0,87	2,9126	2,1
Msi	1,84	1,79	1,86	1,82	1,89	1,85	1,86	1,91	1,95	1,94	1,92	1,976	1,34
MAl	2,02	1,93	2,1	2,06	2,06	2,01	2,6	0,856	0,83	0,91	0,91	0,87	3,8
Liquid phase	32,585	33,365	32,22	32,96	31,94	32,58	1,4	31,48	31,02	31,06	30,93	29,93	1,8
d[mm]	1,9	2,64	3,18	4,53	4,94	6,177	—	1,65	2,63	3,1	4,5	5,627	—
l[mm]	0,693	0,308	0,639	0,6322	0,6286	0,585	—	1,23	1,5	1,38	1,562	1,526	—
$\frac{l}{d}$ [mm/mm]	0,36	0,116	0,2	0,14	0,127	0,095	—	0,745	0,572	0,446	0,347	0,27	—
ES	0,112	0,131	0,088	0,117	0,139	0,194	32,36	0,128	0,153	0,119	0,161	0,147	12,4
$F/M \cdot 10^{-3}$ [N/g]	17,37	7,94	5,09	3,02	1,88	1,41	—	13,65	8,34	6,0	3,88	3,21	—

4/20

M.Dr.Eng.COTEA ION, Dr.Eng.D.PUSCASA, Dipl.Eng.D.NICOLAU
RESEARCH AND DESIGN INSTITUTE FOR BINDER AND ASBESTOS CEMENT INDUSTRY, ROMANIA

Contributions to the clinker grindability physics

Les contributions à la physique de broyage du clinker

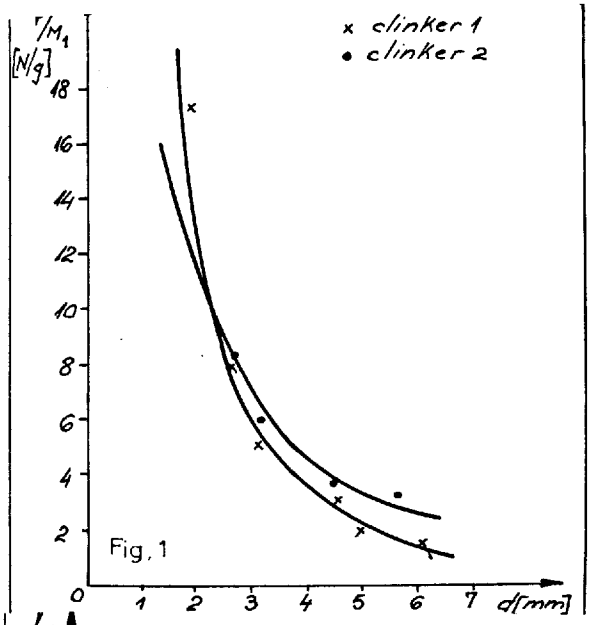

Fig. 1

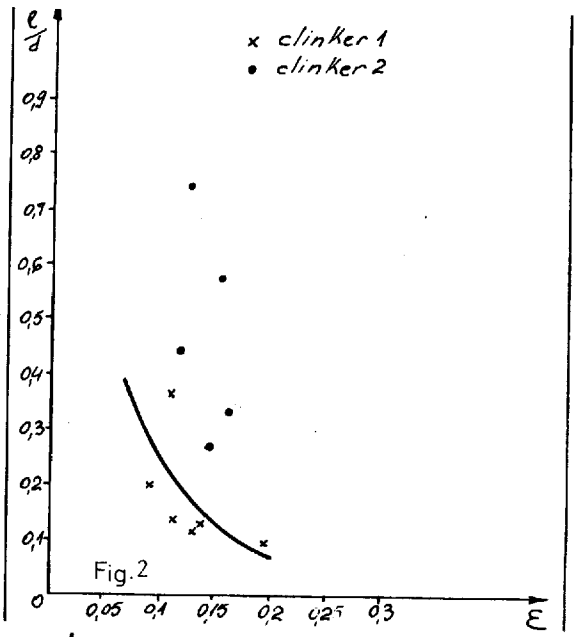

Fig. 2

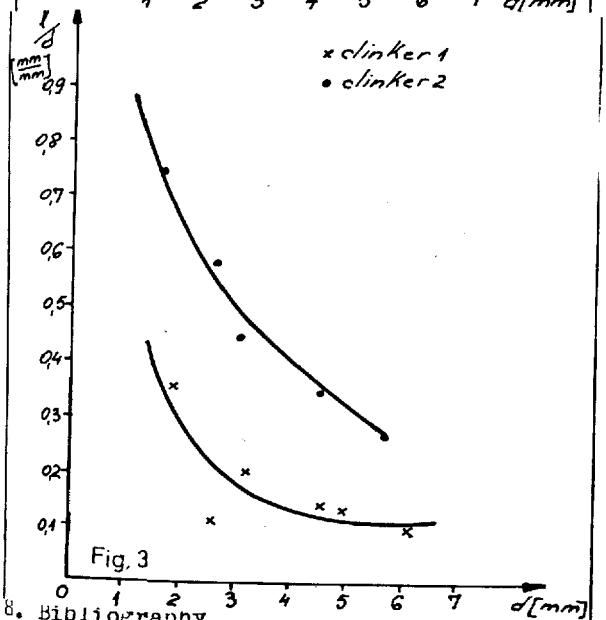

Fig. 3

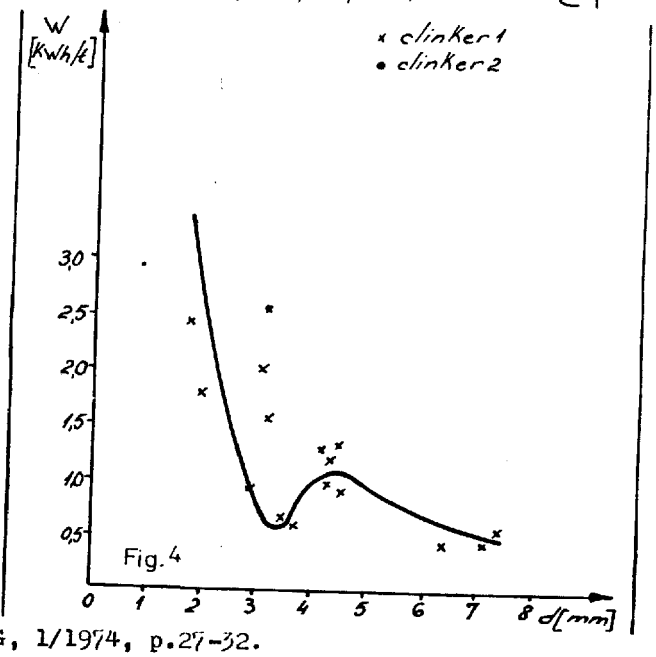

Fig. 4

8. Bibliography

(1) - Butt. Ju.M, Kolbasov. V.M, Melniekij - ZKG, 1/1974, p.27-32.
(2) - Cotea I, Puşcaşu D, Nicolau D, - Consilox, Cluj Napoca, Sept.1984.
(3) - Cotea I, Puşcaşu D, Nicolau D, - Silikonf, Budapest, May 1985.
(4) - Gouda G.R. - Cem.Concr. Res., Vol.9, 1979, p.209-218.
(5) - Petersen I.F. - Cim.Bet.Plat., Ch.,5/1980 p.297-301.
(6) - Scheubel B., Balzer H.J., - ZKG 11/1983 p. 624-627.

dr.eng.IOAN COTEA, eng.NICOLAE BUTUCESCU, eng.LIANA BUCEA, eng.VALERIAN MIHAI

Research and Design Institute for Binder and Asbestos Cement Industry, Romania

STUDY OF THERMAL EFFECTS OBTAINED IN THE CLINKERIZATION PROCESS BY THERMO-DIFFERENTIAL ANALYSIS.

In order to study the way in which the elements of the raw material mix can influence on the thermal effects characteristic to the clinkerization process, there were made a series of experiments with a thermodifferential analysis equipment.

During these experiments the main mineralogical Components of Portland Clinker as well as of common Portland clinkers with variable composition were synthetized.

There were used a Derivatograph MOM Q 1500 D with a kiln of up to 1500°C, with an automatic record of T, TG, DTA, DTG curves at heating and cooling.

In order to make a series of control analysis on the cured specimen with ATD equipment there were suplimentary introduced in the kiln - in the thermocouples space - a big platinum crucible (with a capacity of aprox. 15 g.raw material mix).

In the synthetizing experiment for each of the four Portland clinker components obtained from pure substances, it resulted:

- the formation of each mineralogical component is characterized by one or more thermal effects(exothermic for crystalization, endothermic for phasat transformations, the metting formation) that appear above 1000°C, the carbonate decomposition is accompanied by a thermo-negative effect below 1000°C;

- the heating speed increase makes the maximum thermal effects temperature increase;

- the existence of a level (at maximum heating temperature) has a strong influence on the content increase of the mineral component;

- slow cooling (compared to the rapid one) has the same favpurable influence, too.

The results obtained at the C_3S synthetization from pure substances with some additives, by curing in ATD kiln; the additives are also pure substances (for SO_3, SO_4Ca p.a. was added) are presented in the following table.

TABLE 1

Additive	dosed C_3S by RX analysis	free CaO chemically determined %	Temperature of thermal effects max, °C	
			endothermic	exothermic
1	2	3	4	5
without	5-10	10,29	950 1465 evident	1350, 1365 very low
1% Fe_2O_3 + 1% Al_2O_3	very much	0,14	940 1425 low	1330 at cooling 1310 low
5% Fe_2O_3	very much	0,27	935 1430 intensive	1165, 1200 very low
5% Al_2O_3	35-40	2,23	940 1405,1480 int.	1192 very low
0,5% MgO	tracks	15,53	910 1460 very low	1040,1275 very low

./.

dr.eng.IOAN COTEA, eng.NICOLAE BUTUCESCU,eng.LIANA BUCEA,eng.VALERIAN MIHA. 2
Research and Design Institute for Binder and Asbestos Cement Industry,Romania

P

1		3	4	5
2% MgO	much	5,65	930 1455 intensive	1163, 1210 1265,very low
0,67% K_2O + 0,35% Na_2O	little	7,96	955 1380,1460 very low	
1% MnO_2	tracks	14,83	950 1475 evident	1180 very low
0,5% TiO_2	tracks	13,57	950 1470 low	1155, 1225 very low
1% SO_3	tracks	12,21	950 1395,1455 low	1475 intensive
2,4% SO_3	tracks	13,47	945 1380 very intensive	above 1500

The working conditions were:
- heating rate 7,5°C/minute
- without a level at maximum temperature (1500°C)
- with rapid cooling

The additives were chosen so that they correspond to elements and proportions that are generally found in the raw materials from our cement plants.

Analysing table 1 it results that:

- the additives generally reduce the temperatures for the maximum exothermic effects (corresponding to the C_3S crystalization), except SO_3 additive; the lowest exothermic effects (that is C_3S formation at low temperatures) are for the Al_2O_3 and Fe_2O_3 additive in greater proportion ;
- the endothermic effects, that mark the phasal transformation and liquid phase production, are more intense for additives in higher percentage (Al_2O_3, Fe_2O_3, MgO and SO_3) that mean a more intensive process (for example, a growth of liquid phase quantity) ;
- Fe_2O_3, Al_2O_3 additives contributes to the biggest C_3S quantity formation.

Similar experiments were made on the other main mineralogical components of Portland clinker. There were notised also in these cases same favourable influences of the additives.

Table 2 shows the results obtained on a series of Portland clinkers made from pure substances in a platinum crucible put in the ATD Kiln.

TABLE 2

SK	%CaO free chem. det.	X ray analysis C_3S, C_2S, C_3A, C_4AF				Optical microscopic analysis C_3S dimensions frequency μm		Thermal effects temperature endothermic	exothermic
1	2	3	4	5	6	7	8	9	10
0,98	1,11	60	15-20	10-15	10	60-65	40-60	1375 int. -	1350 intensive
0,98	0,50	60-65	< 15	15	10	60-65	10-40	1380 int. -	1355 very "

./.

dr.eng.IOAN COTEA, eng.NICOLAE BUTUCESCU, eng.LIANA BUCEA, eng.VALERIAN MIHAI

Research and Design Institute for Binder and Asbestos Cement Industry, Romania

1	2	3	4	5	6	7	8	9	10
o,96	o,5o	55-6o	2o-25	1o-15	1o	55-6o	5-25	139o int. -	136o int.
o,95	o,28	6o	<15	15	1o	55-6o	2o-4o	1385 int. -	1365 very int.
o,92	o,28	55-6o	2o-25	1o-15	1o	55	5-2o	1395 med. int. -	137o very intensive
1,o6	1,14	6o	<15	15-2o	5	65	1o-4o	14oo int. -	1375 very int.
o,94	o,49	55-6o	2o	1o-15	1o	5o-55	5-4o	14oo int. -	1365 int.

The temperature for the exothermic maximal effects correspond to the crystalization phase of the C_3S (main clinker component) and the temperature for the endothermal maximal effect (above 1ooo°C) indicates the temperature that makes the liquid phase increase.

The exothermic effects have the maximum between 135o-1375 and the endothermic ones between 1375-14oo°C.

There were made a series of experiments in order to obtain the Portland clinker with a mix of a certain composition in which in the initial composition various oxides were added or taken out; pure substances were used.

The analysis of the obtained data made evident that :

= for a 1% reduction of each silicon, aluminium and iron oxides, the C_3S content is bigger although the free CaO propoftion grows;

- from the other oxides admixtures (MgO, K_2O, Na_2O, MnO_2, TiO_2 and SO_3), the SO_3 additives give the higher percentage of free CaO;

- the thermal effects with the lowest temperatures are obtained for the additives in the highest percentages (sum of o,5% MgO + o,67% K_2O + o,33% Na_2O + 1% MnO_2 + o,5% TiO_2 + 1% SO_3; also 3% SO_3 and 2% MgO), and from the elements the SO_3 additives.

The exothermic effects have temperatures corresponding to their maximal value between 122o and 1365°C and the endothermic ones maximal values between 1o2o and 1415°C.

There were obtained clinkers from $CaCO_3$ mixtures various clay materials (Kaolinite, bentonite, Kaolinite clay, illite, feldspar, etc.) and correction pure oxides for the mixtures to have the same chemical composition.

The obtained clinkers had C_3S 55-65% (more for the kaolinite and bentonite in the initial mixture), freee CaO o,24-1,15%.

The exothermic effects were maximal between 122o and 1295°C (higher for kaolinite) and the endothermic ones 1325-1345°C (generally higher for kaolinite).

There were made some more experiments with raw materials from some deposits of Romanian Cement plants (the clay materials being kaolinite clay, illite, montmorillonite, some with many bad minerals) and the results were as follows:

- the exothermic effects have maximal values between 117o and 1295°C and the endothermic ones between 127o and 134o°C;

./.

- at clinkerization temperature of 1380°C (in ATD equipment) the lowest free CaO content and higher C_3S as well as the maximal thermal effects with the lowest temperatures were obtained from the meals that had clay materials as kaolinite clays; on the pilot-scale experiments these gave the higher mechanical strengths;

- at clinkerization temperature of 1430°C for the clinkers with more kaolinite in the respective meals, there were not obtained contents higher of C_3S, and in the pilot-scale experiments the strengths were lower, indicating a clinker supercombustion.

We can conclude that the experiments made evident the possibility of synthetizing the clinker and mineralogical components with the thermodifferential analysis

The method has some advantages:

- it can correlate the temperature, the nature and the amplitude of the thermal effects in the physical and chemical processes of transformation of the cured mixture, as well as the product quality and quantity resulted after clinkerization;

- it can be appreciated the favourable or harm influences of various additives, as well as the various thermal curing for the respective mixtures;

- it can be evaluated the optimal conditions for a clinkerization at lower temperatures, having as an effect a reduction of fuel consumption in the industrial process;

- the method is easy to apply and offers a satisfactory precision by the good equipment respectibility.

dr.eng.IOAN COTEA,eng.NICOLAE BUTUCESCU,eng.LIANA BUCEA,eng.VALERIAN MIHAI

Research and Design Institute for Binder and Asbestos Cement Industry,Romania

REFERENCES

1. R.Bucchi - The influence of the Raw Material Nature and Preparation on the Raw Mix Reactivity
The works of the 7th International Congress on the Cement Chemistry. Paris (98o, vol.I)

2. I.Butt - Modern Studying Methods for clinker Formation Mechanism and Phasal Composition.Tement, 1975, 2, 12...19

3. A.Dehaeul C.Sinsaillier - Reaction Heat Determination using the Thermodifferential Analysis - Special aplication in the case of Cement Raw Materials - ZKG-1979, 8

4. G.Gouda - Raw material for cement - its Influence on the Fuel Consumption. Rock Products, Oct.1977, pp.6o-64

5. Ed.R.C. Mackenzie - Differential Thermal Analysis (Academic Press - New York 197o)

6. V.G. Ramachandran - Applications of Differential Thermal Analysis in Cement Chemistry (New-Yprk 1969)

7. I.Odler - Separation Possibilities of Portland Cement Individual Components - by Selective Dissolution - ZKG-1979, 1o,5o4...5o7

8. I.Teoreanu - Binder and Concrete Technology. Ed.Didactică şi Pedagogică Bucureşti - 1967

9. I.Teoreanu - And Others,Clinkerization Behaviour of Some Raw Material Mixtures, Materiale de Construcţii 1985,1,42-48

1o. I.Teoreanu - And Other - Influence of some Compositional and Curing Parameters on the Portland Cement Clinker Hydraulic Properties. Materiale de Construcţii, Review, 1985 1, pp.48-51.

11. V.Timashev - Clinkerization Kinetics, clinker structure composition and its phases. The works of the 7th International Congress on Cement Chemistry. Vol.I Paris 198o

12. D.Todor - Mineral Thermal Analysis. Ed.Tehnică,Bucureşti 1972.

M.Eng.I.COTEA, Dipl.Eng.A.ROMANESCU, Dipl.Eng.C.DUMITRESCU

RESEARCH AND DESIGN INSTITUTE FOR BINDER AND ASBESTOS CEMENT INDUSTRY,ROMANIA

Researches Concerning the Harmful Components Elimination from Phosphogypsum for Using it as Cement Setting Time Regulator.

Recherches concernant l'élimination des composants nocifs du phosphogypse en vue de son utilisation comme regulateur de prise du ciment.

I N T R O D U C T I O N

In Romania there are no phosphate deposits that can be economically quarried, the phosphate raw material is imported from the USSR (Kola Apatite), USA (Florida phosphorite), Jordan, Marocco, Togo, Israel.

For the phosphoric acid manufacturing the wet process with dihydrate is used, a precipitate results after filtering, that is the dihydrated calcium sulphate having 25-30% humidity - the phosphogypsum.

According to the phosphate stone nature and to the manufacturing technological parameters of phosphoric acid, the phosphogypsum contains some impurities that, in the case of using it at cement grinding unfavourably influence on the cement physico-mechanical characteristics, as the phosphorous soluble and insoluble compounds [$H_3PO_4 \cdot n H_2O$, $Ca(H_2PO_4)2 \cdot H_2O$, $CaHPO_4 \cdot 2H_2O$, $AlH_3(PO_4)_2 \ 2H_2O$], the flourus (HF, H_2SiF_6, Na_2SiF_6), the organic substances, the magnesium oxide and alkali salts (1,2)

It was found that the negative influence of cement impurities is lower in the case of the slag cements.(3)

This work presents the results obtained as a consequence of the researches made in our institute to eliminate the existing impurities in phosphogypsum, in order to be used as setting regulator for all cement brands manufactured in Romania.

Experimental Data

There were examined 80 phosphogypsum batches sampled in two years period from four chemical fertilizer plants that came from various raw material.

The physico-chemical characteristics of the examined phosphogypsum varied according to the nature of the raw materials used and to the technological parameters of phosphoric acid manufacturing.

In this work the results obtained at phosphogypsum use will be presented ; the physico-chemical characteristics are presented in table 2.

Table 2

CHEMICAL COMPOSITION OF PHOSPHOGYPSUM

Components (%)	Phosphogypsum		
	I_1 (Tunis)	II_1 (Kola)	III_1 (Florida)
P_2O_5 total	0,750	0,898	0,704
P_2O_5 soluble	0,220	0,299	0,194
P_2O_5 syncr.	0,443	0,527	0,424
CaO	32,580	33,010	31,940
SO_4	54,120	55,120	53,124
F^- total	0,503	0,189	0,431
F^- soluble	0,149	0,181	0,207
SiO_2	0,745	0,331	3,340
Fe_2O_3	0,283	0,202	0,250
Al_2O_3	0,047	0,047	0,581
MgO	0,092	0,073	0,140

./.

M.Eng.I.COTEA, Dipl.Eng.A.ROMANESCU, Dipl.Eng.C.DUMITRESCU

RESEARCH AND DESIGN INSTITUTE FOR BINDER AND ASBESTOS CEMENT INDUSTRY,ROMANIA

Researches Concerning the Harmful Components Elimination from Phosphogypsum for Using it as Cement Setting Time Regulator

Recherches concernant l'élimination des composants nocifs du phosphogypse en vue de son utilisation comme regulateur de prise du ciment.

Components (%)	Phosphogypsum I_1 (Tunis)	II_1 (Kola)	III_1 (Florida)
Na_2O	o,o8o	o,o72	o,o67
K_2O	o,oo7	o,o37	o,oo8
Org.	o,395	o,o48	o,o86
humidity 25o°C	18,2o	17,79	18,8o
humidity 45°C	2,4e	2,27	1,8o

For cement manufacturing the clinkers, whose composition is presented in table 3, were used.

Table 3

CLINKER MODULAR MINERALOGICAL COMPOSITION

Clinker	Free CaO %	Modular composition M_{Si}	M_{Al}	C_{St}	Mineralogical composition % C_3S	C_2S	C_3A	C_4AF
1. Normal Portland	o,55	1,93	1,94	o,97	58,74	12,76	12,11	1o,64
2. Ferroportland	o,76	1,83	o,86	o,95	6o,o3	11,87	3,38	17,66

There were made cements with or without furnace granulated slag.

Slag oxidic composition is presented in table 4.

Table 4

SLAG CHEMICAL COMPOSITION

Material	Chemical composition (%) PC	SiO_2	Al_2O_3	Fe_2O_3	CaO	SO_3
slag	o,2o	35,84	12,5e	o,6o	43,27	o,17

Natural gypsum or phosphogypsum as such or purified were used as setting time regulator.

The natural gypsum used as setting regulator had a content of $CaSO_4 \cdot H_2O$ of 81,33% and $CaSO_4$ of 4,84%.

The clinkers were ground with gypsum additive or phosphogypsum with or without slag at a fineness of 3ooo cm2/g Blaine, and the cements obtained were tested from the point of view of the physico-mechanical behaviour, using standard methods.

The chemical and mineralogical composition of phosphogypsum and clinkers, as well as the hydration product nature on hardened pastes were determined using chemical, X-ray analysis, thermodifferential and electronic microscopy methods.

./.

M.Eng.I.COTEA, Dipl.Eng.A.ROMANESCU, Dipl.Eng.C.DUMITRESCU
RESEARCH AND DESIGN INSTITUTE FOR BINDER AND ASBESTOS CEMENT INDUSTRY,ROMANIA

Researches Concerning the Harmful Components Elimination from Phosphogypsum for Using it as Cement Setting Time Regulator

Researches concernant l'élimination des composant nocifs du phosphogypse en vue de son utilisation comme regulateur de prise du ciment.

Results and Discussions

Following the phosphogypsum composition with time there were made evident the wide limits of compositional variation because of the reaction tank conditions and the raw material composition.

From the calculations, on the basis of the chemical analysis (table 2),the possible compounds in the examined phosphogypsum are the ones presented in table 5.

Table 5

POSSIBLE CONSTITUENTS,RESULTED FROM CALCULATIONS BASED ON CHEMICAL ANALYSIS

Constituents	Phosphogypsum I_1	II_1	III_1
$CaSO_4 \cdot 2H_2O$	91,07o	95,78o	93,83o
$MgSO_4$	o,21o	o,06o	o,2o4
H_3PO_4	o,3o4	o,413	o,268
$Ca_5(PO_4)_3F$	o,2o6	o,11o	o,2o2
$CaHPO_4 \cdot 2H_2O$	1,o73	1,276	1,o26
Na_2SiF_6	o,242	o,218	o,2o3
K_2SiF_6	o,o17	o,o86	o,o18
SiO_2	o,663	o,239	3,27o
Other constituents(x	6,21o	1,8oo	1,ooo

x) Other constituents : $Fe(H_2PO_4)3$, $Al(H_2PO_4)_3$, $K_2MgCa_2(SO_4)_4 \cdot 2H_2O$, $CaSO_4$ SiF_6AlF_6 (OH) $12H_2O$, compounds of Tr_2O_3,U TiO_2.

The presence of $CaHPO_4 \cdot 2H_2O$ compound was made evident by 1R spectral analysis, (fig.1) by low uptake from 83o cm^{-1} due to HPO_4^{2-} ion,corresponding to calcium dibasic orthophosphate included in the red.

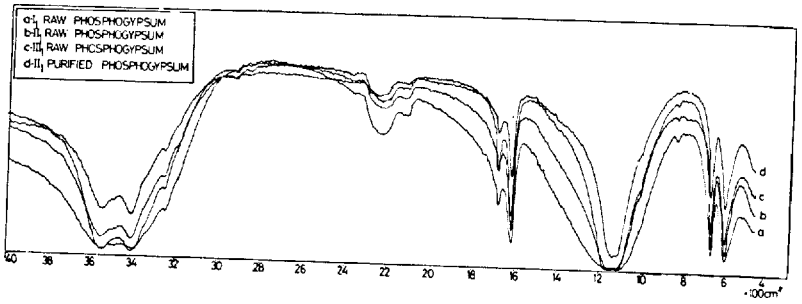

Fig.1 - 1 R Spectres of phosphogypsum.

./.

M.Eng.I.COTEA, Dipl.Eng.A.ROMANESCU, Dipl.Eng.C.DUMITRESCU

RESEARCH AND DESIGN INSTITUTE FOR BINDER AND ASBESTOS CEMENT INDUSTRY,ROMANIA

Researches Concerning the Harmful Components Elimination from Phosphogypsum for Using it as Cement Setting Time Regulator

Researches concernant l'élimination des composant nocifs du phosphogypse en vue de son utilisation comme regulateur de prise du ciment.

The granulometric analysis and the microscopic study shew that the I_1 and III_1 phosphogypsum have long prismatic crystals, the particle proportion of diametre between 15-5o μm, being 51,4% on I_1 sample and 77,1% on II_1 sample. III_1 Phosphogypsum is microgranular agglomerated, the particle proportion of diametre between 15-5o μm being 82,1%.

The analysis of the purified phosphogypsum by washing, neutralization and thermal curing, as it is presented in table 6 and fig.1 lead to the following conclusions:

Table 6

THE PHYSICO-CHEMICAL CHARACTERISTICS OF PURIFIED PHOSPHOGYPSUM

Phosphogypsum	pH	Chemical composition (%)					
		P_2O_5 soluble	P_2O_5 syncr.	F^- total	F^- soluble	Organic substances total	Organic substances (C)
I_1 - washed	4,5	o,o2	o,446	o,54o	o,oo9	o,4	o,28o
- neutralized	6,o	tracks	-	-	-	-	-
- thermal cured	6,o	tracks	o,1o5	o,438	-	-	o,oo6
II_1 - washed	4,5	o,o5	o,55o	o,532	o,o42	o,o2o	o,o42
- neutralized	6,5	tracks	-	-	-	-	-
- thermal cured (x	6,o	tracks	o,o8o	o,5o1	-	-	o,oo5
III_1 - washed	4,5	o,o3	o,426	o,492	o,o71	o,23o	o,o66
- neutralized	6,o	tracks	-	-	-	-	-
- thermal cured (x	6,o	tracks	o,o29	o,444	-	-	o,oo8

x) rehydrated at granulation

- washing and neutralizing lead mainly to a content lowering of soluble substances.
- thermal curing leads to a content lowering of $CaHPO_4 \cdot 2H_2O$ and organic substances.

The physico-mechanical characteristics of cement with raw and purified phosphogypsum are presented in table 7 compared to those of cements with gypsum.

./.

M.Eng.I.COTEA, Dipl.Eng.A.ROMANESCU, Dipl.Eng.C.DUMITRESCU
RESEARCH AND DESIGN INSTITUTE FOR BINDER AND ASBESTOS CEMENT INDUSTRY, ROMANIA

Researches Concerning the Harmful Components Elimination from Phosphogypsum for Using it as Cement Setting Time Regulator.

Researches concernant l'élimination des composant nocifs du phosphogypse en vue de son utilisation comme regulateur de prise du ciment.

Table 7

CEMENT PHYSICO-MECHANICAL CHARACTERISTICS

Cement denomination	Clinker	Additive	SO_3 content (%)	Blaine specific surface (cm2/g)	Setting time (h.min.) i.	f.	Compressive strength (MPa) 2 days	7 days	28 days
1.	1.	gypsum	2,82	3o3o	1.5o	4.o5	19,2	37,3	48,7
2.	2.	gypsum, slag	3,13	3o5o	3,oo	4.5o	16,9	32,4	43,1
3.	2.	gypsum	2,33	3ooo	2,45	4.oo	16,8	29,o	4o,2
4.	1.	raw I_1 phospho-gypsum	2,87	3o6o	5.35	8.oo	14,9	33,3	4o,3
5.	1.	raw II_1 phospho-gypsum	2,92	298o	6.5o	8.35	14,6	34,8	42,o
6.	1.	Raw III_1 phospho-gypsum	3,o1	3o2o	6.oo	8.3o	12,8	33,o	45,8
7.	1.	raw II_1 phospho-gypsum - slag	3,1o	3o5o	3.55	6.5o	15,1	31,o	44,1
8.	2.	raw II_1 phospho-gypsum	2,29	3o3o	6.1o	8.oo	12,6	26,o	38,6
9.	1.	washed and neutralized II_1 phosphogypsum	3,2o	3o4o	3.45	6.15	18,o	35,o	46,3
1o.	1.	washed and neutralized III_1 phosphogypsum - slag	3,19	3ooo	3.3o	5.55	16,8	32,o	41,1
11.	1.	II_1 phospho-gypsum thermal cured and rehydrated at granullating	2,98	3o2o	2.45	4.15	21,4	37,1	47,6
12.	2.	II_1 phospho-gypsum thermal cured and rehydrated at granulating	2,3o	3o5o	3,3o	5.45	17,1	3o,2	41,o

The obtained cements with raw phosphogypsum additive were characterized by longer time settings and lower mechanical strengths, especially for short terms, about 2o-3o% compared to reference standard cement.

There are lower mechanical strengths in the case of cement with slag additive 1o-15% at 2 days.

By using washed and neutralized phosphogypsum cements with physico-chemical characteristics similar to these of reference standard cement, especially with slag additive, are obtained.

./.

M.Eng.I.COTEA, Dipl.Eng.A.ROMANESCU, Dipl.Eng.C.DUMITRESCU
RESEARCH AND DESIGN INSTITUTE FOR BINDER AND ASBESTOS CEMENT INDUSTRY,ROMANIA

Researches Concerning the Harmful Components Elimination from Phosphogypsum for Using it as Cement Setting Time Regulator.

Researches concernant l'élimination des composant nocifs du phosphogypse en vue de son utilisation comme regulateur de prise du ciment.

The washed, neutralized and thermal cured phosphogypsum has the same behaviour as the natural gypsum, leading to the achievement of some cements of superior strengths.

Hydration evolution of cements with phosphogypsum additive compared to these of gypsum additive was examined by RX diffractometre analysis and electronic microscopy (fig.2 and 3).

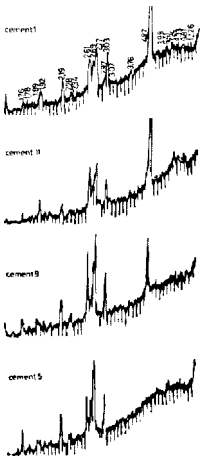

Fig.2. X-Ray analysis of hydrated cements,at 1 day

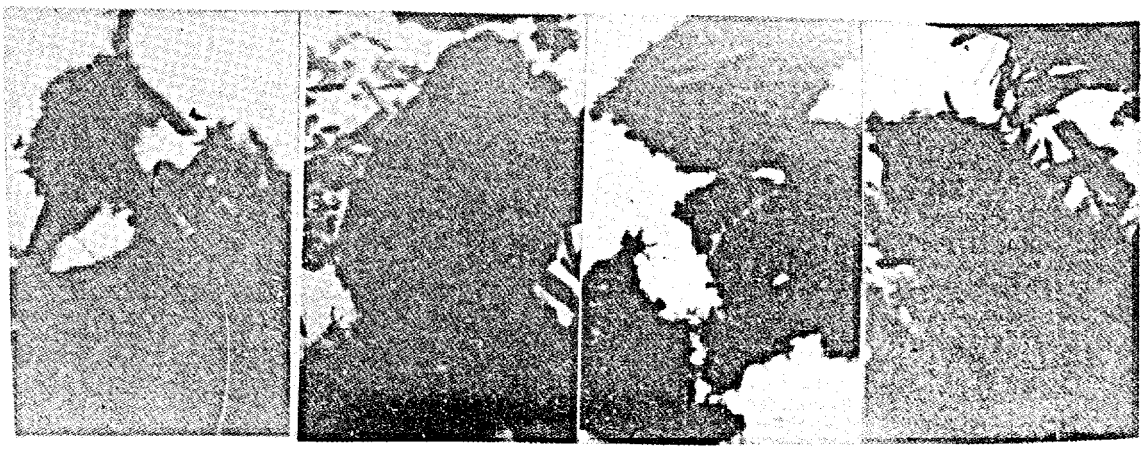

Cement 1 Cement 5 Cement 9 Cement 11

Fig.3. Electronomicroscopic image of hydrated cements, at 1 day.

The process kinetics of hydration-hydrolysis, accompanied by hydration products is slower for cements with raw phosphogypsum and is accelerated for cements with purified phosphogypsum, and in this case the cement behaviour is practically similar to the standard cement.

The results of the researches lead to establishing the solution of eliminating the harm components of phosphogypsum in order to use it as additive at cement grinding.

M.Eng.I.COTEA,Dipl.Eng.A.ROMANESCU, Dipl.Eng.C.DUMITRESCU
RESEARCH AND DESIGN INSTITUTE FOR BINDER AND ASBESTOS CEMENT INDUSTRY,ROMANIA

Researches Concerning the Harmful Components Elimination from Phosphogypsum for Using it as Cement Setting Time Regulator.

Researches concernant l'élimination des composant nocifs du phosphogypse en vue de son utilisation comme regulateur de prise du ciment.

The technological flow of purified phosphogypsum obtaining, used as additive at cement grinding, is presented în fig.4.

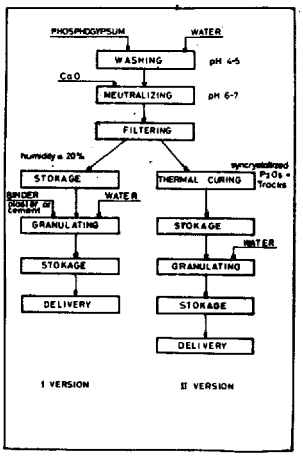

Fig.4. Technological flow of phosphogypsum purification.
I version - for common cement and cements with additive
II version - for superior cements.

C O N C L U S I O N S

From the experimental data, the following important conclusions resulted:

1.- The compositional variation of phosphogypsum that results in Romania in the manufacturing process of phosphoric acid, is in large limits due to the variety of phosphatic stone used and technological conditions, without the possibility of maintening these parametres constant.

2.- The raw phosphogypsum use as time setting regulator lead to lengthening the setting time and to the lowering the mechanical strengths especially at short terms,about 2o-3o%.

At cements with slag additive this shortening of mechanical strengths is only 1o-15%.

3.- The soluble compounds elimination in phosphogypsum by washing and neutralization up to pH=6-7 makes possible the phosphogypsum use as additive for common cement grinding,especially for slag cements.

4.- In the case of superior cements,the phosphogypsum use as setting time regulator is conditioned by P_2O_5 syncrystallized (bound as $CaHPO_4.2H_2O$) presence that imposes a suplementary preparation by thermal curing in order to eliminate it.

R E F E R E N C E S

1. V.Gh.Apreotesei,I.Samoil "Phosphoric Acid Manufacturing" vol.II,(197o).
2. Onoda Engineering and Consulting Co,LTD Japan "Phosphogypsum" leaflet 3o,(1981).
3. M.S.Tolocicova, S.V. Zapolski. " Phosphogypsum Used for setting time regulator", Tement, 3, (1979).

Dipl.eng.DUMITRESCU,CRISTINA, Dipl.eng.NISTOR,GABRIELA
RESEARCH AND DESIGN INSTITUTE FOR BINDER AND ASBESTOS CEMENT INDUSTRY,ROMANIA

Binders of Base-Acid Type Setting Used in Dental Technique.
Liants au durcissement du type base-acide,utilisés dans la technique dentaire.

Introduction

In the phosphate systems, from the orthophosphoric acid-metal oxide interaction it results phosphates with various compositions and structures that determine an adequate process kinetics, binder system properties.

The investigation of the processes that take place at phosphate binder setting leads to the conclusion that the binder properties are determined by the interaction between the two components and sparigly soluble salt formation that give spatial red with low internal pressions. The formation of some sparigly soluble interaction products is not a sufficient condition for the binder properties. A great interaction speed between the two system components leads to the internal tension and to the impossibility of a setting structure; the setting does not take place at very slow setting speed. By retarding or accelerating the process the setting process of the phosphate binders can be adjusted in order to obtain favourable physical and mechanical characteristics (1,2,3).

The researches included in this work refer to the phosphate binders of base-acid setting used in dental technique, namely the zinc phosphate cement.

Experimental data

The zinc phosphate powder was made by burning at 1100, 1200 and 1300°C a mixture of zinc oxide, magnesium oxide, silica dioxide, aluminium oxide, calcium carbonate and calcium fluoride of high purity, in various proportions, ground at a fineness of 0,0 % residue on the sieve with 10.000 mesh/cm^2.

The burning process was achieved at 2-6 hours level and rapid or slow cooling. The burned material was ground at a fineness of 0,0% residue on the sieve with 10000 mesh/cm^2.

The liquid was obtained from partial neutralization of orthophosphoric acid of 89% percentage and 1,75 g/ml density, with aluminium hydroxide and zinc oxide, at laboratory temperature or 80-100°C.

The liquid density was 1,40-1,50 g/ml and was regulated by varying the distilled water ratio .

There were researched the chemical, physical and mechanical properties of powders and liquid mix at standard consistency as well as the setting processes of these masses correlated to above mentioned properties. The chemical physical and mechanical properties examined on cement pastes were : As content, water solubility, film thickness, setting-time and compressive strength (determined by ISO methods) and pH.

The zinc phosphate cement setting was examined by diffractometre analysis.

Results and Discussions

The composition of the zinc phosphate dental cement powder is presented in table 1.

./.

Dipl.eng.DUMITRESCU CRISTINA, Dipl.eng.NISTOR GABRIELA

RESEARCH AND DESIGN INSTITUTE FOR BINDER AND ASBESTOS CEMENT INDUSTRY,ROMANIA

Binders of Base-Acid Type Setting Used in Dental Technique

Liants au durcissement du type base-acide, utilisés dans la technique dentaire

T A B L E ,1.

Powder chemical composition

Compounds	Powder chemical composition Z_1	Z_2	Z_3	Z_4
ZnO	9o,2o	89,oo	88,oo	88,oo
MgO	8,4o	1o,oo	9,oo	8,44
SiO_2	1,4o	1,oo	1,oo	o,5o
Al_2O_3	-	-	2,oo	2,oo
CaO	-	-	-	1,oo
CaF_2	-	-	-	o,o6

As for the composition of the zinc phosphate dental cement powder burned at 13oo°C, 4 hours level, the main component is the zinc oxide made evident at the X-ray analysis in fig.1. Some of the zinc oxide interacts with SiO_2 forming Zn_2SiO_4, with Al_2O_3 forming $ZnAl_2O_4$ and solid solutions with MgO.

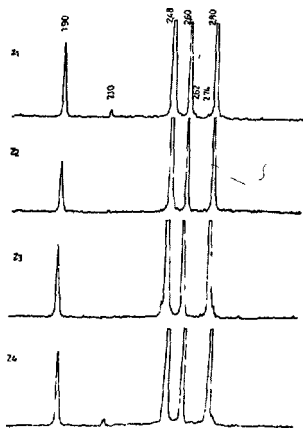

Fig.1. X-ray diagrams of powders burned at 13oo°C, 4 hours level.

By powder burning it results first, the ZnO compaction in order to improve the cement properties; the unburned ZnO reacts rapidly with the liquid that does not permit the strength structure formation.

The liquid resulted from the partial neutralization of orthophosphoric acid had a free acid content of 35-38%.

The water content of the liquid is aprox. 36%.

The chemical, physical and mechanical characteristics of the obtained cements are presented in table 2.

./.

Dipl.eng.DUMITRESCU CRISTINA, Dipl.eng.NISTOR GABRIELA

RESEARCH AND DESIGN INSTITUTE FOR BINDER AND ASBESTOS CEMENT INDUSTRY, ROMANIA

Binders of Base-Acid Type Setting Used in Dental Technique

Liants au durcissement du type base-acide, utilisés dans la technique dentaire

T A B L E 2.

Chemical, physical and mechanical characteristics of zinc phosphate cements.

Cement denomination	As Content (%)	Standard consistency (g /o,5 ml.)	Setting time (min.)	Film thickness (μm)	Compressive strength (MPa)	Soluble material (mgP_2O_5/g)	Cement pH
Z_1	o,oool9	1,2o	4 1/2	3o	75	o,48	4,8o
Z_2	o,oool8	1,3o	6 1/4	2o	9o	o,15	4,8o
Z_3	o,oool8	1,3o	7 1/4	15	98	o,17	5,2o
Z_4	o,oool8	1,35	6 1/2	15	loo	o,o3	5,6o

The increase of MgO content leads to the increase of the cement plasticity and of the mechanical strengths.

SiO_2 presence in a ratio of more than 1% generally contributes to reducing the setting time and to some lowering of burning temperature.

The CaO presence in the raw mix composition, in the presence of Al_2O_3 and SiO_2 leads to increase the plasticity and the mechanical strengths.

The calcium fluoride additive has a mineralizing effect at powder burning.

As for the liquid preparation method (at 8o-loo°C or at 2o°C) and consequently, its composition, examining the diagrams in fig.2, the following conclusions are drawn regarding the cement properties:

- the necessary powder quantity for standard consistency paste is bigger (better plasticity) in the case of the liquid prepared in cold conditions;
- the setting time is shorter for the liquid obtained in cold conditions.
- the compressive strength presents some increase in the case of using the liquid prepared in cold conditions.
- there is an increase of pH at cements made with liquid prepared in cold conditions.

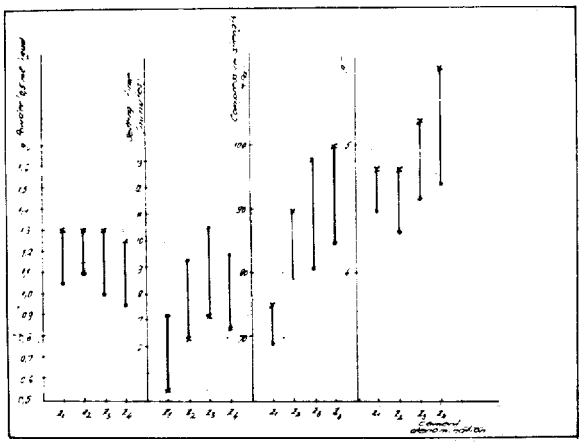

Fig.2. The influence of the liquid preparing method on the zinc phosphate properties.

x - liquid prepared at 2o°C
• - liquid prepared at 8o - loo°C.

Dipl.eng.DUMITRESCU CRISTINA, Dipl.eng.NISTOR GABRIELA

RESEARCH AND DESIGN INSTITUTE FOR BINDER AND ASBESTOS CEMENT INDUSTRY,ROMANIA

Binders of Base-Acid Type Setting Used in Dental Technique

Liants au durcissement du type base-acide, utilisés dans la technique dentaire

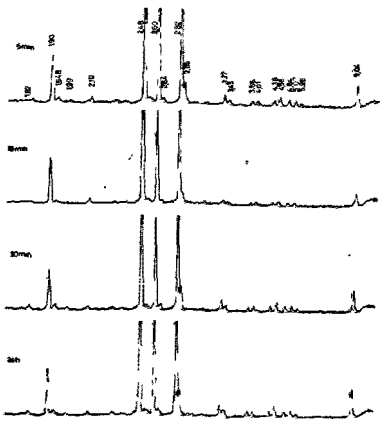

Fig.3. X-ray diagrams of the Z_1 set cement.

The rapid evolution of the reaction can be followed from the pH evolution of paste that has an accentuated growth in the first 3o minutes and then a slower one until 24 hours when the reaction is practically finished.

The structure of the set cement is a structure of composite type ; the unreacted zinc oxide particles are bound with a binder of base-acid type formed in the interaction of ZnO and MgO with H_3PO_4

The interaction of ZnO with H_3PO_4 takes place rapidly, after 5 minutes the neutral zinc phosphate $Zn_3 (PO_4)_2 . 4 H_2O$ is already formed.

Conclusions

From the examination of the experimental data the following conclusions can be drawn:

1. The main component of the zinc phosphate dental cement powder is cured ZnO, with a compact structure. The MgO, SiO_2, Al_2O_3, CaO and CaF_2 modifiers have the role of embettering the cement quality, contributing to the paste plasticity and to the mechanical strengths of the set cement.

2. The use of the liquid prepared at 2o°C, compared to the liquid prepared at 8o-1oo°C leads to the increase of the paste plasticity, the mechanical strengths and pH.

3. A rapid interaction takes place between the powder and the liquid with the final-formation of $Zn_3 (PO_4)_2 . 4 H_2O$, quite unsoluble that has a hardened spatial red that represents the strength structure.

The structure of the set cement is a structure of composite type; the unreacted ZnO particles are bound by the binder of base-acid type hardening formed by interaction of ZnO with H_3PO_4.

./.

Dipl.eng.DUMITRESCU CRISTINA, Dipl.eng.NISTOR GABRIELA

RESEARCH AND DESIGN INSTITUTE FOR BINDER AND ASBESTOS CEMENT INDUSTRY, ROMANIA

Binders of Base-Acid Type Setting Used in Dental Technique
Liants au durcissement du type base-acide, utilisés dans la technique dentaire

REFERENCES

1. S.L.Golîko - Volfson and others., Himiceskie asnovî tehnologhii i primenenia fosfatnîh aviazok i pokrîtii, Moskva, Izd.Himia, (1968)

2. I.Teoreanu and others. - Physico-chemical basis of anorganic binder setting Didactica şi pedagogică Publishing House, Bucharest, (1971).

3. R.Craig - Restorative Dental Materials, (1980).

CONSTANTIN POPESCU, B.E., CONSTANTA ANTONESCU, B.Sc.

Research and Design Institute for Binder and Asbestos Cement Industry, Romania

CLINKER MANUFACTURING WITH ALKALI, CHLORINE AND SULPHUR COMPOUND CONTROLLED CONTENT BY GAS DEVIATION IN STAGES CLINKERIZATION EQUIPMENT.

1.1. The researches made and published especially in the last twenty years made evident the importance of Knowing and controlling the cement content of alkali and sulphur compounds regarding their harm influence on the cement quality and, together with the chlorine and raw materials compounds on the way of flowing the raw mix circulation through the clinkerization equipment, and the necessary measures to be taken in order to avoid aggregat products.

1.2. The causes and the way in which the alkali compounds influence on the raw mix behaviour in the clinkerisation equipment, as well as the measures that can be taken to control the harm effects, are indicated by these components behaviour during heating, at melting temperatures and gasifying point respectively. Heating, behind the melting point has as result the evaporation and volatilization - with or without decomposition - and their passing through the gas flow, situation in which they can react with, for example, the sulphur dioxide coming from the fuel combustion and then, with the raw *mix* after thermal curing, and thus forming the compounds recirculation and formation. [1,2,3,4].

1.3. The gravimetric proportion of the compounds that are released from the raw mix during its heating in the kiln to pass in the gas flow and is named " primary volatilization coefficient" and is noted ε_1 while the " secondary volatilization coefficient" - noted ε_2 represents the gravimetric proportion of the same compounds that are released from the kiln material resulted from their recirculation.

1.4. The compounds from the raw materials and from the fuel as well as those formed from the recirculation, that have the melting point below the clinkerization temperature can generate or encourage the sediment formation on the equipment walls whose development impose periodical interventions for release, generally with working breake.

These phenomena are more pregnant in the case of the clinkerization equipment with technological process fractioning and especially in the case of suspension preheaters, where the temperature system and the intimate contact between gas and powdery raw materials that are found is a suspension date in the connection zone between kiln and preheater that represents special favourable conditions for gas compounds interaction and condensation, the frequency with which it could happen in some cases, in acceptable if there hadn't been forseen adequate measures for adapting the working conditions and the equipment in order to eliminate them.

./.

CONSTANTIN POPESCU B.E., CONSTANTA ANTONESCU B.Sc.
Research and Design Institute for Binder and Asbestos Cement Industry, Romania

P

Because of the up to date character, and practically the generalization of their adoption, at present and in the near future in the cement industry, these equipments-with or without double feeding with fuel (precalcination) - are taken into consideration in the present work.

1.5. Stages clinkerization equipments offer in the same time adequate possibilities for content controlling and adjustment of the respective harmful (noxius) compounds by deviation - regularly partial - of gases at kiln outlet and their evacuation from the equipment, which is known as " alkali valve", Or more general "by pass" as it is shown in fig.1.

1.6. This work establishes the calculation relationings of gas proportion that must be deviated at kiln outlet in order to fit the prescribed limits for eliminating the negative effects on the cement quality and working equipment of chlorine, sulphur or any similar compounds that are brought in the system by the raw material mix and the fuel.

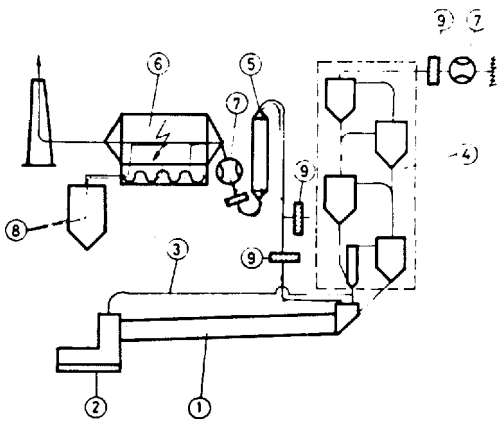

Figure no.1 Diagram of clinkerization equipment with gas deviation

gas
exhausted material

1 Rotary kiln
2 Clinker cooler
3 Tertiary air pipe
4 Raw material mix preheater
5 Tower for exhausted gases conditioning
6 Precipitator
7 Exhauster
8 Deposit for material rich in controlled (+) component (+)
9 Register for gas flow control

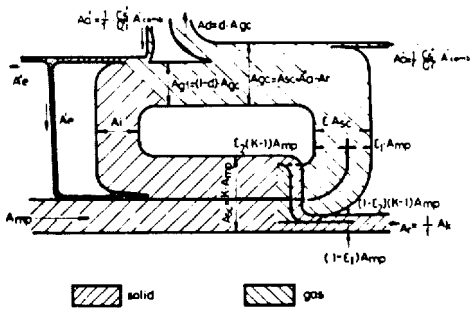

Figure no.2 Diagram of A compound circulation in the clinkerization equipment

./.

CONSTANTIN POPESCU B.E., CONSTANTA ANTONESCU B.Sc.

Research and Design Institute for Binder and Asbestos Cement Industry, Romania

2. Calculation of deviated gas proportion

2.1. Preliminary relations

Volatile compounds circulation and the denominations used are shown in fig.2, from which it results on the one hand Ar expression :

$$Ar = \left[(1 - \mathcal{E}_1) + (K-1)(1 - \mathcal{E}_2) \right] Amp \qquad (1)$$

and on the other hand the element (compound) A balance on the equipment whole :

$$Amp + A'a + A''a = Ar + d\,(K\,Amp + A''a - Ar) \qquad (2)$$

From (1) it results :

$$K = \frac{Ar + (\mathcal{E}_1 - \mathcal{E}_2)\,Amp}{(1 - \mathcal{E}_2)\,Amp} \qquad (3)$$

K elimination between (1) and (2) leads to the relations :

$$Ar = \frac{(1-d)\left[Amp\,(\mathcal{E}_1 - \mathcal{E}_2) + A''a\,(1 - \mathcal{E}_2)\right] + A'a\,(1 - \mathcal{E}_2) + Amp\,(1 - \mathcal{E}_1)}{1 - \mathcal{E}_2\,(1 - d)} \qquad (4)$$

$$d = (1 - \mathcal{E}_2)\,\frac{Amp + A'a + A''a - Ar}{(\mathcal{E}_1 - \mathcal{E}_2)\,Amp + (1 - \mathcal{E}_2)\,A''a + \mathcal{E}_2\,Ar} \qquad (5)$$

By Ar elimination between (1) and (2) another expression is found for d :

$$d = \frac{\left[\mathcal{E}_1 - (K-1)(1-\mathcal{E}_2)\right] Amp + A'a + A''a}{\left[\mathcal{E}_1 + (K-1)\,\mathcal{E}_2\right] Amp + A''a} \qquad (6)$$

and K expression respectively :

$$K = \frac{\left[(\mathcal{E}_2 - \mathcal{E}_1)\,Amp - A''a\right] d + (1 + \mathcal{E}_1 - \mathcal{E}_2)\,Amp + A'a + A''a}{\mathcal{E}_2\,Amp\,d + (1-\mathcal{E}_2)\,Amp} \qquad (7)$$

The minimum residual content is achieved when all gases are deviated at kiln outlet, when relation (4) has d = 1; it results after calculation :

$$\min Ar = (1 - \mathcal{E}_2)\,A'a + (1 - \mathcal{E}_1)\,Amp \qquad (8)$$

2.1.1. In the case of some existing equipment the volatility coefficient $\mathcal{E}_2$ can be calculated using chemical analysis - Amp and Asc - and volatilization aptitudes - $\mathcal{E}_1$ and $\mathcal{E}$ - of the raw material mix and of the solid material at kiln inlet using the relation :

$$\mathcal{E}_2 = \frac{Asc\,\mathcal{E} - Amp\,\mathcal{E}_1}{Asc - Amp} \qquad (9)$$

./.

CONSTANTIN POPESCU B.E., CONSTANTA ANTONESCU B.Sc.

RESEARCH AND DESIGN INSTITUTE FOR BINDER AND ASBESTOS CEMENT INDUSTRY

TABLE NO 1

COMPULSORY CONDITIONS FOR VOLATILE COMPONENTS AND CALCULATION RELATIONS FOR GAS DEVIATION RATIO

HARMFUL COMPONENTS		RESTRICTIVE CONDITIONS			CALCULATION RELATIONS AND FIGURE	COMPULSORY CONDITIONS
		ATM	ADMISSIBLE LIMIT			
			%	VAL.		
Cl^-	max. admissible %	EQUIPEMENT FUNCTIONALITY	%	0,015	$d\alpha(1-\xi_2)\frac{A_{mp}\cdot A_0' - A_0'' \cdot m\alpha A_r}{(\xi_1-\xi_2)A_{mp}\cdot(1-\xi_2)A_0'-\xi_2 m\alpha A_r}$; $C_S = C_{SO}\cdot d(455-507\,\varphi+17\,\varphi^2)$; $C_S = C_{SO}\cdot d(392-350\,\gamma+8\,\gamma^2)$; $K=\frac{m\alpha A_r(\xi_1-\xi_2)A_{mp}}{(1-\xi_2)A_{mp}}$, Fig. No 3	$m\alpha \cdot A_r \leq 0,015\%$ $\xi_2 \neq 1$
			g/Nm³	12	$c\xi_2\gamma_0 d^2\cdot\left\{c\left[\gamma_0(1-\xi_2)-\xi_2(\gamma_0'-\gamma_0)\right]-\xi_1 A_{mp}\cdot A_0'-A_0''\right\}d-\xi_1 A_{mp}\cdot A_0'-A_0''-c(1-\xi_2)(\gamma_0'-\gamma_0)=0$; $C_S = C_{SO}\cdot d(455-507\,\varphi+17\,\varphi^2)$; $C_S = C_{SO}\cdot d(392-350\,\gamma+8\,\gamma^2)$, Fig. No 3	$c\neq 0$ $d\in[0,1]$
Na_2O	max. admissible %	CEMENT QUALITY PROVIDING	%	0,6	$Ad^2+Bd+C=0$ $A=(A_1'-\alpha A_2')\xi_2'\xi_1'-\xi_2'\left[A_{mp}'(\xi_1'-\xi_2')+A_0'(1-\xi_2')\right]\cdot\alpha-\xi_2'\left[A_{mp}''\xi_1'-\xi_2'\right]+A_0''(1-\xi_2')$,	$\alpha_k = 0,58$
K_2O	max. admissible %	EQUIPEMENT FUNCTIONALITY	%	1,0	$B=(A_1'-\alpha A_2')(\xi_2'-\xi_1'-2\xi_1'\xi_2')+(1-2\xi_2')\left[A_{mp}'(\xi_1'-\xi_2')+A_0'(1-\xi_2')\right]\cdot\alpha-(1-2\xi_2')\left[A_{mp}''(\xi_1'-\xi_2')+A_0''(1-\xi_2')\right]+\xi_2'\left[A_{mp}'(1-\xi_1')+A_0'(1-\xi_2')\right]\cdot\alpha+\xi_2'\left[A_{mp}'(1-\xi_1')+A_0'(1-\xi_2')\right]$ Fig No 3	$\alpha < 1$
					$C=\left[(A_1'-\alpha A_2')-(A_0'-\alpha A_0'')\right](1-\xi_2')(1-\xi_1'-\xi_2')$	
SO_3	$C_2H_5^-$ max. admissible %	EQUIPEMENT FUNCTIONALITY	SO_3/ alkalies molar ratio	(+) 1,0	$Ad^2+Bd+C=0$ $A=\xi_2'\xi_1'\left[A_{mp}'(\xi_1'-\xi_2')+A_0'(1-\xi_2')\right]\cdot\alpha-\xi_2'\xi_1'\cdot\left[A_{mp}''(\xi_1'-\xi_2')+A_0''(1-\xi_2')\right]+\beta\cdot\xi_2'\cdot\xi_1'\left[A_{mp}''\xi_1'-\xi_2'\right]+A_0''(1-\xi_2')$	$\alpha<1$ $\beta=1,55$ SO_3 $\beta=1,875$ S
SO_3	max. admissible %				$B=(\xi_2'\cdot\xi_1'-\xi_2'\xi_1')\cdot\left[A_{mp}'(\xi_1'-\xi_2')+A_0'(1-\xi_2')\right]-\alpha(\xi_2'-\xi_1'-2\xi_1'\xi_2')\left[A_{mp}'(\xi_1'-\xi_2')+A_0'(1-\xi_2')\right]-\beta\cdot(\xi_2'\xi_1'-\xi_2'\cdot\xi_1')\left[A_{mp}'(\xi_1'-\xi_2')+A_0'(1-\xi_2')\right]-\xi_2'\xi_1'\left[A_{mp}'(1-\xi_1')+A_0'(1-\xi_2')\right]-\xi_2'\xi_1'\left[A_{mp}'(1-\xi_1')+A_0'(1-\xi_2')\right]\cdot\alpha-\xi_2'\xi_1'\left[A_{mp}'(1-\xi_1')+A_0'(1-\xi_2')\right]\cdot\beta$	
Na_2O	max. admissible %			(+) 1,25	$C=\left[(1-\xi_2')\xi_1'+\xi_2'\xi_1'\right]\left[A_{mp}'\xi_1'\xi_2'+A_0'(1-\xi_2')\right]-\left[(1-\xi_2')\xi_1'+\xi_2'\xi_1'\right]\left[A_{mp}'\xi_1'\xi_2'+A_0'(1-\xi_2')\right]\beta\left[(1-\alpha)\xi_2'\xi_1'+\xi_2'\xi_1'\left[A_{mp}'\xi_1'\xi_2'+A_0'(1-\xi_2')\right]+\xi_2'\xi_1'\left[A_{mp}'\xi_1'\xi_2'+A_0'(1-\xi_2')\right]\right]\beta\xi_2'\xi_1'\xi_2'\xi_1'\left[A_{mp}'\xi_1'\xi_2'+A_0'(1-\xi_2')\right]+\beta\xi_2'\xi_1'\xi_2'\xi_1'\left[A_{mp}'\xi_1'\xi_2'+A_0'(1-\xi_2')\right]$	$\beta<0,97$ SO_3 $\beta\geq 2,42$ S
K_2O	max. admissible %				$D=(1-\xi_2')(1-\xi_1')\left\{\left[A_{mp}'(\xi_1'\xi_2')+A_0'(1-\xi_2')\right]\cdot\alpha-\xi_2'(1-\xi_1')\left\{\left[A_{mp}'(1-\xi_1'\xi_2')+A_0'(1-\xi_2')\right]\right\}\cdot\beta(1-\xi_2')\alpha+\xi_2'\left\{\left[A_{mp}'\xi_1'\xi_2'+A_0'(1-\xi_2')\right]\left[A_{mp}'(1-\xi_1'\xi_2')+A_0'(1-\xi_2')\right]\right\}$ Fig No 3	$\alpha<0,66$

ALKALINE OXIDES EXPRESSED AS Na_2O equivalent

Table no.1 shows the relations for the deviation proportion calculation in various situations taken into consideration.

3. Influence of evacuation gas deviation from the kiln on the specific consumption of fuel at clinker manufacturing.

Gas deviation at kiln outlet and their elimination in the atmosfere has as a result the loss of their physical heat and as a consequence, the achievement of a specific fuel consumption at clinker manufacturing higher than in the case of using the respective gases at raw materials heating, situation taken as standard.

The specific fuel consumption that uses natural gases with inferior caloric power of 8500 Kcal/Nm3, was calculated from the thermal balance for the clinkerization equipment with such dimentions as to work without gas deviation in order to achieve specific fuel consumption - noted as C_{S0} between 760 and 825 Kcal/kg.clinker.

The results are expressed according to the specific reference consumption - C_{SO} - and to the deviation proportion - d - on the one hand, and on the other to the proportion between fuel discharge introduced at the first combustion stage and the total - φ - in the relation :

$$C_S = C_{SO} + d\ (455 - 507\varphi + 17\varphi^2)$$

showed graphically in figure no.3.

./.

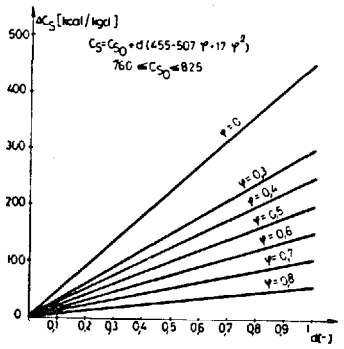

Figure no.3 Specific fuel consumption increase according to the gas deviation proportion at Kiln outlet and to the combusted fuel specific consumptions ratio at first stage and total

R E F E R E N C E

1. Weber, P. — Les problemes relatifs aux alcalis et l'élimination de ceux-ci dans les fours rotatifs par voie sèche economisant la chaleur. Zement-Kalk-Gips,nr.8/1964(broşură Polysius)

2. Duda,H. Walter — Cement -Data - Book (Ed.II) Bauverlag G.M.B.H. Wiesbaden and Berlin Macdonald & Evans, London.

3. Biege,W. Neal Parson,J.Ladd — Bypass systems for preheater and flash calciner kilns Pit and Quarry, July, 1978

4. Norbow, R. Henning — Wet or dry process kiln for your new installation Rock Products, May 1974.

5. Garret, M.H. Murray, J.A. — Improving thermal efficiency-design and operation considerations.Part.IV. Rock products, August 1974

6. Svendsen, J. — Alkaliarmer Zement aus Hochalkali-Rohstoffen mit energie-viertschaftlich günstiger Verfahrenstechnik. Zement-Kalk-Gips, nr.6/1978.

./.

7. Garret, M.Hoke — Energy conservation by the V.S.Cement Industry. Part.I. Pit and Quarry, March, 1976

8. Elkjaer, P.H. — Systèmes de precalcination Cements, betons,platres, nr.723, 2/1980.

9. Gouda, R.G. — Raw mix the key for a successful and profitable cement plant operation. World Cement Technology, nov.1979.

10. Locher, F.W. Sprung, S., Opitz, D. — Comunicare prezentată la Siliconf,Budapesta 1981. Reaktionen im Bereich der Ofengase Zement-Kalk-Gips, nr.1/1972.

11. Rössner, P., Feige, F., Danowski,W. Keiser, J. — Betriebseargebnisse mit dem ZAB-Vorwärmer im Eichofelder. Zementwerke Deuna unter den Bedigungen hoher Alkali-und Chloridbelastungen. Zement-Kalk-Gips, nr.12/1977.

12. Portland Cement Onoda — Informaţii tehnice asupra procedeului R.S.P.

13. Pieczora, Stefan — Zagadnienia alkaliow, chlorkow i siarki w procesie wypalania Klinkiera portlandzkiego w piecach obrotowychna metode sucha Cement, Wapro, Gips nr.8-9/74.

Dipl.Eng.ALEXANDRU ROMANESCU, Dipl.Eng.CRISTINA DUMITRESCU

RESEARCH AND DESIGN INSTITUTE FOR BINDER AND ASBESTOS CEMENT INDU TRY ROMANIA

Considerations Concerning the Hardening Mechanism of the Controlled Expansion Cements

Les considérations en ce qui concerne le mécanisme de renforcement aux ciments à expansion contrôle.

I N T R O D U C T I O N

The gas well cementing requires a special cement that must assure the sealing of drilling and extracting column against the well hole wall in order to avoid gas losses.

The following things were taken into consideration in order to chose this cement type: cement paste fluidity and density must correspond for cementing at high temperature and pressure conditions; the mehcanical strength of the hardened cement must assure the well starting and working; the expansion must be achieved in an optimal period and must assure the sealing up between the column and the well hole wall.

For the specific conditions of gas wells in Romania the cements must have the following physico-mechanical characteristics: thickening time of min.13o minutes at 7o°C and 4oo bars, compressive strength at 1day of min.3,5 MPa and at 3 days of min. 7,o MPa and expansion of o,2 - 1,o%.

The expansion phenomenon of the investigated cements is due to the calcium hydroaluminate sulphates in the hardening process and especially the ettringite formation. The other physico-mechanical characteristics are conditioned by the nature and the relations established among the mineralogical constituents of the material used (1-4).

Experimental data

The investigated expansion cements were made by grinding together the Portland and aluminous clinker, trass or slag and gypsum.

The chemical composition of the raw materials used is presented in table 1.

Table 1

Raw material	Oxidic composition (%)						Mineralogical composition (%)	
	PC	SiO_2	Al_2O_3	Fe_2O_3	CaO	SO_3	C_3S	C_3A
Portland clinker	2,79	21,13	5,oo	5,51	61,96	o,48	54,68	3,94
Aluminous clinker	1,69	2,6o	43,3o	13,73	29,84	-	-	-
Trass	1o,74	56,37	1o,91	2,16	8,87	o,o2	-	-
Slag	o,2o	35,84	12,5o	o,6o	43,27	o,17	-	-
Gypsum	o,o1	o,2o	o,3o	o,o3	32,73	46,49	-	-

The manufacturing formulas of the investigated expansion cements are presented in table 2.

Table 2

Cement symbol	% content of:					Blaine specific surface (cm2/g)
	Portland clinker	Aluminous clinker	Trass	Slag	Gypsum	
a_1 ... a_4	62	12	17	-	9	28oo - 35oo
b_1 ... b_4	6o	1o	2o	-	1o	28oo - 35oo
c_1 ... c_2	39	12	+/- 4o	-	1o	28oo - 3ooo

Dipl.Eng.ALEXANDRU ROMANESCU, Dipl.Eng.CRISTINA DUMITRESCU

RESEARCH AND DESIGN INSTITUTE FOR BINDER AND ASBESTOS CEMENT INDUSTRY,ROMANIA

Considerations Concerning the Hardening Mechanism of the Controlled Expansion Cements

Les considérations en ce qui concerne le mécanisme de renforcement aux ciments à expansion contrôle.

Table 2 /cnt'd

Cement symbol	% content of: Portland clinker	Aluminous clinker	Trass	Slag	Gypsum	Blaine specific surface (cm2/g)
d	62	12	-	17	9	3ooo
e	6o	1o	-	2o	1o	3ooo
f	39	12	-	4o	9	35oo

The cements made were tested from the ysico-mechanical behaviour point of view at high pression and temperature conditions, with or without modifying setting time additive - lignotartrine (L.C.[x])

In order to examine the hydration-hydrolysis processes, chemical,diffractometre and electronomicroscopic analyses were made, on specimens having a w/c ratio of 1 at various hydration periods.

Results and Discussions

The cements made following the formulas given in table 2, of a fineness of 3ooo om2/g Blaine specific surface, were characterized by physico-mechanical properties that are presented in table 3.

Table 3

Cement symbol	Thickening time at 7o°C and 4oo bars (min.)	Linear variation in water at 6o°C (%) 1d	3d	7d	Compressive strength in water at 6o°C (MPa) 1d	3d
a_2	112	o,7o6	o,756	o,769	3,o	9,1
a_2+ LC	15o	o,668	o,747	o,753	1o,4	16,8
b_2	135	o,419	o,412	o,416	3,6	9,9
b_2 + LC	18o	o,612	o,669	o,682	3,8	13,1
C_2	98	o,595	o,587	o,587	4,2	8,3
C_2 + LC	135	o,686	o,69o	o,691	9,2	15,6
d	12o	o,259	o,271	o,271	5,7	9,9
d + LC	17o	o,15o	o,162	o,165	16,6	36,4
e	1o8	o,271	o,283	o,289	6,1	11,8
e + LC	14o	o,183	o,196	o,196	17,5	41,2
f	93	o,571	o,583	o,589	15,4	22,3
f + LC	176	o,o41	o,o34	o,o28	18,6	45,o

Examining the results presented in table 3, the following interpretations can be made:

- The thickening times of no additive cements present values closed to the necessary minimal limit,generally, below this limit.In order to achieve sdequate thickening times lignotartrine- LC was used as retarder.

x) L.C. Calcium lignosulphonate with tartrate.

Dipl.Eng.ALEXANDRU ROMANESCU, Dipl.Eng.CRISTINA DUMITRESCU
RESEARCH AND DESIGN INSTITUTE FOR BINDER AND ASBESTOS CEMENT INDUSTRY,ROMANIA

Considerations Concerning the Hardening Mechanism of the Controlled Expansion Cements

Les considérations en ce qui concerns le mécanism de renforcement aux ciments à expansion contrôle.

- The linear expansion at trass cements as expansion stabilizer had values within the expected limits of o,45 - o,7o%. The L.C. additive at trass cement did not significantly influence the expansion.

The cements made with slag as expansion stabilizer present more reduced expansions, and when are LC added decrease below the limit that is necessary to used them at gas well cementing.

- The compresive mechanical strengths are correlated to the expansion value and are characterized by higher values for slag cements as compared to the ones with trass as expansion stabilizer (5,7 - 15,4 MPa at 1 day as compared to 3,o-4,2 MPa).

The LC additive in cement pastes leads to the increase of the mechanical strengths.

The fineness grinding influence on the physical and mechanical properties of investigated expansion cement was examined for "a" cement and is presented in fig.1.

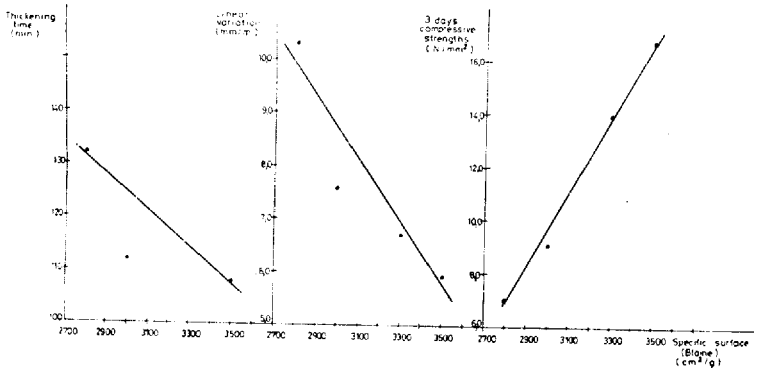

Fig.1. Grinding fineness influence of "a" cement on the physical and mechanical properties.

The increase of the grinding fineness from 28oo to 35oo cm2/g (Blaine Specific Surface) leads to the thickening time and expansion diminution and mechanical strengths increase.

The hardening processes kinetics was studied by determining the ettringite content (table 4), diffractometric analysis (fig.2) and electronic microscopy (fig.3).

Table 4

Cement denomination	a_2		a_2+LC		d		d + LC	
	1 day	3 days	1 day	3 days	1 day	3 days	1 day	3 days
Etringite content	12,18	13,4o	11,9o	11,98	8,1o	9,18	6,o4	6,5o

./.

Dipl.Eng.ALEXANDRU ROMANESCU, Dipl.Eng.CRISTINA DUMITRESCU
RESEARCH AND DESIGN INSTITUTE FOR BINDER AND ASBESTOS CEMENT INDUSTRY,ROMANIA

Considerations Concerning the Hardening Mechanism of the Controlled Expansion Cements

Les considérations en ce qui concerne le mécanism de renforcement aux ciments à expansion contrôle.

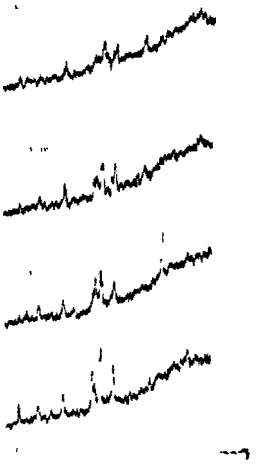

Fig.2.- X-ray diagrams of the hydrated cements, at 1 day.



a_2 Cement a_2 + LC cement d cement d + LC cement

Fig.3.- Electromicroscopic image of the hydrated cements, at 1 day.

Examining the data from table 4 and fig.2 and 3, it is made evident the fact that the hydration - hydrolysis processes kinetics is more accelerated from the first hardening terms at trass cement used as stabilizer as compared to the slag cements. LC additive leads to the slowing of the hydration process.

There can be seen that the calcium hydrosulphate- aluminate mechanism formation, particularly the trisulphate one, correlated to their ratios, the formation kinetics and the equilibrium conditions are determinant factors for expansion.

As a consequence of the obtained results, at present, the expansive cement based on mixture is manufactured and used at gas well cementing, that leads to the elimination of the gas losses by improper sealings that used to happen when common cement was used.

C O N C L U S I O N S

Examining the experimental data the following important conclusions can be drawn:

./.

Dipl.Eng.ALEXANDRU ROMANESCU, Dipl.Eng.CRISTINA DUMITRESCU

RESEARCH AND DESIGN INSTITUTE FOR BINDER AND ASBESTOS CEMENT INDUSTRY,ROMANIA

5

Considerations Concerning the Hardening Mechanism of the Controlled Expansion Cements

Les considérations en ce qui concerne le mécanism de renforcement aux ciments à expansion contrôle.

P

1. There can be made cements with controlled expansion for cementing at high temperature and pression conditions (70°C and respectively 400 bars) by grinding at 3000-3500 cm^2/g (Blaine specific surface) of same mixtures of ferroportland clinker aluminous clinker and gypsum. LC additive is used in order to achieve the thickening time.

2. The cements made with slag as expansion stabilizer present more reduced expansions that with LC additive, lower below the limit necessary to use them at gas well cementing.

3. The expansion is achieved on the basis of the calcium hydrosulphate-aluminate formation, particularly the trisulphatated one, correlated to their rations, their formation kinetics and equilibrium conditions that are formed in the expansive cement.

REFERENCES

1. Mehta P, Polivka M - Expansive Cements (principal rapport),Proc.Sixth.Intern.Cong. Chem.Cements, Moscow (1974).

2. Budnikov, P.P., Kravcenko,I.V. - Expansive Cements (Principal rapport) Proc.Fifth Intern Symp.Chemistry of Cement,Tokio (1968).

3. Teoreanu,I, Dumitresou C, Mechanisms of controlled expansion cements hardening, Cement and concrete Research, 12,141-155, (1982).

4. Teoreanu,I, Munteanu M, - Revue Roumaine de Chimie, 3,135-149 (1985).

eng.ROMANESCU,ALEXANDRU,eng.BUCEA,LIANA,Eng.AMZICA,FLORIN

RESEARCH AND DESIGN INSTITUTE FOR BINDER AND ASBESTOS CEMENT INDUSTRY,ROMANIA

Clinker Compositional Field Modification for Lowering its Formation Temperature.

Romanian researches, as well as researches in other countries (1), (2),(3), aiming at a hydraulic cement obtaining that need less fuel in the manufacturing process tend on the one band to reduce the $CaCO_3$ content in the raw material mix and on the other hand, to the components formation at temperature below 1450°C. These were the reasons for the study of the compositional field of belitic sulphate aluminate clinker.

The laboratory researches proved the existance of cements of a mineralogical composition in a $C_2S - C_4AF - (C_4A_3\bar{S} + C\bar{S})$ ternary diagram. Taking into account the laboratory results the clinker was manufactured in a pilot plant with a rotary kiln of Ø 1,2 m.and L = 17 m.and an output of aprox.o,5 t/h.

The mineralogical composition of the obtained clinker was within these limits:

- β - bilcalcic silicate ($\beta - C_2S$) : 45 -5o%
- tetracalcic sulphatealuminate ($C_4A_3\bar{S}$) : 15-25%
- tetracalcic ferrialuminate (C_4AF) 15-2o%
- calcium sulphate ($C\bar{S}$) : lo-15%

For the SO_3 retention in clinker, the combustion was made in a highly oxidant air and the material temperature in the clinkerization zone was 1250°C.

The results of the determinations for the boundless calcium oxide shows that the clinkerization process determined the complete bound of the oxide up to values of o,o3-o,11% free CaO.

The clinker X-ray analysis indicates the formation of four mineralogical constituents in the mineralogical composition (figure 1).

Figure 1

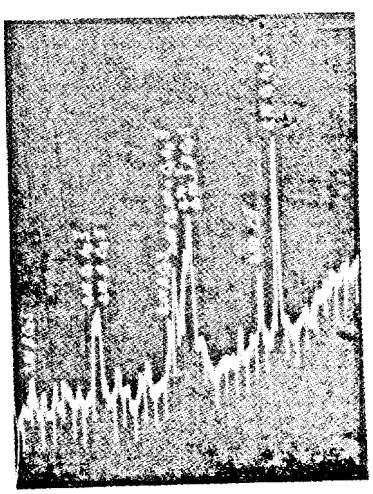

Diafractogram of belite sulphate aluminate clinker obtained in the pilot plant.

The optical microscope analysis made on these clinkers made evident a micro-crystaline structure with crystalized bicalcic silicate with dimensions of.

./.

eng.ROMANESCU ALEXANDRU, eng.BUCEA LIANA, eng.AMZICA FLORIN

Research and Design Institute for Binder and Asbestos Cement Industry,Romania

5-3o microns and tetracalcic sulphatealuminate with dimensions of less than 5 microns, having sometimes up to lo microns.

The ferrialuminate mass is placed in the connate spaces (figure 2 and 3).

Figure 2



Figure 3

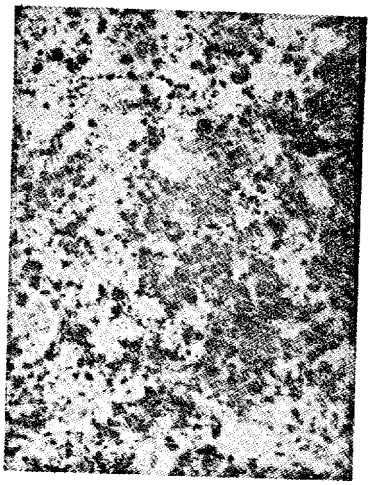

Microphotos of belitic sulphate aluminate clinker obtained in the pilot plant.

The clinkers were ground at a fineness, measured by Blaine specific surface, of about 5ooo cm2/g, without gypsum or other additives, and the cements were tested on plastic mortars.

The results of the physical and mechanical tests for the obtained cements are presented in table 1.

TABLE 1

Specimen no.	Cement curing time (days)	Setting (minutes)		Mechanical strengths on plastic mortars (N/mm2)									
		Initial	Final	Bending					Compression				
				2d	7d	28d	9od	18od	2d	7d	28d	9od	18od
o	1	2	3	4	5	6	7	8	9	1o	11	12	13
1	1-2	11	21	3,5	3,9	6,2	6,9	8,1	21,8	3o,3	4o,4	52,4	59,5
1	9o	-	-	3,3	3,7	6,o	-	-	21,o	29,5	37,2	-	-
2	1-2	12	25	3,8	5,o	6,9	8,1	-	25,1	34,7	44,4	52,6	-
2	6o	-	-	3,7	4,8	6,6	-	-	25,o	34,6	42,8	-	-

T h e s e data show that from the belite sulphate aluminate clinkers there can be obtained cements of rapid setting and hardening with mechanical compressive strength at 2 days of 21-25 N/mm2.and at 28 days of 4o-44 N/mm2.

eng.ROMANESCU ALEXANDRU, eng.BUCEA LIANA, eng.AMZICA FLORIN
Research and Design Institute for Binder and Asbestos Cement Industry,Romania

P

The mechanical strengths increase by 14% from 28 days to 9o days for bending traction and by 19% for compression.

The cement curing for 6o or even 9o days determines mechanical strengths reduction any other problems than average cements.

Belite sulphate aluminate clinker grinding aptitude was determined comparatively to an average Portland clinker on laboratory scale, in a counter mill in order to measure the electric power consumption.

Figure 4

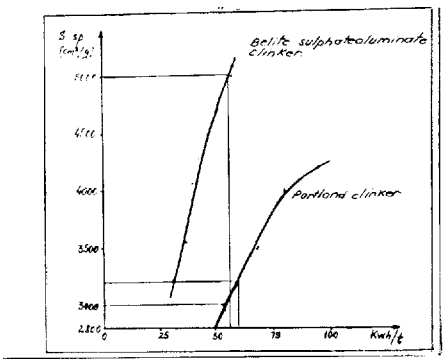

Grinding aptitude of belite sulphate aluminate clinker compared to that of common Portland clinker.

The curves in figure 4 show that this type of clinker has a good clinker aptitude, so that the electric power consumption for the achievement of a 5ooo cm2/g fineness is no higher than the one used for a 3ooo-32oo cm2/g fineness of average Portland cements.

The belite sulphate aluminate cement was tested on concretes and the most important conclusions (table 2) are the following:

- the concrete must be put in work in half an hour from the preparation, it can be used in the prefabricated industry.

- the B.2oo concrete for the 315 kg.cement/m3 dosis for d_{max} = 31 mm.and for 355 Kg Cement/m3 dosis for d_{max} = 16 mm

- the B.25o concrete for the 35o kg.cement/m3 dosis for d_{max}.= 31 mm.and for for 385 kg.cement/m3 dosis for d_{max}.= 16 mm.

TABLE 2

No.	Aggregate d_{max}.	Cement dosis	Water l/m3	Tap-ping	Density Kg/m3.	Compresion strength N/mm2						
						8h	12h	16h	1d	3d	7d	28d
o	1	2	3	4	5	6	7	8	9	1o	11	12
1.	31	315	2oo	5	236o	-	-	-	9,4	13,5	16,3	23,5
2.	31	35o	2oo	5	235o	5,8	8,6	11,o	12,8	15,o	17,5	29,9

./.

o	1	2	3	4	5	6	7	8	9	1o	11	12
3.	16	355	22o	9	231o	3,o	4,3	4,7	5,9	7,6	8,6	23,4
4.	16	385	22o	8	231o	1,8	3,4	4,o	6,6	9,6	11,9	31,2

Taking into account that this clinker is obtained from a raw material mix with a $CaCO_3$ content of aprox.2o% smaller than average clinkers and with a clinkerization temperature of 2oo°C lower, the theoretical heat consumption necessary for the belite sulphate aluminate clinkers was calculated. The obtained value is 3o3 Kcal/Kg clinker compared to 43o-45o Kcal/Kg.clinker for average Portland clinkers.

The low heat consumption, a good grinding aptitude and mechanical strengths at 28 Days of minimum 4o N/mm2 prove the advantages of this type of clinker.

REFERENCES

1. P.K.Meh ta - World Cement Technology, 11, no.4 (198o)
2. G.Sudih, A.O. - Chem.Abstr.9o 1o8911 (1979)
3. I.V.Timaşev, - Tement, no.5 (198o)

Dr.eng.MARIA ENCULESCU

Research and Design Institute for Binder and Asbestos Cement Industry,Romania

CONTRIBUTIONS TO CLINKER FORMING KINETICS.
CONTRIBUTIONS SUR LA CINETIQUE DE LA FORMATION DU CLINKER.

SUMMARY The paper briefly deals with clinkering kinetics of the aluminous and portland clinkers specific mineralogical compounds.

Clinkering ability of the raw meals for white portland clinkers is shown.

It is also shown clinkering ability of the raw meals used for white aluminous refractory clinkers based on calcium monoaluminate and dialuminate.

Finally, clinkering ability of the raw meals based on slag coming from Ferrous Metallurgy Works Galaţi is described.

1 - CLINKERING KINETICS OF THE RAW MEALS

Clinkering kinetics of the raw meals for pure mineralogical compounds specific for the portland clinkers : $3CaO.SiO_2$; $\beta_2 CaO.SiO_2$; $3CaO.Al_2O_3$; $4CaO.Al_2O_3.Fe_2O_3$ as well as for pure mineralogical compounds particular for aluminous refractory clinkers, such as: $CaO.Al_2O_3$; $CaO.2Al_2O_3$; $12CaO.7\ Al_2O_3$; $3CaO.Al_2O_3$ and $CaO.6\ Al_2O_3$ has been studied on ATD + ATG - MOM - HUNGARY apparata by our experts MIHAI VALERIAN, BUTUCESCU NICOLAE and STAMATE IRINA (2,3,4,5,13).

$$C_{C3S} = \frac{3 \times 56}{1 \times 60} = 2.8;\ F\ [\ T(ft)\ ]$$

where: T = burning temperature $[^oC]$

t - burning time - $[h]$

$$C_{C_2S} = \frac{2 \times 56}{1 \times 60} = 1.86;\ F\ [\ T\ (ft)]$$

therefore resulting that $3CaO.SiO_2$ meal basicity having a molar ratio of - 2.8 implies a more difficult, havier as compared to $2CaO.SIO_2$ meals with lower basicity, namely a molar ratio of 1.86.

Thus, as function of their basicity the raw meals having a high content of $3CaO.SiO_2$ shall have more difficult clinkering depending upon molar ratios difference.

$$\Delta\ C = 2.8 - 1.86 = o.94$$

In case of the aluminous refractory meals clinkering kinetics shall develop as function of molar ratios as follows:

./.

Dr.eng.MARIA ENCULESCU

Research and Design Institute for Binder and Asbestos Cement Industry,Romania

P

$$C_{C_3A} = \frac{3 \times 56}{102} = 1.64; \; F\,[T.(ft)]$$

where : T = burning temperature (°C)

t = time (hr.)

$$C_{C_{12}A7} = \frac{12 \times 56}{7 \times 102} = 0.97 \; ; \; F\,[T.(f.t.)]$$

$$C_{CA} = \frac{1 \times 56}{1 \times 102} = 0.55; \; F\,[T.(f.t)]$$

$$C_{CA2} = \frac{1 \times 56}{1 \times 102} = 0.27; \; F\,[T.(f.t)]$$

$$C_{CA6} = \frac{1 \times 56}{6 \times 102} = 0.091 \; ; \; F\,[T.(f.t)]$$

resulting that low basicity meals (low CaO %) and high content of Al_2O_3 (maximum Al_2O_3 %) shall have a maximum clinkering kinetics very difficult one and occuring at high temperature; for instance CaO.6 Al_2O_3 shall be clinkerized in the are furnace at 1820°C; CA_2 shall be clinkerized in the arc furnace at 1722°C; CA shall be clinkerized at 1600°C during abt.6 hr; $C_{12}A_7$ shall be clinkerized at 1400°C during abt.5 hr; C_3A shall be clinkerized at 1395°C during abt.5 hr, thus easier clinkering kinetics at lower temperature depends on higher and more difficult havier basicity at higher temperature depending on Al_2O_3 % in the raw meal composition.

Also, clinkering ability of the raw meals concerning aluminous and portland cements develops as per classical formulas 1-12 more usually being Blaise's formula 6

$$AC = \frac{600}{Co + 2C_1 + 2C_2 + 3C_3 + 4C_4 + 4C_5 + 2C_6}$$

where C_o, C_1, C_2, C_3, C_4, C_5, C_6 stand for CaO % at 1000°C, 1100°C, 1200°C, 1300°C, 1350°C, 1400°C and 1500°C or as simplified by the paper author (2,3,4,5,13)

$$AC = \frac{600}{3C_3 + 4C_4 + 4C_5 + 2C_6}$$

taking into account the fact that at about 1300°C liquid phase begin to occur.

Studies and research work achieved by the author (1,2,3,4,5,13) analyses clinkering kinetics of the raw meals for pure mineralogical compounds, as well as of raw meals for white and coloured aluminous and portland clinkers and the following formulas have been stated:

$$AC_{total\ 1} = \frac{1000 \times n \times \sum_o^n C}{\sum_o^n T}; \; f\,(t)$$

$$AC_{total\ 2} = \frac{\sum_o^n T}{1000 \times n \times \sum_o^n C}; \; f\,(t)$$

./.

Dr.eng.MARIA ENCULESCU
Research and Design Institute for Binder and Asbestos Cement Industry,Romania

P

where T (^{o}C) stands for the temperature at whinch specimen of free CaO have been sampled

C (%) - free CaO
n - number of specimen
t (hours) - clinkering time

Figure no.1 shows clinkering ability of the raw meals for white portland clinkers to be noted as the best ability that one of white clinker with pegmatite.

Figure no.2 indicates clinker ability of the raw meals for aluminous clinkers noticeable being white aluminous clinkers, such as: CaO.2 Al_2O_3 (B) and CaO.Al_2O_3 (Al).

Figure no.3 shows clinkering ability of the raw meals based on slag from GALATI out of which meals with very low content of $3CaO.SiO_2$ and very high content of $2CaO.SiO_2$ may be stand out.

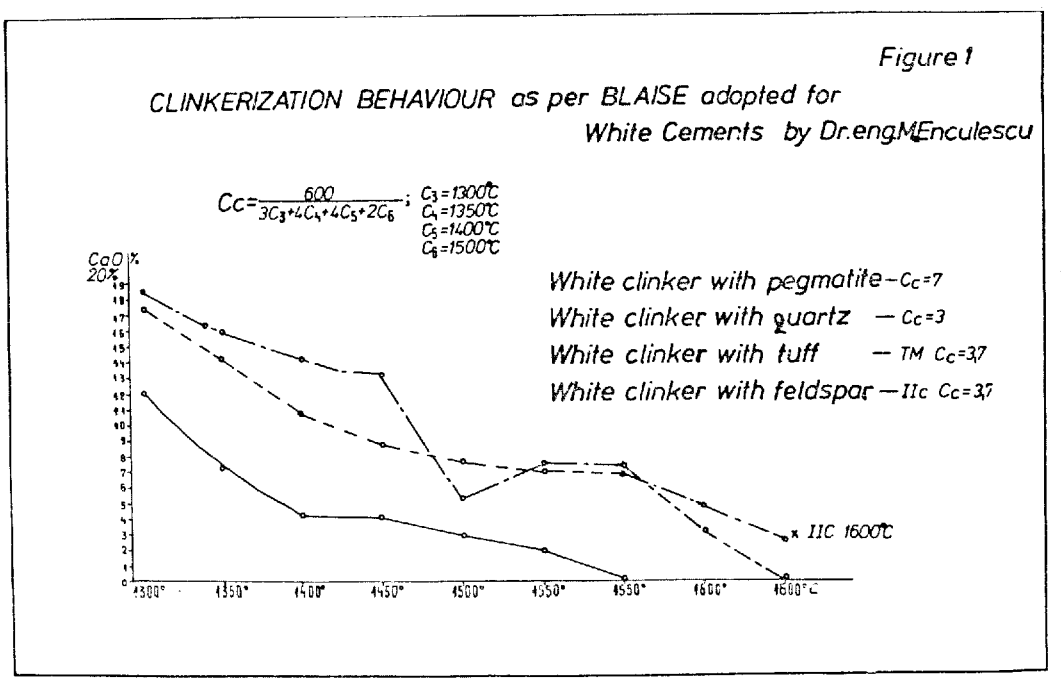

Figure 2

LABORATORY WHITE CEMENTS
Variation of the clinkerization behaviour depending upon the temperature
Formulae BLAISE and Dr.eng.M.Enculescu

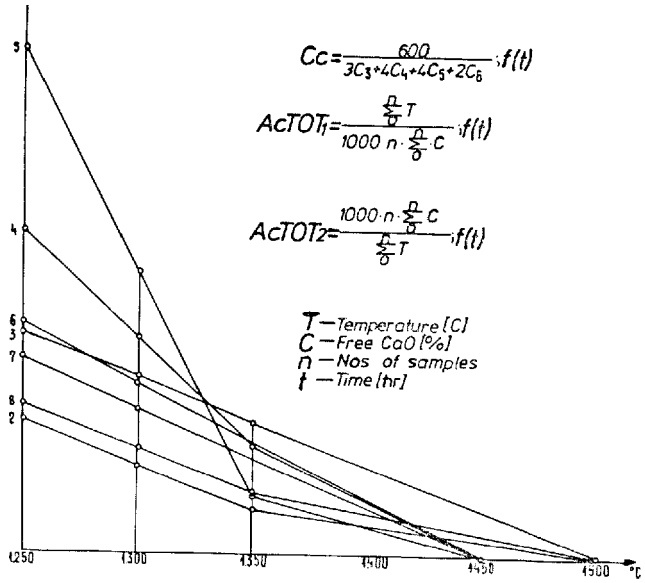

P

Figure 3

CLINKERIZATION BEHAVIOUR

Formulae as per Dr.eng.

M.Enculescu

$$AcTOT_1 = \frac{\sum_0^n T}{1000\, n \sum_0^n C} \cdot f(t)$$

$$AcTOT_2 = \frac{1000\, n \sum_0^n C}{\sum_0^n T} \cdot f(t)$$

T — Temperature [°C]
C — Free CaO [%]
n — Nos of samples
t — Time [hr]

Remarks: The formulae 1.5.8.9.10.11.12. become couspicuous

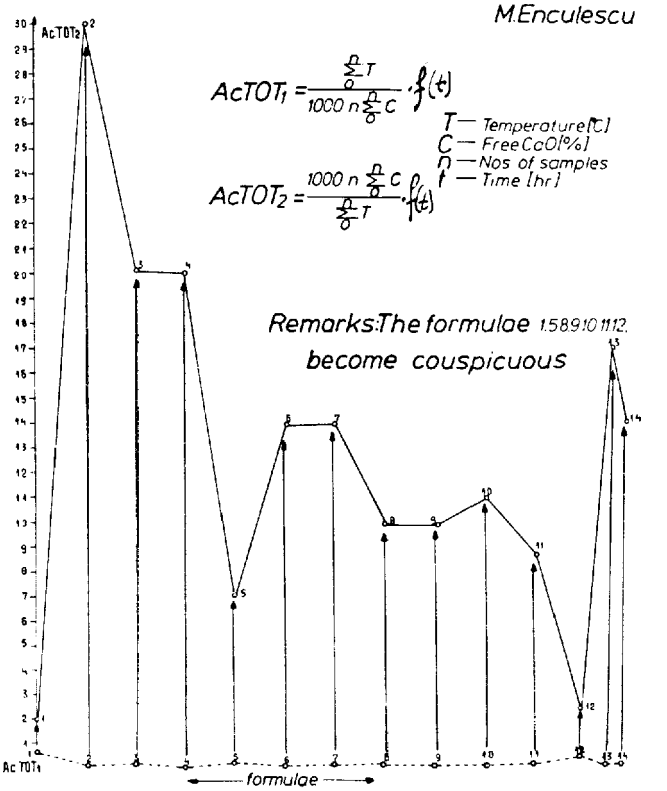

Dr.eng.MARIA ENCULESCU

Research and Design Institute for Binder and Asbestos Cement Industry,Romania

B I B L I O G R A P H Y

1.- S.Solacolu, " Chenistry-physics of the technical silicates" the 2nd edition - Technical Publishing House 1968, Bucharest.

2.- M.Enculescu, "Constributions to obtain the white cement" Technical scientific communication session - ICPILA Bucharest, 21-22 october 1983.

3.- M.Enculescu, "Research concerning determination of the characteristics of the calcium carbonate resulted from chemical industry as regards their usage possibilities in binders industry" Studies - 1st and 2nd phases 1984 - ICPILA Bucharest

4.- M.Enculescu, "Research of the characteristics of slags coming from foundries - furnaces and metalurgy as regards their usage possibilities in the binders industry. Studies - 1st and 2nd stages, 1984 - ICPILA - Bucharest

5.- M.Enculescu, "Contributions for usage of waste materials and by-products resulting from chemical industry and metalurgy in the binders industry - CONSILOX IV - Cluj Napoca, 1984.

6.- R.Blaise, Revue des materials de construction 674-675, nos.11-12 (1971) 287-295

7.- U.Ludwig, Sprechsaal fur Keramik - Baustoffe 6 - 1974 - 231-242

8.- Butt Di-M, SILIC ATTECHNIK - 23 no.3 1972-89

9.- Zur-Strassen H. - Zement-Kalk-Gips, 1o no.1 - 1957 - 1

1o.- x x x Der Theor.warmessedorf der zementa brodes zement 3o - 1941 - 231-25o

11.- Deheul, A.Sinsa Illier - C - Sinsa Illier - C - Zement - Kalk - Gips no.8 1979 - 34o-4oo

12.- C.Popescu, H.Bocan, A.Ichim, Alexandra Tatcu Aniko Fazakas Methods for determination of clinkering ability of raw materials meals for cement" - Building Materials Revue no.3 - 1983, Vol.3

13.- M.Enculescu, "Contributions at usage of waste materials and by-products resulted from chemical industry, as well as calcium carbonates precipitates and phosphogypsum in the binders industry.

The 4-th chemistry and chemical engineering conferrence the 17-th- 18th

October 1985 - Politechnical Institute - Bucharest

Demetrio Gaspar-Tébar et José Luis Sagrera-Moreno - Instituto "Eduardo Torroja" - Spain

L'ACTION DE L'EAU DE MER SUR UN CIMENT PORTLAND DE HAUTE RESISTANCE INITIELLE ET SUR UN CIMENT PORTLAND RESISTANCE AUX SULFATES: INFLUENCE DE L'ADDITION DE LAITIER, ETUDE DE LA CONCENTRATION IONIQUE.

P

1.- Introduction

Le mécanisme des réactions qui ont lieu lorsque le ciment portland hydraté, et surtout de ses mélanges avec des additions naturelles ou artificielles, est soumis à l'action de solutions agressives, est un des problèmes complexes dans le champ de la Chimie Appliqquée. C'est dans le but de contribuer à sa connaissance que nous avons développé ce travail, qui fait partie d'un Projet de Recherche de l'IETcc à long terme, aussi bien à échelle de laboratoire qu'à échelle réelle.

2.- Partie expérimentale

2.1.Matériaux employés:

2.1.1.- Ciments: deux ciments portland industriels ont été utilisés (l'un de haute résistance initielle -ciment 1- et l'autre, résistent aux sulfates -ciment 2-) dont la composition chimique et potentiel le calculée (Bogue), ainsi que la surface spécifique, se trouvent dans le Tableau 1. La fig. 2 contient les DRX des phases cristallines correspondant aux aluminates des résidus en acide salicylique-méthanol de ces ciments.

2.1.2.- Laitier: Nous avons employé le laitier dont l'analyse chimique et le diagramme de rayons X se trouvent dans le Tableau 1 et fig. 2, respectivement.

2.1.3.- Eau de mer artificielle: l'eau de mer artificielle a été préparée d'après le point 6 de la norme ASTM D 1141-75. La teneur en ions, signalée par la suite, et le pH déterminé expérimentalement, son les suivants: Ca(II) = 0,521 g/l; Mg(II) = = 1,347 g/l; SO (II) = 2,928 g/l, Cl(I) = 19,585 g/l et pH = 6,5.

2.2.- Préparation et conservation des éprouvettes de mortier (1:3): nous avons préparé les mélanges suivants: ciment/laitier = 85/15, 65/35, 40/60 et 30/70 (en poids), qui ont été utilisés pour préparer les différentes séries d'éprouvettes de mortier (1:3) de 1 x 1 x 6 cm; la relation a/c a été 0,6. Elles ont été curées 1 jour en chambre humide, à 20 ± 1°C, avec une humidité relative supérieure à 95% et, aprés, sous eau douce pendant 21 jours; par la suite nous avons immergé 12 éprouvettes/1 série/ciment ou mélange/1 âge en 800 ml d'eau douce filtré ou en eau de mer artificielle pendant 56, 90, 180 et 360 jours.

2.3.- Préparation de la phase solide: la nouvelle phases solide formée dans l'eau de mer artificielle où les éprouvettes de mortier ont été immergées a été séparée par filtration après en avoir extrait les éprouvettes de mortier, et elle a été séchée au courant d'azote.

3.- Résultats obtenus

L'évolution des teneurs en Ca(II) et de Mg(II) dans la solution et la nouvelle phase solide on été représentées dans les fig. 3 à 9.

4.- Interprétation des résultats

4.1.- Evolution de la teneur en Ca(II).

L'accroissement de Ca(II) en relation avec la teneur de cet ion dans l'eau de mer artificielle où ont été immergées les éprouvettes de mortier ($1{,}30 \times 10^{-2}$ moles/litre), est dû à la dissolution d'une partie du $Ca(OH)_2$, dont la solubilité dans l'eau à 20°C est 1.230 g/l $\lessgtr$ $1{,}66 \times 10^{-2}$ moles/litre, formé dans les éprouvettes de mortier comme conséquence des réactions d'hydrataion des composants du clinker, d'après la réaction (A):

$$\text{(A)}\quad Ca(OH)_2\text{.solide} \underset{\text{mer}}{\overset{H_2O}{\rightleftharpoons}} Ca(OH)_2\text{.dissous} \underset{\text{mer}}{\overset{H_2O}{\rightleftharpoons}} Ca(II) + 2\,OH(I).$$

donnant lieu encore à un accroissement des groupes OH(I) et ainsi de la valeur du pH, pouvant atteindre des valeurs plus grandes que 11,5 dans les solutions où les éprouvettes en ciment ont été immergées, à 10 pour les éprouvettes élaborées avec mélanges ciment/laitier = 85/15 et 7,5 et inférieur à 9,5 dans ceux correspondant aux séries d'eprouvettes de mortier restante.

Les quantités de $Ca(OH)_2$ dissoutes sont fonction de celles qui vont se former dans les réactions d'hydratation qui, à leur tour, dépendent des mélanges ciment/laitier utilisés dans la fabrication des diverses séries d'éprouvettes de mortier; une partie du $Ca(OH)_2$ formé, réactionne avec le laitier donnant les composants de calcium correspondants, et une autre partie expérimente, dans les éprouvettes, la réaction de carbonatation.

L'équilibre (A) est affecté, en ce cas là, par la présence des ions dans l'eau de mer artificielle non communs, différents du Ca(II) d'une façon spéciale, et encore par l'existance d'autre ions ou composants qui donnent lieu à des réactions de précipitation avec les ions Ca(II) ou avec les ions OH(I) de l'équilibre (A) mentionné, comme il arrive dans les ions Mg(II), SO_4(II) et avec le CO_2, qui forment:

$$\text{(B)}\quad Ca(II) + 2\,OH(I) + CO_2 \rightleftharpoons Ca\,CO_3 \text{ . solide} + H_2O$$

$$\text{(C)}\quad Ca(II) + SO_4(II) \overset{H_2O}{\rightleftharpoons} Ca\,SO_4 \text{ . } 2\,H_2O \text{ . solide}$$

$$\text{(D)}\quad Mg(II) + 2\,OH(I) \rightleftharpoons Mg(OH)_2 \text{ . solide}$$

qui produisent, dans un degré détérminé, la diminution des ions Ca(II) et OH(I) dans la solution favorisant, se même, la solubilité du $Ca(OH)_2$ et la progression des réactions d'hydratation; phénomènes qui, à leur tour, sont fonction du temps de conservation-attaque pour chaque mélange comme on peut l'apprécier dans les fig. 3 et 5. Tous ces phénomènes agissent sur les quantités de $Ca(OH)_2$ dissoutes dans ces systèmes ciment/laitier-eau douce, (fig. 3 et 5).

Les quantités de Ca(II) $\rightleftharpoons$ $Ca(OH)_2$ dissout, qui se trouvent dans la solution et dans la nouvelle phase solide, dans chaque cas, diminuent brusquement, à mesure que la teneur de ciment dans le mélange utilisé pour élaborer les différentes séries d'éprouvettes de mortier diminue (fig. 3 et 5). Si, en plus du Ca(II) mentionné, on tient compte de celui qui existe dans l'eau de mer artificielle ($1{,}04 \times 10^{-2}$ moles/800 ml) -c'est à dire, le Ca(II) présent dans la phase liquide en plus de celui de la phase solide- il apparait que pour chaque âge dans le système ciment 1/laitier-eau de mer artificielle et pour le premier âge dans le système 2/laitier-eau de mer artificielle, ces quantités se trouvent alignées, pratiquement, sur une ligne droitqui unit les points correspondant au $Ca(II)_2$ dissout, des séries d'éprouvettes faites en ciment 1 et 2, sans addition de laitier, plus celui de l'eau de mer, en ordonnées, et celui du mélange théorique ciment/laitier = 0/100, lorsqu'il n'y a pas de ciment en abscisses; il s'agit par conséquent d'un phénomène additif (fig. 4 et 6).

Les quantités totales de Ca(II) <> Ca $(OH)_2$ dissout, pour chaque mélange et pour tous les âges, plus le Ca(II) de l'eau de mer des systèmes estudiés, se trouvent aux environnements représentés dans la figure 7, où son inclues les valeurs moyennes expérimentales pour chaque mélange et les valeurs calculées pour chaque mélange à partir de la valeur moyenne qui correspond au système partial ciment (100%)-eau artificielle. Dans cette figure on peut observer que les quantités de Ca(II) sont fonc

tion de la quantité de ciment dans le mélangé employé pour élaborer les séries d'éprouvettes de mortier et qui, comme il a été signalé précédemment, répondent à une fonction linéaire dont les points d'intersection aux axes des ordonnées et abcisses sont correspondantes à la valeur moyenne expérimentale du système ciment (100%)-eau de mer, et au mélange ciment/laitier = 0/100 (il n'y a pas de ciment).

Pour les DRX, il a été mis en évidence que dans les fractions enrichies (ciment hydraté-attaqué) extraites des éprouvettes de mortier fabriquées avec ciment et avec les mélanges ayant la plus petite teneur en laitier (15%), immergées dans l'eau de mer, les pics du Ca $(OH)_2$ existent, tandis que, dans les autres cas, ceux-ci n'ont pas été détéctés puisque, dès la naissance, l'hydroxide de calcium a partiellement réagi avec le laitier et avec le CO_2 dissout dans l'eau de mer pour donner les composants de calcium correspondants dans l'éprouvettes; le reste s'est dissout dans l'eau de mer.

Comme les quantités de Ca $(OH)_2$ dissoutes -on tient compte de celui qui existe dans l'eau de mer artificielle- répondent quantitativement aux contenus de ciment des mélanges utilisés (figure 7 et Tableau 2), nous considérons que ce phénomène est dû à la progression des réactions d'hydratation qui ont fourni le Ca $(OH)_2$ nécéssaire pour que les réactions mentionnées aient lieu.

Une partie du Ca $(OH)_2$ dissout a réagi, en milieu basique fort, avec le CO_2 de l'eau de mer artificielle d'après l'équilibre (B) parce que le produit de solubilité atteint ($4{,}8 \times 10^{-9}$), précipitant Ca CO_3 comme calcite et comme aragonite en accord avec les conditions du milieu, donnant lieu, en grand partie, à la formation de la nouvelle phase solide, étant donné que le Mg(II) ha précipité en quantités plus petites que $0{,}15 \times 10^{-2}$ moles, ou il n'a pas précipité, comme nous verrons plus tarde. Les quantités de la nouvelle phase solide sont fonction du temps de conservation-attaque pour chaque mélange, et pour un même âge, du mélange utlisé dans la fabrication des séries d'éprouvettes de mortier; en definitive elles dépendent, spécialement, du degré de carbonatation de la solution et, par conséquent, de la quantité de Ca $(OH)_2$ dissoute.

4.2.- Evolution de la teneur en Mg(II)

La teneur en Mg(II) de l'eau de mer artificielle ($4{,}43 \times 10^{-2}$ moles/800 ml), où ont été immergées les éprouvettes de mortier élaborées avec les ciments 1 et 2 et avec les mélanges qui ont le plus petit contenu de laitier (15%), pratiquement, a disparu ayant précipité comme Mg $(OH)_2$, et dans les éprouvettes de mortier et dans la solution, donnant lieu à la nouvelle phase solide, avec la calcite et l'aragonite, comme il a été démontré par DRX.

Le Mg(II) existant dans l'eau de mer artificielle réagit, à pH > 10, avec les ions OH(I) de l'équilibre (A) d'après la réaction (D), qui précipite comme $Mg(OH)_2$ parceque $[Mg(II)]\ [OH(I)]^2 > Ps\ (1{,}8 \times 10^{-11})$; cette réaction a en elle même une diminution du pH. Dans les solutions mentionées plus haut, qui ont un pH $> 10{,}5$, cette réaction s'est produite, ayant détecté le composant cristallin brucite dans la nouvelle phase solide, où se trouve le Mg(II) en quantités plus petites que $1{,}80 \times 10^{-2}$ moles (dans la phase liquide on le trouve en quantités plus petites que $0{,}5 \times 10^{-2}$ moles); le Mg(II) restant a précipité au sein des épruvettes de mortier comme brucite, d'après l'équilibre (E):

(E) $Mg(II) + Ca(OH)_2$.dissout $\rightleftharpoons$ $Mg(OH)_2$. solide + Ca(II)
solution éprouvette éprouvette

de telle sort que pour chaque mol d'ions Mg(II) qui à précipité, un autre de Ca(II) passe à la solution, lequel réagit avec les composants de laitier, ou bien se trouve dans la phase liquide ou dans la nouvelle phase solide. Au contraire, dans les solutions (eau de mer artificielle) où ont été immergées les éprouvettes de mortier fabriquées avec les mélanges ciment/laitier = 65/35, 40/60 et 30/70 (en poids) n'ont pas précipité dans la solution (dans la nouvelle phase solide il n'a pas été détecté) les conditions adéquates n'y étant pas (pH < 10) et n'atteignant pas le Ps; cet ion se trouve dans la solution en quantités inférieures à $2{,}6 \times 10^{-2}$ moles et supérieures à $1{,}0 \times 10^{-2}$ moles pour deux de ces mélanges qui ont des contenus en laitier plus grands (60 et 70% en poids), le reste ayant précipité dans les éprouvettes de mortier, en des quantités telles qu'elles dépendent de la quantité de $Ca(OH)_2$ engendrées dans les réactions d'hydratation (fig. 8 et 9).

4.3.- Evolution des teneurs en Ca(II) et Mg(II)

Dans les figures 8 et 9 nous avons représenté l'evolution des teneurs en ions Ca(II) et Mg(II) dans la solution [Ca(II) procédant du Ca $(OH)_2$ dissout, plus Ca(II) de l'eau de mer] plus dans la nouvelle phase solide, graphiques 1 et 3, en plus du Ca(II) dans la solution plus dans la nouvelle phase solide procédant du $Ca(OH)_2$ dissout, graphique 2, en fonction du mélangé ciment/laitier utilisé pour l'élaboration des séries d'éprouvettes de mortier pour chaque période de conservation-attaque; dans ce figures on apprécie que ces teneurs sont en relation intime de telle façon que lorsque l'une diminue, l'autre augmente et viceversa, existant un point de croisement dans les graphiques 2 et 3 qui correspond aux mélanges ciment 1/laitier = 40/60 (pour deux âges) et 50/50 (pour les autres deux âges) et ciment 2/laitier = 40/60 (pour les quatre âges), où a lieu l'equilibre ionique Ca(II) à la solution $\rightleftharpoons$ Mg(II) qui disparait de la solution, où, pour chaque mol d'ions Ca(II) mis en jeu, un autre d'ions Mg(II) disparait. Dans le cas des éprouvettes fabriquées avec mélanges qui ont des quantités de laitier inférieures à 60% les quantités de Ca(II) sont supérieures à celles de Mg(II), puisque durant l'hydratation une plus grande quantité de $Ca(OH)_2$ se produit, restant libre en partie une plus grande quantité qui facilite la précipitation du Mg(II) et la dissolution du Ca $(OH)_2$; par contre, dans les cas des éprouvettes fabriquées avec des mélanges qui ont des quantités supérieures de laitier (70%) le phénomène est inversé, y restant dans la solution et dans la nouvelle phase solide des teneurs plus grandes de Mg(II) que de Ca(II) parceque il n'y a pas les conditions pour que le ion Mg(II) précipite, n'existant pas une quantité d'ions OH(I) suffisante, étant donné que la quantité nécessaire de $Ca(OH)_2$ ne s'est pas générée. Les faits mentionnés influent dans le degré de résistance chimique des ciments.

4.4.- Evolution de la teneur de SO_4(II) et de Cl(I)

Les teneurs d'ions SO_4(II) et de Cl(I) dans l'eau de mer artificielle, subissent une diminution que est en liaison intime avec les caracteristiques du ciment et du laitier, ainsi que le mélange employé pour élaborer les différentes séries d'éprouvettes de mortier et du temps de conservation-attaque qui influen sur la formation de composants à base de sulfates (gypse secondaire et ettringite) et de chlorures (sel de Friedel) dans les éprouvettes de mortier.

Demetrio Gaspar-Tébar et José Luis Sagrera-Moreno

P

Tableau 1

1.-Analyse chimique (%, e.p.)		Ciments 1	2	Laitier
P.F.	.....	0,4	1,1	0,4
R.I.	.....	3,1	0,2	0,0
SiO_2	.....	19,3	22,0	35,2
Fe_2O_3	.....	3,9	4,1	0,7
Al_2O_3	.....	6,2	1,9	12,0
CaO	.....	61,1	67,9	37,3
MgO	.....	1,5	0,5	6,3
SO_3	.....	4,1	2,3	0,0
Mn (II)	.....	nd	nd	0,8
CaO libre	....	1,0	1,8	-

nd = pas dosé

2.-Composition potentielle (Bogue)			
C_3S	.....	39,2	75,6
C_2S	.....	25,7	6,1
C_3A	.....	9,9	0,0
C_4AF	.....	12,0	12,8

3.-Surface spécifique (Blaine)			
cm^2/g	.....	3.313	3.553

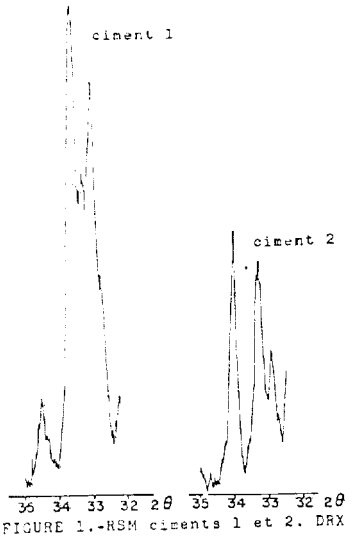

FIGURE 1.-RSM ciments 1 et 2. DRX

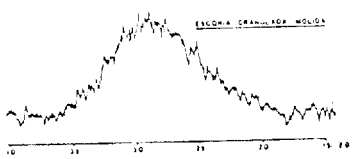

FIGURE 2.- Laitier. DRX

Tableau 2.- Ca (II), teneur total: moles x 10^{-2}

melange: ciment/ laitier	Système: ciment - 1/laitier		ciment - 2/laitier	
	experimental - x	calculée - x	experimental - x	calculée - x
100/0	5,55	5,55	6,35	6,35
85/15	4,60	4,71	5,44	5,40
65/35	3,50	3,60	4,23	4,13
40/60	2,12	2,22	2,75	2,54
30/70	1,85	1,67	2,20	1,91

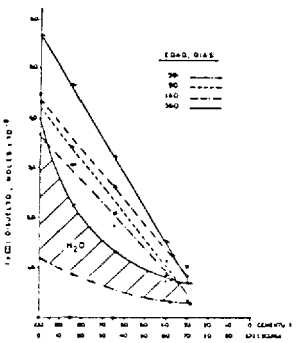

ciment 1/laitier

FIGURE 3

Ca(II) dissout.Evolution teneur

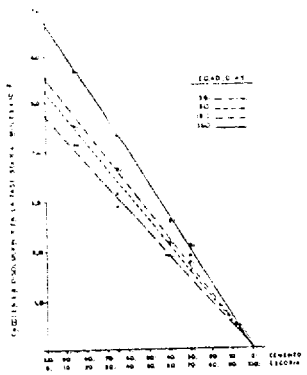

ciment 1/laitier

FIGURE 4

Ca(II) total.Evolution teneur

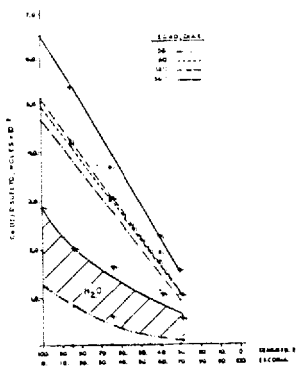

ciment 2/laitier

FIGURE 5

Ca(II) dissout.Evolution total

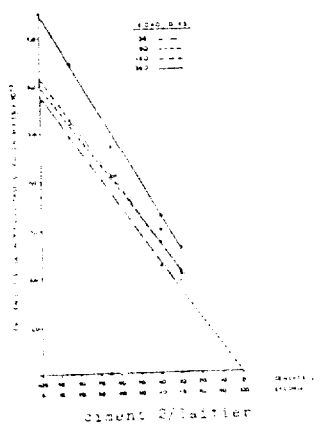

ciment 2/laitier

FIGURE 6

Ca(II) total.Evolution teneur

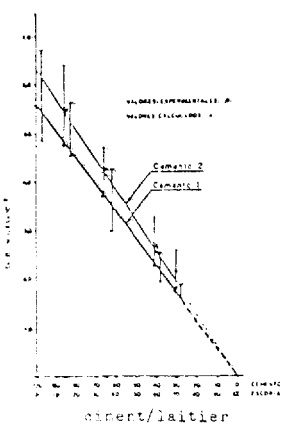

ciment/laitier

FIGURE 7

Ca(II) total.Evolution teneur

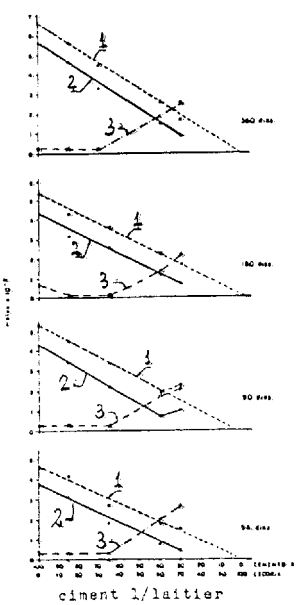

ciment 1/laitier

FIGURE 8

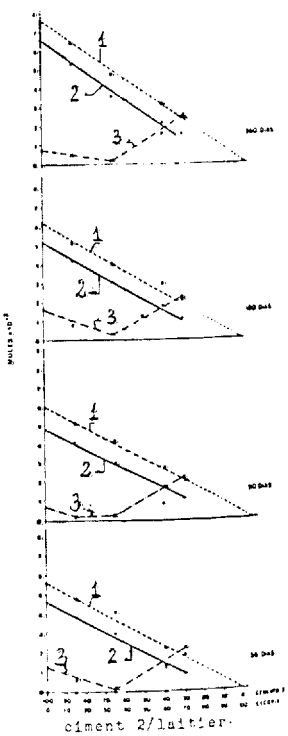

ciment 2/laitier

FIGURE 9

Ca(II) et Mg(II). Evolution teneur

1.-Ca(II) solution + Ca(II) phase solide
Ca(II) solution = Ca(II) eau de mer + Ca(II) dissout
2.-Ca(II) dissout = Ca(II) solution + Ca(II) phase solide
3.-Mg(II) solution + Mg(II) phase solide

Francisca Bermejo-Muñoz, José Luis Sagrera-Moreno et Demetrio Gaspar-Tébar
Instituto "Eduardo Torroja" - Spain

COMPORTMENT D'UN CIMENT PORTLAND RESISTANT AUX SULFATES FACE A L'EAU DEIONISEE ET LES SOLUTIONS DE SULFATE DE SODIUM ET DE SULFATE DE MAGNESIUM.

1.- Introduction

Le comportement de mortiers et bétons soumis à l'action de différentes ambiances agressives à fait l'objet de nombreux travaux comme conséquence du grand nombre d'ouvrages construits dans ces milieux, ce sujet ayant préocupe non seulement d'un point de vue constructif mais encore scientifique pour connaître les causes qui produisent l'attaque chimique; c'est ainsi que, à l'objet d'élargir la connaissance du mécanisme des réactions qui ont lieu lorsque les ciments portland hydratés et surtout de ses mélanges avec des additions naturelles et artificielles, sont soumis à l'action de solutions agressives, ce travail, qui fait partie d'un Projet de Recherche à long terme, a été réalisé aussi bien à échelle de laboratoire comme à échelle réelle.

Dans d'autres travaux présentés dans ce Congrès nous étudions le comportement mécanique-résistant d'un ciment (ciment 2), analogue à celui qui fait l'objet de ce travail, lorsque diverses séries d'éprouvettes de mortier et de béton sont soumises à l'action de différentes solutions agréssives(1), la variation de la concentration ionique de l'eau de mer où les éprouvettes de mortier fabriquées avec deux ciments portland industriels (ciment 1 et ciment 2) ont été immergées, et des ses mélanges avec laitier (2), l'évolution des caractéristiques structurelles des composants cristallins de la fraction enrichie (ciment hydraté-attaqué) extraite de l'une des éprouvettes de mortier faites avec trois ciments (ciment 1, ciment 2 et ciment 3) et de ses mélanges avec laitier, immergées en eau de mer artificielle, ainsi que de la phase solide formée dans cette eau de mer (3).

2.- Partie expérimentale

Dans ce travail nous étudions le comportement d'un ciment portland résistant aux sulphates lorsque les lits fabriqués avec ce ciment, qui s'est hydraté et qui a été conservé pendant 7 ou 28 jours dans atmosphère étanche avec une humidité relative supérieure à 90% et une température de 21 ± 2°C, sont soumis à l'action d'eau déionisée (système ciment 2 hydraté-eau déionisée), d'une solution de sulfate de sodium (système ciment 2 hydraté-solution de sulfate de sodium) et d'une solution de sulfate de magnésium (système ciment 2 hydraté-solution de sulfate de magnésium), determinant la variation de la concentration d'ions Ca (II) et SO_4(II) dans les deux premiers systèmes, et des ions Ca (II), Mg (II) et SO_4(II) dans le troisième système aussi bien dans les solutions comme dans le ciment hydraté du lit, l'évolution du pH et de la conductivité de ces solutions, ainsi que les modifications structurelles expérimentées par le ciment hydraté du lit.

2.1.- Matériaux employés

2.1.1.- Ciment: nous avons utilisé un ciment portland industriel résistent aux sulphates (ciment 2), de fabrication espagnole, dont la composition chimique et potentielle calculée (Bogue), ainsi que la surface spécifique, se trouvent dans le Tableau 1. Dans la fig. 1 sont indiqués les DRX des phases cristallines correspondentes aux aluminates du ciment anhydre et du résidu en acide salicylique-méthanol.

2.1.2.- Solutions agressives: nous avons utilisé les solutions suivantes:

a. eau déionisée,
b. solution de sulfate de sodium (2,1 g/l de Na_2SO_4), avec une concentration de SO_4(II) = 1,42 g/l<>1,48 x 10^{-2} moles /litre, déterminée expérimentalement.

c. solution de sulfate de magnesium (2,76 g/l de $MgSO_4 \cdot 7 H_2O$), avec une concentration de SO_4(II) = 1,076g/l <>1,42 x 10^{-2} moles/litre et de Mg (II) = 0,272 g/l <>1,12 x 10^{-2} moles/litre, déterminées expérimentalement.

2.2.- Préparation des lits de ciment hydraté: le ciment est malaxé avec l'eau de consistence, il est introduit en chambre humide (humidité relative > >90%; t°C = 21 + 2°C) pendant 8 heures, de suite, on fait passer la pâte par un tamis avec une ouverture de 1,5 mm obtenant ainsi un granulé de ciment, que l'on introduit dans un tuyeau en plastique (Ø = 3,5 cm; h = 16 cm), isolée de l'atmosphère avec l'azote.

Les solutions qui se trouvent dans un réservoir nourrice, traversent le lit de ciment, recueillant diverses fractions, en fonction du temps (0,15 - 0,16 l/h), où l'on a effectué les déterminations analytiques mentionnées.

3.- Résultats obtenus

Les résultats obtenus ont été représentés dans les fig. 2 à 10, celles-ci étant inclues.

4.- Interprétation des résultats

4.1.- Evolution de la teneur en Ca (II) dans le système ciment-eau déionisée et ciment-sol. de Na_2SO_4.

Dans ce travail il a été mis en évidence que les quantités de $Ca(OH)_2$ extraites des deux systèmes ciment-eau déionisée et ciment-solution de sulfate de soldium est une fonction exponentielle (fig. 2 et 3), étant asymptote par rapport à la quantité de solution qui traverse le lit, procès qui influence la progression des réactions d'hydratation et la dégradation des composants du ciment, comme on peut l'apprécier dans les DRX des figures 4 et 5.

Le Ca (II) qui apparait dans l'eau déionisée et dans la solution de Na_2SO_4 qui ont traversé les lits de ciment hydraté et granulé procède, fondamentalement, du $Ca(OH)_2$ formé pendant les réactions d'hydratation des composants de la fraction clinker du ciment (étant donné la solubilité des composants de calcium du ciment), en vertu de la réaction (A):

(A) $Ca(OH)_2$. solide $\rightleftharpoons$ $Ca(OH)_2$. dissout $\rightleftharpoons$ Ca (II) + + 2 OH^- (I)

produisant un accroissement brusque du pH (il atteint des valeurs supérieures à 12 dans le cas de l'eau et à 11,5 de la solution de Na_2SO_4). La solubilité du $Ca(OH)_2$ en eau est de 1,230 g/l, à 20°C, (4) ou de 1,230 g/l comme CaO<>1,625 g/l comme $Ca(OH)_2$ (5); les silicates de calcium hydratés sont peu solubles dans l'eau, 50 mg/l comme Ca O (6) (7) <>66 mg/l comme Ca $(OH)_2$; l'ettringite se dissout légèrement, d'après certains auteurs (8)(9) et elle est extrèmement insoluble, d'après les autres (10).

Les concentrations maximales de Ca (II) dans les solutions (2,1 x 10^{-2} moles/litre et 1,6 x 10^{-2} moles/litre) (2,1 x 10^{-2} moles/litre et 1,93 x 10^{-2} moles/litre), ainsi que les valeurs du pH et de la conductivité, ont été obtenues lorsqu'elles ont traversé les lits 0,60 l d'eau déionisée pour le ciment hydraté 7 jours et 0,36 l dans le cas du ciment hydraté 28 jours et 1,01 litres de la solution Na_2SO_4 pour le ciment

hydraté 7 jours et 0,49 pour 28 jours, respectivement.

Dans les extractions suivantes elles décroissent exponentiellement pouvant être plus petites que $0,2 \times 10^{-2}$ moles/litre dans le premier système et $0,4 \times 10^{-2}$ moles/litre dans le second.

Les quantités de Ca (II) $\leftrightarrow$ $Ca(OH)_2$ extraites des lits de ciment sont fonction du pouvoir dissolvant, de la solution et du volume qui a traversé les lits de ciment, d'une part, ainsi que du temps d'hydratation du ciment, de l'autre, comme on peut l'apprécier dans les DRX des figures 4 et 5 et dans le Tableau 2. Ainsi, ces quantités représentent 65,7% et 50,8% pour l'eau déionisée et 34,3% et 32,3% pour la solution de sulfate de sodium (là on doit tenir compte de l'effet salin), selon qu'il s'agisse du ciment hydraté pendant 7 ou 28 jours, respectivement; le reste, reste dans les éprouvettes de mortier sous forme de sels de calcium; tout le $Ca(OH)_2$ a disparu (DRX des fig. 4 et 5). Tous ces phénomènes sont en rapport avec le degré d'hydratation et de carbonatation du ciment, ainsi qu'avec la progression des réactions d'hydratation.

4.2.- Evolution des teneurs en Ca (II) et Mg (II) dans le système ciment-sol. de Mg SO_4.

Dans le système ciment-solution de sulfate de magnesium se produit un ensemble de processus physico-chimiques qui donnent lieau à la formation de composants dans les lits de ciment (7 et 28 jours), d'une nouvelle phase solide dans la solution qui a traversé les lits, et à la dissolution des autres.

Dans le lit de ciment il s'est formé brucite et gypse secondaire (prouvé par DRX, fig. 6), la portlandite a disparu et les composants anhydrides du ciment ont diminué; et aussi, la quantité d'éttringite et de calcite a augmenté.

La solution qui a traversé les lits de ciment a expérimenté des modifications en ce qui concerne les teneurs en Ca (II), Mg (II) et SO_4 (II), ainsi que la valeur du pH et de la conductivité; à leur sein, une nouvelle phase solide s'est formée, composée de brucite et de calcite (DRX de la fig. 7) où elles ont précipité, ayant atteint les Ps correspondents.

Dans ces travaux il a été mis en évidence que le Mg (II) de la solution ($1,12 \times 10^{-2}$moles/litre) disparait totalement ou partiellement lorsqu'il traverse le lit de ciment hydraté, hayant précipité comme $Mg(OH)_2$ sur place, totalement lorsque la concentration de Ca (II) dans la solution, extraite du ciment, est $\geq 1,12 \times 10^{-2}$ moles/litre et le pH $\geq$ 11,5 et, partiellement, lorsque les deux caractéristiques sont plus petites (fig. 8 et 9). Le précipité de $Mg(OH)_2$ dans le lit, produit une diminution de la porosité, arrivant parfois à se colmater et empêchant le passage de la solution (fig. 10); le précipité commence dans la zone supérieure de la colonne du lit de ciment, raison pour laquelle la partie principale d'échange doit descendre à mesure qu'une plus grande quantité de solution de Mg SO_4 s'écoule.

La formation de brucite dans le lit de ciment à lieu d'après la réaction suivante:

$$\underbrace{(B)\ Ca(OH)_2.\text{sólide} \left[\rightleftharpoons Ca(OH)_2.\text{dissout} \rightleftharpoons Ca(II) + 2\,OH(I)\right]}_{\text{lit de ciment}} +$$

$$+\ Mg(II) \underset{\text{solution}}{\rightleftharpoons} \underbrace{Mg(OH)_2.\text{solide} + Ca(II)}_{\text{lit de ciment}}$$

puisque Ps $[Mg(OH)_2] = 1,8 \times 10^{-11} <$ P's $[Ca(OH)_2] = 5,5 \times 10^{-6}$, s'accomplissant d'autre part, $[Mg(II)][OH(I)]^2 >$ Ps ($1,8 \times 10^{-11}$). En ce cas là, pour chaque mol d'ions Mg (II) qui disparait de la solution, il en apparait un autre de Ca (II).

Le $Ca(OH)_2$ du lit de ciment hydraté, se dissout dans la solution de Mg SO_4, d'après l'équilibre (A), arrivant à disparaître (DRX de la fig. 6); dans les premières extractions, la teneur en Ca (II) $Ca(OH)_2$ dissout atteint sa valeur maximale aussi bien dans le lit de ciment hydraté 7 jours ($2,8 \times 10^{-2}$ moles/litre et 28 jours ($2,38 \times 10^{-2}$ moles/litre) lorsque 0,72 l et 0,21 l, respectivement, ont coulé; par la suite, il diminue, atteignant les valeurs minimales ($0,4 \times 10^{-2}$ moles/litre pour le premier lit, augmentant par la suite, et $0,08 \times 10^{-2}$ moles/litre pour le deuxième lit), les teneurs en Ca (II) suivent l'évolution représentée dans les fig. 8 et 9, où nous indiquons aussi, l'évolution des teneurs en Mg (II).

Dans ce système on remarque que l'évolution de la teneur en Mg (II) dans les différentes extractions de la solution est intimement en rapport à celle de Ca (II), de telle façon que, lorsque l'élimination du Mg (II) dans la solution, par précipitation dans le lit de ciment comme $Mg(OH)_2$, est partielle, il y a $[Ca(II)] + [Mg(II)] = cte$ ($\simeq 1,12 \times 10^{-2}$ moles/litre = concentration initielle de Mg (II) dans la solution) de telle façon que pour chaque mol de Mg (II) qui disparait de la solution, un autre Ca (II) apparait, comme il a été signalé auparavant. Dans les points d'intersection des graphiques qui représentent les tenuers en Ca (II) et Mg (II) (fig. 8 et 9), il y a $[Ca(II)] = [Mg(II)] = 0,6 \times 10^{-2}$ moles/litre; c'est à dire, l'équilibre (B) est atteint. Equilibre lié aux réactions d'hydratation du ciment et à la formation de $Ca(OH)_2$, qui se trouvent favorisés par l'élimination d'ions OH (I) et par la dissolution de la portlandite.

Les faits mentionnés prouvent que les quantités de Ca (II) $\leftrightarrow$ $Ca(OH)_2$ extraites des lits de ciment dépendent du temps d'hydratation du ciment et de l'influence du cation Mg (II). Ainsi, dans le cas du lit de ciment hydraté pendant 7 jours, le précipité de $Mg(OH)_2$ a colmaté ce lit, dont 47% a été extrait (Tableau 2), tandis que, dans le cas du lit de ciment hydraté pendant 28 jours, 24,6% en a été estrait (Tableau 2) et 38,9% de Mg (II) s'est déposé, à cause de l'influence de la précipitation de ce Mg (II) qui déplace l'équilibre (B) vers la formation de brucite pour les raisons dont nous avons fait l'exposé auparavant.

Dans la plûpart des extractions, des petites quantités de précipité sont apparues (de l'ordre de mg) qui, groupés, ont permis de déterminer leur composition chimique et de les étudier par DRX (fig. 7), ayant identifié les pics des composants cristallins calcite et brucite, qui ont précipité ayant les conditions favorables pour attiendre les produits de solubilité correspondents.

4.3.- Evolution de la teneur en SO_4(II).

L'eau déionisée dissout, aussi, les sulfates présents dans le ciment, étant fonction du degré d'hydratation et formation de nouveaux composants; ainsi, dans le cas du lit de ciment hydraté pendant 7 jours, 41% des ces composants restent dans le ciment et 53% dans le lit hydraté pendant 28 jours. L'extraction de ces composants diminue exponentiellement, comme dans le cas de Ca (II), avec le passage de l'eau déionisée.

Par contre, dans le cas de la solution de Na_2SO_4, lorsque les premières quantités de cette solution s'écoulent, la concentration de ions SO_4 (II) y diminue (ils sont retenus par le lit du ciment) mais, par la suite, cette concentration se maintient pratiquement constante. En résumé, dès le commencement une partie de la concentration d'ions SO_4 (II), en petite quantité et étant donné les caractéristiques structurelles du ciment, a été retenue par le ciment hydraté du lit, fondamentalement, sous forme de $CaSO_4 . 2H_2O$, ayant Ca (II) -procédent du $Ca(OH)_2$-. Par contre, ayant atteint l'équilibre et n'existant pas de Ca (II) $Ca(OH)_2$, puisqu'il s'est dissout, la formation de ce composant et de l'ettringite s'arrête, la solution de Na_2SO_4 agissant comme dissolvant des composants du ciment.

Dans le système ciment-solution de sulfate de magnesium a lieu un procès analogue à celui de la solution de sulfate de sodium (la teneur en SO_4(II) diminue dans la première extraction et n'expérimente pas, par la suite, de variation); cependant, étant donné les caractéristiques de ce système qui met en jeu des quantités plus grandes de Ca (II), d'après l'équilibre (B), les quantités d'ions SO_4 (II), sont plus grandes (de l'ordre de 10 - 12%, face à 6 - 7% par rapport à la quantité totale mise en jeu), ayant formé $CaSO_4 . 2H_2O$ et ettringite en petite quantité (fig. 6) en accord avec les caractéristiques du ciment.

La formation de $Mg(OH)_2$ (pK = 11,5), la liberation de $Ca(OH)_2$ (pK = 5,3), l'avancement des réactions d'hydratation et la régulation du pH ont favorisé l'obtention de $Ca_2SO_4 . 2H_2O$ (pK= 4,6), qui réactionne avec les aluminates de calcium hydraté du ciment, produisant ettringite en petite quantité; phénomènes qui ont été prouvés par DRX, spécialement dans le ciment du lit hydraté pendant 7 jours.

4.4.- Evolution du pH et de la conductivité

Le pH des différentes fractions extraites de l eau déionisée est gouverné par l'équilibre (A). Dans les premières extractions un accroissement brusque se produit, pouvant atteindre des valeurs supérieures à 12, qui restent pratiquement constantes dans une primière étape; de suite, elles descendent (elles sont supérieures à 9). L'évolution du pH est en accord avec la quantité de $Ca(OH)_2$ dissout, de la même façon que dans le système ciment-dissolution de sulfate de sodium.

Le système ciment - solution de sulfate de magnesium, reçoit l'influence, en outre des procès précedents, de la réaction de précipitation de $Mg(OH)_2$, qui maintient le pH dans la zone comprise entre 10,6 et 10,7 à parti des premières extractions, où il se trouve à environ 11,8.

Quant à la conductivité, qui est fonction des ions présents dans les solutions, elle est gouvernée, spécialement, par l'équilibre (A), subissant une augmentation brusque dans les premières extractions et, par la suite, diminuant exponentiellement d'une façon analogue à celle que subit la quantité de $Ca(OH)_2$ dissout. Les valeurs de conductivité subissent fondamentalement l'influence des ions OH(I) et Ca(II) dans le premier système et, en plus, les ions SO_4(II) et Na (I) dans le second et les ions SO_4 (II) et Mg (II) dans le troisième, dont les conductivités ioniques a 25°C, en $ohm^{-1} . cm^2 . equiv.^{-1}$, son: $\lambda_{OH(I)} = 198,0$; $\lambda_{Ca(II)} = 59,5$; $\lambda_{SO_4(II)} = 80,0$; $\lambda_{Na(I)} = 50,1$ et $\lambda_{Mg(II)} = 53,1$ (à dilution infinie).

5. Conclusions

Première:
Le $Ca(OH)_2$ présent dans les lits de ciment hydraté, qui procèdent des réactions d'hydratation du ciment, se dissout dans l'eau déionisée qui traverse ces lits et en plus petit degré dans la solution de sufate de sodium; de même, les composants à base de sulfates et spécialement l'ettringite, se disolvent (partiellement) dans l'eau déionisée.

Les quantités dissoutes, qui expérimentent une diminution exponentielle en même temps que le volume de la solution qui traverse les lits augmente, sont fonction du temps d'hydratation-conservation du ciment des lits, des caractéristiques de la solution (sans ou avec ions, communs ou non et qui réactionnent avec d'autres ions) et du volume de la solution.

Deuxième:
De même, ce $Ca(OH)_2$ se dissout dans la solution de sulfate de magnesium qui traverse les lits de ciment. La solution de l'hydroxide mentionné est influencée par la présence de Mg (II) dans la solution, qui précipite comme brucite dans les lits, pouvant arriver à le colmater dans des cas détérminés.

L'évolution de la teneur en Mg (II) dans la solution est en rapport étroit avec celle du Ca (II) dans cette solution et viceversa, de telle façon que, lorsque la concentration de l'un augmente, celle de l'autre diminue.

La teneur en Mg (II) dans la solution disparait totalement ou partiellement lorsqu'il traverse les lits de ciment; totalement lorsque $[Ca(II)] \simeq 1,12 \times 10^{-2}$ et pH $> 11,5$. Lorsqu'il y a Mg (II) dans la solution, il y a $[Ca(II)] + [Mg(II)] = cte \simeq 1,12 \times 10^{-2}$ moles/litre = concentration initielle de Mg(II)]

Troisième:
Les ions SO_4 (II) des solutions de Na_2SO_4 et $MgSO_4$ sont retenues partiellement dans les lits de ciment, où a lieu la formation de petites quantités de gypse secondaire et d'ettringite (plus grandes dans le cas de la solution $MgSO_4$); cette rétention diminue en même temps que le volume de la solution qui a traversé les lits augmente. en dépendance à son tour, du temps de conservation du ciment.

Quatrième:
La conductivité et le pH des solutions qui ont traversé les lits de ciment hydraté poursuivent leur évolution, analogue à celle du $Ca(OH)_2$ extrait, étant fonction, d'une façon spéciale, de la concentration d'ions OH(I) présents dans les solutions mentionnées.

Cinquième:
Les composants cristallins du ciment hydraté (ettringite, portlandite et calcite) et de la fraction non hydratée du clinker, expérimentent des changements considérables qui dépendent de la solution (classe et volume) et du temps de conservation du ciment.

6. Bibliographie

(1) GASPAR-TEBAR, D.; SAGRERA-MORENO, J.L. et GONZALEZ-VILA, V.; (1986).- Contribution a l'etude du resistance chimique des ciments. Comportement mecanique-resistant d'un ciment portland (C_3A, calculée = 0%) front diverses solutions agressives. Communication presentée à ce Congrès.

(2) GASPAR-TEBAR, D. et SAGRERA-MORENO, J.L.; (1986).- L'action de l'eau de mer sur un ciment portland de haute resistance initielle et sur un ciemnt portland resistant aux sulfates: influence de l'addition de laitier. Etude de la concentration ionique. Communication presentée à ce Congrés.

(3) GASPAR-TEBAR, D. et SAGRERA-MORENO, J.L.; (1986). L'action de l'eau de mer sur un ciment portland de haute resistance initielle, sur un ciment portland resistante aux sulfates et sur un ciment portland ordinaire: influence de l'addition de laitier. Etude par DRX. Communication presenté à ce Congrés.

(4) BICZOK, I.; (1972).- Corrosión y Protección del Hormigón.- Edic. Urmo; Bilbao.- Pg. 211.

(5) DURIEZ, M. et ARRAMBADI, J.; (1961).- Nouveau traité de Matériaux de Construction; Tome 1.- Edi. Dunod; Paris.- Pgs. 489-490.

(6) ALEGRE, R.; (1978).- Comportement des ciments en milieu agressif.- Annales de l'Institut Technique du Bâtiment et des Travaux Publics (Serie: Sols et Fundations, nº 159); 364, 78.

(7) DEEYFUS, J.; (1960).- La Chimie des Ciments; Tome 1; Edit. Eyrolles; Paris.- Pg. 41.

(8) TAYLOR, H.F.W.; (1964).- The Chemistry of Cements; Vol. 1.- Edit. Acad.Press. Inc.; London. Pg. 228.

(9) LEA. F.M. y DESCH, E.H.; (1960).- Química del Cemento y del Hormigón.- Edit. Tipografía Artistica; Madrid.- Pg. 228.

(10) BOGUE, R.H.; (1962).- La química del Cemento Portland.- Edit. Dossat; Madrid.- Pg. 600.

Remerciements

Nous voudrons exprimer nôtre plus vivie reconaissance aux membres de l'EI "Durabilidad" del IETcc: Amalia Rodríguez, Lucila López, Mª Soledad Cid, Felipe Cantero et Manuel Cantero pour l'aide prêtée dans les réalisation de ce travail.

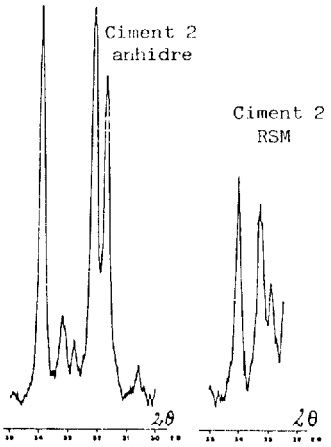

FIGURE 1

Ciment 2: anhidre et RSM. DRX.

Tableau 1

1.- Analyse chimique		%, e. p.
P.F.	.....	1,1
R.I.	.....	0,2
SiO_2	.....	22,0
Fe_2O_3	.....	4,1
Al_2O_3	.....	1,8
CaO	.....	67,9
MgO	.....	0,5
SO_3	.....	2,3
CaO libre	....	1,8
2.- Composition potential (Bogue)		
C_3S	.....	75,6
C_2S	.....	6,1
C_3A	.....	0,0
C_4AF	.....	10,8
3.- Surface spécifique (Blaine)		
cm^2/g	.....	3.553

Tableau 2
Quantité de Ca (II) dans les composants

Composants		Solutions					
		Eau deionisée		Na_2SO_4		$MgSO_4$	
		7 jours	28 jours	7 jours	28 jours	7 jours	28 jours
Ciment	(100,0)	30,0	46,2	57,1	67,7	52,9	73,8
Solution	(0,0)	65,7	50,8	34,3	32,3	47,1	24,6
Somme	100,0	95,7	97,0	91,4	100,0	100,0	98,4

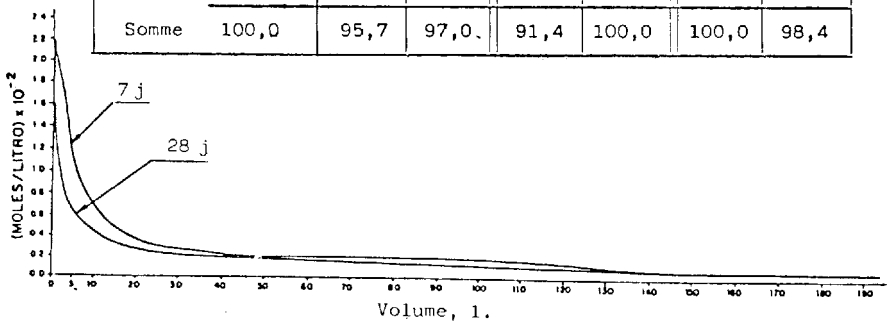

FIGURE 2

Ciment 2 hydraté - eau deionisée: Evolution de la teneur de Ca (II).

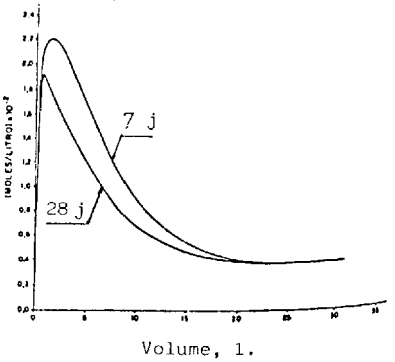

FIGURE 3

Ciment 2 hydraté - sol. Na_2SO_4: Evolution de la teneur de Ca (II).

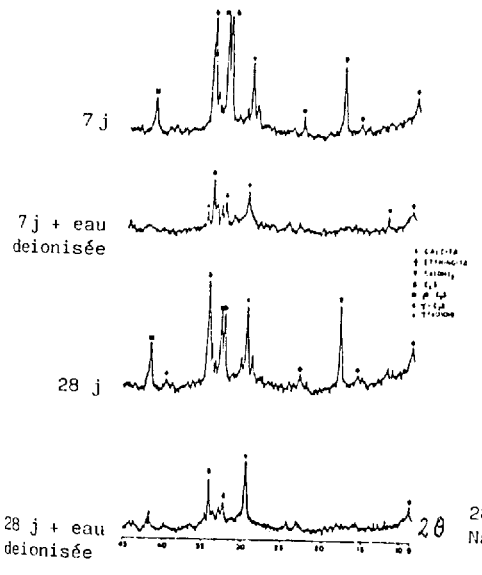

FIGURE 4

Ciment 2 hydraté - eau deionisée:
-Ciment hydraté (7 et 28 j)
-Ciment hydraté (7 + 28 j) + eau deionisée. DRX.

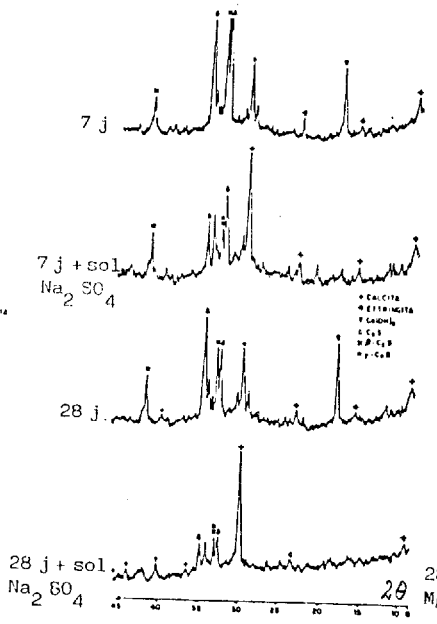

FIGURE 5

Ciment 2 hydraté - sol. Na_2SO_4:
-Ciment hydraté (7 et 28 j). DRX
-Ciment hydraté (7 + 28 j) + sol. Na_2SO_4. DRX.

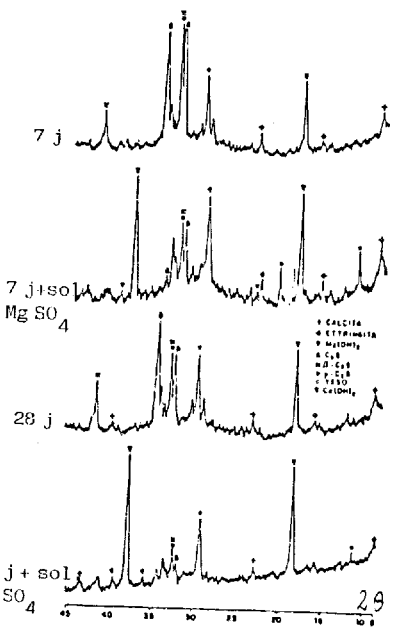

FIGURE 6

Ciment 2 hydraté - sol. Na_2SO_4:
-Ciment hydraté (7 et 28 j). DRX
-Ciment hydraté (7 et 28 j) + sol. $MgSO_4$. DRX.

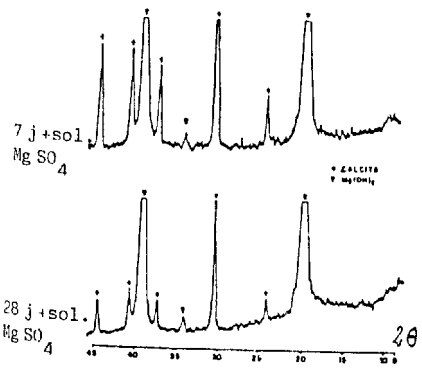

FIGURE 7

Ciment 2 hydraté - sol. $MgSO_4$:
Nouvelle phase solide. DRX.

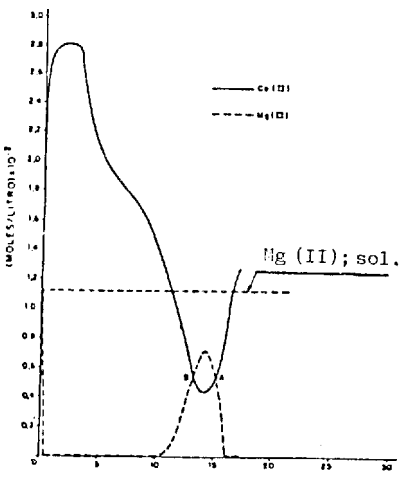

FIGURE 8

Ciment 2 hydraté (7 j) - sol. $MgSO_4$
Evolution des teneurs de Ca (II) et de Mg (II).

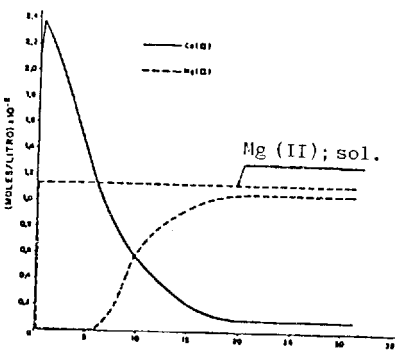

FIGURE 9

Ciment 2 hydraté (28 j) - sol. $MgSO_4$
Evolution des teneurs de Ca (II) et de Mg (II).

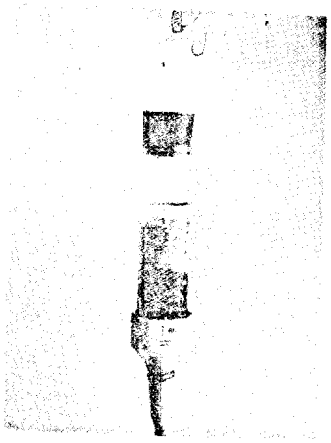

FIGURE 10

Ciment 2 (7 j) - sol. $MgSO_4$. Vue du lit.

M.P. DE LUXAN; M.I. SANCHEZ DE ROJAS; Inst. Constr. Cem. "E. Torroja" (C.S.I.C.). Madrid, Spain
M.T. MARTIN PATINO; C.S.I.C. and Dep. Geol. and Geoquim., Univ. Autónoma. Madrid, Spain.
J. SAAVEDRA; U.E.I. Mineral and Geol. (C.S.I.C.). Salamanca, Spain.

CHARACTERIZATION AND POZZOLANIC PROPERTIES OF SEDIMENTARY OPALINE ROCKS

INTRODUCTION

Among the present trends in the cement industry, the special mention is for the mixed cements.

This has led to the search for materials capable of being incorporated into cement and to the study of their suitability as active additions.

In Spain natural pozzolans and slag has been used for many years, and recently fly ash has come widely into use. However, the way between the source and its use is a basic economic factor which restricts the use of these materials whose cost must be very low. The discovery of the existence of sedimentary opaline rock in the west of the Iberian Peninsula has covered a geographical area where no other material is found that has pozzolanic properties. The present study is concerned with these opaline rocks and their use as active additions to cement.

CHARACTERIZATION OF OPALINE ROCKS

* These sedimentary levels appear on the old meteorized socle of the Central Spanish mountain system.

* Their origin is connected with an exogenic phenomenon linked to meteorization prodesses in a hot climate with alternating dry and humid seasons. The silica set free by meteorization in the humid period concentrates through evaporation in low-relief areas during the dry season and precipitates as the acidity decreases.

* The mineral compounds commonly found in these materials are quartz, opal-CT, opal-A, kaolinite and micas. This composition was established by means of an X-ray diffraction analysis (Fig.1).

FIG.1.- Typical X-ray diffractogram of an opaline rock

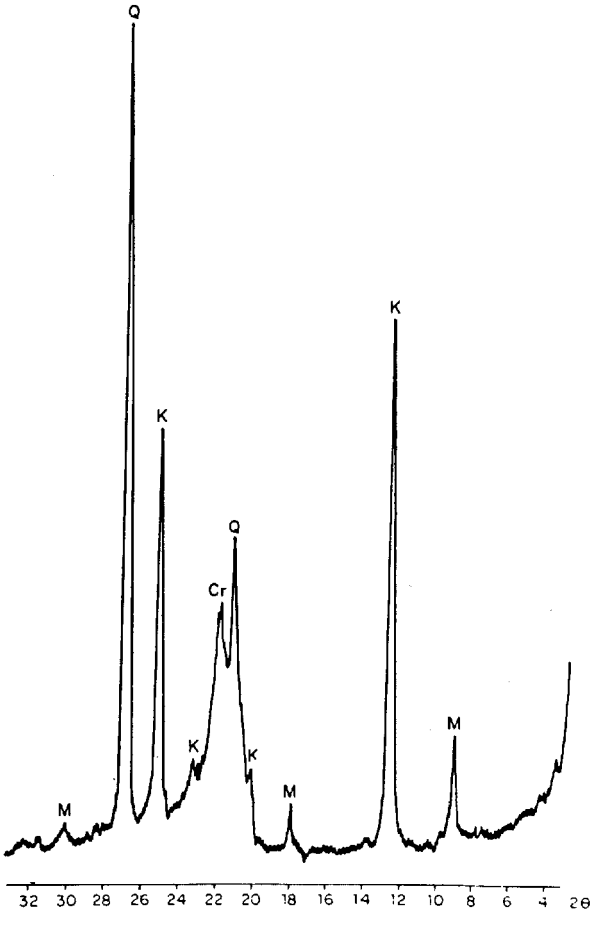

Q: quartz; M: micas; K: kaolinite; Cr: opal C-T

FIG.2.- Typical IR absorption spectrum of an opaline rock

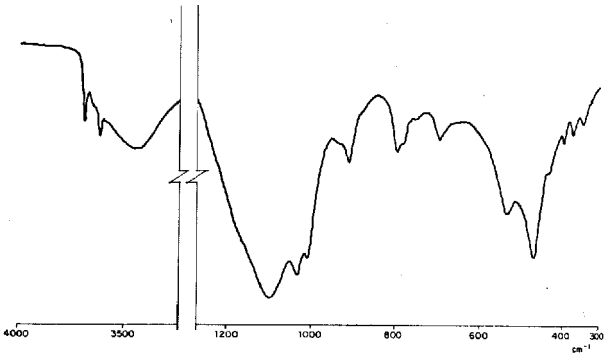

TABLE I

VALUE (%)	CHEMICAL COMPOSITION OF OPALINE ROCKS										
	S	A	F	C	M	N	K	T	$\bar{S}$	LOI	Ins. Res.
MAXIMUM	90,7	15,9	3,7	0,32	0,46	0,17	1,70	0,32	0,09	7,7	89,9
MINIMUM	74,1	5,2	1,0	0,16	0,23	0,03	0,07	0,11	0,03	2,0	83,0
MEAN	82,6	9,5	2,0	0,22	0,32	0,10	0,77	0,19	0,07	4,2	86,5

* By means of infrared absorption spectroscopy (Fig.2) these minerals were confirmed and at 3697 and 3620 cm^{-1} the bands corresponding to stretching vibrations of the -OH groups in kaolinite and micas were observed, while the band for water of hydration was found at 3460 cm^{-1}. Between 1200 and 900 cm^{-1} the Si-O stretching vibrations take place that correspond both to the existing silica as well as the silicates. The double band 798 and 778 cm^{-1} is characteristic for quartz and overlaps with the opal absorption at 790 cm^{-1}. The bending vibrations of the Si-O-Si group at 475 cm^{-1} come from the opal and the dioctahedral minerals.

Sporadically, smaller quantities of other minerals were identified, among them alunite, viseite, baryta,... (1), (2).

* The most frequent micromorphology of the polymorphous silica, observed by means of a scanning electron microscope consists of sheets with serrated edges that penetrate into each other (Fig.3a) or that form spherical compositions, lepispheres, in the empty spaces or hollows (Fig.3b). These crystalline forms cover the surfaces and walls of the pores (Fig.3c).

* The materials which were received in small blocks were ground, a process controlled by the Blaine final specific surface value, around 4500 cm^2/g.

* The chemical composition is shown in Table I, which

M.P. DE LUXAN; M.I. SANCHEZ DE ROJAS; Inst. Constr. Cem. "E. Torroja" (C.S.I.C.). Madrid, Spain.
M.T. MARTIN PATINO; C.S.I.C. and Dep. Geol. and Geoquim., Univ. Autónoma. Madrid, Spain.
J. SAAVEDRA; U.E.I. Mineral. and Geol. (C.S.I.C.). Salamanca, Spain.

gives the maximum, minimum and mean values for the whole range of samples. Chemical analysis was carried out by means of Inductively Coupled Plasma Spectrometry, except the SO_3 content which was determined gravimetrically. The insoluble residue is obtained by HCl $-Na_2CO_3$ attack and later ignition at 975°C.

SAMPLE REACTION CAPACITY

It is the aim of this research to study the suitability of these materials as pozzolanic products. Pozzolanic activity was evaluated by means of an accelerated test of opal/lime mortar, described earlier (3).

FIG.3.- SEM microstructure of opaline rocks



a



b

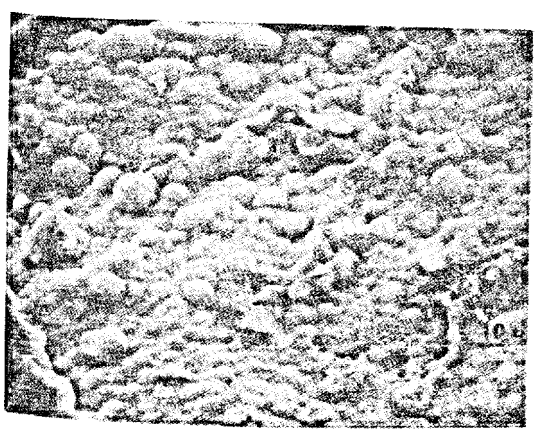

c

The mortar is prepared with 375 g of opal, 125 g of hydrated lime, 1500 g of graded standard sand and 250 cc of water. From each sample, 6 prisms (40x40x160mm) were obtained. The specimens are cured in the moist closet at 21°C for 48 hours and at 50°C for 72 hours. Flexural and compressive results are given in Fig.4.

An absorption of water increase effect is therefore not observed in any of the samples which bears out the contents of other studies concerned with opaline rock, (4).

FIG.4.- Accelerated test

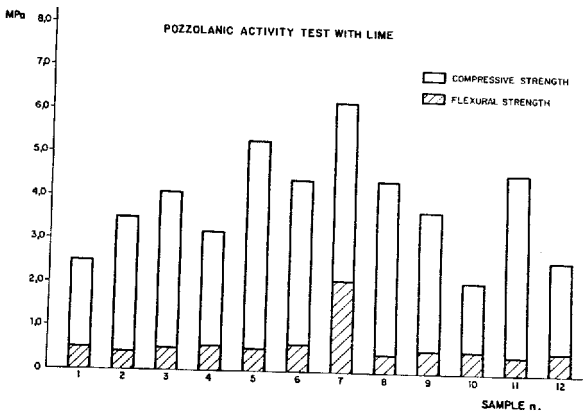

CONCLUSIONS

1. These deposits can be quite productive by using traditional quarry methods. The geotechnical conditions in the production areas are also favourables.

2. The mineralogical analysis has shown the various forms of silica besides stable form (quartz): the almost amorphous opal-A and the disordered opal-CT.

3. The pozzolanic activity test provides a classification of the different materials with regard to their reaction capacity:
   * Samples ns. 1,2,4,9,10 and 12 - low activity.
   * Samples ns. 3,5,6,7, 8 and 11 - good activity.

For these opaline rocks a higher water requirement is not necessary.

4. The pozzolanic behaviour of these materials is similar to that of other products used today as active additions to portland cement.

ACKNOWLEDGEMENT

This study was carried out under the auspices of the Institute for Geology and Mining of Spain (IGME). The authors wish to express their thanks to Mr. G. Gómez Moreno for contributing to the success of this work.

REFERENCES

1.- SAAVEDRA J., MARTIN PATINO M.T.; Rev. Inst. Inv. Geolog., 34, 1980, pp 263 - 270.

2.- SAAVEDRA J., MARTIN PATINO M.T.; Cuadernos Lab. Xeolóxico de Laxe, 2, 1981, pp 253 - 261.

3.- LUXAN M.P. de, SANCHEZ de ROJAS M.I.; Mater. Constr. (IccET), 35, 200, 1985, pp 3 - 13.

4.- GRBA V., BLAZEVIC N. and SOLVIC Z.; Cemento-Hormigón, 588, 1982, pp 973 - 986.

G.Peter, Q. Yang and A. Rosli
Institute for Building Materials, Chemistry of Materials and Corrosion,
Swiss Federal Institute of Technology, Zurich

INFILTRATION OF CHLORIDE UNDER CAPILLARY ACTION

In capillary absorption tests, we measured the penetration depth of a statistically defined liquid front as a function of time. This was accomplished with the help of electrical conductivity and gamma absorption measurements. The absorption of water and a 4% NaCl solution was investigated on concrete discs (200 x 200 x 35 mm) which were cut out of concrete walls (1000x1000x200mm), all at the same level. Two types of Portland cement with differing C_3A content (7% and 12% respectively) were employed. The cement content was 300 kg/m³ and the W/Z value 0.5. The concrete was mixed at two different temperatures (5°C and 20°C respectively) and stored at 20°C/70% R.H. for three months prior to tests. The absorption tests were carried out under two different climatic conditions (5°C, 85%RH and 20°C, 70% R.H.) and covered a period of about 5 weeks for approx. 70mm capillary rise. The original concrete surface against the formwork served as the absorption surface.

The capillary rise of the liquid front closely followed the relationship $h = k.\sqrt{t}$ (t = time). In general, the coefficient k increases with rising temperatures, increasing capillary pore content and decreasing water content in the concrete. In contrast, increased air pore content results in lower k values. The observed values lie in the range of 3-7mm/$h^{1/2}$. For the concrete with a cement of lower C_3A content, the NaCl solution was absorbed noticeably more slowly than the water. At the same time, in the case of the NaCl solution, the blurring of the liquid front decreased with increasing capillary rise. For the concrete with a cement of greater C_3A content however, the salt solution was usually as rapidly (or even more rapidly) absorbed as the pure water. The blurring showed no consistent trend.

The infiltration of chloride in concrete depends on the surface distance. The total chloride content determined after completing the test was higher for the cement type with greater C_3A content. On the other hand, a higher capillary pore content was observed for the concrete types made at 20°C with cement of greater C_3A content. Thus, the k value for the absorption of the salt solution was also higher. It was interesting to observe that for the concrete made at 20°C, the chloride content was propotional to the k value for surface distances of 0-10mm. This was true for both cement types. It also correlates with the practical experience that a carbonation of the concrete surface (which results in a decreased k value) leads mostly to a lower chloride content. The total chloride content of the concrete made at 20°C was independent of the C_3A content of the cement for surface distances of 30-40mm. It lay in the region of 0.15% Cl (referred to cement mass) with an absorption temperature of 5°C and of 0.07% Cl with an absorption temperature of 20°C.

The bound chloride, i.e. the difference between the chloride soluble in nitric acid and in cold water, yielded values clearly above 0.4% Cl referred to cement mass (0.44 - -0.67). This applies to both cement types with surface distances of 0-10mm. Smaller values were found for the bound chloride in the range 0-10mm when the concrete was made at 5°. The influences of the absorption temperature and C_3A content of the cement were small. The concrete made at 5° yielded smaller capillary pore content than the one made at 20°C.

The relationship between the bound chlorid and the total chloride amounted to approx. 0.4, independent of the cement type and the test parameters for surface distances of 0-30mm.

After the salt had exerted its influence, observation with the SEM revealed the formation of new crystals, some of them branched. With EDXRA the crystals showed increased chloride content compared to their surroundings. Even NaCl crystals could be found.

We thank W. Studer (Swiss Federal Laboratories for Materials Testing and Research), P. Wagli and R. Wessicken (Swiss Federal Institute of Technology) for their valued cooperation.

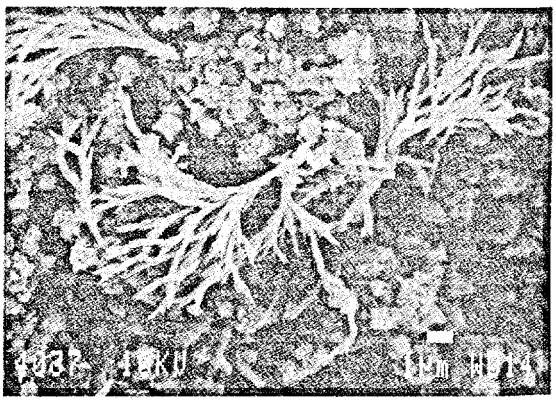

Branched crystals in concrete found after NaCl absorption

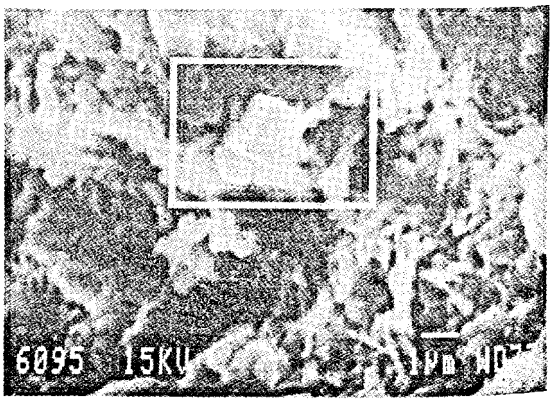

NaCl crystal in concrete

S. Popovics Drexel University - Philadelphia - U.S.A.

MODELING MATHEMATICALLY THE EFFECT OF CURING TEMPERATURE ON THE STRENGTH DEVELOPMENT OF CEMENTS.

P

Introduction

The purpose of the research was the development and calibration of a mathematical cement model for the description of the effect of curing temperature on the hydration of various portland cements as reflected by their strength developments. The term "model" implies the mathematical form of a simplified, hypothetical cement from which many of the factors influencing the hydration and hardening of an actual cement are disregarded; the remaining few variables are combined in a form that can reproduce numerically one, specific cement property which is the compressive strength in this case.

The model presented here considers the hydrations of the C_3S and C_2S as first order reactions in which the C_3A acts as a catalyst.

The investigation included the development of formulas for numerical estimation of several characteristics of the kinetics of hydration. These are, as follows:

age of concrete when the hardening begins;
age when the diffusion control of the hydration starts; and
final strength potential of concrete, that is, the strength after very long proper curing;

for portland cements of various types and various curing temperatures. This investigation is the continuation of the work on the "exponential cement model" that was presented at the 6th and 7th International Congresses on the Chemistry of the Cements. (1)(2)

Origin of the Model

The exponential cement model, probably the first non-linear cement model for the representation of hardening, is much simplier than most of the linear models. It was introduced in 1967 (3). The original mathematical form of this model provides a relationship between the strength developing capability of a portland cement under curing at constant standard temperature (22°C) and its simplified compound composition, as follows:

$$f_{ct} = f_{28} \frac{1 - C_3 e^{-a_1 t} - (1 - C_3) e^{-a_2 t}}{1 - C_3 e^{-28a_1} - (1 - C_3) e^{-28a_2}} \qquad 1)$$

where

f_{ct} = strength of portland cement paste, mortar, or concrete at the age of t, cured at constant standard temperature, MPa
f_{28} = 28-day strength at the same mixture, MPa
t = age of the specimen at testing, days,
C_3 = computed C_3S content of the portland cement, percent/100,
a_1 and a_2 = rates of hardening of the C_3S and the other component which are independent of the strength, age, and C_3S content, but may be a function of the C_3A content, and any other factor that influences the course of hydration (fineness, gypsum content, admixtures, water-cement ratio, temperature, curing and testing methods, etc.), 1/day.

This equation was obtained from the following conditions:

(a) The model consists only of two hardening components; the first component is the C_3S, the second component is a mixture of the other cement ingredients, mainly C_2S.

(b) These two components hydrate simultaneously as first order reactions with differing rates but without any interaction with each other.

(c) The kinetics of hardening is controlled only by the rates of chemical reactions between the two cement compounds and water.

(d) The final strength developed by C_3S is the same as the final strength of the second component.

The proportionality factors, which are the a parameters in Equation 1), represent the specific rates of hardening, that is, (the rate of hardening)/(remaining strength at a given age). The squares of these parameters represent specific decelerations of hardening. The more intensive the early hardening process, the greater is the value of a_1; and the longer and larger is the hardening after 28 days; the smaller becomes the value of a_2 up to a certain limit. In other words, (Eq. 1) describes the strength development when the chemical reactions control the hydration process without any consideration of the diffusion process.

The extension of this model to various constant curing temperatures is based on the recognition that the exponential cement model represents the hardening from the viewpoint of chemical kinetics as the sum of two different first-order reactions. Since experimental data have supported this with standard curing temperature (1)-(4), the logical working hypothesis is that compressive strengths of concretes cured at a constant temperature other than the standard will also be reproducible by the extension of this model. This paper presents a justification of this hypothesis by introducing the extended form and comparing its predicted values to experimental strength results.

Description of the New Model

Although the new model is based on the earlier published exponential cement models, it has two important novel properties: (a) it is extended to include the strength development produced during the period when the diffusion process controls the hydration rather than the rate of chemical reactions; and (b) it is extended to strengths of mixtures that were cured at constant temperature other than the standard 22°C. These two extensions are discussed below.

The strength development of a cement paste, mortar, or concrete can be divided into two consecutive stages from the point of view of kinetics of hydration: (a) the first stage is when the rate of strength development is controlled by the rates of chemical reactions between the cement compounds and water, followed by (b) the second stage, that is the strength development controlled by the speed of diffusion of the aqueous phase in the hardened cement paste to the unhydrated portion of the cement. The dividing point of time between the two stages is marked as t_d. In other words, the first stage of the

strength development, f_{ct}, takes place from the time of beginning of hardening, t_s, up to t_d, whereas the second stage strength, f_{dt}, develops after the beginning of the diffusion control, t_d. Figure 1 shows that the total strength of the concrete, f_t, during the first stage is equal to f_{ct}, whereas the total strength of the concrete in the second stage is equal to the sum of f_{ct} at the age of t_d, which is f_{ctd}, and f_{dt}. The importance of distinguishing between the two stages is that the strengths in the first stage are highly sensitive to the curing temperature, whereas those in the second stage are not.

The new cement model recognizes quantitatively these two stages of strength development. In addition, several other factors are included in the model as variables that influence the kinetics of strength development. These are: compound composition and fineness of the cement; age; and curing temperature.

The mathematical form of this new cement model is as follows:

1. During the first stage of hydration, when the strength development is controlled by the rate of chemical reactions, that is when $t \leq t_d$:

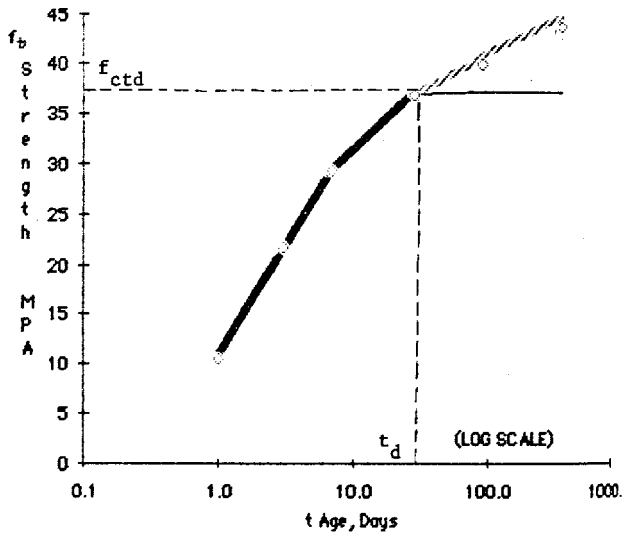

Figure 1. Strength development of concrete with Type I cement cured at 32°C. Points: experimental data; continuous lines: calculated from Eq. 2); cross-hatched line: calculated from Eq. 7).

$$f_{ct} = f_o f_{28} \frac{1 - C_3 \exp\left(-a_1(t - t_s)(S/3000)\right) - (1 - C_3) \exp\left(-a_2(t - t_s)(S/3000)\right)}{1 - C_3 \exp\left(-a_1(28 - t_s)(S/3000)\right) - (1 - C_3) \exp\left(-a_2(28 - t_s)(S/3000)\right)} \quad 2)$$

where

f_o = relative final strength of the cement paste, mortar or concrete, that is, strength after a very long proper curing, percent/100 of the 28-day strength,
t_s = age when the hardening process starts, days,
t_d = age when the speed of diffusion takes over the control of strength development, days
S = Blaine specific surface of the cement, cm^2/g.

The other symbols are identical with the symbols of Eq. 1).

2. During the second stage of hardening, when the strength development is controlled by the speed of diffusion, that is when $t > t_d$:

$$f_t = f_o f_{28} \frac{1 - C_3 \exp\left(-a_1(t_d - t_s)(S/3000)\right) - (1 - C_3) \exp\left(-a_2(t_d - t_s)(S/3000)\right)}{1 - C_3 \exp\left(-a_1(28 - t_s)(S/3000)\right) - (1 - C_3) \exp\left(-a_2(28 - t_s)(S/3000)\right)} + f_{dt} \quad 3)$$

where

f_{dt} = strength developed after the age of t_d by diffusion, MPa.

The other symbols are identical with the symbols of Eqs. 1) and 2).

Using appropriate a_1 and a_2 values, strengths can be calculated from these equations for various cement types at various ages for different but constant curing temperatures. These calculated values were compared to pertinent experimental concrete strengths.

Experimentally Obtained Strengths

The experimental data were taken from a paper by Klieger. (5) Accordingly, ASTM Types I, II and III portland cements were used to make concrete for the determination of their compressive strengths.

Two cements were used for each type. The chemical and physical characteristics of the cements are presented in Table 1. The nominal cement content of the concretes was 310 kg/m^3, the air content was between 4 and 5% and the water content was adjusted for each mixture to produce 5 to 10 cm slump. The concretes were mixed and placed at temperatures of 4.44, 12.78, 22.78, 32.22, 40.5 and 48.86°C. Specimens were prepared for testing at ages of 1, 3, 7 and 28 days, 3 months and 1 year.

For specimens that were broken at the age of 28 days or earlier, all concretes were cured continuously moist at the mixing and placing temperature until testing the strength. After the initial 28 days, the specimens remaining for tests at 3 months and 1 year were cured further continuously moist but at 22.78°C until breaking. The compressive strength tests were performed on beam ends remaining from flexural tests as 15-cm modified cube tests.

TABLE 1 - PHYSICAL AND CHEMICAL CHARACTERISTICS OF CEMENTS (5)

Cement ASTM type	Fineness Specific Surface Blaine cm^2/g	Normal consistency %	Time of Setting Vicat hr. & min. Initial	Final	Alkalies, % Na_2O	K_2O	Total as Na_2O	Calculated Compound Composition % C_3S	C_2S	C_3A	C_4AF	$CaSO_4$	Free CaO
22.78°C and below													
I	3310	25.0	4:00	6:55	0.22	0.67	0.66	42.5	28.8	11.3	8.0	3.61	0.90
III	4840	29.0	1:45	4:00	0.19	0.42	0.47	58.2	13.1	10.3	8.0	4.47	1.71
II	3910	25.0	5:05	8:45	0.14	0.21	0.28	33.9	40.7	6.1	10.2	2.98	1.22
22.78° and above													
I	3120	24.5	3:00	---	0.23	0.63	0.64	41.8	29.4	10.9	8.4	3.66	1.07
III	4730	28.5	2:00	4:00	0.18	0.47	0.49	53.8	17.1	11.5	8.1	4.65	1.08
II	3880	24.0	3:30	5:00	0.20	0.47	0.51	39.1	34.4	7.2	10.4	3.04	0.84

Further details concerning the concrete and tests can be found in Klieger's original paper. (5)

After a stepwise optimization of Eqs. 2) and 3), the compressive strength values calculated by the cement model at ages from 1 day through 1 year for concretes cured at seven different temperatures are presented in Table 2 for Type I portland cement. For the sake of comparison, the experimentally obtained data by Klieger are also presented. It can be seen that the goodness of fit is quite good between the calculated and experimental strength. The compressive strengths developed by Type II and III cements are not presented here due to space restrictions, but the obtained goodness of fit is good also for these cements.

Characteristics of the Kinetics of Hydration

In addition to the good fit to experimental strengths (Table 2), the model provided specific formulas for several characteristics of the kinetics of hydration of portland cements as a function of curing temperature and cement type. For Type I cements used by Klieger these formulas are, as follows:

Beginning of the hardening:

$$t_s = \frac{215}{(t^o + 10)^2} - 0.10 \quad \text{in days} \qquad 4)$$

Beginning of the diffusion control:

$$t_d = 120 \times 10^{-0.01923 t^o} \quad \text{in days} \qquad 5)$$

Compressive strength developed during the diffusion control:

$$f_{dt} = 960 \log(t/t_d) \quad \text{in psi} \qquad 6)$$

$$= 6.62 \log (t/t_d) \quad \text{in MPa} \qquad 7)$$

Final relative compressive strength:

$$f_o = -33 \times 10^{-6}(t^o - 29)^3 + 1.00 \quad \text{in \%/100} \qquad 8)$$

where t^o is the constant curing temperature in °C. The other symbols are identical with the symbols of Eqs. 2) and 3).

Table 2 contains illustrative values of Eqs. 4), 5), and 8) for several temperatures. Similar, although not identical formulas were obtained for cements of Types II and III. These are not presented here; nevertheless they are discussed below.

Interpretation of the Formulas

The above-presented equations for the kinetics of Type I cement as well as the similar equations for Type II and III cements indicate the following:

1. The starting time of hardening, t_s, is decreasing quite rapidly with an increase in the curing temperature. t_s roughly coincides with the time of initial setting of the cement paste. Thus, all the factors that influence the time of setting (fineness, C_3A content, SO_3 content, etc.) also influence the value of t_s. Note that when the curing temperature is -10°C or less, the hardening does not start. The value of t_s affects primarily the very early strengths.

2. The time of transition, t_d from chemical reaction control to diffusion control of the hardening shortens with increasing curing temperatures, but it is also controlled, negatively, with the rate of hardening, that is C_3S content, fineness, etc. of the cement. Similar tendency appears with the strength development of the various cements during the diffusion-controlled period; that is, the higher the rate of hardening, the smaller the strength increase. Note that the diffusion-controlled strength development, f_{dt} is far the less sensitive to the temperature of curing than the chemical reaction-controlled strength development. The t_d and f_{dt} values affect the strength at later ages.

3. f_o and the other factors are functions not only of the curing temperature but also of the cement type. For instance, f_o is highest for Type II cement and lowest for Type III cement indicating the inverse effect of C_3S and C_3A contents on the final strength which has also been demonstrated experimentally. (6) When the curing temperature is close to 29°C, the

TABLE 2 - CALCULATED AND EXPERIMENTAL STRENGTHS OBTAINED AT VARIOUS CURING TEMPERATURES

Cement: Type I

Curing temp °C	Source of strength	a_1 1/d	a_2 1/d	t_d day	f_{ctd} MPa	f_o %/100	Compressive Strength, MPa					
							1	3	7	28	90	365
							day					
4.44	Calc.	0.08	0.014	98.6	55.03	1.49	0.20	5.61	14.36	36.73	53.88	58.85
	Exp.						0.56	5.11	14.98	36.26	49.84	54.11
12.78	Calc.	0.20	0.060	68.1	48.00	1.14	4.12	13.71	25.77	43.83	48.81	52.90
	Exp.						4.06	13.51	26.25	43.75	52.85	55.93
22.78	Calc.	0.48	0.11	43.8	42.56	1.00	9.42	21.52	31.59	41.85	44.67	48.75
	Exp.						9.87	21.84	31.43	42.35	44.52	50.33
22.78	Calc.	0.41	0.13	43.8	38.32	1.00	7.67	18.63	28.75	37.87	40.42	44.51
	Exp.						8.05	18.20	28.42	38.08	42.0	45.15
32.22	Calc.	0.7	0.12	28.8	37.43	0.99	10.65	20.96	28.67	37.37	40.75	44.84
	Exp.						10.43	21.63	29.12	36.68	39.9	43.68
40.56	Calc.	0.95	0.13	19.9	34.72	0.95	12.27	21.38	27.98	35.71	39.12	43.20
	Exp.						12.95	22.40	26.95	33.04	36.75	41.02
48.86	Calc.	3.0	0.20	13.8	27.31	0.74	14.53	19.50	24.44	29.38	32.79	36.87
	Exp.						14.28	19.88	24.08	28.77	33.11	37.24

final strength developed by Type II cement is about 10% higher than that of Types I and III. The f_o equations also show that the final strengths are increasing (or decreasing) faster than linearly as the curing temperature is decreasing (or increasing) from 29°C.

Note that Carino and Lew also reported that the value of f_o decreases with increasing curing temperatures, but they recommended a linear relationship for this function instead of the cubic form of Eqs. 7) and 8). (7)

The value of f_o affects primarily the strength at later ages.

Eqs. 5) through 8) are approximations with restricted limits of validity. The restrictions originate from the intentional simplification of the formulas. For instance, the actual f_o value does not increase indefinitely as the cubic function of Eq. 8) indicates but rather levels off around 0°C as well as above 60°C temperatures, respectively. Such curve, however, would require a much more complicated mathematical form. The t_s values as represented by Eq. 4) also change with the temperature more rapidly than the actual values. Nevertheless, all these formulas seem to be useful tools between 0 and 50°C for the estimation of several characteristics of the kinetics of hardening numerically that we could do only in in qualitative terms up to now.

As far as this writer can tell, formulas similar to Eqs. 5) through 8) have not been published. Nevertheless, the primary importance of these formulas is not so much the actual numbers they provide because these are valid strictly speaking only for the cements used by Klieger in his experiments. It seems more important that they show the general approach for the establishment of similar formulas for other cements and, with further research, for the determination of how the cement characteristics influence the t_d, f_o, etc. values, that is the kinetics of hardening, under various curing conditions.

Conclusions

The new cement model represented by Eqs. 2) and 3) can reproduce the strength development of portland cements of Types I, II and III cured at differring temperatures quite well as demonstrated by the data in Table 2. In addition, the optimization and calibration processes of this model provided formulas for the numerical estimations of several characteristics of the kinetics of hydration as shown by Eqs. 4) through 8).

Acknowledgment

This work was sponsored by the National Science Foundation NSF Grant Nos. CEE-8304382 and CEE-8442765.

References

1. S. Popovics, "Strength Development of Portland Cement Paste," The VI. International Congress on the Chemistry of Cement, Supplementary Paper, Section II, Moscow, September, 1974, p. 20.

2. S. Popovics, "Possibility of a Catalytic Role of C_3A in the Hardening of Portland Cements," 7th International Congress on the Chemistry of Cement, Vol. IV, Editions Septima, Paris, 1980, pp. 602-606.

3. S. Popovics, "A Model for the Kinetics of the Hardening of Portland Cement," Highway Research Record, No. 192, Highway Research Board, Washington, D.C., 1967, pp. 14-35.

4. S. Popovics, "Phenomenological Approach to the Role of C_3A in the Hardening of Portland Cement Pastes," Cement and Concrete Research, Vol. 6, No. 3, May, 1976, pp. 343-350.

5. Klieger, "Effect of Mixing and Curing Temperature on Concrete Strength," ACI Journal, Proc. Vol. 54, June, 1958, pp. 1063-1081.

6. S. Popovics, Concrete Making Materials, McGraw-Hill Book Company, New York, etc. and Hemisphere Publishing Corporation, Washington, etc., 1979, p. 370.

7. N. J. Carino and H. S. Lew, "Temperature Effects on Strength-Maturity Relations of Mortar," ACI Journal, Proc. Vol. 80, No. 3, May-June 1983, pp. 177-182.

Menashi D. Cohen and Barzin Mobasher, Department of Civil Engineering, Northeastern University, Boston, Massachusetts 02115, U.S.A.

PHYSICO-CHEMICAL, MICROSTRUCTURAL, AND MICROMECHANICAL INVESTIGATIONS OF SULFOALUMINATE-TYPE EXPANSIVE CEMENTS

RECHERCHES PHYSICO-CHIMIQUE, MICROSTRUCTURALE, ET MICROMÉCANIQUE SUR UN CIMENT EXPANSIF DU TYPE-SULFOALUMINATE

INTRODUCTION

Portland cement is one of the most widely used materials in the construction industry. One of its disadvantages, however, is its inherent characteristic to shrink upon drying and, owing to its low tensile strength, to crack. Upon cracking, concrete becomes more permeable and allows, with greater ease, the ingress of harmful chemicals to its interior which may lead to loss of strength and ultimate deterioration. This imposes unnecessary maintenance and rehabilitation costs, and becomes a major concern in an industry that accounts for more than 250 billion dollars on GNP per year in the United States.

In response to this concern, expansive cements, in the form of shrinkage-compensating cement, have been developed and used in the field for several decades. When mixed with water, expansive cements expand and create tensile stresses in the reinforcing steels and, therefore, compressive stresses in the concrete. The idea is that upon shrinkage, concrete will simply release some, preferably not all, of its compressive stress, thereby preventing any tension from building up and thus avoiding the formation of cracks.

TYPES

The three types of sulfoaluminate-type expansive cements that have been studied in the United States are differentiated by their supplementary alumina-bearing phases. For example, Type K expansive cement is characterized by $C_4A_3\bar{S}$. Type K expansive cement is usually produced by intergrinding ordinary portland cement clinker, expansive clinker (containing $C_4A_3\bar{S}$), and calcium sulfate (anhydrite or gypsum).

Similarly Type M is characterized by $CA+C_{12}A_7$. Type S has no supplementary alumina-bearing phase, but is characterized by a high percentage of C_3A.

Expansive cements can also be based on the positive volume change associated with the hydration of an oxide such as CaO or MgO. Commercial expansive cements based on CaO ("free lime") exist; cements based on MgO have been studied.

HYDRATION

When water is added to expansive cement, a complex reaction takes place. The silicate phases (C_3S and C_2S) react with water to produce calcium silicate hydrates ($C\bar{S}H$) gel and calcium hydroxide. CSH gel contributes to the strength of the cement. The stoichiometric equations can be generalized as follows:

$$2C_2S + 3H \longrightarrow C_3S_2H_2 + CH \quad ....(1)$$

$$2C_3S + 5H \longrightarrow C_3S_2H_2 + 3CH \quad ...(2)$$

Trisulfate hydrate ($C_6A\bar{S}_3H_{32}$) commonly referred to as ettringite is the principle phase in the C-A-$\bar{S}$-H system that contributes to expansion in sulfoaluminate-type expansive cements. In Types S, K, and M expansive cements, ettringite is assumed to form as follows:

$$\text{TYPE S-}C_3A + 3C\bar{S}H_2 + 26H \longrightarrow C_6A\bar{S}_3H_{32} \quad ..(3)$$

$$\text{TYPE K-}C_4A_3\bar{S} + 8C\bar{S}H_2 + 6CH + 74H \longrightarrow 3C_6A\bar{S}_3H_{32} \quad ..(4)$$

$$\text{TYPE M}\begin{cases} CA + 3C\bar{S}H_2 + 2CH + 20H \longrightarrow C_6A\bar{S}_3H_{32} & ..(5) \\ C_{12}A_7 + 21C\bar{S}H_2 + 9CH + 173H \longrightarrow 7C_6A\bar{S}_3H_{32} & ..(6) \end{cases}$$

The product ettringite ($C_6A\bar{S}_3H_{32}$) has a density of 1.73 g/cm^3 and contains six units of CaO, one of Al_2O_3, three of SO_3, and thirty-two of water. It occurs as hexagonal columns or needles in which the water of crystallization is contained in channels parallel to the c-axis (1). The stoichiometric reactions 1-6 are ideal and the exact reaction equations have not yet been determined.

THEORIES OF EXPANSION

There are two major schools of thought concerning the expansion mechanism: the Crystal Growth Theory and the Swelling Theory.

THE CRYSTAL GROWTH THEORY (1-11)

According to the Crystal Growth Theory, expansion is caused by the growth of ettringite crystals from the surfaces of the expansive particles (topochemical reaction mechanism) or from the solution (through-solution reaction mechanism). The growth of these crystals, commonly referred to as crystal growth, is regarded as producing a 'crystallization pressure', and, hence, the expansive force.

THE SWELLING THEORY (12-15)

According to the Swelling Theory, expansion occurs because of wetting of the ettringite particles that are of colloidal size. These particles have been referred to as gel. This gel has a large surface area, and like CSH gel, takes up water to produce overall expansion by swelling. The formation of this gel occurs by a through-solution mechanism due to the reaction between the expansive particles and the surrounding solution. Moreover, if calcium and hydroxyl ions exist in the solution, ettringite particles will be colloidal in size; but if such ions are absent, ettringite particles will be larger in size. It is only in the former case that expansion can occur. This school of thought, unlike the first, does not consider the size of the expanding particles to be important. Instead, it stresses that it is the existence of calcium ions which affects the size of ettringite crystals and, therefore, the rate and magnitude of expansion.

On the other hand, in order to explain excess expansion observed in an expansion study, it was suggested that water adsorption and interparticle repulsion in ettringite formation (due to high Zeta potential values) act concurrently and significantly with crystal growth thrust during expansion (16).

The above theories of expansion have been discussed in detail in references (17-19).

DISCUSSION OF THE THEORIES

In discussing the review paper (17), B. Mather (18) suggested that the observed increase in dimensions of expansive cements cannot be explained either as crystal growth (first school) or swelling of ettringite (second school). He stated that the crystal size or degree of crystallinity of the ettringite is irrelevant and that expansion needs no explanation other than the increase in volume upon C_3A or $C_4A_3\bar{S}$ to ettringite transformation. In the reply to Mather's discussion (19), based on the equations below:

$$V = N \cdot A \cdot L \quad ..... \quad (7)$$

$$dV = NA.dL + LA.dN + LN.dA \quad ... \quad (8)$$

it was claimed that expansion based on volume change depends on the crystallinity of ettringite (the second term, LA.dN) and thus any explanation of the mechanism of expansion should be based on either or both schools of thought. In equation (7) the parameters V and N are total volume and total number of ettringite crystals produced, and A and L are cross-sectional area and length of a single ettringite crystal. Equation 8 represents the total differential of equation 7. Although expansion by water adsorption has not been ruled out (19), it is believed that its contribution to expansion is insignificant because of the low surface area of ettringite -approximately 8,000-19,000 m^2/kg depending on lime concentration (16).

OBJECTIVES

A fundamental requirement in the successful use and application of expansive cement is the clear understanding of the mechanism of the expansion process and development. This fact has been recognized for some time. Research activities at elucidating the expansion mechanism have been significant and achievements made are encouraging. With all the extensive work done, however, there still is a lack of general consensus regarding the mechanism of expansion including the kinetics and morphology of ettringite formation.

The purpose of this paper is to present results of an investigation aimed at assessing the mechanism of expansion. The results presented herein are based on the physico-chemical, microstructural, and micromechanical studies of the sulfoaluminate-type expansive cements.

EXPERIMENTAL INVESTIGATION

The experimental work included studies of sulfate solubility, microstructure (scanning electron microscopy-SEM), strength, expansion, and shrinkage characteristics.

MATERIALS

The materials used were portland cement p.c. S3210, Type

Menashi D. Cohen and Barzin Mobasher, Department of Civil Engineering,
Northeastern University, Boston, Massachusetts 02115, U.S.A.

3.3 PHYSICO-CHEMICAL, MICROSTRUCTURAL, AND MICROMECHANICAL INVESTIGATIONS OF SULFOALUMINATE-TYPE EXPANSIVE CEMENTS

RECHERCHES PHYSICO-CHIMIQUE, MICROSTRUCTURALE, ET MICROMÉCANIQUE SUR UN CIMENT EXPANSIF DU TYPE-SULFOALUMINATE

K expansive clinkers ECL-103 and TXI-4C, pure $C_4A_3\bar{S}$, pure C_3A, natural gypsum G-1, and a reagent grades gypsum and calcium hydroxide. The physico-chemical characteristics are listed in Table 1.

Oxides	p.c. S3210 wt.%	Expansive ECL-103 wt.%	Clinker TXI-4C wt.%	Pure $C_4A_3\bar{S}$ wt.%	Pure C_3A wt.%	Natural Gyp. G-1 wt.%
SiO_2	21.66	14.7	20.42			1.92
Al_2O_3	4.6	5.9	10.32	49.41	37.07	0.12
Fe_2O_3	3.96	1.9	2.79	0.38	0.02	0.48
CaO	64.81	62.6	57.24	37.58	61.48	31.97
MgO	1.35	3.5	0.67			0.37
SO_3	2.4	8.7	5.1	11.9		46.12
Na_2O	0.2	0.23	0.25			
K_2O	0.24	0.75	0.74			
L.O.I.		0.86	0.63	0.54	0.25	20.68
Free-lime	0.13	5.1	1.34	0.3	0.2	
Equiv Na_2O		0.73	0.74			
Imp.						1.72
TOTAL	99.35	99.34	100.24	100.11	99.0	103.38
Phase	Bogue	Mehta	Mehta	XRD*	XRD*	
C_3S	55.23	76.14	22.71			
C_2S	20.44	-15.29	41.42			
C_3A	5.49				99.8	
C_4AF	12.05	5.78	8.49			
$C_4A_3\bar{S}$		9.35	17.04	99.7		
$C\bar{S}$	4.08	12.7	4.87			77.6
TOTAL	97.29	103.97	94.53	99.7	99.8	

* Estimated value

TABLE 1: Typical percentages of oxides and calculated compound compositions

SULFATE SOLUBILITY

Stoichiometric amounts according to equations 3 and 4 using C_3A (C-coarse and F-fine), $C_4A_3\bar{S}$ (C and F), reagent grade gypsum ($C\bar{S}H_2$) and calcium hydroxide (CH) were blended in individual flasks containing one liter of deionized water. $C_4A_3\bar{S}$-C and $C_4A_3\bar{S}$-F had Blaine specific surface areas of 364 and 972 m^2/kg, respectively. C_3A-C and C_3A-F were 321 and 820 m^2/kg. Sulfate solubility was studied as a function of particle type (C_3A or $C_4A_3\bar{S}$)and fineness (C or F) by measuring the amount of dissolved sulfate consumed daily in suspension hydration at 23 °C for several days. The sulfate consumed went for the production of ettringite. The detailed procedures are described elsewhere (20).

For $C_4A_3\bar{S}$, Fig. 1, from ref.(20),results show fineness does not affect the rate and amount of sulfate depletion even when concentration of C_4A_3S is tripled from 0.25 to 0.75 grams per liter of water. This result is not expected since mass and surface area play important roles in kinetics (6,21,22).

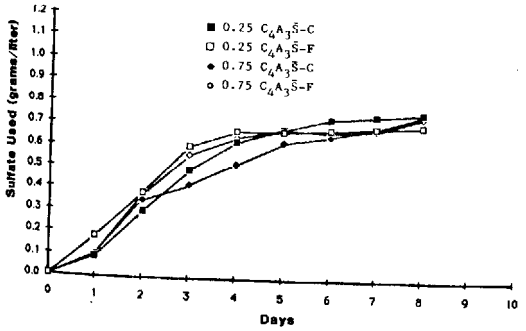

Fig. 1: Daily consumption of sulfates for ettringite production.

Results in general are conflicting but they do suggest that sulfate solubility technique with $BaCl_2$ precipitation is not as sensitive to $C_4A_3\bar{S}$ fineness and amount as it is for C_3A in suspension hydration.

SEM ANALYSIS

Samples of $C_4A_3\bar{S}$ and C_3A were separated by microsieves into two size fractions: particles smaller than 37 microns (-400 mesh) and particles larger than 74 microns (+200 mesh). These particles were dispersed in suspension hydration in flasks as described earlier (6,20,21). At different stages of hydration samples were removed from the flasks and prepared for SEM observations. The purpose of particle separation was to study particle size effect on ettringite morphology. In models developed for sulfoaluminate-type expansive cements (6,22,23) it was predicted that the length of ettringite crystals are directly related to the size of C_3A or $C_4A_3\bar{S}$ particles, and that $C_4A_3\bar{S}$ particles produce longer ettringite crystals than C_3A particles.

SEM micrographs, Figs. 2 and 3, from ref.(20) show that the mode of ettringite formation in suspension hydration is topochemical for both C_3A and $C_4A_3\bar{S}$ particles. Nearly all micrographs showed similar patterns. Generally, $C_4A_3\bar{S}$ particles produce a more defined and radial mode of ettringite crystals (Fig. 2), compared to C_3A particles that produce irregular but defined ettringite crystals (Fig. 3). This could be attributed to differences in the crystalline nature of C_3A and $C_4A_3\bar{S}$ and to differences in solution pH (9.2-10.3 for C_3A and 11.5-11.8 for $C_4A_3\bar{S}$).

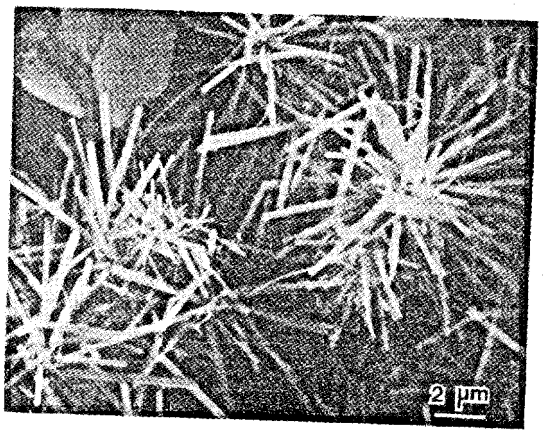

Fig. 2: SEM micrograph of hydrated $C_4A_3\bar{S}$ at 7 days.

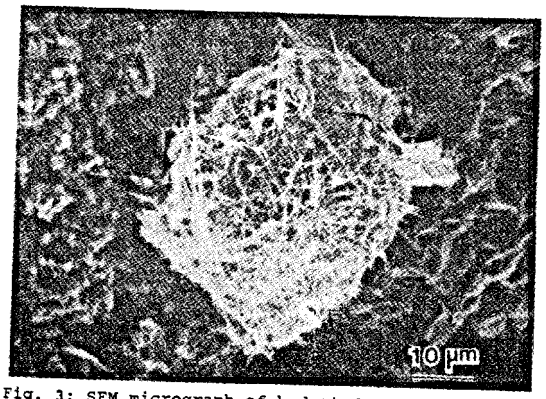

Fig. 3: SEM micrograph of hydrated C_3A at 7 days.

In another approach that utilizes SEM in the study of expansive cements, expansive paste slabs were used (24). Internal restraint was provided by means of uni-directional and bi-directional reinforcement. The expansive cement paste used was 53.33% p.c. S3210, 11.67% reagent grade gypsum, and 35% TXI-4C (2-5 microns). Results of this study indicate that internal restraint by wire reinforcement does not affect the morphology (i.e. size, shape, and preferred orientation) of ettringite produced. However, there was formation of large $Ca(OH)_2$ crystals due to internal restraint, both at the wire-cement interface and in the matrix. Results reported by other investigators on the effects of externally applied constant pressures (16,17,25), however, indicate morphological differences in ettringite. Therefore, different mechanisms may be operative in the two restraining conditions; internal wire-reinforcements which exert time-dependent

Menashi D. Cohen and Barzin Mobasher, Department of Civil Engineering, Northeastern University, Boston, Massachusetts 02115, U.S.A.

3.3 PHYSICO-CHEMICAL, MICROSTRUCTURAL, AND MICROMECHANICAL INVESTIGATIONS OF SULFOALUMINATE-TYPE EXPANSIVE CEMENTS

P

RECHERCHES PHYSICO-CHIMIQUE, MICROSTRUCTURALE, ET MICROMÉCANIQUE SUR UN CIMENT EXPANSIF DU TYPE-SULFOALUMINATE

directional pressures starting at a critical degree of hydration α_{cr} when ettringite crystals surpass surrounding solution layer (3,4,6,8,17,23,24), and externally applied constant pressures starting at the onset of hydration.

STRENGTH-EXPANSION MEASUREMENTS

The free expansion of the blends in saturated lime-water at 23±1 °C was studied by measuring the daily length changes of thin prismatic paste specimens having dimensions 4.8 mm x 15 mm x 80 mm. Procedures for proportioning, mixing, casting, curing, and measurement are described elsewhere (5,6,26).

Strength was measured indirectly from the first mode of resonant frequency of prismatic specimens similar in dimensions to the expansion specimens. The square of this frequency gives a measure of dynamic Young's Modulus and compressive strength (5,6,27-29).

Pure Components

Paste blends of p.c. S3210, gypsum G-1, 2.5% and 5% C_3A (C and F) or $C_4A_3\bar{S}$ (C and F), with extent of reaction %R≥100, were mixed with deionized water at 0.4 w/c. Percent R is an approximate measure of wt% C_3A or $C_4A_3\bar{S}$ that converts to ettringite (4,5,6,23). Percent R>100 indicates excess sulfate. Figs. 4, 5 (from ref.20) and 6 show the expansion-time behaviors of the 2.5% to 5% C_3A (C and F) and $C_4A_3\bar{S}$ (C and F) blends. Results indicate that the behavior of expansion is extremely dependent on the type and amount of expansive component. With the higher content, comparing Figures 4 and 5, the effects of fineness and type become more pronounced. Fig. 5 shows that $C_4A_3\bar{S}$-C and C_3A-C give a higher expansion rate than $C_4A_3\bar{S}$-F and C_3A-F. This is not expected since at early ages tests have shown that finer particles produce expansion at a higher rate. However, this may be explained from Richards-Helmuth's model on expansive cements (4) showing that there is an optimum range of expansion particles 6.8-11 microns, that give the highest expansion. Since more than 50% of the $C_4A_3\bar{S}$-F and C_3A-F particles were smaller than 5 microns compared to 18% and 7% for $C_4A_3\bar{S}$-C and C_3A-C, one can suggest that a greater amount of ettringite formed in the fine particles is being wasted. Figure 6 clearly shows the effect on expansion of a series of blends with increasing content of $C_4A_3\bar{S}$ but constant %R.

Type K Clinker

Paste blends of p.c. S3210, Type K expansive clinker TXI-4C, gypsum G-1, w/c=0.4, and %R=65, were made with varying wt% of Type K expansive clinker form 23%-50%. TXI-4C was ground to a Blaine of 422 m^2/kg. This "whole" clinker was then separated into several size fractions by air-classifier: 2-5 microns (481 m^2/kg), 5-8 microns (450 m^2/kg), 8-13 microns (232 m^2/kg), and +13 microns (89 m^2/kg). Figures 7 and 8 show the expansion time and strength-time relationships. With higher amount of expansive component, 50% clinker in Fig. 7, behavior is "abnormal" (6,31), i.e. double curvature expansion and strength drop. The 35% clinker mix in Fig. 7 and the 2-5 micron mix in Fig. 8 show "normal" (6,31) behavior in their strength-expansion patterns while the mixes containing 50% clinker in Fig. 7 and whole clinker in Fig. 8 show abnormal behavior.

The paste blends containing Type K TXI-4C (whole) tested in free expansion contained 1.34% free lime. Another Type K clinker, ECL-103 was also obtained from a different source and it had a relatively high amount of free lime (5.1%). The clinker was ground either by impact (ECL-103V "whole") or by grinding in a steel ball mill (ECL-103G1 "whole"). ECL-103V "whole" was separated into several size fractions by air-classifier: 2-5 microns (682 m^2/kg), 5-8 microns (417 m^2/kg), 8-13 microns (279 m^2/kg), and +13 microns (138 m^2/kg). The "whole" clinker was 270 m^2/kg. (The Blaine of the steel ball milled clinker, ECL-103G1 "whole" was 426 m^2/kg). Impact grinding gives angular shape particles while steel ball mill grinding gives a more rounded or spherical particle shape.

Two paste blends containing p.c. S3210, gypsum G-1, and 30% ECL-103 (V or G whole), with 0.4 w/c and 75% R were tested in expansion and results clearly indicate that the method of grinding plays a significant role in the expansion behavior, Fig. 9. The Figure shows that the blend containing the expansive clinker ground by impact gives double the expansion of the expansive clinker ground in steel ball mill even though it has the same chemical composition and a significantly smaller surface area. Fig. 10 also shows expansion-time behavior of

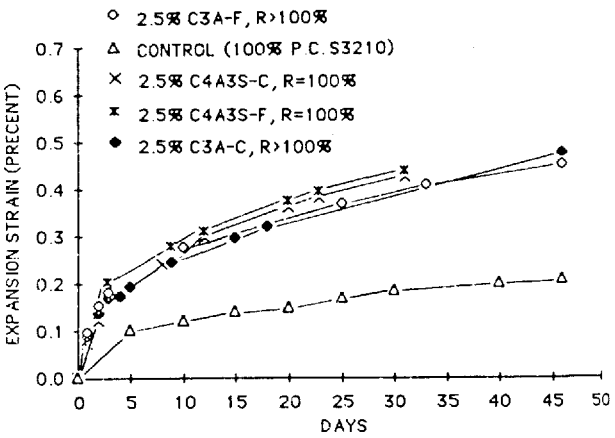

Fig. 4: Effects of type and fineness of expansive component on expansion.

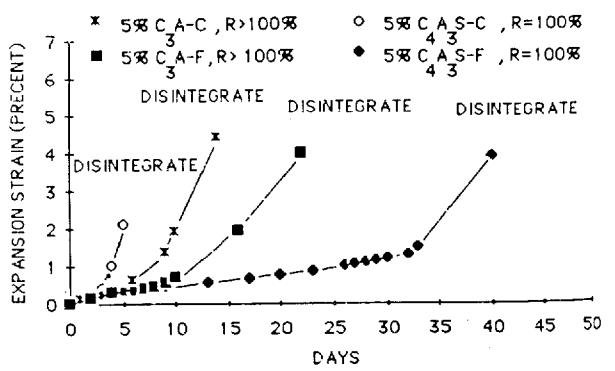

Fig. 5: Effects of type and fineness of expansive component on expansion.

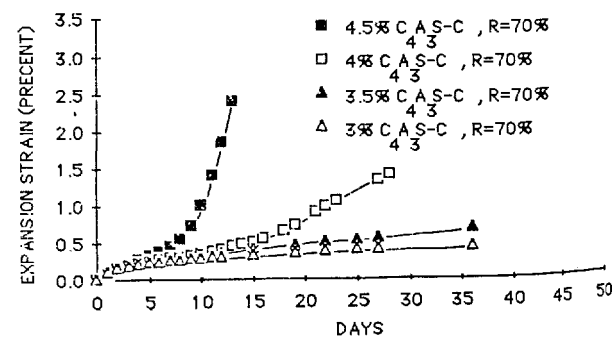

Fig. 6: Effects of increasing content of expansive component on expansion.

several blends containing the impacted clinker ECL-103V (8-13 microns). Comparison of the 15%, 20%, and 35% mixes gives the effect of increasing expansive clinker wt% on expansion while maintaining %R at 70. Clearly, as wt% expansive clinker increases, expansion increases just as shown in previous work (6). Comparing the 30% clinker and the 35% clinker explains the effect of increasing %R on expansion while maintaining constant wt% expansive clinker. In these cases increasing wt.% clinker while maintaining constant %R or increasing %R while maintaining constant wt.% clinker yielded higher expansion rates and magnitudes.

An interesting feature in ECL-103V and ECL-103G1 series is that regardless of mix composition, expansion was virtually completed within the first two days of curing. The 35% clinker in Fig. 10 shows a very peculiar and interesting feature in that expansive cements could accommodate as much as 2.5% expansion strain even as

Menashi D. Cohen and Barzin Mobasher, Department of Civil Engineering,
Northeastern University, Boston, Massachusetts 02115, U.S.A.

3.3 PHYSICO-CHEMICAL, MICROSTRUCTURAL, AND MICROMECHANICAL INVESTIGATIONS OF SULFOALUMINATE-TYPE EXPANSIVE CEMENTS

RECHERCHES PHYSICO-CHIMIQUE, MICROSTRUCTURALE, ET MICROMÉCANIQUE SUR UN CIMENT EXPANSIF DU TYPE-SULFOALUMINATE

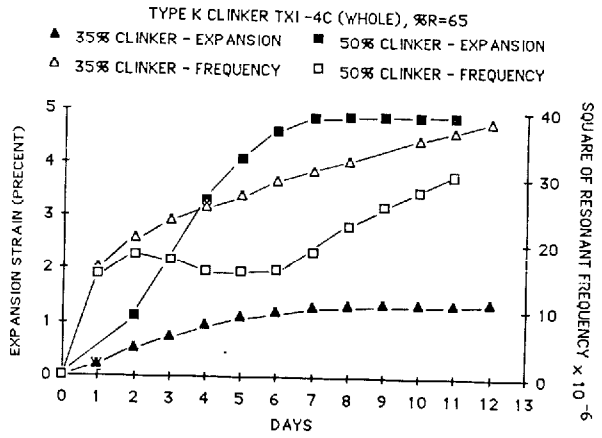

Fig. 7: Strength-Expansion relationship of expansive cement blends: Effects of particle sizes.

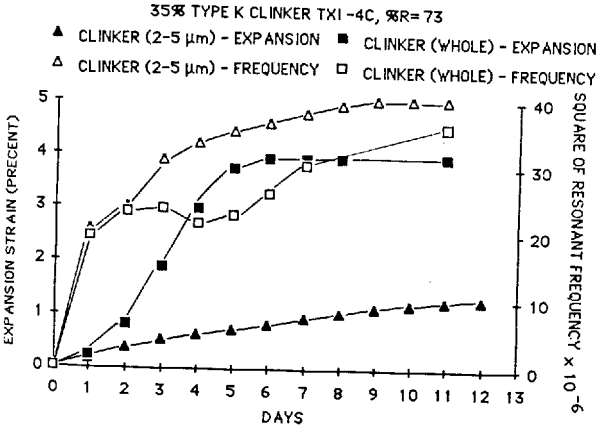

Fig. 8: Strength-Expansion relationship of expansive cement blends: Effects of content of expansive component.

early as two days without disintegrating. Normally this amount of expansion could not have been accommodated so soon if the matrix had not developed such high strength. Moreover, such high expansion magnitude usually leads to disintegration. The very high rate and magnitude of expansion development in only two days and the ability of the mixes to accommodate the expansion can only be attributed to the high amount of free lime and its effect on accelerating ettringite formation. Virtually, in all the blends containing the high free lime Type K expansive clinker ECL-103, expansion was completed in two days.

SHRINKAGE MEASUREMENTS

The shrinkage characteristics (23±1 °C, 45%±3% Rh) of Type K expansive cements, specifically magnitude and rate, were also studied (30). Reinforced and unreinforced expansive cement paste and mortar blends of p.c., S3210, gypsum G-1, and expansive component (pure $C_4A_3\bar{S}$ or ECL-103 V (or G1)) were mixed, casted, and cured for predetermined number of days before shrinkage. For example, many specimens were subjected to shrinkage after different duration of curing, some before developing their full expansion potential. Results, showed that shrinkage characteristics of expansive cements are different from those of portland cement. Generally, expansive cements showed higher shrinkage magnitudes than those of the specific portland cement used but it is cautioned that this finding may vary for other types of portland cements. Although the same factors are involved in the shrinkage process of expansive cement and portland cements, the following processes are of greater significance in expansive cements and render different expansive cement shrinkage

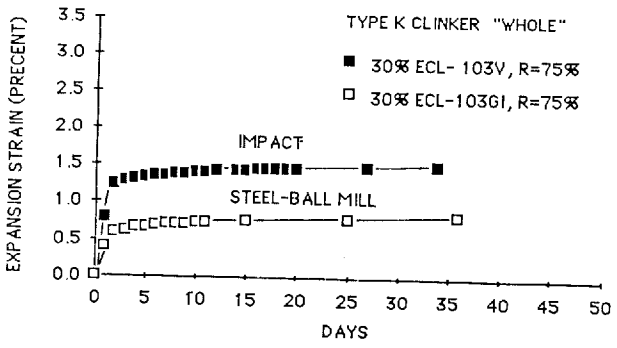

Fig. 9: Effect of grinding method of expansive clinker on expansion.

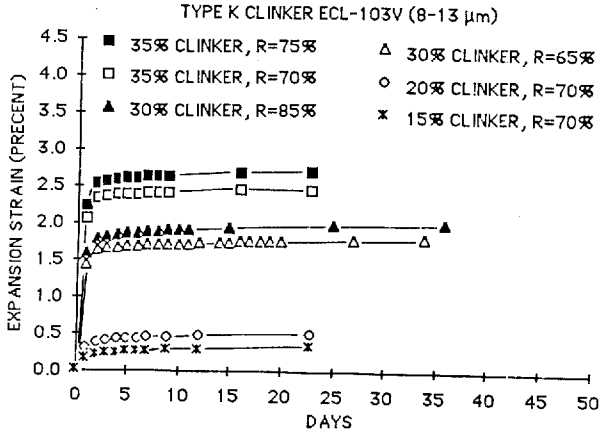

Fig. 10: Expansion behavior of different series of blends.

behavior: formation of pores/microcracks, interaction of expansion and shrinkage, loss of water adsorbed on the surfaces of ettringite, and decomposition of ettringite.

It was also found that large amounts of expansive component resulting in excessive expansion and strength drop could lead to higher shrinkage magnitudes because of excess microcracking. Moreover, although free expansion paste specimens shrink more than restrained expansion paste specimens, they follow a similar shrinkage trend.

The stability of ettringite upon carbonation was also tested and results are close to those of other investigators (31-33). It was shown that ettringite decomposes to gypsum, calcite, and an alumina bearing product. Since CO_2 attack is limited to surface of concrete, smaller specimens are more susceptible to carbonation attack because of their higher surface to volume ratios.

CONCLUSIONS

This research has shown that one can utilize the topochemical Crystal Growth Theory to explain the hydration kinetics and strength-expansion behaviors of sulfoaluminate-type expansive cements.

The sulfate solubility study with $BaCl_2$ precipitation is not as sensitive to $C_4A_3\bar{S}$ fineness and amount as it is for C_3A in suspension hydration. On the other hand, expansion measurements showed that fineness plays a dominant role in expansion behavior.

SEM micrographs of suspension hydration indicate that although crystals grow on the surfaces of both C_3A and $C_4A_3\bar{S}$ particles, there exists some morphological difference between them. This morphological difference made it difficult to check the theory (6,22,23) that $C_4A_3\bar{S}$ particles produce larger ettringite than C_3A crystals. Moreover, because of the large distribution

Menashi D. Cohen and Barzin Mobasher, Department of Civil Engineering, Northeastern University, Boston, Massachusetts 02115, U.S.A.

3.3 PHYSICO-CHEMICAL, MICROSTRUCTURAL, AND MICROMECHANICAL INVESTIGATIONS OF SULFOALUMINATE-TYPE EXPANSIVE CEMENTS
RECHERCHES PHYSICO-CHIMIQUE, MICROSTRUCTURALE, ET MICROMÉCANIQUE SUR UN CIMENT EXPANSIF DU TYPE-SULFOALUMINATE

of $C_4A_3\bar{S}$ and C_3A particle sizes it was difficult to develop an accurate relationship between particle size and length of ettringite crystals. Very narrow and distinct particle size distributions such as 5-10 and 30-35 microns should be used to provide information for developing the relationship.

Analysis of SEM micrographs at high magnification could give the false impression that crystals are dispersed in the matrix. This could lead one to suggest that the mode of ettringite formation is through-solution. SEM micrographs examined at lower magnification, however, suggested that the mode of formation is topochemical.

Internal restraint by directional wire reinforcement does not appear to influence ettringite morphology in expansive cements. Results reported by other investigators on the effects of externally applied constant pressures, however, indicate morphological differences in ettringite. This suggests that different mechanisms may be operative in the two restraining conditions.

The strength-expansion studies showed the sensitivities of expansion and strength development patterns to wt.% and fineness of expansive component, and extent of reaction (%R). Specifically, the effects of fineness and particle size distributions in this study and elsewhere (4,5,6,21,22,23,31) suggest that the mechanism of ettringite formation and subsequent expansion is topochemical Crystal Growth (first school). Higher magnitude and duration of expansion could lead to abnormal behavior, a phenomenon associated with double curvature expansion and strength drop (6,31). Moreover, as expected high free lime content could accelerate formation of ettringite such that all expansion could be completed within the first two days of hydration. The effect of the high free-lime content on accelerating the ettringite formation at the early age seems to enable the cement matrix to accommodate a large magnitude of expansion.

In the shrinkage studies, it was shown that expansive cement shrinks more than portland cement. If expansive cement is subjected to shrinkage before it has fully expanded to its potential, serious problems may arise resulting in loss of strength. In future research more emphasis should be invested at identifying and quantifying the parameters involved during the shrinkage of expansive cements.

Since ettringite readily decomposes upon carbonation, expansive cements may be more durable and provide better service if they have a low surface area to volume ratio.

ACKNOWLEDGMENTS

This research was supported by the U.S. National Science Foundation.

REFERENCES

1. H. E. Shwiete, U. Ludwig, and P. Jager, "Investigation in the System $3CaO-Al_2O_3-CaSO_4-CaO-H_2O$," Symposium on Structure of Portland Cement Paste and Concrete. Special Report 90, pp. 353-367, Highway Research Board, Washington, D.C., 1966.
2. G. L. Kalousek and E. J. Benton, "Mechanism of Seawater Attack on Cement Pastes," ACI Journal No. G7-9, pp. 187-192, 1970.
3. A. Bentur and M. Ish-Shalom, "Properties of Type Expansive Cement of Pure Components. II. Proposed Mechanism of Ettringite Formation and Expansion in Unrestrained Paste of Pure Expansive Component," J. Cement and Research, V. 4, pp. 709-721, 1974.
4. C.W. Richards and R.A. Helmuth, "Expansive Cement Concrete--Micromechanical Models for Free and Restrained Expansion," Technical Report No. 191, Dept. of Civil Eng., Stanford University, Stanford, Ca. 1977.
5. A. Kerdegari, "The Role of Gypsum in Portland Cement and Expansive Cement," Ph.D. Dissertation, Dept. of Civil Eng., Stanford University, Stanford, Ca. 1978.
6. M.D. Cohen, "Micromechanics of Expansive Mechanisms in Expansive Cement Concretes," Ph.D. Dissertation, Dept. of Civil Eng., Stanford University, Stanford, Ca. 1981.
7. K. Ogawa and D.M. Roy, J. Cement and Concrete Research, V.12, pp. 101-109, 1982.
8. M. Ish-Shalom and A. Bentur, "Properties of Type K Expansive Cement of Pure Components. I. Hydration of Unrestrained Paste of Expansive Components-Results," J. Cement and Concrete Research, V. 4, pp. 519-532, 1974.
9. P.P. Budnikov and I.V. Kravchenko, "Expansive Cements. Principal Paper--Expansive Cements," Proc. of the Fifth Int. Symp. on the Chemistry of Cement, V. 4, pp. 319-330, Tokyo, 1968.
10. T. Nakamura, G. Sudoh, and S. Akaiwa, "Mineralogical Composition of Expansive Cement Clinker Rich in SiO_2 and Its Expansibility," Proc. of the Fifth Int. Sym. on the Chemistry of Cement, V. 4, pp. 351-365, Tokyo, 1968.
11. I. Soroka, Portland Cement Paste and Concrete, London and Basingstoke: The MacMillan Press, Ltd., 1979.
12. S. Chen and P.K. Mehta, J. Cement and Concrete Research, V. 12, pp. 257-259, 1982.
13. P.K. Mehta, "Mechanism of Expansion Associate With Ettringite Formation," J. Cement and Concrete Research, V. 3, pp. 1-6, 1973.
14. P.K. Mehta and S. Wang, J. Cement and Concrete Research, V. 12, pp. 121-122, 1982.
15. P.K. Mehta and F. Hu, "Further Evidence for Expansion of Ettringite by Water Adsorption," J. Am. Cer. Soc.-Discussion and Notes, pp. 179-181, 1978.
16. V.A. Rossetti, G. Chiocchio, and A.E. Paolini, "Expansive Properties of the Mixture $C_4A\bar{S}H_{12}$-$2C\bar{S}$. I. An Hypothesis on the Expansion Mechanism," J. Cement and Concrete Research, V. 12, pp. 577-585. 1982.
17. M.D. Cohen, Theories of Expansion in Sulfoaluminate-Type Expansive Cements: Schools of Thought," J. Cement and Concrete Research, V. 13, pp. 809-818, 1983.
18. B. Mather, A discussion of ref. # 17, J. Cement and Concrete Research, V. 14, pp. 603-609, 1984.
19. M.D. Cohen, A reply to the discussion of ref. 18, J. Cement and Concrete Research, V. 14, pp. 610-612, 1984.
20. M.D. Cohen, E. Campbell, and W. Fowle, "Kinetics and Morphology of Ettringite Formation, " Proc. of the VIIth Int. Conf. on Cement Microscopy, pp. 360-381, Fort Worth, 1985.
21. M.D. Cohen, "Microstructural Analysis of Ettringite Formation: Scanning Electron Microscope," Proc. of the 4th Int. Conf. on Cement Microscopy, pp. 204-224, Las Vegas, 1982.
22. M.D. Cohen, "Modeling of Expansive Cements," J. Cement and Concrete Research, V. 13, pp. 519-528, 1983.
23. M.D. Cohen and B.B. Bantimba, "Correlation of Unrestrained Hydration Expansion and Particle Size Distribution of $4CaO.3Al_2O_3.SO_3$," Report No. 1 to National Science Foundation, Tech. Rep. CE-84-1, Dept. Civil Eng., Northeastern University, Boston, Ma. 1984.
24. M.D. Cohen and H. Nayeb Hashemi, "Crystal Morphology Under Pressure," Proc. of the VIIth Int. Conf. on Cement Microscopy, pp. 267-276, Fort Worth, 1985.
25. R. Sh. Mikhail, S.A. Abo-El-Enein, S. Hanofi, and R.J. Good, "Ettringite Formation in Compressed Expansive Cement Pastes," J. Cement and Concrete Research, V. 11, pp. 665-673, 1981.
26. D. A. Burciaga, "Micromechanical Modeling of Expansive Cements," Engineer Thesis, Dept. of Civil Eng., Stanford University, Stanford, Ca. 1977.
27. A.M. Neville, Properties of Concrete, p. 282, New York: John Wiley and Sons. Inc. 1963.
28. S. Spinner and W. Thefft, "A Method for Determining Mechanical Resonance Frequencies and for Calculating Elastic Moduli from their Frequencies," ASTM Proc. 61, pp. 1221-1238, 1961.
29. G. Pickett, "Equations for Computing Elastic Constants form Flexural and Torsional Resonant Frequencies of Vibration of Prisms and Cylinders," ASTM Proc. 45, pp. 846-863, 1945. PCA Res. Bul. 7.
30. M.D. Cohen and B. Mobasher, "Shrinkage of Expansive Cements," Submitted to J. Am. Cer. Soc. 1985.
31. M.D. Cohen and C.W. Richards, "Effects of Particles Sizes of Expansion Clinker on Strength-Expansion Characteristics of Type K Expansive Cements," J. of Cement and Concrete Research, V. 12, pp. 717-725, 1982.
32. J. Calleja, "Durability," Proc. of the 7th Int. Cong. on the Chemistry of Cement, VII-2/1, V. 1, Paris, 1980.
33. D. Gaspar, M. Munoz-Plaza, and T. Vazquez, "Action on CO_2 on a Portland Cement. II.," Mat. de Constr. (IETCC-Spain), (in Spanish), No. 168, 75-87, 1978.
34. D. Gaspar, M. Munoz-Plaza, and F. Trivino, "Action of CO_2 on a Portland Cement. III.," Mat. de Constr. (IETCC-Spain), (in Spanish), No. 169, 63-73, 1978.

V.Klassen BTIBM, Belgorod, U.S.S.R.

INTERACTIONS IN $CaCO_3$-$SiO_2$$R_2CO_3$ (R_2 SO_4) MIXTURES

P

There are domains of solid solutions (shaded areas) in diagrams of $CaCO_3$-Na_2CO_3 and $CaCO_3$-K_2CO_3 state systems previously studied by Niggli, Krüger and others. Under the atmospheric pressure of CO_2 and in opened system as well there exists the possibility to form the $K_2Ca_2(CO_3)_3$ compounds.

Transformations occured in $CaCO_3$-alkali-sulphate systems under air atmosphere have been studied and the state diagrams were plotted. $CaCO_3$+Na_2SO_4 were found to interact and form a number of solid solutions like Kurnakov's bertollides; eutectic temperatures of $5CaCO_3 \cdot 6Na_2SO_4$, $6CaCO_3 \cdot 5K_2SO_4$ and $5CaCO_3 \cdot 4K_3Na(SO_4)_2$ are 825°C, 880°C and 820°C respectively.

Alkali admixtures cause $CaCO_3$ multistage dissociation (up to 7 stages) connected with the formation of complex salts, solid solutions and melts containing carbonate, especially of eutectic composition. Addition of SiO_2 accelerates the reactions of $2CaCO_3$+ $+SiO_2$= $2C_2S$+$2CO_2$ as a result of formation of low-temperature melts. The dissociation of $CaCO_3$ is speeded up to 850°C (the temperature of SiO_2 complete fixing) and then due to formation of $2C_2S \cdot CaCO_3$ and $R_2Ca(CO_3)_2$ is slowed down. The temperature of CO_2 release from the compounds rises in the set: $CaCO_3 \rightarrow 2C_2S \cdot CaCO_3 \rightarrow R_2Ca(CO_3)_2$.

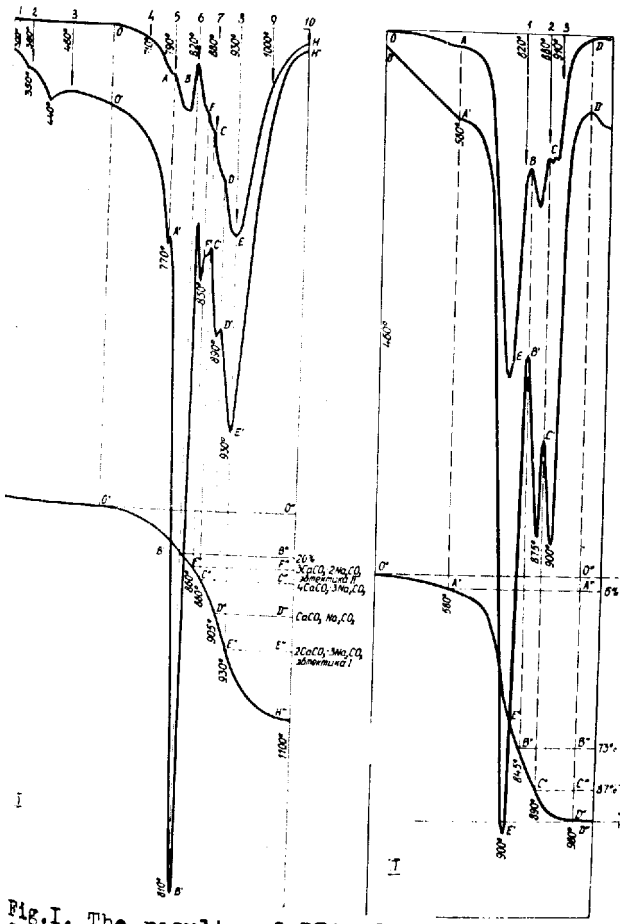

Fig.I. The results of DTA of the mixes $CaCO_3$+Na_2CO_3(I) and $2,7CaCO_3$+SiO_2+8%K_2CO_3 (2) in the open air.

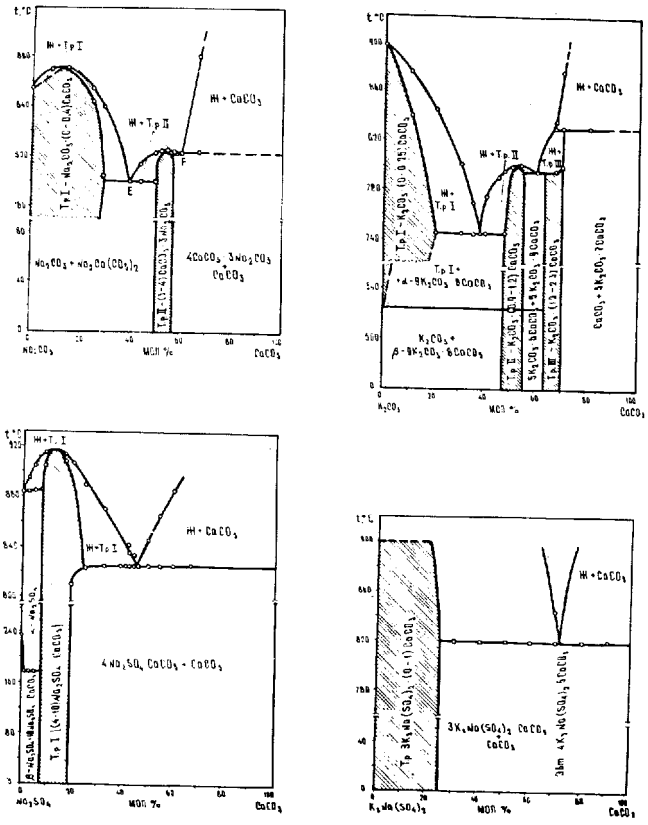

Fig.2. The diagram of the system state at the partial pressure, CO_2 101,3 kPa.

In carbonate mixtures at 900°C I wt % R_2O forms 5-6 wt % melts. According to our data, R_2O content in the zone of decarbonization is 2-4 weight %. It promotes the formation of 10-20 wt % liquid phase at low temperature and, hence, fundamentally changes the conception of solid state reactions taking place in cement kilns.

There are exchange reactions between R_2SO_4 and $CaCO_3$ in atmosphere of combustion products. These reactions produce $2C_2S \cdot CaSO_4$. This compound may be formed by the interaction of fuel oil sulphur with material burned in a kiln. Above 1300°C $2C_2S \cdot CaSO_4$ is being decomposed and reacting with CaO forms low active alite.

P

Table I.

X-ray characteristics of $K_2Ca_2(CO_3)_3$

d,A	I	d,A	I	d,A	I	d,A	I	d,A	I
6,85	8	3,038	95	2,22	I5	2,00	6	I,77	I0
6,60	9	2,948	I00	2,I8	9	I,926	I8	I,7I	9
3,83	I2	2,637	43	2,I6	I2	I,9I5	23	I,69	5
3,44	8	2,539	48	2,II	5	I,873	33	I,53	8
3,26	7	2,468	45	2,07	6	I,84	II	I,5I5	I0
3,I3	II	2,29	I9	2,0I6	I4	I,8I	I9	I,47	7

Table 2.

X-ray characteristics

$Na_2SO_4:CaCO_3$ = I0:I				$Na_2SO_4:CaCO_3$ = 4:I			
d,A	I	d,A	I	d,A	I	d,A	I
4,63	4	2,I96	6	4,60	2	2,I83	8
3,878	70	2,I43	2	3,85	86	2,I3	2
3,559	26	I,937	30	3,558	48	I,923	36
2,952	4	I,784	8	2,926	3	I,775	I2
2,824	7I	I,568	I0	2,805	I00	I,556	I0
2,667	I00	I,54	6	2,644	80	I,52	4
2,309	5	I,48	6	2,289	4	I,473	I0

K.Karibaev
N.Bajirov
A.Patcenko
N.Panina
Institut polytechnique de Kiev, NIICement - Moscow, U.S.S.R.

1

MODIFICATION DE LA STRUCTURE DES SCORIES DE LA DEPHOSPHORATION THERMIQUE ELECTRIQUE.

F

Des scories de déphosphoration thérmique électrique granulées représentent la vitre à composition vollastonitique caractérisée par la structure polymérique. Il est connu que la réactivité de la scorie dépend du degré de la polymérisation des anions silico-oxygéniques. Lors de l'hydratation il se produit la déstruction de la vitre pour le compte de la rupture de liaisons Si-O-Si, donc la variation de la structure anionique est un facteur déterminant l'hydrolicité des scories.

Dans le travail présent nous avons montré que l'introduction dans la scorie fondue à 1723K d'additions contenant de Mg^{2+}, Ca^{2+}, Ba^{2+} augmente la réactivité. L'introduction de ces additions modificatrices provoque des variations de la structure de la scorie qui se fixe ensuite dans la vitre lors de la granulation. Les oxydes MeO diffusant dans le bain fondu sont des donneurs d'ions d'oxygène qui assure la rupture de liaisons entre les tétraèdres de la structure.

Des courbes cinétiques de l'interaction du molybdate d'ammonium avec scorie (fig.I) témoignent de la présence importante dans la scorie modifiée de tétraèdres d'île et d'orthosilicates. Le temps de passage de 99% de SiO_2 total en acide siliceuse molybdénique réduit en 2,5 fois. Le changement des courbes indique sur la haute vitesse de l'hydrolyse de la scorie modifiée et sur la formation du complexe siliceux molybdenique jaune, ce qui est assuré par la dépolymérisation d'anions siliceux oxygénique – résultat de l'action des additions modificatrices.

Selon les données de l'analyse aux rayons X des produits de l'hydratation de la scorie dans la solution de chaux (fig.2), la scorie modifiée a la plus haute réactivité. L'abaissement de la basicité des hydrosilicates lors de l'hydratation de la scorie modifieé dans la solution de chaux est assuré par l'accélération de la lixiviation de SiO_2 par suite de la destruction de la scorie. Ce même fait explique l'augmentation de la quantité de néoformations, ce qui est affirmé par l'accroissement de l'intensité de réflexion.

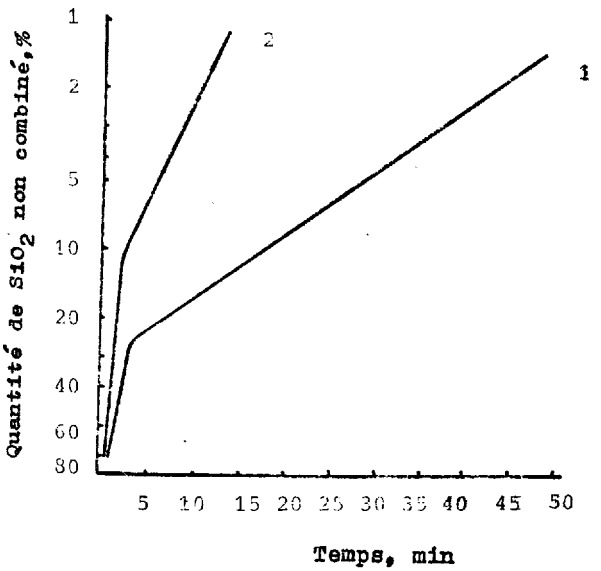

Fig.I. Courbes cinetiques de l'interaction du molybdate d'ammonium avec la scorie de départ (I) et la scorie modifiée (2).

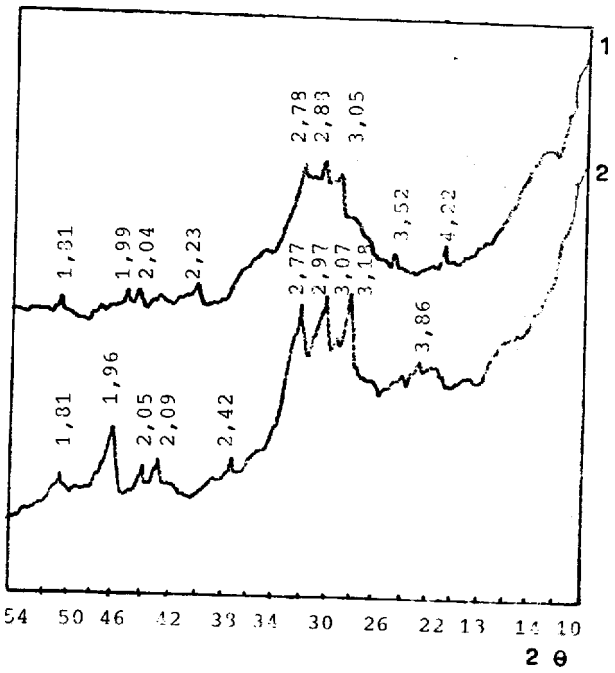

Fig.2. Diffraction à rayons X des produits de l'hydratation des scories dans la solution de chaux I - scorie de départ; 2 -scorie modifiée.

La haute réactivité de la scorie modifiée est confirmée par l'analyse thermique differentielle. La courbe de l'ATD du pré-

cipité se formant lors de l'hydratation de la scorie-témoin dans la solution de chaux (fig.3) montre la présence d'effets faibles endothermiques à 470 et 785°C indicant sur la teneur faible en C_2SH (A) et d'un effet fort exothermique à 940°C indicant sur la teneur prédominante de la vitre non réagie.

Sur la courbe de l'ATD des produits de l'hydratation de la scorie modifiée il ya un effet endothermique profond à 205-220°C indicant sur la quantité accrue de C_2SH_2.

Il est à noter un certaine accroissement de l'effet endothermique à 490 et 780°C, la diminution considérable de l'effet exothermique à 945°C aussi l'augmentation de la perte de masse l'echantillon.

Lors de l'étuvage, la scorie modifiée présente l'aptitude au durcissement avec la formation d'hydrosilicate de calcium faiblement cristallisés à composition CSH(B).

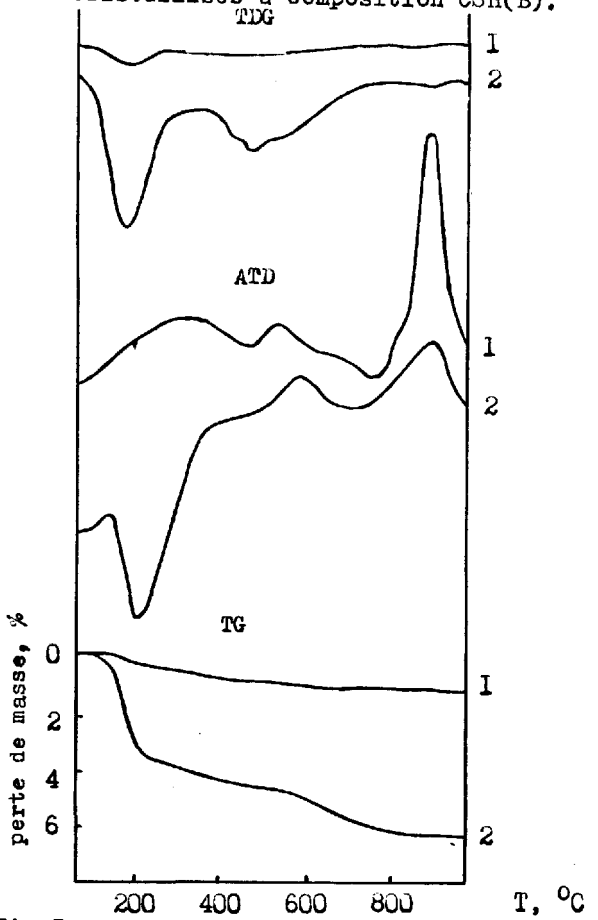

Fig.3. Analyse thermique de produits de l'hydratation
I - scorie de depart; 2 - scorie modifiée.

Les résultats de recherches confirment la possibilité de l'augmentation de la réactivité des scories à l'aide de l'action orientée sur la structure du methasilicate de calcium etant une phase prédominante et la plus inerte des scories.

V.M. KOLBASSOV Institut de Génie chimique D.I. Mendelev, Moscow, U.S.S.R.

MODIFICATION DE LA STRUCTURE HYDRATEE DES CIMENTS

P

La formation de la structure du ciment durci est déterminée essentiellement par l'hydratation du silicate tricalcique accompagnée de la création en quantité prépondérante des produits hydratés à dispersité, morphologie et cristallinité différentes. Les autres composants du ciment y jouent également un rôle déterminé. Cependant, dans un ciment polyminéral c'est le C_3S qui en saturant rapidement la phase liquide d'ions de calcium détermine les conditions du milieu où se déroule également l'hydratation de ces phases de clinker. De cette manière, la présence du C_3S dans le ciment constitue le facteur principal déterminant les propriétés structurales et techniques du ciment durci.

Au cours de l'hydratation de C_3S il se forme à la surface et dans le volume initial de ses grains et se développe dans le temps une couche de nouvelles formations hydratées constituée selon les concepts actuels (1) d'hydrates externe et interne qui diffèrent entre eux par la structure et la morphologie de leurs particules composantes.

Comme l'ont montré les résultats des études à la microscopie électronique (2, 3) réalisées selon une méthode originale permettant d'observer la surface intacte des particules hydratables, dès les premières secondes de l'interaction C_3S - eau à la surface des grains du C_3S commencent à apparaître de nouvelles formations hydratées qui recouvrent certaines zones de la surface de ces grains sous forme des particules à grains fins (diffraction électronique de 1,83 Å) et sous des formes morphologiques plus perfectionnées (sphérolithes, aiguilles de 1 μ). La diffraction électronique de ces formations (1,83; 1,66; 1,53 Å) permet de les identifier comme la phase C-S-H.

Il est à noter qu'une modification de la composition du milieu de durcissement (l'introduction d'adjuvants de gypse dans le système "C_3S + eau") amenait à un changement considérable des indices morphologiques des hydrosilicates de calcium (HSC) de formation initiale. Ce qui est plus typique pour ces conditions c'est une apparition rapide de HSC phanérocristallins ayant également de diverses formes morphologiques.

L'apparition des hydrates primaires dans des zones déterminées de la surface des grains du C_3S est due au fait qu'ils se forment initialement dans les zones les plus actives de la surface (aux endroits de concentration de dislocations, etc.) lesquelles les premières se soumettent à l'hydratation et commencent à des vitesses différentes à saturer d'ions formateurs les volumes locaux proches de la surface de la phase liquide des hydrates. Les résultats des études (2-8) permettent d'estimer que la vitesse de formation, les formes d'accroissement morphologiques, la dispersité de HSC (et d'autres nouvelles formations dans le ciment polyminéral durci) sont déterminées en premier lieu par la composition de la phase liquide et son homogénéité en volume (par la vitesse de saturation en ions formateurs d'hydrates, la valeur et le gradient de leurs concentrations, la valeur de sursaturations). Dans les systèmes "ciment - eau" dépourvus d'adjuvants solubles dans l'eau, ces facteurs sont dus à l'activité d'hydratation de la surface des grains de ciment (y compris de ses zones distinctes) qui détermine l'intensité et la régularité d'arrivée d'ions formateurs d'hydrates à la phase liquide. Lorsqu'on introduit avec l'eau de gâchage des adjuvants solubles dans l'eau, ce sont ces derniers qui y jouent un rôle déterminant. Ainsi, à la mise en contact avec la phase liquide d'une composition homogène dans tout son volume, il se forme de préférence des hydrates à forme arrondie des particules. En revanche, dans les conditions du gradient des concentrations de la phase liquide, il se crée des courants de convection favorisant le développement de cristaux de forme allongée (aciculaires, prismatiques, fibreux). Des sursaturations élevées en Ca^{2+} établies dans le volume intégral de la phase liquide

contribuent à une formation d'hydrates à cristallinité élevée à l'instar de ceux formés à l'aide de la méthode de traitement par chaleur humide ou par suite d'addition de $CaCl_2$. Un haut gradient de concentration que possèdent les volumes locaux de la phase liquide réalisée, en particulier, aux premiers stades d'hydratation du C_3S dans des microvolumes proches de la surface de la phase liquide stimule un accroissement rapide des groupes unitaires d'hydrates cristallins relativement gros. Une formation simultanée d'hydrates sur la base des C_3S et β-C_2S sous diverses formes morphologiques observées dans les ouvrages (2,3) est conséquence d'une inhomogénéité de la phase liquide dans ses microvolumes locaux.

La morphologie et les dimensions des particules hydratées dépendent en grande partie du fait que la formation d'hydrates se produit à des conditions restreintes ainsi qu'en présence d'une surface solide développée laquelle, à des paramètres déterminés du réseau cristallin, peut jouer le rôle de substrat pour la formation de germes et d'hydrates. Dans de pareilles conditions, il se forme une structure dense à haute dispersité, amorphe sous les rayons X /métamicte d'après I.G. Chpinova (9)/ typique pour un hydrate interne (10). Une même structure prédomine dans le ciment durci à un bas rapport liquide - solide additionné d'agents tensio-actifs (ATA).

A leur tour, les hydrates revêtant de diverses formes morphologiques et capables, de ce fait, à fixer, à telle ou telle vitesse, les ions de la phase liquide qui les alimente, modifient également la composition et l'anisotropie de la structure. Par conséquent, la composition de la phase liquide est également sujette à des modifications périodiques tant au niveau des macrovolumes qu'à celui des microvolumes. On peut apprécier ces modifications d'après la morphologie des hydrates qui forment la structure du ciment durci.

Durant l'hydratation du C_3S les nouvelles formations, grâce à une augmentation de leur teneur en volume par rapport au volume des grains initiaux de liant, se propagent sur toute leur surface et remplissent l'espace intergranulaire du ciment durci ainsi que le volume des grains initiaux lequel se rétrécit par suite de l'hydratation.

La surface des grains de ciment avant le début de leur hydratation doit être considérée comme interface des zones de formation des hydrates interne et externe. Ceci est confirmé par le rapport volumétrique des hydrates interne et externe dans le ciment durci (10) ainsi que par une topographie différente de structure des hydrates dans ces zones ce qui est dû à des conditions différentes de leur formation.

Du fait que l'interaction initiale "C_3S - eau" passe à la surface du premier, le front de développement de l'hydrate interne est orienté vers l'intérieur du grain à partir de cette surface tandis que celui de l'hydrate externe vers l'espace intergranulaire. Dès le premier moment d'hydratation du C_3S commence la formation de l'hydrate externe. Des phases hydratées distinctes qui font partie de sa composition apparaissent et se développent sous des formes d'accroissement actives (2) et modifient ainsi la composition et la symétrie de la phase liquide en influant à travers cette dernière sur la morphologie et la dispersité de la portion suivante des hydrates en précipitation.

Des masses d'hydrates à grains fins amorphes sous les rayons X apparaissent par conséquent et se déposent à la surface pour remplir l'espace libre entre les plus grosses particules d'hydrates formées auparavant. Ce dernier phénomène s'accompagne de nouveau par une modification de la composition et de la symétrie de la phase liquide. Il se produit alors une formation alternée de phases hydratées sous diverses formes morphologiques. Cela constitue, apparemment, la cause même de formation d'une texture feuilletée ou à blocs alternés signalée par

les auteurs des ouvrages (11,12). Grâce à la nature métasomatique* de sa formation (12) l'hydrate interne possède une structure plus homogène, dense, submicrocristalline, amorphe sous les rayons X formée dans des conditions restreintes sous les couches de l'hydrate externe formé auparavant.

Une inhomogénéité de la phase liquide est propre dans une plus grande partie à la zone de développement de l'hydrate externe qui remplit l'espace intergranulaire dans le ciment durci.

Plusieurs propriétés techniques du ciment durci dépendent de sa porosité et, en premier lieu, du nombre de gros pores (à un rayon conventionnel de 10^3 Å). Mais les pores pareils ne peuvent se former que dans la zone de l'hydrate externe. Aussi, la zone de développement de l'hydrate externe est-elle la partie la plus faible et friable dans la structure du ciment durci d'où la nécessité d'améliorer la solidité et la densité de cette zone en premier lieu.

Dans une certaine mesure, on peut l'obtenir par voie de régulation du rapport entre les épaisseurs des couches d'hydrates interne et externe grâce au choix de la finesse de broyage du ciment et de la densité d'assemblage de ses grains dans la structure en formation (en améliorant le rapport eau/ciment et le degré de densité). Plus fines sont les particules de clinker, plus minces seront les couches d'hydrate interne formées pendant son hydratation. Plus vaste est l'espace intergranulaire dans le ciment durci, plus grand volume pourra occuper et sera donc plus friable l'hydrate externe qui s'y développe.

Il est possible d'influer avec succès sur la dispersité et la morphologie des particules de l'hydrate externe qui déterminent la quantité et la solidité des contacts entre elles à l'aide d'adjuvants chimiques solubles dans l'eau (6-8).

Les adjuvants les plus efficaces au point de vue formation de la structure de la zone de l'hydrate externe sont ceux du type $NaNO_2$. De tels adjuvants ne permettent pas une formation de complexes avec les phases de clinker contenant de l'aluminium. Ces composés ont l'aspect de cristaux relativement gros qui ne jouent pas toujours un rôle positif dans la formation de la structure optimale du ciment durci. D'autre part, en apportant des modifications à la composition ionique de la phase liquide les adjuvants pareils sont capables d'initier une morphologie déterminée des particules formées au sein de l'hydrate externe. Ainsi, en présence d'adjuvants de nitrite de sodium, une quantité déterminée des particules de l'hydrate externe revêtent l'aspect de formations fibreuses ce qui permet de réaliser le soi-disant "autorenforcement" du ciment durci, en particulier, dans la zone la plus faible de son espace intergranulaire. La germination dans les pores du ciment durci de formations fibreuses s'accompagne d'une augmentation du nombre de contacts entre les particules solides et d'une diminution des dimensions des pores (7) ce qui, comme on le sait, rend plus dense et plus solide la structure en formation.

Les adjuvants de superplastifiants (SP) apportent, eux aussi, des transformations favorables dans la structure de l'hydrate externe. Grâce à leur effet réducteur d'eau, les adjuvants SP réduisent le volume de l'espace intergranulaire dans la pâte de ciment et, par conséquent, créent des conditions plus restreintes pour la formation et au développement de l'hydrate externe. Un rôle important y revient également à l'effet de modification d'adsorption des adjuvants SP. La stabilisation des hydrates obtenue grâce à cet effet en état finement divisé, amorphe sous les rayons X contribue encore davantage à optimiser la structure de l'hydrate externe dans le ciment durci.

* Métasomatose: processus de substitution chimique des minérais les uns par les autres avec la conservation d'anciennes forme, structure et d'autres particularités sous l'action des solutions qui entrent en contact avec les minérais.

Une combinaison de ces deux modes d'action des adjuvants SP approche considérablement la structure d'hydrate externe dans le ciment durci de celle de l'hydrate interne ce qui explique notamment un effet élevé de la résistance à la compression obtenu grâce à ce phénomène. Un rôle déterminé joue également une plus petite valeur des contraintes intérieures enregistrées dans le ciment durci où l'hydrate externe est représenté par des particules finement divisées, amorphes sous les rayons X, d'HSC et de portlandite.

Un moyen optimal d'agir sur la structure et les propriétés du ciment durci (en premier lieu dans la zone qu'y occupe l'hydrate externe) est une utilisation d'adjuvants combinés solubles dans l'eau constitués par des SP et électrolytes inorganiques. Grâce à ce procédé on a réussi à doubler presque la résistance à la compression et à la flexion du ciment durci et de réduire quatre fois sa porosité totale. La porosité d'un tel ciment durci ne constituait que ~ 3 % de volume, les pores à rayon efficace de plus de 10^3 Å étant pratiquement absents.

REFERENCES

1. M. Daimon, S. Neda, R. Kondo, "Morfhological study on hydration of Tricalcium silicate". Cement and Concrete Res., 1971, 1(4), p. 391-401.
2. Ю.М. Бутт, В.М. Колбасов, П.А. Козырева. Фазообразование на ранних стадиях гидратации портландцемента. Труды МХТИ им. Д.И. Менделеева, 1975, вып. 87, с. 48-50 (en russe).
3. Ю.М. Бутт, В.М. Колбасов, Н.А. Козырева. Дискуссия по докладу Г.Л. Калоусека "Процессы гидратации на ранних стадиях твердения цемента", Труды VI Международного конгресса по химии цемента, 1976, т. II, кн. 2, с. 105-107 (en russe).
4. Г.В. Топильский, Ю.М. Бутт, В.М. Колбасов. "К вопросу о составе и свойствах портландита в гидратированных портландцементах". Кристаллография, 1968, т. 13, 5, с. 1083-1088 (en russe).
5. В.М. Колбасов, Г.В. Топильский "Исследование гидратации портландцементных клинкеров", Известия АН СССР "Неорганические материалы", 1970, т. 6, 5, с. 967-970 (en russe).
6. Ю.М. Бутт, В.М. Колбасов "Влияние состава цемента и условий твердения на формирование структуры цементного камня", Труды VI Международного конгресса по химии цемента, 1976, т. II, кн. I, с. 281-283 (en russe).
7. Ю.М. Бутт, В.М. Колбасов "Твердение цементов при пониженных температурах и структурообразующая роль водорастворимых добавок", Труды II Международного симпозиума по зимнему бетонированию, 1975, т. I, с. 6-17 (en russe).
8. Ю.М. Бутт, В.М. Колбасов, Н.В. Фартунина "О влиянии условий среды твердения на структурную плотность цементного камня", Труды конференции "Siliconf", 1977, Будапешт, с. 471-481 (en russe).
9. Л.Г. Шпынова, Н.В. Белов, В.И. Чих "О метамиктности гидросиликатов кальция камня β-C_2S", ДАН СССР, 1979, т. 244, 6, с. 1115-1117 (en russe).
10. Р. Кондо, М. Даймон "Фазовый состав затвердевшего цементного камня", Труды VI Международного конгресса по химии цемента, 1976, т. II, кн. I, с. 244-257 (en russe).
11. Ю.М. Бутт, В.В. Тимашев "Скорость гидратации C_3S и особенности микроструктуры мономинерального камня", Строительные материалы из местного сырья и отходов промышленности Казахстана, 1972, с. 13-35 (en russe).
12. Л.Г. Шпынова, В.И. Чих "Взаимосвязь микроструктур клинкера, цементного порошка и камня", Цемент, 1978, 4, с.6-8 (en russe).

ILYINETS, A.M., SIMONOV, V.I., BIKBAU, M.Ya.
Institute of Crystallography of the Academy of Sciences, NIICement, Moscow, U.S.S.R.

NEW DATA CONCERNING ATOMIC STRUCTURES OF PORTLAND CEMENT SILICATES

P

Extensive physico-chemical investigations of polymorphous modifications of tricalcium silicates which are impotant components of portlandcement clinker, do not provide sufficient data on their crystal structure. The reasons lie in the difficulty of obtaining perfect single crystals of these compounds, particularly the high-temperature modifications stabilized at normal temperature. Up to now investigators failed to refine the structure of the high-temperature rhombohedral modificatio of C_3S, whose idealized model was proposed by Jeffry in 1952 / 1 /.

We obtained single crystals of rhombohedral modification of C_3S in the system $CaO-SiO_2-CaCl_2$ at 1400°C in silicate-chloride melt. Sr atoms were used as a stabilizer, keeping the high-temperature phase at normal temperature. X-ray analysis of crystals confirmed space group R3m / 2 / (unit cell parameters: a_o= 7.0767(9), c = 24.974 (4) Å, V = 1072.5 Å^3) and allowed us to refine the structure, proposed by Jeffry. The basis of structure is formed by Ca-polyhedra layers of two types: Ca1-polyhedra with seven vertices and greatly distorted Ca2, Ca3-octahedra. The packing of Ca-polyhedra in each layer and the manner of their connection with Si-tetrahedra is shown in Fig.1. Projection of structure of C_3S onto the ab-plane:

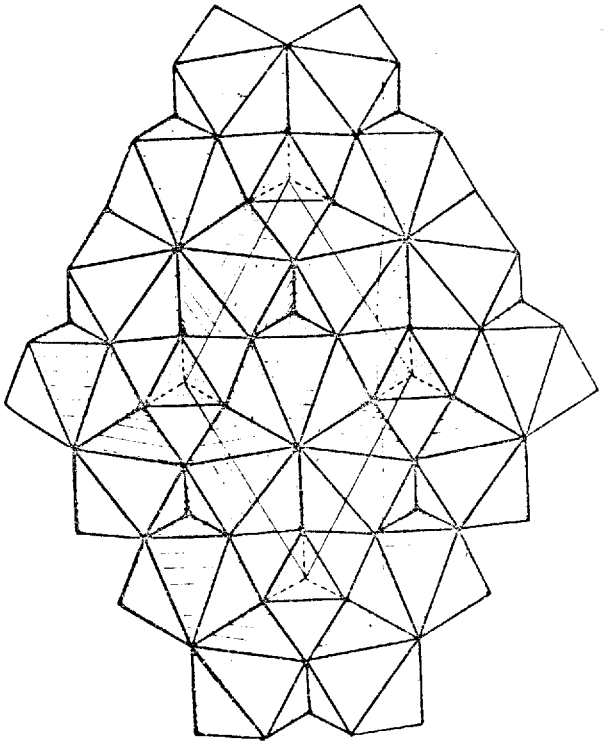

a - a layer of Ca-polyhedra with 7 vertices, z ≈ 0;

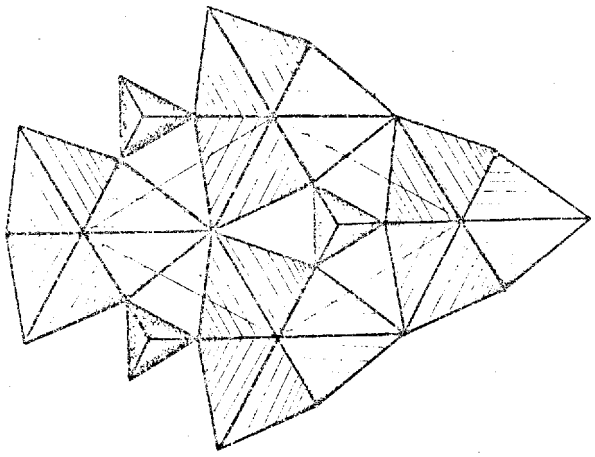

b - a layer of Ca2-octahedra, z ≈ 2/9;

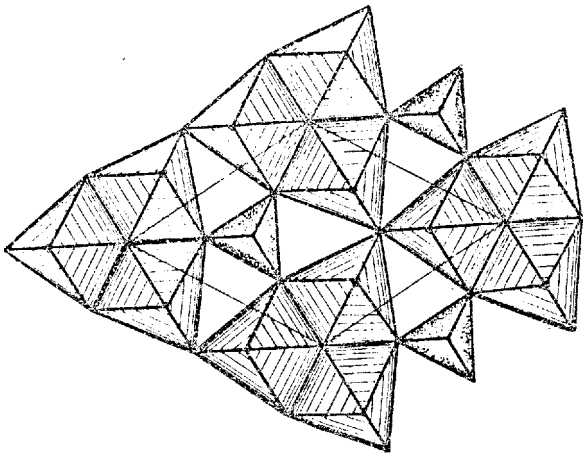

c - a layer of Ca3-octahedra, z ≈ 1/9.

The mutual arrangement of the layers along the c-axis is shown in Fig.2. A comparison with the Jeffry model shown that mutual arrangement of Ca and Si atoms almost coincides, as well as the positions of seven out of 9 oxygen atoms. A change of positions of two atoms is due to reorientation of Si-tetrahedra along the 3-fold axis and rotation of another Si-tetrahedra by 60° about the same axis. A similar change of positions of Si-tetrahedra was reported in / 3 /. It was established in studies of the high-temperature modification of C_3S at 1200°C. However, that paper also reports statistical orientation of Si-tetrahedra along the 3-fold axis: in 30% of cases it coincides with the Jeffry orientation and in 70% - it is just the opposite.

Nishi and Takeuchi in their paper were the first to show a correlation between the structures of the high-temperature rhombohedral modification and the low-temperature triclinic phase, established in / 4 /. The correlation between these two structures can be demonstrated more vividly in the form of a transitio matrix from unit cell parameters of a rhombohedral modification of C_3S, stabilized by us at normal temperature (a = 7.076 and c = 24.974 Å) to cell parameters of the triclinic phase (a = 11.67; b = 14.24; c = 13.72 Å; α = 105.3°, β = 94.2° γ = 90°). This matrix, line by line, has form: 2/3, 4/3, 1/3; -2,0,0; -1/3,-5/3, 1/3. Re-calculated parameters of a rhombohedral unit cell are: a = 11.65; b = 14.11; c = 13.61; α = 105°, β = 95°, γ = 90°; these values are father close to the parameters reported in / 4 /. This transformation allows one to recalculate the atomic coordinates of the triclinic phase to a twice-centered hexagonal unit cell. A comparison of the transformed atomic coordinates of triclinic modification with the atomic coordinates of the initial rhombohedral modification showed that all the cations and 37 oxygen atoms out of 45 are slightly displaced with respect to each other. A non-coincidence of coordinates of the remaining 8 oxygenatoms can be attributed to a reorientation of two Si-tetrahedra out of 9 along the 3-fold axis, including rotation of one of these two tetrahedra by 60° about the 3-fold axis with respect to the position of Si-tetrahedra in the rhombohedral modification / 5 /. One could have supposed that the change of the orientation of 2 out 9 Si-tetrahedra in the triclinic phase is due to statistical orientation of three tetrahedra, found in paper / 3 /. However, this correlation does not exist, because statistically oriented tetrahedra in paper / 3 / correspond to certain tetrahedra in / 2 /, while two reversely oriented tetrahedra in the triclinic phase correspond to other tetrahedra in / 2 /.

Thus, comparing structures of the "high-temperature", the "low-temperature" rhombohedral modifications and the low-temperature triclinic phase, one can come to a conclusion that the main difference between them lies in the orientation of Si-tetrahedra, while positions of Ca, Si atoms and free oxygen remain close. Apparently, the structures of the 5 remaining intermediate modifications of C_3S also differ from each other only by rotations of Si-tetrahedra.

We have also grown α'_L-C_2S single crystals in the same system $CaO-SiO_2-CaCl_2$, also stabilized by Sr atoms at normal temperature. Orthorhombic unit cell parameters are: a = 20.871(2), b = 9.496(1), c = 5.500(1) Å. Similar values of parameters of α_L-C_2S with 3-fold value of one of the parameters, as compared to α'_L-C_2S was reported in paper / 6 /. The differences lie only in setting crystallographic axes. The structure of the α'_L-phase was determined in paper / 7 / and refined to R-factor 7% in space group $Pna2_1$. The basis of the structure is formed by Ca-polyhedra with 8 vertices and Ca(Sr)-polyhedra with 10 vertices positioned along the a-axis. Peculiar is the orientation of Si-tetrahedra along the a-axis. It is assumed that the hexagonal structure of the high-temperature -phase of C_3S has all the Si-tetrahedra oriented in the same direction / 8 /. The transition $\alpha \rightarrow \alpha'$ is due to a possible rotation of Si-tetrahedra. In our case, 4 tetrahedra, out of 6, connected with Ca-polyhedra with 8 vertices, are connected along the a-axis, while two others are oriented in the opposite direction (Fig. 3). Apparently, it is this

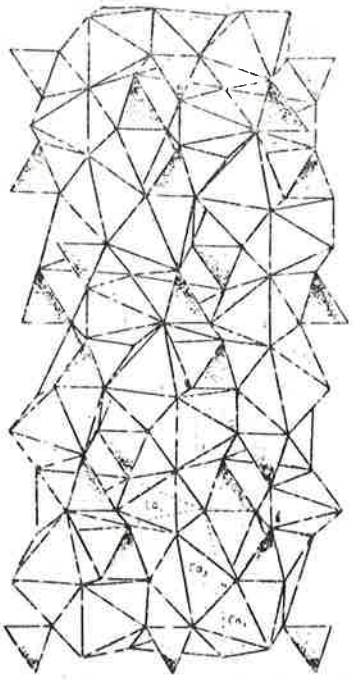

Fig. 2. Structure of rhombohedral modification of C_3S, (110) cut.

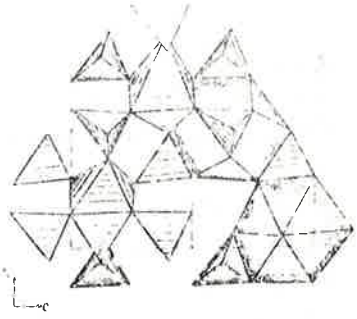

Fig. 3. Structure of α'-C_2S ($Ca(Ca,Sr)SiO_4$): two cuts, perpendicular to (100). The A-A cut shows only Ca-polyhedra with 8 vertices, the B-B cut - only Ca(Sr)-polyhedra with 10 vertices.

change of Si-tetrahedra orientation that leads to a 3-fold value of the parameter a = 20,871 Å (in another setting it is the c-axis). A further clarification of the mechanism of transition $\alpha \rightarrow \alpha'$ in C_2S can be made by means of a direct structure determination of the α-phase, which is complicated by difficulties in obtaining single crystals of this most high-temperature phase of C_2S stabilized at normal temperatures.

Thus, polymorphous transformations of C_2S and C_3S are caused by slight displacements of atoms within the structure and a change of the orientation of Si-tetrahedra. The latter circumstance can be explained by a lower capability of Si-O bonds (in contrast to Ca-O bonds) to accumulate thermal energy, which, in its turn, according / 9 /, on cooling and heating, makes Si-tetrahedra change their position in the structure to a more energetically favourable position. Thus in each temperature range there exists a certain modification. The addition of Sr atoms into the nodal points of the crystal lattice of C_3S and C_2S increases entropy in minerals and contributes to keeping thermodynamical stability, in normal conditions in the form of solid replacement solutins. Sr atoms are suitable for solving the problems of stabilizing the high-temperature modifications, since the Sr^{2+} radius in normal conditions corresponds to the effective Ca^{2+} radius at high temperature in minerals.

REFERENCES

1. J.W.Jeffry, The crystal structure of tricalcium silicate.- Acta Cryst., 1952, v.5, p.26-35
2. Ilyineys A.M., Malinowsky Yu.A., Nevsky N.N. Crystal structure of rhombohedral modification of tricalcium silicate Ca_3SiO_5 - DAN SSSR, 1985, v.281, 2, 332-336
3. F. Nishi, Y. Takeuchi. The rhombohedral structure of tricalcium silicate at 1200°C Zet. Kristallogr., 1984, 168, 3, 197-212.
4. Golovastikov N.I., Matveeva R.G., Belov N.N Crystal structure of tricalcium silicate $3CaO \cdot SiO_2 = C_3S$ - kristallografiya, 1975, 20 4, 721-729.
5. Simonov V.I., Ilyinets A.M. On the uniform structural basis of polymorphous modifications of tricalcium silicate Ca_3SiO_5 (in publication).
6. H. Saafeld. X-ray Investigation of Single Crystals of Ca_2SiO_4 (Larnite) at High Temperatures. - Amer. Mineralog. 1975, 60, 824-827.
7. Ilyinets A.M., Nevsky N.N., Ilukhin V.V., Bikbau M.Ya., Belov N.V. Crystal structure of the α'-modification of dicalcium silicate $Ca(Ca,Sr)SiO_4$ - DAN SSSR, 1982, 267, 3, 641-644.
8. W.Eysel, T.Hahn. Polymorphism and solid solution of Ca_2GeO_4 and Ca_2SiO_4 - Zet. Kristallogr., 1970, v.131, 322-341.
9. Bikbau M.Ya., Butt A.M., Timashev V.V. On the polymorphism and stabilization of dicalcium silicate. - In: Chemistry and technology of silicates. Proceeding of Moscow Mendeleev Chemico-Technological Institute, 1975, 87, 3-9.

L. S. KLUEVA, A. I. MARKOV NIICement, Moscow, U.S.S.R.

MODIFICATION OF CEMENT CONTRACTION DUE TO FALSE SETTING

Premature loss of plasticity, characteristic of the false-setting cements, develops directly after the mixing of the cement paste or mortar and concrete mix is ended. Evident and repeatedly proved is the interdependence of false setting and the presence of dehydrated forms of gypsum in cement content, those of forms of gypsum, which are characterised by the increased solubility comparing to dehydrite.

During the cement hydration there takes place a contraction - decrease in the absolute volume of the system "cement-water" as a result of chemical fixation of the water and its transformation into crystalline hydrates. In this work we used differencial contraction method for the investigation of false-setting cement hydration.

The subject of our inquiry were cements of laboratory comminution (S_{sp}~3000 cm^2/g; gypsum content -2,5% in terms of SO_3), produced on the base of clinkers of different mineralogical composition and alkali content. All of the newly produced cements were characterised by normal setting. The changes in the setting type were reached by means of gypsum dehydration in cement contents after preliminary thermal treatment. Contraction measurements were performed for solutions with cement/sand =I:I at cement/water= 0,35; quartz sand was used as a model system. The compensation of difference of temperatures between the investigated system and the model one was performed to the precesion of 0,I°C.

As for cements containing no additives but gypsum, the degree of false setting is defined mainly by the gypsum dehydration rate during cement comminution, and by the original clinker features, such as alkali content in particular (I). It is seen from the table I, that cements, produced on the base of clinkers with low and moderate alkali content ($\leq$ 0,7% R_2O in terms of Na_2O) after thermal treatment in temperature range of I00-I50°C can develop a false setting both with full (Ist type) and partial premature loss of plasticity. Cements produced on the base of clinkers with elevated alkali content in the conditions of analogical thermal treatment are characterized by exclusively false setting of the 2nd type. Temperature elevation above I70°C in all the cases develops quick setting features. As a rule cements develop quick setting features, if the temperature is above I70°C.

False-setting cements at early ages of hydration are characterized by higher contraction rate than those with normal setting. However the differences of contraction occure immediately after a water-addition with one kind of cements (fig.Ia), while with the others the difference of contraction takes place after about 2 hours of hydration (fig.Ib).

Fig.I. Contraction curves of cements of different setting types, produced on the base of different clinkers:I-normal setting; 2 and 2'- false setting after the primary and secondary mixing correspondingly.

Table I.

Clinkers:	R_2O,%	Anomalsetting types, observed after thermal treatment of cements		
		I00-I30°C:	I50°C:	I70°C and higher
I	0,32	II	I	Quick setting features
2	0,42	II	I	
3	0,49	II	I	
4	0,49	II	I	- " -
5	0,52	II	I	- " -
3a	0,66	II	I	- " -
6	0,85	II	II	- " -
6a	0,92	II	II	- " -
3b	I,06	II	II	- " -
7	I,08	II	II	- " -
8	I,II	II	II	- " -
7a	I,23	II	II	- " -
9	I,33	II	II	- " -
4a	I,44	II	II	- " -

Notes: 3,3a,3b - different clinker samples from one of the producers (identical to 4 and 4a, 6 and 6a, 7 and 7a).

a) Clinker 7 (identical to 4 and 6a).

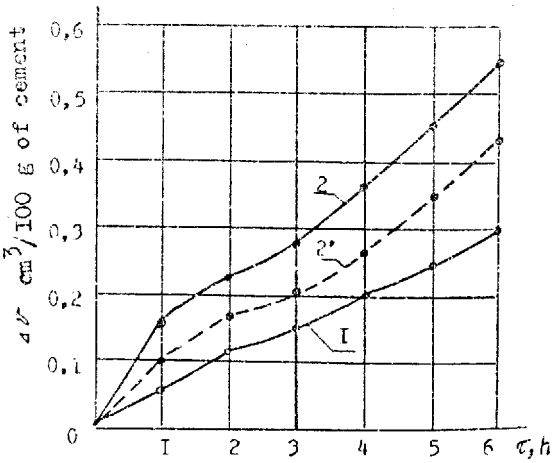

b) Clinker 3b (identical to 3a).

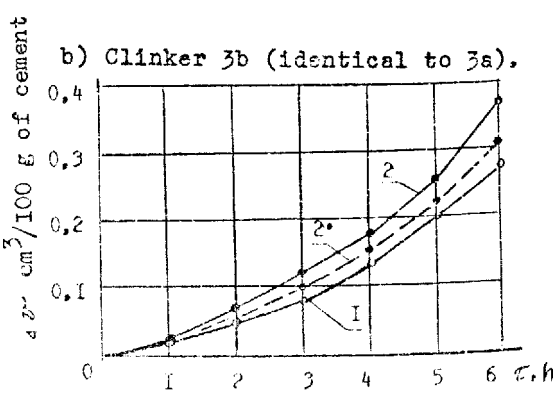

To reveal the reasons of the observed differences we shall consider the phase composition of hydration products. According to the current data: certain setting type of cement at early stages of hydration can cause the dominating crystallization of the following new formations: ettringite (normal setting), $CaSO_4 \cdot 2H_2O$ and ettringite (false setting) and calcium hydroaluminates (quick setting). Table 2 contains calculated data of contraction volume in connection with crystallization of $CaSO_4 \cdot 2H_2O$, ettringite and one of calcium hydroaluminate. The formation of the primary gypsum-ettringite structure, causing the false setting of cements, does not have any advantages over crystallization of ettringite at normal setting from the point of view of contraction effect. The increase of volume of new formations at generation of the primary gypsum-ettringite structure according to our calculations cannot cause such substantial differences in the level of contraction effects of cements with normal and false settings.

Table 2

Reaction scheme	:Changes of :the system :volume,%
$C_3A+3CaSO_4 \cdot 2H_2O+26H_2O \rightarrow C_3A \cdot 3CaSO_4 \cdot 32H_2O$	-6,44
$CaSO_4 \cdot 0,5H_2O+1,5H_2O \rightarrow CaSO_4 \cdot 2H_2O$	-6,98
$C_3A + 6H_2O \rightarrow C_3A \cdot 6H_2O$	-23,78

Analytical results of the previously investigated liquid phase composition (2) can testify the primary supersaturation of the liquid phase of false-setting cements by sulphate ions, with consequent reduction of ion concentration after the development of false setting. Comparing the results of investigated liquid phase composition and the contraction dynamics of cements we can conclude, that $CaSO_4 \cdot 2H_2O$, crystallizing as an element of initial structure of false-setting cements, does not take part in the reaction with aluminous phases of clinker, because $CaSO_4 \cdot 2H_2O$ is already blocked as a result of joint crystallization with ettringite. In connection with this the system revealed a seeming disadvantage of the gypsum for regulating the setting process; this results in the formation of hydroaluminate phase, which elevates the contraction effect of false-setting cements.

The possibility of the formation of hydroaluminate phase at early stages of hydration of false-setting cements is illustrated by fig.2, according to which there takes place the coincidence of contraction curves for false- and quick-setting cements, containing gypsum in the form of semi-hydrate in the first case, and in the second case in the form of dehydrate, but of insufficient volume (SO_3- content in cements on fig.2 is referred to with regard for SO_3 in clinker). In other words the false setting proved identical to quick setting in the given case in terms of contraction effect.

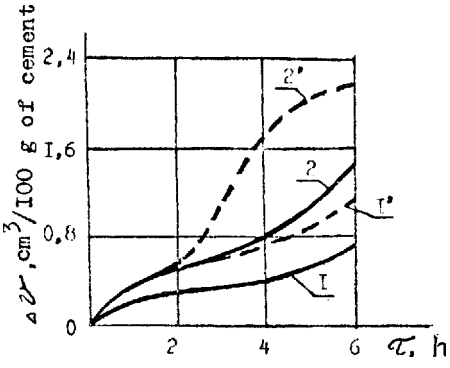

Fig.2. Contraction curves of cements produced on the base of clinker 7; these have different compositions and different gypsum forms: 1 and 1' - correspondingly unheated (normal setting) and heated (false setting of the II type) cement, containing 2,5%SO_3; 2 and 2' - correspondingly unheated and heated cement, containing 1,48% SO_3 which is caracterized in both cases by quick setting.

Comparison of the data on the cement contraction and mineralogical composition of the initial clinkers have shown that in terms of quantity the formation of hydroaluminate phase at early stage of false-setting cements gydration is determined by C_3A - content in the initial clinker.

According to the contraction curves (fig.1), $CaSO_4 \cdot 2H_2O$ is again able to regulate the setting after the failure of initial structure of false-setting cements at the secondary mixing.

So the results of investigations of contraction of cements with different setting types indicate that with dehydrated forms of gypsum present in false-setting cements at early stages of hydration there takes place the crystallization of $CaSO_4 \cdot 2H_2O$ from the liquid phase, supersaturated with sulphate-ions and then $CaSO_4 \cdot 2H_2O$ is blocked in the composition of initial gypsum-ettringite structure; this results in the reduction of gypsum volume which acts as setting regulator and causes the changes in composition of hydrate new formations.

BIBLIOGRAPHY

I. Энтин З.Б., Клюева Л.С., Папиашвили У.И. Исследование особенностей процесса структурообразования цементов с ложным схватыванием.-УП Международный конгресс по химии цемента. Париж, 1980

2. Энтин З.Б., Клюева Л.С. Роль жидкой фазы в явлениях аномального схватывания цементов.-УI Всесоюзное совещание по химии и технологии цемента. М, 1982

N. KOMAROVA,
V. RIASINE,
G. TCHISTIAKOV, NIICement, Moscow, U.S.S.R.
A. KORENGA

STABILISATION ORIENTEE D'UNE COMPOSITION DE PHASES DESEQUILIBREES DU CLINKER BLANC.

Le présent ouvrage traite des particularités propres à la formation de la composition de phase et de la microstructure dans les clinkers blancs à haute teneur en aluminates (tabl. 1) soumis à la cuisson avec blanchiment dans des fours rotatifs industriels (clinkers 1, 2, 3, 4, 5, 6 et 6-H), dans un creuset (clinkers 7 et 7-H) et en laboratoire (clinker 4-T). Les données de la figure 1 relatives à la modification de la composition de phase et du facteur de réflexion (FR) des clinkers en fonction du régime thermique du blanchiment sont obtenues en laboratoire lors de la cuisson avec blanchiment dans l'eau des mélanges bruts utilisés à la fabrication des clinkers dans les fours rotatifs et le creuset ainsi que lors du blanchiment à neuf dans l'eau des clinkers industriels 4 et 5 après leur maintien préalable pendant 20 mn à 1450 °C, la température étant réduite vers le moment du blanchiment à la valeur requise. La détermination de la composition de phase des clinkers a été faite à l'aide de la méthode d'analyse radiographique.

Les particularités propres à la composition de phase des clinkers blancs à haute teneur en aluminates sont les suivantes:

- la formation d'une composition de phase variable déséquilibrée à bas degré d'ordre de la structure des minérais en fonction du régime de refroidissement (de blanchiment) du clinker avec, y compris, une suppression partielle ou à peu près complète de la cristallisation du C_3A (tabl. 1, fig. 1);
- la stabilisation de préférence des formes trigonale et monoclinique à haute température de l'alite à une faible teneur en formes à haute température de la bélite - et $\alpha' - C_2S$;
- une absence totale d'alumoferrite de calcium (tabl. 1, fig. 3);
- la présence dans la composition des minérais de clinker d'impuretés structurales de divers type (1) avec la prédominence de la cristallisation des phases d'alumosilicate suivant le type des cristaux mixtes (des mélanges isomorphes) et la conservation des paramètres radiocristallographiques de l'alite et de la bélite le plus souvent et du C_3A à un plus faible degré. Cela entraîne une modification sélective des caractéristiques radiographiques des phases et aboutit à une perturbation des dépendances de référence adoptées à l'analyse quantitative de phase: quantité de phase - intensité des maximums (la somme des phases ne correspond pas à 100 % au tableau 1, fig. 3);
- l'oxyde de magnésium s'intègre dans la fraction d'alumosilicate en quantités différentes en fonction du régime de refroidissement du clinker sous la forme de périclase ou d'une impureté isomorphe dans le C_3A et exerce une forte influence sur le FR de la fraction d'alumosilicate du clinker (tabl. 2, fig. 2.3);
- la formation pendant la cuisson du clinker de silicates et d'alumosilicates avec une présence du CaO à faible fixation chimique et structurale amène à un entrainement sélectif du CaO au cours de la cuisson et à la formation de portlandite et de $CaCO_3$ au cours du blanchiment;
- pendant la cuisson dans un milieu très réducteur et le blanchiment dans un milieu vapeur-gaz on voit apparaitre dans la composition du clinker des minérais du groupe de γ-bélite ($\gamma-C_2S$, chondrodite de calcium, khilchoanite et $\gamma-C_2S$-hydrate), qui ne sont pas ordinaires pour le ciment Portland.

Le blanchiment des clinkers sous une température de 1150 à 1450 °C ne s'accompagne pas de la réduction du Fe^{3+} au Fe^{2+}. La particularité établie chez les oxydes de fer de ne pas former de phases d'alumoferrites indépendantes (où les ions de fer constituent des chromophores capables de former des variétés et doivent posséder des caractéristiques spectroscopiques stables), mais de s'intégrer en qualité d'impuretés dans les phases d'aluminate et d'alumosilicate principalement en présence d'un entou-

N. KOMAROVA,
V. RIASINE,
G. TCHISTIAKOV,
A. KORENGA

Influence du régime de refroidissement sur la composition de phase du clinker blanc

Tableau 1

Clinker	Régime de refroidissement (de blanchiment)	Teneur en oxydes, % en masse			KS	SM	Composition minéralogique potentielle, % en masse				Composition de phase, % en masse				FR, %
		Fe_2O_3	FeO	MgO			C_3S	C_2S	C_3A	C_4AF	C_3S	C_2S	C_3A	Total	
1	blanchi dans un milieu de vapeur	0,10	0,14	1,64	0,91	4,7	66	18,5	13	0,8	60	30	10	100	88
2	blanchi dans l'eau	0,75	0,14	3,7	0,93	5,5	71,6	12,6	7,9	2,3	68	20	12	100	85
3	blanchi dans un milieu vapeur-gaz	0,17	0,22	2,9	0,89	3,7	56	20,8	14,4	1,3	59	27	13	99	84
4**	blanchi dans un milieu vapeur-gaz	0,43	0,14	0,73	0,93	3,5	67,6	13,6	15,3	1,3	54,5	29	19	102,5	85
4-H	refroidi à l'air	0,58	néant								68	22	16	106	72
4-П	blanchi à neuf dans l'eau à 1450 °C	0,58	néant								80	22	1	103	80
4-TH	refroidi à l'air										68,5	25	19	112,5	72
5	blanchi dans un milieu vapeur-gaz	0,47	0,14	0,79	0,83	4,2	46	36	13,6	1,4	48	35	19	102	83
5-H	refroidi à l'air	0,62	néant								72	20	14	106	69
5-П	blanchi à neuf dans l'eau à 1400 °C	0,47	0,02								72,5	26	1	99,5	80,5
6	blanchi dans l'eau	0,71	0,07	0,93	0,83	4,2	45,8	35,9	12,1	2,2	70	25	4,5	99,5	80
6-H	refroidi à l'air	0,7	0,07	1,72	0,83	4,3	46,3	36,3	12,3	2,1	56	34	I0	I00	62
7	blanchi dans l'eau	0,4	néant	0,97	0,81	3,4	38	38	16	1,2	52	36	10	98	83
7-H	refroidi à l'air	0,44	néant	1,1	0,82	3,3	40,5	35,9	16,3	1,3	55	30	14	99	74

* Les alumoferrites de calcium ne sont décelés dans aucun des clinkers même après que ces derniers ont été débarrassés de silicates de calcium à l'aide de l'acide borique.

** La composition théorique indiquée concerne également les clinkers à indices supplémentaires H, П et TH. Les clinkers 5, 7 et 7-H sont obtenus sur la base des mélanges à KS = 0,93 à 0,92.

rage de ligends différents, prédétermine l'acquisition par les ions de fer de diverses caractéristiques spectroscopiques et de diverses propriétés colorantes. Il s'en suit que le FR des clinkers blancs ne doit pas dépendre directement de la quantité d'oxydes de fer.

Lorsque le blanchiment des clinkers se produit dans l'eau ou dans un milieu vapeur-gaz à une température de 1250 °C et plus basse, on voit se stabiliser dans tous les cas les compositions à haute teneur en C_3A qui est proche ou supérieure à la quantité calculée de ce minérai (tabl. 1, fig. 1). Quant le blanchiment se fait à une température comprise entre 1275 e 1375 °C on observe de différents schémas de cristallisation du C_3A en fonction de la composition

Tableau 2

Caractéristiques de la fraction d'alumosilicate des clinkers blancs

Clinker	Teneur en phase d'alumosilicates, % en masse	FR, %	Composition chimique du clinker, % en masse*							concentration en masse d'oxydes de fer dans les phases d'alumosilicates du clinker, %
			SiO_2	Al_2O_3	Fe_2O_3	FeO	CaO	MgO	MnO	
4	19,1	89	11,69	31,33	2,18		52,35	2,08	0,02	70
4-H	16,3	70	10,73	32,30	2,35	0,03	48,65	5,58	0,09	65
4-П	15,8	80	16,58	31,58	2,54		45,75	3,11	0,01	66,7
5	13,5	89	10,37	33,34	1,89	0,22	52,25	1,73	0,02	46,33
5-H	16,3	77	10,26	32,92	2,32	0,01	49,06	4,91	0,108	61,3
5-П	18,8	83	12,87	31,59	2,77		48,51	3,70	0,003	84

* Dans les échantillons des clinkers 4-H, 5 et 5-H le Cr_2O_3 n'est pas décelé, dans les autres échantillons sa quantité a constitué de 0,007 à 0,011 %.

chimique et de la réactivité du mélange cru. Dans les clinkers obtenus sur la base de mélanges très basiques (FS = 0,93 à 0,92) à une basse réactivité (clinkers 4 et 5) on réussit à supprimer presque complètement la cristallisation du C_3A en opérant le blanchiment à une température de 1375 °C au minimum. Une haute teneur en C_3A a été enregistrée dans de pareils clinkers dès la réduction de la température vers le moment du blanchiment à 1350 °C. On peut supprimer la cristallisation du C_3A dans le clinker 6 en opérant le blanchiment à une température de 1300 °C tandis que dans les clinkers 4-T et 7 on l'obtient à une température de 1350 °C au minimum vers le moment du blanchiment. Il est possible de régler le degré de suppression de la cristallisation du C_3A dans les clinkers 4-T et 7 en faisant varier la température pendant le blanchiment de 1275 à 1350 °C. Simultanément avec la suppression de la cristallisation de la phase du C_3A est observi un accroissement sensible de la teneur totale en phases de silicate par suite de différentes modifications qui surviennent dans les schémas de cristallisation d'alite et de bélite en fonction des conditions concrètes: la quantité d'alite augmente à une suppression de la cristallisation de la bélite ou la quantité de bélite augmente considérablement à une faible réduction de la teneur en alite.

Le déséquilibrage de la composition de phase des clinkers blancs est dû à la stabilisation qui a lieu pendant le blanchiment de clinker à composition des phases à haute température dans des systèmes d'alumosilicate à haute basicité contenant des impuretés de MgO. L'aluminium peut s'intégrer dans les tétraèdres de SiO_4 lorsqu'il est chauffé à 1300 °C et plus, ses paramètres structuraux étant soumis à des modifications en présence de hautes températures (2). La nature de la cristallisation déséquilibrée des phases pendant le blanchiment dépend de la cinétique de fixation du CaO lors de la cuisson dans un intervalle de températures de 1200 à 1350 °C.

Le maximum du FR s'obtient à des températures différentes du clinker vers le moment du blanchiment. Le clinker 7 possède la blancheur maximale à la température de blanchiment de 1200 °C, les clinkers 4 et 4-T à la température de 1300 °C, le clinker 5 à la température de 1350 °C et le clinker 6 à la température de 1450 °C. Une suppression importante ou presque totale de la cristallisation du C_3A est accompagnée, de règle, par une réduction du FR du clinker de 2 à 5 %.

N. KOMAROVA,
V. RIASINE,
G. TCHISTIAKOV,
A. KORENGA

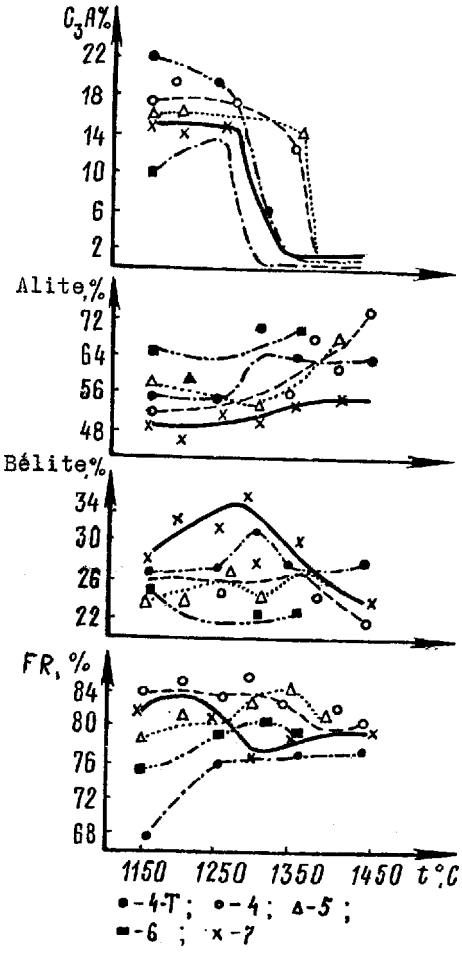

Fig. 1. Composition de phase et FR des clinkers blancs en fonction du régime de blanchiment thermique. La désignation des courbes correspond au marquage des clinkers dans le tableau 1

Dans la fraction d'alumosilicate des clinkers blancs extraite par une dissolution de phases de silicate dans la solution à 5 % d'acide borique, il y a de 10 à 16 % de SiO_2 qui s'y trouve en qualité d'impureté structurale isomorphe (tabl. 2, fig.3). Le changement du régime de refroidissement du clinker entraine une modification sensible du contenu et de la nature de répartition de l'oxyde de magnésium dans la fraction d'alumosilicate du clinker ce qui constitue justement la principale condition de la modification du FR de clinker par suite du blanchiment réalisé de 70 à 89 %.

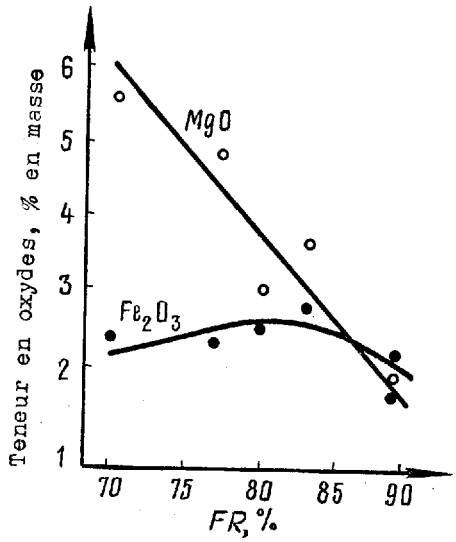

Fig. 2. Influence des oxydes ferriques et de magnésium sur le FR de la fraction d'alumosilicate du clinker blanc

A un accroissement en masse de 2 à 5 % de la fraction du MgO, la blancheur de la fraction d'alumosilicate diminue brusquement (fig. 2). Dans les clinkers à FR le plus haut (fig. 3, clinkers 1 et 2), l'oxyde de magnésium se cristallise sous la forme de périclase indépendamment de la valeur de sa fraction en masse dans le clinker. Une haute teneur des phases d'alumosilicates en oxydes de fer n'influe presque pas directement sur leur coloration.

La fraction d'alumosilicate séparée des clinkers 4-II et 5-II se compose de 94 à 96 % de la phase amorphe sous les rayons X et contient de 4 à 6 % de C_3A cristallin. D'après sa composition chimique, elle ne diffère pas sensiblement des fractions d'alumosilicate à structure cristalline du C_3A séparées d'autres clinkers. Dans les clinkers indiqués a eu lieu apparemment une stabilisation de la phase métamicte amorphe sous les rayons X qui est proche du C_3A d'après sa composition, mais qui possède un niveau énergétique structural élevé dû à une haute concentration d'impuretés et de défauts. La preuve en est la présence d'effets exothermiques sur les courbes d'analyse

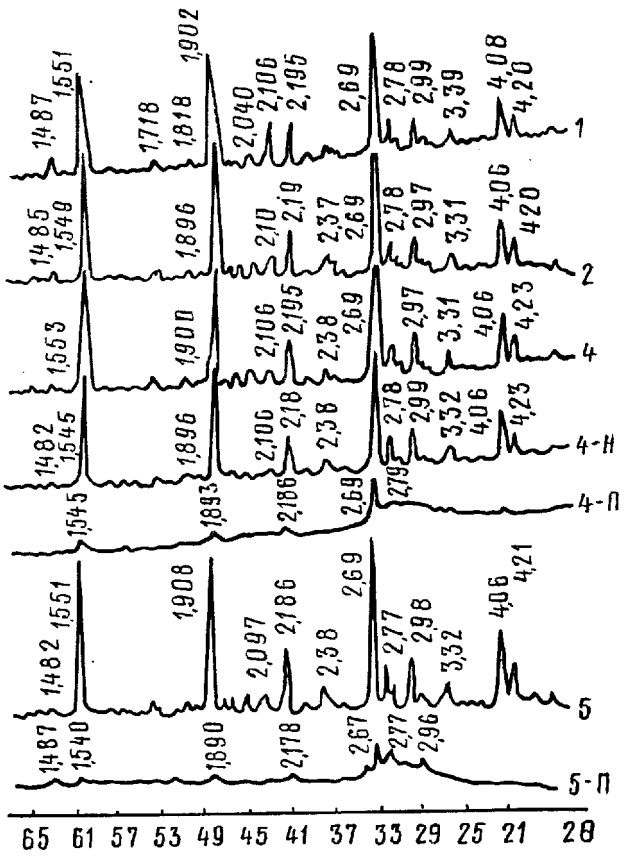

Fig. 3. Spectres de diffraction au rayons X (CuKα) de la fraction d'alumosilicate des clinkers blancs. La désignation des spectres correspond au marquage des clinkers au tableau 1

thermique différentielle avec des maximums à 325 et à 440 °C lesquels sont propres aux processus de "retour" des minérais métamictes à l'état cristallin ordonné (3) ainsi que la présence d'effets exothermiques de cristallisation du C_3A et de la périclase respectivement à 845 et 870 °C (fig. 4).

Des études de la microstructure des clinkers blancs à l'aide de microscopes électroniques à trame et à transmission ont décelé dans tous les clinkers à un haut FR la formation de phases à relief lisse de la surface de clivage. La microstructure du clinker 1 à blancheur maximale est construite selon le principe d'un assemblage dense de cristaux ce qui lui assure une très haute masse spécifique (4350 kg/m^3). Au point de

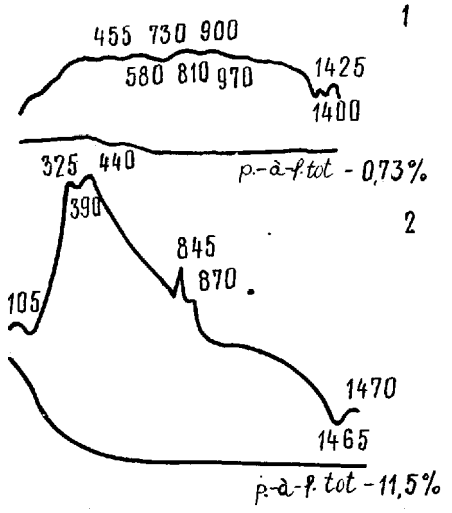

Fig. 4. Dérivatogrammes du clinker 4-(1) et de sa fraction d'alumosilicate séparée (2)

vue d'un haut degré de blancheur, la microstructure du clinker doit assurer après le broyage l'obtention de particules à l'aspect optique homogène, à surface lisse, à basse microporosité et à haute capacité réfléchissante. La détermination de la surface spécifique des clinkers broyés et des clinkers bruts non broyés par méthode d'adsorption d'azote à basse température a montré une faible augmentation (de 20% au maximum) de la surface spécifique après le broyage ce qui témoigne non seulement d'une haute porosité des granules de clinker blanc mais aussi d'un grand nombre de microfissures qui y apparaissent de toute évidence par suite de l'accumulation de dislocations de "scindement" prédéterminant les surfaces de destruction pendant le broyage (4).

Les spectres de réflexion optique dans le domaine visible des clinkers à haute et à basse caractéristiques du FR ont une différence peu sensible au point de vue des centres de coloration d'où vient que le FR des clinkers et des ciments est déterminé en grande partie par le pouvoir réfléchissant des surfaces de particules.

N. KOMAROVA,
V. RIASINE,
G. TCHISTIAKOV,
A. KORENGA

REFERENCES

I. Франк-Каменецкий В.А. Природа структурных примесей в минералах. Издат. Ленинградского ун-та, I964.
2. Лазаренкова Л.Е., Питак М.В., Старшинов Б.Н., Шуляк Р.С. Исследование методом ИК-спектроскопии изменения структуры каолина при нагревании. Сб. Физико-химические процессы производства и применение огнеупоров. Металлургия. М.:,I98I.
3. Белов Н.В. Очерки по структурной минералогии. Недра. М.:, I976.
4. Ван Бюрен. Дефекты в кристаллах. Издат. иностр. лит-ры. М.:, I962.

Z.M.Larionova
I.I.Kourbatova
N.S.Zhelvakova
L.P.Moïsseeva

NIIJB, Moscow, U.S.S.R.

INFLUENCE DES ADDITIONS ORGANIQUES SUR LA FORMATION DE LA STRUCTURE DE LA PIERRE DE CIMENT

Les adjuvants organiques influencent considérablement sur la formation de la structure de la pierre de ciment dans le béton et améliorent ses proprietes constructives. Il est le plus avantageux d'utiliser les adjuvants complexes et les superplastifiants, dont l'emploi rationnel est etroitement lié avec la détermination du mécanisme de leur action. Ces adjuvants changent la cinétique de l'hydratation du liant et les conditions de la formation des phases hydratées étant eux-même très rarement des éléments de la structure du durcissement. Leur influence se manifeste principalement dans les delais initiaux. Les particularités de l'hydratation dans cette période caractérisent le plus entièrement les changements de concentration observés dans la phase liquide. C'est pourquoi, en étudiant en cinétique les compositions des phases liquides, il est possible d'etablir le mécanisme de l'action d'un adjuvant (I). D'apres l'allure des courbes $C_{R^+}(\tau)$, $C_{Na^+}(\tau)$, $C_{K^+}(\tau)$, $C_{Ca^{2+}}(\tau)$, $C_{SO_4^{2-}}(\tau)$ il est possible d'évaluer l'influence de l'adjuvant sur la dissolution du clinker, la cristallisation des phases contenant le calcium et la vitesse de la formation d'ettringite. Si l'adjuvant ralentit la dissolution, alors le passage de R^+ de clinker sera ralenti et, conformement à cela, la concentration de ces ions dans la phase liquide sera plus basse. On peut l'observer en appliquant le superplastifiant C-3 ou le poly-électrolyte soluble dans l'eau sur la base de l'acide salicylique (BPП), ralentissant l'hydratation, et l'adjuvant complexe sur la base de résine d'urée, accélérant l'hydratation (Fig.I).

D'après le changement dans la phase liquide de la concentration d'ions des métaux alcalins il est possible dans certaines cas d'évaluer quantitativement le degree de l'hydratation du ciment.

L'abaissement lent de la concentration d'ions de calcium dans la phase liquide dans la plupart des cas indique le ralentissement de dégagement des phases contenant le calcium, et l'abaissement brusque-indique le surcroit de la vitesse de leur cristallisation. Si, simultanément, on observe aussi l'abaissement brusque de la concentration des sulfates, alors ça temoigne le liage de la masse principale de gypse en ettringite, ce fait est confirmé par les donnee de l'analyse chimique. C-3 se sorbant principalement sur hydro-aluminates ralentit la cristallisation d'ettringite, et BPП ralentit l'hydratation des composants aluminatique et silicique de clinker, c'est pourquoi la concentration de calcium pour le système avec C-3 entre 4 et I6 h et pour le système avec BPП entre 4-48 h abaisse faiblement. L'adjuvant complexe sur la base de résine d'urée influence activement durant 6 h sur la cinetique de dissolution ainsi que sur la cristallisation des phases hydratees. La cristallisation de ces dernières se réalise dans ce

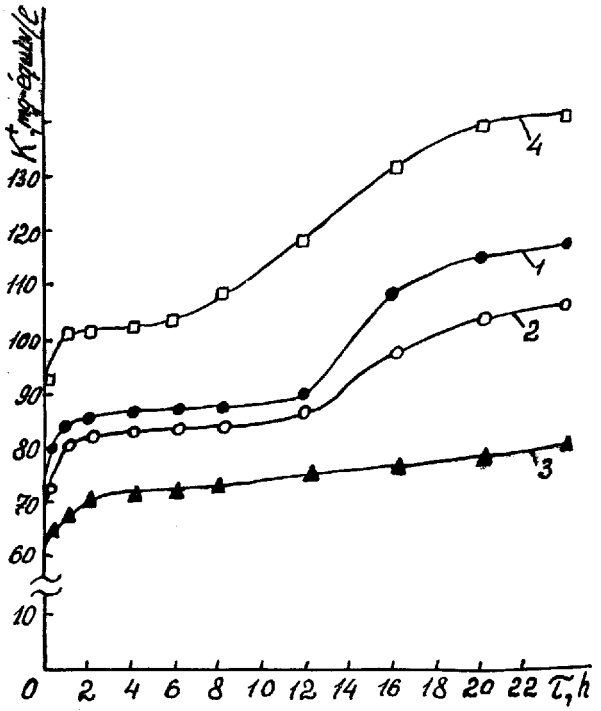

Fig.I. L'influence des adjuvants organiques sur le changement de la concentration de K^+ dans la phase liquide pendant l'hydratation de ciment: I - le ciment a aluminates moyens sans adjuvant; 2 - le même-avec C-3; 3 - le même-avec BPП; 4 - le même-avec l'adjuvant, complexe sur la de résine d'urée.

système plus intensivement (Fig.2).

Pour la détermination du mécanisme de l'action des adjuvants organiques il est rationnel de combiner les études des phases liquides avec les essais de la résistance plastique des systèmes. La formation des films d'adsorption bloquant la surface de la phase solide et ralentissant l'hydratation provoquera la prolongation de la période d'induction, et la cristallisation intensive d'ettringite amenera à un accroissement rapide de la résistance plastique. Le superplastifiant C-3 prolonge la periode d'induction. Au contraire, l'adjuvant complexe sur la base de résine d'urée réduit la période d'induction pour 2 h (de 8 jusqu à 6 h), et aussi assure les valeurs plus hautes de la résistance dans les délais posterieurs (Fig.3). Les études d'adsorption de C-3 sur les minéraux de clinker et les ciments montrentque C_3A et ses hydrates possède une capacite d'adsorption la plus grande et β-C_2S une capacité d'adsorption la plus faible. L'adsorption principale d'adjuvant sur le composant aluminate de clinker s'explique, à ce qu'il parait, par l'accroissement de la surface specifique de C_3A, se hydratant rapidement. Avec cela, il se forme les hydroalumina-

Z.M.Larionova
I.I.Kourbatova
N.S.Zhelvakova
L.P.Moïsseeva

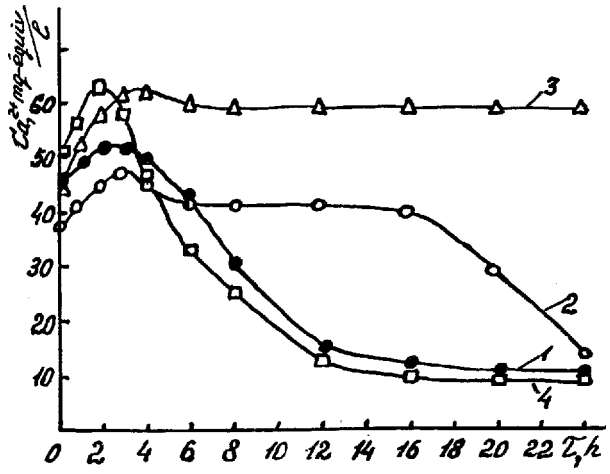

Fig.2. L'influence des adjuvants organiques sur le changement de la concentration de Ca^{2+} dans la phase liquide pendant l'hydratation de ciment.
I - le ciment sans adjuvant; 2 - le même-avec C-3; 3 - le même-avec ВРП; 4 - le même-avec l'adjuvant complexe sur la base de résine d'urée.

tes de calcium avec une grande quantité de l'eau, ce qui amène à une réduction de rapport eau-ciment dans le système. Il en suit qu'ilya lieu une basse efficacité de plastifiant dans le cas d'application des ciments riche en aluminate.
S'adsorbant sur la surface des particules de ciment, C-3 les disperse. Sous le microscope polarisant on voit dans la suspension de ciment-eau sans adjuvant que les particules de ciment forment des grandes agglomérations. Dans la suspension de ciment-eau avec l'adjuvant C-3 en quantité de 0,I-0,3% (de la masse de ciment) on observe une dispersion partielle des particules de ciment, et avec augmentation de la quantité d'adjuvant jusqu' a 0,5-I,0% - leur peptisation ultérieure (2).
Cette propriété de superplastifiant C-3 exerce une influence sur la formation de la pierre de ciment. En comparant sous le microscope des lames transparentes de la pierre de ciment sans adjuvant et celles avec l'adjuvant de 0,5% de C-3, on peut noter que la microstructure de ce dernier est

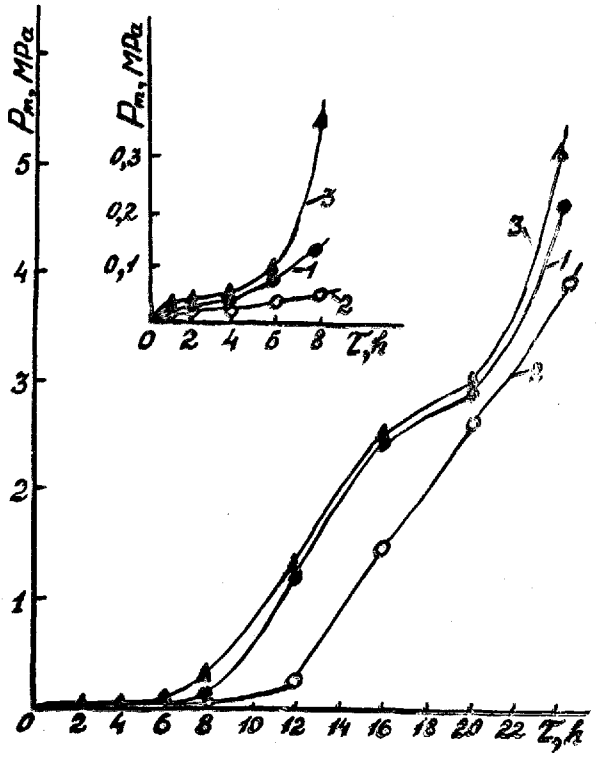

Fig.3. Le changement de la resistance plastique pendant l'hydratation des ciments.
I - le ciment sans adjuvant; 2 - le même - avec C-3; 3 - le même-avec l'adjuvant complexe sur la base de résine d'urée.

plus homogène. Avec cela a lieu l'augmentation de la porosite, conditionnée par l'entrainement de l'adjuvant par l'air. Dans la pierre de ciment avec C-3 on voit les pores arrondis avec limites régulières et le diamètre de 0,04-0,I5 mm (Fig.4). Les échantillons étuvés de la pierre de ciment avec l'adjuvant ont les mêmes caractéristiques structurales que les échantillons d'un durcissement normal.
S'adsorbant sur la surface des particules du ciment, C-3 ralentit leur hydratation dans les premiers jours, pourtant dans

Table

Le dégré de l'hydratation de la pierre de ciment d'après la ligne de C_3S, d = I,76 Å

La composition de la pierre de ciment	Les conditions du durcissement	Les délais de l'hydratation, jours			
		I	3	7	28
Ciment + H_2O	Normales	35,0	54,0	58,0	58,4
Ciment + H_2O + C-3	Normales	28,0	5I,0	57,0	6I,0
Ciment + H_2O	Etuvage	49,9	58,5	60,0	62,2
Ciment + H_2O + C-3	Etuvage	53,7	54,8	59,7	65,7

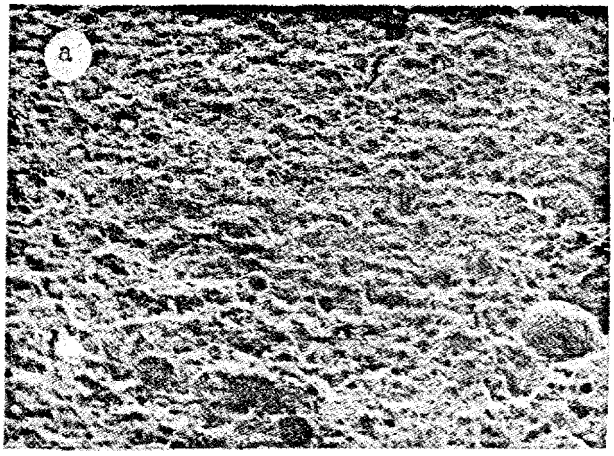

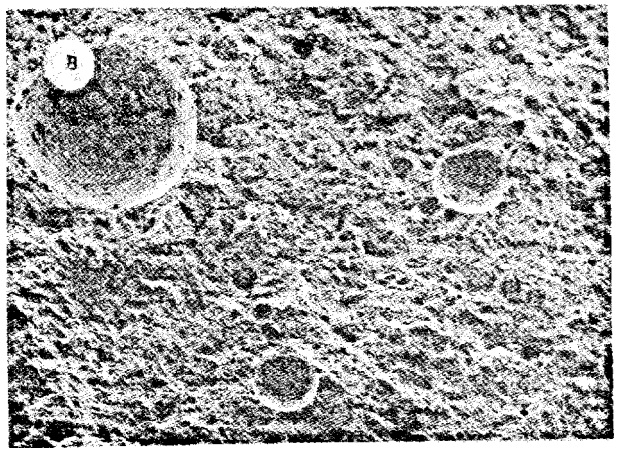

Fig.4. La microstructure de la pierre de ciment, SEMx70
a) - sans adjuvant;
b) - avec C-3.

7 jours les échantillons ont pratiquement le même dégré d'hydratation ce qui confirme les données d'une analyse quantitative radiographique (Tabl.).
Donc, l'application des adjuvants organiques est une des voies de la formation dirigée de structure de la pierre de ciment.

BIBLIOGRAPHIE

I. - И.И.Курбатова (1977) "Химия гидратации портландцемента", М., Стройиздат, (en russe).

2. - Л.П.Моисеева, З.М.Ларионова (1981) Влияние суперпластификатора С-3 на структурообразование цементного камня. "Гидратация и твердение вяжущих", Львов, p.258 (en russe).

L.I.Levin
G.M.Tamarutski VNIIzhelezobeton, NIICement, Moscow, U.S.S.R.

MODIFIED LIGNIN - BASE SUPLONATES IN THE MATERIALS ON CEMENT BASE

The features of the cement-based materials in many aspects are conditioned by their structure, controlled formation of which is possible through the use of superficially-active substances (SAS).

However the main part of the SAS is anion-active and can retard cement hydration as a result of chemisorption of cement particals and formations on the surface of calcium centres. Besides, the application of the SAS rather often is accompanied by over-increase in air-entrapping or water-release which negatively affect the structural and mechanical features of the materials, especially when hardening in the conditions of thermal treatment. Effective additives for cements and concretes, causing no reduction in the rate of hydration (the so-called LSTM - lignum-base sulphonates, technical, modified), are produced as a result of chemical treatment of lignin-base sulphonates by amino-containing substances, after which they acquire the increased capacity for chemisorption on the surfaces of oxigen centres and do not prevent the water from binding with Ca-centres of cement particles surfaces. Modified products are characterized also by optimal molecular/mass distribution, which results in limitation of their air-entrapping capacity and in the increase of their plasticizing activity.

The selected adsorptive-dispersive features of LSTMs make it possible to introduce them both with mixing water and at the production of cement, intensifying its comminution (tabl.1).

The LSTM introduced into comminution process allow to maintain the reasonable proportion of average (5-30 m) and fine (less than 5 m) fractions in the process of production of usual and high-strength cements. So the LSTMs positively affect the consistency and rheology of cement on its hydration and strength characteristics (tabl. 2, fig.1).

Contraction of grain composition with simultaneous limitation of fine fraction are especially important for high-strength plasticized cement, which is often used in concretes with reduced water content (as well as w/c) when there is an increase of the suction of water from the hydration products of the fine fraction; this can lead to the destabilization of the structure of hardened material.

The addition of LSTM effectively plasticizes water-cement systems, essentially reducing vibroviscosity of the cement paste as much as 2-4 times and water requirements of the paste and concrete mix by 15-25% (fig. 1 and 2), both when the addition is injected together with the mixing water, and during the grinding process of cement (curve 3). The use of the additive increases the settling of the concrete mix from 2-4 cm to 15-20 cm without reduction or even with increase in the concrete strength using in the latter case the plasticized cement with increased activity. In addition to that the concrete mixes with LSTM are characterized by the reduced ability for water-release and separation into layers.

The cement stone and concrete with addition of LSTM after normal and hydrothermal hardening are characterized by the fineness of pores of the structure with reduced content of larger pores. This is confirmed by the shift towards smaller sizes of effective radii of the pores in the range of $50 \cdot 10^{-10}$ - $1000 \cdot 10^{-10}$ m, by the reduction of dispersion values of average radii of the pores and by the reduction of macro-pores volume by 10-30% (tabl.3).

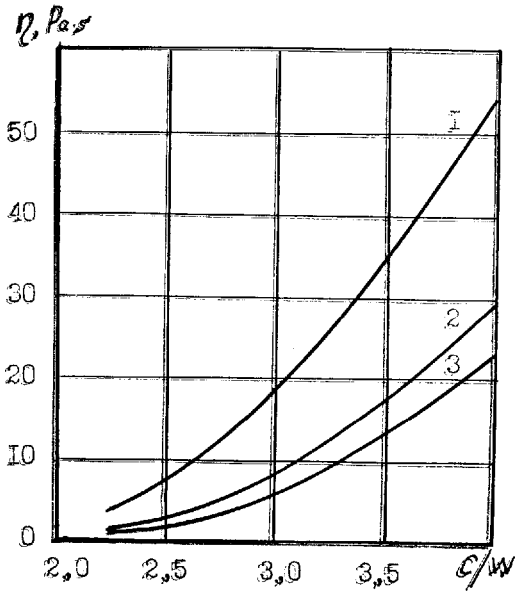

Fig.1. The change of vibriviscosity of the cement paste depending on water-cement proportion: 1- Portland Cement A; 2- Portland Cement A+LSTM with mixing water; 3- plasticized Portland Cement C.

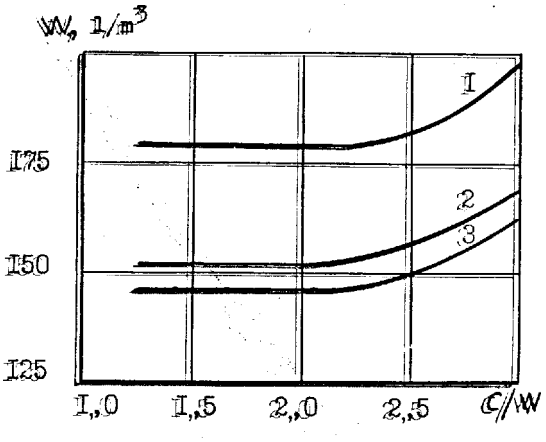

Fig.2. The dependence of water requirement of concrete mixes on the c/w proportion at the settling of the cone by 2-4 cm: 1-3 - the same as in the fig.1.

The influence of LSTM additive on the grain composition of cement.

Table 1

Code	Cement	Specific surface m^2/kg	Grain composition: less then $5 \cdot 10^{-6}$ m	Grain composition: $5 \cdot 10^{-6} - 30 \cdot 10^{-6}$ m
A	Pilot Portland Cement	300,0	1,8	52,4
B	Portland Cement with increased specific surface	365,0	8,2	58,8
C	Plasticized Portland Cement with addition of LSTM	352,0	5,8	65,3

Notes: The cements A,B,C are produced from one and the same clinker (C_3S - 58%; C_2S - 22%; C_3A - 5%; C_4AF - 13%); cements A and C are produced at one and the same grinding conditions; for the purpose of comparison on the same mill there was produced Portland Cement B, having the specific surface as that of the plasticized cement.

Table 2

The influence of the LSTM additive on physico-chemical features of cement.

Code of cement	Rate of hydration of cement stone in terms of C_3S, $d = 1,76 \cdot 10^{-10}$ m: 1 day	28 days	Features of the solution 1:3 (GOST) 310.4-81: Spread of the cone, mm, at w/c=0,40	Strength of the samples, MPa: Samples of normal hardening 28 days	Steamed samples 1 day
A	36,0	83,8	120	57,1	39,8
B	42,4	84,1	122	60,4	42,2
C	46,9	86,0	166	64,4	48,0

Table 3

Characteristic of the porous structure of cement stone

Code of cement	Pore sizes, $10^{-3} m^3/kg$, radius $30 \cdot 10^{-10}$ - $50 \cdot 10^{-10}$ m	$50 \cdot 10^{-10}$ - $1000 \cdot 10^{-10}$ m	$1000 \cdot 10^{-10}$ - $20 \cdot 10^{-6}$ m	Average diameter of the pores 10^{-6} m
A	0,017	0,042	0,021	2,7
B	0,015	0,0438	0,0182	2,4
C	0,021	0,0482	0,0188	2,2

Notes: Micro-porosity (less than $20 \cdot 10^{-6}$m) has been estimated by means of a mercury porometer in the pressure range up to 250 MPa.

Table 4

The influence of the LSTM-additive on the performance features of the concrete mix and concrete with c/w = 2,5.

Cement	Additive	Requirement, kg/m^3		Settling of the cone (cm)	Strength of the concrete, MPa, after steam curing at the age of	
		Cement	Water		1 day	28 days
Portland Cement A	-	450	I80	2 - 3	37	55
the same	LSTM	450	I80	I4 -I6	37	56
Plasticized Portland Cement C with LSTM	-	450	I80	I7 -I9	39	59
Portland Cement A	LSTM	380	I52	2 - 3	38	58
Plasticized Portland Cement C with LSTM	-	368	I47	2 - 3	42	65

The improvement of the porous structure and strengthening of the contact zone between the aggregate and the mortar part at the expence of water-release contributes to increased frost-resistance and strength of the concrete (tabl.4).

BIBLIOGRAPHY:

I. Тарнарупкий Г.М., Юдович Б.Э. О механизме действия пластификаторов в цементно-водных системах. Общие положения. Труды НИИцемента "Новые эффективные виды цемента", М., с.II4.

A.J.Mituzas
V.V.Montvilla
L.V.Petravichys
O.M.Stanylenis
Akmyantsementas, Novye Akmyane, U.S.S.R.

TECNOLOGY OF PRODUCTION OF HIGH ALITE PORTLAND CEMENT CLINKERS

P

One of the ways to utilize the raw dust, collected by the electric filters of the rotary kilns for the burning of Portland Cement clinker, is the injection of the dust through the aggregate head.

The analysis of the collected dust of different plants has shown, that its chemical composition had a wide range. In the most cases the dust was more enriched by acidic components than the standardized raw mix, which is a result of differentiated removal of clay-like and rather dispersive component. This phenomenon spontaneously increases the SC of the main material on its way along the kiln. The recirculation of the collected dust to the hot end of the kiln approximates the real content of the clinker to the present one, and is one of the ways of effective use of the high-temperature flame-zone.

If we take the collected dust and introduce a carbonate component into it till the SC is higher than that of the original raw mix, and then introduce this enriched dust into the kiln head, then it will be possible to produce high-alite clinker and still with higher hydraulic activity.

To study the behaviour of carbonate component in the kiln area we introduced into it Ca^{45} isotope in the form of $CaCO_3$. Then in definite intervals we selected the clinker samples leaving the kiln and examined them by means of radio- and petrographic methods.

On radiographic films of the sample, collected from preparatory zones at the moment of the indicator injection (Fig.I), one can see the uniform blackening of the whole cross-section area which is an evidence of a complete coincidence of Ca^{45} and the main volume of the material, present at this moment in the kiln area. The deposit of high-temperature CaO particles inside the cold end of the kiln increases the speed of physico-chemical transformation of the material both in preparatory zones and the high-temperature zone of calcination.

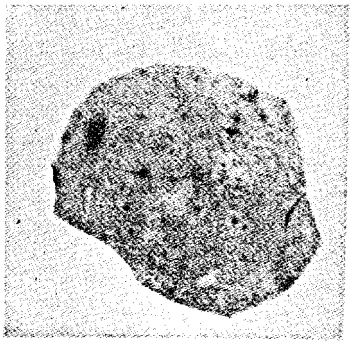

Fig.I. Radiographic film of a granule from a preparatory zone of the kiln.

However a definite part of the carbonate component, introduced jointly with the raw dust, interacts with acidic compounds of the mix and melts in the flame zone, and then leaving the gas stream it deposits

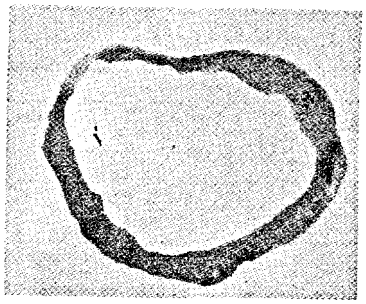

Fig.2. Radiographic film of a granule from the caking zone of the kiln.

on the newly formed clinker granules. On the Fig.2 one can see a radiographic film of the granule in the centre of the caking zone at the moment of injection of the $CaCO_3$-indicator. One can see clearly the deposited material, which has formed the exterior layer of the granule as a result of superficial diffusion.

Under conditions of a definite saturation degree of the raw dust by means of carbonate component and also with its sufficient volume it is possible to produce clinkers with SC≈I. Fig.3,4 show the petrographic films of microsection metallographic specimens of practically "pure" alite clinker, produced according to the above-mentioned method in the rotary kiln ⌀ 4xI50m.

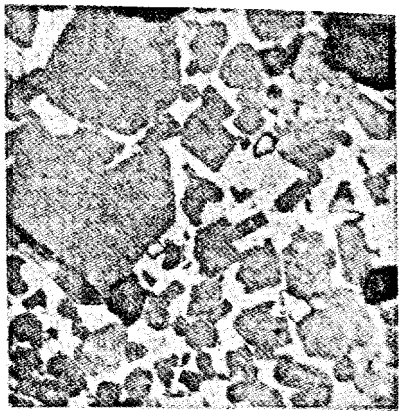

Fig.3. Petrographic film of the periphery layer of a granule (x200).

In the granula cross-section of such a clinker two zones are clearly seen: periphery layer (fig.3), formed by means of material deposit in the caking zone of the rotary kiln, and the central part (fig.4), formed by the material from the cold end of the kiln.

The periphery zone, constituting 8-I0% of the general volume of the granule, contains 60-63% alite, 5-I0% belite and 25-27% intermediate substance, while the central part contains 70+72% alite, 20+22% intermediate substance and isolated grains of belite.

Physico-chemical analysis of the samples, collected from the whole length of

the kiln being simultaneously fed with the carbonate-enriched raw dust showed that the volume of the material, deposited in certain zones of the kiln, depended on dispersivity of the introduced limestone component, on performance conditions of a particular kiln and on technical solutions of the problem of delivery of original components through the kiln-head.

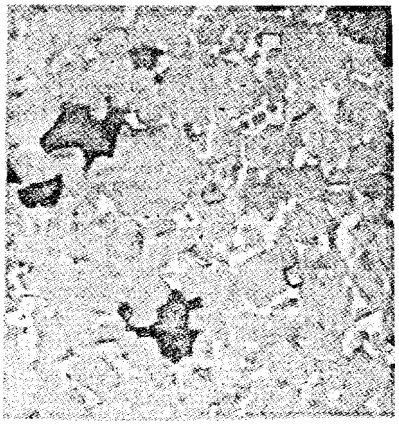

Fig.4. Petrographic film of the central part of a granule (x200).

I.L.Luginina
M.A.Putrenko

Technological Institute of Building Materials, Belgorod, U.S.S.R.

PARTICULARITIES OF CEMENT HYDRATION IN SUSPENSIONS WITH ALCALI ADDITIONS.

Water-release considerably hampers the investigation of hardening cement suspensions with water/cement > 0,5. Adding silicate of sodium into cement suspensions we have managed to investigate the suspension hydration with water/cement=I,0-2,0 having eleminated water-release. We have prevented the quick thickening of the suspensions by adding two-substituted phosphate of sodium. Oil-well pastes can easily penetrate pores and cracks of the rocks and possess the increased anti-filtering and strength features.

There was found and proved the predominant influence of calcium ions concentrations in the suspensions on the hydration and gelation in the system of cement-water-silicate of sodium. In the system without addition of phosphate of sodium not only quick thickening and growth of plastic strength are observable, but also the decrease of strengthening speed at elder ages. Adding some phosphate of sodium to the system we can see that the suspensions thicken in IO-40 min., and after the induction period of strengthening are characterised by the quick growth of strength which is 2-3 times as much as that in the pastes without phosphate of sodium (fig.I).

a)

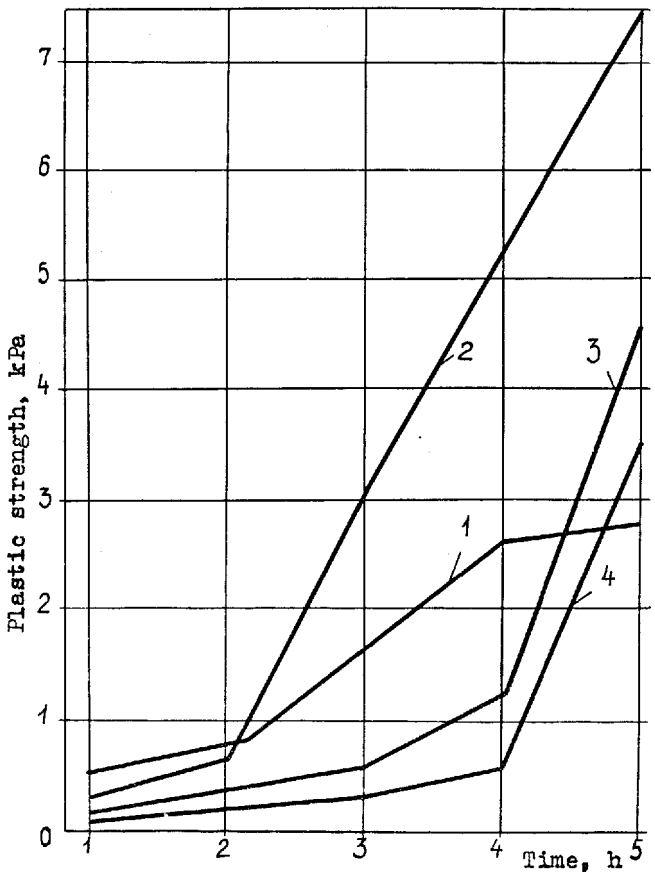

b)

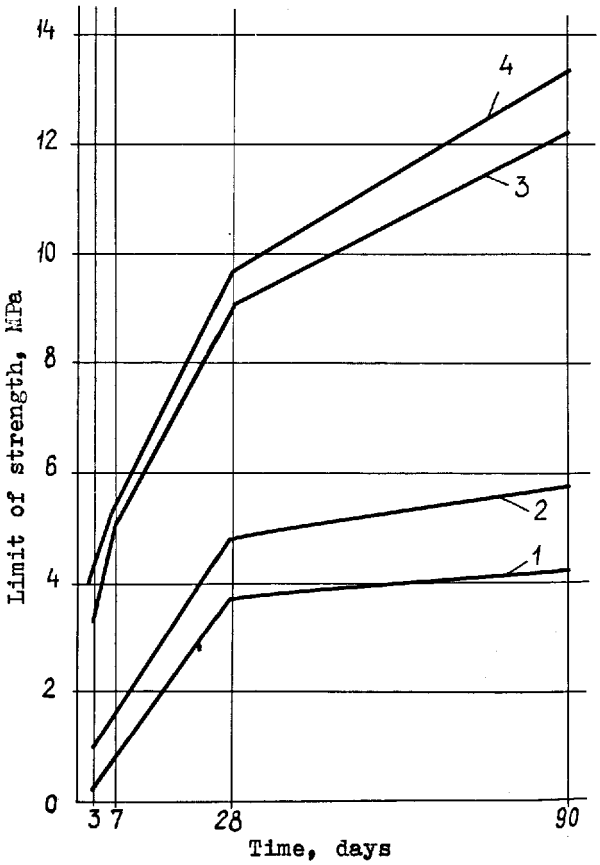

Fig.I. Plastic strength (a) and compressive strength (b) of the cement suspensions (water/cement = 0,I; silicate of sodium -IO%), containing sodium phosphate, % P_2O_5
I - 0; 2 - 0,4; 3 - 0,5; 4 - 0,6.

Electron microscope method has given us a possibility to reveal the differences in the structure of cement stone (fig.2). The first composition develops strong and porous structure with crystals of ettringite, which release on the surface of cement granules. Cement stone of the second composition is characterized by the more dense structure, represented mainly by calcium hydrocilicates with ettringite crystallizing in the pores of cement granules.

a)

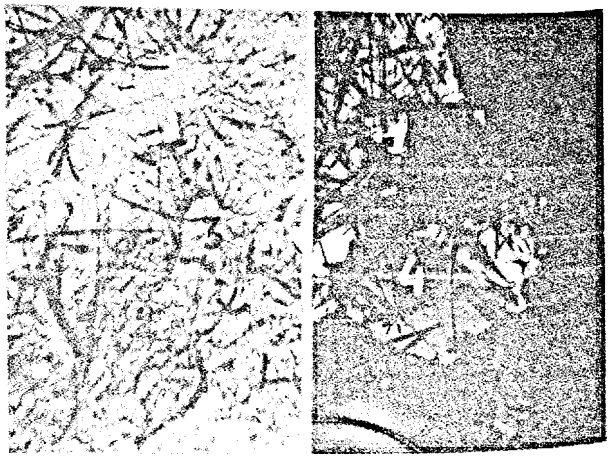



b)







Fig.2. Electron microfilms of the chipped surfaces of cement stone (water/cement = I,0), hydrated during 60 days (x6000) : a) with additive of I0% silicate of sodium; b) with additive of I0% silicate of sodium and 0,5% P_2O_5 in ferm of $Na_2HPO_4 \cdot I2H_2O$. I - ettringite; 2 - fibrous hydrosilicates of calcium; 3 - the residues of unhydrated cement granules; 4-hydroxide of calcium; 5-plate-scaled hydrosilicates of calcium.

These new compositions are used for water-proofing of exploratory workings in pit-construction.

I.L.Luginina
R.G.Nigmadilova
Technological Institute of Building Materials, Belgrad, U.S.S.R.

KINETICS OF ASSIMILATION OF CALCIUM OXIDE IN PRESENCE OF TITANIUM COMPOUNDS.

P

The essencial features of clinkerization in presence of titanium compounds have been described by many investigators. This concern in the problem is quite lawful and conditioned by the occurance of the element in the Earth's crust, and by the titanium chemical nature, analogical to chemical features with oxidization rate = 4 (I). H.Kühl in his fundamental monography "Zemenchemie" (2) pointed out, that the titanium oxides could form compounds not only with the main composites of the raw mixes, but also with alkalies.

We have studied the influence of the titanium dioxide on the dynamics of calcium oxide assimilation in portland raw mixtures.

Chemically pure titanium dioxide of rutile modification were injected into portland raw mixtures of various modular features. The compact samples were burned at the temperatures of 900-I450°C in electric furnace, and in the cake there was estimated the content of free calcium oxide. The results are given in the table.

We suppose that in the portland raw mixtures containing simultaneously both titanium dioxide and alkaline component there exists a possibility of formation of alkaline titanates and their solid solutions which (because their melting temperature is 85-I200°C) stimulate the processes of calcium carbonate dissociation and binding of calcium oxides into clinker minerals. Alkaline compounds of titanium also affect the clinkerization processes at higher temperatures, changing the features of the liquid phase.

The possibility of formation of alkaline titanates was confirmed by our investigation of the systems $CaO-TiO_2-K(Na)_2O$ and $MgO-TiO_2-K(Na)_2O$. At the burning temperatures of 900-II00°C in the burning products there were found titanates of alkaline metals.

So the titanium compounds and alkaline compounds simultaneously present in raw mixtures produce positive effect on the processes of clinkerization.

The free CaO content in the cake

Table

№ cake	TiO_2 content (%) mass	K_2O content (%) mass	Free CaO content (%) at the burning temperatures (°C)						
			900	I000	II00	I200	I300	I400	I450
I	0,0	0,0	32,4	30,7	25,0	22,0	I6,5	I,5	0,0
2	0,5	0,0	33,0	27,5	22,0	I7,0	I4,0	0,0	0,0
3	I,0	0,0	-	32,0	22,0	I5,0	II,0	0,0	0,0
4	2,0	0,0	-	3I,0	22,0	I8,0	7,5	0,0	0,0
5	3,0	0,0	30,0	27,0	24,0	-	7,0	0,0	0,0
6	5,0	0,0	28,0	24,0	I5,0	I5,0	5,0	3,0	2,0
7	8,0	0,0	-	27,5	2I,0	20,0	8,0	3,0	5,0
2-I	0,5	0,5	-	35,0	I9,2	I5,0	I0,8	I,0	0,0
4-I	2,0	0,5	-	27,0	2I,0	I2,3	8,0	0,5	0,0
6-I	5,0	0,75	-	22,5	II,5	I0,0	5,0	I,4	I,6
7-I	8,0	I,0	36,5	30,8	20,5	I6,6	I0,0	2,5	2,0

At the temperatures of 900-I200°C the speed of the binding process of calcium oxide is increased in the case with all concentrations of titanium dioxide. In the field of active mineral formation (I300-I450°C) the effect of titanium dioxide is expressed more clearly: in the presence of 3% content of TiO_2 the speed of the binding of calcium oxide is increased and with the increase of TiO_2-content from 3 to 8% the speed is reduced. The injection of alkaline component (chemically pure potassium oxide) into the raw mixtures, containing titanium dioxide, caused definite changes in the character of calcium oxide assimilation: in the temperature range of 900-I200°C the binding of calcium oxide was more active compared to mixtures without alkalies, but with the adequate volume of TiO_2. There was also noticed essential reduction of free calcium oxide content in the mixtures containing the increased volume of TiO_2 at the concluding stages of clinkerization.

BIBLIOGRAPHY

I. Г.П.Лучинский. Химия титана. "Химия", М. I97I

2. H.Kühl. Zemetchemie. Band II, Berlin, I958

B.Moudelman
A.Clutchariov
G.Galimova
A.Bessmertnykh

NIIstromproek, Tachkent, NIICement, Moscow, U.S.S.R.

PARTICULARITES THERMOCHIMIQUES DU PROCESSUS DE CUISSON DU CLINKER ALINITIQUE

L'utilisation du bain fondu de sel en qualité du milien réactionel assure la baisse de la température de cuisson de 300-350° aussi que les formations intermédiaires et la composition de phases du clinker cuit inordinaires.

Des essais du four rotatif 2,5x75m ont permit d'identifier des transformations physiquo-chimiques pendant la cuisson. L'analyse de phases aux rayons X (fig.I), les méthodes pétrographiques et de la microscopie électronique ont mis en évidence la succession de la formation de minéraux en fonction de la température (tabl.I).

Table I

Succession de la formation de minéraux

Temp.,°C	Minéraux	Q-té,%
500-650	$C_{II}A_7CaCl_2$ - chloraluminate de Ca	2-4
650-750	$CaCO_3 \cdot CaCl_2$ -charbochlorite	8-I2
650-750	$C_{II}A_7CaCl_2$	3-7
	$2\,CaO \cdot SiO_2$ $CaCO_3$-spourrite	35-45
	C_2S - silicate bicalcique	jusqu'à 2
750-850	$C_{II}A_7CaCl_2$	3-7
	$2CaO \cdot SiO_2$ $CaCO_3$	45-55
	C_2S	I2-I8
Zone du cuisson	$C_{II}A_7CaCl_2$	4-5
	C_2S	25-35
	$20CaO \cdot MgO \cdot 6SiO_2 \cdot Al_2O_3 \cdot CaCl_2$- alinite	55-65
clinker	$C_{II}A_7CaCl_2$	3-4
	C_2S	25
	C_2F-ferrite bicalc.	jusqu'à 4
	$20CaO \cdot MgO \cdot 6SiO_2 \cdot Al_2O_3 \cdot CaCl_2$	55-65
	C_3S	3-7

L'analyse thermique différentielle (fig.2) et l'analyse chimique des échantillons pris dans les différents domaines du four ont montré que la décarbonation se passe essentiellement à 970-I070 K. L'absence de la chaux libre témoigne de la haute réactivité du cru.

La circulation du chlore est subite au circuit interne (déchlorage dans les zones chaudes et régénération de $CaCl_2$ dans les froides) comprenant l'issue d'une certaine quantité de chlore entrant dans la structure cristalline de minéraux (fig.3).

Des calculs thermodynamiques selon des données sur les transformations physico-chimiques, aussi que l'analyse de la dissipation de la chaleur ont laissé établir des facteurs assurant la réduction de la consommation spécifique de la chaleur en comparaison avec le procédé classique. Cette réduction peut être de 20% (tabl.2).

Table 2

Facteurs assurant la réduction de la consommation de la chaleur pour la cuisson du clinker alinitique (voie humide)

NN	Facteurs	Part de l'économie totale,%	Article du bilan thermique
I.	Diminution de la basicité du cru	23	Consommation téorique de la chaleur
2.	Augmentation de l'exothermie des réaction de ménaralisation	II	I bid.
3.	Régénération de $CaCl_2$	2	I bid.
4.	Formation de bain fondu	6	I bid.
5.	Déchlorage	-I3	I bid.
6.	Baisse de la température du processus	2	Pertes de chaleur à travers le corps du four
		I2	Pertes de chaleur avec l'air excédant du refroidisseur
7.	Diminution de l'humidité de la pâte crue	II	Consommation de la chaleur pour évaporisation de l'eau
8.	Augmentation de la capacité horaire du four	I6	Pertes de chaleur a travers le corps du four
9.	Diminution de la quantité spécifique du cru (sur l'unité de masse du clinker)	4 5	Consommation théorique de la chaleur Consommation de la chaleur pour évaporisation de l'eau
IO.	Diminution du volume et de la température de gaz perdus	20	Pertes de chaleur avec des gaz perdus
II.	Diminution de la quantité de la poussièrre	I	Pertes de la chaleur avec la poussière

Des calcules et des essais industriels montre que la mise au point de la tecnologie à basse température réduit la consommation thermique (20%) et augmente la capacité horaire des fours rotatifs (30%).

B.Noudelman
A.Clutchariov
G.Galimova
A.Bessmertnykh

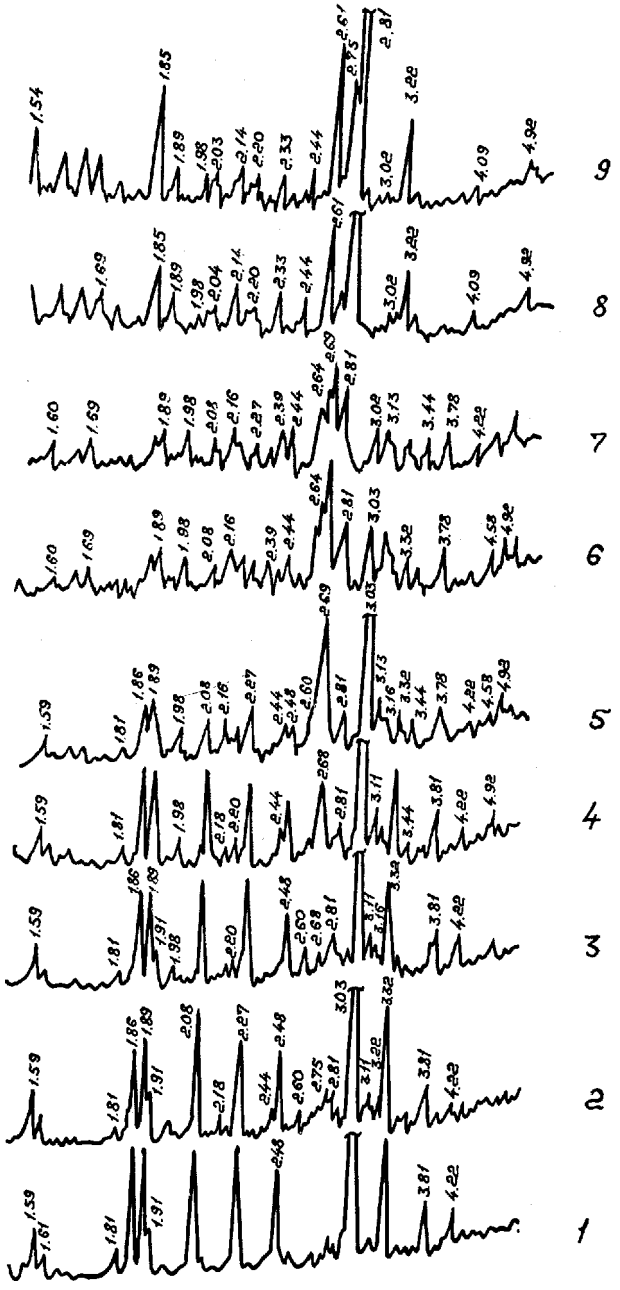

Fig.1. Analyse au rayons X des échantillons:
1 - cru de départ; 2 - 150°C; 3 - 300°C;
4 - 500°C; 5 - 650°C; 6 - 750°C; 7 - 800°C;
8 - zone de cuisson 9 - clinker alinitique

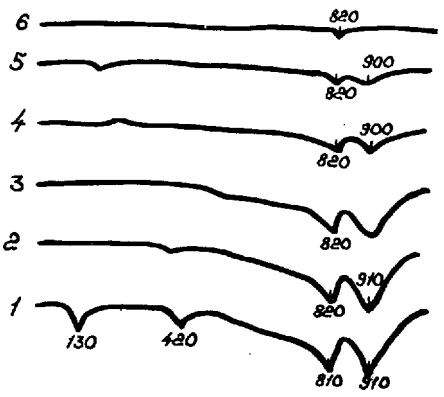

Fig.2. Analyse thermique dif. des échantillons: 1 - zone de chaînes; 2,3,4,5 - température du matériau 500, 650, 750, 800°C; 6 - début de la zone de cuisson

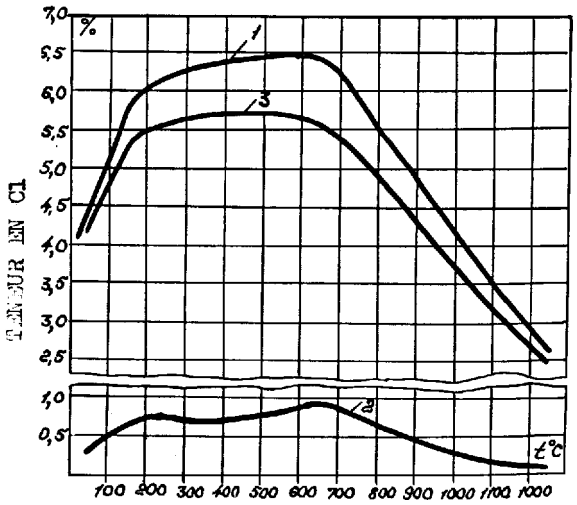

Fig.3. Variation de la teneur en chlore du matériau lors du traitement thermique dans four rotatif 1 - Cl^- total; 2 - Cl^- combiné avec des alcalis (RCl); 3 - Cl^- combiné en $CaCL_2$ et autres combinaisons

A.A. PACHTCHENKO,
E.A. MIASNIKOVA,
V.V. TOKARTCHOUK,
V.V. CHEVTCHENKO

Institut polytechnique de Kiev, U.S.S.R.

PARTICULARITES DE LA CLINKERISATION DES CRUS A COMPOSANTS ALUMINOSILICIEUX A HAUTE REACTIVITE.

L'intensification des processus de clinkérisation peut être obtenue en introduisant dans le mélange cru une matiére naturelle à haute réactivité ou un sous-produit industriel qui a subi au préalable un traitement à haute température et a accumulé une quantité déterminée d'énergie interne. Une baisse supplémentaire de la consommation d'énergie nécessaire à la fabrication du clinker est possible grâce à l'utilisation d'un tel composant à l'état non broyé (1) ou la production sur sa base des clinkers (de bélite) à faible saturation à activité élevée (2).

On a établi l'efficacité d'utilisation des roches effusives, les basaltes, largement répandus dans le monde entier (3) en qualité de composant aluminosilicieux ferrifère è haute réactivité entrant dans le mélange cru du ciment Portland. Ils sont caractérisés (d'après R. Deli) par une composition chimique moyenne suivante, % en masse: SiO_2 - 49,06; TiO_2 - 1,36; Al_2O_3 - 15,7; Fe_2O_3 - 5,38; FeO - 6,37; MnO - 0,31; MgO - 6,17; CaO - 8,95; Na_2O - 3,11; K_2O - 1,52; P_2O_5 - 0,45; H_2O - 1,62. Les basaltes provenant d'un même gisement diffèrent sensiblement au point de vue de la stabilité de composition.

Pour donner une appréciation comparative préalable de l'homogénéité chimico-minéralogique et des intervalles des températures de fusion des basaltes et d'autres minérais aluminosilicieux utilisés traditionnellement dans l'industrie du ciment, on s'est servi du diagramme d'état d'un système à quatre composants SiO_2 - Al_2O_3 - CaO - MgO. Les points figuratifs d'un nombre écrasant de compositions des basaltes se placent à l'intérieur du tétraèdre MS - CMS_2 - CaS_2-S (fig. 1). Cela étant, la température du début de fusion des basaltes constitue (1150±10) °C et celle de la fin de fusion oscille au niveau de 1300 °C en fonction de la teneur en Al_2O_3 (4).

Les compositions d'argiles utilisées dans l'industrie du ciment se caractérisent par une plus grande diversité: les points

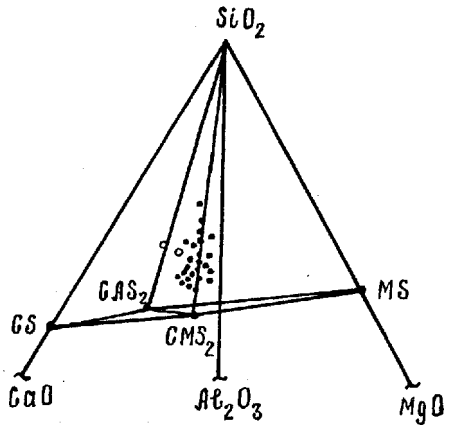

Fig. 1. Disposition des points figuratifs des compositions des basaltes dans les tétraèdres élémentaires du système SiO_2 - Al_2O_3 - CaO - MgO:
(·) - tétraèdre MS-CMS_2-CaS_2-S;
(∘) - tétraèdre CS-CMS_2-CAS_2-S.

figuratifs de ces compositions se placent dans les tétraèdres élémentaires: CS -CMS_2 - CAS_2 - S; MS - CMS_2 - CAS_2 - S; CAS_2 - $M_2A_2S_5$ - MS - S; CAS_2 - A_3S_2 - $M_2A_2S_5$ - S.

L'intervalle des températures de fusion, lui aussi, est soumis respectivement à d'importantes oscillations: la température du début de fusion des argilles de diverses compositions varie de 1135 à 1300 °C et celle de la fin de fusion, de 1400 à 1500 °C. Les laitiers de haut fourneau occupent une position intermédiaire entre les basaltes et les argiles. Les points figuratifs de la masse essentielle de compositions de laitiers se situent dans les tétraèdres élémentaires: C_3S_2 - CS - C_2MS_2 - C_2AS_2; C_2MS_2 - CAS_2 - MA - M_2S; C_2MS_2 - C_2AS_2 - CAS_2 - MA (fig. 2). La température du début de fusion de la majorité des laitiers constitue 1285 à 1290 °C et celle de la fin de fusion est de 1400 à 1500 °C.

Il en résulte que les basaltes ont un plus bas point de fusion que les autres minéraux aluminosilicieux utilisés dans l'industrie du ciment: dans les mélanges crus contenant du basalte la fusion commence à une plus basse température de l'ordre de

A.A. PACHTCHENKO,
E.A. MIASNIKOVA,
V.V. TOKARTCHOUK,
V.V. CHEVTCHENKO

P

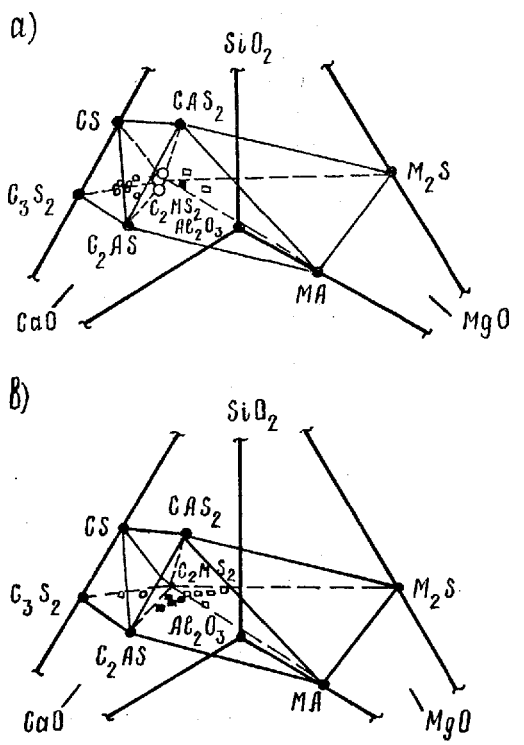

Fig. 2. Disposition des points figuratifs des compositions de laitiers dans les tétraèdres élémentaires du système SiO_2-Al_2O_3-CaO-MgO:
(∘) - tétraèdre C_3S_2-CS-C_2MS_2-C_2AS;
(O) - tétraèdre CS-C_2MS_2-C_2AS-CAS_2;
(■) - tétraèdre C_2MS_2-C_2AS-CAS_2-MA;
(□) - tétraèdre C_2MS_2-CAS_2-MA-M_2S

1150 °C, aux environs de 1180 à 1200 °C la masse essentielle de basalte est en fusion et la quantité de la matière fondue atteint 30 % (5) ce qui est capable d'accélérer sensiblement la formation d'alite. Ce fait a permis de concevoir la possibilité de cuisson des mélanges crus basaltiques non broyés; la formation de minéraux se produit alors grâce à une imprégnation des particules décarbonisées des pierres de carbonate concassées par le basalte en fusion et à une interaction ultérieure de la phase liquide et de l'oxyde de calcium.

Une étude des particularités de formation de la structure du clinker de ciment Portland au cours de la cuisson des mélanges crus à haute dispersite a montré une baisse sensible du rôle des réactions en phase solide grâce à une réduction du nombre de contacts entre les particules et, respectivement, à un rétrécissement du front des réactions (6). Dans le domaine des températures comprises entre le début de fusion du basalte et 1250 °C la vitesse du processus d'imprégnation est faible, la matière fondue pénètre dans la particule de carbonate essentiellement par gros pores principaux. Dans la zone de contact du composant carbonaté avec le basalte on observe une interaction des composants grâce aux processus d'échange de diffusion conduisant à une formation dans la couche de basalte contiguë à la chaux concassée, de cristaux de mélilite, de wollastonite et de bélite. Cependant, les réactions de formation des minéraux possèdent une nature limitée, la profondeur de diffusion des nouvelles formations étant faible. Lorsque la température se porte à une valeur de 1300 à 1350 °C, la viscosité de la matière fondue baisse, elle devient capable de pénétrer dans les micropores (les pores primaires de la matière crue et les pores secondaires dont l'apparition est due à la décarbonisation). Les dimensions des pores augmentent grâce à une action de coincage de la matière fondue et à une dissolution des parois de pores ce qui, à son tour, facilite la progression de la phase liquide à l'intérieur des grains de carbonate. Par suite d'une jonction diffusée d'ions de calcium à la phase liquide, une couche de cristaux de silicate bicalcique apparaît suivant le front de mouvement de l'excès de matière fondue à travers la particule décarbonisée. Avec l'épaississement de la couche, la vitesse de diffusion d'ions de calcium dans la matière fondue ralentit quelque peu tout en restant au-dessus des vitesses de diffusion des autres ions ce qui provoque une modification progressive de la structure de la couche intermédiaire: à la limite de la matière en fusion a lieu un délayage des nouvelles formations et une baisse de leur basicité tandis qu'à la limite de la composan-

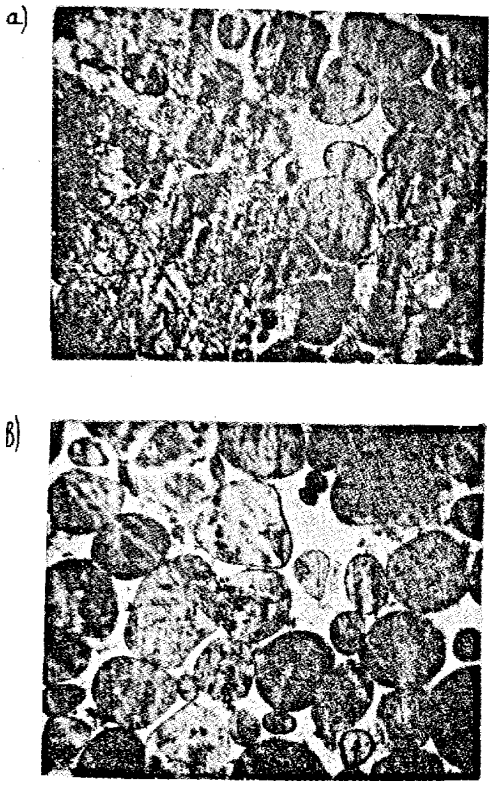

Fig. 3. Microphotographies des clinkers: a) formation de bélite; b) formation d'alite; x 300

te carbonatée se produit une saturation de la couche d'ions de calcium et un accroissement de la basicité des composés jusqu'à la formation du silicate tricalcique. Le processus d'imprégnation une fois terminé, on voit apparaître d'abord dans le clinker des grains de bélite sans formes particulières mais proches du faciès propre à la bélite (fig. 3, a). Par la suite, les cristaux de bélite prennent leur forme habituelle, puis, tout en gardant les formes cristallographiques propres à la bélite, commencent à tourner au clair, le teint propre aux cristaux d'alite dans les sections polies pour se transformer définitivement en cristaux d'alite (fig. 3, b).

Etant donné que tous les processus se produisent en présence de la matière en fusion et, par conséquent, à une grande vitesse, la synthèse des silicates de différentes basicités se déroule pratiquement simultanément. Le clinker obtenu est caractérisé par une structure zonale, un ordre indéterminé de disposition des champs alternés de cristaux d'alite et de bélite dû à une inhomogénéité de la structure du composant carbonaté (irrégularité de disposition des gros pores) étant donné que la thèse ci-dessus est juste pour le nouvement du front de la matière en fusion aussi bien de la surface de la particule que de l'"intérieur' de cette dernière, c'est-à-dire, de la surface de pore. Il s'en suit que la vitesse des processus se déroulant pendant la cuisson des mélanges non broyés dépend sensiblement de la porosité du composant carbonaté de base et, avant tout, de la valeur moyenne du rayon des pores. La cote admissible des particules du composant carbonaté assurant la totalité suffisante des processus d'imprégnation et de synthèse des minéraux de clinker, peut être déterminée d'après l'équation (1):

$$R = -0,03t-1,38r_o^2+0,23\cdot10^{-4}t^2- -0,43\cdot10^{-4}tr_o+0,11\cdot10^{-2}r_o^2t, \quad (1)$$

où: R est la mesure linéaire des particules du carbonate concassé, mm;
r_o est la valeur moyenne du rayon des pores, unités conventionnelles;
t est la température de cuisson, °C.

Les données de calcul sont confirmées par les résultats expérimentaux (v. tableau) (7).

La cuisson de mélanges crus non broyés permet d'obtenir des clinkers qui donnent les ciments des classes 400 et 500 caractérisés par des qualités exothermiques modérées et une résistance aux sulfates élevée. Grâce à un remplacement partiel (à 50 %) de la boue crue par un mélange non broyé de calcaire-basalte, on obtient une économie de chaleur de cuisson de 10 % tandis que le rendement du four rotatif augmente de 19,5 % (8).

Une réduction supplementaire de la consommation d'énergie de cuisson peut être obtenue grâce à l'utilisation de mélanges

Tableau

Type de roche carbonatée	Valeur moyenne du rayon des pores, un. conv.	Cote admissible (mm) des particules du carbonate concassé à la température de cuisson, °C			
		expérim.		equat.(1)	
		1350	1400	1350	1400
terre meuble	5,56	3,9	8,2	4,4	8,9
calcaire coquiller	11,68	9,3	26,8	10,4	23,7
roche sédimentaire	4,30	3,7	7,8	3,9	6,6
roche granulaire cristalline	1,11	1,4	3,6	1,6	3,3

crus contenant du basalte à faible coefficient de saturation destinés à obtenir des clinkers de bélite activés par un produit sulfaté (hopshogypse). La température de cuisson d'un tel clinker ne dépasse pas 1300 à 1350 °C et la résistance atteint 54,8 MPa (9).

REFERENCES

1. Цементы из базальтов/Под общ. ред. А.А. Пащенко. - Киев: Наукова думка, 1983. - 199 с.
2. Stark I. Entwicklungsstand von Belite-Zementen. - Beton-technik, 1982, No. 3, S. 72-80.
3. Йодер Г.С., Тилли К.Э. Происхождение базальтовых магм. - М.: Мир, 1965. - 247 с.
4. Пащенко А.А., Мясников А.А., Мясникова Е.А. Использование диаграммы состояния системы SiO_2-Al_2O_3-CaO-MgO для определения температур плавления основных изверженных горных пород. - Доклады АН УССР, сер. Б, 1981, с. 51-55.
5. О температуре появления расплава при обжиге известково-базальтовых шихт/А.А. Пащенко, А.А. Мясников, Е.А.Мясникова, Н.В. Лукашевич. - Доклады АН УССР, сер. Б., 1981, № 6, с. 73-75.
6. Будников П.П., Гинстлинг А.М. Реакции в смесях твердых веществ. - М.: Стройиздат, 1971. - 488 с.
7. Пащенко А.А., Мясникова Е.А., Токарчук В.В. Влияние характеристик карбонатных пород на процессы пропитки в крупнодисперсных портландцементных смесях. - Доклады АН УССР: сер. Б., 1983, с. 34-37.
8. Островская Н.Д., Мясникова Е.А. Использование базальтов в цементном производстве. - Цемент, 1984, № 6, с. 11.
9. Пащенко А.А., Мясникова Е.А., Шевченко В.А. Фосфогипс-интенсификатор обжига. - Строительные материалы и конструкции, 1983, № 4, с. 19-20.

V.P.Rjazin
Z.B.Entin
N.I.Komarova
N.A.Shebanov

NIICement, Moscow, U.S.S.R.

SOME FEATURES OF MINERAL FORMATION ON THE SAMPLE SURFACE.

Thermodynamic conditions on a calcinating granule surface at the external heat energy supply and abstraction differ considerably from the conditions of the material existence in the granule. This is a result of the further factors' affect:

1) the difference of surface and volume dimensions;
2) the phenomena on the heterogeneous madiums interface (solid phase - gas);
3) the chemical composition difference owing to the diffusive transfer of material through the interface and the exchange with the inner volume;
4) the intergranular pressure and the voltage vectors direction;
5) the temperature and its gradient;
6) the physical and mechanical features of the surface and inner layers (structure, heat and electric conduction, strength, hardness etc.).

Owing to the above mentioned differences the surface layer of a clinker granule considered to be an important object of study. The requisite for the study was also the experimentally established differences in the content of calcium oxyde in superfractions and on the granule surface of white Portland Cement clinker in comparison with large fractions, inner granule volume and the mean clinker mass.

To make reseaches of the phenomena on the surface layer of the Portland Cement clinker with effective thickness of 30 μkm the diffractometer DRON-2 with the high-temperature attachment UVD-2000 has been used. This method provides to obtain in vacuum (where the displacement volume pressure is not more than 10^{-4} mm Hg) the diffraction spectrum from the packed powder surface at temperature up to 2000°C. The scanning electron microscope "Jeol" - JSM-350CF with the spectrometer FCS has been also used.

Indication of the diffractograms has been made after 10-minutes exposure at designed temperature. The error of automatic control of the temperature is $\pm$ 4°.

The following was of the main interest:
- the features of phase formation on the material surface in the conditions of its intensive heat exposure (the heater is a tungsten tape);
- the processes of phase transition on the surface of the calcinating material;
- the changes of phase and chemical composition of the surface layer in the process of heating and cooling of the sample.

At the heating of the packed powder of threewedged C_3S up to 1500°C in the thin surface layer of 50-70 μkm, tricalcium silicate decomposes with α'- C_2S formation, but without calcium oxide extraction; meanwhile the inner volume of the sample does not change and still consists of C_3S.

At the heating of a white clinker powder containing three phases - C_3S, C_2S (β-form), C_3A the material surface undergoes the following changes (fig.I,2):
- alite content in the surface layer has monotonously decreased in the temperature interval 1000÷1400°C, and in the range of 1400 up to 1450°C it has sharply reduced to zero;

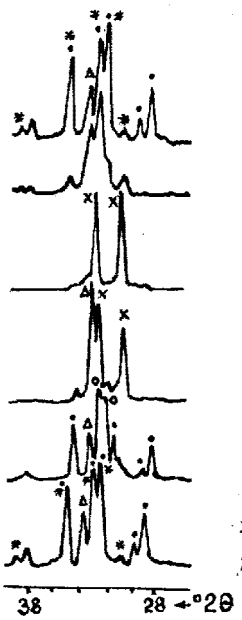

Fig.I. The radiograms' sections of a white clinker powder at its heating up to 1550°C in vacuum.
• - alite, * - β-C_2S, o - α'- C_2S, x - α- C_2S, Δ - C_3A.

- C_3A content in the surface layer being constant at 1000°C up to 1400°C has sharply increased in the temperature interval 1400÷1450°C, and at the further increase of temperature up to 1550°C the content of C_3A has reduced to zero as a result of transition to a liquid phase;

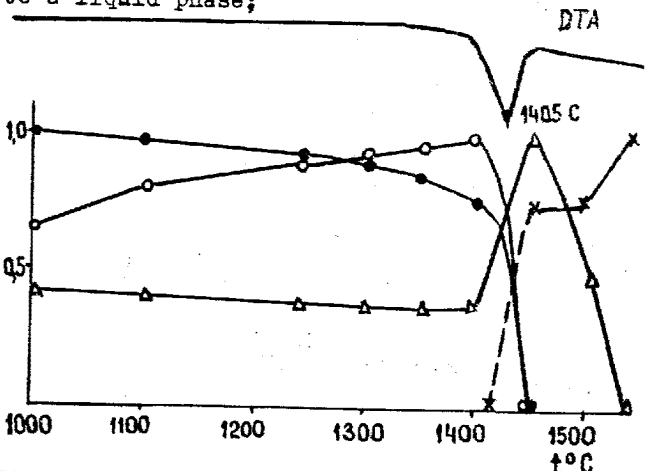

Fig.2. The change of phase composition of the white clinker surface at heating up to 1550°C.
• - alite, * - β- C_2S, o - α'- C_2S, x - α-C_2S, Δ - C_3A.

- C_2S content (in β-form) has monotonously increased from 1000 up to 1400°C in accordance with reduction of C_3S content. At the increase of temperature from 1450 up to 1550°C

α'-form has passed into α-C_2S (endoeffect connected with the transition of α' into α - modification of C_2S on the DTA curve - at 1405°C). The intervals of the more sharp change of the content of alite, C_3A, and the α'-α transition of C_2S practically coincide; - after cooling of the sample reflections of only two phases - C_3A and β- C_2S are displayed on the difractogram of the surface layer. Free calcium oxide is not observed. In the same time the main sample mass gives the typical X-ray photograph of the white clinker with comparatively higher alite content and lower C_3A content than the initial (before calcination) clinker.

The analogous phase composition of the surface has been produced at the calcination (up to 1500°C) of the raw mixture powder of the white clinker, containing 82,5% of limestone, 9,8% of kaolin, 5,9% of sand (fig.3). Under these conditions the sharp increase of C_3A-content and α'-α transition of C_2S in the surface layer has occurred in the interval of 1400°-1500°C. To α'-α transition on the DTA-curves the endoeffect at 1410°C corresponds. Exoeffect at 1345°C, as a result of the initial alite formation, concerns only the inner part of the sample. On the surface of the sample C_2S does not appear in the whole temperature interval up to 1500°C. Small amount of C_3S on the sample surface has been indicated only after its cooling.

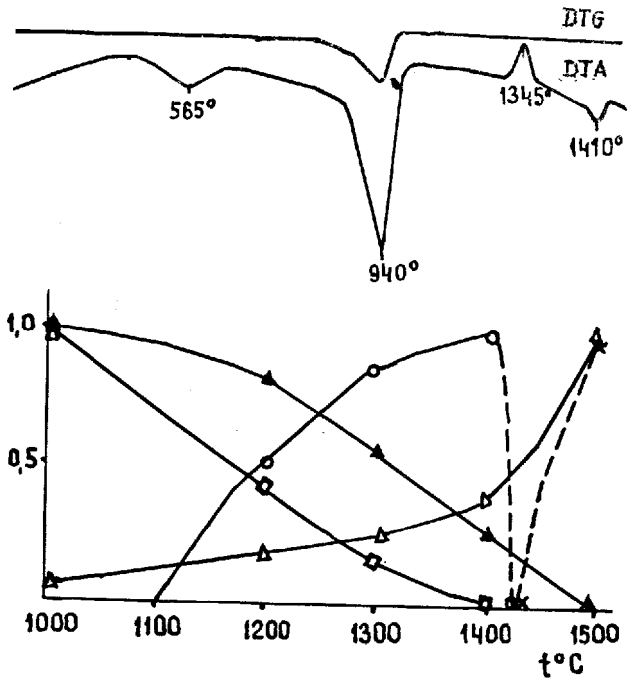

Fig.3. The changes of phase composition of the raw mixture of the white clinker at heating in UVD-2000 kilns and diversition system.
▲ - CaO, □ - SiO_2, o - α'- C_2S, x - α- C_2S, Δ - C_3A.

Alite formation on the surface of the sample at heating has been observed only at the calcination of mixtures with surplus content of calcium oxide. In this case CaO_{fr} crystals are present not only on the surface of the sample but in the inner volume of the sample as well (fig.4).

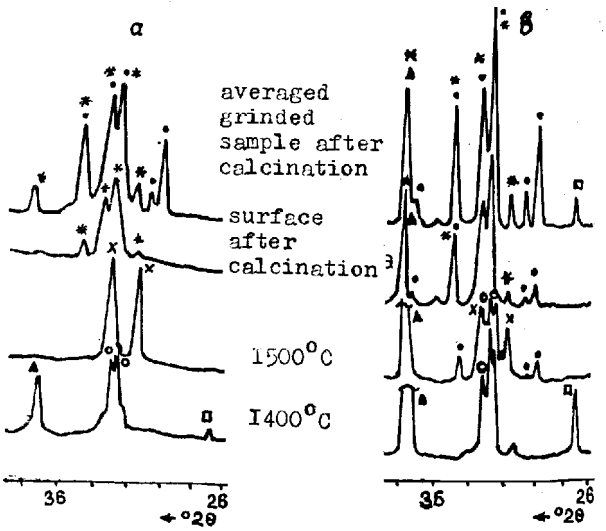

Fig.4. The radiograms' sections on the surface and the averaged grinded sample at calcination of the raw mixture with stoichiometric (a) and with surplus content of CaO (b).

The layer diffraction analysis of the samples has shown the following (fig.5):

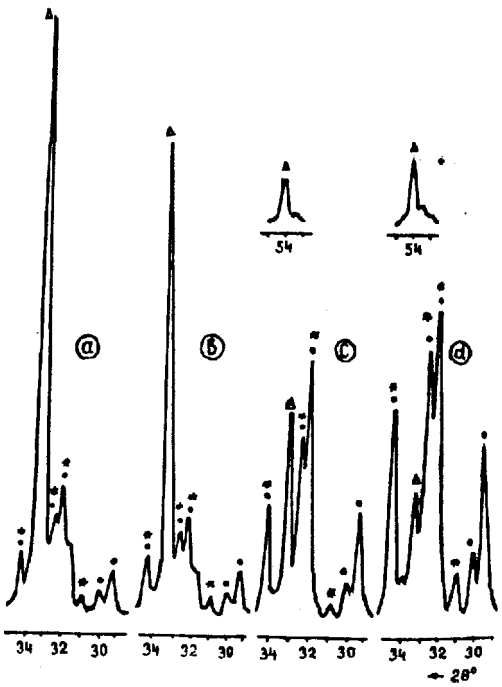

Fig.5. Radiograms of the surface and the adjoining parts of the sample.

a) the surface after calcination;
b) has removed the layer of 40 μkm;
c) has removed the layer of 120 μkm;
d) the averaged grinded sample.

- on the surface - C_3A, β and α'- C_2S, small amount of C_3S;
- to the depth of 50-70μkm the relative reduction of compositions of these phases and increase of alite amount;
- beginning with the depth of 70-100μkm the usual phase composition with high alite content.

It is noted that the opposite surface of the sample which has not been subjected to radiation (X-ray radiation, ultra-violet, luminous, thermal) by phase composition is analogous to the irradiated one.

The sample cut has been studied in the direction from the surface to the centre with the help of electron probe of the size of 2x10 μkm with the step of 2 μkm. The change of characteristic X-radiation intensity of Ca, Si and Al has been observed. It has been indicated that the intensity relation of Ca- and Si-curves on the surface and in the width of the sample is the same. It prevents from explaining the absence of C_3S on the surface by evaporation of calcium oxide from the surface in vacuum or its diffusion inside of the sample. Thus, the absence of alite on the surface at the synchronous absence of free calcium oxide can be explained only by absorption of the large amount of surplus calcium oxide by α-C_2S grating without the change of the grating type. At the cooling of the sample some part of α-C_2S, containing surplus calcium oxide reorganizes with C_3S formation which is fixed on the X-ray photograph of the cooled sample.

As for decimicrone widthes of the surface apparently it is possible to say that aluminium diffuses in the direction of the surface of the sample. It leads to the relative Ca and Si reduction on the surface before the appearance of the melt. The high intensity of C_3A peak on the surface at relatively low intensity of minerals-silicates peaks and comparatively small changes of the relations of intensity of the characteristic curves of Ca, Si, Al in comparison with the sample width indicates the formation of cubic C_3A with isomorphic Si. The cause of the formation of this mineral but not alite is the thermodynamic predilection and "two-dimensionality" of the texture. The irradiation of the sample does not affect the phase composition.

In conclusion it is necessary to say that the high-temperature processes of mineral formation on the surface of the sample considerably differ from those in the whole mass of mineral.

U. Ludwig and C. Urrutia
Institut fur Gesteinshuttenkunde, RWTH, Aacnen, West Germany

INFLUENCE OF SUCROSE ON THE SETTING OF PORTLAND CEMENT.

EXPERIMENTAL PROCEDURES

For the preparation of the portland cements, two industrial clinkers A and B, anhydrite and hemihydrate were employed. The calcium sulphate was added in amounts of 2.5 wt.% SO_3 to both of the cements. The chemical composition of the clinkers is shown in tab. 1. The anhydrite/hemihydrate ratio in the cement was 1.
The setting or rheology of cements has been measured according to DIN 1164, or by means of a coaxial cylinder viscosimeter, at constant water-cement ratios. The sucrose was added together with the mix water directly to the dry cement, or the cement was premixed with water for 4 min. before adding the sucrose. The alteration of the chemical composition of the pore solution that had been squeezed out of mortars according to DIN 1164, were established by Atomic Absorption Spectrophotometry (Ca, Al, Fe, Na, K), colorimetry (Si and sucrose), titration (OH^-), and SO_4^{--} by precipitation as barium sulphate.

Table 1 Chemical composition of the clinkers in wt.%

	Clinker A	Clinker B
SiO_2	22.40	21.50
Al_2O_3	4.52	5.31
Fe_2O_3	2.61	3.21
CaO	68.60	62.40
MgO	1.05	1.13
K_2O	0.18	0.68
Na_2O	0.20	0.20
SO_3	0.02	0.55

RESULTS

As for the cement containing little alkali, the direct addition of sucrose to the mix water does not induce any, dealing with portland cement, however , containing a lot of alkali, a distinct retardation of the initial setting up to 0.2 wt.% sucrose is effected.

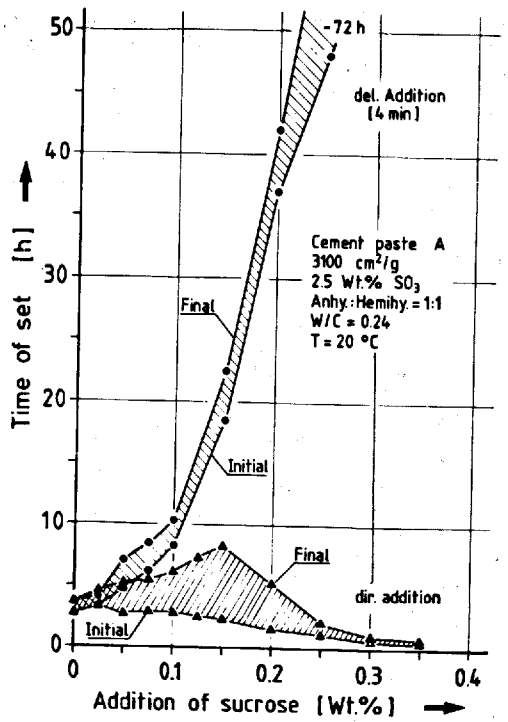

Fig. 1 Setting time of cement paste A vs addition of sucrose (direct or delayed addition of sucrose)

Consequent to that, even here a false set occurs. For both cements the final setting is evidently retarded till the false set takes place coinciding with a prolongation of the setting interval, and then accelerates (see picture 1 and and 2).

In correspondence with the results obtained by measuring the setting, the direct addition of augmenting portions of sucrose affectuates an increasingly accelerated gain of viscosity of cement pastes. The subsequent dosage of sucrose, however, already causes a long-lasting low viscosity, even when dealing with a smaller content of additive. In this respect picture 3 visualizes the shear stress versus time.

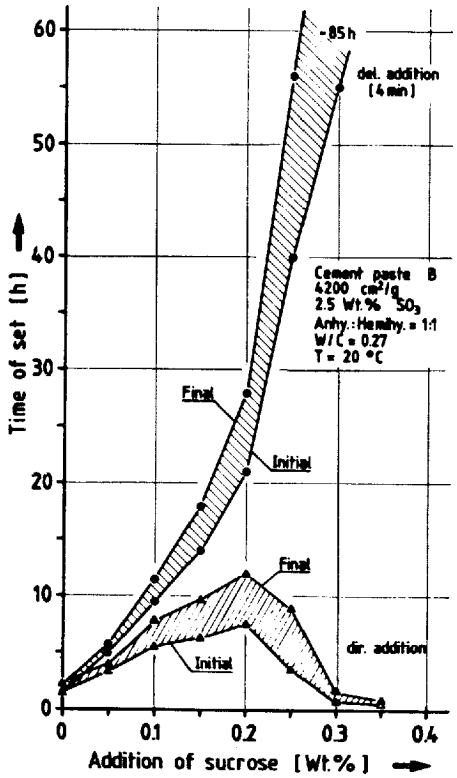

Fig. 2 Setting time of cement paste B vs addition of sucrose (direct or delayed addition of sucrose)

For the time being a particulary fast decrease of the Ca^{++}- and SO_4^{--}-ion concentration within the pore solution is being held responsible for the effect of the directly or subsequently added sucrose to the cement going along with an extremely fast formation of ettringite. Without a retarder or especially in case of delayed addition of sucrose, the respective concentrations are noticably higher (see table 2).
When directly adding sucrose, the aluminate concentration, too, is obviously increased.

sucrose added	content wt.%	Ca^{++} (g/l)	SO_4^{--} (g/l)	Al_2O_3 (mg/l)
without	0.0	1.3	1.4	0.5
directly	0.4	0.6	0.4	9.0
after 4 min	0.4	1.7	2.0	2.0

Tab.2 Calcium-, sulphate-, and aluminate-ion concentration within the pore solution 1 hour after mixing

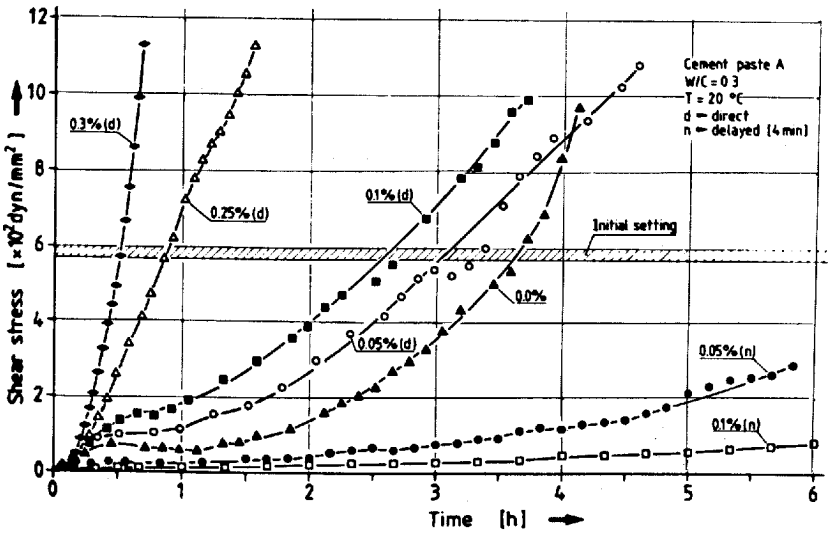

Fig. 3 Variation of shear stress with time measured at a shear rate of 0.02 min^{-1} at several sucrose concentrations

The direct addition of sucrose to cement leads to its evidently accelerated bond to or within the solid phases (see picture 4).

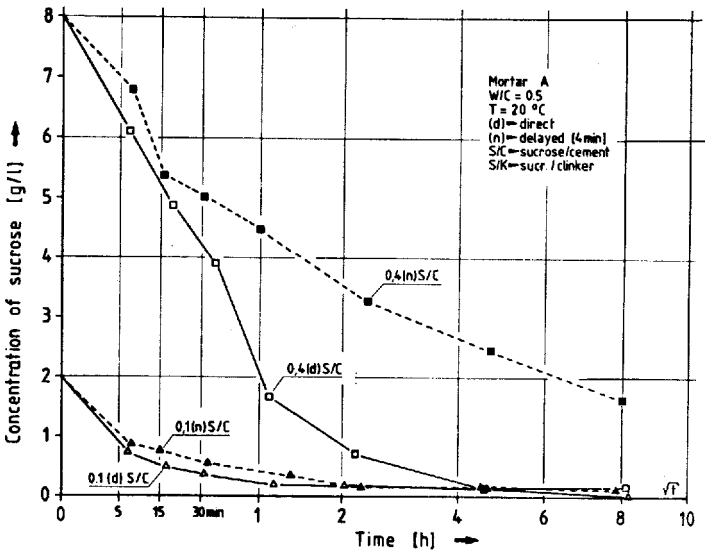

Fig. 4 Concentration of sucrose in the pore solution in cement mortar mixed with 0.1 wt.% and 0.4 wt.% sucrose refered to cement

Everaldo Marciano Jr. (ABCP - Brasil)
Peter Bartha (Refratechnik GmBh) West Germany

CL. CONTRIBUTION TO THE KNOWLEDGE OF THE PHASE COMPOSITION OF DIFFERENT MAGNESIA-CHROME BRICKS AFTER THE ATTACK BY CEMENT CLINKER

1. Introduction and posing the problem

Nowadays mainly magnesia chrome bricks are used as refractory lining in the burning zone of cement rotary kilns. The MgO-content of the bricks vary between approx. 80 and 60 % MgO according to the MgO-raw material and chrome ore ratio. Accordingly the Cr_2O_3 content ranges between 4 and 16 %. Additionally they show considerable differences in type and quantity of the chemical secondary components SiO_2, Al_2O_3 and Fe_2O_3.

Therefore the durability of the magnesia chrome bricks is not only determined by its behaviour towards mechanical load but also by its chemical reaction at high temperatures.

Aim of the following comparative investigations is to determine the chemical-mineralogical changes of four representative magnesia chrome bricks of different chemism after its contact with cement clinker.

2. Character of the applied materials

Two industrial cement raw materials of similar mineralogical composition were chosen for the investigations. Its chemical properties were adjusted regarding the content and composition of the ashes of two different coals (mineral coal and charcoal from Brasilia).

Four in the cement industry applied magnesia chrome bricks with different chemical-mineralogical and physical properties were investigated regarding their phase composition before and after the attack by cement clinker. Above all the magnesia chrome bricks differ in type of the applied dead burnt magnesia and chrome ore, in the ratio of the beforementioned and in the burning temperature during the brick burning process.

In the following sections the applied materials are described in detail.

2.1 Coal ashes

Due to the fact that the Brasilian cement industry recently mainly applies solid fuel, some native current mineral coals and one charcoal were chosen. Table 1 gives the chemical mineralogical composition and the fusing behaviour of the two ashes. The ashes obviously have different Al_2O_3- and CaO-contents as well as different fusing points.

2.2 Raw meals

Table 2 reflects the chemical mineralogical composition, the theoretical clinker phases as well as the burnability index of the raw meals. Please note the significant differences in the MgO-content, in the alumina modulus and in the burnability index.

2.3 Refractory bricks

A characterization regarding chemical analysis, phases and the most important physical properties are shown in table 3 and figure 1

3. Test conditions

By adding the same portion of water the raw meals were pressed into tablets of 20 mm in diameter and 20 mm in length and dried at 110 °C until achieving constant weight. Cubic test specimen of 70 x 70 mm were sawed out of the refractory bricks.

3 tablets each were put on top of a cube and covered with a second cube from the same brick material.

The samples were heated up in a Bickley-laboratory furnace fired with natural gas at 10°C/min up to 1700 °C. Preliminary tests at 1500 and 1600 °C had not resulted in any significant reactions at the contact. The durability reached 5 hours in a homogeneous temperature field.

After slowly cooling off in the furnace the samples were prepared according to the different tests. Fig. 2 schematizes the procedure.

4. Results of the investigations

For a better understanding of the new formations of the phases several test methods were combined:

- Atomic absorption spectroscope
- X-ray phase analysis
- Reflected light microscopy
- Scanning electron microscopy (SEM)

4.1 X-ray phase analysis

Please refer to table 4 for the results. Alite, the compound richest in lime, only occurred in brick D. C_2S was found in every brick. The intensity showed, however, that generally more C_2S was found in combination with raw meal 1 than with raw meal 2.

All brick samples pretreated with raw meal 2 had monticellite and merwinite. Except for sample B which also had a considerable quantity of those silicates with raw meal 1. Forsterite could only be proved in samples B and C under the influence of raw meal 2.

Especially raw meal 1 was responsible for the highest quantities of the phase C_4AF in the brick samples A and C.
Aluminate phase was only found in the brick samples A and B. The combination of brick sample C/raw meal 1, however, produced a phase which - according to the d-values (ASTM-Standards 17-736)- was first identified as calcium-aluminum-magnesium silicate of the formula (CaO, MgO, Al_2O_3). SiO_2.

4.2 Reflected light microscopy

The investigations with the reflected light microscope were carried out in order to control the phases determined by the X-ray phase analysis and to determine their spatial distribution. Due to the fact that the reaction tests were carried out in a homogeneous temperature field there was no clear zonal sequence as can be observed with used bricks in the practice.

Raw meal 1 provoked the formation of the compound belite as silicate phase in all brick samples except for in brick sample B, where a significant quanitity of merwinite and monticellite could be determined.

Brick sample C contained a high quanitity of a prismatic phase hard to etch. It could be proved all over the whole infiltrated brick part. Very small quanitities of prismatic phases were also found in brick sample A.

Calcium-aluminate-ferrite was found in all brick samples: the highest quanitity in brick samples A and C, the lowest in B.

Raw meal 2 caused a different reaction than raw meal 1. Besides of belite there were also the significant phases merwinite and monticellite. Very small quanitities in decreasing sequence could be determined in the brick samples C, B and A.

Calcium-aluminate-ferrite was determined under the impact of raw meal 1 with the same before-mentioned tendency for the respective bricks.

Under the attack of the pure ashes forsterite formed in all bricks, the charcoal additionally caused the formation of monticellite. In general the infiltration evoked by the mineral coal ashes was nearly twice as high as that by the charcoal ashes.

4.3 Scanning electron microscopy (SEM)

The investigations by the SEM were carried out as supplement to the X-ray phase analysis and the microscopical investigations. The SEM indentified the unknown phases, the known phases and determined the exact chemical composition including the incorporated foreign ions.

The results can be summerized as follows:

- The prismatic phase found by the reflected light microscope was identified as a melilite of the ideal composition C_6MA_4S (fig. 3).
- The exclusive formation of alite in brick sample D with both raw meals was confirmed. Furthermore the incorporation of significant quanitities of chrome could be proved. Measured individual values amounted up to 20 and 25 atomic% Cr_2O_3.
- The Cr_2O_3-content in belite varied between 9 and 0 atomic%, the standard value varying between 1 and 4 atomic%.

- According to individual measuring 2 - 4 atomic% of MgOwere determined in belite in all brick samples after their reaction with raw meal 2.

Cr_2O_3 preferably substituted Al_2O_3. Higher quanitities could be determined in the brick samples reacting with raw meal 2 than with raw meal 1. The average doping quanitity was between 2 and 3.5 atomic%, in extreme cases between 15 and 16 atomic%. In these cases the general formula should read $C_4(Al,Cr)F$.

The doping of SiO_2 in calcium-aluminate-ferrite was nearly constant and varied between 4 and 4.5 atomic%.

Titanium and manganese were incorporated in calcium-aluminate-ferrite in samll, varying quanitities. A calcium-titanate-phase tending to C_3T_2 could be determined in very small quanitities with both raw meals. But it still contained between 5.55 and 5.65 atomic% of silicium (fig. 4).

5. Discussion of the results and conclusion

Taking into account that the brick samples were investigated under static conditions in a homogeneous temperature field and at increased temperatures (practical case of thermal overload) the following findings can be learnt from the phases in the slagged brick samples when only considering the chemical-mineralogical impact:

- As noted the bricks generally suffered more under the attack of raw meal 1 than of raw meal 2. As this result cannot only be attributed to the insignificant chemical differences there must also be kinetic causes: the higher burnability index of raw meal 2 together with a coarser grinding.

The less abundant offer of clinker phases with raw meal 2 can also serve as an explanation why merwinite and monticellite, which are less calciferous,formed in all bricks instead of belite in the case of raw meal 1.

- The abundance of calcium-aluminate-ferrite in bricks A and B can be explained by the high content of magnesium ferrite as the matrix forming phase of the bricks.

- In sample C considerably high quanitities of melilite were found of the approximately composition C_6A_4MS. An increased Al_2O_3-content of the brick could be responsible for it as the brick contains a chrome ore with an extremely high quanitity of magnesium-aluminate-spinel. The fact that this phase does not appear in brick sample D with the lowest content of Al_2O_3 underlines our presumption. Furthermore it is known that melilite forms during the wear of magnesia bricks containing MA-spinel.

The bricks B and C with forsteritic matrix react more sensitive in connection with cement clinker, because they enable the formation of the phases monticellite and merwinite which are less calciferous and which have a lower fusing point.

- Alite was only found in sample D, which has a sinter with a CaO/SiO_2 ratio of > 1.87 and is nearly free of iron. Therefore the formation of calcium-aluminate-ferrite can be practically excluded.

- The tested bricks suffer more under the mineral coal ashes than under the charcoal ashes. The mineral coal ashes, however, cause the formation of forsterite instead of forsterite and monticellite which occur in the bricks when attacked by charcoal ashes. This is caused by the different lime content of the two ashes. For the refractoriness forsterite is preferred to monticellite which has a lower fusing point.

- As observed by the SEM the incorporation of chrome into the lattice of alite and belite as well as the substitution of Al by Cr in calcium-aluminate-ferrite indicates the decomposition of the chromite spinel portion of the chrome ore and partly explains the whereabouts of the liberated chromium oxide.

- Striking was the formation of a calcium titanate phase, even if it was only found in small quanitities. It can only be explained by the supply of TiO_2 from the raw meal and the chrome ore.

The following conclusions can be drawn concerning the evaluation of the investigated bricks:

- A high compound of magnesia ferrite in the matrix is undesirable, because, under the attack of the clinker phases it leads to calcium-aluminate-ferrite and a lower fusing point of the brick matrix. Above all this is a typical behaviour towards cement clinker resistant to sulfate.

- A low CaO/SiO_2 ratio in the brick weakens its resistance to clinker phases because monticellite and merwinite lower the fusing point and therefore decrease the refractoriness. This effect is not dangerous as long as the quanitity of forsterite in the brick is only insignificant.

- The Al_2O_3-content of the chrome ore is in so far important for the reaction to cement clinker as increased Al_2O_3-contents might cause the formation of melilite.

- The results with the two raw meals show that besides the chemism the burnability of the raw meals influence intensity and completeness of the phase formation.

Table 1:

	mineral coal ashes	charcoal ashes
SiO_2 (%)	59.01	55.52
Al_2O_3	27.12	11.56
Fe_2O_3	7.16	6.12
CaO	1.71	15.38
MgO	1.06	2.88
K_2O	1.92	3.52
Na_2O	0.17	0.98
Mn_2O_3	0.05	0.29
TiO_2	1.10	-
Cr_2O_3	-	0.03
SO_3	-	-
CaO/SiO_2	0.03	0.28
LSF	0.84	8.85
SM	1.72	2.99
AM	3.76	1.65

	mineral coal ashes	charcoal ashes
softening point (°C)	1400	1220
hemispherical fusing point (°C)	1500	1230
flow point (°C)	1530	1400
Mineralogical composition		
quartz	x	x
silicate phase	x	x
mullite	x	x
calcite	-	x
free lime	-	x
field spar	x	-
haematite	x	x
glimmer	x	-
montmorillinite	x	-

Table 2:

Chem. composition	raw meal 1	raw meal 2
SiO_2	22.32	21.48
Al_2O_3	5.33	4.65
Fe_2O_3	3.40	3.46
CaO	65.83	63.45
MgO	1.97	5.20
K_2O	0.60	0.45
Na_2O	0.10	0.12
SO_3	0.17	0.32
Cl	0.05	0.07
TiO_2	0.21	0.25
Mn_2O_3	0.04	0.17
Rational analysis (according to BOGUE)		
C_3S	57.7	58.9
C_2S	29.5	17.1
C_3A	8.4	6.5
C_4AF	10.4	10.5
LSF	92.4	92.9
LSF (incl. MgO)	93.3	103.3
SM	2.49	2.52
TM	1.61	1.35

Mineralogical composition

	raw meal 1	raw meal 2
glimmer	x	x
montmorillinite	x	x
chlorite	-	x
calcite	x	x
dolomite	x	x
quartz	x	x
haematite	x	x

Table 3:

Refractory bricks(original composition)

	A	B	C	D
MgO	81.41	78.7	81.11	84.94
Cr_2O_3	3.95	6.93	4.64	8.41
Al_2O_3	2.58	2.68	4.73	1.88
Fe_2O_3	7.16	6.66	4.28	2.75
SiO_2	1.84	3.44	3.38	1.09
CaO	2.70	1.24	0.78	0.97
Mn_2O_3	0.36	0.20	0.66	0.15
K_2O	0.02	0.04	0.05	0.01
Na_2O	0.02	0.02	0.02	0.03
CaO/SiO_2	1.47	0.36	0.23	0.89
$CaO+SiO_2$	4.54	4.68	4.16	2.06

Mineralogical composition

periclase	x	x	x	x
chromite	x	x	x	x
MF	x	x	x	x*
M"S	-	x	x	-
CMS	x	x	x	-
C_3MS_2	x	-	-	x
C_2S	-	-	-	x**

x= present *= hardly any **= few

bulk density (g/cm^3)	2.93	2.81	2.85	2.93
apparent porosity(%)	18.85	23.34	21.24	17.70
cold crushing strength (N/mm^2)	60.7	47.2	44.2	57.8

Table 4: X-ray phase analysis

bricks

	A		B		C		D	
raw meal mix	1	2	1	2	1	2	1	2
C_3S							x	pro
C_2S	pos	pos	x	x	x	x	pos	x
C_3MS_2		x	x	x		x		x
CMS			x	x		x		x
M_2S				x		x		
C_3A	x						x	pos
C_6A_4MS					xx	pos		
C_4AF	xx	x	pro	pos	xx	pos	pos	pos
MA					x		x	

X = present
pos = possible
pro = probable

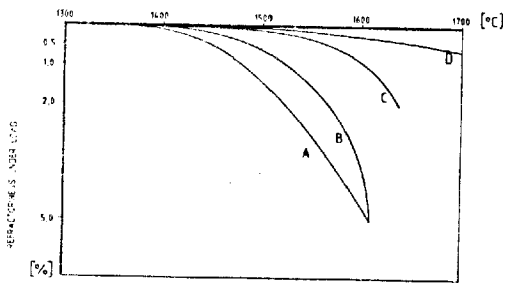

Fig. 1: Refractoriness under load of the investigated bricks according to DIN

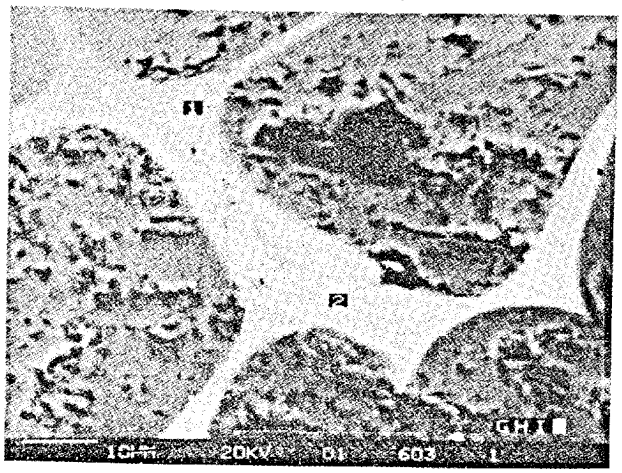

Fig. 3: SEM picture of the prismatic (melilite)-phase

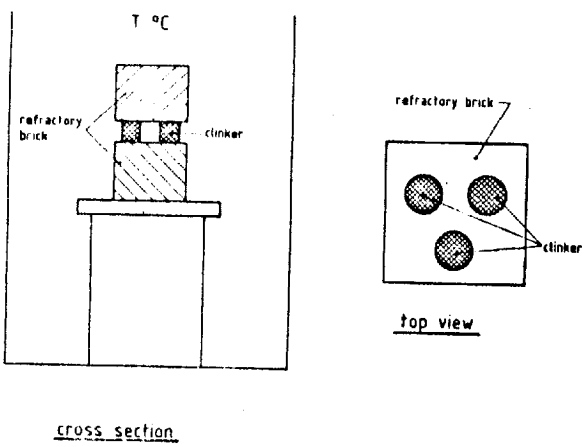

Fig. 2: Experimental arrangement

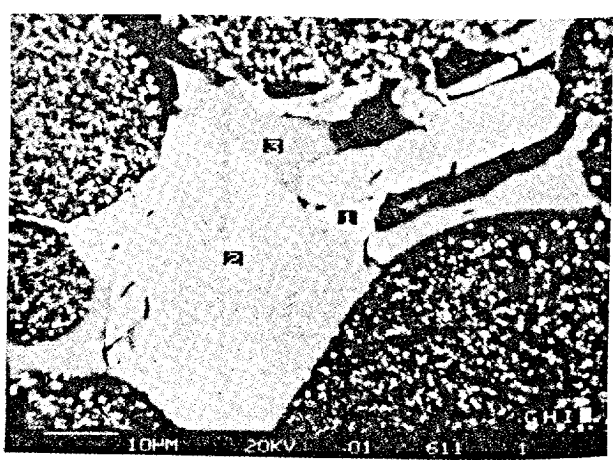

Fig. 4: SEM picture of the calcium-titanate-phase

C. MacInnis, P.P. Hudec and M. Moukwa
University of Windsor, Windsor, Ont., Canada

EFFECT OF MICROCLIMATE ON CONCRETE DETERIORATION

CL

EFFECT OF MICROCLIMATE ON CONCRETE DETERIORATION

SUMMARY

The south facing vertical surface of concrete barrier walls for highways often exhibit considerable scaling which suggests that walls so oriented are subjected to a more severe exposure condition. The objective of this research was to measure and define the microclimate by measuring the temperature, and moisture and salt concentration conditions obtaining at the surface and in the near sub-surface of south and north facing highway barrier walls. Two field exposure sites were included in the study: a south facing wall on a divided highway and two laboratory cast barrier wall panels placed to face north and south respectively at an outdoor site.

The field measurements of temperature and moisture content were obtained on a semi-continuous basis for three winter months. The results showed that a temperature gradient as high as 9C between the concrete surface and the 1 cm depth was common. The rate of freezing and thawing was significantly higher on the south facing wall than on the north facing wall and also the south facing wall was found to undergo a significantly greater number of freeze-thaw cycles. The foregoing findings indicate that a much more severe climate exists on south facing walls. This can be attributed directly to the greater insolation received by such walls.

Introduction

Concrete barrier walls are commonly used along highways in Canada and in and in northern U.S. states. Some have shown rapid deterioration in the form of surface scaling. Typically, the deterioration has tended to be more pronounced on the south facing walls. The purpose of this study was to measure and define the microclimate at such walls. The microclimate elements measured were temperature at the surface and near sub-surface, moisture content and salt content.

Field Instrumentation and Measurements

The microenvironment existing in the surface layer of concrete barrier walls was measured at two distinctly different sites. One site was an existing south facing barrier wall along a heavily travelled divided four-lane highway in South Windsor (Ontario), the E.C. Row Expressway. The results obtained at this site represent only a south facing exposure, and are described elsewhere (1).

The other site was the roof of Essex Hall on the campus of the University of Windsor. The tests results from that site are the subject of this paper. Two panels having the shape and dimensions of concrete barrier wall sections were cast in the laboratory, instrumented, cured for one month and then placed on the roof, one facing north and the other facing south. The concrete used was air-entrained (nominal 5-7%) with a water-cement ratio of 0.47 and maximum aggregate size of 10 mm (3/8"). Copper-constantan thermocouples were used for the temperature measurements. The thermocouples were placed at the surface, and at 10mm depth from the surface. Stainless steel electrodes were embedded at 10mm depth and 10mm apart, and used in the measurement of moisture and salt concentration. The cast panels are shown in Figure 1, and the instrumentation of the panels in Figure 2.

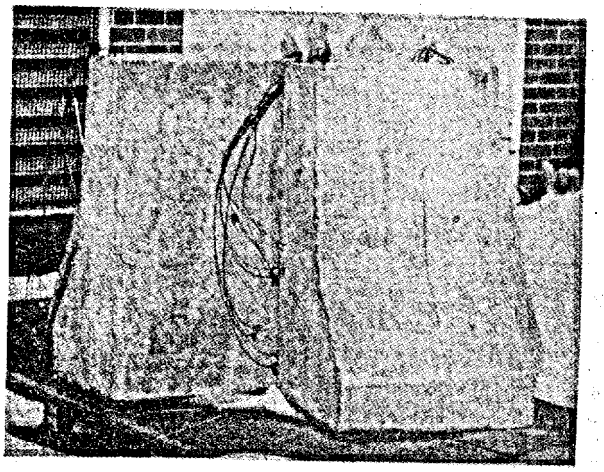

Figure 1: Cast panels. Note electrodes embedded along the center line of the panel and thermocouple wires in the back of the panel.

The panels were sprayed with a 9% NaCl salt solution three times in a manner shown in Fig. 3 to result in three distinct salt concentration zones. Natural moisture content and induced salt content were determined by two methods. The primary method used was the "capacitance effect method" developed by Hudec, MacInnis and Moukwa (1). This method is based on the observation that the capacitance of concrete varies with the degree of saturation. By applying an electrical field through stainless steel electrodes and measuring the resulting current, it was possible to predict the degree of saturation and, to some extent, the salt content. Current readings were taken after each spraying.

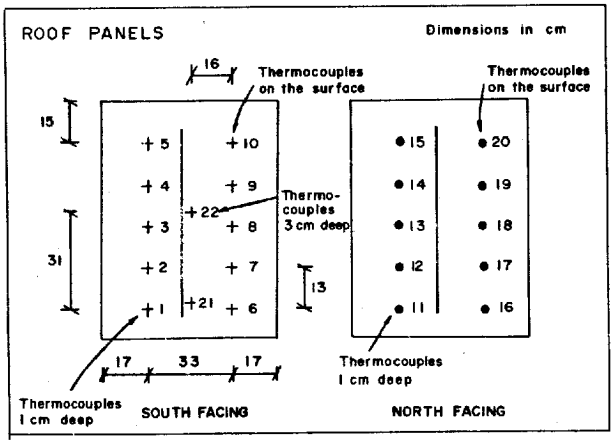

Figure 2. Placement of thermocouples and electrodes in the south and north facing panels.

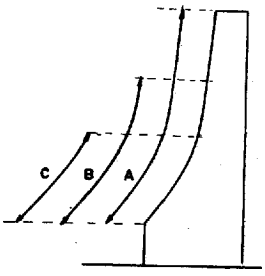

A : sprayed on May 20
B : sprayed on June 2
C : sprayed on June 6

Fig. 3.Spraying of the panels by 3% NaCl solution.

The second method involved physical sampling. Concrete samples were chiseled from the panels at different locations during the period of study to determine the actual degree of saturation and salt content. The degree of saturation was determined gravimetrically. The salt content in the panels was determined chemically by the Berman-Volhard method.

Data collection was initiated in February, 1984. Current readings and temperatures were recorded on a semi-continuous basis for two months. The outside temperature, relative humidity, wind direction and precipitation were obtained from the Windsor Airport weather station. The sunshine record, which was not available from the Windsor Airport, was obtained from the Harrow weather station, some 15 miles distant. Current readings and temperatures were recorded for various types of weather.

Temperature Conditions

The temperature regime existing in the panels depended on the prevailing weather conditions, which can be classified into several distinct types: sunny and cold; sunny and warm; partly sunny and cold; cloudy and cold; cloudy and warm.

Daily Temperature changes

Typical temperature variation in the south facing roof panel for a sunny and cold day are shown in Figure 4. The figure shows that a rapid rise in temperataure occurs in the surface layer when the sun irradiates the concrete. Subsequently, a rapid drop in temperataure takes place in the evening of a sunny day. A maximum warming rate of 16.7 C/h and a maximum cooling rate of 8.6 C/h were recorded in

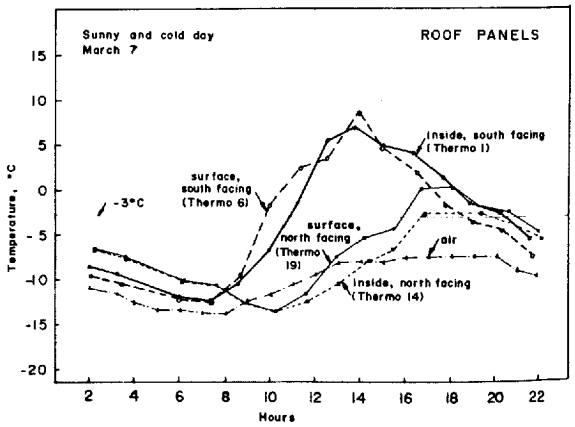

Figure 4. Typical temperature variations in the south-facing roof panel on a cold but sunny day.

the south facing panel for a sunny day. However, tabulation of the frequency of different rates of change in concrete temperature showed that most changes in temperature were at the rate of between 0 and 3 C/h, for both the warming and cooling parts of the cycle.

Temperature gradients with depth

Large difference in temperature was found to exist between the surface and the interior of the concrete face, sometimes on cold and windy days, but especially on sunny days. The largest temperature differential between the surface and the 10 mm depth was found to be 9 C for the south facing roof panel. This typically occurred during sunny afternoons when the sun's radiation coupled with a high air temperature warmed the surface of

the panel. The inverse was true (surface much cooler than the interior) in the evening of a sunny day when the cold ambient temperature cools the surface.

A typical change in the differential temperature (dt) experienced by the thermocouples (1,6) (3,8) and (5, 10) is shown in Figure 5. The "dt" is defined as the difference in concrete temperature between the surface and the 10mm depth.

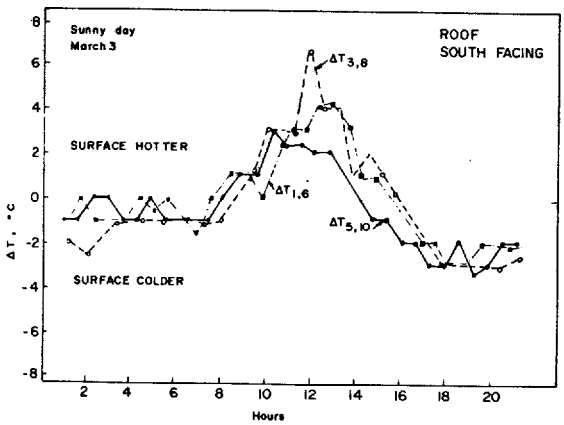

Figure 5. Differential temperature between surface and 10mm depth over 24h period.

Temperature reversals

During partly sunny days, the surface layer of the panel experienced multiple cycles of thermal changes, which undoubtebly would produce significant stresses. For the period of the test, the thermocouples (1,6) and (5,10) experienced, respectively, 68 and 50 changes in dt over a period of 14 days.

Freeze-thaw Cycles

The temperature change from above to below the freezing point can be defined as one cycle of freezing and thawing. Because of pore size considerations, the minimum temperature required to freeze capillary water was taken as -3 C. The number of freeze-thaw cycles per day (with -3 C as the freezing line) for all the thermocouples is given in Figure 6.

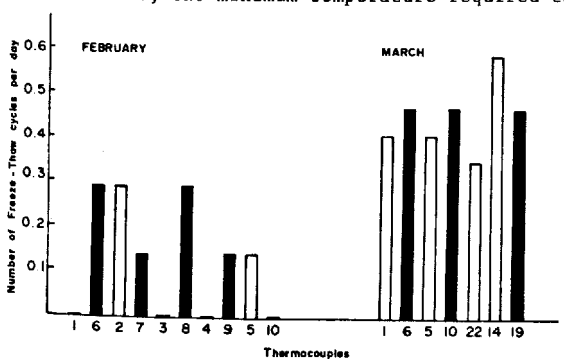

Figure 6. Average number of freeze-thaw cycles per day measured by thermocouples in February and March.

The rate of freezing and thawing ranged from 0.1 to 7 C/h for the roof panels. It was observed that the rates of freezing were lower than that of thawing and, that freezing and thawing proceeded most often at a low rate (between 0 - 3 C/hour) for the roof panels. At the bottom of the panels, freezing proceeded most often at a rate between 6 and 9C/h. Conversely freezing at the top proceeded most often at the lower rate of between 0 and 3 C/hour. Thawing at the top or the bottom of the panel proceeded most often at a rate between 0 and 3 C/h. Freezing occurred first on the surface and half an hour later at the 10mm depth.

Factors Affecting Temperature.

Panel Orientation

The maximum differential temperature on the north facing panel was 5C, while 9.0C was recorded for the south facing panel. The temperature of the north panel was controlled by the air temperature, and not by the sun's rays. Thus, the temperature in the north facing panel frequently remained below -3C for long periods, and experienced fewer freeze - thaw cycles than the south facing panel.

Shape of the Panel

The temperature change observed was affected by the shape of the barrier wall and by the depth of the thermocouples. The maxima rates recorded on the surface were higher than inside the south facing panel. The highest rate of temperature change was recorded on the surface at the bottom of the south facing panel and, also, the lowest rate recorded at the 10 mm depth occurred at the bottom of the panel. The shape of the barrier wall had a relatively small effect on the rate of temperature change in the north facing panel.

High temperatures and high temperature gradients recorded at the bottom of the south facing panel can be explained by the angle of the sun's rays with the surface. On a clear day the bottom part receives and absorbs more solar energy than the top.

Moisture Conditions

Figure 7 gives an example of the degree of saturation and the temperature of the concrete in the roof panels between noon and 2 pm during the cited observation periods in February. Note that the panels are not critically saturated; also note that on Feb. 27, the north-facing panel surface was below freezing, while the south-facing surface was well above freezing.

Although in general, the moisture content in the barrier walls is controlled by wetting and drying, the orientation of the wall also has a significant influence. Since at this geographic location, the prevailing wind direction is from the south, the south facing wall should have higher moisture content due to driving rain. On the other hand,

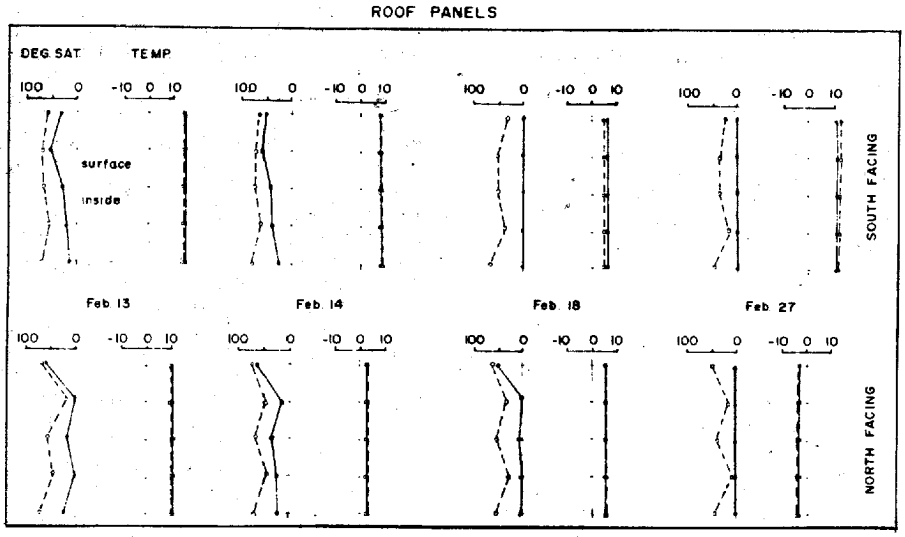

Figure 7. Distribution of temperature and degree of saturation across the south and north facing panels on selected days.

the surface of the south facing panel would dry faster than the north facing panel. The values of average degree of saturation calculated for the roof panels at the surface and at the 10 mm depth, given in Table 1, confirmed this general observation.

Table 1
Degree of Saturation of South and North Panels

Date March	Time	10mm Dept South	10mm Dept North	Surface South	Surface North
6	14:20	53.3	49.9	.0	13.1
10	0:00	85.0	74.0	71.1	63.6
11	13:40	68.9	60.0	36.5	30.4
12	10:50	62.3	56.7	28.1	30.2
13	13:20	65.5	50.0	30.5	21.8
14	8:35	69.8	53.2	44.3	34.2
18	16:40	50.3	48.8	.0	.0
27	10:35	30.2	31.5	.0	.0
Average		60.7	54.3	26.3	24.2

Salt content

The salt content of the panels was calculated from current readings using the frequency-class method described by Hudec, MacInnis and Moukwa (1), and on chiselled samples. The roof panels, at the conclusion of the test, had a salt content equivalent to 2.1, 4.6, and 4.5 percent NaCl solution in the top, middle, and bottom portion of the panel respectively. It is known that freeze-thaw cycles in the presence of a 3 to 4% salt solution produce the most severe scaling (2).

Conclusions

Direct rays of the sun have a pronounced effect on the surface temperature of the concrete, which can be more than 10 degrees higher than the air temperature. On sunny days when the air temperature is below freezing, the concrete surface can be well above freezing. As soon as the sun is obscured by cloud(s), the surface begins to cool rapidly. Thus, on partly cloudy days, the surface can undergo several cycles of freezing and thawing. The rapid temperature changes and differences observed between the surface and the sub-surface of the concrete no doubt set up thermal stresses and contribute to the deterioration of the concrete.

The roof concrete panels were generally not at "critical" saturation levels while undergoing freezing and thawing. This was in marked contrast to E.C. Row highway exposure panels, where snow accumulation and car splash maintained near-critical saturation during most of the winter. However, a limited amount of salt spraying of the roof panels was sufficient to maintain the salt concentration in the 2 to 6% range.

The shape of the panel had a bearing on the moisture and temperature conditions. The lower curved portion was found to have higher, and more frequent changes in these parameters.

It can therefore be concluded that the south-facing concrete barrier walls experience a much harsher climatic environment, and are more prone to deterioration than walls facing in other directions.

Acknowledgments

The authors would like to thank the Ontario Ministry of Transportation and Communications for providing research funds for this work. Thanks are also due to Mr. Peter Feimer of the Civil Engineering Department, University of Windsor, for assistance in the field work.

References

1. Hudec, P., MacInnis, C., and Moukwa, M., "Microclimate of concrete barrier wallls: temperature, moisture, and salt content", in preparation.

2. Hudec, P., MacInnis, C., and Moukwa, M., "The capacitance effect method of measuring moisture and salt content of concrete", in preparation.

3. Litvan, G.G., "Phase transitions of absorbates V: Aqueous sodium chloride solutions absorbed in porous silica glass", National Research Council of Canada, Division of Building Research, Ottawa, Nov. 1972.

J. BARON*, R. GUYOT*
* LAFARGE COPPEE RECHERCHE, France

UN MODELE PHENOMENOLOGIQUE DE L'EVOLUTION DE LA RESISTANCE EN COMPRESSION PARAMETRANT L'INFLUENCE DU CLINKER ET CELLE DES GRANULATS

INTRODUCTION

La finesse de mouture du ciment est le principal paramètre sur lequel le cimentier peut agir pour modifier les propriétés du ciment. A l'origine de cette étude, nous souhaitions connaître, pour chacun de nos clinkers industriels, l'effet d'un accroissement de la surface spécifique sur les résistances aux diverses échéances.

Nous souhaitions obtenir des valeurs chiffrées, utilisables pour notre usage interne et nous ne nous souciions pas d'aboutir à un modèle ayant une valeur générale. Ce n'est qu'à la fin des essais, en dépouillant les résultats que le modèle émergea : en cherchant à représenter l'influence de la surface spécifique, nous nous somme aperçus qu'il était possible de faire ressortir des grandeurs, caractéristiques du clinker lui-même, et d'autres, caractéristiques des granulats du béton.

NATURE DES ESSAIS

Nous avons étudié les résistances en compression à 1, 2, 7 et 28 jours de mortiers AFNOR et de bétons composés à partir de 52 ciments résultant du broyage de 14 clinkers industriels.
Deux séries d'essais ont été faites :

TABLEAU 1

Série 1 sur 4 clinkers (A à D)	Finesse Blaine (cm^2/g) des ciments broyés	2 800	3 650	4 500	—
	Taux de $\bar{S}$ (%) des ciments	2.8	3.2	3.6	—
	Résistances en compression mortier AFNOR à 1, 2, 7 et 28 jours Résistances en compression béton sur cylindres 16 x 32 cm à 1, 2, 7 et 28 jours Granulats siliceux 0 - 10 mm Dosage 425 kg/m^3 Rapport eau/ciment ajusté pour obtenir un affaissement de 5 cm au cône d'Abrams				
Série 2 sur 10 clinkers (E à N)	Finesse Blaine (cm^2/g) des ciments broyés	2 800	3 650	4 500	5 350
	Taux de $\bar{S}$ (%) des ciments	2.8	3.2	3.6	4.0
	Résistances en compression mortier AFNOR à 1, 2 et 28 jours Résistances en compression béton sur cylindres 16 x 32 cm à 1, 2, 7 et 28 jours Granulats siliceux 0 - 10 mm (identiques à ceux de la série 1) Dosage 300 kg/m^3 Rapport eau/ciment ajusté pour obtenir un affaissement de 8 cm au cône d'Abrams				

LE MODELE POUR LES MORTIERS

Ce modèle permet de calculer, pour un clinker donné, connaissant la finesse de mouture du ciment, la résistance en compression du mortier standard à n'importe quelle échéance, entre 1 et 28 jours. Il fait intervenir quatre grandeurs qui, ne dépendant pas de la surface spécifique du ciment, sont caractéristiques du clinker :

- Le Coefficient d'efficacité chimique du broyage : a
- La Résistance de référence à 1 jour : R_{01}
- Le Taux d'accroissement des résistances : r
- Le Dommage : D

Nous allons introduire successivement chacune de ces quatre grandeurs en montrant comment on peut les calculer à partir des résultats expérimentaux.

Le Coefficient d'efficacité chimique du broyage

Dans nos expériences, le développement des résistances R dépend de deux paramètres, le temps t et la surface spécifique S. Le principe du modèle consiste à réunir ces deux paramètres en un seul, appelé "temps équivalent" et noté u ; u est, lui-même, fonction de t et de S. On écrit :

$$R(t,S) = R(u) \text{ avec } u = u(t,S)$$

L'expression de la fonction u est construite en trois étapes A, B, C :

A) On admet que, si le clinker était monophasé, on pourrait écrire :

$$u.S_o = t.S$$

S_o étant une surface spécifique de référence choisie arbitrairement.

B) Pour tenir compte de ce que le clinker est, en fait, polyphasé, on définit une "surface chimiquement équivalente", notée S', telle que :

$$R(t,S) = R(u) \text{ avec } u.S_o = t.S'$$

Ces deux équations permettent de déterminer S' pour chaque valeur de S. En pratique, il est commode de représenter, pour chaque valeur de S, la variation de R en fonction de Log t ; le changement de variable de t à u s'écrit :

$$\text{Log } u = \text{Log } t + \text{Log } S'/S_o$$

et correspond à une translation des courbes parallèlement à l'axe des temps (figure 1).

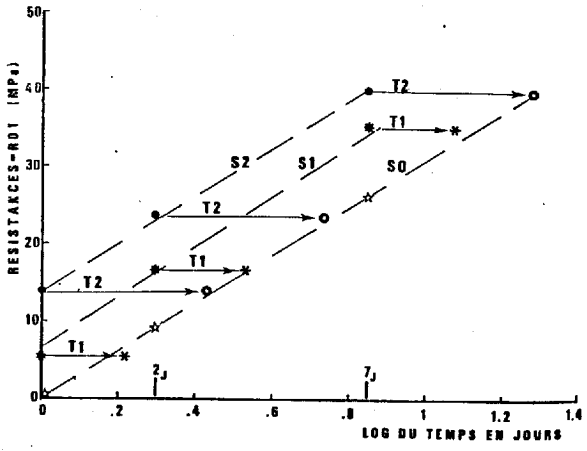

Figure 1 : Construction de la droite représentant la variation de la résistance de compression en fonction du temps indépendamment de la finesse.
Laisser tels quels les points (*) représentant la mouture la plus grossière S_o.
Translater les points (+) représentant la finesse S_1 d'une translation T_1 parallèle à l'axe de temps.
Translater les points (○) représentant la finesse S_2 d'une translation T_2 parallèle à l'axe de temps.
Choisir T_1 et T_2 de telle sorte que l'ensemble des points s'alignent le mieux possible. Le résultat de la construction se trouve figure 2.

On prend comme surface spécifique de référence S_o la valeur correspondant à la mouture la plus grossière ($S_o = 2800\ cm^2/g$). Pour cette finesse de référence on pose par convention que u = t (et donc S' = S_o) ; la courbe R(Log t), correspondant à cette finesse de référence, ne subit aucune translation. Les autres courbes,

J. BARON*, R. GUYOT*
* LAFARGE COPPEE RECHERCHE, France

correspondant aux autres finesses S, sont translatées de $T = \text{Log } S'/S_o$. Les valeurs de T pour chaque S sont calculées statistiquement de manière à optimiser la coïncidence de toutes les courbes.

C) Pour achever la détermination de la fonction u, il suffit de relier S' à S par une relation empirique telle que si $S = S_o$ alors $S' = S$. Les résultats expérimentaux s'accordent approximativement avec la relation linéaire :

$$(S'/S - 1) = (S/S_o - 1).a$$

Le coefficient de cette relation, a, qui suffit à lui seul à définir le temps équivalent u, est appelé Coefficient d'efficacité chimique du broyage ; il est caractéristique du clinker et permet de prévoir l'effet de la finesse sur la vitesse de développement des résistances.

La Résistance de référence à 1 jour et le Taux d'accroissement des résistances

On étudie maintenant la relation $R = R(u)$. La figure 2 montre, à titre d'exemple, la courbe unique, indépendante de la finesse, obtenue pour le clinker C, après le changement de variable de t en u. Entre 1 et 7 jours, cette courbe est linéaire en Log u ; il en est de même pour l'ensemble des courbes correspondant aux 14 clinkers étudiés. Dans tous les cas, on peut écrire:

$$R = R_{o1} + r \text{ Log } u \quad \text{pour} \quad 1 \text{ j} < u < 10 \text{ j}$$

Cette équation définit deux nouvelles grandeurs, caractéristiques de chaque clinker :

R_{o1} : La Résistance de référence à 1 jour (Résistance à 1 jour lorsque le clinker est broyé à la finesse de référence S_o)

r : Taux d'accroissement des résistances (accroissement des résistances entre 1 et 10 jours pour la finesse de référence).

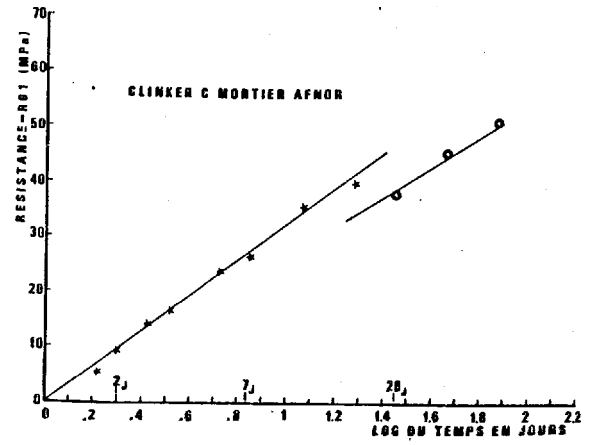

Figure 2 : Variation de la résistance en compression sur mortier AFNOR en fonction du temps équivalent.

Le Dommage

Comme la courbe de la figure 2, toutes les courbes homologues correspondant à l'ensemble des clinkers étudiés, présentent un décrochement qui survient entre 10 et 20 jours. Pour rendre compte de cet effet sans modifier la forme de l'équation précédente on introduit un coefficient (1-D) qui réduit la pente r ; on écrit:

$$R = R_{o1} + (1-D) \cdot r \cdot \text{Log } u \quad \text{pour} \quad u > 20 \text{ j}$$

Par analogie avec le paramètre qui intervient en Mécanique de l'endommagement, le coefficient D qui varie de 0 (aucune réduction) à 1 (accroissement de résistance nul) est appelé le Dommage (Cf, infra : Discussion).

Valeurs des 4 caractéristiques pour les 14 clinkers étudiés

Ces valeurs sont données dans la partie gauche (Mortier) du tableau 2 (page suivante). Elles appellent les commentaires suivants :

a) Il existe une corrélation inverse entre R_{o1} et r (figure 3) ; en général - sauf deux notables exceptions - l'accroissement des résistances après 1 jour est d'autant plus rapide que la résistance à 1 jour est plus faible. On retrouve là un résultat connu mais exprimé, cette fois, indépendamment de la finesse.

b) R_{o1} ou r d'une part, a et D d'autre part, forment un ensemble de trois grandeurs indépendantes, nécessaires pour caractériser le développement des résistances pour n'importe quelle finesse de mouture.

c) Les valeurs de ces caractéristiques varient dans une gamme étendue et, à l'intérieur de cette gamme de variation, toutes les classes intermédiaires sont représentées. Il y a donc, en principe, une grande variété de clinkers possibles.

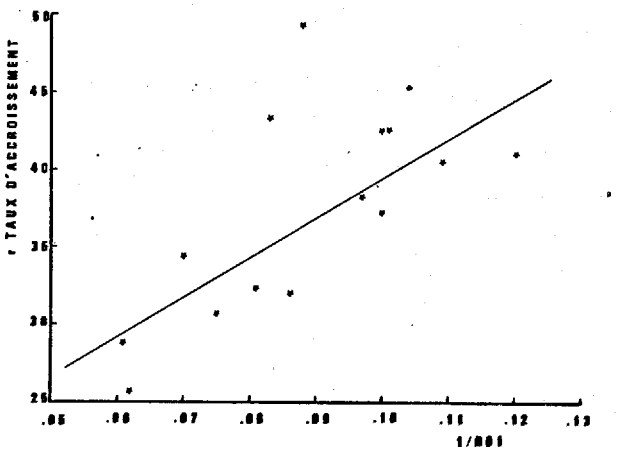

Figure 3 : Relation entre r (taux d'accroissement de la résistance lorsque l'âge est multiplié par 10) et l'inverse de R_{o1}, résistance à 1 jour à la finesse la plus grossière (finesse de référence S_o)

EXTENSION DU MODELE AUX BETONS

Le modèle permet de calculer, pour un clinker et des granulats donnés, connaissant la finesse de mouture du ciment, la résistance en compression à n'importe quelle échéance entre 1 et 28 jours.

Le Coefficient d'efficacité chimique du broyage a, est considéré comme une caractéristique du clinker et prend donc la valeur donnée au tableau 2, indépendamment de la nature des granulats et du rapport E/C.

Les trois autres grandeurs prennent des valeurs qui peuvent dépendre des granulats et du rapport E/C.

J. BARON*, R. GUYOT*
* LAFARGE COPPEE RECHERCHE, France

TABLEAU 2

Valeurs des caractéristiques pour les mortiers et les bétons

	Mortiers				Bétons				
Clinkers	a	R_{o1}	r	D	R_{o1b}	r_b	D_b	k_1	k
		MPa	MPa		MPa	MPa			
Série 1									
A	0,16	8,3	41,1	0,17	5,3	28,2	0,15	0,64	0,69
B	0,80	16,1	25,7	0,09	11,8	18,0	0,14	0,73	0,70
C	0,91	11,6	32,0	0,16	9,2	22,0	0,18	0,79	0,69
D	0,11	10,0	37,2	0,04	8,0	28,8	0,14	0,80	0,77
Moyenne 1							0,15	0,74	0,71
Série 2									
E	-0,06	10,3	38,2	0,00	5,7	27,0	0,06	0,55	0,86
F	1,40	13,4	30,7	0,21	8,4	22,4	0,15	0,63	0,72
G	0,57	12,1	43,3	0,34	6,1	28,2	0,24	0,50	0,65
H	0,76	12,3	32,7	0,19	6,2	23,2	0,04	0,50	0,71
I	-0,26	11,3	49,3	0,31	6,1	27,7	0,08	0,53	0,56
J	0,81	16,5	28,8	0,22	9,0	22,9	0,13	0,55	0,80
K	0,15	9,2	40,5	0,13	6,3	25,0	0,00	0,68	0,62
L	0,05	9,9	42,5	0,16	4,0	27,5	0,06	0,40	0,65
M	0,33	10,0	42,5	0,25	5,4	24,9	0,05	0,54	0,56
N	1,30	14,3	34,4	0,16	8,1	24,9	0,10	0,56	0,72
Moyenne 2							0,09	0,54	0,69
Moyenne 1 + 2				0,24					

Les bétons étudiés ont des rapports E/C variables, différents du rapport E/C = 0,5, qui est celui du mortier standard. Pour s'affranchir de l'influence du rapport E/C on commence par calculer la résistance R qu'aurait le béton si son rapport E/C était égal à 0,5. Ce calcul se fait en appliquant la formule de Féret :

$$(R/R_{exp})^{1/2} = 0,359\ (1-3,15\ (E+V)/C)$$

où :
3,15 est la masse volumique du ciment ; E et C, respectivement les poids d'eau et de ciment ; V, le volume d'air, non mesuré dans nos expériences, est pris égal à 0,30. Le coefficient 0,356 est tel que $R = R_{exp}$ pour les valeurs du mortier standard E/C = 0,5 et V = 0,30

Le modèle est appliqué aux résistances R calculées de cette façon.

La variation de R en fonction de Log u (figure 4) peut être représentée, comme pour le mortier standard, par les équations :

$$R = R_{o1b} + r_b \text{ Log } u \quad \text{pour} \quad 1\ j < u < 10\ j$$

$$R = R_{o1b} + (1-D_b)\ r_b \text{ Log } u \quad \text{pour} \quad u > 20\ j$$

Les grandeurs R_{o1b}, r_b et D_b dépendent du clinker, des granulats et du rapport E/C.

Afin de séparer l'influence du clinker et celle des granulats, on pose :

$$R_{o1b} = k_1\ R_{o1} \quad \text{et} \quad r_b = k\ r$$

R_{o1} et r étant les caractéristiques du clinker définies au paragraphe précédent. Le tableau 2 (dans sa partie droite - Bétons) donne les valeurs obtenues pour les 14 clinkers étudiés.

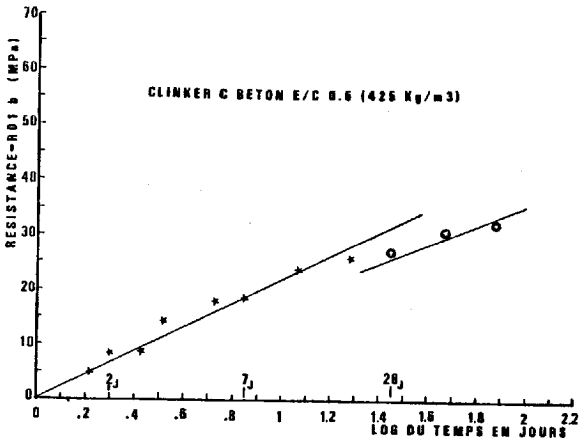

Figure 4 : Variation de la résistance en compression sur béton en fonction du temps équivalent.

On observe que les valeurs des coefficients k_1 et k dépendent peu des clinkers ; ils dépendraient probablement davantage de la nature minéralogique des granulats mais ce facteur n'était pas inclus dans nos expériences. Nous proposons d'appeler :

k : le Coefficient d'auréole
k_1 : le Coefficient d'auréole précoce

Les moyennes des valeurs de k_1 et k sur l'ensemble des clinkers montrent que :

- Le Coefficient d'auréole est, en moyenne, de 0,71 pour la série 1 (E/C voisin de 0,45) et de 0,69 pour la série 2 (E/C voisin de 0,64) Il est donc indépendant de E/C (l'influence du rapport E/C a été prise en compte précédemment en appliquant la formule de Féret aux résultats bruts).

- Le rapport k_1/k est voisin de 1 pour un dosage en ciment de 425 kg/m^3 ; il est de 0,8 pour un dosage en ciment de 300 kg/m^3.

Concernant le Dommage, il ne paraît pas possible de séparer de la même façon l'influence du granulat et celle du clinker ; la corrélation entre les valeurs mesurées sur mortier et sur béton n'est pas significative. En moyenne, le Dommage pour les bétons, diminue avec le dosage en ciment : 0,15 pour 425 kg/m^3 et 0,09 pour 300 kg/m^3. Si l'on compare les valeurs moyennes de Dommage pour les mortiers et pour les bétons, on peut conjecturer qu'elles témoignent de deux effets antagonistes :

a) le mortier est plus riche en ciment (500 contre 425 ou 300 kg/m^3) ce qui tendrait à augmenter le Dommage

b) mais le plus gros granulat du mortier est 5 fois plus fin que celui du béton (2 mm contre 10 mm) ce qui tendrait à réduire le Dommage

COMPARAISON MODELE/EXPERIENCE

Pour une finesse de mouture et pour une échéance donnée, la résistance trouvée expérimentalement est notée $R_{ex.}$ et la valeur calculée par le modèle $R_{th.}$ On calcule le rapport R_{th}/R_{ex}.

La comparaison modèle/expérience consiste à étudier la distribution statistique des valeurs de ce rapport; cette distribution représentée sur la figure 5 pour le mortier standard d'une part et pour les bétons d'autre part est à peu près gaussienne dans les deux cas,

J. BARON*, R. GUYOT*
* LAFARGE COPPEE RECHERCHE, France

avec cependant quelques résultats aberrants en "queues de courbe".

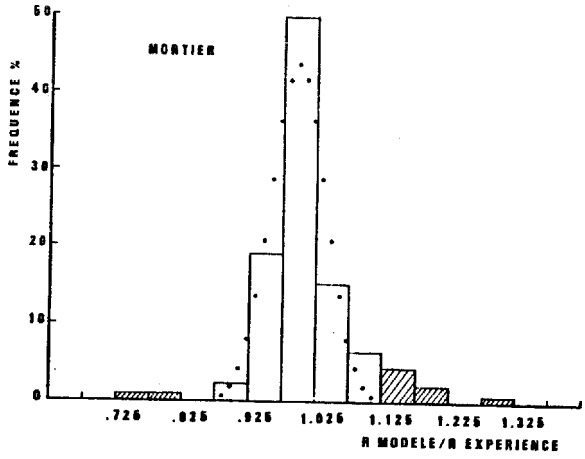

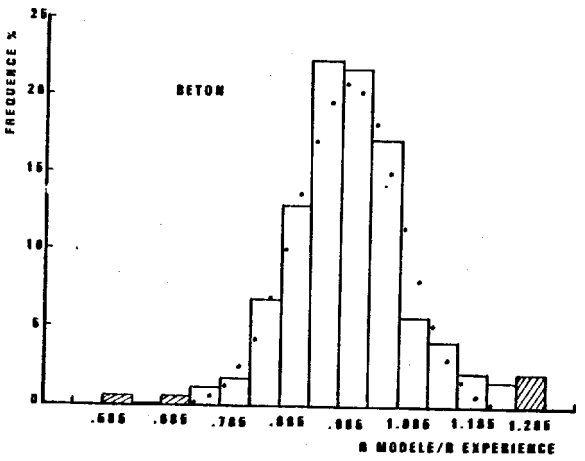

Figures 5 a (Mortiers) et 5 b (Bétons) : Histogramme des valeurs du rapport résistance calculée sur résistance expérimentale pour l'ensemble des valeurs à 1, 2, 7 et 28 jours.
Le tracé en pointillé représente l'ajustement de la distribution à une courbe de Gauss lorsqu'on élimine les résultats représentés dans les parties hachurées.

La comparaison modèle/expérience se résume comme suit :

TABLEAU 3

Distribution du rapport R_{th}/R_{ex}

	Mortier standard	Béton
Nombre de résultats	154	194
Moyenne	1,0	1,0
Coefficient de variation	6 %	9 %
Coefficient de variation dans 1 test de répétabilité	3 %	6 %
Proportion de résultats aberrants	10 %	5 %

Les résultats qualifiés ici "d'aberrants" sont ceux dont la fréquence est supérieure à ce que laisse prévoir la distribution gaussienne.

Dans la majorité des cas, l'imprécision de la prévision suit une loi gaussienne. L'imprécision relative est la somme de la dispersion expérimentale et de l'imprécision strictement due au modèle. La dispersion expérimentale peut être évaluée à partir d'un test de répétabilité ; les valeurs données dans le tableau, 3 % pour les mortiers, 6 % pour les bétons, sont des valeurs pratiquement minimales. Par différence, on peut estimer que l'imprécision proprement due au modèle est de l'ordre de 3 %.

DISCUSSION

Le modèle que nous proposons est semi-empirique. Sa première justification est donc d'être en accord avec les résultats expérimentaux ; néanmoins la signification physique de deux aspects particuliers du modèle doit être discutée : le changement de variable de t en u et l'introduction d'un Dommage D.

Le changement de variable de t en u

Il revient à supposer que la vitesse de développement de la résistance R à un instant donné est :

- fonction de la valeur de la résistance à cet instant ;
- proportionnel à la surface spécifique du ciment anhydre ;

Soit : $\frac{\partial R}{\partial t} = f(R).S$

L'intégration de cette équation différentielle donne une fonction R (tS) où le produit tS forme une variable unique ce qui correspond bien au modèle que nous nous sommes donné.

Le Dommage

L'existence d'une discontinuité dans la courbe R(t) entre 7 et 28 jours peut surprendre et être mise en doute. N'est-ce pas un effet de la transformation opérée sur les courbes ? Pour répondre à cette question il faut étudier l'évolution des résistances sur un même ciment en multipliant les échéances d'essai. S'étant aperçu qu'un tel protocole, malgré sa simplicité, était très rare, le CERILH a fait en 1985 une série d'essais au titre de première vérification de notre hypothèse. Dans cette série le ciment est un CPA pauvre en C3A et les essais sont faits sur mortier standard ; on mesure à la fois la résistance en compression et la contraction Le Chatelier (Chemical shrinkage). Cette dernière caractéristique qui peut être mise en relation avec l'avancement des réactions d'hydratation, ne présente aucune discontinuité significative entre 1 et 90 jours ; en revanche une discontinuité survenant entre 10 et 20 jours est nettement visible dans l'évolution de la résistance (figure 6). Ceci suggère une cause mécanique et peut justifier le terme de "Dommage" que nous avons choisi. Le Dommage pourrait être, pensons nous, une microfissuration résultant des contraintes qui accompagnent nécessairement la formation de la texture (2) ; dans ce cas, on comprendrait qu'il puisse augmenter avec le dosage en ciment et la dimension des plus gros granulats. Ce n'est qu'une hypothèse mais qui pourrait être aisément vérifiée en suivant, par exemple, l'émission acoustique des éprouvettes entre 1 et 90 jours.

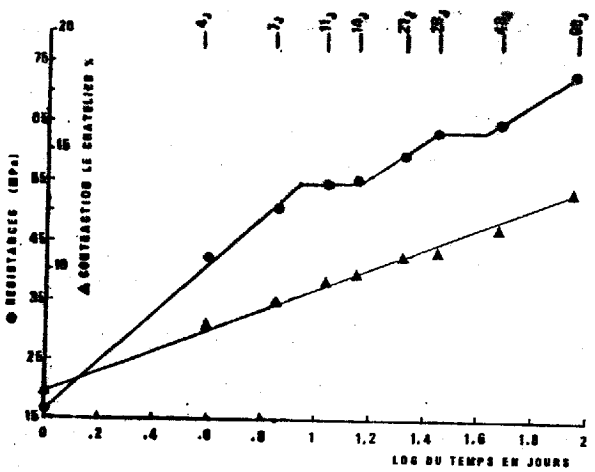

Figure 6 : Variation de la résistance standard d'un mortier AFNOR et de la concentration Le Chatelier en fonction du logarithme du temps en jours pour un même CPA (d'après le CERILH (1))

CONCLUSION

La résistance en compression d'un béton dépend du clinker, de sa finesse, du rapport E/C et du temps. L'intérêt du modèle semi-empirique que nous venons de présenter est de séparer, entièrement (pour les échéances de 1 à 10 jours) ou presque entièrement (au delà de 20 jours), l'influence du clinker et celle des granulats ; ce faisant, il ouvre de nouvelles perspectives d'étude et d'optimisation.

Clinker

A la place de la grandeur unique que constitue la classe de résistance du ciment, le modèle substitue : la finesse de mouture comme paramètre et deux grandeurs indépendantes, caractéristiques du clinker avant mouture (le Coefficient d'efficacité chimique du broyage et le Taux d'accroissement des résistances).

Granulat

Le modèle permet de caractériser l'influence globale des granulats par une seule grandeur (le Coefficient d'auréole) quand le rapport E/C est de l'ordre de 0,5 ou moins, ou, par deux grandeurs, quand le rapport E/C est de 0,6 ou plus. Dans ce dernier cas il faut introduire, en plus, un Coefficient d'auréole précoce, dont la valeur est toujours inférieure à celle du Coefficient d'auréole et qui s'applique aux résistances à 1 jour.

L'interaction clinker/granulat dans le phénomène de Dommage

Nos résultats montrent une discontinuité dans l'évolution des résistances entre 10 et 20 jours. Ce phénomène, s'il était confirmé devrait retenir l'attention ; nous le présentons ici comme une hypothèse, une invitation à des expérimentations complémentaires. Dans le modèle ce Dommage est caractérisé par une grandeur unique dont la valeur dépend indissociablement, du clinker, des granulats et du rapport E/C.

BIBLIOGRAPHIE

(1) L.J HOLLEBECQ Note interne du CERILH aimablement communiquée aux auteurs

(2) J. BARON
Déformations, contraintes et ruptures dans les bétons avant tout chargement in "Mécanique de la rupture" FNB, collège international des sciences de la construction, conseil international de la langue française, 1983

C.BERTRAND, C.BONET, P.GARDE
LAFARGE COPPEE RECHERCHE, France

NOVEL COMBUSTION and VOLATILIZATION DIAGNOSTIC TECHNIQUES in CEMENT KILNS

1 - INTRODUCTION

In recent years, most of the cement factories, for economical reasons, had to shift from fuel oil firing to pulverized fuel firing in their rotary kilns. Among the multiple problems created by this compulsory change, process problems in the kiln were particularly significant, arising from the differences in composition and combustion characteristics between the solid fuels and the liquid fuels previously used.

Moreover, among the pulverized fuels available (coals, petroleum cokes, solid residues), significant differences exist in ash content, volatiles content, sulfur content or calorific value.

On top of that, the transport of pulverized fuels is much more troublesome than the transport of liquid fuels, and fluctuations in the fuel mass flow rate at the tuyere are often the cause of difficulties to keep steady combustion conditions.

Instruments able to quantify the variations of the flame characteristics and shape due to a change in the mass flow rate, the composition, the granulometry or the nature of the fuel are practically absent from the market, if one excepts the classical one-colour pyrometers used to control the clinkerization zone temperature.

Consequently, a change in the combustion and heat transfer characteristics is very often only detected after it has had a significant effect on the clinker quality, or on the frequency of appearance of rings and concretions.

Therefore, LAFARGE COPPEE RECHERCHE has tried to develop its own investigation tools, adapted to the geometry and the conditions prevailing in the clinkerization zone of rotary kilns, and allowing to obtain an instantaneous (or quasi-instantaneous) information on the variations occurring in firing conditions, heat transfer or atmosphere composition in this zone.

For this purpose, three instruments have been constructed at L.C.R., with different external collaborations :

- an ellipsoidal radiometer probe, developed in collaboration with TOTAL-CFR (LE HAVRE, FRANCE).
- a microphone probe, developed with the C.N.R.S. (C.R.C.C.H.T., ORLEANS, FRANCE).
- a spectroradiometric probe, developed with the S.O.P.R.A. (BOIS-COLOMBES, FRANCE) and the C.N.R.S. (C.O.R.I.A., ROUEN, FRANCE).

They were designed to control specifically the following characteristics :

- the flame length (ellipsoidal radiometer and microphone probe) ;
- the emissivity and temperature profiles of the flame, the clinker and the wall (spectroradiometric probe) ;
- the presence in the furnace atmosphere of compounds representative of the volatilization process (spectroradiometric probe).

2 - THE ELLIPSOIDAL RADIOMETER PROBE

Radiation is the dominating heat transfer process in the combustion zone of the rotary kiln. It is well-known that, at fixed power input conditions, the radiative heat transfer profile from the flame to the furnace load exhibits a maximum, appearing more markedly and moving toward the burner mouth when the flame length decreases, i.e. when the combustion intensity increases (1).

From the measurement of the amplitude and the position of this maximum, one can then expect to derive some information on the variations of the flame length when parameters like thrust, primary air mass flow rate or amount of swirl at the tuyere are changed.

The ellipsoidal radiometer, initially developed at the International Flame Research Foundation (2), allows to measure the total radiation heat flux (kW/m2) received at a given location inside a furnace. It is represented on figure 1.

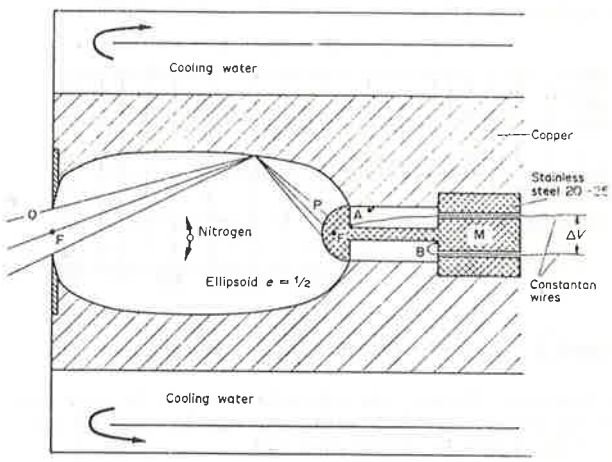

Figure 1 : Schematic diagram of the ellipsoidal radiometer.

Any incident radiation entering the orifice O is reflected by the gold-plated ellipsoidal cavity onto the thermopile P placed at the second focus of the ellipsoid. The power received is measured as the e.m.f. ΔV. The radiometer is first calibrated in a black-body furnace and then allows to measure directly the total radiation heat flux received from the hemisphere surrounding it. Nitrogen flowing in the cavity prevents its internal surface from being spoiled by particulates or condensable gases.

The axis of the ellipsoid is kept perpendicular to the flame axis, and the radiometer is inserted in a water-cooled probe allowing to move it along the furnace axis (Figure 2). The radiation heat transfer profile in the flame zone can then be recorded.

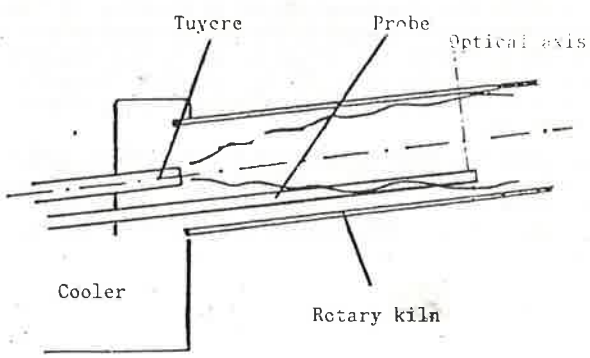

Figure 2 : Experimental set-up.

C.BERTRAND, C.BONET, P.GARDE
LAFARGE COPPEE RECHERCHE, France

NOVEL COMBUSTION and VOLATILIZATION DIAGNOSTIC TECHNIQUES in CEMENT KILNS

Since the kiln rotates, the probe can only be introduced into the furnace from the fixed end near the tuyere. But the flame in a cement kiln is very long (15 - 30 m) and thus, to have a chance to detect the maximum of the radiation heat flux profile, the water-cooled probe used must also be very long. The probe used here is 15 meters long and has a diameter of 0.20 meters.

3 - THE MICROPHONE PROBE

The combustion noise emitted by industrial turbulent flames burning with air is generally characterized by a broadband frequency spectrum in the region 50 - 700 Hz (Figure 3). This noise is most of the time 10 to 20 dB higher than the aerodynamic noise of the unignited jet.

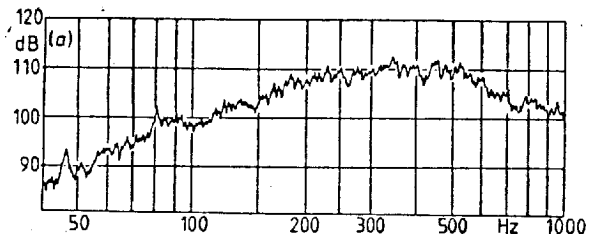

Figure 3 : Frequency spectrum of combustion noise.

In premixed flames, the combustion noise is very sensitive to the fuel/air ratio and can be used to control the flame stoichiometry (3).

In long diffusion flames, the combustion noise intensity does not depend any more on the fuel/air ratio, but depends strongly on the jet velocity (4).

Since the flame length of a cement kiln type flame depends strongly on the thrust of the fuel jet, the idea was to try to detect the variations of the flame length by recording the combustion noise inside the rotary kiln. The advantage of such a method over the one described in section 2 would be a large reduction of the measuring probe size and of the response time, since only one measurement of the acoustic pressure at one location near the flame is necessary.

A microphone probe for combustion noise measurements inside furnaces has already been described in the litterature (5). Its functioning principle is based on the damped Helmholtz resonator : the acoustic pressure is measured through a small duct (providing an efficient protection against the incoming thermal radiation) by a microphone diaphragm placed in a cavity. A 1 mm-thick rubber seal placed in the cavity damps completely the resonance and allows to get a flat response curve of the probe up to 700 Hz, at which frequency it acts as a low-pass filter eliminating the higher frequencies.

This probe has been inserted in a rotary kiln, protected by a double water-cooling system and a refractory head, as shown in figures 4 and 5. The probe used was 2 meters long and had a diameter of 60 mm.

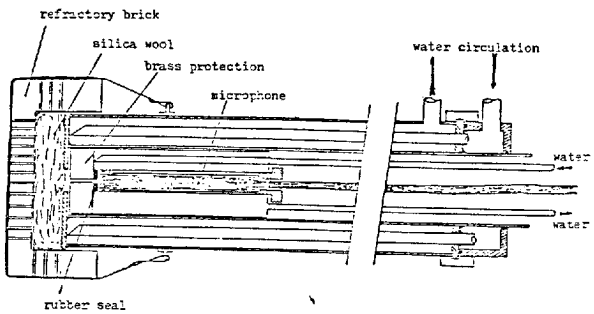

Figure 4 : Diagram of the microphone probe.

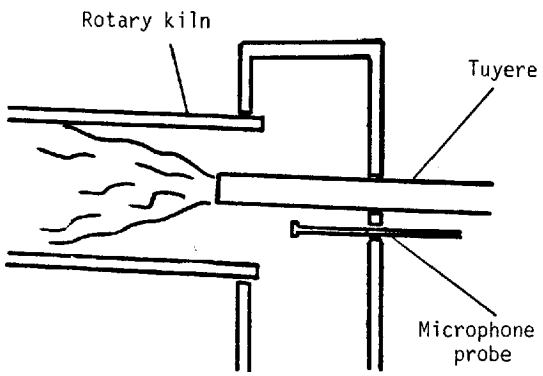

Figure 5 : Experimental set-up.

4 - THE SPECTRORADIOMETRIC PROBE

The ellipsoidal radiometer described in section 2 measures the total radiation received at one location inside the furnace, but does not give any spectral information on it. This spectral information is yet necessary if one is interested also in the measurement of temperature and emissivity profiles of the different parts of the furnace (wall, load, flame), or in the detection of emitting atomic or molecular species present in the furnace gases.

An optical head allowing to perform this kind of measurements is represented on figure 6.

The optical head collects a nearly parallel beam of radiation (2° divergent) and focuses it onto a bundle of three 50 m long optical fibers (diameter of each fiber : 600 µm). It is entirely water-cooled and a continuous flow of air prevents the quartz window from being obscured by particles deposits.

This optical head can replace the ellipsoidal radiometer at the extremity of the 15 meters long probe body represented in figure 2, which allows to extract the radiation, through the optical fibers, out of the rotary kiln.

C.BERTRAND, C.BONET, P.GARDE
LAFARGE COPPEE RECHERCHE, France

C.L

NOVEL COMBUSTION and VOLATILIZATION DIAGNOSTIC TECHNIQUES in CEMENT KILNS

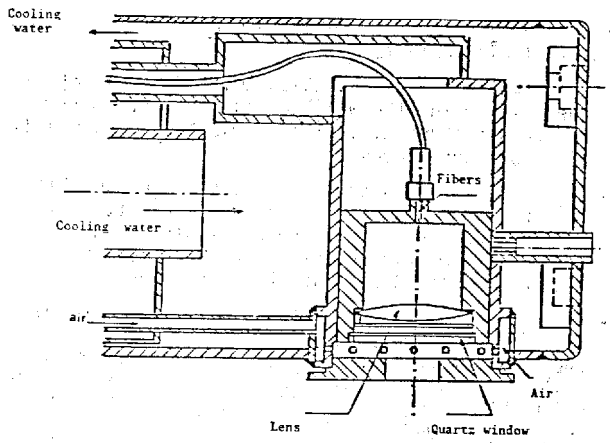

Figure 6 : Sketch of the optical head of the spectro-radiometer.

The bundle of optical fibers is connected to the entrance slit of a grating monochromator with spectral range 0.5 to 1.1 µm (Figure 7).

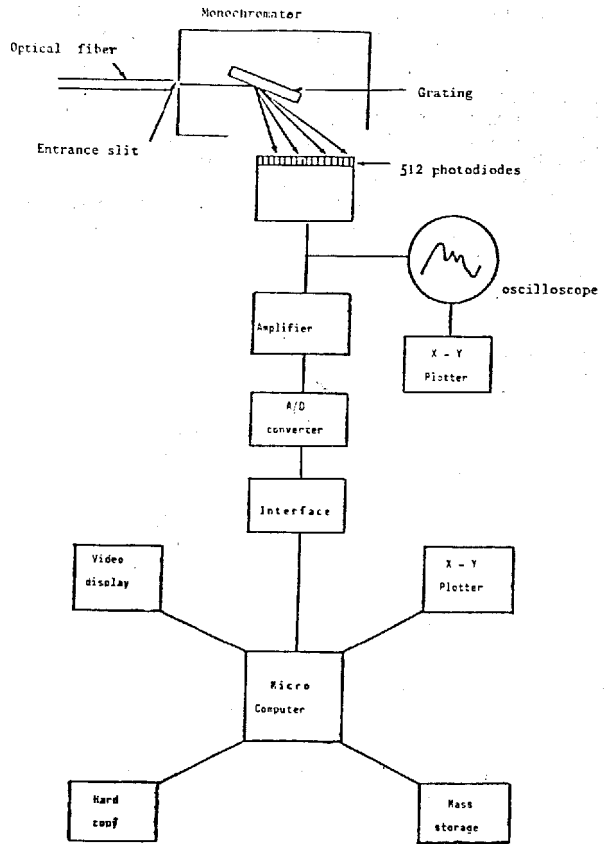

Figure 7 : Signal analysis.

The spectra are detected by an array of 512 photodiodes electronically scanned, and the signal, after amplification and digitalization, can be analysed on-line, or stored on disks through a micro-computer.

The acquisition time of one "instantaneous" spectrum is 32 ms. A preliminary laboratory calibration of the complete system by means of a black-body furnace allows to transform any incoming radiation signal into an absolute radiation intensity.

5 - MEASUREMENT OF THE FLAME LENGTH IN A ROTARY KILN

The measurements have been performed in a 35 meters long rotary kiln of CIMENTS LAFARGE FRANCE, equipped with the original L.C.E.-Tuyere allowing to vary the thrust without changing the mass flow rates of pulverized fuel and transport air. The thrust could be varied from 60 N to 180 N, leading to variable flame lengths from 16 to 12 meters, calculated by using the empirical Ruhland's equation. Different amounts of swirl could be applied via an internal primary air jet.

Both the ellipsoidal radiometer probe and the microphone probe were used in this experimental work. The results followed the expected trend, i.e. an increased amplitude of the peak heat flux, and a shift of its location toward the tuyere for the shortest flames, accompanied by an increase of the combustion noise (the shortest flames correspond to the highest thrusts).

Figure 8 shows the variation of the measured peak heat flux versus the flame length, and figure 9 shows the remarkable correlation obtained between the measured values of the peak heat flux and the recorded acoustic pressure for the entire set of non-swirling flames.

For swirling flames, correlations are less satisfactory, and further work is under way to try to understand the reasons of this different behaviour.

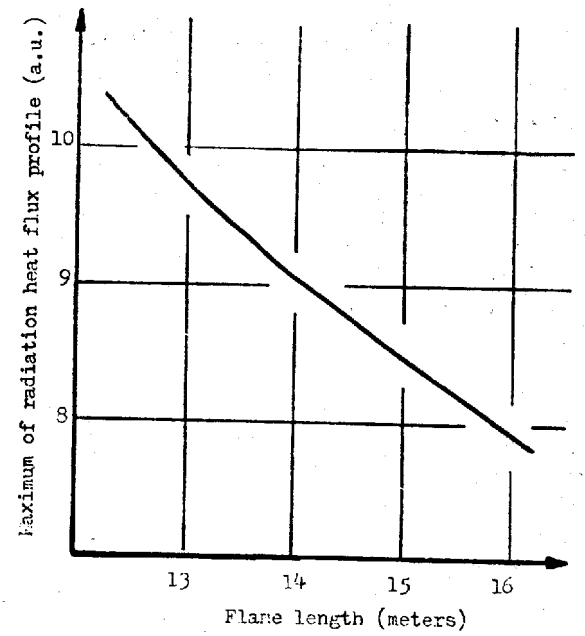

Figure 8 : Measured maximum of the heat flux profile versus calculated flame length.

C.BERTRAND, C.BONET, P.GARDE
LAFARGE COPPEE RECHERCHE, France

NOVEL COMBUSTION and VOLATILIZATION DIAGNOSTIC TECHNIQUES IN CEMENT KILNS

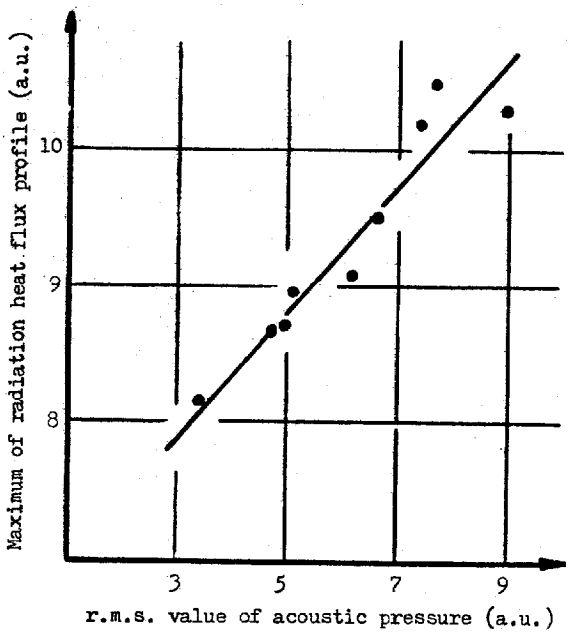

Figure 9 : Measured maximum of the heat flux profile versus measured r.m.s. value of the acoustic pressure.

6 - MEASUREMENT OF THE TEMPERATURE AND EMISSIVITY PROFILES, AND OF THE POTASSIUM CONCENTRATION

These measurements have been performed in a 60 meters long rotary kiln, by using the spectroradiometric probe described in section 4.

Figure 10 shows typical emission spectra taken in the furnace inside and outside the flame. The decay above 800 nm is due to the absorption of the optical fibers.

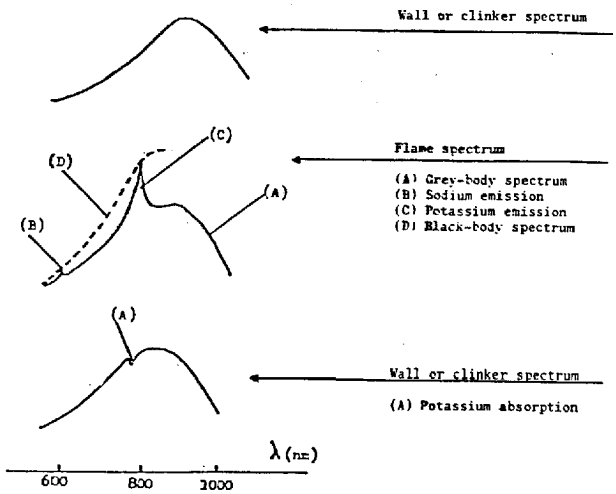

Figure 10 : Typical emission spectra recorded in the rotary kiln.

The observation of the recorded spectra leads to make the following remarks :

- the spectra of the radiation emitted by the flame, the clinker and the wall consist of very similar background spectra, on which emission and absorption lines are superimposed.
- the emission lines present on the flame radiation spectrum at 590 nm and 768 nm are characteristic of the presence in the furnace atmosphere of sodium and potassium, respectively. They are not found in the absence of clinker in the combustion zone.
- the absorption line on the clinker radiation spectrum is found on spectra recorded near the tuyere, where the temperature of the air coming from the cooler is lower (900-1000°C) than the clinker temperature : the radiation emitted by the clinker is absorbed at 768 nm by the relatively cold potassium vapour present in the air.
- the resolution of the monochromator used in this study was 50 Å. The potassium emission line observed is in fact an unresolved doublet of two lines of natural width of the order of 1 Å, separated by 34 Å. Yet, instantaneous half -widths of 100 to 200 Å are often recorded. Self-absorption broadening occurs then strongly, giving a means to derive the potassium concentration in the kiln atmosphere (6).
- It can be calculated, and it has already been mentioned in the litterature (7), that at the usual flame temperatures the potassium emission corresponds to the thermal equilibrium of the emitting excited state. Therefore the radiation intensity of the potassium peak can be considered as a black-body reference at the local flame temperature, allowing to calculate the instantaneous emissivity at this wavelength by the ratio between the radiation intensity of the background spectrum and the radiation intensity of the potassium peak.

Measurement of the temperature profiles

Further analyse of the spectra has shown that fuel-oil, coal and petroleum coke flames in the rotary kiln radiate, in the spectral range investigated, as grey bodies,(i.e. having an emissivity independent of the wavelength) of high emissivity (0.8-0.9). Consequently, axial temperature profiles of the flame can be derived via on-line two-wavelength pyrometry, like the temperatures of the wall or of the clinker, whose emissivities were measured very close to 1.

Figure 11 shows an example of an axial temperature profile measured via two-wavelength pyrometry.

The optical axis is directed downward, so that the temperature measured at the extremity of the kiln is first the clinker bed temperature. Then, as soon as the optical head reaches the combustion zone and is immerged into the flame, the measured temperature is representative of the flame temperature only, which increases up to 1770°C.

C.BERTRAND, C.BONET, P.GARDE
LAFARGE COPPEE RECHERCHE, France

C.L

NOVEL COMBUSTION and VOLATILIZATION DIAGNOSTIC TECHNIQUES in CEMENT KILNS

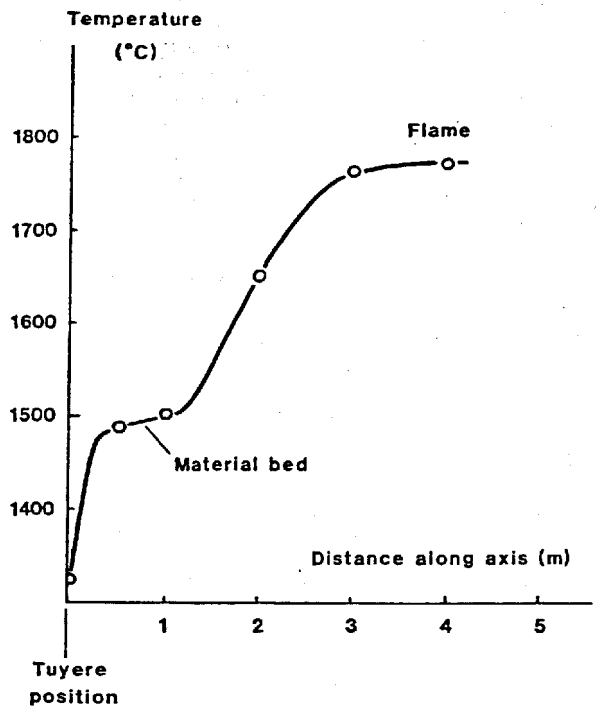

Figure 11 : Axial temperature profile measured in the rotary kiln.

Measurement of the potassium concentration

The self-absorption broadening of an emission line can be related to the concentration N_ℓ of the absorbing species (potassium) by considering the absorption coefficient χ_ν :

$$\chi_\nu = (c^2/8\pi\nu^2)\,(g_u/g_\ell)\,A_{u\ell}\,N_\ell$$

C is the light velocity.

ν is the central frequency of the emission line.

g_u et g_ℓ are the statistical weights of the excited state and the ground state, respectively.

$A_{u\ell}$ is the transition probability.

In an optically thick medium, the relationship linking χ_ν to the half-width of the broadened line depends on the profile of the line. Assuming a Voigt profile, instantaneous volume fractions of potassium as large as 0.5 to 1 % have been computed. They are characteristic of puffs of potassium liberated in the kiln atmosphere by the volatilization process occurring at the clinker surface.

7 - CONCLUSIONS

The recent development of new technologies allows to design investigation tools which can collect useful and accurate information even from very hostile media, like the clinkerization zone of a rotary kiln.

The instruments described here can be labeled as first generation instruments, designed to demonstrate the feasability of a certain type of in-situ measurements. Their development is required to allow the design of a second generation of instruments, generally simplified in order to fulfill only one specific function.

One can think, for instance, to derive from the spectroradiometric probe a more compact instrument able to continuously monitor the presence of potassium in the furnace atmosphere, giving then an information on the intensity of the volatilization process occuring in the combustion zone, and therefore allowing to limit it by an appropriate action on the input parameters of the kiln.

At this stage, these instruments are expected to become part of a more computerized conception of the process control.

ACKNOWLEDGEMENTS :

Part of this work (the development of the spectroradiometric probe) has been carried out with the financial support of the C.O.D.E.T.E.C. (Comité pour le Développement des Technologies d'Emploi du Charbon).

REFERENCES :

(1) S.MICHELFELDER, C.BERTRAND and R.PAYNE, "Transfert de Chaleur et Pollution", Rev. Gén. Therm. Fr., n° 196, pp. 305 - 329 (AVRIL 1978).

(2) J.CHEDAILLE and Y.BRAUD, "Industrial Flames, Vol. 1 : Measurements in Flames", Edward ARNOLD Pub., p. 57, 1972.

(3) C.BERTRAND, "Le Contrôle de la Combustion par la Mesure in-situ du Bruit émis par les Flammes Turbulentes", Rencontre S.F.T. 1984, ONERA-CERT, TOULOUSE , Section III.B, pp. 29 - 37 (28 - 30 MAI 1984).

(4) W.C.STRAHLE, "Combustion Noise", Prog. Energy Combust. Sci., Vol. 4, p. 157 (1978).

(5) C.BERTRAND, "A Microphone Probe for Noise Measurements inside Furnaces", J. Phys. E : Sci. Instrum., Vol. 16, pp. 345-348 (1983).

(6) F.CABANNES et J.CHAPELLE, "Spectroscopic Plasma Diagnostics", in Reactions under Plasma Conditions, M. VENUGOPALAN editor, Vol. 1, pp. 446 - 449, Wiley Inter Science (1971).

(7) P.H.TH.ZEEGERS and C.TH.J.ALKEMADE, "Chemiluminescence of OH-radicals and K-atoms by Radical Recombination in Flames", Tenth Symposium (International) on Combustion, pp. 33 - 40, The Combustion Institute, Pittsburgh (1965).

J. CHAPPUIS, LAFARGE COPPEE RECHERCHE, France

PHYSICAL ELEMENTARY MECHANISMS OF FLUIDIFICATION BY SUPERPLASTICIZERS OR WATER-REDUCING AGENTS.

INTRODUCTION

Our research is aimed at understanding the mechanisms by which water-reducing admixtures and superplasticizers modify the rheology of concrete and mortars.

However, real systems (commercial admixtures and Portland cement) appeared to us to be much too complicated for this study; for instance, it will be shown that there are several elementary mechanisms by which organic molecules can fluidify dense suspensions and that commonly used concrete admixtures act simultaneously through several of these mechanisms. It will also be shown that some of the fluidifying mechanisms are related to the surface properties of the particles and to the intersticial liquid characteristics. But, in the particular case of cement mixed with water, the particles initially have different compositions and the surfaces of these particles are transforming with time ; there are also important changes in the composition and pH of the liquid intersticial medium.

For these reasons, in the present work it was tried to find simple systems for which reliable scientific explanations could be given regarding the phenomenon of fluidification. For instance it was found that concrete fluidifying admixtures are equally efficient on much simpler aqueous suspensions like those in which the particles are made of a single constituent which is unreactive with water. An other degree of simplification has consisted in choosing and studying model molecules which could only operate through a single mechanism. The most part of the work presented in this paper has been performed with suspensions of α alumina in water and the chemical admixtures used have been particularly anionic molecules, non-ionic polymers and surfactants.
A preliminary study was first performed in order to understand the rheological behaviour of the alumina suspensions containing no admixtures.

The first part of this paper is an approach from the literature of the theoretical aspects related to the rheology of suspensions.

The second part summarizes the results of the preliminary study of alumina suspensions containing no admixtures.

Three elementary mechanisms have been identified and their studies are described in each of the three following parts, namely :

- in part 3, the modification of the surface charge of the particles by ionic molecules,

- in part 4, the entropic effects obtained with macromolecules,

- and in part 5, the diminution of the capillary forces obtained when using surfactants, in suspensions with a small water to solid ratio.

1 - THEORETICAL ASPECTS of the RHEOLOGY of SUSPENSIONS

A suspension is a two-phases system in which solid particles are suspended in a liquid medium ; when the particles are inferior to one micrometer the term "dispersion" is preferably used.

Most theories on the rheology of suspensions or dispersions, only take into account the hydrodynamic parameters and suppose that the effect of the interparticle forces are negligible. Such theories will be inadequate to explain the fluidifying effects of admixtures : by adding a small amount of superplasticizer in a suspension we do not change the hydrodynamic parameters of the system, but , of course, we considerably decrease the viscosity. We have then to consider the particle interactions which can have large effects on the rheology of the system, as mentioned in some recent papers like those by P.G. de GENNES (1), W.B. RUSSEL (2) or Th. F. TADROS (3).

In the absence of organic molecules the interparticle forces are of two kinds : van der Waals forces and electrical double layer interactions.

The van der Waals forces arise through the fact that even neutral atoms constitute systems of oscillating charges because of the presence of a positive nucleus and negative electrons. The force between two atoms is always attractive and in a system made of two particles there is an attractive force between every couple of atoms of the system. There is a resulting macroscopic force between the particles. For two particles of radius R, separated by a distance d, the van der Waals force can be expressed, when $d \ll R$, by $F = HR/12\,d^2$, H being the Hamaker coefficient of the system (4). In a liquid medium, when the two particles are made of the same material, the Hamaker coefficient is positive (or null) and the van der Waals force is always attractive, whatever the liquid (5).

The electrical double layer interactions have their origin in the surface electric charge which appears for most substances in contact with an aqueous medium ; with regards to inorganic oxides the electrical double layer at the oxide/water interface is considered to be established by the unequal adsorption of H^+ and OH^- (6). The oxide surfaces are positively charged at low pH and negatively charged at high pH. For each oxide, there is a pH value called PZC (Point of Zero Charge) for which the surface charge is null, but the values of the PZC can be very different for various oxides (7). Two particles, situated in a given liquid, possess surface charges of the same sign, if they are made of the same material : they will then exert between themselves repulsive double layer interactions.

In the case of dispersions of a single solid constituent in water there are hence attractive van der Waals forces and repulsive double layer interactions. It is experimentally known and it has been theoretically demonstrated in the D.L.V.O. theory (8,9) that suspensions are stable when repulsive double layer interactions are larger than van der Waals forces and that there is flocculation in the opposite case.

Regarding the rheological properties, we expect to have good flowing properties when repulsive interparticle forces dominate, that is to say when there is no contact between the particles. On the other hand, we expect to get high viscosities due to the cohesion between the particles when repulsive double layer interactions are smaller than the van der Waals forces. This point of view is supported by the fact that superplasticizers are known to have a dispersing effect as well.

The modification of the flowing properties of a suspension, when using organic molecules, can then be explained as a consequence of the modification of the surface forces between the particles ; in the suspension, the molecules adsorb at the surface of the particles : for this reason, van der Waals forces are reduced, and if the particles are charged the electrical interactions are deeply modified.

Another group of forces between particles are due to

the interaction of long chain molecules adsorbed on the particles (10,11). When two particles, each carrying an adsorbed polymer, come closer to each other such effects can lead to repulsion : each polymer chain, because of unavailability of space, loses its available conformations. Thus the contribution of these chains to the free energy of the system is increased resulting in a repulsive force ("steric" or "entropic" effect).

2 - RHEOLOGICAL BEHAVIOUR of ALUMINA SUSPENSIONS WHEN CONTAINING NO ADMIXTURE

This work, already published elsewhere (12) is merely summarized hereafter.

A alumina ALCOA A 16 S.G. with a mean particle diameter of 0.6 µm has been chosen to magnify the surface force effects. In order to be able to vary the surface charge of the particles, the alumina suspensions have been studied in all the pH range. Adjustement of pH has been done by using adequate quantities of HCl or NaOH. All supensions are prepared 24 hours before measurements, so as to be in physico-chemical equilibrium.

Rheological measurements, sedimentation measurements and electrical characterizations of the surface charge of the alumina particles have been performed on each suspension. According to the different techniques used different concentrations were necessary. In this paper the concentrations of the suspensions are characterized by the ratio W/A (mass of water/mass of alumina powder).

Rheological measurements have been performed with a concentric cylinders viscometer "Rheomat 115". Suspensions having W/A ratios equal to 0.6 have been studied and according to their viscosities three couples of concentric cylinders have been used. All the experimental curves (shear rate vs shear stress) are significative of Bingham fluids. The viscosity was taken as the inverse of the slope of the straight part of each curve.

For the sedimentation test, suspensions with a W/A ratio equal to 10, are poured into test tubes having a one hundred graduations scale. At rest, with unstable suspensions, there appears a sharp interface between the settling part of the suspension and the more or less clear dispersing liquid. The number N of divisions above the sharp interface is plotted as a function of time. The rate of sedimentation is taken as the slope of the initial straight part of the curve.

The electric properties of the surface of the particles were investigated by measuring their electrophoretic mobilities by using a Rank Brothers Mark III zetameter. Measurements have been performed with suspensions containing 10 mg/l of alumina powder, in all the pH range. We have also supplied BALLION and JAFFREZIC-RENAULT (13), in "Laboratoire Pierre Süe" at Saclay, with our alumina samples and they have determined the surface charge of the particles vs pH, by adsorption measurements of radioactive Na^+ and Cl^-.

We reproduce on figure 1 the curve of the surface charge of the particles as a function of pH.

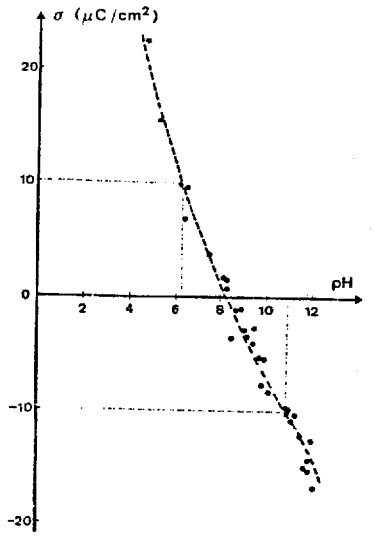

Fig. 1 : Surface charge of the alumina particles vs pH (from ref. 13).

From this work, the point of zero charge is equal to pH 8,5. The particles are positively charged at smaller pH and negatively charged at higher pH. The first results we got from the electrophoretic measurements were erroneous. After modification of a questionable mode of preparation of the very dilute suspensions we could finally get electrophoretic mobilities in agreement with the results of figure 1.

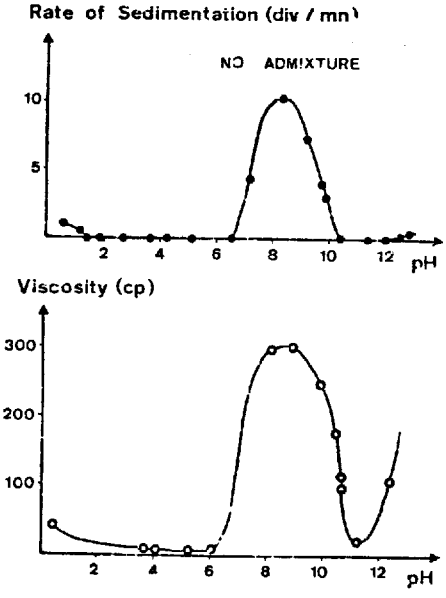

Fig. 2 : Rate of sedimentation and viscosity vs pH of alumina suspensions without any admixture.

On figure 2, the upper curve indicates the rate of sedimentation of alumina suspensions vs pH. These suspensions are unstable for pH between 6.5. an 10.5 that is to say two pH units on every side of the point of zero charge (8.5). The lower curve indicates the viscosities of alumina suspensions vs pH. In the pH range 6.5 - 10.5 the suspensions exhibit high viscosity values.

Refering to the D.L.V.O. theory (8, 9), sedimentation experiments can perfectly be explained if the double layer interactions are small in the high sedimentation pH range ($6,5 < pH < 10,5$). That is in perfect agreement with the results of figure 1 where it can be seen that the absolute value of the surface charge is the same for the two limiting pH values (10 μ C/cm2), that it is smaller inside that pH range and larger outside.

The flocculation for very acid ($pH < 1,5$) or very basic ($pH > 12$) media can be explained in the following way : the ionic strength of the medium, is, in such conditions, very high, and there is a compression of the double layer and hence an important decrease of the repulsive double layer interactions.

Figure 2 indicates that there is a great analogy between sedimentation and rheological behaviours. Hence, we can also explain the rheological behaviour of the suspensions by considering the relative magnitude of the attractive van der Waals forces and of the repulsive double layer interactions : when repulsive interactions are predominant, every particle is separated from the others and the viscosity of the suspenis small ; on the other hand, when attractive interactions are predominant, there are contacts between the particles and the viscosity of the suspension is high.

3 - FLUIDIFICATION of the SUSPENSIONS by IONIC MOLECULES

We have selected for this part of the study the following admixture molecules :

- glucose and triethanolamine which are uncharged molecules,
- tripolyphosphate and a N.F.C. (naphtalene formaldehyde condensate), which are anionic molecules.

Depending on the tests, we have used alumina suspensions containing various admixture concentrations. However, in all the results described below, the admixture concentration was in all cases on the order of 1 to 2 % of the weight of the alumina powder.

On figures 3 to 6, the upper curves indicate the sedimentation behaviour of alumina suspensions having a W/A ratio equal to 10, and the lower curves indicate the rheological behaviour of alumina suspensions having a W/A ratio equal to 0.6. The admixtures used are respectively :

- glucose on figure 3,
- triethanolamine on figure 4,
- tripolyphosphate on figure 5,
- N.F.C. on figure 6.

With the uncharged molecules it can be seen that the suspensions flocculate and have high viscosity values in the pH range 6.5 - 10.5. The curves are very similar to those obtained with alumina suspensions containing no admixture. It is interesting to note that the maximal value of the viscosity is equal to about 300 centipoises without any admixture and is about 100 centipoises with glucose and triethanolamine. These two uncharged molecules have then a fluidifying effect but this effect is not related to a modification of the surface charge of the particles. This effect can merely be explained by a decrease of the van der Waals forces connected to the adsorption of the molecules at the surface of the particles.

With tripolyphosphate there is a pH range for which the suspensions flocculate and have high viscosity values. This pH range is no more centered around the initial point of zero charge (which was 8.5.) but around a new pH value close to 4.

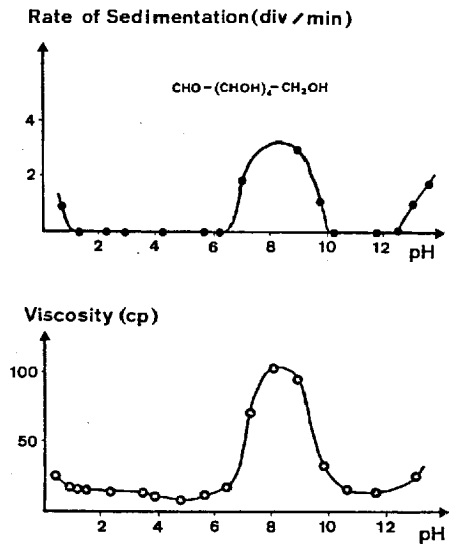

Fig. 3 : Rate of sedimentation and viscosity vs pH of alumina suspensions containing glucose.

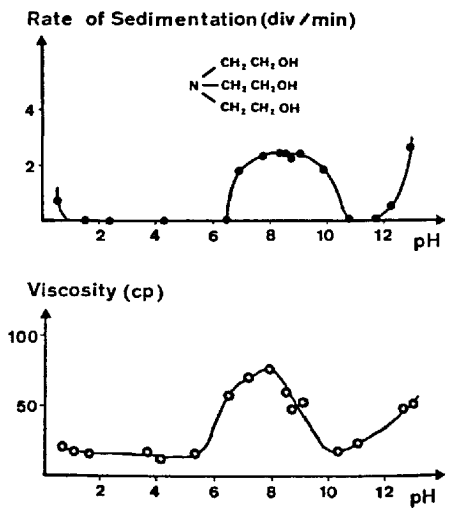

Fig. 4 : Rate of sedimentation and viscosity vs pH of alumina suspensions containing triethanolamine.

The same effect can be observed with the naphtalene formaldehyde condensate (see figure 6). In that case, we notice that for pH smaller than 4 whe have adverse effects probably due to the protonation of the negative groups SO_3^- of the N.F.C. molecule.

We propose to explain the displacement of the pH range where the suspensions flocculate, in the following way : there is a phenomenon of adsorption, that is to say of fixation of the admixture molecules on the solid surface ; when adsorbing at the surface

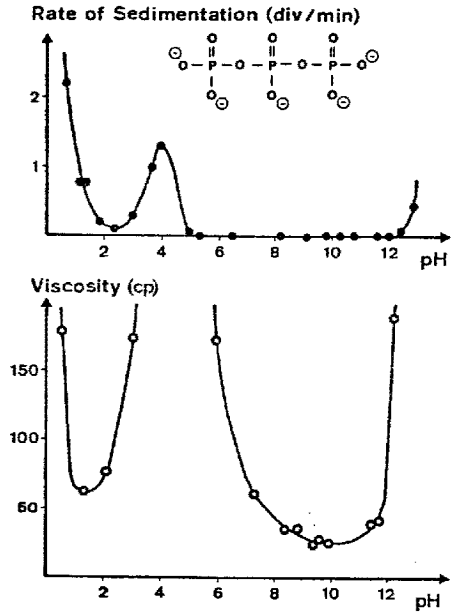

Fig. 5 : Rate of sedimentation and viscosity vs pH of alumina suspensions containing tripolyphosphate.

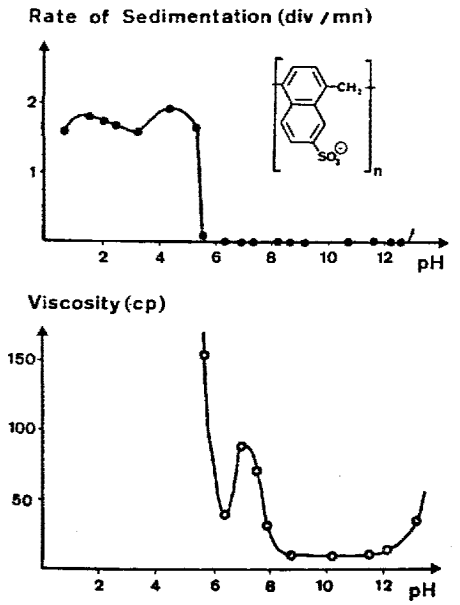

Fig. 6 : Rate of sedimentation and viscosity vs pH of alumina suspensions containing N.F.C. (Naphtalene formaldehyde condensate).

of the particles, the anionic molecules bring about their negative charges. These negative charges must be taken into account with the initial charge, for computing the resulting charge of the particles. In the presence of an anionic admixture, the particles have then a smaller point of zero charge around which the suspensions flocculate and exhibit high viscosity values.

This hypothesis has been confirmed by the following investigation : we have first made adsorption measurements of N.F.C. on alumina at different pH. This has been done by measuring with an ultraviolet spectrometer, and at the wavelength of 290 mμ, the equilibrium concentration of N.F.C. in suspensions containing a known weight of alumina. As the initial concentration of N.F.C. was known, it was then possible to compute for each measurement the adsorbed quantity of N.F.C. per gram or per square meter of alumina. The adsorption isotherms, for 5 different pH, are drawn on figure 7.

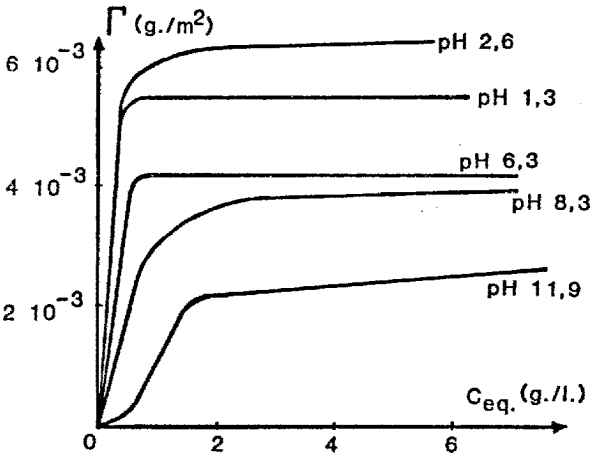

Fig. 7 : Adsorption Isotherms of N.F.C. on α alumina in different pH conditions.

From figure 7 it can be seen that the smaller the pH, the higher the amount adsorbed. This can be explained by considering the electrostatic interaction between the N.F.C. molecules (negatively charged) and the alumina surface, (differently charged according to the pH as indicated on figure 1). The smaller adsorption at pH 1.3 than at pH 2.6 can also be explained by the protonation of the SO_3^- groups in a very acid medium.

As we know that one mole of monomer of N.F.C. has a weight of 240 grams and carries one negative charge that is to say 96500 coulombs, it is possible to know the charge brought about on the surface of alumina by the adsorbed molecules. We have then considered a very simple model in which the surface charge of the particles is equal to the algebric sum of the initial charge of the particles and of the negative charge brought by the adsorbed molecules. From this model and for a given dosage of admixture it is possible to compute the resulting charge of the particles, for the different pH for which the adsorption isotherms have been measured. For instance, figure 8 shows the

computed surface charge of alumina in a given case (W/A = 10, N.F.C./A = 0,015).

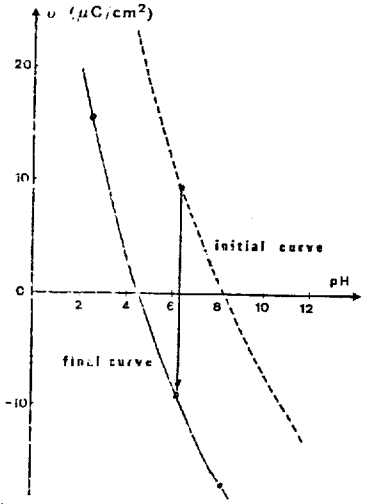

FIG. 8 : Computed charge from our simple additive model of alumina particles vs pH, in the case of a suspension with a W/A equal to 10 and containing an initial dosage of N.F.C. of 1.5 % of the weight of alumina.

It can be seen from figure 8 that there is a new point of zero charge, the value of which is slightly higher than pH 4. This value has been found in good agreement with the pH range in which the suspensions flocculate (see figure 6) and there is a good correlation with a direct measure by microelectrophoresis (see figure 9).

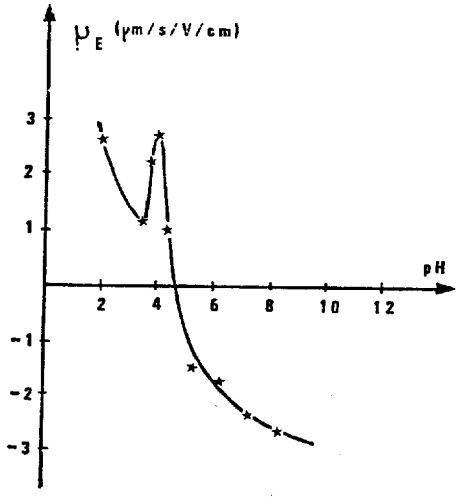

Fig. 9 : Electrokinetic mobility of alumina particles as a function of pH. The dilute suspension has been prepared by using particles and liquid after centrifugation of a suspension with a W/A equal to 10 and containing an initial dosage of N.F.C. of 1.5 % of the weight of alumina.

As a conclusion we think that the fluidifying mechanism of anionic molecules has been elucidated : these molecules, when adsorbing at the surface of the particles modify their surface charge. According to the pH value of the system, the absolute value of the surface charge may be increased or decreased, and the suspension may be respectively fluidified or thickened.

4 - FLUIDIFICATION of the SUSPENSIONS by ENTROPIC EFFECTS

Stabilization of colloidal dispersions by polymer adsorption plays an important role in diverse fields as pigment dispersion in paints, water treatment, mineral processing or cell aggregation. In 1951, MACKOR (14) proposed the first explanation of the stabilizing action of polymers by the decrease in configurational freedom of the segments of adsorbed polymer when the particles approach each other. MACKOR's simple model has since become the basis of the entropic stabilization theory. The theory has later been modified and refined by many investigators and FISCHER (15) was the first to introduce the osmotic repulsion concept. In their monograph on the subject, SATO and RUCH (16) point out that most of the modern theories are based on MACKOR'S or FISCHER'S works. However no universal theory has yet been established.

Entropic effects are usually not mentioned in the literature on admixtures, as a possible fluidifying mechanism. As such a result is however theoretically possible, we have then conducted an experimental study by using two non-ionic polymers, polyethylene glycol (PEG) and polyvinylpyrolidone (PVP). The choice of non-ionic polymers has been made so as to avoid the fluidifying charge effects but, in the practice polyelecrolytes would, of course, be preferable. Polyethyleneglycol of different molecular weights has been used (200, 400, 1500, 4000, 20.000 and 35.000). For polyvinylpyrolidone the molecular weights used were 10.000, 24.000, 40.000 and 360.000. Each of these products has been used at five different concentrations in the range 0-30 g/l, as admixtures of the alumina suspensions in all the pH range. We have then obtained 50 different curves which cannot be reproduced here ; however all theses curves have the same shape (flocculation and high viscosities in the pH range 6.5 - 10.5).

From a careful analysis of this experimental work we have drawn the following conclusions :

- there is a fluidification of the alumina suspensions due to the entropic effect. However, this effect is much smaller than the one due to the charged molecules,

- there is a thickening effect due to the increase of viscosity of the liquid of the suspension. This effect is most marked with high molecular weight polymers and with high concentrations,

- there is an other thickening effect at high molecular weights and low concentrations. As mentionned in the literature (16) such conditions are those which correspond to the bridging of the particles by polymer molecules,

- in the case of PEG and PVP with the studied alumina suspensions, the resulting effect is then a moderate fluidifying action, only in tye case of polymers with a medium molecular weight (in the range 2000-10.000) and only at medium dosages (5-10 g/l).

5 - FLUIDIFICATION of the SUSPENSIONS by DIMINUTION of the CAPILLARY FORCES

The solid volume fraction of the suspensions used in the preceding parts of this study was about 30 % in the case of the suspensions prepared for the rheological tests and about 2,5 % in the case of the suspensions prepared for the sedimentation tests. Such suspensions are two phases systems : they contain the solid particles and the liquid and no air is entrapped. There are no capillary forces in such systems and surfactants have no marked effect as fluidifying admixtures.

If we now consider mortars or concretes, a non-negligible percentage of air is contained in the mix, and this percentage is more important for smaller water to cement ratios. We have then three-phases systems (solid, liquid, air) in which the liquid is in the form of axially symmetrical meniscii between the solid particles. Every meniscus attracts the two particles between which it is situated. When there are such capillary forces between most of the particles of the suspension, its workability is highly reduced.

The capillary force which tends to bring together two particles is the sum of two terms :

- one is due to the surface tension of the liquid which is applied along the three phase line,

- the other is due to a smaller pressure inside the liquid as a consequence of Laplace law. As each of these terms is proportional to the surface tension of the liquid, the resulting force is also proportional to that surface tension. In order to reduce the capillary forces, one has then to use a surfactant, that is to say a product able to reduce considerably the surface tension of water, even when used at small dosages.

When the water to solid ratio is such that there are capillary forces in the suspensions, classical rheological measurements cannot be conducted because the systems are too cohesive. We have then decided to carry workability measurements with a "maniabilimètre à mortier L.C.L." ; the measure consists in determining the necessary time, for a given volume of mortar under vibration, to flow so as to reach a given mark in the apparatus.

A first series of experiments was conducted by using a tabular alumina 28-48 mesh (300-650 µm). For instance, the flowing time fo W/A = 0.20 suspensions was 30 seconds without admixture and 7 seconds when using butanol as a non-foaming surfactant.

Some other experiments have been conducted with normalized mortars (1350 g of normalized sand and 450 g of Portland cement) at different water-cement ratios namely 0.40 0.45 and 0.50. The measurement was made 5 minutes after the end of the mixing operation.

	FLOWING TIME		
W/C	0.40	0.45	0.50
Mortar without admixture	220"	20.1"	8.6"
Mortar with surfactant	81"	14.1"	2.8"

From the lecture of the table, the fluidifying action of the surfactant is obvious. These experiments thus confirm our theoretical approach concerning the diminution of the capillary forces.

6 - EXTRAPOLATION to the REAL CASE of COMMERCIAL ADMIXTURES in CONCRETE or MORTARS

In this study, by taking model systems we have been able to put into evidence three elementary mechanisms of fluidification of suspensions by organic molecules. Some other non-identified elementary mechanism might be detected in the future.

Regarding the practical systems, the different elementary mechanisms we have studied take place simultaneously ; for instance lignosulfonate are anionic, surfactive molecules, the molecular weight of which is appropriate to get an entropic effect. This is probably the major reason for which the earlier studies carried on practical systems, were not appropriate so as to clarify the way superplasticizers work. This also justifies, a posteriori, the proceeding which had been decided for this research.

REFERENCES

1 - P.G. de GENNES, Phys. Chem. Hydrodyn. 2, 31 (1981)

2 - W.B. RUSSEL, J. Rheol. 24, 287 (1980)

3 - Th. F. TADROS, Adv. Coll. and Int. Sci., 12, 141 (1980)

4 - A.W. ADAMSON, *"Physical Chemistry of Surfaces"* p. 331 J. WILEY N.Y. (1967)

5 - H.C. HAMAKER, Physica 4, 1058 (1937)

6 - D.N. FURLONG, D.E. YATE and T.W. HEALY, "Fondamental Properties of the Oxide/Aqueous Solution Interface" in *"Electrodes of Conductive Metallic Oxides"*. Part B.,S.TRASATTI ed., ELSEVIER (1981)

7 - G.A. PARKS, Chem. Rev. 65, 177 (1965)

8 - B. DERJAGUIN and L. LANDAU, Acta Physicochim. 14, 633 (1941)

9 - E. VERWEY and J. Th. G. OVERBEEK, *"Theory of Stability of Lyophobic Colloids"*. ELSEVIER Amsterdam (1948)

10 - T. SATO and R. RUCH, *"Stabilization of Colloidal Dispersions by Polymer Adsorption"*. (Surfactant Science Series V.9). Marcel DEKKER, Inc. N.Y. (1980)

11 - R.H. OTTEWILL, J. Coll. and Int. Sci. 58, 357 (1977)

12 - J. CHAPPUIS in *"Concrete Rheology"* p. 38 ed : J. SKALNY. Materials Research Society (1982)

13 - D. BALLION and N. JAFFREZIC-RENAULT, "Influence de l'adsorption d'acides organiques sur le comportement électrophorétique des dispersions aqueuses d'alumine". 3° Meeting de la Société Générale d'Electrochimie. LYON 6-10 Sept. 1982

14 - E.L. MACKOR, J. Coll. Interf. Sci. 6, 492 (1951)

15 - E.W. FISCHER, Kolloid - Z, 160, 120 (1958)

16 - M.J. ROSEN, In *"Surfactants and Interfacial Phenomena"* p. 265, J. WILEY N.Y. (1978)

Parmi ces applications, nous pouvons citer :
- La prévision du domaine de stabilité des hydrates, lorsque le ciment est au contact d'un milieu réactionnel quelconque, soit dans le cadre de son utilisation (durabilité des bétons), soit au laboratoire, pour des études comme celle de la dissolution sélective des hydrates par des réactifs chimiques appropriés. Dans ce cas, la modélisation peut être étendue avec profit à divers milieux non aqueux.

L'étude des interactions des hydrates et des adjuvants, dont la plupart forment des complexes avec le calcium ou d'autres ions du système ciment-eau.
- Le calcul et le raffinement des constantes d'équilibre des hydrates, dont il manque de nombreux exemplaires pour décrire complètement l'hydratation, ou qui ne sont connues qu'avec une précision insuffisante. Dans ce cadre, il reste à étendre le domaine d'applications du modèle à l'étude des solutions solides comme les CSH ou la série des aluminates hydratés hexagonaux.
- Le calcul du taux de sursaturation de chacun des hydrates dans la séquence des réactions d'hydratation, qui constitue, à travers la relation : $A = R.T.Ln (S / S_x)$, où S est le produit ionique effectif, et S_x le produit de solubilité à l'équilibre, une mesure de l'affinité chimique A, qui est l'une des forces motrices produisant la création de la nouvelle structure au cours de l'hydratation.

A ce titre, les techniques de calcul et les concepts que nous avons développés ici constituent un premier élément d'un ensemble plus vaste, qui doit intégrer les autres forces du système, liées aux processus de diffusion au voisinage de l'interface anhydres-solution, à travers la couche d'hydrates poreuse, ainsi qu'aux gradients de température et éventuellement aux gradients électriques de double couche.

Bien que d'un abord plus difficile, l'approche analytique doit se montrer plus efficace à long terme que les approches empiriques, qui permettent d'établir des relations entre variables résultantes, comme la porosité, la chaleur d'hydratation, la résistance mécanique, mais sans permettre d'en comprendre et donc d'en prévoir les anomalies, ou d'en analyser les composantes.

7 - BIBLIOGRAPHIE

/1/ COURNIL M. ; GALTIER P. ; CONRAD F. ; Journal de chimie physique, 79, n°5, 1982, pp 427-433.

/2/ KARMAZSIN E. ; COMEL C. ; MURAT M. ; "Etude des systèmes $CaSO_4$-H_2O par calorimétrie isotherme. IV - Etablissement d'un modèle cinétique pour la réaction d'hydratation de $CaSO_4$, $1/2H_2O$ -beta pur" Rev."Ciments, bétons, plâtres et chaux", n°740 1/83, pp 47-50.

/3/ BARRET P. "Modélisation et réactivité des matériaux". Ibid., n° 755, 4/85, pp 237-244.

/4/ DRON R. "Mécanisme de la prise du laitier granulé sous activation alcaline" - Rapport de recherche LCPC n°38, Sept.1974.

/5/ BERTANDIE D. "Contribution à l'étude cinétique de la formation des hydrates dans les solutions aqueuses obtenues à partir du ciment alumineux". Thèse Univ. Dijon 15/6/1977.

/6/ MENETRIER D. "Contribution à l'étude cinétique de la période intiiale d'hydratation du silicate tricalcique $3CaO,SiO_2$, constituant principal du ciment portland. Thèse Univ. Dijon, 15/6/77

/7/ BARRET P. ; BERTRANDIE D. ; BEAU D. "Calcium hydrocarboaluminate, carbonate, alumina gel and hydrated aluminates solubility diagram calculated in equilibrium with CO_{2g} and with Na^+_{aq} ions. Cement and concrete research, Vol. 13, 1982, pp 789-800.

/8/ SOUSTELLE M. et coll. "Stabilité thermodynamique des phases dans le système $CaO-Al_2O_3-H_2O$" (Ibid.), Vol.15, 1985, pp 421-430.

/9/ SOUSTELLE M. et coll "Application des propriétés thermodynamiques du système $CaO-Al_2O_3-CO_2-H_2O$ à l'hydratation des ciments alumineux". (Ibid.), vol. 15, 1985, pp 655-661.

/10/ ROSSET R. ; BAUER D. , DESBARRES J. "Chimie analytique des solutions et microinformatique". Ed. Masson, 1979.

/11/ DEFAY R. "Sortir de l'équilibre. Thermodynamique et capillarité". Ed;Univ. libre de Bruxelles;, 1981.

/12/ DEFAY R. ; PRIGOGINE I. ; BELLEMANS A., EVERETT D.H.. "Surface tension and adsoption". Ed. Longmans, Green, 1966.

/13/ BATES R.G. ; BOWER V.E. ; SMITH E.R. "Calcium hydroxyde as a high alkaline pH standard". Jour. of Res. N.B.S., Vol. 56, N°6, June 1956, pp 305-312.

/14/ JONES F.E. "The quaternary system $CaO-Al_2O_3-CaSO_4-H_2O$ at 20°C" TRANS. F. Society, 1939, pp 1484-1510.

/15/ YEATTS Leroy B. ; MARSHALL L. "Aqueous systems at high emperature. XVIII. Activity coefficient behaviour of calcium hydroxyde in aqueous sodium nitrate to the critical temperature of water". J.Phys.Chem., Vol.71,n° 8, 1967, pp 2641-2650.

/16/ JONES F.E. "The quinary system $CaO-Al_2O_3-CaSO_4-K_2O-H_2O$ (1% KOH) at 25°C". Ibid. (1% NaOH), J.Phys.Chem., Vol. 48, N° 6, Nov. 1944

/17/ HANSEN W.C. ; PRESSLER E.E. "Solubility of $Ca(OH)_2$ and $CaSO_4,2H_2O$ in dilute alkali solutions". Ind. and Eng.Chem., Vol.39, n° 10, Oct. 1947.

C. VERNET, Société des CIMENTS FRANCAIS - C.E.R.E.G. (FRANCE)

MODELISATION DES DIAGRAMMES D'EQUILIBRE DE SOLUBILITE DES HYDRATES - INTERACTIONS IONIQUES

C.L.

1 - INTRODUCTION

1.1 - NECESSITE D'UNE APPROCHE ANALYTIQUE ET D'UN MODELE DES REACTIONS D'HYDRATATION

Par suite de la généralisation de l'emploi des ajouts minéraux de toutes origines et des adjuvants organiques, la complexité des phénomènes et des systèmes chimiques mis en jeu au cours de l'hydratation devient de plus en plus grande. Sachant par ailleurs que le ciment portland est un milieu interactif, les approches purement empiriques perdent leur intérêt, car elles conduisent à multiplier sans cesse les plans d'expérience, sans garantie de succès. Il faut donc essayer de prévoir le comportement dynamique des ciments en affinant l'analyse des mécanismes qui en sont la base, et rechercher des modèles plus "physiques que "mathématiques", qui seraient de véritables outils pour le chimiste.

Des modèles de réactions d'hydratation ont été élaborés dans des cas simples, comme celui du plâtre /1/ /2/, prenant en compte les processus de diffusion dans un mécanisme de dissolution-précipitation. On peut donc espérer parvenir au même résultat dans le cas complexe du ciment portland, mais il faudra pour cela faire face à un certain nombre de difficultés, à la fois techniques et conceptuelles /3/.

1.2 - LA MODELISATION DE L'ETAT D'EQUILIBRE, UNE PREMIERE ETAPE VERS UN MODELE DYNAMIQUE DE L'HYDRATATION

Considérons le sytème ciment-eau, non plus comme un système fermé ordinaire, mais comme un ensemble de deux systèmes ouverts, le premier étant constitué des grains anhydres et le second étant constitué de la phase aqueuse et des hydrates. Les deux systèmes vont échanger de la matière (flux de diffusion) et de l'énergie à travers une frontière : l'interface réactionnelle.

La construction d'un modèle dynamique de l'hydratation devra donc intégrer l'évolution dans le temps de la surface de cette interface. Par ailleurs, devant la difficulté posée par la modélisation des régimes convectifs auxquels sont soumises les pâtes immobiles, il faudra se placer dans des conditions de diffusion stationnaire non convective, c'est-à-dire dans un réacteur ouvert, continu, agité, isotherme et isobare /3/.

Ces deux conditions ne sont pas encore totalement réunies aujourd'hui, mais il est possible, dans une première étape, d'étudier séparément le système hydrates-solution, avec l'objectif de modéliser son comportement lorsqu'il est soumis à des contraintes chimiques analogues à celles qui sont produites par le compartiment "anhydres".

Bien que l'hydratation soit un processus irréversible, la démarche précédente implique avant toute autre chose, la connaissance et la modélisation de l'état d'équilibre, qui constitue l'état de référence. Encore faut-il pour cela que le modèle soit suffisamment proche de la réalité physique, c'est-à-dire de la perception que nous pouvons en avoir à travers nos moyens d'investigation.

2 - MODELISATION DES EQUILIBRES DES HYDRATES DES CIMENTS. CONDITIONS POUR QUE LE MODELE SOIT UTILISABLE EN PRATIQUE

Nous pourrons considérer que le modèle satisfait au critère de représentativité physique, s'il permet de prévoir les valeurs expérimentales dans la limite de l'incertitude des mesures. Etudions en premier lieu les conditions qu'il faudra satisfaire pour atteindre cet objectif.

2.1 - PRISE EN COMPTE DES INTERACTIONS

Pour qu'un diagramme d'équilibre soit utilisable en pratique, il faut le construire en tenant compte de toutes les interactions ioniques, afin de déterminer avec une précision suffisante les constantes d'équlibre "pures", c'est-à-dire débarassées de l'influence du milieu. A ce titre, des progrès restent à faire, car on ne trouve dans la bibliographie que des modèles qui, soit négligent l'influence de la force ionique de la solution et assimilent activités et concentrations ioniques /4/, soit négligent la formation des complexes solubles entre les ions du système /5//6//7//8//9/. Compte tenu de l'expression des produits ioniques des hydrates, dans lesquels les activités des ions sont affectées dans la plupart des cas de puissances assez élevées, ces approximations conduisent à des erreurs systématiques sur la valeur des constantes et par voie de conséquence, sur les prévisions données par le modèle. C'est ainsi que, dans le cas de l'ettringite par exemple, pour laquelle le produit ionique apparent s'écrit :

$$(Ca^{2+})^6.(AlO_2^-)^2.(SO_4^{2-})^3.(OH^-)^4 = S'_9$$

le fait de négliger la formation des ions $CaOH^+$ aux environs de pH 12,8, en assimilant (Ca^{2+}) au calcium total, équivaut à surestimer (Ca^{2+}) d'un facteur supérieur à 2 et par suite la constante S'_9 d'un facteur $2^6 = 64$. Compte tenu de la précision avec laquelle sont connues la plupart des constantes de solubilité (rares sont celles qui sont connues à mieux qu'un facteur 10 près), cette erreur, qui semble a priori importante, l'est beaucoup moins que celle que l'on ferait en identifiant activités et concentrations des ions. En effet, le coefficient d'activité moyen de S est ici affecté de la puissance 15, ce qui représente un facteur 1000 à 10000 sur sa valeur, selon la force ionique de la solution.

2.2 - TECHNIQUES DE CALCUL

On conçoit maintenant qu'il soit difficile de prévoir à l'aide d'un modèle trop grossier les domaines de stabilité d'hydrates dont les produits ioniques ne diffèrent que d'une ou deux puissances de 10, ce qui est le cas des aluminates hydratés hexagonaux substitués, comme le monochloro, le monosulfo, et le monocarbo-aluminate. C'est ainsi que l'on est amené à renoncer, non seulement aux approximations faites sur les interactions, mais aussi à celles qui sont faites habituellement dans les calculs pour résoudre plus facilement le système d'équations représentant le système chimique à l'équilibre. Nous rejoignons ici la démarche utilisée par ROSSET /10/, l'un des premiers à prendre le chemin du traitement numérique des systèmes de la chimie analytique des solutions. Les progrès de la micro-informatique, présente aujourd'hui dans tous les laboratoires de recherche, permettent de développer cette technique avec le maximum de rigueur.

2.3 - CHOIX DU SYSTEME D'EQUATIONS

Bien que le système d'équations associé au système chimique ne soit pas linéaire en général, la réalité physique impose l'existence d'au moins une solution réelle, que l'on pourra calculer. Il faut cependant garder à l'esprit qu'une solution ne sera pas nécessairement représentative, car seuls nos acquis expérimentaux nous permettent de choisir le bon système d'équations, en nous indiquant la nature et le nombre de phases solides en équilibre avec un milieu particulier.

Prenons l'exemple du système /CaO, Al_2O_3, SO_3, R_2O, H_2O/, avec les phases solides gypse et ettringite. Supposons que l'on ignore l'existence de la portlandite, qui précipite au-delà d'une certaine valeur du pH : ceci aboutirait à trouver des solutions purement mathématiques et à poursuivre le tracé du diagramme dans un domaine où ce système n'existe plus "en réalité", à l'équilibre (dans le cas présent, le calcul s'avère quand même interessant lorsque le point figuratif de la solution se trouve dans le domaine de sursaturation de la portlandite, au cours de la "période dormante" des ciments).
Notons au passage que la comparaison des résultats expérimentaux conduirait ici à rechercher l'explication des écarts et par conséquent à identifier la phase manquante. Ce n'est donc pas le modèle lui-même qui est fructueux, mais sa confrontation avec les données expérimentales.
L'utilisation de la règle des phases peut s'avérer très utile, en permettant de faire le compte des équations du système : dans l'exemple précédent, avant la précipitation de la portlandite, la variance est égale à 2, pour 5 constituants indépendants, lorsque l'on tend vers l'équilibre à partir de la sursaturation. Par contre, la mise à l'équilibre à partir du domaine sous-saturé introduit une relation supplémentaire entre les variables, car alors la composition initiale de la solution est liée à la stoechiométrie des phases qui se dissocient. La variance devient égale à 1, avec 4 constituants indépendants. Ces 2 cas font évidemment appel à un traitement mathématique différent.

2.4 - COMPOSES NON STOECHIOMETRIQUES

Le problème de la représentativité des calculs se pose de façon particulièrement évidente dans le cas de la "coprécipitation", dont l'approche expérimentale est rendue difficile par le caractère pseudo-colloïdal des précipités, comme les hydroxydes des métaux de transition, les halogénures d'argent et les silicates de calcium hydratés (CSH des ciments). Dans ce dernier cas, en particulier, les moyens actuels d'investigation ne permettent pas de savoir si ce composé non stoechiométrique est un mélange de composés définis de structures voisines ou une solution solide dont la composition serait variable en fonction des conditions locales instantanées de précipitation. La résolution d'un tel système nécessite une relation entre les rapports stoechiométriques du précipité et la composition de la solution :
- dans le cas du mélange, on peut écrire par exemple que la probabilité de précipitation de chaque composé est inversement proportionnelle à sa solubilité, la somme des probabilités étant égale à 1. Cette démarche probabiliste implique la connaissance des produits de solubilité des constituants du mélange que l'on pourrait évaluer à partir des enthalpies libres de formation ;
- le cas des solutions solides exige une généralisation du concept de produit de solubilité, qui jusqu'ici ne s'applique qu'à des composés dont la stoechiométrie est indépendante de la composition de la solution (activité constante dans le solide).
Nous pensons que cette généralisation est possible et que l'on peut calculer l'expression du produit de solubilité généralisé en fonction des coefficients stoechiométriques, ou relier ces derniers aux activités des ions, à l'aide d'un calcul thermodynamique. Ceci fera l'objet d'une publication ultérieure.

2.5 - DEFINITION DE L'ETAT D'EQUILIBRE. DIMENSION DES CRISTAUX

Une autre difficulté d'utilisation du produit de solubilité se manifeste lorsque le précipité subit d'importantes variations de surface spéficique en fonction du temps. Le concept de phase doit être précisé lorsque la surface devient grande par rapport à la masse /11/. Il faut alors introduire une variable extensive supplémentaire (surface) et des variables intensives comme la tension superficielle et le potentiel électrique de surface. Lorsque la solubilité diminue par "vieillissement", le produit ionique est alors une fonction de la dimension des cristaux, que l'on peut représenter à l'aide de plusieurs paramètres, selon la nature de la distribution statistique des diamètres. Le simple bon sens nous indique ici que nous n'avons pas affaire à une situation d'équilibre, puisque le système évolue. Il n'empêche que l'on ne peut évacuer ce problème (en particulier dans le cas des ciments) car il présente de réelles difficultés, lorsqu'il s'agit de comparer les valeurs expérimentales aux valeurs calculées. La théorie de la nucléation /11//12/ nous apprend que dans ce cas, la dimension des cristaux dépend non seulement du temps, mais aussi des conditions chimiques au moment même de la précipitation (influence du taux de sursaturation sur le nombre de germes par unité de volume). C'est pourquoi on peut aboutir, même au bout d'un temps très long, à des états stationnaires différents, si les conditions de précipitation ont été différentes. C'est le cas de la portlandite, qui montre d'importantes différences de solubilité, non seulement en fonction de la dimension des cristaux /13//14/, mais aussi selon leur mode de préparation : la solubilité est plus grande pour des cristaux préparés par réaction $CaO + H_2O$, dans le domaine sursaturé.
La seule possibilité pour le chimiste est ici de réaliser un plan d'expériences qui respecte le mieux possible les conditions de précipitation qui existent dans les ciments, c'est-à-dire d'étudier et de mesurer les constantes des hydrates de synthèse précipités en régime très sursaturé. Dans ces conditions, la comparaison avec les résultats du modèle peut alors être faite, sur la base d'un état stationnaire très proche de l'équilibre, réalisé à partir de conditions initiales standardisées.
Les difficultés rencontrées au cours de cette discussion de la validité du modèle ne sont qu'en partie résolues. La condition ci-dessus fait ressortir par exemple la nécessité de construire un appareillage permettant de réaliser des états très sursaturés en chaux, pendant des temps suffisamment longs.
Du point de vue du physicien, c'est bien dans l'effort pour résoudre ces difficultés que résident toutes les chances de succès de la démarche. Le reste n'est qu'une question de mise en route d'un engrenage mathématique et informatique, le problème du calcul lui-même pouvant d'ailleurs être traité de différentes manières, selon les moyens dont on dispose. La méthode que nous proposons dans la suite de cette communication n'a donc pas la prétention d'être unique ou irremplaçable. Elle s'est simplement avérée très pratique à l'usage. Nous étudions, à l'aide de quelques exemples, les moyens permettant de simplifier le plus possible les algorithmes de calcul, de façon à obtenir des boucles d'itération très rapidement convergentes, adaptées à l'emploi de microprocesseurs beaucoup plus lents que les grosses unités de calcul.

3 - MISE EN EQUATION DES EQUILIBRES DE SOLUBILITE DES HYDRATES

3.1 - GENERALITES

Dans la suite de l'exposé, les systèmes chimiques seront désignés par leurs composants, selon la notation habituelle (le nombre de composants d'un système étant défini comme le plus petit nombre de constituants indépendants à partir desquels on peut déterminer complètement la composition de chaque phase).

3.2 - VARIABLES

Nous prendrons en considération l'ensemble des ions susceptibles d'exister dans la solution interstitielle des bétons, en étendant le domaine de pH (qui se situe habituellement entre 12,3 et 13,3) à la gamme pH 10 à pH 14, qui permet de couvrir un certain nombre d'applications particulières. Seules seront donc considérées comme négligeables les concentrations des espèces comme H_3O^+, HSO_4^- ou H_2CO_3, qui sont inférieures à 10^{-9} au-dessous de pH 10. Pour des raisons pratiques, nous avons choisi de prendre comme variables primaires les molalités (indépendantes de la température). Nous utilisons comme **variables secondaires** la **force ionique** I et les **coefficients d'activité individuels des ions** (*Tableau 1*). Bien que le calcul de ces coefficients individuels ne soient pas parfaitement rigoureux, compte tenu de la difficulté d'évaluation des rayons ioniques, utilisés dans les formules de DEBYE et HUCKEL, nous avons adopté cette méthode qui se montre souple, en permettant de calculer les coefficients d'activité moyens de chacune des constantes d'équilibre, quels que soient le système ou la composition de la solution.

Tableau 1 - Variables utilisées dans le modèle -

Espèces ioniques et moléculaires (Molalités)	Noms	Coefficients d'activité individuels	Rayons ioniques des ions solvatés (Å) (valeurs indicatives)
(Ca 2+)	C2	gC2	5 à 6
(CaOH +)	C1	gC1	4 à 5
(H2SiO4 2-)	H2	gH2	4
(H3SiO4 -)	H3	gH3	4
(H4SiO4 aq)	H4		
(AlO2-)=(H4AlO4-)	A1	gA1	4
(CO3 2-)	G2	gG2	4
(HCO3 -)	G1	gG1	3
(OH -)	OH	gOH	2 à
(Na+)+(K+)	R1	gR1	4
(SO4 2-)	S4	gS4	4
(NaSO4-)+(KSO4-)	RS4	gRS4	4
(CaSO4 aq)	CS4		
(Cl-)(ou anion monovalent d'acide fort)	X1	gX1	2 à 3

(liste non limitative)

N.B. : Les rayons ioniques figurant dans le *Tableau 1* sont en général supérieurs à ceux que l'on pourrait calculer à partir des mobilités électriques, en appliquant la loi de STOKES. Certains peuvent être obtenus par régression, à l'aide des formules de DEBYE et HUCKEL, à partir de bilans ioniques de composés insolubles, en faisant varier la force ionique /15/.

Les diagrammes d'équilibre sont en général construits à l'aide des concentrations ou des molalités TOTALES qui à de rares exceptions prés, sont les seules grandeurs accessibles à l'expérimentation.

Cette méthode présente l'inconvénient de faire disparaître une partie de l'information utile, à savoir la répartition d'un élément chimique, sous ses différentes espèces, complexes ioniques ou moléculaires. Nous avons donc choisi d'utiliser les grandeurs totales (*Tableau 2*) comme variables secondaires, en gardant la possibilité d'effectuer des projections des domaines d'équilibre sur les plans optionnels, en conservant un fichier complet par point du diagramme.

Tableau 2 - Expression des molalités totales

Variables résultantes	variables primaires
CT	C2 + C1 + CS4
ST	H2 + H1 + H4
AT	A1 + A0
GT	G2 + G1
RT	R1 + RS4
S4T	S4 + RS4 + CS4
BT (basicité)	OH + C1

3.2 - SYSTEME D'EQUATIONS

A pression et température constantes, un système de c composants (ou c molalités totales indépendantes), comportant p phases solides et une phase aqueuse, a pour variance : $v = c - p + 1$.

Toutes les molalités sont donc déterminées si l'on se fixe v d'entre elles et ceci quel que soit le nombre d'ions complexes. Le problème va consister à éliminer les inconnues entre $n = (e - v)$ équations, dans un système comportant e espèces en solution. Ces équations sont de 4 types (*Tableau 3*) :

Tableau 3 - Equations et constantes chimique (liste non limitative)
(l'apostrophe désigne les constantes apparentes)

RELATIONS -	Constantes	Valeurs à 25°C indicatives	Coeff. moyen d'activité
Réactions acide-base			
C2.OH/C1 =	K_1'	0,037	$g1 = gC2.gOH/gC1$
H3.OH/H2 =	K_2'	0,0063	$g2 = gH3.gOH/gH2$
H4.OH/H3 =	K_3'	4,31 E-5	$g3 = gOH/gH3$
A0.OH/A1 =	K_5'	3,33.E-5	$g5 = gOH/gA1$
G1.OH/G2 =	K_7'	2.E-4	$g7 = gG1.gOH/gG2$
Complexes sulfate			
C2.S4/CS4 =	K_{12}'	0,01	$g12 = gC2.gS4$
R1.S4/RS4 =	K_{13}'	0,13	$g13 = gR1.gS4/gRS4$
Produits de solubilité			
H4 =	K_4'	1,6.E-3	
A0 =	K_{13}'	1.E-6	
$C2^a.C1^{1-a}.H2^{1-b-c}.H1^{2c}.OH^c.$ =	S_0'	1.E-7,25	gS0
$C2.OH^2.$ =	S_1'	5,3.E-6	gS1
C2. S4 =	S_2'	3,185.E-5	gS2
C2. G2 =	S_3'	4,5.E-9	gS3
$C2^4.A1^2.OH^6.$ =	S_4'	5.E-27	gS4
$C2.^4A1^2.S4.OH^4.$ =	S_5'	1.E-29	gS5
$C2^4.A1^2.X1^2.OH^4.$ =	S_6'	1.E-31	gS6
$C2^4.A1^2.G2.OH^4.$ =	S_7'	5.E-31	gS7
$C2^2.A1^2.OH^2.$ =	S_8'	1.E-14	gS8
$C2.^4A1^2.G4^3.OH^4.$ =	S_9'	1 E-44	gS9

a) L'équation d'électroneutralité : $\Sigma_i z_i C_i = 0$

b) r équations correspondant aux réactions chimiques d'association d'espèces en solution (réactions acide-base, formations de complexes solubles). Ces r équations relient l'ensemble des ct molalités totales à l'ensemble des e espèces en solution, d'où ct = e - r

c) pour p phases solides, p équations obtenues en écrivant les produits de solubilité $_j (c_i)^n i = S'_j = S_j/\gamma \equiv$

d) des équations particulières au nombre de s = n - r - p - 1, reliant certaines des variables lorsqu'il y a dégénérescence du nombre de constituants indépendants (ceci se produit quand l'équilibre est atteint à partir du domaine sous-saturé, ou lorsque le système comporte des phases solides non indépendantes, par exemple dans l'équilibre métastable $C_2AH_8 + C_4AH_{19} + CH$, où la relation restrictive est $(C/A)_{solution} \equiv 4$.
On a alors :
c = ct - s, et c = e - r - s < e - r

4 - PRINCIPE GENERAL DES CALCULS

4.1 - TRAITEMENT NUMERIQUE

Bien que cela soit possible dans un grand nombre de cas, on ne cherchera pas à exprimer les solutions du système sous forme d'expressions algébriques explicites reliant les grandeurs totales. Chaque point d'une courbe d'équilibre sera associé à un domaine-solution D, de la dimension égale à la variance du système. Ce domaine sera représenté par un fichier contenant les valeurs calculées, pour chaque valeur du ou des paramètres choisis selon la variance.

4.2 - EXPRESSION PARAMETRIQUE DES SOLUTIONS CHOIX DES PARAMETRES

Le traitement numérique sera d'autant plus facile et rapide que les expressions à calculer seront moins complexes. On aura donc intérêt à travailler dans des systèmes de variance non nulle. Les points invariants pourront être obtenus en faisant tendre vers zéro l'une des molalités, dans un système où v = 1, contenant un constituant supplémentaire non précipitable.
Inversement, on évitera de traiter des systèmes de variance élevée, ce qui obligerait à stocker un grand nombre de fichiers de gande dimension. L'expérience montre que, dans le cas des ciments, la plupart des équilibres peuvent être traités avec v = 1.
On aura avantage à choisir comme paramètres les molalités des ions intervenant le plus souvent dans les réactions de formation de complexes, comme OH^- et SO_4^{2-}. Ceci permet d'éliminer les r équations correspondantes du système, et de le réduire à un nombre d'équations égal au nombre de molalités totales ct.

4.3 - NIVEAU DE COMPLEXITE DES SYSTEMES

Le système (S) ainsi réduit contient (s + 1) équations linéaires, et p équations non linéaires. Il est bien évident que si l'on peut éviter d'avoir à substituer dans les premières, des expressions non linéaires tirées des secondes, la résolution du système sera très simple. Or ce procédé n'est possible que dans un certain nombre de cas, qu'il faut être capable de prévoir. Pour cela, nous allons considérer le sous-système (SS), constitué des p équations non linéaires (produits de solubilité).
Définition : Nous appellerons MULTIPLICITE m du système SS, le nombre minimum de molalités totales nécessaire pour écrire les p produits de solubilité.

Le système SS comprend m variables et p équations (m > p - 1). Sa résolution directe permet de réduire le système S à un système linéaire constitué de l'équation d'électroneutralité et des éventuelles équations restrictives particulières. Pour que ceci soit possible, il faut disposer de (m - p) variables optionnelles, prises comme paramètres, parmi les variables autorisées par la variance, d'où la condition : v > m - p
Le niveau de complexité du système peut donc être représenté par la variable :
δ = m - p - v = m - c + 1, avec
m> 0 pour tout c, d'où δ > 1 - c
Si v > m - p, alors δ < 0, et le nombre de paramètres dont on dispose est suffisant pour résoudre SS séparément.
Si δ > 0, la résolution se complique : on apporte v paramètres pour résoudre SS, mais il en manque m-p-v. Dans tous les cas, on doit avoir : δ < 1 + s, pour résoudre le système général S. L'étendue des variations possibles de δ est donc donnée par :

$$1 - c < \delta < 1 + s$$

Le nombre optimum de paramètres, c'est à dire le minimum nécessaire à la résolution de SS est obtenu pour δ = 0, soit v = m - p. Dans la mesure du possible, on s'arrangera donc pour se placer dans ces conditions de variance.

Cas défavorable
Lorsque 0 < δ < 1 + s, on est obligé de substituer des expressions non linéaires dans l'équation d'électroneutralité et les équations particulières. Le système S se réduit alors à une équation finale de la forme :
$y = D.X^{-n} + E = X$, avec n > 0 et D > 0

L'exposant n n'est pas nécessairement un entier.
L'équation peut être résolue par itération : la méthode classique des approximations en spirale n'étant utilisable que si ABS (y') < 1, nous utiliserons une autre méthode itérative (méthode de la tangente mobile).

4.7 - CORRECTIONS DUES A LA FORCE IONIQUE

Après avoir obtenu un fichier complet des solutions dans l'espace des molalités, il reste à calculer la force ionique et les coefficients d'activité individuels, à l'aide des formules de DEBYE et HUCKEL étendues. On retourne alors à une nouvelle résolution du système, par une boucle d'itération qui est arrêtée lorsque les valeurs obtenues sont stationnaires. Les coordonnées du point de la courbe d'équilibre ainsi obtenues peuvent alors être envoyées dans une mémoire de stockage, affichées ou éditées dans un graphe, sous la forme d'une projection dans un plan quelconque de l'espace des molalités.

4.8 - ORGANIGRAMME (voir *Fig. 1*)

5 - RESULTATS. EXEMPLE

La méthode précédente nous a permis de modéliser la plupart des systèmes d'hydrates de la chimie du ciment. Les résultats concordent bien avec les données expérimentales, par exemple les coordonnées des points invariants donnés par JONES /16/. Pour juger des performances du modèle, nous donnons les résultats obtenus dans le système [CaO, SO_3, R_2O, H_2O] dans le domaine d'équilibre gypse + portlandite, qui a été étudié par HANSEN et PRESSLER /17/ (*Fig.2*).
L'exactitude des prévisions du modèle ne peut être obtenue ici qu'en tenant compte des complexes sulfate et des réactions acide-base.

Fig 1.

Modélisation des équilibres chimiques des hydrates des ciments.

PROGRAMME SOLUB. Organigramme.

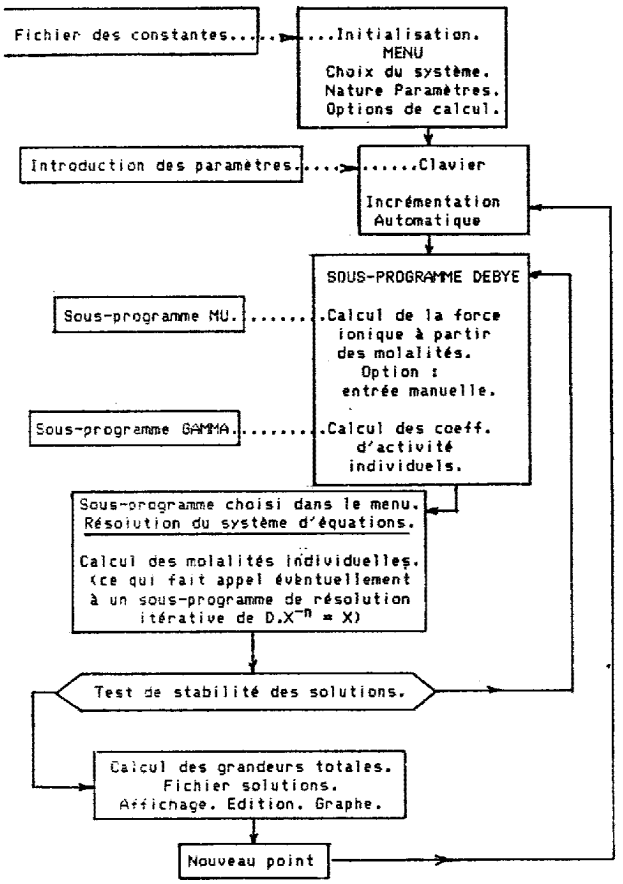

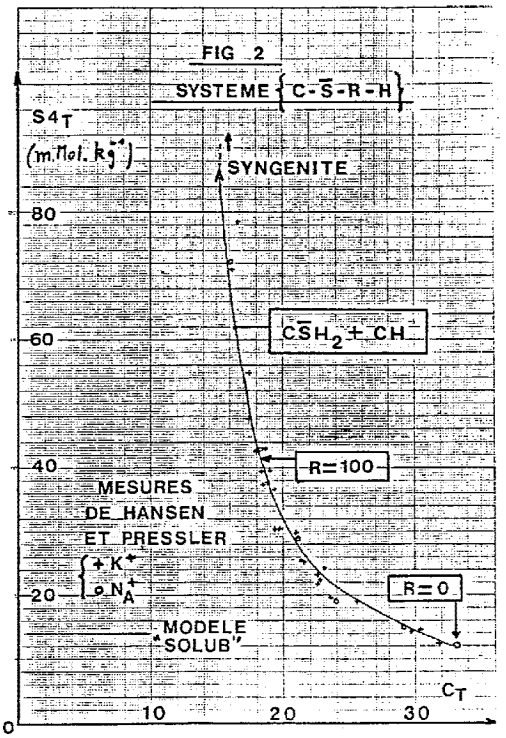

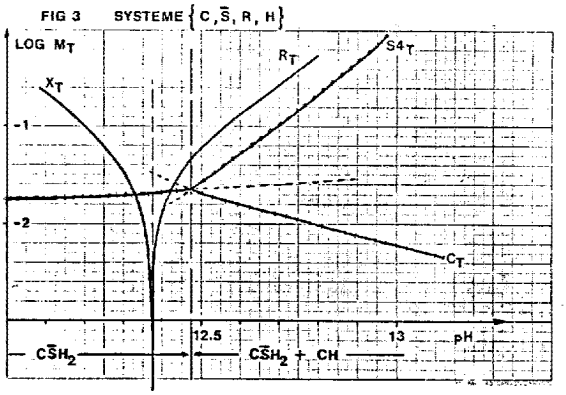

Dans le même système, on peut prévoir le pH de précipitation de la portlandite en présence de gypse et le comportement d'une suspension de gypse dans laquelle on ajoute une base forte R2O (*Fig.3*). La projection du domaine d'équilibre sur un plan /pH,R2O/ montre comment le gypse peut avoir un effet accélérateur de prise des ciments, en abaissant légèrement le pH d'équilibre : le mélange des 2 phases gypse et portlandite se comporte comme un "super tampon" (*Fig.4*).

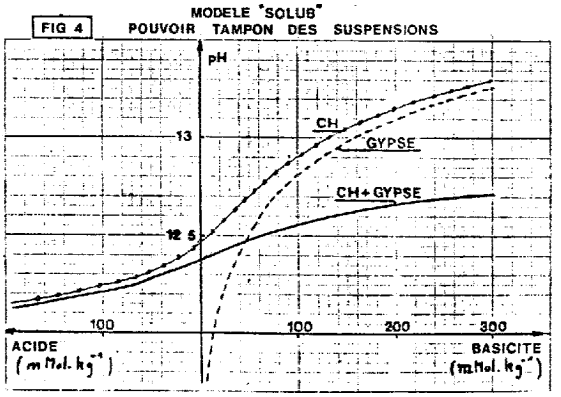

6 - CONCLUSIONS

Le souci de la représentativité physique dans la modélisation des équilibres des hydrates nous a conduit à faire face à toute la complexité de l'approche analytique de l'hydratation. Nous pensons que cet effort se justifie par la grande variété de ses applications , dont le simple exemple qui précède montre déjà la richesse.

F. Indelicato - Dipartimento di Ingegnerie Strutturale, Politecnico di Torino Italia
L. Cussino - Riserca e Sviluppo, Unicem S.p.A., Casale Monferrato, Italia

COMPORTEMENT VISCOÉLASTIQUE À LONG TERME DES BÉTONS DE CIMENT ALUMINEUX

1. INTRODUCTION

L'étude systématique du comportement statique et structurale des bétons à base de ciment alumineux forme l'objet d'une littérature assez nourrie, mais cette dernière tout en étant riche des données et d'études théoriques n'est pas en mesure, pour l'instant, de mettre à la disposition du responsable d'un projet tous les éléments dont il a besoin pour assurer un calcul correct.

A ce sujet et pour nous en tenir tout simplement à la caractéristique la plus significative - la résistance à la rupture par compression - un exemple emblématique est donné par le fait qu'en dépit de la grande abondance d'ouvrages et d'intéressantes études sur son évolution à long terme (1), (2), (3) et bien que les auteurs attribuent d'un commun accord à la conversion la responsabilité de la chute de la résistance dans le temps, bien connue, lorsqu'il s'agit de quantifier cette chute on bute à une grande dispersion des données.

En effet, l'influence qu'exercent les différents paramètres sur l'évolution de la résistance après les premiers jours n'a pas encore été bien définie.

Il a été prouvé, néanmoins, que la nature de l'agrégat (calcaire ou siliceux) peut jouer un rôle déterminant et donner lieu - pour le calcaire - à la formation d'un carbo-aluminate plus stable que les aluminates héxagonaux (4). Le phénomène s'accompagne d'une réduction de la porosité et a, comme suite, une augmentation continue ou, tout au moins, une stabilisation significative - environ aux valeurs maximales obtenues - des résistances observées sur une période de cinq ans (5).

Le contraire se produit pour l'agrégat siliceux.

Un ouvrage récent, étayé par les résultats d'essais réalisés jusqu'à un an après la préparation des échantillons confirme que l'agrégat calcaire exerce une influence favorable sur certaines caractéristiques mécaniques et, en particulier, sur la résistance à la rupture par compression (6).

Quant aux déformations différées et, en particulier au fluage, une caractéristique dont le responsable du projet doit absolument tenir compte pour pouvoir formuler des prévisions correctes au sujet du comportement dans le temps voire de la déformabilité du béton, les données à long terme que nous offre la littérature sont assez moins nombreuses que celles concernant la résistance bien que les premiers ouvrages en la matière remontent aux années '30 (7), (8).

A une époque plus récente, de nouveaux résultats ont été diffusés (9) tandis que ceux disponibles ont été interprétés dans une optique plus moderne (10). Toutefois ce domaine nous semble encore offrir de nombreuses possibilités de recherche.

Ce qui précède pourrait également s'appliquer aux modules d'élasticité encore que ces derniers soient bien documentés par des ouvrages de considérable envergure (2), (6), (11) et à d'autres caractéristiques collatérales qui intéressent en tous cas le responsable du projet, telle que la résistance à la traction.

Dans ce contexte s'inscrit l'étude expérimentale dont il est question qui porte essentiellement sur le fluage à long terme et sur le retrait des bétons à base de ciments alumineux et d'agrégat calcaire ou siliceux.

L'étude est intégrée par des donnés relatives à l'évolution dans le temps des modules d'élasticité et aux résistances à la compression et à la traction de ces bétons.

A partir de ces préalables on se propose:

- de présenter les valeurs de fluage et de retrait des bétons soumis à observation pendant 4 ans;
- d'analyser la possibilité de prévoir ces caractéristiques à l'aide d'essais à court terme;
- d'étudier l'influence exercée par l'agrégat (calcaire ou siliceux);
- de comparer l'effet des différents âges de mise en charge;
- d'élargir le tableau d'ensemble général par de nouvelles données expérimentales concernant la résistance à la compression et à la traction ainsi que les modules d'élasticité.

2. CARACTERISTIQUES DES ECHANTILLONS

Pour la confection des éprouvettes nous avons utilisé deux bétons préparés à partir du même ciment alumineux du commerce ayant la composition chimique pondérale suivante: Al_2O_3 39,3%, CaO 38,3%, Fe_2O_3 11,6%, FeO 5,0%, SiO_2 4,0% avec de faibles quantités de MgO, K_2O et Na_2O.

Le premier type de béton, obtenu en utilisant un agrégat siliceux naturel du Po présentait les caractéristiques suivantes: Ø max. 20 mm; courbe granulométrique continue; dosage du ciment 350 kg/m^3; rapport E/C = 0,52; slump 9,5 cm; tassement par table vibrante; masse volumique au démoulage 2418 kg/m^3.

Le deuxième type était caractérisé par un agrégat calcaire concassé: $CaCO_3$ 99,8; Ø max. 20 mm; courbe granulométrique continue, dosage du ciment 350 kg/m^3; rapport E/C = 0,60; slump 12 cm; tassement par table vibrante; masse volumique au démoulage 2360 kg/m^3.

Les deux bétons ont été préparés à quelques heures de distance l'un de l'autre, dans le même milieu et en utilisant le même appareillage.

Nous avons préparé, avec chaque mélange, des éprouvettes de 10x10x30 cm pour les essais de fluage et de retrait et pour la détermination du module d'élasticité longitudinale, ainsi que des éprouvettes cubiques de 10 cm de large, pour les essais de compression et des éprouvettes cylindriques, pour l'essai brésilien.

Pendant les 7 premiers jours, les éprouvettes ont été stockés en milieux contrôlé, à la température de 20 ± 1°C et à une teneur d'humidité relative de 90% min.

Ensuite elles ont été transférés, pour les essais, dans un milieu contrôlé à la température de 20 ± 1°C et à une humidité relative de 65%.

3. MODALITES D'ESSAI

3.1 Essais de fluage

Les éprouvettes ont été soumises à une charge constante, dans des châssis expréssement prévus à cet effet équipés d'un vérin hydraulique comportant un dispositif de réglage de la pression à air qui assure une stabilité durable de la charge (Fig. 1).

Sur chacune des quatre faces longitudinales de l'éprouvette a été placée une base extensométrique de 100 mm, pour la lecture de la déformation; l'extensomètre utilisé est de type mécanique avec sensibilitè $1 \cdot 10^{-3}$ mm.

Au bout de 7, 28, 92 et 180 jours, les éprouvettes ont été soumises à une charge centrée correspondant à une contrainte de 25 N/mm^2, c'est à dire près de 35% des résistances à la compression à l'échéance de 28 jours, pour les deux types de béton.

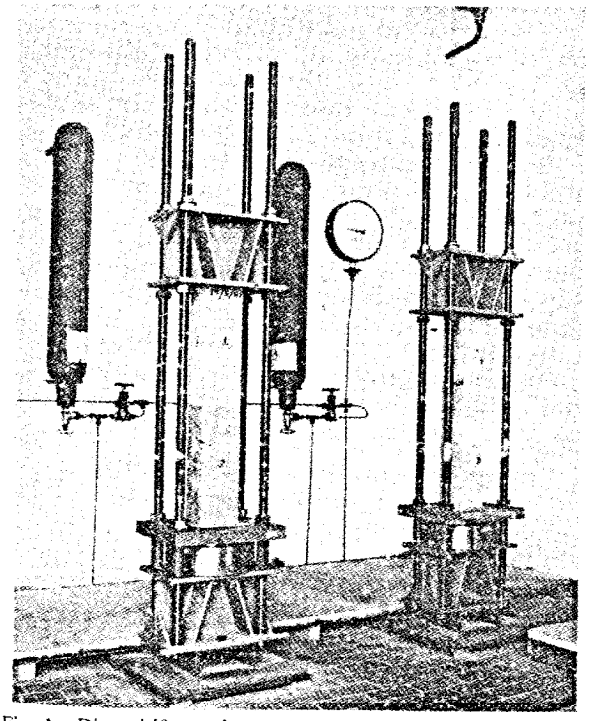

Fig. 1 - Dispositif de mise en charge.

Nous avons utilisé 16 éprouvettes qui ont été mises en charge par groupes de deux, pour chaque essai et pour chaque type de beton.

3.2 Mesure du retrait

Les déformations ont été mesurées à partir de 24 heures après la préparation des bétons, à l'aide d'un extensomètre mécanique, tout comme pour le fluage, en utilisant deux éprouvettes par type de béton.

3.3 Module d'élasticité longitudinale

Les modules sécants E correspondant à une contrainte de compression maximale de 25 N/mm^2 ont été determinés à différentes échéances sur deux éprouvettes de chaque type de béton. L'appareillage extensométrique est le même qui a été utilisé pour le fluage et pour le retrait.

3.4 Résistances à la compression

Elles ont été déterminées à l'aide d'une machine universelle en utilisant 54 éprouvettes testés à neuf échéanches s'échelonnant entre 1 jour et 4 ans.

4. RESULTATS DES ESSAIS ET COMMENTAIRES

4.1 Retrait

Les déformations de retrait ε_r, observées à partir d'un jour après la préparation des éprouvettes sont indiquées à la Fig. 2 qui montre également les déformations différées (fluage + retrait).

On peut remarquer qu'au bout de 4 ans, les ε_r présentent des valeurs très proches de celles que l'on enregistre habituellement pour les bétons à base de ciment Portland, ce qui correspond aux données signalées par Neville (12).

Il y a lieu toutefois de souligner que le retrait du béton à base d'agrégat calcaire est légèrement supérieur à celui du béton à base d'agrégat siliceux.

4.2 Fluage

Les déformations de fluage ε_f (Fig. 2), par suite des modalités d'essai qui ont été adoptées coïncident pratiquement avec celles différées.

Ces préalables ayant été posés, lorsqu'on analyse les valeurs de fluage au bout de 4 ans on peut observer:

— que les valeurs de dilatation maximale pour les deux bétons sont celles qui correspondent à une mise en charge de 7 jours;

— que les valeurs de ε_f des deux bétons diminuent au fur et à mesure qu'augmente la durée de la mise en charge;

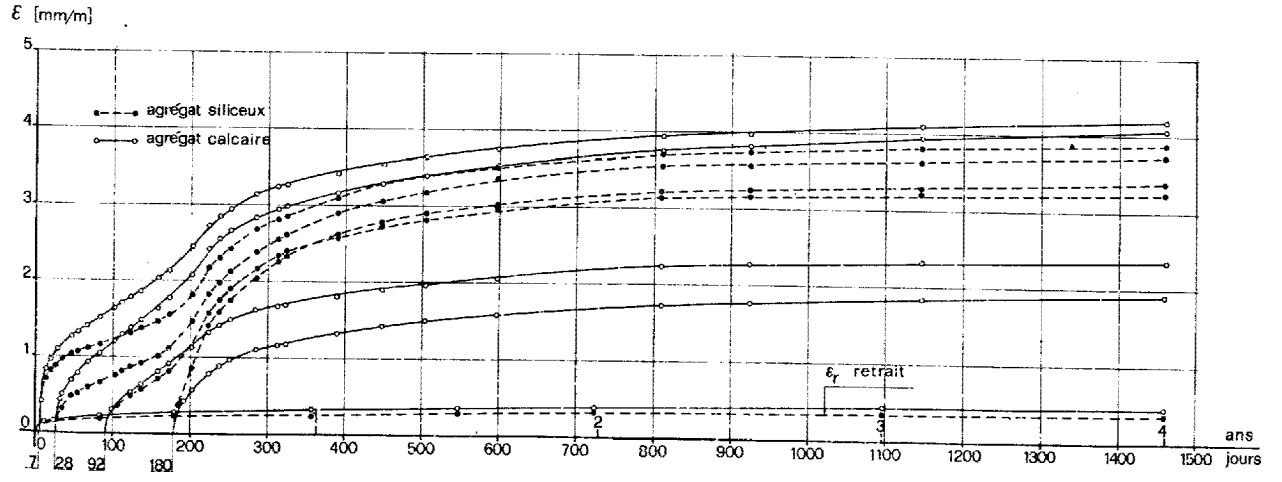

Fig. 2 - Évolution des déformations differées (fluage + retrait) et retrait en fonction du temps.

— que les dilatations des bétons à base d'agrégat calcaire à 7 et à 28 jours de mise en charge dépassent bien qu'en moindre mesure, celles du béton à base d'agrégat siliceux;

— qu'à l'échéance de 92 et de 180 jours, les ε_f du béton à base d'agrégat calcaire sont considérablement inférieures à celles du béton à base d'agrégat siliceux; en particulier, après 180 jours de mise en charge elles ne mesurent que la moitié;

— les ε_f de l'agrégat siliceux tendent à se regrouper autour de la même valeur, indépendamment de l'age de mise en charge (différence de 15% entre les valeurs maximales et minimales);

— l'agrégat calcaire présente, au contraire, une différenciation très nette, caractérisée par deux valeurs de la ε_f: celles à 7 et 28 jours sont élevées et très rapprochées entr'elles tandis qu'au fur et à mesure qu'augmente l'âge de mise en charge on observe une réduction importante de la déformabilité si bien qu'entre les ε_f des échantillons à 7 jours et celles des échantillons à 92 et 180 jours la différence se chiffre approximativement à 45% et à 55%.

Une analyse plus exhaustive pourrait être consacrée à l'évolution du fluage qui présente des aspects intéressants surtout pendant la première année, mais puisqu'une partie des données que nous présentons dans cet ouvrage et qui concerne cette période ont été signalées et discutées en détail (13), (14), nous nous bornerons à mettre l'accent sur quelques aspects essentiels.

Plus particulièrement, il y a lieu de souligner que toutes les courbes, à part celles des échantillons mis en charge à 180 jours, présentent deux points d'infléxion limitant un trajet du diagramme compris entre 70 et 220 jours d'âge des échantillons où la vitesse de croissance de la déformation augmente en mesure considérable et recommence ensuite à diminuer. Ce fait confirme les observations de Swami (9) et, en partie, les commentaires de Neville (10).

L'origine de ce comportement des bétons alumineux doit être probablement attribuée aux phénomènes de nature physico-chimique liés à la cure des éprouvettes. A ce propos nous voudrions souligner le différent comportement des deux matériaux: en effet l'augmentation de la vitesse de déformation des bétons à base d'agrégat calcaire est plus lente, ce qui fait que les inflexions sont moins marquées. Ce fait pourrait être expliqué en admettant que l'interaction chimique entre agrégat calcaire et pâte de ciment (5), à fur et mesure que se développe dans le temps à la dépense des hydrates hexagonaux (4), entraîne un'amélioration progressive de l'adhérence pâte-agrégat calcaire.

Afin d'aboutir à une évaluation plus complète du phénomène du fluage nous avons estimé utile de procéder à une comparaison entre les deux bétons objet de l'étude et un béton structural ordinaire de bonne qualité, de la classe $f_{ck} = 50$ N/mm^2 à base de ciment Portland, testé dans le même laboratoire et dans les mêmes conditions.

Le choix est tombé sur ce béton, du fait que les déformations mesurées montraient une excellente correspondance avec celles calculées par voie théorique, en appliquant les formules proposées par le C.E.B. (15).

Nous avons adopté, comme paramètre de comparaison, le facteur de fluage φ qui est le rapport entre la déformation de fluage et la déformation longitudinale à l'age de 28 jours, notamment:

$$\varphi = \frac{\varepsilon_f}{\varepsilon_{e28}}$$

Les Fig. 3 et 4 montrent une comparaison entre les facteurs de fluage du béton ordinaire et ceux du béton à base d'agrégat siliceux et calcaire.

On peut observer:

— à court terme, les facteurs de fluage des bétons à base de ciment alumineux correspondent approximativement à ceux du béton ordinaire. Plus précisément, les facteurs du béton à base d'agrégat siliceux sont légèrement inférieurs, alors que ceux du béton calcaire sont supérieurs, bien que en moindre mesure;

— au bout de six mois, le coéfficient φ des deux bétons à base de ciment alumineux (calcaire, siliceux) enregistre une augmentation franchement supérieur à celle du coéfficient du béton ordinaire;

— quelque temps avant un an d'âge commence la phase définitive que caractérise une tendance très nette des φ vers des valeurs asymptotiques assez élevées (elles sont 2 à 3 fois plus importantes que celles du bétons ordinaire).

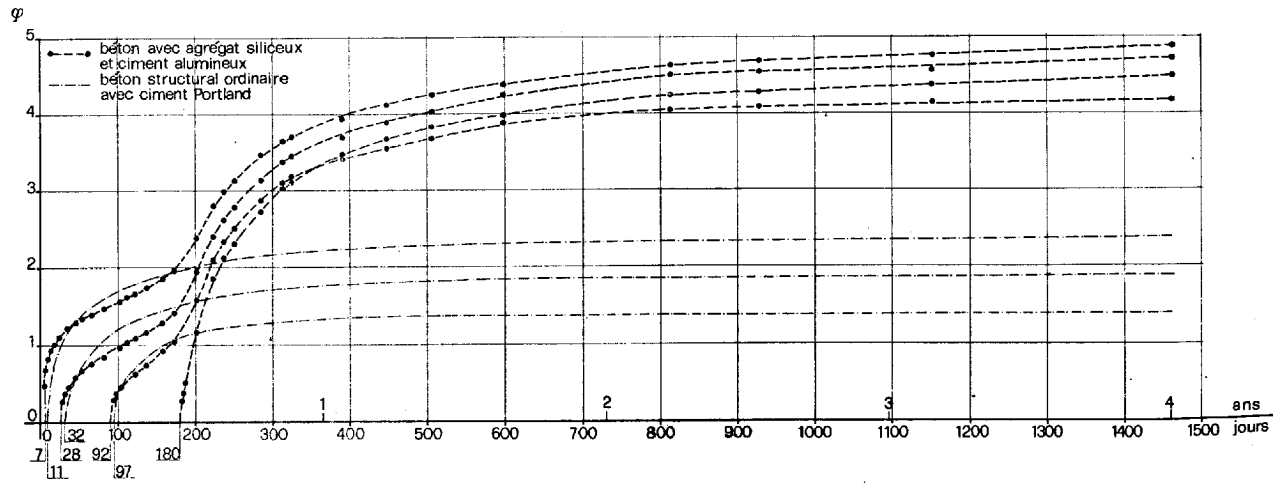

Fig. 3 - Évolution dans le temps des facteurs de fluage du béton alumineux avec agrégat siliceux en fonction de l'âge de mise en charge, et comparaisons avec un béton ordinaire.

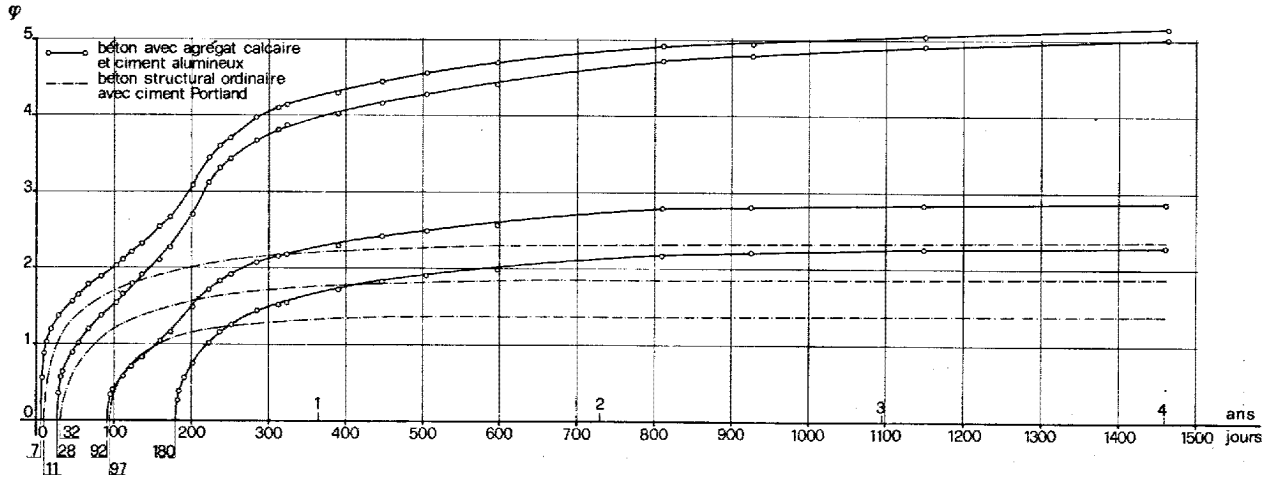

Fig. 4 - Évolution dans le temps des facteurs de fluage du béton alumineux avec agrégat calcaire en fonction de l'âge de mise en charge, et comparaison avec un béton ordinaire.

Une analyse qualitative permet, en tous cas, d'observer, au cours de cette phase, une différence de comportement très nette entre les deux bétons à base de ciment alumineux.

On peut constater, en effet que l'age de mise en charge exerce une faible influence - à l'échéance de quatre ans - sur la φ du béton siliceux.

À noter le rapport $\frac{\varphi \text{ siliceux}}{\varphi \text{ ordinaire}}$ dont la valeur maximale se chiffre à 3.

Dans le béton calcaire, l'âge de mise en charge exerce au contraire, une influence favorable car il engendre une considérable réduction de φ. Le rapport $\frac{\varphi \text{ calcaire}}{\varphi \text{ ordinaire}}$ tout en demeurant défavorable atteint néanmoins une valeur maximale de 2,6.

En dernier lieu on peut encore observer que l'allure des dilatations ε_f et des coéfficients de fluage ne permettent pas - tout au moins pour les types de bétons à base de ciment alumineux examinés - d'extrapoler les résultats des essais de fluage routiniers à court terme, à 90 jours d'âge. En effet, contrairement à ce qui se produit lorsqu'on opère sur les bétons ordinaires, dans ce cas les résultats peuvent ne pas être significatifs et même porter à des conclusions erronées.

4.3 Résistance à la rupture par compression

La résistance à la rupture par compression f_c des éprouvettes à base d'agrégat calcaire et siliceux est reportée à la Fig. 5. L'examen des diagrammes nous suggère quelques remarques:

— à très court terme on obtient des valeurs de résistance très élevés, ce qui d'ailleurs est bien connu pour les bétons à base de ciments alumineux: dans notre cas, les deux matériaux enregistrent au bout de 24 heures, des résistances d'environ 57 N/mm^2;

— la résistance du béton à base d'agrégat siliceux augmente d'abord plus rapidement que celle du matériau calcaire. Ensuite se produit une inversion de comportement si bien qu'à l'écheance d'un an à peu près, les f_c des deux matériaux s'avèrent être égales et se chiffrent à 82 N/mm^2. Cette valeur de la résistance correspond également à la valeur maximum qu'enregistre le béton à base d'agrégat siliceux;

— dans le délai de temps entre un e quatre ans, les valeurs de resistance du béton à base d'agrégat siliceux commencent à diminuer d'abord lentement et ensuite, après une période de stabilisation, en manière plus marquée.
Au bout de 4 ans, la chute de résistance est de 25% vis-à-vis de la valeur maximum;

— dans le même délai, la résistance des bétons à base d'agrégat calcaire ne cesse d'augmenter jusqu'à l'échéance de 2 ans et se stabilise ensuite autour de 87 N/mm^2 maximum.

4.4 Résistance à la traction

Nous avons limité l'étude de la résistance à la traction f_{ct} aux 18 premiers mois. Le Tableau 1 montre les valeurs obtenues avec l'essai brésilien sur des éprouvettes cylindriques ayant les dimensions suivantes: Ø = 15 cm, l = 30 cm. Les valeurs indiquées représentent la moyenne obtenue sur 3 éprouvettes.

Tableau 1 - Variation de la résistance à la traction des bétons alumineux en fonction du temps et du type d'agrégat

Résistance à la traction				
Âge du béton	28 j	180 j	360 j	540 j
Calcaire	3,8 N/mm^2	4,2 N/mm^2	4,6 N/mm^2	4,6 N/mm^2
Siliceux	3,6 N/mm^2	3,8 N/mm^2	3,8 N/mm^2	3,6 N/mm^2

On peut observer un meilleur comportement général du béton à base d'agrégat calcaire.

Il faut néanmoins tenir compte du fait que la forme de l'agrégat pourrait avoir influencé le résultat: l'un étant concassé (celui calcaire), l'autre naturel, de fleuve (celui siliceux).

4.5 Déformation élastique

Le Tableau 2 regroupe les modules d'élasticité secants longitudinales, face à une contrainte de compression maximale de 25 N/mm^2.

On peut observer:

— que pour les deux bétons, E atteint sa valeur maximum à 28 jours;

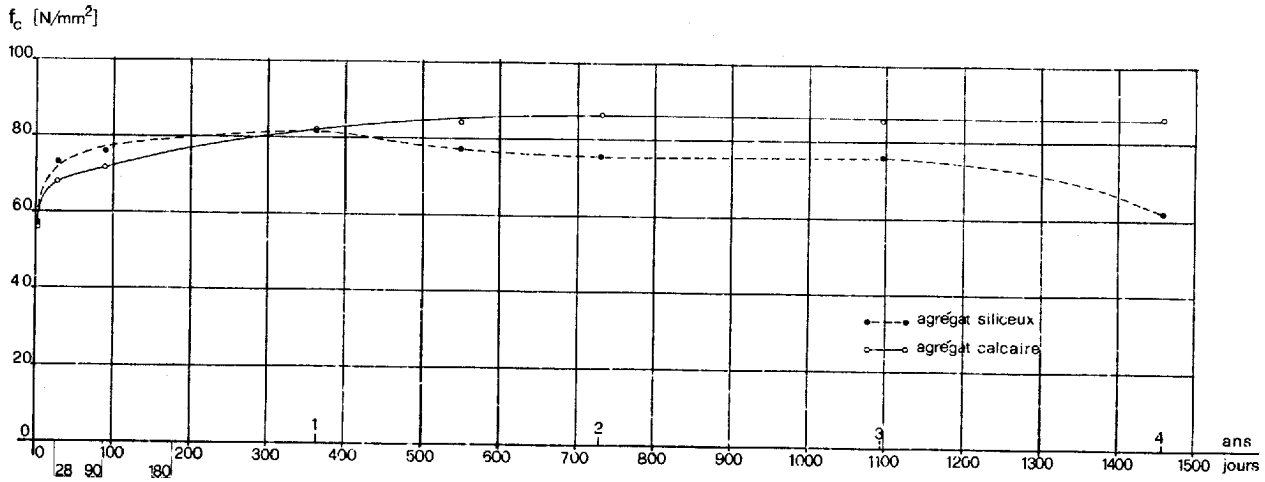

Fig. 5 - Évolution de la résistance à la compression des bétons alumineux en fonction du temps et du type d'agrégat.

— qu'à la même échéance de 28 jours, les valeurs des modules d'élasticité des deux bétons sont (avec une bonne approximation) égaux et proches de ceux que la littérature signale pour les bétons de la classe f_{ck} = 40 N/mm^2 à base de ciment Portland;

— qu'après 28 jours on enregistre une diminution du module d'élasticité, plus accentuée pour le béton à base d'agrégat siliceux (près de 33% à 4 ans) qu'elle ne l'est pour celui à base d'agrégat calcaire (près de 23% à 4 ans).

Tableau 2 - Évolution du module d'élasticité longitudinale en fonction du temps et du type d'agrégat

Module d'élasticité longitudinale E (N/mm^2)		
Âge des échantillons	Agrégat	
	Siliceux	Calcaire
7 j	30.830	32.700
28 j	33.790	33.680
92 j	32.920	31.890
180 j	28.740	28.670
1 a	22.980	27.960
4 a	22.630	25.770

5. CONCLUSIONS

D'après les données obtenues ou peut tirer les conclusions suivantes:

— la déformabilité sous charge des bétons alumineux, quelque se soit le granulat employé, est remarquable en comparaison à la déformabilité des bétons ordinaires;

— à la différence des bétons ordinaires les alumineux montrent entre 70 et 220 jours de cure un'augmentation de la vitesse de déformation sous charge;

— l'influence exercée sur les valeurs finales du fluage par l'agrégat est remarquable. En effet tandis que en présence d'agrégat siliceux le fluage à 4 ans montre des valeurs très peux dispersées, à savoir presque indépendentes de l'âge de mise en charge, en presence de granulat calcaire l'âge de mise en charge joue un rôle importante dans le sens que, lorque elle augmente, le fluage final diminue d'une façon drastique;

— l'influence exercée par l'agrégat sur l'allure des courbes de développement du fluage est elle aussi sensible. Aux courtes échéances l'augmentation de la vitesse de déformation est plus importante dans les bétons siliceux alors que en présence d'agrégat calcaire elle tend à disparaître au croître de l'âge de mise en charge;

— l'allure des courbes du fluage dans les premiers mois empêche de faire des prévisions à long terme sur la base des usuels essais à 90 jours. Les prévisions pourraient être valable seulement dans le cas d'un béton alumineux avec agrégat calcaire mise en charge après 180 jours de cure. En tout cas il nous semble qu'avec les bétons alumineux les données de fluage puissent être extrapolées seulement à partir d'environ 10 mois après démoulage;

— l'effet positif de l'utilisation d'un granulat calcaire en substitution du siliceux est confirmé par l'évolution dans le temps des résistances mécaniques.

6. BIBLIOGRAPHIE

(1) V. MATIC, «*Influence de l'âge sur le béton de ciment alumineux*», Bulletin RILEM, N. 6, pp. 33-38, Mars 1960.

(2) D.C. TEYCHENNÉ, «*Long-term research into the characteristics of high alumina cement concrete*», Magazine of Concrete Research, Vol. 27, N. 91, pp. 78-102, June 1975.

(3) C.M. GEORGE, «*Ciments alumineux. Une synthèse des recents publications (1974-1979)*», VII Cong. Int. Chimie des Ciments, Vol. I, V-1/3-1/26, Paris 1980.

(4) A. NEGRO, L. CUSSINO, A. BACHIORRINI, «*Sur l'hydratation de l'aluminate monocalcique en presence de quartz et de carbonate de calcium*», Il Cemento, N. 3, pp. 285-302, Luglio-Settembre 1978.

(5) L. CUSSINO, A. NEGRO, «*Hyaratation du ciment alumineux en présence d'agrégat siliceux et calcaire*», VII Cong. Int. Chimie des Ciments, Voi. III, V-62-67, Paris 1980.

(6) M.F. HAKIM, «*Étude de l'hydratation du ciment alumineux associé à des granulats calcaires, consequences sur les propriétés mécaniques*», Thèse INSA, Toulouse 1984.

(7) W.H. GLANVILLE, F.G. THOMAS, «*Studies in reinforced concrete - IV: Further investigations on creep or flow of concrete under load*», Dept. Scientific and Industrial Research, Building Research Technical Paper N. 21, 44 pp., London 1939.

(8) W.H. GLANVILLE, «*Studies in reinforced concrete - III: The creep or flow of concrete under load*», Dept. Scientific and Industrial Research, Building Research Technical Paper N. 12, 39 pp., London 1930.

(9) R.N. SWAMI, A.B. IBRAHIM, K.L. ANAND, «*The strength and deformation characteristics of high early strength structural concrete*», Materiaux et Constructions, Vol. 8, N. 48, pp. 413-423, Novembre-Décembre 1975.

(10) A.M. NEVILLE, «*Creep of concrete: plain, reinforced and prestressed*», North-Holland, pp. 622, Amsterdam 1970.

(11) A.R. CUSENS, N. JACKSON, «*Flexural behaviour of higly converted prestressed high-alumina cement concrete*», Magazine of Concrete Research, Vol. 27, N. 91, pp. 103-110, June 1975.

(12) A. NEVILLE, «*High-alumina cement - A current review*», Il Cemento, N. 3, pp. 291-301, Luglio-Settembre 1978.

(13) F. INDELICATO, «*Fluage a breve e medio termine di calcestruzzi confezionati con cemento alluminoso*», Seminaire International sur les Aluminates de Calcium, pp. 231-240, Turin 14-16 Septembre 1982.

(14) F. INDELICATO, «*Bétons à base de ciment alumineux - étude de la déformabilité*», Colloque International Liaisons Pâtes de Ciment - Materiaux Associés, Toulouse 17-19 Novembre 1982.

(15) C.E.B., «*Manuel de calcul: Effets structuraux du fluage et des déformations différées*», Bulletin N. 136, Budapest, Juin 1980.

J.R.L. Dyczek and M.Petri Mining and Metallurgy Academy - Poland

MECHANICAL PROPERTIES OF AUTOCLAVED, MONOMINERAL MATERIALS FROM TOBERMORITE, XONOTLITE AND HILLEBRANDITE.

CL

1. Preparation of the samples.

Semi - dry mixtures of calcium hydroxide and finely ground silica gel were condensed by pressing forming beams 10 x 10 x 60 mm and autoclaved under saturated steam pressure after 24 hrs of autoclaving at 180°C. It was found thet samples with the molar ratio CaO/SiO_2 = 5 : 6 with the addition of 0,5 % Al_2O_3 contain only crystalline 11 Å tobermorite. Samples with the ratio CaO/SiO_2 = 1 : 1 - contain xonotlite, and those with the ratio CaO/SiO_2 = 2 : 1 -contain hillebrandite, after autoclaving for 24 hrs at 240°C.

2. Bending strength and Young's modulus, calculation of the coefficient of the pore shapes.

Young's modulus /E/ and the bending strength /R_b/ of each samples were measured. Particular series of samples from tobermorite, xonotlite and hillebrandite /To, X, H/ were formed at different pressure. Thanks to this in each series the samples had different porosity. The results are shown in Fig.1.

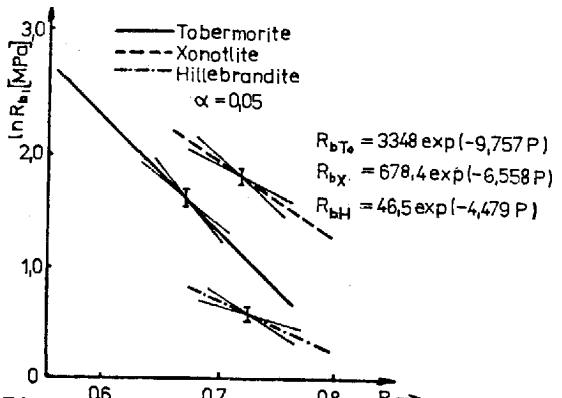

Fig.1. Strength of the examined samples as a function of their porosity

The given fuctions were derived basing on the results of bending tests of 34 samples, the total porosities of which were within the interval 0,762 - 0,546 for tobermorite, bending tests of 36 samples with the porosity from 0,793 to 0,663 for xonotlite and of 30 samples of hillebrandite with the total porosity from 0,797 to 0,678.
The porosity has been given as the volume fraction.

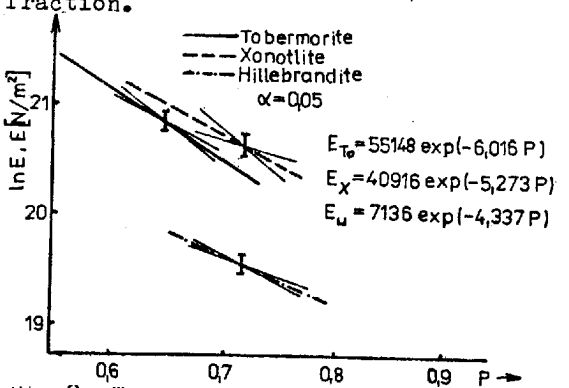

Fig.2. The dependence of Young's modulus on porosity for the exeminated samples.

The general form of the derived equations describing Young's modulus as a function of porosity : $E = E_o \exp(-b_E P)$ /Hashin 1962/ contains the empirical constant b_E, which for different materials may assume values from 2 up to from ten to twenty. It is believed that this constant corresponds to the concentration coefficient of stresses induced around the pores under the influence of the applied external stress. For pores of spheroidal form arranged in the material of the matrix in such a way that the longer axis of the spheroid in two extreme cares in perpendicular or parallel to the direction of stresses, the highest concentration of stresses occurs on the greatest curvature of those pores, the arrangement of which is much that the longer axis of the spheroid is approximately perpendicular to the direction of the tensile stress. Thus these pores will determine the value of the stress concentration coefficient K. The K value for varying ratio of the spheroid axis a/c can be described by a hyperbolic equation :

$$K = \frac{5}{4} \frac{a}{c} + \frac{3}{4}$$

Assuming after Rossi /1968/ that $K = b_E$, the equation explaining the dependence of Young's modulus on porosity will asume the form :

$$E = E_o \exp\left[-\left(\frac{5}{4}\frac{a}{c} + \frac{3}{4}\right)P\right] \qquad /1/$$

In a material containing spherical pores /a/c = 1/, the value of the concentration coefficient of stresses in the matrix $K = b_E = 2$. Higher values of b_E are an evidence of the presence of pores of non - spherical form. Basing on the derived values of b_E /equations from Fig. 2; b_E for tobermorite : 6,0158, b_E for xonotlite : 5,2732, b_E for hillebrandite 4,3369/ - the hypothetical mean ratio of the a/c axis was determined, assuming a spheroidal form of the pores. For the hydrated calcium silicates this ratio was as follows : for tobermorite-4,212, for xonotlite- 3,618, for hillebrandite - 2,869.
The above, derived values of the ratio of the axes of spheroidal pores were confronted with the values calculated by the method proposed by Carniglia /1972/ according to his equation :

$$\log\frac{\sigma}{\sigma_o} = \left(\frac{-b_E P}{4{,}606} - \frac{1}{2}\log\frac{1}{1-P}\right) + S\log\left(\frac{\frac{1}{P^{1/3}} - \frac{11}{16} - \frac{P^{\frac{1}{3}}}{8} - \frac{3P^{\frac{4}{3}}}{16}}{P^{-\frac{1}{3}} - 1}\right) \qquad /2/$$

where : S - shape coefficient of the pores /its value increases with increasing asymetry of the pores/; σ - bending strength; σ_0 - strength at zero porosity /value obtained by extrapolation/; b_E and P - as before /b_E - empirical index exponent as in Fig.2., P - volume fraction of pores/.
In E_g /2/ the effect both of the change in the cross - section area transferring the load /1 st member of the right - hand side of the equation[x]/ and the stress concentration around the pores /the total equation[xx]/ on the strength of the materials have been taken into consideration.
To determine the coefficient S in E_g /2/ the dependence $\log \sigma/\sigma_0 = f/P/$ for different values of S has been plotted as the model curves.
The curve of the anologous function obtained experimentally has been compared with this model.
The course of these dependences is asown in Fig.3 for tobermorite. The derived values of S are as follows : tobermorite $\simeq$ 7 ; xonotlite $\simeq$ 4; hillebrandite $\simeq$ 1,5.

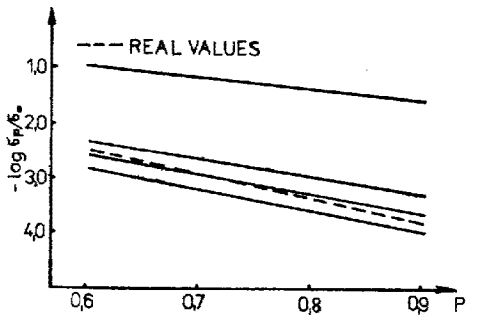

Fig.3. Function $\sigma = f/P/$ according to Carniglia equation for the tobermorite samples.

3. Determination of the critical stress concentration coefficient K_{IC} and the effective fracture energy γ_F for To, X and H.

K_{IC} and γ_F was determined in a three-points bending test of samples notched to different depth under conditions of controlled propagation of the fracture.
Mean measurement values for samples with selected different porosity are put together in Table 1.

Table 1. K_{IC} and γ_F obtained for To,X and H

Material	Porosity	K_{IC} $\left[\frac{MN}{m^{3/2}}\right]$	γ_F $\left[\frac{J}{m^2}\right]$
Tobermorite	0,715	0,120	1,093
	0,669	0,174	4,838
	0,622	0,240	4,231
Xonotlite	0,757	0,179	2,770
	0,721	0,271	5,670
	0,687	0,391	5,568
Hillebrandite	0,739	0,153	4,272
	0,697	0,165	5,448
	0,654	0,238	8,927

4. Discussion of the results and conclusions.

As it should be expected, with increasing volume fraction of pores the mechanical properties of To, X and H samples undergo deterioration. The rate of these changes for the particular minerals is defferent, the differences being possibly due to their different texture. Tobermorite crystallizes in the form of plates with the result that the pores between the grains assume elongated forms / a/c/= 4,212; S $\simeq$ 7/. The asymmetry of pores occurring in materials from X and H, crystallizing in needle-shoped form is smaller /X : a/c = 3,618; S $\simeq$ 4 ; H : a/c = 2,869, S = 1,5/.
In case of all examined materials the values of S are greater than 1. When analyzing the cracking process in these materials the stress concentration around the pores should be taken into consideration. Materials built of needle - like crystals /X, H/ are characterized by relatively greater values of the fracture energy γ_F and of the stress concentration coefficient K_{IC} than materials from tobermorite, althongh their bending strength and Young's modulus at small porosity are smaller than those of the corresponding tobermorite samples.
On the stress - strain curve for xonotlite samples the range of pseudoplastic deformations has been observed, what has already been reported by the authors /Dyczek, Petri 1974/.
Basing on the obtained results it can be assumed that materials from X and H of needle like crystallites reveal greater ability to absorb energy in the cracking process. This refers in particular to xonotlite, provided the process of its formation is not accompanied by the formation of microcracks.

---

x/ corresponding to the curve in Fig.3 denoted as P II

xx/ corresponding to curves in Fig.3 denoted as P I /for S > 0/

References :

1. Z.Hashin, J.Appl.Mech. 29, 1 /1962/
2. R.C.Rossi, J.Amer.Ceram.Soc. 51,8 /1968/
3. S.C.Carniglia, J.Amer.Ceram.Soc. 55,12 /1972/
4. J.Dyczek and M.Petri,"6 Int.Symp.Chem. Cem." Proc.Moscow/1974/

O.Z. CEBECI, W.H. MIRZA and S.I. AL-NOURY- Department of Civil Engineering, King, abdulaziz University Jeddah, Saudi Arabia

CL

STRENGTH DEVELOPMENT OF MORTARS IN HOT AND DRY ENVIRONMENT

INTRODUCTION

Masonry mortars are made by mixing, in certain proportions, one or more types of cement with clean, well-graded sand, and sufficient water is added to produce a plastic, workable mixture. When hardened, mortars must possess adequate strength, durability, and volume stability. Although Portland cement is capable of developing high compressive strength, its fresh mortars, made without plasticizers, lack the desired workability. Therefore, lime is commonly added to cement mortars in order to achieve adequate plasticity (1,2).

While Portland cement must be kept saturated to improve hydration and strength development, lime gains strength primarily by evaporation of the mixing water. Naturally, the ambient temperature and relative humidity at construction sites show considerable variations with climatic and seasonal changes. Although high temperature and low humidity are detrimental for the strength ultimately developed in Portland cement paste, mortar and concrete (3,4), cement-lime mortars may behave differently under these adverse conditions (5).

In this work the strength development in a cement and a high-lime mortar under hot and dry environmental conditions was investigated. The test specimens were made at 20, 35, and 50 C, and were cured at these temperatures in lime saturated water, and 92%, 75%, and 33% relative humidity. The compressive strengths of the mortars (developed in these 12 different media of various temparature-humidity combinations covering the range of common normal and hot weather conditions) were determined.

MATERIALS, TESTS AND RESULTS

A commercial ordinary Portland cement and hydrated lime and a local natural sand, all conforming to standard specifications, and tap water were used for preparing the mortars. The proportions of the solid constituents of masonry mortars are conventionally specified by volume (1); however, weight proportions were adopted in this study, so that the mixes were accurately reproduced in the laboratory. The amount of mixing water for each type of mortar was determined by the standard (ASTM C 109) flow table test, and fixed such that the mixes at different temperatures produced flows in the range 100-110%, thereby, all being at normal consistency. The mix proportions are shown in Table 1. It should be noted that Type O is essentially the "high-lime, low-strength" mortar specified by the same designation in some standards (1).

Table 1. Mix proportions of the mortars

Mortar Designation	Proportions, by weight Cement	Lime	Sand	Water
Type C	1	-	3	0.65
Type O	1	0.8	7.5	1.7

The mortars were mixed and cast in 40x40x160mm molds according to the ISO-RILEM Recommendation R679. The mixer, materials and the molds were kept at 20, 35 and 50 C, and the specimens were stored at these temperatures in humid cabinets for 24 hours. After demolding, some specimens were crushed in order to determine the 1-day strength, others were placed in water baths at 20, 35 and 50 C, or stored in 9 different cabinets at these temperatures and at 92%, 75%, and 33% relative humidity (RH) maintained above saturated salt solutions (6).

The strength development in the cement mortar (designated as Type C) and in the high-lime mortar (designated as Type O) upon curing under various conditions up to 28 days are shown in Fig. 1 and 2, respectively. The specimens were brought to room temperature and crushed at their respective moisture conditions. It should be noted that specimens dried prior to crushing indicate greater strength than similar ones of the same batch tested in the saturated condition (7).

DISCUSSION

The effect of elevated temperature on the compressive strength of Portland cement mortar is demonstrated in Fig. 1(a). It is confirmed that, with increasing curing temperature, the early strength increases at the expense of the ultimate strength. Similar data has been reported in the recent literature (8,9), but Fig. 1(b)-(d) reveal important findings: Regardless of the curing temperature, strength development in 92% RH is about the same as that in water, and strength gain practically ceases within 28 days when the RH is reduced to 33%. At 50 C, the effect of 75% RH is almost as detrimental as 33%, whereas at lower temperatures 75% RH reduces, but does not stop, the strength development.

Fig. 1(a) also shows that the cement mortar (Type C) is much stronger than the high-lime mortar because partial replacement of the Portland cement with lime and increased proportions of sand and water in the latter substantially reduce its compressive strength (1,2).

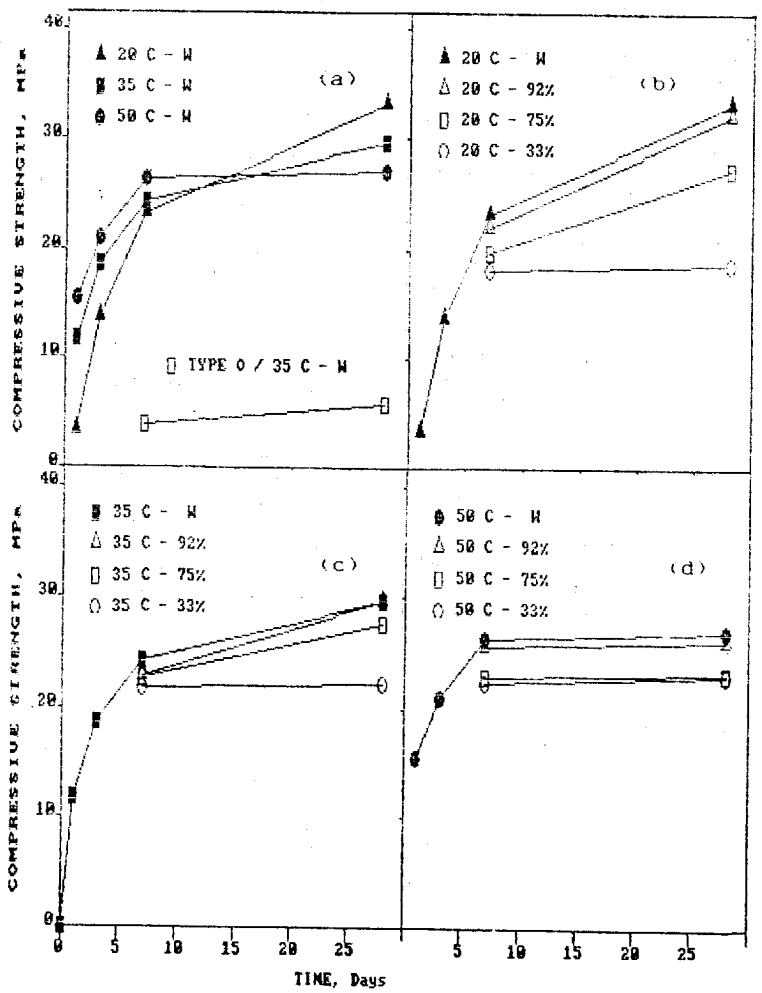

Figure 1- Compressive strength of Portland cement mortars developed under various curing conditions

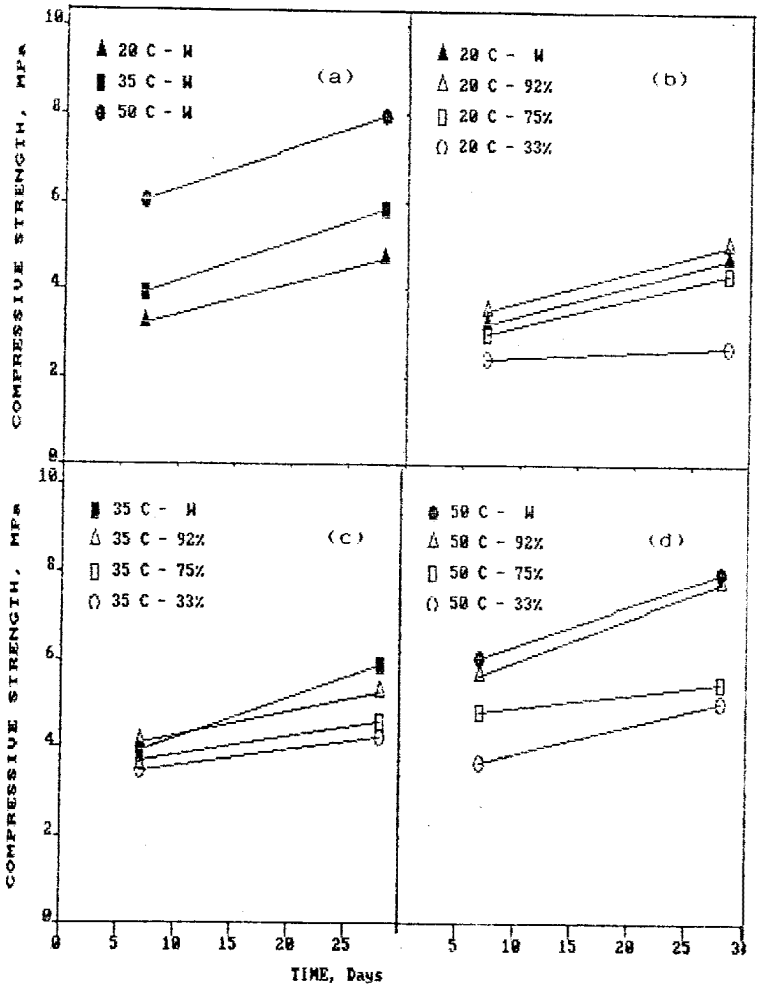

Figure 2- Compressive strength of high-lime mortar developed under various curing conditions

The compressive strength of high-lime mortar increases with increasing temperature throughout 28 days of wet curing, as shown in Fig. 2(a). A similar trend has been observed by Dalziel (8), who investigated the effect of curing temperature on the development of strength of mortar containing fly ash.

From 7 to 28 days, the strength gain in 33% RH is very small at 20 C, while at 35 C, and particularly at 50 C the improvements in the compressive strength achieved in the dry media are not negligible.

The differences between the behavior of cement and high-lime mortars should not imply that the high-lime mortar, a favorite of masons because of its excellent workability and economical cost, may also be the favorite in hot and dry environment, since dry-cured specimens attain about 60-70% of the strength of wet-cured ones.

In 20 C, high-lime mortars cured in 92% RH show slightly more strength than those cured in water, probably due to the effect of the moisture condition of the specimen on the observed strength (Fig. 2(b)). This holds also for the 7-day test results at 35 C (Fig. 2(c)).

CONCLUSION

The present investigation has shown that increasing temperature and decreasing relative humidity influence Portland cement and cement-lime mortars differently.

At normal and high temperature, dry environment is detrimental for the compressive strength of cement mortar. At elevated temperature, prolonged wet curing does not substantially improve the strength whereas at 20 C, it increases the 28-day compressive strength of the specimens almost twice as much as that of the dry-cured ones.

The strength of high-lime mortar increases with increasing temperature and humidity of the curimg media.

ACKNOWLEDGEMENT

This paper is based upon work supported by SANCST, the Saudi Arabian National Center for Science and Technology, under Grant No. AR6-077

REFERENCES

1. F.A. RANDALL, Jr., and W.C. PANARESE (1976), "Concrete masonry handbook", Portland Cement Association, Skokie.

2. C. BEALL (1984), "Masonry design and detailing", Prentice-Hall, Inc., Englewood Cliff.

3. F.M. LEA (1970), "The chemistry of cement and concrete, 3rd ed.", Edward Arnold Publishers Ltd., London.

4. G.J. VERBECK and R.H. HELMUTH (1968), "Structures and physical properties of cement paste", Proc. Fifth Int. Symp. Chem. of Cement, Tokyo, Vol. III, pp. 1-32.

5. W.H. MIRZA and S.I. AL-NOURY (1985), "Mortar in an adverse climate", Concrete International, 7(8)56-59.

6. D.S. CARR and B.L. HARRIS (1949), "Solutions for maintaining constant relative humidity", Ind. Eng. Chem. 41(9)2014-2015.

7. P. BARNES, Ed. (1983), "Structure and performance of cements", Applied Science Publishers, London.

8. J.A. DALZIEL (1980), "The effect of curing temperature on the development of strength of mortar containing fly ash", Proc. Seventh Internat. Conf. Chemistry of Cement, Paris, Vol. III, pp. IV-93-97.

9. N.J. CARINO and H.S. LEW (1983), "Temperature effects on strength-maturity relations of mortar", J. Amer. Concr. Inst., 80,177-182.

K. S. Han and J. Rhee, Professor, Inha University, Inchon, Korea.

Studies on the synthesis of C_3A by Sol-gel process

INTRODUCTION

Nowadays the sol-gel process for preparation of inorganic materials is applying extensively to obtain fibers, coatings and films, porous solids, nuclear fuels and oxide powders (1-3).

In the synthesis of inorganic materials by the sol-gel process, the raw materials are mixed in solution state and reacted lower temperature, and then drying and sintering process of the product are followed. By using this method, one can save energy and obtain highly pure and homogeneous materials.

Therefore, it has many advantages over the conventional method in which solid powder mixture is sintered or melted. In spite of many apparent advantages of the sol-gel process, it has some disadvantages of high cost of raw materials, large shrinkage during processing, residual fine pores, residual hydroxyl and long processing time (3,4).

The C_3A, one of the cement compounds, could be obtain by sintering an oxide powder mixture of C_3A composition at 1365°C for many hours with intermediate grinding, in this study, however, C_3A was synthesized by applying the sol-gel process using aluminium-sec-butoxide as alumina source and calcium nitrate as calcium oxide source.

Hydrolyzation conditions of Al-sec-butoxide and peptizing and gelling conditions for the mixture of hydrolyzed precipitate from the Al-sec-butoxide and the calcium nitrate were examined. And also, the optimum heating conditions for the synthesis of C_3A were investigated carefully. Heat treatment in the air and in the atmosphere of the oxygen-free dried nitrogen were respectively performed to study $C_{12}A_7$ which was produced unexceptionally in the early stage of synthesizing reaction of C_3A.

Besides, C_3A obtained by the conventional method was compared with C_3A from sol-gel method in terms of their reactivity of formation and crystallinity each other.

EXPERIMENTAL

Reagent grade Al-sec-butoxide, $Al(O\text{-}sec\text{-}C_4H_9)_3$, and calcium nitrate, $Ca(NO_3)_2 \cdot 4H_2O$ were used for the study.

Because the Al-sec-butoxide hydrolyze easily even with the moisture in the air to form aluminium hydroxide, the stoichiometric procedure was performed in the glove chamber under the dry nitrogen gas atmosphere.

Yoldas reported that hydrolyzing of Al-sec-butoxide and peptizing of the precipitate was affected considerably by the temperature of hydrolyzing water (5). Consequently, the hydrolysis was done by introducing the alkoxide into 200 fold mole of hot water (85°C) alkoxide under vigorous stirring on the hot plate keeping 90°C for 15 min.. After dispersion of the precipitate the calculated amount of calcium nitrate for C_3A synthesis was dissolved in the solution.

Different amount of HCl in 0.1 N solution, from 0.01 to 0.2 fold mole per mole of $Al(O\text{-}sec\text{-}C_4H_9)_3$, was added and stirred briskly for peptizing and gelling of the mixed solution at 90°C.
The completion of gelling was identified by finding the dispersion of the precipitate and stagnation of bubbles in the solution. The gelled sample was dried at 110°C.

On the other hand, a powder sample for C_3A was prepared by calcining the mixture of $CaCO_3$ and Al_2O_3 with ratio of 3:1 at 1000°C for comparison with sol-gel sample.

The effect of heat treatment on the formation of C_3A was investigated for the dried sol-gel sample and the oxide mixture sample. Both samples were heat-treated at 1100, 1200, 1300 and 1400 °C in the air and in the atmosphere of oxygen-free dried nitrogen respectively. Five times of 10 hours heating at 1100 and 1200 °C were carried out for each sample, but when sintered at 1300 and 1400 °C, 10 hours heating was repeated to complete the formation of C_3A.

Reactivity of C_3A formation was examined quantitatively by X-ray diffraction analysis and represented as the ratio of the amount of $C_{12}A_7$ to C_3A produced during the heat treatment.

Crystallized C_3A size was calculated by Scherrer equation for X-ray diffraction profiles.

The heat evolved by hydration reaction of C_3A in 18 hrs measured by the multicell conduction calorimeter.

RESULTS AND DISCUSSION

When hot water of 85°C was used for the hydrolysis of Al-sec-butoxide, AlO(OH), boemite, was produced and the peptizing and gelling for the mixed solution was performed.

The relation between gelling time of the mixed solution and the amount of HCl added per mole of $Al(O\text{-}sec\text{-}C_4H_9)_3$ was shown in Fig. 1. When more than 0.1 fold mole of HCl was added, the gelling was rapidly occured within 3 hours, but it was not occured when added less than 0.03 fold mole of HCl. Although quite slow gelling was performed by adding 0.05 to 0.08 fold mole of HCl, the enhanced reactivity of C_3A formation was found when gelling for longer time. It was supposed to be caused by high homogeneity of components through longer time. Hence the peptizing and gelling was proceeded by using 0.05 fold mole of HCl at 90°C in this study.

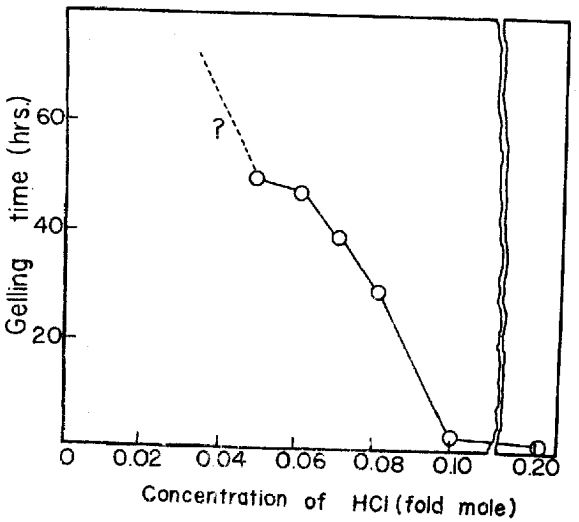

Fig. 1 Gelling time for the mixture solution of AlO(OH) and $Ca(NO_3)_2 \cdot 4H_2O$ with various amount of HCl per mole of $Al(O\text{-}sec\text{-}C_4H_9)_3$.

When the sol-gel sample was heated in the air, $C_{12}A_7$ was started to form after heating at 600°C for 1 hour, and C_3A was appeared after heating at 1000°C for 30 hours. When the oxide mixture sample was sintered in the air, on the other hand, $C_{12}A_7$ and C_3A were started to form after heating at 1000°C for 10 hours and at 1100°C for 10 hours, respectively.

As shown in Fig. 2 and Fig. 3, initial formation of $C_{12}A_7$ from the sol-gel sample heated at 1100 and

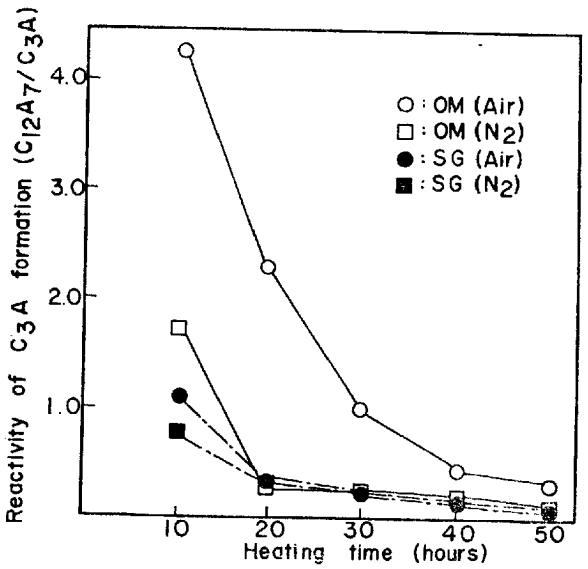

Fig.2 Reactivity of C_3A formation with various heating time at 1100°C.

*SG: Sol-gel sample dried at 110°C.
OM: Oxide mixture sample heat treated at 1000°C for 1 hr.

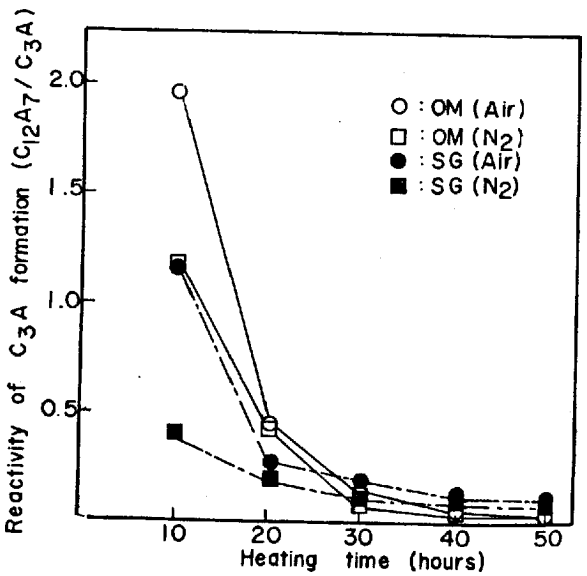

Fig.3 Reactivity of C_3A formation with various heating time at 1200°C.

1200 °C was much better than that of the oxide mixture sample. It is believed that superior reactivity of the sol-gel sample is due to minified fineness and high homogeneity of reacting particles. J. A. Imlach and F. P. Glasser refered that traces of water undoubtedly hasten the formation of $C_{12}A_7$

and the water may act as a catalyst (6).

Furthermore, the oxide mixture sample heated in an atmosphere of oxygen-free dried nitrogen exhibited around the same reactivity with the sol-gel sample heated in the air. It was supposed that $C_{12}A_7$ from the oxide mixture sample was reacted normally to form C_3A without any interrupting of contact to water during heat treatment.

Fig. 4 and Fig. 5 showed that the reactivity of C_3A formation from the oxide mixture sample was superior at 1300 and 1400°C than that from the sol-gel sample. In particular, the reactivity under the atmosphere of oxygen-free dried nitrogen was remarkable.

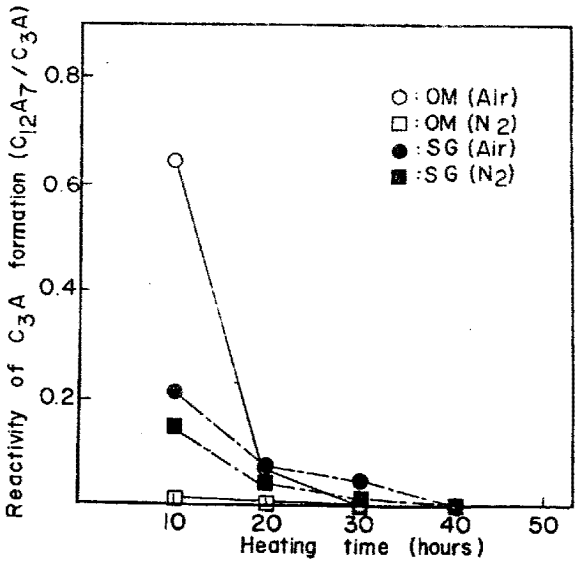

Fig.4 Reactivity of C_3A formation with various heating time at 1300°C.

In the initial heating stage of forming C_3A from the reacting of CaO and Al_2O_3 , $C_{12}A_7$ was inevitably formed as a intermediate product. $C_{12}A_7$ has zeolitic behavior (7) and in the temperature range of 950-1350 °C, it enters into reversible equilibrium with water present in furnace atmosphere and the constitution of the phase is described as $C_{12}A_{14}O_{32}(OH)_2$ (8).

The sol-gel sample showed superior reactivity with initial formation of $C_{12}A_7$ at 600°C and C_3A at 1000°C, but the effect of reactivity to lower $C_{12}A_7/C_3A$ ratio to less than 0.4 was inferior when it was heated repeatedly at lower temperature

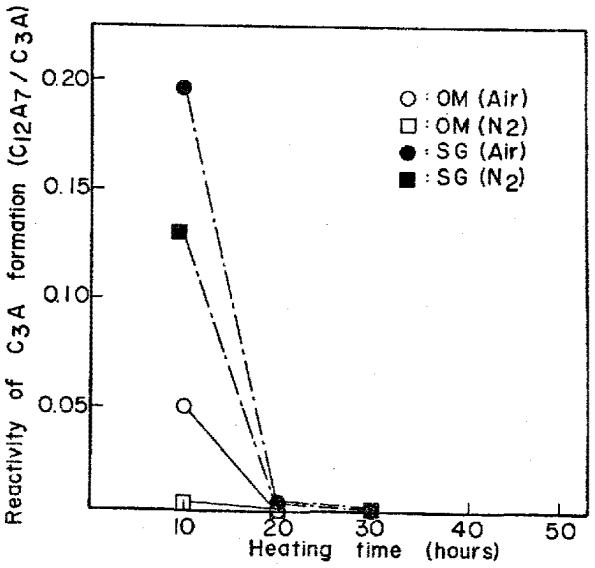

Fig.5 Reactivity of C_3A formation with various heating time at 1400°C.

(1100, 1200°C) and heated at higher temperature (1300, 1400°C). C_3A is formed by diffusion of CaO to $C_{12}A_7$, but the C_3A formation might be prevented when $C_{12}A_7$ become stable by incorporating OH group.

Heating in an atmosphere of oxygen-free dried nitrogen could not eliminate the trouble-some OH group in the stable $C_{12}A_7$ phase. Since the oxide mixture sample could produce $C_{12}A_7$ without OH group, on the contrary, it was presumed to have remarkable effect for formation of C_3A.

Crystallized particle size of C_3A formed by sol-gel and conventional method were both in the range of 63-70 nm.

Since the heat evolved in 18 hours by hydration of C_3A obtained from two different method were in the range of 140-145 cal/gr, the hydration characteristics of them seemed to be almost the same.

CONCLUSION

AlO(OH) was formed from Al-sec-butoxide through hydrolysis with hot water of 85°C.

The gelling process of the mixture solution of AlO(OH) precipitate and $Ca(NO_3)_2 \cdot 4H_2O$ proceeded most favorably when 0.05 fold mole of HCl was added to one mole of Al-sec-butoxide.

Initial formation of $C_{12}A_7$ and C_3A at lower temperature (1100, 1200°C) from sol-gel sample was superior, but complete crystallization of C_3A at higher temperature (1300, 1400°C) was inferior as compared with that from oxide mixture sample.

The formation reactivity of C_3A in an atmosphere of oxygen-free dried nitrogen from oxide mixture sample showed remarkable effect.

The crystallized size and the hydration characteristics of C_3A obtained by different process exhibited around the same results.

The kinetics of this progress will be more fully described in a subsequent paper.

REFERENCES

1) Sumio sakka, K. Kamiya, "Glasses from metal alcoholates", Jour. of Non-Crystalline Solids, Vol. 42, 403-422 (1980).

2) Helmut Dislich, "Glassy and crystalline systems from gels : Chemical basis and technical application", Jour. of Non-Crystalline Solids, Vol. 57, 371-388 (1983).

3) Larry L. Hench and Donald R. Vlrich, "Ultrastructure processing of ceramics, glasses and composites", John Wiley and Sons, New York, pp 15-26 (1984).

4) J. D. Mackenzie, "Glasses from melts and glasses from gels", Jour. of Non-Crystalline Solids, Vol. 48, 1-10 (1982).

5) B. E. Yoldas, "Alumina sol preparation from alkoxides", Amer. Ceram. Soc. Bull., Vol. 54, 289-290 (1975).

6) J. A. Imlach, L. S. Dent Glasser, F. P. Glasser, "Excess oxygen and the stability of $C_{12}A_7$", Cem. and Conc. Res., Vol. 1, 57-61 (1971).

7) D. M. Roy and R. Roy, "Crystalline solubility and zeolitic behavior in garnet phases in the system $CaO-Al_2O_3-SiO_2-H_2O$", Chemistry of Cement, Proc. 4th. Intl. Symp., Washington 1960, National Bureau of Standards, Vol. 1, 307-314 (1962).

8) R. W. Nurse, J. H. Welch and A. J. Majumdar, "The $12CaO \cdot 7Al_2O_3$ phase in the $CaO-Al_2O_3$ system", Trans. Brit. Ceram. Soc., 323-332 (1965).

I.Y. SEO - Research Center of Ssang yong Cement Ind. Co., Ltd.
S.H. CHOI - University, Seoul, Korea

THE UNSTABLE STATE OF ALKALI IN CEMENT CLINKER

Introduction

Though alkalies are minor components of cement clinkers, there have been many researches about them in view point of the significance of their influences on clinker phases and hydration reactions of cement, as well as the alkali-aggregate reaction. However, some conflicting phenomena still occur in empirical data. These may be partially due to the versatile formation reactions of their compounds and their complex behaviors in hydration of cement.

In the previous research[1,2], investigating the existing states of potassium in portland cement clinker, the new concept of alkali, given a name as unstable alkali, was introduced. It was found that the unstable alkalies exist when SO_3 content is below a certain limit, related mainly to alkali content in the clinker. The unstable alkalies, which are readily sloubie with water, react with gypsum to form $Ca(OH)_2$ and syngenite on hydration. As a result, the heat liberation rate of hydration at the early hydration process (first peak) increases remarkably, and the reaction cannot be controlled only by the supplement of gypsum to the cement. A increasing tendency of ignition loss of clinker with increase of unstable alkali content was found.

In this paper, the formation mechanism of the unstable alkalies and their forms occuring in clinker were studied.

Experimental

The raw mixtures added various amount of KOH to the mixture of OPC clinker composition not containing potassium and sulfur were prepared, and they were shaped into pellet-and tablet-types and sintered at 1400° and 1450°X for 30 min. after calcination at 900°C for 1 hr. respectively (P-series). Tablet-type samples were prepared by pressing the calcined raw mixtures. The clinkers were vacuum-dryed at 150°C after measurements of porosity by kerosene (Sp. Gr. : 0.796 at 20°C), and the content of alkalies and water-soluble components of the clinkers were analysed. Also the distributions of potassium and other elements at various parts of the clinkers were analysed by means of SEM-EDX system.

In order to elucidate the fact that the K_2O-Al_2O_3 compounds are some forms of unstable alkalies, the lime-saturated C_3A-K_2O system and K_2CO_3-Al_2O_3 system were examined. The lime-saturated C_3A was prepared from the raw mixture of excess CaO content from stoichiometric composition with chemical pure reagents. The mixture was calcinated at 1000°C for 1 hr. and sintered at 1450°C for 12 hrs after pressing. Remixing, pressing and sintering were repeated until the free CaO content was not changed. Free CaO content of the last C_3A (sample No. K0) was 2.2%. The mixtures of various amount of K_2CO_3 addition to the C_3A were sintered at 1400°C for 1 hr. (K-series). And then K_2O content, changes of free CaO and C_3A content, and the change of lattice parameter (a) of C_3A were analysed by chemical analysis and x-ray diffraction analysis.

The mixtures of K_2CO_3 and Al_2O_3, with various molar ratios of K_2O/Al_2O_3 such as (1) 4.0, (2) 3.0, (3) 2.0; (4) 1.5, (5) 1.2, (6) 1.0 (sample No. : C-1, C-2, C-3, C-4, C-5 and C-6 respectively), were calcined at 600°C and sintered at 1100°C for 20 min. (C-series). Water-soluble K_2O and Al_2O_3 of the syntered samples were analysed and their reaction products were identified by means of x-ray diffraction analysis.

Results and Discussions

1. Formation mechanism of unstable alkalies and their forms.

Fig. 1 is the SEM and characteristic x-ray image of potassium distribution of a P-series clinker with high unstable alkali content and reveals that most of potassium are apt to be concentrated at the liquid phase of clinker. It was found that ignition loss of clinker tends to increase according to unstable alkali content.[2] Volatilized alkalies and SO_3 content of a high-ignition loss clinker were analysed and are listed in table 1. It appears from the result that unstable alkalies have a hygroscopic and easily volatile properties. Fig. 2 shows the correlationships of K_2O content vs. Al_2O_3, Fe_2O_3, CaO and SiO_2 content analysed by EDX at various parts of P-series clinkers. In the results, K_2O content has a positive correlationship only with Al_2O_3 content and no relationship with Fe_2O_3 content. Moreover, water-soluble Al_2O_3 content increases with increase of water-soluble K_2O (unstable alkali

of potassium) content in P-series clinkers, which is shown in Fig. 3. Fig. 4 is the scanning election micrograph which shows potassium aluminate in a P-series clinker. The chemical composition of square part (labelled C) in the photograph was 10.5% of SiO_2, 34.0% of Al_2O_3, 0.0% of Fe_2O_3, 16.7% of CaO, 2.0% of MgO, 4.2% of Na_2O and 32.7% of K_2O.

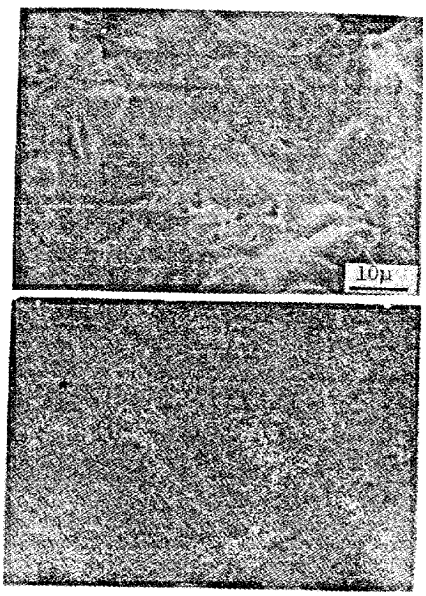

Fig. 1. Scanning electron micrograph and its K Ka-radition photograph.

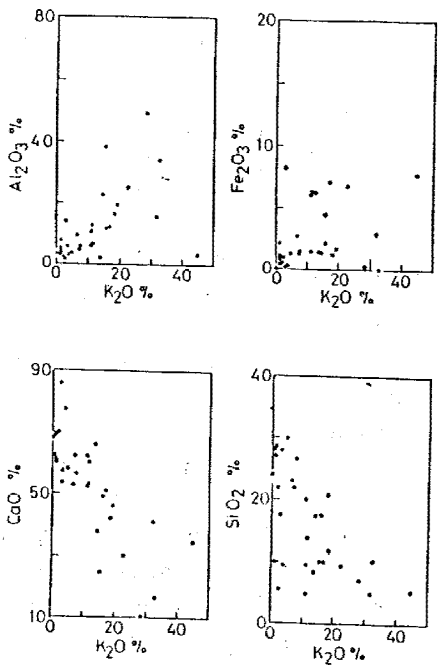

Fig. 2. K_2O content vs. Al_2O_3, Fe_2O_3, CaO and SiO_2 content of various parts of clinkers (P-series).

Fig. 5 shows that porosity of clinker tends to increase on the conditions when unstable alkali content increases. The same result can be found in the Ono's report[3], in which alkali carbonates was used for alkali sources without SO_3 addition. Equations (1), (2) and table 2 represent the results of multiple linear regression analysis about the correlation ship of alkali content and porosity of closed pore with the unstable alkali content of the P-series clinkers.

Table 1. Volatilized alkali and SO_3 content of a high-ignition loss clinker sample.

Temp. range °C	Ig.loss %	Volatilized content %			Remark
		Na_2O	K_2O	SO_3	
20 - 400	0.72	tr	tr	tr	dehydration
400 - 600	0.13	tr	0.01	tr	dehydration of $Ca(OH)_2$
600 - 900	0.46	tr	0.42	tr	volatilization of unstable K_2O

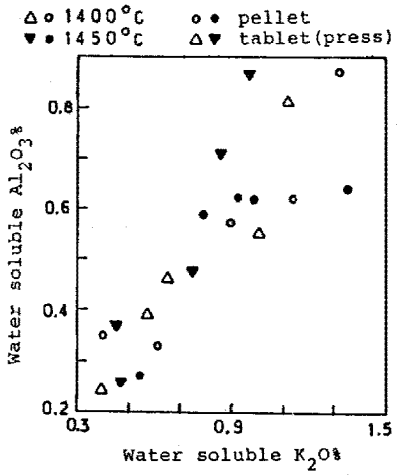

Fig. 3. Water soluble K_2O vs. water soluble Al_2O_3 content in P-series clinkers.

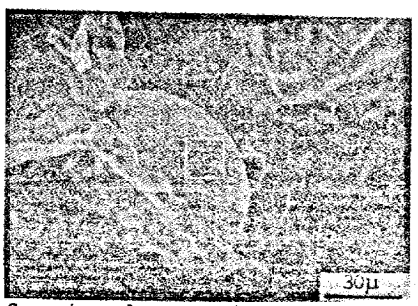

Fig. 4. Scanning electron micrograph showing the K_2O-Al_2O_3 compound formation.

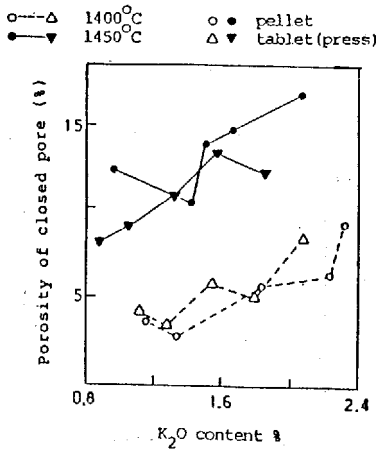

Fig. 5. Change of porosity according to K_2O content of P-series clinkers.

$$S\text{-}\overline{\overline{K}}\% = 0.630\ T\text{-}K_2O\% - 0.294 \quad \ldots\ldots\ldots\ldots\ldots\ldots \quad (1)$$

$$S\text{-}\overline{\overline{K}}\% = 0.608\ T\text{-}K_2O\% + 0.021\ CP\% - 0.437 \quad \ldots\ldots\ldots \quad (2)$$

where, $S\text{-}\overline{\overline{K}}\%$: Unstable alkali content in clinker

$T\text{-}K_2O = K_2O\% + 1.52Na_2O\%$ in clinker

CP% : porosity of closed pore in clinker

Table 2. Results of regression analysis (n=20).

No. of equation	Correlation coefficient	Error of estimate	F-value	F(0.01)
1	0.94	—	133.25**	8.29
2	0.98	0.066	200.93**	6.11

Eq. (2) has higher correlation coefficient and F-value than those of Eq. (1). That means porosity of closed pore may be one of the factors related with unstable alkali formation. Moreover, reguarding that some parts of P-series clinkers have higher K_2O content relatively to the Al_2O_3 content in Fig. 2, it is possible to presume the following explanation for the formation of another types of unstable alkalies. (Refer to Fig. 6.)

The amount of trapped alkali vapor may increase in closed pores of clinker with higher alkali and lower SO_3 content. The alkali vapor will condense on the wall of the closed pores in the cooling process and some of the alkalies will solidify and remain as free alkalies on the wall of the pores.

From the above results, it is reasonable to think that two types of unstable alkalies, compounds of K_2O-Al_2O_3 system and free K_2O, exist in cement clinkers with high alkali and low SO_3 content.

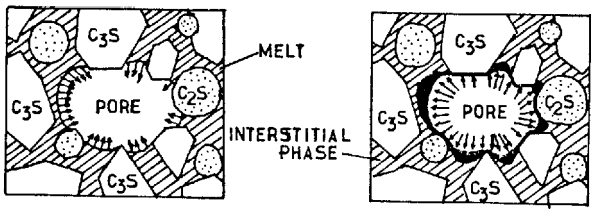

K_2O vaporization at high temperature

condensation when cooling

Fig. 6. Schematic diagram of K_2O vaporization and condensation at closed pore.

2. Compounds of K_2O-Al_2O_3 system

Fig. 7 shows x-ray diffraction patterns of K-series clinkers, and in K3.56 and K10.47 clinkers, some new peaks (marked X) come out at 32.8°, 33.7°, 34.4° and 38.7° (CuKa 2θ). The intensities of the peaks and free CaO content (37.4°) increase according to K_2O content of the clinkers. The figures of the sample names represent the K_2O content of the clinkers. It was confirmed that the new peaks disappear in the x-ray diffraction pattern of the water-extracted residue of K10.47 clinker for 30 seconds. It means that some new mineral or minerals, which are readily soluble with water, exist and the crystal system of C_3A is still cubic at K3.56 and K10.47 clinkers.

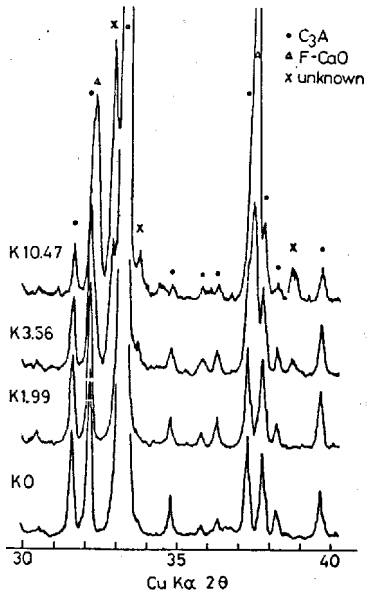

Fig. 7. Change of x-ray diffraction pattern of C_3A according to its K_2O content.

Fig. 8 shows that the lattice parameter (a) of C_3A increases slightly up to about 2.5% of K_2O content and does not change above the K_2O content.

Fig. 9 shows the change of C_3A content analysed by quantitative x-ray diffraction analysis according to the K_2O content in K-series clinkers. Up to about 2.5% of K_2O content, C_3A content is almost unchanged, however above the K_2O content, it decreases inversely with increase of K_2O content. Also the free CaO content in Fig. 10 is almost unchanged up to about 3% of K_2O content and increases linearly above the K_2O content. In K_2O-Al_2O_3 system, the compounds of $3K_2O \cdot Al_2O_3$[4], $K_2O \cdot Al_2O_3$[5], $K_2O \cdot 5Al_2O_3$[6] and $K_2O \cdot 11Al_2O_3$[7] were reported. In C_3A-K_2O system, if the above compounds are produced after sintering, the reaction equations will be same as following models, and CaO/K_2O substitutional molar ratio (m) and C_3A/K_2O molar ratio (n) of each models were calculated in table 3. Comparing the decreasing rate of C_3A content in Fig. 9, n-value equals to about 1 and corresponds to model (2) of $K_2O \cdot Al_2O_3$ formation. In Fig. 10, m-value equals to about 2 and corresponds to the value between model (1) and (2). Fig. 11 shows the x-ray diffraction patterns of K 10.47 clinker and C-series samples, and reveals that the compound $K_2O \cdot Al_2O_3$ is the major mineral in C-6 sample and most of the unknown peaks (labelled X) of K10.47 clinker correspond to the compound. However, some unknown peaks, though their intensities are very low, still remain and m-value does not correspand to model (2). Therefore, according to the composition of liquid phase of each part of clinker, other minerals of K_2O-Al_2O_3 system are thought to form simultaneously.

Model for compound formation of K_2O-Al_2O_3 system.

$$C_3A + xK \rightarrow (1-\frac{x}{3})\ C_3A + \frac{x}{3}\ K_3A + xC \quad \ldots\ldots\ldots\ldots (1)$$

$$C_3A + xK \rightarrow (1-x)\ C_3A + xKA + 3xC \quad \ldots\ldots\ldots\ldots (2)$$

$$C_3A + xK \rightarrow (1-5x)\ C_3A + xKA_5 + 15xC \quad \ldots\ldots\ldots\ldots (3)$$

$$C_3A + xK \rightarrow (1-11x)\ C_3A + xKA + 33xC \quad \ldots\ldots\ldots\ldots (4)$$

where, C = CaO, A = Al_2O_3, K = K_2O.

Table 3. CaO/K_2O substitutional molar ratio(m) and C_3A/K_2O molar ratio(n) of each models.

Model No.	m	n	Remark
1	1	-1/3	model of compound formation of K_2O-Al_2O_3 system
2	3	-1	
3	15	-5	
4	33	-11	

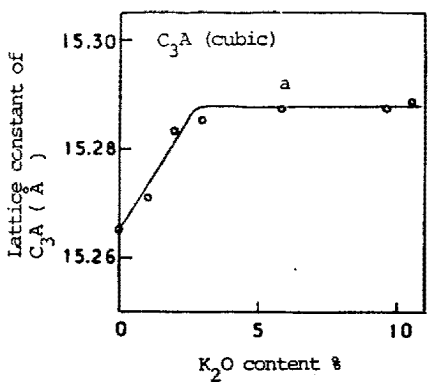

Fig. 8. Change of lattice parameter of lime-saturated C_3A according to its K_2O content.

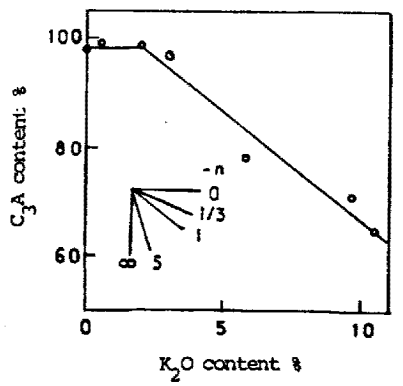

Fig. 9. Change of C_3A content of lime-saturated C_3A according to its K_2O content.

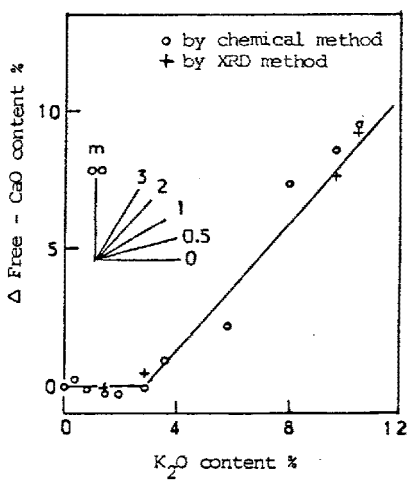

Fig. 10. Change of free-CaO content according to K_2O content of lime-saturated C_3A.

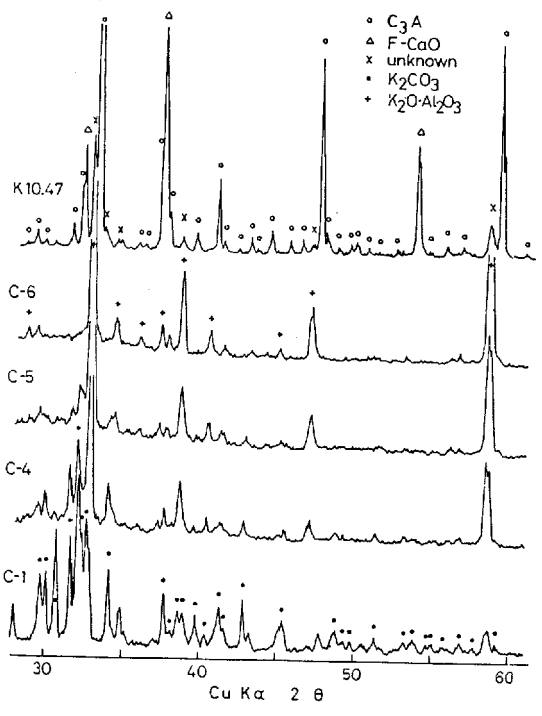

Fig. 11. X-ray diffraction patterns of K10.47 in C_3A-K_2O system and C-1, C-4, C-5 and C-6 in K_2O-Al_2O_3 system.

Conclusions

Two forms of unstable states of potassium, compounds of K_2O-Al_2O_3 system and free K_2O, exist in the clinkers of this experiment. Most of potassium are apt to be concentrated at the liquid phase of clinker and the K_2O-Al_2O_3 compounds are formed in the liquid phase concentrated by K_2O. Therefore, water-soluble Al_2O_3 content is apt to increase according to the unstable alkali content. The compound $K_2O \cdot Al_2O_3$, which was confirmed to be formed easily in the C_3A-K_2O system, is a major mineral among the K_2O-Al_2O_3 compounds. The amount of trapped alkali vapor may increase in closed pores of clinkers with higher alkali and lower SO_3 content. Free K_2O is thought to be the condensed alkali in the pores.

References

1) I.Y. Seo and S.H. Choi, "Influence of Potassium on the Cement Clinker Formation, I.Unstable Free Alkali in Clinker," J. Korean Ceram. Soc., 22 (1) 25-34 (1985).

2) I.Y. Seo and S.H. Choi, "Influence of Potassium on the Cement Clinker Formation, II Factors of Unstable Alkali Formation," ibid, 22 (2) 25-32 (1985).

3) Y. Ono, T. Hidaka and M. Shirasaka, "On the Influence of Na_2O, K_2O and MgO on the Development of Strength of Portland Cement Mortar," Rev. 23rd Gen. Mtg. Japan, 61-65 (1969)

4) ASTM card No. 27-1336.

5) Brown Miller, Am. J. Sci. 29 266 (1935) : by ASTM card No. 2-0897.

6) Yamaguchi and Suzuki, Bull. Chem. Soc. Japan, 41 93 (1968) by ASTM card No. 21-618.

7) ASTM card No. 31-960.

Vázquez, T., Blanco-Varela, M.T., Palomo-Sánchez, A.
Instituto Eduardo Torroja de la Construcción y del Cemento (C.S.I.C.) Madrid- España

LUMPING OF ANHYDROUS PORTLAND CEMENT: STUDY THROUGH IS SPECTROSCOPY

EPAISISSEMENT DU CIMENT PORTLAND ANHYDRE: ETUDIE PAR ESPECTROSCOPIE INFRAROUGE

Introduction

The use of combustibles with a high content in sulfur propiates that during the process of clinkerization several sulfates are formed and afterwards remain incorporated to the clinker. Among these sulfates we can find the K_2SO_4 and the $2CaSO_4.K_2SO_4$ (calcic langbeinite), that have a definite influence in the probable presence of false setting and lumping in cements.

The mechanism that overrule the aparition of both effects is quite similar being the presence of calcic singenite ($CaSO_4\ K_2SO_4.H_2O$) the determinative common cause.

Even when the lumping of the anhydrous cement doesn't damage the hydraulic characteristics of the cement, sometimes it produces great problems of manipulation in operations of unloading in silos or stores where it is conserved. A commong case of serious economic consequences is the lumping produced in holds of ships disposed to carry a heap cement. In the present work it is studied this kind of lumping.

Some considerations about lumping in cements

F. MATOUSCHEK (1) discovers a similar phenomenon as the one studied in the present work: formation of grumes in all the mass of an ensilaged cement, in such a manner that it solidified, needing finally to remove it with shovel and meaning this very high costs.

FOREST (2) in 1962 associated the presence of grumes in anhydrous cements with the formation of syngenite. He indicates that exists a level in the proportion of syngenite; below this level, its action isn't operative. In the experimental works achieved by him, he establishes this limit in 0,65%.

S. SPRUNG (3) attests that the water that comes from the dehydration of gypsum in the silo spreads as vapour to colder zones and reacts with the cement. As a result of the reaction it appears, among other compounds, acicular syngenite that forms a rigid texture.

NIELSEN (4) explains how the water's vapour produced as a consequence of the dehydration of gypsum and a storing of the cement in hot spreads it self through its mass, reacting and producing several chemical reactions "such as the formation of syngenite".

RUIZ DE GAUNA (5) verifies that cement's gypsum can be dehydration to hemihydrate in the silo and that the soluble anhydrite hydration very easily to hemihydrate with water's vapour. The transition from hemihydrate to gypsum requires the presence of water in a liquid condition.

PLIEGO-CUERVO AND GLASSER (6) demonstrate experimentaly the coexistence of CaO, C_3A, C_2S, with $2CaSO_4.\ K_2SO_4$ and K_2SO_4.

T. VAZQUEZ-MORENO and O. FERNANDEZ-PEÑA (7) present the hypothesis that the calcic langbeinite ($2CaSO_4.K_2SO_4$) formed during the clinkerization can be transformed by the effect of wet air in syngenite and very activ $CaSO_4$.

Experimental procedure

Studied samples

It is studied a portland cement that supported a pronounced lumping in the holds of a ship that had carried 5.500 Tm and during its pneumatic unloading, it was necessary an extraction of about 2000 Tm of cement with manual methods, because it was impossible to do it as normally.

For the performance of the present work, 10 samples of the cement (numbered from 1 to 10) were taken in different zones of the ship's holds. They were clasified in three different groups, considering the distinct aspects that the samples presented:

1st. Group: It concerns to sample nº 1 and it is the only one whose appearance and texture is similar as the one that could show up a hidrated and hardened cement. (Photog. 1)

2nd. Gruop: It concerns to the samples numbered: 2-3-4 and 5. They are similar between them, with a very lumped aspect. The photog. 2 of sample 2 it is shown as an example of the appearance that all the ones of this group present.

3rd. Group: It is formed by the samples nº 6-7-8-9 and 10. The appearance of these samples is the one of a quite fluid cement, with nodules of small size, easily brittle with the hand.

Photograph nº 3 concerns to 7th sample, given as an example of the ones belonging to this group.

All the samples were treated with salicylic acid in methanolic medium, with the purpose of removing calcic silicates and to enable the spectroscopic study of the cement's sulphates. They were studied by infra-red spectroscopy before and after the treatment. In all the cases, the results obtained through IR spectroscopy were verified through Differential Thermal Analysis and Thermogravimetric Analysis.

The chemical analysis of the cement is give in Table I.

Results and Discussion

There is a perfect agreement between the form and aspect of the samples and its correspondent IR spectra (figs. 1 - 6).

LUMPING OF ANHYDROUS PORTLAND CEMENT: STUDY THROUGH IR SPECTROSCOPY

EPAISISSEMENT DU CIMENT PORTLAND ANHYDRE: ETUDIE PAR ESPECTROSCOPIE INFRARROUGE

CL

Certainly:

1st Group: The IR spectrum of sample nº 1 gives bands of characteristic compounds of the hydratated cement. So, of portlandite (ν-OH in 3640 cm^{-1}); Tobermorite (νI and ν_3-OH in 3400-3600 cm^{-1}); H-O-H in 1600-1700 cm^{-1}; $\nu_3 SiO_4$ in 940 cm^{-1}...), etc.

2nd Group: The IR spectra of the samples 2-3-4 and 5 are very similar between them. The characteristic bands of syngenite, of $CaSO_4 \cdot \frac{1}{2} H_2O$ and probably of ettringite appear, among others, in all of them.

3rd Group: The IR spectra of the samples 5-6-7-8-9 and 10, are also similar between them. It outstands among other bands, the characteristic ones of $CaSO_4 \cdot \frac{1}{2} H_2O$ and of K_2SO_4. We can also notice with a weak intensity, the specific ones of $CaSO_4 \cdot 2 H_2O$.

Sample nº 1 has been taken from the coating stuck to the walls of the ship's hold, that being the colder part is where the water's vapour has been condensed. The correspondent liquid water reacted with the cement, with whom it was in contact, hydration it and showing the hydration phases detected in the sample.

It is the only sample among the ones studied that has been in contact with liquid water.

The samples that form the 2nd Group were situated in the inside of the mass that formed the stored cement, in places near the central part of the ship's hold, where the temperature of cement was approximately the maximum existent.

The samples that form the 3rd Group were situated near the periphery of the whole mass of stored cement.

According to the results obtained in the study of the samples, the cement's lumping is explained by the following causes:

The cement supported a high temperature during the grinding process, so the gypsum underwent a partial dehydration, according to the following reactions:

$$CaSO_4 \cdot 2 H_2O \rightarrow CaSO_4 + 2 H_2O \quad (1)$$

$$CaSO_4 \cdot 2 H_2O \rightarrow CaSO_4 \cdot \tfrac{1}{2} H_2O + 1{,}5 H_2O \quad (2)$$

The cement, being still hot, was introduced in the holds of the ship that thereinafter had to carry it. In the same holds, the gypsum that wasn't still dehydration continued this dehydration.

The resultant H_2O (V) of the reaction (1) and/or (2) reacted also with the K_2SO_4 that the cement contained and with the $CaSO_4$ and/or with the $CaSO_4 \cdot \frac{1}{2} H_2O$ also produced by these reactions, not only because of the high temperature of the grinding but also as a cause of the high temperature of ensilaged. Definitively syngenite is produced ($CaSO_4 \cdot K_2SO_4 \cdot H_2O$) according to the following reactions:

$$CaSO_4 + K_2SO_4 + H_2O \rightarrow CaSO_4 \cdot K_2SO_4 \cdot H_2O \quad (3)$$

$$CaSO_4 \cdot \tfrac{1}{2} H_2O + K_2SO_4 + \tfrac{1}{2} H_2O \rightarrow CaSO_4 \cdot K_2SO_4 \cdot H_2O \quad (4)$$

The $CaSO_4$ that intervene in reactions (1) and (3) is soluble anhydrite of high reactivity. Probably it is the catalyst of the reaction of $CaSO_4 \cdot \frac{1}{2} H_2O$ - and even of $CaSO_4 \cdot 2H_2O$ - with H_2O and K_2SO_4 for the correspondent formation of syngenite.

The $CaSO_4 \cdot \frac{1}{2} H_2O$ that intervene in the reactions (2) and (4) is also of a high activity, because it is naissant. Its "oldness" would make it notably less reactive.

The IR spectra of the lumping samples (2nd Group) demonstrate the presence of syngenite and the inexistence of K_2SO_4. So, they uphold the mechanism indicated in (3) and (4).

Although, as the IR spectra of the samples that belong to the 2nd Group present characteristic bands of $CaSO_4 \cdot \frac{1}{2} H_2O$ and K_2SO_4, and also weak correspondent to $CaSO_4 \cdot 2H_2O$, it is induced that reactions (3) and (4) haven't been performed, not in a significative form: syngenite hardly exists, the $CaSO_4 \cdot \frac{1}{2} H_2O$ has "grown old" and that is why its reactivity is very low, and a part of $CaSO_4 \cdot 2H_2O$ without dehydrate stays, even being a small part. All this is a consequence of the cement lying in less hot zones than the case of the lumped cement. With laboratory experimentation it was comprobed that the lumping produced in presence of K_2SO_4 happens the same with the calcic langbeinite ($2CaSO_4 \cdot K_2SO_4$). So that, portland cement was mixed up and homogeneized (whose specific surface and chemical analysis are given in table nº 2) with a 1.5% wt of langbeinite. Afterwards the mixture was introduced in a cilindric container of about 25 cm of diameter and 8 cm of height. In the middle of the mass of cement an electric calefactory was introduced surrounded with $CaSO_4 \cdot 2 H_2O$. This is a similar system as the one used by Forest (2).

The temperature reached by the cement was controlled by a dispositive that consisted in a regulator and 6 thermocouples that were introduced inside the cement, placing them all along the diameter of the container. The distance between thermocouple and thermocouple was about 2.5 cm.

The packing case that held in the cement was covered up after that the convenient perforations for the introduction of the heating and control elements were made.

The gradient of temperature reached was from 120ºC to 45ºC; these temperatures persisted constantly during the time the experimentation lasted.

Periodically, the IR spectroscopy of cement's samples taken from the proximities of the thermocouples was done. The whole system can be seen in photograph nº 4.

LUMPING OF ANHYDROUS PORTLAND CEMENT: STUDY THROUGH IR SPECTROSCOPY

EPAISISSEMENT DU CIMENT PORTLAND ANHYDRE: ETUDIE PAR ESPECTROSCOPIE INFRARROUGE

CL

After 15 days the experimentation was finished. The lumped aspect of the cement can be seen in photograph nº 5.

Along the studies done by IR spectroscopy it can be demonstrated the formation of syngenite with a similar mechanism like one already described and that can be summarized in this case in this way:

- The calcic langbeinite added to the cement reacted with the water's vapour generated by the gypsum that sorrounded the calefactor and with the one proceeding from the dehydration that constituted the cement according to:

$2CaSO_4.K_2SO_4 + H_2O \quad CaSO_4.K_2SO_4.H_2O + CaSO_4$

It can be said that syngenite is also formed and it is the responsable of the lumping.

The resultant $CaSO_4$ in the reaction is soluble anhydrite of a high activity.

If K_2SO_4 exists in cement, would react (in presence of water's vapour) easily with it to give syngenite again. Also this $CaSO_4$ helps in the presence of false setting in cements.

Conclusions

One of the causer of portland cement lumping can be explained by a group of concurrent agentes, amoung them the following can be named:

- a high temperature reached in the grinding of cement that makes possible the partial dehydration of gypsum.
- the storage of cement still hot, makes that gypsum continues its dehydration in the same place of storage.
- The presence of K_2SO_4 in the clinker, that reacts with the resultant compounds of the dehydra of gypsum, forming calcic syngenite ($CaSO_4.K_2SO_4.H_2O$).
- probably the pneumatic unloading of cement cooperates in the apparition of the phenomenon.
- the calcic langbeinite ($2CaSO_4.K_2SO_4$) that appears sometimes in portland clinker can react with water's vapour to produce soluble anhydrite and syngenite.

This syngenite is able to produce lumping in the anhydrous cement.

Bibliography

1.- MATOUSCHEK, F.-Zement-Kalk-Gips, nº 8 p. 395 (1972)
2.- FOREST, J. - Rev. Mat. Const. nº 157, p. 35 (1962)
3.- SPRUNG, S.- Zement-Kalk-Gips nº 6, p. 305 (1978)
4.- NIELSEN, H.C.A. - Rock Products nº 2, p. 72 (1974)
5.- RUIZ DE GAUNA, A.- Materiales de Construcción nº 159, p. 13 (1975)
6.- PLIEGO-CUERVO, Y. and GLASSER, F.P. - Cement and Concrete Research V. 9, p.573 (1979)
7.- VAZQUEZ, T. and FERNANDEZ-PEÑA, O. - Materiales de Construcción nº 182, p. 43 (1981)

Table 1

L.I. - 0.8	SO_3	- 2.8	
R.I. - 3.5	Na_2O	- 0.2	
SiO_2 -20.9	K_2O	- 0.8	
Al_2O_3- 5.9	spec.surf (cm^2/g)	-3.360	
Fe_2O_3- 2.4	CaO_f	- 0.7	
CaO -60.5			

Table 2

L.I. - 0.2	SO_3	- 0.6	
R.I. - 0.1	Na_2O	- 0.2	
SiO_2 -21.8	K_2O	- 0.3	
Al_2O_3- 4.6	CaO_f	- 0.9	
Fe_2O_3- 3.7	spec.surf. (cm^2/g)	-3.005	
CaO -65.6			

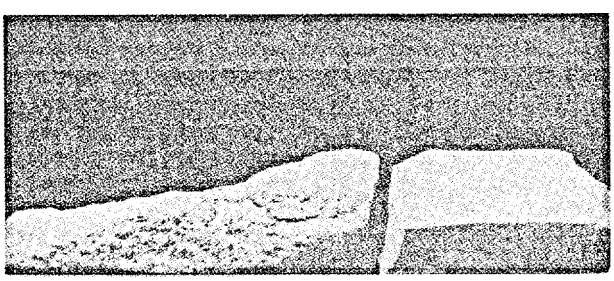

Phot 1 = sample nº 1



Phot. 2 = sample nº 2

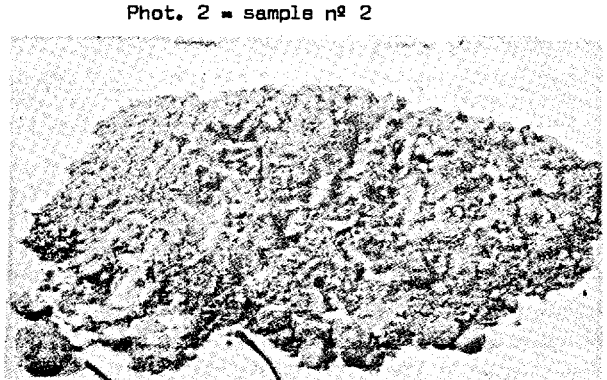

Phot. 3 = sample nº 7

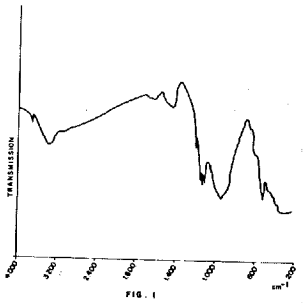

IR spectrum of sample N. 1

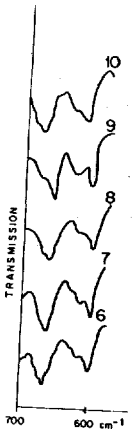

FIG. 5

Some details of IR spectra of samples N. 6 to 10. The band $\nu_3 SO_4$ in 620 cm^{-1}, correspondig to K_2SO_4 can be observed clearly

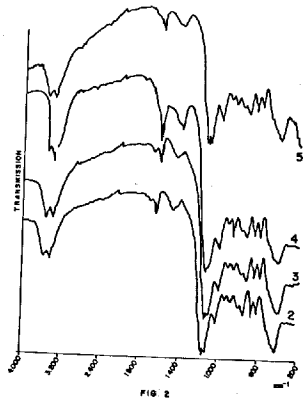

IR spectra of samples N. 2 to 5, after treatment with salicilic-metanol



Some details of IR spectra of samples N. 6 to 10. The bands corresponding to $CaSO_4 \cdot \frac{1}{2}H_2O$ can be observed clearly. The bands corresponding to syngenite are very weak

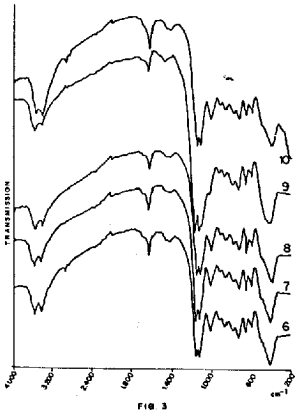

IR spectra of samples N. 6 to 10, after treatment with salicilic-metanol

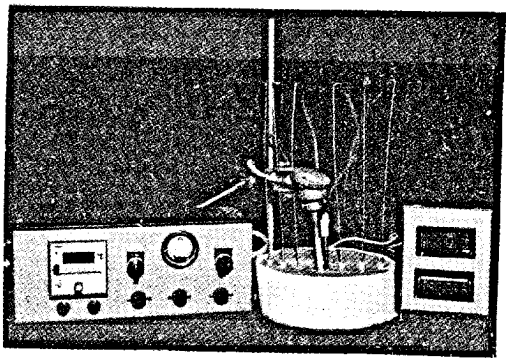

Phot. 4
system of the laboratory y experimentation



Some details of IR spectra of samples N. 2 to 5. The bands corresponding to syngenite can be observed clearly

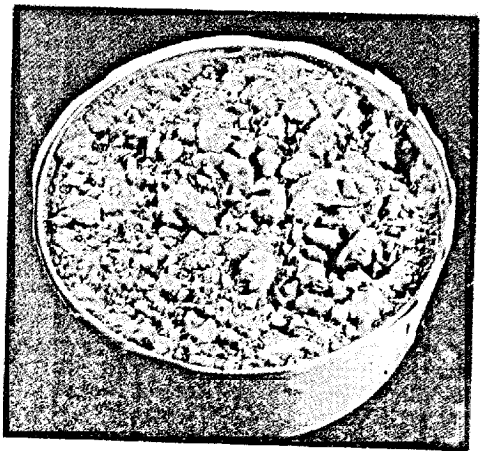

Phot. 5
Aspect of the cement

L.J. Struble - Center for Building Technology, National Bureau of Standards, Gaithersburg, U.S.A.

Synthesis and Characterization of Ettringite and Related Phases

1. Introduction

Ettringite, a naturally occurring mineral and a phase that typically forms during hydration of portland cement, is known to undergo partial dehydration at temperatures as low as 110°C [1,2], and there are indications that this dehydration may be reversible [2-6]. Because a reversible reaction that occurs below 40°C might have application in passive solar energy storage, the present investigation was initiated to explore the potential of ettringite as a phase change material for solar energy storage.

The present paper presents synthesis procedures and various analytical properties of ettringite and a number of isostructural phases, described in more detail in a series of progress reports [7-9]. A separate paper [10] addresses the thermal characteristics as regards energy storage.

The crystal structure of ettringite (fig. 1), as reported by Moore and Taylor [11], consists both of columns whose empirical composition is $[Ca_3Al(OH)_6 \cdot 12H_2O^{3+}]$, and of channel sites, three occupied by sulfate ions and the fourth by two water molecules. This structure is amenable to a number of chemical substitutions [2]. Divalent anions, e.g. carbonate, may substitute for sulfate [12]. Substitution of monovalent anions for sulfate has also been reported, producing phases of the type $[Ca_3Al(OH)_6]_2(Cl)_6 \cdot 26H_2O$ [13,14]. However, Taylor [2] noted that the existence of phases of this type appears to be in conflict with structural requirements, since it would be necessary to accomodate all six monovalent anions in only four available sites. Attempts to prepare these phases in the present study were not sucessful [9]. Other trivalent anions have been substituted for aluminum [15-17], and both the iron and chromium analogs of ettringite were synthesized in the present study. In some instances tetravalent cations can be substituted for aluminum [18,19], and a carbonate- and silicon-substitued phase, thaumasite, was prepared in the present study.

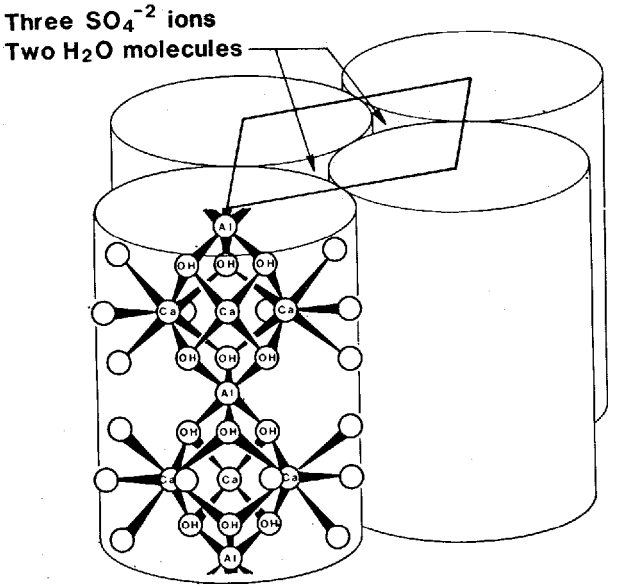

Figure 1. Crystal structure of ettringite, modified from Moore and Taylor [11].

2. Experimental Procedures

2.1 Synthesis

Synthesis procedures were developed to allow reproducible preparation of pure phases that are chemically homogeneous and uniform in particle size. Since these objectives appeared best met by synthesis from solution, a general procedure was followed involving precipitation from a mixture of solutions, one solution containing calcium and the other solution containing the remaining reactants in their stoichiometric proportions. When the two solutions were mixed, a precipitate typically formed immediately, and the mixture could be filtered after approximately one hour to collect the product. Excess amounts of Ca^{+2} and SO_4^{-2} were not used, though both Jones [20] and Lea [1] had reported that an excess of these ions was necessary in the synthesis due to the incongruent solubility of ettringite. Concentrations as high as possible were used, so as to maximize yield. Concentration of the calcium solution was increased by dissolving CaO in a 10 percent sugar solution, a procedure used previously by Carlson and Berman [12].

Phases synthesized by the method described above are listed in table 1. Ettringite was prepared from the calcium solution described above and either a solution of $Al_2(SO_4)_3$, or a solution of $Na_2Al_2O_4$ and Na_2SO_4. Fe-substituted ettringite was synthesized from the calcium solution and a $Fe_2(SO_4)_3$ slurry. The Cr-substituted ettringite was prepared from the calcium solution and a $CrK(SO_4)_2$ solution. The CO_3-substituted ettringite was prepared using the calcium solution and a solution of $Na_2Al_2O_4$ and Na_2CO_3. Thaumasite was prepared from the calcium solution and a solution of Na_2SiO_3, Na_2SO_4, and Na_2CO_3; these solutions were mixed after first cooling to 5°C, the low temperature presumably allowing the necessary 6-fold coordination of silicon [2]. Synthesis of thaumasite required considerably longer reaction times; after a few hours at 5°C, a precipitate had formed that was amorphous to X-rays, but after 5 months of mixing at approximately 5°C, the precipitate was identified as thaumasite. When a similar method was used to synthesize a Cl-substituted ettringite, using a

CL

Table 1. Synthesized phases.

Phase	Formula
ettringite	$[Ca_3Al(OH)_6]_2(SO_4)_3 \cdot 26H_2O$
iron-substituted ettringite	$[Ca_3Fe(OH)_6]_2(SO_4) \cdot 26H_2O$
chromium-substituted ettringite	$[Ca_3Cr(OH)_6]_2(SO_4)_3 \cdot 26H_2O$
carbonate-substituted ettringite	$[Ca_3Al(OH)_6]_2(CO_3)_3 \cdot 26H_2O$
thaumasite, a carbonate- and silicon-substituted ettringite	$[Ca_3Si(OH)_6]_2(SO_4)_2(CO_3)_2 \cdot 24H_2O$

Table 2. Chemical compositions of synthesized phases.

		Substituted Ettringite		
	Ettringite	Fe	Cr	CO_3
Weight percent[a]				
Al_2O_3	7.09	0	0	8.16
SO_3	16.73	17.55	16.67	0.11
CaO	24.32	24.37	23.98	26.54
Cr_2O_3	0	0	10.51	0
Fe_2O_3	0.04	13.97	0.04	0.03
CO_2	0	0	0	11.5
H_2O	50.98	44.19	48.81	52.32
Calculated molar ratios				
Ca	6.0	6.0	6.0	6.0
Al	1.9	0.0	0.0	2.0
Fe	0.0	2.4	0.0	0.0
Cr	0.0	0.0	1.9	0.0
SO_3	2.9	3.0	2.9	0.0
CO_2	0.0	0.0	0.0	3.3
H_2O	39.2	33.9	38.0	36.8

[a]Determined by Inductively Coupled Plasma Emission Spectroscopy except CO_3 and H_2O, which were determined from TGA patterns.

solution of $AlCl_3$, the product was Friedel's salt.

2.2 Characterization

In order to characterize the synthesized phases, samples were analyzed as follows: for qualitative phase composition, by X-ray diffraction (XRD); for bulk chemical composition, using inductively coupled plasma-emission spectroscopy (ICP); for morphology, by scanning electron microscopy (SEM); by infrared spectroscopy (IR); and, for thermal properties, by thermogravimetric analysis (TGA) and differential scanning calorimetry (DSC). Two of the phases, the Cr-substituted ettringite and the thaumasite, were not analyzed by every method.

Chemical analyses following the normal dissolution and analytical procedures required for ICP analysis. The qualitative XRD analysis utilized normal techniques for specimen preparation and data collection. Some phases were also analyzed by XRD to determine the unit cell parameters; these analyses utilized slower scan rates and, in some cases, an internal standard. The SEM examination of the samples employed standard procedures for specimen preparation and analysis, dispersing each powder in alcohol, then evaporating the dispersion onto a carbon grid. The SEM was operated at a voltage of 10, 12, or 20 KeV as necessary to optimize the micrograph. The IR analyses were made using Fourier transform infrared (FTIR), with specimens prepared as mulls of powder in Nujol. Thermal analyses by TGA and DSC utilized ~1 mg specimens in open pans. TGA scans were collected between room temperature and 1000°C at 10° per min. In addition, TGA scans of the low-temperature dehydration reaction were collected between room temperature and 150°C at 0.6° per min. DSC scans were collected between 0 and 150°C at 0.6° per min. Each DSC peak was integrated to determine the change in enthalpy, and examined to determine the onset temperature of the dehydration reaction. Both measurements required determination of the baseline and boundary of each peak, which were determined by visual inspection, assisted by a derivative function.

3. Results and Discussion

Bulk chemical compositions were determined (table 2) for comparison to stoichiometric compositions. In all cases the water contents were higher than expected. Otherwise, the compositions indicate that ettringite and the Cr-substituted ettringite were synthesized with little or no impurity.

CL

The CO_2 content of the CO_3-substituted phase is slightly higher than expected, and the Fe content of the Fe-substituted phase is higher than expected, suggesting possible impurities in these preparations.

X-ray diffraction analysis provided rapid assessment of synthesis procedures. The XRD patterns (fig. 2) indicated that little or no contaminating phases were present, i.e. that each desired phase was the major crystalline constituent.

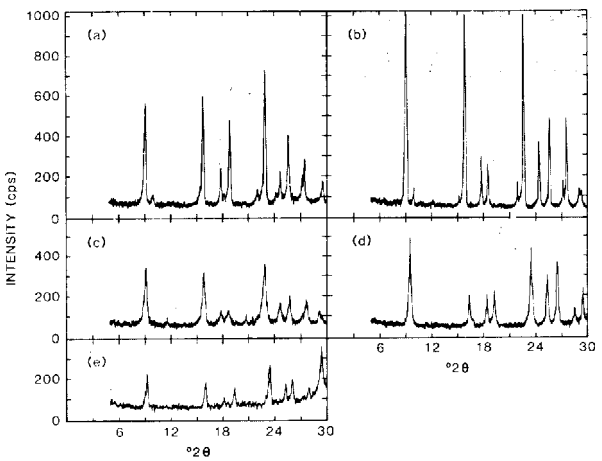

Figure 2. XRD patterns of (a) ettringite, (b) Fe-substituted ettringite, (c) Cr-substituted ettringite, (d) CO_3-substituted ettringite, (e) thaumasite.

Though the XRD patterns vary slightly with chemical composition, each phase appears to have the same or similar crystal structure. Unit cell parameters (table 3) were determined by indexing the powder patterns using the trigonal structure P31c reported for ettringite by Moore and Taylor [11] or for thaumasite using the hexagonal structure $P6_3$ reported by Edge and Taylor [21]. For ettringite and Cr-substituted ettringite, the parameters in table 3 agree within 0.002 nm with values reported by Buhlert and Kuzel [15]. Parameters for the Fe-substituted phase, however, are larger than the reported values [15], 0.002 nm larger in the a-direction and 0.005 nm larger in the c-direction. Parameters for thaumasite in table 3 are slightly larger in both directions (0.003 nm in the a-direction and 0.0024 nm in the c-direction) than the values reported by Effenberger et al. [22]. As expected, the lattice parameters in table 3 vary with chemical composition. In the simplest case, substitution of Cr or Fe for Al is expected to expand the lattice since the ionic radii of Fe and Cr are larger than the radius of Al. However, the lattice parameters with Cr or Fe substitution are larger in the c-direction, but slightly smaller in the a-direction. Thus the effect of these substitution appears to be more complicated than may be explained simply by ionic radii. Since the CO_3 anion is known to be smaller than than the SO_4 anion in thaumasite [22], the substitution of CO_3 for SO_4 in ettringite is expected to reduce the lattice in both directions. This effect was observed.

The morphologies observed by SEM (fig. 3) vary significantly with chemical composition. The ettringite occurs as short, prismatic crystals, variable in cross section between 0.2 and 3 μm, with aspect ratio of 2 or 3. This morphology is different from the morphology of ettringite in hydrated portland cement, where it typically occurs as prismatic, hexagonal needles with aspect ratios between 4 and 10, depending on the available space [23]. The Fe-substituted phase is uniform in size, approximately 3 μm in cross section, with an aspect ratio of approximately 2. The Cr-substituted phase consists of plates with roughly hexagonal outline, lacking the well-developed morphology of the other phases, and highly variable in size, ranging from 0.2 to 9 μm. Finally, the CO_3-substituted phase is composed of clusters or rosettes of prismatic crystals, 0.3 to 1 μm in cross section, with an aspect ratio of approximately 5.

The FTIR spectra (fig. 4) were examined to determine the effects of chemical composition on frequencies of the water bands. It is generally accepted that a shift of IR band to higher frequency indicates a higher strength bond. However, it was argued by Ryskin [24] for the case of $R_3SiOH...B$ complexes (where R and B are organic species) that lowering the OH stretch frequency is accompanied by an increase of the force constant of the Si-O bond. If the spectra for ettringite and substituted phases are interpreted in the same way, a chemical substitution that causes a shift of the OH stretch band to lower frequency is expected to be associated with an increase in the force constant of the Ca-O bond, and thus a greater change in enthalpy with dehydration.

Based on peak assignments of Ryskin [24] and with reference to the ettringite crystal structure (fig. 1), OH bands were assigned either to non-hydrogen-bonded hydroxyl or to hydrogen-bonded hydroxyl. In this case, non-hydrogen-bonded hydroxyl are the hydroxyl ions and the water molecules on the columns, which are bonded to Ca atoms; and hydrogen-bonded hydroxyl are the water molecules in the channels, which are hydrogen-bonded to other water molecules. The frequencies of bands assigned to hydrogen-bonded and non-hydrogen-bonded hydroxyl vary somewhat with composition (table 4). Compared to the unsubstituted ettringite, both the non-hydrogen-bonded and hydrogen-bonded hydroxyl stretching bands are shifted to a slightly lower frequency (20 cm^{-1} for each band) for the Fe-substituted phase. The hydrogen-bonded stretch band is shifted even further (170 cm^{-1} lower) for the CO_3-substituted phase.

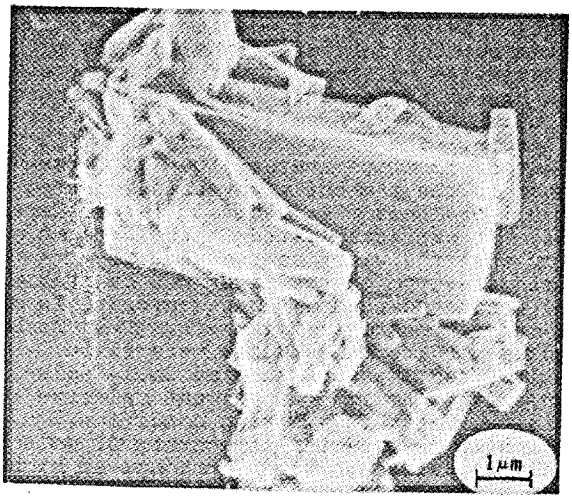

(a)

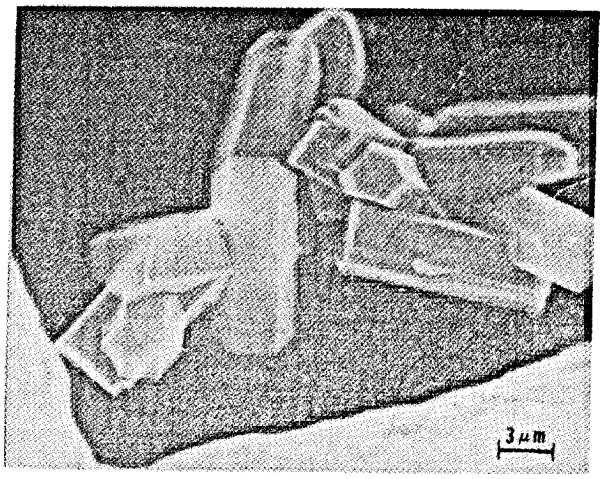

(b)

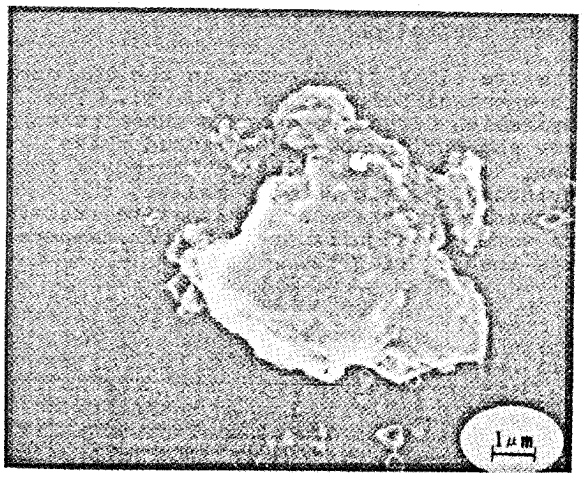

(c)

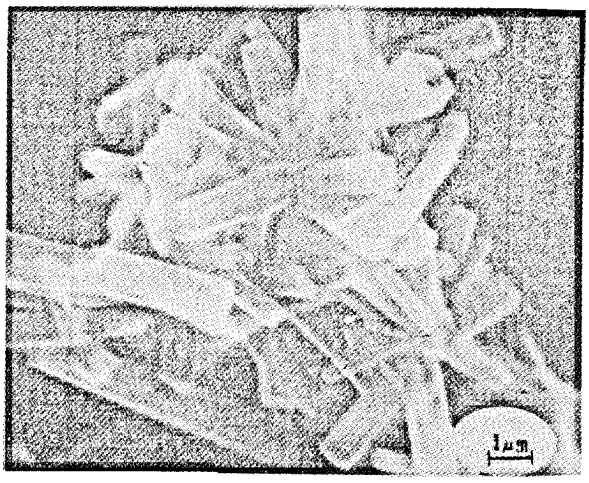

(d)

Figure 3. SEM micrographs of (a) ettringite, (b) Fe-substituted ettringite, (c) Cr-substituted ettringite, (d) CO_3-substituted ettringite.

Table 3. Unit cell parameters[a] of synthesized phases.

Phase	Structure	a (nm)	c (nm)
$[Ca_3Al(OH)_6]_2(SO_4)_3 \cdot 26H_2O$	P31c	1.123	2.150
$[Ca_3Fe(OH)_6]_2(SO_4)_3 \cdot 26H_2O$	P31c	1.1182	2.2008
$[Ca_3Cr(OH)_6]_2(SO_4)_3 \cdot 26H_2O$	P31c	1.119	2.177
$[Ca_3Al(OH)_6]_2(CO_3)_3 \cdot 26H_2O$	P31c	1.0834	2.1250
$[Ca_3Si(OH)_6]_2(SO_4)_2(CO_3)_2 \cdot 24H_2O$	$P6_3$	1.106	1.042

[a]Determined using X-ray powder patterns. Parameters reported with 5 significant figures were determined using an internal standard, and those with 4 significant figures were determined using an external standard.

Thaumasite shows only one broad OH stretch band, assigned to non-hydrogen-bonded hydroxyl stretch because the thaumasite structure has no water in channel positions [2]. This hydroxyl stretch band in thaumasite is shifted to a lower frequency compared to the unsubstituted ettringite. Thus based on FTIR data, it is expected that the enthalpy change on dehydration will rank from low to high according to the following: unsubstituted ettringite,

Fe-substituted phase, CO_3-substituted phase, and thaumasite.

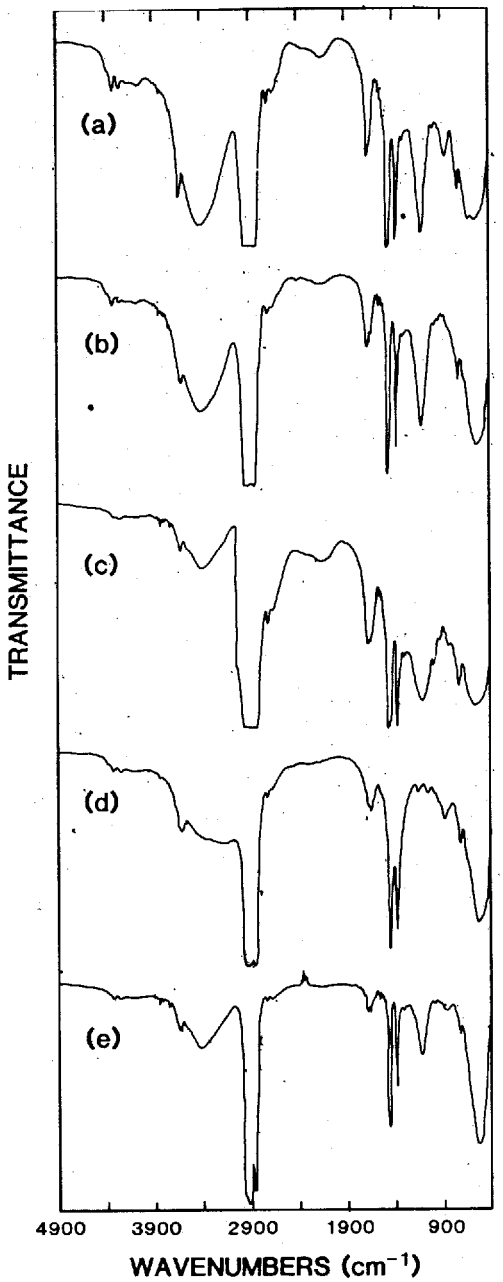

Figure 4. IR patterns of (a) ettringite, (b) Fe-substituted ettringite, (c) Cr-substituted ettringite, (d) CO_3-substituted ettringite, and (e) thaumasite.

For each phase, the amounts of water lost during heating, calculated from the TGA curves and expressed as mol water per mol of each ignited phase, are plotted in figure 5. The major weight loss occurs below approximately 200°C under these conditions, and is probably due to loss of crystalline water. As the temperature is increased, the further weight loss is probably due to loss of hydroxyl. These TGA data may be compared to data for ettringite, the only phase with published TGA data available. The water contents at intermediate temperatures (100-300°C) are higher in the present study than reported by Lea [1] or Jones [20], but similar to Taylor [25]. It was anticipated in the present study that the water contents of the ettringite-type phases might not be stable, i.e., that the phases might dehydrate in dry air and rehydrate in moist air. Therefore, samples for thermal studies were first equilibrated over a saturated $ZnCl_2$ solution, with a nominal 10 percent relative humidity. At this starting condition, ettringite is expected to contain 32 mols of water [1], although water contents as high as 36.5 mols have been reported and attributed to adsorbed water [4]. The water content of ettringite at room temperature in the present study is approximately 40 mols per mol ignited phase.

There are clear differences in the TGA data with chemical composition (fig. 5). The dehydration curves for the Fe-substituted phase and for the CO_3-substituted phase appear to be very similar to the curve for ettringite. The other two phases, the Cr-substituted phase and thaumasite, retain more water at significantly higher temperatures than ettringite.

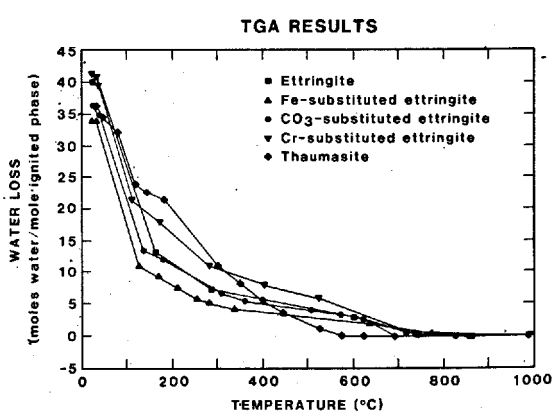

Figure 5. Dehydration data, recalculated from TGA curves.

Data regarding the low-temperature dehydration, some of which have been reported elsewhere [10], are presented in table 5. Enthalpy changes are listed relative to both the amount of the phase and the amount of water lost, the latter allowing comparison of enthalpy changes independent of the amount of water lost. The enthalpy changes on dehydration range from 2.1 to 3.8 kJ per g H_2O. Values for

CL

Table 4. IR wavenumbers (cm^{-1}) of hydroxyl bands[a].

Phase	O-H Stretch		O-H Bend
	Non-hydrogen-bonded	Hydrogen-bonded	Hydrogen-bonded
$[Ca_3Al(OH)_6]_2(SO_4)_3 \cdot 26H_2O$	3640	3420	1670
$[Ca_3Fe(OH)_6]_2(SO_4)_3 \cdot 26H_2O$	3620	3400	1670
$[Ca_3Al(OH)_6]_2(CO_3)_3 \cdot 26H_2O$	3620	3250	1650
$[Ca_3Si(OH)_6]_2(SO_4)_2(CO_3)_2 \cdot 24H_2O$	3410	--	1650

[a]Tentative peak assignments by inspection, based on [24].

Table 5. Dehydration data for synthesized phases[a].

Phase	Loss[b]	Onset Temperature	Enthalpy Change	
	(mols H_2O per mol phase)	(°C)	(kJ per g sample)	(kJ per g H_2O)
$[Ca_3Al(OH)_6]_2(SO_4)_3 \cdot 26H_2O$	19	30	0.59	2.09
$[Ca_3Fe(OH)_6]_2(SO_4)_3 \cdot 26H_2O$	24	6	0.84	2.55
$[Ca_3Cr(OH)_6]_2(SO_4)_3 \cdot 26H_2O$	13	22	0.67	3.73
$[Ca_3Al(OH)_6]_2(CO_3)_3 \cdot 26H_2O$	23	7	0.80	2.55
$[Ca_3Si(OH)_6]_2(SO_4)_2(CO_3)_2 \cdot 24H_2O$	9	33	0.25	1.97

[a]Reported by Struble and Brown [10].
[b]Measured using TGA.
[c]Measured using DSC.

ettringite and thaumasite are nearly equal, while values for both the Fe-substituted phase is considerably higher. It is interesting to note that these values bracket the heat of vaporization of water, which is 2.27 kJ per g. The enthalpy change varied with composition in the order expected based on the previous discussion of FTIR spectra for the unsubstituted ettringite and the Fe- and CO_3-substituted phases, but not for thaumasite.

The change in enthalpy due to dehydration of ettringite and related phases range from 0.4 to 0.8 kJ per g. This range is higher than the enthalpy changes of other materials presently used for solar energy storage. For example, Glauber's salt melts with an enthalpy change of 0.25 kJ per g [27]. The onset temperature for dehydration of ettringite and related phases ranges from 6° to 30°C as measured by DSC. The enthalpy change and dehydration temperature data demonstrate that ettringite and related phases have potential as energy storage materials [10].

4. Conclusions

The following have been concluded regarding synthesis and properties of ettringite and related phases:

1. A general synthesis method using a mixture of two concentrated solutions allowed preparation of the ettringite and related phases with divalent cations.

2. Morphology of the synthesized phases vary with chemical composition. Crystals are generally hexagonal in outline, either short, prismatic crystals, or platey crystals.

3. The IR frequencies of bands assigned to non-hydrogen-bonded and hydrogen-bonded hydroxyl stretching vary with composition. Compared to ettringite, the bands are shifted to a slightly lower frequency for Fe- and CO_3-substituted phases and thaumasite. These shifts are associated with higher changes in enthalpy with dehydration for Fe- and CO_3-substituted phases, but not for thaumasite.

4. Dehydration data, i.e. the amount of water lost, the temperature at which dehydration begins, and the change in enthalpy associated with the low-temperature dehydration vary with composition.

5. Acknowledgements

The project described here was funded by U.S. Department of Energy, Office of Solar Heat Technologies, Passive and Hybrid Solar Energy Division. I am pleased to acknowledge the contributions of K. Galuk, P.W. Brown, and H.F.W. Taylor.

6. References

1. F.M. Lea. The Chemistry of Cement and Concrete. 3rd Edition. 727 pages. New York: Chemical Publishing Company, Inc. (1971).

2. H.F.W. Taylor. Mineral. Mag., 39(304), 377-389 (1973).

3. H.A. Berman and E.S. Newman. In: Proc. Int. Symp. Chem. Cem., 4th, Volume I, Paper III-S1, p. 247-257. Washington: U.S. Department of Commerce (1960).

4. N.N. Skoblinskaya and K.G. Krasilnikov. Cem. Concr. Res., 5(4), 381-394 (1975).

5. N.N. Skoblinskaya, K.G. Krasilnikov, L.V. Nikitina, V.P. Varlamov. Cem. Concr. Res., 5(5), 419-432 (1975).

6. R. Turriziani. Chapter 6 in: The Chemistry of Cements, ed. H.F.W. Taylor, Vol. 1, pp. 233-286. London: Academic Press (1964).

7. J.B. Ings and P.W. Brown. NBSIR 82-2531, 11 pages. Washington: U.S. Department of Commerce (1982).

8. L.J. Struble and P.W. Brown. NBSIR 84-2942, 41 pages. Washington: U.S. Department of Commerce (1984).

9. L.J. Struble and P.W. Brown. Inorganic Compounds for Passive Solar Energy Storage - Solid-State Dehydration Materials and High Specific Heat Materials. Submitted for publication as NBSIR (1986).

10. L.J. Struble and P.W. Brown. Inorganic compounds for passive solar energy storage utilizing a dehydration reaction and specific heat. Submitted to Sol. Energy Mater. (1985).

11. A.E. Moore and H.F.W. Taylor. Acta Crystallogr., B26, 386-393 (1970).

12. E.T. Carlson and H.A. Berman. J. Res. Nat. Bur. Stand., 64A(4), 333-341 (1960).

13. N.N. Serb-Serbina, Yu.A. Savvina, and V.S. Zhurina. Dokl. Akad. Nauk SSSR, 3, 659-662 (1956).

14. H.E. Schwiete, U. Ludwig, and J. Albeck. Zem.-Kalk-Gips, 58 (5), 225-234 (1969).

15. R. Buhlert and H.J. Kuzel. Zem.-Kalk-Gips, 24(2), 83-85 (1971).

16. J. Bensted and S. Prakash Varma. Cem. Technol., 2, 73-76, 100 (1971).

17. I. Odler and S. Abdul-Maula. Cem. Concr. Res., 14(1), 133-141 (1984).

18. S. Prakash Varma and J. Bensted. Silic. Ind., 38(2), 29-32 (1973).

19. W. Lukas. Cem. Concr. Res., 6(2), 225-234 (1976).

20. F.E. Jones. In: Proc. Symp. Chem. Cem., pp. 231-245. Stockholm: Ingeniorsvetenskapsakademien (1938).

21. R.A. Edge and H.F.W. Taylor. Acta Crystallogr., B27, 594-601 (1971).

22. H. Effenberger, A. Kirfel, G. Will, and E. Zobetz. Neues Jahr. Mineral. Monatsch., 2, 60-68 (1983).

23. P.W. Brown et al. The hydration of tricalcium aluminate and tetracalcium aluminoferrite in the presence of calcium sulfate. Report of RILEM Committee 68MMH. Submitted for publication in Mater. Struct. (1986).

24. Ya. I. Ryskin. Chapter 9 in: The Infrared Spectra of Minerals, V.C. Farmer, ed., pp. 137-181. London: Mineralogical Society (1974).

25. H.F.W. Taylor. In: The Chemical and Chemically-Related Properties of Cement, F.P. Glasser, ed., pp. 65-82. Shelton, Stoke-on-Trent: The British Ceramic Society (1984).

27. G.A. Lane. Solar Heat Storage: Latent Heat Material. Volume I, 238 pages. Boca Raton: CRC Press, Inc. (1983).

A. C. Chou, H. C. Eaton[1], F. W. Cartledge and M. E. Tittlebaum, The Hazardous Waste Research Center, Louisiana State University, Baton Rouge, Louisiana 70803 - U.S.A.

A TEM Study of the Interactions Between Certain Organic Hazardous Wastes and Type I Portland Cement

INTRODUCTION

The disposal of hazardous wastes will be one of the major enviromental issues well into the next century. Many of the engineering practices of the past are being questioned by the public. There are serious concerns over potentially adverse health effects which may result from landfilling, deep well injection, incineration, and other methods of disposal which may not be adequately understood. The present paper reports research aimed at understanding the behavior of organic wastes which are solidified prior to disposal by landfilling.

Landfilling refers to the disposal of raw or treated waste in a land based site. Federal regulations prohibit the landfilling of liquids or semiliquids and also require that the leaching potential for certain toxins be reduced to levels which pose no environmental threat. This has resulted in the development of various waste solidification and stabilization technologies. Many of the methods utilize a solidifying matrix composed of relatively inexpensive materials like Portland cement, flyash, kiln dust, or natural pozzolans.

Solidification processes do not necessarily involve chemical interaction between the waste and the matrix materials. For stabilization, or fixation, to occur, however, a reaction must occur. The waste material must be chemically combined with the matrix and exhibit longterm retention under leaching conditions.

Current methods for the development of solidification or stabilization formulae involve treatability studies. Several mixtures, representing a variety of proportions of matrix components, waste and water, are mixed. Physical measurements and leaching experiments are performed and the most effective composition is selected.

Because of the complexity of the systems, there is a poor fundamental understanding of the microchemistry, the microstructure, and the properties of solidified or stabilized wastes. Without this information it is difficult to model the long-term environmental behavior of a hazardous waste landfill.

Recently, Poon et al. (2) used scanning electron microscopy (SEM) and x-ray diffraction to characterize the microstructural evolution of a solidified hazardous waste during leaching. They observed a correlation between the release of zinc ions and a reduction in the amount of ettringite in the hydrated, waste-containing cement. Walsh et al. (3), in a different approach, have used scanning electron microscopy, optical microscopy and x-ray diffraction to determine the mechanisms of interaction between the waste and the cement matrix. It is their contention that leaching and long-term stability can only be understood when the microchemical mechanisms of solidification/stabilization are understood.

Scanning electron microscopy has been widely used in studies of cement microstructure but the results have been difficult to interpret and even more difficult to generalize. Chemical information available from energy dispersive x-ray analysis in the SEM can give the elemental composition of a phase, but compound identification is often difficult. The stoichiometry of the heavy elements can be estimated through careful analytical technique, but light element determination is more difficult.

The transmission electron microscope (TEM) has been used to study ceramic materials and minerals

A. C. Chou, H. C. Eaton[1], F. W. Cartledge and M. E. Tittlebaum, The Hazardous Waste Research Center, Louisiana State University, Baton Rouge, Louisiana 70803

CL

for the past thirty years and several studies of cement have been reported. To the authors' knowledge, however, the TEM has not been applied to studies of solidified hazardous chemical wastes. The main advantage of the TEM is the high spatial resolution, which can exceed 0.2 nanometers in a modern instrument. In addition, the selected area diffraction pattern (SAD) can provide information about the crystal structure and the orientation of crystalline phases. Both of these characteristics are important for waste research.

The specimen suitable for TEM examination must be very thin (100 nm at 100kV) to allow penetration of the electron beam. This thickness can be achieved by replica techniques, by ion thinning or by ultramicrotomy. The replica technique, used in the present study, reproduces the topography of the specimen surface.

Cements are composed of several particle-like phases and its surfaces are porous. Some mineral components of the sample were easily extracted onto the acetate film. Therefore, in addition to the morphological structure being preserved in the carbon film, extracted particles were sometimes observed. Thin crystalline particles were frequently suitable for obtaining electron diffraction patterns.

The present communication reports the use of the TEM in a study of the solidification products resulting from mixing Type I Portland cement with either ethylene glycol or p-bromophenol. Replica methods were used to isolate fine particles of calcium silicate hydrate (CSH) or small particles of other phases embedded in the CSH. Most of the phases were identified as either cement clinker phases or as products of normal cement hydration reactions. Other particles were not identifiable as phases typically occurring in hydrated cement pastes.

SAMPLE PREPARATION AND EXPERIMENTAL PROCEDURE

Type I Portland cement was used as the solidification matrix material. The cement had the composition shown in Table 1. Cement/organic samples were prepared using either pure ethylene glycol or p-bromophenol. Organics were weighed into 20 mL borosilicate glass screw cap vials. Ten grams of cement and 4 mL of deionized water were added to each vial and the mixture was stirred to apparent homogeniety with a glass stirring rod. The organic

Table 1. Percent Composition of Portland Cement

SiO_2	20.6%
Al_2O_3	5.2%
Fe_2O_3	2.4%
CaO	64.9%
MgO	3.3%
K_2O	0.6%
SO_3	2.9%

compounds were added in amounts from 0.2 g to 2.0 g, yielding organic/cement weight ratios of 0.02, 0.04, 0.1, and 0.2. The samples were cured at room temperature (21°-25°C). Control cement samples (i.e. samples of cement and water only) were prepared and stored similarly.

All hydrated cement samples were ground with silicon carbide papers using grit sizes ranging from 180 to 600. Specimens were polished with diamond paste on a rotating wheel using propanol as a lubricant. Rinsing was also with propanol, rather than water, in order to prevent further hydration. The cleaned specimen was replicated by a cellulose acetate tape wetted by acetone. After the plastic tape was dry, it was stripped off the specimen and then coated with carbon in a vacuum evaporator. The carbon film was then cut into small pieces (ca. 9 mm^2) and washed in acetone. After the plastic dissolved, the carbon film was caught on an electron microscope grid for TEM study. A JEOL 100-CX transmission electron microscope was used at 100 kV.

RESULTS

Control Cement Samples

Various morphologies of CSH were observed including fibrous, needle, tubular, and aggregates of small irregular plates. Analyses of many diffraction patterns indicate that although the morphologies differ, the crystal structures are similar with d-spacings of approximately 0.3, 0.28, and 0.18 nm. An example is shown in Fig. 1. This is consistent with previsouly reported work.

In some cases, different diffraction patterns for CSH material were observed. For example, Figure 2 is a diffraction pattern from a specimen with d-spacings of 0.32, 0.28, and 0.16 nm. This structure is similar to afwillite. The particle shown in Figure 3 exhibits a crumpled foil morphology with d-spacings of 0.29, 0.31, and 0.19 nm.

Cement Containing Ethylene Glycol

In cement containing ethylene glycol, the morphology and tobermorite structure of the CSH has been significantly modified. This is consistent with x-ray diffraction studies of the same material (3) where the major peak was weakened and broadened. In some specimens observed in the present work, the surface appeared "glassy" and surrounded by blocky amorphous particles. This is seen in Figure 4. In most other regions, however, CSH appeared as spherical particles embedded in an amorphous material. Some aggregates of spherical particles were amorphous and others crystalline. A variety of morphologies each exhibiting the afwillite structure, with d-spacings of 0.33 and 0.2 nm, were also observed.

Another crystalline structure was frequently observed in the ethylene glycol cement. The structure was crystalline with d-spacings of 0.208, 0.205, 0.201, 0.12, 0.115, 0.103 and 0.1 nm. Morphologies were either aggregates of spherical grains, single irregular plates, or thin flakes. Similar structures were also observed in the pure cement samples, but not to the extent seen in ethylene glycol samples.

Small crystals (15-60 nm) with a cubic structure also were observed. This structure has

not been reported in pure cement and may be a compound of C_3A and ethylene glycol.

Figure 5 shows a $Ca(OH)_2$ crystal. The diffraction pattern shows the characteristic hexagonal structure, however, the diffraction spots are diffuse and tend to form a ring pattern. This implies that the CSH/ethylene glycol is bonded with the $Ca(OH)_2$ forming a thin layer.

Cement Containing p-Bromophenol

The morphologies of the phases contained in cement containing p-bromophenol were also observed to differ from those in hydrated pure cement. Most of the phases appeared as spherical particle aggregates as shown in Figure 6. The number of amorphous aggregates also increased.

The degree of crystallinity of the CSH structure decreased with the addition of p-bromophenol. Large particles having d-spacings characteristic of the CSH(II) structure were observed; however, the particles have retained the shape of the original cement clinker grains. This may imply that the hydration process in this material is different from that in the pure cement. Scanning electron microscopy observations of the same material shown that there are more large distinguishable particles in the p-bromophenol containing material (4).

It was observed that in many CSH regions, the aggregate morphology was unstable under the influence of the electron beam. The particles bubbled significantly, a phenomenon not observed in either the pure cement samples or the cement containing ethylene glycol. Apparently the p-bromophenol, or derivatives of it, were incorporated in the CSH structure, forming an unstable material. The diffraction patterns only showed a single diffuse ring with a d-spacing of approximately 0.29 nm, as illustrated in Figure 7. Similarly, several $Ca(OH)_2$ and $Mg(OH)_2$ crystals were observed. The crystals appeared streaked and diffuse, possibly due to the incorporation of p-bromophenol.

SUMMARY AND CONCLUSIONS

During the course of hydration, a variety of morphological types of CSH have been observed by researchers. Several classifications have been proposed based on SEM and TEM studies. Unfortunately, the compositional and structural differences between these types have not been well defined in the literature. Midgley (5) suggests that CSH may occur in set Portland cement in three forms: (1) fibrous material which sometimes gives diffuse diffraction patterns showing 0.305, 0.208, and 0.18 nm d-spacing of the tobermorite phase; (2) irregular masses of small, distorted plates often giving a single diffuse ring at 0.29-0.3 nm in an SAD pattern; and (3) crumpled foils where no structure was mentioned.

In general, the CSH structure is an amorphous solid body filled with small particles with a variety of morphologies, some having the same crystal structures. In this study, the tobermorite structure is the major crystal structure in CSH. In addition, this study supports Taylor's model (6) that only subcrystalline order exists in the neighborhood of small fragments of Ca-O layers in the CSH structure. The subcrystalline order extends only several hundred nanometers.

The major conclusions of the present study are as follows:

1. The major crystal structure of the CSH in pure cement is tobermorite, but with various morphologies.

2. The addition of ethylene glycol or p-bromophenol to cement change the morphology of the CSH and its crystal structure. Aggregates of small grains are the main morphology and the amount of tobermorite structure has greatly decreased. In addition, various crystal structures with different d-spacings were observed.

3. The amount of amorphous material increases with the addition of either ethylene glycol or p-bromophenol.

4. Ethylene glycol and p-bromophenol may be incorporated into the CSH structure and may exist in the micropores between CSH constituents.

5. Ethylene glycol and p-bromophenol are observed to absorb onto some of the $Ca(OH)_2$ and $Mg(OH)_2$ crystals.

6. Small amounts of fine crystals are found in ethylene glycol and p-bromophenol containing cements. Their d-spacings could be determined but did not correspond to any of the expected products of the hydration of pure cement.

REFERENCES

1. Author to whom correspondence should be addressed.

2. C. S. Poon, A. I. Clark, C. J. Peters and R. Perry, Waste Management and Research 3, 127 (1985).

3. M. B. Walsh, H. C. Eaton, M. E. Tittlebaum and F. K. Cartledge, "The Effect of Two Organic Compounds on a Portland Cement-Based Stabilization Matrix," to appear in Hazard Waste and Hazardous Materials, 1986.

4. D. Skipper, H. C. Eaton, M. E. Tittlebaum and F. K. Cartledge, 7th International Conference on Cement Microscopy, Orlando, Florida, 1986.

5. H. G. Midgley, Structure, Solid Mechanics and Engineering Design, Vol. I, p. 275, 1969.

6. F. H. W. Taylor, Cement Production in Use, Engineering Foundation, New York, p. 107, 1979

A. C. Chou, H. C. Eaton[1], F. W. Cartledge and M. E. Tittlebaum, The Hazardous Waste Research Center, Louisiana State University, Baton Rouge, Louisiana 70803

CL

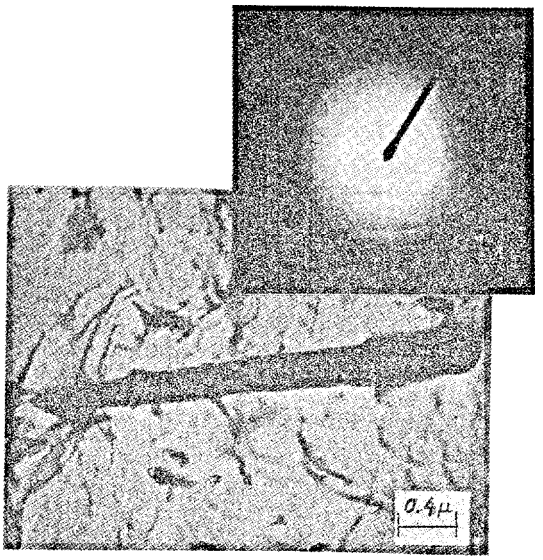

Figure 1. Needle morphology of CSH in pure cement. (Aged 1 month)

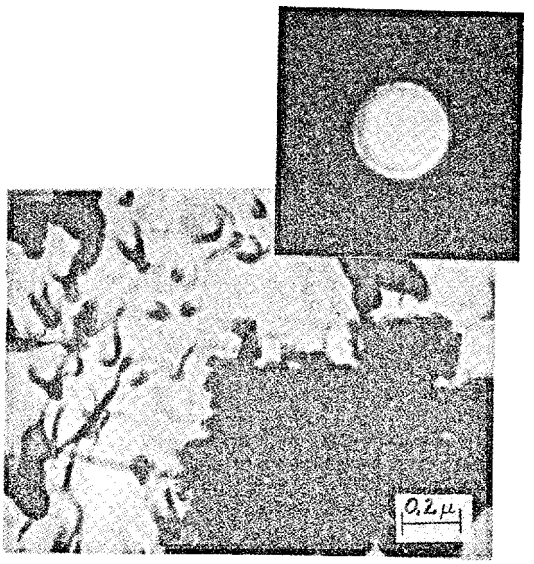

Figure 2. A particle of CSH in pure cement. The diffraction pattern reveals a structure similar to afwillite. (Aged 1 month)

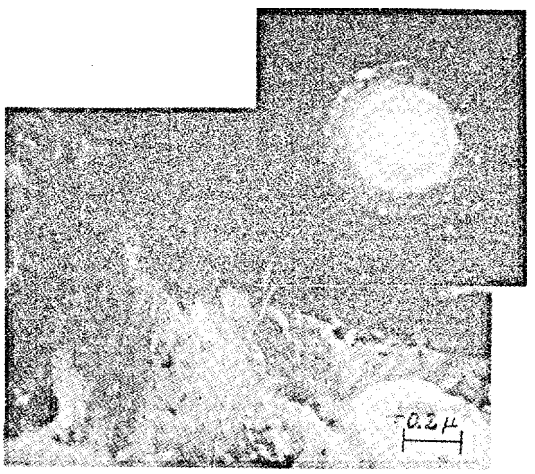

Figure 3. CSH in pure cement. The particle has the crumpled foil morphology. (Aged 1 month)

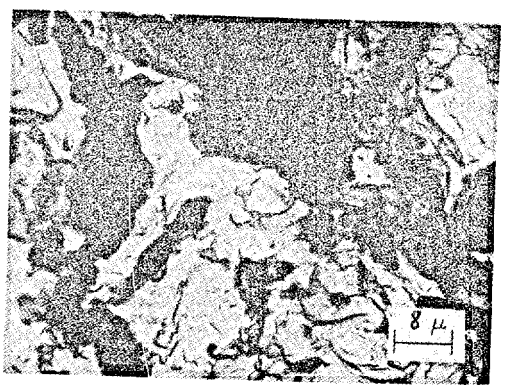

Figure 4. Glassy structure in ethylene glycol cement. Blocky grains surround the thin glassy structure. (Aged 1 month)

A. C. Chou, H. C. Eaton[1], F. W. Cartledge and M. E. Tittlebaum, The Hazardous Waste Research Center, Louisiana State University, Baton Rouge, Louisiana 70803

CL

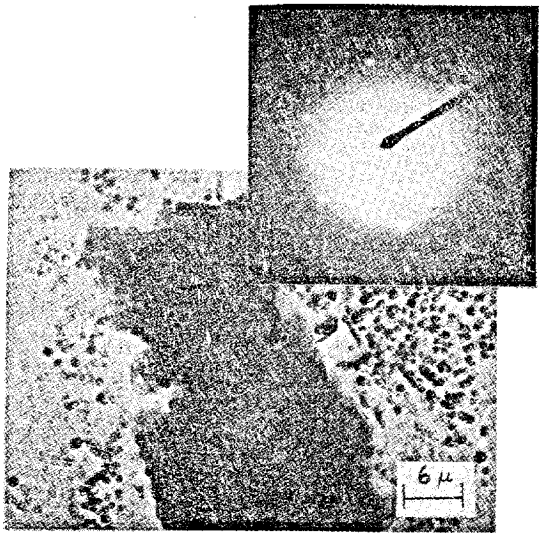

Figure 5. $Ca(OH)_2$ crystals in ethylene glycol cement. The diffraction pattern shows a diffuse ring structure. (Aged 1 month)

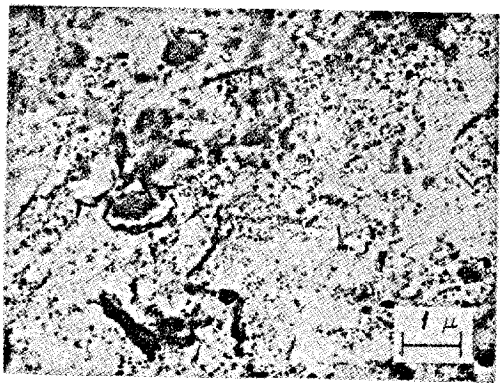

Figure 6. Crystalline spherical aggregates of CSH in p-bromophenol cement aged for 6 months.

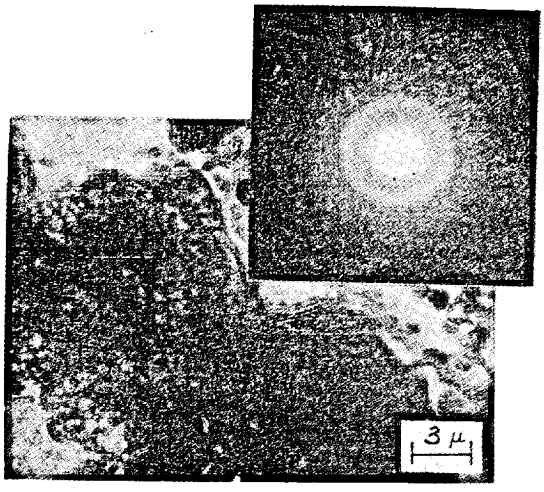

Figure 7. An unstable structure in p-bromophenol cement aged for 6 months.

J. G. Griffin and K. E. Daugherty*, Department of Chemistry, North Texas State University, Denton, Texas 76203. U.S.A.

CL. The Effect of Glass Content on Hydration in the System $CaO-Al_2O_3-MgO-SiO_2$

INTRODUCTION AND EXPERIMENTAL

Because of its importance in many fields, the system $CaO-Al_2O_3-MgO-SiO_2$ has been extensively investigated (1-4). The section of this system containing 5% MgO is of particular importance to the study of high-alumina cement (2). This section contains a field of stability for the quaternary compound, Hexacalcium Tetraalumino Magnesium Silicate (C_6A_4MS), first described by Parker in 1952 (3). Subsequent investigations (5-8) have failed to confirm the formula assigned by Parker; however, as yet, no other formula has been firmly established.

Investigating the composition of the mineral known as "unstable C_5A_3", Parker found that the compound C_6A_4MS occurs as a primary phase in the quaternary system. He found the pure compound to melt incongruently at 1380°C to form CA, MA, and liquid. On further heating to 1400°C, it forms MA and liquid, with final melting occurring at 1420°C. Studying the system further, Parker and Ryder (9) found C_6A_4MS to have definite hydraulic properties, but in general to be a less favorable constituent of high-alumina cement than CA. Their conclusion rested primarily on the slow setting times and poor strength characteristics exhibited by the C_6A_4MS.

It has been suggested that the glass-crystalline ratio of a material may directly influence its hydration behavior (10). Investigations on slags (4,10-13) have shown that this ratio and the chemical composition plays an important role in the hydration process. This investigation was designed to examine the effect of varying the glass-crystalline ratio on the hydration of synthetic samples of composition C_6A_4MS.

Three samples of chemical composition C_6A_4MS were prepared by the high-temperature reaction of $CaCO_3$ with stoichiometric amounts of $MgCO_3$, SiO_2, and $Al(OH)_3$. ACS Reagent grade chemicals were used to prepare a raw mix from which all three samples were synthesized. In order to ensure homogeneity, the raw mix was placed into a porcelain jar with twenty-five stainless steel ball bearings, and tumbled for twenty-four hours on a Norton Mill. The samples were placed in a Lindberg, model 51333, electric furnace and calcined for two hours at 900°C. The temperature was then raised to the firing temperature at a rate of 200°C/h. Firing conditions for the three samples are shown in Table 1. Samples I and III were removed from the furnace and allowed to cool to room temperature in a desiccator. For sample II, however, the furnace temperature was lowered from 1370°C to 900°C at a rate of 100°C/h. When the furnace reached 900°C, the sample was removed from the furnace and allowed to cool to room temperature in a desiccator. All samples were ground to pass a 400-mesh sieve and had identical Blaine surface areas of 2500 cm^2/g. Using the ASTM standard method (14), a small amount of free-lime was detected in sample II. No free-lime was detected in either of the other samples.

TABLE 1

C_6A_4MS Preparation and Analysis

Sample Number	I	II	III
Furnace Temperature	1445°C	1370°C	1420°C
Firing Time	2.25 h	24.5 h	0.5 h
Qualitative XRPD	---	C_6A_4MS, $C_{12}A_7$	C_6A_4MS
Free Lime Content	0.00%	0.14%	0.00%
Specific Gravity	3.08	3.08	3.08
Surface Area (cm^2/g)	2500	2500	2500
Percent Glass	100	73	0

Powder X-ray diffraction was used to confirm the presence of C_6A_4MS (15), as well as to determine the identity of the hydration products. All X-ray powder analyses were conducted on a Philips-Norelco X-ray diffractometer using nickel-filtered Cu Kα radiation at 35KV and 18mA. The goniometer scanning speed was 2°(2θ)/minute.

A combination DTA/TGA, Mettler TA-HE20 thermobalance, was used to follow the hydration of the samples. Samples were run in a flowing air atmosphere from 25°C to 900°C at a rate of 10°C/min. The DTA was set at 200μV for a full scale pen deflection, and the recorder speed was 8cm/h.

The optical microscopy technique used for the determination of the glass-crystalline ratio was a modification of the "South African Procedure", which has been previously decribed by Fulton (16). A portion of each sample, having a particle size of 200-270 mesh was placed on a glass slide and wetted with glycerol. The sample was viewed under both plane and polarized light, with the particles which were visible under the polarized light being counted as crystalline. The glass content was then calculated using the equation:

$$\% \text{ Glass} = \frac{\text{total particles} - \text{crystalline particles}}{\text{total particles}} \times 100$$

Allowances were made for particles which showed only partial crystallinity.

Each sample was mixed with distilled-deionized water at a water-solid ratio of 10/1, and placed in a tightly sealed polyethylene container. Samples were cured at three temperatures (2, 25, and 50°C) and maintained for intervals of 1 to 90 days. In order to stop the hydration, samples were placed in an excess of cold ethanol, and ground with an agate mortar and pestle. They were then filtered using a 10-15μ Hirsch funnel and washed with cold acetone. Finally, each sample was dried at 105°C for

15 minutes.

RESULTS AND DISCUSSION

Figure 1 illustates the changes in the DTA patterns of the amorphous C_6A_4MS sample, hydrated at 50°C, as the hydration proceeds from 1 to 90 days. These DTA patterns are representative of all the DTA patterns obtained, although, in general, the small peak at 300°C was not as prominent in the other samples. This peak is attributed to the presence of gibbsite, AH_3, and in all cases was observed to increase as the hydration time and temperature increased. Attempts to use this correlation to approximate the degree of hydration, however, were unsuccessful, due primarily to the small size of the desired peak and interference from the other much larger peak, centered at 340°C.

Previous studies (4,17-19) have used the percent combined water as an approximation to the degree of hydration. In this study, the percent combined water was calculated from TGA patterns using the equation:

$$\%H_2O = \frac{\text{wt at } 105^\circ C - \text{wt at } 900^\circ C}{\text{wt at } 900^\circ C} \times 100$$

where the weight at each temperature is calculated by subtracting the weight loss at each temperature, as indicated by the TGA, from the initial weight of the sample.

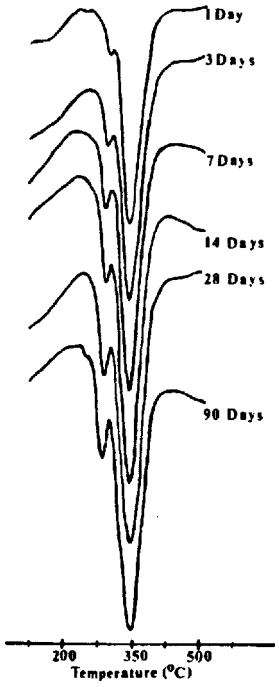

FIG. 1
DTA Patterns for Hydrated C_6A_4MS (100%Glass/50°C)

The relationships between the percent combined water and the plus/minus 1°C curing temperature, for each of these samples, are illustrated in Figures 2 through 4. In Figure 2, the percent combined water of the crystalline C_6A_4MS sample can be seen to increase with increasing temperature. The 90 day samples, which appear to deviate from this behavior, actually reflect the fact that at 50°C, the only species present are C_3AH_6 and AH_3, while at lower temperatures, both C_3AH_{8-12} and C_2AH_6 are also observed.

Figures 3 and 4 show the effect of temperature on the hydration of C_6A_4MS-(I) and C_6A_4MS-(II), respectively. In both cases, the relationship between the 2°C and the 25°C curves is simply the increase in the hydration rate at the higher temperature. The apparent anomalous behavior of the 50°C curves, on the other hand, is explained by the fact that the stable hydrates, C_3AH_6 and AH_3, are the only species present, and contain less combined water than the metastable hydrates found in the lower temperature samples.

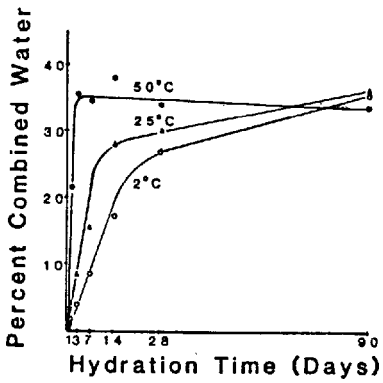

FIG. 2
The Effect of Temperature on the Hydration of C_6A_4MS (100% Crystalline)

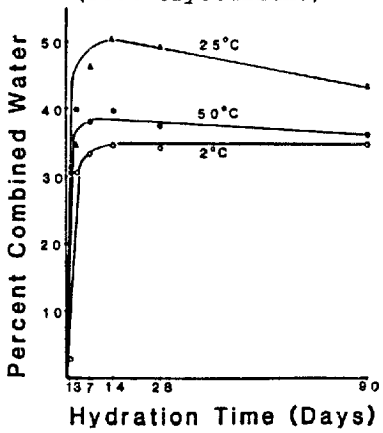

FIG. 3
The Effect of Temperature on the Hydration of C_6A_4MS (100% Glass)

J. G. Griffin and K. E. Daugherty*, Department of Chemistry, North Texas State Univeristy, Denton, Texas 76203

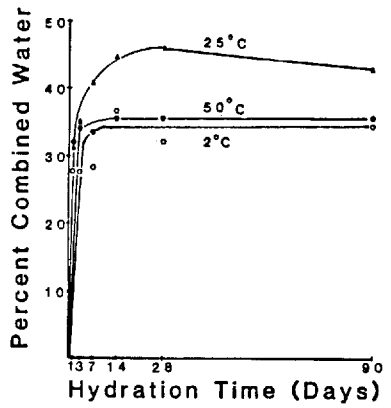

FIG. 4
The Effect of Temperature on the Hydration of C_6A_4MS (73% Glass)

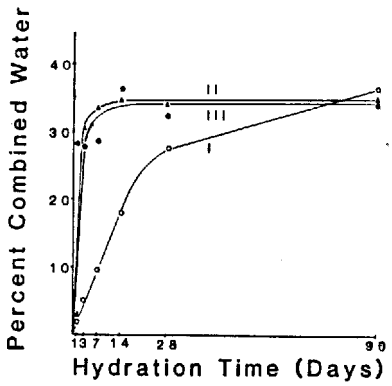

FIG. 5
The Effect of Glass Content on the Hydration of C_6A_4MS (2°C)

The effect of the glass content on the hydration of C_6A_4MS at each of the three curing temperatures studied, is shown in Figures 5 through 7. In Figure 5, which shows the hydration of the C_6A_4MS samples at 2°C, the hydration of the 100% glass sample, and the 73% glass sample appear very similar, while the hydration of the 100% crystalline sample proceeds more slowly. An X-ray examination of these samples, revealed that, although all three samples reacted to form a combination of the metastable calcium aluminate hydrates, C_3AH_{8-12} and C_2AH_6, the crystalline sample did indeed react more slowly. The non-hydrated crystalline C_6A_4MS could still be identified after 28 days of hydration.

In the hydration of C_6A_4MS at 25°C, illustrated in Figure 6, similar results were obtained. The glassy samples reacted with water to form C_3AH_{8-12} and C_2AH_6, with the stable calcium aluminate hydrate, C_3AH_6, appearing after 7 days. The crystalline sample, on the other hand, reacted more slowly, with the non-hydrated crystalline form appearing as late as 14 days after the onset of hydration. The stable hydrate, C_3AH_6, also appeared after 14 days hydration.

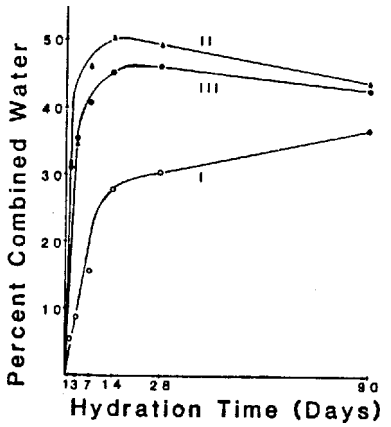

FIG. 6
The Effect of Glass Content on the Hydration of C_6A_4MS (25°C)

Figure 7 shows that at 50°C all of the samples hydrate in much the same way. X-ray examinations of these samples revealed that, with the exception of the very early stages of hydration of the crystalline sample, which showed a small amount of C_3AH_{8-12} present, the only species present in any of the samples are C_3AH_6 and AH_3. In all of these samples, the amount of AH_3 increased with increasing curing time. The correlation between the size of the X-ray peaks of AH_3 and the size of the DTA peak at 300°C appears quite good, although exact measurements could not be made of the DTA peaks.

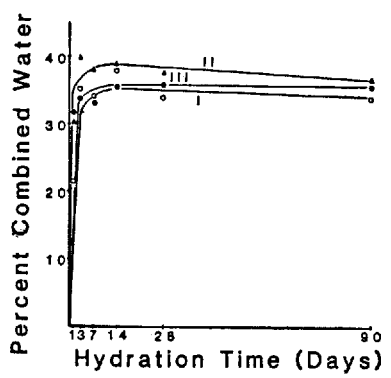

FIG. 7
The Effect of Glass Content on the Hydration of C_6A_4MS (50°C)

From X-ray powder diffraction data, it is possible to construct the hydration pathway for C_6A_4MS, as follows;

$$C_6A_4MS + H_2O \xrightarrow{2^oC;25^oC} C_3AH_{8-12} + C_2AH_6 + \text{others}$$

$$C_3AH_{8-12} \xrightarrow{25^oC} C_3AH_6 + AH_3 + \text{others}$$

$$C_6A_4MS + H_2O \xrightarrow{50^oC} C_3AH_6 + AH_3 + \text{others}$$

The compounds referred to as others were added because no compounds containing either MgO or SiO_2 were observed. Although in several instances, peaks appeared which may have been due to C_2ASH_8, the peaks were very weak and did not appear with any regularity. Two possible explanations for this behavior are: that the amounts of MgO and SiO_2 present are so small that the compounds containing these oxides were present in quantities of less than 3%, and therefore not detectable by X-ray diffraction; or that these oxides may be present in an amorphous form, which also could not be detected by X-ray diffraction.

CONCLUSIONS

The products of the hydration of C_6A_4MS are dependent upon the curing temperature. The metastable calcium aluminate hydrates C_3AH_{8-12} and C_2AH_6 are produced from the hydration at 2°C. At 25°C these products slowly convert to the stable calcium aluminate hydrate, C_3AH_6, and gibbsite, AH_3. At 50°C the metastable hydrates are not observed and C_3AH_6 and gibbsite are formed exclusively. Other hydration products, although not observed, must also be present to account for the presence of MgO and SiO_2. It is possible that these products are either amorphous or present in concentrations too small to be detected by X-ray powder diffraction.

Results indicate that the percent combined water at any given time during the hydration of C_6A_4MS is dependent upon both the curing temperature and the glass content of the sample. At 2°C and 25°C, the glass content has a significant effect on the hydration of C_6A_4MS, with an increase in the glass content being accompanied by a corresponding increase in the percent combined water. At 50°C, however, the glass content has little effect on the percent combined water. It is evident that as the curing temperature is increased, the effect of the glass content, in terms of the percent combined water, is decreased.

REFERENCES

1. H.F.W. Taylor, The Chemistry of Cements, Vol.I, p.69, Academic Press, New York (1964).

2. F.M. Lea, The Chemistry of Cement and Concrete, 3rd. edn., p.69, Chemical Publishing Company, Inc., New York (1971).

3. T.W. Parker, Proceedings of the Third International Symposium on the Chemistry of Cement, London (1952), pp. 485-515.

4. K.E. Daugherty, B. Saad, C. Weirich, and A. Eberendu, Silicates Industriels, 48(4), 107-110 (1983).

5. J.H. Welch, Nature (London), 191, 559-560 (1961).

6. A.J. Majumdar, Trans. Br. Ceram. Soc., 63, 347-364 (1964).

7. H.G. Midgeley, Trans. Br. Ceram. Soc., 67, 1-3 (1968).

8. P. Lhopitallier, Proceedings of the Fourth International Symposium on the Chemistry of Cement, Washington D.C. (1960), pp. 1007-1033.

9. T.W. Parker, and J.F. Ryder, Proceedings of the Third International Symposium on the Chemistry of Cement, London (1952), pp. 524-527.

10. R.H. Bogue, J. Am. Concr. Inst., 26(11), 227-230 (1955).

11. K. Gee, Slag Cement Seminar, University of Alabama, School of Engineering, Special Studies, April 30, 1981.

12. S.M. Royak, Ya.M. Shkol'nik, V.V. Orlov, L.A. Orlov, and V.I. Ermakov, Zh. Prikl. Khim., 48(5), 986-990 (1975).

13. S. Visser, J.E. Kruger, J.H.P. Van Aardt, and M.P. Brandt, CSIR Report BOU(1975), 74 pp.

14. ASTM Designation: C114-58, 1958 ASTM Book of Standards, Part IV, pp. 82-85.

15. H.G. Midgeley, Mag. of Concr. Res., 9 (25), 17-24 (1956).

16. F.S. Fulton, Portland Cement Institute Monograph, Johannesburg (1974), pp. 6-7.

17. C.J. Goodbrake, Ph.D. Dissertation, University of Illinois, Urbana-Champaign, Illinois (1978).

18. Z.Q. Wu, J. Hriljac, C.L. Hwang, and J.F. Young, J. Am. Ceram. Soc., 66(5), C86-C87 (1983).

19. J.G. Griffin, and K.E. Daugherty, Thermochimica Acta, in press.

G. Frohnsdorff, J. Clifton, H. Jennings, P. Brown, L. Struble, National Bureau of Standards, USA
J. Pommershein - Bucknell University, U.S.A.

IMPLICATIONS OF COMPUTER-BASED SIMULATION MODELS, EXPERT SYSTEMS, DATABASES, AND NETWORKS FOR CEMENT RESEARCH

CL

1. INTRODUCTION

The use of new materials, construction practices, and designs have prompted a re-examination of traditional approaches to concrete technology. In addition, concrete structures are often used beyond their planned lifetimes, in functions for which they were not originally intended, or in harsher conditions than originally expected. There is, therefore, a need to develop improved methods and procedures for predicting the performance of cement and concrete. At the same time, rapid growth in the power and availability of computers raises questions about how they might be used to make concrete a more predictable and better performing material. As will be seen, the answers to these questions can suggest alternative ways to plan and organize cement research.

The significance of research on cement, as on other materials, depends on the questions asked, and both the questions and answers are changing because of computers. Paradoxically, the questions in cement research are becoming more oriented towards the end use of cements in concrete and, at the same time, becoming more fundamental. This is because computers can be used as links between technology and science. Thus, it is no longer unrealistic to expect scientific researchers to address such complex technological questions as "How can the performance of concrete be predicted?" which, even ten years ago, were remote from their interests and experience.

The objective of the present paper is to suggest how research questions might be addressed using computers, specifically using a computer-based knowledge system (Fig. 1) consisting of 1) models to simulate chemical and physical relationships, 2) knowledge-based expert systems, and 3) databases. In the figure, the complementary parts of the knowledge system are connected through a global computer network linking collaborating researchers. Although there is other research in this area, we are using specific examples from investigations currently being carried out at the National Bureau of Standards (NBS) to illustrate the technical feasibility of the general approach.

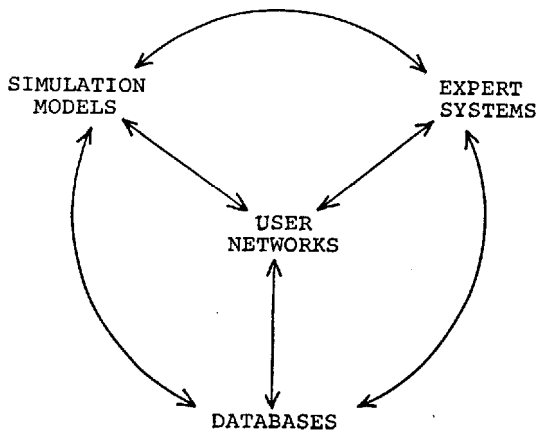

Figure 1. Schematic of a computer-based knowledge system

2. SIMULATION MODELS

Investigations of complex systems, in which the starting conditions are not well-defined and the results depend on many variables, pose serious difficulties. Understanding of such a system may often be advanced by constructing computer-based simulation models intended to represent the system and the phenomena that occur within it. Such models must be based on established scientific principles, possibly supplemented by a small number of intuitive hypotheses. The models can then be tested for their ability to explain observed relationships. Such an approach is being used increasingly in cement and concrete research [1].

In advancing understanding of cement and concrete technology, it is necessary to understand the reactions with water of cement particles, individually and in groups, and the development of microstructure in hardened cement pastes. Much recent research has contributed towards this goal [2], but few of the studies have been directed towards the development of simulation models for hydrating cements. Models are being developed in our laboratory for the hydration of tricalcium silicate (C_3S) particles [3, 4] and for the development of microstructure in C_3S pastes [5]. These are intended to be evolutionary steps towards the development of a "macromodel" [1] to describe the changes that take place when multiphase cements react to form the matrix in hardened concrete, and the subsequent reactions which affect its long term performance.

The microstructure model [5] simulates development of microstructure during the hydration of C_3S following the flow chart in Fig. 2. The model begins by calculating the spatial distribution of a chosen volume of particles in a defined volume. The free space is filled with water and then the water-filled space is gradually filled by hydration products from reactions following predefined rules. The calculations account for all the material in the system at various degrees of reaction; the results are stored in a numerical data file that can be used to produce various types of output. A typical output is a graphical representation of the distribution of the material in a cross-section of the volume (Fig. 3). Such an output may be used for visual comparison with scanning electron micrographs of sections of hardened pastes. The data file contains information about microstructural features that, presumably, govern properties or phenomena of interest, such as porosity, permeability modulus of elasticity, and fracture. The model consists of many subroutines which can be modified as new insights become available. This flexibility opens up many possibilities for collaborative research.

The model simulating development of microstructure is presently being linked to a model for chemical changes taking place during hydration of cements containing polyminerallic particles, thus producing a more comprehensive model for the hydration of portland cements. The combined model will provide an improved representation of the chemical and kinetic aspects of the hydration reactions and their effects on microstructure development.

It is intended that these models will have input from many researchers, either through their direct participation in the model development or through participation in scientific and technical committees on the mathematical modeling of cement hydration,

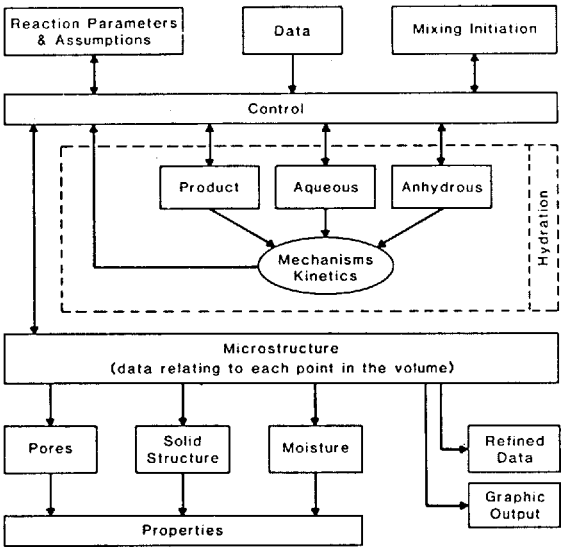

Figure 2. Flow chart for a comprehensive computer simulation model of microstructure and property development of cement pastes. Most of the small boxes represent subroutines which perform operations on different aspects of the microstructure under the control of the control program. Subroutines can be changed to invoke different assumptions and processes. In using the model, the microstructure undergoes incremental small changes at a rate controlled by a kinetics subroutine. The calculated microstructure can be used to produce a graphic output or as input to calculations of bulk properties.

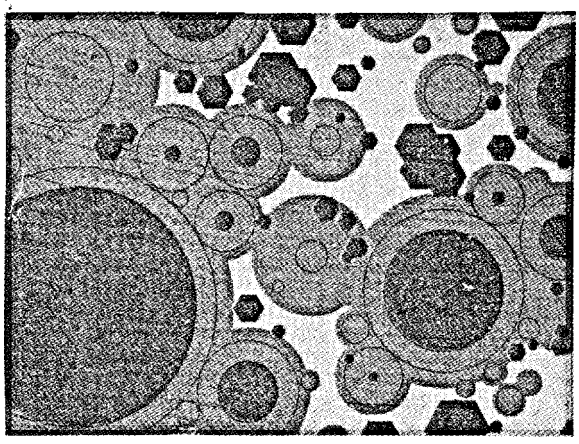

Figure 3. Graphic display of a cross-section of the calculated microstructure from a computer simulation. This cross-section is of a tricalcium silicate paste with w/s = 0.5 and a 42% degree of hydration. Solid black circles represent anhydrous C_3S; grey areas, C-S-H; hexagons, CH crystals (calculated as spheres); and black lines, original boundaries of C_3S particles.

e.g. RILEM Committee 68-MMH [2] and Sub-Committee 225.1 of the American Concrete Institute (ACI). Because constraints on resources make it unlikely that many such models will be developed in the near future, it is desirable that interested researchers should have an opportunity to share in the development and use of the model. How this might be done is discussed further in the section entitled Computer Networking.

3. KNOWLEDGE-BASED EXPERT SYSTEMS

Whereas most chemical and physical simulation models are deterministic, there is growing recognition of the need to develop stochastic models for the representation of real phenomena [6]. Also, much important knowledge falls in the category of expert opinion and, within the last twenty years, substantial progress has been made in developing, for practical application, computer programs incorporating expert opinion. Such programs are referred to as "knowledge-based expert systems" or "expert systems," with pioneering applications being in medical diagnosis and the analysis of mass spectra [7]. Expert systems are difficult and costly to develop, but their potential for improving the quality of decisions is high.

Recently, Clifton, Oltikar, and Johnson [8] developed a prototype expert system, DURCON (from DURable CONcrete), for selecting materials for producing durable concrete. DURCON is an interactive computer program that assists in designing concrete for use in a specified environment and in selecting appropriate materials and proportions for use in a trial mixture. It includes durability as regards freezing and thawing, corrosion of reinforcing steel, chemical attack, and alkali-aggregate reaction. DURCON is based on the American Concrete Institute (ACI) Guide to Durable Concrete [9], the most authoritative document on durable concrete published by the ACI. It is being developed in cooperation with the ACI Committee 201 on Durability, and a number of experts on durability have contributed ideas and critically reviewed the system. It is hoped and expected that the completed expert system will be approved by a consensus of the ACI committee and will be recognized as a standard equivalent to the guide on which it is based.

Among the benefits of an expert system are that it can:

1) provide an easy-to-use representation of expert knowledge,

2) assist in the making of decisions on complex problems,

3) draw attention to gaps in knowledge and to research needs, and

4) provide an educational tool.

NBS has recently begun the development of another expert system, based on the ACI Guide to the Selection and Use of Cements [10]. Like DURCON, this is being developed with the collaboration of an ACI committee, in this case ACI 225 on Hydraulic Cements. This raises the question of whether there should be a

group of complementary expert systems, each representing one or more aspects of concrete technology, which could be used separately or together for solving a specific problem or, perhaps, as a convenient representation of a code of practice, e.g. ACI 318 [11]. Some possible topics for expert systems which might become components of a larger system representing a code of practice for concrete, or a commentary on a code, are: 1) definition of service conditions, 2) materials selection, 3) mixture design, 4) expected life, 5) construction requirements, 6) general requirements, 7) structural systems or elements, 8) condition assessment, 9) protective measures, and 10) repair procedures.

Currently, expert systems depend heavily on the knowledge which experts have gained from experience. However, they have the potential for incorporating simulation models (Fig. 1) to help improve the recommendations they make. Expert systems can also be used to improve the efficiency of simulation models, as by application of pre-established rules to the selection of parameters.

As with simulation models, the large effort required to develop an expert system makes it desirable that many researchers have an opportunity to share in its development, evaluation, and use. Computer networking should facilitate this.

An important question which cannot be overlooked is that of liability for errors in decisions arrived at with the help of an expert system. If the expert system was developed by a consensus process in an authoritative standards organization, then the expert system may be considered as a new type of standard. The users and developers of a standard expert system would, presumably, have similar liabilities for faulty decisions to the developers and users of other standards. The situation could well be much more complicated if a faulty decision was attributed to a less-openly developed expert system.

4. DATABASES

Simulation models and expert systems require data and other knowledge to make them useful. In this paper, "data" refers to information in the form of numerical quantities relating to a material or system, and "knowledge" refers to all forms of information, including text, images, and data. For convenience, "databases" will be used to refer to any computer-based collection of knowledge, not only numerical data. Text and images are often of less certain origin than data, but they may be equally valuable in decision-making. The costs involved in establishing databases have required decisions concerning their scope and usefulness. Although it is evident that much knowledge is worth recording, it is often difficult to justify the cost. However, advances in the recording of sound and images (e.g. laser video-disc recording) and in database management systems [12] are reducing the cost of databases by making them easier to produce and maintain.

Prioritizing and structuring knowledge for possible use in a database may be viewed in terms of its potential usefulness in aiding the development of a simulation model, an expert system, or both. A model or expert system may itself be used to establish priorities and structure. Thus, new knowledge may be checked using a model or expert system for consistency with what is already known.

Examples of NBS contributions to the databases for cement science are the revisions of the phase diagrams for the C-S-H [13, 14] and C-A-S-H [15] systems. This work provides fundamental data needed for simulation models of cement hydration and, possibly, for expert systems. Although the phase diagrams are of great importance as representations of the phase relationships governing the cement hydration reactions, their critical evaluation and improvement have been slow in recent years. Their usefulness will be increased through the use of computers to store and display them in new, more convenient ways.

In addition to the phase diagrams, NBS has a substantial database on the properties and laboratory test performance of cements in the Cement and Concrete Reference Laboratory [16], CCRL, sponsored by the ASTM Committees C-1 on Cements and C-9 on Concrete and Concrete Aggregates. The database consists of many replicate sets of results from ASTM standard tests on carefully-homogenized, commercial portland cements used in the CCRL Proficiency Sample Program [17]. In principle, the database is available for use by standards developing committees, or other interested parties. The database includes only the results of ASTM standard tests, and has no information on the phase compositions of the cements other than calculated potential compound compositions. To help overcome this deficiency of current ASTM tests, task groups on phase analysis of clinkers and cements have been set up in ASTM Subcommittee C-1.23 on Chemical Analysis (of cements). The task groups are developing standard practices for quantitative phase analysis by x-ray diffraction and by light microscopy and have stimulated an NBS project to prepare a standard reference material (SRM) for clinker phase analysis. Results of these activities will strengthen the value of computer databases based on ASTM tests by making it possible to characterize cements more precisely.

5. COMPUTER NETWORKING

The benefits of knowledge increase with its accessibility and reliability. New technology for communication between computers is facilitating the transmission of data between researchers and increasing the possibilities for their participation in reviewing and sharing data. The increased ease and speed of communication will bring new opportunities for world-wide collaboration among cement researchers, and should stimulate greater cooperation in planning research and sharing research results. Such cooperation is likely to have an enormous impact on the collective rate of progress in cement research by helping overcome inefficiences resulting from the limited resources being scattered among many relatively small research groups.

If researchers are willing to avail themselves of the opportunities, it is likely that research activities in different laboratories will become increasingly complementary. This can be

accomplished through the exchange of ideas at the planning stage and through the exchange of data. Through exchanges of this sort, it is possible to envision cement research moving into an era characterized by "hyperintelligence" as defined by Bugliarello [18]. The concept is that groups of individuals may be able to act as though possessing an enhanced intelligence because of ability to share knowledge easily and rapidly.

As a step towards establishment of a computer network among cement and concrete researchers, NBS is operating an electronic bulletin board (EBB) [19] for exchange of information regarding the expert system development. It allows participants to communicate with each other using personal computers connected by the telephone system. In this way, a computer conference can take place with participants commenting on, and recommending improvements to, the expert system. In the same way, the bulletin board may, eventually, provide access to the expert system, or other programs, for purposes of development or practical use.

The possibilities provided by computer networking complement, or multiply, those derived from the development and use of simulation models, expert systems, and databases without such a network.

6. DISCUSSION

Knowledge systems for cement and concrete science and technology depend on knowledge produced in the laboratory and in the field. A system for managing the knowledge facilitates its use and increases its value; however, it cannot be justified without the necessary knowledge. Furthermore, such a system must continue to be supplied with new information through laboratory and field research.

The biggest problem in predicting the performance of concrete is the lack of a sufficient database on field performance. This is an area where computers can be expected to make an important contribution which will be facilitated if a standard format for recording the field performance of structures can be made available.

As the knowledge system becomes better integrated and more coherent, research needs will become more clearly defined. For example, the development of the expert system DURCON has shown where more information on alkali-silica reactions is needed. Thus, improved methods for handling knowledge can increase the need for research by increasing the value of its results. The computer plays a vital role in this process by increasing the sophistication of the measurements and by facilitating the storage and retrieval of data. In view of the great advances in the technology, it seems that the time is now right for a workshop or conference to be held to discuss the planning and implementation of a knowledge system such as is discussed in the present paper. We are planning such a workshop.

7. CONCLUSIONS

The impact of computers on cement research is accelerating. Simulation models for the reactions of cements with water and expert systems relating to cement and concrete are being developed at the same time that database and networking technologies are undergoing rapid growth. Taken together, these developments provide new opportunities for collaboration among cement researchers in activities that will lead to still more rapid progress in cement and concrete science and technology.

8. ACKNOWLEDGEMENTS

The authors wish to acknowledge that very many persons have contributed to the development of the ideas presented in this paper. In particular, they wish to thank Dr. Leslie Parrott, Dr. Karen Scrivener, Dr. H.F.W. Taylor, Mr. Stewart Tresouthick, and Dr. Folker Wittmann, for many thought-provoking discussions, and Dr. Vagn Johanssen and all members of his RILEM Committee 68-MMH on Mathematical Modeling of Cement Hydration for the stimulation provided by their activities.

9. REFERENCES

1. Frohnsdorff, G., and Clifton, J.R., A review of mathematical modeling applied to the manufacture and use of portland cements, Cem. Res. Prog., 1980, pp. 279-304 (1981).

2. Taylor, H.F.W., and 11 others, The hydration of tricalcium silicate, Report of RILEM Committee 68-MMH, Task Group 3, Mater. Constr. (Paris), v. 17, 1984, pp. 457-468.

3. Pommersheim, J.M., and Clifton, J.R., Mathematical modeling of tricalcium silicate hydration, Cem. Concr. Res., v. 9, 1979, pp. 765-770.

4. Pommersheim, J.M., and Clifton, J.R., Mathematical modeling of tricalcium silicate hydration, silicate hydration, Cem. Concr. Res., v. 12, 1982, pp. 765-772.

5. Jennings, H.M., and Johnson, S.K., Simulation of microstructure development during the hydration of a cement compound, J. Amer. Ceram. Soc., (submitted for publication).

6. Martin, J.W., Service life prediction from accelerated aging test results using reliability theory and life testing analysis, in Masters, L.W. (ed.), Problems in Service Life Prediction of Building and Construction Materials, NATO Series E, Applied Science No. 95, Martinus Nijhoff, Dordrecht, Netherlands, 1985, pp. 191-211.

7. Duda, R., and Shortliffe, E.H., Expert Systems Research, Science, v. 220, No. 4594, 1983, pp. 261-268.

8. Clifton, J.R., Oltikar, B.C., and Johnson, S.K., Development of DURCON, an expert system for durable concrete: Part 1, NBSIR 85-3186, Bureau of Standards, Washington, D.C., 1985 (18 pp.)

9. Guide to Durable Concrete, ACI 201.2R-77, Manual of Concrete Practice, v. 1, Am. Concr. Inst., Detroit, 1985 (37 pp.)

10. Guide to the Selection and Use of Hydraulic Cements, ACI 225R-85, J. Am. Concr. Inst., v. 82, 1985, pp. 901-929.

11. Building Code Requirements for Reinforced Concrete, ACI 318-83, Manual of Concrete Practice, v. 3, Detroit, 1985 (111 pp.).

12. Ambler, E., Engineering Property Data: A National Priority, ASTM Standardization News, August 1985, pp. 46-50.

13. Jennings, H.M., Aqueous solubility relationships for two types of calcium silicate hydrate, J. Amer. Ceram. Soc., (in press).

14. Brown, P.W., Franz, E., Frohnsdorff, G., and Taylor, H.F.W., Analysis of the aqueous phase during early C_3S hydration, Cem. Concr. Res., v. 14, 1984, pp. 257-262.

15. Brown, P.W., Barret, P., et al., The hydration of tricalcium aluminate and tetracalcium aluminoferrite in the presence of calcium sulfate, Mater. Constr. (Paris) (submitted for publication).

16. The Cement and Concrete Reference Laboratory - A case history in collaborative standardization, ASTM Mater. Res. Stand., v. 10, 1970.

17. Pielert, J.H., Haverfield, J.W., and Spellerberg, P.A., Application of CCRL data in the formulation of precision estimates for selected cement standards, Cem., Concr., Aggregates, v. 7, 1985, pp. 37-42.

18. Bugliarello, G., Hyperintelligence: The Next Evolutionary Step, The Futurist, v. 18, 1984, pp. 6-11.

19. Kaetzel, L.J., and Clifton, J.R., A bulletin board system for feedback to the DURCON expert system: a description and reference, NBSIR Series Report, National Bureau of Standards (submitted for publication).

V.I. AKUNOV,
S.D. MAKASHEV,
V.A. DMITRIYEVA,
N.V. TSUKANOVA,
B.E. YUDOVICH

USSR

1

CL

MECHANOCHEMICAL ACTIVATION OF MATERIALS IN CEMENT MANUFACTURE

Mechanochemical activation has been reported for a number of materials being subjected to jet grinding, such as sand, limesand mixes, slag portland cement, straight cement, belite slurry, and high alumina cement. Jet grinding has been revealed to improve compressive strength ratings of the cement by 5 to 10 MPa on average. The reason for this increase lies in a more uniform grain size distribution of cement and the modified surface morphology of cement grains which include reentrant angles /1, 2/.

This report is devoted to the mechanochemical activation of cement raw materials and clinkers in jet mills (table 1) operating with two counter streams of material whose particles are accelerated to supersonic speeds by gaseous fluids, air and water steam, carrying them.

The grinding of certain raw materials and their mixes in a model MSP-0.5 jet mill provided an almost 100% yield in the 1-40 μm fraction range (table 2). As a result a 100 °C lower temperature can be afforded in the calcination zone of pilot rotary kilns, as compared with the temperatures needed to calcine the ball-mill ground mixes, the respective clinkering rate constant being also increased 2 to 7 times (table 3). The resultant clinkers exhibited an increased dislocation density on the chippings (table 4) which led to a 28-day compressive strength of this cement being increased by 5 to 15 MPa.

The largest increment of strength was exhibited by cements prepared from the raw mixes in which one component was jet-grinded (carbonaceous or agrillacious) and the other component was ball-mill grinded, the specific surface of the cements being about 3000 cm^2/g (table 5). For higher specific surface figures of 4000 and 5000 cm^2/g, a certain decrease was noted of the positive effect of jet grinding on cement strength ratings. Moreover, a further grinding of clinkers manufactured from jet milled raw materials, performed in a laboratory jet mill, to a fineness of 4000 cm^2/g failed to result in an additional increment of strength as compared with the ball milling of the same clinkers (table 5).

It was found, however, that the jet grinding of cements of diverse compound compositions in steam carrier fluid increased the compressive strength ratings as compared with that of ball-mill grinded cements

Table 1

Technical Data on Soviet Jet Mills MSP-0.5 and MSP-0.05

Description	Units	MSP-0.05	MSP-0.5	
Original lump size	mm	5	7	
Grinding compartment length/diameter	mm	150/180	200/140	
Acceleration ducts length/diameter	mm	20/16	40/32	
Nozzle diameter	mm	4	5	
Classifier type		impinge-swirling		
Carrier fluid		air	air or steam	
Input fluid pressure	atm	4-5	4-5	6-7
Fluid temperature	°C	20-25	20-25	230
Capacity	t/hr	0.05	0.5	
Specific energy requirements for clinker grinding	kWhr/t	300	200	
Fluid rate	m^3/min	1.1	0.7	

Table 2

Size Distribution of Jet Ground Raw Materials

Component	Persentage of fraction range shown			
	5 μ	5-20 μ	20-30 μ	30-40 μ
Chalk	0.3	0.5	8.2	91.0
Clay	0.1	25.0	23.4	51.5
Sand	1.4	3.1	38.1	57.4
Pirite cinder	0.3	0.9	2.6	96.2

Table 3

Kinetics of Lime Assimilation in Raw Mixes of Ball and Jet Grinding Processes

Grind process type	Percent R on 004 sieve	Bound CaO, %, after 30 min conditioning at indicated T, °C				Clinkering rate constant (after Carter-Valency)k x 10^{-4}, at shown T, °C			
		1000	1100	1200	1300	1000	1100	1200	1300
ball	14.4	28.5	18.6	15.2	4.3	5.5	20.0	28.0	96.0
inter-ground jet	1.3	18.9	17.2	14.9	2.8	19.7	23.4	30.0	119.0
separate jet	0.5	18.4	14.9	13.5	2.3	20.3	29.6	34.3	131.0
jet + clay ball chalk	2.2	15.9	15.2	14.3	1.6	27.5	29.8	32.9	150.0

Table 4

Dislocation Density on Chippings of Various Size Clinker Grains

Grind process type	Dislocation count, μ^{-1}, * for indicated grain size, mm						Count level
	1-2	2-3	3-5	5-7	7-10	10	
ball mill	0.84	0.77	0.74	0.70	0.59	0.51	min
	1.83	1.64	1.29	1.96	1.29	1.05	max
	1.34	1.21	1.02	1.33	0.94	0.78	av.
jet mill	0.84	0.70	0.88	1.35	1.20	1.38	min
	2.05	1.38	2.36	2.09	1.88	2.10	max
	1.45	1.04	1.62	1.72	1.54	1.74	av.

*Note: determined by the secant line method for each fraction.

(table 6). The highest effect of the mechanoactivation, 120 MPa, was noted for belite-aluminate cement, the lowest effect was identified for alite cements, independent of their C_3A content. Conversely, for alite jet-mill cements, a 4 to 5 MPa increase in early strength of up to 3 day old mortars dominated over the strength increments of other cements.

One of the reasons why jet grinding of cements increases the compressive strength ratings may be attributed to a growth (up to 80 %) of the yield of the 5-30 μm fraction over the 50 % content of this fraction in the ball grinded product (table 7).

When the carrier fluid was cold air, no effect of mechanoactivation was recorded after jet grinding of both belite and alite clinkers (table 6), which may be traced to a more extensive carbonation of new formations which occur in the grinding under the impact of the air moisture.

Jet grinding is able to promote the cement into the next higher compressive strength brand (due to a 50 kgf/cm^2 increase in the strength) provided the jet fluid is chosen appropriately. In view of a higher water requirement of jet-ground cements, the efficient application of this grinding method calls for a separate study.

V.I. AKUNOV,
S.D. MAKASHEV,
V.A. DMITRIYEVA,
N.V. TSUKANOVA,
B.E. YUDOVICH

Table 5

Physico-mechanical Tests of Ball and Jet Ground Cements

Raw mix grinding process	Strength, MPa, at age (days) indicated							
	bending				compressive			
	1	3	7	28	1	3	7	28
	Ball mill grinding to 3000 cm^2/g fineness							
1 ball	1.7	4.3	5.8	7.3	7.2	28.4	40.9	67.5
2 joint jet	1.9	5.1	6.8	7.2	8.6	31.7	45.8	68.4
3 separate jet	3.7	5.9	6.4	7.9	20.6	43.0	56.6	68.8
4 jet chalk+ball clay	3.3	6.3	7.3	8.6	16.8	41.2	57.6	84.5
5 ball chalk+jet clay	2.8	6.2	7.3	7.9	12.0	38.1	57.3	80.4
	Ball mill grinding to 4000 cm^2/g fineness							
1 ball	2.4	4.3	6.3	7.5	12.0	34.5	46.8	72.7
2 joint jet	4.8	6.2	6.6	7.9	26.0	46.9	59.1	73.7
3 separate jet	5.0	6.7	7.5	8.2	27.1	40.5	59.9	81.0
4 jet chalk+ball clay	3.9	6.5	7.6	7.8	18.5	42.8	59.0	81.5
5 ball chalk+jet clay	3.2	5.3	7.0	8.2	16.8	37.6	55.7	80.0
	Ball-mill grinding to 5000 cm^2/g fineness							
1 ball	2.8	4.3	6.3	7.5	13.6	36.9	47.4	68.4
2 joint jet	5.1	6.8	7.5	7.5	34.6	52.2	62.5	76.7
3 separate jet	5.2	7.0	7.1	7.9	32.5	51.1	62.0	71.9
4 jet chalk+ball clay	5.0	7.0	7.5	8.4	33.5	50.9	64.3	71.2
5 ball chalk+jet clay	4.2	6.0	6.8	8.1	25.6	43.2	52.8	70.0
	Jet grinding to 4000 cm^2"g fineness							
1 ball	2.9	4.3	8.2	9.2	14.7	35.6	55.2	74.1
2 joint jet	3.8	6.7	7.7	9.2	20.8	41.2	55.2	77.6
3 separate jet	2.9	5.9	7.6	8.8	25.8	32.5	51.6	64.4
4 jet chalk+ball clay	3.3	6.6	8.7	8.9	17.6	37.7	58.7	74.1
5 ball chalk+jet clay	2.9	7.3	8.4	8.8	15.1	37.8	61.2	71.9

Table 6

Physico-mechanical Tests of Various Jet and Ball Ground Cements

	Clinker composition, %				Strength, MPa, at age (days) indicated							
					bending				compressive			
No.	C_3S	C_2S	C_3A	C_4AF	1	3	7	28	1	3	7	28
					Ball mill grinding							
1	12	61	6	16	1.3	1.5	1.8	3.8	5.2	7.5	10.0	26.2
2	55	18	9	12	2.9	5.4	5.6	6.8	14.9	34.5	44.1	60.9
3	35	44	3	15	3.0	5.2	5.2	7.7	9.6	26.1	34.1	57.9
4	32	47	9	9	2.7	4.7	5.1	6.9	9.0	21.9	33.1	54.7
5	65	16	4	13	3.3	5.8	6.9	7.9	12.4	31.6	46.8	65.7
6	55	18	10	14	2.6	6.0	6.5	7.4	9.5	30.8	45.6	64.5

V.I. AKUNOV,
S.D. MAKASHEV,
V.A. DMITRIYEVA,
N.V. TSUKANOVA,
B.E. YUDOVICH

Table 6

Clinker No.	Clinker composition, % C_3S	C_2S	C_3A	C_4AF	Strength, MPa, at age (days) indicated: bending 1	3	7	28	compressive 1	3	7	28
					Air-jet grinding							
1	12	61	6	16	1.5	1.7	1.9	3.3	5.2	7.7	9.3	25.1
2	55	18	9	12	3.3	5.3	6.0	7.3	17.2	35.1	42.8	58.9
					Steam-jet grinding							
3	35	44	3	15	2.9	5.7	5.8	8.2	9.4	27.6	30.9	62.4
4	32	47	9	9	3.1	4.9	5.5	8.3	10.5	29.8	38.4	66.6
5	65	16	4	13	5.3	7.3	8.4	8.9	21.8	45.6	54.6	69.7
6	55	18	10	14	4.3	6.9	7.1	8.8	18.1	42.2	57.2	69.9

Table 7

Grain Size Distribution for Various Cements

Clinker No.	Weight percentage for indicated grain size range (μ) 1	1-5	5-7	7-10	10-15	15-20	20-30	30-60	30	60
					Ball mill grinding					
1	7.8	11.7	9.3	13.7	4.9	9.8	15.2	17.7	27.6	9.9
2	7.7	4.4	10.8	7.3	8.3	12.7	17.1	20.5	31.7	11.2
3	22.1	3.9	6.1	3.1	18.3	7.4	4.8	27.3	24.3	7.0
4	20.7	1.3	9.4	9.9	16.6	9.9	3.5	25.4	28.7	3.3
5	19.6	4.0	7.6	9.8	18.3	10.2	11.0	13.1	19.5	6.4
6	19.3	3.0	4.2	8.4	19.3	8.4	8.4	22.6	29.0	6.4
					Jet grinding					
1	4.4	7.5	8.5	17.0	28.7	16.5	2.7	14.2	14.7	0.5
2	9.5	4.6	10.3	9.8	16.0	16.5	7.7	22.5	25.5	3.0
3	19.9	3.1	12.0	15.7	23.1	6.8	17.8	1.6	1.6	-
4	34.6	2.1	2.1	31.4	24.6	4.2	1.0	-	-	-
5	21.5	1.0	14.1	5.8	30.9	20.4	2.1	4.2	4.2	-
6	17.8	6.3	8.4	16.2	28.3	15.2	5.2	2.6	2.6	-

REFERENCES

1. Акунов В.И. Струйные мельницы. М., Машгиз, 1967, 267 с.
2. Акунов В.И., Юдович Б.Э., Литвинов Г.П. и др. Генерация поверхности и зернового состава продуктов измельчения в струйных мельницах. "Цемент", 1980, № 7, с. 11-13.

Y.M. BAZHENOV - MISI Kujbychev, Moscou - U.S.S.R.

EVALUATION OF REOLOGICAL CHARACTERISTICS OF CEMENT PASTE AND CONCRETE WITH HELP OF COMPUTERS

CL

The development of computer technic discovers the possibility to further improvements of technological recalculations to obtain higher quality of production and economic benefits. Computerisation of concrete technology has a great importance, particularly in the conditions of increasing the deviation in properties of raw materials (different chemical and fine-grounded admixtures, secondary industrial raw materials), and complicated technology (application of robots, new ways of mix activation, new casting equipment and ways of concrete set). Operation of technology on the base of wideer computer application will give a guaranteed quality of the fresh concrete mix and a quality of hardened concrete for different conditions of precast concrete constructions.

Additionally computerisation of industry needs a new approach to evaluation of influence of cement, aggregates and other factors on the rheological characteristics of concrete mix. For the first time we are interested not in general estimation of material utility for concrete, but quantitative evaluation of one or another factor on rheological characteristics of concrete, setting time, hardness and concrete strength at particular age.

There are wide applications of mathematical models in technological recalculations in the Soviet Union, which allow to obtain with the help of experiments planning and standard means of materials tests, tests of fresh concrete mix and hardened concrete (1, 2, 3, 5). However, these methods are suitable for accepted conditions and alternation of raw materials and technology needs its great adjustment. Therefore it remains an actual task of discovering a new criterion of evaluation cement and aggregate influence on characteristics of concrete mix and relations, which give us a possibility to describe characteristics of cement paste and concrete mix of different compositions in general form. This is more important in conditions of increased raw material resources for concrete and large utilisation of different water-reducers and complex admixtures on their base.

With addition of water-reducers and superplasticizers to cement paste either efficiency or influence on fluidity (SI) of cement paste and rate of admixture (D) depend on type of admixture and quality of cement. However, the slope of curves Sl=f(D is similar in all cases (Fig. 1), and only parameters of these curves are different. We can see three areas on these curves. At the first area the quantity of water-reducer is yet not enough for an influence on all the cement grains and admixture efficiency is negligible. Slight fluidizing effect is gained at the area 11, when the continuous layer of water-reducer is developed on the cement grains surfaces. Optimum cement rate accounting for technical and economic factors lays in the limits of this area. The efficiency of admixture gradually decreases at the area 111. Physical and chemical factors which determinate the slope and parameters of curves Sl=f(D) for different types of water-reducers are different, however, the slope of curves having a great importance for mathematical prediction of admixture efficiency looks alike. This gives us a possibility to approximate in calculation of the function Sl=f(D) at the area 111 with the help of following expression:

$$Sl = K_1 K_2 (D + a)$$

where: K_1 - coefficient of water-reducer influence on fluidity of cement paste; K_2 - coefficient accounted for the influence of cement; a - constant.

Coefficient K_1 can in some limits give us a characteristic of the water-reducer efficiency; the bigger coefficient, the higher fluidizing effect. Coefficient K_2, in general, determines the possibility of applicating an admixture for a given cement; its increasing shows a higher efficiency of an admixture in the cement paste of a given

cement.

It's recommended to held out comparison tests of small volumes to get useful data for calculations. As a standard one could apply data of a well-known water-reducer or data of agreed standard curve. It's recommended to discuss possible parameters of such a curve at the congress.

However, there are some limits of information concerning influence of water-reducers on cement pastes for prediction of rheological characteristics. One should mention the structure of concrete mix, characteristics of aggregates, quantity of cement. The aggregate influences on rheological characteristics of the mix. This aggregate influence is practically impossible to evaluate on the base of its size, pore volume and other standard characteristics only. The appointed integral criterion - "water consumption of aggregate" - gives a more accurate evaluation and this criterion obtained from estimation of water consumption of cement paste, mortar and concrete mix of equal fluidity determine relative increase of water-cement ratio which applied for comparison of structural role of the aggregate. In account of water consumption of the aggregate it's possible to estimate the efficient water-cement ratio which characterizes the behaviour of the cement paste and the concrete mix (1, 4).

The influence of water-reducing admixtures on rheological characteristics of a concrete mix could be accounted for with the help of a special coefficient the same way as with the cement paste which is determined with comparison tests. It substantially simplifies accounts and gives us a possibility to use one method of prediction of the rheological characteristics of concrete mix for application of different water-reducers.

In the base of this proposal lays an experimentally stated fact that water-reducers don't alter their character of relation between the concrete mix fluidity and water consumption, but alter parameters of relative curves only (Fig. 2, 3). Addition of water-reducer increases fluidity of the concrete mix and decreases water consumption of the concrete mix of equal fluidity. If known that admixture decreases water consumption of the concrete mix by 10 or 20% then we can describe corresponding curves which have the same behaviour as the curve for the concrete mix without an admixture but with different parameters, and determine water consumption with the help of these curves to obtain a given fluidity of the concrete mix. While applying complex chemical admixtures the influence on water consumption of concrete mix is possible to evaluate the type and rate of the water-reducing coponent.

The influence of water-reducing admixtures on water consumption of a concrete mix is possible to evaluate with the coefficient which shows an amount of decreased water content at equal fluidity of mix in the presence of an admixture.

$$\alpha = B_g/B = \frac{100 - {}_{\Delta}B}{100}$$

where B_g - water consumption of concrete mix in the presence of an admixture; B - water consumption of a concrete mix without admixture; B - reduction of water consumption of concrete mix with of an admixture.

Coefficient α determines slope of the curve S1 = (B) and efficiency of admixture. This coefficient depends on the type and rate of an admixture and the quality of an applied cement.

Fluidity of a concrete mix increases with an admixture rate. The behaviour of the curve S1 =(D) is similar to the curve of the cement paste and has same characteristic areas. Optimal admixture rate is usually admitted at the upper side of the area 11 (higher increase of fluidity with the rate of an admixture), but to some limits could be influenced by some other factors: necessity of high development of concrete strength, guarantee of no bleeding of concrete mix, economic benefits, etc.

Comparison of different water-reducing

admixtures in optimal rates gives us a possibility to divide them into several classes by its efficiency of influence on the rheological properties of a concrete mix: water-reducers, which decrease water content

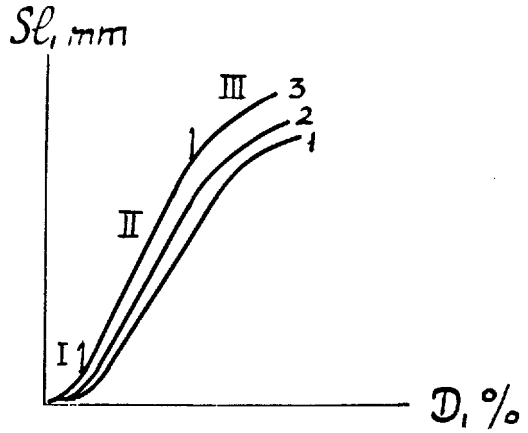

Fig. 1. Influence of water-reducer rate on a slump of cement paste: 1-cement paste with 10% of C_3A in cement and the admixture "40-03"; 2-same as above, but 4% of C_3A; 3-cement paste with 4% oc C_3A and the admixture "10-03"

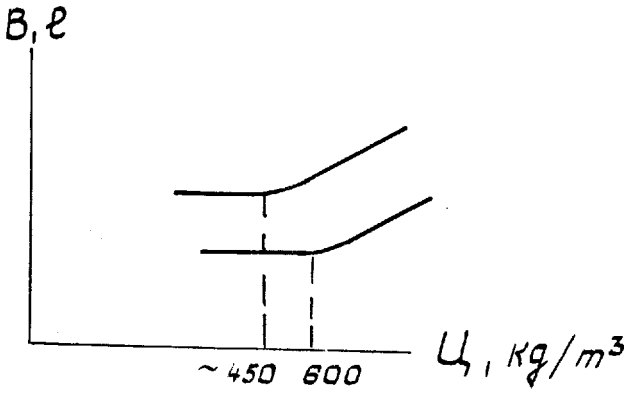

Fig. 2. Influence of the type of water-reducer on water consumption of the concrete mix: 1-concrete mix with superplasticizer C-3; 2-same as above, but with СДБ ; 3-same as above, but without admixture

on 5, 10, 15, 20 and 25% in mixtures of equal fluidity. Coefficient α will be altering the range from 0,95 to 0,75, correspondingly, we need a quantitative value

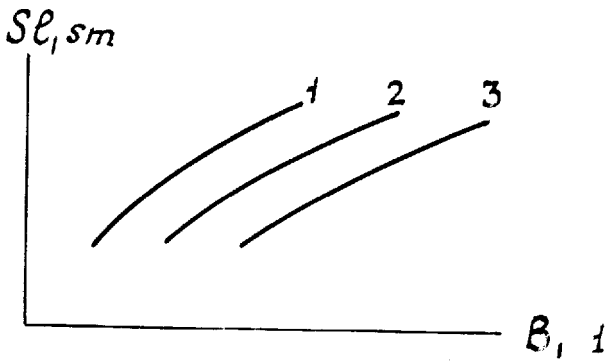

Fig. 3. Influence of the superplasticizer C-3 on the relation between water consumption of the concrete mix and cement consumption: 1-concrete mix in presence of superplasticizer; 2-concrete mix without an admixture

Table 1

Type of superplasticizer	Water-cement ratio	Water reduction in mixes with equal fluidity, %
Reference concrete mix without admixture	0,425	-
C-3 (USSR)	0,32	24,8
30-03 (USSR)	0,315	26,0
KM-30 (USSR)	0,31	27,2
10-03 (USSR)	0,31	27,2
Mighty (Japan)	0,315	26
БП -1 (Bulgary)	0,32	24,8
Melment (FRG)	0,32	24,8
Super (USA)	0,318	25,3

of the coefficient for computer calculations, but not the nature of the admixture. Different admixtures of one class will be presented by one coefficient in calculations.

Experiments have shown that admixtures of the different chemical composition, but one and the same class of influence had a relatively small deviation in the reduced

Table 2

Cement composition, %		Average water reduction in mixes of equal fluidity in the presence of superplasticizer "10-03", %			
C_3S	C_3A	0,5	0,75	1	1,25
49	6	18	23	28	33
40	8	17	22	27	32
33	10	15	19	24	29

water (Table 1).

The comparisons were taken with one rate of superplasticizer 10 and fluidity of the concrete mix 5 cm. Cement consumption was 500 kg/m^3, r = 0,32. Similar results were obtained by the small correlation of admixture rate.

Influence of mineralogical composition of cement on the efficiency of the superplasticizer was smaller then the rate of admixture (Table 2). This can be accepted by coefficient ß excluded in terms of corresponding correlation of admixture rate, e.g. with aluminate cement the quantity of superplasticizer could be increased by 0,1-0,2% of cement weight.

To get proof of the water-reducers efficiency it's necessary to develop a standard method of comparison tests. This gives us a possibility to design mathematical models with application of such arguments as cement paste-consumption, water consumption of aggregate, effective water-cement ratio of the cement paste and concrete mix, coefficients of water-reducer efficiency, α and ß. Experimental calculations show the possibility of accurate prediction of rheological properties of the concrete mix with the help of one model, when different cements, admixtures, and aggregates are applied. Correspondingly the reversal task of concrete mix design in the function of given rheological properties were carried out more accurately and the possibility of effective monitoring of precast concrete and concrete construction process has become a reality. We can immediately react to the slightest alternations in raw materials properties and obtain high quality of construction with minimal consumption of cement and reduced costs with the help of computers.

REFERENCE

1. Bazhenov Y.M., Komar A.A., Technology of concrete and reinforced concrete production. Moscow, Stroyizdat, 1984.
2. Bazhenov Y.M., Voznesenskiy V.A. Perspectives of application of mathematical methods in technology of precast concrete. Moscow, Stroyizdat, 1974.
3. Bazhenov Y.M., Gorchakov G.I., Alimov L.A., Voronin V.V., Improvement of durability of concrete and reinforced concrete constructions in severe conditions. Moscow, Stroyizdat, 1984.
4. Bazhenov Y.M. 7-th Congres International de la Chimie des Cimentas. 1980, Paris, vol. 1V, p. 125.
5. Shein V.I. Mathematical models of alternation of the properties of cement paste with time. 7-th Congres International de la Chimie des Cimentas. Paris, 1980, vol. 1.

L.S. GEIDAROVA, Giprocement, Lëningrade, URSS
M.A. ASTAKHOVA

CERTAINS ASPECTS DE L'ACTIVATION LORS DE L'OBTENTION DU LIANT SANS CLINKER

Il est connu que les substances peu solubles se caractérisent des propriétés déterminées de l'acidité ou basicité de la surface, qui peuvent être renforcées par le traitement thermique à 413-773K [1].

Cette technique été utilisée pour la matière sulfatocalcique - phosphogypse - qu'est sous-produit de la production chimique.

Active par son acidité, la forme du phosphogypse a été étudiée à la température différente du traitement sur des systèmes-modèles - suspensions - de rapport phosphogypse/eau = 1:10, par mesure à l'aide de pH-mètrmillivoltmètre. La variation de la concentration des ions H^+ dans les suspensions en fonction de la température du traitement du phosphogypse montre qu'elle atteint sa valeur maximale à 673K [2].

Les résultats de la spectroscopie infrarouge et de l'analyse des phases aux rayons X ont mis en évidence la déshydration du phosphogypse lors du traitement thermique à 673K et la transformation du réseau cristallin du gypse dihydraté en structure d'anhydrite - apparition de la raie d'absorption 620 cm^{-1}, disparition de la raie 1686 cm^{-1}. On note aussi la présence du sulfate de calcium en forme hydratée - $CaSO_4 \cdot 0,5\ H_2O$ - les raies d'absorption dans la région de 3615, 3546, 1620 cm^{-1}. L'apparition de l'anhydrite est nettement observée sur les diffractogrammes par les raies 3,85; 3,49; 2,83; 1,87; 1,75; $1,65 \cdot 10^{-10}$ m.

La présence du gypse en forme semihydratée 3,48; 3,10; 2,80; 2,35; 1,85; $1,70 \times 10^{-10}$m y est aussi constatée.

Selon les données de l'analyse thermique différentielle le phosphogypse prétraité à 673K par rapport au phosphogypse, révèle un effet endothermique très faible dans la plage de 423- à -473K qui est lié à la déshydratation du gypse semihydraté, présenté en phosphogypse en quantité peu considérable. La perte de l'eau fait ici 0,75%. Les études physicochimiques ont mis en évidence que le phosphogypse traité à 673K est présenté par d'env. 85% de l'anhydrite et par 15% du gypse semihydraté.

L'analyse électronique stéréomicroscopique a montrée que le traitement du phosphogypse à 673K varie entièrement la forme de ses cristaux. Du phosphogypse aux grands cristaux lamellaires il se transforme aux plus petites particules de differentes dimensions, parmi lesquelles on distingue aussi les cristaux lamellaires, mais de moindres dimensions (fig. 1b).

Le nouveau produit obtenu - le phosphoanhydrite - a été utilisé pour l'activation de la pâte de néphéline (sous-produit de la production de l'alumine), comprenant jusqu'à 85% de β-C_2S. L'activation de la pâte de néphéline est nécessitée par l'absence des propriétés liantes, car les grains de β-C_2S, dont elle est composée, sont entourés des enveloppes finement agrégées hydratées. On a introduit de 5 à 15% de l'activateur lors du broyage de la pâte de néphéline. La composition optimale du liant comprend 90% de la pâte de néphéline et 10% du phosphoanhydrite. En résultat des études on a obtenu le liant mixte dont l'activité après 28 jours du durcissement était comprise entre 32 et 36 MPa.

L'analyse physico-chimique (des phases à rayons X, ATD, IR-spectrométrie, électronique-stéréomicroscopique, pétrographique) a montré l'augmentation de la réactivité de la pâte de néphéline en présence du phosphoanhydrite [3]. Sur les diffractogrammes à 3 et 28 jours du durcissement on note en particulier la diminution des raies analytiques du silicate bicalcique: 1,93; 2,02; 2.28; 2,19; 2,41; 2,54; 2,61; 2,74; 2,78; 2,88; $3,04 \times 10^{-10}$ m pour la pâte de néphéline activée par rapport au β-C_2S pur et à la pâte de néphéline inactivée. Après 28 jours du durcissement on note sur les diffractogrammes l'apparition des reflets se rapportant à la phase d'ettringite: 9,6; 5,6; $3,85 \times 10^{-10}$ m. Pour les produits de l'hydratation du liant (de la pâte de néphéline avec phosphoanhydrite) à l'âge de 3 jours on distingue sur les courbes d'ATD l'effet endothermique à 408K et 423K lié

à la perte de l'eau d'adsorption et la décomposition du gel de tobermorite. On peut supposer aussi dans l'échantillon la présence des petites quantités des hydrosilicates mal cristallisés, hautement basiques, pareils au tobermorite, et des hydrosilicates de calcium-sodium (effets endothermiques faibles à 869K et 1003K).

Sur les courbes d'ATD des produits de l'hydration du liant étalon (la pâte de néphéline avec du gypse) on note les effets endothermiques à 423K, 438K, 931K et 1072K. Pour le liant activé les pertes de poids sont plus élevées (1,5 fois) que pour le liant étalon.

Les résultats de la spectrométrie infrarouge prouvent aussi une grande intensité du processus de l'hydratation du liant activé.

Par comparaison au liant étalon l'analyse pétrographique a révélé l'augmentation importante de nouvelles formations dans les produits de l'hydratation du liant de néphéline activé vers 28 jours du durcissement. Les particules de la pâte de néphéline semblent être cristalloamorphes, car elles sont entourées par de masses compactes de nouvelles formations, composées des hydrosilicates, des écailles de $Ca(OH)_2$, des grains du carbonate et d'ettringite.

Les photographies prises au stéréomicroscope électronique des produits de l'hydrations du liant activé après 28 jours du durcissement (fig. 2a) montrent que la structure du liant activé durci se caractérise par les globules du gel C-S-H, liées aux grains de l'ettringite. La structure correspond à la formation de gros agrégats sphériques (ayant quelquefois la forme des disques), qui forment des liaisons avec des particules avoisinantes (germinations aux points de contact par gel C-S-H, ayant une forme morphologique de feuille). La structure du liant étalon (fig. 2b) est globulaire par sa composition, mais friable, la consolidation est assurée par germination aux points de contact du gel, enveloppant les particules de la pierre de néphéline.

Les données d'expérience citées montrent que l'activateur obtenu-phosphoanhydrite - influence la composante siliceuse de la pâte de néphéline et elles permettent de croire possible l'activation des matériaux au caractère inerte par rapport aux propriétés liantes par de certains produits thermiquement traités.

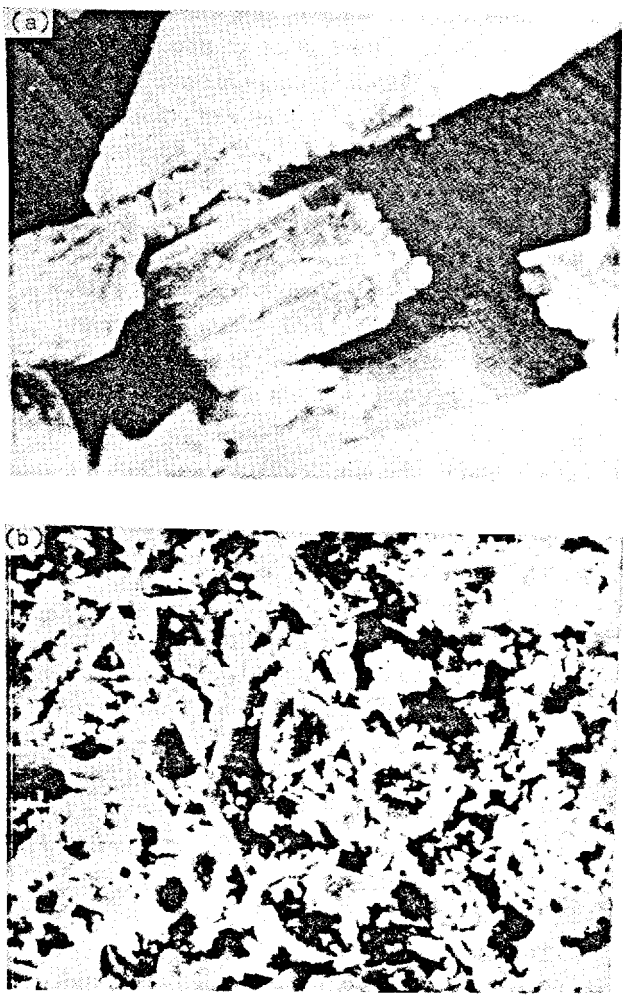

Fig. 1. Structure du phosphogypse (a) et du phosphoanhydrite (b) sous microscope électronique, x1000.

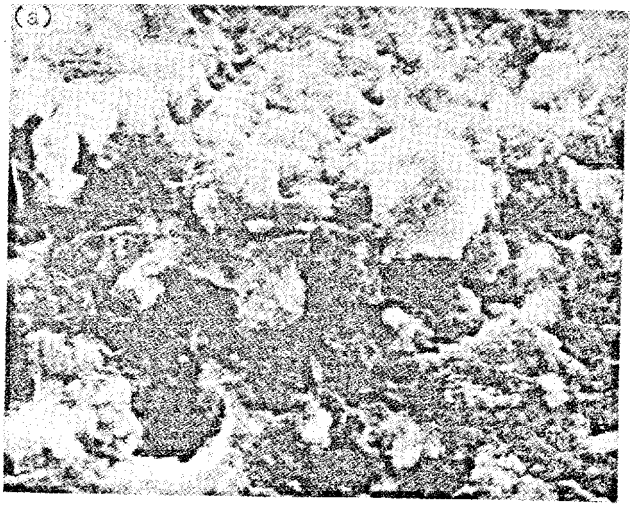

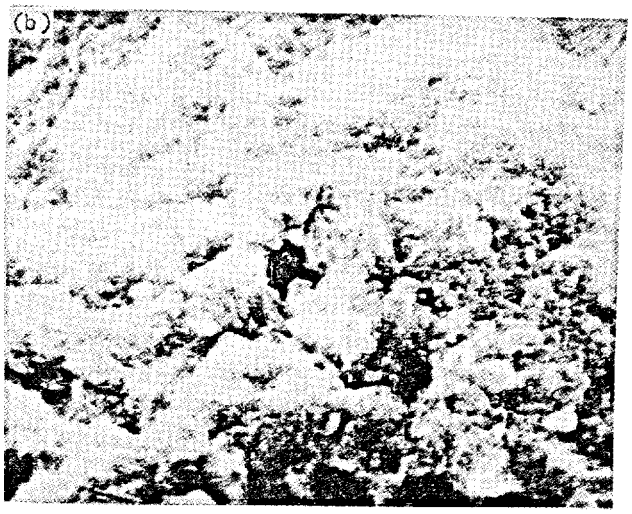

Fig. 2. Microphotographie électronique de la réplique de la surface de la pierre de la pâte de néphéline avec phosphoanhydrite (a) et gypse (b) après 28 jours du durcissement, x3000.

BIBLIOGRAPHIE

I. Танабе К. Твердые кислоты и основания. Изд-во "Мир", Москва, 1973.
2. Сычёв М.М., Гейдарова Л.С., Астахова М.А., Сватовская Л.Б. Активация нефелинового шлама фосфогипсом - Цемент, 1983, № 5.
3. Сычев М.М., Сватовская Л.Б., Астахова М.А., Гайдарова Л.С. Некоторые аспекты активации сульфато-нефелинового вяжущего - Цемент, 1985, № 2.

V.D. GLOUKHOVSKY - Institut des Ingénieurs du bâtiment, Kiev, URSS
P.V. KRIVENKO,
R.F. ROUNOVA

PARTICULARITES DE LA FORMATION DE STRUCTURE DANS LE CIMENT DURCI CONTENANT DES ALCALIS

La manière traditionnelle chimico-minéralogique d'aborder un problème de la synthèse de résistance du ciment durci ne permet pas d'augmenter considérablement l'activité des ciments calciques existants puisque leur base consiste dans la réalisation des propriétés d'hydratation des minéraux de clinker à haute basicité qui est suivie de phénomènes positifs comme négatifs.

L'expérience accumulée pendant plus de 20 ans de recherches et d'exploitation dans le domaine du ciment durci sur la base des systèmes dispersifs ne contenant pas de minéraux à haute basicité et utilisant, à côté de la phase vitreuse, en qualité d'un constituant siliceux, des composés à faible basicité avec C/S $\leq$ 2 montre (1, 2) que le résultat de la formation de structure se distingue qualitativement du résultat traditionnel mentionné. Ces systèmes, par suite de l'augmentation du degré de condensation anionique des tétraèdres d'aluminium et silicium oxygénés, possèdent une résistance élevée à la destruction hydrolytique tandis que l'introduction dans le milieu de gâchage des alcalis ayant une énergie chimique considérable rend ces systèmes très actifs (3).

Les propriétés du ciment durci alcalin se caractérisent par les paramètres suivants: activité lors des essais standartisés - 80...140 MPa; résistance à la flexion - 6...14 MPa; résistance au gel - 700...1000 cycles; imperméabilité à l'eau - B10...B50; résistance à la corrosion dans les milieux de sulfate K_c = 0,9 - 1,2 (4). Suivant l'intensité d'accroissement de résistance (I jour - 25...35 MPa; 3 jours - 65...75 MPa) les ciments se rapportent aux ciments à durcissement super rapide et suivant le dégagement de chaleur - aux ciments à faibles températures.

La présence du cation alcalin conditionne les particularités des processus de la formation de structure des ciments en question (5). A la période d'hydratation initiale, le cation alcalin joue un rôle d'un catalysateur en diminuant la concentration du CaO dans le liquide mère, maintenant les forces ioniques du milieu de gâchage nécessaires à la destruction des liaisons covalentes résistantes et en prenant part à l'évacuation des produits de destruction hors de la réaction grâce aux processus d'échanges des cations. Ces produits sont des gels d'hydrosilicates contenant des agglomérations des hydrosilicates de calcium fibreux à basse basicité d'un aspect commun CSH (B) et des inclusions des hydrogrénats à composition variable ainsi que l'acide silicique précipité.

A mesure du développement des processus de condensation et de condensation-cristallisation, le constituant alcalin devient un des éléments-formateurs de structure du ciment durcissant. Les formations nouvelles alcalines sont analogues aux hydroalumosilicates alcalins de type des zéolites et des hydromicas ainsi qu'aux compositions mixtes alcalines-alcalino-terreuses - analogues aux naturelles ce qui prédétermine leur durabilité et certaines autres propriétés (2). Selon les indices structuraux, ces phases, comme en cas du gel d'hydrosilicate, se trouvent également longtemps en état amorphe se condensant autour de la carcasse hydrosiliceuse dans les pores du ciment durci en augmentant avec cela la densité et l'imperméabilité à l'eau de ce dernier. La porosité du ciment durci contenant des alcalis est caractérisée par une teneur élevée en pores du gel dont le rayon et de 1,0 - 4,0 mm et par une teneur diminuée en pores capillaires.

Selon nos recherches (6), les états amorphes et cristallins métastables de la structure de la matière minérale jouent un rôle particulier dans les processus de la formation de structure du ciment durci. Ce rôle est conditionné par le fait que la matière se trouvant dans l'état mentionné est caractérisée, en comparaison avec la matière cristalline stable, par un pouvoir énergétique maximum et une densité minimum. C'est justement ça qui assure le processus de con-

Tableau

Degré de rétablissement des liaisons structurales de la pierre de ciment obtenue par les formations nouvelles du ciment alcalin

Composition de la phase type gel	Cycles de pressage*	$R_{compr.}$, MPa / ρ, g/cm — Pression, MPa					
		50	100	300	400	500	1000
$0,8CaO \cdot SiO_2 \cdot 2H_2O$	I	21,9 / 1,06	30,4 / 1,09	143,0 / 1,34	192,5 / 1,53	275,6 / 1,65	136,4 / 2,04
	II	23,8 / 1,08	50,0 / 1,09	77,0 / 1,38	68,0 / 1,59	72,2 / 1,63	68,0 / 2,06
	III	24,0 / 1,09	23,4 / 1,11	67,8 / 1,49	71,0 / 1,76	70,0 / 1,90	46,7 / 2,12
$Na_2O \cdot Al_2O_3 \cdot 2SiO_2 \cdot 2H_2O$	I	9,4 / 1,11	22,2 / 1,27	52,1 / 1,58	58,8 / 1,59	67,9 / 1,71	69,1 / 1,80
	II	9,0 / 0,89	20,6 / 1,02	55,8 / 1,34	104,0 / 1,47	123,0 / 1,58	171,0 / 1,77
	III	7,53 / 0,89	17,7 / 1,02	33,3 / 1,34	50,7 / 1,47	58,1 / 1,58	28,1 / 1,77
		33,5	15,8	13,2	12,0	10,8	10,2
		Pertes de l'eau zéolithique, %					

* En cas des mêmes pressions, les échantillons du deuxième pressage ont été préparés à partir de la matière des échantillons du premier pressage et les échantillons du troisième pressage - à partir de la matière des échantillons du deuxième pressage.

densation (formation de structure) et qui se manifeste dans les interactions superficielles, dans l'apparition des contacts de phase entre les particules ainsi que dans la diminution de volume du système pour le compte de l'augmentation de densité de la matière.

Outre la participation dans les processus de formation de structure du ciment durci d'un caractère d'hydratation-condensation, les phases amorphes et métastables se trouvant dans l'état dispersif tendent à la formation de structure du type contact-condensation dont l'essence est montrée dans nos publications aux Congrès précédents (7, 8). La présence de ces phases dans le système dispersif obtenu par l'hydratation en excès du liquide de gâchage détermine les propriétés distinctives des liaisons structurales du ciment durci qu'elles forment.

Selon les notions connues (9), lors du durcissement de la pâte de ciment, la structure de coagulation thixotrope avec des contacts de film hydrolabiles passe en structure type condensation-cristallisation avec des contacts de phase irréversibles résistants à l'eau. Nos expériments montrent que ces derniers portent longtemps un caractère partiellement réversible (voir tableau). Ils

peuvent être détruits, broyés et rétablis ensuite par pressage, c'est-à-dire à la suite du rapprochement réitératif des macroparticules immédiatement après le pressage avec l'obtention d'une pierre résistante à l'eau. Et c'est seulement après le passage de toutes les formations nouvelles hydrosiliceuses dans un état cristallin stable que les contacts de phase prennent un caractère irréversible, et il est impossible d'obtenir la pierre résistante à l'eau par pressage.

Après la destruction, broyage et ensuite le pressage de la pierre, sa résistance se rétablit d'une façon incomplète. Si les cycles de durcissement-destruction-broyage-pressage continuent, alors après chaque cycle, la densité de la pierre augmente tandis que l'énergie superficielle des particules et la résistance de la pierre diminuent. C'est pourquoi, après chaque cycle avec rétablissement des contacts, la résistance de ces derniers diminue (pratiquement à la pression >300 MPa). En cas de l'aluminosilicate sodique, la perte de l'eau zéolitique se superpose sur cette dépendance commune ce qui exerce une influence sur un caractère du changement de densité et sur une consolidation intermédiaire de la pierre.

En général, le processus de la formation de structure du ciment durci sur la base des hydrates dispersifs métastables se produit avec le dégagement d'énergie et est suivi de phénomènes qui peuvent être caractérisés, en termes les plus généraux, comme l'autoorganisation (mise en ordre) de la matière.

Les données ci-dessus concernant les particularités de la formation de structure ouvrent des possibilités pour contrôler les propriétés des ciments alcalins et de la pierre à durcissement de contact (reçue par pressage des hydrates broyés). En premier cas, cela s'obtient par la normalisation de la composition des éléments alcalins, c'est-à-dire des phases aluminosiliceuses, par la teneur en constituant alcalin et son type et par la teneur en additions de modification. Le ciment de laitier alcalin M 400...M 1400 est un exemple de ces ciments. Outre les résultats techniques, l'utilisation de ce ciment favorise la solution des problèmes liés aux gains d'énergie dans la technologie de la production du ciment.

En deuxième cas, cela s'obtient par la répartition dans le temps des processus chimiques et physiques. De ce fait, lors du durcissement, il n'y a pas de changement de composition chimique ou d'état agrégé de la matière. Sans la consommation d'énergie supplémentaire, il devient possible d'utiliser dans la composition des ciments alcalins une série de produits secondaires desquels on obtient dans le système donné les hydrates métastables et ensuite stables (boues de bélite et d'amiante ciment, cendres très calciques d'hydroévacuation, etc.).

References

1.В.Д.Глуховский. Грунтосиликаты. К., 1959.

2.Щелочные и щелочноземельные гидравлические вяжущие и бетоны. Под общ.ред.проф. В.Д.Глуховского. К., 1979.

3.Шлакощелочные бетоны на мелкозернистых заполнителях. Под общ.ред.проф. В.Д.Глуховского. К., 1981.

4. V.D. Glukhovsky, G.S. Rostovskaja, G.V. Rumyna. 7th Int. Congr. on the Chem. of Cem., v. III. Paris, 1980.

5. П.В.Кривенко. "Цемент", № 3, 1985.

6. П.И.Боженов, В.Д.Глуховский, Р.Ф.Рунова Сб. "Строительные материалы. Строительное производство". Л., 1973.

7. В.Д.Глуховский, Р.Ф.Рунова. VI Международный конгресс по химии цемента, т. II, ч. I., 1976.

8. V.D. Glukhovsky, P.V. Krivenko, R.F. Runova. 7th Int. Congr. on the Chem. of Cem., v. II. Paris, 1980.

9. Ребиндер П.А. Физико-химическая механика дисперсных структур. М., 1966.

A.V. VOLJENSKIY -Institut des Ingénieurs du bâtiment de Moscou, URSS

INFLUENCE DE LA CONCENTRATION DES LIANTS EN MELANGE AVEC L'EAU SUR LA RESISTANCE ET DEFORMABILITE DE CE MELANGE LORS DU DURCISSEMENT

Toutes les propriétés techniques des mélanges des liants durcis avec l'eau, y compris la durabilité, sont déterminées par les facteurs principaux suivants:

1. Les propriétés physiques et physico-chimiques des liants et des hydrates se formant lors de l'interaction des liants avec l'eau aux conditions de durcissement adoptées.

2. La concentration du liant par masse en unité de volume du mélange initiale et la valeur limite optimale de cette concentration pour chaque liant et chaque condition de durcissement. Le dépassement de cette valeur favorise la chute de résistance et même l'autodestruction du système dans les conditions d'expansion libre.

3. La microstructure de la phase solide et des pores dans le monolithe durci déterminée par la dispersité et la configuration des particules d'hydrates nouvellement formées.

4. Les propriétés d'adhésion-cohésion et autres propriétés physico-chimiques des particules nouvellement formées.

Avec cela, plus est grand le volume absolu de la phase solide en unité de volume du monolithe durci (jusqu'à la valeur limite) et plus sont intensives les manifestations des propriétés d'adhésion-cohésion des particules constitutives, plus sont dispersives ces particules et par conséquent, plus sont fins les pores - plus est haut le niveau des propriétés de construction du monolithe (à l'exception du paramètre de protection thermique).

La concentration optimale du liant en mélange avec l'eau "C_o" et le rapport nécessaire "eau-liant" sont déterminés par les formules 1 et 2.

$$C_o = \frac{\rho_I}{(I + W_o)(I + V)} \qquad (1)$$

où, ρ_I est la densité réelle de l'hydrate en g/cm^3, W_o est la quantité d'eau invaporable lors du durcissement du liant en g/g de masse du liant initial, V est le volume limite minimal des pores se formant entre les particules de l'hydrate exprimé en cm^3/cm^3 du volume absolu de la masse de l'hydrate.

Le rapport "eau-liant" est déterminé par la formule:

$$(E/L) = \frac{\rho_o - C_o}{\rho_o \cdot C_o} \qquad (2)$$

où ρ_o est la densité réelle du liant initial.

Suivant les études /1, 2/, les mélanges du liant avec l'eau pris au rapport optimal ou au rapport diminué de la quantité du liant sont caractérisés par l'accroissement de résistance normal sans anomalies. Les mélanges contenant le liant en quantité élevée par rapport à la quantité optimale montrent, après l'accroissement de résistance initial normal, la diminution de cette résistance et l'augmentation du volume.

Ce fait est expliqué par la pression des germes nouvellement formés à l'intérieur de la structure formée à l'absence de l'espace nécessaire à l'emplacement des particules nouvelles des hydrates avec les intervalles entre elles. Ce fait peut être observé en cas d'accès supplémentaire dans le système de l'eau sous forme du liquide ou de la vapeur et en cas de l'interaction de cette eau avec les particules du liant non hydratées.

Le rapport "eau-liant", en cas de concentration optimale du liant, est toujours plus grand que le rapport exigé par la stoechiométrie de la réaction de son hydratation (approximativement plus grand de 1,3-1,5 fois).

Le volume limite minimal des intervalles entre les particules des hydrates des différents liants (V) est individuel et dépend également des conditions de leur hydratation.

Suivant nos données, "V" et le rapport optimal "eau/liant" lors de l'hydratation aux conditions normales sont les suivants:

1) le ciment portland: 0,37 cm^3/cm^3 du volume absolu des hydrates; le rapport "eau/ciment" est égal à 0,39;

2) le plâtre semi-hydraté ß: 0,2 cm^3/cm^3

du volume absolu des hydrates; le rapport "eau/plâtre" est égal à 0,24;

3) l'aluminate tricalcique, en cas de formation à partir de celui-ci du C_3AH_6: 0,8 cm^3/cm^3; le rapport "eau/C_3A" est égal à 0,67;

4) l'ettriguite, en cas de sa formation à partir du mélange de l'hydroxyde de calcium, du sulfate d'aluminium et de l'eau: 1,0 cm^3/cm^3; le rapport "eau/liant" est égal à 0,9.

Il en résulte que tout liant à sa concentration optimale dans le mélange avec l'eau et au rapport correspondant "eau-liant" formant un système durcissant ayant des déformations de retrait normales, à la mesure de l'augmentation de concentration et de la diminution du rapport "eau/liant", passera d'abord en classe des "irrétrécissables", ensuite en classe des "expansifs" et même en classe des "autodestructifs", en cas de l'expansion libre lors du durcissement, ou en classe des "contraints" à l'hydratation dans le volume "fermé". L'intensité et la vitesse de développement des déformations correspondantes avec le temps doivent dépendre des propriétés individuelles des liants et des conditions du durcissement.

Avec cela, plus sont grandes les valeurs de l'eau invaporable "W_0" fixée par le liant en cas de l'hydratation complète et des volumes minima entre les particules "V", moins est la résistance du liant dans le système à la concentration optimale "C_0".

Le degré de remplissage du volume libre dans le mélange du liant avec l'eau par les hydrates qui dépend du degré d'hydratation du liant et de la quantité d'eau adsorbée par les hydrates exerce une influence directe sur la résistance et autres propriétés du système. A cette raison, il est utile de déterminer le volume absolu de la phase solide $V_{ph.s}$ pour un ou un autre délai de durcissement du système (sans tenir compte de l'air entrainé et de l'expansion du système) en utilisant la formule 3 /3/.

$$V_{ph.s} = \frac{C_i(I-\alpha)}{\rho_0} + \frac{C_i\alpha(I+W_0)}{\rho_I} \qquad (3)$$

où C_i est la contenance du liant dans le mélange initial exprimée en g/cm^3; α est le degré d'hydratation; ρ_0, ρ_I sont les densités réelles du liant et de l'hydrate en g/cm^3.

A l'aide de la soustraction de la valeur N du volume total du système durci on obtient le volume des pores. La concentration volumique /3/ des hydrates nouvellement formés "N" est déterminée avec une approximation admissible par la formule de A.V. Voljenskiy et U.D. Tshistov:

$$N = \frac{C_i[\rho_0(I+W) - \rho_k(I-\alpha)]}{\rho_k[\rho_0 - C_i(I-\alpha)]} \qquad (4)$$

Dans ce cas, W est la quantité d'eau invaporable en g par g du liant initial; ρ_k est la densité réelle du liant durci pour un ou un autre délai. Pour les autres symboles, voir les formules I, 2 et 3.

Parmi les formules modernes sur la résistance des mélanges durcissants nous ne trouvons pas les formules qui tiendraient compte du passage des indices physico-mécaniques et des autres propriétés par le maximum avec une altération suivante de ces indices et autres propriétés malgré une augmentation monotone de la concentration du liant dans le système.

Les formules de résistances ne traduisent pas également le fait que la diminution du rapport "eau-liant" favorise une augmentation de dispersité des particules nouvellement formées et, par conséquent, un accroissement de résistance /4/.

Les formules existantes peuvent être utilisées avec un degré de confiance différent pour des systèmes ayant un rapport "eau-liant" optimal et plus grand.

Les résultats des études /2/ illustrent les faits mentionnés.

A partir du ciment Portland (ρ_0 = 3,1; W_0 = 25,4%; ρ_I = 2,47 à l'hydratation

complète), on a préparé les échantillons (2x2 et 2x2x2 cm) avec le rapport "eau/ciment" de 0,05; 0,1; 0,15; 0,2 et 0,25. Pendans trois jours on a conservé ces échantillons au-dessus de l'eau et ensuite dans l'eau jusqu'à 6 ans. Aux âges déterminés (3, 7,28 jours; 6 ans) on a analysé la résistance des échantillons, leurs volumes, porosité, degré d'hydratation d'après la teneur en eau invaporable et la concentration volumique des formations nouvelles (N). Les résultats ont montré que la résistance des échantillons de toutes les compositions augmentait jusqu'à l'âge de 1-3 ans et ensuite diminuait autant plus que plus est la diminution du rapport "eau-ciment". Par exemple, la résistance des échantillons préparés avec le rapport "eau/ciment" =0,10 a atteint pendant trois ans 106 MPa, tandis qu'elle a diminué vers 5 ans jusqu'à 90 MPa.

La résistance des échantillons préparés à partir d'un autre ciment (rapport "eau/ciment" = 0,2), ayant atteint vers trois ans 92 MPa, a diminué vers 6 ans jusqu'à 60 MPa.

Le degré d'hydratation des échantillons avec les rapports "eau/ciment" 0,05-0,15 a atteint vers l'âge de 5-6 ans la valeur de 0,45-0,5, et celui des échantillons avec les rapports "eau/ciment" de 0,2-0,25 a été égal à 0,75-0,78.

Les échantillons de toutes les compositions ont montré une augmentation de volume (3-5%) qui a atteint son maximum vers 28-30 jours de durcissement pour les échantillons, préparés avec le rapport "eau-ciment"=0,05; 0,1; 0,15 et 0,3-1% pour les échantillons préparés avec le rapport "eau/ciment"=0,2 et 0,25. Plus tard, les échantillons avec le rapport "eau/ciment"=0,2 et 0,25 ont montré une diminution de volume jusqu'aux valeurs initiales et les échantillons avec le rapport "eau/ciment"=0,05; 10,1 et 0,15 approximativement jusqu'à 2-2,5%. Suivant l'auteur, ce fait est dû à la relaxation de la contrainte dans le système durci ou à la diminution de teneur en eau dans les formation d'hydrates nouvelles ou, enfin, à l'effet conjugué de ces deux facteurs. Le passage des échantillons du gonflement au retrait lors du durcissement de longue durée exige une étude ultérieure car ce phénomène peut être lié avec le comportement des bétons dans les structures contraintes mécaniquement ou à l'aide des éléments de contrainte et exercer une influence indésirable et même dangereuse sur la capacité portante de la structure.

Les essais analogues /5/ ont été effectués sur les échantillons préparés à partir du ciment sulfo-alumineux de laitier (CSAL) contenant 30% de plâtre semi-hydraté, 30, 20, 10% de ciment alumineux, 35, 45, 53% de laitier de haut-fourneau et 5-7% de ciment Portland. Les bétons, en cas de la consommation du CSAL 350-400 kg/m^3 (dureté des mélanges est de 20-30 s), après quatre heures de durcissement à la température de 20°C, ont la résistance de 4-6 MPa, après un jour de durcissement - 12-16 MPa et après 28 jours - 40-50 MPa. Les bétons sur la base du CSAL durcissent à des températures 40-55°C sans diminuer la résistance et atteignent même après quatre heures de durcissement une résistance de 15 MPa et plus. D'après la vitesse d'accroissement de résistance initial ce ciment dépasse le ciment alumineux et il est de 3-4 fois moins cher que ce dernier. La résistance des échantillons préparés à partir du mélange de CSAL avec l'eau (rapport "eau/ciment"-0,1; 0,25 et 0,4) conservés au-dessus de l'eau augmentait continuellement jusqu'à l'âge de 4,5 ans. Ces ciments contenaient 30 et 20% de ciment alumineux (n°n° 1 et 2). Après quatre heures de durcissement, les échantillons avaient la résistance de 15-30 MPa et après un jour de durcissement - 17-37 MPa. Après un an de durcissement, la résistance des échantillons avec le rapport "eau/ciment" égal à 0,1 a atteint son maximum de 90-95 MPa, tandis qu'après 5,5 ans de durcissement elle a diminué jusqu'à 22 MPa (n°I) et jusqu'à 18,5 MPa (n° 2). Le volumé des échantillons des deux compositions a augmenté de 1% pen-

dant 3-6 mois et plus tard, il a diminué jusqu'à la valeur initiale.

Donc, lors du durcissement des échantillons préparés à partir du CSAL, on a observé le même phénomène qu'en cas des échantillons préparés à partir du ciment Portland. Selon ces essais, il est recommandé d'utiliser le CSAL aux rapports "eau/ciment" qui ne sont pas inférieurs à 0,35-0,4. Les extrémums analogues sur les courbes de résistance des échantillons préparés aux rapports "liant-eau" diminués (en comparaison avec les rapports optima) s'observaient en cas de l'aluminate tricalcique, de l'ettringuite et des liants "gypse-ciment-pouzzolane" (IGCP). Le ciment Portland à la chaux contenant une quantité considérable d'oxyde de calcium et d'autres substances est caractérisé par l'absence d'expansion lors de son interaction avec l'eau. Les bétons basés sur ce liant atteignent une résistance de 4-6 MPa après 4-7 heures de durcissement à la température de 20°C et 15-20 MPa et plus à la température de 80-95°C.

Selon les données préliminaires, le rapport eau/liant optimal se trouve dans des limites de 0,35-0,4.

BIBLIOGRAPHIE

I.3. Волженский А.В., Ж. "Строительные материалы", 1979, № 7, 1981, № 8.
2. Волженский А.В., Карпова Т.А., Ж. "Строительные материалы", 1980, № 7.
4. Волженский А.В., Рожкова К.Н., Ж. "Строительные материалы", 1972, № 5.
5. Карпова Т.А., Волженский А.В., Ж. "Строительные материалы", 1982, № 7.

W. Weisweiler - Institut Fur Chemische Technik - West Germany

QUANTIFICATION OF THALLIUM - and LEAD-CYCLES IN CEMENT PLANTS

CL

1. Introduction

Early studies concerning the causes of thallium emissions in the cement production are found in the literature(/1-4/, beginning in 1980). Through controlled discharge of "blood leeting" of the so-called external cycle of a cement kiln plant with fly-ash feedback, a strategy for effectively controlling the thallium cycle extension and emissions was developed by KAMM, OBLÄNDER and WEISWEILER /5/, as shown by industrial results. From all the above cited papers it can be concluded, that material cycles are formed. As an example a plant with cyclone perheater is to be considered operating in a combined mode. In this case a cycle can be delineated following the materials' pathway: Heat exchanger → raw mill → electric filter → silo → heat exchanger. A sharp enrichment level is observed when using pyrite cinder as iron oxide source containing a high thallium concentration.

The purpose of the present work was to determine in a quantitative manner the cycles and enrichment behaviour of thallium and lead in a cement rotary kiln plant; for details see WEISWEILER et el. /6/. The studies were carried out in two parallel running cement production plants (cyclone preheater and LEPOL), typical for Central Europe. Feeding with high-thallium containing pyrite cinder, as iron oxide source, was done as a matter of convenience for sharpening the enrichment level and only during those studies were carried out.

2. Measurement Strategy, Sampling, Mass Streams

The knowledge of the material balances is suggested to be of key importance for understanding the extent and causes of cycles in industrial processes. In this context only the Tl-and Pb-cycles were of interest. The mass streams were calculated on the basis of metallic Tl and Pb. Thallium is found mainly as a mixed crystal halide Tl(Cl,Br) /7/, or as iodide with chloride portions /8/. Lead is also found as chloride but in a basic sulfate or silicate matrix in the clinker.

Preparation of the samples and their parallel determination by means of atomic absorption spectroscopy were discussed by WACHTER and WEISWEILER /9/. The solid specimens were taken from the mass streams described as follows:

A. Rotary kiln with cyclone preheater (measuring period 5 resp. 40 days).

   1) Heavy metal path across the solid material stream

      a) direct operating mode: raw meal (raw material + additives) → kiln meal (raw meal + filter dust) → clinker.

      b) Combined operating mode: raw meal = kiln meal (raw material + additives + filter dust) → clinker.

   2) Heavy metal path across the gas stream: fuel or substitute fuel → dust in raw gas → electric filter dust → dust in clean gas.

B. Rotary kiln with grate-type preheater (measuring period 48 days).

   1) Heavy metal path across the solid material stream: raw meal = kiln meal (raw material + additives) → pellets from drying chamber → pellets from calcining chamber → clinker.

   2) Heavy metal path across the gas stream: fuel or substitute fuel → grate riddlings and dust from the intermediate dust collection → dust in raw gas → electric filter dust → dust in clean gas.

The results from the Tl- and Pb- analyses in the described mass streams were used in preparing the figures of the balances in form of SANKEY-diagrams. For typcial minimal and maximal Tl- and Pb-content values see /6/.

3. Thallium and Lead Balances for the Rotary Kiln with Cyclone Preheater

The symbols used for all heavy metal streams are given as follows. The units in SANKEY-diagram are kg/h.

Symbol	Heavy metal mass stream
B	feeded fuel oil
E	dust emission
Eb	feeded substitute fuel
Fs	filter dust
K	produced clinker
Om	kiln meal before preheating (Fs+S)
Rg	dust in exit gas (raw gas)
S	raw meal from silo; in combined mode: S=Om
Wt/Ok	cycle in heat exchanger/kiln cycle

The results of the corresponding dust measurement in exit gas before and after the electric filter (raw gas resp. clean gas) are given as follows for the direct and combined operating modes. In the combined mode the heat content of the kiln gases, before the dust collection, is used for drying the raw meal mixture in the grinding mill. Dust concentrations were measured with an exhausting device working parallel to the gas stream. Following dust concentrations were measured: in the raw gas 30-50 g/m^3 in direct mode and 14-28 g/m^3 in combined mode operation resp. (15 min, 3.5 m^3/h, 8-32 g dust). In contrast the dust concentrations in the clean gas were found to be 20-40 mg/m^3 in direct mode and 10-20 mg/m^3 in combined mode operation (6-13 h, 10-15 m^3/h, 1.2-4.4 g dust). The thallium concentrations in 15 mean daily samples in the dust of the raw gas were 900-2900 ppm and 100-600 ppm operating in the direct and combined mode respectively, whereas in the dust of the clean gas values of 1500-3600 ppm (direct mode) and 600-1200 ppm (combined mode) were found. The analogous lead concentrations were found to be in the raw gas: 30-70 ppm (direct mode) and 10-70 ppm (combined mode); in the clean gas: 15-75 ppm (direct mode) and 10-75 ppm (combined mode).

KAMM /10/ recently reported overall enrichment factors for Tl of 10 000 and for Pb of 20 assuming a maximum of 0.5 ppm Tl and 25 ppm Tb in raw meal and 5000 ppm Tl and 500 ppm Pb in clean gas. These values were obtained from specimens taken at the plants in the technically encountered conditions. From the results obtained in the present study, mean overall enrichment factors of at best 2500-3500 for Tl and 2-4 for Pb are found for a plant operating with continuously changing modes (direct and combined).

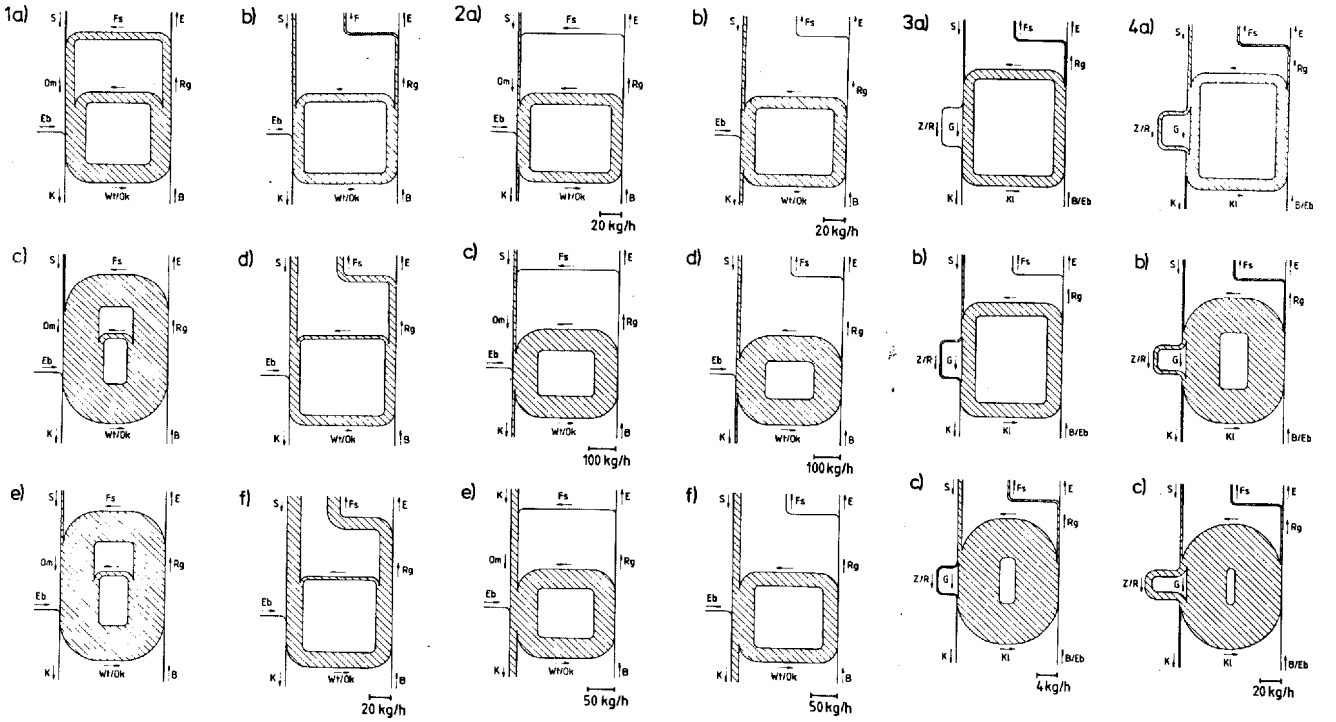

Fig.1: Rotary kiln with cyclone preheater: Thallium mass streams

Fig.no.	1a	1b	1c	1d	1e	1f
operating mode	direct	combined	direct	combined	direct	combined
additive	ore	ore	pyrite cinder	pyrite cinder	pyrite cinder	pyrite cinder
substitute fuel	-	-	-	-	acid sludge	acid sludge

Fig.2: Rotary kiln with cyclone preheater: Lead mass streams

Fig.no.	2a	2b	2c	2d	2e	2f
operating mode	direct	combined	direct	combined	direct	combined
additive	ore	ore	pyrite cinder	pyrite cinder	pyrite cinder	pyrite cinder
substitute fuel	-	-	-	-	acid sludge	acid sludge

Fig.3 and 4: Rotary kiln with grate type preheater: thallium mass streams (Fig.3) and lead mass streams (Fig.4)

Fig.no.	3a	3b	3c	4a	4b	4c
additive	pyrite cinder	pyrite cinder	pyrite cinder	pyrite cinder	pyrite cinder	pyrite cinder
substitute fuel	-	acid sludge	acid sludge	-	acid sludge	acid sludge
period	-	-	6 weeks	-	-	6 weeks

3.1 Thallium Balances

Balances were made for the direct and combined operating mode. Mass streams were determined when feeding with iron ores and with Tl containing pyrite cinder with/without acid sludge. SANKEY-diagrams of the mass streams were prepared for all six variations (Figs. 1a-f); they are based on a mean daily operating period of 12 h in direct/combined mode. Longer operating periods were not considered.

Fig.1a shows the total thallium mass stream within the plant operating in a direct mode, firing with petroleum coke and feeding iron ores (Tl< 5 ppm). A small Tl stream coming from the silo with the raw meal, S, enters the thermal-chemical part of the process. Dust from the electric filter, Fs, is added before entering the cyclone preheater (mass stream Om). An internal Tl-cycle is formed within the heat exchanger due to the volatilization of Tl-compounds and condensation on the dust particles of the countercurrently flowing gas (Tl-stream Wt/Ok). A residual Tl-stream enters the rotary kiln via the partially calcinated materials leaving the cyclone. In the rotary kiln the Tl-compounds finally enter the gas phase and are transported out by the dust charged combustion gases which enter the cyclone; here they condense on the countercurrently entering solids. As can be seen, the Tl-cycle is not limited to the preheating unit but includes the rotary kiln.

The thallium compounds coming with the raw gas from the heat exchanger, Rg, are collected together with the dust, Fs, in the electric filter which in case of a direct operation are added to the raw meal before entering the heat exchanger. In a combined operation this Tl-stream is formed anew in the silo because the dust charged combustion gases from kiln are used for drying the raw meal in the meal. The so formed Tl-stream, Om or S, completes the external cycle.

The back-feeding of the collected dust in the electric filter, Fs, to the preheater has, as is known, a great effect in the heat exchanger cycle. It is remarkable the low Tl-fixation in the clinker. If the electric filter works without failure, a low Tl-emission is found too.

Fig.1b shows the thallium mass streams in the subsequently nocturnal combined operating mode. The same kind of cycles is observed, nevertheless are the mass streams farther reduced because of the greater storage volume available in the raw meal silo.

Fig.1c shows the increase of the Tl-streams, after a one day period, when feeding with pyrite cinder of an 230-310 ppm Tl-content. During a direct operation the Tl-mass streams are found mainly in the external cycle because of the drastic higher Tl-contents in filter dust, Fs. The enrichment level is diminished in the subsequently combined operating mode maintaining the firing of petroleum coke and the feeding of pyrite cinder. The corresponding streams are shown in Fig.1b.

When using acid sludge as substitute feed the same mass streams are practically measured in a direct operation (Fig.1e), whereas in a combined mode a slight increase of the mass stream is observed in the heat exchanger/rotary kiln system (Fig.1f).

3.2 Lead Balances

The lead balances were carried out on the same specimens and under the same conditions as for thallium. During the direct operation a clear increase of the enrichment level is observed in the transition zone between preheater and rotary kiln (Fig.2a). Because of the lower Pb-content in the filter dust the external cycle is less pronounced. The lead content in clinker is almost the same as that of the raw meal, coming from the silo and entering the preheater. When operating in a combined mode (Fig.2b) similar Pb-contents are found in the cycles as well as in the clinker and emissions. With a higher Pb-supply by feeding with pyrite cinders a very sensitive cycle formation is observed (Fig.2c - note scale). The lead content in clinker is increased to 100 ppm. As expected, a change in the levels is not observed in the subsequently combined operation (Fig.2d). Firing with high sulfur cycle although Pb-containing pyrite cinder feeding is maintained. Lead is discharged mainly through the clinker. Low lead emission from the less pronounced external cycle remains unchanged (Fig.2e). During a combined operation relevant changes are neither expected nor they are observed (Fig.2f).

4. Thallium and Lead Balances for a Rotary Kiln with Grate Type Preheater

In the description of the mass streams of a LEPOL-plant, the streams Om, Wt/Ok are not needed, but the following are introduced additionally:

Symbols	Heavy metal stream
G	granulated raw meal
Kl	grate type preheater cycle
Oe	kiln inlet end (partially calcinated solids)
Z/R	intermediate dust collection (Z) and grate riddlings (R)

For a sampling period of 30 days following dust concentrations were found: in raw gas (30 min, 5 m^3/h, 5-15 g) ca. 2-5 g/m^3 and in clean gas (7.5 h, 10 m^3/h, 3-11 g) 50-130 mg/m^3. The heavy metal content was in raw gas dust: 100-800 ppm thallium, resp. 1200-5000 ppm Pb, and in clean gas dust: 160-1050 ppm Tl, resp. 7500-15400 ppm Pb.

As in the case of the heat exchanger plant the analogous enrichment factors were determined and found to be roughly 850 for Tl and 450 for Pb. These values are based on a mean dust content of 430 ppm Tl and 11100 ppm Pb in clean gas, when feeding with heavy metal containing pyrite cinders.

4.1 Thallium Balances

The Tl-streams were determined for the following conditions: feed with pyrite cinder of 230-310 ppm Tl and with/without firing acid sludge as well as after six weeks firing with acid sludge. The corresponding SANKEY-diagrams are given by the figures 3a-c. As is clearly seen, a thallium cycle is formed at preheater and over the rotary kiln (Fig.3a). The external cycle through the collected filter dust, Fs, does not appear when this is not feeded to the kiln. Nevertheless, an external cycle is formed when the dust from the intermediate collection as well as the grade riddlings Z/R are feeded to the kiln. Firing with sulfur containing acid sludge, Eb, increases the thallium cycles about by a half, as is shown in Fig.3b. The Tl-emission and -fixation in clinker remain more or less the same. After a period of six weeks an increase of Tl in the grate type preheater cycle is observed with a feed of pyrite cinder and firing mainly acid sludge (Fig.3c). An increase in thallium content of the raw gas is also observed. Compared with the rotary kiln with cyclone preheater, the contents are already lower: G = 8.4 kg/h (Fig.3c) whereas Om = 34.4 kg/h (Fig.1c).

4.2 Lead Balances

A considerable mass stream supplied by the intermediate collected dust and grate riddlings, Z/R, enters the kiln (Figs. 4a-c, note different scales !). Likewise an increased Pb-stream, Kl, is found between the kiln and grate type preheater. By continuous operation with pyrite cinder (Fig.4a) and additional firing with acid sludge (Fig.5b), the lead content in the cycle between kiln and preheater, Kl, is increased. Nevertheless, the Pb-stream, supplied by intermediate dust and grate riddlings, Z/R, remains the same. The cycle contents after a six weeks operation increased further by about 30 % (Fig.4c).

5. Evaluation of the Balances with Regard to Both Kiln Plants

5.1 Thallium Balances

Rotary kiln with cyclone preheater

Tl-compounds are enriched mainly in the suspension preheater kiln. The high volatility of the halides is responsible for the formation of the internal

cycles. At 1000 K, the vapour pressure of thallium chloride, thallium bromid and thallium iodide are respectively 290, 257 and 300 mbar. At the cyclone the raw meal is heated up to ca. 800 °C by the countercurrently flowing combustion gases leaving the kiln. A condensation maximum is measured in the zone at 450 °C for thallium chloride/thallium iodide /6/. The thallium compounds condense preferentially on the finest dust particles /10/; in their way to the kiln they reach warmer zones, at which they almost completely evaporate and are transported back to the 450 °C zone.

Beside these internal cycles the feed-back of the electric filter dust (about 15 t/h in a 3000 t/day plant) is a cause of the high Tl-rates. As shown by the balances, the emission has a low Tl-content and there is no considerable discharge through clinker, so that almost all of the feeded thallium remains within the process. In view of this, the cement production is also an efficiently process for enriching Tl-compounds.

In contrast to a direct operation, lower Tl-concentrations are found in a combined mode, because most of the thallium is transported to the grinded raw material and to the filter dust in silo. With an increased sulfur feed, e.g. through acid sludge, a reduction of the thallium cycle is not observed.

Rotary kiln with grate type preheater
The LEPOL-plant shows an analogous behaviour in the development of thallium cycles as the heat exchanger plant. Thallium compounds, which evaporate at $T > 450$ °C, condense mainly on the pellet bed of the LEPOL grate, which serves as filter dust. Firing acid sludge was found to have no effect on the internal thallium cycles. Finally, it was found, that the circulating thallium quantity in this plant is lower than the corresponding quantity in a heat exchanger plant related to the produced clinker basis; each plant having a nominal output of 1500 t/d and 3000 t/d respectively.

5.2 Lead Balances

Rotary kiln with cyclone preheater
Lead compounds participate essentially at the internal cycles but only small quantities are transported by the filter dust cycle. The highest Pb-stream is found about a temperature of 800 °C, so that the maximal condensation occurs between the preheater outlet and the kiln inlet. The reason is lying in the volatility of the lead halides; vapour pressures at 1000 K are roughly 45, 71 and 148 mbar for $PbCl_2$, $PbBr_2$ and PbI_2 respectively. Volatility analyses of the filter dust, carried out in the laboratory, showed Pb as $PbCl_2$ together with $AlCl_3$ and KCl portions enclosed in a matrix mainly of calcite /11/. The finer dust particles have a higher Pb-content. The fixation of lead in clinker is greater as for thallium. The correlation between the content in filter and emitted dust is analogous also for lead. The two operating modes (direct and combined) reveal no essential difference of the cycles.

An increase of sulfur by firing acid sludge reduced the lead content in the cycles by about a half; probably the lower volatile basic lead sulfates are formed (at $T < 640$ °C: $PbO \cdot PbSO_4$, 4 $PbO \cdot PbSO_4$; at $T > 640$ °C: 2 $PbO \cdot PbSO_4$ in addition). This was confirmed by laboratory experiments on the sulfatization of PbO /12/.

Rotary kiln with grate type preheater
Lead compounds are found enriched likewise within the preheater/kiln cycle. The feed-back of the intermediate gas dust and grate riddlings has only a minor effect on the built-up of the internal cycle. Firing acid sludge increases appreciably the circulating lead streams. Examined electric filter dusts are rich in syngenite $K_2Ca(SO_4)_2 \cdot H_2O$ and arcanite K_2SO_4.

References

/1/ H. Keinhorst : Staub Reinhalt. Luft 40 (1980) No. 1, 26/29

/2/ H. Keinhorst : Zement-Kalk-Gips 33 (1980) No.12, 648/52

/3/ K. Welzel, H.D. Winkler : Zement-Kalk-Gips 34 (1981) No. 10, 530/34

/4/ S. Sprung : Zementindustrie. VDZ, Düsseldorf, 43 (1983)

/5/ K. Kamm, W. Obländer, W. Weisweiler : Staub-Reinhalt. Luft 43 (1983) No.5, 193/98

/6/ W. Weisweiler, K. Blome, L. Kaeding : Staub-Reinhalt. Luft 45 (1985) No.10, 461/66

/7/ H.U. Bambauer, H. Schäfer: Mineralogie 62 (1984) No. 1, 33/50

/8/ W. Weisweiler, E. Mallonn: Naturwiss. 70 (1983) 304/5

/9/ Ch. Wachter, W. Weisweiler: Mikrochimica Acta/ Wien (1982 I) 307/15

/10/ K. Kamm : Staub-Reinhalt.Luft 45 (1985) No.1, 15/18

/11/ W. Weisweiler, E. Mallon, B. Schwarz : * (in press)

/12/ W. Weisweiler, E. Mallonn, K. Blome : Zement-Kalk-Gips 38 (1985) No. 7, 387/92

W. Weisweiler, B. Schwarz, E. Mallonn - Institut Fur Chemische Technik - West Germany

ISOLATION OF THALLIUM-AND LEAD-HALIDES ORIGINATING FROM ELECTRIC SEPARATOR DUST OF CEMENT PLANTS BY VAPORIZATION ANALYSIS

Introduction

The build-up of thallium and lead halide cycles during cement production leads to considerable enrichment of these heavy metal compounds /1/. This enrichment is found in the kiln dust of the preheating zone, in the electric separator dust, and in the emitted fine dust particles /2,3/. Additionally, the mass streams of thallium /4,5/ and lead exhibit a further increase by recycling dust from electric separator into the raw meal silo /6/.

Vaporization analysis /7/ of electric separator dust from two types of cement plants, one with suspension preheater, the other with grate-type preheater(LEPOL), shows that the trace element iodine is most important concerning the chemical reactions of thallium. One of the sources of iodine /8/ is found to be the fuel. The rotary kiln with suspension preheater was fired with natural coal by addition of 6-10 mass percent of petrol coke. The other rotary kiln with grate-type preheater was fed with pure petrol coke.

Composition of the electric separator dusts

Two types of electric separator dust were used for investigation. One was taken from a cement plant with a suspension preheater (SP). This plant was fired with natural coal containing 6-10 mass percent of petrol coke.

The second dust specimen was taken from a grate-type preheater (LEPOL) which was fired with pure petrol coke. Table 1 summarizes the results of the chemical analysis. The X-ray diffraction analysis proved that the electric separator dust from the cement plant with suspension preheater (SP) was found to be calcite with a relatively high amount of thallium compounds, but less of lead. The LEPOL-electric separator dust was identified as arcanite (K_2SO_4) and syngenite ($K_2Ca(SO_4)_2 \cdot H_2O$). This dust contained a very high amount of lead and less thallium.

Table 1: Chemical and X-ray diffraction analysis of the two electric separator dusts (SP and LEPOL)

element resp. component	SP	LEPOL
	mass percent	
K_2O	1.0	25.09
Na_2O	0.23	0.77
SO_3	0.79	19.50
Cl	0.20	3.07
SiO_2	1.34	10.19
Al_2O_3	3.28	3.04
Fe_2O_3	1.45	1.73
CaO	44.78	31.71
CO_2	36.40	n.d.
loss of ign.	37.42	n.d.
Tl	$2.7 \cdot 10^{-2}$	$7.8 \cdot 10^{-3}$
Pb	$5.7 \cdot 10^{-3}$	$9.97 \cdot 10^{-2}$
X-ray diffraction	calcite	arcanite syngenite

Vaporization analysis

The vaporization analysis apparatus that was used for the experiments was made of quartz (Fig.1). It was modified so that it was possible to determine traces of thallium and lead to enrich the compounds in a preparative scale. The experimental conditions are listed in table 2.

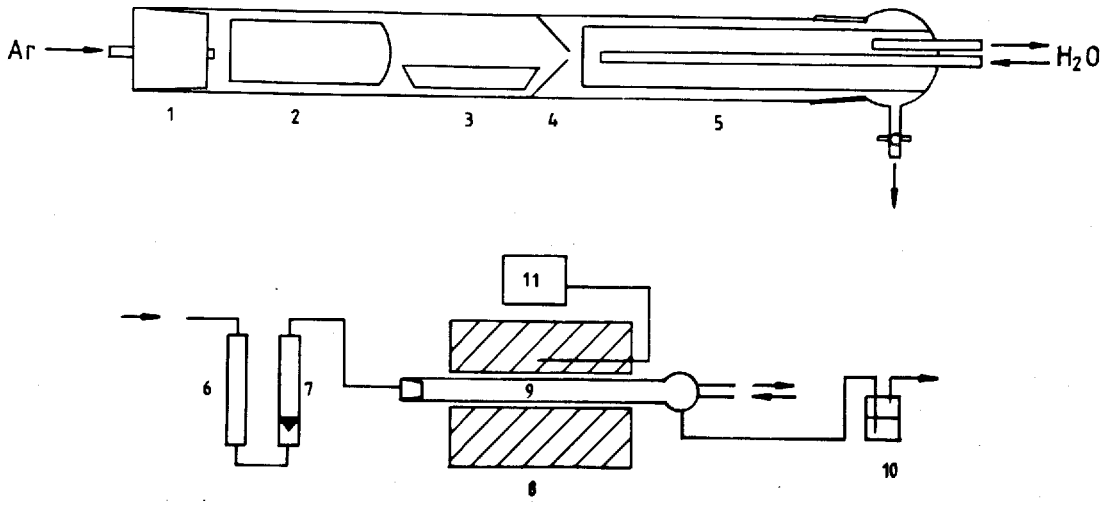

Fig.1: Modified vaporization apparatus

1 Condenser, 2 Nozzle, 3 Nickel boat, 4 Flow resistance, 5 Teflon stopper
6 Drying tube, 7 Flow meter, 8 Furnace, 9 Vaporization tube, 10 Bubble counter

Table 2: Experimental conditions of the used vaporization apparatus

Length of the vaporization tube	580 mm
Diameter of the vaporizattion tube	30 mm
Distance from nozzle to cooler	5 mm
Diameter of the nozzle	3 mm
Length of the nozzle	15 mm
Length of the flow resistance	26 mm
Argon gas stream	120 Nl/h
Maximum mass of the electric filter dust	30 g

The vaporization tube was heated by an electric furnace in order to vaporize the volatile compounds. These compounds were transported by an inert gas stream and condensed on a cooler. For the quantitative analysis of the heavy metals, the condensate was dissolved in HNO_3 (10 %) and analyzed using atomic absorption spectrometry (AAS). For determination of the compounds the X-ray diffraction method was used.

An important parameter of the vaporization analysis was found to be the temperature that was optimized for thallium and for lead compounds. The thallium compounds sublimate at a temperature of 500 °C and the lead compounds at 900 °C. Thus it was possible to separate the thallium compounds from the lead com - pounds.

Identification of the condensates

At 500 °C the vaporization analysis using an inert argon gas stream showed yellow and red sublimates from both electric separator dusts /9/. The condensates were identified as thallium iodide by X-ray diffraction. TlI appeared as the rhombic modification as well as red cubic, high temperature modification. Increasing vaporization time yielded higher concentration of chloride in the sublimate. When the condensation of the thallium compounds at 500 °C was finished, a temperature of 900 °C was applied in order to volatilize the lead compounds. In both cases the condensates could be identified as lead chloride.

A fractionated vaporization analysis of the LEPOL electric separator dust at 900 °C in an inert argon gas stream showed the following results, obtaining by an energy dispersive electron probe microanalyzer (Fig.2).

If an air stream or a gas stream of N_2 with an addition of 1 % HCl was used instead of an inert argon stream white sublimates were found. Instead of TlI the X-ray diffraction analysis showed peaks of TlCl. Iodine was now volatilized as elemental iodine.

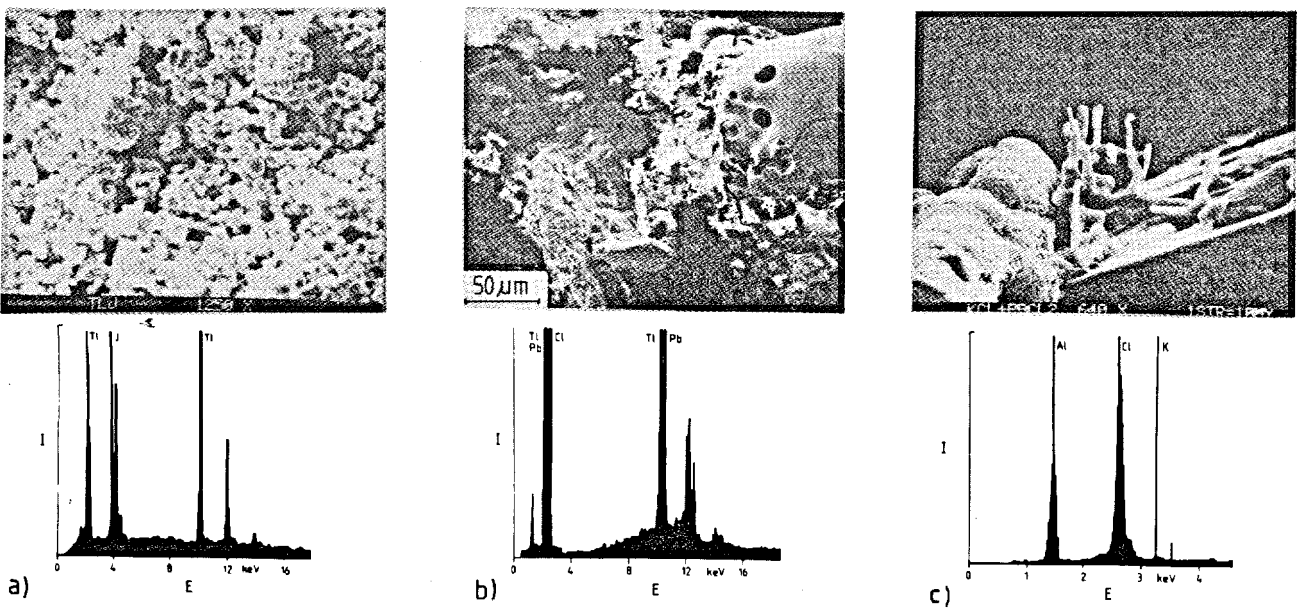

Fig.2: Condensate of LEPOL dust

a) Identified as pure thallium iodide obtained after 20 min vaporization time, the energy dispersive spectrum exhibited peaks of pure TlI

b) The second condensate, derived after a vaporization time of two hours, was identified as $PbCl_2$ with amounts of TlCl

e) After 16 hours vaporization the condensate was analyzed and identified as KCl with parts of $PbCl_2$ and $AlCl_3$

Quantitative determination of the compounds of lead and thallium

The results obtained by the combined methods of vaporization analysis and AAS as well as by wet chemistry operations and AAS /10/ were compared and resulted in good agreement. In addition to the two electric separator dusts, a synthetic dust, i.e. calcite with admixture of thallium chloride (1270 ppm Tl) and lead chloride (1114 ppm Pb) was used.

The electric separator dust (SP) showed the highest volatilization factor W (volatilized elemental mass/ 100% elemental mass) of lead compounds, but only small amounts of total lead concentration. The synthetic dust and the electric separator dust (LEPOL) with high amounts of lead, but in different matrices ($CaCO_3$; arcanite/syngenite), showed similar, but in comparison with electric separator dust (SP) much lower volatilization factors (Fig.3).

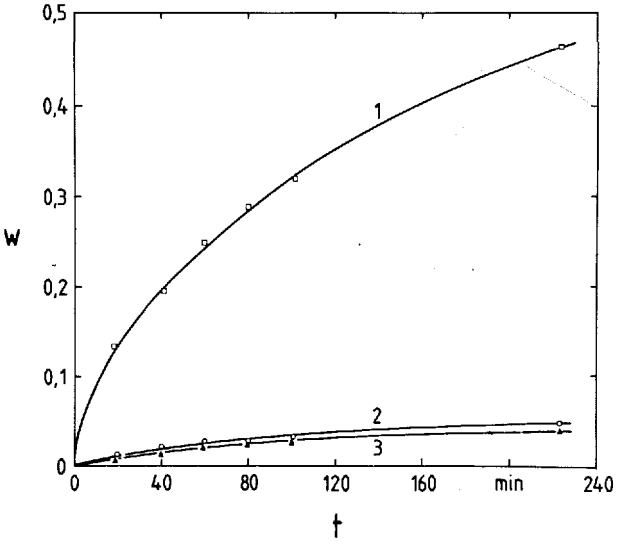

Fig.3: Volatilization factors of lead compounds
1 Electric separator dust (WT)
2 Synthetic dust
3 Electric separator dust (LEPOL)

For the thallium vaporization (Fig.4) the synthetic and the electric filter dust (SP) with their same matrices exhibited nearly the same volatilization factors. Both showed relatively high amounts of thallium. The volatilization factor of the electric filter dust (LEPOL) with its sulphate matrix was found to be smaller.

At a temperature of 500 °C the synthetic and the electric filter dust (LEPOL) showed the same volatilization characteristics, in contrast to the electric filter dust (SP) which had got a smaller volatilization factor (Fig.4).

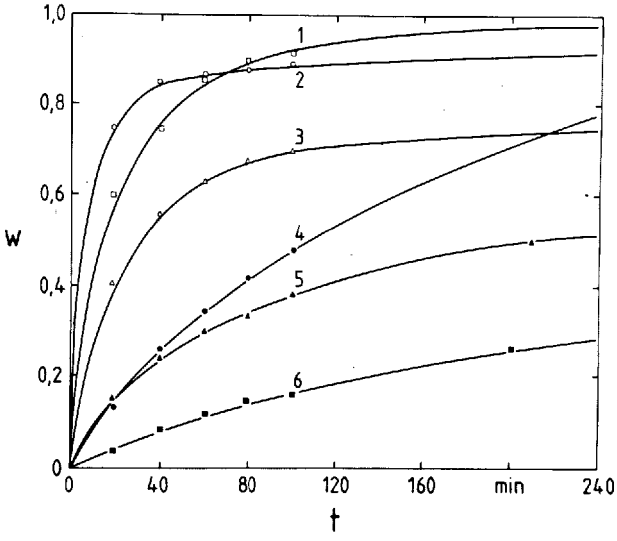

Fig.4: Volatilization factors for thallium compounds

1	Electric filter dust (SP)	900°C
2	Synthetic dust	900°C
3	Electric filter dust (LEPOL)	900°C
4	Synthetic dust	500°C
5	Electric filter dust (LEPOL)	500°C
6	Electric filter dust (SP)	500°C

Reasons for the vaporization of thallium iodide

The vapour pressures of thallium iodide and thallium chloride are nearly the same /11,12,13/. The amount of chlorine in both electric filter dusts was found to be much higher than the amount of iodide, yet the vaporization analysis showed a sublimate of thallium iodide in both cases. For that reason, the vaporization analysis was applied to a mixture of 100 mg TlCl/2 g NaI. Much TlI and only small amounts of TlCl were found in the condensate.

The TlI formed from TlCl/NaI or TlCl/KI which occurs in the preheating zone of the cement production and which is able to react there is thermodynamically favoured. This was also proved by calculations for this system at a temperature of 700-1200 K. Thus it is possible to find TlI in the preheating hone of cement plants.

References

/1/ S. Sprung, Schriftenreihe der Zementindustrie (Düsseldorf) 43 (1982)

/2/ H.U. Bambauer, H. Schäfer. Fortschr. Mineralogie 62 (1984) No. 1,33/50

/3/ B. Haegermann. Diplom-Thesis, University of Clausthal, 1982

/4/ K. Blome, Untersuchungen über das Verhalten von Thallium und Blei bei der Zementherstellung. Ph.D.Thesis, University of Karlsruhe, 1983

/5/ W. Weisweiler, K. Blome, L. Kaeding, Staub-Reinhalt. Luft 45 (1985), No.10, 461/66

/6/ K. Kamm, W. Obländer, W. Weisweiler, Staubh-Reinhalt. Luft 43 (1983) No.5, 193/98

/7/ H. Walk, Die Gehalte der Schwermetalle Cd, Tl, Pb, Bi und weiterer Spurenelemente in natürlichen Böden und ihren Ausgangsgesteinen Südwest-Deutschlands. Ph.D.Thesis, University of Karlsruhe, 1982

/8/ W. Weisweiler, E. Mallonn, K.J. Kohl, Zement-Kalk-Gips (in press)

/9/ W. Weisweiler, E. Mallonn, Naturwiss. 70 (1983) 304/5

/10/ Ch. Wachter, W. Weisweiler, Mikrochimica Acta/Wien (1982 I) 307/15

/11/ Handbook of Chemistry and Physics. 65th Ed. CRC Press, Boca Raton/Florida, USA, 1985

/12/ J. Barin, O. Knacke, Thermochemical Properties of Inorganic Substances. Springer Verlag, Berlin, 1973

/13/ J. Barin, O. Knacke, O. Kubaschewski, Thermochemical Properties of Inorganic Substances, Supplement. Springer Verlag, Berlin, 1977

Opening Session - 22 September 1986 / Séance Inaugurale - 22 Septembre 1986

Dr. JOSÉ ERMÍRIO DE MORAES FILHO

(Presidente do Grupo Votorantim e Presidente do Sindicato Nacional da Indústria do Cimento)

"Na qualidade de Presidente da Comissão Organizadora do Oitavo Congresso Internacional de Química do Cimento e de Presidente do Sindicato Nacional da Indústria do Cimento temos a satisfação de saudar os participantes deste evento, apresentando-lhes as boas vindas ao nosso país, onde esperamos que tenham uma ótima estada.

Sediar este Congresso é, para a Indústria do Cimento do Brasil, além da satisfação e da honra de tê-los conosco, uma rara oportunidade de intensificação do intercâmbio tecnológico que já mantemos, inclusive através de nossa participação nos demais congressos desta série, que já criou uma tradição e se constitui, talvez, no principal evento internacional da indústria do cimento. Assim é que, nos seis anos de intervalo entre essas reuniões, nossos cientistas desenvolvem intenso trabalho de pesquisa, do qual todos participam através de consultas mútuas propiciadas pela intensa correspondência trocada a partir do contato estabelecido durante o congresso.

A Indústria Brasileira do Cimento tem demonstrado ser capaz de enfrentar e vencer um grande número de desafios, sempre agravados pelas condições gerais do país.

Durante as décadas de 60 e 70 teve a nossa indústria que crescer em quantidade e qualidade, em função do aumento da demanda. Nesses vinte e poucos anos passamos de 30 para 56 fábricas e de 5 milhões para 40 milhões de toneladas-ano de capacidade instalada.

O esforço financeiro que essa expansão representou foi realizado com alguma ajuda do capital estrangeiro e com o máximo possível de capital de risco, o que muito nos valeu no recente período recessivo.

A atualização tecnológica acompanhou esse crescimento quantitativo, tendo a nossa indústria incorporado todos os avanços no sentido da otimização do uso da energia elétrica e térmica. Assim é que toda a expansão promovida a partir dos anos 60 foi feita com a adoção do processo seco, com unidades de capacidade instalada mínima de 1.000 toneladas/dia, dotadas dos mais modernos equipamentos de proteção ao meio ambiente.

A substituição do óleo combustível importado pelo carvão mineral nacional, realizada a partir de 1979 e motivada pelas incertezas do abastecimento do petróleo, além do seu alto preço, foi uma demonstração da nossa capacidade técnica, uma vez que passamos a consumir carvões nacionais com 35 e até 55% de cinzas, tendo o programa de substituição sido completado em reduzido prazo.

Embora estejamos em décimo primeiro lugar entre os produtores mundiais, temos ainda elevada capacidade ociosa e são grandes as possibilidades de crescimento do consumo no Brasil. Os estudos de que dispomos indicam que, hoje, o consumo potencial é de 43 milhões de toneladas/ano, montante que teria sido atingido se o país não tivesse sofrido forte recessão durante cinco anos e meio. Aquela cifra nos colocaria como o quinto produtor mundial de cimento e com um consumo per-capita em torno de 300 kg.

Com essas cifras queremos enfatizar a alta significação que tem para este país a realização, entre nós, deste Oitavo Congresso Internacional de Química do Cimento.

Para que possamos fazer uma idéia quantitativa do que representa esse evento, citamos o número de trabalhos apresentados:

Relatórios	24
Comunicações	256
Relatórios Gerais	12
Comunicações dos Seminários	33
Comunicações Livres	23
Posters	43
	391
Outros trabalhos	87
	478

O exame de todo esse acervo foi realizado pelos três Comitês Científicos e está transcrito nos Anais que os senhores estão recebendo.

O elevado nível desses trabalhos nos garante que este congresso será pleno de intenso trabalho e excelentes resultados, inclusive com a extensão da apreciação das matérias aqui propostas por um prazo bem maior do que os dias destinados a este evento.

Declaramos abertos os trabalhos deste Oitavo Congresso Internacional de Química do Cimento, desejando que tenham todos uma boa performance e um ótimo aproveitamento.

Muito obrigado."

Dr. PAULO MÁRIO FREIRE

(Diretor Superintendente da Cia. de Cimento Portland Paraíso - Cimentos Alvorada, Barroso, Goiás e Paraíso)

"Autoridades

Senhoras e Senhores

A responsabilidade da Comissão Organizadora do 8º Congresso começou logo após a sessão de encerramento do congresso de Paris quando os presentes aplaudiram o convite para que comparecessem ao congresso do Rio de Janeiro.

Como bem ressaltou o Dr. José Ermírio de Moraes Filho, em seu discurso na abertura deste congresso, a Indústria do Cimento no Brasil, pelo seu porte, desenvolvimento e perspectivas, poderá aproveitar de forma plena todo o saber que fluiu neste recinto ao longo destes proveitosos dias.

Foram abordados temas de alto interesse para a Indústria do Cimento em todo o mundo e esperamos que esses resultados dêem margem a muitos aperfeiçoamentos tanto para a produção de clínquer e cimento quanto para os utilizadores do produto, principalmente pela indústria da construção civil.

Felizmente a Indústria Brasileira do Cimento conta com o apoio da Associação Brasileira de Cimento Portland, que completa 50 anos de trabalho, e cujos técnicos têm a capacidade de assimilar os ensinamentos contidos nos Anais dos congressos, e transformá-los em conceituações práticas que permitam a sua aplicação pelos produtores e usuários do cimento.

Ao fim desses seis dias de intenso trabalho precisamos tratar de assegurar, para o futuro, a realização de novos congressos internacionais de química do cimento com o mesmo êxito que caracterizou não só o congresso do Rio de Janeiro mas os congressos anteriores.

Para isso, propomos que seja elaborado um regulamento simples que contenha a experiência até agora acumulada na organização desses eventos. Essa tarefa ficaria a cargo de uma Organização dos Congressos Internacionais de Química do Cimento, a ser composta pelos presidentes das Comissões Organizadoras dos congressos realizados.

Quero apresentar, em meu nome e da Indústria Brasileira do Cimento nossos agradecimentos aos três profissionais, responsáveis pelo êxito técnico deste congresso os srs.

J. P. Meric - da Cie. des Ciments Français
Jan Skalny - da W. R. Grace
Francisco de Assis Basílio, Colaborador, assim como aos Drs.
Paulo Monteiro
Yoshiro Kihara
M. S. Marinho
H. Bucher
na organização administrativa tivemos a atuação de:
João Batista Menescal Fiuza - Diretor Administrativo
Gabriel Vianna - Assessor
e todos os técnicos e funcionários do Sindicato Nacional da Indústria de Cimento:

Finalmente, agradeço a todos os especialistas que apresentaram os trabalhos que estão publicados nos 6 volumes dos Anais, a todos os que compareceram ao congresso e especialmente àqueles que cooperaram na condução dos trabalhos nas sessões de Temas e Sub-temas.

Chegamos à hora da despedida certos de que todos hão de se lembrar do Congresso e do Rio de Janeiro, de suas praias e belezas naturais.

Até o 9º Congresso."

PROF. F. A. BASÍLIO (Ingénieur Conseil)

"Mes Dames et Messieurs

En 1980, à Paris, a la soirée du 4 juillet à la séance de clotûre du 7ème Congrès International de la Chimie des Ciments, M. Raymond Poitrat, Président du Syndicat National des Fabricants de Ciments et de Chaux et Président de la Comission du Congrès, annonça la ville de Rio de Janeiro comme siège du congrès suivant, le 8ème. Il savait qu'il prenait une grande responsabilité car il devrait choisir un nouveau siège avec l'assurance d'avoir un autre congrès organisé avec les mêmes caractéristiques des congrès précédents de la chimie des ciments avec un niveau scientifique bien en accord avec la recherche la plus avancée dans ce domaine.

S'il a reussi on non dans le choit qu'il a fait, c'est a vous de la juger, après le congrès que vient de finir, mais la Commission d'Organisation du Congrès de Rio de Janeiro, a fait de son mieux pour être digne de la mission.

En effet, dans le but d'assurer la coopération d'un plus grand nombre des plus importants spécialistes des pays du monde, et éviter des longs déplacements pour eux, on a résolu travailler, dans le choix des Thèmes et Sous-thèmes du congrès, en trois Comités Scientifiques respectivement à Paris (France), à Baltimore (USA) et à Rio de Janeiro (Brésil). Pour assurer la coordination des travaux le Dr. Paulo M. Freire, Vice-Président Éxecutif de la Commission d'Organization du Brésil, et moi même, nous avons été présent à presque toutes les réunions des Comités Scientifiques.

Les Trois Comités ont finalement, après quelques années de travail, presenté la relation des Thèmes et Sous-thèmes pour le 8ème congrès, qui fut approuvé par la Commissiona d'Organization.

En envisageant la situation particulière de l'Amérique du Sud et jugeant d'avantage de discuter un peu plus les sujets des questions posées par les participants du congrès, la Commission d'Organization a approuvé la diminuition du nombre des thèmes, reduit à quatre et alors prendre toute la journée pour chaque théme.

L'organisation technique du congrès a eu de la chance dans le choix des spécialistes pour la présidence des thèmes et des sous-thèmes, et pour présenter le rapport principal, rapport spécial et rapport des communications de chaque thème. Nos invitations furent acceptées et on a pu voir les spécialistes que sont venues à Rio de Janeiro et les excelents travaux presentées. Nous avons a remercier aussi tous les auteurs de Communications Basiques et Communications Libres et qui sont dejà publiées aux annales. Les Communications aux Séminaires seront publicés au sixième volume des Annales.

In apperçu sur le congrés de Rio de Janeiro nous montre que nous avons reçu 398 documents que seront publiés aux Annales du congrès imprimés en six volumes dont cinq vous ont été remis à l'occasion de l'inscription au congrès et le dernier vous sera envoyé par la poste.

Le congrés a reçu environ 600 inscriptions et en plus, à peu près, 100 accompagnants.

Du point de vu technique, on a vu un enorme interêt dans toutes les sessions de thèmes et dans celles des sous-thèmes dont la contribution des membres des tables rondes, et de plusieurs invités ont produit de discussion à haut niveau technique à propos des questions posées par l'audience.

En conséquence, comme pour les annales du congrès de Paris, les Annales du congrès de Rio de Janeiro, seront une référence très importante, pendant des années, pour tous ceux qui s'intéressent à l'évolution des recherches en ce qui concerne la chimie du ciment.

Je remercie vivement à tous ceux qui ont collaboré pour la réussite de ce congrès et je fait les meilleurs voeux pour qu'au prochain congrès ont puisse se rencontrer et prêter une colaboration si utile comme vous vener des prêter au 8ême congrès.

Merci pour l'attention."

PARTICIPANTS' LIST

	NAME	COMPANY	ADRESS	ZIP-CITY-STATE-COUNTRY
001	ARMANDOLA,HAYDEE VIRGINIA	CADIEM LABORATORIOS	N.S.DEL CARMEN 2306	1674-SAENZ PENA-B.A.-ARGENTINA
002	BONFORTE,ANTONINO	CADIEM LABORATORIOS	N.S.DEL CARMEN 2306	1674-SAENZ PENA-B.A.-ARGENTINA
003	GIMENEZ,ANIBAL HORACIO	CEMENTO SAN MARTIN S.A.	DEFENSA 113-9o.PISO	1065-BUENOS AIRES- ARGENTINA
004	FESSIA,SILVER DANIEL	CORPORACION CEMENTERA ARGENTINA S.A.	C.DE CORREO 9	5000-CORDOBA- ARGENTINA
005	MORETTI,RAUL	CORPORACION CEMENTERA ARGENTINA S.A.	AV.ESPANA	5500-MENDOSA- ARGENTINA
006	MELCONIAN,RUBEN	DAREX SAIC (W.R.GRACE)	PRIMEIRA JUNTA 550	1878-BUENOS AIRES- ARGENTINA
007	IDIAZABAL,MIGUEL	KHD-HUMBOLDT WEDAG-DEUTZ ARGENTINA	VALENTIN GOMEZ 577	1706-HAEDO-B.A.- ARGENTINA
008	FAVA,ALBERTO S.C.	INSTITUTO TECNOLOGICO DEL HORMIGON	MIRAVE 2774	1281-BUENOS AIRES- ARGENTINA
009	CABALLERO,JULIO CESAR	INST.DEL CEMENTO PORTLAND ARGENTINO	SAN MARTIN 1137	1004-BUENOS AIRES- ARGENTINA
010	LONGO,ADOLFO	INST.NACIONAL DE TECNOLOGIA INDUSTRIAL	CASILLA CORREO 157	1650-SAN MARTIN- ARGENTINA
011	SONA,JORGE DANIEL	JUAN MINETTI S.A.	ITUZAINGO 87-2o.PISO	5000-CORDOBA- ARGENTINA
012	GALVAN,LUIS ERNESTO	LOMA NEGRA CIASA	AV.PTE.ROQUE SAENZ PENA 634	1035-BUENOS AIRES- ARGENTINA
013	MIRETZKY,BERNARDO	LOMA NEGRA CIASA	AV.PTE.ROQUE SAENZ PENA 634	1035-BUENOS AIRES- ARGENTINA
014	SAIZ,ALBERTO	PETROQUIMICA CRSA	BARRIO DON BOSCO	9003-C.RIVADAVIA- ARGENTINA
015	PREATONI,DANIEL EDUARDO	PROCEM S.A.	RAWSON 1192	1182-BUENOS AIRES- ARGENTINA
016	ORTEGA,PEDRO HECTOR	REFRACTARIOS ARGENTINOS SACIM	TTE.GRAL.JUAN PERON 1669	BUENOS AIRES- ARGENTINA
017	WHITE,CLIFFORD	C.S.H.CONSULTANTS PTY LTD.	RMB 5465-THE RIDGEWAY	2250-HOLGATE- AUSTRALIA
018	GERGER,WOLFGANG	GMUNDNER ZEMENTWERKE	P.O.BOX 6	A-4810-GMUNDEN- AUSTRIA
019	KING.TREVOR	ARAWAK CEMENT COMPANY LTD.	CHECKER HALL	ST.LUCY- BARBADOS
020	LAKSMAN,RAMESH	ARAWAK CEMENT COMPANY LTD.	CHECKER HALL	ST.LUCY- BARBADOS
021	BLONDIAU,LEON-MARIE	CIMENTS D'OBOURG S.A.	RUE DES FABRIQUES 2	7048-MONS-OBOURG- BELGIUM
022	DE RYCKHOLT,ROGER DU BOIS DE BOUNAM	CIE.DES CIMENTS BELGES	GRAND ROUTE 860	7530-TOURNAI- BELGIUM
023	TENOUTASSE,M.	S.A.REDCO	NAAMLOSE VENNOOTSCHAP	2920-KAPELLE- BELGIUM
024	FIERENS,PAUL	UNIVERSITE DE MONS	AVENUE MAISTRIAU 21	B-7000-MONS- BELGIUM
025	DE LEON,LUIS PONCE	CIA BOLIVIANA DE CEMENTO	AV.SAN MARTIN	S-0558-COCHABAMBA- BOLIVIA
026	TORDOYA,LUIS PANDZO	CIA BOLIVIANA DE CEMENTO	AV.SAN MARTIN	S-0558-COCHABAMBA- BOLIVIA
027	VIDOS,DALIBOR CEZAREO	CIA BOLIVIANA DE CEMENTO	AV.SAN MARTIN	S-0558-COCHABAMBA- BOLIVIA
028	DO AMARAL FILHO,EPAMINONDAS MELO	ASSOC.BRAS.DE CIMENTO PORTLAND	R.SILVIA CELESTE CAMPOS 504	05462-S.PAULO-SP- BRASIL
029	BACELLAR,LUIS	ASSOC.BRAS.DE CIMENTO PORTLAND	AV.TORRES DE OLIVEIRA 76	05347-S.PAULO-SP- BRASIL
030	BARRETO,ARGO MENNA	ASSOC.BRAS.DE CIMENTO PORTLAND	AV.TORRES DE OLIVEIRA 76	05347-S.PAULO-SP- BRASIL
031	BATTAGIN,ARNALDO	ASSOC.BRAS.DE CIMENTO PORTLAND	AV.TORRES DE OLIVEIRA 76	05347-S.PAULO-SP- BRASIL
032	BATTAGIN,INES	ASSOC.BRAS.DE CIMENTO PORTLAND	AV.TORRES DE OLIVEIRA 76	05347-S.PAULO-SP- BRASIL
033	BUCHER,HANS	ASSOC.BRAS.DE CIMENTO PORTLAND	AV.TORRES DE OLIVEIRA 76	05347-S.PAULO-SP- BRASIL
034	ESPER,MARIO WILLIAM	ASSOC.BRAS.DE CIMENTO PORTLAND	AV.TORRES DE OLIVEIRA 76	05347-S.PAULO-SP- BRASIL
035	KIHARA,YUSHIRO	ASSOC.BRAS.DE CIMENTO PORTLAND	AV.TORRES DE OLIVEIRA 76	05347-S.PAULO-SP- BRASIL
036	LOPES,CARLOS ALBERTO	ASSOC.BRAS.DE CIMENTO PORTLAND	AV.TORRES DE OLIVEIRA 76	05347-S.PAULO-SP- BRASIL
037	LOPES,CARLOS MANUEL GONCALVES	ASSOC.BRAS.DE CIMENTO PORTLAND	AV.TORRES DE OLIVEIRA 76	05347-S.PAULO-SP- BRASIL
038	MARCIANO,EVERALDO	ASSOC.BRAS.DE CIMENTO PORTLAND	AV.TORRES DE OLIVEIRA 76	05347-S.PAULO-SP- BRASIL
039	MARCIANO,ZULEICA ALVES N.	ASSOC.BRAS.DE CIMENTO PORTLAND	AV.TORRES DE OLIVEIRA 76	05347-S.PAULO-SP- BRASIL
040	RODRIGUES FILHO,HUGO DA COSTA	ASSOC.BRAS.DE CIMENTO PORTLAND	AV.TORRES DE OLIVEIRA 76	05347-S.PAULO-SP- BRASIL
041	RODRIGUES,PAULO	ASSOC.BRAS.DE CIMENTO PORTLAND	AV.TORRES DE OLIVEIRA 76	05347-S.PAULO-SP- BRASIL
042	SCANDIUZZI,LUERCIO	ASSOC.BRAS.DE CIMENTO PORTLAND	AV.TORRES DE OLIVEIRA 76	05347-S.PAULO-SP- BRASIL
043	SUTO,ANTONIA JADRANKA	ASSOC.BRAS.DE CIMENTO PORTLAND	AV.TORRES DE OLIVEIRA 76	05347-S.PAULO-SP- BRASIL
044	TEZUKA,YASUKO	ASSOC.BRAS.DE CIMENTO PORTLAND	AV.TORRES DE OLIVEIRA 76	05347-S.PAULO-SP- BRASIL
045	ZAMPIERI,VALDIR	ASSOC.BRAS.DE CIMENTO PORTLAND	AV.TORRES DE OLIVEIRA 76	05347-S.PAULO-SP- BRASIL
046	RIBEIRO,VOLNEY NASCIMENTO	BRASCEP ENGENHARIA LTDA	R.TEOFILO OTONI 85	20090-R.JANEIRO-RJ- BRASIL
047	BATISTA,ANTONIO CARLOS	BRASILIT S.A.	AV.PROSPERIDADE 380	09250-SANTO ANDRE-SP-BRASIL
048	BIENFAIT,BERNARD	BRASILIT S.A.	AV.PROSPERIDADE 380	09250-SANTO ANDRE-SP-BRASIL
049	FERNANDES,PAULO BASILIO	BRASILIT S.A.	AV.PROSPERIDADE 380	09250-SANTO ANDRE-SP-BRASIL
050	GAUDIOT,JEAN JACQUES	BRASILIT S.A.	AV.PROSPERIDADE 380	09250-SANTO ANDRE-SP-BRASIL
051	ISHII,ROSEMARY SANAE ZAMATARO	BRASILIT S.A.	AV.PROSPERIDADE 380	09250-SANTO ANDRE-SP-BRASIL
052	MARCHI,JOSE EDUARDO	BRASILIT S.A.	AV.PROSPERIDADE 380	09250-SANTO ANDRE-SP-BRASIL
053	DIOGO,FRANCISCO FERNANDES	CAMARGO CORREA INDUSTRIAL S.A.	R.GABRIEL R.DOS SANTOS 1415	18320-APIAI-SP- BRASIL
054	PEREIRA.MANUEL G.L.SIMOES	CAMARGO CORREA INDUSTRIAL S.A.	R.GABRIEL R.DOS SANTOS 1415	18320-APIAI-SP- BRASIL
055	ROSA,JOSE LUIS	CAMARGO CORREA INDUSTRIAL S.A.	R.FUNCHAL 160	04551-S.PAULO-SP- BRASIL
056	CRAIEVICH,ALDO	CBPF/CNPQ-MIN.DE CIENCIA E TECNOLOGIA	R.XAVIER SIGAUD 150	22290-R.JANEIRO-RJ- BRASIL
057	FARIAS,ROBERTO F.S.	CEPED-CENTRO DE PESQUISAS DA BAHIA	ROD.RAPOSO TAVARES 3175 BL.G	05575-S.PAULO-SP- BRASIL
058	SANTOS,MARCOS EDILTO CINTRA	CEPED-CENTRO DE PESQUISAS DA BAHIA	DOD.BR-536,KM 0	42800-CAMACARI-BA- BRASIL
059	SAAD,MIGUEL	CESP-CIA ENERGETICA DE SAO PAULO	AV.PAULISTA 2064	01310-S.PAULO-SP- BRASIL
060	SALLES,FLAVIO MOREIRA	CESP-CIA ENERGETICA DE SAO PAULO	AV.PAULISTA 2086	01310-S.PAULO-SP- BRASIL
061	DA SILVA,JOSE MARIA RANGEL	CIA.AGRO-IND.DE MONTE ALEGRE-CAIMA	EST.DO ALEIXO,KM 10	69000-MANAUS-AM- BRASIL
062	SASAOKA,YOSUKE	CIA.AGRO-IND.DE MONTE ALEGRE-CAIMA	EST.DO ALEIXO,KM 10	69000-MANAUS-AM- BRASIL
063	FALCAO,RICARDO FIGUEIREDO	CIA.CEARENSE DE CIMENTO PORTLAND	R.MADRE DE DEUS 27	50000-RECIFE-PE- BRASIL
064	MIRANDA,ROMULO FABRI	CIA.CIMENTO PORTLAND ITAU	AL.SANTOS 1357	01419-S.PAULO-SP- BRASIL
065	MOURA,GUILHERME	CIA.CIMENTO PORTLAND ITAU	AL.SANTOS 1357	01419-S.PAULO-SP- BRASIL
066	RIBOLDI,ALAYR	CIA.CIMENTO PORTLAND ITAU	AL.SANTOS 1357	01419-S.PAULO-SP- BRASIL
067	SALVADOR,WELDON	CIA.CIMENTO PORTLAND ITAU	AL.SANTOS 1357	01419-S.PAULO-SP- BRASIL
068	SIQUEIRA,ETEOCLES MEIRELLES	CIA.CIMENTO PORTLAND ITAU	AL.SANTOS 1357	01419-S.PAULO-SP- BRASIL
069	SORIA,HUGO GONZALES	CIA.CIMENTO PORTLAND ITAU	AL.SANTOS 1357	01419-S.PAULO-SP- BRASIL
070	AGUIAR,MARCELO ANTONIO	CIA.CIMENTO PORTLAND DE SERGIPE	R.MADRE DE DEUS 27	50000-RECIFE-PE- BRASIL
071	BARRETO,LUIZALPES	CIA.DE CIMENTO ATOL	FAZ.SAO SEBASTIAO S/N	57240-S.M.CAMPOS-AL- BRASIL
072	SALVADOR,REGINA CELIA	CIA.DE CIMENTO ATOL	FAZ.SAO SEBASTIAO S/N	57240-S.M.CAMPOS-AL- BRASIL
073	REZENDE,ALCIONE	CIA.DE CIMENTO ITAMBE	ROD.BR-377,KM 134	83650-BALSA NOVA-PR- BRASIL
074	FERNANDES FILHO,ROMARIO	CIA.DE CIMENTO PORTLAND GAUCHO	ROD.BR-116,KM 256	93250-ESTEIO-RS- BRASIL
075	FONTOURA,MARIO L.FRANCESCHI	CIA.DE CIMENTO PORTLAND GAUCHO	ROD.BR-116,KM 256	93250-ESTEIO-RS- BRASIL

	NAME	COMPANY	ADRESS	ZIP-CITY-STATE-COUNTRY
076	RAMOS,MANUEL BAUTISTA	CIA.DE CIMENTO PORTLAND MARINGA	BARAO DE TAQUARI S/N	18400-ITAPEVA-SP- BRASIL
077	ALVES,HENRIQUE CLEMENTE BAETA	CIA.DE CIMENTO PORTLAND PARAISO	RDD.RJ-166,KM 2,5-VAL DE PALMAS	28500-CANTAGALO-RJ- BRASIL
078	AMERICO,GILMAR MAGNO	CIA.DE CIMENTO PORTLAND PARAISO	AV.RIO BRANCO 103,18o.ANDAR	20041-R.JANEIRO-RJ- BRASIL
079	ARAUJO JUNIOR,ANTENOR	CIA.DE CIMENTO PORTLAND PARAISO	R.TIRADENTES S/N	36205-BARROSO-MG- BRASIL
080	BLATTER,JORG	CIA.DE CIMENTO PORTLAND PARAISO	AV.RIO BRANCO 103,18o.ANDAR	20041-R.JANEIRO-RJ- BRASIL
081	CHAGAS,ROBERTO OLIVEIRA	CIA.DE CIMENTO PORTLAND PARAISO	AV.RIO BRANCO 103,18o.ANDAR	20041-R.JANEIRO-RJ- BRASIL
082	DA SILVA,CARLOS ALBERTO M.P.	CIA.DE CIMENTO PORTLAND PARAISO	AV.RIO BRANCO 103,18o.ANDAR	20041-R.JANEIRO-RJ- BRASIL
083	DE CARVALHO,PEDRO HENRIQUES	CIA.DE CIMENTO PORTLAND PARAISO	AV.RIO BRANCO 103,18o.ANDAR	20041-R.JANEIRO-RJ- BRASIL
084	DIVINO,FRANCISCO EDUARDO GUIMARAES	CIA.DE CIMENTO PORTLAND PARAISO	AV.RIO BRANCO 103,18o.ANDAR	20041-R.JANEIRO-RJ- BRASIL
085	FONTES,ARTHUR	CIA.DE CIMENTO PORTLAND PARAISO	AV.RIO BRANCO 103,18o.ANDAR	20041-R.JANEIRO-RJ- BRASIL
086	FREIRE,EDUARDO	CIA.DE CIMENTO PORTLAND PARAISO	AV.RIO BRANCO 103,18o.ANDAR	20041-R.JANEIRO-RJ- BRASIL
087	FREIRE NETO,MARIO	CIA.DE CIMENTO PORTLAND PARAISO	AV.RIO BRANCO 103,18o.ANDAR	20041-R.JANEIRO-RJ- BRASIL
088	GOULART,BENEDITO DA COSTA	CIA.DE CIMENTO PORTLAND PARAISO	AV.RIO BRANCO 103,18o.ANDAR	20041-R.JANEIRO-RJ- BRASIL
089	ISNARD,CARLOS AUGUSTO	CIA.DE CIMENTO PORTLAND PARAISO	AV.RIO BRANCO 103,18o.ANDAR	20041-R.JANEIRO-RJ- BRASIL
090	LOPES,GERALDO ALMEIDA	CIA.DE CIMENTO PORTLAND PARAISO	RDD.RJ-166,KM 2,5-VAL DE PALMAS	28500-CANTAGALO-RJ- BRASIL
091	MONTEIRO,PAULO JOSE M.	CIA.DE CIMENTO PORTLAND PARAISO	AV.RIO BRANCO 103,18o.ANDAR	20041-R.JANEIRO-RJ- BRASIL
092	MONTENEGRO,CARLOS ALBERTO PINTO	CIA.DE CIMENTO PORTLAND PARAISO	R.1-CIVIT II-LOTES 5 A 8	29160-SERRA-ES- BRASIL
093	OLIVEIRA,JERONIMO TOMAZ FERREIRA	CIA.DE CIMENTO PORTLAND PARAISO	RDD.RJ-166,KM 2,5-VAL DE PALMAS	28500-CANTAGALO-RJ- BRASIL
094	PEDRO,JOSE ALBERTO SALGADO	CIA.DE CIMENTO PORTLAND PARAISO	AV.RIO BRANCO 103,18o.ANDAR	20041-R.JANEIRO-RJ- BRASIL
095	PEREZ,BENITO EDUARDO LOBOS	CIA.DE CIMENTO PORTLAND PARAISO	AV.RIO BRANCO 103,18o.ANDAR	20041-R.JANEIRO-RJ- BRASIL
096	ROSAT,PAULO WILTGEN	CIA.DE CIMENTO PORTLAND PARAISO	AV.RIO BRANCO 103,18o.ANDAR	20041-R.JANEIRO-RJ- BRASIL
097	SILVA,CARLOS CESAR	CIA.DE CIMENTO PORTLAND PARAISO	R.1-CIVIT II-LOTES 5 A 8	29160-SERRA-ES- BRASIL
098	UNANUE,WALTER MARIO GARCIA	CIA.DE CIMENTO PORTLAND PARAISO	AV.RIO BRANCO 103,18o.ANDAR	20041-R.JANEIRO-RJ- BRASIL
099	VITRAL,JOSE ROBERTO CAMARA	CIA.DE CIMENTO PORTLAND PARAISO	R.TIRADENTES S/N	36205-BARROSO-MG- BRASIL
100	LIMA NETO,JORGE	CIA.DE CIMENTO PORTLAND POTY	R.MADRE DE DEUS 27	50000-RECIFE-PE- BRASIL
101	SHDEEN,EUSEBIO MUNHOZ	CIA.DE CIMENTO PORTLAND POTY	R.MADRE DE DEUS 27	50000-RECIFE-PE- BRASIL
102	CERON,CLAIR	CIA.DE CIMENTO PORTLAND RIO BRANCO	R.JOAO NEGRAO 1285	80000-CURITIBA-PR- BRASIL
103	FOSTER,HERBERT	CIA.DE CIMENTO PORTLAND RIO BRANCO	R.JOAO NEGRAO 1285	80000-CURITIBA-PR- BRASIL
104	MONACO,ERNANI	CIA.DE CIMENTO SALVADOR	PONTA DA SAPOCA	40000-S.T.PARIPE-BA- BRASIL
105	ABREU,JOAO BOSCO	CIA.MATERIAIS SULFUROSOS-MATSULFUR	AV.AMAZONAS 311-3o.ANDAR	30180-B.HORIZONTE-MG-BRASIL
106	ABREU,JOSE EDUARDO	CIA.MATERIAIS SULFUROSOS-MATSULFUR	AV.AMAZONAS 311-3o.ANDAR	30180-B.HORIZONTE-MG-BRASIL
107	MACHADO,JOSE EUSTAQUIO	CIA.MATERIAIS SULFUROSOS-MATSULFUR	AV.AMAZONAS 311-3o.ANDAR	30180-B.HORIZONTE-MG-BRASIL
108	RIBEIRO,MARCOS ANTONIO	CIA.MATERIAIS SULFUROSOS-MATSULFUR	AV.AMAZONAS 311-3o.ANDAR	30180-B.HORIZONTE-MG-BRASIL
109	SOARES,ALBERTO LUIZ	CIA.MATERIAIS SULFUROSOS-MATSULFUR	AV.AMAZONAS 311-3o.ANDAR	30180-B.HORIZONTE-MG-BRASIL
110	TIBURCIO,MAURICIO	CIA.MATERIAIS SULFUROSOS-MATSULFUR	AV.AMAZONAS 311-3o.ANDAR	30180-B.HORIZONTE-MG-BRASIL
111	BERTELLI NETO,JOAO	CIA.PARAIBA DE CIMENTO PORTLAND-CIMEPAR	FAZENDA GRACA - C.P.15	58000-JOAO PESSOA-PB-BRASIL
112	VISANI,VITTORIO	CIA.PARAIBA DE CIMENTO PORTLAND-CIMEPAR	FAZENDA GRACA - C.P.15	58000-JOAO PESSOA-PB-BRASIL
113	DA SILVA NETO,JOSE MARIA	CIA.SIDERURGICA DA GUANABARA-COSIGUA	AV.JOAO XXIII,6777	23500-R.JANEIRO-RJ- BRASIL
114	FERREIRA,NELSON AMILCAR	CIMENTO ARATU S.A.	VIA PERIFERICA,S/N	43700-SIMOES FO.-BA- BRASIL
115	OLIVEIRA,MANOEL	CIMENTO CAUE S.A.	ESTACAO DE JOAO CORREA,S/N	35166-MESQUITA-MG- BRASIL
116	RUAS,AMARILIO	CIMENTO CAUE S.A.	AV.CEL.JUVENTINO DIAS,S/N	33600-P.LEOPOLDO-MG- BRASIL
117	SOARES,JARBAS	CIMENTO CAUE S.A.	AV.CEL.JUVENTINO DIAS,S/N	33600-P.LEOPOLDO-MG- BRASIL
118	FEREIRA,ALAOR	CIMENTO E MINERACAO BAGE S.A.	AV.MARIA COELHO AGUIAR,215 BL.A	05804-S.PAULO-SP- BRASIL
119	MOURA,LUIZ EDUARDO G.TAQUECE	CIMENTO IRAJA S.A.	AV.MERITI,4411	21250-R.JANEIRO-RJ- BRASIL
120	PESSOA,FRANCISCO DE PAULA GUSMAO	CIMENTO IRAJA S.A.	AV.MERITI,4411	21250-R.JANEIRO-RJ- BRASIL
121	MOUSSA,MURRIB	CIMENTO ITAU DE CORUMBA S.A.	AV.RIO BRANCO,S/N	79300-CORUMBA-MS- BRASIL
122	SILVA JUNIOR,DARIO	CIMENTO ITAU DE CORUMBA S.A.	AV.RIO BRANCO,S/N	79300-CORUMBA-MS- BRASIL
123	CARVALHO,LUIZ VILAR	CIMENTO ITAU DO PARANA S.A.	R.JOAO NEGRAO 1285	80000-CURITIBA-PR- BRASIL
124	TELES,RICARDO A.DA SILVA	CIMENTO ITAU DO PARANA S.A.	R.JOAO NEGRAO 1285	80000-CURITIBA-PR- BRASIL
125	ANDRADE,JOSE GONCALVES	CIMENTO MAUA S.A.	RDD.MG-424,KM-31	35720-MATOZINHOS-MG- BRASIL
126	BONNAL,PAUL JEAN JOSEPH	CIMENTO MAUA S.A.	AV.ALMTE.BARROSO,52-15o.ANDAR	20031-R.JANEIRO-RJ- BRASIL
127	CATILLON,JEAN DIDIER	CIMENTO MAUA S.A.	RDD.RJ-166,KM-8-FONTE DA SAUDADE	28520-EUCLIDELAND-RJ-BRASIL
128	COSTA,DANIEL TRAVASSOS R.	CIMENTO MAUA S.A.	RDD.RJ-166,KM-8-FONTE DA SAUDADE	28520-EUCLIDELAND-RJ-BRASIL
129	DA SILVA,ARMANDO MARTINS	CIMENTO MAUA S.A.	RDD.RJ-166,KM-8-FONTE DA SAUDADE	28520-EUCLIDELAND-RJ-BRASIL
130	DEJEAN,JEAN	CIMENTO MAUA S.A.	ROD.MG-424,KM-31	35720-MATOZINHOS-MG- BRASIL
131	DEMARS,PATRICK	CIMENTO MAUA S.A.	AV.AFONSO PENA,941-1o.ANDAR	30130-B.HORIZONTE-MG-BRASIL
132	MACHADO NETO,TOBIAS	CIMENTO MAUA S.A.	AV.ALMTE.BARROSO,52-15o.ANDAR	20031-R.JANEIRO-RJ- BRASIL
133	MADRE,BENOIT	CIMENTO MAUA S.A.	AV.ALMTE.BARROSO,52-15o.ANDAR	20031-R.JANEIRO-RJ- BRASIL
134	MATSUSHITA,KAORU	CIMENTO MAUA S.A.	ROD.MG-424,KM-31	35720-MATOZINHOS-MG- BRASIL
135	MATTOSINHO,JOAO BATISTA	CIMENTO MAUA S.A.	ROD.MG-424,KM-31	35720-MATOZINHOS-MG- BRASIL
136	BARRETO,CANDIDO LOPES	CIMENTO PIRINEUS S.A.	ROD.BR-414,KM-70	77135-C.DE GOIAS-GO- BRASIL
137	COELHO,FERNANDO DE BARROS	CIMENTO SANTA RITA S.A.	AV.BRIG.FARIA LIMA,888-12o.ANDAR	01452-S.PAULO-SP- BRASIL
138	DAMICO,GIOVANNI	CIMENTO SANTA RITA S.A.	AV.BRIG.FARIA LIMA,888-12o.ANDAR	01452-S.PAULO-SP- BRASIL
139	MARIANO,ADILSON DORTA	CIMENTO SANTA RITA S.A.	AV.BRIG.FARIA LIMA,888-12o.ANDAR	01452-S.PAULO-SP- BRASIL
140	SANTOS,MANUEL VITOR	CIMENTO SANTA RITA S.A.	AV.BRIG.FARIA LIMA,888-12o.ANDAR	01452-S.PAULO-SP- BRASIL
141	ALMEIDA,JOSE NEWTON R.	CIMENTO TUPI S.A.	VIA SERGIO BRAGA,S/N	27265-V.REDONDA-RJ- BRASIL
142	IVO,LUIZ SANTANA	CIMENTO TUPI S.A.	ROD.BR-040,KM-655	36280-CARANDAI-MG- BRASIL
143	RINELLI,JOSE LUIZ	CIMENTO TUPI S.A.	PRAIA DE BOTAFOGO,228-16o.ANDAR	22250-R.JANEIRO-RJ- BRASIL
144	VIANA,JOSE LEANDRO GARCIA	CIMENTO TUPI S.A.	PRAIA DE BOTAFOGO,228-16o.ANDAR	22250-R.JANEIRO-RJ- BRASIL
145	MESQUITA,GERONCIO	CIMENTOS DO BRASIL S.A.-CIBRASA	ROD.BR-316,KM-150	68700-CAPANEMA-PA- BRASIL
146	MOLLO,EDUARDO	CIMENTOS DO BRASIL S.A.-CIBRASA	ROD.BR-316,KM-150	68700-CAPANEMA-PA- BRASIL
147	MUNHOZ,MIGUEL DIAS	CIMINAS-CIMENTO NACIONAL DE MINAS S.A.	VARGEM ALEGRE,S/N	33600-P.LEOPOLDO-MG- BRASIL
148	VIEIRA,RAIMUNDO NONATO RIBEIRO	CIMINAS-CIMENTO NACIONAL DE MINAS S.A.	VARGEM ALEGRE,S/N	33600-P.LEOPOLDO-MG- BRASIL
149	DE SOUZA JR.,HAMILTON FERREIRA	CIPLAN-CIMENTO PLANALTO S.A.	SCS-ED.BARACAT 11o.ANDAR	70309-BRASILIA-DF- BRASIL
150	MARCOVICH,PAULIN EMILE	CIPLAN-CIMENTO PLANALTO S.A.	SCS-ED.BARACAT 11o.ANDAR	70309-BRASILIA-DF- BRASIL

	NAME	COMPANY	ADRESS	ZIP-CITY-STATE-COUNTRY
151	CASTRO,MANUEL	CLEPLAN-EMPREENDS.E PROJS.INDS.LTDA	ALAMEDA CAMPINAS,463-10o.ANDAR	01404-S.PAULO-SP- BRASIL
152	HELLOFS,LEONARD	CLEPLAN-EMPREENDS.E PROJS.INDS.LTDA	ALAMEDA CAMPINAS,463-10o.ANDAR	01404-S.PAULO-SP- BRASIL
153	GRIJSPEERDT,HENRI	COBRASCOM S.A.	AV.ALMTE.BARROSO,63	20036-R.JANEIRO-RJ- BRASIL
154	DANTAS,RONALDO LUZ	COHIDRO-CIA.DES.RECURSOS HIDRICOS	AV.IVO DO PRADO,840	49000-ARACAJU-SE- BRASIL
155	TARTUCE,RONALDO	CONCREBRAS S.A.ENG.CONCRETO	R.AMERICO BRASILIENSE,633	04715-S.PAULO-SP- BRASIL
156	DE BONIS,BRUNO	CONSULTOR AUTONOMO	R.FERREIRA CARDOSO,37-SALA 101	21050-R.JANEIRO-RJ- BRASIL
157	UGLIARA,WAGNER	COPEBRAS S.A.	PCA.DA REPUBLICA,497-5o.ANDAR	01045-S.PAULO-SP- BRASIL
158	PAMPLONA,AFRODIZIO	D.N.O.C.S.	R.TABAJARAS,11	60000-FORTALEZA-CE- BRASIL
159	VEIGA,ROBSON	ELETROSUL S.A.	OBRA JORGE LACERDA	88700-TUBARAO-SC- BRASIL
160	SPLETTSTOSER JR.,JAIME	ELFUSA-GERAL DE ELETROFUSAO	ESTR.MUNICIPAL P/AGUAI,KM-3	13870-S.J.B.VISTA-SP-BRASIL
161	SPRENGER,CARLOS EDUARDO	ETERNIT S.A.	AV.DOS AUTOMOBILISTAS,1828	06020-OSASCO-SP- BRASIL
162	ANDERSEN,ALLAN	F.L.SMIDTH	R.NEBRASKA,443	04560-S.PAULO-SP- BRASIL
163	BIRCH,ERIK	F.L.SMIDTH	R.NEBRASKA,443	04560-S.PAULO-SP- BRASIL
164	GIUNTOLI.ROLDAND	F.L.SMIDTH	R.NEBRASKA,443	04560-S.PAULO-SP- BRASIL
165	OTSEN,OLE	F.L.SMIDTH	R.NEBRASKA,443	04560-S.PAULO-SP- BRASIL
166	DE OLIVEIRA,JOSE GARIBALDI	FORJAS BRASILEIRAS S.A.	R.MEXICO,111-18o.ANDAR	20031-R.JANEIRO-RJ- BRASIL
167	DE SOUZA,GUERINO A.	FORJAS BRASILEIRAS S.A.	R.MEXICO,111-18o.ANDAR	20031-R.JANEIRO-RJ- BRASIL
168	PEDRAS,GABRIEL LUIZ J.	FORJAS BRASILEIRAS S.A.	R.MEXICO,111-18o.ANDAR	20031-R.JANEIRO-RJ- BRASIL
169	PEIXOTO,PAULO ROBERTO C.	FORJAS BRASILEIRAS S.A.	R.MEXICO,111-18o.ANDAR	20031-R.JANEIRO-RJ- BRASIL
170	FESTGE,REINHOLD	HAVER + BEUMER L.I.C.M.LTDA.	ROD.CAMPINAS/MONTE-MOR,KM-20	13190-S.PAULO-SP- BRASIL
171	GAMBURGO,ADRIAN	HAVER + BEUMER L.I.C.M.LTDA.	ROD.CAMPINAS/MONTE-MOR,KM-20	13190-S.PAULO-SP- BRASIL
172	REMMERT,JOSEF	HAVER + BEUMER L.I.C.M.LTDA.	ROD.CAMPINAS/MONTE-MOR,KM-20	13190-S.PAULO-SP- BRASIL
173	PRISZKULNIK,SIMAO	HIDROSERVICE ENG.PROJETOS LTDA.	R.AFONSO CELSO,235	01419-S.PAULO-SP- BRASIL
174	DUARTE,EDSON	IBACIP-IND.BARB.DE CIMENTO PORT. S.A.	ROD.CE-223,KM-2.5-S/N	63186-BARBALHA-CE- BRASIL
175	MARINHO,MARCELO J.B.DE SOUZA	ICI BRASIL S.A.	R.VERBO DIVINO,1356	04719-S.PAULO-SP- BRASIL
176	CINCOTTO,MARIA ALBA	INST.DE PESQ.TECNOLIGAS DE S.PAULO-IPT	AV.PROF.ALMEIDA PRADO,535	05508-S.PAULO-SP- BRASIL
177	MARQUES,JOAO CARLOS	INST.DE PESQ.TECNOLIGAS DE S.PAULO-IPT	CIDADE UNIVERSITARIA-C.P.7141	05508-S.PAULO-SP- BRASIL
178	TANGO,CARLOS EDUARDO DE S.	INST.DE PESQ.TECNOLIGAS DE S.PAULO-IPT	CIDADE UNIVERSITARIA	05508-S.PAULO-SP- BRASIL
179	UEMOTO,KAI LOH	INST.DE PESQ.TECNOLIGAS DE S.PAULO-IPT	AV.PROF.ALMEIDA PRADO,535	05508-S.PAULO-SP- BRASIL
180	COSTA,BILL JORGE	INST.DE TECNOLOGIA DO PARANA	R.DOS FUNCIONARIOS,1357	80030-CURITIBA-PR- BRASIL
181	CACONIA,ALCINA	INST.NACIONAL DE TECNOLOGIA	AV.VENEZUELA,82	20081-R.JANEIRO-RJ- BRASIL
182	CIANI,MARCIA	INST.NACIONAL DE TECNOLOGIA	AV.VENEZUELA,82	20081-R.JANEIRO-RJ- BRASIL
183	GRECA,MARIA CONCEICAO	INST.NACIONAL DE TECNOLOGIA	AV.VENEZUELA,82	20081-R.JANEIRO-RJ- BRASIL
184	MELO,ELIANE	INST.NACIONAL DE TECNOLOGIA	AV.VENEZUELA,82	20081-R.JANEIRO-RJ- BRASIL
185	MESQUITA,CLAUDIO	INST.NACIONAL DE TECNOLOGIA	AV.VENEZUELA,82	20081-R.JANEIRO-RJ- BRASIL
186	PALAZZO,MARIO	INST.NACIONAL DE TECNOLOGIA	AV.VENEZUELA,82	20081-R.JANEIRO-RJ- BRASIL
187	AZEVEDO JR.,EMERSON	ITABIRA AGRO-INDUSTRIAL S.A.	FAZENDA MONTE LIBANO - C.P.252	29300-C.ITAPEMIRI-ES-BRASIL
188	FERNANDES,AULO	ITABIRA AGRO-INDUSTRIAL S.A.	FAZENDA SUMIDOURO,S/N	18300-C.BONITO-SP- BRASIL
189	NOVAES,ROGERIO	ITABIRA AGRO-INDUSTRIAL S.A.	FAZENDA MONTE LIBANO - C.P.252	29300-C.ITAPEMIRI-ES-BRASIL
190	PARACAMPOS,SERGIO	ITABIRA AGRO-INDUSTRIAL S.A.	FAZENDA MONTE LIBANO - C.P.252	29300-C.ITAPEMIRI-ES-BRASIL
191	BRAGA,JOSE AUGUSTO	ITAIPU BINACIONAL	CANTEIRO DE OBRAS-LAB.DE CONCRETO	85890-F.DO IGUACU-PR-BRASIL
192	FERNANDES NETTO,FRANCILINO	ITAIPU BINACIONAL	CANTEIRO DE OBRAS-C.P.1555	85892-F.DO IGUACU-PR-BRASIL
193	FELIX,ALUIZIO	ITAPESSOCA AGRO-INDUSTRIAL S.A.	ILHA DE ITAPESSOCA,S/N	55900-GOIANA-PE- BRASIL
194	GUEIROS,INALDO	ITAPESSOCA AGRO-INDUSTRIAL S.A.	ILHA DE ITAPESSOCA,S/N	55900-GOIANA-PE- BRASIL
195	KONDO,OSWALDO	ITAPETINGA AGRO-INDUSTRIAL S.A.	AV.CENTENARIO,S/N	59600-MOSSORO-RN- BRASIL
196	MONTENEGRO,MARCOS	ITAPETINGA AGRO-INDUSTRIAL S.A.	AV.CENTENARIO,S/N	59600-MOSSORO-RN- BRASIL
197	TRES,LUIS	ITAPICURU AGRO-INDUSTRIAL S.A.	ROD.BR-316,KM-466	65400-CODO-MA- BRASIL
198	ANDERSEN,VAGN	KHD DO BRASIL LTDA.	AV.PAULISTA,460-11o.ANDAR	01310-S.PAULO-SP- BRASIL
199	BONFIM,MARCOS	MAGNESITA S.A.	PCA.LOUIS ENSCH,240	32210-CONTAGEM-MG- BRASIL
200	DE BRITO,CARLOS BORGES	MAGNESITA S.A.	PCA.LOUIS ENSCH,240	32210-CONTAGEM-MG- BRASIL
201	GARRELL,RICHARD PAUL	MAGNESITA S.A.	PCA.LOUIS ENSCH,240	32210-CONTAGEM-MG- BRASIL
202	GONTIJO,LOURENCO	MAGNESITA S.A.	PCA.LOUIS ENSCH,240	32210-CONTAGEM-MG- BRASIL
203	MOSCI,RICARDO	MAGNESITA S.A.	PCA.LOUIS ENSCH,240	32210-CONTAGEM-MG- BRASIL
204	ORNELAS,PAULO MARCHI	MAGNESITA S.A.	PCA.LOUIS ENSCH,240	32210-CONTAGEM-MG- BRASIL
205	RODRIGUES,ANGELA	MAGNESITA S.A.	PCA.LOUIS ENSCH,240	32210-CONTAGEM-MG- BRASIL
206	VALLE,DENIZ	MAGNESITA S.A.	PCA.LOUIS ENSCH,240	32210-CONTAGEM-MG- BRASIL
207	WAJDOWICZ,ADAM	MAGNESITA S.A.	PCA.LOUIS ENSCH,240	32210-CONTAGEM-MG- BRASIL
208	ZACCARDI,MIGUEL ANGEL	MAGNESITA S.A.	PCA.LOUIS ENSCH,240	32210-CONTAGEM-MG- BRASIL
209	SCHLEISS,RENE	MAGOTTEAUX DO BRASIL	AV.GAL.DAVID SARNOFF,1221	32210-CONTAGEM-MG- BRASIL
210	ARREPIA,AUGUSTO ALFREDO	MATSICA INDUSTRIA E COMERCIO	AV.PAPA JOAO PAULO I,2971	07080-GUARULHOS-SP- BRASIL
211	ABREU,JOSE AUGUSTO ARNAO P.	MAXBETON INDUSTRIA E COMERCIO LTDA.	R.DEBRET,23-SALA 403	20030-R.JANEIRO-RJ- BRASIL
212	ABREU,JOSE AUGUSTO A.K.P.	MAXBETON INDUSTRIA E COMERCIO LTDA.	R.DEBRET,23-SALA 403	20030-R.JANEIRO-RJ- BRASIL
213	GIAMMUSSO,SALVADOR	MAXBETON INDUSTRIA E COMERCIO LTDA.	ALAMEDA SANTOS,1470-SALA 707	01418-S.PAULO-SP- BRASIL
214	PALERMO,GIOVANNI	METRO-SAO PAULO	R.LUIS COELHO,197-9o.ANDAR	01309-S.PAULO-SP- BRASIL
215	HIRTH,HAROLD	MULTIPLUS INFORMATICA S/C LTDA.	R.DR.FLAQUER,115-SALA 1618	04006-S.PAULO-SP- BRASIL
216	ARRIAGADA,LUIS OMAR	O & K - ORENSTEIN & KOPPEL EQUIP.LTDA.	R.CAP.ANTONIO ROSA,376-15o.ANDAR	01443-S.PAULO-SP- BRASIL
217	LEIBLEIN,ELMAR	O & K - ORENSTEIN & KOPPEL EQUIP.LTDA.	R.CAP.ANTONIO ROSA,376-15o.ANDAR	01443-S.PAULO-SP- BRASIL
218	SCHNEIDER,HORST	O & K - ORENSTEIN & KOPPEL EQUIP.LTDA.	R.CAP.ANTONIO ROSA,376-15o.ANDAR	01443-S.PAULO-SP- BRASIL
219	SERBONCINI,AMAURI	O & K - ORENSTEIN & KOPPEL EQUIP.LTDA.	R.CAP.ANTONIO ROSA,376-15o.ANDAR	01443-S.PAULO-SP- BRASIL
220	KASAI,NOBORU	ONODA BRASILEIRA IND.COM.LTDA.	AV.BERNARDINO DE CAMPOS,98	04004-S.PAULO-SP- BRASIL
221	MORAES,MARIA LUIZA	PETROBRAS - CENPES	CID.UNIVERSITARIA-ILHA DO FUNDAO-B.7	21910-R.JANEIRO-RJ- BRASIL
222	NUNES,NEY VIEIRA	PETROBRAS - CENPES	CID.UNIVERSITARIA-ILHA DO FUNDAO-B.7	21910-R.JANEIRO-RJ- BRASIL
223	PARENTE,FERNANDO	PETROBRAS - CENPES	CID.UNIVERSITARIA-ILHA DO FUNDAO-B.7	21910-R.JANEIRO-RJ- BRASIL
224	SILVA,MARIA DAS GRACAS	PETROBRAS - CENPES	CID.UNIVERSITARIA-ILHA DO FUNDAO-B.7	21910-R.JANEIRO-RJ- BRASIL
225	EFTIMIADES,MARIO	POLYSIUS PROJ.IND.LTDA.	AV.BRIG.FARIA LIMA,1885-14o.ANDAR	01451-S.PAULO-SP- BRASIL

	NAME	COMPANY	ADRESS	ZIP-CITY-STATE-COUNTRY
226	GEIB,HERIBERT	POLYSIUS PROJETOS IND.LTDA	AV.BRIG.FARIA LIMA,1885-14o.ANDAR	01451-S.PAULO-SP- BRASIL
227	GONCALEZ,FRANCISCO	POLYSIUS PROJETOS IND.LTDA	AV.BRIG.FARIA LIMA,1885-14o.ANDAR	01451-S.PAULO-SP- BRASIL
228	GRINFEDER,CLAUDE	POLYSIUS PROJETOS IND.LTDA	AV.BRIG.FARIA LIMA,1885-14o.ANDAR	01451-S.PAULO-SP- BRASIL
229	THIEME,KLAUS	POLYSIUS PROJETOS IND.LTDA	AV.BRIG.FARIA LIMA,1885-14o.ANDAR	01451-S.PAULO-SP- BRASIL
230	BURIGO,ARYOVALDO	POZOLANA IND.E COM.LTDA.	AV.PROF.FRANCISCO MORATO,492	05512-S.PAULO-SP- BRASIL
231	ABREU,MIRIAN ANTONIO	SABESP	AV.DO ESTADO,561	01107-S.PAULO-SP- BRASIL
232	DE OLIVEIRA,ROBERTO	SERRANA S.A.DE MINERACAO	CAIXA POSTAL 5	11940-JACUPIRANGA-SP-BRASIL
233	DJANIKIAN,JOAO GASPAR	SERRANA S.A.DE MINERACAO	AV.MARIA COELHO AGUIAR,215-3o.AND.BL-A	05804-S.PAULO-SP- BRASIL
234	GOMES,DURVAL	SERRANA S.A.DE MINERACAO	ROD.BR-116,KM-488	11950-JACUPIRANGA-SP-BRASIL
235	GUIDA,LIVIO	SERRANA S.A.DE MINERACAO	AV.MARIA COELHO AGUIAR,215-3o.AND.BL-A	05804-S.PAULO-SP- BRASIL
236	MARTINS,JOANIEL MUNHOZ	SERRANA S.A.DE MINERACAO	CAIXA POSTAL 5	11940-JACUPIRANGA-SP-BRASIL
237	FERNANDES FILHO,OSCAR	SIKA S.A.PRODUTOS QUIMICOS	ESTRADA DO TIMBO,52	21061-R.JANEIRO-RJ- BRASIL
238	COUTO,TIAGO	SOEICOM S.A.-SOC.DE EMP.IND.,COM.E MIN.	AV.PORTUGAL,700	33200-VESPASIANO-MG- BRASIL
239	WAISBERG,BENAMI	SOEICOM S.A.-SOC.DE EMP.IND.,COM.E MIN.	AV.PORTUGAL,700	33200-VESPASIANO-MG- BRASIL
240	AURICCHIO,ELCIO	S.A.INDUSTRIAS VOTORANTIM	PRACA RAMOS DE AZEVEDO,254	01037-S.PAULO-SP- BRASIL
241	BENEDETTI,NILDO MAXIMO	S.A.INDUSTRIAS VOTORANTIM	PRACA RAMOS DE AZEVEDO,254	01037-S.PAULO-SP- BRASIL
242	FERREIRA FILHO,FRANCISCO DIAS	S.A.INDUSTRIAS VOTORANTIM	PRACA RAMOS DE AZEVEDO,254	01037-S.PAULO-SP- BRASIL
243	MARTINI,CELSO ANTONIO	S.A.INDUSTRIAS VOTORANTIM	AV.SENADOR JOSE E.DE MORAES	28500-CANTAGALO-RJ- BRASIL
244	MARTINS,OSORIO L.SILVEIRA	S.A.INDUSTRIAS VOTORANTIM	PRACA RAMOS DE AZEVEDO,254	01037-S.PAULO-SP- BRASIL
245	MENDES,ROBERTO PEREIRA	S.A.INDUSTRIAS VOTORANTIM	AV.SENADOR JOSE E.DE MORAES	28500-CANTAGALO-RJ- BRASIL
246	MORAES,JOSE ROBERTO	S.A.INDUSTRIAS VOTORANTIM	PRACA RAMOS DE AZEVEDO,254	01037-S.PAULO-SP- BRASIL
247	RESENDE,MARCOS MARRA	S.A.INDUSTRIAS VOTORANTIM	AV.SENADOR JOSE E.DE MORAES	28500-CANTAGALO-RJ- BRASIL
248	SANCHEZ,ISIDRO L.C.CONTRERAS	S.A.INDUSTRIAS VOTORANTIM	PRACA RAMOS DE AZEVEDO,254	01037-S.PAULO-SP- BRASIL
249	BIRINDELLI,LUCY D.	THEMAG ENGENHARIA LTDA.	R.BELA CINTRA,986-12o.ANDAR	01415-S.PAULO-SP- BRASIL
250	KUPERMAN,SELMO	THEMAG ENGENHARIA LTDA.	R.BELA CINTRA,986-12o.ANDAR	01415-S.PAULO-SP- BRASIL
251	CARVALHO,MOACYR	UNIV.DO ESTADO DO RIO DE JANEIRO	R.SAO FRANCISCO XAVIER,524-5o.ANDAR	20550-R.JANEIRO-RJ- BRASIL
252	CARVALHO FILHO,ARNALDO CARDIM	UNIV.DO EST.DE S.PAULO-ESC.POLITECNICA	AV.PROF.ALMEIDA PRADO-TRAV.2,271	05598-S.PAULO-SP- BRASIL
253	VOLLET,DIMAS ROBERTO	UNIV.DO EST.DE S.PAULO-IQA	FRANCISCO DEGNI,S/N - C.P.174	14800-ARARAQUARA-SP- BRASIL
254	CAMPITELI,VICENTE CONEY	UNIV.ESTADUAL DE PONTA GROSSA	PRACA SANTOS ANDRADE,S/N	84100-P.GROSSA-PR- BRASIL
255	PINHEIRO,ALCINA KOENOW	UNIV.FED.RJ-ESCOLA DE ENGENHARIA	R.MARQUES DO PARANA,128-COB.	22230-R.JANEIRO-RJ- BRASIL
256	ZAKON,ABRAHAM	UNIV.FED.RJ-ESCOLA DE QUIMICA	R.GENERAL CANABARRO,79-203	20271-R.JANEIRO-RJ- BRASIL
257	COSTA,DARY WERNECK	UNIV.FED.MS	CIDADE UNIVERSITARIA - CICET	79100-C.GRANDE-MS- BRASIL
258	PINTO,JOSE ANTONIO	UNIV.FED.SANTA MARIA	R.BENJAMIN CONSTANT,1096-CID.UNIVERS.	97050-S.MARIA-RS- BRASIL
259	OLIVEIRA,MARILDA BARRA	UNIV.FED.UBERLANDIA	AV.UNIVERSITARIA,S/N	38400-UBERLANDIA-MG- BRASIL
260	VOLKOV,VASIL	HIGHER INST.OF CHEMISTRY TECHNOLOGY	8 KLIMENT OHRIDSKI	1156-SOFIA-BULGARIA
261	WALDNER,ERWIN	MIRON INC.	2201 CREMAZIE EAST	H1Z 2C1-MONTREAL-QB- CANADA
262	FELDMAN,ROLF F.	NAT.RES.COUNCIL CANADA-INST.RES.CONST.	M-20 MONTREAL ROAD	K1A OR6-OTTAWA-ON- CANADA
263	LITVAN,GERARD	NAT.RES.COUNCIL CANADA-INST.RES.CONST.	M-20 MONTREAL ROAD	K1A OR6-OTTAWA-ON- CANADA
264	AITCIN,P.-C.	UNIV.DE SHERBROOKE-FAC.APPLIED SCI.	DEPT.CIVIL ENG.	J1K 2R1-SHERBROOKE-QB-CANADA
265	MINDESS,SIDNEY	UNIV.OF BRITISH COLUMBIA	DEPT.CIVIL ENG.	V6T 1W5-VANCOUVER-BC- CANADA
266	MACINNIS,CAMERON	UNIV.OF WINDSOR	401 SUNSET AVENUE	N9B 3P4-WINDSOR-ON- CANADA
267	CORNEJO,EDUARDO	CEMENTO MELON S.A.	PEDRO DE VALDIVIA 98	LA CALERA- CHILE
268	PEREZ,MARCELO UBILLA	CEMENTO POLPAICO S.A.	AMUNATEGUI,178-5o.PISO	SANTIAGO- CHILE
269	CUEVAS,ARNOLDO BUCAREY	CEMENTOS BIOBIO S.A.	AV.GRAN BRETANA,1725-93 C - CONCEPCION	TALCAHUANO-CHILE
270	KITTL,PABLO	UNIV.DE CHILE - IDIEM	CASILLA 1420	SANTIAGO- CHILE
271	MONDACA,JORGE MAURICIO OSSA	UNIV.DE CHILE - IDIEM	PLAZA ERCILLA 883	SANTIAGO- CHILE
272	VALENZUELA,PABLO CARRILLO	UNIV.DE CHILE - IDIEM	PLAZA ERCILLA 883	SANTIAGO- CHILE
273	CHEN,QUANDE	THE CHINESE SILICATE SOCIETY	BAI WAN ZHUANG	BEIJING -CHINA
274	HUANG,SHIYUAN	THE CHINESE SILICATE SOCIETY	BAI WAN ZHUANG	BEIJING -CHINA
275	SU,MUZHEN	THE CHINESE SILICATE SOCIETY	BAI WAN ZHUANG	BEIJING -CHINA
276	SUN,GUOKUANG	THE CHINESE SILICATE SOCIETY	BAI WAN ZHUANG	BEIJING -CHINA
277	TONG,DAMAO	THE CHINESE SILICATE SOCIETY	BAI WAN ZHUANG	BEIJING -CHINA
278	WU,ZHONGWEI	THE CHINESE SILICATE SOCIETY	BAI WAN ZHUANG	BEIJING -CHINA
279	YANG,NANRU	THE CHINESE SILICATE SOCIETY	BAI WAN ZHUANG	BEIJING -CHINA
280	YE,RUILUN	THE CHINESE SILICATE SOCIETY	BAI WAN ZHUANG	BEIJING -CHINA
281	CHEN,ZHI-YUAN	TONGJI UNIVERSITY	SHIPING ROAD,1239	200092-SHANGAI -CHINA
282	PING,LU	TONGJI UNIVERSITY	SHIPING ROAD,1239	200092-SHANGAI -CHINA
283	WEI,SHEN	TONGJI UNIVERSITY	SHIPING ROAD,1239	200092-SHANGAI -CHINA
284	LOU,ZONGHAN	ZHEJIANG UNIVERSITY	DEPT.OF MATERIALS SCI.& ENG.	HANGZHOU-CHINA
285	STAMARIA,FERNANDO ARTURO RODRIGUEZ	CEMENTOS DEL CARIBE S.A	VIA 40 - LAS FLORES	AA 2739-BARRANQUILLA-COLOMBIA
286	SUAZA,JAIME	CEMENTOS RIOCLARO S.A.	CRA 46-No.5611-TORREARGOS-P.14	7421-MEDELLIN- COLOMBIA
287	NOGUERA,JAIME COVILLA	CIA.COLOMBIANA DE CLINKER S.A.	MOMONAL	AA 3344-CARTAGENA- COLOMBIA
288	OROZCO,ORLANDO LAFAURIE	TOLTECEMENTO	APDO.AEREO 292	SINCELEJO-SUCRE- COLOMBIA
289	MAINIERI,ENRIQUE ALBERTO ACOSTA	CEMENTOS DEL PACIFICO S.A.	APDO.6559	SAN JOSE-COSTA RICA
290	ALMEBORG,JORN	AALBORG PORTLAND	RORDA SVEJ 44-P.O.BOX 165	9100-AALMORG-DENMARK
291	CHRISTENSEN,JENS TIM	AALBORG PORTLAND	RORDA SVEJ 44-P.O.BOX 165	9100-AALMORG-DENMARK
292	KNUDSEN,TORBEN	DANISH TECHNICAL UNIVERSITY	ANKER ENGELUNDSSVEJ	2800-LYNGBY-DENMARK
293	ENKEGAARD,TORBEN	F.L.SMIDTH & CO.A/S	77 VIGERSLEV ALLE	2500-VALBY-COPENHAGEN-DENMARK
294	FEDDERSEN,OLE FINN	F.L.SMIDTH & CO.A/S	77 VIGERSLEV ALLE	2500-VALBY-COPENHAGEN-DENMARK
295	JOHANSEN,VAGN	F.L.SMIDTH & CO.A/S	77 VIGERSLEV ALLE	2500-VALBY-COPENHAGEN-DENMARK
296	OSBAECK,BJARNE	F.L.SMIDTH & CO.A/S	77 VIGERSLEV ALLE	2500-VALBY-COPENHAGEN-DENMARK
297	IDORN,GUNNAR	GMIDORN CONSULT A/S	ROEJELSKAER 15	2840-HOLTE-DENMARK
298	POLAK,ELZBIETA	BIRKBECK COLLEGE	MALET STREET	WC1 7HX-LONDON-ENGLAND,U.K.
299	GUNSON,ALAN	BLUE CIRCLE INDUSTRIES PLC.	GROUP RESEARCH-305 LONDON ROAD	DA9 9JG-GREENHITHE-ENGLAND,U.K.
300	MOIR,GRAEME K.	BLUE CIRCLE INDUSTRIES PLC.	GROUP RESEARCH-305 LONDON ROAD	DA9 9JD-GREENHITHE-ENGLAND,U.K.

	NAME	COMPANY	ADRESS	ZIP-CITY-STATE-COUNTRY
301	BENSTED,JOHN	BRITISH PETROLEUM,INC.	RESEARCH CENTRE	TW16 7LN-SUNBURY-ENGLAND,U.K.
302	MATTHEWS,JOHN	BUILDING RESEARCH STATION	GARSTON	WD2 7JR-WATFORD-ENGLAND,U.K.
303	LEES,TIMOTHY	CEMENT AND CONCRETE ASSOCIATION	WEXHAM SPRINGS	SL3 6PL-SLOUGH BUCKS-ENGLAND,U.K.
304	POMEROY,CHARLES DUNCAN	CEMENT AND CONCRETE ASSOCIATION	WEXHAM SPRINGS	SL3 6PL-SLOUGH BUCKS-ENGLAND,U.K.
305	BALDIE,KEITH	CESB	CERL,KELVIN AVENUE	KT22 7SE-LEATHERHEAD-ENGLAND,U.K.
306	SCRIVENER,KAREN	IMPERIAL COLLEGE OF SCIENCE AND TECHN.	PRINCE CONSORT ROAD	SW7 2BP-LONDON-ENGLAND,U.K.
307	FORRESTER,JAMES	KING'S COLLEGE LONDON	12 MAYFLOWER WAY	HP9 1JE-BEACONSFIELD-ENGLAND,U.K.
308	RODGER,SALLY	OXFORD UNIVERSITY-DEPT.OF METTALURGY	PARKS ROAD	OX1 3PH-OXFORD-ENGLAND,U.K.
309	MILLS,PETER	PRIVATE INDIVIDUAL	30 SWINBURNE STREET	DERBY-ENGLAND,U.K.
310	JACKSON,PETER	THE RUGBY PORTLAND CEMENT	CENTRAL LABORATORY-PARKFIELD	CV21 1QJ-RUGBY-ENGLAND,U.K.
311	CABRERA,JOSEPH G.	THE UNIVERSITY OF LEEDS	DEPT.OF CIVIL ENGINEERING	LS2 9JT-LEEDS-ENGLAND,U.K.
312	BANFILL,PHILLIP F.G.	THE UNIVERSITY OF LIVERPOOL	DEPT.OF BUILDING ENGINEERING	L69 3BX-LIVERPOOL-ENGLAND,U.K.
313	BAILEY,JOHN	THE UNIVERSITY OF SHEFFIELD	ELMFIELD NORTHUMBERLAND ROAD	S10 2TZ-SHEFFIELD-ENGLAND,U.K.
314	ERIKSSON,BO-ERIK	LOHJA CORPORATION		08700-VIRKKALA-FINLAND
315	PALM,CARL-OLOF	OY PARTEK AB	DEVELOPMENT CENTRE	21600-PARGAS-FINLAND
316	TALLING,BOB	OY PARTEK AB	DEVELOPMENT CENTRE	21600-PARGAS-FINLAND
317	NIEMINEN,PERTTI	TAMPERE UNIVERSITY OF TECHNOLOGY	P.O.BOX 527	33101-TAMPERE-FINLAND
318	COLLIS,HENRY	CEMBUREAU	2 RUE SAINT-CHARLES	75015-PARIS-FRANCE
319	DUTRON,PIERRE	CEMBUREAU	2 RUE SAINT-CHARLES	75015-PARIS-FRANCE
320	SOUKATCHOFF,PASCAL	CENTRE DE RECHERCHES DE PONT	A.MOUSSON-BP 28	54700-PONT A MOUSSON-FRANCE
321	BOMBLED,JEAN-PAUL	CERILH	23 RUE DE CRONSTADT	75015-PARIS-FRANCE
322	FAUVEAU,PIERRE	CERILH	23 RUE DE CRONSTADT	75015-PARIS-FRANCE
323	REGOURD,MICHELINE	CERILH	23 RUE DE CRONSTADT	75015-PARIS-FRANCE
324	LOVICHI,JEAN-PIERRE	CIMENTS LAFARGE FRANCE	30 COURS PIERRE PUGET	13006-MARSEILLE-FRANCE
325	CASTANET,ROBERT	CNRS	3 RUE THIEUX	13008-MARSEILLE-FRANCE
326	BERNAUDAT,FRANCOIS	COMMISSARIAT A L'ENERGIE ATOMIQUE	60-68 AV.DU GENERAL LECLERC-B.P.6	92265-FONTENAY-AUX-ROSES-FRANCE
327	LAMEILLE,JEAN-MICHEL	COMMISSARIAT A L'ENERGIE ATOMIQUE	60-68 AV.DU GENERAL LECLERC-B.P.6	92265-FONTENAY-AUX-ROSES-FRANCE
328	REVERTEGAT,ELIANE	COMMISSARIAT A L'ENERGIE ATOMIQUE	LA80.BETONS-BAT.158-SACLAY	91191-GIF-SUR-YVETTE-FRANCE
329	OBERSTE-PADTBERG,RUDIGER	DOWELL SCHLUMBERGER	B.P.90	42003-SAINT-ETIENNE-FRANCE
330	PARCEVAUX,PHILIPPE	DOWELL SCHLUMBERGER	B.P.90	42003-SAINT-ETIENNE-FRANCE
331	GUILHOT,BERNARD	ECOLE DES MINES	158 COURS FAURIEL	42100-SAINT-ETIENNE-FRANCE
332	SOUSTELLE,MICHEL	ECOLE DES MINES	158 COURS FAURIEL	42023-SAINT-ETIENNE-FRANCE
333	BARRET,PIERRE	FACULTE DES SCIENCES MIRANDE	B.P.138	21004-DIJON-FRANCE
334	AMBROISE,JEAN	INSA	20,RUE ALBERT EINSTEIN	69621-VILLE URBANNE-FRANCE
335	PERRA,JEAN	INSA	20,RUE ALBERT EINSTEIN	69621-VILLE URBANNE-FRANCE
336	GRANDET,JACQUES	INSA-LABORATORIE DE GENIE CICIL	AVENUE DE RANGUEIL	31077-TOULOUSE-FRANCE
337	OLLIVIER,JEAN-PIERRE	INSA-LABORATORIE DE GENIE CICIL	AVENUE DE RANGUEIL	31077-TOULOUSE-FRANCE
338	DRON,ROGER	LABORATORY CENTRAL PONTS & CHAUSSEES	58 BD.LEFEBVRE-CEDEX 15	75732-PARIS-FRANCE
339	RIVES,JEAN	LAFARGE COPPEE	28,RUE EMILE MENIER	75116-PARIS-FRANCE
340	RIVOIRE,CLAUDE	LAFARGE COPPEE	28,RUE EMILE MENIER	75116-PARIS-FRANCE
341	SANTOS,FERNANDO M.OLIVEIRA	LAFARGE COPPEE-DIV.INTERNATIONAL	28,RUE EMILE MENIER	75116-PARIS-FRANCE
342	BARON,JACQUES	LAFARGE COPPEE RECHERCHE	B.P.8	07220-VIVIERS-SUR-RHONE-FRANCE
343	BORREIL,ANDRE	LAFARGE COPPEE RECHERCHE	B.P.8	07220-VIVIERS-SUR-RHONE-FRANCE
344	CHAPPUIS,JACQUES	LAFARGE COPPEE RECHERCHE	B.P.8	07220-VIVIERS-SUR-RHONE-FRANCE
345	SORRENTINO,DANIELLE	LAFARGE COPPEE RECHERCHE	B.P.8	07220-VIVIERS-SUR-RHONE-FRANCE
346	SORRENTINO,FRANCOIS	LAFARGE COPPEE RECHERCHE	B.P.8	07220-VIVIERS-SUR-RHONE-FRANCE
347	HAWTHORN,FRANCK	SOCIETE DES CIMENTS FRANCAIS	TOUR GENERALE 5,PLACE DE LA PYRAMIDE	92088-PARIS LA DEFENSE-FRANCE
348	MARIOT,RENE JEAN	SOCIETE DES CIMENTS FRANCAIS	TOUR GENERALE 5,PLACE DE LA PYRAMIDE	92088-PARIS LA DEFENSE-FRANCE
349	MERIC,JEAN-PAUL	SOCIETE DES CIMENTS FRANCAIS	TOUR GENERALE 5,PLACE DE LA PYRAMIDE	92088-PARIS LA DEFENSE-FRANCE
350	RICHER,FRANCOIS	SOCIETE DES CIMENTS FRANCAIS	CEREG-B.P.01	78930-GUERVILLE-FRANCE
351	VERNET,CHRISTIAN	SOCIETE DES CIMENTS FRANCAIS	CEREG-B.P.01	78930-GUERVILLE-FRANCE
352	VON EUW,MARCEL	SOCIETE DES CIMENTS FRANCAIS	TOUR GENERALE 5,PLACE DE LA PYRAMIDE	92088-PARIS LA DEFENSE-FRANCE
353	FRESSY,MICHEL	VICAT	TOUR GAN - CEDEX 13	92082-PARIS-FRANCE
354	GISAS,KOSTAS	HERACLES G.C.C.	S.VENIZELOU,49-51	14123-ATHENS-GREECE
355	MARINOS,IOANNIS	HERACLES G.C.C.	S.VENIZELOU,49-51	14123-ATHENS-GREECE
356	VASILOUDIS,PASCHALIS	HERACLES G.C.C.	S.VENIZELOU,49-51	14123-ATHENS-GREECE
357	HALSTEAD,PHILIP E.	MATERIALS MEASUREMENT LTD.	GPO BOX 4194	HONG KONG-HONG KONG
358	KOLTAI,IMRE	NIKEX-DEPARTMENT 32	MESZAROS-UTCA 48-54	BUDAPEST-HUNGARY
359	TALABER,JOZSEF	RESEARCH AND DES.INST.SILICATE IND.	BECSI UT 126-128	H-1300-BUDAPEST-HUNGARY
360	TAMAS,FERENC	UNIVERSITY OF VESZPREM	P.O.BOX 158	H-8201-VESZPREM-HUNGARY
361	CHATTERJEE,ANJAN KUMAR	ASSOCIATED CEMENT COMPANIES LTD.	CENTRAL RESEARCH STATION	400604-THANE-SHARTRI MARG-INDIA
362	NARANG,KARTAR CHAND	DALMIA CEMENT(BHARAT)LIMITED	HANSALAYA,15-BHARAKHAMBA RD.-11/12 FLS.	110001-NEW DELHI-INDIA
363	DAS,KESHAB	DEVELOPMENT CONSULTANTS P.LTD.	24 B,PARK STREET	700016-CALCUTTA-INDIA
364	IRANI,DINSHAW BOMANJI	NAT.COUNCIL FOR CEMENT & BUILDING MAT.	M-10 SOUTH EXTENSION PART II	110049-NEW DELHI-INDIA
365	KANURI,HARINADHA BABU	NAT.COUNCIL FOR CEMENT & BUILDING MAT.	M-10 SOUTH EXTENSION PART II	110049-NEW DELHI-INDIA
366	LAXMI,SHOBHAY	NAT.COUNCIL FOR CEMENT & BUILDING MAT.	M-10 SOUTH EXTENSION PART II	110049-NEW DELHI-INDIA
367	RAINA,SHIBAN J.	NAT.COUNCIL FOR CEMENT & BUILDING MAT.	M-10 SOUTH EXTENSION PART II	110049-NEW DELHI-INDIA
368	VIVESVARAYA,HOSAGRAHAR C.	NAT.COUNCIL FOR CEMENT & BUILDING MAT.	M-10 SOUTH EXTENSION PART II	110049-NEW DELHI-INDIA
369	AHSAN,MANZOOR	ORISSA CEMENT LIMITED	B 45/47 CONNAUGHT PLACE-SHIV MAHAL	110001-NEW DELHI-INDIA
370	PANDAKASALA,JACOB ALEXANDER	THE TRAVANCORE CEMENTS LTD.	NATTAKOM KOTTAYAM KERALA	686013-KOTTAYAM-INDIA
371	SOROKA,ITZHAK	TECHNION	TECHNION CITY	32000-HAIFA-ISRAEL
372	AUSTONI,SERGIO	CEMENTI TICINO CETI SPA	VIA BONGIASCA	21020-COMABBIO-ITALY
373	PIAZZA,EUGENIO	CEMENTI VICTORIA	VIA MONTESANTO 13	13039-TRINO VERCELLESE-ITALY
374	FRIGIONE,GIUSEPPE	CEMENTIR	VIA CORDGLIO 71	80124-NAPLES-ITALY
375	BUZZI,SANDRO	FRATELLI BUZZI CEMENTI SPA	CORSO GIOVANE ITALIA 39	15033-CASALE MONFERRATO-ITALY

	NAME	COMPANY	ADRESS	ZIP-CITY-STATE-COUNTRY
376	BUCCHI,RENATO	ITALCEMENTI SPA	VIA G.CAMOZZI 124	24100-BERGAMO-ITALY
377	COSTA,UMBERTO	ITALCEMENTI SPA	VIA G.CAMOZZI 124	24100-BERGAMO-ITALY
378	MASSAZZA,FRANCO	ITALCEMENTI SPA	VIA G.CAMOZZI 124	24100-BERGAMO-ITALY
379	ORTOLANI,VITTORIO	ITALCEMENTI SPA	VIA G.CAMOZZI 124	24100-BERGAMO-ITALY
380	TOGNON,GIAMPIETRO	ITALCEMENTI SPA	VIA G.CAMOZZI 124	24100-BERGAMO-ITALY
381	BIAGINI,STEFANO	MAC SPA	VIA VICINALE CORTI 21	31100-TREVISO-ITALY
382	COLLEPARDI,MARIO	MAC SPA	VIA VICINALE CORTI 21	31100-TREVISO-ITALY
383	GUELLA,SILVIO MAURO	MAC SPA	VIA VICINALE CORTI 21	31100-TREVISO-ITALY
384	INDELICATO,FERDINANDO	POLITECNICO DI TORINO-DIP.DI ING.STRUT.	CORSO DUCA DEGLI ABRUZZI 24	10129-TORINO- ITALY
385	LUCCO-BORLERA,MARIA	POLITECNICO DI TORINO-DIP.DI ING.STRUT.	CORSO DUCA DEGLI ABRUZZI 24	10129-TORINO- ITALY
386	CUSSINO,LUCIANO	UNICEM SPA	VIA CARLO MARENCO 25	10126-TORINO- ITALY
387	NEGRO,ALFREDO	UNICEM SPA	VIA CARLO MARENCO 25	10126-TORINO- ITALY
388	AIELLO,ROSARIO	UNIV.DELLA CALABRIA	ARCAVACATA DI RENDE	87030-COSENZA-ITALY
389	MONDSI,SAVERIA	UNIV.DI ANCONA-DIP.SCIENZE DEI MATER.	VIA DELLE BRESCE BIANCHE	60131-ANCONA- ITALY
390	MORICONI,GIACOMO	UNIV.DI ANCONA-DIP.SCIENZE DEI MATER.	VIA DELLE BRESCE BIANCHE	60131-ANCONA- ITALY
391	PAURI,MARCO	UNIV.DI ANCONA-DIP.SCIENZE DEI MATER.	VIA DELLE BRESCE BIANCHE	60131-ANCONA- ITALY
392	AMICARELLI,VINCENZO	UNIV.DI BARI-FACOLTA DI INGEGNERIA	VIA REDAVID 200	70124-BARI- ITALY
393	MASSIDDA,LUIGI	UNIV.DI CAGLIARI	PIAZZA D'ARMI	09100-CAGLIARI-ITALY
394	SANNA,ULRICO	UNIV.DI CAGLIARI	PIAZZA D'ARMI	09100-CAGLIARI-ITALY
395	MARCHESE,BERNARDO	UNIV.DI NAPOLI-DIP.ING.DEI MATERIALI	PIAZZALE TECCHIO	80125-NAPOLI- ITALY
396	MASCOLO,GIUSEPPE	UNIV.DI NAPOLI-DIP.ING.DEI MATERIALI	PIAZZALE TECCHIO	80125-NAPOLI- ITALY
397	SANTORO,LUCIANO	UNIV.DI NAPOLI	VIA MEZZOCANNONE 4	80134-NAPOLI- ITALY
398	SERSALE,RICCARDO	UNIV.DI NAPOLI-DIP.ING.DEI MATERIALI	PIAZZALE TECCHIO	80125-NAPOLI- ITALY
399	VALENTI,GIAN LORENZO	UNIV.DI NAPOLI	PIAZZALE TECCHIO	80125-NAPOLI- ITALY
400	FESTA,DINA	UNIV.DI PADOVA	VIA MARZOLO 9	35100-PADOVA- ITALY
401	SCARINCI,GIOVANNI	UNIV.DI PADOVA	VIA MARZOLO 9	35100-PADOVA- ITALY
402	CIGNA,RANIERI	UNIV.DI ROMA-DIP.ICMMPM	VIA EUDOSSIANA 18	00184-ROMA- ITALY
403	TURRIIIANI,RENATO	UNIV.DI ROMA-DIP.ICMMPM	VIA EUDOSSIANA 18	00184-ROMA- ITALY
404	MCLEOD,MAURICE	CARIBBEAN CEMENT COMPANY	ROCKFORT	KINGSTON-JAMAICA
405	FUKAYA,YASUBUMI	CHICHIBU CEMENT CO.LTD.	2-1-1,TSUKUMI-CHO	360-KUMAGAYA-SHI-JAPAN
406	TAKANO,YUKIO	CHICHIBU CEMENT CO.LTD.	2-1-1,TSUKUMI-CHO	360-KUMAGAYA-SHI-JAPAN
407	KOIBUCHI,KIYOSHI	DAICHI CEMENT CO.LTD.	1-1,ASANO-CHO,KAWASAKI	KAWASAKI-JAPAN
408	NAKAGAWA,KOJI	DENKI KAGAKU KOGYO CO.LTD.	AOMI-CHO,NISHIKUBIKI-GUN	949-03-NIIGATA-JAPAN
409	HARA,NAOMICHI	GOVERNMENT INDUSTRIAL	RESEARCH INSTITUTE,KYUSHU	841-TOSU-SAGA-KEN-JAPAN
410	HASABA,SHIGEMASA	ISHIKAWA TECHNICAL COLLEGE	TUBATA,KANOKU,	920-ISHIKAWA-JAPAN
411	KAWAMURA,MITSUNORI	KANAZAWA UNIVERSITY-FAC.OF ENGINEERING	40-20,KODATSUNO 2 -CHOME	920-KANAZAWA-JAPAN
412	TORII,KAZUYUKI	KANAZAWA UNIVERSITY-FAC.OF ENGINEERING	40-20,KODATSUNO 2 -CHOME	920-KANAZAWA-JAPAN
413	ASAKURA,ETSURO	MITSUBISHI MINING & CEMENT CO.	2270 YOSOKE-CHO,CHICHIBU-GUN	SAITAMA-KEN-JAPAN
414	MAKI,IWAO	NAGOYA INST.OF TECHNOLOGY	GORISO-CHO,SHOWA-KU	466-NAGOYA-JAPAN
415	MITSUDA,TAKESHI	NAGOYA INST.OF TECHNOLOGY-CERAMICS LAB.	ASAHIGAOKA,TAJIMI	507-GIFU-KEN-JAPAN
416	YAMAZAKI,YUKINORI	NIHON CEMENT CO.LTD.	2-23-1,KIYOSUMI,KOTO-KU	TOKYO-JAPAN
417	AOKI,SHIGEKI	NIHON UNIVERSITY	1-8-14,SURUGA-DAI,KANDA	101- TOKYO-JAPAN
418	TSUYUKI,NAOMITSU	NIHON UNIVERSITY	7-24-1,NARASHINODAI	274-FUNABASHI-SHI-JAPAN
419	TSUJIMATSU,HIROSHI	NIPPON KOKAN K.K.	1-1-2,MARUNOUCHI,CHIYODA-KU	TOKYO-JAPAN
420	HANEHARA,SHUNSUKE	ONODA CEMENT CO.LTD.	1-1-7,TOYOSU,KOTO-KU	135- TOKYO-JAPAN
421	TAKEMOTO,KUNIHIRO	ONODA CEMENT CO.LTD.	1-1-7,TOYOSU,KOTO-KU	135- TOKYO-JAPAN
422	UCHIDA,SHUNICHIRO	ONODA CEMENT CO.LTD.	1-1-7,TOYOSU,KOTO-KU	135- TOKYO-JAPAN
423	UCHIKAWA,HIROSHI	ONODA CEMENT CO.LTD.	1-1-7,TOYOSU,KOTO-KU	135- TOKYO-JAPAN
424	KOBAYASHI,SHIGEHIRO	OSAKA CEMENT CO.LTD.	7-1-49,MINAMI OKAJIMA,TAISHO-KU	OSAKA-JAPAN
425	INOKAWA,HISASHI	SUMITOMO CEMENT CO.LTD.	585,TOYOTOMI-CHO,FUNABASHI	CHIBA-JAPAN
426	KATO,OSAMU	THE CEMENT ASSOCIATION OF JAPAN	17-33-4,TOSHIMA,KITA-KU	TOKYO-JAPAN
427	USHIYAMA,HIROTAKA	TOKUYAMA SODA CO.LTD.	1-1,MIKAGE-CHO	TOKUYAMA-JAPAN
428	GOTO,SEICHI	TOKYO INSTITUTE OF TECHNOLOGY	2-12-1,OOKAYAMA-MEGURO	152- TOKYO-JAPAN
429	NISHIMOTO,NOBUYOSHI	UBE INDUSTRIES,LTD.	1-12-32,NISHIHON-MACHI	755- UBE- JAPAN
430	IKEDA,KO	YAMAGUCHI UNIVERSITY	TOKIWADAI 2557	755- UBE- JAPAN
431	IWABUCHI,TOSHITSUGU	YAMASO CHEMICAL CO.LTD.	25-5-2,CHOME HATCHOBORI CHUO-KU	104- TOKYO-JAPAN
432	DOUMET,JOSEPH	CIMENTERIE NATIONALE S.A.L.	B.P.11	5101- BEYROUTH-LIBAN
433	ULIBARRI,RAMON POD	CEMENTOS MEXICANOS	APDO.POSTAL 392	64520- MONTERREY-MEXICO
434	REGGAD,AHMED	CIMENTERIE DE L'ORIENTAL	B.P.44	OUJDA-MOROCCO
435	AHMOUI,BELKACEM	ASMENT DE TEMARA	AIN ATTIG	TEMARA-MOROCCO
436	VAN KLAVEREN,WILLEM	CEMENTIFABRIEK(CEMIJ)BV	POST BOX 462	1970-AL/IJMUIDEN-NETHERLANDS
437	DE JONG,JAN	ENCI	LAGE KANAALDIJK,115-P.O.BOX 1	6200-AA/MAASTRICHT-NETHERLANDS
438	MELAND,INGER	CEMENT AND CONCRETE INSTITUTE	SINTEF	7034-TRONDHEIM-NORWAY
439	LINDSTAD,JORN	NORCEM A/S	HAAKON 7,GT.2	0114-OSLO 1-NORWAY
440	STOLTENBERG-HANSSON,ERIK	NORCEM A/S		3950-BREVIK-NORWAY
441	GJORV,ODD E.	UNIVERSITY OF TRONDHEIM NTH		7034-TRONDHEIM-NORWAY
442	PITERSON,RAMON ABRAHAM BALID	CEMENTO PANAMA S.A.	P.O.BOX 1755	ZONA 1-PANAMA-PANAMA
443	QUINTERO,GUSTAVO	CEMENTO PANAMA S.A.	P.O.BOX 1755	ZONA 1-PANAMA-PANAMA
444	BAIBE,ISABELINO E.GAMARRA	INDUSTRIA NACIONAL DEL CEMENTO	GENERAL SANTOS-6o.PISO	ASUNCION-PARAGUAY
445	PALACIO,HIGINIO VILLALBA	INDUSTRIA NACIONAL DEL CEMENTO	GENERAL SANTOS-6o.PISO	ASUNCION-PARAGUAY
446	DUARTE,JOSE DOMINGO CARRERAS	ITAIPU BINACIONAL	PARAGUAY-BRASIL	PARAGUAY
447	VERA,CARMELO ACOSTA	ITAIPU BINACIONAL	PARAGUAY-BRASIL	PARAGUAY
448	GONZALES DE LA COTERA,MANUEL ALFONSO	ASOC.DE PRODUCTORES DE CEMENTO	AV.CARLOS VILLARAN,504,STA.CATALINA	LIMA-PERU
449	ARATA,EDUARDO RODRIGUEZ	CEMENTOS LIMA S.A.	LAS BEGONIAS,475-OF.234	LIMA-PERU
450	ARDILES,LUIS ENRIQUE SALINAS	CEMENTOS LIMA S.A.	LAS BEGONIAS,475-OF.234	LIMA-PERU

	NAME	COMPANY	ADRESS	ZIP-CITY-STATE-COUNTRY
451	KURDOWSKI,WIESLAW	AKADEMIA GORNICZO-HUTNICZA	AL.MICKIEWICZA 30	30059-KRAKOW-POLAND
452	GOMES,ALVARO NUNES	CIMPOR-CIMENTOS PORTUGAL EP	R.ALEXANDRE HERCULANO,35	1200-LISBOA-PORTUGAL
453	OLIVEIRA,MARIO MARQUES	CIMPOR-CIMENTOS PORTUGAL EP	R.ALEXANDRE HERCULANO,35	1200-LISBOA-PORTUGAL
454	REIS,MARIA OLINDA BRAGA	LABORATORIO NAC.DE ENGENHARIA CIVIL	AV.BRASIL,101	1799-LISBOA-PORTUGAL
455	AL-NOURY,SOLIMAN	KING ABDULAZIZ UNIVERSITY	P.O.BOX 9027	21413-JEDDAH-SAUDI ARABIA
456	AFSHAR,ALI BEHROOZ	HERIOT-WATT UNIVERSITY	RICCARTON CAMPUS	EH10 4ER-EDINBURGH-SCOTLAND,U.K.
457	MCCARTER,WILLIAM JOHN	HERIOT-WATT UNIVERSITY	RICCARTON CAMPUS	EH10 4ER-EDINBURGH-SCOTLAND,U.K.
458	BARTOS,PETER	PAISLEY COLLEGE	HIGH STREET	PA1 2BE-PAISLEY-SCOTLAND,U.K.
459	GLASSER,FREDRIK PAUL	UNIVERSITY OF ABERDEEN	MESTON WALK	AB9-2UE-OLD ABERDEEN,SCOTLAND,U.K.
460	TAYLOR,HARRY F.W.	UNIVERSITY OF ABERDEEN	DEPT.OF CHEMISTRY,MESTON WALK	AB9-2UE-OLD ABERDEEN,SCOTLAN
461	CREMIEUX,PIERRE	SOCOCIM INDUSTRIES	B.P.29	RUFISQUE-SENEGAL
462	KELLY,R.J.	BLUE CIRCLE LIMITED	P.O.BOX 2484	2000-JOHANNESBURG-SOUTH AFRICA
463	OBERHOLSTER,BERTIE	NATIONAL BUILDING RES.BUILDING	P.O.BOX 395	0001-PRETORIA-SOUTH AFRICA
464	CHOI,SANG-HEUL	HANYIANG UNIVERSITY	17 HAENGDANG-DONG,SUNGDONG-KU	133-SEOUL-SOUTH KOREA
465	HAN,KI-SUNG	INHA UNIVERSITY	253 YONGHYUN-DONG,NAM-KU	160-INCHON-SOUTH KOREA
466	SEO,IL-YOUNG	SSANG-YONG RESEARCH CENTER	YUSEONG-P.O.BOX 12	300-32-DAE-JEON-SOUTH KOREA
467	NAM,KEE DONG	TONG YANG CEMENT CORPORATION	60 DORYOM-DONG CHONGRO-KU	110-SEOUL-SOUTH KOREA
468	GOMA I GINESTA,FERRAN	ASLAND CATALUNIA S.A.	CORSEGA 325	08025-BARCELONA-SPAIN
469	CORONAS,JUAN RAMON BARRAGANO	ASLAND-CIYD	VILLALUENGA DE LA SAGRA	TOLEDO-SPAIN
470	ALONSO,JULIO PEREZ	ASLAND S.A.	ORENSE 81	28020-MADRID-SPAIN
471	REY,PEDRO	ASLAND S.A.	CARRETERA ALMADEN,KM 1	14007-CORDOBA-SPAIN
472	CASTRO,NESTOR	AUXILIAR DE LA CONSTRUCCION	DIAGONAL 534	08006-BARCELONA-SPAIN
473	MURTRA,ISIDORO	AUXILIAR DE LA CONSTRUCCION	DIAGONAL 534	08006-BARCELONA-SPAIN
474	VILA ,VICTORIANO JOSE GONZALEZ	CEMENTOS ATLANTICO S.A.	APARTADO 65	ALCALA DE GUADAIRA-SPAIN
475	FERNANDEZ,MARCOS	CEMENTOS COSMOS S.A.	OURAL	LUGO-SPAIN
476	LONGARELA,ANGEL	CEMENTOS COSMOS S.A.	LUCHANA,23-4o.PISO	28010-MADRID-SPAIN
477	MARTINEZ,ARTURO	CEMENTOS COSMOS S.A.	OURAL	LUGO-SPAIN
478	CEBRIAN,JOSE LUIS	CEMENTOS HONTORIA	VENTA DE BANOS	VALENCIA-SPAIN
479	MONTRAVERA,JUAN PUIG	CEMENTOS MOLINS S.A.	PASEO DE GRACIA,92	BACELONA-SPAIN
480	CARMONA,JOSE MARIA SARDI	CEMENTOS MORATA DE JALON S.A.	PASEO MARI AGUSTIN,4-6	50004-ZARAGOZA-SPAIN
481	HUARTE,GABRIEL	CEMENTOS PORTLAND S.A.	ESTELLA 6,APARTADO 107	31080-PAMPLONA-SPAIN
482	FRADERA,ENRIQUE	CEMENTOS UNILAND S.A.	CORSEGA 299	08008-BARCELONA-SPAIN
483	FERRANDO,JOAQUIM	CIA.VALENCIANA DE CEMENTOS PORTLAND	COLON 68	46004-VALENCIA-SPAIN
484	CALLEJA,JOSE	IECA-OFICEMEN	VELAZQUEZ,23	28001-MADRID-SPAIN
485	ALONSO,MARIA CRUZ ALONSO	INSTITUTO EDUARDO TORROJA	SERRANO GALVACHE S/N.	28033-MADRID-SPAIN
486	ANDRADE,MARIA DEL CARMEM	INSTITUTO EDUARDO TORROJA	SERRANO GALVACHE S/N.	28033-MADRID-SPAIN
487	BLANCO-VARELA,MARIA TERESA	INSTITUTO EDUARDO TORROJA	SERRANO GALVACHE S/N.	28033-MADRID-SPAIN
488	DE LUXAN,MARIA PILAR	INSTITUTO EDUARDO TORROJA	SERRANO GALVACHE S/N.	28033-MADRID-SPAIN
489	GASPAR-TEBAR,DEMETRIO	INSTITUTO EDUARDO TORROJA	SERRANO GALVACHE S/N.	28033-MADRID-SPAIN
490	SORIA,FRANCISCO	INSTITUTO EDUARDO TORROJA	SERRANO GALVACHE S/N.	28033-MADRID-SPAIN
491	TRIVINO,FERNANDO	INSTITUTO EDUARDO TORROJA	SERRANO GALVACHE S/N.	28033-MADRID-SPAIN
492	VAZQUEZ-MORENO,TOMAS	INSTITUTO EDUARDO TORROJA	SERRANO GALVACHE S/N.	28033-MADRID-SPAIN
493	CORDMINA,JORGE	L.A.C. S.A.	APARTADO 56-S.FELIU LLOBREGAT	BARCELONA-SPAIN
494	GIBERT,SANTIAGO	L.A.C. S.A.	APARTADO 56-S.FELIU LLOBREGAT	BARCELONA-SPAIN
495	BRAVO,FRANCISCO	SOCIEDAD FINANCERA Y MINERA	C.TOMAS HEREDIA,27	29001-MALAGA-SPAIN
496	MANCHON,JOSE LUIS MARTINEZ	S.A.E.DE CEMENTOS PORTLAND		45220-YELES(TOLEDO)-SPAIN
497	RUDENIUS,ARNE	ABETONG-SABEMA	BOX 24	VAEXJOE-SWEDEN
498	WARRIS,BIRGER	CEMENTA AB-RESEARCH AND DEVELOPMENT	P.O.BOX 144	S-182 12-DANDERYD-SWEDEN
499	NAREDI,ROBERT	CEMCON	HYLLTORPSGATAN 6	S-216 16-MALMO-SWEDEN
500	CHANDRA,SATISH	CHALMERS UNIVERSITY OF TECHNOLOGY	SVEN HULTINSGATAN 8	S-412 96-GOTHENBURG-SWEDEN
501	NILSSON,LARS-OLOF	CHALMERS UNIVERSITY OF TECHNOLOGY	DIVISION OF BUILDING MATERIALS	S-412 96-GOTHENBURG-SWEDEN
502	HANNAWAYYA,FRANCISA	HANNAWAYYA S.LABORATORY	HUNDHAMRAVAGEN 7-NORSBORY	+ 753 -STOCKOLM-SWEDEN
503	PETERSON,OLOF	LUND INST.OF TECHN.-DIV.OF BUILD.MAT.	P.O.BOX 118	S-221 00-LUND-SWEDEN
504	KLINGSTEDT,GUNNAR	SWEDISH CEMENT & CONCRETE	RESEARCH INSTITUTE	S-100 44-STOCKHOLM-SWEDEN
505	PICCOLI,MARCO BERETTA	CEMENTIA PLANUNGS AG	NUESCHELERSTRSSE 45	CH-8001-ZURICH-SWITZERLAND
506	PETER,GUSTAV	ETH	INSTITUTE BAUSTOFFE	-ZURICH-SWITZERLAND
507	BRAUN,HANS	HOLDERBANK MANAGEMENT & CONSULTING		CH-5113-HOLDERBANK-SWITZERLAND
508	GEBAUER,JURAJ	HOLDERBANK MANAGEMENT & CONSULTING		CH-5113-HOLDERBANK-SWITZERLAND
509	SCHRAEMLI,WERNER	HOLDERBANK MANAGEMENT & CONSULTING		CH-5113-HOLDERBANK-SWITZERLAND
510	KOELLIKER,EMIL	INSTITUTE TECH.RESEARCH	SWISS CEMENT INDUSTRY	CH-5103-WILDEGG-SWITZERLAND
511	LAUBER,JOSEF	PORTLAND CEMENT-WERK	WUERENLINGEN-SIGGENTHAL	CH-5301-ST.SIGGENTHAL-SWITZERLAND
512	BRUNNER,PAUL	VIGIER CEMENT LTD.		CH-4708-LUTERBACH-SWITZERLAND
513	SINGH,RAMJATTAN	TRINIDAD CEMENT LTD.	SOUTHERN MAIN ROAD-CLAXTON BAY	SAN FERNANDO-TRINIDAD & TOBAGO
514	TONAK,TULIN	CEMENT MANUFACT.ASSOC.-CRDC	P.O.BOX 2 - BAKANLIKAR	TR 06582-ANKARA-TURKEY
515	BRUSCHERA,JORGE	ANCAP	C.C.1090	MONTEVIDEO-URUGUAY
516	SUAREZ,JOSE	ANCAP	C.C.1090	MONTEVIDEO-URUGUAY
517	PHILLEO,ROBERT	CONSULTING ENGINEER	7420 ANNANWOOD COURT	22003-ANNANDALE-VA-U.S.A.
518	MAC DOWELL,JOHN F.	CORNING GLASS WORKS	SULLIVAN PARK FR-5	14831-CORNING-NY-U.S.A.
519	COOK LONNIE	DAVENPORT CEMENT COMPANY	P.O.BOX 4049	52808-DAVENPORT-IA-U.S.A.
520	PATZIAS,TERRY	DUNDEE CEMENT CO.	P.O.BOX 122	48131-DUNDEE-MI-U.S.A.
521	KOLAN,ANDREW	ENERGY SERVICES,INC.	205 PINE AVENUE	21146-SAVERNA PK-MD-U.S.A.
522	GUITTON,ETIENNE	GENERAL PORTLAND,INC.	NORTH CENTRAL PLAZA III,SUITE 1700	75248-DALLAS-TX-U.S.A.
523	ROWE,WALT	GENERAL PORTLAND,INC.	3333 FORT WORTH AVENUE	75211-DALLAS-TX-U.S.A.
524	GEORGE,CHARLES	LAFARGE FONDU INTERNATIONAL	18 KOGER EXECUTIVE CENTER	23502-NORFOLK-VA-U.S.A.
525	MOORE,CLYDE W.	LONE STAR INDUSTRIES INC.	515 WEST GREENS ROAD	77067-HOUSTON-TX-U.S.A.

	NAME	COMPANY	ADRESS	ZIP-CITY-STATE-COUNTRY
526	WILLIAMS,CRAIG	MASTER BUILDERS	23700 CHAGRIN BLVD.	44022-CLEVELAND-OH-U.S.A.
527	FROHNSDORFF,GEOFFREY	NATIONAL BUREAU OF STANDARDS	BUILDING 226,ROOM B-368	20899-GAITHERSBURG-MD-U.S.A.
528	DAUGHERTHY,KENNETH	NORTH TEXAS STATE UNIVERSITY	DEPT.OF CHEMISTRY	76203-DENTON-TX-U.S.A.
529	BHATTY,MUHAMMAD	PORTLAND CEMENT ASSOCIATION	5420 OLD ORCHARD ROAD	60648-SKOKIE-IL-U.S.A.
530	DIAMOND,SIDNEY	PURDUE UNIVERSITY	SCHOOL OF CIVIL ENGINEERING	47906-WEST LAFAYETTE-LA-U.S.A.
531	KLEMM,WALDEMAR	SOUTHWESTERN PORTLAND CEMENT CO.	P.O.BOX 937	93392-VICTORVILLE-CA-U.S.A.
532	GRUTZECK,MICHAEL	THE PENNSYLVANIA STATE UNIVERSITY	104 MATERIALS RESEARCH LABORATORY	16802-UNIVERSITY PARK-PA-U.S.A.
533	ROY,DELLA M.	THE PENNSYLVANIA STATE UNIVERSITY	217 MATERIALS RESEARCH LABORATORY	16802-UNIVERSITY PARK-PA-U.S.A.
534	SULLIVAN,PATRICK	UNION CARBIDE CORP.	P.O.BOX 8361	25303-SUTH CHARLESTON-U.S.A.
535	MEHTA,POVINDAR K.	UNIV.OF CALIFORNIA-CIVIL ENG.DEPT.	723 DAVIS HALL	94720-BERKELEY-CA-U.S.A.
536	BUCK,ALAN D.	U.S.CORPS OF ENGINEERS	P.O.BOX 631	39180-VICSBORG-MS-U.S.A.
537	TURK,DANICA	USG CORPORATION	700 N.HIGHWAY 45	60048-LIBERTYVILLE-IL-U.S.A.
538	MATHER,BRYANT	WATERWAYS EXPERIMENT STATION	BOX 631-WESSV-Z	39180-VILKSBURG-MS-U.S.A.
539	MATHER,KATHERINE	WATERWAYS EXPERIMENT STATION	BOX 631-WESSV-Z	39180-VILKSBURG-MS-U.S.A.
540	FARKAS,EMERY	W.R.GRACE & CO.	62 WHITTEMORE AVENUE	02140-CAMBRIDGE-MS-U.S.A.
541	HAYDEN,THOMAS D.	W.R.GRACE & CO.	62 WHITTEMORE AVENUE	02140-CAMBRIDGE-MS-U.S.A.
542	ROBERTS,LAWRENCE R.	W.R.GRACE & CO.	62 WHITTEMORE AVENUE	02140-CAMBRIDGE-MS-U.S.A.
543	SKALNY,JAN	W.R.GRACE & CO.	7379 ROUTE 32	21044-COLUMBIA-MD-U.S.A.
544	STERLING,WILLIAM T.	W.R.GRACE & CO.	1114 AVENUE OF THE AMERICAS	10036-NEW YORK-NY-U.S.A.
545	PETRAVITCHUS,LEOPOLDAS	AKMIARCEMENTAS		235464-NOV.AKMIANE-LITUANIA-U.S.S.R.
546	KOUZNETZOVA,TAMARA	INSTITUT CHEMICO-TECHNOLOGIQUE	PLACE MIOUSKAIA,9	125820-MOSCOW-U.S.S.R.
547	BOIKOVA,ALEXANDRA	INSTITUT DE CHIMIE SILIC.	QUAI MAKAROV,2	199164-LENINGRAD-U.S.S.R.
548	NIKIFOROV,YOURIY	INSTITUT GIPROCEMENT	RUE TCHELIEV,13	193224-LENINGRAD-U.S.S.R.
549	AITMOURATOV,ROUSTEM	INSTITUT NIICEMENT	3,ZOUTCHEVOI PROSEK 12	107014-MOSCOW-U.S.S.R.
550	KHLOUSOV,VLADIMIR	INSTITUT NIICEMENT	3,ZOUTCHEVOI PROSEK 12	107014-MOSCOW-U.S.S.R.
551	MTCHEDLOV-PETROSIAN,OTAR	INSTITUT UJGIPROCEMENT	AVENUE PRADVA,10	310022-KHARKOV-U.S.S.R.
552	KOUSCHIDI,VICTOR	MINISTRY OF BUILDING MATERIALS	PLACE NOGINA,2/5	103713-MOSCOW-U.S.S.R.
553	GOMEZ C.,JESUS M.	C.A.FABRICA NACIONAL DE CEMENTOS	TORRE MADELCA-JESUITAS A.MATURIN/1366	1010-CARACAS-VENEZUELA
554	GOUVEA A.,FLAVIO	C.A.FABRICA NACIONAL DE CEMENTOS	TORRE MADELCA-JESUITAS A.MATURIN/1366	1010-CARACAS-VENEZUELA
555	PERZ,CESAR ARBALAEZ	C.A.VENCEMOS LARA	APARTADO 577	BARQUISIMETO-VENEZUELA
556	LOSADA,JOSE FLORENCIO RAMOS	CEMENTO ANDINO S.A.	CALLE RIO DE JANEIRO	VALERA-VENEZUELA
557	SALAZAR B.,RAMON V.	CEMENTOS GUAYANA S.A.	APARTADO DE CORREO 235	PUERTO ORDAZ-BOLIVAR-VENEZUELA
558	AUMUND,FRANZ	AUMUND FOERDERERBAU GMBH	SAALHOFER STRASSE 17-POST 1261	D-4134-RHEINBERG-WEST GERMANY
559	BEUMER,BERNHARD	BEUMER MASCHINENFABRIK KG	OELDER STRASSE 40	D-4720-BECKUM-WEST GERMANY
560	HAEGERMANN,HANS	BUDERUS AG	MUEHLRAIN 12	633-WETZLAR-WEST GERMANY
561	RUDERT,VOLKHART	DYCKERHOFF AG	RHEINGAUSTRASSE 180	D-6501-WIESBADEN-WEST GERMANY
562	BLUNK,GUENTER	FORSCHUNGSGEM.EISENHUETTERSCH.	BLIERSHEIMER STRASSE 62	41 DUISBURG 14-WEST GERMANY
563	LOCHER,FRIEDRICH	FORSCHUNGSINSTITUT D.ZEMENTINDUSTRIE	TANNENSTRASSE 2-PF 301063	D-4000-DUSSELDORF-WEST GERMANY
564	SPRUNG,SIEGBERT	FORSCHUNGSINSTITUT D.ZEMENTINDUSTRIE	TANNENSTRASSE 2-PF 301063	D-4000-DUSSELDORF-WEST GERMANY
565	WISCHERS,GERD	FORSCHUNGSINSTITUT D.ZEMENTINDUSTRIE	TANNENSTRASSE 2-PF 301063	D-4000-DUSSELDORF-WEST GERMANY
566	HASCHKE,WOLFGANG	HAVER & BOECKER	CARL-HAVER PLATZ	D-4740-OELDE-WEST GERMANY
567	HAVER,RUDOLF	HAVER & BOECKER	CARL-HAVER PLATZ	D-4740-OELDE-WEST GERMANY
568	KROBOTH,KARL	HEIDELBERGER ZEMENT AG	BERLINER STRASSE 6	D-6900-HEIDELBERG-WEST GERMANY
569	LIEBER,WERNER	HEIDELBERGER ZEMENT AG	BERLINER STRASSE 6	D-6900-HEIDELBERG-WEST GERMANY
570	LUEHR,HANS-PETER	INSTITUT FUER BAUTECHNIK	REICHPIETSCHUFER 74-76	D-1000-BERLIN 30-WEST GERMANY
571	TEODORU,GEORGE	INSTITUTE OF TROPICAL TECHNOLOGY	P.O.BOX 250171	D-5000-KOLN 1-WEST GERMANY
572	ODLER,IVAN	INST.FUR NICHTMETALLISCHE WORKSTOFFE	ZEHNTNERSTRASSE 2A	D-3302-CLAUSTHAL-WEST GERMANY
573	WOLTER,ALBRECHT H.	KHD HUMBOLDT WEDAG	POSTFACH 910457	D-5000-KOLN 91-WEST GERMANY
574	SCHEUBEL,BERN	KRUPP POLYSIUS AG	GRAFF GALEN STRASSE 17	D 4720-BECKUM-WEST GERMANY
575	WEBER,PAUL	KRUPP POLYSIUS AG	GRAFF GALEN STRASSE 17	D-4720-BECKUM-WEST GERMANY
576	KUZEL,HANS-JURGEN	MINERALOGISCHES INSTITUT-ERLANGEN UNIV.	SCHLOSSGARTEN 5	D-8520-ERLANGEN-WEST GERMANY
577	POELMANN,HERBERT	MINERALOGISCHES INSTITUT-ERLANGEN UNIV.	SCHLOSSGARTEN 5A	D-8520-ERLANGEN-WEST GERMANY
578	PISTERS,HEINZ	READMIX ZEMENTWERKE GMBH R	CO KG,AM KOLLENBACH 27	D-4720-BECKUM-WEST GERMANY
579	DALDRUP,HEINRICH GROSSE	REFRATECNIK GMBH	RUDOLF-WINKEL STRASSE 1-3	D-3400-GOETTINGEN-WEST GERMANY
580	LUDWIG,UDO	RWTH AACHEN		D-5100-AACHEN-WEST GERMANY
581	BILLHARDT,HERMANN-WOLFRAM	SPENNER ZEMENT KG	P.O.BOX 1126	D-4782-ERWITTE-WEST GERMANY
582	BUNDFUSS,KERSTIN	UNIVERSITAET KARLSRUHE	AM FASANENGARTEN	D-7500-KARLSRUHE-WEST GERMANY
583	WIERIG,HANS-JOACHIM	UNIVERSITAT HANNOVER	HINDENBURGALLEE 31A	D3007-GEHRDEN-WEST GERMANY
584	OSEN,ERNST	UNIVERSITY OF KARLSRUHE	KAISERSTRASSE 12	D-7500-KARLSRUHE-WEST GERMANY
585	WEISWEILER,WERNER	UNIVERSITY OF KARLSRUHE	KAISERSTRASSE 12	D-7500-KARLSRUHE-WEST GERMANY
586	MLAKAR-BEC,VIKTORIJA	CEMENTARNA	KOLODVORSKA 5	TRBOVLJE-YUGUSLAVIA
587	POPOVIC,KRESIMIR	CIVIL ENGINEERING INSTITUTE	JANKA RAKUSE,1	41000-ZAGREB-YUGUSLAVIA
588	DRAGICEVIC,LJUBINKO	INSTITUT ZA PUTEVA	KUMODRASKA 257	11000-BEOGRAD-YUGUSLAVIA
589	ZIVANOVIC,BRANISLAV	INSTITUTE FOR MATERIALS TESTING	BULEVAR VOJV.ODE MISICA 43	11000-BEOGRAD-YUGUSLAVIA
590	DIMIC,DAMIJANA	ZAVOD ZA RAZISKAVO MATERIALA	DIMICEVA 12	61000-LJUBLJANA-YUGUSLAVIA

Abla Gráfica e Editora Ltda.
Rua Júlia Lopes de Almeida, 15 e 15-A
Telefones: 253-6054, 253-6296, 253-6325
Rio de Janeiro – RJ

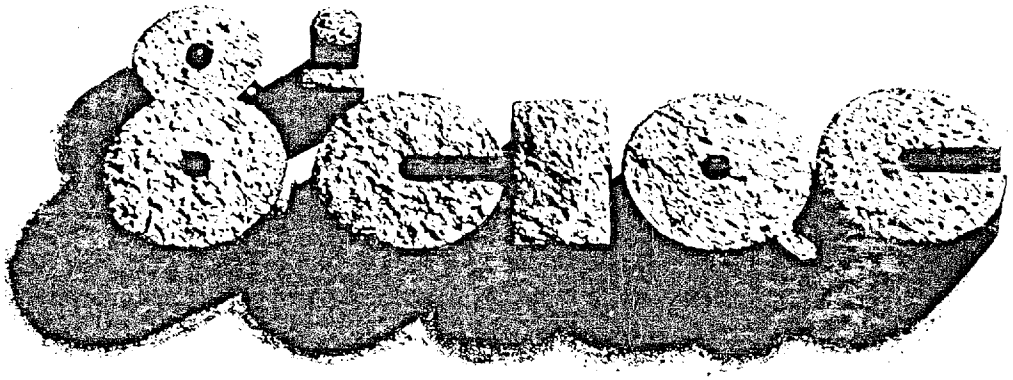

8.º Congresso Internacional de Química do Cimento

8th International Congress on the Chemistry of Cement

8e Congrès International de la Chimie des Ciments

General Reports — Posters — Seminars
Rapports Généraux — Posters — Séminaires
Volume VI

22-27 de setembro de 1986
Rio de Janeiro — Brasil



8.º Congresso Internacional de Química do Cimento

8th International Congress on the Chemistry of Cement

8e Congrès International de la Chimie des Ciments

General Reports — Posters — Seminars
Rapports Généraux — Posters — Séminaires

Volume VI

22-27 de setembro de 1986
Rio de Janeiro — Brasil

Não é permitida a reprodução dos Anais sem prévia autorização da Comissão Organizadora do Congresso.

The Proceedings are not to be reprinted without a previous permission of the Organizing Commission of the Congress.

La reproduction des Annales est interdite sans, au-devant, l'autorisation de la Commission d'Organisation du Congrès.

• • •

A substância e a forma de apresentação dos trabalhos que compõem os Anais do Congresso são de exclusiva responsabilidade de seus autores.

The substance and the form of presentation of the papers that compound the Proceedings of the Congress are exclusive responsability of their authors.

Le fond et la forme de publier les travaux qui composent les Annales du Congrès sont d'exclusive responsabilité de leur auteurs.

Secretaria Geral do 8º CIQC:
Rua da Assembléia, 10 - 40º and. - Gr. 4001
Tel.: 221-6562 – Telex: (021) 33191
20011 Rio de Janeiro – RJ – Brasil

Apoio financeiro da

finep FINANCIADORA DE ESTUDOS E PROJETOS

ORGANIZING COMMISION:

PRESIDENT:	JOSÉ ERMÍRIO DE MORAES FILHO	BRASIL
EXECUTIVE VICE-PRESIDENT:	PAULO MÁRIO FREIRE	BRASIL
TECHNICAL DIRECTOR:	FRANCISCO DE ASSIS BASÍLIO	BRASIL
ADMINISTRATIVE DIRECTOR:	JOÃO BATISTA MENESCAL FIUZA	BRASIL
DIRECTORS:	ALBERTO LUIZ GONÇALVES SOARES	BRASIL
	ENRIQUE GUNTHER DREWES	BRASIL
	EPAMINONDAS MELO DO AMARAL FILHO	BRASIL
	MARCÍLIO DE BRITO	BRASIL
	NEWTON GOULART	BRASIL

SCIENTIFIC COMMITTEES:

– SOUTH AMERICA:		
• PRESIDENT:	FRANCISCO DE ASSIS BASÍLIO	BRASIL
	ALVARO AUGUSTO ALVES PINTO	BRASIL
	DANTE E.J. VERONELLI	ARGENTINA
	FLEMING OEST	BRASIL
	HANS BUCHER	BRASIL
	JOÃO GASPAR DJANIKIAN	BRASIL
	LUIZ ROBERTO MARTINS DE MIRANDA	BRASIL
	MARIA DAS GRAÇAS JAQUÁ	BRASIL
	MARIA LUIZA MOREIRA DE MORAES	BRASIL
	NEY JOSÉ DE SOUZA E SILVA	BRASIL
	PABLO KITTL D.	CHILE
	PAULO RODRIGUES	BRASIL
	ROBERTO R. COELHO	BRASIL
	YASUKO TESUKA	BRASIL
	YUSHIRO KIHARA	BRASIL
– NORTH AND CENTRAL AMERICA, AND FAR EAST:		
• PRESIDENT:	JAN P. SKALNY	U.S.A.
MEMBERS:	DELLA M. ROY	U.S.A.
	GEOFFREY FROHNSDORFF	U.S.A.
	GERARD G. LITVAN	CANADA
	HIROSHI UCHIKAWA	JAPAN
	J. FRANCIS YOUNG	U.S.A
	JORGE MARIO VILLASENOR	MEXICO
	R.E. OBERHOLSTER	SOUTH AFRICA
	SIDNEY DIAMOND	U.S.A.
	S.W. TRESOUTHICK	U.S.A.
	WU ZHONG-WEI	CHINA
– EUROPE, ASIA AND AFRICA:		
• PRESIDENT:	JEAN PAUL MERIC	FRANCE
MEMBERS:	C. CHARRETON	FRANCE
	FRANCO MASSAZZA	ITALY
	FRANÇOIS LE BEL	FRANCE
	FRIEDRICH W. LOCHER	WEST GERMANY
	F. YAGIZ	TURKEY
	H.W.W. POLLITT	ENGLAND, U.K.
	JOSE CALLEJA	SPAIN
	J. TALLABER	HUNGARY
	LABO KADA ABOUBACAR	NIGERIA
	O.P. MTCHEDLOV-PETROSSIAN	U.S.S.R.
	P. DUTRON	FRANCE
	RENATO BUCCHI	ITALY
	S.K. CHOPRA	INDIA
	T.V. KOUZNETSOVA	U.S.S.R.
	WIESLAW KURDOWSKI	POLAND

PRINCIPAL REPORT OF THE SUB-THEME 1.1

Pages

15 F.P. Glasser (Scotland, U.K.) – Kinetics of cement-making reactions.

GENERAL REPORTS OF SUB-THEMES' COMMUNICATIONS:

33	M.S. Marinho	(Brasil)	Sub-theme 1.1
38	Y. Kihara	(Brasil)	Sub-theme 1.2
46	P. Rodrigues	(Brasil)	Sub-theme 1.3
50	Y. Tezuka	(Brasil)	Sub-theme 2.1-a
56	A. Ferreira	(Brasil)	Sub-theme 2.1-b
62	F.A. Basílio	(Brasil)	Sous-thème 2.1-c/d
67	P. Kittl	(Chile)	Sub-theme 2.2
76	P.J.M. Monteiro	(Brasil)	Sub-theme 2.3
80	A.F. Battagin	(Brasil)	Sub-theme 3.1
89	Y. Tezuka	(Brasil)	Sub-theme 3.2
96	H.R.E. Bucher	(Brasil)	Sub-theme 3.3
104	S. Priszkulnik	(Brasil)	Sub-theme 4.1
123	J.G. Djanikian	(Brasil)	Sub-theme 4.2
128	H.V. Armandola	(Argentina)	Sub-theme 4.3

SEMINARS/SÉMINAIRES

SEMINAR/SÉMINAIRE 1
Magnesium Oxide in Portland Cement and Concrete
Oxyde de Magnésium dans le Ciment Portland et dans le Béton
Chairman/Président: Y. NIKIFOROV (U.S.S.R.)

Pages		
143	N.F. Ananenko (U.S.S.R.)	General Report Communications:
149	A. Palomo, J. Vazquez, M.T. Blanco-Varela (Spain)	Influence of MgO on the crystalline microstructure of the liquid phase of portland cement.
154	J. Gebauer (Switzerland)	Effect of high MgO content in cement upon-turn properties of concrete.
158	V.K. Kozlova (U.S.S.R.)	Sur la formation des phases nouvelles dans le clinker lors de la cuisson des mélanges crus à base des produits sécondaires.
164	I.G. Louginina, V.M. Konovalov, L.D. Chaklova, V.A. Beletskai (U.S.S.R.)	Durcissement du ciment portland à teneur elevée en oxyde de magnésium et en autres compositions magnésiennes.

SEMINAR/SÉMINAIRE 2
Cements with Mineral Additions/Ciments Contenant des Additions Minérales
Chairman/Président: M. VON EUW (France)

170	M. Von Euw (France)	Rapport Général Communications:
178	V.S. Ramachandran (Canada), Z. Chun-mei (China)	Cement with calcium carbonate additions.
183	J. Almeborg, J.T. Christensen (Denmark)	Danish portland-fly ash cement.
189	J.P. Ollivier (France)	Rôle des additions minérales sur la formation de l'auréole de transition entre gros granulat et mortier.
198	R. Guyot, R. Ranc, B. Cariou (France)	Utilisation de la potentialité hidraulique du clinker dans les ciments portland avec ajout de fillers calcaires.
204	K. Takemoto (Japan)	The variation of activity index of slag.
207	T.V. Kuznetsova, S.D. Makachev, Z.B. Entin (U.S.S.R.)	Cements with mineral admixtures: state of the art and prospects.
211	Gerd Wischers (West Germany)	Optimization of cements with mineral addictions.

SEMINAR/SÉMINAIRE 3

Effect of the Chemical and the Physico-chemical Properties of Cement Paste and Aggregate Characteristics on the Rheological Behaviour of Mortar and Concrete.

Influence des Propriétés Chimiques et Physico-chimiques de la Pâte et des Caractéristiques des Granulats sur le Comportement Rhéologique des Mortiers et des Bétons.

Chairman/Président: J.P. BOMBLED (France)

217	S. Feneuille, J.P. Bombled (France)	Rapport Général Communications:
223	P.F.G. Banfill, S.M. Gill (England, U.K.)	The rheology of aluminous cement pastes.
228	G.H. Tattersall (England, U.K.)	Components of workability and rheological measurements on mortars and fresh concrete.
239	M. Michaux, R. Oberste-Padtberg (France)	The effect of mix water salinity on cement slurries containing polynaphtalene sulphonate dispersants.
243	J. Orban, P. Parcevaux, D. Guillot (France)	Influence of shear history on the rheological properties of oil well cement slurries.
248	U. Costa, F. Massazza (Italy)	Structure and properties of cement suspensions.
260	F. Basile, S. Biagini, G. Ferrari, M. Collepardi (Italy)	Effect of condensation degree of polymers based on naphthalene on fluidities of cement pastes.
264	F. Basile, S. Biagini, G. Ferrari, M. Collepardi (Italy)	Properties of cement mixes containing naphthalene sulfonated polymers of different molecular weight.
269	S. Grzeszczyk, L. Kucharska (Poland)	The influence of alkallies upon the water demand of early hydration stage cement pastes in the light of rheological studies.
274	J. Mierzwa (Poland)	Thixotropic-plastic-viscous rheological model of cement paste as the result of physical and mineralogical cement properties.
279	S. Sprung (West Germany)	Influence of the composition of clinker and cement on the rheological behaviour of fresh concrete.
284	H.J. Wierig (West Germany)	Influences of cement and temperature on the consistency of fresh concrete.

SEMINAR/SÉMINAIRE 4:

Cement Specifications and Development of Testing Procedure. / Bases Scientifiques des Spécifications pour le Ciment et le Développement des Méthodes d'Essais.

Chairman/Président: P. Dutron (France)

288	P. Dutron (France)	Rapport Général
		Communications:
296	T. Sanduo (China)	Some views on cement specification.
300	P. Terrier (France)	Gestion et assurance de la qualité des essais.
308	A.K. Mullick, K.H. Babu, P. Bhaskara Rao (india)	Evaluation of pozzolanic activity and its impact on specification of blended cements.
312	O. Kato (japan)	Trend of the specification and the method on alkali-silica reaction in Japan.
316	G. Frohnsdorff, P.W. Brown, J.H. Pierlet (U.S.A)	Standard specifications for cements and the role in their development of quality assurance systems for laboratories.
321	E.B. Entin, L.S. Klyueva (U.S.S.R.)	Cement quality: key measures and evaluation techniques.
328	I. Odler, S. Abdul-Maula, U. Hennicke (West Germany)	A new method for determination of cement setting time.

POSTERS

Pages	Authors (Countries)/Auteurs (Pays)	Titles of Papers/Titres de Travaux
331	G. Giaccio, R. Zerbino (Argentina)	Factors affecting cement paste-aggregate bond.
334	J.K. Shukuzawa, H.C. Rodrigues Filho, V.A. Zampieri (Brasil)	Relationship between alite microscopic reactivity and clinker hydraulicity.
337	G. Babachev, K. Kolev (Bulgaria)	The influence of the cement type on the values for light constructive – thermal insulating concrete.
340	T. Ming-shu, X. Zhong-zi, H. Su-fen (China)	Alkali reactivity of glass aggregate.
344	L. Zonghan X. Xianyu, H. Ren, Ch. Yimin (China)	Calcium silico-fluoride phase A and its effects on formation of C_3S.
349	J.A. Forrester, S.A. Jefferis (England, U.K.)	Effects of high shear mixing on hydration behaviour of cement paste and rheological interpretations.
351	M.J. Coole, A.M. Harrisson (England, U.K.)	The effect of simulated large pour curing conditions on the temperature rise and strength growth of PFA containing concrete.
356	C. Vernet (France)	Réactions periodiques lors de l'attaque des ciments par des réactifs chimiques.
358	C. Vernet (France)	Évolution de la microstructure des hydrates des ciments – Aspects théoriques.
361	C. Vernet (France)	Un nouvel instrument pour l'étude des réactions d'hydratation: le GECS (générateur électrochimique de chaux sursaturée).
364	J. Ambroise, J. Péra, M. Murat (France)	Interêt de l'addition de métakaolin au ciment portland pour l'élaboration de matériaux composites renforcés par des fibres de verre.
371	R. Kovács (Hungary)	Rapid method for cement strength prediction.
374	F.D. Tamás, E. Farkas, M. Vörös, (Hungary) D.M. Roy (U.S.A.)	Low-frequency electrical conductivity of cement, clinker and clinker mineral pastes.
381	G. Scarinci, D. Festa, G. Sorarù, G. Grassi, L. Stafferi, C. Badini (Italy)	Portland cement renforced with new alkali-resistant glass fibers.
384	G. Mascolo, P. Pernice, O. Marino (Italy)	Ionic conductivity of lamellar calcium aluminate hydrates.
386	R. Sersale, R. Aiello, G. Frigione (Italy)	Natural zeolites as active additions to the portland clinker.
389	K. Ikeda (Japan)	A new type of pozzolanic cement utilizing red mud and fly ash.
395	K. Isozaki, S. Iwamoto, K. Nakagawa (Japan)	Some properties of alkali activated slag cement.

400	N. Tsuyuki, N. Hirota, K. Miyakawa, J. Kasai (Japan)	The physical properties and the hydration mechanism of C_3A in the presence of $CaSO_4.2H_2O$ and $Ca(OH)_2$.
405	S. Goto, M. Daimon (Japan)	Ion diffusion in cement paste.
410	S. Grzeszczyk (Poland)	C_3A-Na_2O solid solutions in pseudo-two-component system NC_8A_3-C_3A.
413	W. Brylicki (Poland)	Phase composition and morphology of autoclaved γ Ca_2SiO_4 containing pastes.
418	I. Cotea, D. Puscasu, D. Nicolau (Romania)	Contributions to the clinker grindability physics.
422	I. Cotea, N. Butucescu, L. Bucea, V. Mihai (Romania)	Study of thermal effects obtained in the clinkerization process by thermodifferential analysis.
427	I. Cotea, A. Romanescu, C. Dumitrescu (Romania)	Researches concerning the harmful components elimination from phosphogypsum for using it as cement setting time regulator.
434	C. Dumitrescu, G. Nistor (Romania)	Binders of base-acid type setting used in dental technique.
439	C. Popescu, A. Antonescu (Romania)	Clinker manufacturing with alkali, chlorine and sulphur compound controlled contend by gas deviation in stages clinkerization equipment.
445	A. Romanescu, C. Dumitrescu (Romania)	Considerations concerning the hardening mechanism of the controlled expansion cements.
450	A. Romanescu, L. Bucea, F. Amzica (Romania)	Clinker compositional field modification for lowring its formation temperature.
454	M. Enculescu (Romania)	Contributions to clinker forming kinetics.
460	D. Gaspar-Tébar, J.L. Sagrera-Moreno (Spain)	L'àction de l'eau de mer sur un ciment portland de haute résistance initielle et sur un ciment portland résistance aux sulfates: influence de l'addition de laitier, étude de la concentration tonique.
463	F. Bermejo-Muñoz, J.L. Sagrera-Moreno, D. Gaspar-Tébar (Spain)	Comportement d'un ciment portland résistant aux sulfates face à l'eau deionisée et les solutions de sulfate de sodium et de sulfate de magnésium.
468	M.P. de Luxan, M.I. Sanchez de Rojas, M.T. Martin Patino, J. Saavedra (Spain)	Characterization and pozzolanic properties of sedimentary opaline rocks.
470	G. Peter, Q. Yang, A. Rosli (Switzerland)	Infiltration of chloride under capillary action.
471	Sandor Popovics (U.S.A.)	Modeling mathematically the effect of curing temperature on the strength development of cements.
476	M.D. Cohen, B. Mobasher (U.S.A.)	Physico-chemical, microstructural, and micromechanical investigations of sulfoaluminate-type expansive cements.
481	V. Klassen (U.S.S.R.)	Interactions in $CaCO_3$ – $SiO_2R_2CO_3$ (R_2 SO_4) mixtures.
483	K. Karibaev, N. Bajirov, A. Patcenko, N. Panina (U.S.S.R.)	Modification de la structure des scories de la déphosphoration thérmique électrique.
485	V.M. Kolbassov (U.S.S.R.)	Modification de la structure hydratée des ciments.
489	A.M. Ilyinets, V.I. Simonov, M. Ya. Bikbau (U.S.S.R.)	New-data concerning atomic structures of portland cement silicates.
492	L.S. Klueva, A.I. Markov (U.S.S.R.)	Modification of cement contraction due to false setting.
494	N. Komarova, V. Riasine, G. Tchistiakov, A. Korenga (U.S.S.R.)	Stabilisation orientée d'une composition de phases desequilibrés du clinker blanc.

500	Z.M. Larionova, I.I. Kourbatova, N.S. Zhelvakova, L.P. Moiséeva (U.S.S.R.)	Influence des additions organiques sur la formation de la structure de la pierre de ciment.
503	L.I. Levin, G.M. Tarnarutski (U.S.S.R.)	Modified lignin-base sulphonates in the materials on cement base.
506	A.J. Mituzas, V.V. Montvilla, L.V. Petravichys, O.M. Stanylenis (U.S.S.R.)	Technology of production of high alite portland cement clinkers.
508	I.L. Luginina, M.A. Putrenko (U.S.S.R.)	Particularities of cement hydration in suspensions with alcali additions.
510	I.L. Luginina, R.G. Nigmadilova (U.S.S.R.)	Kinetics of assimilation of calcium oxide in presence of titanium compounds.
511	B. Noudelman, A. Clutchariov, G. Galimova, A. Bessmertnykh (U.S.S.R.)	Particularités thermochimiques du processus de cuisson du clinker alinitique.
513	A.A. Pachtchenko, E.A. Miasnikova, V.V. Tokartchouk, V.A. Chevtchenko (U.S.S.R.)	Particularités de la clinkerisation des crus à composants aluminosilicieux à haute réactivité.
517	V.P. Rjazin, Z.B. Entin, N.I. Komarova, N.A. Shebanov (U.S.S.R.)	Some features of mineral formation on the sample surface.
520	U. Ludwig, C. Urrutia (West Germany)	Influence of sucrose on the setting of portland cement.

FREE COMMUNICATIONS / COMMUNICATIONS LIVRES

Pages	Authors (Countries/Auteurs (Pays)	Titles of Papers/Titres de Travaux
523	E. Marciano Jr., (Brasil) P. Bartha (West Germany)	Contribution to the knowledge of the phase composition of different magnesia – chrome bricks after the attack by cement clinker.
529	C. MacInnis, P.P. Hudec, M. Moukwa (Canada)	Effect of microclimate on concrete deterioration.
534	J. Baron, R. Guyot (France)	Um modele phenomenologique de l'evolution de la resistance en compression parametrant l'influence du clinker et celle des granulats.
539	C. Bertrand, C. Bonet, P. Garde (France)	Movel combustion and volatilization deagnostic techniques in cement kilns.
544	J. Chappuis (France)	Physical elementary mechanisms of fluidification by superplasticizers or water-reducing agents.
550	C. Vernet (France)	Modelisation des diagrammes d'equilibre de solubilites des hidrates-interactions ioniques.
556	F. Indelicato, L. Cussino (Italy)	Comportement viscoélastique à long terme des bétons de ciment alumineaux.
562	J.R.L. Dyczek, M. Petri (Poland)	Mechanical properties of autoclaved, monomineral materials from tobermorite, zonotlite and hillebrandite.
565	O.Z. Cebeci, W.H. Mirza, S.I.Al. Noury (Saudi Arabia)	Strength development of mortars in hot and dry environment.
569	K.S. Han, J. Rhee (South Korea)	Etudes sur la synthese de C_3A par le Procede de sol-gel.
573	I.Y. Seo, S.H. Choi (South Korea)	The unstable state of alkali in cement clinker.
578	T. Vazquez, M.T. Blanco- Varela, A. Palomo-Sanchez (Spain)	Lumping of anhydrous portland cement: study through is spectroscopy.
582	L.J. Struble (U.S.A.)	Synthesis and characterization of ettringite and related phases.
589	A.C. Chou, H.C. Eaton, F.M. Cartledge, M.E. Tittlebaum (U.S.A.)	A tem study of the interactions between certain organic hazardous wastes and type in portland cement.
594	J.G. Griffin, K.E. Daugherty (U.S.A.)	The effect of glass content on hidration in the system $CaO-Al_2O_3-MgO-SiO_2$.
598	G. Frohnsdorff, J. Clifton, H. Jennings, P. Brown, L. Struble, J. Pommersheim (U.S.A.)	Implications of computer-based simulation models, expert systems, databases, and networks for cement research.
603	V.I. Akunov, S.D. Makashev, V.A. Dmitriyeva, N.V. Tsukanova, B.E. Yudovich (U.S.S.R.)	Mechanochemical activation of materials in cement manufacture.

607	Y.M. Bazhenov (U.S.S.R.)	Evaluation of reological characteristics of cement paste and concrete with help of computers.
611	L.S. Geidarova, M.A. Astakhova (U.S.S.R.)	Certains aspects de l'activation lors de l'obtention du liant saus clinker.
614	V.D. Gloukhovsky, P.V. Krivenko, R.F. Rounova (U.S.S.R.)	Particularites de la formation de structure dans le ciment durci contenant des alcalis.
617	A.V. Voljenskiy (U.S.S.R.)	Influence de la concentration des liants en melange avec l'eau sur la resistance et deformabilite de cemelange lors du durcissement.
621	W.Weisweiler (West Germany)	Quantification of thallium – and lead – cycles in cement plants.
625	W. Weisweiler, B. Schwarz, E. Mallon (West Germany)	Isolation of thallium – and lead – halides originating from electric separator dust of cement plants by vaporization analysis.

SPEECHES / ALLOCUTIONS
Organizing Commission / Commission d'Organization

Pages

629 Opening Session / Séance Inaugurale
Dr. José Ermírio de Moraes Filho (President/Président)

631 Closing Session / Séance de Clôture
Dr. Paulo Mário Freire (Executive Vice-President/Vice-Président Exécutif)

632 Dr. Francisco de Assis Basílio (Technical Director/Directeur Technique)

635 Participants List / Liste de Participants

F.P. Glasser - Department of Chemistry, University of Aberdeen,
Meston Walk, Old Aberdeen, AB9 2UE, Scotland, U.K.

KINETICS OF CEMENT-MAKING REACTIONS

1. INTRODUCTION

The kinetic aspects of cement clinkering have not been specifically addressed at previous International Cement Congresses, although its proceedings contain many valuable contributions on various aspects of kinetics. The reasons for this absence lie partly in the complexity of cement reactions: it is difficult to analize from the kinetic standpoint complex and ill-understood processes. But partly, the nature of kinetic studies is responsible. Kinetic studies may be contrasted with equilibrium thermodynamic studies; the latter have a coherent and well defined body of theory which serves as a unifying thread. Kinetic studies appear at first sight to lack this unification. The nature of the kinetic treatment has to be varied to suit the particular type of reaction, and a wide range of processes involving solid, liquid and vapour phases occur all of which appear to require special treatments. Moreover, while equilibrium conditions prevailing in the kiln can generally be defined in terms of accessible physiochemical parameters - temperature, composition, etc. - kinetic parameters often seem to be elusive and difficult to evaluate and apply in practice.

The general applicability of kinetic concepts to cement making cannot however be questioned: equilibrium may govern the ultimate nature of the products which can be obtained in a cement kiln, but kinetic factors determine the economics of achieving these ends. We thus recognize that kinetics and equilibrium studies are intertwined. Both aspects are important in determining the process parameters and economics of cement production. It is apparent that continued economic pressures on cement makers will intensify the need to make a more uniform product as well as increasing the performance parameters of concrete systems. It is unlikely that this can be achieved by application of empirical methods alone, hence the need to emphasize fundamental aspects, including process kinetics.

A full review of kinetic theory relevant to cements is beyond the scope of this contribution. However, a number of excellent monographs have appeared, notably those of Budnikova and Ginstling (1968), Kingery et al (1976), Young (1966) Schmalzried (1981) and Doremus (1985). These develop basic concepts, give mathematical treatments and illustrate their application to a wide range of solid state reactions. Cement scientists have perhaps lagged somewhat behind their colleagues engaged in the study of ceramic systems. Yet parallels undoubtedly exist, and are drawn in this review where deemed to be appropriate.

2. SURVEY OF THE KINETICS OF CEMENT MAKING

Cement making raw materials bear little similarity to the final clinker product in terms of phase composition, texture, microstructure, or in the crystal structures, compositions and reactivity towards water of the constituent phases. The lteration in bulk chemical composition is less arked, although substantial: many of the compon-nts of clinker batches are essentially involatile, .g. CaO, $A\ell_2O_3$, SiO_2,and are thus preserved through he cycle, eventually appearing in the solid phases. ther phases are volatile but may condense in part t some stages of the process: examples include SO_x nd alkalis. Yet others are sufficiently volatile o be essentially eliminated in the kiln; CO_2 and H_2O, arising both from fuel and raw materials, are examples.

During cement making, the raw materials undergo a thermal excursion in which they are heated comparatively slowly to $\sim 1450^0$C, maintained briefly for a matter of minutes at the high temperature and finally cooled, typically at a relatively fast rate. It is difficult to construct a typical profile because many modern plants depart from older practice and use a suspension preheaters to raise batch temperatures to $\sim 900^0$C, finishing the partially calcined batch in a short rotary kiln. However, it suffices for present purposes to recall the general features: a progressive heating to temperatures such that partial fusion occurs, followed by comparatively rapid cooling of the product, termed clinker.

The early stages of reaction are characterized by decomposition reactions, of which the most important is the decomposition of calcite, $CaCO_3$. Other important decompositions occur: much of the $A\ell_2O_3$ and Fe_2O_3 contents of the raw meal are present as clays and hydrous oxides, which loose water. At the same time, reaction begins. The vapour atmosphere in contact with the decomposing mass is comparatively rich in S, mainly SO_2, and in CO_2 and H_2O. Moreover, the raw meal contains at this stage large quantities of carbonate (CO_3^{2-}) ions; possibly also sulphate, etc. Secondary reactions occur leading to formation of intermediate phases such as sulphate apatites and silicocarbonates,e.g. spurrite. These intermediate phases may subsequently break down in the higher temperature zones of the kiln, but their role as intermediates to the synthesis of C_3S, C_2S etc. may be important, although not yet fully investigated. Moreover, the presence of low-melting sulphates may lead to transient liquid formation even at the comparatively low temperatures encountered in the decarbonation zones.

During the final stages of clinkering, a melt phase develops which has a vitally important role in the kinetics of the clinkering process. Microstructural evidence obtained on simulate clinker batches suggests that the melt phase is very fluid and strongly wets the solid phases. Development of this liquid phase occurs over a rather narrow temperature range, if transitory premelting phenomena are ignored. The main melting, which results in formation of 15-20% of an oxide melt, occurs at comparatively high temperatures. Lea and Parker (1934) who studied phase equilibrium in the CaO-$A\ell_2O_3$-Fe_2O_3-SiO_2 system determined that a eutectic occurred between C_3S, C_2S, C_3A, ferrite and melt at 1338^0C; its melt composition was given as 54.8 CaO, 22.7 $A\ell_2O_3$, 16.5 Fe_2O_3 and 6.5 SiO_2 (wt %), The phase equilibrium data are not strictly applicable to clinker batches for two reasons. Firstly, the presence of additional components, e.g. MgO, Na_2O, K_2O, TiO_2, alter somewhat the position and temperature of melting; presumably the temperature is shifted to lower values. Secondly, when clinker batches commence melting, they are far from equilibrium and contain as yet much unreacted SiO_2, CaO, etc: C_3S will not yet be present in substantial quantities. Thus melting occurs under metastable conditions. In general, metastable solid phase assemblages commence melting at lower temperatures than would obtain if stable phases were present. Thus both factors work in the same direction, shifting the temperature at which extensive melting occurs to less than 1338^0C. The quantitative extent of the

reduction in the temperature of initial fusion is not known, but is unlikely to be greated than 20-40°C. Thus extensive melting can be expected to occur at or just above 1300°C.

Correspondingly, the composition of the liquid may also be subject to change, both on account of the metastable nature of the melting which affects the solubilities of the major components, but also on account of the solubility of minor components. These minor components do not necessarily dissolve entirely in the melt (indeed, some are probably inaccessible, being locked into undissolved solids) and there are no grounds, based on present evidence, to suppose that the liquid composition differs substantially greatly from that of the equilibrium eutectic.

Once melt develops, with formation of a substantial quantity of oxide liquid, material transport is facilitated. The melt phase dissolves material from phases which are unstable in the new conditions e.g. SiO_2, CaO, and deposits transported species either on those phases which are stable, e.g. C_2S or nucleates stable phases not hitherto present, e.g. C_3S.

The inability of the clinker batch to develop much C_3S in the solid state arises because C_3S itself is only stable at temperatures above 1250° - 1275°C, and this lower limit below which C_3S is unstable, fortuitously lies so close to the partial fusion temperature that the two happenings are practically coincident, in terms of the thermal regime imposed on the batch in the course of its passage through the kiln.

The dissolution of metastable phases is of course of crucial importance. Clinkers which contain substantial quantities of undigested raw materials are apt to be unsatisfactory. The mechanisms of dissolution require to be examined. Fig. 1 shows three of the most important mechanisms involved in dissolution reactions. Fig. 1(a) shows a CaO grain dissolving in a clinker liquid which is undersaturated with respect to CaO but saturated with respect to C_3S. The CaO-melt interface has, however, served as a site for preferential nucleation of C_3S, which now forms a protective barrier around the CaO, thereby retarding further dissolution. Textures of this type are sometimes observed in clinker thin sections, where grains of CaO become isolated from contact with melt by inclusion in C_3S. The remaining two cases are uncomplicated by the appearance of additional solid phases: the kinetic barrier in 1(b) is the rate at which material can diffuse away from the interface. This mechanism operates in the case of SiO_2 grains; adjacent to the interface, the SiO_2 content of the melt rises locally, its viscosity increases and the grain becomes embedded in a sheath of melt having relatively poor transport properties. Thus transport through the liquid and removal of material from the dissolving grain becomes rate-determining. Fig. 1(c) illustrates another type of kinetic control which can operate. In this instance, the surface of the grain is kinetically inert, and becomes the barrier to dissolution. The dissolution of periclase, MgO, in clinker melts is an example. Although the melt phase is normally undersaturated in MgO, and the MgO grains may be quite small, their comparatively unreactive surfaces inhibits dissolution in the course of typical clinkering cycles. Much of the evidence concerning dissolution of reactants in clinkering is indirect, from mineralogical thin

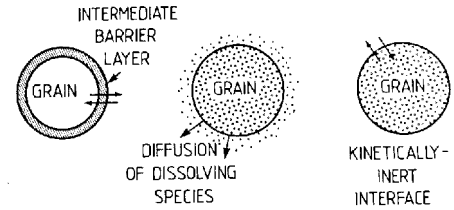

Fig. 1. Kinetic limitations to the dissolution of solid in melt, showing (left) solid barrier layer formation, (centre) sluggish diffusion in the melt and (right) surface control.

sections, and direct experimental verification is thus far lacking.

However, numerous empirical trials of clinker batches, as well as works experience, show that an upper limit of the grain size which can be digested can be established on a purely empirical basis, at least for CaO and SiO_2. These observations correlate well with theory.

Normal clinkering processes attain a sufficiently high temperature that the only phases coexisting stably with melt are C_3S and C_2S. The nucleation of C_3S appears not to be difficult, although clinker microstructures reveal a range of C_3S crystal sizes and habits. Well-burnt clinkers are characterized by relatively large C_3S crystals having well-developed euhedral morphology. However, as noted, this is not invariably the case, and it would be interesting to have better-established the relationship berween clinker microstructure and the nucleation and subsequent growth conditions of C_3S.

Since C_3A and ferrite are not present at peak clinkering temperatures, they originate by crystallization from the melt during clinker cooling. It is of course possible for the liquid phase present during high temperature processing to be preserved as a glass. Indeed, the eutectic composition in the C-A-F-S system can be prepared in laboratory furnaces on a 10g scale and readily preserved to ambient in glassy form by quenching the melt in water. Thus the formation of potential C_3A and ferrite could potentially be suppressed in clinkers in favour of glass. It is not conclusively proved that OPC clinkers do contain glass and since Bogue calculations of the potential compound content generally give reasonable agreement with the actual compound content, as determined by X-ray diffraction, glass must be absent or comparatively scarce. Nevertheless there are cases where Bogue calculations differ significantly from observed phase contents. In this context it is important to note that more rapid cooling, or the presence of more glass stabilizers, or both, could rapidly alter the compound content, by preserving glass mainly at the expense of C_3A and ferrite. Another important consequence of the cooling rate is that it must be sufficiently rapid to retard decomposition of C_3S which, below 1250° ± 25°C, tends to decompose to C_2S and free lime.

This brief survey highlights some of the kinetic aspects of cement making and serves as an introduction. These will be analized in more depth in

subsequent sections, but it is essential that aspects of the kinetics, although treated separately, should be seen to be part of a continuous, integrated process.

3. THE THERMAL ACTIVATION CONCEPT

A salient feature of the cement burning process is the relationship between temperature, thermodynamic state and reactivity. Reactions can occur, in theory, both during rising and falling temperatures. However, the clinker tends to reflect the high temperature state, many reactions occurring more sluggishly on the falling temperature cycle than on the rising temperature cycle. These and other phenomena find more quantitative explanation in terms of the activation energy concept. In order for a reaction to proceed, it must have a favourable driving force, usually defined in terms of the Gibbs free energy, ΔG, the criterion of an energitically feasible reaction being that it has a negative free energy. However, a reaction may not proceed directly, but may proceed through an activated state. Fig. 2 shows the concept applied to a comparatively simple case, in which atom migration results in a phase change. The atom which moves is shown in shading to distinguish it from other atoms which, in the example, remain essentially fixed. Atoms or ions must acquire sufficient energy to attain an activated state in which they can react, yielding a product having a lower free energy than the reactant. The exact nature of the activation barrier in atomistic terms is often not known, but we return to this point subsequently. One way in which the activation barrier may be overcome is by giving atoms, ions, etc. sufficient energy to overcome this barrier. At a fixed temperature, atoms or ions, even if all of the same kind, may vary in energy. This is the Boltzmann distribution, relating the energy spectrum of constituent particles to temperature. Given a system of N particles, in kinetics we are concerned by the number of such particles, N_i, having more than a specific energy, E_i. From the Boltzmann distribution

$$N_i = \frac{N}{Z} \exp\ (-E_i/kT)$$

where Z is the distribution function, k the Boltzmann constant and T the absolute temperature. If

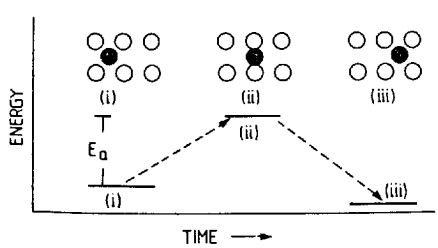

Fig. 2. Schematic view of activation energy showing it (top sequence) in terms of atom migration and (bottom sequence) in terms of energy changes. The overall difference between (i) and (ii) is the activation energy while the thermodynamic driving force is the difference between (i) and (iii)

the critical energy in question is taken to be E_a the activation energy, it can be seen from the shape of the normal distribution curve that the number of particles having greater than the critical energy increases rapidly with temperature.

Further development of the Boltzmann relationship assumes many forms - a result which often but unnecessarily leads to concern over which is the 'right' equation. All, however, contain a factor of the general form $\exp(-E_a/RT)$ where R is the gas constant. From this, a reaction rate constant, K, may be defined such that:

$$K = A \exp\ (-E_a/RT)$$

Most kinetic treatments use these equations, either in the form given here or in some derivative form. It is seen that the number of particles which acquire sufficient energy to become activated, and initiate a reaction, increases rapidly with temperature. Fig. 2 shows the activation for motion for a single ion or atom. This event might occur, for example, in a crystallographic phase transformation. Other events, such as transport to a surface and across an interface, clearly have a more complex activation energy which is the summation of a number of separate processes

$$E_a = \Sigma(E_{a_i} + E_{a_{ii}} + E_{a_{iii}} \ldots.)$$

Whilst it may not be possible to separate these terms, in practice one may be rate-limiting and hence determine the kinetics. If a reaction occurs at some equilibrium temperature, it may be necessary to achieve a substantial driving force in order for the reaction to proceed at a perceptible rate. Jøns (1980) has tabulated driving forces for the reaction:

$$Ca_2SiO_4 + CaO = Ca_3SiO_5$$

Fig. 3 shows schematically the situation. Below the equilibrium temperature, T_E, Ca_2SiO_4 and CaO are the more stable assemblage: above, Ca_3SiO_5 is the more stable. If, however, activation forces are examined at some increment ΔT above and below T_E, the proportion of thermally activated species will be greated at $T_E + \Delta T$ than at $T_E - \Delta T$, so the forward reaction, leading to C S formation, will tend to proceed more rapidly than the back reaction leading to its decomposition. The practical consequences are that reactions leading to C_3S formation occur rather more quickly at clinkering temperatures than in the reverse direction, so that C_3S is not significantly decomposed during clinker cooling. The reaction leading to C_3S formation does, however, have some other noteworthy features. The positive free energy of formation at low temperatures is low: $\Delta G = 0.32$ and 0.16 Kcal mol^{-1} at 1050°C and 1150°C respectively. However, even in its range of stability the driving force is small, only -0.16, -0.30 and -0.27 kcal mol^{-1} at 1350°, 1450° and 1550°C respectively. The rather small driving force for Ca_3S formation from C_2S and CaO is a noteworthy feature of clinkering chemistry. As will be shown, the presence of a liquid phase is important to facilitate material transport.

4. KINETIC ROLE OF DEFECTS AND IMPURITY IN CEMENT MAKING

It has been known for many decades that the migration of atoms in solids, and hence their reactivity, is greatly enhanced by the presence of

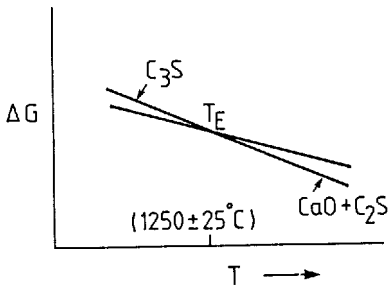

Fig. 3 Free energy changes for the reaction: $CaO + SiO_4 \rightleftharpoons Ca_3SiO_5$ close to the equilibrium temperature, T_E.

defects. Simple atomic defects are readily characterized: atom sites normally occupied may be left vacant (so-called Schottky disorder: in ionic substances, it may be necessary to have charge-equivalent numbers of cation and anion defects) and Frenkel defects, in which extra atoms or ions occupy interstial sites. In fact, these intrinsic defects are best observed in chemically very pure solids. Clinker minerals do not however fit this description, and most of the defects are chemically-induced: these and other related defects are termed 'extrinsic defects'. That is not to say that Schottky and Frenkel defects are absent: they occur, but in numbers which are effectively chemically controlled. An example of a chemically induced defect is in the substitution of $A\ell$ in C_3S; if the substitution occurs for Si, and in the absence of other charge-compensating mechanisms, it would be necessary to introduce $4A\ell^{3+}$ to balance $3Si^{4+}$. Of course in practice other compensatory mechanisms do also exist, so the actual substitutions observed are a complex mixture of isomorphous crystallo-chemical substitutions as well as vacancies and interstitials. The exact balances have not been quantitatively characterized, but it is apparent that the number of extrinsic defects in a typical clinker mineral vastly exceeds the number of intrinsic defects. Moreover, defects in the more general sense need not be confined to points i.e., individual lattice sites or paired vacancy interstitials. Real crystals of cement phases consist of a mosaic of slightly misoriented domains. Moreover, owing to the complex polymorphism of the C_3S and C_2S phases especially, they will have undergone a complete series of polymorphic transformations during cooling. This results in twinning, the creation of polytypes and the accumulation of lattice strain and misfit along domain boundaries arising in part from the progressive lowering of crystal symmetry and lattice misfit which accompanies these events. Groves and colleagues (1984) have recently contributed to crystallographic studies of the polytypism of real C_3S crystals. Although these studies disclose the finer details of the crystal structure, they do not enable the number and type of defects to be calculated nor can their effect on the thermodynamic properties be determined. However, another approach to defect characterization has been taken which allows the number of defects to be integrated over a bulk sample. This method utilizes the principle that the defect content is, in part, metastable at low temperature and can be discharged by low-temperature annealing.

In the course of discharging these defects, many of which serve as electron traps, both thermoluminescence and phosphorescence can be observed. C_3S, for example, has a thermoluminescence peak at -118°C and the rate law for the decay of the subsequent phosphorescence was determined. Theoretical interpretations have enabled the electron depths to be determined, giving insight into the nature at least of the photo-optically-active centres: Descamps (1974) and Firens and Tirlocq (1980). They correlate defect content with reactivity: Maycock, et al. (1974) have also given an account of the role of lattice defects in controlling reactivity.

It therefore appears that the existence of defects in clinker minerals has been established. Crystallographic defects appear to predominate, mainly extended defects and point defects controlled by chemical substitution. We are, however, some way from being able to quantify the absolute number of defects and to control this type and character.

5. DECOMPOSITION REACTIONS

Broadly, decomposition reactions in cement systems can be classified into one of several types. Table 1 shows classification. The early stages of clinkering are associated with events such as the decomposition of calcite and clay minerals, etc. These kinetics have been extensively investigated especially in connection with ceramic processes.

The decomposition of calcite, $CaCO_3$, is an important step in clinkering. In suspension pre-heaters, grains of calcite are essentially in contact with only a gas stream. Under these conditions, the physico-chemical conditions leading to calcite decomposition can be specified in terms of temperature and ambient CO_2 pressure, but the kinetics are still rather complex. Fig.4,5 shows in superposition the equilibrium P-T curve and observed rate data. As the CO_2 pressure rises the minimum temperature necessary to initiate dissociation increases. Once, however, this

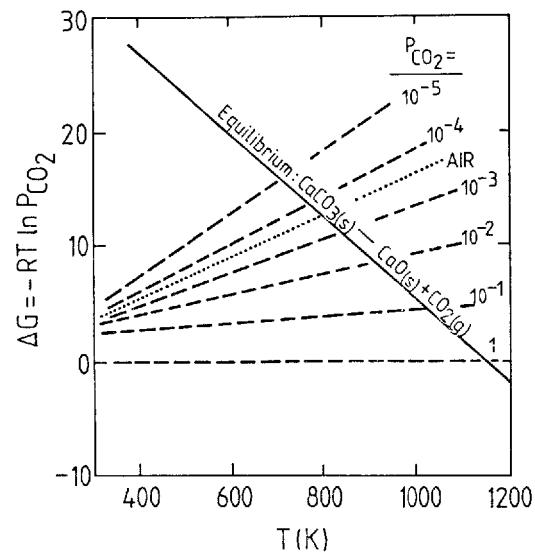

Fig. 4. Free energy changes in the system $CaO-CO_2$. The solid line gives ΔG values, while the corresponding dashed lines indicate equilibrium CO_2 pressures (dotted line, P_{CO_2} in free air) in atmospheres.

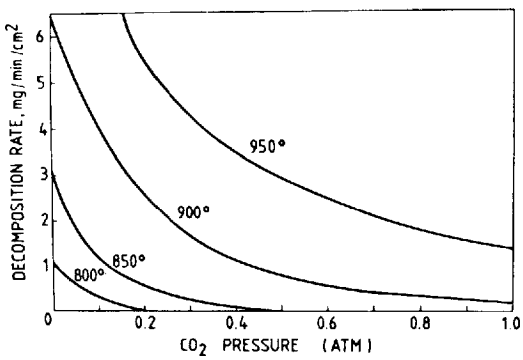

Fig. 5. The decomposition rate shown for successive isotherms. Decomposition can only occur within the limited range of pressure temperature conditions as defined in Fig. 4. However, within these favourable regimes, the rate is still dependent on many factors (see text). In the region for which data are shown, the reaction proceeds such that the kinetics are formally first-order.

decomposition threshold is exceeded it is necessary to consider three factors in order to analize the reaction kinetics. These factors are (i) processes leading to the initiation of reaction, generally termed 'nucleation', (ii) the reaction mechanism of the main (bulk) stage of decomposition and (iii) the energetics and geometry of reaction, including heat flow and mass balance as well as surface area and particle size. Fig. 6a shows the initial stage of reaction. Nucleation of the solid product of decomposition, CaO, is accomplished by loss of CO_2. Since this occurs at the surface, a product layer is quickly established; although nucleation may occur at selected sites, it spreads rapidly. Electron micrographs disclose that the product is adherent but, on account of the large density difference between solid product (CaO) and its substrate consisting of unreacted $CaCO_3$, the product layer is microporous. The kinetics now become controlled by other factors. Firstly, the decomposition is endothermic, so heat must be supplied to make the reaction proceed; ΔH_{298}^{o} is 44.3 kcal mol^{-1} and remains large at all temperatures, so energy input exerts an important control over kinetics. Secondly, reaction must occur through a thickening skin of product. Fig. 6b shows the situation. The material and thermal balance now affects the rate markedly: the CO_2 flux through the product layer experiences a pressure drop, while the thermal flux ensures also that a temperature gradient occurs. Kingery et al (1976) summarizes these balances. The net effect resulting from a thickening product layer is somewhat dependent on temperature: at low temperatures, the kinetics are strongly dependent on geometric surface area, and hence particle size and packing. Increasing surface area favours decomposition while dense powder packings inhibit decomposition by decreasing the effective surface area as well as impeding diffusion of CO_2. Suspension preheaters favour open packings, whereas kiln decomposition occurs partly in packed beds of material, partly in particles being tumbled through a vapour stream. But at

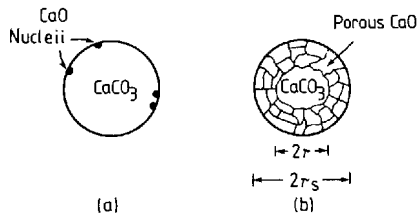

Fig. 6. Showing spatial arrangement of product on decomposing $CaCO_3$ particle at (left) the initial nucleation stage and (right) a shell of undecomposed $CaCO_3$ surrounded by CaO.

higher temperatures, such that the absolute rate of decomposition is more rapid, heat transfer tends to dominate. Not surprisingly, therefore, kinetics studies undertaken by various investigations, differ somewhat in their conclusions, depending on the range of conditions studied. However, experiments on loose powders usually show that the kinetics are first order, i.e., for cylindrical particles of initial radius r_o, α the fraction decomposed in some time t is given by a relation having the form

$$(1-\alpha)^{\frac{1}{2}} = 1-kt/r_o$$

where k is the activation energy: a graph of $1-\alpha$ vs time t produces a straight line relationship for a particular temperature. These conclusions have been verified and expanded for a range of cement-making raw materials. Among the more recent studies are those of Rudolph (1979) who examined process data for vibratory furnace decomposition of $CaCO_3$. The kinetics were also studied by Mueller, et al (1977) who obtained good agreement with previously published data. Parallel studies by Fredericks (1979) and Drozdetskaya and Gropyanov (1977) reached similar conclusions. The data were applied to large-scale reactors by Biernacki and Kowalski (1981). General analyses of the data relevant to clinkering have also been made by Mueller, et al (1979) and Rao and Cutler (1975). This latter study also included an analysis of the role of coal ash in promoting decomposition while Veruto, et al. (1984) examined the surface area of the product and the catalytic role of CO_2. The kinetics are of course influenced by the presence of impurity, and important studies in this area have been undertaken by Talaker, et al (1982) who examined the effect of Ca (as $Ca(NO_3)_2$), $A\ell_3(PO_4)_6$ and CaF_2; calcium nitrate was found to be a powerful accelerator while aluminium phosphate was a retarder. CaF_2, on the other hand, behaved as an accelerator at low temperatures, but retarded at high temperatures. Shearer, et al (1980) studied the effect of $NaC\ell$ on the decomposition. Even trace amounts of $NaC\ell$, insufficient to wet the grains significantly affected the decomposition. Moreover melt temperatures were depressed to as low as 690°C because $CaCO_3$ CaO and $NaC\ell$ have a significantly lower melting point than $NaC\ell$ alone (801°C). In the presence of 2 wt.% $NaC\ell$, sintering of CaO was accelerated and pore sizes grew to 1.5-3.0 μm, contrasted with 0.01-0.02μm in pure limestone (90-99% $CaCO_3$) batches also sintered for 1h at 850°C in a $N_2/O_2/CO_2$ atmosphere.

TABLE 1

DECOMPOSITION REACTIONS INVOLVING A VOLATILE PHASE

Reaction: Example	Features	Comments
$CaCO_3 \rightarrow CaO + CO_2$	One step reaction: solid 1 → solid 2 + gas. Decomposition initiated at surface.	Kinetics approximate to first order. Rate limiting factor varies with temperature and absolute rate of decomposition.
$CaSO_4 \cdot 2H_2O \rightarrow CaSO_4$.	As above, but decomposition occurs in stages. Two intermediate products, α and β hemihydrate possible.	Kinetics approximate to 2nd order but complicated by retention of water in pore structure.
$CaCO_3 \xrightarrow{\text{melt impurity}} CaO + CO_2$	Liquid phase film provides complex interface.	Apt significantly to affect rate of decomposition.
$Al_2Si_2O_5(OH)_4 \xrightarrow{\text{kaolin}}$ "metakaolin" + H_2O	Bulk diffusion of H species (H^+, OH^-) rate controlling: structure of metakaolin is topotactic after kaolin percursor.	Metastable but persistent intermediate phase obtained before final decomposition to mullite and silica.

The kinetics of other decomposition reactions have been studied on account of their technical importance, and are found to differ significantly from $CaCO_3$, whereas the $CaCO_3$ decomposition occurred in a single stage, other examples are known in which decomposition occurs with formation of intermediate solid products. For example, $CaSO_4 \cdot 2H_2O$ decomposes in stages, yielding the so called hemihydrate, ideally $CaSO_4 \cdot \frac{1}{2}H_2O$, before decomposing first to $CaSO_4$ and eventually to $CaO + SO_2 + O_2$. The hemihydrate intermediate occurs in two modifications, the so-called α and β forms. They have not always been accepted as distinct polymorphs, but do appear to differ sufficiently to warrant a distinction on kinetic grounds. The α and β hemihydrate inherit a pore structure which is conditioned in part by the crystal structure of the percursor gypsum, but the extent to which recrystallization occurs appears to depend partly on the rate of water removal, chemical purity of the parent, etc. For example, during subsequent removal of water, the α phase dehydrates sharply over a narrow range of temperatures where β loses the last $^1/_4$ of its water over a wide range of temperatures. Ball and Norwood (1977, 1978) attributed these differences to the smaller pores in β which, it was suggested, trapped liquid water. The retention of water to relatively high temperatures is not, however, believed to reflect on the stoichiometry of the material. The final stage of thermal decomposition, marked by the reaction of $CaSO_4 \rightarrow CaO + SO_2 + O_2$, has been studied recently by Hanic, et al (1985). They distinguished two kinetic conditions: one, which obtained below the $CaO + CaSO_4$ eutectic at 1638K, the other at higher temperatures such that partial melting occurred. Below 1638K, the decomposition was found to obey second-order kinetics of the type $G(\alpha) = 1/(1-\alpha) - 1$ where α = the fraction decomposed, whereas above the eutectic, the kinetics were controlled by a phase boundary reaction in which an interface moves at a constant velocity inward, with $G(\alpha) = 1-(1-\alpha)^{\frac{1}{2}}$. The distinction berween solid state and liquid-phase reactions is of considerable importance and has enabled the authors to show that E_a, the activation energy, decreased from 622 ±7kJ mol^{-1} in the solid state to only 373 ±4kJ mol^{-1} in the presence of liquid. A vast literature exists on the effect of impurities supposedly to catalize $CaSO_4$ decomposition. It is impossible to assess, in modern terms, the worth of these studies. Undoubtedly many of the reactions described occurred under conditions such that partial melting occurred while in others, decomposition occurred simultaneously with solid state reaction, as with SiO_2 to form C_2S.

The decompositions of clays, e.g. kaolin, have also been extensively studied. Kaolin is an interesting example of a special type of decomposition because the decomposition proceeds topotactically, i.e. with preservation of structure. Water is lost in the course of reaction but the oxygens and many of the cations present in kaolin remain on essentially the same positions throughout; this structural control has a profound influence on the kinetics and mechanism of the decomposition, as well as on the structure of the solid decomposition product. The kinetics are controlled essentially by diffusion of OH^- ions in the bulk rather than by surface reaction.

Decomposition reactions thus reveals a wide range of reaction types. Table 1 summarizes these with respect to reactions, all of which are characterized by evolution of a volatile phase. Even in the absence of complicating factors, e.g. reactions with other phases, the reactions are of sufficient complexity as to require application not only of formal kinetic treatments to the data, but also application of other structure sensitive techniques, e.g. X-ray and electron diffraction and microscopy. Given the complex nature of some of the decompositions, and the effect of impurity in clinker batches, it is easy to appreciate that the regime of steadily rising temperatures encountered by material in the kiln leads to a complex series of reactions. Moreover, with rising temperature, the minerals in the raw meal cease to behave as an isolated system of individual particles but instead begin to react with each other. Where reaction occurs with

elimination of a volatile (CO_2, SO_2, H_2O etc.) concomitant chemical reaction may not only be affected by the rate at which reactants are formed from percursors, but the very existence of the reaction may affect the decomposition rates.

6. CLINKER MINERAL FORMATION

6.1. The Industrial Perspective

The study of burning reactions in the cement kiln is largely qualitative on account of the great chemical complexity and physical inhomogeneity of the raw materials. However, more quantitative studies have been made on model systems - chemically simplified, but containing many of the components of real clinker batches. Much valuable information has been obtained from this type of study.

The general question of reactivity of industrial clinkers has been examined on account of its great importance to industrial practice. This aspect has been reviewed at previous Congresses, but subsequent to Paris, important reviews have been made. The calcination behaviour of batches has been studied by Kupper and Tiggeobacumber (1983) using a new laboratory apparatus. The evaluation of the reactivity and burnability has been advanced by Chromy (1985) and Ludwig and Ruchkensteiner (1973) (1976) who showed that increasing the rate of heating of the raw meal above the decomposition temperature required to achieve reaction at the maximum sintering temperature was reduced by as much as 40%. Other studies, notably those of Fundal (1979, 1981) have enabled mathematical expressions for the burnability to be formulated. The information required includes the lime saturation factor, silica modulus and the fractions of acid insoluble quartz > 44 μm and of calcite > 125 μm. These grain sizes seem to correspond to the maximum grain size which can be effectively assimilated in the course of a typical clinkering cycle. Although the sizes were fixed largely on the basis of reaction in model systems, plant trials show that these limits are applicable to typical burning schedules. The continuing importance of grinding as an aid to enhancing batch reactivity was also quantified by Mosikas, et al (1981). The general concept of 'burnability' has also been addressed by Humpola (1981), Krachner (1985) and Teoreanu, et al (1985) and by Ludwig (1981). Special aspects of the burning process have also been investigated; Gouda (1979) examined the relationships between clinker composition and grindability, while the effect of fuel source on batch reactivity was addressed by Vogel (1983) and by Waechtler, et al (1984). Sulphate, present in fuel and raw materials, apparently influences greatly the rate of calcium silicate formation. This aspect was studied by Lim and Park (1983, 1984a, b). The microstructural aspects of clinkering have also been related to composition and burning history in a series of papers by Chatterjee (1979a, 1979b) Sarkar (1979) and Chatterjee, et al. (1980).

The kinetics of reaction have also been studied from a more theoretical standpoint by Mchedlov-Petrosyan et al (1978) and by Chatterjee et al (1980). The importance of minor components, and of low-temperature batch reactions leading to the development of phases intermediate between the starting materials and the high-temperature clinker minerals, are emphasized.

The formation of intermediate phases in cement kilns has long been known from a study of kiln coatings but many of the phases found occurring e.g. spurrite, a calcium silicate carbonate, have been assumed to be oddities. However, it appears that under some conditions they may represent an alternative pathway to the formation of clinker minerals. Spurrite, (to give one example) is actually somewhat more stable at high temperatures with respect to dissociation than is calcite. Mchedlov-Petrosyan et al (1975) has also emphasized the role of thermodynamic metastability and metastable reaction sequences in controlling overall batch reactivity. The effect of furnace atmosphere on reaction kinetics has also been analized by Sylla (1981); reductive burning lowers potential ferrite, but also increases the content and reactivity of C_3A. Mackenzie and Aldridge (1980) have also analized the effect of reducing atmospheres: the differences are partly kinetic and partly due to a shift in equilibrium. The distribution of reactants in clinker batches reflects the statistics of mixing in inhomogeneous particulate systems, and the influence of inhomogeneity on kinetics, as reflected by mix burnability and nodule formation, has been analized by Petersen, et al (1979).

6.2. Reactions between Selected Solid Components

Studies of the reactions between selected components of clinker batches have contributed to understanding the reaction kinetics. We first note that kinetic studies cannot be extended over too wide a range of temperatures without a fundamental change occurring in the nature of the reaction mechanism. For example, Delinge, et al (1977) studied reactions leading to C_3A formation from CaO-$A\ell_2O_3$ mixtures using pure reactants as ca 20 μm grains. The reactants were in a DTA apparatus. At 1300°C, some reaction forming CA and $C_{12}A_7$ occurred, but above 1355°C, metastable melting occurred resulting in rapid transfer of material through the melt and recrystallization of $C_{12}A_7$. This $C_{12}A_7$, persisted only up to 1375°C forming C_3A by reaction of the melt with CaO and $C_{12}A_7$. Formation of C_3A in the solid state has a relatively high activation energy, and is a comparatively slow process relative to $C_{12}A_7$ formation. The formation kinetics of C_3A have been studied by Mackenzie and Bonerjee (1978) and in the presence of SiO_2 as an additional component by Chow and Burnet (1981a, 1981b). The formational kinetics of the monocalcium aluminate have also been studied by Singh and Ali (1980). Tetracalciumalumino ferrite has also been synthesized by solid state reaction, and its formation kinetics have been determined by Mackenzie and Alasti (1978).

Reaction kinetics leading to the formation of C_2S and C_3S have extensively studied by Shrader and Kenhe (1973): calcium aluminates were included, by Ludwig and Wolter (1977) and Odler and Doerr (1977). In the latter study, fine grained chemically pure reactants were heated isothermally at temperatures in the range 1370°C and 1520°C. The velocity of formation was very slow at 1370°C but much more rapid, and relatively comparable at temperatures between 1420° and 1520°C. They tentatively concluded that the reaction rate could not be expressed in terms of a particular order of reaction, or that any simple interpretation could be placed on the kinetic data. They supposed that

the great enhancement of reactivity between 1370°C and 1420°C arose from the greater reactivity between α Ca_2SiO_4, relative to $\alpha'Ca_2SiO_4$ which would be present at 1370°C, and that the sharp retardation with increasing time arose from the formation at high temperatures of diffusional barriers, presumably of C_3S product. After reaction had slowed, the batch was reground and refired. This led to a fresh burst of reactivity, which arose as a consequence of disrupting the barrier layer.

The effect of atmosphere on the reaction has also been investigated by Svetik, et al (1982). Their investigation was in the range 700°-1000°C, so the product of reaction in $CaO-SiO_2$ mixtures was C_2S and to a lesser extent CS and C_3S_2. Reducing atmospheres, generated from mixed CO_2/H_2, accelerated the reaction. This was attributed to water vapour rather than the presence of reducing components, e.g. CO, H_2. Barrier layer formation occurred which retarded reaction rate. Water vapour is of course known to have an appreciable effect on formation of "$C_{12}A_7$". It is well established that at temperatures below 1050°C, appreciable water can be accommodated. However, the status of $C_{12}A_7$ as an anhydrous compound in the $CaO-Al_2O_3$ system is questionable. There seems no doubt that the presence of water vapour acts as a powerful agent to promote its formation, even at 1300°C. The role of the water, whether kinetic or structural both, is not known with certainty.

In an interesting study, Mackenzie and Hadipour (1978) determined the effect of DC voltages on reaction kinetics in the range 950°-1150°C. Electrolysis, particularly at higher applied potential, markedly affects the amount of phases formed. This was explained in terms of the thermal diffusivities and electrical mobility of the ions, the oxygen packing of the matrices through which diffusion occurs and the orientation relative to the applied field of the reactant grains.

6.3. Reactions in the Presence of a Liquid Phase

Studies performed on selected components of cement batches as well as on raw meals show that calcium aluminate- ferrites and to a lesser extent, silicates can form by solid state reaction. However formation of alite, while possible in the solid state, will be preceeded or accompanied by extensive melt formation in commercial kiln feeds. Thus one of the most important steps in the kiln process, development of C_3S (the term as used here embraces alite), is accomplished by sintering in the presence of a reactive liquid. The liquid phase is reactive in the sense that it wets grains, has good transport properties, is capable of dissolving in substantial amounts all major and minor components of clinker batches and, moreover, is present in sufficient quantities not only to bridge adjacent grains but also to facilitate material transport over longer distances. This ability to facilitate long-range transport also enables statistical fluctuation in the local composition of the clinker feed to be averaged out, with the result that the final clinkered product is texturally and mineralogically homogeneous.

During the clinkering process, grain growth also occurs, Initially, when the feed is essentially solid, grains grow by solid state diffusion. Generally, the driving force for recrystallization and hence the rate of grain growth, is inversely proportional to grain size such that if r_o is the radius at time zero, the growth at some time is given by

$$r - r_o = (2k)^{\frac{1}{2}}(t)^{\frac{1}{2}}$$

where k is a constant of the particular system. In relatively pure single-phase materials, when r is plotted *vs* log t, a straight line is obtained whose slope is 0.5. However, impure ceramic materials frequently exhibit phase formation at the surface, so that slopes less than 0.5, ranging as low as 0.1 are frequently obtained. Little work seems to have been done on cement clinkers, but it would appear that grain growth is minimized by fairly rapid heating, so that t is small, (ii) formation of intermediate phases, e.g. Ca_2SiO_4 barrier layer between CaO and SiO_2, which slows grain growth, (iii) premelting, which produces small amounts of liquid which inhibit solid-phase grain growth. Much energy is expended in grinding the raw materials, so grain growth especially of CaO is clearly an important but undesirable phenomenon

Grain growth can also occur by vapour-phase transport. But it would appear that the vapour pressure of clinker constituents is too low to make this an effective means of transporting silicate components. Matsumoto and Sata (1981) examined volatilization of C_3S in the range up to 1749°C (in air) and 1900°C (in vacuo). Although incongruent volatilization occurred, leaving Ca_2SiO_4, the rate at which it occurred was slight except at the highest temperatures, well above those normally encountered in clinkering.

The process of densification of the clinker also proceeds by sintering. It is commonly assumed that densification is associated with grain growth. Indeed, while the two processes often proceed simultaneously, there is not necessarily any connection. The first stages of densification of the clinker are probably aided by condensation of thin films of alkali sulphates, etc., on surfaces occurring at temperatures such that the condensate is liquid; this causes the the grains to stick and be drawn together by capillary forces. The hot consolidation of grains is also assisted by the mechanical compaction arising from the rotatory motion of the kiln. However, low temperature liquid formation may well be a transient phenomenon, the liquid disappearing by evaporation of some of its constituents.

Once a silicate liquid develops, wetting of grains can occur on a large scale. It is characteristic of clinker batches that this liquid content remains close to zero until some critical temperature is attained, following which the proportion of liquid increases rapidly as heat is added over a short temperature range, following which interval the amount of liquid remains relatively insensitive to changing temperature. The critical range of temperatures, over which much (ca 20%) liquid develops is probably in the range 1300-1340°C. The wetting relationships are a complex relationship between competing reactions: grains of solid may react with each other, as well as with liquid. Although of considerable importance to the clinkering process, relatively little systematic study has been made. In general, the situation is as shown in Fig. 7. The microstructure can be quantified in terms of the dihedral angles Ø, between melt and solid and between two

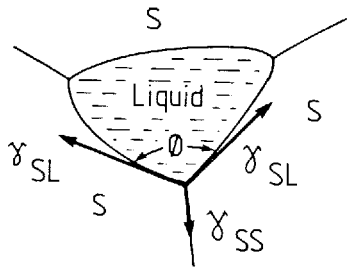

Fig. 7. Interfacial relationships between liquid-solid contacts in a two phase system: γ is the surface tension, S = solid, L = liquid.

solids. The numerical value of the Ø is a function of the interfacial energy, γ, between two phases, γ_{SL} is the interfacial energy between a solid-liquid pair; such that

$$\cos\frac{\emptyset}{2} = \frac{1}{2}\,\frac{\gamma_{SS}}{\gamma_{SL}}$$

We can distinguish several cases, depending on the value of Ø. In cement clinkering, the important cases are shown in Table 2.

TABLE 2

Wetting of Solids by Melt

γ_{SL}/γ_{SS}	Consequences
< 1.0	Ø > 120°: second phase forms isolated pockets.
between 1. and $\sqrt{3}$	Ø between 60° and 120°: some liquid penetration along boundaries.
between $\sqrt{3}$ and 2	Ø less than 60°: extensive wetting.
> 2.0	Ø = 0: solid grains isolated

These wetting relationships are crucial to the ability of the liquid to transport material. In Fig. 7 the value of Ø is fairly high, whereas in a real clinker it is lower. The consequences of this are shown in Fig. 8 which depicts an idealized clinker microstructure in which Ø for C_3S-L pairs are sufficiently low that the C_3S grains are completely wetted by liquid but Ø for C_2S-L pairs is much higher, ca 90°, so incomplete wetting occurs at C_2S-L boundaries. Of course this stage is achieved only towards the end of the clinkering process when a textural equilibrium obtains. Nevertheless, a microstructure shown is generally favourable to densification and nearly maximizes the ability of the liquid to transport material. The physics of this densification may be treated as follows. If two particles are initially in contact, a negative pressure is developed at the small negative radius of curvature, ρ, compared with the free surface of the particles. This results in a spontaneous viscous flow of material into the neck regions. The initial rate of neck growth is given by Kingery (1976) as

$$\frac{x}{r} = \left(\frac{3\gamma}{2\eta\rho}\right)^{\frac{1}{2}} t^{\frac{1}{2}}$$

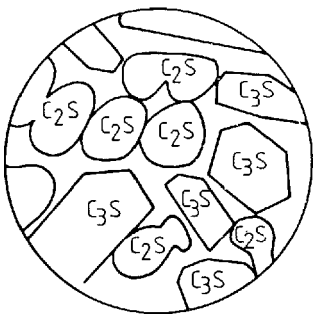

Fig. 8. Idealized clinker microstructure of C_3S and C_2S crystals in liquid.

where the various geometric parameters are designated in Fig. 9; γ is the surface tension, η the viscosity and ρ the negative radius of curvature. The increase of contact diameter is only proportional to $t^{\frac{1}{2}}$, which explains why the initial rate of densification is so much more rapid than the latter stages. Thus, given the comparatively brief sintering period employed in clinkering, many pores persist, especially in the large size range. The smaller pores are reshaped by surface tension and material transport, but the larger pores which depend mainly on viscous flow if they are to shrink, remain relatively unaffected. Indeed, it is fortunate that this should be the case, because their presence greatly facilitates subsequent grinding of the clinker: the larger pores act as flaws, fracture being preferentially initiated between adjacent large pores and propagated through the solid.

Fig. 8 shows schematically differing morphologies for C_3S and C_2S crystals. Cement clinkers vary widely in mean crystal size of the solid phases which are stable at clinkering temperatures, as well as in their morphologies. Nevertheless, microscopists will recognize that a characteristic texture occurs in well-proportioned and well-burnt clinkers. This texture is characterized by having relatively large and well-formed i.e., faceted, C_3S crystals and less well-formed, rounded crystals of C_2S. This texture arises from a variety of

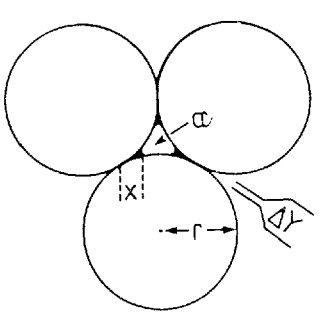

Fig. 9. Contraction of grains resulting from sintering. The grain overlap is ΔY, producing solid-solid contacts, which are available for material transport, along x. The grain radius is r; α is a pore, either empty or liquid-filled.

circumstances. First, sufficient liquid must be present, and the liquid have sufficient wetting power, to achieve this texture. Secondly, growth conditions must permit larger crystals to develop at the expense of smaller. But the development of faceted, rather than rounded morphologies, arises from the difference in energy between various faces of the crystals. These facets are planes which have rational Miller indices, but vary depending on spatial orientation in surface energy, γ. In practice, the function which the crystal strives to minimize is given by

$$\gamma = \Sigma_i A_i \gamma_i$$

where A_i and γ_i are the area and specific surface energy of a plane with indices (i). In practice, the energy driving transport of material from one face to another is comparatively small and the crystal shape is more apt to be determined by rates of growth of different crystal faces, rather than their specific surface energies. The fastest-growing faces tend to grow themselves out of existence leaving behind the slowest-growing faces which ultimately dominate the morphology. The C_2S crystals, with their characteristic rounded morphology, probably reflect growth occurring mainly in the solid state, where material transport is comparatively slow and the impingement of other grains impedes the development of an equilibrium morphology. Thus the texture of a cement clinker reflects the kinetic controls exerted during the firing process, C_2S crystals having typically grown by solid state reaction while the better faceted C_3S crystals reflect growth in the presence of a reactive liquid phase. Variants of the texture described can, of course, occur but while microscopists have frequently noted these, they have not generally been interpreted on a kinetic basis except for certain obvious features, such as the metastable persistence of CaO clusters in the vicinity of former large fragments of calcite, or of undissolved periclase (MgO) on the site of former dolomite grains.

The transport properties of the melt phase are of considerable importance, and have been studied by a number of workers. Diffusion profiles were determined, using a Pt marker to define the original interface, by Kondo and Choi (1968) and Heilmann (1960). Both workers were interested in determining the role of coal ash, and used crucibles fashioned from clinker to contain ash. At 1500°C the ash was fully molten, but the contact between clinker and melt was marked by consecutive zones rich in C_3S (closest to the clinker crucible) and in C_2S. These studies reveal essentially that diffusion proceeds as would be expected from the $CaO-A\ell_2O_3-SiO_2$ phase diagram; if the compositions of the two phases (ash and clinker) are superimposed on the appropriate isothermal section, and the disposition of the tie line connecting the two compositions with respect to the phase regions which it traverses, enables the phase zonation to be predicted. The phase diagram cannot of course predict the relative prominence of the zones, as judged by their thicknesses; this can only be determined by experiments of the type which have been undertaken, for example by Christensen and Simonsen (1970) who made use of an isothermal section technique. Fig. 10 shows a portion of this isotherm. The clinker composition lies at point Cl, while the ash composition lies at A2. The tie line

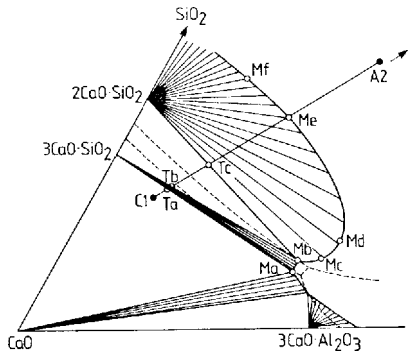

Fig. 10. Part of an isothermal section of the system $CaO-A\ell_2O_3-SiO_2$ at 1500°C. The dashed lines show liquidus phase equilibria. In the example, an ash whose composition lies at A2 is reacting with a clinker at Cl. A tie line is shown and the course of the reaction explained in the text.

connecting the two passes through successive zones of (i) C_3S, CaO and liquid the latter having the composition corresponding to M_a, (ii) C_3S and liquid the latter varying between M_a and M_b, (iii) C_3S, C_2S and liquid which composition lies at point M_b, (iv) C S and liquid, varying between M_b and M_e (M_c, M_d..mark successive tie lines) until at M_c the local composition is completely molten. Interestingly, as C_2S develops in region (1D) upon adding more SiO_2 as ash, and as the liquid composition changes progressively from M_b....M_d, partial freezing occurs: the added "fluxes" actually serve to decrease the amount of liquid present over this composition range. The phase diagram can thus be used to predict the zonation occurring in diffusion couples.

The interfaces between zones do not of course remain stationary but undergo spatial shifts as diffusion proceeds. It is therefore necessary to add to the diffusion equations in order to develop a dynamic model. Fick's equations, as well as a moving boundary condition and a 'tortuosity factor' to allow for the existence of lengthened diffusion paths around crystalline grains, it being assumed that diffusion rates through the crystals were negligible compared to those through the melt, have been incorporated. The necessary equations, while rather cumbersome, appear to give a good fit between experimental data and observation and represent the most comprehensive model developed especially for clinkering reactions.

Studies aimed at correlating kinetic and phase equilibria have also been developed by Christansen and Jepsen (1971) who made diffusion couples of 'sandwiches' composed of discs of selected reactants. These were heated isothermally at temperatures such that a liquid developed. The layer thickness of the intermediate, partially melted zone was found to increase linearly with $t^{\frac{1}{2}}$. An apparent diffusion coefficient, for the diffusion of the CaO component through the liquid, $D_i = 4.37 \times 10^{-7} cm^2 s^{-1}$ was calculated. This value is termed 'apparent'

because the liquid phase composition varies across the interface, hence D could only be a mean value.

One important measure of the kinetics of reaction is the rate at which CaO particles can be dissolved in melt. The liquid phase developed during firing is of course normally undersaturated with respect to the maximum solubility of CaO which can be obtained at saturation so a driving force should be available for its dissolution. The problem has been addressed by Johansen and Jepsen(1978) and Christensen (1981).

The rate of alite formation in clinker sandwiches was determined by Christensen, Jepsen and Johansen (1978). The sandwich construction imposed by the geometry ensured that transport occurred bidirectionally, across the interface. After a period of isothermal annealing, the sandwich was sectioned to determine the rate of alite growth. The width of the alite layer, x, was found to increase with reaction time according to the relation.

$$k^1 = k^1 t$$

The value of k^1 was fixed by the parameters of the reacting system; it was increased by increasing melt content, by increasing temperature, and by substitution of Fe_2O_3 for $A\ell_2O_3$. The effect of increasing temperature is two-fold; it increases somewhat the amount of melt and also lowers its viscosity and increases its wetting power. Substitution of Fe_2O_3 for $A\ell_2O_3$ presumably also contributes to lowering viscosity and surface tension. It has been suggested that small amounts of MgO are beneficial in clinkering, but substitution of MgO up to saturation did not have an appreciable effect on k. In these experiments, lime particles of known size were mixed with a pre-reacted synthetic clinker batch which had the composition $67CaO$, $6A\ell_2O_3$ and $27SiO_2$ (wt.%). The mixture was pressed into cylinders and fired at 1500°C for different times: the amount of CaO added was such that the liquid was under-saturated. After annealing, the samples were quenched and analized for free CaO content. Its rate of disappearance in terms of x, the fraction reacted, as a function of time was found to be expressed in the equation:

$$(1+\beta_x)^{2/3} - {}^{2}/_{3}X = 1 - [(2\alpha\beta D\Delta C)d_1]t/r_o^2$$

where D is the effective binary diffusion co-efficient of 'CaO' in the melt, ΔC the concentration difference of CaO across the reaction layer, α the volume fraction of liquid in the interfacial layer, d_1 the density of CaO, t the time and β a complex constant related to the composition and porosity of the material. The physical significance of the quantities is worth examining: the rate of disappearance of CaO is proportional to $1/r_o^2$ where r_o is the original radius of the particles: hence the importance of particle size reduction. The amount of liquid in clinker probably cannot be greatly increased in practice nor can the value of ΔC which, together with α, is effectively fixed by the nature of the phase equilibria, as expressed by the phase diagram. Calculations made using representative values for α, β and ΔC gave a value for t/r_o^2 of ~2600 min mm^{-2} which, for a burning time of 20 minutes, corresponds to a maximum size for dissolution of 90μm. CaO grains ~90μm would be furnished by $CaCO_3$ grains ~120μm, and this upper limit to the size of CaO grains which can be assimilated agrees with empirical observations. These concepts have continued to be developed in studies of the application of phase diagrams to industrial clinker formation by Johansen (1979) and Petersen (1983), who determined the course of isothermal sintering studies and interperted the kinetics of reaction, and by Odler and Abdul-Maula (1980a) as a prelude to determining the role of mineralizers. The importance of CaO clustering in the isothermal burning stage was also revealed in the kinetic clinkering studies of Chromy (1982) and Chromy and Hrabe (1982) and other kinetic considerations, as elucidated by Teoreanu and Dulamescu (1981).

6.4. Role of Fluxes and Mineralizers.

Many of these studies just described were made on chemically simplified systems. Data have also been accumulated in the role of other components. These may be regarded as either fluxes of mineralizers, or both. Fluxes assist reaction without altering the basic stability of the calcium silicates, etc. whereas mineralizers enter into solid solution in the clinker phase thereby altering significantly the thermodynamic stability of the solids. Mineralizers may also act as fluxes by virtue of their partition between solid and liquid phases. Fluxes and mineralizers are reviewed elsewhere, so we confine ourselves to citing specifically studies in which the kinetic effects are included. Odler and Abdul-Maula (1980b) have analized the mode of action of mineralizers including CaF_2, ZnO, CuO and Co_2O_3; Packter and Zaidi (1981) have examined the role of $CaC\ell_2$ in mineralized batches containing SiO_2 which reacted with dissolved CaO to form βCa_2SiO_4. Luginina, et al (1973) examined the role of naturally-occurring volatile additives; Draynea et al (1976) the role of iron salts in accelerating reactions to form calcium aluminates, while Johansen and Christensen (1979a, 1979b) analized the mineralizing effect of CaF_2. They found that 0.5% CaF_2 increased the rate of reaction by a factor of 2.4 at 1350°C and by 1.2 at 1500°C; a 1% addition was only slightly more effective, increasing the rate by 2.8 and 1.7 at 1350° and 1500°C respectively. The enhancement was interperted in terms of the width of the stability field of C_3S which is greater in the presence of CaF_2 than in the usual case, where only $A\ell_2O_3$ and Fe_2O_3 are present. This in turn increases the ΔC term in the equation above, and hence increases the driving force for the solution of CaO and its reprecipitation from the melt as C_3S. Whilst this explanation is undoubtedly valid, the real picture is perhaps more complex: the presence of F in the melt in place of O^{2-} substantially enhances the solvent and tranport properties of the melt, as well as its wetting power. Moreover, since F^- behaves partly as a mineralizer, inasmuch as it can be incorporated into the C_3S structure and thereby causing it to become the stable phase relative to CaO and C_2S at temperatures less than 1250°C, it may facilitate formation of C_3S in the solid phase even before much melting has occurred. CaF_2 appears to be the only common mineralizer which permits C_3S to be formed essentially by solid state reaction, its formation having been observed at temperatures as low as ~1025°C by Shame and Glasser (1986).

Although the role of mineralizers is of very considerable theoretical interest, it is probably not practicable to incorporate them on an industrial scale. Even F^-, known to be a very effective flux and mineralizer, leads to problems on an industrial

scale on account of its partial volatility, therefore: parallel studies of the classical fluxes used -$A\ell_2O_3$, Fe_2O_3 and to a lesser extent alkalis and MgO, etc.- continue. Many of the advances made in recent years concerning the action of ordinary fluxes have been incorporated into a four-stage model of cement burning by Imlach (1976); valuable data have also been obtained on the mobility of Aℓ and Fe in clinker melts by Osokin, et al. (1973).

6.5. Additional Observations on C_3S Formation.

Many details of the kinetics of C_3S formation in clinker batches seem not to have been completely investigated. The first step in C_3S formation, its nucleation from melts, seems not to have been studied. In many silicate systems, nucleation, particularly of incongruently melting phases (of which C_3S in an example) has proved difficult. However, there is no evidence concerning C_3S; certainly solid surfaces frequently serve as sites for nucleation of silicates and the abundance of crystalline particulate matter present at all stages of the clinkering process could presumably provide potential sites for C_3S nucleation. Many clinkers typically contain comparatively coarse-grained C_3S. This could suggest that nucleation in fact occurs relatively infrequently but that once nucleated, crystal growth had occurred rapidly. On the other hand, this texture could be explained by assuming that nucleation occurred at numerous sites but subsequently unequal growth conditions and rapid material transport favoured assimilation of smaller nucleii by larger crystals. The mathematics of diffusion and transport relevant to these processes have been reviewed by Crank (1975) whose treatise will at least provide the necessary mathematical background to the diffusional aspects. Growth of crystals is, additionally, complicated in this case because it may be facilitated by convective transport as well as diffusion and it appears that a complete analytical solution is not available for cases such as this where both mechanisms operate. If, however, one or the other mechanism is found to dominate, the existing body of theory is adequate. Considering the rate at which C_3S crystals often grow in the high temperature zone - ca0.1-1mm hr - and the large compositional difference which exists between C_3S and the nutrient melt phase - it is tempting to conclude that both convection and diffusion transport work cooperatively to facilitate crystal growth. Goldstein, et al. (1976) have contrasted the differing growth morphologies of calcium silicates obtained from the melt with these obtained by solid state reaction. Space precludes a lengthier description of the background, but the particular problem of competitive growth of crystals, where one nucleus competes with another of the same phase, as well as with other phases having one or more components in common, has been extensively treated in other branches of materials science. Further analysis of the earlier stages of precipitation will be found in papers treatments by Kahlweit (1976) and in numerous texts on crystallization.

The presence at high temperatures of C_3S and C_2S with liquid also implies that C_3A and ferrite are not present. Indeed, this appears to be the case: the liquid phase may be regarded as forming by melting of the $A\ell_2O_3$ and Fe_2O_3 components together with appropriate amounts of CaO and SiO_2. Minor components, such as alkalis, are partitioned between melt and solid phases (C_3S, C_2S). It would not be correct to assume that the minor components are contained exclusively in the melt, nor is equilibrium necessarily attained with respect to their distribution. Clinker liquids are capable of dissolving substantial MgO, although in practice the inert surfaces of MgO grains inhibit solution. This inertness, as well as local clusters of MgO-rich regions and the reduction in solvent power as the melt approaches local saturation, all conspire to ensure that the maximum solvent power of the melt cannot in practice be attained.

6.6. Reactions Occurring During Clinker Cooling. Kinetics of events occurring during clinker cooling.

Many important events occur during clinker cooling. For example, most if not all the C_3A and ferrite develop during cooling. Other possibilities may, however, intervene to prevent these compounds from crystallizing: the melt may fail to crystallize and instead persist as glass. We may first analize the fate of the liquid phase in themodynamic terms, as shown in Fig. 11.

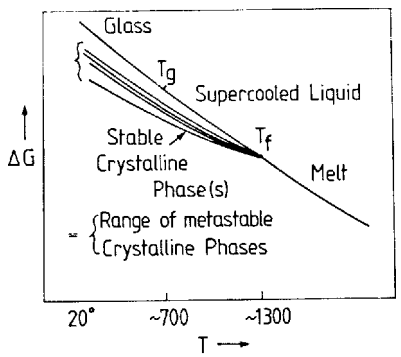

Fig. 11. Free energy - temperature diagrams showing the thermodynamic relationship of a melt and possible products occurring as a consequence of its cooling. T_f is its normal fusion point, T_g the glass transition temperature.

The example depicted strictly relates to precipitation of a single phase, but is in principle applicable to systems of greater complexity. Above ~1300°C, a fully fluid melt exists, It has a fusion point, in this instance close to 1300°C, below which crystalline material develops. In polycomponent systems, freezing occurs over a range of temperatures but is simplified in the diagram to show a definite point. Many oxide melts are distinguished by their tendency to persist as supercooled melts rather than crystallizing. Therefore a metastable prolongation of the free energy curve can be obtained below T_f where the melt still persists as a true liquid. If this melt continues to persist below T_f, with falling temperatures its viscosity increases steadily until eventually it achieves the mechanical properties associated with a rigid solid, below which temperature it is best described as a glass. This transformation temperature, T_g, or strictly range of temperatures, is therefore termed the glass transformation. It was initially defined in terms of viscosity, but in fact thermophysical studies disclose that a variety of

significant changes also occur at an accelerated rate at about this temperature: for example, the free volume available to the liquid suddenly decreases, as evidenced by the concommitant increase in density which occurs at an accelerated rate over a short range of temperatures. It is likely that atomic and ionic motions and structural relaxations occur relatively rapidly above T_g, whereas below T_g these motions are frozen in by quenching. Below T_g, the structural state can be altered only slightly by annealing or very slow cooling. Glasses thus have structural 'memories' for thermal histories below T_g. However, what is of primary concern to cement makers is the preservation or non-preservation of a glassy phase which, if present, must occur at the expense of C_3A and ferrite phases.

If the supercooled liquid is to crystallize, nucleation must occur with only small degrees of undercooling. Nucleation theory is itself in a semi-satisfactory state of development, but if it is assumed that the rate of nucleation I is the rate at which accreting molecules or ions strike the surface of a critical nucleus,

$$I = ZA^X N^X$$

where A^X is the surface area of the critical nucleus Z the collision frequency per unit area and N^X the number of nucleii per unit volume (the theory borrows from condensation of liquid droplets from vapour, where N^X is related to droplet density, the droplets being considered to be the critical nucleus). At small supercooling, critical nucleii form readily and the ionic mobility of species, i.e., Ca, Aℓ and O in the case of a C_3A nucleus, remains high. However, with increasing undercooling the mobility of species in the melt decreases rapidly so while nucleation may still occur, growth rates decrease drastically. Critical undercoolings necessary effectively to suppress growth and hence preserve glass would appear to be in the order of a few hundred degrees, so that supercooled melts preserved to temperatures approaching T_g are unlikely to exhibit bulk crystallization. It would appear that the liquid phase in clinker is not a good potential glass former, but lies on the threshhold of glass formers, given the typical cooling cycles employed in cement production. Of course clinker cooling is far from uniform and the more rapidly cooled fraction, e.g., dusts, is more likely to preserve glass than large lumps of clinker, the interior of which inevitably experience slow cooling. Maki (1979) has specifically discussed the mechanism of glass formation with reference to melt composition and cooling history. He delineated areas of glass formation in the low-silica portions of cement-clinkering systems. Both SiO_2 and $Aℓ_2O_3$ contribute to network formation, which is an essential prerequisite to the formation of a 'structured' liquid. The Aℓ is, however, only partly a network former, so the presence of SiO_2 contributes more significantly to the glass-forming properties of the liquid. Maki measured T_g for a range of compositions and found little variation: T_g ranged between 675 and 704°C. He noted that the viscosity, ν, of the undercooled melt varied with temperature according to the usual relation, $\log \nu = A_\nu + E_\nu/RT$ where E_ν is an activation energy for viscous flow. If crystallization can be suppressed as by rapidly cooling its viscosity rises and the melt is increasingly liable to be retained as glass.

If some crystallization occurs, the principal products - C_3A and ferrite - reject SiO_2, which concentrates in the remaining amorphous phase, thereby also increasing its tendency to persist as glass. This mechanism, supercooling plus fractional crystallization, made it feasible to obtain at least some glass in commercial clinkers.

Once nucleation and growth occur, the nature of the crystalline phases produced may not be that which would be obtained at equilibrium. Two types of phenomena may occur: one is the development of totally new phases, different from those obtained at equilibrium while the other leads to formation of variants of the stable phases. The first seems not to occur in clinker batches, although common in other systems. However, the C_3A phase crystallizing from undercooled melts has been found to differ significantly from C_3A produced under equilibrium conditions. Its crystallization was studied by Han and Glasser (1980) and by Han et al (1980, 1981), with increasing cooling velocities, C_3A crystallized from simulated clinker melts containing CaO, MgO, $Aℓ_2O_3$, Fe_2O_3 and SiO_2, together with incremental alkali additions, was found to differ progressively from ordinary C_3A, obtained by subsolidus isothermal reaction. The crystals became progressively more disordered, resulting in a decrease in intensity of X-ray reflections with $h + k + ℓ \neq 4n$, but also, the range of solid solution in C_3A was greatly enhanced, albeit metastably, to include Si, Mg, Fe, etc., in quantities much in excess of their equilibrium concentrations. This new variety of C_3A, formed proto-C_3A, arises as a consequence of cooling history. Although first isolated in laboratory preparations, it has been encountered in clinker. The consequences of these new types of compositional and structural variations are as yet unclear, but could affect markedly the reactivity of the aluminate phase. Equilibrium substitution of alkali, which lowers the symmetry of C_3A from cubic to orthorhombic or to tetragonal has very little influence on its reactivity with water. But the substitution of substantial quantities of Mg, Si, Aℓ and Fe in proto C_3A could have a more significant effect. Moreover, by incorporating large quantities of these elements in the C_3A structure, the potential for forming other phases, e.g., C_2S and ferrite during clinker cooling is altered. The characterization of proto C_3A has been made by Han and Glasser.

Another potential consequence of the cooling history imposed on clinker is that C_3S, stable at high temperatures, tends to decompose upon cooling. The kinetics of its decomposition were studied systematically by Mohan and Glasser (1970a,b,c). Phase pure C_3S was annealed isothermally. Fig 12 shows a typical decomposition using initially pure C_3S. A prolonged induction period is required, during which nucleii of the decomposition products CaO and Ca_2SiO_4 develop. This gradually gives way to an acceleration in decomposition as nucleii begin to grow. Eventually, geometric impingement slows growth as nucleii coalesce and the reaction rate decreases. The importance of the induction period and its attribution to nucleation, was supported by showing that, if nucleii of the decomposition products were supplied, the time required for nucleation was greatly reduced: the nucleii acted as decompositional catalysts. Analysis of the decompositional reaction was made by the Avrami equation.

1.1

$\delta = 1-\exp(-kt^n)$

where k is a constant and the value of n is related to the mechanism of nucleation.

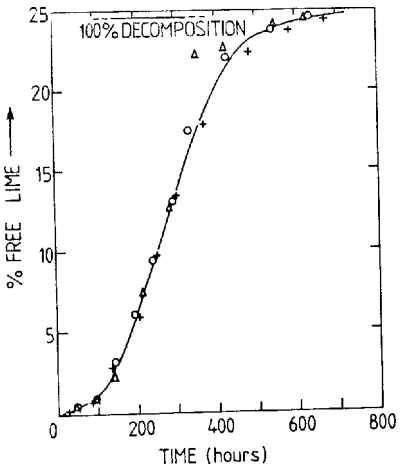

Fig. 12. Kinetics of the decomposition of C_3S at 1175°C, as determined by the rate of free lime production; 100% decompostion corresponds to 24.6% lime content.

For three-dimensional nucleation and growth, $3 \leq n \leq 4$, and for two dimensional nucleation and growth, $2 \leq n \leq 3$. The value of n was determined in this instance by plotting log $[1/1-\delta)]$ against log t: a straight line slope was obtained corresponding to n = 2.59. In this instance, microscopic observations supported the surface growth mechanism. However, some doubts have been expressed as to the validity of inferring mechanisms from the Avrami treatment. It would appear that in cases such as the present where the reactant and product(s) have well-defined stoichiometries the procedure is valid, but its application to other, less straightforward cases, e.g., hydration reactions, may require additional justification. The sensitivity of the surface condition was demonstrated by using water vapour, and it was shown that the rate of decomposition at constant temperature was a linear function of P_{H_2O}; Fig. 13 shows data. In general, if data from various temperatures were to be compared, it was found best to recalculate data in such a way as to plot a family of time-temperature-transformation curves.

The formation of ferrite during undercooling has been observed by Maultzsch and Scholze (1973). They found that during rapid growth, the inner zones of crystals failed to maintain equilibrium with subsequent zones and the crystals were compositionally inhomogeneous with respect to their A/F ratio.

Many events happening during cooling undoubtedly influence clinker properties. Indeed, it has long been believed that cooling rate influences clinker properties; for example, Sylla (1975) has determined the relation between clinker cooling and the

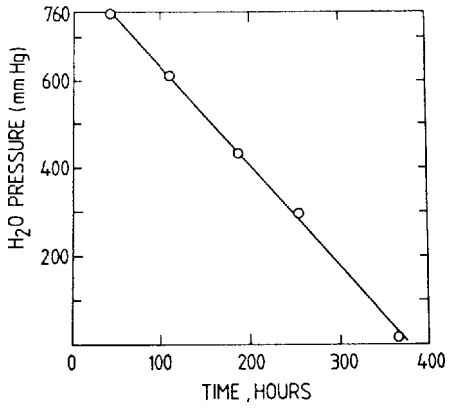

Fig. 13. Influence of H_2O vapour on the decomposition of C_3S at 1025°C. The time shown is that required to attain 50% decomposition.

set and strength gain of cement. However, many kinetically-controlled phenomena can occur during cooling in addition to those described here. There is suspicion that the polymorphism of C_3A is influenced by cooling rate. C_3S has numerous polymorphs; present evidence is that monoclinic and triclinic phases have about the same reactivity, but rhombhedral may be more active. The polymorphs of C_2S differ widely in reactivity, γ being especially inert but having two polymorphs, α' and β, both of which might be present at ambient. The connection between impurity content, cooling history and the preservation of reactive forms of C_2S, C_3A and C_3S is not at present well understood but remains an area fruitful for further work.

6.7. Summary of Clinker Formation.

A satisfactory qualitative account of the overall picture of clinkering kinetics can be given on the basis of the currently-available literature and many aspects can be treated more quantitatively. Nevertheless, it is difficult to fit the seperate quantitative approaches together to obtain an overall quantitative presentation. This is considered to arise because of the many overlapping reactions occurring in the process, which occur competitively. The following general features emerge as a key area of kinetic control.

(i) at temperatures above 600°-700°C decarbonation and dehydroxylation of the clinker feed occurs. Fine-grained, porous and chemically reacted solid decomposition products are formed. The gas phase contains reactive components, such as CO_2, and catalytic components, e.g. H_2O, which assist reaction.

(ii) at these low temperatures, intermediate phases, e.g. carbonate-silicates form. While these phases are subsequently decomposed in the high-temperature zone of the kiln, they may act as important precursors to the formation of C_2S, aluminates and ferrites, etc. Their role in the overall kinetics of formation is yet to be evaluated.

(iii) the high local concentrations of "volatiles" - e.g. chlorides, sulphur oxides, F - reached in modern fuel-efficient kilns may also play an important role in promoting reaction. In particular

high local concentrations of these components may exceed the dew point, resulting in formation of a transient low melting point salt-rich liquid.

(iv) reactions amongst the main components - CaO, $A\ell_2O_3$, Fe_2O_3 and SiO_2-proceed at unequal rates. Formation of calcium aluminates and ferrite seem to occur at lower temperatures, and at more rapid rates, than formation of calcium silicates during the early stages of batch reaction.

(v) the early stages of clinkering are also marked by formation of calcium aluminates, ferrites, silicates etc. which are thermodynamically metastable in terms of the overall batch composition. Examples include aluminates, e.g. $C_{12}A_7$ silicates, e.g. C_2AS (gehlenite), and ferrites e.g. CF. Their formation is conditioned partly by more favourable kinetics, but also by statistical distribution of the chemical components, which give rise to local areas which are enriched relative to the bulk in compounds of the exotic phases. Dicalcium silicate forms at much lower temperatures than tricalcium silicate. The C_2S phase can be developed in the solid state, whereas C_3S for all practical purposes forms only in the presence of a liquid phase.

(vi) Above 1300°C liquid develops and C_3S crystals. In well blended, well fired clinker batches a mineralogical and texture equilibrium is attained. The transport mechanisms via the liquid phase have been extensively studied in recent decades and it is possible to quantify the driving forces leading to C_3S formation, determine in general the role of minor components and mineralizers on the process kinetics.

SUMMARY.

The kinetics of cement making are reviewed. The early stages of calcining are dominated by decomposition reactions, by solid state diffusion leading to formation of calcium aluminates, Ca_2SiO_4 as well as by intermediate phases formed by partially-volatile constituents such as SO_4^{2-} and CO_3^{2-}. The main formation of C_3S occurs later, by sintering in the presence of a reactive liquid which also facilitates compaction of the mass. C_3A and ferrite arise mainly from crystallization of the high temperature liquid.

As a result of recent researches, the kinetics of many of these reaction have been analized in much more detail. Model studies on chemically simplified systems have explained and anticipated many of the kinetic phenomena occurring in chemically more complex batches as are used commercially. Kinetic treatments appropriate to the various stages of reaction are developed on a formal mathematical basis, but it is also essential to have a thorough understanding of the equilibria involved if the kinetic analyses are to be applicable to real problems.

REFERENCES

M.C. BALL and L.S. NORWOOD, (1977) "Surface area and porosity changes in the dehydration of calcium sulphate hydrate". J. Chem. Soc. Faraday Trans.(1) 73 [6] 932-941.

- ibid, (1978) J. Chem. Soc. Faraday Trans., (1) 74 [6] 1477-1487.

D. BERUTO, L. BARCO and A.W. SEARCY (1984) "CO_2 catalized surface area and porosity changes in high surface area CaO aggregates. J. Amer. Ceram. Soc., 67 [1] 512-515.

J. BIERNACKI and I. KOWALSKI (1981) "Calcination of limestones suspended in a gaseous phase." Cem. - Wapno- Gips. No. 6, 154-159.

P.P. BUDNIKOVA and A.M. GINSTLING (1968) "Principles of Solid State Chemistry" (translated by K. Shaw) Maclaren and Sons, London.

K.S. CHOU and G. BURNETT (1981) "Formation of calcium aluminates in the lime-sinter process" Cement Concr. Res. 11 (1) 57-64.

- ibid (1981) 11 (2) 167-174.

J. CRANK (1975) "Mathematics of Diffusion", Oxford University Press, London.

A.K. CHATTERJEE (1979) "Phase Composition Microstructure and Burning of Portland Cement Clinker" World Cem. Tech., 10 (4) 124-127.

T.K. CHATERJEE, A.K. CHATTERJEE and S.N. GOSH.(1980) "Clinkering reactions in Portland cement manufacture - a review of sequence and kinetics." Silicates Industriel. No. 4-5, 81-87.

N.H. CHRISTENSEN (1979) "Burnability of cement raw materials at 1400°C: I. The effect of chemical composition." Cement Concr. Res., 9 [1] 35-44(1979).

- ibid (1979) II "Effect of fineness" Cement Concr. Res., 9 [3] 285-293.

- ibid (1981) World Cement Tech., 12, 238.

N.H. CHRISTENSEN and O.L. JEPSEN, (1971) "Diffusion in three component cement clinkers". J. Amer. Ceram. Soc., 54 208-210.

N.H. CHRISTENSEN, O.L. JEPSEN and V. JOHANSEN (1978) "Role of a formation in clinker sandwiches" Cement Concr. Res., 8 [6] 693-702.

N.H. CHRISTENSEN and K.A. SIMONSEN (1970) "Diffusion in Portland cement clinkers" J. Amer. Ceram. Soc., 53 (1) 361-364.

CHROMY (1982) "Portland clinker formation processes I. Mechanisms. ZKG, Zem-Kalk-Gyps, Ed. A 35 (4) 204-210.

CHROMY, S. (1985) "Evaluation of the reactivity and of burning ability of industrial cement raw materials by a kinetic method" Stavivo 63 (5) 198-204.

DELIGNE, M. FIRENS, P., PICQUET P. et al. (1977) "Mechanism of dynamic synthesis of calcium aluminates." Silic. Ind., 42 (6) 261-266.

DESCAMPS, J., FIRENS, P. and VERHAGEN, J.P. (1974) "Application of thermoluminescence to the study of chemical defects in tricalcium silicate." Silic. Ind. 39 (7-8) (215-227.

DOREMUS, R.H. (1985) "Rates of Phase Transformations" Academic Press.

DRAYNEA, I., MUNTEAN, M. and TEOREANU, I. (1976) "Effect of $FeSO_4$ on burning oxidic mixtures in the system CaO ($CaCO_3$) -$A\ell_2O_3$. Silic. Ind. 41 (9) 357-362.

DROZDETSKAYA, G.V. and GROPYANOV, V.M. (1977) "Calculation of the kinetics of $CaCO_3$ decompostion under nonisothermal conditions. Zhur. Prikl. Khim, 50 (3) 496-499.

FIRENS, P. and TIROCQ, J. (1980) "Phosporescence and thermoluminescence of tricalcium silicate at low temperatures. Silic. Ind. 45 (4-5) 75-79.

FUNDAL, E. (1979) "Burnability of cement raw mixes" World Cem. Technol., 10 (6) 195-196.

FUNDAL, E. (1981). "Burnability of cement raw mixes". Cem.-Wapno-Gips. No.1, 16-21.

GOL'DSHTEIN, L. Ya., SMIRNOVA, L.V. and CHISTYAKOVA, A.A. (1976) "Characteristics of mineral formation during production of Portland cement clinker by melting". Zh. Prik. Khim. 49 (8) 1694-1698.

GOUDA, G.R. (1979) "Effect of clinker composition on grindability." Cem. Concr. Res., 9 (2) 209-218.

GROVES, G.W. and SINCLAIR, W. (1984) "The structure of alites" pp 93-100 in British Ceramic Proceedings No. 35, ed. F.P. Glasser, Stoke-on-Trent,England.

HAN, K.S. and GLASSER, F.P. (1980) "Crystallization of the liquid phase developed during clinkering." Cement Concr. Res. 10 483-489.

HAN, K.S. and GLASSER, F.P. and GARD, J.A., (1980) "Studies of the crystallization of the liquid phase in Portland cement clinker: effects of MgO and Na_2O." Cement Concr. Res. 10 443-448.

HAN,K.S., GARD, J.A. and GLASSER, F.P. (1981) "Composition of stable and metastable C_3A solid solutions crystallized from simulated clinker melts". Cement Concr. Res., 11 79-84.

HANIC, F., GALIKOVA, L., HAVILICA, J. et al. (1985) "Kinetics of thermal decomposition of $CaSO_4$ in air" Brit. Ceramic Trans. Jour. 84 (1) 22-25.

HEILMANN, T. (1960) in "Chemistry of Cement". Vol.1 (Proc. 4th Intl. Conf. on the Chemistry of Cement Washington, D.C.)p87.

HUMPOLA, H. (1981) "Optimization of the reactivity of cement raw material powder." Stavivo, 59 (1) 29-33.

IMLACH, J.A. (1976) "Non-isothermal investigation of the kinetics of reactions occurring during clinker formation" Cement Concr. Res. 6 (6) 747-755.

JOHANSEN, V. (1979) "Application of equilibrium phase diagrams to industrial clinker formation" Zem.-Kalk-Gips, 32 (4) 176-181.

JOHANSEN, V. and CHRISTENSEN (1979) "Role of formation of C_3S in the system CaO-SiO_2-$A\ell_2O_3$-Fe_2O_3-MgO with addition of CaF_2" Cement Concr. Res. 9 (1) 1-5.

JOHANSEN, V., JEPSEN, L., CHRISTENSEN, N.H. et al., (1978) "Ternary diffusion in cement clinker at 1500°C". Cement Concr, Res., 8 (3) 301-309.

JØNS, E.S. (1980) "Thermodynamic driving force for formation of tricalcium silicate

KAHLWEIT, M. (1976) "Kinetics of Crystallization". Ann. Rev. Phys. Chem., 27 59-63.

KINGERY, W.D., BOWEN, H.K. and UHLMANN, D.R. (1976) "Introduction to Ceramics" (2nd Ed.) Wiley Interscience, New York.

KONDO R. and S. CHOI, S. (1968) "Chemistry of Cement Clinker". Vol.1,Proc. 5th Intl. Symp. Chemistry of Cement (Tokyo) p 163.

KRACHNER, A., KEISER, J. and GATHEMANN, B. (1985) Mater. Constr. (Bucharest) 15 (2) 106-108; 111.

KUPPER, D. and TIGGESBAUCUMBER, P. (1983) "Calcination behaviour of cement raw meals". ZKG., Zem.-Kalk.-Gips. Ed. A. 36 (5) 275-280.

LEA, F.M. and PARKER, T.W. (1934) "Investigations of the quaternary system CaO-$A\ell_2O_3$-SiO_2-Fe_2O_3". Phil. Trans. Roy. Soc. (London). Sec. A. 234, 1-41.

LIM. E. -K. and PARK, B.-C. (1983) Jour. Korea Ceram. Soc. 20 (4) 295-304.

- ibid., (1984) 21 (2) 113-120.

- ibid., (1984) 21 (3) 221-230.

LUDWIG, U. (1981) "Influence on the sintering behaviour of cement raw meal", ZKG, Zem-Kalk-Gips. Ed.A. 34 (4) 175-186.

LUDWIG, U. and RUCHENSTEINER, G. (1973) "Firing of cement meals and quality of clinker". Tonind.-Ztg. Keram. Rundsch, 97 (1,2) 313-315.

LUDWIG, U. and WOLTER, A. (1979) "Formation and stability of tricalcium silicate and alites". Zem-Kalk-Gips. Ed. A. 32 (9) 455-459.

MACKENZIE, K.J.D. and ALASTI, H. (1978). "Formation kinetics of Portland cement clinker phases II. Tetracalcium aluminoferrite". Trans. Jour. Brit. Ceram. Soc. 77 (5) 162-167.

MACKENZIE, K.J.D. and ALDRIDGE, L.D. (1980)"Effect of reaction atmosphere on phase development in Portland cement clinker". Trans. Jour. Brit. Ceram. Soc. 79 (2) 29-36.

MACKENZIE, K.J.D. and BANERJEE (1978) "Formation kinetics of Portland cement clinker ". Trans. Jour. Brit. Ceram. Soc., 77 (3) 88-92.

MACKENZIE, K.J.D and HADIPOUR N. (1978) "Formation kinetics of Portland cement clinker, III. β dicalcium silicate and tricalcium silicate". Trans. Jour. Brit. Ceram. Soc. 77 (6) 168-172.

MAKI, I. (1979) "Mechanism of glass formation in Portland cement clinker". Cement Concr. Res. 9 (6) 757-763.

MATSUNOTO, K. and SATO, T. (1981) "Vaporization of tricalcium silicate at high temperatures". Nippon Kagaku Kaishi No. 10, 1676-1680.

MAULTZSCH, M. and SCHOLZE, H. (1973) "Formation of the ferrite clinker phase from the melt", Zem.-Kalk-Gips, 26 (12) 583-587.

MAYCOCK, J.N., SKALNY, J. and KALYONCU, R. (1974) "Crystal defects and hydration. I Influence of lattice defects" Cement Concr. Res. 4 (5) 835-847.

MCHEDLOV-PETROSYAN, O.P., SHCHETKINA T. Yu. and FATALIEV, S.A. (1975) "Role of metastable phases in formation processes of silicates." Silikattechnik 26 (8) 258-260.

MCHEDLOV-PETROSYAN, O.P., SHCHETKINA, T. Yu. and SAPOZHNIKOVA, N.J. (1978) "Development of solid-phase reaction theory and clinker mineral formation" Tsement No.9, 8-9.

MERAIKIB, M. and FRIEDRICHS, H.A. (1979) "Kinetics of limestone calcination". Arch. Eisenhuttenwes. 50, (8) 323-328.

MUELLER, A., DAHM, B. and STARK, J. (1977) "Decomposition kinetics of calcium carbonate" Silikattechnik, 28 (1) 4-7.

MUELLER, A., DAHM, B. and STARK, J. (1979) "Kinetics of calcium carbonate dissociation" Zem.-Kalk-Gips. 32 (2) 78-82.

MOHAN, K. and GLASSER, F.P.G. (1977) "The thermal decomposition of Ca_3SiO_5 at temperatures below 1250°C I. Pure C_3S and influence of excess CaO or Ca_2SiO_4" Cement Concr. Res. 7,1-8.

- ibid., II. The influence of Mg, Fe, Aℓ and Na oxides on the decomposition. 7,269-275.

- ibid., III. The influence of water and sulphate on the decomposition. 7, 379-383.

MOSIKAS, N., HAAG, E. HENIN, J.P., et al. (1981) "Burnability of cement raw materials as a function of their grinding fineness". Cir., Betons, Platres, Chaux. No. 729, 75-78.

ODLER, I. and DOERR, H. (1977) "Tricalcium silicate formation by solid state reactions". Amer. Ceram. Soc. Bull. 56 (12) 1086-1089.

ODLER, I. and ABDUL-MAULA, S. (1980) "Effects of mineralizers on the burning of Portland cement clinkers. I. Kinetics of the process." ZKG, Zem.-Kalk-Gips. Ed. A. 33 (3) 132-136.

- II. Mode of action of the mineralizers. 33 (6) 278-282.

OSOKIN, A.P., BUTT, Yu. M. and TIRNASHEV, V.V. (1973) "Mobility of Aℓ and Fe in clinker melts." Tr.Moscow. Khim-Technol. Inst., No. 72, 108-111,

PACKTER, A. and ZAIDI S.A. (1981) "Heterogeneous reactions of silica powders with calcium oxide solution in calcium chloride melts to form β dicalcium silicate - kinetics and mechanism." Silic. Ind. 46 (9) 173-177.

PETERSEN, I.F. (1983) "Isothermal sintering of Portland cement raw mixes." World Cem. 14 (6) 220-228.

PETERSEN, I.F. and JOHANSEN, V. (1979) "Burnability and clinker nodule formation from a statistical point of view". Cement Concr. Res., 9 (5) 631-639.

RAJA RAO, W. and CUTLER I.B. (1975) "Effects of calcining conditions on the dissociation rate of limestones and properties of lime." Bull. Centr. Glass Ceram. Inst. (Calcutta) 22 (2-3) 66-72.

RAUSCHENFELS, E. (1976) "Clinkerability of cement raw meal". Zem.-Kalk-Gips, 29 (2) 78-85.

RUDOLPH, R. (1979) "Output and process data characteristics for $CaCO_3$ decomposition in vibratory furnaces" Silikattechnik 30 (6) 169-171.

SARKAR, S.L. (1979) "Phase composition, microstructure, quality and burning of Portland cement clinkers" World Cem. Technol. 10 (9) 371. (see also 371-373).

SCHMALZREID, H. (1981) "Solid State Reactions" 2nd Ed. Monographs in Modern Chemistry, Verlag Chemie. (Weinheim).

SHEARER, J.A., JOHNSON, I. and TURNER, C.B. (1980) "Interaction of NaCℓ with limestones during calcination". Amer. Ceram. Soc. Bull., 59 (5) 521-524.

SHRADER, R. and KENKU, K. (1973) "Kinetics of reactions in the systems CaO-SiO_2 and CaO-$Aℓ_2O_3$". Tsement No. 2, 12-13.

SINGH, V.K. and ALI, M.M. (1980) "Formation kinetics of high alumina cement phases. I. Monocalcium aluminate". Trans. Jour. Brit. Ceram. Soc. 79 (5) 112-114.

SYLLA, H.-M. (1975) "Effects of clinker cooling on the setting and strength of cement". Zement-Kalk-Gips. 28 (9) 357-362.

SYLLA, H.-M. (1981) "Influence of reductive burning on the properties of cement clinker" ZKG Zem.-Kalk-Gips, Ed. A. 34 (12) 618-630.

SVETIK, S., JESENAK, V. and HARABE, Z. (1982) "Effect of atmosphere on the rate and mechanism of reactions in the system $CaCO_3$-SiO_2 at low temperatures". Silikaty, 26 (4) 289-298..

TALABER, J. SZNI, F., BERECJ, K. et al. (1982). "Effect of additives on the dissociation rate of calcium carbonate". Epitoanyag 34 (6) 201-206.

TEOREANU, I. and DULAMSCU, D. (1981) "Kinetic considerations concerning the clinkering behaviour of Portland cement raw mixes". Cemento 78 (4) 183-196.

TEOREANU, I., GEORGESCU, M., PURI, A. et al. (1985). "Clinkering potential of some mixes of raw materials" Mater. Constr. (Bucharest) 15 (1) 42-47.

VOGEL, E. (1983) "Reactions between solid fuel and the batch in cement rotary kilns" Baustoffindustrie 26 (1) 5-7.

WAECHTLER, H-.J., GAHRMANN, N., IGNER, R.I., et al. (1984) "Influence of the energy source on cement clinker quality" Silikattechnik 35 (9) 259-263.

YOUNG, D.A. (1966) "Decompositon of solids (Topic 21, in Vol. 1 of The International Encyclopedia of Physical Chemistry and Chemical Physics: Pergamon Press, Oxford).

M.S.MARINHO, ICI BRASIL S.A., SÃO PAULO, BRASIL

COMMUNICATION REPORT - SUB-THEME 1.1.

1- INTRODUCTION

Theme 1 of the congress (President Dr. C.D.Pomeroy - UK) is mainly concerned with studies on clinker formation and properties which are directly connected with the industrial process of cement manufacturing. From those studies in the past, that modern cement plants of today were idealized (short kilns, pre-calcining stages, low-alkali plants, etc.) and also new cements, generally utilizing less energy for its manufacturing than conventional O.P.C.

Sub-Theme 1.1 (President Prof.Mechedlov Petrossian - USSR) is devoted to the kinetic of clinker formation, a subject of considerable complexity, but of enormous importance to the development of clinker burning techniques. However, in the last decade, although many works have arisen on the subject, we are still far on the understanding of reaction kinetics during clinker formation. Mathematical modelling have been exaustively applied in this field to identify reaction mechanisms, but the limitations of such methods, like availability of reliable data and approximations from simpler systems, have led to a general disbelief on such models for the complex cement matrix. Works on pure cement phases especially C_3S have thrown some light to the problem and certainly will help further studies in the future.

At this congress, the communications presented in the sub-theme 1.1 have been divided into two groups: (1) kinetc studies done with industrial or laboratory prepared raw mixes and (2) studies done in pure or a mix of cement phase raw-materials. The author shall only be making a summary of relevant communications, highlighting important and new information, with exemption of any personnal opinion as it is the scope of a communication report.

2- KINETICS OF CLINKER REACTIONS

-Communications

1.0 - Prof. F.P.Glasser (UK)

"Principal report of Sub-theme 1.1"

1.1 - D.Gosch, S.A. Khadilkar, R.K. Agarwal, G.A. Mudhbhatkal and A.K. Chatterjee (India)
"Specific Surface as a parameter for raw mix burnability and its relation with volume change of fired raw mix pellets".

1.2 - F. Petersen (Denmark)
"The Ability of Clinker Nodule Formation".

1.3 - P. Burki and H. Braun (Switzerland)
"Investigations on influence of raw mix reactivity and rate of clinker formation".

1.4 - A. Wolter (West Germany)
"Phase composition of calcined raw meal".

1.5 - R.Costanet and F.P. Sorrentino (France)
"Study of clinkering reactions by high temperature calorimetry".

1.6 - S.J.Raina, P.Bhaskara Rao, S.K.Handoo and George Samuel (India)
"A new approach for estimation of heat requirement for clinkerization".

1.7 - A.Ossokin and E.Potapova (URSS)
"Mineral Formation in the Melt".

1.8 - W.Feng and S.Yu
"A study on the Kinetics of the burning of Portland Cement Clinker in different processes".

An attempt to improve the theoretical prediction of burnability (com.1.1) has been presented. It is a modification from previous theories of Jander (1) and Ginstling (2), which are based on the diffusion mechanism of monodisperse spherical particles, contrasting with the polidisperse nature of industrial mixes.
Firing samples with varying surface area, temperature of reaction and retention time, a equation (a) was derived by multiple regression technique.

$$\alpha = 0.7396+2.158\times10^{-3}\rho_1+6.209\times10^{-4}\rho_2+3.605\times10^{-5}\rho_3-0.013\rho_4 \quad (a)$$

Where α is the lime combinability ratio, ρ_1 the retention time in minutes, ρ_2 the temperature in ^{o}C, ρ_3 the surface area in cm^2/gm and ρ_4 percent total CaO in raw mix after burning.
The equation is valid within a temperature range of 1200-1500°C. This equation was tested with industrial raw mixes, where calculated values of lime combinability were compared with experimental. Calculated values were always lower and that was attributed to the influence of minor elements acting as mineraiizers.
A better qualitative insight to the equation was done by expansion/shrinkage studies on the industrial raw mixes used on the experiments above. Those studies could give some information on lime combinability, solid-state reactions (intermediate phases forming), formation of liquid and compressive strenght of the pellet.
The equation can be used to predict free-lime of a clinker given the surface area of raw mix, temperature of burning and retention time. However, absolute values are far to be obtained and caution must be taken due to interference of minor elements. The shrinkage/expansion experiments are fundamental for better interpretation of results.

A study of nodule size that can survive in the burning zone of a rotatory kiln (com.1.2), had been done utilizing a computer program. A worst case model is assumed where two clinker nodules at a foot of a charge will be consolidated into a permanent contact or sheared apart. By fixing several kiln parameters and physical properties of the mix and varying the capillary pressure and viscosity, a graph of Fraction of contacts surving against nodule diameter was derived. The model seemed sensitive to changes in physical properties, but critical regarding size of nodules that can form permanent contacts.

Two raw meals, with substantial difference in reactivity (measured as % free lime at 1500°C) due to raw-material nature,were studied in view of accessing the influence of a slow and a rapid up-heating (com.1.3). The influence on burnability and microstructure of the clinker were investigated. It has been shown that burnability is better in both raw meals, in the case of a rapid upheating. The suggestion that a gain in reactivity is due to the preservation of small and disordered intermediate minerals up to stage of alite formation (3, 4) has been confirmed by an increase of width and poor peak resolution of belite (XRD) on the reactive meal/rapid upheating sample.
Optical microscopy showed clear differences between the two clinkers formed concerning pore and clinker minerals size. The importance of micro-homogeinity of the meal was stressed, being inherent to the raw components and it is not significantly affected at the grinding fineness, typical of industrial raw mills. The authors point out that further work is needed to a better understanding of process condition, influencing clinker microstructure.
Another work (com.1.4) studied calcined meals extracted from 20 Kiln inlets. Those were thoroughly examined by XRD to identify phases present. Those phases were classified within groups: (1) - non-reacted materials, (2) - new phases formed during calcination, (3) - condensed salts and (4) - dusts.
Interrelation between the formation of new phases and degree of calcination (DCAL) was one of the main aspects of the study. DCAL has been related to various aspects of raw meal composition and free-lime amount.
Attention was also devoted for the exothermal heat, which is liberated in the reaction between free lime and "hydraulic factors", especially SiO_2. The degree of belite formation DC_2S in relation to the heat release in the kiln and degree of calcination have been shown. Subject to complete calcining, the range of exothermic heat liberated in the rotatory kiln varies between a minimum of 30% (very homogeneous meal) and a maximum of 80% (extremely heterogeneous meal). The presence of clinker dust was concluded to be of importance in pre-calcining.

A portfolio of new applications for calcined meal was also suggested (ex.: substitute clinker in fly-ash and slag cement, acting as main component of hydraulic active binders, for solidifying waste material).

High Temperature Isothermal Calorimetry have been used to study the change of enthalphy of all stages of clinkering reaction (com. 1.5). Experimental values were compared with calculated based on several data published in the literature for the enthalphy of formation of different reaction stages.
Results compared well taking into account some factors not included in the studies where data was taken from. The calculations gave at the end, a difference of 77 cal/g. at the exothermic part of the curve (C_2S formation). This could not be explained as no new phase have been detected by XRD. The authors mentioned that studies are underway to investigate such phenomena.

The authors (com.1.6) have suggested a new method of experimental determination of theoretical heat requirement for clinkerization. Zur Straussen (5) formulas, which are widely used, are only suitable to special compositions of the raw meal (limestone rich in calcite, clay minerals made up of equal contributions from the principal clay minerals, etc.). The idea was to develop a method by which no mineralogical composition of the raw meal or the heats of formation of the complex minerals were needed. Five clinkers were submitted to the method based on DTA analysis. Three had the composition suited to Zur Straussen formula and the others scaped quite considerably.
The results between the two methods agreed well for the first three clinkers and as expected were different for the last two. The method seems to work well, but high precision thermal analyser is required.

The effect of several anions and cations in relation to melt formation speed was analysed (com.1.7). A study of the time taken for CaO to be transformed in C_3S against grain size for various additions was presented. An addition of F^-, decreased the time from 52 to 14 minutes for the same grain size. The presence of $CaF_2 + CaSO_4$ decrease the time even further. A formula was finally proposed to calculate the firing time needed for the transformation of CaO into C_3S, depending on the medium grain size of CaO.

A raw mix was submitted to two different burning processes (com.1.8). A rapid and a slow one. The rapid method consisted in placing a pellet into a furnace at a range of 1280° - 1320°C, and the slow at a temperature rise of about 350°C/hr, simulating an industrial kiln operation. The rapid method yielded a lower activation energy and a higher velocity rate constant.

3- REACTION KINETICS OF PURE OR COMBINED CLINKER PHASE

- Communications

1.1 - B.Cottin, A.Rovanet and M.Conjeaud (France)
"Mineralogical changes of lime-silica-alumin raw-materials at 830°C".

1.2 - W.Weisweiler, E.Osen and M.Lemperle
"Effect of Fe_2O_3 and Al_2O_3 admixtures on the reaction kinetics between $CaO-SiO_2$ powder compacts".

1.3 - S.C.Ahluwalia and V.K.Mathur (India)
"Thermal studies on the effect of some transition metal oxides on the kinetics of formation and stabilization of β -Dicalcium Silicate".

1.4 - T.V.Kuznetsova, I.A.Brytov, N.A.Kozreva, B. Ivanov, I.I.Kiselyeva and E.A.Tsukerman (USSR
"Auger electron spectroscopic study of calcium silicates and aluminates".

1.5 - A.V.Bessmertnykh, V.K.Khokhlov and V.V. Sheludko (USSR)
"Thermodynamic study of Decarbonation kinetics".

1.6 - N.F.Fiodorov, A.P.Gavrilov, N.I.Ivanov and O.M.Khalina (USSR)
"Synthesis kinetics of calcium aluminates by the heat treatment in a cast-iron bath".

1.7 - A.Rovanet (France)
"Solid state reactions between lime and alumina".

1.8 - M.Dragicevic (Yugoslavia)
"Prognosis of the physical-mechanical characteristics of Portland Cement".

Four raw mixes with distinct variations on the amounts of C, S and A were studied (com.1.1), regarding decarbonation,degree of reaction ($CaO \rightarrow C_2S$) and phase formation occuring at a fixed temperature of 830°C. The morphology of the treated raw mixes was a varying parameter (simple mixing, compactation(pellets)and micronization in a high efficiency mill).
The influence of CO_2 and water vapour on the velocity of combination and the nature of phases formed has been analysed. The following aspects are interesting to be noted:

Decarbonation
- The sample which has been micronized, because of grain shape, had a remarkable speed of decarbonation.
- The resistance of CO_2 transfer is rather higher in the already decarbonated region of the lime grain, than in the porous region inter-grains.
- The water vapour helps the decarbonation rate through the layer of carbonated material around the grain (catalytic effect due to acceleration of diffusion of CO_2 in water vapour and a change on thermal conductivity of the gas).

Degree of Reaction
- Micronized sample had a superior speed of reaction, due to grain fineness (specific surface area).
- Pelletized sample did not yield a better speed of reaction compared with a simple mixture.
- Water vapour had a good catalytic effect on the samples, which were simply mixed.

Phase Formation (examined by XRD)
- Two equilibrium phases are formed (C_2S and $C_{12}A_7$) and also some non-equilibrium such as CS, C_3A, CA and C_2AS. Various tables in the text showed the results obtained.

Interface phase formation between CaO and SiO_2 in the presence of Al_2O_3 and Fe_2O_3 were studied by diffusion couple technique at high temperatures (com.1.2) and phase formation was analysed by Electron Probe Micro Analysis (EPMA) and optical microscopy. Layer thickness of undoped CaO - SiO_2 mixtures were compared to those with Fe_2O_3 or Al_2O_3 (CaO (Fe_2O_3)/SiO_2, CaO/SiO_2 (Fe_2O_3), CaO (Al_2O_3)/SiO_2 and CaO/SiO_2 (Al_2O_3)).
Additions of Fe_2O_3 either to the CaO or SiO_2 showed a rather similar trend for the curves. Values in the region at 3% by weight Fe_2O_3 in SiO_2 and Fe_2O_3 in CaO, decreased the overall reaction rate. Values above that (especially at high temperatures >1350°C) increased the thickness of total reaction zone. At temperatures below 1450°C, the effect of Fe_2O_3 in SiO_2 beyond 3%, does not contribute for any increase in layer thickness. C_2S is the dominant phase between 1100 - 1400°C. Above 1400°C, CS or a glass phase "CS_2" are predominant.

Additions of Al_2O_3 in CaO gave similar results as above, sharp decrease up to 3% by weight Al_2O_3 and an increase in layer thickness for higher percentages (more pronounced at higher temperatures). In the case of Al_2O_3 in SiO_2, a continuous increase in total layer thickness was observed. Samples with 5-10% by weight Al_2O_3 fired at 1450°C for 15 minutes, complete reaction of the diffusion couple had taken place leaving mainly CS and "CS_2" phases. Explanations about the findings are given based on disorder and vacancies in CaO. Activation energies had also been calculated.

The effect of MnO_2, TiO_2 and Ci_2O_3 on the decomposition of $CaCO_3$ and formation of β-C_2S were studied (com.1.3). Decomposition temperature of $CaCO_3$ was lowered by the presence of three dopants within the range 0.1-1.0%. Formation temperature of β-C_2S is not significantly affected up to 1%, but has been reduced at 5% addition of TiO_2 and MnO_2.

The stabilization of α',β and γ C_2S in the presence of this dopants was also studied.

A mathematical treatment for the decarbonation kinetics of CO_2 and a solid ($CaCO_3$, for example), based on the linear thermodynamics of irreversible processes was given (com.1.5). A final equation for the degree of decarbonation is presented. The limits of validity of such equation is also given.

A report on the production of Alumina and High Alumina cements by immersion on a cast-iron melt was presented (com.1.6). It has been shown that the speed of formation of the phases of Alumina Cements are faster using this method than obtained using conventional rotatory Kiln methods. The quality of the product obtained is also very good. It is suggested that such methods could be used succesfully in industrial scale. Advantages such lack of pollution from combustion products and the elimination of dust from the system are among some of the described in the text.

A study on the kinetics of formation of Calcium Aluminates was done by two different experimental conditions (com.1.7).
In the first, Alumina was melted and cooled slowly to form a compact pellet, which was deeped into $CaCO_3$ powder. The maximum temperature of reaction examined was 1370°C. The interface between the powder and pellet was studied by electron and optical microscopy after etching and also XRD. XRD analysis on the surface of the compact layer showed the existence of $C_{12}A_7$. At more profound regions of the product CA, CA_2 and CA_6 were present. An investigation on the powdered region close to the Alumina block showed only the presence of C_3A.

Secondly, raw mixes of the two oxides in proportions of the existing Calcium-Aluminates were prepared and fired at the same temperatures as above. Several graphs on the kinetics of formation of the different phases are presented and discussed. A relation between time of saturation at each phase with the chemical potencial of the calcium is presented.

Auger Spectroscopy was used as a new technique to analyse cement clinker minerals (com.1.4) and a mathematical model has been described to foresee Potland Cement strenghts values after 3 and 28 days (com.1.8). Although results have a good agreement with experimental data, the author stresses, that due to accuracy of chemical and physical-mechanical investigations, the model gives a good qualitative guidance to work done at cement factories.

REFERENCES

1) W.Jander, Zement 20, 936-39, 951-53 (1931)

2) A.M.Ginstling and B.I.Braunstein, J.Applied Chemistry (USSR), 23, nº 12 (1950)

3) H.Bomas, V.Ludwig, A.Wolter, Tonind. Z tg. 105, 144 (1981)

4) A.Wolter, Zement - Kalk - Gips, 38, 612 (1985)

5) H.Zur Strassen, Zement Kalk Gips 10 (11, 1-12) (1957)

YUSHIRO KIHARA - Associação Brasileira de Cimento Portland

COMMUNICATION REPORT: RELATIONSHIP OF PROCESSING PARAMETERS TO CLINKER PROPERTIES; INFLUENCE OF MINOR COMPONENTS

1 INTRODUCTION

The sub-theme 1.2 *Relationship of processing parameters to clinker properties; influence of minor components* belongs to theme 1 *Clinker formation and properties.*

Dr. Iwao Maki (Japan) is responsible for the Principal Report of sub-theme 1.2, and Dra. A. Boikova (URSS) is in charge of the Special Report, which deals with the topics considered most relevant to deserve the researchers attention in the near future.

Thirty (30) Basic Communications from 16 countries were received in this sub-theme, distributed as following:

URSS	6
China	4
India	4
Italy	4
Brazil, Bulgaria, Czechoslovakia, Denmark, France, Germany, Japan, Poland, Romania, Spain, USA and Yugoslavia .....(each one)	1

Contributions from URSS, China, India and Italy make up 59% of the papers presented in this sub-theme.

The papers presented deal basically with:

1. the influence of processing parameters in the characterization and properties of clinker phases.

2. the crystal chemistry and influence of minor elements in the stabilization and activation of clinker phases.

A critical analysis of the communications allows to notice the general deep concern in presenting well founded data in experimental studies, supported by various analytical techniques (x-ray diffraction, optical microscopy, scanning electron microscopy, energy-dispersive analysis, electron microprobe analysis, differential thermal analysis, thermogravimetry, infrared absorption spectrophotometry, etc.) correlating them with industrial practice. The papers aim a major knowledge in the kinetics of clinkering reactions in the kilns, as well as in the crystal chemistry of phases actived and stabilized by minor elements.

The practical application of the scientific knowledge about the chemistry of cement from sub-theme 1.2 aims:

a) improvement in the quality of the industrial product;

b) energy saving in cement manufacturing processes;

c) activation techniques of clinker phases; and

d) development of new hydraulic binders.

The Basic Communications presented in this sub-theme are listed at the end of this Communication Report.

2 RELATIONSHIP OF PROCESSING PARAMETERS TO CLINKER PROPERTIES

2.1 Fuel and Raw Material

The use of high ash content (35-54%) mineral coal in cement industry has a strong influence over the behaviour of rotary kiln running, as well as modifies clinker characteristics, changing their composition and reactivity, which can extreme situations undermine the quality of the cement so produced. Irregularities in the coal burning and in the assimilation of the ashes by the clinker are shown by the segregate distribution of the C_2S, corrosion and excessive growth of the C_3S, digitation of the C_2S crystals, formation of $C_2S\gamma$ and exsolution in the C_3S crystals, appearence of reduced phases, and variation in the C_3S, C_2S and C_3A contents. This undesirable microstructural features affect the quality of the cement, influencing the setting time, the heat of hydration, the optimal gypsum content, the evolution of mechanical strength and the grindability of the clinker *(Y. KIHARA*[1]*)*.

The use of certain solid fuels in cement kilns may conduct to accidental formation of reduced conditions. *VERNET*[2], studying the burning influence at reduced conditions in the clinker phase stability and hydraulicity, observed that CaO reduction by carbon provoques an improvement in belite content, without free secondary CaO formation. Reduced conditions little affect alite crystal lattice, composition and reactivity, in spite of belite allotropic transformations being accelerated with important changes in their composition and reactivity. The reduction causes improvement in C_3A and C_2S contents and decrease in the C_3S amount, influencing the setting time and the early behaviour of the cement.

MASSAZZA and PEZZUOLI[3] studied the interactions between alkaline vapours and coal ashes. Coal ashes brought to high temperature can fix high amount of K_2O from atmospheres containing potassium carbonate or sulphate vapours. The alkali absorption in the coal ashes and in the coatings present in cement kiln is a complex process, which depends not only on the concentration of the alkaline elements but also on , the composition of the atmosphere on the material present in the kiln , and on the structure of the solid phase.

Variation in raw materials and coal can add alkali sulphate to the clinker. Coal , contributes with a varying percentage of SO_3 and ash, which greatly affects the process and, accordingly, the cement quality. Alkali sulphates are incorporated in the crystal lattice of clinker minerals. Higher amounts of Na, K and S alter the structure of the clinker as the alkali sulphate (thenardite, arcanite, anydrite, aphthitalite and calcium langbeinite) are crystallized and precipitated over the calcium silicate grains as small crystallites and fine polysynthetical stripes. Belite crystals show higher concentration of K and it seems that the structure of C_2S changes to $KC_{23}S_{12}$. The presence of alkali sulphates changes the morphology of the crystals, which results in changed hydration properties, early setting and stiffening, slump loss, early increase and late decrease in strength. The most important parameters influencing strength are the soluble potassium oxide and the alteration of the Ca-silicate grains, especially C_2S *(G.R. GOUDA*[4]*)*.

A new potassium - alumina phase ($K_2O.Al_2O_3$) and free K_2O in clinkers burned with an alkali-rich raw material are described by *FUNDAL*[5]. They have strong hygroscopic properties and can influence the setting behaviour, the storage and the strength properties of the cement. The so-called alkali aluminate forming in alkali-rich clinker by cooling doesn't crystallize by prolonged burning time at normal sintering

temperatures, being gradually substituted by the crystallization of ferrite and aluminate.

SERSALE, AMICARELLI, FRIGIONE and UBBRIACO[6] pointed out that the use of LD steel slag, at a rate of 10%, as partial substitute of limestone in the raw mix of portland clinker, doesn't affect the technical behaviour of the resultant cements and lowers the heat consumption of the clinkering process.

2.2 Burning and Cooling Conditions and Kiln Dynamics

SHEUBEL[7] used microscopic methods to obtain information regarding the thermal hystory of the clinker. A long calcination zone accelerates the recrystallisation of CaO and the formation of large belite crystals, which on their part obstruct the alite formation. This results in a flat distribution curve of alite crystal sizes together with a large mean diameter and a more difficult clinker grindability. The statistical evaluation of the alite crystals diameters or chord lengths permits simple representation of the material temperature profile in the kiln. Given the knowledge of the kiln system and certain raw material parameters, the measured data can be used for improving clinker grindability and quality, as well as for optimizing the burning process.

The currently employed burning and cooling regimes are not optimal, as they imply in a prolonged retention in the high temperature zone, thus leading to the inhibition of the alite formation process in the clinker and decrease in its activity. For producing a portland cement clinker with high hydraulic activity conditioned by an optimal alite content and maximal crystalline disorder, it is necessary to maintain a certain relation between temperature and burning time depending on the nature and composition of the raw material *(B.S. AL'BATS, M.A. VERDIAN, L.S. FILLIPOVA and E.L. LEBEDEVA*[8]*)*.

According to *ODLER, ABDUL-MAULA and ANGELOVA*[9] variations in heating rate, burning temperature, burning time at maximum temperature and cooling rate bring about only small, though distinct variations in the size of alite crystals formed. The average alite crystal size increases distinctly with increasing burning temperature. Variations of other factors such as heating rate, burning time and cooling rate have little effects on alite crystal size. The initial cement hydration is accelerated with increasing heating rate and retarded with increasing burning temperature and burning time. The progress of hydration after about one day and more, just as the strength developement are only little affected by the burning conditions employed.

The increase in the burning degree by changing the heating time causes modifications in the composition and structure of clinker and, therefore, in the properties of the resulting cements. The loss of most volatile elements and the increase in the sizes of alite and belite crystals are the most evident phenomenoms. In some cases the reactivity of the aluminate phases reduces as the burning degree increases, in others it remains inaltered, whereas the alite reactivity shows a general reduction. Significant decreases in the rheological parameters are observed as the burning time lengthens and the reactivity lowers. The reduction in the alite reactivity envolves in its turn the decrease in early strengths *(U. COSTA and F. MASSAZZA*[10]*)*.

PUERTA and TRIVINO[11] studied the influence of different types of quenching (air and water) on various clinkers reheated on the following temperatures: 1000, 1206, 1320 , 1460 and 1576°C, with respect to their phase

formation and mechanical strength. The experimental results obtained do not seem to be in accordance with bibliographic data. In water quenched clinker trigonal alite with Aℓ and Mg in solid solution was characterized, less reactive than monoclinic alite obtained in air quenched clinkers. The mechanical strength was always lower than of those quenched by air, possibly due to trigonal alite. In air quenched clinker monoclinic alite (possibly a mixture of M_1 + M_3 forms) was obtained.

The increase of whiteness of bleached clinkers can be attained by burning at the highest possible temperature, by sharp quenching, and by decreasing time of burning which promotes the fine crystallization of the phases. Quenching by water increases the amount of alite, decreases the amount of aluminate and belite with high impurity contents, favours the glassy phase formation and changes the crystallization features of the minerals. The majority of Fe^{3+} is concentrated in the aluminate and glassy phases and the Fe_2O_3 contents in alite and belite does practically not change in bleached and unbleached clinkers *(A.I. BOIKOVA, O.I. FOMICHEVA and A.P. ZUBEKHIN*[12]*)*.

According to *BHASKARA RAO, HANDOO and SAMUEL*[13] the use of La^{140} with activity, as radiotracer, in a wet process cement rotary kiln shows that the assumptions made in the existing equations defining the material movement phenomenon in rotary kilns are valid only over a very limited length within which the material is in the form of a dry flowing powder without any appreciable physico chemical change. This zone is limited to the conventional preheating zone. The study revealed that the material movement in the transition and burning zone was much faster than that of the fine powdery material which is explained by the fact that nodulization takes place in this zone.

2.3 Prediction of Cement Strength

HARGRAVE, VENKATESWARAN, DESHMUKH and CHATTERJEE[14] proposed an approach for prediction of 28 days cement strength, based on microstructure parameters under reflected light microscopy. The parameters are:

- phase index (PHI)
- crystal size index of alite (CSI-A)
- crystal size index of belite (CSI-B)
- morphology index of alite (MOI-A)
- morphology index of belite (MOI-B)
- twinning index (TWI)
- cluster index (CLI)

By multiple linear regression analysis of microstructural parameters in relation to compressive strength of a large number of data *(Figure 1)* the following equation was obtained:

$$28D\ strength = 0.028 + 98.598(PHI) + 90.571(CSI\text{-}A) + 1.539(CSI\text{-}B) + 61.437(MOI\text{-}A) + 2.943(MOI\text{-}B) + 85.049(TWI) - 84.308(CLI)$$

The coefficient of multiple correlation (r) is 0.836 and the standard error of estimate is 52.794.

The method compared with *ONO*'s technique shows similarities, but it is considered more accurate and with greater potential to predict the 28 days cement strength in short time.

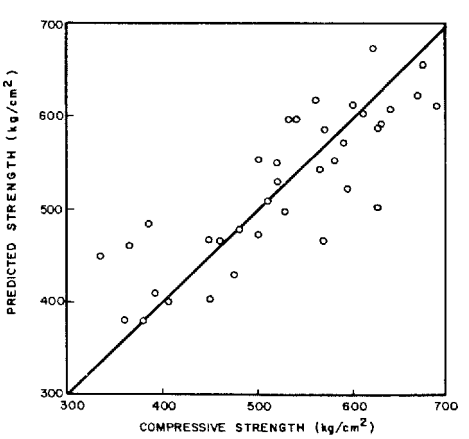

FIGURE 1 - Correlation between 28D cement compressive strength with predicted strength by mycroscopic techniques.

3 CRYSTAL CHEMISTRY OF CLINKER PHASES AND INFLUENCE OF MINOR COMPONENTS

3.1 Crystal Chemistry of Clinker Phases

Mg^{2+}, Na^{+} e S^{6+} ions in structures of clinker phases cause changes and distortions favouring the reactivity. They influence the stabilization of phases and crystal morphology of alites and belites. They modify aluminoferrite contents and the $A\ell_2O_3/Fe_2O_3$ ratio. Till the following limits: 2% MgO; 0,5% SO_3 and 1% Na_2O the clinker reactivity is increased, and surpassing these limits the clinker quality can be altered by the formation of independent phases of MgO, sulphates and alkalies and finally by the modification of the phase relations *(T.V. KOUNETSOVA*[15]*)*.

The modification of alite is influenced by the burning conditions and the MgO content in clinker. Monoclinic alite M_1 is always observed when clinker is burnt for short time or by slow burning. It converts into M_3 with prolonged burning at high temperature. High MgO contents favours the convertion from M_1 to M_3.M_3 alite hydrates more slowly than M_1 alite at early age. After 3 days, the hardened cement containing M_3 is denser than that containing M_1 and the former shows greater strength than the latter *(M.NAGASHIMA, E. ASAKURA, S.UDA and H. KAWABATA*[16]*)*.

The study of belite has received special attention from some researchers dealing with special cements of low energy consumption. The activation of belite by stabilizing more reactive phases (α') employing minor elements (P_2O_5, SO_3, MgO, alkalies,etc.) and by modifying process parameters (burning conditions and temperature) is the subject of *CHOUBINE and KHNYKINE, MATROVIC et alii, KRIVOBORODOV et alii, FENG XIU-JI et alii and SARASWAT et alii's* contributions.

The formation of a βC_2S phase in the $CaCO_3$-SiO_2 system increases with increasing percentage (0.1-1.0 as % Na_2O/K_2O) of Na_2CO_3 5% of dopant give most predominant βC_2S phase alongwith a little α'-C_2S, C_3S and alkali-silicate. Sodium carbonate is found to be most effective in turning down the temperature of formation of most desired α' and β phases than potassium carbonate *(I.P. SARASWAT, V.K. MATHUR and S.C. AHLUWALIA*[17]*)*.

In C_2S doped with phosphates it was observed that solid solution of the α' form develops strength much faster than those in β modification, due to faster hydration. The change of crystal modification and impurity types distributions modify only the rate of hydration *(B. MATKOVIC, V. CARIN, R. HALLE and J.F. YOUNG*[18]*)*.

The positron annihilation technique is used to study changes of microstructure defects in C_2S doped with Na_2O (1-2%) and P_2O_5 (0,5-1,5%). The Na^{+} replaces Ca^{2+} and P^{5+} replaces Si^{4+}, creating vacancies in the C_2S structure. The vacancy concentration and the rate of C_2S formation increases with doped Na^{+} and P^{5+} *(F.XIU-JI, M.S.LONG SHI-ZONG, DING QUING-JUN, HUANG CONG-YUN, S.DE-XUN, TENG MIN-KANG, YIN CHUAN-YUAN*[19]*)*.

White belite portland cements with various MgO (1-10%) and SO_3 (5%) contents and low Fe_2O_3 content were synthesized in laboratory. The positive influence on acceleration of the clinkerization processes is registered when the clinker contains 7% MgO and 5% SO_3. Both the whiteness of the clinkers and the mechanical strength (above 33-35 MPa in 28 days) of the resulting cement are good. Sulphate aluminate compound of the $(C, M)_4A_3\bar{S}$ type was formed and incorporated all MgO in the crystal lattice *(I. TEOREANU, M. MUNTEAN, M. BEDO and T. SUDRIGEAN*[20]*)*.

Modifications of the phases of clinkers with sulphoaluminate and sulpho-ferrites with the aid of admixtures and changes in the thermal regime permit to control the

the hydraulic activity of the phases and the properties of the cement so obtained *(Y. KRIVOBORODOV, O. FOMITCHEVA and A. BOIKOVA*[21]*)*.

The synthesis are oriented towards the stabilization of the α' form with high cooling rates, to guarantee the stability of the high temperature modifications *(V.CHOUBINE and Y.KHNYKINE*[22]*)*.

The solid-state equilibrium relationship between C_3A, $C_{12}A_7$ and the solid solution of calcium aluminoferrite at 1200°C, in the most basic part of $CaO-Al_2O_3-Na_2O-Fe_2O_3$ system was studied by *GILIOLI et alii*[23]. There is no formation of quaternary compounds and sodium preferentially dissolves in calcium aluminates extending their stability inside the quaternary system.

3.2 Influence of Mineralisers

The use of mineralisers in clinker burning lowers the clinkering temperature, increasing the kiln production, and promotes energy saving. Four papers present the fluorine and sulphate influence on clinkering conditions and strength developments.

The use of CaF_2 and $CaSO_4$ in cement clinkering can depress the melting point of the eutectic mix T_2 and reduce the viscosity of the eutectic melt, favouring the clinker formation at lower temperatures (1300-1350°C). $2C_2SCaF_2$ and $3C_3SCaF_2$ can hardly form in the presence of SO_3. The $2C_2SCaSO_4$ occurs only in the mix with $F/SO_3 < 0.158$ and $3C_2S - 3CaSO_4.CaF_2$ forms easily owing to the melting of the eutectic mix *(D. TONG and Z. LIN*[24]*)*.

In clinker doped with CaF_2, the fluorine concentration is highest in the alite phase, lower in the belite phase, and lowest in the intersticial phase. The amount of fluorine dissolved in the silicate increases with the amount of fluorine in the clinker. The fluorine content in the clinker, with an appropriate amount of SO_3 (> 1.35%), prevents the formation of $Ca_{12}Si_4O_{19}F_2$ and favours the increase of alite content, the decrease of its crystal size and its complete crystallization, improving the strength development *(S. WEI and F. MINGFEN*[25]*)*.

The use of fluorite, fluorsilicate and sulphate compound as a mineraliser was studied by *PAGE*[26] et al. in four Indian Plants. The improvement in quality of clinker doped with mineraliser can be primarly attributed to the formation and development of C_3S phase, more than to the incorporation of mineralising ions in the structure of phases. The incorporation of fluorine in C_3S or other clinker phases, by itself, cannot insure better hydraulic potential for a clinker. Complex reactions involving F, SO_3 and P_2O_5 in the structure of C_3S thereby don't improve strength developments.

Addition of gypsum to Na_2O containing raw meals leads to a modification of the clinker structure towards a better developed alite and belite crystals. Reactivity of the raw mix is increased so that more C_3S can be formed and the C_3A phase tends to crystallize in the cubic form, improving the compressive strength of the cement. When more gypsum is added in the raw mix than the optimum content, the compressive strength of resultant cements decreases possibly due to reduction of the hydraulic reactivity of βC_2S *(R.J. SLOTA and A. LEWANDOWSKA - KANAS*[27]*)*.

3.3 Other Contributions

The formation of an intermediate compound containing magnesium has received much attention in the alinite cement process formation. A new compound, $Ca_8Mg(SiO_4)_4Cl_2$ was synthesized in the $CaO-MgO-SiO_2-CaCl_2$ system and the crystal structure study is presented by *Y. RUILUN, W.BOLIN and W. XINRONG*[28].

PEREZ - MENDEZ & FAYOS[29] studied the crystal structure of $K_3Ca_2(SO_4)_3$, a compound identified in coatings on heat recovery cyclones in portland cement kilns. It showed a very distorted structure analogue to apatite $M_5(YO_4)_3X$.

Fluorine compounds present in industrial gypsum - waste used as a cement setting regulator may cause as much as 3 days significative retardation in the growth of initial strengths of cement paste or mortar. Small quantities (1%) of silico fluorides in gypsum, mainly Na_2SiF_6, accelerate considerably the formation of ettringite and reduce the alite hydration degree. NaF exhibits lower retardation effects, whereas CaF_2 shows almost no influence on the initial strengths *(Z. SAUMAN*[30]*)*.

REFERENCES

1 - *Influence of high ash content mineral coal in portland cement clinker characteristics.* Y. KIHARA - Brazil.

2 - *Cuissons reductrices - consequences relatives à la stabilite des phases du clinker.* C. VERNET - France.

3 - *Interactions between alkaline vapours and coal ashes.* F. MASSAZZA and M. PEZZUOLI - Italy.

4 - *Microstructure and properties of high-alkali clinker.* G. R. GOUDA - USA.

5 - *The description of a new potassium-alumina phase in ordinary portland cement.* E. FUNDAL - Denmark.

6 - *A study on the utilization of an italian steel slag.* R. SERSALE, V. AMICARELLI, G. FRIGIONE and P. UBBRIACO - Italy.

7 - *Investigation on the influence of the kiln system on clinker quality.* B. SCHEUBEL - Germany

8 - *Durée de cuisson du clinker et ses propriétés.* B.S. AL'BATS, M. A. VERDIAN, L.S. FILLIPPOVA and E.L. LEBEDEVA - URSS

9 - *The effect of burning conditions on the structure of portland clinker and the reactivity of the resultant cement.* I. ODLER, S.ABDUL-MAULA - Germany, and T.ANGELOVA - Bulgaria

10 - *Influence of the burning degree on the rheological and strength properties of clinkers.* U. COSTE and F. MASSAZZA - Italy.

11 - *Modifications clinker phase and mechanical strength in relation to type of quenching.* F. PUERTAS and F. TRIVIÑO - España

12 - *Chemical composition of phases and phase relations in unbleached and bleached clinkers.* A.I. BOIKOVA, O.I.FOMICHEVA and A.P.ZUBEKHIN - URSS

13 - *Radio tracer technique: a diagnostic method for evaluation of raw meal and clinker movement, in a cement rotary kiln.* P.BHASKARA RAO, S.K. HANDOO and SAMUEL - Inde

14 - *Quantification of OPC clinker microstructure - An approach for prediction of cement strength.* R.V. HARGAVE, D. VENKATESWARAN, V.V. DESHMUKH, and A.K. CHATTERJEE - Inde

15 - *Influence des facteurs differents sur la composition de phase et les propriétés du clinker.* T.V. KOUZNETSOVA - URSS

16 - *Characteristics of alite in portland cement clinker and C_3S solid solution.* M.NAGASHIMA, E.ASAKURA, S. UDA and H.KAWABATA - Japan

17 - *Thermal decomposition and phase transformation studies of $CaCO_3$-SiO_2 (2:1) system in presence of sodium and potassium carbonate.* I.P. SARASWAT, V.K. MATHUR and S.C.AHLUWALIA - Inde

18 - *Dicalcium silicate doped with phosphates.* B.MATKOVIC, V.CARIN, R. HALLE - Yugoslavia and J.F.YOUNG - USA

19 - *Investigation on doped β-C_2S with positron annihilation.* F.XIU-JI, M.S.LONG SHI-ZONG, DING QING-JUN HUANG CONG-YUN, SHEN DE-XUN, TENG MIN-KANG and YIN CHUAN-YUAN - China

20 - *Belitic portland cements with various content of MgO and SO_3.* I.TEOREANU, M.MUNTEAN, M.BEDO and T. SUDRIGEAN Romania

21 - *Composition des phases des clinkers contenant des sulfoaluminates et sulfoferrites.* Y. KRIVOBORODOV, O.FOMITCHEVA and A. BOIKOVA - URSS

22 - *Modification des clinkers de belite.* V.CHOUBINE and Y.KHNYKINE - URSS

23 - *Solid state relationships in the lime-richest part of the CaO-Al_2O_3-Na_2O - Fe_2O_3 system.* C. GILIOLI, F. MASSAZZA and M.PEZZUOLI - Italy

24 - *The role of CaF_2 and $CaSO_4$ in cement clinkering.* D. TONG and Z.LIN - China

25 - *A study of the effects of CaF_2 on clinker doped with compound mineralizer.* S,WEI and F. MINGFEN - China

26 - *Influence of mineralisers on the constitution and properties of industrial clinkers.* C.H. PAGE, D.GHOSH and A.K.CHATTERJEE - Inde

27 - *Modification of clinker phase composition and strength properties of a high - alkali cement clinker by gypsum addition.* R.J.SLOTA and A.LEWANDOWSKA-KANAS - Poland

28 - *The synthesis and crystal structure of a new compound $Ca_8Mg(SiO_4)_4Cl_2$.* Ye. RUILUN, Wu. BOLIN and Wang XINRONG - China

29 - *A very modified apatite-type structure. $K_3Ca_2(SO_4)_3F$.* M.PÉREZ-MÉNDEZ and J.FAYOS - Spain

30 - *Influence of fluorides and silico-fluorides on the hydration of cement.* Z.SAUMAN - Czechoslovakia.

PAULO RODRIGUES - Associação Brasileira de Cimento Portland

SUB-THEME 1.3 - LOW ENERGY CLINKER FORMATION

1 INTRODUCTION

The reduction in energy consumption on clinker manufacture has been taken into account in many aspects, such as changes in industrial process and modification or distortion in the microstructure.

In the papers received concerning the sub-theme 1.3, tendency in emphasizing clinker alinitic and belitic cements was verified.

Secondly, the reexamination of intermediate phases, influence of mineralizers, and modification in raw meals composition were the themes of major authors interest.

It was received 14 research works, being(2) from China, (6) from URSS, (2) from India, (1) from France and (3) from Germany.

The research works were classified in three groups.

Group 1: - Mineralizers utilization

Group 2: - Composition and raw meal modifications

Group 3: - Formation kinetics

2 GROUP 1: MINERALIZERS UTILIZATION

2.1 CHLORIDE SALTS AS REACTION MEDIUM FOR LOW TEMPERATURE CLINKERISATION - A PROBE INTO ALINITE TECHNOLOGY

R.K. Agarwal, S.V.Paralkar and A.K.Chatterjee

The authors compare the morphologic and microstructural characteristics of alinitic clinkers with ordinary portland clinkers.In order to analyse the reactions that occur at various temperatures from 150°C to 1400°C , experiments were made with additions of $CaCl_2$.

The authors tried additions of magnesium salts and non-calcium chloride salts in combination with $CaCl_2$.

It was observed that magnesium salts, irrespective of their froms, when mixed with $CaCl_2$ are more effective as a mineralizer than $CaCl_2$ alone.

It was also observed that $MgCO_3$ and $MgCl_2$ are equally effective in lowering the decarbonation temperature.

The authors concluded that clinkerisation is possible at temperatures lower than 1200°C with the utilization of chloride salts as a reaction medium. The formation temperature of alinite phase seems to be around 900°C under optimum conditions, the phase can be stable up to 1150°C and the clinkers are characterized by the presence of chloride in fixed and free forms.

Moreover the presence of chloride was observed in silicate and aluminate phases.

2.2 SYNTHESIS OF CALCIUM SILICATES AT LOW TEMPERATURES AND INFLUENCES ON THEIR REACTIVITY

D. Bürger and U. Ludwig

The paper shows some results obtained from C_3S and alite production at temperature range of 1150°C - 1350°C and measurements of hydration processes of these synthetics.

The authors obtained correlations among crystal symmetry, burning reactivity, microstructural development dependent on burning conditions and the hydraulic reactivity of the tricalcium silicates with and without additional agents.

The synthetics were obtained by burning pure chemical products and their characterization was realized in the following aspects:

- Microstructure and morphology by means of SEM
- Hydraulic reactivity by means of conduction calorimeter traces (heat liberation) and quantitative X-ray analysis to determine the unreacted C_3S residue.

Other properties were investigated, such as:

- Rheological properties
- Compressive strenght
- Studies of the hydrated phases

Studies on CaF_2 and ZnO influence demonstrated that the temperature decreasing on the formation of the synthetics is correlated with the increasing of the symmetrical properties.

The authors concluded that it is possible to reduce the burning temperature on the synthesis of the calcium silicates and , the economy saving grinding energy, [illegible]

activity or even to increase it.

The use of mineralizers allows the synthesis of alites at 1150°C with CaF_2 and 1250°C with ZnO.

2.3 LOW TEMPERATURE SYNTHESIS OF BELITE REACTIVITY

C. Vernet

By activation with $Ca(NO_3)_2$ and $CaCl_2$, the author produced C_2S at low temperatures.

This research work shows the mechanisms that can conduct to a network distortion at low temperature and so obtain good reactivity.

The studies on the reactivity were performed with the products obtained from pure and impure raw meals.

The author concluded that the multiplicity of melted salts, enclose a very promising investigation field on the synthesis of hydraulic materials at low temperatures.

The study on belite allowed to delimit three temperature ranges where the characteristics of crystallinity and reactivity were differents.

2.4 RESEARCH ON AN EARLY STRENGTH CEMENT CONTAINING HIGH CONTENT OF IRON

Feng Xiuji
Zhu Yufeng

The authors discuss the characteristics of C_4AF, pointing out the possibility of attainning a cement with high early strength from clinker with high content of ferrite phase.

The clinker of such cement besides the high early strength is produced at lower temperatures.

3 GROUP 2: COMPOSITION AND RAW MEAL MODIFICATIONS

3.1 INVESTIGATIONS ON THE PRODUCTION OF LOW LIME PORTLAND CEMENTS

U. Ludwig and R. Pöhlmann

The paper is a review on clinker burning behaviour and clinker reactivity produced with natural raw mixes, with or without sintering admixtures, having their compositions in the range of k = 75 to k = 99.

The experiments were made with the use of the following sintering agents: MgO, SO_3, ZnO, CaF_2 and their combinations.

Based on the results, the authors discussed the theoretical concepts about the mineralizers effect on clinker formation and properties.

From burning investigations it can be detached:

- Favourable influences of CaF_2 and ZnO additions in raw mixes high and low lime standards.
- Porosity and densification of the clinker produced at lower temperatures and influency on grindability.
- Studies on burning temperatures as a function of lime standard and sintering agents.
- Favourable influence of liquid phase on formation of clinker using a higher content of MgO.

Tests made with clinker, produced in laboratory kiln, in order to verify the reactivity showed the following:

- Phase composition and its properties in relation to the lime standard.
- Grindability index of clinkers as a function of burning degree and lime standard.
- Compressive strength development as a function of lime standards.
- Compressive strength development as a function of fine-grinding and burning conditions.
- Compressive strength of portland cement mortars made from clinkers with different lime standards as a function of the burning degree and of a "mineralization".

3.2 CLINKERISATION WITH LOW ENERGY CONSUMPTION DURING THE BURNING OF RAW MIXES CONTAINING NOT GROUND SLAG

N.M. Javoronkov
O.P. Mtchedlov - Petrossian
N.P. Kogan
A.I. Zdorov
Y.G. Ientch

The paper relates a theoretical study on the amount of energy, necessary to attain the clinkerisation by the use of metallurgical slags, compared to the amount needed to produce clinkers having clay as raw meal.

To reach this objective the authors established new coefficients, so energetic estimative can be obtained when such metallurgical slags are used.

According to the authors, the calculations showed that the theoretical energy consumption on the clinker formation where metallurgic slags are used, can be fixed at 1061kj/kg.Cℓ.

3.3 STUDY ON LOW BASICITY CLINKERS

L.G. Soudakas
U.V. Nikiforov
M.V. Kougia
N.A. Sokolova

The paper deals with the reducing of energy consumption by decreasing clinker basicity.

Results on laboratory and semi-industrial researches with clinkers, with KS in the range of 0,76-0,90 and invariable silica and alumina modulus, showed to be possible to save about 8%-12% in the clinkerisation heat.

The authors have syntherized 39 raw mixes and the obtained clinkers were cooled by two ways: rapid and slow.

With the X-ray and microscopic analysis of the clinkers the authors concluded:

- The samples burnt in laboratory and cooled rapidly exhibited the belite in the α'form, while the samples cooled slowly showed the β form.
- In spite of the rapid cooling, in the clinkers obtained by semi-industrial experiments, several samples did not present the $\alpha'C_2S$, although they showed high hydraulic activity.

The clinkers obtained by semi-industrial experiments, having the same phase compostion, but differing on its microstructure, showed different chemical activity during interaction with water, causing differences in compressive strenghts at 28 days.

3.4 MICROSTRUCTURE AN SOLID SOLUTIONS OF LOW TEMPERATURE CLINKERS

S.N. Ghosh
V.K. Mathur
A.K. Parashar

The paper refers to the production of clinker in laboratory furnace and pilot plant using marginal grad plant raw materials, at temperatures lower than ordinary clinker.

With the electronic microscopy SEM-EDXA and tests on compressive strength performed on clinker, the authors concluded that reactive belite cement and low temperature alitic cement, prepared in the laboratory and in the pilot plants have irregular morphology leading to early development of strength.

4 GROUP 3: FORMATION KINETICS

4.1 PHYSICOCHEMICAL ASPECTS ON CHLOROSILICATES CRYSTALLIZATION DURING THE CLINKERISATION AT LOW TEMPERATURES IN SALINE MELT

B.I. Nouldelman
A.J. Gadaev

The research work explains the formation kinetic mechanisms of alinitic clinkers minerals.

The authors found out that the "gas-liquid-solid" interphases play an important role on the mineral formation processes.

Two mechanisms of chlorosilicates crystallization were pointed out. One is associated (to properties of the interphases), and the other with volumetric properties of liquid phase.

It was also verified the presence of two kinds of liquid phase, which are responsible for the formation of a thin superficial layer that activates the crystal formation of chlorinated minerals. This reveals the necessity of creating a well developed interphase in order to obtain high kinetic parameters on formation of alinitic clinker minerals.

4.2 FORMATION, CRYSTAL CHEMISTRY AND PROPERTIES OF ALINITE AND JASMUNDITE

M.Y. Bikbaou

The paper reports the studies on general mechanisms of mineral formation in chloride and sulphide clinker systems, more specifically the formation of high-basicity silicates, alinite and jasmundite.

Studying the crystallization mechanisms of this silicates prepared from pure products, the author concluded:

- The crystallization raté for alinite and jasmundite is 7-8 times greater than that of C_3S, in spite of lowering the synthesis temperature by 300k-400k.
- The activation energies of formation is 83kJ/mol for alinite and 114kJ/mol in the temperature range 1670k-1770k.
- Alinite does not crystallize is a saline melt of calcium chloride, as it was supposed before, but rather in a silicate melt containing some dissolved chloride.
- Jasmundite also crystallizes in a silicate melt containing sulphur as sulphide.

Analysing the F, Cℓ and S effects on the properties of silicate melts, the author concluded that there is a decrease in the formation temperature of the melt, a decrease in its viscosity and surface tension; another effect is an acceleration of the ion exchange processes in the melts, and a more intense solidification of minerals.

Finally, the author presents comparative studies among the hydration of alinite, C_3S and jasmundite, concluding that alinite presents higher hydration rate due to the presence of chloride on its crystal lattice, while the presence of sulphur in the crystal lattice of jasmundite causes a radical reduction in the hydration rate.

4.3 AN INVESTIGATION INTO CEMENT $CaO-SiO_2-A\ell_2O_3-Fe_2O_3-SO_3$ SYSTEM

Wang Yanmou
Deng Jun'An
Su Muzhen

Showing the production of ferroaluminate cement clinkers with $C_4A_3\bar{S}$, C_2S and C_4AF as their main components and the hydration of respective cements, the authors point out the low energy consumption and the higher cement properties.

To obtain the cement clinker ferroaluminate, experiments were made by using pure chemical products and natural raw meals.

Detailed studies on formation of intermediate phases in the $C-A-F-\bar{S}$, $C-A-S-\bar{S}$ and $C-S-A-F-\bar{S}$ systems are presented along with studies on burning phenomena.

With the XRD, DTA, high temperature XRD and SEM-EDAX techniques, the authors studied the phases characterization of clinkers burnt at different temperatures.

The performance tests made on the produced cements, showed that the ferroaluminate

cements exhibit the properties of high early strength, constant increase of strength in frost resistance and excellent impermeability.

The authors conclude that besides the higher properties, the ferroaluminate clinker cements, are produced with low energy consumption. The clinkerisation temperature is low (1250°C), the grindability is high and the content of limestone in its raw meal is much lower than that in the raw meal of ordinary portland cement.

4.4 ALITESULFOALUMINATE CLINKER: PRODUCTION AND PROPERTIES

V.B. Khlousov

The paper presents the simultaneous attainment of alite and sulphoaluminate by the creation of adequate conditions to earlier formation of liquid phase which high reactivity, assuring by this way, the alite formation at lower temperatures.

The sulphoaluminate formation is assured by adjusting raw meal composition wich must contain sufficient amount of $A\ell_2O_3$ and $CaSO_4$.

To obtain the alitesulphoaluminate clinkers, raw mixes were partially prepared from natural raw meals, and partially from industrial wastes rich in $A\ell_2O_3$ and containing fusing materials.

Studying phase formation kinetics, composition and properties of alitesulphoaluminate cements produced in industrial kiln, the author concluded:

- The clinker composition is: alite (C_3S), belite (βC_2S), calcium sulphoaluminate ($C_4A_3\overline{S}$) calcium aluminate |wich depends on raw mixes basicity ($C_{12}A_7$, C_3A)|, calcium ferroaluminate (C_4AF), calcium suphate ($C\overline{S}$) and gehlenite (C_2AS).
- By the intensification of clinkering process it is possible to lower the burning temperature to 1250-1350°C, reducing energy consumption in about 18% and increasing kiln capacity in 27%.
- Sulphoaluminate cements present quick hardening and high compressive strength.

4.5 CONDITIONS OF THE EXISTENCE OF HYDRAULICALLY ACTIVE BELITE CEMENT

J. Stark
A. Müller
R. Seydel
K. Jost

The paper relates the laboratory and pilot plant experiments with the active belite cements, evidencing the studies about the phase composition related do KS and the rate of cooling.

Through the laboratory tests and verifications the authors concluded:

- By thermal and chemical activation, the belite is high influenced so, because of its strength and other structural properties it becomes similar to an ordinary portland cement.
- The cooling is the most important factor for the hydraulic activity where under conditions of rapid cooling, about 727°C/min and cooling temperature range, from 1300°C to 900°C, an active belite clinker can be produced with sufficient early strength, and good strength after 28 days.

The active belite cement allows the production of ordinary portland cement with a specific heat consumption of 320kJ/kg.Cℓ.

4.6 TECHNOLOGICAL ASPECTS OF STRUCTURE REPLICATION IN SILICATES

G.I. Ovcharenko

The paper presents results on studies about structure replication in silicate reactions.

The author studied the interference of sintering agents (on production of binding materials) by melting and sintering.

A crystal chemical model and mechanisms for belit stabilization by lime are given.

YASUKO TEZUKA - Associação Brasileira de Cimento Portland

COMMUNICATION REPORT ON SUB-THEME 2.1 - *PHYSICAL CHEMISTRY OF HYDRATION PROCESS - INFLUENCE OF MINOR COMPONENTS AND ADMIXTURES.*
Group a

1 INTRODUCTION

The 52 basic reports on sub-theme 2.1 - *Physical chemistry of hydration process - Influence of minor components and admixtures* have been broken down into four groups.

a - Hydration of portland cement and individual clinker minerals with admixtures - 18 communications.

b - Hydration of portland cement - 17 communications

c - Hydration of individual clinker minerals - 13 communications

d - Hydration of cement-solid solutions - 4 communications.

2 HYDRATION OF PORTLAND CEMENT AND CLINKER MINERALS WITH ADMIXTURES

The contributions to this topic come from Italy (3), Poland (2), Czechoslovakia (2), China, Belgium Korea, Japan, U.S.A., France, U.R.R.S., Spain, Scotland, Rumania and India (one each).

There seems to be general agreement that, even small additions of inorganic or organic admixtures can change the course of the hydration reaction of portland cement and clinker minerals.

This subject was subdivided into the following three items:

- Inorganic admixtures
- Organic admixtures
- Experimental techniques.

3 INORGANIC ADMIXTURES

The six papers on the influence of the inorganic admixtures on the hydration of portland cement and minerals are as follows:

3.1 *Induction period in calcium silicate hydration in the light of some new experimental results.* W. Kurdowski, W.Nocun Wczelik, K. Miskiewicz, J. Szuba - Poland.

3.2 -Ca_3SiO_4 *hydration in the presence of electrolytes.* M. Gawlicki, W. Nocun Wczelik - Poland.

3.3 *Accelerating effect of chloride salts on the hydration of portland cement.* Guo Chengju - China.

3.4 *Mécanisme réactionnel et cinétique de l'hydratation du silicate tricalcique en présence de chlorure de calcium.* P.Fierens, Y. Kabuema, J. Orszagh, N. Tenoutasse , J. Terloco - Belgium.

3.5 *Extension of setting time by means of mineralized clinkers.* J. R. Baragano , G. Campos - Spain.

3.6 *Alliage d'hydrolicite des ciments* A.M. Dmitriev, A.K. Zapolszky, T.V. Kouznetzova, B.E. Yudovitch, I. D. Ponomarev - U.R.S.S.

Kurdowski and co-worker[3.1], using microcalorimetry, Q x RD and DTA, studied the early stages of the C_3S and $C_2S.CaCl_2$ hydration process in order to elucidate which of the following phenomena is the main factor responsible for the retardation of the process in the induction period

- calcium silicate hydrate nucleation;
- calcium hydroxide or basic calcium chloride nucleation;
- liquid phase supersaturation with Ca^{2+} or other ions in relation to hydration products.

They found that in the hydration process of C_3S and $C_2S.CaCl_2$ with some admixtures acting as Ca^{2+} binding agents, i.e. CH, C-S-H and SiO_2, the liquid phase plays a decisive role as a rate controlling factor acting either directly and indirectly.

This means that the nucleation process is not the decisive factor hindering the reaction in the induction period. The above mentioned admixtures can act as a nucleation barrier eliminating agent but in general they change the reaction in the liquid phase.

When a high amount of SiO_2 or a C-S-H phase is introduced into the hydrating C_3S-H_2O mixture, the complete disappearence of the induction period is observed.

The active silica is the best acceleration as it ensures relatively fast Ca^{2+} ion combination and considerable Ca^{2+} ion supersaturation decrease with a simultaneous C-S-H phase formation.

Jawlicki and Nocun-Wczelik[3.2] investigated the influence of the K_2SO_4, Na_2SO_4, K_2CO_3 and Na_2CO_3 on the hydration of $\beta-C_2S$ at room temperature, in water, and water/solid ratio equal to 50.

They showed that the sodium salts act more strongly than potassium salts, especially at the beginning of the reaction and that the carbonates are better $\beta-C_2S$ hydration accelerators than sulphates. 2% Na_2CO_3 additions rises the degree of $\beta-C_2S$ hydration from about 40% to 80% after 24 hours.

The liquid phase analysis indicated that K_2SO_4 and Na_2SO_4 addition facilitates the calcium and silica leaching into the solutions. Therefore the liquid phase supersaturation occurs earlier than in a suspension without any admixture.

According to Guo Chengju[3.3], the dissolution, diffusion and crystallization of calcium hydroxide are markedly intensified by the calcium chloride, presumably because of the formation of calcium oxychloride.

When cement grains are introduced into the $CaCl_2$ solution, the CH dissolves more rapidly than in pure water, forming a complex solution, which contains less discrete CH than an ordinary saturated or supersaturated CH solution. The dissolved lime bearing substance, probable a basic calcium chloride diffuses far away from the reaction site and crystallize, both at intensified rates. The resulting solid may be either portlandite or calcium oxychloride, depending on the $CaCl_2$ concentration in the pore liquid.

The calcium oxychloride is a metastable phase, which can stand in equilibrium with a solution containing 15-30 parts of $CaCl_2$ in 100 parts of water. In a higher or lower $CaCl_2$ concentration, it decomposes.

Chengju concluded that the role of $CaCl_2$ in accelerating the hydration of portland cement is that of a catalyzer with the oxychloride produced acting as the intermediate product.

Fierens et al.[3.4] reported that the kinetics of C_3S hydration with $CaCl_2$ comply with the Avrami and Jander laws and that the effect

of $CaCl_2$ is expressed by the reduction of the induction period and acceleration of reaction rate.

In the communication[3.5] by Baragans and Campos it is shown that certain minor elements, as components of raw meals may influence the hydration processes and change the setting and hardening of cement pastes.

In the raw meals contained P_2O_5, the setting time become longer with percentages from 0.4% P_2O_5 and increased accordingly on that basis. With 1% P_2O_5, the free lime content decreases, setting times being maintained without any remarkable variation.

Mechanical strengths with 0.4% P_2O_5 increased after 3 days and are greater at 28 days, while with 1% P_2O_5 the strengths are lower up to 7 days, although at 28 days they exceed those of the initial clinker.

The raw meals containing fluorites expressed as F^- ranging from 0.12% to 0.62% showed that free lime decreases according to the greater F^- content, as the setting lengthens. It was observed that when F^- increases, not only the initial setting is lengthened, but also the interval between the initial and the final setting increases.

It was reported that while in the clinker without F^-, the C_3A is in the cubic form, the tetragonal form increasing according to the F^- percentage and the possible presence of $C_{11}A_7CaF_2$ also being detected, which would explain the lengthening of the setting time.

4 ORGANIC ADMIXTURES

There are nine communications on this item, as can see from the following list:

4.1 *Interpretation of the effects of retarding admixtures on pastes of C_3S, C_3A plus gypsum and portland cement.* H.M. Jennings, H. Taleb, G. Frohnsdorff and J. R. Clifton - U.S.A.

4.2 *Retardation of portland cement hydration by citric acid.* N.B. Singh, A.K. Singh and S.P. Singh - India.

4.3 *Effect of alkali content in clinker on the cement hydration with and without sodium gluconate.* G. Moriconi, S. Monosi, M.Pauri and M. Collepardi - Italy.

4.4 *Effect of retarding admixtures on the portland cement hydration.* S. Monosi, G. Moriconi, M. Pauri and M. Collepardi - Italy.

4.5 *Effect of calcium lignosulfonate on the early hydration process of portland cement.* J.Y. Moon, K. S. Han and S.H. Choi - Korea.

4.6 *Effect of triethanolamine on the tricalcium silicate hydration.* M. Pauri, S. Monosi, G. Moriconi and M. Collepardi - Italy.

4.7 *Hardening processes in some C_4AF - additives - water systems.* I. Teoreanu , A. Puri and M. Georgescu - Rumania.

4.8 *Adsorption of superplasticizers on C-S-H(I) and ettringite.* Y. Fukaya and K. Kato - Japan.

4.9 *Effects of molar parameters of sulphonated melamina and formaldehyde polycondensates on mortar properties.* T. Sebok - Czechoslovakia.

In the communication[4.1] by Jennings et al. it is reported that during the short initial period of rapid reaction and in the induction period, the cement paste is plastic, while after the induction period the reaction accelerates and the paste begins to stiffen.

The length of the induction period and the *time of set* is influenced by organic retarders. According to the authors, the reactions between cement and water which end the induction period could occur in any of three positions:

a - on the surface of the anhydrous material or of the hydration product;

b - in the aqueous phase; and

c - in the hydration product.

Although retarders are normally added to the aqueous phase, they could influence reactions in the other two positions by adsorption onto a surface or incorporation into a product.

Studing the effects of the retarders on pastes of C_3S and of C_3A - gypsum systems , they concluded that the two systems have different, possibly independent, influences on the concentrations of retarders in the aqueous phase of a portland cement paste.

In the case of C_3S, some of the retarder is incorporated into the layer of the product which forms around the grains during the early stages of reaction. It appears that a process which controls the induction period occurs within this C-S-H layer and that the incorporation of a retarder somehow slows the process.

The C_3A - gypsum - water system removes a large amount of retarder from the aqueous phase during the early stages of hydration, with the rate of removal falling with time.

It seems probable that, at least for some organic retarders, the effects on the portland cement reaction may be considered to be a combination of separate processes occuring in the C_3S - water and C_3A - gypsum - water systems.

Singh and co-workers[4.2] found that the hydration of both aluminate and alite in the presence of citric acid is retarded at all concentrations. The conversion of ettringite into monosulphate occurs before the hydration of alite. The amount of CH and its crystallinity and compactness is lowered by the addition of citric acid.

Sodium gluconate as a retarder was studied by Moriconi et al.[4.3] and Monosi et al.[4.4]

In communication (4.3) they reported that the addition of sodium gluconate significantly retarded both the ettringite production and the calcium silicates hydration for the three cements: an industrial clinker with 0.22% Na_2O and 0.54% K_2O, the same clinker heated in a laboratory in the presence of 1% Na_2CO_3 (Na_2 content became 0.56%) and the same clinker thermally treated in the absence of Na_2CO_3.

This retarding action was particularly effective in the case of the cement with the higher alkali content.

In the communication (4.4) the authors confirmed the retarding action of gluconate on portland cement.

The retarding effect was much more remarkable on ASTM type V portland cement with nil C_3A content. They also reported that the sodium lignosulfonate has negligible effects on the kinetics of cement hydration.

Moon and co-workers[4.5] also studied the influence of lignosulfonate salt on the early hydration of clinker minerals.

From the results of their experiments they suggested that the retardation in the hydration of clinker minerals when the calcium lignosulfonate is added is related to the amount of C_4AF and gypsum.

The hydration of C_3S in the C_3S-C_3A-C_4AF system varies considerably in accordance with the content of gypsum and lignosulfonate.

They found that the optimum content of SO_3 was 2.0% when 0.25% calcium lignosulfonate is added to portland cement while addition of 0.5% calcium lignosulfate requires 2.5% SO_3.

Pauri et al.[4.6] reported that triethanolamine (0.1%) slightly retarded the early hydration of C_3S paste during the first 6 hours. This retarding effect is almost eliminated when C_3S hydrates in the presence of C_3A or NC_3A and $C\bar{S}H_2$.

Addition of triethanolamine accelerates the early production of ettringite and its conversion into monosulfate. It seems that adsorption of triethanolamine by ettringite can remove them from the aqueous phase and reduce the retarding effect on the C_3S hydration.

Teoreanu et al.[4.7] showed that the addition of an industrial product containing mostly dimethylterephtalate into the C_4AF - $C\bar{S}H_2$ - water system roused moderate retarding effect but did not essentially affect the kinetics of the hydration, conversion processes and the relative amounts of phases formed. The presence of the admixture determined a finer grain size of the hydrated compounds associated with the formation of a compact microcrystalline hardening structure which determines the development of high mechanical strengths.

Fukaya and Kato[4.8] studied the adsorption behaviour of β-naphthalene sulfonate formaldehyde condensates (NSF) on ettringite and C-S-H by use of the acidity or basicity of the solid surface as an index of the surface characteristics of hydrates.

The adsorption of an admixture is considered to have a deep relationship with the crystalline structure or surface characteristics of the hydrate as well as the molecular structure of the admixture. From the relationship between the surface basicity of the hydrates and the amount of adsorption, they found that NSF is adsorbed on the surface of the hydrate in flat form. Also, the NSF is adsorbed on C-S-H (I) in a monolayer while ettringite forms multilayers.

As a result of the study of the effect of various ions coexisting with an admixture in liquid phase, they showed that Na^+ or K^+ ion does not adsorb on ettringite but on C-S-H (I).

The adsorption of these cations did not affect the amount of adsorption of the admixture. On the other hand, they found that Ca^{2+} ion adsorb on either C-S-H (I) or ettringite, and that Ca^{2+} ion has a direct effect on the adsorption mechanism of an admixture.

Sebok[4.9] reported that the efficiency of sulfonated melamine and formaldehyde polycondensates on the rheological properties of cement mortars as well as on the strength after 28 days depend on their molar parameters mainly on the molar weight (M_w) and polydispersity (R_p). He found that the sulfonated melamine and formaldehyde polycondensates slow down hydration of C_3A to a significant extent but their influence on the kinetics of C_3S and β-C_2S hydration is smaller.

5 EXPERIMENTAL TECHNIQUES

Three communications concerning the experimental methods that might provide additional insight into the physico-chemical processes occuring during early hydration of cement paste with admixtures are presented at this Congress.

5.1 *Monitoring the influence of admixtures and composition on the early hydration*

characteristics of cement paste using a.c. electrical response techniques. A.B. Afshar and W.J. McCarter - Scotland.

5.2 *Mécanisme d'action des fluidifiants étudié par RMN du proton.* M. Letellier, H. Van Damme, B. Mortureux, M. Regourd - France.

5.3 *Influence of temperature and admixtures on the C_3S and cement hydration investigated by radiometric emanation method.* V. Balek, J. Kriz, J. Dohnálek - Czechoslovakia.

Afshar and McCarter[5.1] reported that they have developed an a.c. electrical method for monitoring hydration processes by measuring the changes in electrical response during the initial 24 hours after gauging cement with water. In essence, the technique entails accurately monitoring the variation in electrical resistivity and dielectric constant value of the paste.

The initial stages of hydration are characterised by a relatively high dielectric constant value and a low resistivity value, caused by high ionic concentrations, particularly Ca^{2+} and OH^- ions leached from the cement grains. There is a small drop in dielectric value over the initial 30 minutes.

The induction period is terminated by a rapid rise in dielectric value. The sudden drop in dielectric value coincides with the rise in resistivity value and a general increase in rigidity of the mix due to the formation of CH and more stable C-S-H hydrates. The authors postulated that the dielectric constant value and resistivity curves are better indicators of the hydration characteristics during the early hydration of cement of various chemical compositions.

They also concluded that the influence of admixtures on the hydrolysis and hydration processes can be quantified and a required percentage of admixtures for a given setting time can be calculated.

Letellier et al.[5.2] showed that the nuclear magnetic resonance (NMR) is a suitable technique for studying the hidration of cement pastes.

They pointed out that in the hydration of C_3S, the proton relaxation spin-lattice T_1 variation was linear up to about 10 hours and permitted the observation of hydrated surface development.

The interpretation of C_3A hydration seems difficult and is very dependent on the water/solid ratio. In the C_3S-C_3A system the proton relaxation times were essentially influenced by C_3A, and the introduction of the plasticizer into the system, for a same water/solid ratio did not change the average proton relaxation times but the initial reaction was lengthened as the C_3A was reduced.

Balek et al.[5.3] studying the hydration processes, especially those taking place during the early hydration stage, proved that the radiometric emanation method (REM) enabled the investigation of the kinetics of early hydration of C_3S and cement as influenced by temperatures and various admixtures.

The radiometric emanation method is based on the measurement of the radon released from samples, previously labelled by its parent isotopes (Th - 228 and Ra - 224).

They also reported that the experimental results of REM agree fairly well with the theoretical curves obtained by computer simulation on the basis of the theoretical model.

ALAOR FERREIRA - CIMBAGÉ - Cimento e Mineração Bagé S/A

COMMUNICATION REPORT ON SUB-THEME 2.1 - PHYSICAL-CHEMISTRY OF HYDRATION PROCESS - INFLUENCE OF MINOR COMPONENTS AND ADMIXTURES
Group - b

2.1.b The following papers were received for comments:

b.1 Computation of solubility relationships for hydrating cement systems. E. GARTNER, J.P. SKALNY (U.S.A.).

b.2 Conduction calorimetry and hydration kinetics - A thermodynamical and analytical approach of the interactive bahaviour of cements. C. VERNET (France).

b.3 Monitoring chemic-physical changes and microestructure development in OPC during early hydration. W.J. McCARTER, A.B. AFSHAR (Scotland, U.K.).

b.4 Sequence and kinetics of hydration reactions of C_3A with gypsum, lime and calcareous fillers. C. VERNET (France).

b.5 Phénomènes électrochimiques intervenant aux premiers stades d'hydratation et de formation de la structures des pâtes de ciment. A. KOCHMAI, O. P. MITCHEDLOV - PETROSSIAN (U.S.S.R.).

b.6 Hydration study of pure phases of cement and synthetic mixtures by microwave dielectric relaxation. F. HENRY, P. BAILLEUL, B. COURTAULT (France).

b.7 Cement hydratation control. M. M. SYCHEV (U.S.S.R.).

b.8 Étude de la cinétique de l'hydratation du ciment portland par la serie de méthodes nucleaires. E. I. FEDIN, T. V. KOUZNETSOVA, A. V. NEKHOROCHEV, M. A. SOROTSHKIN, A. L. BLUMENFEL'D, A. B. KOUDRIAVTSEV, G. AKIMOV (U.S.S.R.).

b.9 The role of kinetic parameters on the properties of hydrating cement paste. V. MLAKAR (Yugoslavia).

b.10 Rôle des processus de la polycondensation au cours du durcissement d'hydratation des liants siliceux. E. D. CHOUKIN, E. P. ANDREEVA, S. I. KONTOROVITSH, E. A. ALMELINA (U.S.S.R.).

b.11 Certaines nouvelles conceptions sur le mécanisme d'hydratation des liants. A. POLAK (U.S.S.R.).

b.12 Effect of carbonates on early stage of hydration of alite. H. USHIYAMA, Y. KAWANO, N. KAMEGAI (Japan).

b.13 Early hydration of alite at low water to powder ratio. I. MINO, F. FUSHII, E. SAKAI (Japan).

b.14 Vanadium pentoxide effect of cement hydration. L. CUSSINO, L. MONTANARO, A. NEGRO (Italy).

b.15 On the use of limestone to control cement setting. A. NEGRO, G. ABBIATI, L. CUSSINO (Italy).

b.16 Classification des processus de durcissement des liants. O. P. MITCHEDLOV - PETROSSIAN, A. V. OUCHEROY - MARCHARK (U.S.S.R.)

b.17 Cement hydration under partially saturated curing conditions. L.J. PAROTT, D. C. KILLOH, R. G. PATEL (England, U.K.).

i - Chemical reactivity could be handled considering two general aspects: velocity of reactions, (kinetic treatment) and extension of the reactions (thermodynamical treatment).

The velocity of a reaction is controled by the activation energy and by many factors such as temperature, pressure, concentration and catalyst which affect the activation energy therefore will change the velocity of the reaction.

On the other hand, the extension of a reaction is also controled by the system capacity of producing work that is the free energy.

Free energy describes the balance between energy change (entalpy) and entropy change (organization energy).

As a constant temperature, a system tends

to undergo a reaction so that in its final state it has lower energy and higher entropy than in its initial state.

ii - Most of the received communications have handled on hydration reaction concerning kinetics.

iii - GARTNER and Other (b.1) in their paper have written:

Because of limited experimental data, the approach taken in this paper deals only with a few selected aspects of the problem. We will come suggestions by others as to how to extend this approach and improve it.

The lack of comprehensive phase equilibrium data for the cement water system is noted, and further work in this area recommended.

We would like to propose that, in the coming years, a concentrated worldwide emphasis be put on phase equilibrium studies, and that the results of such studies be handled in a special session of the 9th International Symposium on the Chemistry of Cements.

iv - C. VERNET (b.2) in his paper said that:

The possibility of measuring the extension of the reaction of others phases led us into one of the most interesting observation. It seems that during the 3rd period of hydration, all reactions have increased its activities, particularly that of alite dissolution. The extension of oversatured lime is increased and this means that the released energy contributes the equilibrium displacement.

v - On the other hand, POLAK (b.11) in his paper pointed out:

The studies of the last years developped by many authors by means of electronic microscopy and X-rays analyses showed in a apparent manner that following the hydration of initial phases of the binders (PI) - x, there is the formation of one intermediary phase - primary hydrate (HP) - y and then one stable phase - secondary hydrate (HS) - z. Such developing formation process x → y → z needs that positive ratios of chemical potentials according Ostwald ($ux > uy > uz$) and the dissolved phases ($Cx^{\infty} > Cy^{\infty} > Cz^{\infty}$) respectively must be established.

vi - Concerning the several periods of the hydration reaction in general all authors agree. So that C. VERNET (b.2) in his paper points out four periods:

I - Initial period, with fast reaction and high thermic flux.

II - Dormant period, with very weak thermic flux, very slow reaction, during that the solution is saturated in lime.

III - Setting period, starting with the portlandite precipitation ($_2$) $Ca^{2+} + 2\overline{OH} \rightarrow Ca(OH)_2$, with the acceleration of the reaction (I) and the appearance of a second peak of thermic flux.

IV - Period of decreasing activity, concerning the C_3S consumption and the thickening of the hydrate layers.

vii - McCARTER and Other (b.3) in their paper only changed the name of the second period; then it was named induction period.

viii- A. KOCHMAI and Others (b.5) in their paper added one more period that is period of formation of the structure of hardened cement concerning further formation of CSH phases and to the initial process of its polycondensation.

ix - A. VERNET (b.4) in his paper have considered also four periods for the hydration of C_3A as it was for the cement hydration. The fourth period is described as follows:

As soon as the C_3A is finished, only the reaction number (6) continues and the end products being ettringite and carbo-alumina

te.

x - Concerning hydration mechanisms at early ages it shall be emphasized:

xi - McCARTER and Other (b.3) in their paper described how they could correlate changes in conductivity and dielectric constant with hydration mechanisms by using scanning electron microscopy techniques and by application of AC electrical field to cement paste, measuring dielectric constant and resistivity changes.

Thus the authors have described the initial changes in electrical parameters (0 - 50 minutes) as the initial period of chemical activity. At intermediate frequencies (200 Hz - 2kHz) the gradual increase in dielectric constant up to 170 minutes would indicate an increase in charge to grain surfaces, possibly due to dissolution of the grain by imbibition of water through the gelatinous C-S-H coating formed on initial hydration. These changes should be attributed to the dormant stage. The authors have attributed the peak in dielectric constant at ≅ 200 minutes to renewed chemical activity on C_3S phase which leads to a rapid gain in rigidity of the paste. The period 170 - 500 minutes could be visualised as stage 3 of hydration process. The authors also ascribe the period form 500 minutes onwards as stage 4 of hydration process.

xii - HENRY and Others (b.6) have made hydration studies of puere phases and synthetic mixtures by microwave dielectric relaxation.

The used method differs from that of McCARTER because HENRY and Others used much higher frequency up to gigahertz whereas McCARTER and Other used up to 200 kHz frequency.

HENRY and Others have examined three hydration cases: C_3S hydration, C_3A hydration and mixture of 90% C_3S + 10% C_3A. They have concluded that in presence of lime formed by the C_3S hydrolises, the hydration of C_3A produced C_4AH_{13}. The response curves of permitivity (ε'/m) and dielectric loss give us an information on the beginning of the paste after 8h30 minutes. Adding 5% of gypsum to the mixture this time drops to 6 hours.

xiii- KOCHMAI and Others (b.5) have studied the interaction between the hydration and crystallization process and the electrochemical phenomena by examining the electrochemical cell Ag, AgCℓ, KCℓm_1/Cement Paste/ KCℓm_2, AgCℓ, Ag where m_1 e m_2 are the concentrations of KCℓ solutions.
They have measured σs (charge densities)

ρs (osmetic pressures)

ϕm (membrane potentials)

ϕtrm (transmembrane potentials)

through the hydration process and could conclude that the hydration process is running through five stages and the 5th one is the period of structure formation of the hardened cement associated to further formation and polycondensation process of CSH phases. This fact causes a reduction of CSH and starts the dropping of ρel and a reduction of ϕtrm.

xiv - VERNET and Others (b.2)

Studying the cement hydration they concluded:

a - the reactivity concept should be taken into account the interactions, that is, from one side the solid properties and from the other the environment conditions.

b - Each hydration period presents one phase with main reaction which is the fastest of the system. The other reactions do not have its initial development in a independent way; its activation energy changes and then its velocities increase as increasing the rate of the main reaction. This is the principal characteristic of the portland cement hydration; for this reason this subject shall be called: dynamic interactant environment.

c - Besides that, the kinetic behaviour of the cement depends on the interaction of its principal compounds, alite and C_3A.

We can say therefore that there is a real coupling between both phases.

xv - Concerning hydration mechanisms at late ages, the paper of MLAKAR (b.9), the paper of FEDIN et al. (b.8) and the paper of CHOUKIN and Others (b.10) shall be considered.

xvi - MLAKAR (b.9) has figured out the rate constants for the characteristic process of hydration: nucleation and growth of hydration products, phase-boundary interaction, and diffusion through growing hydration layer on a group of commercial cements and a synthetic one by adding alkali sulphates. The kinetic constants were obtained on the basis of kinetic study of alite hydration of these samples, using the method of kinetic parameter determination taking into account the α-t dependence and polydispersity of the examined systems.

xvii- FEDIN et al. (b.8) could determine the thickeness of the hydrated layers and the specific surface in the initial hydration stage. For that, they have used the time changes of spin-lattice relaxation as variation of the thin water layers.

By means of the magnetism it is possible to define the content of solid phase in water. After 24 hours, when the gel quantity is still low they discovered only traces of water in the solid phase; at the fourth day the water content independently of the water/solid ratios is 6.5 to 8% in weight; at 28th day the content increases to 8 - 9%.

For tobermorite gel quality parameter at all hardening ages the authors have taken the ratio between compression strength and hydration degree (R/γ). In presence of low values for the water/solid ratios the R/γ reachs its maximum value. This could be because the formation of the polyhydrated hydrosilicates at initial hydration stage as well as due to polymerization-recrystallization process ocurring intensively at older ages.

xviii - CHOUKIN and Others (b.10) have concluded:

During all period of silicates hydration in water and in calcium chloride solution, there is the formation of polycondensation process of siliceous ions. These processes are produced in such a manner that very soon there is the extration of the calcium hydrosilicates with low polycondensation degree ("n") corresponding n = 1 to 4. During the hydration process we observe an increase of the average value of "n" and of the fraction of high polymerization where the polycondensation degree is equal and higher than 6.5 ($Q_n \geqslant 6.5$) with a decrease of the low polymerization fraction.

xix - Concerning hydration Activation there are two important papers: M.M. SYCHEV's (b.7) and C. VERNET's (b.2).

xx - SYCHEV has pointed out:

Dissociative adsorption involved the following recombination processes

$$\overline{OH} + p^+ \rightarrow OH_{ad}$$
$$H_2O + e^- \rightarrow H_{ad} + OH^-$$
$$H_{ad} + OH_{ad} \rightleftarrows H_2O_{ad}$$

The latter is involved in the rupture of -Ca-O-Si≡ bonds, hydration surface of Ca^{++} ions, and release of these ions + into solution. Thus, the factors that increase the concentration of surface traps and free charge carriers will activate the process of cement setting. This statement is substantiated by correlation of free carrier concentration and length of induction period.

Electrolites can activate not only the surface of cement minerals, thus increasing the concentration of acceptor species, as for example in chromate ion absortion, but also the adhesive interactions of cementi-

tions phases with the structural materials.

By muclear gamma resonance studies of the behavior of oxidizing and reducing species added into the water of mixing SYCHEV could conclude that the activating effect of chromium ions is due to ionsorption, whereas that of manganese or tin compounds is due to oxidation-reduction properties. SYCHEV points out:

Thus, the presence of a solid, finely ground, acidic activator facilitates the appearance of nuclei of high-polymeric hydrosolicate phase-fibrous calcium silicate hydrates of morphological form which positively affects the kinetics of hydration and setting.

xxi - VERNET (b.2) in his paper has written:

The thermic activation is not only a phenomenon of mass heating, although it could be so, if the grains are close enough and therefore the heat transfer will be facilitated. In the case of pure pastes it will be possible to define a global activation energy for each hydration period where we have a process in the same chemical system.

The fineness of grinding is the predominant parameter for increasing the "coupling degree". It facilitates the thermic and ionic transfers. Since the hydration is a surface reaction, the dissolution ionic debits of the phases will be increased; in consequence it will result in higher extension of reactions and in higher velocity of reactions.

xxii - Concerning the hydrations and additives I have selected four papers:

xxiii - H. USHIYAMA and Others (b.12).

It shall be emphasized the conclusion of the authors:

(1) A small amount of carbonates or bicarbonates delays but a large amount accelerates the hydration.

(2) The difference of cation in carbonates or bicarbonates little causes the change of hydration rate.

(3) The degree of delay-effect addition of bicarbonates on hydration is larger than that of carbonates.

xxiv - I. MINO and Others (b.13)

The authors concluded:

The hydration ratio of cement was gradually decreased by the augmentation of packing fraction of particles. In DSP materials, cement particles act as strong internal filler and the source of $Ca(OH)_2$ supply. The total pore volumes of DSP are small and the pore sizes of DSP materials become small compared with conventional cement paste with the increase of packing fraction and the pozzolanic reaction of silica fume. Considering the reaction of cement and silica fume, the control of relation between the packing fraction and the hydrations of hydraulic materials appears to be very important in DSP materials.

xxv - CUSSINO and Others (b.14) have studied the influence of V_2O_5 on nine cements and have concluded:

1 - When V_2O_5 is dissolved into the clinker, mainly into belite, there was not significant changes either in setting or hardening of the cement.

2 - When V_2O_5 is simply added to the cement the settings change; for cement with additions up to 0.25% of V_2O_5 the setting increases as increasing the V_2O_5 content. For V_2O_5 bigger than 0.25% the setting decreases as increasing the V_2O_5 content.

The setting acceleration is due to the thickening of the paste without hydration advancing as it can be seen from calorimetric curves.

The setting delay is, probably due to the formation of calcium vanadate which covers

the cement grains and so hinders hydration.

xxvi - NEGRO and Others (b.15) have concluded:

It is possible to displace 50% of gypsum by limestone without compromissing the cement behaviour.

According to known data, there is a optimum gypsum/limestone ratio which determines the best performance of the cement.

Although the role of the limestone is sometimes limited as setting regulating device, always the limestone reacts with cement producing carbo-aluminate and so proceeding as an active compound of cement.

xxvii - Finally it shall be considered the paper of MITCHEDLOV and Others (b.16) concerning classification of the hardening process of the binders and that of PARROT and Others (b.17), cement hydration under partially saturated curing conditions.

xxviii - MITCHEDLOV and Others (b.16) have proposed to classify the hardening processes of the binders in three types:

a) The first type involves the rapid hardening processes of the most reactive binders: CaO, C_3A, C_4AF. These processes are running with the development of great amount of heat. The hydration induction period is lacking. The maximum hydration rate corresponds to the initial reaction ($\alpha \cong 0.05 - 0.1$).

b) The second type is characteristic for hardening of most of the binders. The accelerated and retarded induction periods are determined through the hydration. The duration of the changes which determine the amounts of heat liberation is not more than one day. The maximum value of hydration rate corresponds to $\alpha \cong 0.3 - 0.5$.

c) The extremely low rate of the reaction with considerable high duration (up to several months) is characteristic of binders like slags, glasses, ashes. In normal conditions the reactivity of those material is practily zero. The maximum reaction velocity and transformation extension correspond to a $\alpha \cong 0.6 - 0.8$.

xxix - PARROTT and Others (b.17) through their paper concluded:

- The results suggested that the rate of cement hydration was related to the amount of water in the layer capillaries rather than the amounts of water in the porous hydrate coatings that surround residual, unhydrated cement grains.
- The effects of relative humidity observed in this study are consistent with reported gradients of microstructure in drying, hydrated cement paste (1). Thus it may be concluded that the surface of prematurely dried concrete will have a low degree of reaction, a higher proportion of large diameter pores and will offer less protection to underlying concrete and any steel reinforcement.

RAPPORT DES COMMUNICATIONS DU SOUS-THÈME 2.1
GROUPE C - HYDRATATION DES CONSTITUANT DU CLINKER

RC
2.1

Les 13 Communications du groupe C ont les titres et auteurs suivants:

T. Mitsuda, S. Kobayakawa et H. Toraya
Caracterisation du C-S-H formé hydrothermiquement

- Il y a plusieurs façon d'obtenir le C-S-H au laboratoire. Les auteurs de la Communication C.1 font reagir l'acide silicique et la chaux aux temperatures superieures a 120°C jusqu'a 210°C. La relation Ca/Si a aussi variée de 0,4 a 3,0 (silicate tri-calcique). Les C-S-H formées se presentèrent sur differentes formes crystallines qui furent examinées en detail par TEM, DRX, IRS, DTA et TG et la superficié specifique par BET.

T. Hara, N. Inoue, H. Noma et T. Hosegawa
Formation et caracterization de la jennite

- Au moin, depuis 1966, d'après les auteurs, de la C.2 la formation de jennite ($Na_2O.8CaO.5SiO_2.11H_2O$) pendant l'hydratation des silicates, a interessé les scientistes. Dans cette Communications, les auteurs font une étude sur les conditions dans lesquelles se forme la jennite. Les auteurs ont montré que un melange de β-C_2S et fumée de silice, en certaines conditions, conduit à la formation de jennite après 91 jours de hydratation a 80°C.

D. Bertrandie et P. Barret
Etapes elementaires interfaciales de l'hydratation des aluminates de calcium, constituants des ciments.

- Malgré le titre de la C.3 en realité elle traite de l'hydration des aluminates et silicates de calcium aussi bien pour des ciments alumineux et ciments portland. Ils disent que "nous avons faite, dans le cas des silicates C_3S et C_2S, un exposé sur nos hypothèses, nos idées et leur rapport experimental et theorique en ce qui concerne les etapes elementaires de l'hydration des principaux aluminates de calcium utilisées dans le ciment". Ils acceptent un processus d'hydratation topochimique preliminaire suivi de la dissolution car "nous postulons l'existance d'une étape irreversible d'hydroxilation superficielle s'accompagnant d'un abaissement d'enthalpie libre susceptible d'expliquer la différence entre la solubilité theorique calculée et les valeurs limites des concentrations observées". Les detailles de l'hydration des silicates et aluminates sont presentées, suivant ses hypothèses, minutieusement.

P. Barret
Mecanisme de l'hydratation des silicates de calcium (C_3S, C_2S) constituant du ciment, vu à travers les concepts generaux de la reactivité des solides.

- La C.4 est bien relationé au travail com-

menté anterieurement de D. Bertrandie et P. Barret. P. Barret dans ce travail présénte encore plus de detailles, sur l'hydratation des silicates, et cherche à complementer et discuter celui que H.F.W. Taylor à presenté à la reunion du Commité 68 de la RILEM, sur formation d'une couche totalement protectrice du grain de ciment, admetant aussi l'existance d'un processus topochimique prealable.

P. W. Brown
Consequences de l'equilibre des phases dans l'hydratation du système C_3S-eau et C_3A-gypse-eau.

- L'auteur la C.5 examine en detail le mechanisme et la cinètique de l'hydratation du C_3S et du C_3A, en presence ou non du gypse, dans la periode de pre-induction de l'hydratation. En ce qui concerne l'hydratation du C_3S il trouve incertain son controle par la variation de la relation C/S. Avec l'aide du MEB il a observé le développement d'une couche de produits d'hydratation sans une forme definie, sur les cristaux de C_3S, pendant la periode de pre-induction. La periode d'induction commence quand la couche à terminé sa formation et finit quand la couche presente des transformations morphologiques avec l'apparition des cristaux en aigüilles de C-S-H. L'hydratation du C_3A est examiné en detail prenant attention à la solubilité du CaO et du Al_2O_3 à la periode de pre-induction, et avec le sulfate quand on etudie le systeme Al_2O_3-$CaSO_4$-H_2O. L'auteur examine les conditions pour la formation du gel AH_3 et a l'ettringite dans la periode de pre-induction.

K. Asaga, M. Daimon, S. Sibata, K. Kishi, K. Yano, P.R. Shrestha
Les effets de l'histoire thermique et des additifs sur l'hydratation du β-C_2S.

Les auteurs de la C.6 ont preparé le β-C_2S par melange de Ca CO_3 et SiO_2 dans la proportion de 2 de CaO et 1 de SiO_2. En suite, le melange est porté a 1.500°C, dans un creuset de platine, pendant 1 a 1,5 heures et refroidi a l'air: on a obtenu la γ-C_2S. Les auteur ont examiné l'influence de l'addition de Fe_2O_3, de Fe_2O_3 + K_2O et de B_2O_3, sur l'inversion β-$C_2S \rightarrow \gamma$ C_2S. Les recherches des auteurs, sur l'hydratation du β-C_2S ont montré que son hydratation est largement affectée par l'histoire thermique de sa preparation (1.000°C ou 1.500°C, par exemple).

Y. Nanru, Z. Baigian et W. Zhanwen
Un β-C_2S actif - Preparation et hydratation

- Les auteurs de la C.7 présentent l'étude de l'hydratation, de ses proprietés de resistances à compression d'un type de β-C_2S preparé à basse temperature, inferieur a 1.123°K. Il s'agit d'une recherche de laboratoire dans le même sens d'autres recherches pour obtenir un β-C_2S actif.
  C'est un minutieux travail de recherches utilisant les techniques modernes pour l'examen de l'evolution de l'hydratation, comme la trimetyl-sililation (TMS), DRX, IR, cromatografie, evolution thermique, et le microscope electronique à balayage.

N.J. Clayden, C.M. Dobson, C.W. Groves et S.A. Rodger
Application des methodes spectroscopique de la resonance magnetique nucleaire (RMN) dans l'état solide pour l'étude de l'hydratation du C_3S.

- Les auteurs de la C.8 ont utilisé l'essai par resonance magnetique necleaire pour l'étude des produits formé par l'hydratation d'un C_3S synthetic pendant les periodes de pre-induction, induction, post-induction accélerée et retardée. Dans la periode de pre-induction, l'indication, à la Fig. 1, du chaleur degagé est significativement petit a cause de l'additif. L'action des additifs comme le Ca Cl_2 et l'acide de maleic "n'ont pas presenté aucun effet

significatif dans la composition chimique ou à la structure du C-S-H. Le seul effet semble être dans la cinetique de l'hydratation". En accompagnant l'hydratation des silicates par RMN, les auteurs ont arrivé à de resultats sur la polymerisation de la silice semblables a ceux obtenus par trimethyl sililation (TMS).

A.R. Ramachandran et M.W. Grutzeck
Hydratation du C_3S a un pH fixé.

- Les auteurs de la C.9 presentent le résultat de la recherche sur l'hydration du C_3S preparé au laboratoire avec un melange de $CaCO_3$ et de la silice colloidale. L'objectif etait de verifier l'influence de la variation du pH (de 8 a 11,5) sur l'hydratation de C_3S en suspension, et à trois temperatures 10°, 25° et 40°C. La variation de la concentration du calcium et de silice en fonction du pH de 8, 10, 11, 11,5 et 12 à 25°C a demontré l'importance de la recherche. Le titre de ce travail ne traduit pas l'importance de la recherche presentée dans la C.10 sur les premiers pas de l'hydratation du C_3S, soit dans la periode de pre-induction et d'induction. Les auteurs ont examiné en detail le mecanisme de la formation initial du gel de silice, en quantifiant la variation de la concentration de calcium en fonction du pH de la solution cette variation conduit à la precipitation du C-S-H avec le pH de 11,5 a 12. Pour arriver a ces conclusions les auteurs ont etudié et discuté en detail la methode de synthese du C-S-H qui conduit à une hydration semblable à l'hydratation reel du C_3S du ciment portland.

Francisa Hannawaya.
Proprietés du C_4AF après 8 années d'hydratation

- L'auteur de la C.11 presente une recherche sur l'hydration du C_4AF synthetic pur et avec l'adition de gypse depuis le periode initial jusqu'a 8 ans. Le melange du CaO (en partant du $CaCO_3$ avec 96 - 98% de pureté), de l'hydroxide d'aluminium (gibbsite) et oxyde ferrique est porté à la temperature de 1.320°C pendant 2 a 3 heures. Le C_4AF en presence d'eau, s'hydrate rapidement et termine la reaction à 28 jours. Les phases crystallines sont: $C_4(A,F)H_n$, $C_3(A,F)H_6$, solutions solides entre les phases precedentes, phase amorphe d'hydroxyde de fer ou d'aluminium et hydroxyde de calcium. Le C_4AF en presence du gypse, s'hydrate plus lentement et donne lieu à la formation d'ettringite qui evolue en monosulfate. Après 8 ans le monosulfate $C_4(A,F)\overline{S}H_{18}$ presente, aux DRX, une plus forte intensité que le $C_4(A,F)\overline{S}H_{12}$.

S. Menosi et M. Collepardi - Italie
Effet de fumée de silice sur les produits d'hydratation du systheme C_3A-$6\overline{S}$ H_2

- Les auteurs de la C.12 ont etudié l'hydration du C_3A synthetic (CaO - de $CaCO_3$ - e Al_2O_3) en melange avec la fumée de silice, avec le gypse et un additif de sulphonate de naphtalene. Ils ont utilisé surtout l'analyse thermogravimetrique (ATG) et l'analyse thermo differentiel (ATD) pour accompagner la cinètique de l'hydratation des differents melanges. Une conclusion importante c'est que l'addition de la fumée de silice accelère la production de l'ettringite et sa conversion en monosulfate.

I.
A.I. Boikova, L.V. Grishchenko, et A.J. Domansky - URSS
Activité d'hydratation des phases contenant du chlore.

- Les auteurs de la C.13 ont étudié l'hydration d'un clinker contenant des phases comme le chloride-silicate de calcium(alunite) et le chlore-aluminate de calcium ($Ca_{11}Al_{14}O_{32}$, $CaCl_2$). Ce clinker contenait

55 - 65% d'alinite et 5 - 10% de chloro-aluminate de calcium. L'etude de la cinêtique de l'hydration de l'alinite pure à montré qu'elle à court terme et à long terme, a une activité beaucoup plus grande que le C_3S. Les auteurs ont etudié, en detail, l'influence de composés mineurs sur l'hydratation.

Groupe D - HYDRATATION DU CIMENT CONTENANT DES SOLUTIONS SOLIDES

Les 4 Communications du groupe D ont les titres et auteurs suivants:

Polman Herbert
Solution solide du complexe d'aluminate de calcium hydraté contenant des anions Cl^-, $(OH)^-$ et CO_3^{2-}

- L'auteur de la C.14 presente une recherche faite sur l'hydratation du C_3A, contenant Cl^-, OH^- et CO_3^{2-}. En plus des aluminates hidratés, il a verifié la formation des hydrates du chlore aluminate de calcium, du carbo-aluminate de calcium, et de l'hydroxide de calcium. En fonction de la composition chimiques des hydrates il y a la formation des solutions solides, étudiées en detail par l'auteur.

R. Wenda et H. J. Kuzel
B^{3+} dans les aluminates de calcium hydratés

- Les auteurs de la C.15 ont fait de recherches sur les effets d'addition de borates sur l'hydratation d'un aluminate monocalcique (CA) synthetic avec l'addition de H_3BO_3 ou de la colemanite $(Ca[B_3O_4(OH)_3].H_2O$ pendant l'hydratation à des temperatures variables de 5° a 60^oC. Ils ont utilisé aussi un "Ciment Fondu" Secar 250. Ils ont detecté quelques nouveaux aluminates de calcium contenant du bore et ont arrivé à la conclusion que le $2CaO.B_2O_3.H_2O$ "est le responsable de la stabilisation des ciments alumineux contenant des borates". Les auteurs indiquent que "l'addition de 5% calemanite, conduit a limiter la formation de 50% des hydrates CAH_{10} et C_2AH_8 qui peuvent avoir de convertion en $C_4A.1/2\ B_2O_3.12H_2O$ et que la transformation de cette fraction en C_3AH_6 est bloquée".

V. Akimov, T. Kouznetsova, A. Koudriavtsev' et V. Paniouchkine - URSS
Defectuosités de structure et activité d'hydratation des mineraux entrant dans le clinker de ciment portland

- Les auteurs de la C.16 ont montrés certains details de l'influence des defectuosités de la structure crystalline des mineraux du clinker, dû à la presence de solutions solides, sur l'activité d'hydratation du ciment portland. Les auteurs ont confirmé que "l'hydratation n'interesse pas toute la surface des cristaux mais essentiellement les centres actifs" et en plus, les défauts superficiels, resultant d'un traitement thermique ou mecanique, des cristaux influent directement sur la durée de la periode d'induction lors de l'hydratation de C_3S". Les auteurs ont largement étudié le phenomène en detail, avec l'utilisation des essais par resonance magnetique nucléaire et d'autres.

T. Kouznetsova et V. Akimov - URSS
Silicate dicalcique et aluminates de calcium

- Les auteurs de la C.17 ont fait de recherches sur l'influence de solutions solides des silicates avec plusieurs substances comme K_2O, B_2O_3, Al_2O_3, Fe_2O_3, Mn_2O_3 et Cr_2O_3 dans l'activation de son hydratation. Les recherches ont été faites en des silicates et aluminates de calcium obtenus au laboratoire. La cinetique de l'hydratation des silicates et aluminates de calcium contenant des solutions solides à été suivi avec l'utilisation des essais par analise microcalorimetrique, analyse des phases par RX et par resonance magnetique nucleaire. En conclusion, les auteurs ont

montré que certaines defectuosites dans les mineraux des clinkers industriel et des phases sinthetiques ont une influence dans le degré d'hydratation et dans la cinetique de l'hydratation des silicates et aluminates de calcium.

P. Kittl, Researcher and Head of the Electron Microscopy Laboratory, Engineering and Material Science Department, IDIEM, Faculty of Physical and Mathematical Sciences, University of Chile, P.O. Box 1420, Santiago, Chile. RC 2.2

Theme 2.- HYDRATION OF THE CLINKER COMPONENTS AND OF THE CEMENTS
Sub-Theme 2.2 - MICROSTRUCTURE OF HARDENED CEMENT PASTE AND ITS EFFECTS ON ITS BEHAVIOUR

1. INTRODUCTION

It is worthwhile to emphasize that in this sub-theme there are a variety in the research, that comes from a work in pure kinetics in a pure phase to a work on fracture mechanics in a hardened hydraulic cement, passing through the morfologic features. So the participation of the different countries, with a maximum of three works to Czechoslovakia and United Kingdom followed by contributions of one work to Brazil, Canada, China, France, Italy, Japan, Poland, Saudi Arabia, U.S.A. and USSR, is also very varied.

In order to make a gradual report of all the works, it was intended an ordenation in the previously shown sense.

Works which deals principally with hydratation kinetics

1.- "Structure and kinetics of formation of the gel phase in hydrated tricalcium silicate".
D. R. VOLLET and A. F. CRAIEVICH - Brazil

2.- "On the hydration of ferrite phase in the presence of lime and gypsum".
A. NEGRO, L. MONTANARO and A. BACHIORRINI - Italy.

3.- "Hydration and porosity of cement paste cured in warm and dry environment".
O. Z. CEBECI - Saudi Arabia

4.- "Phenomenes cristallochimiques intervenant dans l'hydratation des mineraux du ciment".
L. CHPYNOVA, V. ILIOUKHINE, M. SANITSKY et S. MELNIK - U.S.S.R.

Works which deals principally with the morphology of the hydration products

5.- "A study of the microstructure of two old cement pastes".
K. L. SCRIVENER - United Kingdom

6.- "Structure and morphological aspects of calcium silicate hydrates". *1

7.- "Microstructure of hardened pastes of gypsum - free portland and slag cements".
F. SKVARA - Czechoslovakia

8.- "$Ca_3SiO_4Cl_2$ hydration under hydrothermal conditions".
W. KURDOWSKY and K. MISKIEWICZ - Poland

9.- "Behaviour of ettringite in high strength hardened cement paste".
K. ISOZAKI and K. NAKAGAWA - Japan

Works which deals principally with fracture and mechanical properties

10.- "The formation of $C_2SH(A)$ and C_3SH at the hydration of portland cement".
V. LACH - Czechoslovakia

11.- "Relationships between ettringite and chloroaluminate, strength, and expansion in paste mixtures".
A. D. BUCK - U.S.A.

12.- "Pore structure and strengths of hardened cement pastes".
J. JAMBOR - Czechoslovakia

13.- "A study of the intrinsic properties of hardened cement pastes (HCP)".
L. PING and H. YIUN-YUAN - China

14.- "Dependence of degree of silica polymerization and intrinsic mechanical properties of C-S-H on C/S ratio".
J. J. BEAUDOIN and R. F. FELDMAN - Canada and J. BARON and M. CONJEAUD - France

15.- "Crack tip processes and fracture mechanism in hardened hydraulic cements".
N. B. EDEN and J. E. BAILEY - United Kingdom

2. PARTICULAR DISCUSSION OF THE WORKS

2.1 Vollet and Craievich, which are the authors of the first work has been studying the hydration of tricalcium silicate with a small-angle X-ray scattering (SAXS) at different temperatures. The degree of the hydration was determined by quantitative X-ray diffraction analysis (QXDA). The kinetics of setting of the pastes is well described by the Johnson-Mehl equation with n=2

$$J_\infty - J_t = (J_\infty - J_0) \exp \{ - k^n \frac{t^n}{n} \} \qquad (1)$$

where J_t, J_0 and J_∞ are the scattering intensity values, respectively, at time t, extrapolated to t=0 and corresponding to the apparent upper asymtote. k is an empirical velocity constant and n a parameter that is a function of the phase transformation determinant mechanism. The

$\ln\ln \frac{J_\infty - J_0}{J_\infty - J_t}$ vs. $\ln t$ plot must be linear in this

range, with a slope n, which in the graph presented by Vollet and Craievich is quite nearly 2. The Arrhenius plot for the empirical hydration velocity $k \alpha \exp(-\Delta E/RT)$ give an empirical activation energy of $\Delta E = 37.2$ KJ/mol. Analysed the SAXS data they can obtain the mean size parameters l_p and l_s respectively of the pores and the solid gel particles, $\bar{l}_p \simeq 0.80$ nm and $\bar{l}_s \simeq 2.05$ (nm), for the satured samples. In the dried samples l_p and l_s can become 2.5 nm and 6.4 nm respectively. This increases, indicating a clustering of the gel particles and pores, when the tricalcium silicate paste dried. His hydration kinetics studies suggest that the hydrated gel correspond to about one layer of tobermorite type, separated by one or two monolayers of water, on the average.

2.2 The second work by Negro, Montanaro and Bachiorrini, is about the hydration of ferrite phase in the presence of lime and gypsum. It is in general accepted that the ferrite phase is a solid solution of the type $C_2(A_nF_{n-1})$ where $0 < n < 0.7$. From the components of this solid solution C_6A_2F, C_4AF and C_6AF_2. With an addition of CH, $C\bar{S}H_2$, and the siliceous powder, they prepared the mortar where the relation water/solid = 0.3. They measure the expansions after 28 hydratation days of three mortars prepared as it is said before and they are compared with two reference mortar containing C_3A, CH and $C\bar{S}H_2$, for the first, and by C_3A with 5% of F, CH and $C\bar{S}H_2$ for the second. They observed that the expansion of this mortar made of ferrite phase is function of the content of A and they amount a minor quantity that of the mortar made with C_3A. For this C_3A mortar the expansion is lower, when the C_3A is replaced by the C_3A with additions. Differential thermal analysis is used for studying the hydration kinetics of this mortar by the evaluation of the amount of ettringite[*2] that they have. After this results is possible to say that the little quantity of ettringite and expansion shown by the ferrite in relation to C_3A, are doing not only to his mediocre reactivity, but to formation of amorphos ferritiques components which implies a lowered of hydratation. The plates showing scanning electron microscopy of the different stages of the phases are very useful.

2.3 The work of Cebeci, which is the third, is about the hydration and porosity of a cement paste cured in warm and dry environment. In order to accomplish this two differents temperatures 17°C and 37°C were maintained during mixing and in the three different curing media: in lime satured water, 75% and 33% relative humidity. The hydration was determined by ignition at 1050 ±50°C to measure the non evaporable water content. The ratio of this to the nonevaporable water content of the paste completely hydrated with excess water in a ball-mill, indicates the degree of hydration of the specimen. The figures shown by the author in which he describes the hydration kinetics, are quite different from the one of Vollet and Craievich, and it is necessary further studying in order to obtain a coherence between this two important experimental facts. Using their own words: "The degrees of hydration and mercury intrusion pore size distributions of the hardened pastes were determined at various ages from one to ninety days. The results indicated that the deficiency

in the relative humidity of the environment, rather than the increase in the hydration temperature, is the dominant factor affecting the parameters investigated in this study. The cement pastes hydrated at lower humidity attained lower ultimate degree of hydration and greater porosity, particularly in macropores, as compared to the pasted hydrated in water".

2.4 The fourth and last work of the first subdivission of this sub-theme is by Chpynova, Ilioukhine, Sanitsky and Melnik, and deals with the crystallographic fenomenous that participate in hydratation of the clinker phase. They show the influence which perfoms the anisotropy of chemical union in the structural polyedres and the nonsaturation of valence forces in the anions on the hydratation of the clinker minerals. They discuss, in the same way, the possibility of formation, when the C_3S hydratation is taking account, of a hydrosilicate with high basicnees nature, which are analogous to the calcium hidroxide structure. With the calcium silicate they obtain that the procesus which is determinant in the hydration are: the polycondensation of SiO_4 in the hydrosilicate, the lixiviation of CH and his crystallisation in the pores upon the form of portlandite; for the aluminates and the calcium aluminaferrite: the protonisation of all $O^{=}$ and the tranformation of Al^{+3} and Fe^{+3} to the IV in VI coordination with the total destruction of the crystalline structure of the original mineral. So, this authors describe a topochemical reaction where only the CH is dissolved and critalized.

2.5 In this work, the first which uses morphology principally and made by Scrivener, deals with the microstructure of two old cement pastes. They have been examined by backscattered electron (bse) imaging of flat polished section in the SEM. One paste has been hydrated under carefully controlled conditions for 23 years. A cement made by William Aspdin is the other and is mixed with water in 1848. The bse imaging technique allows, that the different phases and porosity in the pastes can be observed. The resolution is about 0.1 μ m. Many features of the original cement can be obtained from the microstructure of the pastes. Many relicts of the original cement grains can be distinguished, and the original particle size distribution can be obtained and the water cement ratio of the paste. As the author said "This study indicates that the net movement of most ionic species during hydration is very small and provides evidence for an in situ reaction mechanism during the latter stages of hydration". This in situ reaction must be correlated with the previously said solid state reaction or a reaction controlled by diffusion, in some previous discussed work.

2.6 The second work which deal principally with morphology is made by Henderson and Bailey and is about the structure and morphological aspects of calcium silicate hydrates. As the authors said the 70% calcium silicate hydrate (C-S-H) have a micro and molecular structure which remains practically uncertain. In order to elucidate this uncertainty of molecular and microstructural characteristics, they prepared various synthetic C-S-H with particular reference to possible structural relationships with the hydrates in portland cement paste. They studied C-S-H formed in a model two phase system, consisting of an aqueous CH solution and an organic layer of hexane containing $(C_2H_5O)_4Si$. The C-S-H prepared in various conditions which give different C/S ratios were observed in TEM. The principal results obtained by the technique are: "The presence of ~1 nm foils extending to 10^2-10^3 nm along the sheet have been directly observed in both amorphous and microcrystalline hydrates, with compositions in the range C/S = 0.9 to 1.75. The ~1 nm thick foils appear to represent the basic core structure of these hydrates, consisting of a CaO_x polyhedral sheet sandwiched between short chain silicate groups. The presence of double ~1 nm foils ~2 nm and less apart, extending over 10^2-10^3 nm are indicative of incipient short range ordering at right angles to the sheet. The non-interfacial C-S-H (C/S = 1.7) was thought to have a fibre-like microstructure when examined at low magnification. However, more detailed microscopy revealed the actual character of this hydrate at a micro and molecular level. Highly directionally orientated foils ~1 nm thick extending some 10^2-10^3 nm were observed. Instead of doublets, multilayered C-S-H foils between ~2 nm and 4 nm apart, consisting

of up to 6 layers, were also observed. In spite of the overall highly directionally orientated character of these foils, conventional electron diffraction contained but two diffuse bands typical of amorphous materials. The thickness of these ~1 nm foils, like similar but more highly curved interfacial C-S-H foils, is again consistent with a basic structural core, consisting of a CaO_x polyhedral sheet sandwiched between silicate groups. The difference in foil character, between the interfacial C-S-H, where they are high curved and the highly directionally orientated non-interfacial hydrate foils, is probably related to the great difference in preparative conditions, rather than to any basic change in their overall sheet-like molecular[*3] level structure, containing CaO_x polyhedral sheets sandwiched between silicate groups of various types; independent of mode of formation, composition or degree of order, strongly suggests that the C-S-H in paste hydrated portland cement, could well, also contain this basic highly orientated layer-like molecular structure."

2.7 The following work, by Skvâra, is about the microstructure of hardened pastes of gypsum-free portland and slag cements. They prepared a ground cement clinker of specific surface 300 to 700 m^2/kg, in which the common setting regulator, the gypsum, is replaced by lignine derivate (or sulphonated polyphenolate) plus alkali carbonate, with w = 0.20. This pastes GF, attain a compressive strenght of 1 to 9 MPA after 1 to 3 hours, and are composed of crystalline and amorphous patterns featuring the ratios C/S = 1 to 5, and C/A = 10 to 50. With SEM it is found that a dense structure is developed in the course of 12 to 24 hours the morphological character of which does not undergo any further changes through the paste strength increases (to 100 MPa and more after 28 days). It is very interesting that this dense structure was not found to contain the crystalline formation typical of hardened PC pastes (portlandite ettringite). A high-lime C-S-H phase (mean C/S ratio = 2.7 $\pm$ 0.1, EDAX analysis) intergrown with very fine CH and highly dispersed hydroaluminates (cubic and hexagonal). The gypsum-free slag cement (GFS) attain a compressive strength of 50 to 90 MPa after 28 days, and over 100 MPa after 180 days. SEM said that his hardened pastes present a dense microstructure composed of the C-S-H phase intergrown with highly dispersed hydroaluminates and hydroalumosilicates. They do not contain CH. The hydrosilicate phase of GF and GFS cements may be classified as C-S-H type III. The major constituent of bonding products in hardened GF cement pastes is mostly the hydrosilicates of the C-S-H II (Taylor) interspersed with very fine CH and highly dispersed hydroaluminates. The major mechanical strength of the hardened GF and GFS cements respect to the PC and SPC ones is the result of the greater bonking capacities of the new hydration products.

2.8 Kurdowsky and Miškiewicz studied the $C_2S \cdot Cl_2Ca$ hydration under hydrothermal conditions. X-ray examination, differential thermal analysis and SEM was used for this investigation. The calcium chlorosilicate which is formed at about 600°C in system C-S-$CaCl_2$, was synthesizes starting from a mixture of calcium carbonate, amorphous silica and calcium chloride with molar ratio 2:1:1, in a laboratory furnace. This calcium chlorosilicate was mixed with amorphous silica in molar proportion 0, 1, 2, which are the samples A, B, C, respectively. The behaviour of this samples in autoclaving is summarized as follows from figures of the authors.

Sample A:

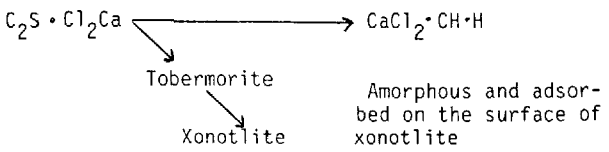

Sample B:

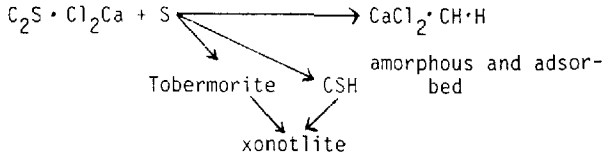

Sample C:

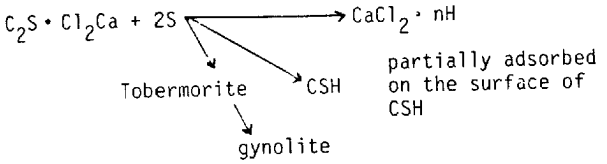

2.9 The last work of this group deals principally with morphology. It was made by Isozaki and Nakagawa and is the behaviour of ettringite in high strength hardened cement paste. They used SEM, mercury pressure porosimetry and powder X-ray diffractometry in order to study the morphology of ettringite and hydrate structure in high strength hardened cement pastes made with normal portland cement containing type II anhydrous calcium sulfate (anhydrite) at long term water curing. The amount of anhydrite added to the normal portland cement were varied from 0 to 20 wt%, w ≈ 0.3, after precuring at 20°C, they were steam cured at 65°C for 4 hrs and inmersed in water at 20°C for forty months. The addition of anhydrite in the high strength hardened cement paste at forty months of age gives a stable ettringite and monosulfate hydrate was not detected. In the SEM figures shown in the work the average shape of ettringite was a needlelike form of 0.2 to 0.8 μm in diameter and 2 to 6 μm in length. Some ettringite crystals can concentrate in the small voids and some times sintered together, growing into a large crystal, this depends on the amount of unreacted anhydrite and the compactness of the matrix of cement paste.

2.10 The work of Lach about the formation of $C_2SH(A)$ and C_3SH at the hydration of portland cement, is the first of the works where the mechanical properties have a very important rol, which go to increase to the last work coomented here. Various methods as X-ray diffractometry, microporosimetry, SEM and, of course, mechanical tests, was used in this work . It is found that the phase composition of microstructure varies significantly with the temperature of autoclaving process (140, 165, 190 and 215°C). At 190 and 215°C temperatures, besides common phases CH and C-S-H gel, the basic hydration products $C_2SH(A)$ and C_3SH were formed according to the reaction:

$$m\ (\text{C-S-H gel}) + nCh \longrightarrow xC_2SH(A) + yC_3SH \qquad (2)$$

In relation to the mechanical properties of hydrated paste, the higher is the crystallinity and basicity of calcium hydrosilicates at the expense of gel and less crystalline ones, the lower is the strength of autoclaved paste. The hydration is not completed even with high autoclaving temperature, and the specimens places in humed atmosphere after autoclaving increased their strength and reduced microporosity. The higher the degree of hydration, the higher the temperature of autoclaving.

2.11 In the work of Buck, the theme is a relationships between ettringite and chloroaluminate, strength, and expansion in paste mixture and this is a part of study of cementitious mixtures for underground sealing and isolation of nuclear wastes. The stability of these phases on such factors as strength and expansion was studies. In order to carry on this objective a serie of paste mixtures using a portland cement, plaster of paris, and two levels of water content with or without the presence of fly ash, ground granulated iron-blast furnace slag, silica fume, or natural pozzolan were made; four mixtures contained sodium chloride instead of plaster of paris were also made. Samples of these mixtures were treated at different temperature and at different age up to one year. The phase composition was studies by X-ray diffraction. Compressive strength and restrained expansion was studied, too. The most significant finding was in his own words: "that since loss of ettringite crystallinity at about 100°C, as determined by XRD, did not affect either compressive strength or expansion significantly, the thermal stability of ettringite in this temperature range do not need to be a concern for repository sealing use of cementitious mixtures. Other findings were: **a)** Some ettringite was destroyed at about 75°C while that in other mixtures persisted to about 100°C. The higher stability seemed to relate to impurity, but this could not be definitely proved by XRD. **b)** If a long-term source of alumina is available and other necessary ingredients are present, new ettringite may continue

to form for at least a year. **c)** Once ettringite had been destroyed by heat, it did not tend to reform under moist storage conditions at room temperature. **d)** When ettringite was destroyed by heat, tetracalcium aluminate monosulfate-12-hydrate (monosulfoaluminate) did not replace it. Instead there was sometimes formation of hydrogarnet after heating to 100°C. **e)** Conversion of ettringite to chloroaluminate in the mixtures containing salt ranged from none to complete at 23°C with some coexistence for a year. In no case did ettringite replace chloroaluminate".

2.12 The third work of the last subdivission is written by Jambor about pore structure and strength of hardened cement paste. Pore structure is an unseparable of the production processes of the cement paste, and in this sense that this work was made, and his principal objective is a connection between strength and porosity. The early works said that the strength decreases very rapidly with increasing porosity. When it is increasing w the unfavorable influence is expressed by the well known formulas of Feret, Abrams, and Bolomey. The influence of porosity in strength are given by the formulae of Powers, Schiller and Ryshkewitch. But because the greath variability of the cement respect to the total porosity and the pore structure which change with time and in dependence on their cure conditions. Porosity and pore structure and his relation to the strength is the aim of this work. A variade group of selected cement pastes with various water-cement ratios was prepared by the author with the effective method of compacting the pastes in various ways. The pore size distributions is analized in a high pressure mercury porosimeter, and presented by the value of his average pores radious. The specific surface of the tested pastes was determined by the BET method and nitrogen was uses as the sorption gas. The values of the bound water in the linding hydration products were determined by the complex thermal analysis and are identical with the ignition loss in the temperature range of 100 to 450°C. Two formulas (3) and (4) allow to predict the changes of the porosity of hardened cement pastes - in dependence of their curing time. Provided no microcracks and additionally created pores in the hardened cement composite are present, its total porosity P in every stage of its hardening way be expressed by formula

$$P = P_o - \Delta V_{hp} \tag{3}$$

where: P_o is the theoretical initial porosity the value of which is given by the sum of the volumes of mixing water (V_w) and air voids (V_v) in a volume unit of the composite inmediately after its compaction, i.e., $P_o = V_w + V_v$ and ΔV_{hp} is the difference between the volume of the developed hydration products (V_{hp}) and the volume share occupied by the hydrated cement in its original unhydrated state in the volume unit of the composite (V_{hc}), i.e., $\Delta V_{hp} = V_{hp} - V_{hc}$. This difference corresponds to the volume increase of the solid phases in the volume unit of the composite due to the hydration process. The results of a great number of hardened cement pastes made of portland cements with different w/c ratios and cured for different time period in water at 20°C showed, that the volume increase of the solid phases due to the cement hydration ΔV_{hp} in the volume unit of hardened cement pastes may be roughly expressed by

$$\Delta V_{hp} = A \cdot w/c \quad - \frac{B}{\sqrt{T} + \frac{B}{A \cdot w/c}} \tag{4}$$

where A is a coefficient depending on the cement composition, the value of which in case of portland cements is approximately 68.4; the product A·w/c is then the maximum possible volume increase of the solid phases that may be achieved in the cement pastes with given w/c after their long term curing in water at 20°C; B is a coefficient depending mainly on the class and fineness of cement, its value for portland cement of class 400 is approximately 17.1; T is time period of curing in water at 20°C in days. Finally the porosity (P)- strength (S) relationship is given by formula (5)

$$S = K \frac{\sqrt{P_o - P}}{P \cdot w/c} \tag{5}$$

where P is the total porosity in the time of test, P_o is the initial porosity as it has been defined above, and K is coefficient, the value of which

depends on the type and activity of cement, on the curing conditions, on the dose of cement in a volume unit of the composite and also on the type of test specimens. The comparison of the experimental and calculated values of the compression strength of the tested cement pastes confirms a satisfactory accuracy of this formula.

2.13 The fourth work of this last subdivission and the thirteenth of the sub-theme is by Ping and Yiun-Yuan and deals with the intrinsic properties of hardened cement pastes (HCP). The fracture strength depends on porosity in a way that the fracture strenght at zero porosity is a parameter in such a well known expression as:

$$\sigma = \sigma_0 (1 - P)^A$$
$$\sigma = \sigma_0 e^{-BP} \qquad (6)$$

where P is the total porosity and σ_0 intrinsic strength at zero porosity, A, B are constant. Or the more recently

$$\sigma = (K_1 K_2^{K_3+K_4}) \left[K_2^{K_3(W-1)} (1-P)^{K_3 W + K_4} \right] \left(\frac{1-P}{1+2P} \right) \qquad (7)$$

where W is the factor of relative specific surface area of the pores, and $K_1 - K_4$ constants depending on intrinsic properties of hardened cement paste, furthermore $K_3+K_4 \approx 3$. Formulaes (6) comes from ceramics, formulae (7) comes from some Weibull statistics consideration, the three formulaes involved the intrinsic strength σ_0 at zero porosity. The objective of this study is to correlate the intrinsic strength σ_0 in hardened cement paste and its mechanical behaviour, σ_0 can be changed by altering the molecular weight distributions of silicate in C-S-H gel by addition of inorganic complex ions and/or organic silane coupling agents to hydrating cement pastes. Low porosity samples was prepared by compactation of a cement with a w/c $\approx$ 0.1 and them cured in water. Gel permeation chromatography, compressive strength, splitting tensile strength, amounts of non-evaporable water, pore size distributions by mercury porosimetry, fracture parameters as G_{IC} (fracture toughness), K_{IC} (critical stress intensity factor) and B (index of brittleness, defined by the irrecoverable dissipated energy of the specimen during the test up to maximum load), SEM and (EPMA) electron microprobe analysis, are the experimental technique used in this work. So it is obtained samples between 5.17 and 1.63 $cm^3/g \cdot 10^2$ total pore vol. The degree of silica polymerization (DSP) did not mean progress of hydration, but can change the intrinsic properties. The conclusions of the authors are: "(1) Both pore structure and intrinsic properties of HCP play an important role on its mechanical characteristics. This intrinsic properties can be modified by the DSP in the microstructure of HCP; (2) The DSP can be increased by addition of inorganic complex ions Fe^{++} and Cu^{++} and organic coupling agents VTES (CH_2=CH-Si $(OC_2H_5)_3$) and MDES ($(CH_3)_2Si(OC_2H_2)_2$) to cement during its hydrating. Mechanical strength develops with increasing the DSP. The lower the porosity of HCP is, the more sensitive is the influence of the changing of DSP on its mechanical strength; (3) The increase of DSP greating improves its index of brittleness. On this basis, they obtained a high strength and low brittleness HCP which is named by their polymerized silicate cement (PSC)."

2.14 The fourteenth work by Beaudoin, Feldman, Baron and Conjeaud is about the dependence of degree of silica polimerization and intrinsic mechanical properties of C-S-H on C/S ratio. Synthetic C-S-H compositions were produced in aqueous solutions containing variable proportions of sodium metasilicate and calcium oxide. The objective of this investigations was to determine in six C-S-H prepared compositions, the degree of polimerization, adsorption characteristcs and intrinsic mechanical properties on C/S ratios. Silica polymerization measurements was made with the method developed by Parrot and Taylor; weight and length change isotherms; porosity measurements, modulus of elasticity measurement, microhardness measurement, was made too. The conclusions obtained by authors are: "1. Degree of polymerization of C-S-H depends on C/S ratio. It decreases as C/S ratio increases. 2. Synthetic C-S-H materials prepared using sodium metasilicate solutions are generally layered systems. Irreversible length and weight change characteristics on exposure

to water vapor are due to intercalation processes and aging phenomena. **3.** Zero porosity values of modulus of elasticity and microhardness for the C-S-H preparations studied appear to be independent of C/S ratio. As microhardness generally correlates with strength, values for intrinsic strength would appear to be independent of C/S ratio over the range studied. **4.** Highest values of modulus of elasticity were obtained for the preparation (C/S = 1.26), which exhibited reversible sorption characteristics in the low pressure region of the water isotherm. Intercalation processes and their effects on the proximity of silicate sheets may have a greater effect on intrinsic mechanical properties than composition and/or degree of poymerization".

2.15 The last work of this sub-theme by Eden and Bailey is about the crack tip processes and fracture mechanism in hardened hydraulic cements. The problem in examining crack tip processes in hardened cement paste is solved utilizing the transluscence of cement pastes and the ability of fine cracks, about 0.1 μm wide to scatter transmitted light. By the use of this technique in conjunction with a straining stage, the following conclusions by the authors are obtained: "**1.** Stable cracking of portland cement materials is observed to proceed in a single, ralatively straight, path. **2.** Fracture mechanics indicate that this stable crack growth is the formation of a process zone, which grows to a characteristic size before failure occurs. **3.** The process zone can be described mathematically in terms of a "tied-crack" model. **4.** The most direct interpretation of this is that fracture of portland cement materials occurs by the parting of two-dimensional hydrate particles, primarily by shear across their interfaces."

3. GENERAL DISCUSSION OF THE WORKS

General objective of science, in order to prove the truth of the models with which they describe a definite branche of phenomenology, is to obtain the same parameters, which describes the models, from independent paths. Here we can have some examples and if it is added the obtention of certain features with technical utility, progress in this branch of the science is secure. In this brief general discussion, we intend to give some examples from the works described and discussed individually before and taken now as a whole.

In the first work (1) by Vollet and Craievich it is suggest that hydration of C_3S paste is controlled by a diffussion mechanism. Another work where hydration kinetics is used is by Cebeci (3) where hydration is studied by the measure of the nonevaporable water content. The figures obtained by Cebeci means a diffussion mechanism with a great velocity in the first stages of production of the hydrated material, which is in contradiction with the model of Vollet and Craievich which means as zero velocity of hydration when at the begining of the reaction. Both facts are in contradiction and further investigation must be made in order to put in accord with some model the experimental facts which always remain. Chpynova, Ilioukhine, Sanitsky and Melnik (4) describe a model of hydratation which is a topochemical reaction governing by diffussion. In his study of the microstructure of a very old cement paste Scrivener (5) describe facts which are in accord with a topochemical reaction governed by diffussion. So we have four coincident opinions about that hydration is governed by a slow diffussion mechanism. This concepts about hydration corresponds to the main phase which is tobermorite, when it is speaking of ferrite phase as Negro, Montanaro and Bachiorrini (2) the model must be another. Because this reaction is very complexe it is necessary further investigations in order to make a quantitative model.

About the mmorphology of the C-S-H the dimensions give by Henderson and Bailey (6) are in accord with the data of Vollet and Craievich (1) and the method of investigations are quite different.

It is an accord that a gypsum-free cement, as it was detected by Skvâra (7), have a hight strength, which can be found in the work of Isozaki and Nakagawa (9).

In this enumeration the work of Kurdowsky and Miškiewicz (8) is isolated, because any other deals with a silica calcium chloride. In the same sense the work of Lach (10) and Buck (11) can not be compared with other in this sub-theme.

Pore structure is treated by Jambor (12) with formulaes which comes from cement investigations, Ping and Yiun-Yuan (13) made an approach that coming from ceramic research, and is necessary further discussion to put in accord this different point of views.

In the work of Eden and Bailey (15) it is find that fracture occurs primarily by shear between the S-C-H particles, where bonding is weak, in consecuence, like Ping and Yiun-Yuan (13) made, strength must be increased by bonding these particles with a polysilicate.

More extense discussion of the very interesting work in this sub-theme must be avoided by a lack of space and time. Words, sentences and paragraphs of the original works must be used, because this lack of time; finally we acknowledge the colaboration of G. Díaz and our secretary M. E. Lillo, without them this discussion can not be written.

Errata: To add in the asterisks:

* 1.- E. HENDERSON and J. E. BAILEY - United Kingdom
* 2.- in function of time. They show that exists a relation between expansion of mortar and the amount of ettringite.
* 3.- structure. The retention of this foil-like molecular

Addenda

After this report was finished, two work arrived, one from Brazil-Japan and the other from Denmark. The two works are:

16.- "The dispersion model for hydration of portland cement.II. The influence of fineness".
T. KNUDSEN - Denmark.

17.- "Hydration characteristics and properties of mixture of cement and high content of calcium*
Y. TEZUKA and J. G. DJANIKIAN - Brazil and
H. UCHIKAWA and S. UCHIDA - Japan.

2.16 In the dispersion model for hydration of portland cement with special emphasis on the influence of fineness Knudsen obtains some interesting results. It is suppose that the hydration of a single grain with size r follow the equation:

$$\alpha(r\ ,\ t) = \exp\ (-r/kt) \qquad (8)$$

where k is the rate - constant corresponding to a linear kinetics reaction mechanism and t is the time, it is suppose too that the particles size distribution followed the Rosin-Rammler's equation

$$F(r) = 1 - \exp\ (\frac{-r}{r_o}) \qquad (9)$$

where r_o is the fineness constant. By integrating over all grain sizes

$$\alpha(t) = \int_o^\infty \alpha(r\ ,\ t)\ d\ F(r) = \frac{t}{t+r/R} \qquad (10)$$

The experimental results are in accord with this formula (10) but with an inicial time t_o

$$\alpha(t) = \frac{t - t_o}{t - t_o + r/R} \qquad (11)$$

t_o is the normal period, which is about 6 $\pm$ 2 hours for w/c= 0.5, k= 0.54 μm/h. This theory, which connect the particles size distribution with a kinetic reaction of a particle, can be put in accord with the others theories of kinetic hydratation discussed before.

2.17 In the work of Tezuka, Djanikian, Uchikawa and Uchida a cement with high content of calcium sulfate was studied, the hydration products detected by powder X-rays diffraction were ettringite monosulfate hydrate and calcium hydroxide. The calcium hydroxide increased with age. With natural gypsum : mixture, no monosulfate detected and ettringite increased with age. On β hemihydrate mixture, the calcium sulfate dehydrate appeared before one day and increased little after this age. With anhydrite mixture, calcium sulfate dehydrate produced increased with age, but even at the age of 28 days, there remained anhydrite still not hydrated. The kinetics of the hydratation studying by the amount of combined water give figures similar to the obtained by Cebeci (3). Unfortunately the largest amount of calcium sulfate produced a fall in the strength, in some cases so much that they have practically non strength. Clear scanning electron micrographs illustrated the work. This work belong to the second group were morfology is the principal aim.

* sulfate".

Paulo J. M. Monteiro Companhia de Cimento Portland Paraíso Brasil

2.3

Communication Report Bond Paste - Aggregate, paste-reinforcement and paste-fibers

The importance of how well a cement paste would "bond" with an associated material has been realized by researchers and practical engineers for some time. However, its study proved to be very complex. It is interesting to note that this difficulty happens in most of the research levels. At the engineering level, the different thermal and elastic properties of the many phases in concrete, create stress concentrations precisely at the interfacial zone. At the microstructural level, the interface between the cement paste and associated materials creates a transition zone in the paste with unique properties.

The difficulty of this topic is again shown by the smaller number of communications than other sub-themes: it takes a long time to develop new methods of analyzing the bond in concrete.

In this section, the following communications were presented:

Distribution of Ca(OH)2 and of the CSH phase in the Oolithic marble/hydrated cement paste interfacial zone; by Chen Zhi-Yuan and Zhang Xio-Zhong.

A preliminary study of the microstructure of the cement/sand bond in mortars; by K.L. Scrivener and P.L. Pratt.

Improvement of paste-aggregate interface by adding silica fume; by Wang Jia, Liu Baoyuan, Xie Songshan and Wu Zhongwei

Improvement of the aggregate-cement paste transition zone by grain refinement of hydration products; by P.J.M. Monteiro and P.K. Mehta.

Effect of pretreatment of aggregate surface on the properties of concrete; by Wu Xuequan, Han Sufen, Bian Qinghan, Tang Mingshu.

Microcracking propagation in flexural loaded portland and high slag cement concretes; by G. Frigione, B. Marchese and R. Sersale.

Durabilite de la liason acier galvanise--pate de ciment portland; by G. Arliguie and J. Grandet.

Investigations on the Zinc/Hydrated cement paste interfacial zone; by Chen Zhi-Yuan and Zhang Xio-Zhong.

Bond in cements reinforced with bundles of fibres; by P. Bartos.

Compatibility of copper fibre with compacted cement and low thermal-shock fatigue thereof; by P. Kittl and G. Dias.

Next some of the main contributions presented by these authors will be highlighted:

Yan and Zhong used the differential scanning calorimetry and the gel chromotography to study the distribution of CH and CSH phase in the Oolithic marble--cement paste transition zone. It was shown that the larger quantities of the hydrate phases are located closer to the interface and the reason is the existence of a water film at the interface. These results seems to support the through--solution type of hydration.

Evidence that the marble reacts with the cement hydration products is given by scanning electron microscopy of the marble surface which is "corroded", indicating a dissolution of the calcite.- An interesting result is that the CH content in the vicinity of the marble surface decreases with longer curing time for pure portland cement paste. No explanation is given to this fact, however the writer would like to mention that this is expected according to Monteiro and Mehta's theory in which the CH reacts with the calcite, with time, in the transition zone.

Additions of silica fume increased the cleavage strength and it was shown that the CH content in the transition zone decreased when silica fume was added.

The data indicated a difference in the degree of the CSH within the transition zone and the bulk paste. In the former the CSH has a higher degree of polymerization than in the bulk paste.

Jia et al. studied the mean size and orientation index of CH and AFt in the transition zone. Also the fracture energy and microhardness at the interface were investigated for pure portland cement and with of silica fume.

The experimental results indicate that the mean size of AFt crystals decreases with increasing distances from the interface. Also the mean size and range of variation decrease with w/c ratio.

Additions of silica fume to the cement paste reduce the size of the CH crystals.- It is shown that with silica fume additions, the microhardness and effective fracture energy increases.

The authors propose that during early cement hydration, the fine particles of silica fume play the same part as nuclei on which CH germs attach. Over time, the silica fume reacts with the CH crystals producing CSH.

Scrivener and Pratt studied the microstructure of the cement paste/sand interface using secondary electrons to analyze the fracture surfaces and backscattered electron imaging to analyze flat polished surfaces. The results indicate that, at early ages, a layer of CSH forms on the

surface of the sand grains by a through--solution mechanism. This same mechanism of hydration is responsible for the precipitation of AFt around the sand grains. This study showed that a much higher concentration of AFt is observed in the interfacial region, in agreement with the published literature. The authors concluded that there is no evidence for the formation of an epitaxial layer of calcium hydroxide around the sand grains. They, also, suggested that the specimen configuration in which cement paste is cast against a large flat piece of aggregate may lead to localized bleeding along the interface, resulting in anomalous results.

Monteiro and Mehta discussed three cases where an improvement of the aggregate-cement paste transition zone was achieved by grain refinement of the hydration products. The main idea is that the strength and durability of concrete could be enhanced if the large grains of calcium hydroxide present in the transition zone are either eliminated or reduced in size.

The first case studied the grain refinement that occurs when condensed silica fume is used. It was shown that the thickness of the transition zone is remarkably decreased when condensed silica fume is used. Also, SEM studies showed the existence of a pozzolanic reaction between the CH film and the condensed silica fume particles.

The second case analyzed the transition zone with type K cement. It was shown that when type K cement is used, small CH crystals are precipitated with a random orientation on the top of a discontinuous CH film. Therefore, there is a CH grain refinement in the interfacial zone.

The third case studied the grain refinement which takes place when instead of silicious rock, carbonate aggregate is used. The authors proposed that the strengthing of concrete, when carbonate aggregate is used, is due to an interaction between CH and calcite, rather than due to the formation of carboaluminates hydrates.They also suggested that the transition zone improvement is due to the replacement of large CH crystals by small crystals of a basic calcium carbonate.

Xuequan et. al. studied the effect of pretreatment of aggregate surface on the properties of concrete. The authors studied the following solutions for aggregate pretreatment: dilute sulphuric acid, alum. solution, sulfuric acid and alum. solution, acidized sodium silicate solution, alum. and water glass solution, sulphuric acidized cement suspension. Silicious and calcareous rocks were used as aggregate.

The results indicate that the mechanical strength of mortars and concretes with pretreated aggreagates are higher than the ones with inert aggregates. This improvement is a result of a combination of physical, chemical and mechanical interlocking effects.

Frigione et al. presents interesting experimental results on the microcracking propagation in portland and high slag cement concretes. Their approach to correlate the mechanical properties of both reinforced and plain concrete to the existing microstructure is commendable and it should be encouraged.

It is shown that high slag cement concretes have a different cracking behavior when compared to pure portland cement concretes. The former has under increasing loads, progressively more cracks with a moderate width ; and the latter develops an approximately number of cracks swiftly growing with stress. It should be mentioned that steam curing decreases these differences.

This cracking behavior may be associated to the different transition zones when high amounts of slag are used. The reduction of the calcium hydroxide in the transition zone for the slag concrete may explain the higher adhesion paste-aggregate. Also, the unreacted slag particles can act as crack-arrestor, causing frequent interruption of the fracture process and preventing the widening of the cracks.

Zhi-Yan and Xio-Zhong studied the zinc/cement paste transition zone using XRD, SEM, EPM and DSC. The results showed that the calcium hydroxyzincate is found mainly in the region 0-10 um from the interface. When silica fume is used the intensity of the Ca-zincate peak declined probably because of a smaller supply of the CH for the formation of the Ca--zincate.

The study of the durability of the galvanized steel and portland cement paste transition zone was studied by Arliguie and Grandet. They showed that a plate of zinc with one extremity embedded in concrete and the other exposed to the atmosphere for six years had a very good bond between the metal and the concrete.

XRD analysis demonstrated that the calcium hydroxyzincate is very stable in an environment containing carbonic gas.- This is an important fact because the penetration of carbonic gas in concrete is one of the main factors of non-galvanized steel corrosion.

The calcium hydroxyzincate is also very stable to the action of chlorides.

TDA analysis of the calcium hydroxyzincate shows that it decomposes in the following sequence:

150-190 C: progressive elimination of the water of hydration

190-200 C: $Zn(OH)_2$ decomposition

480 C: decomposition of CH

Bartos analyzed the pullout modes of failure of glass strands, including aging effects. The experimental program included a comprehensive series of pullout tests for different combinations of matrices, glass fibers, curing conditions and age. The following modes of failure were identified-: (I) complete tensile fracture of the whole strand; (II) complete pullout of the whole strand; (III) intermediate failure mode. The last case could be divided into two different types: (a) combined pullout and tensile failure, (b) telescopic failure. The energy absorption of the fiber bundles failing in these modes was greater than the other failure modes.

It should be mentioned that acrylic polymer increased the bond to such a degree that only very short embedment lengths produced a pullout or a combined failure.- Also, wet curing increased the bond considerably.

The author suggests some criteria to design bundles of fibers to act as reinforcement which can improve both strength and thoughness of the matrix.

Kittl and Diaz studied the compatibility of copper fibers with compacted cement and its low thermal;-shock fatigue resistance. Copper fibers (4% by weight) were mixed with portland cement having a water/cement ratio of 0.04 and compacted by compression.

The authors suggest that the difference in the cement paste and copper thermal expansion coefficients can create microcracks that are able to modify the thermal fatigue behavior, once the can stop the fatigue crack propagation and modify the mean strength. The compacted copper fiber-cement composite withstood 3000 cycles of a thermal shock between 283 K and 373 K with no rupture but only a reduction in the mean strength.

No corrosion was observed in the 2 years old composite samples nor in the ones stored in water at 373 K for 50 hours.

Conclusions

In summary, after analyzing the work presented in this section we can conclude the following:

I) The microstructure of the transition zone created by the interface between the cement paste and a plane of discontinuity (simulating the aggregate) has been well characterized and understood. A summary of the transition zone characteristics for this particular configuration is presented in many review articles, and in this congress it can be found in the principal reports by Massazza and Diamond.

II) The addition of sand particles in the cement paste increases the degree of variables to define the transition zone, because now the interfaces between the cement paste and the rocks have variable radius of curvature and the transition zone around a sand particle may interfere with another transition zone of a neighbor sand particle. Also, because of the sand gradation, it is possible to have distinct localized bleeding around the sand particles, producing transition zones with potentially different microstructures. The understanding of the transition zone existing in mortar is not complete, however the work by Scrivener and Pratt is very promising and more research should be done in this area.

III) The knowledge of the transition zone in concrete is mainly based on the extrapolation of the microstructural knowledge gathered using simplified models. It is expected that some of the basic features already known should apply to the transition zone in concrete: a zone of lower density with a higher concentration of ettringite and calcium hydroxide (some of them with a preferred orientation). However, these hypothesis should be experimentally verified in a more complex system. Besides considering the effect of different sizes and types of aggregates, it is necessary to study the effect of admixtures such as silica fume, slag, fly-ash on the transition zone.

IV) Usually, the aggregate-cement paste interface microstructure tends to receive most of attention. This is somewhat unfair because concrete, in most of civil engineering applications, is used in association with other materials and these interfaces should be equally important. It should be noted, however, that the interface between galvanized steel and cement paste has been well described by the continuous work of the Toulouse research group.

The present writer feels that the study of the transition zone is at a turning point, and, therefore he would like to point out some research areas, where some intense work should be dedicated. Of course, the list is not complete and reflects some of the writer's personal research interests and bias.

I) The interface between the aggregate and the cement paste was studied using very simplified models. The writer feels that the researchers should now take a bold step and analyze the real microstructure existing in concrete. It would be very helpful to understand the kinetics of the transition zone between the paste and the aggregate in a real situation where there is the aggregate gradation, the effect of bleeding, the mutual effect between

aggregates, and air voids.

II) To study the effect of the existing microstructure of the transition zone on the properties of concrete. For instance, it has been taken for granted that the precipitation of CH with a preferential orientation in the transition zone has a deleterious effect on the mechanical properties of concrete because of the "easiness" to cleave along the basal plane; however there is no experimental measurement of this effect in real concrete. Also there is a lack of basic studies on the correlation between the microstructure of the transition zone and the durability of concrete.

III) Most of the work on the transition zone has been on the description of the existing microstructure.- There is a tremendous lack of mathematical modeling. These models are important to establish a scientific framework of study, which can provide sound predictions and guidelines for concrete improvements. The models should also correlate the existing microstructure with the mechanism of crack propagation.

IV) The transition zone with limestone aggregate should be continued to be studied in details, because of the practical applications and because the reaction between the calcite and the hydration products is not yet clear.

V) To study concrete (or mortar) as a complete composite material. The new research should model concrete as a porous-granular material, that is, consisted of discrete particles of rock dispersed in a porous medium. The attraction of this model is that some of the transition zone characteristics (specially a localized higher porosity) could be easily incorporated in the model. Also the inclusion of fibers could be naturally added as another phase, once the pertinent constitutive laws are given.

Finally, it should be understood that concrete is a complex system; one cannot recommend an improvement of a particular property without studying the influence on the other properties. In this sense, concrete improvement has to be dealt as an optimization problem with the adequate constrains. Suppose, for instance, that it is possible to improve the transition zone to such a degree that there is virtually no microcracking there: the concrete most likely will have a greater mechanical strength but the concrete may lose a important energy absorption mechanism and may became brittle. Another example would be the reduction of most of the CH crystals in the transition zone to improve the mechanical properties and creating potential problems of reinforcement corrosion due to the localized PH reduction.

This should not discourage the material scientists and engineers, but, on the contrary, they should unite forces to create a new "material engineering" for concrete.

COMMUNICATION REPORT OF SUB-THEME 3.1: CHARACTERISTICS AND ACTIVATION OF BLENDING COMPONENTS

RC 3.1

1 INTRODUCTION

The sub-theme 3.1 embraces 21 investigations carried out on different materials used as addition to the cement. This fact led us to classify the papers into four different groups according to the type of material. The classification was made only with the purpose of clarifying the comments on the communications.

First Group takes into account the communications about slags, Second Group about fly ashes, Third Group about silica fumes and Fourth Group, about miscellaneous materials. The latter embraces investigations of burnt clays, kiln dust, calcareous filler etc., or two or more types of the former materials.

2 FIRST GROUP: SLAGS

About 48% of the papers were included in this group that deals with investigations on activation of slags, structure and reactivity of slags and slag hydration. The following papers were listed:

- *Dissociation of Aluminium from Slag Glasses and Formation of Ettringite* by LOU ZONGHAN and collaborators, from China.
- *Alkali Activation of Indian Blast Furnace Slags* by P.S.PARAMESWARAN and A.K.CHATTERJEE, from India.
- *Activation of Synthetic Melilite Slags by Alkalies* by J. MALOLEPSZY, from Poland.
- *High Strength Slag-Alkaline Binders* by J.MALOLEPSZY and M.PETRI, from Poland.
- *Hydration of Blast Furnace Slag Particle* by K.SATO and collaborators, from Japan.
- *Some Features about the Slag Structure* by A.A.GOVOROV, from Soviet Union.
- *The Use of Microscopy for Estimating the Basicity of Slags in Slag Cements* by A.F. BATTAGIN, from Brazil.
- *Structure and Reactivity of Glassy Slags* by R. DRON, from France.
- *Physicochemical Principles of the Hydraulic Activity of Blast Furnace Slags* by Y.S. SHKOLNICK, from Soviet Union.
- *The Effect of Hydration Products in Steam Treated Steel Slag on the Hydration of Blended Cement* by WANG YUJI, from China.

2.1 Activation of Slags

LOU ZONGHAN and collaborators suggest that Al_2O_3 plays an important role on slag activity. As Aluminium dissociation and the formation of ettringite are closely related, they consider this fact an important parameter in the study of slag cement hydration mechanism. In a solution with different pH values, Aluminium will exist in the form of AlO_2^- or Al^{3+} or $Al(OH)_3.Al^{3+}$ ions in the slag glasses are four fold co-ordinated but after

the slag is attacked by alkalies, the co-ordination state of Al^{3+} changes to six fold co-ordination. Simultaneously, bridging Oxygen in glass network changes into non-bridging Oxygen. As a result, the network structure is broken. After the slag glass is attacked, the hydrate products, ettringite and C-S-H gel will form rapidly by the surface reaction between the slag glass and alkaline solution and this fact will promote the dissociation of slag glass. According to the authors, the change in the state of co-ordination of Aluminium is a result of alkaline activation. As only after this change of Aluminium co-ordination ettringite will form by the sulphate activation, the authors concluded that sulphate activation factually does not exist.

PARAMESWARAN and CHATTERJEE reported studies on alkali activated Indian slags with high alumina contents (20-24%) and low lime contents (30-35%). Experimental results showed that strength development patterns depend on the slag glass content, slag fineness and on optimisation of the activator dosage. They concluded from an exhaustive study that for the slags under consideration, an activator mix of 1% Na_2CO_3 + Na_2SO_4 + hydrated lime is practically as effective as the optimum dosage of the caustic NaOH, the former being easily handled and used.

Investigations of *MALOLEPSZY* revealed that compressive strength of hardened slag pastes depends first of all on the type of alkaline activator. Tests carried out on synthetic melilite slags with different compositions showed that Na_2CO_3 is especially suitable for activation of melilite slags rich in C_2MS_2 (akermanite) and NaOH for activation of melilite slags rich in C_2AS (gehlenite). It was also concluded that autoclaved pastes made from gehlenite slags attained the highest strengths.

In other communication, *MALOLEPSZY and NOCUN* showed by means of X-Ray Analysis and Scanning Electron Microscopy (SEM) that reaction products of Na_2CO_3 activated slag are C-S-H, calcite and a zeolite-type mineral. Using a water glass as activator, the same products were obtained but the stage of slag reaction was higher. Consequently, the contents of C-S-H phase and zeolites were also higher. The more compact structure of C-S-H gel and smaller porosity assure the higher values of compressive and bending strength in the case of water-glass activation.

SATO and collaborators investigated the factors affecting the hydration of slag particles, as for example, the particle size, the surface area and the kind of activator. They pulverized a slag to a Blaine specific surface of 3720 cm^2/g and separated it into five samples. The thickness of the hydrated layer with respect to each sample was evaluated by means of the particle size distribution and the rate of hydration. The latter was obtained after the activation of the slags by NaOH, $Ca(OH)_2$ or OPC and the dissolution of the hydrated parts by a salicylic acide-acetone-methanol solution. They concluded that the thickness of the hydrated layer on slag particles does not depend on the particle size. The rate of hydration depends only on the total surface area. It was also suggested that the difference between NaOH and $Ca(OH)_2$ in activating capacity is not noticeable up to 3 days but the NaOH effectivity is greater after 7 days. On the other hand, OPC activating capacity is always greater, especially in the early stages.

2.2 Structure and Reactivity of Slags

GOTOH reported experiences carried out on many slag samples that confirmed the important role of potential crystalline phases (related to the vitreous matrix) and its structure as factors that influence the slag hydraulic activity. Effectively, through the equilibrium diagram for the quaternary system $CaO-MgO-Al_2O_3-SiO_2$, the chemical

composition and the potential mineralogical composition, the author determined the S + A contents (percent by mol). Four different technological slag types were classified according to their S + A contents, that is, Martin process slags presented less than 40% S + A; blast furnace slags and slags produced in the manufacture of phosphorous, between 40% and 50% S + A; acid steel slags and slags from the smelting of copper and nickel with more than 50% S + A. By means of potential mineralogical composition determination and infrared analysis, *GOVOROV* found out that in slags with 40-50% S + A contents, the structural unit was the $Si_2O_7^{6-}$ (melilite, mainly), with 50-60% the structural unit was $Si_3O_9^{6-}$ (pseudowollastonite, mainly), with 60-65%, it was the anorthitic chain $Si_2Al_2O_8^{2-}$ or pyroxenitic SiO_3^{2-}. In slags with more than 65% S + A, the structural unit was the silica tetrahedron (tridymite). Therefore, the S + A contents are related not only to the different technological kinds of slags but also to their structural units. Different structural elements and different S + A contents influence the rate of silica dissolution under water action and the compressive strength.

BATTAGIN reported the existence of a close relationship between the chemical composition and the refractive index of granulated blast furnace slags. The determination of the latter may give information concerning the basicity of the slags, base of the most current methods of slag quality control. By means of the linear regression analysis, an attempt of correlating the refractive index of slags to the most usual chemical moduli resulted in correlation coefficients ranging from 0.96 to 0.99. Simultaneously, r values of 0.91, 0.86 and 0.87 were obtained correlating the refractive index of slags to the compressive strength of laboratory slag cements at 7, 28 and 90 days, respectively. In addition, the method proved to be advantageous due to the fact that it can be applied to slag cement samples, where chemical methods are limited, requiring previous and laborious slag separation.

DRON studied the slag structure by means of Raman Spectroscopy Analysis carried out on sinthetic glasses obtained after fusion at 1600°C and quenching of mixtures of pure oxides. He suggests that the glass structure is an instantaneous configuration image of the liquid after the quenching. The author proposes the concept of acid-base, that is, the characterization of the mean liquid by the parameter pO^{2-} that is similar to the pH of water solution. The pO^{2-} can be deduced from Raman Spectroscopy Analysis which originates bands that are typical of the structural elements SiO_2 (X), $SiO_{2,5}$ (Y), SiO_3^{2-} (E), $SiO_{3,5}^{3-}$ (Z) and SiO_4^{4-} (S). The glassy slag structure is characterized by a silicatic anionic *sub-network* made of SiO_3^{2-} units between $SiO_{2,5}^{-}$ and $SiO_{3,5}^{3-}$. The bond between the silicium and bridging or non-bridging oxygen atoms is covalent. Calcium, Magnesium and Aluminium (AlO^{+}) form, in their turn, cationic *sub-networks*, without internal bonds. They are self connected by electrovalent bonds. The two *sub-networks* form together the vitreous network whose bond are made by the Silicium, Calcium, Magnesium and Aluminium atoms. These atoms are bound by means of Oxygen atoms. Thus, the type of bond can be covalent or electrovalent. The latter constitutes the weaker points of the network and plays an important role in the slag reactivity. The reactivity of the glassy slag is due to its solubility in basic solutions, generally higher than the solubility of the hydrated phase originated from the hydration itself. The reactivity can be measured by means of slag solubilization in an aqueous 0.04N Sodium Hydroxide solution. On the other hand, it can be also known through the index:

$$R' = \frac{Al_2O_3.CaO}{(Al_2O_3 + SiO_2)^2},$$

which presents a good correlation to both the slag solubility and the compressive

strength. A slag of satisfactory quality has a reactivity index higher than 0.18.

According to *SHKOLNICK*, in modern methods of producing granulated slags, water cooling is mainly used. As a result, the hydrolysis of Calcium Sulphide occurs, with losses that might be up to 20-30% of initial sulphur content in the melt. Experiments carried out by adding different amounts of S^{2-} into slag samples at constant $\frac{CaO}{SiO_2}$ ratio showed an influence on slag reactivity. This influence is advantageous up to 2 - 2,5% of S^{2-}, that is, its solubility range. A further increase in its content has no effect on hydration. *SHKOLNICK* explained in his communication that this fact might be attributed to S^{2-} entrance into glassy slag structure. Within its solubility range, S^{2-} forms Si-O-Ca-S groups in which the binding energy Si-O-Ca is reduced because of the most covalent character of Ca-S bond. He concludes *In view of this it seems desirable to use air or, still better, inert gases for cooling slag melts*. Due to the reduction of sulphur losses, this would improve both the slag quality and the environmental conditions.

2.3 Slag Hydration

WANG YUJI presented the results of an investigation carried out on steel slags and blended cements made from these slags. To prevent unsoundness due to free lime hydration, slags must be treated by steams or water. By means of *SEM*, the author found out that steel slags treated in steams under different pressures for different periods originate, in their turn, different amounts of $Ca(OH)_2$ and C-S-H with different morphologies. Irregular round particles of $Ca(OH)_2$ were found under lower pressures and shorter time. With the increase of pressure and time, $Ca(OH)_2$ crystals enlarge in size and gradually change from irregular into regular hexagonal shape. Calcium silicate hydrates are chiefly fibrous and needle-like.

When the treated steel slag is used for making blended cement, the hydrates formed during the steam treatment process will decrease the cement initial hydration rate. On the other hand, they will promote the hydration of unhydrated particles of blended cement in later stages. As a result, the compactness of the hardened cement paste will increase and, therefore, the strength at later stages also will increase. The optimum condition of steam treatment for steel slag is supposed to be 1-3 atm pressure of satured steam for a time below 3 hours. In such condition most of free lime will hydrate while the degree of hydration of slag silicates will be inexpressive.

3 SECOND GROUP: FLY ASHES.

About 14% of the papers were included in this group that deals with investigations on fly ash reactivity, activation and hydration. The following papers were listed:

- *The Evaluation of Pozzolanic Reactivity of Fly Ashes* by H. SHIYUAN and C. JIPING, from China.
- *Effects of Fly Ash Grinding on the Hydration and Strength Development of Fly Ash Cements* by H. CHENG, from China and B. OSBAECK, from Denmark.
- *Reaction Process and Microstructure in Compacted Fly Ash and Fly Ash-Chemical Additive Mixtures* by M.KAWAMURA and collaborators, from Japan.

3.1 Fly Ash Reactivity

SHIYUAN and JIPING have investigated seven fly ash samples selected from various Chinese power stations. By dissolving mixtures of fly ash - CaO (ratio 4:1) and fly ash - cement (ratio 3:7) into 2N hydrochloric aqueous solution at different times, they calculated the fly ash reaction degree. The fly ash reaction degree, that is, the amount

of dissolved fly ash at a defined time, seems to possess a good correlation with the strength of fly ash - $Ca(OH)_2$ and fly ash - cement pastes. Although the fly ash reaction degree has a good correlation with the fly ash-cement paste strength, its determination demands a long time. Thus the method is not suitable for practical uses. However, the pH value of the liquid in fly ash suspension in deionized water was found to have some correlation with the fly ash reaction degree and in its turn, with the compressive strength. Measurements of pH values of fly ash suspensions might be taken as a simple and rapid method for comparative evaluation of the pozzolanic reactivity of fly ashes.

3.2 Fly Ash Activation and Hydration

CHENG and OSBAECK reported experiments carried out on a Danish coarse fly ash (specific surface of about $200m^2/kg$) that was ground to $450m^2/kg$ and $650m^2/kg$. The three materials were tested on fly ash - cement mixes with 10, 20 and 30% of fly ash replacement. When fly ash was ground, three major changes in its physical caracter were detected: its fineness was increased, there was an increase in the density due to the crushing of hollow particles and there was a change in particle shape, running away from the predominant spherical shape. These changes affected cement properties and characteristics like setting, water requirement, strength development, etc. With regard to the latter, it was shown that fly ash grinding can lead to an expressive increase of fly ash cement strength at all ages. This fact is probably due to an enhancement of the rapid aluminate reaction taking place just after the induction period, an increased pozzolanic reaction corresponding to the lime consumption, a decreased content of air entrained and a reduced intrinsic porosity of the fly ash.

KAWAMURA and collaborators investigated the microstructure of three fly ashes produced from the burning of pulverized bituminous coals. The investigations were made by means of *SEM*, X-Ray Diffraction Analysis, Differential Thermal Analysis and pore size distribution determined by Mercury Porosimeter. When usual bituminous fly ashes were compacted at an appropriate moisture condition, they exhibited a slow hardening property, the same occuring to fly ash - chemical additives mixtures. From the results obtained in their study, the authors concluded that the hardening property exhibited by compacted fly ashes was supposed to be derived from the free lime and anhydrite contained originally in the fly ash. The reaction for the formation of ettringite actively occurred in compacted fly ashes. The addition of hydrated lime and gypsum effectively promoted the formation of ettringite in compacted mixtures. The strength of compacted fly ash--hydrated lime and fly ash-hydrated lime--gypsum mixtures is closely related to the amount of ettringite and to the changes in pore size distribution. However, there was a poor correlation between strength and the amount of ettringite in compacted fly ash-portland cement mixtures. The needle-like crystals of ettringite produced on the surface of fly ash particles appear to contribute to the strength development of compacted fly ash mixtures due to the densification of their structure.

4 THIRD GROUP: SILICA FUMES

About 10% of the papers were included in this group that deals with investigations on silica fume characteristics and reactivity. The following papers were listed:

Influence of Elements (Si, Al, K, Na, Ca, Cl, C) in the Reactivity of Condensed Silica Fume by P.C.AITCIN, from Canada and A. CARLES - GIBERGUE, N. OUDJIT and A. VAQUIER, from France.

. *Blended and Special Cements Incorporating Condensed Silica Fume* by K. POPOVIC, from Yugoslavia.

4.1 Condensed Silica Fume (CSF) Characteris tics and Reactivity

AITCIN and collaborators studied 18 silica fumes from different origins. The materials are by-products of manufacture of silicon, ferrosilicon and other silicon alloys and have different chemical composition (SiO_2 ranging from 96% to 23%). Physical properties are also variable, specific surface area ranging between 7500 and 24000 m^2/kg and bulk density between 125 and 600 kg/m^2. The authors concluded that both the CSF dissolution by pure water and the pozzolanic activity (amount of fixed lime in mortar) depend mainly on the glassy silica contents. The specific surface area influences very little the rate of pozzolanic reaction. Three samples did not exhibit typical pozzolanic behaviour. CSF-16 is an inert material due to its low glass contents. CSF-8 has a low pozzolanic degree due to the presence of carbon recovering the reactive silica glassy phase, this fact promoting the decrease of the reaction rate. The elimination of carbon by heating improved the pozzolanic activity. CSF-15, due to its low silica contents and low vitrification degree, showed a low capacity of fixing hydrated lime. On the other hand, it showed a typical behaviour of hydraulic binder due to the presence of hydrated lime and dicalcium silicate in its composition.

POPOVIC and collaborators carried out experiments to find out the influence of different forms of condensed silica fume on cement properties. By comparing test results of cement samples prepared by addition of original very fine silica dust to portland cement, ground pellets of CSF to portland cement, predensed dust to portland cement and laboratory and industrial interground PC clinker and CSF pellets, they concluded that the silica fume has a positive influence on cement properties. Although some previous experiments had showed that specific surface of predensed dust was approximately one half of the original fine dust surface (for ground pellets even one third of dust) and that the pozzolanic activities of these two forms were reduced in the same proportion, the increase in cement later strengths was still significant. In addition to this, the water requirement and drying shrinkage of such cements were not so high as those caused by very fine original silica dust. This material also presented problems of handling and transport due to its inconvenient physical characteristics. According to the authors the more acceptable properties of cements incorporating ground pellets or predensed dust can be explained by the particle agglomeration. This fact reduces the active surface of silica particles and therefore their water requirement. It seems, however, that the bonds among silica particles in agglomerated grains are not so strong to hinder the pozzolanic reaction which contributes to strength and durability of hydrated cement pastes.

5 FOURTH GROUP: MISCELLANY

About 29% of the papers were included in this group that deals with investigations on blended cement composition, particle size distribution of calcareous filler, clay mineral activation, properties of blended cements with kiln dust mixtures, etc. The following papers were listed:

. *Generalized Method for the Determination of the Composition of Portland Cement Mixtures with Additions* by F.GOMA, from Spain.

. *Particle Size Distribution in Blended Cements* by D.M. SORRENTINO, from France.

. *Particle Size Distribution and Specific Surface Measurements of Components of Co-ground Blended Cements: Application to Fillers and Slags* by J.P. BOMBLED and collaborators, from France.

. *Various Activation Means of Potentially Pozzolanic Materials: Application to Lime-Pozzolana Cements* by J.P. BOMBLED, from France.

. *The Different Activation Processes of Clay Minerals to Obtain Pozzolanic Binders with Optimal Strengths* by M. MURAT and collaborators, from France.

. *Properties of Blended Cements Made with Portland Cement, Cement Kiln Dust, Fly Ash and Slag* by M. BHATTY, from U.S.A.

5.1 Blended Cement Composition Determination

GOMA has proposed a method for the determination of the composition of portland cement with additions. His method is based on the dissolution of cement samples by means of an aqueous solution of 10% hydrochloric acid (cold). The composition of soluble fraction was determined (main oxides) and a triangular diagram (SiO_2-CaO-R_2O_3) was used. Portland cements without additions from different origins gave a narrow location area. This point is technically useful when the type of cement is unknown. Different types of addition (slags, pozzolans, fly ashes, basalt rock, calcareous) gave location areas on the diagram that were sufficiently isolated to be identified very easily. So, the type of cement can be recognized. In addition, when we have the materials which make up a binary mixture, it is possible to determine the proportion of addition.

5.2 Particle Size Distribution of Blended Cements

SORRENTINO, investigating the particle size distribution in blended cements developed a method based on sieving and sedimentation with Andreasen's pippetes. He dedicated special attention to the cements with calcareous filler, in the particular case where clinker and filler are industrially produced by co-grinding. In order to obtain the respective grain size distribution of the clinker and the calcareous filler, besides the granulometric analysis, a simultaneous $CaCO_3$ content determination in each fraction was addopted. At first, the method was tested with success on three laboratory cements, since the grain size distribution of each component was previously known before the blend was made. In the three industrial blended cements, the author concluded that calcareous filler contained a high amount of very small grains. The mean ranged between 2,7 and 7,5µm. On the other hand, in the three cements, clinker contained a large proportion of large size grains, that is, 20.1, 30.9 and 35.1% of particles above 45µm. *SORRENTINO* concludes: *These grains are not easily hydrated and do not take part in the development of early strength. Thus, co-grinding is not the most well adapted process in the case where the filler of the C.P.J. (French blended cement) is calcareous, since it partially counteracts the beneficial effects brought by the addition of limestone.*

BOMBLED and collaborators also applied an interaction of sedimentation by Andreasen's pippetes and X-Ray Diffraction Analysis to investigate the particle size distribution in blended cements. Phase analysis by X-ray diffraction was truely used to crystalline materials as, for example, calcareous filler. On the other hand, when the material blended to the clinker is amorphous (case of slags), the authors suggest the use of Atomic Absortion or Plasma Spectrometry Analysis, for the determination of a trace element, like for example, Manganese in slags. Table 3 of their communication shows a complete size distribution of calcareous filler and clinker in a blended cement with 25% of filler. As

an example of this distribution we can mention the case of granulometric fraction nº 7 (diameter below 7μm) that was enriched in calcareous filler, having a 50%/50% ratio clinker/calcareous filler. Another example, the fraction nº 11 of the same blended cement, with particle diameter below 1μm, has a 10%/90% ratio clinker/calcareous filler.

5.3 Activation of Pozzolanic Materials

BOMBLED showed in his communication, results of different means of activation of various potentially pozzolanic materials from different origins. Most tests were carried out on samples of laterite, kaolin, basalt, bauxite, silica fume, pozzolan from Volvic (France) etc. To increase the pozzolanic reaction rate of mixtures of lime/pozzolan (ratio 20:80), several activation means were addopted: thermal treatment, chemical additives to improve the burning, mechanical procedure (fine grinding), chemical activation and rheological means (decrease of water contents, compactation).

The thermal treatment increases the pozzolanic activity of materials mainly due to the dehydration of clay minerals, crystallographic changes and increase of surface area (microfissuration, porosity). There is always an *optimum* temperature which enables the material to obtain a *maximum* strength. Mortar strength increased for most samples, except for the basalt and the pozzolan from Volvic. The use of chemical additives to improve the burning, like sodium and calcium carbonates, calcium, sodium and potassium sulphates etc. modifies the kinetics of temperature activation and consequently increases the compressive strength of pozzolan-lime mortar. It is remarkable in the laterite the increase of strength with the use of sodium silicate in the raw material, followed by burning at 800°C. However, a larger increase of strength is reached, in both laterite and kaolin, when these materials are burnt at 800°C and then chemically activated by sodium hydroxide or sodium silicate.

MURAT and collaborators have also investigated the activation processes but related specifically to clay materials. The use of clay materials as pozzolanic binders requires previous activation processes that are classified into chemical, thermal and mechanical activation. The chemical activation takes into account the existence of OH^- and Ca^{2+} ions in solution as elements that are able to modify or to destroy the structure of a natural or burnt clay and consequently to originate hydration products. These hydration products are responsable for the hardening properties of the pozzolanic binders. When the chemical activator is calcium hydroxide, the main hydration product in the kaolinite is the C-S-H. In montmorillonite, hydrated calcium aluminate is more frequently observed.

The thermal activation is promoted by burning some clays at temperatures between 600 and 900°C. As a result, the clay crystalline structure is more or less destroyed. Under these conditions, the burnt clay is more active than the natural clay, but it also demands the use of chemical activator to produce a material with hardening properties. A typical case of thermal activation is the kaolinite dehydration at 700-800°C that originates the metakaolinite. The metakaolinite activated by calcium hydroxide originates the C-S-H, hydrogehlenite (C_2ASH_8) and lesser amounts of C_4AH_{13}. By comparing the activity of burnt clay mineral to the natural clay mineral, the authors found significative differences. The following growing order is supposed to occur in burnt material: kaolinite > montmorillonite > illite > crystallized mica, while in natural clay mineral it was found: montmorillonite > illite > kaolinite.

Mechanical activation of clay mineral is got by grinding the thermally activated clays.

The increase of the hardening rate of these materials is due to the formation of surface defects during the grinding that increase, in their turn, the material activity.

5.4 Blended Cements Properties

BHATTY showed in his communication, results of tests carried out on three cement kiln dusts with different chemical compositions, two fly ashes and one slag. By preparing blended cement with binary, ternary and quaternary mixes, he compared some properties of blended cements to those of portland cements. Some of his main conclusions were:

- *At addition levels of 10% and 20% in binary and ternary blends, fly ashes were much better inhibitors of sulphate expansion than slag but at higher addition levels both fly ashes and slag behaved similarly in reducing the expansion significantly compared to cement alone.*

- *All ternary blends made with cement, kiln dusts and slag or fly ash showed higher autoclave expansion than cement alone except the ternary blends made with cement, high sulphate dust and Class F fly ash.*

- *Most ternary blends made from cement, high sulphate or high chloride kiln dust and slag or Class F and Class C fly ash developed significantly higher strengths than cement alone at 1 day. One year strengths of most ternary blends were higher than cement.*

- *At later ages, ternary blends containing kiln dusts and slag produced higher strengths than ternary blends containing kiln dust and either Class F or Class C fly ash.*

- *Alkali-aggregate mortar bar expansions of binary cement-kiln dust, cement-slag and cement-Class F fly ash blends were comparable to cement alone. However, binary cement-Class C fly ash blends showed much higher expansions at one year when these blends contained 20% and 30% Class C fly ash.*

YASUKO TEZUKA, Associação Brasileira de Cimento Portland

RC 3.2

COMMUNICATION REPORT ON SUB-THEME 3.2 - EFFECT OF BLENDING COMPONENTS ON HYDRATTION AND STRUCTURE FORMATION

1 INTRODUCTION

There are one principal report by H. Uchikawa, one special report by J. Calleja and 23 basic reports on sub-theme 3.2 - *Effect of blending components on hydration and structure formation.*

The 23 basic reports are coming from Japan(4), England(4), Italy(3), France(3), U.S.A.(3), China, Hungary, U.R.S.S., Poland, Yugoslavia and Argentine, (one each) as we can see in the following list:

1 - *Zeta potencial and rheological behavior of slag cement pastes.*
R.I.A. Malek, M. Silsbee and D.M. Roy - U.S.A.

2 - *Rhéologie du béton frais.*
J. P. Bombled - France.

3 - *Influence of character of blending component on the diffusion of* Na^+ *and* Cl^- *ions in hardened blended cement.*
H. Uchikawa, S. Uchida, K. Ogawa - Japan.

4 - *Measurement of* OH^- *ion concentrations of pore fluids and expansion due to alkali-silica reaction in composite cement mortars.*
J.J. Kollek, S.P. Varma, C. Zaris - England.

5 - *Hydration of alite and* C_3A *and changes of some structural characteristics of cement pastes by addition of silica fume.*
D. Andrija - Yugoslavia.

6 - *Action d'un fluidifiant et d'une fumée de silice condensée réactive aux courtes échéances sur la liaison gros granulat-mortier.*
J.P. Ollivier, J. Grandet, B. Hanna - France.

7 - *Properties of very fine blast furnace slag prepared by classification.*
K.Sato, E.Konishi, K.Fukaya - Japan.

8 - *Effect of fine mineral admixtures on the properties of hardened cement pastes.*
C.Atzeni, A.Marcialis, L.Massidda, U.Sanna - Italy.

9 - *Texture et performance des ciments fillerises.*
P. Gegout, H. Hornain, B. Thuret, B. Mortureux, J. Voland, M. Regourd - France.

10 - *Activity of fly ashes used as a pozzolanic admixtures to cement.*
W. Roszczynialski, K. Gustaw - Poland.

11 - *Behavior of Italian fly ash in portland cement mortars.*
G. L. Valenti, R. Cioffi, R. Sersale - Italy.

12 - *Effect of cement composition on the strength contribution of fly ash.*
Z.Z.Gu, B.W. Zhou, M.L. Yue, T.F. Tang, W.J. Wang - China.

13 - *Effect of* $Ca(OH)_2$ *and* $CaSO_4.2H_2O$ *on the strength of fly ash cement pastes.*
S.B. Wang, R.L. Berger - U.S.A.

14 - *The effect of the curing temperature on the pozzolanic reaction in fly ash blended cement.*
Y. Halse, H.V. Jensen, P.L. Pratt - England.

15 - *Composition of pore fluids extruded from slag cement pastes.*
M. Silsbee, R.I.A. Malek, D.M. Roy - U.S.A.

16 - *Effect of the addition of blast-furnace slag on the physical and mechanical properties of mortars cured at high temperatures.*
A.I. Elola, A.S. Szteinberg, R. J. Torrent - Argentine.

17 - *Interfacial microstructural alterations of mature blast furnace cement pastes.*
B. Marchese - Italy.

18 - *Ciments multicomposants a base des laitiers de metallurgie des metaux non ferreux.*
P.I. Bojenov, B.A. Grigor'ev - URSS.

19 = *Research on making cements of improved sulfate resistance and watertightness.* L. Opoczky, I. Vincze - Szekely, L. Szatura - Hungary.

20 = *Effect of character of glass phase in blending components on their reactivity in calcium hydroxide mixture.* H. Uchikawa, S. Uchida, S. Hanehara - Japan.

21 = *An examination of some pure and composite portland cement pastes using scanning electron microscopy with X-ray analytical capability.* A.M. Harrison, N.B. Winter, H.F.W. Taylor - England.

22 = *Effect of polymer modifications on the mechanical properties of calcium silicate and calcium aluminate cements.* N.B. Eden, J.E. Bailey - England.

23 = *Influence of kind of calcium sulfate on hardening of cement paste mixed with humic acid.* Y. Takano, Y. Mizukami - Japan.

The basic reports on sub-theme 3.2 can be classified as follows:

a) Effect of fly ashes	5
b) Effect of blast furnace slag	6
c) Effect of silica fume	3
d) Effect of mineral fillers	3
e) Effect of polymer	1
f) Effect of calcium sulfate	1
g) Methods of investigation	2
h) Influence of blending component on the durability	2
	23

Many communications pointed out that the substitution of various kinds of blending components (fly ashes, blast furnace slags, silica fume, mineral fillers etc.) for part of portland cement is interesting not only because it can improve certain properties of cement, eg. lowering the heat of hydration, lessening alkali-aggregate reaction, improving sulphate and sea water resistance but also saves energy and resources and safeguard the environment.

The effect of the blending components on the hydration characteristics of the blending cements was examined by:

- physical and mechanical tests;
- scanning electron microscopy (SEM)
- electron probe microanalyser (EPMA)
- energy disperson X-ray spectrometry (EDXRA)
- X-ray diffractometer (XRD)
- thermogravimeter (DTA)
- mercury porosimeter
- Na_2 adsorption method
- pore fluid analysis
- conduction calorimeter
- trimethylsililation method
- molybdate method
- zeta meter
- viscosimeter.

2 FLY ASH

2.1 Pozzolanic Activity

The determination of the pozzolanic activity of fly ashes is important for deciding whether a given type of fly ashes can be applied as addition to cements.

However, the measure of the pozzolanic activity of fly ashes seems to be hard because very often the various methods for determining the pozzolanic activity do not characterize this activity unequivocally.

Four communications were presented about this subject.

Uchikawa, Uchida and Hanehara[20] suggest that the simple but effective method to evaluate the pozzolanic reactivity of fly ash is amount of acid soluble $SiO_2 + Al_2O_3$.

Since fly ashes with larger amount of glass phase and higher glass basicity has higher pozzolanic reactivity, date of soluble amount of glass phase, could be considered to reflect their character.

Weakly bonded SiO_2 and Al_2O_3 with comparatively high reactivity was easily dissolved by Na_2CO_3 solution after boiled in conc. HCl (acid soluble part).

Acid soluble part per specific surface area of blending component is considered to correspond to their basicity and condensation degree of silica ion.

Wang and Berger[13] observed that the fly ash with 8% monomer and about 90% dimer and polymer, exhibited very low reactivity, only 7-12% reaction degree at 60 days. This lower reactivity is probably associated with small amount at monomer in fly ash.

Roszczynialski and Gustaw[10] report that the most reliable method of pozzolanic activity of fly ashes consists in determining the content of SiO_2 and Al_2O_3 (ASTM C 593-69) and compressive strength (method proposed by Fratini and Lea); additional determination of carbon content in ashes can be usefull. They found that carbon content above 3% renders the fly ash unapplicable as addition to cement.

In the communication[11] by Valente, Cioffi and Sersale it is shown that particle size

distribution of fly ash and their calcium oxide content are the main factors that influence the performance of fly ash in portland cement.

2.2 Hydration

The hydration of cement containing fly ash was studied by the authors by means of heat of hydration and phase composition of cement pastes.

a) Heat of hydration

Roszczynialski and Gustaw[10] found that the fly ash addition to cement diminishes the heat evolution and retards the appearance of the maximal heat corresponding to the hydration of alite and C_3A.

Those results are confirmed by Halse, Jensen and Pratt[11]. They studied the influence of the temperature on the hydration of portland cement containing 30% fly ash.

Conduction calorimeter measurements show that increasing the temperature to 40°C advances and enhances the hydration substantially, while decreasing to 10°C extends the induction period, broadens the peaks and lowers the peak rate of heat output substantially. Despite the inicial retardation of hydration, clearly the fly ash has enhanced the amount of hydration in the first 2-3 days at all temperatures.

b) Phase composition

Halse, Jensen and Pratt[14] observed that in the initial wetting and induction period, short rods of AF_t are seen to form over the surface of both cement and fly ash particles. During the acceleratory period the surfaces of both cement and fly ashes become covered with small crystals of CH and type I C-S-H, engulfing the short rods of AF_t, and AF_m phase appear as a large hexagonal platelets.

Uchikawa, Uchida and Ogawa[3] report that the ordinary portland paste had dense C-S-H around alite and large layer agglomeration of CH while fly ash cement paste contained fine C-S-H around fly ash particles and locally produced CH and AF_m phase; this later phase was increaser in fly ash cement when compared with ordinary portland cement. The amount of CH in hardened fly ash cement was decreased with the increasing amount of fly ash.

In the communication[21], Harrisson, Winter and Taylor show that in the fly ash cement, additional C-S-H is formed not only in space occupied previously by fly ash or pore solution, but also in space previously occupied by CH.

The C-S-H forming as a result of CH reacting with fly ash has a higher Aℓ/Ca ratio than that formed as inner product of alite or belite.

Harrison et al.[21] and Uchikawa et al.[3] in their communications, report that the presence of fly ashs seems to affect not only the composition of C-S-H formed close it or as its own inner products, but also that of the C-S-H formed as inner product of alite or belite, but to a lesser extent.

Habe et al.[14] found for the ordinary port land cement the Ca/Si ratio of C-S-H between 1.89 and 2.00. The inner product of either alite or belite were substantially pure C-S-H. The outer product, somewhere also pure C-S-H, but others were mixtures of C-S-H with AF_m phase or CH.

In pastes with fly ash the Aℓ/Ca and Si/Ca ratios were higher and it is likely that etrantligite (C_2ASH_8) was formed.

Uchikawa et al.[3] also show that for ordinary portland cement paste the Ca/Si ratio of C-S-H was 1.90 and for cement with fly ash addition 1.32.

2.3 Compressive Strength

According to Gu, Zhow, Yue, Tand and Wang[12], cement composition influences significantly the strength contribution of fly ash.

They report that fly ash cements, with 17 typical clinker ground to the same specific surface area, gypsum content same as that in the factors and 30% fly ash, exhibited at 7 and 28 days decreased compressive strength and increased compressive strength at 90 days when compared with cements without fly ash addition.

For the suitable clinker the strength of fly ash cement was reduced only by 10% at 28 days and increased by 15% at 90 days.

Using the regressive analyses, the authors suggest that the K_2O, C_3S and KH of cement are directly proportional to the strength, while $CaSO_4$ and C_2S are inversely proportional to that.

The C_2S is desadvantageous to the strength contribution of fly ash because the hydration rate of C_2S is very slow at earlier ages. $CaSO_4$ was inversely proportional to the strength of fly ash cement at 28 and 90 days; it might result from that the $A\ell_2O_3$ in fly ash had speed up the transformation of AF_t to AF_m.

K_2O of cement accelerated the hydration of C_2S when fly ash was added and increased the solubility of acid oxides in fly ash.

Halse, Jensen and Pratt[14] studied the influence of the temperature on the strength

and found that the highest 28 days strenght for the fly ash cement was obtained at 40°C curing, but, by 180 days curing at 20°C gives higher strength than at 40°C. Curing at 8°C appears to slow down the strength.

Wang and Berger[13] report the effect of CH and $C\bar{S}H_2$ on the strength of fly ash cement pastes. The strength decreases with the addition of CH at early ages and the more CH addition, the lower the compressive strength.

It seems that only about 10% of CH added react with fly ash, 90% of CH added exists as fine aggregate.

$C\bar{S}H_2$ added to fly ash cement decreases the strength at early ages but increases the strength at later ages.

The contribution of $C\bar{S}H_2$ added to the strength lies in the reaction of $C\bar{S}H_2$ with C_3A or with $A\ell_2O_3$ from fly ash to form ettringite in the capillary and densification of the structure of the paste at later age by the pozzolanic reaction of fly ash with CH to form C-S-H gel.

Most of ettringite were formed before 14 days and was consumed up at 28 days indicating that the contribution of $C\bar{S}H_2$ to strength was limited within 28 days.

2.4 Durability

Kolleck, Varma and Zaris[4], using the techniques of pore fluid extraction from pastes and mortar bar expansion, studied the effect of fly ash upon the potential for alkali-silica reaction.

They concluded that if the pore fluid OH^- ion concentration of fly ash cement is less than 0.3M at 180 days, a deleterious expansion with opal is unlikely to occur.

In the communication[10], Roszczyniashi and Gustaw shown that fly ash addition increases the resistance of the fly ash cement to sulphate corrosion.

Uchikawa, Uchida and Ogawa[3] studied the effect of fly ash on the depression of concrete deterioration by alkali-aggregate reaction and by chloride attack to reinforcement.

They found that the diffusion coefficient of Na and Cℓ ion through ordinary portland cement was largest while fly ash cement was smaller.

The diffusion of Cℓ ion was about ten times as large as that of Na ion.

In the fly ash cement, the diffusion of ions appears to become difficult with increasing pore volume ratio of 5-50 nm in spite of its high total porosity.

Because of fly ash cement had larger total porosity and pore volume ratio of 5-50 nm than ordinary portland cement, it is considered that fly ash cement have resistance to the diffusion of alkali ion and Cℓ ion than ordinary portland cement paste.

3 BLAST FURNACE SLAG

3.1 Hydration

Uchikawa, Uchida and Hanehara[20] consider that the hydration of slag is based on the elution of the chain structure of SiO_4^{4-} and $A\ell O_4^{5-}$ in slag by the attack of OH^-.

They found that the hydration degree of slag with high crystalline phase (15-28%) was small and that of slags with less than 5% crystalline phase, was not related to glass phase content. The hydration degree of slag was related to the amount of SiO_2 eluted by 0.1N NaOH solution.

Slags with lower content of crystalline phase and higher ratio of monomer/dimer had higher reactivity.

In the communication[21], Harrison and Winter report that reactions rims around the larger slag grains were barely detectable at 28 days old slag cement paste, but the 180 days old paste showed well developed rims up to 10μm wide. Fully reacted relics of smaller grains were also abundant.

At 180 days old slag cement paste there was a matrix apparently of C-S-H closely mixed with AF_m phase, in which were embedded the partly and fully reacted slag grains, together with relies of clinker phases, regions of CH, occasional unreacted clinker phases, and aggregats of AF_m crystals up to 30μm in size.

The slag rims and relics contained substantial amount of MgO, $A\ell_2O_3$, SiO_2 and CaO.

Uchikawa, Uchida and Ogawa[3] also report that the blastfurnace slag cement had dense C-S-H complicated with AF_m.

3.2 Compressive Strength

According to Sato, Konishi, Fukaya, Koibuchi, Ishikawa and Iijima[7], the low early strength caused by addition of granulated blast furnace slag can be improved by making it finer.

The authors shown that the strength of cement with slag 7000 cm^2/g fineness was higher than that of pure cement and considerably higher than ordinary slag cement.

Elola, Szteinberg and Torrent[16] studied the effect of high temperature curing on the strength of blas furnace slag cements.

They report that no significant acceleration of the reaction was found between mortars cured at 40°C and 80° for the portland cement, while for the slag cement, some acceleration in strength development was observed in mortars cured at 80°C when compared with those cured at 40°C. The different strength behaviour of slag cement and portland cement when the curing temperature was raised from 40°C to 80°C can be explained by the change in pore structure.

For the slag cement, the high temperature leads to a strong refinement of the pore structures.

Bojenov and Grigor'ev[18] report the use of slag from the pyrometallurgic treatment of the coppernickel agglomeration as a blending component of cement. They showed that the strength at early ages was lower than pure cement but at late ages was similar to that.

3.3 Durability

Kollek, Varma and Zais[4] and Silsbee, Malek and Roy[15] used the method of pore fluid extraction from cement pastes to analyse the effect of slag addition to cement concerning about alkali-aggregate reactions and the passivation of steel in concrete.

Kolleck et al.[4] found that blastfurnace slag invariably contribute to the OH^- ion concentration of pore fluid. This contribution depends on the alkali content of the slag and on its reactivity.

The authors concluded that the damaging effect of alkali silica reaction can be effectively reduced at higher levels of cement substitution by slag. An ON^- ion concentration of 0.5M appears to be a threshold for damaging reaction at 180 days with blast furnace slag cements.

Also, according to Silsbee et al.[15], additions of slag always lowered the alkali levels substantially from that found in the pure cements.

Tests conducted by Silsbee et al.[15] show that in the slag cement, generally the calcium levels an somewhat lower than for the corresponding pure cement, because lower calcium content of the cement and increased consuption of the calcium by the relatively silica-rich slag cement.

The sulfate levels in the slag cement remained relatively constant, while in the portland cement tended to pass through a minimum and then increase. This behaviour suggests early ettringite formation (low SO_4^- in solution) followed by release of sulfate to solution along with Ca and Al.

The authors also show that the reduction in pH values of the pore fluids extracted from the samples caused by additions of blast furnace slag is not likely to cause major deleterious effects. In all cases, the slag cements contained much lower chlorid levels in the pore solution than the pure cement.

Additionally, Silsbee et al.[15] report that the diffusion rates of ions through blast furnace slag cement paste are much lower than for portland cement pastes, diminishing the rate of penetration of harmful species from the environment.

Uchikawa, Uchida and Ogawa[3] also have concluded that the diffusion coefficient of Cl and Na ions through blastfurnace slag cement paste was smaller than for pure cement.

They observed that blastfurnace slag cement with 70% of slag tended to have larger total porosity and pore volume ratio less than 5nm whereas cement with 40% slag had smaller total porosity and larger pore volume ratio less than 5nm.

The diffusion coefficient of ions in the blastfurnace slag cement became smaller with increase in pore volume ratio less than 5nm.

Sato, Konishi, Fukaya, Koibuchi, Ishikawa and Iijima[7] confirm that the addition of granulated blastfurnace slag is effective in preventing the alkali-aggregate reaction and durability against sea water.

They report that the higher the slag content, the shallower the permeation depth of Cl^- ion.

Marchese[17] studied the microstructural modifications of reinforced slag cement past at crack surfaces and steel/cement pastes interfaces cured 6 months and then immersed for 3 years in natural sea water.

They found that the contact between static sea water and mature slag cement paste has not presented apparently alterations after long time.

The pre cracking patterns have not changed in the number and width of the cracks.

When cracks were formed in the mature paste, the sea water penetrated in them and arouse the latent chemical reactivity.

The second generation products observed were: honeycombe or reticulated C-S-H, leaf-shaped aragonite, granular Ca-rich form; flat fish shaped form, presumably of an organic nature; hexagonal lamallae of CH and fibres of ettringite type I, in pre-existing cavities.

The crack that forms at the interface paste/steel consists of two distinct surfaces. The paste surface shows a typical compact cristalline microstructure where Mg, Si,

Cℓ and Fe are present in notable quantities. Sensible larger grains of calcite are distributed in it. The steel surface shows compact areas beside extremely porous ones, both indicative of high degree of corrosion.

Malek, Silsbee and Roy[1] using the microelectrophoresis technique concluded that the zeta potential value of slag particles reflects its agglomeration tendency, the more negative its value the more dispersed the slag. Thus a negative zeta potential slag was found to exhibit favorable workability.

4 SILICA FUME

A number of investigations have reported that the silica fume a by product from the silica metal and ferro-silicon alloys production in electric arc furnaces has been mixed with portland cement from the view point of improving strengths, preventing alkali-aggregate expansion and chemical attack.

The silica fume or microsilica is a very active material with high amount of amorphous SiO_2, particles with submicron size and very high total specific surface area.

4.1 Hydration

Opczky, Vincze, Szekely and Szatura[19] verified in their investigations that silica fume reacts with CH formed at the hydration of cement. The formation of C-S-H is evident even after 3 days.

The hydration process of cement is accelerated by silica fume because even at the early stage of hardening Ca^{2+} ions are adsorbed by it and high specific surface area is ensured for the formation of hydrates. Due to the reaction between silica fume and CH, high amount of C-S-H is formed in some capillary pores thus compacting the pore structure of the cement paste.

During the hydration of cement with silica fume C-S-H phase is occuring first in form of islands of small equant grains at 3 days, then it exhibits at 7 and 28 days, elongated and fibrous morphology.

The heat of hydration for cement with silica fume is higher than that of the pure cement.

Uchikawa et al.[3] report that the cement with silica fume was rich in C-S-H, poor in Aℓ bearing hydrates; the amount of AF_m and CH was remarkably small than that in cement paste with ordinary fly ash.

According to Uchikawa et al.[20] reactivity of silica fume was dominantly controlled by specific surface area and glass phase content. The hydration degree could be evaluated by reacted $Ca(OH)_2$ and SiO_2.

Andrija[5] reports that in the cement paste containing silica fume the acceleration of alite was detected at entire 28 days period and the acceleration of hydration of the C_3A was relatively retarded at 3 days.

Because CH diminishing continue at 7 and 28 days hydration, the author suggests that the alite hydration acceleration takes place not predominantly by hydrolysis equilibrium shift due to pozzolanic lime consumption.

Olliver, Grandet and Hanna[6] studied the effect of silica fume on the interface mortar/coarse aggregate.

They found that the addition of silica fume modify the structure of the transition rims. It was not observed the preferencial orientation of the C-S-H near the coarse grains and the adhesion between the interface mortar/coarse aggregate was enhanced.

4.2 Compressive Strength

Opoczky, Vincze, Szekely and Szatura[19] report that the compressive strength of the cement increased 20-40% by addition of 15-25% silica fume.

Also, Andriga[5] report that the compressive strength of hardened cement with silica fume were increased in comparing with them of the pure cement.

4.3 Durability

Uchikawa et al.[3] showed that the cement with silica fume have smaller diffusion coefficient of alkali ions than the pure cement, and the total porosity and pore volume ratio less than 5nm increased compared with ordinary portland cement.

Opsczky et al.[19] report that the characteristic pore size in cement silica fume added is shifted from 100nm to 10 nm. They also shown that the cement with silica fume has an enhanced watertightness compared with that of pure cement and that the sulfate resistance increased 80-90% by 15-25% silica fume additions.

5 MISCELLANESUS

5.1 Filler

According to Bombled[2] the mineral fillers when added in the cement could play many roles: to replace the deficient fine grains in the size distribution curve, to fill the capillary pores, to modify the rheological properties and accidentaly to participate in hydration reactions of the cement pastes.

He reports the influence of the filler addition less than 25% to cement on the

rheology and water content was small compared with pure cement. If any influence exists, the plasticity and the cohesion was enhanced and somewhat pseudo-acceleration of the setting time observed.

Gegout, Hornain, Thuret, Mortureux, Voland and Regourd[9] report that the mechanical performance and porous texture of the hardened cement paste with up to 15% addition of limestone filler was similar to that of pure cement.

They found that the compressive strenght is proportional to the solid volume increased during the hydration of cement paste for one initial porosity.

Atzeni, Marcialis, Massidda and Sanna[8] in their experiments found that the strength properties depends not only on total pore volume but also on a new parameter related to pore distribution defined as mean distribution radius.

5.2 Polymers

Eden and Bailey[22] report the effect of polymer on the properties of calcium silicate and calcium aluminate cements.

They found that the polymers affect the hydration reaction to varying degrees, depending on their own reactivity and this may lead to a complex polymer/hydrate gel or even a chemically cross-linked polymer, rather than hydrate particle alone being the main binding agent.

The effect of reaction between the polymer and hydrates in the calcium silicate system may be limited by the presence of conventional hydrates, but in the calcium aluminates the formation of the conventional crystalline hydrates is strongly suppressed by the presence of large amount of polymer.

The mechanical properties and the durability of the polymer modified cements are influenced by the polymer content, water content, and the nature of any polymer/cement interation.

5.3 Calcium Sulfate

Takano and Mizukami[23] studied the influence of the type of calcium sulfate on the initial hydration of cement paste mixed with humic acid.

It seems that if the amount of dissolved humic acid is great with low $[Ca^{2+}] \cdot [SO_4^{2-}]$ saturation ratio in the liquid phase, as is seem when the 5% humic acid is added to cement with anhydrite, more humic acid is adsorbed on fine hydrate formed at the initial age. Thus the crystallization and conversion of initial hydrates are hampered. This retardation ends with the decrease in the dissolved amount of humic acid and the rise in $[Ca^{2+}] \cdot [SO_4^{2-}]$ saturation ratio.

At the initial age, the $[Ca^{2+}] \cdot [OH^-]^2$ saturation ratio depends on the kind of calcium sulfate added to cement and free lime of cement.

They found that the $[Ca^{2+}] \cdot [OH^-]^2$ saturation ratio decreses as the elution of Ca^{2+} from alite is hampered as a result of adsorption of humic acid thereon.

HANS ROMAN EDMUNDO BUCHER - Associação Brasileira de Cimento Portland

COMMUNICATIONS REPORT: SPECIAL CEMENTS, HIGH-ALUMINA CEMENT AND OTHER NON-SILICATIC CEMENTS

1 INTRODUCTION

The meaning and content of the chapter *Special Cements* has been always changing in the course of the last succeeding International Congresses on the Chemistry of Cements. Traditionally, only cements differing from straigth portland were considered *special* or *all others excluding portland*. Later on, any binder whose manufacture and/or use and application had a special intrinsic nature or a specific performance were considered *special*. Actually as the best-known *special cements* may be considered:

- High-alumina cement
- Expansive cement
- Oilwell cement
- Magnesium Oxychloride cement (Sorel)
- Decorative purposes cement (mainly white)
- Miscellaneous cements (phosphate, activated belitic, alunitic, anhydrite-based, etc.)

To the present Congress, 28 papers were submitted covering the following areas:

9 papers on high-alumina cement,
6 papers on expansive cement,
2 papers on oilwell cement,
2 papers on fast setting and hardening cement,
2 papers on decorative purposes cement,
1 paper on magnesium oxychloride cement, and
3 papers on unclassified subjects.

2 HIGH-ALUMINA CEMENT

The nine papers on high-alumina cement came from the following countries: Spain (1), France (2), United Kingdom (2), Hungary (1), Italy (2) and Poland (1), and have the following indicated titles and authors

(2.1) The Development of Microstructure in High-alumina Cement, by Halse, Y. and Pratt, P.L.;

(2.2) The Effect of Superplasticisers in the Hydration of Aluminous Cement, by Gill, S.M., Banfill, P.F.G. and El-Jazairi, B.;

(2.3) Hydration of Monocalcium Aluminate with Calcite, by Bachiorrini, A., Guilhot, B. Murat, M., Negro, A., Soustelle, M., and Fournier, A.A.;

(2.4) Stability of the Compond C_5A_3 in the System $CaO-Al_2O_3$, by Lucco, M.B.,and Brisi, C.;

(2.5) Aluminous Cement: How to Avoid Degrading of Mechanical Strength, by Trivino, F.;

(2.6) The Effect of Synthesis and Cooling Conditions on Phase Properties of the $C_{12}A_7$, by Grzymek, J. Derdacka-Grzymek, A., Konik, Z., Pyzalski, M., Stok, A., and Iwanciw, J.;

(2.7) A Summary of Experiences on Estimating the Expectable Changes of Strength of Concrete made with High Alumina Cement, by Revay, M.;

(2.8) The Setting and Hardening Characteristics of Calcium Aluminate Cements: Studies of the Systems $C_{12}A_7$ - C_3A and $C_{12}A_7$ - CA, by Menestrier-Sorrentino, D., George, C.M., and Sorrentino,F.P., and

(2.9) Alumina Cement Hydration in Pure Water and in Sulphate Solution in the Presence of Siliceous or Calcareous Aggregate, by Bachiorrini, A. and Cussino, L.

High-alumina cement has traditionally been a

point of concurrent interest in light of contributions sent to the last 3 International Congresses on the Chemistry of Cement: 15 papers were sent to Paris in 1980, 6 were sent to Moscow in 1974 and 9 to the 5th Congress in Tokyo in 1968. Besides these specific papers, a considerable amount of new scientific and technological knowledge has been widespread in the last decades on this subject in specialized publications. Recent advances in the field are resumed in the Principal Paper in a more comprehensive way.

Subdividing the main subject *High-alumina Cement* into the following three items:

a) formation, composition and structure;

b) hydration and hardening; and

c) properties and uses, the content of the supplementary papers received may be summarized as follows:

2.1 Formation, Composition and Structure

The authors of *Stability of the Compound C_5A_3 in the System $CaO-Al_2O_3$* (2,4) intend to prove that this compound, firstly described by Shepard, Rankin and Wright in 1909, is really a phase forming part of thermodynamical equilibrium of the $CaO-Al_2O_3$ system. They believe the compound that can be in fact considered as instable is $C_{12}A_7$ with which C_5A_3 used to be confounded in the past. Moreover, from their experimental work they conclude that pentacalcium trialuminate is far more stable at 1200°C than the mixture of C_3A plus CA. By this way of reasoning, C_5A_3 may not be just considered as transition product between these two compounds.

Another study (2.6) on the equilibrium of the $CaO-Al_2O_3$ system belongs to Grzymek and refers to the existence of two polimorphisms of dodecacalcium heptaluminate. These polimorphisms are in his opinion of isotropic and anisotropic optical nature an their transition temperature for changing from the γ to the α form can be established as 1673°K. According to his results, the researcher suggests that the *d* values, in Å, currently assigned to this compound and published in technical literature corresponds in reality to the property of a mixture of both α and γ polimorphs.

2.2 Hydration and Hardening

As could be expected in the case if high-alumina cement, this is the most interest awaking subject of all papers devoted to this kind of cement. In the last decades there has been an ever increasing attraction of the mechanism of hydration and hardening whose origin lies in the *Conversion* of hydration products and resulting in drop of mechanical strength.

The authors of paper (2.8) *The Setting and Hardening Characteristic of Calcium Aluminate Cements: Studies of the Systems $C_{12}A_7$ - C_3A and $C_{12}A_7$ - CA*, synthetized experimental high-alumina cements composed predominantly by calcium rich aluminates by fusion at 1450°C and slow cooling.

These mixtures covered a wide range of the $CaO-Al_2O_3$ interval which compound composition varied for $C_{12}A_7$ between 24 and 93% , for C_3A content was between 6 and 28% and, finally, monocalcium aluminate extended from 7,1 to 27%. Hydration of the most representative of these experimental cements revealed to the authors that reaction speed with water increases with $C_{12}A_7$ and C_3A. On the other hand, continous substitution of C_3A for CA results in predominant hydration products changing from C_2AH_8 to CAH_{10}. This constitutes a means for directing hydration compounds in a specific way.

High-alumina cements present the pecularity that the composition of their hydration products do not depend solely on the

initial anhydrous mineralogical composition, but also on water: cement ratio and temperature of the reacting media. In consequence, another way of directioning the hydration process is based on the selection of a water: cement ratio that is equal or less than the so-called *critical value*. Nevertheless it isn't always possible to fix such a value in practice by the fact that the fresh mixture has to fulfill at the same time a certain specificied workability. In accordance with this line of thought, the paper (2.2) by Gill, Banfill and El-Jazairi suggests the use of chemical additives to attain this condition in mortar and concrete with high-alumina cement. The authors used as water reducing additives high range superplasticizers jointly with water:cement ratios between 0,3 and 0,4 in the experimental temperature range from 5 to 40°C. The tendency of the additive in promoting the retarding of hydration was compensated by the researchers by adding a lithium salt. The mechanical strength of the specimens — measured indirectly by means of ultrasound pulse velocity — was considerably higher in the 5 to 20°C temperature range than in the 30 to 40°C. Unfortunately, the authors do not show results on the effect of both additives on the consistency of pastes and mortars used.

Paper (2.1) deals with the hydration process of high-alumina cement pastes during their first 12 hours cured at 8,23 and 40°C in a thermostatic bath. The authors compare pastes mixed with tap water and with sea water by means of S.E.M. complemented with X-ray diffraction and D.T.A. analysis. They also describe the evolution of the structure with time and especially accompanying alumina gel transformation besides hydration products responsible for mechanical strength. They conclude that hydration reaction speed rises with temperature but the onset of structure formation occurs first at 8 and 40°C then at 23°C. Sea water used as mixing water retarded high-alumina cement hydration.

Papers (2.3), (2.5), (2.7) an (2.9) covered specifically the *conversion* problem characterized by the transformation of the initially formed hexagonal hydrates into the cubic form with a corresponding loss in strength by the significant increase in porosity.

Révay (2.7), complementing a paper presented for the first time at the Moscow Congress in 1974, establishes equations by which he can estimate the relative strength evolution with time of concrete structures built in Hungary with high-alumina cement. By extensive sampling and testing the composition of site concretes in order tc determine the level of hydration, the extension of conversion and the degree of carbonation, he may estimate the relative stage of the strength evolution in any particular structure. In the authors opinicn, these formulas should be useful in foresighting the time by which the maximum drop in strength will occur in any specific structure unde the Hungarian prevailing conditions.

In (2.3) under *Hydration of Monocalcium Aluminate with Calcite*, the authors studied the modifications accomplished by monocalcium aluminate hydration in the presence of calcite. An analysis of the thermodynamic stability of the different possible phases present during hydration of CA and the study of the formation kinetics of the hydration products, permits the authors to conclude about the mechanism of monocarboaluminate formation. The scheme idealized here accounts for sharp differences in ionic concentrations in the solution at the calcite interface. In this way, the precipitation of carboaluminate in the neighborhood of calcite surface implies an alteration in the proportions of the hydrates formed: CAH_{10} and C_2AH_8. The increase of calcite concentration and their fineness is responsible for higher or lower amounts of monocarbonate formation. On the other hand, agitation during hydration and higher

water:cement ratios is the main cause in diminishing monocarboaluminate precipitation. Consequently, fixing calcium aluminate as tabular $C_4A\bar{C}H_{11}$ during reaction of high-alumina cement with water contributes to significantly reduce the hexagonal hydrates and their conversion.

In more or less the same way, Bachiorrini and Cussino (2.9) follow the hydration of mortar and concrete specimens during 5 and 7 years. As the title suggests, the authors compare the performance of specimens molded with calcareous or siliceous fillers and aggregates and conclude on the fundamental importance of calcium carbonate in promoting carboaluminate formation and altering pore size distribution. Micropore promotion instead of macrosizes contributes to enhance dimensional stability by reducing penetration of sulphate solution that may provoke expansion.

Finally, the contribution of paper (2.5) *Aluminous Cement: How to Avoid the Degrading of Mechanical Resistance* is the last on the conversion subject. The author focuses conversion counteraction in a multiple way in order to conclude about the more convenient remedy. The use of up to 20% calcium carbonate (fineness is not shown) in pastes and mortars in combination with different curing treatments (temperature, humidity and low pressure CO_2) is the way the researcher considers more appropriate to avoid the formation of cubic C_3AH_6 and promote AH_3, $C\bar{C}$ and $C_4A_3\bar{C}H$ instead. The only trouble of this procedure is that the more efficient curing conditions are cumbersome from the practical point of view: 15 to 72 hour duration under 70 to 105°C temperature.

3 EXPANSIVE CEMENT

Six papers were accepted from the following countries: Peoples Rep. of China (2) and one each of Bulgaria, Italy, Japan and U.S.S.R., whose titles and authors are:

(3.1) Effect of Alkali on the Expansive Properties of Sulfoaluminate Cement Pastes, by Shan-Ba, W., Shang-Xing, J., Yin-Jang, L. and Ke-Yong, H.;

(3.2) *Hydrogarnet and Calcium Hydrocarboaluminate Based Cements*, by Korneer, V.I., Andreew, V.V. and Niliforow, U.V.;

(3.3) *Calcium Sulfoaluminate made from Phosphogypsum and its Hydration Properties*, by Santoro, L., Garofano, R., and Valenti, G.L.

(3.4) *Expansive Cement With Hydroxyde Expanding Phase on Admixture's Basis* by Djabarrow, N.B.

(3.5) *Mechanism of Expansibe Pressure Development with Hydration of CaO* by Yamazaki, Y. and Sakakibara, Y.

(3.6) *Study on High Self-Stressing Aluminate Cement* by Jungan, X., Xueli, T. Wenhao, Ch., Jizhi, X., Yaozhong, X. and Yiyu, Z.

Of these six papers, two refer to type K expansive cement based on sulphoaluminates: (3.1) and (3.3). One treats about tipe M expansive cement based on high-alumina plus calcium sulphate (3.6); another handles a kind of type S expansive cement (3.2); a fifth refers to an expansive agent based on calcium oxide (3.5), and the last describes an expansive addition based on an unidentified metalic hydroxide (3.4).

Paper (3.1) is devoted to study the influence of alkali on the hydration of an expansive cement based on a mixture of high $C_4A_3\bar{S}$ clinker with gypsum. Using 0,06M up to 0,7M NaOH solution as the mixing water (w/c ratio = 0,36), the authors succeed in accelerating crystaline ettringite formation even at pH of 13,3. In this way, it is possible to reach higher expansions and

higher strength in a shorter period of time comparatively to speciments molded only with pure water. However, at later ages the mechanical strength of specimens molded with water is higher than those with the alkali solution.

The researchers of the University of Naples show in their paper (3.3) that the formation of $C_4A_3\bar{S}$ in expansive clinker by firing a mixture of calcium carbonate, alumina and gypsum is much eased when the calcium sulphate dihydrate is substituted by phosphogypsum containing fluor and phosphate. The burning temperature and the clinkering time are significantly reduced by the catalytic action of the minute impurities contained in the synthetic gypsum. According to the authors findings, there are no noticeable differences in the hydration of both clinkers.

The soviet writers of paper (3.2) describe the production of a binder based on the pyroprocessing of hydrogarnets and calcium hidrocarboaluminate rejects coming from alumina manufacture. The material can be added to cement in order to produce, among others, expansive cements.

In *Study of High Self-Stress Aluminate Cement* (3.6) the authors present the expansive characteristics of high-alumina cement combined with calcium sulfate and analyze its performance as a function of parameters like an alkalinity coefficient, SO_3 level and curing temperature. The hydration products of this cement are basically ettringite and alumina gel. The authors conclude that the hydrated cement has a high long time stability and a highly compact structure that makes this kind of cement especially suitable for concrete for hydraulic tubes or penstocks.

The use of CaO as an expansive agent is thoroughly studied in paper (3.5). The authors use a mixture of calcium oxide, ground quartz and a retarding additive for composing a product usually employed as demolition agent. The paper shows the evolution of pressure and volume increase with time of hydration and comment on the change of the crystalline structure of $Ca(OH)_2$.

4 OILWELL CEMENT

The two papers received were: one from Brazil and the other from United Kingdom and the summary of both follows.

(4.1) *The Effect of the Hemihydrated and Dihydrated Crystalline Forms of the Calcium Sulphate on the Thickening Time, Rheological Properties and Compressive Strength of the Oilwell Cement Slurries* by Silva, M.G.P., de Moraes, de Moraes, M.L.M. and Abdel--Rehim, H.A.A. the paper compares the influence of different amounts of gypsum and plaster of Paris on the specific properties of oilwell cement slurries made with three different portland clinkers for API type G oilwell cements. The authors conclude that in comparison to dihydrate, plaster of Paris raises the yield point and the apparent viscosity and may increase plastic viscosity of slurries made with the same clinker. At the same time, hemihydrate gives higher strength and delays slurry thickening up to a certain amount.

(4.2) The paper *Infrared Spectral Examination of Oilwell Cements* by Bensted, O. is centered on infrared identification of calcium sulphate forms and detection of aeration influences on type H and G oilwell cement waveband spectra in order to advance some indication of slurry performance alteration. According to the author .... *such an infrared spectroscopic examination is no substitute for the usual quality examination of oilwell cements.*

5 MAGNESIUM OXICHLORIDE CEMENT

(5.1) *Investigations on the System MgO - $MgCl_2$ - H_2O, and Hydration of Sorel Cement* by Menetrier - Sorrentino, D., Barret, P. and Saqout, S. Although Sorel cement is almost 120 years old, continously appear new works on this kind of binder, like basic research by present authors. The paper analyses kinetic behaviour of MgO + MCℓ reaction in aquous solution and the thermodynamic equilibrium of the four possible hydrates by which can be predicted outdoor exposure performance in any particular case.

6 DECORATIVE PURPOSE CEMENT

(6.1) *Peculariities of Mineral Formation and Hydration Phenomena of Decorative and High-Iron Content Cements* by Gaidjouvov, P. The author devoted his work to estabilish optimum condition for bleaching white cement clinker during pyroprocessing. By means of a (gas + plus wate vapor) mixture treatment for reduction of ferric oxides, decarbonation is enhanced, liquid formation is accelerated and whitening is favoured. On the other hand, the author gives some general outlines on a calcium-ferric clinker production for decorative application.

(6.2) *New Aspects of White Cement Physico-Chemistry* by Zoubekhin, A.P. This paper deals with the cristallochemical transformations of titanium, manganese and iron oxidizing which influence chromaticity and reflection coefficients of while cements. The author also discusses the weakening or strengthening of whiteness index by combination of these chromophoric oxides in reducing or oxyding burning atmosphere with slow cooling or quenching condition.

7 QUICK-SETTING AND HARDENING CEMENT

(7.1) *Shrinkage Problem of Quick-setting Cement* by Hosek, J., Kolar, K. and Novotny, J. The authors describe technical characteristics of quick--setting and rapid-hardening cements made in Checoslovaquia by high--fineness grinding of portland cement clinker with addition of ligninsulphonate as grinding-aid and sodium carbonate as set-retarding addition. The paper also details the way used to measure the true early shrinkage of low w/c paste, free from thermal expansion or mechanical restrain.

(7.2) *Development of a Fast Setting High Strength Cement Composite* by Lasmi , S., Mandal, P.K., Ghosh, R. and Subba RaO, V.V. The paper describes a cement which composition is based on a mixture (not indicated) of high strength portland cement, high-alumina cement, anhydrous calcium sulphate, fused calcium chloride and ground sand for special rapid setting and hardening applications (like plugging, anchoring or grouting). The material hardens in 15 minutes, attains around 10 MPa in one hour and approximately 75 MPa in one day. Heat of hydration, X-ray diffration curves, scanning electron micrographs at different hydration periods and strength development at various ages are given.

8 MISCELLANEOUS CEMENTS

Under this classification enter all binders who have in common only the word cement. A brief review of the three papers coming from India (1), U.S.S.R. (1) and U.S.A. (1) is given bellow.

(8.1) *Non-alitic Cement from Calcium Sulpho aluminate Clinker - Optimization for High-strength and Low-temperature*

Application, by Mudbhatkal, G.A., Parmeswaran, P.S., Heble, A.S., Pai, B.V.B., and Chatterjee, A.K.. These researchers optimized clinker with a mineralogical composition in the $C_4A_3\bar{S}$ - C_2S field as principal compounds and C_2AS, CA, CS, C_4AF, etc. as eventual accessory minerals. They covered in experimental trial batches firing the compositional interval of $3,6<A/S<4,0$ and $2,0<A/\bar{S}<3,0$ at L.S.F. (sulphoaluminate) equal to 1,0 at burning temperatures in the 1200 - 1300°C range. The composition with the best compromise between good mechanical strength and low clinkering temperature was later materialized in pilot plant scale in order to produce cement for field concrete evaluation. According to the authors conclusion, the non-alitic cement performed well up to 4 years exposure to site conditions showing good initial strength, no longtime reversion in mechanical resistance, good sulphate attack and corrosion performance, and excellent low-temperature behavoir during initial hydration.

(8.2) *Sulphate Resistant Alinite Cement*, by Poulatov, Z.P. and Noudelman, B.I. The paper makes a general description of composition and some properties of this kind of cement produced in the Soviet Union on industrial scale. Emphasis is given on the excellent properties against sulphate attack and data is presented on flexural strength and linear expansion of specimen stored up to approximately 2 years.

(8.3) *Hydrogarnet - Gehlenite Hydrate Cements from CaO - Al_2O_3 - SiO_2 Glasses*, by Mac Dowell, J.F. The author presents the results of a comprehensive research about the hydration of CaO - Al_2O_3 - SiO_2 glasses, which composition hasn't been much studied yet. The main feature of this work is establishing that the hydration products of these *glassy-cements* are stable hydrogarnet und gehlenit-hydrate, presenting low porosity and high mechanical strength in a fast-hardening way. The potential practical value of this research lead the author to file a patent application.

9 MISCELLANEOUS SUBJECTS

Three papers handle different aspects which are not readily grouped in foregoning subjects and are listed followingly.

(9.1) *Cement of Thermally Activated Laterites. Role of Iron Oxydes on the Strength Development*, by Pera, J. Ambroise, M., Murat, M. and Silveira, M. This contribution belongs to the subject more properly covered by the pozzolanic materials. The authors submitted different laterites to heat treatment at 750°C in order to activate their kaolinitic minerals. Best pozzolanity was achieved with materials containing less than 50% quartz and whose kaolin has a minimum of 10% iron oxyde.

(9.2) *The Behavoir of Certain Compositions Belonging to the $3CaO.SiO_2$ - $2CaO.SiO_2$ - $2BaO.SiO_2$ System During Hardening*, by Teoreanu, I., and Andreonescu, E.. The authors have synthesized different mixtures containing CaO, BaO and SiO_2 with the aim of producing mineral compounds of the form indicated in the title of the paper. The experimental cements were tested in order to evaluate some of their physical properties in pastes at the initial hydration period and the evolution of hardening by means of compressive strength up to 21 days. According to the authors, the introduction of BaO contributes to stabilize C_2S ss in the α' form during pyro-

processing and to enhance the reactivity with water with a positive effect on hardening by raising mechanical strength.

(9.3) *The influence of Some Additions on the Hydration and Hardening of Tricalcium Aluminate*, by Teoreanu, I. Georgescu, M. and Puri, A.. The paper describes through XRD and DTA data the behavoir of C_3A during hydration in the presence of gypsum and dimethylterephtalate (DMTP).

S. PRISZKULNIK

RC
4.1

Le sous-thème 4.1 "STRUCTURE DES PORES, PERMÉABILITÉ ET DIFFUSION EN RAPPORT À LA DURABILITÉ"a été enrichi par la présentation des 12 travaux suivants:

1. "Microfissuration des bétons", par H.HORNAIN et M.REGOURD.

2. "Le rapport entre la microstructure et la durabilité des ciments avec ajouts", par N.TENOUTASSE et A.M.MARION.

3. "À l'égard de l'analyse de la structure poreuse du ciment durci", par G.BOZHINOV et N.BAROVSKI.

4. "Sur la distribution de chlorure dans la pâte de ciment durcie et sa solution poreuse", par G.BLUNK, P.GUNKEL et H.G.SMOLCZYK.

5. "Rôle de la porosité dans la durabilité des liants hydrauliques", par E.REVERTEGAT et F.BERNAUDAT.

6. "Relation entre la lixiviation d'éléments traces (Cs,Sr et Co) et la microstructure au cours du vieillissement d'un mortier à base de CPA", par J.M.LAMEILLE, R.CHIAPPINI, G.GOUTIÈRE, J.C.PETIT et M.REGOURD.

7. "Modélisation des phénomènes de transport dans les mécanismes d'altération d'une pâte de ciment", par F.BERNAUDAT et E.REVERTEGAT.

8. "Structure poreuse et diffusion ionique aux systèmes adjuvant-ciment Portland avec ajouts", par AMITABHA KUMAR et DELLA M.ROY.

9. "Influence des cendres volantes, ajoutées au ciment, sur les changements de la structure des pores dans les mortiers conservés dans des solutions de NaCl", par S.KRISHNAMOORTHY et N.K.JAIN.

10. "Résistance au gel des ciments aux fillers", par P.GEGOUT, H.HORNAIN, B.THURET et M.REGOURD.

11. "Influence des conditions de durcissement sur la durabilité de la pâte de ciment et du béton", par G.TEODORU.

12. "Le mesurage de la perméabilité", par C.D.LAWRENCE.

La quantification du réseau microfissural des bétons fait l'objet du travail nº 1.

Le travail nº 2 concerne l'évolution de l'hydratation des ciments Portland avec ajouts de cendre volante et inclut un modèle pour le mecanisme de la réaction pouzzolanique.

Le travail nº 3 présent un modèle physique pour l'analyse de la structure poreuse de la pâte de ciment.

Le travaux nº 4 à 9 présentent l'évolution de la diffusion ionique dans la structure poreuse des pâtes de ciments sans et avec ajouts minéraux, ayant en vue soit la résistance à la corrosion de l'acier soit l'interaction avec des déchets atomiques.

La rélation entre la résistance mécanique et la structure poreuse avec la tenue au gel fait l'objet des travaux nº 10 et 11.

Finalement, le travail nº 12 présente une cellule pour mésurer la perméabilité et la diffusion de gas et la perméabilité à l'eau des bétons.

La qualité et l'actualité des cex travaux exigent la présentation et la discussion de chacun d'eux. La restriction du temps a determiné ce resumé que, malheuresement, ne transmet pas avec fidelité leurs précieuses idées.

S. PRISZKULNIK

Dans l'étude intitulé" MICROFISSURATION DES BÉTONS", M.HORNAIN et M.REGOURD ont observé et quantifié le réseau microfissural de bétons.

Les techniques microscopiques et stéréologiques ont été appliquées à l'étude de deux bétons avant et après chargement: l'un de granulats silico-calcaries et l'autre de granulats légers.

Les observations ont été effectuées à 3 échelles (niveaux de structure I, II e III).

À l'échelle centimétrique (niveau de structure I), les exames ont été faits sur plaques polies de béton 10x10 cm, aux gradissement 4 à 40 à l'aide d'une loupe binoculaire qui permet l'observation des distributions et orientations préférentielles des granulats et des interfaces.

À l'échelle millimétrique (niveau de structure II), l'observation a été faite sur sections polies, lames minces ou de répliques, à l'aide du microscope optique ou au microscope électronique à balayage (M.E.B.) à des grandissements compris entre 300 et 1000 environ.

En plus, à l'échelle micrométrique (niveau de structure III), les auteurs ont utilisés le MEB sur fractures, aux grandissements 1000 à 10.000.

Les auteurs discutent les techniques de traitement préalable des échantillons, et le risque que ces opérations peuvent engendrer des contraintes mécaniques, donc des microfissures. Un certain nombre de précautions sont recommandées: échantillons suffisament épais, sciage ménagé, plissage progressif, et contrôle de la déshydration des échantillons destinés aux observations microscopiques.

Pour la visualisation et observation des microfissures, au niveau de structure I, les auteurs utilisent la coloration du béton à l'aide d'une solution alcoolique d'un colorant insoluble dans l'eau (rouge Irgacete par example).

La méthode par imprégnation de résine (epóxy, méthyl-métacrylate...) est surtout utilisée pour caractériser le niveau de structure II. La fractographie au MEB permet la caractérisation du faciès des hydrates et de leur mode de rupture, l'étude des interfaces pâtes de ciment-granulat; l'observation du mode de rupture des granulats et autres inclusions.

La technique des répliques a été aussi developpée et utilisée, permettant l'observation soit au microscope optique en transmisson ou en reflexion, et au MEB après métallisation à des grandissements ne dépassant pas 1000.

Pour la quantification du réseau microfissural, les auteurs ont utilisé la stéréologie, par laquelle ils ont mesuré le nombre d'intersections des microfissures avec un réseau de sécants aléatoires ou orientées.

L'application de ces méthodes a un béton de granulats silico-calcaires et aussi un de granulats légers de schiste expansé a permis d'extraire les conclusions suivantes:

a) avant chargement, au niveau de structure I, dans les deux bétons , des zones de moindre cohésion assimilables à des fissures se manifestant par la pénétration ou la diffusion du colorant, existent aux interfaces pâte de ciment durcie-granulats. Leur quantification montre que leur densité est plus faible dans le béton de granulats légers, la différence étant due à une meilleure liaison entre le liant hydraté et les granulats de schistes expansés.

b) après chargement, les observations faites au niveau de structure I, mettent en évidence

dans les deux bétons la formation d'une fissure principale sous forme d'une bande étroite microfissurée, de quelques centaines de microns de largeur, tortueuse souvent oblique par rapport à la direction de contrainte.

Sous chargement contrôlé, la fracture des deux bétons est essentiellement intergranulaire, sauf localement ou les granulats étaient préfissurés. Dans le béton silico-calcaire, la trace des différentes microfissures constituant la fissure principale est nette et bien dessinée; par contre, elle apparaît plus diffuse dans le béton de granulats légers, dont les propriétés mécaniques (module d'Young en particulier) sont plus proches de celles de la pâte. Cet aspect plus diffus paraît correspondre a un microendommagement de la pâte de ciment proprement dite sur le trajet de la fissure.

S. PRISZKULNIK

Au travail de N.Tenoutasse et A.M.Marion, sous-titre "LE RAPPORT ENTRE LA MICROSTRUCTURE ET LA DURABILITE DE CIMENTS AVEC AJOUTS", il a été etudiée l'évolution de l'hydratation des ciments composés d'un ciment Portland et de cendre volante, aussi bien que discuté le mécanisme de la réaction pouzzolanique et son rapport avec l'inhibition de la réaction alcalis-granulats.

Les auteurs ont employé un ciment Portland du type I de l'ASTM et une cendre volante de la classe F de l'ASTM, avec lesquels ils ont préparés des ciments contenant de 0 a 80% de cendre, dont l'hydration a été examinée par microscopie électronique à balayage avec le spectre de diffraction des rayons X par énergie dispersive, dès l'âge de 3 jours jusqu'à 2 ans.

La solubilité des alcalis de la cendre a été analysée encore par spéctrométrie d'absorption atomique.

A propos de la solubilité des alcalis de la cendre dans l'eau et dans des solutions saturées de chaux, des essais ont été faits au ciment Portland et au ciment avec ajout de 25% de cendre, pour la détermination de la composition chimique de la solution poreuse dès 5 minutes jusqu'à 8 h.

Les résultats montrent la basse solubilité du K_2O de la cendre, sa libération étant plus facilité à partir du ciment. En relation au Na_2O, aucune altération significative a été observée par la présence de la cendre dans la composition du ciment, ce qui confirme la plus basse solubilité des alcalis de la cendre.

Les micrographies électroniques de l'hydratation des ciments avec ajouts montrent, déjà à l'âge de 14 jours, l'activité pouzzolanique de quelques particules de la cendre volante, à cause de l'occurrence des cristaux typiques de mullite sur ses surfaces. Cependant, la présence de chaux libre et le comportement mécanique de tels ciments composés ne permet la caractérisation d'une importante réaction pouzzolanique à cet âge.

Les auteurs signalent la persistance des particules des cendres intactes après 2 ans d'hydratation, même aux ciments composés avec 10% de cendre, ce qui révèle la profonde hétérogéneité de la réaction pouzzolanique, liée à l'histoire thermique de chaque grain de cendre.

La réaction évoluant, des macropores se font visibles à la surface des particules de cendre, pourtant ils sont invisibles sur les particules intactes.

Au dernier stage de la réaction, les particules se desintègrent.

La réaction pouzzolanique cause la formation massive de silicate de calcium hydraté. La diffraction des rayons X par énergie dispersive révèle la présence de teneurs pas méprisables d'aluminium au silicate, ce qui bien démontre la réaction pouzzolanique entre la phase vitreuse silico-alumineuse de la cendre et l'hydroxide de calcium.

Après des longues périodes de temps d'hydratation, la microscopie électronique ne montre dans la pâte de ciment aucun trait de cristaux de mullite, tandis que la diffraction des rayons X révèle un spectre typique de mullite. On obsèrve, aussi, le monosulfoaluminate de calcium (MSA), mieux cristallisé que dans la pâte pure.

Un aspect notable dans les micrographies concerne la présence des plaques bien cristallisées au ciment composé, avec une morphologie qui rappele celle du $Ca(OH)_2$ et/ou du MSA, mais la diffraction des rayons X par énergie dispersive présente des hautes teneurs de silice et d'alumine et un contenu apreciable de potassium. Le numéro des plaques paraît être proportionnel au contenu de cendre dans la pâte durcie.

S. PRISZKULNIK

La présence de potassium démontre que les alcalis de la cendre sont maintenus dans les produits hydratés qui résultent de la ráction pouzzolanique.

L'analyse des résultats a été, alors, étendue à la réaction alcalis-silice, attribuant l'action bénéfique de la cendre à la facilité de mobilisation du calcium dans les particules siliceuses reactives, ce qui amène à la formation du gel avec haute concéntration en calcium. De la réaction du complèxe alcalis-silice avec le $CA(OH)_2$ résulte le complèxe blanc et opaque d'hydroxide de calcium hydroxide alcalin-silice, non expansible.

Les observations effectuées ont permis, encore, la présentation d'un mécanisme originel pour expliquer la réaction pouzzolanique, incluant les 3 stages suivants:

- diffusion de la phase aqueuse à travers de la pâte de ciment et ou des macropores des particules de cendre aux locaux actives;

- précipitation de $Ca(OH)_2$ au local active (interne ou externement) pour former des masses circulaires de $Ca(OH)_2$;

- réaction entre les masses et la phase vitreuse silico-alumineuse des particules de cendre, amenant à la formation du gel de silicate de calcium-hydraté contenant de l'aluminium (et le potassium en quelques cas), et du silicoaluminate de calcium bien cristallisé contenant du potassium.

S. PRISZKULNIK

Dans le travail intitulé "À L'ÉGARD DE L'ANALYSE DE LA STRUCTURE POREUSE DU CIMENT DURCI", G.BOZHINOV et N.BAROVSKY proposent un modèle physique pour définir et illustrer les principaux caractéristiques de la pâte de ciment.

Les auteurs signalent les suivants facteurs qui intérviennent à l'origine des pores:

a) Immédiatement après le mélange du ciment avec l'eau, le volume absolu de la pâte resulte des parties des volumes du ciment, de l'eau de gâchage et éventuellement par des bulles d'air. Les parties de l'eau et les bulles composent ce qui est appelé volume libre de la pâte du ciment qui est premièrement disponible pour l'augmentation des produits d'hydratation dy ciment.

b) Pendant l'hydratation, ce volume libre augmente par conséquence de la réaction du ciment avec l'eau ayant une partie remplie en même temps avec les produits d'hydratation. Ainsi la quantité d'eau de la pâte est une des principales sources des pores et l'état de l'eau dans le système durci est très important.

c) Les produits d'hydratation présentent des formes et dimensions variées avec plus ou moins d'embriquement entre les particules dont la phase liquide présente des propriétés specifiques au système durci.

Le volume absolu des hydrates est plus grand que celui des grains anhydres, mais il est plus petit que le total des volumes absolus des grains anhydres et de l'eau d'hydratation. Comme, pendant l'hydratation, le facteur E/C en plus de celui strictement demandé par les réactions ne change pas le volume initial de la pâte, le résultat de cet équilibre cause les pores de contraction.

d) La structure complexe des hydrates, ayant des surfaces specifiques, des capacités d'absorption et adhérence extrêmement developpées, outre de la distribution reciproque et de la cohésion entre les particules, predéterminent les conditions à la formation d'une structure poreuse typique.

Dans ce contexte une partie de l'eau est combinée dans les produits d'hydratation, une partie est absorbée aux surface solides et une partie reste hors des champs de force des surfaces solides (eau capillaire). Ces espèces d'eau, présentent des densités diverses et, par conséquent, sont différents quant à leur volumes specifiques, à la force d'adhérence à la phase solide et la volabilité. Sont les espèces que Powers a appelé l'eau évaporable et non évaporable

Ainsi, l'éspace occupé par l'eau évaporable dans la pâte durcie du ciment corréspond au volume total des pores, lequel contient les pores du gel et les pores capillaires. Les pores du gel sont differenciés par Kando et Daiman en intercrystallite et intracrystallite.

On obtient alors que le volume total des pores peut-être presenté par la partie durcie à un certain âge et le volume absolu de la phase solide au même âge, pourvu que le contenu d'air ne soit pas consideré. Dans certains cas la porosité de contraction doit être specialement considerée et traitée comme une partie en separée du volume total des pores.

Pour quantifier les parties des volumes de pores du gel, pores de contraction et pores capillaires, les auteurs proposent, alors, un modèle physique pour la pâte de ciment.

Le concept basique du modèle est que l'origine et l'évolution dans le temps de la structure poreuse sont relacionnées à l'état initial de la pâte et suivent le procès d'hydratation du ciment. Il tient en compte que la contraction est due principalement au gel d'aluminates de calcium hydratés et occupe une partie de l'éspace intra-gel rempli par l'eau capillaire. Les pores du

S. PRISZKULNIK

gel sont relacionnées au gel des silicates de calcium hydratés.

La validité du modèle est limitée aux conditions suivantes:

- le clinker du ciment reçoit seulement l'addition de gypse;
- l'hydrataion a lieu dans un tube d'essai, à la température d'ambiance, de manière à éviter l'évaporation;
- l'hydratation des composés du clinker ne diffère pas de l'hydratation des minéraux purs, le principe de superposition d'effets étant valide;
- le gypse réagit completement avec le C_3A pour former l'ettringite pendant la période initiale d'hydratation;
- le mot gel se refère au gel de silicate de calcium hydraté;
- la teneur en air de la pâte de ciment n'est pas considerée.

Pour le calcul des différentes parties de volumes de pores, sont considerées la composition minéralogique du ciment et les équations chimiques correspondentes aux réactions d'hydratation.

Pour essayer le modèle proposé, les auteurs ont preparé des pâtes de ciment, avec des rapports E/C = 0,30-0,35-0,40-0,45 et 0,50, et ils les ont mises dans de tubes de verre, maintenus hermetiquement fermés à la température d'ambiance, pour les essayer aux âges de 1,3,7,28 et 180 jours.

La quantité d'eau combinée a éte mesurée par analyse thermique différentiel; le volume total des pores a été estimé sur la base de la masse volumique et du poids spécifique de la pâte durcie. La distribution des pores entre 5 et 10^4 nm a été mesurée par le porosimètre à mercure, pour évaluer les pores de contraction et capillaires. La capacité d'absorption a éte mesurée par la méthode d'absorption d'eau.

Les résultats ont confirmé la tendance générale du développement de la structure poreuse avec la réduction progressive du volume total des pores au cours du temps et la conséquente rédistribution des parties des volumes des pores, c'est à dire l'augmentation des volumes des pores du gel et de contraction et décroissement des volumes des pores capillaires et bulles d'air.

Comparant les valeurs estimées selon le modèle, les auteurs ont confirmé une bonne approximation avec le volume total des pores, tandis que la prévision des parties des volumes éxige une confirmation expérimental additionelle.

S. PRISZKULNIK

Au travail intitulé "SUR LA DISTRIBUTION DE CHLORURE DANS LA PÂTE DE CIMENT DURCIE ET SA SOLUTION POREUSE", les auteurs G.Blunk, P. Gunkel et H.G. Smolczyk, ont appliqué de pressions jusqu'à 500 N/mm² (MPa) pour l'extraction de la solution contenue dans les pores des pâtes de ciments, aux phases de prise et de durcissement, ayant pour objet l'étude de l'évolution de la concentration des chlorures de sodium et de calcium.

Ils ont été utilisés plusieurs ciments Portland et de laitier, aussi bien que les minéraux purs du ciment C_3S et C_3A. Le C_3A a été mélangé avec le $CaSO_4$. H_2O et $Ca(OH)_2$ dans la rélation moléculaire 1:1:0,3.

Les pâtes des ciments et celle contenant le minéral C_3S ont été préparées avec un rapport E/C de 0,60, tandis que la pâte du minéral C_3A a été preparée avec E/C de 0,90.

Pour l'étude à la phase de prise, le chlorure a éte ajouté à l'eau de gâchage des pâtes en teneurs variables de 0,2 a 3,0% par rapport au poids du matériau sans perte au feu.

Pour l'étude à la phase du durcissement, ils ont broyé et tamisé des pâtes sans chlorures et ont conservé les grains compris entre 0,5 et 1 mm dans une solution de chlorure, pendant 28 jours, pour les essais de diffusion.

Les résultats ont montré que le mélange du C_3A fixe une grande partie des chlorures, aussi bien que du calcium et sodium.

Les essais avec C_3S ont montré que les chlorures sont fixés aux ciments non seulement chimiquement pour les aluminates, mais aussi pour les silicates hydratés. En effet, les ciments fixent des teneurs de chlorure compris entre ceux fixés par les minéraux C_3A et C_3S.

Le C_3S a une capacité de fixer les chlorures inférieure à celle du C_3A. Particulièrement, le chlorure de calcium est fixé en grande quantité par le C_3S, tandis que pour le chlorure de sodium elle est limitée, de manière que, au cas du chlorure de sodium, la teneur de chlorure restante en solution est plus grande, comparativement au chlorure de calcium. En même temps, selon les mesures effectuées dans la solution contenue aux pores, le pH accroît avec de chlorure de sodium et decroît avec celui de calcium, par rapport au pH de la solution sans chlorures.

Considérant, alors, la rélation d'ions Cl^-/OH^-, importante pour la corrosion de l'acier, les auteurs l'ont calculée à partir des valeurs mesurées dans des solutions contenues aux pores des pâtes dont l'eau de gâchage a reçu l'addition de 1% de chlorure.

Les résultats ont montré que le désavantage de la plus grande concentration de chlorure de sodium dans la solution est contrebalancé par l'alcalinité supérieure. Ainsi, le chlorure de calcium doit être également consideré ou, bien encore, moins favorable à la corrosion de l'acier par rapport à celui de sodium.

Pour complémenter, ils ont calculé la rélation d'ions Cl^-/OH^- pour des solutions contenues aux pores des pâtes dont l'eau de gâchage a reçu l'addition de chlorure de sodium et qui ont été préparées sans et avec l'addition de sulfates de calcium et de sodium et d'hydroxide de sodium, à la proportion de 0,10 mol par kg de ciment.

Par rapport à la solution sans addition, les résultats ont montré que l'addition de sulfate de calcium augmente un peu la teneur de chlorure soluble, tandis que l'addition d'une quantité equivalente d'hydroxide de sodium augmente d'un tiers la teneur de chlorure soluble et, finalement, l'addition de sulfate de sodium double cette teneur.

Comme les deux additions, de NaOH et Na_2SO_4, augmentent la concentration de OH^- dans la même échelle, les auteurs montrent que, au cas du sulfate de sodium, les deux anions OH^- et SO_4^- diminuent la fixation de chlorure.

S. PRISZKULNIK

Le rapport presenté par E.Revertegat et F. Bernaudat sous-titre "ROLE DE LA POROSITÉ DANS LA DURABILITÉ DES LIANTS HYDRAULIQUES" fait part d'une étude de la prévision de la durabilité des liants hydrauliques utilisés dans les stockages des déchets radioactifs pour la fabrication de l'infrastructure des conteneurs et des matrices d'enrobage.

Pour justifier une durabilité sur 300 ans de ces liants, deux types d'essais sont menés en parallèle:

- mise en évidence des interactions chimiques entre les pâtes de ciment et diverses solutions aggressives(chlorure, sulfate, acides carboniques et humiques) qui peuvent être présents dans l'eau souterraine dans un site de stockage de déchets;

- détermination des paramètres régissant le transport des ions en solution dans la pâte de ciment et, en particulier, mesure des coefficients de diffusion.

Le travail présente les premiers résultats concernant les ciments CPA et CLC, agressés par des solutions de NaCl.

Les éprouvettes utilisées dans l'etude des mécanismes d'interactions chimiques sont des plaquettes rondes de 4 mm d'épaisseur et de 70mm de diamètre. Le rapport E/C des pâtes est de 0,37. Après conservation des plaques pendant 3 mois dans une eau saturée en chaux, elles sont immergées dans des bacs, dont la concentration em ions Cl^- est respectivement de 0- 0,2- 2et 20g/l. Pour chaque concentration, deux valeurs de pH sont étudiées: 11,5 et 13.

A chaque échéance (0-1-3-6 mois) les mesures et analyses suivantes ont éte réalisées: resistance mécanique en flexion; porosité au mercure et à l'eau; teneur en $Ca(OH)_2$par thermogravimétrie; analyse chimique des éléments par fluorescence X; profil de diffusion du chlore par microanalyse électronique; étude microstructurale par diffraction des rayons X et microscopie électronique à balayage.

L'étude de la diffusion est réalisée en cellule de diffusion sur des éprouvettes de 4mm et 1,5mm d'épaisseur . Le pH de la solution dans chaque compartiment est égal à 13. La concentration en ions Cl^-dans le compartiment "amont" présente les valeurs 0,2, 2 et 20g/l, et la teneur en ions chlorure qui diffusent dans le compartiment "aval" est analysée par chromatographie en phase liquide.

Les auteurs présentent les conclusions suivantes:

La principale dégradation observée dans une pâte de ciment CPA, soumise à l'agression d'une eau chlorée, ne sera pas due à l'apparition des chloroaluminates, mais à une augmentation de la porosité engendrée par la solubilisation de l'ettringite et essentiellment de la chaux. Ce phénomène de solubilisation et de lixiviation de $Ca(OH)_2$ est d'autant plus important que le pH de l'eau de contact est faible et que la concentration en ions Cl^- est élevée.

Pour une pâte de ciment CLC les differences essentielles de comportement avec la pâte de ciment CPA sont les suivantes:

- une distribuition de pores à l'origine plus fine et qui ne pourra que s'accentuer lors de l'hydratation progressive de produits siliceux. Par conséquence le ciment CLC possède un chemin diffusionnel, pour les ions agressifs ou radioactifs, plus fins que le ciment CPA;

- une quantité de $Ca(OH)_2$ a l'origine plus faible et qui ne peut que décroître lors de l'hydratation. Par conséquence un ciment soumis à l'action des chlorures étant

essentiellement affecté par la disparition de la chaux, le ciment CLC sera plus résistant qu'un ciment CPA;

- après attaque, l'augmentation de la porosité totale est nettement inférieure (+ 18% au lieu de 62% pour les ciments CPA à l'echéance de six mois dans une solution à 20 g/l de Cl^-). La quantité de chaux qui réagi avec les chlorures et qui s'est lixiviée est nettement moins importante que celle d'un ciment CPA;

- absence d'un domaine poreux entre 0,06 µm et 0,90 µm, observé sur les ciments CPA après attaque, et qui a été attribué à la lixiviation de la chaux;

- bien qu'un retard dans l'hydratation des produits siliceux a été observé à pH = 11,5 un début de cloisonnement de la fine porosité apparaît pour les fortes concentration en chlorure. Ce phénomène est probablement dû à l'apparition abondante de chloroaluminate dans une structure peu lixiviée. Pour de ciment CPA il y a à la fois cloisonnement et augmentation de la fine porosité, sous la double action de l'appartition des chloroaluminates et de la lixiviation importante de la chaux et de l'ettringite.

Lorsque les ions Cl seront véhiculés dans une eau interstitielle de pH = 13 la modification de la matrice du ciment CLC sera pratiquement inexistante. Il n'existe donc pas une barrière "protectrice", comme dans le ciment CPA, qui pourrait freiner la lixiviation des radioéléments vers l'extérieur du béton. Reste à savoir comment évoluera cette "barrière" lorqu'elle sera atteinte par le front de dégradation.

S. PRISZKULNIK

Le travail sous-titre "RELATION ENTRE LA LIXIVIATION D'ELEMENTS TRACES (Cs, Sr et Co) ET LA MICROSTRUCTURE AU COURS DU VIEILLISSEMENT D'UN MORTIER A BASE DE CPA", presenté par J-M.Lameille, R.Chiappini, G.Goutière, J-C.Petit et M.Regourd concerne les relations existentes entre les relâchements de certains radioéléments (60 Co, 90 Sr et 137 Cs) sous l'action du lessivage par l'eau et l'évolution des caractéristiques cristallochimiques et microstructurales de la matrice cimentée à base de ciment Portland artificiel (CPA) dans laquelle certains déchets radioactifs sont solidifiées, en vue de leur stockage.

L'étude a envisagé les 2 types possibles d'altération affectant le confinement des radioéléments, soit la déstruction directe de la matrice due aux différentes aggressions physiques et chimiques, et les modifications minéralogiques, structurales ou textures qui pourraient conduire à une augmentation excessive des relâchements de radioactivité.

Le mortier utilisé comme enrobé avait la composition suivante: 1000 kg de ciment, 750 kg de sable, 400 l de concentrât d'evaporateur, c'est à dire d'une solution contenant principalement des borates de sodium (~25.000 ppm de bore) et 60 kg de chaux, ce qui donne un rapport E/C de 0,4. La chaux introduite sert à stabiliser les borates sous forme calcique et donc à diminuer leur effet retardateur.

Ce mortier a été utilisé pour la confection des éprouvettes 2 x 2 x 16 cm, qui ont été placées sous une couverture de 2 cm d'argile, recouverte par 2 cm d'eau.

En plus d'une étude en "temps réel" à 10°C (température interne du site) qui sert de reférence, les auteurs ont choisi d'accélérer les cinétiques tout en évitant de dégrader trop brusquement et articiellement la matrice. Ceci a été réalisé en augmentant la température de conservation des éprouvettes jusqu'à 60°C. A chaque échéance, ils ont mesuré sur les différentes éprouvettes les paramètres physiques suivants: résistances mécaniques en compression, porosités, masses et gonflements. La microstructure a été étudiée au moyen d'un microscope électronique à balayage (MEB), d'une microsonde électronique et de la diffraction des rayons X.

Les éprouvettes dopées au césium 137 ou au cobalt 60 sont des orthocylindres carottés de 2 cm. Elles ont été ensuite stockées à 10°C, 40°C ou 60°C pendant un temps donné, puis lixiviées à 10°C dans de l'eau déminéralisée. Les lixiviations ont été menées en dynamique, c'est-à-dire avec renouvelement de l'eau: 3 fois la première journée, chaque jour la première semaine, chaque semaine le premier mois, chaque mois le premier semestre et enfin tous les semestres. Un enrobé n'ayant pas subi de vieillissement (lixivié immédiatement après la cure en atmosphère humide) sert de referénce. Les mesures de radioactivité dans les lixiviats on été effectuées au moyen d'un spectromètre muni d'un détecteur NaI ou GeLi.

Lors des expériences d'hydratation des composés simples, il a été étudié la rétention de chaque élement trace au cours des hydratations de C_3S, de C_3S + C_3A puis de C_3S + C_3A + gypse avec un rapport e/s ~10. La filtration a été effectuée sur filtre millipore de 0,45 µm et l'hydratation a été stoppée par trois lavages à l'éther et par cryosublimation. Le solide a été ensuite examiné au cours du temps au moyen de diverses techniques physiques d'analyse complémentaires (MEB, DRX, microsonde électronique et ionique etc...). La solution a été analysée soit par volumétrie et par absorption atomique.

La principale observation de cette étude est qu'il n'existe pas de lien directe entre les variations, au cours du vieillissement,

S. PRISZKULNIK

des caractéristiques macroscopiques de la matrice cimentée (résistances mécaniques, porosité, texture etc...) et les taux de lixiviation du césium et du cobalt. En fait, cette matrice se comporte comme un CPA classique du faite que le borate de sodium est stalibisé par de l'hydroxyde de calcium et que sa teneur dans la formulation est maintenue à une valeur suffisamment faible (<25.000 ppm dans la solution de gâchage). Compte tenu des concentrations en radioéléments introduites (Cs: ~4,1.10^{-3} ppm; Co: ~1,6.10^{-3} ppm), il est vraisemblable que les composés incorporant effectivement ces radioéléments représentent une très faible fraction de la masse totale de la matrice. Il est donc normal que la formation et/ou l'évolution au cours du temps de ces composés n'induisent pas de modifications des proprietés macroscopiques de la matrice.

Par contre, les caractéristiques de lixiviation de ces élements sont directement liées à la forme chimique sous laquelle ils sont présents. En particulier, les courbes de lixiviation suggèrent l'existence de deux étapes: dans un premier temps la fraction des radioéléments restée dans l'eau interstitielle (~30%) est relâchée par diffusion; cette fraction est déterminée par le coefficient de partage solide/liquide lors de la prise du ciment. Ceci se produit lorsque les conditions physico:chimiques sont peu agressives. La durée de cette première étape, qui est effectivement observée expérimentalement, diminue lorsque la température de vieillissement des échantillons augmente. Par exemple à une transformation des composés incorporant le radioélément soit à leur corrosion par la solution lorsque celle-ci est suffisament aggressive.

Les auteurs ont discuté les comportements spécifiques du Cs et du Co et ont presenté les conclusions suivantes:

- la température induit des variations microstructurales importantes de la matrice. Toutefois, les taux de lixiviation observés ne peuvent être directement corrélés à ces modifications physiques mais plutôt aux formes chimiques de rétention des radioéléments. La température influe également fortement sur la transformation au cours du temps de ces composés. Par exemple, la transformation des aluminates en leur forme stable induit le piégeage d'environ 10% de césium supplémentaire et, après 6 mois à 60°C, 80% du césium se trouve dans les aluminates. A long terme, seule leur transformation ou leur destruction sous l'action de l'environnement peut permettre la libération du césium. De même la fraction du cobalt piégé dès la prise est ~99,8%; la destruction de l'hydroxychlorure formé initialement entraîne l'incorporation de cet élément dans les CSH qui gouverneront donc son relâchement à long terme.

Toutefois, compte tenu des périodes de temps (300 ans) sur lesquelles une évaluation du relâchement des radioéléments doit être effectuée, il est nécessaire de poursuivre ce type d'étude sur des durées beaucoup plus longues (plusieurs années), au moins jusqu'à ce qu'un état stationnaire soit observé. L'identification des composés dans lesquels s'incorporent les divers radioéléments, ainsi que la connaissance de leurs propriétés thermodynamiques, est un élément clef d'une telle étude. Par conséquent, le confinement des déchets nucléaires dans des matrices à base de ciment est un problème auquel la chimie des ciments, et en particulier des éléments traces, doit apporter une contribution décisive.

S. PRISZKULNIK

Au travail intitulé "MODELISATION DES PHENOMENES DE TRANSPORT DANS LES MECANISMES D'ALTERATION D'UNE PATE DE CIMENT", F. Bernaudat et E. Revertegat étudent une modélisation pour la prédiction du comportement d'un liant hydraulique en présence d'eau chargée d'ions dans le cadre d'un stockage de déchets radioactifs, dont la durée de vie est de 300 ans

L'approche expérimental entreprise a été décomposée en trois séries d'essais: des essais d'attaque de pâtes de ciment par des ions agressifs (ciments CPA et CLC, attaque par des ions chlorure et sulfate); des essais en cellule de diffusion permettant de mesurer le coefficient de diffusion d'ions agressifs. La troisième série d'essais a permis de mesurer les paramètres du transport des éléments radioactifs tels que le césium, et l'eau tritiée.

Dans un premier temps les auteurs ont cherché à interpréter les expériences de diffusion par un modèle simple faisant intervenir un transport par loi de Fick dans un milieu poreux. Dans les cas où un transfert a pu être détecté, ils ont montré qu'un phénomène d'adsorption-désorption quelquefois réversible se superpose à la diffusion, et cela même pour l'eau tritiée. De plus, le régime permanent qui est atteint au cors de ces essais n'est qu'apparent. Au bout d'un temps assez long après le passage en régime permanent, les points expérimentaux ne s'alignent plus sur la courbe théorique.

Dans d'autres cas, la seule loi de Fick, même avec adsorption réversible, ne permet pas d'expliquer les résultats. C'est ce qu'on obsèrve avec un ciment très poreux comme le CLC (porosité ~32%) lequel ne laisse pratiquement rien diffuser alors qu'un CPA (~25%) donne un résultat tout à fait interprétable.

Un autre modèle a donc été développé. Celui-ci fait intervenir à la fois des phénomes de transport par diffusion (avec ou sans adsorption) et des équilibres chimiques dans la solution interstitielle de la pâte de ciment. L'équation de diffusion a été modifiée de façon à tenir compte des variations de porosité dues à la formation ou à la disparition de précipités. Les équations "chimiques" sont résolues par une méthode de Newton-Raphson. L'ensemble permet d'interpréter aussi bien des essais de diffusion que des essais d'agression.

Le modèle résout simultanément et à chaque pas de temps:

- Une équation de diffusion, pour chaque espèce en solution dont on aura déterminé le coefficient de diffusion et le taux de retard,
- Un système d'équations que l'on peut diviser en deux types:
  - des équilibres chimiques
  - des équations de conservation.

S. PRISZKULNIK

Le travail presenté par Amitabha Kumar et Della M. Roy, sous titre"STRUCTURE POREUSE ET DIFFUSION IONIQUE AUX SYSTÈME ADJUVANT-CIMENT PORTLAND AVEC AJOUTS", concerne l' invetigation sur matériaux cimentés durcis saturés de l'eau des mécanismes de diffusion d'éspèces ioniques et son rapport aux propriétés basiques des matériaux, ayant pour but reveler les effets de la porosité et de la distribution des dimensions des pores sur la diffusion ionique dans ces matériaux.

L'étude expérimentale s'est developpé en pâtes preparées avec du ciment Portland type I de l'ASTM sans et avec l'addition de laitier de haut fourneau, cendre de basse teneur en calcium, silice amorphe ulrafine et grains fins de quartz . Le rapport E/C de ces pâtes a varié de 0,30 a 0,40 et une partie d'elles a reçu l'addition d'un superfluidifiant, au dosage de 0,331% par rapport au poids des solides.

Des éprouvettes cylindriques de 3,5 cm de diamètre et 1,7 ou 3,2mm de hauteur ont été moulées et conservées pour le premier jour sous l'eau déminéralisée et, après démoulage, dans une solution saturée d'hydroxide de calcium, aux temperatures de 27°, 38° et 60° C.

La diffusion de chlorure de cesium a été étudiée après 7, 28, 90, 180 et 365 jours. 4 éprouvettes de chaque hauteur pour chacune pâte ont été essayées a chaque âge.

Les éprouvettes on été preparées un jour avant le début de l'essai. Elles ont été retirées des bacs de conservation, lavées sous l'eau déminéralisée et polies aux deux faces avec feuille de carbure de silicium, pour l'obtention de disques de 1,68± 0,05 ou 3,18± 0,05mm d'épaisseur. Ces disques se sont constitués en cellules de diffusion saturées de solution d'hydroxide de calcium.

A chaque semaine, un disque de chaque épaisseur a été retiré du bac pour la détermination des teneurs de Cs^+ et Cl^-présents dans la solution contenue dans la cellule.

L'analyse de Cs^+a été faite par absorption atomique, tandis que le Cl^-a été mesuré avec un électrode ionique spécifique.

Des disques semblables ont été soumis aux essays en porosimètre à mercure. Avant les essais, les éprouvettes ont été sechées a - 80°C et 2,67MPa. La porosité et la distribuition des dimensions de de pores entre 7,5 µm et 1,9 nm ont été mesurées par l'emploi de mercure sous pression jusqu'à 386 MPa et le calcul a été fait sur la base d'un angle de 140° pour le contact entre le mercure et la pâte sèche.

Les resultats obtenus montrent que la porosité des pâtes de ciment Portland decroît de 3 à 5% avec la réduction de 0,05 au rapport E/C. A mesure que l'âge avance, la porosité diminue, la différence étant supérieure à 27°C et inférieure à 60°C. La dimension moyenne des pores augmente avec l'âge pour les rapports E/C plus élevés et augmente toujours entre 6 mois et 1 an d'hydratation, la porosité diminuant quand même.

L'addition de laitier provoque une réduction à la porosité et aux dimensions des pores. Pour la silice amorphe finement broyée les pores ont des dimensions inférieures, tandis que la porosité est nominalement supérieure. La pâte avec du quartz finement broyé présente un comportement semblable à celle de réference a 27°C, tandis qu'à 60°C elle présente une porosité inférieure et des pores plus petits. La cendre volante produit des porosités supérieures à 7 et 28 jours, mais la distribution des dimensions de pores à 28 jours preuve qu'il y a eu une augmentation des pores plus fins.

L'accroissement des pores plus fins élève la tortuosité ou l'entreliaison des pores, aménant le délai de la diffusion ionique, ce qui a été confirmé pour les résultats d'essais.

L'essai de diffusion ionique des pâtes de ciments Portland a permit démontrer qu'une augmentation du rapport E/C accroît le coefficient effective de diffusion d'ions Cl^+et Cs^-.

Les résultats montrent encore que la diffusion du cation est en général rallenti par rapport à celle de

l'anion, ce qui permet de considérer la pâte de ciment Portland comme une mebrane électronegative.

En particulier, le laitier de haut founeau retarde effectivement la diffusion du Cl^-, tandis que la diffusion du Cs^+ est exceptionnellement basse quand la pâte est préparée avec de la silice amorphe finement broyée.

Ces résultats ont une application directe à la protection des aciers contre la corrosion et à l'enrobage des déchets nucléaires.

S. PRISZKULNIK

Le travail de S.Krishnamoorthy et N.K.Jain, intitulé "INFLUENCE DES CENDRES VOLANTES, AJOUTÉES AUX CIMENTS, SUR LES CHANGEMENTS DANS LA STRUCTURE DES PORES LES MORTIERS CONSERVÉS DANS DES SOLUTIONS DE NaCl", concerne l'étude de l'influence de l'addition de cendre volante à 2 ciments Portland, en vue de déterminer la nature des changements au grandeur des pores des pâtes durcies et son influence sur la durabilité des éprouvettes de mortiers preparés avec ces ciments.

A propos de la composition chimique pontentiel de Bogue, un des ciments présente 3,63% de C_3S et l'autre 33%. Deux autres ciments composés ont été préparés par l'addition de 25% de cendre volante à chacun de ces ciments Portland.

En utilisant un motier mélangé avec 1 partie de ciment, 3 de sable normal et 0,4 de l'eau distillée, des éprouvettes prismatiques de 40x40x160mm' ont été moulées. Elles sont restées pendant 24 heures sous un tissus de jute mouileé et, après, sous l'eau courante et dans de solutions à 3% et 6% de chlorure de sodium, pour des essais en 7, 28, 90, 180 et 365 jours.

Les éprouvettes prismatiques ont été soumises à la détermination de la résistance à la flexion et, ensuite, les respectives parties ont été essayées à la compression. Après la rupture, des pétits échantillons ont été retirés, traités avec acétone, sechés à 105°C et conservés dans un déssiccateur à vacuum pour arrêter l'hydratation.

Des mesures en porosimètre à mercure ont été faites aux échantillons ainsi traités, avec de pressions jusqu'à 407 MPa.

Par la fragmentation des échantillons, les grains passants par le tamis de 45 μm ont été separés en vue de l'obtention de difractogrammes de rayons X, en relation à l'étalon de platine.

Les résultats obtenus ont montré:

a) les mortiers de ciment curés dans des solutions de NaCl présentent une résistance mécanique inférieure que ceux maintenus sous l'eau courante, étant la chute de résistance plus accentuée au ciment avec moins de C_3S. L'addition de la cendre volante attenue cette chute;

b) l'attaque des mortiers de ciment Portland par le chlorure de sodium provoque une augmentation de la grandeur des pores, à cause de la dissolution de la pâte durcie, liée à la formation de chlorure de calcium et de chloroaluminate de calcium. L'addition de la cendre volante à ces ciments inhibe la formation de pores plus grands, au cas de la cure faite dans des solutions de NaCl;

c) les difractogrammes de rayons X indiquent la formation d'une grande quantité de $Ca(OH)_2$ aux mortiers préparés avec les deux ciments portland et curés à l'eau courante. Quand ces mortiers sont curés dans des solutions de NaCl, il est observé la formation de chloroaluminate de calcium, avec la reduction considérable de $Ca(OH)_2$.

Pour les épprouvettes préparées avec les ciments composés avec de la cendre volante des petits teneurs en $Ca(OH)_2$ sont observés. Pourvu que le $Ca(OH)_2$ a été consumé dans la réaction pouzzolanique avec la cendre volante et qu'une autre partie a reagi pour former le chloroaluminate de calcium, la possibilité de lixiviation de produits solubles est sensiblement diminuée.

S. PRISZKULNIK

Le rapport de P.Gegout, H.Hornain, B.Thuret et M.Regourd sous-titre "RESISTANCE AU GEL DES CIMENTS AUX FILLERS" a pour objet caractériser l'influence d'un filler calcaire sur la tenue au gél des mortiers de ciment Portland avec ajouts (CPJ).

Deux ciments, contenant respectivement 15% et 30% de filler calcaire, ont été préparés par mélange d'un CPA industriel et d'un calcaire (98% de $CaCO_3$) broyés séparément à 3.500 et 3.700 cm^2/g respectivement.

Des prismes de mortiers 4x4x16cm ont été gâchés avec différents rapports E/C dans le but de comparer leur comportement soit à E/C constant, soit à E/(CPA contenu dans le mélange) constant.

Des quantités variables d'entraîneur d'air ont été ajoutées à l'eau de gâchage afin d'obtenir des quantités d'air différentes et des bulles plus ou moins espacées.

Les prismes ont été conservés dans l'eau à 20°C.

Après 7 jours, le module d'Young a été determiné à partir des mesures de résonance en flexion, sur les 9 prismes de chaque série. Le prisme présentant la valeur médiane a été sélectionné pour le compactage des bulles d'air et le calcul du facteur d'éspacement de ces bulles, par la technique des traversées linéaires. Les 8 autres prismes ont été conservés dans l'eau a 20°C jusqu'à 105 jours.

A 105 jours, 4 prismes sur 8, présentant le module d'Young le plus proche de la valeur médiane, ont été introduits dans l' enceinte de gel, et les 4 autres ont été soumis à la détermination de la résistance mécanique en compression.

Les prismes ont subi 300 cycles au total, restant chacun 3h à l'air à une temperature de -20°C et 1h dans l'eau à une temperature de +20°C, étant de l'ordre de 10°C/h la vitesse de refroidissement.

En plus, il a été calculé a l'espacement moyen critique des bulles d'air ($\bar{L}cr$), définie comme l'espacement au-delà duquel un matériau donné ne résiste pas aux conditions de gel imposés. Cette valeur a été déterminé après 100 cycles.

Les principaux résultats obtenus ont permis de mettre en évidence les points suivants:

Avant gel:

- A E/C égal, les résistances mécaniques diminuent quand la teneur en filler augmente.

- La diminution des résistances est due dans ce cas, à l'accroissement de la proportion d'eau disponible relativement à la quantité de CPA proprement dit dans le ciment fillérisé. Pour un rapport E/C constant, le rapport"E/CPA" augmente avec la teneur en filler.

- Une correction du rapport E/C tenant compte de l'excès de l'eau engendré par la présence de filler, permet d'obtenir des résistances comparables à celles des CPA.

Après gel:

- L'addition d'entraîneur d'air permet d'introduire dans les mortiers un réseau de bulles susceptibles d'améliorer leur comportement au gel.

- En fonction du rapport E/C et de la teneur en filler, il est possible de déterminer un espacement moyen critique des bulles d'air ($\bar{L}cr$), au-delà duquel le mortier devient gélif dans les conditions expérimentales choisies.

- Pour un même ciment, $\bar{L}cr$ diminue quand E/C augmente.

- Toutefois la correction du E/C tenant compte de l'excès de l'eau apporté par la présence de filler permet d'obtenir des $\bar{L}cr$, donc des résistantes au gel, comparables à celles des CPA.

- L'abaissement des résistances mécaniques dans le cas des fortes teneurs en air entreiné, ($\bar{L}$ faible), n'a pas d'incidence néfaste sur la tenue au gel des mortiers dont les $\bar{L}$ restent inférieurs aux $\bar{L}cr$.

S. PRISZKULNIK

Le rapport de M.George Teodoru, intitulé "INFLUENCE DES CONDITIONS DE DURCISSEMENT SUR LA DURABILITÉ DE LA PÂTE DE CIMENT ET DU BÉTON", présente les recherches sur des composants minéralogiques purs du ciment Portland, sur des ciments et bétons, en vue d'expliquer qu'une haute résistance mécanique n'est pas un indice suffisant pour un béton durable, mas c'est surtout sa structure qui est déterminante.

Les recherches entreprises incluent d'abord des examens aux microscopes, optique et électroctronique, sur les silicates tricalcique (C_3S) et dicalcique (C_2S),l'aluminate tricalcique (C_3A), l'aluminoferrite tétracalcique (C_4AF) et sur suspensions de ciment, pour deux conditions d'hydratation: l'une à 20°C et l'autre par l'autoclavage.

La suspension de C_3S après autoclavage présente après 6h la formation de grands "éventails" vigoureux ayant comme point de départ les granules de C_3S. Le champ reste presque vide, ou peuplé par des petits fragments. Le développement des cristaux après traitement est réduit, le processus étant presque terminé à ce moment-là. On trouve dans les suspensions après autoclavage de moins nombreux cristaux de portlandite.

L'autoclavage augmente fortement la vitesse d'hydratation du C_2S, plus que dans le cas du C_3S. Cette constatation est confirmée aussi par l'action favorable de l'autoclavage sur les résistances en compression par rapport aux résistances à 28 jours de durcissement des pâtes de C_2S pur.

Pour le C_3A, le traitement à l'autoclave est le plus défavorable, parce qu'il freine l'hydratation, la résistance en compression après autoclavage étant presque nulle.

Sous le traitement en autoclave, le C_4AF s'hydrate plus intensément que dans le cas du durcissement à 20°C et donne de grandes quantités d'hydroxide de calcium et d'hydroxide de fer.

En général, les formations cristallines qui résultent de l'autoclavage possèdent des dimensions beaucoup plus petites que celles obtenues par les traitements hydrothérmiques sans pression et par conséquent un grand degré de dispersion, ce qui mène à un haut niveau d'énergie potentielle de surface.

L'auteur a utilisé aussi la vitesse de propagation longitudinale et l'atténuation des ultrasons ayant comme but l'obtention des informations plus globales sur un grand volume de béton caractérisé par une répartition aléatoire des phénomènes remarqués à microéchelle.

Les résultats laissent entrevoir l'existence des défauts sur la structure des bétons traités à l'autoclave. Malgré les très grandes résistances du béton autoclavé, les vitesses des ultrasons sont basses par rapport aux valeurs obtenus pour le béton durci dans de conditions normales.

La présence de ces défauts dans la structure des bétons autoclavés influence la durabilité, comme il a été verifié par l'auteur à travers des essais sur des prismes de béton 10x10x55cm³ après saturation à l'eau, en mesurant la variation de:
- module d'élasticité dynamique par l'excitation des oscillations longitudinales;
- décrément logarithmique des oscillations forcées de la courbe de résonance;
- décrément logarithmique des oscillations libres mesuré de la courbe de décroissance des amplitudes, suite à l'exposition aux cycles de gel-dégel.

Les résultats obtenus montrent pour le béton durci dans des conditions standard une résistance au gel-dégel beaucoup plus grande que pour celui autoclavé.

S. PRISZKULNIK

Le travail de C.D. Lawrence, sous le titre de "LE MESURAGE DE LA PERMEABILITÉ" décrit le projet et les essais entrepris pour la mise en service d'une cellule de perméabilité, en utilisant des éprouvettes de 150 mm de diamètre et 50 mm de hauteur.

Pratiquement, la même cellule permet la réalisation des essais de perméabilité et de diffusion au gas et de perméabilité à l'eau.

Au cours des essais de perméabilité au gas oxygène, l'auteur identifique la grande influence de l'humidité relative des échantillons, qui doit être soigneusement équilibrés avant l'essai, et propose un période de 4 semaines pour la conservation des éprouvettes en béton commun.

Ces essais ont permis, encore, montrer une correlation entre la perméabilité à l'oxygène et la résistance à la compression de bétons curés à 20°C sous l'eau, préparés avec du ciment Portland ou bien avec de remplacement partiel de laitiers granulés de haut fourneau ou de cendres volantes.

Pour le mesurage de la diffusion d'oxygène, la cellule exige une modification pour permettre l'entrée et la sortie du gas à travers des surfaces planes des éprouvettes. Une autre modification necéssaire est à respect de la ceinture d'etancheité, cas il a éte verifié que la ceinture de PVC a presenté une légère absorption de l'oxygène, alors elle a été substituée par du polyuréthane.

Pour la mesure de petites concentrations d'oxygène au courant de gas nitrogène il a été employée une cellule électrochimique contenant un diaphragme chauffé d'oxide de zirconium.

Les essais ont permis démontrer une correlation entre la perméabilité et la diffusion de l'oxygène, au cas des éprouvettes conservées à 55% d'humidité relative.

La mesure de la perméabilité à l'eau est faite avec une cellule semblable, mais la longue durée de l'essai a exigée des précautions aditionnelles incluant la ceinture d'étancheité en polyuréthane et l'enveloppement du tube interne avec un gros tissus de nylon pour libérer des très petites quantités de gas sous pression qui diffusent à travers des parois du tube interne, sous-peine d'intérferer à l'écoulement de l'eau par l'épprouvette.

JOÃO GASPAR DJANIKIAN - Serrana S/A de Mineração

COMMUNICATIONS REPORT ON SUB-THEME 4.2 - MECANISMS OF CEMENT PASTE DEGRADATION DUE TO CHEMICAL AND PHYSICAL PROCESSES

I - INTRODUCTION

Eighteen communications received by the Congress were classified as relating to subtheme 4.2 and proceeded from France (4), West Germany (3), URSS (2), Spain (2), China, Switzerland, New Zealand, Japan, Yugoslavia, Czechoslovakia and Egypt (one from each country).

In a previous appreciation of described subjects, the works can be distributed as follows: sulfate attack (6), decomposition by heat treatment (3), CO_2 corrosion (3) and other studies (6).

1. Sulfate attack

1.1 - "The influence of alite content on the sulfate resistance of Portland cement."
D. DIMIC and S. DROLJC - Yugoslavia

1.2 - "Contribution to the study of the chemical resistance of cements. Behaviour mechanical - resistance of a Portland cement (with a content calculated of C_3A null) opposite to diverse aggressive solution".
D.G. TEBAR, J.L.S. MORENO, V.G. VILA Spain.

1.3 - "A contribution to the study of ettringite caused expansion".
R.DRON, F. BRIVOT - France

1.4 - "Sur le role de la phase siliceuse dans les processus de destruction de la pierre de ciment dans les milieux de sulfate."
F.F. ALKSNIS, V.I. ALKSNE - URSS

1.5 - "Destruction of historical buildings by the formation of ettringite or thaumasite".
U. LUDWIG and S. MEHR - West Germany

1.6 - "The sulphate resistant Portland cement are not ultimate answer to the problem of sulphate attack"
R.T. MORALES - Spain

On the work 1.1, of DIMIC and DROLJC, the authors investigate six sulfate-resisting Portland cements and one ordinary Portland cement, with different mineralogical composition, in regard to their sulfate resistance by the Koch-Steinegger method. The results show that mortar prepared from ordinary Portland cement with a high content of C_3A (10,3%), as expected, deteriorated significantly in the 10% w/v solution of Na_2SO_4 . 10 H_2O.

Comparison of sulfate-resisting Portland cements shows that the cements with relatively low C_3A content and with a C_3S content lower than 60% could be declared as sulfate resistant, while cements with higher content of C_3S (77,0% and 66,5%) and at the same time lower C_3A(3,2% and 3,4%)

content reacted more strongly with sulfate ions, forming ettringite and gypsum, as showed by X-ray analysis.

On the basis of test results and field experience they conclude that for better sulfate resistance of a Portland cement, the C_3S content is also an important factor, besides the C_3A content, and propose a revision on Yugoslav Standard.

On the work 1.2, TEBAR et al. present the results of a long-therm laboratory study of submitting a industrial sulfate-resisting

Portland cement, of calculated Bogue potencial composition of C_3A null, C_4AF 10,8%, C_3S 75,6% and C_2S 6,1% to solutions of gypsum, sodium and magnesium sulfate during 1.800 days, in mortar samples of 1x1x6 cm, 4x4x16 cm, 7x7x28 cm and concrete samples of 10x10x40 cm.

The results show that the Koch-Steinegger coefficient is higher than 0,70 on all cases and the evolution of mechanical strength is function of the solution composition.

On the work 1.3, DRON and BRIVOT propose a model for studying the ettringite expansion by calcining at 1000°C a stechiometric mixture of aluminum sulfate and pure calcium hydroxide.

The hydration of this calcined ettringite, to the form with 32 H_2O, is accompained by a type Calvet microcalorimeter and the expansion mesured by an apparatus properly developed (p.4).

The rehydration of a pure paste is completed within 2 hours, having a linear expansion near of 10%, without restriction.

The greatest pressure is given by the cristallization forces; the application of a unilateral restriction, even near of 0,1 MPa neutralizes completely the expansion in the correspondent direction, pointing out that the expansion pressure is not significant, when compared to cristallization pressure.

On the work 1.4, of ALKSNIS and ALKSNE, the authors show that in environment conditions, in presence of SO_4^{2-} and $CO_3$2-, besides the transformation of aluminous phase in ettringite, thaumasite formation will be expected, by transformation of siliceous phase; and more, the mechanism of this reaction depends on ambient temperature. Over 20°C ettringite is detected and bellow 10°C, thaumasite.

On sample with composition $(CaO)_3.Al_2O_3$: : $CaSO_4.0,5\ H_2O$: $CaCO_3$ = 1:4,7 : 3 (molar parts) was observed a complete desapearence of ettringite, 6 months after the action of CO_2 of environment.

Although this thaumasite formation mechanism is not sufficiently clear, the material behaviour control at low temperatures, besides sulfate resistance determination, would be considered as mandatory requirement.

On the work 1.5, of LUDWIG and MEHR, the formation of ettringite ($C_3A.Cs_3.H_{32}$) and thaumasite ($Cc.Cs.CS.H_{14,5}$) is identified through the mineralogical examination of damages on historical buildings, as due to incompatibility of high alkaline aluminate binders with gypsum or lime-gypsum mortars.

Mortars with higher sulfate resistant cement, in excess of gypsum and calcite, are instable at temperatures of 2 to 40°C, caused by ettringite formation.

At a later stage, on temperatures below 20°C, thaumasite is formed with decomposition of the initially formed ettringite, by combining the unreacted gypsum and calcite. After 120 days, the specimens stored at 2°C are destroyed.

On mortars with C_3S and C_2S as starting materials, and molar ratio SiO_2:$CaSO_4$ = 1, thaumasite was formed, without expansion, when stored at 2°C under water, but the original CSH-phase is destroyed and structure is strongly weakened.

On the work 1.6, MORALES presents a study

of two Portland cements type V, PY-4 and PY-6, and four mixture cements with pozzolan D (diatomite) by the Le Chatelier - Anstett Method.

By XRD investigation on cracked tarts, thaumasite was detected after 3 years, in mixtures where C_3S content are: 79,43% (PY-6) 63,54% (PY-6/D80/20) and 58,19% (PY-4).
On mixture with C_3S below 56% cracks have not occured.

2. Decompcsition by heat treatment

2.1 - "Mechanism of subsequent ettringite formation in mortars and concretes after heat treatment".
D. HEINZ and U. LUDWIG - West Germany

2.2 - "Thermal decomposition of hydrated cement pastes"
A.ZURZ, I. ODLER, S. ABDUL-MAULA - West Germany.

2.3 - "Evolution of strength and structure of concretes heated up to 1.100°C"
J. VOLANT and H. HORNAIN - France

On the work 2.1, HEINZ and LUDWIG to justify damages occured in precast units, that had been heat treated during production and subjected for several years to open-air weathering, study the influence of heat treatment, ranging between 20% and 100°C, in mortars made with PZ55 cement (C_3A at about 12%) and SO_3 3,8%; parallelly study a finely ground clinker with adding anhydrite, to have the SO_3 amount ranged from 2 to 8,6%, to investigate the influence of molar ratio of sulfate and aluminate.

It is verified by X-ray analysis, that at increased temperatures, there is a decreasing formation of calcium aluminate hydrate and it is concluded that, aluminate and sulfate ions get bound within the CSH-gel, and, in the subsequent storage under water, are available as reaction partners for an Aft-phase formation, resulting in expansion and a diminution of strength.

On the work 2.2, ZURZ et al. present a study of prepared cements, grinding industrial clinkers and raw materials with amounts of gypsum corresponding to 3% SO_3, in a laboratory ball mill, to a specific surface area of 3.000 cm^2/g (Blaine). Specimens 10x10x60 cm of pure cement pastes, water/solids ratios between 0,26 and 0,30, hydrated for at least one year at 20°C in a satured water vapor atmosphere, were heat up in an eletric furnace to temperatures between 100 and 1.000°C.

By X-ray diffraction was determined that the phase composition after heating consisted of free CaO and β-dicalcium silicate, for pure tricalcium silicate and non-blended cements; C_2 (A,F) for the OPC and antisulfate cements; C_3A for the white cement; melilite for blast furnace cement; β-dicalcium silicate and no free lime for fly ash-Portland cement, gehlenite for the pozzolan-Portland cement and wollastonite for the silica fume system. In addition, an increase in porosity and average pore size was observed, with loss of strength, as the temperature increased, partially related to a loss of bound water.

On the work 2.3, VOLANT and HORNAIN show that concretes prisms of 7x7x28 cm made with cements CPA, CHF and CPJ, have had weight losses of 5%, when heated up to 1.100°C.

At 105°C, the ettringite is transformed into monosulfo-aluminate and at 390°C, the structure became porous with loss of strength. At 550°C, the Ca $(OH)_2$ is strongly dehydrated, being fissurated and causing separation of material. The cements poor in lime (CPJ with fly ash or slag, CHF) have better strength due to less fissuration.

3. CO_2 Corrosion

3.1 - "Skins of calciumcarbonate and their significance for the corrosion of concrete".
E. KOELLIKER - Switzerland

3.2 - "CO_2 corrosion of geothermal cement

grouts"
N.B. MILESTONE, D.A. ST. JOHN, J.H. ABBOTT, L.P. ALDRIDGE - New Zealand

3.3 - "Investigation into the carbonation of autoclaved aerated concrete (AAC)"
Z. YUPING, L. DEDONG and S. GUOKUANG - China

On the work 3.1, KOELLIKER submits mortars prism of 40x40x160 mm to the action of concentrated solutions of calcium hydroxide, moist air of 90 - 100% r.h. and air of 70% r.h., both to 20°C.

SEM investigation revealed that in water, crystals of calcite had well developed faces and sizes from 1-10 μ diameter. On the other hand, in the air was observed a finer structure and grains not well crystallized, estimated of about 0,5 μ.

On the work 3.2, MILESTONE et al. presents a study of cement grouts corrosion in wells casings, exposed to conditions of CO_2^- rich, acidic or alkaline fluids, respectivelly. On the first condition, rapid carbonation and corrosion from HCO_3^- put doubt if any Portland cement system could withstand it. On the second condition, grouts are carbonating only.

It was observed that when silica is added to the formulations, the grouts are less durable and rates of attack are increased. It is hypothesized that without added silica, the HCO_3^- reacts with the CH for producing calcite, that has a larger molar volume, reducing the porosity; on the contrary, with added silica, the HCO_3^- attack must be directly on the hydrated calcium silicate (tobermorite and xonotlite) giving aragonite, that leads to an increase in porosity.

On the work 3.3, YUPING et al. present the study of three types of autoclaved aereted concrete: cement-lime-sand, cement-slag-sand and cement-lime-fly ash submitted to natural and artificial carbonation.

Mercury intrusion porosimetry shows that carbonation leads to a drop in the percentage of small pores and an increase in larger ones.

Strength tests show retrogression for all three types in artificial environment, although in natural, C-L-S and C-S-S presented an increase after one year exposure.

Concrete of C-L-F has a higher rate of carbonation as compared with C-L-S and C-S-S.

SEM shows that carbonation mechanism in artificial and natural environment is different; in the former, there is a serious build up of calcite on air pores of all concretes, not seen in the last.

4 - Other studies

4.1 - "Evolution of the microstructure of concrete during the ASTM Test for freezing and thawing"
C. VERNET - France

4.2 - "Influence of ionic species on alkali-aggregate reaction"
M. SHIZAWA, Y. JOE and H.KOTANI - Japan

4.3 - "Degradation of hydrated cements by chloride brines"
R. OBERSTE - PADTBERG - France

4.4 - "The stability of the calcium sulfoaluminate hydrates in aqueous solutions"
H.Y. GHORAB and E.A. KISHAR - Egypt

4.5 - "Contraintes internes dans le beton et sa durabilité"
Z. TSILOSSANI, I. PANTSKHAVA, K. KVARTSKHAVA - URSS

4.6 - "Corrosion of hardened cement pastes by NH_4NO_3 solutions"
A. BAJZA, I. ROUSEKOVA and O. VRANA Czechoslovakia

On the work 4.1, VERNET study the freezing and thawing action by ASTM 666-80-B Method and observe that the microcraks developed to sample center, passing by big size cappilary pores, the transition aureola of aggregates and big portlandite crystals. The subsequent stage, when cracks reach a certain dimension, chemical process of redissolution of hydrates speed the destruction.

By SEM investigation of hydrates orientation, it is assumed that concrete acts like a pump, resulting that thawing action being more destructive in water than in air.

On the work 4.2, SHIZAWA et al. using ASTM C227 Method, in order to investigate the effect of alkali ionic species and coexisting anionic species, upon the expansion due to alkali-aggregate reactions, conclude that the expansion was accelerated by sodium and potassium, but not lithium.

In relation to coexisting anionic species, the degree of expansion was decreased in following order: chloride, sulfate, hydroxide and carbonate.

Sodium ion has larger effect than potassium ion, at same content of total alkali and with same anionic species.

On the work 4.3, OBERSTE-PADTBERG show the study on degradation of hydrated high sulfate resistant oilwell class G cement, introducing samples of disks pastes (h=20mm; d=40mm) in saturated brines of KCl, $CaCl_2$ and $MgCl_2$, for a reaction period of 3 months at 55°C. The pastes were prepared with fresh water and also with 30% NaCl containing water (as commonly applied in the field of oil well cementing).

SEM investigation shows that salt water cement paste is attacked for all brines severally. The degrading mechanism is explained by the formation of alkali hydroxides and silicates, and the related pH decrease that leads to C-S-H instability.

On the work 4.4, GHORAB and KISHAR, studying the stability of calcium sulfoaluminate hydrates in water and NaOH solutions, at temperatures up to 100°C, and by XRD patterns of solids obtained, show that ettringite is found to be stable in water at 30°C and 60°C, the resulting solution having a pH value of 11,2: it persists alkaline solutions of concentration up to 0,2M at 30°C; it converts to the monosulfate hydrate on water at 100°C and in 0,08M NaOH at 60°C. On the other hand, monosulfate hydrate is unstable on water at 30°C, but it stability is greatly enhanced in alkaline solutions.

On the work 4.5, TSILOSSANI et al. measuring the internal effort by means of magnetic - elastic catchings put into concrete prisms of 7x7x21 cm, suggest a model to make statements for prevision the longevity of concrete, under the effect of temperature and humidity.

On the work 4.6, BAJSA et. al on a study of deterioration of concrete in agricultural conditions, submitting cement pastes in cylindrical samples (d = 30mm), to 0,5, 3 and 5% NH_4NO_3 solutions, for period close to 1 year, show that the hydration products are the same as those formed by water curing plus $C_3A.Ca(NO_3)_2 . 10\ H_2O$, causing expansion, decrease in density and strength, and increase in porosity.

SUB - THEME 4.3

CEMENT PASTE COMPATIBILITY WITH AGGREGATES AND CONCRETE REINFORCEMENTS INCLUDING ELECTROCHEMICAL CORROSION

BY MRS. HAYDEE ARMANDOLA

INTRODUCTION:

The contents of the sub-theme we are going to tackle in this 8th. International Congress on the Chemistry of Cement, as well as those of sub-theme IV - 1 and sub-theme IV - 2, under a slightly different title, carry on with certain subjects already dealt with in the VII Theme of the 7th. Congress: "Interface reactions between cement and aggregate in concrete and mortar", "Durability" "Bond Strength". It is probably called differently due to the fact that the present title further focusses on this problem by aiming at an approach to the traditional essence of these Congresses, i.e. "The Chemistry of Cement".

But it is downright obvious that even if the contents of some of the communications only give an incomplete answer to the essence, we cannot disregard the complex problem of durability, so long as its crucial consequences in the fields of Technology and Economy, make it unavoidable; let alone when there is a well-founded opinion that the new advances in concrete durability must have cement chemistry research as the driving force.

Undoubtedly, technological aspects are predominant in most of the reports submitted dealing with this subject, but effects are analized without taking into account causes or mechanisms, and neither research is carried out nor is there any conclussion grounded on a scientific basis, thus in most cases Empirism prevails.

Mr. J. Calleja (1) has been working hard on this subject that undoubtedly springs from the inherent features of the theme already dealt with. The problems brought about by research work on durability make it highly complex and usually impossible to simplify. It includes certain interacting factors of a very different nature and sometimes the effects of those factors have no close links with their relevance.

In his Research Paper, Mr. J. Calleja has carried out a deep survey of different viewpoints on the theme of durability, but at the same time bearing in mind its own limits and keeping it within the fields of chemistry of cement and Plain Concrete.

The 8th. Congress brings in the question of corrosion-passivation in reinforcements in sub-theme IV - 3. What has been said about the durability of plain concrete holds good when it refers to the durability of stressed or prestressed metallic reinforcements embedded in concrete.

Thus all the factors are linked with the electrochemical degradation of metals embedded in concretes of different characteristics deriving from its components and its technology and those springing from the environment.

COMMUNICATIONS

The chairman of sub-theme IV - 3 has been sent twelve Communications from nine countries:

IV-3.1 ALKALI - REACTIVITY OF GRANITIC ROCK AGGREGATES. H.C. Visvesvaraya, A.K. Mullick, George Samuel, S.K. Sinha and R.C. Wason. INDIA.

IV-3.2 INFLUENCE OF REACTIVE AND ALKALI COMPOUNDS ON EXPANSION OF ALKALI-SILICA REACTION. Kin-ichi Nakano, Shigehiro Kobayashi and Seiichi Nagaoka. JAPAN.

IV-3.3 ON THE BEHAVIOUR OF ALKALI IN ALKALI-AGGREGATE REACTION. W. Kobayashi, N. Kataoka and Y. Tsutsumi. JAPAN.

IV-3.4 CHEMICAL AND SWELL PROPERTIES OF THE ALKALI-SILICA REACTION PRODUCT. G. Davies and R.E. Oberholster. SOUTH AFRICA.

IV-3.5 FIRST STEPS OF CONCRETE HYDRATION AND GEL FORMATION IN SURFACE CONTACT WITH AGGREGATES. Z.M. Larionova and I.I. Kourbatova. U.S.S.R.

IV-3.6 EFFECT OF DEGREE OF COMPATIBILITY OF CEMENT AND AGGREGATES ON CONCRETE DURABILITY UNDER CONDITIONS OF HIGH TEMPERATURE ACTION. V.I. Kadlecek and S. Modry. CZECHOSLOVAKIA.

IV.3-7 THERMOMECHANICAL COMPATIBILITY OF AGGREGATES IN AUTOCLAVED VERY HIGH STRENGTH CONCRETES. G.P. Tognon, S. Cangiano and G. Coppetti. ITALY.

IV.3-8 THE COMPATIBILITY BETWEEN AN EXPANSIVE GROUT AND ITS RESTRAINING ENVIRONMENT. R.I.A. Malek, P.H. Licastro and O.M. Roy. U.S.A.

IV.3.9 CORROSION BEHAVIOUR OF STEEL DURING ACCELERATED CARBONATION OF SOLUTIONS WHICH SIMULATE THE PORE CONCRETE SOLUTION. C.Andrade, C. Alonso, P. Santos and A. Macías. SPAIN.

IV.3.10 CHEMICAL POTENTIOSTATIC PROTECTION OF REINFORCING STEEL IN CONCRETE. J. Wisniewski, J. Karys, J. Czaja. POLAND.

IV.3.11 EFFECT OF ZINC OXIDE ADMIXTURE ON CORROSION INHIBITION OF IRON IN CEMENT MORTAR CONTAINING SEA WATER. C. Tashiro and Y. Fukushima. JAPAN.

IV.3.12 CORROSION BEHAVIOUR OF TAD, DIFFUSED REINFORCEMENT CONCRETE TUBES. M. Arpaia, ... Cigna and R. Turrizia-ni. ITALY.

After surveying the different papers, it was deemed convenient to group them according to the themes developed in them.

1. Cement - aggregate reaction

It is well-known that the chemical reactions of aggregates with concrete can affect the performance of concrete. Some reactions may be beneficial but others result in serious damage to concrete by causing abnormal expansion, loss of strength and cracking. During the 7th. International Congress the main paper (1) and the General Report on Theme VII (2) showed a comprehensive and critical review of the complex problem and accumulated knowledge in this field.

Both papers are backed up by plenty of bibliography by referring to the different kinds of reactions, their ocurrence, materials involved, mechanisms developed, identification by laboratory tests and criteria for judging reactivity and recommended procedures to minimize the effects of the reaction. Contradictions found in some of the research works are also mentioned.

Summing up, we can state that degradation is caused by the simultaneous influence of factors such as:

* The alkali content in cement, but also the alkali liberated by some aggregates or any other concrete component.
* Type of cement (rate of transport).
* The content and type of unstable minerals in the natural aggregates: "pessimum content" and grain size.
* Reactivity of aggregate, which is based on the presence of amorphous or partly crystallized silica.
* The humidity of the surrounding environment.
* The wet and dry cycling.
* Exposure conditions (external amount of aggressive substance).
* The temperature.

The interface (cement-aggregates) begins to be created when thin films of wa-

ter are formed on aggregate surfaces during the mixing of concrete. Alkalies from the cement dissolve immediately in the liquid, and lime commences to be released by the hydration reactions. From this outset, with its concurrent creation of strong OH-concentrations, any of the following cement-aggregate reactions may proceed in the interface-zone, dependent upon the available constituents and the conditions for mass-transport and energy-conversion in the system: pore - liquid - interface - interior of aggregate particles. Thus, according to different cases, there are different reactions: siliceous-aggregate; silicate-aggregate; dolomithic-aggregate; calcium-carbonate aggregates.

The mechanism in each reaction has often been analysed by different researchers (2). It is not a priori possible to evaluate such reactions as converging towards increased performance quality and equilibrium, or as contributions to deterioration, and also the position of cracks, for instance in a zonal interface system, ought to be cautiously interpreted at the present stage of knowledge.

The communication IV-3.1 presents the results of an investigation of alkali silica reaction in concrete containing granitic aggregates, possible mechanisms of deleterious reaction and its impact on cement specifications. Compatibility of siliceous aggregates with the alkalies in cement has been an important factor in durability of concrete. In addition to conventional reactants like opal, chert, chalcedony or volcanic glasses, it is now held that presence of "stained" quartz in siliceous aggregates could also cause alkali silica reaction (ASR).

Granite aggregates in a 25 year old concrete gravity dam contained mainly quartz and alkali feldspars, with varying quantities of biotite and muscovite 50-80 % of quartz showed strain effect with undulatory extinction angle 25-30°. Alkali feldspars included orthoclase, plagioclase, microcline and microcline-perthite.

The dam manifested typical external signs of distress associated with alkali-silica reaction, scanning electron microscope (SEM) and energy dispersive analysis of X-rays (EDAX) studies revealed the predominant presence of alkalies in the reaction rims on aggregates altering their borders, which consisted of fluffy, amorphous gel formation. Occasionally the reaction products were crystalline. The presence of typical white gel deposits in the concrete was less frequent.

In addition to the presence of strained quartz, the role of alkali feld spars were investigated. Microscopic studies indicated the alteration of alkali feld spars to clay minerals and sericite. X-ray diffractogram (XRD) studies confirmed changes in the crystal structure and mineral composition.

These results tend to support the hypothesis that alkali feldspar can themselves release alkalies in the presence of calcium hydroxide to participate in ASR. Should that be the case, merely stipulating a low alkali level in the cement may not be adequate and depletion of calcium hydroxide would assume importance.

The role of active siliceous pezzolan and hydraulic slags have been advocated for alleviating ASR. In addition to lowering the total soluble alkali content in the concrete to the extent cement is replaced by these additives, they also combine with the calcium hydroxide (CH) liberated during the hydration of cement. It has been reported that if the CH liberated can be fully consumed by large proportions of slags, ASR would not take place.

In the context of above, modified cement compositions having no C_3S phase or lower amount of C_3S phase merit consideration. In these cement systems, the amounts of CH liberated upon hydration are considerably lower. Authors point out that the use of such cements with known reactive aggregates are presently under investigation and the results will be reported subsequently.

The communication IV-3.2 refers to deleterious cracks in concrete structures considered to be caused by alkali-silica reaction. These have been often found in Japan from about 1975.

In this study, investigation was carried on the factors affecting expansion of mortar bar, that is, types of reactive aggregate, alcali contents of portland cement, types of alkali compouds as several sources of alkali, amount of alkalis and types of chemical admixtures.

The present work includes studies with 9 kinds of normal portland cement and 5 aggregates. The tests were effected by using ASTM techniques (Petrographic Examination of Aggregates; Potential Reactivity by

Chemical Method; and Mortar Bar Method).

Results show that even though the total alkali content is the same amount, the expansion increases with increase of afterwards additional alkali.

Low alkali cement with large amount of adding alkali shows more expansion than that of high alkali cement with small amount alkali addition if their total Na_2O equ. is same. Furthermore these tendency was more pronounced in the case of NaCl addition.

These results assess that expansion of mortar bars was largely influenced by water soluble alkali content. These results indicated that even though equivalent Na_2O contents were the same, extent of expansion varied widely dependent upon the kind of alkali ions. Furthermore sodium compounds affected more than potassium compounds.

The influence of chemical admixtures on expansion was examined using low alkali cement.

The total alkali as Na_2O equ. was adjusted to 0.60, 1,20 and 2.00% by adding NaCl to low alkali cement.

Even though the total alkali content is the same amount, the expansion increased with the increase of afterwards adding alkali. It is technologically important that alkali introduced afterwards shows remarkable influence for mortar bar expansion comparing with intrinsic alkali in cement.

The communication IV-3.3 sets out to carry on research works effected by one of the authors, who studied on the chemistry of alkali-aggregate reaction by using silica gel-sodium hydroxide model (3) (4).

In the case siliceous aggregate is immersed in NaOH solution, the following reactions occur:

(1) adsorption of NaOH to silanol groups of aggregate

(2) rupture of surface siloxane bridge of aggregate by attack of NaOH and dissolution of SiO_2.

(3) rupture of inside siloxane bridge of aggregate and loosing of its structure

(4) adsorption of NaOH to inside silanol groups made by reaction (3)

If the siliceous aggregate is well-crystallised, the attack of NaOH takes place mainly at the surface and only reaction (1) and (2) occur.

On the other hand, in the case of poorly crystallised silica, NaOH penetrates into it and reaction (3) and (4) occur too. Reaction (3) looses the network of silica and produces a cross-linked polyelectrolyte containing Na^+. This type of structure, in contact with water, sets up an inhibition pressure and because the silicon-oxigen framework is partly disrupted the material swells.

In this paper, the behaviour of alkali in mortar bar which expands caused by alkali - aggregate reaction is discussed based on the above hypothesis.

In the research works carried out Perex glass, four reactive aggregates and a non-reactive aggregate were used. High alkali Portland cement was used. Experiments included immersion test in NaOH, mortar bar structure formation and analysis of pore solution obtained from cured and crushed-out mortar bars.

The immersion tests were effected in NaOH solution according to ASTM-C-289. The quantity of silanol group in residual aggregate was measured. The method followed is stated in the work. Mortar bar test was carried out according to ASTM-C-227.

Test and analysis results are stated and drawn up in charts. After discussion of those, the following conclusions were agreed upon.

On the aggregate immersed in NaOH solution, there is close relation between the quantity of alkali adsorbed to ruptured inside siloxane bridges. On the mortar bar, the quantity of alkali adsorbed to ruptured inside siloxane bridge/unit reactive aggregate is tightly related to expansion.

From these results, the rupture of inside siloxane bridge by the attack of alkali seems to be a cause of the expansion by alkaly-aggregate reaction.

The communication IV-3.4 deals with the identification of the alkali-silica reaction product (ASRP) in deteriorated concrete, considering it as a positive way of diagnosing alkali-silica reaction (ASR). Confirmation of ASR is usually obtained by performing scanning election microscopy (SEM) combined with electronic diffraction x-ray analysis (EDAX), or x-ray diffraction analysis (XRD), or both, on reaction product. However, characterisation of the ASRP mineralogically and morphologically as well as chemically and physically , can assist in elucidating the mechanism of the reaction and thereby contribute to the

prevention of the problem.

The possibility also exists that the ASRP observed in concrete and characterised in the laboratory is a harmless end product and is in itself not deleterious that it cannot exert swell pressure.

The present work includes a complete bibliography on this theme and a thorough series of charts to illustrate what has been stated.

Recently the authors of the present work have submitted extensive XRD and SEM-EDAX data on the ASRP. They described two amorphous phases, and a number of morphologically distinct crystalline phases, three of which are very widely distributed.

X-ray diffraction data on reaction products have revealed at least two crystalline phases, one with a characteristic peak at 12 Å and the other with one at 8 Å. A third phase with a characteristic peak at 2.90 Å has also been suggested. A characteristic of the 12 Å phase is that the 12 Å peak shifts progressively down to 8.26 Å when heated to between 40 and 110° C. This shift is reversible.

The ARSP is a multicomponent system. Included with the different crystalline and amorphous phases are contaminants such as quartz and various forms of calcium carbonate. Although whole sample analysis naturally give the combined composition of all the different phases plus contaminants, the advantage of this type of analysis is that the amount of water and CO_2 in the reaction product can be determined.

A semi-quantitative EDX analysis can be obtained from a non-polished surface and is very useful to characterise the different phases. However, x-ray scattering and absorption severely hamper the reliability and reproductibility of the analysis.

Quantitative microprobe analysis are the most suitable for obtaining the composition of the different phases in the ARSP. However, the fact that a flat well-polished surface is required means that the morphology, whereby the phase is characterised, is largely destroyed. Consequently, it is often difficult to distinguish between amorphous gels and crystalline phases and impossible to recognise different morphologies. In addition, water and usually carbon are not determined by microprobe analysis.

The more common phases on the ASRP in concrete from affected structures are a massive, amorphous gel and three distinct crystalline phases, namely rod-like, blade-like and rosette-like crystals. Although the quality and reproductibility of standardless EDX analysis are poor, a good indication of the chemical composition of the various phases can be obtained.

The massive gel is very often associated with rosette-like crystals. It has a much higher Ca and lower K content than the crystalline phases. The composition of the crystalline phases is much less variable than that of the amorphous gel. All three crystalline phases are characterised by the presence of Si, K and Ca. Small amounts of Na can be found in the blade-like and rosette-like crystals but this element is consistently present only in the rod-like crystals. Other elements that may be present in minor amounts are Al, Fe, and very occasionally, Mg. The rosette-like crystals are not only the most common crystalline phase observed in affected concrete but are generally chemically the most consistent and have the highest CaO content of the three.

Close to the contact with the aggregate, the alkali-silica reaction product found in voids alongside with the aggregate is highest in Si. These appears to be a depletion of Ca in the cement paste at the boundary with the reaction product.

No measurable swell pressures were produced by either the 12 Å phase and the 8 Å phase separated from concrete of deteriorated structures.

The communication IV-3.5 refers to the fact that a concrete structure is determined by a set of physicochemical processes taking place during binder-hardening and its possible reactions when they come into contact with aggregates. The first steps in binder-hardening constitute the period which conditions the resistance; deformation and other characteristics in the executed concrete.

The present work states that by means of studying variables according to the time of liquid-phase formation in concretes, we can assess the influence of different factors (such as temperature, additives, etc.) on cement hydration.

It also points out the influence on the liquid-phase composition by the clinker mine

ralogical structure, its alkali content, plaster included and admixtures added. Special reference is made as regards a superplastifying formed by naftalen-formol resins.

It is also stated that different aggregates adsorb hydrogels of a certain composition. This has been checked by using an electronic microscope. Different observations and verifications on this theme are given in detail.

2. Surface deterioration of concrete.

The communication IV-3.6 deals with this complex problem. Rate of the surface deterioration of concrete in natural exposure under normal temperature and moisture conditions is usually very slow. That is the reason why it is useful to study the deterioration phenomenon under more severe model conditions in laboratory. Results of such laboratory experimental project, which was realized a time ago are presented in this paper.

The aim of the experimental programme was to determine the extent of surface deterioration and besides, to compare the resistance of concrete with aggregates of different thermal expansion to the repeated action of high temperatures. For this purpose limestone and quartz were chosen as main representatives.

The work includes details related to materials used; their grain size; the way in which test probes have been used, steps making up the cycles to which they are submitted; studies of temperature gradient in and on the surface of test probes, and so on.

For the evaluation of the extent of surface deterioration of cycled concrete specimens (temperature difference was approx. 125 or 140°C respectively and the total number of temperature cycles was fifteen) some test methods have been used. Changing of properties of concrete has been assessed by tensile splitting strength test, adsorption and penetration of indication solution of sodium chloride on cubes and length changes (dilation), ultrasonic speed and pull-off strength on deteriorated surface of prisms.

The experimental programme constitutes an interesting example carried out in a laboratory since it takes into account both traditional and modern techniques to evaluate the behaviour of concretes of a specific composition.

Results obtained have shown pronounced structure deterioration of concrete in the surface layers after first several temperature loading cycles. Development of deterioration was more intensive in the case of concrete with limestone aggregate and also was more pronounced in the case of partially humid concrete in comparison with a fully saturated one. From the results it was evident that properties of quartz aggregates are more compatible with limestone aggregates.

Finally, the used test methods show different sensitivity for evaluation of the extent of deteriorated structure of exposed concrete surface.

It is obvious that as it usually happens with most models including cycles with temperature conditions more demanding than the normal ones, quantitative conclusions gathered from those prompt experiments can only be applied to similar situations to those simulated. So that we should be aware of rushing to conclusions. On the whole it would be highly interesting to research not only the effects but also physicochemical as well as chemical changes taking place during the experiment.

3. Compatibility of mixes of different aggregates

The communication IV-3.7 analyses the effect of the thermal and elastic compatibility of binary mixes of different types of aggregates on the properties of autoclaved very-high-strength-concretes.

The mechanical properties of autoclaved very-high-strength-concretes made with quartz aggretate and aggregates differently interacting with the cement matrix, were studied in previous works (5) (6) (7).

The trends of compresive strengths and moduli of elasticity versus the aggregate of maximum diameter were observed in autoclaved concretes made with aggregate consisting of limestone, quartz and a 50 % mix of the two. The investigation was extended to concretes with aggregate of maximum diameter up to 20 mm formed of basalt, jasper, granite and porphyry as well as 50 % binary mixes of these aggregates, besides of limestone and quartz mixes with the above materials.

The work assesses the characteristics of materials used in concrete mixes; the composition of the concrete mixes; the hydrother-

mal cycles applied to the autoclaved concretes; the tests made and results obtained.

It could be noticed that the moduli of elasticity of concretes where the aggregate consists of 50 % binary mix of the two materials depend on the moduli of elasticity of the mix constituents and their thermal compatibility related to the respective coefficient α .

The most interesting phenomena appear when limestone is present in the mix aggregates. Depending on the ratio of the modulus of elasticity of limestone to the aggregate with which it is mixed and as a function of the difference between the thermal expansion coefficient α of limestone and that of the aggregate, more or less marked deviations of the modulus of elasticity from the theoretical value are noticed.

In the case of concrete autoclaving, it can be useful to use only one type of aggregate rather than choose a mix of materials having different thermomechanical properties. In fact in rather large temperature ranges, such as those found in the hydrothermal treatment, the difference in the moduli of elasticity and thermal expansion coefficients relevant to aggregates affects strengths and, above all, the modulus of elasticity of the relative concretes.

The use of aggregate mixes containing limestone can involve a drop in the modulus of elasticity. However it is expected from the compressive strength values that follow an intermediate trend beween those of concretes with aggregate consisting of only one component.

In rather wide temperature ranges such as those related to the concrete autoclaving, in the case an aggregate mix is used, a study on the thermal and elastic compatibility between them and the cement matrix seems necessary to foresee the mechanical and elastic properties of the relative concretes.

4. Mechanical properties and durability of cement-based plug-seals

The communication IV-3.8 deals with this subject. Cementitious materials are used to seal access shafts and boreholes in many underground systems e.g. radioactive-waste repositories. Their primary function is to provide a tight seal at the interface.

Successful performance in this respect could be dependent almost entirely on expansivity of the plug relative to the restraining forces of the surrounding host rock.

In cementitious formulations, whether ettringite or salt (ClNa) is the principal expansive component the degree of restraint offered by the surrounding rock mass is of importance in the development of interfacial stress. Information exists on unrestrained and standard restrained expansion for mortars and concrete, however, most do not permit calculation of actual interface stresses under the existing restraining forces of actual borehole geometry.

A system to determine the radial stresses of the grout/concrete on the host enviroment, which permits stimulation of the surrounding rock mechanical properties was designed. A brief description of the system is presented together with typical data, and their implications on seal durability.

It consists of a strain gage instrumented cell and its associated signal conditioner/amplifier. The test cell used in the system is unique in that it provides for direct calibration of the complete system. It is versatile in that the cell material and dimensions can be selected to stimulate restraint of a given host material under a geostatic load reflecting depth.

Samples can be run under a range of temperature and pressure conditions, with the latter simulating either inyection pressure or hydrostatic load conditions. Details of the design and grading of the apparatus employed are pinted out in the paper.

Two ettringite-based expansive formulations have been chosen for the present study. Formulation I (F-I) a mortar based on type K expansive cement and formulation II (F-II), a grout based on class H cement with added calcium sulphate hemihydrate. A third, salt (NaCl)-based formulation (F-III) was also tested. This is a mortar containing much smaller hemihydrate than F-I and F-II and mixed with supersaturated NaCl solution. F-II was found to give the highest stresses, whereas F-III gave the lowest stresses.

Three distinct phases of expansion were found: the first is a thermal phase occuring with early heat liberation, the second occurs after the cement reaches its thermal maximum when simultaneous cooling and crystallisation of expansive componets takes place, and the

third phase occurs after total relief of thermal stresses.

In numerous field applications of expansive cements and seal materials, it is neccesary to attain chemical compatibility between the concrete formulation and the surrounding enviroment. In salt-host sites (largely in oil and gas industry as well as radioactive waste repositories) it was found that the use of saturated salt solution as a mixing fluid instead of water is necessary to prevent salt migration and subsequent adverse effects on seal durability. One salt-containing formulation (F-III) has been tested in the present investigation. This formulation contains 2.6 % hemihydrate in addition to salt (NaCl). The mixed expansive functions of sulphate and salt has an important significance in field applications in conjuntion with tempeature effects on stability of the seal material.

Although the restraining forces in a salt environment may differ from those of tuff rock (for ettringite-based formulations), the same restraining forces were applied to the salt-based formulation in order to establish a basis for comparison. A simple mathematical relationship can be applied to transform the resulting data into actual stresses in a salt environment.

The normalized expansive stress curve (at 38°C) for this formulation (F-III) reflects the general expansive characteristics explained. The expansion is partly due to Friedel's salt and ettringite. However, crystallization of salt with curing (water consumption in hydration process) may be the primary cause of expansion. The micrograph salt crystals growing inside pores of cement matrix. Crystallization starts at the walls and progresses to the center exerting pressure on the pore walls.

5. Corrosion-passivation in reinforcements

Metallic corrosion is always a heterogeneous reaction taking place in an interface metal-environment. Metallic corrosion arises due to the trend in metals to return to their original state i.e. as compounds which are more stable and have minimum potential energy.

The mechanism in a corrosive process consists of a spreading oxidation i.e. a loss of electrons on the part of the corroding metal.

Most of the corrosive processes fall within the electrochemical type, which implies the generation of an electric current or the flow of electrons from one part of the metal to the other. There is micro or macrocell formation, thus resulting in metal dissolution which always takes place in the anode. That trend to lose electrons varies according to the respective metal and it is influenced by the harmful environment or the electrolyte where the reaction of the corroding metal takes place.

When a metal comes into contact with a dissolution of its own cations, apart from the trend to bring about ion-production by the respective metal which becomes negatively charged (electrolytical dissolution), there is a driving force that leads cations to discharge on the metal, thus turning into neutral atoms and charging the metal positively. This driving force is measured by the osmotic pressure of dissolving cations.

A metal coming into contact with its own ion-dissolution becomes a voltaic hemi-cell electrode. Its own potential value should be measured by referring to another reference electrode. Thus, isolated potentials are relative, not absolute, and they are expressed according to an hemi-cell which is assigned a zero potential value by agreement. By that we mean, for eg. the hydrogen electrode and the choice of which to use depends on the electrolyte where the reaction (for eg. a corrosive reaction) takes place. Metallic potential (for eg. that of a corroding metal) should be expressed according to a reference electrode.

Usually bare steel exposed to the air or in contact with soils, water or any other aggresive environment, is prone to corrosion.

Simplified, the corrosion process can be separated into two single processes, the cathodic and the anodic process. The anodic process is the real dissolution of iron. Positively charged iron ions pass into solution:

$$Fe \longrightarrow Fe^{++} + 2e^{-}$$

The surplus electrons in the steel will combine at the cathode with water and oxigen to form hydroxil ions: $2e^{-} + \frac{1}{2}O_2 + H_2O \longrightarrow 2OH^{-}$

After some intermediate stages, the ion and hydroxide ion will combine to form rust which at least theoretically, can be written as Fe_2O_3.

Under practical conditions, rust product are more or less water-containing compounds. This means, that only oxigen is consumed to form rust product. This oxigen must normally diffuse towards the metal. Water is only necessary to enable the electrolytic process to take place. On the contrary, steel in concrete is protected against corrosion by passivation.

The reason for this passivation is the alkalinity of concrete (the pH-value of the pore-water runs up to pH $>$ 12,5) and relatively high electrical resistivity in atmospheric exposure.

In the case of such high pH values, a microscopic oxide layer is formed on the steel surface, the so-colled passive film, which prevents the anodic dissolution of iron. Thus, corrosion of reinforcement is impossible, even if all other preconditions for corrosion are fulfilled (mainly the presence of mositure and oxygen).

If this pH value drops below pH=9 due to carbonation, or the chloride content exceeds a certain critical value, the passivated coating and, consequently, the corrosion protection will be lost locally or in even grater surface areas.

Corrosion of the reinforcement will only be possible after carbonatation or a harmful amount of aggressive substances has reached the surface of the reinforcement or when said substances belong to the concrete mass surrounding the reinforcement. That is the case of chlorides being added to the concrete mix.

Varied and multiple causes may bring about corrosion in reinforcements. Among them we can mention the carbonation of concrete, this being a matter of permanent concern, because many structures have their concrete surface directly exposed to the action of the atmosphere and the standard allow relatively little depth of cover of reinforcements.

As is already well known "carbonation" means the reaction between the atmospheric CO_2 with the solid phases of the cement paste.

The $Ca(OH)_2$, Na (OH) and K(OH) dissolved in the pore water of the concrete and, possibly, the soluble alkali of the aggregates provide the pore water with a pH between 12,5 and 13.5.

As different authors have stated the final state of this process consists of amorphous SiO_2,$Al(OH)_3$, $SO_4Ca.2H_2O$, CO_3Ca in different polymorphic varieties and H_2O. Thus, the initial alkaline pH in the pore concrete solution is neutralized. This neutralization allows the corrosion of reinforcements if a minimum of moisture and oxygen are present.

This reaction requires small amounts of water, as dry concrete will not carbonate. The highest rate of carbonation will be found in air with a relative humidity of 50-60 %. Under conditions of higher atmospheric humidity, diffusion of the CO_2 will be inhibited by the water that has accumulated in the pore cavities.

After all the Na(OH), K(OH) and $Ca(OH)_2$ in the pore cavities has been re-dissolved and carbonated, the pH will commence to decrease. At the same time the calcium silicates will partly pass into solution and also react with the CO_2 of the air. As soon as the hardened cement has been completely carbonated, a pH of about 8.3 will develop under normal partial pressure of the CO_2.

The chemical reaction, illustrated in simplified terms, will at a certain moment take place not in a specific depth, but rather in a certain range of depth.

The alkalinity interface does not run exactly parallel to the concrete surface but will vary more or less in relation to the inhomogeneities of the conrete.

Carbonation of the concrete may, besides other methods, be rendered visible by simply spraying colour indicators onto the fresh concrete surfaces. The essence of this procedure is that such colour indicators show different colours in different pH regions. For investigations on the carbonation of concrete phenolphtalein, among others, proved useful as it appears colourless with a pH below 9, but shows an intensive red with a pH above 9.

The carbonation rate of the concrete and/or the rate at which the alkalinity interface, which is of major importance with respect to corrosion protection, will enter the interior of the concrete, depends on the following factors:

- partial pressure of the CO_2 (normal CO_2 content of the air, 0.03%)
- concrete permeability (w/c-ratio, curing, concrete humidity, cement content, grain size distribution curve)
- amount of substance capable of reacting with CO_2 (cement content, type of cement applied).

As this is a diffusion process, calculations in very simplified terms first exhibit a so-called $\sqrt{t}$ dependence, i.e. the alkalinity interface penetrates into the interior of the concrete almost linearly with the square root of the concrete age.

This holds true for relatively low environmental humidity, e.g. indoor conditions. However, for out_door constructions more precise bases of calculation reveal that due to subsequent hardening of the concrete, $Ca(OH)_2$ diffusion from the interior of the concrete, changing humidity near the surface and some other influences, the alkalinity interface will penetrate into the interior of the concrete at an increasingly slower rate than a $\sqrt{t}$ function would suggest, approaching an ultimate value over a very extended period of time.

In the region of cracks in concrete, the penetration rate of carbonation down a crack into the interior of the concrete is considerably higher than in uncracked concrete. Influencing factors of major importance are:

- crack widths
- permeability of concrete
- humidity of concrete

If the passivation on the steel surface is destroyed within a strictly confined area, i.g. within the region of cracks in concrete or peaks of carbonation that reach to the surface of the reinforcement, then the situation and distribution of anodically and cathodically acting bar regions will become an important factor with regard to the rate of corrosion.

In the region of cracks in concrete it should further be considered that owing to the slip existing between steel and concrete, the active steel surface will not be confined to the actual cross-section of the crack.

Depending on the specific environmental and concrete conditions, the maximum corrosion rate can be assumed in the range between 60 and 200 μ/year. (9) (10).

The minimum values of uncracked concrete cover as indicated in the CEB-FIP Model Code 1978 are sufficient to assure that the carbontion of concrete exposed to the open air, even during a very long period of time, will not reach the surface of the reinforcement in uncracked regions. However, this applies only to concrete which has been properly composed, compacted and cured. Only in very dry environmental conditions carbonation may penetrate deeper, exceeding the concrete cover. In such cases, however, the moisture content will, as a rule, not be high enough to produce any significant corrosion. The concrete covers given by the Model Code thus guarantee sufficient durability of the steel in uncracked concrete of structures exposed to the open air.

Within the region of cracks carbonation can penetrate to the reinforcement at a substancially higher rate than in uncracked concrete. In reinforced concrete construction the width of cracks cannot be limited to such an extent that corrosion during the whole service life of the structure could be completely ruled out. Yet, the width of cracks is no longer to be regarded as a major factor in corrosion protection of the reinforcement. Carbonation in the region of smaller cracks, will reach the reinforcement only at a later time than in that of wider cracks. From this point, however, the rate of corrosion is almost independent of the crack width, as the diffusion of oxygen is in general not influenced by the width of cracks. Corrosion normally tends to cause only a small reduction of the bar diameter so that a sufficiently long service life is to be expected, provided that the bars applied are not too thin. (11)(12).

The thickness of concrete cover is of major importance due to the fact that with increasing thickness of cover the risk of concrete being spalled off by corrosion products will be substantially reduced.

The state of knowledge with respect to cracks transverse to the reinforcement is illustrated diagrammatically.

There are not very reliable findings available as regards the situation in the region of longitudinal cracks (stirrups in webs,

two-ways slabs, etc.). But here, too, it is obvious that an increased concrete cover may substantially reduce the risk of spalling. In view of the considerable importance of this problem, investigations in this field are felt to be urgently required.

The communication IV-3.9 lets us know about results obtained from works carried out by the authors as part of a research project initiated some years ago adressed to the question of how and up to what extent the corrosion of reinforcement occurs during carbonation. The ascertaining of the corrosion rates of the steel would permit the calculation of the residual service life of the structure.

The only common statement in carbonated concrete is that pH value decreases and the reinforcements corrode. Only authors who have studied the effect of cracks and have measured the decrease in diameter of the bars due to carbonation in the region of cracks give an approximate to a medium value of the corrosion rate at these points.

Some years ago a research project was initiated in our Institute to study this gap in knowledge and some results have already been published. The experimental work mainly dealt with the study of the corrosion parameters of reinforcements embedded in hardened carbonated mortar of concrete and immersed in carbonated solutions that reproduce the composition of the pore concrete solution.

But the system used for carbonating in these experiments was one accelerated by pure CO_2 gas. This method produces a saturation of CO_2 in the solution or in the carbonation chamber and may lead to different phenomena from those which occurs when carbonation is produced naturally (the proportion of CO_2 in the atmosphere is about 0.03 %). This point is analyzed in the present paper and is taken into account in the future experimental work.

This paper sets out changes in the chemical composition of like-pore concrete solutions during accelerated and natural carbonation (by air) and also the results of simultaneous changes of corrosion potentials and corrosion rates of reinforcements. The results confirm the previously published hypothesis giving a new insight into the phenomenon.

Random behaviours related with the changes in the corrosion rate of steel during accelerated carbonation of cement mortars have suggested the need to study the process in a more simple medium which allows the isolation of the different parameters. Thus, saturated $Ca(OH)_2$-base solutions with different additions of KOH and NaOH have been used to simulate the real pore concrete solution.

In the present work, simultaneous changes in the pH value, corrosion potential and corrosion rate (measured by means of the determination of the Polarization Resistance) of steel roads have been monitored during accelerated carbonation produced by a constant flux through the solution of CO_2 gas and/or air.

Some clear differences in these variables have been established beween solutions with and without Na^+ and K^+ ions, which may clarify the different corrosion behaviours observed in mortar made with different types of cements. Because CO_3Ca is insoluble, the solution not containing alkalies are carbonated more quickly than those containing them. Final pH values in the case of a saturated $Ca(OH)_2$ alkali-free solution are always near neutrality (pH 6-7), but solutions containing alkalies may have a final pH value of about 10,4 where a buffer of $CO_3^=/HOC_3$ is established. Only when an excess of CO_2 gas is passed through the solution are all sodium and potasium carbonates transformed into bicarbonates and the final pH value is about neutrality.

These results lead to an apparent contradiction between the final pH values of real carbonated concretes and those carbonated in an accelerated form.

Concerning the corrosion behaviour, the previous hypothesis is confirmed using air as the carbonating agent. The corrosion potential of steel rises simultaneously with the decrease in pH value is until a limit is reached and depassivation occurs. After this moment corrosion starts and the corrosion rate is dependent on the final pH value of the solution and, therefore, its bicarbonate content.

The passive layer disappears from steel at pH - 8, as Pourbaix has stated many years ago. When $NaNO_2$ is present, the passive layer remains in spite of the lowering of the pH value.

The communication IV-3.10 describes experiments carried out to complete the natural passivation that concrete produces to embedded reinforcements.

Although high quality portland cement concrete offers an adequate protection to embedded reinforcements, sometimes the access to metallic reinforcements of aggressive substances and gases determines that the measures taken may not be sufficient to ensure appropriate durability.

Especially in the case of severe attack it is frequent to try and improve protection of reinforcements by applying supplimentary measures. Among them we can mention:

* outer surface protection of concrete with different coatings
* recoating reinforcements with synthetic resin, bitumen or others
* anodic or cathodic protection
* addition of inhibitors to mortar
* galvanic reinforcement

The present communication describes the experiments carried out to obtain passivation of reinforcements with the aid of anodic polarization through a cement of a specific density together with organic inhibitors consisting of an abietic and adepic acid mix.

We have aimed at determining the propierties of the passive film resulting on the surface of the reinforcement embedded in cement paste and portland cement mortar. We have determined the relationship between changes in active resistivity and reinforcement potential during cement paste hardening. Test probes which had 4 % of the abietic and adepic acid mix were measured similarly. The equipment employed in this experimental project was especially devised by the authors.

The influence of concrete composition was studied by using different qualities as well as different values in concrete-water relationship. Porosity and resistance to corrosion by cement paste and mortars were measured. We chose as an indicating parameter of passivation the time after which the aggressive environment (ClH) reaches the surface of the reinforcement, at that time determining an active resistance of the coat and the electric potential of the reinforcement.

The conclusions we gather are that by applying inhibitors to reinforcement coatings as an abietic and adepic acid mix together with the creation of a passive film devised constitute good protection to concrete reinforcements exposed to aggressive environmets. Condictions stated for the creation of a passive film and the electric system devised allow a prompt and easy protective method.

Among other procedures tested to improve on passivation and corrosion resistance to steel embedded in cement paste, reinforcement galvanization stands out. As zinc dust, zinc chloride or zinc oxide, this metal has been used with this aim. In a work presented in the 7th. Congress (8), the adherence between the cement paste in concrete and reinforcement bars was discussed with zinc and cement paste as special experimental materials. Implicitly referring to the possible passivating role of zinc-coating on steel reinforcement bars. The development of calcium hydroxyzincate is found as the interface reaction product in lime-solutions, whereas the presence of alkalis promote the formation of zinc-oxides and soluble zincates are formed in pure alkaline solutions.

The communication IV-3.11 describes the experiments carried out to complete with addition of zinc oxide the natural passivation that concrete produces to embedded reinforcements.

The passivation or corrosion of iron plates embedded in ordinary portland cement mortar containing a small amount (0.2%) of zinc oxide powder. The cement mortar was made with cement to sand ratio of 1:3, and water to cement ratio of 0.8. Sweet water and sea water were used as mixing water and steam curing was used for acceleration of corrosion for 90 days.

The spontaneous potential of specimens was measured, using silver chloride electrode as a reference electrode.

The rust area was measured on the iron plate after crushing the specimens. Tne measurements were made at 7, 14, 28, 56 and 90 days.

The cement hydration products in contact with the iron plate were investigated using a scanning electron microscope. The pore size distribution of the cement mortars were measured by means of mercury penetration poro-

simeter analysis. When sweet water was used, corrosion was not observed in any of the specimens. It seems that the amount of corrosion was not appreciable under the conditions of water/cement ratio, thickness of mortar cover and the accelerated curing used in this study. On the other hand, when sea water was used, the corrosion was observed in the control specimen (without zinc oxide).

Namely the rusted area of the control specimen was over 80% at 90 days. However, when zinc oxide was used no corrosion was observed.

When the specimens were mixed with sweet water (specimens with or without zinc oxide) the spontaneous potential was about -100 mv. When the specimens contained sea water (specimens with or without zinc oxide), the spontaneous potential was about -300 mv at early stage after mixing. In the former case the potential was negatively larger with curing time (-400 mv), but in the latter case it became negatively smaller with curing time. It remained at about -150 mv after curing for 30 to 35 days.

The scanning electron micrographs of the hydration products on the iron plate in 28 days old specimens, may be grouped into two types. The hydration products in plate with zinc and sweet water, zinc and sea water and cement and sweet water consisted of CSH and calcium hydroxide, and the texture was compact. On the other hand, the hydratation products in control specimen mixed with sea water, consisted mainly of large hexagonal crystal of calcium hydroxide formed in the interfacial region between the iron plate and the cement mortar. The texture in this case was porous.

In the case of zinc oxide addition, probably this compound $Ca(Zn(OH)_3.H_20)_2$ may have formed.

In spite of differences in the type of mixing water, the total pore volumen of specimens containing the zinc oxide admixture, were slightly smaller than the control. The zinc oxide admixture affected the microstructure of the cement mor tar in a beneficial manner which is related to prevention of diffusion of oxigen and other harmful constituents.

It was concluded that the zinc oxide admixture was very effective as a corrosion inhibitor for iron in cement mortar containing sea water.

It should be pointed out that the conclusion is valid as to test conditions. Now, one should be careful in trying to extend it to other situations. It is also important to bear in mind that the addition of zinc to mortar and concrete above certain concentrations may change the hardening process. Consequently, besides research as regards its effect on embedded reinforcement passivation in an all-round work on the theme, said effects should be mentioned and enlarged upon.

The communication IV-3.12 sets out to study the corrosive process in a special type of reinforced concrete tubes.

The corrosion behaviour of steel embedded in concrete is alleged to be very good, due to the passivity given to it by the alkaline environment which forms after the clinker components hydration processes.

Therefore reinforced concrete pipelines, like the other structures in civil engineering, should be and usually are sufficiently safe, from the point of view of the corrosion phenomena concerning the reinforcement.

Unfortunately many failures have recently occurred, either because of incorrect design and manufacturing, or because of the strong aggressivity of the environment, with consequent relevant costs, whose magnitude have been adequately underlined. Several preventive countermeasures may therefore be suggested whenever the possibility of steel depassivation is forecasted.

The reinforced concrete tubes, which constitutes the object of study in the present communication, are manufactured in such a way that very dense concrete is obtained, usually with a rather thin cover.

Maximum aggregate dimension is 3 mm, cement content is 650 kg/m3, water/cement ratio is 0.3; the cover of the pipe used in this experiment is 0.5 cm. The use of such pipes for water transportation is

spreading rapidly, even if their reinforcement corrosion behaviour has not yet been studied in depth.

The tubes tested were "new material" as far as corrosion behaviour is concerned: it was therefore believed necessary to conduct an in-depth investigation in various experimental conditions. The experiments started about two years ago and are still continuing.

The corrosion determination methods were the corrosion potential measurement, the polarization resistance or corrosion rate CR determination, and visual observations.

The specimens obtained from a tube were used for the following experimentations:

A - exposure of specimens to various environments. The tested environments were tap water, magnesium chloride and sodium chloride solutions, sand containing NaCl solution, clay and sand;

B - exposure to various environments of specimens with artificial scratches on the external cover, made in order to leave bare some superficial wires;

C - exposure to soils of scratched specimens prepared in order to measure the current of the corrosion couple generated between bare wires and concrete covered wires.

A few wires, disposed on three parallel layers along the specimen thickness, were partly liberated from concrete in order to allow electrical measurements on superficial wires, medium wires and deep wires.

The investigation was carried out with the adoption of both traditional measuring techniques (spontaneous corrosion potential measurement, visual examination) and electrochemical techniques (polarization resistance or CR and polarization curve determination).

The results of experiments of over approximately two years showed that with the specimens, even with a rather small concrete cover (0.5 cm) no corrosion phenomena were observed at all, probably due to the low porosity of the tube, in the presence of scratches artificially made over the outer surface in order to simulate an erroneous handling of the pipe; it was observed that the corrosive attack remained strictly localized in the part of the wires directly in contact with the aggressive environment, and did not spread into the concrete.

Moreover, in the presence of soils with different permeability (sand and clay) the results of the tests showed again the good corrosion behaviour of the reinforcement.

Several points emerge from the results of about two years investigation on corrosion behaviour of specimens cut from tubes, exposed to several corrosive environments (tap water, 3,5 % NaCl solution, sand humidified with NaCl solution, clay, sand).

(1) Results of six month-experiments on specimens exposed to all corrosive environments tested, show that there was no corrosion of reinforcing wires. The spontaneous potentials of wires lay in the range of steel passivity state;

(2) In the presence of artificial scratches on the outer concrete cover (scratches made to leave bare surface wires in order to simulate an erroneous handling of the tubes); it was observed that the corrosive attack remained strictly localized on the wire surface directly in contact with the aggressive environment, while there was no corrosion propagation on adjacent wire surface embedded in concrete;

(3) for scratched specimens exposed to different soils (clay and sand); corrosion couple, generated between the bare surface of wires directly exposed to the soil and the surface of the wires covered with concrete, gives rise to mean corrosion penetration rates of 0.04 mm/y for bare wires exposed to clay and of 0.08 mm/y for those exposed to sand. In this case too, attack was strictly restricted to the bare area. Stifling during the corrosion attack is due to protective effects of corro-

sion products in anodic areas.

(4) Investigations are still continuing to verify the long-time behaviour of tube reinforcement.

The communication presented explains a complete methodology as to how a new product should be studied, in this case a concrete reinforced tube, in order to evaluate the corrosion behaviour of the embedded steel.

--- 0 ---

REFERENCES

1.- CALLEJA, J., "Durability". Principal paper. Theme VII, sub-theme 2. 7th. International Congress on the Chemistry of Cement, 1980.

2.- IDORN, G.H., "Interface reactions between cement and aggregate in concrete and mortar". General report. Theme VII. 7th. International Congress on the Chemistry of Cement, 1980.

3.- GLASSER, L.S.D., and KATAOKA, N., (1981), "The Chemistry of Alkali-aggregate reaction". 5th. Int. Conf. Alkali-Aggregate Reaction in Concrete, 5252/22.

4.- GLASSER,L.S.D. and KATAOKA, N., (1981). "The Chemistry of Alkali-aggregate reaction", Com. Concr. Res. 11, 1-9.

5.- TOGNON, G.P., COPETTI, G., URSELLA, P., 9 Internationaler Kongress der Beton- und Fertigteilindustrie (Wien, 8 - 13 Oktober 1978), 39-46.

6.- TOGNON, G.P., URSELLA, P., COPPETTI, G., J.Am. Concr. Inst., 1980, 77 (3), 171-178.

7.- TOGNON, G.P., URSELLA, P., COPPETTI, G. 7th. Int. Congress Chem. Cem (Paris, 30 juin - 5 juillet, 1980), VII - 75-80.

8.- ARLIGUIE, G., GRANDET, J., and DURAL, R., "Study of the contact zone between zinc and Portland cement paste". 7th. International Congress on the Chemistry of Cement, 1980.

9.- SCHIESSL, P., Zur Frage der Zulassigen RiBbreite und der erforderlichen Betondeckung im Stahlbetonbau unter besonderer beruckrichtigung der Karbonatisierung der Betons. Deutscher Ausschub fur Stahlbeton, Heft 255, Berlin 1976.

10.- TUUTTI, K., Corrosion of Steel in Concrete. CBI forskning 4/82. Cement-och Betonginstitutet, Stockholm.

11.- BEEBY, A.W., Concrete in the Oceans. Cracking and Corrosion. Technical Report Nro.1 CIRIA/VEG, Cement and Concrete Association, Department of Energy, 1978.

12.- TUUTTI, K., Craks and Corrosion. Cement-och Betonginstitutet, Fo 6:78, Stockholm 1978.

--- 0 ---

N.F. ANANENKO, Guiprocement, Leningrad, USSR

MAGNESIUM OXIDE IN PORTLAND CEMENT

The problem on the maximum permissible MgO content in Portland cement clinker is up to now one of important matters of concern in cement chemistry and technology.

For the first time commercial production of magnesia clinker with clinker burning in rotary kilns was organized by V.V. Serov (1). On the basis of extensive experiments V.V. Serov established appropriate requirements for the chemical and mineralogical composition of magnesia clinker and developed specifications for cement soundness tests. With magnesia clinker as the basis there was organized manufacturing of magnesia slag portland cement specifications for which were also standardized. The mentioned above types of cement were manufactured for a long time at one of cement plants in the USSR (2).

The investigations of V.V. Serov were further continued and developed by P.P. Bydnikov (3), N.A. Toropov (4), S.M. Royak (5-6), L.Yu. Astansky (7) and by other Soviet scientists.

The publications on problems in researching and obtaining cements with elevated and high MgO content within the period from the VII-th International Congress on the Chemistry of Cement (Paris, 1980) were concerned mainly with magnesium oxide effect of clinker structure, alite polymorphism, mineral formation processes at various temperatures (8-10).

In the recent years there have been published a number of works aimed at further investigation of constructional and engineering properties of cements with various MgO contents to ensure soudness of cement (11-12).

Certain countries have introduced alterations into their standards as regards the permissible MgO content increasing it to 6% (USA, India) (13). Table 1 gives values for MgO content and methods of test for cement soundness in international standards.

The amount of magnesium oxide acceptable in clinker is in the range from 3 to 6.5%. The minimum MgO content in cement can be ascribed to absence of the necessity to revise the traditions.

The requirement for cement soundness is envisaged in standards of all the countries (13), but the methods used for testing are various: boiling test or cold water pat test, expansion measuring on cement paste samples in boiling or wet stored (Le Chatelier test), autoclave test under 2 MPa to detect sample expansion.

The Le Chatelier test is most extensively employed as it permits to give a quantitative estimation of the cement expansion value. But this method doesn't allow to detect unsoundness due to periclase hydration and hence it can be only used with cements of low MgO contents.

The autoclave test has been standardized in 9 countries inclusive of USA, Canada, Belgium, Finland. The acceptable linear expansion being from 0.5 (Venezuela) to 1.3 (Argentina, Belgium).

In the USSR practice when carrying out scientific and research works (14) for quality assessment of cement featuring elevated MgO content, the linear deformation of bar specimens is determined through autoclave tests after previous 4-hour boiling. In our opinion, such a method of expansion assessement makes it possible to reveal the effect of both magnesium oxide and calcium oxide on this particular characteristic.

Special investigations of prof. I.G. Luginina on magnesia cement stone expansion in autoclave tests disclosed that volume deformation manifests itself during isothermal curing.

The alterations in the steaming conditions consist in lowering the maximum pressure, on achieving it, within the time interval of 1-1.5 hour, down to 0.6-0.7 MPa and then raising it again to the maximum one and retaining it constant during 3-4 hours. Within the initial stage intensive hydration of clinker minerals and crystallization of the hydration products take place, that strengthen the cement stone

Table 1

Magnesium Oxide Contents and Methods for Cement Soundness Tests in Different National Standards

Country	MgO content limit in clinkers, %	Soundness, h	
		Method	Permissible expansion
Austria	5.0		
Great Britain	4.0	Le Chatelier test	10 mm
Brazil	6.5	Le Chatelier test	5 mm
Denmark	3.0	Le Chatelier test	10 mm
India	6.0	Le Chatelier test autoclave test (at MgO 3%)	10 mm 0.8%
Italy	4.0	Le Chatelier test	10 mm
Canada	5.0	Autoclave test	1%
France	5.0	Le Chatelier test or 7 days water storage	10 mm
FRG	5.0	Boiling test	
Czechoslovakia	6.0 4.0	Boiling test	
Rumania	2.5-5.0	Le Chatelier test	10 mm
USA	6.0	Autoclave test	0.8%
USSR	5.0	Boiling test	no cracks
Japan	5.0	Boiling test	no cracks

structure prior to periclase hydration. The subsequent curing under 2 MPa pressure has practically no effect on the value of the linear deformation of the cement specimens. The proposed conditions simulate cement hardening more exactly.

The question on the method for soundness tests and the criterion for its assessment with cements featuring an elevated and high MgO content deserve special study and discussion.

When working out chemical and technological technique which would assist in obtaining cement withstanding autoclave tests at elevated MgO contents, some investigators aimed at binding magnesium oxide into chemical compounds and thus to neutralize its detrimental effect on hydration. In doing this various additives were introduced into the raw mixture, burning temperature was changed. The results obtained were rather contradictive and therefore couldn't be used in production.

To clear out the possibilities in formation of magnesium-containing compounds in the field of Portland cement clinker compositions, special investigations were carried out to study products of clinker formation within the temperature interval from 700°C to 1300°C (15) .

The raw mixtures contained magnesium oxide (on clinker basis) in amounts of 1-10%. The control raw mixture containing no magnesian component was also investigated. The burning products underwent X-ray phase analysis in a DRON-1 apparatus. For identification of X-ray photographs use was made of the data from the ASTM roentgenometry file.

No interference lines which would indicate the presence of magnesium silicates or spinel in the burning products were found on any of the diffractograms in the whole of the temperature interval investigated, free magnesium oxide was identified in the burning products of raw mixtures containing MgO. No other magnesium containing compounds were found. Thus it was proved once and again that MgO is present mainly in a free form from the moment of magnesium carbonate decomposition till completion of clinker formation.

The research in magnesium oxide effect on clinker phase composition and its microstructure under various burning conditions 16 have disclosed that the nature of MgO effect on clinker microstructure is closely connected with the gaseous atmosphere during burning. At clinker burning in a neutral atmosphere presence of magnesium oxide in amounts of 3% and above noticeably affects the microcrystalline structure - the alite and belite crystals acquire an indefinite form.

Clinker burning in a reducing medium impairs its microstructure, as compared to the control clinker containing no magnesium oxide, only when MgO content reaches 5% and above. The alite and belite crystals of clinkers with 2-3% of magnesium oxide present had in contrast a more regular form.

Both the phase composition of clinkers and their microcrystalline structure change under the effect of magnesium oxide depending on the burning conditions. It has been found out that with an increase in magnesium oxide content in clinkers of neutral atmosphere burning the proportion between the aluminate and aluminoferrite phases changes so that the portion of C_3A reduces while the portion of $C_2A_xF_{1-x}$ increases. This change has no monotonous character but reaches a maximum when magnesium oxide content is about 3%. With a further increase in MgO content the amount of C_3A again begins to grow.

In clinkers obtained in a reducing atmosphere this regularity has somewhat another character: - the shift maximum is observed at MgO content of about 2%, and the relative value of the phase shift decreases.

The investigations on assessement of the effect of simultaneous presence in the raw mixture of a mineralizing (CaF_2) and alloying (MgO) components have shown that the latters produce a noticeable influence on clinker phase composition causing an elevated alite and intermediate phase contents (17, 18). An increase in magnesium oxide content above 3.0% results in a decrease in the amount of high-basic calcium silicate.

Incorporation of magnesium oxide in amounts up to 3.0% in fluor-containing clinkers favourably effects crystallization of alite forming mainly a high symmetrical modification.

The investigations on admixture distribution among the basic clinker phases, carried out in the "Camebaks" plant, have demonstrated, that magnesium oxide is concentrated mainly in the aluminate and aluminoferrite constituents.

One of technological methods making it possible to reduce the adverse effect of an elevated magnesium oxide content on cement quality as regards its soundness is introduction of active mineral additives into the binder composition.

The favourable effect of active mineral additives on the results of autoclave tests of cements featuring an elevated MgO content is accounted by the fact that silica present in the additive partially binds periclase into magnesium hydrosilicates. Besides, during hydrothermal treatment of cement in presence of ash one can notice a retardation in periclase hydration due to an elevated density of the cement stone.

The technological method of introduction of active additives into cement with elevated MgO content has been studied and examined by a number of authors (19-20). Since autoclave treatment doesn't simulate cement hardening under normal conditions, the data on hardening high magnesian cements obtained for many years are of great interest for revealing possible consequences due to retarded hydration of periclase.

Table 2 represents the results of determining linear deformations of cements with 6-6.5% magnesium oxide contents which were water-stored during 20 years (19). The linear deformations of the cements no matter whether they contain or not a mineral additive are rather insignificant. Thus, expansion of plain cement on the basis of clinker with 6.03% MgO content after 20 years of storage in water was only 0.29%, the linear expansion for the last five years increased in this case only by 0.01%. Cement obtained from clinker having a 6.5% MgO content without active mineral additives in 10 years of hardening showed linear expansion as high as 0.30% and in 15 years - 0.31%. It should be noted that this cement failed autoclave tests on soundness (expansion being 12.2%).

Introduction of a 15% mineral additives

Table 2

Cement Soundness and Linear Deformation under Normal Hardening Conditions

Description of Cement Additive	Linear Expansion, %						
	Autoclave test at 2 MPa	Hardening Duration, years					
		1	3	5	10	15	20
	Clinker of pilot plant burning at MgO = 6.54%						
Plain cement	12.2	0.13	0.22	0.25	0.30	0.31	0.32
Tripoli earth	0.33	0.06	0.09	0.10	0.13	0.14	0.15
Fly ash	0.43	0.08	0.13	0.14	0.15	0.15	0.17
Tuf	0.16	0.10	0.15	0.16	0.18	0.18	0.20
	Commercial clinker MgO = 6.03%						
Plain cement	11.3	0.10	0.16	0.19	0.25	0.28	0.29
Tripoli earth	0.11	0.07	0.11	0.14	0.17	0.20	0.20
Fly ash	0.07	0.06	0.11	0.13	0.16	0.17	0.18
	Commercial clinker MgO = 5.22%						
Plain cement	5.28	0.13	0.20	0.24	0.29	0.33	0.34
Tripoli earth	0.15	0.06	0.10	0.15	0.19	0.20	0.21
Fly ash	0.16	0.07	0.12	0.14	0.17	0.17	0.17
	Commercial clinker MgO = 1.13						
Plain cement	0.02	0.07	0.09	0.09	0.12	0.13	0.13

(Tripoli earth, tuf, fly ash) into cements as seen from Table 2 noticeably diminished linear deformation of cements both under water hardening and in autoclave treatment.

For example, expansion of plain cement obtained of clinker with a 5.22% MgO content after 20 years amounted to 0.29%, and with Tripoli earth and fly ash introduction the same 0.20 and 0.18%, respectively.

The 20-year storage specimens of cements produced on the basis of clinker with 6.03% magnesium oxide content were studied using roentgenographic and derivatographic methods of analysis. The data obtained point to the presence of unhydrated periclase (reflection 2.09-2.10 Å) in the hardening products along with magnesium hydroxide (reflection values 2.35-2.36; 1.570-1.574 Å). By application of calibration mixtures featuring various magnesium oxide contents the amount of residual periclase in the cement stone of plain cement and cement with a 15% Tripoli earth additive was determined. It comprised 1.64 (±0.1%). The degree of periclase hydration in 20 years of cement hardening constituted 72% in the first case and 68% in the second case.

The X-ray photographs show no interferentional lines which could be attributed to magnesium hydrosilicates. The possibility of formation of the latters (chrysotile-type) in hardening under normal conditions cements with addition of the ash, Tripoli earth, trass and other siliceous materials has been marked in publication (22).

No magnesium hydrosilicates were either found in specimens of cement stone by a derivatographic analysis. The whole of the thermograms irrespective of additives present in cement show endothermal effects at 150°C (calcium hydrosilicates), 420-430°C (magnesium hydroxide), 545-550°C (portlándit) and at 820°C (hydrosilicates and cal-

cium corbonate). With the help of infrared spectroscopy calcium carbonate was detected in hardening products (lines at 713, 875 and 1430 cm^{-1}).

Electron-microscope investigations on specimens at 20 years storage in water in a scanning microscope provided no means to reveal the variations in cement stone structure depending on active mineral additives present in the cement.

The cement stone on the basis of the control cement (plain) only features more pores which are larger than those in specimens of cements with fly ash and Tripoli earth additives. The whole of cement stone specimens are characterized by a dense mass and pores partially or completely filled with hydration products in a form of plates and needle-like crystals.

Investigations carried out by Dr. S.S. Rehsi have made it possible to look into the composition, soundness, strength of high-magnesis cement (up to 15% MgO) with a fly ash additive (20-40%) (20, 21) at 14 years hardening.

It has been ascertained that incorporation of fly ash in high-magnesia cement has an efficient stabilizing influence on technical characteristics of such a binder. The compressive strength as well as the tensile strength of high-magnesia cement without fly ash appreciably falls even after 90 days of storage in water at 27±2°C, while introduction of 30% fly ash ensures a steady strength development during the first five years whereupon it remains constant. The expansion of high-magnesia cements containing fly ash and without it at 14 years storage in water was 0.239 and 1.833%, respectively. Incorporation of fly ash brings about no changes in the composition of the hydration products of high-magnesia cements, so in specimens of 14 years storage in water CSH, ettringite, $Mg(OH)_2$, $Ca(OH)_2$, $CaCO_3$ and residual inhydrated MgO were indentified.

Practically the whole of investigations on the effect of hydraulic additives on magnesian cements properties points to their favourable action. This technological method would assure obtaining of high-quality magnesian cements and application of dolomite limestones.

The production practice has proved that magnesium oxide impedes obtaining of high-quality cement. In view of this technological methods aimed at raising the product quality are under development at cement plants. Significant works in this field have been carried out by M.A. Teixeira de Castro (23).

As mentioned above, according to the Brazil standards the permissible magnesium oxide content in cement is up to 6.5%. Therefore the problem on provision of manufacturing high-quality magnesian cement is of great urgency.

The major recommendations on improvement of the quality of high-magnesia cements are as follows:

- fine grinding of raw mixture;
- thorough mixing of raw mixture;
- sharp burning of clinker in oxidizing atmosphere;
- fine (possibly repeated) cement grinding;
- clinker should feature:
  a) as high tricalcium silicate content as possible;
  b) elevated iron content

For each plant and its raw base the mentioned conditions should naturally be refined, but they are obligatory to a certain degree. Unfortunately the work under consideration doesn't touch upon the subject of cement soundness provision by autoclave tests, but adduces data obtained in Le Chatelier tests.

Currently the problems on the phase composition of clinkers featuring various magnesium oxide contents as well as the effect of chemical and technological factors (chemical composition and fineness of raw mixtures, cement fineness etc.) on the properties of magnesian cements have been studied fully enough (24, 25).

However there are no data on organization of commercial magnesian cement manufacture. Different standards for assessment of cement soundness not always allow to compare characteristics of cements obtained and investigated. Moreover, there is no unified opinion on suitability of autoclave cement test since, as it has been found, its results are influenced by some other factors.

The results of physicomechanical tests and linear expansion values obtained on long-term hardening under normal conditions have evidently a great importance in solving the problems under consideration. These data for 25-30 years of cement hardening would allow to evaluate cement characteristics and methods for cement testing.

REFERENCES

1. Serov V.V. Tsement No. 1, 1934; No. 7, 1935.
2. Getchert I.E., Zhukov M.P. Trudy Giprotsementa, vyp. 16, Promstroiizdat, 1963.
3. Budnikov P.P., Vorobev H.S. Tsement No. 1, 1960.
4. Toropov N.A., Merkov L.D., Shishakov N.A. Tsement No. 1, 1937.
5. Royak S.M., Myshlyaeva V.V., Trudy NIITsementa, vyp. 7, Promstroiizdat, 1953.
6. Royak S.M., Myshlyaeva V.V. Vliyanie povyshennogo soderzhaniya okisi magnia na svoistva tsementov. Promstroiizdat, 1956 (MPSM SSSR, TsBTI Tekhnicheskoe Upravlenie, Informatsionnoe soobshchenie).
7. Astanskii L.Yu. Issledovanie rezhima okhlazhdenia tsementnogo klinkera. Ufa, 1959.
8. Y.V. Nikiforov, R.A. Zozoulia. 7-th International Congress on the Chemistry of Cement. V. II, Paris, 1980, p. 1-34.
9. R. Bucchi. 7-th International Congress on the Chemistry of Cement. V. I, Paris, 1980, p. 1-1/3.
10. V.V. Timashev. 7-th International Congress on the Chemistry of Cement. V. I, Paris, 1980, p. 1-3/1.
11. G. Goswami, S.K. Mohanty, J.D. Panda. Cement and Concrete Research. Vol. 14, p.p. 407-412, 1984.
12. Mangelnde Raumbeständigkeit im Autoklaven von Klinkern mit niedrigen MgO-Gehalten. Reports. Zement-Kalk-Gips, 1982, Nr. 9, S. 508.
13. Cement Standards of the World. Cembureau. The European Cement Association.
14. Kogan L.S., Nikiforov Y.V. Trudy instituta Giprocement, vyp. 24, 1962, L.
15. Nikiforov Y.V., Zozoulia R.A. Trudy Instituta NIITsement, vyp. 63, M., 1982, S. 123-132.
16. Kuznetsova T.V., Soboleva K.L. Tsement, 1979, No. 12, S. 12-13.
17. Nikiforov Y.V., Svatovskaia M.B. Tsement, 1983, No. 1, S. 14-16.
18. Nikiforov Y.V., Svatovskaia M.B., Tsintsiper M.S., Milovanov Y.A. Tsement, No. 8, 1983.
19. Nikiforov Y.V., Zozoulia R.A. Trudy instituta NIITsement, No. 77, M., 1983, S. 64-70.
20. S.S. Rehsi. Magnesium Oxide in Portland Cement. Adv. Cem. Technol., Crit. Rev. and Stud. Manuf. Qual. Contr., Optimizat. and Use, Oxford e.a. 1983, p. 467-483.
21. S.S. Rehsi, Garg S.K. "Durabil. Build. Mater.", 1985, 2, No. 3, 265-273.
22. Rosa J. Stavivo, 1961, No. 12.
23. M.A. Teixierde de Castro. Tecnica, 1981, 41, No. 458, 263-273.
24. Dreizler J., Knöfel D. Zement-Kalk-Gips, 1982, Nr. 10, S. 537-550.
25. Chr. Rott., D. Knöfel, J. Dreizler. Zement-Kalk-Gips, 1984, Nr. 4, S. 195-199.

PALOMO, A.; VAZQUEZ, T. and BLANCO-VARELA, M.T.

Instituto Eduardo Torroja de la Construcción y del Cemento (C.S.I.C.) Madrid (España)

INFLUENCE OF MgO ON THE CRYSTALLINE MICROSTRUCTURE OF THE LIQUID PHASE OF PORTLAND CEMENT

S1

INFLUENCE DE MgO SUR LA MICROSTRUCTURE CRISTALLINE DE LA PHASE LIQUIDE DU CEMENT DE PORTLAND

Introduction

Due to the pernicious effect that the magnesium oxide effectuates on the stability of the concrete's volume, generally the contents of Mg in Portland cement are restrained in the legislation of the countries of the world. Although, the presence of Mg in raws mixes can also generate important benefits. The MgO, for example, is a well known fluxing agent, and it improves the burnability of raws; and it also accelerates the rate of combiantion of lime. Besides this, if the formation of periclase in the clinker could be diminished or delayed, there would be the important chance of using in the elaboration of the cement big calcareous beds useless nowadays by problems of dolomitization; and many times with important increases of costs due to the provision of lime stone with less contents in magnesium oxide, worked out in more grievous conditions.

In the present work a special emphasis has been put in the study of the modifications that the compo - nents of the liquid phase of the clinker (aluminatas and ferrites) undergo, and the micro-structures that are generated by the presence of a certain quantity of MgO.

Bibliography about this subject isn't abundant. Nevertheless, we can consider the studies of Müller-Hesse and Shwiete (1), Midgley (2), Woermann et al. (3), Locher (4), and Miyazawa and Tomita (5) about the capacity of aluminates and ferrites to incorporate MgO in their crystalline lattices, and the studies of Dreizler et al. (6), Christensen (7), Bucchi (8), Budnikow and Worobjew (9), Guye (10), Ramachandrán (11), and Nikiforov et al. (12) about different aspects of the role of MgO in Portland cement.

Experimental Procedure

The materials used in the realization of this work have been laboratory reactives of a high degree of purity (99%): $CaCO_3$, Al_2O_3, Fe_2O_3 and MgO. The procedure to whom these compounds were submitted is described in the following way:

- Five mixtures in correspondence with five compositions of the ternary system C-A-F (see Table 1) were prepared.
- A study by Differential Thermal Analysis of each compositions was made.
- Pellets, of about 0.4 gr. belonging to each composition, were made using for it a 7 mm - internal diameter cylindric mould and an hydraulic press that was activated to a pressure of 4 free tons.
- The tablets, introduced in tiny platinum crucibles were submitted to a thermic programmed treatment (similar to the DTA) in a vertical laboratory furnace with an attached programmer controller of temperature. This thermic treatment (identical for all the compositions except in the final temperature that was reached) consisted in the preservation of the sample up to 1100ºC during 25 minutes, heat it inmediatelly up to 1500ºC (at a velocity of 40ºC/min.), preserve it 10 minutes at that temperature and finally cool it at a velocity of 8ºC/min. until it reached the required temperatures. These temperatures were different for each composition and they depended on the results obtained before by DTA. Table 2 shows the list of temperatures selected in each case.

Table 1

	CaO (wt%)	Al_2O_3 (wt%)	Fe_2O_3 (wt%)
composition 1	42,1	23,7	34,2
composition 2	53,1	28,2	18,7
composition 3	49,5	35,0	15,5
composition 4	41,8	34,9	23,3
composition 5	44,9	45,3	9,8

Table 2

compositions	temperatures of treatment (ºC)
1 and 1+ MgO	1390 - 1230 1050
2 and 2+ MgO	1355 - 1265 1210
3 and 3+ MgO	1325 - 1185
4 and 4+ MgO	1370 - 1290 1242 - 1145
5 and 5+ MgO	1280 - 1190 1130

- Once the required temperature was reached, the sample was kept during an hour at that same temperature and inmediatelly after it was taken out of the furnace and quenched in an air current.
- The quenched samples were analysed by infra-red spectroscopy and by X-ray diffraction (Table 3 resumes the data obtained with these methods). They also were prepared for its observation through reflected light optical microscopy.
- All the stages described up to here, were repeated one by one with the same compositions given in Table 1, but all of them doped with 6.5% of MgO.

Results and Discussion

In figures 1 and 2 the results obtained in the study by DTA about the thermic behaviour of the five chosen compositions are shown.

In the DTA curves (in the section corresponding to the heating), compositions 1, 2 and 3 show a double peak that indicates consecutives meltings. The first of these peaks presents its maximum at about 1315ºC and the second one presents it in a range of temperature that goes from 1340ºC to 1375ºC.

Compositions 4 and 5 present an only peak assignable to the melt with the maximum over 1320ºC.

Concerning with the cooling, all the compositions, except number 3, show two peaks corresponding to consecutive solidifications. The first one in a range

PALOMO, A.; VAZQUEZ, T. and BLANCO-VARELA, M.T.

INFLUENCE OF MgO ON THE CRYSTALLINE MICROSTRUCTURE OF THE LIQUID PHASE OF PORTLAND CEMENT S1

INFLUENCE DE MgO SUR LA MICROSTRUCTURE CRISTALLINE DE LA PHASE LIQUIDE DU CEMENT DE PORTLAND

of temperatures between 1321 and 1239ºC and the second one between 1225ºC and 1132ºC. Composition No 3 presents an only peak of solidification with a minimum at 1282ºC.

With the base of these data it is described and explained the results obtained for each composition:

Composition No.1

From micrographs 1 and 2 and from Table 3 it is infered the evolution of this composition when the temperature falls: First the ferritic phase crystalizes in needles shapes, and among the needles a poorly crystalized material, rich in Al, solidifies. As the essay temperature decreases, the kind of texture doesn't change, but the material that initially was nearly vitreous, has been transformed into a heap of tiny crystals of CA that rest upon a whitish base of ferritic nature though clearly different from the already mentioned ferritic needles. This reveals that two ferritic phases with different contents in Fe and in Al have been formed; this is logic if it is considered that when CA crystallizes from a rich in Al melted phase, segregations are produced; this helps to form a second ferritic phase poorer in Al than the primary needles. The IR spectroscopy sustain these deductions, because the bands of absorption in the 650-730 cm^{-1} zone (characteristic of vibrations FeO_4) wouldn't be observed as continuous if it existed one only phase; an only ferritic phase would produce definite bands in determinate frequencies. The same thing can be said about the band in 570 cm^{-1}, attributed to Al-O vibrations of ferritic phase that do not appear single and clear and this because surely existes an overlapping of Al-O bands due to more than one ferritic phase.

The IR spectroscopy is also in agree with the existence, at a high temperature of aluminates that aren't crystallized because in 780-800 cm^{-1} zone (characteristic of AlO_4 vibr.), it is observed a difusse absorption. By XRD the presence of a little amount of crystallized CA is detected, it really corresponds to some crystalline nucleus of the monoaluminate.

Table 3
IR and X-ray examination

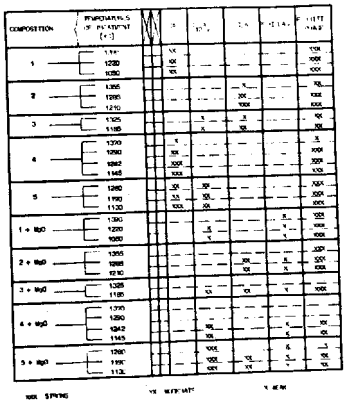

The composition No. 1 lies down upon the primary field of crystallization of C_2Fss and upon the area of compatibility CA-C_2Fss; this corroborates that the

Fig. 1

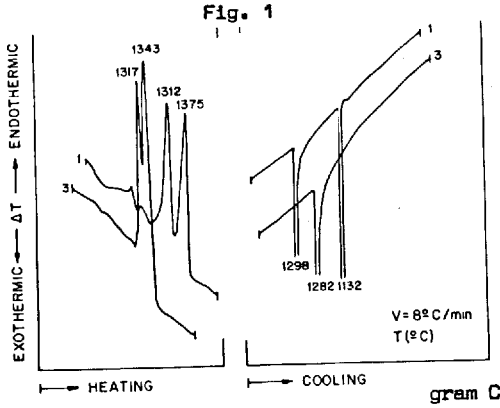

crystallization sequence described for this composition is in agree with the equilibrium established in the ternary diagram C-A-F.

Fig. 2

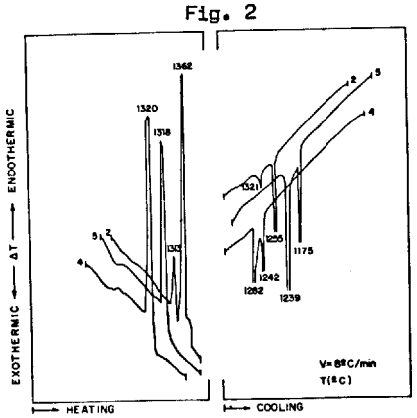

Composition No.2

Composition 2 lies upon the primary crystallization field of the CaO and upon the triangle of compatibility C-C_3A-C_2Fss. This composition presents at the highest temperature of treatment a vitreous solidification that on the microscope is seen as an uniform and grayish mass. Although not only the IR spectroscopy but also the XRD (see Table 3) discovers the presence of C_3A traces and a little of ferritic phase (type C_6A_2F). When the treatment temperature diminishes, a texture like the one of micrograph 3 is found. In this microstructure, that doesn't have posterior changes, it is observed a great number of dark and long crystals of C_3A that are homogeneously distributed upon a surface of clear colour and of ferritic nature. Decreasing the treatment temperature a little bit more, it is observed that the degree of crystallization of the phases improves. The ferritic phase gets on being rich in Al.

Composition No. 3

This composition presents a microstructure as the ones of micrographs 4 and 5. Apparently, two only phases appear but the presence of 3 phases is deduced through XRD and IR spectroscopy $C_{12}A_7$, C_3A and ferritic phase. Ferritic phase (the clearest one) is rich in Al and crystallizes in shape of small needles that are partially cut by aluminates (tinier crystalls but longer). Composition 3 shows us a case where the proximity of the succesive temperatures of crystallization, don't allow the observation of intermediate stages. This composition lies upon the primary field of crystallization of the C_3A, near the boundary that separates this field with that of C_2Fss and also near the ternary eutectic C_3A - C_2Fss - $C_{12}A_7$. This justifies the similitude between the texture

PALOMO, A.; VAZQUEZ, T. and BLANCO-VARELA, M.T.

INFLUENCE OF MgO ON THE CRYSTALLINE MICROSTRUCTURE OF THE LIQUID PHASE OF PORTLAND CEMENT S1

INFLUENCE DE MgO SUR LA MICROSTRUCTURE CRISTALLINE DE LA PHASE LIQUIDE DU CEMENT DE PORTLAND

MIC. 1 comp. 1 (1390ºC)

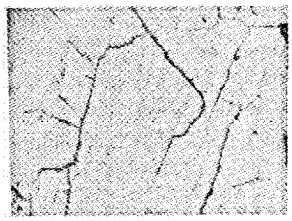

MIC. 2 comp. 1 (1050ºC)

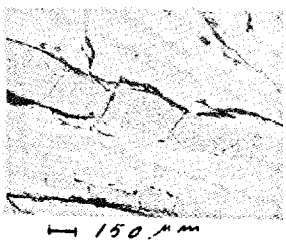

MIC. 3 comp. 2 (1285ºC)

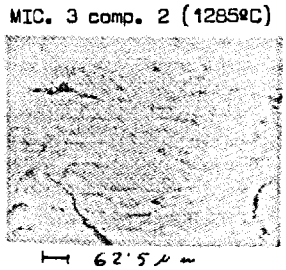

MIC. 4 comp. 3 (1185ºC)

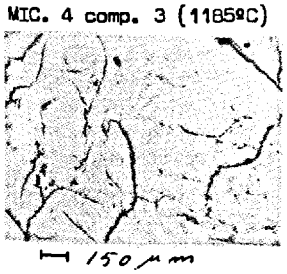

MIC. 5 comp. 3 (1185ºC)

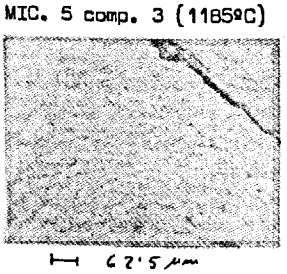

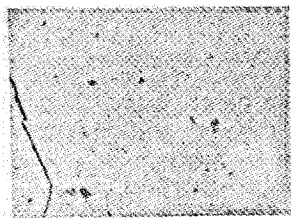

MIC. 6 comp. 4 (1370ºC)

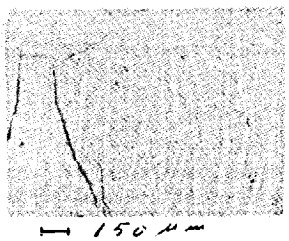

MIC. 7 comp. 4 (1290ºC)

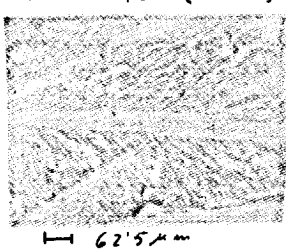

MIC. 8 comp. 4 (1145ºC)

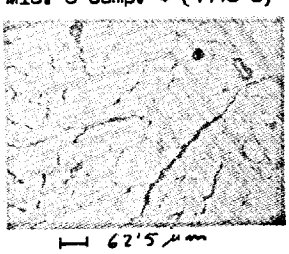

MIC. 9 comp. 5 (1280ºC)

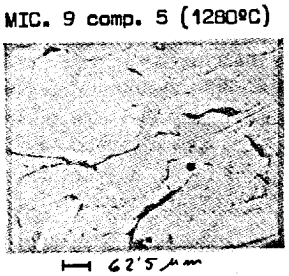

MIC.10 comp. 5 (1130ºC)

found in this composition and the typical texture of the compositions that lie upon the primary crystallization field of C_2Fss, because the early crystallization of the C_2Fss, when the amount of crystallized C_3A isn't big yet, enables the formation of this kind of texture.

Composition No. 4

Microscopy (micrographs 6,7 and 8), XRD and, IR spectroscopy give the following data about the development of this composition with the temperature. In a first stage, ferritic crystals with needle shape solidity and among them, an amorphous material rich in Al. In an ulterior stage, the vitreous material crystallizes in the shape of tiny crystals of CA at the same time that the ferritic needles grow slighty. Finally, all the crystals (ferrites and aluminates) grow and increase their degree of crystallinity considerably, locating the CA crystals upon a base of ferritic origin that on the micriscope presents a lighter colour than the one of the ferritic needles; so that two ferritic phases with different proportions of Fe and Al are formed.

This composition shows a great similitude with composition 1 and this is logica because composition 4 is also localetd upon the primary crysta

MIC. 11 comp 1 M (1390ºC)

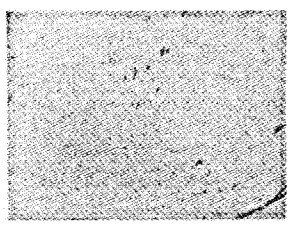

MIC. 12 comp 1 M (1050ºC)

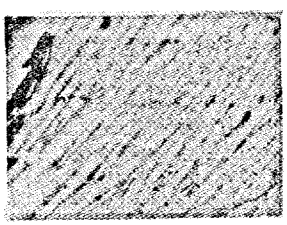

MIC. 13 comp 4 M (1145ºC)

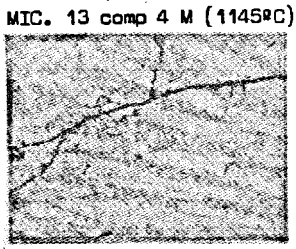

MIC. 14 comp 2 M (1285ºC)



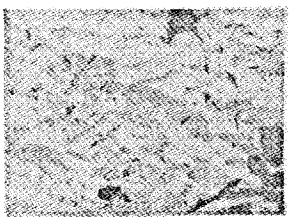

MIC. 15 comp 2 M (1285ºC)

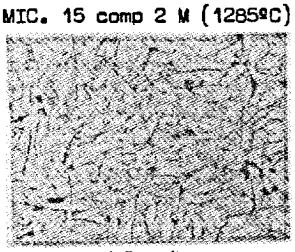

MIC. 16 comp 3 M (1185ºC)

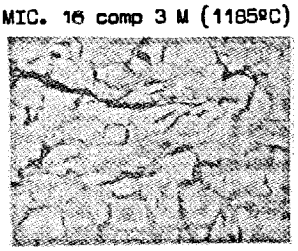

MIC. 17 comp 3 M (1185ºC)

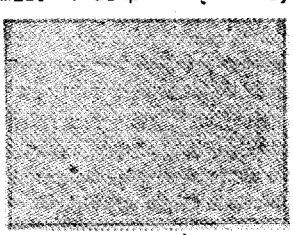

MIC. 18 comp 5 M (1280ºC)

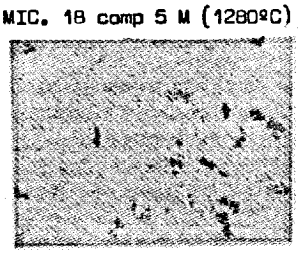

MIC. 19 comp 5 M (1190ºC)

INFLUENCE OF MgO ON THE CRYSTALLINE MICROSTRUCTURE OF THE LIQUID PHASE OF PORTLAND CEMENT S1

INFLUENCE DE MgO SUR LA MICROSTRUCTURE CRISTALLINE DE LA PHASE LIQUIDE DU CEMENT DE PORTLAND

llization field of the C_2Fss and upon the compatibility area CA - C_2Fss. The only difference between both compositions is that composition 4 is richer in Al and it is nearer to the boundary CA - C_2Fss; this makes that this composition will have a bigger proportion of CA and a less proportion of ferritic primary phase . The rest of the resultants are interpreted exactly the same as in composition 1.

Composition No.5

The solidification of this composition can be described in the following way: First dendritic crystals of $C_{12}A_7$ begin to nucleate and grow (this crystals that lie upon a slightly devitrified and rich in Al base can be seen in micrograph 9); afterwards and due to the annealing it can be observed an increasing in the dendrites size together with an eutectic crystallization where $C_{12}A_7$, CA and a ferritic phase rich in Fe solidify simultaneously (see micrograph 10). The facts described for composition 5, are in good agree with the situation of this composition in the equilibrium diagram. Composition 5 lies upon the primary field of crystallization of the $C_{12}A_7$ and upon the triangle of compatibility $C_{12}A_7$ - C_2Fss -CA.

Effects of the MgO

The addition of a 6.5% of MgO to each one of these compositions produces a group of effects that can be described in the following way:

In composition 1, the MgO acts upon the nature of the phases and upon the evolution of microstructure (see Table 3 and micrographs 11 and 12). Concerning with the nature of the phases, MgO helps to form $C_{12}A_7$ in detriment of monocalcic aluminate and favours the formation of an only ferritic phase; concerning to the evolution of the microstructure, MgO alters the temperatures when the phases begin to crystallize.

When it is added to composition 1, 6.5% of MgO, it is observed that at a high temperature ferritic phase with a little of periclase crystallizes (crystalline aluminates aren't detected). When the temperature diminishes, together with the ferrites, it crystallizes a tiny amount of $C_{12}A_7$. The final texture found is similar as the one of composition 1 without MgO, although the stages of crystallization are produced in lower temperatures, this gives us an idea of the fluxing action of MgO.

The presence of $C_{12}A_7$ instead of CA, gives also an idea of the power of Mg to replace the Ca atoms in the lattice of $C_{12}A_7$, producing $(C_{1-x}M_x)_{12}A_7$.

The ferritic phase is also affected by the presence of MgO, because it appears an only ferritic phase, rich in Fe (richer than C_4AF). This is infered by IR spectroscopy, because of the situation of the band that appears in 705 cm^{-1}.

As it was mentioned before, composition 4 has many things in common with composition 1: its final microstructure scarcely changes with the presence of MgO (see micrograph 13); what logicallychanges, are the temperatures of the stages of crystallization.

Also, and the same as it happened with composition 1, in presence of MgO, the only aluminate that crystallizes in composition 4 is the $C_{12}A_7$. Also there is an only one feritic phase.

The differences between compositions 1 and 4 with addition of MgO, are due to the positions of each of these compositions in the diagram C-A-F.

Being composition 4 richar in Al we found more amount of aluminate and also a ferritic phase richer in Al (type C_6A_2F), hipothesis based on the position of a band found in the IR spectra near to 720 cm^{-1}.

Besides this, with respect to the effect of MgO on composition 4, there is an important detail in relationship with the fluxing power of the compound and is the vitreous solidification of the sample quenched at the highest temperature. Composition 2 doesn't change appreciably by the presence of MgO in relation to the nature of the phases that are formed in the different tested stages, but at 1350ºC the fluxing effect of the MgO and the primary crystallization of ferrite are observed.

From the microstructural point of view there are changes that deserve being mentioned (see micrographs 14 and 15); in composition 2 predominates an eutectic crystallization, but in presence of MgO a very clear separation between ferrites and aluminates is observed (aluminates have a considerable size); besides due to the aspect of aluminates (it is observed a union of tiny crystals) it can be said that an eutectic crystallization happened though not in the magnitude when MgO wasn't present. About the ferritic phase it can be said that is a rich in Al one.

Micrographs 16 and 17 show the microstructural evolution of composition 3 in presence of MgO. Textures are similar when MgO wasn't present; nevertheless the presence of this oxide makes crystals have a grater size. What before were ferritic needles, very well formed, now they are crystals withan indefinite shape. Aluminates conserved its lengthened shape. It is also observed with a great clearness aggroupments of tiny crystals separated by ferritic phase.

It is important to express again the fluxing power of the MgO (the sample of high temperature with MgO is amorphous).

Finally, and concerning to composition No. 5, we have to say that MgO effectuates a quite perceptible action principally from the point of view of the nature of the phases.

In presence of MgO isn't detected anything of CA but although it is found much $C_{12}A_7$ and also some C_3A. Logically this has a repercussion over the studied microstructures. The kind of texture is similar but when the nature of the aluminates is changed, diffe

rences are detected (see micrographs 18 and 19), such as the exposure that the crystalline mass presents, fact that is surely connected with the data that the IR spectroscopy adduces about the $C_{12}A_7$ found in the sample of 1280ºC, that has a big symmetry.

To finish this study it is suitable to appoint that the amount of periclase found in almost the total cases, has never passed the traces.

Conclusions

- If it is added 6.5% wt of MgO to the compositions of the system C-A-F studied in this work, the MgO comes into the lattice of the aluminates in substitution of calcium, generating $(C_{1-x}M_x)_{12}A_7$ in the compositions that being absent Mg produce CA and $(C_{1-x}M_x)_3A$ in those where it is formed $C_{12}A_7$. And also the Mg gets into the lattice of the ferritic phase.
- The modifications observed in the microstructures by the effect of adding MgO is generally justifiable by the fluxing action of this compound and/or by the modifications that magnesium oxide introduces in the equilibrium of the phases.
- The Mg incorporated to the primary $C_{12}A_7$, lattice improves notably its structural order.

References

1.- Müller-Hesse, H. and Schwiete, H.E. - Zement-Kalk - Gips nº 9, p. 386 (1956)
2.- Midgley, H. - Proc. 5th Intern. Symp. on Chem. of Cement. Paper nº 1-12, S-230. Tokyo (1968)
3.- Woerman, E. Hahn, Th. and Eysel, W. - Zement Kalk - Gips nº 16 p. 370 (1963); nº 20, p. 385 (1967); nº 21 p. 241 (1968); nº 22 y 235 (1969)
4.- Locher, F.W. - Proc. 4th Intern. Symp. on Chem. of Cement. Paper II - S5. Washington (1960)
5.- Miyazawa, K. and Tomita, K. - Zement-Kalk-Gips nº 19, p. 82 (1966)
6.- Dreizler, I. and Knöfel, D. - Zement-Kalk-Gips nº 10 p. 237 (1982)
7.- Christenssen, N.H. - World Cement Technology p. 223 October (1978)
8.- Bucchi, R. - World Cement Technology p. 210 June (1981); p. 258 July/August (1981)
9.- Budnikow, P.P. and Worobjew, Ch. S. - Silikattechnik nº 4 p. 158 (1958)
10.- Guye, F. Revue des Materiaux de Construction nº 567 p. 333 (1962)
11.- Ramachandran, V.S. - Il Cemento nº 3 p. 159 (1980)
12.- Nikiforow, Ш. V. - Proc. 6th Intern. Symp. on Chem. of Cement, S - 110 Moscow (1974)

J. Gebauer, "Holderbank" Management and Consulting Ltd., Switzerland

EFFECT OF HIGH MgO CONTENT IN CEMENT UPON-TERM PROPERTIES OF CONCRETE

1. Introduction

The various national cement standards, prescribing the permissible limits for magnesia in cement, list maximum values from 3.0 up to 6.5 %. This limitation of the MgO content is due to the potential negative effect of uncombined magnesia (periclase) on concrete durability.

Any increase of the permitted magnesia content in cement would be of great practical importance, offering a considerably increased choice of raw materials for cement manufacture.

Up to date, there is no firm evidence that cements with 7 - 8 % MgO in clinker cause any deterioration of concrete specimens either in laboratory tests or in practice. Most of the investigations on MgO expansion are carried out on neat cement paste or mortar specimens and only very limited data exist on either concrete specimens or concrete constructions. To our knowledge, the only long-term tests in concrete were carried out by Gonnermann et al (2) and showed no strength loss for concrete cylinders made with autoclave- unsound cements with 7 - 10 % MgO even after 15 years of water storage.

A quick and reliable performance test would make the stringent MgO limitatations superfluous. The only standardized performance test available and used in practice, the ASTM autoclave test, has been subjected to serious criticism. The main objections against this autoclave test have been summarized by Mehta (1):

> The autoclave test conditions force the crystalline MgO to hydrate and expand whereas in normally cured concrete, the MgO hydrates at a rate too slow to be of any consequence
>
> The magnitude of the expansion in neat cement bars caused by hydration of free MgO or CaO may be high, but in corresponding concretes it is not even high enough to cause cracking
>
> No correlation has ever been shown between the autoclave test specification limits and the soundness of concrete.

In 1981 a research program was initiated at the Technical Center of "Holderbank" Management and Consulting Ltd. on the long-term properties of concrete produced with cements containing an elevated amount of MgO to classify the relevance of the autoclave test from the viewpoint of concrete as well as the justification of the low limiation of the MgO content in cement. Besides Portland cement, blended Portland cements - a cement type which has recently been gaining in importance - were also included in the investigation. In the following, the presently available results of our long-term research program are presented and discussed.

2. Experimental work

2.1. Materials used

An industrially produced ordinary Portland cement and three blended cements, prepared from ordinary Portland cement and various hydraulically active additives, were used for the investigations.

The ordinary Portland cement's clinker, containing 7.5 % MgO, was produced in a wet process kiln under normal operating conditions in order to achieve the maximum autoclave unsoundness for the given MgO content. As microscopical observations showed, the clinker contained a large amount of coarse, crystalline periclase as well as large clusters of periclase.

The blended cements were produced by blending ordinary Portland cement with 20 % additives, namely preground blast furnace slag, natural pozzolan and fly ash.

The chemical composition and fineness of the ordinary Portland cement and of the hydraulically active additives are shown in table 1.

The Bogue mineralogical composition of the ordinary Portland cement, the free lime content and the periclase content are shown in table 2. The periclase content was determined by means of the X-ray diffraction method using the principal reflection at d = 2'106 A.

Table 1: Chemical composition of cement and additives

	Portland Cement	Fly ash	Slag	Pozzolan
L.o.i. (%)	0.87	3.2	1.0	4.4
SiO_2	18.4	50.8	34.3	70.7
Al_2O_3	5.8	25.2	9.0	13.1
Fe_2O_3	3.3	7.8	0.92	1.5
CaO	59.7	3.2	43.7	1.8
MgO	7.1*)	2.1	5.6	0.31
SO_3	1.92	1.8	3.5	0.05
K_2O	1.3	3.9	0.66	3.4
Na_2O	0.14	0.53	0.51	3.9
TiO_2	0.31	0.86	0.45	0.19
Mn_2O_3	0.10	0.10	0.39	0.05
P_2O_5	0.23	0.19	0.03	0.09
Cl	0.01	0.01	0.02	0.06
Blaine (cm^2/g)	3210	4060	3240	4950

*) MgO content in clinker = 7.5 %

Table 2: Mineralogical composition of Portland cement

C_3S	54.1 %
C_2S	12.0 %
C_3A	9.8 %
C_4AF	10.1 %
Periclase (XRDA)	5.8 % (in clinker 6.1 %)
Free lime (acc to ASTM)	1.9 % (in clinker 2.0 %)

2.2. Preparation and testing

The cements included in the long-term program were tested on concrete slabs. The slabs, 100 x 50 x 7 cm in size, were prepared from concrete mixes containing a constant 300 kg cement per m^3 of concrete and natural aggregate of 32 mm maximum grain size. The water content of the concrete was as required to reach a concrete consistency of 7.5 ± 1 cm slump. The concrete slabs were cured for up to 7 days in a curing room at 20°C and 95 % relative humidity. Thereafter, one slab of each concrete mix was deposited at the outdoor testing facilities in Holderbank, Switzerland, while the other one was kept in the curing room. The outdoor storage of slabs is shown in Fig. 1.

The slabs were tested after 28 days, 0.5, 1, 2, 3 and 4 years. Further tests are foreseen after 5, 10 and 20 years. In addition, concrete cores from the 4 year old slabs were exposed to autoclave treatment according to the ASTM procedure and tested thereafter.

On the concrete slabs, the following tests were carried out:

Compressive strength tests on cores (dia. 50 mm and h = 5.6 mm) drilled from the slabs; each strength test result quoted represents the average of 6 cores.

Ultrasonic pulse velocity measurements with the aid of a Pundit apparatus.

Periclase and microstructure investigation by means of light microscopy on polished cross-sections of cores.

Determination of the periclase content by means of X-ray diffraction, using the mortar fraction of the cores. The content of periclase was recalculated as a percentage of the total concrete mix, including ccarse aggregate and assuming no hydration of periclase in the reference 1-day old concrete.

The cements were also tested on standard soundness tests according to the Le Chatelier and ASTM autoclave method.

3. Discussion of the results

The autoclave expansion of the cements is - with the exception of pozzolanic cement - excessive and higher than that specified in ASTM. The high autoclave expansion is due to the high periclase content and the elevated amount of free lime in the cement (table 3).

The concrete, however, shows after four years no signs of deterioration, and a continuous strength gain can be observed over the entire 4 year testing period in all concrete slabs stored indoor (Fig. 2). The ultrasonic pulse velocity measurement confirms these findings. At the outdoor facilities, some degradation of the concrete due to freezing/thawing cycles is observed as the concrete had not been air-entrained and thus is not sufficiently frost resistant.

Table 3: Physical properties of cements and concrete slabs

Cement	PC		PC/FA		PC/SL		PC/POZZ	
Proportioning	100		80/20		80/20		80/20	
Blaine (cm^2/g)	3210		3380		3180		3580	
ASTM autocl.(%)	7.14		8.00		6.39		0.45	
Le Chatelier(mm)	1.75		0.75		1.00		2.25	
Concrete slab								
W/C ratio	0.56		0.56		0.56		0.58	
Strength(N/mm^2)	I	O	I	O	I	O	I	O
28 days	35.9	35.0	34.7	32.4	36.5	36.5	33.8	29.8
0.5 year	51.1	46.4	45.5	42.8	49.9	46.0	43.2	39.3
1 year	53.6	44.8	45.9	44.2	52.4	48.8	44.0	38.2
2 years	56.2	51.4	48.1	45.7	54.8	53.5	45.5	43.4
3 years	58.7	55.0	50.2	46.0	58.2	55.2	46.0	44.0
4 years	60.7	57.6	52.5	46.6	60.8	55.0	46.9	42.9
4 years and autoclave	65.1		55.9		69.3		56.8	
UPV (m/sec)								
28 days	4700	4645	4667	4560	4711	4560	4571	4433
0.5 year	4837	4733	4861	4768	4849	4678	4756	4612
1 year	4849	4814	4397	4837	4849	4802	4745	4711
2 years	4875	4802	4897	4849	4873	4825	4768	4733
3 years	4921	4802	4945	4791	4873	4791	4837	4685
4 years	4958	4766	4929	4745	4890	4779	4795	4633

I = Indoors (curing room)
O = Outdoor facilities
UPV = Ultrasonic pulse velocity

Table 4: Periclase in Portland cement concrete (XRD analysis)

Age of concrete	% of reference	periclase content in concrete (%)
1 day (reference)	100	0.73
4 years	70	0.51
4 years and autoclave	40	0.29

The microscopical investigation and X-ray diffraction analysis of the concrete shows that part of the periclase has hydrated within the four years without any harmful expansion. The microphotograph of the 4-year old concrete shows the position of a periclase containing clinker particle which has partially hydrated. Periclase crystals can be seen also in the hydrated zone of the clinker particle (Fig. 3).

During the autoclave treatment, periclase is further hydrated, again without any negative effect on concrete properties. On the contrary, the concrete experienced a substantial strength gain. Part of the periclase remains unreacted, even after the severe autoclave treatment as shown in the microphotograph (Fig. 4) and confirmed by X-ray diffraction analysis. The results of the X-ray diffraction analysis of concrete made with the Portland cement are shown in table 4 and figure 5, indicating the reduction of periclase content in concrete during

the 4 years of normal curing and autoclave treatment.

These findings suggest that the periclase is hydrating very slowly at normal curing conditions in concrete and without impairing the concrete properties.

The main reasons for the absence of any detrimental effect of periclase in concrete in contrast to the ASTM autoclave test are the lower percentage of periclase in concrete compared to neat cement paste and the slower rate of periclase hydration in concrete under normal curing conditions compared to the autoclave curing. The stresses developed by slow hydration of the smaller amount of periclase begins to act after the mature concrete has gained sufficient strenth. On the contrary, in the autoclave test the sudden development of expansive forces due to periclase hydration easily surpasses the cohesive forces of the relatively immature and weak cement paste. The autoclave test has therefore no practical significance for the performance of concrete in practice.

4. Conclusions

Both Portland cement and blended Portland cements produced with a clinker of 7.5 % MgO content show satisfactory properties in 4-year old concrete, even when the major part of the MgO is present as coarse crystalline periclase. It can thus be concluded that the current cement standard specifications regarding the permissible MgO content in cement are not adequate and even hinder the economical use of cement raw material resources. The investigations confirm the irrelevance of the ASTM autoclave test for the performance of concrete in practice, already stated already by other investigations.

Literature

(1) P.K. Mehta: History and status of performance tests for evaluathion of soundness of cements ASTM Publication, STP 663, 1953, pp 35 - 55

(2) H.F. Gonnermann, W. Lerch and W.M. Whiteside: PCA, Research Laboratory Bulletin No. 45, 1953, pp 1 - 168

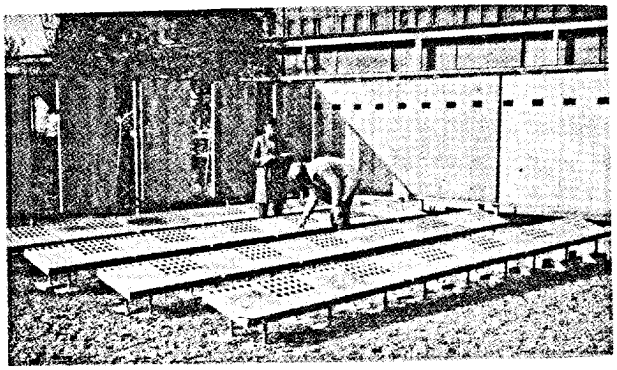

Fig. 1: Outdoor stored slabs at the testing station in Holderbank, Switzerland



Fig. 3: 4 year old Portland cement concrete, arrows indicate periclase crystals

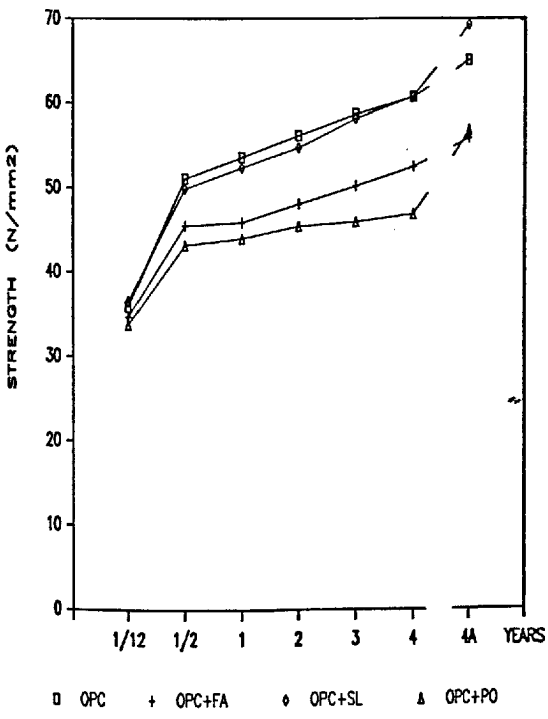

Fig. 2: Strength development of concrete

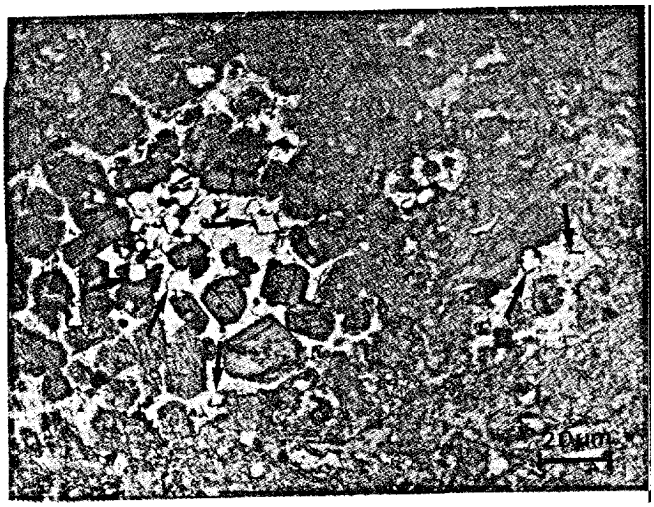

Fig. 4: 4 year old concrete, autoclaved, arrows indicate periclase crystals

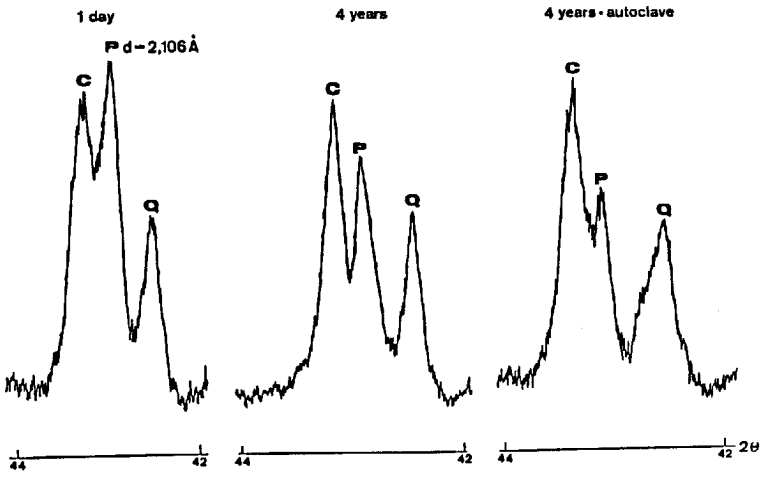

Fig. 5: X-ray diffraction analysis of concrete (C = calcite, P = periclase, Q = quartz)

V.K. KOZLOVA - Institut Polytechnique Altaique I.I. Polzounov, U.R.S.S.

SUR LA FORMATION DES PHASES NOUVELLES DANS LE CLINKER LORS DE LA CUISSON DES MELANGES CRUS A BASE DES PRODUITS SECONDAIRES

Lors de la planification du développement ultérieur de la cimenterie, une attention toujours croissante est faite à l'utilisation des produits secondaires et des déchets des autres industries.

A présent, les particularités des propriétés des mélanges crus et celles des processus de formation du clinker, en cas de l'utilisation des laitiers et des cendres d'une nature différente en qualité du constitant alumosilicate ou de l'addition de correction, sont étudiées en détail.

La plupart des laitiers, des cendres et des autres produits secondaires se distinguent du constituant argileux utilisé dans la production du ciment par une teneur élevée en sesquioxydes, en particulier, en oxyde d'aluminium. Les particularités des processus de formation des minéraux lors de la cuisson des mélanges crus basés sur les produits secondaires sont déterminées justement par cette distinction.

Les recherches des dernières années montrent que lors de la cuisson des charges de ciment crues dans lesquelles le constituant argileux se trouve remplacé par le laitier ou les cendres, il est utile d'obtenir les clinkers en vue de la production du ciment Portland particulier: ciment à haute teneur en alumine, ciment ferreux, ciment à durcissement rapide sur la base des sulfoaluminates ou des fluroaluminates (en cas de la présence d'une quantité nécessaire de sulfates ou de fluorures).

Les systèmes de sulfates et de fluorures jouent un rôle toujours croissant en vue de produire les ciments contenant les minéraux dans la composition desquels entrent les sulfates et les fluorures, en particulier, les minéraux se formant sur la base des sesquoxydes (plus souvent de l'oxyde d'aluminium) et sur la base des composés mentionnés.

Il est naturel que la particularité de la production des ciments de ce type consiste dans l'utilisation du cru riche en sesquioxydes ce qui est typique pour une série des produits secondaires les plus employés.

Au cours de l'étude des propriétés d'un grand nombre de clinkers et de ciments obtenus à partir des charges crues dans lesquelles on a utilisé, en qualité du constituant alumosilicate, les cendres provenant du charbon minéral avec une introduction simultanée des adjuvants de modification en sulfates ou en fluorures, nous avons établi la possibilité d'obtenir les ciments répondant aux exigences du "TOCT" (norme d'Etat) à une augmentation considérable de la teneur en oxyde de magnésium dans le constituant carbonate.

Les normes de tous les pays concernant les ciments ont une exigence nécessaire pour la quantité maximum admissible de MgO dans le clinker de ciment Portland. Cette teneur limite en MgO correspond à 3-5 %. La cause principale de ces limitations est un danger de l'expansion tardive du ciment lors de l'hydratation du MgO est une parte de résistance qui y est directement liée. Les limitations de la teneur en MgO dans la composition du clinker rétrécissent considérablement les ressources de matières premières de la cimenterie et compliquent l'exploitation des gisements isolés, puisque l'oxyde de magnésium entre en grandes quantités dans la composition des roches carbonatées des plusieurs gisements sous forme des inclusions des calcaires magnésiens et dolomitiques.

Les recherches des procédés en vue l'obtenir les ciments de haute qualité avec une teneur élevée en oxydes de magnésium dans la composition du clinker ont une grande importance pratique. A présent, on considère comme le fait établi avec une précision assez suffisante que l'oxyde de magnésium est représenté dans la composition du clinker de ciment Portland essentiellement sous forme de la périclase. Certaine sa quantité se trouve en état de dissolution dans le constituant vitreux du clinker. Une part déterminée de MgO, grâce aux substitutions isomorphes, entre dans la composition des minéraux principaux du clinker. Par exemple,

jusqu'à 1,5 % de MgO se trouve dans l'alite, 1-3 % - dans les alumoferrites de calcium, jusqu'à 2,5 % - dans l'aluminate tricalcique et 6 % - dans la phase vitreuse.

Une série d'essais montre que lors du refroidissement rapide du clinker la quantité d'oxyde de magnésium dans la composition de la phase vitreuse augmente. Par conséquent, sa quantité plus faible reste sous la forme de la périclase et les grains de cette dernière ont des dimensions plus petites par rapport au régime normal de refroidissement (1, 2). La périclase sous forme finement dispersée est capable de s'hydrater simultanément avec les autres minéraux de clinker et ne cause pas de grandes contraintes locales lors du processus de durcissement. Les garanties d'une cristallisation plus fine de la périclase et sa distribution plus homogène dans le clinker peuvent être considérées comme des mesures permettant d'augmenter la quantité admissible du MgO dans le ciment. Selon les données des auteurs de l'étude (3), l'utilisation d'un minéralisateur fluoritique lors de la cuisson favorise la formation des cristaux plus fins de la périclase et leur distribution homogène dans la masse de clinker.

La possibilité d'augmenter la teneur en oxyde de magnésium dans la composition du mélange cru a été observée lors de la caractéristique des particularités portant sur la composition et les propriétés des clinkers obtenus à l'aide des cendres utilisées en qualité du constituant alumosilicate de la charge (4). En cas de la teneur en MgO du mélange cru allant jusqu'à 6 %, l'expansion d'autoclave du ciment préparé sur la base du clinker de cendre constitue 0,8 %. En cas de l'utilisation de l'argile, le clinker ayant les mêmes valeurs du coefficient de saturation (CS) et le même module alumine est caractérisé par une expansion de 6,5 %, déjà à la teneur en MgO égale à 5,5 %.

Pour résoudre les problèmes d'obtention du ciment Portland standard avec une teneur élevée en oxyde de magnésium, beaucoup de chercheurs ont été orientés vers le choix de la composition minéralogique optimum du clinker et vers l'introduction des certains adjuvants.

Les résultats des essais (5) montrent qu'aux autres conditions égales et à la quantité équivalente de MgO dans les clinkers, l'expansion d'autoclave des ciments diminue considérablement à mesure de l'augmentation de la teneur en SO_3 dans le clinker. Selon l'opinion de l'auteur, l'introduction des sulfates peut neutraliser l'effet négatif sur les propriétés des clinkers dû à une teneur élevée en MgO. En cas de la présence des sulfates, on peut obtenir un ciment se caractérisant par une stabilité de volume si le clinker contient jusqu'à 6 % de MgO. Pour calculer la quantité nécessaire du SO_3 dans la composition de clinker, on propose la formule suivante:

$$\% SO_3 = 0{,}67 (\% MgO - 2)$$

En cas de la teneur en MgO jusqu'à 2 %, son influence négative se neutralise par le fait qu'il entre dans la composition des phases de clinker. Pusque l'utilisation des cendres en qualité du constituant cru rend utile l'obtention des ciments à partir des ciments à haute teneur en alumine jusqu'aux ciments ferritiques ainsi que des ciments à base des clinkers contenant les adjuvants des sulfates et des fluorures, nous avons étudié la possibilité de fabrication des ciments mentionnés avec une teneur élevée en MgO dans la composition du cru. A cette fin, on a préparé quatre types des clinkers ayant une haute teneur en MgO. Les mélanges crus n°n° 1, 2, 3 (tableau I) s'approchent, d'après leurs compositions, du mélange cru destiné à la fabrication du ciment Portlant normal. Dans ce mélange cru, le constituant argileux a été complètement remplacé par la cendre. Les compositions des mélanges crus n°n° 4, 5, 6 correspondent à la composition du mélange cru destiné à la fabrication du clinker ferritique. Les mé-

langes crus pour les clinkers n° 7, 8, 9 contiennent 3,5 % de gypse. Les mélanges crus destinés aux clinkers n°n° 10, 11, 12 ont eu 1,5 % de CaF_2. Lors de la fabrication de tous les clinkers, on a utilisé en qualité du constituant alumosilicate les cendres prevenant des charbons minéraux. La composition chimique des cendres est la suivante: SiO_2 - 52,46%, Al_2O_3 - 28,54%; Fe_2O_3 - 9,96%; CaO - 6,24%. Pour augmenter la teneur en MgO, on a introduit dans tous les mélanges crus une quantité différente de magnésite. La température de cuisson des clinkers a été de 1350-1380°C. La cuisson a été faite selon un régime lent, et le refroidissement a été effectué dans l'air.

Les analyses pétrographiques montrent que tous les clinkers se caractérisent par une distribution homogène de la périclase par la masse des grains. Dans les clinkers n° 1-6, la masse principale des grains de périclase a des dimensions de 3 à 17μ . Dans les clinkers obtenus avec les adjuvants de gypse ou de fluorure de calcium, les dimensions moyennes des grains de périclase sont de I - 10μ. La quantità de périclase dans ces clinkers est un peu plus petite que dans les autres clinkers. La teneur en oxyde de magnésium non lié a été déterminé selon la méthodologie de l'Institut "Giprocement" (6).

La détermination de la composition minéralogique des clinkers obtenus par la méthode d'analyse chimique rationnelle n'a pas permis de fixer une variation qulques peu considérable en quantité des minéraux isolés, à l'exception d'une certaine augmentation de la teneur en CaO libre. Sur la base des clinkers obtenus, é l'aide du broyage en commun avec l'adjuvant de gypse (3-5%), on a fabriqué les ciments pour lesquels on a déterminé l'expansion linéaire après le traitement d'autoclave à 2,1 MPa et la limite de compression (tableau 2). Lors de la fabrication des ciments à base dés clinkers contenant du SO_3, l'addition de gypse a constitué 3 %, tandis que pour tous les autres ciments cette dernière a été de 5 %. La surface spécifique des ciments a été de 2900 - 3100 cm^2/g. Les ciments préparés avec l'utilisation des cendres en qualité du constituant alumosilicate ont une stabilité de volume à la teneur en MgO jusqu'à 6,0 - 8,0 %. En cas de la fabrication du clinker de ciment Portland normal sur la base des mélanges crus dans lesquels on a utilisé la cendre en qualité du constituant alumosilicate, il est possible d'augmenter la teneur en MgO jusqu'à 6 %. Si on introduit dans la composition des mélanges crus préparés avec l'utilisation des cendres, des adjuvants supplémentaires de correction ou de modification, en vue d'obtenir des ciments Portland particuliers, on peut augmenter la quantité de MgO admissible jusqu'à 8 % et plus. Le clinker de ciment Portland ordinaire obtenu avec l'utilisation des cendres provenant des charbons minéraux se distingue par une quantité élevé de la phase vitreuse alumoferritique (25-28 %). La quantité de cette phase augmente de plus dans les clinkers du type ferritique (jusqu'à 40 %). C'est pourquoi, l'augmentation de la teneur admissible en MgO de ces clinkers peut être expliquée par la présence d'une plus grande quantité de cet oxyde sous forme des solutions solides dans la composition de la phase vitreuse alumoferritique.

La cause de l'influence favorable des additions de fluorures et de sulfates sur les propriétés des clinkers avec une teneur élevée en MgO n'est pas suffisamment claire à présent. A première vue, une influence positive des additions des sulfates, en cas de l'obtention des ciments avec une teneur élevée en MgO, pourrait être expliquée par une formation, due aux réactions d'échanges, du $MgSO_4$ dont la température de la dissociation est de 1135°C. Donc, lors de la cuisson jusqu'à la température mentionnée, une partie de MgO peut se trouver dans la composition du sulfate de magnésium ce qui favoriserait l'inhibition du processus de recristallisation accumulative de la périclase. Cependant, un tel mécanisme chimique

Tableau 1

Clinker, numéro	n	p	CS	Teneur totale en MgO, %	Quantité de MgO libre, %
1	0,99	1,15	0,89	4,5	2,27
2	0,99	1,15	0,89	5,5	3,18
3	0,99	1,15	0,89	6,0	3,98
4	0,73	0,63	0,89	6,0	2,85
5	0,73	0,63	0,89	7,0	3,65
6	0,73	0,63	0,89	8,0	4,43
7	1,76	2,50	0,82	6,0	2,35
8	1,76	2,50	0,82	7,0	3,15
9	1,76	2,50	0,82	8,0	3,53
10	1,29	2,53	0,77	6,0	2,57
11	1,29	2,53	0,77	7,0	3,45
12	1,29	2,53	0,77	8,0	3,90

Tableau 2

Ciment, numéro	Teneur en MgO, %	Expansion linéaire des échantillons-poutrelles, %	Limite de résistance à la compression, MPa		
			3 jours	7 jours	28 jours
1	4,5	0,26	17,5	32,1	40,6
2	5,5	0,37	16,3	31,0	39,1
3	6,0	0,52	15,8	29,7	38,4
4	6,0	0,19	17,4	24,3	42,5
5	7,0	0,28	16,0	20,8	39,5
6	8,0	0,45	14,7	21,9	40,5
7	6,0	0,13	23,1	31,1	40,7
8	7,0	0,21	21,9	29,8	39,4
9	8,0	0,30	22,2	29,3	38,6
10	6,0	0,17	34,1	42,9	49,3
11	7,0	0,26	31,7	41,1	48,1
12	8,0	0,29	30,3	39,7	47,5

de l'influence des sulfates exigerait leur quantité considérable pour former $MgSO_4$. L'action des sulfates pourrait être expliquée également par une formation en leur présence du composé $3Ca{\cdot}MgSO_4$ dans la composition duquel une partie de MgO est fixée sous forme du $MgSO_4$. Dans le travail (7) on parle de la possibilité de formation d'un tel composé lors de la cuisson des mélanges $C_3A + MgSO_4$. Pourtant, il est nécessaire d'avoir dans ce cas dans la composition du clinker une quantité élevée de SO_3 et de Al_2O_3 pour neutraliser l'influence négative du MgO. Les données expérimentales disponibles (5) montrent que la quantité nécessaire de SO_3 est beaucoup plus petite par rapport à celle dont on a besoin pour former $MgSO_4$. Apparemment, en présence des adjuvants des sulfates lors de la cuisson des clinkers avec une teneur élevée en MgO, des composés se forment se caractérisant par une grande valeur du rapport MgO/SO_3. C'est pourquoi, nous avons effectué des recherches supplémentaires ayant pour but une étude de l'interaction dans les systèmes $MgO - Al_2O_3 - MgSO_4$ et $MgO - SiO_2 - MgSO_4$. Selon nos données, on n'a pas effectué des recherches sur des systèmes semblables ainsi qu'on n'a pas mentionné une formation des composés quelconques relatifs aux systèmes ci-dessus en cas de la cuisson du clinker de ciment Portland à une teneur élevée en MgO.

La formation du sulfoaluminate de calcium ($3Ca{\cdot}CaSO_4$) dans le système $CaO-Al_2O_3-CaSO_4$ (7, 8, 9) et du sulfoaluminate de baryum ($4BaO{\cdot}Al_2O_3{\cdot}BaSO_4$) dans le système $BaO-Al_2O_3-BaSO_4$ (10) permet de supposer la formation du sulfoaluminate de magnésium dans le système $MgO-Al_2O_3-MgSO_4$. L'analyse chimique et à rayons X des produits de la cuisson à double reprise des mélanges $MgCO_3$, Al_2O_3 et $MgSO_4$ (cuisson effectuée dans les fours électriques à la température de 1000-1300°C et avec le maintien de 2 heures) témoigne de la présence de l'interaction chimique avec une formation d'une phase nouvelle qui se décompose progressivement en cas de l'augmentation de température ultérieure. La composition de la combinaison qui se forme s'approche de $3(MgO{\cdot}Al_2O_3){\cdot}MgSO_4$. Il est à noter que la formation de la combinaison nouvelle s'effectue plus complètement en cas de la cuisson des mélanges se composant du $MgCO_3$, Al_2O_3, $MgSO_4$ par rapport à la cuisson des mélanges $MgSO_4$, $MgO{\cdot}Al_2O_3$ synthétisé préalab-

lement. Selon les données préliminaires, le sulfoaluminate de magnésium qui se forme n'a pas de propriétés liantes. Lors de la formation du composé mentionné, 1 % de SO_3 fixe environ 2 % de MgO et 1,3 % de Al_2O_3.

Nous n'avons pas examiné l'interaction dans le système $MgO-Al_2O_3-MgF_2$, mais par analogie avec le même système contenant CaO, on peut supposer la probabilité de la formation du fluoraluminate de magnésium en présence des fluorures. La possibilité de formation du sulfoaluminate de magnésium lors de la cuisson des clinkers avec une haute teneur en MgO (pour le compte du SO_3 se trouvant dans la composition du clinker) est en bonne concordance avec les publications concernant l'influence du MgO sur la composition minéralogique du ciment (II) qui montrent qu'en cas de l'augmentation de la teneur en MgO, la quantité du C_3A dans le clinker diminue tandis que la quantité d'alite s'accroît. La quantité de C_3A peut diminuer grâce à la fixation du Al_2O_3 en sulfo aluminate de magnésium. A la diminution de la quantité de C_3A, une quantité supplémentaire de CaO se dégage pour former C_3S.

Selon les données des auteurs de la recherche (II), les silicates de magnésium et les spinelles ne se forment pas lors de la cuisson des charges crues contenant une quantité élevée de MgO. La quantité principale de MgO se trouve dans le clinker sous forme de la périclase. En cas de l'introduction du fluorure calcique dans la charge, on ne fixe pas également une formation des composés quelquonques. On n'observe qu'une variation du caractère de cristallisation de la périclase disponible. En même temps, G.D. Ouryvaéva montre dans ses recherches (12) la présence d'une certaine quantité des silicates de magnésium: montitshellite ($CaO \cdot MgO \cdot SiO_2$), okermanite ($2CaO \cdot MgO \cdot SiO_2$), mervinite ($3CaO \cdot MgO \cdot 2SiO_2$) dans les clinkers à une quantité élevée de MgO cuits à des températures de 1200-1300°C. Si la température de cuisson est portée jusqu'à 1400-1500°C, la quantité des silicates de magnésium diminue, et la teneur en périclase augmente. Apparemment, la cause des divergences des données disponibles consiste dans la détermination de la composition minéralogique aux différents stades de cuisson. Il est possible que les silicates de magnésium ci-dessus représentent des composés intermédiaires qui se forment lors de la cuisson du clinker de ciment Portland ayant une telle composition.

Nous avons supposé que la formation des silicates de magnésium mentionnés est la conséquence de l'existence, à des températures plus basses, des autres composés intermédiaires sur la base desquels, en cas de l'augmentation de température de cuisson et de la présence du CaO, l'apparition des montitshellites, des okermanites et des mervinites est possible. En présence des adjuvants de sulfates et de fluorures lors de la cuisson du clinker de ciment Portland ayant une quantité élevée de MgO à des températures de 800-1200°C, des sulfosilicates ou des fluosilicates de magnésium peuvent se former en qualité des combinaisons intermédiaires dont la composition chimique hypothétique, par analogie avec les sulfosilicates et les fluosilicates de calcium peut être écrite comme la suivante: $2(MgO \cdot SiO_2)MgSO_4$ et $2(MgO \cdot SiO_2)MgF_2$.

L'analyse des mélanges $MgCO_3 + SiO_2 + CaSO_4$ et des mélanges $MgCO_3 + SiO_2 + MgSO_4$ cuits à des températures de 800-1300°C confirme l'existence de l'interaction qui peut être appréciée d'après la dynamique de la fixation et du dégagement du groupe de sulfate. Les combinaisons qui se forment commencent à se décomposer même à des températures dépassant 1100°C.

En tenant compte des faits mentionnés, on peut représenter le schéma de formation d'une partie de la périclase qu'on peut détecter dans les clinkers cuits de la façon suivante:

$$2(MgO \cdot SiO_2) \cdot MgSO_4 \xrightarrow{\text{environ } 1100^\circ C} 2(MgO \cdot SiO_2) + MgSO_4$$

$$MgSO_4 \xrightarrow{1155^\circ C} MgO + SO_3$$

$2(MgO \cdot SiO_2) + 2CaO \longrightarrow 2(CaO \cdot MgO \cdot SiO_2)$ ou

$2(MgO \cdot SiO_2) + 2CaO \rightarrow 2CaO \cdot MgO \cdot 2SiO_2 + MgO$ ou

$2(MgO \cdot SiO_2) + 3CaO \rightarrow 3CaO \cdot MgO \cdot 2SiO_2 + MgO$

Si la température de cuisson augmente, il se produit une substitution ultérieure du MgO par CaO dans la composition des silicates de magnésium:

$$CaO \cdot MgO \cdot SiO_2 + CaO \xrightarrow{1300-1400^\circ C} 2CaO \cdot SiO_2 + MgO \text{ ou}$$

$2CaO \cdot MgO \cdot 2SiO_2 + 2CaO \longrightarrow 2(2CaO \cdot SiO_2) + MgO$ ou

$3CaO \cdot MgO \cdot 2SiO_2 + CaO \longrightarrow 2(2CaO \cdot SiO_2) + MgO$

D'une façon analogue doivent se dérouler les réactions de formation des silicates de magnésium et de leurs transformations en silicates de calcium avec le dégagement du MgO si le composé intermédiaire initial est un fluosilicate de magnésium.

Selon le schéma proposé sur le déroulement des réactions, on peut voir qu'en présence des adjuvants des fluorures ou des sulfates dans le cru, la composition minéralogique des matières cuites à une large gamme de températures (de 800 à 1400°C) se caractérise par une teneur considérable en oxyde de magnésium dans la composition des combinaisons intermédiaires. La formation de la périclase s'effectue progressivement, à mesure de la décomposition de ces combinaisons. La formation de la périclase suivant ce schéma peut expliquer sa distribution homogène et la cristallisation sous forme des grains fins en cas de la présence des adjuvants de gypse et de fluorine dans le cru. Ce fait est illustré dans la recherche (II) et est confirme par nos propres données.

Pour résoudre la question sur la possibilité de la conservation partielle des combinaisons intermédiaires mentionnées dans la composition du clinker cuit, des essais supplémentaires sont nécessaires.

REFERENCES

1. Астреева О.М., Лопатникова Л.Я. О растворимости трехкальциевого алюмината в алюмоферритах кальция. Труды НИИЦемента, 1952, вып. 5.
2. Рояк С.М. Определение фазового состава портландцементного клинкера и глиноземистого цемента химическим методом. Научные сообщения НИИЦемента, 1958, № 2(33).
3. Коган С.Л., Никифоров Ю.В., Окороков С.Д. Труды Гипроцемента, 1963, вып.XXIX.
4. Рехси С.С., Гарт С.К. Производство клинкера с использованием золы-уноса. Шестой Международный конгресс по химии цемента. Стройиздат, М., 1976.
5. Шмидт-Хенко К. Содержание оксида магния в клинкере, автоклавные испытания и прочность. Шестой Международный конгресс по химии цемента. Стройиздат, М., 1976, т. I.
6. Богданова И.В., Ситчикова В.А. Химический метод количественного определения оксида магния в различных фазах цементного клинкера и доменного шлака. Труды Гипроцемента, 1969, вып. 34.
7. Окороков С.Д., Голынко-Вольфсон С.Л., Саталкина М.А. О взаимодействии алюминатов кальция с сульфатами элементов II группы периодической системы Д.И. Менделеева при их спекании. ЖПХ, т. 36, вып. 10, 1968.
8. Рагозина Т.А. Взаимодействие сульфата кальция с алюминатами при 1200 °С. ЖПХ, т. 30, вып. 11, 1957.
9. Рагозина Т.А. Влияние $CaSO_4$ на фазовый состав силикатов и алюминатов кальция при обжиге. Узбекский химический журнал, 1952, № 2.
10. Волков В.В., Вербенова Х.И., Сычев М.М., Касьянова Г.Н. Образование сульфоалюмината бария при получении бариевых цементов. Цемент, 1972, № 5.
11. Никифоров Ю.В. Влияние оксида магния на свойства и качество клинкера и цемента. Цемент, 1975, № 6.
12. Урываева Г.Д. Цементы из шламов. Издательство "Наука", Новосибирск, 1970, стр. 82.

I.G. LOUGININA,
V.M. KONOVALOV,
L.D. CHAKHOVA,
V.A. BELETSKAIA, Institut technologique des matériaux de construction, Belgorod, U.R.S.S.

DURCISSEMENT DU CIMENT PORTLAND A TENEUR ELEVEE EN OXYDE DE MAGNESIUM ET EN AUTRES COMPOSITIONS MAGNESIENNES

L'Institut technologique de Belgorod présente une étude concernant les compositions à haute teneur magnésienne qui sont proches des compositions de ciment Portland et des compositions liantes, pareilles au ciment Sorel. Le but de cette recherche est d'utiliser les calcaires dolomitiques à haute teneur magnésienne dans la technologie du ciment Portland et d'emplouer plus largement les compositions liantes à haute teneur magnésienne en conférant à ces dernières des propriétés différentes.

Tout d'abord, nous avons tâché d'obtenir le ciment de bonne qualité à partir du calcaire dolomitique en cas de la concentration de l'oxyde de magnésium dans le clinker plus de 5 % en masse et d'étudier l'influence des régimes différents et des conditions de durcissement sur la régularité du changement de volume lors du durcissement.

Nous avons étudié les mélanges crus d'une large gamme de compositions avec des coefficients de saturation de 0,85 à 0,93 à module alumine - 1,3 - 2,2 et à module silicique 2,1 - 2,2. Ces mélanges crus contenaient dans le clinker 5-10 % en masse d'oxyde de magnésium, des impuretés des composés des alcalis, du fluor, du phosphore et du soufre. Les adjuvants minéralisants accélèrent les processus de formation des silicates à des températures de 1100 à 1350°C, stabilisent les solutions solides du silicate dicalcique, type α et α' et diminuent la température de l'apparition du clinker fondu de 30-70°C. Si la température de cuisson est de 1100 - 1300°C, des solutions solides se forment s'échelonnant entre le mervinite et le silicate dicalcique et ayant la structure α' - C_2S. Aux températures mentionnées, il est possible la formation dans ces charges des Ca_2MgSiO_8, $Ca_3MgAl_4O_4$, $MgFe_2O_4$. La décomposition des phases contenant du magnésium s'effectue à des températures supérieures à 1350°C. La diminution de l'intensité de réflexion du périclase a été observéée lors de l'introduction des adjuvants complexes qui favorisaient simultanément la cristallisation de gros cristaux d'alite (jusqu'à 100 μ). On observe l'augmentation de la teneur en minéraux (par rapport à la teneur calculée), en particulier, de la teneur en aluminoferrite de calcium. Les paramètres de résistance des ciments (1:0 tableau I) obtenus à partir des clinkers avec les minéralisateurs complexes témoignent de leur haute qualité. Pour tous les délais de durcissement, le ciment magnésien avec les adjuvants complexes a montré une résistance plus haute et un accroissement relativement plus actif de cette résistance.

Tableau 1

Résistance des ciments durcissant dans l'eau, 20°C

n° du ciment	Teneur en oxyde de magnésium	Addition du minéralisateur	Résistance à la compression, MPa, à l'âge de			
			3 jours	7 jours	28 jours	1100 jours
1	0	0	34	46	74	82
2	10	0	26	53	62	77
3	10	1	38	54	63	110
4	10	2	42	66	106	136

Le vaporisage dans l'autoclave des échantillons de ciment avec une haute teneur en oxyde de magnésium est inséré dans les normes de la majorité des pays. Cependant, le traitement d'autoclave ne simule pas le durcissement des ciments dans les conditions normales correspondant au service du béton. C'est pourquoi, nous avons observé pendant quelques années le durcissement des ciments magnésiens en vue de déterminer les conséquences possibles dues à l'hydratation tardive du périclase.

Les déformations linéaires des échantillons prismatiques faits de la pâte de ciment (10x10x60 mm) qui ont durci dans l'eau pendant 6 années sont montrées sur la figure 1. L'examen de ces échantillons ne détecte pas de défauts sous forme des fissures, des incurvations des prismes, de l'écaillage de surface. Vers six ans de

I.G. LOUGININA,
V.M. KONOVALOV,
I.D. CHAKHOVA,
V.A. BELETSKAIA

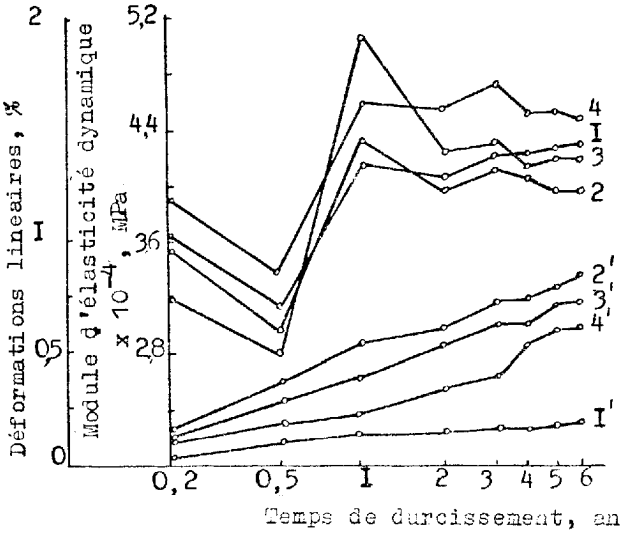

Fig. 1. Changement de module d'élasticité (1-4) et de déformations linéaires (1'-4') de la pierre de ciment durcissant dans l'eau à 20°C. Pour les désignations, voir Tableau 1

cissement, les déformations linéaires du ciment n°2 atteignent 0,98 %. L'allongement maximum est observé chez le ciment fait à partir du clinker obtenu sans minéralisateur. Le degré d'hydratation du périclase dans le ciment calculé selon les données de l'analyse thermogravimétrique atteint vers 6 ans de durcissement 12,6 - 13,4 %.

Les essais d'autoclave ont été effectués selon la norme de magnésium. Tous les ciments contenant MgO jusqu'à 10 % ont montré un changement de volume irrégulier. La valeur d'expansion des échantillons prismatiques du ciment variait de 10,65 à 31,00 %. Cependant, le degré d'hydratation du périclase après le vaporisage dans l'autoclave a été de 87 - 96 %.

Nous avons établi que la déformation des ciments magnésiens dépendait de la durée et des conditions de leur durcissement. Un durcissement suffisant de la structure de la pierre de ciment avant le traitement hydrothermal favorise la diminution de l'expansion magnésienne.

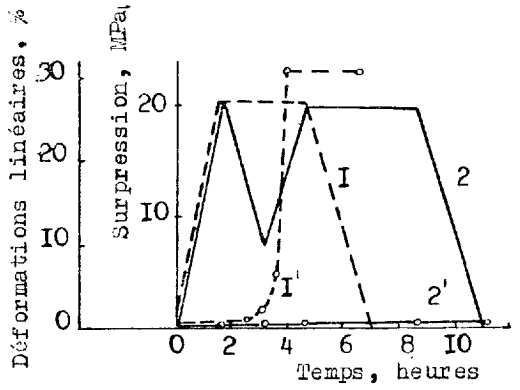

Fig. 2. Régime comun (I) et régime proposé (2) du traitement d'autoclave. Déformations linéaires des échantillons de ciment vaporisés selon les régimes 1(1') et 2(2')

Il est connu que les produits d'hydratation aux périodes initiales de durcissement ne sont pas stables. Cela est confirmé par les variations en temps des propriétés élastiques et de déformation de la pierre de ciment (figure 1). La cristallisation des hydrosilicates dans la pierre de ciment durcissante est accompagnée d'une chute de résistance. Cependant, dans deux ans de durcissement, si en juger d'après les variations peu considérables du module d'élasticité dynamique, l'équilibre s'établit, et à l'avenir, la pierre gagne des propriétés stables.

Les ciments qui ont montré un changement de volume irrégulier un jour après le gâchage (expansion 6-10 % en cas de la teneur en oxyde de magnésium de 6,5 - 7 % en masse) ont subi les essais d'autoclave à l'âge de 2 ans de durcissement dans l'eau. Dans ce cas, les ciments sur la base des clinkers avec les minéralisateurs complexes possédaient une plus haute résistance (3 à 5 fois).

On estime que l'essai des ciments magnesiens par le vaporisage (2 MPa, 3 heures) assure l'hydratation complète du périclase. En déterminant le degré d'hydratation du périclase pour les ciments fabriqués à l'usine (teneur en MgO - 4,5 - 5,0 % en masse) et pour les ciments de laboratoire (teneur en MgO - 5 - 6 % en masse) qui ont subi les essais normalisés, on a constaté que la

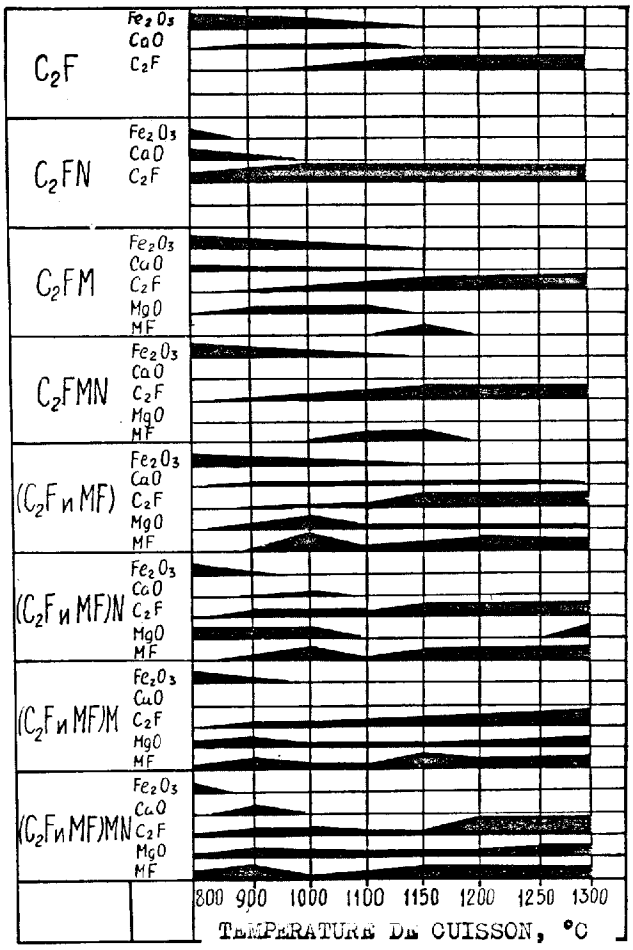

Fig. 3. Variation de l'intensité des pics de diffraction des minéraux sur les diffractogrammes des charges en fonction de la température et des additions. C_2F - charge comptée sur la formation du $2CaO \cdot Fe_2O_3$; N et M - - additions sous forme des carbonates Na_2CO_3 et $MgCO_3$; C_2F et MF - - charge comptée sur la formation du $2CaO \cdot Fe_2O_3$ et $MgFe_2O_4$ à rapport 1:1

quantité de l'oxyde de magnésium passé en brucite était limité de 30-45 %.

Une étude spéciale sur l'expansion magnésienne de la pierre de ciment dans l'autoclave montre que les déformations de volume se manifestent à la période du maintien isothermique (fig. 2). Le régime modifié du vaporisage consiste dans le fait qu'après l'obtention de la pression maximale, on la diminue pendant 1 - 1,5 heures jusqu'à 0,6 - 0,7 MPa, après quoi, elle est reportée à la valeur maximale et est maintenue constante pendant 3 - 4 heures. Dans ce cas, à la période initiale, il y a une hydratation intense des minéraux de clinker et une cristallisation des produits d'hydratation qui mènent au durcissement de la structure de la pierre de ciment avant le début d'hydratation du périclase. Le maintien ultérieur à 2 MPa n'influe pas pratiquement sur les valeurs des déformations linéaires des échantillons de ciment. Le régime proposé simule plus précisément les processus de durcissement du ciment dans les conditions normales et il est recommandé, au lieu du régime existant, pour les essais des ciments contenant du magnésium en vue de déterminer la régularité du changement de volume.

Par conséquent, si on assure un degré d'hydratation assez haut à l'aide de la structure solide de la pierre de ciment qui rend plus difficile l'accès de l'eau au périclase et qui est capable de résister à l'expansion magnésienne, on peut garantir un changement de volume régulier à des concentrations plus hautes en oxyde de magnésium par rapport à celles prévues par les normes.

Dans la deuxième partie de notre recherche, nous avons tâché d'utiliser la dolomite en qualité du constituant cru obligatoire. L'utilisation des roches carbonatées à haute teneur magnésienne en qualité du constituant de départ lors de la production des ciments spéciaux augmente les ressources de matières premières.

Actuellement, on travaille activement dans le domaine de la création du liant efficace pour l'agglomération des concentrés de minerai de fer finement dispersés. Des liants obtenus à partir des concentrés de minerais de fer et du constituant du flux contenant de l'oxyde de magnésium peuvent être les plus perspectifs. Dans la métallurgie, on utilise largement la dolomite en

I.G. LOUGININA,
V.M. KONOVALOV,
L.D. CHAKHOVA,
V.A. BELETSKAIA

qualité du flux.

Le but de cette recherche est d'obtenir le liant susceptible d'augmenter la fluidité et le pouvoir de désulfuration du laitier de haut fourneau ce qui est assuré à l'aide de l'oxyde de magnésium contenant dans les flux. Cependant, les normes de tous les pays limitent la teneur en oxyde de magnésium dans le ciment Portland.

Nous avons réussi à synthétiser le liant ferreux contenant de l'oxyde de magnésium jusqu'à 18 % en masse. Dans le système la série $CaO-SiO_2-Al_2O_3-Fe_2O_3-MgO$ on a choisi à cinq constituants la série des minéraux suivants: $C_2F-C_2S-C_4AF-MF-MgO$. La quantité d'oxydes acides de silicium et d'aluminium est limitée dans le système ce qui est une condition nécessaire de la composition optimum.

Les charges crues ont été obtenues sur la base des calcaires à différente teneur en oxyde de magnésium, de la dolomite et du concentré de minerai de fer. Le silicate dicalcique (forme β), les aluminoferrites et la solution solide du fer magnésifère dans le périclase constituaient les minéraux principaux des compositions synthétisées. Dans les agglomérés ferreux on a trouvé de nouvelles ferrites calciques-magnésiques - $Ca_mMg_n(Fe_2O_6)$. La composition des formations nouvelles dépend des conditions de cuisson et du rapport des agents. Le liant nouveau durcit à l'air. L'activité d'hydratation dépend de la composition minéralogique où une influence décisive est exercée par la ferrite calcique-magnésique et les fers magnésifères.

Les mélanges comptés sur la formation des ferrites calciques et magnésiques à rapport $C_2F:MF = I$ ont été analysés par la méthode de phase à rayons X. On a établi la suite de formation de la ferrite dicalcique en cas de l'introduction des additions catalytiques, de l'oxyde de magnésium à des températures de 800 à 1300°C. La variation de l'intensité des réfexiońs principales est montrée sur le diagramme (fig. 3).

L'introduction des combinaisons alcalines mène à la formation des carbonates magnésiques et calciques doubles qui conditionnent l'apparition des matières fondues eutectiques perturbant la topochimie de formation des minéraux.

L'oxyde de magnésium de la dolomite comptée sur la formation de la ferrite dicalcique favorise l'apparition du fer magnésifère qui passe ensuite en bain fondu. La ferrite calcique-magnésique $Ca_2Mg(Fe_2O_6)$ apparaît dans le bain fondu.

En cas d'une teneur considérable en oxyde de fer dans le bain fondu, la formation des ferrites calciques-magnésiques est ralentie à cause de la diminution de solubilité de l'oxyde de calcium. Les combinaisons alcalines diminuent la viscosité des matières ferreuses-magnésiques en fusion ce qui favorise la formation des minéraux et diminue l'intervalle de température de la cristallisation. En présence des minéralisateurs, l'assimilation de l'oxyde de fer s'achève presque dans toutes les charges à une températures diminuée de 100-200°C. Apparemment, cela est conditionné par la formation des ferrites alcalines.

Il résulte de la figure 3 que le minéralisateur se trouvant dans la charge comptée sur la synthèse des ferrites dicalciques et magnésiques fait varier les conditions de formation des minéraux, de solubilité de la ferrite de magnésium et celles de cristallisation de la ferrite calcique-magnésique à partir du bain fondu. En présence du minéralisateur, à la température de 1100°C, les oxydes de magnésium, de calcium et de fer passent complètement dans le bain, et le fer magnésifère y passe partiellement. La cristallisation simultanée des ferrites calciques et magnésiques est accompagnée à la température de 1300°C par un dégagement d'une grande quantité de périclase.

Dans la charge $(C_2F + MF)M$, le fer magnésifère se forme à la température de 800°C, la quantité maximale est observée à la température de 900°C, la matière fondue apparaît à une température diminuée de

I.G. LOUGININA,
V.M. KONOVALOV,
L.D. CHAKHOVA,
V.A. BeLeTSKAIA

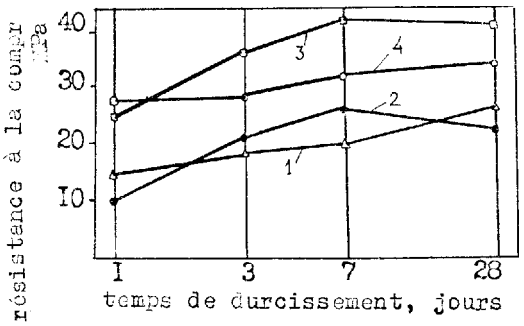

Fig. 4. Influence des compositions des ferrites calciques sur la résistance des échantillons hydratés.
1 - C_2F; 2 - C_2FN
3 - C_2FM; 4 - C_2FMN

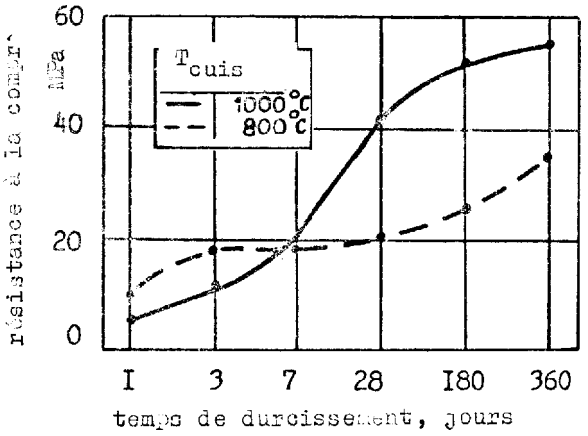

Fig. 5. Cinétique de durcissement de l'oxyde de magnésium gâché par la solution de l'aluminate de sodium

100°C et a une plus large intervalle de température en ce qui concerne la stabilité. Le fer magnésifère se cristallise le premier, ensuite c'est la ferrite calcique-magnésique qui se dégage. L'introduction du minéralisateur dans la charge mène à une assimilation précoce de l'oxyde de fer, à l'apparition du bain fondu et à une formation relativement à des basses températures de la ferrite dicalcique. La quantité de ferrite dicalcique reste à un même niveau à des températures de 1000-1150°C. A la température de 1200°C, un dégagement rapide et complet de la ferrite calcique-magnésique est observé.

L'accroissement de résistance des compositions synthétisées avec le temps est montré sur la figure 4. On a essayé les echantillons préparés de la pâte à rapport L/S = 0,26. La ferrite calcique-magnésique se distingue de la ferrite dicalcique par une plus haute activité d'hydratation. La diminution de résistance des compositions C_2FN et C_2FMN s'explique par une hydratation ralentie des minéraux en cas d'addition des minéralisateurs.

A l'aide de la spectroscopie à résonance γ-nucléaire, on a déterminé la distribution des ions selon les positions cristallographiques. Les valeurs calculées des rapports des ions de fer se trouvant dans les positions octaédriques et tétraédriques sont en bonne corrélation avec les données sur la résistance à l'âge d'un mois.

Les recherches effectuées ont permis d'élaborer les paramètres technologiques en vue d'obtenir un ciment ferreux spécial avec une teneur en oxyde de magnésium jusqu'à 18 % en masse sur la base des roches à haute teneur magnésienne.

On a étudié également les propriétés liantes de l'oxyde de magnésium gâché par la solution d'aluminate de sodium contenant de l'alcali. La matière de gâchage est constituée de résidus industriels.

Les matières de départ pour synthétiser le liant ont été représentées par l'oxyde de magnésium cuit aux températures de 800 et 1000°C et par la solution d'aluminate de sodium d'une densité élevée. La détermination de la résistance des échantillons s'effectuait à l'aide des essais des poutrelles 10x10x60 mm, I:0 lors du durcissement à l'air et après le traitement thermique à des températures de 100 - 140°C.

L'oxyde de magnésium gâché par la solution de l'aluminate de sodium forme une pâte plastique. La cinétique du durcissement de l'oxyde de magnésium gâché par l'aluminate de sodium est montrée sur la figure 5.

I.A. [illegible]GININA,
V.M. [illegible]KOVALOV,
L.D. [illegible]CHANOVA,
V.A. [illegible]SKAIA

Em faisant varier la concentration de la solution de gâchage, on peut régler le processus de durcissement du liant obtenu. Si on augmente la densité de la solution d'aluminate de sodium, l'hydratation et la cristallisation de l'hydroxyde de magnésium sont accélérées.

La vitesse de cristallisation et de durcissement de l'hydroxyde de magnésium gélatinisé peut être augmentée par le traitement thermique à des température de 110-120°C. A l'âge de deux heures, la résistance augmente jusqu'à 39,5 MPa et devient commensurable avec la résistance à l'âge de 28 jours de durcissement à l'air. Le traitement thermique permet d'atteindre la résistance du liant magnésien jusqu'à 80 - 100 MPa. Sur les radiogrammes du liant durcissant lors du chauffage, outre les lignes analytiques de l'hydroxyde de magnésium, on voit apparaître les pics de diffraction supplémentaires appartenant à $NaAlCO_3(OH)_2$.

La microscopie électronique du liant durci a montré que les cristaux de l'hydrocarbonate aluminosodique avaient une forme aciculaire et se trouvaient à la surface des gros grains de l'hydroxyde de magnésium.

Par conséquent, lors du gâchage de la magnésite caustique par la solution de l'aluminate de sodium on a reçu un nouveau liant magnésien durcissant à l'air même à la température de 110 - 120°C. La formation de structure du durcissement est accompagnée par le dégagement et la cristallisation de l'hydroxyde de magnésium et de l'hydroxycarbonate aluminosodique. Le degré de radoucissement du liant obtenu à la température de 500 - 900°C est beaucoup plus petit par rapport au ciment d'oxychlorure magnésien qu'on utilise jusqu'à présent. Lors de la cuisson à des températures supérieures à 1200°C, le liant atteint une résistance considérable (100 - 150 MPa). Le liant magnésien proposé peut être utilisé en qualité d'un réfractaire.

M. VON EUW Societé des Ciments Français - Paris, France

CIMENTS CONTENANT DES ADDITIONS MINERALES

1. INTRODUCTION

Le ciment portland artificiel est unanimement classé en tête de liste des liants hydrauliques. Cela ne veut cependant pas dire qu'il est apte à résoudre tous les problèmes de formulation des bétons, que ce soit dans le domaine du batiment ou dans celui des travaux publics.

Les caractéristiques des bétons prises en compte selon les emplois concernés se regroupent essentiellement dans les thèmes suivants :

- rhéologie des bétons frais
- évolution des résistances en fonction du temps
- évolution du dégagement de chaleur pendant le durcissement
- résistances aux divers types de corrosion des bétons durcis.

Pour parvenir à satisfaire les exigences à l'emploi, on demande souvent aux ciments d'avoir des propriétés contradictoires, ce qui conduit le fabricant à proposer une palette plus ou moins large de produits.

Dans le cas le plus simple il fabrique un seul clinker et le broie à diverses finesses; mais s'il se rend maître des résistances mécaniques, il risque de faire apparaître des différences rhéologiques et il ne résoud pas simultanément les problèmes liés à la corrosion chimique.

Cela veut dire que les cimenteries ne produisant que du ciment portland sont très souvent obligées de fabriquer deux clinkers :

- un clinker à saturation élevée pour ciment à hautes résistances mécaniques et fort dégagement de chaleur, mais à faible résistance chimique,

- un clinker peu saturé pour ciment à forte résistance à la corrosion chimique et faible dégagement de chaleur, mais à résistances mécaniques limitées.

La cimenterie moderne est conçue de préférence en une seule ligne de fabrication de clinker pour optimiser les investissements et les frais d'exploitation.
Par ailleurs, dans l'intérêt général aussi bien que dans la recherche du meilleur prix de revient, les cimentiers sont incités à économiser l'énergie et à consommer des sous-produits.

Pour ces deux raisons, on observe une tendance à ne fabriquer qu'un seul clinker, potentiellement très performant, et à le broyer avec des additions minérales de provenances diverses. En choisissant convenablement ces constituants secondaires, on peut résoudre les deux problèmes essentiels que sont la classe de résistance mécanique et l aptitude à résister aux attaques chimiques des bétons.

Les matériaux utilisés varient en premier lieu selon les ressources naturelles et le développement industriel régional, c'est-à-dire la mise à disposition de sous-produits.

L'industrie cimentière est ainsi amenée à consommer couramment des laitiers de haut-fourneau, des cendres de charbon, des pouzzolanes naturelles ou des matières douées d'activité pouzzolanique. Dans certains pays on utilise également des roches calcaires comme addition minérale.

En consultant les recueils de norme, on dénombre :

35 pays prévoyant des ciments au laitier
14 pays prévoyant des ciments aux cendres
31 pays prévoyant des ciments à la pouzzolane
15 pays prévoyant des ciments au filler calcaire.

En Europe 19 pays utilisent ces additions dans des ciments binaires ou composés avec plusieurs constituants. La France a innové dans ce domaine en développement fortement la consommation de filler calcaire en co-broyage à la cimenterie avec le clinker, seul ou avec le laitier ou les cendres de charbon.
En 1984, les quantités absorbées par les cimenteries françaises s'élevaient à :

2 086 000 tonnes de laitier granulé
719 000 tonnes de cendres volantes
93 000 tonnes de pouzzolanes
855 000 tonnes de fillers.

C'est en raison de la longue expérience française dans ce domaine que le Comité d'Organisation du 8 ème Congrès International de la Chimie du Ciment m'a confié la présidence de ce Séminaire. Je le remercie de sa confiance, et j'ai maintenant l'honneur de vous présenter les personnalités qui vont animer notre réunion par l'apport de leurs connaissances et la participation aux discussions qui suivront la présentation de leurs rapports :

Dr. Baron, de Lafarge Coppée - France
Dr. Christensen, de Aalborg Cement - Danemark
Dr. Ghosh, de Cement Research Institut - Inde
Pr. Ollivier, de l'Institut National des Sciences Appliquées - France
Dr. Ramachandran, du Conseil National de la Recherche - Canada.
Dr. Takemoto, de Onoda Cement - Japon
Pr. Wishers, du V.D.Z. - République Féd. Allemande.

Le précédent Congrès tenu à Paris en 1980 avait consacré un thème entier aux ciments avec laitiers et un autre aux ciments avec pouzzolanes. Les fillers calcaires n'avaient pas été pris en considération. Le programme de l'actuel Congrès comprend dans son thème 2 l'influence des matières d'addition sur le processus d'hydratation, et dans son thème 3 les effets de leurs composants sur l'hydratation et la structure.

Pour éviter trop de répétitions, il m'a donc semblé opportun d'orienter nos travaux vers les aspects techniques dérivant des connaissances scientifiques. Dans ce but, nous essaierons de faire une synthèse basée sur les propriétés d'usage des ciments. Une telle synthèse doit faire apparaître les comportements et les phénomènes particuliers liés à la présence des laitiers, des matériaux pouzzolaniques et des fillers calcaires. Les deux premiers ont donné lieu depuis longtemps à de nombreuses recherches, en revanche les fillers calcaires, en raison ce leur utilisation plus récente, occupent une place nouvelle et encore peu développée dans les programmes de recherches.

Comme c'est souvent le cas, les résultats de certains essais paraitront contradictoires. Il en est ainsi par exemple de la comparaison des résistances mécaniques en essais normalisés des ciments portland additionnés de diverses poudres minérales, et de celles obtenues par broyage du mélange de l'ensemble des constituants.

Je souhaiterais être clair à ce sujet:

Quelle que soit la propriété d'usage que l'on veuille examiner, la comparaison ne peut valablement être faite qu'entre des ciments de même classe de résistance. Cette notion est d'ailleurs d'autant plus facile à appliquer que les normes nationales définissent les classes de résistance entre des limites inférieures et supérieures : c'est le cas par exemple pour l'Allemagne Fédérale et pour la France depuis plusieurs années et ce le sera à l'avenir pour l'ensemble des pays européens qui établissent actuellement un projet de normes communes.

Un autre point essentiel sur lequel je dois attirer l'attention est celui du choix de l'addition minérale. Là encore il peut y avoir contradiction entre les résultats de certains chercheurs et ceux de l'industrie cimentière; il y a en effet une grande différence de conception entre la revue systématique d'un ensemble de minéraux et la sélection faite par les industriels à l'aide de critères engageant leur responsabilité. On peut par exemple trouver dans une étude de laboratoire des fillers qui diminuent la maniabilité ou la résistance au gel mais ce sont précisément de tels minéraux qui sont rejetés pour un emploi industriel.

Ces deux réserves étant faites, les caractéristiques essentielles retenues pour la commercialisation des ciments doivent à la fois être conformes aux normes et satisfaire les exigences des emplois.

2. NORMES

D'une manière générale, les normes nationales donnent une définition plus ou moins précise des constituants, suivie d'un classement des liants en fonction des proportions admises pour chaque constituant. Un autre classement est ensuite ouvert à ces divers types de ciments en fonction de leur classe de résistance, puis des spécifications particulières, principalement d'ordre chimique, sont imposées à certaines catégories.

Cette conception des normes peut faire l'objet de certains commentaires :

2.1. DEFINITION DES CONSTITUANTS

Doit-on normaliser les constituants, c'est-à-dire leur donner une définition précise assortie de tests de qualité et de spécifications chiffrées ? Cette question est très controversée. Pour certains, des normes de sous-produits tels que les laitiers et les cendres, ou de produits pouzzolaniques ou calcaires, n'auraient pas de sens puisque ce ne sont pas des produits élaborés. Pour d'autres, la normalisation serait sécurisante; c'est ainsi que plusieurs pays étudient un projet de normes pour les cendres volantes. A mon avis, ce projet ne peut intéresser que les bétonniers, qui ne disposent pas des moyens d'optimisation qu'ont les cimentiers.

2.2. COMPOSITION DES CIMENTS

Je voudrais citer l'exemple des normes françaises devant le projet de normalisation européenne (CEN). L'Institut Français de Normalisation a mis en application en 1979 ses normes P 15 300 et P 15 301 en créant une catégorie de ciments composés appelés CPj pouvant contenir jusqu'à 35 % d'additions minérales, prises individuellement ou par mélange de plusieurs constituants, sans imposer à ces produits de spécifications chiffrées. Evidemment les additions choisies par le cimentier sous sa responsabilité ne doivent pas perturber les caractéristiques des bétons.

En 1980, ces normes ont été complétées par l'introduction d'un ciment CLC pouvant contenir entre 40 et 75 % d'un mélange de laitier et de cendres et constituant un produit intermédiaire entre les CHF ayant des proportions semblables de laitier seul et les CLK renfermant au minimum 80 % de laitier.

Alors que les CPJ sont destinés à réaliser sans difficultés et en économisant l'énergie, des ciments qui répondent aux besoins les plus courants, les CLC, les CHF et les CLK sont fabriqués pour résister aux corrosions d'origine chimique, telle que l'eau de mer et les terrains gypseux.

Dans ces conditions, les éléments composés occupent dans le marché français des liants hydrauliques une place prépondérante ainsi que le montre la répartition suivante pour l'année 1984:

CPA = 23,8 %
CPJ = 63,2 %
CHF, CLK, CLC = 5,9 %
Autres liants = 7,1

La proposition faite par la France d'introduire dans le projet de normes européennes les ciments du type CPj, s'est d'abord heurtée à une opposition basée sur le manque d'informations concernant la durabilité des bétons de CPj, mais il faut savoir qu'en réalité les difficultés rencontrées sont de divers ordres :

- Les approvisionnements en additions minérales sont à caractère régional,
- les règlements de sécurité concernant les constructions sont nationaux,
- les procédures de certification de conformité sont nationales,
- la reconnaissance mutuelle des contrôles n'est pas acquise.

Malgré ces difficultés et devant l'intérêt, si ce n'est l'obligation, de supprimer les entraves techniques à la libre circulation des marchandises entre les pays du Marché Commun Européen, des études ont été effectuées pour aboutir à une caractérisation satisfaisante des constituants, notamment des fillers calcaires. La durabilité des bétons de ciments fillérisés a ainsi été vérifiée par des essais en commun. Le Pr. WISCHERS, responsable de ces questions au sein du Comité Européen de Normalisation fera le point de l'optimisation des additions minérales dans les ciments (1).

Je voudrais simplement préciser que les cimentiers disposent de moyens importants et efficaces pour sélectionner leurs approvisionnements, les homogénéiser, les contrôler :

- les pouzzolanes sont choisies en tenant compte des possibilités d'obtenir une efficacité régulière avec le clinker auquel elles sont ajoutées.
- les cendres volantes subissent en particulier un contrôle de régularité de leur teneur en carbone imbrulé(2).
- les laitiers sont souvent homogénéisés, par exemple, sur parc après avoir subi un contrôle d'hydraulicité avec le clinker.

- les fillers calcaires sont choisis à partir de tests de composition basés notamment sur une faible teneur en argile et en matières organiques. Leur sélection est complètée par une étude du comportement rhéologique et de la durabilité des ciments auxquels ils sont incorporés.

De toute façon, après avoir optimisé la composition de ses ciments, le cimentier s'assure de la régularité des performances et il a les meilleurs moyens d'y parvenir par un pilotage bien contrôlé des doseurs et des broyeurs.

3. SATISFACTION A L'EMPLOI

Les ciments sont livrés à la clintèle par classes de résistance en fonction de l'échéance de durcissement en milieu humide; mais un premier écueil auquel on se heurte selon que l'on se réfère au respect des normes ou à la satisfaction de l'utilisateur est lié au rapport eau/ciment : en effet, les essais normalisés sont faits en mortier ISO à E/C = 0,5 alors que les bétons de chantiers sont généralement confectionnés à maniabilité définie, ce qui revient à ajuster le rapport E/C pour tenir compte des caractéristiques rhéologiques.

Un second écueil est celui de l'évolution des résistances en fonction du temps, laquelle dépend à la fois de la nature des constituants et de leur finesse.

L'optimisation d'un ciment renfermant une ou plusieurs additions minérales conduit donc le fabricant à une étude complexe portant sur le choix des constituants, leur mode de broyage, la granularité du ciment et son taux de gypsage.

3.1. RHEOLOGIE

La maniabilité des bétons frais conditionne la mise en place, c'est-à-dire les moyens, l'économie des procédés et en définitive la qualité des bétons; c'est pourquoi elle constitue en particulier pour le choix des fillers un critère des plus sévères. Les laboratoires attachent donc un grand intérêt aux contrôles rhéologiques en vue d'obtenir l'ouvrabilité optimale avec la régularité maximale. J.P. BOMBLED rappelle quels sont les facteurs intervenant sur la maniabilité et rend compte de l'influence des fillers notamment dans la pâte interstitielle (3).

Il faut tout de suite préciser que les appareils de mesure sont fort différents selon que l'on fait des études sur pâtes de ciment, sur mortiers ou sur bétons. Dans les deux premiers cas, on utilise des viscosimètres à cylindres coaxiaux ou des pénétromètres à aiguille ou à sonde, alors que les contrôles sur bétons sont effectués avec des méthodes adaptées au type de béton. Il faut savoir que la maniabilité du béton est dépendante de toute l'étendue granulaire; c'est pourquoi on n'observe pas systématiquement de concordance entre les essais sur pâte de ciment et ceux sur béton. Par ailleurs, les appareils de contrôle rhéologique des bétons diffèrent selon la consistance:

- flow test pour les bétons fluidifiés,
- slump test (ASTM) et maniabilimètre LESAGE-LCPC pour les bétons à consistance molle,
- coefficient de serrage de WALZ (DIN) pour les bétons de consistance sèche.

Ces déterminations sont indispensables pour mettre au point la fabrication d'un nouveau ciment car l'utilisateur n'admet pas les changements d'ouvrabilité dûs à des variations de qualité du ciment. De plus, il ne faut pas se contenter de rechercher une demande en eau acceptable au malaxage mais il faut s'assurer que la variation de la rhéologie dans le temps ne conduit pas à remalaxer le béton de centrale avec une addition d'eau à l'arrivée sur chantier, ce qui se ferait au détriment de la résistance.

L'expérience a montré des comportements sensiblement différents selon l'origine des cendres de centrales thermiques ou celle des fillers calcaires.

La nature du régulateur de prise(gypse, plâtre, anhydrite, gypse chimique) influence la maniabilité et il faut savoir que des comportements anormaux peuvent être observés en présence de fluidifiants : des difficultés sérieuses ont été rencontrées sur des chantiers importants, par exemple avec des ciments au laitier.

L'introduction des fillers calcaires dans les ciments CPj fabriqués en France a succédé à de nombreuses études dans lesquelles la demande en eau et la maniabilité des bétons ont eu une place importante. La synthèse des résultats obtenus par les laboratoires cimentiers permet de conclure que le comportement rhéologique des bétons, à classe de résistance égale, n'est pas affecté par l'emploi de ciments renfermant moins de 30 % de filler calcaire, si la pureté du filler répond au test d'absorption du bleu de méthylène qui caractérise la teneur limite acceptable en argile.

Contrairement à certaines idées reçues, ces mêmes études ont montré que les variations de finesse des constituants de ces CPj au calcaire n'ont pratiquement pas d'influence sur la demande en eau.

L'ouvrabilité et son évolution ne sont pas les seules caractéristiques à prendre en compte; le ressuage et le retrait, responsables de la microfissuration, ont des conséquences que nous examinerons dans le cadre de la durabilité.

3.2. CINETIQUE DE L'HYDRATATION ET DEVELOPPEMENT DES RESISTANCES

Toutes les études à caractère scientifique, aussi bien que les essais visant à comparer les résistances en fonction de l'addition minérale, montrent une participation aux réactions physico-chimiques d'hydratation, plus ou moins rapide pour les laitiers et les pouzzolanes, mais non négligeable pour les fillers calcaires.

La finesse des constituants en présence joue un rôle essentiel dans la vitesse des réactions. Selon les aptitudes comparées au broyage on obtient des ciments dans lesquels les surfaces spécifiques des constituants peuvent être extrêmement différentes. L'étendue des plages granulaires a des conséquences multiples sur le déroulement des phénomènes physico-chimiques du durcissement.

3.2.1. Laitiers

Les phénomènes de durcissement des ciments au laitier sont maintenant assez bien connus. Nous avions à ce sujet retenu du Congrès de Paris, d'abord le rôle de la structure du verre de laitier, structure non pas désordonnée, mais organisée à très courte distance. Nous savons

aussi que pour obtenir cette structure où le silicium forme des tétraèdres SiO_4^{4-} plus ou moins polymérisés, les cavités laissées libres dans le réseau sont occupées par les cations Ca, K, Na. Plus la part de ces cations est importante, plus les tétraèdres SiO_4^{4-} sont isolés et plus le verre est instable donc chimiquement actif. C'est là l'explication de l'utilisation en cimenterie des seuls laitiers vitreux de composition chimique basique.

Les études récentes du mécanisme de l'hydratation, en particulier celles de VERNET , en on mis en évidence les différentes phases par le suivi de l'évolution des concentrations ioniques de la solution interstitielle et la simultanéité des pics de flux thermique (4).

Il a été démontré que dans le système clinker-laitier-gypse-eau les réactions s'influencent par différents couplages. Ces réactions débutent par la chimisorption de l'eau, suivie de la rupture des liaisons à la surface des grains, puis de la solvatation; elles aboutissent à la précipitation de l'éttringite, du CHS et de la portlandite. Après épuisement du gypse l'éttringite se transforme en monosulfoaluminate puis l'excès d'aluminates précipite sous forme de C_4AH_{13}.

Le laitier joue un rôle actif dès les premiers instants du contact avec l'eau, ce qui a été facilement démontré par Mme REGOURD, mais ce n'est qu'après la période dormante et l'épuisement du gypse que s'accélère l'hydratation du laitier(5).

Les travaux de VERNET expliquent que les courbes de croissance des résistances des ciments au laitier varient non seulement avec le laitier mais avec le clinker utilisé. Cette particularité avait été mise en évidence par HAWTHORN. Elle fait l'objet du rapport du Dr. TAKEMOTO et plaide en faveur de l'emploi du laitier. à la cimenterie (6) (7).

3.2.2. Pouzzolanes et cendres

Alors que les laitiers doivent leur hydraulicité précoce à leur teneur relativement élevée en ions Ca dans leur propre structure, les pouzzolanes ne peuvent participer au durcissement des ciments que très lentement en réagissant avec la chaux du milieu aqueux auquel elles sont incorporées.

La pouzzolanicité est une qualité difficile à quantifier; initialement attachée à des roches éruptives de structure vitreuse finement divisées, elle a été étendue à des matériaux siliceux sédimentaires ou encore d'origine organogène, ainsi qu'à des produits artificiels tels que les argiles cuites et à des sous-produits comme les cendres de houille et les fumées de silice.

Le taux et la vitesse de fixation de la chaux par le matériau pouzzolanique sont fonction de sa composition chimique acide (SiO_2 + Al_2O_3 + Fe_2O_3 > 75 %), de sa structure vitreuse ou amorphe, de sa surface spécifique et de sa porosité, ainsi que de la quantité de chaux et de sulfate disponibles dans le milieu; l'élévation de température permet d'accélérer les réactions, très lentes à la température ordinaire.

On a essayé de définir l'activité pouzzolanique par diverses méthodes, principalement chimiques, basées sur le taux de fixation de chaux ou la solubilité de la silice et de l'alumine dans la soude ou la potasse.

La fixation de la chaux, si elle est indispensable, n'est malheureusement pas suffisante pour développer des résistances mécaniques; les zéolithes, par exemple, ne doivent pas être confondues avec les pouzzolanes.

Le cimentier n'a donc pas d'autres moyens pratiques que de procéder à deux types d'essais complémentaires pour choisir un matériau à usage pouzzolanique. Le premier, très rapide consiste à chiffrer l'aptitude à fixer la chaux pour éliminer les matériaux non réactifs, le second est destiné à suivre les résistances mécaniques de mortiers expérimentaux en fonction du temps par comparaison à des mortiers de référence.

La structure vitreuse ou tout au moins amorphe de la pouzzolane donne lieu à des phénomènes physico-chimiques en présence d'eau, de chaux et de sulfates, comparables à ceux observés avec les laitiers, à savoir : chimisorption, hydrolyse, lixiviation lente de la masse, solvatation des ions libérés, puis précipitation et cristallisation des espèces hydratées en sursaturation dans la solution interstitielle.

Comme dans le cas des laitiers, la présence de germes cristallins dans la structure favorise la précipitation des hydrates sous forme de fibrilles, aiguilles et plaquettes enchevêtrées, indispensables à une bonne cohésion et à de grandes résistances.

Ces hydrates sont pratiquement les mêmes que ceux observés avec les ciments de laitier, mais ils se forment très lentement à partir de la pouzzolane car les tétraèdres SiO_4^{4-} de la masse anhydre y sont moins indépendants.

Les résistances à court et moyen termes, contrairement aux ciments de laitier, ne sont dues qu'à l'hydratation du clinker dans les ciments et la pouzzolane; la pouzzolanicité n'intervient qu'au-delà de 90 jours et se poursuit très longtemps à la condition de rester en milieu humide.

Le type d'ouvrage et le milieu de conservation sont donc déterminants dans l'utilisation des ciments à la pouzzolane.

Le Docteur GHOSH fera un exposé sur les recherches expliquant la faveur croissante des utilisateurs pour les ciments avec additions de laitiers et de pouzzolanes (8). Puis MM. CHRISTENSEM et ALMEBORG feront part des résultats de leurs recherches pour valoriser les ciments aux cendres volantes au Danemark (9).

3.2.3. Fillers calcaires

La pratique courante depuis une dizaine d'années, de l'addition de fillers calcaires à la fabrication de ciments normalisés, est considérée en Europe comme une initiative française, bien que quelques autres pays dans le monde l'aient adoptée par exemples le Canada, le Chili; la Chine, l'Espagne la Finlande.

La fabrication de ces ciments est généralement faite par co-broyage des constituants, mais ils peuvent également être produits par broyage séparé et homogénéisation.

Le cobroyage d'éléments de dureté très différente comme les clinkers et certains calcaires conduit à des ciments dont l'étendue et

la répartition granulaires diffèrent évidemment de celles de chaque constituant.

BOMBLED et al consacrent une communication à ces mesures sélectives de finesse et montrent que l'on atteint des différences très significatives qui conditionnent les performances (10).

Je voudrais faire remarquer que cela constitue un degré de liberté dont use le cimentier pour ajuster la qualité de son produit.

R. GUYOT et al présentent d'ailleurs à ce sujet une communication qui met bien en valeur la possibilité d'utiliser la potentialité hydraulique du clinker dans les ciments fillérisés au calcaire. Ils montrent que pour une même classe de résistance définie à 28 jours, le clinker du ciment fillérisé est broyé plus fin que dans un ciment pur et, de ce fait, développe aux courtes échéances une quantité d'hydrates plus importante. Ils expliquent ainsi que l'on trouve toujours des résistances plus élevées pendant les premiers jours pour des résistances identiques à 28 jours. Nous verrons cependant que le calcaire participe lui aussi à ces résistances précoces (11).

Pour comprendre les réactions d'hydratation des ciments fillérisés au calcaire nous disposons de quelques études récentes à caractère scientifique :

- le Pr OLLIVIER montre le rôle des fines particules d'additions minérales dans la formation de l'auréole de transition entre les grains fins de la pâte et les granulats du béton. Il rappelle que cette auréole qui constitue la zone de liaison pâte-granulats est le point faible des bétons en raison de l'orientation préférentielle des cristaux et de la forte porosité qui favorise le passage des agents de corrosion (12).

Les additions minérales, et particulièrement les calcaires, peuvent modifier favorablement les paramètres de l'auréole de transition et améliorer ainsi les caractéristiques du béton.

Les fillers calcaires se distinguent des autres additions minérales par leur réaction avec les aluminates de calcium pour former du carboaluminate, concurremment à la réaction de formation du sulfo-aluminate à partir du gypse.

- Cette activité chimique des fillers calcaires a été montrée par M. REGOURD et al (13). Elle fait l'objet du rapport du Dr. RAMACHANDRAN (14) qui a étudié séparément les trois systèmes :

- silicate tricalcique-carbonate de calcium-eau
- aluminate tricalcique-gypse-carbonate de calcium -eau
- ciment portland-carbonate de calcium-eau.

Le Dr. RAMACHANDRAN exposera son important travail dans un instant, mais je retiendrai dès maintenant que ses résultats permettent de réfuter le classement des fillers calcaires dans la catégorie des additions inertes. En mettant en évidence leur participation aux réactions chimiques d'hydratation des aluminate et silicate tricalciques, le Dr. RAMACHANDRAN fait des fillers calcaires des constituants actifs des ciments, qui en accélèrent le durcissement.

- Le travail du Dr. RAMACHANDRAN trouve un complément particulièrement constructif dans la communication de C. VERNET consacrée à la cinétique de l'hydratation de l'aluminate tricalcique en présence de gypse, chaux et filler calcaire. C. VERNET applique sa méthode de suivi des concentrations ioniques et de mesure des flux thermiques pour comparer les séquences de l'hydratation sans $CaCO_3$ et avec diverses proportions $CaCO_3$/gypse. Il montre ainsi comment se succèdent les phases ettringite carbo-aluminate. Ses observations au MEB et ses mesures par DRX lui permettent de situer la formation du carboaluminate au voisinage des grains de C_3A et de différencier la réactivité des fillers en fonction de la consommation des ions carbonates pour donner du carboaluminate (15).

La conséquence pratique que l'on peut déduire de telles études est essentiellement le rôle de régulateur de prise joué par la calcite. En optimisant le gypsage en présence de filler calcaire, le cimentier dispose d'un moyen subtil pour moduler la vitesse de dégagement de chaleur et la progression des résistances.

3.3. DURABILITE

La durabilité d'un matériau est son aptitude à résister pendant longtemps à des agressions d'ordre mécanique et chimique. C'est certainement la qualité faisant l'objet à la fois des plus grandes exigences et des spécifications les moins significatives. La raison en est simple: elle fait avant tout intervenir le temps et cette donnée n'est pas rigoureusement remplaçable par des essais accélérés.

Quels sont les paramètres qui interviennent dans la capacité d'un béton de ciment à résister à la corrosion ? J'aurais tendance à répondre qu'il n'y en a qu'un seul : la compacité; malheureusement il n'y a pas de béton réellement compact et si l'on veut le protéger efficacement il faut lui donner, avant l'application des forces de destruction, une résistance mécanique élevée et une composition chimique adaptée.

Si l'on voulait approfondir la connaissance des phénomènes de dégradation il faudrait examiner en détails deux groupes de paramètres, ceux qui caractérisent le béton et ceux qui définissent l'agent agressif:

béton		agent agressif	
	composition		nature ou composition
	âge		intensité ou concentration
	taux d'hydratation		instant d'application
	compacité		

Je ne pourrai bien entendu m'arrêter au cours de mon exposé qu'aux observations essentielles permettant de situer le comportement des additions minérales dans ce vaste contexte.

Au double point de vue de la composition du béton et de la nature de l'agent agressif il suffit de rappeler que les clinkers à la fois les moins saturés en chaux et les plus pauvres en aluminate sont les plus résistants chimiquement et les moins résistants mécaniquement. Dans chaque pays il existe des normes et des règlements pour cette catégorie de ciments à base de clinker spéciaux.

Ce qui nous intéresse plus ici c'est l'usage en cimenterie des laitiers, pouzzolanes et fillers en regard de la durabilité. Deux groupes de ciments devraient être examinés séparément :

- les ciments spéciaux à fortes proportions d'additions, tels que les ciments pouzzolaniques,

pouzzolano-métallurtiques, ce haut-fourneau et à très fortes teneurs en laitier.

- les ciments portland composés, à teneurs limitées en additions, dont les CPJ fabriqués en France constituent un des groupes les plus importants.

Les additions à activité pouzzolanique et les laitiers offrent l'intérêt de réaliser des bétons moins basiques que les portlands, donc de s'opposer à la corrosion d'origine chimique. Nous ne pouvons nous étendre sur cet aspect du problème qui est traité dans d'autres thèmes du Congrès.

La compacité étant l'impératif essentiel, je trouve opportun de réfléchir sur les défauts de compacité, à savoir la porosité et la microfisssuration.

3.3.1. Porosité initiale et évolution

La porosité initiale dépend de la granularité des constituants, du dosage en eau du béton et de l'air entraîné. Le ciment complète la courbe granulaire en tant que filler, ce qui nécessite un dosage optimal. Les micropores aqueux sont d'autant plus nombreux que la courbe est discontinue dans le domaine des fins et ultrafins et que la demande en eau est élevée. Les fines particules d'additions minérales permettent d'étendre et de compléter cette courbe, d'où une diminution du volume des pores à colmater par les hydrates, ce qui donne un avantage aux ciments composés.

L'évolution de la porosité en l'absence d'agression dépend de la rapidité de formation des hydrates et de la quantité de ces hydrates. Dans ce cas GUYOT et al ont fait des mesures comparatives de porosité avec des ciments portland et des ciments fillérisés au calcaire, de même classe de résistance à 28 jours. Ils ont accompagné ces mesures d'un suivi de l'eau liée au cours de l'hydratation et de la dimension des pores de la pâte.

La conclusion de l'étude remarquable de GUYOT est que les deux types de ciment, malgré leur différence de teneur en clinker, mais grâce à leur différence de finesse produisent les mêmes quantités d'hydrates pour aboutir à la même résistance et à la même compacité (11).

En ce qui concerne les autres additions minérales, on retiendra que les laitiers ont les taux de réaction les plus élevés ; l'hydratation précoce des laitiers contribue donc à donner un matériau compact au jeune âge. En revanche, dans le cas des cendres volantes et des pouzzolanes naturelles, la porosité diminue moins vite, mais de façon continue pour arriver tardivement à la même valeur à résistance égale.

Ce processus se déroule régulièrement tant que le béton est maintenu en milieu humide et en l'absence d'agressions.

Comme les micropores et les microfissures, l'auréole de transition faisant l'objet du rapport du Pr. OLLIVIER constitue une zone de fragilité où s'accumulent des contraintes mécaniques qui s'ajoutent aux sollicitations d'ordre chimique. Les additions consommatrices de chaux -laitiers et pouzzolanes- contribuent à diminuer cette fragilité en agissant favorablement sur l'orientation de la portlandite et en emplissant progressivement les pores.

3.3.2. Microfissuration

La microfissuration résulte des tensions créées au cours du premier et du second retraits, c'est-à-dire avant et pendant la prise.

Les microfissures qui apparaissent les premières sont liées au ressuage ; les suivantes sont dépendantes de la contraction chimique ou LE CHATELIÉR, et au phénomène d'échauffement suivi de refroidissement.

Comment interviennent les additions minérales dans ce processus ?

Il est connu que le laitier à cause de sa structure a une tendance à augmenter le ressuage donc les risques de microfissuration avant prise, alors que les pouzzolanes et les fillers calcaires ont un effet plutôt bénéfique.

Les additions minérales les moins réactives pendant la période de prise sont les matières pouzzolaniques ; ce sont celles qui sont conseillées pour les ouvrages où les phénomènes d'origine thermique sont les plus gênants.

Les ciments composés au filler calcaire ont un comportement intermédaire entre ceux aux pouzzolanes et ceux au laitiers.

Dans tous les cas, les risques de microfissuration sont plus faibles qu'avec les portlands ordinaires, étant données les différences de flux thermique pour des ciments de même classe de résistance.

3.3.3. Résistances à la corrosion

Quelle que soit l'origine des forces de destruction - lixiviation - développement de cristaux expansifs d'origine chimique - gel, dégel de la solution interstitielle - on assiste toujours à une compétition entre l'action de destruction et une action réparatrice se manifestant par la cicatrisation des microfissures tant que le milieu humide permet la croissance des hydrates.

Les ciments fillérisés au calcaire ne font pas exception et se comportent aussi bien que leurs homologues au laitier ou aux pouzzolanes.

J. BARON rend compte à ce sujet d'essais comparatifs de durabilité à l'eau de mer entre des CPJ à 10 et 20 % de calcaire et des CPA, tous les ciments étant faits avec du clinker de composition chimique résistant à la mer. Pour la même classe de résistance, il n'observe pas de différence de comportement (16).

Les cimentiers européens se sont particulièrement penchés sur les épreuves de résistance au gel-dégel des ciments au filler calcaire. Après avoir confronté avec beaucoup de difficultés les résultats d'essais effectués dans des conditions pas toujours comparables, ils sont arrivés à la conclusion que les ciments commercialisés avec addition de calcaire avaient une tenue au gel-dégel satisfaisante. De très nombreux clichés au M.E.B. ont d'ailleurs bien

illustré le comportement de ces ciments.

Dans sa communication intitulée "Evolution de la microstructure des bétons au cours du test ASTM de gel-dégel", C. VERNET rend compte de ses observations résultant d'un plan d'expérience basé sur l'examen au M.E.B. de 25 bétons de ciments Portland et de ciments fillérisés. Il met particulièrement bien en évidence les processus destructeurs et réparateurs et montre le bon comportement des ciments aux fillers calcaires, alors que les cendres volantes sont génératrices de dégradations (17).

Nous avons vu que les calcaires étaient sélectionnés pour garantir une bonne compacité initiale des bétons et que la formation relativement rapide de carboaluminate venait s'ajouter au CSH et à la portlandite pour renforcer les liaisons entre les grains ; il est donc logique que les bétons correspondant aient une bonne durabilité. En revanche, C. VERNET a montré que les cendres volantes ne développent leurs liaisons que très tardivement et qu'elles introduisent une porosité de dimension élevée, d'où leur comportement médiocre.

Le rôle des bulles d'air dans le mécanisme de dégradation au gel-dégel a d'abord été étudié par T.C. POWERS qui a émis la notion de "facteur d'espace critique" ; puis Monsieur PIGEON a montré que ce facteur critique d'espacement des bulles d'air varie en fonction de la vitesse de refroidissement.

M. REGOURD et al ont étudié les conséquences favorables de l'addition d'un entraîneur d'air qui ramène l'espacement moyen des bulles d'air à moins de 100 microns pour tous les ciments, c'est-à-dire, largement au-dessous de la valeur critique. Ceci veut dire que le choix du ciment pour la tenue des bétons au gel-dégel ne constitue pas un réel problème, et que l'emploi d'un entraîneur d'air résoud à coup sûr les cas litigieux (18).

3.3.4. Protection des armatures

Je ne voudrais pas omettre d'évoquer, au titre de la durabilité, le problème de la protection des armatures.

Il est bien connu que la pâte de ciment protège les armatures de la corrosion électrochimique grâce à sa forte basicité. En présence de l'excès de chaux libérée par l'hydratation du clinker, le pH de la solution interstitielle est d'environ 12,5 , cette valeur est vérifiée pour tous les ciments, sauf pour ceux qui sont très riches en laitier. Si le pH descend au-dessous de 10, la protection n'est plus assurée ; cette situaation peut résulter d'une pénétration du CO_2 atmosphérique par les pores ouverts et les microfissures.

Les risques de carbonatation sont donc essentiellement dépendants de la compacité du béton ; ceci nous ramène donc aux résultats de C. GUYOT, à savoir qu'à résistance égale, au même âge, la compacité est pratiquement la même pour les ciments fillérisés que pour les ciments purs. J. BARON en a vérifié les conséquences favorables en mesurant les profondeurs de pénétration de la carbonatation sur des mortiers standards après un an de conservation : que ce soit en Portland pur ou avec 15 et 30 % de filler calcaire, les résultats étaient les mêmes, et bien meilleures qu'avec le laitier (16).

4. CONCLUSION

Les pouzzolanes et les laitiers de haut-fourneau sont bien connus pour les propriétés qu'ils confèrent à certaines catégories de ciments à haute résistance chimique. Leur utilisation en proportions modérées comme additif au clinker permet en outre de moduler facilement la palette des ciments par classe de résistances mécaniques.

Les fillers calcaires peuvent, sans inconvénients, être utilisés pour ce même usage visant à économiser le clinker.

La participation de ces diverses additions minérales au processus de durcissement n'est évidemment pas la même, mais chacune d'entre elles fait preuve d'une activité chimique que le cimentier est à même de contrôler pour produire des ciments de qualité régulière.

Les aspects scientifiques des différents processus intervenant dans la confection et la mise en place des bétons, puis dans leur durcissement et leur aptitude à résister aux divers types de corrosion, ont été abordés dans le but d'être discutés par les spécialistes réunis dans notre séminaire.

5. BIBLIOGRAPHIE

1. G. WISCHERS - VDZ : Optimisation of cements with mineral admixtures (ce congrès).

2. M. VON EUW - Société des Ciments Français: L'utilisation des Cendres Volantes en cimenterie. VII Congrès ERMCO - LONDRES, mai 1983.

3. JP. BOMBLED - CERILH - Rhéologie du béton frais. Influence de l'ajout de fillers aux ciments (ce congrès).

4. C. VERNET. Société des Ciments Français : Etude de la cinétique des réactions d'hydratation des ciments artificiels. Thèse CNAM, chap. 2.2, Octovre 1982.

5. M. REGOURD, JH THOMASSIN, P. BAILLIF and JC. TOURAY : Blast Furnace Slag Hydration Surface Analysis. Cement Concrete Research, 13, 549-556 (1983).

6. F. HAWTHORN, E. DEMOULIAN, P. GOURDIN, C. VERNET. Société des Ciments Français : Laitiers et Clinkers - Influences réciproques. Paris 1980, thème III-145.

7. K. TAKEMOTO - ONODA Cement. Japon : Variation of Activity Index of Slag(ce congrès).

8. S.N. GHOSH. Nat. Council for Cement and Building Materials. Indian : Chemical Composition vis-à-vis Optimal Addition of Minerals to Cement (ce congrès).

9. J. ALMEBORG and JT. CHRISTENSEN - Aalborg Portland Denmark : Danish Portland. Fly Ash Cement (ce congrès).

10. JP. BOMBLED, G. BELLINA et B. MORTUREUX -

CERILH - : Détermination des courbes granulométriques et des aires massiques des constituants de mélanges cobroyés - applications aux fillers et aux laitiers. (ce congrès).

11. R. GUYOT, R. RANC, B. CARIOU - Lafarge Coppée : Utilisation de la potentialité hydraulique du clinker dans les ciments portland avec ajout de filler calcaire (ce congrès).

12. JP. OLLIVIER - I.N.S.A. - UPS - Toulouse, France : Rôle des additions minérales sur la formation de l'auréole de transition entre gros granulats et mortier (ce congrès).

13. M. REGOURD, B. MORTUREUX, H. HORNAIN - CERILH. Liaison pâte de ciment filler dans les ciments composés. Colloque International Toulouse. France nov. 1982. A. 64-A-72.

14. V.S. RAMACHANDRAN and ZHANG CHUN-MEI - Nat. Research Council Canada : Cement with calcium carbonate additions (ce congrès).

15. C. VERNET. Société des Ciments Français : Séquence et cinétique des réactions d'hydratation de l'aluminate tricalcique en présence de gypse, de chaux et de fillers calcaires. (ce congrès).

16. J. BARON - Lafarge Coppée Recherche - France : The Durability of Limestone Composite Cements in the Context of the French Specifications. Communication to International Seminar on some Aspects of Admixtures and Industrial by-products on the Durability of Concrete (avril 1986 Chalmers University of Technology Sweden).

17. C. VERNET. Société des Ciments Français : Evolution de la Microstructure des Bétons au cours du Test ASTM de gél-dégel (ce congrès).

18. P. GEGOUT, H. HORNAIN, B. THURET, M. REGOURD-CERILH- Résistance au gel des ciments aux fillers calcaires.

V.S. Ramachandran, Division of Building Research, National Research Council Canada;
Zhang Chun-mei, Nanjing Institute of Technology, Nanjing, The People's Republic of China

CEMENT WITH CALCIUM GARBONATE ADDITIONS

INTRODUCTION

Limestone is used for various purposes in concrete technology, viz, as raw material for clinker production, partial replacement of gypsum, and as coarse or fine aggregate. Limestone dust produced in quarrying operations poses disposal and environmental problems and has been suggested for use as an additive to portland cement. Some standards do allow the use of calcium carbonate as an additive in cement provided the properties of concrete made with such a cement are not adversely affected. Work carried out on its effect on hydrating cement shows that the physical and mechanical characteristics are influenced to different extents.

Some work has been carried out on the effect of $CaCO_3$ on cement paste, but there is no general agreement on the relative effects of different amounts of it on the cement paste properties (1-9). This may be mainly due to differences in the characteristics of the materials and the methods used. The objective of the present work is to assess the effect of various amounts of $CaCO_3$ on the hydration of C_3S and C_3A in order to explain the physico-chemical changes occurring during hydration of portland cement.

EXPERIMENTAL

Type 1 portland cement containing C_3A 12.8%, C_4AF 6.6%, C_3S 51.5%, C_2S 19.8%, and $CaSO_4$ 5.1% was used. C_3A and C_3S were supplied by the Tetratech Co. and Portland Cement Association, respectively. The C_3S had a Blaine surface area of 3600 cm^2/g. Gypsum and calcium carbonate (N_2 surface area 6.5 m^2/g), both of reagent quality, were supplied by Fisher Scientific Co. and Anachemia Chemical Co., respectively.

Conduction calorimetry, differential scanning calorimetry (DSC), thermogravimetry (TGA), differential thermal analysis (DTA), X-ray diffraction (XRD), scanning electron microscopy (SEM), and high-pressure Hg porosimetry were used in this work and have been described elsewhere (10-13).

Cement pastes containing various amounts of $CaCO_3$ were subjected to compressive strength measurements using 2-cm cubes. The setting times were determined according to ASTM C191-82. Samples were prepared as follows:

1. C_3S was mixed with 0, 5, 10, 15 and 50% $CaCO_3$ (with respect to the total weight of C_3S + $CaCO_3$) at a water/solid ratio of 0.4 or 0.7. The pastes were hydrated in capped polyethylene vials for specified intervals of time, then subjected to drying under vacuum for one day before being examined.
2. C_3A and 0, 12.5 and 25% gypsum/$CaCO_3$ or 12.5% gypsum + 12.5% $CaCO_3$ or 25% gypsum + 12.5% $CaCO_3$ (based on the weight of C_3A) were mixed with water at a water/C_3A ratio of 4. All were hydrated in closed containers for specified intervals of time; cold methanol was used to terminate hydration. The pastes formed from C_3A + gypsum or C_3A + gypsum + $CaCO_3$ were dried at room temperature under vacuum and others at 50°C under vacuum.
3. Samples of cement containing 0, 5, 10, 15 and 50% $CaCO_3$ with respect to the total weight of cement + $CaCO_3$ were mixed with water at a water/solid ratio of 0.4 or 1.0. Those for TGA were prepared from cubes tested for compressive strength; some of the broken pieces were ground and dried for one day under vacuum.

RESULTS AND DISCUSSION

Hydration characteristics of C_3S

Tricalcium silicate was hydrated in the presence of 0, 5, 10, 15 and 50% $CaCO_3$ at a water/solid ratio of 0.4 or 0.7. The resulting products were examined by TGA, DTA, SEM and conduction calorimetry. Strength and shrinkage data were also obtained. The $Ca(OH)_2$ formed at different times is shown in Figure 1. The results are calculated on the basis of C_3S to avoid dilution effect. The amount of lime formed at 0% $CaCO_3$ increases from 8.9% at 1 day to 23.2% at 28 days. Addition of $CaCO_3$ increases the amount of $Ca(OH)_2$ at all times of hydration, indicating that $CaCO_3$ increases the rate of hydration of C_3S. At 28 days addition of 0, 5 and 15% $CaCO_3$ yields 23.2, 24.0 and 25.5% $Ca(OH)_2$, respectively. The results also indicate that 15% $CaCO_3$ shows a greater accelerating effect than 5% $CaCO_3$.

The conduction calorimetric curves showing the rate of heat development of C_3S during hydration up to 24 h are given in Fig. 2. The onset of the accelerating period representing the hydration of C_3S does not seem to be affected, but the intensity of the peak increases as the amount of added $CaCO_3$ is increased. The total heat developed at 24 h decreases in the following manner: C_3S - 15% $CaCO_3$ > C_3S - 10% $CaCO_3$ > C_3S - 5% $CaCO_3$ > C_3S - 0% $CaCO_3$. The conduction calorimetric curves also show the accelerating effect of $CaCO_3$.

Results were also obtained for the non-evaporable water and C_3S contents for C_3S pastes hydrated to different times. At any time of hydration the non-evaporable water content was higher and the unhydrated C_3S lower in pastes containing $CaCO_3$, confirming that hydration rate is increased in the presence of $CaCO_3$.

Thermogravimetric analysis of the C_3S + $CaCO_3$ + H_2O system revealed that as hydration proceeded the peak due to $CaCO_3$ decomposition at about 750°C diminished. This indicated that some $CaCO_3$ was consumed during the reaction. Figure 3 shows the amount of free $CaCO_3$ remaining at different times of hydration. In the C_3S - $CaCO_3$ mixture containing 15% and 5% $CaCO_3$ the amount of $CaCO_3$ that was combined or incorporated into the hydrating C_3S was 2.4 and 1.3 percentage points, respectively.

The SEM photograph of C_3S paste hydrated for 1 day in the presence of 50% $CaCO_3$ is shown in Fig. 4. Fibrous particles of C-S-H grow on both the C_3S (marked by C) and $CaCO_3$ (marked by L) particles. It is possible that $CaCO_3$ acts as a nucleating agent. Another possibility is that C-S-H containing $CaCO_3$ forms on the C_3S particles having higher

permeability than that occurring with 0% $CaCO_3$; this would result in an increase in the rate of reaction.

Other effects of $CaCO_3$ on C_3S pastes included increase in modulus of elasticity, microhardness, C/S ratio of the C-S-H phase, rate of shrinkage, and development of smaller diameter pores up to 7 days of hydration.

Hydration of C_3A

The hydration of C_3A alone and of that containing 12.5 or 25% $CaCO_3$, 12.5 or 25% gypsum, and a mixture of $CaCO_3$ and gypsum hydrated to different times was followed by DSC. The C_3A samples formed hexagonal aluminate hydrates at earlier times, identified by endothermal peaks at about 150 and 250°C. Both peaks increased in intensity up to 4 h, then decreased until at 1 day there was only an intense peak at 314°C, indicating formation of cubic C_3AH_6. It is difficult to conclude from DSC just when the formation of C_3AH_6 was initiated; thermograms indicate, however, that almost all of the hexagonal phase was converted to the cubic phase within 7 h. SEM examination revealed the formation of cubic aluminate at 4 h and X-ray indicated C_3AH_6 even after 1 h of hydration.

By adding $CaCO_3$ to C_3A the endothermal peak at 160-165°C and another at 235-250°C developed even at 5 min. They increased in intensity with time and are ascribed to the carboaluminate hydrate, mixed perhaps with hexagonal aluminate hydrates. The formation of the cubic phase was suppressed for up to 2 days.

Unhydrated C_3A + $C\bar{S}H_2$ mixtures containing 25% $C\bar{S}H_2$ indicated an endothermic effect at 135°C (due to $C\bar{S}H_2$). This peak decreased with hydration. One representing the formation of ettringite was observed at about 100°C after as little as 5 min. Most gypsum was consumed in the first hour. At 2 h the formation of monosulfoaluminate was evidenced by an endothermal peak at 165°C.

By the addition of 12.5% $CaCO_3$ to the C_3A + 25% $C\bar{S}H_2$ mixture the rate of consumption of $C\bar{S}H_2$ increased. Practically no $C\bar{S}H_2$ remained even at 30 min. Consequently, the rate of ettringite formation is increased, as is also the rate of conversion of ettringite to monosulfoaluminate.

Conduction calorimetric curves of C_3A + 12.5% $C\bar{S}H_2$ and C_3A + 12.5% $C\bar{S}H_2$ + 12.5% $CaCO_3$ are shown in Fig. 5. The C_3A + 12.5% $C\bar{S}H_2$ mixture developed heat as soon as it came into contact with water. A peak at about 3 min represents the maximum rate of formation of ettringite. In the presence of $CaCO_3$ the earlier peak becomes more intense and occurs at about 5 min. Simultaneous formation of carboaluminate and ettringite results in a more intense peak than that for ettringite alone formed by the C_3A + 12.5% $C\bar{S}H_2$ mixture. DSC curves show that at 5 min both ettringite and carboaluminate (peak at about 160-170°C) are formed. There was also indication that more ettringite was formed in the C_3A + 12.5% $C\bar{S}H_2$ + 12.5% $CaCO_3$ mixture than in the C_3A + 12.5% $C\bar{S}H_2$ mixture. After 20 min there was an additional peak at about 180°C, indicating the presence of monosulfoaluminate. Comparison of thermograms for different times showed that formation of ettringite and its conversion to monosulfoaluminate is accelerated in the presence of $CaCO_3$. Such results suggest that $CaCO_3$ existing as a complex layer on the surface of hydrating C_3A is more permeable than that formed by gypsum and accelerates formation of ettringite and monosulfoaluminate.

Hydration of cement

Figure 6 compares the amounts of $Ca(OH)_2$ formed at different times in cement pastes hydrated with 0, 5, 10 and 15% $CaCO_3$. Results are reported on the basis of cement content to avoid dilution effect by $CaCO_3$. At all periods from 3 h to 28 days there is evidence that $CaCO_3$ promotes formation of $Ca(OH)_2$. The amount of CH formed is increased in cements containing larger amounts of $CaCO_3$. This is particularly significant at earlier times. Calcium hydroxide is derived from the hydration of C_3S and C_2S, and the results indicate that C_3S and C_2S phases in cement may be accelerated by $CaCO_3$. Hydration of pure C_3S is accelerated by $CaCO_3$, as shown in Fig. 1.

The rate of heat development in cement containing 0, 5, 10, 15 and 50% $CaCO_3$ is shown in Fig. 7. Although the time for the onset of heat evolution is not changed significantly in the samples containing different amounts of $CaCO_3$, heat evolution is accelerated. At 50% $CaCO_3$ the amplitude of the peak occurs 3½ h earlier than in that hydrated without $CaCO_3$. Figure 8 shows the total heat developed in these pastes for up to 24 h. The curves demonstrate that at all dosages of $CaCO_3$ more heat is developed, signifying the accelerating effect of $CaCO_3$. In pure C_3S pastes there is a similar accelerating effect (Fig. 2). The total heat developed in cement containing 15% $CaCO_3$ is 8 and 28 cal/g at 4 and 8 h, respectively; the corresponding values for C_3S containing 15% $CaCO_3$ are 6 and 22 cal/g. If this heat is derived mainly from the C_3S portion of cement (52% C_3S), the heat evolution in cement should be far lower than the values determined. The higher values signify that either the accelerating influence of $CaCO_3$ on C_3S is more significant in cement or that part of the heat should be attributed to the hydration of the C_3A or C_4AF phases.

It has been shown that in the C_3S-$CaCO_3$-H_2O system some $CaCO_3$ is incorporated into the C-S-H phase (Fig. 3). In portland cement C_3A reacts with $CaCO_3$ to form carboaluminate, and some $CaCO_3$ is incorporated also into the hydrated C_3S phase. Figure 3 compares the relative amounts of free, unreacted $CaCO_3$ with hydrating portland cement or C_3S initially containing 5 or 15% $CaCO_3$. Generally, more $CaCO_3$ seems to be incorporated into cement paste than into C_3S paste. This can be explained by consumption of some $CaCO_3$ by the C_3A phase in cement. It would be expected that part of C_3A reacts with the $C\bar{S}H_2$ and part with the $CaCO_3$.

Because of the accelerating influence of $CaCO_3$ on the hydration sequence of C_3A and C_3S it would be expected that $CaCO_3$ would influence the setting property of cement. Figure 9 gives the initial and final setting times of cement prepared at a w/s = 0.4, or at the same consistency. Setting time decreases as the amount of added $CaCO_3$ is increased. The acceleration of setting time at 15% $CaCO_3$ varies

between 0.8 and 1.5 h. Setting times, even at 15% $CaCO_3$, exceed the minimum limit requirements of the Canadian standard (14). Comparison of setting time with calorimetric and TGA results (Figs. 5, 6 and 7) suggests that at time of setting C_3A and C_3S have hydrated to different extents. The accelerated setting can therefore be explained by the acceleration of hydration of C_3A to form sulfoaluminate and of C_3S to form C-S-H and CH in cement.

The rates of strength development in cement pastes containing 0, 5, 10 and 15% $CaCO_3$ are given in Fig. 10. Up to 1 day the strength seems to be higher in pastes containing $CaCO_3$. Later strengths at 7 and 28 d indicate lower strengths in paste containing 10-15% $CaCO_3$. At 28 days they are as follows: cement - 5% $CaCO_3$ > cement - 0% $CaCO_3$ > cement - 10% $CaCO_3$ > cement - 15% $CaCO_3$. The decrease in strength at dosages of 10-15% $CaCO_3$ at 28 days may be due partly to lower degree of hydration (based on the weight of cement paste containing $CaCO_3$); the amount of CH in cement pastes with 0, 5, 10 and 15% $CaCO_3$ is, respectively, 12.9, 12.6, 11.9 and 11.5 at 28 days. The porosity values show that total porosity of paste with 15% $CaCO_3$ is higher than that containing 0% $CaCO_3$ at 28 days, the values being 30.9 and 25.5%, respectively (Fig. 11). Higher porosity in pastes containing 15% $CaCO_3$ may be responsible for the decrease. A part of $CaCO_3$ that remains unreacted may act as a diluent. That not all added $CaCO_3$ acts as a diluent is evident from the results for mortars. If strengths of mortars containing cement + quartz and cement + $CaCO_3$ are compared, higher strengths are obtained with $CaCO_3$, indicating that it participates in forming bonds in the paste (3). Microstructural studies indicate this possibility (Fig. 4). At 90 days cements with 0, 5 and 10% $CaCO_3$ have about the same strength. Further long-term strength development studies in pastes containing 15% $CaCO_3$ will have to be carried out to examine whether, at this dosage, strength will eventually reach the same value as that for the paste containing 0% $CaCO_3$.

CONCLUSIONS

Hydration of $C_3A + C\bar{S}H_2$ in the presence of $CaCO_3$ results in accelerated formation of ettringite and its conversion to monosulfoaluminate hydrate. This is probably due to the formation of highly permeable carboaluminate on the hydrating surface of C_3A.

Calcium carbonate accelerates the hydration of C_3S and is partially incorporated into the C-S-H phase. The modified surface of the hydrating C_3S and nucleation on the $CaCO_3$ particles are two mechanisms that could produce this effect.

Hydration of cement is also accelerated by $CaCO_3$. In the paste, $CaCO_3$ is incorporated into the hydrating C_3A and C_3S phases. Setting times are reduced owing to accelerated formation of ettringite and C-S-H. Earlier strengths of cement pastes are increased by the addition of $CaCO_3$, but at 28 days strengths decrease in the presence of 10 and 15% $CaCO_3$. At 90 days the strength for 15% $CaCO_3$ is lower than that of the other mixes. There is evidence that all added $CaCO_3$ does not act as an inert additive in terms of chemical reaction and strength development.

ACKNOWLEDGEMENTS

The authors are very grateful to J. Clark and G.M. Polomark for experimental assistance. The paper is a contribution from the Division of Building Research, National Research Council of Canada.

REFERENCES

1. Soroka, I., Stern, N.: "Calcareous fillers and the compressive strength of portland cement", Cem. Concr. Res., 6, No. 3, 367-376 (1976).

2. Soroka, I., Setter, N.: "The effect of fillers on strength of cement mortars", Cem. Concr. Res., 7, No. 4, 449-456 (1977).

3. Mortureux, B., Hornain, H., Regourd, M.: "Cement paste-fillers bond in blended cements", presented at Conference of CERILH, 1-9 (1982).

4. Bensted, J.: "Some hydration investigations involving portland cement - effect of calcium carbonate substitution of gypsum", World Cement Technology, 11, No. 8, 395-406 (1980).

5. Bensted, J.: "Further hydration investigations involving portland cement and the substitution of limestone for gypsum", World Cement Technology, 14, No. 10, 383-392 (1983).

6. Timashev, V.V., Kolbasov, V.M.: "Properties of cements with carbonate additives", (Rus.). C.R., URSS, No. 10, 10-12 (1981).

7. Lyubimova, T. Yu., Nismevich, M.L., Levkova, N.S., Mikhailov, N.V.: "Structure formation kinetics during hardening of cements in the presence of carbonate fillers", Kolloidnyi Zhurnal, 34, No. 6, 868-877 (1972).

8. Spohn, E., Lieber, W.: "Reactions between calcium carbonate and portland cement, Contributions to the systems C_3A-$CaCO_3$-H_2O and C_4AF-$CaCO_3$-H_2O", Zement-Kalk-Gips, 18, No. 9, 483-485 (1965).

9. Tong, S.D., Fang, D.R.: "Blended cement using zeolite and limestone as fine fillers", Silicates Industriels, 48, No. 6, 127-132 (1983).

10. Ramachandran, V.S., Polomark, G.M.: "Extraction of $Ca(OH)_2$ from portland cement and $3CaO.SiO_2$ pastes", J. Chem. Tech. Biotechnol., 32, No. 10, 946-952 (1982).

11. Traetteberg, A., Ramachandran, V.S., Grattan-Bellew, P.E.: "A study of the microstructure and hydration characteristics of tricalcium silicate in the presence of calcium chloride", Cem. Concr. Res., 4, No. 2, 203-221 (1974).

V.S. Ramachandran, Division of Building Research, National Research Council Canada;
Zhang Chun-mei, Nanjing Institute of Technology, Nanjing, The People's Republic of China

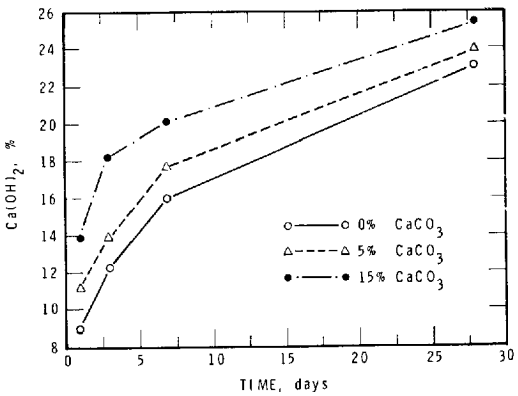

Figure 1. Formation of $Ca(OH)_2$ in C_3S pastes containing different amounts of $CaCO_3$ (C_3S basis)

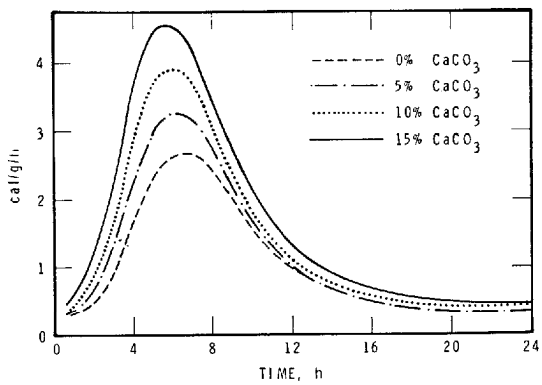

Figure 2. Conduction calorimetric curves of C_3S hydrated with different amounts of $CaCO_3$ (C_3S basis)

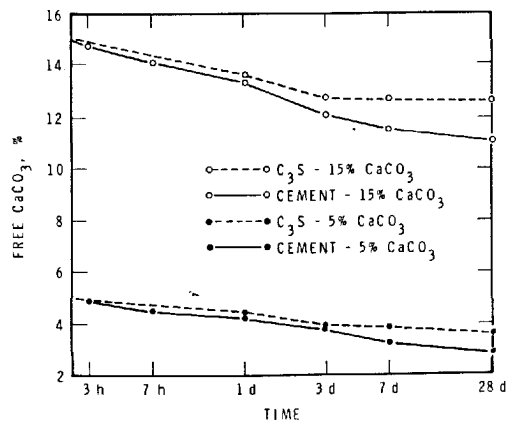

Figure 3. Free $CaCO_3$ remaining in the C_3S and cement pastes at different times of hydration (based on C_3S + $CaCO_3$ or cement + $CaCO_3$)

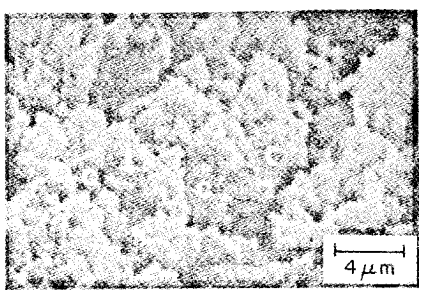

Figure 4. Micrograph of C_3S paste containing 50% $CaCO_3$ hydrated for 1 day (w/s = 0.7) C: growth on C_3S; L: growth on $CaCO_3$

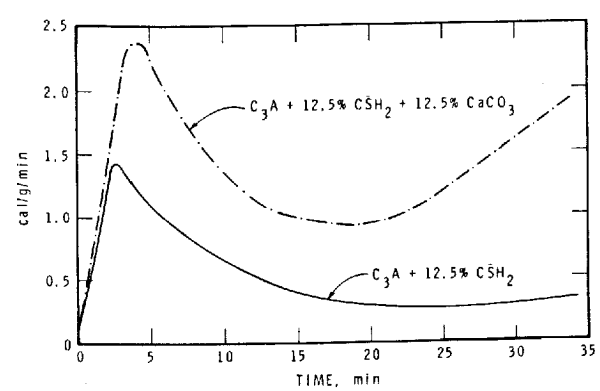

Figure 5. Conduction calorimetric curves of C_3A hydrated with $C\bar{S}H_2$ and $CaCO_3$

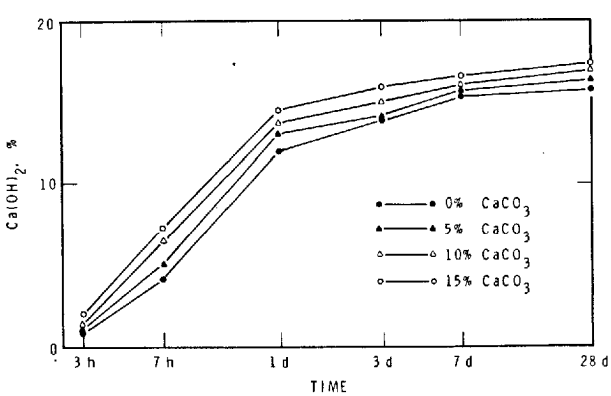

Figure 6. Formation of $Ca(OH)_2$ in cement pastes containing different amounts of $CaCO_3$ (cement basis)

12. Ramachandran, V.S., Beaudoin, J.J.: "Significance of water:solid ratio and temperature on the physico-mechanical characteristics of hydrating $4CaO.Al_2O_3.Fe_2O_3$", J. Mater. Scie., 11, 1893-1910 (1976).

13. Ramachandran, V.S.: "Estimation of tricalcium silicate through polymorphic transformation", J. Thermal Analysis, 3, 181-190 (1971).

14. Canadian Standards Associates: "Portland Cements", CAN3-AS-M83 (1983).

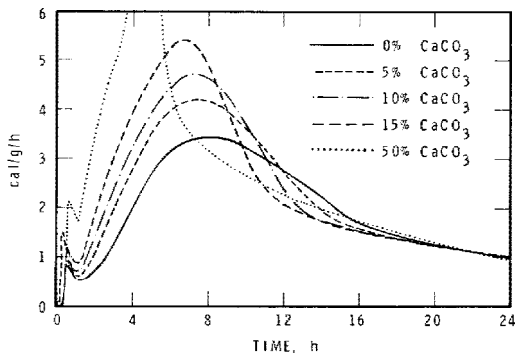

Figure 7. Conduction calorimetric curves of cement hydrated with different amounts of $CaCO_3$ (cement basis)

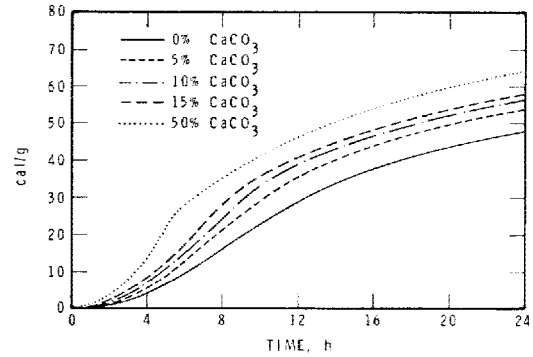

Figure 8. Heat developed in the hydration of cement containing different amounts of $CaCO_3$ (cement basis)

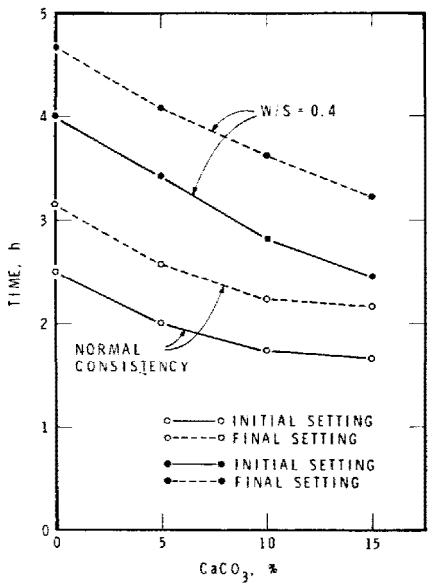

Figure 9. Setting times of cement pastes with different amounts of $CaCO_3$

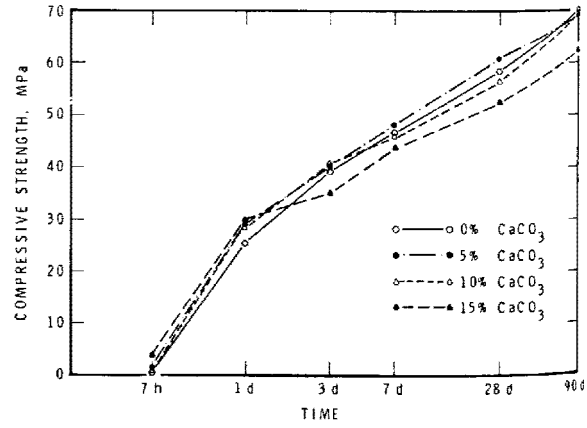

Figure 10. Compressive strength of cement pastes containing different amounts of $CaCO_3$

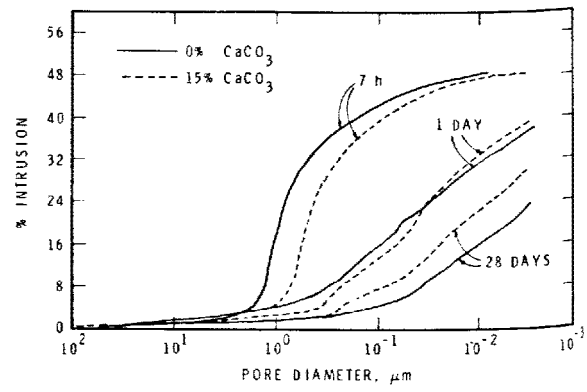

Figure 11. Pore size distribution curves of cement pastes containing 0 and 15% $CaCO_3$

J. Almeborg and J. T. Christensen, Aalborg Portland, Denmark

Danish Portland-Fly Ash Cement

Introduction

Before the oil crisis in 1973/74, only 25% of the electric power used in Denmark came from coal fired power plants and the production of fly ash was less than 0.3 million tonnes per year.

By 1980 the use of coal had increased to 75% of the total fuel consumption and the fly ash production had reached 1.0 million tonnes per year.

Part of this fly ash is used by Aalborg Portland - the only cement manufacturer in Denmark - in three different ways:

- As a substitute for clay in the raw mix. The fly ash is insufflated into the burning zone of the cement kilns at a rate of up to 12% of clinker output.
- For manufacture of rapid hardening portland cement containing up to 5% of fly ash.
- For manufacture of portland-fly ash cement containing about 24% of fly ash.

Production of portland-fly ash cement

The portland-fly ash cement was designed to fulfil the requirements of the Danish cement standard, DS 427, and the future European standard for cement, EN 197. Furthermore, it was decided that the new cement should have a compressive strength at any age not lower than for Danish ordinary portland cement. Laboratory investigations and grinding tests in the plant revealed that these requirements would be met by a cement containing about 24% fly ash and having a specific surface of 450 m^2/kg.

Production of portland-fly ash cement takes place on mill installations as shown in Figure 1.

The 24% of fly ash for portland-fly ash cement is extracted directly from the storage silo to weight feeders. The feed control to the cement mills is based on the loss in weight principle. The shape of the feed bin and its mechanical stirrers were important design features for maintaining steady flow of fly ash to the cement mill.

As a further control fly ash, material from the primary grinder, and material from the secondary grinder are analyzed by XRF every 4 hours and the amount of fly ash in the portland-fly ash cement is calculated.

The fly ash used comes from different power plants and from coal of different origin but the fly ash always complies with the requirements set out in Table 8.

The portland-fly ash cement produced has average properties as shown in Table 1.

As illustrated by Table 2 it was possible to discontinue production af ordinary portland cement shortly after the introduction of the portland-fly ash cement. This does, however, not mean that ordinary portland cement has simply been substituted by portland-fly ash cement. For example has the portland-fly ash cement substituted some of the use of rapid hardening portland cement for certain purposes, especially in concrete products (slabs, pipes). In this connection it should also be mentioned that some ordinary portland cement has been replaced by a combination of rapid hardening portland cement and fly ash mixed at the concrete plants.

Research projects

At the design stage several research projects were initiated, all aiming at providing information on important subjects related to the use of portland-fly ash cement. Summaries of results of the projects are given below.

Water penetration

Water penetration was measured in accordance with ISO 7031 on concretes differing in the type of cement used and the cement content. All concretes were air-entrained (air content 4-7%) [1,2]. The samples were cured 28 days in water (20^0C), 14 days in air (20^0C, >65%RH) and finally 14 days in water (20^0C) before testing. The results are given in Table 3.

The results, although not unambiguous, indicate that at this testing age the two types of cement will yield the same level of resistance to water penetration provided that the concretes are cured properly.

Alkali-silica reactivity

The effect of substituting 30% by weight of ordinary portland cement containing either 0.68 or 1.14% Na_2O eq. with two Danish fly ashes (Composition as shown in Table 4) on alkali-silica reactivity was tested according to ASTM C 441 (expansion of mortar bars at 37.8^0C).

The result shown in Figure 2 clearly demonstrates the beneficial effect of fly ash 0029 on expansion caused by alkali-silica reaction. Similar results were obtained with fly ash 0038. Similar results were also obtained with both fly ashes when tested according to the modified methods described by Brotschi and Mehta [3].

Diffusion of chloride

The effect of cement type, w/c ratio, temperature and curing time on the diffusion of chloride through cement paste has been studied at The Danish Corrosion Centre [4]. The technique used for diffusion measurements is outlined in Figure 3.

From the results of Table 5 the superior behaviour of portland-fly ash cement compared with the behaviour of rapid hardening and sulfate resistant portland cement is noted.

Carbonation

Based on a literature survey, Justesen and Nepper-Christensen [5] have expressed the following opinion concerning carbonation of concrete containing portland-fly ash cement:

- The carbonation proceeds faster in an initial period which may be of a duration of about one year. The rate of carbonation depends to a high degree on the curing conditions, particularly on the protection of the concrete against drying-out at the very early stage of hardening.
- At later ages the difference in carbonation depth seems to be rather independent of the type of cement used.

The results from a long term durability project (25 years) commenced in 1983 in order to evaluate the durability of concrete with mineral admixtures (fly ash, microsilica) support the first of these conclusions. The concrete structures included in the testing project are still too young to give evidence for the second conclusion, see Table 6 [6].

Freeze/thaw resistance

The long term project [6] referred to above also includes testing the concretes for freeze/thaw resistance according to ISO 4846. 28 days old slabs and 2 year old drilled cores were tested with the result (Table 7) that good freeze/thaw resistance (scaling less than 0.5 kg/m^2) was obtained for all concretes, irrespective of cement type, which were designed to provide frost resistance (marked with * in Table 7).

Since 1976 many thousands of square metres of concrete pavement were made with concrete containing fly ash or from portland-fly ash cement in Denmark and they have been exposed to severe freeze/thaw conditions during the winters. The experience gained is that air-entrained concrete (4-6% air) produced with a strength (>30 MPa) and a w/c ratio (<0.5) corresponding to the specifications for concrete in aggressive environment in Dansk Ingeniørforenings Code of Practice [7] will have excellent freeze/thaw resistance.

Wear resistance

Following some cases of unsatisfactory wear resistance of concrete floors (laid in pigsties) made with portland-fly ash cement an investigation of the influence of cement type and the use/non-use of a curing membrane on this property was taken up. The wear resistance was measured by sand blasting the concrete surface with a sand-water slurry according to a method developed by The Danish Agricultural Engineering Institute [8].

Only minor differences in wear resistance could be attributed to the cement type whereas both the use/non-use of curing membrane and the compressive strength were found to be important parameters, see Figure 4 [9].

Quality of fly ash

As part of the quality control of fly ash used by the cement and concrete industry in Denmark the chemical and physical properties are tested on monthly average samples from 8 major power plants. The control also comprises preparation of a blended cement (70w% Rapid hardening portland cement + 30w% fly ash) which is tested for compressive strength, setting time and soundness.

The quality control requirements for fly ash, the average test results and standard deviations for the years 1983-85 are shown in Table 8.

Taking into account that the data of Table 8 represent fly ashes produced at different power plants from coal of different origin the resulting strengths of the blended samples show remarkable uniformity.

The standard deviations shown in Table 1 for portland-fly ash cement also confirm that it is possible to manufacture uniform cement from fly ashes from different power plants and from different coals.

Thus it has not been found necessary to introduce further requirements for fly ash used for manufacturing portland-fly ash cement in Denmark.

Conclusion

Portland-fly ash cement has been marketed in Denmark for 5 years and covers a market share of 35-40% of the total cement consumption.

Danish research projects concerning water permeability, alkali-silica reactivity, chloride diffusion, carbonation, freeze/thaw resistance and wear resistance confirm that portland-fly ash cement has similar or better properties in those respects than ordinary portland cement.

J. Almeborg and J. T. Christensen, Aalborg Portland, Denmark

Danish Portland-Fly Ash Cement

References

1. Geiker, M.: Standardbetons frostbestandighed og vandtæthed, Aalborg Portland, Internal Report, December 1984

2. Bækmark, K.: Betons vandtrykpermeabilitet efter ISO 7031, Aalborg Portland, Internal Report, September 1984

3. Brotschi, J. & Mehta, P. K.: Test methods for determining potential alkali-silica reactivity in cements, Cement and Concrete Research, Vol. 8, pp. 191-200, 1978.

4. Hansson, C. M., Strunge, H., Markussen, J. B. & Frølund, T.: The effect of cement type on the diffusion of chloride, Nordic Concrete Research, Publication no. 4, pp. 70-80, Oslo 1985.

5. Justesen, C. F. & Nepper-Christensen, P.: Portlandflyveaskecement, Aalborg Portland, Internal Report, August 1985.

6. Rasmussen, T. H.: Langtidsforsøg vedrørende holdbarheden af beton med flyveaske og mikrosilica, Aalborg Portland, Internal report, November 1984.

7. Dansk Ingeniørforenings Code of Practice for the Structural Use of Concrete, DS 411, 3. edition, March 1984.

8. Pedersen, S.: Metode til karakterisering af staldgulve, Danish Agricultural Engineering Institute, Orientering nr. 8, 1981.

9. Pedersen, S. & Johansen, P.: Undersøgelse over forskellige betontyper til svinestalde, Danish Agricultural Engineering Institute, Orientering nr. 32, 1985.

Tables

Chemical properties	
M	1.3 +/- 0.3 %
$\bar{S}$	2.6 +/- 0.2 %
Loss on ignition	2.5 +/- 0.2 %
Fly ash	24 +/- 1.5 %
Physical properties	
Setting time	
Initial	130 +/- 16 minutes
Final	165 +/- 18 minutes
Soundness	0 +/- 0 mm
Compressive strength	
1 day	14 +/- 1.8 MPa
2 days	24 +/- 1.8 MPa
7 days	37 +/- 2.0 MPa
28 days	49 +/- 2.2 MPa

Table 1. Average properties and standard deviations of Danish portland-fly ash cement. Testing performed according to the methods of Danish Standard 427 which closely resemble the methods of ISO R 679 and R 680.

Type of cement	1980	1981	1982	1983	1984	1985
Ordinary portland cement	40	36	24	14	0	0
Portland-fly ash cement	0	6	23	31	40	35
Rapid hardening portland cement	56	52	46	49	52	60
Special cements	4	6	7	6	8	5

Table 2. Use of different cement types (%) in Denmark.

Type of cement	Cement content kg/m^3	w/c ratio	Compressive strength MPa	Water penetration min - max mm	Water penetration average mm	Test series no.
Rapid hardening portland cement	288	0.49	25	0 - 13	3	1
	300	0.46	33		16	2
	348	0.41	35	0 - 23	4	1
Portland-fly ash cement	289	0.48	30	0 - 10	1	1
	325	0.43	32		8	2
	348	0.42	32	0 - 15	3	1
	350	0.44	35		4	2

Table 3. Water penetration for concretes differing in cement type and cement content. Compressive strength results refer to 28 days curing. Averages refer to 6 samples in series 1 and 3 in series 2.

Oxides		Danish ordinary portland cement	High alkali portland cement	Fly ash 0038	Fly ash 0029
S	%	21.2	20.3	49.5	50.7
A	%	4.7	4.5	22.4	24.9
F	%	2.8	2.9	10.1	7.7
C	%	64.2	63.4	6.3	5.4
M	%	1.2	2.3	3.6	2.5
$\bar{S}$	%	2.6	3.2	0.7	0.7
LOI	%	1.3	0.9	3.2	3.9
Na_2O	%	0.33	0.40	0.59	0.93
K_2O	%	0.53	1.13	2.64	3.80
Na_2O eq	%	0.68	1.14	2.33	3.43

Table 4. Composition of cements and fly ashes used in alkali-silica reactivity tests.

Cement type	Temperature °C	Curing time 28 days w/c ratio 0.40	0.50	0.60	90 days w/c ratio 0.40	0.50	0.60
Rapid hardening portland cement	20	–	122	–	–	100	–
	30	67	132	263	45	125	257
	50	–	289	–	–	284	–
Low alkali sulfate resistant portland cement	20	–	151	–	–	140	–
	30	106	193	279	83	171	160
	50	–	370	–	–	388	–
Portland-fly ash	20	–	92	–	–	29	–
	30	41	116	139	5.8	37	88

Table 5. Effective diffusion coefficients for cement pastes, 10^{-13} m^2/s.

Type of cement	Cement content kg/m^3	w/c ratio	Compressive strength MPa (28 days)	Depth of carbonation mm average	std.dev.	Age years
Rapid hardening portland cement	260	0.54	22	2.1	1.0	2.0
	340	0.43	37	1.3	0.5	1.8
Low alkali sulfate resistant portland cement	260	0.52	29	3.0	1.2	2.0
	340	0.42	36	<0.5	–	1.8
	390	0.36	51	0.8	0.4	1.8
Portland-fly ash cement	260	0.54	29	2.7	1.4	1.7
	340	0.44	30	2.8	0.8	2.0
	390	0.42	35	1.8	0.7	1.8

Table 6. Depth of carbonation for concretes with different cement types.

Cement type	Cement content kg/m^3	w/c ratio	Air content %	Compressive strength 28 days MPa	Scaling, 25 cycles Slabs 28 days kg/m^2	Drilled cores 2 years kg/m^2
Rapid hardening portland cement	261	0.54	5.5	28	0.11	0.00
	255	0.53	6.0	32	0.03	
*	334	0.43	5.0	38	0.15	0.00
Low alkali sulfate resistant portland cement	264	0.52	5.0	25	2.60	0.03
	262	0.51	5.5	32	0.33	
*	340	0.42	6.0	40	0.06	0.01
*	390	0.36	5.0	48	0.07	0.00
Portland-fly ash cement	257	0.52	4.5	28	0.68	
	261	0.54	5.5	27	0.31	0.32
*	333	0.44	5.0	32	0.09	0.00
*	341	0.45	5.0	33	0.15	
*	397	0.42	3.0	38	0.11	0.02

Table 7. Freeze/thaw resistance according to ISO 4846 of concretes with different cement types.

J. Almeborg and J. T. Christensen, Aalborg Portland, Denmark

Danish Portland-Fly Ash Cement

		Requirements	Power plant no. 1	2	3	4	5	6	7	8	All
S	%	>40.0	53.2 3.3	54.5 2.9	54.0 8.0	51.0 2.9	56.3 3.9	51.8 2.3	52.3 2.4	53.2 3.7	53.3 4.5
A	%		25.1 1.9	29.7 2.1	32.0 4.6	30.7 3.6	28.3 3.2	30.6 3.3	32.2 0.7	32.4 3.5	29.7 4.0
F	%		9.3 1.5	6.7 1.2	4.9 1.4	7.2 1.8	6.3 1.4	6.6 1.8	5.2 0.8	6.0 2.6	6.7 2.1
C	%	<12.0	5.2 0.9	4.8 1.3	6.5 2.5	6.1 1.4	4.6 2.8	6.3 1.1	7.3 1.3	5.1 1.9	5.7 1.9
M	%	<5.0	3.2 0.6	1.9 0.5	1.4 0.5	2.2 1.1	1.6 0.5	2.3 1.1	1.8 0.5	1.4 0.8	2.0 1.0
$\bar{S}$	%	<3.0	1.0 0.3	0.6 0.2	0.5 0.2	0.8 0.3	0.6 0.2	0.6 0.2	0.6 0.2	0.5 0.2	0.7 0.3
LOI	%	<5.0	3.0 0.6	1.3 0.3	3.2 0.7	2.6 0.5	2.7 0.7	3.2 0.6	3.1 0.6	2.5 0.4	2.7 0.8
Avail. Na_2O eq.	%	<1.5	0.8 0.1	0.4 0.1	0.2 0.1	0.5 0.2	0.5 0.1	0.4 0.2	0.3 0.1	0.4 0.2	0.5 0.2
Residue on 45µm	%	<40.0	26.3 3.7	23.6 3.6	30.7 4.3	25.5 3.7	20.7 5.8	20.8 2.4	26.6 2.1	22.8 2.8	24.7 5.0
Compr. strength DS 427 MPa											
1 day			10.3 0.9	10.0 0.9	9.3 1.1	9.8 1.0	10.7 1.1	9.6 0.9	9.6 1.0	10.4 0.8	10.0 1.1
7 days			30.9 1.8	30.9 1.6	29.8 2.0	30.5 2.3	30.9 1.9	30.2 2.0	29.2 2.4	32.3 0.8	30.6 2.0
28 days			41.8 2.2	42.1 1.5	40.3 2.6	41.3 2.9	42.5 2.3	40.9 2.3	40.2 1.9	43.3 1.5	41.6 2.4
56 days			52.1 2.7	51.3 1.9	48.8 3.0	50.6 3.3	53.0 3.3	50.7 3.1	49.5 2.1	53.4 1.4	51.2 3.2
Setting time min.											
Initial			180 20	188 20	203 33	202 28	178 16	201 21	209 37	190 24	193 27
Final			213 22	222 25	236 38	239 33	208 19	234 23	241 39	224 27	226 30
Number of samples			31	18	26	30	27	23	11	16	182

Table 8. Average(first line) and standard deviation(second line) for chemical and physical data for samples from 8 Danish power plants. Compressive strengths and setting times are measured on a mix of 70% rapid hardening portland cement and 30% fly ash. Soundness of all mixes was 0 mm. Requirements not shown in the table: Moisture <1.5%, S+A+F >70%, Cl^- <0.1%.

J. Almeborg and J. T. Christensen, Aalborg Portland, Denmark

Danish Portland-Fly Ash Cement

Figures

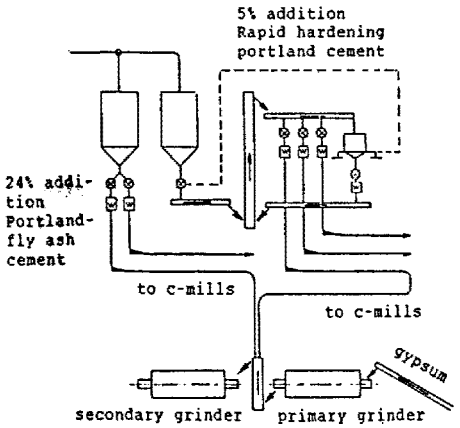

Figure 1. Diagram of mill installations for production of portland-fly ash cement

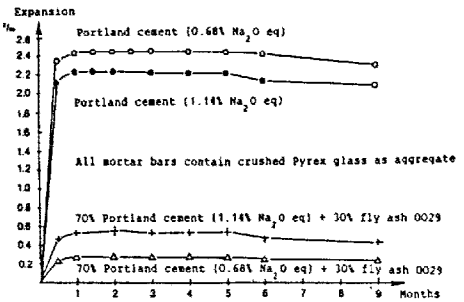

Figure 2. Time-expansion curves for mortar bars (ASTM C 441)

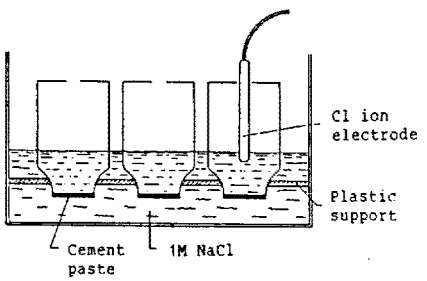

Figure 3. Schematic drawing of experimental arrangement for diffusion measurements

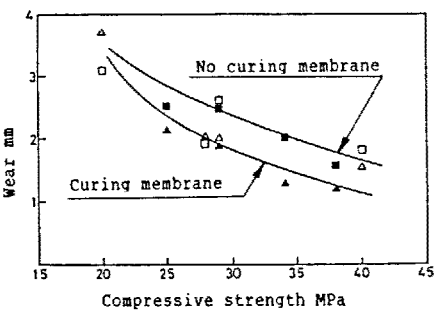

Figure 4. Effect of curing membrane and compressive strength on wear resistance

- △ Portland-fly ash cement, curing membrane
- □ Portland-fly ash cement, no curing membrane
- ▲ Rapid hardening portland cement, curing membrane
- ■ Rapid hardening portland cement, no curing membrane

J.P. OLLIVIER - Laboratoire de Génie Civil - I.N.S.A-U.P.S.-Toulouse - France

RÔLE DES ADDITIONS MINÉRALES SUR LA FORMATION DE L'AUREOLE DE TRANSATION ENTRE GROS GRANULAT ET MORTIER

La structuration de l'auréole de transition, zone de liaison entre la pâte de ciment et les granulats, a fait l'objet de nombreuses études dans le cas des ciments portland. C'est en effet le point faible des bétons puisqu'elle présente une forte porosité et une morphologie cristalline qui lui confèrent de mauvaises caractéristiques mécaniques et en font un chemin privilégié pour la migration des agents aggressifs.

Les additions minérales utilisées dans les ciments agissent sur certains paramètres qui commandent la formation de l'auréole de transition : l'arrangement granulaire au voisinage de l'interface avec les granulats, la vitesse d'hydratation, la fluidité de la pâte et le contrôle de l'hydratation du C_3A. Nous avons donc axé notre contribution sur les modifications de la zone de liaison apportées par diverses additions minérales.

Une première partie est consacrée à des additions dont la granularité est voisine de celle des grains de clinker et qui peuvent être utilisées comme filler sans fluidifiant (cendres volantes, laitier, calcaire).

Dans une seconde partie nous présentons l'action de la fumée de silice de granularité très inférieure à celle du clinker dont l'emploi comme ajout nécessite l'usage d'un fluidifiant. Nous étudions en particulier le rôle de la nature de la silice sur la structuration de l'auréole de transition.

I - METHODE EXPERIMENTALE

L'auréole de transition formée au voisinage des gros granulats d'un béton est étudiée au moyen d'une éprouvette mixte constituée d'un bloc de marbre plan poli contre lequel est coulé un mortier ou une pâte pure de ciment. Après rupture au voisinage immédiat de l'interface, les deux demi-éprouvettes sont observées au microscope électronique à balayage (MEB). La structuration de la phase liante (pâte ou mortier) est analysée par diffraction de rayons X (DRX) selon la méthode d'abrasion progressive (1). Cette méthode permet :

- de caractériser l'orientation préférentielle des cristaux de portlandite qui se développent avec leur axe c perpendiculaire au gros granulat. On défini à cet effet un indice I d'orientation dont on étudie la variation avec la distance δ à l'interface ;

- de connaître la répartition des phases anhydres ou hydratées cristallisées depuis la surface de rupture jusqu'au coeur de l'éprouvette.

II - RAPPEL SUR LA STRUCTURATION DE LA PATE DE CIMENT PORTLAND NON FILLERISEE AU VOISINAGE D'UN GROS GRANULAT

La variation de l'indice d'orientation des cristaux de CH varie typiquement en fonction de la distance à l'interface selon la courbe de la figure 1.

On rappelle que :

$$I = \frac{\text{intensité raie (00.1)}/\text{intensité raie (10.1)}}{0,74}$$

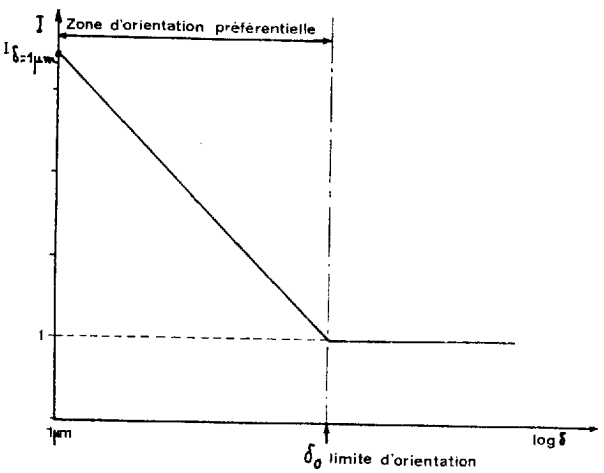

Figure 1 - Schéma caractéristique de l'orientation des cristaux de CH au voisinage d'un gros granulat.

L'orientation préférentielle de la portlandite et l'hydratation particulière de la pâte sont interprêtées par l'existence d'un gradient de teneur en eau dû à un effet de paroi entre le gros granulat et les grains de ciment (2). L'amplitude de l'orientation des premiers cristaux voisins de l'interface est déterminée par les conditions d'hydratation du C_3A et du C_3S selon le schéma de la figure 2 dans le cas d'un granulat inerte.

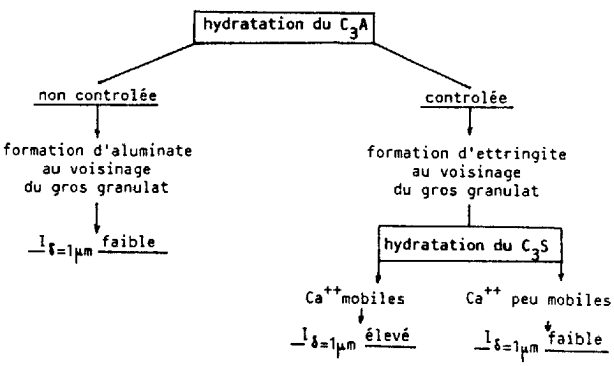

Figure 2 - Analyse schématique de la croissance des cristaux de portlandite dans l'auréole de transition

Dans le cas d'un gros granulat calcaire, l'orientation des premiers cristaux de CH est notablement diminuée si la calcite réagit précocement avec les aluminates de calcium hydratés c'est-à-dire si la réaction du C_3A n'est pas efficacement contrôlée par les sulfates.

La limite d'orientation δ_o augmente avec les possibilités de migration des ions Ca^{++} dans la pâte de ciment. Dans le cas des pâtes pures δ_o est ainsi une fonction croissante de la teneur en eau de gâchage et du temps de début de prise.

III - INFLUENCE D'ADDITIONS MINERALES DE DE GRANULARITE VOISINE DE CELLE DU CIMENT SUR LA FORMATION DE L'AUREOLE DE TRANSITION

Les additions minérales jouent un rôle physique sur le comportement rhéologique de la pâte fraîche de ciment et chimique sur son hydratation. Leur présence peut donc agir sur la formation de l'auréole de transition. Ceci a été vérifié avec des cendres et des laitiers par CARLES et al (3, 4) dont nous résumons tout d'abord les principaux résultats. Nous présenterons par la suite d'autres résultats plus partiels obtenus avec des fillers calcaires (5).

Les études avec cendres et laitiers ont été conduites au moyen d'éprouvettes mixtes confectionnées avec des pâtes à base d'un ciment CPA 55 R gachées à une concentration volumique $\gamma = \frac{c}{c+e} = 0{,}527$ sur un marbre de carrare (teneur en $CaCO_3 > 99$ %). Trois ajouts ont été utilisés au taux unique de substitution de 30 %. Il s'agit :

- d'une cendre volante de houille n°1 (395 $m^2 kg^{-1}$ Blaine) ;
- d'une cendre volante de lignite n°2 (210 $m^2 kg^{-1}$ Blaine) ;
- d'un laitier de fonte Thomas granulé broyé à 350 $m^2 kg^{-1}$ Blaine.

La composition chimique du ciment (320 $m^2 kg^{-1}$ Blaine) et des additions est indiquée au tableau 1

	SiO_2	Al_2O_3	Fe_2O_3	CaO	MgO	Na_2O	K_2O	SO_3	Perte au feu
ciment	21,4	5,3	2,3	64,0	1,4	0,04	0,49	2,98	1,02
cendre n°1	54,8	27,1	8,8	3,3	2,1	0,3	2,6	0,9	3,6
cendre n°2	24,8	14,9	10,1	50,7*	3,7	0,8	1,0	9,1	0,4
laitier	33,1	11,4	FeO = 1,9 0	42,4	8,3	0,6			

* dont 28 % de chaux libre

TABLEAU 1

Composition chimique du ciment, des cendres et du laitier

La croissance des cristaux de CH aux premiers ages peut être analysée au moyen des courbes de la figure 3.

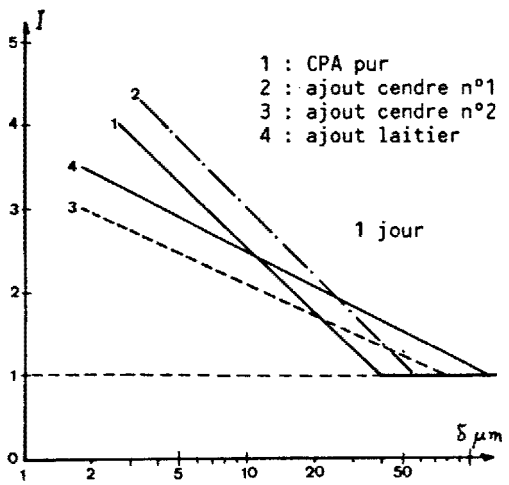

Figure 3 - Croissance préférentielle des cristaux de portlandite dans des ciments fillérisés au voisinage d'un gros granulat.

La limite d'orientation δ_o est d'autant plus grande que la ressuée est importante après la mise en place. Celle-ci augmente si le pourcentage de grains irréguliers, la porosité ouverte ou la surface spécifique des grains de l'ajout diminuent. La valeur de δ_o et l'orientation préférentielle des cristaux de CH formés au voisinage immédiat de l'interface, caractérisée par $I_{\delta=1\mu m}$, peuvent être analysées comme suit d'après les indications de la figure 2.

* cendre de houille n°1 :

La grande porosité (7%) explique que cet ajout n'ait qu'un faible rôle fluidifiant. La valeur de δ_o est donc peu accrue par rapport à celle de la pâte pure (65 µm au lieu de 40 µm). Cette cendre apporte des sulfates rapidement solubles qui contribuent à la formation d'ettringite autour des grains de C_3A. Il n'apparaît donc pas d'aluminate hydraté et la surface du gros granulat de marbre cemeurant inattaquée et plane, les cristaux de portlandite ont un indice d'orientation élevé.

* cendre de lignite n°2 :

La faible surface spécifique, ajoutée à la forme sphérique de nombreux grains et à l'inexistence d'une porosité ouverte notable font que cette cendre est un excellent fluidifiant. La limite d'orientation δ_o est donc notablement accrue (de 40 μm à 90 μm).

La composition chimique de cette cendre est remarquable par ses hautes teneurs en sulfate et en chaux avec une fraction importante de cette dernière sous forme de CaO libre. La désorientation des cristaux de portlandite au voisinage du gros granulat s'explique ici par l'existence de germes de cristallisation homogène formés autour des grains de cendre par l'extinction de la chaux vive qu'ils contiennent. Un résultat analogue a été obtenu par l'utilisation de germes de CaO ou de $Ca(OH)_2$ mélangés au ciment : cette activation cristallochimique conduit à une forte désorientation des cristaux de portlandite dans l'auréole de transition (6).

* laitier de fonte :

Le laitier granulé a une action fluidifiante sur la pâte de ciment ce qui se traduit par une augmentation de la valeur de δ_o. Dans l'auréole de transition le rapport eau/clinker est accru par rapport au cas des CPA purs. Les seuls sulfates présents provenant de la dissolution du gypse, le contrôle de l'hydratation du C_3A est alors insuffisant pour éviter la formation d'aluminates de calcium hydratés au voisinage du gros granulat. Les cristaux de portlandite formés sont alors plus faiblement orientés, la modification étant encore plus importante au voisinage des granulats calcaires qui sont corrodés avec la formation de carboaluminate.

Le laitier et les cendres utilisés dans ces essais ne sont pas des additions inertes ; leur réaction contribue donc au remplissage progressif de la porosité de l'auréole de transition comme de celle de la masse de la pâte. Au fur et à mesure du temps l'évolution de l'orientation préférentielle des cristaux de portlandite près de l'interface est très faible : légèrement croissante avec le laitier et décroissante avec les cendres. Enfin la faible pouzzolanicité des cendres utilisées n'a pas permis de mettre en évidence la consommation de la portlandite par DRX avant 6 mois ni dans la pâte, ni dans l'auréole de transition.

* Fillers calcaires:

Comme les additions précédentes les fillers calcaires utilisés comme ajout ont une surface spécifique de l'ordre de celle du clinker qu'ils remplacent. Par conséquent l'effet de paroi entre grains de ciment et gros granulat ne devrait pas être notablement modifié. On constate effectivement que l'orientation des cristaux de portlandite est peu affectée par l'ajout de filler calcaire (5).

Des études morphologiques de faciès de rupture d'éprouvettes mixtes ont montré l'existence d'un film dense d'hydrates, essentiellement constitué de portlandite, déposé sur le granulat (7). Ce film est analogue à celui observé avec des ciments portland non fillérisés ou contenant des ajouts de cendre volante ou de laitier. Avec un filler silico-calcaire cette morphologie est modifiée : il se forme alors davantage d'ettringite bien cristallisée au voisinage de l'interface.

Les fillers calcaires se distinguent des cendres et laitiers par leur réaction avec les aluminates de calcium qui conduit à la formation du carboaluminate $C_3A.CaCO_3.11H_2O$ (8). Dans l'auréole de transition comme dans le coeur de la pâte cette réaction de la calcite se fait concurremment avec celle du gypse (7). Ainsi, près de l'interface, la forte teneur locale en eau due à l'effet de paroi entraîne un développement plus abondant des aluminates hydratés (9) qui réagissent avec le filler calcaire pour former davantage de carboaluminate (5). Cette activité chimique des fillers calcaires a des conséquences favorables sur la résistance mécanique et la porosité des pâtes de ciment ou des mélanges C_3A + $CaCO_3$ (10). Puisqu'elle y est plus intense qu'à coeur on peut penser que ses conséquences sont encore plus importantes dans l'auréole de transition.

IV - INFLUENCE DE LA FUMEE DE SILICE CONDENSEE SUR LA FORMATION DE L'AUREOLE DE TRANSITION

La fumée de silice se distingue des additions précédentes par sa grande surface spécifique (de l'ordre de 20 000 m^2kg^{-1}) et sa réaction pouzzolanique rapide. Comme l'ont noté récemment Carles-Gibergues et al. (11) et Oudjit (12) il y a lieu de considérer que la fumée de silice ne présente pas la même réactivité quelle que soit sa provenance et qu'en particulier sa teneur en impuretés, notamment en carbone, joue un très grand rôle.

Nous avons indiqué par ailleurs (13) le rôle d'une fumée de silice sur la formation de l'auréole de transition ; nous présentons ici l'influence de la nature de la fumée de silice sur cette zone de contact dans la continuité des travaux de Carles-Gibergues.

Les études ont été effectuées au moyen d'éprouvettes mixtes associant un gros granulat de marbre de carrare et un mortier préparé avec un rapport liant/sable calcaire = 1,5. Ce rapport est choisi conformément au dosage du mortier retenu dans les bétons de haute résistance préparés avec 700 kg de ciment par m^3. Nous présentons tout d'abord les résultats obtenus en l'absence de fluidifiant comme dans le chapitre précédent. Dans l'optique d'une application à l'analyse du comportement des bétons de haute résistance nous présenterons ensuite l'influence de la nature de la fumée de silice en présence de naphtalène sulfonate.

Les caractéristiques des silices choisies sont reportées au tableau 2. Nous avons choisi une silice réactive (n°1) et une autre contenant un pourcentage élevé de carbone qui la rend moins réactive aux jeunes âges (n°2). Nous avons également utilisé la silice n° 2 chauffée à 550°C de façon à brûler son carbone résiduel : après traitement, elle est repérée silice n°3 dans nos résultats.

	SiO_2	Na_2O	MgO	Al_2O_3	CaO	MnO	K_2O	Fe_2O_3	SO_3	Cl^-	C 500°C	Perte au feu
Silice n°1	93,4	0,4	1,9	0,8	0,3	'	1,3	0,9	0,7	0,2	0,1	3,9
Silice n°2	81	0,5	2,5	0,8	0,1	0,1	3	1,5	0,4		5	10,2

Silice n°1 S_s BET = 19 000 $m^2 kg^{-1}$

Silice N°2 S_s BET = 23 000 $m^2 kg^{-1}$

TABLEAU 2

Caractéristiques des fumées de silice

IV - 1- Influence de la nature de la fumée de silice en l'absence de fluidifiant

Les différents mortiers sont préparés avec une teneur pondérale en eau (eau/ciment + silice) = 0,40

Les courbes de la figure 4 illustrent la croissance préférentielle des cristaux de portlandite dans le mortier au voisinage du gros granulat. Les deux silices dosées à 10 % en poids de liant conduisent à une réduction notable de l'indice d'orientation. Ceci peut s'expliquer par la diminution de la porosité près de l'interface due au remplissage des vides intergranulaires par les grains de fumée de silice qui jouent également le rôle de germe de cristallisation pour la portlandite. En outre il y a lieu de noter que la silice n°1 accélère l'hydratation du ciment et diminue la fluidité ce qui contrarie le libre développement des cristaux de portlandite. La silice n°2 entraîne au contraire un retard aux jeunes âges mais il se forme une plus grande quantité d'aluminates hydratés dans l'auréole de transition.

Comme dans le cas des échantillons préparés avec du ciment pur, on peut enfin remarquer que l'ettringite se forme en plus grande quantité au voisinage du gros granulat avec la silice comme l'indiquent les courbes de la figure 5. Ceci s'explique par la diffusion des ions SO_4^{--} vers l'interface due à l'existance d'un gradient de teneur en eau. En outre, dans le cas de la silice n°2 la quantité d'ettringite est plus importante que pour les autres échantillons. Il semble donc que le C_3A s'hydrate plus rapidement avec cet ajout puisque nous avons mentionné précédemment que la quantité d'aluminate hydraté était elle aussi plus importante.

L'examen du MEB indique que la morphologie des faces de rupture des éprouvettes mixtes n'est pas affectée par l'addition de silice aux jeunes âges. On retrouve, côté granulat (figure 6), des dépots de portlandite analogues à ceux présentés dans le cas des éprouvettes mixtes préparées sans silice (figure 7).

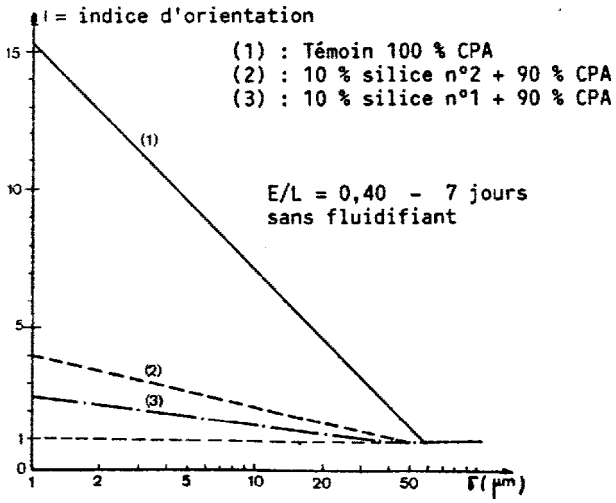

Figure 4 - Orientation des cristaux de portlandite dans les mortiers au voisinage d'un gros granulat : influence de la nature de la silice en l'absence de fluidifiant.

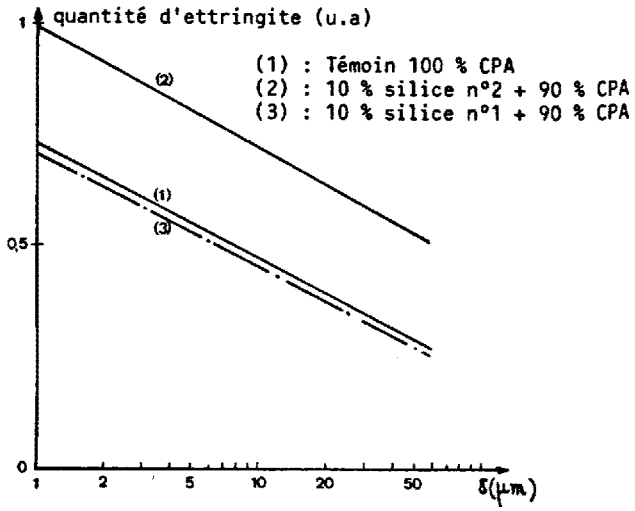

Figure 5 - Formation de l'ettringite au voisinage d'un gros granulat dans des mortiers préparés sans fluidifiant (E/L = 0,40 - 7 jours)

La figure 8 illustre le faciès de rupture côté mortier d'une éprouvette préparée avec de la silice n°2 âgée de 7 jours. Sous le film dense de portlandite l'ettringite finement cristallisée s'est développée de façon plus abondante que dans les autres éprouvettes ce qui confirme les analyses par DRX.

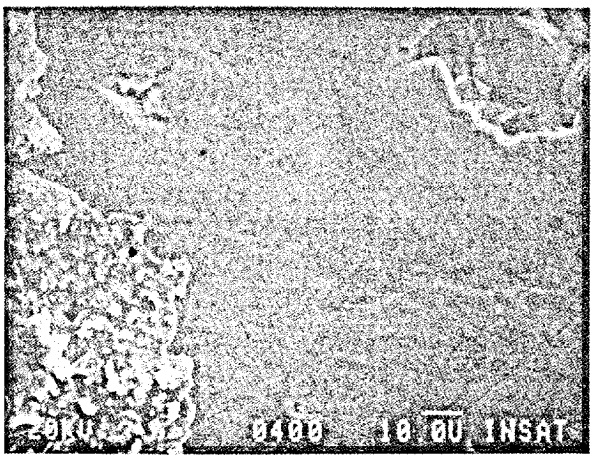

Figure 6 - Face de rupture côté granulat d'une éprouvette mixte préparée avec un mortier contenant de la silice n°2 (10% du liant) sans fluidifiant (E/L = 0,40 - 7 jours)



Figure 7 - Face de rupture côté granulat d'une éprouvette mixte préparée avec un mortier sans silice et sans fluidifiant (E/L = 0,40 - 7 jours)

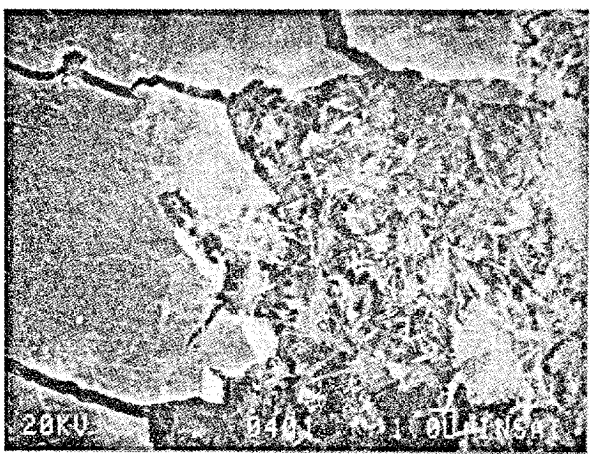

Figure 8 - Eprouvette analogue à celle de la figure 7 face de rupture côté mortier

IV -2- Influence de la nature de la fumée de silice en présence de fluidifiant

IV -21- Hydratation des mortiers en présence de fluidifiant

La cinétique d'hydratation a été analysée par calorimétrie adiabatique sur des mortiers 1/3. Les courbes de la figure 9 indiquent la variation des instants d'apparition du maximum du flux thermique en fonction du dosage en fluidifiant.

Avec la silice n°1 l'hydratation aux jeunes âges est toujours accélérée par rapport au témoin ne contenant pas de silice pour un dosage en fluidifiant inférieur à 4 %. Ce résultat n'est pas vérifié quelque soit le dosage en fluidifiant ; nous avons en effet pu vérifier que pour une valeur de 10 % il y avait au contraire un retard par rapport au témoin.

Avec la silice n°2 le changement de comportement se produit à un dosage beaucoup plus faible en fluidifiant (de l'ordre de 4%) qui correspond à une valeur extrême utilisée dans la fabrication des bétons de haute résistance. Buil |14| a déjà mentionné que la silice pouvait avoir ce rôle retardateur aux forts dosages en fluidifiant. Nous indiquons ici que toutes les silices ne se comportent pas de la même manière et nous pensons que ceci peut être attribué aux impuretés présentes. En effet avec la silice n°3 (silice n°2 réchauffée à 550°C) et 4% de fluidifiant, le maximum de flux thermique apparaît au bout de 10 heures comme dans le cas de la silice n°1 au lieu de 14,5 heures avant le réchauffage.

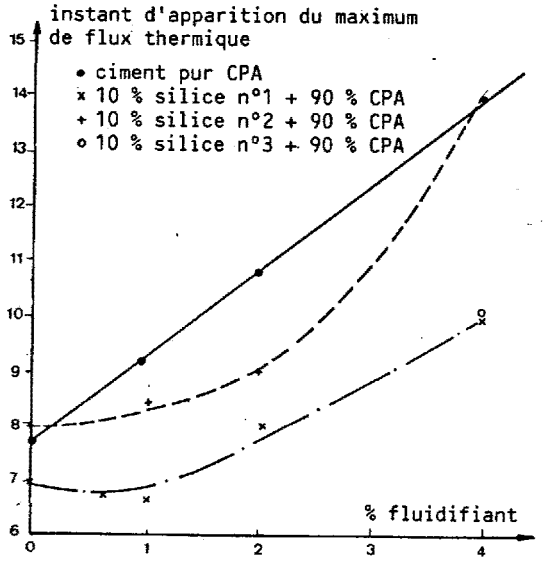

Figure 9 - Influence de la nature de la fumée de silice et du dosage en naphtalène sulfonate sur l'hydratation des mortiers.

IV -22- Formation de l'auréole de transition

Les courbes des figures 10, 11 et 12 représentent l'orientation préférentielle des cristaux de portlandite au voisinage d'un gros granulat dans des mortiers préparés respectivement avec 1% de fluidifiant et diverses silices dosées à 10%, 4% de fluidifiant et diverses silices dosées à 10%, 4% de fluidifiant et divers dosages de la silice n°1.

En l'absence de silice et comme nous l'avons indiqué par ailleurs |13| les cristaux de portlandite restent bien orientés au voisinage du gros granulat.

Au contraire, la présence de fumée de silice conduit à une désorientation des cristaux de portlandite dans la zone interfaciale quelque soit le dosage en fluidifiant. Les courbes de la figure 13 permettent de vérifier l'une des hypothèses formulées précédemment pour expliquer ceci : le rôle de remplissage des grains de silice. Lorsque le dosage en silice augmente (à teneur en eau constante) on observe une désorientation progressive des cristaux de portlandite dans l'auréole de transition. Par ailleurs la répartition des cristaux d'ettringite dans cette zone est modifiée à cause de la diminution du gradient de teneur en eau (figure 13). Les vides intergranulaires sont progressivement comblés par les quantités croissantes de silice bien dispersée au voisinage du gros granulat. De même que pour les ions SO_4^{--}, la migration des ions Ca^{++} vers l'interface est alors plus faible et les cristaux de portlandite sont faiblement orientés malgré la bonne fluidité des mortiers

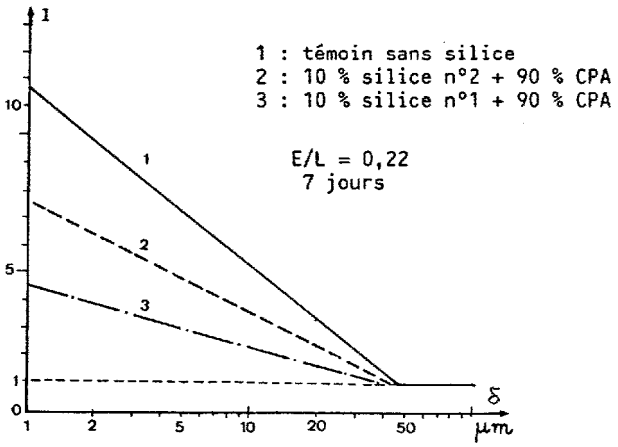

Figure 10 - Orientation des cristaux de portlandite dans les mortiers au voisinage d'un gros granulat : influence de la nature de la silice en présence de fluidifiant (1% en poids de ciment)

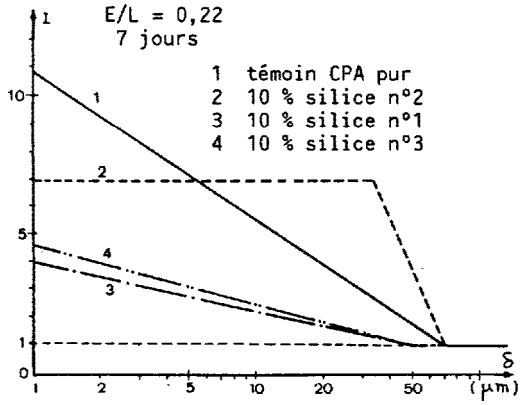

Figure 11 - Orientation des cristaux de portlandite dans les mortiers au voisinage d'un gros granulat : influence de la nature de la silice en présence de fluidifiant (4%)

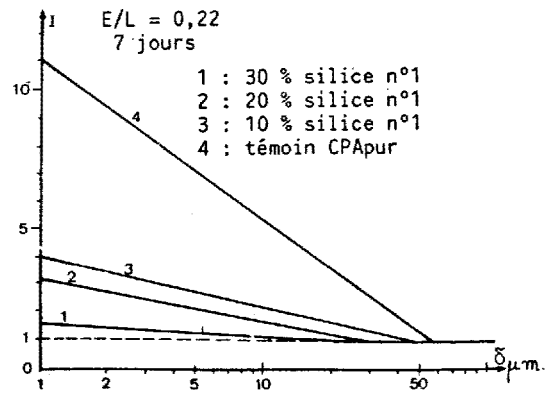

Figure 12 - Orientation des cristaux de portlandite dans les mortiers au voisinage d'un gros granulat : influence de la teneur en silice en présence de 4% de fluidifiant

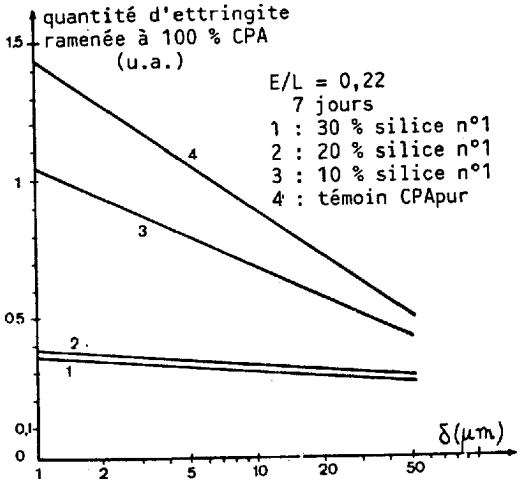

Figure 13 - Quantité d'ettringite formée dans les mortiers au voisinage d'un gros granulat : influence de la quantité de silice en présence de fluidifiant

Les figures 10 et 11 confirment l'influence relative des deux fumées de silice sur le développement des cristaux de portlandite au voisinage d'un gros granulat. Comme en l'absence de fluidifiant, la silice n°1 modifie davantage l'orientation préférentielle que la silice n°2. Ceci est probablement dû, comme l'indique la figure 9, à une accélération plus importante de l'hydratation.

Avec un dosage de 4% en fluidifiant la courbe de la figure 11 relative à la silice n°1 présente un palier. Nous avons déjà noté une telle forme de courbe dans le cas des pâtes pures de ciment portland gâchées avec de fortes teneurs en eau |15|. On constate également un développement des cristaux de portlandite avec orientation constante dans une zone de 10 à 20 µm voisine de l'interface avec de très forts dosages en fluidifiant (10%) et avec ou sans la fumée de silice n°1. L'existence de ce palier n'est donc pas causée par la seule présence de fumée de silice bien que l'ajout d'une silice qui, par sa teneur en impuretés, retarde l'hydratation puisse permettre une telle croissance de la portlandite à de plus faibles dosages en fluidifiant. La teneur en impureté, notamment en carbone, peut effectivement être mise en cause car si on remplace la silice n°2 par la silice n°3 la courbe calorimétrique (cf. figure 9) et le développement des cristaux de CH (cf. la figure 10) sont pratiquement analogues à ceux obtenus avec la silice n°1.

L'examen au MEB des faciès de rupture des éprouvettes mixtes permet de compléter l'analyse de l'influence des silices.

Pour un dosage de 4% en fluidifiant les figures 14a et 14b représentent respectivement la face granulat et la face mortier d'une éprouvette âgée de 7 jours. Au voisinage immédiat du granulat la portlandite se développe sous forme de gros cristaux selon la face (00.1) parallèle à l'interface. La figure 14b montre que de petits cristaux de CH, bien formés mais plus petits, se développent à distance de l'interface de façon plus désordonnée.

Avec le même dosage en fluidifiant et 10% de la fumée de silice n°2 les figures 15a et 15b présentent des faces de rupture côté mortier également après 7 jours de conservation. De gros cristaux de portlandite se développent encore au voisinage de l'interface mais leur faciès est tout à fait différent : la croissance est beaucoup moins orientée qu'en l'absence de silice.

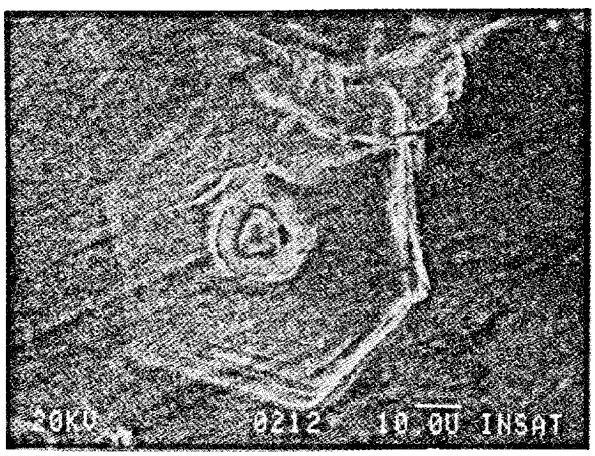

a - face granulat

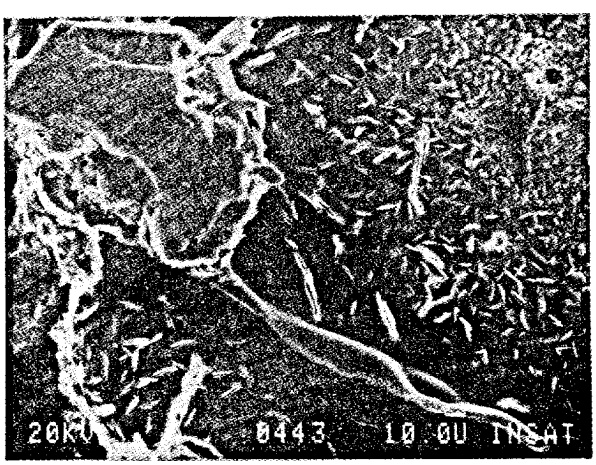

b - face mortier

Figure 14 - Faciès de rupture d'une éprouvette mixte le mortier est préparé avec 4% de fluidifiant sans silice (E/liant = 0,22 - 7 jours)

Enfin avec la silice n°1 les figures 16 a et b illustrent un troisième mode de croissance à faible orientation préférentielle (faces de rupture côté mortier).

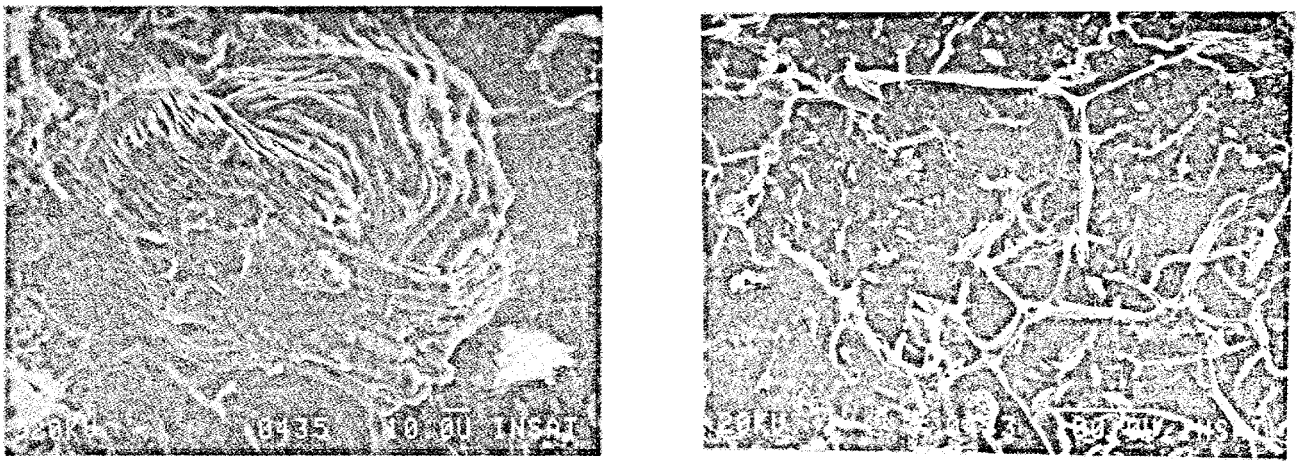

Figure 15 - Faciès de rupture d'une éprouvette mixte côté mortier : 4% fluidifiant, 10% silice n°2, E/liant = 0,22 = 7 jours

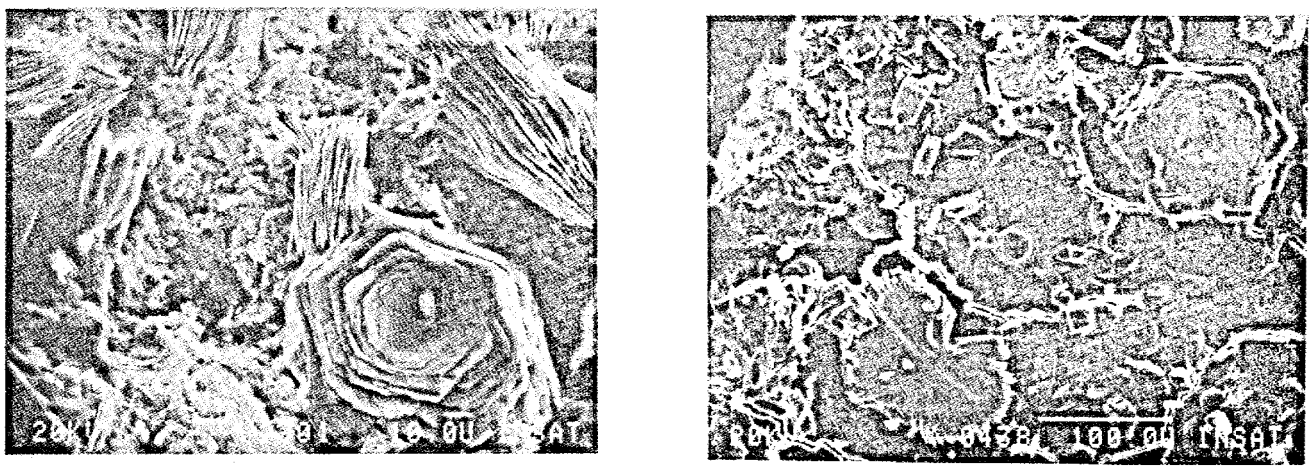

Figure 16 - Faciès de rupture d'une éprouvette mixte coté mortier : 4% de fluidifiant, 10% de silice n°1, eau/liant = 0,22, 7 jours

Ces clichés montrent que l'addition de fumée de silice modifie le développement de la portlandite vraisemblablement parce que ses grains constituent des germes de cristallisation. L'orientation préférentielle est alors logiquement plus faible mais il y a lieu de noter que la taille des cristaux formés au voisinage de l'interface n'est pas réduite. Nous pouvons enfin remarquer des structures filamenteuses sur les faces de rupture : nous pensons qu'elles sont dues à la condensation des molécules de naphtalène sulfonate qui, en migrant vers le granulat, ont saturé la zone de contact.

La microstructure de l'auréole de transition évolue considérablement entre 7 jours et 28 jours du fait de la réactions pouzzolanique. Celle-ci se manifeste par une diminution de l'intensité des pics de diffraction et par une modification du faciès des hydrates : les gros cristaux formés à l'interface se transforment en un gel de texture plus dense (figure 17).

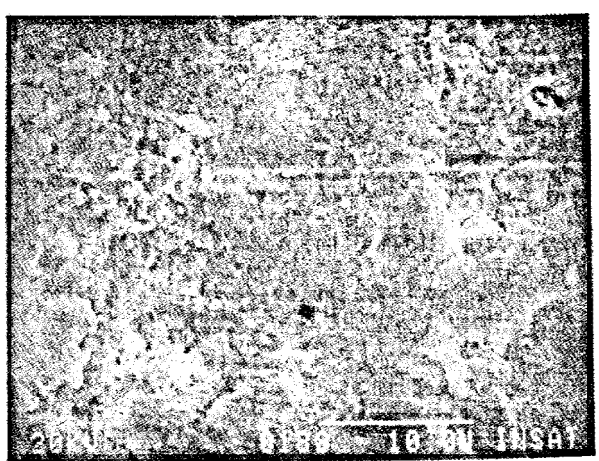

Figure 17 - face de rupture d'une éprouvette mixte côté granulat - mortier âgé de 28 jours 10% silice n°1

V - CONCLUSIONS

Les additions minérales agissent sur la formation de l'auréole de transition par leur présence physique et leur activité chimique.

Lorsque la granularité de l'ajout est voisine de celle des grains de clinker l'effet de paroi n'est pas notablement affecté. Cependant l'épaisseur de l'auréole de transition augmente si les additions minérales accroissent la fluidité de la pâte.
Lorsque la granularité de l'ajout est beaucoup plus faible que celle du clinker, la compacité au voisinage des interfaces avec les granulats augmente comme dans le reste de la phase liante. Un dosage suffisant en particules fines peut annihiler les caractéristiques néfastes de l'auréole de transition : gradient de teneur en eau et orientation préférentielle des cristaux de portlandite.

Les réactions chimiques des ajouts peuvent avoir des conséquences à la fois sur la formation de l'auréole de transition puis sur son évolution dans le temps.

Leur influence aux jeunes âges est essentiellement liée à la cristallogénèse des hydrates : ils peuvent constituer des germes de cristallisation (cas de la silice et des cendres contenant de la chaux vive) ou modifier la cinétique d'hydratation du clinker. A ce propos, il y a lieu de noter l'importance de leur action sur le contrôle de l'hydration du C_3A.

L'influence des additions minérales dans l'auréole de transition aux plus longues échéances n'est pas notablement différente de ce qu'elle est dans la masse du liant sauf lorsque l'environnement particulier favorise leur réaction. C'est le cas du filler calcaire avec les grandes quantités d'aluminates hydratés formés dans leur voisinage, près des interfaces. C'est aussi celui des fumées de silice qui peuvent réagir plus rapidement près de l'interface où la teneur en eau est localement plus élevée.

En conclusion lors du choix de la nature et des caractéristiques d'une addition minérale il est opportun de considérer son rôle spécifique dans l'auréole de transition. En effet si certaines additions contribuent à diminuer les performances du ciment, leur action bénéfique sur la zone de liaison pâte - granulat peut se traduire par une altération moins significative des qualités du béton. Les études aux interfaces et sur bétons doivent de ce fait constituer l'un des éléments d'analyse pour l'optimisation des additions minérales.

Remerciements :

Le document présenté ici constitue une synthèse de travaux dont la plupart ont été effectués au laboratoire de Génie Civil I.N.S.A.-U.P.S. de Toulouse. En plus des chercheurs cités dans ce texte je souhaite remercier M. HANNA pour la part prise dans l'étude des fumées de silice.

BIBLIOGRAPHIE

(1) J. GRANDET, J.P. OLLIVIER. Nouvelle méthode d'étude des interfaces ciment-granulat. 7ème Congrès Int. de la Chimie des Ciments. VII.85. Paris 1980.

(2) J.P. OLLIVIER, J. GRANDET. Processus de formation de l'auréole de transition. Liaisons pâtes de ciment - matériaux associés. Colloque Int. Toulouse 17-19 novembre 1982.

(3) A. CARLES-GIBERGUES, J. GRANDET, J.P. OLLIVIER. Modification of the ciment paste-aggregate interfacial region due to addition of fly ash or silica fume in mortars of portland cement. MRS Meeting Boston, novembre 1981.

(4) A. CARLES-GIBERGUES, J. GRANDET, J.P. OLLIVIER. Evolution dans le temps de l'auréole de transition de pâte contenant des ajouts. Ib (2).

(5) ESCADEILLAS. communication personnelle.

(6) J.P. OLLIVIER, J. GRANDET. Désorientation des cristaux de portlandite dans l'auréole de transition. Ib (2).

(7) B. MORTUREUX, H. HORNAIN, M. REGOURD. Liaison pâte de ciment - filler dans les ciments composés. Ib (2).

(8) J. FARRAN. Contribution minéralogique à l'étude de l'adhérence entre les constituants hydratés du ciment et les matériaux enrobés. Revue des matériaux de construction. n°S 490 - 491 - 492, 1956.

(9) J. GRANDET, J.P. OLLIVIER. Etude de la formation du monocarboaluminate de calcium hydraté au contact d'un granulat calcaire dans une pâte de ciment portland. Cem. concr. Res. vol. 10, pp. 759 - 770, 1980.

(10) J. JAMBOR. Binding capacity of calcium aluminate hydrates containing other ions. Ib (2).

(11) P.C. AITCIN, A. CARLES-GIBERGUES, N. OUDJIT, A. VAQUIER. Influence des éléments autres que Si sur la réactivité des fumées de silice. Congr. Int. Ch. des Ciments Rio 1986.

(12) M. N. OUDJIT. Réactivité des fumées de silice condensées en présence de chaux ou de ciment portland. Thèse D.I. I.N.S.A. de Toulouse 1986.

(13) J.P. OLLIVIER, B. HANNA. Action d'un fluidifiant et d'une fumée de silice condensée réactive sur la formation de la liaison gros granulat-mortier Congr. Int. Chimie des Ciments Rio 1986.

(14) M. BUIL, A.M. PAILLERE, B. ROUSSEL. High strength mortars containing condensed silica fume. Cem. and Concr. Res. Vol. 14. pp.693 704 , 1984.

(15) J.P. OLLIVIER. Contribution à l'étude de l'hydratation de la pâte de ciment portland au voisinage des granulats. Thèse d'Etat. Toulouse 1981.

(16) Ph. PINSONNEAULT. Influence des fumées de silice sur les propriétés physiques et chimiques des bétons et des mortiers. Université de Sherbrooke 1983.

R.GUYOT, R.RANC, B.CARIOU
LAFARGE COPPEE RECHERCHE, FRANCE

UTILISATION DE LA POTENTIALITE HIDRAULIQUE DU CLINKER DANS LES CIMENTS PORTLAND AVEC AJOUT DE FILLERS CALCAIRES

1 - INTRODUCTION

Les ciments avec ajout calcaire se sont développés en France depuis 1979, date à partir de laquelle la Normalisation Française a autorisé leur fabrication et leur commercialisation en même temps qu'elle établissait des exigences très strictes au niveau des performances et de la régularité.

Le respect des exigences de performances imposées par la Règlementation et l'adéquation du produit aux besoins réels du marché ont conduit à des ciments dont le taux d'ajout calcaire se situe actuellement entre 10 et 25 % suivant les classes de résistances, mais plus généralement autour d'un taux de 20 % d'ajout calcaire.

En 1983, sur vingt-trois millions de tonnes de ciment consommées en France, il y en a 16,5 millions de tonnes ayant un taux d'ajout compris entre 5 et 35 % qui se distribuent ainsi : 7,7 millions de tonnes de ciment, où rentrent des ajouts de filler calcaire, soit seuls, soit en association avec du laitier, des cendres ou des pouzzolanes ; 4,8 millions de tonnes de ciment avec ajout de laitier seul ; 2,8 millions de tonnes de ciment avec ajout de cendres ou pouzzolanes seules et 1,2 millions de tonnes de ciment avec ajout mixte laitier-cendres. Ceci montre la part importante des ciments avec ajout et en particulier de ceux qui ont comme constituants des fillers calcaires.

Pour que ces ciments à taux d'ajout calcaire relativement élevé puissent se développer commercialement et avoir la part de marché qu'ils occupent actuellement, il était nécessaire de bien montrer qu'un ciment Portland avec ajout de filler calcaire (CPJ) possède les mêmes propriétés que le ciment Portland pur sans ajout (CPA) issu du même clinker et appartenant à la même classe de résistance en compression à vingt-huit jours.

Il arrive en effet que ce point soit contesté en tenant le raisonnement spécieux suivant : "Lorsqu'un ciment Portland pur (CPA) et un ciment Portland avec ajout de filler calcaire (CPJ) appartenant à la même classe de résistance à vingt-huit jours sont gâchés au même rapport eau sur ciment, le rapport eau sur clinker du CPJ étant plus élevé que celui du CPA, il en résulte une porosité plus grande de la pâte hydratée du CPJ avec tous les risques qu'entraînerait cette conséquence".

S'il est vrai, par définition même, qu'il y a moins de clinker dans un ciment avec ajout calcaire que dans un ciment Portland pur, il est tout aussi évident que dans chacun des cas ce clinker ne pourra agir et développer ses résistances que s'il est suffisamment broyé. Ce qui importe donc, ce n'est pas tant la quantité de clinker présente que l'activité hydraulique de ce clinker. Celle-ci se développe grâce au broyage et se traduit, après gâchage, par la formation d'hydrates qui donneront les résistances et la réduction progressive de la porosité du matériau.

2 - VALORISATION du POTENTIEL HYDRAULIQUE du CLINKER par AJOUT de FILLER INERTE

En France, comme dans de nombreux pays, les classes de ciments sont définies par le niveau des résistances mécaniques à vingt-huit jours en mortier ISO à 20°C. La classe de résistance la plus demandée est la classe 45 c'est-à-dire celle pour laquelle les ciments doivent avoir en moyenne une résistance à 28 jours en mortier ISO proche de 45 MPa ; elle représente près de 65 % des demandes des utilisateurs.

La finesse de broyage nécessaire pour obtenir 45 MPa de résistance en compression à vingt-huit jours varie suivant les clinkers. Une expérience faite sur une population de quatorze clinkers industriels de provenances différentes et donnant les résistances à vingt-huit jours en mortier AFNOR en fonction de la finesse Blaine de broyage (figure 1) montre que :

- La finesse de broyage nécessaire pour obtenir 45 MPa à vingt-huit jours est toujours inférieure à 2700 $cm^2\ g^{-1}$.
- Pour près de la moitié des clinkers, la finesse de broyage pour obtenir 45 MPa est même inférieure à 2000 cm^2/g^{-1}.

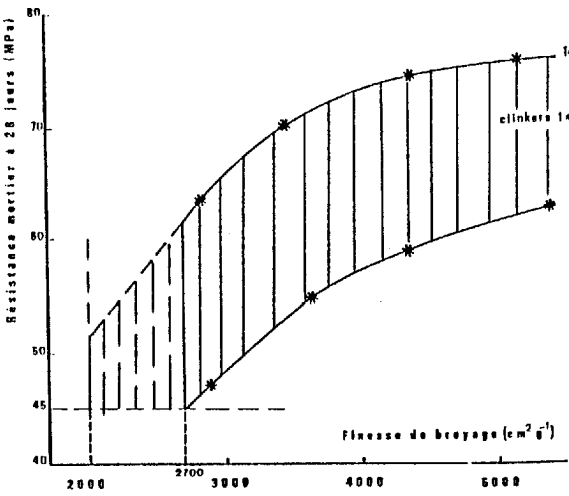

Figure 1 : Résistances à vingt-huit jours obtenues en mortier AFNOR à partir de quatorze clinkers en fonction de leur finesse de broyage (la partie hachurée entre les courbes enveloppes (1) et (14) est la zone où se situe l'ensemble des courbes résistances-finesses des quatorze ciments.

On voit donc que pour obtenir la classe de résistance 45 la plus couramment demandée, le clinker ne devra être que grossièrement broyé si on veut un ciment Portland pur sans ajout. La fraction granulaire la plus grossière du ciment obtenu est alors constituée de grains de clinker qui ne s'hydratent pas et qui sont donc, en grande partie, inutiles pour le développement des propriétés hydrauliques.

On conçoit donc bien que la seule façon de valoriser le potentiel hydraulique du clinker est de le broyer plus finement tout en ajoutant un filler inerte pour maintenir la résistance à vingt-huit jours du ciment à la valeur nominale de la classe de résistance demandée.

3 - EXPERIMENTATION et CARACTERISTIQUES des CIMENTS

Pour montrer que dans un ciment Portland avec ajout calcaire le résultat de l'activité hydraulique du

clinker est au moins égal à celui du CPA de même classe, malgré un taux de clinker moins important mais grâce à une finesse de broyage plus poussée, nous avons suivi le développement des hydrates et l'évolution de la porosité de quatre ciments issus d'un même clinker :

. CPA 55 : ciment Portland sans ajout ayant une résistance à vingt-huit jours de 58,3 MPa.

. CPJ 55 : ciment Portland avec 15 % d'ajout calcaire ayant une résistance à vingt-huit jours de 57,3 MPa à peu près identique au précédent.

Ces deux ciments, avec et sans ajout, appartiennent tous deux à la classe de résistance 55.

. CPA 45 : ciment Portland sans ajout ayant une résistance à vingt-huit jours de 49,9 MPa.

. CPJ 45 : ciment Portland avec 27 % d'ajout calcaire ayant une résistance à vingt-huit jours de 48,7 MPa, donc très proche de celle du CPA 45 précédent.

Ces deux ciments, avec et sans ajout, appartiennent tous deux à la classe de résistance 45.

Les ciments CPA 55 et CPA 45 ont été obtenus en broyant le clinker d'origine aux finesses Blaine respectives de 3340 cm^2g^{-1} et 2250 cm^2g^{-1}.

Les ciments CPJ 55 et CPJ 45 ont été obtenus en ajoutant respectivement 15 et 27 % d'un même filler calcaire à un CPA du même clinker broyé à une finesse Blaine de 3970 cm^2g^{-1}. Il est à remarquer que la finesse de broyage du clinker dans le CPJ 45 est plus élevée que celle du CPA 55.

Les caractéristiques de ces quatre ciments figurent au tableau 1.

	Finesse Blaine du ciment (cm^2g^{-1})	Finesse Blaine clinker seul (cm^2g^{-1})	Finesse Blaine du calcaire (cm^2g^{-1})	Taux d'ajout calcaire (%)
CPA 55	3340	3340	-	0
CPJ 55	4180	3970	5400	15
CPA 45	2550	2550	-	0
CPJ 45	4360	3970	5400	27
	Résistance compression mortier AFNOR (MPa)			
	1 j	2 j	7 j	28 j
CPA 55	15,1	25,5	43,8	58,3
CPJ 55	18,4	27,9	45,0	57,3
CPA 45	11,2	19,8	35,4	49,9
CPJ 45	14,9	23,3	37,3	48,7

Tableau 1 : Caractéristiques des quatre ciments étudiés.

On peut noter que dans chaque classe de ciment, pour des résistances à vingt-huit jours équivalentes en CPA et CPJ, les résistances initiales à un et deux jours des deux CPJ sont supérieures à celles des CPA correspondants. On retrouve là un caractère général qui est la supériorité des résistances initiales du CPJ par rapport à celles du CPA de même classe.

Cela s'explique si l'on sait que l'effet de la finesse de broyage du clinker se fait beaucoup plus sentir sur les résistances initiales que sur les résistances à vingt-huit jours alors que l'effet de l'ajout se fait sentir d'une façon égale sur les résistances initiales et sur les résistances à vingt-huit jours.

4 - SUIVI de l'EAU LIEE au COURS de l'HYDRATATION

L'eau liée déterminée sur les pâtes pures hydratées à E/C 0,5 et 0,28 de chacun des quatre ciments à différentes échéances après stoppage d'hydratation à l'acétone éther, permet de suivre l'évolution des taux d'hydratation de huit heures à quatre-vingt dix jours (tableau 2).

Malgré une certaine dispersion des résultats obtenus, on voit très nettement que le clinker des CPJ s'hydrate plus rapidement que celui des CPA car :

- à huit heures, l'eau liée des CPJ est toujours plus élevée que celle des CPA correspondants de même classe ;
- à un, deux, sept et vingt-huit jours, les valeurs de l'eau liée sont très voisines entre le CPJ et le CPA de même classe ;
- à quatre-vingt dix jours, la quantité d'eau liée des CPJ a tendance, trois cas sur quatre, à être sensiblement inférieure à celle des CPA correspondants.

	E/C = 0,50			
	CPA 55	CPJ 55	CPA 45	CPJ 45
8 h	4,5	7,0	4,6	6,4
1 j	15,2	15,3	14,0	13,8
2 j	18,8	17,2	16,2	15,5
7 j	22,0	22,0	19,8	19,5
28 j	24,6	23,6	24,4	22,5
90 j	27,0	24,6	26,2	23,1
	E/C = 0,28			
8 h	7,4	8,4	5,9	7,0
1 j	15,1	14,2	13,2	13,0
2 j	16,8	15,8	15,5	15,0
7 j	18,9	18,2	17,2	17,5
28 j	20,6	19,5	18,9	19,6
90 j	20,6	19,5	18,9	19,6

Tableau 2 : Pourcentage d'eau liée à différentes échéances de chacun des quatre ciments hydratés en pâte pure à E/C = 0,5 et à E/C = 0,28.

Ainsi les CPJ, bien que contenant moins de clinker que les CPA de même classe, ont grâce à la plus grande fi-

nesse du clinker un taux d'hydratation d'abord plus élevé aux très courtes échéances, puis identique à celui des CPA jusqu'à vingt-huit jours et légèrement inférieur de vingt-huit à quatre-vingt dix jours, période pendant laquelle l'évolution du taux d'hydratation s'est aussi stabilisée.

Il est à remarquer par ailleurs que cette stabilité est plus vite acquise tant pour les CPJ que pour les CPA, au E/C de 0,28 qu'au E/C de 0,5. Nous pouvons expliquer cela par le fait qu'à un rapport E/C de 0,28 les quantités d'eau disponibles pour l'hydratation deviennent rapidement plus faibles et la vitesse d'hydratation se ralentit.

5 - EVOLUTION de la POROSITE

La porosité des pâtes pures hydratées à E/C de 0,5 et de 0,28 pour chacun des quatre ciments entre un et quatre-vingt dix jours a été mesurée au moyen d'un porosimètre à mercure. Celui-ci permet d'obtenir (tableau 3) la porosité comprise entre 0,0075 micromètres (75 Å) et 120 micromètres.

	E/C = 0,50			
	CPA 55	CPJ 55	CPA 45	CPJ 45
1 j	41	40	44	42
2 j	38	38	40	40
7 j	32	32	34	34
28 j	26	26	27	30
90 j	21	23	23	26
	E/C = 0,28			
1 j	22	21	23	25
2 j	16	18	17	19
7 j	13	13	14	15
28 j	9	10	10	12
90 j	7	7	9	9

Tableau 3 : Mesure de la porosité (exprimée en pourcentage de volume) à différentes échéances de chacun des quatre ciments hydratés en pâte pure à E/C = 0,5 et à E/C = 0,28.

Avant chaque mesure, l'échantillon de pâte hydratée a été :

- concassé à une dimension de 5 à 10 mm ;
- mis sous vide pendant cinq minutes ;
- soumis pendant six heures à un échange eau-méthanol ;
- séché à l'air pendant une demi-heure, puis à l'étuve à 40° pendant douze heures.

D'une façon tout à fait analogue à ce que nous avons remarqué précédemment pour la teneur comparée en eau liée des CPA et CPJ de même classe, on voit que :

- à un jour, la porosité des CPJ a tendance (trois cas sur quatre) à être moins élevée que celle des CPA de même classe ;
- à deux, sept et vingt-huit jours, les valeurs des porosités sont très voisines entre le CPJ et le CPA correspondant de même classe ;
- à quatre-vingt dix jours, la porosité des CPJ a tendance (uniquement pour les pâtes hydratées à un rapport E/C de 0,5) à être sensiblement plus élevée que celle des CPA de même classe.

L'évolution de la porosité se stabilise également au cours de cette période et plus particulièrement en pâtes hydratées au E/C = 0,28.

En résumé, on constate donc qu'entre CPA et CPJ de même classe, les porosités sont très voisines avec toutefois une tendance pour les CPJ à avoir une porosité légèrement plus faible à un jour et un peu plus élevée après vingt-huit jours.

L'examen des spectres de porosité de chacun de ces quatre ciments hydratés en pâte pure à E/C = 0,5 montre, de la même manière, que la répartition des pores en fonction de leur dimension est la même pour les ciments purs que pour les ciments avec ajout de filler calcaire (figures 2 a,b,c).

La dimension des pores de la pâte hydratée est essentiellement fonction de l'avancement de l'hydratation ; c'est pourquoi à vingt-huit et quatre-vingt dix jours, les pores se situent respectivement à partir de 0,1 micromètres et 0,05 micromètres quel que soit le ciment alors qu'à deux jours la dimension des pores est un peu plus élevée pour le CPA 45 que pour le CPA 55 et les deux CPJ, ce qui traduit bien l'avancement plus poussé de l'hydratation des deux CPJ aux jeunes âges.

6 - POROSITE - RESISTANCE

Les corrélations entre les résistances en mortier AFNOR et les porosités en pâte pure à E/C = 0,5 sont excellentes (tableau 4).

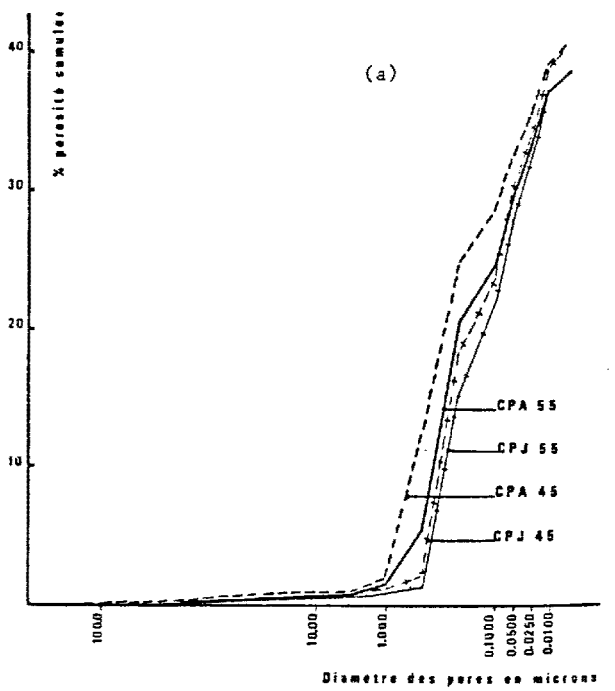

R.GUYOT, R.RANC, B.CARIOU
LAFARGE COPPEE RECHERCHE, FRANCE

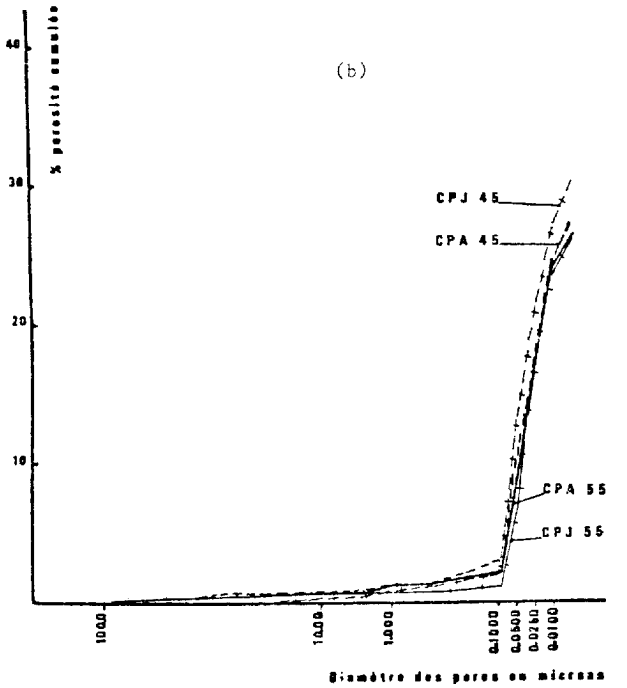

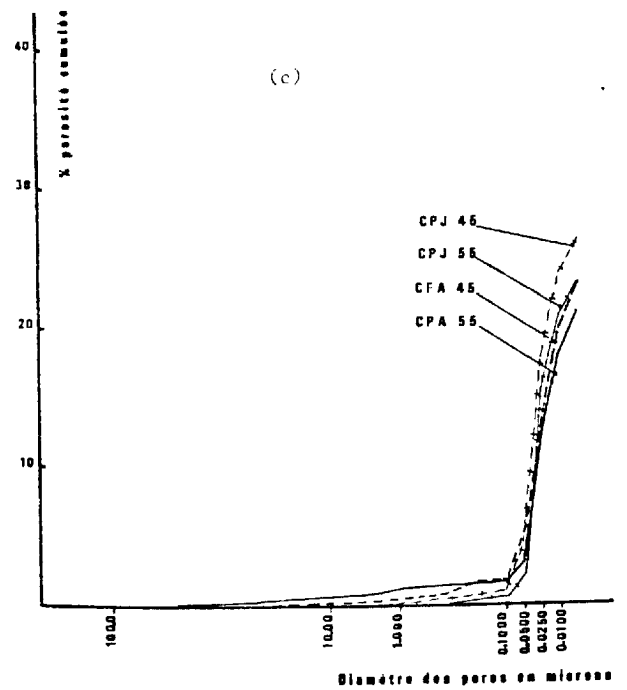

Figure 2(a) (b) (c) : Répartition de la porosité en pâte pure à E/C = 0,5 aux échéances de : (a) 2 jours ; (b) 28 jours ; (c) 90 jours.

Pour les huit valeurs de CPA (deux CPA, quatre échéances), le coefficient ρ de corrélation simple résistance-porosité est égal à -0,991 (il est même égal à 0,996 si on écarte l'échéance à vingt-huit jours du CPA 45).

Pour les huit valeurs de CPJ (deux CPJ, quatre échéances), le coefficient ρ de corrélation simple résistance-porosité est égal à -0,993.

Lorsqu'on groupe les huit valeurs de CPJ et les sept valeurs de CPA, cette corrélation reste excellente et le coefficient de corrélation reste inchangé ρ = -0,994 (figure 3).

Echéance	1 jour		2 jours		7 jours		28 jours	
	P	R	P	R	P	R	P	R
CPA 55	41	15,1	38	25,5	32	43,8	26	58,3
CPA 45	41	11,2	40	19,8	34	35,4	(27	49,9)
CPJ 55	40	18,4	38	27,9	32	45,0	26	57,3
CPJ 45	42	14,9	40	23,3	34	37,3	30	48,7

	Coefficient de corrélation multiple	
CPA 55	Pour les 8 couples de valeurs ρ = -0,991	Pour les 15 couples de valeurs ρ = -0,994
CPA 45	Pour les 7 couples de valeurs (1) ρ = -0,996	
CPJ 55	Pour les 8 couples de valeurs ρ = -0,993	
CPJ 45		

P = % porosité pâte pure E/C = 0,5
R = résistance mortier AFNOR en MPa

(1) en ne prenant pas en compte l'échéance à vingt-huit jours du CPA 45.

Tableau 4 : Corrélation Résistance mortier AFNOR/ Porosité pâte pure à E/C = 0,5.

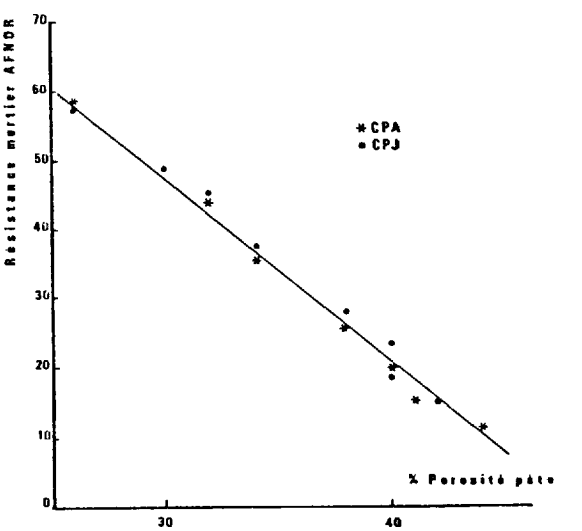

Figure 3 : Corrélation Résistance mortier AFNOR et porosité pâte pure à E/C = 0,5.

Ce qui indique bien qu'un CPJ présente la même porosité qu'un CPA pour une même résistance mortier.

R.GUYOT, R.RANC, B.CARIOU
LAFARGE COPPEE RECHERCHE, FRANCE

7 - SUIVI du TAUX de PORTLANDITE en COURS d'HYDRATATION

Le taux de Portlandite $Ca(OH)_2$ déterminé par analyse thermo-pondérale (ATP) sur pâte pure à E/C = 0,5 (tableau 5) est également un moyen de suivre le taux d'hydratation comme nous l'avons fait précédemment avec le taux d'eau liée. Il est intéressant de noter tout d'abord qu'il y a effectivement une très bonne cohérence entre le taux d'eau liée et le taux de Portlandite aussi bien pour les CPA que pour les CPJ avec ajout calcaire (tableau 6). Le rapport % eau liée/% Portlandite est le même pour le CPJ que pour le CPA.

Les conclusions que l'on peut tirer du suivi des taux de la Portlandite sont donc les mêmes que celles établies avec l'eau liée : teneurs en $Ca(OH)_2$ très voisines entre CPA et CPJ de même classe, donc même taux d'hydratation jusqu'à vingt-huit jours.

Echéances	CPA 55	CPJ 55	CPA 45	CPJ 45
7 j	12	12	13	12
28 j	14	14	15	13
90 j	16	15	16	14

Tableau 5 : Taux de Portlandite mesuré par ATD sur pâte pure à E/C = 0,5 à différentes échéances.

Echéances	CPA 55	CPJ 55	CPA 45	CPJ 45
7 j	1,8	1,8	1,5	1,6
28 j	1,8	1,7	1,6	1,7
90 j	1,7	1,6	1,6	1,7

Tableau 6 : Valeurs du rapport % eau liée/% Portlandite à différentes échéances pour les quatre ciments.

8 - EVOLUTION de la DECROISSANCE du C3S par DIFFRACTION X

Les mesures de diffraction ont été faites pour suivre la disparition des anhydres : C3S (raie à 1.77 Angström) au cours de l'hydratation en pâte pure à E/C = 0,5 et à E/C = 0,28 de chacun des quatre ciments (tableau 7).

De même que nous avions observé un développement plus rapide des hydrates en CPJ qu'en CPA, nous retrouvons une diminution plus rapide du C3S dans le CPJ comparativement au CPA de même classe.

Cette diminution plus rapide du C3S dans les CPJ est particulièrement nette avec les ciments de classe 45 où la différence de finesse du clinker entre CPA et CPJ est la plus grande.

Il est à noter que dans les deux CPA hydratés en pâte pure à E/C = 0,5, il reste après vingt-huit jours encore près de 10 % du C3S initial non combiné alors que dans le CPJ le C3S s'est entièrement hydraté.

Au-delà de vingt-huit jours, le C3S des CPA continue de s'hydrater en partie mais il en reste d'une façon visible à quatre-vingt dix jours et vraisemblablement au-delà sans peut-être ne jamais se combiner, ni donner de résistance car insuffisamment broyé.

Echéances	E/C = 0,50			
	CPA 55	CPJ 55	CPA 45	CPJ 45
Anhydre	62	56	60	49
8 h	-	50	50	36
1 j	30	28	30	15
2 j	27	23	24	11
7 j	13	6	14	3
28 j	5	traces	6	traces
90 j	2	traces	traces	traces
	E/C = 0,28			
Anhydre	62	56	60	49
8 h	57	46	57	33
1 j	32	25	30	19
2 j	22	20	23	13
7 j	20	13	23	6
28 j	17	10	17	4
90 j	12	10	15	4

Tableau 7 : Evolution des hauteurs de pics (raie à 1,77 Å) du C3S dans les pâtes hydratées à E/C = 0,5 et E/C = 0,28 des quatre ciments.

Le comportement est analogue à E/C = 0,28 mais, à partir de sept jours, la diminution du C3S se ralentit encore plus fortement et à quatre-vingt dix jours la quantité de C3S initial demeure encore relativement importante.

9 - ALUMINATE TRICALCIQUE et FORMATION de MONOCARBOALUMINATE

Les mesures de diffraction X ont permis également de suivre la disparition du C3A (raie à 2,7 Angström) au cours de l'hydratation en pâte pure à E/C = 0,5 et à E/C = 0,28 (tableau 8).

	E/C = 0,50			
	CPA 55	CPJ 55	CPA 45	CPJ 45
Anhydre	32	39	32	33
8 h	33	35	32	27
1 j	26	27	22	20
2 j	15	22	14	16
7 j	5	5	9	4
28 j	traces	traces	2	traces
90 j	traces	traces	traces	traces
	E/C = 0,28			
Anhydre	32	39	32	33
8 h	29	31	28	25
1 j	23	23	23	20
2 j	16	18	18	14
7 j	13	12.	13	5
28 j	9	8	9	4
90 j	7	8	9	4

Tableau 8 : Evolution des hauteurs de pics (raie à 2,7 Å) du C3A dans les pâtes hydratées à E/C = 0,5 et E/C = 0,28 des quatre ciments.

P.GUYOT, R.RANC, B.CARIOU
LAFARGE COPPEE RECHERCHE, FRANCE

Le pic du C_3A étant moins important, il est plus difficile d'observer une différence significative entre CPA et CPJ.

Cette différence cependant apparaît encore assez nettement avec la classe 45 où l'on retrouve la diminution plus rapide du C_3A dans le CPJ.

A E/C = 0,28, la diminution du taux d'aluminate tricalcique se ralentit fortement à partir de sept jours comme pour le C_3S ; à quatre-vingt dix jours la quantité de C_3A initial demeure encore relativement importante.

Les mesures de diffraction X montrent à l'échéance de sept jours l'apparition de monocarboaluminate de chaux : C_3A, $CO_3Ca.11H_2O$ (raie à 7,63 Å) dans chacun des deux CPJ (tableau 9). Il est difficile de donner une estimation en pourcentage des quantités formées mais elles paraissent sensiblement identiques dans chacun des deux CPJ qui, rappelons-le, sont constitués du même clinker broyé à la même finesse et ne diffèrent que par la quantité de l'ajout calcaire plus élevé dans le CPJ 55 que le CPJ 45.

Le filler calcaire n'est donc pas véritablement un inerte puisqu'il réagit avec l'aluminate tricalcique pour donner du carboaluminate comme cela a déjà été montré par d'autres chercheurs(1). Malgré l'intérêt que présente cette réactivité du filler, nous ne pensons pas qu'elle soit déterminante dans les propriétés du CPJ et, compte tenu de ce que nous avons vu précédemment, ce sont avant tout les hydrates développés par la finesse de broyage du clinker qui sont les éléments déterminants de la qualité et des performances des ciments avec ajout calcaire.

	E/C = 0,50			
	CPA 55	CPJ 55	CPA 45	CPJ 45
8 h	0	0	0	0
1 j	0	0	0	0
2 j	0	0	0	0
7 j	0	11	0	11
28 j	0	19	0	28
90 j	0	38	0	39
	E/C = 0,28			
8 h	0	0	0	0
1 j	0	0	0	0
2 j	0	0	0	0
7 j	0	3	0	5
28 j	0	7	0	10
90 j	0	6	0	12

Tableau 9 : Evolution des hauteurs de pics par diffraction X (raie à 7.63 Å) du monocarboaluminate de chaux dans les pâtes hydratées à E/C = 0,5 et E/C = 0,28 des quatre ciments.

CONCLUSION

Nous avons ainsi montré que lorsqu'un ciment Portland pur (CPA) et un ciment Portland avec ajout de fillers calcaires (CPJ) appartenant tous deux à la même classe de résistance à vingt-huit jours sont gâchés au même rapport eau sur ciment (eau/CPA = eau/CPJ), on obtient des pâtes hydratées de même porosité ; les propriétés en mortiers et bétons qui en découlent seront donc identiques pour chacun des deux ciments.

Ce résultat est obtenu par un broyage plus poussé du clinker dans le CPJ que dans le CPA, ce qui permet d'obtenir avec le CPJ des quantités d'hydrates identiques à celles du CPA bien qu'il y ait moins de clinker dans le ciment CPJ avec ajout que dans le ciment pur CPA.

L'intérêt de l'incorporation d'un filler calcaire dans un ciment apparaît ainsi très clairement : en utilisant moins de clinker mais en développant mieux le potentiel hydraulique de ce clinker par un broyage approprié, on obtient un ciment avec ajout qui aura en tout point les mêmes propriétés que celles d'un ciment Portland pur habituel. Il pourra répondre aux mêmes exigences car la composition et la structure de la pâte liante obtenue après hydratation sont identiques.

En corollaire, il faut souligner toute l'importance qu'il y a à contrôler et à maîtriser la finesse réelle de broyage du clinker dans le ciment avec ajout car c'est la finesse de broyage du clinker qui est l'élément déterminant de la qualité du CPJ au filler calcaire.

REFERENCES

(1) Liaison pâte de ciment-filler dans les ciments composés. B.MORTUREUX - H.HORNAIN - M.REGOURD - Colloque International Liaison Pâte de Ciment - Matériaux Associés - TOULOUSE - Novembre 1982.

K. TAKEMOTO Onoda Cement Co, Ltd, - Japan

THE VARIATION OF ACTIVITY INDEX OF SLAG

1. Introduction

The sum of blast furnace slag produced in Japan was 24.8×10^6 ton in 1984. The share of water-quenched granulated slag was 46.6%. The gradually-cooled slag was used mainly for subbase of road, and the use of granulated slag was mainly for slag cement. The production of slag cement was 8.6×10^6 ton, which holds 12.3% of total production of all cements, and is estimated to hold 20% in near future.

The method of manufacture of slag cement is mostly separate-grinding of slag with gypsum, and then mixing with ordinary portland cement (OPC) at cement plant. The blending ratio is around 50 : 50.

The slag activity index is one of the method of evaluation for the latent hyraulicity of slag. But, the author shows that the slag activity index varies not only with slag, also with OPC used.

2. Slag Activity Index

The slag activity index (A.I)(1) is calculated as follows;

$$A.I = S_1/S_0 \times 100 \qquad --1)$$

where S_1 and S_0 is strength of blended cement and OPC, respectively.

On the other hand, the basicity (2) of slag is also used for evaluating the hydraulicity of slag.

$$\text{Basicity} = (A+C+M)/S \qquad --2)$$

where A, C, M and S is Al_2O_3, CaO, MgO and SiO_2, respectively.

Fig. 1 shows the relation between A.I. and basicity. The slags were 13 kinds, which came from 13 different iron works, and mixed with one of OPC in laboratiry mixer. The mixing ratio was 50 : 50. The strength test was done by JISR5201, which uses 1 : 2 mortar and water-cement ratio of 65%. The specimen was cured up to 28 days in water at 293°K. Then, compressive strength was tested. The relation is better with considering the fineness of slag.

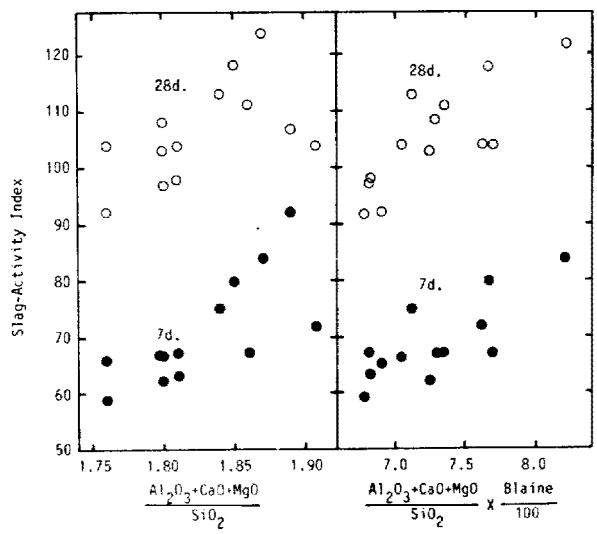

Fig. 1 Activity Index and Basicity of Slag

Table 1 Chemical composition of slag ground with Gypsum

slag	chemical analysis (%)								basicity	glass content(%)	Blaine (cm^2/g)
	SiO_2	Al_2O_3	Fe_2O_3	CaO	MgO	SO_3	Na_2O	K_2O			
A	31.7	14.2	0.5	41.1	6.2	2.8	0.22	0.33	1.88	100	3,580
B	32.1	13.4	0.5	40.9	6.0	3.4	0.15	0.27	1.80	100	3,840
C	31.9	13.1	0.8	39.1	7.1	3.3	0.22	0.37	1.79	100	3,950
D	31.6	11.9	0.4	41.7	8.5	3.1	0.15	0.24	1.90	98	4,090
E	31.8	12.2	0.4	41.1	5.4	3.1	0.20	0.34	1.78	99	4,230

Table 2 Chemical composition of ordinary portland cement

OPC No.	chemical analysis (%)										Blaine (cm^2/g)
	Loss	Insol	SiO2	Al_2O_3	Fe_2O_3	CaO	MgO	SO_3	Na_2O	K_2O	
1	0.6	0.1	22.1	5.3	3.0	63.6	1.8	2.0	0.39	0.56	3,520
2	1.0	0.1	21.9	5.4	2.8	63.9	1.5	2.0	0.33	0.71	3,170
3	0.5	0.1	21.4	5.5	3.6	64.5	1.1	1.9	0.28	0.54	3,030
4	0.8	0.1	22.0	5.8	3.0	63.8	1.7	2.0	0.29	0.51	3,300
5	0.7	0.2	21.6	5.5	3.0	64.0	1.2	2.1	0.40	0.51	3,480
6	0.5	0.1	22.2	5.5	2.8	63.7	1.6	2.1	0.26	0.64	3,230
7	1.1	0.4	21.7	5.1	3.0	63.5	1.6	2.0	0.49	0.45	3,200
8	0.8	0.1	22.3	5.9	2.7	63.2	1.7	2.0	0.26	0.26	3,120
9	0.7	0.1	22.4	5.0	3.1	64.2	0.9	2.1	0.31	0.56	3,270

3. Strength of Slag Cement

To evaluate the A.I., mortar strength of blended cements, which are the mixtures of 5 kinds of slag and 9 kinds of OPC., were tested. All of them came from different iron works and cement plants. The chemical compositions and fineness were shown in **Table 1 and 2.** The mixing ratio of slag to OPC was 50 : 50.

Fig. 2 is the results of strength tests. The 7 days-strength of slag cement depends mainely on the strength of OPC. The 28 days-strength is not parallel to that of OPC. This means that slag contributes to the later-age strength of slag cement. Here, the author emphasizes that the 28 days-strength of a slag cement is influenced by the OPC used. For example, the slag cements made with OPC NO.1 and 3 show the better strength development. On the other hand, the slag cements made with OPC NO.6 and 8 show the worse strength development. This means that the capability of OPC as activator to the hydraulicity of slag differs between OPCs. The specification (1) informs such phenomena in its Appendix. F.Schroeder and R.Vinkeloe (3) mentioned two examples which clinkers having high lime contents gave good influence to the strength of slag cements. R. Kondo (4) found early that the strength distribution of synthetic slags differs by the kind of activator, such as $Ca(OH)_2$ and $CaSO_4$.

The author tried to find the factors to dominate the activation capability of OPC, but could not succeed.

4. Variation of Slag Activity Index

The above mentioned results bring on the fear that the slag activity index varies with slag, also with OPC used. **Table 3** shows the slag activity index calculated from **Fig. 2.** The coefficient of variation of A.I. between slags is Cs = 8.4% in average, and that between OPC is Cp = 4.4%. Namely, the slag-activity index is influenced considerably with OPC used. This fact was confirmed statistically in **Table 4** of analysis of variance, which shows that OPC is highly significant to A.I., just as slag is so.

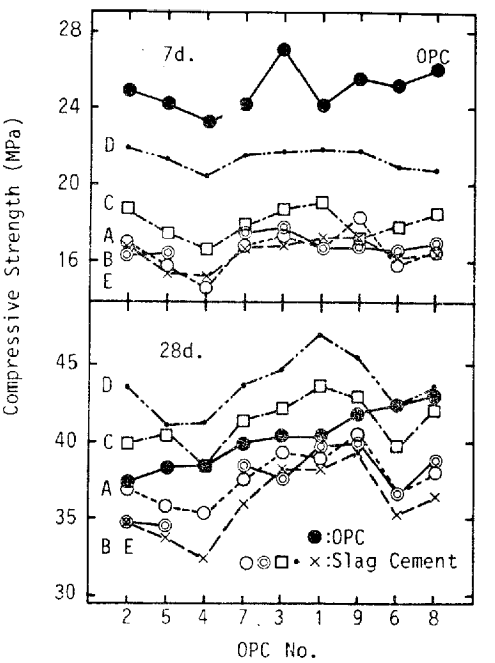

Fig. 2 Mortar Strength of OPC and Slag Cement (Slag /OPC=50/50)

Table 4 Analysis of variance for activity index

factor	sum of squares	degrees of freedom	variance	variances ratio
slag	2004.42	4	501.10	40.61**
OPC	672.02	8	84.00	6.81**
residual	394.89	32	12.34	
total	3071.33	44		

Table 3 Slag activity index and its variation (28d.)

slag	OPC 1	2	3	4	5	6	7	8	9	statistics $\bar{x}_p$	σ_p	C(%)
A	95.4	98.9	97.1	92.1	93.6	86.5	94.5	88.8	96.7	93.7	3.37	4.0
B	95.1	93.1	94.7	84.6	88.7	83.4	90.3	84.9	94.8	90.0	4.49	5.0
C	107.8	107.1	104.4	99.7	105.9	93.7	104.0	98.2	102.6	102.6	4.35	4.2
D	115.5	116.4	110.2	106.9	107.2	99.8	110.0	101.4	108.7	108.5	5.28	4.9
E	98.5	94.2	92.7	-	90.5	86.7	96.3	90.6	95.5	93.3	3.59	3.8
$\bar{x}_s$	102.5	101.9	99.8	95.8	97.2	90.0	99.0	92.8	99.7	$\bar{\bar{x}}$	$\bar{\sigma}_p$	$\bar{c}_p$
σ_s	8.76	10.00	7.51	10.83	7.94	7.04	8.45	7.08	5.97	97.6	4.22	4.4
C_s(%)	8.5	9.8	7.5	11.3	8.2	7.8	8.5	7.6	6.0			
$\bar{C}_s$(%)	8.4											

$\bar{x}$: mean
σ : standard deviation
c : coefficient of variation

5. Quality control of Slag Cement

The fact above mentioned means that the slag activity index is not useful to control the strength development of slag cement. Actually, the control at cement plant depends on the basicity and fineness of slag, and clinker quality and fineness of OPC, and also mixing ratio. They can control the quality of slag cement at real time.

In U.K., some of the ready-mixed concrete plant mix the ground slag in replacement of OPC (5)(6). But, they have not so many factors at ready mixed-concrete plant site, as at cement plant site, to control the quality of slag cement. The author claims such ready-mixed slag concrete should not be applied in general use.

6. Conclusion

The slag activity index varies not only with slag, but also with OPC. The activation capability of OPC to the hydraulicity of slag differs between OPCs. The author feels the difficulty in controling the quality of slag-replacement ready-mixed concrete.

Acknowledgement

The author appreciates the Laboratory of Cement Association of Japan permited him to use the test results on slag cement.

Literature

(1) ASTM C989-85

(2) JIS R5211-1964

(3) Schroeder, F and Vinkeloe, R., (1968) Proc. of Vth international Symposium on the Chemistry of Cement, part IV, p.177, Tokyo.

(4) Kondo, R., (1952) Semento-Gijutsu-Nenpo, VI, pp.180-186.

(5) Reeves, C.M., (1982) The Use of Ground Granulated Blastfurnace Slag for within-mixer Production of Portland-Blastfurnace Cement Concrete:Background and Development of the System in the U.K., Silicates Industriels, pp. 109-113.

(6) Jones, P.R., Reeves, C.M. and Dewae, J.D., (1982 Progress in the Use of Ground Granulated Blastfurnace Slag by the U.K. Ready Mixed Concrete Industry, Silicate Industriels, pp.253 -258.

T.V. KUZNETSOVA, S.D. MAKACHEV,
Z.B. ENTIN, Cement Research Institute, Moscow, USSR

CEMENTS WITH MINERAL ADMIXTURES: STATE OF THE ART AND PROSPECTS

Although the manufacturing and use of cements with mineral admixtures had been known from the beginning of this century it were only the last one or two decades that saw an increasing interest to this cements in all industrial countries aroused in connection with multipled fuel costs. The report by Dutron /1/ predicts that the average content of admixtures in cement will increase by 1990 to as much as 23% in Western Europe, to 12% in the United States, and to 10% in Japan. By 2000, the proportion of admixtures in cement will increase, on the average, 1.5 or 2 times above this level.

1. Classification of admixtures. Standards concerning classification of admixtures used in cement manufacture and/or specifications for such admixtures have been developed in many countries, including, for example, the USA, West Germany, Romania, and East Germany. One of the more complete classifications may be found in the Soviet standard GOST 24640-81 /2/. It categorizes the admixtures into active mineral, fillers, technological, and those controlling the main and special properties of cement.

This report will survey the experience which has been accumulated in using cements with mineral admixtures.

2. Specifications and estimation of effectiveness of mineral admixtures. Despite the vast literature on the chemistry and properties of cements with admixtures /3-5/ there has not been elaborated so far a suitable method of direct quantitative estimation of activity of admixtures which could substitute for the existing empirical techniques. Indeed, the data on chemical and mineralogical composition of an admixture, degree of crystallization, content of vitreous phase, etc., enable one to characterize the material as an active mineral admixture only with some probability, but to issue an accurate conclusion direct testing is needed.

According to the Soviet standard, an admixture is categorized as active provided it meets the requirements as follows:

- for a cement paste of normal consistency prepared of the mix of the finely ground material with hydrated lime in the 4:1 proportion with a small addition of gypsum, the final set is not later than 7 days after mixing with water;
- the specimen immersed in water after the final set is not washed out and retains clear cut edges for at least 3 days;
- for blended portland cement containing 30% or 40% of the characterized material (depending on the type of admixture), the setting concentration of calcium hydroxide in the liquid phase should be at least 0.5 mmol/l below the saturation isoterm.

For artificial admixtures, the latter test is replaced by the strength tests for rod specimens prepared from a mix of the material being defined with hydrated lime and gypsum and steam cured to some specified procedure. The bending strength of these specimens should be at least 1 MPa, and the compressive strength at least 3 MPa.

A simple and convenient criterion to estimate the effectiveness of an admixture is the coefficient of relative clinker requirement for a concrete defined as the ratio

$$K_{cl} = \frac{BC\ (100 - A)}{100\ PC}$$

where BC stands for blended cement (with admixture) requirement in kg/m^3; A for the percentage of admixture; and PC for plain cement requirement in kg/m^3.

An admixture is claimed efficient if $K_{cl} \leqslant 0.95$.

3. Nomenclature of active mineral admixtures. In the USSR 28 to 30 million tons of various materials, mainly industrial wastes, is annually used as admixtures in cements. These materials include metallurgical slags (blast-furnace and thermophosphorous), bergmeal, metallurgical molding sand, diatomite, belite slurry, flyash and cinder. The list of admixtures in use is being expanded but the main proportion falls to blast furnace granulated slags which are completely uti-

lized in this country.

The quality of slags is assessed mainly by their chemical analysis. The reactive components of slag are CaO and Al_2O_3 added by MgO given its content not exceeds 10 wt %. The passive components include SiO_2, TiO_2, MnO and a proportion of MgO in excess of 10%.

When the MgO content of slag exceeds 14-15%, there is a risk of magnesial expansion and the quality of slag is markedly lower. Therefore, the Soviet standard GOST 3476-74 puts the upper limit on MgO content at 15%. It allows, however, a higher contents of MgO up to the highest level met in industrial slags (16-17%) provided the material simultaneously contains exceedingly high percentage of Al_2O_3, up to 12-15%. A high MgO content increases the activity of Al^{3+} ions and facilitates their transition into an octahedral coordination with oxygen. As a result the mobility of the Al-O bond increases and this compensates to a large degree of decrease of CaO in the slag. Higher proportions of Al_2O_3, an oxide of intermediate basicity, leads also to a narrow field of primary crystallisation of MgO and increases its solubility in slags glass. This prevents magnesial expansion of the cement.

Thermophosphorous slags of electric steelmaking primarily contain glass of vollastonite composition. The activity of O^{2-} in these slags is lower than in blast furnace slags, and the degre of polymerisation of the anionic sceleton is higher in accordance with the lower ratio O^{2-}/S^{4+}. Accordingly, equal strength cements with thermophosphorous slags contains 10% to 15% smaller proportions of admixture than blast-furnace slag cements.

An advantage of thermophosphorous slag cements is due to their enhanced sulphate resistance, which results from almost complete absence of Al_2O_3 in the slag. This quality have led to an industrial technology which uses these slags and ordinary clinker to yield high quality, sulfate-resistant, slag portland cement which excels in quality the sulfate-resistant portland cement and is much cheaper to produce and with lesser energy requirements.

The slags of nonferrous metallurgy contain large proportions of ferrous oxides in the form of Fe_2O_3 and FeO. Granulation virtually does not improve their activity, but has a bearing on their hardness and grindability. When these slags are hydrated in an alkali medium, FeO is gradually oxidized by air oxygen into Fe_2O_3 so that the initial ratio of FeO/Fe_2O_3 almost does not affect the slag activity. By their effect on the cement strength, the ferrous slags are inferior to blast furnace and thermophosphorous slags, and are about equivalent to pozzolans. No loss of strength was noted in a prolonged hydration of cement containing portland cement clinker, gypsum, and ferriferous slag from copper-melting manufacture in a proportion of 30 wt %. After one year of setting the cement stone exhibited low basicity hydrosilicates, hydroferrites, and iron hydroxide. There was no evidence of ferrous compounds similar to calcium sulfoaluminate hydrates.

A remarkable property of nonferrous slag cements is due to the high degree of protection they offer to steel reinforcement elements. They consume oxygen which penetrates into the cement stone by oxidizing FeO to Fe_2O_3. This property of the slags to inhibit oxygen agressive action is even higher than that of the known inhibitor - sodium nitrite-nitrate.

Coal slags containing CaO in proportions of 25-40% approach in their basicity to electric thermophosphorous slags, but differ from the latter by a greater activity of the glass which they contain in lesser proportions. With 30 to 40% coal slags interground with clinker, the resultant cement exhibits a 28-day compressive strength of up to 35-40 MPa.

The quality of belite slime is governed by the residual content of alkali oxides, basically Na_2O. Given the residual content

of R_2O in slag not exceeds 1.0-1.2% (expressed as the Na_2O equivalent of the total alkalies), the belite slime is a valuable component for portland cement clinker and an effective admixture to cement. The 28-day compressive strength of cements with up to 15-20% of belite slime amounts to 40-50 MPa. Where the slag contains a higher proportions of R_2O, special precautions should be considered to protect the concrete from cement bleeding and alkali corrosion.

Acid flyash as admixture has received a rather thorough treatment and is widdly utilized in many contries, including Hungary, France, Poland, and the Soviet Union.

A considerable interest is attracted to basic flyash containing higher proportions of free CaO. In the USSR, such flyash has been utilized to produce a self-stressing cement with a self-stress energy is excess of 2.0 MPa, a non-shrinking cement, and a cement with controlled linear expansion.

Scanning electron microscopy has revealed that the expansive properties of a cement are conditioned by the shape of ettringite formations that occur in hydration of the flyash cement. If the cement stone exhibits formless star-like clusters of subfine-crystalline fibres of ettringite, it will possess excessive expansion and the flyash cement will not pass a soundness test. Where ettringite forms into long prismatic crystals, these reinforce the setting cement paste and give it an increased strength and density. Such cements exhibit linear expansion within 0.5-2%, pass soundness tests, and demonstrate a 28-day compressive strength of 40-50 MPa at a self stressing of 2.0-3.0 MPa. Prolonged tests of complex reinforced concrete structures made with these cements have confirmed their high durability.

The most general and definitive property of all active mineral admixtures is in their lower basicity as compared with portland cement clinker. Therefore, admixtures enter acid-basic interactions with minerals of clinker and facilitate more full utilization of its chemical energy. The intensity of the interaction defines the activity of the admixture, being controlled by many factors such as chemical composition, the degree of vitreous phase, fineness, surface morphology of grains, and such.

In hydration of admixtures a significant role is played by alkali oxides entering into the liquid phase from the admixture proper and from portland cement clinker. At the initial stage, movable alkali ions accumulate near the surface of the particle and diffuse along the microcracks and phase interfaces. These ions interact with the admixture, demolish the surface layer of the glass and yield soluable but immobile alkali silicates and aluminates. This in turn increases the osmotic pressure in the reaction zone causing an influx of water so that the particle of admixture finds itself surrounded by a liquid envelope separating it from the rest cement paste at the initial setting stage.

The aforementioned process can be readily observed in electron micrographs recorded in the hydration of flyash cements owing to a right spherical shape of flyash particles. In further stages of setting, the substitution of alkali ions with calcium ions leads to the formation of hydrosilicates, hydroaluminates, and hydroferrites of calcium, dense integration of the particle into the cement stone and consolidation of the stone.

The outlined mechanism satisfactorily explains the principle engineering properties of cement with mineral admixtures, namely, a decreased early strength, ability of prolonged strength development, lower frost resistance, increased sulfate resistance, increased shrinkage deformations in setting on air, and such. This mechanism also defines the directions for further improvements of additive cement qualities. The principal direction concerns with the acceleration of the rate of setting to enhance the strength of these cements to the

level of plain cements, retaining all the specific engineering properties of these cements and their low power requirements in manufacture. One of the important trends to produce the most effective cements of this kind, as it was shown by the special researches, is the utilization of clinker with rational chemico-mineralogical composition, which fully corresponds to physico-chemical properties and composition of the admixtures to be used.

REFERENCES

1. Дютрон "Настоящее и будущее цементов, предназначенных для бутона заводского производства". П-й Международный конгресс по бетону заводского производства, Лондон, сентябрь 1934.
2. В.И. Сатарин "Шлакопортландцемент". УІ Международный конгресс по химии цемента, т. 3, 45-56, Москва, 1976.
3. M. Daimon "Mechanism and kinetics of slag cement hydration" VII Intern. Congress on the Cem. of Cem., v. 1, Theme III - 2/1, Paris, 1980.
4. R. Sersale "Structure and characterization of pozzolanas and of fly ashes" VII Intern. Congress on the Cem. of Cem., v. 1, Theme IV - 1/3, Paris, 1980.
5. K. Takemoto, H. Uchikawa "Hydration of pozzolanic cement". VII Intern. Congress on the Cem. of Cem., v. I, Theme IV - 2/1, Paris, 1980.

Gerd Wischers - Research Institute of the German Cement Industry, Dusseldorf, West Germany

OPTIMIZATION OF CEMENTS WITH MINERAL ADDICTIONS

In general the optimization of an industrial product denotes the attainment of a particularly favourable ratio between its performance and its cost of manufacture. An improvement in the performance/cost ratio can be achieved by, for example, raising the quality while keeping the cost unchanged or by lowering the manufacturing cost while keeping the quality unchanged. However, an improvement may also be obtained when, in conjunction with a slight lowering of quality, the cost is substantially reduced.

The quality of a product is judged by the properties which are of decisive importance with regard to its utilization. In the case of cement its quality must therefore be judged by its performance in concrete. Optimization moreover always presupposes a standard of comparison to which both the performance and the price can be referred. In the case of the optimization of cements with mineral additions it is obviously meaningful to judge them with reference to the cement which is most extensively manufactured and used worldwide and with which therefore most experience has been gained, namely, portland cement.

1. Functions of cement in concrete

Cement always has a number of functions to perform in concrete, some of which are essential in all cases, e.g., attainment of a sufficiently high strength, and some that are required only for special purposes, e.g., adequate resistance to sea-water. The functions that cement in concrete always has to perform include:

- satisfactory rheological properties for good workability;
- satisfactory strength development and sufficiently high 28-day strength;
- satisfactory durability of the concrete under usual environmental conditions;
- lasting corrosion protection of the reinforcing steel.

In addition to these basic requirements there may be other requirements which, though not applicable worldwide, have the character of basic requirements in some countries. These include, for example, adequate freeze-thaw resistance in countries where all external structural components are frequently exposed to frost action in the normal course of things. Besides for special purposes cements with pronounced special properties can give better service and higher performance, which justify higher cost and higher prices. These include, for example, particular rheological properties of grout, particularly rapid hardening for prestressed precast concrete units, or a particular chemico-mineralogical composition to withstand chemical attack. To keep within the allotted time, the following treatment of the subject will confine itself to the above-mentioned basic requirements and, in addition, to freeze-thaw resistance.

2. Mineral additions

The principal constituents of cement can, with regard to their properties, be divided into four groups, namely, hydraulic constituents, latently hydraulic constituents, pozzolanic constituents, and fillers. Furthermore, cement always contains additions of calcium sulphate as a setting time controlling agent and sometimes additives such as grinding aids, for example.

2.1 Hydraulic constituents

Hydraulic constituents, e.g., portland cement clinker, consist predominantly of calcium silicates with a lime/silica ratio distinctly higher than 2.0. In finely ground form they react relatively rapidly with the mix water, i.e., they set and harden rapidly. The hydration products - in the case of complete hydration - occupy about twice as large a volume as the original clinker particles, and in this way they have both a strength-developing and a pore-filling action.

2.2 Latently hydraulic constituents

Latently hydraulic constituents such as, for example, granulated blastfurnace slag likewise consist predominantly of calcium silicates, but their lime/silica ratio is much lower, usually between only 1.0 and 1.5. Therefore they react only at a slow rate with the mix water and require activation - e.g., by alkalies, calcium hydroxide or sulphates - in order to harden more rapidly. In so far as they achieve complete hydration, which requires moist curing for a relatively long time, their hydration products also occupy about twice as large a volume as the original particles of granulated blastfurnace slag.

2.3 Pozzolanic constituents

Pozzolanic constituents such as, for example, natural pozzolanas or certain fly-ashes from coal-fired power stations consist in part of reactive silica or reactive aluminates, the remainder usually being inert matter. In contrast to hydraulic and latently hydraulic constituents, they cannot harden on their own, but need for this the presence of calcium hydroxide in solution, e.g., calcium hydroxide which is split off in the hydration process of portland cement clinker. The chemico-mineralogical reaction of pozzolanas with calcium hydroxide proceeds at a distinctly slower rate than the hydration of hydraulic and latently hydraulic constituents. Because of the content of inert matter the reaction products moreover occupy less than twice as large a volume as the original pozzolana or fly-ash particles.

2.4 Fillers

Fillers are finely divided mineral substances which do not react, or react only very slightly, with the mix water or with other constituents of the cement. If they are of suitable fineness, they can so complement the particle size distribution of the cement that the rheological properties (water demand, workability) are distinctly improved and a space-filling and stabilizing effect is achieved within the structure of the cement paste. Because fillers have no, or only very little, chemico-mineralogical reaction, they yield no reaction products which reduce the porosity existing after the concrete has been mixed and compacted. Limestone with a high content of calcium carbonate is particularly suitable as filler. The proportion of clayey constituents in the filler must be limited, otherwise the water demand of the cement will be greatly increased and the resistance to freeze-thaw cycles drastically diminished.

3. Cement-technological measures

In principle, all the above-mentioned initial materials are suitable for making cements with approximately equal properties. However, they require the application of cement-technological measures duly suited to the individual constituents. It is up to the cement manufacturer so to choose these measures that with the use of mineral additions an optimum is attained with regard to the ratio of performance to manufacturing cost. The first condition for such optimization is not of a technical but of an economic nature, namely, that the mineral additions in question supplied "free to cement plant", i.e., inclusive of the frequently very high freight charges for transporting them from their source, should be distinctly cheaper than the cement clinker produced in the cement plant. They should be cheaper because the technological operations for making cement with mineral additions are often more expensive than those for making portland cement. If such mineral substances are cheaply available, it will then be necessary to check their performance, e.g., as regards workability and strength, and to investigate whether they contain harmful matter which may, for example, accelerate carbonation or impair frost resistance. For cement manufacture there are then essentially three technological

measures available, which will be described below.

3.1 Composition of the cement

All cements made with mineral additions contain portland cement clinker. In comparison with portland cement containing - along with calcium sulphate and admixtures - 100 % clinker a portland cement with up to, say, 5 % mineral additions may have distinctly better properties with regard to constructional technology, e.g., workability, bleeding, or uniformity of colour. As to the proportion of the various mineral additions a distinction should be drawn between the highest possible and the optimum proportion. Purely scientific publications often give information on the highest possible proportion of mineral additions. Although it is possible largely or entirely to compensate for their effect on the properties by means of other cement-technological measures, e.g., higher fineness of grinding, there are technical and economic limits to such compensation. For optimizing the ratio of performance to manufacturing cost it must therefore be considered what change in the cement properties as compared with portland cement is brought about by mineral additions, what degree of change the makers of concrete - i.e., the cement manufacturer's customers - can accept, by what cement-technological measures the influence of the mineral additions upon the cement properties can be wholly or partly compensated, and what extra burden this will place upon the cost of manufacture. The result of such considerations will very probably vary from one cement plant to another, from one country to another and most notably from one continent to another. In this context the prices of fuel for clinker production and the rates charged by electricity suppliers, as well as the availability and prices of the mineral additions, play a major part. In the last 15 years, which have been characterized by a drastic rise in fuel and electricity costs, an optimum with regard to the composition of cement with mineral additions has emerged in Western Europe, as represented in Table 1.

Table 1: Optimum proportions of mineral additions

Mineral addition	Optimum proportion of addition in % by weight	Significant changes in properties as compared with portland cement
Limestone filler	15 ± 5	-
Natural pozzolana	25 ± 10	Slower hardening longer curing
Coal fly-ash	25 ± 10	Slower hardening longer curing
Granulated blastfurnace slag	25 ± 10	-
	60 ± 15	Slower hardening longer curing

3.2 Chemical optimization

Various substances can accelerate the rates of hydraulic and pozzolanic reactions. Because the mineral additions either do not react at all (fillers) or react much more slowly than cement clinker, there is good reason to activate the reactivity of latently hydraulic and pozzolanic added substances. Particularly reactive clinkers with relatively high alkali and tricalcium aluminate content can stimulate granulated blastfurnace slag, pozzolana and fly-ash to react notable more rapidly. It has been found suitable to relieve the clinker of too high a content of alkalies by appropriate measures applied in the burning process and to add the alkali-enriched substances thus obtained to the cement with slowly reacting mineral additions. A procedure of this kind is in accordance with the cement standards of several Western European countries and is to be included also in the future European cement standard. Calcium chloride is likewise able effectively to activate slowly reacting mineral additions, but in many countries the addition of substances containing chloride is banned be-

cause of their corrosion-promoting effect on reinforcing steel.

3.3 Fineness and particle size distribution

Besides the composition of the cement and its chemical optimization, its fineness of grinding and particle size distribution are of major influence on the properties of the cement, namely, the rheological properties as well as hardening and imperviousness. The specific surface area measured by the Blaine method is often used as the measure of fineness. This characteristic value is relatively simple to determine and can suitably be used for cement production monitoring. The Blaine value is, however, an integral value with only very limited informative usefulness as to the cement properties. More information is provided by the particle size distribution such as can now be determined fairly simply with a laser granulometer and which is represented as the cumulative line for the particle sizes in a special granulometric diagram called the Rosin-Rammler-Sperling-Bennet or RRSB diagram. For cement the particle size cumulative line generally appears as a straight line. As an example, Fig. 1 shows the cumulative line for a normal portland cement plotted in the RRSB diagram.

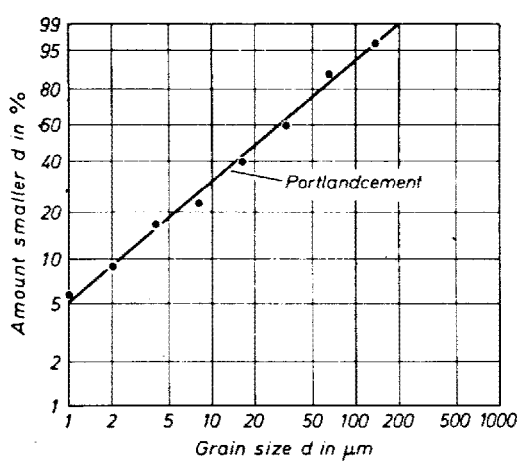

Fig. 1: Example of a grain size distribution diagram

If cement of the same composition is ground to a somewhat greater or less fineness in the same grinding plant, the straight lines in the RRSB diagram undergo an approximately parallel shift, as shown schematically in Fig. 2. Only if the cement is ground very fine does the slope of the lines change.

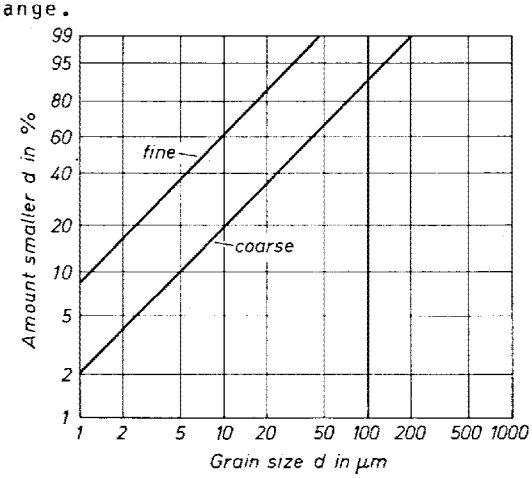

Fig. 2: Grain size distribution curves of fine and coarse cement

The slope of the lines (gradient) can be varied within certain limits by modifications to the grinding plant, e.g., by changing over to a differently composed ball charge in the mill or by altering the circulating load in a closed-circuit plant. The nature and quantity of the mineral additions also affect the slope of the lines: such added substances which are more easily grindable than cement clinker - limestone fillers, for example - cause them to slope less steeply, whereas substances which are more difficult to grind - granulated blast-furnace slag, for example - cause them to slope more steeply. Fig. 3 schematically represents two cements with approximately equal specific surface areas but with different slopes of their respective particle size cumulative lines.

The position and slope of the particle size cumulative lines are manifested in the properties of the ciment and in the cost of

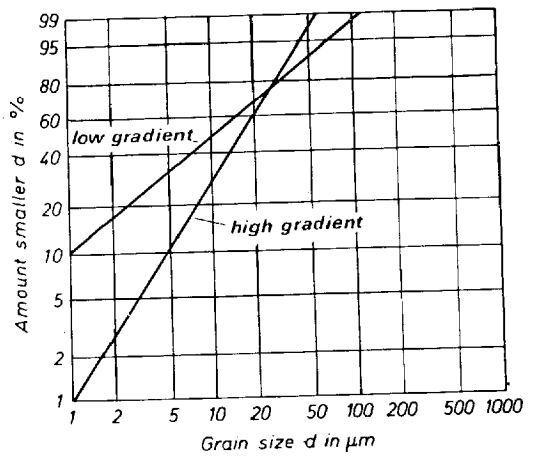

Fig. 3: Grain size distribution diagrams with different slopes

grinding. If cement of a given composition is merely ground to a greater fineness (straight line in Fig. 2 shifts to the left), the strenght increases in consequence, the water demand usually increases a little, but overall there is little change in workability. Greater fineness involves higher grinding cost, however. Since the contribution of the mineral additions to strength is in general distinctly less than that of portland cement clinker, cements made with such added substances always have to be more finely ground. For example, as against a Blaine value of 3000 cm^2/g for portland cement, a blastfurnace cement with a slag content of 60 % will have to be ground to approximately 4000 cm^2/g.

The slope of the particle size cumulative lines has opposite effects on the rheological properties and on the strength. The steeper the slope, the higher is the strength attained for equal specific surface area. The less steep the slope, the lower is the water demand and the better the workability. An addition of 10 - 15 % of limestone filler will make the cumulative line become less steep when grinding is performed in the same plant. Because the filler makes little contribution to the 28-day strength, such cement must be ground more finely in order to attain the same strength as it would attain without the filler. At the same time, however, the reduced steepness of the cumulative line results in lower demand and better workability despite the greater fineness of grinding.

4. Uniformity

For the concrete maker it is very important that the cement properties should vary as little as possible. That is why this problem receives the cement manufacturer's particular attention. Now cement clinker and, even more so, the mineral additions always show a certain amount of variation, which is sometimes very considerable and which must be smoothed as much as possible in the process of cement manufacture, as is schematically represented in Fig. 4.

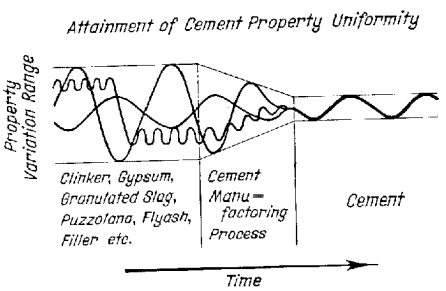

Fig. 4: Homogenization of cement properties

If, as is sometimes required by cement consumers, in the manufacture of cement with mineral additions the composition and fineness thereof are kept constant, the variations in the properties of the cement will fully manifest themselves. Therefore the properties of the cement constituents must be permanently monitored. With the aid of suitable control technology it can be ensured that there is the least possible variation in the cement properties overall. Such control, however, presupposes that - within certain limits - the composition of

the cement made with mineral additions, its chemical optimization, its fineness and, if necessary, also its particle size distribution are allowed to be changed. Most national cement standards allow scope for such control, and it is also to be incorporated in the future European cement standard.

J.P. BOMBLED - Centre d'Etudes et de Recherches de l'Industrie des Liants Hydrauliques, Paris - France
S. Feneuille - Lafarge Coppée - Paris, France

INFLUENCE DES PROPRIÉTÉS CHIMIQUES ET PHYSICO-CHIMIQUES DE LA PÂTE ET DES CARACTÉRISTIQUES DES GRANULATS SUR LE COMPORTEMENT RHÉOLOGIQUE DES MORTIERS ET DES BÉTONS.

1. INTRODUCTION

Le sujet de ce séminaire n'est certes pas nouveau puisque, sous une forme ou sous une autre, il figurait déjà dans le programme des précédents congrès internationaux de la chimie des ciments. En outre, les phénomènes physico-chimiques de base qui gouvernent la rhéologie des mortiers et des bétons ont été depuis longtemps reconnus (voir par exemple les références 1) et ils ont été eux-mêmes très largement étudiés sur des systèmes modèles permettant d'isoler l'effet de tel ou tel d'entre-eux.

Pourquoi alors éprouver le besoin de refaire le point sur ce sujet?. La réponse à cette question doit être vraisemblablement recherchée dans l'impossibilité qui subsiste encore aujourd'hui de modéliser ces matériaux très complexes que sont les bétons, les mortiers et même les pâtes pures de ciment, qu'ils soient à base de ciments Portland ou de ciments alumineux .

Certes, l'on sait maintenant expliquer *a priori* le comportement rhéologique de tel ou tel mélange contenant un liant hydraulique en cours d'hydratation mais l'on ne sait pas prévoir quantitativement les propriétés de mise en place d'un mortier ou d'un béton à partir des paramètres physico-chimiques qui permettent de caractériser ses différents constituants . Peut-être d'ailleurs parce que l'on ne sait pas définir précisément ce que sont ces propriétés de mise en place. En outre, la simple caractérisation du comportement rhéologique intrinsèque du matériau reste encore aujourd'hui un sujet de controverse puisque les résultats obtenus dépendent en général de la méthode et même des instruments de mesure utilisés.

Et pourtant, l'on ne saurait se satisfaire de cette situation car les professionnels du béton sont journellement confrontés à des problèmes qui trouvent leur origine dans les propriétés rhéologiques du matériau. Ainsi, pour tenter de résoudre ces problèmes, se sont développées dans les laboratoires de recherche industrielle de nombreuses études purement empiriques . Leur objectif se réduit dans la plupart des cas à mettre en évidence des corrélations entre deux paramètres et, comme il arrive souvent dans ce type d'approche, les résultats obtenus sont peu significatifs, parfois même contradictoires. Ils ne permettent pas de construire les connaissances solides qui seraient nécessaires pour résoudre, autrement que par des palliatifs, les problèmes pratiques rencontrés .

Est-ce à dire que rien ne se passe dans ce domaine et que les choses n'y progressent que très lentement. Une façon de répondre à cette question est de commencer par rappeler quelle était la situation au terme du précédent congrès international de la chimie des ciments qui s'est tenu à Paris en 1980. Ensuite, nous tenterons de dégager les faits importants ou les tendances qui ont caractérisé l'apport au sujet de ces cinq dernières années. Enfin, nous donnerons un bref résumé des contributions présentées à ce séminaire et nous indiquerons quelques voies qui, peut-être, mériteraient d'être explorées à l'avenir .

2. RAPPEL DE LA SITUATION DU SUJET EN 1980.

Le sujet de ce séminaire n'était pas explicité sous la même forme dans le programme du dernier congrès international de la chimie des ciments. Toutefois, le thème VI présidé par S. Diamond[2] et intitulé : "Les pâtes de ciment : rhéologie, évolution des propriétés et des structures" présentait de larges plages de recouvrement et nombre de communications ont concerné directement ce sujet .

En 1980, les questions fondamentales restaient les suivantes :

- comment caractériser de façon appropriée le comportement rhéologique d'une pâte de ciment donnée?,

- quelles sont les modifications apportées dans ce comportement par un changement des caractéristiques du ciment ou par l'incorporation d'ajouts minéraux ou d'adjuvants chimiques, de superplastifiants en particulier?.

En effet, les méthodes de mesure des caractéristiques rhéologiques, et plus précisément de la relation déformation/effort de cisaillement, s'étaient progressivement sophistiquées au cours des années 70 mais, pour la plupart, elles modifiaient les paramètres qu'elles étaient censées mesurer et, en conséquence, les résultats correspondants étaient souvent incohérents sinon contradictoires .

Ces difficultés méthodologiques n'avaient pas empêché cependant de répondre, au moins partiellement, à la seconde des deux questions précédentes. Depuis longtemps déjà, en particulier, les principaux facteurs gouvernant la rhéologie des pâtes de ciment avaient été identifiés : géométrie et granulométrie des grains de ciment, constitution chimique et minéralogique des clinkers, éléments mineurs, teneur en eau, nature des ajouts, etc...

En outre, les phénomènes physico-chimiques correspondants avaient été également reconnus et avaient déjà donné lieu à des investigations parfois très poussées. C'est ainsi que l'origine (rupture des liaisons chimiques lors du broyage, différence de taille entre les anions et les cathions solubilisés) et les conséquences (floculation, thixotropie) de l'existence de charges électriques sur les particules solides étaient déjà bien comprises, en présence d'adjuvants notamment ; il en était de même de l'enchevêtrement des grains et de la dilatance ou encore de la tension superficielle et de la composition de l'eau interstitielle.

Les apports du congrès de 1980 ont avant tout :

- confirmé le comportement approximativement binghamien des pâtes de ciment;

- proposé quelques relations fonctionnelles permettant de déterminer le seuil de cisaillement ou la viscoplasticité apparente à partir des deux caractéristiques essentielles de la pâte : finesse ou surface spécifique du ciment , rapport eau/ciment[3] ;

- établi le rôle déterminant des sulfates[4] et celui, plus limité, de la teneur en aluminate tricalcique.

Comme l'indiquait le titre du thème VI, ces contributions ne concernaient pratiquement que les pâtes de ciment pures ou les mortiers . Certes le thème VII était intitulé :"Réaction aux interfaces entre ciment et granulat dans les bétons et les mortiers" mais aucune contribution à ce thème n'eut à voir vraiment avec les propriétés rhéologiques .

Toutefois, on savait bien déjà qu'il est impossible de décrire le béton frais comme un milieu homogène, et que les plus simples des modèles rhéologiques doivent faire intervenir au moins deux phases (pâte et granulat par exemple, ou dans d'autres conditions, phase liquide et particules solides) de comportement rhéologique différent, interagissant d'une façon inhomogène et évolutive dans le temps . En conséquence, la possibilité de relier scientifiquement des lois d'écoulement aux tests de maniabilité utilisés pour caractériser l'aptitude d'un béton à être mis en oeuvre était considérée de toute façon comme hors d'atteinte. Dans ces conditions, la tendance était de réserver les études "scientifiques" aux pâtes pures pour n'aborder le béton qu'au travers d'études purement empiriques orientées vers le pragmatisme des chantiers[5].

3. LES PRINCIPALES CONTRIBUTIONS DE 1980 A 1986

Dans le domaine considéré, les cinq dernières années ont été principalement marquées par deux événements. Tout d'abord en 1982, à Boston, la Materials Research Society a organisé un colloque sur l'effet des phénomènes de surface et des phénomènes colloïdaux sur les propriétés du béton frais; les comptes rendus de ce colloque ont été édités par Skalny[6]. Ensuite, en 1983, a paru le livre de Tattersall et Banfill intitulé : "The Rheology of Fresh Concrete"[7].

On pourrait également noter la parution de l'ouvrage sur "Le Béton Hydraulique" publié sous la direction de Baron et Sauterey[8], ainsi que les comptes rendus, publiés dans "il cemento", d'une journée de travail de l'A.I.T.E.C. sur la rhéologie des pâtes de ciment, des mortiers et des bétons[9,10,18,22] .

Les principales contributions que l'on peut trouver dans ces différents ouvrages indiquent bien les tendances qui caractérisent les recherches menées dans ce domaine durant la période considérée :

- effets des conditions expérimentales sur les propriétés rhéologiques mesurées ;

- influences respectives des propriétés rhéologiques du fluide interstitiel et de la friction entre aggrégats ;

- mécanisme d'action des adjuvants et effets des ajouts minéraux .

Concernant le premier point, un grand nombre d'études a encore concerné les conditions de validité et de fiabilité des mesures effectuées sur les viscosimètres à cylindres coaxiaux[10,11,12]. Si l'on excepte le cas favorable des pâtes pures soumises à des contraintes suffisamment faibles pour éviter tout glissement, les résultats correspondants ont été souvent décevants. Dans le cas des bétons en vérité, il semble bien que seul le recours à des méthodes anciennes plus ou moins empiriques puisse conduire à des mesures significatives. A cet égard, on peut citer notamment celles qui sont basées sur la puissance requise pour mélanger un béton frais. Leur utilisation ne devient simple cependant qu'à condition d'admettre un comportement de Bingham pouvant être décrit au moyen de deux paramètres seulement[7] . La nécessité de définir des procédés de mélanges standardisés est en tout cas soulignée par plusieurs auteurs. D'autres tests de propriétés rhéologiques ont été également discutés [13,14].

Le second point a été examiné notamment dans trois articles dont la synthèse permet, presqu'à elle seule, d'apprécier l'état actuel des connaissances dans ce domaine . Ainsi, Lawrence et Singh[15] ont analysé en grand détail l'apparition dans le temps des divers phénomènes physico-chimiques qui permettent de décrire qualitativement les propriétés rhéologiques des bétons frais .

Massazza et Costa[9] ont analysé l'influence des trois principaux facteurs qui conditionnent les propriétés rhéologiques des pâtes de ciment, des mortiers et des bétons : la cohésion, la friction entre particules solides et la viscosité de la phase interstitielle . Ils se sont intéressés en particulier aux effets de la répartition granulométrique des différentes particules solides et à ceux de l'hydratation .

Enfin, Hattori et Izumi[16] ont modifié la définition newtonnienne de la viscosité en utilisant le concept de friction intermoléculaire et après avoir obtenu la relation entre viscosité et nombre de points de friction, ils ont déduit de la théorie du taux de coagulation de Verwey et Overbeek[17] les équations de la viscosité dépendant du temps. Les applications de cette théorie restent pour l'instant assez limitées mais l'apport conceptuel est sans doute important .

Le dernier point a donné lieu durant ces cinq dernières années à une abondante littérature et à plusieurs articles de revue concernant les effets, tant des adjuvants chimiques[18,19], que des ajouts minéraux[20] cendres volantes notamment. Dans la plupart des cas, ces ajouts minéraux ont des effets bénéfiques sur la rhéologie du béton frais, en particulier lorsqu'ils sont utilisés en conjonction avec des superplastifiants . Au niveau des phénomènes physico-chimiques qui sont à l'origine des effets observés, une grande attention a continué d'être portée aux forces d'interaction électrique entre particules, notamment dans les suspensions denses[21], et à l'adsorption des fluidifiants sur les différents composés chimiques (silicates et aluminates) du ciment[22]. Enfin, les effets des adjuvants sur les propriétés rhéologiques de pâtes de clinker finement broyé mais non gypsé ont donné lieu à quelques études essentiellement empiriques[23].

4. LES COMMUNICATIONS PRESENTEES A CE CONGRES.

Pour la plupart, les différents points évoqués précédemment apparaissent d'une manière ou d'une autre dans l'ensemble des rapports et communications présentés à ce congrès .

C'est ainsi que Costa et Massazza[24] rappellent que le comportement et les propriétés rhéologiques des suspensions concentrées résultent d'un état d'équilibre entre, d'une part, des interactions ioniques et électriques (entre les grains eux-mêmes ou entre ceux-ci et les ions présents dans le liquide interstitiel) et, d'autre part, des actions purement mécaniques (forces capillaires, frottements internes, etc...).

Les interactions électrocinétiques expliquent en grande partie le fait, observé par tous, que l'état floculé est l'état habituel, en l'absence naturellement d'adjuvants défloculants, d'un ciment dans l'eau. On comprend également ainsi que l'architecture correspondante contribue à l'existence de la cohésion, du seuil de cisaillement et du comportement thixotrope des pâtes de ciment. L'action de nombreux fluidifiants s'interprète à partir des mêmes concepts[25].

Beaucoup de chercheurs continuent d'ailleurs d'aborder l'étude des propriétés rhéologiques par celle des phénomènes électrocinétiques au travers notamment de la zétamétrie . Cette approche connaît un succès certain pour des suspensions de grains quasi inertes comme celles d'alumine par exemple[25], mais le problème s'est révélé très difficile pour un matériau évolutif toujours loin de l'équilibre comme le sont les suspensions de ciment dans l'eau[26]. Il semble que l'on ait eu quelques déceptions dans ce domaine et que beaucoup d'efforts devront y être encore consacrés si l'on veut progresser significativement .

La maniabilité des bétons et ses diverses composantes, cohésion, viscosité de la pâte interstitielle et frottement interne des granulats ne semblent pas donner lieu à des divergences d'interprétation[27]. Toutefois, on peut regretter qu'aucune étude ne soit présentée sur l'action "lubrifiante" de la pâte interstitielle qui est fournie par l'eau et les particules solides les plus fines . Il nous semble y avoir là un domaine qui mériterait un complément d'investigation . L'on sait en tous cas que la présence ou l'absence d'interface eau/air dans l'espace intergranulaire induit des comportements rhéologiques très différents qui ne peuvent être approchés de la même façon, notamment au niveau des mesures[28] .

Le comportement pratiquement binghamien du béton, au repos ou sous de faibles vitesses de cisaillement, est à nouveau confirmé par plusieurs auteurs[24,27] de même que le comportement quasi newtonien dans certaines conditions (vibration énergique, défloculation poussée, addition de résines) . Néanmoins, ce comportement est très souvent affecté par des transformations réversibles (thixotropie) ou irréversibles (sédimentation, hydratation) voire, dans certaines conditions par l'apparition de dilatance .

Concernant la mesure des coefficients rhéologiques des pâtes de ciment, différents travaux semblent montrer que finalement l'appareil le mieux adapté est le viscosimètre à cylindres coaxiaux à condition naturellement que n'apparaisse aucun phénomène de glissement, mais il faut noter que subsistent des variantes de réalisation ou d'exploitation des résultats[27]. Pour les bétons, les méthodes utilisées restent trop différentes dans leur principe et dans leur réalisation pour tenter de chercher de bonnes corrélations entre les différents résultats obtenus . Il reste difficile de passer de la pâte au béton[29] même si l'on peut signaler d'intéressantes tentatives tenant compte de plusieurs paramètres[24,30]. Au niveau des mesures, on peut noter une tentative, à la suite de nombreux travaux déjà existants, de suivre par ultra-sons l'évolution du seuil de cisaillement et la vitesse de prise[31].

Comme cela a déjà été souligné ci-dessus, l'on sait depuis longtemps que les caractéristiques rhéologiques des pâtes, des mortiers et des bétons frais dépendent non seulement de la composition du ciment (clinker, gypse et ajouts) mais aussi de facteurs liés à la préparation du béton (rapport eau/ciment, énergie de malaxage, température, etc...) et aux adjuvants éventuels. Comme il s'agit des premières minutes de la vie du matériau, ce sont évidemment les constituants les plus rapidement solubles (aluminate tricalcique, sulfates et alcalins) qui ont la plus grande influence. Ce point est confirmé dans plusieurs communications[29,32,33,34].

L'influence déterminante des sulfates de calcium incorporés au ciment sur le comportement rhéologique du béton frais est rappelée dans plusieurs communications[29,32]. Cette influence dépend bien sûr de la vitesse de dissolution de ces sulfates qui est liée à leur nature et qui permet de brider plus ou moins rapidement les premières liaisons qui pourraient se développer pendant la période de mise en oeuvre. A noter que, dans certaines conditions, le calcaire peut être substitué aux sulfates comme régulateur de prise[35].

Les ajouts (laitiers, cendres, pouzzolanes, etc...) ont en général une influence favorable sur la rhéologie; les facteurs importants étant l'écart de broyabilité avec le clinker ainsi que la géométrie des grains. Le cas des fillers calcaires, beaucoup moins étudié que les précédents, est discuté par Bombled[28].

L'on sait également que les facteurs granulométriques du ciment et des granulats (forme, état de surface et répartition de taille des grains), par le fait même qu'ils conditionnent le nombre de points de contact intergranulaires où s'exercent des forces de liaison, jouent eux aussi un rôle essentiel. Il est donc normal que l'étude de ces facteurs apparaisse dans plusieurs contributions. Ainsi, l'influence de la finesse du ciment est abordée par Costa et Massazza[24] ; celle des conditions de broyage dans le cas de ciments aux ajouts (broyage séparé ou cobroyage) et des différences de broyabilité des divers composants du ciment sont aussi discutées[28,29].

Parmi les conditions de préparation du béton, la température joue également un rôle; celui-ci est discuté par Wierig[32].

Enfin, un des points de grande importance actuelle est l'action de défloculants fluidifiants et l'évolution dans le temps de leur efficacité, ces fluidifiants étant d'ailleurs souvent utilisés comme réducteurs d'eau. Les recherches sur les mécanismes d'actions de ces adjuvants, l'influence de leur structure (et en particulier, de leur degré de polymérisation) et de leur composition ainsi que celle du ciment (présence d'éléments rapidement solubles, sulfates notamment) continuent d'être très actives[25,36,37] mais manifestement beaucoup reste encore à faire. Les effets de la salinité de l'eau interstitielle sont également un sujet d'intérêt[38].

Pour terminer l'examen des communications, il faut noter que les liants spéciaux, liants alumineux[39,40] et ciments pour forage pétrolier[38,41] n'ont pas été oubliés.

En conclusion, ce rapide survol semble montrer que les travaux conduits actuellement dans le domaine couvert par ce séminaire ont pour but avant tout de confirmer et d'approfondir des connaissances déjà acquises antérieurement plutôt que d'apporter des éclairages radicalement nouveaux. La progression est lente, ce qui confirme la difficulté du sujet.

5. QUELQUES PISTES POUR L'AVENIR

Il semble à présent que tous les phénomènes pouvant affecter la rhéologie des pâtes, des mortiers et des bétons sont assez bien compris individuellement. Peu d'entre eux cependant ont été analysés de manière quantitative et il reste vraisemblablement beaucoup de travail à faire dans ce domaine. Cette analyse quantitative supposera dans certains cas l'utilisation de nouvelles connaissances de base et, plus que jamais, seules les démarches pluridisciplinaires auront quelque chance de conduire au succès.

Ainsi, le concept d'objet fractal[42] a permis récemment de renouveler l'approche d'un grand nombre de phénomènes dans l'ensemble des sciences de la matière et il a été récemment appliqué à la structure des gels de ciment[43] ; on peut à juste titre se poser la question de savoir par exemple si l'introduction d'une dimension fractale pour caractériser la "rugosité" des granulats ne permettrait pas de quantifier plus aisément leur enchevêtrement.

Par ailleurs, de nombreuses équipes de recherches de base ont récemment reconsidéré la rhéologie des suspensions concentrées (voir par exemple la référence[44]) en utilisant des systèmes modèles, des simulations sur ordinateur[45] et les théories de la mécanique statistique comme la percolation[46,47] par exemple. Les phénomènes d'aggrégation dans les suspensions concentrées ont été également étudiées d'un point de vue géométrique en utilisant la notion de dimension fractale[48]. Ici aussi, sans doute serait-il utile de rechercher l'impact que pourraient avoir les résultats obtenus sur les questions abordées dans ce séminaire. Dans la même perspective, on peut se poser la question de savoir s'il ne serait pas intéressant de chercher à relier les propriétés rhéologiques[49] des solutions concentrées au problème du remplissage de l'espace par des grains de tailles diverses, problème dont les solutions ont récemment progressé, au moins sur des systèmes modèles[50,51,52].

Enfin, et de façon plus générale, on peut se demander si les méthodes de simulation qui ont été mises au point par et pour le génie chimique ne pourraient pas résoudre ce problème très délicat du caractère non additif des très nombreux phénomènes qui sont à prendre en considération si l'on veut élaborer un modèle rhéologique prédictif d'une pâte pure de ciment ou d'un béton adjuvanté. Bien entendu, cela ne veut dire en aucune manière que les phénomènes purement chimiques n'auront pas à être pris en compte ; cela signifie au contraire qu'ils auront à être intégrés dans une approche plus générale qui ne devra retenir que l'essentiel si elle veut être réellement efficace.

BIBLIOGRAPHIE

[1]J.-P. Bombled, "Rhéologie des mortiers et des bétons frais", Mater. Constr. (Paris), 688, 137-55, 1974 ; C. Legrand, "Contribution à l'étude de la rhéologie du béton frais", Mater. et Constr. (RILEM) 5, 275-95, 379-93.

[2]S. Diamond, "Cement pastes:rheology and evolution of properties and structures", 7ème Congrès International de la Chimie des Ciments (Paris), Vol. I, 113-23, 1980.

[3]R.A. Helmuth, "Structure and rheology of fresh cement paste", 7ème Congrès International de la Chimie des Ciments (Paris), Vol. III, VI-0/1-30, 1980.

[4]J.-P. Bombled, "Influence des sulfates sur les comportements rhéologiques des pâtes de ciment et sur leur évolution", 7ème Congrès International de la Chimie des Ciments (Paris), Vol. III, VI-164-69, 1980.

[5]M. Maultzsch et U. Meinhold, "Testing methods for the set of pastes and mortars", 7ème Congrès International de la Chimie des Ciments (Paris), Vol. III, VI-158-63, 1980.

[6]J. Skalny (ed.), "Concrete Rheology", Proc. Symp. M, Mater. Res. Soc. Ann. Mtg, Boston, MA, Nov. 1982, Mat. Res. Soc., (Pittsburgh, PA 15237), 233pp, 1982.

[7]G.H. Tattersall et P.F.G. Banfill, "The Rheology of Fresh Concrete", Pitman Books Limited (Londres), 356 pp, 1983.

[8]J. Baron et R. Sauterey (eds.), "Le Béton Hydraulique", Presses de l'Ecole Nationale des Ponts et Chaussées (Paris), 560pp, 1982.

[9]F. Massazza et U. Costa, "Rheological problems related to the use of cement", Il Cemento, 79 (4), 217-42, 1982.

[10]R. Lapasin, "Rheology of cement pastes", Il Cemento, 79 (4), 243-60, 1982.

[11]D.M. Roy, "Predicting fresh cement paste properties", in "Characterization and Performance Prediction of Cement and Concrete", J.F. Young (ed.), Engineering Foundation, New York, 219 pp, 151-4, 1983.

[12]R. Lapasin, A. Papo et S. Rajgelj, "Flow behaviour of fresh cement pastes. A comparaison of different rheological instruments and techniques", Cem. Concr. Res. 13(3), 349-56, 1983.

[13]C. Dulieu, "Rheology of fresh cement pastes and their variation with time testing methods", Cim., Bétons, Plâtres, Chaux (737), 230-5, 1982.

[14]J. Murata, "Flow and deformation of fresh concrete", Mater. Constr. (Paris), 17(98), 117-29, 1984.

[15]C.D. Lawrence et K.S.W. Sing, "The development of microstructure in fresh concrete", in ref.6, 2-13.

[16]K. Hattori et K. Izumi, "New rheological theory of concentrated suspensions", in ref. 6, 14-28.

[17]E.J.W. Verwey et J.Th.G. Overbeek, "Theory of the Stability of Lyophobic Colloids", Elsvier Publishing Co. Ltd, p 139-69, 1948.

[18]M. Collepardi, "Influence of admixtures on rheological properties of concrete", Il Cemento 79(4), 289-316, 1982.

[19]J.F. Young, "Effects of chemical admixtures on the rheological properties of fresh concrete", in ref. 6, 120-38.

[20]D.M. Roy, J. Skalny et S. Diamond, "Effects of blending materials on the rheology of cement pastes and concrete", in ref. 6, 152-73.

[21]J. Chappuis, "Relation of the rheological properties of dense suspensions to interparticle forces", in ref. 6, 38-45.

[22]U. Costa, F. Massazza et A. Barrila, "Adsorption of superplasticizers on C_3S. Changes in Zeta potential and rheology of pastes", Il Cemento 79(4), 323-6, 1982.

[23]F. Skvara et M. Rybinova, "The systems ground clinker-polyphenol sulphonate-alkali metal salts", Cem. Concr. Res. 15, 1013-21, 1985.

[24]U. Costa et F. Massazza, "Structure and properties of cement suspensions", ce congrès.

[25]J. Chappuis "Physical elementary mechanisms of fluidification by superplasticizers or mater-reducing agents", ce congrès.

[26]A. Zelver, "Interférences entre particules solides en suspension diluée", ce congrès(poster).

[27]G.H. Tattersall, "Components of workability and rheological measurements on mortars and fresh concrete", ce congrès.

[28]J.-P. Bombled, "Rhéologie du béton frais : l'influence de l'ajout de filler aux ciments", ce congrès.

[29]S. Sprung, "Influence des conditions de mise en place sur la rhéologie du béton frais", ce congrès.

[30]Y.M. Bazhenov, "Evaluation of rheological characteristics of cement paste and concrete with help of computers".

[31]I. Odler, S. Abdul-Maula et U. Hennicke, "A new method for determination of cement setting time", ce congrès.

[32]H.-J. Wierig, "Influence of cement and temperature on the consistency of fresh concrete", ce congrès.

[33]S. Grzeszczyk et L. Kucharska, "The influence of alkalies upon the water demand of early hydratation stage cement pastes in the light of rheological studies", ce congrès.

[34]J. Mierzwa, "Thixotropic-plastic-viscous rheological model of cement paste as the result of physical and mineralogical cement properties", ce congrès.

[35]A. Negro, G. Abbiati et L. Cussino, "Sur l'emploi du calcaire comme régulateur de prise du ciment", ce congrès.

[36]T. Sebök, "Effects of the molar parameters of sulphonated melamine and formaldehyde polycondensates on mortar properties", ce congrès.

[37]F. Basile, S. Biagini, G. Ferrari et M. Collepardi, "Properties of cement mixes containing naphtalene sulfonated polymers of different molecular weight" ; "Effect of condensation degree of polymers based on naphtalene sulfonate on fluidities of cement pastes" ; "Effect of the gypsum state in industrial cements on the action of superplasticizers", ce congrès.

[38]M. Michaux et R. Oberste-Padtberg, "The effect of mix water salinity on cement slurries containing polynaphtalene dispersants", ce congrès.

[39]P.F.G. Banfill et S.M. Gill, "The rheology of aluminous cement pastes", ce congrès.

[40]S.M. Gill, P.F.G. Banfill et B. El-Jazairi, "The effect of superplasticizers on the hydratation of aluminous cement", ce congrès.

[41]J. Orban, P. Parcevaux et D. Guillot, "Influence of shear history on the rheological properties of oil well cement slurries", ce congrès.

[42]B. Mandelbrot, "Les Objets Fractals", Flammarion (Paris), 203 pp, 1984.

[43]A.J. Allen et P. Schofield, "Possible fractal structure of cement gels", NATO ASI on "Scaling Phenomenon in Disordered Systems", Geilo, Norvège avril 1985, à publier par Plenum Publishing Company Ltd.

[44]R. Blanc, "Rheology of concentrated dispersions", à paraître dans le Journal de Physique (Paris), colloque Science of Ceramics 13, 1986.

[45]J.F. Brady et Bossis G., "The rheology of concentrated suspensions of spheres in simple shear of flow by numerical simulations", J. Fluid Mech. 155, 105-29, 1985.

[46]P.-G. de Gennes, "Conjonctures on transition from Poiseuille to plug flow in suspensions", J. Physique (Paris) 40, 783-7, 1979.

[47]P.G. de Gennes, "Dynamics of concentrated dispersions", Phys. Chem. Hydr. II, 1, 31-44, 1981.

[48]P. Meakin, "Diffusion-controlled cluster formation in 2-6 dimensional space", Phys. Rev. A 27, 1495-507, 1983.

[49]P.K. Haff, "Grain flow as a fluid-mechanical phenomenon", J. Fluid. Mech. 134, 404-30, 1983.

[50]R. Omnès, "Sur l'empilement aléatoire d'un système de sphères de rayons différents", J. Physique (Paris) 46, 139-45, 1985.

[51]M. Suzuki et T. Oshima, "Coordination number of a multicomponent randomly packed bed of spheres with size distribution", Powder Technology 44, 213-8, 1985.

[52]T. Stovall, F. de Larrard et M. Buil, "Linear packing density model of grain mixtures", à paraître dans Powder Technology.

P.F.G. BANFILL, S.M. GILL
School of Architecture and Building Engineering - The University of Liverpool
England, U.K.

THE RHEOLOGY OF ALUMINOUS CEMENT PASTES

INTRODUCTION

The rheology of cement pastes has been studied over several decades, but work has concentrated almost entirely on Portland cement (1), and no information seems to be available on aluminous cement pastes. In view of the industrial importance of Ciment Fondu grouts, particularly in marine applications where their superior durability and rapid strength gain are advantageous, it is useful to compare the rheology of Ciment Fondu pastes with that of ordinary Portland cement. This paper reports work carried out with a typical Ciment Fondu to provide this information.

RHEOLOGY OF CEMENT PASTES

The principal features of the rheology of cement pastes have been described in detail elsewhere (1), but may be briefly summarised as follows:

1. The flow curve of cement paste has been described in terms of various models:

Bingham $\tau = \tau_o + \mu\dot{\gamma}$

Hershel-Bulkely $\tau = \tau_o + A\dot{\gamma}^B$

Robertson-Stiff $\tau = A(\dot{\gamma}+C)^B$

Ostwald-De Waele $\dot{\gamma} = B\sinh(\tau - \tau_o)/A$

with associated observations in each case of shear thinning behaviour at high shear rates (τ shear stress, $\dot{\gamma}$ shear rate).

2. The existence of a yield value indicates that structure exists in the paste, due to the interactions between cement particles in the suspension. This structure breaks down on shearing because the energy input to the links between particles is sufficient to break the bonds. This structural breakdown manifests itself in two ways. Firstly, the yield value and plastic viscosity of the paste decrease with prolonged mixing, so that the method of preparing the paste affects the measured rheological parameters. Secondly, the torque, T, exerted by the paste on a continuously rotating cylinder or cone in a rotational viscometer decreases with time, t, according to an exponential relationship of the form

$$T - T_e = ke^{-bt}$$

where Te is the torque reached at equilibrium and k and b constants. The latter effect was treated theoretically by Tattersall (2) in terms of the number of links between particles in the paste.

3. The structural breakdown can also account for the variation in the reported flow curve shapes.

Banfill and Saunders (3) found that when the time taken to complete an up and down cycle in a coaxial cylinders viscometer was short the flow curve showed a hysteresis loop with the downcurve falling to lower shear stresses than the upcurve (structural breakdown), whereas when the cycle time was long the loop was reversed. At intermediate cycle times flow curves with more than one loop were obtained. Furthermore the cycle times producing these types of curve varied from cement to cement. Only at cycle times of two minutes or less were the loop shapes consistent. They explained this in terms of the competition between shear-induced structural breakdown and the buildup of structure due to continuing hydration reactions. In addition, prolonged mixing results in reversible flow curves (up- and downcurves superimposable).

4. Variations in yield value over a 20-fold range and in plastic viscosity over a 50-fold range have been reported by different workers and can be explained by differences in experimental technique (4). In addition to the effect of mixing on the structural breakdown, cement pastes slip at the walls of the viscometer. This is assumed to be overcome by profiling or serrating the surfaces but no-one has shown conclusively that this is so. Nevertheless, Mannheimer showed that slippage could result in a sixfold reduction in the measured yield value of a cement paste (5).

5. Because of the variation of shear stress across the gap of a coaxial cylinders viscometer fluids with a yield value exhibit plug flow at low shear rates where the stress does not exceed the yield value at all points in the fluid, as shown by the Reiner-Rivlin equation:

$$\Omega = \frac{T}{4\pi\mu h}\left(\frac{1}{R_b^2} - \frac{1}{R_c^2}\right) - \frac{\tau_o}{\mu}\ln\frac{R_b}{R_c}$$

only when $T/2\pi R_b^2 h \geq \tau_o$ does all the fluid flow. This may be taken account of in the evaluation of data, but Tattersall and Dimond found that plug flow also occurred at much higher shear rates and stresses in conditions of steady continuous shear (6). They observed discontinuities in the exponential decay of torque with time which on visual examination of the paste were found to coincide with the times at which a solid plug of material broke up. When the observed width of the sheared zone was used in calculations instead of the instrument gap width, previously irreconcilable data on the effect of shear rate on the structural breakdown kinetics could be understood.

This complex behaviour of Portland cement pastes forms the background against which the rheology of Ciment Fondu pastes must be compared.

EXPERIMENTAL DETAILS

All experiments were carried out using a typical Ciment Fondu with the composition and other properties given in Table 1. The viscometer used in this work was a Haake Rotovisco RV2 with PG142 external speed programmer. Two coaxial cylinders geometries were used: (i) the Haake system MVIIP with inner cylinder radius 18.4mm, outer cylinder radius 21mm, height 60mm, both cylinders profiled with vertical ribs of 0.1mm square section, spaced 2mm apart round the circumference; (ii) the system S13/15 used by Tattersall and Dimond with inner cylinder radius 13mm, outer cylinder radius 15mm, height 50mm, both cylinders profiled with vertical serrations of 0.5mm square section, spaced 0.5mm apart round the circumference.

Pastes were prepared in batches of not more than 250g measured by weight and blended either by hand mixing with a spatula in a beaker for one minute or in a propellor type laboratory mixer at a speed of 1000 rpm for a predetermined time. Time and temperature were carefully controlled; all mixes were prepared and tested at 20 C.

The experimental programme studied the following: the effect of cycle time on flow curve shape; the effects of mixing time, concentration in water and age after mixing; and the behaviour under continuous shear.

Table 1 Properties of the Ciment Fondu

Setting time (BS 915): Initial	280 min
Final	293 min
90 μm residue (%)	3.8
Surface Area (Blaine) (m^2/kg)	276
Chemical Composition (%):	

SiO_2	Al_2O_3	Fe_2O_3	FeO	TiO_2	CaO	Na_2O	K_2O	SO_3	CO_2
4.14	28.67	10.43	5.63	1.98	38.5	0.06	0.04	0.19	0.42

RESULTS

EFFECT OF CYCLE TIME ON FLOW CURVE SHAPE

Pastes of 0.325 w/c were hand mixed and tested in the MVIIP geometry with shear starting 2.5 minutes after the first contact of cement and water. The total cycle time was varied from one minute to one hour and the maximum speed of rotation was 500 rpm. Figure 1 shows the three types of flow curve obtained, classified according to Banfill and Saunders, and Table 2 gives the cycle times at which these occurred. The relationship between speed and torque shown by the section XX in Figure 1, whether downcurve or upcurve, was independent of cycle time and conformed to the Reiner-Rivlin equation for a Bingham fluid. In view of these results the cycle time in all subsequent experiments was kept short to produce Type 1 flow curves, from the downcurve of which the yield value and plastic viscosity were calculated using that equation.

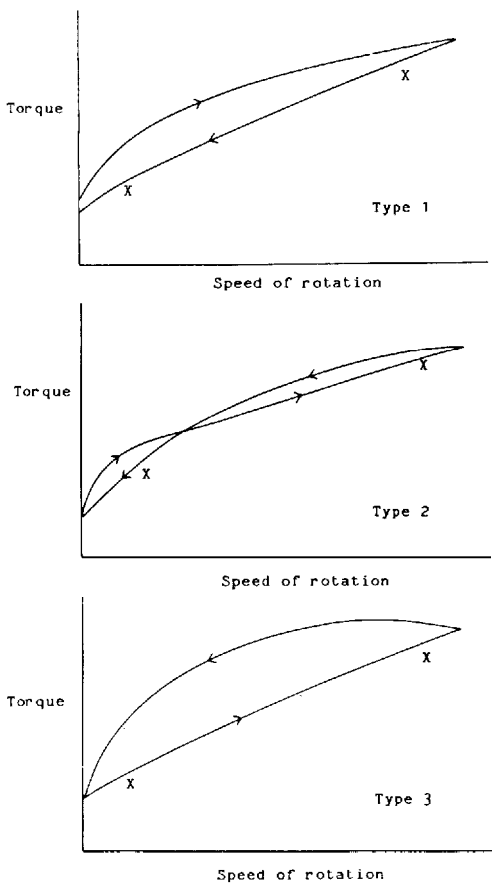

FIGURE 1 - Classification of flow curve types.

Table 2 Variation in flow curve with cycle time

Cycle time (min)	1	2	5	9.8	12	24	36	48	60
Flow curve type	1	1	1	1	2	3	3	3	3

EFFECT OF MIXING TIME

Pastes of 0.3 and 0.4 w/c were mechanically stirred for up to 10 minutes and tested in the MVIIP geometry with shear starting one minute after the end of stirring (i.e. up to 11 minutes from first contact of cement and water). The maximum speed was 500 rpm and the cycle time one minute. Figure 2 shows the effect of mixing time on the yield value and plastic viscosity.

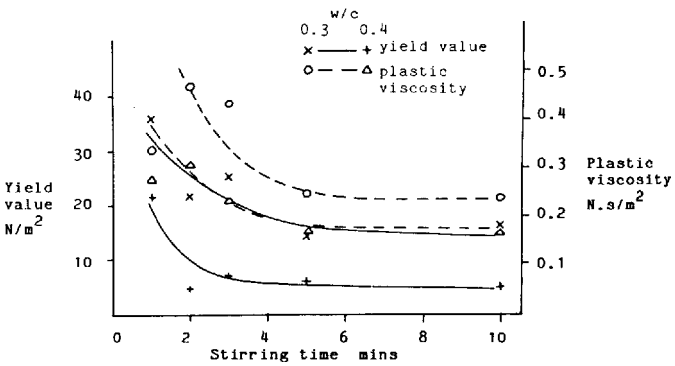

FIGURE 2 - Effect of mixing time on the rheology of Ciment Fondu pastes.

EFFECT OF CONCENTRATION OF PASTE

Pastes of different w/c ratios were mechanically mixed for 5 minutes then tested in the MVIIP geometry to a maximum speed of 999 rpm and in the S13/15 geometry to 500 rpm, in both cases with a one minute cycle time. This mixing time was chosen in the light of the results in Figure 2. Separate paste samples were prepared for each test in both geometries. Figure 3 shows the variation in yield value and plastic viscosity with w/c ratio with comparative information on Portland cements drawn from Tattersall and Banfill's survey of the literature (1).

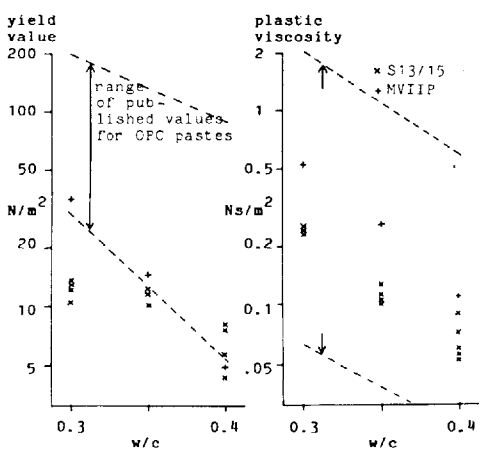

FIGURE 3 - Effect of w/c ratio on the rheology of Ciment Fondu and Portland cement pastes.

EFFECT OF AGE

Separate samples of paste at 0.3 w/c ratio were mechanically mixed for 5 minutes then left to stand for up to 90 minutes before testing in the S13/15 geometry to a maximum speed of 999 rpm or in the MVIIP geometry to 500 rpm with a one minute cycle time. Figure 4 shows the variation with age in yield value and plastic viscosity calculated as before.

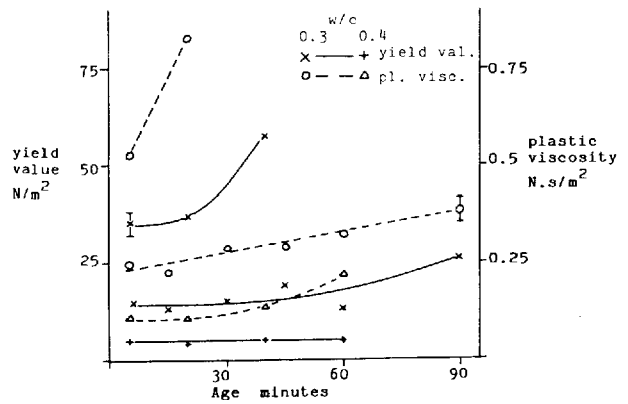

FIGURE 4 - Variation of yield value and plastic viscosity of Ciment Fondu pastes with standing time.

STRUCTURAL BREAKDOWN IN STEADY SHEAR

Hand mixed and mechanically mixed pastes of 0.3 and 0.4 w/c ratio were sheared in both geometries at several speeds of rotation. Typical torque-time behaviour observed in both geometries, as recorded on a continuous chart trace, is shown in Figure 5. However, plug flow taking the form of a stationary zone of paste up to 1mm thick adjacent to the stationary outer cylinder was observed in the MVIIP geometry but never in the S13/15 geometry. It occurred only in the pastes of 0.3 w/c, which suggests that it may be related to the stiffness of the paste. Because of the quantitative uncertainties introduced by this plug flow, only those results obtained in the S13/15 system will be reported here, but it must be borne in mind that the results from the two systems show close qualitative agreement. Table 3 summarises the results.

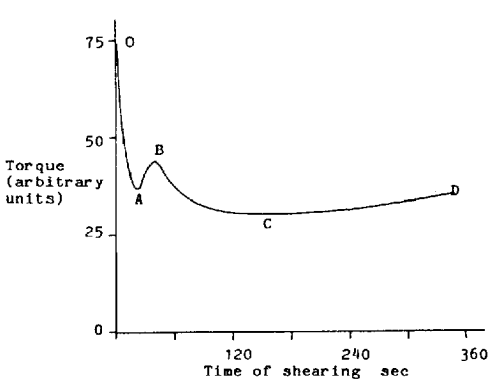

FIGURE 5 - Variation in torque with time during continuous steady shearing of Ciment Fondu paste.

DISCUSSION

Most of the features of the rheology of Portland cement pastes described earlier have been observed in these experiments on Ciment Fondu pastes, but some novel features are also present.

FLOW CURVES

Ciment Fondu pastes may be described by the Bingham model provided it is also realised that structural breakdown occurs on shearing which may distort the flow curve and give apparent shear thinning behaviour. Structural breakdown results in the greater effect on the yield value than on the plastic viscosity (Figure 2), exactly as is observed in Portland cements (7).

The changing flow curve/hysteresis loop pattern shown in Figure 1 follows the same sequence as for Portland cements. Loops indicative of structural breakdown are obtained at short cycle times, while the sense of the loop is reversed at long cycle times. At intermediate times of 10-20 minutes curves with more than one loop are observed. While Banfill and Saunders (3) attribute this to the competition in Portland cement between shear induced breakdown and hydration causing buildup, this cannot apply to Ciment Fondu because of the different chemistry involved. The hydration of Ciment Fondu proceeds via a "through solution" mechanism with dissolution of calcium aluminates. Structure development is delayed until their subsequent precipitation when the saturation level is exceeded (8). In contrast, in Portland cement the growth and interlocking of hydration products takes place from the first contact of cement and water (9). Therefore the observed changes in flow curve/hysteresis loop shape in both types of cement are probably due to physical effects arising from flocculation and deflocculation processes. Hattori and Izumi have explained the hysteresis loops by a theoretical model based on these considerations (10).

EFFECT OF CONCENTRATION AND AGE

Figure 3 shows that the yield value and plastic viscosity of Ciment Fondu pastes are related to w/c ratio in a similar way to Portland cement pastes but that the values determined are somewhat lower. Consequently a Ciment Fondu grout will be easier to pump but may show a slightly greater tendency to bleed. It also accounts for the well known harshness of Ciment Fondu concretes (11).

Because of the low rate of reaction between Ciment Fondu and water during the induction period, the relatively slow increase in yield value and plastic viscosity of undisturbed paste with time (Figure 4) is not surprising. There is a marked difference between results obtained in the two geometries which may be explained by the occurrence of plug flow in the MVIIP system as noted above. This would increase the effective shear rate in the paste and cause the apparently higher yield value and plastic viscosity which have been calculated from the instrument dimensions for Figure 4. In view of the observation of plug flow during continuous shear experiments this must be considered a plausible explanation.

STRUCTURAL BREAKDOWN AND BUILDUP

In general the structural breakdown behaviour of Ciment Fondu pastes is similar to that of Portland cement pastes, but this is the first time that observations of a double minimum in the torque-time behaviour have been reported.

Table 3 Structural breakdown under steady shear (S13/15 geometry)

Experimental Conditions					Torque (Nmm) at				Time (sec) from 0 to			Slope of semi-log plot (sec^{-1})	
W/C	Mixing method	Time (min)	Shearing speed (rpm)		0	A	B	C	A	B	C	OA	BC
0.3	Hand	1	200	)mean	35.7	16.9	19.3	12.9	22	41	175	10.3	1.84
	(4 replicates)			)s.d.	1.9	0.8	0.5	1.5	2.3	2	33	1.7	0.23
0.3	Hand	1	400		>46	19.7	21.2	18.6	45	72	160	3.7	0.73
0.3	Hand	1	500		>46	20.6	21.6	20.3	40	55	120	5.7	0.70
0.3	Machine	5	500		35.4	-	-	17.7	-	-	135	-	1.37
0.3	Machine	10	500		34.5	-	-	16.7	-	-	160	-	1.18
0.4	Hand	1	200		16.9	4.6	6.0	5.5	40	72	140	4.3	*
0.4	Hand	1	400		25.6	6.4	-	-	40	-	-	4.8	-
0.4	Hand	1	500		23.0	6.1	7.4	6.7	20	45	100	3.9	*
0.4	Machine	5	500		28.1	7.1	-	-	65	-	-	7.6	-
0.4	Machine	10	500		26.2	6.9	-	-	60	-	-	4.6	-

* The differences between the torques at points B and C are too small to allow accurate calculation of the slope of the semi-logarithmic graph.

The general form of the torque-time relationship under conditions of steady continuous shear is shown in Figure 5. The main features are the rapid initial decrease to a minimum at point A followed by a small peak B and another minimum C, after which torque steadily rises (D). When the torque reading, T, taken from the chart record is plotted in the form log(T-TeA) or log(T-TeC) against time, where TeA and TeC are the torques at the two minima A and C respectively, both portions fit a straight line relationship (Figure 6). The peak after the initial rapid fall in torque is generally well defined and two minima are clearly evident. However, in some experiments, particularly in mechanically mixed and less concentrated pastes the double minimum tends to merge into a single shallow one (Table 3). In the S13/15 geometry the second minimum is always below the first, but in the MVIIP geometry it is normally at the same torque or slightly above. This could be due to differences in the relative rates of breakdown and buildup at the higher shear rates prevailing in the MVIIP geometry when plug flow is taking place.

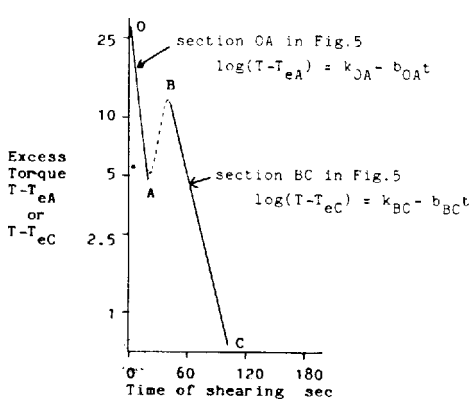

FIGURE 6 - Exponential form of the relationship between torque and time in continuous steady shear.

The linear relationship between log(T-TeA) and time is exactly as first reported by Tattersall for Portland cement pastes (2). However the slopes of the semilogarithmic plots shown in Figure 6 are different for the two portions of the torque-time curve. For the initial breakdown OA (Figure 5) the slope is 5-10 times that of the portion BC. There are insufficient data to confirm Tattersall's observations that the slope of the semilogarithmic plot is steeper at higher shear rates. The slope of the portion OA is not significantly affected by w/c ratio. No conclusion can be drawn about section BC because at 0.4 w/c the second minimum is either not present or so shallow that it is not possible to produce a semilogarithmic plot of the data.

Increasing the w/c ratio moves the whole curve to lower torques but has no significant effect on the times to any of points A, B or C. Mechanical mixing has the same effect but results in a single minimum, the position of which depends on w/c ratio (Table 3). At 0.3 w/c ratio the overall shape of the single minimum is shallow with the lowest torque occurring at times corresponding to point C of the curves with double minima, whereas at 0.4 w/c the minimum is sharply defined with the lowest torque corresponding in time to point A.

These observations tend to support the hysteresis loop behaviour. If the buildup of structure were of chemical origin the time after initial contact of water and cement would be critical whereas mechanical mixing for 10 minutes leaves the shape of the torque-time relationship unchanged. Thus the critical time is that from the start of shearing in the viscometer and the explanation of structural buildup must be sought in physical, flocculation changes.

STRUCTURAL MODEL

Tattersall's model for the structural breakdown of Portland cement pastse was proposed on the basis of the work done in a rotational viscometer (i) in overcoming normal viscous forces, (ii) in breaking linkages and (iii) in keeping them broken (2). Since he observed no rebuilding of structure, item (iii) was not considered. His model correctly predicts the exponential form of the experimental relationship between the excess torque (T-Te) and

time and gives the breakdown constant as

$$b = \frac{2\pi K}{n_0 \psi} w(w - w_1)$$

where w is the shear rate, n_0 and ψ are structural parameters - the initial number of linkages present and their strength repectively, and K, w_1 constants. Hattori and Izumi's structural model (10) explicitly allowed structural rebuilding or reflocculation and, as already noted, this accounted for the observed flow curve/hysteresis loop shapes.

If it is considered that the new structure which forms has different structural parameters then it too will undergo structural breakdown but at the same shear rate the value of the breakdown constant, b, will be different. For example, stronger linkages or more of them, perhaps arising from a different geometrical arrangement in the new structure, will result in a smaller constant b.

The existence of different types of flocculation structure in clay suspensions is well known and documented (12). The flat particles may associate through edge-edge, face-face or edge-face linkages and these types of linkage have different strengths arising from the different arrangements of atoms in the surface layers in these parts of the particles. These structural variations produce different rheological properties. Bombled (13) and Legrand (14) consider that the charge distribution on a grain of cement is not uniform. Ridges and other points where there are abrupt changes in direction of the surface are thought to be charged differently from flat faces. Consequently there is the possibility of face-ridge association relying on electrostatic charges. Because of the heterogeneity of cement particles the strength of this association may well depend on the relative orientation of the particle contacts.

The following model is therefore a plausible suggestion to account for the observed rheological behaviour of Ciment Fondu pastes. Particles are in contact when they are first mixed with water and remain together in the form of flocs, where the interparticle attraction is the resultant of attractive Van der Waals forces and the mutual repulsion of the electrical double layers around each charged particle in water. The particles in a floc are arranged randomly with some strong and some weak linkages. Shear breaks these flocs down, reduces the apparent viscosity of the suspension and individual particles can flow past one another and reorientate themselves. Particles collide but because of their freedom of movement are able to take up relative positions such that only the strongest linkages are formed. This results in a net increase in the strength of the structure, which is then followed by further breakdown, but at a lower rate because of the stronger linkages.

The model is somewhat speculative at this stage but further experimental evidence in support is provided by the effect of superplasticisers, to be described in a later publication. These admixtures remove the second minimum in the torque-time relationship, as would be expected for materials which adsorb all over the particle surfaces thereby obliterating any differences in the charge distributions. Consequently a single type of structure only is involved.

CONCLUSIONS

The rheology of Ciment Fondu pastes is broadly similar to that of Portland cement pastes. They show Bingham type behaviour with slightly lower yield value and plastic viscosity. They exhibit structural breakdown in the form of a dependence on the time of mixing. The flow curves show similar hysteresis loop behaviour to that shown by Portland cement pastes and which can be explained by the competition between structural breakdown and buildup due to flocculation.

In continuous steady shear experiments the behaviour shows novel features in the form of a double minimum in the torque-time curve. This behaviour can also be explained by a change in the flocculation structure upon shearing.

ACKNOWLEDGEMENTS

We gratefully ackowledge the financial support of the Science and Engineering Research Council and FEB (Great Britain) Ltd; provision of materials by Lafarge Aluminous Cement Co Ltd; and the experimental assistance of Miss P. Hooper.

REFERENCES

1. G.H. TATTERSALL, P.F.G. BANFILL (1983), The Rheology of Fresh Concrete, London, Pitman.
2. G.H. TATTERSALL (1955), Brit. J. Appl. Phys. 6 (5), 165-7.
3. P.F.G. BANFILL, D.C. SAUNDERS (1981), Cem. Concr. Res. 11, 363-70.
4. P.F.G. BANFILL (1985), 4th Nat. Conf. on Mechanics and Technology of Composite Materials, Varna, Bulgaria, 423-6.
5. R.J. MANNHEIMER (1983), Oil and Gas J. Dec 5, 144-7.
6. G.H. TATTERSALL, C.R. DIMOND (1976), Hydraulic Cement Pastes, Publicn. 15.121, Slogh, Cement and Concrete Association, 118-33.
7. P.F.G. BANFILL (1981), Mag. Concr. Res. 33 (114), 37-47.
8. F.M. LEA (1970), Chemistry of Cement and Concrete, London, Arnold.
9. D.D. DOUBLE, S.J. PERRY, A. HELLAWELL (1978), Proc. Roy. Soc. Lond. A 359,435-51.
10. K. HATTORI, K.IZUMI (1982), J. Dispersion Sci. Tech. 3 (2), 129-45; 147-67; 169-93.
11. T.D. ROBSON (1962), High Alumina Cements and Concretes, London, Contractors Record Ltd.
12. H. VAN OLPHEN (1977), An Introduction to Clay Colloid Chemistry, New York, Wiley.
13. J.P. BOMBLED (1974), Revue des Materiaux de Construction (688), 137-55.
14. C. LEGRAND (1981), Cahiers de la Groupe Francaise de Rheologie, (Special Number) October, 129-36.

G. H. TATTERSALL - University of Sheffield - England, U.K.

COMPONENTS OF WORKABILITY AND RHEOLOGICAL MEASUREMENTS ON MORTARS AND FRESH CONCRETE
COMPOSANTES DE LA MANIABILITE ET MESURES RHEOLOGIQUES SUR MORTIERS ET BETONS FRAIS

Introduction

The fact that the number of proposed methods for the measurement of workability is well into three figures (1) illustrates the importance attached to the subject, but it also demonstrates that except in the tautological, and therefore not very helpful, sense that the workability of concrete is its ability to be worked, there is not even a universally accepted definition of the term, as pointed out by Neville (2) in his summary of the differing views expressed at a conference in 1973. The situation has improved a little since then, but not much.

Workability seems to be a very complex property because it embraces a number of what might be called constituent properties, as follows.

(i) ability to undergo satisfactory mixing, to produce a homogeneous product.

(ii) ability to flow to fill a mould or formwork, which might be of a difficult shape and might contain congested reinforcement.

(iii) ability to be compacted to remove air so that the hardened concrete may achieve its maximum potential strength.

(iv) ability to resist segregation and excessive bleeding.

(v) ability to provide a satisfactory surface finish, either direct from the mould or as a result of some mechanical processing of a free surface.

(vi) ability to be transported by any one or more of a variety of methods including dumper truck, conveyor belt, pumping, tremieing, etc.

(vii) behaviour in response to various mechanical processes such as application of pressure or vibration.

The situation is further complicated by the necessity to deal with a very wide range of workabilities, from the very high workability of the flowing and almost self levelling concretes at one end of the scale, to the extremely low workabilities of the semi-dry mixes such as are used, for example, for extrusion processes, at the other end.

The workability of a concrete mix is affected by

(i) mix proportions (i.e. of cement, cement replacements, aggregates, and water)

(ii) chemical and physical properties of the cement

(iii) physical properties of the aggregates (particularly shape, particle size distribution and water absorption, and, to a lesser extent, surface texture)

(iv) presence and quantity of any admixtures

(v) age

and there are interactions between these variables. It might also be remarked that there are considerable difficulties in imposing on these variables a control that is adequate for the obtaining of good reproducibility of nominally identical mixes, even in the laboratory.

In terms of sophistication, though certainly not chronologically, the history of the development of tests for the measurement of workability can be considered as having taken place in a series of stages. The earliest stage is that of the very simple tests that were purely empirical and made no pretence of being otherwise, some of which have survived to the present day because of their simplicity rather than because of their usefulness. They include the best known of all, the slump test, and also a whole variety of penetration tests, drop tests and deforming tests. That this approach has still not been abandoned is demonstrated by the recent inclusion, in the latest edition of British Standard 1881, of the flow table test for high workability concretes.

A later stage of development is represented by tests that are based on the idea of isolating one of the constituent properties of workability listed above, and attempting to assess it separately. The compacting factor test of Glanville, Collins and Matthews (3) is an example of this class, and it has probably not been sufficiently appreciated that the authors themselves did not consider it to be an adequate measure of workability in general. A more recent example in this class is the 'efflux rheometer' of Bartos (4) which has been commented on elsewhere (5, 6). Other tests that were intended to imitate practical placing processes, such as that described by Baron (7) and the similar one proposed by Angles (8) some years later, may also be regarded as coming in this category.

These empirical tests have been listed and discussed elsewhere (1); serious criticisms may be made of each one individually but the defect they possess as a group is that any one of them may classify as identical in workability two concretes that are subsequently found to behave very differently on the job. Progress beyond this point became possible only when consideration was given to the question of the behaviour of fresh concrete under defined conditions of stress and/or strain. Early attempts to do this include the experiments of L'Hermite (9) with his annular shear box, and of Berthier (10) with his deforming cubical mould, but most of the work is more recent and includes that to be discussed below.

Tassios (11) has discussed the qualitative relationships between the constituent properties of workability and fundamental properties of the concrete which can, at least in principle, be measured, such as yield stress, yield strain, plastic viscosity and cohesion.

In spite of their obvious, and not so obvious defects, the various empirical tests have contributed to the development of mix design techniques, and in other ways. Nevertheless, any critical review of the field of workability measurement forces the conclusion that a great deal of time and effort has been wasted by some workers who quite clearly have not taken the trouble to study previous work, as is shown, for example, by the several instances that could be quoted of proposals for what purports to be a new test that is in fact similar in all essentials to one that was proposed perhaps 20 or 30 years earlier. In addition, considerable confusion has been caused by the careless and slipshod use of terminology so that, for example, words such as viscosity, mobility and fluidity, to which are properly attached rigorous definitions in terms of fundamental quantities (12), have been used to describe the results of measurements made with quite arbitrary apparatus.

Definition of workability

Attention has already been drawn to the existence of a wide range of opinions on the matter of the definition of the term workability, and these have included proposals for considering it not as a property of the fresh concrete alone but as one that necessitates a consideration of the placing process concerned, or the development of properties measured on the hardened concrete. For example Baron and Lesage (13) suggested a definition based on assessment of the porosity of concrete that had been laid in a given way.

It is clear that general development will be difficult, if not impossible, until there is a generally agreed acceptance of at least the approach to a definition. There seems to be no valid reason why that approach should not be the same as that used successfully for any other physical property, and that means (14, 15)

(i) workability is a property of the fresh concrete, and of the fresh concrete alone

(ii) workability can be defined as being measured by a set of constants W_i and, together, the constants in this set must provide a unique description. The number of constants required to achieve this, that is, the number of constants in the set W_i, is not known a priori.

(iii) the numerical value of each of the constants in the set should be independent of the method by which it is measured, that is, it should be expressible in fundamental units.

It seems reasonable to suggest that the validity of any proposed method of measurement should be judged in terms of how well these criteria are met. Every one of the methods incorporated in the various national standards, as well as every one of the many other methods proposed, fails conspicuously when judged in this way. In violation of condition (iii), results depend markedly on details of the apparatus used and in many cases depend also on details of just how it is used, i.e. they are operator sensitive.

More importantly, from the practising engineer's point of view, any one of the tests may classify as being identical in workability two concretes which are subsequently found to behave very differently in practice. For example, it is well known that two concretes of the same slump may exhibit quite different workabilities as assessed in terms of the job to be done, and this defect in the test has been responsible for some very expensive mistakes.

The detailed definition and determination of the constants W_i involves an investigation of a rheological nature, since rheology is defined as 'the science of the deformation and flow of matter' (12), and that means a consideration of the relationships between stress, strain, strain rate, and time, and perhaps the whole strain history of the material. The end result should be a rheological model, described in mathmatical terms, and obtained either experimentally or obtained theoretically with subsequent experimental verification.

Acceptance of the statement made above, that workability is a property of the fresh concrete alone, does not, of course, mean that the properties of the hardened concrete should be ignored. It has been pointed out previously that the former is important only in relation to the latter. Bombled (16) has commented 'one must never forget that the search for optimal rheological properties (of the fresh concrete) is not an end in itself and it would be disastrous if obtaining them were to be to the detriment of the ultimate properties of the hardened concrete'.

Rheology of cement pastes

Since concrete consists of aggregates, cement and water, it may be regarded as either a suspension of inert particles in a matrix of cement paste, or as inert particles coated with cement paste, and it is reasonable to suppose that a thorough understanding of the rheology of the paste must be obtained before satisfactory progress can be made in the study of the concrete of which it is a constituent. Such an argument was put forward some 30 years ago (17). More recently, Bombled (16) has argued that 'the cement has a predominant role to play in the rheology of the fresh concrete'.

In fact, limited work carried out later on the effect of cement properties on fresh concrete properties, by Dimond (18) and An-Keat Yeoh (19) indicates that this statement needs some qualification, but there is no denying the obvious importance of the cement paste.

Experiments with a coaxial cylinders viscometer, reported in 1954, (17, 20) showed

(i) at low shear rates cement pastes behaved according to the Bingham model

(ii) at low shear rate both the yield value and the plastic viscosity were related approximately exponentially to the water content of the paste

(iii) under higher shear rates plastic viscosity decreased with time while yield value appeared to remain approximately constant

(iv) there was little or no tendency for a rebuilding of structure to take place, at least in times considerably greater than those required for an experiment, so the change could not be classified as thixotropic

(v) at constant rate of shear, the structural breakdown as measured by decrease in torque could be well represented by a simple exponential equation.

A simple theory of breakdown was presented which explained quantitatively the main results.

These findings, which can be explained qualitatively (14) on the basis of Double's membrane theory of hydration (21), have on the whole been confirmed by the considerable amount of work that has been published subsequently, but several difficulties have become apparent. The main ones may by summarised as

(i) results obtained by various workers differ by orders of magnitude

(ii) many different types of hysteresis loop have been found, including positive and negative hysteresis and even figure of eight loops (22)

(iii) decay of torque at constant shear rate cannot always be described by a simple exponential law (23, 24). There may be a discontinuity which has been explained (25) by the presence of a plug whose existence is not predicted from normal plug flow considerations.

These matters have been dealt with fully elsewhere (14) and further discussion is outside the scope of the present paper as are also studies, such as those by Bombled (26) or by Hannant (27) which are intended to aid in the elucidation of hydration mechanisms. It is sufficient to make two observations about the use of the coaxial cylinders viscometer for experiments in cement past rheology, which, it is suggested, should be taken into account in future work.

(i) the finding of a plug, whose existence is so far unexplained, is sufficient to call into question all the results reported from coaxial cylinders viscometer measurements. Observations should be made of the nature of the flow pattern and experiments should be carried out with more than one experimental set-up.

(ii) as was pointed out over 30 years ago (17), the obtaining of hysteresis loops is useful in preliminary work but is not a satisfactory approach for quantitative considerations, because the results depend so markedly on details of experimental procedure. (Of course, it follows that the reporting of hysteresis loops is quite useless if experimental details are not reported at all, or inadequately.) Cheng and Evans have pointed out (28) that it is not possible to deduce the form of a rheological model from experiments carried out at varying shear rates, and Worrall and Tuliani (29) have shown experimentally that two suspensions of quite different thixotropic properties can give similar hysteresis loops.

Another, perhaps cynical, comment may be made and that is that while it can be useful to carry out measurements on fully broken down pastes, that should not be done simply because it is easier.

However, the main conclusion to be drawn, so far as a study of concrete rheology is concerned, is that the whole field of cement paste rheology is in such a state of confusion and uncertainty that to wait for it to be resolved before proceeding with work on the very practical problems relating to concrete, would be to impose a quite unacceptable delay.

Preliminary considerations for concrete

The fact that cement paste rheology is so little understood therefore implies that it is worthwhile carrying out investigations on concrete itself, but there are also some other implications. The first of these is that the approach should be an experimental one, because it is clear that any theoretical treatment would necessarily be based on inadequate information and is therefore unlikely to be successful. The only recent attempt (30) at a theoretical treatment resulted in a prediction of the effect of aggregate grading on workability in the opposite sense to the data given in Road Note 4, which was firmly established on practical experience and experiment. The theory itself was severely criticised (31) but this outstanding disagreement with practice is alone sufficient to condemn it.

The second implication, taking into account also the history of attempts to measure workability, is that a simple empirical approach is not likely to yield any further useful information, and the experiments to be carried out must involve studies of concrete behaviour under reasonably well known conditions of stress and strain or strain rate.

This suggests two possibilities; the first is by using the methods of soil mechanics and the second is by using techniques that have been established for investigating the rheological properties of suspensions. Several workers, including L'Hermite (9), Tassios (11), Ritchie (32), Uzomaka (33) and Mamillan (34) have adopted the first approach and this work has been reviewed elsewhere (1). More recently, Ukraincik (35) has carried out measurements with a type of shear box in investigations which also involved the use of rheological methods. However, the object in all this work was not the development of a practical workability test, because the methods are too cumbersome and time consuming for there to be much hope of their being sufficiently modified for use on site or even for control in a laboratory. A more promising approach seems to be to attempt to apply established rheological methods because they do offer the possibility of being so modified and also, some of them have the advantage of applying continuous shear which seems appropriate in relation to the practical use of fresh concrete.

Ordinary casual observation shows immediately that there is some limiting stress below which a given fresh concrete does not flow, as indicated for example by the mere fact that it is possible to measure a slump value, and this means that the material possesses a yield value. The nature and meaning of yield value have been the subject of some discussion (14, 36) but there is no doubt that from the practical engineering point of view it does exist.

It follows that the flow properties of concrete must be described by an equation of the type

$$\tau = \tau_o + f(\gamma, \dot{\gamma}, t) \qquad (1)$$

where τ is the shear stress at shear strain γ and time t, and τ_o is the yield stress. The simplest possible form of this equation is

$$\tau = \tau_o + \mu\dot{\gamma} \qquad (2)$$

where μ is the plastic viscosity, which is the equation of the Bingham model. It follows immediately that, in order to determine the two constants needed for a full description, measurements must be made at not fewer than two different shear rates. Any test in which only one measurement is made cannot in principle provide sufficient information, no matter how complicated the test procedure or how sophisticated the treatment of the results. This criticism applies to all the standard tests and explains why each of them suffers from the defect that it can classify as identical two concretes that are subsequently found to behave quite differently.

Bombled (37) has proposed that, in accordance with Coulomb's Law as applied in the treatment of results from the soil mechanics shear box, the yield value may be written as

$$\tau_o = c + k.\tan\phi \qquad (3)$$

where c is the cohesion and ϕ is the angle of friction; he considers that the former is provided essentially by the interstitial paste, and the friction by interference between large particles of aggregate.

The coaxial cylinders viscometer is an obvious possible apparatus for a rheological investigation and has been used on high workability concretes by Uzomaka (38), Murata and Kikukawa (39), and Sakuta, Yamane, Kasami and Sakamoto (40). In each case, the results indicated that the flow properties of fresh concrete fit the Bingham model, but the values of yield value and plastic viscosity obtained differed by orders of magnitude. Bloomer (41) has discussed in detail the requirements for the design of a viscometer suitable for measurements on concrete and has pointed out that

(i) the annular gap, $R_c - R_b$ should be not less than 10 times the maximum aggregate size d

(ii) the ratio of the radius of the outer cylinder R_c, to that of the inner cylinder R_b, should be not greater than 1.2 in order to reduce the variation in shear rate across the gap and to reduce the range of speeds in which plug flow occurs.

(iii) the ratio of the height of the inner cylinder, h_b, to the radius, should be not less than unity, in order to reduce end effects.

(iv) to avoid slippage, asperities should be provided on the surfaces of both cylinders and the depth of these asperities, a, should be not less than the maximum aggregate size, d.

Table I shows that all the viscometers fail in respect of gap size and some of them fail in other ways too.

Table I Dimensions of coaxial cylinders viscometers

Quantity	Value Desired	Value in apparatus of U	M&K	S et al
$(R_b-R_c)/d$	$\geq$ 10	1.6	2.25	3
R_c/R_b	$\leq$ 1.2	1.3	1.6	2.5
h_b/R_b	$\geq$ 1	0.8	3.4	2.5
a/d	$\geq$ 1	0.9 1.3	0	0

The only way of reconciling the conflicting requirements listed by Bloomer is to build a large apparatus; he estimates that a satisfactory one would have a sample volume of $2\frac{1}{2}m^3$ and would require a 4 h.p. motor to drive it. This is clearly impractical; an alternative possibility is to consider a mixer method.

Measurements using a mixer

Quite apart from any theoretical considerations, the attractions of attempting to use a mixer for measurements on a material such as concrete are obvious, and several workers have done so certainly as early as 1928. However, in all but two cases measurements were made at only one speed, and in the two cases (42, 43) in which a range of speeds was used, no attempt was made to plot a flow curve. This was first done in 1970 (44) from experiments with a food mixer, in which power consumption was measured at each of the three speeds of which the mixer was capable, and torque was calculated as net power divided by speed. It was found that when plotted as torque against speed, the three points fell close to a straight line which had an intercept on the torque axis, thus indicating that the flow properties of fresh concrete approximated to the Bingham model.

The equation to the line may be written as

$$T = g + hN \qquad (4)$$

where T is the torque at speed N, g is the intercept on the torque axis, and h is the reciprocal of the slope of the line. This equation is obviously analogous to the equation for the Bingham model and it seems apparent that the constant g is a measure of yield value while the constant h is a measure of plastic viscosity. Theoretical justification for this conclusion will be summarised later.

This result which was obtained before the coaxial cylinders work referred to above was published, was a very surprising one, in view of the known complexity of cement paste behaviour. Of course, an experimental result based on only three points is somewhat questionable but it has been amply confirmed since by a very large volume of work. It is now thought that the explanation of this simple behaviour is that the shear rates in the mixing process are substantially higher than those used in the test and the cement paste has already been subjected to structural breakdown so that the paste itself exhibits Bingham properties. It can now be regarded as firmly established that, over a range of shear rates that are important in practice, the flow

properties of fresh concrete are described by the simple Bingham model, and therefore can be characterised in terms of the two constants yield value and plastic viscosity. Whether this is the whole story will be discussed later.

Scullion (45) improved the original apparatus and used it in investigations on the effect on workability of the properties and proportions of mix constituents but further intensive investigations showed that its disadvantages were such that it should be abandoned in favour of a new apparatus that was developed.

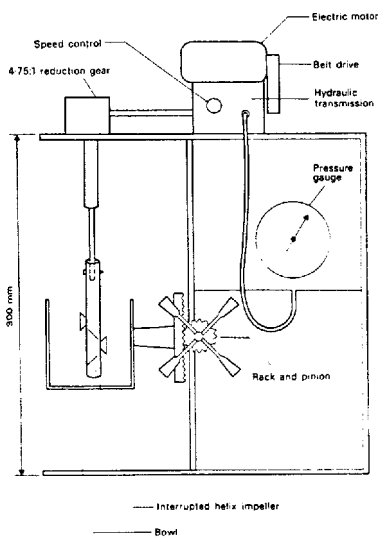

Figure 1 The two-point workability apparatus

The new apparatus, the development and construction of which have been described in detail elsewhere (46, 14), is shown diagrammatically in Figure 1. A suitable impeller is immersed in the concrete under test which is contained in a cylindrical bowl, and is rotated about its own axis by means of an electric motor driving through an infinitely variable hydraulic transmission. The torque required at each of a range of speeds is measured by monitoring the pressure of the oil in the hydraulic transmission. When net torque (that is, the difference between the torques when the bowl contains concrete and when it is empty) is plotted against rotational speed, the points are found to fit to the linear Bingham relationship with a correlation coefficient usually in excess of 0.99.

The apparatus in this form was developed specifically for high workability concretes and has been found to be suitable for a range from about 75mm slump to flowing concrete. For low workabilities it is unsuitable, because the concrete is found to move to the sides of the bowl and fail to fall back, so that the impeller then rotates in the hole it has made. For such concretes an alternative form was developed in which an impeller of a different shape is caused to rotate in planetary motion, and in this form it can be used for low workability concretes down to about 25mm slump. The apparatus can readily be changed from one form to the other; together, therefore, they can cover almost the whole range of practical workabilities, with the exception of extremely low workabilities.

The apparatus has been called the two-point workability apparatus because it satisfies the condition of providing measurements at the required minimum number of two different shear rates. In practice, more speeds are used in order to reduce experimental error.

Practical use of the apparatus

Two practical problems may arise in the use of the apparatus and were considered during the development work.

The first is that, because of trapping of coarse aggregate, the torque reading is not steady. Typically, the torque oscillates about a mean value by a few percent but on this oscillation are imposed larger 'kicks' which are due to aggregate trapping and should be ignored. The extent of the oscillation is reduced by introducing damping into the measuring system but not to such an extent that the response is sluggish. In practice, it is a relatively easy matter to adjust the damping to the right level and to 'learn' to ignore the kicks so that the mean of the small oscillations can be read. A previously inexperienced operator can be taught, or can teach himself, in about quarter of an hour. Of course, the process can be made even easier by automatic recording of torque as a function of time (at a given speed) when a trace of the form shown in Figure 2 is obtained, provided the chart speed is appropriate. The simple insertion of a pressure transducer in the hydraulic line permits this method to be used, and this was done by Gjorv and co-workers (47). An alternative approach, which was considered during the early stages of development of the apparatus, is to take signals from strain gauges fixed on the drive shaft and such a development has been reported recently by Cabrera and Hopkins (48). The disadvantages are that it is considerably more expensive and requires the provision of slip rings whose performance might be affected by even small amounts of dirt. Cabrera reports (49) that no such problem has been experienced but it may still be thought that the system is too vulnerable to be used on an apparatus that has been designed for operation under site and plant conditions.



Figure 2 Oscillation of torque

The second problem is that of the possible occurrence of segregation during the test, and much effort was devoted to trials of impellers of various shapes (41, 50) to reduce this problem to a minimum. The result is that for a wide range of mixes it is clear from ordinary visual observation that the difficulty does not arise, but for some mixes there may be a separation of coarse particles on top of the concrete, or the development of a compacted layer at the bottom of the bowl. However, Wallevik and Banfill (51) have shown that even in such cases during a single test, taking a few minutes, 'the aggregate grading in the zone sheared by the impeller is unchanged'. This has been confirmed by other unreported experiments.

In practice therefore the concrete should be agitated only during loading (at low speed) and the actual carrying out of the test. Under these conditions segregation sufficient to affect the results should not occur; if it does, it is suggested that questions should be raised about the suitability of the mix in general and whether it is likely to segregate in the practical use for which it is intended.

The time needed for a test is under 3 minutes if 7 points are obtained, or under 2 minutes for the 4 points that are usually sufficient for site work. Sugden (52) who used the apparatus on site in both the uniaxial and the planetary form, reported that the time for a test, including loading, was 5 minutes, which he compared with the 3 minutes needed for a slump test.

A much more fundamental difficulty was raised by Ukraincik, (35) who questioned the validity of the straight line relationship for normal concretes and claimed to have obtained three different types of torque/speed curve. However, a plot of the numerical results he gave suggested that his curves had been much over-idealised and the only reasonable conclusion to be drawn was the restricted one that he had observed a curvature towards the origin (53). Even so, this does, as he points out, raise questions about the determination of yield value from linear extrapolation. The apparatus he used was of the food mixer type and one of the reasons that this apparatus has been abandoned, and is now regarded as obsolescent, is that Bloomer showed that the relationship between speed and average shear rate is not constant over the range of speeds used, so that a material whose shear stress/shear rate relationship is linear may well give a torque/speed line that is curved. Unfortunately, Ukraincik does not give any other information about his apparatus so a proper comparison of his results with those of others cannot be carried out, but measurements with the planetary form of the apparatus described above over a greater range than is normally used, showed that a lowest speed comparable with that used by Ukraincik there was no evidence of a curvature towards the origin. In no case has such behaviour been reported by any other worker, except when the concrete in the bowl was vibrated.

It may also be pointed out the criticisms concerning inadequate gap size, that were emphasised in the discussion of coaxial cylinders viscometers, may, with some modification, be levelled at both forms of the apparatus described here. It is necessary to attempt to reconcile what is theoretically desirable with what is practicable, and so to restrict sample size to a reasonable amount. The extent to which the compromise is acceptable must be judged on whether

(a) the method works in practice and yields results that are more useful than those from previous methods and

(b) the results of measurements comply with the theoretical treatment.

It has been shown that the evidence is very encouraging.

Accuracy and sensitivity

Banfill (54) has pointed out that in dealing with a material as variable as concrete, valid estimates of experimental error can be obtained only from properly designed experiments whose results can be processed statistically. For the usual empirical single point tests this involves very lengthy investigations and then the result, when obtained, applies only to the test in general and not specifically to a particular set of measurements. From factorial experiments by Orr (77), in which compacting factor was measured, and similar experiments by himself for slump and vebe, Banfill quotes standard deviations for slump as 11mm, compacting factor as 0.024, and for vebe time as 0.25 times the reading. The practical error figure taken for the slump test is $\pm$ 25mm.

In contrast, the experimental error in the two-point method can be readily calculated for each individual test by considering the variance about the line $T = g + hN$. Bloomer (41) has shown that the standard error in h is given by

$$\frac{\alpha_h}{h} = \sqrt{\left[\left(\frac{1-r^2}{r^2}\right)\cdot\left(\frac{1}{n-2}\right)\right]} \qquad (5)$$

where r is the correlation coefficient and n is the number of experimental points, and the standard error for g is given by

$$\frac{\alpha_g}{g} = 0.95\,\frac{h}{g}\left(\frac{\alpha_h}{h}\right) \qquad (6)$$

where the numerical factor (in this case 0.95) is fixed by the particular choice of speeds used in the test. The error at any chosen level of significance can be found by multiplying these values by the appropriate value of Student's t. The error on h is read off a graph (14) and that on g easily calculated. Typical errors on g and h are of the order of 10% at the 90% confidence level.

The fact that errors can be calculated for each individual test and that the error is usually around only 10%, has the consequence that small effects that would be undetected by other tests can be observed. For example, Bloomer (41) found effects of the variation of fines content that would have remained undetected by the slump test, and Saeed (59) demonstrated the variability caused by variations in water content of a moist aggregate. Recently, Ellis (56), in work on concretes containing ground granulated blast furnace slag, showed that the test was better at detecting significant changes in workability of GGBRS/OPC concretes relative to their OPC controls than any of the British Standard test methods. Waddicor (57) stated that he had been able to assess the performance of plasticising admixtures

more critically than previously. Crossley (58), who used the apparatus for evaluating cements, reported that correlation coefficients were always very high and that repeatability between nominally identical concrete mixes was such that the flow curves lay within bounds that were equivalent to a change in water/cement ratio of about 0.01.

Theoretical considerations

It has been stated earlier that the constants g and h are measures respectively of the yield value and plastic viscosity of the concrete, but the only justification offered so far is that of analogy between the equation of the flow curve and that of the Bingham model. Theoretical support can be provided by considering behaviour in the mixing process and it can also be shown how, following suitable calibration of the apparatus, the constants g and h can be converted to measures of yield value and plastic viscosity in fundamental units. This has been discussed in detail elsewhere (14, 59) and will only be summarised here.

It is first of all necessary to show that the apparatus is operating in the region of laminar flow. This was done by Bloomer using heavy oils (41) and by Saeed (50) using Newtonian polybutene solutions, who each demonstrated close adherence to the relationship

$$N_p = B.Re^{-1} \qquad (7)$$

up to a Reynolds number of 10, where N_p is the power number and Re is the Reynolds number. Then, on the basis of the postulate by Metzner and Otto (60) that the average shear rate in a mixer may be regarded as being simply proportional to the speed, it can be shown that the equation for a Bingham material is

$$T = (G/K)\tau_o + G\mu N \qquad (8)$$

where G is a constant obtained by calibration with Newtonian liquids, and K is a constant obtained by calibration with non-Newtonian liquids whose apparent viscosities vary with shear rate in a known way, determined by separate experiments using a conventional viscometer.

By comparison of equations (4) and (8) it is apparent that

$$\tau_o = (K/G).g \qquad (9)$$

$$\mu = (1/G).h \qquad (10)$$

and hence both yield value and plastic viscosity can readily be expressed in fundamental units (14, 46). The calibration process is somewhat tedious and in practice it is quite satisfactory to express results simply in terms of g and h, which are simply proportional to τ_o and μ respectively.

For two nominally identical apparatuses, A and B, the constants K and G should of course be the same, but, if they are not, corrections may be made by writing

$$g_A = g_B \cdot \frac{G_A K_B}{G_B K_A} \text{ and } h_A = h_B \cdot \frac{G_A}{G_B} \qquad (11)$$

Figures have been published (46) to show that what was already good agreement between results from two nominally identical apparatuses could be improved further in this way; Banfill (61) has only recently applied the method again.

More importantly, it is possible to use the equations for comparison of results from different forms of apparatus, and in particular, from the uniaxial and planetary forms, with a view to establishing a single scale to cover almost the whole range of workabilities. Such a study was made by Bloomer (41) and later extended by Dimond (62) who used the same apparatuses but a greater number of mixes. Dimond found the agreement between experiment and theory to be very promising but to depend to some extent on a somewhat arbitrary choice from equally plausible assumptions about the nature of the calibration curves. The difficulty arises from the results obtained on the non-Newtonian liquids used in the determination of the constant K.

It would be very desirable to use a material whose properties are similar to those of the materials for which the apparatus is to be used, that is, one that conforms to the Bingham model. Unfortunately it has not been possible to find a suitable material, even after publication of an appeal (63); several that have been described by other workers as Binghams were tried but all were found to suffer from structural breakdown under shear. It was therefore necessary to use aqueous carboxymethyl cellulose solutions which are pseudo-plastics of the power law type and whose flow curve may therefore be described as

$$\tau = r\dot{\gamma}^s \qquad (12)$$

Unfortunately, detailed work has shown that, for the solutions used, the constant s is in fact dependent on shear rate to an extent that introduces uncertainties into the interpretation. Saeed (50) has made a thorough study of this problem but further work is needed before it is completely resolved.

Factors affecting workability

The two-point workability apparatus has been used by a number of workers in investigations of the effects of various factors on workability, as follows:-

Mix proportions and aggregate type - Scullion (45), Bloomer (41) and Saeed (50)

Cement properties - Dimond (62) and An-Keat Yeoh (64)

Plasticisers - Scullion (45), Waddicor (65), Banfill (66), Rixom and Waddicor (67), Bloomer (41), Edmeades and Hewlett (68) and Carlisle (69)

Air entrainment - Banfill (14)

Fly ash - Ellis (70)

Blast furnace slag - Arnold (71), Crowter (72), and Ellis (56)

Steel fibres - Urbanowicz and Dimond (73)

Fine dredged sand - Carr and Banfill (74)

A full discussion of this work is beyond the scope of the present paper but the main general results may be summarised as follows.

(i) There is in general no correlation between the values of g and h so it is necessary to measure both of them, and suggestions such as that of Hobbs (30), in support of single point tests are shown to be invalid (31).

(ii) There is strong interaction between the effects of the variables. For example the effect of a change in fines content depends very much on the values of other parameters such as water/cement ratio and aggregate/cement ratio.

(iii) For some factors interactions are less strong and generalisations may be made. For example, an increase in water content always reduces both g and h, an increase in plasticiser content decreases g but has very little effect on h, while an increase in air entraining agent content decreases h with little effect on g. Replacement of cement by ground granulated blast furnace slag has little effect on either g or h.

These results lead to two very important conclusions. The first is that measurement of the two quantities g and h readily provides a means of differentiating between concretes that are wrongly judged to be similar by other tests. The second conclusion is that because changes that affect workability affect g and h in different ways according to the causative agent, the two-point test presents possibilities for a control method that have not been available previously. It can not only detect that workability has changed, but can give strong indicators as to the cause of the change. This possibility has been discussed in detail elsewhere (75, 76).

Banfill (77) has produced the diagram shown in Figure 3 as a simplified guide to show in general terms the effect of increases in concentration of various components, on g and h. Of course, for control purposes, much more specific diagrams are needed but they can be readily constructed.

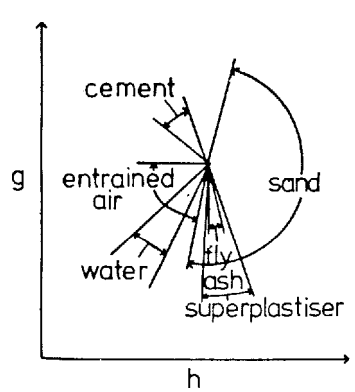

Figure 3 Effect of increase in quantity of various mix constituents

Effect of vibration on workability

The use of vibrators for the placing and compaction of concrete is a long established practice, yet the design of the equipment is still on a very much ad hoc basis. Early work on the effect of vibration was based mainly on assessments of the properties of the hardened concrete except for some empirical flow tests and some shear box experiments by L'Hermite (9) on fresh concrete. Clearly, it is the effect on flow properties of fresh concrete that is of major interest.

Just as ordinary casual observation shows that fresh concrete possesses a yield value, as mentioned earlier, so it is also obvious that when vibration is applied to concrete, the effective yield value is at least very much reduced, perhaps even to zero. This is indicated by the fact that the concrete flows easily under its own weight.

Reduction in yield value was studied in an interesting series of experiments by Lasalle and Legrand (78) in which they measured the minimum torque required to turn a paddle located at various distances from a vibrating source. They state that when a critical amplitude is exceeded the yield value is reduced to zero but the radius of effectiveness of a vibrator decreases as frequency increases, because of increased damping. They describe the existence of three zones, in relation to an internal vibrator:

Zone 1 near the source, where turbulence occurs and operates against satisfactory compaction

Zone 2 further away, where yield value is practically destroyed and compaction takes place satisfactorily

Zone 3 further still, where the vibration is damped to an extent that yield value is not sufficiently decreased, and satisfactory compaction does not occur.

The positions of the boundaries between these zones are conditioned by the amplitude and frequency of the vibration but in Zone 2 the parameters of vibration have little influence on rheological characteristics. It should be noted that they measured only yield value and, more importantly, that to avoid difficulties of change with time they used calcite pastes. This does raise a question about the validity of the application of the results to cement pastes and (even further removed) to concretes.

Because it is easy to mount the bowl of the two-point test apparatus on a vibrating table, it becomes possible to obtain the flow curve for a material when it is not being vibrated and of the same material when it is being vibrated. Preliminary experiments on these lines, using a concrete in which all the cement had been replaced by pulverised fuel ash, and a table vibrator actuated by a commercial shutter vibrator, have already been reported (14). Little was expected from these experiments because of the complex waveform of the vibrator, except an indication as to whether experiments with more expensive apparatus would be worthwhile, and these experiments have now been carried out (79).

The bowl of the workability apparatus was mounted on an electromagnetic vibrator whose amplitude and frequency could be controlled

independently, and which was capable of 70 kN peak thrust. A flow curve for unvibrated concrete was obtained in the normal way, then the impeller was run at its top speed and the vibrator was switched on at the chosen amplitude and frequency, resulting in a very rapid drop in torque followed by a slower rise, which was attributed to the occurrence of compaction. The minimum torque observed was taken as a measure of the effect on workability, and gave one point on the flow curve of the concrete under vibration. The concrete was then remixed, replaced in the bowl, and measurements repeated at a lower speed setting to give another point. In this way four points were obtained and the vibrated flow curve was constructed. Experiments of this type were carried out on two different mixes of 75mm slump at six frequencies from 15 to 100 Hz and four accelerations from $2\frac{1}{2}$ to 10g.

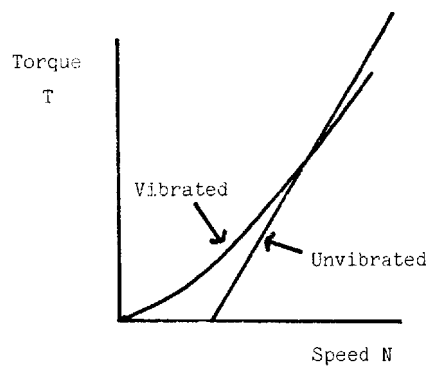

Figure 4 Effect of vibration on flow curve

The results were of the form shown in Figure 4. The flow curve for the vibrated concrete appeared to start from the origin and could be well represented by a power law equation of the type

$$T = A_v N^{B_v} \qquad (13)$$

This means that yield value has been reduced to zero but the flow curve has been changed from a straight line to a curve which crosses the original unvibrated line, so that at the higher shear rates the application of vibration actually reduces the workability of the concrete. Experimental points to confirm this were obtained, but whether any practical process operates in a shear rate range where the effect is important is not known. It can be shown that the straight line $T = g + hN$ for the unvibrated concrete can also be approximated very closely over the shear rate range covered in the test, by a power law relationship, so the effect of applying vibration may be presented in the form

$$(T_v/T) = (A_v/A).N^{B_v-B} \qquad (14)$$

There was some evidence that (A_v/A) was an exponential function of acceleration, and (B_v-B) an exponential function of velocity.

The indication that the curve pases through the origin means that at low shear rates, such as those produced by flow under self weight, concrete under vibration can be regarded as a Newtonian whose flow properties can be characterised by the viscosity η or its reciprocal, the fluidity ϕ, which may be found from the slope of the tangent from the origin. For both mixes studied it was found that the results fitted a relationship of the form

$$\phi = c_1(1 - \exp(c_2 A(f-F_c))) \qquad (15)$$

where A is amplitude, f is frequency and F_c is some small critical frequency that must be exceeded for there to be any effect at all. Note that, since velocity is proportional to the product of frequency and amplitude, this shows that the effect of vibration is to be measured in terms of the maximum velocity of the vibration.

The obtaining of the evidence that at low shear rates concrete under vibration behaves as a Newtonian prompts the carrying out of experiments that would have been unjustified in the absence of such evidence. Apparatus was set up to study the rate of fall of a column of concrete contained in a 100m dia. vertical pipe when vibration was applied at the bottom, where the concrete was allowed to flow out into a containing bowl. If the material behaves as a Newtonian the height H would be expected to decrease according to

$$dH/dt = -bH \qquad (16)$$

where b is proportional to the fluidity. The simplicity of this arrangement permits the carrying out of a large number of experiments and observations were made on six mixes at ten frequencies from 15 to 200 Hz and eight accelerations from 0.85 to 8.9 g. All the results were found to fit the relationship proposed and further, for each mix, to fit a relationship of the form

$$b = c_3.(A - A_o).\ln(1 - f/F) \qquad (17)$$

where A_o is a small critical amplitude and F is a large critical frequency in excess of 200 Hz. While the actual value of F is in some doubt, its existence is not, as was confirmed by subsidiary experiments at frequencies up to 1000 Hz. If the values of A and f are well away from the critical values, this expression again reduces to a simple function of velocity. Finally, a good correlation was found between ϕ from the two-point apparatus experiments and b from the quite different vertical pipe experiments.

The importance of velocity was also confirmed by experiments on cement pastes using a smaller scale version of the two-point apparatus, and this work has already been reported (80).

Other applications of the two-point apparatus

The two-point apparatus has been shown (81) to be satisfactory for measurements on grouts of the type used for filling prestressing ducts, provided the impeller is modified to produce greater values of net torque. It has also been used for mortars although in this case peculiar results have been obtained on several occasions, when the flow curve

has been found to have a negative slope. This is not yet explained, but in the case of mortars the requirements for gap width of a coaxial cylinders viscometer are obviously much less demanding than for concrete, so Banfill (61) has substituted a serrated cylinder for the normal impeller and has obtained satisfactory results.

The apparatus is also useful at a smaller scale (2/5) for investigations of cement pastes at low shear rates, but then the impeller and container are used in conjunction with a normal viscometer head and drive unit. This arrangement was used in the vibration experiments on cement paste, referred to above and has also been used by An-Keat Yeoh (64) in his investigation of the effect of cement properties. Yeoh found that for pastes made from a given cement with varying water contents, the ratio g/h was a constant and could be useful in looking for correlations between rheological properties and factors in the composition of the paste. It is interesting that Bombled has independently suggested the use of this ratio of yield value to plastic viscosity to characterise pastes, although his suggested term 'intrinsic plasticity' might be criticised.

A difficulty in using coaxial cylinders for cement pastes is that at the water/cement ratios normal in concrete heavy sedimentation occurs in the paste. Bhatty and Banfill (82) showed that using the helical geometry of the scaled down two-point apparatus, sedimentation, as measured by their sedimentation index, was only about 6% of that for coaxial cylinders, and even at a water/ cement ratio of 1.0, the difference in solids concentration from top to bottom of the sample was only 5%.

Conclusions

It can now be taken as established that, at the low rates of shear important in practice, the flow properties of concrete in the low to very high workability range, conform to the Bingham model, and can therefore be assessed in terms of yield value and plastic viscosity. This is not an assumption, as some authors seem to think; it is a statement well attested by a large volume of experimental results obtained by a large number of independent workers.

The two-point test apparatus is capable of measuring the two parameters and of ascribing an estimated experimental error to each determination. As a result, it can differentiate between concretes wrongly judged by other tests to be similar and it can form the basis of a production control system.

The knowledge now available leads to a greater understanding of the existing standard tests (83, 50, 14), and of processes such as pumping (14) and the application of vibration. Of course, there are still large gaps; the test itself might be improved by development of new impellers and further study is needed on the calibration with non-Newtonians, and certainly much more work is needed on the effects of various factors on g and h.

The test is not capable of dealing with extremely low workability concretes, which cannot even be regarded as a continuum so the approach must be different, and it cannot give information at stresses below the shear stress.

However, it can be claimed that it has already served in elucidating previously intractable problems and can do much more. Finally, it was never intended to be only a laboratory tool and it is believed that its use on site, or at the ready mixed concrete plant, would lead to substantial savings by avoiding disputes and lost production and by preventing expensive mistakes.

References

1. Tattersall, G.H. The Workability of Concrete, C&CA 1976.
2. Neville, A.A. RILEM, Chairman's Summary.
3. Glanville, W.H., Collins, A.R. and Matthews, D.D., Road Research Technical Paper No. 5, HMSO, 1947.
4. Bartos, P. Concrete, 12, (10), 28-30, 1978.
5. Tattersall, G.H., Concrete, 12,(12),15, 1978.
6. Banfill, P.F.G., Concrete 13 (1), 16, 1979.
7. Baron, J., RILEM, Vol. 1, 2D1-1.
8. Angles, J.G., Concrete 8 (12), 26, 1974.
9. L'Hermite, R., CERILH Pub. Tech. No. 1, 1948.
10. Berthier, R.M., Rev. des Mater. de Constr. et de Trav. Pub. (417), 187-9, 1950.
11. Tassios, T.P., RILEM Vol. 1, 1.3-1 to 1.3-36.
12. British Standard BS5168; 1975.
13. Baron, J. & Lesage, R., RILEM, 1.1-1 to 1.1-27.
14. Tattersall, G.H. & Banfill, P.F.G., The Rheology of Fresh Concrete, Pitman, London, 1983.
15. Tattersall, G.H., Proc. Symp. M. Annual Meeting Mater. Res. Soc., 1982, 78-97.
16. Bombled, J.P., Rev. des Mater. de Constr.(688), 137-155, 1974.
17. Tatersall, G.H., M.Sc., Thesis, University of London, 1954.
18. Dimond, C.R., Unpublished Report, University of Sheffield, Reported in Ref. 14.
19. Yeoh, An-Keat, M.A. Thesis, University of Sheffield, 1982.
20. Tattersall, G.H., Brit. J. Appl. Phys., 6, (5) 165-7, 1955.
21. Double, D.D., Perry, S.J. and Hellawell, A., Proc. Roy. Soc. A., 359, 435-451.
22. Banfill, P.F.G. and Saunders, D.C., C&CR, 11, 363-370, 1981.
23. Tirona, E.E., M. Eng. Thesis, SEATO Graduate School Engng, 1964.
24. Nessim, A.A. and Wajda, R.L., MCR, 17 (51), 59-68, 1965.
25. Tattersall, G.H. and Dimond, C.R., Proc. Conf. Hydraulic Cement Pastes, 118-133, C&CA, 1976.
26. Bombled, J.P., CERILH Pub. No. 213 & Rev.des Mater.de Constr. 1971.
27. Hannant, D.J. & Keating,J., C&CR, 15, 605-612, 1985.
28. Cheng, D.C. & Evans, F., Brit. J. Appl. Phys., 16, (11), 1599-1617, 1965.
29. Worrall, W.E. & Tuliani S., Trans. Brit. Ceram. Soc., 63 (4), 167-186, 1964.
30. Hobbs, D.W., MCR 28 (97), 191-202, 1976.
31. Tattersall, G.H. & Dimond, C.R., MCR 29 (101), 225-7, 1977.
32. Ritchie, A.G.B., MCR 14 (40), 37-42, 1962.
33. Uzomaka, O.J., MCR 23 (75-76), 111-8, 1971.
34. Mamillan, M., Suppl. Ann. de. L'inst. Bat. et Trav.Pub. (201), 912-952, 1964.
35. Ukraincik, V., C&CR 10, 203-212, 1980.
36. Cheng, D.C.H., Bull. Brit. Soc. Rheol., 21 (4), 60-5, 1978.

37. Bombled, J.P., Rheologie du Beton Frais et influence des Fillers; Synthese des Etudes 1982/4. CERILH.
38. Ujomaka, O.J., Rheol. Acta 13, 12-21, 1974.
39. Murata, J. & Kikukawa, H., RILEM Vol. 1, 1.2-1 to 1.2-33.
40. Sakuta, M., Yamane, S., Kasami, H. & Sakamoto, A., Proc. Conf. Quality Control Concrete, Vol. 2, 125-132, 1979, Stockholm.
41. Bloomer, S.J., Ph.D. Thesis, University of Sheffield, 1979.
42. Purrington, W. & Loring, H.C., Proc. ASTM 30 Pt. II, 654-673, 1930.
43. Harrison, O.J., Tech.Rep.27, Ready Mixed Concrete (UK) Ltd.
44. Tattersall, G.H., Paper to Conf. E. Midlands Region Concrete Soc., Nottingham, 1971.
45. Scullion, T., M.A. Thesis University of Sheffield, 1975.
46. Tattersall, G.H. & Bloomer, S.J., MCR 31 (109), 202-210, 1979.
47. Gjorv, O.E., Private Communication Jan. 1983.
48. Cabrera, J.G. & Hopkins, C.J., MCR 36 (129), 237-240, 1984.
49. Cabrera, J.G., Private Communication.
50. Saeed Ahmad, Ph.D. Thesis, University of Sheffield, 1982.
51. Wallevik, O. & Banfill, P.F.G., Internal Rep. University of Liverpool, 1983.
52. Sugden, A., Unpublished Report, 1981. Reported in Ref. 14.
53. Tattersall, G.H. C&CR 11, 485-7, 1981.
54. Banfill, P.F.G., MCR 29 (100), 156-7, 1977.
55. Orr, D.M.F., J.A.C.I. Proc. 69, (10), 619-624, 1972.
56. Ellis, C. Paper presented at Workshop on blast furnace slag cements and concretes, York, Oct. 1985.
57. Waddicor, M.J., MCR 32 (113), 244, 1980.
58. Crossley, A.N., Reported in Report BS74, University of Sheffield.
59. Cheng, D.C.H., Bull. Brit. Soc. Rheol. 21 (4), 60-5, 1978.
60. Metzner, A.B. & Otto, R.E., J. Amer. Inst. Chem. Engs. 3, 3-10, 1957.
61. Banfill, P.F.G., Private communication.
62. Dimond, C.R., Unpublished report. Reported in Ref.14.
63. Anon. Technical enquiry. Bull. Brit. Soc. Rheol. 21, 23, 1978.
64. Yeoh, An-Keat, M.A. Thesis, University of Sheffield, 1982.
65. Waddicor, M.J., Private communication to P.F.G. Banfill, Nov. 1980.
66. Banfill, P.F.G., MCR 32 (110), 17-27, 1980.
67. Rixom, M.R. & Waddicor, M.J., in Developments in the use of superplasticisers, Pub. SP-68, ACI 1981, pp. 359-380.
68. Edmeades, R.M. & Hewlett, P.C., Proc. Admixtures Cong. CI80 49-72, 1980.
69. Carlisle, J.S., B.Sc. Project, Sheffield City Polytech. 1981.
70. Ellis, C., MCR 33 (117), 233-5, 1981.
71. Arnold, S.R., Private communication to P.F.G. Banfill, Aug. 1981.
72. Crowter, G., B.Sc. Project, University of Sheffield. Reported in Ref. 14.
73. Urbanowicz, C., M.A. Thesis, University of Sheffield 1973.
74. Carr, M.P. & Banfill, P.F.G., Research Report, University of Liverpool, 1985.
75. Tattersall, G.H., Concrete 16 (3), 21-4, 1982.
76. Tattersall, G.H., Proc. Symp. M. Annual Meeting Mater. Res. Soc., 1982, 78-97.
77. Banfill, P.F.G., Proc. Conf. Mech. & Techny. of Composite Materials Varna, Bulgaria, 1985. pp. 443-6.
78. Lassalle, A. & Legrand, C., Mater. et Constr. (76), 315-322.
79. Tattersall, G.H. & Baker P.H., To be published.
80. Tattersall, G.H., Proc. Conf. Mech. & Techny of Composite Materials Varna, Bulgaria, 1985, pp. 419-422.
81. Tattersall, G.H., Unpublished report, Nov. 1984.
82. Bhatty, J.I. & Banfill, P.F.G., C&CR 13, 69-78, 1982.
83. Tattersall, G.H., MCR 28 (96), 143-7, 1976.

Abbreviations

MCR	Magazine of Concrete Research
C&CR	Cement and Concrete Research
RILEM	Proc. RILEM Seminar on Fresh Concrete : Important Properties and the measurement. Leeds 1973.

MICHAUX M.
OBERSTE - PADTBERG R. - Etudes et Fabrications Deowell Schlumberger - Saint Etienne - France

THE EFFECT OF MIX WATER SALINITY ON CEMENT SLURRIES CONTAINING POLYNAPHTALENE SULPHONATE.

S3

INTRODUCTION

Wherever cement slurries or concrete grouts are pumped, their rheological properties are of interest. In order to adjust a slurry at a given water to cement (W/C) ratio for pumpability, dispersants, also called superplasticizers, are added. The most frequently applied dispersants are of the naphtalene sulfonate formaldehyde condensate (NSFC) type. In the oil well cementing industry, they are exclusively applied in fresh water and low salinity water. For salt rich cementing slurries, as frequently designed for salt zone cementing, NSFC is reported to be of no use, and even to deteriorate the rheological behavior of the slurries.

In the present study the effect of both, mix water salinity and dispersant content on slurry rheology and NSFC adsorption on cement particles is reported. A model for salt - NSFC interactions in a Portland cement slurry is developed.

LITERATURE REVIEW

Many articles in the literature deal with the adsorption of NSFC on cement surfaces in fresh water based slurries. The cement to NSFC interactions in salt water based systems have not yet been studied. Usually, pseudo adsorption isotherms are determined for a particular cement and correlated with properties such as sedimentation velocity [1], zeta potential [2-6], or different kinds of rheology [3], [7]. Here, we should also refer to comprehensive studies by Tattershall and Banfill [8]. Michaux et al [9] studied the interaction between NSFC and fresh water mixed oil well cement slurry by zeta potential and adsorption measurements and correlated these results to the rheological slurry properties.

EXPERIMENTAL

1. Slurry preparation

All slurries were prepared according to the API specification N° 10 [10] at 25°C and agitated subsequently for 20 mn in an atmospheric consistometer before carrying out the measurements. For all tests a (water + NSFC)/cement ratio of 0.44 was maintained.

2. Chemicals

One single batch of cement and one single batch of dispersant solution (solid content = 40%) were used. The free Na_2SO_4 content of the NSFC, determined as described in [9] was less than 1% by weight of liquid (bwol).

3. Measurements

The determination of the adsorbed NSFC was done by UV absorption as described in [9]. Rheology tests were done according to [9] and [10].
Conductimetric measurements were also done on salt water solutions containing different concentrations in NSFC.
For turbidimetric tests, different amounts in NSFC were added to 10 cc of a cement slurry's interstitial water, filtrated 20 mn after mixing. This solution was left under static conditions for 48 h and subsequently tested for absorbance at 650 nm before and after filtration.

RESULTS

Fig.1 shows the evolution of the yield value (YV) of cement slurries with various low amounts in NSFC as a function of their mix water (NaCl) salinity. For the 1 and 2% by weight of cement (bwoc) NSFC containing cement slurries, salt has a highly viscosifying effect.

In Fig.2, we see the YV evolution as a function of NSFC concentration for three different salinities. For all three cases, we can see that a NSFC addition effects a slurry viscosification that, after a maximum YV, will result in a well dispersed slurry. These maxima occur at different NSFC concentrations, depending on the mix water salinity, and are of differing importance; compared to a NSFC free system the YV in the fresh water system increases only by about 20%, whereas for the 30% NaCl slurry by more than 500%. The high salinity cement goes between 7.2 and 7.8% bwol NSFC through a minimum (overdispersed).

Parallel to the increased NSFC demand for a well dispersed cement slurry with increasing salinity, we also experienced an increasing NSFC adsorption on both, cement particles after 20 mn hydration and synthesized calcium silicate hydrates (CSH) with higher slurry mix water salinity (see fig.3 and 4).

In order to determine the effect of both, cations and anions on the NSFC-cement interaction, we measured the dispersant adsorption in the presence of two other soluble salts, having a common ion with NaCl : KCl and $NaNO_3$ (see fig.5) in the presence of 2% bwoc NSFC. Both alkali chlorides influenced the NSFC adsorption in the same way: the dispersant adsorption increased drastically with increasing salinities (up to 95% adsorption). The $NaNO_3$ showed hardly any effect on the NSFC to cement interaction.

Conductimetric tests showed that at increasing water salinities NSFC additions had decreasing effects on the conductance of the resulting solution (see fig.6).

DISCUSSION

In the scope of the present tests, it was experienced for the first time that NSFC can be applied as salt cement slurry dispersant. It was shown that increasing mix water salinity increases the NSFC demand for a well dispersed slurry.
Adsorption tests revealed that the increase in dispersant demand for a well dispersed cement slurry is related to an increase in NSFC adsorption as soon as cement slurries are mixed with NaCl or KCl rich water.

This can be, partly, attributed to the formation of different initial hydration products (chloroaluminates, Na^+, K^+, and Cl^- containing CSH) with an increased specific surface in a NaCl rich system compared to a fresh water one. It was shown, however, that sodium chloride effects the NSFC adsorption on pure CSH phases in the same way. This means, that a specific surface modification of a cement during initial cement - water contact due to salinity variations cannot be exclusively responsible for the observed phenomenon.

A deactivation of the NSFC, leading to a higher dispersant demand, can be explained by the formation of ion pairs: the negatively charged sulfonate group of

the NSFC will interact with positively charged ions according to :

$$R - SO_3^- + Na^+ \rightleftharpoons [R - SO_3^- \ldots {}^+Na]^0$$

with R being the naphtalenic group.

This unity has no external electrical charge and its formation will be promoted if, for a given alkali activity, the NSFC concentration increases.

If this were the main mechanism responsible for the increased NSFC demand for constant slurry dispersion, the effect of NaCl replacement by $NaNO_3$ should have the same effect on polymer adsorption. This is not the case (see fig.5).

A possible mechanism for the increased NSFC adsorption on cement grains with increasing alkali chloride concentrations can also be due to a compaction of the NSFC unities as an effect of an increased electrolyte activity. Thus, the single dispersant molecules could have been agglomerated in the form of micelles (see fig.7). The quantity, size, and form of the micelles is reported to depend on the nature and concentration of electrolytes [11] . This could explain the differences in NSFC adsorption at different alkali salts.

The agglomeration of a certain number of micelles may finally lead to a precipitate. In fact, in the scope of additional tests, it was observed that, if NSFC was added up to a certain concentration into an interstitial salt cement slurry water (mix water salinity : 30% NaCl), a precipitate was formed. This precipitate disappeared when NSFC was added in excess (shown in fig.8).
Interstitial waters from cement slurries of lower mix water salinity ($\leq$ 26% NaCl) did not produce this precipitate.

The initial increase in YV for salt free as well as salt rich cement slurries, at low NSFC concentrations (see fig.2) can be explained by the patch model as described by Michaux et al. [9] .
The positive charge observed on cement particles without dispersants is a global charge. The actual charge is probably composed of positive patches separated by neutral or even negative regions. Therefore particles will tend to orientate themselves to align positive and neutral or negative patches. This will result in attractive forces creating a tridimensional structure. This strength is measured macroscopically by YV determination and is somehow proportional to the product of the average number of positive (n^+) and negative (n^-) patches on the particles.

For the neat formulation, $n_0^+ \gg n_0^-$. As we now increase the dispersant concentration, n^- increases and n^+ decreases.
Only a fraction of the sulfonate groups of the dispersant chains neutralizes the positive site. The rest brings an excess k of negative charges. Therefore we obtain :

$$n^- n^+ = (n_0^+ - km)\,[n_0^- + (\alpha - k)m]$$

where :

m is the average number of adsorbed dispersant molecules per cement particle surface unit.

α is the average number of sulfonate groups per dispersant molecule.

This product must go with increasing NSFC concentrations through a maximum and so must the YV.

This patch model is supposed to be responsible for the slight YV increases as soon as initial NSFC amounts are added to the 0 and 18% NaCl cement slurries. The main factor for the drastic YV increase and subsequent decrease in the high salinity cement slurry at NSFC concentrations between 0 and 7% bwol is supposed to be the formation and subsequent disappearance (see fig.8) or the dispersion of the precipitate observed with increasing NSFC amounts added to a high salinity interstitial water. However, within a cement slurry, we cannot differentiate between adsorbed and flocculated NSFC.

CONCLUSIONS

In order to disperse a cement slurry by NSFC, its molecules have to adsorb on cement surfaces. This will decrease attractive interparticle forces.

Salt water cement slurries of a W/C ratio of about 0.44 need for a YV close to zero by far more dispersant than fresh water mixed ones. The reason is that with increasing water salinities an increased NSFC amount is adsorbed on both, cement particles and pure CSH phases.
The mechanism for this can be explained by a deactivation of the NSFC at high electrolyte activities due to the formation of ion pairs. The compaction of NSFC layers, being adsorbed on the cement particles, may lead to the adsorption of additional NSFC.

Micellation is postulated, and agglomeration due to both, mix water salinity and NSFC addition could be observed. The appearance and subsequent disappearance or dispersion of a precipitate in slurry's interstitial water, prepared with 30% NaCl mix water, can explain the pronounced YV increase for a salt water slurry with increasing NSFC amounts.

LITERATURE

[1] Kondo,R. ; Daimon,M. ; Sakai,E. ; Il Cemento, V.3, pp 225-230 (1978)

[2] Daimon,M. ; Roy,D. ; J. Cem. Conc. Res., V.8, pp 753-764 (1978)

[3] Daimon, M. ; Roy,D. ; J. Cem. Conc. Res. V.9, pp 103-109 (1979)

[4] Suzuki, K. ; Nichikawa,T. , Kato,K. ; Hayashi,H; Ibo,S. ; J. Cem. Conc. Res. V.11, pp 759-764 (1981)

[5] Collepardi, M. : Il Cemento, V.4, p 298 (1983)

[6] Pauri, M. ; Ferrari,G. ; Collepardi, M.; J. Cem. Conc. Res., V.13, pp 61-68 (1983)

[7] Kishitani,K. ; Tomosana,F. ; Oka, S. ; ACI Publ. Sp 68-24, pp 423-439 (1979)

[8] Tattershall, G. ; Banfill, P/F/G. ;The Rheology of Fresh Concrete ; Pitman Publishing, London (1983)

[9] Michaux,M. ; Defosse, C. ; J. Cem. Conc. Res. V.16 (1986)

[10] API Specification for Materials and Testing for Well Cements, Spec. 10 ; American Petroleum Institute, Washington DC (1984)

[11] Hall, D.G. ; Tiddy, G.J.T. ; Anionic Surfactants - Physical Chemistry of Surfactant Action ; Lucassen & Reynders (Editors), pp 55-108 (1981)

FIG.1 INFLUENCE OF NSFC CONCENTRATION ON YIELD VALUE

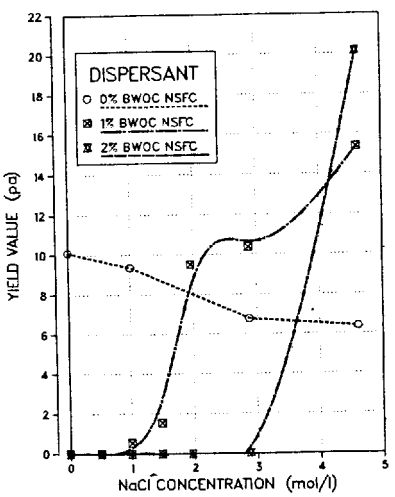

FIG.2 INFLUENCE OF SODIUM CHLORIDE CONCENTRATION ON YIELD VALUE

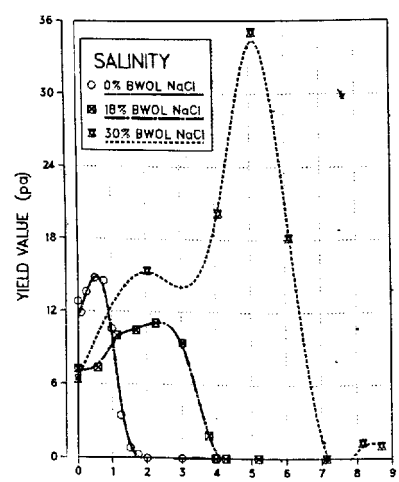

FIG.3 NSFC ADSORPTION ISOTHERM AS A FUNCTION OF SODIUM CHLORIDE CONCENTRATION

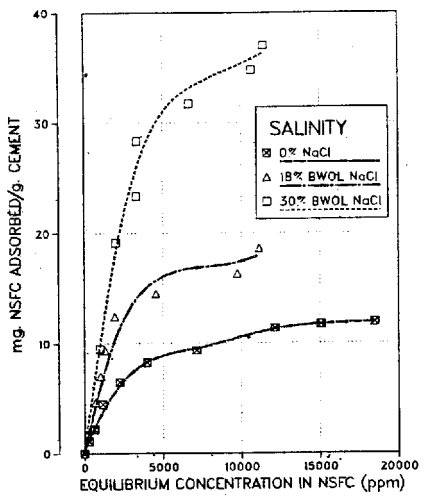

FIG.4 NSFC ADSORPTION ISOTHERMS ON CEMENT AND CSH

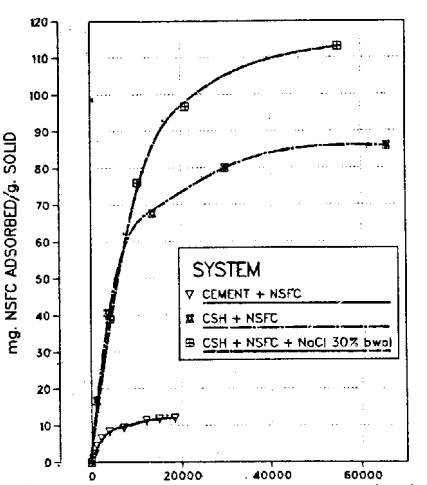

MICHAUX M.
OBERSTE - PADTBERG R.

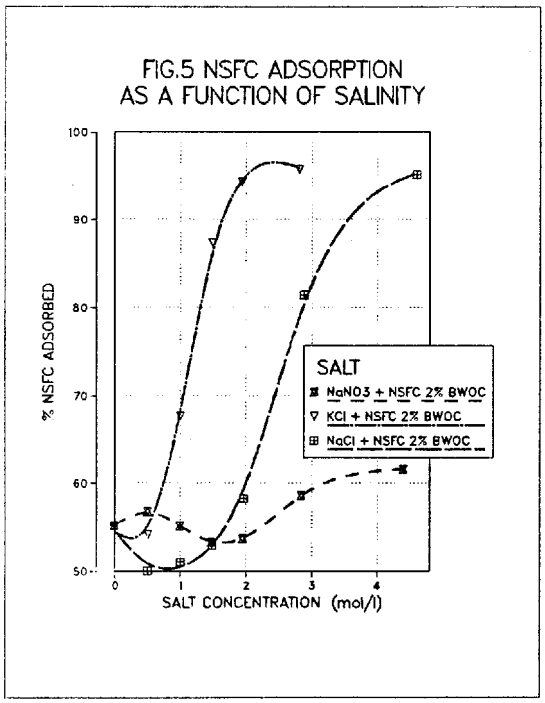

Fig. 7 : The Hartley spherical micelle showing surfactant ion of dubious status. (The representation of surfactant chains as rods is highly idealized.)

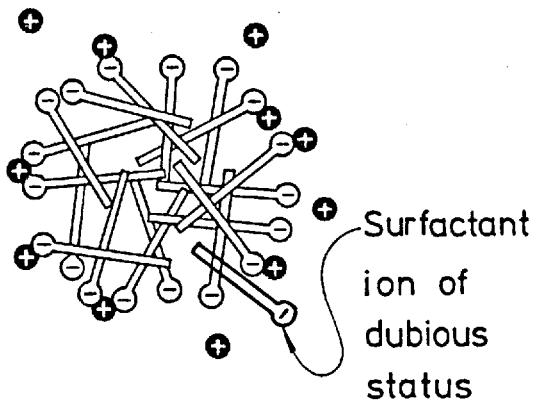

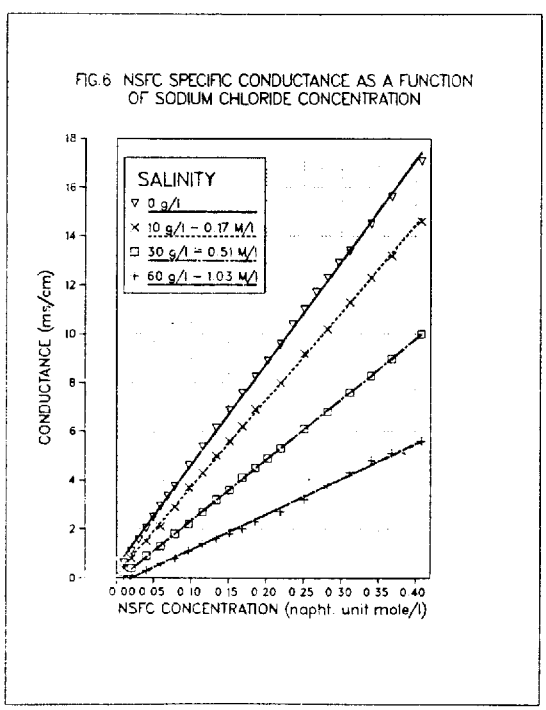

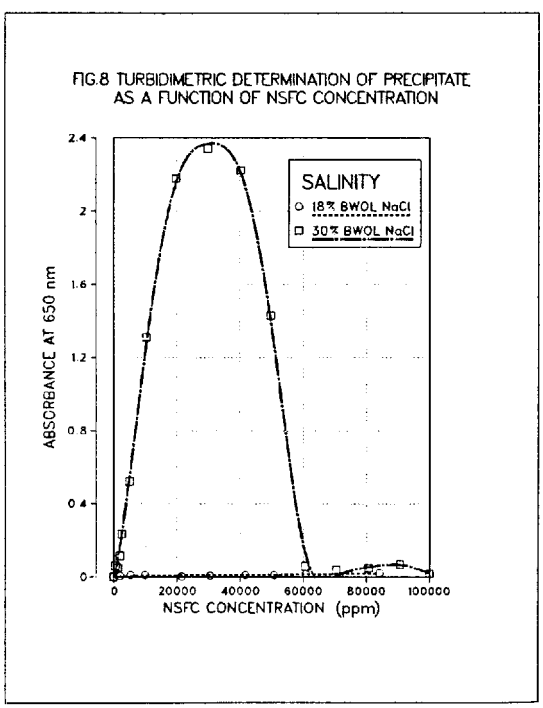

ORBAN,J.
PARCEVAUX, P.
GUILLOT, D.

Etudes et Fabrications Dowell Schlumberger - Saint Etienne - France

INFLUENCE OF SHEAR HISTORY ON THE RHEOLOGICAL PROPERTIES OF OIL WELL CEMENT SLURRIES

INTRODUCTION

Cement slurries are commonly considered to exhibit a shear dependent behavior. This is particularly true from a rheological point of view. In the construction industry and in civil engineering, Tattersall and Banfill [1] , and Lapasin and al. [2] , have analyzed this shear dependence. Lapasin proposed a thixotropic model to characterize slurry rheology. Banfill analyzed the influence of mixing conditions on the rheological behavior. He suggested the use of a Bingham Plastic model to characterize the equilibrium flow condition in most common situations.

In oil well cementing, cement slurry rheology plays an important role on the effectiveness of a cement job. A major problem is that job design is done from laboratory tests performed on slurry samples mixed in conditions, as per the API specification 10 [3] , that do not systematically simulate those of field mixing.

The influence of shearing not only should account for mixing, but also for pumping the cement slurry into the casing and displacing it into the casing to formation annulus. Here as well, the similarity between laboratory agitation in a consistometer [3], and field pumping is of utmost importance.

Finally, following to mixing and stirring, the cement slurry is rheologically characterized using a viscometer. A thixotropic model was proposed in [2], which mainly accounts for API Class A or ASTM type 1 cements which produce reasonably high levels of ettringite very soon after mixing. In fact, most API Class G or H cements show lower levels of thixotropy. However, the rheological test itself should not perturbate the fluid sample. This problem was analyzed by Batty and Banfill in [4] . It was concluded that rotational viscometers with coaxial cylinders are suitable to measure the rheology of a slurry the water to cement ratio of which is higher than 0.35, as sedimentation occurs during the test.

Up to now, the shear dependency of cement slurries has then been described as a function of several interdependent parameters, like time, shear rate, shear stress, flow regime, but no attempt has been made to combine all these factors into a single one that would biunivocally describe this shear dependency. The main objective of this work has consequently been to define such an independent parameter. Furthermore, as there is a large difference between laboratory and field or industrial mixing conditions, it has been attempted to compare both scales.

RHEOLOGICAL PROCEDURE AND CHARACTERIZATION

In this study two coaxial cylinder viscometers have been used :

the FANN 35 SA/SR12 with R1B1 geometry, a constant speed apparatus with a Couette fixture, standard in the oil industry [3] ,

the CARRI-MED CS100, a constant stress apparatus with a Searl fixture, with the CA 1809 geometry.

The Bingham Plastic model was used to characterize the rheological behavior of the slurries, as only equilibrium characteristics under shear were examined. Furthermore, wall slippage was not taken into account, although its influence is sometimes not negligeable for absolute measurements [5] .
Wall slippage was here ignored because only comparison between results obtained with the same viscometer and the same geometry has been performed.

Preconditioning of the slurry was achieved with the standard API atmospheric consistometer [3] . The slurry consistency increase versus time is related to the appearance of a gel structure, most of the time related to cement hydration, in the slurry. It is commonly accepted that a fluid that generates a consistency of at least 40 Bc (arbitrary unit of torque on the consistometer) is unpumpable with oil field equipment.

SLURRY MIXING AND VOLUMETRIC SHEARING ENERGY

- Experimental -

The first part of this study was performed with the API standard laboratory mixer [3] . This mixer has an impeller that can rotate with a controlled speed up to 12000 RPM under load. Mixing conditions were varied by controlling the impeller speed and the mixing time.

The second part of the study was performed with a standard oil field mixer, also called jet mixer This mixer works on the following principle : water is jetted at high speed, and cement powder falls by gravity into the high velocity zone. This permits the wetting of the cement powder by water, and some small shearing after wetting. Additional shearing was added into the slurry with different shearing devices or by pumping it through different orifices and at different pumping rates.

On all mixing devices, the shearing power could be determined through the measurement of torque and speed for a rotating system, or pressure and flow rate for orifices.

Cement slurries were composed of CEMOIL API Class G cement with 44% water by weight, with or without polynaphtalene sulfonate superplasticizer.

- Characterization of Mixing Conditions -

Bingham Plastic parameters were evaluated versus several factors that can characterize the mixing conditions, like the maximum shear rate, the shearing time, the typical Reynolds number if available, and the specific shearing energy.

This specific shearing energy Se, e.g. in fact the total mechanical energy given to a unit volume of slurry during the mixing process, can be expressed by :

$$Se = \frac{1}{V} \int_0^t P(t)\,dt \qquad (1)$$

where V is the slurry volume, P(t) the power and t the time.

When a laboratory type mixer is used, Se is obtained using the following equation:

$$Se = \frac{1}{V.d} \int_o^t T(t).S(t)dt \qquad (2)$$

where T is the torque measured between the motor of the mixer and the mixing bowl, S is the rotational speed of the impeller, d the diameter of the impeller's blade, V the volume of the slurry, and dt the unit mixing time.

The torque due to the friction in the packing and the bearing of the mixing bowl was calibrated versus speed. It was then possible to determine the torque really applied on the impeller only to shear the slurry.

With a field type mixer, the total specific shearing power put in the slurry was evaluated through the measurement of the pressure drop and flow rate (Q) when the shearing is produced through small orifices, or torque (T) and speed (S) for rotating shearing devices, as per the following equations [6] :

orifice :

$$Se = \frac{\rho.Q^2}{2K^2A^2} \qquad (3)$$

rotating :

$$Se = \int_o^t \frac{T(t).S(t)}{Q(t)} dt \qquad (4)$$

where ρ is the slurry density, Q the flow rate, A the orifice area, and K the efficiency of the orifice

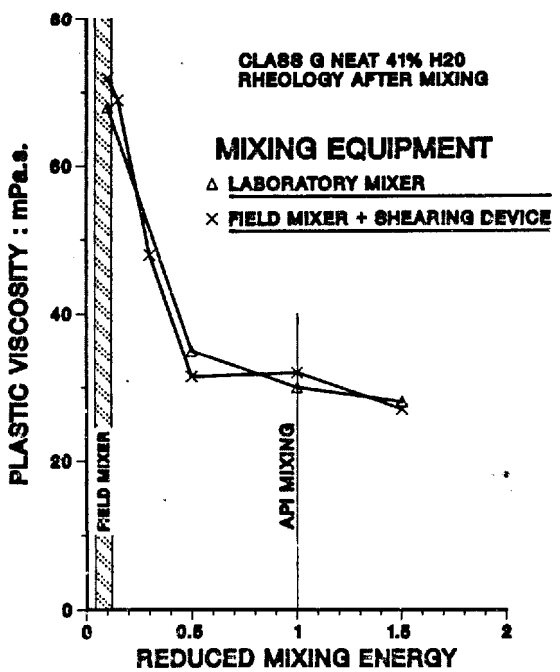

Fig.1: Comparison between field and laboratory mixer Plastic viscosity

In order to facilitate comparisons, the specific shearing energy was then adimensionalized by the energy level corresponding to the API laboratory mixing energy.

A clear dependence of the rheological behavior on the specific shearing energy during mixing is observed (see figures 1 and 2). The plastic viscosity regularly decreases when the specific shearing energy increases, while the yield stress first decreases at low energy levels, and then increases. The mixing technique, and the scale, laboratory or industrial, have only secondary effects on the slurry behavior. A similar type of dependency was already described in [1] , pages 268 to 271.

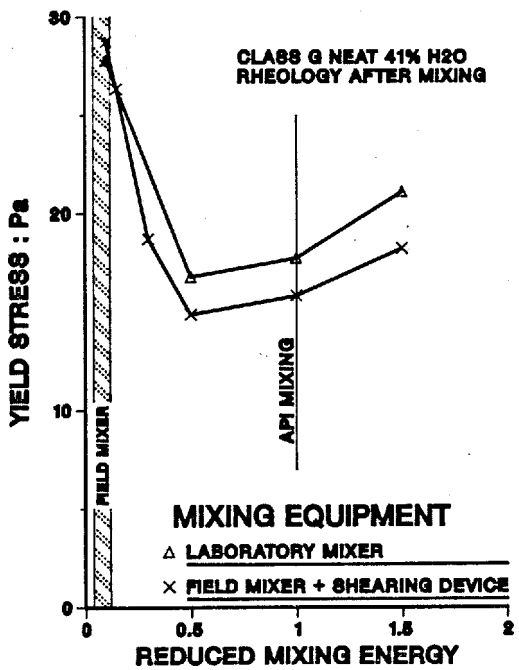

Fig.2 : Comparison between field and laboratory mixer Yield stress

_ Discussion On Mixing -

This influence of shearing during mixing was also analyzed using cement slurries containing some organic superplasticizer (see fig. 3) of the polynaphtalene sulfonate condensate (PNS) family. Mixing was performed with a laboratory type mixer. The plastic viscosity shows the same dependence on the mixing energy as in the case of a neat slurry. Conversely, the yield stress stays close to a minimum value up to a critical specific energy. At this point, the yield stress increases quickly with the energy. Consequently, the efficiency of the superplasticizer is reduced by the mixing. This phenomenon was already observed by Vom Berg as described in [7] .

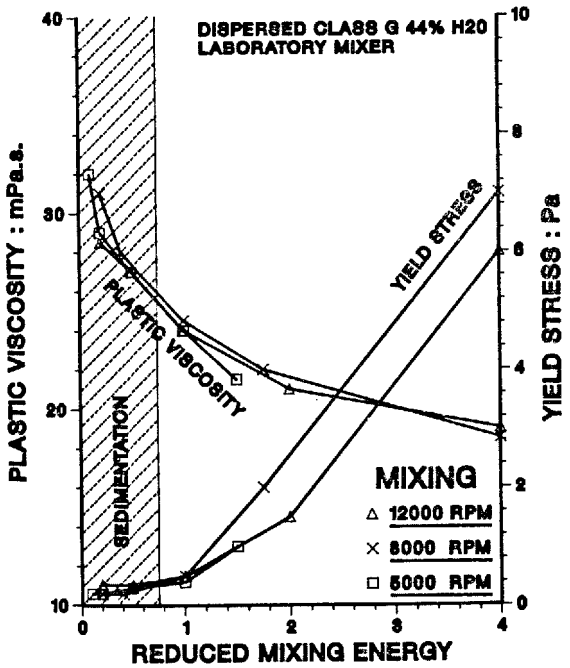

Fig.3: Influence of mixing energy on the rheology of dispersed cement slurry

The mechanism of action of polynaphtalene sulfonate dispersants has been described by Michaux and al. in [8] and [9] , through an adsorption model.

Furthermore, any cement powder being composed of agglomerates of cement particles linked through electrostatic forces, the action of the mixing process is, first, the deflocculation of these agglomerates and the wetting of residual particle flocs by the mixing water, and, second, the erosion of cement grains and possible generation of some colloidal particles.

A possible explanation for this influence of the specific shearing energy on cement slurry rheology is, then, that the average size of cement flocs and possibly of cement particles is reduced when the specific shearing energy increases, thereby promoting a better contact between water and cement, and increasing the cement specific surface area available to the dispersant, this artificially impairing the dispersant's efficiency.

A reduction in cement particle size is pretty well in line with the effect on rheology, as smaller particles in suspension are known to generate lower viscosities [7] , but will also promote higher yield stresses because of an increased surface activity. A secondary factor that tends to promote this mechanism is the reduction of bleeding with increasing specific shearing energy, as shown in table 1.

Table 1 : Influence of shearing energy on free water development, with a Class G Cemoil mixed with 1.8% PNS and 42% water by weight of cement.

Spec. Energy	0.15		1		3	
Temperature deg.C	20	85	20	85	20	85
Free water in mL/250mL	1	22	2	5	1	3

However no evidence to support this hypothesis could yet be found, neither through particle size determination, nor through microstructural investigations.

EVALUATION OF THE FLOW REGIME

After being mixed on surface, oilwell cement slurries are pumped with high pressure triplex displacement pumps, down a casing and up the casing to formation annulus. The exhibited flow regime can then range between fully developed turbulent flow and very low laminar, depending on flow geometry, slurry rheology and density, and pump rates.

Experimental

In the laboratory, the standard API atmospheric consistometer [3] used to simulate agitation produces a very good turbulent flow regime. At the other extreme, laminar flow conditions were simulated in the laboratory by the rotational viscometer.

The experimental study was then performed in the laboratory as follows: after standard API mixing at 20 deg.C, and a given agitation time in the consistometer (turbulent flow) at 80 deg.C, a rheological test was performed also at 80 deg.C. Laminar shearing was simulated by a given time at a given shear rate in the rotational viscometer.

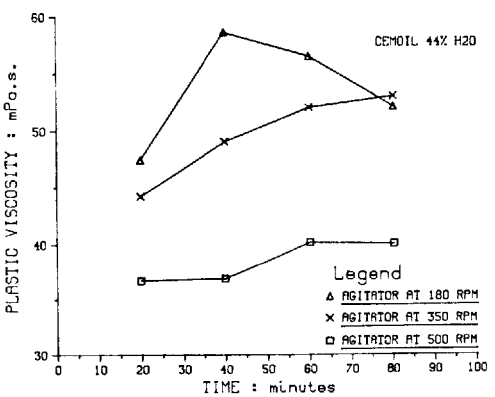

Fig.4 : Influence of turbulent stirring on cement rheology . Plastic viscosity

Discussion

As can be observed on fig.4 and 5, the influence of time is not very relevant for turbulent agitation, while the level of energy or turbulence is a predominant factor affecting the plastic viscosity. It is important to notice that the yield stress is not very much affected by turbulent agitation.

In contrast, in a laminar flow regime (see fig.6 and 7), both plastic viscosity and yield stress increase drastically with time, while the influence of the level of energy or shear rate does not follow a definite trend. Slurries in totally static conditions exhibit similar behavior to those in the laminar dynamic state.

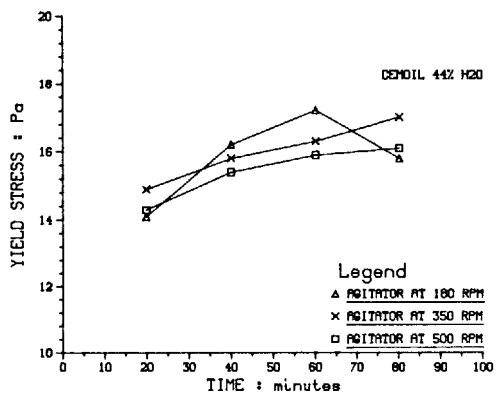

Fig. 5 : Influence of turbulent stirring on cement rheology. Yield stress

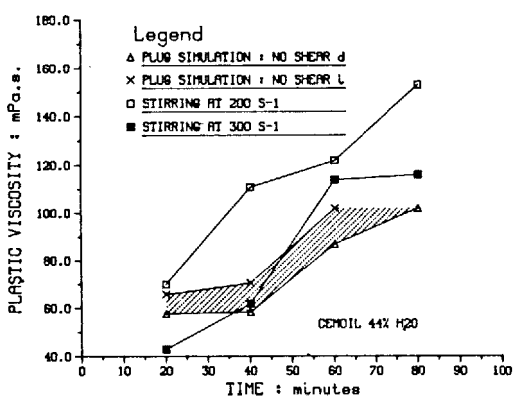

Fig. 6 : Influence of laminar stirring on cement rheology. Plastic viscosity

EVOLUTION OF SLURRY RHEOLOGY DURING THE RHEOLOGICAL TEST

Not only true or simulated pumping operations affect cement slurry rheological behavior, but the rheological test itself induces additional shearing in the slurry sample. This can modify the measurement, as any additional shearing energy would do. The specific shearing energy input by the viscometer can obviously be determined through equation (3).

Experimental

The influence of the test routine was then investigated, by varying either the time steps T at each shear rate, the number of steps, or the maximum rotational speed. Then the results were analyzed as a function of the shearing energy, or as a function of the maximum shear rate. For this study only neat Cemoil Class G slurry mixed with 44% fresh water by weight of cement was used. All experiments, from mixing the slurry till the end of the rheological test, were performed at a temperature of 20 deg.C.

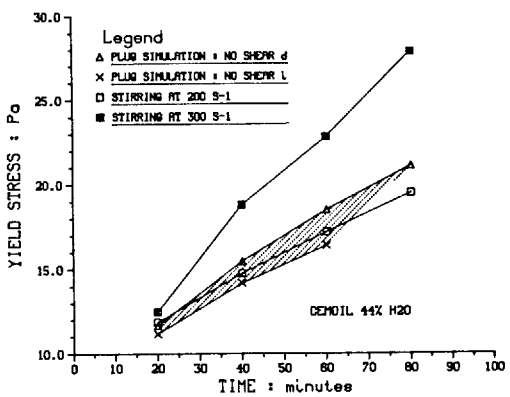

Fig. 7 : Influence of laminar stirring on cement rheology. Yield stress

Discussion

Test results presented in table 2 and in figure 8, show a strong dependence of cement slurry rheology on both the specific shearing energy and the maximum shear rate input during the rheological experiment.

Table 2: Influence of the test routine on slurry rheology

Specific energy M J/m^3	Plastic Viscosity m Pa.s.	Yield Stress Pa
0.03	61.7	12.1
0.28	47.2	13.4
0.68	40.5	13.9
1.20	40.0	15.0
2.00	39.0	19.0
4.00	39.0	19.0
6.80	38.0	19.0

When the test shearing energy increases, the plastic viscosity decreases while the yield stress increases. This is in agreement with the previous results. However, at very high levels of energy, both parameters

tend to reach a stable plateau. The same dependency is observed with increasing the maximum shear rate. Such a similar result is not surprising as the maximum shear rate accounts for a large part in the total specific energy.

The conclusion is that the test routine has a strong influence in the rheological measurements. As the test itself should disturb the sample as little as possible, it seems necessary to limit both the specific shearing energy and the maximum shear rate during the test.

The total shearing energy produced by the test should stay as small as possible in comparison with the shearing energy already put into the sample through mixing and preconditioning.

CONCLUSIONS

Cement slurry rheology dramatically depends on the shear history of the sample. Slurry mixing, dynamic conditioning, and the rheological test itself have a strong influence on the measured rheological parameters. This influence could be described by a single parameter, the specific shearing energy. The results obtained from laboratory and industrial conditions are then in good accordance.

Laboratory mixing procedure should be optimized to match the industrial specific mixing energy, and the laboratory dynamic conditioning should respect the flow regime expected in the field.

In order for the measured rheological parameters to be representative of the dynamic behavior of a given slurry sample, the rheological test itself should feature the minimum shearing energy possible, e.g. maximum shear rate, time step, and number of steps should be limited.

REFERENCES

[1] G.H TATTERSALL and P.F.G BANFILL "The rheology of fresh concrete", Pittman Advanced Publishing Program, 356 pages, 1983.

[2] R. LAPASSIN,A. PAPO,S. RAJGELJ, "The phenomenological description of the thixotropic behavior of fresh cement pastes", Rheologica Acta 22, pp. 410-416, 1983.

[3] API Specification 10 for Materials and testing for well cements, API production department, Second edition, June 15, 1984.

[4] J.I. BHATTY and P.F.G BANFILL " Sedimentation behavior in cement pastes subjected to continuous shear in rotational viscometers", Journal of Cement and Concrete Research Vol 12, pp. 69-78, 1982.

[5] R.J. MANNHEIMER "Effect of slip on the flow properties can flaw resistance calculations", Oil and Gas Journal, Dec.5,pp 144-147, 1983.

[6] R. BYRON, W.E. STEWARD and E.N. LIGHTFOOT "Transport phenomena", John Wiley & Sons Inc. Horwood Limited, 447 pages, 1980.

[7] R.W. WHORLOW "Rheological Techniques", Ellis

[8] M. MICHAUX and C. DEFOSSE "Oil well cement slurries. Microstructural approach of their rheology" Journal of Cement and Concrete Research, Vol 16, Jan. 1986.

[9] M. MICHAUX and R.O. PADTBERG "The effect of mix water salinity on polynaphtalene sulfonate containing cement slurries", to be presented at the 8th International Congress on the Chemistry of Cement, Rio de Janeiro, Sept. 1986.

[10] H. SCHLICHTING "Boundary Layer Theory", Mc Graw-Hill Book Company, 817 pages, 1979.

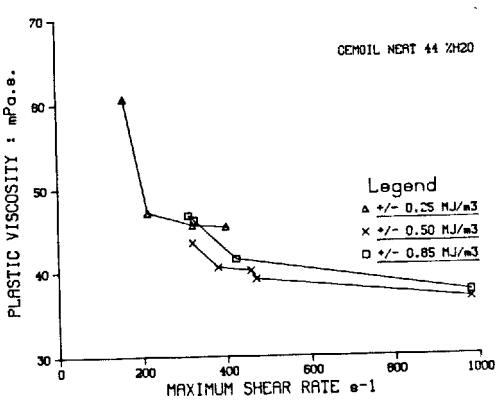

Fig. 8 : Influence of the maximum shear rate on cement rheology

U. COSTA and F. MASSAZZA
Dr. of Chemistry and Prof. of Applied Chemistry (ITALCEMENTI- BERGAMO - ITALY)

STRUCTURE AND PROPERTIES OF CEMENT SUSPENSIONS
STRUCTURE ET PROPRIÉTÉS DES SUSPENSIONS DE CIMENT

1. INTRODUCTION

Fresh mortar and concrete can be considered as aggregate dispersions in a matrix formed of cement paste. According to this model the system deforms when it is submitted to stresses and the aggregate grains move in a deformable medium composed of the cement paste. Therefore the rheological behaviour of concrete could quite be explained if the rheological properties of paste and the interactions between these and aggregate were completely defined.
In the last few years many studies were devoted to the cement paste rheology but only few were carried out on the relationships between paste and concrete properties, owing to the difficulty of recognizing and evaluating all the parameters which characterize concrete. Difficulties were encountered also in defining the rheological state equations for concrete on account of the experimental difficulties related to the complexity of the material.
This report reviews the latest acquisitions on the cement dispersions and their influence on the interpretation of the behaviour of mortars and concretes.

2. RHEOLOGICAL MODELS

2.1 Methodological problems

The behaviour of fresh cement paste submitted to shear stresses can be classified into 3 fundamental types: Newtonian, viscoplastic (shear thinning) or dilatant (shear thickening) **(1)**. These behaviours depend on the suspension structure on which concentration, specific surface, particle size distribution and solid shape act **(2)**. As figure 1 shows, a mortar behaviour passes from shear thinning to Binghamian and shear thickening, as the solid concentration increases. In figure 2 the pseudoplastic behaviour of a mortar having angular grains changes to Newtonian when grains are spherical.
Under a constant shear rate the cement pastes show a rheological dependance on time, generally of thixotropic type **(4)(5)**. The experimental preparation methodologies or the instrumental measuring techniques modify the paste structure so as they become preminent with respect to the factors involved in properties of the dispersed materials. This is a general problem concerning the rheological measurements carried out on thick suspensions whose macroscopic flowing properties are sensitive to the arrangement of the particles in the viscometer cell. Thick suspensions have viscosity or rheological flowing behaviours strictly dependent on the used measuring instrument and working conditions **(6)**. In fact the results of the rheological tests largely depend on the geometry of the flow channel, the speed as well as the dimensional and shape properties of particles. Furthermore, the results can vary, even though the same instruments and working conditions are employed in repeated tests, since the paste does not take the same structure.

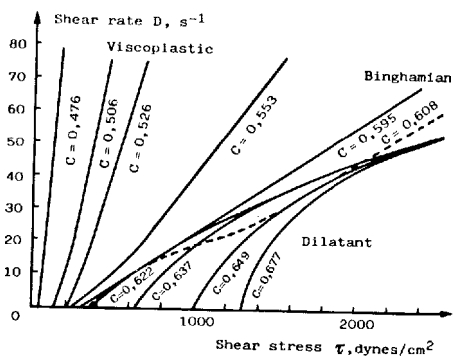

FIG. 1: Flow curves of mortars with different solid concentrations (c) **(3)**

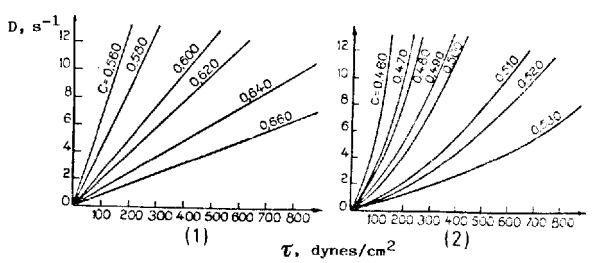

FIG. 2: Influence of the grain shape on the flow-curves of mortars **(3)** *: 1) spherical grains 2) angular grains*

A complete description of the rheological behaviour would demand also observations of the cement paste under the microscope (for example by light scattering techniques) to point out the changes undergone by the particle movement, in connection with the shape and amplitude of the flowing channel, and to determine

the type of flow (laminar, elongational, a.s.o.) (6). Therefore to obtain results expressing the real behaviour of the suspensions it is necessary to respect some design feature of the apparatus, and the experimental procedure. For example the annular section between the coaxial cylinders must be fixed with great attention. It must be limited to avoid settling phenomena and it must be wide enough with respect to the maximum particle size of the dispersed solid to obtain a laminar flow (7).

The behaviour of similar pastes transforms from thixotropic into antithixotropic when the measurement cycle time varies (fig. 3). This fact is explained by the competition occurring between the breakdown and reconstruction processes, the latter due to the cement particle hydration (8). The rotation speed of the rotor can affect the results in a different way. If the speed is slow, a slipping can occur between rotor surface and paste but, if it is fast, a centrifugation occurs (9). Figure 4 shows that the flow curves change appreciably when the acceleration of the shear rate varies.

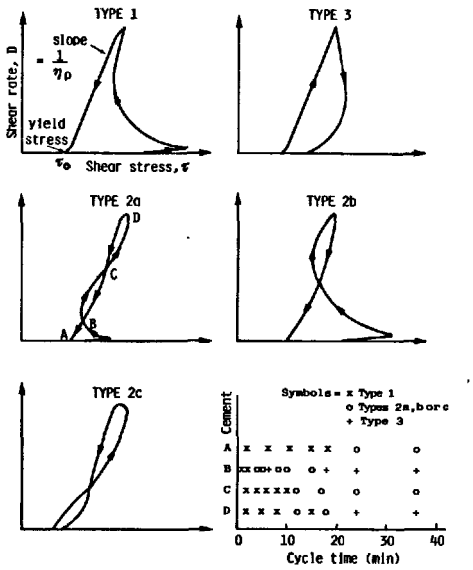

FIG. 3: Effect of the cycle time on the type of flow curves obtained on cement pastes (8)

The viscometric studies on cement pastes are generally carried out by using shear rates which are largely slower than the critical one for which Reynolds number exceeds the calculated value separating the laminar from the turbulent flow (11). Nevertheless, conditions of turbulent flow were observed at shear rates, D, equal to 1800 s^{-1} and 1065 s^{-1}, by using rotors with smooth or grooved surface respectively(10). This phenomenon takes place because the turbulence in suspension occurs for lower shear rates than those in pure dispersion medium (12).

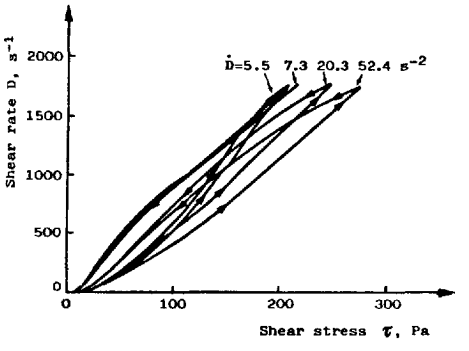

FIG. 4: Flow curves at different acceleration of shear rate $\dot{D}$ (10)

The most common procedures of the shear rate application to the paste are of 4 types: a) constant rate, b) step-increasing rate, c) step-decreasing rate, d) continuously varying rate. Procedure a) gives values corresponding to equilibrium conditions between applied stress and resistance to flow. The step-procedures have the advantage, compared with the previous one, that they allow measurements to be taken on a wider range of D values, by working on the same paste sample (13). The last procedure is unable to characterize quantitatively the "shear-dependent" behaviour of the paste (14) and it often shows hysteresis loops. By working with pastes made with 0.6-0.7 w/c ratios, the settling phenomena in the viscometer can become very important if helicoidal rotors are not used(15).

2.2 Rheological behaviours

The rheological characterization of a thick suspension demand two complementary descriptive elements. The former is the flow curve representing the equilibrium conditions between applied stress and shear rate (shear-dependent analysis). The latter is the structural strain curve versus time obtained by submitting the paste to a constant flow rate (time-dependent analysis). The formulation of the mathematical models interpreting the experimental curves allows the essential rheological parameters (viscosity, yield value, thixotropic breakdown energy, a.s.o.) related to the suspension structure,to be obtained.

2.2.1 "Shear-dependent" behaviour

Fresh cement pastes can comply with the linear models of simple fluids, such as Newton's or Bingham's, when the shear rate is limited and the structural demolition during mixing is complete. However, the relationship between shear rate D and shear stress τ is not generally linear and therefore the above models cannot be used in any case. Attempts to interpret mathematically the complex behaviours of the cement pastes date back to the end of the 70s and a great researching effort was made on this aspect of rheology.

Table 1 shows several proposed models, starting from Jones and Taylor's (16) who used two different equations (eq. 1 and 2). The former, composed of the combined Bingham and power law, derived directly from the classical Herschel-Bulkley's equation used for the first time to study benzene-rubber system (17). The latter equation, based on the model proposed by Robertson and Stiff (18), showed an excellent compliance with the experimental data. The results of these Authors pointed out that the cement paste was shear thickening at w/c ratios < 0.4, shear thinning

at w/c ratios ≥ 0.4 and behaved in a Binghamian manner at w/c ratios = 0.40.
In a following work the linear term of Bingham equation was replaced by a hyperbolic function (eq. 3 of table 1). The model showed a good agreement with flow curves of paste in the rotational viscometer, up to D values of about 380 s^{-1} **(19)**. Functions of this type were proposed by Eyring to interpret the behaviour of fluids as gelatin and cellulose dispersions **(20)**.

TABLE 1: Rheological models proposed for the fresh cement pastes

MODEL			RHEOLOGICAL BEHAVIOUR
1) $\tau = \tau_0 + kD^n$	**(17)**	utilized by **(16)**	n>1 Dilatant n<1 Viscoplas.
2) $\tau = A(D+C)^B$	**(18)**		B>1 Dilatant B<1 Viscoplas.
3) $\tau = \tau_0 + B\sinh^{-1}(D/C)$	**(19)**		Viscoplastic
4) $D = \alpha\tau^2 + \beta\tau + \delta$	**(21)**		Viscoplastic
5) $D = k_1\tau + k_2\tau^n$	**(23)**	utilized by **(22)**	Pseudoplastic
6) $\tau^{\frac{1}{2}} = \tau_0^{\frac{1}{2}} + k_1 D^{\frac{1}{2}}$	**(24)**		Viscoplastic
7) $\tau = \sum_{i=1}^{n} A\sinh^{-1}(DB_i)$	**(20)**		Pseudoplastic
8) $\tau = \eta D$			Newtonian
9) $\tau = \tau_0 + \eta_{pl} D$			Binghamian

τ = shear stress; η = viscosity; τ_0 = yield stress; η_{pl} = plastic viscosity; D = shear rate
A,B,C,k,k_1,k_2, α, β, δ = constants

More recently the descending branch of the second isteresis loop was interpolated by a parabola equation (eq. 4 of table 1). This model allows two important rheological parameters to be obtained easily, that is yield value τ_0 and viscosity coefficient η_{pl} **(21)**.
The compliance of different models with the description of the viscometric flow of cement pastes, having w/c ratios between 0.30 and 0.45, was evaluated in a recent work **(22)**. For this analysis some other classical models applicable to the rheology of simple fluids and suspensions (given by equations 5, 6, 7 of table 1) were considered. By using statistical and iterative procedures it was possible to calculate the parameters of each equation giving the best agreement with the experimental flow curves. The compliance of the model was evaluated by the difference between the shear rate values calculated by the corresponding equation and the experimental ones. Good correlations resulted for Eyring's, Herschel-Bulkley's and parabolic models. The two last are constitutionally related, since Herschel-Bulkley equation becomes a parabola when exponent B is 2.
It is interesting to notice that the proposed equations generally show a constant term, which corresponds to the yield stress, and a second term of exponential type. In some cases also a linear term in D appears. The physical interpretation of this analytical formulation leads to assume, similarly to what found also for other rheological systems **(20)**, that the cement pastes consist of Newtonian and non-Newtonian units. The latter would identify with the flocculа formed from the aggregation of the particles that, during motion, undergo a structural breakdown. Therefore, as D increases, the motion resistance tends to decrease in an exponential manner.
An attempt to interpret the flow curves according to a more general model based on physical principles, considered different types of friction which determine the suspension viscosity **(25)**. In the interactions between components three types of friction liquid-liquid, liquid-particle, particle-particle were distinguished. Therefore viscosity was expressed on the basis of the number of molecular friction points per unit of shear plane according to

$$\eta = B_1 n_1^{2/3} + B_2 n_2^{2/3} + B_3 (n_3 u)^{2/3} \qquad 10)$$

where n_1, n_2, n_3 are number of friction points of the three species in question on the shear plane and **u** is dimentionless factor varying from 0 to 1.
Factor **u** expresses the ratio of the number of friction points to the initial number of non-agglomerated particles and it takes value 1 when agglomeration is complete. If **u** is constant as the shear rate varies, η is constant too and therefore the flow is Newtonian. Generalized flow curves can be derived by introducing the η expression in the Newton classic equation (eq. 8 in table 1).
Factor **u**, which determines the viscosity and therefore the material flow, was deduced by considering the competitive effects of coagulation and dissociation caused by the mechanical stresses acting during the flow. Unlike the previous models, this approach allows also the time factor to be introduced into the state equation. In this way it was possible to explain mathematically the changes in the shape of the curves shown in figure 3, depending on the variation of the test duration.

2.2.2 "Time-dependent" behaviour and thixotropy

When the shear rate is constant, the cement suspensions show shear stress-time transient characterized by 3 stages, as indicated in fig. 5. An initial stage, where τ reaches a maximum (τ_{max}) quickly, a period of stress decrease as far as a minimum value (τ_e), a third stage represented by a slight increase in τ.
In some cases the appearance of an additional maximum was observed during the third stage **(13)**.
The trend of τ-t transient results from different phe

nomena having opposite actions. The demolition of the particle agglomeration caused by the shear stress **(4)**, and the grain orientation as a function of the lower hydrodynamic resistance during motion **(3)** cause a viscosity decrease with time. At the same time the hydration process of cement introduces new bonds among the dispersed particles, which increases the dispersion viscosity **(27)**. The paste viscosity depends on the inner structure resulting from the chemical-physical forces which act among particles. These forces react elastically at weak stresses, but if the stress becomes high enough, they fail and the structure degrades and flocs form which offer a lower resistance to flow. The change in the flocculation degree of the paste was considered to be the base of the thixotropic behaviour **(4)**.

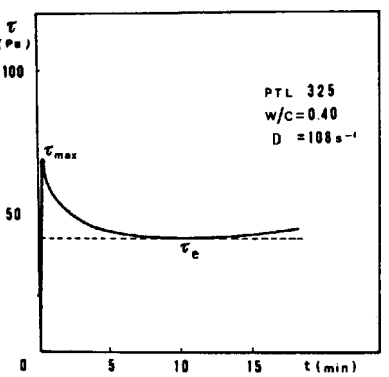

FIG. 5: A typical transient behaviour shear stress vs time at constant shear rate **(26)**

The quantitative measurement of thixotropy is not a simple question since a thixotropic material is sensitive to stress conditions and rheological hystory. The phenomenon is affected by rheological and experimental factors. The rheological ones include the rate constant and the order of the demolition process, in their turn related to the elastic energy and the relaxation time of the structure. The experimental variables concern temperature and shear rate.
It is practically impossible from a single τ-t curve to explain all these dependences, so thixotropy is generally measured by using empiric coefficients which express the aggregation degree of the dispersion. For instance, the coefficient of thixotropy is the ratio **(28)**

$$\lambda = \frac{\tau_{max} - \tau_e}{\tau_{max}} \qquad 11)$$

where τ_{max} is the peak stress corresponding to the initial degradation of the structure and τ_e is the stress required to keep the configuration in equilibrium. Thixotropy is also expressed by a similar coefficient given by the ratio

$$r = \frac{\tau_{max}}{\eta_e} \qquad 12)$$

where η_e is the equilibrium viscosity **(29)**.
The process of thixotropic demolition can be studied through the analysis of the $\tau = f(t)$ curves. A recent work **(30)** illustrated the mathematical method to derive the rheological state equation and to interpret the kinetics of the structural breakdown to obtain the rate constant and the process order. The rheological equation was expressed in the general form:

$$\tau = f_0(D) + \lambda' f_1(D) \qquad 13)$$

where D = shear rate

$$\lambda' = \frac{\tau - \tau_e}{\tau_{max} - \tau_e} \quad \text{structural parameter} \qquad 14)$$

Vom Berg's model (n° 3 of table 1) was used for the functions $f_0(D)$ and $f_1(D)$.
By means of a procedure of curve fitting, simultaneously applied to values τ_{max} and τ_e obtained with different shear rates, the parameters of equations $f_0(D)$ and $f_1(D)$ were calculated. The same data allowed the variation of parameter λ' with time to be analyzed and, therefore, the modification of the system thixotropy could be expressed through the deduction of the constant rate **k** and the order **n** of the breakdown process. The data obtained on cement pastes of different type are given in table 2 from which it results that **k** varies as the shear rate changes, according to a hyperbolic relation whose parameters considerably depend on the type of cement. On the contrary the changes in order **n** of the process with the type of cement are more limited.

TABLE 2: Parameters of the breakdown rate equation: $\frac{d\lambda'}{dt} = -k(D)\lambda'^{n}$ 15) **(30)**

CEMENT	w/c	n	a (s^{-1})	b
325 Ptl	0.40	1.36	678	26
425 Ptl	0.40	1.00	1356	62.4
425 Ptl	0.45	1.09	2634	27

λ' = structural parameter given by 14) equation
n = order of breakdown process
a,b = parameters of the equation : $k(D) = \frac{D}{a+b \cdot D}$ 16)
where D = shear rate

The influence of the shear rate on the kinetics of the demolition process was particularly examined in another study **(10)**. It was observed that, for $D < 1065 s^{-1}$, the τ-t curves are descending and can be described by an equation including two exponential terms. The need to introduce two terms instead of one, as in Tattersall equation **(4)**, is due to that the breakdown process can be subdivided into two stages: a primary which occurs very quickly and finishes in 5 seconds at the latest and a secondary which is much slower. The introduction of a third term into the equation became necessary to interpret the reascending of τ when shear rate D exceeds $1065 s^{-1}$. Tests performed by replacing the paste with water showed that a turbulent motion can be established with so high shear rates. Therefore this increase in τ and paste viscosity should not be interpreted as a rheopexy phenomenon and, hence, as a real change in the inner structure,

but as the consequence of the flow transition from laminar to turbulent.

2.2.3 Models and paste structure

The examination of the equations proposed to interpret the shear-dependent or time-dependent behaviours of cement suspensions showed that only some are based on physical hypotheses, whereas most of them derive from procedures of curve fitting applied to experimental data. This trend is rather common in rheological studies and can be attributed to three fundamental reasons **(31)**. The first is to sum up the experimental data with a small number of parameters. In this way it is possible to establish quantitative relationships between the rheological parameters and the different chemical-physical factors affecting them: concentration, fineness, composition of cement, a.s.o. A second one is to extrapolate the experimental data outside the range of shear rate or solid concentration considered in the tests, especially to apply the results to the practice. Finally, the third reason it to correlate the rheological behaviour with the chemical-physical processes which occur, on a microscopic scale, among the suspension constituents.
However, the factors and interactions determining the rheological behaviour of suspensions are many and complex and therefore it becomes difficult to consider all of them to establish models of general validity.

3. STRUCTURE OF PASTES

3.1 Structure factors

The structure, and therefore the suspension rheology, are affected by several chemical-physical factors concerning both the dispersed solid phase and the liquid.

3.1.1 Solid phase properties

Specific surface, particle size distribution and shape of grains are factors of primary importance since these parameters determine the number of the contact points between particles which result in frictions and agglomeration forces. Bombled **(2)** expressed the flow resistance (f) per surface unit of the suspension versus the grain number n_s, the number of contacts per grain λ^* and adherence A, which represents the sum of the intergrain forces (frictional, Coulomb's, Van der Wall's), by equation

$$f = n_s \lambda^* A \qquad 17)$$

Since the number of contacts per grain increases exponentially as the specific surface increases **(32)**, equation 17) justifies the exponential-type relationships found experimentally between the paste viscosities or yield stress and the specific surface of cement **(2)(33)**. It was also found that monogranular particles result in pastes having poor rheological properties **(34)**. The improvement of these properties is chiefly related to the achievement of the particle size and shape favorable to the maximum filling of the empty space. Continuous particle size distributions represent the optimum about the matter **(35)**. Also the particle shape plays an important role, as was pointed out by a study on hydrated lime suspensions **(36)**. This property, together with the particle size distribution, appeared to affect the rheology of these suspensions more significantly than the electrokinetic potential of particles. The particle size distribution and the surface extension have also other indirect effects on the rheology of pastes.
In fact the particle size distribution determines the permeability of the granular whole, whereas the specific surface conditions the extent of the forces acting among the surface electric charges. As permeability decreases, the rheological behaviour can transform from shear thinning into thickening owing to the resistance that water finds when it flows inside the paste **(2)**.
As the specific surface increases, the particle agglomeration caused by the electric charges induced by the clinker comminution process **(37)** and the cement hydration **(38)**, increases.
These factors related to the physical state of the solid add to others of chemical nature. The mineralogical composition of clinker and the reactivity of phases affect the hydration process. Therefore, they can act on the paste rheology through the bonds forming between the hydrated products **(39)** and the changes in the solution ionic equilibria affecting the double-layer forces **(40)(41)**. The mineralogical composition of clinker can affect the rheological behaviours also indirectly owing to the different grindabilities shown by the constituents **(42)**.

3.1.2 Liquid phase properties

The mechanical properties of the liquid phase, that is surface tension and viscosity, and the chemical-physical properties such as affinity for surface and the dielectric constant, are other factors affecting rheology. In particular, the strong surface tension of water, together with the affinity for surface of the cement grains, cause intense capillary forces when the intergranular space is not quite saturated with water. Under these conditions air-liquid menisca form and a negative pressure P, given by the following Laplace formula, creates in the liquid:

$$P = -4 \frac{A}{r} \qquad 18)$$

where r = curvature radius of meniscus
and A = surface tension of water

This pressure is equilibrated by compressive forces acting in the grains. The paste cohesion reduces appreciably when the amount of water exceed that necessary for saturation, since the capillary forces cease **(43)**. The dielectric constant affects the Coulomb and Van der Walls interactions acting between grains **(44)**.

3.1.3 Solid-liquid interactions

The interactions occurring between the dispersed solid and the liquid can be subdivided into three categories:
- *hydrodynamic actions that cause a viscosity in -*

crease in the liquid;
- *attractions between particles that lead to the formation of floccula and aggregates and a continuous agglomerated structure;*
- *contacts between particles that create frictions during the motion.*

Cheng **(31)** tried to summarize, in a scheme given in fig. 6, the relationships between the categories of interactions and the factors conditioning them. The double-pointed arrows mean that the factor in question determines the appearance of the interaction but, in its turn, it is simultaneously affected by the interaction itself. Each of the fundamental interactions acquires a different importance depending on the solid concentration in the solution.

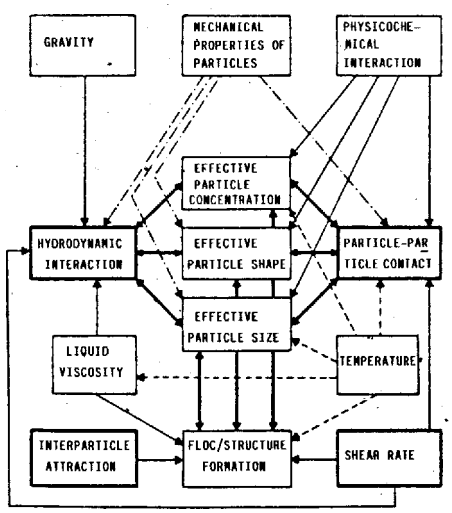

FIG. 6: Interplay of the three categories of interactions and factors affecting suspension viscosity **(31)**

For example, the contribution of the hydrodynamic factors increases at medium or low concentrations, the attractive forces predominate at medium-high concentrations and the friction between particles plays the main role at very high concentrations. In any case the predominant interaction determines the rheological behaviour of the suspension.

Figure 7 is a tentative to represent the rheological behaviours of the suspensions as a function of three fundamental types of interactions. A shift along axis **y** shows that, in the absence of attraction forces among the particles, the suspension behaviour varies from Newtonian to non-Newtonian as the solid concentration passes from low to medium values. Contacts predominate at a very high concentration, so the behaviour becomes at first dilatant as far as to transform into a more complex one (granulo-viscous).

If also the attraction forces among particles are considered, an increase in the suspension viscosity is observed in any case, since the dispersed solid tends to form floccula or aggregations. As the forces increase in dispersions having medium-low solid concentrations, the behaviours pass from pseudoplastic to viscoplastic and plastic. When the attraction forces are weak, floccula are broken easily but, as they become stronger, floccula become more resistant and can endure a certain stress without breaking. At this point the suspension shows a certain elasticity as far as a given threshold stress which represents the yield value and indicates the transition from pseudoplasticity to viscoplasticity.

This picture explains how it is difficult to interpret the macroscopic rheological behaviour of pastes in terms of structure. For example the same rheological response can be obtained by combining a low attraction force with a high solid concentration or a medium attraction with a low concentration. Therefore, to define the physical models of the structure of the concentrated cement suspensions, it becomes very important to examine the forces acting among particles and their variations as a function of the solid concentration.

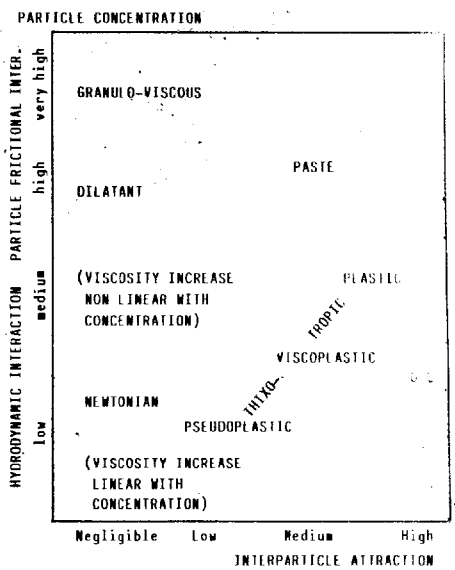

FIG. 7: Relation between different types of rheological behaviour and the three categories of interactions **(31)**

3.2 Forces among particles

3.2.1 Equilibria among particles

The main forces acting on a group of particles are Van der Wall's, generally attractive, and the electrostatic ones, generally repulsive. Moreover there are forces resulting from the presence of water films adsorbed on particles, referred to as "structural forces", which cause a repulsive effect known as "disjoining pressure" **(45)**. Finally, if systems containing particles with sizes above the colloidal ones are considered, also capillary forces can occur when air-water interfaces create in the system.

Table 3 summarizes the different types of acting forces and the dimensional range of the particles on which the action of each of them prevails.

TABLE 3: Forces acting between particles **(46)(62)**

TYPE OF FORCES	SIZE OF PARTICLES (mm)	EFFECT OF FORCES	ACTION DISTANCE (mm)
Capillary	1 - 0.1	Attraction	-
Van der Walls	0.1 -10^{-4}	Attraction	5-20·10^{-7}
Coulomb (double layer)	10^{-2} -10^{-6}	Repulsion	10-50·10^{-7}
Disjoining pressure	10^{-2} -10^{-6}	Repulsion	5-30·10^{-7}

The nature of the forces acting between particle was examined in several reviews **(43)**. Van der Walls forces result from electromagnetic interactions, between the atomic electron clouds, which give rise to orientation, dispersion and induction effects. These effects contribute to the cohesion of the materials.
The electrostatic forces derive from ionic double layers that, in water, surround the particles and can be quantitatively evaluated by the measurement of zeta potential. The structural forces, i.e. disjoining pressure, derive from the water adsorbed on the particles which has different chemical-physical properties from water in bulk. Water shows a certain degree of structural order and for this reason creates a physical and thermodinamyc barrier that hinders the contact between particles **(46)**.
According to DVLO classical theory **(40)(41)**, the stability of a colloidal suspension is determined by the balance between Van der Walls attraction forces (V_A) and the repulsive ones among the electrical double layers on the particles (V_R). The trend of V_A,V_R and the total potential energy $V_T = V_A+V_R$, expressed as a function of the distance between two particles, can be seen in figure 8.
The attraction and repulsion increase quickly starting from a certain distance, as the particles approach each other. The total energy curve passes through a maximum (V_{max}) that forms a barrier opposing the particle adhesion. The lower this barrier the higher the number of particles which agglomerate by taking the potential interaction energy corresponding to the primary minimum V_{1min}. V_{max} depends on the sizes of the particles and their surface charge. With relatively big particles the total potential energy curve can show a secondary minimum at a wider separation distance. If this secondary minimum is rather deep, 2-3 times the Brownian kinetic energy of the particle, it causes flocculation. The particle association due to flocculation is different from that occurring with the primary minimum since it is reversible and easily destroyed by shaking. Only if this secondary minimum were deeper than the primary one, a stable suspension could be obtained.

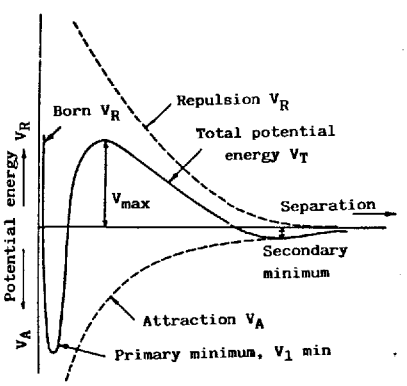

FIG. 8: Potential energy diagram for two particles **(47)**

These concepts have been taken from Powers who included in the balance among forces also those resulting from the disjoining pressure **(43)**. The relative energy of two quartz plates subject to Van der Walls forces (V_A) and the disjoining pressure (V_R) is shown in figure 9. The latter is calculated on the basis of thickness values of the water films adsorbed on hardened cement paste. It can be noticed that in this case the secondary minimum falls at about 25 Å. The floccula forming when the particles approach this distance remain isolated if the solid concentration is limited, but they can link by forming a continuous structure (flocculent state), when the particle compaction is as highest as possible.
The system cohesion increases if the water is reduced. In this case the interstitial spaces are no longer completely filled with water. Air-water interfaces cause capillary forces between particles.

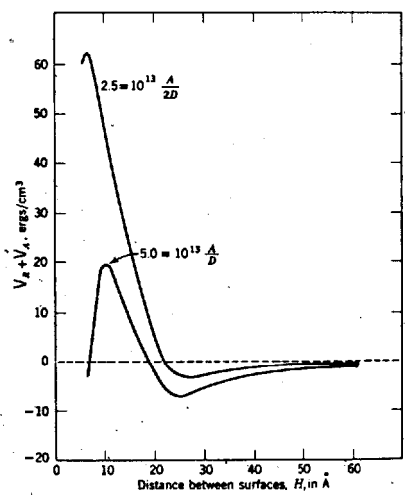

FIG. 9: Calculated potential energy of two parallel silica plates in water versus distance H. Curves refer to 2 values of parameter A/D of Van der Walls attraction force V_A **(43)**

The curves shown in figure 8 indicate two possibilities to prevent the particles from coagulating and, therefore, to obtain suspensions with good flowing properties. The former is to rise the height of the potential barrier V_{max} by intensifying the repulsion. The latter is to avoid the particles from approaching a lower distance than that corresponding to the secondary minimum of energy. Both effects can be attained by using plasticizers and superplasticizers that have a strong deflocculating action of the cement grains. They increase the absolute value of the surface charge (zeta potential) as well as they create a steric hindrance to the particle approach **(48)**. The possibility given by the theory to modify the flocculated structure of the suspension by acting on the double layer repulsion are applied in the concrete technology.

3.2.2 Zeta potential

The particles of inorganic oxydes are carriers of unequilibrated electrical charges from the non-compensation of positive and negative valencies of the surface atoms (accidental charges). Other charges can derive from isomorphic substitutions in the lattices between atoms of difference valence (inherent charges). Another contribution can come from the hydrolysis of the amphoteric hydroxyl groups **(49)** shown in figure 10. Therefore the surface has an electrical poten -

tial ψ_0 compared with that of bulk solution considered as zero.

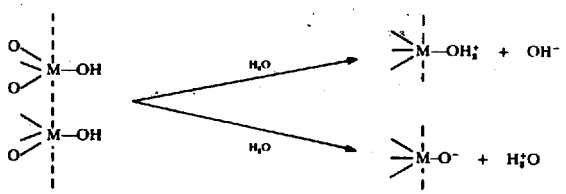

FIG. 10: Hydrolysis reactions of the surface hydroxyl groups **(49)**

The surface charges attract opposite-sign ions, present in the solution, which form a layer adjacent to the surface. This layer extends from the surface as far as a distance **d** (fig. 11). The trend of the electrical potential shows a linear reduction as far as distance **d**, which corresponds to the limit of the adsorbed ion layer (Stern's rigid layer). Beyond this limit, the decay is exponential in the so-called diffused ionic layer. Potential ψ_0, corresponding to the limit of the rigid layer, cannot be measured easily whereas a parameter strictly related to ψ_d, that is ζ potential, can be calculated. This is determined by microscopic observations of the electrophoretic mobility **u** of the suspended particles subject to an electric field. Mobility **u** is related to ζ by the expression

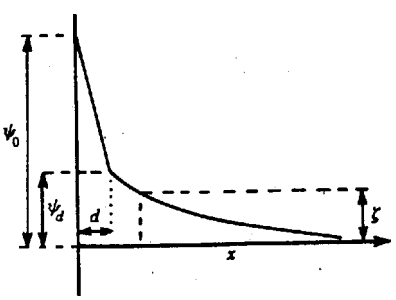

FIG. 11: Schematic illustration of the electrical double layer **(49)**

$$u = (\varepsilon_r \cdot \varepsilon_0 \cdot \zeta / \eta) \cdot f(ka, \zeta) \qquad 19)$$

where ε_r and ε_0 = permittivities of the solution phase and free space

η = viscosity of the medium

$f(ka, \zeta)$ = numerical factor

The oxide surface, by participating in the acid-base equilibria given in figure 10, show considerable changes in their surface charge and, therefore, in their zeta potential as a function of pH of the medium. Figure 12 exemplifies the electrophoretic mobilities obtained in alumina and silica suspensions as a function of pH **(49)**. It can be observed that silica particle charges become increasingly negative over a wide pH range. On the contrary alumina is charged positively as far as pH 9 and negatively above this value. The same figure shows that the increase in the ionic force of the medium reduces the potential owing to the compression of the double layer, but it does not modify its course. These systems where it is possible to modify zeta potential, as a function of pH of the medium, are suitable to check the correlations provided by DVLO theory between the rheological properties of the suspension and zeta potential. When the surface potential is high, and therefore the repulsion forces prevail on Van der Walls attraction ones, a low viscosity must be expected. On the contrary, the aptitude for flow will be limited when the double layer interactions are poor and the cohesion between particles is high. These remarks have been confirmed experimentally in latest works **(50)**, always concerning alumina concentrated suspensions that showed the viscosity values versus pH given in fig. 13.

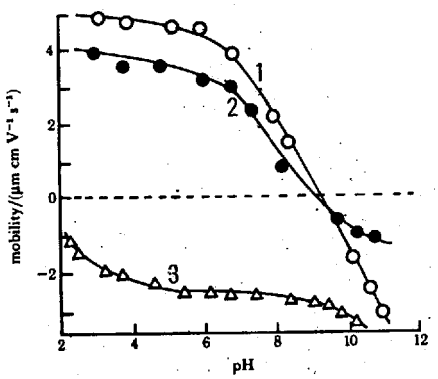

FIG. 12: Mobility against pH **(49)**
1) alumina in 10^{-3} mol/dm^3 NaCl
2) alumina in 10^{-1} mol/dm^3 NaCl
3) silica in 10^{-3} mol/dm^3 NaCl

The comparison of figures 12 and 13 shows how the suspension viscosity attains a maximum value at the point of zero charge of the surfaces.

In these systems, where stable equilibria establish between the solution and the surface, the value of zeta potential has a well defined physical meaning. When the cement-water system is considered, the application of the classical model of the electric double layer becomes questionable since the interfaces in this case are not in thermodynamic equilibrium. When the cement surface come in contact with water, it reacts by producing ions and sur-

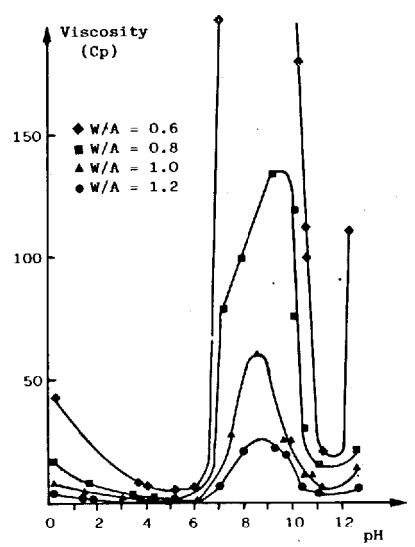

FIG. 13: Viscosities of alumina suspensions vs pH. The concentrations are expressed by W/A (mass of water/mass of alumina) **(50)**

... charges in a large amount. These ions caused by hydration add to those already present in water and contribute to a large extent to the formation of the ionic envelope around the particles (38). The ionic envelop differ from a normal double layer in that the inner part is being transformed continuously.
It was proposed to replace the classic concept of zeta potential with that of dynamic potential which evolves continuously with the hydration time and takes into account the ionic parameters of the contact solution (51).
The evolutionary nature of zeta potential of the cement particles suspended in water is shown in fig.14. ζ potential decreases and then reaches a stable value after 25 minutes. pH reaches the value 10, as a result of the dissolution of calcium and alkaline hydroxides.

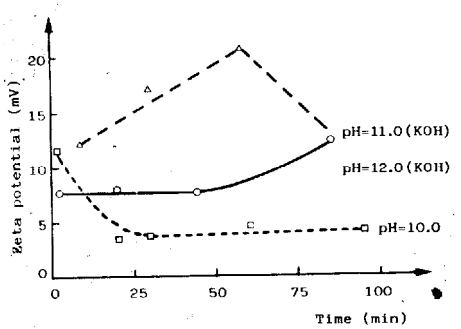

FIG. 14: Zeta-potential of portland cement as a function of time and initial pH-value (38)

When KOH is added to the cement suspension, the ζ potential shows increasing or decreasing trends according to the pH increase. However these behaviours have not found a rigorous explanation but, in any case, they testify a change in the surface composition with time. Nevertheless these composition changes, during the induction period or more advanced stages of the hydration process, have appeared as relatively slow. As a consequence, it is possible to detect a well defined zeta potential associated to a double layer that can be described by models derived from the classical Stern-Grahame's (52)(53), as that given in figure 15. The correlation between zeta potential and rheological behaviour is complicated by that ζ measurements are carried out in diluted suspensions whereas viscosimetry utilizes pastes or concentrated suspensions. Moreover, in the rheological measurements the pastes are in a dynamic state that modifies the double layer structure and therefore the value of zeta potential, compared with that generally measured at the rest state (63).

4. STRUCTURAL MODELS

At the present state-of-art the structural models proposed for fresh cement pastes are essentially qualitative. They are based on concepts of the colloid chemistry.
One of the first models for the flocculated state of the paste dates back to Powers (43) who imagined that fresh cement pastes made at the usual w/c ratio were composed of floccula. The mixing mechanical action produces hydraulic forces which tend to separate the individual particles and to create an uniform dispersion state. Only when the mixing action ceases, a continuous structure forms.
This is considered as a hypothetical single flocculus that involves the whole paste. The density of the floccula varies with the w/c ratio since the thixotropic structure forms very quickly when the mixing action has ceased, therefore the particles cannot reach the equilibrium position. Helmuth (1) resuming these concepts, represented the cement paste in the model of fig. 16, where the cement grains are considered as spherical in first approximation. This model points out the dispersing and stabilizing effect on the structure exerted by the disjoining pressure caused by the adsorbed water films. If the mixing action is strong enough, the thickness of the adsorbed water film tends to equalize as far as to take the value of the so-called hydraulic radius.

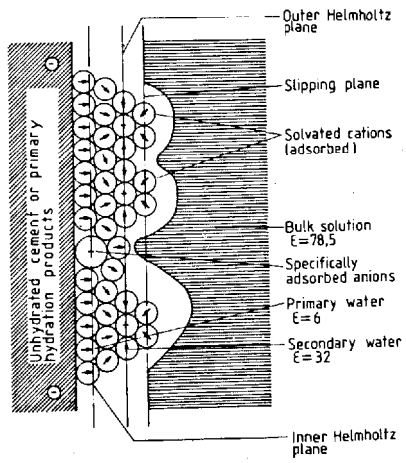

FIG. 15: Model of electrical double layer
ε = dielectric constant

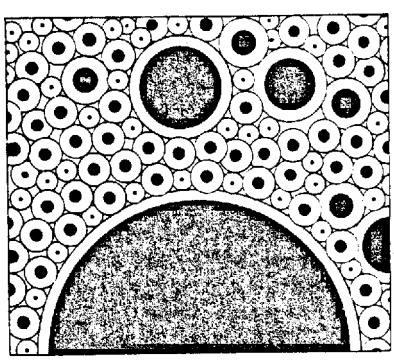

FIG. 16: Simplified model of spherical particles of fresh cement paste structure. a/c ratio = 0.5. Cement specific surface 430 m^2/kg (1)

The above-mentioned models are based on assumptions that simplify appreciably the real characteristics of the cement paste. First of all the shape of the cement grains is not spherical but angular and this morphologic feature can strongly affect the equilibria of the structure, as indicated in the model proposed by Legrand shown in fig. 17 (55). In this model the formation of the continuous network of floccula in the cement paste becomes possible chiefly owing to the formation of direct tip-to-tip or tip-to-face coulomb

bonds between grains. These bonds, according to Bom - bled (2), are the result of the incomplete neutraliza tion from "counterions", in the aqueous medium, of the electric charges gathered in the tips and corners of the grains. These attraction forces, strengthened

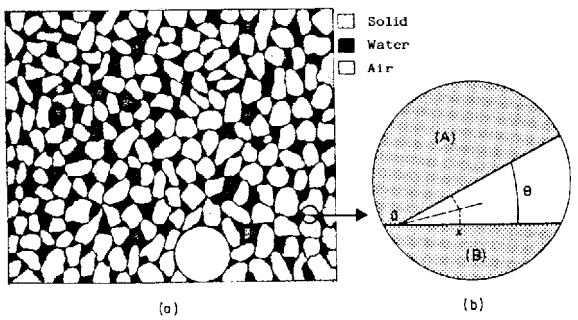

FIG. 17: Schematic model of fresh cement paste flocculent state (55)

in the association point by Van der Walls forces, act on a limited surface. There fore it can be assumed that the contact area behaves as an articulated joint. On the surface of the grains adjacent to "articulated joint" the repulsion forces act. There are the disjoining pressure caused by the adsorbed water films and the interaction of the dou ble ionic layers. These repulsion forces tend to en - large the contact angle Θ if the surrounding structure does not prevent it. The presence of unavoidable air bubbles entrained during mixing creates discontinui - ties in the structure and it gives rise to capillar y forces. Of course on the grains the gravity force acts. To conclude the structure is supported by local equi- libria between the repulsion and attraction forces.
This model allows the interpretation of some aspects of the rheological behaviour such as plasticity, thixotropy and viscosity, which affect considerably the workability of fresh cement paste. The grain displacement in the flocculated structure is possible only if the shear stress attains a suffi - cient value to break the intergrain bonds. In this ca se the paste behaviour is called plastic. Once attain ed the flowing threshold, it can happen that the mo - tion resistance of paste decreases with time: the known phenomenon of thixotropy takes place. Also this phenomenon is the result of the progressive breakdown of the bonds between grains. In any case, even though during the motion the primary bonds are broken, the grains still feel the so-called first, second- and third-type electroviscous effects caused by the ionic diffused layers (56). Moreover, also the interstitial liquid flowing between the grains will show a resi - stance depending on both its own viscosity and the permeability of the granular whole. Therefore all the se factors contribute to make viscosity higher than that belonging to a suspension of non-interacting ele ments.

5. RELATIONSHIPS BETWEEN PASTE AND CONCRETE

The previous paragraphs showed that fresh cement pastes, made at normal w/c ratios, have prevailingly viscopla stic behaviours and can be characterized by the two fundamental parameters τ_0 and η_{pl}.
Tests performed by means of rheometers with helicoi - dal rotor showed that the rheological behaviour of fresh concrete is of viscoplastic-Binghamian type (57). The refore also this system can be characterized by two rheological parameters (two point test), that is yield value and coefficient of viscosity. The analogy bet - ween the two systems is not casual but can be consi - dered as the result of the two essential roles that the interstitial paste plays in the concrete rheology, that is the cohesion and lubrication towards the ag - gregate. The former can be considered as directly de rived from the yield value, the latter from the paste viscosity.
The attempts made to establish quantitative relation- ships between the paste rheological properties and the mortar and concrete workability have not been nu merous so far. To establish a correlation between wor kability of fresh concrete and rheology of cement pa- ste, it is necessary to know the effective w/c ratio given by the formula

$$(w/c)_{eff} = \frac{w-(k_s \cdot s + k_g \cdot g)}{c} \qquad 20)$$

and the effective water content expressed by

$$p_{eff} = \frac{c}{1000}\left[\frac{1}{\varrho} - (w/c)_{eff}\right] \qquad 21)$$

where the coefficients k_s and k_g represent the increa se in the water content required to obtain the same workability when sand or coarse aggregate is added to the paste (58). The terms w, s, g and c represen t the water, sand, coarse aggregate and cement contents (kg) of concrete and ϱ the cement density.
The values of slump and flowtable spread of mortars having different composition were correlated with a parameter X_η calculated by equation

$$X_\eta = \frac{\varrho \cdot g}{\eta \frac{(s/c)^2}{\psi}} \qquad 22)$$

where η is the viscosity coefficient of the paste mea sured by the rotational viscometer, s/c is the sand/ /cement ratio, ψ is the paste volume per surface u- nit of the sand, g the gravity and ϱ the mortar den sity (59). The empirical parameter X_η includes both the terms of the mortar composition and the rheologi- cal properties of the paste having the same w/c ra - tio. In the case of mortars with s/c ratios ranging between 2.1 and 3.9 it was found only a correlation curve bet ween the slump or flowtable values and the parameter X_η. When superplasticizers are present, the workabi- lity data, represented as a function of X_η, lie on different curves depending on the considered s/c ra- tios. To establish a more general correlation bet - ween paste and mortar properties, also valid in the presence of admixture, it would have been necessary

to introduce other parameters concerning the admixture-aggregate interaction, the entrained air a.s.o.
The model which consider fresh concrete in its whole as a dispersion, even though it includes a large dimensional range of grains, was the base of recent attempts aiming at characterizing the concrete behaviour in a rational manner.
The viscosity of mortars and concretes was calculated by an equation whose essential terms were the effective volume concentration of the solid phase and the maximum one permitted by particle size distribution and shape of the aggregate.
The obtained data were in good agreement with the experimental ones derived from rotoviscometric tests for a large range of mix composition **(60)**.
Good results were obtained **(61)** by applying an equation deduced by Roscoe **(12)** for suspensions of stiff spheres. This equation includes fineness modulus, volumetric percentage related to the total solid content in concrete and volumetric concentration of the coarser part of the aggregate.

6. CONCLUSIONS

As a rule, the study of fresh cement paste rheology can give important information about the component interactions and the structure. Nevertheless the interpretation of the rheological behaviour is not simple because it depends not only on many factors concerning the chemical-physical properties of the cement or the liquid phase but also on the techniques and the experimental measuring instruments.
The development of the rheological studies on pastes allowed progress to be made in the rigorous interpretation of the flow curves by means of sophisticated mathematical calculations. These analysis methods allows a more accurate study of the influence of some chemical-physical factors. The possibility of establishing models of general validity is in conflict with the difficulty of expressing quantitatively the factors that show a very large variability, such as size, shape and mineralogical composition of the cement grains.
Another uncertainty reason lies in the imperfect knowledge of all the types of interactions solid-solid and liquid-solid.
Finally, the check of the assumptions by direct tridimensional observations of a suspension as the cement paste having high consistency and submitted to a chemical-physical evolution, presents great difficulties.
Therefore at the present state-of-art it is possible to make only a schematic description of the structure based on simplified assumptions that can explain qualitatively the rheological properties of the material.
The models proposed on the basis of the equilibria of the attraction and repulsion forces acting between particles can explain the existence of a yield value, a viscosity varying with the duration of the applied stress (thixotropy) and the admixture effect.
However the understanding of the phenomena concerning the paste rheology has not yet reached a sufficient level to interpret the most complex "suspension" formed of fresh concrete.

REFERENCES

(1) R.A. HELMUTH, *7th Int. Congr. on the Chem. of Cement (Paris, June 1980), vol. III, VI-0/16*

(2) J.P. BOMBLED, *Rev. Mat. Constr. 1974,(688), 137*

(3) C. LEGRAND, *Cem. Concr. Res. 1972, 2 (1), 17*

(4) G.H. TATTERSALL, *Nature 1955, 175, 166*

(5) R. LAPASIN, V. LONGO, S. RAJGELJ, *Cem.Concr.Res. 1979, 9 (3), 309*

(6) D.C.-H. CHENG, *Powder Technology 1984, 37, 255*

(7) R. LAPASIN, V. LONGO, S. RAJGELJ, *Il Cemento 1976, (2), 91*

(8) P.F.G. BANFILL, D.C. SAUNDERS, *Cem. Concr. Res. 1981, 11 (3), 363*

(9) K. WESCHE, H. FLATTEN, W. VOM BERG, *RILEM Seminar "Fresh Concrete: Important Properties and their Measurement" (Leeds, March 1973),vol.1, 2.10-1*

(10) W. VOM BERG, *VIII Int. Congr. on Rheology (Napoli, Sept. 1980), vol. 3, 665*

(11) E.L. WHITE, D.M. ROY, *Symp. M "Effect of Surface and Colloid Phenomena on Properties of Fresh Concrete" (Boston, Nov. 1982), 108*

(12) R. ROSCOE, *Brit. J. Appl. Phys. 1952, 3, 267*

(13) B. CAUFIN, A. PAPO, *Zement Kalk Gips 1984,(12),656*

(14) R. LAPASIN, *Il Cemento 1982, (4), 243*

(15) J.I.BHATTY, P.F.G. BANFILL, *Cem.Concr.Res. 1982, 12 (1), 69*

(16) T.E.R. JONES, S. TAYLOR, *Mag. Concr. Res. 1977, 29 (101), 207*

(17) W.H. HERSCHEL, R. BULKLEY, *ASTM Proc.1926,26, 621*

(18) R.E. ROBERTSON, H.A. STIFF Jr., *J. Soc. Petrol. Engin. 1976, 16, 31*

(19) W. VOM BERG, *Mag. Concr. Res. 1979, 31 (109),211*

(20) H. EYRING, *J. of Chem. Phys. 1936, 4, 283*

(21) C. ATZENI, L. MASSIDDA, U. SANNA, *Il Cemento 1983, (3), 141*

(22) C. ATZENI, L. MASSIDDA, U. SANNA, *Cem.Concr.Res. 1985, 15 (3), 511*

(23) S.B. ELLIS, *Thesis 1927, Lafayette College, Pa.*

(24) N. CASSON, *in Rheology of Disperse Systems 1959, Pergamon Press, 84*

(25) K. HATTORI, K. IZUMI, *Symp. M "Effect of Surface and Colloid Phenomena on Properties of Fresh Concrete" (Boston, Nov. 1982), 14*

(26) R. LAPASIN, A. PAPO, S. RAJGELJ, *Cem.Concr. Res. 1983, 13 (3), 349*

(27) Y. OTSUBO, S. MIYAI, K. UMEYA, *Cem. Concr. Res. 1980, 10 (5), 631*

(28) O.C.C. LIN, *Chemtech 1975, 5 (1), 51*

(29) C. LEGRAND, *7th Int. Congr. on the Chem. of Cement (Paris, June 1980), vol. IV, 124*

(30) R. LAPASIN, V. LONGO, S. RAJGELJ, *VIII Int.Congr. on Rheology (Napoli, Sept. 1980), vol. 3, 659*

(31) D.C.-H. CHENG, *Chemistry and Industry 1980, (10),403*

(32) C. LEGRAND, *Le Béton Hydraulique by J. Baron and R. Sauterey, Presses de l'Ecole Nationale des Ponts et Chaussées 1982, 115*

(33) K. RENDCHEN, *Beton 1976, (9), 321*

(34) V. SAINT-ETIENNE, *Ciment Betons Platres Chaux 1984, (747), 107*

(35) F. SKVARA, K. KOLAR, J. NOVOTNY, Z. ZADAK, *Cem. Concr. Res. 1981, 11 (2), 247*

(36) U. WITTNEBEN, *Zement Kalk Gips 1980, (10), 526*

(37) J. FRIPIAT, J. CHAUSSIDON, A. JELLI, *Chimie-Physique des Phenomènes de Surface, Masson et Cie Ed., Paris 1971*

(38) E. NÄGELE, *Cem. Concr. Res. 1985, 15 (3), 453*

(39) Y. IVONOV, E. STANOEVA, *Silic. Ind. 1979, 14 (9), 199*

(40) B.V. DERJAGUIN, L. LANDAU, *Acta Physicochim. (USSR) 1941, 14, 633*

(41) E.J.W. VERWEY, J.TH. G. OVERBEEK, *Theory of the Stability of Lyophobic Colloids, Elsevier Publ. Co., Amsterdam 1948*

(42) M. REGOURD, *Le Béton Hydraulique by J. Baron and R. Sauterey, Presses de l'Ecole Nationale des Ponts et Chaussées, 1982, 193*

(43) T.C. POWERS, *The Properties of Fresh Concrete, J. Wiley & Sons, Inc., N.Y., 1968*

(44) J. TH. G. OVERBEEK, *Powder Technology 1984, 37, 195*

(45) W. DROST-HANSEN, *Ind. and Eng. Chem. 1969, 61 (11), 10*

(46) B.W. NINHAM, *The J. of Phys. Chem. 1980, 84 (12), 1423*

(47) T. SATO, R. RUCH, *Stabilization of Colloidal Dispersions by Polymer Adsorption, Marcel Dekker Inc., N.Y., 1980*

(48) F. MASSAZZA, *Advances in Cement Technology ed.by S.N. Ghosh, Pergamon Press, Oxford, 1983, 569*

(49) R.H. OTTEWILL, *Phil. Trans. R. Soc. Lond. 1983, A 310, 67*

(50) J. CHAPPUIS, *Symp. M "Effect of Surface and Colloid Phenomena on Properties of Fresh Concrete" (Boston, Nov. 1982), 38*

(51) A. ZELWER, *Ciments Bétons Plâtres Chaux 1984, (749), 213*

(52) O. STERN, *Z. Elektrochemie 1934, 30, pp. 508*

(53) D.C. GRAHAME, *ChemRev. 1947, 41, 44*

(54) J.O'.M. BOCKRIS et al., *Proc. Phys. Soc. 1963, London, 274, 55*

(55) C. LEGRAND, *Le Béton Hydraulique by J. Baron and R. Sauterey, Presses de l'Ecole Nationale des Ponts et Chaussées, 1982, 99*

(56) E.M. PETRIE, *Ind. Eng. Chem., Prod. Res. Dev. 1976, 15 (4), 242*

(57) G.H. TATTERSALL, P.F.G. BANFILL, *The Rheology of Fresh Concrete, Pitman Advanced Publ. Program, Boston 1983*

(58) YU. M. BAZHENOV, *7th Int. Congr. on the Chem. of Cement (Paris, June 1980), vol. IV, 125*

(59) C. ATZENI, L. MASSIDDA, U. SANNA, *AITEC 25°: Il Cemento ed il Calcestruzzo negli Anni'80 (Parma, October 1985), 217*

(60) S. KAKUTA, M. FUJII, T. AKASHI, *The Cem. Ass. of Japan - Review of the Thirty-Third Gen. Meet. (Tokyo, June 1979), 129*

(61) H. KIKUKAWA, *The Cem. Ass. of Japan - Review of the Thirty-Eighth Gen. Meet.(Tokyo, May 1984), 192*

(62) P.C. KREIJGER, *Concrete International 80 - Proc. of the Int. Congr. on Admix. (London, April 1980), 1*

(63) A. ZELWER, G. JUNGERS, *Internal Report of CERILH, Paris, pp. 91*

F. Basile, S. Biagini, G. Ferrari - MAC, R&D Laboratories, Treviso, Italy
M. Collepardi - Universitu of Ancona, Italy

EFFECT OF CONDENSATION DEGREE OF POLYMERS BASED ON NAPHTHALENE ON FLUIDITIES OF CEMENT PASTES.

Introduction

The modern technology makes extensive use of superplasticizers in order to improve the strength of hardened concrete by reducing the amount of water added to the fresh mix.

The phenomena associated with the fluidifying action of superplasticizers are quite complex and involve the adsorption of the macromolecules of the polymer onto the cement grains, the modification of the electrostatic charges on the surface of the cement particles and the modification of the kinetic of hydration of the various constituents of the cement.

It has been shown that, in the case of naphthalene sulfonate condensates, there is a relationship between the effectiveness as superplasticizer and the degree of polymerization, expressed by viscosity measurements (1).

Gel Permeation Chromatography (GPC) has been used by various authors to determine the molecular weight of superplasticizers based on condensates of naphthalene sulfonic acids with formaldehyde (2,3,4).

Recently, the influence of the molecular weight of naphthalene based polymers on the rheological properties of mixes made with different cements has been studied. It has been shown that the fluidity of the mixes increases up to a maximum value, which occurs at different values of the molecular weight of the polymer, depending on the cement used. Moreover, with polymers having extremely high values of molecular weight, a decrease in the fluidity of cement mixes has been observed (5).

In the present work, GPC and ultrafiltration have been used to study the effect of the degree of condensation of polymers based on naphthalene sulfonate on the fluidity of cement pastes, in a range for which an increase of the molecular weight of the condensate causes an increase in the fluidity of the cement mixes. In particular, the purpose of the present work is to examine whether the increase in the effectiveness of the superplasticizer with its degree of condensation is due either to the reduction in the low molecular weight fraction or to the change in the molecular weight distribution of the highly condensed polimeric fraction.

Experimental

Materials

Synthesis of naphthalene sulfonate based superplasticizer

Pure naphthalene (10.00 kg) was charged in a glass reactor and heated at 120°C. Then 8.36 kg of 98% H_2SO_4 ($H_2SO_4/C_{10}H_8$ molar ratio = 1.07) were added and the temperature was raised at 165 °C. This temperature was mantained for two hours to complete the sulfonation of naphthalene. The sulfonation mixture was diluted with 5.97 kg of water and then 7.81 kg of 36% formaldehyde solution ($HCHO/C_{10}H_8$ molar ratio = 1.20) were added. The condensation was carried out at 112°C for 14 hours and 7 samples of polymer were collected (one every 2 hours) having increasing degree of condensation. The samples, after neutralization with sodium hydroxide, had a total solids content of about 40% by weight.

Cement

Type I Portland cement with Blaine fineness of about 0.4 m^2/g has been used. The chemical composition of the cement is shown in Table 1.

Table 1 Chemical analysis of the cement used

CONSISTUENT	PERCENTAGE
SiO_2	21.56
Al_2O_3	4.88
Fe_2O_3	2.30
CaO	60.64
MgO	2.15
K_2O	0.66
Na_2O	0.39
SO_3	3.37
LOSS ON IGNITION	3.87

Techniques

Gel Permeation Chromatography

The samples of naphthalene sulfonic acid formaldehyde condensate to be analyzed were dissolved in 0.55 M KNO_3 aqueous solution to obtain concentrations of 3.0 g/100 ml.

The samples were analyzed using 0.55 M KNO_3 aqueous solution as eluant at a flow rate of 1 ml/min.

Shodex Ionpak S-803/S (exclusion limit 50,000 dalton) and Shodex Ionpak S-804/S (exclusion limit 500,000 dalton) coupled columns, made by semirigid crosslinked styrene-divinylbenzene sulfonate gel, were employed.

Columns were kept in a thermostatic oven at 68°C and all the samples were analyzed at this temperature.

Samples of monodisperse polystyrene sulfonate of different molecular weights (4,400-6,500-17,400-39,900-104,000), naphthalene 2-sulfonate and naphthalene 1,5-disulfonate were used as calibration standards for the columns.

Analyses were performed with a Perkin-Elmer liquid chromatograph equipped with pump mod. Series 4 and Perkin-Elmer ultraviolet detector mod. LC75 at a wavelength of 292 nm.

Chromatographic data were collected and processed by a Perkin-Elmer Data Station mod. 3600 equipped with Chromatographics 2 and GPC4 programs, both by Perkin-Elmer, used for data collection and data processing, respectively.

Ultrafiltration

Samples withdrawn after 4 and 14 hours of condensation were ultrafiltered in order to remove the monomer and the lower molecular weight products. Amicon stirred cell mod. 8200 and Amicon ultrafiltration membrane mod. YM2 having a nominal cut-off of 1,000 dalton, were employed.

Mini-slump test

The fluidity of fresh cement pastes (water/cement ratio = 0.35) in the presence of the condensates (0.4% of dry product by weight of cement) was evaluated by the mini-slump test, after five minutes of mixing. The results were expressed in cm^2 by measuring the area of the circular path described by the fresh cement paste, after having picked-up the cone (6).

Results and Discussion

In Fig. 1 the progressive development of the condensation reaction is shown, as it results from the GPC analyses at different condensation times.

According to the GPC theory, the higher molecular weight fractions elute at first, followed by the lower molecular weight fractions and the monomer (naphthalene 2-sulfonate). From Fig. 1 it is possible to recognize that, by increasing the condensation time, the monomer and the lower molecular weight fractions decrease and conversely the higher molecular weight fractions increase.

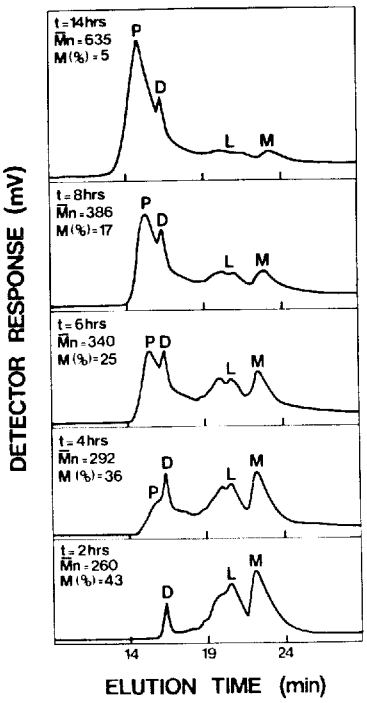

Fig.1 GPC chromatograms of some condensation products at different times (t) of reaction and different number average molecular weight ($\bar{M}n$). P = Polymer; M = Monomer; L = Low molecular weight fraction; D = Naphthalene disulfonate.

Fig. 2 shows the fluidity of fresh cement pastes as a function of the monomer content in the superplasticizer. It can be seen that there is a strong negative influence of the monomer content in the superplasticizer on the fluidity of cement pastes. This agrees with the results of authors who found that naphthalene 2-sulfonate does not exert any fluidifying effect (7).

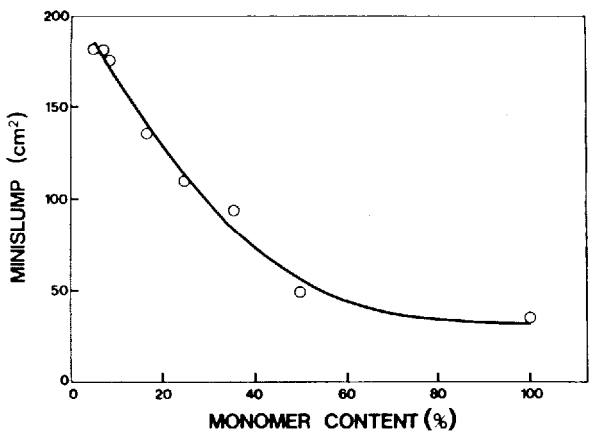

FIg.2 Effect of monomer content in the condensation product on the fluidity (mini-slump) of the cement pastes.

In Fig. 3 the mini-slump values are plotted versus the number average molecular weight ($\overline{Mn}$) of the condensate. This Figure shows that, with the cement used in the present work, the fluidity increases by increasing the $\overline{Mn}$ value up to about 600.

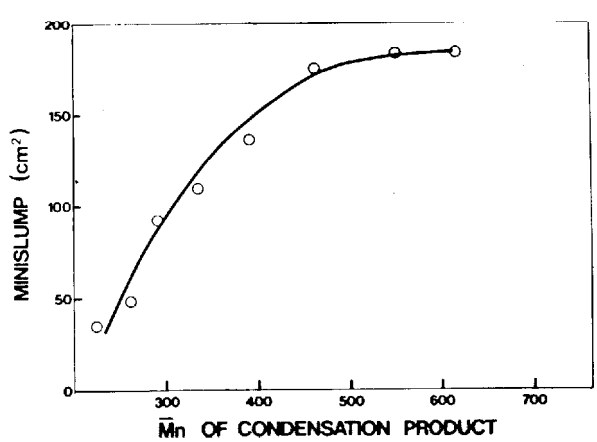

Fig.3 Effect of $\overline{Mn}$ of the condensation product on the fluidity (mini-slump) of the cement pastes.

By comparing the sample condensed for 4 hours ($\overline{Mn}$ = 292) with that condensed for 14 hours ($\overline{Mn}$ = 635), the latter appears to be much more effective as superplasticizer (Fig. 3). One cannot know whether the 14hr-condensate sample is better for the lower content in monomer and "L" fraction or for the higher molecular weight of the "P" fraction (Fig. 1). To clarify this point, both the samples were subjected to ultrafiltration process in order to remove the monomer and the "L" fraction. Figure 4 shows the GPC chromatograms of the two samples before and after ultrafiltration process. The mini-slump values of the cement pastes treated with condensation products before and after the ultrafiltration are shown in Table 2. The results show that, although the ultrafiltered products have different $\overline{Mn}$ values, their fluidifying effect is substantially the same. This demonstrates that, at least for the range of molecular weights considered in the present work, the "P" fraction content and not its molecular weight is determining the fluidifying effect of naphthalene based condensates.

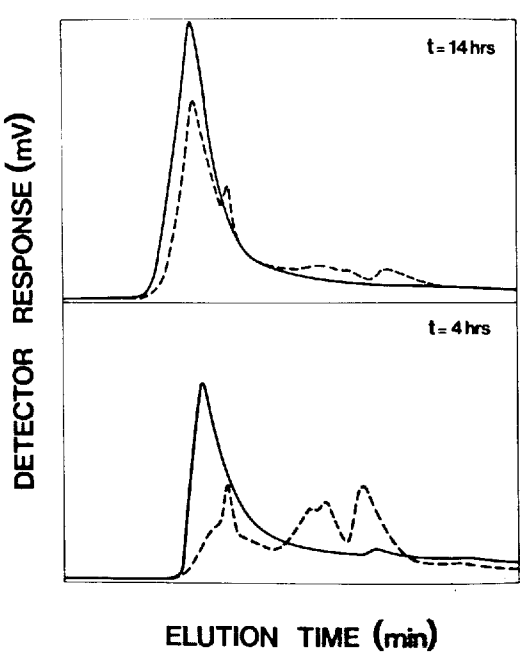

Fig. 4 GPC chromatograms of superplasticizer samples condensed for 4 hrs and 14 hrs before (dotted line) and after ultrafiltration.

Table 2 Effect of ultrafiltration on $\bar{M}n$ and minislump.

	CONDENSATION TIME	$\bar{M}n$	MINI-SLUMP (cm^2)
BEFORE ULTRAFILTRATION	4 HOURS	292	75
	14 HOURS	635	185
AFTER ULTRAFILTRATION	4 HOURS	435	185
	14 HOURS	735	185

Conclusions

It is possible to conclude that, for the range of $\bar{M}n$ of the condensate examined in the present work, the effectiveness of naphthalene sulfonate polymer as superplasticizer is in relation to the content of the monomer and the lower molecular weight fraction, while the molecular weight value of the highly condensed polymeric fraction of the condensate is not determining the effectiveness of the superplasticizer. By using different cements, or by varying the range of $\bar{M}n$ of the polymer examined, different results may be obtained, as previously reported (5).

References

(1) M. Collepardi, M. Corradi and M. Valente, "Developments in the use of Superplasticizers", pg 485, Publ. SP-68, Am. Concr. Inst., Detroit (1981).

(2) M.G. Garvey and T.F. Tadros, Kolloid-Z. u.Z. Polymere 250, 967 (1972).

(3) D.M. Roy, G. Varadi, F.D. Tamàs, G. Pàlyi and B. Bartha, Cem. Concr. Res., Vol. 14, 439 (1984).

(4) H. Edelstein, "Aqueous Gel Permeation Chromatography of Some Naphthalene Sulfonic Acid Formaldehyde Condensates", Mini-Symposium of the North Jersey Chromatography Group Subsection of the A.C.S., March 6, 1978, at Hoffman La Roche Auditorium, Clifton, New Jersey.

(5) G. Ferrari, F. Basile, A. Dal Bo', A. Mantoni, "The Influence of Molecular Weight of Beta-Naphthalene Based Polymers on the Rheological Properties of Cement Mixes", Symposium of the A.I.T.E.C., , October, 1985, Parma, Italy.

(6) L.M. Meyer, W.F. Perenchio, Concrete International, 36-43, January 1979.

(7) M. Collepardi, M. Corradi, G. Baldini, M. Pauri, 7th International Congress on the Chemistry of Cement, Vol. III, pg. VI- 20, Paris (1980).

F. Basile, S. Biagini, G. Ferrari - MAC, R&D Laboratories, Treviso, Italy
M. Collepardi - University of Ancona, Italy

PROPERTIES OF CEMENT MIXES CONTAINING NAPHTHALENE SULFONATED POLYMERS OF DIFFERENT MOLECULAR WEIGHT

Introduction

Sulfonated Naphthalene-formaldehyde polymers are the basic materials for the production of a class of superplasticizers, which are today extensively used to manufacture cement concretes and mortars. While a large amount of work has been devoted to examine the properties of fresh and hardened concretes containing superplasticizers (1,2), relatively few papers have been published to examine the effect of superplasticizers on the chemical characteristics of polymers and cement mixes (3-6).

This investigation was therefore carried out in order to correlate performances of cement mixes (including mortars), with the physico-chemical characteristics of cement pastes, manufactured with and without the addition of Naphtalene based superplasticizers.

In particular the work was carried out with a series of different superplasticizers based on sulfonated Naphthalene, in order to evaluate the effect of the polymer molecular weight on the hydration of cement and the performances of cement mixes.

Experimental

Materials

Four samples of sulfonated Naphthalene polymers of different molecular weight were obtained by a process described in an other work (7), where the final condensation step was maintained for 2, 4, 10 and 14 hrs respectively, at a temperature of 112°C.

The Number Average Molecular Weight ($\overline{M}n$) of condensated superplasticizers was determined by use of Gel Permeation Chromatography (8) and specific values for each sample of polymer are given in Table 1.

Table 1 Number Average Molecular Weight ($\overline{M}n$) of different samples of condensated Naphthalene sulfonate.

SAMPLE	CONDENSATION TIME (hrs)	$\overline{M}n$
A	2	260
B	4	290
C	10	480
D	14	640

A type I ASTM Portland cement was used, and its chemical analysis is given in Table 2.

Table 2 Chemical analysis of Portland cement

	%w
L.O.I.	1.20
SiO_2	21.05
Al_2O_3	5.20
Fe_2O_3	3.12
CaO	63.70
MgO	0.75
Na_2O	0.20
K_2O	0.37
SO_3	1.90
Blaine fineness (m^2/gr)	0.380

Techniques

Polymer adsorption, zeta potential, minislump, heat evolution rate, differential thermogravimetry (DTG) were carried out on cement pastes (water/cement ratio = 0.40) hydrated at 20°C by following the techniques described in previous papers (5,6). Polymer adsorption, zeta potential and minislump were determined after 5 min of mixing. Moreover ASTM (with only 5 days) flow table, air-entrainment measurement and compressive strength on mortar mixes at 20°C (sand/cement ratio = 3) were carried out at a given water/cement ratio (0.45) or at a given flowability (flow cone = 70%).

The superplasticizer dosage was 0.4% of dry polymer by weight of cement.

Discussion of results

Fig.1 shows the polymer adsorbed on cement (by percentage of the original amount of polymer) as a function of its Number Molecular Weight ($\overline{M}n$). By increasing $\overline{M}n$ the polymer adsorption increases up to 70%. Beyond an $\overline{M}n$ value of about 600 it seems that there is no significant increase in the polymer adsorption.

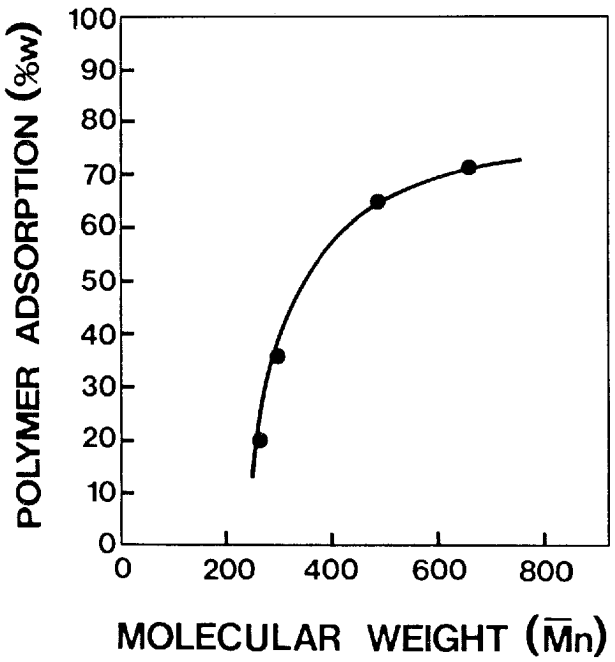

Fig.1 Adsorption of Naphthalene sulfonate polymers on cement paste as a function of the Number Molecular Weight ($\bar{M}n$) of polymers.

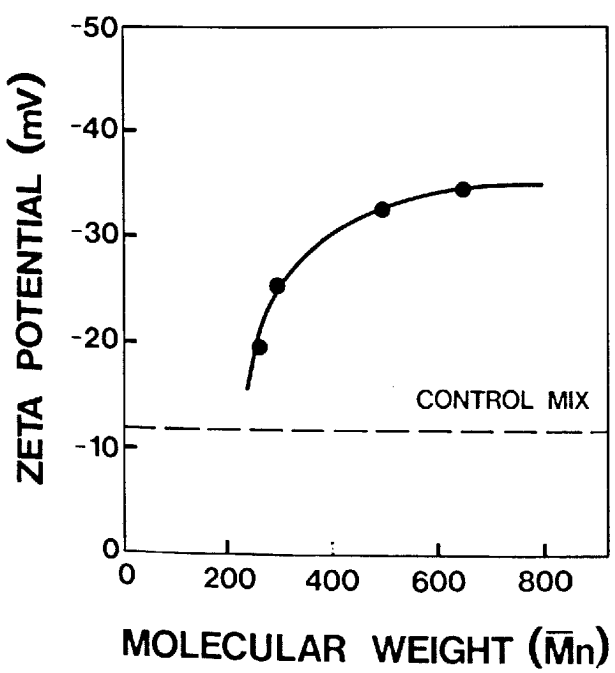

Fig.2 Zeta potential of cement pastes with and without Naphthalene polymers of different Molecular Weight ($\bar{M}n$).

A similar trend was recorded for the zeta potential vs $\bar{M}n$ curve (fig. 2). Also in this case it seems that there is no substantial increase in zeta potential for $\bar{M}n$ values higher than 600.

Figure 3 shows that the fluidifying effect of the polymer increases by increasing the polymer $\bar{M}w$ value. Also in this case it seems that the effect does not substantially change with polymers having $\bar{M}n$ value higher than about 600.

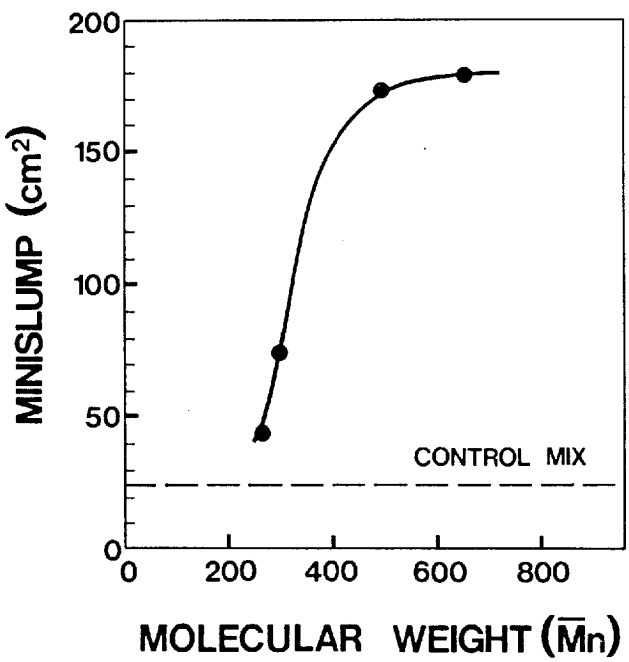

Fig.3 Minislump of cement pastes prepared with and without addition of Naphthalene polymers of different Molecular Weight ($\bar{M}n$).

Curves of heat evolution rate as a function of hydration time up to 24 hrs with and without superplasticizers are shown in Fig. 4. In the presence of those admixtures both the induction period and the time corresponding to the maximum in the heat evolution curve are increased with respect to the control mix without admixture. This indicates a retarding effect of the polymer on the early cement hydration. The higher the polymer $\bar{M}n$ value, the more effective the retarding action of the polymer.

In order to obtain more information about the effect of the polymer on the cement hydration, the percentage of $Ca(OH)_2$ produced from 8 hrs to 28 days was

determined by DTG (Table 3). At 8 hrs the percentage of $Ca(OH)_2$ decreases in the presence of polymers with respect of control mix. The higher the polymer $\overline{Mn}$ value, the more effective is the retarding action on the early cement hydration, thus confirming the results obtained by the calorimetry technique (Fig. 4). On the other hand, at longer ages, such as a 7 and 28 days, the polymer addition increases the cement hydration degree and the effect becomes more remarkable by increasing the molecular weight of the polymer.

Table 3 $Ca(OH)_2$ (% by weight of anhydrous cement) in pastes cured with and without Naphthalene polymers of different Molecular Weight ($\overline{Mn}$)

MOLECULAR WEIGHT OF POLYMER ($\overline{Mn}$)	$Ca(OH)_2$ (%w) after:			
	8 hrs	1day	7days	28days
CONTROL	2.0	7.3	9.0	10.5
260	1.8	6.6	9.5	10.7
290	1.7	6.5	10.5	11.2
480	1.6	6.7	11.0	12.1
640	1.5	6.8	12.0	15.2

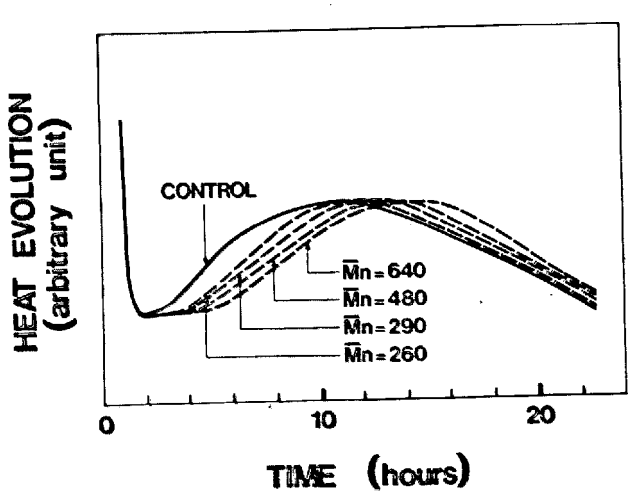

Fig.4 Heat evolution curves of cement pastes with and without addition of naphthalene sulfonate polymers of different Molecular Weight ($\overline{Mn}$).

Table 4 and 5 show the results on mortars at a given w/c ratio and at a given flowability respectively. For the tests at a given w/c ratio, the superplasticizer addition causes an increase in the flow table of the mortar. The fluidifying effect increases by increasing the polymer $\overline{Mn}$ value. On the other hand the polymer addition causes an increase in the air-entrainment. This effect is greatest with the polymer having $\overline{Mn}$ value of 290. It would seem that the air-entrainment decreases with the molecular weight of the polymer and increase with the fluidity of the mortar, so that the highest increase in the air-entrainment is caused by the polymer with an intermediate $\overline{Mn}$ value such as 290 in the present work. Because of the high increase in the air-entrainment, the strengths of mortars with polymers having $\overline{Mn}$ values of 260 and 290 are lower than the strength of the plain mortar, in spite of a higher cement hydration degreee at 7 and 28 days of the superplasticized cement mixes with respect to the control mix (Table 3). For the polymers with $\overline{Mn}$ of 480 and 640 causing a lower increase in the air-entrainment, the strength of the superplasticized mortars at later ages (7 and 28 days) are slightly higher than the control mortar.

Table 4 Characteristics of mortars (water/cement = 0.45; sand/cement = 3) prepared with and without Naphthalene sulfonate polymers of different Molecular Weight ($\overline{Mn}$).

$\overline{Mn}$ OF POLYMER	FLOW *	ENTRAINED AIR	COMPRESSIVE STRENGTH (MPa)		
		%v	1day	7days	28days
CONTROL	65	5.0	13.5	42.0	52.5
260	80	9.0	12.5	37.0	47.5
290	90	12.0	10.5	33.0	44.0
480	110	8.5	12.0	43.0	53.0
640	120	7.5	13.0	44.0	55.5

* ASTM C 109 - 5 drops only

The effect of the polymer $\overline{Mn}$ value on the air-entrainment in superplasticized mortars appears clearer in the tests at a given flowability (Table 5). In this case the increase in the air volume caused by the superplasticizer decreases by increasing the polymer $\overline{Mn}$ value from 280 to 640. The increase in strength is remarkable with the polymers having the highest $\overline{Mn}$ value (480 and 640) since there is the greatest reduction in the w/c ratio (Table 5), the highest increase in the cement hydration degree (Table 3) with a negligible or no increase at all in the air volume. For the polymers having lower $\overline{Mn}$ value (260 and 240), both the reduction in the w/c ratio (Table 5) and the increase in the cement hydration degree (Table 3) are much lower, so that the increase in the air volume with respect to the control mortar substantially reduces the above beneficial effects and no significant increase in strength is obtained in superplasticizerd mortars.

Table 5 Characteristics of mortars with a given flow prepared with and without Naphthalene sulfonate polymers of different Molecular Weight ($\overline{Mn}$).

Mn OF POLYMER	WATER/CEMENT RATIO	FLOW (*)	ENTRAINED AIR (%v)	COMPRESSIVE STRENGTH 1day	7days	28days
CONTROL	0.45	70	5.0	12.0	42.0	52.5
260	0.43	70	8.0	13.0	42.0	51.0
290	0.42	70	8.2	13.0	43.5	53.0
480	0.40	70	6.5	18.0	52.0	63.0
640	0.39	70	5.0	18.5	52.5	64.0

(*) ASTM C 109 - 5 drops only

Conclusions

By increasing the Molecular Weight of sulfonated Naphthalene polymer the fluidifying effect of the superplasticizer increases. This effect is accompanied with an increase in the zeta potential of cement pastes and in the amount of polymer adsorbed on hydrated cement. For the cement used in the present work no significant increase in fluididity, zeta potential and adsorption appears for Number Molecular Weight ($\overline{Mn}$) of the polymer higher than about 600.

By increasing the molecular weight of the polymer, the degree of cement hydration is reduced at earlier ages and increased at later ages. The retarding effect on the early cement hydration, which could be ascribed to the adsorption of polymer molecules on cement particles, seems to be advantageous to reduce slump loss in concrete mixes. The increase of the hydration degree at later ages could be ascribed to a better dispersion of cement particles, as a result of a higher zeta potential which increases by increasing the molecular weight of the polymer.

The molecular weight of the polymer significantly affects also the increase in the volume of entrained air in cement mixes. This volume decreses by increasing the molecular weight of the polymer. With $\overline{Mn}$ value higher than about 600 no substantial increase in the air volume is found with respect to the control mix. Consequently the increase in strength caused by polymers with $\overline{Mn}$ higher than a certain value (about 600 for the cement used in the present work) becomes very effective as the reduction in the w/c ratio and the increase in the degree of cement hydration are not counteracted by any increase in the volume of entrained air.

References

(1) Proceedings of International Symposium on "Superplasticizers in Concrete", ACI, SP-62, May 1978, Ottawa, Canada.

(2) Proceeding of International Conference on "Development in the use of Superplasticizers", ACI,SP-68, (1981), Ottawa, Canada.

(3) R. Kondo, M. Daimon, E. Sakai "Interaction Between Cement and Organic Polyelectrolytes". Il Cemento, 75, 225-230, (1978).

(4) D.M. Roy et al., "Rheological Properties of Cement Mixes", Cem. Concr. Res. 8, 758-764, (1978); 9,

103-110, (1979); 9, 731-740, (1979); 10, 287-295, (1980).

(5) M. Collepardi, M. Corradi, G. Baldini, M. Pauri, "Influence of Sulfonated Naphtalene on Fluidity of Cement Pastes", Proc. 7th Int. Congress on the Chemistry of Cement, Vol. III, pg 20-25, Paris 1980.

(6) M. Collepardi, M. Corradi, M. Valente, "Influence of Polymerization of Sulfonated Naphtalene Condensate and its Interaction with Cement", in ref. (2)

(7) F. Basile, S. Biagini, G. Ferrari and M.Collepardi, "Effect of Condensation Degree of Polymers Based on Naphthalene Sulfonate on Fluidities of Cement Pastes", This Symposium.

(8) G. Ferrari, F. Basile, A. Dal Bo', A. Mantoni, "L'influenza del peso molecolare dei polimeri a base di beta-naftalensolfonato sulle proprietà reologiche degli impasti cementizi", in "Il Cemento ed il Calcestruzzo negli anni 80", pg 251-259, Parma, Italy, (1985).

Stefania Grzeszczyk, Dr., Institute of Cementing Building Materials, Opole, Poland
Leokadia Kucharska, Asst. Prof., D.Sc., Technical University of Wrocław, Poland

THE INFLUENCE OF ALKALIES UPON THE WATER DEMAND OF EARLY HYDRATION STAGE CEMENT PASTES IN THE LIGHT OF RHEOLOGICAL STUDIES

INTRODUCTION

The influence of cement paste alkalies upon mechanical quantities is considered to result from the changes in the liquid phase composition caused by sodium and potassium sulphates and from the changes in the hydraulic activity of clinker minerals due to the building-in of alkalies into the crystal lattice of minerals. The influence of alkalies upon the solution composition through the changes of clinker phase and gypsum solubility shows impact upon the water demand and the rheological qualities of cement pastes. According to Odler and others (1) the rheological qualities of cement pastes depend primarily on w/c, hydration time, mixing intensity and fine-graininess. The chemical and mineral composition is considered less important. The effects of Gebauer's and Schramla's (2) studies point to the significant influence of the following factors upon the water demand: C_3A content, the total content of alkalies and the content of 10 - 30 μm grains.

It has been proved that, of all parameters under investigation, the water demand of cements is linearly correlated with the water-demand of concretes made from these cements. Johansen's tests on cement pastes, as cited Jawed and Skalny (3), showed that the amount of water bound during the three minutes' hydration is negatively correlated with the twenty-eight days' strenght. This suggests that reactions occurring during very early contact of cement and water have a significant influence upon the forthcoming development of strenght. The practical consequence of early cement hydration reactions can be found in the rheological qualities of the paste.

The consistence of fresh cement pastes results from the overlapping of effects that flocculate and delay the early hydration of aluminates by means of gypsum. The impact of gypsum is modified by the presence of alkalies. According to Bombled (4), the sulphates of alkalies decrease the paste deformability, shorten considerably the time of setting, K > Na, and weaken the strenght. Ish-Shalom and Greenberg (5) have proved that alkalies, while having little influence upon the plastic viscosity of cement pastes, increase greatly the yield value, in proportion to the content of alkalies.

This paper presents the results of the research work into the influence of alkalies upon the rheological qualities of clinker and cement pastes during the first hour of hydration with regard to the kind and origin of alkalies.

EXPERIMENTAL

The tests were carried out with the aid of the RV-2 rotary viscometer-coaxial cylinders (made in the GDR), in which the geometry of both cylinder surfaces was modified to reduce sedimentation and slip.

The experiments were performed on industrial as well as laboratory-synthesized clinkers and cements. The clinkers for preparing the experimental cements were synthesized out of chemically pure ones containing Na_2O (0 - 1.3 %) or K_2O (0.8 %) and main clinker oxides. Various amounts of Na_2O or K_2O (in the form of carbonates) were being added to a standard raw meal.

The synthesis of clinker with no content of alkalies was repeated three times using the same composition and maintaining identical conditions. The chemical composition of synthesized and industrial clinkers is shown in Table 1.

Table 1.
The chemical composition of synthesized and industrial clinkers under investigation.

clinker	K_1	K'_1	K''_1	K_2	K_3	K_4	K_5	K_6	P_1	P_2	P_3
IgLoss	0.20	0.20	0.30	0.45	0.30	0.30	0.20	0.20	0.60	0.40	0.60
Insoluble	0.00	0.10	0.10	0.10	0.10	0.10	0.20	0.10	0.10	0.32	0.22
SiO_2	23.10	23.00	22.90	22.90	22.40	22.45	22.45	22.90	20.60	22.50	20.90
Fe_2O_3	3.85	3.85	3.75	3.75	4.00	4.15	4.15	4.15	4.40	2.60	2.45
Al_2O_3	7.90	7.80	7.80	7.85	7.60	7.70	7.50	7.60	6.30	5.80	7.40
CaO	63.70	63.60	63.70	63.00	63.05	63.30	63.65	63.30	64.80	65.20	65.10
MgO	1.40	1.30	1.30	1.30	1.20	1.20	1.10	1.20	1.00	1.80	1.00
SO_3	—	—	—	—	—	—	—	—	0.70	0.50	0.70
Na_2O	—	—	—	0.75	0.80	0.90	1.30	—	0.10	0.10	0.17
K_2O	—	—	—	—	—	—	—	0.80	0.70	1.20	1.20
Free CaO	0.40	0.60	0.75	0.95	0.80	1.00	0.80	0.80	0.97	1.72	1.95

The synthesized clinkers contained no SO_3 and alkalies were embodied in clinker phases. The identyfication (X-ray diffractometry and optical microscopy) of the synthesis products showed that sodium concentrates mainly in the C_3A phase and the increase in its amount in the clinker system produces a change in the symmetry of the Na_2O-in-C_3A solid solution, a regular one for a non-sodium clinker sample and a monoclinic one for the samples with 0.90 % and 1.30 % by weight of Na_2O.

Taking into account the content of SO_3 in the tested industrial clinkers, one may assume that some of their alkali contents are found in the form of sulphates and some, that are not bound into sulphates, remain built in the clinker phases. All the clinkers and cements used in the tests were ground to cover the identical area of 300± 20 m^2/kg in compliance with Blaine'a. The cements contained 5 % of gypsum ($CaSO_4 \cdot 2H_2O$). The way of preparing the samples for the rheological measurements was identical for all clinkers.

Test procedure:

The pastes were made by mixing the clinker or the cement with distilled water or with water containing 0.90 % of Na_2O or K_2O in the form of NaOH, Na_2SO_4 or K_2SO_4. The mixing was done by hand for 4 minutes, which was followed by a minute's mixing at 243 rpm. For clinker suspensions w/c was equal to 0.6, while cement pastes had the equivalent of 0.4. The flow curves were determined after 10 minutes from the moment of clinker or cement contact with water. The time of determining flow curve is 20 minutes. The stress in time at the constant shear rate of 46 s^{-1} was measured for the period of 60 minutes.

Stefania Grzeszczyk, Dr., Institute of Cementing Building Materials, Opole, Poland
Leokadia Kucharska, Asst. Prof., D.Sc., Technical University of Wrocław, Poland

RESULTS AND DISCUSSION

The flow curves of clinker pastes with no alkali content and with built-in alkalies are presented in Fig. 1, while Fig. 2 shows the flow curves of cement pastes with regard to the amount of built-in sodium.

The positions of the flow curves of non-alkali clinker pastes K_1, K_1', K_1'' point to varied reactivity of the said clinkers.

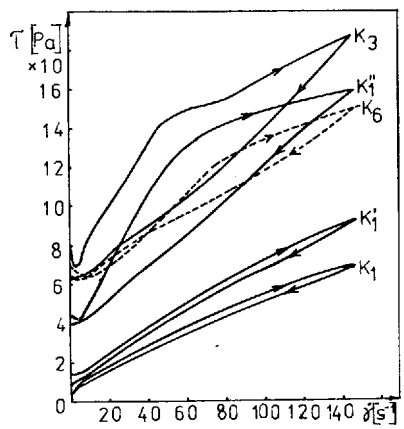

Fig. 1. The flow curves of clinker pastes with no alkali content (K_1, K_1', K_1'') and containing 0.8 % Na_2O (K_3) and 0.8 % K_2O (K_6).

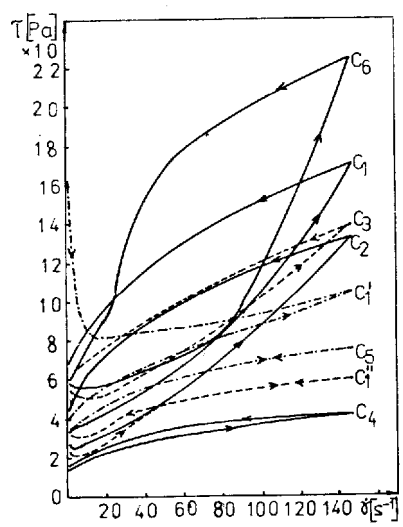

Fig. 2. The flow curves of cement pastes made from non-sodium clinkers C_1, C_1', C_1'' and from clinkers containing sodium (C_2 - 0.75, C_3 - 0.80, C_4 - 0.90, C_5 - 1.30 % Na_2O) and potassium (C_6 - 0.80 % K_2O).

The results show that increased activity of non-alkali clinker, reflected in the shift of the flow curves towards greater stresses, i.e.:

$$K_1'' > K_1' > K_1 \xrightarrow{\text{consistence decrease}},$$

is related to greater consistence decrease of the cement pastes made from the said clinkers:

$$C_1 > C_1' > C_1'' \xrightarrow{\text{consistence decrease}},$$

The analysis of the built-in sodium impact upon the dynamic yield value and viscosity (Fig. 3), deducted from the setting curves of tested suspensions, suggests that built-in sodium brings about the decrease in yield value and viscosity when compared with non-alkali cement C_1.

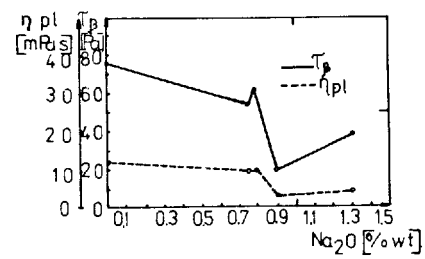

Fig. 3. The influence of built-in sodium upon the dynamic yield values (τ_β) and viscosity (η_{pl}) of cement pastes.

In the light of Hiroshi Uchikawa's and others' research results (6), the indicated differences in the reactivity of non-alkali cements may be connected with the differences in the reactivity of C_3S.

Taking into consideration the test results of non-alkali C_1' and C_1'' cement suspensions, which may also stand as a point of reference for the suspensions made from sodium-containing clinkers, it is possible to state that the influence of sodium built in clinker phases upon the water demand of the cement paste in the early hydration stage does not exceed the changes in the water demand linked to a varying degree of clinker phase crystallization if identical raw meal composition and synthesis conditions are preserved.

According to Shine and Glaser (7), sodium released during the hydration, decreases the content of Al^{+3} ions in the solutions and delays the hydration itself. This may justify the observed decrease in viscosity. Showing the lack of significant influence of built-in sodium upon the water-demand is consistent with the conclusions of several authors stating the lack or little positive impact of built-in sodium upon the cement strenght.

The position and course of the flow curve for the cement paste containing potassium suggests that some amount of potassium that is not bound with C_2S, due to the increased reactivity of the phases in which it occurs, has impact on the solubility of gypsum.

Stefania Grzeszczyk, Dr., Institute of Cementing Building Materials, Opole, Poland
Leokadia Kucharska, Asst. Prof., D.Sc. Technical University of Wrocław, Poland

As a result it affects the paste flow by showing an increased effect of the shear rate and clearly visible hysteresis anti - loop.

The effect of built - in alkalies reveals itself more clearly during the measurements of stresses in time. A considerable increase of stresses in time (Fig. 4) was observed both in clinker and in cement pastes, the growth being higher for the samples with sodium than the ones with potassium. The above research results are in keeping with the results obtained by other authors and suggest that sodium lessens clinker activity and thus weakens the efficiency of regulating the setting with gypsum. The great growth of stress in time for built-in sodium cement pastes may be justified by the greater reactivity of C_3A_{ss} if compared with C_2S_{ss}.

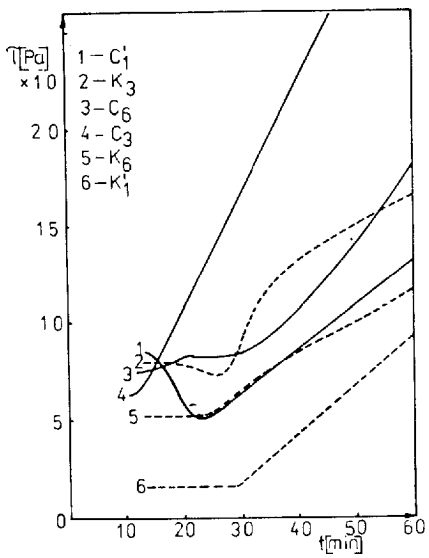

Fig. 4. The diagram of stress variation in time ($\dot{\gamma}$ = 46 s^{-1}) for the non-alkali clinker and cement pastes (K'_1, C'_1), the pastes containing 0.8% Na_2O (K_3, C_3) and the ones with 0.8% K_2O (K_6, C_6).

Bringing sodium as NaOH into the batch water (Fig. 5) causes an increased consistence of clinker pastes while the influence of NaOH upon cement pastes is dependent on clinker reactivity. The more reactive clinker is , the lesser impact of NaOH upon the cement paste consistence.

The effect of sodium added as NaOH is observed in the early stage of hydration (up till 30 minutes) as a change in the paste consistence. In the later stage (Fig. 6) this sodium does not affect changes of stresses in time streight lines in the stress - time system for samples without and with NaOH are parallel.

The constant concentration of NaOH in the solution reduces the amount of coagulating Al^{+3} ions- the precipitation of $Ca(OH)_2$ on the surface of C_3A grains at the initial stage and the reaction with the aluminium ions found in the solution contribute to the formation of C_4AH_6 mainly in non - gypsum suspensions. In accordance with Shine's and Glasser's research results the presence of gypsum reduces the amount of Al^{+3} ions in the solutions to 50 % of that in non - gypsum ones. The source of sodium does not affect the solution composition in the presence of gypsum. Reducing the number of ions coagulating in the solution does affect the paste consistence and its changes in time.

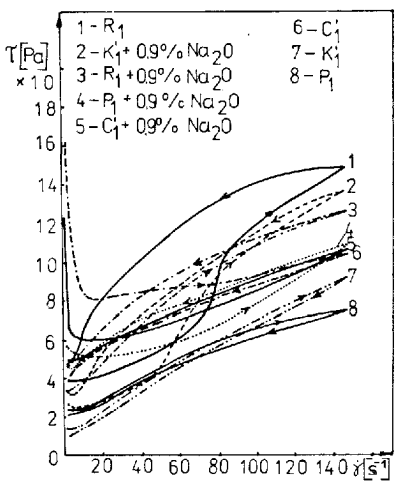

Fig. 5. Flow curves of clinker and cement pastes without and with 0.9 % Na_2O in the form of NaOH (K'_1 , C'_1 - synthesized clinker and cement P_1 , R_1 - industrial clinker and cement).

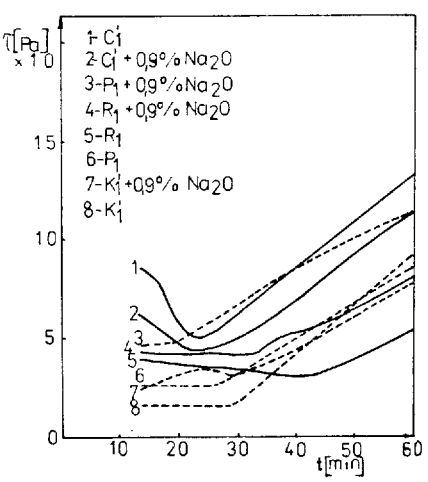

Fig. 6. The diagram of stress variation in time ($\dot{\gamma}$ = 46 s^{-1}) for clinker and cement pastes without and with sodium as NaOH .

Stefania Grzeszczyk, Dr., Institute of Cementing Building Materials, Opole, Poland
Leokadia Kucharska, Asst. Prof., D.Sc. Technical University of Wrocław, Poland

The results of rheological research work in the initial period (till 30 minutes) help reach the similar conclusion. In the presence of gypsum changes in both cases (i.e. cements with sodium embodied and introduced as NaOH) point to little influence of gypsum upon the paste consistence. However, changes in time for suspensions with sodium built-in and introduced as NaOH reveal diverse behaviour of C_3A_{ss} and C_3A in the presence of gypsum.

The research work into the impact of alkali sulphates (Na_2SO_4 , K_2SO_4) introduced into the batch water of clinker and cement pastes showed that, in both cases, sulphates increase consistence (Fig. 7).

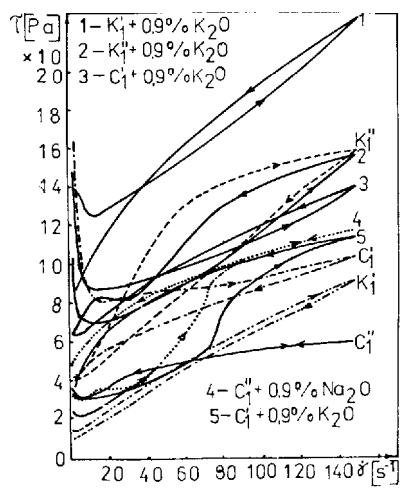

Fig. 7. Flow curves of non - alkali clinker and cement pastes (K'_1 , K''_1 , C'_1 , C''_1) whose batch water contained no or 0.9 % Na_2O or K_2O in the form of K_2SO_4 and Na_2SO_4 .

The quantity of changes is dependent upon clinker reactivity (compare K'_1 and K''_2 , Fig. 7) . The influence of sulphates is particulary clearly indicated at the initial stage of hydration.

Measuring stresses in time (Fig. 8) proved that sulphates in clinker pastes cause heavy coagulation, which means a significant growth of consistence during early hydration. In the later period of hydration, over 30 minutes, one observes a considerable decrease in the influence of alkali sulphates on the clinker consistence in particular.

Cement pastes containing K_2SO_4 or Na_2SO_4 show increased consistence and greater changes in time for K_2SO_4 . This is consistent with the research results (8) which attribute greater influence of K_2SO_4 to the formation of syngenite and calcium sulphate.

Rheological investigations of industrial cements confirmed the results obtained for synthesized ones (Fig. 9) .

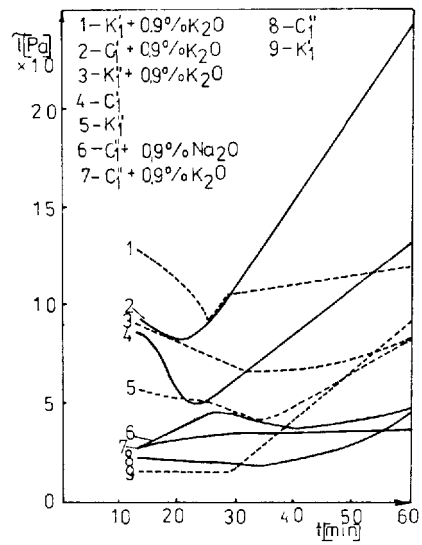

Fig. 8. The diagram of stress variation in time ($\dot{\gamma} = 46\ s^{-1}$) for clinker and cement pastes without or with Na_2SO_4 and K_2SO_4 to the amount of 0.9 % Na_2O or K_2O .

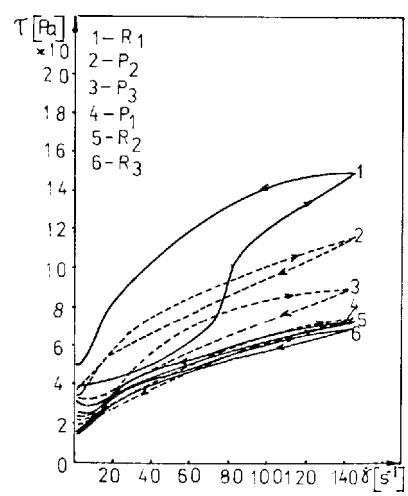

Fig. 9. Flow curves of industrial clinker and cement pastes.

The analysis of flow curves of clinker and cement pastes coupled with the analysis of the mineralogical composition of the said clinkers makes it possible to conclude that differences in the rheological behaviour of cement pastes at the early stage of hydration are related to clinker reactivity. In case of the weaker reactivity of P_1 clinker the efficiency of gypsum influence is smaller. The reverse is true for P_2 clinker , in which an efficient reaction of gypsum with C_3A is revealed by a decrease in the paste consistence.

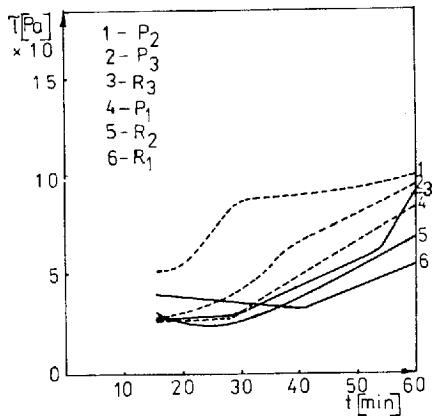

Fig. 10. Curves of stress variation in time ($\dot{\gamma}$ = 46 s^{-1}) for industrial clinker and cement pastes.

At the later stage of hydration (Fig. 10) the course of stress variation, though less intensive, is similar to that represented in Fig. 8 (the influence of potassium sulphate). The SO_3 and K_2O content in industrial clinkers suggests that part of potassium is found in the form of sulphate whose amount in P_1 clinker is greater. The cement paste made from the said clinker is characterized by more intensive growth of stresses in time.

CONCLUSIONS

1. The rheological method has been used to show that the more reactive clinker is the lesser water demand of the cement paste obtained from it.

2. It has been proved that the efficiency of gypsum influence as a setting regulator is dependent on the clinker reactivity. Increasing the clinker reactivity, even with the constant content C_3A , leads to decreasing the consistence of the cement paste.

3. Built in alkalies decrease the efficiency of regulating the paste setting by adding gypsum.

4. The more reactive clinker, the lesser impact of alkalies that are not built in clinker phases upon the consistence of cement pastes and the consistence changes in time.

5. The greatest changes of consistence in time occur in the cement pastes containing built - in sodium. On the other hand , potassium sulphate exerts the greatest influence upon the increase in consistence.

REFERENCES

1. I. Odler, T. Becker, B. Weiss : Rheological Properties of Cement Pastes. Il Cemento , No 3, 303-309 (1978) .

2. J. Gebauer, W. Schramli : Variations in Water Requirement of Industrially Produced Portland Cements. Bull. Am. Ceram. Soc., vol.52, No 2, 161-168 (1974) .

3. I. Jawed, J. Skalny : Alkalies in Cement : a Review II. Effects of Alkalies on Hydration and Performace of Portland Cement. Cem. Concr. Res., vol. 8, No 1, 37-52 (1978) .

4. J.P. Bombled : Influence of sulphates on the rheological behaviour of cement pastes and their evolution. Proc. of 7th International Congress on the Chemistry of Cements, vol. III , Paris, Editions Septima, VI 164-169 (1980)

5. M. Ish-Shalom, S.A. Greenberg : The Rheology of Fresh Portland Cement Pastes. Proc, 4th International Symposium on the Chemistry of Cements. Washington, vol. II, 731-748 (1960) .

6. Hiroshi Uchikawa, Kenji Ogawa, Shunichiro Uchida : Influence of Character of Clinker on the Early Hydration Process and Rheological Property of Cement Paste. Cem. Concr. Res., vol. 15, No 4, 561-572 (1985) .

7. G.Y. Shin, F.P. Glasser : Chemistry of Cement. Pore Fluids. I . Suspension Reactions of $Ca_{3-x}Na_{2x}Al_2O_6$ Solid Solutions with and without Gypsum Additions. Cem. Concr. Res., vol. 13, No 3, 366-376 (1983) .

8. I. Odler, R. Wonnemann : Effect of Alkalies on Portland Cement Hydration. II. Alkalies Present in from of Sulphates. Cem. Concr. Res., vol. 13, No 6, 771-777 (1983) .

J. MIERZWA, Technical University of Cracow, Poland

Thixotropic - plastic - viscous rheological model of cement paste as the result of physical and mineralogical cement properties

1. INTRODUCTION

Development of industrial production and processing of concrete particularly intensive in the last period of twenty years sests larger and larger demands for scientific technology of concrete. One of these demands is a necessity of precise description of behaviour of fresh concrete during mixing, transportation and forming. That behaviour is a result of components properties as well as of kinematic-dynamic parameters of interactions of a certaing process of treatment.
To solve the problem the rheological methods obtained from the mechanics of continuous mediums have been applied.
Unfortunatelly, as the investigations which have been carried on till now have proved, fresh concrete have turned out to be anextremely complex real rheological body.

One of the ways which may lead to a solution is an attempt to describe rheological properties of cement paste which is a basic component of concrete. A wide interest connected with the rheological issue of concrete in the world is confirmed by large amount of publications. Their number, beginning from the first of Powers Wiler /in 1941/ includes now about 350 to 400 of items. More then half of them are works dedicated to the rheology of cement paste. On the one hand it ocknowleges the range of difficulties to encounter, on the other the essential significance of this issue for rheology of fresh concrete.

2. THE CURRENT STATE OF RESEARCH

The research works on rheology of cement pastes which have been carried on hitherto have proved the great complexity of the issue. Recapitulations of these works made in papers [1, 2, 3] have shown that the issue of cement paste rheology focuses on three topics:
a/ the influence of methodology of testing, measuring apparatus and physical state of sample in time of testing on the result of the test,
b/ the influence of physical, chemical and mineralogical characteristic of cement and solids concentration of paste on rheological characteristics,
c/ the influence of additions and admixtures on rheological characteristic of cement paste.

Publicated results of investigation diversify very seriously and thus their synthesis is practically impossible. This fact is caused by a paste characteristic. A fresh paste as an unstable body is continuously changing in time. So every act of shearing which has the aim of establishing τ-$\dot{\gamma}$ in relation to variable time "t" must destroy the current state of the structure. Therefore every established rheological value is a result of "history" of sample shearing in previous period. The method applied for testing and the way of initial preparation of sample influences therefore essentially the result of test. For instance, as the examinations have confirmed, a certain program of $\dot{\gamma}$-t in a sample enables to obtain a respectively optional shape, thereby, rheological nature of flow curve [4, 5].

On the present stage of development of research of cement paste and concrete rheology and of possibilities of practical applications one can assume that there is a vital need to create the system of comparable tests results of different research-centres all over the world [3]. So there is a need of standardization of rheological methodology of cement paste. It certainly doesn't exclude the possibility of carrying on other optional research programs according to certain needs.
At the Technical University in Cracov a wide program has been taken up on that issue at the beginning of this decade and the results obtained are going to be put forward in the following part of the paper.

3. "STANDARD" METHODOLOGY OF MEASUREMENT OF RHEOLOGICAL CEMENT PASTES PROPERTIES

Calculation of flow-curve /rheogram/ of rheostablie bodies resowes itself into determining their dependency in the system of variables τ-$\dot{\gamma}$/shear stress-shear rate/. In tests of cement paste which is treated as a rheologically unstable medium the test t is unsatisfactory because there is necessery to identify the function in relation to variable of time. There are two methods being put to this end: hysteresis loop method and the "equilibrium" curve method, suggested originaly by J.Pawlowski [6].

Keeping up the criticall opinion of D.C. Cheng, F.Evans and P.S.Worralland S.Tulliani on the hysteresis concept particularly in the light of tests results [4, 5], as the most adequate for rheological identification of paste the equilibrium curve method has been accepted. The method assumes realization of shear test with constant shear rate $\dot{\gamma}_i$ = constans, calculating values τ, as τ_{max} and τ_m as a minimal shear stress carried over by the struoture.

A set of curves calculated on the same sample paste enables to calculate the general dependence τ-$\dot{\gamma}$-t. It has been found that the most advisable time for calculating τ-t

with $\dot{\gamma}_i$ = const. Ranges from 10 to 10^2 min. which is the period of reaction induction in portlnad cements after the water is added 7. Taking into account a particular significance of initial preparation of a sample the standardized program of mixing with the use of lab mixer /ISO/ has been applied the program consists of: t_1 = 60 s mixing with n_1 = = 140 rpm + t_2 = 30 s with n_2 = 285 rpm + 90 s pause + t_3 = 60 s with n_3 = 285+600 s pause + + t_4 = 15 s with n_4 = 140 + t_5 = 15s with n_5 = = 285 rpm /total 15 min./.
During the next 45-55 min a series of curves τ-t was performed with denotation τ_1/τ_{max} and τ_m/τ_{min} with different $\dot{\gamma}_i$ = const each. Tests have proved that for applied "standard" program of measurements the results dispersion does not exceed 12% when upper limit of time of testing does not exceed 0,65 of time of the initial setting period /Vicat/.

On the basis of testing over 680 curves τ-t which were obtained from testing of 20 different cements it may bestated that to establish a precise dependence τ-$\dot{\gamma}$-t it is enough to take 6 levels of constant shear rate $\dot{\gamma}_i$ from intervals $\dot{\gamma}_1$ = 0,5÷3 s^{-1}, $\dot{\gamma}_2$=6÷10 s^{-1}, $\dot{\gamma}_3$=25÷30s^{-1}, $\dot{\gamma}_4$=70÷80s^{-1}, $\dot{\gamma}_5$=140÷160s^{-1}, $\dot{\gamma}_6$=400÷500s^{-1}.

The location of minimum of τ-t function on the time axis at the point t_m corresponding τ_{min} depends on concentration of paste solid phase c_v /and also w/c / and shear rate $\dot{\gamma}_i$. In lesser degree it depends on the surface area of cement and its mineralogical characteristic. For pastes with w/c= 0,37-0,75 values of t_m were on an average 6-8 min.
In Fig. 1 the exemplary series of curves τ-t for pastes with different w/c ratio and different shear rate $\dot{\gamma}_i$ = const. is shown.
The complex problem of establishing of the real value $\dot{\gamma}_i$ caused by heterogeneousnes of shear in the clearance of a viscometer /Bingham's flow/, according to the error analysis results /by Maron Krieger/ can be ignored /allowing an error up to 10%/ if the apparatus fulfius the condition $s = R_z/R_w < 1{,}05$ and the clearance $\Delta R = R_z - R_w > 1$ mm /for paste/.

4. EXPERIMENTS

Program of experiments included 20 clear - clinker cements with five different mineralogical compositions and appropriate amounts of gypsum /shown in Tab. 1/.

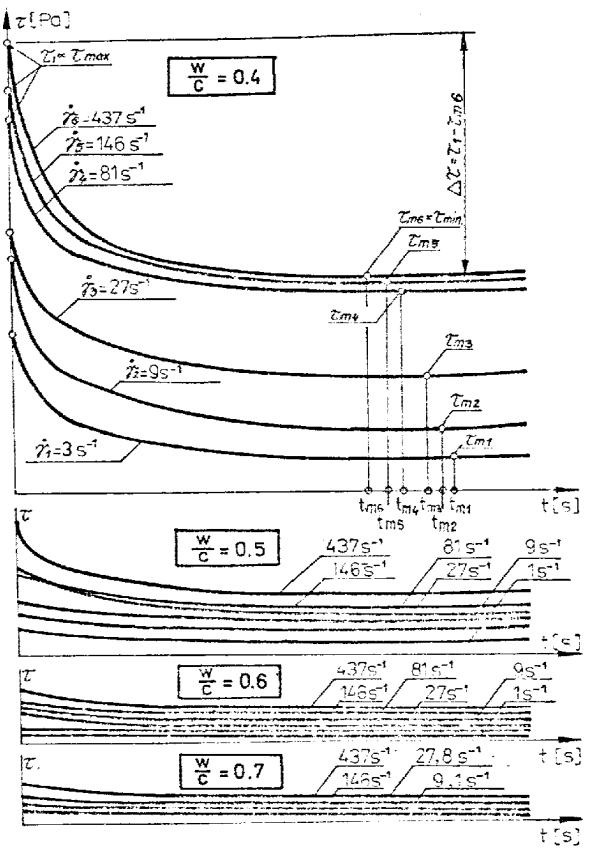

Fig.1. Series of "equilibrium" corves τ-t of flow for pastes with different w/c and constat shear ratio.

Table 1.

Cement series	Proportional amounts of certain mineralogical components Amount /%/				Gypsum %
	C_3S	C_2S	C_3A	C_4AF	
"G"	58	21	6	10	5,3
"P"	66	14	8	8	6,4
"C"	51	25	10	7	6,4
"Oz"	42	33	10	8	4,2
"Od"	50	20	16	9	6,0

Each of the cements with the same mineralogical composition was powdered up to four different levels of surface areas F_B = 300, 350, 400 and 450 m^2/kg. Every cement was used, according to "standard" program, to form cement pastes with w/c ratio = 0,4 0,5 0,6 and 0,7. Experiments were made on Rheotest RV2 type rotating coaxial cylinder with serrated surfaces /ΔR= 0,97 mm/. The full cycle of test included calculation of curves series

τ-t for each w/c and measurement of each following curve $\dot{\gamma}_i$= const was preceded by repeated mixing for 10 s with n = 140 min^{-1}.

5. THE GENERAL RHEOLOGICAL MODEL OF CEMENT PASTE

Realization of such a vast program of investigations has given a basis to take up an attempt to establish the general rheological model of cement paste within the range of variation of its w/c ratio 0,4<w/c<0,70, that is the most interestig from the technological point of view. Lack of rheostability of cement paste and manifested by it the thixotropical efect of flowing with simultaneous separated thixotropy from the efect of plastic-viscous flow /according to def. of Trapeznikow [8]/ imposes the necessity of approximation of rheological paste model in the three variables system $\tau-\dot{\gamma}-t$. The analysis of test results has demonstrated that as the most typical function in graphic formulation the plane layer for the exponential type function should be taken on /Fig. 2/.

of paste, connecting in its first part in form:

$$\tau_{HB} = \tau_o + \eta_{pn} \cdot \dot{\gamma}^n \qquad /2/$$

the Herschel-Bulkley's model with functional coefficient of thixotropy:

$$\theta = t^A \cdot e^{B(t-1)} \qquad /3/$$

It is the five-parameter model where τ-shear stress [Pa], τ_o- liquid limit [Pa], η_{pn}- nonlinear plastic viscosity [Pa·s^n], n - coefficient of flow speed [-], $\dot{\gamma}$- shear rate [s^{-n}], t - value corresponding to shear time [-], A B - coefficients qualifying thixotropic predispositions of paste [-]. Qualification of the rheological parameters of the model is done by graduate analysis, where stationary state gained by paste in the proces of constant mixing with speed $\dot{\gamma}_i$= const. after time t= t_m is a starting point. For this moment coefficient of thixotropy θ= 1,0 and shear stress achieves its minimum /$\tau = \tau_m$/ for the structure is totally destroyed. Correlation analysis of rheological parameters of the equation /1/ resolves itself into analy-

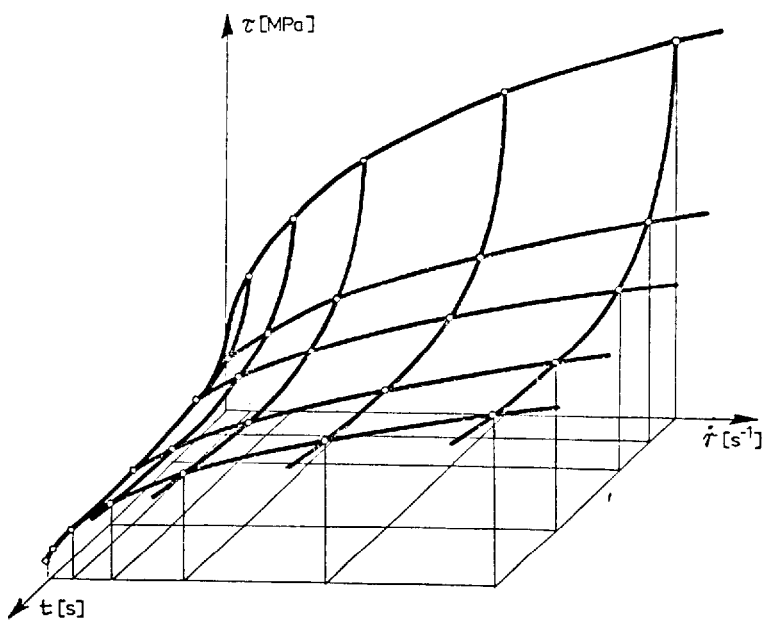

Fig. 2. Graphical image of function $\tau-\dot{\gamma}-t$ which models rheological properties of cement pastes according to equation /1/.

In a satisfactory precise manner it is described by the equation:

$$\tau = (\tau_o + \eta_{pn} \cdot \dot{\gamma}^n) \cdot t^A \cdot e^{B(t-1)} \qquad /1/$$

The structure of the equation /1/ underlines both the plastic-viscuous properties /Bingham's nonlinear/ and thixotropic properties

sis of equation /2/ or directly into linearized for technical application of Bingham's equation with parameters τ_o, η_p. They can be calculated either in three-parameter step-correlation assuming as an optimum the coefficient of the accuracy of correlation r or by the simple two-parameter method of least squares. Coefficients A, B of the functional

factor of thixotropy can be obtained by the method of succesive approximations on the ground of analysis of curves τ-t where value $t = t_m$ is known from experiments and extremum of the function ϑ is placed at the point:

$$\frac{d\vartheta}{dt} = 0 \longrightarrow t_m = -\frac{A}{B}$$

6. SOME PRACTICAL ASPECTS OF INFLUENCE OF PHYSICAL AND MINERALOGICAL CHARACTERISTICS ON THE RHEOLOGICAL PROPERTIES OF CEMENT PASTE

It is impossible to present fully the influence of mineralogical composition, surface area, grain composition of cement and additions on rheological parameters of pastes so interesting from the scientific point of view in the paper. The results of investigations on cement paste rheology has proved to be very useful in selcting composition od pastes for injections. When for certain technical mixing conditions of pastes for injections the thixotropical coefficient is calculated, the basic parameters of linearized /for technical applications/ of rheological equation /2/ is the liquid limit τ_o and viscous plasticity η_p. Experiments also shown that they are connected both with a cement surface area F_B and its mineralogical composition expressed by the coefficient M_α in the following equations:

$$\tau_o = (16.5 - 2M_\alpha) \cdot c_v^{(8+0.5 F_B^2 \cdot 10^5)} \cdot 10^4 \ [Pa] \qquad /4/$$

$$\eta_p = 3.3 \cdot c_v^{(17+0.27 M_\alpha) F_B^{-0.125}} \cdot 10^2 \ [Pa \cdot s] \qquad /5/$$

As an enough precise and useful measure of mineralogical predispositions of cement the factor resulting from a proportional composition of clinker can be assumed:

$$M_\alpha = \frac{C_3S + C_2S}{C_3A + C_4AF} \qquad /6/$$

Its value in ordinary portland cements oscillates in the range from 2,8 to about 5,6 and shows inconsiderable fluktuations in the years production of a certain cement plant and is in a way its characteristic value. The index of volume concentration of solids c_v is connected with the coefficient w/c or paste by the dependence:

$$c_v = \frac{1}{1 + \frac{w}{c} \cdot \varrho_c} \qquad /7/$$

where ϱ_c denotes specific density of cement.

Equations /4/ and /5/ similarly like the respective dependences of J.P.Bombled [1], G. Wischers, K.Rendchen [9], W. von Berg [10], H.P.Backes, W. von Berg [11] has confirmed also as a significant the influence of mineralogical composition and surface area of cement on paste rheology. Qualification of these dependencies and adequate equation of sedimentation makes easier the selection of composition of injecting pastes. As it results from Fig. 3 the influence of a quality of cement when its clinker mineralogical composition is taken into account /if the value of additions does not exceed 10-15%/ can play a significant role in optimal shaping of the parameters for injection in cable-canals of prestressed constructions.

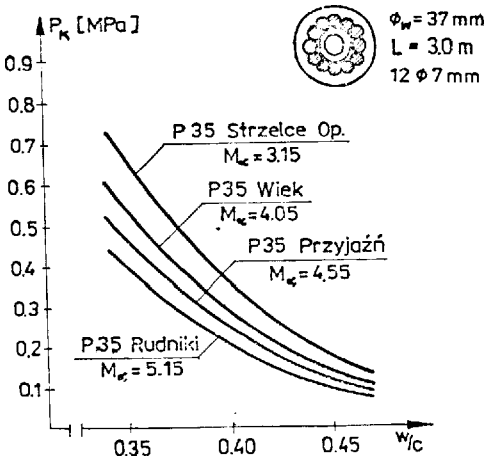

Fig. 3. Influence of mineralogical composition of cements from different cement plants /Rudniki, Przyjaźń, Wiek, Strzelce Opolskie/ on the parameters of the process of paste injection in cable-canals $\varnothing$ = 37 mm filling 12$\varnothing$7 mm, lenght 30 m [12].

7. CONCLUSION

In the paper an attempt of describing of the cynthetic rheological model of cement paste has been taken up. The research program was preceded by the selection of standardized methodology, apparatus and conditions of initial preparation of paste. Results of tests have demonstrated that in relation to properties in flow stage cement paste reveals characteristic of a thixotropic, nonlinear, plastic-viscouse body which is precisely qualified by five rheological parameters such as: τ_o, η_{pn}, n, A, B.
For technical applications this model /1/ can take on a simplified, linearized form. Values of rheological parameters in this model are under the influence of solids concen-

tration, of paste and mineralogical composition of cement with its surface area.

REFERENCES

[1] J.P.Bombled - RILEM Sem. Leeds 1973.

[2] G.H.Tattersall - The workability of concrete. Cem. Con. Assoc. 1976.

[3] R.A.Helmuth - 7-th Congr. Chem. Cem. Paris 1980. S.-T. VI-0.

[4] D.M.Roy, K.Asaga - Cem. Con. Res.9/1979.

[5] P.F.G.Banfil, D.C.Saunders - Cem. Con. Res. 11/1981.

[6] J.Pawlowski - Chem. Ing. Techn. 28/791/ 1956.

[7] R.Kondo, M.Daimon - 6-th Congr. Chem. Cem. Moscow 1976, V. II. B 1.

[8] A.A.Trapeznikow - VII-th Int. Congr. Rheology, Getheborg. 23-27.VIII.1976.

[9] G.Wischers, K.Rendchen - RILEM Semin. Leeds 1973.

[10] W. von Berg - Mag. Con. Res. Vol 31, Nr 109 Dec. 1979.

[11] H.P.Beckes, W. von Berg - IX Int. Congr. Rheology, Mexico 1984.

[12] J.Mierzwa - XXXI Konf. Nauk. KILiW PAN KN PZITB Krynica 1985.

[13] J.Mierzwa - II Konf. Nauk.-Techn. "Proj. i Realizacja Zbiorników", Kraków 1985.

S. Sprung - Research Institute of the German Cement Industry, Dusseldorf, West Germany

Influence of the composition of clinker and cement on the rheological behaviour of fresh concrete

1. Introduction

Ready-mixed concrete should in general remain workable for a longer time than concrete made on the construction site. The consistency of the fresh concrete and its change with time will, for given mix composition, grading curve and type of aggregate, depend to a great extent on the chemical and physical properties of the cement paste. Raised temperature of the fresh concrete accelerates hydration and hastens early stiffening in many cases. The evaporation of mix water, the increase in water demand due to absorption by the aggregate, the presence of fine particles due to aggregate abrasion or fine-grained additives, and the inexpert use of admixtures above all have an effect on the consistency of fresh concrete (1, 2, 3).

Hydration of the cement begins immediately after the mix water has been added. At first, tricalcium aluminate (C_3A) and readily water-soluble calcium sulphates are virtually the only substances that participate in the hydration reactions (4). The initial hydration reactions take place at the surfaces of the cement particles. At this stage their extent depends chiefly on the reactivity and the amount of the C_3A in the clinker, on the surface area and particle size distribution of the cement and on the temperature of the cement paste. Other cement clinker phases participate only to a minor degree in the initial hydration reactions. The first stage of hydration ends after a few minutes. Then follows the dormant period, lasting 2 - 6 hours. The resumption of hydration at the end of the dormant period results in hardening of the cement.

The extent of hydration up to the beginning of the dormant period as well as the amount and morphology of the hydration products which are formed up to that point of time determine the water demand for adjusting the initial consistency of the cement paste. During the dormant period the paste undergoes further stiffening. When the consistency has attained a certain condition, the cement begins to set, according to the standard definition. After the end of setting, the hardening phase of the cement paste commences (1).

Research in recent years has shown that the consistency of the fresh concrete changes in a manner similar to that of the cement paste (5, 6). In the first minutes after the mixing of the concrete its workability, measured for example in terms of spread in the DIN 1048 flow table test, decreases. The decline in workability depends largely on the amount and on the morphology of the hydration products formed in the cement paste. During the dormant period the consistency of the fresh concrete undergoes only little change if optimized cement is used for making the concrete and if the optimization of the cement achieved in the grinding process in the cement plant is not subsequently nullified by additives, admixtures and the working procedures applied in making the concrete. The relatively stable level of consistency is established after at most 10 minutes and has therefore proved useful in practice for characterizing the initial consistency of fresh concrete (a_{10}).

The consistency of cement paste and of fresh concrete depends on the water film thickness on the surface of the cement particles and on the thickness of the cement paste coating on the surface of the aggregate particles. Model calculations, which were confirmed by investigations on concretes as commonly used in practice, have revealed this (6). The thickness of the water film that forms on the individual cement particles depends at given surface area and voids between the particles primarily on the water/cement ratio. For constant water cement ratio the rheological effectiveness is influenced more particularly by the amount and morphology of the hydrate phases formed. Accordingly, the water film thickness is the governing factor for the initial consistency and for the change that the consistency of the cement paste undergoes with the passage of time. The importance of the composition, surface area and particle size distribution of the cement for the progressive change in the consistency of cement paste will be summarizingly discussed, on the basis of a large number of research results, in the following sections.

Similar relationships apply to the consistency of fresh concrete. For constant cement content, a stiffer consistency develops as time passes, but especially with decreasing water/cement ratio or if the cement has a marked tendency to early stiffening.

The consistency of fresh concrete depends furthermore also on the thickness of the cement paste coating on the aggregate particles. With diminishing thickness of the water film and correspondingly stiffer initial consistency of the cement paste, the desired consistency of the fresh concrete can be obtained by increasing the cement content and thus the amount of paste while leaving the water/cement ratio unchanged (6). That is the reason why the result of the consistency mearsurement performed on cement paste is not directly applicable to fresh concrete, despite similarity of behaviour in principle.

2. Composition

2.1 Clinker

The properties of cement clinker are to a great extent influenced by the composition of the raw mix and of the fuels, as well as by the burning and cooling conditions. Important with regard to the processes associated with early stiffening and with setting is the proportion of C_3A that undergoes hydration in the first minutes after the addition of the mix water and up to the beginning of the dormant period. It is referred to as C_3A conversion (ΔC_3A). Inves-

tigations have shown that the C_3A conversion of industrial cement clinkers of normal composition can amount to about 0.4 - 2.0 wt.-%. As a rule, the C_3A conversion is greater according as the clinker contains more C_3A and as more alkalies are combined in the clinker (7).

To diminish the influence of the C_3A conversion on stiffening and setting the C_3A content of the clinker can be reduced to a limited extent by a lowering of the alumina/iron ratio. The heightened reactivity of C_3A due to incorporation of alkalies can moreover be reduced. To achieve this, the alkalies must be bound in the form of alkali sulphate (sulphatization), e.g., as a result of the controlled use of inexpensive sulphur-rich fuels. With a fairly high total alkali content a degree of sulphatization of 40 - 70 %, and with a fairly low total alkali content a degree of sulphatization of up to 90 %, has been found to be advantageous for reasons of plant operation, emission and product quality (8, 9).

Besides the composition of the process materials, the kiln atmosphere and the rate of cooling of the clinker have a major effect on the C_3A content and on the reaction capability of the C_3A. The C_3A content and reactivity increase if the clinker is burned under reducing conditions and is cooled slowly from the clinkering temperature to around 1 300 °C (7). An increase in the C_3A content is also to be expected if, as a result of using coal with a very high ash content and of slow cooling of the clinker in the high-temperature zone of the kiln, the proportion of clinker melt is increased and its composition changed (9).

2.2 Cement

The C_3A content and the reaction capability of the C_3A determine the reactivity of the clinker. It can be gauged and monitored by measurement of the C_3A conversion. Closer monitoring in the context of industrial quality control would appear to be particularly appropriate if, during the manufacturing process, the clinker properties vary in consequence of using raw materials and fuels of varying composition, or because of irregular kiln operation or because the cooling rate is not properly adjusted to the composition of the kiln feed. In the cement grinding process the variations in the properties of the clinker can be taken into account by optimum adjustment of the added calcium sulfates to the C_3A conversion at any given time, in order to produce cement with uniform workability and strength development. In this connection the surface area and particle size distribution of the cement must moreover be taken into consideration.

An optimum dosage of calciumsulfates is achieved if the cement contains just so much readily water-soluble sulphate in the form of hemihydrate ($CaSO_4 \cdot 1/2H_2O$) or anhydrite III ($CaSO_4$ III) that the C_3A which undergoes hydration in the first few minutes can react with this sulphate to form fine-grained ettringite. The ettringite is deposited on the surfaces of the cement particles, as a result of which a structure is formed in which the hydration products do not yet bridge the water film between the cement particles. Fig. 1 is a scanning electron micrograph showing the stucture formed in the cement paste after 5 minutes hydration time.

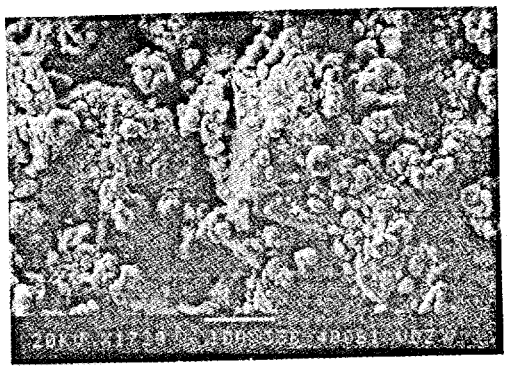

Fig. 1: Scanning electron micrograph of cement paste after 5 minutes hydration (W/C ∿ 0,4).

The nature and quantity as well as the crystal shape and size of hydrate phases formed in the first minutes affect the consistency of the cement paste and the water demand. The relationships are represented schematically in Fig. 2, based on a model conceived by J. Krell (6). The left-hand diagram relates to cement paste made from an optimized, the right-hand diagram to paste made from a non-optimized portland cement. In both examples the paste is of standard consistency. The cements have been made from the same clinker, have equal surface area and particle size distribution and therefore equal C_3A conversion.

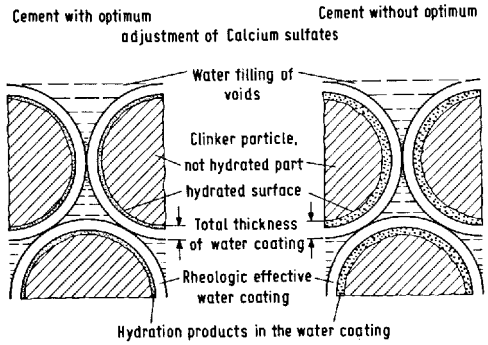

Fig. 2: Influence of optimization of the added calcium sulfates upon the water demand for obtaining the standard consistency.

Besides the proportion of the mix water which is chemically bound in the hydrate phases, the water serves primarily to fill the voids between the clinker particles and to form a water film on the surfaces of the incipiently hydrated clinker particles. The volume of these voids depends on the particle size distribution. The quantitative division of the mix water between what is needed for chemical binding in the hydration products and what is needed for rheological reasons is shown in Fig. 4 in Section 3. As model calculations indicate, the overall thickness of the water film on the surfaces of the clinker particles in a paste of standard consistency is of the order of less than 0.5 micron (6). The hydrate phases formed during the initial hydration grow more or less far into the enveloping water film. The remaining rheologically effective part of the film enables the clinker particles to slide along one another and is therefore of governing importance with regard to the consistency of the cement paste. For a particular thickness of the water film the paste possesses standard consistency.

With optimized cement the fine-grained ettringite which is formed as a result of the C_3A conversion is deposited on the surfaces of clinker particles and only slightly reduces the thickness of the water film (finely dotted area in left-hand diagram). If the water/cement ratio is not changed and there is a little C_3A conversion, only little stiffening of the cement paste occurs. With more C_3A conversion and correspondingly lager amounts of ettringite a stiffer consistency develops. In order to obtain a more plastic consistency, the amount of mix water and thus the effective water film thickness must be appropriately increased.

The recrystallization of the ettringite which begins during the dormant period will normally cause a slow stiffening of the cement paste. But if, with higher alkali content in the solution, the ettringite recrystallizes more rapidly and the lager crystals grow farther into the water film, this brings about early and rapid stiffening or manifests itself in an appreciably higher water demand for obtaining the standard consistency (8, 11,12).

If there is a deficiency of sulphate in the solution, coarsely tabular monosulphate is in part formed instead of ettringite. If there is an excess of sulphate, secondary gypsum and also syngenite are formed. Within a few minutes these hydrate phases build up a rigid interlocking structure of relatively large crystals which protrude far into the enveloping water film and which restrict the free mobility of the clinker particles (coarsely dotted area in right-hand diagram). In consequence of this the cement paste quickly stiffens if the water/cement ratio is left unchanged. To obtain the standard consistency, the rheologically effective water film thickness must therefore be increased to the requisite thickness for this purpose by the addition of substantially more mix water. The effect that deficient optimization of the calcium sulfates in the cement has upon the water demand is apparent from the experimental results represented in Fig. 3 (Section 3).

3. Surface area and particle size distribution

Besides the composition, the surface area and particle size distribution of the cement are particularly important with regard to the water demand and to the stiffening and the setting of cement paste (13, 14, 15). In Fig. 3 these relationships are represented for two cements which were ground from the same industrial clinker to mass related surface areas of 3 570 cm^2/g and 5 465 cm^2/g (Blaine) respectively. For equal slope n of the RRSB particle size distribution the two cements moreover differ in their position parameter x' (14, 15). In the lower diagram the C_3A conversion, and in the upper diagram the water demand of the cements measured in accordance with DIN 1164, are represented as functions of the proportion of the added calcium sulfates anhydrite II ($CaSO_4$ II) and hemihydrate ($CaSO_4 \cdot 1/2H_2O$). The total sulphate content is approximately 3.2 wt.-% of SO_3.

From the diagrams it appears, first, that the more coarsely ground cement displays less C_3A conversion (about 1.1 wt.-%) than the more finely ground cement does (1.6 wt.-%). The C_3A conversion is independent of the mix proportions of the calcium sulphates.

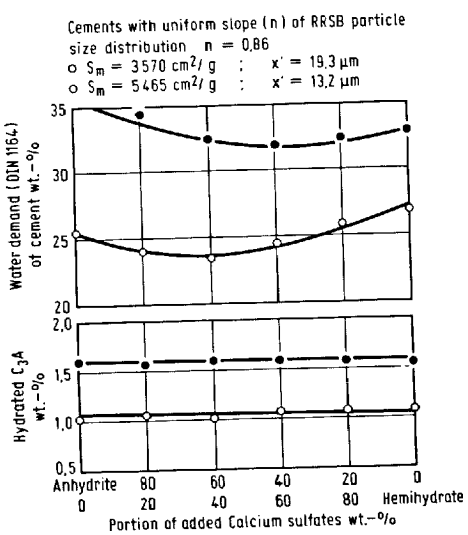

Fig. 3: C_3A conversion and water demand (Din 1164) of portland cements with different surface areas, as functions of the composition of the added calcium sulfates.

If the mixture of these substances is optimally adjusted to the C_3A conversion, a min-

imum water demand for obtaining the standard consistency is achieved for both cements. For this, however, the finer cement with the higher C_3A conversion requires a higher proportion of hemihydrate (about 80 %) than the coarser cement does (about 30 %). Besides, the water demand for standard consistency in conjunction with optimum dosage of calcium sulphates increases from about 23 wt.-% for the coarser to about 32 wt.-% for the finer cement. Investigations have shown that the surface area and the particle size distribution parameters affect the cement paste consistency more strongly according as the clinker contains more C_3A and/or the reaction capability of the C_3A is greater.

One of the causes of the higher water demand of the finer cement therefore is the greater amount of ettringite which, with optimum dosage of calcium sulphates, is formed as a result of the higher proportion of C_3A conversion that occurs (see also Section 2). In general, the water demand increases distinctly for non-optimized as compared with optimized cements. This is due to the fact that, for equal C_3A conversion, the water demand over and above the chemically combined portion depends very considerably on the morphological condition of the hydrate phases. The amount of water needed for wetting and for filling the voids between ettringite and monosulphate or ettringite and secondary gypsum is withdrawn from the rheologically effective water film and must therefore be replaced in order to give the cement paste the standard consistency.

As compared with the clinker and cement composition as factors affecting the water demand, however, the surface area as well as the position parameter x' and the slope n of the particle size distribution have the greater influence on the water demand of the cement (15). This emerged from investigations on cements which had been produced from one and the same industrially manufactured clinker. The nature and quantity of the added calcium sulfates were optimally adjusted to the different amounts of C_3A conversion associated with these cements. These relationships are shown schematically in Fig. 4 for cements with different values of the position parameter x' and constant slope n in the RRSB granulometric diagram.

It appears from this diagram that the water demand for obtaining the standard consistency increases with increasing proportion of fine particles or with decreasing value of the position parameter x'. The water demand is composed of three portions. The portion combined chemically in the hydrate phases before the beginning of the dormant period is the smallest (represented by the hatched area). In general, it increases with higher C_3A content of the clinker, higher reaction capability of the C_3A and, as shown in this diagram, with higher content of fine particles in the cement. This is also the case if the cement, for constant surface area, has a higher value of the slope of the particle

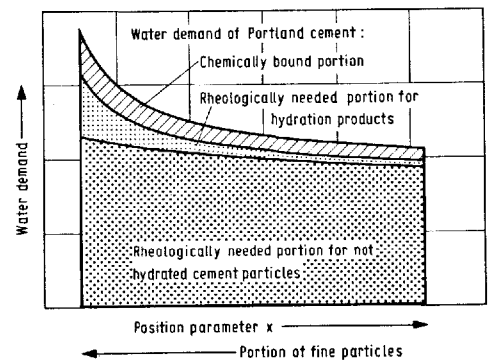

Fig. 4: Influence of the particle size distribution on the binding of water in portland cement at standard consistency.

size distribution. In all, however, at most only about 10 % of the total mix water amount is needed for chemical combining in the hydrate phases. This proportion decreases in the case of cements which contain dense and non-absorbent interground additions such as, for example, blastfurnace slag or limestone. These additions do not participate in the hydration reactions that occur before the dormant period begins. They behave like inert substances by which the clinker component of the cement is diluted. The C_3A conversion decreases roughly in proportion to the amount of interground additions contained in the cement (16).

The largest portion of the mix water (indicated by the dotted area) is necessary for rheological reasons to obtain the standard consistency. A smaller part of this water (finely dotted) serves to wet the hydration products and fill the voids between the hydrate phases. This portion increases more than proportionally according as more hydrate phases with increasingly high content of fine particles are formed in the cement. In the case of optimized cements this portion displays a minimum, as the research results represented in Fig. 3 show.

The major part of the water (coarsely dotted) serves to fill the voids between the clinker particles - just as it would with any inert finely divided material of equal surface area and particle size distribution - and to form the rheologically effective water film. In this case it corresponds roughly to a water cement ratio of 0.2. The rheologically necessary portion of the water demand increases drastically if the cement, for equal content of fine particles, has a steeper particle size distribution so that the volume of the voids between the clinker particles becomes larger.

When cements are interground with additions, the more easily grindable materials such as limestone or pozzolana may enrich in higher concentrations in the fine particle size

fraction. They are thus able to reduce the larger volume of voids of a clinker if the later has been ground in such a way as to have a steep particle size distribution. Because of this voids volume reduction and the dilution of the clinker component of the cement, the water demand for obtaining the standard consistency of the cement alltogether is reduced. On the other hand, if the volumetric proportion of the fine fraction derived from a more easily grindable addition because of overgrinding substantially exceeds the existing voids volume of the clinker, or if, in the event of poorer grindability, it has a very narrow particle size distribution so that the voids volume of the pulverized product as a whole is increased, the water demand becomes greater with increasing proportion of interground additions. It also becomes greater if the additive has a high inherent porosity of its own (16).

References

1. Wischers, G.: Ansteifen und Erstarren von Zement und Beton. Betontechn. Berichte 1980/81, pp. 145-167, Beton-Verlag GmbH, Düsseldorf, 1982.

2. Richartz, W.: Einfluß von Zusätzen auf das Erstarrungsverhalten von Zement. Betontechn. Berichte 1982/83, pp. 169-198, Beton-Verlag GmbH, Düsseldorf, 1984.

3. Krell, J.: Einfluß chemisch-mineralogischer Reaktionen des Zements auf das Ansteifen von Zementleim und Beton. beton 35 (1985), No. 12, pp. 465-472.

4. Locher, F.W., Richartz, W. und S. Sprung: Erstarren von Zement, Teil 1: Reaktion und Gefügebildung. Zement-Kalk-Gips 29 (1976), No. 10, pp. 435-442.

5. Rendchen, K.: Einfluß der Granulometrie von Zement auf die Eigenschaften des Frischbetons und auf das Festigkeits- und Verformungsverhalten des Festbetons. Schriftenreihe der Zementindustrie, No. 45, Beton-Verlag GmbH, Düsseldorf, 1985.

6. Krell, J.: Die Konsistenz von Zementleim, Mörtel und Beton und ihre zeitliche Veränderung. Schriftenreihe der Zementindustrie, No. 46, Beton-Verlag GmbH, Düsseldorf, 1985.

7. Locher, F.W., Richartz, W., Sprung, S. und H.-M. Sylla: Erstarren von Zement, Teil 3: Einfluß der Klinkerherstellung. Zement-Kalk-Gips 35 (1982), No. 12, pp. 669-676.

8. Locher, F.W., Richartz, W., Sprung, S. und W. Rechenberg: Erstarren von Zement, Teil 4: Einfluß der Lösungszusammensetzung. Zement-Kalk-Gips 36 (1983), No. 4, pp. 224-231.

9. Sprung, S.: Emissionsprognosen beim Einsatz von Abfallbrennstoffen. Zement-Kalk-Gips 37 (1984), No. 10, pp. 519-522.

10. Sprung, S.: Einflüsse der Verfahrenstechnik auf die Zementeigenschaften. Zement-Kalk-Gips 38 (1985), No. 10, pp. 577-585.

11. Mehta, P.K.: Effect of lime on hydration of pastes containing gypsum and calcium aluminates or calcium sulfoaluminates. J. Amer. Ceram. Soc. 56 (1973), No. 6, pp. 315-319.

12. Mehta, P.K.: Scanning electron micrographic studies of ettringite formation. Cem. Concr. Res. 6 (1976), No. 2, pp. 169-182.

13. Meric, J.P.: Influence of grinding and storage of clinker. Principal Report Sub-Theme I-4, 7. Intern. Congr. Chem. Cem., Paris, 1980, pp. I-4/1-4/16.

14. Kuhlmann, K., Ellerbrock, H.-G. und S. Sprung: Korngrößenverteilung und Eigenschaften von Zement, Teil 1: Festigkeit von Portlandzement. Zement-Kalk-Gips 38 (1985), No. 4, pp. 169-178.

15. Sprung, S., Kuhlmann, K. und H.-G. Ellerbrock: Korngrößenverteilung und Eigenschaften von Zement, Teil 2: Wasseranspruch von Portlandzement. Zement-Kalk-Gips 38 (1985), No. 9, pp. 528-534.

16. Ellerbrock, H.-G., Sprung, S. und K. Kuhlmann: Einfluß von Zumahlstoffen auf die Eigenschaften von Zement. Zement-Kalk-Gips 38 (1985), No. 10, pp. 586-588.

H.-J. Wierig - University of Hanover, West Germany

INFLUENCES OF CEMENT AND TEMPERATURE ON THE CONSISTENCY OF FRESH CONCRETE

As a result of the impetuous development of the ready mixed concrete industry in the past years, questions of fresh concrete technology have become increasingly important /1/. If we intend to keep a tight control on ready mixed concrete production, we need a qualitative and quantitative comprehension of the main factors effecting the quality of fresh concrete, especially the initial consistency and the temporal changes in consistency. This includes knowledge of the amount of water required by each single compound of the mix. To date considerations were often concentrated on the amount of water required by the aggregates, and the influence of cement and other compounds were in general neglected. Various research programmes, carried out at the Institut für Baustoffkunde und Materialprüfung der Universität Hannover were aimed at examining possiblities of grasping the influence of cement on the consistency of fresh concrete and stiffening under various temperatures.

Concretes with three different mixes, containing 16 various cements in normal commercial use, were tested at 3 temperatures. The concretes varied in their water/cement ratios (w/c = 0,75, 0,63 and 0,57) and in the grading of their aggregates. The cements were chosen along the lines of various sorts of cement, various compressive strengths and chemical composition. Detailed results of the examination will be published soon /2/. Fig. 1 shows an example to illustrate how the initial spreads according to the German flow table test of one of the concretes tested is set against temperature of fresh concrete. Each point stands for one concrete mix containing one cement. Fig. 2 shows the changes in consistency of the same concrete mixes in the first 45 minutes after production. Taking into consideration the varying scales of the ordinate the two figures show that the influence of the cement on the initial spread is, with its range of roughly 16 cm much stronger than on the changing spread with its range of only about 5 cm.

In order to grasp the influence of cement on consistency by material characteristics, various evaluation methods were employed. We came to the conclusion that it is not possible to describe this influence by way of one single characteristic, be it the amount of water required for standard consistency (Wa) according to DIN 1164, the specific surface (O), or the spread (a) of the standard mortar. But if we combine several of these cement properties to form one new characteristic, then relatively good relationships between the cement characteristic and the concrete spread values can be found, as seen in fig. 3. When evaluating the results shown in fig. 3 we have to consider that the deviation on repeating a flow table test is about ± 2 cm /3/.

The influence of temperature on spread becomes clear if we join the points of a concrete and its particular cement. For the sake of better understanding this is illustrated in fig. 4 with an example of 4 chosen concretes. In contrast to information such as in /4/ we found that fresh concretes containing various cements often showed widely varying "temperature characteristics" in the initial consistency.

In order to go into the influence of the initial consistency, the change in consistency and the temperature characteristic, additional tests were carried out using laboratory cements. These cements were ground in a laboratory mill from large-scale-produced portland cement clinker, slag and fly ash. Based on the investigations of Locher, Richartz and Sprung /6/, anhydrite and hemihydrate were added as sulphate-bearing agents, in various dosages. Setting, the amount of water necessary for standard consistency, the spread of standard mortar, the change in spread and other qualities were examined. The results of these examinations will too be appearing shortly in detail /5/. Figures 5 to 7 show some exemplary results. Firstly fig. 5 shows how, using laboratory cements from a single clinker, by way of varying the sulphate concentration from hemihydrate (HH) to

anhydrite (AH), the temperature characteristic of the mortar spread may be intentionally varied. As well as gradual lines, curves with distinct minima and maxima are formed.

Fig. 6a and 6b demonstrate that two cement characteristics (e.g. spread of standard mortar and water requirement for standard consistency) can independantly of each other be influenced by variation in the mixing proportion of the sulphate-bearing agents; this being carried out with laboratory cements, using two different clinkers. Fig. 7a and 7b also demonstrate that a change in dosage of calcium sulphate bearer must not necessarily have an affinitive effect on two cement properties; here, the initial setting and mortar spread. Thus it may be concluded that the "optimation" of a cement cannot be undertaken with an eye on only one characteristic (e.g. setting), but, rather by "system optimation" of several characteristics.

An explanation for the discovered phenomena is to be sought in the fact that the rheological behaviour of cement pastes, plastic cement mortars and concretes is similar to that of a Bingham model /7/, /8/, /9/. However, the rheogramm of a Bingham model shows two values which are independant of one another. Thus it is understandable that the influence on properties of fresh cement pastes, cement mortars and concretes can in general form only be described by two values in each case. These do not have to be physically exactly defined values. Any customary methods used for testing mortar and concrete are suitable, as long as their results do not correlate closely to one another; i. e. in as much as they describe different fields of rheological behaviour.

References

/1/ Wierig, H.-J., E. Scholz und H. Nelskamp: Zu offenen Fragen der Frischbetontechnologie, Betonwerk + Fertig- teil-Technik, Heft 11, 1984, S. 733-741

/2/ Wierig, H.-J. und B. Restorff: Ansteifen des Frischbetons (to appear shortly)

/3/ Wierig, H.-J. und H. Nelskamp: Meßstreuungen bei der Prüfung der Frischbetonkonsistenz, beton 33 (1983), S. 380-384

/4/ U.S. Bureau of Reclamation, Concrete Manual, 8th Ed. (Denver 1975)

/5/ Scholz, E.: Zum Einfluß von Temperatur und Calciumsulfat-Art im Zement auf die Ausgangskonsistenz und das Ansteifen von Normmörteln sowie andere Zementeigenschaften (to appear shortly)

/6/ Locher, F.W., W. Richartz, S. Sprung: Erstarren von Zement, Teil II: Einfluß des Calciumsulfatzusatzes, Zement-Kalk-Gips, Heft 6, 1980, S 271-277

/7/ Wesche, K. und W. vom Berg: Rheologische Eigenschaften von Zementleim und Frischbeton, Betontechnische Berichte 1973, S. 21-40, Beton-Verlag GmbH, Düsseldorf

/8/ Tattersall, G.H.: The workability of concrete, Cement & Concrete Association, Wexham Springs 1976, A Viewpoint Publication

/9/ Murata, J.: Flow and deformation of fresh concrete Matériaux et Constructions, Vol. 17 - No 98, 1984, S. 117-129

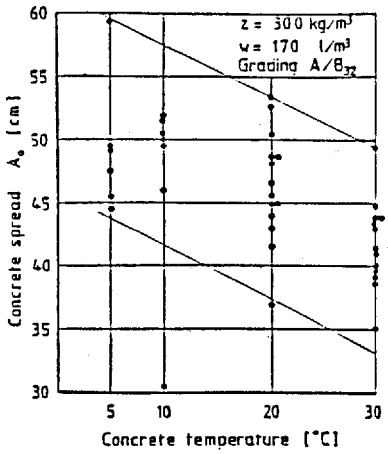

Fig. 1. Influence of cement and temperature on concrete spread A_o

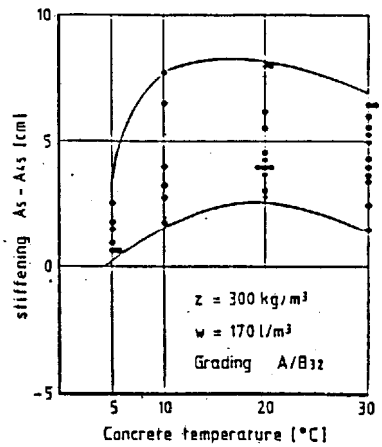

Fig. 2. Influence of cement and temperature on stiffening

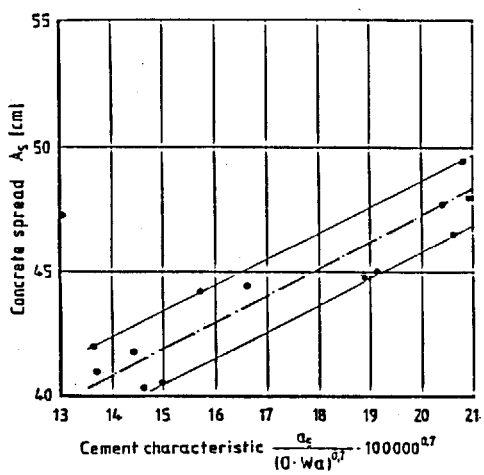

Fig. 3. Influence of cement on concrete spread
a_5 = spread of standard mortar
O^5 = specific surface of cement
Wa = water required

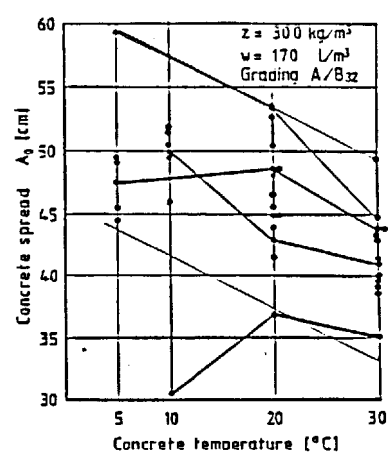

Fig. 4. Influence of cement and temperature on concrete spread A_o

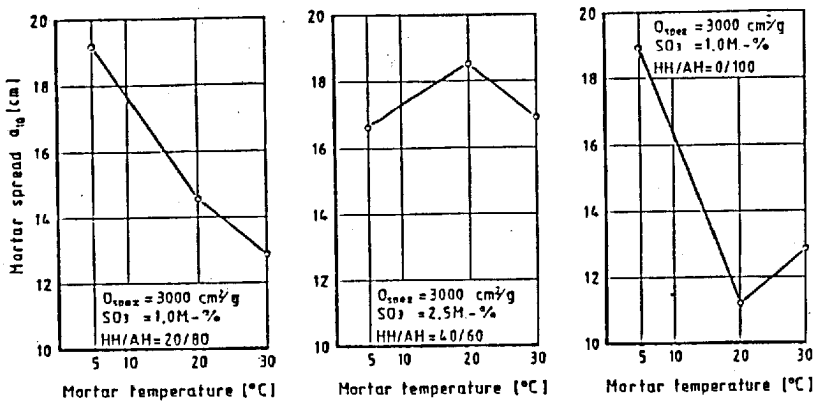

Fig. 5. Temperature characteristics of standard mortars made from clinker B (selected examples)

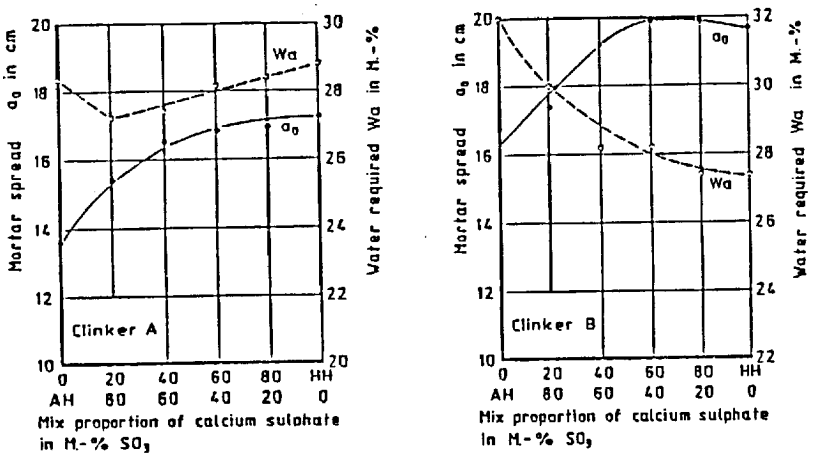

Fig. 6a. Fig. 6b.

Fig. 6. Influence of type of calcium sulfate on the amount of water required to reach standard consistency and the spread of the standard mortar

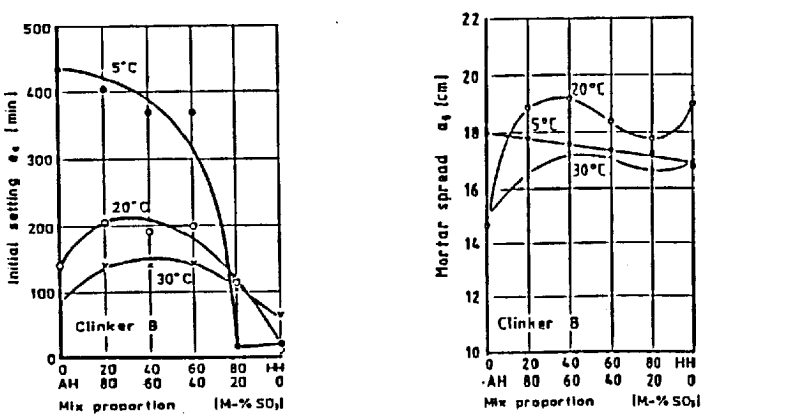

Fig. 7a. Fig. 7b.

Fig. 7. Influence of type of calcium sulfate on initial setting of cement pastes and spread of standard mortar

Pierre DUTRON, Cembureau

RAPPORT INTRODUCTIF AU 4ème SÉMINAIRE - BASES SCIENTIFIQUES DES SPÉCIFICATIONS POUR LE CIMENT ET LE DÉVELOPPEMENT DES MÉTHODES D'ESSAIS. S4

L'objet de ce rapport est de dresser un inventaire des principaux essais de caractérisation des ciments qui sont couramment utilisés et qui sont repris pour la plupart dans les normes nationales et internationales.

Nous établirons tout d'abord un classement de ces essais en les groupant en quatre catégories en fonction du type d'information recherchée. Nous verrons ensuite quelles sont, pour chacun de ces essais, la ou les méthodes utilisées et dans quelle mesure les résultats apportés par ces méthodes répondent aux besoins des producteurs et des utilisateurs.

Le rapport se terminera par quelques considérations en matière de vérification, voire de certification, de la conformité des ciments aux spécifications des normes.

1. Tentative de classification des essais du ciment

1.1 Vérification de la composition des ciments

On peut ranger dans cette catégorie :

- des mesures physiques indirectes telles que celle de la masse spécifique du ciment Portland ; cet essai tend toutefois à disparaître des normes ;
- des mesures chimiques parmi lesquelles la perte au feu et le résidu insoluble, destinées à déceler la présence dans le ciment Portland d'additions non autorisées ;
- des mesures chimiques, physiques ou physico-chimiques ayant pour but de déterminer la teneur en divers constituants (clinker, cendres volantes, pouzzolanes), dans les ciments composés ; ce type d'essai voit son importance croître avec le développement de ces ciments.

1.2 Appréciation des caractéristiques des ciments qui exercent une influence sur les propriétés des bétons frais

Il s'agit essentiellement de l'ouvrabilité et de son évolution qui peut être évaluée par la mesure

- de la demande en eau caractérisée par la détermination de la consistance normale ,
- du début et de la fin de prise.

Notons l'importance de ces caractéristiques pour la mise en oeuvre des bétons.

1.3 Appréciation des caractéristiques conférées par le ciment aux bétons au cours de leur durcissement

Ceci couvre :

- les résistances mécaniques, essentiellement à la compression, mesurées sur mortier normal ; c'est le maître-essai des ciments ;
- les variations de volume, d'origine hygrothermique, telles que le retrait ;
- certaines propriétés particulières telles que la chaleur d'hydratation.

1.4 Appréciation des caractéristiques des ciments qui exercent une influence sur les propriétés des bétons durcis

Il s'agit de s'assurer que le ciment est susceptible de garantir la durabilité du béton

- sous des conditions d'exposition normales au moyen d'essais physiques (Le Chatelier, autoclave, ...) et chimiques (MgO, SO_3, ...),

. sous des conditions plus sévères telles que des agressions de caractère chimique en fixant certaines caractéristiques de composition des ciments (teneur en C_3A, laitier, ...).

2. Examen critique des méthodes utilisées et en cours d'expérimentation

Remarques préliminaires

Inévitablement, le contenu d'une norme est le résultat d'un compromis équilibré entre les points de vue des diverses parties concernées.

En matière de méthodologie, ceci conduit à faire choix de méthodes de référence relativement simples, pas trop coûteuses, notamment au point de vue de l'équipement, et ceci explique que le plus souvent ce n'est pas le dernier cri de la technique qui est retenu dans les textes officiels. On a toutefois tenté de remédier à cette situation en autorisant dans les normes l'utilisation de méthodes plus modernes ou plus élaborées, le recours à la méthode de référence ne restant impératif qu'en cas de litige.

2.1 Vérification de la composition des ciments

Il est normal que l'organisme de certification, ou encore l'utilisateur, soit en mesure de vérifier si la composition d'une production ou d'une livraison de ciment correspond bien à la dénomination annoncée ou commandée.

Cette vérification revêt une importance croissante au cours de ces dernières années car, si l'on excepte le monde anglo-saxon, la part du ciment Portland pur est en diminution au profit des ciments Portland composés.

C'est donc un domaine où un effort particulier a été fait en matière de méthodes, notamment dans le cadre du CEN (Comité Européen de Normalisation), en définissant des essais basés soit sur un examen microscopique, soit sur une séparation des constituants en mettant à profit leurs différences de densité, ou encore leurs différences de dissolution dans certains solvants.

On peut dire que des résultats probants sont dès à présent obtenus pour les ciments binaires (mélanges de clinker et d'un autre constituant) mais que des études restent nécessaires pour les ciments ternaires, voire quaternaires.

Tout ceci constitue un progrès vis-à-vis des mesures plus rudimentaires telles que la masse spécifique, la perte au feu, ou le résidu insoluble, qui sont appelées à disparaître progressivement des normes.

2.2 Mesure des caractéristiques des mélanges frais

Il faut reconnaître l'importance capitale que représentent pour les utilisateurs du ciment la mesure et, de ce fait, la connaissance, voire même la préestimation de l'évolution rhéologique des bétons frais. Ce besoin d'information est devenu plus aigu par suite du développement remarquable du béton prêt à l'emploi.

Il faut tout autant reconnaître que les méthodes de mesure définies dans les normes ne répondent que très imparfaitement à ce besoin. L'appréciation de la demande en eau par la détermination de la consistance normale donne tout au plus une indication au temps t_0 sans qu'on puisse suivre l'évolution de cette demande dans le temps ; cette méthode d'essai n'est d'ailleurs plus guère prévue dans les normes et n'est accompagnée d'aucune exigence chiffrée.

L'essai de vitesse et de durée de prise (qu'il s'agisse de la méthode Vicat ou, plus rarement, de la méthode Gillmore) est certes respectable par son ancienneté mais il ne donne que des informations conventionnelles et ponctuelles, laissant de côté la période initiale de début de rigidification, si importante pour apprécier l'aptitude du béton à être compacté et moulé.

Cette lacune ne provient pas d'un manque d'études de caractère méthodologique ; la littérature scientifique fourmille de références sur des rapports de recherche touchant ce domaine. Des techniques de mesures continues faisant appel à la pénétrométrie ou encore à la viscosimétrie ont été mises au point et permettent de suivre avec plus de précision l'évolution dans le temps de ces phénomènes rhéologiques. Des tentatives ont également été faites en vue d'établir une corrélation entre cette évolution rhéologique et la variation de certaines propriétés physiques des pâtes de ciment telles que la vitesse de transmission des sons ou la conductivité électrique. Mais tous ces travaux n'ont pas encore abouti au point de permettre une évolution du contenu des normes. Les raisons en sont multiples :

Souvent ces nouvelles techniques font appel à des modes opératoires plus sophistiqués se prêtant mal à un emploi fréquent dans le cadre d'un contrôle de routine.

En général, ces méthodes d'essai sont applicables à des pâtes de ciment, rarement à des mortiers, et exceptionnellement à des bétons, car la présence d'un squelette pierreux dans le béton constitue un obstacle difficilement surmontable.

- La corrélation entre l'évolution rhéologique de la pâte de ciment et celle du béton est loin d'être simple à apprécier, d'autant plus que les essais de laboratoire peuvent difficilement tenir compte des conditions de chantier : forme et compacité des granulats, teneur en ciment et en eau des bétons, température et durée de mise en oeuvre, ...

En conclusion, voilà certes un domaine où des progrès sont attendus.

2.3 Mesure des caractéristiques des ciments en voie de durcissement

On considérera ci-après essentiellement la mesure des résistances mécaniques qui constitue la caractéristique du ciment la plus importante, mesure qui est presque partout effectuée sur des éprouvettes de mortier, ce qui constitue un compromis technico-économique entre l'essai sur pâte et celui sur béton.

Sans vouloir faire preuve de chauvinisme européen, on croit pouvoir dire que la mise au point dans les années 60 de la méthode dite "RILEM-CEMBUREAU" qui a fait l'objet de la Recommandation ISO R 679 de 1967, puis tout récemment de la norme CEN 196-1, a constitué un progrès très important pour les raisons suivantes :

Elle est déjà reprise dans plus de 30 normes nationales, couvrant la majeure partie de l'Europe (Ouest et Est) et de l'Amérique du Sud et commence à s'implanter en Afrique et en Asie. De nombreux pays examinent l'opportunité d'y recourir de sorte que, sans être prophète, on peut escompter qu'elle deviendra d'ici la fin du siècle la méthode universellement reconnue avec comme conséquence que lorsqu'on citera des chiffres de résistance, tout le monde ou presque parlera le même langage.

La conception de son mode opératoire est telle qu'elle donne des résultats relativement peu dispersés qui supportent avantageusement la comparaison avec les autres méthodes les plus connues, comme cela fut déjà exposé au Congrès de Moscou en 1974.

La composition de son mortier, qui est presque un micro-béton, est telle que les valeurs obtenues donnent une indication assez proche des résistances que le ciment conférerait à des bétons de composition courante.

Tout ceci est-il de nature à donner entière satisfaction ? La réponse à cette question doit être négative en ce sens qu'il y a lieu d'être plus ambitieux et de sortir d'une certaine attitude routinière. En effet, la mesure directe de la résistance par des essais destructifs implique plusieurs sujétions dont il serait bon d'être dégagé :

- La préparation, la conservation et l'essai d'éprouvettes de mortier représentent un travail long et coûteux.

  La réponse à la question posée, à savoir quelle sera la résistance du ciment (et conséquemment du béton) à divers âges , vient toujours trop tard, c'est-à-dire quand le béton est mis en oeuvre et qu'on ne peut plus guère réagir.

  On a, bien entendu, essayé de trouver une solution à cet état de choses de deux manières. On a d'abord conservé le principe de l'essai direct sur éprouvettes, mais en accélérant par voie physique (température et quelquefois pression) le développement des résistances de manière à pouvoir estimer, après quelques heures, le niveau des résistances à 7 ou 28 jours d'âge. Il existe à cet égard une littérature abondante et cette technique a reçu certaines applications, surtout dans des cas privilégiés où la composition du béton et de chacun de ses constituants est tout-à-fait constante. Par contre, dans la pratique courante, l'essai de résistance accéléré ne s'est guère développé au cours des dernières années, d'autant plus que la multiplication des types de ciment à plusieurs constituants apporte un élément perturbateur ; en effet, certains de ces ciments peuvent présenter une même allure de développement des résistances sous une température normale, tout en réagissant différemment sous un régime thermique accélérant l'hydratation.

  L'autre solution consiste à remplacer la mesure des résistances par une estimation indirecte de celles-ci en faisant appel à d'autres caractéristiques du ciment qui sont censées régir le développement de l'hydratation et du durcissement. On a songé, pour le ciment Portland tout au moins, à établir une relation entre résistance et composition minéralogique du clinker. On pourrait aussi avoir recours à la détermination de certaines caractéristiques physico-chimiques mesurées sur la pâte de ciment au cours de l'hydratation et établir sur cette base des modèles mathématiques permettant une préestimation de la résistance.

  Même si l'on est encore loin de pouvoir abandonner dans les normes l'essai classique de compression, ce séminaire devrait permettre de faire le point des progrès réalisés dans ce domaine et des lacunes qui restent à combler.

  Il y a d'autres caractéristiques du ciment qui intéressent l'utilisateur par l'effet qu'elles peuvent avoir sur les bétons au cours de leur durcissement. Retenons-en deux qui nous paraissent plus importantes, à

savoir le retrait et la chaleur d'hydratation.

Le retrait d'hydratation et surtout de dessiccation de la pâte de ciment constitue sans nul doute un point faible du ciment auquel on ne peut échapper, si l'on excepte le cas de quelques ciments spéciaux. La mesure de ce retrait effectuée sur pâte ou mortier de ciment ne se retrouve qu'exceptionnellement dans les normes nationales qui fixent, dans ce cas, une réduction maximale de longueur à un certain âge ; il faut dire que cet essai, assez conventionnel, est délicat et que les résultats présentent une dispersion non négligeable. Dans la mesure où l'on serait en droit d'associer la notion de retrait à celle de la finesse du ciment, on notera que les normes prévoient encore souvent l'essai de tamisage avec, toutefois, une prescription donnant une limite maximale plutôt que minimale au refus sur un tamis donné ; ce type d'essai a tendance à disparaître des normes car il n'apporte guère d'information utile, notamment parce que la majeure part des grains de ciment ont une dimension nettement inférieure aux mailles des tamis les plus fins. Tout au plus permet-il parfois de déceler l'absence ou la présence de certaines matières d'addition. Par contre, l'essai le plus courant est la mesure de la surface spécifique du ciment par perméabilimétrie qui donne une appréciation globale de la finesse ; encore une fois, on impose à cet égard plus souvent une valeur minimale que maximale. Il ne faut d'ailleurs pas demander à cet essai de fournir plus d'indications qu'il ne peut en donner. Disons qu'il permet surtout d'apprécier la régularité d'un ciment tant que sa composition ne subit aucune modification.

Un progrès substantiel, réalisé il y a plus d'une décennie, a consisté dans la mesure rapide et précise de la composition granulométrique, caractéristique qui conditionne bien des propriétés du ciment. Toutefois, la technique du granulomètre au laser reste essentiellement réservée aux recherches, voire pour l'auto-contrôle du producteur,mais elle n'est pas reprise dans les normes et l'on conçoit d'ailleurs qu'il serait pour le moins hasardeux de fixer une exigence, par exemple en définissant un fuseau granulométrique à respecter.

La mesure de la chaleur d'hydratation est d'application courante pour caractériser les ciments dits "à faible chaleur dégagée" destinés à la construction d'ouvrages massifs. C'est presque toujours la mesure par voie isotherme, issue de l'ASTM et utilisant le calorimètre à dissolution, qui est prévue dans les normes. On fait appel beaucoup plus rarement à la voie semi-adiabatique de la bouteille Thermos, ou encore à la méthode par conduction opérant en conditions isothermes, cette dernière convenant d'ailleurs mieux pour mesurer à court terme (quelques heures à 3 jours) le dégagement de chaleur de ciments à durcissement relativement rapide.

Si l'on peut ainsi estimer être bien armé pour les mesures sur ciment, par contre, on ne dispose pas encore de méthode satisfaisante pour apprécier le dégagement de chaleur ou plus simplement l'augmentation de température au sein d'une masse de béton en cours de durcissement, ce qui correspond au problème rencontré sur chantier. Voici encore un domaine pour lequel des études paraissent nécessaires.

2.4 Mesure des caractéristiques des ciments qui peuvent influencer le comportement à long terme des ouvrages en béton

Un certain nombre d'essais plus ou moins conventionnels sont prévus et normalisés dans le but de garantir aux utilisateurs que les

ouvrages en béton réalisés avec le ciment testé gardent dans le temps leurs qualités de stabilité dimensionnelle et de résistances mécaniques, ce dans des conditions d'exposition normales, c'est-à-dire non particulièrement agressives.

C'est le cas de certains essais physiques (Le Chatelier, autoclave, ...) et chimiques (MgO, SO_3, ...). Il ne semble pas qu'il y ait une grande évolution dans ce domaine, ni que cela donne lieu à des difficultés de la part des utilisateurs. Il faut toutefois être conscient que dans certains cas -nous songeons à l'essai à l'autoclave -, les informations obtenues par les mesures sont significatives s'il s'agit de ciments Portland pour lesquels ils avaient d'ailleurs été conçus mais qu'il n'en est pas nécessairement de même lorsque l'on se trouve en présence de ciments composés.

Par contre, si l'on aborde l'aspect de la durabilité des ouvrages en béton ayant à supporter des conditions d'exposition plus sévères, on peut se demander si l'on est aujourd'hui suffisamment pourvu en méthodes d'essai et en critères quantitatifs pour garantir au mieux le bon comportement de ces ouvrages dans le temps.

Nous nous limiterons à trois aspects qui se présentent plus ou moins fréquemment dans la pratique, à savoir le comportement au gel, la protection des armatures contre la corrosion et la résistance aux agressions chimiques. De quoi dispose-t-on tout d'abord pour s'assurer qu'un ciment donné est capable de fournir des bétons suffisamment résistants à l'action des cycles de gel-dégel ? On ne peut évidemment pas se baser sur la seule composition de ce ciment, et des essais de gel-dégel sur des pâtes ou des mortiers n'étant pas représentatifs, la seule possibilité retenue actuellement est de conduire ces essais sur bétons.

On est toutefois loin d'être au bout de ses peines puisque, suivant la composition du béton choisi (notamment sa teneur en ciment, en eau et en air) et le type de cycle retenu (notamment gel-dégel sous eau ou à l'air), on peut aux deux extrêmes obtenir des résultats satisfaisants ou désastreux avec n'importe quel ciment. On est donc conduit à choisir des conditions d'essai médianes et de comparer les résultats obtenus sur le ciment étudié avec ceux que donne le même béton contenant un ciment dit de référence, c'est-à-dire un ou plusieurs ciments pour lesquels on dispose d'une longue expérience attestant qu'ils permettent la réalisation de bétons durables.

Devons-nous nous satisfaire de cette façon de faire pragmatique et empirique, ou bien ne conviendrait-il pas de pousser plus avant les études pour aboutir à des solutions plus scientifiquement élaborées ?

Le problème de la protection des armatures est une question de toute première importance puisque on peut considérer que le phénomène de corrosion de ces armatures est le plus souvent à la base du mauvais comportement dans le temps des structures en béton.

A première vue, c'est évidemment aux spécifications relatives à la composition et à la mise en oeuvre du béton qu'il appartient de fixer les règles de bonne exécution dosage avec un rapport E/C relativement faible et une teneur minimale en ciment, épaisseur de recouvrement des aciers suffisante et bien contrôlée, protection adéquate de béton frais contre la dessiccation.

Si toutes ces règles sont respectées, il n'y a plus de problème de corrosion. Toutefois, l'expérience nous montre que, souvent, il

n'en est pas ainsi et ceci a conduit les experts en ciment à se pencher sur cette question.

Nous songeons par exemple aux mesures de l'évolution de la profondeur de carbonatation déterminées sur des éprouvettes de mortier de ciment. La relation entre corrosion et carbonatation est en effet bien connue et on sait également que la vitesse de carbonatation est liée à la rapidité de développement des résistances du ciment, cette rapidité pouvant à son tour dépendre de la composition et de la classe de résistance du ciment.

Si l'on en vient aux agressions chimiques, les spécifications qui figurent dans les normes concernent le plus souvent la résistance aux sulfates et fixent des exigences en matière de composition des ciments basées sur l'expérience des décennies précédentes. Pour le ciment Portland, il s'agit de fixer des limites pour les teneurs en C_3A, Al_2O_3, C_4AF, ..., tandis que pour les ciments composés, on exige une teneur minimale en certains constituants tels que le laitier. Pour les autres agressions chimiques, telles que, par exemple, les eaux pures, on se limite le plus souvent à des recommandations générales.

On a pourtant essayé maintes fois dans le passé de mettre au point des essais d'appréciation directe portant sur le comportement d'éprouvettes de pâtes, mortiers ou bétons, immergées totalement ou partiellement, de manière continue ou discontinue, dans des solutions contenant l'agent agressif à des concentrations plus ou moins fortes pour accélérer le processus de dégradation éventuelle.

Force est de constater qu'aucune de ces études n'a débouché sur la mise au point d'une méthode largement acceptée et permettant une appréciation directe des performances du ciment et qu'on en est donc resté aux exigences de caractère descriptif mentionnées plus haut.

Conc

1.

Ceci est devenu d'autant plus nécessaire que, si certains essais bien connus de longue date, tel l'essai Le Chatelier-Anstett-Blondiau, étaient en mesure de donner des indications valables dans le cas de ciment Portland pur, ils risquent souvent d'induire en erreur lorsqu'ils sont utilisés sur des ciments composés.

2.

3. Conformité des ciments aux spécifications des normes

Un certain nombre d'éléments nouveaux tels que les progrès en matière d'interprétation statistique des résultats, les possibilités offertes à l'égard du calcul des risques encourus par le producteur comme par l'utilisateur sont à la base d'une évolution marquée dans le domaine de la vérification de la conformité d'une production globale ou d'une livraison particulière de ciment vis-à-vis des exigences de la norme. Bien souvent, cette vérification donne droit en corrolaire à une certification, c'est-à-dire à l'attribution d'une marque de qualité certifiée par un organisme indépendant.

3.

On constate de plus en plus que les méthodes de certification s'appuient, comme dans les industries les plus avancées, sur une vérification de la valeur de l'assurance qualité à l'intérieur des entreprises, en d'autres termes, de l'auto-contrôle industriel.

Cela implique un renforcement de la responsabilité des industriels, en l'occurrence des cimentiers, l'existence d'organismes indépendants et crédibles,

capables de vérifier la valeur de cette assurance qualité.

Conclusions

1. Il ne faut pas retenir de ce rapport introductif que tout va mal en matière d'essais et de spécifications pour les ciments. Les connaissances acquises et les réglementations en vigueur sont de nature à garantir à l'utilisateur que le ciment qu'il met en oeuvre lui permet de réaliser des bétons de qualité.

2. Ceci n'empêche pas que, pour chacun des domaines considérés plus haut, les progrès en équipement et techniques de mesures scientifiques sont tels qu'ils peuvent et doivent conduire à une évolution de la méthodologie appliquée aux ciments et aux bétons au plus grand bénéfice des producteurs et des utilisateurs.

3. Formons le voeu que ce séminaire, comme d'ailleurs le 8ème Congrès International de la Chimie des Ciments, nous permette d'avancer dans cette voie.

Tong Sanduo
Standardization Institute of Building Materials, Beijing, China

SOME VIEWS ON CEMENT SPECIFICATION

1. INTRODUCTION

For assuring cement and concrete quality chemical, physical and mechanical requirements as well as cement constituents are stipulated in all cement specifications. Most of stipulations are necessary, but some of them are so strict that the application of natural resources are restricted. In order to make good use of mineral resources it is reasonable to revise some of requirements under the prerequisite for ensuring cement performance and stability.

2. EXTEND THE MgO LIMIT

The main purpose of stipulating MgO limit in cement specifications is to avoid the unsoundness of hardened concrete in long term. The presence of excessive amounts of MgO in cement clinker may lead to expansion and crack development and cause the structure failure since the conversion of MgO to $Mg(OH)_2$ involves a volume expansion of 117% and it may take several years for its hydration. In order to prevent this harmful expansion the MgO content should not exceed a certain value, mostly 5.0%, in all specifications. As a result of this restriction some of limestones partially containing dolomite can not be well used thus the mineral resources are shortened. Our test results show that the MgO content could be extended to 6.0% or even more, e.g. 7.0%, the performance of the portland cement are unchanged and the cement pastes remain stable in long term. The long term strength of cement mortars with various MgO contents in clinker are shown in Table 1.

It has been proved that the MgO amount in clinker by chemical analysis cannot indicate the long term soundness of cement exactly, since MgO exists in clinker in the form of various morphology. Except for certain amount in the amorphous form and in the crystalline lattice of cement compounds, MgO exists predominantly in the form of periclase crystals with different sizes, and it is the periclase that cause harmful expansion. For clinker containing nearly same amount of MgO the autoclave expansion will be greater as the amount of periclase and free lime increase and the sizes of periclase become larger (Table 2).

Table 2 Autoclave expansion of the cement with different content of MgO

Plant	MgO %	fcao %	Periclase %	aver. diameter of periclase (μ)	autoclave expansion %
A	4.50	0.60	2.10	5.10	0.23
B	4.50	1.83	3.12	5.27	2.54
C	5.11	0.25	2.80	4.60	0.22
D	5.25	0.63	-	-	0.46
C	6.25	slight	3.30	4.80	0.30
E	6.08	0.39	-	-	failure

Appropriate measures have been taken in the process in plant C to control the free lime content and growing of periclase content as MgO increases, the cements remain sound under the autoclave test (Table 3). It can be concluded that the permissible MgO content might be extended to 7%.

Table 1 Strength development of cement with various MgO contents

Sample No.	MgO in clinker %	Compressive strength (MPa)					Tensile strength (MPa)				
		28days	6months	1year	3years	10years	28days	6months	1year	3years	10years
1	1.04	67.2	81.8	81.8	89.7	97.0	3.3	3.8	4.2	4.2	4.2
2	5.11	72.3	85.6	89.3	94.3	99.0	3.3	3.2	3.4	3.9	4.2
3	6.25	68.5	81.4	86.7	93.6	101.3	3.3	3.3	3.6	3.8	4.1
4	7.26	66.9	79.5	82.3	87.5	97.6	3.3	3.5	3.5	3.8	4.3
5	7.53	71.8	84.4	87.3	92.1	101.0	3.3	3.4	3.6	3.6	4.1

Tor.g Sanduo
Standardization Institute of Building Materials, Beijing, China

Table 3 Relation between MgO and periclase content for cement produced in same plant

MgO %	fcao %	Periclase %	Autoclave expansion %
5.11	0.25	2.80	0.22
6.25	slight	3.30	0.18
6.50	0.29	3.60	0.19
7.28	0.30	3.90	0.60
7.53	0.26	4.30	0.48

3. LIMESTONE CAN BE USED AS CEMENT ADDITION

Limestone used as mineral addition togather with blastfurnace slag and pozzolana in cement has good effect on the cement performance. In most of cement specifications limestone is defined as a filler and can only be added to cement within a few hundredths, except for French standard (AFNOR) in which more than 5% of limestones can be allowed in type CPJ cement. Our research shows that limestone can be used not only as a filler but a good secondary constituent in cement. Suitable amount of limestone blended with blastfurnace slag, pozzolana or fly ash in cement can improve the cement performance and get the energy saving effect. In the current standards in China 10% of limestones are permissible in blastfurnace slag portland cement and fine filler pozzolana (or fly ash) portland cement.

Limestone as a compound addition in cement has the following benefits:

(1) Reduce the water requirement and improve the workability (Fig.1).
(2) Shorten the setting time (Fig.2).
(3) Increase the early strength [Fig.3(a), 3(b)].
(4) Regulate the strength development (Fig.4).

The reason why limestone has above effects is that it gives good physical and chemical functions in cement hardening. It physically plays a role of a filler and has the water-reducing effect, besides there is chemical reaction between $CaCO_3$ and cement hydrates, $C_3A \cdot CaCO_3 \cdot 11H_2O$ can be formed after 3 days. Fig.5(a), 5(b), shows the XRD. Patterns of the pastes of the cement with limestone hydrated at 3 days.

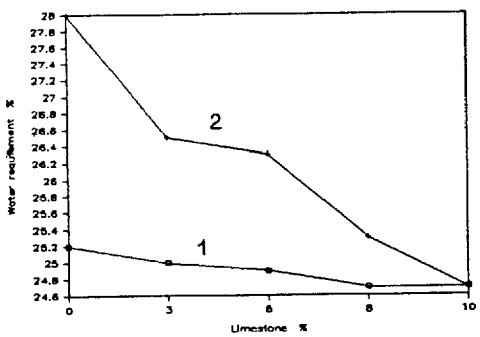

1. Protland slag cement
2. Portland pozzolana cement

Fig.1 Effect of limestone contents on the water requirement of cements

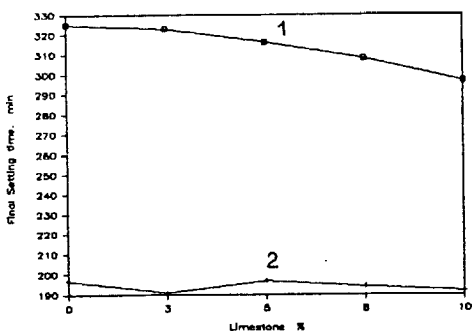

1. Portland slag cement
2. Portland pozzolana cement

Fig.2 Effect of limestone contents on the final setting time of cements

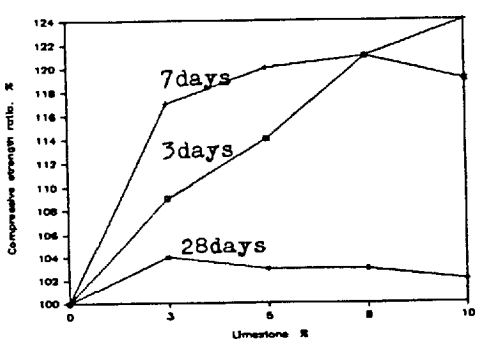

Fig.3 (a) Effect of limestone contents on the early strength of porltnad slag cement

Tong Sahduo
Standardization Institute of Building Materials, Beijing, China

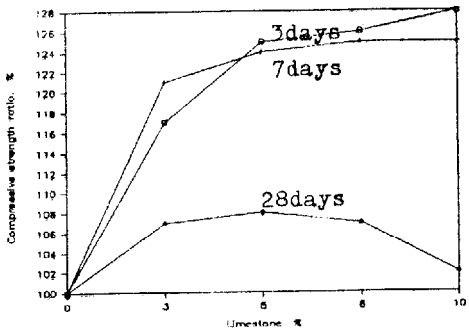

Fig.3 (b) Effect of limestone contents on the early strength of portland pozzolana cement

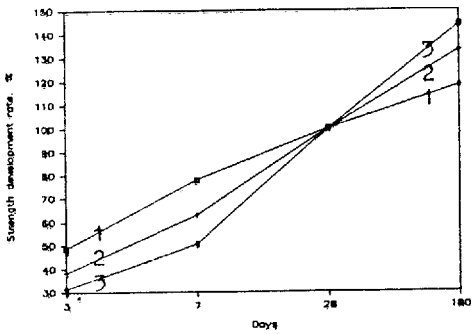

1. Ordinary portland cement
2. Portland slag cement with limestone
3. Portland Blastfurnace slag cement

Fig.4 The strength development rate of the portland slag cement

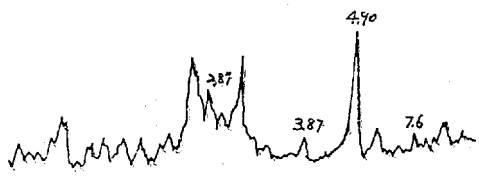

Fig.5 (a) XRD pattern of the paste of the portland slag cement with limestone hydrated at 3 days

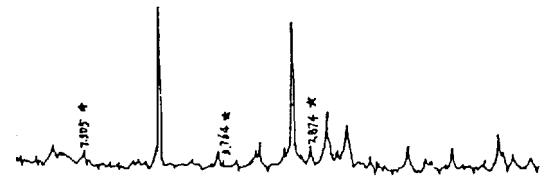

Fig.5 (b) XRD pattern of the paste of the portland pozzolana cement with limestone hydrated at 3 days

4. KILN DUST CAN BE USED AS A FILLER

Kiln dust as a waste was ejected into atmosphere or collected and dischanged. It pollutes surroundings. Our test results indicate that suitable amounts of kiln dust as an addition incorporated into cement are of no influance on the cement performance. In certain circumstances it can even improve the early strength, therefore using kiln dust as a filler in cement is in favor of saving amount of clinker thus saving energy. It is possible to define this stipulation in specification.

The constituents of kiln dust are changed apparently as the raw materials and fuel changes. It also varies with the kiln type and process. Table 4 shows the average chemical composition of kiln dust and its fluctuation ranges for 38 cement plants. But as to the same plant if the operation is stable the compositions of kiln dust are not changed so much.

From optic microscope observation and X-ray examination there are 16 types of mineral constituents in kiln dust, namely, calcium carbonate, dolomite, orthoclase, quartz, mica, slag residue (when slag used as raw materials), glass, Carbon, free lime, β-C_2S, C_2F, C_4AF, mullite, dehydrated clay, gypsum, alkali Sulphate. Those minerals come from decomposition and conbination of raw materials as well as fuel combustion. Among them some are inert materials, others belong to clinker minerals and pozzolanic materials. They are not harmful to cement performance, except that free lime should be noticed. As we know free lime in clinker might cause cement unsoundness, but free lime in kiln

Tong Sanduo
Standardization Institute of Building Materials, Beijing, China

Table 4 Chemical compositions of kiln dust (%)

	LOi	SiO_2	Ai_2O_3	Fe_2O_3	CaO	MgO	SO_3	K_2O	Na_2O	fCaO	TiO_2	S
Average	20.42	16.69	5.12	3.59	45.75	2.03	3.54	2.19	0.30	8.07	0.31	0.35
Range	5.72 ∫ 31.81	11.22 ∫ 24.55	2.83 ∫ 10.68	2.05 ∫ 7.29	37.65 ∫ 57.54	0.73 ∫ 5.86	0.18 ∫ 16.43	0.59 ∫ 7.71	0.12 ∫ 0.64	0.33 ∫ 21.73	0.16 ∫ 0.72	0 ∫ 2.83

dust stands in different condition. Most of them are finely dispersed and hardly appear as inclusion. They are not in a dead-burnt state, so free limes in kiln dust are not affected apparently on cement soundness as in clinker. Small amount of kiln dust incorporated in cement will not cause unsoundness.

Kiln dust presents certain reactivity during cement hardening process. By comparing cement with 30% kiln dust to the same cement with 30% quartz it shows that the compressive strength ratio at 3 months are greater than 100% (Table 5).

Table 5 Reactivity of kiln dust

Sample	Compressive strength at 3 months (MPa)	3M strength ratio %
Kiln dust A	46.6	113
Kiln dust B	51.7	125
Kiln dust C	42.4	102
Fly ash	48.8	117
Slag	46.3	112
Pozzolana	48.2	116
Quartz	41.5	100

Table 6 presents the compressive strength of ordinary portland cement and blast-furnace portland cement with 5% and 8% kiln dust respectively in comparison with corresponding cement without kiln dust addition. It proves that the strength of cements with kiln dust continously develop in long term. Other performance such as shrinkage, permeability and frozen resistance have been proved not to be changed as well, so it is considered that kiln dust can be used as a filler to incorporate into cement.

Table 6 Compressive strength of cements with kiln dust

Plant No.	Cement type	Kiln dust %	Compressive strength (MPa)					Relative value %				
			3days	7days	28days	6months	5years	3days	7days	28days	6months	5years
L	ordinary	0	17.4	28.4	42.1	68.0	78.0	100	100	100	100	100
	ordinary	5	19.1	31.2	45.3	69.4	83.6	110	110	108	102	107
	Blast-furnace slag	0	18.2	27.6	43.4	68.4	78.8	100	100	100	100	100
	Blast-furnace slag	8	17.9	28.4	45.3	72.0	85.4	98	103	104	105	108
G	ordinary	0	14.7	26.3	42.6	64.9	72.9	100	100	100	100	100
	ordinary	5	17.5	29.4	46.3	69.9	76.4	119	112	109	108	105
	Blast-furnace slag	0	15.4	25.7	45.1	68.8	80.8	100	100	100	100	100
	Blast-furnace slag	8	15.1	26.6	45.0	67.7	80.3	98	104	100	98	99

PIERRE TERRIER - C.E.R.I.L.H., France

GESTION ET ASSURANCE DE LA QUALITE DES ESSAIS.

La passation des marchés de fourniture, ou d'une façon plus simple la vente, a pour objet le transfert à l'utilisateur des produits ou composants aptes à satisfaire ses besoins. L'aptitude en question est mesurée par le moyen des essais, contemporains (essais de réception) ou préalables au contrat (marque de qualité) ; les essais sur des prélèvements conservatoires permettant éventuellement la vérification ultérieure de la qualité de la fourniture. Dans tous les cas, les essais associent à des échantillons représentatifs d'un produit, ici le ciment, des caractéristiques définies, mesurées sur l'échantillon lui-même ou sur des corps d'épreuve préparés spécialement, en mortier le plus souvent ; la mesure étant effectuée dans des conditions spécifiées, conformément à un document : la norme d'essai. (La norme de produit rattache, par ailleurs, la caractéristique mesurée lors de l'essai à la performance impliquée par l'application, c'est-à-dire le béton.

En milieu industriel, seule la pratique régulière des essais permet, en permanence, le pilotage des fabrications au voisinage de l'optimum économique. "Sans essais, pas de qualité" pourrait-on dire, cet aphorisme ne doit pas en cacher un autre : "pas d'essais sans qualité" qui est la cheville ouvrière de ma contribution.

La qualité est l'aptitude objective à satisfaire les besoins de l'utilisateur. Il faut distinguer la qualité de l'utilité, bien qu'elles soient quelquefois égales ; elles le sont quand nous offrons une chaise confortable à un homme fatigué mais remarquons que si nous offrons une deuxième chaise de même qualité, son utilité est à peu près nulle. La satisfaction n'est pas toujours proportionnelle à l'utilité (l'air est plus utile que l'or). En outre, sauf à vivre isolé, pour chaque individu, à la satisfaction de sa propre fonction d'utilité, peut s'ajouter (ou se retrancher) celle qu'il retire de la satisfaction de la fonction d'utilité d'autrui, c'est ce que PARETO a nommé l'ophélimité.

La qualité, qui seule retient notre attention, ne peut s'apprécier que par rapport à des critères objectifs.

Dans le domaine des essais où il y a peu de tris, pratiquement ni rebut ni retouche et pas d'après-vente, les défaillances ne sont généralement pas mesurables directement. La qualité ne peut être que constitutive et contemporaine de l'essai, elle n'est maitrisable que par la mise en place effective d'un système de gestion de la qualité recouvrant trois fonctions : définition, obtention et vérification de la qualité. L'assurance de la qualité apporte ensuite la preuve d'une bonne gestion et fait la démonstration que la qualité est obtenue. Pour cela, quelques actions sont nécessaires et suffisantes ; à l'occasion de son accréditation par le Réseau Nationale d'Essais, le C.E.R.I.L.H. les a mises en oeuvre ou développées.

Sur la base des dispositions du guide ISO/IEC25-1982 "Prescriptions générales concernant la compétence technique des laboratoires d'essais", une politique de gestion de la qualité est manifestée par l'existence d'un système dont les bases sont :

- un responsable, agissant par délégation de la Direction Générale doté du pouvoir et des moyens nécessaires pour que soient identifiés les problèmes liés à la qualité et pour provoquer et contrôler les actions correctives opportunes. Chargé du suivi de la qualité telle qu'elle est formalisée (manuel, plans qualité) et vécue (audits), il prépare le rapport annuel et l'échéancier Assurance qualité, propose les actions de formation et d'information et assure les relations avec les organismes d'accréditation et les partenaires extérieurs.

un Manuel Qualité. Document qui explicite les dispositions générales prises par le laboratoire pour obtenir et garantir la qualité des prestations d'essai ; rédigé dans un climat de participation des intervenants et révisable.

des Plans Qualité, spécifiques aux différents groupes d'essais : physiques et mécaniques, chimiques, calorimétriques. Ils indiquent les modes opératoires, les matériels d'essais ainsi que les précautions prises pour l'obtention effective de la qualité requise.

Responsable, Manuel, Plans sont les seules obligations de moyens, les autres obligations qui s'expriment en termes de résultat, sont résumées au tableau I et développées dans ce qui suit.

Tableau I . Le programme de gestion et d'assurance de la qualité.

ACTION	FONCTION	DOMAINE
1. Prévoir dans le détail toutes les modalités qui affectent la qualité, dégager les facteurs d'influence.	Définition de la qualité	Gestion de la qualité
2. Rédiger les dispositions prises en vue d'obtenir la qualité.	Obtention de la qualité	
3. Attribuer les rôles, désigner les responsables et obtenir des conduites conformes aux dispositions spécifiées.		
4. Organiser l'autocontrôle	Vérification de la qualité	
5. Analyser les défaillances, traiter les anomalies et les réclamations.	Démonstration de la qualité	Assurance de la qualité
6. Participer à des essais interlaboratoires.		
7. Déclencher des audits internes. Préparer et suivre un échéancier d'assurance qualité.		
8. Appartenir à un réseau d'accréditation et se soumettre aux audits externes.		

Pierre TERRIER
C.E.R.I.L.H.,FRANCE

S4

1. DEFINITION DE LA QUALITE.

La définition de la qualité passe par la prévision dans le détail de toutes les modalités qui affectent la qualité des essais comme cela se déduit de l'analyse des facteurs d'influence. Cette action est à la charge des commissions de normalisation, elle constitue un préalable à la rédaction de la norme. Elle a été pleinement assumée par le CEN TC 51 pour les normes d'essais, par exemple le projet EN 196 parti I "Détermination des résistances mécaniques" est un modèle du genre.

Dans ce domaine des essais mécaniques, FERET a proposé des 1892 l'éprouvette 4x4x16 cm Au Congrès International tenu en 1900 pendant l'exposition universelle, la FRANCE a préconisé le mortier plastique 1/3. En 1943, dans un article en forme de "suggestions au sujet des méthodes normales d'essai des liants hydrauliques", FERET a rappelé l'essentiel de ce qui lui paraissait recommandable :

- un mortier de composition granulométrique étendue,
- des prismes 4x4x16 cm,
- l'adoption d'une quantité fixe d'eau de gâchage,
- une température uniforme de 20° C dans les locaux,
- une mécanisation du gâchage.

Dans les années 50, un comité mixte RILEM -CEMBUREAU a rédigé, sur ces principes, une méthode d'essai en compression du mortier, présentée par M. DUTRON, adoptée par CEMBUREAU à HELSINKI en août 1956 et par la RILEM à la Convention Permanente de Munich de septembre 1956, cette méthode a été retenue par le Comité ISO/TC/71 dans sa recommandation ISO.R 679 de 1968 (révisée en 1982) avant d'être reprise, complétée et précisée par le CEN : projet EN 158 d'octobre 1980 devenu en août 1982 le projet EN 196 partie I.

2. DISPOSITIONS A PRENDRE.

Des dispositions sont prises pour que les locaux aient des caractéristiques en rapport avec les exigences des essais. Dans certaines salles ou enceintes, la température et l'humidité relative de l'air doivent être régulées et enregistrées. La vitesse de circulation de l'air peut être limitée (inférieure à 0,5 m/s pour les mesures calorimétriques selon la norme P 15 - 436).

Les instruments font l'objet lors de l'acquisition d'une évaluation de leurs performances, leurs qualités métrologiques sont qualifiées par comparaison avec les exigences des normes. Ils sont étalonnés périodiquement et les grandeurs sont rattachées aux étalons nationaux. Le Bureaux National de Métrologie (B.N.M.) ayant mis en place un système cohérent de dissémination des unités de mesure, les laboratoires d'essais pensent faire étalonner leurs instruments par des centres agrés B.N.M. qui garantissent le raccordement aux étalons nationaux (figure 2). Les réetalonnages sont réalisés selon un planning préétabli, consignés par écrit, matérialisés par des étiquettes qui peuvent comporter les constantes mesurées (figure 3).

Dans les mesures comparatives, un produit de référence est utilisé pour l'étalonnage: ciment étalon français, disponible au CERILH ou ciment étalon américain, disponible au NBS.

Suite à la résolution 76, prise à ROME en 1982, la constitution d'un stock de sable européen de référence est actuellement préparée par le CEN. Ce sable doit permettre d'étalonner les sables nationaux.

Les produits à essayer, les prélèvements faits, les éprouvettes préparées en vue des essais, les corps d'épreuve sont référencés et marqués de façon à se rattacher au lot d'origine. La gestion du système de référence permet de situer les en-cours géographiquement (salle de conservation dans l'eau, armoire humide) et par rapport au temps (temps légal et âge des essais). Cette traçabilité permet, notamment en cas d'anomalie, la mise en cause d'essais effectués dans un local identifié à une époque déterminée (coupure du courant par exemple).

L'obtention de la qualité commence donc par la rédaction des dispositons ci-dessus aptes à la mise en pratique des spécifications des normes. Dans cet esprit, un document de référence dont il conviendra de tenir compte pour les essais relatifs à la résistance mécanique est le guide rédigé sous l'égide de CEMBUREAU pour un groupe animé par le Docteur KOELIKER (Manual for Testing of strength of Cement draft 1981) pour l'application de la norme CEN.

3. ATTRIBUTION DES ROLES.

Les opérateurs doivent être formés à :

- conduire les essais conformément au Plan Qualité,
- rendre compte de toute anomalie,
- ne déroger aux dispositions du Plan Qualité qu'avec l'accord de l'encadrement,
- enregistrer les mesures et les identifications utiles de façon à formaliser le suivi des essais et permettre eventuellement le traitement des non conformités.

Les spécifications des modes opératoires impliquent la compétence de l'opérateur, les dispositions prises ne doivent pas être un obstacle à la confiance qui lui est faite ni le décharger de la responsabilité de la tâche qu'il accomplit.

Un des rôles du responsable qualité est précisemment d'animer l'ensemble des personnes impliquées par l'organisation de la qualité en vue d'obtenir l'adhésion complète à l'état d'esprit qualité ; mais l'adhésion n'est pas tout, l'entretien et l'acquisition des connaissances ne doivent pas être sous estimés non plus

Pierre TERRIER
C.E.R.I.L.H., FRANCE

que les moyens matériels mis à la disposition de chacun.

MATERIELS DE MESURE ET D'ESSAI

Ce tableau précise l'identification, la situation, les caractéristiques et le mode d'étalonnage ainsi que sa fréquence de chacun des appareils et instruments de mesure utilisés. Les responsables du matériel considéré sont aussi indiqués.

DESIGNATION	IDENTIFICATION	CARACTERISTIQUES SPECIFICATION D'ACHAT	MAINTENANCE	ETALONNAGE	RESPONSABLES
Balance analytique digitale.	SARTORIUS type 2474 Pièce 207	portée 160 g au 0,01 mg	Entretien annuel par fournisseur OSI	Vérification trimestrielle au moyen des poids étalonnés	Mme B. M. P.
Balance de précision digitale	SARTORIUS type 2257 pièce 207	portée 1600 g au 0,01 g	Entretien annuel par founisseur OSI	IDEM	Mme B. M. P.
Boite de poids RP1 étalonnés	PROLABO n°34924 pièce 209	masses 100 à 1 g et divisionnaires	Mise à disposition par Chef Section	Rattaché BNM Certificat LNE n° 408 211/1	Mme B. Mme B.
Four électrique réglable à ventilation naturelle	PIEZO CERAM type TH4 pièce 201	température maximum 1300°C 4000W	Intervention du fournisseur en cas de besoin	Vérification mensuelle de la température 1000±25°C et après chaque intervention	M. P.
Four électrique réglable à ventilation naturelle	PIEZO CERAM type TTSOP 33 P palier 2e étage	température maximum 1600°C 3500W	IDEM	IDEM 1200 ± 25° C	M. P.

TABLEAU II - EXTRAIT D'UN TABLEAU DE MAINTENANCE ET D'ÉTALONNAGE

RÉSEAU NATIONAL D'ESSAIS



FIGURE 1. LE LOGO RNE

Pierre TERRIER
C.E.R.I.L.H., FRANCE

LABORATOIRE NATIONAL D'ESSAIS
Département
Métrologie et Instruments de Mesure

CENTRE D'ÉTALONNAGE MÉCANIQUE
1, rue Gaston-Boissier — 75015 PARIS
Tél.: (1) 532.29.89
Télex: LNE 202 319 F

Centre d'étalonnage agréé
par le
BUREAU NATIONAL DE MÉTROLOGIE
chaîne d'étalonnage unités mécaniques

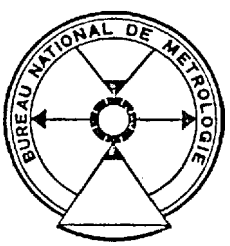

FIGURE 2
En tête d'un certificat d'étalonnage émis par un centre d'étalonnage agrée BNM (arrêté du 11 mars 1977)

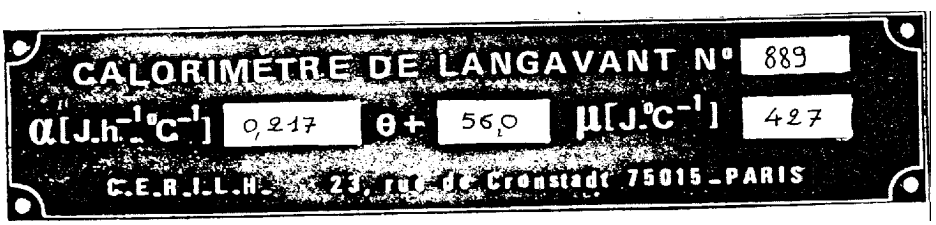

FIGURE 3
Modèle d'étiquette pour un calorimètre avec l'indication des constantes de l'appareil.

Pierre TERRIER
C.E.R.I.L.H., FRANCE

4. EXERCICE DE L'AUTOCONTROLE.

Dès lors que l'opérateur sait ce qu'on attend de lui, peut mesurer si ce qu'il fait correspond à ce qu'on attend de lui, peut agir sur le déroulement de l'essai l'autocontrôle est possible et peut-être organiser par :

- des essais à blanc pour tester l'appareillage.
- des essais de répétabilité,
- le recours à des échantillons types,
- la comparaison des méthodes, dans certains cas,
- la cohérence des résultats.

5. TRAITEMENT DES ANOMALIES.

Avec le traitement formalisé des anomalies commence l'assurance de la qualité.

Tout écart par rapport à une situation prévue, décelé au laboratoire, constitue une anomalie. Toute anomalie est traitée, en particulier l'anomalie de fonctionnement des matériels ou conditions d'essais fait remonter l'arbre des causes, provoque la remise en question des réglages, de l'entretien, de l'étalonnage avec mise hors service éventuelle jusqu'à conformité.

Il est utile de distinguer les modes de défaillances puis de classer leurs conséquences (mineure, significative, critique, catastrophique). L'analyse des risques doit être conduite dans l'esprit d'une prévention adaptée (maintenance des groupes de froid à l'entrée de la saison chaude).

6. ESSAIS INTERLABORATOIRES.

Les résultats d'une mesure sont entachés, par rapport à la valeur vraie, m, de la grandeur, d'erreurs provenant de deux sources : une erreur de répétition et une erreur de laboratoire. Le résultat d'une mesure peut être représenté de la façon suivante :

$$x_{i,k} = m + l_i + e_{i,k}$$

l_i est l'erreur entre les laboratoires,

$i = 1, 2, \ldots, p$

p est le nombre de laboratoires.

La valeur moyenne de cette erreur l_i est nulle mais sa variance n'est pas nulle. Celle-ci a pour expression $V(L)$ ou $\sigma^2(L)$. C'est la variance de laboratoire.

$e_{i,k}$ est l'erreur de répétition dans un même laboratoire d'indice i

$k = 1, 2, \ldots n$

n est le nombre de résultats ou d'essais dans le laboratoire.

La valeur moyenne de l'erreur $e_{i,k}$ est nulle mais sa variance n'est pas nulle. Elle a pour expression : $V(r)$ ou $\sigma^2(r)$. C'est la variance de répétabilité.

L'ensemble des np résultats est caractérisé par une moyenne $\bar{X}$ et une variance $V(R)$ ou $\sigma^2(R)$. Celle-ci est la variance de reproductibilité qui caractérise la distribution de l'ensemble des mesures.

On a : $V(R) = V(L) + V(r)$

que l'on peut écrire $\sigma^2(R) = \sigma^2(L) + \sigma^2(r)$

en général $\sigma(R)$ est beaucoup plus grand que $\sigma(r)$

La valeur vraie, m, est en général, sinon toujours, différente de la valeur moyenne $\bar{X}$. Toutefois, on peut estimer la valeur maximale de l'erreur $|m - \bar{X}|$. En effet si l'on se donne un petit nombre, α, appelé seuil des probabilités significatives ou niveau de signification, on peut trouver deux nombres λ_1 et λ_2 tels que la probabilité que l'on ait : $\lambda_1 \leqslant m \leqslant \lambda_2$ soit égale ou supérieure à $1 - \alpha$

L'intervalle entre les 2 nombres λ_1 et λ_2 est l'intervalle de confiance bilatérale. $1 - \alpha$ est appelé niveau de confiance, c'est la probabilité pour que l'intervalle calculé contienne la valeur vraie.

Selon le fascicule de documentation X 06-041 de la collection des normes françaises, l'intervalle de confiance bilatérale, au niveau de confiance $1 - \alpha = 0{,}95$ pour la valeur vraie m, est l'intervalle :

$$\bar{X} \pm 1{,}96\sqrt{\frac{\sigma^2(R)}{p} - \left(1 - \frac{1}{n}\right)\frac{\sigma^2(r)}{p}}$$

Lorsque l'on a pu déterminer par un essai interlaboratoires les caractéristiques des lois de reproductibilité, $\sigma(R)$, et de répétabilité, $\sigma(r)$, il est possible de connaître l'intervalle de confiance lié à une moyenne de résultats d'une autre mesure de même nature. Cette autre mesure peut être effectuée par un nombre de laboratoires inférieur au nombre p de l'essai interlaboratoires et chacun d'eux peut avoir obtenu un nombre de résultats différent de n.

De même, on peut, d'après $\sigma(R)$ et $\sigma(r)$, estimer l'écart maximal admissible entre les moyennes des mesures de deux laboratoires qui effectueraient un essai différent de l'essai interlaboratoires et dont l'un aurait obtenu n_1 et l'autre n_2 résultats.

En effet, d'après le fascicule X 06-041, au seuil de $\alpha = 5\ \%$ ou $(1 - \alpha) = 0{,}95$, on doit avoir :

$$|\bar{X}_1 - \bar{X}_2| \leqslant 1{,}96\sqrt{2\left[\sigma^2(R) - \left(1 - \frac{1}{2n_1} - \frac{1}{2n_2}\right)\sigma^2(r)\right]}$$

si $n_2 = n_1 = 1$

$$|X_1 - X_2| \leqslant 1{,}96\sqrt{2\sigma^2(R)} = 2{,}77\sigma(R)$$

Ce mode d'utilisation ultérieure des caractéristiques de la dispersion d'une méthode d'essai, qui ont été déterminées au cours de l'essai interlaboratoires, est très utile (Tableau III).

Pierre TERRIER
C.E.R.I.L.H., FRANCE

Ces essais en commun conduits par le C.E.R.I.L.H. depuis 1949 ont été étendus en 1960 à l'ensemble des essais courants du ciment. Ils regroupent maintenant environ cent cinquante participants. Ils permettent chaque année aux laboratoires de confronter leurs résultats à l'ensemble des mesures.

7. PRATIQUE DE L'AUDIT INTERNE.

Un audit interne est déclenchée dans chaque unité technique (chimie, calorimétrie, etc..) une fois par an par le Responsable Qualité avec la participation du responsable technique.

TABLEAU III. APPLICATION DES ESSAIS INTERLABORATOIRES AUX MESURES DE CHALEUR D'HYDRATATION.

A. Les résultats des mesures de chaleur d'hydratation sont fournis à diverses échéances jusqu'à cinq jours. A titre indicatif les échéances de 12h, 1j, 3j, 5j, peuvent être retenues.
Les écarts types de répétabilité (r) et de reproductibilité (R) déterminés selon le fascicule de documentation X06-041 "Fidélité d'une méthode d'essai. Guide pour les essais interlaboratoires", sont les suivants :

t	12 h	1 j	3 j	5 j
(r) ($J.g^{-1}$)	10	10	10	10
(R) ($J.g^{-1}$)	15	15	20	20
Valeurs moyennes ($J.g^{-1}$) obtenues lors des essais interlaboratoires (à titre indicatif).	150 à 250	285 à 360	350 à 400	360 à 410

B. Intervalles de confiance bilatéraux, en $J.g^{-1}$, rapportés à un résultat ou à la moyenne de deux ou quatre résultats.

Cas retenus		Vis-à-vis du laboratoire	Vis-à-vis de l'ensemble des laboratoires	
		12 h, 1 j	12 h et 1 j	3 j et 5 j
1 résultat dans 1 laboratoire		± 20	± 30	± 40
2 résultats dans 1 laboratoire		± 14	± 26	± 37
Entre 2 laboratoires	1 résultat par laboratoire	± 20	± 21	± 28
	2 résultats par laboratoire	± 14	± 18	± 26

C. Ecarts admissibles entre les résultats de deux mesures ou de deux moyennes en $J.g^{-1}$

Cas retenus		12 h	1 j	3 j	5 j
2 résultats dans 1 laboratoires : $\lvert X_1 - X_2 \rvert$		28	28	28	28
ENTRE DEUX LABORATOIRES	1 résultat par laboratoire : $\lvert X_1 - X_2 \rvert$	42	42	55	55
	2 résultats par laboratoire : $\lvert X_1 - X_2 \rvert$	37	37	52	52

Pierre TERRIER
C.E.R.I.L.H., FRANCE

L'audit a pour but de déceler les risques de non qualité dans le laboratoire. C'est un examen méthodique qui vise à caractériser principalement :

- l'efficacité des modes opératoires,
- l'efficacité des procédures,
- le respect des procédures et des modes opératoires.

L'audit doit être conduit en se plaçant autant qu'on peut sur le terrain (et non comme un scribe installé sur les gradins et qui critique les phases du combat dans l'arène !) Le but de l'audit est de supprimer les imperfections en décelant les points d'application des actions correctives et en identifiant les opportunités pour l'amélioration. A l'occasion de l'audit on vérifie que les actions préventives ou correctives prises antérieurement ont porté les effets escomptés.

8. ACCREDITATION.

Le réseau national d'essais RNE dispose d'une méthode d'investigation qui lui permet d'évaluer le degré de conformité de l'organisation interne du laboratoire avec les exigences du référentiel. L'audit lui permet, par l'information préalable (questionnaire), l'interview, la consultation de documents et la visite des installations de constater que pour les différentes activités élémentaires, l'action à mener est bien prise en compte, la procédure décrivant ce qu'il faut faire et par qui le faire existe et est complète et que son application est vérifiée.

L'accréditation par le réseau matérialisée par le droit d'usage d'un logo (figure 1) correspond pour le laboratoire à la reconnaissance de sa capacité technique à réaliser pour le compte de tiers les prestations d'essais pour lesquelles il est accrédité.

La création du Réseau National d'Essais permet la création d'un pôle de cohérence et de compétence en matière d'essais. Un réseau de laboratoire dont la crédibilité ne puisse être mise en doute, c'est aussi un moyen de répondre au besoin des utilisateurs qui exigent des assurances quant à la qualité des essais par lesquels ils orientent leurs décisions. En outre, l'accréditation est reçue avec fierté par chacun des intervenants du laboratoire ce qui contribue à développer l'esprit Qualité. La satisfaction du personnel résulte du double sentiment de bien faire et de faire quelque chose d'utile. A mesure que cette aptitude s'accroit et que des progrès sont réalisés, d'autres deviennent accessibles et sont souhaités. La recherche de la qualité est alors qualifiante pour l'individu. Les différents systèmes nationaux d'accréditation coordonnent leurs efforts au sein de l'ILAC. Dans le domaine des matériaux cette concertation s'effectue principalement par la RILEM laquelle participe depuis 1977 aux travaux de l'ILAC.

Le principe d'un nouveau Comité Technique sur les Procédures d'Evaluation pour les Laboratoires de référence du ciment et du béton au sein de la Rilem a été retenu à la réunion du Conseil Général à WASHINGTON, en septembre 1985 à l'initiative de M FROHNSDORFF (ETATS-UNIS) et du Dr. BASILIO (BRESIL). Dans un large domaine couvrant : l'harmonisation des méthodes d'essais, la reconnaissance mutuelle des contrôles, la mise en place des systèmes d'assurance de la qualité, les essais d'intercomparaison, l'audit et l'accréditation des laboratoires, ce comité peut entreprendre en 1986 Le recensement des procédures, la tenue d'un symposium pour la confrontation des expériences en 1987 et ultérieurement la préparation d'un guide de bonne pratique.

* * * *

Au terme de cette communication, il importe peut être de bien distinguer d'une part, la gestion de la qualité des produits attestée par la certification, et d'autre part, la gestion de la qualité des essais dont témoigne l'accrédition. Pourtant un certain parallélisme existe entre les deux démarches, comme cela apparaît au tableau IV.

La certification des produits met désormais en oeuvre trois niveaux de contrôles : contrôle de fabrication (niveau 1) autocontrôle (niveau 2) et contrôle par le service de vérification (niveau 3). L'attribution du droit d'usage de la marque NF-VP des ciments, laquelle est gérée par le Comité de la Marque, s'appuie sur les essais réalisés aux niveaux 2 et 3 aux conditions suivantes, relatives à la résistance, à la compression :

a) VERIFICATION DU BON ETALONNAGE.

Les prélèvements effectués au titre du contrôle NF-VP (12 par an au minimum) sont chacun divisés en deux parts égales, l'une étant essayée par le laboratoire du Service de Vérification (ville de Paris) donne un résultat x_i , l'autre essayée par le laboratoire du fabricant un résultat y_i.

On s'assure d'abord que les différences $d_i = y_i - x_i$ ne sont pas éxagérement dispersées. A cette fin, on vérifie que la valeur e_m définie par la formule ci-dessous est inférieure à un seuil $e_o = 1$ MPa

$$e_m = 1/n \sqrt{\Sigma(y_i - x_i)^2 - 1/n\left[\Sigma(y_i - x_i)\right]^2} = \frac{\sigma_d}{\sqrt{n}}$$

n devant être au moins égal à 12.

b) VERIFICATION DE L'HOMOGENEITE DE L'AUTOCONTROLE.

La vérification ci-dessus étant faite, il convient de s'assurer que les essais d'étalonnage du fabricant (sur prélèvement Ville de Paris) appartiennent, avec une forte probabilité, à la même distribution statistique que l'ensemble des résultats de l'autocontrôle. A cette fin, on calcule :

$$u = \frac{|M - m|\sqrt{n}}{\sigma}$$

formule dans laquelle M est la moyenne de l'ensemble des résultats du fabricant et leur écart-type, m la moyenne de ses n essais d'étalonnage (12 en principe).

Pour $u > 2{,}58$ on serait conduit à conclure à la non identité de deux populations avec un

Pierre TERRIER
C.E.R.I.L.H, FRANCE

risque d'erreur de 1 %.

c) CORRECTION D'ETALONNAGE.

Dans le processus de vérification de la conformité aux normes par utilisation des résultats de l'autocontrôle ces derniers sont introduits dans les calculs après avoir effectué la correction d'étalonnage. En pratique le paramètre M (moyenne) de la distribution statistique de l'autocontrôle est remplacé par :

M + m' - m (où M est la moyenne de l'autocontrôle, m' la moyenne des essais NF-VP de l'étalonnage et m la moyenne des essais d'étalonnage du fabricant.

Ces vérifications et correction étant faites, la distribution des valeurs de l'autocontrôle doit satisfaire aux conditions fixées pour les limites nominales des classes de la norme NF.P.15-301 avec les probabilités suivantes :

. 90 % pour les valeurs minimales à 2 jours
. 99 % pour les valeurs minimales à 28 jours
. 90 % pour les valeurs maximales à 28 jours

Une certaine analogie apparait à cet égard entre les principaux systèmes européens de certification des produits permettant d'envisager entre les pays une reconnaissance mutuelle des procédures de certification (projet du sous-comité du CEN animé par M. VAN KLAVEREN).

L'accréditation s'applique déjà en FRANCE aux laboratoires qui interviennent au niveau 3 pour le béton et ses constituants (ciment, adjuvants, etc..) progressivement, elle peut concerner ceux du niveau 2. Elle qualifie, comme nous l'avons vu, une organisation et une aptitude à gérer la qualité des essais. Elle implique notamment le rattachement des grandeurs principales aux étalons nationaux. Elle correspond, elle aussi à trois niveaux de contrôle : l'autocontrôle, par l'unité technique (niveau I), l'audit interne et l'assurance de la qualité (niveau II) et l'audit externe (niveau III). Géré par le Réseau National d'Essais pour la FRANCE (par des Commissions sectorielles spécialisées : bâtiment Génie Civil etc...), la procédure s'inscrit dans une perspective de reconnaissance mutuelle de l'accréditation des laboratoires au sein de l'ILAC (International Laboratory Accreditation Conference).

CERTIFICATION DE QUALITE	ACCREDITATION
Niveau 1 contrôle de fabrication Niveau 2 autocontrôle du fabricant Niveau 3 contrôle du service de vérification	Niveau I autocontrôle par l'unité technique Niveau II audit interne et assurance de la qualité Niveau III audit externe par l'organisme accréditeur
Implique des conditions de prise en compte des résultats	Implique des conditions de réalisation des essais
Gérée par le Comité de Marque	Gérée par le Réseau National d'Essais
Evolution vers la reconnaissance mutuelle des certifications (CEN)	Evolution vers la reconnaissance mutuelle des accréditations (ILAC).

TABLEAU IV

A.K. MULLICK, K.H. BABU
P. BHASKARA RAO
National Council for Cement and Building Materials, New Delhi - India

EVALUATION OF POZZOLANIC ACTIVITY AND ITS IMPACT ON SPECIFICATION OF BLENDED CEMENTS.

INTRODUCTION

India has a long tradition in manufacture and use of blended cements, which presently comprise nearly three-fourth of the total cement production. Portland pozzolana cements (PPC), which comprise nearly half the total production, are made with flyashes and/or calcined clay pozzolana (CCP), mostly interground with cement clinker and gypsum.

Like in many other countries, cement specifications in India have some prescriptive and some performance requirements; characteristics and permissible proportion of pozzolana being such prescriptive requirements. In an effort to make the cement specifications as much performance-oriented as possible, the need of separate tests for pozzolanic materials in specifications of portland pozzolana cement (IS : 1489-1976) has been questioned. While the debate continues, it is held that, in order to ensure special properties of PPC claimed in standard specifications, viz better resistance to leaching, aggressive waters and alikali-reactive aggregates and reducing unsoundness due to free lime and magnesia hydration, some test to ensure its adequate reactivity to lime-systems is necessary. Such tests are also necessary to distinguish a pozzolana from a totally inert additive, for which performance requirements in terms of setting and compressive strength are not adequate. With this as a background, this paper reviews the characteristics of pozzolana and portland pozzolana cements in the country and makes recommendation for improvements in the cement specifications and methods of evaluation of pozzolanic materials.

CURRENT SPECIFICATIONS

IS: 1489-1976 permit addition of 10 to 25 percent pozzolana material in the manufacture of PPC. Being used as an all-purpose cement for plain and reinforced concrete interchangeably with ordinary portland cement, the specification requirements of compressive strength at 3, 7 and 28 days and setting times, in case of both types of cements, are identical. However, no tests for durability which may have a bearing on the long-term performance are prescribed. The pozzolanic materials are required to conform to requirements of IS: 3812 (Part I) - 1981 in case of flyashes and IS: 1344-1981 in case of CCP. As is common in many other countries (1,2), these requirements are in terms of chemical composition, fineness, drying shrinkage, lime-reactivity test (8 days at 50°C) as well as minimum 80 percent strength at 28 days in cement activity test with 20 percent replacement of cement by the pozzolanic material.

Out of these, pozzolanic activity has been found to have poor correlation with broad limits of chemical requirements specified, especially because the pozzolana used are essentially silica-and alumina-bearing, and pozzolana with sizeable calcium oxide content are seldom encountered. Fineness in terms of specific surface area (Blaine's) is important, but particle-size-distribution (fractions below 10 μm) is found to correlate better with pozzolanic activity (3). In order to evaluate the pozzolanic activity, one has, therefore, to fall back upon the physical tests involving reactivity to lime, e.g. lime-reactivity and cement activity tests.

CHARACTERISTICS OF POZZOLANA AND CEMENTS

Large number of samples of pozzolana materials, clinkers and cements produced with these (both OPC and PPC) in different cement plants were evaluated periodically. A summary of results of lime-reactivity (LR) and cement activity tests of pozzolana are described in Fig. 1 & 2 respectively. It is seen that the pozzolana used in about 30 percent

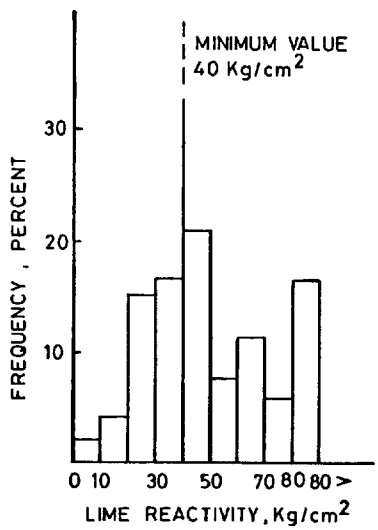

Fig. 1 : Histogram of lime-reactivity of pozzolana materials.

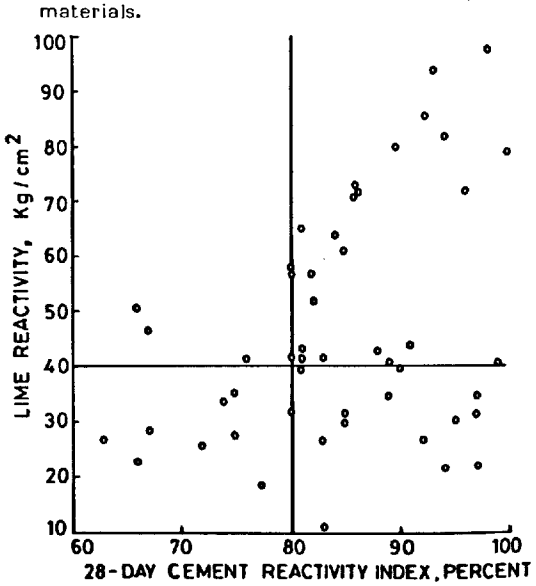

Fig. 2 : LR and Cement activity of pozzolana.

samples did not satisfy the requirement of minimum 40 kg/cm^2 lime-reactivity (Fig. 1). However, most of the samples satisfied the requirement of 80 percent cement activity and correlation with lime-reactivity was poor and the trend erratic (Fig. 2).

Reasons for this are not difficult to seek. Replacement of 20 percent cement amounts to a corresponding increase in the water-cement ratio and the resultant strength, in absence of any contribution from the pozzolana upto 28 days, could be of the order of 75 to 80 percent of the control (Fig. 3). Further modifications in the

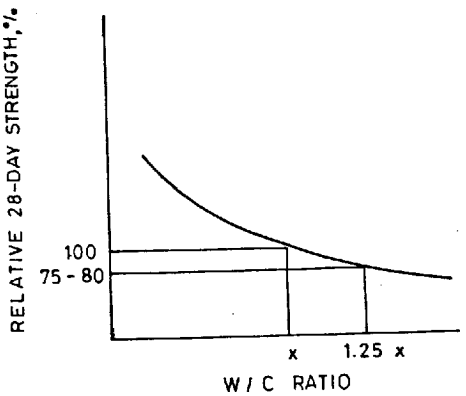

Fig. 3 : Effect of increasing w/c ratio by 20% on relative strength.

strength result due to the effect of granulometry of the pozzolana material in water requirement for the constant flow (105 percent). These are corroborated by the results in Table 1.

TABLE - 1

REACTIVITY OF INERT ADDITIVES WITH LIME AND CEMENT

Sl No *	Fineness cm^2/g	Lime reactivity kg/cm^2	Cement reactivity k.g/cm^2	Increase (+) or decrease (-) in water requirement %
A_1	3085	1.5	80	- 0.7
A_2	3290	1.4	74	0
A_3	3590	1.2	70	+ 0.7
B_4	3010	1.5	60	+ 3.5
B_5	3350	1.8	55	+ 4.1
B_6	3475	2.3	52	+ 4.8

* A_1 to A_3 limestone, B_4 to B_6 sand

where 20 percent cement was replaced by inert additives like ground limestone and sand. It is seen that the resultant strength was of the order of 52-80 percent of the control, depending mainly on the modification of water demand. On the other hand, some pozzolana material having relatively high LR were found to have resulted in cement activity lower than 80 percent, because of increased water demand (Fig. 2).

The dosage of pozzolana material used in manufacture of PPC in India usually ranges between 10 to 15 percent. Data on strengths of PPC and OPC obtained from the clinker used in the manufacture, whenever ground to comparable finenesses, are given in Table 2.

TABLE - 2

STRENGTHS OF PPC AND OPC - PLANT DATA

Cement Plant	Fineness cm^2/g		Ratio of Strength PPC / OPC	
	OPC	PPC	7 days	28 days
1	3755	3800	0.65	0.74
	4090	4355	0.61	0.74
2	2755	3325	0.92	0.85
3	2965	3000	0.96	0.94
4	3086	3473	0.98	0.95
5	2855	3863	0.88	0.97
	2519	3293	0.89	0.87
	3074	3872	-	0.87
6	3474	3608	0.72	0.63
7	2871	3413	0.91	0.87
8	2941	3504	0.87	0.90
9	3546	3782	0.89	0.90
10	3453	3826	1.24	1.02
11	3726	3826	1.00	1.06
12	3050	3453	0.52	0.70
13	3293	3696	0.82	0.78
14	3826	3896	0.78	0.74
15	4659	4684	0.90	1.03
16	3765	3750	0.80	0.79
17	3300	3655	0.98	1.02
18	2822	3252	1.10	1.10
19	3395	3375	0.78	0.83
20	3020	3128	0.91	1.07
21	3113	3273	0.87	0.91

It would be seen that inspite of somewhat lower percentage of pozzolana in industrial production, the strength ratios were more or less similar to cement-activity indices and age of testing (7 or 28 days) did not make much difference. This would point to the fact that not much of pozzolanic reaction was taking place upto 28 days. This is corroborated by X-ray diffraction studies carried out in the manner suggested by Costa and Massazza (4). Typical results indictated that the reduction of CH upto 28 days in the presence of pozzolana was not high. Typical scanning electron micrographs upto 28 days' hydration (Fig. 4 & 5), showed substantial proportion of unreacted flyash or CCP-particles with some hydration products.

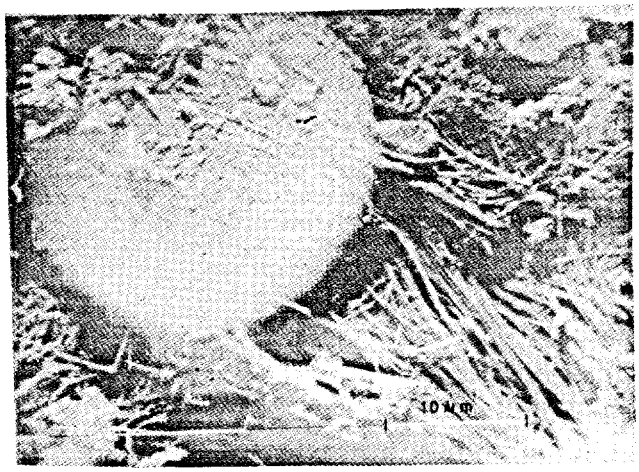

Fig. 4 : Electron micrograph showing unreacted fly ash particle.

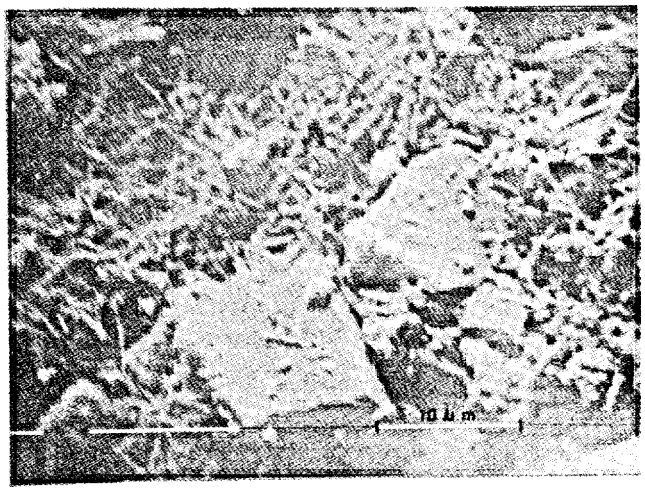

Fig. 5 : Electron micrograph showing unreacted CCP particle.

MODIFICATIONS IN CEMENT ACTIVITY TESTS

From the above it will be clear that the cement activity test does not serve the purpose of properly characterising a pozzolan or to distinguish it from an inert additive, mainly because the limit of 80 percent is not a stringent one, and secondly, not much of pozzolanic activity can be expected during 28 days hydration specially with pozzolana of marginal reactivities. On the other hand, variation in water content for constant flow introduces additional variability in results (5).

Lime reactivity test would seem to be preferable in that one of the reactants e.g. lime is constant and responses obtained with different pozzolana material help in evaluating and characterising them. Helmuth has discussed in detail the relevant reaction chemistry and the effects of amount of lime involved in evaluating pozzolana of both high and low reactivities (5). Although, the products of reaction in lime-pozzolana systems are essentially calcium silicate hydrates, there could be differences in the morphology and C/S molar ratio than what is expected in hydration with cements. It is for this reason that many tend to question the reliability of lime reactivity test under thermally activated regime in simulating the reaction of the same pozzolana with cements under normal conditions of curing.

Keeping these criticisms in view, attempts were made to assess the potential of strength contribution of a pozzolana to the cement under normal condition of curing in a more direct manner. For this, the standard cement sand mortar was tested for compressive strength at 28 days in the usual manner, except the water-cement ratio was kept constant at 0.5. Two other mixes were then tested; one with 20 percent extra cement (by weight) in the mix and the other with 20 percent pozzolana by weight in the mix with the water content same as in control. Since the water content was adequate to accommodate the increase in fines, no modification in the sand content was necessary. The contribution of the pozzolana to the strength development (PI), expressed as a proportion of an equal weight of cement was given by;

$$PI = \frac{C-A}{B-A}$$

where A is the cement strength in the control and B and C are the strength in mixes with additional cement and addition of pozzolan respectively.

Results of tests on different pozzolana samples are given in Fig. 6. Obviously the chemical composition

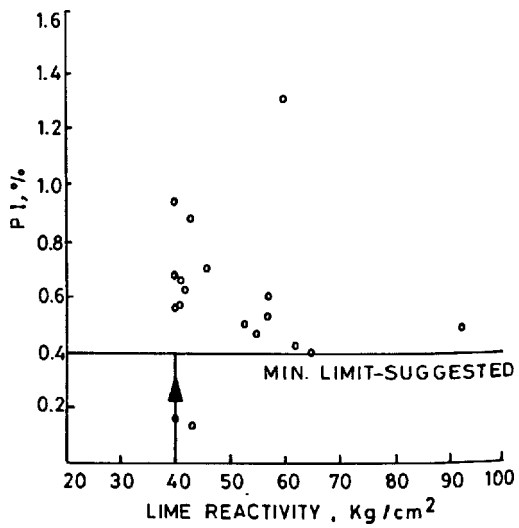

Fig. 6 : Relation between pozzolanacity index and lime-reactivity.

and fineness of cement would be important parameters and a strict comparison would have called for a "standard" cement to be used in each case, similar to a standard "lime" being used in lime-reactivity test. However, from the standardisation point of view, it would require that such a standard cement be used in all the laboratories and cement plants in the country. The cement used in this exploratory tests were, therefore, purposely chosen at random. Although there was considerable scatter in the test results in Fig. 6, it would appear that a pozzolana activity index (PI) of around 40 percent and above corresponded the lime reactivity value of 40 kg/cm^2.

These results point to the possibility of improving the cement activity test and set a realistic strength limit. In absence of any strength contribution by the pozzolana, a 20 percent cement replacement can cause 20 percent lowering of strength due to increase in water-cement ratio, i.e. 80 percent relative strength. Complete pozzolanic reaction, on the other hand, would result in strength equal to that of control (i.e. 100 percent relative strength), may be at a later age. Between these two extremes, since pozzolana materials of satisfactory lime-reactivity were found to contribute about 40-50 percent strength as of cement of equal weight, a 20 percent replacement of cement should correspond to atleast 90 percent relative strength upto 28 days when tested in constant water content.

CONCLUSIONS

Based on these investigations, the following suggestions are made for incorporation in specifications of blended cements;

i) While attemptes to make cement specifications more performance-oriented should continue, characterisation of additives in blended cements is necessary.

ii) Lime-reactivity tests are better suited to characterise a pozzolana and distinguish it from inert additives.

iii) Cement-activity tests should be carried out at constant water content and a minimum 90 percent relative strength for 20 percent cement replacement would ensure satisfactory pozzolanic activity.

ACKNOWLEDGEMENTS

This paper is a contribution from the Centre for Standardisation, Calibration, Testing and Quality Control at the National Council for Cement and Building Materials and based on data available with the Centre. The paper is published with the permission of Chairman and Director General of the Council.

REFERENCES

1.- OSCAR E. MANZ (1983), "Review of international specifications for use of flyash in portland cement concrete", Flyash, Silica Fume, Slag and other Mineral By-Products in Concrete, Vol. 1, Publication SP-79, ACI, pp 187-200.

2.- EDDIE ROSSOUW and JAPIE KRUGER (1983), "Review of specifications for use of flyash in portland cement concrete", Ibid, pp 201-220.

3.- P.K. MEHTA (1985), "Influence of flyash Characteristics on the Strength of portland-flyash mixtures", Cem. Concr. Res., 15(4), 669-674.

4.- U. COSTA and F. MASSAZZA (1983), "Some properties of pozzolanic cements containing fly ashes", Flyash, Silica Fume, Slag and other Mineral By-Products in Concrete, Vol. 1, Publication SP-79, ACI, pp 235-254.

5.- RICHARD HELMUTH (1983), "Some questions concerning ASTM standards and methods of testing fly ash for use with portland cement", Cement, concrete and aggregates, 5(2), 103-110.

OSAMU KATO - THE CEMENT ASSOCIATION OF JAPAN - R&D LABORATORY OF THE CEMENT ASSOCIATION OF JAPAN

TREND OF THE SPECIFICATION AND THE METHOD ON ALKALI - SILICA REACTION IN JAPAN

Numbers of cracks were found in the concrete piers of highways in Osaka City in 1982. Core specimens were extracted from the concrete piers and tested. As a result, the cause of the cracks was determined to be alkali-silica reaction.
Committee of Research on alkali-aggregate reaction of Japan Concrete Institute conducted a nation-wide survey of concrete constructions in the later years, and the results revealed several deteriorated concrete structures, whose cause was suspected alakli-aggregate reaction.

In Japan the examples of alkali-aggregate reaction were hitherto unknown, thus, the specification and test method had not been formed. Since 1984 much has been discussed as to set the specification for low-alkali cement and test method to determine alkali reactivity of aggregate in a somewhat hasten manner.

Japanese Industrial Standard Specification (JIS) for low-alkali cement was issued on February 1, 1986. The specification defines the alkali content of low alkali Portland cement to be below 0.6%. In respect to the test method for concrete aggregate, there is no authorized test method in Japan.

1. Establishment of JIS Specification on Low-Alkali Portland Cement

The Cement Association of Japan prepared a draft proposal for evaluation of alkali content of low-alkali Portland cement in order to set the criteria. However, it was found difficult at that time to establish the standard value of alkali content which ascertained the ground and gained a strong consensus, because of the lack of sufficient data showing correlation between alkali content and concrete expansion of alkali-reactive aggregate. Therefore, the Cement Association of Japan decided to propose low-alkali Portland cement should contain less than 0.6% of alkali with the reference to ASTM C150 /1/ and other references /2, 3, & 4/. Agency of Industrial Science and Technology reviewed the proposal, and revised JIS R5210 /5/ to add specification for low-alkali Portland cement. The newly issued alkali content of low alkali Portland cement was defined as $Na_2O(\%) + 0.658K_2O(\%)$ to be below 0.6%, and it was published officially on February 1, 1986. (Note. 1)

Note. 1: Analysis for Na_2O and K_2O is defined by JIS R5202 /6/, and they are determined by atomic absorption spectrophotometry or flame spectrophotometry.

2. Study of the Test Methods for Potential Reactivity of Aggregate

There is no official test method in Japan that determines alkali reactivity of concrete aggregate at present. The Cement Association of Japan, Japan Concrete Institute, General Building Research Corporations, and Public Works Research Institute of Ministry of Construction are currently undertaking a research to formulate the test method. The outline of these test methods is summarized as follows :

1. The test method that determines alkali reactivity of aggregate with the use of chemical method.
2. The test method to determine expansion of mortar specimen or concrete specimen.
3. The test method to determine dynamic Young's modulus and ultrasonic pulse velocity of mortar specimen or concrete specimen.

It is envisaged that the test method with the application of chemical method (1), and one with

Osamu Kato
The Cement Association of Japan

the determination of expansion of mortar bar (2) shall be approved as the standard test method for alkali reactivity determination in the near future.

2.1 Chemical Method

ASTM C289 /7/ was partly modified to construct the test method with the application of chemical method. The flow chart of this method is shown in Fig. 1.

The difference of this method with ASTM C289 is:

1. Perchloric acid is used in the determination of dissolved silica.
2. Atomic absorption spectrophotometry is adopted, while ASTM C289 doesn't include the two devices.

The advantages of the test method are shortening of analysis period and minimization of analytical error.

It is considered the chart (Fig. 2) of ASTM C289, "Illustration of Division Between Innocuous and Deleterious Aggregates on Basis of Reduction in Alkalinity Test" can be applied to determining alkali reactivity of Japanese andesite. Chert, however, is subject to consideration as sufficient data are not available for this aggregate.

2.2 Mortar Bar Method

For mortar bar method, a prism specimen of 4 x 4 x 16 cm (see Fig.2) is recommended. The mix proportion for this test method is similar to the one defined by ASTM C227 /8/. The total alkali content (Na_2O eq.) must be controlled at 1.2% to form a mortar specimen.

This specimen is easy to handle, as it does not destroy its form when casted off the mold. Nor does it twist or deform while it is preserved in the container. In addition, our experience tells that the measurement precision is notable with this method.

Fig. 3. shows the comparison of expansion ratio of a 4 x 4 x 16 cm specimen with a Stanton's bar. The mix proportion of the two specimens is identical. The results are congenial at large.

3. Future Schedule

At present, several institutions are undertaking the research of alkali-aggregate reaction. Yet, the vital issue is where to locate the responsibility of such a test method and to standardize it. In short, determining the standard value of total alkali content of 1 m^3 concrete is indispensable. In such a case, alkali content of water reducing agent and other admixtures, and mixing water must be tested integrally.

References:

1. ASTM C150-85 Standard Specification for Portland Cement.
2. Report of a Working Party of the Cement and Concrete Association, Minimizing the Risk of Alkali-Silica Reaction, Guidance Notes. (1983)
3. Vorbeugende Massnahmen gegen schädigende Alkalireaktion im Beton, Vorläufige Richtlinie. (1974)
4. NBR 5732-1977 Portland comum cemento.
5. JIS R5210-1979 Portland Cement
6. JIS R5202-1981 Method for Chemical Analysis of Portland Cement
7. ASTM C289-81 Standard Test Method for Potential Reactivity of Aggregates (Chemical Method)
8. ASTM C227-81 Standard Test Method for Potential Alkali Reactivity of Cement-Aggregate Combinations (Mortar-Bar Method)

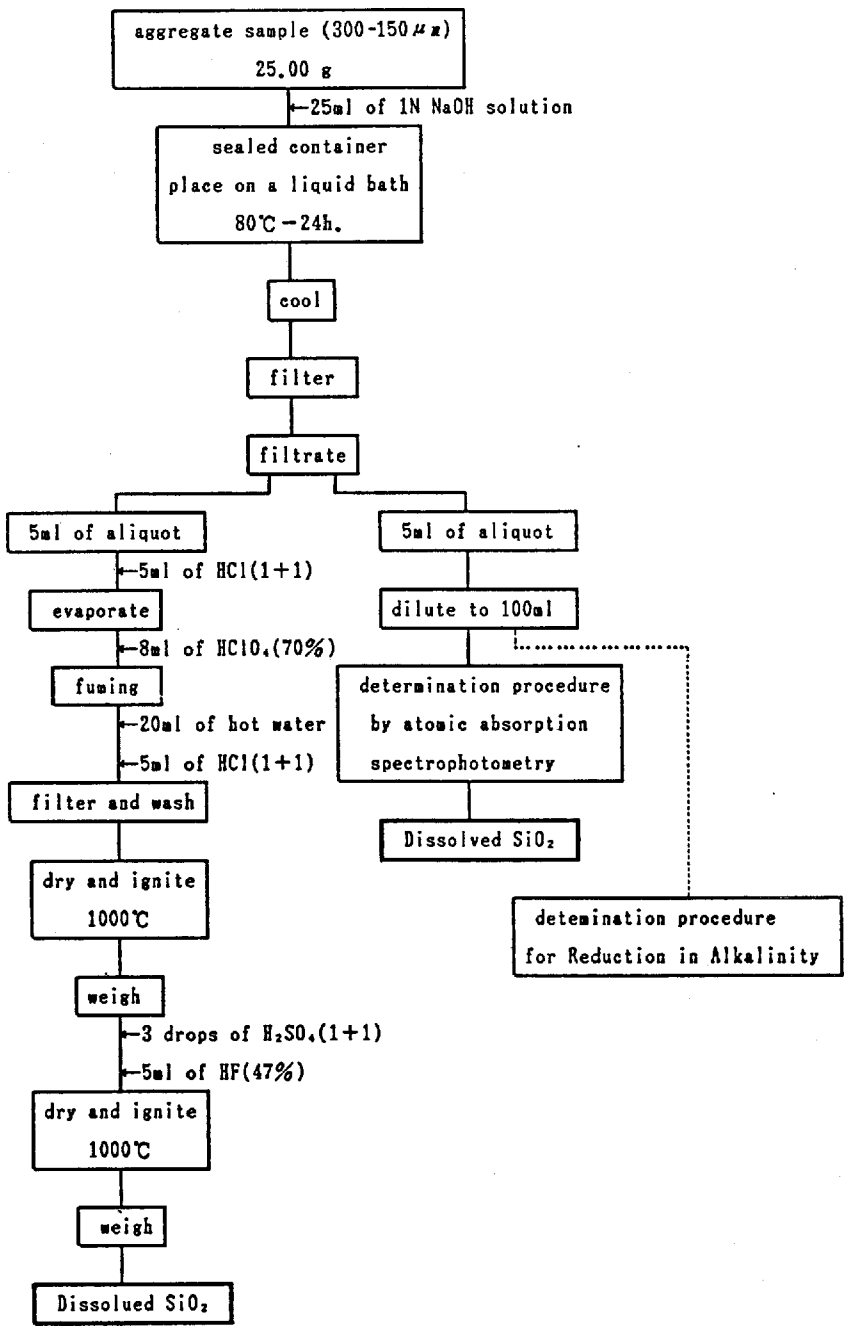

Fig.1 Flowchart of determination procedure of Dissolved Silica

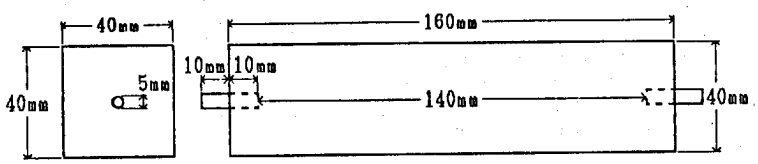

Fig.2 40×40×160mm Prism Specimen for Mortar bar test.

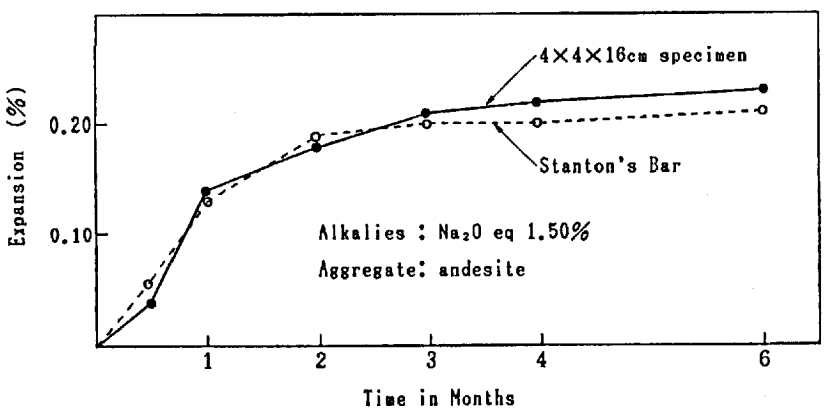

Fig. 3 A Example of Comparison of Expansion Ratio between the Stanton's Bar and 4×4×16cm Mortar Specimen

GEOFFREY FROHNSDORFF, PAUL W. BROWN AND JAMES H. PIELERT
CENTER FOR BUILDING TECHNOLOGY, U.S. NATIONAL BUREAU OF STANDARDS, GAITHERSBURG, MD 20899

STANDARD SPECIFICATIONS FOR CEMENTS AND THE ROLE IN THEIR DEVELOPMENT OF QUALITY ASSURANCE SYSTEMS FOR LABORATORIES.

1. INTRODUCTION

In recent years, there have been increasing pressures to broaden standard specifications for cements, particularly because of concern about conservation of fuels and other resources [1]. Concern is appropriate because, at least in the United States, cement manufacture is one of the largest industrial users of energy [2]. Whether or not changing cement specifications will have a significant effect on energy use, a number of important questions have been raised by the need to ensure that specifications do not unnecessarily hinder innovation in cement formulation. Unfortunately, these questions often end up as unresolved debates on the advantages and disadvantages of performance specifications, as opposed to prescriptive specifications.

In this paper, we discuss the purposes of standard specifications for cements, the types of specifications, the shortcomings of present specifications, the stimuli for changing the forms of cement specifications, the development of performance specifications for cements in ASTM, and the possibility of including optional prescriptive requirements in a performance specification. We also discuss the roles of quality assurance systems for cement testing laboratories and speculate about cement specifications of the future.

2. PURPOSES OF STANDARD SPECIFICATIONS FOR CEMENTS

The main purpose of a specification is to facilitate commercial transactions by defining a product in suitably precise terms acceptable to both the buyer and seller. In the case of a cement specification, it also facilitates the building design process by informing the designer and construction specifier about essential characteristics of the cement and helps protect public safety by defining materials which are likely to perform predictably and safely under normal conditions. Because most cements are commodities -- materials produced in large quantities which are sufficiently similar to each other for the products from different manufacturers to be interchangeable -- specifications must reflect their commodity nature. This requires specifications to address questions of quality, including aspects of performance and uniformity which affect interchangeability. In addition, specifications are usually expected to define minimum acceptable levels of performance, preferably through simple, short-term tests which have a strong, clearly-apparent, correlation with performance in common end uses. It is seldom considered essential for specifications to define maximum levels of performance, though maximum levels may be defined.

3. PRESCRIPTIVE AND PERFORMANCE SPECIFICATIONS FOR CEMENTS

Specifications are often discussed in terms of two extreme types -- prescriptive specifications and performance specifications [3]. A prescriptive specification defines a product in terms of its constituents and their relationships to each other, while a performance specification defines a product solely in terms of the functions it is to perform. Because it relies on measures of performance to assure the suitability of a product, a performance specification defines the product less narrowly, at least in terms of the constituents, than a prescriptive specification.

While it is useful to analyze specifications in terms of the extent to which they exhibit features of prescriptive and performance specifications, it often seems to be unrealistic to try to write specifications solely in either prescriptive or performance terms. On one hand, a purely prescriptive specification may require some knowledge which is not yet available, such as the relationship between composition and rate of strength development, or some analyses which are too sophisticated to be practical; on the other hand, a performance specification may require tests, such as tests for sulfate resistance, which are too complicated, time-consuming, and expensive for routine use. As a result, most product specifications have both prescriptive and performance requirements. Though such specifications are sometimes referred to as mixed specifications, they are still prescriptive.

In principle, a performance specification is less likely to inhibit development of new products since it gives a clear statement of the performance required and how a product's performance is to be evaluated. However, because of the frequent difficulty and slowness of performance testing, particularly where durability is concerned, compromises are often made. In view of the need to facilitate innovation, it is important to ensure that the elements in a specification, whether prescriptive or performance, are not unnecessarily restrictive.

Cement specifications differ greatly in the primary classification schemes used. For example, the main classification used in naming a cement may be in terms of strength (as in specifications in many European countries), of performance requirements other than strength (as in the ASTM C-150 Standard Specification for Portland Cements), or of the type and quantity of ingredients in the cement (as in the ASTM C-595 Standard Specification for Blended Hydraulic Cements).

4. SHORTCOMINGS OF PRESENT CEMENT SPECIFICATIONS

Cement specifications reflect the course of their evolution. Thus, a requirement in the current version of a specification may have been added long ago -- so long ago that the reason for the limit established, or even the precise reason for the requirement, may not be known by the active membership of the responsible committee. Such a requirement probably achieved its immediate purpose when first introduced though, possibly, at the expense of adding new restrictions on composition or performance which may now prove difficult to change. Also, prescriptive specifications are often vague, or completely silent, on the performance the products are intended to provide. In prescriptive specifications, the goal is usually to define the composition in unambiguous terms. For cements, this is not yet possible because of lack of adequate methods for determination of phase composition and particle size distribution.

Ideally, a specification should state explicitly what essential aspects of performance can be expected from the product. For example, a specification for a cement for use in reinforced concrete should indicate its ability to provide adequate corrosion protection for the reinforcing steel in general concrete construction. The specification should also state how compliance with necessary performance requirements can be demonstrated, whether by compositional analysis or by performance tests; in cases where performance tests for essential aspects of performance would take too long for routine use, or would be too expensive, provision should be made for alternative tests which will provide an equal or higher level of confidence that the required performance will be achieved. A list of performance characteristics which the authors recommend be considered in the preparation of a cement specification is given in Table 1.

Table 1. Performance Characteristics for Possible Inclusion in Performance Specifications for Cements

- o Strength at a given age
- o Dimensional stability
- o Flow properties (workability)
- o Setting time
- o Heat evolution
- o Sulfate resistance
- o Deleterious reactions with aggregates and reinforcement
- o Corrosion protection for steel
- o Response to air-entraining and other admixtures
- o Resistance to water
- o Uniformity of performance
- o Rate of strength gain at specified temperatures
- o Resistance to chemical attack
- o Color
- o Permeability to fluids
- o Electrical conductivity

Two of the most important characteristics in the list are often taken for granted, probably because they are always provided by portland cements. These are i) resistance to water, and ii) corrosion protection of steel. Although these characteristics are not specified in present cement specifications, they should be included in any performance specification for cements which are to be used in place of portland cements.

5. STIMULI FOR CHANGING THE FORMS AND CONTENTS OF SPECIFICATIONS

Cement specifications used in different countries have significant differences. This shows that there can be much flexibility in the formulation of cement specifications. It also suggests that few, if any, cement specifications are optimal. While cement specifications have been reasonably effective in meeting the normal, slowly-changing needs of most cement manufacturers and users, several new factors now suggest more urgent needs for changing the forms and contents of cement specifications. These include:

- o International agreements to encourage and support the use of international standards [4]
- o Governmental policies encouraging the development of performance specifications [5]
- o The need for conservation of the world's non renewable resources, e.g. fuels and industrial minerals used in cement manufacture
- o The need for minimizing detrimental effects on the environment of unused waste and by-product materials which are potentially useful as ingredients of cements, e.g. fly ash and by-product gypsum
- o Improvements which have been made in fundamental understanding of the factors affecting the performance of cements and concretes, e.g., factors affecting alkali-aggregate reactions [6]
- o Improvement which have been made in test methods and methods of materials characterization, e.g., X-ray diffraction
- o Possibilities for using knowledge-based expert systems to aid selection of concrete materials
- o Growing interest in providing comprehensive data bases to support the construction process and facilitate failure analyses.

These factors are stimulating critical reviews of cement specifications. As a result, changes are likely to be made and it is the responsibility of cement and concrete technologists to ensure the changes are rational.

6. INCLUSION OF OPTIONAL PRESCRIPTIVE REQUIREMENTS IN PERFORMANCE SPECIFICATIONS

It has already been mentioned that prescriptive specifications pose barriers to innovation because they put unnecessary limits on the range of permitted compositions. On the other hand, prescriptive specifications can reduce the risks which might arise from an unrestricted range of compositions, particularly when there is uncertainty about the adequacy of the available performance tests. Prescriptive specifications also, frequently, have the benefit of depending on analyses which can be carried out more rapidly than performance tests.

Performance specifications are usually believed to encourage innovation since they specify precisely what a product is intended to do and how its ability to perform satisfactorily may be assessed. They do not put unnecessary restrictions on factors such as composition or source of origin. Unfortunately, performance specifications may be inadequate in the choice of criteria intended to evaluate performance, and the performance tests, particularly ones relating to durability, may take a long time to carry out. This is a serious problem if the product cannot be used until a test is completed.

Because of the shortcomings of each of the extreme types of specification, practicality suggests that cement specifications should have both prescriptive and performance components, as is usually the case. However, to reduce the barriers to innovation, it is desirable that the specification include a complete performance specification, thereby establishing a logical basis for development of prescriptive criteria which may be needed as alternative, optional, criteria of compliance with the specification. A scheme of this type can be represented as in Figure 1.

In this scheme, the first four steps, 1 through 4, are the formulation of the performance specification; the next three, 5 through 7, are the conversion of some or all of the performance criteria into optional prescriptive criteria for acceptance testing; and the last two, 8 and 9, represent the generation and feedback of information on performance-in-use to the standards-writing body. At present, the feedback mechanism is usually too weak to have much effect on the standards-writing process, except when very severe problems are recognized. However, the scheme presented here can provide a model upon which to base the development of future performance specifications for cements. In essence, it describes the approach being taken in the development of a performance specification for blended cements in ASTM Committee C-1 on Cements.

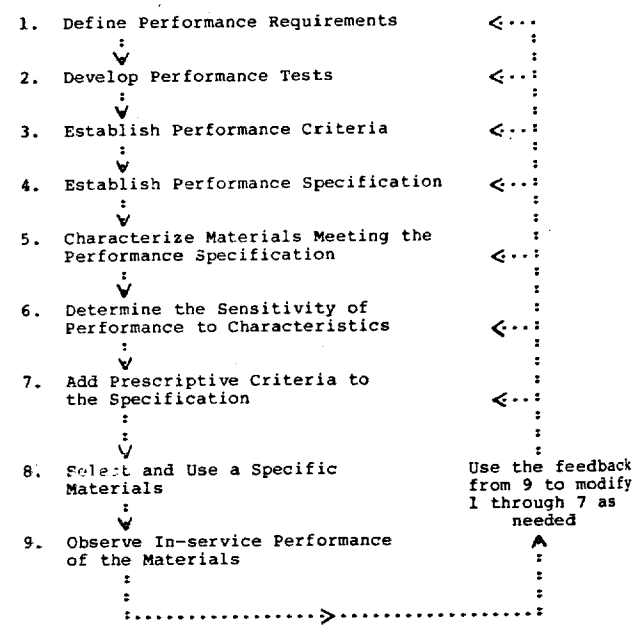

Figure 1. Scheme for Development of a Performance-Based Specification with Optional Prescriptive Criteria

7. THE ROLE OF A QUALITY ASSESSMENT SYSTEM IN THE EVOLUTIONARY DEVELOPMENT OF CEMENT STANDARDS

In many countries, a system for quality assessment of cement testing laboratories has been established. An example is the Cement and Concrete Reference Laboratory (CCRL) at the U.S. National Bureau of Standards (NBS). The CCRL is sponsored by ASTM Committees C-1 on Cements and C-9 on Concrete and Concrete Aggregates and managed for ASTM by NBS. Financial support for the CCRL is provided mostly by the fees charged for its services. The functions of the CCRL as related to cement [13], in decreasing order of importance, are:

i) Voluntary inspection of laboratories which use ASTM cement tests to identify, for the benefit of the laboratory managers, deviations from the correct procedures in the use of the standard tests;

ii) Provision of proficiency samples of cements for use by laboratories which wish to participate in an interlaboratory test program using ASTM cement tests; this gives laboratory managers a way of comparing their cement test results with those of other participants;

iii) Identification of problems with ASTM cement standards and bringing them to the attention of ASTM Committee C-1; and,

iv) Conduct of research needed for improvement of ASTM cement standards.

Quality assessment programs, such as the CCRL, can provide a powerful mechanism for improvement of cement standards through the feedback they provide on the effectiveness of the standards. For example, the databases they develop from interlaboratory cooperative test programs can be used for analysis of the variances in test results obtained using the standard tests; also, research on reasons for unexpectedly large variances can draw attention to problems with the standards. Because the quality assessment organization is constantly in touch with a large number of laboratories, it can develop an especially high sensitivity to the problems encountered; also if, as is the case with the CCRL, the organization is under the oversight of the standards committee, it can provide an effective means for feedback about the problems to the committee and its subcommittees. For these reasons concerning improvement of cement standards, it is strongly recommended that a high level of cooperation be maintained between quality assessment systems for cement testing laboratories and cement standards committees.

8. CEMENT STANDARDS OF THE FUTURE

In the future, increasing demands are likely to be placed on cement specifications. Because of the growing demands of some users for more information, there could be divergent needs for specifications between different types of users. Some users may only want the minimum assurance of quality while others may want precise data for use in predictive calculations and addition to databases. Further, depending on whether they are national or international, the specifications may have to meet the relatively narrow needs of individual countries, or the needs of groups of countries in different states of development. Nevertheless, it seems possible that a single specification could be prepared which could be used, in whole or in part, to meet the needs of different countries. Where the commodity nature of cements is emphasized, performance should be able to be defined in relatively precise terms, with lower and, possibly, upper limits being placed on acceptable performance for a given type of cement. In other cases, where there are many sophisticated users, emphasis might be placed on precise definition of the physical and chemical characteristics of a cement so that the user can apply his knowledge to predict how the cement will behave under diverse conditions.

It does not seem to be unrealistic to think in terms of prediction of the performance of a cement in concrete using computer-based mathematical models [7]. If and when this is achieved, the cement specification may require the manufacturer to transfer to the user data which is needed for predictive calculations.

Specifications sometimes show logical inconsistencies. To prevent this, the logic of each specification may, in the future, be subjected to computer analysis using techniques for standards analysis, synthesis, and expression [8, 9]. Also, recognizing the ever-present desire to use materials at close to their full potential, it is to be expected that computer-based systems to aid selection of the ingredients of concrete will be developed and standardized. An indication of this is that the American Concrete Institute (ACI) Committee 201 on Durability has established a subcommittee on knowledge-based expert systems. The National Bureau of Standards is working with the subcommittee in the development of a prototype expert system, DURCON [10], for selecting concretes for durability. The expert system is based on the ACI Guide to Durable Concrete [11]. Its development is proving valuable in drawing attention to gaps in the knowledge base available for selecting durable concrete. This should lead to more highly-focused research to improve our ability to make high quality decisions in the selection of cements and other building materials. It may provide a new incentive for specifications to include optional requirements for more information about cements to be transfered between manufacturer and user.

Overall, we must expect some cement specifications to develop as adjuncts to computer-integrated construction. This must include the establishment of integrated project information systems [12] whose lives will extend beyond those of the structures to which they apply. They must include the most relevant information about the materials used in the structures. In the case of concretes, it must be supposed that it will include information on the phase analysis and compositions of the cements and mineral admixtures used, together with the concrete mixture design. Thus, for reasons beyond those of performance specification, the future cement specification will probably require precise description of the cement in physical and chemical terms, whether or not explicit limits are set on physical and chemical properties.

9. CONCLUSIONS

As a result of a growing need of some users for more information, two distinct sets of needs seem to be developing for cement specifications. They are for specifications with which compliance can be shown by relatively simple tests based on, and logically traceable to, performance criteria; and specifications requiring the characterization of cements in the most precise chemical and physical terms so as to provide

the basis for prediction of performance using mathematical models. The growth in the power and availability of computers is likely to have several effects on specifications. For example, computers may be used for checking the logical consistency of specifications and for storing specified data about concrete materials used in individual construction projects. They may also employ specified data for predicting the performance of cements in concretes and mortars using mathematical models and for aiding decision-making on the selection of concrete materials using knowledge-based expert systems. Databases incorporating cement test results from quality assurance programs will aid the formulation of mathematical models and the development of expert systems. All of these foreseeable developments must be expected to cause further evolution of cement specifications.

10. REFERENCES

1. NMAB Report 361, The Status of Cement and Concrete R&D in the United States, National Materials Advisory Board, National Academy of Sciences, Washington DC, 1980, 105 pp.

2. Energy Consumption in Manufacturing, A Report to the Energy Policy Project of the Ford Foundation, Ballinger Publishing Co., Cambridge, MA, 1974, 610 pp.

3. B.E. Foster (ed.), Performance Concept in Buildings, Proceedings of the Joint RILEM-ASTM-CIB Symposium, NBS SP 361, 2 vol., National Bureau of Standards, Washington DC, 1972.

4. U.S. Trade Agreements Act of 1979, Statements of Administrative Action, Title IV - Technical Barriers to Trade (Standards), House Document No. 96-153, Part II, U.S. Government Printing Office, Washington, DC, 1979.

5. Circular A-119 (Revised), Federal Participation in the Development and Use of Voluntary Standards, Office of Management and Budget, Washington DC, October 26, 1982; see Federal Register, V. 47, No. 211, November 1, 1982, pp. 49497-49499.

6. G. Frohnsdorff, J.R. Clifton and P.W. Brown, History and Status of Standards Relating to Alkalies in Hydraulic Cements, in Cement Standards -- Evolution and Trends, ASTM STP 663, P.K. Mehta (ed.), American Society for Testing and Materials, Philadelphia, 1978, pp. 16-34.

7. G. Frohnsdorff and J.R. Clifton, A Review of Mathematical Modeling Applied to the Manufacture and Use of Cements, Cements Research Progress --1980, American Ceramic Society, 1981, pp. 279-298.

8. J.R. Harris and R.N. Wright, Organization of Building Standards: Systematic Techniques for Scope and Arrangement, Building Science Series Report BSS 136, National Bureau of Standards, Washington, DC, September 1981, 267 pp.

9. F.I. Stahl, R.N. Wright, S.J. Fenves and J.R. Harris, Expressing Standards for Computer-Aided Building Design, Computer Design, V. 15, 1983, pp. 329-334.

10. J.R. Clifton, B.C. Oltikar and S.K. Johnson, Development of DURCON, An Expert System for Durable Concrete; Part I, NBSIR 85-3186, National Bureau of Standards, Washington DC, July 1985, 18 pp.

11. Guide to Durable Concrete, J. American Concrete Institute, Detroit, 1977, pp. 573-609; also published as Section ACI 201.2R-77 in the Manual of Concrete Practice, Part 1, Materials and General Properties of Concrete.

12. R.N. Wright, Computers in Building -- A Strategy for Building Research, Building Research and Practice, V. 12, 1984, pp. 14-20.

13. J.H. Pielert, J.W. Haverfield, and P.A. Spellerberg, Application of CCRL Data in the Formulation of Precision Estimates for Selected Cement Standards, Cement, Concrete, and Aggregates, V. 7, Summer 1985, pp. 37-42.

E.B. ENTIN,
L.S. KLYUEVA, Cement Research Institute, Moscow, USSR

CEMENT QUALITY: KEY MEASURES AND EVALUATION TECHNIQUES

Specification of portland cement and its modifications is normally effected in conformity with the relevant ISO recommendations, national standards or SEV* standards (in the East European countries) as a set of widely agreed and practically significant performance measures, such as fineness of grinding, setting times, soundness, compressive strength and its development rate, and resistance to certain environments for special cements.

The most important figure of merit, from both engineering and cost-effectiveness viewpoints, is the 28-day compressive strength of a cement (specified in the USSR as the cement brand in kgf cm^{-2}) measured after 28 days of normal setting. However, this characteristic may vary for the same cement in wide range depending on the composition of standard test samples and the procedure of their preparation. Observing that cement is a semi-product, say, of concrete, it should be the principal, and more meaningful, requirement of cement testing techniques that there exist a strong correlation between the strength of cement and concrete.

The cement testing procedures, standardized in the industrial countries and widely used in the market and research practice, differ from each other by the sieve analysis of sand, composition and consistency of the mortar, and the size and consolidation of the test specimens.

A thorough review of the most widely used cement testing procedures has been reported by Dutron et al. /6/, another survey of relevant standards has been presented later by the World CEMBUREAU /7/. To date most countries have reconsidered their national standards for cement testing methods, but with no significant alterations. The Socialist countries have introduced a new standard SEV 3920-82: "Cement. Methods of testing for physical and mechanical properties" /8/.

In what follows we would like to examine certain general aspects of cement testing methodology.

Void content of sand and the composition of a standard cement mortar

Standard sands used in cement testing are normally natural quartz sands from a certain quarry for the country or a group of countries. Some national standards dictate the use of the so-called one-fraction sands with narrow sieve analyses of 0.15-0.60 mm in the USA, 0.50-0.90 mm in the USSR, 0.60-0.85 mm in Great Britain, and 0.10-0.30 mm in Japan. A common disadvantage of sands with narrow size distributions is an increased void content. For example, the void content of the one-fraction sand subject to the USSR cement testing standard amounts to 40-42% in a bulk state, 36-37% in a vibration consolidated state, and about 33% in a moist vibration consolidated state.

The structure of cement-sand mortars used in cement strength tests is consistent with a dense type in which the grains of sand are segregated by cement paste. The batch of cement paste naturally has to fill the intergrain voids and envelop sand grains thus separating them with a layer of paste.

Specimens of mortars prepared with the use of one-fraction sand are characterized by an increased macroporosity which depends not only on the void content of the sand but also on the composition of the standard mortar and, to a certain degree, on the consolidating means used. The standard mortar composition of the cement/sand ratio 1:3 should be recognized as unsatisfactory from the void-content spandpoint. Theoretical analysis of mortars conforming to the Soviet standard GOST 310.4-81 indicates that for a water/cement ratio of 0.40, the cement paste yield is hardly adequate to fill the voids

* SEV is the Russian acronium for the Council of Mutual Economic Assistance (CMEA or COMICON).

of the sand. For a collection of cements examined (compositionally different: straight and with admixtures of slag and flayash in proportions of 5, 12, and 20 wt. %), the coefficient showing excess of the cement paste varies predominantly between 1.11 and 1.13 growing as high as 1.14-1.16 for cements with an admixture of bergmeal and metallurgical sand. Accordingly, for cement test specimens by GOST 310.4-81, the macroporosity, defining the quality of the placement of the specimens, is about 4% /10/.

The unsatisfactory placement of specimens may degrade the normal profile of the strength versus W/C ratio dependence. At a constant W/C ratio, the strength of standard specimens can be increased by some technological means increasing the yield of cement paste. The increase in strength for such specimens will not be achieved in concretes made of these cements, that is, the correlation between the strength of cement in the mortar and concrete will be upset.

It is quite obvious, therefore, that a standard mortar should be prepared with such a ratio of cement and sand that would provide a warranted excess of the cement paste over the amount needed to fill the voids in the sand. For one-fraction sand mortars, the calculated macroporosity of specimens reduces in coming from 1:3 mortars to 1:2 mortars from 4-5% down to 1.5-2% (given isoplacticity of the mortars).

Comparison of variances for the ratio of concrete strength to cement strength, determined for isoplastic mortars with cement-sand proportions of 1:3, 1:2-3/4, 1:2-1/2, and 1:2 prepared at a constant cement consumption rate of 300 kg/m^3, indicates that the correlation of strength tests for cement and concrete improves for mortars of 1:2-1/2 and 1:2 proportionings (the level of significance for the variances being different is, respectively, 25, 25, 5, and 2.5%).

Thus, with one-fraction sand, one may achieve a considerable improvement of cement testing conditions by employing isoplastic mortars of 1:2-1/2 and 1:2 cement-sand ratios, which approach in their composition to the pastes of concrete mixes.

The recommendations of ISO and CMEA prescribe the use of sands with complex size distribution, the so-called three-fraction sands, of grain size measuring from 0.08 to 2.00 mm across. These sands exhibit a lower void content as compared with one-fraction sands (about 35% in a bulk state and 28% in a vibration consolidated state). The theoretical macroporosity of standard specimens in this case is small and amounts to about 0.7% for 1:3 composition mortars at a water/cement ratio of 0.50 /10/.

Comparison tests indicate, however, that the results may differ markedly if sands of a standard sieve analysis are from different sources. The respective tests with three-fraction sands of Polish and Czech origin, meeting the requirements of ISO and SEV recommendations, are summarized in Table 1. A perusal of the content of this table indicates that the 28-day strengths of specimens prepared with different-source sands and the same cement sample can differ from 4.0 to 11.7 MPa. It should be noted that these discrepances in compressive strength exceed both the laboratory and interlaboratory systematic errors resulted from using a standard sand of the same source.

Water/cement ratio and the consistency of standard mortars

Specification of cements as to the value of compressive strength is carried out by testing speciments of cement mortars prepared either with a constant water/cement ratio (ISO and CMEA recommendations, poly-fractional sand procedure, national standards of Great Britain, Japan and some other countries) or with a constant consistency of the mortar (national standards of the USSR and the USA).

We have mentioned already that the qua-

E.B. ENTIN,
L.S. KLYUEVA

Table 1

Effect of Three-Fraction Sands on Cement Strength Tests

Test place	No. of specim's	Sand source	Compressive strength, MPa for setting age (days) indicated			
			1	3	7	28
USSR	51	Poland	4.5	11.3	19.0	31.5
		CSSR	5.2	14.0	22.3	37.1
Hungary	26	Poland	6.0	13.0	21.0	39.0
		CSSR	9.0	19.0	28.0	43.0
Bulgaria	14	Poland	4.6	12.8	21.3	32.9
		CSSR	7.0	18.6	30.3	44.6

Table 2

Correlation Coefficients of 28-day Strength Tests by GOST 310.4-81 and SEV 3920-82

Test place	GOST vs SEV with three fraction sands from		Within SEV method on Polish and Czech. 3-fraction sands
	Poland	Czechoslovakia	
USSR	0.86	0.87	0.95
Hungary	0.78	0.83	
Bulgaria	0.88	0.80	

lity of a cement manifests itself in the final run by the cement behavior in concrete. Proceeding from this standpoint, two cements may be recognized as having identical quality if, given equal cement requirement and flowability of concrete mixes, they result in concretes of equal strength. Experience suggests, however, that these conditions of quality testing are impossible to meet if cement strength tests are carried out at a constant W/C ratio without taking account of mortar's flowability.

Constant W/C ratio tests are incapable of adequately revealing high engineering properties of cements with enhanced plasticity or decreased water requirements. These cements, however, are advantageous, if correctly specified, in that they open up the way for cement savings since a given placeability can be achieved at a lower W/C ratio than for cements of the same brand (28-day compressive strength) but unsatisfatory plasticity. From the viewpoint of cement quality testing, it is immaterial whether the difference in cement requirement occurred in manufacturing equally strong concretes of a given placeability has been caused by reduced activity or increased water requirement and unsatisfatory plasticity.

In cement specification, water requirements are estimated (simultaneously giving an indirect indication of rheological properties) with the normal consistency index of cement paste. Statistical processing of the data covering Soviet industrial cements suggests that there exists an approximately linear dependence between the normal consistency index and the W/C ratio of constant consistency mortars (Fig. 1), the correlation coefficient being 0.94. At an equal water requirement estimated with the normal consistency index, individual cements may, however, considerably differ in the W/C ratio of constant consistency mortar. Nonetheless, even with account of this remark, from the standpoint of cement behavior in concrete, the quality estimate is more objective in the case of tests with a constant mortar consistency rather than with a constant W/C ratio.

A constant consistency of mortar is not of that much significance in testing purely clinker cements which are characterized by close water requirements, but it is significant for cements with admixtures whose production is increasing by many cement producers.

Correlation of standard strength extimates from one- and three-fraction sand tests

Bulgaria, Hungary, and the Soviet Union carried out comparative tests of national cements by two methods as prescribed in the CMEA standard SEV 3920-82 and in the Soviet standard GOST 310.4-81. In the tests by GOST 310.4-81, all the countries used one-fraction sand in conformity with another

Table 3

Comparative Tests of Cements /11, 12/

Test place; method; cement	Participants (n) and reproducibility	Specific surface cm^2/g		Normal consistency,%		Initial set, min		Compressive strength, MPa for setting age (days) indicated											
								Laboratory (L)				Interlaboratory (IL)				International			
		L	IL	L	IL	L	IL	1	2	7	28	1	2	7	28	1	2	7	28
USSR;	n	10	19	10	19	10	19	10	10	10	10	19	19	19	19				
GOST	x	3428	3501	25.53	23.87	168	164	18.4	34.4*	45.6	57.8	14.7	29.2*	39.2	50.5				
310.4-81;	s	228	334	0.4	0.9	43.3	39.2	0.8	3.1	2.8	3.1	3.6	3.5	3.8	5.3				
portland	v, %	6.7	9.5	1.7	3.8	25.7	23.8	4.5	9.2	6.1	5.3	24.4	12.0	9.8	10.4				
cem.																			
France,	n		56		57		60	25	25	25	25	53	57	57	58	114	122	128	126
under	x		4253		30.2		150	18.1	28.2	40.0	53.2	18.1	28.2	40	53.4	18.1	28.2	39.9	52.9
CERILH	s		80		1.3		21	0.3	0.4	0.5	0.8	1.5	1.1	1.5	2.0	1.5	1.5	1.9	2.4
1982/83	v, %		1.87		4.33		14.0	1.85	1.35	1.21	1.43	8.03	3.96	3.71	3.66	8.3	5.32	4.71	4.86
ISO R 679, C.P.A. class 55-R																			

Note (*) 3-day compressive strength

Table 4

Physical Characteristics of Cements with Normal and False Sets

Portland cement producer	Setting type	NC, %	Setting test (hr-min)		W/C	Cone spread, mm	Compressive strength, MPa for setting age (days) indicated				
							normal setting				steam cure
			beg.	end			1	3	7	28	1
Brjansk cement plant	normal	24.00	2-35	4-30	0.36	113	10.8	22.7	36.5	48.0	26.2
	false type 1	27.25	2-30	4-35	0.38	112	11.5	25.7	37.8	51.4	26.2
Punane Kunda works	normal	25.25	2-50	4-50	0.37	113	17.0	31.4	39.7	50.0	34.5
	false type 2	26.50	2-45	4-40	0.40	113	12.5	25.0	35.4	47.1	29.7

Soviet standard GOST 6139-78. The tests by SEV 3920-82 were carried out with three-fraction sands from Poland and Czechoslovakia. These sands conformed to the standard but somewhat differed from one another by the surface morphology of the grains and the voids content (35% and 38% for Polish and Czech sands, respectively).

The correlation coefficients for the results of two testing methods are summarized in Table 2. As can be seen, the values of the coefficient are rather high (from 0.78 to 0.88 for international data), though somewhat lower than when one method of testing was employed on two different sands. However, the absolute value of the difference in the test results by two different methods does not exceed the test data difference in one method but with different sands. This allowed the following approximate relationship to be established between the classes of strength resulting from the two methods:

60, 55, 50, 40, and 30 MPa (GOST 310.4-81, 1-fraction sand)

55, 50, 45, 35, and 25 MPa (SEV 3920-82, 3-fraction sand)

Accordingly, the standard SEV 3920-82 "Cement. Methods of testing for physical and mechanical properties", superseding RS 138-73, allows for equal use of methods with one- and three-fraction sands. From January 1, 1985, Bulgaria, Hungary, Poland, and the Soviet Union have introduced this standard into commercial, industrial, and scientific spheres.

Assessing accuracy of cement testing methods

This purpose is served by systematically run comparison interlaboratory tests both within certain countris and on an international scale.

The comparative test data presented in Table 3 indicate that in general the physico-mechanical testing techniques are inaccurate, and the reason for this we see as follows. In the process of preparation and setting of specimens, a number of environmental and test parameters, such as setting temperature, stiffening amplitude, mass, etc, varies, although within the narrow limits specified by the standard, yet at random. Accordingly, the error of the test is in considerable degree due to the stochastic nature of the test procedure rather than to the properties of cement being evaluated.

False setting

False set relates to the properties of cement which affect the specification test results in a random way.

Abnomal phenomena at early setting age intervals may be broadly categorized into false sets of type 1 and 2 (respectively

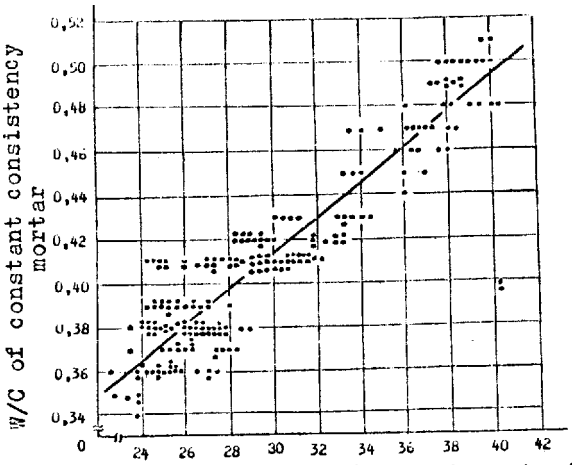

Fig. 1. Water/cement ratio of constant consistency mortar versus water requirement of cements. r = 0.94 for W/C = 0,008 (NC+21,6)

reflecting complete or partial premature loss of plasticity after mixing), and characterized by a trend to quick set and the quick set proper.

Transition from normal setting to false setting and from one false set type to the other is connected directly or indirectly with the change in the forms of gypsum in the cement. The trend to quick set, which manifests itself in degrading the initial set, and the quick set proper may be traced to both the lack of gypsum for setting control and a deep dehydration of gypsum in cement grinding. With the existing technology of cement manufacturing involving bihydrated gypsum as set retarder, the false set of 1 or 2 type and the trend to quick set are typical of industrial cements.

It is important to note that some cements exhibit both types of false set, whereas other cements give no evidence of type 1. Whether one or the other type of false set predominates depends primarily on the alkali content in the clinker /13/. With a moderate alkali content of a clinker (about up to 0.7% expressed as the Na_2O equivalent of the total alkalies), the cement having been heated in the mill to 100-150°C can exhibit both types of false set. With a higher alkali percentage of clinker than indicated, cements exhibit the false set of type 2 exclusively. An increase in temperature in the mill up to 170°C inescapably results in quick set properties.

The contact of cement with the environmental moisture in handling, shipment and storage may cause rehydration of the gypsum dehydrated in grinding, thereby eliminating the false set of type 1. The false set of type 2 is harder to eliminate.

Experience also exists on false set cases in shipment and storage of cements with initially normal setting properties. This is connected with the fact that the normal setting cements containing, as fresh from manufacturing, only bihydrate gypsum acquire in storage semihydrate gypsum whose content can vary both sides, increasing and decreasing. The appearance of semihydrate gypsum in storage in air may be attributed to surfase hydration in which both ambient moisture and gypsum crystal water take part.

The aforementioned variations of cement rheology that occur both in cement manufacturing and storage cast a shadow of randomness onto the specification of some cement performance measures, such as the normal consistency index, setting time, strength development rates, etc.

Choice of cements for steam curing

The methods of accelerated testing are well treated in /6/ devoted to the analysis of cement test methods. The lack of sufficient correlation between the strength test data at normal setting and various accelerated test methods bars the standartization of an accelerated test method. At the same time, a complete refusal of the common testing methods with 28-day compressive strength in favor of an accelerated test procedure would be undeserable due to a considerable proportion of cement being consumed in concretes not subjected to steam curing not to mention a need for rewriting the respective documentation involved in civil engineering procedures.

Summary

The consideration of cement testing methods in compliance with the Soviet State standard GOST 310.4-81 and the ISO and CMEA recommendations oriented to the use of sands which differ in sieve analysis indicates that all the methods are not free from shortcomings. The use of one-fraction sand inflicts a substantial shortcoming in the form of increased macroporosity of the specimens due to a shortage of cement paste which compounds the effect of random factors on the repeatability of the particular test method. With three-fraction sand, the reproducibility of the test method somewhat improves, but the test methods fail to take account of various water requirements of tested cements. Another shortcoming of the latter approach is its sensitivity to the sand, which is connected with the sand grain surface morphology and inconsistency of size distributions, in polyfractional sands.

An improvement of cement testing methods should be sought on the lines of using sands with a narrow sieve analysis and employing isoplastic mortars with a cement/sand ratio of about 1:2. The development of such a method and its promotion as a widely adopted approach is a challenge in the cement testing field. Achievement of this objective would considerably improve the correlation of strength test data from mortars and concretes.

REFERENCES

1. Organisation Internationale de Standartisation. Methode d'essais mechanique des ciments. Recommendation ISO R679, 1968.
2. Recommendation for standartization SEV RS 138-73 "Cements. Methods of physical and mechanical testing". Berlin, 1972.
3. The USSR State standard GOST 310.4-81 "Cements. Bending and compressive strength testing methods".
4. British Standard BS 4550: 1978 "Methods of Cement Testing".
5. ASTM C 109-80 "Cement hydraulic mortars". Methods of compressive strength testing with 2-in. specimens"
6. P. Dutron, K. Bang Peterson, S. Cral: Modern methods of mechanical tests for cement. In: The 4th International Congress on the Chemistry of Cement (Stroyizdat, Moscow 1976) in Russian.
7. Cement Standards of the World CEMBUREAU. The European Cement Association Library. Paris 1980.
8. Standard SEV 3920-82 "Cement. Methods of testing of physical and mechanical properties". The permanent CMEA committee on cooperation in standartization. Poland 1982.
9. USSR standard GOST 6139-78 "Normal sand for cement testing. Specification".
10. Z.B. Entin, L.S. Klyueva: in: The 4th International congress on the chemistry of cement (Stroyizdat, Moscow 1976) in Russian.
11. Z.B. Entin, Oleinikova, G.A. Rudneva, T.V. Kuznetsova: Estimation of accuracy for physico-mechanical cement tests. Tsement No. 5 (1978).
12. Centre d'Etudes at de Recherches de l'Industrie des Liants Hydrauliques. Essais Interlaboratores 1982/1983. Rapport General. Paris 1984.
13. Z.B. Entin, L.S. Klyueva: Liquid phase in anomalous setting of cements. Theses to 4th All-Union Conference on Cement Chemistry and Technology (Moscow 1982).

I. Odler, S. Abdul-Maula and U. Hennicke. Technical University Clausthal, D-3392 Clausthal-Zellerfeld, Federal Republic of Germany.

A NEW METHOD FOR DETERMINATION OF CEMENT SETTING TIME

For cement setting time determination the Vicat needle penetration method (1,2) and its numerous modifications (3) are most widely used. In addition to that the Gillmore method has been widely accepted in the USA (4). All these methods are arbitrary ones as the obtained results depend-in addition to the setting characteristics of the studied binder-also on the employed initial water-solid ratio, the diameter of the needle, the weight applied on the needle and other experimental factors.

In our work on acoustic properties of cementitious materials we observed consistently a very low initial acoustic conductivity of such systems right after mixing,which increased rather suddenly by several orders of magnitude after a period of time. We assumed, that this sudden increase in acoustic conductivity may be related to the setting of the system. To test this hypothesis we performed the tests reported.

EXPERIMENTAL

The set-up of the equipment employed is shown in Fig. 1. Electric impulses of preset frequency and intensity are produced in an impuls generator. They are converted into an acoustic signal of constant intensity using an ultrasonic generator equiped with piezoelectric transformers made from barium titanate. The fresh cement paste or mortar is placed between the generator and sensor. In the latter one the acoustic signal, which passed the paste or mortar, is converted again into an electric signal. The amplitude of the obtained signal, which indicates the fraction of acoustic energy not absorbed by the sample,is registered by the aid of an analog-digital-convertor. The data obtained this way are stored in a computer, and may be depicted graphically using a plotter.

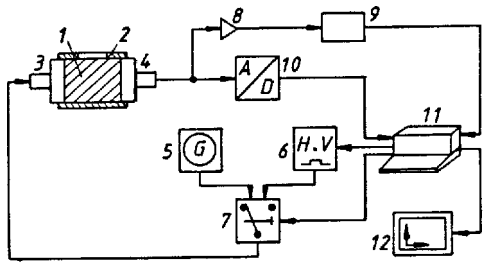

1. binder sample
2. sample holder
3. ultrasound generator
4. ultrasound sensor
5. frequency generator
6. impuls generator
7. switcher
8. amplyfier
9. digital chronometer
10. analog-digital-convertor
11. computer
12. plotter

FIG. 1: Set-up of the experimental equipment

RESULTS

To compare our acoustic data with results of other methods the setting time of a single portland cement paste (normal consistency ASTM C 187, DIN 1164 T 5) was determined using the following approaches:

1. Vicat method using a needle Ø = 1,13 mm and a load of 300 g (1,2)
2. Same - with a needle Ø = 2 mm
3. Same - with a needle Ø = 3 mm
4. Gillmore method (4)
5. Acoustic method using a frequency of 75 KHz. The gap width between generator and sensor was varied between 20 and 40 mm
6. Acoustic method using a frequenc of 160 KHz and a gap width of 20 mm

In Fig. 2a the distance from the bottom at which the needle became stuck in the paste is shown as function of time for all three needles employed. Expectedly, the time at which the needle ceased to penetrate to the bottom, just as the time at which it ceased to penetrate into the paste, shifted to shorter times with increasing diameter of the needle. The beginning and end of setting as determined by the Gillmore method is shown in the Figure with arrows designated G_b (beginning) and G_e (end).

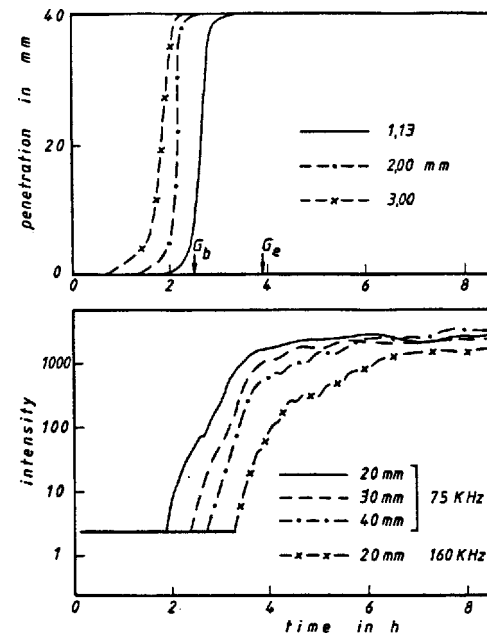

FIG 2: Setting data of an OPC obtained with
a) the Vicat and Gillmore methods and
b) the acoustic method

Fig. 2b shows the intensity of the measured acoustic signal as function of time. The time at which the signal became detectable increased with increasing

I. Odler, S. Abdul-Maula and U. Hennicke. Technical University Clausthal, D-3392 Clausthal-Zellerfeld, Federal Republic of Germany.

distance between the sonic generator and sensor and with its increasing frequency. It can be seen that the "setting time" determined acoustically lied within the range of setting time values determined by the classical methods, used for comparison. In subsequent experiments a constant frequency of 75 KHz and a gap between the generator and sensor of 20 mm were maintained. The data obtained this way were compared with those determined with the Vicat method using a 1,13 mm needle.

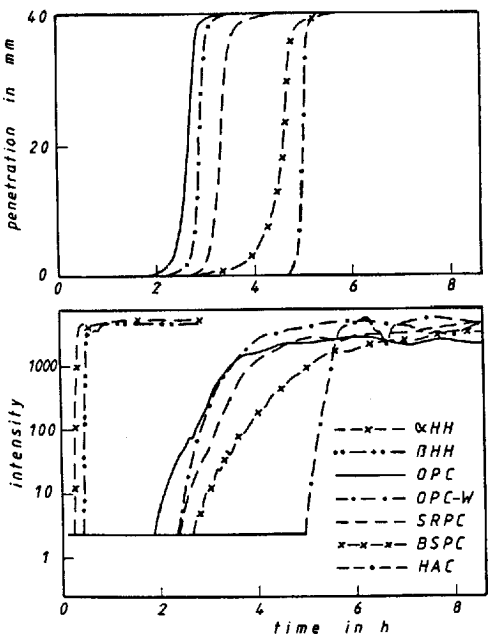

FIG. 3: Setting data for different kinds of inorganic binders a) Vicat method b) acoustic method

Fig. 3 shows data obtained on a series of various cements i. e. an ordinary portland cement (OPC), a "white" portland cement with no Fe_2O_3 (OPC - W), a "sulphate resistant" portland cement (ASTM type V) with increased Fe_2O_3 content (SRPC), a blast furnance slag portland cement (BSPC), a high alumina cement (HAC) and on two types of plaster of Paris (α HH and β HH). It can be seen that the orders in which the Vicat needle ceased to penetrate to the bottom and that in which the acoustic conductivity started to increase were identical.

Fig. 4 shows data obtained on our OPC cement with different chemical admixtures added. It appears that a setting acceleration brought about by an addition of $CaCl_2$ could be detected with both methods just as a retardation brought about by ZnO or sucrose.

Fig. 5 shows the effect of variations of the water-cement ratio on the obtained data. It appears, that the Vicat method is distinctly more sensitive to such variations than the acoustic one.

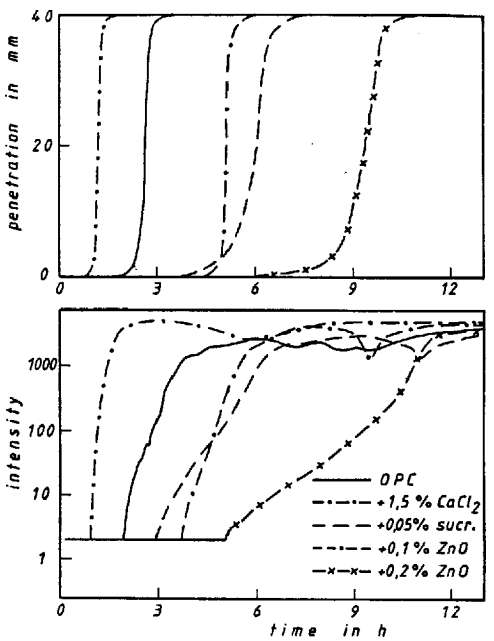

FIG. 4: Effect of chemical admixtures on setting a) Vicat method b) acoustic method

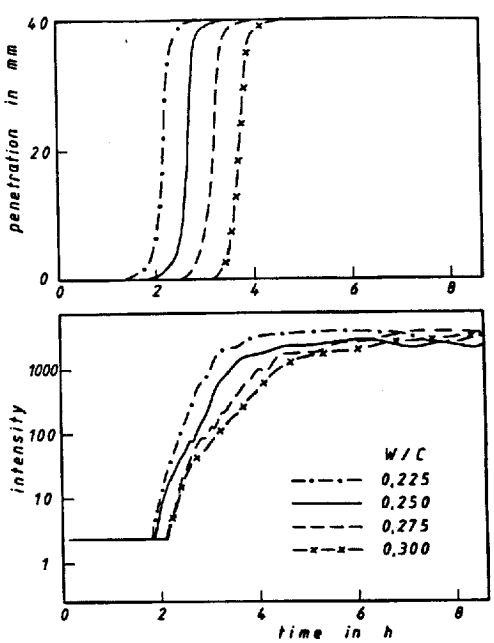

FIG. 5: Effect of water-solid ratio variation on setting a) Vicat method b) acoustic method

I. Odler, S. Abdul-Maula and U. Hennicke. Technical University Clausthal, D-3392 Clausthal-Zellerfeld, Federal Republic of Germany.

Finally, Fig. 6 demonstrates the possibility of the use of the acoustic method also in systems for which penetration methods are not suitable. It can be seen that the "setting time" of a pure cement paste was identical with that of a mortar with quartz sand made from the same cement with the same w/s (0.3). A mortar with a higher w/s(0.5)exhibited a retarded setting time; the measured setting time remained virtually unchanged if either quartz or expanded perlite were added as aggregate. An addition of glass fibers resulted in a retardation of setting whose origin is not obvious. Finally, a very significant retardation of setting was determined in a cement - pine wood chip blend, apparently due to the carbohydrate compounds present in the wood mass.

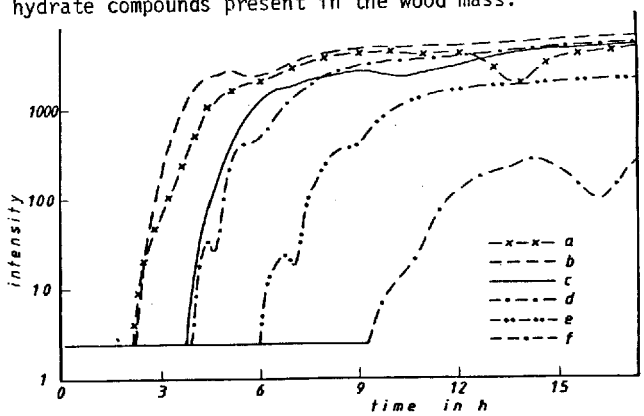

a. Paste OPC w/c 0,3 - d. Mortar OPC:Perlite 10:1 w/c 0,5
b. Mortar OPC:Sand 1:1 w/c 0,3 e. Mortar OPC:Glass Fibers10:1 w/c 0,5
c. Mortar OPC:Sand 1:3 w/c 0,5 f. Mortar OPC:Wood Chips10:1 w/c 0,5

FIG. 6: Setting characteristics of pastes and mortars made from same cement using different aggregates (acoustic method)

DISCUSSION

From the obtained data it becomes obvious, that the increase of acoustic conductivity observed in cementitious systems is due to the setting of the present binder. The phenomenon appears to be independent on the quality of the binder employed as an increase, of acoustic conductivity at the time of setting can be detected even if binders of different chemical nature are employed.

The origin of the increase of acoustic conductivity is not obvious at this time. We assume, that the solid framework formed in the paste at the time of setting causes - in addition to the ceasing of plastic deformability of the system - also its increased acoustic conductivity.

Just like in other methods, the exact setting time determined by our new method depends, to a certain degree, also on the conditions of testing. We assume that the obtained variations are due to different amounts of acoustic energy lost if signals of different frequency are employed or if the distance to be passed by the acoustic signal varies. It is of importance, however, that variations of setting time,such as those due to binder quality or to the effect of chemical additions, can be well detected acoustically if constant conditions of testing are employed. On the other hand the method is less sensitive to variations of the water-solid ratio which affect significantly the rheology of the cement paste and thus the outcome of measurements made with a penetrations method.

A special advantage of our new method is the possibility of its use in systems for which penetration methods are not, or only little suitable. Our experience shows that the acoustic method may be succesfully employed not only in ordinary cement pastes and mortars but even in glass or organic fibers or wood chips reinforced systems, not suitable for testing by any penetration method.

Our experiments were limited, so far, to systems that could be placed in a gap of maximum 40 mm, due to a limited output of our sonic generator. We believe, however, that the method may be employed even for concrete mixes, if the intensity of the entering acoustic signal will be increased appropriately.

CONCLUSIONS

A new method for setting time determination of cement pastes or mortars was developed in which the setting is determined on the basis of a sudden increase of acoustic conductivity of the system at the time of setting. The method is insensitive to the nature of the binder employed and little sensitive to variations in the rheology of the mix. The method may be employed also in mixes in which penetration methods cannot be employed due to the presence of foreign components, such as fibers, light weight aggregates, or wood chips.

REFERENCES

1. ASTM C 191-82
Test Method for Time of Setting of Hydraulic Cement by Vicat Needle.

2. DIN 1164 T 5
Test Method for Time of Setting of Hydraulic Cement by Vicat Needle (in German).

3. M. Maultzsch. Needle apparatus has existed for 100 years (in German). Zement-Kalk-Gips 36, 558-581 (1983).

4. ASTM C 266-77
Test Method for Time of Setting of Hydraulic Cement by Gillmore Needles.

G.GIACCIO (CIC-LEMIT) and R. ZERBINO (CONICET) - Argentina

FACTORS AFFECTING CEMENT PASTE-AGGREGATE BOND

P

1. INTRODUCTION

There is a general concense about the influence of cement paste-aggregate bond on the behaviour of concrete. It is recognized that the transition zone (interface) is the weakest link of the composite material and the one which directly affects mechanical properties and durability. In this way, the interest in factors that affect cement paste-aggregate bond, continuosly increases.

Adherence is partly due to mechanical interlocking produced by aggregate irregularities and to van der Waals forces which cause the adhesion between aggregates and cement hydration products. Besides there may be some slow chemical reactions that contribute to bond development.

This paper analyzes the influence of many factors on bond strength by mechanical tests. To do this, pastes with different water-cement ratios, chemical admixtures (a water reducing and two superplasticizers additives), expansive addition, and fly ash incorporation were used. Four types of rocks with different surface texture were included. Test age was also considered as a variable.

This study was complemented by SEM observations performed on fracture surfaces, for a qualitative analysis of interfaces and cement pastes.

2. EXPERIENCES

2.1 Test method:

The aggregate-hydrated cement paste bond strength was evaluated by flexure tests with mid-point loading system. Figure 1 shows a scheme of specimens.In every case, modulus of rupture of the corresponding cement paste were measured. Samples were cured in water until testing age.

A deformation-controlled testing machine was employed with a rate of 2 mm/minute.

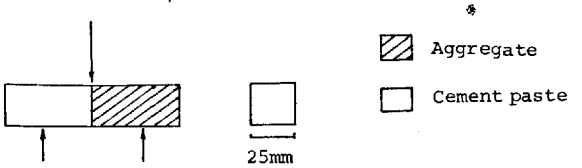

Figure 1: Cement paste-aggregate specimen and loading scheme.

2.2 Discussion of results:

Aggregate surface texture is one of the most important factors that affects bond strength, as it causes mechanical interlocking.

Meanwhile, fracture is preferentially produced at the interface in smooth surfaces, crack path can also develop through the paste and even sometimes, including aggregate grains in rough or broken surfaces.

Aggregates usually employed in concrete elaboration, present different surface texture, due to their porosity, grain size, cleavage plans, hardness, and also external factors as weathering.

Two textures for each aggregate were studied: natural fractured and swan surfaces. Table 1 shows the relationship Interface modulus of rupture (If_r) / Cement paste modulus of rupture (Pf_r). Bond strength is lower than paste strength, ranging from 20 to 62 %. It must be noted that fractured surfaces have always greater adherence than sawn surfaces.

Table 1. Influence of surface texture on aggregate-cement paste bond strength.(2)

Rock	Interface bond strength / Cement paste strength		sawn / fractured
	fractured surface	sawn surface	
SANDSTONE	0.40	0.32	0.80
MARBLE A	0.30	0.20	0.67
GRANITE B	0.46	0.20	0.43
BASALT	0.62	0.20	0.32

w/c ratio=0,40. Age:28 days.Paste strength= 12 MPa.

Although sawn surfaces are similar, when comparing many aggregates, their bond strength can be very different. In this case, the high bond developed by sandstone may be principally attributed to rock porosity. At the same time, variations produced by changes in surface texture for the same aggregate can be higher than those due to changes in aggregate type. Then, it becomes difficult to compare petrography influence as their effects are usually superposed.

To study other factors affecting bond strength, a unique surface texture was adopted. Marble or granitic aggregates were used with a grounded surface obtained by sanded.

Figure 2 shows the influence of water-cement ratio on bond strength. It appears that If_r variability is lightly lower than Pf_r; the relationship If_r/Pf_r trends to increase with high w/c ratios.

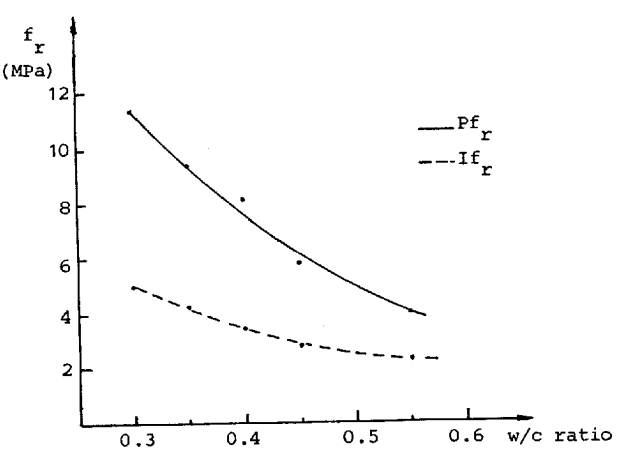

Figure 2: Influence of water-cement ratio on bond strength (If_r) and cement paste modulus of rupture (Pf_r)

If_r/Pf_r relationship is also modified by cement strength evolution rate. Generally strength gain takes place more slowly in interface than in cement paste. Table 2 shows the effect of age on bond and paste strength employing marble and granite, and a high early strength cement. It can be seen the significative differential evolution of interface and cement paste.

For normal cement or specially low heat cement the effect of age on If_r/Pf_r relationship is smaller.

If_r / Pf_r ratio prcbably changes because voids volume and size at the interface are larger than into the cement paste,(1) with time these voids are progressively filled, and, consequently, If_r / Pf_r ratio is modified.

Table 2. Effect of age on bond and paste strength.

Age (days)	Modulus of rupture (MPa) Interface: If_r Marble A	Granite A	Paste: Pf_r	If_r / Pf_r Marble A	Granite A
10	3.4	---	11.0	0.31	---
28	4.1	3.7	12.0	0.34	0.31
90	5.8	5.7	12.0	0.48	0.48
180	6.3	6.4	12.3	0.51	0.52

Grounded surfaces. w/c ratio = 0.40
Cement: C_3S:56%, C_2S:19%, C_3A:0.2%, C_4AF:15.8%.

To study influence of admixtures and additions series with w/c: 0.30 ahd 0.40 were made. Pastes included different types of superplasticizers (Naphtalene and Melamine basis, water reducing (lignosulfonate basis) expansive and fly ash addition.

Table 3 shows the obtained results of bond and paste modulus of rupture. As it can be seen some admixtures incorporate important air quantities as a secondary effect.

Air incorporation affects in different grade inter - faces and bulk paste behaviour. Pf_r decreases in a higher percentage than If_r by air presence, being the relationship If_r/Pf_r strongly increased.

Comparing NS with NSA (Table 3), air incorporation re duced paste strength in 41% and 26% at 7 and 60 days respectively; bond strength was only 10% lower at 7 days and it remains the same at 60 days.

All these experiences were made with vertical inter- faces, the effects of air bubbles could be different on horizontal interfaces.

Superplasticizers did not modify significatively If_r and Pf_r. Their principal effects appear by means of air incorporation. Naphtalene superplasticizer which did not entrained air gave almost the same If_r. Pf_r is higher at early ages probably due to the better dispersion of cement particles.

Melamine superplasticizer (MS) produced a small re- duction of strength at 7 days, However, it can be seen that at 60 days there is a little increment in bond strength for every superplasticizer.

Generally interfaces marble B-cement paste are slight ly weaker than granite's B.

The presence of this water reducing admixture, (which also incorporates air) produced higher If_r but smaller Pf_r. It appears again that interface is less sensi - tive than bulk paste, to air presence.

A modified behaviour was observed when fly ash was incorporated. Paste with 20% weight replacement of fly ash (Class F) finer than cement, was used. It may be seen that at 7 days paste strength decreased but bond strength wasn't affected. At 60 days If_r with fly ash is higher and Pf_r is still a bit small. Then If_r/Pf_r relationship is increased for fly ash blends, being the effect more evident at advanced ages.

Strength gain (7 to 60 days) is also more pronunciated at interfaces: while series $C_{0.4}$ increased bond and paste strength 50 and 37% respectively, this evolution for FA series was 100 and 61%. (Table 3).

It must be mentioned that there is a qualitative im- provement of interface, as fracture in 60 days FA bond tests was always through the paste nearly interface while for the corresponding control series($C_{0.4}$) only a small amount of paste remains adhered on the aggre- gate surface.

Fly ash reaction contributes to develop bond strength filling voids, that are originally larger at inter - face, and reducing large $Ca(OH)_2$ crystals concentra- tion. These crystals have lower adhesion capacity(van der Waals forces) and apport preferred cleavage plans.

SEM micrograph (Figure 3) shows a fly ash-cement paste -granite aggregate interface.Oriented $Ca(OH)_2$ crystals are clearly distinguished.Big crystals are often found close to interfaces probably due to a greater space for growth.

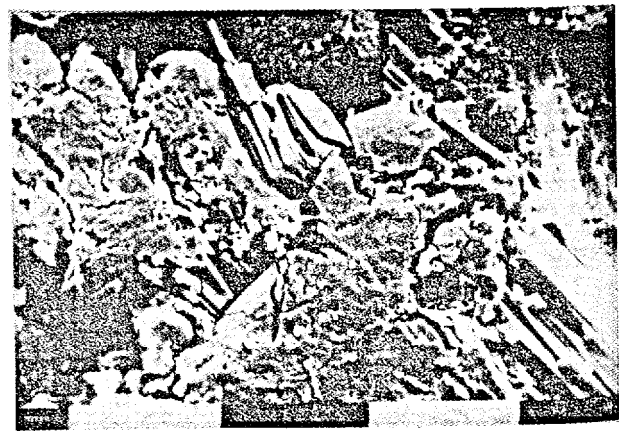

Figure 3: SEM micrograph of fly ash-cement paste-gran- ite B interface, view from aggregate(split along inter_ face). (Age: 60 days). Bar = 10 m. X 2700.

Table 3. Influence of additions or chemical admixtures on bond and cement paste strength.

Addition or chemical admixtures	Symbol	w/c	Air incorpo ration	Rock	Modulus of rupture (MPa) Interface: If_r 7 days	60 days	Paste: Pf_r 7 days	60 days	If_r / Pf_r 7 days	60 days
None	$C_{0.3}$	0.3	no	g	4.9	5.9	11.0	12.3	0.44	0.48
				m	4.6	5.4			0.42	0.44
Superplasticizer Naphtalene	NS		no	g	5.0	6.4	12.0	12.5	0.42	0.51
	NSA		yes	g	4.5	6.4	7.1	9.2	0.63	0.70
				m	3.8	6.5			0.54	0.71
Superplasticizer Melamine	MS		no	g	4.0	6.5	10.0	12.8	0.40	0.51
				m	4.0	6.0			0.40	0.47
None	$C_{0.4}$	0.4	no	g	3.6	5.4	8.4	11.5	0.43	0.47
Water reducing	WRA		yes	g	4.2	5.7	6.3	7.8	0.67	0.73
Fly ash(4200cm^2/g)	FA		no	g	3.4	6.8	6.7	10.8	0.51	0.63
Expansive	E		no	g	2.9	6.3	8.8	11.6	0.33	0.54

Rocks: Granite B(g), Marble B(m). Cement: 2860 cm^2/g. (C_3S:30%, C_2S:41%, C_3A:9.5%, C_4AF:10.9%).

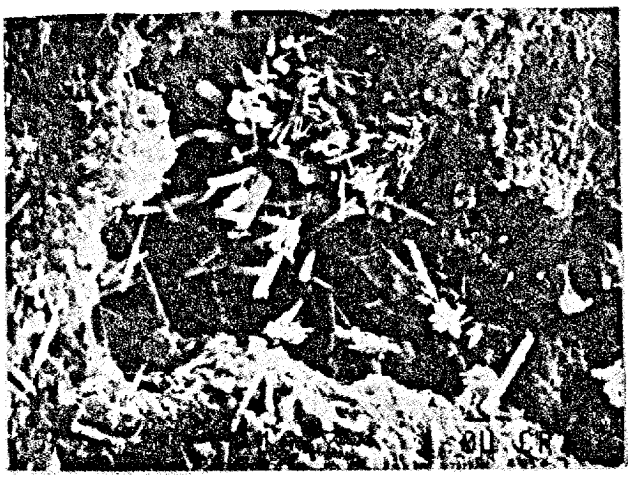

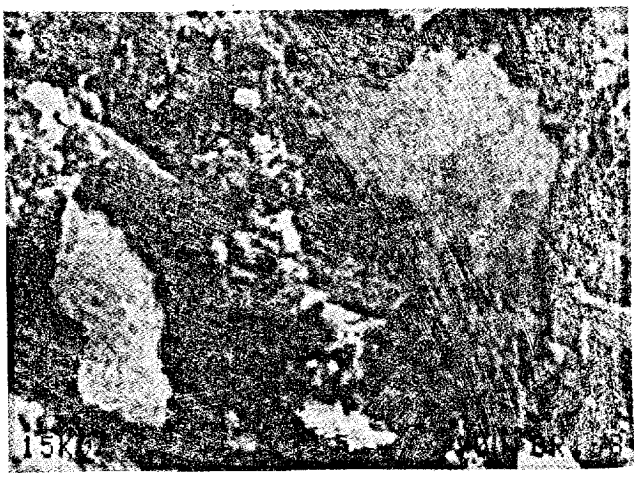

Figure 4: SEM micrographs of cement paste with expansive addition. (age: 100 days). a)(left):interface view from aggregate (split along interface). X4000. b)(right): bulk paste. X6000.

Paste incorporating 12% cement weight expansive addition was mixed. Expansion of bars inmersed continuosly in water were 44 /tm/m and 54 /tm/m at 7 and 60 days respectively. Pf_r was always similar to control paste ($C_{0.4}$). (Specimens had free expansion conditions)

Bond reduction at early ages and bond increment at advanced ages were found. Then If_r/Pf_r relationship had a strong evolution with time.

Figures 4.a and 4.b show respectively interface and interior paste characteristics of series including expansive addition. Bulk paste appears very compact, meanwhile bigger voids and crystals are observed at interface.

3. CONCLUSIONS

The principal conclusions extracted from these experiences can be summarized as follows:

- Surface texture is one of the most important factors affecting bond strength, and consequently If_r/Pf_r relationship. Rough surfaces had always higher bond than sawn surfaces. For practical purposes physical aspects, as mechanical interlocking, have more influence than petrographic aggregate characteristics.
- If_r/Pf_r ratio is modified by maturity. Interface bond develops more slowly than paste strength.Cement with high hydration rate showed clearly this phenomenon.
- It is confirmed that bond is less sensitive to w/c ratio than paste strength(mainly with high w/c ratio)
- Air presence affects in different magnitude interface and paste strength. While there is a substantial decrease in paste modulus of rupture (Pf_r), the effects on bond are very small.
- Fly ash incorporation modified If_r/Pf_r relationship. Fly ash reaction (60 days) produced an increase in bond (26%) while paste strength was still a bit lower than control (6%), and also a different crack path was observed.
- There weren't found important changes on cement paste-aggregate bond produced by the water reducing agent and the superplasticizers. Only melamine superplasticizer reduced stregth at 7 days. Nevertheless paste strength can be affected by air entrainment caused by these admixtures.
- Expansive addition, in this dosage, did not affect paste strength, however it modified bond development. It reduced bond at early ages and increased bond at advanced ages.

4. REFERENCES

(1). MASO,J.C.(1980) La liaison entre les granulats et la pate de ciment hydraté, VII Int.Cong.on the Chem.of cement.Vol 1. París.

(2). GIACCIO,G. ZERBINO,R. and GIOVAMBATTISTA,A.(1985) "Adherencia agregado-matriz".Colloquia 85.Vol 1. RILEM. Buenos Aires. Argentina.

J.K. Shukuzawa, H.C. Rodrigues Filho, V.A. Zampieri
Associação Brasileira de Cimento Portland

RELATIONSHIP BETWEEN ALITE MICROSCOPIC REACTIVITY AND CLINKER HYDRAULICITY

P

1 INTRODUCTION

The technique of etching polished section is an essential process for the reflected light microscopy studying of clinker. Because of the similar reflecting power of clinker minerals, it is only possible to observe of microscopic textures and structures through the etching of polished section by adequate chemical substances.

The thickness of coating of the reaction products formed in the crystal surface, determines the color observed by reflected light. The color is a result of light refraction and varies according to Newton's Series, while the thickness of coating grows [1]. So, as the color is closely related to the reaction rate of crystal with the etchant, it can be used as a crystal reactivity.

In order to check the relation between the alite crystals color and the clinker hydraulic activity, microscopic studies performed in industrial clinker samples are shown.

2 NH_4Cl ETCHING

The following aspects were obtained as a result of previous microscopic observations performed in clinkers from different plants, using NH_4Cl as etchant:

a) NH_4Cl must always be used in an aqueous solution, in concentrations about 0.1%, and when the room temperature is 22°C, the ideal etching time would be about 20 seconds.

b) with the increasing of the etching time, the alite crystals color changes progressively into the following degrees:

light brown
dark brown
dark blue
light green-blue
greenish-yellow
orange-yellow

↓ increasing of the etching time

c) the same color and tonality can be obtained, even after a new polishing and etching, because of the good repeatibility of the method.

d) with NH_4Cl the reaction rate is affected by the alite crystallographic orientation. With polished thin sections it was possible to see that the perpendicular section to crystallographic C-axis shows low reactivity, while parallel section shows a high one.
This etching anisotropy is closely related to the optical anisotropy. The optically less anisotropic alite sections are those that have minor reactivity.
The more anisotropic sections are the more reactives.
This reactivity increases with the growing of the optical anisotropy.

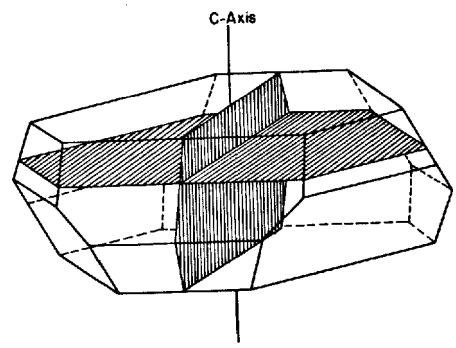

FIGURE 1- Sketch of a single cristal by Yamaguchi and Ono [2]

e) according to ONO [3], alite crystals of clinkers burned at high temperatures show greater birrefringence and are hydraulically more active. These alite crystals when submitted to reflected light microscopy show elongated forms and high reactivity to NH_4Cl.

f) small alite crystals are more reactive to NH_4Cl than the large crystals. In the same clinker nodule, it is observed that while the smaller crystals reach blue color, the large ones remain brown. These observations are in accordance with the results attained by other authors [3,4,5] that obtained a greater hydraulic activity for the small crystals in relation to the large crystals.

g) alite crystals with thin belite lamellae are usually observed in industrial clinkers burned in reducing environment. They occur in three different sets with strict crystallographic orientation with respect to the host [6]. This texture results from an oxidation of Fe^{2+}, which replaces part of Ca^{2+} in the alite crystal lattice. Less frequently, in some parts of the clinker alite crystals appear without fine lamellae and decomposition structure.
Fe^{2+} is probably still in the lattice, since droplets of metallic iron and high frequency of C_3A can be observed in the nearness. Reactivities of alite crystal with lamellae and alite crystal without decomposition structure are very different. While the first one keeps the brown color, the second shows a light blue color. The behavior of these two types of alite after the NH_4Cl etching agrees with Woermann's observations. This author points out the incorporation of Fe^{2+} into alite crystal lattice to be responsible for the high crystal instability and thus for its reactivity.

h) alite idiomorphic crystals from quick cooling rate clinkers, are more reactive than irregular crystals from slower cooling clinkers. According to Dorn [1], cooling rate is supposed to be the most important factor in crystal color development.

3 ALITE REACTIVITY AND CLINKER HYDRAULICITY

By means of NH_4Cl etching of clinker polished sections an attempt was made with the purpose of correlating the alite microscopical reactivity to the clinker hydraulic activity. Three samples of industrial clinker from the same raw mix and burnt into the same rotary kiln (1,000 ton/day) were selected. Phase quantification by microscopy showed similar compositions, mainly with regard to the alite content. This fact lead us to conclude how insignificant is the influence of its content in the difference of hydraulic activity among the clinkers.

A method based on Dalziel's[7] proposition and adjusted by Ferreira[8] was used in order to evaluate the clinker hydraulic activity. This method consists in the determination of the compressive strength of 20mm diameter x 30mm high mini-cylinders. Powdered clinkers with a specific surface area (Blaine) of about 340 $m^2.kg^{-1}$ were dry pressed till a porosity of 35%. Then, the dry specimens were submitted to a vacuum lower than 0,60 mbar, during ten minutes inside a vacuum chamber. Under this condition the entering of water occurs without a significant alteration on the chamber interior negative pressure. After the vacuum application a sufficient amount of water was added, so that the specimens could be completely submerged; then the pressure was lightened in order to let the water enter. The submerged mini-cylinders were cured in a water temperature of 23°C, for 18 hours and 28 days, respectively, when finally tested. The final result of the test was obtained through arithmetic mean of four test specimens, with within coefficient of variation between 0,0 and 5,0%.

Due to the fact this method is not standarded and considering the comparative aim of this study, relative strengths were prefered.
Sample B with 36,4MPa at 18 hours and 147,0 MPa at 28 days was taken as reference (100%). According to *Figure 2*, the three samples were packed in the same polished section in order to make the etching acts in an uniform way. This procedure reduces differences during the etching time.
The polished surface was etched with NH_4Cl (0,1%) during 20 seconds just washed with water and dried.

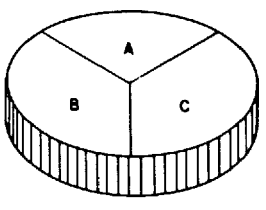

FIGURE 2 - Polished section with three samples of clinker

As it was discussed before, the alite reactivity depends on, among other factors, the crystallographic section. So, on the polished surface of a unique clinker fragment it is possible to recognize different alite sections, with a variety of colors. In addition varieties of crystal sizes and the heterogeneity of industrial clinker fragments, make it difficult to evaluate the color of alite in clinker as a whole.

In order to make this evaluation less subjective, the alite crystals were classified, according to color, in four types and the frequency of each one was determined by crystal microscopical counting, under a magnification of 250 times.

TABLE 1 - MICROSCOPICAL AND PHYSICAL CHARACTERISTICS OF CLINKERS

	COMPONENT		CLINKER A	CLINKER B	CLINKER C
PHASE COMPOSITION BY MICROSCOPY	ALITE (%)		61.6	65.4	65.5
	BELITE (%)		21.1	17.9	15.3
	C_3A (%)		4.2	2.0	2.3
	C_4AF (%)		12.0	13.4	15.8
	FREE LIME (%)		1.1	1.3	1.1
ALITE	SIZE (μm)		50-60	30-40	25-30
	BIRREFRINGENCE		0.0045-50	0.0045-50	0.0045-50
	FORM		subidiomorphic	idiomorphic	idiomorphic
	COLOR TYPE	I (%)	82	25	8
		II (%)	13	27	24
		III (%)	4	32	49
		IV (%)	1	16	19
BLAINE ($m^2.kg^{-1}$)			346	334	336
18 HOURS STRENGTH (%)			49	100*	122
28 DAYS STRENGTH (%)			92	100**	106

* 36,4 MPa
** 147,0 MPa

TYPE	COLOR
I	BROWN CRYSTALS
II	CRYSTALS OF BLUE COLOR IN THEIR CORE AND BROWN IN THEIR RIM (BROWN PREDOMINANCE)
III	CRYSTALS OF BLUE COLOR IN THEIR CORE AND BROWN IN THEIR RIM (BLUE PREDOMINANCE)
IV	BLUE CRYSTALS

Table 1 shows a good accordance between the alite color and the relative strength of clinkers. Differences among individual values of relative strength at 28 days decreased in relation to 18 hours values. However the same general tendency was kept. Clinker C not only showed the biggest strength but also the most content of types III and IV reactive alite crystals. On the other hand, in clinker A, with the lowest strength, most crystals are type I, in others words, the least reactivity.

In these three samples, the alite reactivity is mainly related to their size. In clinker A, besides of the alite biggest size, it seems that the alite irregular shape and the exsolution texture found in various crystals contributed to decrease its reactivity.

The birrefringence values of the alite crystals showed that the burning temperature was the same in the three clinkers. It means in this specific case that the reactivity was not influenced by this factor.

4 CONCLUSIONS

The alite crystal color after etching is a parameter that can be used to predict the reactivity. It can replace other parameters like crystal shape and size, birrefringence, incorporation of minor elements, cooling rate etc. that were known by their remarkable effect on clinker reactivity.

Although we haven't had yet enough data to correlate statistically the mini-cylinder strength to standarded method strength, results of research showed an inter dependence between alite microscopic reactivity and clinker hidraulicity.

We believe this kind of study and future advances like the belite reactivity evaluation will lead us to a better prediction of cement behaviour.

REFERENCES

1. DORN, J. *Theory of etch color development in portland cement.* In: BAYLES, J. ed. *Proceedings of the sixt International Conference on Cement Microscopy,* Albuquerque, 1984. p.421-26.

2. YAMAGUCHI, G. & ONO, Y. *Mikroskopische Untersuchungen am Alit des Portland zementklinkers. Zement-Kalk-Gips,* Wiesbaden, 20 (9):390-94, 1966.

3. ONO, Y. *Microscopical estimation of burning condition and quality of clinker.* In: *INTERNATIONAL Congress on the Chemistry of Cement,* 7th, Paris, 1980. v.2,

4. LONG, G.R. *Clinker quality characterisation by reflected light techniques.* In: GOUDA, R.G., ed. *Proceedings of the fourth International Conference on Cement Microscopy,* Las Vegas, 1982. p.92-109.

5. CAVENY, W.J. & WIGAND, W. & BAILEY, D.E. *Microscopic method helps assess cement performance. Oil & Gas Journal,* Tulsa, : 90-93, Sept. 26, 1983.

6. WOERMANN, E. *Decomposition of alite in technical portland cement clinker.* In: *INTERNATIONAL Congress on the Chemistry of Cement,* 4th, Washington, D.C., 1960. v.1, p.119-29.

7. DALZIEL, J.A. *A mini-cylinder test for the rapid determination of cement quality. Cement Technology,* London, 2(4): 105-12, July/aug. 1971.

8. FERREIRA Jr., S. *Um método de ensaio acelerado para determinar a resistência à compressão do cimento na temperatura normal.* In: ASSOCIAÇÃO BRASILEIRA DE CIMENTO PORTLAND (ABCP). *Reunião de Técnicos da Indústria do Cimento,* 34ª, São Paulo, 1983. (*paper avaiable only by contacting author*).

G. Babachev, K. Kolev - Sofia Bulgaria

THE INFLUENCE OF THE CEMENT TYPE ON THE VALUES FOR LIGHT CONSTRUCTIVE-THERMAL INSULATING CONCRETE.

P

The method for experiment planning and mathematic modelling (active experiment) is used to evaluate and to optimize the properties of the light concrete by varying factors on three levels according the type of the concrete - portland cement 20 PZ 350, fly-ash cement, shlake portland cement.

The following main receipt factors are selected to be investigated:

- Cement amount per 1 m^3 concrete (X_1), varying on three levels: 250, 300 and 350 kg/m^3. These limits are selected so that to be obtained a wider concrete range with properties and parameters, varying in a relatively wide range in order to meet the practice requirements;

- Water content per 1 m^3 concrete (X_2) varying on three levels: 190, 205 and 220 kg/m^3. The limits for the variation of the last factor are been so selected that to be obtained concrete mixes which are not hardly processed or startfying, considering also the necessary water content for the used additives.

- The ratio of the amounts for the coarse and fine additives (by volume) (X_3), varying on three levels: 0.7, 0.85 and 1.0. The reason to select the above limit values is based on the results of the preliminary research and investigations - in such manner the advisability of the above limit values has been proved.

On the basis of preliminary investigations and references about the possible kind of the mathematic relations, the type of the goal-function was selected as a full polynom of second degree, as follows:

$$Y = B_o + \sum_{i=1}^{3} B_i X_i + \sum_{i=1}^{3} B_{ii} X_i + \sum_{i<j} B_{ij} X_i X_j$$

where the symbol $\sum_{i<j}$ means a sum of all possible different $X_i X_j$ members.

In order to avoid difficulties in respect of the factors' dimensions, a coding procedure has been selected - as using non-dimensional values in limits of -1 to +1 according the following relation:

$$x_i = \frac{X_i - X_o}{0.5(X_{i\,max} - X_{i\,min})}$$

where:

$X_{i\,min}$ is the low limit for factor variation

$X_{i,o}$ is the middle (average) value of the factor in the investigated range

$X_{i\,max}$ is the top limit for factor variation.

To obtain maximum information from the mathematic model at lowest influence of the unknown or disturbing factors, an experiment plant is used - this plan of the experiment is near to D-optimal plan of type B_3, as shown in Table 1. for natural factor coordinates.

Table 1.

No.	Natural coordinates		
	X_1	X_2	X_3
I	350	190	0.7
II	250	220	0.7
III	250	190	1.0
IV	350	220	1.0
V	350	190	1.0
VI	250	220	1.0
VII	350	220	0.7
VIII	250	190	0.7
IX	350	205	0.85
X	250	205	0.85
XI	300	220	0.85
XII	300	190	0.85
XIII	300	205	1.0
XIV	300	205	0.7
XV	300	205	0.85

For goal-functions (Y) are selected: the consistency of the concrete mix, measured by technical viscosity meter; compressive strength after thermal traetment on the first day R_{H}^{II} 1; tensile strength at bending on the first day R_{OI}^{II} 1; compressive strength at normal setting or hardening conditions on the seventh day; voluminary density of the concrete after steam treatment $\rho_{o,w}^{II}$.

The experiment was performed by portland cement 20 PZ 350 with 37.5 MPa activity. As a light additional material a shlake-ash mix was used - from the "Bobov Dol" thermal power station, with voluminal density of the grain equal to 1335 kg/m^3 . As a coarse additional material is used a ceramsyte gravel with 20mm maximal diameter of the grains and 860kg/m^3 voluminal density of grains. Part of the samples were thermally treated by steam at atmospheric pressure and T = 358 $\pm$ 5°K temperature of isothermal heating mode: 2.5 + 1.5 + 5 + 2 = 11 Hours

and the other part of the samples are at normal setting or hardening conditions.

Before introducing the test results in order to develop the relevant mathematic models a stochastical processing is necessary to determine mean arithmetic value, root-mean-square deviation, variation factor, to check for random errors with a significant deviation from the mean value, to determine the mean dispersion for the experimental cement bloc.

After the preliminary stohastical treatment/ processing the test results for every propery of the light concrete are introducing in the computer. By means of the relevant computer programmes are calculated and checked for valuability (weight) factors in the models, checked for adequatity according the Fisher criteria. The properties of the light constructive-thermal insulating concrete, experimentally determined, are show in Table 2. On the basis of the experimental results (Table 2) are calculated mathematical models with the following expressions (after the adequatity check for the relevant properties):

1/ Consistency (acc. the measurements by technical viscosity meter) - S

$$S = 8.3 + 0.6X_1 + 0.8X_3 - 2.7X_2 + 0.8X_1X_2 - 1.2X_2X_3 + 0.7X_2^2 - 2.5X_1^2 .$$

2/ Compressive strength after steam treatment- R_HII 1

$$R_H\text{II } 1 = 13.6 + 1.5X_1 - 0.8X_2 + 0.6X_3 - 1.6X_3^2 + 0.7X_1X_3$$

3/ Tensile strength at bending after steam treatment - R_{OI}II 1

$$R_{OI}\text{II } 1 = 1.45 - 0.12X_2 - 0.08X_3 - 0.19X_3^2 - 0.12X_2X_3$$

4/ Compressive strength after 7-day setting time R_H7:

$$R_H7 = 11.5 + 1.7X_1 - 0.5X_2 - 1.2X_1^2$$

5/ Voluminal density after steam treatment $\rho_{o,w}$II

$$\rho_{o,w}\text{II} = 1213 + 36X_1 + 12X_3 + 30X^2$$

Table 2.

No.	S sec.	R_OIII1 MPa	R_HIII1 MPa	R_H7 MPa	ρ_{o,w_3}II kg/m^3
I	9	1.45	13.6	12.7	1262
II	4	1.44	10.1	8.6	1183
III	3.5	1.44	11.0	9.1	1211
IV	9	1.16	14.2	11.2	1293
V	12	1.39	14.8	13.3	1302
VI	4	0.77	9.0	7.4	1194
VII	4.5	1.30	10.7	10.7	1244
VIII	6	1.27	11.0	9.1	1231
IX	4.5	1.31	15.0	12.3	1292
X	7	1.52	12.1	8.9	1211
XI	4	1.72	13.3	12.2	1227
XII	14	1.38	14.9	10.8	1193
XIII	10	1.17	13.6	13.0	1241
XIV	7	1.24	11.3	11.5	1198
XV	8	1.34	12.5	10.0	1204

All models meet the requirements of the criteria for adequatity of the description and can be used to analyse the properties of the light concrete.

A full polynom is obtained for the influence of the cement amount on the consistency, i.e. all investigated factors (members of the mix) has influence on the possibility of the concrete mix.

A prevailing factor is the cement amount. The influence of the last factor on the consistency of the concrete mix is non-linear and is realized by means of the other two investigated factors with relatively poor effects of mutual influence. The increasing of the cement amount up to certain limit causes increasing of the consistency i.e. in the investigated limits the optimal cement amount relating the consistency is 250 kg/m^3.

At selected thermal treatment mode the most important effect for the light concrete grades has the amount of the used cement - in order to increase the compressive strength after steam treatment. The maximal increasing of the compressive strength can be obtained at cement amount of 350 kg/m^3. The effect of the compressive strength increasing is more with higher shlake-ash mix: ceramsyte equal to 1.0. The mutual influence of these two factors is positive in respect of the compressive strength and can be used to produce light concrete with increased compressive strength values.

The influence of the concrete amount per 1 m^3 light constructive-thermal insulating concrete on the compressive strength is in the limits of the experiment's error and is not reported by means of the mathematic model. Possibly this mechanical factor is poor sensitive in respect of cement amount, as can be assured that the disturbance of the material is happened mainly from the light additional substances and the increasing of the cement amount is helpful to composite strengthening or consolidation.

The compressive strength of the light concrete after 7-day setting period at normal conditions is determined mainly by the cement amount. The increasing of the last factor in the limits of 250 to 350 kg/m^3 at the same other conditions causes compressive strength increasing by 5 MPa or at water content of 190 kg/m^3 is achieved maximal compressive strength of 12.7 MPa. At more cement amount the compressive strength is not increased.

References:

1/ Babachev, G.N. "Ash and Shlake - Valuable materials", Sofia, "Technika" 1984

2/ Voznesenskij V.A. "Statistical Methods for Experiment Planning in Technical-Economical Investigation". Moskow, "Finansi i Statistika"1981

Tang Ming-shu, Xu Zhong-zi and Han Su-fen
Nanjing Institute of Chemical Technology, China

ALKALI REACTIVITY OF GLASS AGGREGATE

Introduction

The properties of aggregate are vitally important to the performance of concrete, especially the durability. To date, the deterioration cases due to the alkali-aggregate reaction have been discovered in more than twenty countries. Due to the gradual lack of natural rock resources and the presence of enormous quantities of industrial solid wastes, the trend to use the solid wastes as aggregate will be increasing for the time to come. The blast furnace slag and coal cinder have been used as aggregates for many years. Besides, millions of tons of refuse glass are generated annually(1). The problem associated with the use of waste glass is the chemical composition of glass, which are responsible for the alkali-aggregate reaction. In volcanic glass, the relationship of their alkali reactivities to chemical compositions has also not yet been fully established. Until now, only R.G. Pike(2) and J.W.Figg(3) have investigated the alkali reactivities of glass aggregate, but the chemical compositions studied by Pike are only limited to binary systems. We made now nearly hundred samples of glass to study the relationship of chemical compositions to aggregate reactivities. The chemical compositions include in three ternary systems, N-A-S, N-C-S, C-A-S and a quaternary system N-C-A-S. The results obtained can be used to examine the alkali reactivities of volcanic glass and industrial glass waste.

Experimental Method

Glass samples were made from quartz sand, pure limestone, Al_2O_3 and Na_2CO_3 . The raw materials were first ground to particles finer than 0.08 mm, then the mixes were melted in an electric furnace. Afterwards, the melts were allowed to flow into cool water for quenching. Some mixes which were difficult to melt were moulded into bars and then melted oy oxygen-acetylene flame, the melts were also allowed to flow into cool water for quenching.

The alkali reactivities of glass aggregates were determined by rapid autoclave mortar bar test suggested by us(4): the size of aggregate: 0.15-0.75 mm, cement: aggregate = 10:1, w/c=0.30 and the alkali content of cement is 1.5% eqv. Na_2O. The mortar bars were removed from the molds after one-day curing in moist chamber, then precured in 100°C steam for 4 hours. After that, they were placed in a 10% KOH solution and autoclave-treated at 150°C for 6 hours. This method has been repeatedly proved to be effective to determine the alkali reactivity of aggregate of alkali-silica type.

Experimental Results

1. N-A-S System

18 glass samples of this system were made. The ranges of chemical compositions (in mol%) of these samples are: SiO_2 41.49-87.60, Al_2O_3 6.32-34.97, Na_2O 2.89-50.34. As the content of Na_2O was over 40 mol%, the products after melting and cooling was a xerogel, not a glass. Mortar bar test proved that the glass aggregates were non-reactive as the content of Al_2O_3 was over 24 mol%(Fig.1). The relations between the expansion values of mortar bars and the ratios A/(S+N)(mol) are shown in Fig.2. It shows that the values of expansion increase sharply as A/(S+N)=0.15, when the ratio A/(S+N) is higher than 0.3, the aggregates are non-reactive.

The experimental results proved that the value of expansion was almost maximum as the ratio N/S=0.5. On account of this result and the relationship of alkali reactivities to A/(S+N), the following formula was obtained by regression analysis. The coefficient of correlation of regression R=0.96.

$$\%e=0.025\,EXP(0.3416((A/(S+N))^{-1}-((N/S)-0.5)^2)) \qquad (1)$$

Where
%e—value of expansion of mortar bar
N,A,S—respective mol% of Na_2O, Al_2O_3, SiO_2 in glass-sample compositions

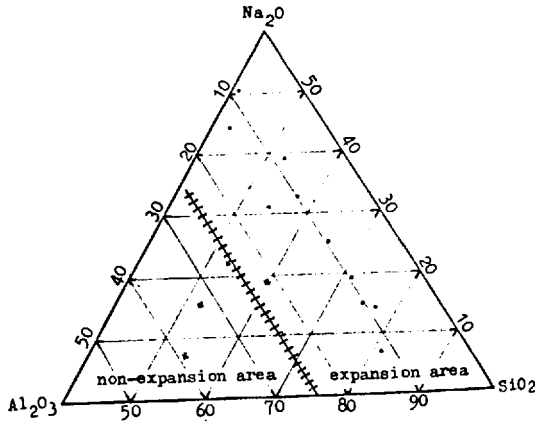

Fig.1 The expansion area and non-expansion area of glass aggregates in N-A-S system (mol %)

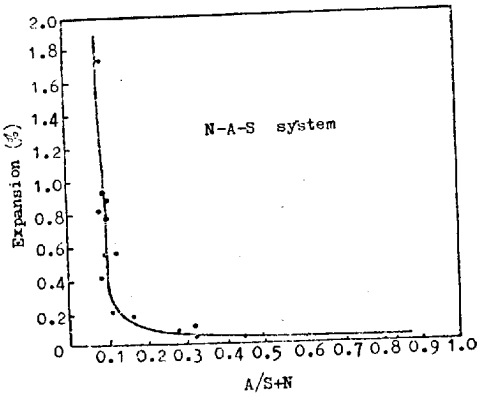

Fig.2 Relation between expansion and A/(S+N)(mol ratio)

2. N-C-S system

In this system, 15 glass samples were made by melting. The ranges of chemical compositions(mol%) of these glass samples are: SiO_2 39.19-71.62, CaO 6.60-44.60, Na_2O 8.97-40.68. In Fig.3, it shows that the aggregates are non-reactive when their CaO contents exceed 22 mol%. The expansion increases sharply as $C/(S+N)\leq 0.2$ and stops as $C/(S+N)\geq 0.3$(see Fig.4). Similarly, the following formula is obtained after regression analasis. The coefficient of correlations R=0.96.

$$\%e=0.0251\ EXP(0.4912((C/(S+N))^{-1}-((N/S)-0.5)^2)) \qquad (2)$$

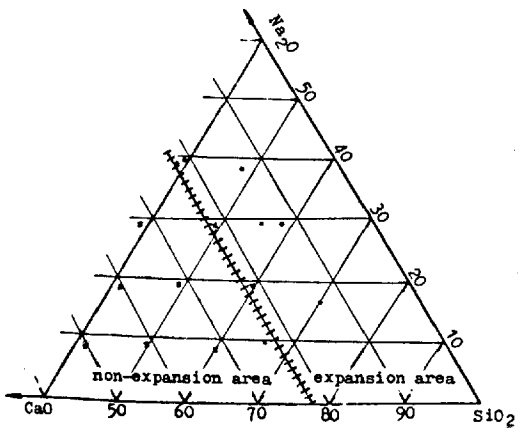

Fig.3 The expansion area and non-expansion area of glass aggregates in N-C-S System

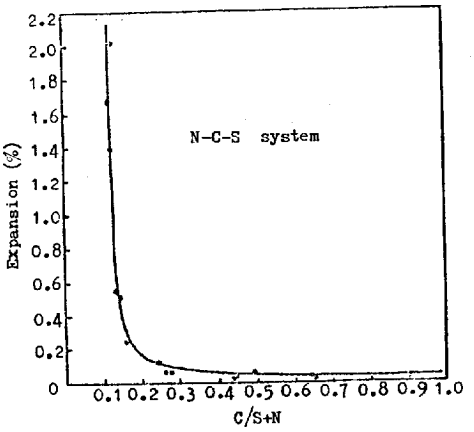

Fig.4 Relation between expansion and C/(S+N) (mol ratio)

3. C-A-S system

For this system, 16 glass samples were made. The ranges of chemical compositions (mol%) of these samples are: SiO_2 42.51-100, CaO 0-35.53, Al_2O_3 0-35.60. It is proved that in this system the value of expansion increases with increase of SiO_2 content (see Fig.6). In Fig.5, it shows that the aggregates are non-reactive when the content (mol%) of silica is less than 66 mol%. The equation of regression which represents the relation of chemical composition to value of expansion is shown in formula(3), the coefficient of correlation R=0.99.

$$\%e=0.0472+3.624\times10^{-4}(SiO_2-55)^2 \qquad (3)$$

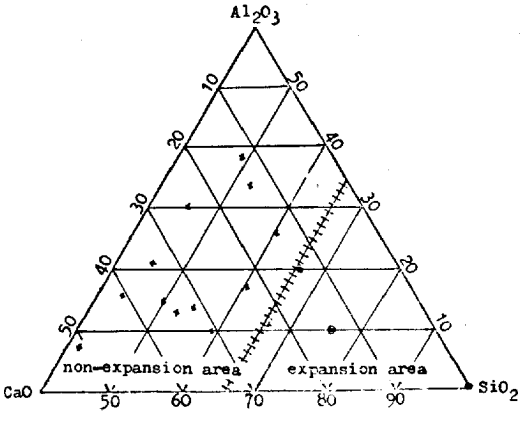

Fig.5 The expansion area and non-expansion area of glass aggregates in C-A-S system (in mol%)

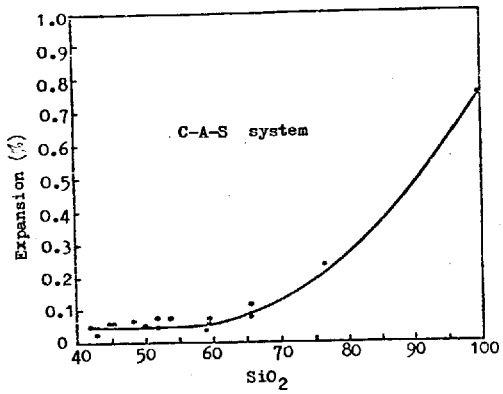

Fig.6 Relationship of expansion to S(in mol%)

4. N-C-A-S system

42 glass samples were made for this system. The ranges of chemical compositions (mol%) of these samples are: SiO_2 46.89-87.60, CaO 1.07-33.39, Al_2O_3 0.62-12.86, Na_2O 1.29-28.97. Similar to the above three systems, the value of expansion increases with the increase of S+N(mol%) contents, and decreases with the increase of C+A contents. In Fig.7, it shows that the region of expansion exists in the cone of the SiO_2 vertex. As shown in Fig.8, the value of expansion decreases with increase of ratio (C+A)/(S+N). The glass aggregates are reactive as this ratio is less than 0.2, and non-reactive as it is higher than 0.3. There is uncertainly in (C+A)/(S+N)=0.2-0.3. Formula(4) is the equation of regression, the coefficient of correlation R is 0.92.

$$\%e=0.0092\,EXP(0.5124((C+A)/(S+N))^{-1}-((N/S)-0.5)^2)) \qquad (4)$$

It is worth mentioning, When we put C=0 or A=0 in equation(4), the results seem to be not consistent with equation (1) or (2), maybe the reason is that there are influence from one another i the chemical compositions, it is not a simple additive relation between them.

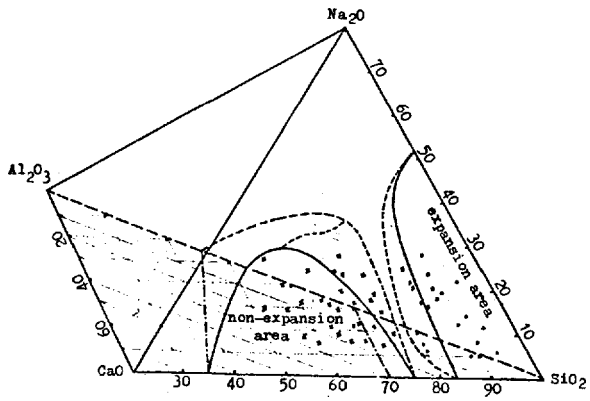

Fig.7 The expansion area and non-expansion area of glass aggregates in N-C-A-S system(mol%)

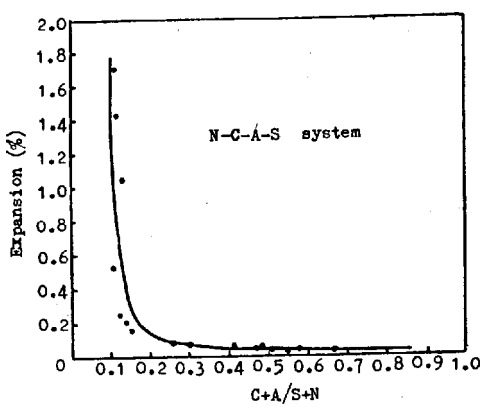

Fig.8 Relation of expansion to (C+A)/(S+N)(mol ratio)

Applications of the Reactive Index K

The alkali reactivities of some rocks of volcanic glass and industrial glass waste were determined by mortar bar test or chemical method. The comparison of these results to reactive index K((C+A)/(S+N)) is shown in Table I, it illustrates that all the rocks are reactive when K is less than 0.134. On the contrary, as K=0.471 or 1.390, the aggregates are expectedly not reactive. Therefor, we can use the reactivve index to predict the alkali reactivity of these kinds of rocks.

Table I Relationship of alkali reactivities of glass rocks to their reactivity index

Rocks	Chemical Compositions (in mol%)							Expansion %	K**	
	SiO_2	Al_2O_3	Fe_2O_3	CaO	MgO	K_2O	Na_2O			
perlite(1)	71.33	11.93	1.75	1.96		3.35	1.65	0.254	0.130	Reactive
perlite(2)	70.43	12.22	1.40	2.21		4.70	2.00	0.391	0.134	Reactive
perlite(3)	72.56	11.49	1.78	0.88		4.07	3.90	0.605	0.106	Reactive
perlite(4)	71.27	12.74	3.67	0.74	0.62	3.61	3.55	*	0.132	Reactive
pichstone	72.70	11.29	1.78	0.81	0.10	3.30	3.15	0.383	0.107	Reactive
obsiden(1)	73.60	11.74	1.16	0.81		3.80	4.50	*	0.102	Reactive
obsiden(2)	70.90	12.73	2.94	0.73	0.21	4.25	3.35	0.105	0.128	Reactive
cinder	55.73	23.42	14.14	5.16	1.41	0.97	0.50	0.034	0.471	Non-reactive
slag	34.73	9.88	1.05	37.85	4.96	3.97	1.80	*	1.390	Non-reactive

*Proved to be reactivity determined by ASTM C289 (chemical method)

**In calculation of K, CaO includes MgO, Al_2O_3 includes Fe_2O_3

Discussion

Three processes are present in alkali-silica reaction, they are: process of reaction, process of imbibition of water and process of swelling. It must be mentioned that all these glass aggregates made by us might react with the pore solution of cement paste, therefore, the difference in expansion of aggregates must be attributed to their different abilities of water imbibition and the swelling of their reaction products. The relationship of these abilities to chemical compositions of glass aggregates deserves to be studied further.

Conclusion

The alkali reactivities of glass aggregates depend on their chemical compositions. The reactivities increase with the increase of S+N contents, and correspondingly decrease with the increase of C+A contents. So far the alkali reactivities of glass aggregates can be predicted by reactive index $K((C+A)/(S+N))$(in mol%). The reactivity sharply increases as K is less than 0.1-0.2. On the contrary, they are not reactive as K is more than 0.3.

Acknowledgements

The authors gratefully acknowledge Professor Wang Zhong-jun and Dr. P.E. Grattan-Bellew for their valuable suggestions.

References

(1) S.N. Ghosh, Advances in cement technology, p.663(1982).
(2) R.G. Pick, Binary silicate glasses in the study of alkali silicate reaction, Highway Research Board Bulletin, No.275, pp39-44(1960).
(3) J.W. Figg, Reaction between cement and artificial glass in concrete, Proc. of 5th International Conference on Alkali-Aggregates Reaction in Concrete, Cape Town, 1981.
(4) Tang Ming-shu, Han Su-fen and Zhen Shihua, A rapid method for identification of alkali reactivity of aggregate, Cem. Conc. Res. Vol.13, No.3,417-422(1983).

LOU Zonghan, Professor, XU Xianyu, HAN Ren and CHENG Yimin, Lecturers
Zhejiang University, P. R. China

Calcium Silico-Fluoride Phase A and Its Effects on Formation of C_3S

For saving energy, the addition of CaF_2 or CaF_2 and $CaSO_4$ to the raw materials is often used in the burning of cement clinker in cement works. In this case, four transitional minerals may emerge in the burning process of cement clinker in kilns. They are calcium silico-fluoride phase A ($C_{19}S_7 \cdot 2CaF_2$), calcium silico-fluoride phase B ($2C_2S \cdot CaF_2$), calcium sulfo-silicate ($2C_2S \cdot CaSO_4$) and fluor-ellestadite ($3C_2S \cdot 3CaSO_4 \cdot CaF_2$). Many researches on these minerals have been done, but the research is far from over and some results of them are contradictious/1/,/2/,/3/,/4/,/5/,/6/. Calcium silico-fluoride phase A is the most important among the four transitional minerals. The present paper will describe its formation and decomposition, and its effects on the formation of C_3S.

1. The Formation of $C_{19}S_7 \cdot 2CaF_2$

Calcium silico-fluoride phase A was prepared by three methods with C_2S which was prepared beforehand, CaO, $CaCO_3$, SiO_2 and CaF_2 in c.p. grade, i.e., sample A with the mole ration of $CaO:SiO_2:CaF_2=19:7:2$; sample B with the mole ratio of $CaCO_3:SiO_2:CaF_2=19:7:2$; sample C with the mole ratio of $C_2S:SiO_2:CaF_2=7:5:2$.

Eight groups of sample A and sample C were burned at 1000°C for 15 min., then heated to 1080, 1090, 1100, 1110, 1140, 1160, 1170 and 1200°C respectively and at these temperatures for 15 min. The results of free CaO and XRD of them are shown in Fig. 1, Fig. 2, Fig. 3 and Fig. 4.

It can be found from these results that $C_{19}S_7 \cdot 2CaF_2$ exist at the temperature range of 1100-1170°C in sample A and of 1070-1170°C in sample C. In both sample free CaO decreases obviously and $C_{19}S_7 \cdot 2CaF_2$ increases obviously at 1110 C. That means the amount of $C_{19}S_7 \cdot 2CaF_2$ formed reaches maximum at this temperature.

From these results it can also be found that the formation rates of $C_{19}S_7 \cdot 2CaF_2$ are different in the two samples. C_2S which was prepared beforehand has a promo-

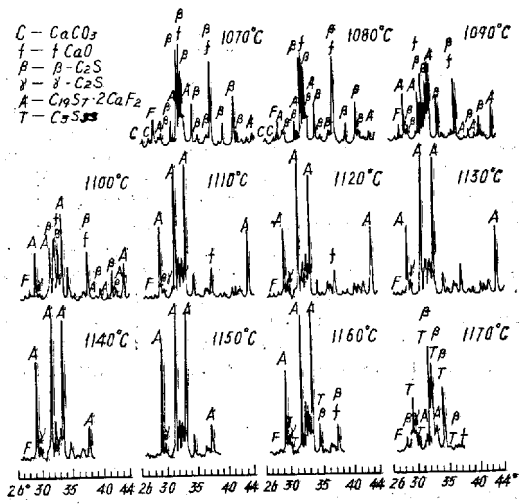

Fig. 2 XRD patterns of sample C at different temperature for 15 min.

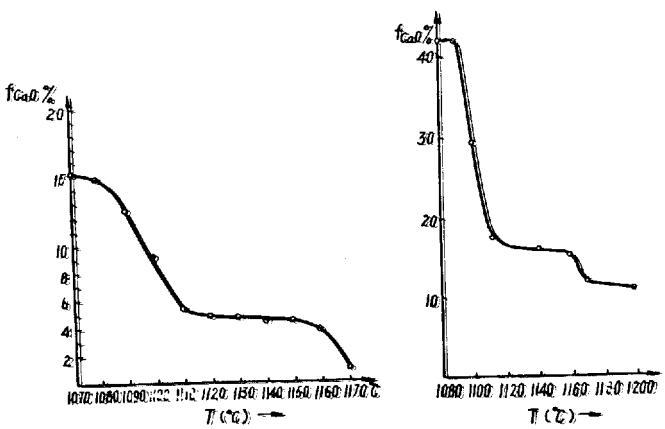

Fig. 1 Percentage of f-CaO of sample C at different temperature

Fig. 3 Percentage of f-CaO of sample A at different temperature

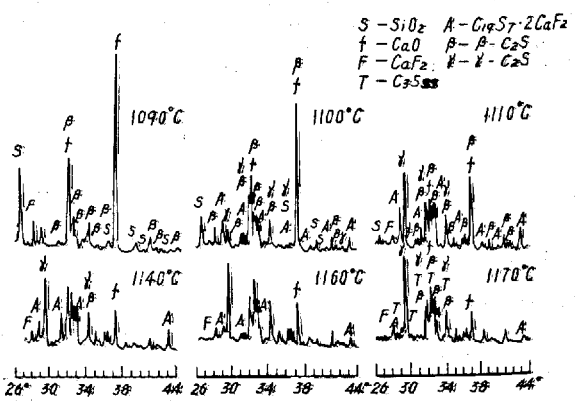

Fig. 4 XRD patterns of sample A at different temperature for 15 min.

tive effect on the formation of $C_{19}S_7 \cdot 2CaF_2$. W. Gutt has described that $C_{19}S_7 \cdot 2CaF_2$ is formed by C_2S, CaO and CaF_2/7/. The result of thermodynamic calculation also indicates this trend.

To investigate the formation rate of $C_{19}S_7 \cdot 2CaF_2$, five sample C's were burned at 1000°C for 15 min. and then heated to 1080, 1090, 1100, 1110 and 1120°C respectively and at these temperatures for 1, 5, 10, 15, 20, 30 and 60 min. respectively. The samples were cooled with liquid nitrogen, then free CaO of each sample was determined. The results are shown in Fig. 5.

In DTA curve of sample B shown in Fig. 7, the endothermic peak in 573°C represents the polymorphic transformation of quartz, in 843°C the decomposition of $CaCO_3$. The endothermic peak in 1179°C indicates that $C_{19}S_7 \cdot 2CaF_2$ melts incongruently at this temperature. According to the phase diagrams of the CaO-C_2S-CaF_2 system made by J. Mukerji/8/. W. Gutt/9/ and Mitsuo Tanaka/10/, in which there is a ternary eutectic at 1110°C, liquidoid should emerge at 1111°C. The exothermic peaks in 1101 and 1118°C represent the formation of $C_{19}S_7 \cdot 2CaF_2$. They should be a single peak, which is divided into two by the endothermic peak liquidoid emerged at 1111°C. The peak temperature of the exothermic peak of formation of $C_{19}S_7 \cdot 2CaF_2$ represents the temperature at which the formation rate of $C_{19}S_7 \cdot 2CaF_2$ is maximal.

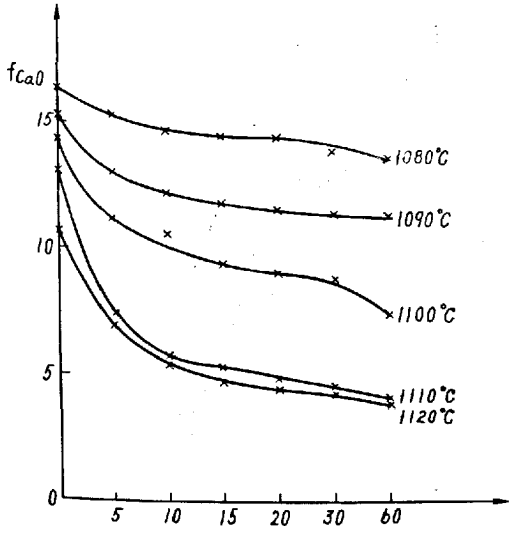

Fig. 5 Relationship between f·CaO of sample C and time at different temperature

The results shown in Fig. 5 were processed by Ginstring Equation, $f(G)=1-\frac{2}{3}(G)-(1-G)^{2/3}-Kt$. The relationship between f(G) and T is shown in Fig. 6. From Fig. 6 it can be shown that $C_{19}S_7 \cdot 2CaF_2$ formed through solid reaction below 1100°C, and through liquidoid above 1100°C, at which liquidoid emerges.

All the results obtained show that the amount of free CaO in sample C is maximal when the sample was burned at 1080°C, and reduces in order of 1090→1100→1110°C. But in the samples burned at 1110 and 1120°C the amount of free CaO is almost the same. So it can be inferred that both the amount and the formation rate of $C_{19}S_7 \cdot 2CaF_2$ formed at 1110°C are maximal.

2. Decomposition of $C_{19}S_7 \cdot 2CaF_2$

To examine whether calcium silico-fluoride phase A decomposes, sample B was burned at 1000°C for 15 min. making $CaCO_3$ decomposition, and at 1110°C for 30 min.

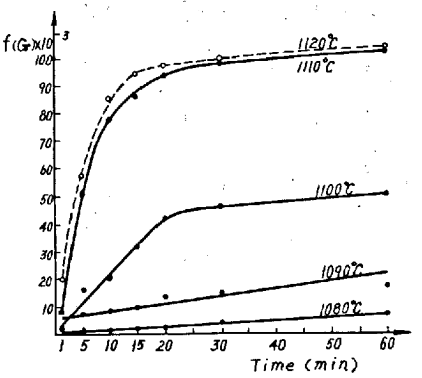

Fig. 6 Relationship between f(G) and time for sample C

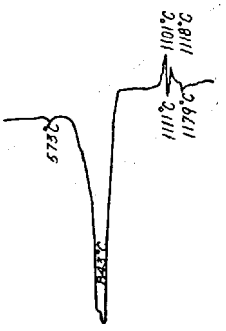

Fig. 7 DTA curve of sample B

making $C_{19}S_7 \cdot 2CaF_2$ formation, then heated to 1120, 1140, 1160, 1180 and 1200°C respectively and at these temperatures for 1, 5, 15, 30 and 60 min. respectively, then cooled with liquid nitrogen.

XRD semiquantitive analysis of these samples was carried out (Fig. 8). The peak intensity ratio of the characteristic peaks of $C_{19}S_7 \cdot 2CaF_2$ at d=2.087$^{o}_{A}$ and $Al(OH)_3$ at d=4.85$^{o}_{A}$, which was added as a reference, is shown in Fig. 9. The determination result of free CaO of these samples is shown in Fig. 10.

From these results, it can be found that the amount of $C_{19}S_7 \cdot 2CaF_2$ decreases with the increase of temperature and burning time, and almost disappears at 1170°C, and

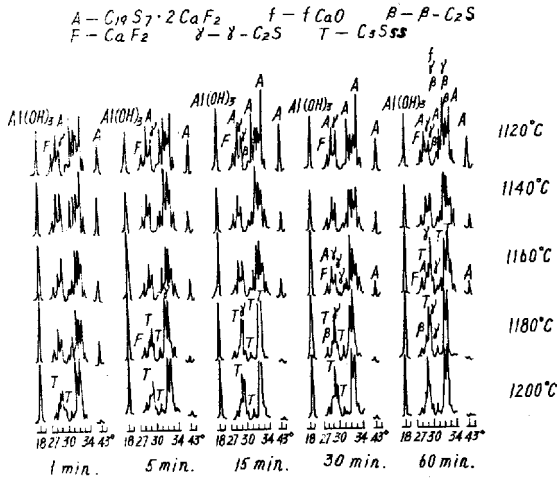

Fig. 8 Semiquantitive XRD patterns of $C_{19}S_7 \cdot 2CaF_2$

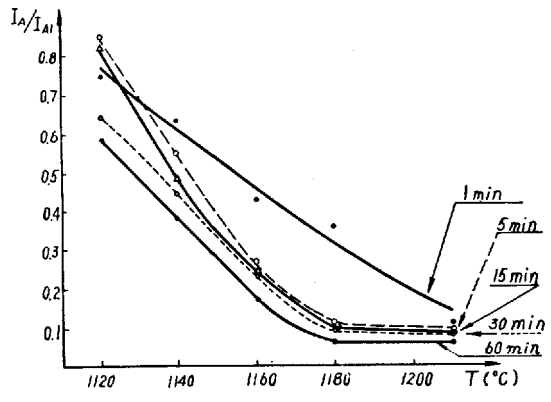

Fig. 9 Peak intensity ratio of $C_{19}S_7 \cdot 2CaF_2$ and $Al(OH)_3$ after the decomposition of $C_{19}S_7 \cdot 2CaF_2$

the amount of free CaO decreases at the same time and decreases rapidly at 1170°C. But in the samples burned at 1120°C, the amount of $C_{19}S_7 \cdot 2CaF_2$ increases for the time of 1 min. and 5 min. In the samples burned at 1120, 1140 or 1160°C, the amount of free CaO increases during the first 15 min. All these results indicate that $C_{19}S_7 \cdot 2CaF_2$ decomposes at these conditions.

The formation reaction of $C_{19}S_7 \cdot 2CaF_2$ is exothermic, so the increase of temperature is favorable to the decomposition of $C_{19}S_7 \cdot 2CaF_2$. Moreover, C_3S_{ss} can be found in the sample B burned at 1140°C for 18 hrs.

To sum up, the process of the formation and decomposition of $C_{19}S_7 \cdot 2CaF_2$ can be suggested as the following. In this process, there are two reactions. One is the formation of $C_{19}S_7 \cdot 2CaF_2$ by C_2S, CaO and CaF_2, the other is the decomposition of $C_{19}S_7 \cdot 2CaF_2$ to promote the formation of C_3S_{ss}. 1110°C is the eutectic in the C_2S-CaO-CaF_2 system and is the critical point of the formation reaction. 1170°C is the temperature at which $C_{19}S_7 \cdot 2CaF_2$ melts incongruently and is the critical point of decomposition reaction. Below 1110°C, $C_{19}S_7 \cdot 2CaF_2$ formed slowly through the solid reaction. in this case, formation reaction is the main reaction. Liquidoid emerges at 1110°C, and the amount and formation rate of $C_{19}S_7 \cdot 2CaF_2$ reach maximum. Above 1110°C, decomposition is dominant. At 1179°C, $C_{19}S_7 \cdot 2CaF_2$ disappears because it melts incongruently.

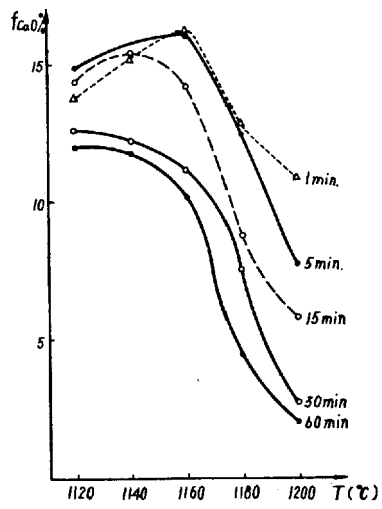

Fig. 10 Curve of f·CaO at different temperature after the formation of $C_{19}S_7 \cdot 2CaF_2$

3. The Effects of $C_{19}S_7 \cdot 2CaF_2$ on the Formation of C_3S_{ss}

To investigate the effects of $C_{19}S_7 \cdot 2CaF_2$ on the formation of C_3S_{ss}, a sample was prepared with $CaCO_3$ and SiO_2 according to the ratio of CaO/SiO_2=3:1. In addition, 3.68% CaF_2 was added into the sample. When all the CaF_2 was consumed, the percentage of $C_{19}S_7 \cdot 2CaF_2$ in the sample was 50%. The sample was burned at 1000°C for 15 min., and at 1110°C for 30 min., then heated to 1160, 1170, 1180, 1200, 1250, 1320 and 1350°C respectively and at these temperatures for 30 and 60 min. respectively. The results of determination of free CaO and XRD are shown in Fig. 11 and Fig. 12.

By means of XRD, C_3S_{ss} can be found in the sample burned at 1160°C. A large amount of C_3S_{ss} will emerge in the sample burned at 1180°C. In correspondence with that, at about 1170°C, the amount of free CaO decreases rapidly and $C_{19}S_7 \cdot 2CaF_2$ disappears finally. There is a lot of C_3S_{ss} "group" in $C_{19}S_7 \cdot 2CaF_2$/4/, so decomposition of $C_{19}S_7 \cdot 2CaF_2$ will promotes the formation of C_3S_{ss} by the nucleating and crystallizing process. This promoting effect will be more obvious when $C_{19}S_7 \cdot 2CaF_2$ incongruently melts at 1170°C.

As well known, through the solid reaction between $CaCO_3$ and SiO_2, only a little C_3S can form at such a high temperature as 1600°C. By the ordinary burning of clinker C_3S can not form until 1280°C. However, by the formation of transitional mineral, $C_{19}S_7 \cdot 2CaF_2$, a large amount of C_3S can form at 1170°C. The forming temperature of C_3S is 100°C below that in the clinker burned ordinarily and 400°C below that through the solid reaction. That indicates $C_{19}S_7 \cdot 2CaF_2$ has a obvious effect on promoting the formation of C_3S.

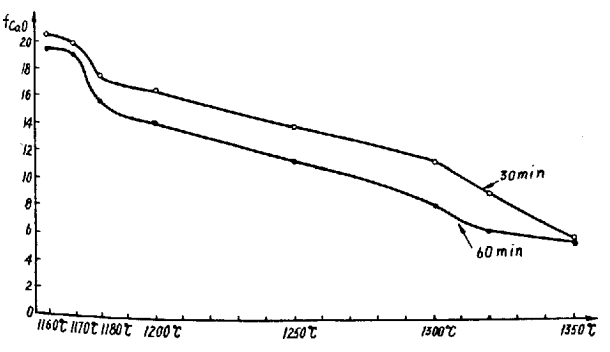

Fig. 11 Percentage of f·CaO of sample prepared with $3CaCO_3+SiO_2$+3.68 wt.% CaF_2

Calcium silico-fluoride phase B ($2C_2S \cdot CaF_2$) and calcium sulfo-silicate ($2C_2S \cdot CaSO_4$) are only related to the formation of C_2S/11/. The effect of fluor-ellestadite ($3C_2S \cdot 3CaSO_4 \cdot CaF_2$) is neccesary to be examined. $3C_2S \cdot 3CaSO_4 \cdot CaF_2$ and $C_{19}S_7 \cdot 2CaF_2$ can not coexist/3/. It is also proved by our experiments. Samples was prepared with $CaCO_3$ and SiO_2 according to the CaO/SiO_2 ratio=3:1, and 30% $3C_2S \cdot 3CaSO_4 \cdot CaF_2$ was added. They were burned at 1200, 1240, 1260, 1270, 1280, 1300 and 1350°C respectively for 30 or 60 min. The free CaO and XRD results of them are shown in Fig. 13 and Fig. 14.

From these results, it can be found that C_3S_{ss} doesn't emerge until 1250°C, and in correspondence with it, free CaO decreases rapidly and $3C_2S \cdot 3CaSO_4 \cdot CaF_2$ disappears at 1250°C. Compared with the results of the samples prepared with $3CaCO_3+SiO_2$+3.68% CaF_2, it can be found that the temperature at which C_3S emerges is 80°C higher. Obviously, it is the liquidoid, which emerges by the congruent melt of $3C_2S \cdot 3CaSO_4 \cdot CaF_2$ at 1250°C, that promotes the reaction of C_2S and CaO to form C_3S_{ss}. Actually, $3C_2S \cdot 3CaSO_4 \cdot CaF_2$ is a mineral with lower melt temperature, its effect mechanism on the formation of C_3S is different from that of $C_{19}S_7 \cdot 2CaF_2$.

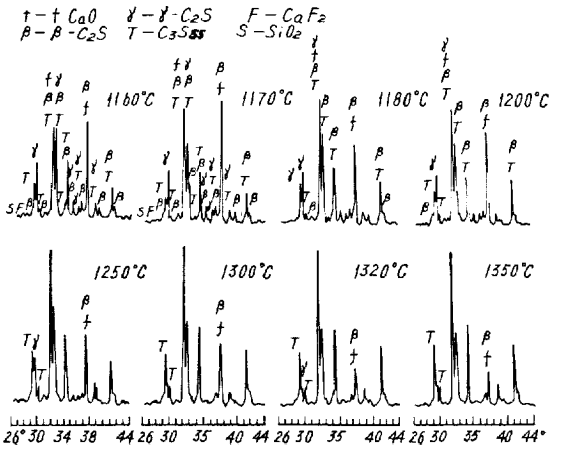

Fig. 12 XRD patterns of samples prepared with $3CaCO_3+SiO_2$+3.68 wt.% CaF_2 at different temperature for 60 min.

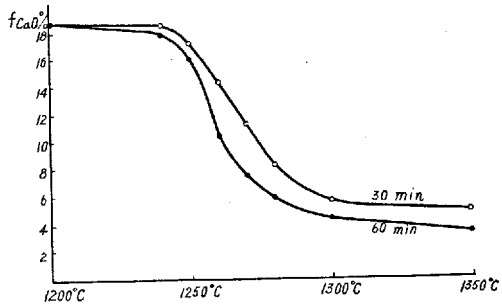

Fig. 13 Percentage of f-CaO of samples prepared with $3CaCO_3+SiO_2$+30% $3C_2S\cdot3CaSO_4\cdot CaF_2$ at different temperature

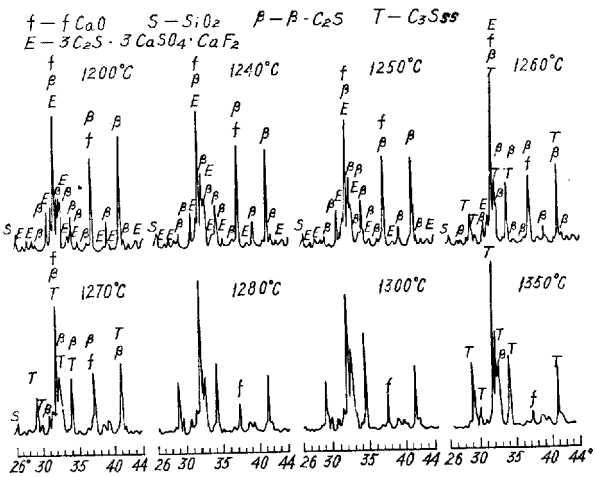

Fig. 14 XRD patterns of samples prepared with $3CaCO_3+SiO_2$+30% $3C_2S\cdot3CaSO_4\cdot CaF_2$ at different temperature for 60 min.

4. Conclusions

1). $C_{19}S_7\cdot2CaF_2$ forms at a temperature range of 1070-1160°C. At about 1110°C, the formation rate of $C_{19}S_7\cdot2CaF_2$ is maximal. The amount of $C_{19}S_7\cdot2CaF_2$ formed is almost maximal.

2). $C_{19}S_7\cdot2CaF_2$ is unstable at the temperature range at which it forms. Its formation and decomposition occur at the same time. Below 1110°C, the formation is the main trend, but above 1110°C, the decomposition is dominant. $C_{19}S_7\cdot2CaF_2$ disappears at 1170°C.

3). There is a lot of C_3S_{ss} "group" in $C_{19}S_7\cdot2CaF_2$. The decomposition of $C_{19}S_7\cdot2CaF_2$ promotes the formation of C_3S_{ss}. When $C_{19}S_7\cdot2CaF_2$ melts incongruently at 1170 °C, this promoting effect is more obvious. Its promoting mechanism is different from $3C_2S\cdot3CaSO_4\cdot CaF_2$, which is a mineral with a lower melt temperature and at 1250°C provides the liquidoid which is neccesary for the formation of C_3S.

REFERENCES:

1. PEIZHI FENG, DAMAO TONG, HONGFENG YI, "Study on the Promoting Effect of CaF_2 and $CaSO_4$ on the Formation of C_3S", 1984, (unpublished)
2. XIUJI FENG, BIN WU, "Study on the Reaction of Ferrari Cement Clinker with CaF_2 and $CaSO_4$, and the Forming Regularity of Their Main Phases", Cement, No. 8, 1983, pp. 7-16
3. C. GILIOLI, F. MASSAZZA, M. PEZZUOLI, "Study on Clinker Calcium silicates Bearing CaF_2 and $CaSO_4$", Cem. Concr. Res., 9(1), 1979, pp. 51-55
4. SHUZHEN YANG, "Study on the Composition and Character of Calcium Silico-Fluoride Phase A, and Phase Diagram of $CaO-C_2S-CaF_2$ System", M.Sc. Thesis, Wuhan Institute of Building Materials, 1982
5. BOLIN WU, "Formation Mechanism and Reaction Dynamics of Calcium Silico-Fluoride Phase A", M.Sc. Thesis, Wuhan Institute of Building Materials, 1982
6. RUILON YE, BOLIN WU, WEIDONG MA, "New Probe on the Mineralizing Mechanism of CaF_2", 1983, (unpublished)
7. W. GUTT, "Manufacture of Portland Cement from Phosphatic Raw Materials", Proc. 5th Int. Symp. Chem. Cem., Tokyo, 1968, Vol. I, pp. 93-105
8. J. MUKERJI, "Phase Equilibriam Diagram $CaO-CaF_2-C_2S$", J. of American Society, 48(4), 1965, p. 210
9. W. GUTT, G. J. OSBORNE, "The System C_2S-CaF_2", Trans. of the British Ceramic Society, 65(9), 1966
10. MITSUO TANAKA, GIICHI SODOH, SHIGEO AKAIWA, "New Compound $Ca_{12}Si_4O_{19}F_2$ in the System $CaO-SiO_2-CaF_2$ and the Role of CaF_2 in the burning of Cement Clinker", Proc. 5th Int. Symp. Chem. Cem., Tokyo, 1968, pp. 77-88
11. XIANGTAI REN, SHIFEN ZHOU, "Study on the Formation Mechanism of Calcium Silicate in $CaO-C_2S-CaF_2-CaSO_4$ System", Prof. Conf. Cem., 1983, pp. 185-194

P

EFFECTS OF HIGH SHEAR MIXING ON HYDRATION BEHAVIOUR OF CEMENT PASTE AND RHEOLOGICAL INTERPRETATIONS

EFFETS DU MELANGE DE HAUTE TURBULENCE SUR L'HYDRATATION DE LA PATE DE CIMENT ET L'INTERPRETATION RHEOLOGIQUE

J.A. FORRESTER, Senior Research Fellow, King's College London
Formerly Chief Chemist, Cement & Concrete Association, U.K.

and

S.A. JEFFERIS, Lecturer in Civil Engineering
King's College London

The application of mechanical shear to a water cement mixture has a profound effect in the rate of hydration. The shear action also generates a product that modifies the rheological characteristic. These two functions add additional consideration to the chemistry of hydraulic cement hydration.

Mechanical shear can be considered as a slicing or grinding action on the surface of hydrating cement and can be said to exist in all concretes where shear action can arise from the impact of aggregate to aggregate contact. In special ways mechanical shear can be induced by purpose designed mixers. These usually incorporate rotor-stator geometries where a cement slurry will receive a strong shear action as it passes through the gap.

Cement hydration can be considered initially to be controlled by a through solution mechansim and later with deposits of hydrate products on cement surfaces the controlling action is by nucleation and diffusion control. The contribution to the mechanics of hydration introduced by mechanical shear is two fold. Firstly the removal of immediate colloidal hydrate products generates ideal nucleation sites for the deposit of through solution reaction products. Such sites act as alternatives to the cement particles themselves and hence deposition of retarding coatings is reduced. Secondly the physical removal of coatings allows access to fresh unhydrated cement surfaces.

The dispersion of colloidal particles of hydrated cement by shear action creates a liquid phase with unique properties that contribute to the rheological characteristics of cement water pastes or concrete.

The changes to the chemical kinetics are demonstrated by conduction calorimetry and rate of formation of hydration products. These are illustrated in the poster where it is shown that mechanical shear increases the rate and amount of silicate reaction and also shortens the time of reaction of aluminate with sulphate. The increase in amount of silicate reacted is confirmed by an increase in the rate of formation of calcium hydroxide. The effect on the sulphate reaction is similar to that induced by sulphate concentration. This similarity is to be expected as the rate has been shown to be a function of availability of reactants and shear can be expected to facilitate this availability.

The action of shear on rheological properties is demonstrated by the decrease in setting time and by the generation of thixotropic properties. An acceleration in the development of shearing threshold is demonstrated by measurements with a cone penetrometer and a Contraves viscometer. The latter indicates the creation of thixotropy. The generation of a gel like characteristic in the liquid phase increases cohesion and hence reduces tendency to bleed. This is a most desirable feature in grouting operations.

Examples of the practical applications of high shear mixing in grouting, waste disposal, self-draining concrete, cut-off wall construction, etc. are given in the poster.

Before rheological properties can be considered it is necessary to understand measurement procedures. In this note only two indicators of rheology/stiffening have been considered:
(i) rotational viscometry (ii) penetration testing. These techniques are not entirely separate but perhaps represent a continuum with rotational viscometry providing data at large strains possibly on an established failure surface and penetration testing providing data at generally much smaller strains and strain rates on a developing failure surface. However, as a result of the different processes involved the strength measured in a penetration test is quite distinct from the yield point determined by rotational viscometry. Considering first rotational viscometry:

If continuous rotation is employed then the rotation may establish a zone of preferred shear. Clearly such a zone cannot be produced in a pure liquid but in a particulate material it is quite normal and furthermore moisture migration to this zone is to be expected. Such moisture migration is well documented, for example in soil mechanics, and tends to reduce the shearing stresses. The migration is consistent with Le Chatelier's principle and may be regarded as a general phenomenon. Therefore, a simple rotational viscometry test is unlikely to measure the bulk properties of a paste but rather will measure the properties of an undefineable continuously sheared zone of water/cement ratio above the bulk value. A simple demonstration of this behaviour can be obtained using a viscometer with a stationary cup and rotating bob with torque measurement on the bob. The test requires a series of sleeves which can be inserted in the cup to reduce the bob to cup gap. With a Newtonian liquid reduction in the gap will increase the measured torque in a regular manner. However, for a series of cement pastes of water cement ratio 0.3 to 0.5 no effect was observed until the gap was reduced to less than 0.5mm at which point there was clearly audible grinding of the grains. Of course, insensitivity to the gap can be explained by a simple Bingham model. However, for the test situation equally simple calculations showed that this was not the case.

Thus in a rotational viscometry test one may have two distinct materials in the annular space between bob and cup: a fluid region of relatively high water/cement ratio adjacent to the moving surface and a stationary region of relatively lower water/cement ratio. These two materials will be rheologically distinct and it will not be possible to calculate the position of the interface between them from the rheological properties of the fluid region. The two materials will also show distinct development of properties with time and there may be further moisture migration.

A further demonstration of the complexity of water migration can be obtained by the use of serrated bobs. In a series of tests two bobs of identical overall diameter were used. One bob had a smooth stainless steel finish and the other had serrations 0.5mm deep. In general one might expect a serrated bob to tend to homogenise the mix and thus show higher shear stresses than a smooth bob. In practice the reverse was observed. Clearly the pumping action of the small serrations accentuated migration rather than reduced it. With deeper serrations homogenisation might be achieved. The fundamental point relating to rotational viscometry is that the system must be evaluated prior to the evaluation of results. External geometry seldom defines the internal behaviour except perhaps for very fluid mixes but for these settlement becomes a problem.

Considering now penetration testing:
Penetration tests can be operated at very low shear rates and continually expose new shear surface. At low shear rates viscous effects are negligible and the test thus measures solid type properties. As new surface is continually exposed the test tends to measure peak stresses rather than residual stresses. Whereas in rotational viscometry, even at very low strain rates, the actual magnitude of the strain will be large and hence the stress measured will be a post failure stress, that is residual stress. In a cementing material residual stresses must be expected to be significantly lower than the peak values.

As a detail of the test procedure consideration of the shape of the failure surface suggests that that data from cone penetration should be more straightforward to analyse than that from penetration of cylindrical rods and tests have shown this to be the case. In particular the relationship:

$$\text{penetration load} = ksh^2$$

where s is the shear strength of the paste,
h is the depth of penetration and
k is a constant related to the cone angle

has been demonstrated to be valid for cone penetration into cement pastes.

No satisfactory continuous function has been identified between the penetration resistance, s and h for penetration of rods except for narrow ranges of penetraton.

The introduction of controlled stress rheometers now means that stress build up prior to establishment of rotation can be studied. Hence both peak and residual stresses can be measured. Such results should be of great value in interpreting strength development results generally.

Having briefly considered the problems relating to rheological measurements it is now possible to discuss the effects of high shear mixing on rheology. High shear mixing changes the nature of a cement paste. A low shear mix is a two phase system of cement grains and water. High shear mixes tend towards a single phase material. The mixes contain sufficient colloid sized material to mask the effect of any remaining grains. As a simple analogy one may say that shearing converts a cement paste which would behave rather as a mix of very fine sand and water to the equivalent of a mix of clay and water with occasional fine sand grains. This change in paste structure is reflected in the development of cohesion and thixotropy of the mix and the suppression of settlement. Cohesion and thixotropy can be demonstrated by viscometric testing but great care must be paid to the selection of test geometries and shear rates. There is a vogue for the study of hysteresis loops for cement paste. Newcomers should be warned that even an empty viscometer will show an hysteresis loop due to the inertia of the system if rapid changes in shear rate are made.

M.J. COOLE and A.M. HARRISSON, Blue Circle Industries PLC, Research Division, Greenhithe, Kent.

THE EFFECT OF SIMULATED LARGE POUR CURING CONDITIONS ON THE TEMPERATURE RISE AND STRENGTH GROWTH OF PFA CONTAINING CONCRETE.

P

1. INTRODUCTION

The hydration of cement is an exothermic reaction which, in the case of large pours, can cause a considerable temperature rise in the concrete placed. When concrete is poured in a large quantity, it is necessary to be able to predict the temperature rise which may occur inside the mass because of the effect this may have on the ultimate properties of the hardened concrete. It is known that elevated temperatures may have a detrimental effect on the strength growth pattern of the concrete and that if the difference in temperature between the centre and surroundings of a pour exceeds 20 to 25°C cracking may occur[1,2,3]. Whether cracking occurs depends both on the magnitude of the temperature induced stress and the capacity of the concrete to accommodate the strain. The need to be able to predict these temperature rises is greater with composite cements, containing pfa or blast furnace slag, where the use of an extender introduces an additional uncertainty as to the effect of increased temperature on the development of strength with time. In the past, various methods have been employed to try to ascertain these effects, such as the adiabatic calorimeter and the vacuum flask calorimeter[4], but none of these methods is able to simulate the typical temperature-time profile of a large pour of concrete. In situ temperature measurement, using thermocouples placed at specific depths in the concrete, can be adopted and may be used to control an auxiliary cube curing bath thereby enabling internal strength values to be obtained[5&6]. This, of course is a retrospective method which can only give an indication of temperature profiles, and their effect on strength, in a structure when it is too late to undertake any corrective action.

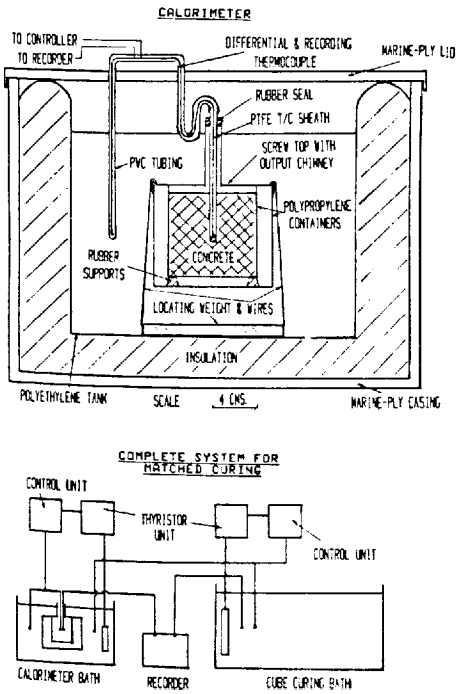

Fig. 1 Calorimeter and matched curing system

The calorimeter described in this paper (fully described by ref.7) is designed to simulate any size of pour of concrete, and to supply information on the associated temperature profile to a cube curing bath which follows the temperature of the main concrete sample by thermocouple control. Cubes from the curing bath can then be used to determine the development of strength in the simulated pour. This system (shown in Figure 1) only requires about 4 kg of cement to supply enough concrete for the control calorimeter and 12 (100mm) cubes. The equipment can therefore be used to explore the behaviour of a range of concrete mixes and composites, with regard to temperature rise and strength development, before undertaking a large pour on site.

2. EXPERIMENTAL

A pure Portland cement (OPC) and a Portland pfa cement (marketed in the UK as Phoenix), manufactured by intergrinding the same clinker with 25% pfa, were used to produce two 11 cube batches of concrete according to BS 4550. See Table 1 for chemical and physical characteristics. This provided enough concrete for the control calorimeter and for two 100mm cubes to be tested at ages of 1,3,7,28 and 91 days. The tests were carried out on both concretes with the control calorimeter set to give simulated pour sizes of 0.8,1.5 and 3 metres depth. Reference cubes were also cured at 20°C using the BS 4550 test procedure.

Small amounts of the Phoenix cement pastes were also stored with the cubes, in sealed plastic vials, so that the hydration could be stopped at the various curing ages in order to determine the amount of unreacted pfa, by a method of solution in diluted HCl (1:49). It was also thought useful to simulate the internal pressure experienced in a 3 metre pour, arising from the mass of concrete above, by mechanically loading the cubes. This was done by removing about 5mm of concrete from each cube mould and placing a steel plate (13mm thick), that was just able to slide within the 100mm mould, on top of the freshly mixed concrete. This plate was then loaded to 70 kPa uniaxially by placing a lead weight on top. On removal from underwater storage for testing, the cubes were also weighed and measured in order to determine the density of compaction. This was done after the saturated cubes had been surface dried.

After the strength tests were completed at the various stages of curing, the inside of each cube was sampled and hydration was stopped by dropping the sample into acetone. It was then prepared for examination by scanning electron microscopy. The sample was first dried under vacuum, then fractured, and the fracture surface was mounted on a stub and given a thin gold coating.

3. RESULTS

Figures 2,3 and 4 show the temperature rises obtained at the centre of simulated pours of 0.8, 1.5 and 3 metres deep respectively for both the OPC and the Phoenix mixes.

These show that as the pour size increased, although the Phoenix mix displayed a lower peak temperature than the OPC mix at all sizes, the time

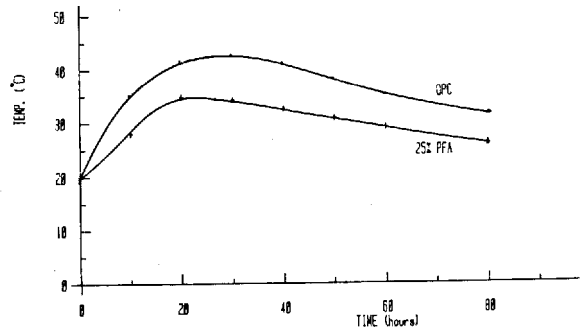

Fig.2 Temperature rise at centre of 0.8m pour

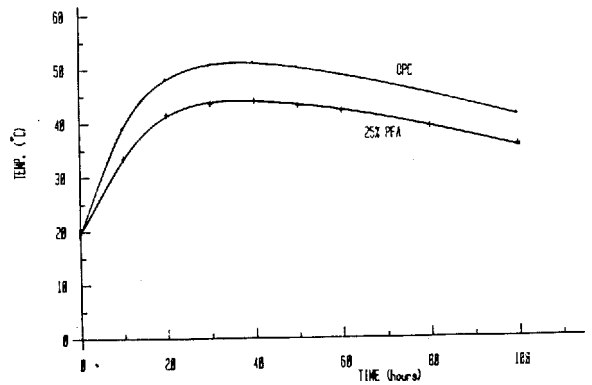

Fig.3 Temperature rise at centre of 1.5m pour

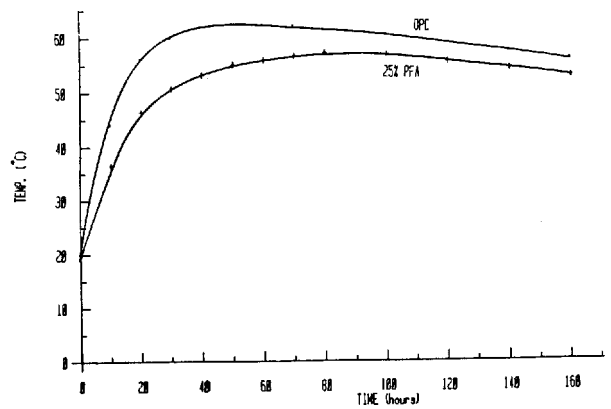

Fig.4 Temperature rise at centre of 3m pour

taken for the Phoenix mix to reach this maximum gradually increased, with respect to the OPC, until at 3 metres the time taken was nearly twice as long. It appears that once the higher temperatures of a 3 metre pour were reached, although the OPC hydration rate was accelerated as expected, the dilution effect of the pfa combined with increased reaction between the pfa and hydration products of the OPC, produced a lower early temperature rise but one which continued as the pfa reactivity increased to produce a much later peak temperature. This was also reflected in the strength growth of the concrete cured under the 3 metre simulated pour conditions (fig 5) as compared with concrete cured at standard 20°C conditions (fig 6).

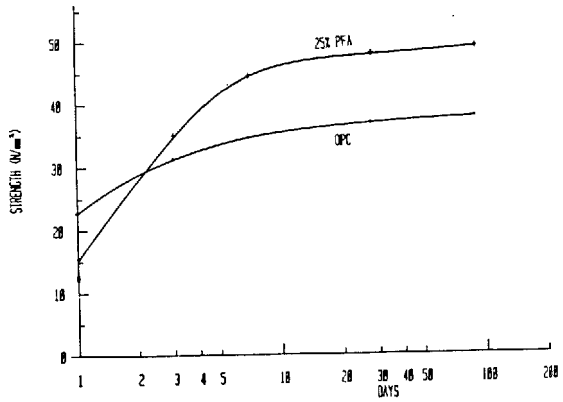

Fig.5 Strength at centre of 3m pour

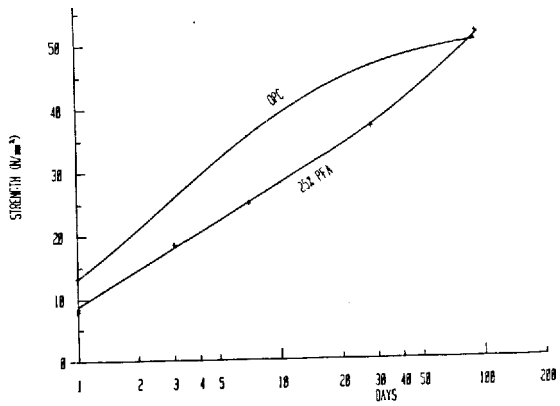

Fig.6 Strength cured at 20°C

With the OPC the rapid increase in temperature rise, and hence hydration rate, caused hydrates to grow in a rapid and perhaps disorganised manner, giving higher early strengths but eventually reduced later strengths. In contrast, the Phoenix concrete under these conditions produced a slower, more prolonged reaction which, together with reaction products between the pfa and OPC combined to give strength growth superior to that of the OPC concrete after 2½ days. Figures 7 and 8 show the strength growth in intermediate sized pours.

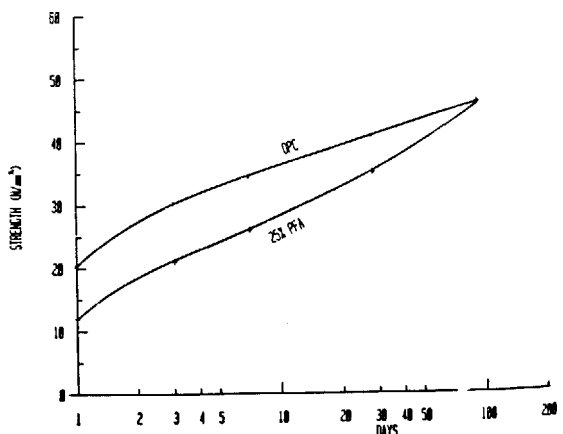

Fig.7 Strength at centre of 0.8m pour

P

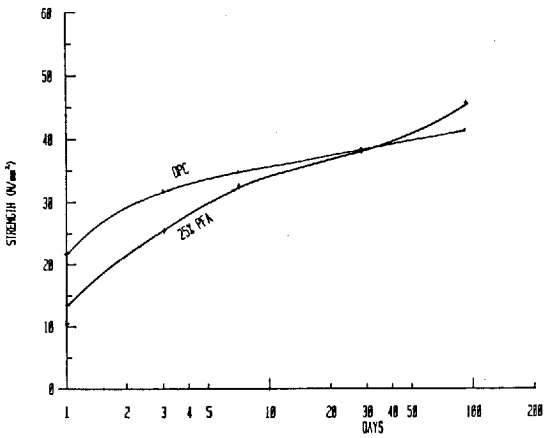

Fig.8 Strength at centre of 1.5m pour

The way in which the temperature has affected the strength growth of the Phoenix concrete, compared with the OPC concrete, is demonstrated in figures 9 and 10 where strength has been plotted against pour size at 1,3,7,28 and 91 days. This shows quite clearly the fall off in strength with increasing pour size for the OPC concrete after 7 days, whereas the Phoenix concrete was only slightly affected after 91 days.

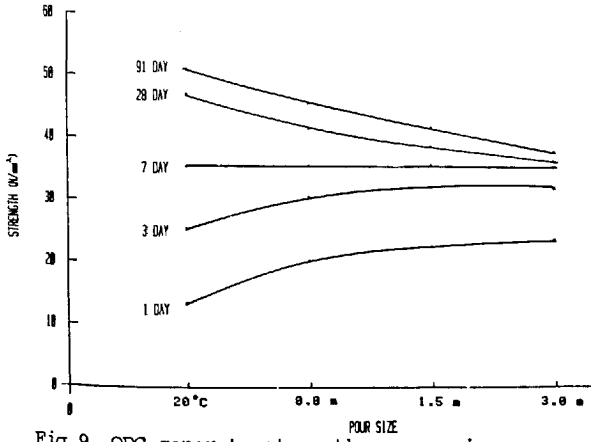

Fig.9 OPC concrete strength-v-pour size

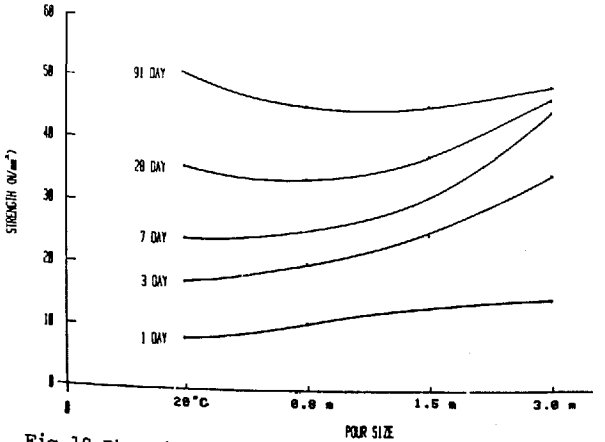

Fig.10 Phoenix concrete strength-v-pour size

The reaction rate of the pfa was determined at various ages, for each of the curing regimes mentioned, by arresting the hydration with acetone and measuring the amount of unreacted pfa by dissolving the ground sample in 1:49 hydrochloric acid (about 0.25N).

From these results (fig 11) it can be seen that the pfa reaction rate rapidly increases, in the larger pours, when a temperature of about 40°C or more is attained. This shows that in a 3 metre pour the amount of pfa reacted after 2-3 days can be expected to be similar to that reacted after 100 days curing at 20°C.

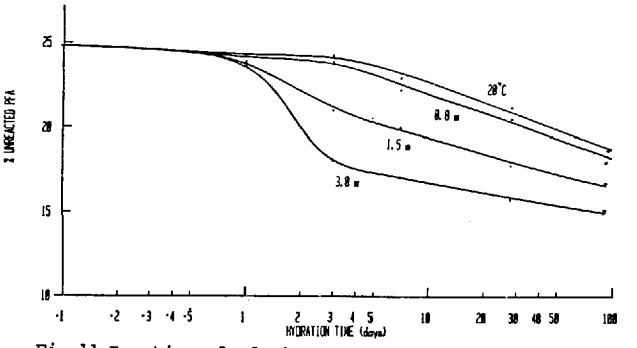

Fig.11 Reaction of pfa in hydrated Phoenix

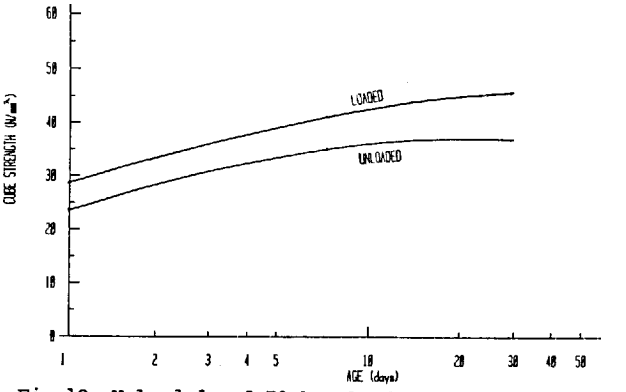

Fig.12 Unloaded and 70 kPa loaded cube strengths OPC concrete

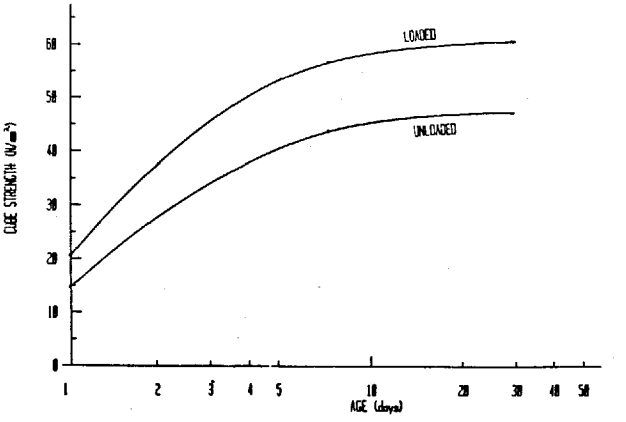

Fig.13 Unloaded and 70 kPa loaded cube strengths Phoenix concrete

The results of the tests in a simulated 3 metre pour with the 100mm cubes being loaded to 70 kPa are shown in figures 12 and 13. The strength results at 1,7 and 28 days show that loading the cubes improved the strengths for both OPC and Phoenix cement concrete. Fig 14 shows the predicted variation in 28 day strength with depth, through a 3 metre pour, as a consequence of both temperature and pressure effects.

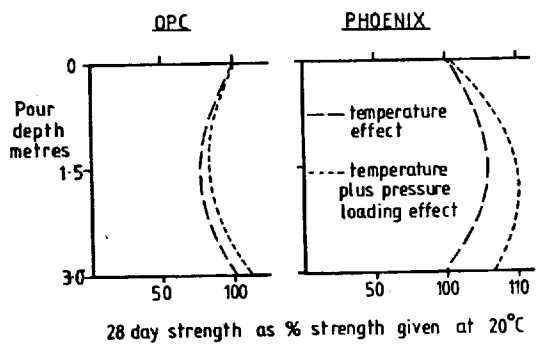

Fig.14 Predicted effect of temperature and pressure loading on 28 day strengths through a 3 metre pour.

Comparison between figures 12 and 13 shows that the concrete containing the Phoenix cement seemed to benefit most from this compaction. This could be a consequence of the better workability of the Phoenix concrete, resulting in a larger loss of expressed water, but may also be related to better hydrate morphology under load. Concrete w/c ratios could be adjusted to minimise any associated increase in bleeding.

In general, the results of the examination by scanning electron microscopy (SEM) reflect the concrete cube strength results. It is possible to relate the strength at a given age or in a given pour size to the observed degree of hydration of the pfa, and the maturity of the hydrate phases. The photographs shown as Figs 15-20 were selected as being representative of the degree of hydration in the concretes at 1,7 and 91 days. Figs 15,16 and 17 are from the 0.8m Phoenix concrete and Figs 18, 19 and 20 are from the 3.0m Phoenix concrete. At 1 day, the degree of reaction of the pfa spheres was limited to a similar extent in both size pours. The spheres was coated with calcium silicate hydrate (C-S-H) of an immature type but the sphere surfaces appeared uncorroded and the C-S-H resulted from precipitation of the outer product from the cement clinker phases.

By 7 days, the pfa in the 0.8m pour was still virtually unreacted, the smooth surface being visible through the now more mature C-S-H. In the 3.0m, concrete, the reaction of the pfa had proceeded to a considerably more advanced stage. Fig.19 shows the spherical shape of a pfa relief which has been almost all replaced by C-S-H, having a radial appearance characteristic of inner product from pfa spheres. The difference in compressive strengths of the two concretes directly reflects the differences seen in the photographs, the 0.8m concrete having a strength of 26.0 Nmm^{-2} and the 3.0m concrete, 42.1 Nmm^{-2}.

The two 91 day concretes show marked similarities and the two photographs given as Figs 17 and 20 show that spheres have reacted to a considerable extent in both concretes. The 0.8m pour has now caught up both in microscopic appearance and strength, the two values being 45.9 Nmm^{-2} for the 0.8m concrete, and 45.2 Nmm^{-2} for the 3.0m pour.

The white line displayed on all the photographs shown below represents 1 μm.

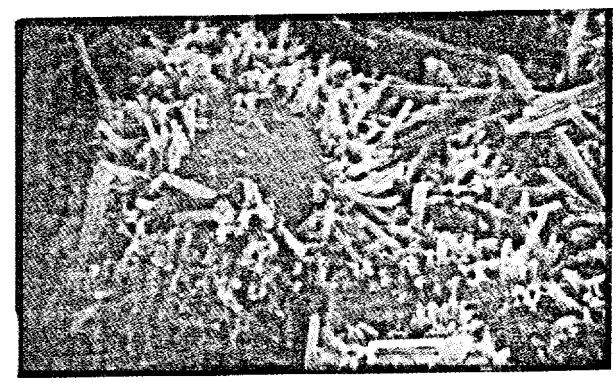

Fig.15 Phoenix, 1 day (0.8m)

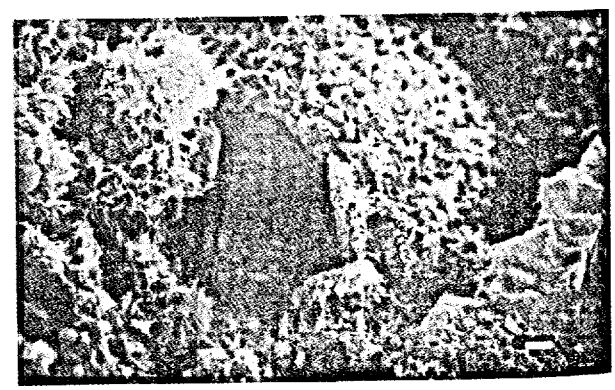

Fig.16 Phoenix, 7 day (0.8m)

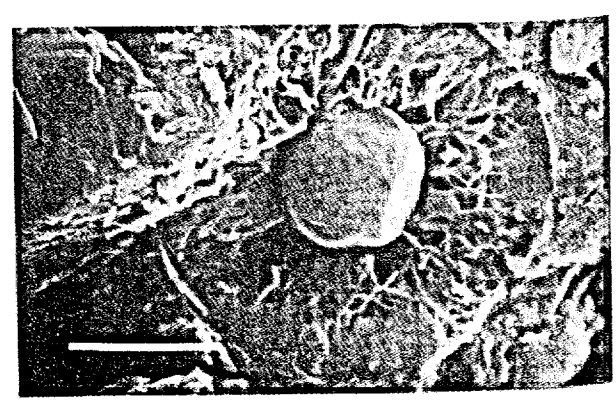

Fig.17 Phoenix, 91 days (0.8m)

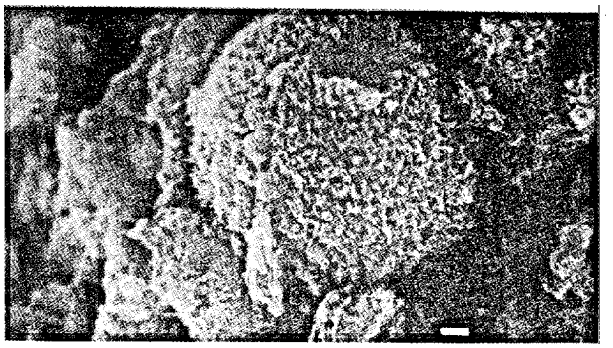

Fig.18 Phoenix, 1 day (3.0m)

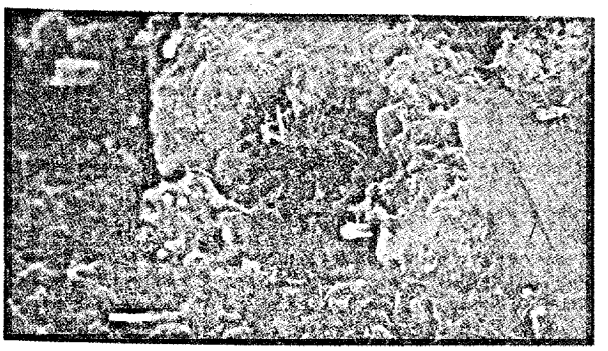

Fig.19 Phoenix, 3 day (3.0m)

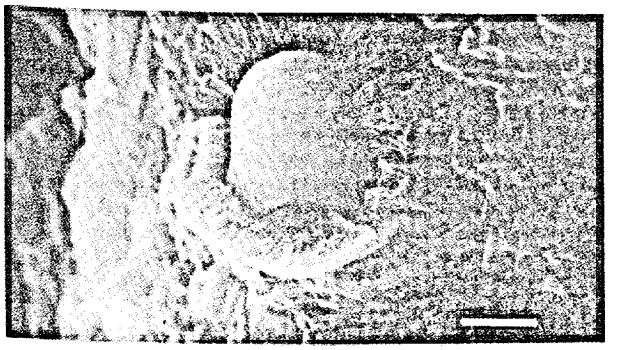

Fig.20 Phoenix, 91 day (3.0m)

Table 1 - Chemical and Physical Characteristics

	O.P.C.	Phoenix Cement	P.F.A
SiO_2	20.1	28.4	51.3
I.R.	0.57		
Al_2O_3	4.7	10.4	27.4
Fe_2O_3	2.5	4.2	9.2
Mn_2O_3	0.18	0.13	0.07
P_2O_5	0.12	0.15	0.23
TiO_2	0.22	0.41	0.97
CaO	64.4	48.6	1.2
MgO	2.1	2.0	1.6
SO_3	2.6	2.4	0.92
L.O.I.	1.4	1.3	2.0
K_2O	0.72	1.4	4.1
Na_2O	0.20	0.36	1.2
F	0.10	0.07	-
Free Lime	2.5	1.8	-
SSA	405	397	-
45 μ res.	9.3	5.3	8.4

4. CONCLUSIONS

1. The results show that Portland pfa cement can produce increased core strength in mass concrete pours where the temperature rise would normally reduce the strength of an OPC concrete to about 70% of its expected value.

2. From the temperature profiles of the simulated pours it can be seen that the interground pfa cement produced lower temperature rises, at later ages, than the OPC, so reducing the thermally induced stresses within a large pour.

3. Although the pfa was slow to react with OPC at standard curing conditions, once the curing temperature exceeded 40°C the reaction rate increased markedly. The extent of this acceleration is such that at the centre of a 3 metre pour, the amount of pfa reacted after 2-3 days can be expected to be similar to that reacted following 100 days curing at 20°C.

4. Simple mechanical loading of the sample cubes showed that, at 28 days, the pressure generated by the mass of concrete above can be expected to reduce the strength loss at the centre of the large OPC pours and further enhance the strength of Portland-pfa pours. Consequently, a full simulation of large pour conditions should include this loading factor.

5. ACKNOWLEDGEMENTS

The authors would like to thank both Dr.G.K. Moir and J.J. Kollek for their assistance and Blue Circle Industries PLC for permission to publish this work.

6. REFERENCES

1. DUNSTAN, M.R.H., MITCHELL, P.B. Results of a thermocouple study in mass concrete in the Upper Tamar Dam. Proc. Inst. Civ. Engrs. Part 1, 60, Feb, Feb.27-52, (1976).

2. FITZGIBBON, M.E. Joint free construction in rich concretes 20 or 2000 m^3. Appraisal decision and thermal control. Symposium (1973).

3. FITZGIBBON, M.E. Large pours 2. Heat generation and control. Current practice sheet 35, Concr. Mag. (1976).

4. ALEGRE, R. La Calorimetrie des ciments au C.E.R.I.L.H. Revue des Materiaux.

5. BLAKEY, H. Temperature matching curing bath - an aid to earlier formwork striking. Concrete (1976).

6. CANNON, R.P. Measurement of the in situ strength and temperature development of concretes containing Portland and Portland blastfurnace cements. Silicates Industriels (1982).

7. COOLE, M.J. Calorimetric Studies of the Hydration Behaviour of Extended Cements, British Ceramic Preceedings No.35 (1984).

REACTIONS PERIODIQUES LORS DE L'ATTAQUE DES CIMENTS PAR DES REACTIFS CHIMIQUES

C. VERNET - SOCIETE DES CIMENTS FRANCAIS C.E.R.E.G.

P

1 - INTRODUCTION

Ce travail se situe dans le cadre d'une recherche à long terme sur les mécanismes réactionnels à l'interface ciment-eau, ayant pour but d'en déterminer les différentes étapes élémentaires. Pour cela, on s'intéresse, non seulement au milieu aqueux, mais aussi aux milieux non aqueux, qui permettent de faire varier les propriétés du solvant ou l'activité de l'eau et peuvent déboucher sur des applications intéressantes dans le domaine du dosage des phases par dissolution sélective.

Au cours d'une étude sur l'attaque acide de l'alite en milieu méthanol, en circuit ouvert, (extension de la méthode de TAKASHIMA), nous avons remarqué des fluctuations des concentrations en espèces dissoutes. Nous précisons ici les conditions dans lesquelles apparaissent ces fluctuations périodiques, qui sont faciles à mettre en évidence à l'aide des moyens modernes de la chromatographie HPLC.

2 - MONTAGE EXPERIMENTAL - PRINCIPE

Le montage dérive d'un système de chromatographie HPLC avec programmateur de gradients, dans lequel on a remplacé la colonne par un filtre en ligne, contenant un disque de poudre compactée de l'échantillon à étudier. A travers ce disque, on peut donc faire circuler à l'aide des pompes haute pression, un réactif de composition déterminée par le programmateur de gradients (FIG. 1).

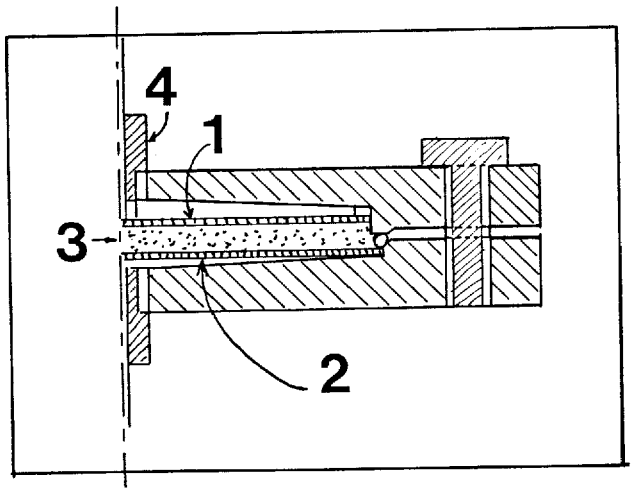

FIG. 1 - SCHEMA DU FILTRE EN LIGNE

1 Diffuseur
2 Grille support de filtre
3 Poudre compactée
4 Connecteur d'alimentation

Le passage en solution du composé étudié est détecté par une sonde conductimétrique à circulation, reliée à un système d'enregistrement.

La seule difficulté technique de la mesure réside dans la manière de réaliser le disque de poudre compactée, de façon à obtenir une répartition uniforme de la matière et éviter ainsi des passages préférentiels de réactif, qui pourraient s'accentuer jusqu'au percement du disque. Pour cela, il est bon de saupoudrer l'échantillon sur le filtre, en interposant un tamis de maille voisine de 160 microns.

3 - RESULTATS

Nous donnons ici quelques résultats obtenus pour les constituants des clinkers, soumis à une percolation par une solution d'acide acétique dans le méthanol, préparée par mélange automatique d'une solution mère à 1 Mol/l avec du méthanol pur. Le programmateur était réglé pour effectuer des paliers successifs de la proportion d'acide, entre 0 et 30 %, de façon à mesurer la période des fluctuations en fonction de la concentration en acide.

Cas de l'alite

On peut constater (Fig. 2), que le régime périodique se déclenche à partir d'un seuil situé vers 4 % de solution 1 M, pour une pastille de 47 mm de diamètre contenant 3 g d'alite broyée, de surface spécifique voisine de 3500 cm^2/g, traversée par un débit de réactif de 3 ml/mn. La fréquence et l'amplitude des fluctuations augmentent pour chacun des paliers de concentration en acide. La fréquence est proportionnelle à la concentration de l'acide acétique :

$$F = 3,8\ C$$

avec : F = Fréquence en mn - 1
C = Concentration molaire de l'acide acétique.

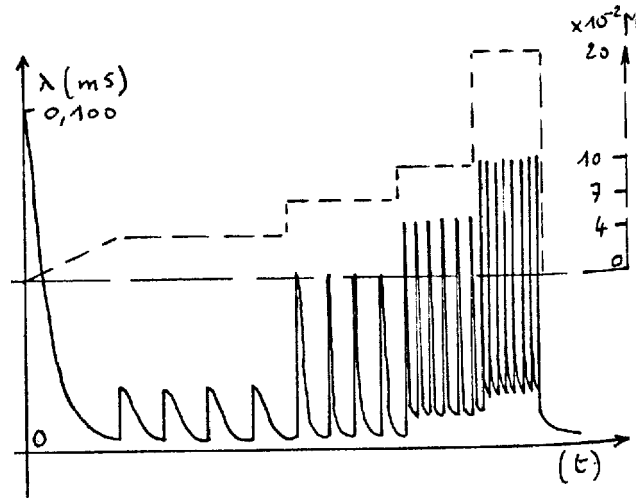

FIG. 2 - ALLURE DES FLUCTUATIONS PERIODIQUES

---- Gradient d'acide acétique
____ Signal conductimétrique

C. VERNET - SOCIETE DES CIMENTS FRANCAIS - C.E.R.E.G.

Les pics périodiques de conductivité ont une forme assymétrique. On observe une montée très rapide, correspondant à un passage en solution très rapide, puis une décroissance d'allure exponentielle.
La hauteur h des pics, traduisant la quantité d'ions libérés, montre une discontinuité en fonction de la concentration d'acide. Le graphe h = f(C) se présente comme une courbe de titrage conductimétrique, avec deux segments de droite de pentes différentes, le point d'intersection se situant vers c = 0,1 Mol/l (Fig. 3).

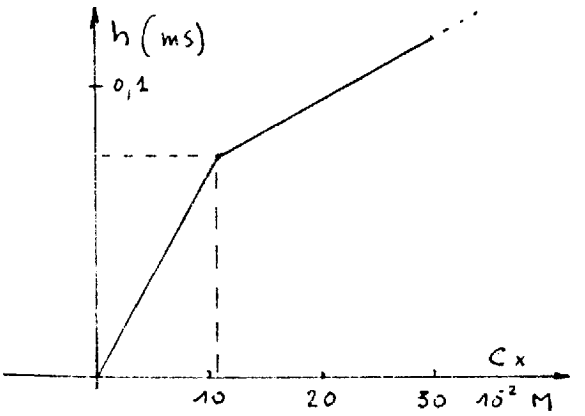

FIG. 3 - EVOLUTION DE LA HAUTEUR DES PICS

LE LONG DU GRADIENT

Autres constituants du clinker

Un comportement identique est constaté pour les autres constituants du clinker. La fréquence et l'amplitude des fluctuations sont beaucoup plus faibles pour les produits peu réactifs, comme la bélite et l'aluminoferrite, que pour le silicate et l'aluminate tricalcique.

4 - INTERPRETATION

Nous ne pouvons tenter ici une analyse détaillée de ces phénomènes périodiques, sur la base des premiers résultats expérimentaux. Leur interprétation nécessite des informations complémentaires, comme la composition chimique de la solution à la sortie du détecteur conductimétrique, ce dernier n'apportant qu'une information globale sur les concentrations en espèces dissoutes. La forme des pics et la discontinuité de l'évolution de la hauteur des pics semblent montrer que le mécanisme réactionnel comporte au moins deux étapes, dont la première est extrêmement rapide.

Dans l'interprétation du mécanisme, l'utilisation de la thermodynamique des processus irréversibles (T.P.I.) devrait se montrer intéressante. En effet, ce type de réactions périodiques n'est habituellement observé que dans des systèmes chimiques ouverts, appelés "structures dissipatives chimiques", où des couplages se manifestent entres diverses forces motrices (force chimique, force de diffusion, force électrocinétique) et les flux qui en résultent (taux de réaction, flux de diffusion, variation des charges électriques superficielles).

Les phénomènes observés ici présentent des analogies frappantes avec des réactions périodiques du type ZHABOTINSKI, de même qu'avec les réactions de précipitation dans des gradients de diffusion (anneaux de LIESEGANG), dont l'étude est du domaine de la T.P.I.

EVOLUTION DE LA MICROSTRUCTURE DES HYDRATES DES CIMENTS - ASPECTS THEORIQUES

C. VERNET - SOCIETE DES CIMENTS FRANCAIS C.E.R.E.G.

1 - INTRODUCTION

Depuis la thèse d'Henry LE CHATELIER, au début du siècle, de nombreuses études ont été publiées au sujet des mécanismes de l'hydratation des ciments. Il semble bien établi aujourd'hui que, au moins aux premiers âges, l'hydratation soit gouvernée par des processus de dissolution-précipitation, dont on cherche encore à décomposer les étapes élémentaires. Les lois qui régissent la croissance cristalline des hydrates seraient donc, d'une part, celles de la diffusion des espèces ioniques à partir des surfaces des grains, et d'autre part, les équations de vitesse des réactions de précipitation, traduisant les phénomènes de germination-croissance.

Si l'on cherche à donner un formalisme mathématique à ces mécanismes, dans le but de construire un modèle physique, on rencontre de grandes difficultés par exemple, devant le problème de la diffusion convective, qui est celui de pâtes de ciment immobiles. Dans le cas plus abordable de la diffusion régulière, où l'on peut faire entrer les suspensions agitées régulièrement, les solutions des systèmes différentiels issus de la combinaison des lois de FICK et des équations de vitesse des réactions, ne sont pas toujours stationnaires. La diffusion dans un gel peut par exemple produire des structures périodiques comme "les anneaux de LIESEGANG", découverts en 1896. En observant que la complexité de ces cas est liée surtout à celle du formalisme des équations de vitesse (par exemple lorsque le mécanisme comporte une étape autoctalytique), nous nous proposons d'étudier ici quelques modèles mathématiques très simplifiés, où nous envisagerons des équations de vitesse de forme simple, dans le cas de la diffusion plane unidimensionnelle. Bien que ces hypothèses de travail soient extrêmement réductrices de la réalité physique, quelques remarques peuvent en être tirées, concernant des particularités connues de la microstructure des hydrates.

2 - MISE EN EQUATIONS

Soit une réaction de précipitation de la forme :

$$A + nB \xrightarrow{} AB_n \qquad (1)$$

Pour que cette réaction se poursuive, il faut que le taux de sursaturation, c'est-à-dire le rapport du produit ionique effectif au produit ionique à l'équilibre :

$$\tau_s = S_p / S^*_p = \frac{(A)(B)^n}{S^*_p}$$

soit supérieur à 1. L'enthalpie libre de la réaction (1) est alors négative :

$$\Delta G_p = - RT \, Ln \, \tau_s$$

La modification des gradients de diffusion des espèces A et B, que l'on suppose générées par la dissolution de grains anhydres va dépendre des vitesses relatives de diffusion et de précipitation.

Nous écrirons que le régime stationnaire auquel nous nous intéressons, est obtenu lorsque dans un intervalle de temps dt, la quantité des espèces apportées par diffusion, dQd, est égale à la quantité dQp consommée par la précipitation.

Pour chacune des espèces, dQd est tiré des lois de FICK :

$$dQd_i = - D_i S \, \partial C_i / \partial x \, . \, dt$$

où D est le coefficient de diffusion, S la surface de l'interface génératrice et C la concentration à la distance x de cette interface.

dQp est tirée de l'équation de vitesse de la réaction (1) :

$$dQp_i = A.V. \, f(C_i). \, dt$$

où f(Ci) est la fonction de vitesse, V le volume de solution et $A = A_o \, e^{-E/RT}$ est la constante de vitesse de la réaction (1).

Dans le cas de la diffusion plane unidimensionnelle, l'égalité de dQd et dQp s'écrit :

$$\frac{dC_i}{f(C_i)} = - \frac{AV}{D.S} \, . \, dx$$

C'est donc la forme de la fonction de vitesse f(C) qui va déterminer la forme des solutions. Deux cas particuliers simples peuvent être envisagés :

- Précipitation très rapide, limitée uniquement par la diffusion de l'ion de concentration C. On peut poser :

  $f(C_i) \sim k(C_i - C_i^*)$

  où C* est la concentration loin de l'interface.

- Précipitation lente, limitée par la cinétique de germination-croissance du précipité. On posera alors :

  $f(C_i) = B. \, \tau_s$

  où τ_s est le taux de sursaturation et B une constante.

3 - RESULTATS

Nous nous limiterons ici au cas où f(C) a une expression linéaire (précipitation rapide). Deux situations peuvent alors se présenter :

- les ions formant le précipité sont issus de la même interface (cas de l'alite donnant des CSH)

- les ions proviennent de la dissolution de 2 minéraux distincts (formation d'ettringite).

C. VERNET - SOCIETE DES CIMENTS FRANCAIS C.E.R.E.G.

1er cas. Ions de même origine

Les solutions sont de la forme :

$$(C - C^*) = (C_o - C^*) \exp\left(-\frac{V.A.}{D.S} . k.x\right)$$

où C* est la concentration loin de l'interface et C_o la concentration à l'interface.

Il est pratique d'utiliser les paramètres habituels des ciments, surface spécifique s et rapport eau/solide r, au lieu du rapport V/S qui devient V/S = r/s.

Dans le cas ci-dessus, le taux de sursaturation est maximum à l'interface génératrice, qui sera donc un site privilégié de précipitation et l'on obtiendra des hydrates précipitant plus loin de l'interface lorsque les gradients seront plus faibles, c'est-à-dire lorsque s sera élevé, r faible et le rapport A/D des constantes de vitesse et de diffusion sera faible (Fig. 1).

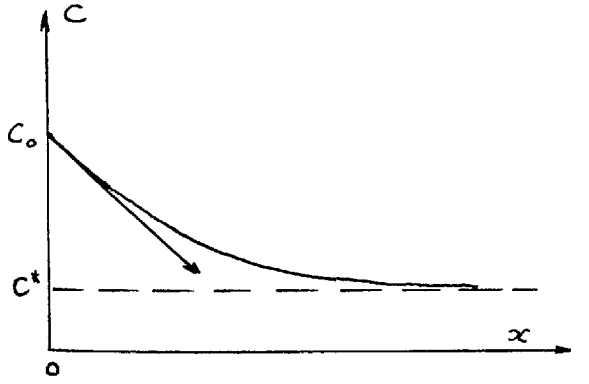

FIG. 1 -GRADIENT DE CONCENTRATION AVEC PRECIPITATION

L'interface génératrice est à l'abcisse x = 0

On constate que ce premier schéma très grossier est cohérent avec les données expérimentales sur l'évolution de la microstructure des silicates hydratés, en particulier l'obtention de fibres plus longues aux faibles E/S et les différences observées en fonction de la composition de la solution interstitielle.

2ème cas. Ions diffusant en sens inverse à partir de 2 interfaces génératrices (Fig. 2).

Les gradients des deux espèces ioniques s'écrivent à l'aide du formalisme précédent :

$$y = (C_1 - C_1^*) = (C_{o1} - C_1^*) \exp\left(-\frac{V.A_1}{S.D_1} . x\right)$$

$$z = (C_2 - C_{o2}) = (C_2^* - C_{o2}) \left[1 - \exp\left(-\frac{V.A_2}{S.D_2} .x\right)\right]$$

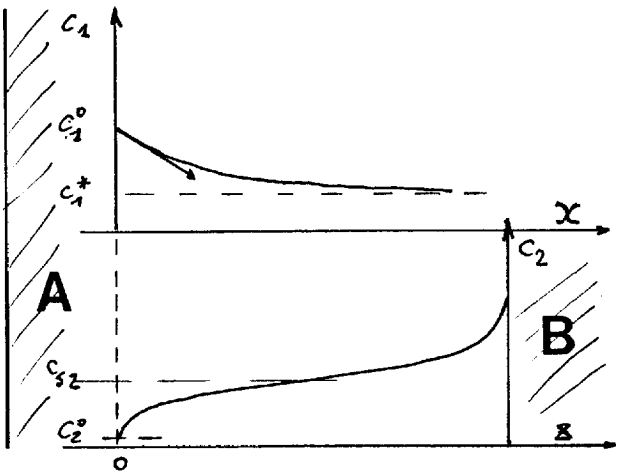

FIG. 2 - DIFFUSION INVERSE AVEC PRECIPITATION

La phase A génère l'ion de concentration C_1.
La phase B génère l'ion de concentration C_2.

On pose : $y = y_o \exp(-k_1 x)$

$$z = z_o . [1 - \exp(-k_2 . x)]$$

L'expression du taux de sursaturation sera la suivante :

$$\tau_s(x) = \frac{y.z^n}{S^*}$$

Posons $u(x) = S^*.\tau_s$

$$= \exp(-k_1 x) [1 - \exp(- k_2 . x)]^n$$

La fonction du/dx s'annule pour :

$$x_m = \frac{1}{k_2} . \ln\left(n \frac{k_2}{k_1} + 1\right)$$

C. VERNET - SOCIETE DES CIMENTS FRANCAIS C.E.R.E.G.

Le taux de sursaturation passe donc par un maximum, à une distance xm de l'interface (Fig. 3). Cette distance est liée uniquement aux constantes thermodynamiques et cinétiques, dans l'hypothèse de travail qui avait été choisie, soit une expression linéaire des constantes de vitesse (Il n'en serait pas de même avec les expressions non linéaires).

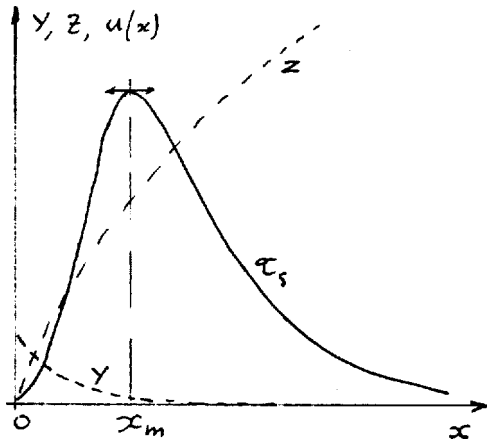

FIG. 3 - TAUX DE SURSATURATION DANS LE CAS DE LA DIFFUSION INVERSE

Ces résultats semblent également cohérents vis-à-vis des observations de la microstructure : l'existence de "coquilles d'ettringite" ou "grains de HADLEY" autour des cristaux de C_3A a été rapportée plusieurs fois.

4 - CONCLUSIONS

Ces quelques exemples simplifiés à l'extrême montrent tout l'intérêt de la modélisation des processus d'élaboration de la microsctructure. Nous sommes encore très loin de pouvoir établir une relation formelle explicite entre l'évolution des taux de réaction et l'évolution des résistances mécaniques et notre démarche théorique donne la mesure des difficultés qu'il faudra vaincre pour y parvenir. Mais nous pouvons remarquer que la microstructure des hydrates ne s'établit pas totalement au hasard et qu'elle obéit aux lois habituelles des processus irréversibles. On peut donc espérer des progrès dans la compréhension de ces phénomènes, en comptant sur les moyens informatiques modernes, qui nous apportent une aide appreciable pour la résolution numérique des systèmes différentiels.

UN NOUVEL INSTRUMENT POUR L'ETUDE DES REACTIONS D'HYDRATATION : LE GECS (GENERATEUR ELECTROCHIMIQUE DE CHAUX SURSATUREE)

C.VERNET - SOCIETE DES CIMENTS FRANCAIS C.E.R.E.G.

1 - INTRODUCTION

Les réactions d'hydratation des ciments se déroulent en général dans le domaine sursaturé de la portlandite $Ca(OH)_2$. Ceci constitue un obstacle à la reconstitution en laboratoire des conditions réelles de la formation et de la croissance des hydrates, telles qu'elles se produisent dans les mortiers et bétons. En effet, l'instabilité des solutions sursaturées rend leur étude expérimentale difficile, et il n'existe pas de méthode fiable, permettant de créer un état de sursaturation déterminé, pendant un temps suffisamment long.

Le développement d'un appareillage répondant à cette question se justifie par exemple dans les applications suivantes :

- Etude de la période dormante, des phénomènes de germination-croissance de la portlandite et du CSH
- Etude des adjuvants des bétons et des modificateurs de la diffusion des ions à l'interface solide-liquide.
- Etude du mécanisme de l'hydratation de C_3S, grâce à la séparation des variables (flux de dissolution et de précipitation).
- Etude des diagrammes d'équilibre des hydrates dans le domaine sursaturé en chaux.
- Synthèse des hydrates en régime de sursaturation contrôlé.
- Mesure de la réactivité des matières pouzzolaniques et des ajouts minéraux.

Malgré ces applications nombreuses et importantes, seules quelques tentatives ont été faites dans ce domaine. La génération de solutions sursaturées en utilisant des résines échangeuses d'ions n'a pas permis de résoudre le problème, car cette technique présente l'inconvénient de libérer des impuretés anioniques et ne permet pas de maintenir un taux de sursaturation élevé pendant un temps suffisamment long, ni de faire varier ce taux en système fermé.
Nous avons donc tenté une nouvelle approche du problème en nous orientant vers les méthodes électrochimiques qui répondent bien aux impératifs techniques des mesures.

2 - IMPERATIFS TECHNIQUES DU SYSTEME

- La technique de sursaturation ne doit pas faire appel à la dissolution d'une phase solide, dont la surface réactive ou les propriétés évolueraient en fonction du temps.
- Le générateur doit être capable de fournir une solution très sursaturée en chaux, dont la concentration atteigne par exemple 40.10^{-3} $Mol.kg^{-1}$ avec une vitesse de sursaturation équivalente à celle de l'alite des ciments, soit 1 à 4.10^{-2} $Mol.kg^{-1}.h^{-1}$.
- La quantité de solution de travail soit être suffisante pour effectuer tous prélèvements et dosages, soit 100 à 500 ml.
- On s'orientera de préférence vers un système permettant de régler à volonté le débit de calcium fourni et, au besoin, de réaliser des asservissements à l'aide de capteurs, dans le but d'effectuer une régulation automatique du degré de sursaturation.

3 - PRINCIPE (FIG.1)

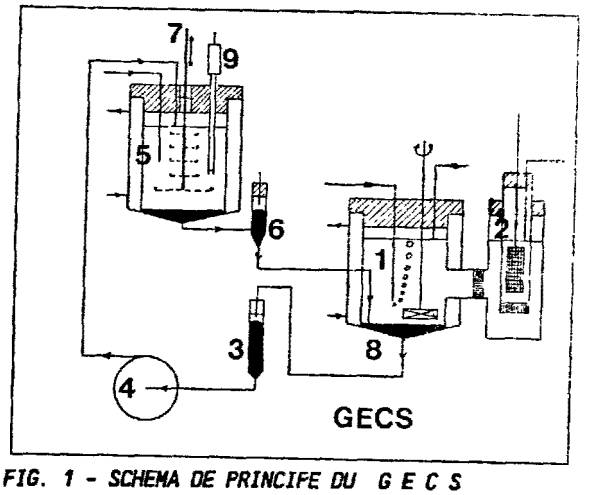

FIG. 1 - SCHEMA DE PRINCIPE DU G E C S

1 Cellule d'électrolyse Compartiment cathodique
2 Cellule d'électrolyse Compartiment anodique
3 Décanteur
4 Pompe
5 Cellule d'hydrolyse
6 Siphon
7 Tige du vibreur
8 Amalgame liquide de calcium
9 Sonde conductimétrique

Nous avons choisi un générateur de type coulométrique, constitué d'une cellule d'électrolyse, où l'on produit une solution de calcium métallique dans le mercure, selon l'équation :

$$Ca^{2+} + 2\ e^{-} + Hg \rightarrow Ca(Hg)$$

Cet amalgame liquide est introduit en continu dans une cellule d'hydrolyse, où le calcium est libéré au contact de l'eau, en produisant la solution de chaux, selon l'équation :

$$Ca(Hg) + 2\ H_2O \rightarrow Ca^{2+} + 2\ OH^{-} + H^2 + Hg$$

A la sortie de la cellule d'hydrolyse, le mercure est recyclé en continu vers la cellule d'électrolyse, où il se recharge en calcium.

4 - FONTIONNEMENT. ASPECTS TECHNIQUES

4.1 - CELLULE D'ELECTROLYSE (FIG. 1)

Le potentiel de décharge des ions calcium sur la nappe de mercure est inférieur au potentiel de réduction de l'eau. Ceci va limiter le rendement électrochimique du générateur. On peut faire reculer le "mur du solvant" en augmentant le pH de l'électrolyte, mais il ne faut pas dépasser le produit de solubilité de la portlandite, ce qui ferait chuter l'activité du calcium, qui doit rester la plus élevée possible, pour faciliter la diffusion. En pratique, l'électrolyte étant constitué d'une solution molaire d'acétate de calcium, le pH optimum se situe vers 11. Au cours de l'électrolyse, le pH a tendance à s'élever, à cause de la réduction cathodique de l'eau :

$$2\ H_2O + 2\ e^{-} \rightarrow 2\ OH^{-} + H_2$$

Cette variation est éliminée en établissant une circulation d'électrolyte tamponné dans la cellule d'électrolyse. L'excès d'électrolyte est pompé au niveau du compartiment anodique, ce qui présente l'avantage d'éviter la rétrodiffusion de l'oxygène libéré à l'anode, vers le compartiment cathodique. Cette rétrodiffusion peut être également diminuée par l'utilisation d'une anode oxydable de grande surface (mercure, fer, carbone).

- A la sortie de la cellule, l'amalgame traverse un décanteur, qui sert à éliminer les traces d'électrolyte entrainées par capillarité, à réaliser l'isolation galvanique et à permettre des prélèvements d'amalgame à des fins analytiques.
- L'amalgame est ensuite pompé vers la cellule d'hydrolyse. La forte variation de la viscosité en fonction de la teneur en calcium du mercure oblige à utiliser un asservissement de débit.

En régime stationnaire, la concentration en calcium de l'amalgame à la sortie du décanteur peut s'écrire :

$C1 = C2 + rI/2d.F$ où

C2 est la concentration en calcium du mercure entrant dans la cellule (recyclage)
r est le rendement d'électrolyse,
I est le courant de génération,
d est le débit de mercure,
F est le Faraday

4.2 - CELLULE D'HYDROLYSE (FIG.1)

Cette cellule est thermostatée et équipée d'une sonde conductimétrique permettant de mesurer en continu la concentration en chaux de la solution.

Le rendement d'hydrolyse dépend de la concentration en chaux dans la cellule, de la surface d'échange amalgame-solution et du régime de diffusion du calcium à l'interface.

- Le premier de ces paramètres n'intervient que faiblement dans le domaine très sursaturé, au-delà de 25 mMol/kg. En effet, l'hydrolyse se produit hors de l'équilibre et la concentration en chaux dans la cellule agit principalement sur la valeur du gradient de diffusion à l'interface.
- Pour augmenter au maximum la surface d'échange, la cellule est équipée d'un système de plateaux perforés, sur lesquels ont fait arriver l'amalgame. Les plateaux horizontaux sont fixés sur une tige verticale, actionnée par un vibreur, ce qui permet de pulvériser l'amalgame en fines gouttelettes. Le fond de la cellule constitue un décanteur où se forme une large nappe de mercure, dont la surface vient s'ajouter à celles des gouttes. Le mercure est évacué en continu par un siphon et retourne vers la cellule d'électrolyse.
- Le régime de diffusion à l'interface mercure-solution est stationnaire tant que l'on ne dépasse pas un taux de sursaturation trop élevé. Dans ce cas, la vitesse d'hydrolyse reste constante et pour un courant de génération constant, la concentration en chaux de la solution augmente linéairement avec le temps. Pour une densité de courant d'électrolyse de 20 mA/cm^2, un débit de mercure de 200 g/mn, cette augmentation est de l'ordre de 20 mMol/kg.h, valeur satisfaisante comparativement à la vitesse de libération de chaux par l'alite.

Dans le domaine très sursaturé, la précipitation de la portlandite a tendance à s'amorcer dans un film de solution qui s'insère par capillarité entre le mercure et la paroi du récipient. Cet inconvénient est difficile à éviter. Un bon échange du calcium des gouttelettes et l'utilisation de parois hydrophobes sont donc indispensables.

5 - RESULTATS

Les courbes de conductivité obtenues pour des courants de génération constants sont très semblables à celles que l'on observe pour les suspensions d'alite (fig. 2).

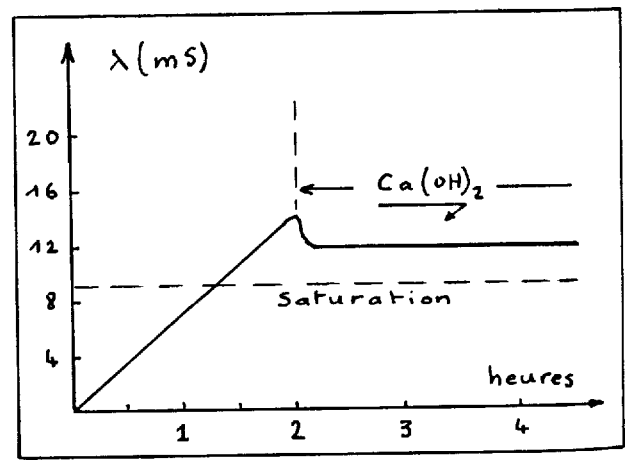

FIG. 2 - COURBE DE CONDUCTIVITE TYPIQUE, OBTENUE DANS LA CELLULE D'HYDROLYSE

- Après une montée pratiquement linéaire, la courbe s'infléchit, puis passe par un maximum pour lequel le taux de sursaturation semble dépendre uniquement de la température, indépendamment du courant de génération. Le facteur d'excès, c'est-à-dire le rapport entre concentration en chaux mesurée et concentration à l'équilibre, est de l'ordre de 1,6 à 1,7 lorsque l'on se trouve au maximum de conductivité. La précipitation de la portlandite produit alors une chute brutale de la concentration, suivie d'un palier traduisant l'établissement d'un régime stationnaire où la consommation de chaux par précipitation est égale à l'apport par le générateur. Ce palier stationnaire se trouve dans le domaine sursaturé de la portlandite. Le facteur d'excès est alors de l'ordre de 1,2 et varie en fonction du courant de génération.

6 - CONCLUSIONS

Ces tous premiers résultats obtenus avec le GECS suffisent à illustrer son utilité pour l'étude du domaine sursaturé de la portlandite et des mécanismes de l'hydratation. Nous avons montré ici que la réalisation d'un tel système est faisable, malgré les obstacles techniques liés à la génération électrochimique de l'amalgame de calcium et aux risques d'oxydation et de pollution de ce dernier par l'oxygène ou des éléments provenant du générateur lui-même. Ceci laisse entrevoir d'intéressantes perspectives pour les applications citées en introduction.

Par exemple, la grande similitude des courbes de conductance obtenues ici, avec celles des suspensions d'alite peut laisser à penser que l'allure de ces dernières n'est pas liée à des effets de barrière interfaciale, mais uniquement à l'existence d'un régime dynamique de dissolution-précipitation, qui est celui du GECS. Il reste à étudier le rôle que peut jouer la couche initiale de CSH sur le flux de dissolution et donc la durée de la période dormante, de même le rôle inverse que peut jouer la germination, de la portlandite sur la perméabilité de cette couche.

P. Ambroise, J. Péra et M. Murat.
Institut National des Sciences Appliquées de Lyon - France

INTERÊT DE L'ADDITION DE MÉTAKAOLIN AU CIMENT PORTLAND POUR L'ELABORATION DE MATÉRIAUX COMPOSITES RENFORCÉS PAR DES FIBRES DE VERRE.

I. INTRODUCTION.

Le renforcement des liants minéraux de type ciments et bétons par des fibres de verre a fait l'objet de très nombreux travaux (1-9) mais tous les problèmes relevant de cette technologie n'ont pas encore été résolus. Il en est ainsi du renforcement des ciments portlands artificiels par la fibre de verre E. En effet ce type de verre borosilicaté (7 à 9 % de B_2O_3) riche en silice (53 à 54 % de SiO_2) ne résiste pas dans un milieu basique tel que celui résultant de la réaction d'hydratation des silicates de calcium anhydres, réaction qui conduit à la formation d'un milieu riche en chaux amenant rapidement le pH à une valeur de l'ordre de 12,5.

La fibre de verre E est en effet attaquée en milieu basique avec destruction du réseau silicique et formation d'une couche superficielle perméable de silicate de calcium hydraté (1-4), couche poreuse permettant ainsi à l'attaque de se poursuivre jusqu'à dissolution complète du verre à long terme.

Ce phénomène est très préjudiciable au renforcement car il provoque très rapidement un abaissement notable des résistances mécaniques du composite.

Différents moyens ont été proposés pour remédier à cet état de fait (7) :

1. Modifier la composition de la fibre pour améliorer sa résistance chimique en milieu alcalin : fibres CEMFIL par exemple (1-3) mais dont le prix est très élevé par rapport à la fibre de verre E (30 F/kg au lieu de 9 F/kg).

2. Protéger la fibre par un dépôt organique ou minéral, procédé utilisant des technologies sophistiquées.

3. Diminuer l'humidité relative du milieu de conservation ou d'utilisation du composite.

4. Abaisser le pH du milieu cimentaire en cours de consolidation.

C'est cette quatrième solution que nous avons adoptée, conséquence d'une recherche plus générale sur la mise au point de liants pouzzolaniques de synthèse à partir de minéraux argileux thermiquement activés (10,11, 15-17).

II. PROCESSUS D'HYDRATATION COMPARES DU CIMENT PORTLAND ARTIFICIEL ET DES LIANTS POUZZOLANIQUES DE SYNTHESE.

Le phénomène d'hydratation et de consolidation des liants pouzzolaniques de synthèse à base de minéraux argileux thermiquement activés (cuisson de la matière première à 700-800°C pendant 5 heures dans un réacteur à lit fixe) nécessite l'addition d'un activateur chimique, en l'occurence l'hydroxyde de calcium $Ca(OH)_2$ qui apporte les ions calcium nécessaires pour former une solution sursaturée à partir de laquelle vont précipiter les différents hydrates responsables du développement des résistances mécaniques. Il est bien évident que l'activateur $Ca(OH)_2$ va être consommé au cours du temps, la vitesse de disparition étant fortement tributaire des conditions expérimentales.

En se fixant des conditions optimales de conservation des éprouvettes (10,11) on peut, par utilisation de l'analyse thermique différentielle (ATD), déterminer de façon semi-quantitative la nature et l'évolution des quantités d'hydrates formés au cours du durcissement, et détecter en particulier la présence ou l'absence de chaux résiduelle dans le matériau.

Dans le cas de l'hydratation de la métakaolinite par exemple (produit d'activation thermique de la kaolinite), les hydrates formés au cours de la consolidation sont essentiellement le silicate de calcium hydraté ou CSH_I de la classification de Taylor (12) et la géhlénite hydratée $2CaO.Al_2O_3.SiO_2.8H_2O$ (13-15). Ces deux hydrates sont caractérisés par les pics endothermiques notés respectivement C et G sur les courbes ATD (Fig. 1). La présence de chaux résiduelle est caractérisée par la présence du pic endothermique, noté CH, vers 550°C.

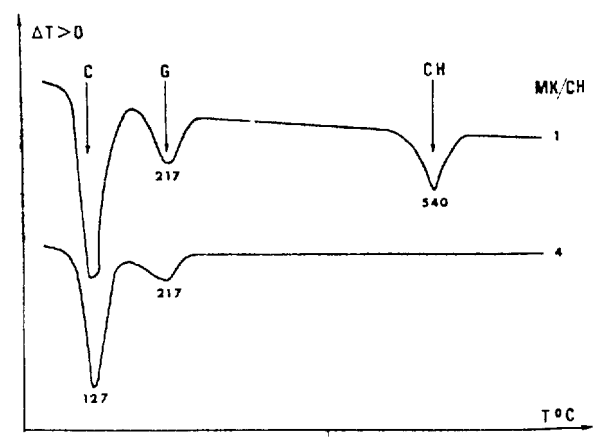

Figure 1. Exemple de courbes ATD des produits d'hydratation de métakaolinite en présence de chaux, à 28 jours, en fonction de la valeur du rapport "Métakaolinite/Hydroxyde de calcium" (MK/CH). Hydratation à E/S = 0,55.

Si on trace, à l'échéance de 28 jours, la hauteur des pics ATD (C, G, et CH) en fonction de la valeur du rapport massique initial Métakaolinite/Hydroxyde de calcium (rapport noté MK/CH), on constate que pour (MK/CH) > 2, il n'y a plus de chaux résiduelle dans le matériau (Fig. 2).

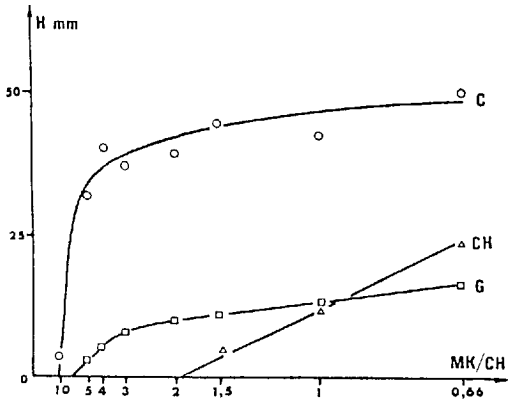

Figure 2. Variation de la hauteur des pics ATD de CSH_I(C), de géhlénite hydratée (G) et de l'hydroxyde de calcium (CH) à 28 jours en fonction de MK/CH.

De même, si on trace la hauteur de ces mêmes pics à différentes échéances d'hydratation, on constate que pour (MK/CH) = 1, la chaux n'est jamais totalement consommée, même à 90 jours (Fig. 3) bien que la formulation choisie corresponde aux conditions théoriques optimales de transformation stoéchiométrique de la métakaolinite en CSH_I et géhlénite hydratée.

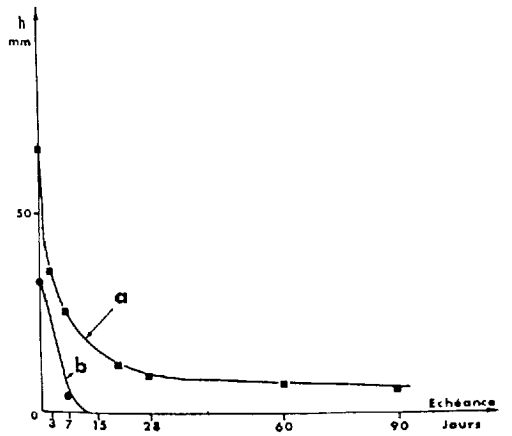

Figure 3. Variation de la hauteur du pic ATD caractéristique de l'hydroxyde de calcium (CH) en fonction de l'échéance d'hydratation pour deux compositions initiales de liants de métakaolinite + chaux : (MK/CH) = 1 (courbe a) et (MK/CH) = 3 (courbe b).

Par contre, pour (MK/CH) = 3, condition correspondant à l'obtention de résistances en compression optimales à 28 jours (de 25 à 35 MPa), la chaux a totalement disparu à l'échéance de 15 jours (Fig. 3).

Dans le cas de la consolidation du ciment portland artificiel, l'hydratation met en jeu les silicates de calcium anhydres (silicates bi- et tricalcique) et conduit à une formation quasi-continue de chaux selon des réactions du type :

$$3CaO.SiO_2 + H_2O \rightarrow CaO.SiO_2.xH_2O + 2\ Ca(OH)_2 \quad [1]$$

$$2CaO.SiO_2 + H_2O \rightarrow CaO.SiO_2.xH_2O + Ca(OH)_2 \quad [2]$$

La réaction [1] est beaucoup plus rapide que la réaction [2]. Par ailleurs le caractère nettement basique de la phase liquide intersticielle est renforcé par la solubilisation des alcalins présents initialement dans le ciment anhydre, phénomène qui conduit à la formation de bases libres (KOH, NaOH) (18) lesquelles sont également très agressives vis-à-vis des fibres de verre.

La différence flagrante entre les comportements respectifs à l'hydratation de ces deux types de liants, avec consommation rapide de la chaux pour les liants pouzzolaniques de synthèse, moyennant une valeur assez élevée du rapport pouzzolane/chaux, et apparition quasi-continue de chaux dans le ciment portland artificiel, nous a conduits tout naturellement à étudier le comportement de la fibre de verre E dans ces milieux cimentaires en cours de consolidation. L'emploi de liants pouzzolaniques de synthèse à base de minéraux argileux thermiquement activés et leur association au ciment portland artificiel, dans lesquels ils trouveront l'activateur chimique nécessaire sous forme de chaux naissante (Fig. 4) doivent permettre de réaliser un renforcement sans altération notable de la fibre de verre E, contrairement à ce qui se passe avec une pâte de CPA pur (19-21).

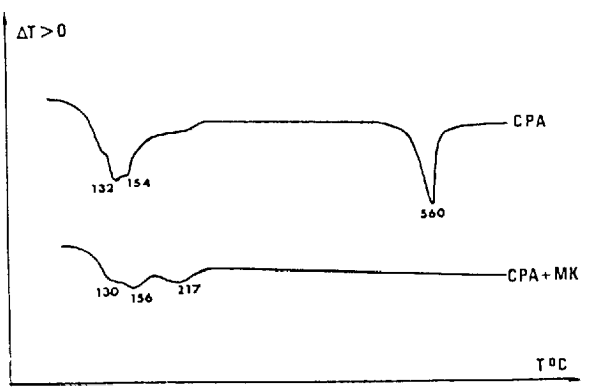

Figure 4. Courbes ATD du produit d'hydratation du ciment portland artificiel (CPA) pur et d'un mélange CPA/Métakaolinite (50/50 en masse) à 28 jours. Dans le cas du mélange CPA + MK on n'observe plus le pic caractéristique de la chaux vers 560°C

car la chaux naissante formée au cours de l'hydratation du CPA est consommée au fur et à mesure de sa formation pour réaliser l'hydratation de la métakaolinite.

On doit signaler cependant que l'idée d'ajouter au ciment portland un solide susceptible d'entrer en réaction avec la chaux au cours de la formation de celle-ci, n'est pas nouvelle : elle a été à la base de l'élaboration des ciments portlands aux pouzzolanes (anciennement CPAZ devenus CPJ ou "ciments aux ajouts" dans la nouvelle nomenclature). Mais les essais concernant le comportement de la fibre de verre E dans ce type de liant, les pouzzolanes ajoutées étant des cendres volantes, ont conduit à des résultats moins performants que ceux effectués avec les fibres à la zircone type CEMFIL (4). Par ailleurs, les résultats obtenus dans le cas du renforcement par les fibres CEMFIL sont très variables selon les caractéristiques chimiques et minéralogiques de la cendre volante utilée (22). L'addition de poussières de silice a également fait l'objet de travaux récents (23).

III. RESULTATS EXPERIMENTAUX ET INTERPRETATION.

La consommation de chaux dans le mélange CPA/MK a été suivie par diffraction des rayons X (Figure 5). Cette figure met clairement en évidence qu'à 28 jours, la chaux est totalement consommée pour le mélange 50/50 en masse.

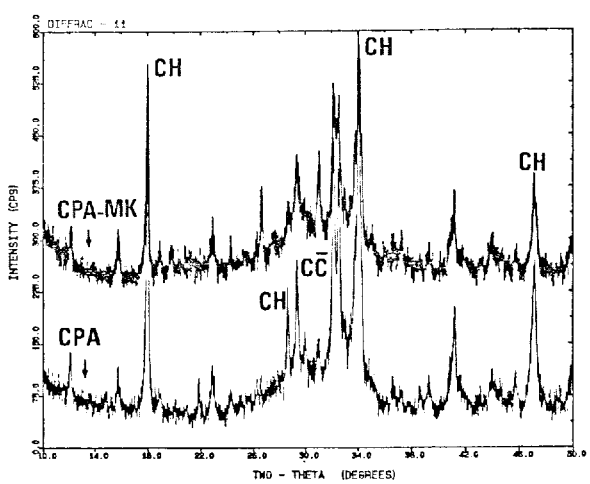

a

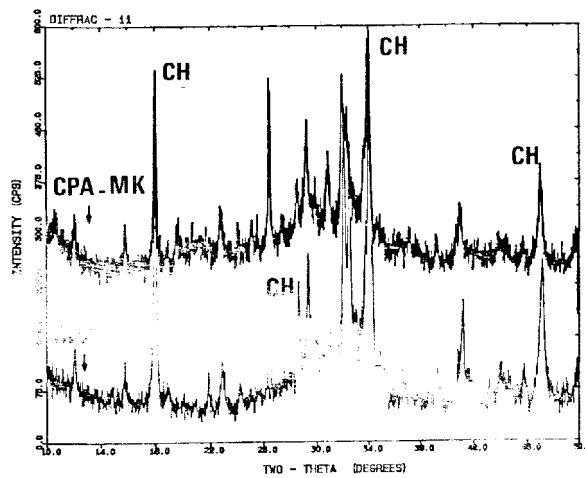

b

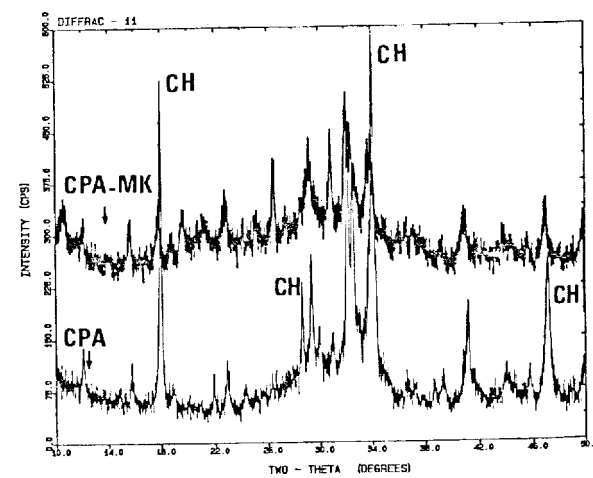

c

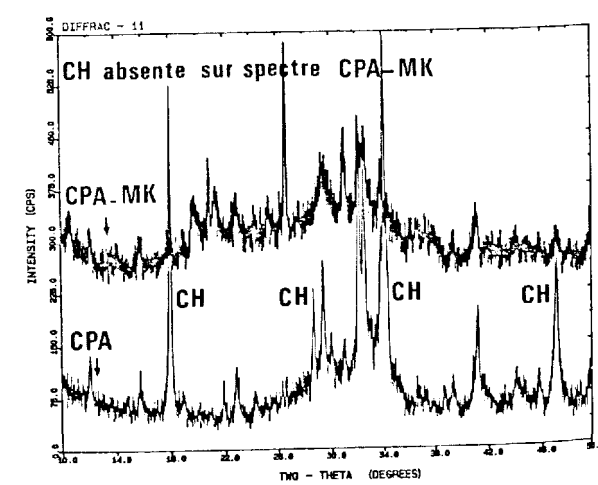

d

Figure 4. Etude de la consommation de chaux à 28 jours pour des mélanges CPA/MK en masse égaux à :

a. 80/20.
b. 70/30
c. 60/40
d. 50/50

Afin de suivre le comportement d'une fibre de verre E, des plaques de matériau composite, de dimensions 500x250x13 mm ont été réalisées à partir de trois types de liants :
- un ciment portland artificiel CPA 55 gâché avec un taux de gâchage E/S (rapport Eau/Solide) de 0,3,
- un liant pouzzolanique de synthèse, constitué de métakaolinite (MK), (obtenue par calcination d'une kaolinite pure pendant 5 heures à 750°C) additionnée d'hydroxyde de calcium pur (CH) dans un rapport massique (MK/CH) = 3. Le gâchage avec l'eau a été réalisé avec un rapport E/S = 0,6.
- un liant mixte "CPA 55 - Métakaolinite", en proportions massiques 50/50 gâché à E/S = 0,4.

Ces plaques, lors de leur élaboration, sont armées avec de la fibre de verre E à raison de 37,4 g de fibre par plaque, la fibre étant orientée dans le sens longitudinal de chaque plaque. Les composites ainsi obtenus sont conservés sous eau à 20°C jusqu'à l'échéance (J-1) jours, puis séchés 24 heures à 20°C dans une chambre de conservation à 60 % d'humidité relative avant de réaliser les essais mécaniques. Les plaques, après essais en flexion 3 points, sont ensuite conservées à la température ambiante pour observation des fibres par Meb à 160 jours et à 1 an.

Les essais en flexion centrée sont réalisés à l'échéance de 36 jours. Les lois de comportement jusqu'à rupture sont représentées sur la Figure 6. Le Tableau I fournit les résistances en compression (R_C) et en traction (R_T) pures des différents liants ainsi que les charges et les flèches ultimes des plaques renforcées par la fibre de verre.

de la plaque de liant de métakaolinite-chaux (colonne 2) n'est pas significatif (de l'ordre de 15 %) alors que les résistances respectives en traction de ces liants varient du simple au triple. La présence de pouzzolanes de synthèse dans les différents liants permet d'empêcher la rupture fragile des plaques comme le montrent les résultats obtenus dans le Tableau I et sur la Figure 6.

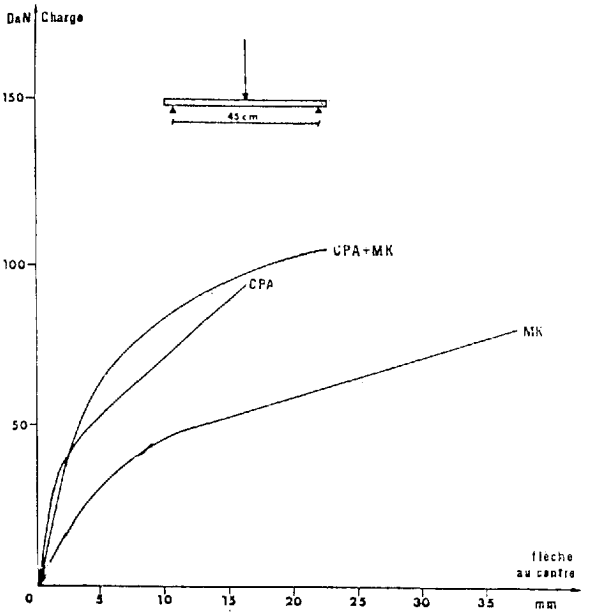

Figure 6. Courbes "charge-flèche" des plaques composites jusqu'à rupture.

TABLEAU I

Caractéristiques mécaniques des liants en pâte pure et des composites.

Propriétés mécaniques	Nature du liant		
	Pâte pure de CPA	MK + CH (3/1)	CPA + MK (1/1)
Pâte pure :			
· résistance en compression (MPa)	62	30	41
· résistance en traction (MPa)	6,9	2,3	3,7
Plaques composites :			
· résistance en traction par flexion (MPa)	15,2	12,8	16,8
· flèche ultime (mm)	16	37	25

Ce tableau met en évidence que, pour pour le liant mixte CPA+MK, la métakaolinite peut servir à consommer la chaux formée dans le ciment portland artificiel (colonne 3) et que l'écart observé entre les charges de rupture de la plaque de CPA pur et

Les fibres extraites des plaques après essais mécaniques à 36 jours ont été examinées en microscopie électronique à balayage (MeB) (utilisation d'un appareil CAMECA MeB 07) après avoir été recouvertes d'une mince couche d'or par métallisation sous

sous vide pour éviter les phénomènes de charge.

On constate très nettement, à l'échéance de 36 jours, que la fibre incorporée au ciment portland artificiel au cours de la consolidation en pâte pure présente un état de surface caractéristique d'une altération chimique et d'une dégradation très prononcée (Fig. 7). D'ailleurs la résistance mécanique propre de cette fibre a presque totalement disparu comme on peut le constater au simple toucher : les fibres émergentes du composite se désolidarisent très facilement de la plaque.

Par contre, les fibres incorporées au liant pouzzolanique de synthèse (métakaolite + chaux) ou au liant (CPA + MK), présentent une surface qui ne semble pas avoir été concernée par une altération chimique due à la chaux (Fig. 7). Les portions de fibre émergeant en bout de plaque sont très résistantes et ne se désolidarisent pas du composite.

L'observation des fibres à des échéances de 160 jours et de 1 an conduisent aux mêmes résultats (Fig. 8)

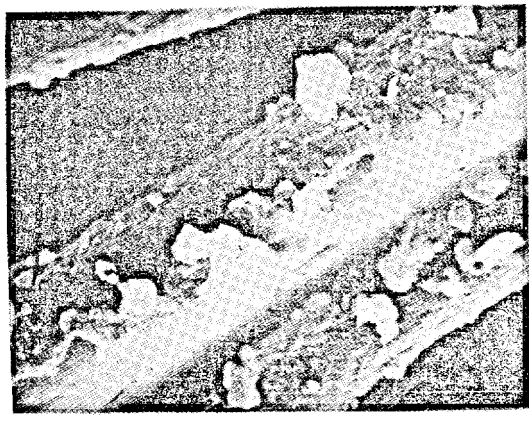

1

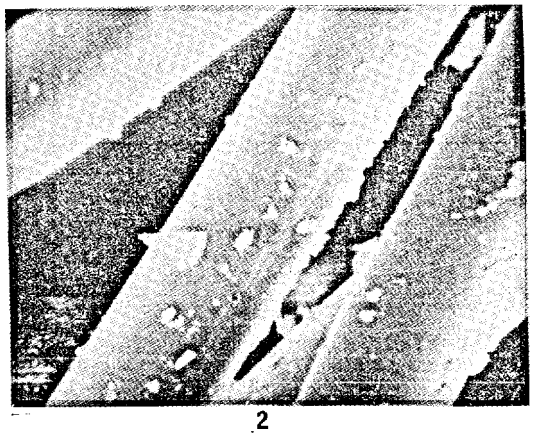

2

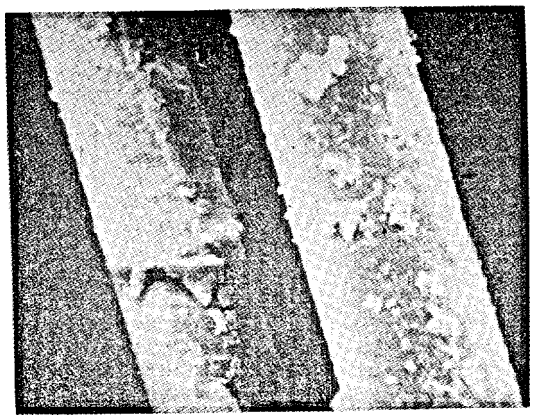

3

Figure 7. Comportement comparé de la fibre de verre E, à 36 jours, après incorporation dans les différents liants suivants (grossissement 2000) :
1) Ciment portland artificiel (CPA)
2) Métakaolin + chaux (MK + CH)
3) Ciment portland artificiel + métakaolin (CPA + MK).

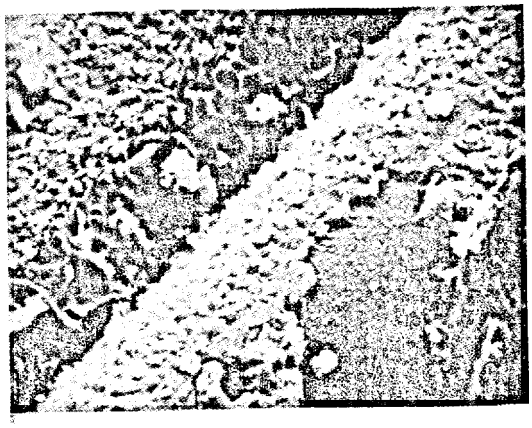

1

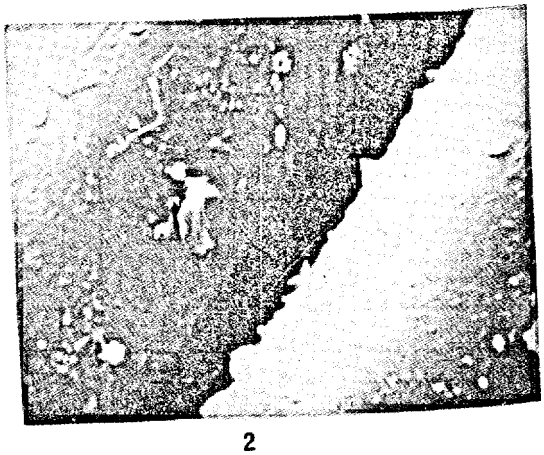

2

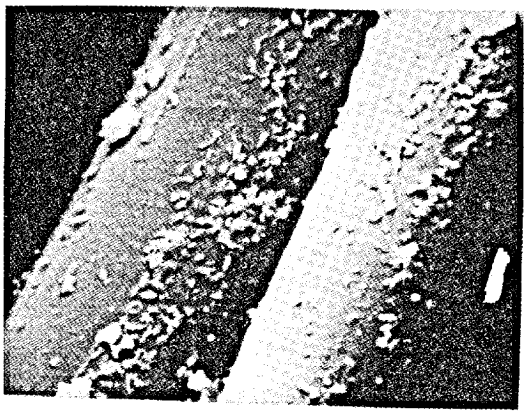

3

Figure 8. Comportement comparé de la fibre de verre E, à 365 jours, après incorporation dans les différents liants suivants (grossissement 4000) :
1) Ciment portland artificiel (CPA)
2) Métakaolin + Chaux (MK + CH)
3) Ciment portland artificiel + Métakaolin (CPA + MK).

IV. CONCLUSION.

Il apparaît donc qu'une solution relativement aisée pour réaliser des matériaux composites à base de liants minéraux renforcés par de la fibre de verre E consiste à utiliser une matrice dont la phase liquide intersticielle ne présente pas de caractère basique prononcé au cours du processus de consolidation. Les deux solutions proposées sont (19) :

- soit l'emploi de liants pouzzolaniques de synthèse (minéraux argileux thermiquement activés) dans des conditions telles que l'activateur chimique (chaux) soit consommé à des échéances raisonnables (une à deux semaines), le liant devant cependant développer des résistances mécaniques élevées à court terme (28 jours),

- soit l'association de ces liants pouzzolaniques de synthèse à du ciment portland artificiel, l'hydroxyde de calcium formé au cours de l'hydratation du second liant jouant le rôle d'activateur chimique pour le premier, donc étant consommé au fur et à mesure de sa formation.

Références.

(1) - MAJUMDAR A.J. and RYDER J.F., "Glass Reinforcement of Cement Products". Glass Technology, 9, (1968) p. 78-84

(2) - STEELE B.R., "Glass Fiber Reinforced Cement", Proc. Inter. Building Exhibition Conf. on Prospects for Fiber Reinforced Construction Materials, Building Research Etablishment, 1972, p. 29-39.

(3) - MAJUMDAR A.J. and TALLENTIRE, "Glass Fiber Reinforced Cement", Int. Symp. on Applications of Fiber Reinforced Concrete, Canada, 1973.

(4) - MAJUMDAR A.J., "The role of the Interface in Glass Fiber Reinforced Cement" Cem. Concr. Res., 4 (1974), p.247-266

(5) - NEVILLE A., (Editor), Proc.RILEM Symp. "Fiber Reinforced Cement and Concrete" The Construction Press, 1975

(6) - LARNER L.J., SPEAKMAN K. and MAJUMDAR A.J "Chemical Interactions between Glass Fibers and Cement", J. Non Crystalline Solids, 20, (1976)

(7) - SHIN Woo Seung,"Recent Development in Alkali-Resistant Fibers at the Battelle Institute", Proc. Inter. Congr.GRC in the 80s, V. BLAKE Ed., The glass Fiber Reinforced Cement Association, U.K., 1982, p. 351-374.

(8) - ROY D.M. MAJUMDAR A.J., SHAH S.P. and MANSON J.A. (Editors), "Advances in Cement-Matrix Composites". Materials Research Society, 1980.

(9) - ROTWELL K.P. and WARRIOR D.A., "Chemical Resistance of GRC", Proc. Intern. Congress GRC in the 80s, V. BLAKE Ed., The Glass Fiber Reinforced Cement Association, U.K., 1982, p. 100-112.

(10) - AMBROISE J., "Elaboration de liants pouzzolaniques à moyenne température et étude de leurs propriétés physico-chimiques et mécaniques". Thèse de Doctorat d'Etat, Lyon, Juillet 1984.

11) - AMBROISE J., MURAT M. and PERA J.,"HYdration and Hardening of calcined clays and related minerals. IV-Experimental conditions for strength improvment on metakaolinite minicylinders". Cem. Concr. Res., 15, (1985), p. 83-88.

(12) - TAYLOR H.F.W., "The Chemistry of Cement", Acad. Press, London and New-York, Vol. I, (1964), p. 167-232.

(13) - STRATLING W., "Die Reaktion zwischen gebranntem Kaolin und Kalk in wâseriger Lösung", Zement Verlag, Berlin, 1938.

(14) - TURRIZIANI R. and SCHIPPA G., "Analisi termica differenziale dei productti di reazione del caolino disidrato con idrato di calcio", Ricer.Scientif. Ital. 24, (1954), 2, p. 366-374.

(15) - MURAT M., "Hydration and Hardening of calcined clays and related minerals. I. Preliminary investigations on metakaolinite". Cem. Concr. Res., 13, (1983), 2,p. 259-266

(16) - AMBROISE J., MURAT M. and PERA J., "Hydration and Hardening of calcined clays and related minerals. V- Extension of the research and general conclusions". Cem. Concr. Res., 15 (1985) p. 261-268.

(17) - AMBROISE J., BACOT J., MURAT M. et PERA J., "Valorisation de la latérite en tant que matériau de construction dans un habitat économique". Premier Congr. Intern. de Géomécanique des Sols Tropicaux et Saprolitiques, Brasilia (Brésil), 1985, Ed. ISSFME, Vol. II, (1985), p. 395-406.

(18) - LONGUET P., BURGLEN L. et ZELWER A., "La phase liquide du ciment hydraté". Rev. Mat. Constr., 678, (1973), 1, p. 35-41.

(19) - AMBROISE J., MURAT M. et PERA J., Brevet Anvar n° 85/00474 déposé le 10.01.1985.
(20) - AMBROISE J., MURAT M. and PERA J., "Durability of E-glass fiber in portland cement-metakaolinite matrix" Intern. Symp. Durability of GFRC, Chicago, Il, Nov. 1985.
(21) - AMBROISE J., MURAT M. et PERA J., "Durabilité des fibres de verre dans différents milieux cimentaires en cours de consolidation. Etude d'une fibre de verre E". VERRES ET REFRACTAIRES, N° 6, Nov. Déc. 1985.
(22) - LEONARD S. and BENTUR A., "Improvment of the Durability of Glass Fiber Reinforced Cement using Blended Cement Matrix". Cem. Concr. Res., 14, (1984), p. 717-728
(23) - BENTUR A., Communication à l'Intern., Symp. Durability of GFRC, Chicago, Nov. 1985.

Remerciements.

Les auteurs remercient la Société VETROTEX (France) qui a fourni les échantillons de verre E, ainsi que Mle BARDOT et Mme CHATELUT (E.R.A. CNRS n° 300, Université Claude Bernard Lyon I) pour les clichés de microscopie électronique à balayage.

R. Kovács
Central Research and Design Institute for Silicate Industry - Hungary

RAPID METHOD FOR CEMENT STRENGTH PREDICTION.

P

Elaboration of the method

Preliminary determination of cement strength has been dealt with for a long time. Forester and Keen /1960/, Leczner and Bernoff /1961/ recommended several methods the essence of lied in accelerating the process of hardening. Most of these methods apply steam curing at atmospheric pressure or above it. However, since the behaviour of various type cements under steam-curing is different, these methods cannot be equally applied to all the cements and don't supply directly comparable results. Besides in the course of steamcuring, especially that, carried out in autoclaves under enhanced pressure, the macro-and microstructure of hardened cement stone as well as the composition of arising hydration products changes considerably. According to methods proposed by Gaca/1963/ and Lawrence /1969/ specimens are prepared either from dry cement powder with the addition of some lubricant or from cement-paste or mortar by pressing The acceleration of hardening in this case is achieved by the closen arrangement of the hydrating cement particles. Yet, wider use of these methods was mindered by several factors. For instance the lubricant /alcohol, ethylene glycol/ applied affected the following hydration, while the preparation of specimens and ensurance of their homogeneity turned to be extremely difficult and connected with a significant subjective error because of the very low water:cement ratio /in the range of 0,1/. At the same time various water requirement of different cement types as well as the amount and composition of dissolved components leached out with the pressed-out water influencing further hydration is not taken into account at all. This is why as Nagy /1969/ had shown these methods have a rather wide variation in results.

Weighing out portions from the moist mixture before pressing is time-consuming and in exact, while drying up of the mixture during this operation also contributes to higher scatter of results. Dabriel /1971/ and lately Relis and Soroka /1974/ used vacuum, too, for the acceleration of hydration of the specimens but they did not suceed to eliminate all the abovementioned error-sources. To all this one can add that the known and widely used standard methods for cement-strength determination posess a lot of shortcomings/disadvantages/ explaining why, up to now no common agreement could be achieved in introducing a worldwide acceptable universal testing method, some of these disadvantages are as follows:

- the sand or aggregate used for the preparation of specimens cannot be exactly defined,
- the prescribed water cement factor leaves the factual water requirement of the cement out of consideration,
- the conditions of preparing the specimens /weighing out portions of the moist mixture, filling them into the moulds, compaction, smoothing their surface etc/ give place to a number of subjective errors

As a consequence the permitted scatter of results for the majority of known standard methods amounts to $\pm$10 % with a poor reproducibility and reliability of results. Besides, the results determining the real quality of the product appear only after 28 days when the cement referred to had been already used up so that no correction is to be made as to its dosage /proportioning/.

Outgoing from all above described in elaborating our new methods we paid special attention to the followings·

-utilization of the experience obtained by known standard and accelerated testing methods
-getting results in a short time with little materials- and labor requirement
-possible minimal scatter of results with possible maximal elimination of subjective factors and other error sources /like the use of sand or aggregates, variable w/c ratio etc/
-applicability for all cement types and possibility of the use of ordinary laboratory equipment,
-simlicity of operations with the possibility of succeeding automation,
-the hydration parameters and -products should not substantially differ from those obsrved in case of normal hardening

After years of investigation and continuous development a new rapid method /now patented under N°181334/ has been outlined the main featured of which are shown below

A rapid method for cement strength prediction

The essence of the method lies in weighing out portions of the dry cement sample to be tested each 25 g out of which cylinder shaped specimens of a determined porosity and are moulded by two-stage pressing These specimens undergo hydration by capillary moistening at ambient temperature in a water-vapour saturated room and are tested after 7-24 hours of hardening. Under the given circumstances- because of the close dislocation of the cement particles - the hardening process takes place very intensively the compressive strength of the specimens achives in 4 hours about 1o MPa, in 8 hours about 2o MPa and in 24 hours about 6o-8o MPa depending on the cement quality. By this time the density of the specimens is in the range of 2,8-2,9 g/cm^3, the porosity between 2o-22%, the moisture and bound water content being 7-9 % and 5-7% respectively.

Usually 6 specimens are prepared for one testing and after a certain experience is gained by the personnel the coefficient of variation of the results is less than 5% ordinaly being even less than 3 % This can be explained by the almost complete elimination of the subjective factors.

The strength results obtained by the new method are in good correlation with the 3, 7, 28 days or any other age strengths of the cement sample as determined by standard methods.

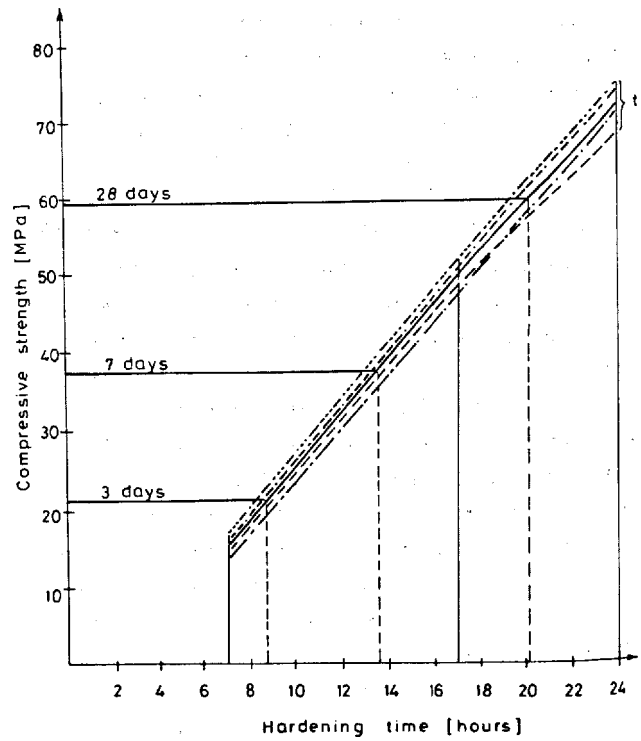

Figure 1
Calibration curve

Based upon these results a calibration curve is drown up /fig.1/ upon which the 3, 7,and 28 days strength values of the same cement samples /determined by standard methods / are marked. To the following it is sufficient to determine the strength of a given cement sample by the rapid method to be able to predict -using the calibration curve- the expect-

able standard strength at any age with a reliability meeting practical requirements /e g ±3 MPa/.
The new method can be applied on one hand in plant laboratories for systematic quality control and on the other hand at cement consumers where - by quick determination of the expectable factual strength of cement - it makes possible the optimal proportioning of the latter at concrete mixing plants and thereby contributes to a cement economy of at least 5-1o % with a more uniform concrete quality at the same time.
The new method is regularly applied at one of the prefabricated concrete plants in Hungary since the beginning of 1986.
More detailed information can be obtained at the institute SZIKKTI, Budapest

References

Debriel,J.A.: Cement Technology 2 N°4 1-8 1971.
Forrester, J.A.- Keen,R A. J.of Applied Chem N°9,358-365 196o.
Gaca,W.:Cement-Wapno-Gips 28 N°78,141-149. 1963.
Lawrence,C.D.: Tl properties of cement paste under high pressure Res.Report. N°19, CCA, 1969, London,21.
Nagy,A : Építőanyag,21, N°12, 45o-458 1969
Leczner,F.J.-Barnoff, R.: J. of the Amer. Concr. Inst.Proc. 57, N°8, 973-975 1961
Relis, M.- Soroka,I : Materiaux et Construction 7 , N°38, 1o3-1o9. 1974.

F.D. Tamás, E. Farkas, M. Vörös (University of Veszprém - Hungary) 1
D.M. Roy (The Pennsylvania State University - U.S.A.)

LOW-FREQUENCY ELECTRICAL CONDUCTIVITY OF CEMENT, CLINKER AND CLINKER MINERAL PASTES.

P

INTRODUCTION

This paper deals with the time function of electrical conductance (or specific conductance = conductivity) of pastes made of portland cements, clinkers or clinker minerals. The effect of some variables (e.g. grinding fineness, temperature, measuring frequency, admixtures etc.) was studied. All tests reported here were made in the state of setting and early hardening and measured at relatively low A.C. frequencies (100 Hz - 10 kHz); this means that the changes in electrical conductance can be attributed to changes in the number or mobility (or both) of charge carrying ions. Other experimental circumstances (as e.g. high-frequency measurements, non-portland cements, suspensions rather than pastes) are excluded.

Regrettably almost no references exist in this narrow field, although the test is simple, yet informative. The first reported conductance measurements on cement pastes date back to 1936 /1/. More extensive research was made by Calleja /2,3,4/ and by Hammond and Robson /5/. Nikkanen /6/ examined the temperature- and moisture dependence of electrical conductance in cement paste and concrete specimens. Ana /7/ tried to utilise the conductivity method for the determination of setting time of oil-well cements. Monfore /8/ examined the change in electrical conductance of cement paste in the setting period and the same was done by Náray-Szabó and Szuk /9, 10, 11/ for normal and steam-cured concrete. Some data were published by Kolbasov et al. /12/, by Batalov and Klyusov /13/ and by Efimenko /14/. Reference is given to the D.C. electrical conductivity of fresh concrete in the booklet by Henning and Oelschläger /15/. Results of recent research by the authors were published in 1982 /16/ and presented at various scientific meetings /17, 18, 19/.

Most researchers agree that the electrical conductance of portland cement pastes increases shortly after mixing with water, followed by a continuous decrease. The increasing period can be interpreted as the liberation of various ions (mainly calcium-, hydroxide-, sulfate- and alkali-ions, etc.) due to hydrolysis; these ions are later immobilised in the lattice of new formations, thus decreasing their mobility and number, and, in turn, the conductance of the paste.

Some researchers found besides this general trend one or two additional, short-lived increases on the descending section of the conductance vs. time plot (to be cassed hereinafter: conductogram) (Fig. 1).

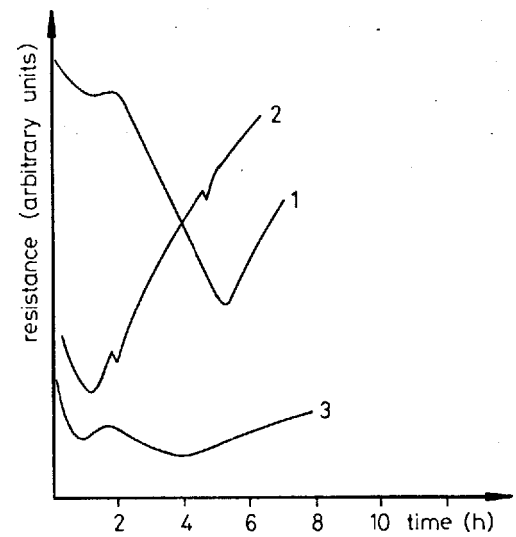

FIG. 1.
Sample conductograms published by Calleja /2/ (Curve 1), Szuk /11/ (Curve 2) and by Henning and Oelschläger /15/ (Curve 3)

In the recent work by Tamas /16/ it is shown that one, sharp, transient conductance maximum appears, the time of which depends on the temperature and w/c ratio of the paste. Retarders and accelerators affect the time and the intensity of this transient maximum, and it can be decreased, or fully eliminated by admixing gypsum to the cement. Later it was shown /17/ that not all cements behave in a similar way: clinker pastes and the majority of cement pastes exhibit no transient maximum on the conductogram, the descending section is usually smooth, with no maximum (although slight inflections or breakpoints max occur). However, by adding

a definite, critical amount of gypsum (for most clinkers approx. 2.5% $CaSO_4.2H_2O$, on the basis of dry cement mass) the transient maximum definitely appears. Adding slightly more or slightly less gypsum than this critical amount, the maximum would be converted into an inflection or breakpoint on the conductogram, while well over or under the critical gypsum content the descending section of the conductogram becomes smooth again /17, 18/.

EXPERIMENTAL

Most experiments were carried out at the Institute of Silicate Chemistry and -Technology of Veszprém University, Hungary. Some control tests, including the frequency variation method were made at the Materials Research Laboratory of the Pennsylvania State University, U.S.A.

Materials

Clinker minerals, clinkers and portland cements of different origin were used. The clinker minerals were prepared from pure reagents by multiple firing and regrinding. After final control (by chemical analysis and XRD) all substances were ground to the desired fineness (0.3 $\pm$ 0.005 m^2/g Blaine, unless otherwise stated). Some control tests were made with quartz sand ground to the same fineness.

Clinkers and cements were industrial products, their composition and moduli given elsewhere /17/. Gypsum was natural rock, its $CaSO_4.2H_2O$ content over 96%. Admixtures were CP grade reagents. De-ionised water was used in all experiments.

Method

The finely ground solids were weighed, transferred to a beaker, water added to give a paste of plastic consistency and thoroughly hand-mixed for one min. After this the paste was transferred to a conductance cell (Fig. 2.), carefully filled to assure a good contact between the paste and the electrodes.

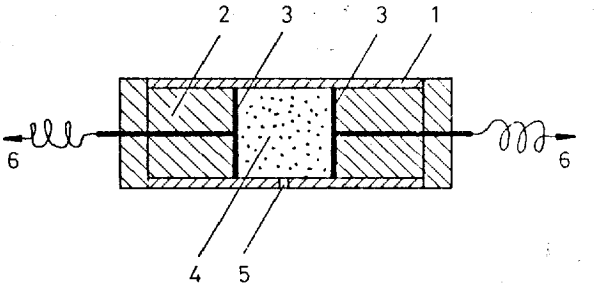

FIG. 2.
The conductance cell. 1 hard PE tube, 2 PTFE cylinder, 3 stainless steel electrodes, 4 cement paste, 5 opening for excess paste, 6 to conductometer and recorder

Excess paste protruded through opening 5. Electrodes were polished before each experiment. Measurement commenced exactly six minutes after the first contact with water; this is zero time on the conductograms. The temperature of the paste was kept constant at 32°C during the experiment with the aid of a flowthrough vessel of a conventional thermostat. Electrodes were hooked to a bridge-type electronic conductometer, the output of which was continuously recorded. In Veszprém a RADELKIS OK 102/1 conductometer (operating at 3 kHz frequency) and a RADELKIS OH 814/1 recorder was used. At MRL-PSU a HP 4274A LCR-meter (operating 0,1 - 100 kHz frequencies) was used, controlled by a HP 9825 computer. Measurements were made at one-minute intervals and recorded by a HP 9872A plotter. Conductances were measured in Siemens, the SI unit of conductance. Conductivity (i.e. specific conductance) values were calculated from the measured conductance by the known dimensions of the cell.

RESULTS AND DISCUSSION

In the following some sample conductograms are shown. The abscissa scale is time (in hours) while the ordinate is conductivity,

expressed in S/m and marked γ according to the rules of the International System.

If an inert material (quartz sand) is mixed with water or admixture solutions to make a paste, its conductogram is straight. A slight decrease of conductivity can be attributed to the adsorption of charge-carrying ions on the surface of the solid (Fig. 3.).

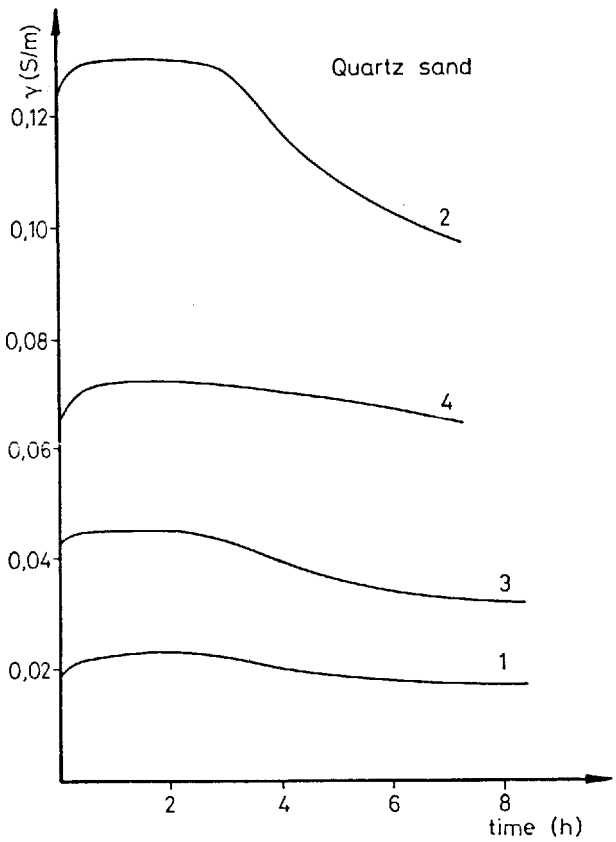

FIG. 3.

Conductograms of quartz sand. 1 no admixture, 2 0.1% Na-formate, 3 0.1% citric acid, 4 0.2% citric acid

All clinkers and the majority of cements investigated so far give only one conductivity maximum (Fig. 4.). Some cements however show a very characteristic second, transient maximum on the descending section of the conductogram, the intensity of which may reach, and (esp. at low measuring frequencies) even exceed that of the first maximum (Fig. 5.).

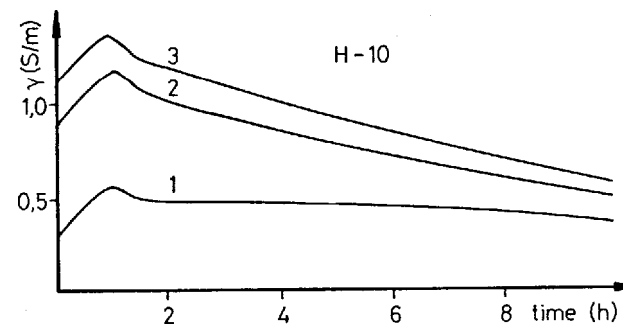

FIG. 4.

Conductograms of H-10 cement; the effect of measuring frequency. No transient maximum occurs. 1=100 Hz, 2=1 kHz, 3=3 kHz

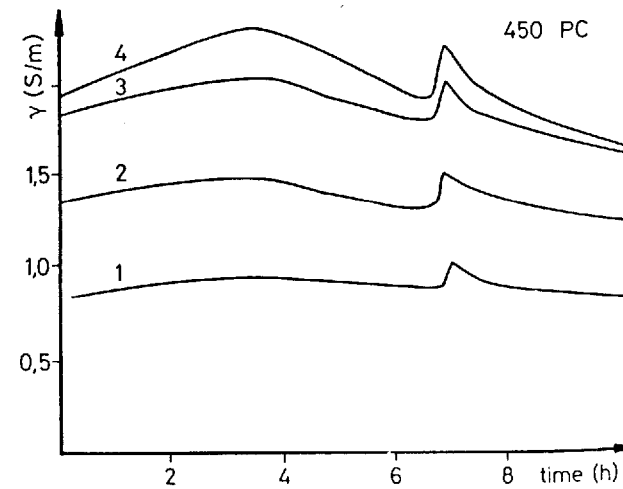

FIG. 5.

Conductograms of 450 cement; the effect of measuring frequency. A transient maximum can be observed. 1=100 Hz, 2=500 Hz, 3=1 kHz, 4=5 kHz

Both plots clearly show that conductivity increases with increasing measuring frequency, but the general "look" of the conductogram remains unchanged.

However, if gypsum is admixed to the clinker, a transient conductivity maximum appears in all clinkers investigated so far, if the amount corresponds to a "critical" value. If slightly higher or lower, the intensity of the transient maximum would diminish; still more or still less gypsum causes an inflexion or breakpoint on the descending branch of the conductogram rather than a

maximum. Well before or beyond the critical gypsum contents the conductogram becomes regular again, with no sign of maximum or inflection. In Figs. 6. and 7. two sample sets of conductograms are shown.

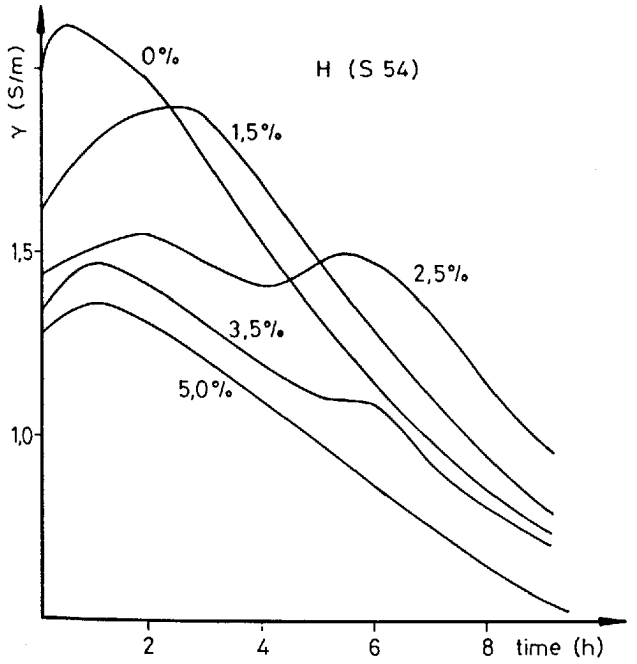

FIG. 6.

Conductograms of HS-54 clinker in the presence of various amounts of gypsum

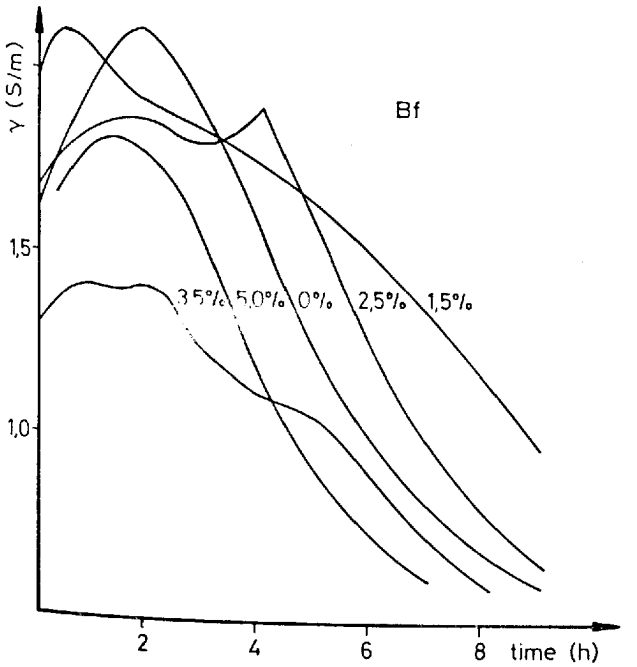

Conductograms of Bf clinker in the presence of various amounts of gypsum

Shape of the plot and values of conductivity of clinkers and cements depend highly on the composition of the particular material (although general trends can be found) and are influenced by several factors, as. e.g. temperature, grinding fineness (surface area), carbonation, and, most strikingly, by admixtures (accelerators, retarders, etc.).

Upon increasing temperature, the first conductivity maximum remains almost unchanged while the second, transient one appears earlier, at 8:10 hr. and 4:45 hr. from beginning, at 32°C and 50°C, respectively (Fig. 1. in /16/).

The effect of aftergrinding is shown in Fig. 8.

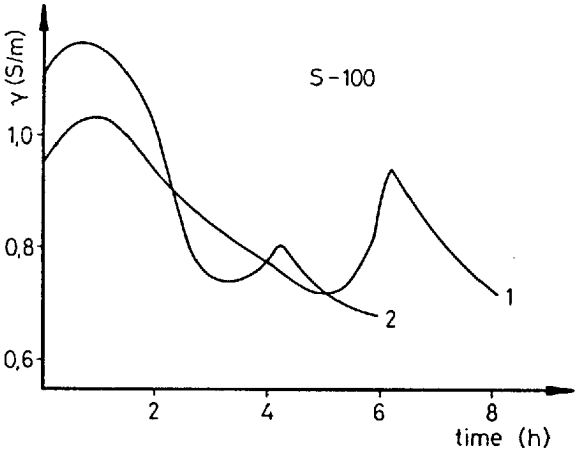

FIG. 8.

Conductograms of S-100 cement pastes - the effect of aftergrinding. Curve 1 surface area 0.337 m^2/g, curve 2 surface area 0.393 m^2/g

The intensity of the first maximum is increased, that of the transient one decreased by aftergrinding. This effect could obviously be attributed to the increase of surface area, but to a partial carbonation as well. To investigate this possibility in more detail the same sample which gave curve 1 in Fig. 8. was put to a desiccator filled with dry carbon dioxide. Results are plotted in Fig. 9. It is clearly visible that CO_2-treatment affects primarily the intensity of the first maximum.

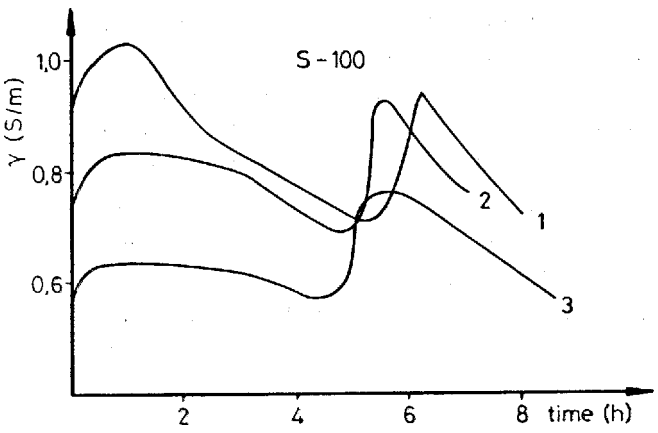

FIG. 9.
Conductograms of S-100 cement pastes - the effect of carbonation. Curve 1: no carbonation, curve 2: after 2 days of carbonation, curve 3: after 14 days of carbonation

The effect of accelerating and retarding admixtures has been described earlier /16/. Citric acid, a well-known retarder has given the most dramatic effects: the time of the first conductivity maximum remained practically unchanged, but its intensity decreased and its shape flattened. The transient maximum on the conductogram however appeared at much later times (in case of the original, no-admixture cement paste this occured at 8:45 hr., and was shifted to 12:00, 18:30 and 41:45 hr., upon adding 0.035%, 0.07% and 0.15% citric acid, resp. but ist shape remained almost unchanged as shown in Fig. 3. of /16/).

Clinker minerals

Conductograms of clinker mineral pastes without admixtures are shown in Fig. 10. It can be readily seen that all four clinker minerals show smooth curves with no transient changes in conductivity, although a slight inflection can be reproducibly observed on the conductogram of C_3S at the age of 1:25 hr. In case of C_4AF some irregularity were found at the beginning period. This phenomenon will be discussed later.

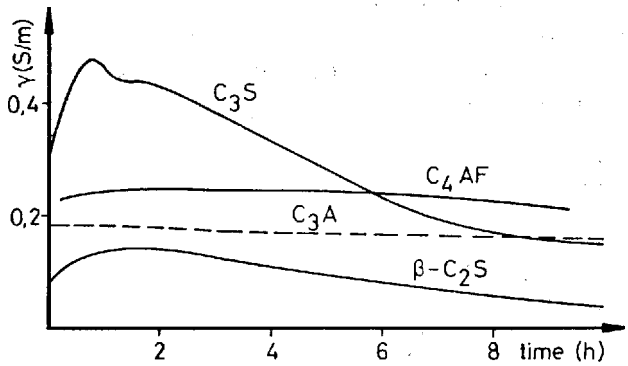

FIG. 10.
Conductograms of clinker mineral pastes

Conductivities of the two alumina-bearing phases change only slightly with time, while the ascending and descending branches are clearly visible on the conductograms of the silica-bearing minerals before and after the first maximum. Conductivity of C_3S pastes is obviously higher than that of the β-C_2S paste, which yields less ions than its more basic counterpart. (It should be mentioned that curves plotted here are not conform in every detail with earlier ones /16/, when other, less pure minerals were used).

The effect of accelerating and retarding admixtures on the conductance behavior is shown in the following figures. In Fig. 11. the conductograms of C_3S pastes are shown (here and subsequently curve 1 refers to the original, no-admixture paste the conductogram of which was already shown in Fig. 10). The addition of an accelerating agent, as sodium formate or calcium chloride increases the intensity of the first maximum (an that of the following inflection), but do not "accelerate" its development. Citric acid, on the other hand is a real retarder. The same can be seen in case of β-C_2S pastes in Fig. 12. (Here the scale of the vertical axis is changed to express phenomena in more detail. The intensity-increasing effect of sodium formate is evident. Calcium chloride has a similar effect, increasing the intensity of the first maximum to 0.8 S/m, without changing its time but this curve was omitted from the figure

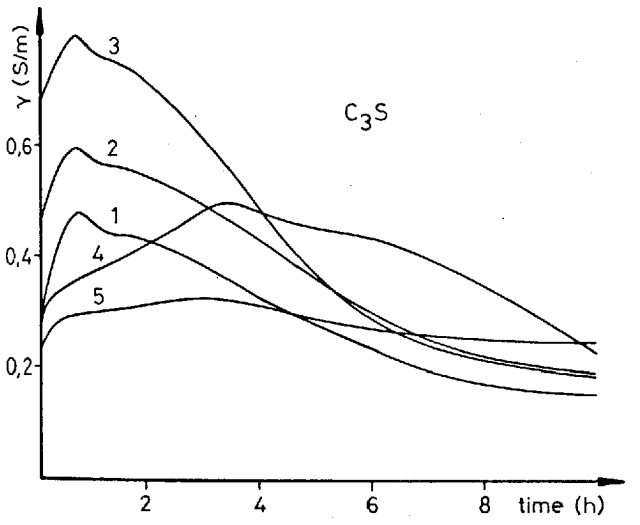

FIG. 11.

Conductograms of tricalcium silicate pastes - the effect of admixtures. Curve 1: no admixture, curve 2: 0.1% sodium formate, curve 3: 0.5% calcium chloride, curve 4: 0.05% citric acid, curve 5: 0.1% citric acid

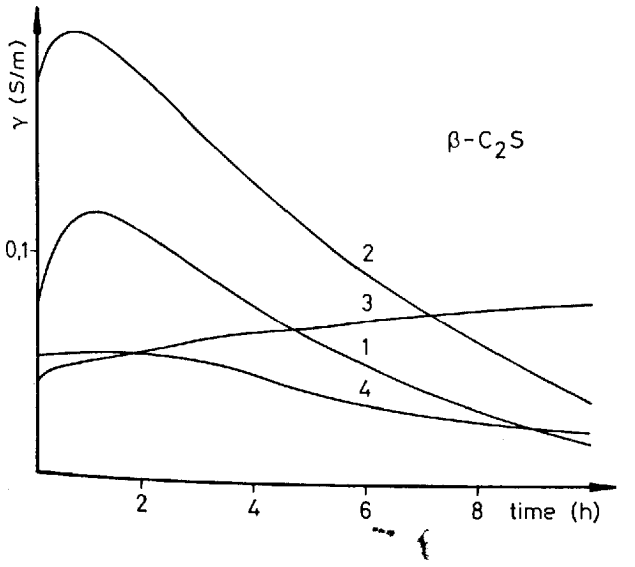

FIG. 12.

Conductograms of β-dicalcium silicate pastes - the effect of admixtures. Curve 1: no admixture, curve 2: 0.1% sodium formate, curve 3: 0.1% citric acid, curve 4: 0.2% citric acid

due to the lack of space. The retarding effect of citric acid is thus documented in the case of β-C_2S too.

The irregularities in the conductogram of C_4AF pastes have already been mentioned earlier. As the measurement of conductance prior to 6 minutes after first contact with water is impossible in our experimental setup, we tried to utilise the retarding effect of citric acid also in this case. Results are plotted in Fig. 13.

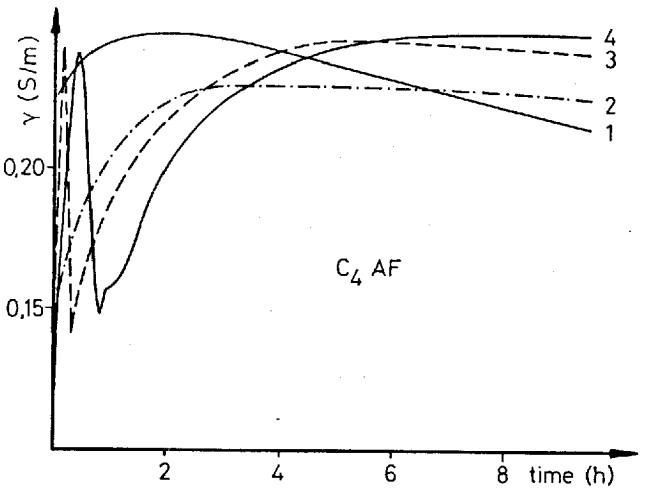

FIG. 13.

Conductograms of tetracalcium aluminate ferrite pastes - the effect of admixtures. Curve 1: no admixture, curve 2: 0.1% citric acid, curve 3: 0.2% citric acid, curve 4: 0.3% citric acid

It is seen on the curves that at the very beginning of hydration conductance is increased sharply, followed by a sudden decrease and a slow increase again. The presence of a short-lived maximum and minimum on the curves was observed reproducibly in each case as the retarding effect of citric acid has rendered these phenomena measurable.

Comments

In this paper only some representative examples were shown from the more than 800 individual tests carried out in the two laboratories. By repeated tests it can be stated that the reproducibility of the absolute conductance values is ± 20%, if the same

raw material batch is used and sample preparation (e.g. adjusting the w/c ratio, mixing, etc.) is done with care. The time of the transient conductivity peak can be reproduced within a few minutes. The general run, the "appearance" of the conductogram is fully reproducible.

It must, however, be borne in mind that - as shown in the paper and in earlier ones - several external factors may affect the conductance behavior of cement or clinker pastes. The evaluation of observations therefore requires great care and multiple parallel tests are recommended. The most frequent artifact, the loss of contact between the paste and the electrodes however is easily recognised by the sudden drop of conductance. (The newly designed cell, with steel clamps has already minimised this source of error).

The interpretation of results is not easy. The first conductivity maximum is undoubtably a consequence of hydrolysis, as stated earlier and the effect of carbonation can be explained by the immobilisation of calcium ions in the lattice of calcium carbonate.

The most interesting feature on conductograms, the appearance of the second, transient maximum on the descending section of the plot in case of near-critical gypsum-to-clinker ratios can only be tentatively explained by the ettringite → monosulfate transformation (no dramatic differences can be observed on XRD patterns of pastes cured to times shortly before and after the transient maximum, respectively). Alternately one could hypothesize protective layers around ettringite grains, which, when disrupted by osmotic pressure release sulfate and other ions into the environment is a transient way.

Experiments are continued to find better arguments for the role of gypsum in the appearance of the transient conductivity maximum in case of near-critical gypsum-to-clinker ratios; to collect correlations between critical gypsum content and the phase composition of clinker; for the utilisation of electrical phenomena in the interpretation of processes taking place during the setting and hardening of cements; and, last not least, the practical application of conductometry to replace empirical time-of-setting determinations.

ACKNOWLEDGEMENT

A part of this work was carried out under grant NSF-INT-80-11922. Some of the clinker minerals were donated by the Department of Binders, Mendeleev Institute of Technology, Moscow, USSR. The help of both organisations is gratefully acknowledged.

REFERENCES

/1/ Boast, W.B.: J. Amer. Concrete Inst. 33, 131 (1936)
/2/ Calleja, J.: J. Amer. Concrete Inst. 23, 525 (1952)
/3/ Calleja, D.: J. Amer. Concrete Inst. 24, 329 (1952)
/4/ Calleja, D.: J. Amer. Concrete Inst. 25, 249 (1953)
/5/ Hammond, E. - Robson, T.: The Engineer 1955 No. 4, 78
/6/ Nikkanen, P.: Valtion Teknillinen Tutkimuslaitos, Ser. 3, No. 60 (1962)
/7/ Ana, I.: Chem. Oil Gas Roman. 6 130 (1970)
/8/ Monfore, G.E.: PCA Res. Dev. Lab. 1968 35
/9/ Náray-Szabó, I. - Szuk, G.: Acta Geol. Acad. Sci. Hung. 3 105 (1955)
/10/ Szuk, G. - Náray-Szabó, I.: Acta Tech. Acad. Sci. Hung. 22, 83 (1958)
/11/ Szuk, G.: Acta Tech. Acad. Sci. Hung. 46 317 (1964)
/12/ Kolbasov, V.M. - Levshin, A.M. - Ptitsin, V.V.: Trudy Mosk. Khim.-Tekh. Inst. 92 138 (1976)
/13/ Batalov, D.M. - Klyusov, A.A.: Trudy Zapadno. Sibir. Nauchno-Issled. Geol. Neft. Inst. 86 (1975)
/14/ Efimenko, Yu. V.: Zh. Prikl. Khim. 48 1135 (1975)
/15/ Henning, O. - Oelschläger, A.: Bindebaustoff-Taschenbuch, Vol. 1, p. 305 (1984)
/16/ Tamás, F.D.: Cement Concr. Res. 12 115 (1982)
/17/ Tamás, F.D. - Salem, T.H. - Mikhail, R. Sh.: Paper presented at the 84th Annual Meeting of the Amer. Ceram. Soc., Cincinnati, Ohio, 1984
/18/ Tamás, F.D. - Farkas, E. - Roy, D.M.: British Ceram. Proc. No. 36, p. 237 (1984)
/19/ Farkas, E. - Tamás, F.D.: Tagungsbericht 9. IBAUSIL, Vol. 1, p. 163 (1985)

G.Scarinci*, D.Festa*, G.Sorarù*, G.Grassi°, L.Stafferi°, C.Badini°
* Istituto di Chimica Industriale, Facoltà di Ingegneria, Università di Padova
° Dipartimento di Scienza dei Materiali e Ingegneria Chimica, Politecnico di Torino

PORTLAND CEMENT RENFORCED WITH NEW ALKALI-RESISTANT GLASS FIBERS

1. Introduction

Glass fibers, to be used for cement reinforcement, should have good resistance toward alkaline attack (portland cement during hydration has a pH value of 12 to 13). Commercially available A and E glass fibers lose their strength rapidly in an alkaline enviroment because alkali attacks directly the silica network and completely dissolves the glass. The hydroxyl ion of the alkali breaks the Si-O-Si linkages according to equation:

$$-Si-O-Si- + OH^- \text{ ----- } Si-OH + Si-O^-$$

alkali resistant glass fibers, with high zirconia content (Cem-fil), developed as a reinforcement over the last few years, are expensive and difficult to fabricate because of their high melting and drawing temperature, thus cheaper compositions are required. This work relates the results obtained with glass fibers (about 15 μm in diameter) of different compositions from various systems obtained from a single nozzle drawing apparatus (table 1). For comparison purpose type E and Cem-fil glass fibers (N° 2 and 10 respectively) there also fabricated and tested.

2. Alkaline durability

Alkaline corrosion tests there carried out according to the following procedure. Five grams of fibers there introduced in a plastic bottle containing 200 ml of a satured solution of $Ca(OH)_2$, flushed with nitrogen to expell air and to avoid contamination of the liquor by CO_2. The bottle was immersed in a costant-temperature bath and mantained at 60 °C.
Tests were carried out for 8, 28, 60 and, sometimes, 90 days in triplicate and results averaged. The fibers there filtered through an alkali-resistant filter paper and washed with 50 ml of 2N-acetic acid and 200 ml of water and dried at 100 °C. The weight loss of fibers was expressed as a function of their exposed surface determined by measuring glass fibers density and diameter (tab 2).
The fibers behaviour in the $Ca(OH)_2$ is quite different, because for some compositions progressive degradation has been observed, whereas for others the corrosive process is gradually lessened (N°5) or stopped at a definite losses level (N°6,8,10). Such a different behaviour is certainly related to the different stability of the various oxides in the highly alkaline enviroment. The individual glass fibers components are not leached to the same extent nor do they all form alkali soluble species; microscopical examination by SEM has revealed the formation of a surface layer of corrosion products which can sometimes behave as a protective coating to limit further corrosion. The relative permeability of this coating to the diffusion of ionic species will be determining factor to promote or hinder the development of the corrosive attack.

3. Composite fabrication

On the ground of chemical durability tests, fibers N°6 and 8, and for comparison fibers N°2 (E glass type) and 10 (Cem-fil type), have been used for the manufacturing of composites. Prismatic samples (20 x 40 x 160 mm) have been made, by means of the pre-mix method, using glass fibers (30 mm long) and Portland cement (425). From preliminary tests the ratio w/c has been fixed at 0.35: this value allowed a good workability of cement slurry containing 3%wt glass fibers. All the operations of fabrication have been made at 20 °C and with a relative humidity not inferior at 75%. Storage has been made in water at 20 °C. After 7,28,60 and 90 days the samples have been broken in three point flexure by means of a LOSENHAUSENWERK apparatus. Obtained values (average of at least 8 tests) are plotted in Fig.1.

Components	Fiber N°									
	1	2	3	4	5	6	7	8	9	10
SiO_2	50.0	54,3	42.5	62.0	54.0	54.0	53.2	52.0	51.8	63.1
CaO	30.0	21.8	13.4	--	--	--	--	--	--	4.9
Al_2O_3	5.0	14.2	10.5	18.0	15.0	15.0	15.0	14.7	14.7	--
Na_2O	3.0	0.1	9.9	--	--	--	--	--	--	15.2
Li_2O	--	--	--	8.0	3.5	3.5	3.5	3.5	3.5	--
K_2O	2.0	0.3	1.3	2.0	2.0	2.0	2.0	2.0	2.0	--
ZnO	2.0	--	--	4.0	24.5	22.0	21.6	17.5	14.0	--
BaO	3.0	--	--	--	--	--	--	--	--	--
MgO	--	0.7	5.3	3.0	--	--	--	--	--	--
FeO	--	--	5.2	--	--	--	--	--	--	--
Fe_2O_3	--	0.2	3.3	--	--	--	2.4	6.8	6.8	--
MnO_2	--	--	--	--	--	--	1.3	2.5	6.2	--
TiO_2	1.0	0.1	5.8	--	--	2.5	--	--	--	--
ZrO_2	1.2	--	2.2	--	1.0	1.0	1.0	1.0	1.0	16.2
P_2O_5	2.8	--	0.6	--	--	--	--	--	--	--
B_2O_3	--	8.0	--	--	--	--	--	--	--	--
F	--	0.4	--	--	--	--	--	--	--	--
SrO	--	0.2	--	--	--	--	--	--	--	--

Table 1 : chemical composition of fibres, wt%

G.Scarinci*, D.Festa*, G.Sorarù*, G.Grassi°, L.Stafferi°, C.Badini°
* Istituto di Chimica Industriale, Facoltà di Ingegneria, Università di Padova
° Dipartimento di Scienza dei Materiali e Ingegneria Chimica, Politecnico di Torino

FIBER N°	FIBER CORROSION (weight loss in g cm^{-2} of fiber surface, X 10^6)			
	8 days	28 days	60 days	90 days
1	183.0	401.0	--	--
2	105.0	130.0	155.6	165.8
3	23.9	129.8	--	--
4	29.0	56.7	--	--
5	19.8	59.8	73.4	--
6	7.3	39.2	37.4	--
7	17.2	59.2	103.0	--
8	5.9	40.3	40.7	--
9	10.2	71.2	122.4	--
10	8.3	20.0	22.0	21.0

Table 2: fibers corrosion

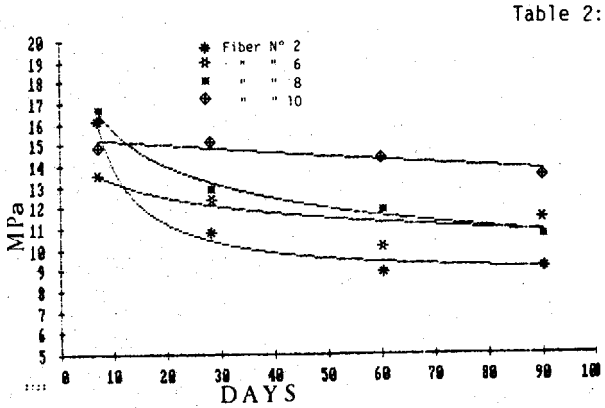

Fig.1 Bending strength vs hydration time for GRC

4. Porosity determination

Porosity of Portland cement paste and of glass fibers composites was determined after 7,28,60 and 90 days curing in water at 20°C.

1.5 g cubic samples were cutted from every specimen, dehydrated by ethil alcohol and ether and then cleaned by a 20' ultrasonic process in order to remove dust from pores. Porosity values were obtained by a Carlo Erba 200 mercury porosimeter which allows pores evaluation in the range from 75,000 to 35 A.

The data have been elaborated using an appropriate software, assuming cylindrical shaped pores, a 140° contact angle and a 480 dine/cm Hg surface tension. The Hg cumulative volume corresponding to the total porosity of one gram of sample and the total surface area of the pores included in every gram of material are reported in Tab.3.

It is well known that porosity is the main factor governing the compressive strength of an hardened cement paste (1). Bending strength, on the contrary, can't be related to porosity, being only determined by the size of the greatest void in the material according to Griffith's theory (2).

Actually the results obtained for only cement pastes are quite spread for every curing time and follow unusual hardening trends. The addition of a few percent of glass fibers causes a remarkable change: bending strength values for every time interval are spread within a more narrowed range, they are much more reproducible and show a reasonable trend with the developing of hydration . This is due to the fact that fibers in a cement matrix reduce average cracks length by stress re-distribution in the matrix.

On examining the porosimeter data for a only-cement made paste, it may be seen that, according to other Authors (1,3),porosity diminishes with increasing hydration times (particularly during the first month) and the pores become smaller. For E glass fiber composites, on the contrary, porosity increases during the first month of hydration perhaps because these fibers are much more susceptible to chemical attack which give rise to new pores. For the other glass fiber composites porosity progressively decrease with hydration time: fibers are scarcely attacked and porosity gradually lowers owing to the increase of volume due to the cement hydration products.

From the strength vs hydration time plotsit may be noticed that the curves referring to the fibers N°6 and N°8 reach similar values at 90 days. Such values are well above the ones obtained with the fiber N° 2. It may therefore be stated that even if the fibers N° 6 and 8 don't give a reinforcement comparable to the one obtained with the zirconia fibers, anyhow they constitute a remarkable progress toward developing alkali resistant fibers.

G.Scarinci*, D.Festa*, G.Sorarù*, G.Grassi°, L.Stafferi°, C.Badini°
* Istituto di Chimica Industriale, Facoltà di Ingegneria, Università di Padova
° Dipartimento di Scienza dei Materiali e Ingegneria Chimica, Politecnico di Torino

Fiber N°	Time (days)	Average strength (MPa)	Cumulative volume ($cm^3/g\ 10^{-3}$)	Surface area (m^2/g)
2	7	15.67	58.61	6.76
2	28	10.82	67.07	8.47
2	60	8.80	51.91	6.04
2	90	9.01	37.46	5.99
6	7	13.50	59.62	6.82
6	28	12.37	53.53	7.05
6	60	10.20	56.79	6.24
6	90	11.45	36.91	6.57
8	7	16.68	68.89	7.65
8	28	12.85	64.30	8.65
8	60	11.86	45.51	5.36
8	90	10.66	37.08	5.16
10	7	14.81	51.86	5.74
10	28	15.11	45.45	5.36
10	60	14.42	39.10	4.42
10	90	13.54	35.72	5.56
Cement	7	---	55.39	5.57
Cement	28	---	28.38	6.81
Cement	60	---	34.67	6.56
Cement	90	---	26.72	6.71

Tab.3 : Average flexural strength and porosimeter data of composites studied

Bibliografy

1) Robbler,M. and Odler,I.
Cement and Concrete Research, 15, (1985), 320

2) Birkall,J.D.; Howard,A.J. and Kendall,K.
Nature, 289, (1981), 388

3) Winsolw,D.N. and Diamond,S.
A.S.T.M. Journal Materials, 5, (1970), 564

G. MASCOLO, P. PERNICE AND O. MARINO.
Dipartimento di Ingegneria dei Materiali e della Produzione, Universita' di Napoli, Italy

IONIC CONDUCTIVITY OF LAMELLAR CALCIUM ALUMINATE HYDRATES.

Introduction

It is well known that calcium aluminate hydrates of AFm type play a primary role in the hydration process of cement especially in relation to the additive employment.

The typical and lamellar structure of such compounds was widely described by Allmann (1), Kuzel (2) and Taylor (3). They are characterized by the general formula $[Ca_2Al(OH)_6][(1/n)X^{-n}(H_2O)_y]$ whose structure is made up by positively-charged layers $[Ca_2Al(OH)_6]^+$ balanced by a negatively-charged interlayer variable with the anion type X^{-n} and with the number of water molecules.

The AFm phases have an aptitude for anionic exchange with a rate, besides, depending on the selectivity of the anion (4).

Analogous structures of the type $[Zn_2Cr(OH)_6]X\cdot mH_2O$ have been studied in relation to their ionic conductivity. Their high values were explained considering the anionic interlayer as a concentrated semi-liquid or frozen solution (5,6).

The aim of the present work is that to extend such measures to the analogous phases of AFm type. The experiments were also carried out at different degree of relative humidity (RH) as it affects the hydration state of the AFm phases and in particular that of the prototype $[Ca_2Al(OH)_6][OH\cdot 3H_2O]$ whose basal spacing c', as we know, increases by increasing the degree of RH (7).

Experimental

The AFm type samples, characterized by interlayer anions such as OH^-, Cl^- and Br^-, were prepared with freshly ignited CaO, alumina gel, a Ca-salt of the corresponding anion and previously distilled and boiled water. The reaction suspension was shaken in a teflon container for ten days at room temperature. The reaction products were filtered under CO_2-free condition and dried by evacuation of the washing liquids which were acetone and ether.

The reaction products were characterized by: x-ray powder diffraction analysis using a Guinier de Wolff camera, TG and DTA analyses and density.

The powders, conditioned to 100% of RH under CO_2-free conditions, were pressed in a cilindrical die whose diameter was 18 mm at 16 MPa obtaining 5 mm in thickness disks. The compacts were analyzed in the relative density after drying on silica gel.

Electrical conductivity measures were carried out both on contact liquid of suspension containing the AFm phase and on the compacts conditioned for 7 days in a prefixed RH environment. The ionic conductivity was determined, keeping the compact under a prefixed RH, by the complex impedance measure employing a Solartron 1250 FRA and a Solartron 1286 Electrochemical interface, interfaced to a Hewlett-Packard 86 B desktop computer. Silver electrodes were painted onto the specimen faces. The signal applied across the sample was 30 mV.

Results and Discussion

Table 1 reports the results concerning the characterization of AFm phases as: basal spacing c', density, water molecules of the interlayer, the last one determined by TG with isoterm at 125 °C, and free $CaCO_3$ content. These results well match with the literature data (8,9).

Table 1 - Basal spacing c', interlayer H_2O molecules, density and free $CaCO_3$ content of AFm phases

Interlayer anion	c'(A)	$(H_2O)_y$	d (g/cc)	Free $CaCO_3$(%)
OH^-	7.95	3	2.04	-
Cl^-	7.80	2	1.90	4.5
Br^-	8.20	2	2.01	4.5

The electrical conductivity of the contact solution of AFm phases ranges between a minimum of $1.5\cdot10^{-3}\,\Omega^{-1}\cdot cm^{-1}$ for the bromide-form and a maximum of $2.7\cdot10^{-3}\,\Omega^{-1}\cdot cm^{-1}$ for the hydroxide-form. The relative density of the compacts ranges between 75 and 78%.
The a.c. conductivities of compacted samples were carried out taking into account that the complex impedance can be written as:

$$Z_{cell} = Z_{sample} + Z_F \qquad (a)$$

Z_{sample} is the impedance of the sample including also the contribute of geometrical capacitance (10), while Z_F is the impedance associated with electrode interface. According to Mayer (11) Z_{sample} may be represented by:

$$Z^{(\omega)}_{sample} = Z' + jZ'' = \frac{R_b}{1 + j\omega R_b C_g} \qquad (b)$$

with $\omega = 2\pi f$, f = frequency, R_b = bulk resistance and C_g = geometrical capacitance. Such an impedance, representable in the Nyquist diagram by a semi-circle, whose diameter R_b has $1/R_bC_g$ as maximum angular frequency, is responsable of the dispersion at the highest frequencies. So the electrical conduction has been obtained by measuring the complex impedance at 6 KHz frequency at which Z_F may be neglected.
From eq. (b) the bulk resistance has been obtained according to:

$$R_b = Z' \frac{(Z'/Z'')^2 + 1}{(Z'/Z'')^2}$$

G. MASCOLO, P. PERNICE AND O. MARINO.
Dipartimento di Ingegneria dei Materiali e della Produzione, Universita' di Napoli, Italy.

P

Fig. 1 reports the conductivities of AFm phases as a function of the relative humidity. The hydroxide-form shows higher values of conductivity in all the range of the RH than those of the chloride and bromide-forms. This behaviour matches well with data of Lal and Howe (5) regarding the hydroxide-form of Zn-Cr salt . The presence, in fact, of disordered H_2O/OH^- pairs arranged in the interlayer (12) improves the proton mobility responsable of the semiconducting properties of such compounds. The conductivity variation results low in the 0 ÷ 80% of RH; this involves that the contribute to the conduction, related with intercrystalline regions, is to be considered negligible and that the bulk conduction is to be mainly attributable to the mobility of the interlayer species.

The remarkable increase of conductivity in the 80 ÷ 100% range of RH could be esplained, expecially for the hydroxide-form, by the further addition of water molecules in the interlayer that, as it is well known, involves an increase in the basal spacing c' (7). The conseguent major distance between the positively-charged layers $|Ca_2Al(OH)_6|^+$, acting on the interlayer anions, could increase the mobility of the interlayer species because of the minor intensity of the field of electrostatic forces.

The bromide-containing AFm phase shows a greater change in conductivity in the 0 ÷ 80% range of RH; this may be due to a conducting contribute of intercrystalline regions.

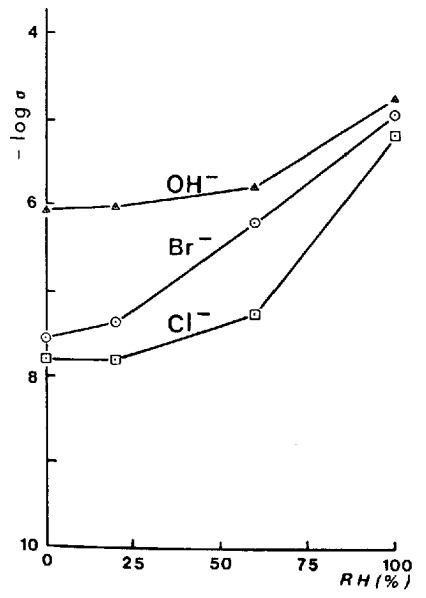

Fig. 1 Bulk conductivity of AFm phases, characterized by different interlayer anions, as a function of relative humidity.

The lower conductivities, observed for the AFm phases respect to those reported by Lal and Howe (5,6) for Zn, Cr samples, could be attributed both to the different methods in measuring the electrical conductivity and to the different composition of the samples and to their different degree of carbonatation. This effect, in fact, reduces the bulk conductivity (5).

Conclusions

The observed semiconduction of the AFm phases is mainly attributable to the mobility of the interlayer species. The hydroxide-form shows, in fact, the highest value of conductivity due to the high mobility of proton jumping from H_2O to OH^- of the interlayer.

The conductivities of the compacts are lower than those of the corresponding parent wash solutions.

The evaluating of an eventual anisotropy in the bulk conduction is not to be neglected because of the lamellar crystalline habitus of such compounds.

In the continuation of this study we intend to evaluate more deeply the impedance variations as a function of the frequency with the pourpose to find out both eventual distribution of relaxing constants and diffusional contributes to the impedance of the samples.

References

1. R. Allmann, Chimia (1970) 24, 99.
2. H. J. Kuzel, Proc. 5th Int. Symp. Chem. Cement, Tokyo, Vol. II, (1968) p. 92.
3. H. F. W. Taylor, Min. Mag. (1973) 39, 377.
4. G. Mascolo and M. Marroccoli, Cem. Concr. Res. 1986 (in press).
5. M. Lal and A. T. Howe, J. Chem. Soc. Chem. Comms. (1980) 737.
6. M. Lal and A. T. Howe, J. Solid State Chem. (1981) 39, 377. Ibidem (1981) 39, 368.
7. M. H. Roberts, Proc. 5th Int. Symp. Chem. Cement, Tokyo, Vol. II, (1968) p. 104.
8. H. J. Kuzel, N. Jb. Miner. mh. (1966) 193.
9. S. J. Ahmed, L. S. Dent Glasser and H. F. W. Taylor, Proc. 5th Int. Symp. Chem. Cement, Tokyo, Vol. II (1968) p. 118.
10. G. W. Jordan and M. F. Berard, J. Electrochemical Soc. (1985) 132, 464.
11. J. Maier, Z. für Phys. Chem. Neue Folge (1984) 140, 191.
12. S. J. Ahmed and H. F. W. Taylor, Nature (1967) 215, 622.

R. SERSALE , University of Naples, Italy
R. AIELLO , University of Calabria, Italy
G. FRIGIONE , University of Calabria, Italy

NATURAL ZEOLITES AS ACTIVE ADDITIONS TO THE PORTLAND CLINKER

INTRODUCTION

The problem of manufacturing blended cements represents since long a subject of very interesting researches, owing to the peculiar properties of such hydraulic binders (1).
Besides the interest of its manufacture with regards to the energy saving, chemical resistance, low heat of hydration , the property of minimizing the expansion following the reaction of the alkalies towards some reactive ingredients, sometimes present in the aggregates for concrete, suggest the use of this type of cement for many important works.
In the sphere of "pozzolanic" cements, several researches on samples manufactured with true pozzolanas, with the "trass" or with different products endowed with pozzolanic behaviour, as fly ashes for example (2), gave evidence of the peculiar characteristics of such binders.
This experimental investigation intends in turn to demonstrate the possibility and opportunity of utilizing also natural zeolites as active additions to the Portland clinker (3), with reference both to the opening of a new field of utilization of these interesting products, very abundant in the central-southern part of Italy, and to the advantages attainable in comparison to the equivalent binders manufactured with true pozzolanas.

EXPERIMENTAL

Neapolitan yellow tuff with a phillipsite content of about 80% has been employed as natural zeolitic product, whereas the true alkali-trachytic phlegraean pozzolana-representing the unzeolited counterpart of the above mentioned tuff - has been used as amorphous addition.
Both the active additions have been added to an industrial clinker in amount varying from 15 to 40%. The chemical compositions of all the product used are reported in Tab. 1

Tab. 1: Chemical composition of the products used for the manufacture of the "pozzolanic" cements.

	Neapolitan yellow tuff	Phlegraean Pozzolan	Clinker
SiO_2 %	54.68	57.00	21.31
$Al_2O_3+TiO_2+Mn_3O_4$	17.70	18.34	3.59
Fe_2O_3	3.82	2.20	4.50
FeO	0.29	2.14	-
CaO	3.66	3.15	65.31
MgO	0.95	0.97	1.04
Na_2O	3.43	4.18	0.70
K_2O	6.38	8.05	1.70
CO_2	-	-	-
SO_3	-	-	2.10
l.o.i.			0.11
Na_2O equiv.	-	-	1.80

The active additions in tab. 1, ground until a 10±2% residue remains on a 32 μm sieve have been added in the above mentioned ratios, to a sample of industrial clinker, typical of the current italian production, having a specific surface area Blaine of 370 m^2/kg. Before grinding the clinker , 5% natural gypsum, with a $CaSO_4 \cdot 2H_2O$ higher than 95%, has been added.

Stated by means of the pozzolanicity test (4) that all the samples, also for compositions poor in addition, can be classified as pozzolanic cements, its technical behaviour has been examined.

EXPERIMENTAL

Compressive strenght tests.

Have been performed on ISO-RILEM mortars (5) aged 3,7, 28, 90 days. Fig. 1 reports strenght progress as a function of addition content and age.

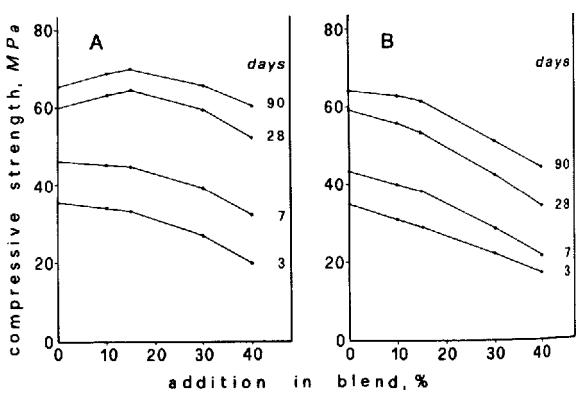

Fig. 1: Compressive strenght progress on mortars.
A = tuff - cement; B = pozzolana - cement.

It is to be seen that, at equal conditions, the zeolitic cements (A), particularly at long ages, show strength values generally higher than those of the typical pozzolanic cements (B).

Workability of the mixtures .

In order to define also the contribution of the zeolitic product to the workability of the mixtures, the flow test on ISO-RILEM mortars (6) with the same water cement ratio has been performed. It is in fact well known that the lower the water the higher the strength of the works.
Stated in advance that any kind of addition definitely decreases the workability of the single clinker, fig.2 reports per cent flow values as a function of the addition amount in the blend and shows that the workability decrease is lower for the vitreous pozzolanic addition (B) and a little bit higher for the zeolitic one (A), owing to its finer texture. The higher water requirement of the zeolitic cements however does not diminish the good results of compressive tests, so that

strenght progress remains at a higher level in comparison to that of the typical pozzolanic cements.

Potential alkali-reactivity.

Has been evaluated from the expansion, after suitable aging, of a series of mortar bars prepared with both the cements and using Pyrex glass as a siliceous reactive ingredient (7).

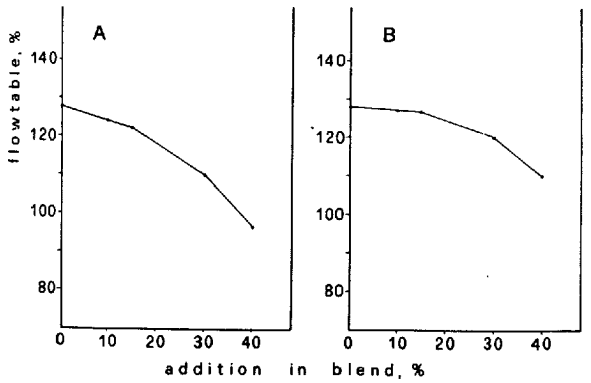

Fig. 2: Flow course of mortars.
A = tuff - cement; B = pozzolana - cement.

Fig. 3 reports the expansion values as a function of addition content and age (180 days) and emphasizes the specific role of the zeolitic addition (A) on the minimization of the expansion phenomenon.
A further improvement of this result can be reached after thermal activation treatment of the zeolitic product at temperature of about 500 °C.

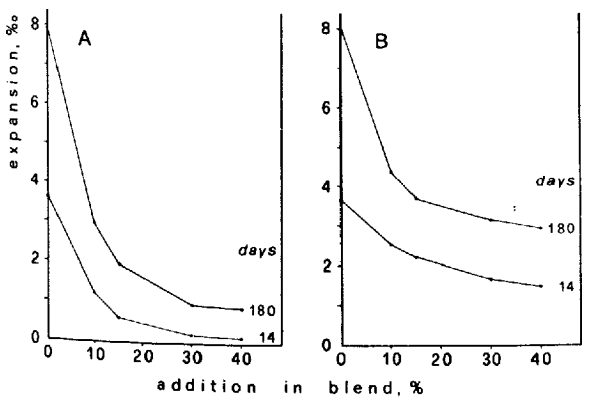

Fig. 3: Potential alkali reactivity tests on mortar bars.
A = tuff - cement; B = pozzolana - cement.

Fig. 4 shows X-ray diffraction diagrams of the untreated Neapolitan yellow tuff (a) and after thermal treatment at 600 °C (b) and Fig. 5 shows the expansion values course for mortar bars manufactured with cements containing as active addition the zeolitic tuff previously treated at 600 °C for one hour (A), and phlegraean pozzolan (B), respectively treated at the same temperature for the same time.

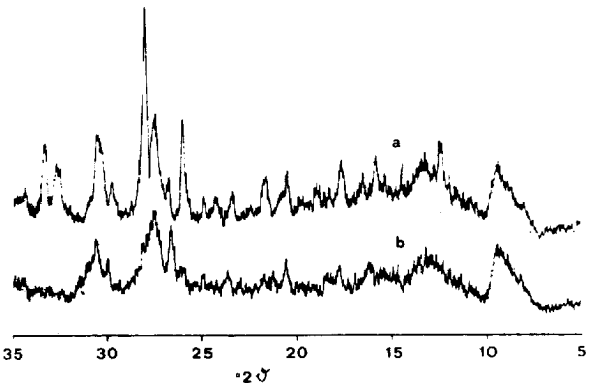

Fig. 4: X-ray diffraction diagrams.
a) untreated phillipsite tuff;
b) same sample treated at 600 °C.

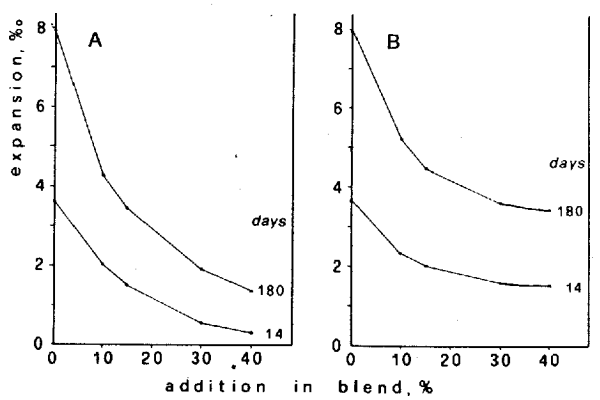

Fig. 5: Potential alkali reactivity tests on mortar bars.
A= blended cement with tuff treated at 600 °C.
B= blended cement with pozzolana treated at 600 °C.

It is to be seen that the use of the zeolitic product thermally activated, reduces by about 40% the expansion values measured, at equal conditions, on mortar bars manufactured with the typical pozzolanic cements.

DISCUSSION AND CONCLUSION.

The whole of the experimental results and of the deductions that can reasonably be drawn, strengthen the interest of the utilization of natural zeolitic product, after proper grinding, for the manufacture of blended cements endowed with special technical performances.
It has been emphasized in fact that mortars prepared with blended cements containing as active addition a powdered phillipsite tuff, show strength progress pretty higher than those of mortars manufactured with blended cements containing the unzeolitized counterpart (the phlegraean pozzolan) and that the zeolitic addition minimizes the more the expansion following alkali-aggregate reaction.
To this end the influence of a thermal treatment of the zeolitic addition as been emphasized and it has been demonstrated that the same thermal treatment does not influence the behaviour of a vitreous natural product when used as active addition to the clinker.
The behaviour of a zeolitic product when used as active addition to the Portland clinker, better than those of the unzeolitized counterpart, is to be brought back to a higher reactivity owing to the peculiar structure of the zeolitic minerals. The pores and channels running throughout the solid reasonably could in fact be responsible for a more rapid and complete attack under the action of the lime solution with a neo-formation as much rapid and complete of the hydration products.
To this higher reactivity is to be attributed the abatement of the expansion following alkali-aggregate reaction, too. A more rapid and complete neo-formation of poorly crystalline, low basicity hydrated calcium silicate, affordsin fact the possibility of incorporating large amounts of alkalies, which otherwise would be available for the deletereous reaction.
With reference to the further minimization of the expansion phenomenon due to thermal activation treatment of the zeolitic product, it is to be hypotesized that owing to the collapse of the structure of the fine-grained zeolitic mineral diffused in the cementing ground mass of the tuff, a quasi-amorphous solid, with specific surface area larger than that of the bubbly pozzolanic glass, owing to the pre-existing pores and channels, is formed, in this way favouring an easier breaking of the Si-O-Si bonds under the attack of the alkaline solution. Furthermore the evolution of the combined water following the thermal treatment promotes, in turn, the neo-formation of free surface bonds which share in the activation of the solid, even though such an activation, to a lesser extent, concerns the vitreous counterpart, too.

REFERENCES

1. SERSALE R. (1980), "Structure et caractérisation des pouzzolanes et des cendres volantes", 7th Int. Congr. on the Chem. of Cement, Paris I, pp IV-1/3-1/21.

- SERSALE R. (1983), "Aspects of the chemistry of additions". In "Advances in Cement Technology" Ed. Ghosh S.N., Pergamon Press, (Oxford) pp 537-567.

2. VALENTI G.L., CIOFFI R., SERSALE R., (1986), "Production and utilization of fly ash in Italy", Canmet/ACI Int. Conf. I, Ed. Malhotra V.M., American Concrete Inst., Detroit, pp 741-762.

3. SERSALE R., FRIGIONE G., (1985), "Natural zeolites as constituents of blended cements", Chimica e Industria, 67, 4, pp 177-180.

- SERSALE R., FRIGIONE G., (1985), "Blended cements manufactured with activated zeolitic additions", Chimica e Industria, 67, 10, pp 537-541.

4. FRATINI N., (1950), Ann. Chim., 40, 461.

5. ISO Recommendation R.679, March (1968).

6. ANSI/ASTM C 230-68.

7. ANSI/ASTM C 441-69.

Ko IKEDA, Department of Mining and Mineral Engineering, Yamaguchi University, 755 Ube, JAPAN.

A new type of pozzolanic cement utilizing red mud and fly ash.

Un nouveau type de ciment pozzolanique utilisant de la boue rouge et de la cendre volante.

SUMMARY: Bauxite from Australia contains boehmite which remains intact in the red mud after extraction of alumina. Therefore,this kind of red mud can be used as cement without clinkering process. Gypsum and/or portlandite were introduced to the red mud as activators. Two series of cement mixtures were prepared. One is blended with the activators for nearly stoichiometric compositions to produce ettringite and/or C_4AH_{13}. The other is blended with the activators of double amount for the stoichiometric compositions. These cement mixtures are called the red mud mixes and are hydraulic themselves. However,they are no use as cements due to the unstable hydration strength. To improve this defect fly ash was added to the red mud mixes to gether with 7 percent portlandite to the fly ash. Thus,moderately high strength cements were obtained, resulting compressive strength up to 9.7,16.4 and 20.1 MPa at 7,28 and 91-day age,respectively, when cured in water. However,deteriorations of strength were encountered in some specimens cured in air after 28-day water curing caused by the disintegration of ettringite,C_4AH_{13} and/or $C_4A\bar{C}H_{12}$.

1. INTRODUCTION

Alumina is usually manufactured from bauxite by the Bayer process,smelting with sodic solution in autoclaves. After extraction of alumina from the raw material,there remains huge amount of waste called "red mud",mainly composed of hematite. The annual production of this by-product reaches 2 million tons in Japan/1/,although full operation is now restricted due to international price competition.

Australian bauxite imported to Japan comprises some amount of boehmite,$Al_2O_3.H_2O$,in addition to gibbsite,$Al_2O_3.3H_2O$,as Al-bearing mineral due to weak metamorphism of ores. Accordingly,boehmite remains intact in the red mud because of the incapability of dissolving this mineral by the Bayer process completely. Therefore,pozzolanic type of cement can be produced from this kind of red mud by introducing some effective activators into the red mud to react with boehmite.

Since energy crisis of petroleum,construction of coal combustible power stations has been becoming popular in Japan and the production of by-product fly ash is estimated to become 12 million tons near the end of this century in Japan/2/. We should,therefore,pay attention to the effective use of the fly ash as well as the red mud.

The possibility of the production of this kind of pozzolanic cement utilizing red mud and fly ash has been already reported in the previous work in which stress was placed on the SEM observations/3/ and it was pointed out that this new type of pozzolanic cement is apt to deteriorate in long term,especially in air(partly unpublished). In this paper mixing range with more activators will be studied and the optimum conditions of mixing will be investigated.

2. EXPERIMENTAL

2.1 Red mud

The red mud used in this study is soda-reduced red mud commercially sold from Mitsui Alumina Company. They wash the soda-rich red mud with water,employing 7-stage anticurrent thickenners to reduce soda content down to 3 percent. It is generally said that the soda content of red mud is around 10 percent in alumina factories. According to XRD following minerals were identified in small amount

Table 1. Chemical compositions of the red mud and the fly ash.

	SiO_2	TiO_2	Al_2O_3	Fe_2O_3	MnO	CaO	MgO	Na_2O	K_2O	SO_3	Ig. loss
Red mud	9.14	8.55	19.88	48.86	-	2.47	-	3.02	-	-	8.51 %
Fly ash	58.00	1.10	21.40	5.22	0.04	2.84	2.64	1.40	2.29	0.18	4.40*

* Mainly carbon.

in addition to hematite and boehmite: sodalite, $2Na_2O.1.7Al_2O_3.3SiO_2.nH_2O$/4/, quartz, kaolinite, calcite and vaterite/3/. The latter two minerals are not essential ones, but are secondary precipitates during washing process, since the washing water dissolves some slaked lime as precipitating agent.

chemical composition of the soda-reduced red mud is given in Table 1. The amount of boehmite is estimated to be 13.7 percent in the red mud by calculation, neglecting the very small presence of quartz.

2.2 Fly ash

The fly ash used in this study is general one produced from domestic coal in Kyuden Sangyo Company. Chemical composition is given in Table 1. Small amount of quartz and mullite were found as crystalline phases in the glassy matrices of the fly ash by the X-ray diffractometry.

2.3 Activators

Chemical gypsum and portlandite (slaked lime) of JIS first grade were employed as activators. Physical characteristics are given in Table 2 as well as those of the other raw materials.

2.4 Red mud mixes

As shown in Fig. 1 two series and 10 mixtures were prepared by mixing red mud with gypsum and/or portlandite. These red mud mixes are hydraulic themselves. The series P is the same as investigated in the previous work/3/ and is represented here again for convenience. Mixing proportions of each series were determined on the basis of those for series P. First of all, mixes of two extremes, mix-100 and mix-0 were determined to give maximum formations of ettringite and C_4AH_{13} at 7-day age, respectively. The other mixes, 75, 50 and 25 were determined by simply dividing the amount of activators between the two extremes into proportions, 3 : 1 (75), 1 : 1 (50) and 1 : 3 (25). Gypsum and portlandite act reversely each other. detailed mixing proportions are given in Table 3.

Table 2. Physical characteristics of raw materials.

	Fineness, Blaine	S.G.
Red mud	8,600 cm^2/g	3.33
Gypsum	1,900	2.32
Portlandite	11,600	2.2
Fly ash	-	-

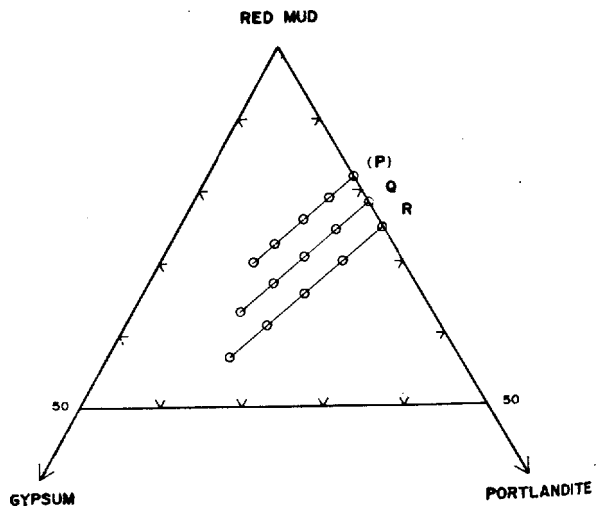

Fig. 1. Triangular representation of the mixing proportions of the red mud mixes.

Table 3. Mixing proportions of the red mud and the activators.

		Mix-100	Mix-75	Mix-50	Mix-25	Mix-0
Series (P)*	Red mud	70.0	73.0	76.0	78.9	81.9 %
	Gypsum	18.4	13.8	9.2	4.6	-
	Portlandite	11.6	13.2	14.8	16.5	18.1
Series Q	Red mud	63.3	67.1	70.9	74.6	78.3 %
	Gypsum	23.3	17.5	11.6	5.8	-
	Portlandite	13.4	15.4	17.5	19.6	21.7
Series R	Red mud	56.8	61.3	65.8	70.3	74.8 %
	Gypsum	28.1	21.1	14.0	7.0	-
	Portlandite	15.1	17.6	20.2	22.7	25.2

* Previous work/3/ and the base of mixing.

P

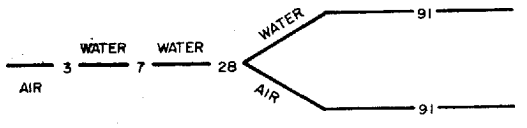

Fig. 2. Curing scheme of present cements.

2.5 Red mud mixes with fly ash

In order to improve long term strenght of the red mud mixes,fly ash blended with 7 percent portlandite was added to the red mud mixes in proportions of 1 : 1(1),2 : 1(2) and 3 : 1(3) in the increasing order of the fly ash. This portlandite acts as an extra activator in appearance. The contents of these mixtures are given in Table 4.

2.6 Curing and testing

Cements of the red mud mixes were tested on flexural and compressive strengths at 3, 7, 28 and 91-day age. Small scale test pieces were prepared in the molds of 1 x 1 x 4 cm dimension in the state of paste with W/C 0.40,i.e.,two pieces for flexural atrength and derived four for compressive strength. Demolding af er 3-day curing in humid air with R.H.90 percent,the test pieces were cured in water in semi-airtight plastic containers at ambient temperature. As illustrating in Fig. 2,the test pieces were divided into two groups at the age of 28-days. The water curing was continued for one group, whereas air curing was carried out in R.H. 90 percent condition for the other group. The air circulates spontenously and the object of this curing is to study the influence of carbon dioxide in air.

Table 5. Flexural and compressive strengths for the red mud mixes.

3	7	28	91	—days—	3	7	28	91
3.9	3.1	1.7	1.6	Q100-0*	8.3	8.1	8.6	6.4
			(1.5)					(6.8)
5.4	3.2	5.1	4.1	75-Q	10.1	10.4	13.9	16.4
			(1.7)					(13.6)
3.8	5.6	3.7	2.6	50-0	13.9	17.4	17.3	15.6
			(1.3)					(19.6)
2.6	3.2	2.5	2.3	25-0	7.7	8.8	9.3	8.9
			(0.5)					(6.0)
0.9	1.3	0.5	0.6	0-0	2.4	3.2	4.1	2.6
			(0.2)					(2.5)
3.1	2.6	2.1	2.3	R100-0*	8.2	6.9	5.8	5.1
			(2.1)					(7.4)
3.1	2.3	2.3	2.2	75-0	7.8	7.2	7.2	5.9
			(1.9)					(6.7)
4.7	4.2	3.8	3.8	50-0	10.4	12.2	11.6	12.3
			(-)					(6.8)
3.6	3.4	3.1	2.7	25-0	8.3	11.6	10.8	11.9
			(-)					(8.4)
1.1	1.0	0.2	1.0	0-0	1.8	2.5	2.7	3.4
			(0.4)					(2.6)

Mean values in MPa. () air curing. * 0 indicating no fly ash.

Table 4. Contents of the red mud mixes with fly ash

	1 : 1	2 : 1	3 : 1	
Red mud mix	50.0	33.3	25.0	%
Fly ash	46.8	62.3	70.1	
Portlandite ——extra	3.2	4.4	4.9	

2.7 Identification of hydrates

Test pieces after the strength test were preserved in acetone and served for the identification of hydrates by means of the X-ray diffractometry,using Mn-filtrated FeKα radiation at 30KV and 10mA.

3. RESULTS AND DISCUSSION

3.1 Strength for the red mud mixes

Results of the strength test are summarized in Table 5. For both of series Q and R decreasing of flexural strength is remarkable,especially in later age as noticed in series P in previous work/3/. This trend is also observed on compressive strength in some specimens. The mixes 0-0 of both series contain no gypsum and show low strength.

For series Q mixes 75-0 and 50-0 give rise generally good results. However,at 91-day age depression is noticed on these mixes cured in air and cured in water,respectively. Though the compressive strength is higher for 50-0 cured in air,the flexural strength becomes very low,i.e.,specimens become brittle. The mix 25-0 shows unstable strength with great deviation,when cured in air at 91 day age.

For series R mixes 50-0 and 25-0 show the saturation of strength,probably due to the exhaution of boehmite reacted with the sufficient amount of activators and depressions take place at 91-day age,when cured in air. Besides,cracking occurred on these specimens at 91-day age,when cured in air and the flexural strength was unable to determine.

3.2 Strength for the red mud mixes with fly ash

Results of the strength test are summarized in Table 6. For both of series Q and R decreasing of flexural strength is not marked but seen, especially in air curing and the strength is dependent on the content of fly ash,i.e.,more fly ash makes the strength decrease.

For series Q abrupt depression of flexural and compressive strengths are observed at 91-day age for the specimens of 75-1,75-2, 75-3 and 100-3 cured in air. For specimens of 0-2 depression is also noticed at 91-day age,when cured in water. On the whole mixes 50-1,50-2,25-1 and 25-2 are superior to the others and no depression of compressive strength was encountered.

For series R abrupt depression of flexural and compressive strengths are observed at 91-day age for the specimens of 100-1, 100-2 and 100-3,when cured in air. In this time no depression is noticed on the specimens 0-2 cured in air at 91-day age. On the whole, the mixes 50-1,50-2,50-3,25-1 and

Table 6. Flexural and compressive strengths for the red mud mixes with fly ash.

3	7	28	91	—days—	3	7	28	91
-	1.7	4.6	4.0 (2.3)	Q100-1*	-	3.5	10.1	15.1 (12.9)
-	4.3	5.0	2.9 (1.2)	75-1	-	9.4	13.2	18.5 (6.0)
-	4.1	4.3	3.1 (2.8)	50-1	-	8.1	12.2	16.8 (15.1)
-	2.6	2.7	3.7 (2.8)	25-1	-	7.2	15.2	16.6 (15.6)
-	1.6	2.8	3.2 (2.4)	0-1	-	6.9	12.0	14.0 (13.0)
-	0.8	3.8	3.3 (1.8)	Q100-2*	-	1.8	7.1	11.2 (10.3)
-	2.8	3.9	3.6 (0.3)	75-2	-	5.6	8.8	13.5 (2.4)
-	2.5	3.5	3.2 (2.1)	50-2	-	5.0	9.0	14.2 (11.3)
-	2.0	3.0	3.8 (2.6)	25-2	-	4.7	8.7	12.0 (11.8)
-	1.3	3.4	3.3 (2.1)	0-2	-	4.8	10.4	7.8 (10.8)
-	0.6	2.6	2.4 (0.6)	Q100-3*	-	1.2	4.8	8.1 (4.2)
-	1.9	2.7	2.7 (0.3)	75-3	-	4.2	7.1	11.3 (3.0)
-	1.5	2.5	2.3 (0.8)	50-3	-	3.2	5.6	9.6 (8.2)
-	0.8	2.4	3.2 (2.1)	25-3	-	2.9	7.3	9.4 (8.4)
-	1.4	2.4	2.7 (2.0)	0-3	-	3.4	8.3	9.2 (7.8)

3	7	28	91	—days—	3	7	28	91
-	1.6	3.2	5.7 (0.8)	R100-1*	-	3.3	5.2	15.2 (2.8)
-	1.8	4.5	3.7 (2.5)	75-1	-	4.0	10.1	14.9 (16.0)
-	4.6	4.4	3.8 (5.0)	50-1	-	9.7	16.4	20.1 (18.8)
-	4.1	4.4	4.6 (3.3)	25-1	-	9.2	13.0	17.7 (17.7)
-	3.1	3.1	3.3 (3.3)	0-1	-	6.5	12.1	14.6 (13.4)
-	0.8	3.4	3.8 (0.6)	R100-2*	-	1.7	7.0	13.9 (3.9)
-	0.9	3.3	2.6 (2.2)	75-2	-	1.9	6.4	13.6 (12.3)
-	2.8	3.6	3.8 (3.8)	50-2	-	6.0	11.3	14.6 (16.9)
-	3.0	3.0	3.6 (3.5)	25-2	-	5.1	9.4	11.4 (11.4)
-	2.9	3.1	3.3 (2.5)	0-2	-	4.3	9.0	11.4 (11.2)
-	0.5	3.6	3.6 (0.4)	R100-3*	-	1.2	6.5	10.7 (2.9)
-	0.8	2.3	2.6 (2.0)	75-3	-	1.8	5.5	11.2 (10.1)
-	1.7	2.7	2.9 (2.8)	50-3	-	4.1	9.2	12.0 (12.8)
-	1.8	2.4	2.8 (2.4)	25-3	-	3.3	6.3	10.5 (8.9)
-	1.9	2.3	3.0 (2.1)	0-3	-	3.3	8.0	10.5 (8.7)

Mean values in MPa. () air curing. * Numerals 1, 2 and 3 indicating the ratios 1 : 1, 2 : 1 and 3 : 1, respectively.

25-2 are superior. Although, the mix 0-2 is good in strength, it may be difficult to use in practice owing to low workability of the paste/3/.

3.3 Hydrates

3.3.1 For the red mud mixes

Hydrates encountered are summarized in Table 7 only limiting at 91-day age for saving space. When gypsum is present, formation of ettringite prevails as seen in the mixes 100-0 and 75-0. However, C_4AH_{13} begins to form gradually with increasing the content of portlandite as seen in the mixes 50-0, 25-0 and 0-0 with occasional carbonation and finally no ettringite exists in the mix 0-0 containing no gypsum. It is curious that no C_4AH_{13} forms in the mixes 100-0 and 75-0 having some potential of C_4AH_{13}. This may be explained to consider the limited solid solution series of $C_6A\bar{S}_3H_{32}$–C_6AH_{32}/5,6/. Sometimes C_4AH_{13} (strictly this should be $C_4A\bar{C}_{0.5}H_{12}$/7/) converts to $C_4A\bar{C}H_{12}$ by carbonation, especially in later age. Disintegration of ettringite takes place in some specimens cured in air. This will be discussed later in detail. Calcite exists from the begining of curing, since the red mud contains some calcite and vaterite. However, most of the calcite would be derived from portlandite due to carbonation. Much calcite is detected in the specimens cured in air at 91-day age. Formation of Ca-monosulphate was scarcely observed. Presence of type II C-S-H was reported in the previous work/3/ by means of SEM. C-S-H probably formed after the reaction of quartz and other silicates contained in the red mud was not clearly identified. Judging from the amount of activators left in specimens cured in water at 91-day age, gypsum is wanting except 100-0, while portlandite is sufficient for reaction for series Q. For series R gypsum is also wanting except 100-0, while portlandite is in excess except 50-0. No distinct relations between hydrates and strength were found except the specimens of 75-0 and 25-0 in series R where disintegrations of ettringite, C_4AH_{13} and $C_4A\bar{C}H_{12}$ were seen.

3.3.2 For the red mud mixes with fly ash

Hydrates identified are summarized in Table 7 for mixes 1 : 1, 2 : 1 and 3 : 1, respectively. Hydrates are similar to those of the red mud mixes. When gypsum is present, ettringite forms preferencially. With increasing the content of portlandite, C_4AH_{13} as well as $C_4A\bar{C}H_{12}$ is observed. Since these mixes comprise fly ash blended with 7 percent portlandite, increasing of the content of portlandite takes place into two directions. One is the direction from mix 100 to mix 0 via mixes 75, 50 and 25. The other is the direction from mix 1 : 1 to mix 3 : 1 via mix 2 : 1. Therefore, formations of C_4AH_{13} and $C_4A\bar{C}H_{12}$ become common, when compared with

Table 7. Hydrates identified in present cements in relation to gypsum and portlandite. Listed only for 91-day age with relative amounts.

	Q100-0	Q75-0	Q50-0	Q25-0	Q0-0
E	++++	++++	++++	++	-
	(++++)	(++++)	(++++)	(+++)	(-)
H13	-	-	-	++	++
	(-)	(-)	(-)	(-)	(+)
$\bar{C}$H12	-	-	++	++++	++++
	(-)	(-)	(-)	(-)	(++)
C$\bar{C}$	++	+	+	+	+
	(+++)	(++++)	(++++)	(++++)	(++++)
G	+	-	-	-	-
	(++)	(-)	(-)	(-)	(-)
P	+	+	+	+	-
	(+)	(+)	(+)	(-)	(-)

	R100-0	R75-0	R50-0	R25-0	R0-0
E	++++	++++	++++	+++	-
	(++++)	(++)	(++++)	(++)	(-)
H13	-	-	-	++	++
	(-)	(-)	(-)	(-)	(++)
$\bar{C}$H12	-	-	+	++	++++
	(-)	(-)	(-)	(-)	(+++)
C$\bar{C}$	+	+	+	+	+
	(++++)	(++)	(++++)	(++++)	(++++)
G	++++	-	-	-	-
	(++++)	(+)	(-)	(-)	(-)
P	++	++	+	++	++
	(+)	(+)	(-)	(+)	(-)

	Q100-2	Q75-2	Q50-2	Q25-2	Q0-2
E	+++	+++	++	+	-
	(+++)	(-)	(++)	(+)	(-)
H13	-	++	++	+++	++
	(-)	(-)	(-)	(++)	(+)
$\bar{C}$H12	-	-	-	+	++
	(-)	(-)	(-)	(+)	(+)
C$\bar{C}$	+	+	+	+	+
	(++)	(++++)	(++)	(+++)	(+++)
G	-	-	-	-	-
	(-)	(++)	(-)	(-)	(-)
P	-	+	+	+	-
	(+)	(-)	(-)	(-)	(-)

	R100-2	R75-2	R50-2	R25-2	R0-2
E	++++	+++	+++	+	-
	(-)	(+++)	(++)	(+)	(-)
H13	-	+	++	++	++
	(-)	(-)	(+)	(+)	(+)
$\bar{C}$H12	-	-	-	+	++
	(-)	(-)	(-)	(+)	(+)
C$\bar{C}$	+	+	+	+	+
	(++)	(++)	(++)	(++)	(+++)
G	-	-	-	-	-
	(+++)	(-)	(-)	(-)	(-)
P	+	+	-	-	+
	(-)	(-)	(-)	(-)	(-)

() air curing. E:ettringite,H13:C_4AH_{13},$\bar{C}H_{12}$:$C_4A\bar{C}H_{12}$,C$\bar{C}$:calcite,G:gypsum,P:portlandite. Peak height of X-ray, ++++:large,+++:medium, ++:small,+:detectable,-:undetectable.

	Q100-1	Q75-1	Q50-1	Q25-1	Q0-1
E	++++	++++	+++	++	-
	(++++)	(+)	(+++)	(++)	(-)
H13	-	-	++	+++	++
	(-)	(-)	(+)	(+)	(+)
$\bar{C}$H12	-	-	-	+	++
	(-)	(-)	(-)	(+)	(+)
C$\bar{C}$	+	+	+	+	+
	(++)	(+++)	(+++)	(+++)	(+++)
G	-	-	-	-	-
	(-)	(++)	(-)	(-)	(-)
P	+	+	+	+	-
	(+)	(-)	(+)	(-)	(-)

	R100-1	R75-1	R50-1	R25-1	R0-1
E	++++	++++	+++	++	-
	(+)	(++++)	(+++)	(++)	(-)
H13	-	-	+	++	++
	(-)	(-)	(+)	(++)	(+)
$\bar{C}$H12	-	-	-	++	++
	(-)	(-)	(-)	(+)	(+)
C$\bar{C}$	+	+	+	+	+
	(+++)	(++)	(++++)	(++)	(++++)
G	-	-	-	-	-
	(++++)	(-)	(-)	(-)	(-)
P	+	-	-	-	-
	(-)	(-)	(+)	(-)	(-)

	Q100-3	Q75-3	Q50-3	Q25-3	Q0-3
E	+++	+++	++	+	-
	(++)	(+)	(++)	(+)	(-)
H13	+	+++	++	+++	+
	(-)	(+)	(+)	(++)	(+)
$\bar{C}$H12	-	-	-	+	+
	(-)	(-)	(-)	(+)	(+)
C$\bar{C}$	+	+	+	+	+
	(++)	(++++)	(++)	(++)	(++)
G	-	-	+	-	-
	(+)	(++)	(-)	(-)	(-)
P	+	+	-	-	+
	(-)	(-)	(-)	(-)	(-)

	R100-3	R75-3	R50-3	R25-3	R0-3
E	++++	+++	++	++	-
	(-)	(+++)	(++)	(+)	(-)
H13	-	+	++	++	++
	(-)	(-)	(+)	(+)	(+)
$\bar{C}$H12	-	-	-	+	++
	(-)	(-)	(+)	(+)	(+)
$\bar{C}$C	+	+	+	+	+
	(++)	(++)	(+++)	(++)	(+++)
G	-	-	-	-	-
	(+++)	(-)	(-)	(-)	(-)
P	-	-	-	-	-
	(-)	(+)	(+)	(-)	(-)

the hydration of the red mud mixes,especially in mixes 2 : 1 and 3 : 1. Formation of Ca-monosulphate is scarce and not distinct generally. Calcite exists from the beginning more or less and much formation of this mineral is seen in specimens cured in air at 91-day age. Disintegration of ettringite as well as C_4AH_{13} and $C_4A\bar{C}H_{12}$ is worthy to note and this phenomenon is closely related to the depression of strength at 91-day age, when cured in air as seen in the specimens 75-1,75-2,75-3 and 100-3 in series Q, and 100-1,100-2 and 100-3 in series R. The rate of consumption of gypsum is great and the amount is generally wanting,while that of portlandite is sluggish and is generally sufficient. Portlandite is apt to convert to calcite especially in air curing at 91-day age. C-S-H probably formed due to the hydration of the fly ash as well as quartz and other silicates included in the red mud was not clearly identified/8/. However,this may be present as reported previously by the observation of SEM/3/.

3.3.3 Disintegration of ettringite, C_4AH_{13} and $C_4A\bar{C}H_{12}$

As seen in Fig. 3 as well as Table 7, disintegration of these minerals occurs partly or completely in some specimens cured in air at 91-day age. Judging from the X-ray results,following reactions would take place in the course of curing.

For ettringite:

$$C_6A\bar{S}_3H_{32} + 3\bar{C} = 3C\bar{S}H_2 + AH_3 + 3C\bar{C} + 23H$$

Consequently,ettringite disintegrates into gypsum,gibbsite and calcite in addition to water and the gibbsite can be hardly detected due to the amorphous nature in the early stage of formation.

For C_4AH_{13} and $C_4A\bar{C}H_{12}$:

$$C_4AH_{13} + \bar{C} = C_4A\bar{C}H_{12} + H$$

$$C_4A\bar{C}H_{12} + 3\bar{C} = AH_3 + 4C\bar{C} + 9H$$

Consequently,the both minerals disintegrate into gibbsite and calcite in addition to water. If these reactions take place independently or simultanously,great depressions of strength are induced. However,it is quite curious that no depressions of strength were found in haüyne-belite cement cured in steam, in which ettringite and C-S-H are essential hydrates and disintegration of the ettringite occurs,when subjected to air after the steam curing. In this case the C-S-H derives from the hydration of C_2S and there may be fundamental difference of C-S-H between the haüyne-belite cement and the present red mud cement/9/.

4. SUMMARY AND CONCLUSION

Red mud cement can be made from soda-reduced red mud,when activated with gypsum and/or portlandite. Boehmite included in the red mud plays an important role in this kind of cement which is regarded as a type of pozzolanic cement,since boehmite cannot be a cement mineral by itself. Many kinds of cement are manufactured,varying the proportion of the red mud and the activators. However, these cements are generally unstable in

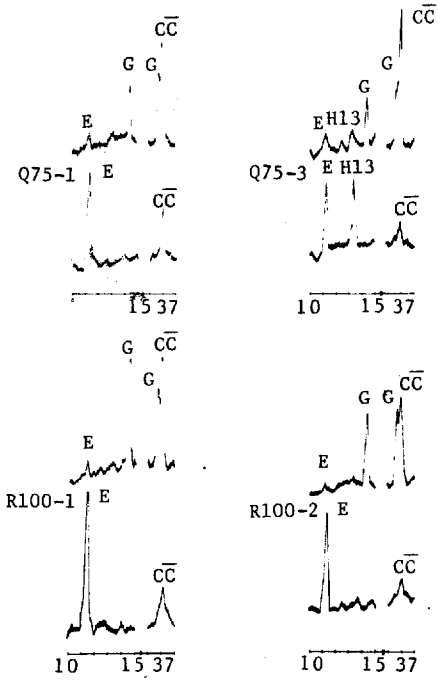

Fig. 3. Powder X-ray diagrams showing the disintegration of hydrates. Top,air curing,and bottom, water curing for each. Other notations, see Table 7. (FeKα).

strength. This defect is improved by introducing fly ash with 7 percent extra portlandite. Thus,hardened cement materials,for instance,having 9.7,16.4 and 20.1 MPa compressive strength at 7, 28 and 91-day age were obtained. However,some specimens show the deterioration of strength,when cured in air after 28-day water curing. This is caused by the disintegration of ettringite,C_4AH_{13} and/or $C_4A\bar{C}H_{12}$ which are the essential hydrates in present cement,probably in addition to C-S-H. Further investigation is necessary to make clear the disintegration of these minerals in various conditions of curing.

REFERENCES

1) The Asahi,No.37146,1984.
2) The Science News,No.1940,1082.
3) Ikeda, K.,Proc. Beijin Inter. Symp. Chem. Cem. Concr.,1985,(in Press).
4) Materials of Mitsui Alumina Co.,LTD.,1978.
5) Taylor, H.F.W.,The chemistry of cement, Academic Press,1,272,1965.
6) Midgley,H.G.,Rosaman,D.,Proc. 4th Inter. Symp. Chem. Cem.,Washington,1,259,1962.
7) Fischer, R.,Kuzel, H.-J.,Cem. Concr. Res., 12,517,1982.
8) Uchuikawa,R.,Uchida, S.,Proc. 7th Inter. Sym. Chem. Cem.,Paris.,3,IV-24,1980.
9) Ikeda, K.,Tashiro, C.,Techn. Repor. Yamaguchi University,2,522,1981.

K. Isozaki, S. Iwamoto and K. Nakagawa
Denki Kagaku Kogyo Co., Ltd, - Japan

SOME PROPERTIES OF ALKALI ACTIVATED SLAG CEMENT

I. INTRODUCTION

In recent years, alkali metal salt activated blast furnace slag cement containing no ordinary portland cement has attracted attention in regard to energy conservation and industrial by-product use as well as properties of high strength development, chemical resistance and heat resistance. However, some reports by other authors appear to fail to provide adequate data regarding the basic properties of this cement. (for example (1), (2)) In this paper, some properties of pastes made with blast furnace slag and NaOH were systematically studied.

II. EXPERIMENTAL

The chemical composition, basicity and glass content of blast furnace slag (BFS) used are shown in Table I.

TABLE I
Chemical composition, basicity and glass content of blast furnace slag (BFS)

Chemical composition (wt%)	
ig.loss	0.15
insol.	0.03
SiO_2	34.22
Al_2O_3	14.93
Fe_2O_3	0.03
CaO	41.76
MgO	7.7
SO_3	0.05
Na_2O	0.24
K_2O	0.44
Total	99.60

Specific gravity... 2.90

Basicity... $\frac{CaO+MgO+Al_2O_3}{SiO_2}$ = 1.88

Glass content... 90%
(determined by an optical microscope)

BFS was ground into blaine specific surface areas of 147, 220, 273, 407, 565 and 654 m^2/kg. The added amounts of NaOH to BFS were 0, 1.6, 3.3, 5.0, 7.5, 10.0, 20.0 and 30.0 wt%. The water to BFS ratios were 0.3, 0.4, 0.6 and 0.7.

The superplasticizers used were the sodium lignosulfonate (LS) and formalin condensates of β-naphthalene sodium sulfonate (NS). These admixtures were high commercial grade water reducing agents for cement. AS reference material, ordinary portland cement (OPC) was used. Table II shows its chemical composition.

TABLE II
Chemical composition of ordinary portland cement (OPC)

Chemical composition (wt%)	
ig.loss	0.7
insol.	0.4
SiO_2	22.1
Al_2O_3	5.0
Fe_2O_3	2.0
CaO	64.6
MgO	1.2
SO_3	2.0
Na_2O	0.41
K_2O	0.42
f-CaO	0.6
Total	99.43

Blaine specific surface area ... 305 (m^2/kg)

Each paste specimen (4x4x16 cm beam) was cured at 20°C, 80 %rh and subjected to a compressive strength test at a predetermined age. The crushed specimens were treated by D-dry method for 48 hrs and used as samples to be studied by a mercury pressure porosimeter, powder X-ray diffractometer, thermal analysis (DTA, TG) and SEM observation. The heat liberation curve of hydration was obtained using a conduction calorimeter. Rheological properties were measured with a coaxial cylinder viscosimeter. The pastes to be tested were prepared by mixing the cement with water or a NaOH solution in a beaker for 2 min by hand. Immediately following mixing, the pastes thus obtained were transferred into a measuring cell. During the experiment, the rotating bob speed increased in one minute from 0 to 350 rpm and in the next, resumed 0 rpm. This method was repeated at each age without interruption from the time each paste was placed in the cell untill completion of the test.

III. RESULTS AND DISCUSSION

III-1 STRENGTH DEVELOPMENT AND HEAT OF HYDRATION

The compressive strengths of the paste specimens increased in proportion to the fineness of BFS on adding 7.5 wt% NaOH. (Fig. 1) Fig.2 shows the relation between the added amount of NaOH and strength development in BFS having a 565 m^2/kg blaine specific surface area. The compressive strengths of the paste specimens increased with NaOH content being maximum at a 10 wt% addition.

OPC has a dormanant period at the early stage of hydration but is nonexistent in the hydration of NaOH activated BFS. (Fig. 3)

P

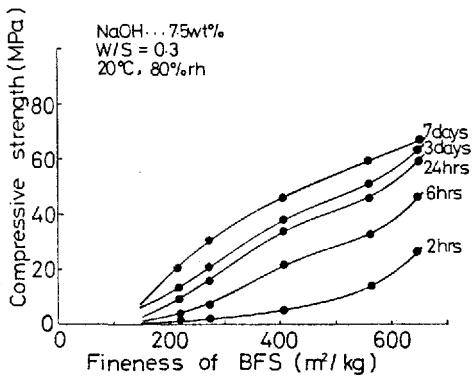

Fig. 1 Effect of fineness of BFS on strength development.

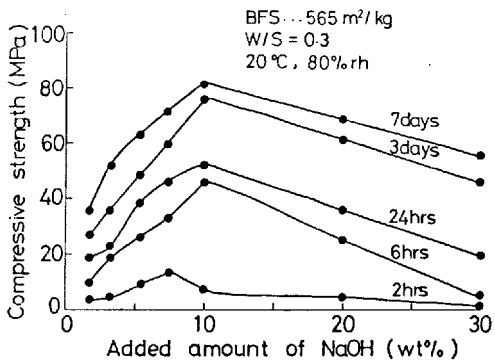

Fig. 2 Effect of added NaOH on strength development.

This should depend on the difference in their hydration mechanisms. The hydration of portland cement occurs mainly by a topochemical reaction and that of alkali activated BFS cement by a solution reaction. With increase in NaOH content and fineness of BFS, the rate of BFS dissolution was found to increase, resulting in enhancement of the hydration of BFS.

The compressive strength of each specific surface area of BFS is plotted as a function of the heat of hydration in Fig. 4. A nearly satisfactory linear plot was obtained for each amount of NaOH added. The 7.5 wt% and 10.0 wt% additions of NaOH to BFS seemed too much for effective strength development. The relation between compressive strength and heat of hydration for the 1.6 wt% addition of NaOH was similar to that of OPC.

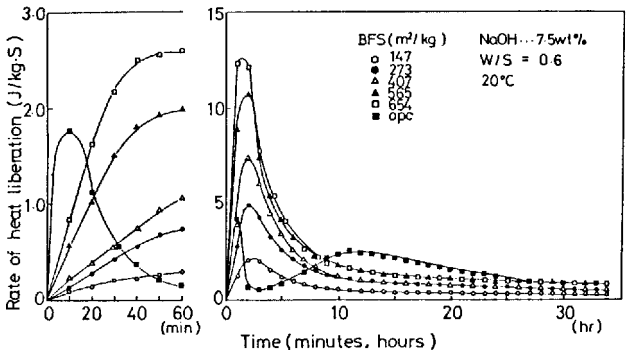

Fig. 3 Heat liberation curves of hydration as a function of time.

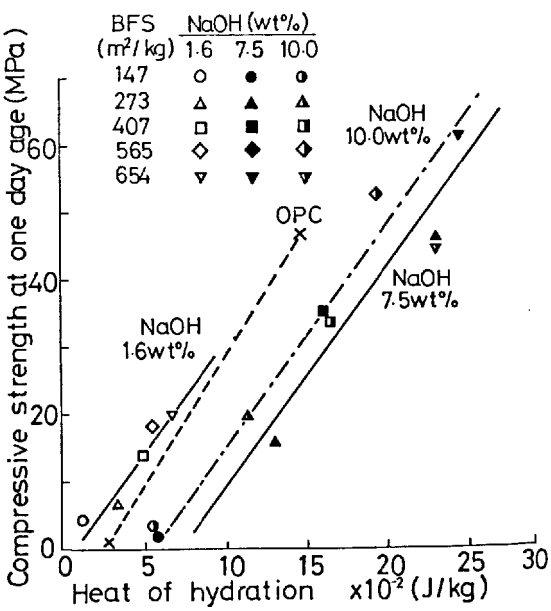

Fig. 4 Relation between heat of hydration and compressive strength for various surface areas of BFS.

Therefore, the optimum amount of NaOH addition is generally assumed to be a few wt%. (3)

III-2 HYDRATION PRODUCTS AND PASTE STRUCTURES

The X-ray diffraction pattern of BFS paste admixed with 7.5 wt% NaOH at 28 days of age is shown in Fig. 5. A broad peak with a maximum was found in the vicinity of 30° (Cu Kα, 2θ), and apparently C-S-H (I). (4)

P

The peaks at 11.7° and 30.4° were identified as $C_3A\ CaCO_3H_{11}$ and C_3ASH_8, respectively. (5)(6) No traces of $Ca(OH)_2$ dehydration in either the DTA or TG curves (Fig. 6) could be found. The endthermic peak at 170°C was regarded as the dehydration of C-S-H (I). (7)

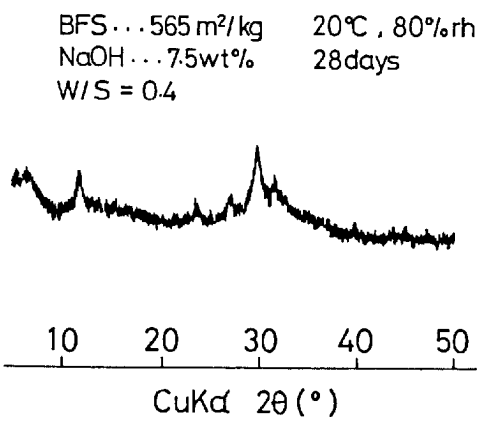

Fig. 5 Powder X-ray diffraction pattern of hardened paste.

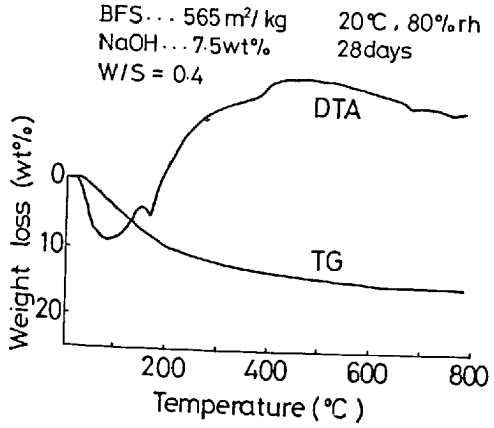

Fig. 6 Thermal analysis curves of hardened paste.

Fig. 7 shows the morphology of the hydrates as determined by SEM. The hydrate structures appeared to be homogeneous and dense compared with those of OPC. Correspondingly we can consider the result of mercury pressure porosimetry. Pore volumes of BFS paste ranging from 107 to 750 nm pore radii were extremely smaller than those of OPC paste. (Fig. 8)



(A) BFS paste (565 m^2/kg, NaOH... 7.5 wt%)



(B) OPC paste

Fig. 7 SEM photograph of hardened pastes at 14 days of age. (W/S = 0.4, 20°C, 80 %rh)

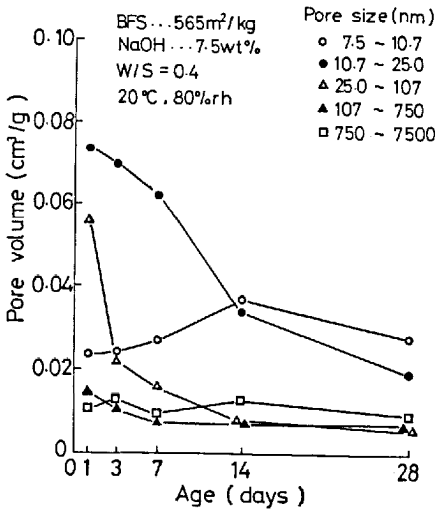

(A) BFS paste

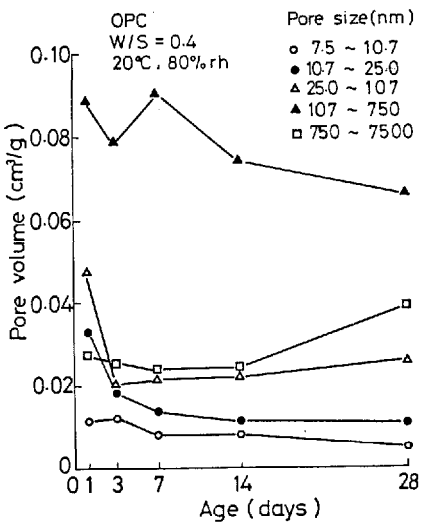

(B) OPC paste

Fig. 8 Pore size distribution of hardened paste as a function of time.

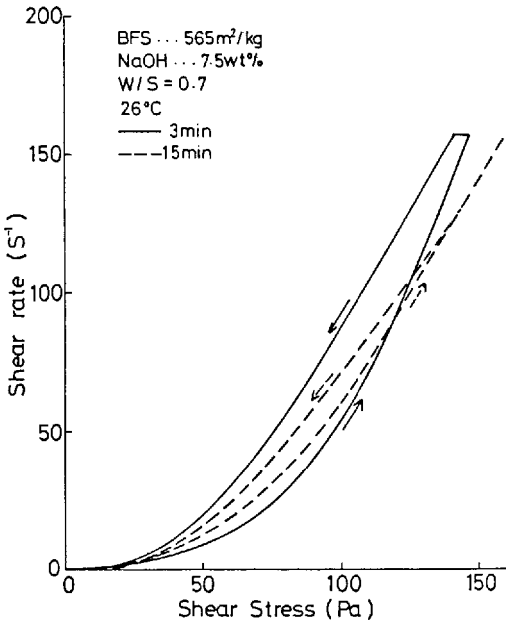

Fig. 9 Flow curves of fresh paste.

III-3 INFLUENCE OF SUPERPLASTCIZER ON RHEOLOGYCAL PROPERTIES

The flow curves obtained 3 and 15 min after the first cement-water contact are shown in Fig. 9 and are pseudoplastic type and thixotropically in reversible character. (8) (9)

A comparison of the effects of the superplasticizers (Fig. 10) indicated differences between LS and NS. LS exhibited strong plasticizing effects on the system of BFS only and the system of BFS admixed with NaOH. However, systems admixed with NS showed the same viscosity as those without superplasticizers since LS retards cement hydration but not NS. In Fig. 3, no dormanant period is present early in the hydration of BFS pastes, thus indicating that hydration strongly proceeds from the first contact of cement with water. Without a delay in hydration, NS is completely consumed at the start of hydration, as was confirmed by examination of the concentration of NS in the liquid phase. (10)

The yield values indicate the workability of fresh pastes. On adding NaOH and superplasticizers, paste behavior was noted to change considerably. (Fig. 11) This point warrants further investigation.

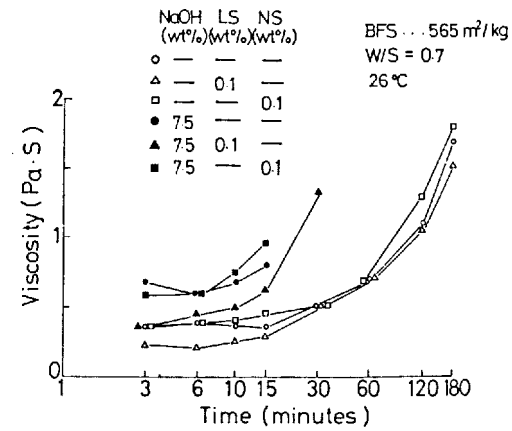

Fig. 10 Viscosity of fresh paste as a function of time.

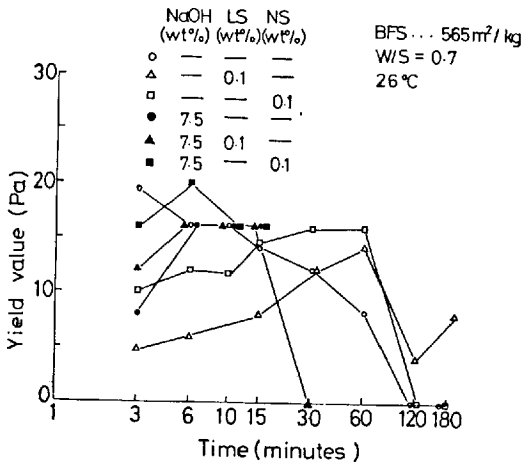

Fig. 11 Yield value of fresh paste as a function of time.

IV. CONCLUSIONS

(1) The optimum amount of NaOH to add to BFS is generally a few wt%. The compressive strengths of NaOH activated BFS paste specimens increases in proportion to the fineness of BFS.

(2) No formation of $Ca(OH)_2$ occurs in the hydration of BFS. The morphology of hydrates is relatively homogeneous and the paste structure is dense compared with that of ordinary portland cement.

(3) The flow curves of NaOH activated BFS pastes are of the pseudoplastic type and thixotropic in character. Sodium lignosulfonate is effective as a superplasticizer for NaOH activated BFS cement but not the formalin condensates of β-naphthalene sodium sulfonate.

REFERENCES

1.- T. Hakkinen and J. Ruohomaki (1985), "Alkali activated slag and blended cement research in Finland" Workshop on blastfurnace slag cements and concretes, York.

2.- V. Glukhovskij, Yy. Zaitsev and V. Pokhomov (1983), "Slag-alkaline cements and concretes-structure, properties, technological aspects of the use" Silicates Industriels, 4-5, 123-127.

3.- J. Metso and E. Kajaus (1983), "Activation of blast furnace slag by some inorganic materials", 1st Inter. Confer. on the use of fly ash, silica fume, slag and others mineral by-products in concrete, 2, 1059-1073.

4.- M. Daimon, C.T. Song, A. NISHITA, O. Yamaguchi and C.E. Kim (1982), "Change in the liquid concentration during the hydration of granulated blast furnace slag" Gypsum & Lime, 176, 3-8.

5.- M.H. Roberts (1969), "Calcium aluminate hydrates and related basic salt solid solutions" Proc. 5th Inter. Symp. Chem. Cement, Tokyo, SP II-29, 104-117.

6.- C.H. Schmidt (1960), Proc. 4th Inter. Symp. Chem. Cement, Washington, 2, 244.

7.- V.S. Ramachandran (1969), "Applications of differential thermal analysis in cement chemistry" Chemical publishing Company, INC. New York, 86.

8.- I. Odler, T. Becker and B. Weiss (1979), "Rheological properties of cement pastes " Il Cemento, 3, 303-310.

9.- R.A. Helmuth (1980), "Structure and rheology of fresh cement paste", 7th Inter. Symp. Chem. Cement, Paris, VI-0, 16-30.

10.- M. Daimon and D.M. Roy (1978), "Rheological properties of cement mixes; I. Method, preliminary experiments and adsorption studies", Cem. Concr. Res.,8, 753-764.

N. Tsuyuki, N. Hirota, T. Miyakawa and J. Kasai
Nikon University - Japan

THE PHYSICAL PROPERTIES AND THE HYDRATION MECHANISM OF C_3A IN THE PRESENCE OF $CaSO_4.2H_2O$ and $Ca(OH)_2$.

INTRODUCTION

On the retardation mechanism of C_3A in the presence of $C\bar{S}H_2$, Mehta[1] suggested that it was coated by gel-like form of ettringite. Corstanje et al. have deduced that the primary cause of C_3A retardation is not SO_4^{2-} but the precipitation of amorphous $Al(OH)_3$ on the surface of the C_3A grain. Tadros et al. suggested that the primary retardation of the dissolution was caused by the formation of an Al-rich layer, and that the induction period represented the process responsible for the removal of the Al-rich layer. The retardation was greatest when both $C\bar{S}H_2$ and CH were present. the authors have recently questioned the role of ettringite in the retardation of C_3A by SO_4^{2-}. The study aimed to clarify the physical properties of C_3A and the mechanism of the excessive retardation. When C_3A was dispersed in suspension of $C\bar{S}H_2$ and CH, the interaction between solid and liquid phases as a function of hydration time was investigated[2].

EXPERIMENTAL

(1) Two kinds of C_3A was synthesized to clarify the characterization. it was the pure C_3A, and other hand, the melt of C_3A composition ($G\text{-}C_3A$) which was synthesized by rapid quenching after fusion. The melt ($G\text{-}C_3A$) involved the slight presence of SiO_2 Various physical properties was measured.

(2) Pure solution and suspensions of $C\bar{S}H_2$, C and mixing both $C\bar{S}H_2$ and CH were prepared. After the synthesized pure C_3A of 2.5 g was dispersed into 125 ml of various suspensions. these were fully shaken in incubater at 25℃. A lot of poly-bottles containing suspension were prepared, these were filtrated by 17G-4 glass filter for each prescribed times. The concentration of Ca^{2+}, $Al(OH)_4^-$ and SO_4^{2-} which eluted from C_3A and pH in the filtrate were measured. On the other hand, after the each residue were stopped the hydration by CH_3OH and CH_3COCH_3, it was dried in the desiccator. XRD and SEM of each specimens which correspond to hydration time were identified and observed.

RESULTS

(1) The physical properties of synthesized pure C_3A and the melt of C_3A composition ($G\text{-}C_3A$) were shown in Table 1. Surface binding energy[3] of C_3A and $G\text{-}C_3A$ by ESCA were shown in Fig.1.2. Fig.1 is wide scanning, and Fig.2 is narrow scanning about Ca.Al. From the results of measurements by Fig.2, the chemical shift of

Table 1. Physical properties of C_3A and the melt ($G\text{-}C_3A$).

	$G\text{-}C_3A$	C_3A
lattice const. (Å)	15.22	15.26
specific gravity	2.98	3.04
specific surface area (m^2/g)	1.38	0.75
free CaO (wt %)	2.44	0.17

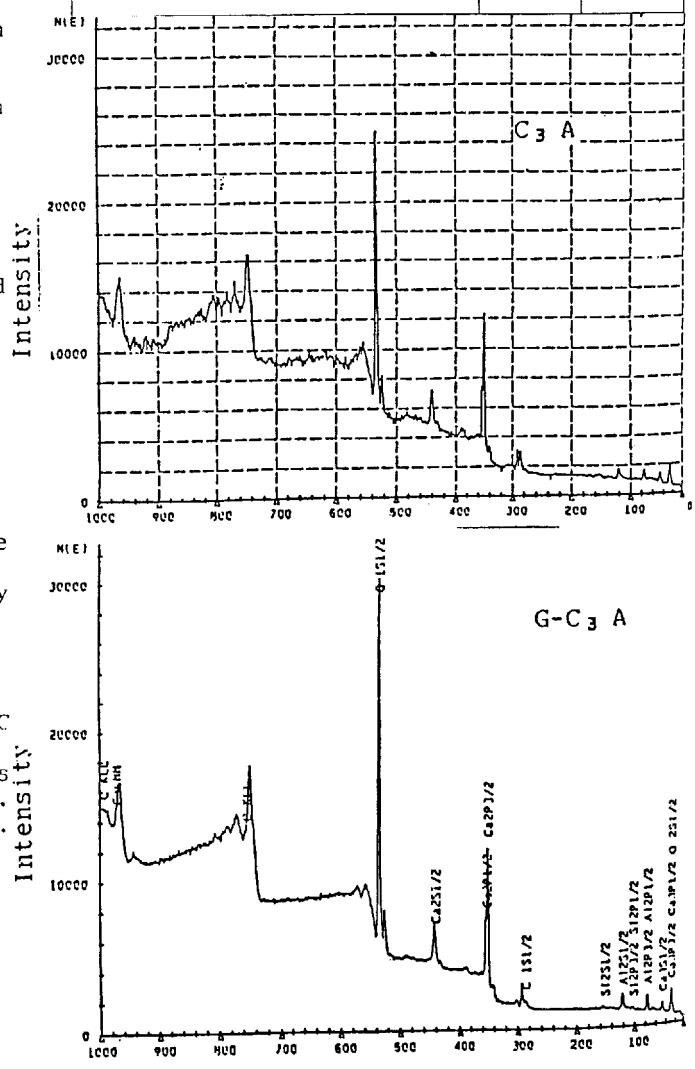

Fig.1. Binding energy of C_3A and the melt ($G\text{-}C_3A$) by XPS (ESCA).

binding energy were obtained about Ca-O. Al-O bond. The results are shown in Table 2.

(2) (i) Conduction calorimetric curves of C_3A and the melt ($G\text{-}C_3A$) which hydrated with pure water were shown in Fig. 3. W/solid ratio is 5. The appearance of the second peak was characterized in the melt ($G\text{-}C_3A$)-H system. Similarly, rate of heat liberation of C_3A which hydrated with various addtions of $C\bar{S}H_2$ and CH were shown in Fig. 4.

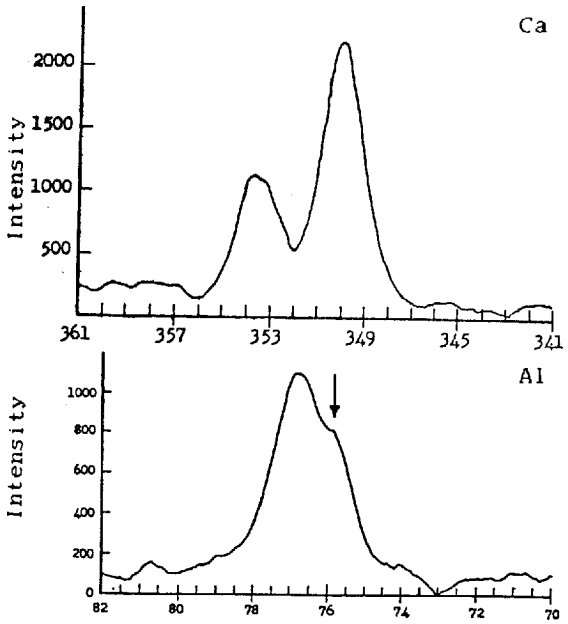

Fig.2. Binding energy of Ca-O, Al-O in C_3A by ESCA.

In case of higher ratio of CH to C_3A over 10%, rate of heat liberation were depressed, the appearance time of the second order peak was dependent on amount of $C\bar{S}H_2$.

(ii) When C_3A was dispersed into aqua solution, the concentration of Ca^{2+} and $Al(OH)_4^-$ which eluted from C_3A and pH in liquid phase were measured by ICP instrument. The result makes as CaO and Al_2O_3 is shown in Fig. 5. Similarly, when C_3A was dispersed into suspension of mixing both $C\bar{S}H_2$ and CH, the concentration of Ca^{2+} .$Al(OH)_4^-$ .SO_4^{2-} and pH were obtained. The results are given in Fig. 6.

Although Ca^{2+} and $Al(OH)_4^-$ were immediately eluted after C_3A hydration, its C/A mole ratio in liquid phase was depend on hydration time. C/A=2 until 5min. C/A=4 until 3hr, C/A=1 after 3hr. pH is almost constant during this period. On C_3A-$C\bar{S}H_2$ -CH system, the concentration of Ca^{2+} and SO_4^{2-} in the presence of $C\bar{S}H_2$ and CH and no C_3A is 1.80g CaO/l, 1.02g SO_3 /l, respectively, it isn't obeys to the common ion effect. The retention period at the highest concentration of SO_4^{2-} is depends on the amounts of $C\bar{S}H_2$ and CH.

(iii) XRD intensity of solid phase corresponds to hydration time was plotted for each hydrates. The results are indicated in Fig.7. Furthermore, SEM photographs are shown in Fig.8.

On C_3A-H system, XRD intensity of C_3A unhydrate rapidly fell, consequently, C_3AH_6 hydrate was growing with hydration progress. However, amorphous C_4AH_{13} hydrate was immediately confirmed by SEM as card-house

Table 2. Chemical shift of binding energy by ESCA.

atom	orbital	G-C_3A	C_3A	shift
Ca	2P	347.5 eV	346.7 eV	0.8 eV
Al	2P	74.1	73.4	0.7
Si	2P	101.7	——	——
O	1S	531.8	531.1	0.7

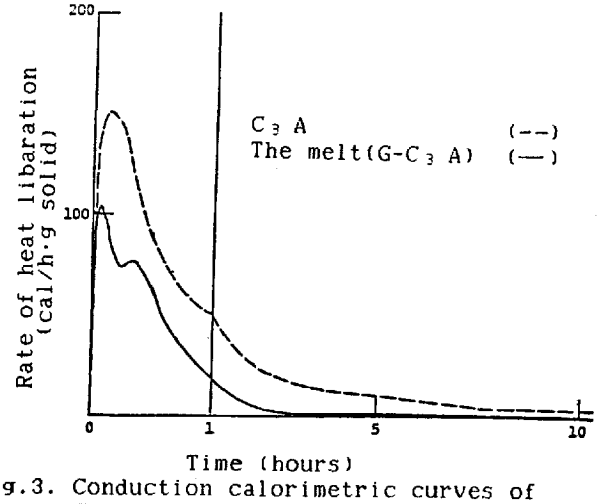

Fig.3. Conduction calorimetric curves of C_3A and the melt (G-C_3A) (W/solid=5).

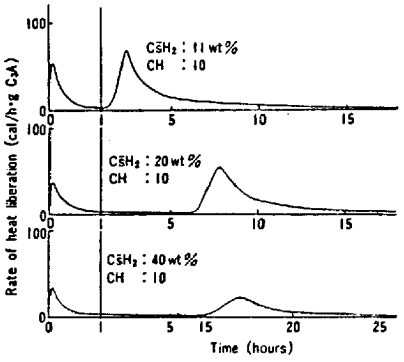

Fig.4. Conduction calorimetric curves of C_3A hydrated with various additions of $C\bar{S}H_2$ and CH (W/C_3A=5).

structure after contact with aqua solution. On C_3A-$C\bar{S}H_2$ -CH-H system, it is difficult to confirm the formation of ettringite by XRD in spite of consumption of SO_4^{2-}. Monosulfate and C_4AH_{13} hydrate were remarkably growing with hydration progress.

DISCUSSION

(1) It is thought that the factor which controlled the hydration of C_3A is caused

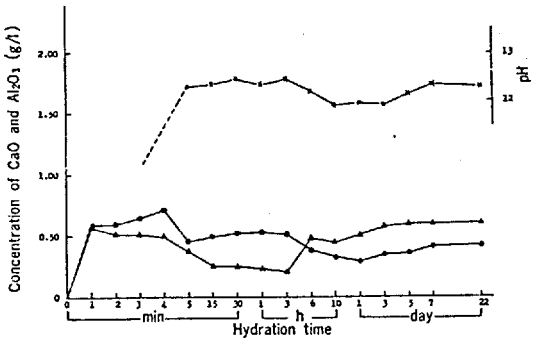

Fig.5. The concentration of CaO(●) Al_2O_3 (▲) and pH(✱) in liquid phase of C_3A-H system as a function of hydration time at 25℃ (W/solid=50).

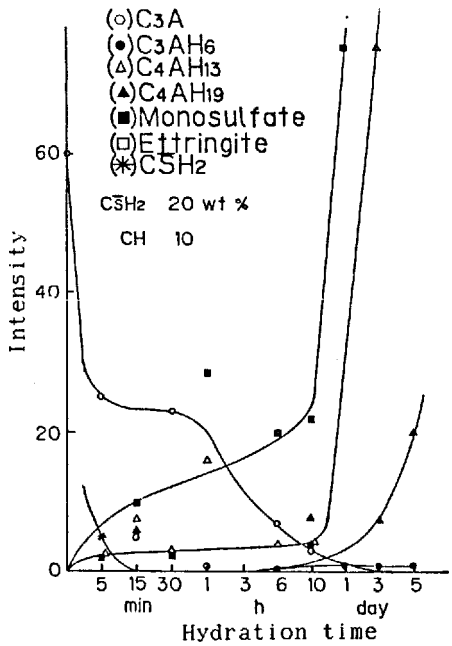

Fig.7. The changes in diffraction intensity of various hydrates as a function of hydration time at 25℃ (W/solid=50).

to binding energy of inner shell electron of Ca, Al and Si combined with O(oxygen). The satellite peak of Al shown in Fig.2 exhibits to become the shoulder by different binding distance of Al-O. The binding energy of C_3A which was synthesized by two different methods was clarified from Table 2. consequently, active C_3A on hydration is 0.7~0.8 eV lower than the melt (G-C_3A). Therefore, the hydration of C_3A is quicker than the melt (G-C_3A).

(2) CaO/Al_2O_3 mole ratio of Ca^{2+} ,$Al(OH)_4$ which eluted from C_3A after contact with aqua solution isn't 3. it is 2 until 15 min. Because of unhydrate C_3A is attacked by the eluted Ca^{2+} ,C_4AH_{13} is formed. resulting Ca^{2+} is consumed. unhydrate C_3A is coated by

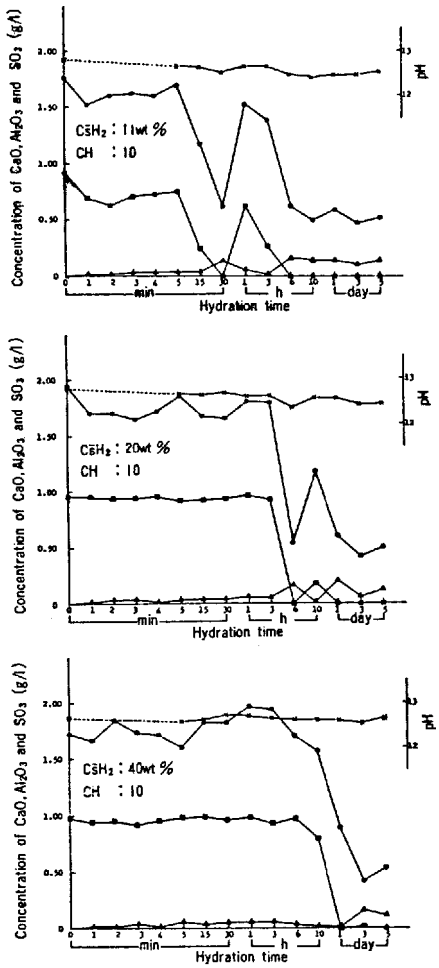

Fig.6. The concentration of CaO(●), Al_2O_3 (▲), SO_3 (■) and pH(✱) in liquid phase of C_3A-$C\bar{S}H_2$ -CH-H system as a function of hydration time at 25℃ (W/solid=50).

hexagonal plate hydrate of C_4AH_{13}. C_4AH_{13} is instantly converted into C_3AH_6, while eluting Ca^{2+}. Particularly, C_3AH_6 is formed rapidly 5 minutes after the addition of water. At this time, the Ca^{2+} concentration in the liquid phase is increased and $Al(OH)_4^-$ is consumed for hydration. Accordingly, there may be such cases in which a C/A of 4 or above is obtained.

In the rapid hydration of C_3A, the above-mentioned reactions proceed continuously, liberating large quantities of heat from the start of hydration. Immediately after the addition of water, the surface of C_3A is covered with two layers: a layer of C_4AH_{13} and a stable layer of C_3AH_6. As a result, the elution of Ca^{2+} and $Al(OH)_4^-$ from C_3A is

remarkably reduced and the hydration is stopped. liberating only a small quantity of heat. In the liquid phase, Ca^{2+} and $Al(OH)_4^-$ are in equilibrium with C/A=1.

(3)In the solution of $C\bar{S}H_2$ and CH only, the concentration of SO_4^{2-} is about 1.02g SO_3 /l. regardless of the mixing ratio of $C\bar{S}H_2$ and CH and the presence or absence of CH. On the other hand, the concentration of Ca^{2+} does not follow the common ion effect but increases sharply to about 1.80g CaO/l. Now, let us study the concentration in a suspension produced by dispersing C_3A in the solution containing $C\bar{S}H_2$ and CH in excess of the saturation level. In this suspension, the total concentration of Ca^{2+} in the liquid phase is calculated by adding the amounts of Ca^{2+} eluted from $C_3A.C\bar{S}H_2$ and CH. Accordingly,

Total CaO=CaO(C_3A)+CaO($C\bar{S}H_2$)+CaO(CH) from Fig.6.

Total CaO≒1.70～1.90g CaO/l here.

CaO($C\bar{S}H_2$)+CaO(CH)≒1.80g CaO/l that is,

CaO(C_3A)≒0.0～±0.10g CaO/l

The amounts of Ca^{2+} and $Al(OH)_4^-$ eluted from C_3A are very small. In this case, the retention time at the highest concentration means the period of time in which the concentrations of 1.80g CaO/l and 1.02g SO_3 /l in the liquid phase are maintained so far as the suspension contains $C\bar{S}H_2$ and CH in excess of the saturation level.

Therefor, the added fully $C\bar{S}H_2$ and CH describes two roles as follows:

(A) $C\bar{S}H_2$ and CH are required to keep at the highest concentration of Ca^{2+} and SO_4^{2-} in liquid phase.
(B) The remained $C\bar{S}H_2$ and CH except for above (A) is present.

Since $C\bar{S}H_2$ and CH corresponding to above (B) is reacted with C_3A, AFt and AFm phases are immediately formed. the resulting C_3A surface is partly coated by these phases. However, C_3A is covered by the highest concentration of $C\bar{S}H_2$ and CH corresponding to above (A).

In this period, the reactions are stopped apparently and the hydration is remarkably retarded. After film formation, the elution of Ca^{2+} and $Al(OH)_4^-$ from C_3A is very small and hydrates are not formed. This finding agrees with the results reported by Mori et al[4]. At the end of the retention period at the highest concentration, $C\bar{S}H_2$ and CH described in (A), and C_3A coprecipitate, forming a thick film rapidly. This film is a solid solution of monosulfate-C_4AH_x system shown as 7.6～9.6Å phase. The retention period at the highest concentration is greatly affected by the mixing amount of $C\bar{S}H_2$ and CH. After the formation of a

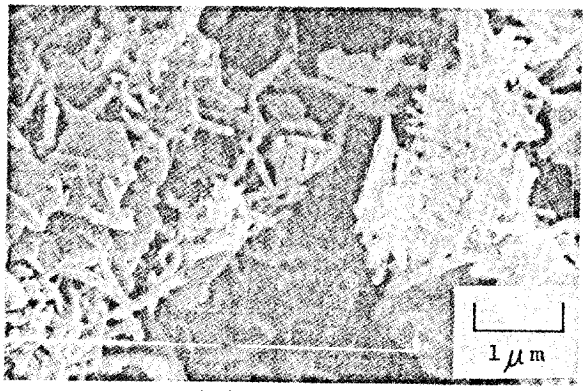

(a)

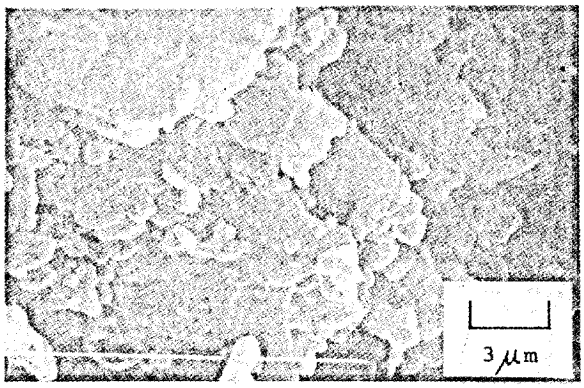

(b)

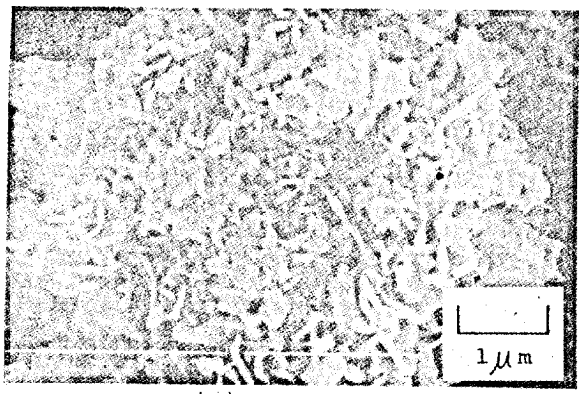

(c)

Fig.8. SEM of C_3A hydrated with addition of $C\bar{S}H_2$ .CH by various hydration time:(W/solid=50).

Mixing ratio against C_3A.			Time
(a) $C\bar{S}H_2$	20wt%		15min
(b) $C\bar{S}H_2$	20wt%		5d
(c) $C\bar{S}H_2$	20wt%,	CH 10wt%	30min

coprecipitate, the concentration of Ca^{2+} and SO_4^{2-} increase slightly again. It is, however,not clear whether this increase in concentration is attributable to the conversion of the ettringite formed immediately after the addition of water into monosulfate or to the formation of a solid solution.

Fig.8(a) and (b) show SEM of C_3A

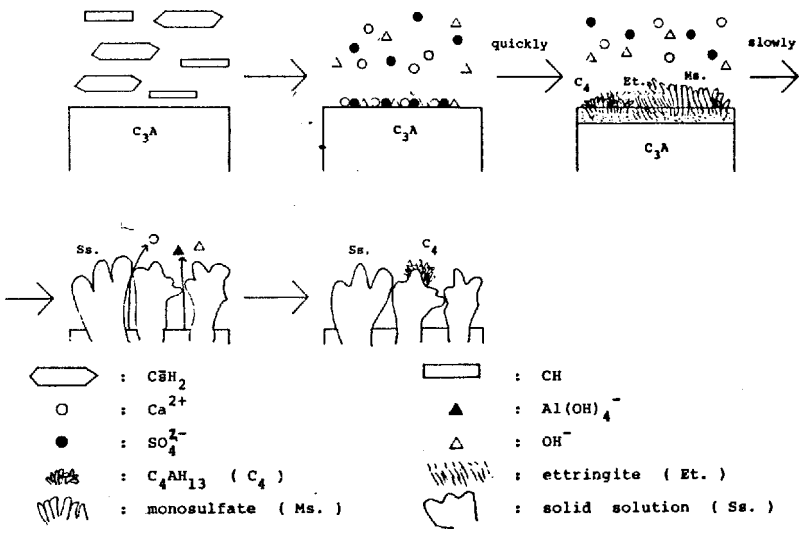

Fig.9. The illustration of C_3A-$C\bar{S}H_2$-CH system hydration process.

hydrated with $C\bar{S}H_2$ for 15 minutes and 5 days, respectively. Fig.8(c) is SEM of C_3A hydrated with $C\bar{S}H_2$ and CH for 30 minutes. Fig.8 shows that the properties of ettrigite and C_4AH_χ formed before the end of the retention period at the highest concentration may differ from those of ettringite and C_4AH_χ formed after the end of the retention time. Before the end of the retention time, ettringite and C_4AH_χ are observed as amorphous acicular ettringite and plate-state C_4AH_χ of card-house structure, respectively. After the end of the retention time, however, they are observed as thick plate-state crystals because of the formation of a solid solution.

The hydration process as described above is schematically shown in Fig.9. Based on this process, the authors would like to propose the following interpretation for the rate of heat liberation shown in Fig.4. Namely, the first peak of the curves corresponds to the start of the formation of ettringite, monosulfate and C_4AH_χ as described in (B) and the second peak corresponds to the start of the formation of a solid solution or the formation of C_3AH_6 in some cases by $C\bar{S}H_2$ and CH as described in (A), respectively.

CONCLUSIONS

The retardation was greatest when both $C\bar{S}H_2$ and CH were present, the authors have recently questioned the role of ettringite in the retardation of C_3A by SO_4^{2-}. Since $C\bar{S}H_2$ and CH is reacted with C_3A, AFt and AFm phases are immediatly formed, the resulting C_3A surface is partly coated by these phase. However, this cause was not essentially on the excessive retardation. Because C_3A is covered by the highest concentration of $C\bar{S}H_2$ and CH, consequently, during this period, the elution of Ca^{2+} and $Al(OH)_4^-$ from its surface has not been able to recognized. Therefore, it is concluded that the hydrates is not produced, and the hydration stops apparently.

REFERENCES

1) P.K.Mehta, J.Am.Ceram.Soc.,56,315-19 (1973).
2) N.Tsuyuki, N.Hirota, T.Miyakawa and J.Kasai, Yogyo-kyokai-shi, 92, 554-61 (1984).
3) N.Tsuyuki, H.Otake, T.Miyakawa and J.Kasai, Yogyo-kyokai-shi, 94, (1986).
4) H.Mori and K.Minegishi, Semento-Gijutsu-Nenpo, XXIX,89-94(1975).

Seishi Goto, Masaki Daimon
(Department of Inorganic Materials,
Tokyo Institute of Technology, Japan)

ION DIFFUSION IN CEMENT PASTE

1. Introduction

The diffusion of ion through hardened cement paste (HCP) takes an important role in the durability of concrete especially in marine construction. When ions penetrate into hardened cement body, the ions sometimes react with hydrates or reinforced steel and the deterioration of concrete will be resulted. A part of the penetrated ions react with hydrates, another part of that ion remains in pore to increase the concentration of pore solution and the rest diffuses into more inner part of HCP. The chemical composition of cement and pporosity of HCP have been discussed in many literatures as main factor which affects to the ion diffusivity in HCP.

The effect of chemical composition of cement on the durability of concrete had been well discussed[1-4]. It is thought that free lime and calcium aluminate hydrates are most undesiarable component for durability of concrete. It is resulted to develop sulfate resisting portland cement and acid resisting portland cement.

The apparent diffusion coefficient (Dap) is affected by the porosity and pore size distribution, because the ions diffuse in pore solution. The pore structure of HCP has been well examed[5-10] by mercury intrusion porosimeter, gas adsorption, permeability, small angle scattering X-ray diffraction and so on. But the discussion of the relationships between pore size distribution and the ion diffusivity is not sufficient[11-14]. Authors[13, 15-16] have shown that there are good co-relations between Dap and the amount of small pore with radius less than 2 nm, even when the hardened body was made from different type of cement or when it was made under different condition such as usual temperature curing or autoclaving. Hughes[14] also suggested that smaller pore may be more important in the consideration of permeability and ion diffusivity.

In this paper, measurement of Cl^- ion diffusivity are mentioned at first. The effects of many factors such as porosity, pore size distribution, chemical composition and ion species on the diffusion are discussed, in the second part. The states of Cl^- ion will also be discussed. We assume two states of Cl^- ion in HCP. One is the Cl^- ion that is in hydrates and the other is that in pore solution.

2. Methods to measure ion diffusivity

There are many mothods to determine the ion diffusivity in HCP ; to measure the depth where the pore solution has a particuler concentration of the diffusing ion[3, 17], to measure the distribution of total concentration of the ion[4, 17, 18], and to determine the amount of diffused ion through a plate of HCP[19, 12].

When HCP sample is immersed in some solution, it is better to seal all except one surface by something such as paraffine (Fig. 1a), because the result of one directional diffusion is easily analyzed mathmatically.

2-1 Colorimetric measurement of Cl^- ion penetrated depth: A sample immersed in a solution is cut parallel to the direction of ion diffusion. A groove is cut with 1-2mm in width on the surface with the same direction of diffusion (Fig. 1b). The groove is painted with aqueous solution of 1% fluorescein sodium salt and aqueous

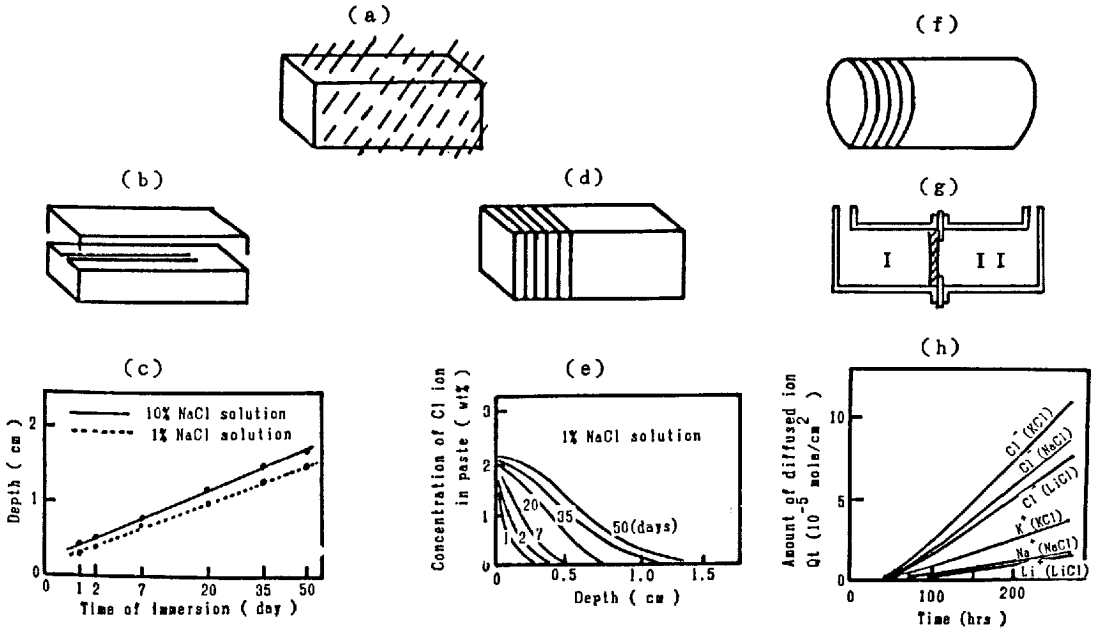

Fig.1 Measurement of ion diffusivity and typical results

Seishi Goto, Masaki Daimon
(Department of Inorganic Materials,
Tokyo Institute of Technology, Japan)

solution of 0. 1N AgNO3. Where the concentration of Cl^- ion is more than a certain value, white crystals of AgCl precipitate. When the concentration is lower than that value, the liquid presents a color of reddish brown. Point where the color changes shows that the pore solution has a concentration of Cl^- ion. The depth of this point from surface contacted with solution during immersion is measured as penetration depth. A typical result is shown in Fig. 1c[17]. We can get a straight line, but the line does not always cross original point, when diffusion proceeds with reaction.

2-2 Analysis with fluorescent X-ray spectroscopy :
A sample immersed in a solution for a period is cut at some distance (Fig. 1d) and make powder to analyse the contents of Cl^- ion by fluorescent X-ray spectroscopy. Total amount of Cl^- ion is measured by this mewthod. A typical result is shown in Fig. 1e[17]. The concentration distribution is almost same as that obeyed to the Fick's law, because the amounts of reacted Cl^- ion with hydrate are roughly proportional to the concentration of pore solution.

2-3 Measurement of the amount of Cl^- ion penetrated through a HCP plate : Fresh paste is degassed by rotary pump just after cement and water mixed, in order to aboid large voids. Cured sample are cut with diamond saw to make plates with 2-3mm in thickness (Fig. 1f). The plate is set in a diffusion cell which is divided to two rooms (Fig. 1g). Room I is filled with solution and room II is filled with distilled water. 25ml of solution is sampled from room II at required time and the same volume of distilled water put back into room II. When n-th sampling had been done at time t, the total amount of Cl^- ion (Qt) diffused thruogh a plate from room I to room II can be calculated as,

$$Qt=(Cn+dV/VII)\cdot\sum_{n=1}^{n-1}Cn\cdot VII$$

where VII is the volume of room II, dV is the volume of sampling at each time. Cn is the concentration of Cl^- ion in the sample. A typical result is shown in Fig. 1h[19]. In the early stage, Qt is not proportional to time, because of unsteady state. But in later stage, the relation betweem Qt and time shows almost strate line. Dap can be calculated from this slope.

3. Effects of ion species and co-exsisting ions[17, 19]

The rate of diffusion of ion in HCP varies with ion species, and is also affected with co-existing ion. Differences in the ion diffusivity of several ion species are shown in Fig. 2, as an example. This is a result obtained by measuring the amount of ion pass through a plate. The solution filled room I of diffusion cell was a mixed solution of LiCl, NaCl and KCl, where the concentration of Li^+, Na^+, $K^+$and Cl^-ion were 1/8-N, 1/8-N, 1/8-N and 1/2-N, respectively. The values of amount of diffused ion in Fig. 2 were calculated as the same concentration for that of bulk solution. There are differences in ion diffusivity in cations and it is clear that anion has larger diffusivity than cations. It is due to the positive charge of hydrates surface, and detailed discussion will be made later.

The rate of diffusion of Cl^- ion in HCP was affected by the co-existing ion, such as Li, Na, K and Mg ion. A result was shown in Fig. 3. This was also a result of the experiment using a plate of HCP and filled room I with each solution of LiCl, NaCl, KCl and MgCl2. The rate of difusion for cation decreases as $K^+>Na^+>Li^+$, but that of Cl^- ion increases as NaCl<KCl<LiCl<MgCL2. When Mg ion attacks HCP, it becomes porous because Mg(OH)2 is precipitates on the surface of HCP and free lime in HCP is desolved. Then the rate oif diffusion of Cl^- ion using MgCl2 solution was largest in these results.

The effect of SO_4^{2-} ion on the concentration distribution of Cl ion are shown in Fig. 4. This is a result of using a block immersed in solution and analysed the concentration distribution with fluorescent X-ray spectrometer. The concentration distribution of the sample immersed in 10% NaCl solution for 35 days and immersed in artificial sea water were similar in the inner parts and that of the samples immersed in 1% NaCl solution for 1 day and artificial sea water for 7 days were similar. But there are much differences in the concentration distribution at the part near the surface. When SO_4^{2-} ion coexisted, the concentration of Cl^- ion near the surface becomes lower with immersing time. It is due to that SO_4^{2-} ion

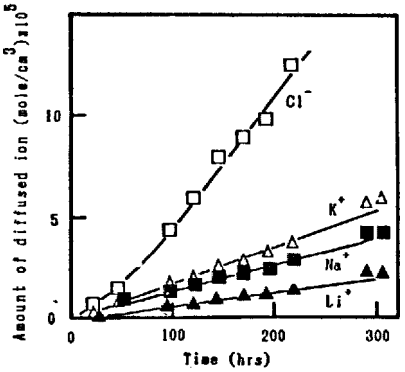

Fig.2 Effect of ion species.

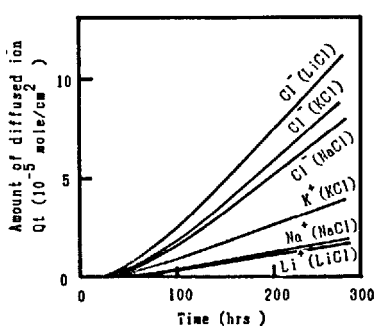

Fig.3 Effect of ion coexisting(1).

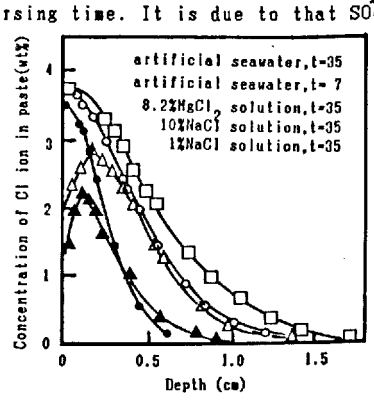

Fig.4 Effect of ion coexisting(2).

Seishi Goto, Masaki Daimon
(Department of Inorganic Materials,
Tokyo Institute of Technology, Japan)

has smaller diffusion coefficient and that calcium alumino sulfate hydrate has lower solbility than that of calcium alomino chloride hydrate.

4 Effect of pore size distribution

4-1. Pore size distribution of HCP[13]

Total porosity (Vt) and bulk density were calculated from the weight of water-saturated and dried sample and the weight in water. The pore volume between 7.5 μm and 7.5 nm measured by mercury intrusion porosimeter (VMIP), and the pore volume between 7.5 nm and 2 nm in radius was measured by N2 gas adsorption (VN2), calculated with Model-less method. Volume of pore with radius under 2 nm (Vs) was calculated from these pore volume.

Mercury intrusion porosimetric pore size distribution indicated that HCP had no pore with radius larger than 430 nm, since it was degassed by rotary pump before molded. Therefore Vs was able to be calculated by the equation of

$$Vs=Vt-(VMIP+VN2)$$

Pore size distribution of HCP are shown in Fig.5. Vt were mainly affected by water/cement ratio, and not by the kinds of cement Vs of PC, BF and SR decreased with the increase of water/cement ratio and with rising of curing temperature. But that of HCP autoclaved has very small volume of V2.

4-2. Relationships between Da and pore size distribution[13]

Dap were measured by the way as mentioned in 2-3. In Fig.6, Dap for ordinally portland cement were plotted with total pore volume. There are low corelationships between them.

Dap for Cl^- ion and Na ion are well correlated with Vs, as shown in Fig.7, even when cement and curing condition changed. Following equations were obtained by least square method.

For Cl^- ion ; log Da =- 6.3Vs - 5.84

For Na^+ ion ; log Da =-13.5Vs - 5.66

It was noticed that Da of Cl^- ion was larger than that of Na^+ ion, and that the gradient of the relation for Na ion was steeper than that of Cl^- ion. This is explained by electric double layer. Surface of the hydrates are positively charged by adsrption of Ca^{2+} ion. Then anion can diffuse in electric double layer but cation can not diffuse in that layer, as shown in Fig.8.

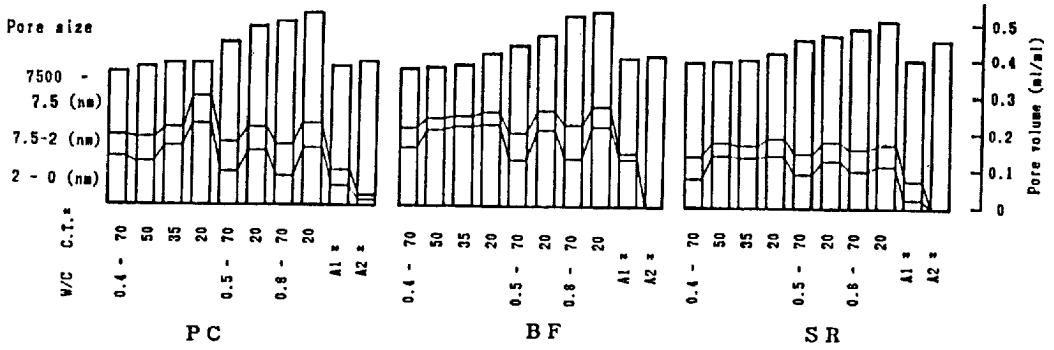

Fig.5 Pore size distribution of portland cement(PC), blastfurnace slag cement(BF) and sulfate resisting portland cement(SR). C.T. : curing temperature(℃), A1 : autoclaved at 180℃ for 3 h, A2 : autoclaved at 180 ℃ for 7 d.

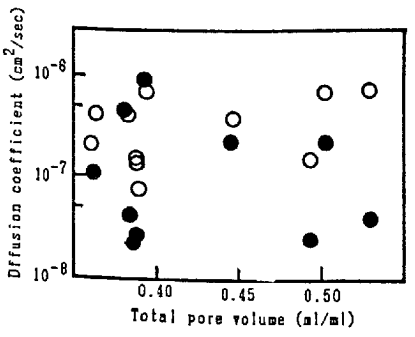

Fig.6 Relationships between total pore volume and apparent diffusion coefficient (Dap). ● Na^+ ○ Cl^-

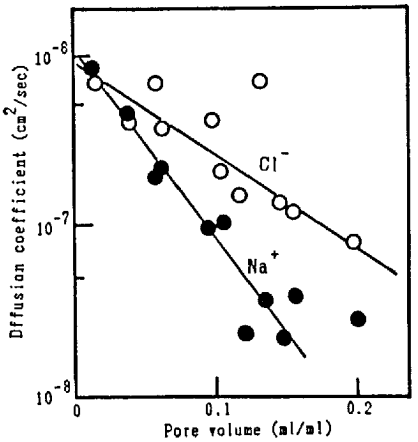

Fig.7 Relationships between pore volume with radius less than 2 nm and Dap.

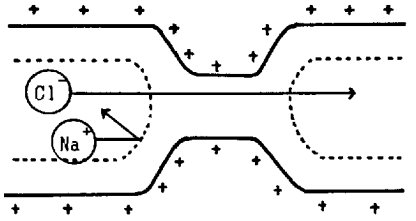

Fig.8 A model of ion diffusion in pore.

Seishi Goto, Masaki Daimon
(Department of Inorganic Materials,
Tokyo Institute of Technology, Japan)

5. Distribution coefficient and total amount of ion in HCP[15]

The amount of soluble ion in HCP and total amount of ion in HCP were measured by using samples which were immersed in the solution for 28 days. Time distribution coefficients between bulk solution and pore solution were calculated from Vt and the amount of soluble ion in HCP. Relationships between distribution coefficient and Vs are shown in Fig.9. The coefficients for Cl^- ion are larger than 1 and increase with Vs. Contrary, those of Na^+ ion are smaller than 1 and decrease with Vs. The surface of hydrates were positively charged because of adsorption of Ca^{2+} ion. And electric double layer could attract anion towards the surface. Then Cl^- ion can easily enter into the micro-pore. The effect of elecric double layer on ion diffusion is mainly due to the changes in distribution coefficient of solution in pore.

Total amounts of Cl^- ion are increased with the concentration in the pore solution as shown in Fig.10. But the total amount of ion has not so good correlation with Vs, because the Al2O3 content of cement is also important factor.

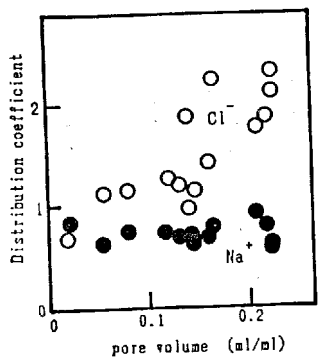

Fig.9 Relationships between distribution coefficient of Na^+ and Cl^- ion and pore volume with radius less than 2 nm.

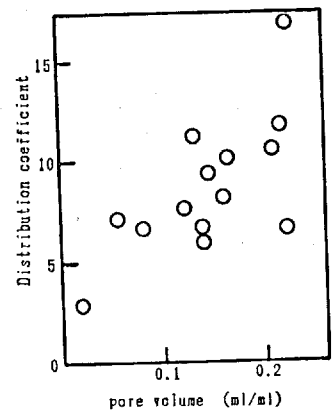

Fig.10 Relationships between distribution coefficient of Cl^- ion and pore volume with radius less than 2 nm.

6. Estimation of ion distribution in HCP[15]

Diffusion of reactive ion in semi infinit body are presented as following equation, which is derived from Fick's 2nd law.

$$Dd^2c/dx^2 = d(c+f(c,t))/dt$$

where f(c,t) is the amount of reacted ion and it is assumed that the reaction is very fast comparing with diffusion and that the amount of reacted ion is proportional to the concentration of solution. Then f(c,t) is presented as αc. Consequently, the ion concentration at position x and time t, CT(x,t), can be obtained as,

$$CT(x,t) = CoT\{1- erf(x/2(Dat/\epsilon kT)^{1/2}\}$$

where CoT is total amount of ion at surface and this is constant. Da is apparent diffusion coefficient. ϵ is total pore volume. kT is distribution coefficient for total amount of ion. In the steady state of diffusion through a plate, relationships among concentration of total ion, concentration of pore solution and concentration of bulk solution are schematically shown in Fig.11.

The ion distribution in HCP can be calculated, by assuming that HCP have been immersed in 1N NaCl solution for 10 years, assuming that HCP samples were

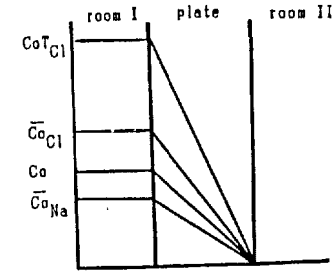

Fig.11 Distribution of ion concentration at steady state.
1: total chloride ion
2: ion in pore solution
3: apparent distribution
4: Na ion in pore solution

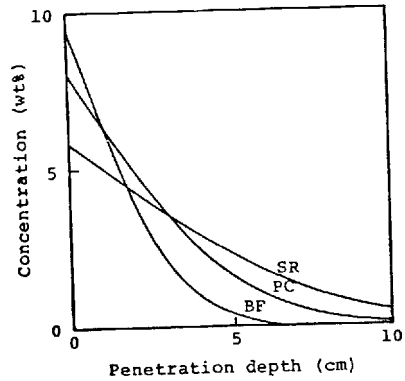

Fig.12 Calculated distribution of ion concentration for PC, BF and SR.

made of PC, BFand SR with water/cement ratio of 0.40, and cured at 35 ℃.

Results are shown in Fig.12. The total amount of Cl^- ion at the surface for BF is highest and that of SR is lowest. But that of BF at inner part is lowest and that of SR is highest. This means that the amount of reacted ion for BF is largest and Da for BF is smallest. This is due to the high content of Al2O3 and the large volume of Vs in BF paste. Contrary, Al2O3 content is lowest and Da is largest in SR paste. Properties of PC are between them. These results are well agreed with the results shown by Gjorv et al[4].

Seishi Goto, Masaki Daimon
(Department of Inorganic Materials,
Tokyo Institute of Technology, Japan)

7. Conclusions

Concerning with ion diffusion in hardened cement paste, many factors such as ion species, porosity, pore size distribution and distribution coefficient of ions were discussed. Ion diffusivity in HCP was measured by many method such as colorimetric method, fluorescent X-ray analysis and a method using thin plate. Pore size distribution was measured by means of mercury intrusion porosimeter and N2 gas adsorption. Pore structure were characterized with a volume of pore with radius less than 2 nm. Distribution coefficient of ion between bulk solution and pore solution and total amount of ion in HCP were also measured. Relationships between the distribution coefficient and pore structure were discussed. Following results are obtained.

1) Ion diffusivity changes with ion species. Anion have larger apparent diffusion coefficient (Dap) than cation. Ion diffusivity is also affected by the ion coexisting.
2) Dap of ions are well correlated to the pore volume with radius less than 2 nm, even when the hardened cement was made from different type of cement and also made under the different conditiuon such as room temperature curing and autoclaving.
3) Distribution coefficient of ion between bulk solution and pore solution is also well correlated to the pore volume with radius less than 2 nm.
4) Composition of cement affects mainly to the total amount of ion in hardened cement paste and the development of pore structure.
5) Finally, the distribution of ion concentration in pastes which had been immersed in NaCl solution for 10 years was calculated from the data of the relation between volume of pore with radius less than 2 nm and apparent diffusion coefficient, distribution coefficient and amount of reacted Cl^- ion. The calculated results has a good agreement with the distribution measured.

References

1)G.L.Kalousek and E.J.Benston, "Mechanism of seawater attack on cement paste", ACI Jour., 67(9),189-192(1970)
2)H.G.Smolczyk, "Chemical reactions of strong chloride-solutions with concrete", Proc.5th Int'l Symp. Chem. Cement, Tokyo 1968, Vol. III, 274-280
3)M.Collepardi, A.Marcialis and R.Turriziani,"The penetration of de-icing agents in cement pastes", Il Cemento, 3/1972, 143-150
4)O.E.Gjorv, O.Vennesland, "Diffusion of chloride ions from seawater into concrete", Cement and Concrete Res., 9, 229-238(1979)
5)R.F.Feldman and H.Cheng-yi, "Properties of portland cement-silica fume pastes. I. Porosity and surface properties", Cement and Concrete Res.,15,765- 774(1985)
6)T.C.Powers, "Physical properties of cement paste", Proc. 4th Int'l Symp. Chem. Cement, Washington,D.C.,1960, Vol.II, 577-613
7)P.K.Mehta and D.Monmohan, "Pore size distribution and permeability of hardened cement paste", Proc. 7th Int'l Cong. Chem. Cement, Paris 1980, Vol. III, VII-1-5
8)B.K.Nyame and J.M.Illston, "Capillary pore structure and permeability of hardened cement paste", Proc. 7th Int'l Cong. Chem. Cement, Paris 1980, Vol.III,VI-181-185
9)S.Goto and D.M.ROY, "The effect of W/C ratio and curing temperature on the permeability of hardened cement paste", Cement and Concrete Res., 11, 575-579(1981)
10)M.Daimon,S.A.Abo-El-Enein,G.Hosaka,S.Goto and R. Kondo, "Pore structure of calcium silicate hydrate in hydrated tricalcium siliate", J. Am. Cer. Soc.,60, 110-114(1977)
11)H.G.Midgley and J.M.Illston, "Effect of chloride penetration on the properties of hardened cement paste", Proc.7th Int'l Cong.Chem.Cement, Paris 1980,Vol.III, VII-101-103
12)C.L.Page,N.R.Short and A.El.Tarras, "Diffsion of chloride ion in hardened cement pastes", Cement and Concrete Res., 11, 395-406(1981)
13)S.Goto, K.Shigeru, T.Takagi and M.Daimon, "Effect of pore size distribution on diffusion of ion through hardened cement paste", Semento Gijutsu Nenpo,36 49-52 (1982)
14)D.C.Hughes, "Sulphate resistance of OPC, OPC/fly ash and SRPC pastes: Pore structure and permeability", Cement and Concrete Res., 15, 1003-1012(1985)
15)K.Shigeru, T.Takagi, S.Goto and M.Daimon, "Diffusion of ion through hardened paste of various cement", Semento Gijutsu Nenpo, 37, 112-116(1983)
16)T.Takagi, S.Goto and M.Daimon, "Diffusion of I ion through hardened cement paste", Semento Gijutsu Nenpo, 38, 78-81(1984)
17)S.Goto, M.Tsunetani, H.Yanagida and R.Kondo, "Diffusion of chloride ion in hardened cement paste", Yogyo-Kyokai -Shi, 87, 126-133(1979)
18)M.Collepardi, A.Marcialis and R.Turriziani,"Penetration of chloride ions into cement paste and concrete", J.Am.Cer.Soc., 55, 534-535(1972)
19)H.Ushiyama and S.Goto, "Diffusion of various ions in hardened portland cement paste", Proc. 6th Int'l Cong. Chem. Cement, Moscow 1974, Vol.II-1, 331-337

Stefania Grzeszczyk
Institute of Cementing Building Materials
45-641 Opole, Oświęcimska 21, Poland

C_3A-Na_2O solid solutions in pseudo-two-component system NC_8A_3-C_3A

P

SUMMARY: It was indicated in the paper that sdlid solutions are formed in the pseudo-two-cpmponent NC_8A_3-C_3A system, the symmetry of which is similar with the symmetry of Na_2O solid solutions in C_3A containing comparable quantities of sodium. It was confirmed that NC_8A_3 compound can not be synthesized out of reaction mixture whose composition corresponds to its stoichiometry. The value of η ratio between intensities of diffractions lines for which d= 1.889 Å and 1.916 Å found on X-ray diffractograms of solid solutions in pseudo-two-component system NC_8A_3-C_3A and solid solutions Na_2O in C_3A changes proportionally to the changes of sodium content in the structure of C_3A, and may constitute the criterion in distinguishing the polymorphic modifications of solid solution Na_2O in C_3A.

INTRODUCTION

According to currently assumed research results concerning C_3A-Na_2O solid solutions, the content of sodium equal to 5.7 % by wieght concentration of Na_2O constitutes the solubility limit of sodium in C_3A [1]. The presence of Si^{+4} ions increases the range of solubility of Na_2O in C_3A. In this case it is possible for the solid solution to form itself as NC_8A_3 [2] There were attempts aiming at synthesizing pure phase of NC_8A_3, but these produced no satisfactory results [3, 4]. The final product of the reaction usually contained small quantities of free CaO [4].

This paper presents results of the research on synthesizing NC_8A_3 phase as well as on solid solutions in pseudo-two-component system NC_8A_3-C_3A.

EXPERIMENTAL

The synthesis of NC_8A_3 compound was carried out in welded crucibles at 1400°C for 20 hrs, and at 1475°C for 5 hrs - similarly as in other works [4, 5]. Before, the reaction mixture corresponding to stoichiometric composition of NC_8A_3 phase containing an excess of Na_2O subjected to repeated thermal treatment at 1000°C until the moment the mixture contained 7.6 % by weight concentration of sodium. The synthesis product obtained at 1400°C contained 1.8 % by weight concentration of free CaO, whereas the one burnt at 1475°C contained considerable quantities of CaO and sodium aluminate NA.

For the experimental study of solid solutions in pseudo-two-component system NC_8A_3-C_3A, the NC_8A_3 phase was used and synthesized at 1400°C.

The synthesis of pseudo-two-component systems NC_8A_3 was carried out at 1300°C for 2 hrs. The following systems were subject of synthesis: NC_8A_3 and $0.5C_3A$, NC_8A_3 and C_3A, NC_8A_3 and $2C_3A$, NC_8A_3 and $3C_3A$ and NC_8A_3 and $4C_3A$. Additionally, the synthesis of sodium oxide solid solutions in tricalcium aluminate was performed. The syntheses consisted in roasting the tricalcium aluminate mixture together with appropriate additions of sodium carbonate at 1250°C The synthesized solid solutions contained the following quantities of sodium in C_3A: 1.8, 3.5, 4.2, 5.2, 5.7 % by weight concentration of Na_2O.

Stefania Grzeszczyk
Institute of Cementing Building Materials
45-641 Opole, Oświęcimska 21, Poland

C_3A-Na_2O solid solutions in pseudo-two-component system NC_8A_3-C_3A

RESULTS AND DISCUSSION

The identification research of synthesized compounds was performed by means of absorption infrared spectroscopy and X-ray diffraction. The infrared spectrum of synthesized NC_8A_3 phase is identical with the spectrum of C_3A-Na_2O solid solution sample containing 5.7 % by weight concentration of Na_2O. Fig.1 shows the infrared spectra of reaction mixtures samples of NC_8A_3 and C_3A compounds, Fig. 2 shows the spectra of synthesized systems of these compounds.

The analysis of infrared spectra of mixtures of NC_8A_3 and xC_3A compounds indicated that on synthesizing the mixtures of compounds where x equals 0.5, 1, 2 and 3 there is a monoclinic compound whose spectrum is identical with the spectrum of C_3A-Na_2O solid solution sample containing 5.7 % Na_2O in C_3A [6]. The spectra of these samples have their bands situated at 483, 513, 533, 720, 790, 867 and 923 cm^{-1}, with the increase of C_3A contet, however the intensity of these bands decreases.

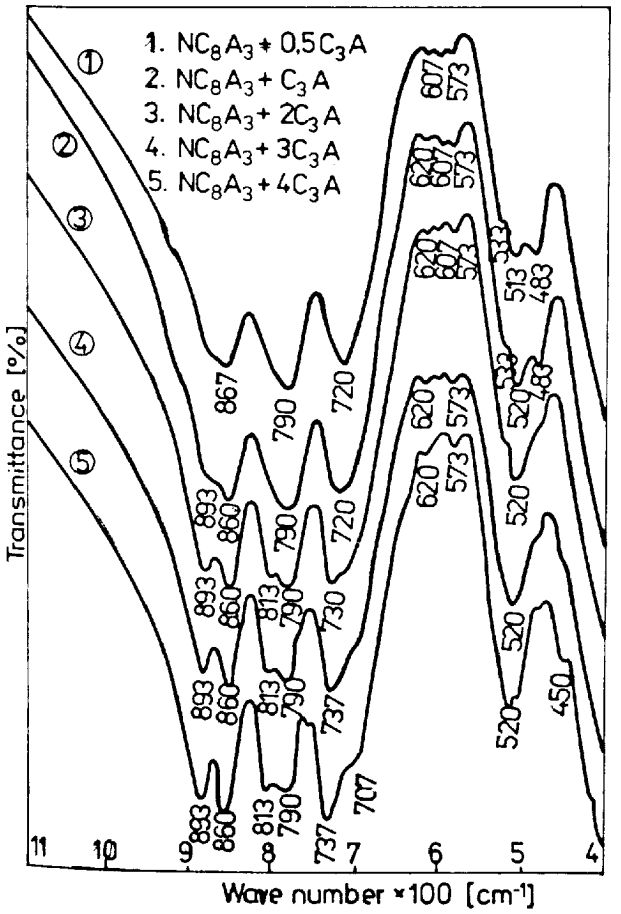

Fig. 1 Infrared spectra of mixture samples of NC_8A_3 and C_3A compounds.

The analysis of spectra of reaction mixtures samples of NC_8A_3 and xC_3A where x equals : 0.5, 1, 2, 3 and 4 indicated that proportionally to the increase of C_3A content in the mixtures, the spectra reveal the appearance and increase of intensity lines characteristic of this compound 520, 737, 813, 860 and 893 cm^{-1}. Alongside there is a decrease of intensity and disappearance of lines characteristic of synthesized phase NC_8A_3.

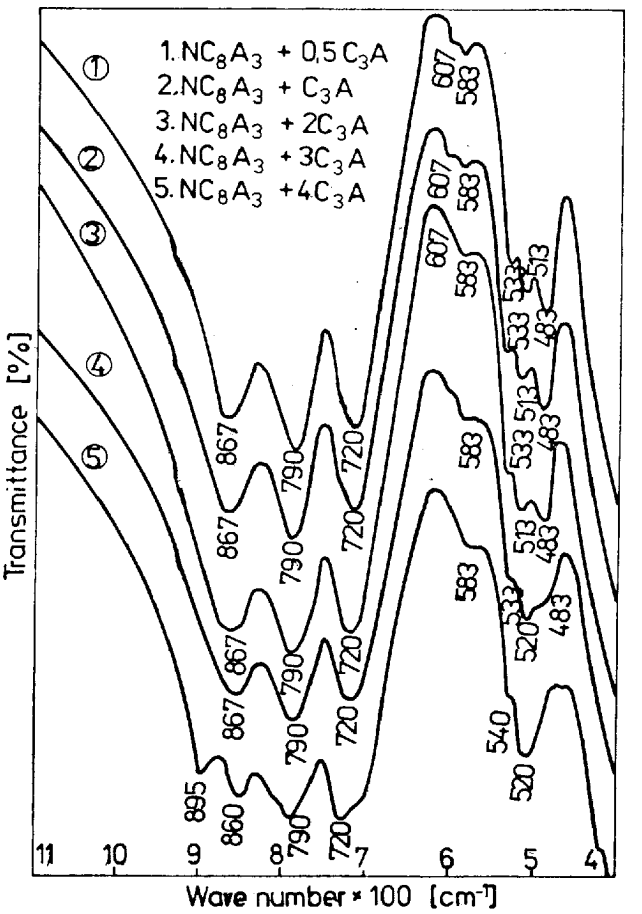

Fig. 2 Infrared spectra of samples of synthesized systems of NC_8A_3 and C_3A compounds.

The spectrum of NC_8A_3 and $4C_3A$ compounds mixture, apart from the bands characteristic of monoclinic modification of solid solution C_3A-Na_2O, also reveals characteristic bands of regular C_3A located at wave frequencies 520, 860 and 893 cm^{-1}.

The X-ray analysis of synthesized mixtures of NC_8A_3 and xC_3A compounds where x= 0.5, 1, 2, 3 and 4 indicated that X-ray diffractograms of the samples for which x= 0.5, 1, 2 and 3 are qualitatively similar to each other

Stefania Grzeszczyk
Institute of Cementing Building Materials
45-641 Opole, Oświęcimska 21, Poland

and reveal lines whose values are characteristic of the orthorhombic and monoclinic phase of solid solution C_3A-Na_2O [6].
It was also observed that as C_3A increases in the burnt compound mixture, i.e. when $x \longrightarrow 3$, the sample X-ray diffractograms reveal a decrease of intensity of lines whose value equals d= 1.889 Å in comparison with the intensity of the lines whose value equals d= 1.918 Å.

The values of η ratio between the intensities of diffraction lines for d= 1.889 Å and d= 1.916 Å for synthesized compounds are given in Table 1.

Table 1.

Values of η ratio between intensities of diffraction lines for d= 1.889 and d= 1.916 Å for NC_8A_3 and C_3A systems.

Stoichiometric composition of NC_8A_3 and C_3A compounds	Ratio values η	Sodium content [% wt]
$NC_8A_3+0.5C_3A=NC_{9.5}A_{3.5}$	0.57	6.5
$NC_8A_3+C_3A = NC_{11}A_4$	0.51	5.7
$NC_8A_3+2C_3A = NC_{14}A_5$	0.50	4.6
$NC_8A_3+3C_3A = NC_{17}A_6$	0.45	3.8
$NC_8A_3+4C_3A = NC_{20}A_7$	-	3.3

The research performed using infrared spectroscopy and X-ray diffraction indicated that following the reaction taking place in the pseudo-two-component system NC_8A_3 and xC_3A, there emerges a solid solution whose symmetry is similar to the symmetry typical of C_3A — Na_2O solid solution containing camparable quantities of sodium. It is worth noting that η ratio values are similar in the case of tested solid solutions Na_2O in C_3A and NC_8A_3 and C_3A compounds system, in which the percentage of Na_2O are similar.

Thus, for the tested pseudo-two-component system NC_8A_3 and C_3A containing 3.8 % Na_2O the value of η equals 0.45, whereas for the solid solution Na_2O in C_3A containing 3.3 % Na_2O η equals 0.41. For the systems NC_8A_3 and C_3A containing 5.7 % Na_2O the value of intensity of diffraction lines is 0.51, whereas for solid solution Na_2O in C_3A containing 5.2 % Na_2O the η value is 0.50.

Additionally to that, the research proved that is the tested system NC_8A_3 and $4C_3A$ apart from orthorhombic and monoclinic modification of C_3A-Na_2O solid solution, there is a presence of regular C_3A.

CONCLUSIONS

It was indicated in the paper that solid solutions are formed is the pseudo-two-component NC_8A_3-C_3A system, the symmetry of which is similar with the symmetry of Na_2O solid solutions in C_3A containing comparable quantities of sodium.

It was confirmed that NC_8A_3 compound can not be synthesized out of reactions mixture whose composition corresponds to its stoichiometry.

The value of η ratio between intensities of diffraction lines for which d= 1.889 Å and 1.916 Å found on X-ray diffractograms of solid solutions in pseudo-two-component system NC_8A_3-C_3A and solid solutions Na_2O in C_3A changes proportionally to the changes of sodium content in the structure of C_3A, and may constitute the criterion in distinguishing the polymorphic modifications of solid solution Na_2O in C_3A.

REFERENCES

1. M.Regourd, S.Chromy, L.Hjorth, B.Mortureux, E.A.Guinier : Polymorphysme des solides du Sodium dans L'Aluminate Tricalcique. Jornal of Applied Cryst., 6 , 355-364, 1973.

2. I.Maki : Nature of the prismatic darc interstitial material in portland cement clinker. Cem. Concr. Res., vol. 3, No 3, 295-313, 1973.

3. J.A.Conwicke, D.E.Day : Crystalline Solubility of Soda in Tricalcium Aluminate. J. Am. Ceramic Soc., 47 , No 12, 654-655, 1964.

4. A.I.Boikowa, W.A.Paramonowa, A.I.Domański: Sostaw i gidratacjonnaja aktywnost aljuminatnoj fazy klinkiera. Cement, 8 , 20-22, 1976.

5. Y.Suzukawa: Die Alkaliphasen im Portlandzement. Part I: Die Natriumphase. Zement-Kalk-Gips, 8 , 345-351, 1956.

6. S.Grzeszczyk: Influence of sodium on phase composition and hydratation activity of calcium aluminates and Portland cement clinker. /In Polish/, Raport PRE 6/83, 126, Technical University of Wrocław, Wrocław, 1983.

W. BRYLICKI, University of Mining and Metallurgy, Cracow, Poland

PHASE COMPOSITION AND MORPHOLOGY OF AUTOCLAVED γC_2S CONTAINING PASTES

P

1. INTRODUCTION

There is a commonly known opinion that under the normal conditions of hydration, γC_2S essentially does not reveal its binding properties /1/. Though the change of the isobaric-isothermal potential ΔG_{298} of hydration reaction γC_2S have a negative value /-2.91 kJ/mol according to /2/, /-5.82 kJ/mol according to /3/ /, kinetics of hydration is low and does not have an essential meaning for technology. However, the observed lack of binding properties of γC_2S under the normal conditions is caused only by kinetic factors. Changing the hydration conditions, e.g. increasing the temperature and pressure in the reaction medium causes the increasing of γC_2S hydration capacity /4, 5/. According to the prevalent opinion of many investigators, during the hydration of γC_2S under hydrothermal conditions the following compounds are created : hydrated calcium silicates with the structure derivative from γC_2S /kilchoanite, phase "P" and calcium chondrodite/ /6, 7, 8, 9/. The investigations on hydration of slurry containing γC_2S in autoclaved mixtures of C/S molar ratio less than 2 proved /6, 7, 10, 11, 12, 13, 14, 15/ that addition of SiO_2 to γC_2S under the appropriate conditions makes it possible to synthesize almost all hydrated calcium silicates existing in the CSH system. G.L. Kalousek /16/ synthesized hydrated calcium silicates from the mixtures γC_2S-SiO_2-H_2O of molar ratio C/S = 0.83 in the presence of 0 - 8% Al_2O_3 as hydrargillite and obtained the phase CSH$_I$ and 11.3 Å tobermorite. The investigations carried out by Kurbus and Jelenic /17/, as well as Kalousek /16/ showed that in the presence of CO_2 in autoclaved mixtures γC_2S-SiO_2-H_2O of molar ratio C/S < 2, some amounts of scawtite were created very easily. During the production of alumina by the Grzymek sintering-selfdisintegrating method, after the extraction of calcium aluminates with 6% sodium carbonate the solid post-extraction residue containing mainly γC_2S is formed from the selfdisintegrating sinter /18/. Except for γC_2S and traces of βC_2S this residue called the postextraction slurry obtained under the industrial conditions contains also $CaCO_3$ - calcite, alkalies, residual aluminates and calcium aluminoferrite and other components. The paper presents the results of the investigations of γC_2S hydration, the model-synthetic post-extraction slurry and industrial slurry "Groszowice", from which the mixtures of different molar ratios were prepared.

2. DESCRIPTION OF EXPERIMENT.

2.1. The preparation of the initial substances.

γC_2S /sample A/ was synthesized from calcium carbonate /pure for analysis/ and silica gel /pure for analysis/. The right course of the synthesis was checked by the chemical, X-ray and infra-red spectroscopic analyses, as well as by the determination of the content of unbound CaO with the Frankie method /CaO_w = 0.108% by weight/. The fineness degree of γC_2S mesured by specific surface with the use of the Blaine device was 8200 cm^2/g. To obtain the synthetic-model post-extraction residues the following selfdisintegrating sinters were synthesized under the laboratory conditions : CaO-SiO_2-Al_2O_3 /calculated phase composition: C_2S - 70.86%, $C_{12}A_7$ - 29.14%/ - sample B and CaO-SiO_2-Al_2O_3-Fe_2O_3 /calculated phase composition : C_2S - 67.25 %, $C_{12}A_7$ - 26.67%, C_4AF - 6.08 %/ - sample C. The right course of the synthesis was checked by the methods of chemical, X-ray and microscopic analyses, using the scanning electron microscope. The sample of γC_2S and dust obtained during the disintegration of the selfdisintegrating sinters B and C were submitted to the 3-stage extraction with the use of soda aqueous solution ; concentration 60 g Na_2CO_3 per liter. The extraction were the same as the industrial ones. In this way, the synthetic post-extraction residues A', B' and C' were obtained, Moreover, the sample of the industrial post-extraction slurry "Groszowice" was taken and denoted as G. The phase chemical composition was determined by the RTG, DTA, DTG and TG methods, as well as morphology of the extraction products with the use of the scanning electron microscope. Table 1 presents the results of the chemical analysis of the initial samples.

On the basis of the phase composition analyses carried out by the above-mentioned methods and the accepted simplifying assumptions, the approximate quantitative phase composition of the initial substances was determined. The calculated phase composition is shown in Table 2.

The substances A, A', B', C and G were used to prepare the mixtures of different molar ratios C/S = 2.0 ; 1.0 ; 0.83; 0.60, where the ratio quantity C/S was corrected only on the basis of the calculated content of γC_2S. In the case of the samples A, A', B' and C' the ground quarz sand of high purity /99.6% SiO_2, specific surface according to Blaine - 5500 cm^2/g/ was used to correct the molar ratio quantity C/S, As far as the same correction is concerned in the post-extraction slurry "Groszowice" - sample G, the waste silica dust was used. It came from "Łaziska" plant and contained mainly β quarz, its specific surface determined by the BET method was 17.500 cm^2/g and chemical composition : SiO_2 - 93.20% ; Fe_2O_3 - 2.50% ; Al_2O_3 - 1.30% ; CaO - 1.75%; MgO - 1.20%.

The prepared initial substances A, A', B', C' and G were dry mixed with the appropriate amounts of silica additives in the planetary agate mill /produced by Fritsch Co./ during 4 hours. The homogenized mixtures were wetted with 5% distilled water and after mixing pressed into pellets under the pressure 30 MPa. The samples of the powdered slurry were put in the laboratory autoclaves, then into the laboratory drier. The temperature in the autoclaves was increasing simultaneously with the temperature in the drier. The required temperature 200°C in the drier was reached within 2 hours. When the isothermal cycle of heating was over /8, 12, 24 and 36 hours, respectively/, the autoclaves were put out of

P

Table 1

Determined component	$\alpha'C_2S$ - sample A /%/	Extracted $\alpha'C_2S$ - sample A' /%/	Extracted dust, composition C-A-S -sample B' /%/	Extracted dust, composition C-A-S-F -sample C' /%/	Post-extraction slurry "Groszowice" - sample G /%/
CaO	66.80	59.60	57.90	55.40	53.59
SiO_2	33.20	26.40	23.30	21.50	21.00
Al_2O_3	-	-	2.2	1.90	5.76
Fe_2O_3	-	-	-	1.60	1.95
Na_2O	-	0.90	0.73	1.13	0.85
K_2O	-	-	-	-	0.24
MgO	-	-	-	-	0.81
SO_3	-	-	-	-	0.49
ignition loss	-	12.90	14.40	17.25	15.10
total	100.00	99.90	98.53	98.78	99.79

Table 2

Phase comp.	A /%/	A' /%/	B' /%/	C' /%/	G /%/
$\alpha'C_2S$	100	91	71	70	65
$CaCO_3$	-	6	22	23	12
$Na_2SiO_3 \cdot 6H_2O$	-	3	2	2	2.5
$C_{12}A_7$	-	-	4	4	4
$C_3A.0.4S.4.7H$	-	-	-	-	10
$C_3A.CaCO_3.12H$	-	-	-	-	.5
total /%/	100	100	99	99	98.5



Fig. 1 - SEM. The post-extraction residue C, /enlarged 3000 X/.



Fig. 2 - SEM. The post-extraction slurry "Groszowice" G /enlarged 3000 X/.

the drier and cooled in the air. Then the samples of slurry were flooded with acetone what interrupted further hydration. The samples of slurry assigned for rentgenographic and thermal analyses were rubbed with acetone, while the samples for scanning electron microscope were in the shape of lumps. When hydration was stopped, the samples were treated with ether and dried in the vacuum drier at 65° C to the constant mass. The samples of hydrated slurry were kept in weighing vessels sealed up with stearin.

2.2. Testing equipment.

The diffractional determinations were accomplished by the Debay-Sherrer-Hull powder method by means of the diffractometer of the type TUR-61 /prod. People's Republic of Germany/ and Philips /The Netherlands/. In all measurements C_uK_α radiation and nickel filter were used. The thermal tests were

W. BRYLICKI, University of Mining and Metallurgy, Cracow, Poland

P

Table 3

C/S	2.0					1.0				
Time /h/	A	A'	B'	C'	G	A	A'	B'	C'	G
8	γC_2S P	γC_2S Ca,P Ch,Sk αC_2SH	γC_2S Ca,P Ch,T $C_{12}A_7$	γC_2S Ca,P Ch,T $C_{12}A_7$	γC_2S Ca,H $C_{12}A_7$ UKs	γC_2S K,Ks P	γC_2S K,Ca T,P Sk	K,Ca T,G Sk UKs	K,Ca T,G Sk UKs	γC_2S K,Ca H,T,G Sk
12	P Ch	γC_2S Ca,P Ch,Sk αC_2SH	γC_2S Ca,P Ch,T $C_{12}A_7$	γC_2S Ca,P Ch,T $C_{12}A_7$	γC_2S Ca,H $C_{12}A_7$ UKs	Ks,K Ch	Ca T,Sk FB UKs	K,Ca T,Sk UKs	K Ca T,Sk UKs	γC_2S K,Ca H,T Sk
24	P Ch	Ca P,Ch Sk αC_2SH	Ca P,Ch T $C_{12}A_7$	Ca P,Ch T $C_{12}A_7$	γC_2S Ca,H P,Ch UKs	Ks K Ch	Ca T,Sk UKs FB	Ca T,Sk UKs	K,Ca H,T Sk G	K,Ca H,T Sk G
36	P Ch	Ca P,Ch Sk αC_2SH	Ca P,Ch T,Sk $C_{12}A_7$	Ca P,Ch T,Sk $C_{12}A_7$	Ca H,P Ch Sk	Ks K Ch	Ca,T Sk UKs FB	Ca,T Sk UKs	Ca,T Sk UKs	Ca H T Sk

Table 4

C/S	0.83					0.60				
Time /h/	A	A'	B'	C'	G	A	A'	B'	C'	G
8	Ks K,T Sk	γC_2S K,Ca,T Sk,UKs	T,Sk K,Ca UKs	T,Sk K,Ca UKs	γC_2S K,Ca T,H	K,Sk Ks,G	γC_2S, K,Ca UKs	γC_2S K,Ca UKs	γC_2S K,Ca UKs	γC_2S K,T,H Ca,UKs
12	Ks,T Sk,K G	K,Ca T,Sk UKs	K,Ca T,Sk UKs	K,Ca T,Sk UKs	K,Ca,T G,Sk,H UKs	K,Ks G,Sk	K,G Ca,Sk UKs	γC_2S K,Ca T,UKs	γC_2S K,Ca T,UKs	K,Ca T,Sk H,UKs
24	Ks,T Sk,K	K,Ca T,Sk UKs	K,Ca T,Sk UKs	K,Ca T,Sk UKs	K,Ca T,Sk H,UKs	K,Ks G,Sk	K,G Ca,Sk UKs	K,Ca T,Sk UKs	K,Ca T,Sk UKs	K,Ca T,Sk UKs
36	Ks,T Sk,K	K,Ca T,Sk UKs	K,Ca T,Sk UKs	K,Ca T,Sk UKs	K,Ca T,Sk H,UKs	K,Ks G,Sk	K,G Ca,Sk UKs	K,Ca T,Sk G,UKs	K,Ca T,Sk G,UKs	K,Ca T,Sk H,UKs

carried out with the use of "Derivatograph" type OD-102 of the Paulik-Erdey system, made in Hungary. The testing of the texture and morphology of hydration products was accomplished by the scanning electron microscope Jeol, type IXA-50A, Japanese production and British, type Cambridge. The observations were made with 1000 - 30.000 enlargement.

3. THE TESTING RESULTS AND DISCUSSION.

In Table 3 and 4 the results of the phase composition tests for slurry of different molar ratios C/S were presented. The results were obtained by the diffractional and complex thermal methods. The Table comprises the following symbols : P - phase "P", Ch - - calcium chondrodite, Sk - scawtite, T - - tobermorite 11.3Å, UKs - hydrated sodium silicate, H - hydrogarnet, Ks - ksonotlite, K - quarz, FB - Bezjak "3, 15" phase, G - - gyrolite, Ca - $CaCO_3$.

Pure γC_2S, which is the component of the pastes of different molar ratios undergoes the total analysis after 12 hours resulting with the formation of the phase "P" and calcium chondrodite /C/S = 2/, ksonotlite /C/S = 1/, the mixture of ksonotlite and tobermorite 11.3Å /C/S = 0.83/, and the mixture of ksonotlite and gyrolite /C/S = 0.60/. The presence of Na^+ ions and particularly Al^{3+} ions in the substances A', B', C' and G independently of the C/S quantity strongly influences the stabilization of the tobermorite phase, which remains the main component of the examined pastes. In the presence of calcite in the pastes of C/S = 1.0 ; 0.83 and 0.60, a big amount of scawtite phase is formed. Simultaneously with the increase of shares of $CaCO_3$ and other components of the post-extraction slurry, e.g. hydrogarnets, the rate of hydrolysis and hydration of γC_2S decreases. It is particularly evident in case of the industrial slurry "Groszowice". The reason for the delayed hydration of γC_2S lies in the precipitation of the secondary calcite and other products of the extraction of calcium aluminates with the soda solution on γC_2S grains, which makes it difficult for water to reach them and decreases the reaction surface. It is visible particularly on the photographs 1 and 2. The carried out investigation revealed that the slurry "Groszowice" may be used to obtain insulating and insulating-constructional materials of the tobermorite and scawtite composition.

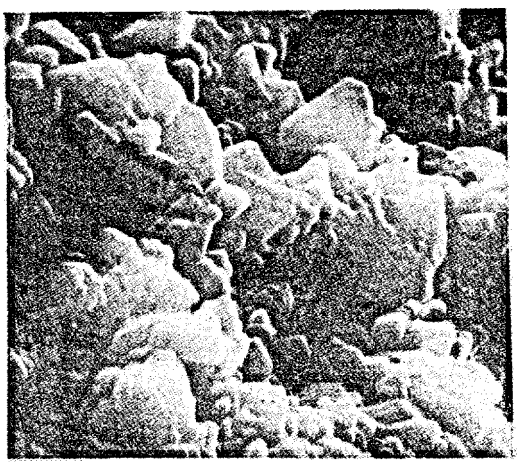

Fig. 3 - SEM. The pastes autoclaved for 12 hours, sample A, temp. 200°C, C/S = 2. Enl. 6000 X.

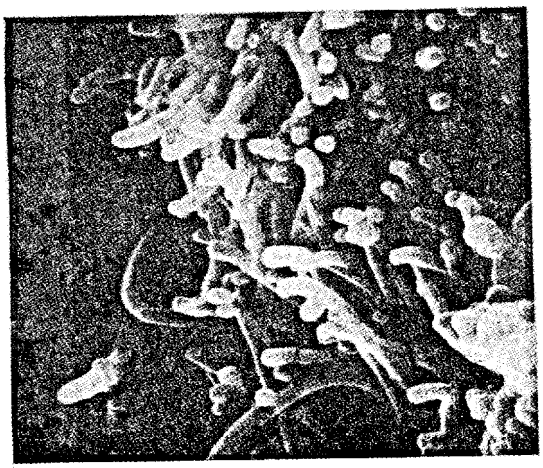

Fig. 4 - SEM. The pastes autoclaved for 12 hours, sample A, temp. 200°C, C/S = 1, Enl. 6000 X.

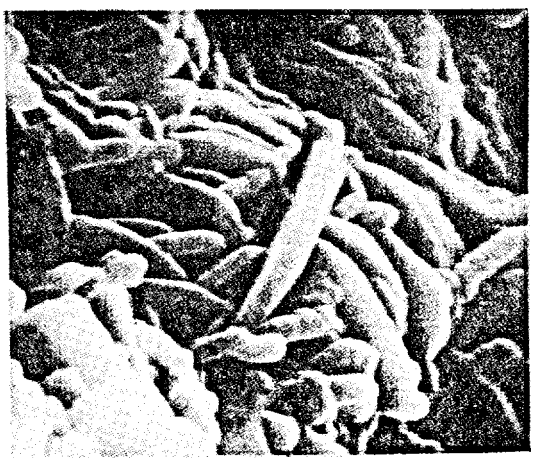

Fig. 5 - SEM. The pastes autoclaved for 8 hours, sample G, temp. 200°C, C/S = 1. Enl. 11 000 X.



Fig. 6 - SEM. The pastes autoclaved for 12 hours, sample A, temp. 200°C, C/S = 0.83. Enl. 10 000 X.

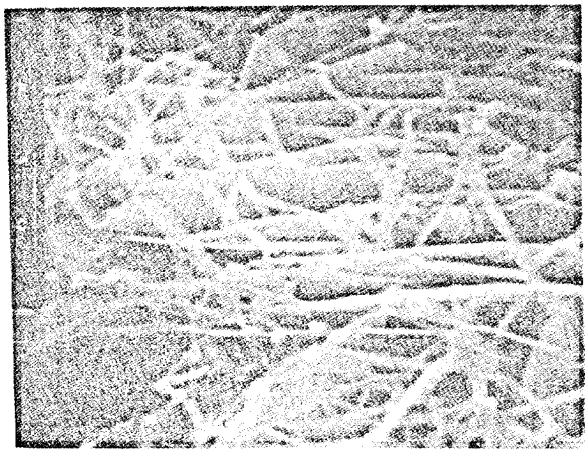

Fig. 7 - SEM. The pastes autoclaved for 12 hours sample G, temp. 200°C, C/S = 0.83. Enl. 10 000 X.

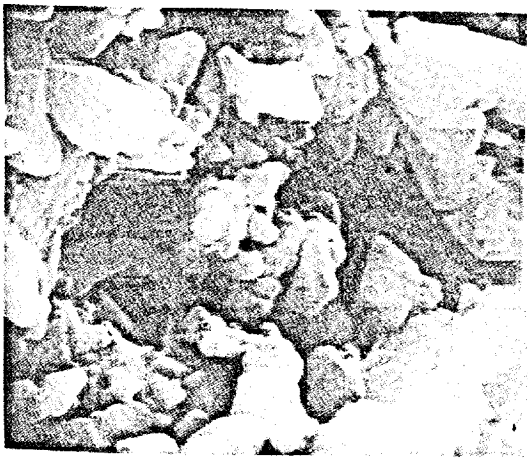

Fig. 8 - SEM. The pastes autoclaved for 12 hours sample A, temp. 200°C, C/S = 0.60. Enl. 5500 X.

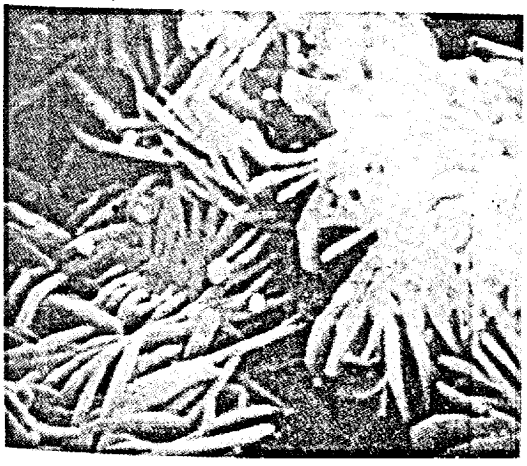

Fig. 9 - SEM. The pastes autoclaved for 12 hours, sample G, temp. 200°C, C/S = 0.60. Enl. 6400 X.

The observations of the pastes accomplished by means of electron scanning microscope revealed the essential differences in morphology of the products of γC_2S hydrolysis and hydration. In the pastes prepared from pure γC_2S /C/S = 2/ the presence of calcium chondrodite and phase "P" in plate forms was discovered. Their morphology confirms their close affinity with γC_2S. Ksonotlite obtained in the paste of molar ratio C/S = 1.0 crystallizes in the shape of long thin fibres /Fig. 4/, rather not typical and essentially different from ksonotlite crystals in the paste of C/S = 0.83 /Fig. 6/. In the paste of molar ratio C/S = 0.6 the typical plate crystals of gyrolite phase are visible /Fig.8/ Essentially different phase composition of the pastes A', B', C' and G causes that the tobermorite phase predominates on the photographs /Fig. 5, 7 and 9/. Apart from this phase, needle-shaped crystals covering tobermorite crystals are visible /Fig. 7/.

4. BIBLIOGRAPHY

1. H.F.W. TAYLOR, The chemistry of cements" Academic Press. London, New York 1964.
2. O.P. MCZEDŁOW-PETROSJAN and W.I.BABUSZKIN, 6th Int. Congr.on the Chem. of Cem. Part II/I 6-16, Moscow 1974.
3. J.M. BUTT and W.I. KAUSZANSKIJ, Nieorg. Mat. t. 10 nr 5/1974 p.947-948 /rus/.
4. M.M. SYCZEW, W.I. KORNIEJEW, E.N. KAZANSKAJA and J.N. MIEDWIEDIEWA, Journ.Prikł. Chim.3, 1973, p. 502-506 /rus/.
5. W.I. KAUSZANSKIJ, Journ. Prikł.Chim.8,1977 p. 1688-1692. /rus/.
6. T. MITSUDA and A. FUKUO, Min. Jour. Vol. 6 Nos 1/2 p. 17-35.
7. K. SPEAKMEN, H.F.W. TAYLOR, J.M. BENNETT and J.A. GARD, J.Chem.Soc. /A/, p. 1052--1060, 1967.
8. H.F.W. TAYLOR, 6th Int. Congr.on the Chem. of Cem. Moscow 1974, Part II/I p.192-207.
9. H.F.W. TAYLOR and D.M. ROY, 7th Int.Congr. on the Chem. of Cem., Paris 1980 s. II-2/2 - II 2/13.
10. J. JERNEJCIC and J. JELENIC, Int. Symp. Aut. Build. Mat. Utrecht 1973, Moscow, 1974, p. 135-146 /rus/.
11. J. JELENIC, J. JERNEJCIC and B. KORBUS, Vest. slov.kem.drustwa XVIII, nr 1-4, 1971 p. 43.
12. A. BEZJAK, Int.Symp.Aut.Build.Mat. Utrecht 1973, Moscow, 1974 p. 124-132.
13. A. BEZJAK, J. JELENIC and J. JERNEJCIC, Nature 248, 1974 Vol. 3 p. 581-582.
14. G.L. KALOUSEK and E.B. NELSON, Cem. Concr. Res. 8, 1978, p. 283-290.
15. K. LUKE, H.F.W. TAYLOR and G.L. KALOUSEK, Amer.Ceram.Soc.Bull. 59, 1979, p.334.
16. G.L. KALOUSEK, Cem. and Concr. Res. 6, 1976, p. 417-418.
17. B.KURBUS and J. JELENIC, Cement /Zagreb/ Br 2/1980-81, p.126-127.
18. J. GRZYMEK, Mat. Sci. Acad.Min. and Met. Cracow, Poland, Cer. Mat.nr 247-part.14, 1969, p. 191-211.

M.Dr.Eng. IOAN COTEA, Dr.Eng.D.PUSCASU, Dipl.Eng.D.NICOLAU

RESEARCH AND DESIGN INSTITUTE FOR BINDER AND ASBESTOS CEMENT INDUSTRY,ROMANIA

Contributions to the clinker grindability physics.

Les contributions à la physique de broyage du clinker.

1. Introduction

The problem of the clinker composition relationship has been studied by many researchers (1), (4), (5), (6), the results obtained being partly contradictory or non-comparable due to the criterion chosen as grindability measurement (work index, Zeisel method etc.)

In this paper, the authors present the results obtained at the trial of the clinker grains by quasistationary (slow) compression, a way of approach presented in previous papers as well (2), (3).

2. Experiments and work methods

Two sorts of clinker have been chosen; these two sorts have different chemical and mineralogical composition (table 1); they have been divided into granulometric classes. The grains, (of a shape almost spherical,) have been individually, subjected to a very slow (quasistatical) compression process.

Besides the chemical and mineralogical composition and the various relationships between the components, the study also involved the density, the liquid phase quantity, the void ratio.

The crushing force, the piston movement up to the crushing, the specific primary crushing energy have been measured and recorded.

The problem referring to the correlation between the crushing energy and the reduction ratio has been previously dealt with (2), (3).

3. The correlation between the specific crushing force and the diameter

The crushing force related to the grain mass, the mean quantity per colectivity (granulometric class) has been correlated with the mean diameter of the grains colectivity.

For both types of clinker, it has been noticed that the specific crushing force lessens with the mean diameter of the grain and that this variation on the d = 2 - 5 mm interval it is practically independent from the chemical and mineralogical composition, the liquid phase percentage and the void ratio (fig.1).

The processing of all the experimental methods by the smallest square method leads to the following:

$$(\mathcal{F} / M)_1 = 39{,}134.10^3 . e^{-0{,}572.d} \quad ; r = 0{,}975$$

$$(\mathcal{F} / M)_2 = 22{,}24.10^3 . e^{-0{,}372.d} \quad ; r = 0{,}979$$

The difference between the coefficients and the exponents of the two relations can be due to the different chemical compositions, according to (4).

4. The correlation between the adimensional ratio (l/d), the mean diameter and the void ratio.

The two types of clinkers have been chosen in such a way as mainly the $(\overline{l/d}) = f(d)$ correlation can be studied within one of them (type 2), f ree from the influence of the porosity (ε) - which, in this case, bars a confined variation whole, within the second one (type 1), the influence of the two factors can be studied.

M.Dr.Eng.IOAN COTEA, Dr.Eng.D.PUSCASU, Dipl.Eng.D.NICOLAU
RESEARCH AND DESIGN INSTITUTE FOR BINDER AND ASBESTOS CEMENT INDUSTRY ROMANIA

Contributions to the clinker grindability physics
Les contributions à la physique de broyage du clinker

4.1. The (1/ d) = f (d) correlation

Within it, (clinker 2), in which the porosity varies relatively in confined limits, the mechanism of the primary crushing is not structurally affected by this factor. The multiple regression analysis reveals in this case the (1/d) ratio lessens with the diameter and increases with the increase of the porosity, fig.2,3. The analytical relation is the following:

$$(1 / d) = o,6. e^{-o,28 d}. e^{4,842 \varepsilon} ; \quad r = o,931$$

4.2. The (1 / d) = f (d, ε) correlation

Within it (type 1 clinker) the variation of the porosity is sensibly increased.

Besides the above mentioned influences, the effect of a higher variation of the porosity inducing structural modifications in the crushing mechanism is also added.

In this respect, according to the Griffith's theory, a more porous body is more friable than a less porous one.

The multiple regression analysis reveals a variation which is contrary to the type 2 clinker, as for as the (1 / d) ratio lessening with the porosity increasing is concerned.

The contradictory effect of the porosity is also shown in the lessening of the correlation coefficient. The analytical relation is the following:

$$(1/d) = o.47. e^{-o,17 d} . e^{-3,36 \varepsilon} ; r = o,8$$

5. The w = f (d, ε) correlation

The primary crushing energy is connected with the values shown by the (2, 3) relation.

$$W = 1.4.1o^{-2} \left(\frac{F}{m.}\right) .1$$

The relations ensured for the two types of clinkers are:

$$W_1 = 328,73. e^{-o,852 d} . d . e^{4,842 \varepsilon}$$
$$W_2 = 146,34. e^{-o,542 d} . d . e^{-3,36 \varepsilon}$$

If considering the mean porosity $\bar{\varepsilon}$ = o.142, equal for the 2 types of clinker, the following relations one obtained:

$$W\ 1/_{\varepsilon=\bar{\varepsilon}} = 6.53,8 \cdot d . e^{-o,852 d}$$
$$W\ 2/_{\varepsilon=\bar{\varepsilon}} = 9o,81 \cdot d . e^{-o,542 d}$$

Which explain the variation form of the crushing energy with the diameter (fig.4).

6. Conclusions

For the 2 analysed clinkers, the variation of the specific primary crushing force mainly depends on the grain diameter, the analytical function being of the following type :

$$(F/M) = A. e^{-Bd.}$$

M.Dr.Eng.IOAN COTEA, Dr.Eng.D.PUSCASU, Dipl.Eng.D.NICOLAU
RESEARCH AND DESIGN INSTITUTE FOR BINDER AND ASBESTOS CEMENT INDUSTRY,ROMANIA

P

Contributions to the clinker grindability physics
Les contributions à la physique de broyage du clinker

the A, B coefficients being able to be in relationship with the chemical and mineralogical composition :

The (l/d) ratio decreases exponentially with the diameter increase and the porosity moulds it in a compley way.

The experiments carried out and the analytical relations established can be an explanatori for the contradictory results regarding the " grindability" and its correlation with the porosity, the liquid phase content the chemical and mineralogical composition.

7. Notations

F = crushing force (N)
M_1 = mass of the clinker grain before the crushing (g)
F/M_1 = specific crushing force (N/g)
d = mean diameter of the clinker grains (mm)
l - movement of the press punch up to the crushing (mm)
l/d - specific movement (mm/mm)
ε - porosity, void ratio/adimensionally
γ = correlation coefficient
W = crushing energy (kWhr/to)

Tabel no. 1

Granulometric fraction [mm]	clinker no. 1							clinker no.2					
	1-2	2-3	3-4	4-5	5-6	6-7	Cv[%]	1-2	2-3	3-4	4-5	5-6	Cv[%]
Loss ignition	0,63	0,83	0,6	0,7	0,83	0,65	14,1	1,01	0,97	0,74	0,67	0,68	20,1
SiO_2 + ins.	20,14	20,12	20,30	20,43	20,38	20,06	0,7	21,26	21,46	21,31	21,18	21,10	0,6
Al_2O_3	7,30	7,39	7,39	7,56	7,25	7,24	1,6	5,13	4,99	5,24	5,25	4,98	2,5
Fe_2O_3	3,62	3,82	3,51	3,67	3,52	3,60	2,9	5,09	5,09	5,76	5,76	5,70	2,3
CaO	65,22	64,80	65,9	65,60	65,50	65,60	0,54	63,20	63,23	63,65	64,21	64,65	1,0
MgO	1,27	1,27	0,81	0,71	0,92	1,35	23,00	1,56	1,56	1,40	1,25	1,20	12,1
SO_3	0,29	0,19	0,19	0,12	0,14	0,24	30,00	0,59	0,49	0,51	0,60	0,48	10,6
Na_2O	0,48	0,48	0,49	0,46	0,45	0,45	3,70	0,26	0,26	0,25	0,26	0,25	2,0
K_2O	0,79	0,85	0,85	0,89	0,87	0,96	6,0	0,79	0,75	0,73	0,71	0,71	4,5
TiO_2	0,24	0,23	0,32	0,35	0,36	0,19	24,0	0,18	0,21	0,24	0,20	0,21	10,4
Total	99,98	99,98	100,32	100,49	100,22	100,34	—	99,97	99,92	99,85	100,00	99,75	—
ins.	0,11	0,31	0,3	0,37	0,34	0,2	35,9	0,55	0,53	0,41	0,27	0,24	35,8
C_4AF	10,0	10,0	10,0	10,0	15,0	10,0	17,0	15÷20	15÷20	15÷20	15÷20	15÷20	0
C_3S	60÷65	60	65	60÷65	65	60÷65	3,6	50÷55	50÷55	50	55÷60	55÷60	5,7
C_2S	10	< 15	10	10	10	10	17	20÷55	15÷20	20÷25	≈ 15	15÷20	16,1
C_3A	15	15	15	15	15	15	0	≈5	≈5	≈5	≈5	≈5	0
γ	3,044	2,985	3,125	3,03	2,955	2,764	5,4	2,985	2,8925	3,015	0,87	2,9126	2,1
MSi	1,84	1,79	1,86	1,82	1,89	1,85	1,86	1,91	1,95	1,94	1,92	1,976	1,34
MAl	2,02	1,93	2,1	2,06	2,06	2,01	2,6	0,856	0,83	0,91	0,91	0,87	3,8
Liquid phase	32,585	33,365	32,22	32,96	31,94	32,58	1,4	31,48	31,02	31,06	30,93	29,93	1,8
$\bar{d}$ [mm]	1,9	2,64	3,18	4,53	494	6,177	—	1,65	2,63	3,1	4,5	5,627	—
$\bar{l}$ [mm]	0,693	0,308	0,639	0,6322	0,6286	0,585	—	1,23	1,5	1,38	1,562	1,526	—
$\frac{\bar{l}}{\bar{d}}$ [mm/mm]	0,36	0,116	0,2	0,14	0,127	0,095	—	0,745	0,572	0,446	0,347	0,27	—
Es	0,112	0,131	0,088	0,117	0,139	0,194	32,36	0,128	0,153	0,119	0,161	0,147	12,4
$F/M \cdot 10^{-3}$ [N/g]	17,37	7,94	5,09	3,02	1,88	1,41	—	13,65	8,34	6,0	3,88	3,21	—

420

M.Dr.Eng.COTEA ION, Dr.Eng.D.PUSCASA, Dipl.Eng.D.NICOLAU
RESEARCH AND DESIGN INSTITUTE FOR BINDER AND ASBESTOS CEMENT INDUSTRY, ROMANIA

Contributions to the clinker grindability physics

Les contributions à la physique de broyage du clinker

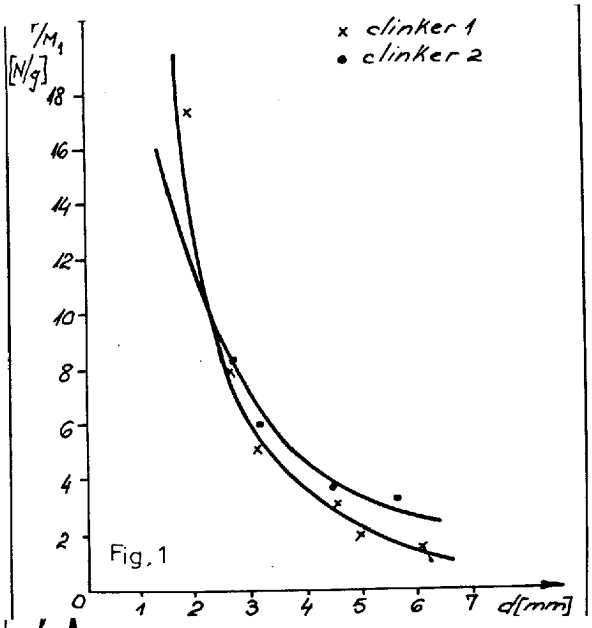

Fig. 1

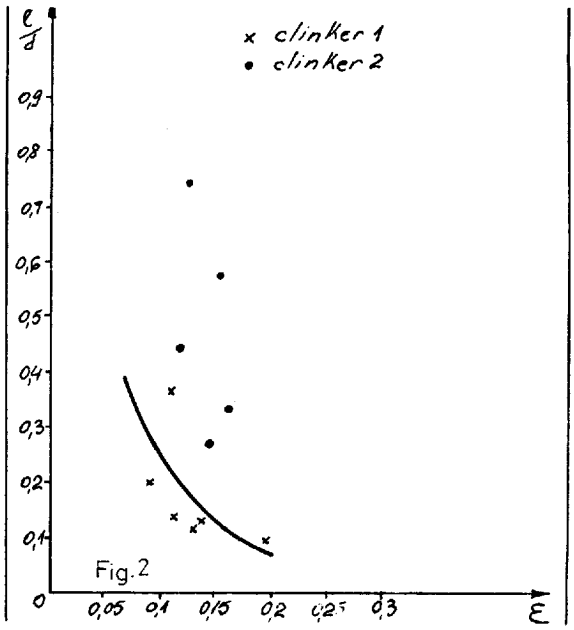

Fig. 2

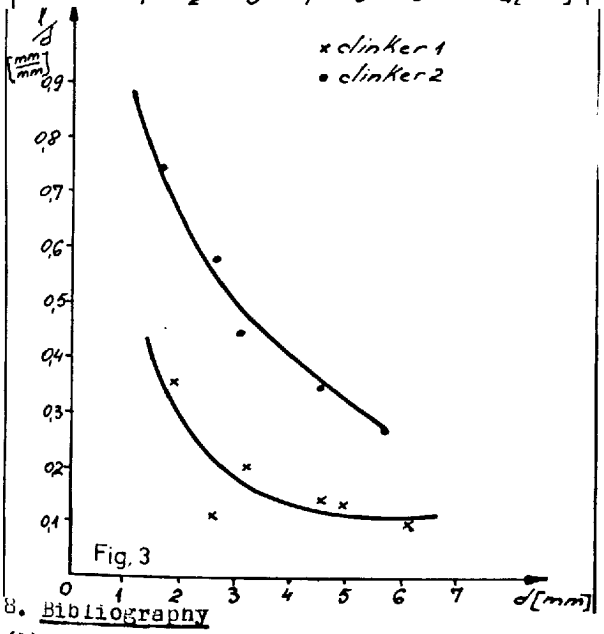

Fig. 3

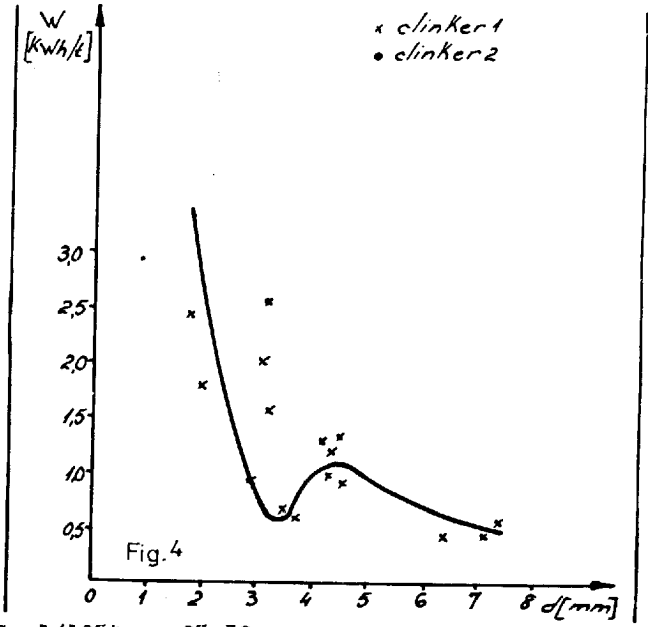

Fig. 4

8. Bibliography

(1) - Butt. Ju.M, Kolbasov. V.M, Melniekij - ZKG, 1/1974, p.27-32.
(2) - Cotea I, Puşcaşu D, Nicolau D, - Consilox, Cluj Napoca, Sept.1984.
(3) - Cotea I, Puşcaşu D, Nicolau D, - Silikonf, Budapest, May 1985.
(4) - Gouda G.R. - Cem.Concr. Res., Vol.9, 1979, p.209-218.
(5) - Petersen I.F. - Cim.Bet.Plat., Ch.,5/1980 p.297-301.
(6) - Scheubel B., Balzer H.J., - ZKG 11/1983 p. 624-627.

dr.eng.IOAN COTEA, eng.NICOLAE BUTUCESCU, eng.LIANA BUCEA, eng.VALERIAN MIHAI

Research and Design Institute for Binder and Asbestos Cement Industry, Romania

STUDY OF THERMAL EFFECTS OBTAINED IN THE CLINKERIZATION PROCESS BY THERMO-DIFFERENTIAL ANALYSIS.

In order to study the way in which the elements of the raw material mix can influence on the thermal effects characteristic to the clinkerization process, there were made a series of experiments with a thermodifferential analysis equipment.

During these experiments the main mineralogical Components of Portland Clinker as well as of common Portland clinkers with variable composition were synthetized.

There were used a Derivatograph MOM Q 1500 D with a kiln of up to 1500°C, with an automatic record of T, TG, DTA, DTG curves at heating and cooling.

In order to make a series of control analysis on the cured specimen with ATD equipment there were suplimentary introduced in the kiln - in the thermocouples space - a big platinum crucible (with a capacity of aprox. 15 g.raw material mix).

In the synthetizing experiment for each of the four Portland clinker components obtained from pure substances, it resulted:

- the formation of each mineralogical component is characterized by one or more thermal effects (exothermic for crystalization, endothermic for phasat transformations, the melting formation) that appear above 1000°C, the carbonate decomposition is accompanied by a thermo-negative effect below 1000°C;

- the heating speed increase makes the maximum thermal effects temperature increase;

- the existence of a level (at maximum heating temperature) has a strong influence on the content increase of the mineral component;

- slow cooling (compared to the rapid one) has the same favpurable influence, too.

The results obtained at the C_3S synthetization from pure substances with some additives, by curing in ATD kiln; the additives are also pure substances (for SO_3, SO_4Ca p.a. was added) are presented in the following table.

TABLE 1

Additive	dosed C_3S by RX analysis	free CaO chemically determined %	Temperature of thermal effects max. °C	
			endothermic	exothermic
1	2	3	4	5
without	5-10	10,29	950 1465 evident	1350, 1365 very low
1% Fe_2O_3 + 1% Al_2O_3	very much	0,14	940 1425 low	1330 at cooling 1310 low
5% Fe_2O_3	very much	0,27	935 1430 intensive	1165, 1200 very low
5% Al_2O_3	35-40	2,23	940 1405,1480 int.	1192 very low
0,5% MgO	tracks	15,53	910 1460 very low	1040,1275 very low

./.

dr.eng.IOAN COTEA, eng.NICOLAE BUTUCESCU, eng.LIANA BUCEA, eng.VALERIAN MIHA.
Researoh and Design Institute for Binder and Asbestos Cement Industry, Romania

P

1		3	4	5
2% MgO	much	5,65	93o 1455 intensive	1163, 121o 1265, very low
o,67% K_2O + o,35% Na_2O	little	7,96	955 138o, 146o very low	
1% MnO_2	tracks	14,83	95o 1475 evident	118o very low
o,5% TiO_2	tracks	13,57	950 147o low	1155, 1225 very low
1% SO_3	tracks	12,21	95o 1395, 1455 low	1475 intensive
2,4% SO_3	tracks	13,47	945 138o very intensive	above 15oo

The working conditions were:
- heating rate 7,5°C/minute
- without a level at maximum temperature (15oo°C)
- with rapid cooling

The additives were chosen so that they correspond to elements and proportions that are generally found in the raw materials from out cement plants.

Analysing table 1 it results that:

- the additives generally reduce the temperatures for the maximum exothermic effects (corresponding to the C_3S crystalization), except SO_3 additive; the lowest exothermic effects (that is C_3S formation at low temperatures) are for the Al_2O_3 and Fe_2O_3 additive in greater proportion ;
- the endothermic effects, that mark the phasal transformation and liquid phase production, are more intense for additives in higher percentage (Al_2O_3, Fe_2O_3, MgO and SO_3) that mean a more intensive process (for example, a growth of liquid phase quantity) ;
- Fe_2O_3, Al_2O_3 additives contributes to the biggest C_3S quantity formation.

Similar experiments were made on the other main mineralogical components of Portland clinker. There were noticed also in these cases some favourable influences of the additives.

Table 2 shows the results obtained on a series of Portland clinkers made from pure substances in a platinum crucible put in the ATD Kiln.

TABLE 2

SK	%CaO free chem. det.	X ray analysis C_3S, C_2S, C_3A, C_4AF			Optical microscopic analysis		Thermal effects temperature	
					C_3S dimensions frequency / μm		endothermic	exothermic
1	2	3	4	5	6	7	8	9	10
o,98	1,11	6o	15-2o	1o-15	1o	6o-65	4o-6o	1375 int. -	135o intensive
o,98	o,5o	6o-65	< 15	15	1o	6o-65	1o-4o	138o int. -	1355 very "

./.

dr.eng.IOAN COTEA, eng.NICOLAE BUTUCESCU,eng.LIANA BUCEA,eng.VALERIAN MIHAI

Research and Design Institute for Binder and Asbestos Cement Industry,Romania

1	2	3	4	5	6	7	8	9	10
o,96	o,5o	55-6o	2o-25	1o-15	1o	55-6o	5-25	139o int. -	136o int.
o,95	o,28	6o	<15	15	1o	55-6o	2o-4o	1385 int. -	1365 very int.
o,92	o,28	55-6o	2o-25	1o-15	1o	55	5-2o	1395 med. int. -	137o very intensive
1,o6	1,14	6o	<15	15-2o	5	65	1o-4o	14oo int. -	1375 very int.
o,94	o,49	55-6o	2o	1o-15	1o	5o-55	5-4o	14oo int. -	1365 int.

The temperature for the exothermic maximal effects correspond to the crystalization phase of the C_3S (main clinker component) and the temperature for the endothermal maximal effect (above looo°C) indicates the temperature that makes the liquid phase increase.

The exothermic effects have the maximum between 135o-1375 and the endothermic ones between 1375-14oo°C.

There were made a series of experiments in order to obtain the Portland clinker with a mix of a certain composition in which in the initial composition various oxides were added or taken out; pure substances were used.

The analysis of the obtained data made evident that :

= for a 1% reduction of each silicon, aluminium and iron oxides, the C_3S content is bigger although the free CaO propoftion grows;

- from the other oxides admixtures (MgO, K_2O, Na_2O, MnO_2, TiO_2 and SO_3), the SO_3 additives give the higher percentage of free CaO;

- the thermal effects with the lowest temperatures are obtained for the additives in the highest percentages (sum of o,5% MgO + o,67% K_2O + o,33% Na_2O + 1% MnO_2 + o,5% TiO_2 + 1% SO_3; also 3% SO_3 and 2% MgO), and from the elements the SO_3 additives.

The exothermic effects have temperatures corresponding to their maximal value between 122o and 1365°C and the endothermic ones maximal values between 1o2o and 1415°C.

There were obtained clinkers from $CaCO_3$ mixtures various clay materials (Kaolinite, bentonite, Kaolinite clay, illite, feldspar,etc.) and correction pure oxides for the mixtures to have the same chemical composition.

The obtained clinkers had C_3S 55-65% (more for the kaolinite and bentonite in the initial mixture), freee CaO o,24-1,15%.

The exothermic effects were maximal between 122o and 1295°C (higher for kaolinite) and the endothermic ones 1325-1345°C (generally higher for kaolinite).

There were made some more experiments with raw materials from some deposits of Romanian Cement plants (the clay materials being kaolinite clay, illite, montmorillonite, some with many bad minerals) and the results were as follows:

- the exothermic effects have maximal values between 117o and 1295°C and the endothermic ones between 127o and 134o°C;

./.

dr.eng. IOAN COTEA, eng.NICOLAE BUTUCESCU, eng.LIANA BUCEA,eng.VALERIAN MIHAI
Research and Design Institute for Binder and Asbestos Cement Industry,Romania

- at clinkerization temperature of 1380°C (in ATD equipment) the lowest free CaO content and higher C_3S as well as the maximal thermal effects with the lowest temperatures were obtained from the meals that had clay materials as kaolinite clays; on the pilot-scale experiments these gave the higher mechanical strengths;

- at clinkerization temperature of 1430°C for the clinkers with more kaolinite in the respective meals, there were not obtained contents higher of C_3S, and in the pilot-scale experiments the strengths were lower, indicating a clinker supercombustion.

We can conclude that the experiments made evident the possibility of synthetizing the clinker and mineralogical components with the thermodifferential analysis

The method has some advantages:

- it can correlate the temperature, the nature and the amplitude of the thermal effects in the physical and chemical processes of transformation of the cured mixture, as well as the product quality and quantity resulted after clinkerization;

- it can be appreciated the favourable or harm influences of various additives, as well as the various thermal curing for the respective mixtures;

- it can be evaluated the optimal conditions for a clinkerization at lower temperatures, having as an effect a reduction of fuel consumption in the industrial process;

- the method is easy to apply and offers a satisfactory precision by the good equipment respectibility.

dr.eng.IOAN COTEA,eng.NICOLAE BUTUCESCU,eng.LIANA BUCEA,eng.VALERIAN MIHAI

Research and Design Institute for Binder and Asbestos Cement Industry,Romania

REFERENCES

1. R.Bucchi - The influence of the Raw Material Nature and Preparation on the Raw Mix Reactivity
The works of the 7th International Congress on the Cement Chemistry. Paris (98o, vol.I)

2. I.Butt - Modern Studying Methods for clinker Formation Mechanism and Phasal Composition.Tement, 1975, 2, 12...19

3. A.Dehoeul C.Sinsaillier - Reaction Heat Determination using the Thermodifferential Analysis - Special aplication in the case of Cement Raw Materials - ZKG-1979, 8

4. G.Gouda - Raw material for cement - its Influence on the Fuel Consumption. Rock Products, Oct.1977, pp.6o-64

5. Ed.R.C. Mackenzie - Differential Thermal Analysis (Academic Press - New York 197o)

6. V.G. Ramachandran - Applications of Differential Thermal Analysis in Cement Chemistry (New-York 1969)

7. I.Odler - Separation Possibilities of Portland Cement Individual Components - by Selective Dissolution - ZKG-1979, 1o,5o4...5o7

8. I.Teoreanu - Binder and Concrete Technology. Ed.Didactică şi Pedagogică Bucureşti - 1967

9. I.Teoreanu - And Others,Clinkerization Behaviour of Some Raw Material Mixtures, Materiale de Construcţii 1985,1,42-48

1o. I.Teoreanu - And Other - Influence of some Compositional and Curing Parameters on the Portland Cement Clinker Hydraulic Properties. Materiale de Construcţii, Review, 1985 1, pp.48-51.

11. V.Timashev - Clinkerisation Kinetics, clinker structure composition and its phases. The works of the 7th International Congress on Cement Chemistry. Vol.I Paris 198o

12. D.Todor - Mineral Thermal Analysis. Ed.Tehnică,Bucureşti 1972.

M.Eng.I.COTEA, Dipl.Eng.A.ROMANESCU, Dipl.Eng.C.DUMITRESCU

RESEARCH AND DESIGN INSTITUTE FOR BINDER AND ASBESTOS CEMENT INDUSTRY,ROMANIA

Researches Concerning the Harmful Components Elimination from Phosphogypsum for Using it as Cement Setting Time Regulator.

Recherches concernant l'élimination des composants nocifs du phosphogypse en vue de son utilisation comme regulateur de prise du ciment.

I N T R O D U C T I O N

In Romania there are no phosphate deposits that can be economically quarried, the phosphate raw material is imported from the USSR (Kola Apatite), USA (Florida phosphorite), Jordan, Marocco, Togo, Israel.

For the phosphoric acid manufacturing the wet process with dihydrate is used, a precipitate results after filtering, that is the dihydrated calcium sulphate having 25-30% humidity - the phosphogypsum.

According to the phosphate stone nature and to the manufacturing technological parameters of phosphoric acid, the phosphogypsum contains some impurities that, in the case of using it at cement grinding unfavourably influence on the cement physico-mechanical characteristics, as the phosphorous soluble and insoluble compounds [$H_3PO_4 \cdot n H_2O$, $Ca(H_2PO_4)_2 \cdot H_2O$, $CaHPO_4 \cdot 2H_2O$, $AlH_3(PO_4)_2 \cdot 2H_2O$], the flourus ($HF$, H_2SiF_6, Na_2SiF_6), the organic substances, the magnesium oxide and alkali salts (1,2)

It was found that the negative influence of cement impurities is lower in the case of the slag cements.(3)

This work presents the results obtained as a consequence of the researches made in our institute to eliminate the existing impurities in phosphogypsum, in order to be used as setting regulator for all cement brands manufactured in Romania.

Experimental Data

There were examined 80 phosphogypsum batches sampled in two years period from four chemical fertilizer plants that came from various raw material.

The physico-chemical characteristics of the examined phosphogypsum varied according to the nature of the raw materials used and to the technological parameters of phosphoric acid manufacturing.

In this work the results obtained at phosphogypsum use will be presented ; the physico-chemical characteristics are presented in table 2.

Table 2

CHEMICAL COMPOSITION OF PHOSPHOGYPSUM

Components (%)	Phosphogypsum		
	I_1 (Tunis)	II_1 (Kola)	III_1 (Florida)
P_2O_5 total	0,750	0,898	0,704
P_2O_5 soluble	0,220	0,299	0,194
P_2O_5 syncr.	0,443	0,527	0,424
CaO	32,580	33,010	31,940
SO_4	54,120	55,120	53,124
F^- total	0,503	0,189	0,431
F soluble	0,149	0,181	0,207
SiO_2	0,745	0,331	3,340
Fe_2O_3	0,283	0,202	0,250
Al_2O_3	0,047	0,047	0,581
MgO	0,092	0,073	0,140

./.

M.Eng.I.COTEA, Dipl.Eng.A.ROMANESCU, Dipl.Eng.C.DUMITRESCU

RESEARCH AND DESIGN INSTITUTE FOR BINDER AND ASBESTOS CEMENT INDUSTRY,ROMANIA

Researches Concerning the Harmful Components Elimination from Phosphogypsum for Using it as Cement Setting Time Regulator

P

Recherches concernant l'élimination des composants nocifs du phosphogypse en vue de son utilisation comme regulateur de prise du ciment.

Components (%)	Phosphogypsum I_1 (Tunis)	II_1 (Kola)	III_1 (Florida)
Na_2O	o,o8o	o,o72	o,o67
K_2O	o,oo7	o,o37	o,oo8
Org.	o,395	o,o48	o,o86
humidity 25o°C	18,2o	17,79	18,8o
humidity 45°C	2,4e	2,27	1,8o

For cement manufacturing the clinkers, whose composition is presented in table 3, were used.

Table 3

CLINKER MODULAR MINERALOGICAL COMPOSITION

Clinker	Free CaO %	Modular composition M_{Si}	M_{Al}	C_{St}	Mineralogical composition % C_3S	C_2S	C_3A	C_4AF
1. Normal Portland	o,55	1,93	1,94	o,97	58,74	12,76	12,11	1o,64
2. Ferroportland	o,76	1,83	o,86	o,95	6o,o3	11,87	3,38	17,66

There were made cements with or without furnace granulated slag. Slag oxidic composition is presented in table 4.

Table 4

SLAG CHEMICAL COMPOSITION

Material	Chemical composition (%) PC	SiO_2	Al_2O_3	Fe_2O_3	CaO	SO_3
slag	o,2o	35,84	12,5o	o,6o	43,27	o,17

Natural gypsum or phosphogypsum as such or purified were used as setting time regulator.

The natural gypsum used as setting regulator had a content of $CaSO_4 \cdot H_2O$ of 81,33% and $CaSO_4$ of 4,84%.

The clinkers were ground with gypsum additive or phosphogypsum with or without slag at a fineness of 3ooo cm2/g Blaine, and the cements obtained were tested from the point of view of the physico-mechanical behaviour, using standard methods.

The chemical and mineralogical composition of phosphogypsum and clinkers, as well as the hydration product nature on hardened pastes were determined using chemical, X-ray analysis, thermodifferential and electronic microscopy methods.

./.

M.Eng.I.COTEA, Dipl.Eng.A.ROMANESCU, Dipl.Eng.C.DUMITRESCU
RESEARCH AND DESIGN INSTITUTE FOR BINDER AND ASBESTOS CEMENT INDUSTRY,ROMANIA

Researches Concerning the Harmful Components Elimination from Phosphogypsum for Using it as Cement Setting Time Regulator

Researches concernant l'élimination des composant nocifs du phosphogypse en vue de son utilisation comme regulateur de prise du ciment.

Results and Discussions

Following the phosphogypsum composition with time there were made evident the wide limits of compositional variation because of the reaction tank conditions and the raw material composition.

From the calculations, on the basis of the chemical analysis (table 2),the possible compounds in the examined phosphogypsum are the ones presented in table 5.

Table 5

POSSIBLE CONSTITUENTS,RESULTED FROM CALCULATIONS BASED ON CHEMICAL ANALYSIS

Constituents	Phosphogypsum I_1	II_1	III_1
$CaSO_4 \cdot 2H_2O$	91,07o	95,78o	93,83o
$MgSO_4$	o,21o	o,06o	o,2o4
H_3PO_4	o,3o4	o,413	o,268
$Ca_5(PO_4)_3F$	o,2o6	o,11o	o,2o2
$CaHPO_4 \cdot 2H_2O$	1,o73	1,276	1,o26
Na_2SiF_6	o,242	o,218	o,2o3
K_2SiF_6	o,o17	o,o86	o,o18
SiO_2	o,663	o,239	3,27o
Other constituents(x	6,21o	1,8oo	1,ooo

x) Other constituents : $Fe(H_2PO_4)3$, $Al(H_2PO_4)_3$, $K_2MgCa_2(SO_4)_4 \cdot 2H_2O$, $CaSO_4$ SiF_6AlF_6 (OH) $12H_2O$, compounds of Tr_2O_3,U, TiO_2.

The presence of $CaHPO_4 \cdot 2H_2O$ compound was made evident by 1R spectral analysis, (fig.1) by low uptake from 83o cm^{-1} due to HPO_4^{2-} ion,corresponding to calcium dibasic orthophosphate included in the red.

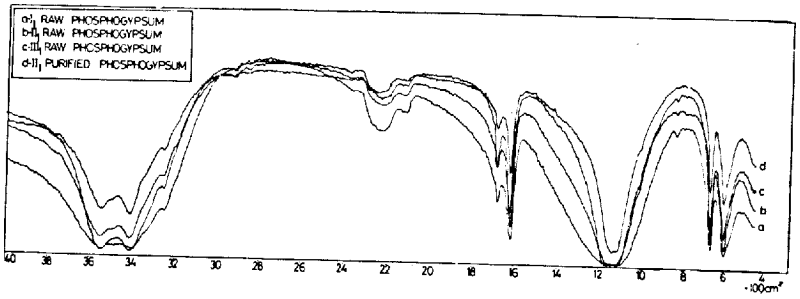

Fig.1 - 1 R Spectres of phosphogypsum.

./.

M.Eng.I.COTEA, Dipl.Eng.A.ROMANESCU, Dipl.Eng.C.DUMITRESCU

RESEARCH AND DESIGN INSTITUTE FOR BINDER AND ASBESTOS CEMENT INDUSTRY,ROMANIA

Researches Concerning the Harmful Components Elimination from Phosphogypsum for Using it as Cement Setting Time Regulator

Researches concernant l'élimination des composant nocifs du phosphogypse en vue de son utilisation comme regulateur de prise du ciment.

The granulometric analysis and the microscopic study show that the I_1 and III_1 phosphogypsum have long prismatic crystals, the particle proportion of diametre between 15-5o μm, being 51,4% on I_1 sample and 77,1% on II_1 sample. III_1 Phosphogypsum is microgranular agglomerated, the particle proportion of diametre between 15-5o μm being 82,1%.

The analysis of the purified phosphogypsum by washing, neutralization and thermal curing, as it is presented in table 6 and fig.1 lead to the following conclusions:

Table 6

THE PHYSICO-CHEMICAL CHARACTERISTICS OF PURIFIED PHOSPHOGYPSUM

Phosphogypsum	pH	Chemical composition (%)					
		P_2O_5		F^-		Organic substances	
		soluble	syncr.	total	soluble	total	(C)
I_1 - washed	4,5	o,o2	o,446	o,54o	o,oo9	o,4	o,28o
- neutralized	6,o	tracks	-	-	-	-	-
- thermal cured	6,o	tracks	o,1o5	o,438	-	-	o,oo6
II_1 - washed	4,5	o,o5	o,55o	o,532	o,o42	o,o2o	o,o42
- neutralized	6,5	tracks	-	-	-	-	-
- thermal(x cured	6,o	tracks	o,o8o	o,5o1	-	-	o,oo5
III_1 - washed	4,5	o,o3	o,426	o,492	o,o71	o,23o	o,o65
- neutralized	6,o	tracks	-	-	-	-	-
- thermal(x cured	6,o	tracks	o,o29	o,444	-	-	o,oo3

x) rehydrated at granulation

- washing and neutralizing lead mainly to a content lowering of soluble substances.

- thermal curing leads to a content lowering of $CaHPO_4 . 2H_2O$ and organic substances.

The physico-mechanical characteristics of cement with raw and purified phosphogypsum are presented in table 7 compared to those of cements with gypsum.

./.

M.Eng.I.COTEA, Dipl.Eng.A.ROMANESCU,Dipl.Eng.C.DUMITRESCU
RESEARCH AND DESIGN INSTITUTE FOR BINDER AND ASBESTOS CEMENT INDUSTRY,ROMANIA

5

Researches Concerning the Harmful Components Elimination from Phosphogypsum for Using it as Cement Setting Time Regulator.

P

Researches concernant l'élimination des composant nocifs du phosphogypse en vue de son utilisation comme regulateur de prise du ciment.

Table 7

CEMENT PHYSICO-MECHANICAL CHARACTERISTICS

Cement denomination	Clinker	Additive	SO_3 content (%)	Blaine specific surface (cm2/g)	Setting time (h.min.) i.	f.	Compressive strength (MPa) 2 days	7 days	28 days
1.	1.	gypsum	2,82	3o3o	1.5o	4.o5	19,2	37,3	48,7
2.	2.	gypsum,slag	3,13	3o5o	3.oo	4.5o	16,9	32,4	43,1
3.	2.	gypsum	2,33	3ooo	2,45	4.oo	16,8	29,o	4o,2
4.	1.	raw I_1 phospho-gypsum	2,87	3o6o	5.35	8.oo	14,9	33,3	4o,3
5.	1.	raw II_1 phospho-gypsum	2,92	298o	6.5o	8.35	14,6	34,8	42,o
6.	1.	Raw III_1 phospho-gypsum	3,o1	3o2o	6.oo	8.3o	12,8	33,o	45,8
7.	1.	-raw II_1 phospho-gypsum - slag	3,1o	3o5o	3.55	6.5o	15,1	31,o	44,1
8.	2.	raw II_1 phospho-gypsum	2,29	3o3o	6.1o	8.oo	12,6	26,o	38,6
9.	1.	washed and neutralized II_1 phosphogypsum	3,2o	3o4o	3.45	6.15	18,o	35,o	46,3
1o.	1.	-washed and neutralized III_1 phosphogypsum - slag	3,19	3ooo	3.3o	5.55	16,8	32,o	41,1
11.	1.	II_1 phospho-gypsum thermal cured and rehydrated at granullating	2,98	3o2o	2.45	4.15	21,4	37,1	47,6
12.	2.	II_1 phospho-gypsum thermal cured and rehydrated at granulating	2,3o	3o5o	3,3o	5.45	17,1	3o,2	41,o

The obtained cements with raw phosphogypsum additive were characterized by longer time settings and lower mechanical strengths, especially for short terms, about 2o-3o% compared to reference standard cement.

There are lower mechanical strengths in the case of cement with slag additive 1o-15% at 2 days.

By using washed and neutralized phosphogypsum cements with physico-chemical characteristics similar to these of reference standard cement, especially with slag additive, are obtained.

./.

M.Eng.I.COTEA, Dipl.Eng.A.ROMANESCU, Dipl.Eng.C.DUMITRESCU
RESEARCH AND DESIGN INSTITUTE FOR BINDER AND ASBESTOS CEMENT INDUSTRY,ROMANIA

Researches Concerning the Harmful Components Elimination from Phosphogypsum for Using it as Cement Setting Time Regulator.

Researches concernant l'élimination des composant nocifs du phosphogypse en vue de son utilisation comme regulateur de prise du ciment.

The washed, neutralized and thermal cured phosphogypsum has the same behaviour as the natural gypsum, leading to the achievement of some cements of superior strengths.

Hydration evolution of cements with phosphogypsum additive compared to these of gypsum additive was examined by RX diffractometre analysis and electronic microscopy (fig.2 and 3).

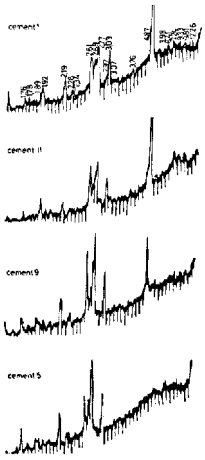

Fig.2. X-Ray analysis of hydrated cements,at 1 day

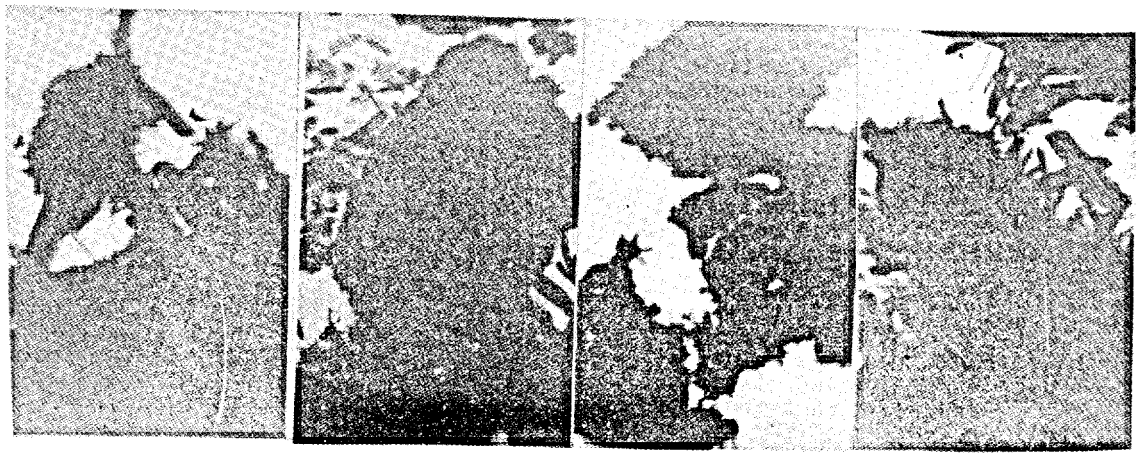

Cement 1 Cement 5 Cement 9 Cement 11

Fig.3. Electronomicroscopic image of hydrated cements, at 1 day.

The process kinetics of hydration-hydrolysis, accompanied by hydration products is slower for cements with raw phosphogypsum and is accelerated for cements with purified phosphogypsum, and in this case the cement behaviour is practically similar to the standard cement.

The results of the researches lead to establishing the solution of eliminating the harm components of phosphogypsum in order to use it as additive at cement grinding.

M.Eng.I.COTEA,Dipl.Eng.A.ROMANESCU, Dipl.Eng.C.DUMITRESCU
RESEARCH AND DESIGN INSTITUTE FOR BINDER AND ASBESTOS CEMENT INDUSTRY,ROMANIA

7

Researches Concerning the Harmful Components Elimination from Phosphogypsum for Using it as Cement Setting Time Regulator.

Researches concernant l'élimination des composant nocifs du phosphogypse en vue de son utilisation comme regulateur de prise du ciment.

P

The technological flow of purified phosphogypsum obtaining, used as additive at cement grinding, is presented în fig.4.

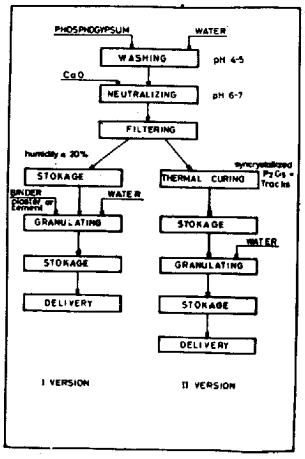

Fig.4. Technological flow of phosphogypsum purification.
I version - for common cement and cements with additive
II version - for superior cements.

C O N C L U S I O N S

From the experimental data, the following important conclusions resulted:

1.- The compositional variation of phosphogypsum that results in Romania in the manufacturing process of phosphoric acid, is in large limits due to the variety of phosphatic stone used and technological conditions, without the possibility of maintening these parametres constant.

2.- The raw phosphogypsum use as time setting regulator lead to lengthening the setting time and to the lowering the mechanical strengths especially at short terms,about 2o-3o%.

At cements with slag additive this shortening of mechanical strengths is only 1o-15%.

3.- The soluble compounds elimination in phosphogypsum by washing and neutralization up to pH=6-7 makes possible the phosphogypsum use as additive for common cement grinding,especially for slag cements.

4.- In the case of superior cements,the phosphogypsum use as setting time regulator is conditioned by P_2O_5 syncrystallized (bound as $CaHPO_4.2H_2O$) presence that imposes a suplementary preparation by thermal curing in order to eliminate it.

R E F E R E N C E S

1. V.Gh.Apreotesei,I.Samoil "Phosphoric Acid Manufacturing" vol.II,(197o).
2. Onoda Engineering and Consulting Co,LTD Japan "Phosphogypsum" leaflet 3o,(1981).
3. M.S.Tolocicova, S.V. Zapolski. " Phosphogypsum Used for setting time regulator", Tement, 3, (1979).

Dipl.eng.DUMITRESCU,CRISTINA, Dipl.eng.NISTOR,GABRIELA
RESEARCH AND DESIGN INSTITUTE FOR BINDER AND ASBESTOS CEMENT INDUSTRY,ROMANIA

Binders of Base-Acid Type Setting Used in Dental Technique. P
Liants au durcissement du type base-acide,utilisés dans la technique dentaire.

I n t r o d u c t i o n

In the phosphate systems, from the orthophosphoric acid-metal oxide interaction it results phosphates with various compositions and structures that determine an adequate process kinetics, binder system properties.

The investigation of the processes that take place at phosphate binder setting leads to the conclusion that the binder properties are determined by the interaction between the two components and sparigly soluble salt formation that give spatial red with low internal pressions. The formation of some sparigly soluble interaction products is not a sufficient condition for the binder properties. A great interaction speed between the two system components leads to the internal tension and to the impossibility of a setting structure; the setting does not take place at very slow setting speed. By retarding or accelerating the process the setting process of the phosphate binders can be adjusted in order to obtain favourable physical and mechanical characteristics (1,2,3).

The researches included in this work refer to the phosphate binders of base-acid setting used in dental technique, namely the zinc phosphate cement.

Experimental data

The zinc phosphate powder was made by burning at 1100, 1200 and 1300 ^{o}C a mixture of zinc oxide, magnesium oxide, silica dioxide, aluminium oxide, calcium carbonate and calcium fluoride of high purity, in various proportions, ground at a fineness of 0,0 % residue on the sieve with 10.000 mesh/cm^2.

The burning process was achieved at 2-6 hours level and rapid or slow cooling. The burned material was ground at a fineness of 0,0% residue on the sieve with 10000 mesh/cm^2.

The liquid was obtained from partial neutralization of orthophosphoric acid of 89% percentage and 1,75 g/ml density, with aluminium hydroxide and zinc oxide, at laboratory temperature or 80-100 ^{o}C.

The liquid density was 1,40-1,50 g/ml and was regulated by varying the distilled water ratio .

There were researched the chemical, physical and mechanical properties of powders and liquid mix at standard consistency as well as the setting processes of these masses correlated to above mentioned properties. The chemical physical and mechanical properties examined on cement pastes were : As content, water solubility, film thickness, setting-time and compressive strength (determined by ISO methods) and pH.

The zinc phosphate cement setting was examined by diffractometre analysis.

Results and Discussions

The composition of the zinc phosphate dental cement powder is presented in table 1.

./.

Dipl.eng.DUMITRESCU CRISTINA, Dipl.eng.NISTOR GABRIELA

RESEARCH AND DESIGN INSTITUTE FOR BINDER AND ASBESTOS CEMENT INDUSTRY,ROMANIA

Binders of Base-Acid Type Setting Used in Dental Technique

Liants au durcissement du type base-acide, utilisés dans la technique dentaire

T A B L E .1.

Powder chemical composition

Compounds	Powder chemical composition Z_1	Z_2	Z_3	Z_4
ZnO	9o,2o	89,oo	88,oo	88,oo
MgO	8,4o	1o,oo	9,oo	8,44
SiO_2	1,4o	1,oo	1,oo	o,5o
Al_2O_3	-	-	2,oo	2,oo
CaO	-	-	-	1,oo
CaF_2	-	-	-	o,o6

As for the composition of the zinc phosphate dental cement powder burned at 13oo°C, 4 hours level, the main component is the zinc oxide made evident at the X-ray analysis in fig.1. Some of the zinc oxide interacts with SiO_2 forming Zn_2SiO_4, with Al_2O_3 forming $ZnAl_2O_4$ and solid solutions with MgO.

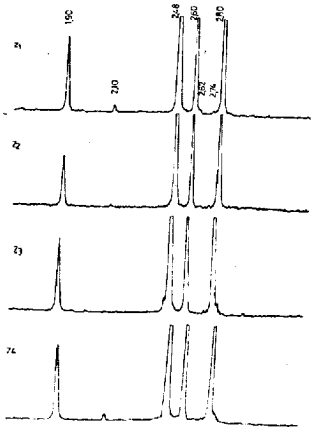

Fig.1. X-ray diagrams of powders burned at 13oo°C, 4 hours level.

By powder burning it results first, the ZnO compaction in order to improve the cement properties; the unburned ZnO reacts rapidly with the liquid that does not permit the strength structure formation.

The liquid resulted from the partial neutralization of orthophosphoric acid had a free acid content of 35-38%.

The water content of the liquid is aprox. 36%.

The chemical, physical and mechanical characteristics of the obtained cements are presented in table 2.

./.

Dipl.eng.DUMITRESCU CRISTINA, Dipl.eng.NISTOR GABRIELA

RESEARCH AND DESIGN INSTITUTE FOR BINDER AND ASBESTOS CEMENT INDUSTRY,ROMANIA

TABLE .2.

Chemical, physical and mechanical characteristics of zinc phosphate cements.

Cement denomination	As Content (%)	Standard consistency (g /o,5 ml.)	Setting time (min.)	Film thickness (μm)	Compressive strength (MPa)	Soluble material (mgP_2O_5/g)	Cement pH
Z_1	o,oool9	1,2o	4½	3o	75	o,48	4,8o
Z_2	o,oool8	1,3o	6¼	2o	9o	o,15	4,8o
Z_3	o,oool8	1,3o	7¼	15	98	o,17	5,2o
Z_4	o,oool8	1,35	6½	15	loo	o,o3	5,6o

The increase of MgO content leads to the increase of the cement plasticity and of the mechanical strengths.

SiO_2 presence in a ratio of more than 1% generally contributes to reducing the setting time and to some lowering of burning temperature.

The CaO presence in the raw mix composition, in the presence of Al_2O_3 and SiO_2 leads to increase the plasticity and the mechanical strengths.

The calcium fluoride additive has a mineralizing effect at powder burning.

As for the liquid preparation method (at 8o-loo°C or at 2o°C) and consequently, its composition, examining the diagrams in fig.2, the following conclusions are drawn regarding the cement properties:

- the necessary powder quantity for standard consistency paste is bigger (better plasticity) in the case of the liquid prepared in cold conditions;
- the setting time is shorter for the liquid obtained in cold conditions.
- the compressive strength presents some increase in the case of using the liquid prepared in cold conditions.
- there is an increase of pH at cements made with liquid prepared in cold conditions.

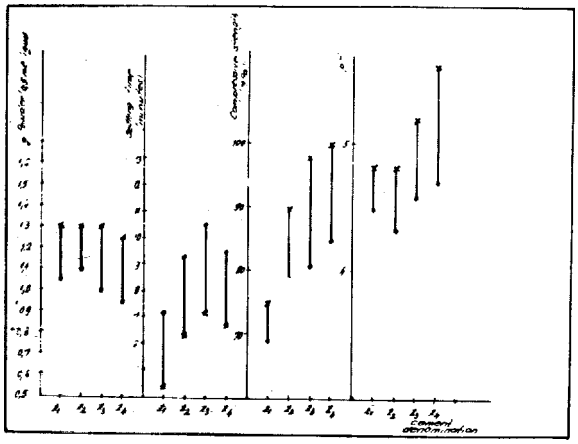

Fig.2. The influence of the liquid preparing method on the zinc phosphate properties.

x - liquid prepared at 2o° C
. - liquid prepared at 8o - loo°C.

Dipl.eng.DUMITRESCU CRISTINA, Dipl.eng.NISTOR GABRIELA

RESEARCH AND DESIGN INSTITUTE FOR BINDER AND ASBESTOS CEMENT INDUSTRY,ROMANIA

Binders of Base-Acid Type Setting Used in Dental Technique

Liants au durcissement du type base-acide, utilisés dans la technique dentaire

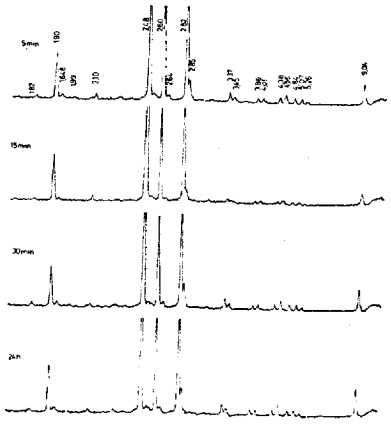

Fig.3. X-ray diagrams of the Z_1 set cement.

The rapid evolution of the reaction can be followed from the pH evolution of paste that has an accentuated growth in the first 3o minutes and then a slower one until 24 hours when the reaction is practically finished.

The structure of the set cement is a structure of composite type ; the unreacted zinc oxide particles are bound with a binder of base-acid type formed in the interaction of ZnO and MgO with H_3PO_4

The interaction of ZnO with H_3PO_4 takes place rapidly, after 5 minutes the neutral zinc phosphate $Zn_3 (PO_4)_2 \cdot 4 H_2O$ is already formed.

Conclusions

From the examination of the experimental data the following conclusions can be drawn:

1. The main component of the zinc phosphate dental cement powder is cured ZnO, with a compact structure. The MgO, SiO_2, Al_2O_3, CaO and CaF_2 modifiers have the role of embettering the cement quality, contributing to the paste plasticity and to the mechanical strengths of the set cement.

2. The use of the liquid prepared at 2o°C, compared to the liquid prepared at 8o-1oo°C leads to the increase of the paste plasticity, the mechanical strengths and pH.

3. A rapid interaction takes place between the powder and the liquid with the final-formation of $Zn_3 (PO_4)_2 \cdot 4 H_2O$, quite unsoluble that has a hardened spatial red that represents the strength structure.

The structure of the set cement is a structure of composite type; the unreacted ZnO particles are bound by the binder of base-acid type hardening formed by interaction of ZnO with H_3PO_4.

./.

Dipl.eng.DUMITRESCU CRISTINA, Dipl.eng.NISTOR GABRIELA

RESEARCH AND DESIGN INSTITUTE FOR BINDER AND ASBESTOS CEMENT INDUSTRY,ROMANIA

Binders of Base-Acid Type Setting Used in Dental Technique
Liants au durcissement du type base-acide,utilisés dans la technique dentaire

R E F E R E N C E S

1. S.L.Golîko - Volfson and others., Himiceskie asnovî tehnologhii i primenenia fosfatnîh aviazok i pokrîtii, Moskva,Izd.Himia,(1968)

2. I.Teoreanu and others. - Physico-chemical basis of anorganic binder setting Didactica şi pedagogică Publishing House, Bucharest, (1971).

3. R.Craig - Restorative Dental Materials, (1980).

CONSTANTIN POPESCU, B.E., CONSTANTA ANTONESCU, B.Sc.

Research and Design Institute for Binder and Asbestos Cement Industry, Romania

CLINKER MANUFACTURING WITH ALKALI, CHLORINE AND SULPHUR COMPOUND CONTROLLED CONTENT BY GAS DEVIATION IN STAGES CLINKERIZATION EQUIPMENT.

1.1. The researches made and published especially in the last twenty years made evident the importance of Know-ing and controlling the cement content of alkali and sulphur compounds regarding their harm influence on the cement quality and, together with the chlorine and raw materials compounds on the way of flowing the raw mix circulation through the clinkerization equipment, and the necessary measures to be taken in order to avoid aggregat products.

1.2. The causes and the way in which the alkali compounds influence on the raw mix behaviour in the clinkerisation equipment, as well as the measures that can be taken to control the harm effects, are indicated by these components behaviour during heating, at melting temperatures and gasifying point respectively. Heating, behind the melting point has as result the evaporation and volatilization - with or without decomposition - and their passing through the gas flow, situation in which they can react with, for example, the sulphur dioxide com_ing from the fuel combustion and then, with the raw *mix* after thermal curing, and thus forming the compounds recirculation and formation. [1,2,3,4].

1.3. The gravimetric proportion of the compounds that are released from the raw mix during its heating in the kiln to pass in the gas flow and is named " primary volatilization coefficient" and is noted ε_1 while the " secondary volatilization coefficient" - noted ε_2 represents the gravimetric proportion of the same compounds that are released from the kiln material resulted from their recirculation.

1.4. The compounds from the raw materials and from the fuel as well as those formed from the recirculation, that have the melting point below the clinkerization temperature can generate or encourage the sediment formation on the equipment walls whose development impose periodical interventions for release, generally with working breake.

These phenomena are more pregnant in the case of the clinkerization equipment with technological process fractioning and especially in the case of suspension preheaters, where the temperature system and the intimate contact between gas and powdery raw materials that are found is a suspension date in the connection zone between kiln and preheater that represents special favourable conditions for gas compounds interaction and condensation, the frequency with which it could happen in some cases, in acceptable if there hadn't been forseen adequate measures for adapting the working conditions and the equipment in order to eliminate them.

./.

CONSTANTIN POPESCU B.E., CONSTANTA ANTONESCU B.Sc.
Research and Design Institute for Binder and Asbestos Cement Industry, Romania

P

Because of the up to date character, and practically the generalization of their adoption, at present and in the near future in the cement industry, these equipments-with or without double feeding with fuel (precalcination) - are taken into consideration in the present work.

1.5. Stages clinkerization equipments offer in the same time adequate possibilities for content controlling and adjustment of the respective harmful (noxius) compounds by deviation - regularly partial - of gases at kiln outlet and their evacuation from the equipment, which is known as " alkali valve", Or more general "by pass" as it is shown in fig.1.

1.6. This work establishes the calculation relationings of gas proportion that must be deviated at kiln outlet in order to fit the prescribed limits for eliminating the negative effects on the cement quality and working equipment of chlorine, sulphur or any similar compounds that are brought in the system by the raw material mix and the fuel.

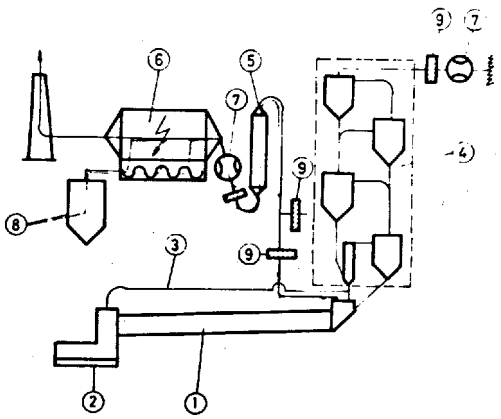

Figure no.1 Diagram of clinkerization equipment with gas deviation

gas
exhausted material

1 Rotary kiln
2 Clinker cooler
3 Tertiary air pipe
4 Raw material mix preheater
5 Tower for exhausted gases conditioning
6 Precipitator
7 Exhauster
8 Deposit for material rich in controlled $^{(+i)}$ component $^{(+i)}$
9 Register for gas flow control

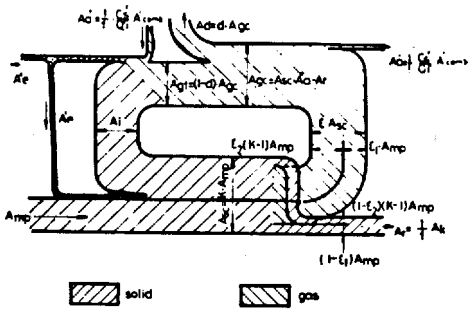

Figure no.2. Diagram of A compound circulation in the clinkerization equipment

./.

CONSTANTIN POPESCU B.E., CONSTANTA ANTONESCU B.Sc.

Research and Design Institute for Binder and Asbestos Cement Industry, Romania

2. Calculation of deviated gas proportion

2.1. Preliminary relations

Volatile compounds circulation and the denominations used are shown in fig.2, from which it results on the one hand Ar expression :

$$Ar = \left[(1 - \mathcal{E}_1) + (K-1) (1 - \mathcal{E}_2) \right] Amp \qquad (1)$$

and on the other hand the element (compound) A balance on the equipment whole :

$$Amp + A'a + A''a = Ar + d\ (K\ Amp + A''a - Ar) \qquad (2)$$

From (1) it results :

$$K = \frac{Ar + (\mathcal{E}_1 - \mathcal{E}_2)\ Amp}{(1 - \mathcal{E}_2)\ Amp} \qquad (3)$$

K elimination between (1) and (2) leads to the relations :

$$Ar = \frac{(1-d) \left[Amp\ (\mathcal{E}_1 - \mathcal{E}_2) + A''a\ (1 - \mathcal{E}_2) \right] + A'a\ (1 - \mathcal{E}_2) + Amp\ (1 - \mathcal{E}_1)}{1 - \mathcal{E}_2 (1 - d)} \qquad (4)$$

$$d = (1 - \mathcal{E}_2)\ \frac{Amp + A'a + A''a - Ar}{(\mathcal{E}_1 - \mathcal{E}_2)\ Amp + (1 - \mathcal{E}_2)\ A''a + \mathcal{E}_2\ Ar} \qquad (5)$$

By Ar elimination between (1) and (2) another expression is found for d :

$$d = \frac{\left[\mathcal{E}_1 - (K-1) (1 - \mathcal{E}_2) \right] Amp + A'a + A''a}{\left[\mathcal{E}_1 + (K-1)\ \mathcal{E}_2 \right] Amp + A''a} \qquad (6)$$

and K expression respectively :

$$K = \frac{\left[(\mathcal{E}_2 - \mathcal{E}_1)\ Amp - A''a \right] d + (1 + \mathcal{E}_1 - \mathcal{E}_2)\ Amp + A'a + A''a}{\mathcal{E}_2\ Amp\ d + (1 - \mathcal{E}_2)\ Amp} \qquad (7)$$

The minimum residual content is achieved when all gases are deviated at kiln outlet, when relation (4) has d = 1; it results after calculation :

$$\min\ Ar = (1 - \mathcal{E}_2)\ A'a + (1 - \mathcal{E}_1)\ Amp \qquad (8)$$

2.1.1. In the case of some existing equipment the volatility coefficient $\mathcal{E}_2$ can be calculated using chemical analysis - Amp and Asc - and volatilization aptitudes - $\mathcal{E}_1$ and $\mathcal{E}$ - of the raw material mix and of the solid material at kiln inlet using the relation :

$$\mathcal{E}_2 = \frac{Asc\ \mathcal{E} - Amp\ \mathcal{E}_1}{Asc - Amp} \qquad (9)$$

./.

CONSTANTIN POPESCU B.E., CONSTANTA ANTONESCU B.Sc.

RESEARCH AND DESIGN INSTITUTE FOR BINDER AND ASBESTOS CEMENT INDUSTRY

COMPULSORY CONDITIONS FOR VOLATILE COMPONENTS AND CALCULATION RELATIONS FOR GAS DEVIATION RATIO — TABLE NO. 1

HARMFUL COMPONENTS		RESTRICTIVE CONDITIONS: AIM	ADMISSIBLE LIMITS		CALCULATION RELATIONS AND FIGURE	COMPULSORY CONDITIONS
Cl^-	max. admissible limit in material	EQUIPEMENT FUNCTIONALITY	%	0,015	$d\alpha(1-\xi_2)\frac{A_{mp}\cdot A_0'-A_0''\cdot \max A_r}{(\xi_1-\xi_2^2)A_{mp}\cdot(1-\xi_2)A_0'+\xi_2\max A_r}$; $C_S = C_{SO}\cdot d(455-507\,\varphi+17\,\varphi^2)$; $C_S = C_{SO}\cdot d(392-350\,\gamma+8\,\gamma^2)$; $K=\frac{\max A_r\cdot(\xi_1-\xi_2)A_{mp}}{(1-\xi_2)A_{mp}}$, Fig. No 1	$\max A_r \le 0{,}015\%$ $\xi_2 \neq 1$
			g/Nm³	12	$c\xi_2 V_0 d^2\cdot\left\{c\left[V_0(1-\xi_2)-\xi_2(V_0-V_0')\right]-\xi_1 A_{mp}\cdot A_0'\right\}d-\xi_1 A_{mp}\cdot A_0'\cdot A_0'-c(1-\xi_2)V_0\cdot V_0'=0$; $C_S = C_{SO}\cdot d(455-507\,\varphi+17\,\varphi^2)$; $C_S = C_{SO}\cdot d(392-350\,\gamma+8\,\gamma^2)$, Fig. No 3	$c=0{,}012$ $d\le[2,1]$
Na_2O	max. admissible limit in material	CEMENT QUALITY PROVIDING	%	0,6	$Ad^2+Bd+C=0$; $A=(A_r'-\alpha A_r'')\xi_2^2\xi_1^2-\xi_2^2\left[A_{mp}'(\xi_1^2-\xi_2^2)\alpha A_0''(1-\xi_2^2)\right]-\alpha\xi_2^2\left[A_{mp}''(\xi_1^2-\xi_2^2)+A_0''^2(1-\xi_2^2)\right]$,	$\alpha_c = 0{,}56$
K_2O	max. admissible limit in material	EQUIPEMENT FUNCTIONALITY		1,0	$B=(A_r'-\alpha A_r'')\xi_2^2(\xi_1^2-\xi_2^2-2\xi_2^2\xi_1^2)+(1-2\xi_2^2)\cdot\left[A_{mp}'(\xi_1^2-\xi_2^2)+A_0''(1-\xi_2^2)\right]\cdot\alpha-(1-2\xi_2^2)\left[A_{mp}''(\xi_1^2-\xi_2^2)+A_0''^2(1-\xi_2^2)\right]\cdot\xi_2^2\left[A_{mp}'(1-\xi_1^2)+A_0'(1-\xi_1^2)\right]\cdot\alpha\xi_2^2\cdot\left[A_{mp}''(1-\xi_1^2)+A_0''^2(1-\xi_2^2)\right]$ Fig. No 3 ; $C=\left[(A_r'-\alpha A_r'')-(A_0'-\alpha A_0'')+(A_{mp}'-\alpha A_{mp}'')-(A_0'-\alpha A_0'')\right](1-\xi_2^2)$	$\alpha_c = 1$
SO_3 (SO₃ admissible limit in material)		EQUIPEMENT FUNCTIONALITY	mol/ alkalies molar ratio	(*) 1,0	$Ad^2+Bd+C=0$; $A=\xi_2^2\xi_1^2\left[A_{mp}'(\xi_1^2-\xi_2^2)+A_0''(1-\xi_2^2)\right]-\alpha\xi_2^2\xi_1^2\cdot\left[A_{mp}'(\xi_1^2-\xi_2^2)+A_0''^2(1-\xi_2^2)\right]+\beta\xi_1^2\cdot\xi_2^2\left[A_{mp}'(\xi_1^2-\xi_2^2)+A_0''^2(1-\xi_2^2)\right]$	$\alpha=1{,}55$ SO_3 $\beta=1{,}32$
SO_3 (max. admissible limit in material)					$B=(\xi_2^2-\xi_1^2+2\xi_2^2\xi_1^2)\cdot\left[A_{mp}'(\xi_1^2-\xi_2^2)+A_0''(1-\xi_2^2)\right]-\alpha\xi_2^2\cdot\xi_1^2+2\xi_2^2\cdot\left[A_{mp}'(\xi_1^2-\xi_2^2)+A_0''^2(1-\xi_2^2)\right]-\beta(\xi_1^2\cdot\xi_2^2+2\xi_2^2\cdot\xi_1^2)\cdot\left[A_{mp}'(\xi_1^2-\xi_2^2)+A_0''^2(1-\xi_2^2)\right]+\xi_2^2\cdot\xi_1^2\left[A_{mp}'(1-\xi_1^2)+A_0'(1-\xi_1^2)\right]-\alpha\xi_2^2\xi_1^2\left[A_{mp}'(1-\xi_1^2)+A_0'(1-\xi_1^2)\right]+\xi_2^2\xi_1^2\left[A_{mp}'(1-\xi_1^2)+A_0''^2(1-\xi_2^2)\right]+\beta\xi_1^2\xi_2^2\left[A_{mp}'(1-\xi_1^2)+A_0''^2(1-\xi_2^2)\right]$	$\alpha=0{,}85$ $\beta=1{,}075$ S
Na_2O (max. admissible limit in material)				(**) 1,25	$C=\left[1-2\xi_2^2+2\xi_2^2\xi_1^2\right]\left[A_{mp}'\xi_1^2\xi_2^2+A_0''(1-\xi_2^2)\right]-\left[-2\xi_2^2\xi_1^2+2\xi_2^2\xi_1^2\right]\left[A_{mp}'\xi_1^2\xi_2^2+A_0''(1-\xi_2^2)\right]+\beta\left[-2\xi_2^2\xi_1^2+2\xi_1^2\xi_2^2\right]\left[A_{mp}'\xi_1^2\xi_2^2+A_0''(1-\xi_2^2)\right]+\xi_2^2\xi_1^2\left[A_{mp}'\xi_1^2\xi_2^2+A_0''(1-\xi_2^2)\right]-\alpha\xi_2^2\xi_1^2\left[A_{mp}'\xi_1^2\xi_2^2+A_0''(1-\xi_2^2)\right]+\xi_2^2\xi_1^2\left[A_{mp}'(1-\xi_1^2)+A_0''(1-\xi_2^2)\right]+\beta\xi_1^2\xi_2^2\left[A_{mp}'(1-\xi_1^2)+A_0''(1-\xi_2^2)\right]$	$\beta=1{,}97$ SO_3 $\alpha=0{,}66$ $\beta=2{,}62$ S
K_2O					$D=(1-\xi_2^2)(1+\xi_2^2)\left[A_{mp}'\xi_1^2\xi_2^2+A_0''(1-\xi_2^2)\right]\cdot A_{mp}'(1-\xi_1^2)\cdot A_0''(1-\xi_2^2)\Big]-\alpha(1-\xi_2^2)\cdot\xi_1^2\cdot\left\{\left[A_{mp}'\xi_1^2\cdot\xi_2^2+A_0''(1-\xi_2^2)\right]\left[A_{mp}'(1-\xi_1^2)+A_0''^2(1-\xi_2^2)\right]\right\}+\beta(1-\xi_2^2)\cdot\xi_1^2\left\{\left[A_{mp}'\xi_1^2\cdot\xi_2^2+A_0''(1-\xi_2^2)\right]\left[A_{mp}'(1-\xi_1^2)+A_0''(1-\xi_2^2)\right]\right\}$ Fig. No 3	

(*) alkaline oxides expressed as (a) Na_2O equivalent (**) effective

2.2. Calculation relations

Table no.1 shows the relations for the deviation proportion calculation in various situations taken into consideration.

3. Influence of evacuation gas deviation from the kiln on the specific consumption of fuel at clinker manufacturing.

Gas deviation at kiln outlet and their elimination in the atmosfere has as a result the loss of their physical heat and as a consequence, the achievement of a specific fuel consumption at clinker manufacturing higher than in the case of using the respective gases at raw materials heating, situation taken as standard.

The specific fuel consumption that uses natural gases with inferior caloric power of 8500 Kcal/Nm3, was calculated from the thermal balance for the clinkerization equipment with such dimentions as to work without gas deviation in order to achieve specific fuel consumption - noted as C_{S0} between 760 and 825 Kcal/kg.clinker.

The results are expressed according to the specific reference consumption - C_{SO} - and to the deviation proportion - d - on the one hand, and on the other to the proportion between fuel discharge introduced at the first combustion stage and the total - φ - in the relation :

$$C_S = C_{SO} + d\ (455 - 507\varphi + 17\varphi^2)$$

showed graphically in figure no.3.

./.

CONSTANTIN POPESCU B.E., CONSTANTA ANTONESCU B.Sc.

RESEARCH AND DESIGN INSTITUTES FOR BINDER AND ASBESTOS CEMENT INDUSTRY

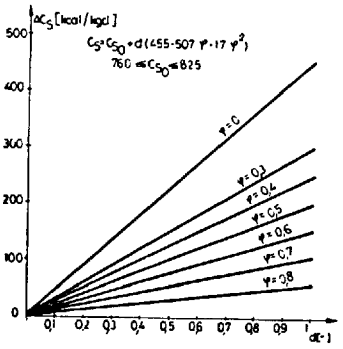

Figure no.3 Specific fuel consumption increase according to the gas deviation proportion at Kiln outlet and to the combusted fuel specific consumptions ratio at first stage and total

R E F E R E N C E

1. Weber, P. — Les problemes relatifs aux alcalis et l'élimination de ceux-ci dans les fours rotatifs par voie sèche economisant la chaleur. Zement-Kalk-Gips, nr.8/1964 (broşură Polysius)

2. Duda, H. Walter — Cement -Data - Book (Ed.II) Bauverlag G.M.B.H. Wiesbaden and Berlin Macdonald & Evans, London.

3. Biege, W. Neal Parson, J.Ladd — Bypass systeme for preheater and flash calciner kilns Pit and Quarry, July, 1978

4. Norbow, R. Henning — Wet or dry process kiln for your new installation Rock Products, May 1974.

5. Garret, M.H. Murray, J.A. — Improving thermal efficiency-design and operation considerations. Part.IV. Rock products, August 1974

6. Svendsen, J. — Alkaliarmer Zement aus Hochalkali-Rohstoffen mit energie-viertschaftlich günstiger Verfahrenstechnik. Zement-Kalk-Gips, nr.6/1978.

./.

7. Garret, M.Hoke — Energy conservation by the V.S.Cement Industry. Part.I. Pit and Quarry, March, 1976

8. Elkjaer, P.H. — Systèmes de precalcination Cements, betons,platres, nr.723, 2/1980.

9. Gouda, R.G. — Raw mix the key for a successful and profitable cement plant operation. World Cement Technology, nov.1979.

10. Locher, F.W. Sprung, S., Opitz, D. — Comunicare prezentată la Siliconf,Budapesta 1981. Reaktionen im Bereich der Ofengase Zement-Kalk-Gips, nr.1/1972.

11. Rössner, P., Feige, F., Danowski,W. Keiser, J. — Betriebseargebnisse mit dem ZAB-Vorwärmer im Eichofelder. Zementwerke Deuna unter den Bedigungen hoher Alkali-und Chloridbelastungen. Zement-Kalk-Gips, nr.12/1977.

12. Portland Cement Onoda — Informaţii tehnice asupra procedeului R.S.P.

13. Pieczora, Stefan — Zagadnienia alkaliow, chlorkow i siarki w procesie wypalania Klinkiera portlandzkiego w piecach obrotowychna metode sucha Cement, Wapro, Gips nr.8-9/74.

Dipl.Eng.ALEXANDRU ROMANESCU, Dipl.Eng.CRISTINA DUMITRESCU

RESEARCH AND DESIGN INSTITUTE FOR BINDER AND ASBESTOS CEMENT INDU TRY ROMANIA

Considerations Concerning the Hardening Mechanism of the Controlled Expansion Cements

Les considérations en ce qui concerne le mécanisme de renforcement aux ciments à expansion contrôle.

I N T R O D U C T I O N

The gas well cementing requires a special cement that must assure the sealing of drilling and extracting column against the well hole wall in order to avoid gas losses.

The following things were taken into consideration in order to chose this cement type: cement paste fluidity and density must correspond for cementing at high temperature and pressure conditions; the mehcanical strength of the hardened cement must assure the well starting and working; the expansion must be achieved in an optimal period and must assure the sealing up between the column and the well hole wall.

For the specific conditions of gas wells in Romania the cements must have the following physico-mechanical characteristics: thickening time of min.13o minutes at 7o°C and 4oo bars, compressive strength at 1day of min.3,5 MPa and at 3 days of min. 7,o MPa and expansion of o,2 - 1,o%.

The expansion phenomenun of the investigated cements is due to the calcium hydroaluminate sulphates in the hardening process and especially the ettringite formation. The other physico-mechanical characteristics are conditioned by the nature and the relations established among the mineralogical constituents of the material used (1-4).

Experimental data

The investigated expansion cements were made by grinding together the Portland and aluminous clinker, trass or slag and gypsum.

The chemical composition of the raw materials used is presented in table 1.

Table 1

Raw material	Oxidic composition (%)						Mineralogical composition (%)	
	PC	SiO_2	Al_2O_3	Fe_2O_3	CaO	SO_3	C_3S	C_3A
Portland clinker	2,79	21,13	5,oo	5,51	61,96	o,48	54,68	3,94
Aluminous clinker	1,69	2,6o	43,3o	13,73	29,84	-	-	-
Trass	1o,74	56,37	1o,91	2,16	8,87	o,o2	-	-
Slag	o,2o	35,84	12,5o	o,6o	43,27	o,17	-	-
Gypsum	o,o1	o,2o	o,3o	o,o3	32,73	46,49	-	-

The manufacturing formulas of the investigated expansion cements are presented in table 2.

Table 2

Cement symbol	% content of:					Blaine specific surface (cm2/g)
	Portland clinker	Aluminous clinker	Trass	Slag	Gypsum	
a_1 ... a_4	62	12	17	-	9	28oo - 35oo
b_1 ... b_4	6o	1o	2o	-	1o	28oo - 35oo
c_1 ... c_2	39	12	./. 4o	-	1o	28oo - 3ooo

Dipl.Eng.ALEXANDRU ROMANESCU, Dipl.Eng.CRISTINA DUMITRESCU

RESEARCH AND DESIGN INSTITUTE FOR BINDER AND ASBESTOS CEMENT INDUSTRY,ROMANIA

Considerations Concerning the Hardening Mechanism of the Controlled Expansion Cements

Les considérations en ce qui concerne le mécanisme de renforcement aux ciments à expansion contrôle.

Table 2 /cnt'd

Cement symbol	% content of: Portland clinker	Aluminous clinker	Trass	Slag	Gypsum	Blaine specific surface (cm2/g)
d	62	12	-	17	9	3ooo
e	6o	1o	-	2o	1o	3ooo
f	39	12	-	4o	9	35oo

The cements made were tested from the ysico-mechanical behaviour point of view at high pression and temperature conditions, with or without modifying setting time additive - lignotartrine (L.C.[x])

In order to examine the hydration-hydrolysis processes, chemical, diffractometre and electronomicroscopic analyses were made, on specimens having a w/c ratio of 1 at various hydration periods.

Results and Discussions

The cements made following the formulas given in table 2, of a fineness of 3ooo cm2/g Blaine specific surface, were characterized by physico-mechanical properties that are presented in table 3.

Table 3

Cement symbol	Thickening time at 7o°C and 4oo bars (min.)	Linear variation in water at 6o°C (%) 1d	3d	7d	Compressive strength in water at 6o°C (MPa) 1d	3d
a_2	112	o,7o6	o,756	o,769	3,o	9,1
a_2 + LC	15o	o,668	o,747	o,753	1o,4	16,8
b_2	135	o,419	o,412	o,416	3,6	9,9
b_2 + LC	18o	o,612	o,669	o,682	3,8	13,1
C_2	98	o,595	o,587	o,587	4,2	8,3
C_2 + LC	135	o,686	o,69o	o,691	9,2	15,6
d	12o	o,259	o,271	o,271	5,7	9,9
d + LC	17o	o,15o	o,162	o,165	16,6	36,4
e	1o8	o,271	o,283	o,289	6,1	11,8
e + LC	14o	o,183	o,196	o,196	17,5	41,2
f	93	o,571	o,583	o,589	15,4	22,3
f + LC	176	o,o41	o,o34	o,o28	18,6	45,o

Examining the results presented in table 3, the following interpretations can be made:

- The thickening times of no additive cements present values closed to the necessary minimal limit, generally, below this limit. In order to achieve adequate thickening times lignotartrine- LC was used as retarder.

x) L.C. Calcium lignosulphonate with tartrate.

Dipl.Eng.ALEXANDRU ROMANESCU, Dipl.Eng.CRISTINA DUMITRESCU
RESEARCH AND DESIGN INSTITUTE FOR BINDER AND ASBESTOS CEMENT INDUSTRY,ROMANIA

Considerations Concerning the Hardening Mechanism of the Controlled Expansion Cements

Les considérations en ce qui concerne le mécanism de renforcement aux ciments à expansion contrôle.

- The linear expansion at trass cements as expansion stabilizer had values within the expected limits of o,45 - o,7o%. The L.C. additive at trass cement did not significantly influence the e pansion.

The cements made with slag as expansion stabilizer present more reduced expansions, and when are LC added decrease below the limit that is necessary to used them at gas well cementing.

- The compresive mechanical strengths are correlated to the expansion value and are characterized by higher values for slag cements as compared to the ones with trass as expansion stabilizer (5,7 - 15,4 MPa at 1 day as compared to 3,o-4,2 MPa).

The LC additive in cement pastes leads to the increase of the mechanical strengths.

The fineness grinding influence on the physical and mechanical properties of investigated expansion cement was examined for "a" cement and is presented in fig.1.

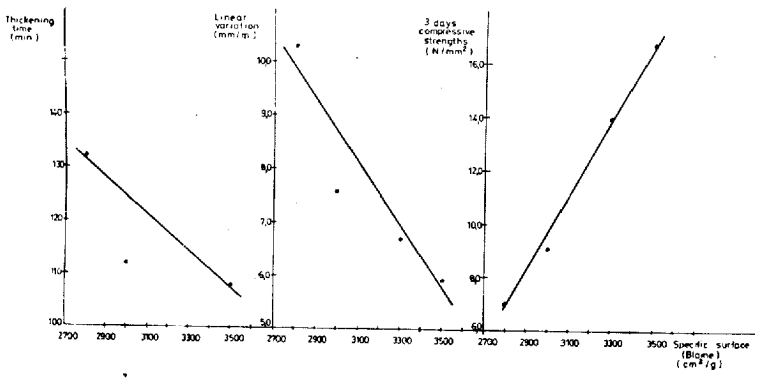

Fig.1. Grinding fineness influence of "a" cement on the physical and mechanical properties.

The increase of the grinding fineness from 28oo to 35oo cm2/g (Blaine Specific Surface) leads to the thickening time and expansion diminution and mechanical strengths increase.

The hardening processes kinetics was studied by determining the ettringite content (table 4), diffractometric analysis (fig.2) and electronic microscopy (fig.3).

Table 4

Cement denomination	a_2		a_2+LC		d		d + LC	
	1 day	3 days	1 day	3 days	1 day	3 days	1 day	3 days
Etringite content	12,18	13,4o	11,9o	11,98	8,1o	9,18	6,o4	6,5o

./.

Dipl.Eng.ALEXANDRU ROMANESCU, Dipl.Eng.CRISTINA DUMITRESCU
RESEARCH AND DESIGN INSTITUTE FOR BINDER AND ASBESTOS CEMENT INDUSTRY,ROMANIA

Considerations Concerning the Hardening Mechanism of the Controlled Expansion Cements

Les considérations en ce qui concerne le mécanism de renforcement aux ciments à expansion contrôle.

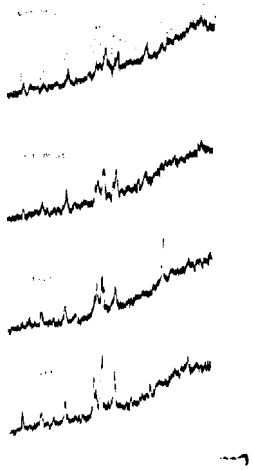

Fig.2.- X-ray diagrams of the hydrated cements, at 1 day.

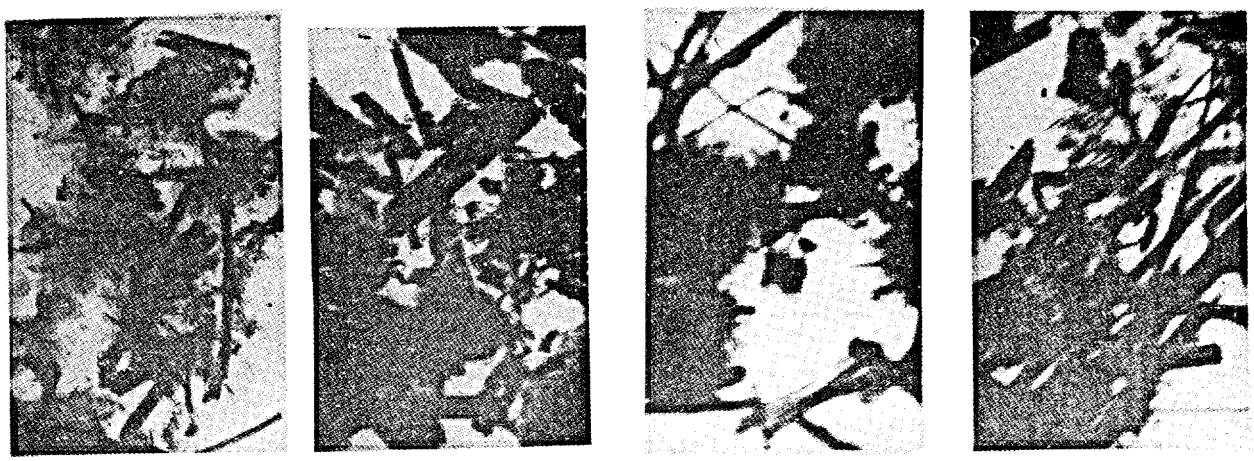

a_2 Cement a_2 + LC cement d cement d + LC cement

Fig.3.- Electromicroscopic image of the hydrated cements, at 1 day.

Examining the data from table 4 and fig.2 and 3, it is made evident the fact that the hydration - hydrolysis processes kinetics is more accelerated from the first hardening terms at trass cement used as stabilizer as compared to the slag cements. LC additive leads to the slowing of the hydration process.

There can be seen that the calcium hydrosulphate- aluminate mechanism formation, particularly the trisulphate one, correlated to their ratios, the formation kinetics and the equilibrium conditions are determinant factors for expansion.

As a consequence of the obtained results, at present, the expansive cement based on mixture is manufactured and used at gas well cementing, that leads to the elimination of the gas losses by improper sealings that used to happen when common cement was used.

C O N C L U S I O N S

Examining the experimental data the following important conclusions can be drawn:

./.

Dipl.Eng.ALEXANDRU ROMANESCU, Dipl.Eng.CRISTINA DUMITRESCU

RESEARCH AND DESIGN INSTITUTE FOR BINDER AND ASBESTOS CEMENT INDUSTRY,ROMANIA

Considerations Concerning the Hardening Mechanism of the Controlled Expansion Cements

Les considérations en ce qui concerne le mécanism de renforcement aux ciments à expansion contrôle.

1. There can be made cements with controlled expansion for cementing at high temperature and pression conditions (7o°C and respectively 4oo bars) by grinding at 3ooo-35oo cm^2/g (Blaine specific surface) of some mixtures of ferroportland clinker aluminous clinker and gypsum. LC additive is used in order to achieve the thickening time.

2. The cements made with slag as expansion stabilizer present more reduced expansions that with LC additive, lower below the limit necessary to use them at gas well cementing.

3. The expansion is achieved on the basis of the calcium hydrosulphate-aluminate formation, particularly the trisulphatated one, correlated to their rations, their formation kinetics and equilibrium conditions that are formed in the expansive cement.

R E F E R E N C E S

1. Mehta P, Polivka M - Expansive Cements (principal rapport),Proc.Sixth.Intern.Cong. Chem.Cements, Moscow (1974).

2. Budnikov, P.P., Kravcenko,I.V. - Expansive Cements (Principal rapport) Proc.Fifth Intern Symp.Chemistry of Cement,Tokio (1968).

3. Teoreanu,I, Dumitrescu C, Mechanisms of controlled expansion cements hardening, Cement and concrete Research, 12,141-155, (1982).

4. Teoreanu,I, Munteanu M, - Revue Roumaine de Chimie, 3,135-149 (1985).

eng.ROMANESCU, ALEXANDRU, eng.BUCEA, LIANA, Eng.AMZICA, FLORIN

RESEARCH AND DESIGN INSTITUTE FOR BINDER AND ASBESTOS CEMENT INDUSTRY, ROMANIA

Clinker Compositional Field Modification for Lowering its Formation Temperature.

Romanian researches, as well as researches in other countries (1), (2),(3), aiming at a hydraulic cement obtaining that need less fuel in the manufacturing process tend on the one band to reduce the $CaCO_3$ content in the raw material mix and on the other hand, to the components formation at temperature below 1450°C. These were the reasons for the study of the compositional field of belitic sulphate aluminate clinker.

The laboratory researches proved the existance of cements of a mineralogical composition in a $C_2S - C_4AF - (C_4A_3\bar{S} + C\bar{S})$ ternary diagram. Taking into account the laboratory results the clinker was manufactured in a pilot plant with a rotary kiln of Ø 1,2 m. and L = 17 m. and an output of aprox. 0,5 t/h.

The mineralogical composition of the obtained clinker was within these limits:

- β - bilcalcic silicate ($\beta - C_2S$) : 45 -5o%
- tetracalcic sulphatealuminate ($C_4A_3\bar{S}$) : 15-25%
- tetracalcic ferrialuminate (C_4AF) 15-2o%
- calcium sulphate ($C\bar{S}$) : lo-15%

For the SO_3 retention in clinker, the combustion was made in a highly oxidant air and the material temperature in the clinkerization zone was 1250°C.

The results of the determinations for the boundless calcium oxide shows that the clinkerization process determined the complete hound of the oxide up to values of o,o3-o,11% free CaO.

The clinker X-ray analysis indicates the formation of four mineralogical constituents in the mineralogical composition (figure 1).

Figure 1

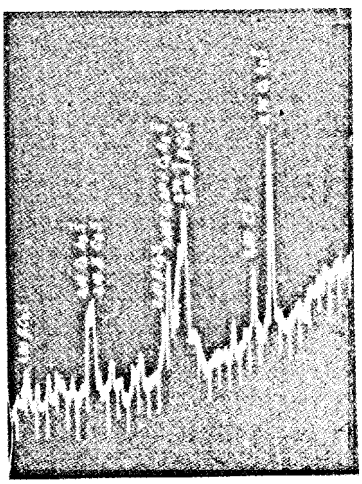

Diafractogram of belite sulphate aluminate clinker obtained in the pilot plant.

The optical microscope analysis made on these clinkers made evident a micro-crystaline structure with crystalized bicalcic silicate with dimensions of.

./.

5-3o microns and tetracalcic sulphatealuminate with dimensions of less than 5 microns, having sometimes up to lo microns.

The ferrialuminate mass is placed in the connate spaces (figure 2 and 3).

Figure 2



Figure 3



Microphotos of belitic sulphate aluminate clinker obtained in the pilot plant.

The clinkers were ground at a fineness, measured by Blaine specific surface, of about 5ooo cm2/g, without gypsum or other additives, and the cements were tested on plastic mortars.

The results of the physical and mechanical tests for the obtained cements are presented in table 1.

TABLE 1

Specimen no.	Cement curing time (days)	Setting (minutes)		Mechanical strengths on plastic mortars (N/mm2)									
				Bending					Compression				
		Initial	Final	2d	7d	28d	9od	18od	2d	7d	28d	9od	18od
o	1	2	3	4	5	6	7	8	9	1o	11	12	13
1	1-2	11	21	3,5	3,9	6,2	6,9	8,1	21,8	3o,3	4o,4	52,4	59,5
1	9o	-	-	3,3	3,7	6,o	-	-	21,o	29,5	37,2	-	-
2	1-2	12	25	3,8	5,o	6,9	8,1	-	25,1	34,7	44,4	52,6	-
2	6o	-	-	3,7	4,8	6,6	-	-	25,o	34,6	42,8	-	-

T h e s e data show that from the belite sulphate aluminate clinkers there can be obtained cements of rapid setting and hardening with mechanical compressive strength at 2 days of 21-25 N/mm2.and at 28 days of 4o-44 N/mm2.

Research and Design Institute for Binder and Asbestos Cement Industry,Romania

P

The mechanical strengths increase by 14% from 28 days to 9o days for bending traction and by 19% for compression.

The cement curing for 6o or even 9o days determines mechanical strengths reduction any other problems than average cements.

Belite sulphate aluminate clinker grinding aptitude was determined comparatively to an average Portland clinker on laboratory scale, in a counter mill in order to measure the electric power consumption.

Figure 4

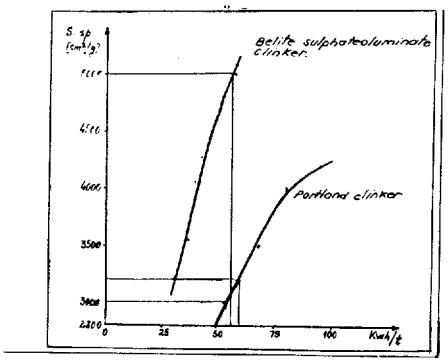

Grinding aptitude of belite sulphate aluminate clinker compared to that of common Portland clinker.

The curves in figure 4 show that this type of clinker has a good clinker aptitude, so that the electric power consumption for the achievement of a 5ooo cm2/g fineness is no higher than the one used for a 3ooo-32oo cm2/g fineness of average Portland cements.

The belite sulphate aluminate cement was tested on concretes and the most important conclusions (table 2) are the following:

- the concrete must be put in work in half an hour from the preparation, it can be used in the prefabricated industry.

- the B.2oo concrete for the 315 kg.cement/m3 dosis for ^{d}max = 31 mm.and for 355 Kg Cement/m3 dosis for ^{d}max = 16 mm

- the B.25o concrete for the 35o kg.cement/m3 dosis for $^{d}max.$= 31 mm.and for for 385 kg.cement/m3 dosis for d max.= 16 mm.

TABLE 2

No.	Aggregate $d_{max.}$	Cement dosis	Water l/m3	Tapping	Density Kg/m3.	Compresion strength N/mm2						
						8h	12h	16h	1d	3d	7d	28d
o	1	2	3	4	5	6	7	8	9	1o	11	12
1.	31	315	2oo	5	236o	-	-	-	9,4	13,5	16,3	23,5
2.	31	35o	2oo	5	235o	5,8	8,6	11,o	12,8	15,o	17,5	29,9

./.

eng.ROMANESCU ALEXANDRU, eng.BUCEA LIANA, eng.AMZICA FLORIN
Research and Design Institute for Binder and Asbestos Cement Industry, Romania

P

o	1	2	3	4	5	6	7	8	9	1o	11	12
3.	16	355	22o	9	231o	3,o	4,3	4,7	5,9	7,6	8,6	23,4
4.	16	385	22o	8	231o	1,8	3,4	4,o	6,6	9,6	11,9	31,2

Taking into account that this clinker is obtained from a raw material mix with a $CaCO_3$ content of aprox.2o% smaller than average clinkers and with a clinkerization temperature of 2oo°C lower, the theoretical heat consumption necessary for the belite sulphate aluminate clinkers was calculated. The obtained value is 3o3 Kcal/Kg clinker compared to 43o-45o Kcal/Kg.clinker for average Portland clinkers.

The low heat consumption, a good grinding aptitude and mechanical strengths at 28 Days of minimum 4o N/mm2 prove the advantages of this type of clinker.

REFERENCES

1. P.K.Mehta - World Cement Technology, 11, no.4 (198o)
2. G.Sudih, A.O. - Chem.Abstr.9o 1o8911 (1979)
3. I.V.Timaşev, - Tement, no.5 (198o)

Dr.eng.MARIA ENCULESCU

Research and Design Institute for Binder and Asbestos Cement Industry,Romania

P

CONTRIBUTIONS TO CLINKER FORMING KINETICS.
CONTRIBUTIONS SUR LA CINETIQUE DE LA FORMATION DU CLINKER.

SUMMARY The paper briefly deals with clinkering kinetics of the aluminous and portland clinkers specific mineralogical compounds.

Clinkering ability of the raw meals for white portland clinkers is shown.

It is also shown clinkering ability of the raw meals used for white aluminous refractory clinkers based on calcium monoaluminate and dialuminate.

Finally, clinkering ability of the raw meals based on slag coming from Ferrous Metallurgy Works Galaţi is described.

1 - CLINKERING KINETICS OF THE RAW MEALS

Clinkering kinetics of the raw meals for pure mineralogical compounds specific for the portland clinkers : $3CaO.SiO_2$; $\beta_2 CaO.SiO_2$; $3CaO.Al_2O_3$; $4CaO.Al_2O_3.Fe_2O_3$ as well as for pure mineralogical compounds particular for aluminous refractory clinkers, such as: $CaO.Al_2O_3$; $CaO.2Al_2O_3$; $12CaO.7\ Al_2O_3$; $3CaO.Al_2O_3$ and $CaO.6\ Al_2O_3$ has been studied on ATD + ATG - MOM - HUNGARY apparata by our experts MIHAI VALERIAN, BUTUCESCU NICOLAE and STAMATE IRINA (2,3,4,5,13).

$$C_{C_3S} = \frac{3 \times 56}{1 \times 60} = 2.8;\ F\ [\ T(ft)\ ]$$

where: T = burning temperature $[^oC]$

t - burning time - $[h]$

$$C_{C_2S} = \frac{2 \times 56}{1 \times 60} = 1.86;\ F\ [\ T\ (ft)]$$

therefore resulting that $3CaO.SiO_2$ meal basicity having a molar ratio of - 2.8 implies a more difficult, havier as compared to $2CaO.SIO_2$ meals with lower basicity, namely a molar ratio of 1.86.

Thus, as function of their basicity the raw meals having a high content of $3CaO.SiO_2$ shall have more difficult clinkering depending upon molar ratios difference.

$$\Delta\ C = 2.8 - 1.86 = 0.94$$

In case of the aluminous refractory meals clinkering kinetics shall develop as function of molar ratios as follows:

./.

Dr.eng.MARIA ENCULESCU

Research and Design Institute for Binder and Asbestos Cement Industry,Romania

P

$$C_{C_3A} = \frac{3 \times 56}{102} = 1.64;\ F\ [\ T.(ft)\ ]$$

where : T = burning temperature (°C)

t = time (hr.)

$$C_{C_{12}A7} = \frac{12 \times 56}{7 \times 102} = 0.97\ ;\ F\ [\ T.(f.t.)\ ]$$

$$C_{CA} = \frac{1 \times 56}{1 \times 102} = 0.55;\ F\ [\ T.(f.t)\ ]$$

$$C_{CA2} = \frac{1 \times 56}{1 \times 102} = 0.27;\ F\ [\ T.\ (f.t)\ ]$$

$$C_{CA6} = \frac{1 \times 56}{6 \times 102} = 0.091\ ;\ F\ [\ T.(f.t)\ ]$$

resulting that low basicity meals (low CaO %) and high content of Al_2O_3 (maximum Al_2O_3 %) shall have a maximum clinkering kinetics very difficult one and occuring at high temperature; for instance CaO.6 Al_2O_3 shall be clinkerized in the are furnace at 1820°C; CA_2 shall be clinkerized in the arc furnace at 1722°C; CA shall be clinkerized at 1600°C during abt.6 hr; $C_{12}A_7$ shall be clinkerized at 1400°C during abt.5 hr; C_3A shall be clinkerized at 1395°C during abt.5 hr, thus easier clinkering kinetics at lower temperature depends on higher and more difficult havier basicity at higher temperature depending on Al_2O_3 % in the raw meal composition.

Also, clinkering ability of the raw meals concerning aluminous and portland cements develops as per classical formulas 1-12 more usually being Blaise's formula 6

$$AC = \frac{600}{Co + 2C_1 + 2C_2 + 3C_3 + 4C_4 + 4C_5 + 2C_6}$$

where C_o, C_1, C_2, C_3, C_4, C_5, C_6 stand for CaO % at 1000°C, 1100°C, 1200°C, 1300°C, 1350°C, 1400°C and 1500°C or as simplified by the paper author (2,3,4,5,13)

$$AC = \frac{600}{3C_3 + 4C_4 + 4C_5 + 2C_6}$$

taking into account the fact that at about 1300°C liquid phase begin to occur.

Studies and research work achieved by the author (1,2,3,4,5,13) analyses clinkering kinetics of the raw meals for pure mineralogical compounds, as well as of raw meals for white and coloured aluminous and portland clinkers and the following formulas have been stated:

$$AC_{total\ 1} = \frac{1000 \times n \times \sum_o^n C}{\sum_o^n T};\ f\ (t)$$

$$AC_{total\ 2} = \frac{\sum_o^n T}{1000 \times n \times \sum_o^n C};\ f\ (t)$$

./.

Dr.eng.MARIA ENCULESCU
Research and Design Institute for Binder and Asbestos Cement Industry,Romania

P

where T (^{o}C) stands for the temperature at whinch specimen of free CaO have been sampled

C (%) - free CaO
n - number of specimen
t (hours) - clinkering time

Figure no.1 shows clinkering ability of the raw meals for white portland clinkers to be noted as the best ability that one of white clinker with pegmatite.

Figure no.2 indicates clinker ability of the raw meals for aluminous clinkers noticeable being white aluminous clinkers, such as: CaO.2 Al_2O_3 (B) and CaO.Al_2O_3 (Al).

Figure no.3 shows clinkering ability of the raw meals based on slag from GALATI out of which meals with very low content of $3CaO.SiO_2$ and very high content of $\beta 2CaO.SiO_2$ may be stand out.

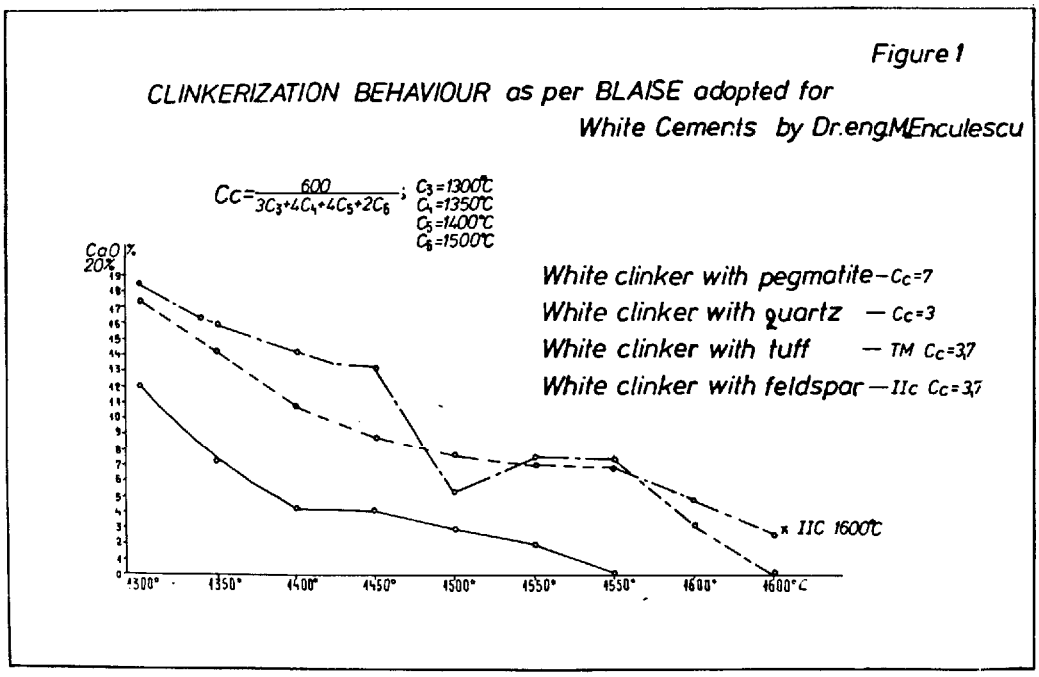

Figure 2

LABORATORY WHITE CEMENTS
Variation of the clinkerization behaviour
depending upon the temperature
Formulae BLAISE and Dr.eng.M.Enculescu

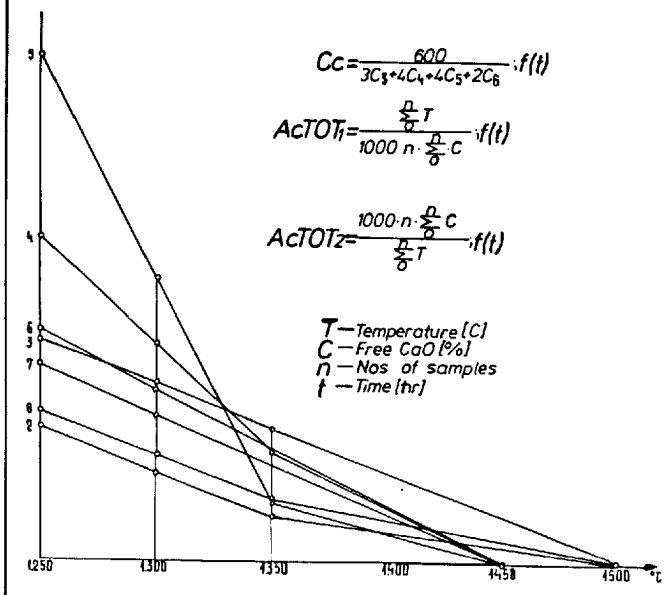

P

Figure 3

CLINKERIZATION BEHAVIOUR

Formulae as per Dr.eng.

M.Enculescu

$$AcTOT_1 = \frac{\sum_0^n T}{1000\, n \sum_0^n C} \cdot \int f(t)$$

$$AcTOT_2 = \frac{1000\, n \sum_0^n C}{\sum_0^n T} \cdot \int f(t)$$

T — Temperature [°C]
C — Free CaO [%]
n — Nos of samples
t — Time [hr]

Remarks: The formulae 1.5.8.9.10.11.12. become couspicuous

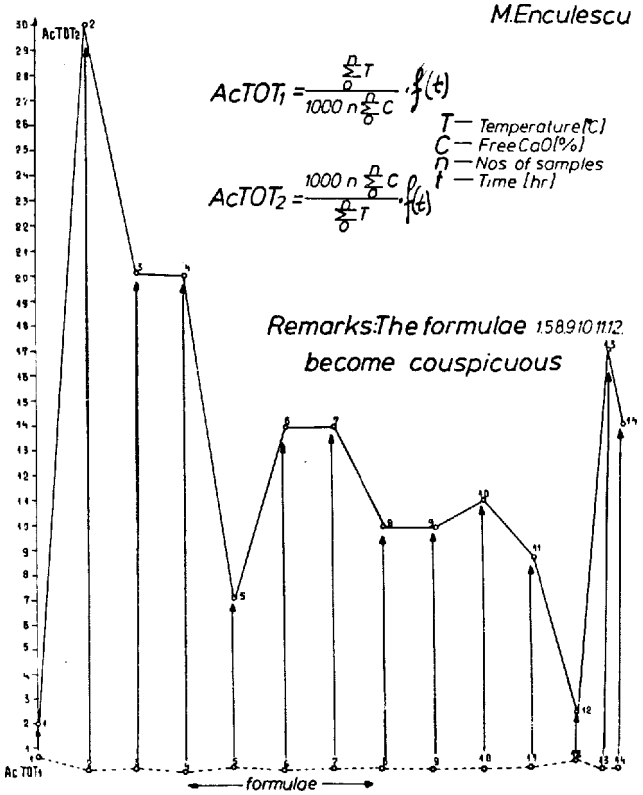

Dr.eng.MARIA ENCULESCU

Research and Design Institute for Binder and Asbestos Cement Industry,Romania

B I B L I O G R A P H Y

1.- S.Solacolu, " Chenistry-physics of the technical silicates" the 2nd edition - Technical Publishing House 1968, Bucharest.

2.- M.Enculescu, "Constributions to obtain the white cement" Technical scientific communication session - ICPILA Bucharest, 21-22 october 1983.

3.- M.Enculescu, "Research concerning determination of the characteristics of the calcium carbonate resulted from chemical industry as regards their usage possibilities in binders industry" Studies - 1st and 2nd phases 1984 - ICPILA Bucharest

4.- M.Enculescu, "Research of the characteristics of slags coming from foundries - furnaces and metalurgy as regards their usage possibilities in the binders industry. Studies - 1st and 2nd stages, 1984 - ICPILA - Bucharest

5.- M.Enculescu, "Contributions for usage of waste materials and by-products resulting from chemical industry and metalurgy in the binders industry - CONSILOX IV - Cluj Napoca, 1984.

6.- R.Blaise, Revue des materials de construction 674-675, nos.11-12 (1971) 287-295

7.- U.Ludwig, Sprechsaal fur Keramik - Baustoffe 6 - 1974 - 231-242

8.- Butt Di-M, SILIC ATTECHNIK - 23 no.3 1972-89

9.- Zur-Strassen H. - Zement-Kalk-Gips, 1o no.1 - 1957 - 1

1o.- x x x Der Theor.warmessedorf der zementa brodes zement 3o - 1941 - 231-25o

11.- Deheul, A.Sinsa Illier - C - Sinsa Illier - C - Zement - Kalk - Gips no.8 1979 - 34o-4oo

12.- C.Popescu, H.Bocan, A.Ichim, Alexandra Tatou Aniko Fazakas Methods for determination of clinkering ability of raw materials meals for cement" - Building Materials Revue no.3 - 1983, Vol.3

13.- M.Enculescu, "Contributions at usage of waste materials and by-products resulted from chemical industry, as well as calcium carbonates precipitates and phosphogypsum in the binders industry.

The 4-th chemistry and chemical engineering conferrence the 17-th- 18th

October 1985 - Politechnical Institute - Bucharest

Demetrio Gaspar-Tébar et José Luis Sagrera-Moreno - Instituto "Eduardo Torroja" - Spain

L'ACTION DE L'EAU DE MER SUR UN CIMENT PORTLAND DE HAUTE RESISTANCE INITIELLE ET SUR UN CIMENT PORTLAND RESISTANCE AUX SULFATES: INFLUENCE DE L'ADDITION DE LAITIER, ETUDE DE LA CONCENTRATION IONIQUE.

P

1.- Introduction

Le mécanisme des réactions qui ont lieu lorsque le ciment portland hydraté, et surtout de ses mélanges avec des additions naturelles ou artificielles, est soumis à l'action de solutions agressives, est un des problèmes complexes dans le champ de la Chimie Appliqquée. C'est dans le but de contribuer à sa connaissance que nous avons développé ce travail, qui fait partie d'un Projet de Recherche de l'IETcc à long terme, aussi bien à échelle de laboratoire qu'à échelle réelle.

2.- Partie expérimentale

2.1.Matériaux employés:

2.1.1.- Ciments: deux ciments portland industriels ont été utilisés (l'un de haute résistance initielle -ciment 1- et l'autre, résistent aux sulfates -ciment 2-) dont la composition chimique et potentiel le calculée (Bogue), ainsi que la surface spécifique, se trouvent dans le Tableau 1. La fig. 2 contient les DRX des phases cristallines correspondant aux aluminates des résidus en acide salicylique-méthanol de ces ciments.

2.1.2.- Laitier: Nous avons employé le laitier dont l'analyse chimique et le diagramme de rayons X se trouvent dans le Tableau 1 et fig. 2, respectivement.

2.1.3.- Eau de mer artificielle: l'eau de mer artificielle a été préparée d'après le point 6 de la norme ASTM D 1141-75. La teneur en ions, signalée par la suite, et le pH déterminé expérimentalement, son les suivants: Ca(II) = 0,521 g/l; Mg(II) = = 1,347 g/l; SO (II) = 2,928 g/l, Cl(I) = 19,585 g/l et pH = 6,5.

2.2.- Préparation et conservation des éprouvettes de mortier (1:3): nous avons préparé les mélanges suivants: ciment/laitier = 85/15, 65/35, 40/60 et 30/70 (en poids), qui ont été utilisés pour préparer les différentes séries d'éprouvettes de mortier (1:3) de 1 x 1 x 6 cm; la relation a/c a été 0,6. Elles ont été curées 1 jour en chambre humide, à 20 $\pm$ 1°C, avec une humidité relative supérieure à 95% et, aprés, sous eau douce pendant 21 jours; par la suite nous avons immergé 12 éprouvettes/1 série/ciment ou mélange/1 âge en 800 ml d'eau douce filtré ou en eau de mer artificielle pendant 56, 90, 180 et 360 jours.

2.3.- Préparation de la phase solide: la nouvelle phases solide formée dans l'eau de mer artificielle où les éprouvettes de mortier ont été immergées a été séparée par filtration après en avoir extrait les éprouvettes de mortier, et elle a été séchée au courant d'azote.

3.- Résultats obtenus

L'évolution des teneurs en Ca(II) et de Mg(II) dans la solution et la nouvelle phase solide on été représentées dans les fig. 3 à 9.

4.- Interprétation des résultats

4.1.- Evolution de la teneur en Ca(II).

L'accroissement de Ca(II) en relation avec la teneur de cet ion dans l'eau de mer artificielle où ont été immergées les éprouvettes de mortier ($1{,}30 \times 10^{-2}$ moles/litre), est dû à la dissolution d'une partie du $Ca(OH)_2$, dont la solubilité dans l'eau à 20°C est 1.230 g/l $\lessgtr$ $1{,}66 \times 10^{-2}$ moles/litre, formé dans les éprouvettes de mortier comme conséquence des réactions d'hydrataion des composants du clinker, d'après la réaction (A):

$$\text{(A)}\quad Ca(OH)_2\,\text{.solide} \overset{H_2O\ mer}{\rightleftharpoons} Ca(OH)_2\,\text{.dissous} \overset{H_2O\ mer}{\rightleftharpoons} Ca(II) + 2\,OH(I)$$

donnant lieu encore à un accroissement des groupes OH(I) et ainsi de la valeur du pH, pouvant atteindre des valeurs plus grandes que 11,5 dans les solutions où les éprouvettes en ciment ont été immergées, à 10 pour les éprouvettes élaborées avec mélanges ciment/laitier = 85/15 et 7,5 et inférieur à 9,5 dans ceux correspondant aux séries d'eprouvettes de mortier restante.

Les quantités de $Ca(OH)_2$ dissoutes sont fonction de celles qui vont se former dans les réactions d'hydratation qui, à leur tour, dépendent des mélanges ciment/laitier utilisés dans la fabrication des diverses séries d'éprouvettes de mortier; une partie du $Ca(OH)_2$ formé, réactionne avec le laitier donnant les composants de calcium correspondants, et une autre partie expérimente, dans les éprouvettes, la réaction de carbonatation.

L'équilibre (A) est affecté, en ce cas là, par la présence des ions dans l'eau de mer artificielle non communs, différents du Ca(II) d'une façon spéciale, et encore par l'existance d'autre ions ou composants qui donnent lieu à des réactions de précipitation avec les ions Ca(II) ou avec les ions OH(I) de l'équilibre (A) mentionné, comme il arrive dans les ions Mg(II), SO_4(II) et avec le CO_2, qui forment:

$$\text{(B)}\quad Ca(II) + 2\,OH(I) + CO_2 \rightleftharpoons Ca\,CO_3\,\text{. solide} + H_2O$$

$$\text{(C)}\quad Ca(II) + SO_4(II) \overset{H_2O}{\rightleftharpoons} Ca\,SO_4\,.\,2\,H_2O\,\text{. solide}$$

$$\text{(D)}\quad Mg(II) + 2\,OH(I) \rightleftharpoons Mg(OH)_2\,\text{. solide}$$

qui produisent, dans un degré détérminé, la diminution des ions Ca(II) et OH(I) dans la solution favorisant, se même, la solubilité du $Ca(OH)_2$ et la progression des réactions d'hydratation; phénomènes qui, à leur tour, sont fonction du temps de conservation-attaque pour chaque mélange comme on peut l'apprécier dans les fig. 3 et 5. Tous ces phénomènes agissent sur les quantités de $Ca(OH)_2$ dissoutes dans ces systèmes ciment/laitier-eau douce, (fig. 3 et 5).

Les quantités de Ca(II) $\rightleftharpoons$ $Ca(OH)_2$ dissout, qui se trouvent dans la solution et dans la nouvelle phase solide, dans chaque cas, diminuent brusquement, à mesure que la teneur de ciment dans le mélange utilisé pour élaborer les différentes séries d'éprouvettes de mortier diminue (fig. 3 et 5). Si, en plus du Ca(II) mentionné, on tient compte de celui qui existe dans l'eau de mer artificielle ($1{,}04 \times 10^{-2}$ moles/800 ml) -c'est à dire, le Ca(II) présent dans la phase liquide en plus de celui de la phase solide- il apparait que pour chaque âge dans le système ciment 1/laitier-eau de mer artificielle et pour le premier âge dans le système 2/laitier-eau de mer artificielle, ces quantités se trouvent alignées, pratiquement, sur une ligne droitqui unit les points correspondant au $Ca(II)_2$ dissout, des séries d'éprouvettes faites en ciment 1 et 2, sans addition de laitier, plus celui de l'eau de mer, en ordonnées, et celui du mélange théorique ciment/laitier = 0/100, lorsqu'il n'y a pas de ciment en abscisses; il s'agit par conséquent d'un phénomène additif (fig. 4 et 6).

Les quantités totales de Ca(II) <> Ca $(OH)_2$ dissout, pour chaque mélange et pour tous les âges, plus le Ca(II) de l'eau de mer des systèmes estudiés, se trouvent aux environnements représentés dans la figure 7, où son inclues les valeurs moyennes expérimentales pour chaque mélange et les valeurs calculées pour chaque mélange à partir de la valeur moyenne qui correspond au système partial ciment (100%)-eau artificielle. Dans cette figure on peut observer que les quantités de Ca(II) sont fonc

tion de la quantité de ciment dans le mélangé employé pour élaborer les séries d'éprouvettes de mortier et qui, comme il a été signalé précédemment, répondent à une fonction linéaire dont les points d'intersection aux axes des ordonnées et abcisses sont correspondantes à la valeur moyenne expérimentale du système ciment (100%)-eau de mer, et au mélange ciment/laitier = 0/100 (il n'y a pas de ciment).

Pour les DRX, il a été mis en évidence que dans les fractions enrichies (ciment hydraté-attaqué) extraites des éprouvettes de mortier fabriquées avec ciment et avec les mélanges ayant la plus petite teneur en laitier (15%), immergées dans l'eau de mer, les pics du Ca $(OH)_2$ existent, tandis que, dans les autres cas, ceux-ci n'ont pas été détectés puisque, dès la naissance, l'hydroxide de calcium a partiellement réagi avec le laitier et avec le CO_2 dissout dans l'eau de mer pour donner les composants de calcium correspondants dans l'éprouvettes; le reste s'est dissout dans l'eau de mer.

Comme les quantités de Ca $(OH)_2$ dissoutes -on tient compte de celui qui existe dans l'eau de mer artificielle- répondent quantitativement aux contenus de ciment des mélanges utilisés (figure 7 et Tableau 2), nous considérons que ce phénomène est dû à la progression des réactions d'hydratation qui ont fourni le Ca $(OH)_2$ nécéssaire pour que les réactions mentionnées aient lieu.

Une partie du Ca $(OH)_2$ dissout a réagi, en milieu basique fort, avec le CO_2 de l'eau de mer artificielle d'après l'équilibre (B) parce que le produit de solubilité atteint ($4,8 \times 10^{-9}$), précipitant Ca CO_3 comme calcite et comme aragonite en accord avec les conditions du milieu, donnant lieu, en grand partie, à la formation de la nouvelle phase solide, étant donné que le Mg(II) a précipité en quantités plus petites que $0,15 \times 10^{-2}$ moles, ou il n'a pas précipité, comme nous verrons plus tarde. Les quantités de la nouvelle phase solide sont fonction du temps de conservation-attaque pour chaque mélange, et pour un même âge, du mélange utlisé dans la fabrication des séries d'éprouvettes de mortier; en definitive elles dépendent, spécialement, du degré de carbonatation de la solution et, par conséquent, de la quantité de Ca $(OH)_2$ dissoute.

4.2.- Evolution de la teneur en Mg(II)

La teneur en Mg(II) de l'eau de mer artificielle ($4,43 \times 10^{-2}$ moles/800 ml), où ont été immergées les éprouvettes de mortier élaborées avec les ciments 1 et 2 et avec les mélanges qui ont le plus petit contenu de laitier (15%), pratiquement, a disparu ayant précipité comme Mg $(OH)_2$, et dans les éprouvettes de mortier et dans la solution, donnant lieu à la nouvelle phase solide, avec la calcite et l'aragonite, comme il a été démontré par DRX.

Le Mg(II) existant dans l'eau de mer artificielle réagit, à pH > 10, avec les ions OH(I) de l'équilibre (A) d'après la réaction (D), qui précipite comme Mg$(OH)_2$ parceque $[Mg(II)]\,[OH(I)]^2 > Ps\ (1,8 \times 10^{-11})$; cette réaction a en elle même une diminution du pH. Dans les solutions mentionées plus haut, qui ont un pH $> 10,5$, cette réaction s'est produite, ayant détecté le composant cristallin brucite dans la nouvelle phase solide, où se trouve le Mg(II) en quantités plus petites que $1,80 \times 10^{-2}$ moles (dans la phase liquide on le trouve en quantités plus petites que $0,5 \times 10^{-2}$ moles); le Mg(II) restant a précipité au sein des épruvettes de mortier comme brucite, d'après l'équilibre (E):

(E) $Mg(II) + Ca(OH)_2$ dissout $\rightleftharpoons$ $Mg(OH)_2$ solide + Ca(II)
solution éprouvette éprouvette

de telle sort que pour chaque mol d'ions Mg(II) qui à précipité, un autre de Ca(II) passe à la solution, lequel réagit avec les composants de laitier, ou bien se trouve dans la phase liquide ou dans la nouvelle phase solide. Au contraire, dans les solutions (eau de mer artificielle) où ont été immergées les éprouvettes de mortier fabriquées avec les mélanges ciment/laitier = 65/35, 40/60 et 30/70 (en poids) n'ont pas précipité dans la solution (dans la nouvelle phase solide il n'a pas été détecté) les conditions adéquates n'y étant pas (pH $<$ 10) et n'atteignant pas le Ps; cet ion se trouve dans la solution en quantités inférieures à $2,6 \times 10^{-2}$ moles et supérieures à $1,0 \times 10^{-2}$ moles pour deux de ces mélanges qui ont des contenus en laitier plus grands (60 et 70% en poids), le reste ayant précipité dans les éprouvettes de mortier, en des quantités telles qu'elles dépendent de la quantité de Ca$(OH)_2$ engendrées dans les réactions d'hydratation (fig. 8 et 9).

4.3.- Evolution des teneurs en Ca(II) et Mg(II)

Dans les figures 8 et 9 nous avons représenté l'evolution des teneurs en ions Ca(II) et Mg(II) dans la solution [Ca(II) procédant du Ca $(OH)_2$ dissout, plus Ca(II) de l'eau de mer] plus dans la nouvelle phase solide, graphiques 1 et 3, en plus du Ca(II) dans la solution plus dans la nouvelle phase solide procédant du Ca$(OH)_2$ dissout, graphique 2, en fonction du mélangé ciment/laitier utilisé pour l'élaboration des séries d'éprouvettes de mortier pour chaque période de conservation-attaque; dans ce figures on apprécie que ces teneurs sont en relation intime de telle façon que lorsque l'une diminue, l'autre augmente et viceversa, existant un point de croisement dans les graphiques 2 et 3 qui correspond aux mélanges ciment 1/laitier = 40/60 (pour deux âges) et 50/50 (pour les autres deux âges) et ciment 2/laitier = 40/60 (pour les quatre âges), où a lieu l'equilibre ionique Ca(II) à la solution $\rightleftharpoons$ Mg(II) qui disparait de la solution, où, pour chaque mol d'ions Ca(II) mis en jeu, un autre d'ions Mg(II) disparait. Dans le cas des éprouvettes fabriquées avec mélanges qui ont des quantités de laitier inférieures à 60% les quantités de Ca(II) sont supérieures à celles de Mg(II), puisque durant l'hydratation une plus grande quantité de $Ca(OH)_2$ se produit, restant libre en partie une plus grande quantité qui facilite la précipitation du Mg(II) et la dissolution du Ca $(OH)_2$; par contre, dans les cas des éprouvettes fabriquées avec des mélanges qui ont des quantités supérieures de laitier (70%) le phénomène est inversé, y restant dans la solution et dans la nouvelle phase solide des teneurs plus grandes de Mg(II) que de Ca(II) parceque il n'y a pas les conditions pour que le ion Mg(II) précipite, n'existant pas une quantité d'ions OH(I) suffisante, étant donné que la quantité nécessaire de $Ca(OH)_2$ ne s'est pas générée. Les faits mentionnés influent dans le degré de résistance chimique des ciments.

4.4.- Evolution de la teneur de SO_4(II) et de Cl(I)

Les teneurs d'ions SO_4(II) et de Cl(I) dans l'eau de mer artificielle, subissent une diminution que est en liaison intime avec les caractéristiques du ciment et du laitier, ainsi que le mélange employé pour élaborer les différentes séries d'éprouvettes de mortier et du temps de conservation-attaque qui influen sur la formation de composants à base de sulfates (gypse secondaire et ettringite) et de chlorures (sel de Friedel) dans les éprouvettes de mortier.

Tableau 1

1.-Analyse chimique (%, e.p.)		Ciments 1	2	Laitier
P.F.	.....	0,4	1,1	0,4
R.I.	.....	3,1	0,2	0,0
SiO_2	.....	19,3	22,0	35,2
Fe_2O_3	.....	3,9	4,1	0,7
Al_2O_3	.....	6,2	1,8	17,0
CaO	.....	61,1	67,9	37,3
MgO	.....	1,5	0,5	6,3
SO_3	.....	4,1	2,3	0,0
Mn (II)	.....	nd	nd	0,8
CaO libre	....	1,0	1,8	-

nd = pas dosé

2.-Composition potentielle (Bogue)			
C_3S	.....	39,2	75,6
C_2S	.....	25,7	6,1
C_3A	.....	9,9	0,0
C_4AF	.....	12,0	10,8

3.-Surface spécifique (Blaine)			
cm^2/g	.....	5.313	3.553

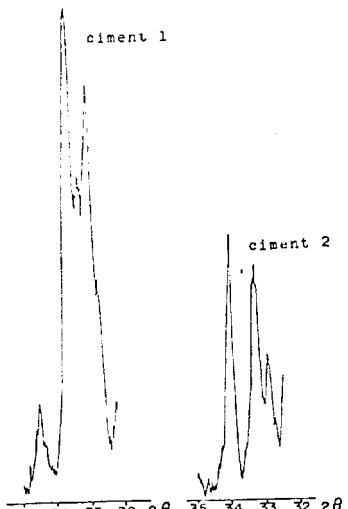

FIGURE 1.-RSM ciments 1 et 2. DRX

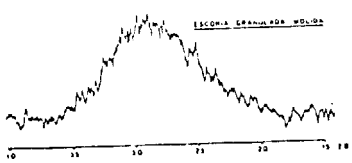

FIGURE 2.- Laitier. DRX

Tableau 2.- Ca (II), teneur total; moles x 10^{-2}

melange: ciment/ laitier	Syatème ciment - 1/laitie		ciment - 2/laitier	
	experi mental - x	calcu lée - x	experi mental - x	calcu lée - x
100/0	5,55	5,55	6,35	6,35
85/15	4,60	4,71	5,44	5,40
65/35	3,50	3,60	4,23	4,13
40/60	2,12	2,22	2,75	2,54
30/70	1,85	1,67	2,20	1,91

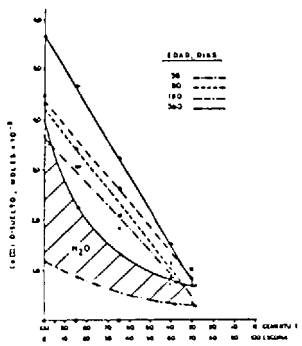

ciment 1/laitier

FIGURE 3

Ca(II) dissout.Evolution teneur

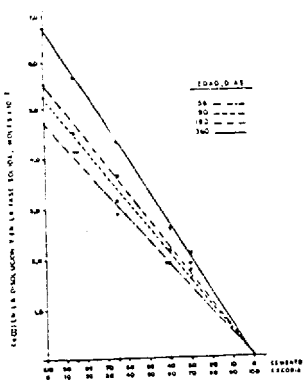

ciment 1/laitier

FIGURE 4

Ca(II) total.Evolution teneur

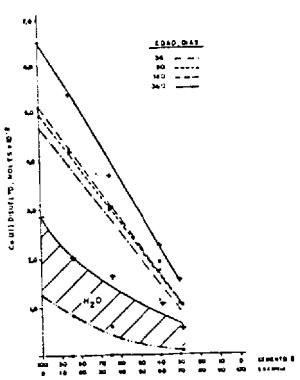

ciment 2/laitier

FIGURE 5

Ca(II) dissout.Evolution total

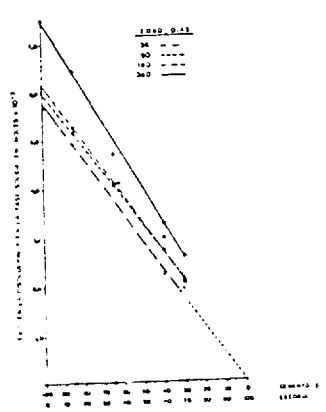

ciment 2/laitier

FIGURE 6

Ca(II) total.Evolution teneur

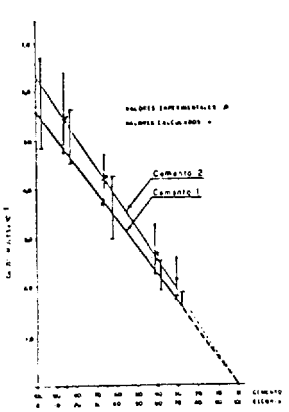

ciment/laitier

FIGURE 7

Ca(II) total.Evolution teneur

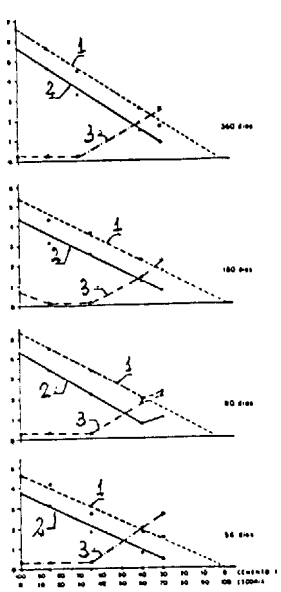

ciment 1/laitier

FIGURE 8

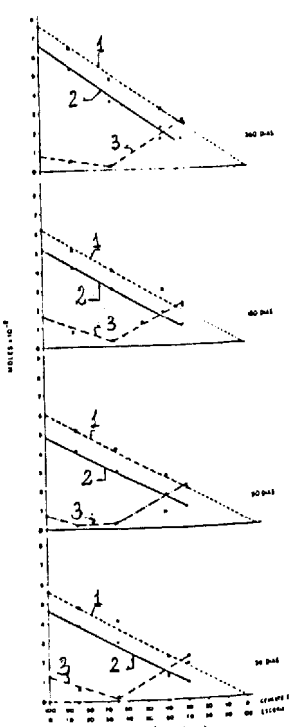

ciment 2/laitier-

FIGURE 9

Ca(II) et Mg(II). Evolution teneur

1.-Ca(II) solution + Ca(II) phase solide
Ca(II) solution = Ca(II) eau de mer + Ca(II) dissout
2.-Ca(II) dissout = Ca(II) solution + Ca(II) phase solide
3.-Mg(II) solution + Mg(II) phase solide

Francisca Bermejo-Muñoz, José Luis Sagrera-Moreno et Demetrio Gaspar-Tébar
Instituto "Eduardo Torroja" - Spain

COMPORTMENT D'UN CIMENT PORTLAND RESISTANT AUX SULFATES FACE A L'EAU DEIONISEE ET LES SOLUTIONS DE SULFATE DE SODIUM ET DE SULFATE DE MAGNESIUM.

P

1.- Introduction

Le comportement de mortiers et bétons soumis à l'action de différentes ambiances agressives a fait l'objet de nombreux travaux comme conséquence du grand nombre d'ouvrages construits dans ces milieux, ce sujet ayant préocupe non seulement d'un point de vue constructif mais encore scientifique pour connaître les causes qui produisent l'attaque chimique; c'est ainsi que, à l'objet d'élargir la connaissance du mécanisme des réactions qui ont lieu lorsque les ciments portland hydratés et surtout de ses mélanges avec des additions naturelles et artificielles, sont soumis à l'action de solutions agressives, ce travail, qui fait partie d'un Projet de Recherche à long terme, a été réalisé aussi bien à échelle de laboratoire comme à échelle réelle.

Dans d'autres travaux présentés dans ce Congrès nous étudions le comportement mécanique-résistant d'un ciment (ciment 2), analogue à celui qui fait l'objet de ce travail, lorsque diverses séries d'éprouvettes de mortier et de béton sont soumises à l'action de différentes solutions agréssives(1), la variation de la concentration ionique de l'eau de mer où les éprouvettes de mortier fabriquées avec deux ciments portland industriels (ciment 1 et ciment 2) ont été immergées, et des ses mélanges avec laitier (2), l'évolution des caractéristiques structurelles des composants cristallins de la fraction enrichie (ciment hydraté-attaqué) extraite de l'une des éprouvettes de mortier faites avec trois ciments (ciment 1, ciment 2 et ciment 3) et de ses mélanges avec laitier, immergées en eau de mer artificielle, ainsi que de la phase solide formée dans cette eau de mer (3).

2.- Partie expérimentale

Dans ce travail nous étudions le comportement d' un ciment portland résistant aux sulphates lorsque les lits fabriqués avec ce ciment, qui s'est hydraté et qui a été conservé pendant 7 ou 28 jours dans atmosphère étanche avec une humidité relative supérieure à 90% et une température de 21 ± 2°C, sont soumis à l'action d'eau déionisée (système ciment 2 hydraté-eau déionisée), d'une solution de sulfate de sodium (système ciment 2 hydraté-solution de sulfate de sodium) et d'une solution de sulfate de magnésium (système ciment 2 hydraté-solution de sulfate de magnésium), determinant la variation de la concentration d'ions Ca (II) et SO_4(II) dans les deux premiers systèmes, et des ions Ca (II), Mg (II) et SO_4(II) dans le troisième système aussi bien dans les solutions comme dans le ciment hydraté du lit, l'évolution du pH et de la conductivité de ces solutions, ainsi que les modifications structurelles expérimentées par le ciment hydraté du lit.

2.1.- Matériaux employés

2.1.1.- Ciment: nous avons utilisé un ciment portland industriel résistent aux sulphates (ciment 2), de fabrication espagnole, dont la composition chimique et potentielle calculée (Bogue), ainsi que la surface spécifique, se trouvent dans le Tableau 1. Dans la fig. 1 sont indiqués les DRX des phases cristallines correspondentes aux aluminates du ciment anhydre et du résidu en acide salicylique-méthanol.

2.1.2.- Solutions agressives: nous avons utilisé les solutions suivantes:

a. eau déionisée,
b. solution de sulfate de sodium (2,1 g/l de Na_2SO_4), avec une concentration de SO_4(II) = 1,42 g/l <> 1,48 x 10^{-2} moles /litre, déterminée expérimentalement.
c. solution de sulfate de magnesium (2,76 g/l de $MgSO_4 \cdot 7\ H_2O$), avec une concentration de SO_4(II) = 1,076g/l <> 1,42 x 10^{-2} moles/litre et de Mg (II) = 0,272 g/l <> 1,12 x 10^{-2} moles/litre, déterminées expérimentalement.

2.2.- Préparation des lits de ciment hydraté: le ciment est malaxé avec l'eau de consistence, il est introduit en chambre humide (humidité relative > > 90%; t°C = 21 + 2°C) pendant 8 heures, de suite, on fait passer la pâte par un tamis avec une ouverture de 1,5 mm obtenant ainsi un granulé de ciment, que l'on introduit dans un tuyeau en plastique (Ø = 3,5 cm; h = 16 cm), isolée de l'atmosphère avec l'azote.

Les solutions qui se trouvent dans un réservoir nourrice, traversent le lit de ciment, recueillant diverses fractions, en fonction du temps (0,15 - 0,16 l/h), où l'on a effectué les déterminations analytiques mentionnées.

3.- Résultats obtenus

Les résultats obtenus ont été représentés dans les fig. 2 à 10, celles-ci étant inclues.

4.- Interprétation des résultats

4.1.- Evolution de la teneur en Ca (II) dans le système ciment-eau déionisée et ciment-sol. de Na_2SO_4.

Dans ce travail il a été mis en évidence que les quantités de Ca $(OH)_2$ extraites des deux systèmes ciment-eau déionisée et ciment-solution de sulfate de soldium est une fonction exponentielle (fig. 2 et 3), étant asymptote par rapport à la quantité de solution qui traverse le lit, procès qui influence la progression des réactions d'hydratation et la dégradation des composants du ciment, comme on peut l'apprécier dans les DRX des figures 4 et 5.

Le Ca (II) qui apparait dans l'eau déionisée et dans la solution de Na_2SO_4 qui ont traversé les lits de ciment hydraté et granulé procède, fondamentalement, du Ca $(OH)_2$ formé pendant les réactions d'hydratation des composants de la fraction clinker du ciment (étant donné la solubilité des composants de calcium du ciment), en vertu de la réaction (A):

(A) $Ca(OH)_2$. solide $\rightleftharpoons$ $Ca(OH)_2$. dissout $\rightleftharpoons$ Ca (II) + + 2 OH^- (I)

produisant un accroissement brusque du pH (il atteint des valeurs supérieures à 12 dans le cas de l'eau et à 11,5 de la solution de Na_2SO_4). La solubilité du Ca $(OH)_2$ en eau est de 1,230 g/l, à 20°C, (4) ou de 1,230 g/l comme CaO <> 1,625 g/l comme Ca $(OH)_2$ (5); les silicates de calcium hydratés sont peu solubles dans l'eau, 50 mg/l comme Ca O (6) (7) <> 66 mg/l comme Ca $(OH)_2$; l'ettringite se dissout légèrement, d'après certains auteurs (8)(9) et elle est extrêmement insoluble, d'après les autres (10).

Les concentrations maximales de Ca (II) dans les solutions (2,1 x 10^{-2} moles/litre et 1,6 x 10^{-2} moles/litre) (2,1 x 10^{-2} moles/litre et 1,93 x 10^{-2} moles/litre), ainsi que les valeurs du pH et de la conductivité, ont été obtenues lorsqu'elles ont traversé les lits 0,60 l d'eau déionisée pour le ciment hydraté 7 jours et 0, 36 l dans le cas du ciment hydraté 28 jours et 1,01 litres de la solution Na_2SO_4 pour le ciment

hydraté 7 jours et 0,49 pour 28 jours, respectivement.

Dans les extractions suivantes elles décroissent exponentiellement pouvant être plus petites que $0,2 \times 10^{-2}$ moles/litre dans le premier système et $0,4 \times 10^{-2}$ moles/litre dans le second.

Les quantités de Ca (II) $\leftrightarrow$ Ca $(OH)_2$ extraites des lits de ciment sont fonction du pouvoir dissolvant, de la solution et du volume qui a traversé les lits de ciment, d'une part, ainsi que du temps d'hydratation du ciment, de l'autre, comme on peut l'apprécier dans les DRX des figures 4 et 5 et dans le Tableau 2. Ainsi, ces quantités représentent 65,7% et 50,8% pour l'eau déionisée et 34,3% et 32,3% pour la solution de sulfate de sodium (là on doit tenir compte de l'effet salin), selon qu'il s'agisse du ciment hydraté pendant 7 ou 28 jours, respectivement; le reste, reste dans les éprouvettes de mortier sous forme de sels de calcium; tout le Ca $(OH)_2$ a disparu (DRX des fig. 4 et 5). Tous ces phénomènes sont en rapport avec le degré d'hydratation et de carbonatation du ciment, ainsi qu'avec la progression des réactions d'hydratation.

4.2.- Evolution des teneurs en Ca (II) et Mg (II) dans le système ciment-sol. de Mg SO_4.

Dans le système ciment-solution de sulfate de magnesium se produit un ensemble de processus physico-chimiques qui donnent lieau à la formation de composants dans les lits de ciment (7 et 28 jours), d'une nouvelle phase solide dans la solution qui a traversé les lits, et à la dissolution des autres.

Dans le lit de ciment il s'est formé brucite et gypse secondaire (prouvé par DRX, fig. 6), la portlandite a disparu et les composants anhydrides du ciment ont diminué; et aussi, la quantité d'éttringite et de calcite a augmenté.

La solution qui a traversé les lits de ciment a expérimenté des modifications en ce qui concerne les teneurs en Ca (II), Mg (II) et SO_4 (II), ainsi que la valeur du pH et de la conductivité; à leur sein, une nouvelle phase solide s'est formée, composée de brucite et de calcite (DRX de la fig. 7) où elles ont précipité, ayant atteint les Ps correspondents.

Dans ces travaux il a été mis en évidence que le Mg (II) de la solution ($1,12 \times 10^{-2}$moles/litre) disparait totalement ou partiellement lorsqu'il traverse le lit de ciment hydraté, hayant précipité comme Mg $(OH)_2$ sur place, totalement lorsque la concentration de Ca (II) dans la solution, extraite du ciment, est $\geqslant 1,12 \times 10^{-2}$ moles/litre et le pH $\geqslant$ 11,5 et, partiellement, lorsque les deux caractéristiques sont plus petites (fig. 8 et 9). Le précipité de Mg $(OH)_2$ dans le lit, produit une diminution de la porosité, arrivant parfois à se colmater et empêchant le passage de la solution (fig. 10); le précipité commence dans la zone supérieure de la colonne du lit de ciment, raison pour laquelle la partie principale d'échange doit descendre à mesure qu'une plus grande quantité de solution de Mg SO_4 s'écoule.

La formation de brucite dans le lit de ciment à lieu d'après la réaction suivante:

$$(B)\ \underbrace{Ca(OH)_2.\text{sólide} \left[\rightleftharpoons Ca(OH)_2.\text{dissout} \rightleftharpoons Ca(II) + 2\,OH(I)\right]}_{\text{lit de ciment}} +$$

$$+\ Mg(II) \rightleftharpoons \underbrace{Mg(OH)_2.\text{solide}}_{\text{lit de ciment}} + Ca(II)$$

$$\text{solution}$$

puisque Ps $[Mg(OH)_2] = 1,8 \times 10^{-11} <$ P's $[Ca(OH)_2] = 5,5 \times 10^{-6}$, s'accomplissant d'autre part, $[Mg(II)][OH(I)]^2 >$ Ps $(1,8 \times 10^{-11})$. En ce cas là, pour chaque mol d'ions Mg (II) qui disparait de la solution, il en apparait un autre de Ca (II).

Le Ca $(OH)_2$ du lit de ciment hydraté, se dissout dans la solution de Mg SO_4, d'après l'équilibre (A), arrivant à disparaître (DRX de la fig. 6); dans les premières extractions, la teneur en Ca (II) Ca $(OH)_2$ dissout atteint sa valeur maximale aussi bien dans le lit de ciment hydraté 7 jours ($2,8 \times 10^{-2}$ moles/litre et 28 jours ($2,38 \times 10^{-2}$ moles/litre) lorsque 0,72 l et 0,21 l, respectivement, ont coulé; par la suite, il diminue, atteignant les valeurs minimales ($0,4 \times 10^{-2}$ moles/litre pour le premier lit, augmentant par la suite, et $0,08 \times 10^{-2}$ moles/litre pour le deuxième lit), les teneurs en Ca (II) suivent l'évolution représentée dans les fig. 8 et 9, où nous indiquons aussi, l'évolution des teneurs en Mg (II).

Dans ce système on remarque que l'évolution de la teneur en Mg (II) dans les différentes extractions de la solution est intimement en rapport à celle de Ca (II), de telle façon que, lorsque l'élimination du Mg (II) dans la solution, par précipitation dans le lit de ciment comme Mg $(OH)_2$, est partielle, il y a $[Ca(II)] + [Mg(II)] = \text{cte} (\simeq 1,12 \times 10^{-2}$ moles/litre = concentration initielle de Mg (II) dans la solution) de telle façon que pour chaque mol de Mg (II) qui disparait de la solution, un autre Ca (II) apparait, comme il a été signalé auparavant. Dans les points d'intersection des graphiques qui représentent les tenuers en Ca (II) et Mg (II) (fig. 8 et 9), il y a $[Ca(II)] = [Mg(II)] = 0,6 \times 10^{-2}$ moles/litre; c'est à dire, l'équilibre (B) est atteint. Equilibre lié aux réactions d'hydratation du ciment et à la formation de Ca $(OH)_2$, qui se trouvent favorisés par l'élimination d'ions OH (I) et par la dissolution de la portlandite.

Les faits mentionnés prouvent que les quantités de Ca (II) $\leftrightarrow$ Ca $(OH)_2$ extraites des lits de ciment dépendent du temps d'hydratation du ciment et de l'influence du cation Mg (II). Ainsi, dans le cas du lit de ciment hydraté pendant 7 jours, le précipité de Mg $(OH)_2$ a colmaté ce lit, dont 47% a été extrait (Tableau 2), tandis que, dans le cas du lit de ciment hydraté pendant 28 jours, 24,6% en a été estrait (Tableau 2) et 38,9% de Mg (II) s'est déposé, à cause de l'influence de la précipitation de ce Mg (II) qui déplace l'équilibre (B) vers la formation de brucite pour les raisons dont nous avons fait l'exposé auparavant.

Dans la plûpart des extractions, des petites quantités de précipité sont apparues (de l'ordre de mg) qui, groupés, ont permis de déterminer leur composition chimique et de les étudier par DRX (fig. 7), ayant identifié les pics des composants cristallins calcite et brucite, qui ont précipité ayant les conditions favorables pour attiendre les produits de solubilité correspondents.

4.3.- Evolution de la teneur en SO_4(II).

L'eau déionisée dissout, aussi, les sulfates présents dans le ciment, étant fonction du degré d'hydratation et formation de nouveaux composants; ainsi, dans le cas du lit de ciment hydraté pendant 7 jours, 41% des ces composants restent dans le ciment et 53% dans le lit hydraté pendant 28 jours. L'extraction de ces composants diminue exponentiellement, comme dans le cas de Ca (II), avec le passage de l'eau déionisée.

Par contre, dans le cas de la solution de Na_2SO_4, lorsque les premières quantités de cette solution s'écoulent, la concentration de ions SO_4 (II) y diminue (ils sont retenus par le lit du ciment) mais, par la suite, cette concentration se maintient pratiquement constante. En résumé, dès le commencement une partie de la concentration d'ions SO_4 (II), en petite quantité et étant donné les caractéristiques structurelles du ciment, a été retenue par le ciment hydraté du lit, fondamentalement, sous forme de $CaSO_4 . 2H_2O$, ayant Ca (II) -procédent du $Ca(OH)_2$-. Par contre, ayant atteint l'équilibre et n'existant pas de Ca (II) $Ca(OH)_2$, puisqu'il s'est dissout, la formation de ce composant et de l'ettringite s'arrête, la solution de Na_2SO_4 agissant comme dissolvant des composants du ciment.

Dans le système ciment-solution de sulfate de magnesium a lieu un procès analogue à celui de la solution de sulfate de sodium (la teneur en SO_4(II) diminue dans la première extraction et n'expérimente pas, par la suite, de variation); cependant, étant donné les caractéristiques de ce système qui met en jeu des quantités plus grandes de Ca (II), d'après l'équilibre (B), les quantités d'ions SO_4 (II), sont plus grandes (de l'ordre de 10 - 12%, face à 6 - 7% par rapport à la quantité totale mise en jeu), ayant formé $CaSO_4 . 2H_2O$ et ettringite en petite quantité (fig. 6) en accord avec les caractéristiques du ciment.

La formation de Mg $(OH)_2$ (pK = 11,5), la liberation de $Ca(OH)_2$ (pK = 5,3), l'avancement des réactions d'hydratation et la régulation du pH ont favorisé l'obtention de $Ca_2SO_4 . 2H_2O$ (pK= 4,6), qui réactionne avec les aluminates de calcium hydraté du ciment, produisant ettringite en petite quantité; phénomènes qui ont été prouvés par DRX, spécialement dans le ciment du lit hydraté pendant 7 jours.

4.4.- Evolution du pH et de la conductivité

Le pH des différentes fractions extraites de l eau déionisée est gouverné par l'équilibre (A). Dans les premières extractions un accroissement brusque se produit, pouvant atteindre des valeurs supérieures à 12, qui restent pratiquement constantes dans une primière étape; de suite, elles descendent (elles sont supérieures à 9). L'évolution du pH est en accord avec la quantité de Ca $(OH)_2$ dissout, de la même façon que dans le système ciment-dissolution de sulfate de sodium.

Le système ciment - solution de sulfate de magnesium, reçoit l'influence, en outre des procès précedents, de la réaction de précipitation de Mg $(OH)_2$, qui maintient le pH dans la zone comprise entre 10,6 et 10,7 à parti des premières extractions, où il se trouve à environ 11,8.

Quant à la conductivité, qui est fonction des ions présents dans les solutions, elle est gouvernée, spécialement, par l'équilibre (A), subissant une augmentation brusque dans les premières extractions et, par la suite, diminuant exponentiellement d'une façon analogue à celle que subit la quantité de Ca $(OH)_2$ dissout. Les valeurs de conductivité subissent fondamentalement l'influence des ions OH(I) et Ca (II) dans le premier système et, en plus, les ions SO_4(II) et Na (I) dans le second et les ions SO_4 (II) et Mg (II) dans le troisième, dont les conductivités ioniques a 25°C, en $ohm^{-1} . cm^2 . equiv.^{-1}$, son: $\lambda_{OH(I)} = 198,0$; $\lambda_{Ca(II)} = 59,5$; $\lambda_{SO_4(II)} = 80,0$; $\lambda_{Na(I)} = 50,1$ et $\lambda_{Mg(II)} = 53,1$ (à dilution infinie).

5. Conclusions

Première:
Le $Ca(OH)_2$ présent dans les lits de ciment hydraté, qui procèdent des réactions d'hydratation du ciment, se dissout dans l'eau déionisée qui traverse ces lits et en plus petit degré dans la solution de sufate de sodium; de même, les composants à base de sulfates et spécialement l'ettringite, se disolvent (partiellement) dans l'eau déionisée.

Les quantités dissoutes, qui expérimentent une diminution exponentielle en même temps que le volume de la solution qui traverse les lits augmente, sont fonction du temps d'hydratation-conservation du ciment des lits, des caractéristiques de la solution (sans ou avec ions, communs ou non et qui réactionnent avec d'autres ions) et du volume de la solution.

Deuxième:
De même, ce $Ca(OH)_2$ se dissout dans la solution de sulfate de magnesium qui traverse les lits de ciment. La solution de l'hydroxide mentionné est influencée par la présence de Mg (II) dans la solution, qui précipite comme brucite dans les lits, pouvant arriver à le colmater dans des cas détérminés.

L'évolution de la teneur en Mg (II) dans la solution est en rapport étroit avec celle du Ca (II) dans cette solution et viceversa, de telle façon que, lorsque la concentration de l'un augmente, celle de l'autre diminue.

La teneur en Mg (II) dans la solution disparait totalement ou partiellement lorsqu'il traverse les lits de ciment; totalement lorsque $[Ca(II)] \simeq 1,12 \times 10^{-2}$ et pH $> 11,5$. Lorsqu'il y a Mg (II) dans la solution, il y a $[Ca(II)] + [Mg(II)] = cte \simeq 1,12 \times 10^{-2}$ moles/litre = concentration initielle de Mg(II)]

Troisième:
Les ions SO_4 (II) des solutions de Na_2SO_4 et $MgSO_4$ sont retenues partiellement dans les lits de ciment, où a lieu la formation de petites quantités de gypse secondaire et d'ettringite (plus grandes dans le cas de la solution $MgSO_4$); cette rétention diminue en même temps que le volume de la solution qui a traversé les lits augmente. en dépendance à son tour, du temps de conservation du ciment.

Quatrième:
La conductivité et le pH des solutions qui ont traversé les lits de ciment hydraté poursuivent leur évolution, analogue à celle du $Ca(OH)_2$ extrait, étant fonction, d'une façon spéciale, de la concentration d'ions OH(I) présents dans les solutions mentionnées.

Cinquième:
Les composants cristallins du ciment hydraté (ettringite, portlandite et calcite) et de la fraction non hydratée du clinker, expérimentent des changements considérables qui dépendent de la solution (classe et volume) et du temps de conservation du ciment.

6. Bibliographie

(1) GASPAR-TEBAR, D.; SAGRERA-MORENO, J.L. et GONZALEZ-VILA, V.; (1986).- Contribution a l'etude du resistance chimique des ciments. Comportement mecanique-resistant d'un ciment portland (C_3A, calculée = 0%) front diverses solutions agressives. Communication presentée à ce Congrès.

(2) GASPAR-TEBAR, D. et SAGRERA-MORENO, J.L.; (1986).- L'action de l'eau de mer sur un ciment portland de haute resistance initielle et sur un ciemnt portland resistant aux sulfates: influence de l'addition de laitier. Etude de la concentration ionique. Communication presentée à ce Congrés.

(3) GASPAR-TEBAR, D. et SAGRERA-MORENO, J.L.; (1986). L'action de l'eau de mer sur un ciment portland de haute resistance initielle, sur un ciment portland resistante aux sulfates et sur un ciment portland ordinaire: influence de l'addition de laitier. Etude par DRX. Communication presenté à ce Congrés.

(4) BICZOK, I.; (1972).- Corrosión y Protección del Hormigón.- Edic. Urmo; Bilbao.- Pg. 211.

(5) DURIEZ, M. et ARRAMBADI, J.; (1961).- Nouveau traité de Matériaux de Construction; Tome 1.- Edi. Dunod; Paris.- Pgs. 489-490.

(6) ALEGRE, R.; (1978).- Comportement des ciments en milieu agressif.- Annales de l'Institut Technique du Bâtiment et des Travaux Publics (Serie: Sols et Fundations, nº 159); 364, 78.

(7) DEEYFUS, J.; (1960).- La Chimie des Ciments; Tome 1; Edit. Eyrolles; Paris.- Pg. 41.

(8) TAYLOR, H.F.W.; (1964).- The Chemistry of Cements; Vol. 1.- Edit. Acad.Press. Inc.; London. Pg. 228.

(9) LEA. F.M. y DESCH, E.H.; (1960).- Química del Cemento y del Hormigón.- Edit. Tipografía Artistica; Madrid.- Pg. 228.

(10) BOGUE, R.H.; (1962).- La química del Cemento Portland.- Edit. Dossat; Madrid.- Pg. 600.

Remercíements

Nous voudrons exprimer nôtre plus vivie reconaissance aux membres de l'EI "Durabilidad" del IETcc: Amalia Rodríguez, Lucila López, Mª Soledad Cid, Felipe Cantero et Manuel Cantero pour l'aide prêtée dans les réalisation de ce travail.

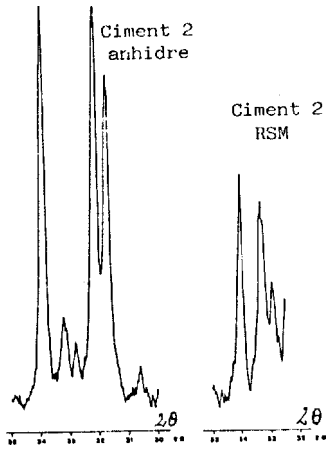

FIGURE 1

Ciment 2:
anhidre et RSM. DRX.

Tableau 1

1.- Analyse chimique %, e. p.

P.F.	.....	1,1
R.I.	.....	0,2
SiO_2	.....	22,0
Fe_2O_3	.....	4,1
Al_2O_3	.....	1,8
CaO	.....	67,9
MgO	.....	0,5
SO_3	.....	2,3
CaO libre	....	1,8

2.- Composition potential (Bogue)

C_3S	.....	75,6
C_2S	.....	6,1
C_3A	.....	0,0
C_4AF	.....	10,8

3.- Surface spécifique (Blaine)

cm^2/g	.....	3.553

Tableau 2
Quantité de Ca (II) dans les composants

Composants		Solutions					
		Eau deionisée		Na_2SO_4		$MgSO_4$	
		7 jours	28 jours	7 jours	28 jours	7 jours	28 jours
Ciment	(100,0)	30,0	46,2	57,1	67,7	52,9	73,8
Solution	(0,0)	65,7	50,8	34,3	32,3	47,1	24,6
Somme	100,0	95,7	97,0	91,4	100,0	100,0	98,4

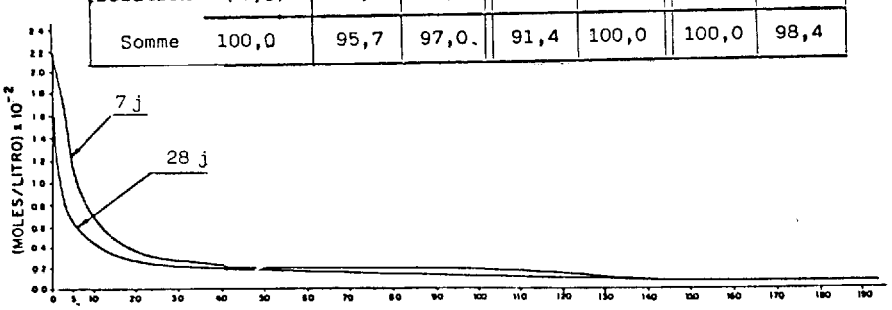

FIGURE 2

Ciment 2 hydraté - eau deionisée: Evolution de la teneur de Ca (II).

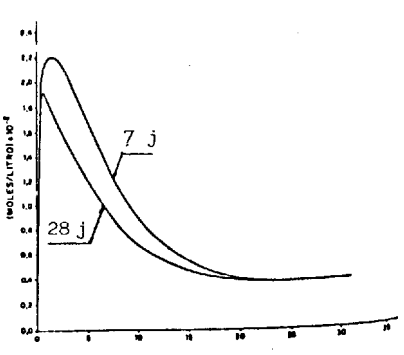

FIGURE 3

Ciment 2 hydraté - sol. Na_2SO_4: Evolution de la teneur de Ca (II).

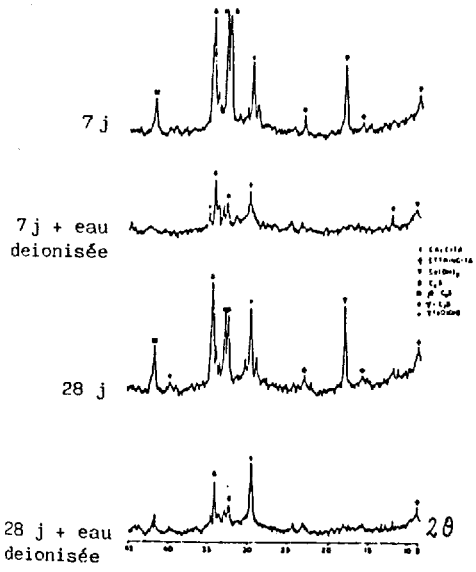

FIGURE 4

Ciment 2 hydraté - eau deionisée:
-Ciment hydraté (7 et 28 j)
-Ciment hydraté (7 + 28 j) + eau deionisée. DRX.

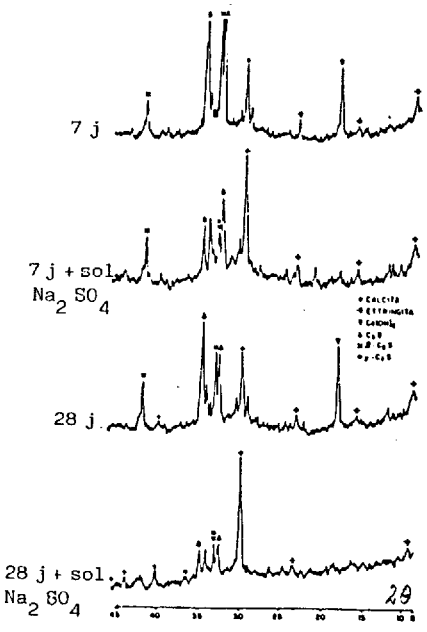

FIGURE 5

Ciment 2 hydraté - sol. Na_2SO_4:
-Ciment hydraté (7 et 28 j). DRX
-Ciment hydraté (7 + 28 j) + sol. Na_2SO_4. DRX.

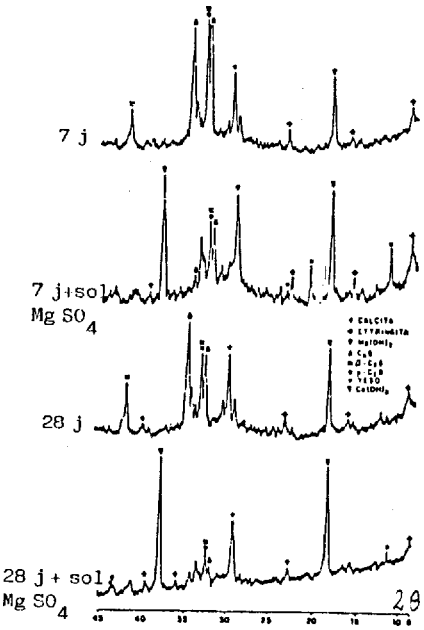

FIGURE 6

Ciment 2 hydraté - sol. Na_2SO_4:
-Ciment hydraté (7 et 28 j). DRX
-Ciment hydraté (7 et 28 j) + sol. $Mg\,SO_4$. DRX.

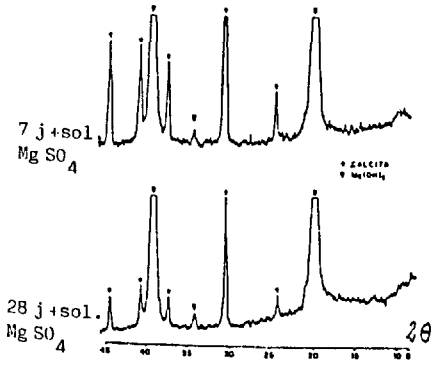

FIGURE 7

Ciment 2 hydraté - sol. $Mg\,SO_4$:
Nouvelle phase solide. DRX.

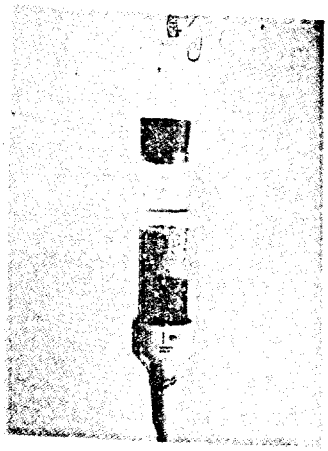

FIGURE 10

Ciment 2 (7 j) - sol. $Mg\,SO_4$. Vue du lit.

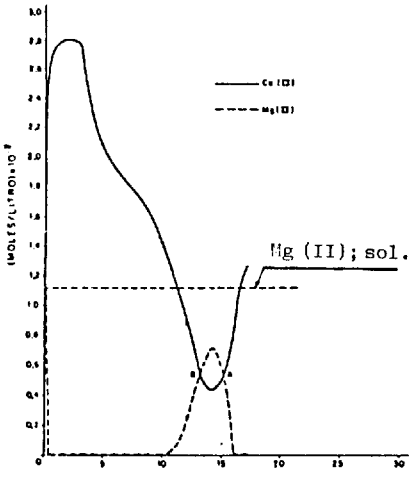

FIGURE 8

Ciment 2 hydraté (7 j) - sol. $Mg\,SO_4$
Evolution des teneurs de Ca (II) et de Mg (II).

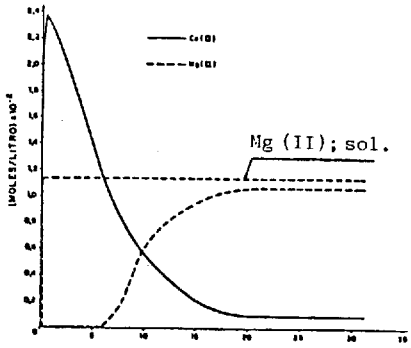

FIGURE 9

Ciment 2 hydraté (28 j) - sol. $Mg\,SO_4$
Evolution des teneurs de Ca (II) et de Mg (II).

M.P. DE LUXAN; M.I. SANCHEZ DE ROJAS; Inst. Constr. Cem. "E. Torroja" (C.S.I.C.). Madrid, Spain
M.T. MARTIN PATINO; C.S.I.C. and Dep. Geol. and Geoquim., Univ. Autónoma. Madrid, Spain.
J. SAAVEDRA; U.E.I. Mineral and Geol. (C.S.I.C.). Salamanca, Spain.

CHARACTERIZATION AND POZZOLANIC PROPERTIES OF SEDIMENTARY OPALINE ROCKS

INTRODUCTION

Among the present trends in the cement industry, the special mention is for the mixed cements.

This has led to the search for materials capable of being incorporated into cement and to the study of their suitability as active additions.

In Spain natural pozzolans and slag has been used for many years, and recently fly ash has come widely into use. However, the way between the source and its use is a basic economic factor which restricts the use of these materials whose cost must be very low. The discovery of the existence of sedimentary opaline rock in the west of the Iberian Peninsula has covered a geographical area where no other material is found that has pozzolanic properties. The present study is concerned with these opaline rocks and their use as active additions to cement.

CHARACTERIZATION OF OPALINE ROCKS

* These sedimentary levels appear on the old meteorized socle of the Central Spanish mountain system.

* Their origin is connected with an exogenic phenomenon linked to meteorization prodesses in a hot climate with alternating dry and humid seasons. The silica set free by meteorization in the humid period concentrates through evaporation in low-relief areas during the dry season and precipitates as the acidity decreases.

FIG.1.- Typical X-ray diffractogram of an opaline rock

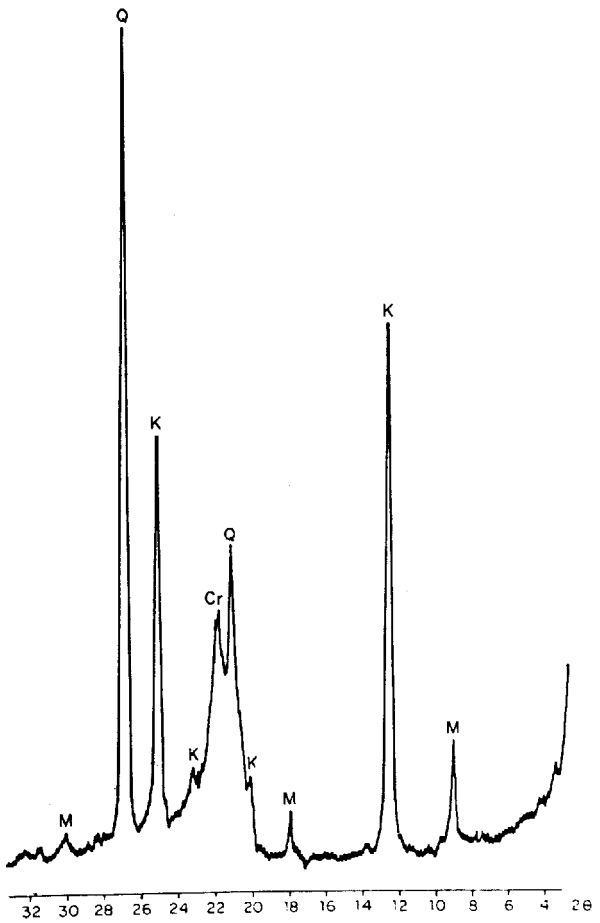

Q: quartz; M: micas; K: kaolinite; Cr: opal C-T

FIG.2.- Typical IR absorption spectrum of an opaline rock

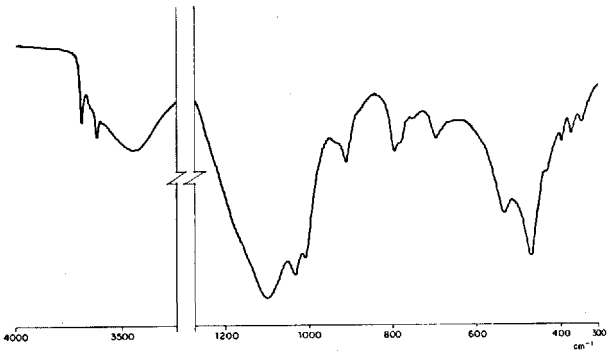

* The mineral compounds commonly found in these materials are quartz, opal-CT, opal-A, kaolinite and micas. This composition was established by means of an X-ray diffraction analysis (Fig.1).

TABLE I

VALUE (%)	CHEMICAL COMPOSITION OF OPALINE ROCKS										
	S	A	F	C	M	N	K	T	$\bar{S}$	LOI	Ins. Res.
MAXIMUM	90,7	15,9	3,7	0,32	0,46	0,17	1,70	0,32	0,09	7,7	89,9
MINIMUM	74,1	5,2	1,0	0,16	0,23	0,03	0,07	0,11	0,03	2,0	83,0
MEAN	82,6	9,5	2,0	0,22	0,32	0,10	0,77	0,19	0,07	4,2	86,5

* By means of infrared absorption spectroscopy (Fig.2) these minerals were confirmed and at 3697 and 3620 cm^{-1} the bands corresponding to stretching vibrations of the -OH groups in kaolinite and micas were observed, while the band for water of hydration was found at 3460 cm^{-1}. Between 1200 and 900 cm^{-1} the Si-O stretching vibrations take place that correspond both to the existing silica as well as the silicates. The double band 798 and 778 cm^{-1} is characteristic for quartz and overlaps with the opal absorption at 790 cm^{-1}. The bending vibrations of the Si-O-Si group at 475 cm^{-1} come from the opal and the dioctahedral minerals.

Sporadically, smaller quantities of other minerals were identified, among them alunite, viseite, baryta,... (1), (2).

* The most frequent micromorphology of the polymorphous silica, observed by means of a scanning electron microscope consists of sheets with serrated edges that penetrate into each other (Fig.3a) or that form spherical compositions, lepispheres, in the empty spaces or hollows (Fig.3b). These crystalline forms cover the surfaces and walls of the pores (Fig.3c).

* The materials which were received in small blocks were ground, a process controlled by the Blaine final specific surface value, around 4500 cm^2/g.

* The chemical composition is shown in Table I, which

M.P. DE LUXAN; M.I. SANCHEZ DE ROJAS; Inst. Constr. Cem. "E. Torroja" (C.S.I.C.). Madrid, Spain.
M.T. MARTIN PATINO; C.S.I.C. and Dep. Geol. and Geoquim., Univ. Autónoma. Madrid, Spain.
J. SAAVEDRA; U.E.I. Mineral. and Geol. (C.S.I.C.). Salamanca, Spain.

gives the maximum, minimum and mean values for the whole range of samples. Chemical analysis was carried out by means of Inductively Coupled Plasma Spectrometry, except the SO_3 content which was determined gravimetrically. The insoluble residue is obtained by HCl $-Na_2CO_3$ attack and later ignition at 975°C.

SAMPLE REACTION CAPACITY

It is the aim of this research to study the suitability of these materials as pozzolanic products. Pozzolanic activity was evaluated by means of an accelerated test of opal/lime mortar, described earlier (3).

FIG.3.- SEM microstructure of opaline rocks

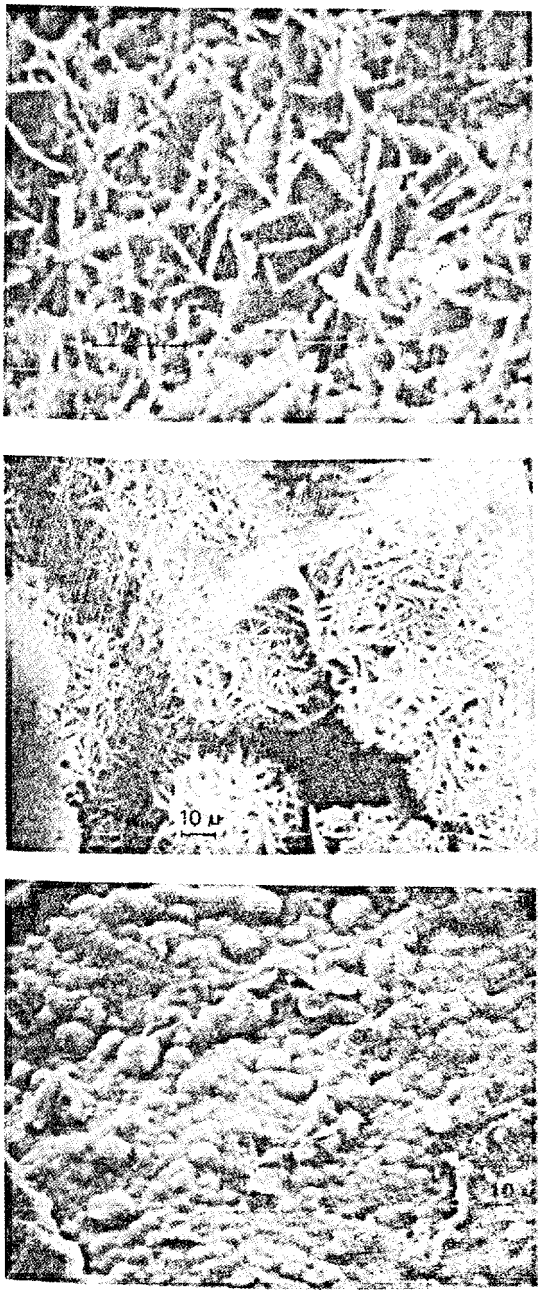

a

b

c

The mortar is prepared with 375 g of opal, 125 g of hydrated lime, 1500 g of graded standard sand and 250 cc of water. From each sample, 6 prisms (40x40x160mm) were obtained. The specimens are cured in the moist closet at 21°C for 48 hours and at 50°C for 72 hours. Flexural and compressive results are given in Fig.4.

An absorption of water increase effect is therefore not observed in any of the samples which bears out the contents of other studies concerned with opaline rock, (4).

FIG.4.- Accelerated test

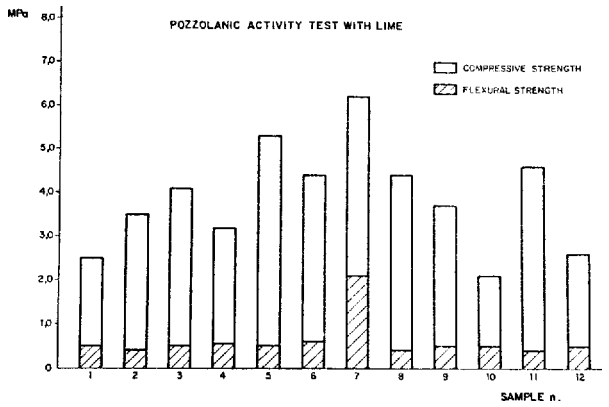

CONCLUSIONS

1. These deposits can be quite productive by using traditional quarry methods. The geotechnical conditions in the production areas are also favourables.

2. The mineralogical analysis has shown the various forms of silica besides stable form (quartz): the almost amorphous opal-A and the disordered opal-CT.

3. The pozzolanic activity test provides a classification of the different materials with regard to their reaction capacity:
   * Samples ns. 1,2,4,9,10 and 12 - low activity.
   * Samples ns. 3,5,6,7, 8 and 11 - good activity.

For these opaline rocks a higher water requirement is not necessary.

4. The pozzolanic behaviour of these materials is similar to that of other products used today as active additions to portland cement.

ACKNOWLEDGEMENT

This study was carried out under the auspices of the Institute for Geology and Mining of Spain (IGME). The authors wish to express their thanks to Mr. G. Gómez Moreno for contributing to the success of this work.

REFERENCES

1.- SAAVEDRA J., MARTIN PATINO M.T.; Rev. Inst. Inv. Geolog., 34, 1980, pp 263 - 270.

2.- SAAVEDRA J., MARTIN PATINO M.T.; Cuadernos Lab. Xeolóxico de Laxe, 2, 1981, pp 253 - 261.

3.- LUXAN M.P. de, SANCHEZ de ROJAS M.I.; Mater. Constr. (IccET), 35, 200, 1985, pp 3 - 13.

4.- GRBA V., BLAZEVIC N. and SOLVIC Z.; Cemento-Hormigón, 588, 1982, pp 973 - 986.

G.Peter, Q. Yang and A. Rosli
Institute for Building Materials, Chemistry of Materials and Corrosion,
Swiss Federal Institute of Technology, Zurich

INFILTRATION OF CHLORIDE UNDER CAPILLARY ACTION

P

In capillary absorption tests, we measured the penetration depth of a statistically defined liquid front as a function of time. This was accomplished with the help of electrical conductivity and gamma absorption measurements. The absorption of water and a 4% NaCl solution was investigated on concrete discs (200 x 200 x 35 mm) which were cut out of concrete walls (1000x1000x200mm), all at the same level. Two types of Portland cement with differing C_3A content (7% and 12% respectively) were employed. The cement content was 300 kg/m³ and the W/Z value 0.5. The concrete was mixed at two different temperatures (5°C and 20°C respectively) and stored at 20°C/70% R.H. for three months prior to tests. The absorption tests were carried out under two different climatic conditions (5°C, 85%RH and 20°C, 70% R.H.) and covered a period of about 5 weeks for approx. 70mm capillary rise. The original concrete surface against the formwork served as the absorption surface.

The capillary rise of the liquid front closely followed the relationship $h = k.\sqrt{t}$ (t = time). In general, the coefficient k increases with rising temperatures, increasing capillary pore content and decreasing water content in the concrete. In contrast, increased air pore content results in lower k values. The observed values lie in the range of 3-7mm/$h^{1/2}$. For the concrete with a cement of lower C_3A content, the NaCl solution was absorbed noticeably more slowly than the water. At the same time, in the case of the NaCl solution, the blurring of the liquid front decreased with increasing capillary rise. For the concrete with a cement of greater C_3A content however, the salt solution was usually as rapidly (or even more rapidly) absorbed as the pure water. The blurring showed no consistent trend.

The infiltration of chloride in concrete depends on the surface distance. The total chloride content determined after completing the test was higher for the cement type with greater C_3A content. On the other hand, a higher capillary pore content was observed for the concrete types made at 20°C with cement of greater C_3A content. Thus, the k value for the absorption of the salt solution was also higher. It was interesting to observe that for the concrete made at 20°C, the chloride content was propotional to the k value for surface distances of 0-10mm. This was true for both cement types. It also correlates with the practical experience that a carbonation of the concrete surface (which results in a decreased k value) leads mostly to a lower chloride content. The total chloride content of the concrete made at 20°C was independent of the C_3A content of the cement for surface distances of 30-40mm. It lay in the region of 0.15% Cl (referred to cement mass) with an absorption temperature of 5°C and of 0.07% Cl with an absorption temperature of 20°C.

The bound chloride, i.e. the difference between the chloride soluble in nitric acid and in cold water, yielded values clearly above 0.4% Cl referred to cement mass (0.44 - -0.67). This applies to both cement types with surface distances of 0-10mm. Smaller values were found for the bound chloride in the range 0-10mm when the concrete was made at 5°. The influences of the absorption temperature and C_3A content of the cement were small. The concrete made at 5° yielded smaller capillary pore content than the one made at 20°C.

The relationship between the bound chlorid and the total chloride amounted to approx. 0.4, independent of the cement type and the test parameters for surface distances of 0-30mm.

After the salt had exerted its influence, observation with the SEM revealed the formation of new crystals, some of them branched. With EDXRA the crystals showed increased chloride content compared to their surroundings. Even NaCl crystals could be found.

We thank W. Studer (Swiss Federal Laboratories for Materials Testing and Research), P. Wagli and R. Wessicken (Swiss Federal Institute of Technology) for their valued cooperation.

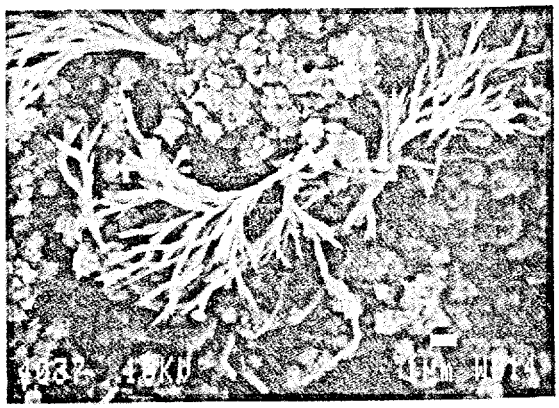

Branched crystals in concrete found after NaCl absorption

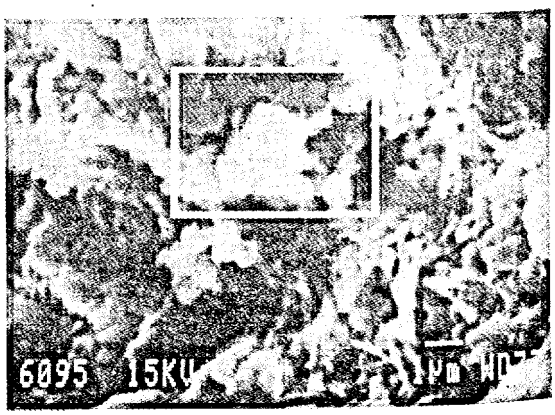

NaCl crystal in concrete

S. Popovics Drexel University - Philadelphia - U.S.A.

MODELING MATHEMATICALLY THE EFFECT OF CURING TEMPERATURE ON THE STRENGTH DEVELOPMENT OF CEMENTS.

P

Introduction

The purpose of the research was the development and calibration of a mathematical cement model for the description of the effect of curing temperature on the hydration of various portland cements as reflected by their strength developments. The term "model" implies the mathematical form of a simplified, hypothetical cement from which many of the factors influencing the hydration and hardening of an actual cement are disregarded; the remaining few variables are combined in a form that can reproduce numerically one, specific cement property which is the compressive strength in this case.

The model presented here considers the hydrations of the C_3S and C_2S as first order reactions in which the C_3A acts as a catalyst.

The investigation included the development of formulas for numerical estimation of several characteristics of the kinetics of hydration. These are, as follows:

age of concrete when the hardening begins;
age when the diffusion control of the hydration starts; and
final strength potential of concrete, that is, the strength after very long proper curing;

for portland cements of various types and various curing temperatures. This investigation is the continuation of the work on the "exponential cement model" that was presented at the 6th and 7th International Congresses on the Chemistry of the Cements. (1)(2)

Origin of the Model

The exponential cement model, probably the first non-linear cement model for the representation of hardening, is much simplier than most of the linear models. It was introduced in 1967 (3). The original mathematical form of this model provides a relationship between the strength developing capability of a portland cement under curing at constant standard temperature (22°C) and its simplified compound composition, as follows:

$$f_{ct} = f_{28} \frac{1 - C_3 e^{-a_1 t} - (1 - C_3) e^{-a_2 t}}{1 - C_3^{-28a_1} - (1 - C_3) e^{-28a_2}} \qquad 1)$$

where

f_{ct} = strength of portland cement paste, mortar, or concrete at the age of t, cured at constant standard temperature, MPa
f_{28} = 28-day strength at the same mixture, MPa
t = age of the specimen at testing, days,
C_3 = computed C_3S content of the portland cement, percent/100,
a_1 and a_2 = rates of hardening of the C_3S and the other component which are independent of the strength, age, and C_3S content, but may be a function of the C_3A content, and any other factor that influences the course of hydration (fineness, gypsum content, admixtures, water-cement ratio, temperature, curing and testing methods, etc.), 1/day.

This equation was obtained from the following conditions:

(a) The model consists only of two hardening components; the first component is the C_3S, the second component is a mixture of the other cement ingredients, mainly C_2S.

(b) These two components hydrate simultaneously as first order reactions with differing rates but without any interaction with each other.

(c) The kinetics of hardening is controlled only by the rates of chemical reactions between the two cement compounds and water.

(d) The final strength developed by C3S is the same as the final strength of the second component.

The proportionality factors, which are the a parameters in Equation 1), represent the specific rates of hardening, that is, (the rate of hardening)/(remaining strength at a given age). The squares of these parameters represent specific decelerations of hardening. The more intensive the early hardening process, the greater is the value of a_1; and the longer and larger is the hardening after 28 days; the smaller becomes the value of a_2 up to a certain limit. In other words, (Eq. 1) describes the strength development when the chemical reactions control the hydration process without any consideration of the diffusion process.

The extension of this model to various constant curing temperatures is based on the recognition that the exponential cement model represents the hardening from the viewpoint of chemical kinetics as the sum of two different first-order reactions. Since experimental data have supported this with standard curing temperature (1)-(4), the logical working hypothesis is that compressive strengths of concretes cured at a constant temperature other than the standard will also be reproducible by the extension of this model. This paper presents a justification of this hypothesis by introducing the extended form and comparing its predicted values to experimental strength results.

Description of the New Model

Although the new model is based on the earlier published exponential cement models, it has two important novel properties: (a) it is extended to include the strength development produced during the period when the diffusion process controls the hydration rather than the rate of chemical reactions; and (b) it is extended to strengths of mixtures that were cured at constant temperature other than the standard 22°C. These two extensions are discussed below.

The strength development of a cement paste, mortar, or concrete can be divided into two consecutive stages from the point of view of kinetics of hydration: (a) the first stage is when the rate of strength development is controlled by the rates of chemical reactions between the cement compounds and water, followed by (b) the second stage, that is the strength development controlled by the speed of diffusion of the aqueous phase in the hardened cement paste to the unhydrated portion of the cement. The dividing point of time between the two stages is marked as t_d. In other words, the first stage of the

strength development, f_{ct}, takes place from the time of beginning of hardening, t_s, up to t_d, whereas the second stage strength, f_{dt}, develops after the beginning of the diffusion control, t_d. Figure 1 shows that the total strength of the concrete, f_t, during the first stage is equal to f_{ct}, whereas the total strength of the concrete in the second stage is equal to the sum of f_{ct} at the age of t_d, which is f_{ctd}, and f_{dt}. The importance of distinguishing between the two stages is that the strengths in the first stage are highly sensitive to the curing temperature, whereas those in the second stage are not.

The new cement model recognizes quantitatively these two stages of strength development. In addition, several other factors are included in the model as variables that influence the kinetics of strength development. These are: compound composition and fineness of the cement; age; and curing temperature.

The mathematical form of this new cement model is as follows:

1. During the first stage of hydration, when the strength development is controlled by the rate of chemical reactions, that is when $t \leq t_d$:

$$f_{ct} = f_o f_{28} \frac{1 - C_3 \exp\left(-a_1(t - t_s)(S/3000)\right) - (1 - C_3) \exp\left(-a_2(t - t_s)(S/3000)\right)}{1 - C_3 \exp\left(-a_1(28 - t_s)(S/3000)\right) - (1 - C_3) \exp\left(-a_2(28 - t_s)(S/3000)\right)} \qquad 2)$$

where

f_o = relative final strength of the cement paste, mortar or concrete, that is, strength after a very long proper curing, percent/100 of the 28-day strength,
t_s = age when the hardening process starts, days,
t_d = age when the speed of diffusion takes over the control of strength development, days
S = Blaine specific surface of the cement, cm^2/g.

The other symbols are identical with the symbols of Eq. 1).

2. During the second stage of hardening, when the strength development is controlled by the speed of diffusion, that is when $t > t_d$:

$$f_t = f_o f_{28} \frac{1 - C_3 \exp\left(-a_1(t_d - t_s)(S/3000)\right) - (1 - C_3) \exp\left(-a_2(t_d - t_s)(S/3000)\right)}{1 - C_3 \exp\left(-a_1(28 - t_s)(S/3000)\right) - (1 - C_3) \exp\left(-a_2(28 - t_s)(S/3000)\right)} + f_{dt} \qquad 3)$$

where

f_{dt} = strength developed after the age of t_d by diffusion, MPa.

The other symbols are identical with the symbols of Eqs. 1) and 2).

Using appropriate a_1 and a_2 values, strengths can be calculated from these equations for various cement types at various ages for different but constant curing temperatures. These calculated values were compared to pertinent experimental concrete strengths.

Experimentally Obtained Strengths

The experimental data were taken from a paper by Klieger. (5) Accordingly, ASTM Types I, II and III portland cements were used to make concrete for the determination of their compressive strengths.

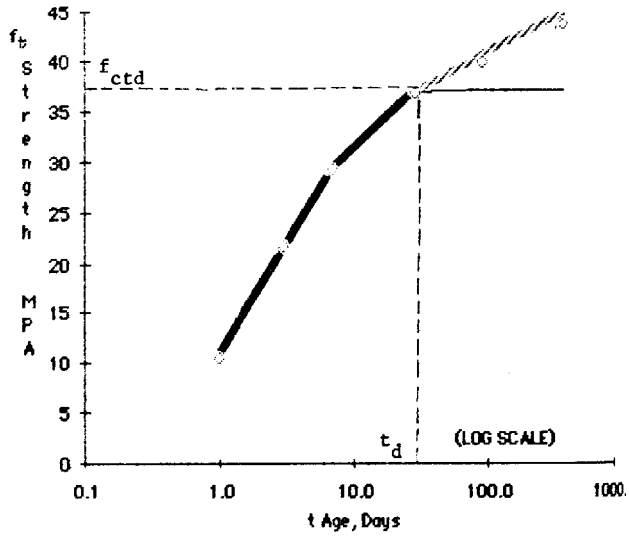

Figure 1. Strength development of concrete with Type I cement cured at 32°C. Points: experimental data; continuous lines: calculated from Eq. 2); cross-hatched line: calculated from Eq. 7).

Two cements were used for each type. The chemical and physical characteristics of the cements are presented in Table 1. The nominal cement content of the concretes was 310 kg/m^3, the air content was between 4 and 5% and the water content was adjusted for each mixture to produce 5 to 10 cm slump. The concretes were mixed and placed at temperatures of 4.44, 12.78, 22.78, 32.22, 40.5 and 48.86°C. Specimens were prepared for testing at ages of 1, 3, 7 and 28 days, 3 months and 1 year.

For specimens that were broken at the age of 28 days or earlier, all concretes were cured continuously moist at the mixing and placing temperature until testing the strength. After the initial 28 days, the specimens remaining for tests at 3 months and 1 year were cured further continuously moist but at 22.78°C until breaking. The compressive strength tests were performed on beam ends remaining from flexural tests as 15-cm modified cube tests.

TABLE 1 - PHYSICAL AND CHEMICAL CHARACTERISTICS OF CEMENTS (5)

Cement ASTM type	Fineness Specific Surface Blaine cm^2/g	Normal consistency %	Time of Setting Vicat hr. & min. Initial	Final	Alkalies, % Na_2O	K_2O	Total as Na_2O	Calculated Compound Composition % C_3S	C_2S	C_3A	C_4AF	$CaSO_4$	Free CaO
22.78°C and below													
I	3310	25.0	4:00	6:55	0.22	0.67	0.66	42.5	28.8	11.3	8.0	3.61	0.90
III	4840	29.0	1:45	4:00	0.19	0.42	0.47	58.2	13.1	10.3	8.0	4.47	1.71
II	3910	25.0	5:05	8:45	0.14	0.21	0.28	33.9	40.7	6.1	10.2	2.98	1.22
22.78° and above													
I	3120	24.5	3:00	---	0.23	0.63	0.64	41.8	29.4	10.9	8.4	3.66	1.07
III	4730	28.5	2:00	4:00	0.18	0.47	0.49	53.8	17.1	11.5	8.1	4.65	1.08
II	3880	24.0	3:30	5:00	0.20	0.47	0.51	39.1	34.4	7.2	10.4	3.04	0.84

Further details concerning the concrete and tests can be found in Klieger's original paper. (5)

After a stepwise optimization of Eqs. 2) and 3), the compressive strength values calculated by the cement model at ages from 1 day through 1 year for concretes cured at seven different temperatures are presented in Table 2 for Type I portland cement. For the sake of comparison, the experimentally obtained data by Klieger are also presented. It can be seen that the goodness of fit is quite good between the calculated and experimental strength. The compressive strengths developed by Type II and III cements are not presented here due to space restrictions, but the obtained goodness of fit is good also for these cements.

Characteristics of the Kinetics of Hydration

In addition to the good fit to experimental strengths (Table 2), the model provided specific formulas for several characteristics of the kinetics of hydration of portland cements as a function of curing temperature and cement type. For Type I cements used by Klieger these formulas are, as follows:

Beginning of the hardening:

$$t_s = \frac{215}{(t^o + 10)^2} - 0.10 \quad \text{in days} \qquad 4)$$

Beginning of the diffusion control:

$$t_d = 120 \times 10^{-0.01923 t^o} \quad \text{in days} \qquad 5)$$

Compressive strength developed during the diffusion control:

$$f_{dt} = 960 \log(t/t_d) \quad \text{in psi} \qquad 6)$$

$$= 6.62 \log (t/t_d) \quad \text{in MPa} \qquad 7)$$

Final relative compressive strength:

$$f_o = -33 \times 10^{-6}(t^o - 29)^3 + 1.00 \quad \text{in \%/100} \qquad 8)$$

where t^o is the constant curing temperature in °C. The other symbols are identical with the symbols of Eqs. 2) and 3).

Table 2 contains illustrative values of Eqs. 4), 5), and 8) for several temperatures. Similar, although not identical formulas were obtained for cements of Types II and III. These are not presented here; nevertheless they are discussed below.

Interpretation of the Formulas

The above-presented equations for the kinetics of Type I cement as well as the similar equations for Type II and III cements indicate the following:

1. The starting time of hardening, t_s, is decreasing quite rapidly with an increase in the curing temperature. t_s roughly coincides with the time of initial setting of the cement paste. Thus, all the factors that influence the time of setting (fineness, C_3A content, SO_3 content, etc.) also influence the value of t_s. Note that when the curing temperature is -10°C or less, the hardening does not start. The value of t_s affects primarily the very early strengths.

2. The time of transition, t_d from chemical reaction control to diffusion control of the hardening shortens with increasing curing temperatures, but it is also controlled, negatively, with the rate of hardening, that is C_3S content, fineness, etc. of the cement. Similar tendency appears with the strength development of the various cements during the diffusion-controlled period; that is, the higher the rate of hardening, the smaller the strength increase. Note that the diffusion-controlled strength development, f_{dt} is far the less sensitive to the temperature of curing than the chemical reaction-controlled strength development. The t_d and f_{dt} values affect the strength at later ages.

3. f_o and the other factors are functions not only of the curing temperature but also of the cement type. For instance, f_o is highest for Type II cement and lowest for Type III cement indicating the inverse effect of C_3S and C_3A contents on the final strength which has also been demonstrated experimentally. (6) When the curing temperature is close to 29°C, the

TABLE 2 - CALCULATED AND EXPERIMENTAL STRENGTHS OBTAINED AT VARIOUS CURING TEMPERATURES

Cement: Type I

Curing temp °C	Source of strength	a_1 1/d	a_2 1/d	t_d day	f_{ctd} MPa	f_o %/100	Compressive Strength, MPa 1 day	3	7	28	90	365
4.44	Calc.	0.08	0.014	98.6	55.03	1.49	0.20	5.61	14.36	36.73	53.88	58.85
	Exp.						0.56	5.11	14.98	36.26	49.84	54.11
12.78	Calc.	0.20	0.060	68.1	48.00	1.14	4.12	13.71	25.77	43.83	48.81	52.90
	Exp.						4.06	13.51	26.25	43.75	52.85	55.93
22.78	Calc.	0.48	0.11	43.8	42.56	1.00	9.42	21.52	31.59	41.85	44.67	48.75
	Exp.						9.87	21.84	31.43	42.35	44.52	50.33
22.78	Calc.	0.41	0.13	43.8	38.32	1.00	7.67	18.63	28.75	37.87	40.42	44.51
	Exp.						8.05	18.20	28.42	38.08	42.0	45.15
32.22	Calc.	0.7	0.12	28.8	37.43	0.99	10.65	20.96	28.67	37.37	40.75	44.84
	Exp.						10.43	21.63	29.12	36.68	39.9	43.68
40.56	Calc.	0.95	0.13	19.9	34.72	0.95	12.27	21.38	27.98	35.71	39.12	43.20
	Exp.						12.95	22.40	26.95	33.04	36.75	41.02
48.86	Calc.	3.0	0.20	13.8	27.31	0.74	14.53	19.50	24.44	29.38	32.79	36.87
	Exp.						14.28	19.88	24.08	28.77	33.11	37.24

final strength developed by Type II cement is about 10% higher than that of Types I and III. The f_o equations also show that the final strengths are increasing (or decreasing) faster than linearly as the curing temperature is decreasing (or increasing) from 29°C.

Note that Carino and Lew also reported that the value of f_o decreases with increasing curing temperatures, but they recommended a linear relationship for this function instead of the cubic form of Eqs. 7) and 8). (7)

The value of f_o affects primarily the strength at later ages.

Eqs. 5) through 8) are approximations with restricted limits of validity. The restrictions originate from the intentional simplification of the formulas. For instance, the actual f_o value does not increase indefinitely as the cubic function of Eq. 8) indicates but rather levels off around 0°C as well as above 60°C temperatures, respectively. Such curve, however, would require a much more complicated mathematical form. The t_s values as represented by Eq. 4) also change with the temperature more rapidly than the actual values. Nevertheless, all these formulas seem to be useful tools between 0 and 50°C for the estimation of several characteristics of the kinetics of hardening numerically that we could do only in in qualitative terms up to now.

As far as this writer can tell, formulas similar to Eqs. 5) through 8) have not been published. Nevertheless, the primary importance of these formulas is not so much the actual numbers they provide because these are valid strictly speaking only for the cements used by Klieger in his experiments. It seems more important that they show the general approach for the establishment of similar formulas for other cements and, with further research, for the determination of how the cement characteristics influence the t_d, f_o, etc. values, that is the kinetics of hardening, under various curing conditions.

Conclusions

The new cement model represented by Eqs. 2) and 3) can reproduce the strength development of portland cements of Types I, II and III cured at differring temperatures quite well as demonstrated by the data in Table 2. In addition, the optimization and calibration processes of this model provided formulas for the numerical estimations of several characteristics of the kinetics of hydration as shown by Eqs. 4) through 8).

Acknowledgment

This work was sponsored by the National Science Foundation NSF Grant Nos. CEE-8304382 and CEE-8442765.

References

1. S. Popovics, "Strength Development of Portland Cement Paste," The VI. International Congress on the Chemistry of Cement, Supplementary Paper, Section II, Moscow, September, 1974, p. 20.

2. S. Popovics, "Possibility of a Catalytic Role of C_3A in the Hardening of Portland Cements," 7th International Congress on the Chemistry of Cement, Vol. IV, Editions Septima, Paris, 1980, pp. 602-606.

3. S. Popovics, "A Model for the Kinetics of the Hardening of Portland Cement," Highway Research Record, No. 192, Highway Research Board, Washington, D.C., 1967, pp. 14-35.

P

4. S. Popovics, "Phenomenological Approach to the Role of C_3A in the Hardening of Portland Cement Pastes," Cement and Concrete Research, Vol. 6, No. 3, May, 1976, pp. 343-350.

5. Klieger, "Effect of Mixing and Curing Temperature on Concrete Strength," ACI Journal, Proc. Vol. 54, June, 1958, pp. 1063-1081.

6. S. Popovics, Concrete Making Materials, McGraw-Hill Book Company, New York, etc. and Hemisphere Publishing Corporation, Washington, etc., 1979, p. 370.

7. N. J. Carino and H. S. Lew, "Temperature Effects on Strength-Maturity Relations of Mortar," ACI Journal, Proc. Vol. 80, No. 3, May-June 1983, pp. 177-182.

Menashi D. Cohen and Barzin Mobasher, Department of Civil Engineering, Northeastern University, Boston, Massachusetts 02115, U.S.A.

PHYSICO-CHEMICAL, MICROSTRUCTURAL, AND MICROMECHANICAL INVESTIGATIONS OF SULFOALUMINATE-TYPE EXPANSIVE CEMENTS

RECHERCHES PHYSICO-CHIMIQUE, MICROSTRUCTURALE, ET MICROMECANIQUE SUR UN CIMENT EXPANSIF DU TYPE-SULFOALUMINATE

INTRODUCTION

Portland cement is one of the most widely used materials in the construction industry. One of its disadvantages, however, is its inherent characteristic to shrink upon drying and, owing to its low tensile strength, to crack. Upon cracking, concrete becomes more permeable and allows, with greater ease, the ingress of harmful chemicals to its interior which may lead to loss of strength and ultimate deterioration. This imposes unnecessary maintenance and rehabilitation costs, and becomes a major concern in an industry that accounts for more than 250 billion dollars on GNP per year in the United States.

In response to this concern, expansive cements, in the form of shrinkage-compensating cement, have been developed and used in the field for several decades. When mixed with water, expansive cements expand and create tensile stresses in the reinforcing steels and, therefore, compressive stresses in the concrete. The idea is that upon shrinkage, concrete will simply release some, preferably not all, of its compressive stress, thereby preventing any tension from building up and thus avoiding the formation of cracks.

TYPES

The three types of sulfoaluminate-type expansive cements that have been studied in the United States are differentiated by their supplementary alumina-bearing phases. For example, Type K expansive cement is characterized by $C_4A_3\bar{S}$. Type K expansive cement is usually produced by intergrinding ordinary portland cement clinker, expansive clinker (containing $C_4A_3\bar{S}$), and calcium sulfate (anhydrite or gypsum).

Similarly Type M is characterized by $CA+C_{12}A_7$. Type S has no supplementary alumina-bearing phase, but is characterized by a high percentage of C_3A.

Expansive cements can also be based on the positive volume change associated with the hydration of an oxide such as CaO or MgO. Commercial expansive cements based on CaO ("free lime") exist; cements based on MgO have been studied.

HYDRATION

When water is added to expansive cement, a complex reaction takes place. The silicate phases (C_3S and C_2S) react with water to produce calcium silicate hydrates (CSH) gel and calcium hydroxide. CSH gel contributes to the strength of the cement. The stoichiometric equations can be generalized as follows:

$$2C_2S + 3H \longrightarrow C_3S_2H_2 + CH \quad ....(1)$$

$$2C_3S + 5H \longrightarrow C_3S_2H_2 + 3CH \quad ...(2)$$

Trisulfate hydrate ($C_6A\bar{S}_3H_{32}$) commonly referred to as ettringite is the principle phase in the C-A-$\bar{S}$-H system that contributes to expansion in sulfoaluminate-type expansive cements. In Types S, K, and M expansive cements, ettringite is assumed to form as follows:

$$\text{TYPE S-}C_3A + 3C\bar{S}H_2 + 26H \longrightarrow C_6A\bar{S}_3H_{32} \quad ..(3)$$

$$\text{TYPE K-}C_4A_3\bar{S} + 8C\bar{S}H_2 + 6CH + 74H \longrightarrow 3C_6A\bar{S}_3H_{32} \quad ..(4)$$

$$\text{TYPE M}\begin{cases} CA + 3C\bar{S}H_2 + 2CH + 20H \longrightarrow C_6A\bar{S}_3H_{32} & ..(5) \\ C_{12}A_7 + 21C\bar{S}H_2 + 9CH + 173H \longrightarrow 7C_6A\bar{S}_3H_{32} & ..(6) \end{cases}$$

The product ettringite ($C_6A\bar{S}_3H_{32}$) has a density of 1.73 g/cm^3 and contains six units of CaO, one of Al_2O_3, three of SO_3, and thirty-two of water. It occurs as hexagonal columns or needles in which the water of crystallization is contained in channels parallel to the c-axis (1). The stoichiometric reactions 1-6 are ideal and the exact reaction equations have not yet been determined.

THEORIES OF EXPANSION

There are two major schools of thought concerning the expansion mechanism: the Crystal Growth Theory and the Swelling Theory.

THE CRYSTAL GROWTH THEORY (1-11)

According to the Crystal Growth Theory, expansion is caused by the growth of ettringite crystals from the surfaces of the expansive particles (topochemical reaction mechanism) or from the solution (through-solution reaction mechanism). The growth of these crystals, commonly referred to as crystal growth, is regarded as producing a 'crystallization pressure', and, hence, the expansive force.

THE SWELLING THEORY (12-15)

According to the Swelling Theory, expansion occurs because of wetting of the ettringite particles that are of colloidal size. These particles have been referred to as gel. This gel has a large surface area, and like CSH gel, takes up water to produce overall expansion by swelling. The formation of this gel occurs by a through-solution mechanism due to the reaction between the expansive particles and the surrounding solution. Moreover, if calcium and hydroxyl ions exist in the solution, ettringite particles will be colloidal in size; but if such ions are absent, ettringite particles will be larger in size. It is only in the former case that expansion can occur. This school of thought, unlike the first, does not consider the size of the expanding particles to be important. Instead, it stresses that it is the existence of calcium ions which affects the size of ettringite crystals and, therefore, the rate and magnitude of expansion.

On the other hand, in order to explain excess expansion observed in an expansion study, it was suggested that water adsorption and interparticle repulsion in ettringite formation (due to high Zeta potential values) act concurrently and significantly with crystal growth thrust during expansion (16).

The above theories of expansion have been discussed in detail in references (17-19).

DISCUSSION OF THE THEORIES

In discussing the review paper (17), B. Mather (18) suggested that the observed increase in dimensions of expansive cements cannot be explained either as crystal growth (first school) or swelling of ettringite (second school). He stated that the crystal size or degree of crystallinity of the ettringite is irrelevant and that expansion needs no explanation other than the increase in volume upon C_3A or $C_4A_3\bar{S}$ to ettringite transformation. In the reply to Mather's discussion (19), based on the equations below:

$$V = N \cdot A \cdot L \quad ..... \quad (7)$$

$$dV = NA.dL + LA.dN + LN.dA \quad ... \quad (8)$$

it was claimed that expansion based on volume change depends on the crystallinity of ettringite (the second term, LA.dN) and thus any explanation of the mechanism of expansion should be based on either or both schools of thought. In equation (7) the parameters V and N are total volume and total number of ettringite crystals produced, and A and L are cross-sectional area and length of a single ettringite crystal. Equation 8 represents the total differential of equation 7. Although expansion by water adsorption has not been ruled out (19), it is believed that its contribution to expansion is insignificant because of the low surface area of ettringite -approximately 8,000-19,000 m^2/kg depending on lime concentration (16).

OBJECTIVES

A fundamental requirement in the successful use and application of expansive cement is the clear understanding of the mechanism of the expansion process and development. This fact has been recognized for some time. Research activities at elucidating the expansion mechanism have been significant and achievements made are encouraging. With all the extensive work done, however, there still is a lack of general consensus regarding the mechanism of expansion including the kinetics and morphology of ettringite formation.

The purpose of this paper is to present results of an investigation aimed at assessing the mechanism of expansion. The results presented herein are based on the physico-chemical, microstructural, and micromechanical studies of the sulfoaluminate-type expansive cements.

EXPERIMENTAL INVESTIGATION

The experimental work included studies of sulfate solubility, microstructure (scanning electron microscopy-SEM), strength, expansion, and shrinkage characteristics.

MATERIALS

The materials used were portland cement p.c. S3210, Type

Menashi D. Cohen and Barzin Mobasher, Department of Civil Engineering, Northeastern University, Boston, Massachusetts 02115, U.S.A.

3.3 PHYSICO-CHEMICAL, MICROSTRUCTURAL, AND MICROMECHANICAL INVESTIGATIONS OF SULFOALUMINATE-TYPE EXPANSIVE CEMENTS

RECHERCHES PHYSICO-CHIMIQUE, MICROSTRUCTURALE, ET MICROMÉCANIQUE SUR UN CIMENT EXPANSIF DU TYPE-SULFOALUMINATE

K expansive clinkers ECL-103 and TXI-4C, pure $C_4A_3\bar{S}$, pure C_3A, natural gypsum G-1, and a reagent grades gypsum and calcium hydroxide. The physico-chemical characteristics are listed in Table 1.

Oxides	p.c. S3210 wt.%	Expansive ECL-103 wt.%	Clinker TXI-4C wt.%	Pure $C_4A_3\bar{S}$ wt.%	Pure C_3A wt.%	Natural Gyp. G-1 wt.%
SiO_2	21.66	14.7	20.42			1.92
Al_2O_3	4.6	5.9	10.32	49.41	37.07	0.12
Fe_2O_3	3.96	1.9	2.79	0.38	0.02	0.48
CaO	64.81	62.6	57.24	37.58	61.48	31.97
MgO	1.35	3.5	0.67			0.37
SO_3	2.4	8.7	5.1	11.9		46.12
Na_2O	0.2	0.23	0.25			
K_2O	0.24	0.75	0.74			
L.O.I.		0.86	0.63	0.54	0.25	20.68
Free-lime	0.13	5.1	1.34	0.3	0.2	
Equiv Na_2O		0.73	0.74			
Imp.						1.72
TOTAL	99.35	99.34	100.24	100.11	99.0	103.38
Phase	Bogue	Mehta	Mehta	XRD*	XRD*	
C_3S	55.23	76.14	22.71			
C_2S	20.44	-15.29	41.42			
C_3A	5.49				99.8	
C_4AF	12.05	5.78	8.49			
$C_4A_3\bar{S}$		9.35	17.04	99.7		
$C\bar{S}$	4.08	12.7	4.87			77.6
TOTAL	97.29	103.97	94.53	99.7	99.8	

* Estimated value

TABLE 1: Typical percentages of oxides and calculated compound compositions

SULFATE SOLUBILITY

Stoichiometric amounts according to equations 3 and 4 using C_3A (C-coarse and F-fine), $C_4A_3\bar{S}$ (C and F), reagent grade gypsum ($C\bar{S}H_2$) and calcium hydroxide (CH) were blended in individual flasks containing one liter of deionized water. $C_4A_3\bar{S}$-C and $C_4A_3\bar{S}$-F had Blaine specific surface areas of 364 and 972 m^2/kg, respectively. C_3A-C and C_3A-F were 321 and 820 m^2/kg. Sulfate solubility was studied as a function of particle type (C_3A or $C_4A_3\bar{S}$) and fineness (C or F) by measuring the amount of dissolved sulfate consumed daily in suspension hydration at 23 °C for several days. The sulfate consumed went for the production of ettringite. The detailed procedures are described elsewhere (20).

For $C_4A_3\bar{S}$, Fig. 1, from ref.(20), results show fineness does not affect the rate and amount of sulfate depletion even when concentration of C_4A_3S is tripled from 0.25 to 0.75 grams per liter of water. This result is not expected since mass and surface area play important roles in kinetics (6,21,22).

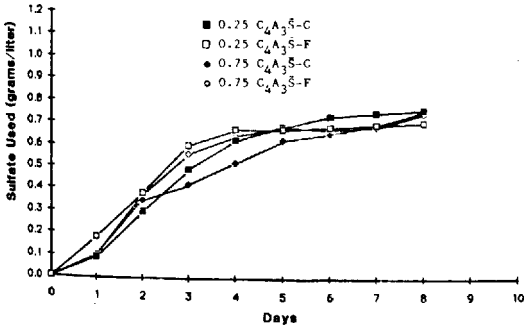

Fig. 1: Daily consumption of sulfates for ettringite production.

Results in general are conflicting but they do suggest that sulfate solubility technique with $BaCl_2$ precipitation is not as sensitive to $C_4A_3\bar{S}$ fineness and amount as it is for C_3A in suspension hydration.

SEM ANALYSIS

Samples of $C_4A_3\bar{S}$ and C_3A were separated by microsieves into two size fractions: particles smaller than 37 microns (-400 mesh) and particles larger than 74 microns (+200 mesh). These particles were dispersed in suspension hydration in flasks as described earlier (6,20,21). At different stages of hydration samples were removed from the flasks and prepared for SEM observations. The purpose of particle separation was to study particle size effect on ettringite morphology. In models developed for sulfoaluminate-type expansive cements (6,22,23) it was predicted that the length of ettringite crystals are directly related to the size of C_3A or $C_4A_3\bar{S}$ particles, and that $C_4A_3\bar{S}$ particles produce longer ettringite crystals than C_3A particles.

SEM micrographs, Figs. 2 and 3, from ref.(20), show that the mode of ettringite formation in suspension hydration is topochemical for both C_3A and $C_4A_3\bar{S}$ particles. Nearly all micrographs showed similar patterns. Generally, $C_4A_3\bar{S}$ particles produce a more defined and radial mode of ettringite crystals (Fig. 2), compared to C_3A particles that produce irregular but defined ettringite crystals (Fig. 3). This could be attributed to differences in the crystalline nature of C_3A and $C_4A_3\bar{S}$ and to differences in solution pH (9.2-10.3 for C_3A and 11.5-11.8 for $C_4A_3\bar{S}$).

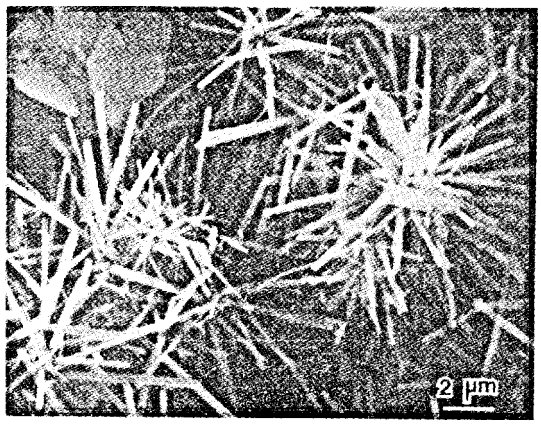

Fig. 2: SEM micrograph of hydrated $C_4A_3\bar{S}$ at 7 days.

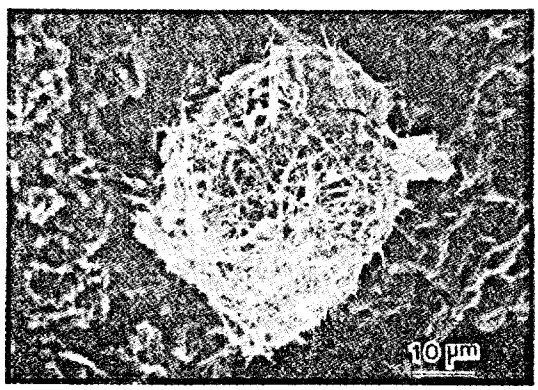

Fig. 3: SEM micrograph of hydrated C_3A at 7 days.

In another approach that utilizes SEM in the study of expansive cements, expansive paste slabs were used (24). Internal restraint was provided by means of uni-directional and bi-directional reinforcement. The expansive cement paste used was 53.33% p.c. S3210, 11.67% reagent grade gypsum, and 35% TXI-4C (2-5 microns). Results of this study indicate that internal restraint by wire reinforcement does not affect the morphology (i.e. size, shape, and preferred orientation) of ettringite produced. However, there was formation of large $Ca(OH)_2$ crystals due to internal restraint, both at the wire-cement interface and in the matrix. Results reported by other investigators on the effects of externally applied constant pressures (16,17,25), however, indicate morphological differences in ettringite. Therefore, different mechanisms may be operative in the two restraining conditions; internal wire-reinforcements which exert time-dependent

Menashi D. Cohen and Barzin Mobasher, Department of Civil Engineering,
Northeastern University, Boston, Massachusetts 02115, U.S.A.

3.3 PHYSICO-CHEMICAL, MICROSTRUCTURAL, AND MICROMECHANICAL INVESTIGATIONS OF SULFOALUMINATE-TYPE EXPANSIVE CEMENTS

RECHERCHES PHYSICO-CHIMIQUE, MICROSTRUCTURALE, ET MICROMÉCANIQUE SUR UN CIMENT EXPANSIF DU TYPE-SULFOALUMINATE

directional pressures starting at a critical degree of hydration α_{cr} when ettringite crystals surpass surrounding solution layer (3,4,6,8,17,23,24), and externally applied constant pressures starting at the onset of hydration.

STRENGTH-EXPANSION MEASUREMENTS

The free expansion of the blends in saturated lime-water at 23±1 °C was studied by measuring the daily length changes of thin prismatic paste specimens having dimensions 4.8 mm x 15 mm x 80 mm. Procedures for proportioning, mixing, casting, curing, and measurement are described elsewhere (5,6,26).

Strength was measured indirectly from the first mode of resonant frequency of prismatic specimens similar in dimensions to the expansion specimens. The square of this frequency gives a measure of dynamic Young's Modulus and compressive strength (5,6,27-29).

Pure Components

Paste blends of p.c. S3210, gypsum G-1, 2.5% and 5% C_3A (C and F) or $C_4A_3\bar{S}$ (C and F), with extent of reaction %R≥100, were mixed with deionized water at 0.4 w/c. Percent R is an approximate measure of wt% C_3A or $C_4A_3\bar{S}$ that converts to ettringite (4,5,6,23). Percent R>100 indicates excess sulfate. Figs. 4, 5 (from ref.20) and 6 show the expansion-time behaviors of the 2.5% to 5% C_3A (C and F) and $C_4A_3\bar{S}$ (C and F) blends. Results indicate that the behavior of expansion is extremely dependent on the type and amount of expansive component. With the higher content, comparing Figures 4 and 5, the effects of fineness and type become more pronounced. Fig. 5 shows that $C_4A_3\bar{S}$-C and C_3A-C give a higher expansion rate than $C_4A_3\bar{S}$-F and C_3A-F. This is not expected since at early ages tests have shown that finer particles produce expansion at a higher rate. However, this may be explained from Richards-Helmuth's model on expansive cements (4) showing that there is an optimum range of expansion particles 6.8-11 microns, that give the highest expansion. Since more than 50% of the $C_4A_3\bar{S}$-F and C_3A-F particles were smaller than 5 microns compared to 18% and 7% for $C_4A_3\bar{S}$-C and C_3A-C, one can suggest that a greater amount of ettringite formed in the fine particles is being wasted. Figure 6 clearly shows the effect on expansion of a series of blends with increasing content of $C_4A_3\bar{S}$ but constant %R.

Type K Clinker

Paste blends of p.c. S3210, Type K expansive clinker TXI-4C, gypsum G-1, w/c=0.4, and %R=65, were made with varying wt% of Type K expansive clinker form 23%-50%. TXI-4C was ground to a Blaine of 422 m^2/kg. This "whole" clinker was then separated into several size fractions by air-classifier: 2-5 microns (481 m^2/kg), 5-8 microns (450 m^2/kg), 8-13 microns (232 m^2/kg), and +13 microns (89 m^2/kg). Figures 7 and 8 show the expansion time and strength-time relationships. With higher amount of expansive component, 50% clinker in Fig. 7, behavior is "abnormal" (6,31), i.e. double curvature expansion and strength drop. The 35% clinker mix in Fig. 7 and the 2-5 micron mix in Fig. 8 show "normal" (6,31) behavior in their strength-expansion patterns while the mixes containing 50% clinker in Fig. 7 and whole clinker in Fig. 8 show abnormal behavior.

The paste blends containing Type K TXI-4C (whole) tested in free expansion contained 1.34% free lime. Another Type K clinker, ECL-103 was also obtained from a different source and it had a relatively high amount of free lime (5.1%). The clinker was ground either by impact (ECL-103V "whole") or by grinding in a steel ball mill (ECL-103G1 "whole"). ECL-103V "whole" was separated into several size fractions by air-classifier: 2-5 microns (682 m^2/kg), 5-8 microns (417 m^2/kg), 8-13 microns (279 m^2/kg), and +13 microns (138 m^2/kg). The "whole" clinker was 270 m^2/kg. (The Blaine of the steel ball milled clinker, ECL-103G1 "whole" was 426 m^2/kg). Impact grinding gives angular shape particles while steel ball mill grinding gives a more rounded or spherical particle shape.

Two paste blends containing p.c. S321G, gypsum G-1, and 30% ECL-103 (V or G whole), with 0.4 w/c and 75% R were tested in expansion and results clearly indicate that the method of grinding plays a significant role in the expansion behavior, Fig. 9. The Figure shows that the blend containing the expansive clinker ground by impact gives double the expansion of the expansive clinker ground in steel ball mill even though it has the same chemical composition and a significantly smaller surface area. Fig. 10 also shows expansion-time behavior of

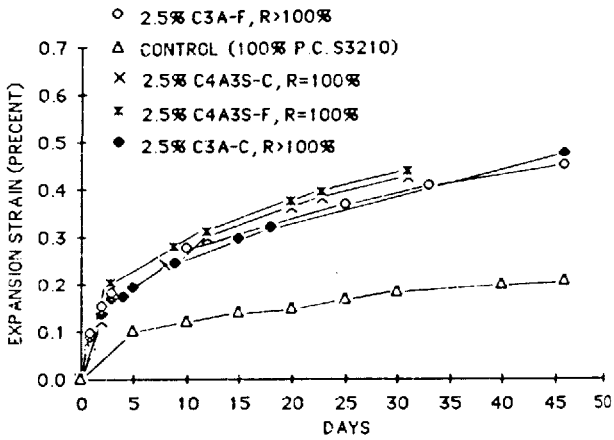

Fig. 4: Effects of type and fineness of expansive component on expansion.

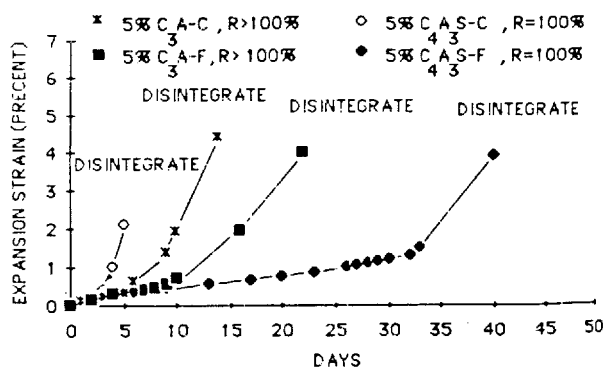

Fig. 5: Effects of type and fineness of expansive component on expansion.

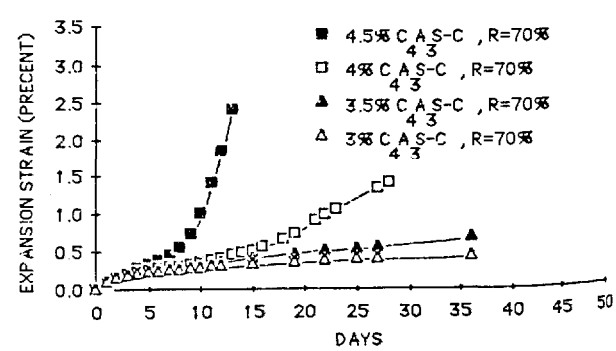

Fig. 6: Effects of increasing content of expansive component on expansion.

several blends containing the impacted clinker ECL-103V (8-13 microns). Comparison of the 15%, 20%, and 35% mixes gives the effect of increasing expansive clinker wt% on expansion while maintaining %R at 70. Clearly, as wt% expansive clinker increases, expansion increases just as shown in previous work (6). Comparing the 30% clinker and the 35% clinker explains the effect of increasing %R on expansion while maintaining constant wt% expansive clinker. In these cases increasing wt.% clinker while maintaining constant %R or increasing %R while maintaining constant wt.% clinker yielded higher expansion rates and magnitudes.

An interesting feature in ECL-103V and ECL-103G1 series is that regardless of mix composition, expansion was virtually completed within the first two days of curing. The 35% clinker in Fig. 10 shows a very peculiar and interesting feature in that expansive cements could accommodate as much as 2.5% expansion strain even as

Menashi D. Cohen and Barzin Mobasher, Department of Civil Engineering, Northeastern University, Boston, Massachusetts 02115, U.S.A.

3.3 PHYSICO-CHEMICAL, MICROSTRUCTURAL, AND MICROMECHANICAL INVESTIGATIONS OF SULFOALUMINATE-TYPE EXPANSIVE CEMENTS

RECHERCHES PHYSICO-CHIMIQUE, MICROSTRUCTURALE, ET MICROMÉCANIQUE SUR UN CIMENT EXPANSIF DU TYPE-SULFOALUMINATE

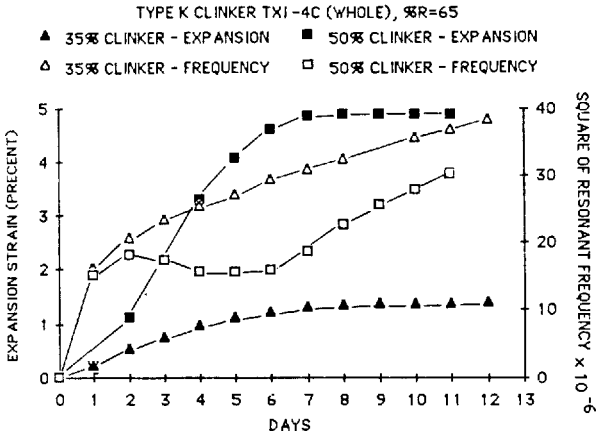

Fig. 7: Strength-Expansion relationship of expansive cement blends: Effects of particle sizes.

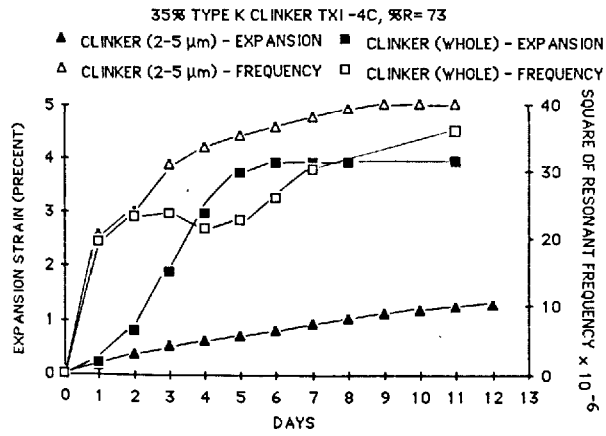

Fig. 8: Strength-Expansion relationship of expansive cement blends: Effects of content of expansive component.

early as two days without disintegrating. Normally this amount of expansion could not have been accommodated so soon if the matrix had not developed such high strength. Moreover, such high expansion magnitude usually leads to disintegration. The very high rate and magnitude of expansion development in only two days and the ability of the mixes to accommodate the expansion can only be attributed to the high amount of free lime and its effect on accelerating ettringite formation. Virtually, in all the blends containing the high free lime Type K expansive clinker ECL-103, expansion was completed in two days.

SHRINKAGE MEASUREMENTS

The shrinkage characteristics (23±1 °C, 45%±3% Rh) of Type K expansive cements, specifically magnitude and rate, were also studied (30). Reinforced and unreinforced expansive cement paste and mortar blends of p.c. S3210, gypsum G-1, and expansive component (pure $C_4A_3\bar{S}$ or ECL-103 V (or G1)) were mixed, casted, and cured for predetermined number of days before shrinkage. For example, many specimens were subjected to shrinkage after different duration of curing, some before developing their full expansion potential. Results, showed that shrinkage characteristics of expansive cements are different from those of portland cement. Generally, expansive cements showed higher shrinkage magnitudes than those of the specific portland cement used but it is cautioned that this finding may vary for other types of portland cements. Although the same factors are involved in the shrinkage process of expansive cement and portland cements, the following processes are of greater significance in expansive cements and render different expansive cement shrinkage

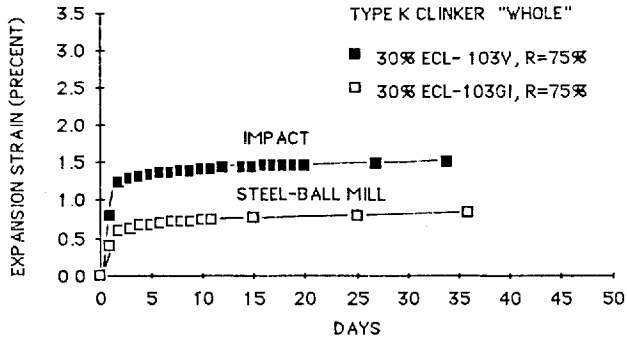

Fig. 9: Effect of grinding method of expansive clinker on expansion.

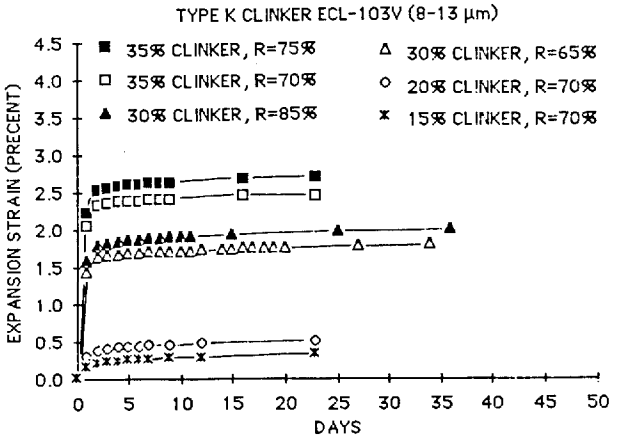

Fig. 10: Expansion behavior of different series of blends.

behavior: formation of pores/microcracks, interaction of expansion and shrinkage, loss of water adsorbed on the surfaces of ettringite, and decomposition of ettringite.

It was also found that large amounts of expansive component resulting in excessive expansion and strength drop could lead to higher shrinkage magnitudes because of excess microcracking. Moreover, although free expansion paste specimens shrink more than restrained expansion paste specimens, they follow a similar shrinkage trend.

The stability of ettringite upon carbonation was also tested and results are close to those of other investigators (31-33). It was shown that ettringite decomposes to gypsum, calcite, and an alumina bearing product. Since CO_2 attack is limited to surface of concrete, smaller specimens are more susceptible to carbonation attack because of their higher surface to volume ratios.

CONCLUSIONS

This research has shown that one can utilize the topochemical Crystal Growth Theory to explain the hydration kinetics and strength-expansion behaviors of sulfoaluminate-type expansive cements.

The sulfate solubility study with $BaCl_2$ precipitation is not as sensitive to $C_4A_3\bar{S}$ fineness and amount as it is for C_3A in suspension hydration. On the other hand, expansion measurements showed that fineness plays a dominant role in expansion behavior.

SEM micrographs of suspension hydration indicate that although crystals grow on the surfaces of both C_3A and $C_4A_3\bar{S}$ particles, there exists some morphological difference between them. This morphological difference made it difficult to check the theory (6,22,23) that $C_4A_3\bar{S}$ particles produce larger ettringite than C_3A crystals. Moreover, because of the large distribution

Menashi D. Cohen and Barzin Mobasher, Department of Civil Engineering, Northeastern University, Boston, Massachusetts 02115, U.S.A.

3.3 PHYSICO-CHEMICAL, MICROSTRUCTURAL, AND MICROMECHANICAL INVESTIGATIONS OF SULFOALUMINATE-TYPE EXPANSIVE CEMENTS

RECHERCHES PHYSICO-CHIMIQUE, MICROSTRUCTURALE, ET MICROMÉCANIQUE SUR UN CIMENT EXPANSIF DU TYPE-SULFOALUMINATE

of $C_4A_3\bar{S}$ and C_3A particle sizes it was difficult to develop an accurate relationship between particle size and length of ettringite crystals. Very narrow and distinct particle size distributions such as 5-10 and 30-35 microns should be used to provide information for developing the relationship.

Analysis of SEM micrographs at high magnification could give the false impression that crystals are dispersed in the matrix. This could lead one to suggest that the mode of ettringite formation is through-solution. SEM micrographs examined at lower magnification, however, suggested that the mode of formation is topochemical.

Internal restraint by directional wire reinforcement does not appear to influence ettringite morphology in expansive cements. Results reported by other investigators on the effects of externally applied constant pressures, however, indicate morphological differences in ettringite. This suggests that different mechanisms may be operative in the two restraining conditions.

The strength-expansion studies showed the sensitivities of expansion and strength development patterns to wt.% and fineness of expansive component, and extent of reaction (%R). Specifically, the effects of fineness and particle size distributions in this study and elsewhere (4,5,6,21,22,23,31) suggest that the mechanism of ettringite formation and subsequent expansion is topochemical Crystal Growth (first school). Higher magnitude and duration of expansion could lead to abnormal behavior, a phenomenon associated with double curvature expansion and strength drop (6,31). Moreover, as expected high free lime content could accelerate formation of ettringite such that all expansion could be completed within the first two days of hydration. The effect of the high free-lime content on accelerating the ettringite formation at the early age seems to enable the cement matrix to accommodate a large magnitude of expansion.

In the shrinkage studies, it was shown that expansive cement shrinks more than portland cement. If expansive cement is subjected to shrinkage before it has fully expanded to its potential, serious problems may arise resulting in loss of strength. In future research more emphasis should be invested at identifying and quantifying the parameters involved during the shrinkage of expansive cements.

Since ettringite readily decomposes upon carbonation, expansive cements may be more durable and provide better service if they have a low surface area to volume ratio.

ACKNOWLEDGMENTS

This research was supported by the U.S. National Science Foundation.

REFERENCES

1. H. E. Shwiete, U. Ludwig, and P. Jager, "Investigation in the System $3CaO-Al_2O_3-CaSO_4-CaO-H_2O$," Symposium on Structure of Portland Cement Paste and Concrete. Special Report 90, pp. 353-367, Highway Research Board, Washington, D.C., 1966.
2. G. L. Kalousek and E. J. Benton, "Mechanism of Seawater Attack on Cement Pastes, " ACI Journal No. G7-9, pp. 187-192, 1970.
3. A. Bentur and M. Ish-Shalom, "Properties of Type Expansive Cement of Pure Components. II. Proposed Mechanism of Ettringite Formation and Expansion in Unrestrained Paste of Pure Expansive Component," J. Cement and Research, V. 4, pp. 709-721, 1974.
4. C.W. Richards and R.A. Helmuth, "Expansive Cement Concrete--Micromechanical Models for Free and Restrained Expansion," Technical Report No. 191, Dept. of Civil Eng., Stanford University, Stanford, Ca. 1977.
5. A. Kerdegari, "The Role of Gypsum in Portland Cement and Expansive Cement," Ph.D. Dissertation, Dept. of Civil Eng., Stanford University, Stanford, Ca. 1978.
6. M.D. Cohen, "Micromechanics of Expansive Mechanisms in Expansive Cement Concretes," Ph.D. Dissertation, Dept. of Civil Eng., Stanford University, Stanford, Ca. 1981.
7. K. Ogawa and D.M. Roy, J. Cement and Concrete Research, V.12, pp. 101-109, 1982.
8. M. Ish-Shalom and A. Bentur, "Properties of Type K Expansive Cement of Pure Components. I. Hydration of Unrestrained Paste of Expansive Components-Results," J. Cement and Concrete Research, V. 4, pp. 519-532, 1974.
9. P.P. Budnikov and I.V. Kravchenko, "Expansive Cements. Principal Paper--Expansive Cements," Proc. of the Fifth Int. Symp. on the Chemistry of Cement, V. 4, pp. 319-330, Tokyo, 1968.
10. T. Nakamura, G. Sudoh, and S. Akaiwa, "Mineralogical Composition of Expansive Cement Clinker Rich in SiO_2 and Its Expansibility," Proc. of the Fifth Int. Sym. on the Chemistry of Cement, V. 4, pp. 351-365, Tokyo, 1968.
11. I. Soroka, Portland Cement Paste and Concrete, London and Basingstoke: The MacMillan Press, Ltd., 1979.
12. S. Chen and P.K. Mehta, J. Cement and Concrete Research, V. 12, pp. 257-259, 1982.
13. P.K. Mehta, "Mechanism of Expansion Associate With Ettringite Formation," J. Cement and Concrete Research, V. 3, pp. 1-6, 1973.
14. P.K. Mehta and S. Wang, J. Cement and Concrete Research, V. 12, pp. 121-122, 1982.
15. P.K. Mehta and F. Hu, "Further Evidence for Expansion of Ettringite by Water Adsorption," J. Am. Cer. Soc.-Discussion and Notes, pp. 179-181, 1978.
16. V.A. Rossetti, G. Chiocchio, and A.E. Paolini, "Expansive Properties of the Mixture $C_4A\bar{S}H_{12}$-$2C\bar{S}$. I. An Hypothesis on the Expansion Mechanism," J. Cement and Concrete Research, V. 12, pp. 577-585. 1982.
17. M.D. Cohen, Theories of Expansion in Sulfoaluminate-Type Expansive Cements: Schools of Thought," J. Cement and Concrete Research, V. 13, pp. 809-818, 1983.
18. B. Mather, A discussion of ref. # 17, J. Cement and Concrete Research, V. 14, pp. 603-609, 1984.
19. M.D. Cohen, A reply to the discussion of ref. 18, J. Cement and Concrete Research, V. 14, pp. 610-612, 1984.
20. M.D. Cohen, E. Campbell, and W. Fowle, "Kinetics and Morphology of Ettringite Formation, " Proc. of the VIIth Int. Conf. on Cement Microscopy, pp. 360-381, Fort Worth, 1985.
21. M.D. Cohen, "Microstructural Analysis of Ettringite Formation: Scanning Electron Microscope," Proc. of the 4th Int. Conf. on Cement Microscopy, pp. 204-224, Las Vegas, 1982.
22. M.D. Cohen, "Modeling of Expansive Cements," J. Cement and Concrete Research, V. 13, pp. 519-528, 1983.
23. M.D. Cohen and B.B. Bantimba, "Correlation of Unrestrained Hydration Expansion and Particle Size Distribution of $4CaO.3Al_2O_3.SO_3$," Report No. 1 to National Science Foundation, Tech. Rep. CE-84-1, Dept. Civil Eng., Northeastern University, Boston, Ma. 1984.
24. M.D. Cohen and H. Nayeb Hashemi, "Crystal Morphology Under Pressure," Proc. of the VIIth Int. Conf. on Cement Microscopy, pp. 267-276, Fort Worth, 1985.
25. R. Sh. Mikhail, S.A. Abo-El-Enein, S. Hanofi, and R.J. Good, "Ettringite Formation in Compressed Expansive Cement Pastes," J. Cement and Concrete Research, V. 11, pp. 665-673, 1981.
26. D. A. Burciaga, "Micromechanical Modeling of Expansive Cements," Engineer Thesis, Dept. of Civil Eng., Stanford University, Stanford, Ca. 1977.
27. A.M. Neville, Properties of Concrete, p. 282, New York: John Wiley and Sons. Inc. 1963.
28. S. Spinner and W. Thefft, "A Method for Determining Mechanical Resonance Frequencies and for Calculating Elastic Moduli from their Frequencies," ASTM Proc. 61, pp. 1221-1238, 1961.
29. G. Pickett, "Equations for Computing Elastic Constants form Flexural and Torsional Resonant Frequencies of Vibration of Prisms and Cylinders," ASTM Proc. 45, pp. 846-863, 1945. PCA Res. Bul. 7.
30. M.D. Cohen and B. Mobasher, "Shrinkage of Expansive Cements," Submitted to J. Am. Cer. Soc. 1985.
31. M.D. Cohen and C.W. Richards, "Effects of Particles Sizes of Expansion Clinker on Strength-Expansion Characteristics of Type K Expansive Cements," J. of Cement and Concrete Research, V. 12, pp. 717-725, 1982.
32. J. Calleja, "Durability," Proc. of the 7th Int. Cong. on the Chemistry of Cement, VII-2/1, V. 1, Paris, 1980.
33. D. Gaspar, M. Munoz-Plaza, and T. Vazquez, "Action on CO_2 on a Portland Cement. II.," Mat. de Constr. (IETCC-Spain), (in Spanish), No. 168, 75-87, 1978.
34. D. Gaspar, M. Munoz-Plaza, and F. Trivino, "Action of CO_2 on a Portland Cement. III.," Mat. de Constr. (IETCC-Spain), (in Spanish), No. 169, 63-73, 1978.

V.Klassen BTIBM, Belgorod, U.S.S.R.

INTERACTIONS IN $CaCO_3$-$SiO_2$$R_2CO_3$ (R_2 SO_4) MIXTURES

P

There are domains of solid solutions (shaded areas) in diagrams of $CaCO_3$-Na_2CO_3 and $CaCO_3$-K_2CO_3 state systems previously studied by Niggli, Krüger and others. Under the atmospheric pressure of CO_2 and in opened system as well there exists the possibility to form the $K_2Ca_2(CO_3)_3$ compounds.

Transformations occured in $CaCO_3$-alkali-sulphate systems under air atmosphere have been studied and the state diagrams were plotted. $CaCO_3$+Na_2SO_4 were found to interact and form a number of solid solutions like Kurnakov's bertollides; eutectic temperatures of $5CaCO_3 \cdot 6Na_2SO_4$, $6CaCO_3 \cdot 5K_2SO_4$ and $5CaCO_3 \cdot 4K_3Na(SO_4)_2$ are 825°C, 880°C and 820°C respectively.

Alkali admixtures cause $CaCO_3$ multistage dissociation (up to 7 stages) connected with the formation of complex salts, solid solutions and melts containing carbonate, especially of eutectic composition. Addition of SiO_2 accelerates the reactions of $2CaCO_3$+ $+SiO_2 = 2C_2S+2CO_2$ as a result of formation of low-temperature melts. The dissociation of $CaCO_3$ is speeded up to 850°C (the temperature of SiO_2 complete fixing) and then due to formation of $2C_2S \cdot CaCO_3$ and $R_2Ca(CO_3)_2$ is slowed down. The temperature of CO_2 release from the compounds rises in the set: $CaCO_3 \rightarrow 2C_2S \cdot CaCO_3 \rightarrow R_2Ca(CO_3)_2$.

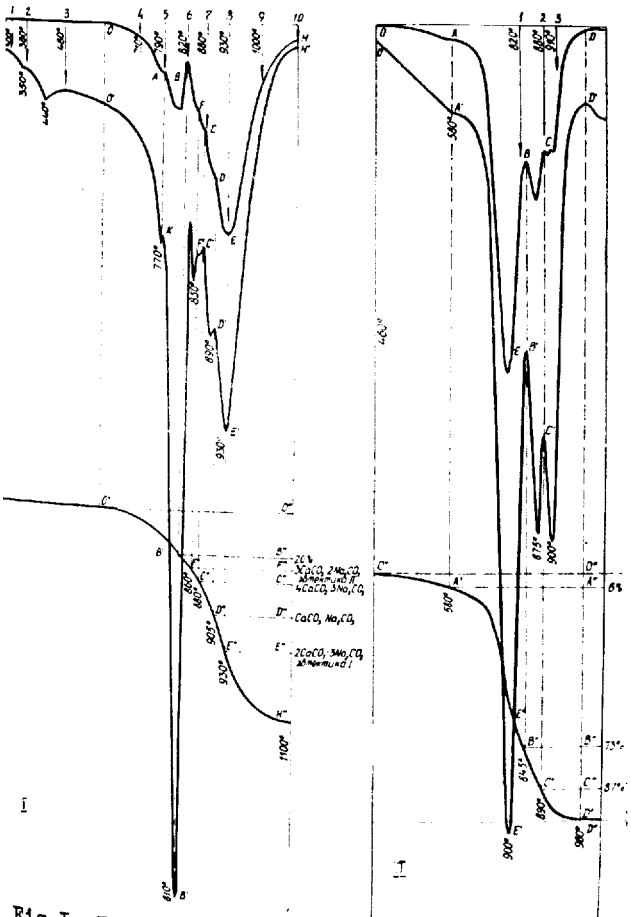

Fig.I. The results of DTA of the mixes $CaCO_3$+Na_2CO_3(I) and $2,7CaCO_3$+SiO_2+8%K_2CO_3 (2) in the open air.

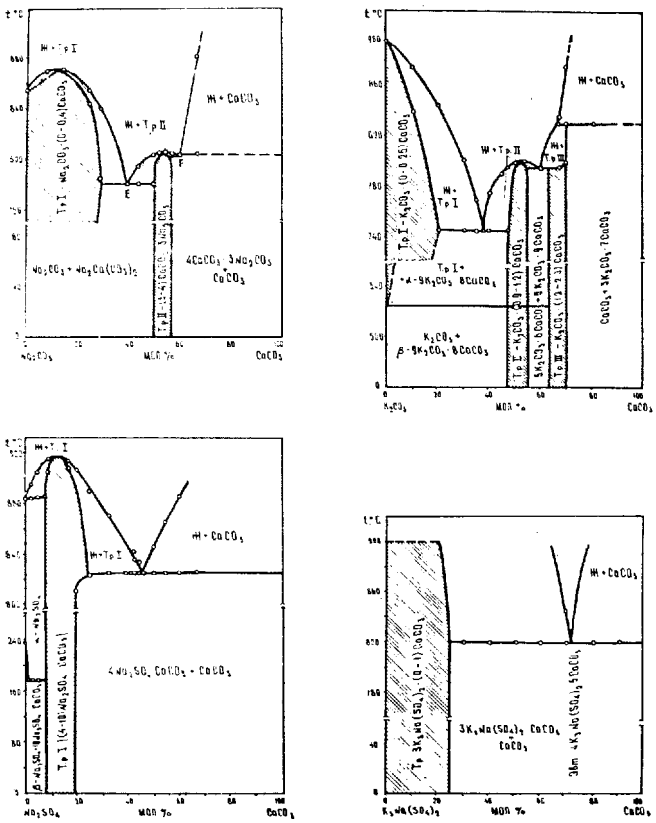

Fig.2. The diagram of the system state at the partial pressure, CO_2 101,3 kPa.

In carbonate mixtures at 900°C I wt % R_2O forms 5-6 wt % melts. According to our data, R_2O content in the zone of decarbonization is 2-4 weight %. It promotes the formation of 10-20 wt % liquid phase at low temperature and, hence, fundamentally changes the conception of solid state reactions taking place in cement kilns.

There are exchange reactions between R_2SO_4 and $CaCO_3$ in atmosphere of combustion products. These reactions produce $2C_2S \cdot CaSO_4$. This compound may be formed by the interaction of fuel oil sulphur with material burned in a kiln. Above 1300°C $2C_2S \cdot CaSO_4$ is being decomposed and reacting with CaO forms low active alite.

P

Table I.

X-ray characteristics of $K_2Ca_2(CO_3)_3$

d,A	I	d,A	I	d,A	I	d,A	I	d,A	I
6,85	8	3,038	95	2,22	I5	2,00	6	I,77	I0
6,60	9	2,948	I00	2,I8	9	I,926	I8	I,7I	9
3,83	I2	2,637	43	2,I6	I2	I,9I5	23	I,69	5
3,44	8	2,539	48	2,II	5	I,873	33	I,53	8
3,26	7	2,468	45	2,07	6	I,84	II	I,5I5	I0
3,I3	II	2,29	I9	2,0I6	I4	I,8I	I9	I,47	7

Table 2.

X-ray characteristics

Na_2SO_4:$CaCO_3$ = I0:I				Na_2SO_4:$CaCO_3$ = 4:I			
d,A	I	d,A	I	d,A	I	d,A	I
4,63	4	2,I96	6	4,60	2	2,I83	8
3,878	70	2,I43	2	3,85	86	2,I3	2
3,559	26	I,937	30	3,558	48	I,923	36
2,952	4	I,784	8	2,926	3	I,775	I2
2,824	7I	I,568	I0	2,805	I00	I,556	I0
2,667	I00	I,54	6	2,644	80	I,52	4
2,309	5	I,48	6	2,289	4	I,473	I0

K.Karibaev
N.Bajirov
A.Patcenko
N.Panina
Institut polytechnique de Kiev, NIICement - Moscow, U.S.S.R.

MODIFICATION DE LA STRUCTURE DES SCORIES DE LA DEPHOSPHORATION THERMIQUE ELECTRIQUE.

Des scories de déphosphoration thermique électrique granulées représentent la vitre à composition vollastonitique caractérisée par la structure polymérique. Il est connu que la réactivité de la scorie dépend du degré de la polymérisation des anions silico-oxygéniques. Lors de l'hydratation il se produit la déstruction de la vitre pour le compte de la rupture de liaisons Si-O-Si, donc la variation de la structure anionique est un facteur déterminant l'hydrolicité des scories.

Dans le travail présent nous avons montré que l'introduction dans la scorie fondue à 1723K d'additions contenant de Mg^{2+}, Ca^{2+}, Ba^{2+} augmente la réactivité. L'introduction de ces additions modificatrices provoque des variations de la structure de la scorie qui se fixe ensuite dans la vitre lors de la granulation. Les oxydes MeO diffusant dans le bain fondu sont des donneurs d'ions d'oxygène qui assure la rupture de liaisons entre les tétraèdres de la structure.

Des courbes cinétiques de l'interaction du molybdate d'ammonium avec scorie (fig.I) témoignent de la présence importante dans la scorie modifiée de tétraèdres d'île et d'orthosilicates. Le temps de passage de 99% de SiO_2 total en acide siliceuse molybdénique réduit en 2,5 fois. Le changement des courbes indique sur la haute vitesse de l'hydrolyse de la scorie modifiée et sur la formation du complexe siliceux molybdénique jaune, ce qui est assuré par la dépolymérisation d'anions siliceux oxygénique - résultat de l'action des additions modificatrices.

Selon les données de l'analyse aux rayons X des produits de l'hydratation de la scorie dans la solution de chaux (fig.2), la scorie modifiée a la plus haute réactivité. L'abaissement de la basicité des hydrosilicates lors de l'hydratation de la scorie modifieé dans la solution de chaux est assuré par l'accélération de la lixiviation de SiO_2 par suite de la destruction de la scorie. Ce même fait explique l'augmentation de la quantité de néoformations, ce qui est affirmé par l'accroissement de l'intensité de réflexion.

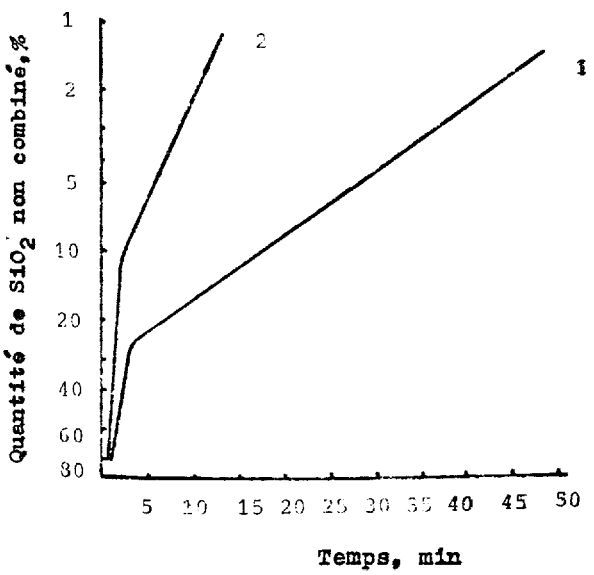

Fig.I. Courbes cinetiques de l'interaction du molybdate d'ammonium avec la scorie de départ (I) et la scorie modifiée (2).

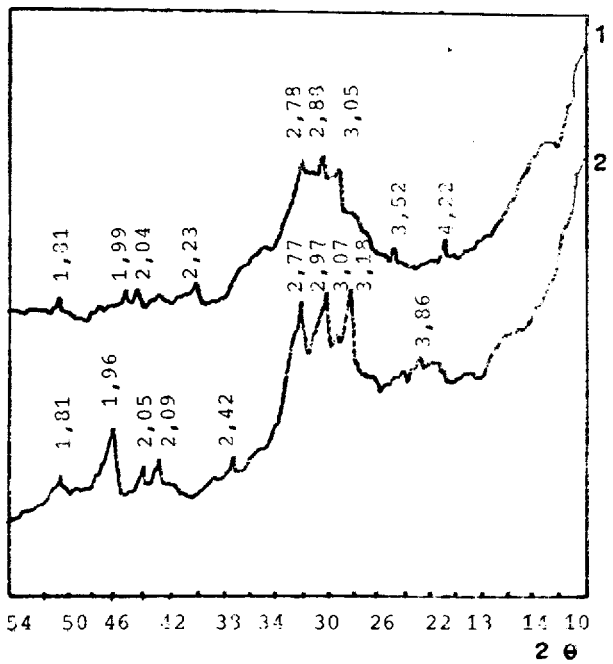

Fig.2. Diffraction à rayons X des produits de l'hydratation des scories dans la solution de chaux I - scorie de départ; 2 -scorie modifiée.

La haute réactivité de la scorie modifiée est confirmée par l'analyse thermique differentielle. La courbe de l'ATD du pré-

cipité se formant lors de l'hydratation de la scorie-témoin dans la solution de chaux (fig.3) montre la présence d'effets faibles endothermiques à 470 et 785°C indicant sur la teneur faible en C_2SH (A) et d'un effet fort exothermique à 940°C indicant sur la teneur prédominante de la vitre non réagie.

Sur la courbe de l'ATD des produits de l'hydratation de la scorie modifiée il ya un effet endothermique profond à 205-220°C indicant sur la quantité accrue de C_2SH_2.

Il est à noter un certaine accroissement de l'effet endothermique à 490 et 780°C, la diminution considérable de l'effet exothermique à 945°C aussi l'augmentation de la perte de masse l'echantillon.

Lors de l'étuvage, la scorie modifiée présente l'aptitude au durcissement avec la formation d'hydrosilicate de calcium faiblement cristallisés à composition CSH(B).

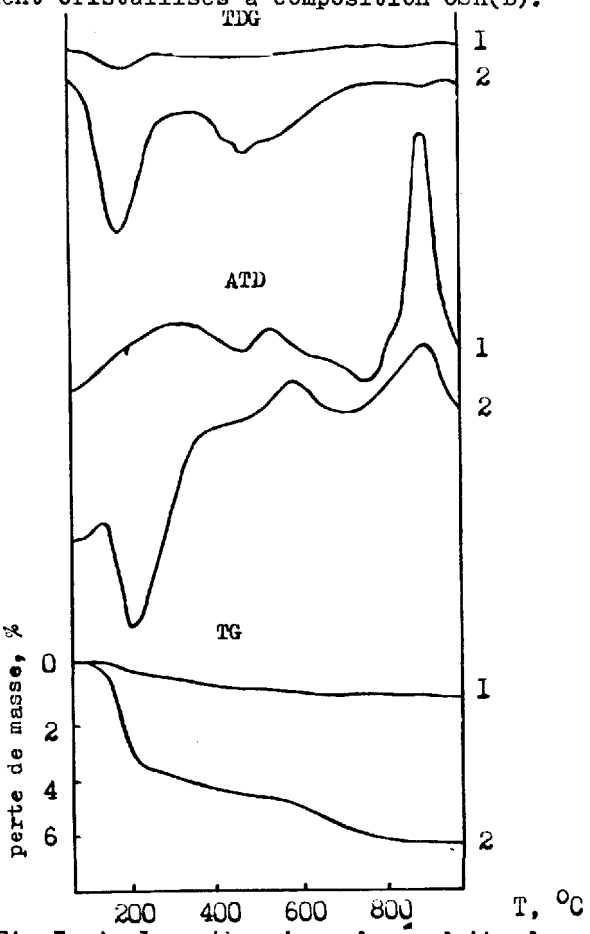

Fig.3. Analyse thermique de produits de l'hydratation
I - scorie de depart; 2 - scorie modifiée.

Les résultats de recherches confirment la possibilité de l'augmentation de la réactivité des scories à l'aide de l'action orientée sur la structure du methasilicate de calcium etant une phase prédominante et la plus inerte des scories.

V.M. KOLBASSOV Institut de Génie chimique D.I. Mendelev, Moscow, U.S.S.R. 1

MODIFICATION DE LA STRUCTURE HYDRATEE DES CIMENTS

P

La formation de la structure du ciment durci est déterminée essentiellement par l'hydratation du silicate tricalcique accompagnée de la création en quantité prépondérante des produits hydratés à dispersité, morphologie et cristallinité différentes. Les autres composants du ciment y jouent également un rôle déterminé. Cependant, dans un ciment polyminéral c'est le C_3S qui en saturant rapidement la phase liquide d'ions de calcium détermine les conditions du milieu où se déroule également l'hydratation de ces phases de clinker. De cette manière, la présence du C_3S dans le ciment constitue le facteur principal déterminant les propriétés structurales et techniques du ciment durci.

Au cours de l'hydratation de C_3S il se forme à la surface et dans le volume initial de ses grains et se développe dans le temps une couche de nouvelles formations hydratées constituée selon les concepts actuels (1) d'hydrates externe et interne qui diffèrent entre eux par la structure et la morphologie de leurs particules composantes.

Comme l'ont montré les résultats des études à la microscopie électronique (2, 3) réalisées selon une méthode originale permettant d'observer la surface intacte des particules hydratables, dès les premières secondes de l'interaction C_3S - eau à la surface des grains du C_3S commencent à apparaître de nouvelles formations hydratées qui recouvrent certaines zones de la surface de ces grains sous forme des particules à grains fins (diffraction électronique de 1,83 Å) et sous des formes morphologiques plus perfectionnées (sphérolithes, aiguilles de 1 μ). La diffraction électronique de ces formations (1,83; 1,66; 1,53 Å) permet de les identifier comme la phase C-S-H.

Il est à noter qu'une modification de la composition du milieu de durcissement (l'introduction d'adjuvants de gypse dans le système "C_3S + eau") amenait à un changement considérable des indices morphologiques des hydrosilicates de calcium (HSC) de formation initiale. Ce qui est plus typique pour ces conditions c'est une apparition rapide de HSC phanérocristallins ayant également de diverses formes morphologiques.

L'apparition des hydrates primaires dans des zones déterminées de la surface des grains du C_3S est due au fait qu'ils se forment initialement dans les zones les plus actives de la surface (aux endroits de concentration de dislocations, etc.) lesquelles les premières se soumettent à l'hydratation et commencent à des vitesses différentes à saturer d'ions formateurs les volumes locaux proches de la surface de la phase liquide des hydrates. Les résultats des études (2-8) permettent d'estimer que la vitesse de formation, les formes d'accroissement morphologiques, la dispersité de HSC (et d'autres nouvelles formations dans le ciment polyminéral durci) sont déterminées en premier lieu par la composition de la phase liquide et son homogénéité en volume (par la vitesse de saturation en ions formateurs d'hydrates, la valeur et le gradient de leurs concentrations, la valeur de sursaturations). Dans les systèmes "ciment - eau" dépourvus d'adjuvants solubles dans l'eau, ces facteurs sont dus à l'activité d'hydratation de la surface des grains de ciment (y compris de ses zones distinctes) qui détermine l'intensité et la régularité d'arrivée d'ions formateurs d'hydrates à la phase liquide. Lorsqu'on introduit avec l'eau de gâchage des adjuvants solubles dans l'eau, ce sont ces derniers qui y jouent un rôle déterminant. Ainsi, à la mise en contact avec la phase liquide d'une composition homogène dans tout son volume, il se forme de préférence des hydrates à forme arrondie des particules. En revanche, dans les conditions du gradient des concentrations de la phase liquide, il se crée des courants de convection favorisant le développement de cristaux de forme allongée (aciculaires, prismatiques, fibreux). Des sursaturations élevées en Ca^{2+} établies dans le volume intégral de la phase liquide

contribuent à une formation d'hydrates à cristallinité élevée à l'instar de ceux formés à l'aide de la méthode de traitement par chaleur humide ou par suite d'addition de $CaCl_2$. Un haut gradient de concentration que possèdent les volumes locaux de la phase liquide réalisés, en particulier, aux premiers stades d'hydratation du C_3S dans des microvolumes proches de la surface de la phase liquide stimule un accroissement rapide des groupes unitaires d'hydrates cristallins relativement gros. Une formation simultanée d'hydrates sur la base des C_3S et β-C_2S sous diverses formes morphologiques observées dans les ouvrages (2,3) est conséquence d'une innomogenéité de la phase liquide dans ses microvolumes locaux.

La morphologie et les dimensions des particules hydratées dépendent en grande partie du fait que la formation d'hydrates se produit à des conditions restreintes ainsi qu'en présence d'une surface solide développée laquelle, à des paramètres determinés du réseau cristallin, peut jouer le rôle de substrat pour la formation de germes et d'hydrates. Dans de pareilles conditions, il se forme une structure dense à haute dispersité, amorphe sous les rayons X /métamicte d'après I.G. Chpinova (9)/ typique pour un hydrate interne (10). Une même structure prédomine dans le ciment durci à un bas rapport liquide - solide additionné d'agents tensio-actifs (ATA).

A leur tour, les hydrates revêtant de diverses formes morphologiques et capables, de ce fait, à fixer, à telle ou telle vitesse, les ions de la phase liquide qui les alimente, modifient également la composition et l'anisotropie de la structure. Par conséquent, la composition de la phase liquide est également sujette à des modifications périodiques tant au niveau des macrovolumes qu'a celui des microvolumes. On peut apprécier ces modifications d'après la morphologie des hydrates qui forment la structure du ciment durci.

Durant l'hydratation du C_3S les nouvelles formations, grâce a une augmentatio de leur teneur en volume par rapport au volume des grains initiaux de liant, se propagent sur toute leur surface et remplissent l'espace intergranulaire du ciment durci ainsi que le volume des grains initiaux lequel se rétrécit par suite de l'hydratation.

La surface des grains de ciment avant le début de leur hydratation doit être con sidérée comme interface des zones de forma tion des hydrates interne et externe. Ceci est confirmé par le rapport volumétrique des hydrates interne et externe dans le ci ment durci (10) ainsi que par une topographie différente de structure des hydrates dans ces zones ce qui est dû à des conditions différentes de leur formation.

Du fait que l'interaction initiale "C_3S - eau" passe a la surface du premier, le front du développement de l'hydrate interne est orienté vers l'interieur du grain à partir de cette surface tandis que celui de l'hydrate externe vers l'espace intergranulaire. Dès le premier moment d'hydratation du C_3S commence la formation de l'hydrate externe. Des phases hydratées distinctes qui font partie de sa composition apparaissent et se développent sous des formes d'accroissement actives (2) et modifient ainsi la composition et la symétrie de la phase liquide en influant à travers cette dernière sur la morphologie et la dispersité de la portion suivante des hydrates en précipitation.

Des masses d'hydrates à grains fins amorphes sous les rayons X apparaissent par conséquent et se déposent à la surface pour remplir l'espace libre entre les plus grosses particules d'hydrates formées auparavant. Ce dernier phénomène s'accompagne de nouveau par une modification de la composition et de la symétrie de la phase liquide. Il se produit alors une formation alternée de phases hydratées sous diverses formes morphologiques. Cela constitue, apparemment, la cause même de formation d'une texture feuilletée ou à blocs alternés signalée par

les auteurs des ouvrages (11,12). Grâce à la nature métasomatique* de sa formation (12) l'hydrate interne possede une structure plus homogène, dense, submicrocristalline, amorphe sous les rayons X formée dans des conditions restreintes sous les couches de l'hydrate externe formé auparavant.

Une inhomogénéité de la phase liquide est propre dans une plus grande partie à la zone de développement de l'hydrate externe qui remplit l'espace intergranulaire dans le ciment durci.

Plusieurs propriétés techniques du ciment durci dépendent de sa porosité et, en premier lieu, du nombre de gros pores (à un rayon conventionnel de 10^3 Å). Mais les pores pareils ne peuvent se former que dans la zone de l'hydrate externe. Aussi, la zone de développement de l'hydrate externe est-elle la partie la plus faible et friable dans la structure du ciment durci d'où la nécessité d'améliorer la solidité et la densité de cette zone en premier lieu.

Dans une certaine mesure, on peut l'obtenir par voie de régulation du rapport entre les épaisseurs des couches d'hydrates interne et externe grâce au choix de la finesse de broyage du ciment et de la densité d'assemblage de ses grains dans la structure en formation (en améliorant le rapport eau/ciment et le degré de densité). Plus fines sont les particules de clinker, plus minces seront les couches d'hydrate interne formées pendant son hydratation. Plus vaste est l'espace intergranulaire dans le ciment durci, plus grand volume pourra occuper et sera donc plus friable l'hydrate externe qui s'y développe.

Il est possible d'influer avec succès sur la dispersité et la morphologie des particules de l'hydrate externe qui déterminent la quantité et la solidité des contacts entre elles à l'aide d'adjuvants chimiques solubles dans l'eau (6-8).

Les adjuvants les plus efficaces au point de vue formation de la structure de la zone de l'hydrate externe sont ceux du type $NaNO_2$. De tels adjuvants ne permettent pas une formation de complexes avec les phases de clinker contenant de l'aluminium. Ces composés ont l'aspect de cristaux relativement gros qui ne jouent pas toujours un rôle positif dans la formation de la structure optimale du ciment durci. D'autre part, en apportant des modifications à la composition ionique de la phase liquide les adjuvants pareils sont capables d'initier une morphologie déterminée des particules formées au sein de l'hydrate externe. Ainsi, en présence d'adjuvants de nitrite de sodium, une quantité déterminée des particules de l'hydrate externe revêtent l'aspect de formations fibreuses ce qui permet de réaliser le soi-disant "autorenforcement" du ciment durci, en particulier, dans la zone la plus faible de son espace intergranulaire. La germination dans les pores du ciment durci de formations fibreuses s'accompagne d'une augmentation du nombre de contacts entre les particules solides et d'une diminution des dimensions des pores (7) ce qui, comme on le sait, rend plus dense et plus solide la structure en formation.

Les adjuvants de superplastifients (SP) apportent, eux aussi, des transformations favorables dans la structure de l'hydrate externe. Grâce à leur effet réducteur d'eau, les adjuvants SP réduisent le volume de l'espace intergranulaire dans la pâte de ciment et, par conséquent, créent des conditions plus restreintes pour la formation et au développement de l'hydrate externe. Un rôle important y revient également à l'effet de modification d'adsorption des adjuvants SP. La stabilisation des hydrates obtenue grâce à cet effet en état finement divisé, amorphe sous les rayons X contribue encore davantage à optimiser la structure de l'hydrate externe dans le ciment durci.

* Métasomatose: processus de substitution chimique des minérais les uns par les autres avec la conservation d'anciennes forme, structure et d'autres particularités sous l'action des solutions qui entrent en contact avec les minérais.

Une combinaison de ces deux modes d'action des adjuvants SP approche considérablement la structure d'hydrate externe dans le ciment durci de celle de l'hydrate interne ce qui explique notamment un effet élevé de la résistance à la compression obtenu grâce à ce phénomène. Un rôle déterminé joue également une plus petite valeur des contraintes intérieures enregistrées dans le ciment durci où l'hydrate externe est représenté par des particules finement divisées, amorphes sous les rayons X, d'HSC et de portlandite.

Un moyen optimal d'agir sur la structure et les propriétés du ciment durci (en premier lieu dans la zone qu'y occupe l'hydrate externe) est une utilisation d'adjuvants combinés solubles dans l'eau constitués par des SP et électrolytes inorganiques. Grâce à ce procédé on a réussi à doubler presque la résistance à la compression et à la flexion du ciment durci et de réduire quatre fois sa porosité totale. La porosité d'un tel ciment durci ne constituait que ~ 3 % de volume, les pores à rayon efficace de plus de 10^3 Å étant pratiquement absents.

REFERENCES

1. M. Daimon, S. Neda, R. Kondo, "Morfhological study on hydration of Tricalcium silicate". Cement and Concrete Res., 1971, 1(4), p. 391-401.
2. Ю.М. Бутт, В.М. Колбасов, П.А. Козырева. Фазообразование на ранних стадиях гидратации портландцемента. Труды МХТИ им. Д.И. Менделеева, 1975, вып. 87, с. 48-50 (en russe).
3. Ю.М. Бутт, В.М. Колбасов, Н.А. Козырева. Дискуссия по докладу Г.Л. Калоусека "Процессы гидратации на ранних стадиях твердения цемента", Труды VI Международного конгресса по химии цемента, 1976, т. II, кн. 2, с. 105-107 (en russe).
4. Г.В. Топильский, Ю.М. Бутт, В.М. Колбасов. "К вопросу о составе и свойствах портландита в гидратированных портландцементах". Кристаллография, 1968, т. 13, 5, с. 1083-1088 (en russe).
5. В.М. Колбасов, Г.В. Топильский "Исследование гидратации портландцементных клинкеров", Известия АН СССР "Неорганические материалы", 1970, т. 6, 5, с. 967-970 (en russe).
6. Ю.М. Бутт, В.М. Колбасов "Влияние состава цемента и условий твердения на формирование структуры цементного камня", Труды VI Международного конгресса по химии цемента, 1976, т. II, кн. 1, с. 281-283 (en russe).
7. Ю.М. Бутт, В.М. Колбасов "Твердение цементов при пониженных температурах и структурообразующая роль водорастворимых добавок", Труды II Международного симпозиума по зимнему бетонированию, 1975, т. I, с. 6-17 (en russe).
8. Ю.М. Бутт, В.М. Колбасов, Н.В. Фартунина "О влиянии условий среды твердения на структурную плотность цементного камня", Труды конференции "Siliconf", 1977, Будапешт, с. 471-481 (en russe).
9. Л.Г. Шпынова, Н.В. Белов, В.И. Чих "О метамиктности гидросиликатов кальция камня β-C_2S", ДАН СССР, 1979, т. 244, 6, с. 1115-1117 (en russe).
10. Р. Кондо, М. Даймон "Фазовый состав затвердевшего цементного камня", Труды VI Международного конгресса по химии цемента, 1976, т. II, кн. 1, с. 244-257 (en russe).
11. Ю.М. Бутт, В.В. Тимашев "Скорость гидратации C_3S и особенности микроструктуры мономинерального камня", Строительные материалы из местного сырья и отходов промышленности Казахстана, 1972, с. 13-35 (en russe).
12. Л.Г. Шпынова, В.И. Чих "Взаимосвязь микроструктур клинкера, цементного порошка и камня", Цемент, 1978, 4, с.6-8 (en russe).

ILYINETS, A.M., SIMONOV, V.I., BIKBAU, M.Ya.
Institute of Crystallography of the Academy of Sciences, NIICement, Moscow, U.S.S.R.

NEW DATA CONCERNING ATOMIC STRUCTURES OF PORTLAND CEMENT SILICATES

Extensive physico-chemical investigations of polymorphous modifications of tricalcium silicates which are impotant components of portlandcement clinker, do not provide sufficient data on their crystal structure. The reasons lie in the difficulty of obtaining perfect single crystals of these compounds, particularly the high-temperature modifications stabilized at normal temperature. Up to now investigators failed to refine the structure of the high-temperature rhombohedral modificatio of C_3S, whose idealized model was proposed by Jeffry in 1952 / 1 /.

We obtained single crystals of rhombohedral modification of C_3S in the system $CaO-SiO_2-CaCl_2$ at 1400°C in silicate-chloride melt. Sr atoms were used as a stabilizer, keeping the high-temperature phase at normal temperature. X-ray analysis of crystals confirmed space group R3m / 2 / (unit cell parameters: a_o= 7.0767(9), c = 24.974 (4) Å, V = 1072.5 Å^3) and allowed us to refine the structure, proposed by Jeffry. The basis of structure is formed by Ca-polyhedra layers of two types: Ca1-polyhedra with seven vertices and greatly distorted Ca2, Ca3-octahedra. The packing of Ca-polyhedra in each layer and the manner of their connection with Si-tetrahedra is shown in Fig.1. Projection of structure of C_3S onto the ab-plane:

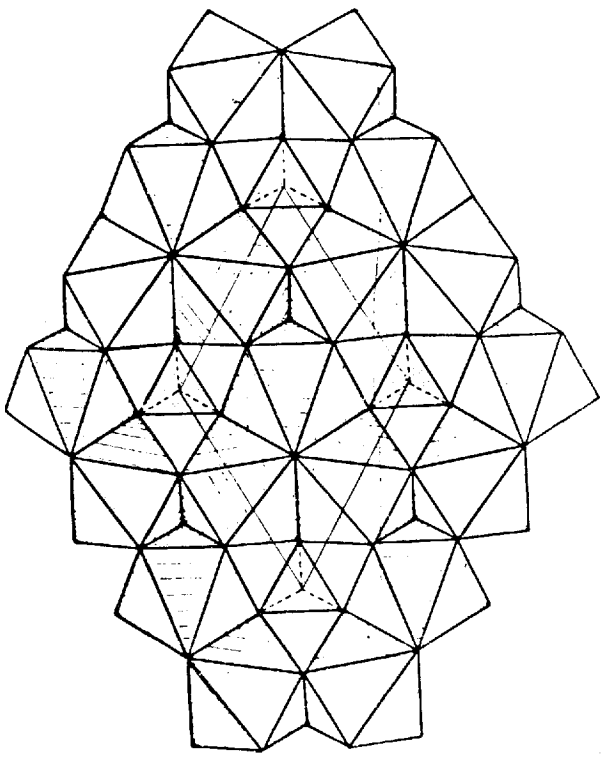

a - a layer of Ca-polyhedra with 7 vertices, z ≈ 0;

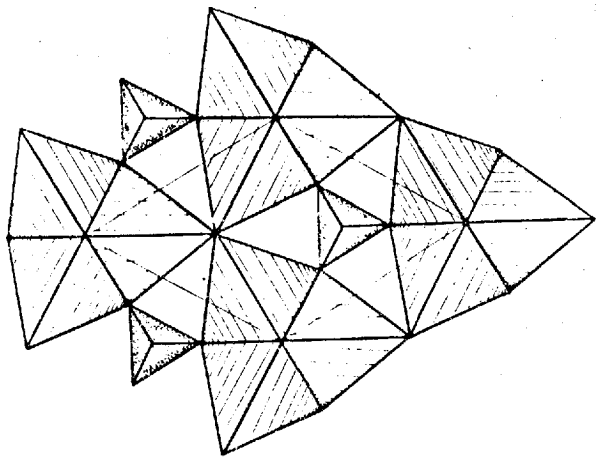

b - a layer of Ca2-octahedra, z ≈ 2/9;

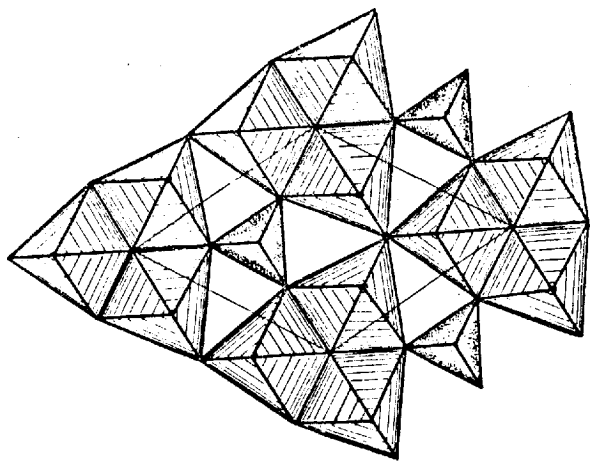

c - a layer of Ca3-octahedra, z ≈ 1/9.

The mutual arrangement of the layers along the c-axis is shown in Fig.2. A comparison with the Jeffry model shown that mutual arrangement of Ca and Si atoms almost coincides, as well as the positions of seven out of 9 oxygen atoms. A change of positions of two atoms is due to reorientation of Si-tetrahedra along the 3-fold axis and rotation of another Si-tetrahedra by 60° about the same axis. A similar change of positions of Si-tetrahedra was reported in / 3 /. It was established in studies of the high-temperature modification of C_3S at 1200°C. However, that paper also reports statistical orientation of Si-tetrahedra along the 3-fold axis: in 30% of cases it coincides with the Jeffry orientation and in 70% - it is just the opposite.

Nishi and Takeuchi in their paper were the first to show a correlation between the structures of the high-temperature rhombohedral modification and the low-temperature triclinic phase, established in / 4 /. The correlation between these two structures can be demonstrated more vividly in the form of a transitio matrix from unit cell parameters of a rhombohedral modification of C_3S, stabilized by us at normal temperature (a = 7.076 and c = 24.974 Å) to cell parameters of the triclinic phase (a = 11.67; b = 14.24; c = 13.72 Å; γ = 105.3°, β = 94.2° γ = 90°). This matrix, line by line, has form: 2/3, 4/3, 1/3; -2,0,0; -1/3,-5/3, 1/3. Re-calculated parameters of a rhombohedral unit cell are: a = 11.65; b = 14.11; c = 13.61, α = 105°, β = 95°, γ = 90°; these values are father close to the parameters reported in / 4 /. This transformation allows one to recalculate the atomic coordinates of the triclinic phase to a twice-centered hexagonal unit cell. A comparison of the transformed atomic coordinates of triclinic modification with the atomic coordinates of the initial rhombohedral modification showed that all the cations and 37 oxygen atoms out of 45 are slightly displaced with respect to each other. A non-coincidence of coordinates of the remaining 8 oxygenatoms can be attributed to a reorientation of two Si-tetrahedra out of 9 along the 3-fold axis, including rotation of one of these two tetrahedra by 60° about the 3-fold axis with respect to the position of Si-tetrahedra in the rhombohedral modification / 5 /. One could have supposed that the change of the orientation of 2 out 9 Si-tetrahedra in the triclinic phase is due to statistical orientation of three tetrahedra, found in paper / 3 /. However, this correlation does not exist, because statistically oriented tetrahedra in paper / 3 / correspond to certain tetrahedra in / 2 /, while two reversely oriented tetrahedra in the triclinic phase correspond to other tetrahedra in / 2 /.

Thus, comparing structures of the "high-temperature", the "low-temperature" rhombohedral modifications and the low-temperature triclinic phase, one can come to a conclusion that the main difference between them lies in the orientation of Si-tetrahedra, while positions of Ca, Si atoms and free oxygen remain close. Apparently, the structures of the 5 remaining intermediate modifications of C_2S also differ from each other only by rotations of Si-tetrahedra.

We have also grown α'_L-C_2S single crystals in the same system $CaO-SiO_2-CaCl_2$, also stabilized by Sr atoms at normal temperature. Orthorhombic unit cell parameters are: a = 20.871(2), b = 9.496(1), c = 5.500(1) Å. Similar values of parameters of α_L- C_2S with 3-fold value of one of the parameters, as compared to α'_L-C_2S was reported in paper / 6 /. The differences lie only in setting crystallographic axes. The structure of the α'_L-phase was determined in paper / 7 / and refined to R-factor 7% in space group $Pna2_1$. The basis of the structure is formed by Ca-polyhedra with 8 vertices and Ca(Sr)-polyhedra with 10 vertices positioned along the a-axis. Peculiar is the orientation of Si-tetrahedra along the a-axis. It is assumed that the hexagonal structure of the high-temperature -phase of C_2S has all the Si-tetrahedra oriented in the same direction / 8 /. The transition $\alpha \rightarrow \alpha'$ is due to a possible rotation of Si-tetrahedra. In our case, 4 tetrahedra, out of 6, connected with Ca-polyhedra with 8 vertices, are connected along the a-axis, while two others are oriented in the opposite direction (Fig. 3). Apparently, it is this

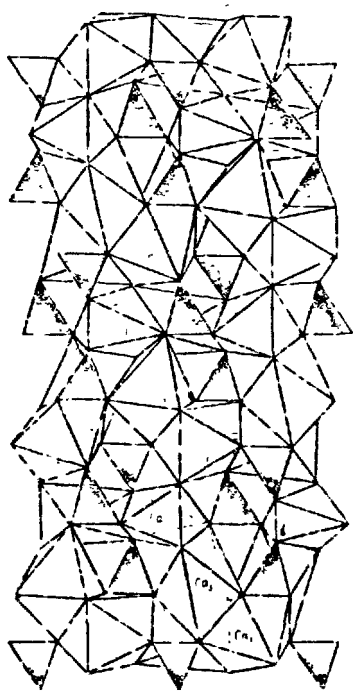

Fig.2. Structure of rhombohedral modification of C_3S, (110) cut.

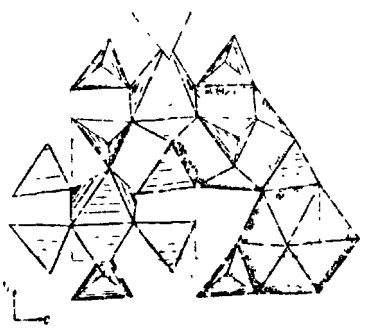

Fig. 3. Structure of α'-C_2S ($Ca(Ca,Sr)SiO_4$): two cuts, perpendicular to (100). The A-A cut shows only Ca-polyhedra with 8 vertices, the B-B cut - only Ca(Sr)-polyhedra with 10 vertices.

change of Si-tetrahedra orientation that leads to a 3-fold value of the parameter a = 20.871 Å (in another setting it is the c-axis). A further clarification of the mechanism of transition $\alpha \rightarrow \alpha'$ in C_2S can be made by means of a direct structure determination of the α-phase, which is complicated by difficulties in obtaining single crystals of this most high-temperature phase of C_2S stabilized at normal temperatures.

Thus, polymorphous transformations of C_2S and C_3S are caused by slight displacements of atoms within the structure and a change of the orientation of Si-tetrahedra. The latter circumstance can be explained by a lower capability of Si-O bonds (in contrast to Ca-O bonds) to accumulate thermal energy, which, in its turn, according / 9 /, on cooling and heating, makes Si-tetrahedra change their position in the structure to a more energetically favourable position. Thus in each temperature range there exists a certain modification. The addition of Sr atoms into the nodal points of the crystal lattice of C_3S and C_2S increases entropy in minerals and contributes to keeping thermodynamical stability, in normal conditions in the form of solid replacement solutions. Sr atoms are suitable for solving the problems of stabilizing the high-temperature modifications, since the Sr^{2+} radius in normal conditions corresponds to the effective Ca^{2+} radius at high temperature in minerals.

REFERENCES

1. J.W.Jeffry, The crystal structure of tricalcium silicate. - Acta Cryst., 1952, v.5, p.26-35
2. Ilyinets A.M., Malinowsky Yu.A., Nevsky N.N. Crystal structure of rhombohedral modification of tricalcium silicate Ca_3SiO_5 - DAN SSSR, 1985, v.281, 2, 332-336
3. F.Nishi, Y.Takeuchi. The rhombohedral structure of tricalcium silicate at 1200°C Zet.Kristallogr., 1984, 168, 3, 197-212.
4. Golovastikov N.I., Matveeva R.G., Belov N.N Crystal structure of tricalcium silicate $3CaO \cdot SiO_2 = C_3S$ - kristallografiya, 1975, 20 4, 721-729.
5. Simonov V.I., Ilyinets A.M. On the uniform structural basis of polymorphous modifications of tricalcium silicate Ca_3SiO_5 (in publication).
6. H. Saafeld. X-ray Investigation of Single Crystals of Ca_2SiO_4 (Larnite) at High Temperatures. - Amer. Mineralog. 1975, 60, 824-827.
7. Ilyinets A.M., Nevsky N.N., Ilukhin V.V., Bikbau M.Ya., Belov N.V. Crystal structure of the α'-modification of dicalcium silicate $Ca(Ca,Sr)SiO_4$ - DAN SSSR, 1982, 267, 3, 641-644.
8. W.Eysel, T.Hahn. Polymorphism and solid solution of Ca_2GeO_4 and Ca_2SiO_4 - Zet. Kristallogr., 1970, v.131, 322-341.
9. Bikbau M.Ya., Butt A.M., Timashev V.V. On the polymorphism and stabilization of dicalcium silicate. - In: Chemistry and technology of silicates. Proceeding of Moscow Mendeleev Chemico-Technological Institute, 1975, 87, 3-9.

L. S. KLUEVA, A. I. MARKOV NIICement, Moscow, U.S.S.R.

MODIFICATION OF CEMENT CONTRACTION DUE TO FALSE SETTING

Premature loss of plasticity, characteristic of the false-setting cements, develops directly after the mixing of the cement paste or mortar and concrete mix is ended. Evident and repeatedly proved is the interdependence of false setting and the presence of dehydrated forms of gypsum in cement content, those of forms of gypsum, which are characterised by the increased solubility comparing to dehydrite.

During the cement hydration there takes place a contraction - decrease in the absolute volume of the system "cement-water" as a result of chemical fixation of the water and its transformation into crystalline hydrates. In this work we used differencial contraction method for the investigation of false-setting cement hydration.

The subject of our inquiry were cements of laboratory comminution (S_{sp} ~3000 cm^2/g; gypsum content ~2,5% in terms of SO_3), produced on the base of clinkers of different mineralogical composition and alkali content. All of the newly produced cements were characterised by normal setting. The changes in the setting type were reached by means of gypsum dehydration in cement contents after preliminary thermal treatment. Contraction measurements were performed for solutions with cement/sand =I:I at cement/water= 0,35; quartz sand was used as a model system. The compensation of difference of temperatures between the investigated system and the model one was performed to the precesion of 0,I°C.

As for cements containing no additives but gypsum, the degree of false setting is defined mainly by the gypsum dehydration rate during cement comminution, and by the original clinker features, such as alkali content in particular (I). It is seen from the table I, that cements, produced on the base of clinkers with low and moderate alkali content (≤ 0,7% R_2O in terms of Na_2O) after thermal treatment in temperature range of I00-I50°C can develop a false setting both with full (Ist type) and partial premature loss of plasticity. Cements produced on the base of clinkers with elevated alkali content in the conditions of analogical thermal treatment are characterized by exclusively false setting of the 2nd type. Temperature elevation above I70°C in all the cases develops quick setting features. As a rule cements develop quick setting features, if the temperature is above I70°C.

False-setting cements at early ages of hydration are characterized by higher contraction rate than those with normal setting. However the differences of contraction occure immediately after a water-addition with one kind of cements (fig.Ia), while with the others the difference of contraction takes place after about 2 hours of hydration (fig.Ib).

Fig.I. Contraction curves of cements of different setting types, produced on the base of different clinkers:I-normal setting; 2 and 2'- false setting after the primary and secondary mixing correspondingly.

Table I.

Clinkers:	R_2O,%	Anomalsetting types, observed after thermal treatment of cements		
		I00-I30°C:	I50°C:	I70°C and higher
I	0,32	II	I	Quick setting features
2	0,42	II	I	
3	0,49	II	I	
4	0,49	II	I	- " -
5	0,52	II	I	- " -
3a	0,66	II	I	- " -
6	0,85	II	II	- " -
6a	0,92	II	II	- " -
3b	I,06	II	II	- " -
7	I,08	II	II	- " -
8	I,II	II	II	- " -
7a	I,23	II	II	- " -
9	I,33	II	II	- " -
4a	I,44	II	II	- " -

Notes: 3,3a,3b - different clinker samples from one of the producers (identical to 4 and 4a, 6 and 6a, 7 and 7a).

a) Clinker 7 (identical to 4 and 6a).

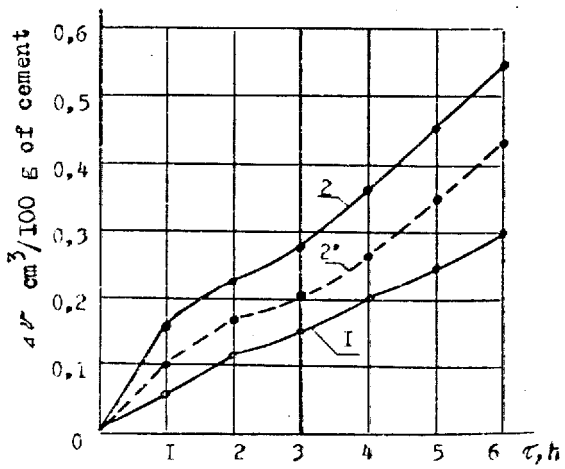

b) Clinker 3b (identical to 3a).

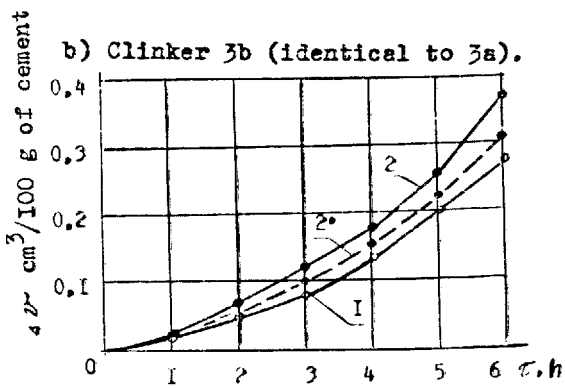

To reveal the reasons of the observed differences we shall consider the phase composition of hydration products. According to the current data certain setting type of cement at early stages of hydration can cause the dominating crystallization of the following new formations: ettringite (normal setting), $CaSO_4 \cdot 2H_2O$ and ettringite (false setting) and calcium hydroaluminates (quick setting). Table 2 contains calculated data of contraction volume in connection with crystallization of $CaSO_4 \cdot 2H_2O$, ettringite and one of calcium hydroaluminate. The formation of the primary gypsum-ettringite structure, causing the false setting of cements, does not have any advantages over crystallization of ettringite at normal setting from the point of view of contraction effect. The increase of volume of new formations at generation of the primary gypsum-ettringite structure according to our calculations cannot cause such substantial differences in the level of contraction effects of cements with normal and false settings.

Table 2

Reaction scheme	:Changes of :the system :volume,%
$C_3A+3CaSO_4 \cdot 2H_2O+26H_2O \rightarrow C_3A \cdot 3CaSO_4 \cdot 32H_2O$	-6,44
$CaSO_4 \cdot 0,5H_2O+1,5H_2O \rightarrow CaSO_4 \cdot 2H_2O$	-6,98
$C_3A + 6H_2O \rightarrow C_3A \cdot 6H_2O$	-23,78

Analytical results of the previously investigated liquid phase composition (2) can testify the primary supersaturation of the liquid phase of false-setting cements by sulphate ions, with consequent reduction of ion concentration after the development of false setting. Comparing the results of investigated liquid phase composition and the contraction dynamics of cements we can conclude, that $CaSO_4 \cdot 2H_2O$, crystallizing as an element of initial structure of false-setting cements, does not take part in the reaction with aluminous phases of clinker, because $CaSO_4 \cdot 2H_2O$ is already blocked as a result of joint crystallization with ettringite. In connection with this the system revealed a seeming disadvantage of the gypsum for regulating the setting process; this results in the formation of hydroaluminate phase, which elevates the contraction effect of false-setting cements.

The possibility of the formation of hydroaluminate phase at early stages of hydration of false-setting cements is illustrated by fig.2, according to which there takes place the coincidence of contraction curves for false- and quick-setting cements, containing gypsum in the form of semi-hydrate in the first case, and in the second case in the form of dehydrate, but of insufficient volume (SO_3- content in cements on fig.2 is referred to with regard for SO_3 in clinker). In other words the false setting proved identical to quick setting in the given case in terms of contraction effect.

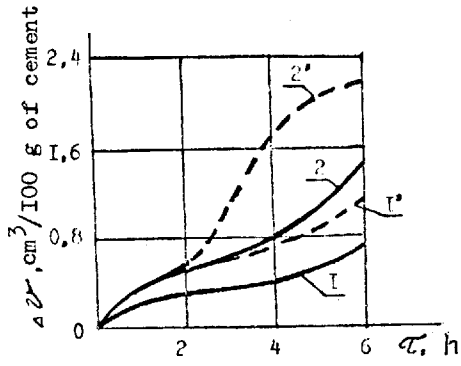

Fig.2. Contraction curves of cements produced on the base of clinker 7; these have different compositions and different gypsum forms: 1 and 1' - correspondingly unheated (normal setting) and heated (false setting of the III type) cement, containing 2,5%SO_3; 2 and 2' - correspondingly unheated and heated cement, containing 1,48% SO_3 which is caracterized in both cases by quick setting.

Comparison of the data on the cement contraction and mineralogical composition of the initial clinkers have shown that in terms of quantity the formation of hydroaluminate phase at early stage of false-setting cements gydration is determined by C_3A - content in the initial clinker.

According to the contraction curves (fig.1), $CaSO_4 \cdot 2H_2O$ is again able to regulate the setting after the failure of initial structure of false-setting cements at the secondary mixing.

So the results of investigations of contraction of cements with different setting types indicate that with dehydrated forms of gypsum present in false-setting cements at early stages of hydration there takes place the crystallization of $CaSO_4 \cdot 2H_2O$ from the liquid phase, supersaturated with sulphate-ions and then $CaSO_4 \cdot 2H_2O$ is blocked in the composition of initial gypsum-ettringite structure; this results in the reduction of gypsum volume which acts as setting regulator and causes the changes in composition of hydrate new formations.

BIBLIOGRAPHY

I. Энтин З.Б., Клюева Л.С., Папиашвили У.И. Исследование особенностей процесса структурообразования цементов с ложным схватыванием.-УП Международный конгресс по химии цемента. Париж, 1980

2. Энтин З.Б., Клюева Л.С. Роль жидкой фазы в явлениях аномального схватывания цементов.-УI Всесоюзное совещание по химии и технологии цемента. М, 1982

N. KOMAROVA,
V. RIASINE,
G. TCHISTIAKOV, NIICement, Moscow, U.S.S.R.
A. KORENGA

STABILISATION ORIENTEE D'UNE COMPOSITION DE PHASES DESEQUILIBREES DU CLINKER BLANC.

Le présent ouvrage traite des particularités propres à la formation de la composition de phase et de la microstructure dans les clinkers blancs à haute teneur en aluminates (tabl. 1) soumis à la cuisson avec blanchiment dans des fours rotatifs industriels (clinkers 1, 2, 3, 4, 5, 6 et 6-H), dans un creuset (clinkers 7 et 7-H) et en laboratoire (clinker 4-T). Les données de la figure 1 relatives à la modification de la composition de phase et du facteur de réflexion (FR) des clinkers en fonction du régime thermique du blanchiment sont obtenues en laboratoire lors de la cuisson avec blanchiment dans l'eau des mélanges bruts utilisés à la fabrication des clinkers dans les fours rotatifs et le creuset ainsi que lors du blanchiment à neuf dans l'eau des clinkers industriels 4 et 5 après leur maintien préalable pendant 20 mn à 1450 °C, la température étant réduite vers le moment du blanchiment à la valeur requise. La détermination de la composition de phase des clinkers a été faite à l'aide de la méthode d'analyse radiographique.

Les particularités propres à la composition de phase des clinkers blancs à haute teneur en aluminates sont les suivantes:

- la formation d'une composition de phase variable déséquilibrée à bas degré d'ordre de la structure des minérais en fonction du régime de refroidissement (de blanchiment) du clinker avec, y compris, une suppression partielle ou à peu près complète de la cristallisation du C_3A (tabl. 1, fig. 1);
- la stabilisation de préférence des formes trigonale et monoclinique à haute température de l'alite à une faible teneur en formes à haute température de la bélite - et $\alpha' - C_2S$;
- une absence totale d'alumoferrite de calcium (tabl. 1, fig. 3);
- la présence dans la composition des minérais de clinker d'impuretés structurales de divers type (1) avec la prédominence de la cristallisation des phases d'alumosilicate suivant le type des cristaux mixtes (des mélanges isomorphes) et la conservation des paramètres radiocristallographiques de l'alite et de la bélite le plus souvent et du C_3A à un plus faible degré. Cela entraîne une modification sélective des caractéristiques radiographiques des phases et aboutit à une perturbation des dépendances de référence adoptées à l'analyse quantitative de phase: quantité de phase - intensité des maximums (la somme des phases ne correspond pas à 100 % au tableau 1, fig. 3);
- l'oxyde de magnésium s'intègre dans la fraction d'alumosilicate en quantités différentes en fonction du régime de refroidissement du clinker sous la forme de périclase ou d'une impureté isomorphe dans le C_3A et exerce une forte influence sur le FR de la fraction d'alumosilicate du clinker (tabl. 2, fig. 2.3);
- la formation pendant la cuisson du clinker de silicates et d'alumosilicates avec une présence du CaO à faible fixation chimique et structurale amène à un entrainement sélectif du CaO au cours de la cuisson et à la formation de portlandite et de $CaCO_3$ au cours du blanchiment;
- pendant la cuisson dans un milieu très réducteur et le blanchiment dans un milieu vapeur-gaz on voit apparaitre dans la composition du clinker des minérais du groupe de γ-bélite (γ-C_2S, chondrodite de calcium, khilchoanite et γ-C_2S-hydrate), qui ne sont pas ordinaires pour le ciment Portland.

Le blanchiment des clinkers sous une température de 1150 à 1450 °C ne s'accompagne pas de la réduction du Fe^{3+} au Fe^{2+}. La particularité établie chez les oxydes de fer de ne pas former de phases d'alumoferrites indépendantes (où les ions de fer constituent des chromophores capables de former des variétés et doivent posséder des caractéristiques spectroscopiques stables), mais de s'intégrer en qualité d'impuretés dans les phases d'aluminate et d'alumosilicate principalement en présence d'un entou-

N. KOMAROVA,
V. RIASINE,
G. TCHISTIAKOV,
A. KORENGA

Tableau 1

Influence du régime de refroidissement sur la composition de phase du clinker blanc

Clinker	Régime de refroidissement (de blanchiment)	Teneur en oxydes, % en masse			KS	SM	Composition minéralogique potentielle, % en masse				Composition de phase, % en masse				FR, %
		Fe_2O_3	FeO	MgO			C_3S	C_2S	C_3A	C_4AF	C_3S	C_2S	C_3A	Total	
1	blanchi dans un milieu de vapeur	0,10	0,14	1,64	0,91	4,7	66	18,5	13	0,8	60	30	10	100	88
2	blanchi dans l'eau	0,75	0,14	3,7	0,93	5,5	71,6	12,6	7,9	2,3	68	20	12	100	85
3	blanchi dans un milieu vapeur-gaz	0,17	0,22	2,9	0,89	3,7	56	20,8	14,4	1,3	59	27	13	99	84
4**	blanchi dans un milieu vapeur-gaz	0,43	0,14	0,73	0,93	3,5	67,6	13,6	15,3	1,3	54,5	29	19	102,5	85
4-H	refroidi à l'air	0,58	néant								68	22	16	106	72
4-П	blanchi à neuf dans l'eau à 1450 °C	0,58	néant								80	22	1	103	80
4-TH	refroidi à l'air										68,5	25	19	112,5	72
5	blanchi dans un milieu vapeur-gaz	0,47	0,14	0,79	0,83	4,2	46	36	13,6	1,4	48	35	19	102	83
5-H	refroidi à l'air	0,62	néant								72	20	14	106	69
5-П	blanchi à neuf dans l'eau à 1400 °C	0,47	0,02								72,5	26	1	99,5	80,5
6	blanchi dans l'eau	0,71	0,07	0,93	0,83	4,2	45,8	35,9	12,1	2,2	70	25	4,5	99,5	80
6-H	refroidi à l'air	0,7	0,07	1,72	0,83	4,3	46,3	36,3	12,3	2,1	56	34	I0	I00	62
7	blanchi dans l'eau	0,4	néant	0,97	0,81	3,4	38	38	16	1,2	52	36	10	98	83
7-H	refroidi à l'air	0,44	néant	1,1	0,82	3,3	40,5	35,9	16,3	1,3	55	30	14	99	74

* Les alumoferrites de calcium ne sont décelés dans aucun des clinkers même après que ces derniers ont été débarrassés de silicates de calcium à l'aide de l'acide borique.

** La composition théorique indiquée concerne également les clinkers à indices supplémentaires H, П et TH. Les clinkers 5, 7 et 7-H sont obtenus sur la base des mélanges à KS = 0,93 à 0,92.

rage de ligends différents, prédétermine l'acquisition par les ions de fer de diverses caractéristiques spectroscopiques et de diverses propriétés colorantes. Il s'en suit que le FR des clinkers blancs ne doit pas dépendre directement de la quantité d'oxydes de fer.

Lorsque le blanchiment des clinkers se produit dans l'eau ou dans un milieu vapeur-gaz à une température de 1250 °C et plus basse, on voit se stabiliser dans tous les cas les compositions à haute teneur en C_3A qui est proche ou supérieure à la quantité calculée de ce minérai (tabl. 1, fig. 1). Quant le blanchiment se fait à une température comprise entre 1275 e 1375 °C on observe de différents schémas de cristallisation du C_3A en fonction de la composition

Tableau 2

Caractéristiques de la fraction d'alumosilicate des clinkers blancs

Clinker	Teneur en phase d'alumosilicates, % en masse	FR, %	Composition chimique du clinker, % en masse*							concentration en masse d'oxydes de fer dans les phases d'alumosilicates du clinker, %
			SiO_2	Al_2O_3	Fe_2O_3	FeO	CaO	MgO	MnO	
4	19,1	89	11,69	31,33	2,18		52,35	2,08	0,02	70
4-H	16,3	70	10,73	32,30	2,35	0,03	48,65	5,58	0,09	65
4-П	15,8	80	16,58	31,58	2,54		45,75	3,11	0,01	66,7
5	13,5	89	10,37	33,34	1,89	0,22	52,25	1,73	0,02	46,33
5-H	16,3	77	10,26	32,92	2,32	0,01	49,06	4,91	0,108	61,3
5-П	18,8	83	12,87	31,59	2,77		48,51	3,70	0,003	84

* Dans les échantillons des clinkers 4-H, 5 et 5-H le Cr_2O_3 n'est pas décelé, dans les autres échantillons sa quantité a constitué de 0,007 à 0,011 %.

chimique et de la réactivité du mélange cru. Dans les clinkers obtenus sur la base de mélanges très basiques (FS = 0,93 à 0,92) à une basse réactivité (clinkers 4 et 5) on réussit à supprimer presque complètement la cristallisation du C_3A en opérant le blanchiment à une température de 1375 °C au minimum. Une haute teneur en C_3A a été enregistrée dans de pareils clinkers dès la réduction de la température vers le moment du blanchiment à 1350 °C. On peut supprimer la cristallisation du C_3A dans le clinker 6 en opérant le blanchiment à une température de 1300 °C tandis que dans les clinkers 4-T et 7 on l'obtient à une température de 1350 °C au minimum vers le moment du blanchiment. Il est possible de régler le degré de suppression de la cristallisation du C_3A dans les clinkers 4-T et 7 en faisant varier la température pendant le blanchiment de 1275 à 1350 °C. Simultanément avec la suppression de la cristallisation de la phase du C_3A est observi un accroissement sensible de la teneur totale en phases de silicate par suite de différentes modifications qui surviennent dans les schémas de cristallisation d'alite et de bélite en fonction des conditions concrètes: la quantité d'alite augmente à une suppression de la cristallisation de la bélite ou la quantité de bélite augmente considérablement à une faible réduction de la teneur en alite.

Le déséquilibrage de la composition de phase des clinkers blancs est dû à la stabilisation qui a lieu pendant le blanchiment de clinker à composition des phases à haute température dans des systèmes d'alumosilicate à haute basicité contenant des impuretés de MgO. L'aluminium peut s'intégrer dans les tétraèdres de SiO_4 lorsqu'il est chauffé à 1300 °C et plus, ses paramètres structuraux étant soumis à des modifications en présence de hautes températures (2). La nature de la cristallisation déséquilibrée des phases pendant le blanchiment dépend de la cinétique de fixation du CaO lors de la cuisson dans un intervalle de températures de 1200 à 1350 °C.

Le maximum du FR s'obtient à des températures différentes du clinker vers le moment du blanchiment. Le clinker 7 possède la blancheur maximale à la température de blanchiment de 1200 °C, les clinkers 4 et 4-T à la température de 1300 °C, le clinker 5 à la température de 1350 °C et le clinker 6 à la température de 1450 °C. Une suppression importante ou presque totale de la cristallisation du C_3A est accompagnée, de règle, par une réduction du FR du clinker de 2 à 5 %.

N. KOMAROVA,
V. RIASINE,
G. TCHISTIAKOV,
A. KORENGA

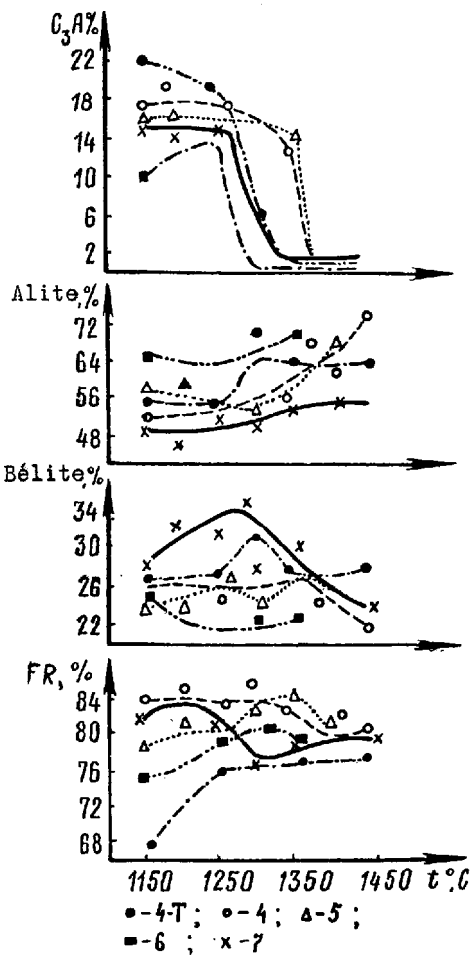

Fig. 1. Composition de phase et FR des clinkers blancs en fonction du régime de blanchiment thermique. La désignation des courbes correspond au marquage des clinkers dans le tableau 1

Dans la fraction d'alumosilicate des clinkers blancs extraite par une dissolution de phases de silicate dans la solution à 5 % d'acide borique, il y a de 10 à 16 % de SiO_2 qui s'y trouve en qualité d'impureté structurale isomorphe (tabl. 2, fig.3). Le changement du régime de refroidissement du clinker entraine une modification sensible du contenu et de la nature de répartition de l'oxyde de magnésium dans la fraction d'alumosilicate du clinker ce qui constitue justement la principale condition de la modification du FR de clinker par suite du blanchiment réalisé de 70 à 89 %.

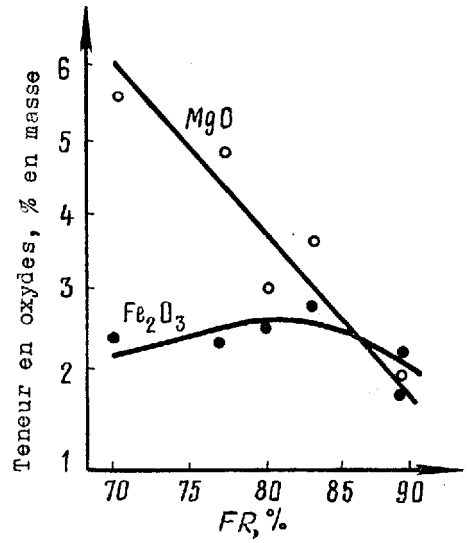

Fig. 2. Influence des oxydes ferriques et de magnésium sur le FR de la fraction d'alumosilicate du clinker blanc

A un accroissement en masse de 2 à 5 % de la fraction du MgO, la blancheur de la fraction d'alumosilicate diminue brusquement (fig. 2). Dans les clinkers à FR le plus haut (fig. 3, clinkers 1 et 2), l'oxyde de magnésium se cristallise sous la forme de périclase indépendamment de la valeur de sa fraction en masse dans le clinker. Une haute teneur des phases d'alumosilicates en oxydes de fer n'influe presque pas directement sur leur coloration.

La fraction d'alumosilicate séparée des clinkers 4-II et 5-II se compose de 94 à 96 % de la phase amorphe sous les rayons X et contient de 4 à 6 % de C_3A cristallin. D'après sa composition chimique, elle ne diffère pas sensiblement des fractions d'alumosilicate à structure cristalline du C_3A séparées d'autres clinkers. Dans les clinkers indiqués a eu lieu apparemment une stabilisation de la phase métamicte amorphe sous les rayons X qui est proche du C_3A d'après sa composition, mais qui possède un niveau énergétique structural élevé dû à une haute concentration d'impuretés et de défauts. La preuve en est la présence d'effets exothermiques sur les courbes d'analyse

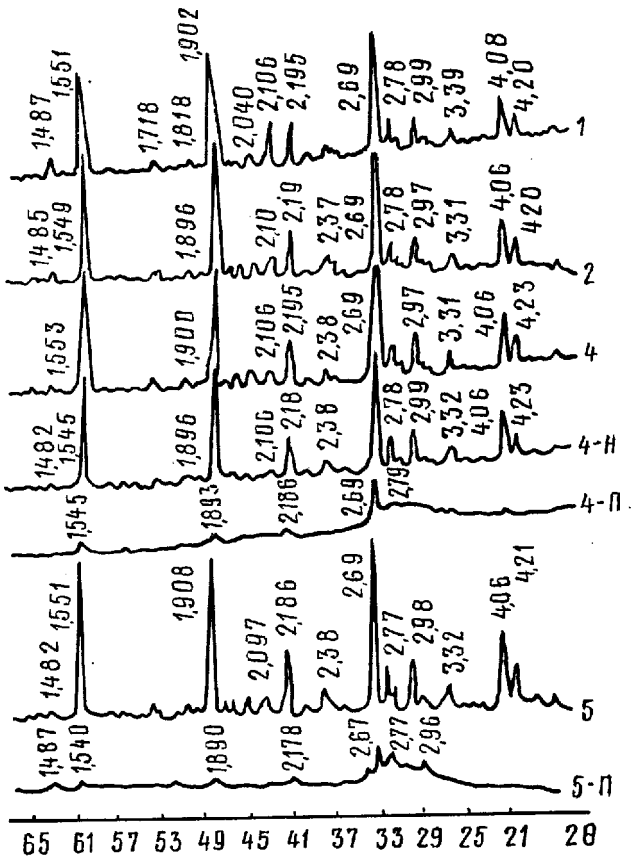

Fig. 3. Spectres de diffraction au rayons X (CuKα) de la fraction d'alumosilicate des clinkers blancs. La désignation des spectres correspond au marquage des clinkers au tableau 1

thermique différentielle avec des maximums à 325 et à 440 °C lesquels sont propres aux processus de "retour" des minérais métamictes à l'état cristallin ordonné (3) ainsi que la présence d'effets exothermiques de cristallisation du C_3A et de la périclase respectivement à 845 et 870 °C (fig. 4).

Des études de la microstructure des clinkers blancs à l'aide de microscopes électroniques à trame et à transmission ont décelé dans tous les clinkers à un haut FR la formation de phases à relief lisse de la surface de clivage. La microstructure du clinker 1 à blancheur maximale est construite selon le principe d'un assemblage dense de cristaux ce qui lui assure une très haute masse spécifique (4350 kg/m^3). Au point de

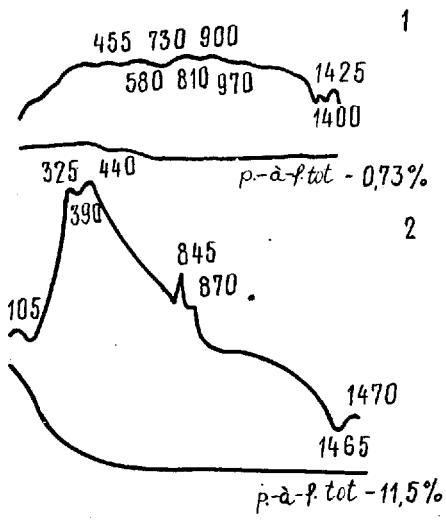

Fig. 4. Dérivatogrammes du clinker 4- (1) et de sa fraction d'alumosilicate séparée (2)

vue d'un haut degré de blancheur, la microstructure du clinker doit assurer après le broyage l'obtention de particules à l'aspect optique homogène, à surface lisse, à basse microporosité et à haute capacité réfléchissante. La détermination de la surface spécifique des clinkers broyés et des clinkers bruts non broyés par méthode d'adsorption d'azote à basse température a montré une faible augmentation (de 20% au maximum) de la surface spécifique après le broyage ce qui témoigne non seulement d'une haute porosité des granules de clinker blanc mais aussi d'un grand nombre de microfissures qui y apparaissent de toute évidence par suite de l'accumulation de dislocations de "scindement" prédéterminant les surfaces de destruction pendant le broyage (4).

Les spectres de réflexion optique dans le domaine visible des clinkers à haute et à basse caractéristiques du FR ont une différence peu sensible au point de vue des centres de coloration d'où vient que le FR des clinkers et des ciments est déterminé en grande partie par le pouvoir réfléchissant des surfaces de particules.

N. KOMAROVA,
V. RIASINE,
G. TCHISTIAKOV,
A. KORENGA

REFERENCES

I. Франк-Каменецкий В.А. Природа структурных примесей в минералах. Издат. Ленинградского ун-та, I964.
2. Лазаренкова Л.Е., Питак М.В., Старшинов Б.Н., Шуляк Р.С. Исследование методом ИК-спектроскопии изменения структуры каолина при нагревании. Сб. Физико-химические процессы производства и применение огнеупоров. Металлургия. М.:,I98I.
3. Белов Н.В. Очерки по структурной минералогии. Недра. М.:, I976.
4. Ван Бюрен. Дефекты в кристаллах. Издат. иностр. лит-ры. М.:, I962.

Z.M.Larionova
I.I.Kourbatova
N.S.Zhelvakova
L.P.Moĭsseeva

NIIJB, Moscow, U.S.S.R.

INFLUENCE DES ADDITIONS ORGANIQUES SUR LA FORMATION DE LA STRUCTURE DE LA PIERRE DE CIMENT

Les adjuvants organiques influencent considérablement sur la formation de la structure de la pierre de ciment dans le béton et améliorent ses proprietes constructives. Il est le plus avantageux d'utiliser les adjuvants complexes et les superplastifiants, dont l'emploi rationnel est etroitement lié avec la détermination du mécanisme de leur action. Ces adjuvants changent la cinétique de l'hydratation du liant et les conditions de la formation des phases hydratées étant eux-même très rarement des éléments de la structure du durcissement. Leur influence se manifeste principalement dans les delais initiaux. Les particularités de l'hydratation dans cette periode caractérisent le plus entièrement les changements de concentration observés dans la phase liquide. C'est pourquoi, en étudiant en cinétique les compositions des phases liquides, il est possible d'etablir le mécanisme de l'action d'un adjuvant (I). D'apres l'allure des courbes $C_{R^+}(\tau)$, $C_{Na^+}(\tau)$, $C_{K^+}(\tau)$, $C_{Ca^{2+}}(\tau)$, $C_{SO_4^{2-}}(\tau)$ il est possible d'évaluer l'influence de l'adjuvant sur la dissolution du clinker, la cristallisation des phases contenant le calcium et la vitesse de la formation d'ettringite. Si l'adjuvant ralentit la dissolution, alors le passage de R^+ de clinker sera ralenti et, conformement à cela, la concentration de ces ions dans la phase liquide sera plus basse. On peut l'observer en appliquant le superplastifiant C-3 ou le poly-électrolyte soluble dans l'eau sur la base de l'acide salicylique (BPП), ralentissant l'hydratation, et l'adjuvant complexe sur la base de résine d'urée, accélérant l'hydratation (Fig.I).

D'après le changement dans la phase liquide de la concentration d'ions des métaux alcalins il est possible dans certaines cas d'évaluer quantitativement le degree de l'hydratation du ciment.

L'abaissement lent de la concentration d'ions de calcium dans la phase liquide dans la plupart des cas indique le ralentissement de dégagement des phases contenant le calcium, et l'abaissement brusque-indique le surcroit de la vitesse de leur cristallisation. Si, simultanément, on observe aussi l'abaissement brusque de la concentration des sulfates, alors ça temoigne le liage de la masse principale de gypse en ettringite, ce fait est confirmé par les donnee de l'analyse chimique. C-3 se sorbant principalement sur hydro-aluminates ralentit la cristallisation d'ettringite, et BPП ralentit l'hydratation des composants aluminatique et silicique de clinker, c'est pourquoi la concentration de calcium pour le système avec C-3 entre 4 et I6 h et pour le système avec BPП entre 4-48 h abaisse faiblement. L'adjuvant complexe sur la base de résine d'urée influence activement durant 6 h sur la cinetique de dissolution ainsi que sur la cristallisation des phases hydratees. La cristallisation de ces dernières se réalise dans ce

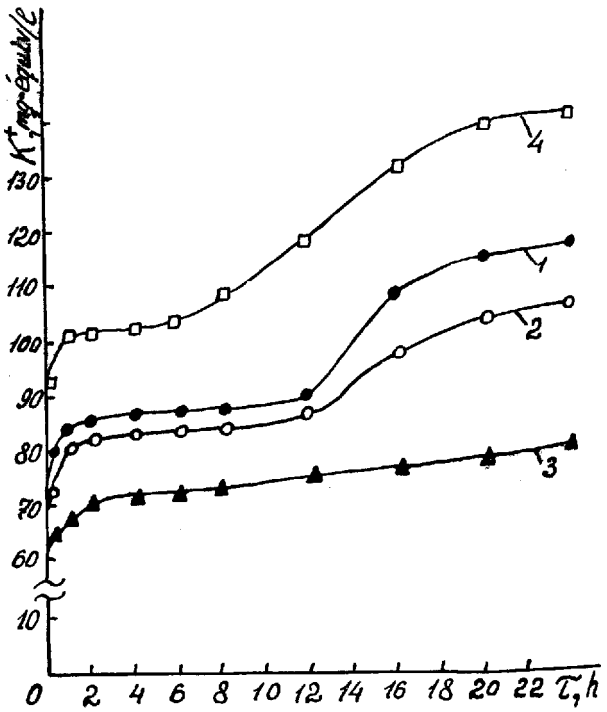

Fig.I. L'influence des adjuvants organiques sur le changement de la concentration de K^+ dans la phase liquide pendant l'hydratation de ciment: I - le ciment a aluminates moyens sans adjuvant; 2 - le même-avec C-3; 3 - le même-avec BPП; 4 - le même-avec l'adjuvant, complexe sur la de résine d'urée.

système plus intensivement (Fig.2).

Pour la détermination du mécanisme de l'action des adjuvants organiques il est rationnel de combiner les études des phases liquides avec les essais de la résistance plastique des systèmes. La formation des films d'adsorption bloquant la surface de la phase solide et ralentissant l'hydratation provoquera la prolongation de la période d'induction, et la cristallisation intensive d'ettringite amenera à un accroissement rapide de la résistance plastique. Le superplastifiant C-3 prolonge la periode d'induction. Au contraire, l'adjuvant complexe sur la base de résine d'urée réduit la période d'induction pour 2 h (de 8 jusqu à 6 h), et aussi assure les valeurs plus hautes de la résistance dans les délais posterieurs (Fig.3). Les études d'adsorption de C-3 sur les minéraux de clinker et les ciments montrentque C_3A et ses hydrates possède une capacite d'adsorption la plus grande et β-C_2S une capacité d'adsorption la plus faible. L'adsorption principale d'adjuvant sur le composant aluminate de clinker s'explique, à ce qu'il parait, par l'accroissement de la surface specifique de C_3A, se hydratant rapidement. Avec cela, il se forme les hydroalumina-

Z.M.Larionova
I.I.Kourbatova
N.S.Zhelvakova
L.P.Moïsseeva

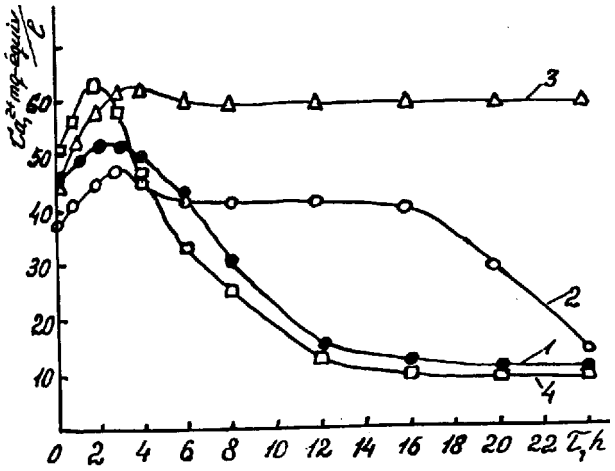

Fig.2. L'influence des adjuvants organiques sur le changement de la concentration de Ca^{2+} dans la phase liquide pendant l'hydratation de ciment.
I - le ciment sans adjuvant; 2 - le même-avec C-3; 3 - le même-avec ВРП; 4 - le même-avec l'adjuvant complexe sur la base de résine d'urée.

tes de calcium avec une grande quantité de l'eau, ce qui amène à une réduction de rapport eau-ciment dans le système. Il en suit qu'ilya lieu une basse efficacité de plastifiant dans le cas d'application des ciments riche en aluminate.
S'adsorbant sur la surface des particules de ciment, C-3 les disperse. Sous le microscope polarisant on voit dans la suspension de ciment-eau sans adjuvant que les particules de ciment forment des grandes agglomérations. Dans la suspension de ciment-eau avec l'adjuvant C-3 en quantité de 0,I-0,3% (de la masse de ciment) on observe une dispersion partielle des particules de ciment, et avec augmentation de la quantité d'adjuvant jusqu' a 0,5-I,0% - leur peptisation ultérieure (2).
Cette proprieté de superplastifiant C-3 exerce une influence sur la formation de la pierre de ciment. En comparant sous le microscope des lames transparentes de la pierre de ciment sans adjuvant et celles avec l'adjuvant de 0,5% de C-3, on peut noter que la microstructure de ce dernier est

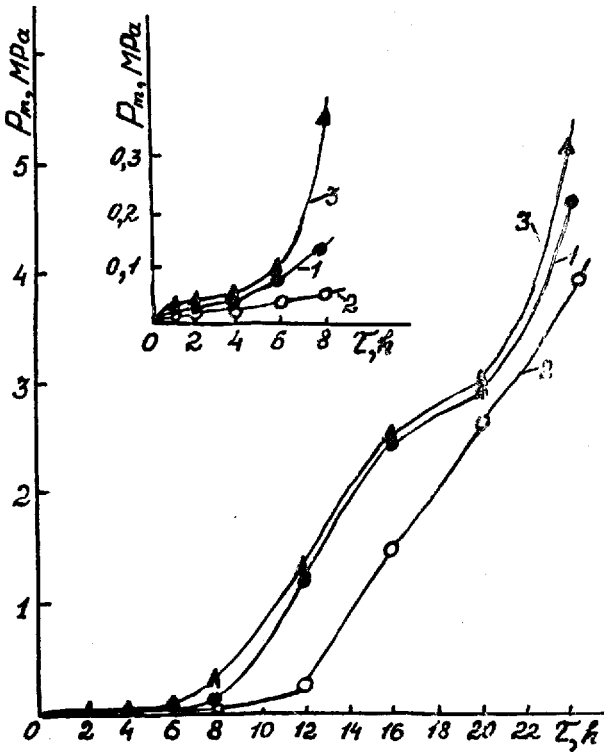

Fig.3. Le changement de la resistance plastique pendant l'hydratation des ciments.
I - le ciment sans adjuvant; 2 - le même - avec C-3; 3 - le même-avec l'adjuvant complexe sur la base de résine d'urée.

plus homogène. Avec cela a lieu l'augmentation de la porosite, conditionnée par l'entrainement de l'adjuvant par l'air. Dans la pierre de ciment avec C-3 on voit les pores arrondis avec limites régulières et le diamètre de 0,04-0,I5 mm (Fig.4). Les échantillons étuvés de la pierre de ciment avec l'adjuvant ont les mêmes caractéristiques structurales que les échantillons d'un durcissement normal.
S'adsorbant sur la surface des particules du ciment, C-3 ralentit leur hydratation dans les premiers jours, pourtant dans

Table

Le dégré de l'hydratation de la pierre de ciment d'après la ligne de C_3S, d = I,76 Å

La composition de la pierre de ciment	Les conditions du durcissement	Les délais de l'hydratation, jours			
		I	3	7	28
Ciment + H_2O	Normales	35,0	54,0	58,0	58,4
Ciment + H_2O + C-3	Normales	28,0	5I,0	57,0	6I,0
Ciment + H_2O	Etuvage	49,9	58,5	60,0	62,2
Ciment + H_2O + C-3	Etuvage	53,7	54,8	59,7	65,7

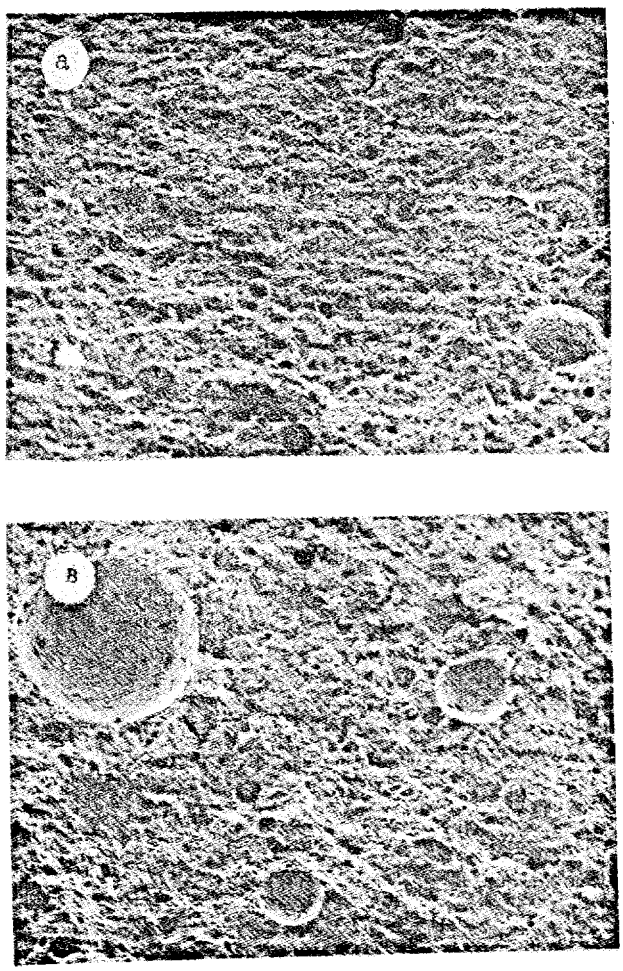

Fig.4. La microstructure de la pierre de ciment, SEMx70
a) - sans adjuvant;
b) - avec C-3.

7 jours les echantillons ont pratiquement le même dégré d'hydratation ce qui confirme les données d'une analyse quantitative radiographique (Tabl.).
Donc, l'application des adjuvants organiques est une des voies de la formation dirigée de structure de la pierre de ciment.

BIBLIOGRAPHIE

I. - И.И.Курбатова (1977) "Химия гидратации портландцемента", М., Стройиздат, (en russe).

2. - Л.П.Моисеева, З.М.Ларионова (1981) Влияние суперпластификатора С-3 на структурообразование цементного камня. "Гидратация и твердение вяжущих", Львов, p.258 (en russe).

L.I.Levin
G.M.Tamarutski VNIIzhelezobeton, NIICement, Moscow, U.S.S.R.

MODIFIED LIGNIN - BASE SUPLONATES IN THE MATERIALS ON CEMENT BASE

The features of the cement-based materials in many aspects are conditioned by their structure, controlled formation of which is possible through the use of superficially-active substances (SAS).

However the main part of the SAS is anion-active and can retard cement hydration as a result of chemisorption of cement particals and formations on the surface of calcium centres. Besides, the application of the SAS rather often is accompanied by over-increase in air-entrapping or water-release which negatively affect the structural and mechanical features of the materials, especially when hardening in the conditions of thermal treatment. Effective additives for cements and concretes, causing no reduction in the rate of hydration (the so-called LSTM - lignum-base sulphonates, technical, modified), are produced as a result of chemical treatment of lignin-base sulphonates by amino-containing substances, after which they acquire the increased capacity for chemisorption on the surfaces of oxigen centres and do not prevent the water from binding with Ca-centres of cement particles surfaces. Modified products are characterized also by optimal molecular/mass distribution, which results in limitation of their air-entrapping capacity and in the increase of their plasticizing activity.

The selected adsorptive-dispersive features of LSTMs make it possible to introduce them both with mixing water and at the production of cement, intensifying its comminution (tabl.1).

The LSTM introduced into comminution process allow to maintain the reasonable proportion of average (5-30 m) and fine (less than 5 m) fractions in the process of production of usual and high-strength cements. So the LSTMs positively affect the consistency and rheology of cement on its hydration and strength characteristics (tabl. 2, fig.1).

Contraction of grain composition with simultaneous limitation of fine fraction are especially important for high-strength plasticized cement, which is often used in concretes with reduced water content (as well as w/c) when there is an increase of the suction of water from the hydration products of the fine fraction; this can lead to the destabilization of the structure of hardened material.

The addition of LSTM effectively plasticizes water-cement systems, essentially reducing vibroviscosity of the cement paste as much as 2-4 times and water requirements of the paste and concrete mix by 15-25% (fig. 1 and 2), both when the addition is injected together with the mixing water, and during the grinding process of cement (curve 3). The use of the additive increases the settling of the concrete mix from 2-4 cm to 15-20 cm without reduction or even with increase in the concrete strength using in the latter case the plasticized cement with increased activity. In addition to that the concrete mixes with LSTM are characterized by the reduced ability for water-release and separation into layers.

The cement stone and concrete with addition of LSTM after normal and hydrothermal hardening are characterized by the fineness of pores of the structure with reduced content of larger pores. This is confirmed by the shift towards smaller sizes of effective radii of the pores in the range of $50 \cdot 10^{-10}$ - $1000 \cdot 10^{-10}$ m, by the reduction of dispersion values of average radii of the pores and by the reduction of macro-pores volume by 10-30% (tabl.3).

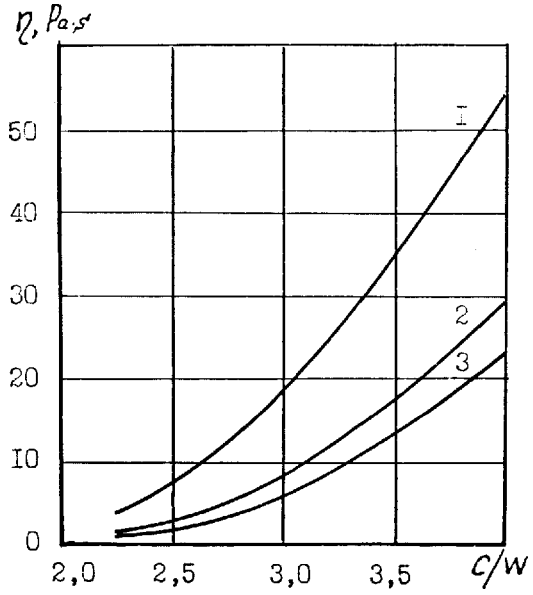

Fig.1. The change of vibriviscosity of the cement paste depending on water-cement proportion: 1- Portland Cement A; 2- Portland Cement A+LSTM with mixing water; 3- plasticized Portland Cement C.

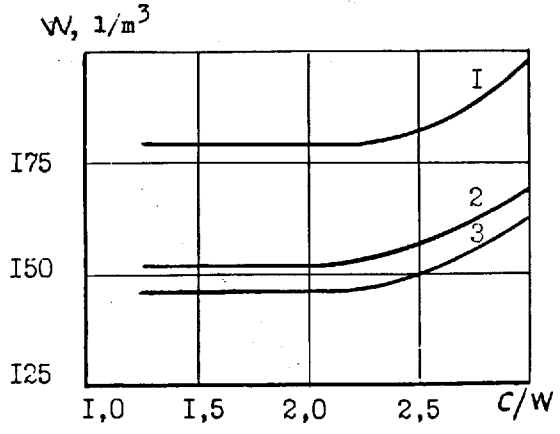

Fig.2. The dependence of water requirement of concrete mixes on the c/w proportion at the settling of the cone by 2-4 cm: 1-3 -the same as in the fig.1.

The influence of LSTM additive on the grain composition of cement.

Table 1

Code	Cement	Specific surface m^2/kg	Grain composition: less then $5 \cdot 10^{-6}$ m	Grain composition: $5 \cdot 10^{-6}$ – $30 \cdot 10^{-6}$ m
A	Pilot Portland Cement	300,0	1,8	52,4
B	Portland Cement with increased specific surface	365,0	8,2	58,8
C	Plasticized Portland Cement with addition of LSTM	352,0	5,8	65,3

Notes: The cements A,B,C are produced from one and the same clinker (C_3S - 58%; C_2S - 22%; C_3A - 5%; C_4AF - 13%); cements A and C are produced at one and the same grinding conditions; for the purpose of comparison on the same mill there was produced Portland Cement B, having the specific surface as that of the plasticized cement.

Table 2

The influence of the LSTM additive on physico-chemical features of cement.

Code of cement	Rate of hydration of cement stone in terms of C_3S, $d = 1,76 \cdot 10^{-10}$ m: 1 day	28 days	Features of the solution 1:3 (GOST) 310.4-81: Spread of the cone, mm, at w/c=0,40	Strength of the samples, MPa: Samples of normal hardening 28 days	Steamed samples 1 day
A	36,0	83,8	120	57,1	39,8
B	42,4	84,1	122	60,4	42,2
C	46,9	86,0	166	64,4	48,0

Table 3

Characteristic of the porous structure of cement stone

Code of cement	Pore sizes, $10^{-3} m^3/kg$, radius $30 \cdot 10^{-10}$ – $50 \cdot 10^{-10}$ m	$50 \cdot 10^{-10}$ – $1000 \cdot 10^{-10}$ m	$1000 \cdot 10^{-10}$ – $20 \cdot 10^{-6}$ m	Average diameter of the pores, 10^{-6} m
A	0,0I7	0,042	0,02I	2,7
B	0,0I5	0,0438	0,0I82	2,4
C	0,02I	0,0482	0,0I88	2,2

Notes: Micro-porosity (less than $20 \cdot 10^{-6}$m) has been estimated by means of a mercury porometer in the pressure range up to 250 MPa.

Table 4

The influence of the LSTM-additive on the performance features of the concrete mix and concrete with c/w = 2,5.

Cement	Additive	Requirement, kg/m^3		Settling of the cone (cm)	Strength of the concrete, MPa, after steam curing at the age of	
		Cement	Water		1 day	28 days
Portland Cement A	-	450	I80	2 - 3	37	55
the same	LSTM	450	I80	I4 -I6	37	56
Plasticized Portland Cement C with LSTM	-	450	I80	I7 -I9	39	59
Portland Cement A	LSTM	380	I52	2 - 3	38	58
Plasticized Portland Cement C with LSTM	-	368	I47	2 - 3	42	65

The improvement of the porous structure and strengthening of the contact zone between the aggregate and the mortar part at the expence of water-release contributes to increased frost-resistance and strength of the concrete (tabl.4).

BIBLIOGRAPHY:

I. Тарнаруцкий Г.М., Юдович Б.Э. О механизме действия пластификаторов в цементно-водных системах. Общие положения. Труды НИИЦемента "Новые эффективные виды цемента", М., с.II4.

A.J.Mituzas
V.V.Montvilla
L.V.Petravichys
O.M.Stanylenis
Akmyantsementas, Novye Akmyane, U.S.S.R.

TECNOLOGY OF PRODUCTION OF HIGH ALITE PORTLAND CEMENT CLINKERS

One of the ways to utilize the raw dust, collected by the electric filters of the rotary kilns for the burning of Portland Cement clinker, is the injection of the dust through the aggregate head.

The analysis of the collected dust of different plants has shown, that its chemical composition had a wide range. In the most cases the dust was more enriched by acidic components than the standardized raw mix, which is a result of differentiated removal of clay-like and rather dispersive component. This phenomenon spontaneously increases the SC of the main material on its way along the kiln. The recirculation of the collected dust to the hot end of the kiln approximates the real content of the clinker to the present one, and is one of the ways of effective use of the high-temperature flame-zone.

If we take the collected dust and introduce a carbonate component into it till the SC is higher than that of the original raw mix, and then introduce this enriched dust into the kiln head, then it will be possible to produce high-alite clinker and still with higher hydraulic activity.

To study the behaviour of carbonate component in the kiln area we introduced into it Ca^{45} isotope in the form of $CaCO_3$. Then in definite intervals we selected the clinker samples leaving the kiln and examined them by means of radio- and petrographic methods.

On radiographic films of the sample, collected from preparatory zones at the moment of the indicator injection (Fig.I), one can see the uniform blackening of the whole cross-section area which is an evidence of a complete coincidence of Ca^{45} and the main volume of the material, present at this moment in the kiln area. The deposit of high-temperature CaO particles inside the cold end of the kiln increases the speed of physico-chemical transformation of the material both in preparatory zones and the high-temperature zone of calcination.

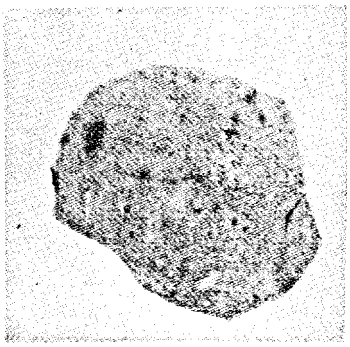

Fig.I. Radiographic film of a granule from a preparatory zone of the kiln.

However a definite part of the carbonate component, introduced jointly with the raw dust, interacts with acidic compounds of the mix and melts in the flame zone, and then leaving the gas stream it deposits

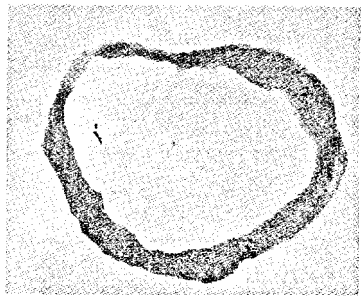

Fig.2. Radiographic film of a granule from the caking zone of the kiln.

on the newly formed clinker granules. On the Fig.2 one can see a radiographic film of the granule in the centre of the caking zone at the moment of injection of the $CaCO_3$-indicator. One can see clearly the deposited material, which has formed the exterior layer of the granule as a result of superficial diffusion.

Under conditions of a definite saturation degree of the raw dust by means of carbonate component and also with its sufficient volume it is possible to produce clinkers with SC≈I. Fig.3,4 show the petrographic films of microsection metallographic specimens of practically "pure" alite clinker, produced according to the above-mentioned method in the rotary kiln ⌀ 4xI50m.

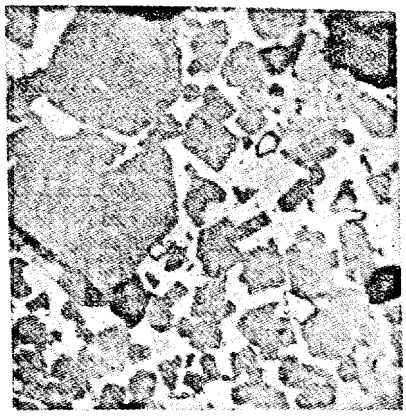

Fig.3. Petrographic film of the periphery layer of a granule (x200).

In the granula cross-section of such a clinker two zones are clearly seen: periphery layer (fig.3), formed by means of material deposit in the caking zone of the rotary kiln, and the central part (fig.4), formed by the material from the cold end of the kiln.

The periphery zone, constituting 8-I0% of the general volume of the granule, contains 60-63% alite, 5-I0% belite and 25-27% intermediate substance, while the central part contains 70+72% alite, 20+22% intermediate substance and isolated grains of belite.

Physico-chemical analysis of the samples, collected from the whole length of

the kiln being simultaneously fed with the carbonate-enriched raw dust showed that the volume of the material, deposited in certain zones of the kiln, depended on dispersivity of the introduced limestone component, on performance conditions of a particular kiln and on technical solutions of the problem of delivery of original components through the kiln-head.

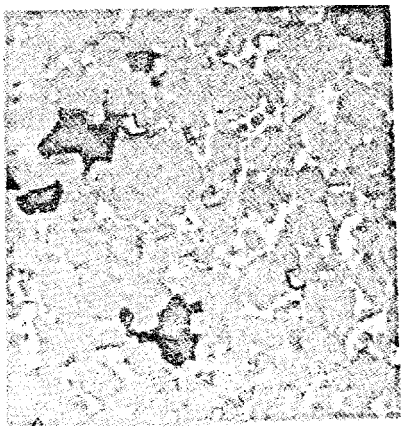

Fig.4. Petrographic film of the central part of a granule (x200).

I.L.Luginina
M.A.Putrenko

Technological Institute of Building Materials, Belgorod, U.S.S.R.

PARTICULARITIES OF CEMENT HYDRATION IN SUSPENSIONS WITH ALCALI ADDITIONS.

P

Water-release considerably hampers the investigation of hardening cement suspensions with water/cement > 0,5. Adding silicate of sodium into cement suspensions we have managed to investigate the suspension hydration with water/cement=I,0-2,0 having eleminated water-release. We have prevented the quick thickening of the suspensions by adding two-substituted phosphate of sodium. Oil-well pastes can easily penetrate pores and cracks of the rocks and possess the increased anti-filtering and strength features.

There was found and proved the predominant influence of calcium ions concentrations in the suspensions on the hydration and gelation in the system of cement-water-silicate of sodium. In the system without addition of phosphate of sodium not only quick thickening and growth of plastic strength are observable, but also the decrease of strengthening speed at elder ages. Adding some phosphate of sodium to the system we can see that the suspensions thicken in I0-40 min., and after the induction period of strengthening are characterised by the quick growth of strength which is 2-3 times as much as that in the pastes without phosphate of sodium (fig.I).

a)

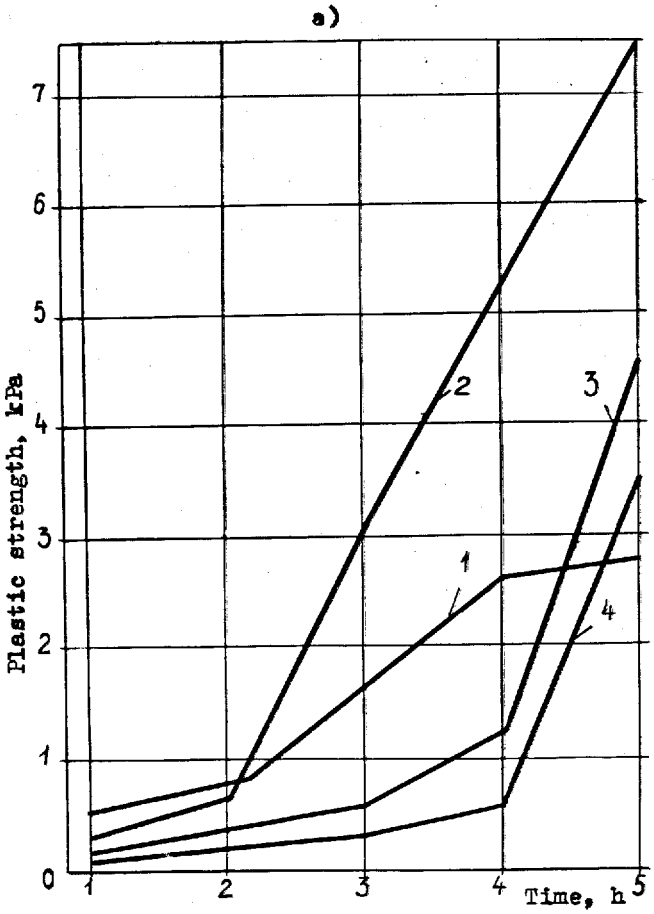

b)

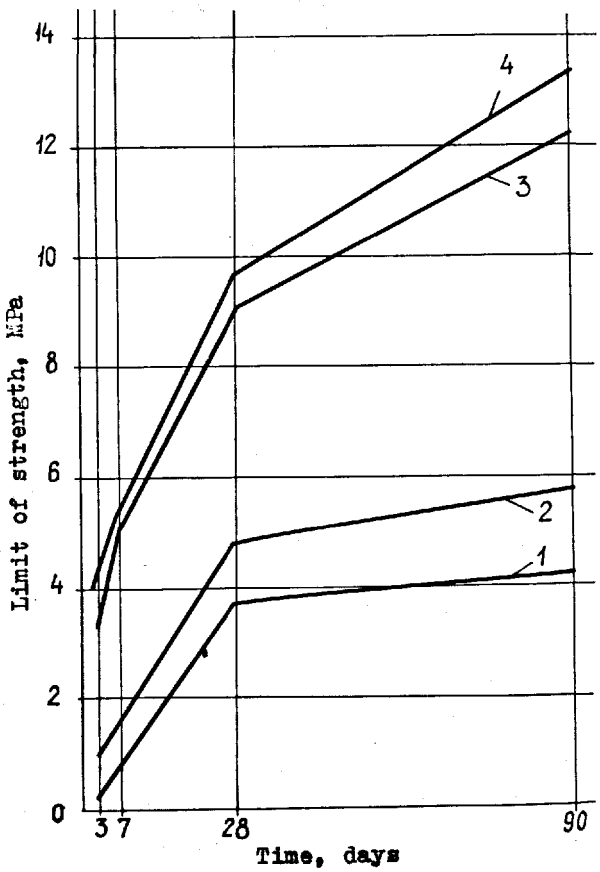

Fig.I. Plastic strength (a) and compressive strength (b) of the cement suspensions (water/cement = 0,I; silicate of sodium -I0%), containing sodium phosphate, % P_2O_5
I - 0; 2 - 0,4; 3 - 0,5; 4 - 0,6.

Electron microscope method has given us a possibility to reveal the differences in the structure of cement stone (fig.2). The first composition develops strong and porous structure with crystals of ettringite, which release on the surface of cement granules. Cement stone of the second composition is characterized by the more dense structure, represented mainly by calcium hydrocilicates with ettringite crystallizing in the pores of cement granules.

a)

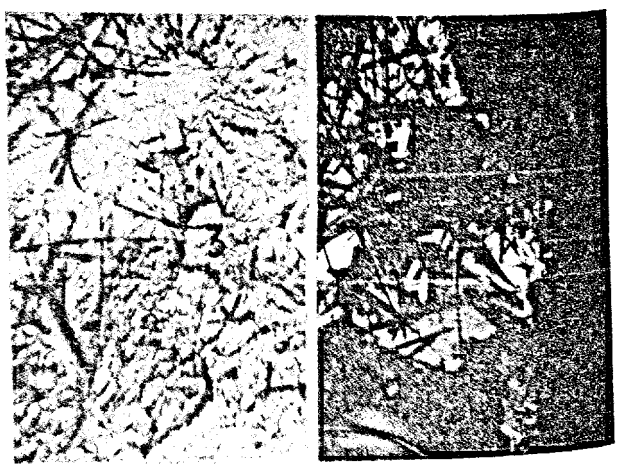

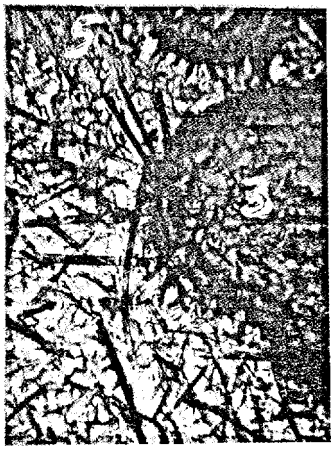

b)

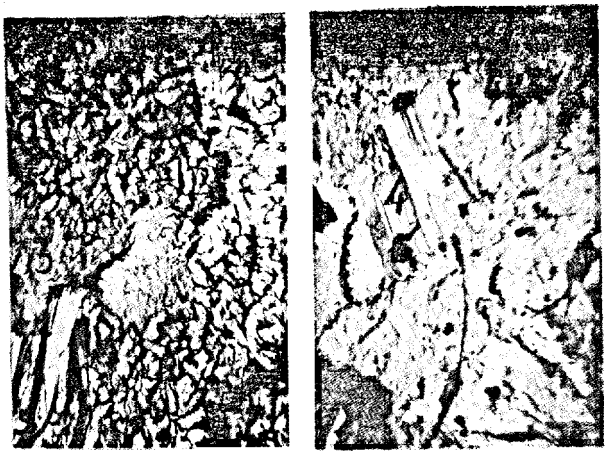



Fig.2. Electron microfilms of the chipped surfaces of cement stone (water/cement = I,0), hydrated during 60 days (x6000) : a) with additive of I0% silicate of sodium; b) with additive of I0% silicate of sodium and 0,5% P_2O_5 in form of $Na_2HPO_4 \cdot I2H_2O$. I - ettringite; 2 - fibrous hydrosilicates of calcium; 3 - the residues of unhydrated cement granules; 4-hydroxide of calcium; 5-plate-scaled hydrosilicates of calcium.

These new compositions are used for water-proofing of exploratory workings in pit-construction.

I.L.Luginina Technological Institute of Building Materials, Belgrad, U.S.S.R.
R.G.Nigmadilova

KINETICS OF ASSIMILATION OF CALCIUM OXIDE IN PRESENCE OF TITANIUM COMPOUNDS.

P

The essencial features of clinkerization in presence of titanium compounds have been described by many investigators. This concern in the problem is quite lawful and conditioned by the occurance of the element in the Earth's crust, and by the titanium chemical nature, analogical to chemical features with oxidization rate = 4 (I). H.Kühl in his fundamental monography "Zementchemie" (2) pointed out, that the titanium oxides could form compounds not only with the main composites of the raw mixes, but also with alkalies.

We have studied the influence of the titanium dioxide on the dynamics of calcium oxide assimilation in portland raw mixtures.

Chemically pure titanium dioxide of rutile modification were injected into portland raw mixtures of various modular features. The compact samples were burned at the temperatures of 900-I450°C in electric furnace, and in the cake there was estimated the content of free calcium oxide. The results are given in the table.

We suppose that in the portland raw mixtures containing simultaneously both titanium dioxide and alkaline component there exists a possibility of formation of alkaline titanates and their solid solutions which (because their melting temperature is 85-I200°C) stimulate the processes of calcium carbonate dissociation and binding of calcium oxides into clinker minerals. Alkaline compounds of titanium also affect the clinkerization processes at higher temperatures, changing the features of the liquid phase.

The possibility of formation of alkaline titanates was confirmed by our investigation of the systems $CaO-TiO_2-K(Na)_2O$ and $MgO-TiO_2-K(Na)_2O$. At the burning temperatures of 900-II00°C in the burning products there were found titanates of alkaline metals.

So the titanium compounds and alkaline compounds simultaneously present in raw mixtures produce positive effect on the processes of clinkerization.

The free CaO content in the cake — Table

№ cake	TiO_2 content (%) mass	K_2O content (%) mass	Free CaO content (%) at the burning temperatures (°C)						
			900	I000	II00	I200	I300	I400	I450
I	0,0	0,0	32,4	30,7	25,0	22,0	I6,5	I,5	0,0
2	0,5	0,0	33,0	27,5	22,0	I7,0	I4,0	0,0	0,0
3	I,0	0,0	-	32,0	22,0	I5,0	II,0	0,0	0,0
4	2,0	0,0	-	3I,0	22,0	I8,0	7,5	0,0	0,0
5	3,0	0,0	30,0	27,0	24,0	-	7,0	0,0	0,0
6	5,0	0,0	28,0	24,0	I5,0	I5,0	5,0	3,0	2,0
7	8,0	0,0	-	27,5	2I,0	20,0	8,0	3,0	5,0
2-I	0,5	0,5	-	35,0	I9,2	I5,0	I0,8	I,0	0,0
4-I	2,0	0,5	-	27,0	2I,0	I2,3	8,0	0,5	0,0
6-I	5,0	0,75	-	22,5	II,5	I0,0	5,0	I,4	I,6
7-I	8,0	I,0	36,5	30,8	20,5	I6,6	I0,0	2,5	2,0

At the temperatures of 900-I200°C the speed of the binding process of calcium oxide is increased in the case with all concentrations of titanium dioxide. In the field of active mineral formation (I300-I450°C) the effect of titanium dioxide is expressed more clearly: in the presence of 3% content of TiO_2 the speed of the binding of calcium oxide is increased and with the increase of TiO_2-content from 3 to 8% the speed is reduced. The injection of alkaline component (chemically pure potassium oxide) into the raw mixtures, containing titanium dioxide, caused definite changes in the character of calcium oxide assimilation: in the temperature range of 900-I200°C the binding of calcium oxide was more active compared to mixtures without alkalies, but with the adequate volume of TiO_2. There was also noticed essential reduction of free calcium oxide content in the mixtures containing the increased volume of TiO_2 at the concluding stages of clinkerization.

BIBLIOGRAPHY

I. Г.П.Лучинский. Химия титана. "Химия", М. I97I
2. H.Kühl. Zemetchemie. Band II, Berlin, I958

B.Noudelman
A.Clutchariov
G.Galimova
A.Bessmertnykh

NIIstromproek, Tachkent, NIICement, Moscow, U.S.S.R.

PARTICULARITES THERMOCHIMIQUES DU PROCESSUS DE CUISSON DU CLINKER ALINITIQUE

L'utilisation du bain fondu de sel en qualité du milien réactionel assure la baisse de la température de cuisson de 300-350° aussi que les formations intermédiaires et la composition de phases du clinker cuit inordinaires.

Des essais du four rotatif 2,5x75m ont permit d'identifier des transformations physiquo-chimiques pendant la cuisson. L'analyse de phases aux rayons X (fig.I), les méthodes pétrographiques et de la microscopie électronique ont mis en évidence la succession de la formation de minéraux en fonction de la température (tabl.I).

Table I

Succession de la formation de minéraux

Temp.,°C	Minéraux	Q-té,%
500-650	$C_{II}A_7CaCl_2$ - chloralumi-nate de Ca	2-4
650-750	$CaCO_3 \cdot CaCl_2$ -charbochlo-rite	8-I2
650-750	$C_{II}A_7CaCl_2$	3-7
	$2\,CaO \cdot SiO_2\ CaCO_3$-spour-rite	35-45
	C_2S - silicate bicalcique	jusqu'à 2
750-850	$C_{II}A_7CaCl_2$	3-7
	$2CaO \cdot SiO_2\ CaCO_3$	45-55
	C_2S	I2-I8
Zone du cuisson	$C_{II}A_7CaCl_2$	4-5
	C_2S	25-35
	$20CaO \cdot MgO \cdot 6SiO_2 \cdot Al_2O_3 \cdot CaCl_2$ - alinite	55-65
clinker	$C_{II}A_7CaCl_2$	3-4
	C_2S	25
	C_2F-ferrite bicalc.	jusqu'à 4
	$20CaO \cdot MgO \cdot 6SiO_2 \cdot Al_2O_3 \cdot CaCl_2$	55-65
	C_3S	3-7

L'analyse thermique différentielle (fig.2) et l'analyse chimique des échantillons pris dans les différents domaines du four ont montré que la décarbonation se passe essentiellement à 970-I070 K. L'absence de la chaux libre témoigne de la haute réactivité du cru.

La circulation du chlore est subite au circuit interne (dé-chlorage dans les zones chaudes et régénération de $CaCl_2$ dans les froides) comprenant l'issue d'une certaine quantité de chlore entrant dans la structure cristalline de minéraux (fig.3).

Des calculs thermodynamiques selon des données sur les transformations physico-chimiques, aussi que l'analyse de la dissipation de la chaleur ont laissé établir des facteurs assurant la réduction de la consommation spécifique de la chaleur en comparaison avec le procédé classique. Cette réduction peut être de 20% (tabl.2).

Table 2

Facteurs assurant la réduction de la consommation de la chaleur pour la cuisson du clinker alinitique (voie humide)

MN	Facteurs	Part de l'économie totale,%	Article du bilan thermique
I.	Diminution de la basicité du cru	23	Consommation téorique de la chaleur
2.	Augmentation de l'exothermie des réaction de ménaralisation	II	I bid.
3.	Régénération de $CaCl_2$	2	I bid.
4.	Formation de bain fondu	6	I bid.
5.	Déchlorage	-I3	I bid.
6.	Baisse de la température du processus	2	Pertes de chaleur à travers le corps du four
		I2	Pertes de chaleur avec l'air excédant du refroidisseur
7.	Diminution de l'humidité de la pâte crue	II	Consommation de la chaleur pour évaporisation de l'eau
8.	Augmentation de la capacité horaire du four	I6	Pertes de chaleur a travers le corps du four
9.	Diminution de la quantité spécifique du cru (sur l'unité de masse du clinker)	4 5	Consommation théorique de la chaleur Consommation de la chaleur pour évaporisation de l'eau
I0.	Diminution du volume et de la température de gaz perdus	20	Pertes de chaleur avec des gaz perdus
II.	Diminution de la quantité de la poussièrre	I	Pertes de la chaleur avec la poussière

Des calcules et des essais industriels montre que la mise au point de la tecnologie à basse température réduit la consommation thermique (20%) et augmente la capacité horaire des fours rotatifs (30%).

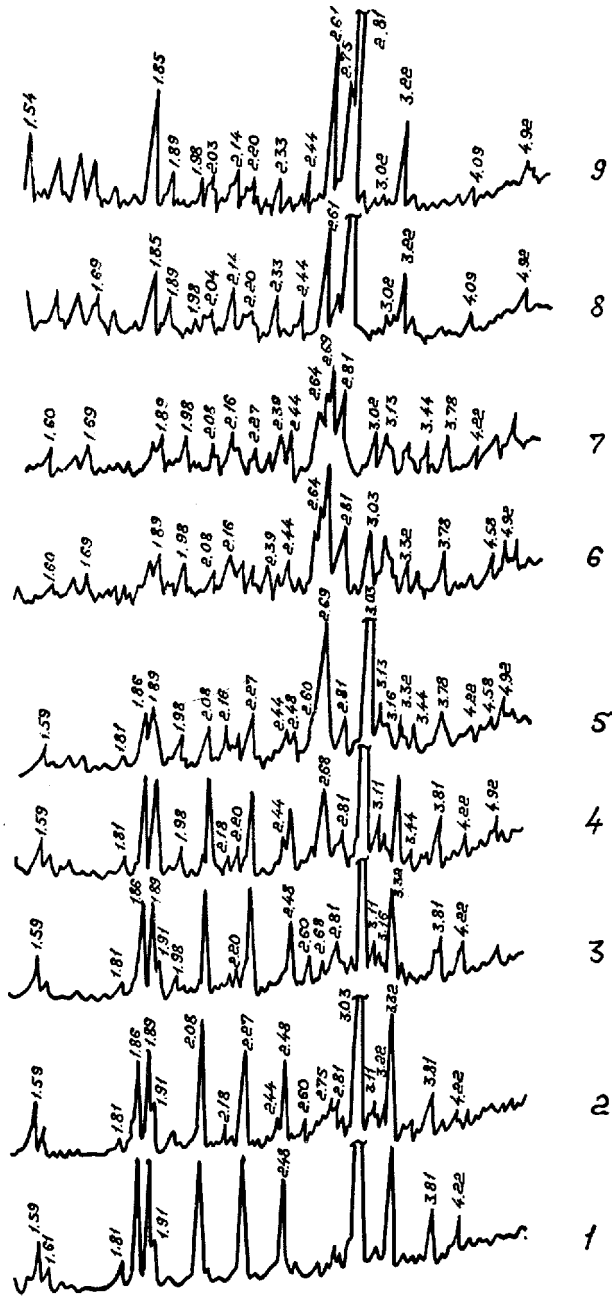

Fig.1. Analyse au rayons X des échantillons:
1 - cru de départ; 2 - 150°C; 3 - 300°C;
4 - 500°C; 5 - 650°C; 6 - 750°C; 7 - 800°C;
8 - zone de cuisson 9 - clinker alinitique

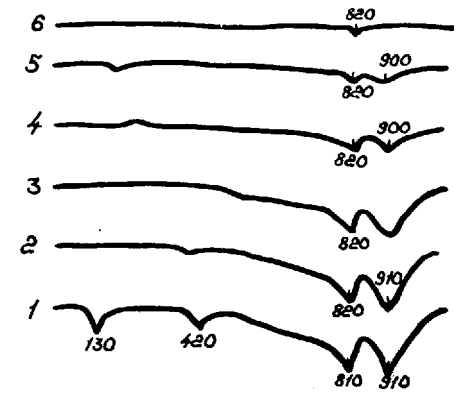

Fig.2. Analyse thermique dif. des échantillons: 1 - zone de chaînes; 2,3,4,5 - température du matériau 500, 650, 750, 800°C; 6 - début de la zone de cuisson

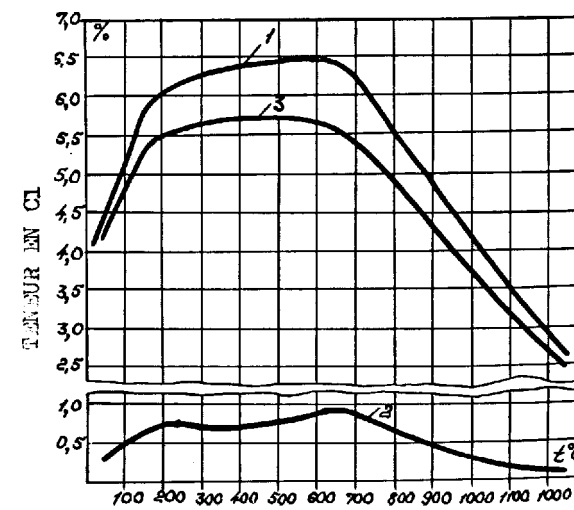

Fig.3. Variation de la teneur en chlore du matériau lors du traitement thermique dans four rotatif 1 - Cl^- total; 2 - Cl^- combiné avec des alcalis (RCl); 3 - Cl^- combiné en $CaCL_2$ et autres combinaisons

A.A. PACHTCHENKO,
E.A. MIASNIKOVA,
V.V. TOKARTCHOUK,
V.V. CHEVTCHENKO

Institut polytechnique de Kiev, U.S.S.R.

PARTICULARITES DE LA CLINKERISATION DES CRUS A COMPOSANTS ALUMINOSILICIEUX A HAUTE REACTIVITE.

L'intensification des processus de clinkérisation peut être obtenue en introduisant dans le mélange cru une matiére naturelle à haute réactivité ou un sous-produit industriel qui a subi au préalable un traitement à haute température et a accumulé une quantité déterminée d'énergie interne. Une baisse supplémentaire de la consommation d'énergie nécessaire à la fabrication du clinker est possible grâce à l'utilisation d'un tel composant à l'état non broyé (1) ou la production sur sa base des clinkers (de bélite) à faible saturation à activité élevée (2).

On a établi l'efficacité d'utilisation des roches effusives, les basaltes, largement répandus dans le monde entier (3) en qualité de composant aluminosilicieux ferrifère è haute réactivité entrant dans le mélange cru du ciment Portland. Ils sont caractérisés (d'après R. Deli) par une composition chimique moyenne suivante, % en masse: SiO_2 - 49,06; TiO_2 - 1,36; Al_2O_3 - 15,7; Fe_2O_3 - 5,38; FeO - 6,37; MnO - 0,31; MgO - 6,17; CaO - 8,95; Na_2O - 3,11; K_2O - 1,52; P_2O_5 - 0,45; H_2O - 1,62. Les basaltes provenant d'un même gisement diffèrent sensiblement au point de vue de la stabilité de composition.

Pour donner une appréciation comparative préalable de l'homogénéité chimico-minéralogique et des intervalles des températures de fusion des basaltes et d'autres minérais aluminosilicieux utilisés traditionnellement dans l'industrie du ciment, on s'est servi du diagramme d'état d'un système à quatre composants SiO_2 - Al_2O_3 - CaO - MgO. Les points figuratifs d'un nombre écrasant de compositions des basaltes se placent à l'intérieur du tétraèdre MS - CMS_2 - CaS_2-S (fig. 1). Cela étant, la température du début de fusion des basaltes constitue (1150±10) °C et celle de la fin de fusion oscille au niveau de 1300 °C en fonction de la teneur en Al_2O_3 (4).

Les compositions d'argiles utilisées dans l'industrie du ciment se caractérisent par une plus grande diversité: les points

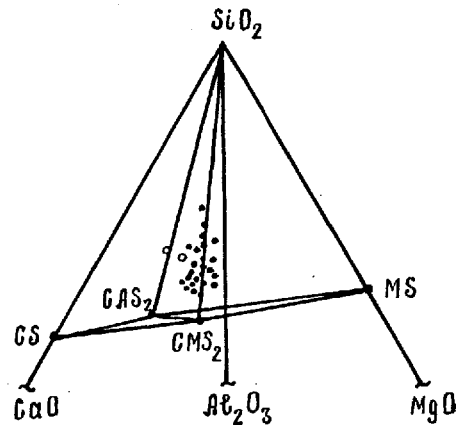

Fig. 1. Disposition des points figuratifs des compositions des basaltes dans les tétraèdres élémentaires du système SiO_2 - Al_2O_3 - CaO - MgO:
(·) - tétraèdre MS-CMS_2-CaS_2-S;
(∘) - tétraèdre CS-CMS_2-CAS_2-S.

figuratifs de ces compositions se placent dans les tétraèdres élémentaires: CS -CMS_2 - CAS_2 - S; MS - CMS_2 - CAS_2 - S; CAS_2 - $M_2A_2S_5$ - MS - S; CAS_2 - A_3S_2 - $M_2A_2S_5$ - S.

L'intervalle des températures de fusion, lui aussi, est soumis respectivement à d'importantes oscillations: la température du début de fusion des argilles de diverses compositions varie de 1135 à 1300 °C et celle de la fin de fusion, de 1400 à 1500 °C. Les laitiers de haut fourneau occupent une position intermédiaire entre les basaltes et les argiles. Les points figuratifs de la masse essentielle de compositions de laitiers se situent dans les tétraèdres élémentaires: C_3S_2 - CS - C_2MS_2 - C_2AS_2; C_2MS_2 - CAS_2 - MA - M_2S; C_2MS_2 - C_2AS_2 - CAS_2 - MA (fig. 2). La température du début de fusion de la majorité des laitiers constitue 1285 à 1290 °C et celle de la fin de fusion est de 1400 à 1500 °C.

Il en résulte que les basaltes ont un plus bas point de fusion que les autres minéraux aluminosilicieux utilisés dans l'industrie du ciment: dans les mélanges crus contenant du basalte la fusion commence à une plus basse température de l'ordre de

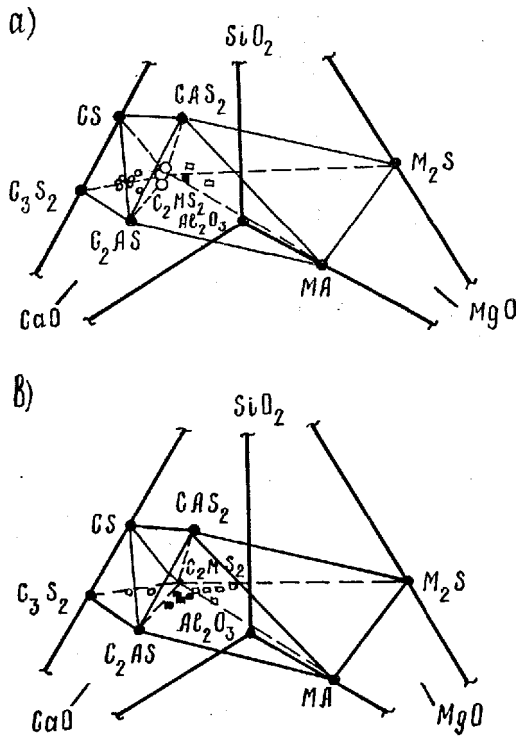

Fig. 2. Disposition des points figuratifs des compositions de laitiers dans les tétraèdres élémentaires du système SiO_2-Al_2O_3-CaO-MgO:
(∘) - tétraèdre C_3S_2-CS-C_2MS_2-C_2AS;
(○) - tétraèdre CS-C_2MS_2-C_2AS-CAS_2;
(▪) - tétraèdre C_2MS_2-C_2AS-CAS_2-MA;
(▫) - tétraèdre C_2MS_2-CAS_2-MA-M_2S

1150 °C, aux environs de 1180 à 1200 °C la masse essentielle de basalte est en fusion et la quantité de la matière fondue atteint 30 % (5) ce qui est capable d'accélérer sensiblement la formation d'alite. Ce fait a permis de concevoir la possibilité de cuisson des mélanges crus basaltiques non broyés; la formation de minéraux se produit alors grâce à une imprégnation des particules décarbonisées des pierres de carbonate concassées par le basalte en fusion et à une interaction ultérieure de la phase liquide et de l'oxyde de calcium.

Une étude des particularités de formation de la structure du clinker de ciment Portland au cours de la cuisson des mélanges crus à haute dispersite a montré une baisse sensible du rôle des réactions en phase solide grâce à une réduction du nombre de contacts entre les particules et, respectivement, à un rétrécissement du front des réactions (6). Dans le domaine des températures comprises entre le début de fusion du basalte et 1250 °C la vitesse du processus d'imprégnation est faible, la matière fondue pénètre dans la particule de carbonate essentiellement par gros pores principaux. Dans la zone de contact du composant carbonaté avec le basalte on observe une interaction des composants grâce aux processus d'échange de diffusion conduisant à une formation dans la couche de basalte contiguë à la chaux concassée, de cristaux de mélilite, de wollastonite et de bélite. Cependant, les réactions de formation des minéraux possèdent une nature limitée, la profondeur de diffusion des nouvelles formations étant faible. Lorsque la température se porte à une valeur de 1300 à 1350 °C, la viscosité de la matière fondue baisse, elle devient capable de pénétrer dans les micropores (les pores primaires de la matière crue et les pores secondaires dont l'apparition est due à la décarbonisation). Les dimensions des pores augmentent grâce à une action de coinçage de la matière fondue et à une dissolution des parois de pores ce qui, à son tour, facilite la progression de la phase liquide à l'intérieur des grains de carbonate. Par suite d'une jonction diffusée d'ions de calcium à la phase liquide, une couche de cristaux de silicate bicalcique apparaît suivant le front de mouvement de l'excès de matière fondue à travers la particule décarbonisée. Avec l'épaississement de la couche, la vitesse de diffusion d'ions de calcium dans la matière fondue ralentit quelque peu tout en restant au-dessus des vitesses de diffusion des autres ions ce qui provoque une modification progressive de la structure de la couche intermédiaire: à la limite de la matière en fusion a lieu un délayage des nouvelles formations et une baisse de leur basicité tandis qu'à la limite de la composan-

a)



b)



Fig. 3. Microphotographies des clinkers: a) formation de bélite; b) formation d'alite; x 300

te carbonatée se produit une saturation de la couche d'ions de calcium et un accroissement de la basicité des composés jusqu'à la formation du silicate tricalcique. Le processus d'imprégnation une fois terminé, on voit apparaître d'abord dans le clinker des grains de bélite sans formes particulières mais proches du faciès propre à la bélite (fig. 3, a). Par la suite, les cristaux de bélite prennent leur forme habituelle, puis, tout en gardant les formes cristallographiques propres à la bélite, commencent à tourner au clair, le teint propre aux cristaux d'alite dans les sections polies pour se transformer définitivement en cristaux d'alite (fig. 3, b).

Etant donné que tous les processus se produisent en présence de la matière en fusion et, par conséquent, à une grande vitesse, la synthèse des silicates de différentes basicités se déroule pratiquement simultanément. Le clinker obtenu est caractérisé par une structure zonale, un ordre indéterminé de disposition des champs alternés de cristaux d'alite et de bélite dû à une inhomogénéité de la structure du composant carbonaté (irrégularité de disposition des gros pores) étant donné que la thèse ci-dessus est juste pour le nouvement du front de la matière en fusion aussi bien de la surface de la particule que de l'"intérieur' de cette dernière, c'est-à-dire, de la surface de pore. Il s'en suit que la vitesse des processus se déroulant pendant la cuisson des mélanges non broyés dépend sensiblement de la porosité du composant carbonaté de base et, avant tout, de la valeur moyenne du rayon des pores. La cote admissible des particules du composant carbonaté assurant la totalité suffisante des processus d'imprégnation et de synthèse des minéraux de clinker, peut être déterminée d'après l'équation (1):

$$R = -0{,}03t - 1{,}38r_o^2 + 0{,}23\cdot10^{-4}t^2 - 0{,}43\cdot10^{-4}1^{r}o + 0{,}11\cdot10^{-2}r_o^2t, \qquad (1)$$

où: R est la mesure linéaire des particules du carbonate concassé, mm;
r_o est la valeur moyenne du rayon des pores, unités conventionnelles;
t est la température de cuisson, °C.

Les données de calcul sont confirmées par les résultats expérimentaux (v. tableau) (7).

La cuisson de mélanges crus non broyés permet d'obtenir des clinkers qui donnent les ciments des classes 400 et 500 caractérisés par des qualités exothermiques modérées et une résistance aux sulfates élevée. Grâce à un remplacement partiel (à 50 %) de la boue crue par un mélange non broyé de calcaire-basalte, on obtient une économie de chaleur de cuisson de 10 % tandis que le rendement du four rotatif augmente de 19,5 % (8).

Une réduction supplementaire de la consommation d'énergie de cuisson peut être obtenue grâce à l'utilisation de mélanges

Tableau

Type de roche carbonatée	Valeur moyenne du rayon des pores, un. conv.	Cote admissible (mm) des particules du carbonate concassé à la température de cuisson, °C			
		expérim.		equat.(1)	
		1350	1400	1350	1400
terre meuble	5,56	3,9	8,2	4,4	8,9
calcaire coquiller	11,68	9,3	26,8	10,4	23,7
roche sédimentaire	4,30	3,7	7,8	3,9	6,6
roche granulaire cristalline	1,11	1,4	3,6	1,6	3,3

crus contenant du basalte à faible coefficient de saturation destinés à obtenir des clinkers de bélite activés par un produit sulfaté (hopshogypse). La température de cuisson d'un tel clinker ne dépasse pas 1300 à 1350 °C et la résistance atteint 54,8 MPa (9).

REFERENCES

1. Цементы из базальтов/Под общ. ред. А.А. Пащенко. - Киев: Наукова думка, 1983. - 199 с.
2. Stark I. Entwicklungsstand von Belite-Zementen. - Beton-technik, 1982, No. 3, S. 72-80.
3. Йодер Г.С., Тилли К.Э. Происхождение базальтовых магм. - М.: Мир, 1965. - 247 с.
4. Пащенко А.А., Мясников А.А., Мясникова Е.А. Использование диаграммы состояния системы SiO_2-Al_2O_3-CaO-MgO для определения температур плавления основных изверженных горных пород. - Доклады АН УССР, сер. Б, 1981, с. 51-55.
5. О температуре появления расплава при обжиге известково-базальтовых шихт/А.А. Пащенко, А.А. Мясников, Е.А.Мясникова, Н.В. Лукашевич. - Доклады АН УССР, сер. Б., 1981, № 6, с. 73-75.
6. Будников П.П., Гинстлинг А.М. Реакции в смесях твердых веществ. - М.: Стройиздат, 1971. - 488 с.
7. Пащенко А.А., Мясникова Е.А., Токарчук В.В. Влияние характеристик карбонатных пород на процессы пропитки в крупнодисперсных портландцементных смесях. - Доклады АН УССР: сер. Б., 1983, с. 34-37.
8. Островская Н.Д., Мясникова Е.А. Использование базальтов в цементном производстве. - Цемент, 1984, № 6, с. 11.
9. Пащенко А.А., Мясникова Е.А., Шевченко В.А. Фосфогипс-интенсификатор обжига. - Строительные материалы и конструкции, 1983, № 4, с. 19-20.

V.P.Rjazin
Z.B.Entin
N.I.Komarova NIICement, Moscow, U.S.S.R.
N.A.Shebanov

SOME FEATURES OF MINERAL FORMATION ON THE SAMPLE SURFACE.

Thermodynamic conditions on a calcinating granule surface at the external heat energy supply and abstraction differ considerably from the conditions of the material existence in the granule. This is a result of the further factors' affect:
I) the difference of surface and volume dimensions;
2) the phenomena on the heterogeneous mediums interface (solid phase - gas);
3) the chemical composition difference owing to the diffusive transfer of material through the interface and the exchange with the inner volume;
4) the intergranular pressure and the voltage vectors direction;
5) the temperature and its gradient;
6) the physical and mechanical features of the surface and inner layers (structure, heat and electric conduction, strength, hardness etc.).

Owing to the above mentioned differences the surface layer of a clinker granule considered to be an important object of study. The requisite for the study was also the experimentally established differences in the content of calcium oxyde in superfractions and on the granule surface of white Portland Cement clinker in comparison with large fractions, inner granule volume and the mean clinker mass.

To make reseaches of the phenomena on the surface layer of the Portland Cement clinker with effective thickness of 30 μkm the diffractometer DRON-2 with the high-temperature attachment UVD-2000 has been used. This method provides to obtain in vacuum (where the displacement volume pressure is not more than 10^{-4} mm Hg) the diffraction spectrum from the packed powder surface at temperature up to 2000°C. The scanning electron microscope "Jeol" - JSM-350CF with the spectrometer FCS has been also used.

Indication of the diffractograms has been made after 10-minutes exposure at designed temperature. The error of automatic control of the temperature is $\pm$ 4°.

The following was of the main interest:
- the features of phase formation on the material surface in the conditions of its intensive heat exposure (the heater is a tungsten tape);
- the processes of phase transition on the surface of the calcinating material;
- the changes of phase and chemical composition of the surface layer in the process of heating and cooling of the sample.

At the heating of the packed powder of threewedged C_3S up to 1500°C in the thin surface layer of 50-70 μkm, tricalcium silicate decomposes with α- C_2S formation, but without calcium oxide extraction; meanwhile the inner volume of the sample does not change and still consists of C_3S.

At the heating of a white clinker powder containing three phases - C_3S, C_2S (β-form), C_3A the material surface undergoes the following changes (fig.I,2):
- alite content in the surface layer has monotonously decreased in the temperature interval 1000÷1400°C, and in the range of 1400 up to 1450°C it has sharply reduced to zero;

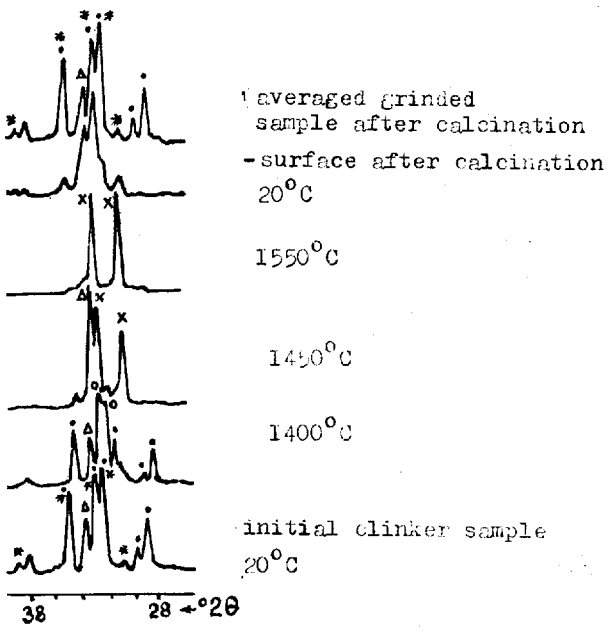

Fig.I. The radiograms' sections of a white clinker powder at its heating up to 1550°C in vacuum.
• - alite, * - β-C_2S, o - α'- C_2S, x - α- C_2S, Δ - C_3A.

- C_3A content in the surface layer being constant at 1000°C up to 1400°C has sharply increased in the temperature interval 1400÷1450°C, and at the further increase of temperature up to 1550°C the content of C_3A has reduced to zero as a result of transition to a liquid phase;

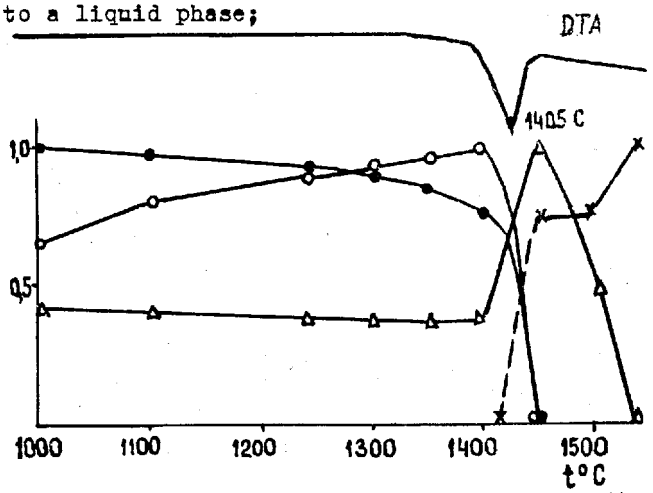

Fig.2. The change of phase composition of the white clinker surface at heating up to 1550°C.
• - alite, * - β- C_2S, o - α'- C_2S, x - α-C_2S, Δ - C_3A.

- C_2S content (in β-form) has monotonously increased from 1000 up to 1400°C in accordance with reduction of C_3S content. At the increase of temperature from 1450 up to 1550°C

V.P.Rjazin
Z.B.Entin
N.I.Komarova
N.A.Shebanov

α'-form has passed into α-C_2S (endoeffect connected with the transition of α' into α - modification of C_2S on the DTA curve - at 1405°C). The intervals of the more sharp change of the content of alite, C_3A, and the α'-α transition of C_2S practically coincide; - after cooling of the sample reflections of only two phases - C_3A and β- C_2S are displayed on the difractogram of the surface layer. Free calcium oxide is not observed. In the same time the main sample mass gives the typical X-ray photograph of the white clinker with comparatively higher alite content and lower C_3A content than the initial (before calcination) clinker.

The analogous phase composition of the surface has been produced at the calcination (up to 1500°C) of the raw mixture powder of the white clinker, containing 82,5% of limestone, 9,8% of kaolin, 5,9% of sand (fig.3). Under these conditions the sharp increase of C_3A-content and α'-α transition of C_2S in the surface layer has occurred in the interval of 1400°-1500°C. To α'-α transition on the DTA-curves the endoeffect at 1410°C corresponds. Exoeffect at 1345°C, as a result of the initial alite formation, concerns only the inner part of the sample. On the surface of the sample C_2S does not appear in the whole temperature interval up to 1500°C. Small amount of C_3S on the sample surface has been indicated only after its cooling.

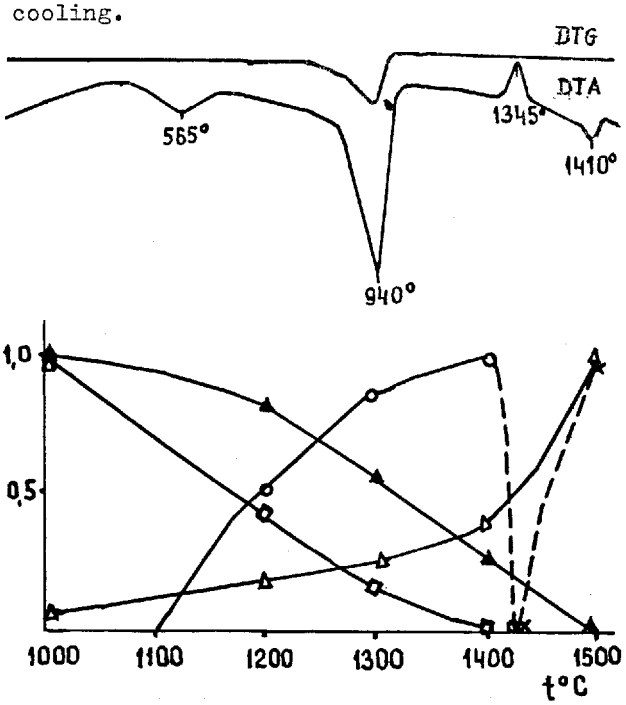

Fig.3. The changes of phase composition of the raw mixture of the white clinker at heating in UVD-2000 kilns and diversition system.
▲ - CaO, □ - SiO_2, o - α'- C_2S, x - α- C_2S, Δ - C_3A.

Alite formation on the surface of the sample at heating has been observed only at the calcination of mixtures with surplus content of calcium oxide. In this case $CaO_{fr.}$ crystals are present not only on the surface of the sample but in the inner volume of the sample as well (fig.4).

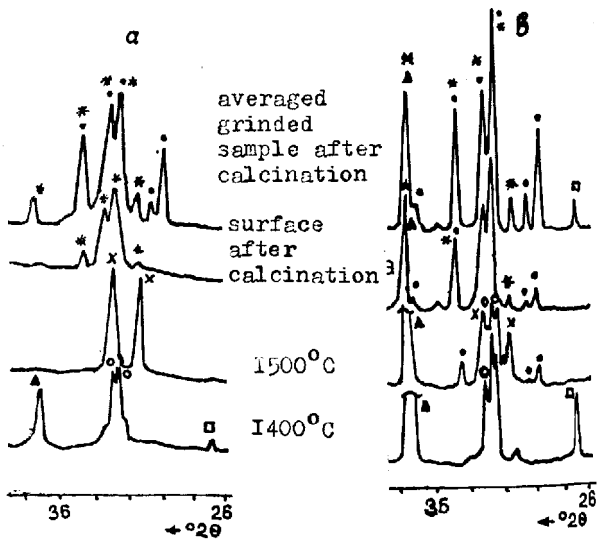

Fig.4. The radiograms' sections on the surface and the averaged grinded sample at calcination of the raw mixture with stoichiometric (a) and with surplus content of CaO (b).

The layer diffraction analysis of the samples has shown the following (fig.5):

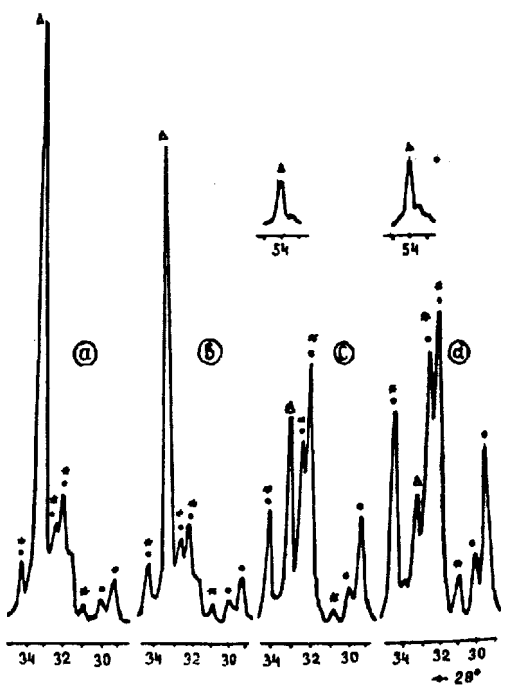

Fig.5. Radiograms of the surface and the adjoining parts of the sample.

a) the surface after calcination;
b) has removed the layer of 40 μkm;
c) has removed the layer of 120 μkm;
d) the averaged grinded sample.

- on the surface - C_3A, β and α'- C_2S, small amount of C_3S;
- to the depth of 50-70 μkm the relative reduction of compositions of these phases and increase of alite amount;
- beginning with the depth of 70-100 μkm the usual phase composition with high alite content.

It is noted that the opposite surface of the sample which has not been subjected to radiation (X-ray radiation, ultra-violet, luminous, thermal) by phase composition is analogous to the irradiated one.

The sample cut has been studied in the direction from the surface to the centre with the help of electron probe of the size of 2x10 μkm with the step of 2 μkm. The change of characteristic X-radiation intensity of Ca, Si and Al has been observed. It has been indicated that the intensity relation of Ca- and Si-curves on the surface and in the width of the sample is the same. It prevents from explaining the absence of C_3S on the surface by evaporation of calcium oxide from the surface in vacuum or its diffusion inside of the sample. Thus, the absence of alite on the surface at the synchronous absence of free calcium oxide can be explained only by absorption of the large amount of surplus calcium oxide by α-C_2S grating without the change of the grating type. At the cooling of the sample some part of α-C_2S, containing surplus calcium oxide reorganizes with C_3S formation which is fixed on the X-ray photograph of the cooled sample.

As for decimicrone widthes of the surface apparently it is possible to say that aluminium diffuses in the direction of the surface of the sample. It leads to the relative Ca and Si reduction on the surface before the appearance of the melt. The high intensity of C_3A peak on the surface at relatively low intensity of minerals-silicates peaks and comparatively small changes of the relations of intensity of the characteristic curves of Ca, Si, Al in comparison with the sample width indicates the formation of cubic C_3A with isomorphic Si. The cause of the formation of this mineral but not alite is the thermodynamic predilection and "two-dimensionality" of the texture. The irradiation of the sample does not affect the phase composition.

In conclusion it is necessary to say that the high-temperature processes of mineral formation on the surface of the sample considerably differ from those in the whole mass of mineral.

U. Ludwig and C. Urrutia
Institut fur Gesteinshuttenkunde, RWTH, Aacnen, West Germany

INFLUENCE OF SUCROSE ON THE SETTING OF PORTLAND CEMENT.

EXPERIMENTAL PROCEDURES

For the preparation of the portland cements, two industrial clinkers A and B, anhydrite and hemihydrate were employed. The calcium sulphate was added in amounts of 2.5 wt.% SO_3 to both of the cements. The chemical composition of the clinkers is shown in tab. 1. The anhydrite/hemihydrate ratio in the cement was 1.
The setting or rheology of cements has been measured according to DIN 1164, or by means of a coaxial cylinder viscosimeter, at constant water-cement ratios. The sucrose was added together with the mix water directly to the dry cement, or the cement was premixed with water for 4 min. before adding the sucrose. The alteration of the chemical composition of the pore solution that had been squeezed out of mortars according to DIN 1164, were established by Atomic Absorption Spectrophotometry (Ca, Al, Fe, Na, K), colorimetry (Si and sucrose), titration (OH^-), and SO_4^{--} by precipitation as barium sulphate.

Table 1 Chemical composition of the clinkers in wt.%

	Clinker A	Clinker B
SiO_2	22.40	21.50
Al_2O_3	4.52	5.31
Fe_2O_3	2.61	3.21
CaO	68.60	62.40
MgO	1.05	1.13
K_2O	0.18	0.68
Na_2O	0.20	0.20
SO_3	0.02	0.55

RESULTS

As for the cement containing little alkali, the direct addition of sucrose to the mix water does not induce any, dealing with portland cement, however , containing a lot of alkali, a distinct retardation of the initial setting up to 0.2 wt.% sucrose is effected.

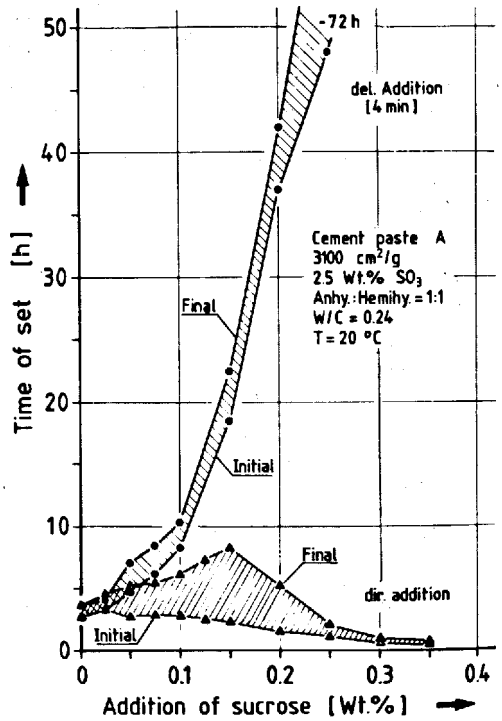

Fig. 1 Setting time of cement paste A vs addition of sucrose (direct or delayed addition of sucrose)

Consequent to that, even here a false set occurs. For both cements the final setting is evidently retarded till the false set takes place coinciding with a prolongation of the setting interval, and then accelerates (see picture 1 and and 2).

In correspondence with the results obtained by measuring the setting, the direct addition of augmenting portions of sucrose affectuates an increasingly accelerated gain of viscosity of cement pastes. The subsequent dosage of sucrose, however, already causes a long-lasting low viscosity, even when dealing with a smaller content of additive. In this respect picture 3 visualizes the shear stress versus time.

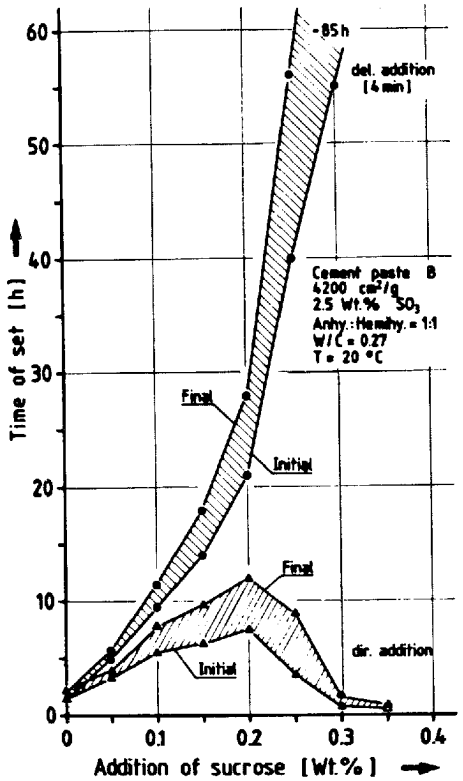

Fig. 2 Setting time of cement paste B vs addition of sucrose (direct or delayed addition of sucrose)

For the time being a particulary fast decrease of the Ca^{++}- and SO_4^{--}-ion concentration within the pore solution is being held responsible for the effect of the directly or subsequently added sucrose to the cement going along with an extremely fast formation of ettringite. Without a retarder or especially in case of delayed addition of sucrose, the respective concentrations are noticably higher (see table 2).
When directly adding sucrose, the aluminate concentration, too, is obviously increased.

sucrose added	content wt.%	Ca^{++} (g/l)	SO_4^{--} (g/l)	Al_2O_3 (mg/l)
without	0.0	1.3	1.4	0.5
directly	0.4	0.6	0.4	9.0
after 4 min	0.4	1.7	2.0	2.0

Tab.2 Calcium-, sulphate-, and aluminate-ion concentration within the pore solution 1 hour after mixing

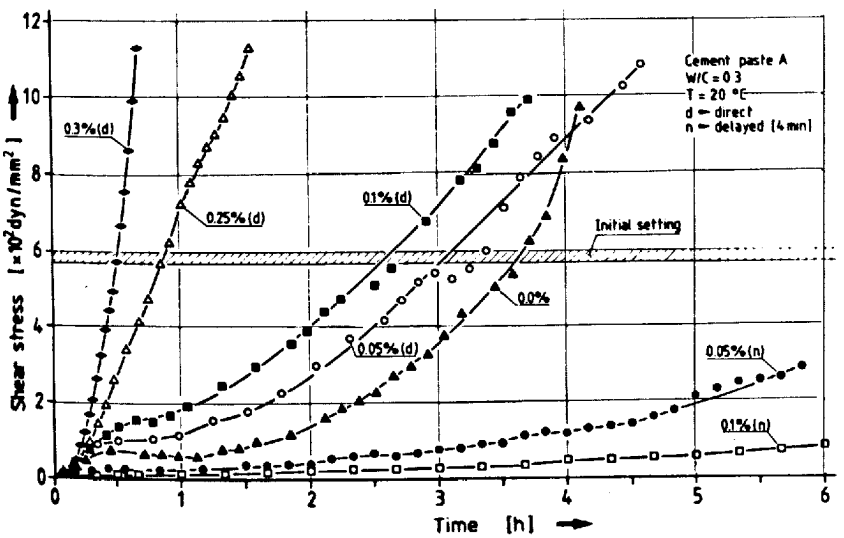

Fig. 3 Variation of shear stress with time measured at a shear rate of 0.02 min^{-1} at several sucrose concentrations

The direct addition of sucrose to cement leads to its evidently accelerated bond to or within the solid phases (see picture 4).

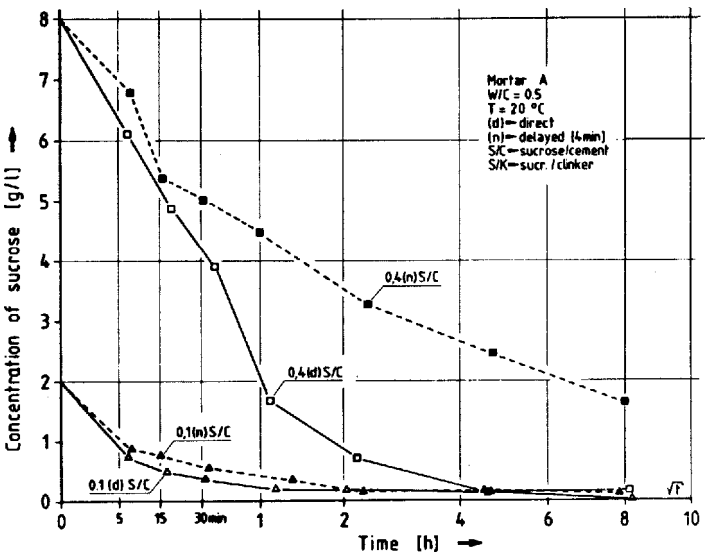

Fig. 4 Concentration of sucrose in the pore solution in cement mortar mixed with 0.1 wt.% and 0.4 wt.% sucrose refered to cement

Everaldo Marciano Jr. (ABCP - Brasil)
Peter Bartha (Refratechnik GmBh) West Germany

CL. CONTRIBUTION TO THE KNOWLEDGE OF THE PHASE COMPOSITION OF DIFFERENT MAGNESIA-CHROME BRICKS AFTER THE ATTACK BY CEMENT CLINKER

1. Introduction and posing the problem

Nowadays mainly magnesia chrome bricks are used as refractory lining in the burning zone of cement rotary kilns. The MgO-content of the bricks vary between approx. 80 and 60 % MgO according to the MgO-raw material and chrome ore ratio. Accordingly the Cr_2O_3 content ranges between 4 and 16 %. Additionally they show considerable differences in type and quantity of the chemical secondary components SiO_2, Al_2O_3 and Fe_2O_3.

Therefore the durability of the magnesia chrome bricks is not only determined by its behaviour towards mechanical load but also by its chemical reaction at high temperatures.

Aim of the following comparative investigations is to determine the chemical-mineralogical changes of four representative magnesia chrome bricks of different chemism after its contact with cement clinker.

2. Character of the applied materials

Two industrial cement raw materials of similar mineralogical composition were chosen for the investigations. Its chemical properties were adjusted regarding the content and composition of the ashes of two different coals (mineral coal and charcoal from Brasilia).

Four in the cement industry applied magnesia chrome bricks with different chemical-mineralogical and physical properties were investigated regarding their phase composition before and after the attack by cement clinker. Above all the magnesia chrome bricks differ in type of the applied dead burnt magnesia and chrome ore, in the ratio of the beforementioned and in the burning temperature during the brick burning process.

In the following sections the applied materials are described in detail.

2.1 Coal ashes

Due to the fact that the Brasilian cement industry recently mainly applies solid fuel, some native current mineral coals and one charcoal were chosen. Table 1 gives the chemical mineralogical composition and the fusing behaviour of the two ashes. The ashes obviously have different Al_2O_3- and CaO-contents as well as different fusing points.

2.2 Raw meals

Table 2 reflects the chemical mineralogical composition, the theoretical clinker phases as well as the burnability index of the raw meals. Please note the significant differences in the MgO-content, in the alumina modulus and in the burnability index.

2.3 Refractory bricks

A characterization regarding chemical analysis, phases and the most important physical properties are shown in table 3 and figure 1

3. Test conditions

By adding the same portion of water the raw meals were pressed into tablets of 20 mm in diameter and 20 mm in length and dried at 110 °C until achieving constant weight. Cubic test specimen of 70 x 70 mm were sawed out of the refractory bricks.

3 tablets each were put on top of a cube and covered with a second cube from the same brick material.

The samples were heated up in a Bickley-laboratory furnace fired with natural gas at 10°C/min up to 1700 °C. Preliminary tests at 1500 and 1600 °C had not resulted in any significant reactions at the contact. The durability reached 5 hours in a homogeneous temperature field.

After slowly cooling off in the furnace the samples were prepared according to the different tests. Fig. 2 schematizes the procedure.

4. Results of the investigations

For a better understanding of the new formations of the phases several test methods were combined:

- Atomic absorption spectroscope
- X-ray phase analysis
- Reflected light microscopy
- Scanning electron microscopy (SEM)

4.1 X-ray phase analysis

Please refer to table 4 for the results. Alite, the compound richest in lime, only occurred in brick D. C_2S was found in every brick. The intensity showed, however, that generally more C_2S was found in combination with raw meal 1 than with raw meal 2.

All brick samples pretreated with raw meal 2 had monticellite and merwinite. Except for sample B which also had a considerable quantity of those silicates with raw meal 1. Forsterite could only be proved in samples B and C under the influence of raw meal 2.

Especially raw meal 1 was responsible for the highest quantities of the phase C_4AF in the brick samples A and C.
Aluminate phase was only found in the brick samples A and B. The combination of brick sample C/raw meal 1, however, produced a phase which - according to the d-values (ASTM-Standards 17-736)- was first identified as calcium-aluminum-magnesium silicate of the formula $(CaO, MgO, Al_2O_3) . SiO_2$.

4.2 Reflected light microscopy

The investigations with the reflected light microscope were carried out in order to control the phases determined by the X-ray phase analysis and to determine their spatial distribution. Due to the fact that the reaction tests were carried out in a homogeneous temperature field there was no clear zonal sequence as can be observed with used bricks in the practice.

Raw meal 1 provoked the formation of the compound belite as silicate phase in all brick samples except for in brick sample B, where a significant quanitity of merwinite and monticellite could be determined.

Brick sample C contained a high quanitity of a prismatic phase hard to etch. It could be proved all over the whole infiltrated brick part. Very small quanitities of prismatic phases were also found in brick sample A.

Calcium-aluminate-ferrite was found in all brick samples: the highest quanitity in brick samples A and C, the lowest in B.

Raw meal 2 caused a different reaction than raw meal 1. Besides of belite there were also the significant phases merwinite and monticellite. Very small quanitities in decreasing sequence could be determined in the brick samples C, B and A.

Calcium-aluminate-ferrite was determined under the impact of raw meal 1 with the same before-mentioned tendency for the respective bricks.

Under the attack of the pure ashes forsterite formed in all bricks, the charcoal additionally caused the formation of monticellite. In general the infiltration evoked by the mineral coal ashes was nearly twice as high as that by the charcoal ashes.

4.3 Scanning electron microscopy (SEM)

The investigations by the SEM were carried out as supplement to the X-ray phase analysis and the microscopical investigations. The SEM indentified the unknown phases, the known phases and determined the exact chemical composition including the incorporated foreign ions.

The results can be summerized as follows:

- The prismatic phase found by the reflected light microscope was identified as a melilite of the ideal composition C_6MA_4S (fig. 3).

- The exclusive formation of alite in brick sample D with both raw meals was confirmed. Furthermore the incorporation of significant quanitities of chrome could be proved. Measured individual values amounted up to 20 and 25 atomic% Cr_2O_3.

- The Cr_2O_3-content in belite varied between 9 and 0 atomic%, the standard value varying between 1 and 4 atomic%.

- According to individual measuring 2 - 4 atomic% of MgOwere determined in belite in all brick samples after their reaction with raw meal 2.

Cr_2O_3 preferably substituted Al_2O_3. Higher quanitities could be determined in the brick samples reacting with raw meal 2 than with raw meal 1. The average doping quanitity was between 2 and 3.5 atomic%, in extreme cases between 15 and 16 atomic%. In these cases the general formula should read $C_4(Al,Cr)F$.

The doping of SiO_2 in calcium-aluminate-ferrite was nearly constant and varied between 4 and 4.5 atomic%.

Titanium and manganese were incorporated in calcium-aluminate-ferrite in samll, varying quanitities. A calcium-titanate-phase tending to C_3T_2 could be determined in very small quanitities with both raw meals. But it still contained between 5.55 and 5.65 atomic% of silicium (fig. 4).

5. Discussion of the results and conclusion

Taking into account that the brick samples were investigated under static conditions in a homogeneous temperature field and at increased temperatures (practical case of thermal overload) the following findings can be learnt from the phases in the slagged brick samples when only considering the chemical-mineralogical impact:

- As noted the bricks generally suffered more under the attack of raw meal 1 than of raw meal 2. As this result cannot only be attributed to the insignificant chemical differences there must also be kinetic causes: the higher burnability index of raw meal 2 together with a coarser grinding.

The less abundant offer of clinker phases with raw meal 2 can also serve as an explanation why merwinite and monticellite, which are less calciferous, formed in all bricks instead of belite in the case of raw meal 1.

- The abundance of calcium-aluminate-ferrite in bricks A and B can be explained by the high content of magnesium ferrite as the matrix forming phase of the bricks.

- In sample C considerably high quanitities of melilite were found of the approximately composition C_6A_4MS. An increased Al_2O_3-content of the brick could be responsible for it as the brick contains a chrome ore with an extremely high quanitity of magnesium-aluminate-spinel. The fact that this phase does not appear in brick sample D with the lowest content of Al_2O_3 underlines our presumption. Furthermore it is known that melilite forms during the wear of magnesia bricks containing MA-spinel.

The bricks B and C with forsteritic matrix react more sensitive in connection with cement clinker, because they enable the formation of the phases monticellite and merwinite which are less calciferous and which have a lower fusing point.

- Alite was only found in sample D, which has a sinter with a CaO/SiO_2 ratio of > 1.87 and is nearly free of iron. Therefore the formation of calcium-aluminate-ferrite can be practically excluded.

- The tested bricks suffer more under the mineral coal ashes than under the charcoal ashes. The mineral coal ashes, however, cause the formation of forsterite instead of forsterite and monticellite which occur in the bricks when attacked by charcoal ashes. This is caused by the different lime content of the two ashes. For the refractoriness forsterite is preferred to monticellite which has a lower fusing point.

- As observed by the SEM the incorporation of chrome into the lattice of alite and belite as well as the substitution of Al by Cr in calcium-aluminate-ferrite indicates the decomposition of the chromite spinel portion of the chrome ore and partly explains the whereabouts of the liberated chromium oxide.

- Striking was the formation of a calcium titanate phase, even if it was only found in small quanitities. It can only be explained by the supply of TiO_2 from the raw meal and the chrome ore.

The following conclusions can be drawn concerning the evaluation of the investigated bricks:

- A high compound of magnesia ferrite in the matrix is undesirable, because, under the attack of the clinker phases it leads to calcium-aluminate-ferrite and a lower fusing point of the brick matrix. Above all this is a typical behaviour towards cement clinker resistant to sulfate.

- A low CaO/SiO_2 ratio in the brick weakens its resistance to clinker phases because monticellite and merwinite lower the fusing point and therefore decrease the refractoriness. This effect is not dangerous as long as the quanitity of forsterite in the brick is only insignificant.

- The Al_2O_3-content of the chrome ore is in so far important for the reaction to cement clinker as increased Al_2O_3-contents might cause the formation of melilite.

- The results with the two raw meals show that besides the chemism the burnability of the raw meals influence intensity and completeness of the phase formation.

Table 1:

	mineral coal ashes	charcoal ashes
SiO_2 (%)	59.01	55.52
Al_2O_3	27.12	11.56
Fe_2O_3	7.16	6.12
CaO	1.71	15.38
MgO	1.06	2.88
K_2O	1.92	3.52
Na_2O	0.17	0.98
Mn_2O_3	0.05	0.29
TiO_2	1.10	-
Cr_2O_3	-	0.03
SO_3	-	-
CaO/SiO_2	0.03	0.28
LSF	0.84	8.85
SM	1.72	2.99
AM	3.76	1.65

	mineral coal ashes	charcoal ashes
softening point (°C)	1400	1220
hemispherical fusing point (°C)	1500	1230
flow point (°C)	1530	1400
Mineralogical composition		
quartz	x	x
silicate phase	x	x
mullite	x	x
calcite	-	x
free lime	-	x
field spar	x	-
haematite	x	x
glimmer	x	-
montmorillinite	x	-

Table 2:

Chem. composition	raw meal 1	raw meal 2
SiO_2	22.32	21.48
Al_2O_3	5.33	4.65
Fe_2O_3	3.40	3.46
CaO	65.83	63.45
MgO	1.97	5.20
K_2O	0.60	0.45
Na_2O	0.10	0.12
SO_3	0.17	0.32
Cl	0.05	0.07
TiO_2	0.21	0.25
Mn_2O_3	0.04	0.17
Rational analysis (according to BOGUE)		
C_3S	57.7	58.9
C_2S	29.5	17.1
C_3A	8.4	6.5
C_4AF	10.4	10.5
LSF	92.4	92.9
LSF (incl. MgO)	93.3	103.3
SM	2.49	2.52
TM	1.61	1.35

Mineralogical composition

	raw meal 1	raw meal 2
glimmer	x	x
montmorillinite	x	x
chlorite	-	x
calcite	x	x
dolomite	x	x
quartz	x	x
haematite	x	x

Table 3:

Refractory bricks(original composition)

	A	B	C	D
MgO	81.41	78.7	81.11	84.94
Cr_2O_3	3.95	6.93	4.64	8.41
Al_2O_3	2.58	2.68	4.73	1.88
Fe_2O_3	7.16	6.66	4.28	2.75
SiO_2	1.84	3.44	3.38	1.09
CaO	2.70	1.24	0.78	0.97
Mn_2O_3	0.36	0.20	0.66	0.15
K_2O	0.02	0.04	0.05	0.01
Na_2O	0.02	0.02	0.02	0.03
CaO/SiO_2	1.47	0.36	0.23	0.89
$CaO+SiO_2$	4.54	4.68	4.16	2.06

Mineralogical composition

periclase	x	x	x	x
chromite	x	x	x	x
MF	x	x	x	x*
M"S	-	x	x	-
CMS	x	x	x	-
C_3MS_2	x	-	-	x
C_2S	-	-	-	x**

x= present *= hardly any **= few

bulk density (g/cm^3)	2.93	2.81	2.85	2.93
apparent porosity(%)	18.85	23.34	21.24	17.70
cold crushing strength (N/mm^2)	60.7	47.2	44.2	57.8

Table 4: X-ray phase analysis

bricks

	A		B		C		D	
raw meal mix	1	2	1	2	1	2	1	2
C_3S							x	pro
C_2S	pos	pos	x	x	x	x	pos	x
C_3MS_2		x	x	x		x		x
CMS			x	x		x		x
M_2S				x		x		
C_3A	x						x	pos
C_6A_4MS					xx	pos		
C_4AF	xx	x	pro	pos	xx	pos	pos	pos
MA					x		x	

X = present
pos = possible
pro = probable

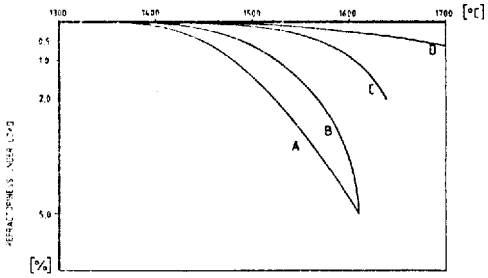

Fig. 1: Refractoriness under load of the investigated bricks according to DIN

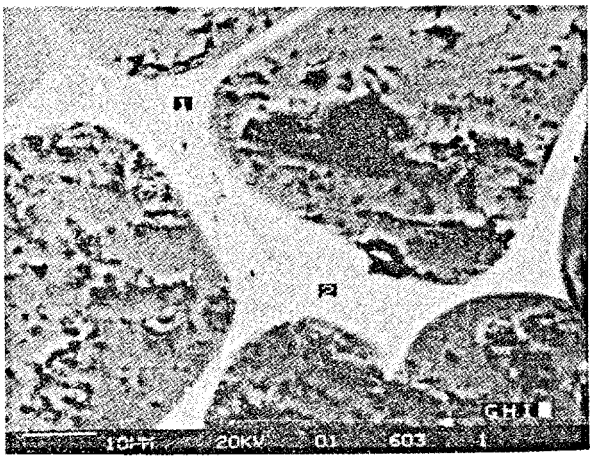

Fig. 3: SEM picture of the prismatic (melilite)-phase

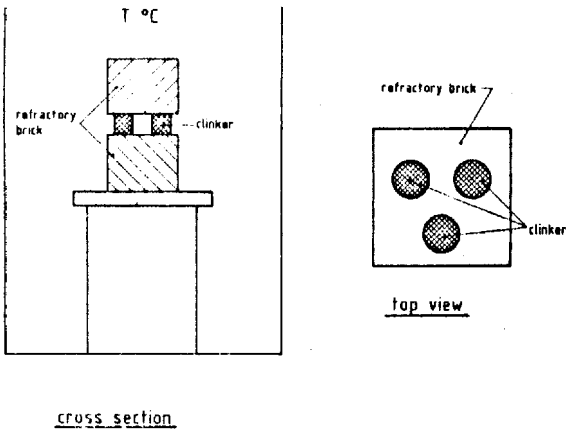

Fig. 2: Experimental arrangement

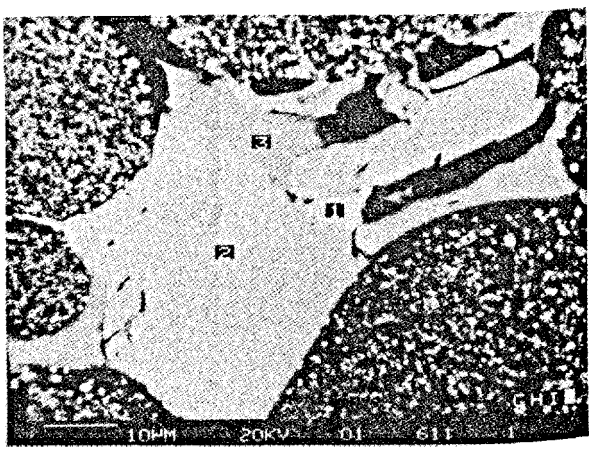

Fig. 4: SEM picture of the calcium-titanate-phase

C. MacInnis, P.P. Hudec and M. Moukwa
University of Windsor, Windsor, Ont., Canada

EFFECT OF MICROCLIMATE ON CONCRETE DETERIORATION

SUMMARY

The south facing vertical surface of concrete barrier walls for highways often exhibit considerable scaling which suggests that walls so oriented are subjected to a more severe exposure condition. The objective of this research was to measure and define the microclimate by measuring the temperature, and moisture and salt concentration conditions obtaining at the surface and in the near sub-surface of south and north facing highway barrier walls. Two field exposure sites were included in the study: a south facing wall on a divided highway and two laboratory cast barrier wall panels placed to face north and south respectively at an outdoor site.

The field measurements of temperature and moisture content were obtained on a semi-continuous basis for three winter months. The results showed that a temperature gradient as high as 9C between the concrete surface and the 1 cm depth was common. The rate of freezing and thawing was significantly higher on the south facing wall than on the north facing wall and also the south facing wall was found to undergo a significantly greater number of freeze-thaw cycles. The foregoing findings indicate that a much more severe climate exists on south facing walls. This can be attributed directly to the greater insolation received by such walls.

Introduction

Concrete barrier walls are commonly used along highways in Canada and in and in northern U.S. states. Some have shown rapid deterioration in the form of surface scaling. Typically, the deterioration has tended to be more pronounced on the south facing walls. The purpose of this study was to measure and define the microclimate at such walls. The microclimate elements measured were temperature at the surface and near sub-surface, moisture content and salt content.

Field Instrumentation and Measurements

The microenvironment existing in the surface layer of concrete barrier walls was measured at two distinctly different sites. One site was an existing south facing barrier wall along a heavily travelled divided four-lane highway in South Windsor (Ontario), the E.C. Row Expressway. The results obtained at this site represent only a south facing exposure, and are described elsewhere (1).

The other site was the roof of Essex Hall on the campus of the University of Windsor. The tests results from that site are the subject of this paper. Two panels having the shape and dimensions of concrete barrier wall sections were cast in the laboratory, instrumented, cured for one month and then placed on the roof, one facing north and the other facing south. The concrete used was air-entrained (nominal 5-7%) with a water-cement ratio of 0.47 and maximum aggregate size of 10 mm (3/8"). Copper-constantan thermocouples were used for the temperature measurements. The thermocouples were placed at the surface, and at 10mm depth from the surface. Stainless steel electrodes were embedded at 10mm depth and 10mm apart, and used in the measurement of moisture and salt concentration. The cast panels are shown in Figure 1, and the instrumentation of the panels in Figure 2.

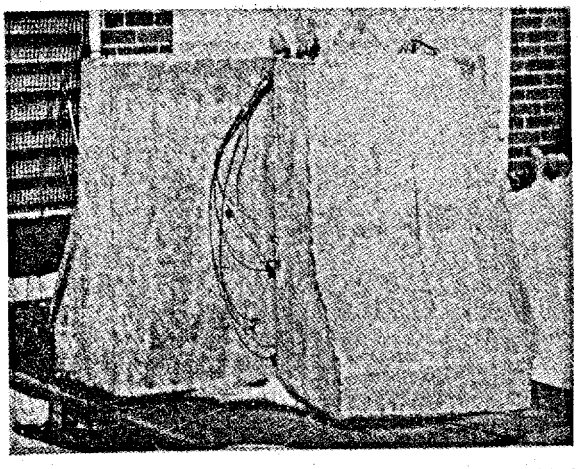

Figure 1: Cast panels. Note electrodes embedded along the center line of the panel and thermocouple wires in the back of the panel.

The panels were sprayed with a 9% NaCl salt solution three times in a manner shown in Fig. 3 to result in three distinct salt concentration zones. Natural moisture content and induced salt content were determined by two methods. The primary method used was the "capacitance effect method" developed by Hudec, MacInnis and Moukwa (1). This method is based on the observation that the capacitance of concrete varies with the degree of saturation. By applying an electrical field through stainless steel electrodes and measuring the resulting current, it was possible to predict the degree of saturation and, to some extent, the salt content. Current readings were taken after each spraying.

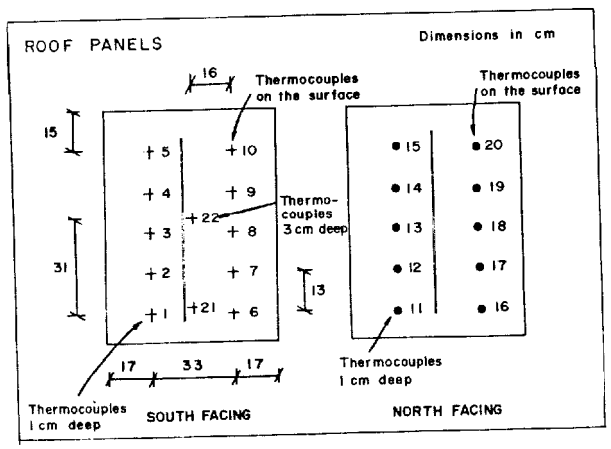

Figure 2. Placement of thermocouples and electrodes in the south and north facing panels.

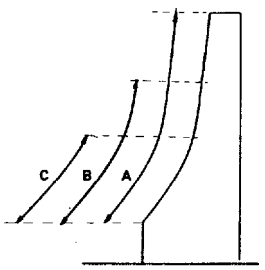

A : sprayed on May 20
B : sprayed on June 2
C : sprayed on June 6

Fig. 3.Spraying of the panels by 3% NaCl solution.

The second method involved physical sampling. Concrete samples were chiseled from the panels at different locations during the period of study to determine the actual degree of saturation and salt content. The degree of saturation was determined gravimetrically. The salt content in the panels was determined chemically by the Berman-Volhard method.

Data collection was initiated in February, 1984. Current readings and temperatures were recorded on a semi-continuous basis for two months. The outside temperature, relative humidity, wind direction and precipitation were obtained from the Windsor Airport weather station. The sunshine record, which was not available from the Windsor Airport, was obtained from the Harrow weather station, some 15 miles distant. Current readings and temperatures were recorded for various types of weather.

Temperature Conditions

The temperature regime existing in the panels depended on the prevailing weather conditions, which can be classified into several distinct types: sunny and cold; sunny and warm; partly sunny and cold; cloudy and cold; cloudy and warm.

Daily Temperature changes

Typical temperature variation in the south facing roof panel for a sunny and cold day are shown in Figure 4. The figure shows that a rapid rise in temperataure occurs in the surface layer when the sun irradiates the concrete. Subsequently, a rapid drop in temperataure takes place in the evening of a sunny day. A maximum warming rate of 16.7 C/h and a maximum cooling rate of 8.6 C/h were recorded in

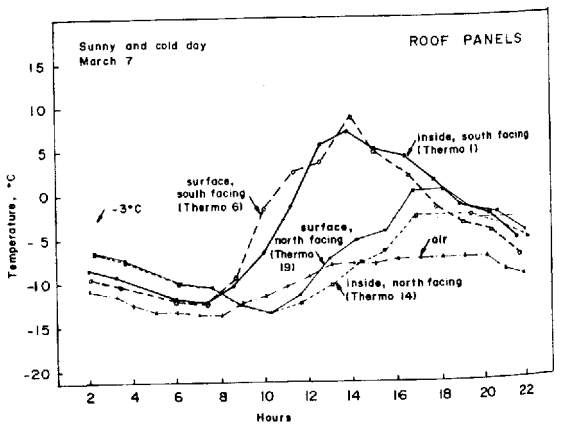

Figure 4. Typical temperature variations in the south-facing roof panel on a cold but sunny day.

the south facing panel for a sunny day. However, tabulation of the frequency of different rates of change in concrete temperature showed that most changes in temperature were at the rate of between 0 and 3 C/h, for both the warming and cooling parts of the cycle.

Temperature gradients with depth

Large difference in temperature was found to exist between the surface and the interior of the concrete face, sometimes on cold and windy days, but especially on sunny days. The largest temperature differential between the surface and the 10 mm depth was found to be 9 C for the south facing roof panel. This typically occurred during sunny afternoons when the sun's radiation coupled with a high air temperature warmed the surface of

the panel. The inverse was true (surface much cooler than the interior) in the evening of a sunny day when the cold ambient temperature cools the surface.

A typical change in the differential temperature (dt) experienced by the thermocouples (1,6) (3,8) and (5, 10) is shown in Figure 5. The "dt" is defined as the difference in concrete temperature between the surface and the 10mm depth.

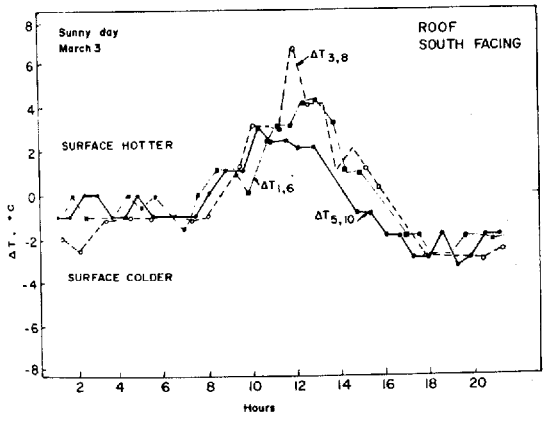

Figure 5. Differential temperature between surface and 10mm depth over 24h period.

Temperature reversals

During partly sunny days, the surface layer of the panel experienced multiple cycles of thermal changes, which undoubtebly would produce significant stresses. For the period of the test, the thermocouples (1,6) and (5,10) experienced, respectively, 68 and 50 changes in dt over a period of 14 days.

Freeze-thaw Cycles

The temperature change from above to below the freezing point can be defined as one cycle of freezing and thawing. Because of pore size considerations, the minimum temperature required to freeze capillary water was taken as -3 C. The number of freeze-thaw cycles per day (with -3 C as the freezing line) for all the thermocouples is given in Figure 6.

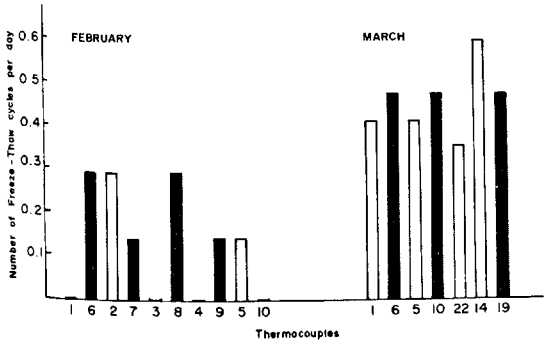

Figure 6. Average number of freeze-thaw cycles per day measured by thermocouples in February and March.

The rate of freezing and thawing ranged from 0.1 to 7 C/h for the roof panels. It was observed that the rates of freezing were lower than that of thawing and, that freezing and thawing proceeded most often at a low rate (between 0 - 3 C/hour) for the roof panels. At the bottom of the panels, freezing proceeded most often at a rate between 6 and 9C/h. Conversely freezing at the top proceeded most often at the lower rate of between 0 and 3 C/hour. Thawing at the top or the bottom of the panel proceeded most often at a rate between 0 and 3 C/h. Freezing occurred first on the surface and half an hour later at the 10mm depth.

Factors Affecting Temperature.

Panel Orientation

The maximum differential temperature on the north facing panel was 5C, while 9.0C was recorded for the south facing panel. The temperature of the north panel was controlled by the air temperature, and not by the sun's rays. Thus, the temperature in the north facing panel frequently remained below -3C for long periods, and experienced fewer freeze - thaw cycles than the south facing panel.

Shape of the Panel

The temperature change observed was affected by the shape of the barrier wall and by the depth of the thermocouples. The maxima rates recorded on the surface were higher than inside the south facing panel. The highest rate of temperature change was recorded on the surface at the bottom of the south facing panel and, also, the lowest rate recorded at the 10 mm depth occurred at the bottom of the panel. The shape of the barrier wall had a relatively small effect on the rate of temperature change in the north facing panel.

High temperatures and high temperature gradients recorded at the bottom of the south facing panel can be explained by the angle of the sun's rays with the surface. On a clear day the bottom part receives and absorbs more solar energy than the top.

Moisture Conditions

Figure 7 gives an example of the degree of saturation and the temperature of the concrete in the roof panels between noon and 2 pm during the cited observation periods in February. Note that the panels are not critically saturated; also note that on Feb. 27, the north-facing panel surface was below freezing, while the south-facing surface was well above freezing.

Although in general, the moisture content in the barrier walls is controlled by wetting and drying, the orientation of the wall also has a significant influence. Since at this geographic location, the prevailing wind direction is from the south, the south facing wall should have higher moisture content due to driving rain. On the other hand,

CL

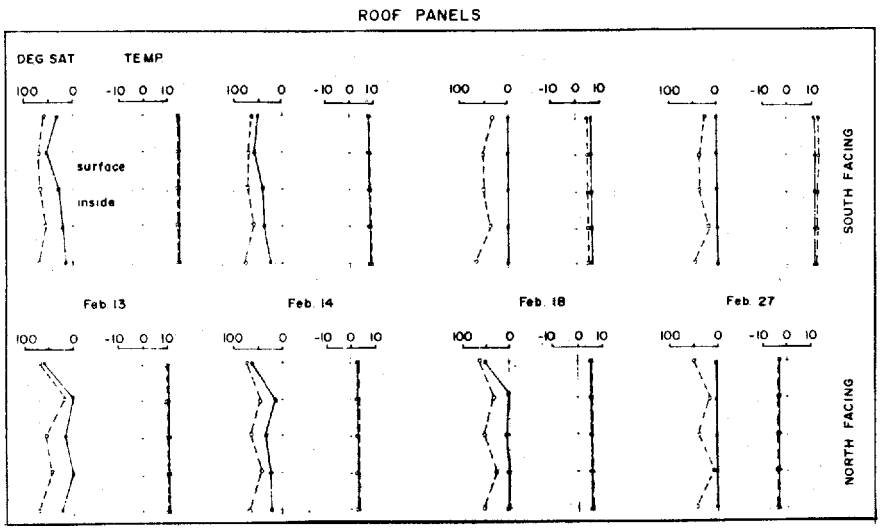

Figure 7. Distribution of temperature and degree of saturation across the south and north facing panels on selected days.

the surface of the south facing panel would dry faster than the north facing panel. The values of average degree of saturation calculated for the roof panels at the surface and at the 10 mm depth, given in Table 1, confirmed this general observation.

Table 1
Degree of Saturation of South and North Panels

Date March	Time	10mm Dept South	10mm Dept North	Surface South	Surface North
6	14:20	53.3	49.9	.0	13.1
10	0:00	85.0	74.0	71.1	63.6
11	13:40	68.9	60.0	36.5	30.4
12	10:50	62.3	56.7	28.1	30.2
13	13:20	65.5	50.0	30.5	21.8
14	8:35	69.8	53.2	44.3	34.2
18	16:40	50.3	48.8	.0	.0
27	10:35	30.2	31.5	.0	.0
Average		60.7	54.3	26.3	24.2

Salt content

The salt content of the panels was calculated from current readings using the frequency-class method described by Hudec, MacInnis and Moukwa (1), and on chiselled samples. The roof panels, at the conclusion of the test, had a salt content equivalent to 2.1, 4.6, and 4.5 percent NaCl solution in the top, middle, and bottom portion of the panel, respectively. It is known that freeze-thaw cycles in the presence of a 3 to 4% salt solution produce the most severe scaling (2).

Conclusions

Direct rays of the sun have a pronounced effect on the surface temperature of the concrete, which can be more than 10 degrees higher than the air temperature. On sunny days when the air temperature is below freezing, the concrete surface can be well above freezing. As soon as the sun is obscured by cloud(s), the surface begins to cool rapidly. Thus, on partly cloudy days, the surface can undergo several cycles of freezing and thawing. The rapid temperature changes and differences observed between the surface and the sub-surface of the concrete no doubt set up thermal stresses and contribute to the deterioration of the concrete.

The roof concrete panels were generally not at "critical" saturation levels while undergoing freezing and thawing. This was in marked contrast to E.C. Row highway exposure panels, where snow accumulation and car splash maintained near-critical saturation during most of the winter. However, a limited amount of salt spraying of the roof panels was sufficient to maintain the salt concentration in the 2 to 6% range.

The shape of the panel had a bearing on the moisture and temperature conditions. The lower curved portion was found to have higher, and more frequent changes in these parameters.

It can therefore be concluded that the south-facing concrete barrier walls experience a much harsher climatic environment, and are more prone to deterioration than walls facing in other directions.

Acknowledgments

The authors would like to thank the Ontario Ministry of Transportation and Communications for providing research funds for this work. Thanks are also due to Mr. Peter Feimer of the Civil Engineering Department, University of Windsor, for assistance in the field work.

References

1. Hudec, P., MacInnis, C., and Moukwa, M., "Microclimate of concrete barrier wallls: temperature, moisture, and salt content", in preparation.
2. Hudec, P., MacInnis, C., and Moukwa, M., "The capacitance effect method of measuring moisture and salt content of concrete", in preparation.
3. Litvan, G.G., "Phase transitions of absorbates V: Aqueous sodium chloride solutions absorbed in porous silica glass", National Research Council of Canada, Division of Building Research, Ottawa, Nov. 1972.

J. BARON*, R. GUYOT*
* LAFARGE COPPEE RECHERCHE, France

UN MODELE PHENOMENOLOGIQUE DE L'EVOLUTION DE LA RESISTANCE EN COMPRESSION PARAMETRANT L'INFLUENCE DU CLINKER ET CELLE DES GRANULATS

INTRODUCTION

La finesse de mouture du ciment est le principal paramètre sur lequel le cimentier peut agir pour modifier les propriétés du ciment. A l'origine de cette étude, nous souhaitions connaître, pour chacun de nos clinkers industriels, l'effet d'un accroissement de la surface spécifique sur les résistances aux diverses échéances.

Nous souhaitions obtenir des valeurs chiffrées, utilisables pour notre usage interne et nous ne nous souciions pas d'aboutir à un modèle ayant une valeur générale. Ce n'est qu'à la fin des essais, en dépouillant les résultats que le modèle émergea : en cherchant à représenter l'influence de la surface spécifique, nous nous sommes aperçus qu'il était possible de faire ressortir des grandeurs, caractéristiques du clinker lui-même, et d'autres, caractéristiques des granulats du béton.

NATURE DES ESSAIS

Nous avons étudié les résistances en compression à 1, 2, 7 et 28 jours de mortiers AFNOR et de bétons composés à partir de 52 ciments résultant du broyage de 14 clinkers industriels.
Deux séries d'essais ont été faites :

TABLEAU I

Série 1 sur 4 clinkers (A à D)	Finesse Blaine (cm^2/g) des ciments broyés	2 800	3 650	4 500	—
	Taux de $\bar{S}$ (%) des ciments	2.8	3.2	3.6	—
	Résistances en compression mortier AFNOR à 1, 2, 7 et 28 jours Résistances en compression béton sur cylindres 16 x 32 cm à 1, 2, 7 et 28 jours Granulats siliceux 0 – 10 mm Dosage 425 kg/m^3 Rapport eau/ciment ajusté pour obtenir un affaissement de 5 cm au cône d'Abrams				
Série 2 sur 10 clinkers (E à N)	Finesse Blaine (cm^2/g) des ciments broyés	2 800	3 650	4 500	5 350
	Taux de $\bar{S}$ (%) des ciments	2.8	3.2	3.6	4.0
	Résistances en compression mortier AFNOR à 1, 2 et 28 jours Résistances en compression béton sur cylindres 16 x 32 cm à 1, 2, 7 et 28 jours Granulats siliceux 0 – 10 mm (identiques à ceux de la série 1) Dosage 300 kg/m^3 Rapport eau/ciment ajusté pour obtenir un affaissement de 8 cm au cône d'Abrams				

LE MODELE POUR LES MORTIERS

Ce modèle permet de calculer, pour un clinker donné, connaissant la finesse de mouture du ciment, la résistance en compression du mortier standard à n'importe quelle échéance, entre 1 et 28 jours. Il fait intervenir quatre grandeurs qui, ne dépendant pas de la surface spécifique du ciment, sont caractéristiques du clinker :

- Le Coefficient d'efficacité chimique du broyage : a
- La Résistance de référence à 1 jour : R_0
- Le Taux d'accroissement des résistances : r
- Le Dommage : D

Nous allons introduire successivement chacune de ces quatre grandeurs en montrant comment on peut les calculer à partir des résultats expérimentaux.

Le Coefficient d'efficacité chimique du broyage

Dans nos expériences, le développement des résistances R dépend de deux paramètres, le temps t et la surface spécifique S. Le principe du modèle consiste à réunir ces deux paramètres en un seul, appelé "temps équivalent" et noté u ; u est, lui-même, fonction de t et de S. On écrit :

$$R(t,S) = R(u) \text{ avec } u = u(t,S)$$

L'expression de la fonction u est construite en trois étapes A, B, C :

A) On admet que, si le clinker était monophasé, on pourrait écrire :

$$u.S_o = t.S$$

S_o étant une surface spécifique de référence choisie arbitrairement.

B) Pour tenir compte de ce que le clinker est, en fait, polyphasé, on définit une "surface chimiquement équivalente", notée S', telle que :

$$R(t,S) = R(u) \text{ avec } u.S_o = t.S'$$

Ces deux équations permettent de déterminer S' pour chaque valeur de S. En pratique, il est commode de représenter, pour chaque valeur de S, la variation de R en fonction de Log t ; le changement de variable de t à u s'écrit :

$$\text{Log } u = \text{Log } t + \text{Log } S'/S_o$$

et correspond à une translation des courbes parallèlement à l'axe des temps (figure 1).

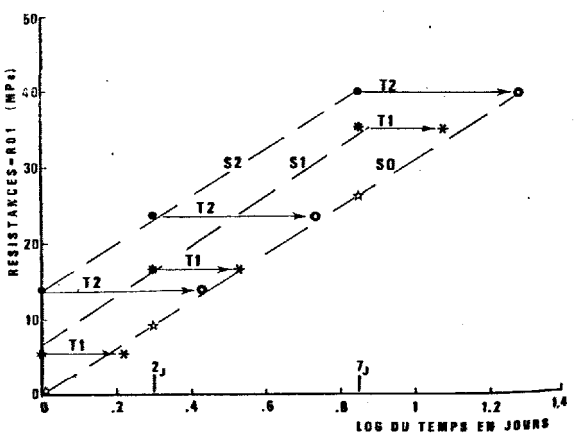

Figure 1 : Construction de la droite représentant la variation de la résistance de compression en fonction du temps indépendamment de la finesse.
Laisser tels quels les points (*) représentant la mouture la plus grossière S_o.
Translater les points (+) représentant la finesse S_1 d'une translation T_1 parallèle à l'axe de temps.
Translater les points (○) représentant la finesse S_2 d'une translation T_2 parallèle à l'axe de temps.
Choisir T_1 et T_2 de telle sorte que l'ensemble des points s'alignent le mieux possible. Le résultat de la construction se trouve figure 2.

On prend comme surface spécifique de référence S_o la valeur correspondant à la mouture la plus grossière (S_o = 2800 cm^2/g). Pour cette finesse de référence on pose par convention que u = t (et donc S' = S_o) ; la courbe R(Log t), correspondant à cette finesse de référence, ne subit aucune translation. Les autres courbes

J. BARON*, R. GUYOT*
* LAFARGE COPPEE RECHERCHE, France

correspondant aux autres finesses S, sont translatées de $T = \text{Log } S'/S_o$. Les valeurs de T pour chaque S sont calculées statistiquement de manière à optimiser la coïncidence de toutes les courbes.

C) Pour achever la détermination de la fonction u, il suffit de relier S' à S par une relation empirique telle que si $S = S_o$ alors $S' = S$. Les résultats expérimentaux s'accordent approximativement avec la relation linéaire :

$$(S'/S - 1) = (S/S_o - 1).a$$

Le coefficient de cette relation, a, qui suffit à lui seul à définir le temps équivalent u, est appelé Coefficient d'efficacité chimique du broyage ; il est caractéristique du clinker et permet de prévoir l'effet de la finesse sur la vitesse de développement des résistances.

La Résistance de référence à 1 jour et le Taux d'accroissement des résistances

On étudie maintenant la relation R = R(u). La figure 2 montre, à titre d'exemple, la courbe unique, indépendante de la finesse, obtenue pour le clinker C, après le changement de variable de t en u. Entre 1 et 7 jours, cette courbe est linéaire en Log u ; il en est de même pour l'ensemble des courbes correspondant aux 14 clinkers étudiés. Dans tous les cas, on peut écrire:

$$R = R_{o1} + r \text{ Log } u \quad \text{pour} \quad 1 \text{ j} < u < 10 \text{ j}$$

Cette équation définit deux nouvelles grandeurs, caractéristiques de chaque clinker :

R_{o1} : La Résistance de référence à 1 jour (Résistance à 1 jour lorsque le clinker est broyé à la finesse de référence S_o)

r : Taux d'accroissement des résistances (accroissement des résistances entre 1 et 10 jours pour la finesse de référence).

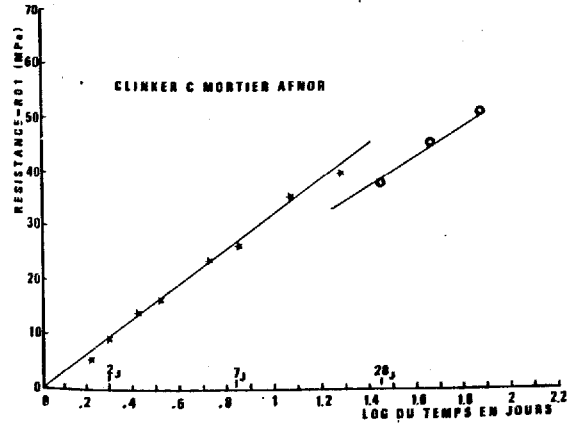

Figure 2 : Variation de la résistance en compression sur mortier AFNOR en fonction du temps équivalent.

Le Dommage

Comme la courbe de la figure 2, toutes les courbes homologues correspondant à l'ensemble des clinkers étudiés, présentent un décrochement qui survient entre 10 et 20 jours. Pour rendre compte de cet effet sans modifier la forme de l'équation précédente on introduit un coefficient (1-D) qui réduit la pente r ; on écrit:

$$R = R_{o1} + (1-D) \, . \, r \, . \, \text{Log } u \quad \text{pour} \quad u > 20 \text{ j}$$

Par analogie avec le paramètre qui intervient en Mécanique de l'endommagement, le coefficient D qui varie de 0 (aucune réduction) à 1 (accroissement de résistance nul) est appelé le Dommage (Cf, infra : Discussion).

Valeurs des 4 caractéristiques pour les 14 clinkers étudiés

Ces valeurs sont données dans la partie gauche (Mortier) du tableau 2 (page suivante). Elles appellent les commentaires suivants :

a) Il existe une corrélation inverse entre R_{o1} et r (figure 3) ; en général - sauf deux notables exceptions - l'accroissement des résistances après 1 jour est d'autant plus rapide que la résistance à 1 jour est plus faible. On retrouve là un résultat connu mais exprimé, cette fois, indépendamment de la finesse.

b) R_{o1} ou r d'une part, a et D d'autre part, forment un ensemble de trois grandeurs indépendantes, nécessaires pour caractériser le développement des résistances pour n'importe quelle finesse de mouture.

c) Les valeurs de ces caractéristiques varient dans une gamme étendue et, à l'intérieur de cette gamme de variation, toutes les classes intermédiaires sont représentées. Il y a donc, en principe, une grande variété de clinkers possibles.

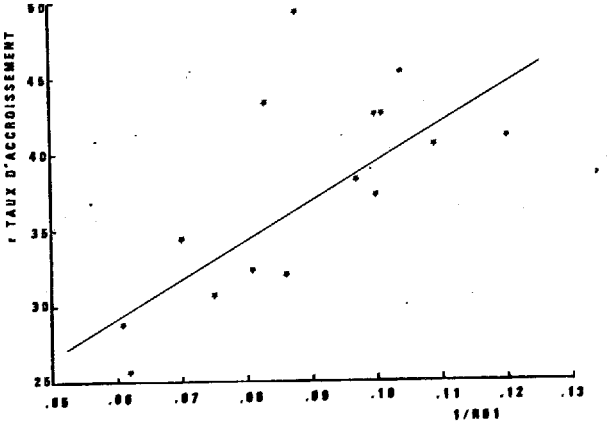

Figure 3 : Relation entre r (taux d'accroissement de la résistance lorsque l'âge est multiplié par 10) et l'inverse de R_{o1}, résistance à 1 jour à la finesse la plus grossière (finesse de référence S_o)

EXTENSION DU MODELE AUX BETONS

Le modèle permet de calculer, pour un clinker et des granulats donnés, connaissant la finesse de mouture du ciment, la résistance en compression à n'importe quelle échéance entre 1 et 28 jours.

Le Coefficient d'efficacité chimique du broyage a, est considéré comme une caractéristique du clinker et prend donc la valeur donnée au tableau 2, indépendamment de la nature des granulats et du rapport E/C.

Les trois autres grandeurs prennent des valeurs qui peuvent dépendre des granulats et du rapport E/C.

J. BARON*, R. GUYOT*
* LAFARGE COPPEE RECHERCHE, France

TABLEAU 2

Valeurs des caractéristiques pour les mortiers et les bétons

	Mortiers				Bétons				
Clinkers	a	R_{o1}	r	D	R_{o1b}	r_b	D_b	k_1	k
		MPa	MPa		MPa	MPa			
Série 1									
A	0,16	8,3	41,1	0,17	5,3	28,2	0,15	0,64	0,69
B	0,80	16,1	25,7	0,09	11,8	18,0	0,14	0,73	0,70
C	0,91	11,6	32,0	0,16	9,2	22,0	0,18	0,79	0,69
D	0,11	10,0	37,2	0,04	8,0	28,8	0,14	0,80	0,77
Moyenne 1							0,15	0,74	0,71
Série 2									
E	-0,06	10,3	38,2	0,00	5,7	27,0	0,06	0,55	0,86
F	1,40	13,4	30,7	0,21	8,4	22,4	0,15	0,63	0,72
G	0,57	12,1	43,3	0,34	6,1	28,2	0,24	0,50	0,65
H	0,76	12,3	32,7	0,19	6,2	23,2	0,04	0,50	0,71
I	-0,26	11,3	49,3	0,31	6,1	27,7	0,08	0,53	0,56
J	0,81	16,5	28,8	0,22	9,0	22,9	0,13	0,55	0,80
K	0,15	9,2	40,5	0,13	6,3	25,0	0,00	0,68	0,62
L	0,05	9,9	42,5	0,16	4,0	27,5	0,06	0,40	0,65
M	0,33	10,0	42,5	0,25	5,4	24,9	0,05	0,54	0,56
N	1,30	14,3	34,4	0,16	8,1	24,9	0,10	0,56	0,72
Moyenne 2							0,09	0,54	0,69
Moyenne 1 + 2				0,24					

Les bétons étudiés ont des rapports E/C variables, différents du rapport E/C = 0,5, qui est celui du mortier standard. Pour s'affranchir de l'influence du rapport E/C on commence par calculer la résistance R qu'aurait le béton si son rapport E/C était égal à 0,5. Ce calcul se fait en appliquant la formule de Féret :

$$(R/R_{exp})^{1/2} = 0,359\ (1-3,15\ (E+V)/C)$$

où :
3,15 est la masse volumique du ciment ; E et C, respectivement les poids d'eau et de ciment ; V, le volume d'air, non mesuré dans nos expériences, est pris égal à 0,30. Le coefficient 0,356 est tel que $R = R_{exp}$ pour les valeurs du mortier standard E/C = 0,5 et V = 0,30

Le modèle est appliqué aux résistances R calculées de cette façon.

La variation de R en fonction de Log u (figure 4) peut être représentée, comme pour le mortier standard, par les équations :

$$R = R_{o1b} + r_b \text{ Log } u \quad \text{pour} \quad 1\ j < u < 10\ j$$

$$R = R_{o1b} + (1-D_b)\ r_b \text{ Log } u \quad \text{pour} \quad u > 20\ j$$

Les grandeurs R_{o1b}, r_b et D_b dépendent du clinker, des granulats et du rapport E/C.

Afin de séparer l'influence du clinker et celle des granulats, on pose :

$$R_{o1b} = k_1\ R_{o1} \quad \text{et} \quad r_b = k\ r$$

R_{o1} et r étant les caractéristiques du clinker définies au paragraphe précédent. Le tableau 2 (dans sa partie droite - Bétons) donne les valeurs obtenues pour les 14 clinkers étudiés.

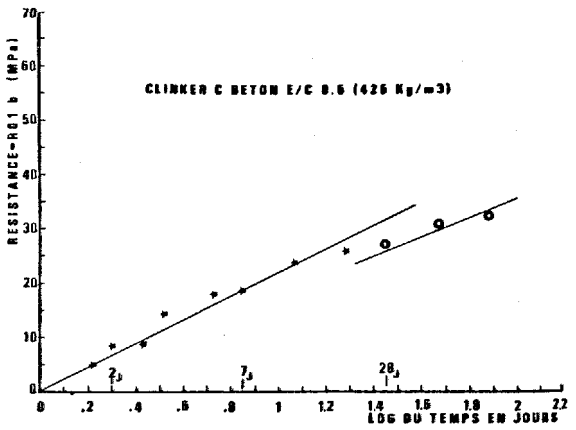

Figure 4 : Variation de la résistance en compression sur béton en fonction du temps équivalent.

On observe que les valeurs des coefficients k_1 et k dépendent peu des clinkers ; ils dépendraient probablement davantage de la nature minéralogique des granulats mais ce facteur n'était pas inclus dans nos expériences. Nous proposons d'appeler :

k : le Coefficient d'auréole
k_1 : le Coefficient d'auréole précoce

Les moyennes des valeurs de k_1 et k sur l'ensemble des clinkers montrent que :

- Le Coefficient d'auréole est, en moyenne, de 0,71 pour la série 1 (E/C voisin de 0,45) et de 0,69 pour la série 2 (E/C voisin de 0,64) Il est donc indépendant de E/C (l'influence du rapport E/C a été prise en compte précédemment en appliquant la formule de Féret aux résultats bruts).

- Le rapport k_1/k est voisin de 1 pour un dosage en ciment de 425 kg/m^3 ; il est de 0,8 pour un dosage en ciment de 300 kg/m^3.

Concernant le Dommage, il ne paraît pas possible de séparer de la même façon l'influence du granulat et celle du clinker ; la corrélation entre les valeurs mesurées sur mortier et sur béton n'est pas significative. En moyenne, le Dommage pour les bétons, diminue avec le dosage en ciment : 0,15 pour 425 kg/m^3 et 0,09 pour 300 kg/m^3. Si l'on compare les valeurs moyennes de Dommage pour les mortiers et pour les bétons, on peut conjecturer qu'elles témoignent de deux effets antagonistes :

a) le mortier est plus riche en ciment (500 contre 425 ou 300 kg/m^3) ce qui tendrait à augmenter le Dommage

b) mais le plus gros granulat du mortier est 5 fois plus fin que celui du béton (2 mm contre 10 mm) ce qui tendrait à réduire le Dommage

COMPARAISON MODELE/EXPERIENCE

Pour une finesse de mouture et pour une échéance donnée, la résistance trouvée expérimentalement est notée $R_{ex.}$ et la valeur calculée par le modèle $R_{th.}$ On calcule le rapport R_{th}/R_{ex}.

La comparaison modèle/expérience consiste à étudier la distribution statistique des valeurs de ce rapport; cette distribution représentée sur la figure 5 pour le mortier standard d'une part et pour les bétons d'autre part est à peu près gaussienne dans les deux cas,

J. BARON*, R. GUYOT*
* LAFARGE COPPEE RECHERCHE, France

avec cependant quelques résultats aberrants en "queues de courbe".

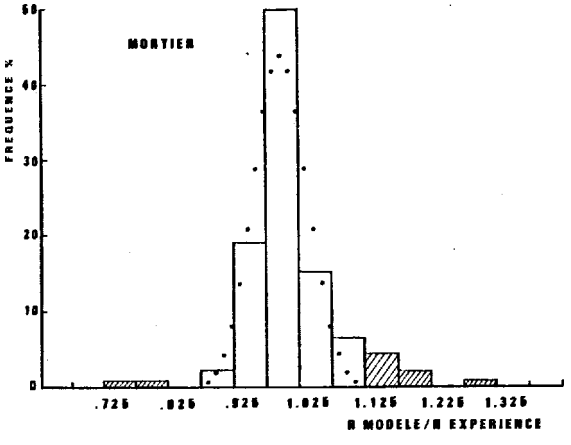

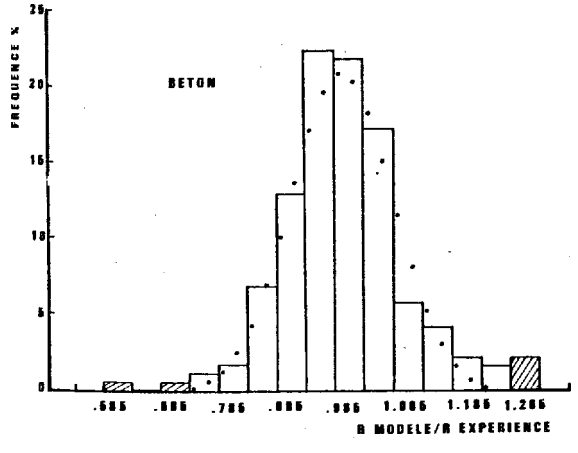

Figures 5 a (Mortiers) et 5 b (Bétons) : Histogramme des valeurs du rapport résistance calculée sur résistance expérimentale pour l'ensemble des valeurs à 1, 2, 7 et 28 jours.
Le tracé en pointillé représente l'ajustement de la distribution à une courbe de Gauss lorsqu'on élimine les résultats représentés dans les parties hachurées.

La comparaison modèle/expérience se résume comme suit :

TABLEAU 3

Distribution du rapport R_{th}/R_{ex}

	Mortier standard	Béton
Nombre de résultats	154	194
Moyenne	1,0	1,0
Coefficient de variation	6 %	9 %
Coefficient de variation dans 1 test de répétabilité	3 %	6 %
Proportion de résultats aberrants	10 %	5 %

Les résultats qualifiés ici "d'aberrants" sont ceux dont la fréquence est supérieure à ce que laisse prévoir la distribution gaussienne.

Dans la majorité des cas, l'imprécision de la prévision suit une loi gaussienne. L'imprécision relative est la somme de la dispersion expérimentale et de l'imprécision strictement due au modèle. La dispersion expérimentale peut être évaluée à partir d'un test de répétabilité ; les valeurs données dans le tableau, 3 % pour les mortiers, 6 % pour les bétons, sont des valeurs pratiquement minimales. Par différence, on peut estimer que l'imprécision proprement due au modèle est de l'ordre de 3 %.

DISCUSSION

Le modèle que nous proposons est semi-empirique. Sa première justification est donc d'être en accord avec les résultats expérimentaux ; néanmoins la signification physique de deux aspects particuliers du modèle doit être discutée : le changement de variable de t en u et l'introduction d'un Dommage D.

Le changement de variable de t en u

Il revient à supposer que la vitesse de développement de la résistance R à un instant donné est :

- fonction de la valeur de la résistance à cet instant ;
- proportionnel à la surface spécifique du ciment anhydre ;

Soit : $\frac{\partial R}{\partial t} = f(R).S$

L'intégration de cette équation différentielle donne une fonction R (tS) où le produit tS forme une variable unique ce qui correspond bien au modèle que nous nous sommes donné.

Le Dommage

L'existence d'une discontinuité dans la courbe R(t) entre 7 et 28 jours peut surprendre et être mise en doute. N'est-ce pas un effet de la transformation opérée sur les courbes ? Pour répondre à cette question il faut étudier l'évolution des résistances sur un même ciment en multipliant les échéances d'essai. S'étant aperçu qu'un tel protocole, malgré sa simplicité, était très rare, le CERILH a fait en 1985 une série d'essais au titre de première vérification de notre hypothèse. Dans cette série le ciment est un CPA pauvre en C3A et les essais sont faits sur mortier standard ; on mesure à la fois la résistance en compression et la contraction Le Chatelier (Chemical shrinkage). Cette dernière caractéristique qui peut être mise en relation avec l'avancement des réactions d'hydratation, ne présente aucune discontinuité significative entre 1 et 90 jours ; en revanche une discontinuité survenant entre 10 et 20 jours est nettement visible dans l'évolution de la résistance (figure 6). Ceci suggère une cause mécanique et peut justifier le terme de "Dommage" que nous avons choisi. Le Dommage pourrait être, pensons nous, une microfissuration résultant des contraintes qui accompagnent nécessairement la formation de la texture (2) ; dans ce cas, on comprendrait qu'il puisse augmenter avec le dosage en ciment et la dimension des plus gros granulats. Ce n'est qu'une hypothèse mais qui pourrait être aisément vérifiée en suivant, par exemple, l'émission acoustique des éprouvettes entre 1 et 90 jours.

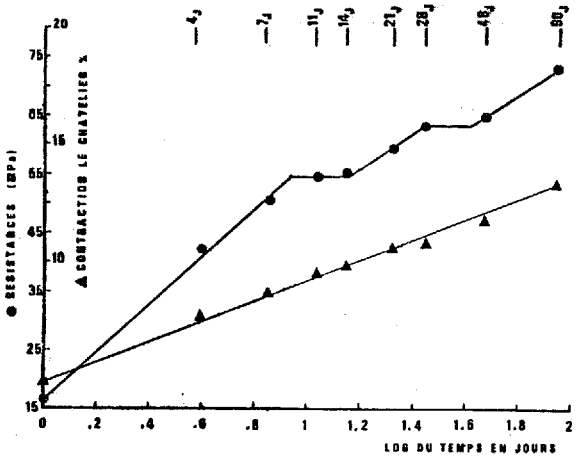

Figure 6 : Variation de la résistance standard d'un mortier AFNOR et de la concentration Le Chatelier en fonction du logarithme du temps en jours pour un même CPA (d'après le CERILH (1))

CONCLUSION

La résistance en compression d'un béton dépend du clinker, de sa finesse, du rapport E/C et du temps. L'intérêt du modèle semi-empirique que nous venons de présenter est de séparer, entièrement (pour les échéances de 1 à 10 jours) ou presque entièrement (au delà de 20 jours), l'influence du clinker et celle des granulats ; ce faisant, il ouvre de nouvelles perspectives d'étude et d'optimisation.

Clinker

A la place de la grandeur unique que constitue la classe de résistance du ciment, le modèle substitue : la finesse de mouture comme paramètre et deux grandeurs indépendantes, caractéristiques du clinker avant mouture (le Coefficient d'efficacité chimique du broyage et le Taux d'accroissement des résistances).

Granulat

Le modèle permet de caractériser l'influence globale des granulats par une seule grandeur (le Coefficient d'auréole) quand le rapport E/C est de l'ordre de 0,5 ou moins, ou, par deux grandeurs, quand le rapport E/C est de 0,6 ou plus. Dans ce dernier cas il faut introduire, en plus, un Coefficient d'auréole précoce, dont la valeur est toujours inférieure à celle du Coefficient d'auréole et qui s'applique aux résistances à 1 jour.

L'interaction clinker/granulat dans le phénomène de Dommage

Nos résultats montrent une discontinuité dans l'évolution des résistances entre 10 et 20 jours. Ce phénomène, s'il était confirmé devrait retenir l'attention ; nous le présentons ici comme une hypothèse, une invitation à des expérimentations complémentaires. Dans le modèle ce Dommage est caractérisé par une grandeur unique dont la valeur dépend indissociablement, du clinker, des granulats et du rapport E/C.

BIBLIOGRAPHIE

(1) L.J HOLLEBECQ Note interne du CERILH aimablement communiquée aux auteurs

(2) J. BARON
Déformations, contraintes et ruptures dans les bétons avant tout chargement in "Mécanique de la rupture" FNB, collège international des sciences de la construction, conseil international de la langue française, 1983

C.BERTRAND, C.BONET, P.GARDE
LAFARGE COPPEE RECHERCHE, France

NOVEL COMBUSTION and VOLATILIZATION DIAGNOSTIC TECHNIQUES in CEMENT KILNS

1 - INTRODUCTION

In recent years, most of the cement factories, for economical reasons, had to shift from fuel oil firing to pulverized fuel firing in their rotary kilns. Among the multiple problems created by this compulsory change, process problems in the kiln were particularly significant, arising from the differences in composition and combustion characteristics between the solid fuels and the liquid fuels previously used.

Moreover, among the pulverized fuels available (coals, petroleum cokes, solid residues), significant differences exist in ash content, volatiles content, sulfur content or calorific value.

On top of that, the transport of pulverized fuels is much more troublesome than the transport of liquid fuels, and fluctuations in the fuel mass flow rate at the tuyere are often the cause of difficulties to keep steady combustion conditions.

Instruments able to quantify the variations of the flame characteristics and shape due to a change in the mass flow rate, the composition, the granulometry or the nature of the fuel are practically absent from the market, if one excepts the classical one-colour pyrometers used to control the clinkerization zone temperature.

Consequently, a change in the combustion and heat transfer characteristics is very often only detected after it has had a significant effect on the clinker quality, or on the frequency of appearance of rings and concretions.

Therefore, LAFARGE COPPEE RECHERCHE has tried to develop its own investigation tools, adapted to the geometry and the conditions prevailing in the clinkerization zone of rotary kilns, and allowing to obtain an instantaneous (or quasi-instantaneous) information on the variations occurring in firing conditions, heat transfer or atmosphere composition in this zone.

For this purpose, three instruments have been constructed at L.C.R., with different external collaborations :

- an ellipsoidal radiometer probe, developed in collaboration with TOTAL-CFR (LE HAVRE, FRANCE).
- a microphone probe, developed with the C.N.R.S. (C.R.C.C.H.T., ORLEANS, FRANCE).
- a spectroradiometric probe, developed with the S.O.P.R.A. (BOIS-COLOMBES, FRANCE) and the C.N.R.S. (C.O.R.I.A., ROUEN, FRANCE).

They were designed to control specifically the following characteristics :

- the flame length (ellipsoidal radiometer and microphone probe) ;
- the emissivity and temperature profiles of the flame, the clinker and the wall (spectroradiometric probe) ;
- the presence in the furnace atmosphere of compounds representative of the volatilization process (spectroradiometric probe).

2 - THE ELLIPSOIDAL RADIOMETER PROBE

Radiation is the dominating heat transfer process in the combustion zone of the rotary kiln. It is well-known that, at fixed power input conditions, the radiative heat transfer profile from the flame to the furnace load exhibits a maximum, appearing more markedly and moving toward the burner mouth when the flame length decreases, i.e. when the combustion intensity increases (1).

From the measurement of the amplitude and the position of this maximum, one can then expect to derive some information on the variations of the flame length when parameters like thrust, primary air mass flow rate or amount of swirl at the tuyere are changed.

The ellipsoidal radiometer, initially developed at the International Flame Research Foundation (2), allows to measure the total radiation heat flux (kW/m2) received at a given location inside a furnace. It is represented on figure 1.

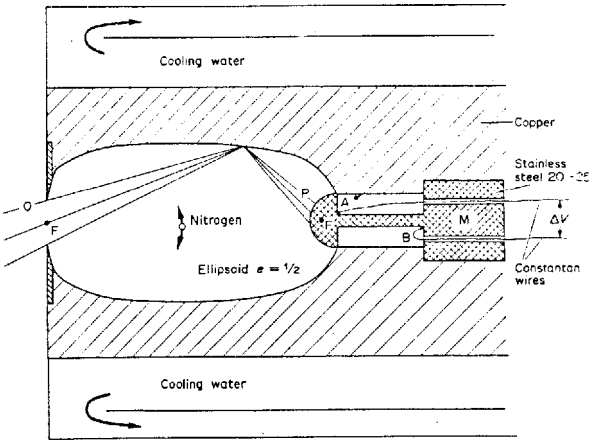

Figure 1 : Schematic diagram of the ellipsoidal radiometer.

Any incident radiation entering the orifice O is reflected by the gold-plated ellipsoidal cavity onto the thermopile P placed at the second focus of the ellipsoid. The power received is measured as the e.m.f. ΔV. The radiometer is first calibrated in a black-body furnace and then allows to measure directly the total radiation heat flux received from the hemisphere surrounding it. Nitrogen flowing in the cavity prevents its internal surface from being spoiled by particulates or condensable gases.

The axis of the ellipsoid is kept perpendicular to the flame axis, and the radiometer is inserted in a water-cooled probe allowing to move it along the furnace axis (Figure 2). The radiation heat transfer profile in the flame zone can then be recorded.

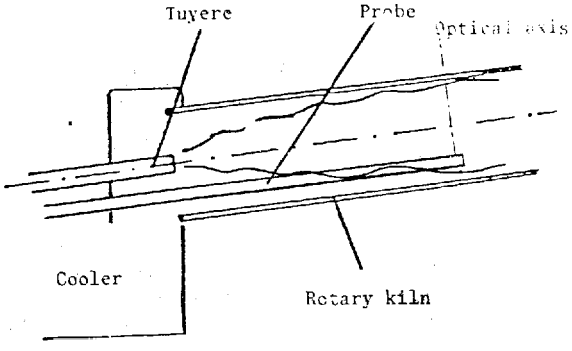

Figure 2 : Experimental set-up.

C.BERTRAND, C.BONET, P.GARDE
LAFARGE COPPEE RECHERCHE, France

C.L

NOVEL COMBUSTION and VOLATILIZATION DIAGNOSTIC TECHNIQUES in CEMENT KILNS

Since the kiln rotates, the probe can only be introduced into the furnace from the fixed end near the tuyere. But the flame in a cement kiln is very long (15 - 30 m) and thus, to have a chance to detect the maximum of the radiation heat flux profile, the water-cooled probe used must also be very long. The probe used here is 15 meters long and has a diameter of 0.20 meters.

3 - THE MICROPHONE PROBE

The combustion noise emitted by industrial turbulent flames burning with air is generally characterized by a broadband frequency spectrum in the region 50 - 700 Hz (Figure 3). This noise is most of the time 10 to 20 dB higher than the aerodynamic noise of the unignited jet.

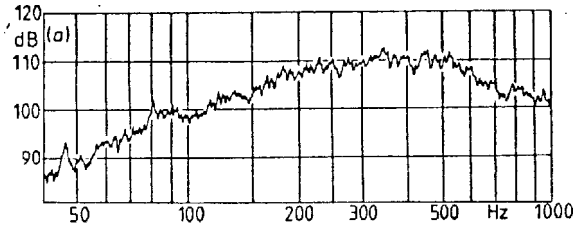

Figure 3 : Frequency spectrum of combustion noise.

In premixed flames, the combustion noise is very sensitive to the fuel/air ratio and can be used to control the flame stoichiometry (3).

In long diffusion flames, the combustion noise intensity does not depend any more on the fuel/air ratio, but depends strongly on the jet velocity (4).

Since the flame length of a cement kiln type flame depends strongly on the thrust of the fuel jet, the idea was to try to detect the variations of the flame length by recording the combustion noise inside the rotary kiln. The advantage of such a method over the one described in section 2 would be a large reduction of the measuring probe size and of the response time, since only one measurement of the acoustic pressure at one location near the flame is necessary.

A microphone probe for combustion noise measurements inside furnaces has already been described in the litterature (5). Its functioning principle is based on the damped Helmholtz resonator : the acoustic pressure is measured through a small duct (providing an efficient protection against the incoming thermal radiation) by a microphone diaphragm placed in a cavity. A 1 mm-thick rubber seal placed in the cavity damps completely the resonance and allows to get a flat response curve of the probe up to 700 Hz, at which frequency it acts as a low-pass filter eliminating the higher frequencies.

This probe has been inserted in a rotary kiln, protected by a double water-cooling system and a refractory head, as shown in figures 4 and 5. The probe used was 2 meters long and had a diameter of 60 mm.

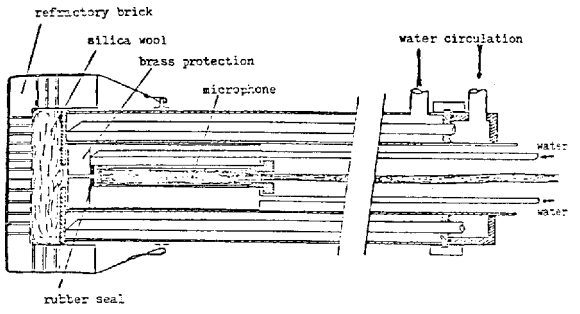

Figure 4 : Diagram of the microphone probe.

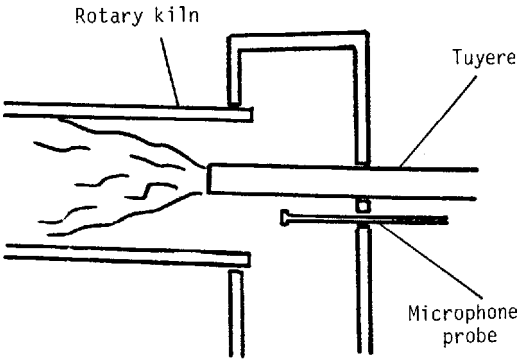

Figure 5 : Experimental set-up.

4 - THE SPECTRORADIOMETRIC PROBE

The ellipsoidal radiometer described in section 2 measures the total radiation received at one location inside the furnace, but does not give any spectral information on it. This spectral information is yet necessary if one is interested also in the measurement of temperature and emissivity profiles of the different parts of the furnace (wall, load, flame), or in the detection of emitting atomic or molecular species present in the furnace gases.

An optical head allowing to perform this kind of measurements is represented on figure 6.

The optical head collects a nearly parallel beam of radiation (2° divergent) and focuses it onto a bundle of three 50 m long optical fibers (diameter of each fiber : 600 µm). It is entirely water-cooled and a continuous flow of air prevents the quartz window from being obscured by particles deposits.

This optical head can replace the ellipsoidal radiometer at the extremity of the 15 meters long probe body represented in figure 2, which allows to extract the radiation, through the optical fibers, out of the rotary kiln.

C.BERTRAND, C.BONET, P.GARDE
LAFARGE COPPEE RECHERCHE, France

C.L

NOVEL COMBUSTION and VOLATILIZATION DIAGNOSTIC TECHNIQUES in CEMENT KILNS

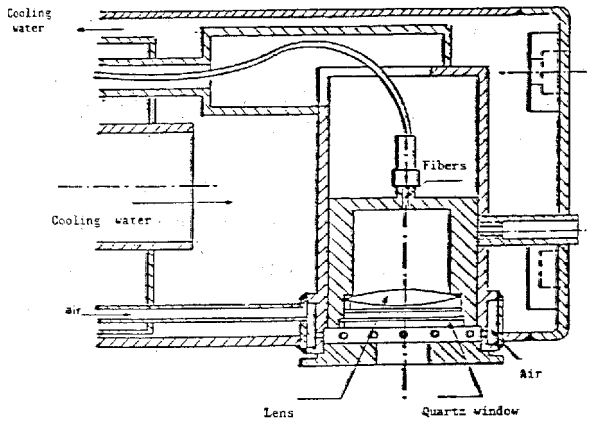

Figure 6 : Sketch of the optical head of the spectro-radiometer.

The bundle of optical fibers is connected to the entrance slit of a grating monochromator with spectral range 0.5 to 1.1 µm (Figure 7).

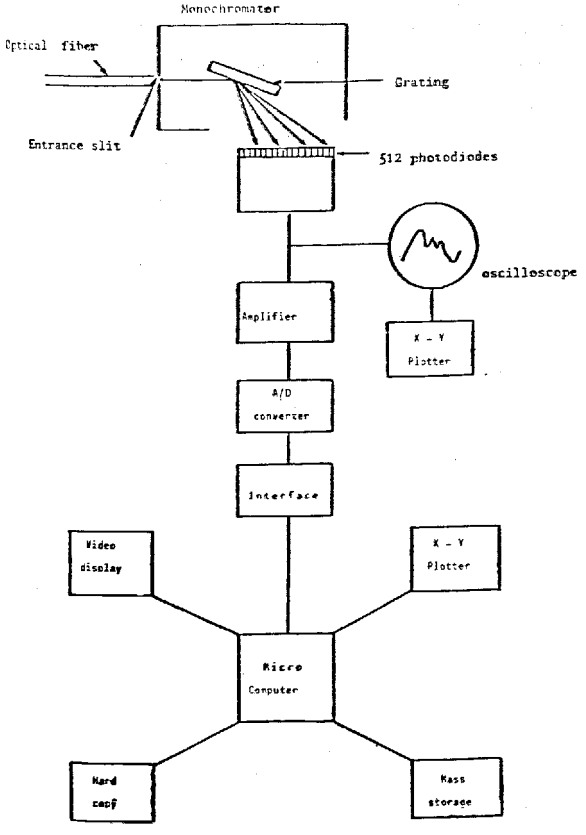

Figure 7 : Signal analysis.

The spectra are detected by an array of 512 photodiodes electronically scanned, and the signal, after amplification and digitalization, can be analysed on-line, or stored on disks through a micro-computer.

The acquisition time of one "instantaneous" spectrum is 32 ms. A preliminary laboratory calibration of the complete system by means of a black-body furnace allows to transform any incoming radiation signal into an absolute radiation intensity.

5 - MEASUREMENT OF THE FLAME LENGTH IN A ROTARY KILN

The measurements have been performed in a 35 meters long rotary kiln of CIMENTS LAFARGE FRANCE, equipped with the original L.C.E.-Tuyere allowing to vary the thrust without changing the mass flow rates of pulverized fuel and transport air. The thrust could be varied from 60 N to 180 N, leading to variable flame lengths from 16 to 12 meters, calculated by using the empirical Ruhland's equation. Different amounts of swirl could be applied via an internal primary air jet.

Both the ellipsoidal radiometer probe and the microphone probe were used in this experimental work. The results followed the expected trend, i.e. an increased amplitude of the peak heat flux, and a shift of its location toward the tuyere for the shortest flames, accompanied by an increase of the combustion noise (the shortest flames correspond to the highest thrusts).

Figure 8 shows the variation of the measured peak heat flux versus the flame length, and figure 9 shows the remarkable correlation obtained between the measured values of the peak heat flux and the recorded acoustic pressure for the entire set of non-swirling flames.

For swirling flames, correlations are less satisfactory, and further work is under way to try to understand the reasons of this different behaviour.

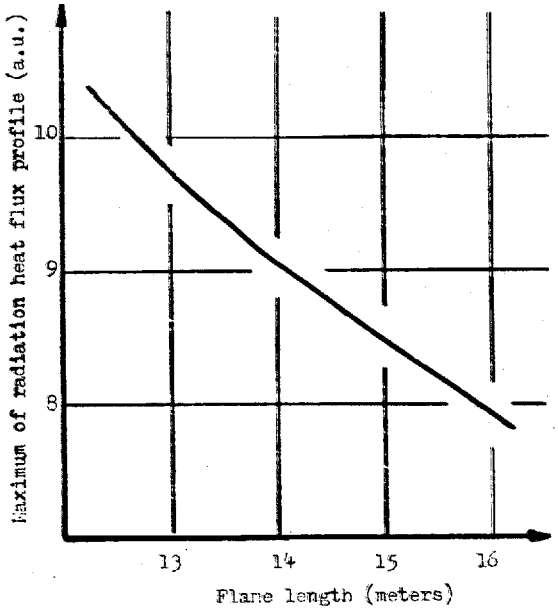

Figure 8 : Measured maximum of the heat flux profile versus calculated flame length.

C.BERTRAND, C.BONET, P.GARDE
LAFARGE COPPEE RECHERCHE, France

C.L

NOVEL COMBUSTION and VOLATILIZATION DIAGNOSTIC TECHNIQUES IN CEMENT KILNS

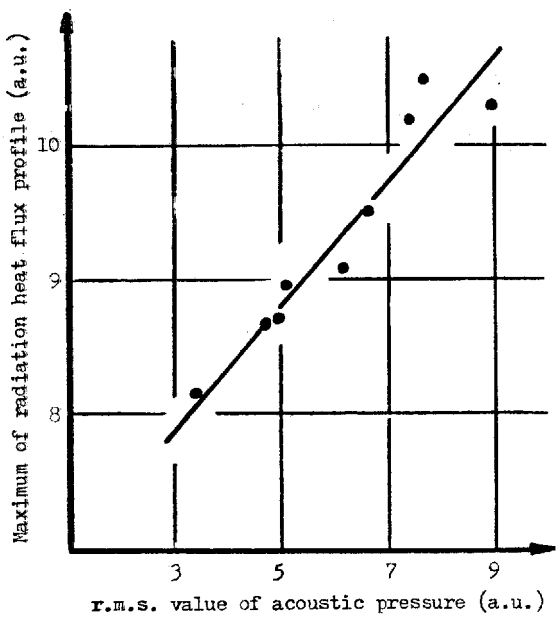

Figure 9 : Measured maximum of the heat flux profile versus measured r.m.s. value of the acoustic pressure.

6 - MEASUREMENT OF THE TEMPERATURE AND EMISSIVITY PROFILES, AND OF THE POTASSIUM CONCENTRATION

These measurements have been performed in a 60 meters long rotary kiln, by using the spectroradiometric probe described in section 4.

Figure 10 shows typical emission spectra taken in the furnace inside and outside the flame. The decay above 800 nm is due to the absorption of the optical fibers.

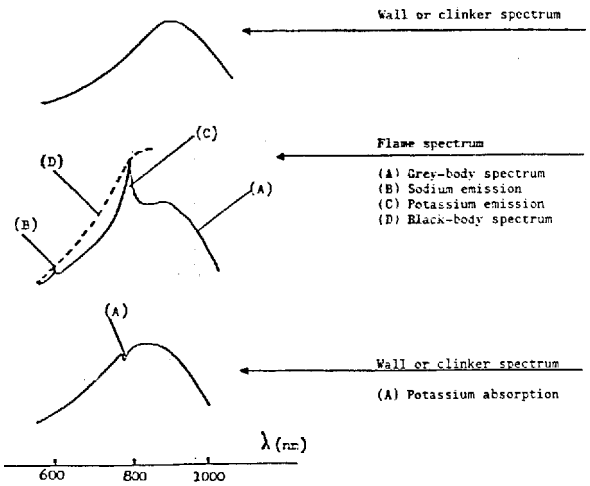

Figure 10 : Typical emission spectra recorded in the rotary kiln.

The observation of the recorded spectra leads to make the following remarks :

- the spectra of the radiation emitted by the flame, the clinker and the wall consist of very similar background spectra, on which emission and absorption lines are superimposed.
- the emission lines present on the flame radiation spectrum at 590 nm and 768 nm are characteristic of the presence in the furnace atmosphere of sodium and potassium, respectively. They are not found in the absence of clinker in the combustion zone.
- the absorption line on the clinker radiation spectrum is found on spectra recorded near the tuyere, where the temperature of the air coming from the cooler is lower (900-1000°C) than the clinker temperature : the radiation emitted by the clinker is absorbed at 768 nm by the relatively cold potassium vapour present in the air.
- the resolution of the monochromator used in this study was 50 Å. The potassium emission line observed is in fact an unresolved doublet of two lines of natural width of the order of 1 Å, separated by 34 Å. Yet, instantaneous half -widths of 100 to 200 Å are often recorded. Self-absorption broadening occurs then strongly, giving a means to derive the potassium concentration in the kiln atmosphere (6).
- It can be calculated, and it has already been mentioned in the litterature (7), that at the usual flame temperatures the potassium emission corresponds to the thermal equilibrium of the emitting excited state. Therefore the radiation intensity of the potassium peak can be considered as a black-body reference at the local flame temperature, allowing to calculate the instantaneous emissivity at this wavelength by the ratio between the radiation intensity of the background spectrum and the radiation intensity of the potassium peak.

Measurement of the temperature profiles

Further analyse of the spectra has shown that fuel-oil, coal and petroleum coke flames in the rotary kiln radiate, in the spectral range investigated, as grey bodies, (i.e. having an emissivity independent of the wavelength) of high emissivity (0.8-0.9). Consequently, axial temperature profiles of the flame can be derived via on-line two-wavelength pyrometry, like the temperatures of the wall or of the clinker, whose emissivities were measured very close to 1.

Figure 11 shows an example of an axial temperature profile measured via two-wavelength pyrometry.

The optical axis is directed downward, so that the temperature measured at the extremity of the kiln is first the clinker bed temperature. Then, as soon as the optical head reaches the combustion zone and is immerged into the flame, the measured temperature is representative of the flame temperature only, which increases up to 1770°C.

C.BERTRAND, C.BONET, P.GARDE
LAFARGE COPPEE RECHERCHE, France

C.L

NOVEL COMBUSTION and VOLATILIZATION DIAGNOSTIC TECHNIQUES in CEMENT KILNS

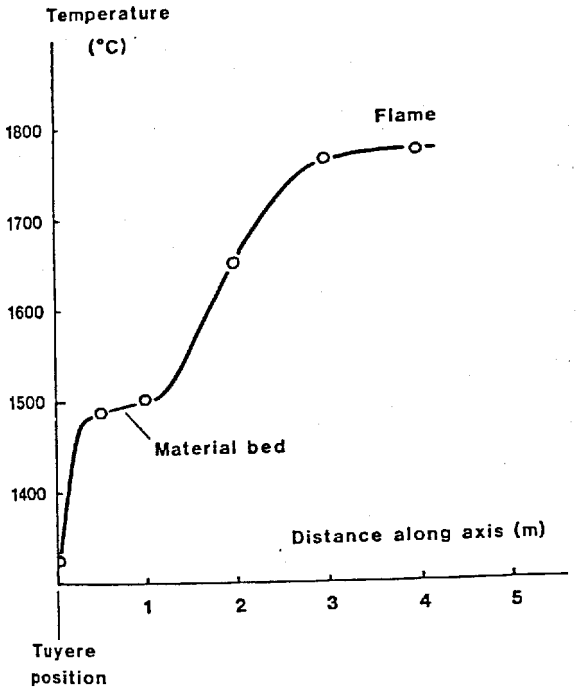

Figure 11 : Axial temperature profile measured in the rotary kiln.

Measurement of the potassium concentration

The self-absorption broadening of an emission line can be related to the concentration N_ℓ of the absorbing species (potassium) by considering the absorption coefficient χ_ν :

$$\chi_\nu = (c^2/8\pi\nu^2)\,(g_u/g_\ell)\,A_{u\ell}\,N_\ell$$

c is the light velocity.

ν is the central frequency of the emission line.

g_u et g_ℓ are the statistical weights of the excited state and the ground state, respectively.

$A_{u\ell}$ is the transition probability.

In an optically thick medium, the relationship linking χ_ν to the half-width of the broadened line depends on the profile of the line. Assuming a Voigt profile, instantaneous volume fractions of potassium as large as 0.5 to 1 % have been computed. They are characteristic of puffs of potassium liberated in the kiln atmosphere by the volatilization process occurring at the clinker surface.

7 - CONCLUSIONS

The recent development of new technologies allows to design investigation tools which can collect useful and accurate information even from very hostile media, like the clinkerization zone of a rotary kiln.

The instruments described here can be labeled as first generation instruments, designed to demonstrate the feasability of a certain type of in-situ measurements. Their development is required to allow the design of a second generation of instruments, generally simplified in order to fulfill only one specific function.

One can think, for instance, to derive from the spectroradiometric probe a more compact instrument able to continuously monitor the presence of potassium in the furnace atmosphere, giving then an information on the intensity of the volatilization process occuring in the combustion zone, and therefore allowing to limit it by an appropriate action on the input parameters of the kiln.

At this stage, these instruments are expected to become part of a more computerized conception of the process control.

ACKNOWLEDGEMENTS :

Part of this work (the development of the spectroradiometric probe) has been carried out with the financial support of the C.O.D.E.T.E.C. (Comité pour le Développement des Technologies d'Emploi du Charbon).

REFERENCES :

(1) S.MICHELFELDER, C.BERTRAND and R.PAYNE, "Transfert de Chaleur et Pollution", Rev. Gén. Therm. Fr., n° 196, pp. 305 - 329 (AVRIL 1978).

(2) J.CHEDAILLE and Y.BRAUD, "Industrial Flames, Vol. 1 : Measurements in Flames", Edward ARNOLD Pub., p. 57, 1972.

(3) C.BERTRAND, "Le Contrôle de la Combustion par la Mesure in-situ du Bruit émis par les Flammes Turbulentes", Rencontre S.F.T. 1984, ONERA-CERT, TOULOUSE , Section III.B, pp. 29 - 37 (28 - 30 MAI 1984).

(4) W.C.STRAHLE, "Combustion Noise", Prog. Energy Combust. Sci., Vol. 4, p. 157 (1978).

(5) C.BERTRAND, "A Microphone Probe for Noise Measurements inside Furnaces", J. Phys. E : Sci. Instrum., Vol. 16, pp. 345-348 (1983).

(6) F.CABANNES et J.CHAPELLE, "Spectroscopic Plasma Diagnostics", in Reactions under Plasma Conditions, M. VENUGOPALAN editor, Vol. 1, pp. 446 - 449, Wiley Inter Science (1971).

(7) P.H.TH.ZEEGERS and C.TH.J.ALKEMADE, "Chemiluminescence of OH-radicals and K-atoms by Radical Recombination in Flames", Tenth Symposium (International) on Combustion, pp. 33 - 40, The Combustion Institute, Pittsburgh (1965).

J. CHAPPUIS, LAFARGE COPPEE RECHERCHE, France

PHYSICAL ELEMENTARY MECHANISMS OF FLUIDIFICATION BY SUPERPLASTICIZERS OR WATER-REDUCING AGENTS.

INTRODUCTION

Our research is aimed at understanding the mechanisms by which water-reducing admixtures and superplasticizers modify the rheology of concrete and mortars.

However, real systems (commercial admixtures and Portland cement) appeared to us to be much too complicated for this study; for instance, it will be shown that there are several elementary mechanisms by which organic molecules can fluidify dense suspensions and that commonly used concrete admixtures act simultaneously through several of these mechanisms. It will also be shown that some of the fluidifying mechanisms are related to the surface properties of the particles and to the intersticial liquid characteristics. But, in the particular case of cement mixed with water, the particles initially have different compositions and the surfaces of these particles are transforming with time ; there are also important changes in the composition and pH of the liquid intersticial medium.

For these reasons, in the present work it was tried to find simple systems for which reliable scientific explanations could be given regarding the phenomenon of fluidification. For instance it was found that concrete fluidifying admixtures are equally efficient on much simpler aqueous suspensions like those in which the particles are made of a single constituent which is unreactive with water. An other degree of simplification has consisted in choosing and studying model molecules which could only operate through a single mechanism. The most part of the work presented in this paper has been performed with suspensions of α alumina in water and the chemical admixtures used have been particularly anionic molecules, non-ionic polymers and surfactants.
A preliminary study was first performed in order to understand the rheological behaviour of the alumina suspensions containing no admixtures.

The first part of this paper is an approach from the literature of the theoretical aspects related to the rheology of suspensions.

The second part summarizes the results of the preliminary study of alumina suspensions containing no admixtures.

Three elementary mechanisms have been identified and their studies are described in each of the three following parts, namely :

- in part 3, the modification of the surface charge of the particles by ionic molecules,

- in part 4, the entropic effects obtained with macromolecules,

- and in part 5, the diminution of the capillary forces obtained when using surfactants, in suspensions with a small water to solid ratio.

1 - THEORETICAL ASPECTS of the RHEOLOGY of SUSPENSIONS

A suspension is a two-phases system in which solid particles are suspended in a liquid medium ; when the particles are inferior to one micrometer the term "dispersion" is preferably used.

Most theories on the rheology of suspensions or dispersions, only take into account the hydrodynamic parameters and suppose that the effect of the interparticle forces are negligible. Such theories will be inadequate to explain the fluidifying effects of admixtures : by adding a small amount of superplasticizer in a suspension we do not change the hydrodynamic parameters of the system, but , of course, we considerably decrease the viscosity. We have then to consider the particle interactions which can have large effects on the rheology of the system, as mentioned in some recent papers like those by P.G. de GENNES (1), W.B. RUSSEL (2) or Th. F. TADROS (3).

In the absence of organic molecules the interparticle forces are of two kinds : van der Waals forces and electrical double layer interactions.

The van der Waals forces arise through the fact that even neutral atoms constitute systems of oscillating charges because of the presence of a positive nucleus and negative electrons. The force between two atoms is always attractive and in a system made of two particles there is an attractive force between every couple of atoms of the system. There is a resulting macroscopic force between the particles. For two particles of radius R, separated by a distance d, the van der Waals force can be expressed, when $d \ll R$, by $F = HR/12\,d^2$, H being the Hamaker coefficient of the system (4). In a liquid medium, when the two particles are made of the same material, the Hamaker coefficient is positive (or null) and the van der Waals force is always attractive, whatever the liquid (5).

The electrical double layer interactions have their origin in the surface electric charge which appears for most substances in contact with an aqueous medium ; with regards to inorganic oxides the electrical double layer at the oxide/water interface is considered to be established by the unequal adsorption of H^+ and OH^- (6). The oxide surfaces are positively charged at low pH and negatively charged at high pH. For each oxide, there is a pH value called PZC (Point of Zero Charge) for which the surface charge is null, but the values of the PZC can be very different for various oxides (7). Two particles, situated in a given liquid, possess surface charges of the same sign, if they are made of the same material : they will then exert between themselves repulsive double layer interactions.

In the case of dispersions of a single solid constituent in water there are hence attractive van der Waals forces and repulsive double layer interactions. It is experimentally known and it has been theoretically demonstrated in the D.L.V.O. theory (8,9) that suspensions are stable when repulsive double layer interactions are larger than van der Waals forces and that there is flocculation in the opposite case.

Regarding the rheological properties, we expect to have good flowing properties when repulsive interparticle forces dominate, that is to say when there is no contact between the particles. On the other hand, we expect to get high viscosities due to the cohesion between the particles when repulsive double layer interactions are smaller than the van der Waals forces. This point of view is supported by the fact that superplasticizers are known to have a dispersing effect as well.

The modification of the flowing properties of a suspension, when using organic molecules, can then be explained as a consequence of the modification of the surface forces between the particles ; in the suspension, the molecules adsorb at the surface of the particles : for this reason, van der Waals forces are reduced, and if the particles are charged the electrical interactions are deeply modified.

Another group of forces between particles are due to

the interaction of long chain molecules adsorbed on the particles (10,11). When two particles, each carrying an adsorbed polymer, come closer to each other such effects can lead to repulsion : each polymer chain, because of unavailability of space, loses its available conformations. Thus the contribution of these chains to the free energy of the system is increased resulting in a repulsive force ("steric" or "entropic" effect).

2 - RHEOLOGICAL BEHAVIOUR of ALUMINA SUSPENSIONS WHEN CONTAINING NO ADMIXTURE

This work, already published elsewhere (12) is merely summarized hereafter.

α alumina ALCOA A 16 S.G. with a mean particle diameter of 0.6 µm has been chosen to magnify the surface force effects. In order to be able to vary the surface charge of the particles, the alumina suspensions have been studied in all the pH range. Adjustement of pH has been done by using adequate quantities of HCl or NaOH. All suspensions are prepared 24 hours before measurements, so as to be in physico-chemical equilibrium.

Rheological measurements, sedimentation measurements and electrical characterizations of the surface charge of the alumina particles have been performed on each suspension. According to the different techniques used different concentrations were necessary. In this paper the concentrations of the suspensions are characterized by the ratio W/A (mass of water/mass of alumina powder).

Rheological measurements have been performed with a concentric cylinders viscometer "Rheomat 115". Suspensions having W/A ratios equal to 0.6 have been studied and according to their viscosities three couples of concentric cylinders have been used. All the experimental curves (shear rate vs shear stress) are significative of Bingham fluids. The viscosity was taken as the inverse of the slope of the straight part of each curve.

For the sedimentation test, suspensions with a W/A ratio equal to 10, are poured into test tubes having a one hundred graduations scale. At rest, with unstable suspensions, there appears a sharp interface between the settling part of the suspension and the more or less clear dispersing liquid. The number N of divisions above the sharp interface is plotted as a function of time. The rate of sedimentation is taken as the slope of the initial straight part of the curve.

The electric properties of the surface of the particles were investigated by measuring their electrophoretic mobilities by using a Rank Brothers Mark III zetameter. Measurements have been performed with suspensions containing 10 mg/l of alumina powder, in all the pH range. We have also supplied BALLION and JAFFREZIC-RENAULT (13), in "Laboratoire Pierre Süe" at Saclay, with our alumina samples and they have determined the surface charge of the particles vs pH, by adsorption measurements of radioactive Na^+ and Cl^-.

We reproduce on figure 1 the curve of the surface charge of the particles as a function of pH.

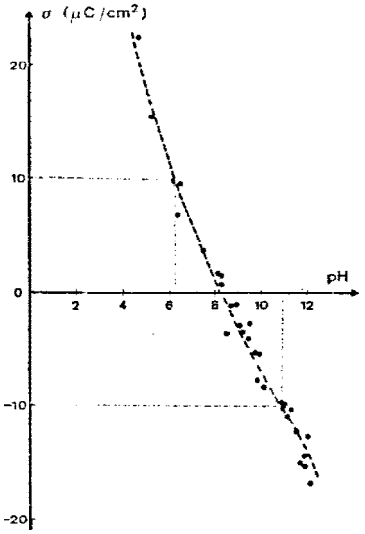

Fig. 1 : Surface charge of the alumina particles vs pH (from ref. 13).

From this work, the point of zero charge is equal to pH 8,5. The particles are positively charged at smaller pH and negatively charged at higher pH. The first results we got from the electrophoretic measurements were erroneous. After modification of a questionable mode of preparation of the very dilute suspensions we could finally get electrophoretic mobilities in agreement with the results of figure 1.

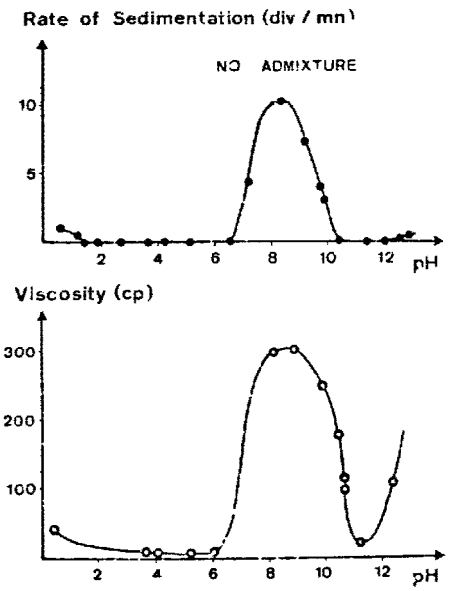

Fig. 2 : Rate of sedimentation and viscosity vs pH of alumina suspensions without any admixture.

On figure 2, the upper curve indicates the rate of sedimentation of alumina suspensions vs pH. These suspensions are unstable for pH between 6.5. an 10.5 that is to say two pH units on every side of the point of zero charge (8.5). The lower curve indicates the viscosities of alumina suspensions vs pH. In the pH range 6.5 - 10.5 the suspensions exhibit high viscosity values.

Refering to the D.L.V.O. theory (8, 9), sedimentation experiments can perfectly be explained if the double layer interactions are small in the high sedimentation pH range ($6,5 < pH < 10,5$). That is in perfect agreement with the results of figure 1 where it can be seen that the absolute value of the surface charge is the same for the two limiting pH values (10 μ C/cm2), that it is smaller inside that pH range and larger outside.

The flocculation for very acid ($pH < 1,5$) or very basic ($pH > 12$) media can be explained in the following way : the ionic strength of the medium, is, in such conditions, very high, and there is a compression of the double layer and hence an important decrease of the repulsive double layer interactions.

Figure 2 indicates that there is a great analogy between sedimentation and rheological behaviours. Hence, we can also explain the rheological behaviour of the suspensions by considering the relative magnitude of the attractive van der Waals forces and of the repulsive double layer interactions : when repulsive interactions are predominant, every particle is separated from the others and the viscosity of the suspen- is small ; on the other hand, when attractive interactions are predominant, there are contacts between the particles and the viscosity of the suspension is high.

3 - FLUIDIFICATION of the SUSPENSIONS by IONIC MOLECULES

We have selected for this part of the study the following admixture molecules :

- glucose and triethanolamine which are uncharged molecules,
- tripolyphosphate and a N.F.C. (naphtalene formaldehyde condensate), which are anionic molecules.

Depending on the tests, we have used alumina suspensions containing various admixture concentrations. However, in all the results described below, the admixture concentration was in all cases on the order of 1 to 2 % of the weight of the alumina powder.

On figures 3 to 6, the upper curves indicate the sedimentation behaviour of alumina suspensions having a W/A ratio equal to 10, and the lower curves indicate the rheological behaviour of alumina suspensions having a W/A ratio equal to 0.6. The admixtures used are respectively :

- glucose on figure 3,
- triethanolamine on figure 4,
- tripolyphosphate on figure 5,
- N.F.C. on figure 6.

With the uncharged molecules it can be seen that the suspensions flocculate and have high viscosity values in the pH range 6.5 - 10.5. The curves are very similar to those obtained with alumina suspensions containing no admixture. It is interesting to note that the maximal value of the viscosity is equal to about 300 centipoises without any admixture and is about 100 centipoises with glucose and triethanolamine. These two uncharged molecules have then a fluidifying effect but this effect is not related to a modification of the surface charge of the particles. This effect can merely be explained by a decrease of the van der Waals forces connected to the adsorption of the molecules at the surface of the particles.

With tripolyphosphate there is a pH range for which the suspensions flocculate and have high viscosity values. This pH range is no more centered around the initial point of zero charge (which was 8.5.) but around a new pH value close to 4.

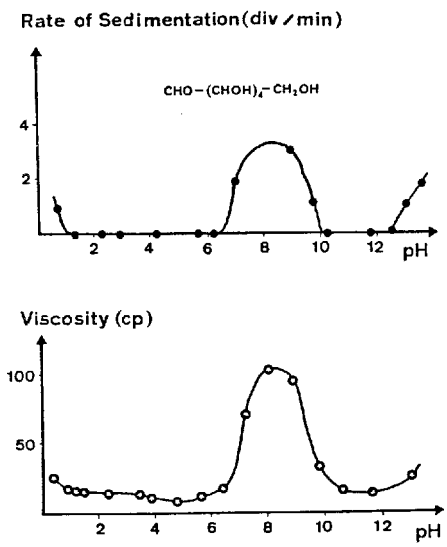

Fig. 3 : Rate of sedimentation and viscosity vs pH of alumina suspensions containing glucose.

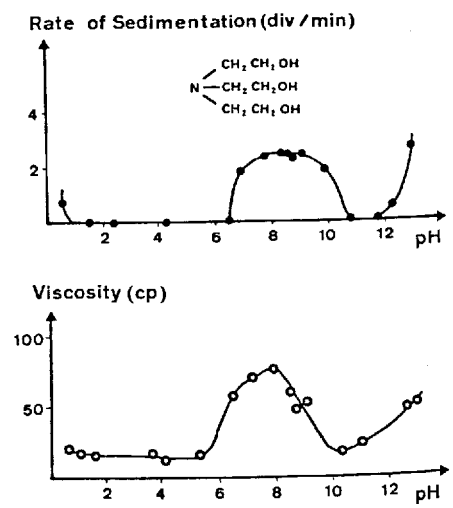

Fig. 4 : Rate of sedimentation and viscosity vs pH of alumina suspensions containing triethanolamine.

The same effect can be observed with the naphtalene formaldehyde condensate (see figure 6). In that case, we notice that for pH smaller than 4 whe have adverse effects probably due to the protonation of the negative groups SO_3^- of the N.F.C. molecule.

We propose to explain the displacement of the pH range where the suspensions flocculate, in the following way : there is a phenomenon of adsorption, that is to say of fixation of the admixture molecules on the solid surface ; when adsorbing at the surface

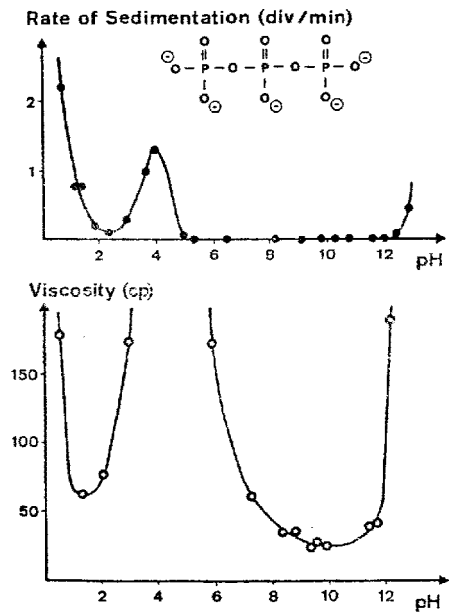

Fig. 5 : Rate of sedimentation and viscosity vs pH of alumina suspensions containing tripolyphosphate.

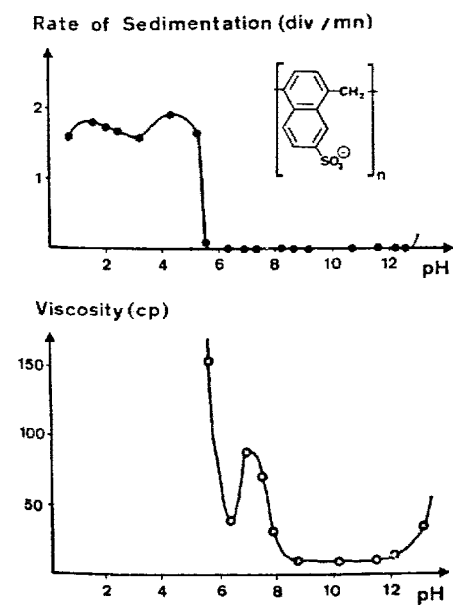

Fig. 6 : Rate of sedimentation and viscosity vs pH of alumina suspensions containing N.F.C. (Naphtalene formaldehyde condensate).

of the particles, the anionic molecules bring about their negative charges. These negative charges must be taken into account with the initial charge, for computing the resulting charge of the particles. In the presence of an anionic admixture, the particles have then a smaller point of zero charge around which the suspensions flocculate and exhibit high viscosity values.

This hypothesis has been confirmed by the following investigation : we have first made adsorption measurements of N.F.C. on alumina at different pH. This has been done by measuring with an ultraviolet spectrometer, and at the wavelength of 290 mμ, the equilibrium concentration of N.F.C. in suspensions containing a known weight of alumina. As the initial concentration of N.F.C. was known, it was then possible to compute for each measurement the adsorbed quantity of N.F.C. per gram or per square meter of alumina. The adsorption isotherms, for 5 different pH, are drawn on figure 7.

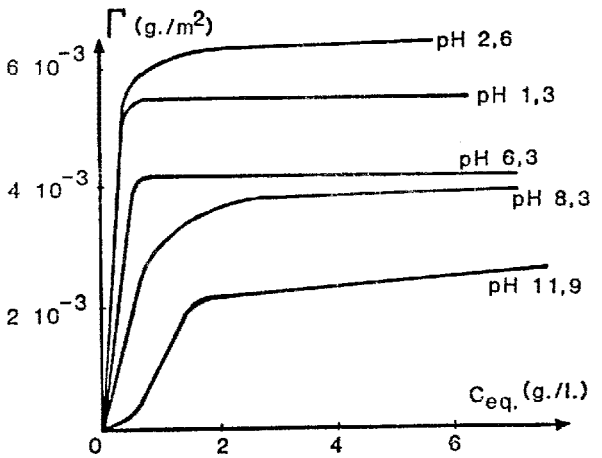

Fig. 7 : Adsorption Isotherms of N.F.C. on α alumina in different pH conditions.

From figure 7 it can be seen that the smaller the pH, the higher the amount adsorbed. This can be explained by considering the electrostatic interaction between the N.F.C. molecules (negatively charged) and the alumina surface, (differently charged according to the pH as indicated on figure 1). The smaller adsorption at pH 1.3 than at pH 2.6 can also be explained by the protonation of the SO_3^- groups in a very acid medium.

As we know that one mole of monomer of N.F.C. has a weight of 240 grams and carries one negative charge that is to say 96500 coulombs, it is possible to know the charge brought about on the surface of alumina by the adsorbed molecules. We have then considered a very simple model in which the surface charge of the particles is equal to the algebric sum of the initial charge of the particles and of the negative charge brought by the adsorbed molecules. From this model and for a given dosage of admixture it is possible to compute the resulting charge of the particles, for the different pH for which the adsorption isotherms have been measured. For instance, figure 8 shows the

computed surface charge of alumina in a given case (W/A = 10, N.F.C./A = 0,015).

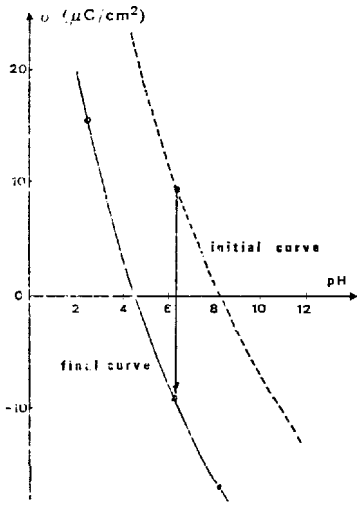

FIG. 8 : Computed charge from our simple additive model of alumina particles vs pH, in the case of a suspension with a W/A equal to 10 and containing an initial dosage of N.F.C. of 1.5 % of the weight of alumina.

It can be seen from figure 8 that there is a new point of zero charge, the value of which is slightly higher than pH 4. This value has been found in good agreement with the pH range in which the suspensions flocculate (see figure 6) and there is a good correlation with a direct measure by microelectrophoresis (see figure 9).

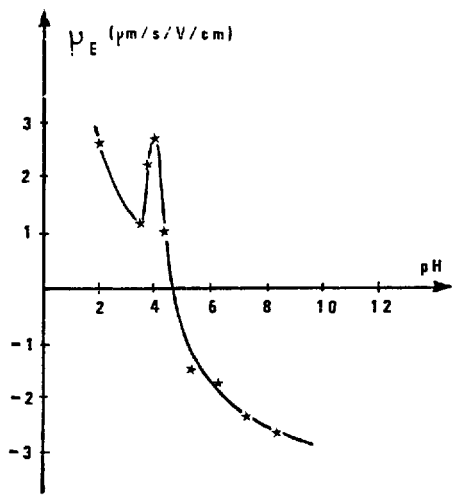

Fig. 9 : Electrokinetic mobility of alumina particles as a function of pH. The dilute suspension has been prepared by using particles and liquid after centrifugation of a suspension with a W/A equal to 10 and containing an initial dosage of N.F.C. of 1.5 % of the weight of alumina.

As a conclusion we think that the fluidifying mechanism of anionic molecules has been elucidated : these molecules, when adsorbing at the surface of the particles modify their surface charge. According to the pH value of the system, the absolute value of the surface charge may be increased or decreased, and the suspension may be respectively fluidified or thickened.

4 - FLUIDIFICATION of the SUSPENSIONS by ENTROPIC EFFECTS

Stabilization of colloidal dispersions by polymer adsorption plays an important role in diverse fields as pigment dispersion in paints, water treatment, mineral processing or cell aggregation. In 1951, MACKOR (14) proposed the first explanation of the stabilizing action of polymers by the decrease in configurational freedom of the segments of adsorbed polymer when the particles approach each other. MACKOR's simple model has since become the basis of the entropic stabilization theory. The theory has later been modified and refined by many investigators and FISCHER (15) was the first to introduce the osmotic repulsion concept. In their monograph on the subject, SATO and RUCH (16) point out that most of the modern theories are based on MACKOR'S or FISCHER'S works. However no universal theory has yet been established.

Entropic effects are usually not mentioned in the literature on admixtures, as a possible fluidifying mechanism. As such a result is however theoretically possible, we have then conducted an experimental study by using two non-ionic polymers, polyethylene glycol (PEG) and polyvinylpyrolidone (PVP). The choice of non-ionic polymers has been made so as to avoid the fluidifying charge effects but, in the practice polyelecrolytes would, of course, be preferable. Polyethyleneglycol of different molecular weights has been used (200, 400, 1500, 4000, 20.000 and 35.000). For polyvinylpyrolidone the molecular weights used were 10.000, 24.000, 40.000 and 360.000. Each of these products has been used at five different concentrations in the range 0-30 g/l, as admixtures of the alumina suspensions in all the pH range. We have then obtained 50 different curves which cannot be reproduced here ; however all theses curves have the same shape (flocculation and high viscosities in the pH range 6.5 - 10.5).

From a careful analysis of this experimental work we have drawn the following conclusions :

- there is a fluidification of the alumina suspensions due to the entropic effect. However, this effect is much smaller than the one due to the charged molecules,

- there is a thickening effect due to the increase of viscosity of the liquid of the suspension. This effect is most marked with high molecular weight polymers and with high concentrations,

- there is an other thickening effect at high molecular weights and low concentrations. As mentionned in the literature (16) such conditions are those which correspond to the bridging of the particles by polymer molecules,

- in the case of PEG and PVP with the studied alumina suspensions, the resulting effect is then a moderate fluidifying action, only in tye case of polymers with a medium molecular weight (in the range 2000-10.000) and only at medium dosages (5-10 g/l).

5 - FLUIDIFICATION of the SUSPENSIONS by DIMINUTION of the CAPILLARY FORCES

The solid volume fraction of the suspensions used in the preceding parts of this study was about 30 % in the case of the suspensions prepared for the rheological tests and about 2,5 % in the case of the suspensions prepared for the sedimentation tests. Such suspensions are two phases systems : they contain the solid particles and the liquid and no air is entrapped. There are no capillary forces in such systems and surfactants have no marked effect as fluidifying admixtures.

If we now consider mortars or concretes, a non-negligible percentage of air is contained in the mix, and this percentage is more important for smaller water to cement ratios. We have then three-phases systems (solid, liquid, air) in which the liquid is in the form of axially symmetrical meniscii between the solid particles. Every meniscus attracts the two particles between which it is situated. When there are such capillary forces between most of the particles of the suspension, its workability is highly reduced.

The capillary force which tends to bring together two particles is the sum of two terms :

- one is due to the surface tension of the liquid which is applied along the three phase line,

- the other is due to a smaller pressure inside the liquid as a consequence of Laplace law. As each of these terms is proportional to the surface tension of the liquid, the resulting force is also proportional to that surface tension. In order to reduce the capillary forces, one has then to use a surfactant, that is to say a product able to reduce considerably the surface tension of water, even when used at small dosages.

When the water to solid ratio is such that there are capillary forces in the suspensions, classical rheological measurements cannot be conducted because the systems are too cohesive. We have then decided to carry workability measurements with a "maniabilimètre à mortier L.C.L." ; the measure consists in determining the necessary time, for a given volume of mortar under vibration, to flow so as to reach a given mark in the apparatus.

A first series of experiments was conducted by using a tabular alumina 28-48 mesh (300-650 µm). For instance, the flowing time fo W/A = 0.20 suspensions was 30 seconds without admixture and 7 seconds when using butanol as a non-foaming surfactant.

Some other experiments have been conducted with normalized mortars (1350 g of normalized sand and 450 g of Portland cement) at different water-cement ratios namely 0.40 0.45 and 0.50. The measurement was made 5 minutes after the end of the mixing operation.

	FLOWING TIME		
W/C	0.40	0.45	0.50
Mortar without admixture	220"	20.1"	8.6"
Mortar with surfactant	81"	14.1"	2.8"

From the lecture of the table, the fluidifying action of the surfactant is obvious. These experiments thus confirm our theoretical approach concerning the diminution of the capillary forces.

6 - EXTRAPOLATION to the REAL CASE of COMMERCIAL ADMIXTURES in CONCRETE or MORTARS

In this study, by taking model systems we have been able to put into evidence three elementary mechanisms of fluidification of suspensions by organic molecules. Some other non-identified elementary mechanism might be detected in the future.

Regarding the practical systems, the different elementary mechanisms we have studied take place simultaneously ; for instance lignosulfonate are anionic, surfactive molecules, the molecular weight of which is appropriate to get an entropic effect. This is probably the major reason for which the earlier studies carried on practical systems, were not appropriate so as to clarify the way superplasticizers work. This also justifies, a posteriori, the proceeding which had been decided for this research.

REFERENCES

1 - P.G. de GENNES, Phys. Chem. Hydrodyn. 2, 31 (1981)

2 - W.B. RUSSEL, J. Rheol. 24, 287 (1980)

3 - Th. F. TADROS, Adv. Coll. and Int. Sci., 12, 141 (1980)

4 - A.W. ADAMSON, *"Physical Chemistry of Surfaces"* p. 331 J. WILEY N.Y. (1967)

5 - H.C. HAMAKER, Physica 4, 1058 (1937)

6 - D.N. FURLONG, D.E. YATE and T.W. HEALY, "Fondamental Properties of the Oxide/Aqueous Solution Interface" in *"Electrodes of Conductive Metallic Oxides"*. Part B., S.TRASATTI ed., ELSEVIER (1981)

7 - G.A. PARKS, Chem. Rev. 65, 177 (1965)

8 - B. DERJAGUIN and L. LANDAU, Acta Physicochim. 14, 633 (1941)

9 - E. VERWEY and J. Th. G. OVERBEEK, *"Theory of Stability of Lyophobic Colloids"*. ELSEVIER Amsterdam (1948)

10 - T. SATO and R. RUCH, *"Stabilization of Colloidal Dispersions by Polymer Adsorption"*. (Surfactant Science Series V.9). Marcel DEKKER, Inc. N.Y. (1980)

11 - R.H. OTTEWILL, J. Coll. and Int. Sci. 58, 357 (1977)

12 - J. CHAPPUIS in *"Concrete Rheology"* p. 38 ed : J. SKALNY. Materials Research Society (1982)

13 - D. BALLION and N. JAFFREZIC-RENAULT, "Influence de l'adsorption d'acides organiques sur le comportement électrophorétique des dispersions aqueuses d'alumine". 3° Meeting de la Société Générale d'Electrochimie. LYON 6-10 Sept. 1982

14 - E.L. MACKOR, J. Coll. Interf. Sci. 6, 492 (1951)

15 - E.W. FISCHER, Kolloid - Z, 160, 120 (1958)

16 - M.J. ROSEN, In *"Surfactants and Interfacial Phenomena"* p. 265, J. WILEY N.Y. (1978)

Parmi ces applications, nous pouvons citer :
- La prévision du domaine de stabilité des hydrates, lorsque le ciment est au contact d'un milieu réactionnel quelconque, soit dans le cadre de son utilisation (durabilité des bétons), soit au laboratoire, pour des études comme celle de la dissolution sélective des hydrates par des réactifs chimiques appropriés. Dans ce cas, la modélisation peut être étendue avec profit à divers milieux non aqueux.

L'étude des interactions des hydrates et des adjuvants, dont la plupart forment des complexes avec le calcium ou d'autres ions du système ciment-eau.
- Le calcul et le raffinement des constantes d'équilibre des hydrates, dont il manque de nombreux exemplaires pour décrire complètement l'hydratation, ou qui ne sont connues qu'avec une précision insuffisante. Dans ce cadre, il reste à étendre le domaine d'applications du modèle à l'étude des solutions solides comme les CSH ou la série des aluminates hydratés hexagonaux.
- Le calcul du taux de sursaturation de chacun des hydrates dans la séquence des réactions d'hydratation, qui constitue, à travers la relation : $A = R.T.Ln (S / S_x)$, où S est le produit ionique effectif, et S_x le produit de solubilité à l'équilibre, une mesure de l'affinité chimique A, qui est l'une des forces motrices produisant la création de la nouvelle structure au cours de l'hydratation.

A ce titre, les techniques de calcul et les concepts que nous avons développés ici constituent un premier élément d'un ensemble plus vaste, qui doit intégrer les autres forces du système, liées aux processus de diffusion au voisinage de l'interface anhydres-solution, à travers la couche d'hydrates poreuse, ainsi qu'aux gradients de température et éventuellement aux gradients électriques de double couche.

Bien que d'un abord plus difficile, l'approche analytique doit se montrer plus efficace à long terme que les approches empiriques, qui permettent d'établir des relations entre variables résultantes, comme la porosité, la chaleur d'hydratation, la résistance mécanique, mais sans permettre d'en comprendre et donc d'en prévoir les anomalies, ou d'en analyser les composantes.

7 - BIBLIOGRAPHIE

/1/ COURNIL M. ; GALTIER P. ; CONRAD F. ; Journal de chimie physique, 79, n°5, 1982, pp 427-433.

/2/ KARMAZSIN E. ; COMEL C. ; MURAT M. ; "Etude des systèmes $CaSO_4$-H_2O par calorimétrie isotherme. IV - Etablissement d'un modèle cinétique pour la réaction d'hydratation de $CaSO_4$,1/2H_2O -beta pur" Rev."Ciments, bétons, plâtres et chaux", n°740 1/83, pp 47-50.

/3/ BARRET P. "Modélisation et réactivité des matériaux". Ibid., n° 755, 4/85, pp 237-244.

/4/ DRON R. "Mécanisme de la prise du laitier granulé sous activation alcaline" - Rapport de recherche LCPC n°38, Sept.1974.

/5/ BERTANDIE D. "Contribution à l'étude cinétique de la formation des hydrates dans les solutions aqueuses obtenues à partir du ciment alumineux". Thèse Univ. Dijon 15/6/1977.

/6/ MENETRIER D. "Contribution à l'étude cinétique de la période intiiale d'hydratation du silicate tricalcique $3CaO,SiO_2$, constituant principal du ciment portland. Thèse Univ. Dijon, 15/6/77

/7/ BARRET P. ; BERTRANDIE D. ; BEAU D. "Calcium hydrocarboaluminate, carbonate, alumina gel and hydrated aluminates solubility diagram calculated in equilibrium with CO_{2g} and with Na^+_{aq} ions. Cement and concrete research, Vol. 13, 1982, pp 789-800.

/8/ SOUSTELLE M. et coll. "Stabilité thermodynamique des phases dans le système $CaO-Al_2O_3-H_2O$" (Ibid.), Vol.15, 1985, pp 421-430.

/9/ SOUSTELLE M. et coll "Application des propriétés thermodynamiques du système $CaO-Al_2O_3-CO_2-H_2O$ à l'hydratation des ciments alumineux". (Ibid.), vol. 15, 1985, pp 655-661.

/10/ ROSSET R. ; BAUER D. , DESBARRES J. "Chimie analytique des solutions et microinformatique". Ed. Masson, 1979.

/11/ DEFAY R. "Sortir de l'équilibre. Thermodynamique et capillarité". Ed;Univ. libre de Bruxelles;, 1981.

/12/ DEFAY R. ; PRIGOGINE I. ; BELLEMANS A., EVERETT D.H.. "Surface tension and adsoption". Ed. Longmans, Green, 1966.

/13/ BATES R.G. ; BOWER V.E. ; SMITH E.R. "Calcium hydroxyde as a high alkaline pH standard". Jour. of Res. N.B.S., Vol. 56, N°6, June 1956, pp 305-312.

/14/ JONES F.E. "The quaternary system $CaO-Al_2O_3-CaSO_4-H_2O$ at 20°C" TRANS. F. Society, 1939, pp 1484-1510.

/15/ YEATTS Leroy B. ; MARSHALL L. "Aqueous systems at high emperature. XVIII. Activity coefficient behaviour of calcium hydroxyde in aqueous sodium nitrate to the critical temperature of water". J.Phys.Chem., Vol.71,n° 8, 1967, pp 2641-2650.

/16/ JONES F.E. "The quinary system $CaO-Al_2O_3-CaSO_4-K_2O-H_2O$ (1% KOH) at 25°C". Ibid. (1% NaOH), J.Phys.Chem., Vol. 48, N° 6, Nov. 1944

/17/ HANSEN W.C. ; PRESSLER E.E. "Solubility of $Ca(OH)_2$ and $CaSO_4,2H_2O$ in dilute alkali solutions". Ind. and Eng.Chem., Vol.39, n° 10, Oct. 1947.

C. VERNET, Société des CIMENTS FRANCAIS - C.E.R.E.G. (FRANCE)

MODELISATION DES DIAGRAMMES D'EQUILIBRE DE SOLUBILITE DES HYDRATES - INTERACTIONS IONIQUES

C.L.

1 - INTRODUCTION

1.1 - NECESSITE D'UNE APPROCHE ANALYTIQUE ET D'UN MODELE DES REACTIONS D'HYDRATATION

Par suite de la généralisation de l'emploi des ajouts minéraux de toutes origines et des adjuvants organiques, la complexité des phénomènes et des systèmes chimiques mis en jeu au cours de l'hydratation devient de plus en plus grande. Sachant par ailleurs que le ciment portland est un milieu interactif, les approches purement empiriques perdent leur intérêt, car elles conduisent à multiplier sans cesse les plans d'expérience, sans garantie de succès. Il faut donc essayer de prévoir le comportement dynamique des ciments en affinant l'analyse des mécanismes qui en sont la base, et rechercher des modèles plus "physiques que "mathématiques", qui seraient de véritables outils pour le chimiste.

Des modèles de réactions d'hydratation ont été élaborés dans des cas simples, comme celui du plâtre /1/ /2/, prenant en compte les processus de diffusion dans un mécanisme de dissolution-précipitation. On peut donc espérer parvenir au même résultat dans le cas complexe du ciment portland, mais il faudra pour cela faire face à un certain nombre de difficultés, à la fois techniques et conceptuelles /3/.

1.2 - LA MODELISATION DE L'ETAT D'EQUILIBRE, UNE PREMIERE ETAPE VERS UN MODELE DYNAMIQUE DE L'HYDRATATION

Considérons le sytème ciment-eau, non plus comme un système fermé ordinaire, mais comme un ensemble de deux systèmes ouverts, le premier étant constitué des grains anhydres et le second étant constitué de la phase aqueuse et des hydrates. Les deux systèmes vont échanger de la matière (flux de diffusion) et de l'énergie à travers une frontière : l'interface réactionnelle.

La construction d'un modèle dynamique de l'hydratation devra donc intégrer l'évolution dans le temps de la surface de cette interface. Par ailleurs, devant la difficulté posée par la modélisation des régimes convectifs auxquels sont soumises les pâtes immobiles, il faudra se placer dans des conditions de diffusion stationnaire non convective, c'est-à-dire dans un réacteur ouvert, continu, agité, isotherme et isobare /3/.

Ces deux conditions ne sont pas encore totalement réunies aujourd'hui, mais il est possible, dans une première étape, d'étudier séparément le système hydrates-solution, avec l'objectif de modéliser son comportement lorsqu'il est soumis à des contraintes chimiques analogues à celles qui sont produites par le compartiment "anhydres".

Bien que l'hydratation soit un processus irréversible, la démarche précédente implique avant toute autre chose, la connaissance et la modélisation de l'état d'équilibre, qui constitue l'état de référence. Encore faut-il pour cela que le modèle soit suffisamment proche de la réalité physique, c'est-à-dire de la perception que nous pouvons en avoir à travers nos moyens d'investigation.

2 - MODELISATION DES EQUILIBRES DES HYDRATES DES CIMENTS. CONDITIONS POUR QUE LE MODELE SOIT UTILISABLE EN PRATIQUE

Nous pourrons considérer que le modèle satisfait au critère de représentativité physique, s'il permet de prévoir les valeurs expérimentales dans la limite de l'incertitude des mesures. Etudions en premier lieu les conditions qu'il faudra satisfaire pour atteindre cet objectif.

2.1 - PRISE EN COMPTE DES INTERACTIONS

Pour qu'un diagramme d'équilibre soit utilisable en pratique, il faut le construire en tenant compte de toutes les interactions ioniques, afin de déterminer avec une précision suffisante les constantes d'équlibre "pures", c'est-à-dire débarassées de l'influence du milieu. A ce titre, des progrès restent à faire, car on ne trouve dans la bibliographie que des modèles qui, soit négligent l'influence de la force ionique de la solution et assimilent activités et concentrations ioniques /4/, soit négligent la formation des complexes solubles entre les ions du système /5//6//7//8//9/. Compte tenu de l'expression des produits ioniques des hydrates, dans lesquels les activités des ions sont affectées dans la plupart des cas de puissances assez élevées, ces approximations conduisent à des erreurs systématiques sur la valeur des constantes et par voie de conséquence, sur les prévisions données par le modèle. C'est ainsi que, dans le cas de l'ettringite par exemple, pour laquelle le produit ionique apparent s'écrit :

$$(Ca^{2+})^6.(AlO_2^-)^2.(SO_4^{2-})^3.(OH^-)^4 = S'_9$$

le fait de négliger la formation des ions $CaOH^+$ aux environs de pH 12,8, en assimilant (Ca^{2+}) au calcium total, équivaut à surestimer (Ca^{2+}) d'un facteur supérieur à 2 et par suite la constante S'_9 d'un facteur $2^6 = 64$. Compte tenu de la précision avec laquelle sont connues la plupart des constantes de solubilité (rares sont celles qui sont connues à mieux qu'un facteur 10 près), cette erreur, qui semble a priori importante, l'est beaucoup moins que celle que l'on ferait en identifiant activités et concentrations des ions. En effet, le coefficient d'activité moyen de S est ici affecté de la puissance 15, ce qui représente un facteur 1000 à 10000 sur sa valeur, selon la force ionique de la solution.

2.2 - TECHNIQUES DE CALCUL

On conçoit maintenant qu'il soit difficile de prévoir à l'aide d'un modèle trop grossier les domaines de stabilité d'hydrates dont les produits ioniques ne diffèrent que d'une ou deux puissances de 10, ce qui est le cas des aluminates hydratés hexagonaux substitués, comme le monochloro, le monosulfo, et le monocarbo-aluminate. C'est ainsi que l'on est amené à renoncer, non seulement aux approximations faites sur les interactions, mais aussi à celles qui sont faites habituellement dans les calculs pour résoudre plus facilement le système d'équations représentant le système chimique à l'équilibre. Nous rejoignons ici la démarche utilisée par ROSSET /10/, l'un des premiers à prendre le chemin du traitement numérique des systèmes de la chimie analytique des solutions. Les progrès de la micro-informatique, présente aujourd'hui dans tous les laboratoires de recherche, permettent de développer cette technique avec le maximum de rigueur.

2.3 - CHOIX DU SYSTEME D'EQUATIONS

Bien que le système d'équations associé au système chimique ne soit pas linéaire en général, la réalité physique impose l'existence d'au moins une solution réelle, que l'on pourra calculer. Il faut cependant garder à l'esprit qu'une solution ne sera pas nécessairement représentative, car seuls nos acquis expérimentaux nous permettent de choisir le bon système d'équations, en nous indiquant la nature et le nombre de phases solides en équilibre avec un milieu particulier.

Prenons l'exemple du système /CaO, Al_2O_3, SO_3, R_2O, H_2O/, avec les phases solides gypse et ettringite. Supposons que l'on ignore l'existence de la portlandite, qui précipite au-delà d'une certaine valeur du pH : ceci aboutirait à trouver des solutions purement mathématiques et à poursuivre le tracé du diagramme dans un domaine où ce système n'existe plus "en réalité", à l'équilibre (dans le cas présent, le calcul s'avère quand même interessant lorsque le point figuratif de la solution se trouve dans le domaine de sursaturation de la portlandite, au cours de la "période dormante" des ciments).
Notons au passage que la comparaison des résultats expérimentaux conduirait ici à rechercher l'explication des écarts et par conséquent à identifier la phase manquante. Ce n'est donc pas le modèle lui-même qui est fructueux, mais sa confrontation avec les données expérimentales.
L'utilisation de la règle des phases peut s'avérer très utile, en permettant de faire le compte des équations du système : dans l'exemple précédent, avant la précipitation de la portlandite, la variance est égale à 2, pour 5 constituants indépendants, lorsque l'on tend vers l'équilibre à partir de la sursaturation. Par contre, la mise à l'équilibre à partir du domaine sous-saturé introduit une relation supplémentaire entre les variables, car alors la composition initiale de la solution est liée à la stoechiométrie des phases qui se dissocient. La variance devient égale à 1, avec 4 constituants indépendants. Ces 2 cas font évidemment appel à un traitement mathématique différent.

2.4 - COMPOSES NON STOECHIOMETRIQUES

Le problème de la représentativité des calculs se pose de façon particulièrement évidente dans le cas de la "coprécipitation", dont l'approche expérimentale est rendue difficile par le caractère pseudo-colloïdal des précipités, comme les hydroxydes des métaux de transition, les halogénures d'argent et les silicates de calcium hydratés (CSH des ciments). Dans ce dernier cas, en particulier, les moyens actuels d'investigation ne permettent pas de savoir si ce composé non stoechiométrique est un mélange de composés définis de structures voisines ou une solution solide dont la composition serait variable en fonction des conditions locales instantanées de précipitation. La résolution d'un tel système nécessite une relation entre les rapports stoechiométriques du précipité et la composition de la solution :
- dans le cas du mélange, on peut écrire par exemple que la probabilité de précipitation de chaque composé est inversement proportionnelle à sa solubilité, la somme des probabilités étant égale à 1. Cette démarche probabiliste implique la connaissance des produits de solubilité des constituants du mélange que l'on pourrait évaluer à partir des enthalpies libres de formation ;
- le cas des solutions solides exige une généralisation du concept de produit de solubilité, qui jusqu'ici ne s'applique qu'à des composés dont la stoechiométrie est indépendante de la composition de la solution (activité constante dans le solide).
Nous pensons que cette généralisation est possible et que l'on peut calculer l'expression du produit de solubilité généralisé en fonction des coefficients stoechiométriques, ou relier ces derniers aux activités des ions, à l'aide d'un calcul thermodynamique. Ceci fera l'objet d'une publication ultérieure.

2.5 - DEFINITION DE L'ETAT D'EQUILIBRE. DIMENSION DES CRISTAUX

Une autre difficulté d'utilisation du produit de solubilité se manifeste lorsque le précipité subit d'importantes variations de surface spécifique en fonction du temps. Le concept de phase doit être précisé lorsque la surface devient grande par rapport à la masse /11/. Il faut alors introduire une variable extensive supplémentaire (surface) et des variables intensives comme la tension superficielle et le potentiel électrique de surface. Lorsque la solubilité diminue par "vieillissement", le produit ionique est alors une fonction de la dimension des cristaux, que l'on peut représenter à l'aide de plusieurs paramètres, selon la nature de la distribution statistique des diamètres. Le simple bon sens nous indique ici que nous n'avons pas affaire à une situation d'équilibre, puisque le système évolue. Il n'empêche que l'on ne peut évacuer ce problème (en particulier dans le cas des ciments) car il présente de réelles difficultés, lorsqu'il s'agit de comparer les valeurs expérimentales aux valeurs calculées. La théorie de la nucléation /11//12/ nous apprend que dans ce cas, la dimension des cristaux dépend non seulement du temps, mais aussi des conditions chimiques au moment même de la précipitation (influence du taux de sursaturation sur le nombre de germes par unité de volume). C'est pourquoi on peut aboutir, même au bout d'un temps très long, à des états stationnaires différents, si les conditions de précipitation ont été différentes. C'est le cas de la portlandite, qui montre d'importantes différences de solubilité, non seulement en fonction de la dimension des cristaux /13//14/, mais aussi selon leur mode de préparation : la solubilité est plus grande pour des cristaux préparés par réaction $CaO + H_2O$, dans le domaine sursaturé.
La seule possibilité pour le chimiste est ici de réaliser un plan d'expériences qui respecte le mieux possible les conditions de précipitation qui existent dans les ciments, c'est-à-dire d'étudier et de mesurer les constantes des hydrates de synthèse précipités en régime très sursaturé. Dans ces conditions, la comparaison avec les résultats du modèle peut alors être faite, sur la base d'un état stationnaire très proche de l'équilibre, réalisé à partir de conditions initiales standardisées.
Les difficultés rencontrées au cours de cette discussion de la validité du modèle ne sont qu'en partie résolues. La condition ci-dessus fait ressortir par exemple la nécessité de construire un appareillage permettant de réaliser des états très sursaturés en chaux, pendant des temps suffisamment longs.
Du point de vue du physicien, c'est bien dans l'effort pour résoudre ces difficultés que résident toutes les chances de succès de la démarche. Le reste n'est qu'une question de mise en route d'un engrenage mathématique et informatique, le problème du calcul lui-même pouvant d'ailleurs être traité de différentes manières, selon les moyens dont on dispose. La méthode que nous proposons dans la suite de cette communication n'a donc pas la prétention d'être unique ou irremplaçable. Elle s'est simplement avérée très pratique à l'usage. Nous étudions, à l'aide de quelques exemples, les moyens permettant de simplifier le plus possible les algorithmes de calcul, de façon à obtenir des boucles d'itération très rapidement convergentes, adaptées à l'emploi de microprocesseurs beaucoup plus lents que les grosses unités de calcul.

3 - MISE EN EQUATION DES EQUILIBRES DE SOLUBILITE DES HYDRATES

3.1 - GENERALITES

Dans la suite de l'exposé, les systèmes chimiques seront désignés par leurs composants, selon la notation habituelle (le nombre de composants d'un système étant défini comme le plus petit nombre de constituants indépendants à partir desquels on peut déterminer complètement la composition de chaque phase).

3.2 - VARIABLES

Nous prendrons en considération l'ensemble des ions susceptibles d'exister dans la solution interstitielle des bétons, en étendant le domaine de pH (qui se situe habituellement entre 12,3 et 13,3) à la gamme pH 10 à pH 14, qui permet de couvrir un certain nombre d'applications particulières. Seules seront donc considérées comme négligeables les concentrations des espèces comme H_3O^+, HSO_4^- ou H_2CO_3, qui sont inférieures à 10^{-9} au-dessous de pH 10. Pour des raisons pratiques, nous avons choisi de prendre comme variables primaires les molalités (indépendantes de la température). Nous utilisons comme variables secondaires la force ionique I et les coefficients d'activité individuels des ions (*Tableau 1*). Bien que le calcul de ces coefficients individuels ne soient pas parfaitement rigoureux, compte tenu de la difficulté d'évaluation des rayons ioniques, utilisés dans les formules de DEBYE et HUCKEL, nous avons adopté cette méthode qui se montre souple, en permettant de calculer les coefficients d'activité moyens de chacune des constantes d'équilibre, quels que soient le système ou la composition de la solution.

Tableau 1 - Variables utilisées dans le modèle -

Espèces ioniques et moléculaires (Molalités)	Noms	Coefficients d'activité individuels	Rayons ioniques des ions solvatés (A) (valeurs indicatives)
(Ca 2+)	C2	gC2	5 à 6
(CaOH +)	C1	gC1	4 à 5
(H2SiO4 2-)	H2	gH2	4
(H3SiO4 -)	H3	gH3	4
(H4SiO4 aq)	H4		
(AlO2-)=(H4AlO4-)	A1	gA1	4
(CO3 2-)	G2	gG2	4
(HCO3 -)	G1	gG1	3
(OH -)	OH	gOH	2 à
(Na+)+(K+)	R1	gR1	4
(SO4 2-)	S4	gS4	4
(NaSO4-)+(KSO4-)	RS4	gRS4	4
(CaSO4 aq)	CS4		
(Cl-)(ou anion monovalent d'acide fort)	X1	gX1	2 à 3

(liste non limitative)

N.B. : Les rayons ioniques figurant dans le *Tableau 1* sont en général supérieurs à ceux que l'on pourrait calculer à partir des mobilités électriques, en appliquant la loi de STOKES. Certains peuvent être obtenus par régression, à l'aide des formules de DEBYE et HUCKEL, à partir de bilans ioniques de composés insolubles, en faisant varier la force ionique /15/.

Les diagrammes d'équilibre sont en général construits à l'aide des concentrations ou des molalités TOTALES qui à de rares exceptions près, sont les seules grandeurs accessibles à l'expérimentation.

Cette méthode présente l'inconvénient de faire disparaître une partie de l'information utile à savoir la répartition d'un élément chimique, sous ses différentes espèces, complexes ioniques ou moléculaires. Nous avons donc choisi d'utiliser les grandeurs totales (*Tableau 2*) comme variables secondaires, en gardant la possibilité d'effectuer des projections des domaines d'équilibre sur les plans optionnels, en conservant un fichier complet par point du diagramme.

Tableau 2 - Expression des molalités totales

Variables résultantes	variables primaires
CT	C2 + C1 + CS4
ST	H2 + H1 + H4
AT	A1 + A0
GT	G2 + G1
RT	R1 + RS4
S4T	S4 + RS4 + CS4
BT (basicité)	OH + C1

3.2 - SYSTEME D'EQUATIONS

A pression et température constantes, un système de c composants (ou c molalités totales indépendantes), comportant p phases solides et une phase aqueuse, a pour variance : $v = c - p - 1$.

Toutes les molalités sont donc déterminées si l'on se fixe v d'entre elles et ceci quel que soit le nombre d'ions complexes. Le problème va consister à éliminer les inconnues entre $n = (e - v)$ équations, dans un système comportant e espèces en solution. Ces équations sont de 4 types (*Tableau 3*) :

Tableau 3 - Equations et constantes chimique (liste non limitative)
(l'apostrophe désigne les constantes apparentes)

RELATIONS -	Constantes	Valeurs à 25°C indicatives	Coeff. moyen d'activité
Réactions acide-base			
C2.OH/C1 =	K_1'	0,037	$g1 = gC2.gOH/gC1$
H3.OH/H2 =	K_2'	0,0063	$g2 = gH3.gOH/gH2$
H4.OH/H3 =	K_3'	6,31 E-5	$g3 = gOH/gH3$
A0.OH/A1 =	K_5'	3,33.E-5	$g5 = gOH/gA1$
G1.OH/G2 =	K_7'	2.E-4	$g7 = gG1.gOH/gG2$
Complexes sulfate			
C2.S4/CS4 =	K_{12}'	0,01	$g12 = gC2.gS4$
R1.S4/RS4 =	K_{13}'	0,13	$g13 = gR1.gS4/gRS4$
Produits de solubilité			
H4 =	K_4'	1,6.E-3	
A0 =	K_{13}'	1.E-6	
$C2^a.C1^{1-a}.H2^{1-b-c}.H1^{2c}.OH^c.$ =	S_0'	1.E-7,25	gS0
$C2.OH^2.$ =	S_1'	5,3.E-6	gS1
C2. S4 =	S_2'	3,185.E-5	gS2
C2. G2 =	S_3'	4,5.E-9	gS3
$C2^4.A1^2.OH^6.$ =	S_4'	5.E-27	gS4
$C2.^6A1^2.S4.OH^4.$ =	S_5'	1.E-29	gS5
$C2^6.A1^2.X1^2.OH^6.$ =	S_6'	1.E-31	gS6
$C2^6.A1^2.G2.OH^4.$ =	S_7'	5.E-31	gS7
$C2^2.A1^2.OH^2.$ =	S_8'	1.E-14	gS8
$C2.^6A1^2.S4^3.OH^6.$ =	S_9'	1 E-44	gS9

a) L'équation d'électroneutralité : $\Sigma_i z_i C_i = 0$

b) r équations correspondant aux réactions chimiques d'association d'espèces en solution (réactions acide-base, formations de complexes solubles). Ces r équations relient l'ensemble des ct molalités totales à l'ensemble des e espèces en solution, d'où ct = e - r

c) pour p phases solides, p équations obtenues en écrivant les produits de solubilité $\prod_j (c_i)^{n_i} = S'_j = S_j/\gamma \equiv$

d) des équations particulières au nombre de s = n - r - p - 1, reliant certaines des variables lorsqu'il y a dégénérescence du nombre de constituants indépendants (ceci se produit quand l'équilibre est atteint à partir du domaine sous-saturé, ou lorsque le système comporte des phases solides non indépendantes, par exemple dans l'équilibre métastable $C_2AH_8 + C_4AH_{19} + CH$, où la relation restrictive est $(C/A)_{solution} = 4$.

On a alors :

c = ct - s, et c = e - r - s < e - r

4 - PRINCIPE GENERAL DES CALCULS

4.1 - TRAITEMENT NUMERIQUE

Bien que cela soit possible dans un grand nombre de cas, on ne cherchera pas à exprimer les solutions du système sous forme d'expressions algébriques explicites reliant les grandeurs totales. Chaque point d'une courbe d'équilibre sera associé à un domaine-solution D, de la dimension égale à la variance du système. Ce domaine sera représenté par un fichier contenant les valeurs calculées, pour chaque valeur du ou des paramètres choisis selon la variance.

4.2 - EXPRESSION PARAMETRIQUE DES SOLUTIONS CHOIX DES PARAMETRES

Le traitement numérique sera d'autant plus facile et rapide que les expressions à calculer seront moins complexes. On aura donc intérêt à travailler dans des systèmes de variance non nulle. Les points invariants pourront être obtenus en faisant tendre vers zéro l'une des molalités, dans un système où v = 1, contenant un constituant supplémentaire non précipitable. Inversement, on évitera de traiter des systèmes de variance élevée, ce qui obligerait à stocker un grand nombre de fichiers de gande dimension. L'expérience montre que, dans le cas des ciments, la plupart des équilibres peuvent être traités avec v = 1.

On aura avantage à choisir comme paramètres les molalités des ions intervenant le plus souvent dans les réactions de formation de complexes, comme OH^- et SO_4^{2-}. Ceci permet d'éliminer les r équations correspondantes du système, et de le réduire à un nombre d'équations égal au nombre de molalités totales ct.

4.3 - NIVEAU DE COMPLEXITE DES SYSTEMES

Le système (S) ainsi réduit contient (s + 1) équations linéaires, et p équations non linéaires. Il est bien évident que si l'on peut éviter d'avoir à substituer dans les premières, des expressions non linéaires tirées des secondes, la résolution du système sera très simple. Or ce procédé n'est possible que dans un certain nombre de cas, qu'il faut être capable de prévoir. Pour cela, nous allons considérer le sous-système (SS), constitué des p équations non linéaires (produits de solubilité).

Définition : Nous appellerons MULTIPLICITE m du système SS, le nombre minimum de molalités totales nécessaire pour écrire les p produits de solubilité.

Le système SS comprend m variables et p équations (m > p - 1). Sa résolution directe permet de réduire le système S à un système linéaire constitué de l'équation d'électroneutralité et des éventuelles équations restrictives particulières. Pour que ceci soit possible, il faut disposer de (m - p) variables optionnelles, prises comme paramètres, parmi les variables autorisées par la variance, d'où la condition : v > m - p

Le niveau de complexité du système peut donc être représenté par la variable :

$\delta = m - p - v = m - c + 1$, avec

m > 0 pour tout c, d'où $\delta > 1 - c$

Si v > m - p, alors $\delta < 0$, et le nombre de paramètres dont on dispose est suffisant pour résoudre SS séparément.

Si $\delta > 0$, la résolution se complique : on apporte v paramètres pour résoudre SS, mais il en manque m-p-v. Dans tous les cas, on doit avoir : $\delta < 1 + s$, pour résoudre le système général S. L'étendue des variations possibles de δ est donc donnée par :

$$1 - c < \delta < 1 + s$$

Le nombre optimum de paramètres, c'est à dire le minimum nécessaire à la résolution de SS est obtenu pour $\delta = 0$, soit v = m - p. Dans la mesure du possible, on s'arrangera donc pour se placer dans ces conditions de variance.

Cas défavorable

Lorsque $0 < \delta < 1 + s$, on est obligé de substituer des expressions non linéaires dans l'équation d'électroneutralité et les équations particulières. Le système S se réduit alors à une équation finale de la forme :

$y = D.X^{-n} + E = X$, avec n > 0 et D > 0

L'exposant n n'est pas nécessairement un entier.

L'équation peut être résolue par itération : la méthode classique des approximations en spirale n'étant utilisable que si ABS (y') < 1, nous utiliserons une autre méthode itérative (méthode de la tangente mobile).

4.7 - CORRECTIONS DUES A LA FORCE IONIQUE

Après avoir obtenu un fichier complet des solutions dans l'espace des molalités, il reste à calculer la force ionique et les coefficients d'activité individuels, à l'aide des formules de DEBYE et HUCKEL étendues. On retourne alors à une nouvelle résolution du système, par une boucle d'itération qui est arrêtée lorsque les valeurs obtenues sont stationnaires. Les coordonnées du point de la courbe d'équilibre ainsi obtenues peuvent alors être envoyées dans une mémoire de stockage, affichées ou éditées dans un graphe, sous la forme d'une projection dans un plan quelconque de l'espace des molalités.

4.8 - ORGANIGRAMME (voir *Fig. 1*)

5 - RESULTATS. EXEMPLE

La méthode précédente nous a permis de modéliser la plupart des systèmes d'hydrates de la chimie du ciment. Les résultats concordent bien avec les données expérimentales, par exemple les coordonnées des points invariants donnés par JONES /16/. Pour juger des performances du modèle, nous donnons les résultats obtenus dans le système [CaO, SO_3, R_2O, H_2O] dans le domaine d'équilibre gypse + portlandite, qui a été étudié par HANSEN et PRESSLER /17/ (*Fig.2*).

L'exactitude des prévisions du modèle ne peut être obtenue ici qu'en tenant compte des complexes sulfate et des réactions acide-base.

Fig 1.

Modélisation des équilibres chimiques des hydrates des ciments.

PROGRAMME SOLUB. Organigramme.

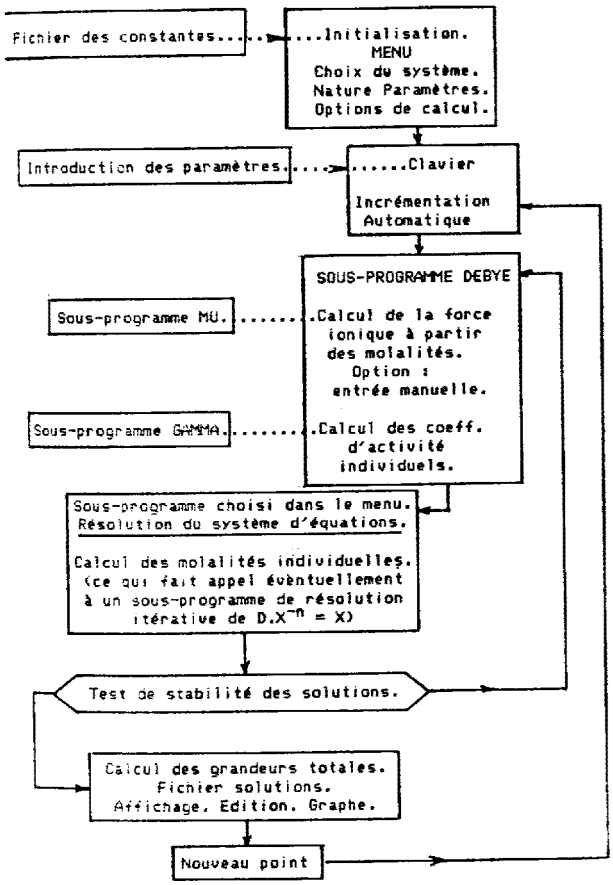

Dans le même système, on peut prévoir le pH de précipitation de la portlandite en présence de gypse et le comportement d'une suspension de gypse dans laquelle on ajoute une base forte R2O (*Fig.3*). La projection du domaine d'équilibre sur un plan /pH,R2O/ montre comment le gypse peut avoir un effet accélérateur de prise des ciments, en abaissant légèrement le pH d'équilibre : le mélange des 2 phases gypse et portlandite se comporte comme un "super tampon" (*Fig.4*).

6 - CONCLUSIONS

Le souci de la représentativité physique dans la modélisation des équilibres des hydrates nous a conduit à faire face à toute la complexité de l'approche analytique de l'hydratation. Nous pensons que cet effort se justifie par la grande variété de ses applications , dont le simple exemple qui précède montre déjà la richesse.

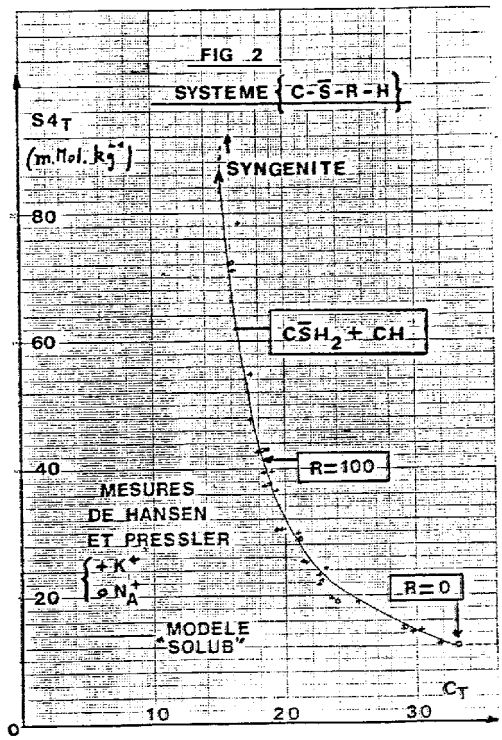

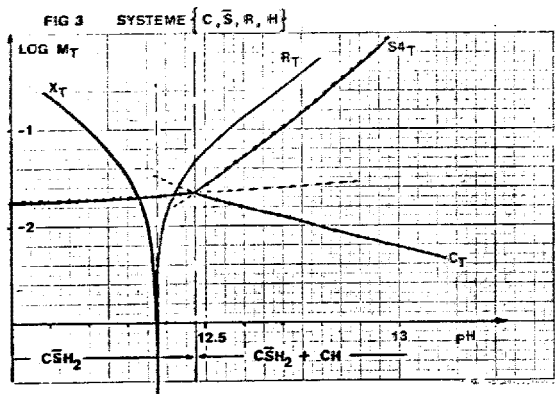

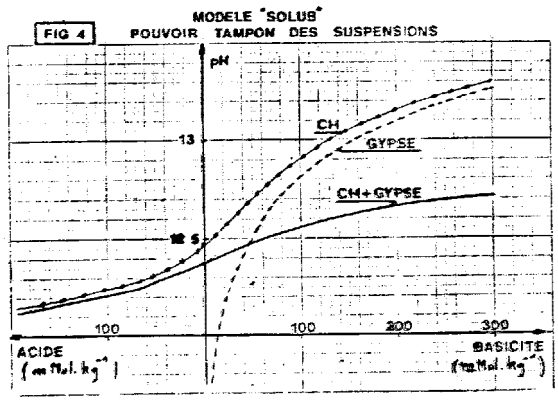

F. Indelicato - Dipartimento di Ingegnerie Strutturale, Politecnico di Torino Italia

L. Cussino - Riserca e Sviluppo, Unicem S.p.A., Casale Monferrato, Italia

COMPORTEMENT VISCOÉLASTIQUE À LONG TERME DES BÉTONS DE CIMENT ALUMINEUX

1. INTRODUCTION

L'étude systématique du comportement statique et structurale des bétons à base de ciment alumineux forme l'objet d'une littérature assez nourrie, mais cette dernière tout en étant riche des données et d'études théoriques n'est pas en mesure, pour l'instant, de mettre à la disposition du responsable d'un projet tous les éléments dont il a besoin pour assurer un calcul correct.

A ce sujet et pour nous en tenir tout simplement à la caractéristique la plus significative - la résistance à la rupture par compression - un exemple emblématique est donné par le fait qu'en dépit de la grande abondance d'ouvrages et d'intéressantes études sur son évolution à long terme (1), (2), (3) et bien que les auteurs attribuent d'un commun accord à la conversion la responsabilité de la chute de la résistance dans le temps, bien connue, lorsqu'il s'agit de quantifier cette chute on bute à une grande dispersion des données.

En effet, l'influence qu'exercent les différents paramètres sur l'évolution de la résistance après les premiers jours n'a pas encore été bien définie.

Il a été prouvé, néanmoins, que la nature de l'agrégat (calcaire ou siliceux) peut jouer un rôle déterminant et donner lieu - pour le calcaire - à la formation d'un carbo-aluminate plus stable que les aluminates héxagonaux (4). Le phénomène s'accompagne d'une réduction de la porosité et a, comme suite, une augmentation continue ou, tout au moins, une stabilisation significative - environ aux valeurs maximales obtenues - des résistances observées sur une période de cinq ans (5).

Le contraire se produit pour l'agrégat siliceux.

Un ouvrage récent, étayé par les résultats d'essais réalisés jusqu'à un an après la préparation des échantillons confirme que l'agrégat calcaire exerce une influence favorable sur certaines caractéristiques mécaniques et, en particulier, sur la résistance à la rupture par compression (6).

Quant aux déformations différées et, en particulier au fluage, une caractéristique dont le responsable du projet doit absolument tenir compte pour pouvoir formuler des prévisions correctes au sujet du comportement dans le temps voire de la déformabilité du béton, les données à long terme que nous offre la littérature sont assez moins nombreuses que celles concernant la résistance bien que les premiers ouvrages en la matière remontent aux années '30 (7), (8).

A une époque plus récente, de nouveaux résultats ont été diffusés (9) tandis que ceux disponibles ont été interprétés dans une optique plus moderne (10). Toutefois ce domaine nous semble encore offrir de nombreuses possibilités de recherche.

Ce qui précède pourrait également s'appliquer aux modules d'élasticité encore que ces derniers soient bien documentés par des ouvrages de considérable envergure (2), (6), (11) et à d'autres caractéristiques collatérales qui intéressent en tous cas le responsable du projet, telle que la résistance à la traction.

Dans ce contexte s'inscrit l'étude expérimentale dont il est question qui porte essentiellement sur le fluage à long terme et sur le retrait des bétons à base de ciments alumineux et d'agrégat calcaire ou siliceux.

L'étude est intégrée par des donnés relatives à l'évolution dans le temps des modules d'élasticité et aux résistances à la compression et à la traction de ces bétons.

A partir de ces préalables on se propose:

— de présenter les valeurs de fluage et de retrait des bétons soumis à observation pendant 4 ans;
— d'analyser la possibilité de prévoir ces caractéristiques à l'aide d'essais à court terme;
— d'étudier l'influence exercée par l'agrégat (calcaire ou siliceux);
— de comparer l'effet des différents âges de mise en charge;
— d'élargir le tableau d'ensemble général par de nouvelles données expérimentales concernant la résistance à la compression et à la traction ainsi que les modules d'élasticité.

2. CARACTERISTIQUES DES ECHANTILLONS

Pour la confection des éprouvettes nous avons utilisé deux bétons préparés à partir du même ciment alumineux du commerce ayant la composition chimique pondérale suivante: Al_2O_3 39,3%, CaO 38,3%, Fe_2O_3 11,6%, FeO 5,0%, SiO_2 4,0% avec de faibles quantités de MgO, K_2O et Na_2O.

Le premier type de béton, obtenu en utilisant un agrégat siliceux naturel du Po présentait les caractéristiques suivantes: Ø max. 20 mm; courbe granulométrique continue; dosage du ciment 350 kg/m^3; rapport E/C = 0,52; slump 9,5 cm; tassement par table vibrante; masse volumique au démoulage 2418 kg/m^3.

Le deuxième type était caractérisé par un agrégat calcaire concassé: $CaCO_3$ 99,8; Ø max. 20 mm; courbe granulométrique continue, dosage du ciment 350 kg/m^3; rapport E/C = 0,60; slump 12 cm; tassement par table vibrante; masse volumique au démoulage 2360 kg/m^3.

Les deux bétons ont été préparés à quelques heures de distance l'un de l'autre, dans le même milieu et en utilisant le même appareillage.

Nous avons préparé, avec chaque mélange, des éprouvettes de 10x10x30 cm pour les essais de fluage et de retrait et pour la détermination du module d'élasticité longitudinale, ainsi que des éprouvettes cubiques de 10 cm de large, pour les essais de compression et des éprouvettes cylindriques, pour l'essai brésilien.

Pendant les 7 premiers jours, les éprouvettes ont été stockés en milieux contrôlé, à la température de 20 ± 1°C et à une teneur d'humidité relative de 90% min.

Ensuite elles ont été transférés, pour les essais, dans un milieu contrôlé à la température de 20 ± 1°C et à une humidité relative de 65%.

3. MODALITES D'ESSAI

3.1 Essais de fluage

Les éprouvettes ont été soumises à une charge constante, dans des châssis expréssement prévus à cet effet équipés d'un vérin hydraulique comportant un dispositif de réglage de la pression à air qui assure une stabilité durable de la charge (Fig. 1).

Sur chacune des quatre faces longitudinales de l'éprouvette a été placée une base extensométrique de 100 mm, pour la lecture de la déformation; l'extensomètre utilisé est de type mécanique avec sensibilité $1 \cdot 10^{-3}$ mm.

Au bout de 7, 28, 92 et 180 jours, les éprouvettes ont été soumises à une charge centrée correspondant à une contrainte de 25 N/mm^2, c'est à dire près de 35% des résistances à la compression à l'échéance de 28 jours, pour les deux types de béton.

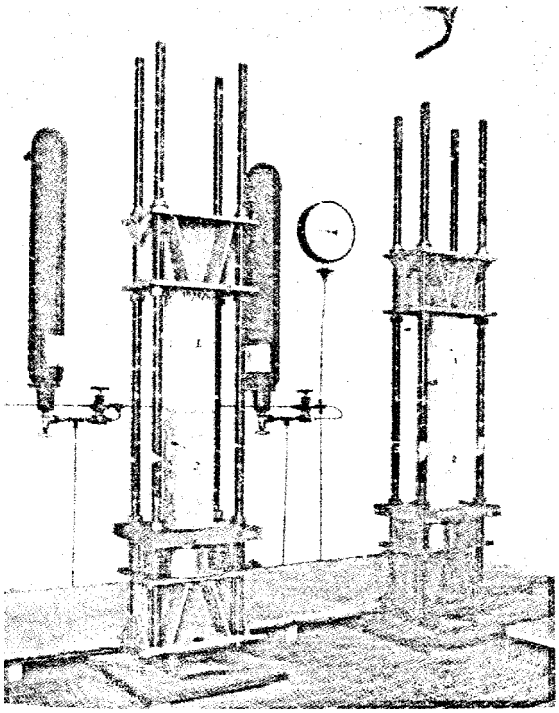

Fig. 1 - Dispositif de mise en charge.

Nous avons utilisé 16 éprouvettes qui ont été mises en charge par groupes de deux, pour chaque essai et pour chaque type de beton.

3.2 Mesure du retrait

Les déformations ont été mesurées à partir de 24 heures après la préparation des bétons, à l'aide d'un extensomètre mécanique, tout comme pour le fluage, en utilisant deux éprouvettes par type de béton.

3.3 Module d'élasticité longitudinale

Les modules sécants E correspondant à une contrainte de compression maximale de 25 N/mm^2 ont été déterminés à différentes échéances sur deux éprouvettes de chaque type de béton. L'appareillage extensométrique est le même qui a été utilisé pour le fluage et pour le retrait.

3.4 Résistances à la compression

Elles ont été déterminées à l'aide d'une machine universelle en utilisant 54 éprouvettes testés à neuf échéances s'échelonnant entre 1 jour et 4 ans.

4. RESULTATS DES ESSAIS ET COMMENTAIRES

4.1 Retrait

Les déformations de retrait ε_r, observées à partir d'un jour après la préparation des éprouvettes sont indiquées à la Fig. 2 qui montre également les déformations différées (fluage + retrait).

On peut remarquer qu'au bout de 4 ans, les ε_r présentent des valeurs très proches de celles que l'on enregistre habituellement pour les bétons à base de ciment Portland, ce qui correspond aux données signalées par Neville ([12]).

Il y a lieu toutefois de souligner que le retrait du béton à base d'agrégat calcaire est légèrement supérieur à celui du béton à base d'agrégat siliceux.

4.2 Fluage

Les déformations de fluage ε_f (Fig. 2), par suite des modalités d'essai qui ont été adoptées coïncident pratiquement avec celles différées.

Ces préalables ayant été posés, lorsqu'on analyse les valeurs de fluage au bout de 4 ans on peut observer:

— que les valeurs de dilatation maximale pour les deux bétons sont celles qui correspondent à une mise en charge de 7 jours;

— que les valeurs de ε_f des deux bétons diminuent au fur et à mesure qu'augmente la durée de la mise en charge;

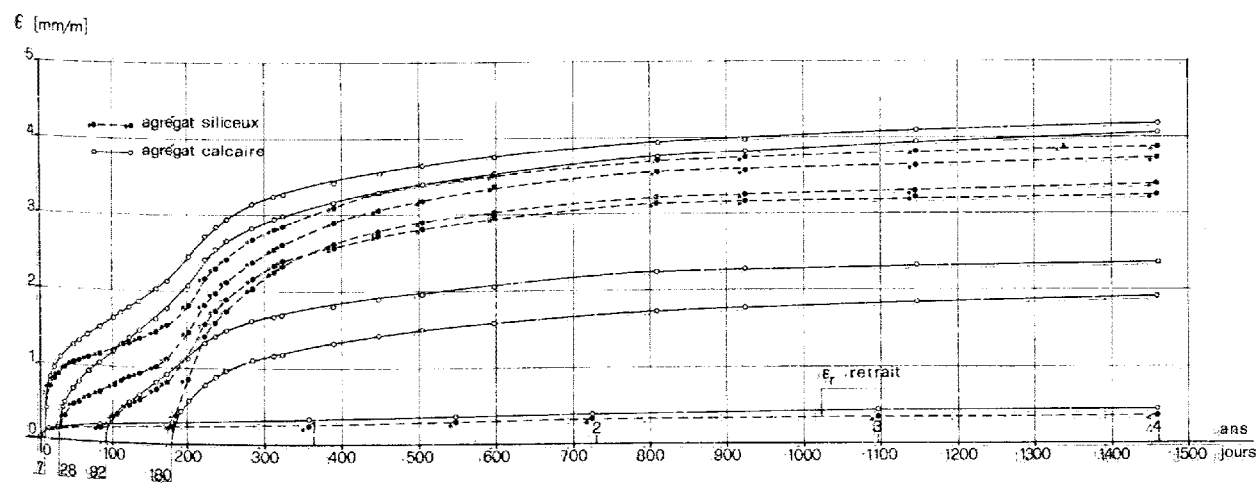

Fig. 2 - Évolution des déformations différées (fluage + retrait) et retrait en fonction du temps.

— que les dilatations des bétons à base d'agrégat calcaire à 7 et à 28 jours de mise en charge dépassent bien qu'en moindre mesure, celles du béton à base d'agrégat siliceux;

— qu'à l'échéance de 92 et de 180 jours, les ε_f du béton à base d'agrégat calcaire sont considérablement inférieures à celles du béton à base d'agrégat siliceux; en particulier, après 180 jours de mise en charge elles ne mesurent que la moitié;

— les ε_f de l'agrégat siliceux tendent à se regrouper autour de la même valeur, indépendamment de l'age de mise en charge (différence de 15% entre les valeurs maximales et minimales);

— l'agrégat calcaire présente, au contraire, une différenciation très nette, caractérisée par deux valeurs de la ε_f: celles à 7 et 28 jours sont élevées et très rapprochées entr'elles tandis qu'au fur et à mesure qu'augmente l'âge de mise en charge on observe une réduction importante de la déformabilité si bien qu'entre les ε_f des échantillons à 7 jours et celles des échantillons à 92 et 180 jours la différence se chiffre approximativement à 45% et à 55%.

Une analyse plus exhaustive pourrait être consacrée à l'évolution du fluage qui présente des aspects intéressants surtout pendant la première année, mais puisqu'une partie des données que nous présentons dans cet ouvrage et qui concerne cette période ont été signalées et discutées en détail (13), (14), nous nous bornerons à mettre l'accent sur quelques aspects essentiels.

Plus particulièrement, il y a lieu de souligner que toutes les courbes, à part celles des échantillons mis en charge à 180 jours, présentent deux points d'inflexion limitant un trajet du diagramme compris entre 70 et 220 jours d'âge des échantillons où la vitesse de croissance de la déformation augmente en mesure considérable et recommence ensuite à diminuer. Ce fait confirme les observations de Swami (9) et, en partie, les commentaires de Neville (10).

L'origine de ce comportement des bétons alumineux doit être probablement attribuée aux phénomènes de nature physico-chimique liés à la cure des éprouvettes. A ce propos nous voudrions souligner le différent comportement des deux matériaux: en effet l'augmentation de la vitesse de déformation des bétons à base d'agrégat calcaire est plus lente, ce qui fait que les inflexions sont moins marquées. Ce fait pourrait être expliqué en admettant que l'interaction chimique entre agrégat calcaire et pâte de ciment (5), à fur et mesure que se développe dans le temps à la dépense des hydrates hexagonaux (4), entraîne un'amélioration progressive de l'adhérence pâte-agrégat calcaire.

Afin d'aboutir à une évaluation plus complète du phénomène du fluage nous avons estimé utile de procéder à une comparaison entre les deux bétons objet de l'étude et un béton structural ordinaire de bonne qualité, de la classe $f_{ck} = 50$ N/mm^2 à base de ciment Portland, testé dans le même laboratoire et dans les mêmes conditions.

Le choix est tombé sur ce béton, du fait que les déformations mesurées montraient une excellente correspondance avec celles calculées par voie théorique, en appliquant les formules proposées par le C.E.B. (15).

Nous avons adopté, comme paramètre de comparaison, le facteur de fluage φ qui est le rapport entre la déformation de fluage et la déformation longitudinale à l'age de 28 jours, notamment:

$$\varphi = \frac{\varepsilon_f}{\varepsilon_{e28}}$$

Les Fig. 3 et 4 montrent une comparaison entre les facteurs de fluage du béton ordinaire et ceux du béton à base d'agrégat siliceux et calcaire.

On peut observer:

— à court terme, les facteurs de fluage des bétons à base de ciment alumineux correspondent approximativement à ceux du béton ordinaire. Plus précisément, les facteurs du béton à base d'agrégat siliceux sont légèrement inférieurs, alors que ceux du béton calcaire sont supérieurs, bien que en moindre mesure;

— au bout de six mois, le coéfficient φ des deux bétons à base de ciment alumineux (calcaire, siliceux) enregistre une augmentation franchement supérieur à celle du coéfficient du béton ordinaire;

— quelque temps avant un an d'âge commence la phase définitive que caractérise une tendance très nette des φ vers des valeurs asymptotiques assez élevées (elles sont 2 à 3 fois plus importantes que celles du bétons ordinaire).

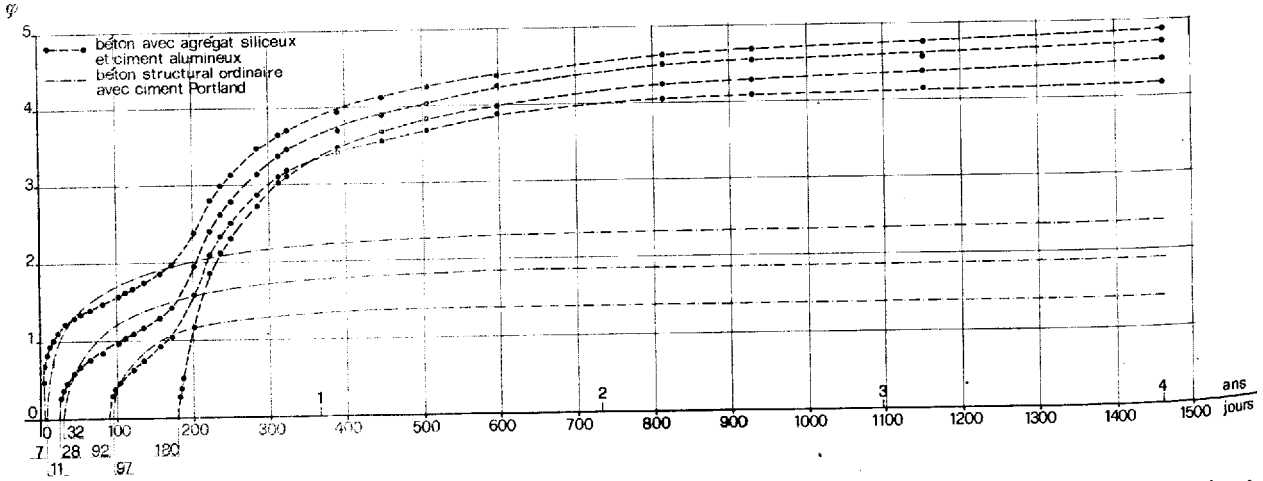

Fig. 3 - Évolution dans le temps des facteurs de fluage du béton alumineux avec agrégat siliceux en fonction de l'âge de mise en charge, et comparaisons avec un béton ordinaire.

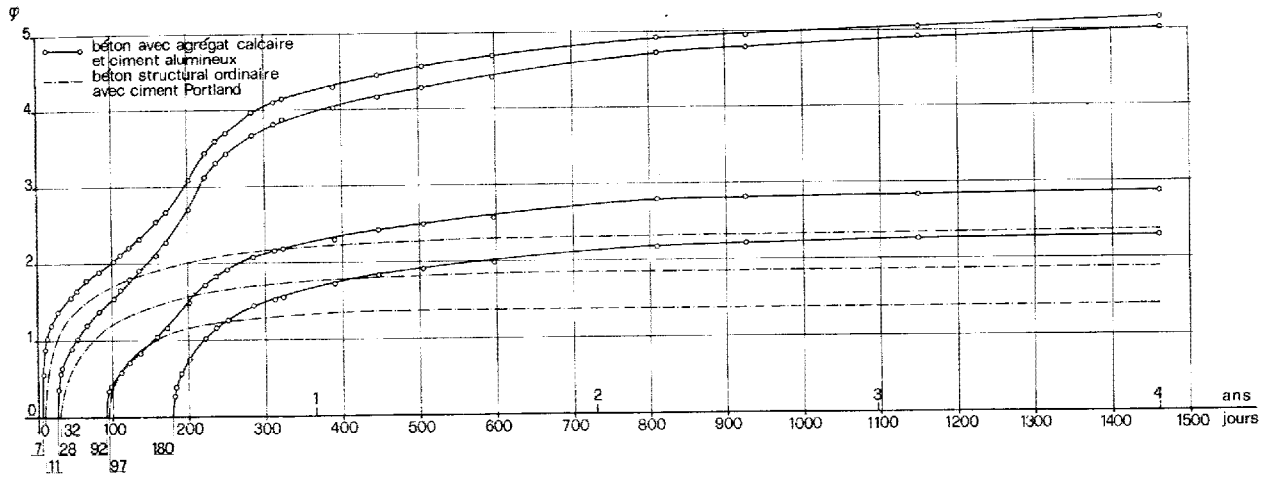

Fig. 4 - Évolution dans le temps des facteurs de fluage du béton alumineux avec agrégat calcaire en fonction de l'âge de mise en charge, et comparaison avec un béton ordinaire.

Une analyse qualitative permet, en tous cas, d'observer, au cours de cette phase, une différence de comportement très nette entre les deux bétons à base de ciment alumineux.

On peut constater, en effet que l'age de mise en charge exerce une faible influence - à l'échéance de quatre ans - sur la φ du béton siliceux.

À noter le rapport $\frac{\varphi \text{ siliceux}}{\varphi \text{ ordinaire}}$ dont la valeur maximale se chiffre à 3.

Dans le béton calcaire, l'âge de mise en charge exerce au contraire, une influence favorable car il engendre une considérable réduction de φ. Le rapport $\frac{\varphi \text{ calcaire}}{\varphi \text{ ordinaire}}$ tout en demeurant défavorable atteint néanmoins une valeur maximale de 2,6.

En dernier lieu on peut encore observer que l'allure des dilatations ε_f et des coéfficients de fluage ne permettent pas - tout au moins pour les types de bétons à base de ciment alumineux examinés - d'extrapoler les résultats des essais de fluage routiniers à court terme, à 90 jours d'âge. En effet, contrairement à ce qui se produit lorsqu'on opère sur les bétons ordinaires, dans ce cas les résultats peuvent ne pas être significatifs et même porter à des conclusions erronées.

4.3 Résistance à la rupture par compression

La résistance à la rupture par compression f_c des éprouvettes à base d'agrégat calcaire et siliceux est reportée à la Fig. 5. L'examen des diagrammes nous suggère quelques remarques:

- à très court terme on obtient des valeurs de résistance très élevés, ce qui d'ailleurs est bien connu pour les bétons à base de ciments alumineux: dans notre cas, les deux matériaux enregistrent au bout de 24 heures, des résistances d'environ 57 N/mm^2;
- la résistance du béton à base d'agrégat siliceux augmente d'abord plus rapidement que celle du matériau calcaire. Ensuite se produit une inversion de comportement si bien qu'à l'écheance d'un an à peu près, les f_c des deux matériaux s'avèrent être égales et se chiffrent à 82 N/mm^2. Cette valeur de la résistance correspond également à la valeur maximum qu'enregistre le béton à base d'agrégat siliceux;
- dans le délai de temps entre un e quatre ans, les valeurs de resistance du béton à base d'agrégat siliceux commencent à diminuer d'abord lentement et ensuite, après une période de stabilisation, en manière plus marquée.

  Au bout de 4 ans, la chute de résistance est de 25% vis-à-vis de la valeur maximum;
- dans le même délai, la résistance des bétons à base d'agrégat calcaire ne cesse d'augmenter jusqu'à l'échéance de 2 ans et se stabilise ensuite autour de 87 N/mm^2 maximum.

4.4 Résistance à la traction

Nous avons limité l'étude de la résistance à la traction f_{ct} aux 18 premiers mois. Le Tableau 1 montre les valeurs obtenues avec l'essai brésilien sur des éprouvettes cylindriques ayant les dimensions suivantes: Ø = 15 cm, l = 30 cm. Les valeurs indiquées représentent la moyenne obtenue sur 3 éprouvettes.

Tableau 1 - Variation de la résistance à la traction des bétons alumineux en fonction du temps et du type d'agrégat

	Résistance à la traction			
Âge du béton	28 j	180 j	360 j	540 j
Calcaire	3,8 N/mm^2	4,2 N/mm^2	4,6 N/mm^2	4,6 N/mm^2
Siliceux	3,6 N/mm^2	3,8 N/mm^2	3,8 N/mm^2	3,6 N/mm^2

On peut observer un meilleur comportement général du béton à base d'agrégat calcaire.

Il faut néanmoins tenir compte du fait que la forme de l'agrégat pourrait avoir influencé le résultat: l'un étant concassé (celui calcaire), l'autre naturel, de fleuve (celui siliceux).

4.5 Déformation élastique

Le Tableau 2 regroupe les modules d'élasticité secants longitudinales, face à une contrainte de compression maximale de 25 N/mm^2.

On peut observer:

- que pour les deux bétons, E atteint sa valeur maximum à 28 jours;

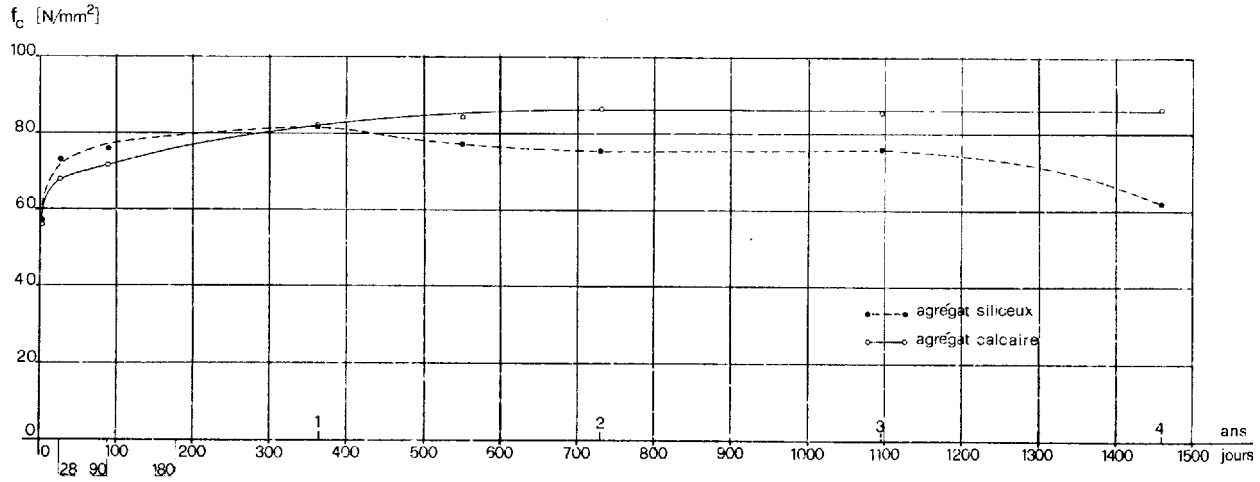

Fig. 5 - Évolution de la résistance à la compression des bétons alumineux en fonction du temps et du type d'agrégat.

— qu'à la même échéance de 28 jours, les valeurs des modules d'élasticité des deux bétons sont (avec une bonne approximation) égaux et proches de ceux que la littérature signale pour les bétons de la classe f_{ck} = 40 N/mm² à base de ciment Portland;

— qu'après 28 jours on enregistre une diminution du module d'élasticité, plus accentuée pour le béton à base d'agrégat siliceux (près de 33% à 4 ans) qu'elle ne l'est pour celui à base d'agrégat calcaire (près de 23% à 4 ans).

Tableau 2 - Évolution du module d'élasticité longitudinale en fonction du temps et du type d'agrégat

Module d'élasticité longitudinale E (N/mm²)		
Âge des échantillons	Agrégat	
	Siliceux	Calcaire
7 j	30.830	32.700
28 j	33.790	33.680
92 j	32.920	31.890
180 j	28.740	28.670
1 a	22.980	27.960
4 a	22.630	25.770

5. CONCLUSIONS

D'après les données obtenues ou peut tirer les conclusions suivantes:

— la déformabilité sous charge des bétons alumineux, quelque se soit le granulat employé, est remarquable en comparaison à la déformabilité des bétons ordinaires;

— à la différence des bétons ordinaires les alumineux montrent entre 70 et 220 jours de cure un'augmentation de la vitesse de déformation sous charge;

— l'influence exercée sur les valeurs finales du fluage par l'agrégat est remarquable. En effet tandis que en présence d'agrégat siliceux le fluage à 4 ans montre des valeurs très peux dispersées, à savoir presque indépendentes de l'âge de mise en charge, en presence de granulat calcaire l'âge de mise en charge joue un rôle importante dans le sens que, lorque elle augmente, le fluage final diminue d'une façon drastique;

— l'influence exercée par l'agrégat sur l'allure des courbes de developpement du fluage est elle aussi sensible. Aux courtes écheances i'augmentation de la vitesse de déformation est plus importante dans les bétons siliceux alors que en présence d'agrégat calcaire elle tend à disparaître au croître de l'âge de mise en charge;

— l'allure des courbes du fluage dans les premiers mois empêche de faire des prévisions à long terme sur la base des usuels essais à 90 jours. Les prévisions pourraient être valable seulement dans le cas d'un béton alumineux avec agrégat calcaire mise en charge après 180 jours de cure. En tout cas il nous semble qu'avec les bétons alumineux les données de fluage puissent être extrapolées seulement à partir d'environ 10 mois après démoulage;

— l'effet positif de l'utilisation d'un granulat calcaire en substitution du siliceux est confirmé par l'évolution dans le temps des résistances mécaniques.

6. BIBLIOGRAPHIE

(1) V. MATIC, «*Influence de l'âge sur le béton de ciment alumineux*», Bulletin RILEM, N. 6, pp. 33-38, Mars 1960.

(2) D.C. TEYCHENNÉ, «*Long-term research into the characteristics of high alumina cement concrete*», Magazine of Concrete Research, Vol. 27, N. 91, pp. 78-102, June 1975.

(3) C.M. GEORGE, «*Ciments alumineux. Une synthèse des recents publications (1974-1979)*», VII Cong. Int. Chimie des Ciments, Vol. I, V-1/3-1/26, Paris 1980.

(4) A. NEGRO, L. CUSSINO, A. BACHIORRINI, «*Sur l'hydratation de l'aluminate monocalcique en presence de quartz et de carbonate de calcium*», Il Cemento, N. 3, pp. 285-302, Luglio-Settembre 1978.

(5) L. CUSSINO, A. NEGRO, «*Hyaratation du ciment alumineux en présence d'agrégat siliceux et calcaire*», VII Cong. Int. Chimie des Ciments, Vol. III, V-62-67, Paris 1980.

(6) M.F. HAKIM, «*Étude de l'hydratation du ciment alumineux associé à des granulats calcaires, consequences sur les propriétés mécaniques*», Thèse INSA, Toulouse 1984.

(7) W.H. GLANVILLE, F.G. THOMAS, «*Studies in reinforced concrete - IV: Further investigations on creep or flow of concrete under load*», Dept. Scientific and Industrial Research, Building Research Technical Paper N. 21, 44 pp., London 1939.

(8) W.H. GLANVILLE, «*Studies in reinforced concrete - III: The creep or flow of concrete under load*», Dept. Scientific and Industrial Research, Building Research Technical Paper N. 12, 39 pp., London 1930.

(9) R.N. SWAMI, A.B. IBRAHIM, K.L. ANAND, «*The strength and deformation characteristics of high early strength structural concrete*», Materiaux et Constructions, Vol. 8, N. 48, pp. 413-423, Novembre-Décembre 1975.

(10) A.M. NEVILLE, «*Creep of concrete: plain, reinforced and prestressed*», North-Holland, pp. 622, Amsterdam 1970.

(11) A.R. CUSENS, N. JACKSON, «*Flexural behaviour of higly converted prestressed high-alumina cement concrete*», Magazine of Concrete Research, Vol. 27, N. 91, pp. 103-110, June 1975.

(12) A. NEVILLE, «*High-alumina cement - A current review*», Il Cemento, N. 3, pp. 291-301, Luglio-Settembre 1978.

(13) F. INDELICATO, «*Fluage a breve e medio termine di calcestruzzi confezionati con cemento alluminoso*», Seminaire International sur les Aluminates de Calcium, pp. 231-240, Turin 14-16 Septembre 1982.

(14) F. INDELICATO, «*Bétons à base de ciment alumineux - étude de la déformabilité*», Colloque International Liaisons Pâtes de Ciment - Materiaux Associés, Toulouse 17-19 Novembre 1982.

(15) C.E.B., «*Manuel de calcul: Effets structuraux du fluage et des déformations différées*», Bulletin N. 136, Budapest, Juin 1980.

J.R.L. Dyczek and M.Petri Mining and Metallurgy Academy - Poland

MECHANICAL PROPERTIES OF AUTOCLAVED, MONOMINERAL MATERIALS FROM TOBERMORITE, XONOTLITE AND HILLEBRANDITE.

CL

1. Preparation of the samples.

Semi - dry mixtures of calcium hydroxide and finely ground silica gel were condensed by pressing forming beams 10 x 10 x 60 mm and autoclaved under saturated steam pressure after 24 hrs of autoclaving at 180°C. It was found thet samples with the molar ratio CaO/SiO_2 = 5 : 6 with the addition of 0,5 % Al_2O_3 contain only crystalline 11 Å tobermorite. Samples with the ratio CaO/SiO_2 = 1 : 1 - contain xonotlite, and those with the ratio CaO/SiO_2 = 2 : 1 -contain hillebrandite, after autoclaving for 24 hrs at 240°C.

2. Bending strength and Young's modulus, calculation of the coefficient of the pore shapes.

Young's modulus /E/ and the bending strength /R_b/ of each samples were measured. Particular series of samples from tobermorite, xonotlite and hillebrandite /To, X, H/ were formed at different pressure. Thanks to this in each series the samples had different porosity. The results are shown in Fig.1.

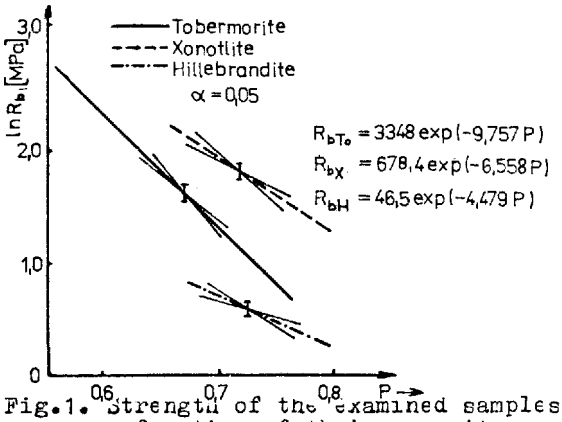

Fig.1. Strength of the examined samples as a function of their porosity

The given fuctions were derived basing on the results of bending tests of 34 samples, the total porosities of which were within the interval 0,762 - 0,546 for tobermorite, bending tests of 36 samples with the porosity from 0,793 to 0,663 for xonotlite and of 30 samples of hillebrandite with the total porosity from 0,797 to 0,678.
The porosity has been given as the volume fraction.

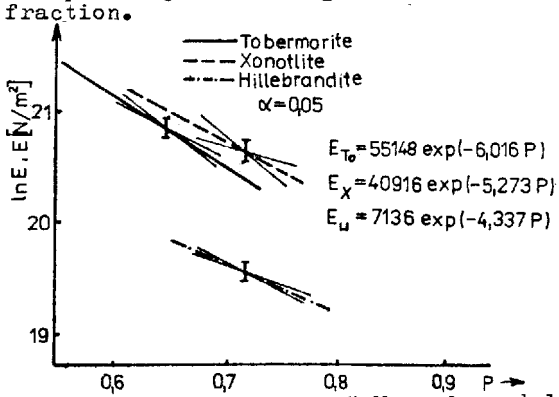

Fig.2. The dependence of Young's modulus on porosity for the exeminated samples.

The general form of the derived equations describing Young's modulus as a function of porosity : $E = E_o \exp /-b_E P/$ /Hashin 1962/ contains the empirical constant b_E, which for different materials may assume values from 2 up to from ten to twenty. It is believed that this constant corresponds to the concentration coefficient of stresses induced around the pores under the influence of the applied external stress. For pores of spheroidal form arranged in the material of the matrix in such a way that the longer axis of the spheroid in two extreme cares in perpendicular or parallel to the direction of stresses, the highest concentration of stresses occurs on the greatest curvature of those pores, the arrangement of which is much that the longer axis of the spheroid is approximately perpendicular to the direction of the tensile stress. Thus these pores will determine the value of the stress concentration coefficient K. The K value for varying ratio of the spheroid axis a/c can be described by a hyperbolic equation :

$$K = \frac{5}{4}\,\frac{a}{c} + \frac{3}{4}$$

Assuming arter Rossi /1968/ that $K = b_E$, the equation explaining the dependence of Young's modulus on porosity will asume the form :

$$E = E_o \exp\left[-\left(\frac{5}{4}\,\frac{a}{c} + \frac{3}{4}\right)P\right] \qquad /1/$$

In a material containing spherical pores /a/c = 1/, the value of the concentration coefficient of stresses in the matrix $K = b_E = 2$. Higher values of b_E are an evidence of the presence of pores of non - spherical form. Basing on the derived values of b_E /equations from Fig. 2; b_E for tobermorite : 6,0158, b_E for xonotlite.: 5,2732, b_E for hillebrandite 4,3369/ - the hypothetical mean ratio of the a/c axis was determined, assuming a spheroidal form of the pores. For the hydrated calcium silicates this ratio was as follows : for tobermorite-4,212, for xonotlite- 3,618, for hillebrandite - 2,869.
The above, derived values of the ratio of the axes of spheroidal pores were confronted with the values calculated by the method proposed by Carniglia /1972/ according to his equation :

$$\log \frac{G}{G_o} = \left(\frac{-b_E P}{4{,}606} - \frac{1}{2}\log\frac{1}{1-P}\right) + \frac{4}{5}\left(\frac{P^{\frac{1}{3}} - \frac{11}{16} - \frac{P^{\frac{1}{3}}}{8} - \frac{3P^{\frac{3}{3}}}{16}}{P^{-\frac{1}{3}} - 1}\right) \qquad /2/$$

CL

where : S - shape coefficient of the pores /its value increases with increasing asymetry of the pores/; σ - bending strength; σ_o - strength at zero porosity /value obtained by extrapolation/; b_E and P - as before /b_E - empirical index exponent as in Eq.2., P - volume fraction of pores/.
In E_x /2/ the effect both of the change in the cross - section area transferring the load /1 st member of the right - hand side of the equation[x]/ and the stress concentration around the pores /the total equation[xx]/ - on the strength of the materials have been taken into consideration.
To determine the coefficient S in E_x /2/ the dependence $\log \sigma/\sigma_o = f/P/$ for different values of S has been plotted as the model curves.
The curve of the anologous function obtained experimentally has been compared with this model.
The course of these dependences is asown in Fig.3 for tobermorite. The derived values of S are as follows : tobermorite $\simeq$ 7 ; xonotlite $\simeq$ 4; hillebrandite $\simeq$ 1,5.

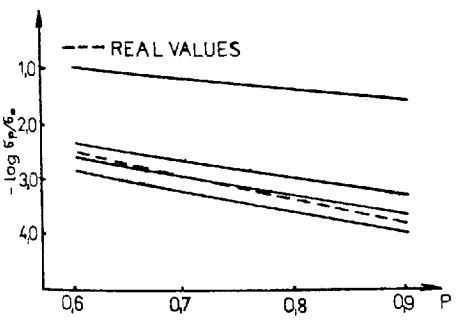

Fig.3. Function $\sigma = f/P/$ according to Carniglia equation for the tobermorite samples.

3. Determination of the critical stress concentration coefficient K_{IC} and the effective fracture energy γ_F for To, X and H.

K_{IC} and γ_F was determined in a three-points bending test of samples notched to different depth under conditions of controlled propagation of the fracture.
Mean measurement values for samples with selected different porosity are put together in Table 1.

Table 1. K_{IC} and γ_F obtained for To, X and H

Material	Porosity	K_{IC} $\left[\frac{MN}{m^{3/2}}\right]$	γ_F $\left[\frac{J}{m^2}\right]$
Tobermorite	0,715	0,120	1,093
	0,669	0,174	4,838
	0,622	0,240	4,231
Xonotlite	0,757	0,179	2,770
	0,721	0,271	5,670
	0,687	0,391	5,568
Hillebrandite	0,739	0,153	4,272
	0,697	0,165	5,448
	0,654	0,238	8,927

4. Discussion of the results and conclusions.

As it should be expected, with increasing volume fraction of pores the mechanical properties of To, X and H samples undergo deterioration. The rate of these changes for the particular minerals is defferent, the differences being possibly due to their different texture. Tobermorite crystallizes in the form of plates with the result that the pores between the grains assume elongated forms / a/c/= 4,212; S $\cong$ 7/. The asymmetry of pores occurring in materials from X and H, crystallizing in needle-shoped form is smaller /X : a/c = 3,618; S $\cong$ 4 ; H : a/c = 2,869, S = 1,5/.
In case of all examined materials the values of S are greater than 1. When analyzing the cracking process in these materials the stress concentration around the pores should be taken into consideration.
Materials built of needle - like crystals /X, H/ are characterized by relatively greater values of the fracture energy γ_F and of the stress concentration coefficient K_{IC} than materials from tobermorite, althongh their bending strength and Young's modulus at amall porosity are smaller than those of the corresponding tobermorite samples.
On the stress - strain curve for xonotlite samples the range of pseudoplastic deformations has been observed, what has already been reported by the authors /Dyczek, Petri 1974/.
Basing on the obtained results it can be assumed that materials from X and H of needle like crystallites reveal greater ability to absorb energy in the cracking process. This refers in particular to xonotlite, provided the process of its formation is not accompanied by the formation of microcracks.

---

x/ corresponding to the curve in Fig.3 denoted as P II
xx/ corresponding to curves in Fig.3 denoted as P I /for S > 0/

References :

1. Z.Hashin, J.Appl.Mech. 29, 1 /1962/
2. R.C.Rossi, J.Amer.Ceram.Soc. 51,8 /1968/
3. S.C.Carniglia, J.Amer.Ceram.Soc. 55,12 /1972/
4. J.Dyczek and M.Petri,"6 Int.Symp.Chem. Cem." Proc.Moscow/1974/

O.Z. CEBECI, W.H. MIRZA and S.I. AL-NOURY- Department of Civil Engineering, King, abdulaziz University Jeddah, Saudi Arabia

STRENGTH DEVELOPMENT OF MORTARS IN HOT AND DRY ENVIRONMENT

INTRODUCTION

Masonry mortars are made by mixing, in certain proportions, one or more types of cement with clean, well-graded sand, and sufficient water is added to produce a plastic, workable mixture. When hardened, mortars must possess adequate strength, durability, and volume stability. Although Portland cement is capable of developing high compressive strength, its fresh mortars, made without plasticizers, lack the desired workability. Therefore, lime is commonly added to cement mortars in order to achieve adequate plasticity (1,2).

While Portland cement must be kept saturated to improve hydration and strength development, lime gains strength primarily by evaporation of the mixing water. Naturally, the ambient temperature and relative humidity at construction sites show considerable variations with climatic and seasonal changes. Although high temperature and low humidity are detrimental for the strength ultimately developed in Portland cement paste, mortar and concrete (3,4), cement-lime mortars may behave differently under these adverse conditions (5).

In this work the strength development in a cement and a high-lime mortar under hot and dry environmental conditions was investigated. The test specimens were made at 20, 35, and 50 C, and were cured at these temperatures in lime saturated water, and 92%, 75%, and 33% relative humidity. The compressive strengths of the mortars (developed in these 12 different media of various temparature-humidity combinations covering the range of common normal and hot weather conditions) were determined.

MATERIALS, TESTS AND RESULTS

A commercial ordinary Portland cement and hydrated lime and a local natural sand, all conforming to standard specifications, and tap water were used for preparing the mortars. The proportions of the solid constituents of masonry mortars are conventionally specified by volume (1); however, weight proportions were adopted in this study, so that the mixes were accurately reproduced in the laboratory. The amount of mixing water for each type of mortar was determined by the standard (ASTM C 109) flow table test, and fixed such that the mixes at different temperatures produced flows in the range 100-110%, thereby, all being at normal consistency. The mix proportions are shown in Table 1. It should be noted that Type O is essentially the "high-lime, low-strength" mortar specified by the same designation in some standards (1).

Table 1. Mix proportions of the mortars

Mortar Designation	Proportions, by weight			
	Cement	Lime	Sand	Water
Type C	1	-	3	0.65
Type O	1	0.8	7.5	1.7

The mortars were mixed and cast in 40x40x160mm molds according to the ISO-RILEM Recommendation R679. The mixer, materials and the molds were kept at 20, 35 and 50 C, and the specimens were stored at these temperatures in humid cabinets for 24 hours. After demolding, some specimens were crushed in order to determine the 1-day strength, others were placed in water baths at 20, 35 and 50 C, or stored in 9 different cabinets at these temperatures and at 92%, 75%, and 33% relative humidity (RH) maintained above saturated salt solutions (6).

The strength development in the cement mortar (designated as Type C) and in the high-lime mortar (designated as Type O) upon curing under various conditions up to 28 days are shown in Fig. 1 and 2, respectively. The specimens were brought to room temperature and crushed at their respective moisture conditions. It should be noted that specimens dried prior to crushing indicate greater strength than similar ones of the same batch tested in the saturated condition (7).

DISCUSSION

The effect of elevated temperature on the compressive strength of Portland cement mortar is demonstrated in Fig. 1(a). It is confirmed that, with increasing curing temperature, the early strength increases at the expense of the ultimate strength. Similar data has been reported in the recent literature (8,9), but Fig. 1(b)-(d) reveal important findings: Regardless of the curing temperature, strength development in 92% RH is about the same as that in water, and strength gain practically ceases within 28 days when the RH is reduced to 33%. At 50 C, the effect of 75% RH is almost as detrimental as 33%, whereas at lower temperatures 75% RH reduces, but does not stop, the strength development.

Fig. 1(a) also shows that the cement mortar (Type C) is much stronger than the high-lime mortar because partial replacement of the Portland cement with lime and increased proportions of sand and water in the latter substantially reduce its compressive strength (1,2).

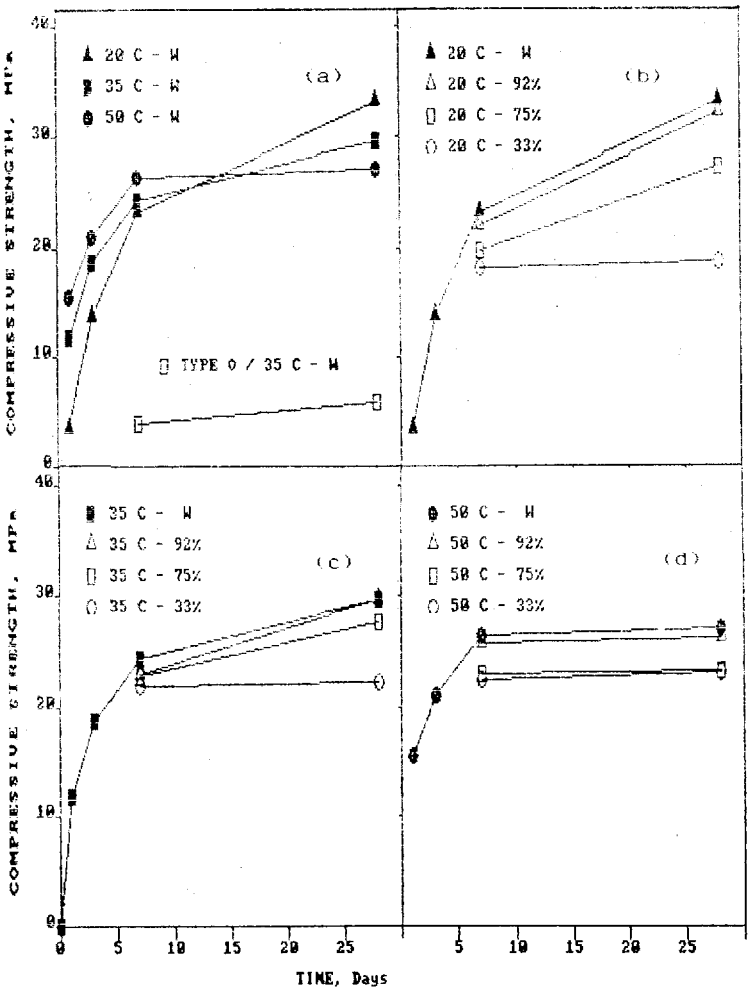

Figure 1- Compressive strength of Portland cement mortars developed under various curing conditions

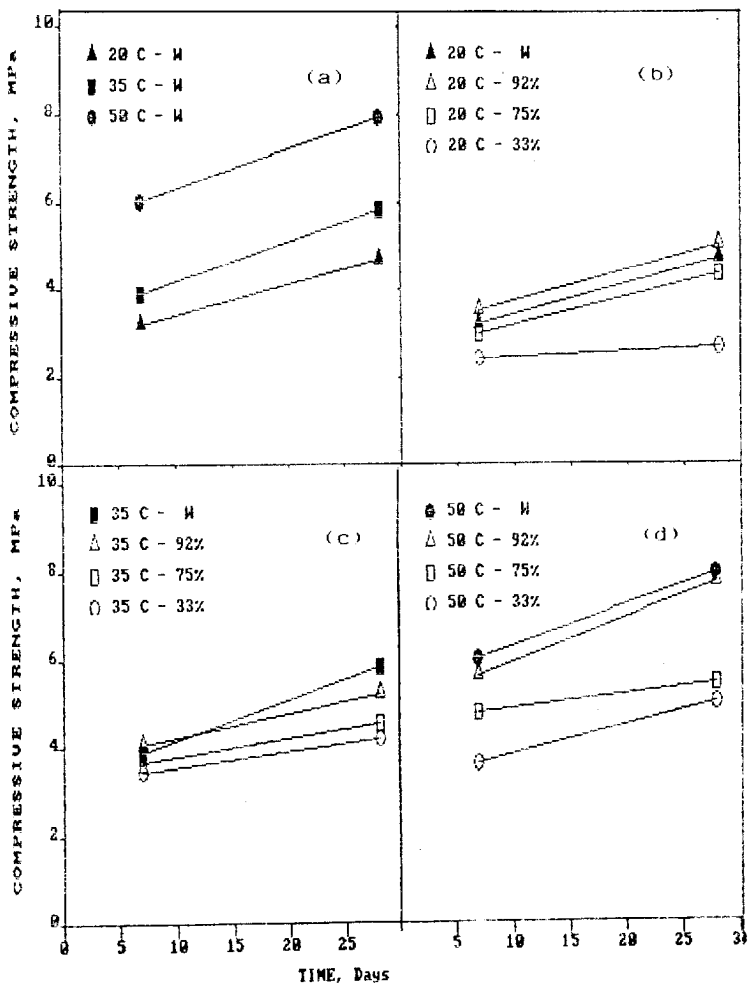

Figure 2- Compressive strength of high-lime mortar developed under various curing conditions

The compressive strength of high-lime mortar increases with increasing temperature throughout 28 days of wet curing, as shown in Fig. 2(a). A similar trend has been observed by Dalziel (8), who investigated the effect of curing temperature on the development of strength of mortar containing fly ash.

From 7 to 28 days, the strength gain in 33% RH is very small at 20 C, while at 35 C, and particularly at 50 C the improvements in the compressive strength achieved in the dry media are not negligible.

The differences between the behavior of cement and high-lime mortars should not imply that the high-lime mortar, a favorite of masons because of its excellent workability and economical cost, may also be the favorite in hot and dry environment, since dry-cured specimens attain about 60-70% of the strength of wet-cured ones.

In 20 C, high-lime mortars cured in 92% RH show slightly more strength than those cured in water, probably due to the effect of the moisture condition of the specimen on the observed strength (Fig. 2(b)). This holds also for the 7-day test results at 35 C (Fig. 2(c)).

CONCLUSION

The present investigation has shown that increasing temperature and decreasing relative humidity influence Portland cement and cement-lime mortars differently.

At normal and high temperature, dry environment is detrimental for the compressive strength of cement mortar. At elevated temperature, prolonged wet curing does not substantially improve the strength whereas at 20 C, it increases the 28-day compressive strength of the specimens almost twice as much as that of the dry-cured ones.

The strength of high-lime mortar increases with increasing temperature and humidity of the curimg media.

ACKNOWLEDGEMENT

This paper is based upon work supported by SANCST, the Saudi Arabian National Center for Science and Technology, under Grant No. AR6-077

REFERENCES

1. F.A. RANDALL, Jr., and W.C. PANARESE (1976), "Concrete masonry handbook", Portland Cement Association, Skokie.

2. C. BEALL (1984), "Masonry design and detailing", Prentice-Hall, Inc., Englewood Cliff.

3. F.M. LEA (1970), "The chemistry of cement and concrete, 3rd ed.", Edward Arnold Publishers Ltd., London.

4. G.J. VERBECK and R.H. HELMUTH (1968), "Structures and physical properties of cement paste", Proc. Fifth Int. Symp. Chem. of Cement, Tokyo, Vol. III, pp. 1-32.

5. W.H. MIRZA and S.I. AL-NOURY (1985), "Mortar in an adverse climate", Concrete International, 7(8)56-59.

6. D.S. CARR and B.L. HARRIS (1949), "Solutions for maintaining constant relative humidity", Ind. Eng. Chem. 41(9)2014-2015.

7. P. BARNES, Ed. (1983), "Structure and performance of cements", Applied Science Publishers, London.

8. J.A. DALZIEL (1980), "The effect of curing temperature on the development of strength of mortar containing fly ash", Proc. Seventh Internat. Conf. Chemistry of Cement, Paris, Vol. III, pp. IV-93-97.

9. N.J. CARINO and H.S. LEW (1983), "Temperature effects on strength-maturity relations of mortar", J. Amer. Concr. Inst., 80,177-182.

K. S. Han and J. Rhee, Professor, Inha University, Inchon, Korea.

Studies on the synthesis of C_3A by Sol-gel process

INTRODUCTION

Nowadays the sol-gel process for preparation of inorganic materials is applying extensively to obtain fibers, coatings and films, porous solids, nuclear fuels and oxide powders (1-3).

In the synthesis of inorganic materials by the sol-gel process, the raw materials are mixed in solution state and reacted lower temperature, and then drying and sintering process of the product are followed. By using this method, one can save energy and obtain highly pure and homogeneous materials.

Therefore, it has many advantages over the conventional method in which solid powder mixture is sintered or melted. In spite of many apparent advantages of the sol-gel process, it has some disadvantages of high cost of raw materials, large shrinkage during processing, residual fine pores, residual hydroxyl and long processing time (3,4).

The C_3A, one of the cement compounds, could be obtain by sintering an oxide powder mixture of C_3A composition at 1365°C for many hours with intermediate grinding, in this study, however, C_3A was synthesized by applying the sol-gel process using aluminium-sec-butoxide as alumina source and calcium nitrate as calcium oxide source.

Hydrolyzation conditions of Al-sec-butoxide and peptizing and gelling conditions for the mixture of hydrolyzed precipitate from the Al-sec-butoxide and the calcium nitrate were examined. And also, the optimum heating conditions for the synthesis of C_3A were investigated carefully. Heat treatment in the air and in the atmosphere of the oxygen-free dried nitrogen were respectively performed to study $C_{12}A_7$ which was produced unexceptionally in the early stage of synthesizing reaction of C_3A.

Besides, C_3A obtained by the conventional method was compared with C_3A from sol-gel method in terms of their reactivity of formation and crystallinity each other.

EXPERIMENTAL

Reagent grade Al-sec-butoxide, $Al(O\text{-}sec\text{-}C_4H_9)_3$, and calcium nitrate, $Ca(NO_3)_2 \cdot 4H_2O$ were used for the study.

Because the Al-sec-butoxide hydrolyze easily even with the moisture in the air to form aluminium hydroxide, the stoichiometric procedure was performed in the glove chamber under the dry nitrogen gas atmosphere.

Yoldas reported that hydrolyzing of Al-sec-butoxide and peptizing of the precipitate was affected considerably by the temperature of hydrolyzing water (5). Consequently, the hydrolysis was done by introducing the alkoxide into 200 fold mole of hot water (85°C) alkoxide under vigorous stirring on the hot plate keeping 90°C for 15 min.. After dispersion of the precipitate the calculated amount of calcium nitrate for C_3A synthesis was dissolved in the solution.

Different amount of HCl in 0.1 N solution, from 0.01 to 0.2 fold mole per mole of $Al(O\text{-}sec\text{-}C_4H_9)_3$, was added and stirred briskly for peptizing and gelling of the mixed solution at 90°C.
The completion of gelling was identified by finding the dispersion of the precipitate and stagnation of bubbles in the solution. The gelled sample was dried at 110°C.

On the other hand, a powder sample for C_3A was prepared by calcining the mixture of $CaCO_3$ and Al_2O_3 with ratio of 3:1 at 1000°C for comparison with sol-gel sample.

The effect of heat treatment on the formation of C_3A was investigated for the dried sol-gel sample and the oxide mixture sample. Both samples were heat-treated at 1100, 1200, 1300 and 1400 °C in the air and in the atmosphere of oxygen-free dried nitrogen respectively. Five times of 10 hours heating at 1100 and 1200 °C were carried out for each sample, but when sintered at 1300 and 1400 °C, 10 hours heating was repeated to complete the formation of C_3A.

Reactivity of C_3A formation was examined quantitatively by X-ray diffraction analysis and represented as the ratio of the amount of $C_{12}A_7$ to C_3A produced during the heat treatment.

Crystallized C_3A size was calculated by Scherrer equation for X-ray diffraction profiles.

The heat evolved by hydration reaction of C_3A in 18 hrs measured by the multicell conduction calorimeter.

RESULTS AND DISCUSSION

When hot water of 85°C was used for the hydrolysis of Al-sec-butoxide, AlO(OH), boemite, was produced and the peptizing and gelling for the mixed solution was performed.

The relation between gelling time of the mixed solution and the amount of HCl added per mole of $Al(O\text{-}sec\text{-}C_4H_9)_3$ was shown in Fig. 1. When more than 0.1 fold mole of HCl was added, the gelling was rapidly occured within 3 hours, but it was not occured when added less than 0.03 fold mole of HCl. Although quite slow gelling was performed by adding 0.05 to 0.08 fold mole of HCl, the enhanced reactivity of C_3A formation was found when gelling for longer time. It was supposed to be caused by high homogeneity of components through longer time. Hence the peptizing and gelling was proceeded by using 0.05 fold mole of HCl at 90°C in this study.

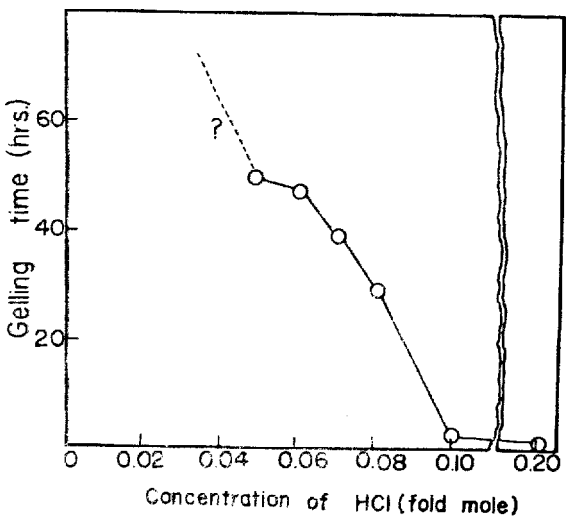

Fig. 1 Gelling time for the mixture solution of AlO(OH) and $Ca(NO_3)_2 \cdot 4H_2O$ with various amount of HCl per mole of $Al(O\text{-}sec\text{-}C_4H_9)_3$.

When the sol-gel sample was heated in the air, $C_{12}A_7$ was started to form after heating at 600°C for 1 hour, and C_3A was appeared after heating at 1000°C for 30 hours. When the oxide mixture sample was sintered in the air, on the other hand, $C_{12}A_7$ and C_3A were started to form after heating at 1000°C for 10 hours and at 1100°C for 10 hours, respectively.

As shown in Fig. 2 and Fig. 3, initial formation of $C_{12}A_7$ from the sol-gel sample heated at 1100 and

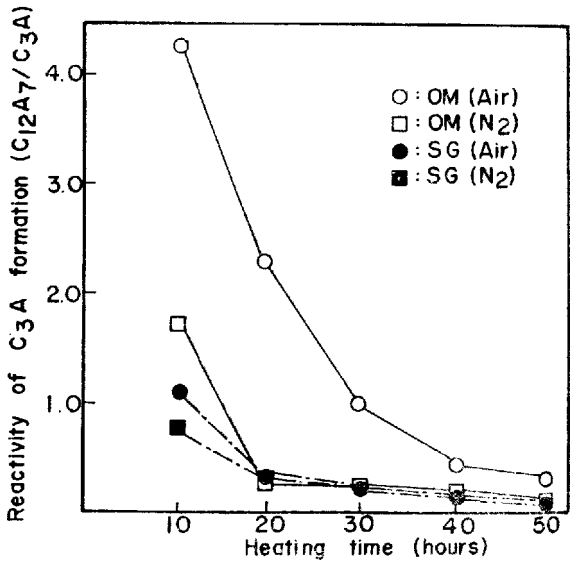

Fig.2 Reactivity of C_3A formation with various heating time at 1100°C.

*SG: Sol-gel sample dried at 110°C.
OM: Oxide mixture sample heat treated at 1000°C for 1 hr.

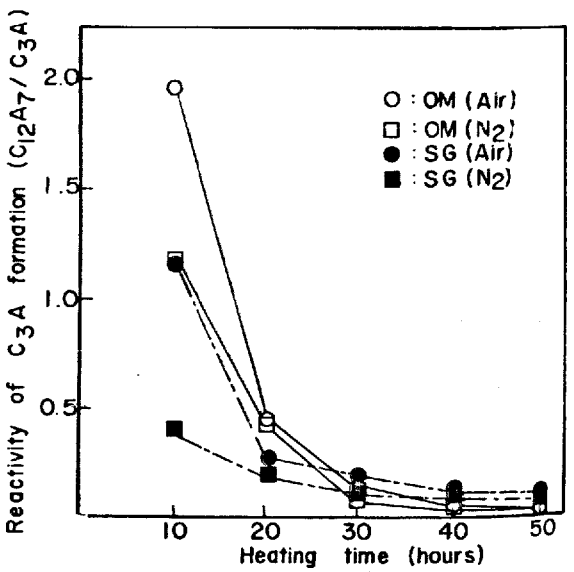

Fig.3 Reactivity of C_3A formation with various heating time at 1200°C.

1200 °C was much better than that of the oxide mixture sample. It is believed that superior reactivity of the sol-gel sample is due to minified fineness and high homogeneity of reacting particles. J. A. Imlach and F. P. Glasser refered that traces of water undoubtedly hasten the formation of $C_{12}A_7$

and the water may act as a catalyst (6).

Furthermore, the oxide mixture sample heated in an atmosphere of oxygen-free dried nitrogen exhibited around the same reactivity with the sol-gel sample heated in the air. It was supposed that $C_{12}A_7$ from the oxide mixture sample was reacted normally to form C_3A without any interrupting of contact to water during heat treatment.

Fig. 4 and Fig. 5 showed that the reactivity of C_3A formation from the oxide mixture sample was superior at 1300 and 1400°C than that from the sol-gel sample. In particular, the reactivity under the atmosphere of oxygen-free dried nitrogen was remarkable.

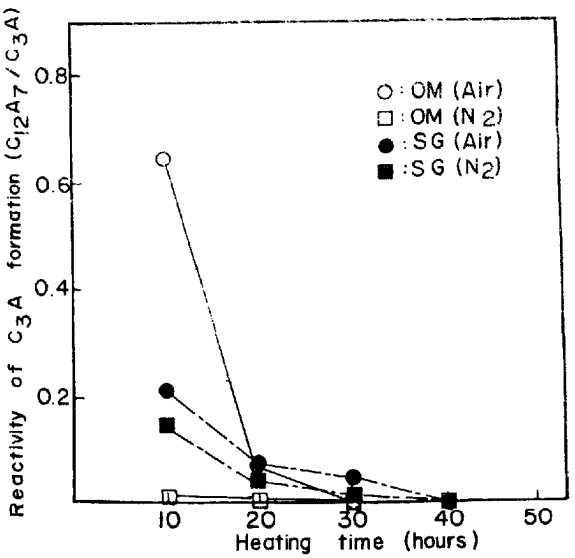

Fig.4 Reactivity of C_3A formation with various heating time at 1300°C.

In the initial heating stage of forming C_3A from the reacting of CaO and Al_2O_3 , $C_{12}A_7$ was inevitably formed as a intermediate product. $C_{12}A_7$ has zeolitic behavior (7) and in the temperature range of 950-1350 °C, it enters into reversible equilibrium with water present in furnace atmosphere and the constitution of the phase is described as $C_{12}A_{14}O_{32}(OH)_2$ (8).

The sol-gel sample showed superior reactivity with initial formation of $C_{12}A_7$ at 600°C and C_3A at 1000°C, but the effect of reactivity to lower $C_{12}A_7/C_3A$ ratio to less than 0.4 was inferior when it was heated repeatedly at lower temperature

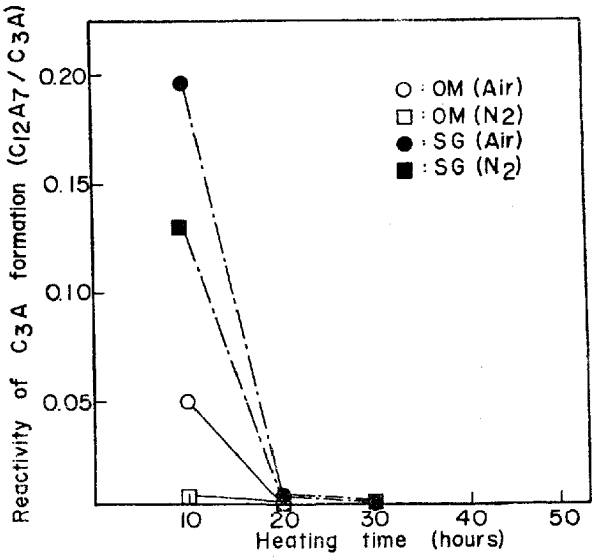

Fig.5 Reactivity of C_3A formation with various heating time at 1400°C.

(1100, 1200°C) and heated at higher temperature (1300, 1400°C). C_3A is formed by diffusion of CaO to $C_{12}A_7$, but the C_3A formation might be prevented when $C_{12}A_7$ become stable by incorporating OH group.

Heating in an atmosphere of oxygen-free dried nitrogen could not eliminate the trouble-some OH group in the stable $C_{12}A_7$ phase. Since the oxide mixture sample could produce $C_{12}A_7$ without OH group, on the contrary, it was presumed to have remarkable effect for formation of C_3A.

Crystallized particle size of C_3A formed by sol-gel and conventional method were both in the range of 63-70 nm.

Since the heat evolved in 18 hours by hydration of C_3A obtained from two different method were in the range of 140-145 cal/gr, the hydration characteristics of them seemed to be almost the same.

CONCLUSION

AlO(OH) was formed from Al-sec-butoxide through hydrolysis with hot water of 85°C.

The gelling process of the mixture solution of AlO(OH) precipitate and $Ca(NO_3)_2 \cdot 4H_2O$ proceeded most favorably when 0.05 fold mole of HCl was added to one mole of Al-sec-butoxide.

Initial formation of $C_{12}A_7$ and C_3A at lower temperature (1100, 1200°C) from sol-gel sample was superior, but complete crystallization of C_3A at higher temperature (1300, 1400°C) was inferior as compared with that from oxide mixture sample.

The formation reactivity of C_3A in an atmosphere of oxygen-free dried nitrogen from oxide mixture sample showed remarkable effect.

The crystallized size and the hydration characteristics of C_3A obtained by different process exhibited around the same results.

The kinetics of this progress will be more fully described in a subsequent paper.

REFERENCES

1) Sumio sakka, K. Kamiya, "Glasses from metal alcoholates", Jour. of Non-Crystalline Solids, Vol. 42, 403-422 (1980).

2) Helmut Dislich, "Glassy and crystalline systems from gels : Chemical basis and technical application", Jour. of Non-Crystalline Solids, Vol. 57, 371-388 (1983).

3) Larry L. Hench and Donald R. Vlrich, "Ultrastructure processing of ceramics, glasses and composites", John Wiley and Sons, New York, pp 15-26 (1984).

4) J. D. Mackenzie, "Glasses from melts and glasses from gels", Jour. of Non-Crystalline Solids, Vol. 48, 1-10 (1982).

5) B. E. Yoldas, "Alumina sol preparation from alkoxides", Amer. Ceram. Soc. Bull., Vol. 54, 289-290 (1975).

6) J. A. Imlach, L. S. Dent Glasser, F. P. Glasser, "Excess oxygen and the stability of $C_{12}A_7$", Cem. and Conc. Res., Vol. 1, 57-61 (1971).

7) D. M. Roy and R. Roy, "Crystalline solubility and zeolitic behavior in garnet phases in the system $CaO-Al_2O_3-SiO_2-H_2O$", Chemistry of Cement, Proc. 4th. Intl. Symp., Washington 1960, National Bureau of Standards, Vol. 1, 307-314 (1962).

8) R. W. Nurse, J. H. Welch and A. J. Majumdar, "The $12CaO \cdot 7Al_2O_3$ phase in the $CaO-Al_2O_3$ system", Trans. Brit. Ceram. Soc., 323-332 (1965).

I.Y. SEO - Research Center of Ssang yong Cement Ind. Co., Ltd.
S.H. CHOI - University, Seoul, Korea

THE UNSTABLE STATE OF ALKALI IN CEMENT CLINKER

Introduction

Though alkalies are minor components of cement clinkers, there have been many researches about them in view point of the significance of their influences on clinker phases and hydration reactions of cement, as well as the alkali-aggregate reaction. However, some conflicting phenomena still occur in empirical data. These may be partially due to the versatile formation reactions of their compounds and their complex behaviors in hydration of cement.

In the previous reserch[1,2], investigating the existing states of potassium in portland cement clinker, the new concept of alkali, given a name as unstable alkali, was introduced. It was found that the unstable alkalies exist when SO_3 content is below a certain limit, related mainly to alkali content in the clinker. The unstable alkalies, which are readily slouble with water, react with gypsum to form $Ca(OH)_2$ and syngenite on hydration. As a result, the heat liberation rate of hydration at the early hydration process (first peak) increases remarkably, and the reaction cannot be controlled only by the supplement of gypsum to the cement. A increasing tendency of ignition loss of clinker with increase of unstable alkali content was found.

In this paper, the formation mechanism of the unstable alkalies and their forms occuring in clinker were studied.

Experimental

The raw mixtures added various amount of KOH to the mixture of OPC clinker composition not containing potassium and sulfur were prepared, and they were shaped into pellet-and tablet-types and sintered at 1400° and 1450°X for 30 min. after calcination at 900°C for 1 hr. respectively (P-series). Tablet-type samples were prepared by pressing the calcined raw mixtures. The clinkers were vacuum-dryed at 150°C after measurements of porosity by kerosene (Sp. Gr. : 0.796 at 20°C), and the content of alkalies and water-soluble components of the clinkers were analysed. Also the distributions of potassium and other elements at various parts of the clinkers were analysed by means of SEM-EDX system.

In order to elucidate the fact that the K_2O-Al_2O_3 compounds are some forms of unstable alkalies, the lime-saturated C_3A-K_2O system and K_2CO_3-Al_2O_3 system were examined. The lime-saturated C_3A was prepared from the raw mixture of excess CaO content from stoichiometric composition with chemical pure reagents. The mixture was calcinated at 1000°C for 1 hr. and sintered at 1450°C for 12 hrs. after pressing. Remixing, pressing and sintering were repeated until the free CaO content was not changed. Free CaO content of the last C_3A (sample No. K0) was 2.2%. The mixtures of various amount of K_2CO_3 addition to the C_3A were sintered at 1400°C for 1 hr. (K-series). And then K_2O content, changes of free CaO and C_3A content, and the change of lattice parameter (a) of C_3A were analysed by chemical analysis and x-ray diffraction analysis.

The mixtures of K_2CO_3 and Al_2O_3, with various molar ratios of K_2O/Al_2O_3 such as (1) 4.0, (2) 3.0, (3) 2.0; (4) 1.5, (5) 1.2, (6) 1.0 (sample No. : C-1, C-2, C-3, C-4, C-5 and C-6 respectively), were calcined at 600°C and sintered at 1100°C for 20 min. (C-series). Water-soluble K_2O and Al_2O_3 of the syntered samples were analysed and their reaction products were identified by means of x-ray diffraction analysis.

Results and Discussions

1. Formation mechanism of unstable alkalies and their forms.

Fig. 1 is the SEM and characteristic x-ray image of potassium distribution of a P-series clinker with high unstable alkali content and reveals that most of potassium are apt to be concentrated at the liquid phase of clinker. It was found that ignition loss of clinker tends to increase according to unstable alkali content.[2] Volatilized alkalies and SO_3 content of a high-ignition loss clinker were analysed and are listed in table 1. It appears from the result that unstable alkalies have a hygroscopic and easily volatile properties. Fig. 2 shows the correlationships of K_2O content vs. Al_2O_3, Fe_2O_3, CaO and SiO_2 content analysed by EDX at various parts of P-series clinkers. In the results, K_2O content has a positive correlationship only with Al_2O_3 content and no relationship with Fe_2O_3 content. Moreover, water-soluble Al_2O_3 content increases with increase of water-soluble K_2O (unstable alkali

of potassium) content in P-series clinkers, which is shown in Fig. 3. Fig. 4 is the scanning election micrograph which shows potassium aluminate in a P-series clinker. The chemical composition of square part (labelled C) in the photograph was 10.5% of SiO_2, 34.0% of Al_2O_3, 0.0% of Fe_2O_3, 16.7% of CaO, 2.0% of MgO, 4.2% of Na_2O and 32.7% of K_2O.

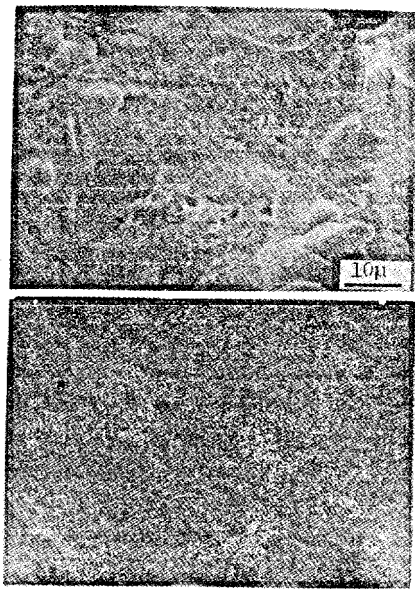

Fig. 1. Scanning electron micrograph and its K Ka-radition photograph.

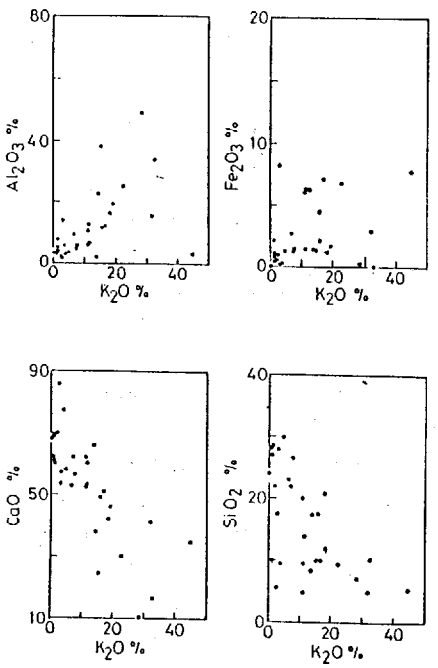

Fig. 2. K_2O content vs. Al_2O_3, Fe_2O_3, CaO and SiO_2 content of various parts of clinkers (P-series).

Fig. 5 shows that porosity of clinker tends to increase on the conditions when unstable alkali content increases. The same result can be found in the Ono's report[3], in which alkali carbonates was used for alkali sources without SO_3 addition. Equations (1), (2) and table 2 represent the results of multiple linear regression analysis about the correlation ship of alkali content and porosity of closed pore with the unstable alkali content of the P-series clinkers.

Table 1. Volatilized alkali and SO_3 content of a high-ignition loss clinker sample.

Temp. range °C	Ig.loss %	Volatilized content %			Remark
		Na_2O	K_2O	SO_3	
20 - 400	0.72	tr	tr	tr	dehydration
400 - 600	0.13	tr	0.01	tr	dehydration of $Ca(OH)_2$
600 - 900	0.46	tr	0.42	tr	volatilization of unstable K_2O

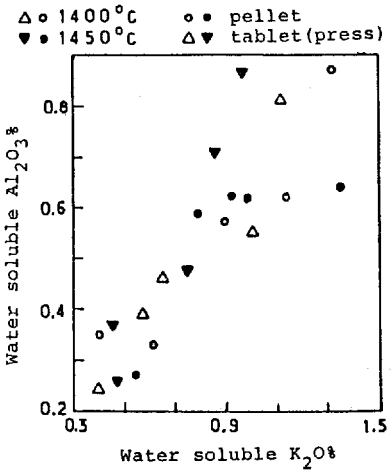

Fig. 3. Water soluble K_2O vs. water soluble Al_2O_3 content in P-series clinkers.

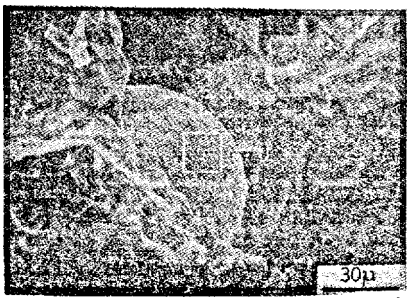

Fig. 4. Scanning electron micrograph showing the K_2O-Al_2O_3 compound formation.

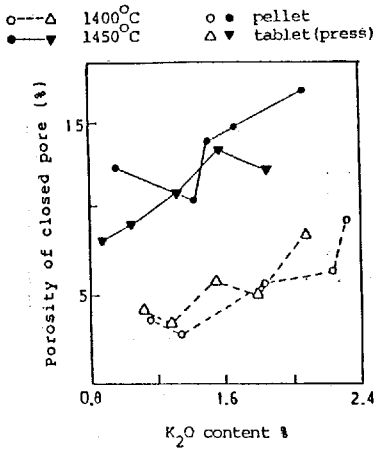

Fig. 5. Change of porosity according to K_2O content of P-series clinkers.

$$S\text{-}\bar{\bar{K}}\% = 0.630\ T\text{-}K_2O\% - 0.294 \quad \ldots\ldots\ldots\ldots\ldots\ (1)$$

$$S\text{-}\bar{\bar{K}}\% = 0.608\ T\text{-}K_2O\% + 0.021\ CP\% - 0.437 \quad \ldots\ldots\ (2)$$

where, $S\text{-}\bar{\bar{K}}\%$: Unstable alkali content in clinker

$T\text{-}K_2O = K_2O\% + 1.52Na_2O\%$ in clinker

CP% : porosity of closed pore in clinker

Table 2. Results of regression analysis (n=20).

No. of equation	Correlation coefficient	Error of estimate	F-value	F(0.01)
1	0.94	—	133.25**	8.29
2	0.98	0.066	200.93**	6.11

Eq. (2) has higher correlation coefficient and F-value than those of Eq. (1). That means porosity of closed pore may be one of the factors related with unstable alkali formation. Moreover, reguarding that some parts of P-series clinkers have higher K_2O content relatively to the Al_2O_3 content in Fig. 2, it is possible to presume the following explanation for the formation of another types of unstable alkalies. (Refer to Fig. 6.)

The amount of trapped alkali vapor may increase in closed pores of clinker with higher alkali and lower SO_3 content. The alkali vapor will condense on the wall of the closed pores in the cooling process and some of the alkalies will solidify and remain as free alkalies on the wall of the pores.

From the above results, it is reasonable to think that two types of unstable alkalies, compounds of K_2O-Al_2O_3 system and free K_2O, exist in cement clinkers with high alkali and low SO_3 content.

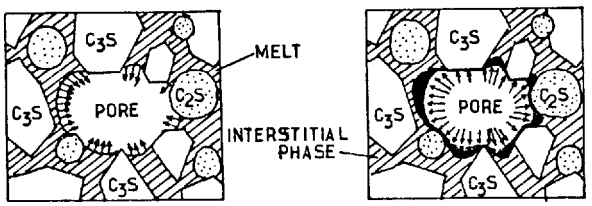

Fig. 6. Schematic diagram of K_2O vaporization and condensation at closed pore.

2. Compounds of K_2O-Al_2O_3 system

Fig. 7 shows x-ray diffraction patterns of K-series clinkers, and in K3.56 and K10.47 clinkers, some new peaks (marked X) come out at 32.8°, 33.7°, 34.4° and 38.7° (CuKa 2θ). The intensities of the peaks and free CaO content (37.4°) increase according to K_2O content of the clinkers. The figures of the sample names represent the K_2O content of the clinkers. It was confirmed that the new peaks disappear in the x-ray diffraction pattern of the water-extracted residue of K10.47 clinker for 30 seconds. It means that some new mineral or minerals, which are readily soluble with water, exist and the crystal system of C_3A is still cubic at K3.56 and K10.47 clinkers.

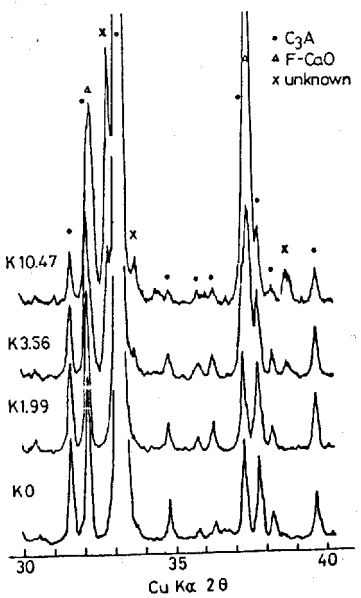

Fig. 7. Change of x-ray diffraction pattern of C_3A according to its K_2O content.

Fig. 8 shows that the lattice parameter (a) of C_3A increases slightly up to about 2.5% of K_2O content and does not change above the K_2O content.

Fig. 9 shows the change of C_3A content analysed by quantitative x-ray diffraction analysis according to the K_2O content in K-series clinkers. Up to about 2.5% of K_2O content, C_3A content is almost unchanged, however above the K_2O content, it decreases inversely with increase of K_2O content. Also the free CaO content in Fig. 10 is almost unchanged up to about 3% of K_2O content and increases linearly above the K_2O content. In K_2O-Al_2O_3 system, the compounds of $3K_2O \cdot Al_2O_3$[4], $K_2O \cdot Al_2O_3$[5], $K_2O \cdot 5Al_2O_3$[6] and $K_2O \cdot 11Al_2O_3$[7] were reported. In C_3A-K_2O system, if the above compounds are produced after sintering, the reaction equations will be same as following models, and CaO/K_2O substitutional molar ratio (m) and C_3A/K_2O molar ratio (n) of each models were calculated in table 3. Comparing the decreasing rate of C_3A content in Fig. 9, n-value equals to about 1 and corresponds to model (2) of $K_2O \cdot Al_2O_3$ formation. In Fig. 10, m-value equals to about 2 and corresponds to the value between model (1) and (2). Fig. 11 shows the x-ray diffraction patterns of K 10.47 clinker and C-series samples, and reveals that the compound $K_2O \cdot Al_2O_3$ is the major mineral in C-6 sample and most of the unknown peaks (labelled X) of K10.47 clinker correspond to the compound. However, some unknown peaks, though their intensities are very low, still remain and m-value does not correspand to model (2). Therefore, according to the composition of liquid phase of each part of clinker, other minerals of K_2O-Al_2O_3 system are thought to form simultaneously.

Model for compound formation of K_2O-Al_2O_3 system.

$C_3A + xK \rightarrow (1-\frac{x}{3})\, C_3A + \frac{x}{3}\, K_3A + xC$ ..... (1)

$C_3A + xK \rightarrow (1-x)\, C_3A + xKA + 3xC$ ..... (2)

$C_3A + xK \rightarrow (1-5x)\, C_3A + xKA_5 + 15xC$ ..... (3)

$C_3A + xK \rightarrow (1-11x)\, C_3A + xKA + 33xC$ ..... (4)

where, C = CaO, A = Al_2O_3, K = K_2O.

Table 3. CaO/K_2O substitutional molar ratio(m) and C_3A/K_2O molar ratio(n) of each models.

Model No.	m	n	Remark
1	1	-1/3	model of compound formation of K_2O-Al_2O_3 system
2	3	-1	
3	15	-5	
4	33	-11	

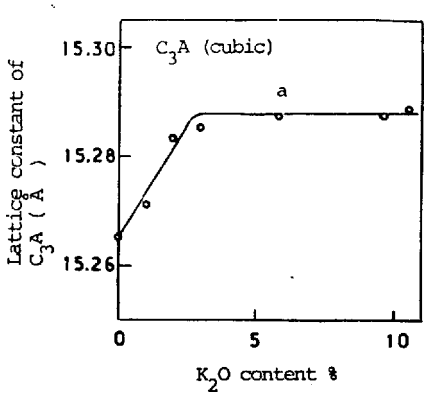

Fig. 8. Change of lattice parameter of lime-saturated C_3A according to its K_2O content.

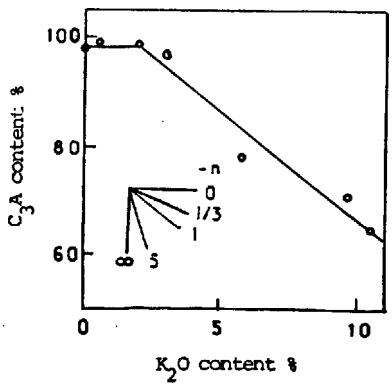

Fig. 9. Change of C_3A content of lime-saturated C_3A according to its K_2O content.

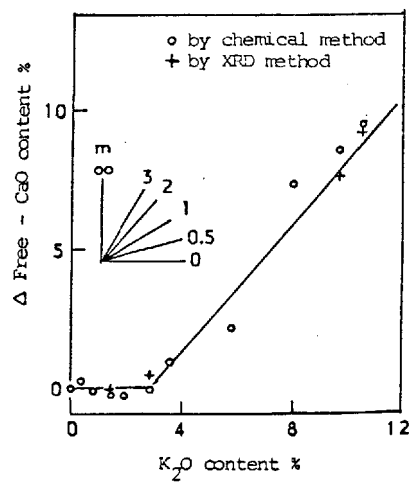

Fig. 10. Change of free-CaO content according to K_2O content of lime-saturated C_3A.

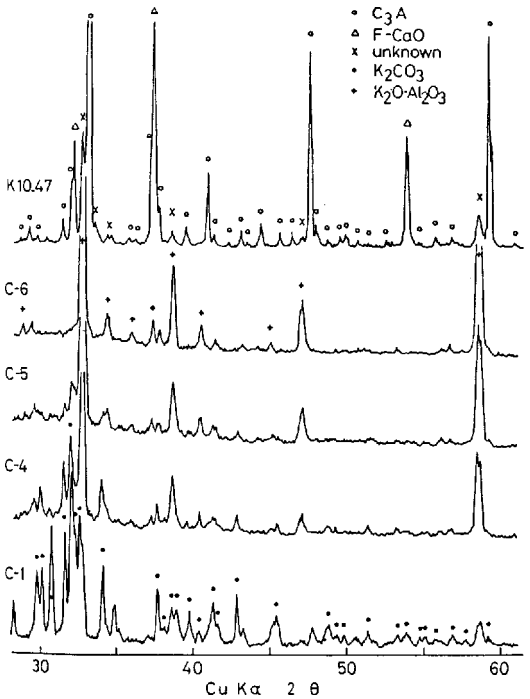

Fig. 11. X-ray diffraction patterns of K10.47 in C_3A-K_2O system and C-1, C-4, C-5 and C-6 in K_2O-Al_2O_3 system.

Conclusions

Two forms of unstable states of potassium, compounds of K_2O-Al_2O_3 system and free K_2O, exist in the clinkers of this experiment. Most of potassium are apt to be concentrated at the liquid phase of clinker and the K_2O-Al_2O_3 compounds are formed in the liquid phase concentrated by K_2O. Therefore, water-soluble Al_2O_3 content is apt to increase according to the unstable alkali content. The compound $K_2O \cdot Al_2O_3$, which was confirmed to be formed easily in the C_3A-K_2O system, is a major mineral among the K_2O-Al_2O_3 compounds. The amount of trapped alkali vapor may increase in closed pores of clinkers with higher alkali and lower SO_3 content. Free K_2O is thought to be the condensed alkali in the pores.

References

1) I.Y. Seo and S.H. Choi, "Influence of Potassium on the Cement Clinker Formation, I.Unstable Free Alkali in Clinker," J. Korean Ceram. Soc., 22 (1) 25-34 (1985).

2) I.Y. Seo and S.H. Choi, "Influence of Potassium on the Cement Clinker Formation, II Factors of Unstable Alkali Formation," ibid, 22 (2) 25-32 (1985).

3) Y. Ono, T. Hidaka and M. Shirasaka, "On the Influence of Na_2O, K_2O and MgO on the Development of Strength of Portland Cement Mortar," Rev. 23rd Gen. Mtg. Japan, 61-65 (1969)

4) ASTM card No. 27-1336.

5) Brown Miller, Am. J. Sci. 29 266 (1935) : by ASTM card No. 2-0897.

6) Yamaguchi and Suzuki, Bull. Chem. Soc. Japan, 41 93 (1968) by ASTM card No. 21-618.

7) ASTM card No. 31-960.

Vázquez, T., Blanco-Varela, M.T., Palomo-Sánchez, A.
Instituto Eduardo Torroja de la Construcción y del Cemento (C.S.I.C.) Madrid- España

LUMPING OF ANHYDROUS PORTLAND CEMENT: STUDY THROUGH IS SPECTROSCOPY

EPAISISSEMENT DU CIMENT PORTLAND ANHYDRE: ETUDIE PAR ESPECTROSCOPIE INFRAROUGE

C L

Introduction

The use of combustibles with a high content in sulfur propiates that during the process of clinkerization several sulfates are formed and afterwards remain incorporated to the clinker. Among these sulfates we can find the K_2SO_4 and the $2CaSO_4.K_2SO_4$ (calcic langbeinite), that have a definite influence in the probable presence of false setting and lumping in cements.

The mechanism that overrule the aparition of both effects is quite similar being the presence of calcic singenite ($CaSO_4\ K_2SO_4.H_2O$) the determinative common cause.

Even when the lumping of the anhydrous cement doesn't damage the hydraulic characteristics of the cement, sometimes it produces great problems of manipulation in operations of unloading in silos or stores where it is conserved. A commong case of serious economic consequences is the lumping produced in holds of ships disposed to carry a heap cement. In the present work it is studied this kind of lumping.

Some considerations about lumping in cements

F. MATOUSCHEK (1) discovers a similar phenomenon as the one studied in the present work: formation of grumes in all the mass of an ensilaged cement, in such a manner that it solidified, needing finally to remove it with shovel and meaning this very high costs.

FOREST (2) in 1962 associated the presence of grumes in anhydrous cements with the formation of syngenite. He indicates that exists a level in the proportion of syngenite; below this level, its action isn't operative. In the experimental works achieved by him, he establishes this limit in 0,65%.

S. SPRUNG (3) attests that the water that comes from the dehydration of gypsum in the silo spreads as vapour to colder zones and reacts with the cement. As a result of the reaction it appears, among other compounds, acicular syngenite that forms a rigid texture.

NIELSEN (4) explains how the water's vapour produced as a consequence of the dehydration of gypsum and a storing of the cement in hot spreads it self through its mass, reacting and producing several chemical reactions "such as the formation of syngenite".

RUIZ DE GAUNA (5) verifies that cement's gypsum can be dehydration to hemihydrate in the silo and that the soluble anhydrite hydration very easily to hemihydrate with water's vapour. The transition from hemihydrate to gypsum requires the presence of water in a liquid condition.

PLIEGO-CUERVO AND GLASSER (6) demonstrate experimentaly the coexistence of CaO, C_3A, C_2S, with $2CaSO_4.\ K_2SO_4$ and K_2SO_4.

T. VAZQUEZ-MORENO and O. FERNANDEZ-PEÑA (7) present the hypothesis that the calcic langbeinite ($2CaSO_4.K_2SO_4$) formed during the clinkerization can be transformed by the effect of wet air in syngenite and very activ $CaSO_4$.

Experimental procedure

Studied samples

It is studied a portland cement that supported a pronounced lumping in the holds of a ship that had carried 5.500 Tm and during its pneumatic unloading, it was necessary an extraction of about 2000 Tm of cement with manual methods, because it was impossible to do it as normally.

For the performance of the present work, 10 samples of the cement (numbered from 1 to 10) were taken in different zones of the ship's holds. They were classified in three different groups, considering the distinct aspects that the samples presented:

1st. Group: It concerns to sample nº 1 and it is the only one whose appearance and texture is similar as the one that could show up a hidrated and hardened cement. (Photog. 1)

2nd. Gruop: It concerns to the samples numbered: 2-3-4 and 5. They are similar between them, with a very lumped aspect. The photog. 2 of sample 2 it is shown as an example of the appearance that all the ones of this group present.

3rd. Group: It is formed by the samples nº 6-7-8-9 and 10. The appearance of these samples is the one of a quite fluid cement, with nodules of small size, easily brittle with the hand.

Photograph nº 3 concerns to 7th sample, given as an example of the ones belonging to this group.

All the samples were treated with salicylic acid in methanolic medium, with the purpose of removing calcic silicates and to enable the spectroscopic study of the cement's sulphates. They were studied by infra-red spectroscopy before and after the treatment. In all the cases, the results obtained through IR spectroscopy were verified through Differential Thermal Analysis and Thermogravimetric Analysis.

The chemical analysis of the cement is give in Table I.

Results and Discussion

There is a perfect agreement between the form and aspect of the samples and its correspondent IR spectra (figs. 1 - 6).

LUMPING OF ANHYDROUS PORTLAND CEMENT: STUDY THROUGH IR SPECTROSCOPY

EPAISISSEMENT DU CIMENT PORTLAND ANHYDRE: ETUDIE PAR ESPECTROSCOPIE INFRARROUGE CL

Certainly:

1st Group: The IR spectrum of sample nº 1 gives bands of characteristic compounds of the hydratated cement. So, of portlandite (ν-OH in 3640 cm^{-1}); Tobermorite (νI and ν_3-OH in 3400-3600 cm^{-1}); H-O-H in 1600-1700 cm^{-1}; $\nu_3 SiO_4$ in 940 cm^{-1}...), etc.

2nd Group: The IR spectra of the samples 2-3-4 and 5 are very similar between them. The characteristic bands of syngenite, of $CaSO_4 \cdot \frac{1}{2} H_2O$ and probably of ettringite appear, among others, in all of them.

3rd Group: The IR spectra of the samples 5-6-7-8-9 and 10, are also similar between them. It outstands among other bands, the characteristic ones of $CaSO_4 \cdot \frac{1}{2} H_2O$ and of K_2SO_4. We can also notice with a weak intensity, the specific ones of $CaSO_4 \cdot 2\ H_2O$.

Sample nº 1 has been taken from the coating stuck to the walls of the ship's hold, that being the colder part is where the water's vapour has been condensed. The correspondent liquid water reacted with the cement, with whom it was in contact, hydration it and showing the hydration phases detected in the sample.

It is the only sample among the ones studied that has been in contact with liquid water.

The samples that form the 2nd Group were situated in the inside of the mass that formed the stored cement, in places near the central part of the ship's hold, where the temperature of cement was approximately the maximum existent.

The samples that form the 3rd Group were situated near the periphery of the whole mass of stored ce - ment.

According to the results obtained in the study of the samples, the cement's lumping is explained by the following causes:

The cement supported a high temperature during the grinding process, so the gypsum underwent a partial dehydra - tion, according to the following reactions:

$$CaSO_4 \cdot 2\ H_2O \rightarrow CaSO_4 + 2\ H_2O \quad (1)$$

$$CaSO_4 \cdot 2\ H_2O \rightarrow CaSO_4 \cdot \tfrac{1}{2}\ H_2O + 1{,}5\ H_2O \quad (2)$$

The cement, being still hot, was introduced in the holds of the ship that thereinafter had to carry it. In the same holds, the gypsum that wasn't still dehydration continued this dehydration.

The resultant H_2O (v) of the reaction (1) and/or (2) reacted also with the K_2SO_4 that the cement contained and with the $CaSO_4$ and/or with the $CaSO_4 \cdot \frac{1}{2} H_2O$ also produced by these reactions, not only because of the high temperature of the grinding but also as a cause of the high temperature of ensilaged. Definitively syngenite is produced ($CaSO_4 \cdot K_2SO_4 \cdot H_2O$) according to the following reactions:

$$CaSO_4 + K_2SO_4 + H_2O \rightarrow CaSO_4 \cdot K_2SO_4 \cdot H_2O \quad (3)$$

$$CaSO_4 \cdot \tfrac{1}{2} H_2O + K_2SO_4 + \tfrac{1}{2} H_2O \rightarrow CaSO_4 \cdot K_2SO_4 \cdot H_2O \quad (4)$$

The $CaSO_4$ that intervene in reactions (1) and (3) is soluble anhydrite of high reactivity. Probably it is the catalyst of the reaction of $CaSO_4 \cdot \frac{1}{2} H_2O$ - and even of $CaSO_4 \cdot 2H_2O$ - with H_2O and K_2SO_4 for the correspondent formation of syngenite.

The $CaSO_4 \cdot \frac{1}{2} H_2O$ that intervene in the reactions (2) and (4) is also of a high activity, because it is naissant. Its "oldness" would make it notably less reactive.

The IR spectra of the lumping samples (2nd Group) demonstrate the presence of syngenite and the inexistence of K_2SO_4. So, they uphold the mechanism indicated in (3) and (4).

Although, as the IR spectra of the samples that belong to the 2nd Group present characteristic bands of $CaSO_4 \cdot \frac{1}{2} H_2O$ and K_2SO_4, and also weak correspondent to $CaSO_4 \cdot 2H_2O$, it is induced that reactions (3) and (4) haven't been performed, not in a significative form: syngenite hardly exists, the $CaSO_4 \cdot \frac{1}{2} H_2O$ has "grown old" and that is why its reactivity is very low, and a part of $CaSO_4 \cdot 2H_2O$ without dehydrate stays, even being a small part. All this is a consequence of the cement lying in less hot zones than the case of the lumped cement. With laboratory experimentation it was comprobed that the lumping produced in presence of K_2SO_4 happens the same with the calcic langbeinite ($2CaSO_4 \cdot K_2SO_4$). So that, portland cement was mixed up and homogeneized (whose specific surface and chemical analysis are given in table nº 2) with a 1.5% wt of langbeinite. Afterwards the mixture was introduced in a cilindric container of about 25 cm of diameter and 8 cm of height. In the middle of the mass of cement an electric calefactory was introduced surrounded with $CaSO_4 \cdot 2\ H_2O$. This is a similar system as the one used by Forest (2).

The temperature reached by the cement was controlled by a dispositive that consisted in a regulator and 6 thermocouples that were introduced inside the cement, placing them all along the diameter of the container. The distance between thermocouple and thermocouple was about 2.5 cm.

The packing case that held in the cement was covered up after that the convenient perforations for the introduction of the heating and control elements were made.

The gradient of temperature reached was from 120ºC to 45ºC; these temperatures persisted constantly during the time the experimentation lasted.

Periodically, the IR spectroscopy of cement's samples taken from the proximities of the thermocouples was done. The whole system can be seen in photograph nº 4.

LUMPING OF ANHYDROUS PORTLAND CEMENT: STUDY THROUGH IR SPECTROSCOPY

EPAISISSEMENT DU CIMENT PORTLAND ANHYDRE: ETUDIE PAR ESPECTROSCOPIE INFRARROUGE

CL

After 15 days the experimentation was finished. The lumped aspect of the cement can be seen in photograph nº 5.

Along the studies done by IR spectroscopy it can be demonstrated the formation of syngenite with a similar mechanism like one already described and that can be summarized in this case in this way:

- The calcic langbeinite added to the cement reacted with the water's vapour generated by the gypsum that sorrounded the calefactor and with the one proceeding from the dehydration that constituted the cement according to:

$$2CaSO_4.K_2SO_4 + H_2O \qquad CaSO_4.K_2SO_4.H_2O + CaSO_4$$

It can be said that syngenite is also formed and it is the responsable of the lumping.

The resultant $CaSO_4$ in the reaction is soluble anhydrite of a high activity.

If K_2SO_4 exists in cement, would react (in presence of water's vapour) easily with it to give syngenite again. Also this $CaSO_4$ helps in the presence of false setting in cements.

Conclusions

One of the causer of portland cement lumping can be explained by a group of concurrent agentes, amoung them the following can be named:

- a high temperature reached in the grinding of cement that makes possible the partial dehydra - tion of gypsum.
- the storage of cement still hot, makes that gypsum continues its dehydration in the same place of storage.
- The presence of K_2SO_4 in the clinker, that reacts with the resultant compounds of the dehydra of gypsum, forming calcic syngenite ($CaSO_4.K_2SO_4.H_2O$).
- probably the pneumatic unloading of cement coopera- tes in the apparition of the phenomenon.
- the calcic langbeinite ($2CaSO_4.K_2SO_4$) that appears sometimes in portland clinker can react with water's vapour to produce soluble anhydrite and syngenite.

This syngenite is able to produce lumping in the anhydrous cement.

Bibliography

1.- MATOUSCHEK, F.-Zement-Kalk-Gips, nº 8 p. 395 (1972)
2.- FOREST, J. - Rev. Mat. Const. nº 157, p. 35 (1962)
3.- SPRUNG, S.- Zement-Kalk-Gips nº 6, p. 305 (1978)
4.- NIELSEN, H.C.A. - Rock Products nº 2, p. 72 (1974)
5.- RUIZ DE GAUNA, A.- Materiales de Construcción nº 159, p. 13 (1975)
6.- PLIEGO-QUERVO, Y. and GLASSER, F.P. - Cement and Concrete Research V. 9, p.573 (1979)
7.- VAZQUEZ, T. and FERNANDEZ-PEÑA, O. - Materiales de Construcción nº 182, p. 43 (1981)

Table 1

L.I. - 0.8	SO_3	- 2.8	
R.I. - 3.5	Na_2O	- 0.2	
SiO_2 -20.9	K_2O	- 0.8	
Al_2O_3- 5.9	spec.surf		
Fe_2O_3- 2.4	(cm^2/g)-3.360		
CaO -60.5	CaO_f	- 0.7	

Table 2

L.I. - 0.2	SO_3	- 0.6	
R.I. - 0.1	Na_2O	- 0.2	
SiO_2 -21.8	K_2O	- 0.3	
Al_2O_3- 4.6	CaO_f	- 0.9	
Fe_2O_3- 3.7	spec.surf.		
CaO -65.6	(cm^2/g)-3.005		



Phot 1 = sample nº 1



Phot. 2 = sample nº 2

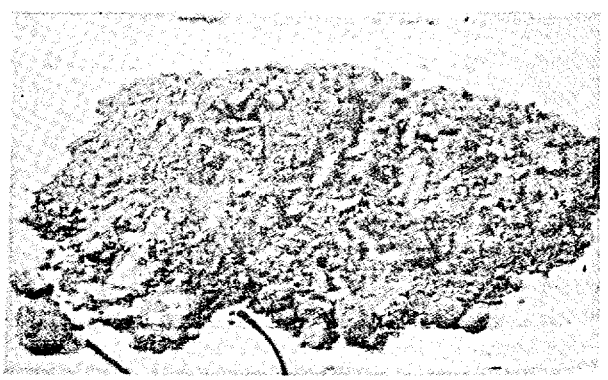

Phot. 3 = sample nº 7



FIG. 1

IR spectrum of sample N. 1

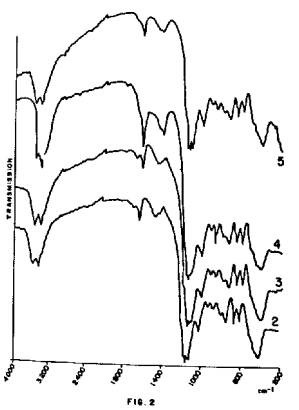

FIG. 2

IR spectra of samples N. 2 to 5, after treatment with salicilic-methanol

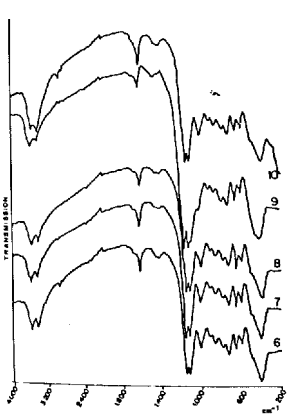

FIG. 3

IR spectra of samples N. 6 to 10, after treatment with salicilic-methanol

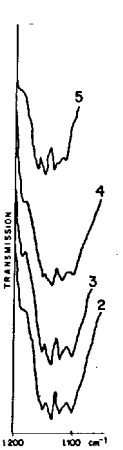

FIG. 4

Some details of IR spectra of samples N. 2 to 5. The bands corresponding to syngenite can be observed clearly

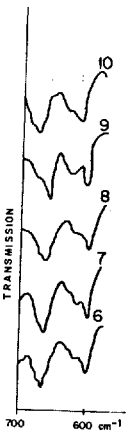

FIG. 5

Some details of IR spectra of samples N. 6 to 10. The band $\nu_3 SO_4$ in 620 cm^{-1}, correspondig to K_2SO_4 can be observed clearly



FIG. 6

Some details of IR spectra of samples N. 6 to 10. The bands corresponding to $CaSO_4 \cdot \frac{1}{2}H_2O$ can be observed clearly. The bands corresponding to syngenite are very weak

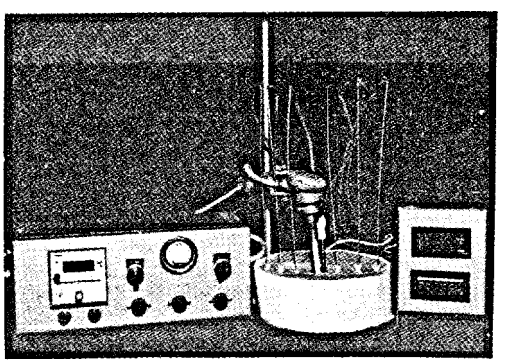

Phot. 4
system of the laboratory y experimentation

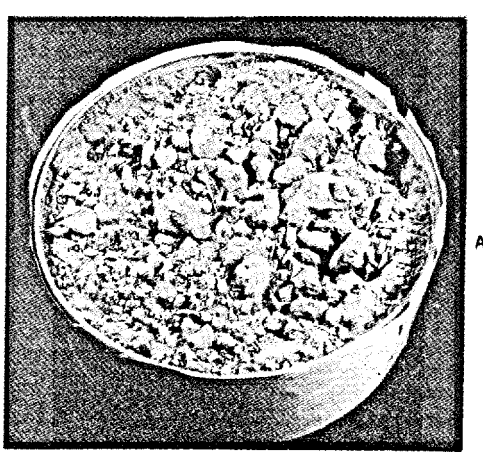

Phot. 5
Aspect of the cement

L.J. Struble - Center for Building Technology, National Bureau of Standards, Gaithersburg, U.S.A.

Synthesis and Characterization of Ettringite and Related Phases

1. Introduction

Ettringite, a naturally occurring mineral and a phase that typically forms during hydration of portland cement, is known to undergo partial dehydration at temperatures as low as 110°C [1,2], and there are indications that this dehydration may be reversible [2-6]. Because a reversible reaction that occurs below 40°C might have application in passive solar energy storage, the present investigation was initiated to explore the potential of ettringite as a phase change material for solar energy storage.

The present paper presents synthesis procedures and various analytical properties of ettringite and a number of isostructural phases, described in more detail in a series of progress reports [7-9]. A separate paper [10] addresses the thermal characteristics as regards energy storage.

The crystal structure of ettringite (fig. 1), as reported by Moore and Taylor [11], consists both of columns whose empirical composition is $[Ca_3Al(OH)_6 \cdot 12H_2O^{3+}]$, and of channel sites, three occupied by sulfate ions and the fourth by two water molecules. This structure is amenable to a number of chemical substitutions [2]. Divalent anions, e.g. carbonate, may substitute for sulfate [12]. Substitution of monovalent anions for sulfate has also been reported, producing phases of the type $[Ca_3Al(OH)_6]_2(Cl)_6 \cdot 26H_2O$ [13,14]. However, Taylor [2] noted that the existence of phases of this type appears to be in conflict with structural requirements, since it would be necessary to accomodate all six monovalent anions in only four available sites. Attempts to prepare these phases in the present study were not sucessful [9]. Other trivalent anions have been substituted for aluminum [15-17], and both the iron and chromium analogs of ettringite were synthesized in the present study. In some instances tetravalent cations can be substituted for aluminum [18,19], and a carbonate- and silicon-substitued phase, thaumasite, was prepared in the present study.

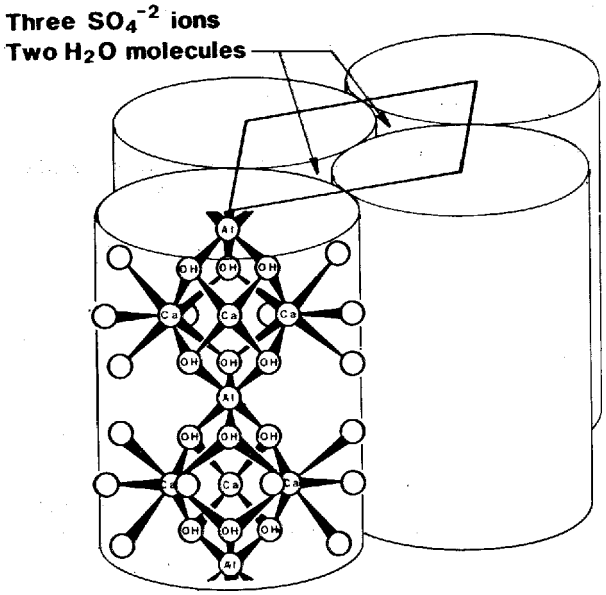

Figure 1. Crystal structure of ettringite, modified from Moore and Taylor [11].

2. Experimental Procedures

2.1 Synthesis

Synthesis procedures were developed to allow reproducible preparation of pure phases that are chemically homogeneous and uniform in particle size. Since these objectives appeared best met by synthesis from solution, a general procedure was followed involving precipitation from a mixture of solutions, one solution containing calcium and the other solution containing the remaining reactants in their stoichiometric proportions. When the two solutions were mixed, a precipitate typically formed immediately, and the mixture could be filtered after approximately one hour to collect the product. Excess amounts of Ca^{+2} and SO_4^{-2} were not used, though both Jones [20] and Lea [1] had reported that an excess of these ions was necessary in the synthesis due to the incongruent solubility of ettringite. Concentrations as high as possible were used, so as to maximize yield. Concentration of the calcium solution was increased by dissolving CaO in a 10 percent sugar solution, a procedure used previously by Carlson and Berman [12].

Phases synthesized by the method described above are listed in table 1. Ettringite was prepared from the calcium solution described above and either a solution of $Al_2(SO_4)_3$, or a solution of $Na_2Al_2O_4$ and Na_2SO_4. Fe-substituted ettringite was synthesized from the calcium solution and a $Fe_2(SO_4)_3$ slurry. The Cr-substituted ettringite was prepared from the calcium solution and a $CrK(SO_4)_2$ solution. The CO_3-substituted ettringite was prepared using the calcium solution and a solution of $Na_2Al_2O_4$ and Na_2CO_3. Thaumasite was prepared from the calcium solution and a solution of Na_2SiO_3, Na_2SO_4, and Na_2CO_3; these solutions were mixed after first cooling to 5°C, the low temperature presumably allowing the necessary 6-fold coordination of silicon [2]. Synthesis of thaumasite required considerably longer reaction times; after a few hours at 5°C, a precipitate had formed that was amorphous to X-rays, but after 5 months of mixing at approximately 5°C, the precipitate was identified as thaumasite. When a similar method was used to synthesize a Cl-substituted ettringite, using a

CL

Table 1. Synthesized phases.

Phase	Formula
ettringite	$[Ca_3Al(OH)_6]_2(SO_4)_3 \cdot 26H_2O$
iron-substituted ettringite	$[Ca_3Fe(OH)_6]_2(SO_4) \cdot 26H_2O$
chromium-substituted ettringite	$[Ca_3Cr(OH)_6]_2(SO_4)_3 \cdot 26H_2O$
carbonate-substituted ettringite	$[Ca_3Al(OH)_6]_2(CO_3)_3 \cdot 26H_2O$
thaumasite, a carbonate- and silicon-substituted ettringite	$[Ca_3Si(OH)_6]_2(SO_4)_2(CO_3)_2 \cdot 24H_2O$

Table 2. Chemical compositions of synthesized phases.

		Substituted Ettringite		
	Ettringite	Fe	Cr	CO_3
Weight percent[a]				
Al_2O_3	7.09	0	0	8.16
SO_3	16.73	17.55	16.67	0.11
CaO	24.32	24.37	23.98	26.54
Cr_2O_3	0	0	10.51	0
Fe_2O_3	0.04	13.97	0.04	0.03
CO_2	0	0	0	11.5
H_2O	50.98	44.19	48.81	52.32
Calculated molar ratios				
Ca	6.0	6.0	6.0	6.0
Al	1.9	0.0	0.0	2.0
Fe	0.0	2.4	0.0	0.0
Cr	0.0	0.0	1.9	0.0
SO_3	2.9	3.0	2.9	0.0
CO_2	0.0	0.0	0.0	3.3
H_2O	39.2	33.9	38.0	36.8

[a]Determined by Inductively Coupled Plasma Emission Spectroscopy except CO_3 and H_2O, which were determined from TGA patterns.

solution of $AlCl_3$, the product was Friedel's salt.

2.2 Characterization

In order to characterize the synthesized phases, samples were analyzed as follows: for qualitative phase composition, by X-ray diffraction (XRD); for bulk chemical composition, using inductively coupled plasma-emission spectroscopy (ICP); for morphology, by scanning electron microscopy (SEM); by infrared spectroscopy (IR); and, for thermal properties, by thermogravimetric analysis (TGA) and differential scanning calorimetry (DSC). Two of the phases, the Cr-substituted ettringite and the thaumasite, were not analyzed by every method.

Chemical analyses following the normal dissolution and analytical procedures required for ICP analysis. The qualitative XRD analysis utilized normal techniques for specimen preparation and data collection. Some phases were also analyzed by XRD to determine the unit cell parameters; these analyses utilized slower scan rates and, in some cases, an internal standard. The SEM examination of the samples employed standard procedures for specimen preparation and analysis, dispersing each powder in alcohol, then evaporating the dispersion onto a carbon grid. The SEM was operated at a voltage of 10, 12, or 20 KeV as necessary to optimize the micrograph. The IR analyses were made using Fourier transform infrared (FTIR), with specimens prepared as mulls of powder in Nujol. Thermal analyses by TGA and DSC utilized ~1 mg specimens in open pans. TGA scans were collected between room temperature and 1000°C at 10° per min. In addition, TGA scans of the low-temperature dehydration reaction were collected between room temperature and 150°C at 0.6° per min. DSC scans were collected between 0 and 150°C at 0.6° per min. Each DSC peak was integrated to determine the change in enthalpy, and examined to determine the onset temperature of the dehydration reaction. Both measurements required determination of the baseline and boundary of each peak, which were determined by visual inspection, assisted by a derivative function.

3. Results and Discussion

Bulk chemical compositions were determined (table 2) for comparison to stoichiometric compositions. In all cases the water contents were higher than expected. Otherwise, the compositions indicate that ettringite and the Cr-substituted ettringite were synthesized with little or no impurity.

The CO_2 content of the CO_3-substituted phase is slightly higher than expected, and the Fe content of the Fe-substituted phase is higher than expected, suggesting possible impurities in these preparations.

X-ray diffraction analysis provided rapid assessment of synthesis procedures. The XRD patterns (fig. 2) indicated that little or no contaminating phases were present, i.e. that each desired phase was the major crystalline constituent.

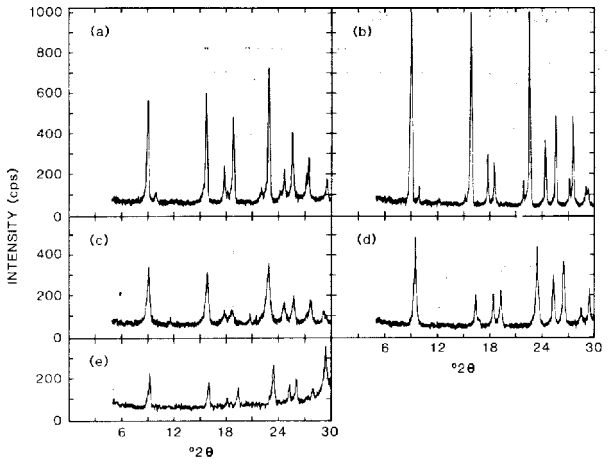

Figure 2. XRD patterns of (a) ettringite, (b) Fe-substituted ettringite, (c) Cr-substituted ettringite, (d) CO_3-substituted ettringite, (e) thaumasite.

Though the XRD patterns vary slightly with chemical composition, each phase appears to have the same or similar crystal structure. Unit cell parameters (table 3) were determined by indexing the powder patterns using the trigonal structure P31c reported for ettringite by Moore and Taylor [11] or for thaumasite using the hexagonal structure $P6_3$ reported by Edge and Taylor [21]. For ettringite and Cr-substituted ettringite, the parameters in table 3 agree within 0.002 nm with values reported by Buhlert and Kuzel [15]. Parameters for the Fe-substituted phase, however, are larger than the reported values [15], 0.002 nm larger in the a-direction and 0.005 nm larger in the c-direction. Parameters for thaumasite in table 3 are slightly larger in both directions (0.003 nm in the a-direction and 0.0024 nm in the c-direction) than the values reported by Effenberger et al. [22]. As expected, the lattice parameters in table 3 vary with chemical composition. In the simplest case, substitution of Cr or Fe for Al is expected to expand the lattice since the ionic radii of Fe and Cr are larger than the radius of Al. However, the lattice parameters with Cr or Fe substitution are larger in the c-direction, but slightly smaller in the a-direction. Thus the effect of these substitution appears to be more complicated than may be explained simply by ionic radii. Since the CO_3 anion is known to be smaller than than the SO_4 anion in thaumasite [22], the substitution of CO_3 for SO_4 in ettringite is expected to reduce the lattice in both directions. This effect was observed.

The morphologies observed by SEM (fig. 3) vary significantly with chemical composition. The ettringite occurs as short, prismatic crystals, variable in cross section between 0.2 and 3 μm, with aspect ratio of 2 or 3. This morphology is different from the morphology of ettringite in hydrated portland cement, where it typically occurs as prismatic, hexagonal needles with aspect ratios between 4 and 10, depending on the available space [23]. The Fe-substituted phase is uniform in size, approximately 3 μm in cross section, with an aspect ratio of approximately 2. The Cr-substituted phase consists of plates with roughly hexagonal outline, lacking the well-developed morphology of the other phases, and highly variable in size, ranging from 0.2 to 9 μm. Finally, the CO_3-substituted phase is composed of clusters or rosettes of prismatic crystals, 0.3 to 1 μm in cross section, with an aspect ratio of approximately 5.

The FTIR spectra (fig. 4) were examined to determine the effects of chemical composition on frequencies of the water bands. It is generally accepted that a shift of IR band to higher frequency indicates a higher strength bond. However, it was argued by Ryskin [24] for the case of $R_3SiOH...B$ complexes (where R and B are organic species) that lowering the OH stretch frequency is accompanied by an increase of the force constant of the Si-O bond. If the spectra for ettringite and substituted phases are interpreted in the same way, a chemical substitution that causes a shift of the OH stretch band to lower frequency is expected to be associated with an increase in the force constant of the Ca-O bond, and thus a greater change in enthalpy with dehydration.

Based on peak assignments of Ryskin [24] and with reference to the ettringite crystal structure (fig. 1), OH bands were assigned either to non-hydrogen-bonded hydroxyl or to hydrogen-bonded hydroxyl. In this case, non-hydrogen-bonded hydroxyl are the hydroxyl ions and the water molecules on the columns, which are bonded to Ca atoms; and hydrogen-bonded hydroxyl are the water molecules in the channels, which are hydrogen-bonded to other water molecules. The frequencies of bands assigned to hydrogen-bonded and non-hydrogen-bonded hydroxyl vary somewhat with composition (table 4). Compared to the unsubstituted ettringite, both the non-hydrogen-bonded and hydrogen-bonded hydroxyl stretching bands are shifted to a slightly lower frequency (20 cm^{-1} for each band) for the Fe-substituted phase. The hydrogen-bonded stretch band is shifted even further (170 cm^{-1} lower) for the CO_3-substituted phase.

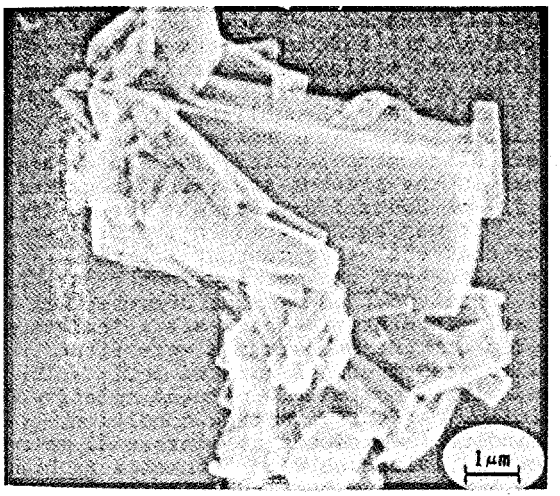

(a)

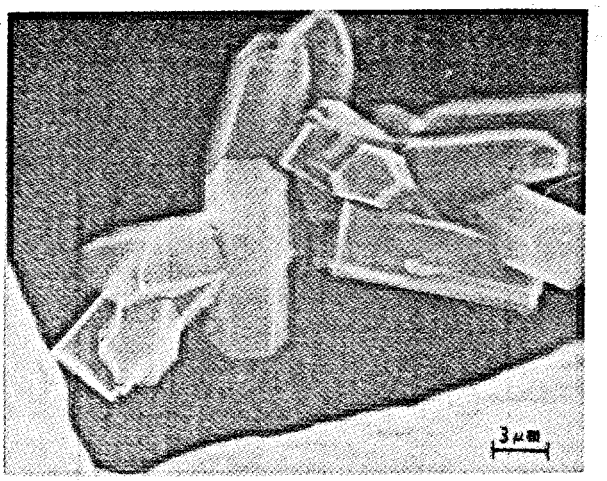

(b)

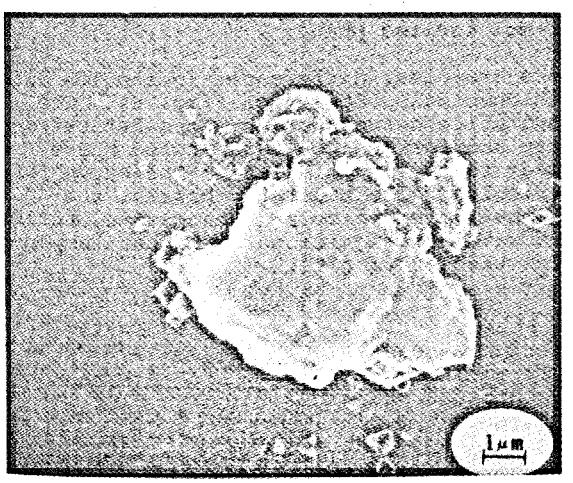

(c)

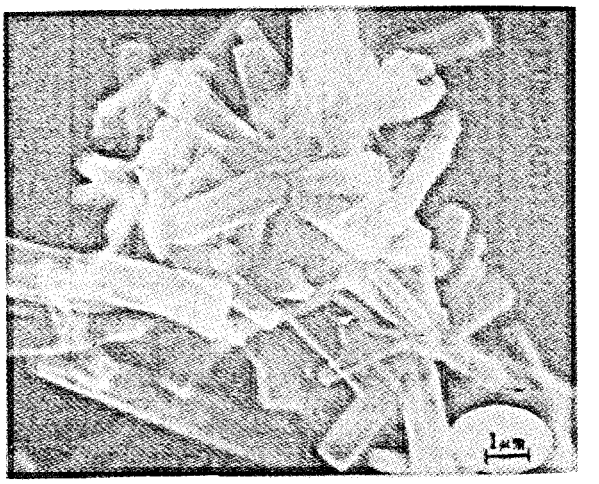

(d)

Figure 3. SEM micrographs of (a) ettringite, (b) Fe-substituted ettringite, (c) Cr-substituted ettringite, (d) CO_3-substituted ettringite.

Table 3. Unit cell parameters[a] of synthesized phases.

Phase	Structure	a (nm)	c (nm)
$[Ca_3Al(OH)_6]_2(SO_4)_3 \cdot 26H_2O$	P31c	1.123	2.150
$[Ca_3Fe(OH)_6]_2(SO_4)_3 \cdot 26H_2O$	P31c	1.1182	2.2008
$[Ca_3Cr(OH)_6]_2(SO_4)_3 \cdot 26H_2O$	P31c	1.119	2.177
$[Ca_3Al(OH)_6]_2(CO_3)_3 \cdot 26H_2O$	P31c	1.0834	2.1250
$[Ca_3Si(OH)_6]_2(SO_4)_2(CO_3)_2 \cdot 24H_2O$	$P6_3$	1.106	1.042

[a]Determined using X-ray powder patterns. Parameters reported with 5 significant figures were determined using an internal standard, and those with 4 significant figures were determined using an external standard.

Thaumasite shows only one broad OH stretch band, assigned to non-hydrogen-bonded hydroxyl stretch because the thaumasite structure has no water in channel positions [2]. This hydroxyl stretch band in thaumasite is shifted to a lower frequency compared to the unsubstituted ettringite. Thus based on FTIR data, it is expected that the enthalpy change on dehydration will rank from low to high according to the following: unsubstituted ettringite,

Fe-substituted phase, CO_3-substituted phase, and thaumasite.

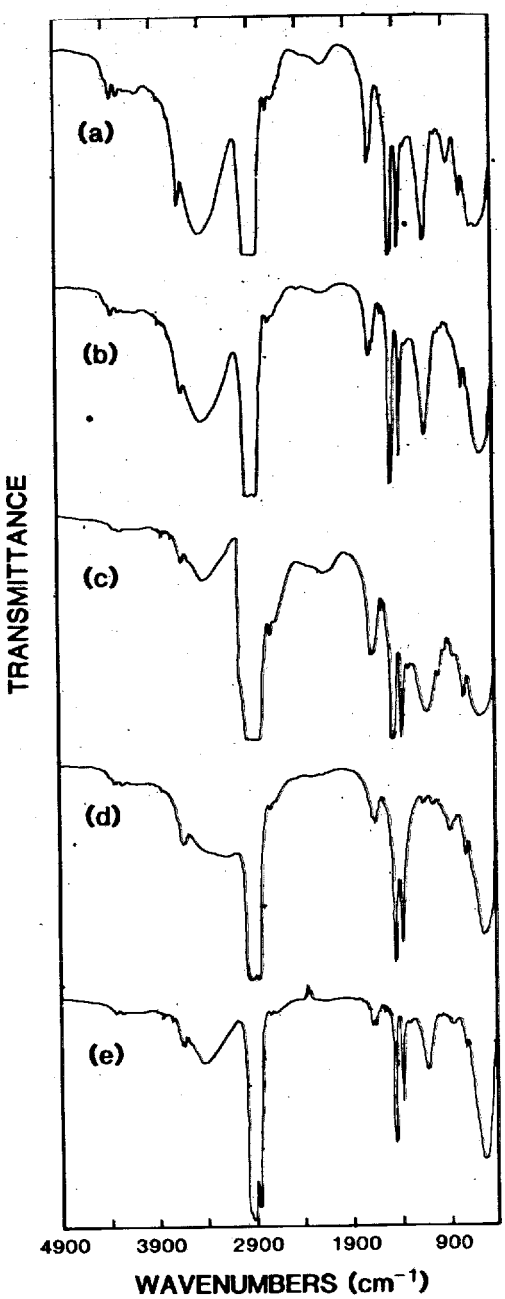

Figure 4. IR patterns of (a) ettringite, (b) Fe-substituted ettringite, (c) Cr-substituted ettringite, (d) CO_3-substituted ettringite, and (e) thaumasite.

For each phase, the amounts of water lost during heating, calculated from the TGA curves and expressed as mol water per mol of each ignited phase, are plotted in figure 5. The major weight loss occurs below approximately 200°C under these conditions, and is probably due to loss of crystalline water. As the temperature is increased, the further weight loss is probably due to loss of hydroxyl. These TGA data may be compared to data for ettringite, the only phase with published TGA data available. The water contents at intermediate temperatures (100-300°C) are higher in the present study than reported by Lea [1] or Jones [20], but similar to Taylor [25]. It was anticipated in the present study that the water contents of the ettringite-type phases might not be stable, i.e., that the phases might dehydrate in dry air and rehydrate in moist air. Therefore, samples for thermal studies were first equilibrated over a saturated $ZnCl_2$ solution, with a nominal 10 percent relative humidity. At this starting condition, ettringite is expected to contain 32 mols of water [1], although water contents as high as 36.5 mols have been reported and attributed to adsorbed water [4]. The water content of ettringite at room temperature in the present study is approximately 40 mols per mol ignited phase.

There are clear differences in the TGA data with chemical composition (fig. 5). The dehydration curves for the Fe-substituted phase and for the CO_3-substituted phase appear to be very similar to the curve for ettringite. The other two phases, the Cr-substituted phase and thaumasite, retain more water at significantly higher temperatures than ettringite.

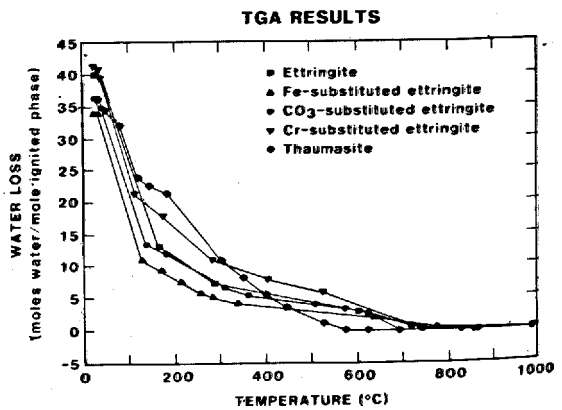

Figure 5. Dehydration data, recalculated from TGA curves.

Data regarding the low-temperature dehydration, some of which have been reported elsewhere [10], are presented in table 5. Enthalpy changes are listed relative to both the amount of the phase and the amount of water lost, the latter allowing comparison of enthalpy changes independent of the amount of water lost. The enthalpy changes on dehydration range from 2.1 to 3.8 kJ per g H_2O. Values for

CL

Table 4. IR wavenumbers (cm^{-1}) of hydroxyl bands[a].

Phase	O-H Stretch		O-H Bend
	Non-hydrogen-bonded	Hydrogen-bonded	Hydrogen-bonded
$[Ca_3Al(OH)_6]_2(SO_4)_3 \cdot 26H_2O$	3640	3420	1670
$[Ca_3Fe(OH)_6]_2(SO_4)_3 \cdot 26H_2O$	3620	3400	1670
$[Ca_3Al(OH)_6]_2(CO_3)_3 \cdot 26H_2O$	3620	3250	1650
$[Ca_3Si(OH)_6]_2(SO_4)_2(CO_3)_2 \cdot 24H_2O$	3410	--	1650

[a]Tentative peak assignments by inspection, based on [24].

Table 5. Dehydration data for synthesized phases[a].

Phase	Loss[b]	Onset Temperature	Enthalpy Change	
	(mols H_2O per mol phase)	(°C)	(kJ per g sample)	(kJ per g H_2O)
$[Ca_3Al(OH)_6]_2(SO_4)_3 \cdot 26H_2O$	19	30	0.59	2.09
$[Ca_3Fe(OH)_6]_2(SO_4)_3 \cdot 26H_2O$	24	6	0.84	2.55
$[Ca_3Cr(OH)_6]_2(SO_4)_3 \cdot 26H_2O$	13	22	0.67	3.73
$[Ca_3Al(OH)_6]_2(CO_3)_3 \cdot 26H_2O$	23	7	0.80	2.55
$[Ca_3Si(OH)_6]_2(SO_4)_2(CO_3)_2 \cdot 24H_2O$	9	33	0.25	1.97

[a]Reported by Struble and Brown [10].
[b]Measured using TGA.
[c]Measured using DSC.

ettringite and thaumasite are nearly equal, while values for both the Fe-substituted phase is considerably higher. It is interesting to note that these values bracket the heat of vaporization of water, which is 2.27 kJ per g. The enthalpy change varied with composition in the order expected based on the previous discussion of FTIR spectra for the unsubstituted ettringite and the Fe- and CO_3-substituted phases, but not for thaumasite.

The change in enthalpy due to dehydration of ettringite and related phases range from 0.4 to 0.8 kJ per g. This range is higher than the enthalpy changes of other materials presently used for solar energy storage. For example, Glauber's salt melts with an enthalpy change of 0.25 kJ per g [27]. The onset temperature for dehydration of ettringite and related phases ranges from 6° to 30°C as measured by DSC. The enthalpy change and dehydration temperature data demonstrate that ettringite and related phases have potential as energy storage materials [10].

4. Conclusions

The following have been concluded regarding synthesis and properties of ettringite and related phases:

1. A general synthesis method using a mixture of two concentrated solutions allowed preparation of the ettringite and related phases with divalent cations.

2. Morphology of the synthesized phases vary with chemical composition. Crystals are generally hexagonal in outline, either short, prismatic crystals, or platey crystals.

3. The IR frequencies of bands assigned to non-hydrogen-bonded and hydrogen-bonded hydroxyl stretching vary with composition. Compared to ettringite, the bands are shifted to a slightly lower frequency for Fe- and CO_3-substituted phases and thaumasite. These shifts are associated with higher changes in enthalpy with dehydration for Fe- and CO_3-substituted phases, but not for thaumasite.

4. Dehydration data, i.e. the amount of water lost, the temperature at which dehydration begins, and the change in enthalpy associated with the low-temperature dehydration vary with composition.

5. Acknowledgements

The project described here was funded by U.S. Department of Energy, Office of Solar Heat Technologies, Passive and Hybrid Solar Energy Division. I am pleased to acknowledge the contributions of K. Galuk, P.W. Brown, and H.F.W. Taylor.

6. References

1. F.M. Lea. The Chemistry of Cement and Concrete. 3rd Edition. 727 pages. New York: Chemical Publishing Company, Inc. (1971).

2. H.F.W. Taylor. Mineral. Mag., 39(304), 377-389 (1973).

3. H.A. Berman and E.S. Newman. In: Proc. Int. Symp. Chem. Cem., 4th, Volume I, Paper III-S1, p. 247-257. Washington: U.S. Department of Commerce (1960).

4. N.N. Skoblinskaya and K.G. Krasilnikov. Cem. Concr. Res., 5(4), 381-394 (1975).

5. N.N. Skoblinskaya, K.G. Krasilnikov, L.V. Nikitina, V.P. Varlamov. Cem. Concr. Res., 5(5), 419-432 (1975).

6. R. Turriziani. Chapter 6 in: The Chemistry of Cements, ed. H.F.W. Taylor, Vol. 1, pp. 233-286. London: Academic Press (1964).

7. J.B. Ings and P.W. Brown. NBSIR 82-2531, 11 pages. Washington: U.S. Department of Commerce (1982).

8. L.J. Struble and P.W. Brown. NBSIR 84-2942, 41 pages. Washington: U.S. Department of Commerce (1984).

9. L.J. Struble and P.W. Brown. Inorganic Compounds for Passive Solar Energy Storage - Solid-State Dehydration Materials and High Specific Heat Materials. Submitted for publication as NBSIR (1986).

10. L.J. Struble and P.W. Brown. Inorganic compounds for passive solar energy storage utilizing a dehydration reaction and specific heat. Submitted to Sol. Energy Mater. (1985).

11. A.E. Moore and H.F.W. Taylor. Acta Crystallogr., B26, 386-393 (1970).

12. E.T. Carlson and H.A. Berman. J. Res. Nat. Bur. Stand., 64A(4), 333-341 (1960).

13. N.N. Serb-Serbina, Yu.A. Savvina, and V.S. Zhurina. Dokl. Akad. Nauk SSSR, 3, 659-662 (1956).

14. H.E. Schwiete, U. Ludwig, and J. Albeck. Zem.-Kalk-Gips, 58 (5), 225-234 (1969).

15. R. Buhlert and H.J. Kuzel. Zem.-Kalk-Gips, 24(2), 83-85 (1971).

16. J. Bensted and S. Prakash Varma. Cem. Technol., 2, 73-76, 100 (1971).

17. I. Odler and S. Abdul-Maula. Cem. Concr. Res., 14(1), 133-141 (1984).

18. S. Prakash Varma and J. Bensted. Silic. Ind., 38(2), 29-32 (1973).

19. W. Lukas. Cem. Concr. Res., 6(2), 225-234 (1976).

20. F.E. Jones. In: Proc. Symp. Chem. Cem., pp. 231-245. Stockholm: Ingeniorsvetenskapsakademien (1938).

21. R.A. Edge and H.F.W. Taylor. Acta Crystallogr., B27, 594-601 (1971).

22. H. Effenberger, A. Kirfel, G. Will, and E. Zobetz. Neues Jahr. Mineral. Monatsch., 2, 60-68 (1983).

23. P.W. Brown et al. The hydration of tricalcium aluminate and tetracalcium aluminoferrite in the presence of calcium sulfate. Report of RILEM Committee 68MMH. Submitted for publication in Mater. Struct. (1986).

24. Ya. I. Ryskin. Chapter 9 in: The Infrared Spectra of Minerals, V.C. Farmer, ed., pp. 137-181. London: Mineralogical Society (1974).

25. H.F.W. Taylor. In: The Chemical and Chemically-Related Properties of Cement, F.P. Glasser, ed., pp. 65-82. Shelton, Stoke-on-Trent: The British Ceramic Society (1984).

27. G.A. Lane. Solar Heat Storage: Latent Heat Material. Volume I, 238 pages. Boca Raton: CRC Press, Inc. (1983).

A. C. Chou, H. C. Eaton[1], F. W. Cartledge and M. E. Tittlebaum, The Hazardous Waste Research Center, Louisiana State University, Baton Rouge, Louisiana 70803 - U.S.A.

A TEM Study of the Interactions Between Certain Organic Hazardous Wastes and Type I Portland Cement

INTRODUCTION

The disposal of hazardous wastes will be one of the major enviromental issues well into the next century. Many of the engineering practices of the past are being questioned by the public. There are serious concerns over potentially adverse health effects which may result from landfilling, deep well injection, incineration, and other methods of disposal which may not be adequately understood. The present paper reports research aimed at understanding the behavior of organic wastes which are solidified prior to disposal by landfilling.

Landfilling refers to the disposal of raw or treated waste in a land based site. Federal regulations prohibit the landfilling of liquids or semiliquids and also require that the leaching potential for certain toxins be reduced to levels which pose no environmental threat. This has resulted in the development of various waste solidification and stabilization technologies. Many of the methods utilize a solidifying matrix composed of relatively inexpensive materials like Portland cement, flyash, kiln dust, or natural pozzolans.

Solidification processes do not necessarily involve chemical interaction between the waste and the matrix materials. For stabilization, or fixation, to occur, however, a reaction must occur. The waste material must be chemically combined with the matrix and exhibit longterm retention under leaching conditions.

Current methods for the development of solidification or stabilization formulae involve treatability studies. Several mixtures, representing a variety of proportions of matrix components, waste and water, are mixed. Physical measurements and leaching experiments are performed and the most effective composition is selected.

Because of the complexity of the systems, there is a poor fundamental understanding of the microchemistry, the microstructure, and the properties of solidified or stabilized wastes. Without this information it is difficult to model the long-term environmental behavior of a hazardous waste landfill.

Recently, Poon et al. (2) used scanning electron microscopy (SEM) and x-ray diffraction to characterize the microstructural evolution of a solidified hazardous waste during leaching. They observed a correlation between the release of zinc ions and a reduction in the amount of ettringite in the hydrated, waste-containing cement. Walsh et al. (3), in a different approach, have used scanning electron microscopy, optical microscopy and x-ray diffraction to determine the mechanisms of interaction between the waste and the cement matrix. It is their contention that leaching and long-term stability can only be understood when the microchemical mechanisms of solidification/stabilization are understood.

Scanning electron microscopy has been widely used in studies of cement microstructure but the results have been difficult to interpret and even more difficult to generalize. Chemical information available from energy dispersive x-ray analysis in the SEM can give the elemental composition of a phase, but compound identification is often difficult. The stoichiometry of the heavy elements can be estimated through careful analytical technique, but light element determination is more difficult.

The transmission electron microscope (TEM) has been used to study ceramic materials and minerals

A. C. Chou, H. C. Eaton[1], F. W. Cartledge and M. E. Tittlebaum, The Hazardous Waste Research Center, Louisiana State University, Baton Rouge, Louisiana 70803

for the past thirty years and several studies of cement have been reported. To the authors' knowledge, however, the TEM has not been applied to studies of solidified hazardous chemical wastes. The main advantage of the TEM is the high spatial resolution, which can exceed 0.2 nanometers in a modern instrument. In addition, the selected area diffraction pattern (SAD) can provide information about the crystal structure and the orientation of crystalline phases. Both of these characteristics are important for waste research.

The specimen suitable for TEM examination must be very thin (100 nm at 100kV) to allow penetration of the electron beam. This thickness can be achieved by replica techniques, by ion thinning or by ultramicrotomy. The replica technique, used in the present study, reproduces the topography of the specimen surface.

Cements are composed of several particle-like phases and its surfaces are porous. Some mineral components of the sample were easily extracted onto the acetate film. Therefore, in addition to the morphological structure being preserved in the carbon film, extracted particles were sometimes observed. Thin crystalline particles were frequently suitable for obtaining electron diffraction patterns.

The present communication reports the use of the TEM in a study of the solidification products resulting from mixing Type I Portland cement with either ethylene glycol or p-bromophenol. Replica methods were used to isolate fine particles of calcium silicate hydrate (CSH) or small particles of other phases embedded in the CSH. Most of the phases were identified as either cement clinker phases or as products of normal cement hydration reactions. Other particles were not identifiable as phases typically occurring in hydrated cement pastes.

SAMPLE PREPARATION AND EXPERIMENTAL PROCEDURE

Type I Portland cement was used as the solidification matrix material. The cement had the composition shown in Table 1. Cement/organic samples were prepared using either pure ethylene glycol or p-bromophenol. Organics were weighed into 20 mL borosilicate glass screw cap vials. Ten grams of cement and 4 mL of deionized water were added to each vial and the mixture was stirred to apparent homogeniety with a glass stirring rod. The organic

Table 1. Percent Composition of Portland Cement

SiO_2	20.6%
Al_2O_3	5.2%
Fe_2O_3	2.4%
CaO	64.9%
MgO	3.3%
K_2O	0.6%
SO_3	2.9%

compounds were added in amounts from 0.2 g to 2.0 g, yielding organic/cement weight ratios of 0.02, 0.04, 0.1, and 0.2. The samples were cured at room temperature (21°-25°C). Control cement samples (i.e. samples of cement and water only) were prepared and stored similarly.

All hydrated cement samples were ground with silicon carbide papers using grit sizes ranging from 180 to 600. Specimens were polished with diamond paste on a rotating wheel using propanol as a lubricant. Rinsing was also with propanol, rather than water, in order to prevent further hydration. The cleaned specimen was replicated by a cellulose acetate tape wetted by acetone. After the plastic tape was dry, it was stripped off the specimen and then coated with carbon in a vacuum evaporator. The carbon film was then cut into small pieces (ca. 9 mm^2) and washed in acetone. After the plastic dissolved, the carbon film was caught on an electron microscope grid for TEM study. A JEOL 100-CX transmission electron microscope was used at 100 kV.

RESULTS

Control Cement Samples

Various morphologies of CSH were observed including fibrous, needle, tubular, and aggregates of small irregular plates. Analyses of many diffraction patterns indicate that although the morphologies differ, the crystal structures are similar with d-spacings of approximately 0.3, 0.28, and 0.18 nm. An example is shown in Fig. 1. This is consistent with previsouly reported work.

In some cases, different diffraction patterns for CSH material were observed. For example, Figure 2 is a diffraction pattern from a specimen with d-spacings of 0.32, 0.28, and 0.16 nm. This structure is similar to afwillite. The particle shown in Figure 3 exhibits a crumpled foil morphology with d-spacings of 0.29, 0.31, and 0.19 nm.

Cement Containing Ethylene Glycol

In cement containing ethylene glycol, the morphology and tobermorite structure of the CSH has been significantly modified. This is consistent with x-ray diffraction studies of the same material (3) where the major peak was weakened and broadened. In some specimens observed in the present work, the surface appeared "glassy" and surrounded by blocky amorphous particles. This is seen in Figure 4. In most other regions, however, CSH appeared as spherical particles embedded in an amorphous material. Some aggregates of spherical particles were amorphous and others crystalline. A variety of morphologies each exhibiting the afwillite structure, with d-spacings of 0.33 and 0.2 nm, were also observed.

Another crystalline structure was frequently observed in the ethylene glycol cement. The structure was crystalline with d-spacings of 0.208, 0.205, 0.201, 0.12, 0.115, 0.103 and 0.1 nm. Morphologies were either aggregates of spherical grains, single irregular plates, or thin flakes. Similar structures were also observed in the pure cement samples, but not to the extent seen in ethylene glycol samples.

Small crystals (15-60 nm) with a cubic structure also were observed. This structure has

CL

not been reported in pure cement and may be a compound of C_3A and ethylene glycol.

Figure 5 shows a $Ca(OH)_2$ crystal. The diffraction pattern shows the characteristic hexagonal structure, however, the diffraction spots are diffuse and tend to form a ring pattern. This implies that the CSH/ethylene glycol is bonded with the $Ca(OH)_2$ forming a thin layer.

Cement Containing p-Bromophenol

The morphologies of the phases contained in cement containing p-bromophenol were also observed to differ from those in hydrated pure cement. Most of the phases appeared as spherical particle aggregates as shown in Figure 6. The number of amorphous aggregates also increased.

The degree of crystallinity of the CSH structure decreased with the addition of p-bromophenol. Large particles having d-spacings characteristic of the CSH(II) structure were observed; however, the particles have retained the shape of the original cement clinker grains. This may imply that the hydration process in this material is different from that in the pure cement. Scanning electron microscopy observations of the same material shown that there are more large distinguishable particles in the p-bromophenol containing material (4).

It was observed that in many CSH regions, the aggregate morphology was unstable under the influence of the electron beam. The particles bubbled significantly, a phenomenon not observed in either the pure cement samples or the cement containing ethylene glycol. Apparently the p-bromophenol, or derivatives of it, were incorporated in the CSH structure, forming an unstable material. The diffraction patterns only showed a single diffuse ring with a d-spacing of approximately 0.29 nm, as illustrated in Figure 7. Similarly, several $Ca(OH)_2$ and $Mg(OH)_2$ crystals were observed. The crystals appeared streaked and diffuse, possibly due to the incorporation of p-bromophenol.

SUMMARY AND CONCLUSIONS

During the course of hydration, a variety of morphological types of CSH have been observed by researchers. Several classifications have been proposed based on SEM and TEM studies. Unfortunately, the compositional and structural differences between these types have not been well defined in the literature. Midgley (5) suggests that CSH may occur in set Portland cement in three forms: (1) fibrous material which sometimes gives diffuse diffraction patterns showing 0.305, 0.208, and 0.18 nm d-spacing of the tobermorite phase; (2) irregular masses of small, distorted plates often giving a single diffuse ring at 0.29-0.3 nm in an SAD pattern; and (3) crumpled foils where no structure was mentioned.

In general, the CSH structure is an amorphous solid body filled with small particles with a variety of morphologies, some having the same crystal structures. In this study, the tobermorite structure is the major crystal structure in CSH. In addition, this study supports Taylor's model (6) that only subcrystalline order exists in the neighborhood of small fragments of Ca-O layers in the CSH structure. The subcrystalline order extends only several hundred nanometers.

The major conclusions of the present study are as follows:

1. The major crystal structure of the CSH in pure cement is tobermorite, but with various morphologies.

2. The addition of ethylene glycol or p-bromophenol to cement change the morphology of the CSH and its crystal structure. Aggregates of small grains are the main morphology and the amount of tobermorite structure has greatly decreased. In addition, various crystal structures with different d-spacings were observed.

3. The amount of amorphous material increases with the addition of either ethylene glycol or p-bromophenol.

4. Ethylene glycol and p-bromophenol may be incorporated into the CSH structure and may exist in the micropores between CSH constituents.

5. Ethylene glycol and p-bromophenol are observed to absorb onto some of the $Ca(OH)_2$ and $Mg(OH)_2$ crystals.

6. Small amounts of fine crystals are found in ethylene glycol and p-bromophenol containing cements. Their d-spacings could be determined but did not correspond to any of the expected products of the hydration of pure cement.

REFERENCES

1. Author to whom correspondence should be addressed.

2. C. S. Poon, A. I. Clark, C. J. Peters and R. Perry, Waste Management and Research 3, 127 (1985).

3. M. B. Walsh, H. C. Eaton, M. E. Tittlebaum and F. K. Cartledge, "The Effect of Two Organic Compounds on a Portland Cement-Based Stabilization Matrix," to appear in Hazard Waste and Hazardous Materials, 1986.

4. D. Skipper, H. C. Eaton, M. E. Tittlebaum and F. K. Cartledge, 7th International Conference on Cement Microscopy, Orlando, Florida, 1986.

5. H. G. Midgley, Structure, Solid Mechanics and Engineering Design, Vol. I, p. 275, 1969.

6. F. H. W. Taylor, Cement Production in Use, Engineering Foundation, New York, p. 107, 1979

A. C. Chou, H. C. Eaton[1], F. W. Cartledge and M. E. Tittlebaum, The Hazardous Waste Research Center, Louisiana State University, Baton Rouge, Louisiana 70803

CL

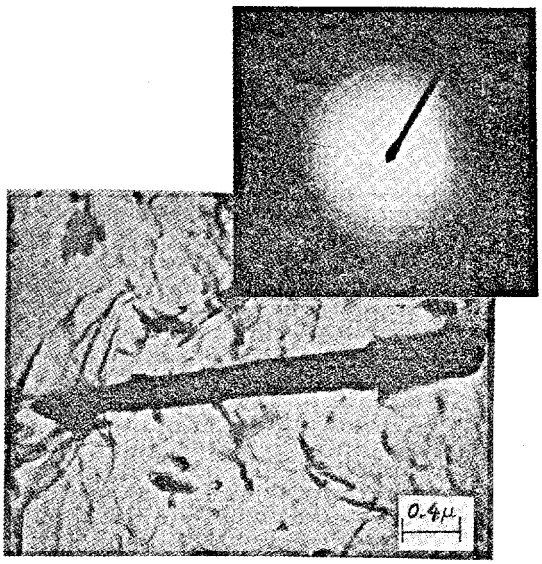

Figure 1. Needle morphology of CSH in pure cement. (Aged 1 month)

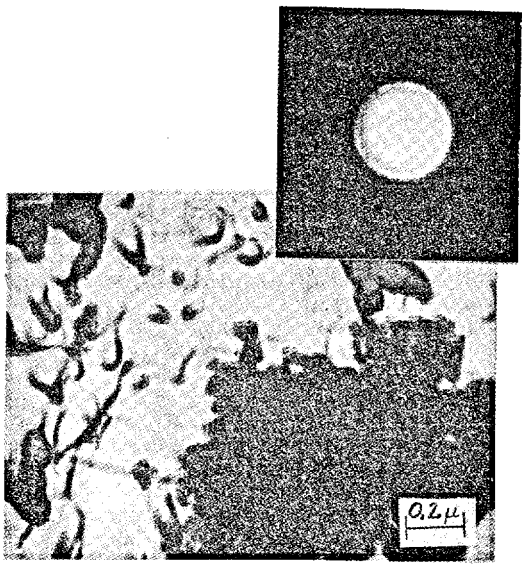

Figure 2. A particle of CSH in pure cement. The diffraction pattern reveals a structure similar to afwillite. (Aged 1 month)

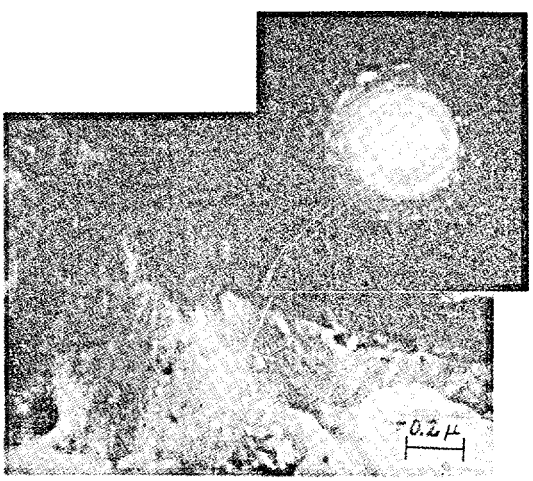

Figure 3. CSH in pure cement. The particle has the crumpled foil morphology. (Aged 1 month)



Figure 4. Glassy structure in ethylene glycol cement. Blocky grains surround the thin glassy structure. (Aged 1 month)

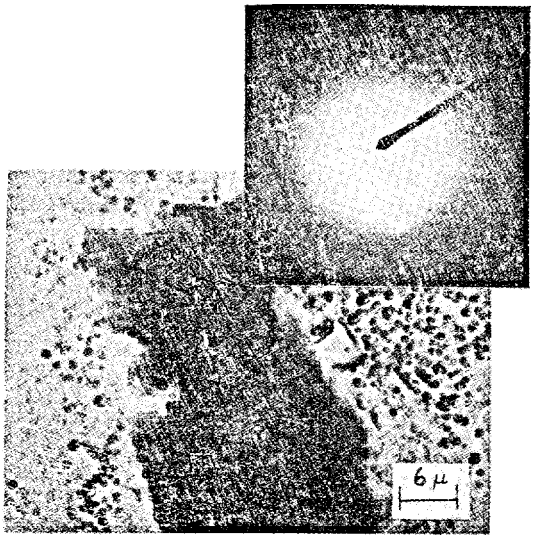

Figure 5. $Ca(OH)_2$ crystals in ethylene glycol cement. The diffraction pattern shows a diffuse ring structure. (Aged 1 month)

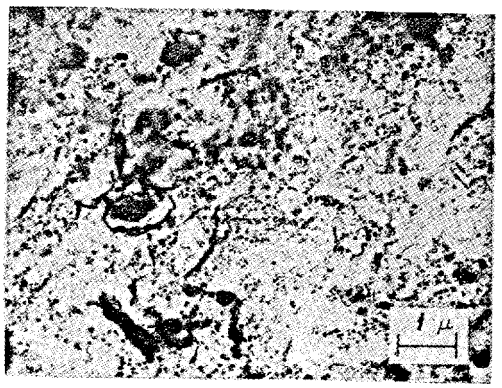

Figure 6. Crystalline spherical aggregates of CSH in p-bromophenol cement aged for 6 months.

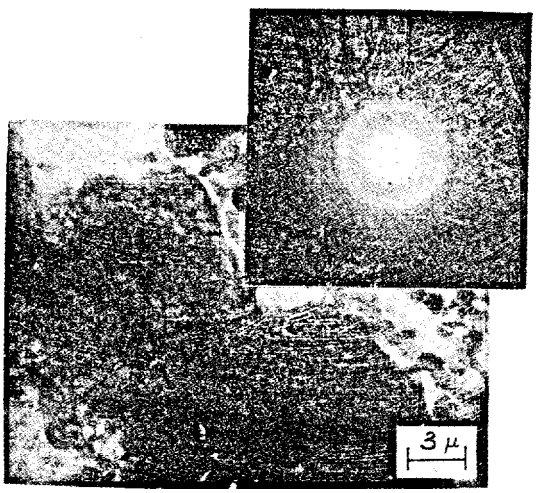

Figure 7. An unstable structure in p-bromophenol cement aged for 6 months.

J. G. Griffin and K. E. Daugherty*, Department of Chemistry, North Texas State University, Denton, Texas 76203. U.S.A.

CL. The Effect of Glass Content on Hydration in the System $CaO-Al_2O_3-MgO-SiO_2$

INTRODUCTION AND EXPERIMENTAL

Because of its importance in many fields, the system $CaO-Al_2O_3-MgO-SiO_2$ has been extensively investigated (1-4). The section of this system containing 5% MgO is of particular importance to the study of high-alumina cement (2). This section contains a field of stability for the quaternary compound, Hexacalcium Tetra-alumino Magnesium Silicate (C_6A_4MS), first described by Parker in 1952 (3). Subsequent investigations (5-8) have failed to confirm the formula assigned by Parker; however, as yet, no other formula has been firmly established.

Investigating the composition of the mineral known as "unstable C_5A_3", Parker found that the compound C_6A_4MS occurs as a primary phase in the quaternary system. He found the pure compound to melt incongruently at 1380°C to form CA, MA, and liquid. On further heating to 1400°C, it forms MA and liquid, with final melting occurring at 1420°C. Studying the system further, Parker and Ryder (9) found C_6A_4MS to have definite hydraulic properties, but in general to be a less favorable constituent of high-alumina cement than CA. Their conclusion rested primarily on the slow setting times and poor strength characteristics exhibited by the C_6A_4MS.

It has been suggested that the glass-crystalline ratio of a material may directly influence its hydration behavior (10). Investigations on slags (4,10-13) have shown that this ratio and the chemical composition plays an important role in the hydration process. This investigation was designed to examine the effect of varying the glass-crystalline ratio on the hydration of synthetic samples of composition C_6A_4MS.

Three samples of chemical composition C_6A_4MS were prepared by the high-temperature reaction of $CaCO_3$ with stoichiometric amounts of $MgCO_3$, SiO_2, and $Al(OH)_3$. ACS Reagent grade chemicals were used to prepare a raw mix from which all three samples were synthesized. In order to ensure homogeneity, the raw mix was placed into a porcelain jar with twenty-five stainless steel ball bearings, and tumbled for twenty-four hours on a Norton Mill. The samples were placed in a Lindberg, model 51333, electric furnace and calcined for two hours at 900°C. The temperature was then raised to the firing temperature at a rate of 200°C/h. Firing conditions for the three samples are shown in Table 1. Samples I and III were removed from the furnace and allowed to cool to room temperature in a desiccator. For sample II, however, the furnace temperature was lowered from 1370°C to 900°C at a rate of 100°C/h. When the furnace reached 900°C, the sample was removed from the furnace and allowed to cool to room temperature in a desiccator. All samples were ground to pass a 400-mesh sieve and had identical Blaine surface areas of 2500 cm^2/g. Using the ASTM standard method (14), a small amount of free-lime was detected in sample II. No free-lime was detected in either of the other samples.

TABLE 1

C_6A_4MS Preparation and Analysis

Sample Number	I	II	III
Furnace Temperature	1445°C	1370°C	1420°C
Firing Time	2.25 h	24.5 h	0.5 h
Qualitative XRPD	---	C_6A_4MS, $C_{12}A_7$	C_6A_4MS
Free Lime Content	0.00%	0.14%	0.00%
Specific Gravity	3.08	3.08	3.08
Surface Area (cm^2/g)	2500	2500	2500
Percent Glass	100	73	0

Powder X-ray diffraction was used to confirm the presence of C_6A_4MS (15), as well as to determine the identity of the hydration products. All X-ray powder analyses were conducted on a Philips-Norelco X-ray diffractometer using nickel-filtered Cu Kα radiation at 35KV and 18mA. The goniometer scanning speed was 2°(2θ)/minute.

A combination DTA/TGA, Mettler TA-HE20 thermobalance, was used to follow the hydration of the samples. Samples were run in a flowing air atmosphere from 25°C to 900°C at a rate of 10°C/min. The DTA was set at 200μV for a full scale pen deflection, and the recorder speed was 8cm/h.

The optical microscopy technique used for the determination of the glass-crystalline ratio was a modification of the "South African Procedure", which has been previously decribed by Fulton (16). A portion of each sample, having a particle size of 200-270 mesh was placed on a glass slide and wetted with glycerol. The sample was viewed under both plane and polarized light, with the particles which were visible under the polarized light being counted as crystalline. The glass content was then calculated using the equation:

$$\% \text{ Glass} = \frac{\text{total particles} - \text{crystalline particles}}{\text{total particles}} \times 100$$

Allowances were made for particles which showed only partial crystallinity.

Each sample was mixed with distilled-deionized water at a water-solid ratio of 10/1, and placed in a tightly sealed polyethylene container. Samples were cured at three temperatures (2, 25, and 50°C) and maintained for intervals of 1 to 90 days. In order to stop the hydration, samples were placed in an excess of cold ethanol, and ground with an agate mortar and pestle. They were then filtered using a 10-15μ Hirsch funnel and washed with cold acetone. Finally, each sample was dried at 105°C for

J. G. Griffin and K. E. Daugherty*, Department of Chemistry, North Texas State University, Denton, Texas 76203

15 minutes.

RESULTS AND DISCUSSION

Figure 1 illustates the changes in the DTA patterns of the amorphous C_6A_4MS sample, hydrated at 50°C, as the hydration proceeds from 1 to 90 days. These DTA patterns are representative of all the DTA patterns obtained, although, in general, the small peak at 300°C was not as prominent in the other samples. This peak is attributed to the presence of gibbsite, AH_3, and in all cases was observed to increase as the hydration time and temperature increased. Attempts to use this correlation to approximate the degree of hydration, however, were unsuccessful, due primarily to the small size of the desired peak and interference from the other much larger peak, centered at 340°C.

Previous studies (4,17-19) have used the percent combined water as an approximation to the degree of hydration. In this study, the percent combined water was calculated from TGA patterns using the equation:

$$\%H_2O = \frac{\text{wt at } 105^oC - \text{wt at } 900^oC}{\text{wt at } 900^oC} \times 100$$

where the weight at each temperature is calculated by subtracting the weight loss at each temperature, as indicated by the TGA, from the initial weight of the sample.

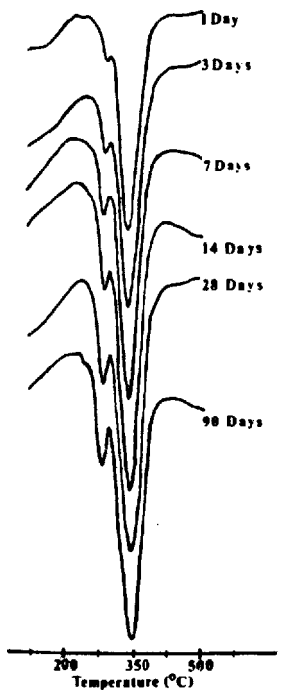

FIG. 1
DTA Patterns for Hydrated C_6A_4MS (100%Glass/50°C)

The relationships between the percent combined water and the plus/minus 1°C curing temperature, for each of these samples, are illustrated in Figures 2 through 4. In Figure 2, the percent combined water of the crystalline C_6A_4MS sample can be seen to increase with increasing temperature. The 90 day samples, which appear to deviate from this behavior, actually reflect the fact that at 50°C, the only species present are C_3AH_6 and AH_3, while at lower temperatures, both C_3AH_{8-12} and C_2AH_6 are also observed.

Figures 3 and 4 show the effect of temperature on the hydration of C_6A_4MS-(I) and C_6A_4MS-(II), respectively. In both cases, the relationship between the 2°C and the 25°C curves is simply the increase in the hydration rate at the higher temperature. The apparent anomalous behavior of the 50°C curves, on the other hand, is explained by the fact that the stable hydrates, C_3AH_6 and AH_3, are the only species present, and contain less combined water than the metastable hydrates found in the lower temperature samples.

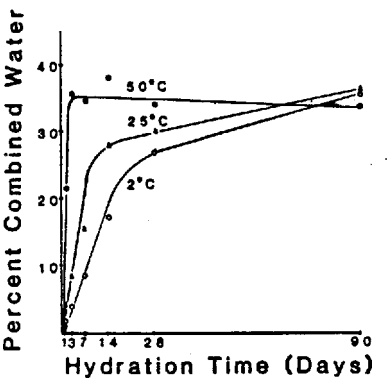

FIG. 2
The Effect of Temperature on the Hydration of C_6A_4MS (100% Crystalline)

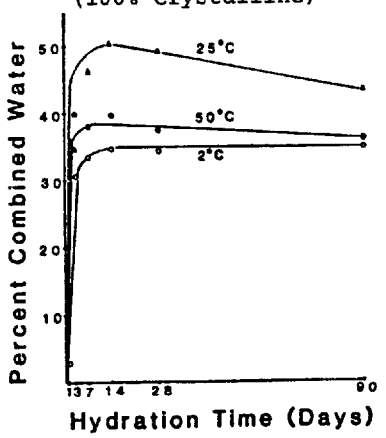

FIG. 3
The Effect of Temperature on the Hydration of C_6A_4MS (100% Glass)

J. G. Griffin and K. E. Daugherty*, Department of Chemistry, North Texas State Univeristy, Denton, Texas 76203

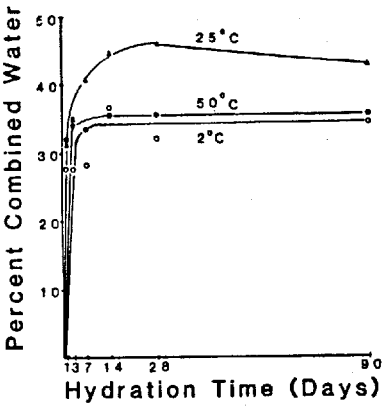

FIG. 4
The Effect of Temperature on the Hydration of C_6A_4MS (73% Glass)

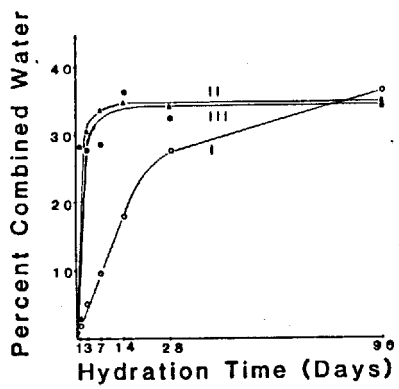

FIG. 5
The Effect of Glass Content on the Hydration of C_6A_4MS (2^oC)

The effect of the glass content on the hydration of C_6A_4MS at each of the three curing temperatures studied, is shown in Figures 5 through 7. In Figure 5, which shows the hydration of the C_6A_4MS samples at 2^oC, the hydration of the 100% glass sample, and the 73% glass sample appear very similar, while the hydration of the 100% crystalline sample proceeds more slowly. An X-ray examination of these samples, revealed that, although all three samples reacted to form a combination of the metastable calcium aluminate hydrates, C_3AH_{8-12} and C_2AH_6, the crystalline sample did indeed react more slowly. The non-hydrated crystalline C_6A_4MS could still be identified after 28 days of hydration.

In the hydration of C_6A_4MS at 25^oC, illustrated in Figure 6, similar results were obtained. The glassy samples reacted with water to form C_3AH_{8-12} and C_2AH_6, with the stable calcium aluminate hydrate, C_3AH_6, appearing after 7 days. The crystalline sample, on the other hand, reacted more slowly, with the non-hydrated crystalline form appearing as late as 14 days after the onset of hydration. The stable hydrate, C_3AH_6, also appeared after 14 days hydration.

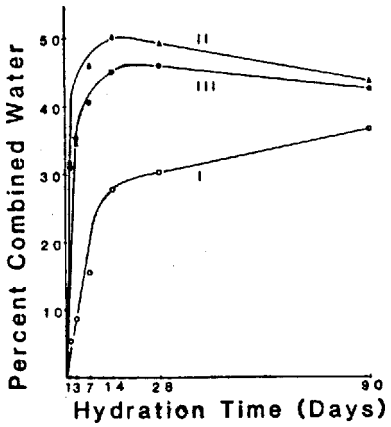

FIG. 6
The Effect of Glass Content on the Hydration of C_6A_4MS (25^oC)

Figure 7 shows that at 50^oC all of the samples hydrate in much the same way. X-ray examinations of these samples revealed that, with the exception of the very early stages of hydration of the crystalline sample, which showed a small amount of C_3AH_{8-12} present, the only species present in any of the samples are C_3AH_6 and AH_3. In all of these samples, the amount of AH_3 increased with increasing curing time. The correlation between the size of the X-ray peaks of AH_3 and the size of the DTA peak at 300^oC appears quite good, although exact measurements could not be made of the DTA peaks.

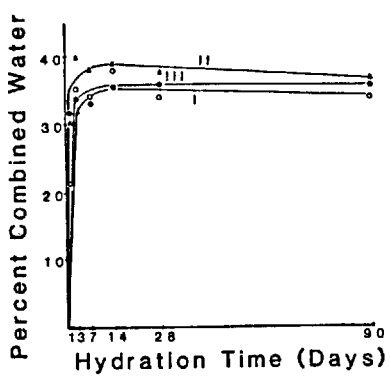

FIG. 7
The Effect of Glass Content on the Hydration of C_6A_4MS (50^oC)

From X-ray powder diffraction data, it is possible to construct the hydration pathway for C_6A_4MS, as follows;

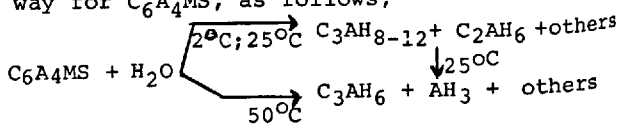

The compounds referred to as others were added because no compounds containing either MgO or SiO_2 were observed. Although in several instances, peaks appeared which may have been due to C_2ASH_8, the peaks were very weak and did not appear with any regularity. Two possible explanations for this behavior are: that the amounts of MgO and SiO_2 present are so small that the compounds containing these oxides were present in quantities of less than 3%, and therefore not detectable by X-ray diffraction; or that these oxides may be present in an amorphous form, which also could not be detected by X-ray diffraction.

CONCLUSIONS

The products of the hydration of C_6A_4MS are dependent upon the curing temperature. The metastable calcium aluminate hydrates C_3AH_{8-12} and C_2AH_6 are produced from the hydration at 2°C. At 25°C these products slowly convert to the stable calcium aluminate hydrate, C_3AH_6, and gibbsite, AH_3. At 50°C the metastable hydrates are not observed and C_3AH_6 and gibbsite are formed exclusively. Other hydration products, although not observed, must also be present to account for the presence of MgO and SiO_2. It is possible that these products are either amorphous or present in concentrations too small to be detected by X-ray powder diffraction.

Results indicate that the percent combined water at any given time during the hydration of C_6A_4MS is dependent upon both the curing temperature and the glass content of the sample. At 2°C and 25°C, the glass content has a significant effect on the hydration of C_6A_4MS, with an increase in the glass content being accompanied by a corresponding increase in the percent combined water. At 50°C, however, the glass content has little effect on the percent combined water. It is evident that as the curing temperature is increased, the effect of the glass content, in terms of the percent combined water, is decreased.

REFERENCES

1. H.F.W. Taylor, The Chemistry of Cements, Vol.I, p.69, Academic Press, New York (1964).

2. F.M. Lea, The Chemistry of Cement and Concrete, 3rd. edn., p.69, Chemical Publishing Company, Inc., New York (1971).

3. T.W. Parker, Proceedings of the Third International Symposium on the Chemistry of Cement, London (1952), pp. 485-515.

4. K.E. Daugherty, B. Saad, C. Weirich, and A. Eberendu, Silicates Industriels, 48(4), 107-110 (1983).

5. J.H. Welch, Nature (London), 191, 559-560 (1961).

6. A.J. Majumdar, Trans. Br. Ceram. Soc., 63, 347-364 (1964).

7. H.G. Midgeley, Trans. Br. Ceram. Soc., 67, 1-3 (1968).

8. P. Lhopitallier, Proceedings of the Fourth International Symposium on the Chemistry of Cement, Washington D.C. (1960), pp. 1007-1033.

9. T.W. Parker, and J.F. Ryder, Proceedings of the Third International Symposium on the Chemistry of Cement, London (1952), pp. 524-527.

10. R.H. Bogue, J. Am. Concr. Inst., 26(11), 227-230 (1955).

11. K. Gee, Slag Cement Seminar, University of Alabama, School of Engineering, Special Studies, April 30, 1981.

12. S.M. Royak, Ya.M. Shkol'nik, V.V. Orlov, L.A. Orlov, and V.I. Ermakov, Zh. Prikl. Khim., 48(5), 986-990 (1975).

13. S. Visser, J.E. Kruger, J.H.P. Van Aardt, and M.P. Brandt, CSIR Report BOU(1975), 74 pp.

14. ASTM Designation: C114-58, 1958 ASTM Book of Standards, Part IV, pp. 82-85.

15. H.G. Midgeley, Mag. of Concr. Res., 9 (25), 17-24 (1956).

16. F.S. Fulton, Portland Cement Institute Monograph, Johannesburg (1974), pp. 6-7.

17. C.J. Goodbrake, Ph.D. Dissertation, University of Illinois, Urbana-Champaign, Illinois (1978).

18. Z.Q. Wu, J. Hriljac, C.L. Hwang, and J.F. Young, J. Am. Ceram. Soc., 66(5), C86-C87 (1983).

19. J.G. Griffin, and K.E. Daugherty, Thermochimica Acta, in press.

G. Frohnsdorff, J. Clifton, H. Jennings, P. Brown, L. Struble, National Bureau of Standards, USA
J. Pommershein - Bucknell University, U.S.A.

IMPLICATIONS OF COMPUTER-BASED SIMULATION MODELS, EXPERT SYSTEMS, DATABASES, AND NETWORKS FOR CEMENT RESEARCH

1. INTRODUCTION

The use of new materials, construction practices, and designs have prompted a re-examination of traditional approaches to concrete technology. In addition, concrete structures are often used beyond their planned lifetimes, in functions for which they were not originally intended, or in harsher conditions than originally expected. There is, therefore, a need to develop improved methods and procedures for predicting the performance of cement and concrete. At the same time, rapid growth in the power and availability of computers raises questions about how they might be used to make concrete a more predictable and better performing material. As will be seen, the answers to these questions can suggest alternative ways to plan and organize cement research.

The significance of research on cement, as on other materials, depends on the questions asked, and both the questions and answers are changing because of computers. Paradoxically, the questions in cement research are becoming more oriented towards the end use of cements in concrete and, at the same time, becoming more fundamental. This is because computers can be used as links between technology and science. Thus, it is no longer unrealistic to expect scientific researchers to address such complex technological questions as "How can the performance of concrete be predicted?" which, even ten years ago, were remote from their interests and experience.

The objective of the present paper is to suggest how research questions might be addressed using computers, specifically using a computer-based knowledge system (Fig. 1) consisting of 1) models to simulate chemical and physical relationships, 2) knowledge-based expert systems, and 3) databases. In the figure, the complementary parts of the knowledge system are connected through a global computer network linking collaborating researchers. Although there is other research in this area, we are using specific examples from investigations currently being carried out at the National Bureau of Standards (NBS) to illustrate the technical feasibility of the general approach.

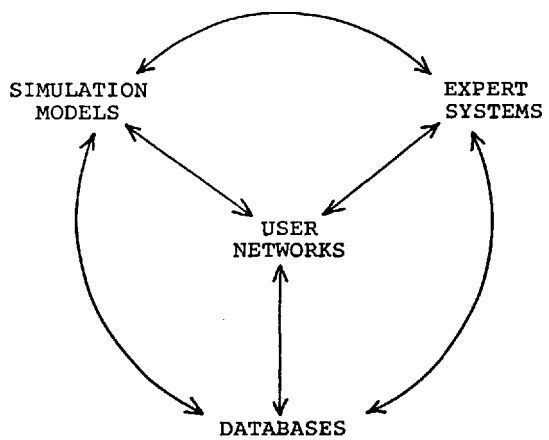

Figure 1. Schematic of a computer-based knowledge system

2. SIMULATION MODELS

Investigations of complex systems, in which the starting conditions are not well-defined and the results depend on many variables, pose serious difficulties. Understanding of such a system may often be advanced by constructing computer-based simulation models intended to represent the system and the phenomena that occur within it. Such models must be based on established scientific principles, possibly supplemented by a small number of intuitive hypotheses. The models can then be tested for their ability to explain observed relationships. Such an approach is being used increasingly in cement and concrete research [1].

In advancing understanding of cement and concrete technology, it is necessary to understand the reactions with water of cement particles, individually and in groups, and the development of microstructure in hardened cement pastes. Much recent research has contributed towards this goal [2], but few of the studies have been directed towards the development of simulation models for hydrating cements. Models are being developed in our laboratory for the hydration of tricalcium silicate (C_3S) particles [3, 4] and for the development of microstructure in C_3S pastes [5]. These are intended to be evolutionary steps towards the development of a "macromodel" [1] to describe the changes that take place when multiphase cements react to form the matrix in hardened concrete, and the subsequent reactions which affect its long term performance.

The microstructure model [5] simulates development of microstructure during the hydration of C_3S following the flow chart in Fig. 2. The model begins by calculating the spatial distribution of a chosen volume of particles in a defined volume. The free space is filled with water and then the water-filled space is gradually filled by hydration products from reactions following predefined rules. The calculations account for all the material in the system at various degrees of reaction; the results are stored in a numerical data file that can be used to produce various types of output. A typical output is a graphical representation of the distribution of the material in a cross-section of the volume (Fig. 3). Such an output may be used for visual comparison with scanning electron micrographs of sections of hardened pastes. The data file contains information about microstructural features that, presumably, govern properties or phenomena of interest, such as porosity, permeability modulus of elasticity, and fracture. The model consists of many subroutines which can be modified as new insights become available. This flexibility opens up many possibilities for collaborative research.

The model simulating development of microstructure is presently being linked to a model for chemical changes taking place during hydration of cements containing polymineralllic particles, thus producing a more comprehensive model for the hydration of portland cements. The combined model will provide an improved representation of the chemical and kinetic aspects of the hydration reactions and their effects on microstructure development.

CL

It is intended that these models will have input from many researchers, either through their direct participation in the model development or through participation in scientific and technical committees on the mathematical modeling of cement hydration,

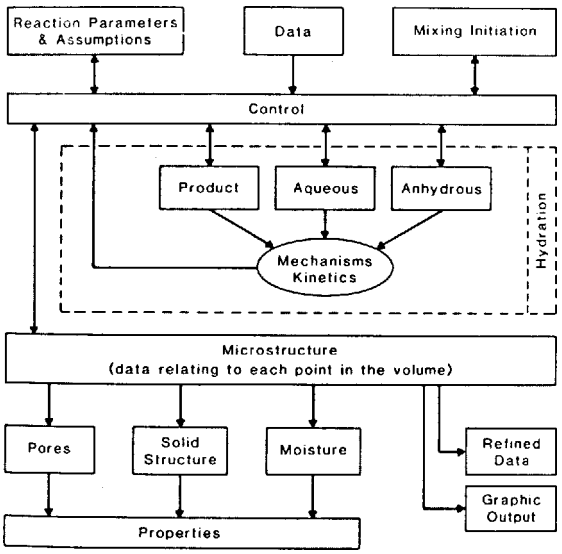

Figure 2. Flow chart for a comprehensive computer simulation model of microstructure and property development of cement pastes. Most of the small boxes represent subroutines which perform operations on different aspects of the microstructure under the control of the control program. Subroutines can be changed to invoke different assumptions and processes. In using the model, the microstructure undergoes incremental small changes at a rate controlled by a kinetics subroutine. The calculated microstructure can be used to produce a graphic output or as input to calculations of bulk properties.

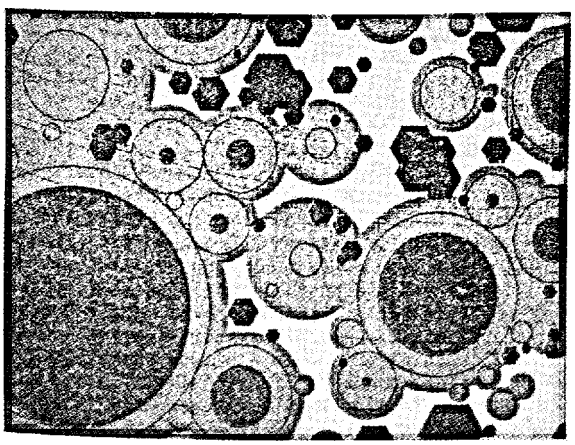

Figure 3. Graphic display of a cross-section of the calculated microstructure from a computer simulation. This cross-section is of a tricalcium silicate paste with w/s = 0.5 and a 42% degree of hydration. Solid black circles represent anhydrous C_3S; grey areas, C-S-H; hexagons, CH crystals (calculated as spheres); and black lines, original boundaries of C_3S particles.

e.g. RILEM Committee 68-MMH [2] and Sub-Committee 225.1 of the American Concrete Institute (ACI). Because constraints on resources make it unlikely that many such models will be developed in the near future, it is desirable that interested researchers should have an opportunity to share in the development and use of the model. How this might be done is discussed further in the section entitled Computer Networking.

3. KNOWLEDGE-BASED EXPERT SYSTEMS

Whereas most chemical and physical simulation models are deterministic, there is growing recognition of the need to develop stochastic models for the representation of real phenomena [6]. Also, much important knowledge falls in the category of expert opinion and, within the last twenty years, substantial progress has been made in developing, for practical application, computer programs incorporating expert opinion. Such programs are referred to as "knowledge-based expert systems" or "expert systems," with pioneering applications being in medical diagnosis and the analysis of mass spectra [7]. Expert systems are difficult and costly to develop, but their potential for improving the quality of decisions is high.

Recently, Clifton, Oltikar, and Johnson [8] developed a prototype expert system, DURCON (from DURable CONcrete), for selecting materials for producing durable concrete. DURCON is an interactive computer program that assists in designing concrete for use in a specified environment and in selecting appropriate materials and proportions for use in a trial mixture. It includes durability as regards freezing and thawing, corrosion of reinforcing steel, chemical attack, and alkali-aggregate reaction. DURCON is based on the American Concrete Institute (ACI) Guide to Durable Concrete [9], the most authoritative document on durable concrete published by the ACI. It is being developed in cooperation with the ACI Committee 201 on Durability, and a number of experts on durability have contributed ideas and critically reviewed the system. It is hoped and expected that the completed expert system will be approved by a consensus of the ACI committee and will be recognized as a standard equivalent to the guide on which it is based.

Among the benefits of an expert system are that it can:

1) provide an easy-to-use representation of expert knowledge,

2) assist in the making of decisions on complex problems,

3) draw attention to gaps in knowledge and to research needs, and

4) provide an educational tool.

NBS has recently begun the development of another expert system, based on the ACI Guide to the Selection and Use of Cements [10]. Like DURCON, this is being developed with the collaboration of an ACI committee, in this case ACI 225 on Hydraulic Cements. This raises the question of whether there should be a

group of complementary expert systems, each representing one or more aspects of concrete technology, which could be used separately or together for solving a specific problem or, perhaps, as a convenient representation of a code of practice, e.g. ACI 318 [11]. Some possible topics for expert systems which might become components of a larger system representing a code of practice for concrete, or a commentary on a code, are: 1) definition of service conditions, 2) materials selection, 3) mixture design, 4) expected life, 5) construction requirements, 6) general requirements, 7) structural systems or elements, 8) condition assessment, 9) protective measures, and 10) repair procedures.

Currently, expert systems depend heavily on the knowledge which experts have gained from experience. However, they have the potential for incorporating simulation models (Fig. 1) to help improve the recommendations they make. Expert systems can also be used to improve the efficiency of simulation models, as by application of pre-established rules to the selection of parameters.

As with simulation models, the large effort required to develop an expert system makes it desirable that many researchers have an opportunity to share in its development, evaluation, and use. Computer networking should facilitate this.

An important question which cannot be overlooked is that of liability for errors in decisions arrived at with the help of an expert system. If the expert system was developed by a consensus process in an authoritative standards organization, then the expert system may be considered as a new type of standard. The users and developers of a standard expert system would, presumably, have similar liabilities for faulty decisions to the developers and users of other standards. The situation could well be much more complicated if a faulty decision was attributed to a less-openly developed expert system.

4. DATABASES

Simulation models and expert systems require data and other knowledge to make them useful. In this paper, "data" refers to information in the form of numerical quantities relating to a material or system, and "knowledge" refers to all forms of information, including text, images, and data. For convenience, "databases" will be used to refer to any computer-based collection of knowledge, not only numerical data. Text and images are often of less certain origin than data, but they may be equally valuable in decision-making. The costs involved in establishing databases have required decisions concerning their scope and usefulness. Although it is evident that much knowledge is worth recording, it is often difficult to justify the cost. However, advances in the recording of sound and images (e.g. laser video-disc recording) and in database management systems [12] are reducing the cost of databases by making them easier to produce and maintain.

Prioritizing and structuring knowledge for possible use in a database may be viewed in terms of its potential usefulness in aiding the development of a simulation model, an expert system, or both. A model or expert system may itself be used to establish priorities and structure. Thus, new knowledge may be checked using a model or expert system for consistency with what is already known.

Examples of NBS contributions to the databases for cement science are the revisions of the phase diagrams for the C-S-H [13, 14] and C-A-S-H [15] systems. This work provides fundamental data needed for simulation models of cement hydration and, possibly, for expert systems. Although the phase diagrams are of great importance as representations of the phase relationships governing the cement hydration reactions, their critical evaluation and improvement have been slow in recent years. Their usefulness will be increased through the use of computers to store and display them in new, more convenient ways.

In addition to the phase diagrams, NBS has a substantial database on the properties and laboratory test performance of cements in the Cement and Concrete Reference Laboratory [16], CCRL, sponsored by the ASTM Committees C-1 on Cements and C-9 on Concrete and Concrete Aggregates. The database consists of many replicate sets of results from ASTM standard tests on carefully-homogenized, commercial portland cements used in the CCRL Proficiency Sample Program [17]. In principle, the database is available for use by standards developing committees, or other interested parties. The database includes only the results of ASTM standard tests, and has no information on the phase compositions of the cements other than calculated potential compound compositions. To help overcome this deficiency of current ASTM tests, task groups on phase analysis of clinkers and cements have been set up in ASTM Subcommittee C-1.23 on Chemical Analysis (of cements). The task groups are developing standard practices for quantitative phase analysis by x-ray diffraction and by light microscopy and have stimulated an NBS project to prepare a standard reference material (SRM) for clinker phase analysis. Results of these activities will strengthen the value of computer databases based on ASTM tests by making it possible to characterize cements more precisely.

5. COMPUTER NETWORKING

The benefits of knowledge increase with its accessibility and reliability. New technology for communication between computers is facilitating the transmission of data between researchers and increasing the possibilities for their participation in reviewing and sharing data. The increased ease and speed of communication will bring new opportunities for world-wide collaboration among cement researchers, and should stimulate greater cooperation in planning research and sharing research results. Such cooperation is likely to have an enormous impact on the collective rate of progress in cement research by helping overcome inefficiences resulting from the limited resources being scattered among many relatively small research groups.

If researchers are willing to avail themselves of the opportunities, it is likely that research activities in different laboratories will become increasingly complementary. This can be

accomplished through the exchange of ideas at the planning stage and through the exchange of data. Through exchanges of this sort, it is possible to envision cement research moving into an era characterized by "hyperintelligence" as defined by Bugliarello [18]. The concept is that groups of individuals may be able to act as though possessing an enhanced intelligence because of ability to share knowledge easily and rapidly.

As a step towards establishment of a computer network among cement and concrete researchers, NBS is operating an electronic bulletin board (EBB) [19] for exchange of information regarding the expert system development. It allows participants to communicate with each other using personal computers connected by the telephone system. In this way, a computer conference can take place with participants commenting on, and recommending improvements to, the expert system. In the same way, the bulletin board may, eventually, provide access to the expert system, or other programs, for purposes of development or practical use.

The possibilities provided by computer networking complement, or multiply, those derived from the development and use of simulation models, expert systems, and databases without such a network.

6. DISCUSSION

Knowledge systems for cement and concrete science and technology depend on knowledge produced in the laboratory and in the field. A system for managing the knowledge facilitates its use and increases its value; however, it cannot be justified without the necessary knowledge. Furthermore, such a system must continue to be supplied with new information through laboratory and field research.

The biggest problem in predicting the performance of concrete is the lack of a sufficient database on field performance. This is an area where computers can be expected to make an important contribution which will be facilitated if a standard format for recording the field performance of structures can be made available.

As the knowledge system becomes better integrated and more coherent, research needs will become more clearly defined. For example, the development of the expert system DURCON has shown where more information on alkali-silica reactions is needed. Thus, improved methods for handling knowledge can increase the need for research by increasing the value of its results. The computer plays a vital role in this process by increasing the sophistication of the measurements and by facilitating the storage and retrieval of data. In view of the great advances in the technology, it seems that the time is now right for a workshop or conference to be held to discuss the planning and implementation of a knowledge system such as is discussed in the present paper. We are planning such a workshop.

7. CONCLUSIONS

The impact of computers on cement research is accelerating. Simulation models for the reactions of cements with water and expert systems relating to cement and concrete are being developed at the same time that database and networking technologies are undergoing rapid growth. Taken together, these developments provide new opportunities for collaboration among cement researchers in activities that will lead to still more rapid progress in cement and concrete science and technology.

8. ACKNOWLEDGEMENTS

The authors wish to acknowledge that very many persons have contributed to the development of the ideas presented in this paper. In particular, they wish to thank Dr. Leslie Parrott, Dr. Karen Scrivener, Dr. H.F.W. Taylor, Mr. Stewart Tresouthick, and Dr. Folker Wittmann, for many thought-provoking discussions, and Dr. Vagn Johanssen and all members of his RILEM Committee 68-MMH on Mathematical Modeling of Cement Hydration for the stimulation provided by their activities.

9. REFERENCES

1. Frohnsdorff, G., and Clifton, J.R., A review of mathematical modeling applied to the manufacture and use of portland cements, Cem. Res. Prog., 1980, pp. 279-304 (1981).

2. Taylor, H.F.W., and 11 others, The hydration of tricalcium silicate, Report of RILEM Committee 68-MMH, Task Group 3, Mater. Constr. (Paris), v. 17, 1984, pp. 457-468.

3. Pommersheim, J.M., and Clifton, J.R., Mathematical modeling of tricalcium silicate hydration, Cem. Concr. Res., v. 9, 1979, pp. 765-770.

4. Pommersheim, J.M., and Clifton, J.R., Mathematical modeling of tricalcium silicate hydration, silicate hydration, Cem. Concr. Res., v. 12, 1982, pp. 765-772.

5. Jennings, H.M., and Johnson, S.K., Simulation of microstructure development during the hydration of a cement compound, J. Amer. Ceram. Soc., (submitted for publication).

6. Martin, J.W., Service life prediction from accelerated aging test results using reliability theory and life testing analysis, in Masters, L.W. (ed.), Problems in Service Life Prediction of Building and Construction Materials, NATO Series E, Applied Science No. 95, Martinus Nijhoff, Dordrecht, Netherlands, 1985, pp. 191-211.

7. Duda, R., and Shortliffe, E.H., Expert Systems Research, Science, v. 220, No. 4594, 1983, pp. 261-268.

8. Clifton, J.R., Oltikar, B.C., and Johnson, S.K., Development of DURCON, an expert system for durable concrete: Part 1, NBSIR 85-3186, Bureau of Standards, Washington, D.C., 1985 (18 pp.)

9. Guide to Durable Concrete, ACI 201.2R-77, Manual of Concrete Practice, v. 1, Am. Concr. Inst., Detroit, 1985 (37 pp.)

10. Guide to the Selection and Use of Hydraulic Cements, ACI 225R-85, J. Am. Concr. Inst., v. 82, 1985, pp. 901-929.

11. Building Code Requirements for Reinforced Concrete, ACI 318-83, Manual of Concrete Practice, v. 3, Detroit, 1985 (111 pp.).

12. Ambler, E., Engineering Property Data: A National Priority, ASTM Standardization News, August 1985, pp. 46-50.

13. Jennings, H.M., Aqueous solubility relationships for two types of calcium silicate hydrate, J. Amer. Ceram. Soc., (in press).

14. Brown, P.W., Franz, E., Frohnsdorff, G., and Taylor, H.F.W., Analysis of the aqueous phase during early C_3S hydration, Cem. Concr. Res., v. 14, 1984, pp. 257-262.

15. Brown, P.W., Barret, P., et al., The hydration of tricalcium aluminate and tetracalcium aluminoferrite in the presence of calcium sulfate, Mater. Constr. (Paris) (submitted for publication).

16. The Cement and Concrete Reference Laboratory - A case history in collaborative standardization, ASTM Mater. Res. Stand., v. 10, 1970.

17. Pielert, J.H., Haverfield, J.W., and Spellerberg, P.A., Application of CCRL data in the formulation of precision estimates for selected cement standards, Cem., Concr., Aggregates, v. 7, 1985, pp. 37-42.

18. Bugliarello, G., Hyperintelligence: The Next Evolutionary Step, The Futurist, v. 18, 1984, pp. 6-11.

19. Kaetzel, L.J., and Clifton, J.R., A bulletin board system for feedback to the DURCON expert system: a description and reference, NBSIR Series Report, National Bureau of Standards (submitted for publication).

V.I. AKUNOV,
S.D. MAKASHEV,
V.A. DMITRIYEVA,
N.V. TSUKANOVA,
B.E. YUDOVICH

USSR

MECHANOCHEMICAL ACTIVATION OF MATERIALS IN CEMENT MANUFACTURE

Mechanochemical activation has been reported for a number of materials being subjected to jet grinding, such as sand, limesand mixes, slag portland cement, straight cement, belite slurry, and high alumina cement. Jet grinding has been revealed to improve compressive strength ratings of the cement by 5 to 10 MPa on average. The reason for this increase lies in a more uniform grain size distribution of cement and the modified surface morphology of cement grains which include reentrant angles /1, 2/.

This report is devoted to the mechanochemical activation of cement raw materials and clinkers in jet mills (table 1) operating with two counter streams of material whose particles are accelerated to supersonic speeds by gaseous fluids, air and water steam, carrying them.

The grinding of certain raw materials and their mixes in a model MSP-0.5 jet mill provided an almost 100% yield in the 1-40 μm fraction range (table 2). As a result a 100 °C lower temperature can be afforded in the calcination zone of pilot rotary kilns, as compared with the temperatures needed to calcine the ball-mill ground mixes, the respective clinkering rate constant being also increased 2 to 7 times (table 3). The resultant clinkers exhibited an increased dislocation density on the chippings (table 4) which led to a 28-day compressive strength of this cement being increased by 5 to 15 MPa.

The largest increment of strength was exhibited by cements prepared from the raw mixes in which one component was jet-grinded (carbonaceous or agrillacious) and the other component was ball-mill grinded, the specific surface of the cements being about 3000 cm^2/g (table 5). For higher specific surface figures of 4000 and 5000 cm^2/g, a certain decrease was noted of the positive effect of jet grinding on cement strength ratings. Moreover, a further grinding of clinkers manufactured from jet milled raw materials, performed in a laboratory jet mill, to a fineness of 4000 cm^2/g failed to result in an additional increment of strength as compared with the ball milling of the same clinkers (table 5).

It was found, however, that the jet grinding of cements of diverse compound compositions in steam carrier fluid increased the compressive strength ratings as compared with that of ball-mill grinded cements

Table 1

Technical Data on Soviet Jet Mills MSP-0.5 and MSP-0.05

Description	Units	MSP-0.05	MSP-0.5	
Original lump size	mm	5	7	
Grinding compartment length/diameter	mm	150/180	200/140	
Acceleration ducts length/diameter	mm	20/16	40/32	
Nozzle diameter	mm	4	5	
Classifier type		impinge-swirling		
Carrier fluid		air	air or steam	
Input fluid pressure	atm	4-5	4-5	6-7
Fluid temperature	°C	20-25	20-25	230
Capacity	t/hr	0.05	0.5	
Specific energy requirements for clinker grinding	kWhr/t	300	200	
Fluid rate	m^3/min	1.1	0.7	

Table 2

Size Distribution of Jet Ground Raw Materials

Component	Persentage of fraction range shown			
	5 μ	5-20 μ	20-30 μ	30-40 μ
Chalk	0.3	0.5	8.2	91.0
Clay	0.1	25.0	23.4	51.5
Sand	1.4	3.1	38.1	57.4
Pirite cinder	0.3	0.9	2.6	96.2

Table 3

Kinetics of Lime Assimilation in Raw Mixes of Ball and Jet Grinding Processes

Grind process type	Percent R on 004 sieve	Bound CaO, %, after 30 min conditioning at indicated T, °C				Clinkering rate constant (after Carter-Valency) k x 10^{-4}, at shown T, °C			
		1000	1100	1200	1300	1000	1100	1200	1300
ball	14.4	28.5	18.6	15.2	4.3	5.5	20.0	28.0	96.0
inter-ground jet	1.3	18.9	17.2	14.9	2.8	19.7	23.4	30.0	119.0
separate jet	0.5	18.4	14.9	13.5	2.3	20.3	29.6	34.3	131.0
jet + clay ball chalk	2.2	15.9	15.2	14.3	1.6	27.5	29.8	32.9	150.0

Table 4

Dislocation Density on Chippings of Various Size Clinker Grains

Grind process type	Dislocation count, μ^{-1}, * for indicated grain size, mm						Count level
	1-2	2-3	3-5	5-7	7-10	10	
	0.84	0.77	0.74	0.70	0.59	0.51	min
ball mill	1.83	1.64	1.29	1.96	1.29	1.05	max
	1.34	1.21	1.02	1.33	0.94	0.78	av.
	0.84	0.70	0.88	1.35	1.20	1.38	min
jet mill	2.05	1.38	2.36	2.09	1.88	2.10	max
	1.45	1.04	1.62	1.72	1.54	1.74	av.

*Note: determined by the secant line method for each fraction.

(table 6). The highest effect of the mechanoactivation, 120 MPa, was noted for belite-aluminate cement, the lowest effect was identified for alite cements, independent of their C_3A content. Conversely, for alite jet-mill cements, a 4 to 5 MPa increase in early strength of up to 3 day old mortars dominated over the strength increments of other cements.

One of the reasons why jet grinding of cements increases the compressive strength ratings may be attributed to a growth (up to 80 %) of the yield of the 5-30 μm fraction over the 50 % content of this fraction in the ball grinded product (table 7).

When the carrier fluid was cold air, no effect of mechanoactivation was recorded after jet grinding of both belite and alite clinkers (table 6), which may be traced to a more extensive carbonation of new formations which occur in the grinding under the impact of the air moisture.

Jet grinding is able to promote the cement into the next higher compressive strength brand (due to a 50 kgf/cm^2 increase in the strength) provided the jet fluid is chosen appropriately. In view of a higher water requirement of jet-ground cements, the efficient application of this grinding method calls for a separate study.

V.I. AKUNOV,
S.D. MAKASHEV,
V.A. DMITRIYEVA,
N.V. TSUKANOVA,
B.E. YUDOVICH

Table 5

Physico-mechanical Tests of Ball and Jet Ground Cements

Raw mix grinding process	Strength, MPa, at age (days) indicated							
	bending				compressive			
	1	3	7	28	1	3	7	28
	Ball mill grinding to 3000 cm^2/g fineness							
1 ball	1.7	4.3	5.8	7.3	7.2	28.4	40.9	67.5
2 joint jet	1.9	5.1	6.8	7.2	8.6	31.7	45.8	68.4
3 separate jet	3.7	5.9	6.4	7.9	20.6	43.0	56.6	68.8
4 jet chalk+ball clay	3.3	6.3	7.3	8.6	16.8	41.2	57.6	84.5
5 ball chalk+jet clay	2.8	6.2	7.3	7.9	12.0	38.1	57.3	80.4
	Ball mill grinding to 4000 cm^2/g fineness							
1 ball	2.4	4.3	6.3	7.5	12.0	34.5	46.8	72.7
2 joint jet	4.8	6.2	6.6	7.9	26.0	46.9	59.1	73.7
3 separate jet	5.0	6.7	7.5	8.2	27.1	40.5	59.9	81.0
4 jet chalk+ball clay	3.9	6.5	7.6	7.8	18.5	42.8	59.0	81.5
5 ball chalk+jet clay	3.2	5.3	7.0	8.2	16.8	37.6	55.7	80.0
	Ball-mill grinding to 5000 cm^2/g fineness							
1 ball	2.8	4.3	6.3	7.5	13.6	36.9	47.4	68.4
2 joint jet	5.1	6.8	7.5	7.5	34.6	52.2	62.5	76.7
3 separate jet	5.2	7.0	7.1	7.9	32.5	51.1	62.0	71.9
4 jet chalk+ball clay	5.0	7.0	7.5	8.4	33.5	50.9	64.3	71.2
5 ball chalk+jet clay	4.2	6.0	6.8	8.1	25.6	43.2	52.8	70.0
	Jet grinding to 4000 cm^2"g fineness							
1 ball	2.9	4.3	8.2	9.2	14.7	35.6	55.2	74.1
2 joint jet	3.8	6.7	7.7	9.2	20.8	41.2	55.2	77.6
3 separate jet	2.9	5.9	7.6	8.8	25.8	32.5	51.6	64.4
4 jet chalk+ball clay	3.3	6.6	8.7	8.9	17.6	37.7	58.7	74.1
5 ball chalk+jet clay	2.9	7.3	8.4	8.8	15.1	37.8	61.2	71.9

Table 6

Physico-mechanical Tests of Various Jet and Ball Ground Cements

Clinker composition, %					Strength, MPa, at age (days) indicated							
					bending				compressive			
No.	C_3S	C_2S	C_3A	C_4AF	1	3	7	28	1	3	7	28
					Ball mill grinding							
1	12	61	6	16	1.3	1.5	1.8	3.8	5.2	7.5	10.0	26.2
2	55	18	9	12	2.9	5.4	5.6	6.8	14.9	34.5	44.1	60.9
3	35	44	3	15	3.0	5.2	5.2	7.7	9.6	26.1	34.1	57.9
4	32	47	9	9	2.7	4.7	5.1	6.9	9.0	21.9	33.1	54.7
5	65	16	4	13	3.3	5.8	6.9	7.9	12.4	31.6	46.8	65.7
6	55	18	10	14	2.6	6.0	6.5	7.4	9.5	30.8	45.6	64.5

Table 6

Clinker composition, %					Strength, MPa, at age (days) indicated							
					bending				compressive			
No.	C_3S	C_2S	C_3A	C_4AF	1	3	7	28	1	3	7	28
					Air-jet grinding							
1	12	61	6	16	1.5	1.7	1.9	3.3	5.2	7.7	9.3	25.1
2	55	18	9	12	3.3	5.3	6.0	7.3	17.2	35.1	42.8	58.9
					Steam-jet grinding							
3	35	44	3	15	2.9	5.7	5.8	8.2	9.4	27.6	30.9	62.4
4	32	47	9	9	3.1	4.9	5.5	8.3	10.5	29.8	38.4	66.6
5	65	16	4	13	5.3	7.3	8.4	8.9	21.8	45.6	54.6	69.7
6	55	18	10	14	4.3	6.9	7.1	8.8	18.1	42.2	57.2	69.9

Table 7

Grain Size Distribution for Various Cements

Clinker No.	Weight percentage for indicated grain size range (μ)									
	1	1-5	5-7	7-10	10-15	15-20	20-30	30-60	30	60
					Ball mill grinding					
1	7.8	11.7	9.3	13.7	4.9	9.8	15.2	17.7	27.6	9.9
2	7.7	4.4	10.8	7.3	8.3	12.7	17.1	20.5	31.7	11.2
3	22.1	3.9	6.1	3.1	18.3	7.4	4.8	27.3	24.3	7.0
4	20.7	1.3	9.4	9.9	16.6	9.9	3.5	25.4	28.7	3.3
5	19.6	4.0	7.6	9.8	18.3	10.2	11.0	13.1	19.5	6.4
6	19.3	3.0	4.2	8.4	19.3	8.4	8.4	22.6	29.0	6.4
					Jet grinding					
1	4.4	7.5	8.5	17.0	28.7	16.5	2.7	14.2	14.7	0.5
2	9.5	4.6	10.3	9.8	16.0	16.5	7.7	22.5	25.5	3.0
3	19.9	3.1	12.0	15.7	23.1	6.8	17.8	1.6	1.6	-
4	34.6	2.1	2.1	31.4	24.6	4.2	1.0	-	-	-
5	21.5	1.0	14.1	5.8	30.9	20.4	2.1	4.2	4.2	-
6	17.8	6.3	8.4	16.2	28.3	15.2	5.2	2.6	2.6	-

REFERENCES

1. Акунов В.И. Струйные мельницы. М., Машгиз, 1967, 267 с.
2. Акунов В.И., Юдович Б.Э., Литвинов Г.П. и др. Генерация поверхности и зернового состава продуктов измельчения в струйных мельницах. "Цемент", 1980, № 7, с. 11-13.

Y.M. BAZHENOV - MISI Kujbychev, Moscou - U.S.S.R.

EVALUATION OF REOLOGICAL CHARACTERISTICS OF CEMENT PASTE AND CONCRETE WITH HELP OF COMPUTERS

The development of computer technic discovers the possibility to further improvements of technological recalculations to obtain higher quality of production and economic benefits. Computerisation of concrete technology has a great importance, particularly in the conditions of increasing the deviation in properties of raw materials (different chemical and fine-grounded admixtures, secondary industrial raw materials), and complicated technology (application of robots, new ways of mix activation, new casting equipment and ways of concrete set). Operation of technology on the base of wideer computer application will give a guaranteed quality of the fresh concrete mix and a quality of hardened concrete for different conditions of precast concrete constructions.

Additionally computerisation of industry needs a new approach to evaluation of influence of cement, aggregates and other factors on the rheological characteristics of concrete mix. For the first time we are interested not in general estimation of material utility for concrete, but quantitative evaluation of one or another factor on rheological characteristics of concrete, setting time, hardness and concrete strength at particular age.

There are wide applications of mathematical models in technological recalculations in the Soviet Union, which allow to obtain with the help of experiments planning and standard means of materials tests, tests of fresh concrete mix and hardened concrete (1, 2, 3, 5). However, these methods are suitable for accepted conditions and alternation of raw materials and technology needs its great adjustment. Therefore it remains an actual task of discovering a new criterion of evaluation cement and aggregate influence on characteristics of concrete mix and relations, which give us a possibility to describe characteristics of cement paste and concrete mix of different compositions in general form. This is more important in conditions of increased raw material resources for concrete and large utilisation of different water-reducers and complex admixtures on their base.

With addition of water-reducers and superplasticizers to cement paste either efficiency or influence on fluidity (SI) of cement paste and rate of admixture (D) depend on type of admixture and quality of cement. However, the slope of curves Sl=f(D is similar in all cases (Fig. 1), and only parameters of these curves are different. We can see three areas on these curves. At the first area the quantity of water-reducer is yet not enough for an influence on all the cement grains and admixture efficiency is negligible. Slight fluidizing effect is gained at the area 11, when the continuous layer of water-reducer is developed on the cement grains surfaces. Optimum cement rate accounting for technical and economic factors lays in the limits of this area. The efficiency of admixture gradually decreases at the area 111. Physical and chemical factors which determinate the slope and parameters of curves Sl=f(D) for different types of water-reducers are different, however, the slope of curves having a great importance for mathematical prediction of admixture efficiency looks alike. This gives us a possibility to approximate in calculation of the function Sl=f(D) at the area 111 with the help of following expressions:

$$Sl = K_1 K_2 (D + a)$$

where: K_1 - coefficient of water-reducer influence on fluidity of cement paste; K_2 - coefficient accounted for the influence of cement; a - constant.

Coefficient K_1 can in some limits give us a characteristic of the water-reducer efficiency; the bigger coefficient, the higher fluidizing effect. Coefficient K_2, in general, determines the possibility of applicating an admixture for a given cement; its increasing shows a higher efficiency of an admixture in the cement paste of a given

cement.

It's recommended to held out comparison tests of small volumes to get useful data for calculations. As a standard one could apply data of a well-known water-reducer or data of agreed standard curve. It's recommended to discuss possible parameters of such a curve at the congress.

However, there are some limits of information concerning influence of water-reducers on cement pastes for prediction of rheological characteristics. One should mention the structure of concrete mix, characteristics of aggregates, quantity of cement. The aggregate influences on rheological characteristics of the mix. This aggregate influence is practically impossible to evaluate on the base of its size, pore volume and other standard characteristics only. The appointed integral criterion - "water consumption of aggregate" - gives a more accurate evaluation and this criterion obtained from estimation of water consumption of cement paste, mortar and concrete mix of equal fluidity determine relative increase of water-cement ratio which applied for comparison of structural role of the aggregate. In account of water consumption of the aggregate it's possible to estimate the efficient water-cement ratio which characterizes the behaviour of the cement paste and the concrete mix (1, 4).

The influence of water-reducing admixtures on rheological characteristics of a concrete mix could be accounted for with the help of a special coefficient the same way as with the cement paste which is determined with comparison tests. It substantially simplifies accounts and gives us a possibility to use one method of prediction of the rheological characteristics of concrete mix for application of different water-reducers.

In the base of this proposal lays an experimentally stated fact that water-reducers don't alter their character of relation between the concrete mix fluidity and water consumption, but alter parameters of relative curves only (Fig. 2, 3). Addition of water-reducer increases fluidity of the concrete mix and decreases water consumption of the concrete mix of equal fluidity. If known that admixture decreases water consumption of the concrete mix by 10 or 20% then we can describe corresponding curves which have the same behaviour as the curve for the concrete mix without an admixture but with different parameters, and determine water consumption with the help of these curves to obtain a given fluidity of the concrete mix. While applying complex chemical admixtures the influence on water consumption of concrete mix is possible to evaluate the type and rate of the water-reducing coponent.

The influence of water-reducing admixtures on water consumption of a concrete mix is possible to evaluate with the coefficient which shows an amount of decreased water content at equal fluidity of mix in the presence of an admixture.

$$\alpha = B_g/B = \frac{100 - \Delta B}{100}$$

where B_g - water consumption of concrete mix in the presence of an admixture; B - water consumption of a concrete mix without admixture; B - reduction of water consumption of concrete mix with of an admixture.

Coefficient α determines slope of the curve S1 = (B) and efficiency of admixture. This coefficient depends on the type and rate of an admixture and the quality of an applied cement.

Fluidity of a concrete mix increases with an admixture rate. The behaviour of the curve S1 =(D) is similar to the curve of the cement paste and has same characteristic areas. Optimal admixture rate is usually admitted at the upper side of the area 11 (higher increase of fluidity with the rate of an admixture), but to some limits could be influenced by some other factors: necessity of high development of concrete strength, guarantee of no bleeding of concrete mix, economic benefits, etc.

Comparison of different water-reducing

admixtures in optimal rates gives us a possibility to divide them into several classes by its efficiency of influence on the rheological properties of a concrete mix: water-reducers, which decrease water content

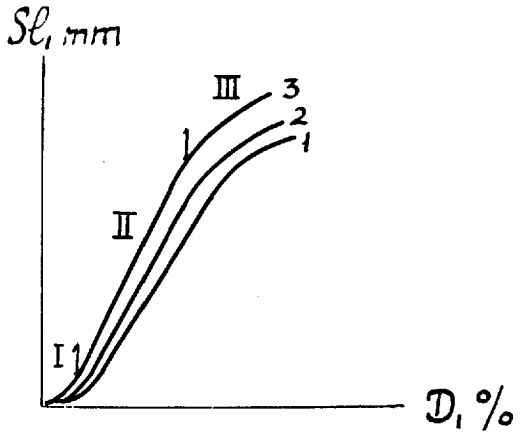

Fig. 1. Influence of water-reducer rate on a slump of cement paste: 1-cement paste with 10% of C_3A in cement and the admixture "40-03"; 2-same as above, but 4% of C_3A; 3-cement paste with 4% oc C_3A and the admixture "10-03"

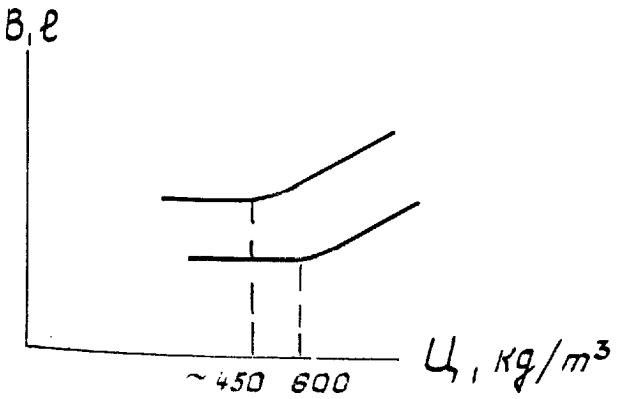

Fig. 2. Influence of the type of water-reducer on water consumption of the concrete mix: 1-concrete mix with superplasticizer C-3; 2-same as above, but with СДБ ; 3-same as above, but without admixture

on 5, 10, 15, 20 and 25% in mixtures of equal fluidity. Coefficient α will be altering the range from 0,95 to 0,75, correspondingly, we need a quantitative value

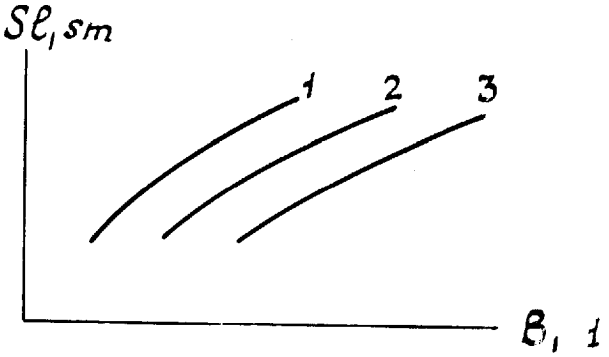

Fig. 3. Influence of the superplasticizer C-3 on the relation between water consumption of the concrete mix and cement consumption: 1-concrete mix in presence of superplasticizer; 2-concrete mix without an admixture

Table 1

Type of superplasticizer	Water-cement ratio	Water reduction in mixes with equal fluidity, %
Reference concrete mix without admixture	0,425	-
C-3 (USSR)	0,32	24,8
30-03 (USSR)	0,315	26,0
KM-30 (USSR)	0,31	27,2
10-03 (USSR)	0,31	27,2
Mighty (Japan)	0,315	26
БП -1 (Bulgary)	0,32	24,8
Melment (FRG)	0,32	24,8
Super (USA)	0,318	25,3

of the coefficient for computer calculations, but not the nature of the admixture. Different admixtures of one class will be presented by one coefficient in calculations.

Experiments have shown that admixtures of the different chemical composition, but one and the same class of influence had a relatively small deviation in the reduced

Table 2

Cement composition, %		Average water reduction in mixes of equal fluidity in the presence of superplasticizer "10-03", %			
C_3S	C_3A	0,5	0,75	1	1,25
49	6	18	23	28	33
40	8	17	22	27	32
33	10	15	19	24	29

water (Table 1).

The comparisons were taken with one rate of superplasticizer 10 and fluidity of the concrete mix 5 cm. Cement consumption was 500 kg/m^3, r = 0,32. Similar results were obtained by the small correlation of admixture rate.

Influence of mineralogical composition of cement on the efficiency of the superplasticizer was smaller then the rate of admixture (Table 2). This can be accepted by coefficient ß excluded in terms of corresponding correlation of admixture rate, e.g. with aluminate cement the quantity of superplasticizer could be increased by 0,1-0,2% of cement weight.

To get proof of the water-reducers efficiency it's necessary to develop a standard method of comparison tests. This gives us a possibility to design mathematical models with applicationof such arguments as cement paste-consumption, water consumption of aggregate, effective water-cement ratio of the cement paste and concrete mix, coefficients of water-reducer efficiency, α and ß. Experimental calculations show the possibility of accurate prediction of rheological properties of the concrete mix with the help of one model, when different cements, admixtures, and aggregates are applied. Correspondingly the reversal task of concrete mix design in the function of given rheological properties were carried out more accurately and the possibility of effective monitoring of precast concrete and concrete construction process has become a reality. We can immediately react to the slightest alternations in raw materials properties and obtain high quality of construction with minimal consumption of cement and reduced costs with the help of computers.

REFERENCE

1. Bazhenov Y.M., Komar A.A., Technology of concrete and reinforced concrete production. Moscow, Stroyizdat, 1984.
2. Bazhenov Y.M., Voznesenskiy V.A. Perspectives of application of mathematical methods in technology of precast concrete. Moscow, Stroyizdat, 1974.
3. Bazhenov Y.M., Gorchakov G.I., Alimov L.A., Voronin V.V., Improvement of durability of concrete and reinforced concrete constructions in severe conditions. Moscow, Stroyizdat, 1984.
4. Bazhenov Y.M. 7-th Congres International de la Chimie des Cimentas. 1980, Paris, vol. 1V, p. 125.
5. Shein V.I. Mathematical models of alternation of the properties of cement paste with time. 7-th Congres International de la Chimie des Cimentas. Paris, 1980, vol. 1.

L.S. GEIDAROVA, Giprocement, Léningrade, URSS
M.A. ASTAKHOVA

CERTAINS ASPECTS DE L'ACTIVATION LORS DE L'OBTENTION DU LIANT SANS CLINKER

Il est connu que les substances peu solubles se caractérisent des propriétés déterminées de l'acidité ou basicité de la surface, qui peuvent être renforcées par le traitement thermique à 413-773K [1].

Cette technique été utilisée pour la matière sulfatocalcique - phosphogypse - qu'est sous-produit de la production chimique.

Active par son acidité, la forme du phosphogypse a été étudiée à la température différente du traitement sur des systèmes-modèles - suspensions - de rapport phosphogypse/eau = 1:10, par mesure à l'aide de pH-mètrmillivoltmètre. La variation de la concentration des ions H^+ dans les suspensions en fonction de la température du traitement du phosphogypse montre qu'elle atteint sa valeur maximale à 673K [2].

Les résultats de la spectroscopie infrarouge et de l'analyse des phases aux rayons X ont mis en évidence la déshydration du phosphogypse lors du traitement thermique à 673K et la transformation du réseau cristallin du gypse dihydraté en structure d'anhydrite - apparition de la raie d'absorption 620 cm^{-1}, disparition de la raie 1686 cm^{-1}. On note aussi la présence du sulfate de calcium en forme hydratée - $CaSO_4 \cdot 0,5\ H_2O$ - les raies d'absorption dans la région de 3615, 3546, 1620 cm^{-1}. L'apparition de l'anhydrite est nettement observée sur les diffractogrammes par les raies 3,85; 3,49; 2,83; 1,87; 1,75; $1,65 \cdot 10^{-10}$ m.

La présence du gypse en forme semihydratée 3,48; 3,10; 2,80; 2,35; 1,85; $1,70 \times 10^{-10}$m y est aussi constatée.

Selon les données de l'analyse thermique différentielle le phosphogypse prétraité à 673K par rapport au phosphogypse, révèle un effet endothermique très faible dans la plage de 423- à -473K qui est lié à la déshydratation du gypse semihydraté, présenté en phosphogypse en quantité peu considérable. La perte de l'eau fait ici 0,75%. Les études physicochimiques ont mis en évidence que le phosphogypse traité à 673K est présenté par d'env. 85% de l'anhydrite et par 15% du gypse semihydraté.

L'analyse électronique stéréomicroscopique a montrée que le traitement du phosphogypse à 673K varie entièrement la forme de ses cristaux. Du phosphogypse aux grands cristaux lamellaires il se transforme aux plus petites particules de differentes dimensions, parmi lesquelles on distingue aussi les cristaux lamellaires, mais de moindres dimensions (fig. 1b).

Le nouveau produit obtenu - le phosphoanhydrite - a été utilisé pour l'activation de la pâte de néphéline (sous-produit de la production de l'alumine), comprenant jusqu'à 85% de β-C_2S. L'activation de la pâte de néphéline est nécessitée par l'absence des propriétés liantes, car les grains de β-C_2S, dont elle est composée, sont entourés des enveloppes finement agrégées hydratées. On a introduit de 5 à 15% de l'activateur lors du broyage de la pâte de néphéline. La composition optimale du liant comprend 90% de la pâte de néphéline et 10% du phosphoanhydrite. En résultat des études on a obtenu le liant mixte dont l'activité après 28 jours du durcissement était comprise entre 32 et 36 MPa.

L'analyse physico-chimique (des phases à rayons X, ATD, IR-spectrométrie, électronique-stéréomicroscopique, pétrographique) a montré l'augmentation de la réactivité de la pâte de néphéline en présence du phosphoanhydrite [3]. Sur les diffractogrammes à 3 et 28 jours du durcissement on note en particulier la diminution des raies analytiques du silicate bicalcique: 1,98; 2,02; 2.28; 2,19; 2,41; 2,54; 2,61; 2,74; 2,78; 2,88; $3,04 \times 10^{-10}$ m pour la pâte de néphéline activée par rapport au β-C_2S pur et à la pâte de néphéline inactivée. Après 28 jours du durcissement on note sur les diffractogrammes l'apparition des reflets se rapportant à la phase d'ettringite: 9,6; 5,6; $3,85 \times 10^{-10}$ m. Pour les produits de l'hydratation du liant (de la pâte de néphéline avec phosphoanhydrite) à l'âge de 3 jours on distingue sur les courbes d'ATD l'effet endothermique à 408K et 423K lié

à la perte de l'eau d'adsorption et la décomposition du gel de tobermorite. On peut supposer aussi dans l'échantillon la présence des petites quantités des hydrosilicates mal cristallisés, hautement basiques, pareils au tobermorite, et des hydrosilicates de calcium-sodium (effets endothermiques faibles à 869K et 1003K).

Sur les courbes d'ATD des produits de l'hydration du liant étalon (la pâte de néphéline avec du gypse) on note les effets endothermiques à 423K, 438K, 931K et 1072K. Pour le liant activé les pertes de poids sont plus élevées (1,5 fois) que pour le liant étalon.

Les résultats de la spectrométrie infrarouge prouvent aussi une grande intensité du processus de l'hydratation du liant activé.

Par comparaison au liant étalon l'analyse pétrographique a révélé l'augmentation importante de nouvelles formations dans les produits de l'hydratation du liant de néphéline activé vers 28 jours du durcissement. Les particules de la pâte de néphéline semblent être cristalloamorphes, car elles sont entourées par de masses compactes de nouvelles formations, composées des hydrosilicates, des écailles de $Ca(OH)_2$, des grains du carbonate et d'ettringite.

Les photographies prises au stéréomicroscope électronique des produits de l'hydrations du liant activé après 28 jours du durcissement (fig. 2a) montrent que la structure du liant activé durci se caractérise par les globules du gel C-S-H, liées aux grains de l'ettringite. La structure correspond à la formation de gros agrégats sphériques (ayant quelquefois la forme des disques), qui forment des liaisons avec des particules avoisinantes (germinations aux points de contact par gel C-S-H, ayant une forme morphologique de feuille). La structure du liant étalon (fig. 2b) est globulaire par sa composition, mais friable, la consolidation est assurée par germination aux points de contact du gel, enveloppant les particules de la pierre de néphéline.

Les données d'expérience citées montrent que l'activateur obtenu-phosphoanhydrite - influence la composante siliceuse de la pâte de néphéline et elles permettent de croire possible l'activation des matériaux au caractère inerte par rapport aux propriétés liantes par de certains produits thermiquement traités.

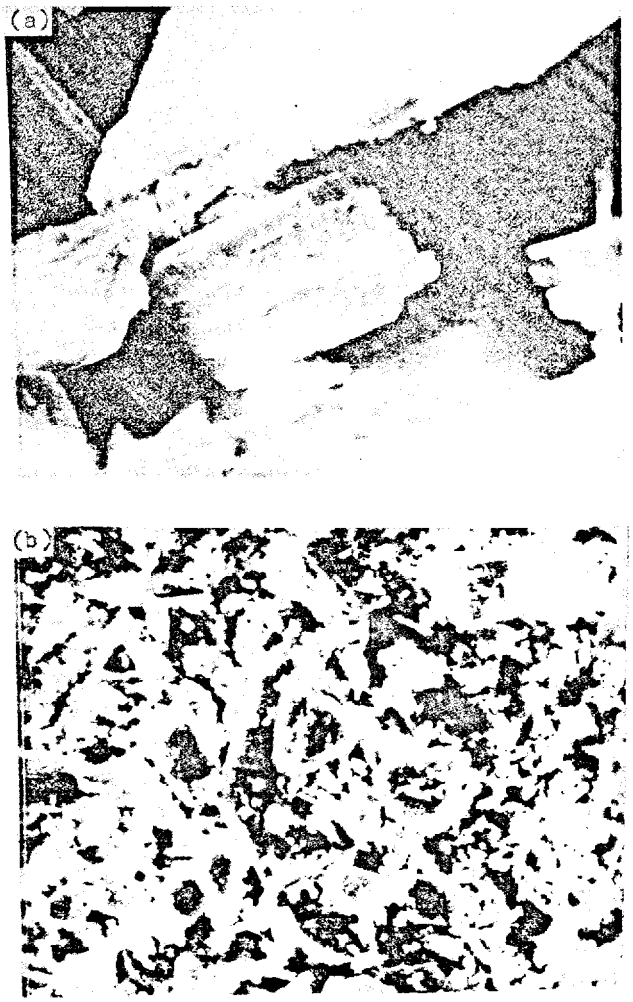

Fig. 1. Structure du phosphogypse (a) et du phosphoanhydrite (b) sous microscope électronique, x1000.

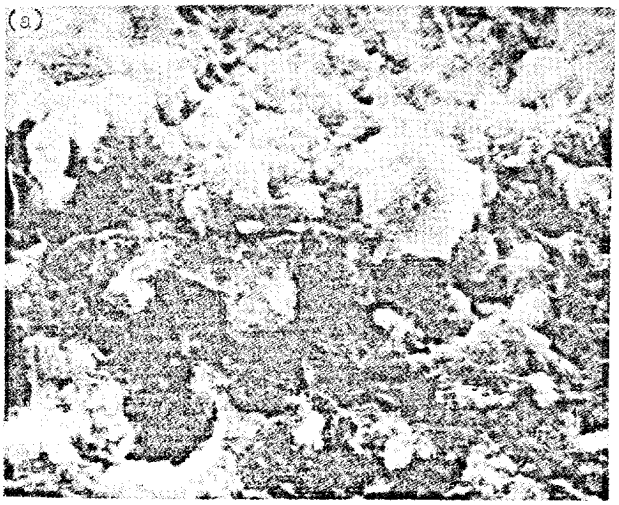



Fig. 2. Microphotographie électronique de la réplique de la surface de la pierre de la pâte de néphéline avec phosphoanhydrite (a) et gypse (b) après 28 jours du durcissement, x3000.

BIBLIOGRAPHIE

I. Танабе К. Твердые кислоты и основания. Изд-во "Мир", Москва, 1973.
2. Сычёв М.М., Гейдарова Л.С., Астахова М.А., Сватовская Л.Б. Активация нефелинового шлама фосфогипсом - Цемент, 1983, № 5.
3. Сычев М.М., Сватовская Л.Б., Астахова М.А., Гайдарова Л.С. Некоторые аспекты активации сульфато-нефелинового вяжущего - Цемент, 1985, № 2.

V.D. GLOUKHOVSKY - Institut des Ingénieurs du bâtiment, Kiev, URSS
P.V. KRIVENKO,
R.F. ROUNOVA

PARTICULARITES DE LA FORMATION DE STRUCTURE DANS LE CIMENT DURCI CONTENANT DES ALCALIS

La manière traditionnelle chimico-minéralogique d'aborder un problème de la synthèse de résistance du ciment durci ne permet pas d'augmenter considérablement l'activité des ciments calciques existants puisque leur base consiste dans la réalisation des propriétés d'hydratation des minéraux de clinker à haute basicité qui est suivie de phénomènes positifs comme négatifs.

L'expérience accumulée pendant plus de 20 ans de recherches et d'exploitation dans le domaine du ciment durci sur la base des systèmes dispersifs ne contenant pas de minéraux à haute basicité et utilisant, à côté de la phase vitreuse, en qualité d'un constituant siliceux, des composés à faible basicité avec C/S $\leq$ 2 montre (1, 2) que le résultat de la formation de structure se distingue qualitativement du résultat traditionnel mentionné. Ces systèmes, par suite de l'augmentation du degré de condensation anionique des tétraèdres d'aluminium et silicium oxygénés, possèdent une résistance élevée à la destruction hydrolytique tandis que l'introduction dans le milieu de gâchage des alcalis ayant une énergie chimique considérable rend ces systèmes très actifs (3).

Les propriétés du ciment durci alcalin se caractérisent par les paramètres suivants: activité lors des essais standartisés - 80...140 MPa; résistance à la flexion - 6...14 MPa; résistance au gel - 700...1000 cycles; imperméabilité à l'eau - B10...B50; résistance à la corrosion dans les milieux de sulfate K_c = 0,9 - 1,2 (4). Suivant l'intensité d'accroissement de résistance (I jour - 25...35 MPa; 3 jours - 65...75 MPa) les ciments se rapportent aux ciments à durcissement super rapide et suivant le dégagement de chaleur - aux ciments à faibles températures.

La présence du cation alcalin conditionne les particularités des processus de la formation de structure des ciments en question (5). A la période d'hydratation initiale, le cation alcalin joue un rôle d'un catalysateur en diminuant la concentration du CaO dans le liquide mère, maintenant les forces ioniques du milieu de gâchage nécessaires à la destruction des liaisons covalentes résistantes et en prenant part à l'évacuation des produits de destruction hors de la réaction grâce aux processus d'échanges des cations. Ces produits sont des gels d'hydrosilicates contenant des agglomérations des hydrosilicates de calcium fibreux à basse basicité d'un aspect commun CSH (B) et des inclusions des hydrogrénats à composition variable ainsi que l'acide silicique précipité.

A mesure du développement des processus de condensation et de condensation-cristallisation, le constituant alcalin devient un des éléments-formateurs de structure du ciment durcissant. Les formations nouvelles alcalines sont analogues aux hydroalumosilicates alcalins de type des zéolites et des hydromicas ainsi qu'aux compositions mixtes alcalines-alcalino-terreuses - analogues aux naturelles ce qui prédétermine leur durabilité et certaines autres propriétés (2). Selon les indices structuraux, ces phases, comme en cas du gel d'hydrosilicate, se trouvent également longtemps en état amorphe se condensant autour de la carcasse hydrosiliceuse dans les pores du ciment durci en augmentant avec cela la densité et l'imperméabilité à l'eau de ce dernier. La porosité du ciment durci contenant des alcalis est caractérisée par une teneur élevée en pores du gel dont le rayon et de 1,0 - 4,0 mm et par une teneur diminuée en pores capillaires.

Selon nos recherches (6), les états amorphes et cristallins métastables de la structure de la matière minérale jouent un rôle particulier dans les processus de la formation de structure du ciment durci. Ce rôle est conditionné par le fait que la matière se trouvant dans l'état mentionné est caractérisée, en comparaison avec la matière cristalline stable, par un pouvoir énergétique maximum et une densité minimum. C'est justement ça qui assure le processus de con-

Tableau

Degré de rétablissement des liaisons structurales de la pierre de ciment obtenue par les formations nouvelles du ciment alcalin

Composition de la phase type gel	Cycles de pressage*	$\frac{R_{compr.}, MPa}{\rho, g/cm^3}$ / Pression, MPa					
		50	100	300	400	500	1000
$0,8CaO \cdot SiO_2 \cdot 2H_2O$	I	21,9 / 1,06	30,4 / 1,09	143,0 / 1,34	192,5 / 1,53	275,6 / 1,65	136,4 / 2,04
	II	23,8 / 1,08	50,0 / 1,09	77,0 / 1,38	68,0 / 1,59	72,2 / 1,63	68,0 / 2,06
	III	24,0 / 1,09	23,4 / 1,11	67,8 / 1,49	71,0 / 1,76	70,0 / 1,90	46,7 / 2,12
$Na_2O \cdot Al_2O_3 \cdot 2SiO_2 \cdot 2H_2O$	I	9,4 / 1,11	22,2 / 1,27	52,1 / 1,58	58,8 / 1,59	67,9 / 1,71	69,1 / 1,80
	II	9,0 / 0,89	20,6 / 1,02	55,8 / 1,34	104,0 / 1,47	123,0 / 1,58	171,0 / 1,77
	III	7,53 / 0,89	17,7 / 1,02	33,3 / 1,34	50,7 / 1,47	58,1 / 1,58	28,1 / 1,77
		33,5	15,8	13,2	12,0	10,8	10,2
		Pertes de l'eau zéolithique, %					

* En cas des mêmes pressions, les échantillons du deuxième pressage ont été préparés à partir de la matière des échantillons du premier pressage et les échantillons du troisième pressage - à partir de la matière des échantillons du deuxième pressage.

densation (formation de structure) et qui se manifeste dans les interactions superficielles, dans l'apparition des contacts de phase entre les particules ainsi que dans la diminution de volume du système pour le compte de l'augmentation de densité de la matière.

Outre la participation dans les processus de formation de structure du ciment durci d'un caractère d'hydratation-condensation, les phases amorphes et métastables se trouvant dans l'état dispersif tendent à la formation de structure du type contact-condensation dont l'essence est montrée dans nos publications aux Congrès précédents (7, 8). La présence de ces phases dans le système dispersif obtenu par l'hydratation en excès du liquide de gâchage détermine les propriétés distinctives des liaisons structurales du ciment durci qu'elles forment.

Selon les notions connues (9), lors du durcissement de la pâte de ciment, la structure de coagulation thixotrope avec des contacts de film hydrolabiles passe en structure type condensation-cristallisation avec des contacts de phase irréversibles résistants à l'eau. Nos expériments montrent que ces derniers portent longtemps un caractère partiellement réversible (voir tableau). Ils

peuvent être détruits, broyés et rétablis ensuite par pressage, c'est-à-dire à la suite du rapprochement réitératif des macroparticules immédiatement après le pressage avec l'obtention d'une pierre résistante à l'eau. Et c'est seulement après le passage de toutes les formations nouvelles hydrosiliceuses dans un état cristallin stable que les contacts de phase prennent un caractère irréversible, et il est impossible d'obtenir la pierre résistante à l'eau par pressage.

Après la destruction, broyage et ensuite le pressage de la pierre, sa résistance se rétablit d'une façon incomplète. Si les cycles de durcissement-destruction-broyage-pressage continuent, alors après chaque cycle, la densité de la pierre augmente tandis que l'énergie superficielle des particules et la résistance de la pierre diminuent. C'est pourquoi, après chaque cycle avec rétablissement des contacts, la résistance de ces derniers diminue (pratiquement à la pression > 300 MPa). En cas de l'aluminosilicate sodique, la perte de l'eau zéolitique se superpose sur cette dépendance commune ce qui exerce une influence sur un caractère du changement de densité et sur une consolidation intermédiaire de la pierre.

En général, le processus de la formation de structure du ciment durci sur la base des hydrates dispersifs métastables se produit avec le dégagement d'énergie et est suivi de phénomènes qui peuvent être caractérisés, en termes les plus généraux, comme l'autoorganisation (mise en ordre) de la matière.

Les données ci-dessus concernant les particularités de la formation de structure ouvrent des possibilités pour contrôler les propriétés des ciments alcalins et de la pierre à durcissement de contact (reçue par pressage des hydrates broyés). En premier cas, cela s'obtient par la normalisation de la composition des éléments alcalins, c'est-à-dire des phases aluminosiliceuses, par la teneur en constituant alcalin et son type et par la teneur en additions de modification. Le ciment de laitier alcalin M 400...M 1400 est un exemple de ces ciments. Outre les résultats techniques, l'utilisation de ce ciment favorise la solution des problèmes liés aux gains d'énergie dans la technologie de la production du ciment.

En deuxième cas, cela s'obtient par la répartition dans le temps des processus chimiques et physiques. De ce fait, lors du durcissement, il n'y a pas de changement de composition chimique ou d'état agrégé de la matière. Sans la consommation d'énergie supplémentaire, il devient possible d'utiliser dans la composition des ciments alcalins une série de produits secondaires desquels on obtient dans le système donné les hydrates métastables et ensuite stables (boues de bélite et d'amiante ciment, cendres très calciques d'hydroévacuation, etc.).

References

1.В.Д.Глуховский. Грунтосиликаты. К., 1959.

2.Щелочные и щелочноземельные гидравлические вяжущие и бетоны. Под общ.ред.проф. В.Д.Глуховского. К., 1979.

3.Шлакощелочные бетоны на мелкозернистых заполнителях. Под общ.ред.проф. В.Д.Глуховского. К., 1981.

4. V.D. Glukhovsky, G.S. Rostovskaja, G.V. Rumyna. 7th Int. Congr. on the Chem. of Cem., v. III. Paris, 1980.

5. П.В.Кривенко. "Цемент", № 3, 1985.

6. П.И.Боженов, В.Д.Глуховский, Р.Ф.Рунова Сб. "Строительные материалы. Строительное производство". Л., 1973.

7. В.Д.Глуховский, Р.Ф.Рунова. УI Международный конгресс по химии цемента, т. II, ч. I., 1976.

8. V.D. Glukhovsky, P.V. Krivenko, R.F. Runova. 7th Int. Congr. on the Chem. of Cem., v. II. Paris, 1980.

9. Ребиндер П.А. Физико-химическая механика дисперсных структур. М., 1966.

A.V. VOLJENSKIY -Institut des Ingénieurs du bâtiment de Moscou, URSS

INFLUENCE DE LA CONCENTRATION DES LIANTS EN MELANGE AVEC L'EAU SUR LA RESISTANCE ET DEFORMABILITE DE CE MELANGE LORS DU DURCISSEMENT

Toutes les propriétés techniques des mélanges des liants durcis avec l'eau, y compris la durabilité, sont déterminées par les facteurs principaux suivants:

1. Les propriétés physiques et physico-chimiques des liants et des hydrates se formant lors de l'interaction des liants avec l'eau aux conditions de durcissement adoptées.

2. La concentration du liant par masse en unité de volume du mélange initiale et la valeur limite optimale de cette concentration pour chaque liant et chaque condition de durcissement. Le dépassement de cette valeur favorise la chute de résistance et même l'autodestruction du système dans les conditions d'expansion libre.

3. La microstructure de la phase solide et des pores dans le monolithe durci déterminée par la dispersité et la configuration des particules d'hydrates nouvellement formées.

4. Les propriétés d'adhésion-cohésion et autres propriétés physico-chimiques des particules nouvellement formées.

Avec cela, plus est grand le volume absolu de la phase solide en unité de volume du monolithe durci (jusqu'à la valeur limite) et plus sont intensives les manifestations des propriétés d'adhésion-cohésion des particules constitutives, plus sont dispersives ces particules et par conséquent, plus sont fins les pores - plus est haut le niveau des propriétés de construction du monolithe (à l'exception du paramètre de protection thermique).

La concentration optimale du liant en mélange avec l'eau "C_o" et le rapport nécessaire "eau-liant" sont déterminés par les formules 1 et 2.

$$C_o = \frac{\rho_I}{(I + W_o)(I + V)} \qquad (1)$$

où, ρ_{I_3} est la densité réelle de l'hydrate en g/cm^3, W_o est la quantité d'eau invaporable lors du durcissement du liant en g/g de masse du liant initial, V est le volume limite minimal des pores se formant entre les particules de l'hydrate exprimé en cm^3/cm^3 du volume absolu de la masse de l'hydrate.

Le rapport "eau-liant" est déterminé par la formule:

$$(E/L) = \frac{\rho_o - C_o}{\rho_o \cdot C_o} \qquad (2)$$

où ρ_o est la densité réelle du liant initial.

Suivant les études /1, 2/, les mélanges du liant avec l'eau pris au rapport optimal ou au rapport diminué de la quantité du liant sont caractérisés par l'accroissement de résistance normal sans anomalies. Les mélanges contenant le liant en quantité élevée par rapport à la quantité optimale montrent, après l'accroissement de résistance initial normal, la diminution de cette résistance et l'augmentation du volume.

Ce fait est expliqué par la pression des germes nouvellement formés à l'intérieur de la structure formée à l'absence de l'espace nécessaire à l'emplacement des particules nouvelles des hydrates avec les intervalles entre elles. Ce fait peut être observé en cas d'accès supplémentaire dans le système de l'eau sous forme du liquide ou de la vapeur et en cas de l'interaction de cette eau avec les particules du liant non hydratées.

Le rapport "eau-liant", en cas de concentration optimale du liant, est toujours plus grand que le rapport exigé par la stoechiométrie de la réaction de son hydratation (approximativement plus grand de 1,3-1,5 fois).

Le volume limite minimal des intervalles entre les particules des hydrates des différents liants (V) est individuel et dépend également des conditions de leur hydratation.

Suivant nos données, "V" et le rapport optimal "eau/liant" lors de l'hydratation aux conditions normales sont les suivants:

1) le ciment portland: 0,37 cm^3/cm^3 du volume absolu des hydrates; le rapport "eau/ciment" est égal à 0,39;

2) le plâtre semi-hydraté ß: 0,2 cm^3/cm^3

du volume absolu des hydrates; le rapport "eau/plâtre" est égal à 0,24;

3) l'aluminate tricalcique, en cas de formation à partir de celui-ci du C_3AH_6: 0,8 cm^3/cm^3; le rapport "eau/C_3A" est égal à 0,67;

4) l'ettriguite, en cas de sa formation à partir du mélange de l'hydroxyde de calcium, du sulfate d'aluminium et de l'eau: 1,0 cm^3/cm^3; le rapport "eau/liant" est égal à 0,9.

Il en résulte que tout liant à sa concentration optimale dans le mélange avec l'eau et au rapport correspondant "eau-liant" formant un système durcissant ayant des déformations de retrait normales, à la mesure de l'augmentation de concentration et de la diminution du rapport "eau/liant", passera d'abord en classe des "irrétrécissables", ensuite en classe des "expansifs" et même en classe des "autodestructifs", en cas de l'expansion libre lors du durcissement, ou en classe des "contraints" à l'hydratation dans le volume "fermé". L'intensité et la vitesse de développement des déformations correspondantes avec le temps doivent dépendre des propriétés individuelles des liants et des conditions du durcissement.

Avec cela, plus sont grandes les valeurs de l'eau inveporable "W_0" fixée par le liant en cas de l'hydratation complète et des volumes minima entre les particules "V", moins est la résistance du liant dans le système à la concentration optimale "C_0".

Le degré de remplissage du volume libre dans le mélange du liant avec l'eau par les hydrates qui dépend du degré d'hydratation du liant et de la quantité d'eau adsorbée par les hydrates exerce une influence directe sur la résistance et autres propriétés du système. A cette raison, il est utile de déterminer le volume absolu de la phase solide $V_{ph.s}$ pour un ou un autre délai de durcissement du système (sans tenir compte de l'air entrainé et de l'expansion du système) en utilisant la formule 3 /3/.

$$V_{ph.s} = \frac{C_i(I-\alpha)}{\rho_0} + \frac{C_i\alpha(I+W_0)}{\rho_I} \qquad (3)$$

où C_i est la contenance du liant dans le mélange initial exprimée en g/cm^3; α est le degré d'hydratation; ρ_0, ρ_I sont les densités réelles du liant et de l'hydrate en g/cm^3.

A l'aide de la soustraction de la valeur N du volume total du système durci on obtient le volume des pores. La concentration volumique /3/ des hydrates nouvellement formés "N" est déterminée avec une approximation admissible par la formule de A.V. Voljenskiy et U.D. Tshistov:

$$N = \frac{C_i[\rho_0(I+W) - \rho_k(I-\alpha)]}{\rho_k[\rho_0 - C_i(I-\alpha)]} \qquad (4)$$

Dans ce cas, W est la quantité d'eau inevaporable en g par g du liant initial; ρ_k est la densité réelle du liant durci pour un ou un autre délai. Pour les autres symboles, voir les formules I, 2 et 3.

Parmi les formules modernes sur la résistance des mélanges durcissants nous ne trouvons pas les formules qui tiendraient compte du passage des indices physico-mécaniques et des autres propriétés par le maximum avec une altération suivante de ces indices et autres propriétés malgré une augmentation monotone de la concentration du liant dans le système,

Les formules de résistances ne traduisent pas également le fait que la diminution du rapport "eau-liant" favorise une augmentation de dispersité des particules nouvellement formées et, par conséquent, un accroissement de résistance /4/.

Les formules existantes peuvent être utilisées avec un degré de confiance différent pour des systèmes ayant un rapport "eau-liant" optimal et plus grand.

Les résultats des études /2/ illustrent les faits mentionnés.

A partir du ciment Portland (ρ_0 = 3,1; W_0 = 25,4%; ρ_I = 2,47 à l'hydratation

complète), on a préparé les échantillons (2x2 et 2x2x2 cm) avec le rapport "eau/ciment" de 0,05; 0,1; 0,15; 0,2 et 0,25. Pendans trois jours on a conservé ces échantillons au-dessus de l'eau et ensuite dans l'eau jusqu'à 6 ans. Aux âges déterminés (3, 7,28 jours; 6 ans) on a analysé la résistance des échantillons, leurs volumes, porosité, degré d'hydratation d'après la teneur en eau invaporable et la concentration volumique des formations nouvelles (N). Les résultats ont montré que la résistance des échantillons de toutes les compositions augmentait jusqu'à l'âge de 1-3 ans et ensuite diminuait autant plus que plus est la diminution du rapport "eau-ciment". Par exemple, la résistance des échantillons préparés avec le rapport "eau/ciment" =0,10 a atteint pendant trois ans 106 MPa, tandis qu'elle a diminué vers 5 ans jusqu'à 90 MPa.

La résistance des échantillons préparés à partir d'un autre ciment (rapport "eau/ciment" = 0,2), ayant atteint vers trois ans 92 MPa, a diminué vers 6 ans jusqu'à 60 MPa.

Le degré d'hydratation des échantillons avec les rapports "eau/ciment" 0,05-0,15 a atteint vers l'âge de 5-6 ans la valeur de 0,45-0,5, et celui des échantillons avec les rapports "eau/ciment" de 0,2-0,25 a été égal à 0,75-0,78.

Les échantillons de toutes les compositions ont montré une augmentation de volume (3-5%) qui a atteint son maximum vers 28-30 jours de durcissement pour les échantillons, préparés avec le rapport "eau-ciment"=0,05; 0,1; 0,15 et 0,3-1% pour les échantillons préparés avec le rapport "eau/ciment"=0,2 et 0,25. Plus tard, les échantillons avec le rapport "eau/ciment"=0,2 et 0,25 ont montré une diminution de volume jusqu'aux valeurs initiales et les échantillons avec le rapport "eau/ciment"=0,05; 10,1 et 0,15 approximativement jusqu'à 2-2,5%. Suivant l'auteur, ce fait est dû à la relaxation de la contrainte dans le système durci ou à la diminution de teneur en eau dans les formation d'hydrates nouvelles ou, enfin, à l'effet conjugué de ces deux facteurs. Le passage des échantillons du gonflement au retrait lors du durcissement de longue durée exige une étude ultérieure car ce phénomène peut être lié avec le comportement des bétons dans les structures contraintes mécaniquement ou à l'aide des éléments de contrainte et exercer une influence indésirable et même dangereuse sur la capacité portante de la structure.

Les essais analogues /5/ ont été effectués sur les échantillons préparés à partir du ciment sulfo-alumineux de laitier (CSAL) contenant 30% de plâtre semi-hydraté, 30, 20, 10% de ciment alumineux, 35, 45, 53% de laitier de haut-fourneau et 5-7% de ciment Portland. Les bétons, en cas de la consommation du CSAL 350-400 kg/m^3 (dureté des mélanges est de 20-30 s), après quatre heures de durcissement à la température de 20°C, ont la résistance de 4-6 MPa, après un jour de durcissement - 12-16 MPa et après 28 jours - 40-50 MPa. Les bétons sur la base du CSAL durcissent à des températures 40-55°C sans diminuer la résistance et atteignent même après quatre heures de durcissement une résistance de 15 MPa et plus. D'après la vitesse d'accroissement de résistance initial ce ciment dépasse le ciment alumineux et il est de 3-4 fois moins cher que ce dernier. La résistance des échantillons préparés à partir du mélange de CSAL avec l'eau (rapport "eau/ciment"-0,1; 0,25 et 0,4) conservés au-dessus de l'eau augmentait continuellement jusqu'à l'âge de 4,5 ans. Ces ciments contenaient 30 et 20% de ciment alumineux (n°n° 1 et 2). Après quatre heures de durcissement, les échantillons avaient la résistance de 15-30 MPa et après un jour de durcissement - 17-37 MPa. Après un an de durcissement, la résistance des échantillons avec le rapport "eau/ciment" égal à 0,1 a atteint son maximum de 90-95 MPa, tandis qu'après 5,5 ans de durcissement elle a diminué jusqu'à 22 MPa (n°I) et jusqu'à 18,5 MPa (n° 2). Le volumé des échantillons des deux compositions a augmenté de 1% pen-

dant 3-6 mois et plus tard, il a diminué jusqu'à la valeur initiale.

Donc, lors du durcissement des échantillons préparés à partir du CSAL, on a observé le même phénomène qu'en cas des échantillons préparés à partir du ciment Portland. Selon ces essais, il est recommandé d'utiliser le CSAL aux rapports "eau/ciment" qui ne sont pas inférieurs à 0,35-0,4. Les extrémums analogues sur les courbes de résistance des échantillons préparés aux rapports "liant-eau" diminués (en comparaison avec les rapports optima) s'observaient en cas de l'aluminate tricalcique, de l'ettringuite et des liants "gypse-ciment-pouzzolane" (IGCP). Le ciment Portland à la chaux contenant une quantité considérable d'oxyde de calcium et d'autres substances est caractérisé par l'absence d'expansion lors de son interaction avec l'eau. Les bétons basés sur ce liant atteignent une résistance de 4-6 MPa après 4-7 heures de durcissement à la température de 20°C et 15-20 MPa et plus à la température de 80-95°C.

Selon les données préliminaires, le rapport eau/liant optimal se trouve dans des limites de 0,35-0,4.

BIBLIOGRAPHIE

I.3. Волженский А.В., Ж. "Строительные материалы", 1979, № 7, 1981, № 8.
2. Волженский А.В., Карпова Т.А., Ж. "Строительные материалы", 1980, № 7.
4. Волженский А.В., Рожкова К.Н., Ж. "Строительные материалы", 1972, № 5.
5. Карпова Т.А., Волженский А.В., Ж. "Строительные материалы", 1982, № 7.

W. Weisweiler - Institut Fur Chemische Technik - West Germany

QUANTIFICATION OF THALLIUM - and LEAD-CYCLES IN CEMENT PLANTS

CL

1. Introduction

Early studies concerning the causes of thallium emissions in the cement production are found in the literature(/1-4/, beginning in 1980). Through controlled discharge of "blood leeting" of the so-called external cycle of a cement kiln plant with fly-ash feedback, a strategy for effectively controlling the thallium cycle extension and emissions was developed by KAMM, OBLÄNDER and WEISWEILER /5/, as shown by industrial results. From all the above cited papers it can be concluded, that material cycles are formed. As an example a plant with cyclone perheater is to be considered operating in a combined mode. In this case a cycle can be delineated following the materials' pathway: Heat exchanger → raw mill → electric filter → silo → heat exchanger. A sharp enrichment level is observed when using pyrite cinder as iron oxide source containing a high thallium concentration.

The purpose of the present work was to determine in a quantitative manner the cycles and enrichment behaviour of thallium and lead in a cement rotary kiln plant; for details see WEISWEILER et el. /6/. The studies were carried out in two parallel running cement production plants (cyclone preheater and LEPOL), typical for Central Europe. Feeding with high-thallium containing pyrite cinder, as iron oxide source, was done as a matter of convenience for sharpening the enrichment level and only during those studies were carried out.

2. Measurement Strategy, Sampling, Mass Streams

The knowledge of the material balances is suggested to be of key importance for understanding the extent and causes of cycles in industrial processes. In this context only the Tl-and Pb-cycles were of interest. The mass streams were calculated on the basis of metallic Tl and Pb. Thallium is found mainly as a mixed crystal halide Tl(Cl,Br) /7/, or as iodide with chloride portions /8/. Lead is also found as chloride but in a basic sulfate or silicate matrix in the clinker.

Preparation of the samples and their parallel determination by means of atomic absorption spectroscopy were discussed by WACHTER and WEISWEILER /9/. The solid specimens were taken from the mass streams described as follows:

A. Rotary kiln with cyclone preheater (measuring period 5 resp. 40 days).

   1) Heavy metal path across the solid material stream

      a) direct operating mode: raw meal (raw material + additives) → kiln meal (raw meal + filter dust) → clinker.

      b) Combined operating mode: raw meal = kiln meal (raw material + additives + filter dust) → clinker.

   2) Heavy metal path across the gas stream: fuel or substitute fuel → dust in raw gas → electric filter dust → dust in clean gas.

B. Rotary kiln with grate-type preheater (measuring period 48 days).

   1) Heavy metal path across the solid material stream: raw meal = kiln meal (raw material + additives) → pellets from drying chamber → pellets from calcining chamber → clinker.

   2) Heavy metal path across the gas stream: fuel or substitute fuel → grate riddlings and dust from the intermediate dust collection → dust in raw gas → electric filter dust → dust in clean gas.

The results from the Tl- and Pb- analyses in the described mass streams were used in preparing the figures of the balances in form of SANKEY-diagrams. For typcial minimal and maximal Tl- and Pb-content values see /6/.

3. Thallium and Lead Balances for the Rotary Kiln with Cyclone Preheater

The symbols used for all heavy metal streams are given as follows. The units in SANKEY-diagram are kg/h.

Symbol	Heavy metal mass stream
B	feeded fuel oil
E	dust emission
Eb	feeded substitute fuel
Fs	filter dust
K	produced clinker
Om	kiln meal before preheating (Fs+S)
Rg	dust in exit gas (raw gas)
S	raw meal from silo; in combined mode: S=Om
Wt/Ok	cycle in heat exchanger/kiln cycle

The results of the corresponding dust measurement in exit gas before and after the electric filter (raw gas resp. clean gas) are given as follows for the direct and combined operating modes. In the combined mode the heat content of the kiln gases, before the dust collection, is used for drying the raw meal mixture in the grinding mill. Dust concentrations were measured with an exhausting device working parallel to the gas stream. Following dust concentrations were measured: in the raw gas 30-50 g/m^3 in direct mode and 14-28 g/m^3 in combined mode operation resp. (15 min, 3.5 m^3/h, 8-32 g dust). In contrast the dust concentrations in the clean gas were found to be 20-40 mg/m^3 in direct mode and 10-20 mg/m^3 in combined mode operation (6-13 h, 10-15 m^3/h, 1.2-4.4 g dust). The thallium concentrations in 15 mean daily samples in the dust of the raw gas were 900-2900 ppm and 100-600 ppm operating in the direct and combined mode respectively, whereas in the dust of the clean gas values of 1500-3600 ppm (direct mode) and 600-1200 ppm (combined mode) were found. The analogous lead concentrations were found to be in the raw gas: 30-70 ppm (direct mode) and 10-70 ppm (combined mode); in the clean gas: 15-75 ppm (direct mode) and 10-75 ppm (combined mode).

KAMM /10/ recently reported overall enrichment factors for Tl of 10 000 and for Pb of 20 assuming a maximum of 0.5 ppm Tl and 25 ppm Tb in raw meal and 5000 ppm Tl and 500 ppm Pb in clean gas. These values were obtained from specimens taken at the plants in the technically encountered conditions. From the results obtained in the present study, mean overall enrichment factors of at best 2500-3500 for Tl and 2-4 for Pb are found for a plant operating with continuously changing modes (direct and combined).

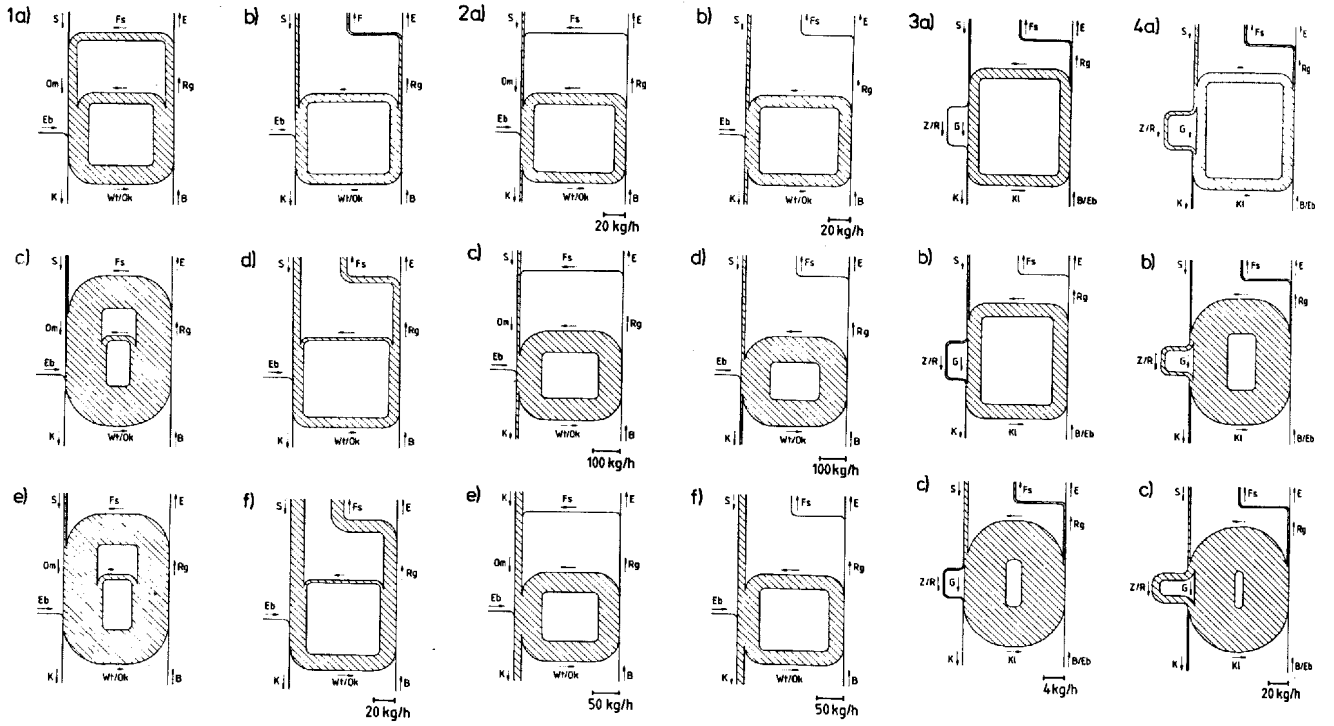

Fig.1: Rotary kiln with cyclone preheater: Thallium mass streams

Fig.no.	1a	1b	1c	1d	1e	1f
operating mode	direct	combined	direct	combined	direct	combined
additive	ore	ore	pyrite cinder	pyrite cinder	pyrite cinder	pyrite cinder
substitute fuel	-	-	-	-	acid sludge	acid sludge

Fig.2: Rotary kiln with cyclone preheater: Lead mass streams

Fig.no.	2a	2b	2c	2d	2e	2f
operating mode	direct	combined	direct	combined	direct	combined
additive	ore	ore	pyrite cinder	pyrite cinder	pyrite cinder	pyrite cinder
substitute fuel	-	-	-	-	acid sludge	acid sludge

Fig.3 and 4: Rotary kiln with grate type preheater: thallium mass streams (Fig.3) and lead mass streams (Fig.4)

Fig.no.	3a	3b	3c	4a	4b	4c
additive	pyrite cinder	pyrite cinder	pyrite cinder	pyrite cinder	pyrite cinder	pyrite cinder
substitute fuel	-	acid sludge	acid sludge	-	acid sludge	acid sludge
period	-	-	6 weeks	-	-	6 weeks

3.1 Thallium Balances

Balances were made for the direct and combined operating mode. Mass streams were determined when feeding with iron ores and with Tl containing pyrite cinder with/without acid sludge. SANKEY-diagrams of the mass streams were prepared for all six variations (Figs. 1a-f); they are based on a mean daily operating period of 12 h in direct/combined mode. Longer operating periods were not considered.

Fig.1a shows the total thallium mass stream within the plant operating in a direct mode, firing with petroleum coke and feeding iron ores (Tl< 5 ppm). A small Tl stream coming from the silo with the raw meal, S, enters the thermal-chemical part of the process. Dust from the electric filter, Fs, is added before entering the cyclone preheater (mass stream Om). An internal Tl-cycle is formed within the heat exchanger due to the volatilization of Tl-compounds and condensation on the dust particles of the countercurrently flowing gas (Tl-stream Wt/Ok). A residual Tl-stream enters the rotary kiln via the partially calcinated materials leaving the cyclone. In the rotary kiln the Tl-compounds finally enter the gas phase and are transported out by the dust charged combustion gases which enter the cyclone; here they condense on the countercurrently entering solids. As can be seen, the Tl-cycle is not limited to the preheating unit but includes the rotary kiln.

The thallium compounds coming with the raw gas from the heat exchanger, Rg, are collected together with the dust, Fs, in the electric filter which in case of a direct operation are added to the raw meal before entering the heat exchanger. In a combined operation this Tl-stream is formed anew in the silo because the dust charged combustion gases from kiln are used for drying the raw meal in the meal. The so formed Tl-stream, Om or S, completes the external cycle.

The back-feeding of the collected dust in the electric filter, Fs, to the preheater has, as is known, a great effect in the heat exchanger cycle. It is remarkable the low Tl-fixation in the clinker. If the electric filter works without failure, a low Tl-emission is found too.

Fig.1b shows the thallium mass streams in the subsequently nocturnal combined operating mode. The same kind of cycles is observed, nevertheless are the mass streams farther reduced because of the greater storage volume available in the raw meal silo.

Fig.1c shows the increase of the Tl-streams, after a one day period, when feeding with pyrite cinder of an 230-310 ppm Tl-content. During a direct operation the Tl-mass streams are found mainly in the external cycle because of the drastic higher Tl-contents in filter dust, Fs. The enrichment level is diminished in the subsequently combined operating mode maintaining the firing of petroleum coke and the feeding of pyrite cinder. The corresponding streams are shown in Fig.1b.

When using acid sludge as substitute feed the same mass streams are practically measured in a direct operation (Fig.1e), whereas in a combined mode a slight increase of the mass stream is observed in the heat exchanger/rotary kiln system (Fig.1f).

3.2 Lead Balances

The lead balances were carried out on the same specimens and under the same conditions as for thallium. During the direct operation a clear increase of the enrichment level is observed in the transition zone between preheater and rotary kiln (Fig.2a). Because of the lower Pb-content in the filter dust the external cycle is less pronounced. The lead content in clinker is almost the same as that of the raw meal, coming from the silo and entering the preheater. When operating in a combined mode (Fig.2b) similar Pb-contents are found in the cycles as well as in the clinker and emissions. With a higher Pb-supply by feeding with pyrite cinders a very sensitive cycle formation is observed (Fig.2c - note scale). The lead content in clinker is increased to 100 ppm. As expected, a change in the levels is not observed in the subsequently combined operation (Fig.2d). Firing with high sulfur cycle although Pb-containing pyrite cinder feeding is maintained. Lead is discharged mainly through the clinker. Low lead emission from the less pronounced external cycle remains unchanged (Fig.2e). During a combined operation relevant changes are neither expected nor they are observed (Fig.2f).

4. Thallium and Lead Balances for a Rotary Kiln with Grate Type Preheater

In the description of the mass streams of a LEPOL-plant, the streams Om, Wt/Ok are not needed, but the following are introduced additionally:

Symbols	Heavy metal stream
G	granulated raw meal
Kl	grate type preheater cycle
Oe	kiln inlet end (partially calcinated solids)
Z/R	intermediate dust collection (Z) and grate riddlings (R)

For a sampling period of 30 days following dust concentrations were found: in raw gas (30 min, 5 m^3/h, 5-15 g) ca. 2-5 g/m^3 and in clean gas (7.5 h, 10 m^3/h, 3-11 g) 50-130 mg/m^3. The heavy metal content was in raw gas dust: 100-800 ppm thallium, resp. 1200-5000 ppm Pb, and in clean gas dust: 160-1050 ppm Tl, resp. 7500-15400 ppm Pb.

As in the case of the heat exchanger plant the analogous enrichment factors were determined and found to be roughly 850 for Tl and 450 for Pb. These values are based on a mean dust content of 430 ppm Tl and 11100 ppm Pb in clean gas, when feeding with heavy metal containing pyrite cinders.

4.1 Thallium Balances

The Tl-streams were determined for the following conditions: feed with pyrite cinder of 230-310 ppm Tl and with/without firing acid sludge as well as after six weeks firing with acid sludge. The corresponding SANKEY-diagrams are given by the figures 3a-c. As is clearly seen, a thallium cycle is formed at preheater and over the rotary kiln (Fig.3a). The external cycle through the collected filter dust, Fs, does not appear when this is not feeded to the kiln. Nevertheless, an external cycle is formed when the dust from the intermediate collection as well as the grade riddlings Z/R are feeded to the kiln. Firing with sulfur containing acid sludge, Eb, increases the thallium cycles about by a half, as is shown in Fig.3b. The Tl-emission and -fixation in clinker remain more or less the same. After a period of six weeks an increase of Tl in the grate type preheater cycle is observed with a feed of pyrite cinder and firing mainly acid sludge (Fig.3c). An increase in thallium content of the raw gas is also observed. Compared with the rotary kiln with cyclone preheater, the contents are already lower: G = 8.4 kg/h (Fig.3c) whereas Om = 34.4 kg/h (Fig.1c).

4.2 Lead Balances

A considerable mass stream supplied by the intermediate collected dust and grate riddlings, Z/R, enters the kiln (Figs. 4a-c, note different scales !). Likewise an increased Pb-stream, Kl, is found between the kiln and grate type preheater. By continuous operation with pyrite cinder (Fig.4a) and additional firing with acid sludge (Fig.5b), the lead content in the cycle between kiln and preheater, Kl, is increased. Nevertheless, the Pb-stream, supplied by intermediate dust and grate riddlings, Z/R, remains the same. The cycle contents after a six weeks operation increased further by about 30 % (Fig.4c).

5. Evaluation of the Balances with Regard to Both Kiln Plants

5.1 Thallium Balances

Rotary kiln with cyclone preheater

Tl-compounds are enriched mainly in the suspension preheater kiln. The high volatility of the halides is responsible for the formation of the internal

cycles. At 1000 K, the vapour pressure of thallium chloride, thallium bromid and thallium iodide are respectively 290, 257 and 300 mbar. At the cyclone the raw meal is heated up to ca. 800 °C by the countercurrently flowing combustion gases leaving the kiln. A condensation maximum is measured in the zone at 450 °C for thallium chloride/thallium iodide /6/. The thallium compounds condense preferentially on the finest dust particles /10/; in their way to the kiln they reach warmer zones, at which they almost completely evaporate and are transported back to the 450 °C zone.

Beside these internal cycles the feed-back of the electric filter dust (about 15 t/h in a 3000 t/day plant) is a cause of the high Tl-rates. As shown by the balances, the emission has a low Tl-content and there is no considerable discharge through clinker, so that almost all of the feeded thallium remains within the process. In view of this, the cement production is also an efficiently process for enriching Tl-compounds.

In contrast to a direct operation, lower Tl-concentrations are found in a combined mode, because most of the thallium is transported to the grinded raw material and to the filter dust in silo. With an increased sulfur feed, e.g. through acid sludge, a reduction of the thallium cycle is not observed.

Rotary kiln with grate type preheater

The LEPOL-plant shows an analogous behaviour in the development of thallium cycles as the heat exchanger plant. Thallium compounds, which evaporate at T >450 °C, condense mainly on the pellet bed of the LEPOL grate, which serves as filter dust. Firing acid sludge was found to have no effect on the internal thallium cycles. Finally, it was found, that the circulating thallium quantity in this plant is lower than the corresponding quantity in a heat exchanger plant related to the produced clinker basis; each plant having a nominal output of 1500 t/d and 3000 t/d respectively.

5.2 Lead Balances

Rotary kiln with cyclone preheater

Lead compounds participate essentially at the internal cycles but only small quantities are transported by the filter dust cycle. The highest Pb-stream is found about a temperature of 800 °C, so that the maximal condensation occurs between the preheater outlet and the kiln inlet. The reason is lying in the volatility of the lead halides; vapour pressures at 1000 K are roughly 45, 71 and 148 mbar for $PbCl_2$, $PbBr_2$ and PbI_2 respectively. Volatility analyses of the filter dust, carried out in the laboratory, showed Pb as $PbCl_2$ together with $AlCl_3$ and KCl portions enclosed in a matrix mainly of calcite /11/. The finer dust particles have a higher Pb-content. The fixation of lead in clinker is greater as for thallium. The correlation between the content in filter and emitted dust is analogous also for lead. The two operating modes (direct and combined) reveal no essential difference of the cycles.

An increase of sulfur by firing acid sludge reduced the lead content in the cycles by about a half; probably the lower volatile basic lead sulfates are formed (at T< 640 °C: $PbO \cdot PbSO_4$, 4 $PbO \cdot PbSO_4$; at T >640 °C: 2 $PbO \cdot PbSO_4$ in addition). This was confirmed by laboratory experiments on the sulfatization of PbO /12/.

Rotary kiln with grate type preheater

Lead compounds are found enriched likewise within the preheater/kiln cycle. The feed-back of the intermediate gas dust and grate riddlings has only a minor effect on the built-up of the internal cycle. Firing acid sludge increases appreciably the circulating lead streams. Examined electric filter dusts are rich in syngenite $K_2Ca(SO_4)_2 \cdot H_2O$ and arcanite K_2SO_4.

References

/1/ H. Keinhorst : Staub Reinhalt. Luft 40 (1980) No. 1, 26/29

/2/ H. Keinhorst : Zement-Kalk-Gips 33 (1980) No.12, 648/52

/3/ K. Welzel, H.D. Winkler : Zement-Kalk-Gips 34 (1981) No. 10, 530/34

/4/ S. Sprung : Zementindustrie. VDZ, Düsseldorf, 43 (1983)

/5/ K. Kamm, W. Obländer, W. Weisweiler : Staub-Reinhalt. Luft 43 (1983) No.5, 193/98

/6/ W. Weisweiler, K. Blome, L. Kaeding : Staub-Reinhalt. Luft 45 (1985) No.10, 461/66

/7/ H.U. Bambauer, H. Schäfer: Mineralogie 62 (1984) No. 1, 33/50

/8/ W. Weisweiler, E. Mallonn: Naturwiss. 70 (1983) 304/5

/9/ Ch. Wachter, W. Weisweiler: Mikrochimica Acta/ Wien (1982 I) 307/15

/10/ K. Kamm : Staub-Reinhalt.Luft 45 (1985) No.1, 15/18

/11/ W. Weisweiler, E. Mallon, B. Schwarz : * (in press)

/12/ W. Weisweiler, E. Mallonn, K. Blome : Zement-Kalk-Gips 38 (1985) No. 7, 387/92

W. Weisweiler, B. Schwarz, E. Mallonn - Institut Fur Chemische Technik - West Germany

ISOLATION OF THALLIUM-AND LEAD-HALIDES ORIGINATING FROM ELECTRIC SEPARATOR DUST OF CEMENT PLANTS BY VAPORIZATION ANALYSIS

Introduction

The build-up of thallium and lead halide cycles during cement production leads to considerable enrichment of these heavy metal compounds /1/. This enrichment is found in the kiln dust of the preheating zone, in the electric separator dust, and in the emitted fine dust particles /2,3/. Additionally, the mass streams of thallium /4,5/ and lead exhibit a further increase by recycling dust from electric separator into the raw meal silo /6/.

Vaporization analysis /7/ of electric separator dust from two types of cement plants, one with suspension preheater, the other with grate-type preheater(LEPOL), shows that the trace element iodine is most important concerning the chemical reactions of thallium. One of the sources of iodine /8/ is found to be the fuel. The rotary kiln with suspension preheater was fired with natural coal by addition of 6-10 mass percent of petrol coke. The other rotary kiln with grate-type preheater was fed with pure petrol coke.

Composition of the electric separator dusts

Two types of electric separator dust were used for investigation. One was taken from a cement plant with a suspension preheater (SP). This plant was fired with natural coal containing 6-10 mass percent of petrol coke.

The second dust specimen was taken from a grate-type preheater (LEPOL) which was fired with pure petrol coke. Table 1 summarizes the results of the chemical analysis. The X-ray diffraction analysis proved that the electric separator dust from the cement plant with suspension preheater (SP) was found to be calcite with a relatively high amount of thallium compounds, but less of lead. The LEPOL-electric separator dust was identified as arcanite (K_2SO_4) and syngenite ($K_2Ca(SO_4)_2 \cdot H_2O$). This dust contained a very high amount of lead and less thallium.

Table 1: Chemical and X-ray diffraction analysis of the two electric separator dusts (SP and LEPOL)

element resp. component	SP	LEPOL
	mass percent	
K_2O	1.0	25.09
Na_2O	0.23	0.77
SO_3	0.79	19.50
Cl	0.20	3.07
SiO_2	1.34	10.19
Al_2O_3	3.28	3.04
Fe_2O_3	1.45	1.73
CaO	44.78	31.71
CO_2	36.40	n.d.
loss of ign.	37.42	n.d.
Tl	$2.7 \cdot 10^{-2}$	$7.8 \cdot 10^{-3}$
Pb	$5.7 \cdot 10^{-3}$	$9.97 \cdot 10^{-2}$
X-ray diffraction	calcite	arcanite syngenite

Vaporization analysis

The vaporization analysis apparatus that was used for the experiments was made of quartz (Fig.1). It was modified so that it was possible to determine traces of thallium and lead to enrich the compounds in a preparative scale. The experimental conditions are listed in table 2.

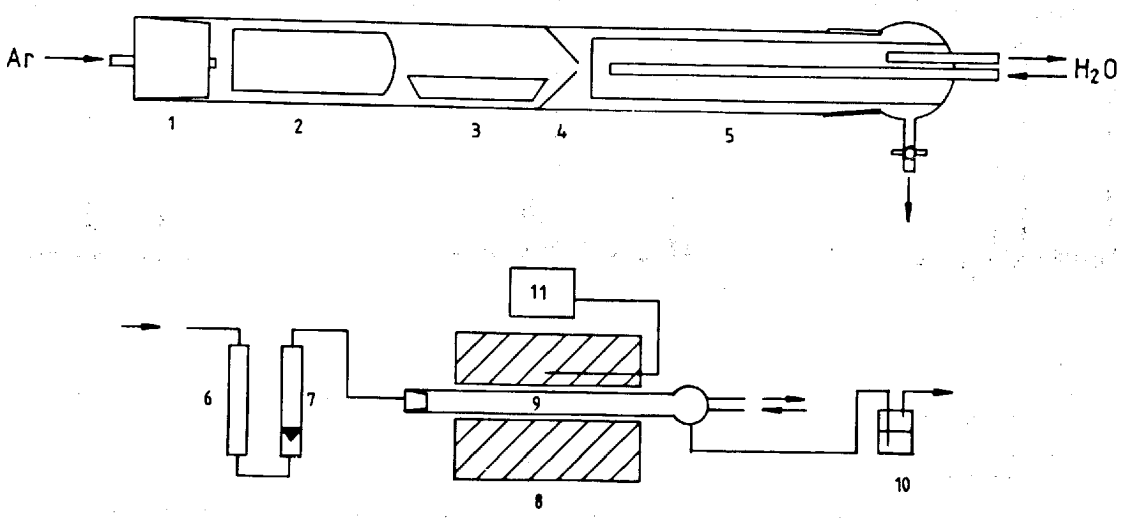

Fig.1: Modified vaporization apparatus

1 Condenser, 2 Nozzle, 3 Nickel boat, 4 Flow resistance, 5 Teflon stopper
6 Drying tube, 7 Flow meter, 8 Furnace, 9 Vaporization tube, 10 Bubble counter

Table 2: Experimental conditions of the used vaporization apparatus

Length of the vaporization tube	580 mm
Diameter of the vaporizattion tube	30 mm
Distance from nozzle to cooler	5 mm
Diameter of the nozzle	3 mm
Length of the nozzle	15 mm
Length of the flow resistance	26 mm
Argon gas stream	120 Nl/h
Maximum mass of the electric filter dust	30 g

The vaporization tube was heated by an electric furnace in order to vaporize the volatile compounds. These compounds were transported by an inert gas stream and condensed on a cooler. For the quantitative analysis of the heavy metals, the condensate was dissolved in HNO_3 (10 %) and analyzed using atomic absorption spectrometry (AAS). For determination of the compounds the X-ray diffraction method was used.

An important parameter of the vaporization analysis was found to be the temperature that was optimized for thallium and for lead compounds. The thallium compounds sublimate at a temperature of 500 °C and the lead compounds at 900 °C. Thus it was possible to separate the thallium compounds from the lead compounds.

Identification of the condensates

At 500 °C the vaporization analysis using an inert argon gas stream showed yellow and red sublimates from both electric separator dusts /9/. The condensates were identified as thallium iodide by X-ray diffraction. TlI appeared as the rhombic modification as well as red cubic, high temperature modification. Increasing vaporization time yielded higher concentration of chloride in the sublimate. When the condensation of the thallium compounds at 500 °C was finished, a temperature of 900 °C was applied in order to volatilize the lead compounds. In both cases the condensates could be identified as lead chloride.

A fractionated vaporization analysis of the LEPOL electric separator dust at 900 °C in an inert argon gas stream showed the following results, obtaining by an energy dispersive electron probe microanalyzer (Fig.2).

If an air stream or a gas stream of N_2 with an addition of 1 % HCl was used instead of an inert argon stream white sublimates were found. Instead of TlI the X-ray diffraction analysis showed peaks of TlCl. Iodine was now volatilized as elemental iodine.

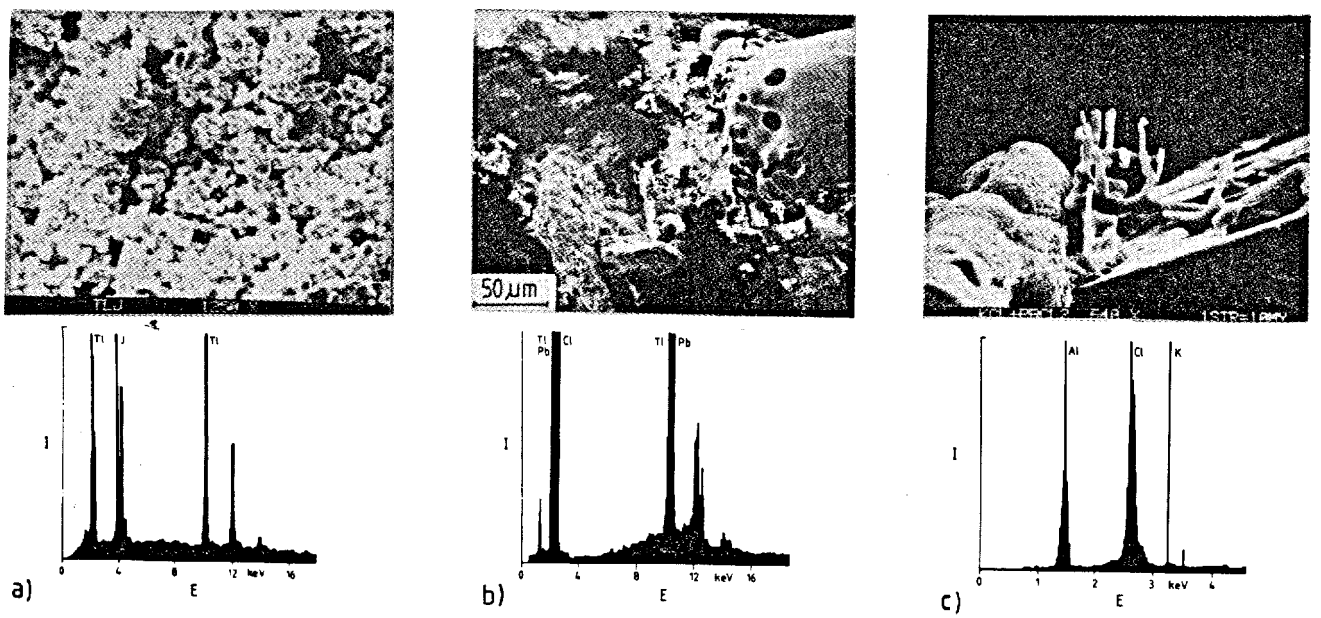

Fig.2: Condensate of LEPOL dust

a) Identified as pure thallium iodide obtained after 20 min vaporization time, the energy dispersive spectrum exhibited peaks of pure TlI

b) The second condensate, derived after a vaporization time of two hours, was identified as $PbCl_2$ with amounts of TlCl

e) After 16 hours vaporization the condensate was analyzed and identified as KCl with parts of $PbCl_2$ and $AlCl_3$

Quantitative determination of the compounds of lead and thallium

The results obtained by the combined methods of vaporization analysis and AAS as well as by wet chemistry operations and AAS /10/ were compared and resulted in good agreement. In addition to the two electric separator dusts, a synthetic dust, i.e. calcite with admixture of thallium chloride (1270 ppm Tl) and lead chloride (1114 ppm Pb) was used.

The electric separator dust (SP) showed the highest volatilization factor W (volatilized elemental mass/ 100% elemental mass) of lead compounds, but only small amounts of total lead concentration. The synthetic dust and the electric separator dust (LEPOL) with high amounts of lead, but in different matrices ($CaCO_3$; arcanite/syngenite), showed similar, but in comparison with electric separator dust (SP) much lower volatilization factors (Fig.3).

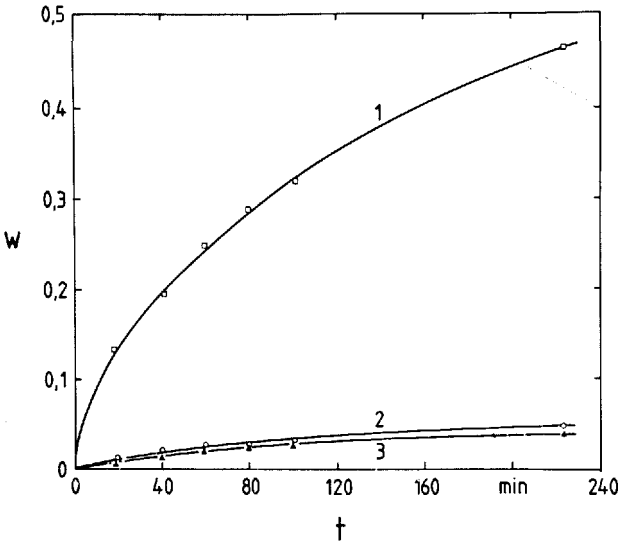

Fig.3: Volatilization factors of lead compounds
1 Electric separator dust (WT)
2 Synthetic dust
3 Electric separator dust (LEPOL)

For the thallium vaporization (Fig.4) the synthetic and the electric filter dust (SP) with their same matrices exhibited nearly the same volatilization factors. Both showed relatively high amounts of thallium. The volatilization factor of the electric filter dust (LEPOL) with its sulphate matrix was found to be smaller.

At a temperature of 500 °C the synthetic and the electric filter dust (LEPOL) showed the same volatilization characteristics, in contrast to the electric filter dust (SP) which had got a smaller volatilization factor (Fig.4).

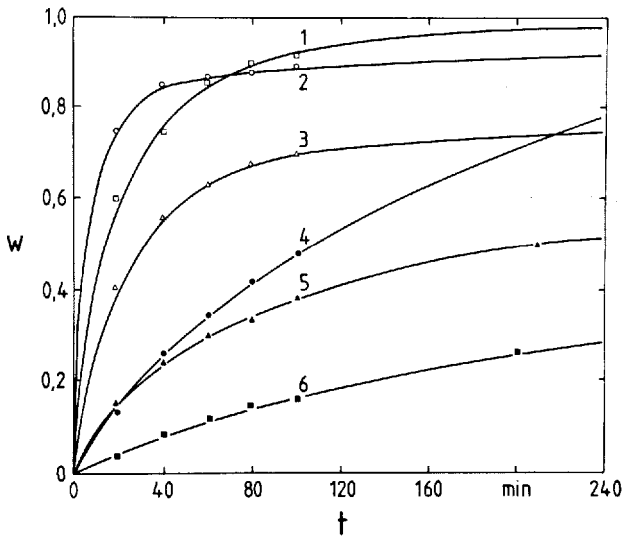

Fig.4: Volatilization factors for thallium compounds

1	Electric filter dust (SP)	900°C
2	Synthetic dust	900°C
3	Electric filter dust (LEPOL)	900°C
4	Synthetic dust	500°C
5	Electric filter dust (LEPOL)	500°C
6	Electric filter dust (SP)	500°C

Reasons for the vaporization of thallium iodide

The vapour pressures of thallium iodide and thallium chloride are nearly the same /11,12,13/. The amount of chlorine in both electric filter dusts was found to be much higher than the amount of iodide, yet the vaporization analysis showed a sublimate of thallium iodide in both cases. For that reason, the vaporization analysis was applied to a mixture of 100 mg TlCl/2 g NaI. Much TlI and only small amounts of TlCl were found in the condensate.

The TlI formed from TlCl/NaI or TlCl/KI which occurs in the preheating zone of the cement production and which is able to react there is thermodynamically favoured. This was also proved by calculations for this system at a temperature of 700-1200 K. Thus it is possible to find TlI in the preheating hone of cement plants.

References

/1/ S. Sprung, Schriftenreihe der Zementindustrie (Düsseldorf) 43 (1982)

/2/ H.U. Bambauer, H. Schäfer. Fortschr. Mineralogie 62 (1984) No. 1,33/50

/3/ B. Haegermann. Diplom-Thesis, University of Clausthal, 1982

/4/ K. Blome, Untersuchungen über das Verhalten von Thallium und Blei bei der Zementherstellung. Ph.D.Thesis, University of Karlsruhe, 1983

/5/ W. Weisweiler, K. Blome, L. Kaeding, Staub-Reinhalt. Luft 45 (1985), No.10, 461/66

/6/ K. Kamm, W. Obländer, W. Weisweiler, Staubh-Reinhalt. Luft 43 (1983) No.5, 193/98

/7/ H. Walk, Die Gehalte der Schwermetalle Cd, Tl, Pb, Bi und weiterer Spurenelemente in natürlichen Böden und ihren Ausgangsgesteinen Südwest-Deutschlands. Ph.D.Thesis, University of Karlsruhe, 1982

/8/ W. Weisweiler, E. Mallonn, K.J. Kohl, Zement-Kalk-Gips (in press)

/9/ W. Weisweiler, E. Mallonn, Naturwiss. 70 (1983) 304/5

/10/ Ch. Wachter, W. Weisweiler, Mikrochimica Acta/Wien (1982 I) 307/15

/11/ Handbook of Chemistry and Physics. 65th Ed. CRC Press, Boca Raton/Florida, USA, 1985

/12/ J. Barin, O. Knacke, Thermochemical Properties of Inorganic Substances. Springer Verlag, Berlin, 1973

/13/ J. Barin, O. Knacke, O. Kubaschewski, Thermochemical Properties of Inorganic Substances, Supplement. Springer Verlag, Berlin, 1977

Dr. JOSÉ ERMÍRIO DE MORAES FILHO

(Presidente do Grupo Votorantim e Presidente do Sindicato Nacional da Indústria do Cimento)

"Na qualidade de Presidente da Comissão Organizadora do Oitavo Congresso Internacional de Química do Cimento e de Presidente do Sindicato Nacional da Indústria do Cimento temos a satisfação de saudar os participantes deste evento, apresentando-lhes as boas vindas ao nosso país, onde esperamos que tenham uma ótima estada.

Sediar este Congresso é, para a Indústria do Cimento do Brasil, além da satisfação e da honra de tê-los conosco, uma rara oportunidade de intensificação do intercâmbio tecnológico que já mantemos, inclusive através de nossa participação nos demais congressos desta série, que já criou uma tradição e se constitui, talvez, no principal evento internacional da indústria do cimento. Assim é que, nos seis anos de intervalo entre essas reuniões, nossos cientistas desenvolvem intenso trabalho de pesquisa, do qual todos participam através de consultas mútuas propiciadas pela intensa correspondência trocada a partir do contato estabelecido durante o congresso.

A Indústria Brasileira do Cimento tem demonstrado ser capaz de enfrentar e vencer um grande número de desafios, sempre agravados pelas condições gerais do país.

Durante as décadas de 60 e 70 teve a nossa indústria que crescer em quantidade e qualidade, em função do aumento da demanda. Nesses vinte e poucos anos passamos de 30 para 56 fábricas e de 5 milhões para 40 milhões de toneladas-ano de capacidade instalada.

O esforço financeiro que essa expansão representou foi realizado com alguma ajuda do capital estrangeiro e com o máximo possível de capital de risco, o que muito nos valeu no recente período recessivo.

A atualização tecnológica acompanhou esse crescimento quantitativo, tendo a nossa indústria incorporado todos os avanços no sentido da otimização do uso da energia elétrica e térmica. Assim é que toda a expansão promovida a partir dos anos 60 foi feita com a adoção do processo seco, com unidades de capacidade instalada mínima de 1.000 toneladas/dia, dotadas dos mais modernos equipamentos de proteção ao meio ambiente.

A substituição do óleo combustível importado pelo carvão mineral nacional, realizada a partir de 1979 e motivada pelas incertezas do abastecimento do petróleo, além do seu alto preço, foi uma demonstração da nossa capacidade técnica, uma vez que passamos a consumir carvões nacionais com 35 e até 55% de cinzas, tendo o programa de substituição sido completado em reduzido prazo.

Embora estejamos em décimo primeiro lugar entre os produtores mundiais, temos ainda elevada capacidade ociosa e são grandes as possibilidades de crescimento do consumo no Brasil. Os estudos de que dispomos indicam que, hoje, o consumo potencial é de 43 milhões de toneladas/ano, montante que teria sido atingido se o país não tivesse sofrido forte recessão durante cinco anos e meio. Aquela cifra nos colocaria como o quinto produtor mundial de cimento e com um consumo per-capita em torno de 300 kg.

Com essas cifras queremos enfatizar a alta significação que tem para este país a realização, entre nós, deste Oitavo Congresso Internacional de Química do Cimento.

Para que possamos fazer uma idéia quantitativa do que representa esse evento, citamos o número de trabalhos apresentados:

Relatórios	24
Comunicações	256
Relatórios Gerais	12
Comunicações dos Seminários	33
Comunicações Livres	23
Posters	43
	391
Outros trabalhos	87
	478

O exame de todo esse acervo foi realizado pelos três Comitês Científicos e está transcrito nos Anais que os senhores estão recebendo.

O elevado nível desses trabalhos nos garante que este congresso será pleno de intenso trabalho e excelentes resultados, inclusive com a extensão da apreciação das matérias aqui propostas por um prazo bem maior do que os dias destinados a este evento.

Declaramos abertos os trabalhos deste Oitavo Congresso Internacional de Química do Cimento, desejando que tenham todos uma boa performance e um ótimo aproveitamento.

Muito obrigado."

Dr. PAULO MÁRIO FREIRE
(Diretor Superintendente da Cia. de Cimento Portland Paraíso - Cimentos Alvorada, Barroso, Goiás e Paraíso)

"Autoridades

Senhoras e Senhores

A responsabilidade da Comissão Organizadora do 8º Congresso começou logo após a sessão de encerramento do congresso de Paris quando os presentes aplaudiram o convite para que comparecessem ao congresso do Rio de Janeiro.

Como bem ressaltou o Dr. José Ermírio de Moraes Filho, em seu discurso na abertura deste congresso, a Indústria do Cimento no Brasil, pelo seu porte, desenvolvimento e perspectivas, poderá aproveitar de forma plena todo o saber que fluiu neste recinto ao longo destes proveitosos dias.

Foram abordados temas de alto interesse para a Indústria do Cimento em todo o mundo e esperamos que esses resultados dêem margem a muitos aperfeiçoamentos tanto para a produção de clínquer e cimento quanto para os utilizadores do produto, principalmente pela indústria da construção civil.

Felizmente a Indústria Brasileira do Cimento conta com o apoio da Associação Brasileira de Cimento Portland, que completa 50 anos de trabalho, e cujos técnicos têm a capacidade de assimilar os ensinamentos contidos nos Anais dos congressos, e transformá-los em conceituações práticas que permitam a sua aplicação pelos produtores e usuários do cimento.

Ao fim desses seis dias de intenso trabalho precisamos tratar de assegurar, para o futuro, a realização de novos congressos internacionais de química do cimento com o mesmo êxito que caracterizou não só o congresso do Rio de Janeiro mas os congressos anteriores.

Para isso, propomos que seja elaborado um regulamento simples que contenha a experiência até agora acumulada na organização desses eventos. Essa tarefa ficaria a cargo de uma Organização dos Congressos Internacionais de Química do Cimento, a ser composta pelos presidentes das Comissões Organizadoras dos congressos realizados.

Quero apresentar, em meu nome e da Indústria Brasileira do Cimento nossos agradecimentos aos três profissionais, responsáveis pelo êxito técnico deste congresso os srs.

J. P. Meric - da Cie. des Ciments Français
Jan Skalny - da W. R. Grace
Francisco de Assis Basílio, Colaborador, assim como aos Drs.
Paulo Monteiro
Yoshiro Kihara
M. S. Marinho
H. Bucher
na organização administrativa tivemos a atuação de:
João Batista Menescal Fiuza - Diretor Administrativo
Gabriel Vianna - Assessor
e todos os técnicos e funcionários do Sindicato Nacional da Indústria de Cimento:

Finalmente, agradeço a todos os especialistas que apresentaram os trabalhos que estão publicados nos 6 volumes dos Anais, a todos os que compareceram ao congresso e especialmente àqueles que cooperaram na condução dos trabalhos nas sessões de Temas e Sub-temas.

Chegamos à hora da despedida certos de que todos hão de se lembrar do Congresso e do Rio de Janeiro, de suas praias e belezas naturais.

Até o 9º Congresso."

PROF. F. A. BASÍLIO (Ingénieur Conseil)

"Mes Dames et Messieurs

En 1980, à Paris, a la soirée du 4 juillet à la séance de clotûre du 7ème Congrès International de la Chimie des Ciments, M. Raymond Poitrat, Président du Syndicat National des Fabricants de Ciments et de Chaux et Président de la Comission du Congrès, annonça la ville de Rio de Janeiro comme siège du congrès suivant, le 8ème. Il savait qu'il prenait une grande responsabilité car il devrait choisir un nouveau siège avec l'assurance d'avoir un autre congrès organisé avec les mêmes caractéristiques des congrès précédents de la chimie des ciments avec un niveau scientifique bien en accord avec la recherche la plus avancée dans ce domaine.

S'il a reussi on non dans le choit qu'il a fait, c'est a vous de la juger, après le congrès que vient de finir, mais la Commission d'Organisation du Congrès de Rio de Janeiro, a fait de son mieux pour être digne de la mission.

En effet, dans le but d'assurer la coopération d'un plus grand nombre des plus importants spécialistes des pays du monde, et éviter des longs déplacements pour eux, on a résolu travailler, dans le choix des Thèmes et Sous-thèmes du congrès, en trois Comités Scientifiques respectivement à Paris (France), à Baltimore (USA) et à Rio de Janeiro (Brésil). Pour assurer la coordination des travaux le Dr. Paulo M. Freire, Vice-Président Êxecutif de la Commission d'Organization du Brésil, et moi même, nous avons été présent à presque toutes les réunions des Comités Scientifiques.

Les Trois Comités ont finalement, après quelques années de travail, presenté la relation des Thèmes et Sous-thèmes pour le 8ème congrès, qui fut approuvé par la Commissiona d'Organization.

En envisageant la situation particulière de l'Amérique du Sud et jugeant d'avantage de discuter un peu plus les sujets des questions posées par les participants du congrès, la Commission d'Organization a approuvé la diminuition du nombre des thèmes, reduit à quatre et alors prendre toute la journée pour chaque thême.

L'organisation technique du congrès a eu de la chance dans le choix des spécialistes pour la présidence des thèmes et des sous-thèmes, et pour présenter le rapport principal, rapport spécial et rapport des communications de chaque thème. Nos invitations furent acceptées et on a pu voir les spécialistes que sont venues à Rio de Janeiro et les excelents travaux presentées. Nous avons a remercier aussi tous les auteurs de Communications Basiques et Communications Libres et qui sont dejà publiées aux annales. Les Communications aux Séminaires seront publicés au sixième volume des Annales.

In apperçu sur le congrés de Rio de Janeiro nous montre que nous avons reçu 398 documents que seront publiés aux Annales du congrès imprimés en six volumes dont cinq vous ont été remis à l'occasion de l'inscription au congrès et le dernier vous sera envoyé par la poste.

Le congrés a reçu environ 600 inscriptions et en plus, à peu près, 100 accompagnants.

Du point de vu technique, on a vu un enorme interêt dans toutes les sessions de thèmes et dans celles des sous-thèmes dont la contribution des membres des tables rondes, et de plusieurs invités ont produit de discussion à haut niveau technique à propos des questions posées par l'audience.

En conséquence, comme pour les annales du congrès de Paris, les Annales du congrès de Rio de Janeiro, seront une référence très importante, pendant des années, pour tous ceux qui s'intéressent à l'évolution des recherches en ce qui concerne la chimie du ciment.

Je remercie vivement à tous ceux qui ont collaboré pour la réussite de ce congrès et je fait les meilleurs voeux pour qu'au prochain congrès ont puisse se rencontrer et prêter une colaboration si utile comme vous vener des prêter au 8éme congrès.

Merci pour l'attention."

PARTICIPANTS' LIST

	NAME	COMPANY	ADRESS	ZIP-CITY-STATE-COUNTRY
001	ARMANDOLA,HAYDEE VIRGINIA	CADIEM LABORATORIOS	N.S.DEL CARMEN 2306	1674-SAENZ PENA-B.A.-ARGENTINA
002	BONFORTE,ANTONINO	CADIEM LABORATORIOS	N.S.DEL CARMEN 2306	1674-SAENZ PENA-B.A.-ARGENTINA
003	GIMENEZ,ANIBAL HORACIO	CEMENTO SAN MARTIN S.A.	DEFENSA 113-9o.PISO	1065-BUENOS AIRES- ARGENTINA
004	FESSIA,SILVER DANIEL	CORPORACION CEMENTERA ARGENTINA S.A.	C.DE CORREO 9	5000-CORDOBA- ARGENTINA
005	MORETTI,RAUL	CORPORACION CEMENTERA ARGENTINA S.A.	AV.ESPANA	5500-MENDOSA- ARGENTINA
006	MELCONIAN,RUBEN	DAREX SAIC (W.R.GRACE)	PRIMEIRA JUNTA 550	1878-BUENOS AIRES- ARGENTINA
007	IDIAZABAL,MIGUEL	KHD-HUMBOLDT WEDAG-DEUTZ ARGENTINA	VALENTIN GOMEZ 577	1706-HAEDO-B.A.- ARGENTINA
008	FAVA,ALBERTO S.C.	INSTITUTO TECNOLOGICO DEL HORMIGON	MIRAVE 2774	1281-BUENOS AIRES- ARGENTINA
009	CABALLERO,JULIO CESAR	INST.DEL CEMENTO PORTLAND ARGENTINO	SAN MARTIN 1137	1004-BUENOS AIRES- ARGENTINA
010	LONGO,ADOLFO	INST.NACIONAL DE TECNOLOGIA INDUSTRIAL	CASILLA CORREO 157	1650-SAN MARTIN- ARGENTINA
011	SONA,JORGE DANIEL	JUAN MINETTI S.A.	ITUZAINGO 87-2o.PISO	5000-CORDOBA- ARGENTINA
012	GALVAN,LUIS ERNESTO	LOMA NEGRA CIASA	AV.PTE.ROQUE SAENZ PENA 634	1035-BUENOS AIRES- ARGENTINA
013	MIRETZKY,BERNARDO	LOMA NEGRA CIASA	AV.PTE.ROQUE SAENZ PENA 634	1035-BUENOS AIRES- ARGENTINA
014	SAIZ,ALBERTO	PETROQUIMICA CRSA	BARRIO DON BOSCO	9003-C.RIVADAVIA- ARGENTINA
015	PREATONI,DANIEL EDUARDO	PROCEM S.A.	RAWSON 1192	1182-BUENOS AIRES- ARGENTINA
016	ORTEGA,PEDRO HECTOR	REFRACTARIOS ARGENTINOS SACIM	TTE.GRAL.JUAN PERON 1669	BUENOS AIRES- ARGENTINA
017	WHITE,CLIFFORD	C.S.H.CONSULTANTS PTY LTD.	RMB 5465-THE RIDGEWAY	2250-HOLGATE- AUSTRALIA
018	GERGER,WOLFGANG	GMUNDNER ZEMENTWERKE	P.O.BOX 6	A-4810-GMUNDEN- AUSTRIA
019	KING,TREVOR	ARAWAK CEMENT COMPANY LTD.	CHECKER HALL	ST.LUCY- BARBADOS
020	LAKSMAN,RAMESH	ARAWAK CEMENT COMPANY LTD.	CHECKER HALL	ST.LUCY- BARBADOS
021	BLONDIAU,LEON-MARIE	CIMENTS D'OBOURG S.A.	RUE DES FABRIQUES 2	7048-MONS-OBOURG- BELGIUM
022	DE RYCKHOLT,ROGER DU BOIS DE BOUNAM	CIE.DES CIMENTS BELGES	GRAND ROUTE 860	7530-TOURNAI- BELGIUM
023	TENDUTASSE,M.	S.A.REDCO	NAAMLOSE VENNOOTSCHAP	2920-KAPELLE- BELGIUM
024	FIERENS,PAUL	UNIVERSITE DE MONS	AVENUE MAISTRIAU 21	B-7000-MONS- BELGIUM
025	DE LEON,LUIS PONCE	CIA BOLIVIANA DE CEMENTO	AV.SAN MARTIN	S-0558-COCHABAMBA- BOLIVIA
026	TORDOYA,LUIS PANOZO	CIA BOLIVIANA DE CEMENTO	AV.SAN MARTIN	S-0558-COCHABAMBA- BOLIVIA
027	VIDOS,DALIBOR CEZAREO	CIA BOLIVIANA DE CEMENTO	AV.SAN MARTIN	S-0558-COCHABAMBA- BOLIVIA
028	DO AMARAL FILHO,EPAMINONDAS MELO	ASSOC.BRAS.DE CIMENTO PORTLAND	R.SILVIA CELESTE CAMPOS 504	05462-S.PAULO-SP- BRASIL
029	BACELLAR,LUIS	ASSOC.BRAS.DE CIMENTO PORTLAND	AV.TORRES DE OLIVEIRA 76	05347-S.PAULO-SP- BRASIL
030	BARRETO,ARGO MENNA	ASSOC.BRAS.DE CIMENTO PORTLAND	AV.TORRES DE OLIVEIRA 76	05347-S.PAULO-SP- BRASIL
031	BATTAGIN,ARNALDO	ASSOC.BRAS.DE CIMENTO PORTLAND	AV.TORRES DE OLIVEIRA 76	05347-S.PAULO-SP- BRASIL
032	BATTAGIN,INES	ASSOC.BRAS.DE CIMENTO PORTLAND	AV.TORRES DE OLIVEIRA 76	05347-S.PAULO-SP- BRASIL
033	BUCHER,HANS	ASSOC.BRAS.DE CIMENTO PORTLAND	AV.TORRES DE OLIVEIRA 76	05347-S.PAULO-SP- BRASIL
034	ESPER,MARIO WILLIAM	ASSOC.BRAS.DE CIMENTO PORTLAND	AV.TORRES DE OLIVEIRA 76	05347-S.PAULO-SP- BRASIL
035	KIHARA,YUSHIRO	ASSOC.BRAS.DE CIMENTO PORTLAND	AV.TORRES DE OLIVEIRA 76	05347-S.PAULO-SP- BRASIL
036	LOPES,CARLOS ALBERTO	ASSOC.BRAS.DE CIMENTO PORTLAND	AV.TORRES DE OLIVEIRA 76	05347-S.PAULO-SP- BRASIL
037	LOPES,CARLOS MANUEL GONCALVES	ASSOC.BRAS.DE CIMENTO PORTLAND	AV.TORRES DE OLIVEIRA 76	05347-S.PAULO-SP- BRASIL
038	MARCIANO,EVERALDO	ASSOC.BRAS.DE CIMENTO PORTLAND	AV.TORRES DE OLIVEIRA 76	05347-S.PAULO-SP- BRASIL
039	MARCIANO,ZULEICA ALVES N.	ASSOC.BRAS.DE CIMENTO PORTLAND	AV.TORRES DE OLIVEIRA 76	05347-S.PAULO-SP- BRASIL
040	RODRIGUES FILHO,HUGO DA COSTA	ASSOC.BRAS.DE CIMENTO PORTLAND	AV.TORRES DE OLIVEIRA 76	05347-S.PAULO-SP- BRASIL
041	RODRIGUES,PAULO	ASSOC.BRAS.DE CIMENTO PORTLAND	AV.TORRES DE OLIVEIRA 76	05347-S.PAULO-SP- BRASIL
042	SCANDIUZZI,LUERCIO	ASSOC.BRAS.DE CIMENTO PORTLAND	AV.TORRES DE OLIVEIRA 76	05347-S.PAULO-SP- BRASIL
043	SUTO,ANTONIA JADRANKA	ASSOC.BRAS.DE CIMENTO PORTLAND	AV.TORRES DE OLIVEIRA 76	05347-S.PAULO-SP- BRASIL
044	TEZUKA,YASUKO	ASSOC.BRAS.DE CIMENTO PORTLAND	AV.TORRES DE OLIVEIRA 76	05347-S.PAULO-SP- BRASIL
045	ZAMPIERI,VALDIR	ASSOC.BRAS.DE CIMENTO PORTLAND	AV.TORRES DE OLIVEIRA 76	05347-S.PAULO-SP- BRASIL
046	RIBEIRO,VOLNEY NASCIMENTO	BRASCEP ENGENHARIA LTDA	R.TEOFILO OTONI 85	20090-R.JANEIRO-RJ- BRASIL
047	BATISTA,ANTONIO CARLOS	BRASILIT S.A.	AV.PROSPERIDADE 380	09250-SANTO ANDRE-SP-BRASIL
048	BIENFAIT,BERNARD	BRASILIT S.A.	AV.PROSPERIDADE 380	09250-SANTO ANDRE-SP-BRASIL
049	FERNANDES,PAULO BASILIO	BRASILIT S.A.	AV.PROSPERIDADE 380	09250-SANTO ANDRE-SP-BRASIL
050	GAUDIOT,JEAN JACQUES	BRASILIT S.A.	AV.PROSPERIDADE 380	09250-SANTO ANDRE-SP-BRASIL
051	ISHII,ROSEMARY SANAE ZAMATARO	BRASILIT S.A.	AV.PROSPERIDADE 380	09250-SANTO ANDRE-SP-BRASIL
052	MARCHI,JOSE EDUARDO	BRASILIT S.A.	AV.PROSPERIDADE 380	09250-SANTO ANDRE-SP-BRASIL
053	DIOGO,FRANCISCO FERNANDES	CAMARGO CORREA INDUSTRIAL S.A.	R.GABRIEL R.DOS SANTOS 1415	18320-APIAI-SP- BRASIL
054	PEREIRA,MANUEL G.L.SIMOES	CAMARGO CORREA INDUSTRIAL S.A.	R.GABRIEL R.DOS SANTOS 1415	18320-APIAI-SP- BRASIL
055	ROSA,JOSE LUIS	CAMARGO CORREA INDUSTRIAL S.A.	R.FUNCHAL 160	04551-S.PAULO-SP- BRASIL
056	CRAIEVICH,ALDO	CBPF/CNPQ-MIN.DE CIENCIA E TECNOLOGIA	R.XAVIER SIGAUD 150	22290-R.JANEIRO-RJ- BRASIL
057	FARIAS,ROBERTO F.S.	CEPED-CENTRO DE PESQUISAS DA BAHIA	ROD.RAPOSO TAVARES 3175 BL.G	05575-S.PAULO-SP- BRASIL
058	SANTOS,MARCOS EDILTO CINTRA	CEPED-CENTRO DE PESQUISAS DA BAHIA	DOD.BR-536,KM 0	42800-CAMACARI-BA- BRASIL
059	SAAD,MIGUEL	CESP-CIA ENERGETICA DE SAO PAULO	AV.PAULISTA 2064	01310-S.PAULO-SP- BRASIL
060	SALLES,FLAVIO MOREIRA	CESP-CIA ENERGETICA DE SAO PAULO	AV.PAULISTA 2086	01310-S.PAULO-SP- BRASIL
061	DA SILVA,JOSE MARIA RANGEL	CIA.AGRO-IND.DE MONTE ALEGRE-CAIMA	EST.DO ALEIXO,KM 10	69000-MANAUS-AM- BRASIL
062	SASAOKA,YOSUKE	CIA.AGRO-IND.DE MONTE ALEGRE-CAIMA	EST.DO ALEIXO,KM 10	69000-MANAUS-AM- BRASIL
063	FALCAO,RICARDO FIGUEIREDO	CIA.CEARENSE DE CIMENTO PORTLAND	R.MADRE DE DEUS 27	50000-RECIFE-PE- BRASIL
064	MIRANDA,ROMULO FABRI	CIA.CIMENTO PORTLAND ITAU	AL.SANTOS 1357	01419-S.PAULO-SP- BRASIL
065	MOURA,GUILHERME	CIA.CIMENTO PORTLAND ITAU	AL.SANTOS 1357	01419-S.PAULO-SP- BRASIL
066	RIBOLDI,ALAYR	CIA.CIMENTO PORTLAND ITAU	AL.SANTOS 1357	01419-S.PAULO-SP- BRASIL
067	SALVADOR,WELDON	CIA.CIMENTO PORTLAND ITAU	AL.SANTOS 1357	01419-S.PAULO-SP- BRASIL
068	SIQUEIRA,ETEOCLES MEIRELLES	CIA.CIMENTO PORTLAND ITAU	AL.SANTOS 1357	01419-S.PAULO-SP- BRASIL
069	SORIA,HUGO GONZALES	CIA.CIMENTO PORTLAND ITAU	AL.SANTOS 1357	01419-S.PAULO-SP- BRASIL
070	AGUIAR,MARCELO ANTONIO	CIA.CIMENTO PORTLAND DE SERGIPE	R.MADRE DE DEUS 27	50000-RECIFE-PE- BRASIL
071	BARRETO,LUIZALPES	CIA.DE CIMENTO ATOL	FAZ.SAO SEBASTIAO S/N	57240-S.M.CAMPOS-AL- BRASIL
072	SALVADOR,REGINA CELIA	CIA.DE CIMENTO ATOL	FAZ.SAO SEBASTIAO S/N	57240-S.M.CAMPOS-AL- BRASIL
073	REZENDE,ALCIONE	CIA.DE CIMENTO ITAMBE	ROD.BR-377,KM 134	83650-BALSA NOVA-PR- BRASIL
074	FERNANDES FILHO,ROMARIO	CIA.DE CIMENTO PORTLAND GAUCHO	ROD.BR-116,KM 256	93250-ESTEIO-RS- BRASIL
075	FONTOURA,MARIO L.FRANCESCHI	CIA.DE CIMENTO PORTLAND GAUCHO	ROD.BR-116,KM 256	93250-ESTEIO-RS- BRASIL

	NAME	COMPANY	ADRESS	ZIP-CITY-STATE-COUNTRY	
076	RAMOS,MANUEL BAUTISTA	CIA.DE CIMENTO PORTLAND MARINGA	BARAO DE TAQUARI S/N	18400-ITAPEVA-SP-	BRASIL
077	ALVES,HENRIQUE CLEMENTE BAETA	CIA.DE CIMENTO PORTLAND PARAISO	ROD.RJ-166,KM 2,5-VAL DE PALMAS	28500-CANTAGALO-RJ-	BRASIL
078	AMERICO,GILMAR MAGNO	CIA.DE CIMENTO PORTLAND PARAISO	AV.RIO BRANCO 103,18o.ANDAR	20041-R.JANEIRO-RJ-	BRASIL
079	ARAUJO JUNIOR,ANTENOR	CIA.DE CIMENTO PORTLAND PARAISO	R.TIRADENTES S/N	36205-BARROSO-MG-	BRASIL
080	BLATTER,JORG	CIA.DE CIMENTO PORTLAND PARAISO	AV.RIO BRANCO 103,18o.ANDAR	20041-R.JANEIRO-RJ-	BRASIL
081	CHAGAS,ROBERTO OLIVEIRA	CIA.DE CIMENTO PORTLAND PARAISO	AV.RIO BRANCO 103,18o.ANDAR	20041-R.JANEIRO-RJ-	BRASIL
082	DA SILVA,CARLOS ALBERTO M.P.	CIA.DE CIMENTO PORTLAND PARAISO	AV.RIO BRANCO 103,18o.ANDAR	20041-R.JANEIRO-RJ-	BRASIL
083	DE CARVALHO,PEDRO HENRIQUES	CIA.DE CIMENTO PORTLAND PARAISO	AV.RIO BRANCO 103,18o.ANDAR	20041-R.JANEIRO-RJ-	BRASIL
084	DIVINO,FRANCISCO EDUARDO GUIMARAES	CIA.DE CIMENTO PORTLAND PARAISO	AV.RIO BRANCO 103,18o.ANDAR	20041-R.JANEIRO-RJ-	BRASIL
085	FONTES,ARTHUR	CIA.DE CIMENTO PORTLAND PARAISO	AV.RIO BRANCO 103,18o.ANDAR	20041-R.JANEIRO-RJ-	BRASIL
086	FREIRE,EDUARDO	CIA.DE CIMENTO PORTLAND PARAISO	AV.RIO BRANCO 103,18o.ANDAR	20041-R.JANEIRO-RJ-	BRASIL
087	FREIRE NETO,MARIO	CIA.DE CIMENTO PORTLAND PARAISO	AV.RIO BRANCO 103,18o.ANDAR	20041-R.JANEIRO-RJ-	BRASIL
088	GOULART,BENEDITO DA COSTA	CIA.DE CIMENTO PORTLAND PARAISO	AV.RIO BRANCO 103,18o.ANDAR	20041-R.JANEIRO-RJ-	BRASIL
089	ISNARD,CARLOS AUGUSTO	CIA.DE CIMENTO PORTLAND PARAISO	AV.RIO BRANCO 103,18o.ANDAR	20041-R.JANEIRO-RJ-	BRASIL
090	LOPES,GERALDO ALMEIDA	CIA.DE CIMENTO PORTLAND PARAISO	ROD.RJ-166,KM 2,5-VAL DE PALMAS	28500-CANTAGALO-RJ-	BRASIL
091	MONTEIRO,PAULO JOSE M.	CIA.DE CIMENTO PORTLAND PARAISO	AV.RIO BRANCO 103,18o.ANDAR	20041-R.JANEIRO-RJ-	BRASIL
092	MONTENEGRO,CARLOS ALBERTO PINTO	CIA.DE CIMENTO PORTLAND PARAISO	R.1-CIVIT II-LOTES 5 A 8	29160-SERRA-ES-	BRASIL
093	OLIVEIRA,JERONIMO TOMAZ FERREIRA	CIA.DE CIMENTO PORTLAND PARAISO	ROD.RJ-166,KM 2,5-VAL DE PALMAS	28500-CANTAGALO-RJ-	BRASIL
094	PEDRO,JOSE ALBERTO SALGADO	CIA.DE CIMENTO PORTLAND PARAISO	AV.RIO BRANCO 103,18o.ANDAR	20041-R.JANEIRO-RJ-	BRASIL
095	PEREZ,BENITO EDUARDO LOBOS	CIA.DE CIMENTO PORTLAND PARAISO	AV.RIO BRANCO 103,18o.ANDAR	20041-R.JANEIRO-RJ-	BRASIL
096	ROSAT,PAULO WILTGEN	CIA.DE CIMENTO PORTLAND PARAISO	AV.RIO BRANCO 103,18o.ANDAR	20041-R.JANEIRO-RJ-	BRASIL
097	SILVA,CARLOS CESAR	CIA.DE CIMENTO PORTLAND PARAISO	R.1-CIVIT II-LOTES 5 A 8	29160-SERRA-ES-	BRASIL
098	UNANUE,WALTER MARIO GARCIA	CIA.DE CIMENTO PORTLAND PARAISO	AV.RIO BRANCO 103,18o.ANDAR	20041-R.JANEIRO-RJ-	BRASIL
099	VITRAL,JOSE ROBERTO CAMARA	CIA.DE CIMENTO PORTLAND PARAISO	R.TIRADENTES S/N	36205-BARROSO-MG-	BRASIL
100	LIMA NETO,JORGE	CIA.DE CIMENTO PORTLAND POTY	R.MADRE DE DEUS 27	50000-RECIFE-PE-	BRASIL
101	SHOEEN,EUSEBIO MUNHOZ	CIA.DE CIMENTO PORTLAND POTY	R.MADRE DE DEUS 27	50000-RECIFE-PE-	BRASIL
102	CERON,CLAIR	CIA.DE CIMENTO PORTLAND RIO BRANCO	R.JOAO NEGRAO 1285	80000-CURITIBA-PR-	BRASIL
103	FOSTER,HERBERT	CIA.DE CIMENTO PORTLAND RIO BRANCO	R.JOAO NEGRAO 1285	80000-CURITIBA-PR-	BRASIL
104	MONACO,ERNANI	CIA.DE CIMENTO SALVADOR	PONTA DA SAPOCA	40000-S.T.PARIPE-BA-	BRASIL
105	ABREU,JOAO BOSCO	CIA.MATERIAIS SULFUROSOS-MATSULFUR	AV.AMAZONAS 311-3o.ANDAR	30180-B.HORIZONTE-MG-	BRASIL
106	ABREU,JOSE EDUARDO	CIA.MATERIAIS SULFUROSOS-MATSULFUR	AV.AMAZONAS 311-3o.ANDAR	30180-B.HORIZONTE-MG-	BRASIL
107	MACHADO,JOSE EUSTAQUIO	CIA.MATERIAIS SULFUROSOS-MATSULFUR	AV.AMAZONAS 311-3o.ANDAR	30180-B.HORIZONTE-MG-	BRASIL
108	RIBEIRO,MARCOS ANTONIO	CIA.MATERIAIS SULFUROSOS-MATSULFUR	AV.AMAZONAS 311-3o.ANDAR	30180-B.HORIZONTE-MG-	BRASIL
109	SOARES,ALBERTO LUIZ	CIA.MATERIAIS SULFUROSOS-MATSULFUR	AV.AMAZONAS 311-3o.ANDAR	30180-B.HORIZONTE-MG-	BRASIL
110	TIBURCIO,MAURICIO	CIA.MATERIAIS SULFUROSOS-MATSULFUR	AV.AMAZONAS 311-3o.ANDAR	30180-B.HORIZONTE-MG-	BRASIL
111	BERTELLI NETO,JOAO	CIA.PARAIBA DE CIMENTO PORTLAND-CIMEPAR	FAZENDA GRACA - C.P.15	58000-JOAO PESSOA-PB-	BRASIL
112	VISANI,VITTORIO	CIA.PARAIBA DE CIMENTO PORTLAND-CIMEPAR	FAZENDA GRACA - C.P.15	58000-JOAO PESSOA-PB-	BRASIL
113	DA SILVA NETO,JOSE MARIA	CIA.SIDERURGICA DA GUANABARA-COSIGUA	AV.JOAO XXIII,6777	23500-R.JANEIRO-RJ-	BRASIL
114	FERREIRA,NELSON AMILCAR	CIMENTO ARATU S.A.	VIA PERIFERICA,S/N	43700-SIMOES FO.-BA-	BRASIL
115	OLIVEIRA,MANOEL	CIMENTO CAUE S.A.	ESTACAO DE JOAO CORREA,S/N	35166-MESQUITA-MG-	BRASIL
116	RUAS,AMARILIO	CIMENTO CAUE S.A.	AV.CEL.JUVENTINO DIAS,S/N	33600-P.LEOPOLDO-MG-	BRASIL
117	SOARES,JARBAS	CIMENTO CAUE S.A.	AV.CEL.JUVENTINO DIAS,S/N	33600-P.LEOPOLDO-MG-	BRASIL
118	PEREIRA,ALAOR	CIMENTO E MINERACAO BAGE S.A.	AV.MARIA COELHO AGUIAR,215 BL.A	05804-S.PAULO-SP-	BRASIL
119	MOURA,LUIZ EDUARDO G.TAQUECE	CIMENTO IRAJA S.A.	AV.MERITI,4411	21250-R.JANEIRO-RJ-	BRASIL
120	PESSOA,FRANCISCO DE PAULA GUSMAO	CIMENTO IRAJA S.A.	AV.MERITI,4411	21250-R.JANEIRO-RJ-	BRASIL
121	MOUSSA,MURRIB	CIMENTO ITAU DE CORUMBA S.A.	AV.RIO BRANCO,S/N	79300-CORUMBA-MS-	BRASIL
122	SILVA JUNIOR,DARIO	CIMENTO ITAU DE CORUMBA S.A.	AV.RIO BRANCO,S/N	79300-CORUMBA-MS-	BRASIL
123	CARVALHO,LUIZ VILAR	CIMENTO ITAU DO PARANA S.A.	R.JOAO NEGRAO 1285	80000-CURITIBA-PR-	BRASIL
124	TELES,RICARDO A.DA SILVA	CIMENTO ITAU DO PARANA S.A.	R.JOAO NEGRAO 1285	80000-CURITIBA-PR-	BRASIL
125	ANDRADE,JOSE GONCALVES	CIMENTO MAUA S.A.	ROD.MG-424,KM-31	35720-MATOZINHOS-MG-	BRASIL
126	BONNAL,PAUL JEAN JOSEPH	CIMENTO MAUA S.A.	AV.ALMTE.BARROSO,52-15o.ANDAR	20031-R.JANEIRO-RJ-	BRASIL
127	CATILLON,JEAN DIDIER	CIMENTO MAUA S.A.	ROD.RJ-166,KM-8-FONTE DA SAUDADE	28520-EUCLIDELAND-RJ-	BRASIL
128	COSTA,DANIEL TRAVASSOS R.	CIMENTO MAUA S.A.	ROD.RJ-166,KM-8-FONTE DA SAUDADE	28520-EUCLIDELAND-RJ-	BRASIL
129	DA SILVA,ARMANDO MARTINS	CIMENTO MAUA S.A.	ROD.RJ-166,KM-8-FONTE DA SAUDADE	28520-EUCLIDELAND-RJ-	BRASIL
130	DEJEAN,JEAN	CIMENTO MAUA S.A.	ROD.MG-424,KM-31	35720-MATOZINHOS-MG-	BRASIL
131	DEMARS,PATRICK	CIMENTO MAUA S.A.	AV.AFONSO PENA,941-1o.ANDAR	30130-B.HORIZONTE-MG-	BRASIL
132	MACHADO NETO,TOBIAS	CIMENTO MAUA S.A.	AV.ALMTE.BARROSO,52-15o.ANDAR	20031-R.JANEIRO-RJ-	BRASIL
133	MADRE,BENOIT	CIMENTO MAUA S.A.	AV.ALMTE.BARROSO,52-15o.ANDAR	20031-R.JANEIRO-RJ-	BRASIL
134	MATSUSHITA,KAORU	CIMENTO MAUA S.A.	ROD.MG-424,KM-31	35720-MATOZINHOS-MG-	BRASIL
135	MATTOSINHO,JOAO BATISTA	CIMENTO MAUA S.A.	ROD.MG-424,KM-31	35720-MATOZINHOS-MG-	BRASIL
136	BARRETO,CANDIDO LOPES	CIMENTO PIRINEUS S.A.	ROD.BR-414,KM-70	77135-C.DE GOIAS-GO-	BRASIL
137	COELHO,FERNANDO DE BARROS	CIMENTO SANTA RITA S.A.	AV.BRIG.FARIA LIMA,888-12o.ANDAR	01452-S.PAULO-SP-	BRASIL
138	DAMICO,GIOVANNI	CIMENTO SANTA RITA S.A.	AV.BRIG.FARIA LIMA,888-12o.ANDAR	01452-S.PAULO-SP-	BRASIL
139	MARIANO,ADILSON DORTA	CIMENTO SANTA RITA S.A.	AV.BRIG.FARIA LIMA,888-12o.ANDAR	01452-S.PAULO-SP-	BRASIL
140	SANTOS,MANUEL VITOR	CIMENTO SANTA RITA S.A.	AV.BRIG.FARIA LIMA,888-12o.ANDAR	01452-S.PAULO-SP-	BRASIL
141	ALMEIDA,JOSE NEWTON R.	CIMENTO TUPI S.A.	VIA SERGIO BRAGA,S/N	27265-V.REDONDA-RJ-	BRASIL
142	IVO,LUIZ SANTANA	CIMENTO TUPI S.A.	ROD.BR-040,KM-655	36280-CARANDAI-MG-	BRASIL
143	RINELLI,JOSE LUIZ	CIMENTO TUPI S.A.	PRAIA DE BOTAFOGO,228-16o.ANDAR	22250-R.JANEIRO-RJ-	BRASIL
144	VIANA,JOSE LEANDRO GARCIA	CIMENTO TUPI S.A.	PRAIA DE BOTAFOGO,228-16o.ANDAR	22250-R.JANEIRO-RJ-	BRASIL
145	MESQUITA,GERONCIO	CIMENTOS DO BRASIL S.A.-CIBRASA	ROD.BR-316,KM-150	68700-CAPANEMA-PA-	BRASIL
146	MOLLO,EDUARDO	CIMENTOS DO BRASIL S.A.-CIBRASA	ROD.BR-316,KM-150	68700-CAPANEMA-PA-	BRASIL
147	MUNHOZ,MIGUEL DIAS	CIMINAS-CIMENTO NACIONAL DE MINAS S.A.	VARGEM ALEGRE,S/N	33600-P.LEOPOLDO-MG-	BRASIL
148	VIEIRA,RAIMUNDO MONATO RIBEIRO	CIMINAS-CIMENTO NACIONAL DE MINAS S.A.	VARGEM ALEGRE,S/N	33600-P.LEOPOLDO-MG-	BRASIL
149	DE SOUZA JR.,HAMILTON FERREIRA	CIPLAN-CIMENTO PLANALTO S.A.	SCS-ED.BARACAT 11o.ANDAR	70309-BRASILIA-DF-	BRASIL
150	MARCOVICH,PAULIN EMILE	CIPLAN-CIMENTO PLANALTO S.A.	SCS-ED.BARACAT 11o.ANDAR	70309-BRASILIA-DF-	BRASIL

	NAME	COMPANY	ADRESS	ZIP-CITY-STATE-COUNTRY
151	CASTRO,MANUEL	CLEPLAN-EMPREENDS.E PROJS.INDS.LTDA	ALAMEDA CAMPINAS,463-10o.ANDAR	01404-S.PAULO-SP- BRASIL
152	HELLOFS,LEONARD	CLEPLAN-EMPREENDS.E PROJS.INDS.LTDA	ALAMEDA CAMPINAS,463-10o.ANDAR	01404-S.PAULO-SP- BRASIL
153	GRIJSPEERDT,HENRI	COBRASCOM S.A.	AV.ALMTE.BARROSO,63	20036-R.JANEIRO-RJ- BRASIL
154	DANTAS,RONALDO LUZ	COHIDRO-CIA.DES.RECURSOS HIDRICOS	AV.IVO DO PRADO,840	49000-ARACAJU-SE- BRASIL
155	TARTUCE,RONALDO	CONCREBRAS S.A.ENG.CONCRETO	R.AMERICO BRASILIENSE,633	04715-S.PAULO-SP- BRASIL
156	DE BONIS,BRUNO	CONSULTOR AUTONOMO	R.FERREIRA CARDOSO,37-SALA 101	21050-R.JANEIRO-RJ- BRASIL
157	UGLIARA,WAGNER	COPEBRAS S.A.	PCA.DA REPUBLICA,497-5o.ANDAR	01045-S.PAULO-SP- BRASIL
158	PAMPLONA,AFRODIZIO	D.N.O.C.S.	R.TABAJARAS,11	60000-FORTALEIA-CE- BRASIL
159	VEIGA,ROBSON	ELETROSUL S.A.	OBRA JORGE LACERDA	88700-TUBARAO-SC- BRASIL
160	SPLETTSTOSER JR.,JAIME	ELFUSA-GERAL DE ELETROFUSAO	ESTR.MUNICIPAL P/AGUAI,KM-3	13870-S.J.B.VISTA-SP-BRASIL
161	SPRENGER,CARLOS EDUARDO	ETERNIT S.A.	AV.DOS AUTOMOBILISTAS,1828	06020-OSASCO-SP- BRASIL
162	ANDERSEN,ALLAN	F.L.SMIDTH	R.NEBRASKA,443	04560-S.PAULO-SP- BRASIL
163	BIRCH,ERIK	F.L.SMIDTH	R.NEBRASKA,443	04560-S.PAULO-SP- BRASIL
164	GIUNTOLI.ROLDANO	F.L.SMIDTH	R.NEBRASKA,443	04560-S.PAULO-SP- BRASIL
165	OTSEN,OLE	F.L.SMIDTH	R.NEBRASKA,443	04560-S.PAULO-SP- BRASIL
166	DE OLIVEIRA,JOSE GARIBALDI	FORJAS BRASILEIRAS S.A.	R.MEXICO,111-18o.ANDAR	20031-R.JANEIRO-RJ- BRASIL
167	DE SOUZA,GUERINO A.	FORJAS BRASILEIRAS S.A.	R.MEXICO,111-18o.ANDAR	20031-R.JANEIRO-RJ- BRASIL
168	PEDRAS,GABRIEL LUIZ J.	FORJAS BRASILEIRAS S.A.	R.MEXICO,111-18o.ANDAR	20031-R.JANEIRO-RJ- BRASIL
169	PEIXOTO,PAULO ROBERTO C.	FORJAS BRASILEIRAS S.A.	R.MEXICO,111-18o.ANDAR	20031-R.JANEIRO-RJ- BRASIL
170	FESTGE,REINHOLD	HAVER + BEUMER L.I.C.M.LTDA.	ROD.CAMPINAS/MONTE-MOR,KM-20	13190-S.PAULO-SP- BRASIL
171	GAMBURGO,ADRIAN	HAVER + BEUMER L.I.C.M.LTDA.	ROD.CAMPINAS/MONTE-MOR,KM-20	13190-S.PAULO-SP- BRASIL
172	REMMERT,JOSEF	HAVER + BEUMER L.I.C.M.LTDA.	ROD.CAMPINAS/MONTE-MOR,KM-20	13190-S.PAULO-SP- BRASIL
173	PRISZKULNIK,SIMAO	HIDROSERVICE ENG.PROJETOS LTDA.	R.AFONSO CELSO,235	01419-S.PAULO-SP- BRASIL
174	DUARTE,EDSON	IBACIP-IND.BARB.DE CIMENTO PORT. S.A.	ROD.CE-223,KM-2.5-S/N	63186-BARBALHA-CE- BRASIL
175	MARINHO,MARCELO J.B.DE SOUZA	ICI BRASIL S.A.	R.VERBO DIVINO,1356	04719-S.PAULO-SP- BRASIL
176	CINCOTTO,MARIA ALBA	INST.DE PESQ.TECNOLIGAS DE S.PAULO-IPT	AV.PROF.ALMEIDA PRADO,535	05508-S.PAULO-SP- BRASIL
177	MARQUES,JOAO CARLOS	INST.DE PESQ.TECNOLIGAS DE S.PAULO-IPT	CIDADE UNIVERSITARIA-C.P.7141	05508-S.PAULO-SP- BRASIL
178	TANGO,CARLOS EDUARDO DE S.	INST.DE PESQ.TECNOLIGAS DE S.PAULO-IPT	CIDADE UNIVERSITARIA	05508-S.PAULO-SP- BRASIL
179	UEMOTO,KAI LOH	INST.DE PESQ.TECNOLIGAS DE S.PAULO-IPT	AV.PROF.ALMEIDA PRADO,535	05508-S.PAULO-SP- BRASIL
180	COSTA,BILL JORGE	INST.DE TECNOLOGIA DO PARANA	R.DOS FUNCIONARIOS,1357	80030-CURITIBA-PR- BRASIL
181	CACONIA,ALCINA	INST.NACIONAL DE TECNOLOGIA	AV.VENEZUELA,82	20081-R.JANEIRO-RJ- BRASIL
182	CIANI,MARCIA	INST.NACIONAL DE TECNOLOGIA	AV.VENEZUELA,82	20081-R.JANEIRO-RJ- BRASIL
183	GRECA,MARIA CONCEICAO	INST.NACIONAL DE TECNOLOGIA	AV.VENEZUELA,82	20081-R.JANEIRO-RJ- BRASIL
184	MELO,ELIANE	INST.NACIONAL DE TECNOLOGIA	AV.VENEZUELA,82	20081-R.JANEIRO-RJ- BRASIL
185	MESQUITA,CLAUDIO	INST.NACIONAL DE TECNOLOGIA	AV.VENEZUELA,82	20081-R.JANEIRO-RJ- BRASIL
186	PALAZZO,MARIO	INST.NACIONAL DE TECNOLOGIA	AV.VENEZUELA,82	20081-R.JANEIRO-RJ- BRASIL
187	AZEVEDO JR.,EMERSON	ITABIRA AGRO-INDUSTRIAL S.A.	FAZENDA MONTE LIBANO - C.P.252	29300-C.ITAPEMIRI-ES-BRASIL
188	FERNANDES,AULO	ITABIRA AGRO-INDUSTRIAL S.A.	FAZENDA SUMIDOURO,S/N	18300-C.BONITO-SP- BRASIL
189	NOVAES,ROGERIO	ITABIRA AGRO-INDUSTRIAL S.A.	FAZENDA MONTE LIBANO - C.P.252	29300-C.ITAPEMIRI-ES-BRASIL
190	PARACAMPOS,SERGIO	ITABIRA AGRO-INDUSTRIAL S.A.	FAZENDA MONTE LIBANO - C.P.252	29300-C.ITAPEMIRI-ES-BRASIL
191	BRAGA,JOSE AUGUSTO	ITAIPU BINACIONAL	CANTEIRO DE OBRAS-LAB.DE CONCRETO	85890-F.DO IGUACU-PR-BRASIL
192	FERNANDES NETTO,FRANCILINO	ITAIPU BINACIONAL	CANTEIRO DE OBRAS-C.P.1555	85892-F.DO IGUACU-PR-BRASIL
193	FELIX,ALUIZIO	ITAPESSOCA AGRO-INDUSTRIAL S.A.	ILHA DE ITAPESSOCA,S/N	55900-GOIANA-PE- BRASIL
194	GUEIROS,INALDO	ITAPESSOCA AGRO-INDUSTRIAL S.A.	ILHA DE ITAPESSOCA,S/N	55900-GOIANA-PE- BRASIL
195	KONDO,OSWALDO	ITAPETINGA AGRO-INDUSTRIAL S.A.	AV.CENTENARIO,S/N	59600-MOSSORO-RN- BRASIL
196	MONTENEGRO,MARCOS	ITAPETINGA AGRO-INDUSTRIAL S.A.	AV.CENTENARIO,S/N	59600-MOSSORO-RN- BRASIL
197	TRES,LUIS	ITAPICURU AGRO-INDUSTRIAL S.A.	ROD.BR-316,KM-466	65400-CODO-MA- BRASIL
198	ANDERSEN,VAGN	KHD DO BRASIL LTDA.	AV.PAULISTA,460-11o.ANDAR	01310-S.PAULO-SP- BRASIL
199	BONFIM,MARCOS	MAGNESITA S.A.	PCA.LOUIS ENSCH,240	32210-CONTAGEM-MG- BRASIL
200	DE BRITO,CARLOS BORGES	MAGNESITA S.A.	PCA.LOUIS ENSCH,240	32210-CONTAGEM-MG- BRASIL
201	GARRELL,RICHARD PAUL	MAGNESITA S.A.	PCA.LOUIS ENSCH,240	32210-CONTAGEM-MG- BRASIL
202	GONTIJO,LOURENCO	MAGNESITA S.A.	PCA.LOUIS ENSCH,240	32210-CONTAGEM-MG- BRASIL
203	MOSCI,RICARDO	MAGNESITA S.A.	PCA.LOUIS ENSCH,240	32210-CONTAGEM-MG- BRASIL
204	ORNELAS,PAULO MARCHI	MAGNESITA S.A.	PCA.LOUIS ENSCH,240	32210-CONTAGEM-MG- BRASIL
205	RODRIGUES,ANGELA	MAGNESITA S.A.	PCA.LOUIS ENSCH,240	32210-CONTAGEM-MG- BRASIL
206	VALLE,DENIZ	MAGNESITA S.A.	PCA.LOUIS ENSCH,240	32210-CONTAGEM-MG- BRASIL
207	WAJDOWICZ,ADAM	MAGNESITA S.A.	PCA.LOUIS ENSCH,240	32210-CONTAGEM-MG- BRASIL
208	ZACCARDI,MIGUEL ANGEL	MAGNESITA S.A.	PCA.LOUIS ENSCH,240	32210-CONTAGEM-MG- BRASIL
209	SCHLEISS,RENE	MAGOTTEAUX DO BRASIL	AV.GAL.DAVID SARNOFF,1221	32210-CONTAGEM-MG- BRASIL
210	ARREPIA,AUGUSTO ALFREDO	MATSICA INDUSTRIA E COMERCIO	AV.PAPA JOAO PAULO I,2971	07080-GUARULHOS-SP- BRASIL
211	ABREU,JOSE AUGUSTO ARNAO P.	MAXBETON INDUSTRIA E COMERCIO LTDA.	R.DEBRET,23-SALA 403	20030-R.JANEIRO-RJ- BRASIL
212	ABREU,JOSE AUGUSTO A.K.P.	MAXBETON INDUSTRIA E COMERCIO LTDA.	R.DEBRET,23-SALA 403	20030-R.JANEIRO-RJ- BRASIL
213	GIANNUSSO,SALVADOR	MAXBETON INDUSTRIA E COMERCIO LTDA.	ALAMEDA SANTOS,1470-SALA 707	01418-S.PAULO-SP- BRASIL
214	PALERMO,GIOVANNI	METRO-SAO PAULO	R.LUIS COELHO,197-9o.ANDAR	01309-S.PAULO-SP- BRASIL
215	HIRTH,HAROLD	MULTIPLUS INFORMATICA S/C LTDA.	R.DR.FLAQUER,115-SALA 1618	04006-S.PAULO-SP- BRASIL
216	ARRIAGADA,LUIS OMAR	O & K - ORENSTEIN & KOPPEL EQUIP.LTDA.	R.CAP.ANTONIO ROSA,376-15o.ANDAR	01443-S.PAULO-SP- BRASIL
217	LEIBLEIN,ELMAR	O & K - ORENSTEIN & KOPPEL EQUIP.LTDA.	R.CAP.ANTONIO ROSA,376-15o.ANDAR	01443-S.PAULO-SP- BRASIL
218	SCHNEIDER,HORST	O & K - ORENSTEIN & KOPPEL EQUIP.LTDA.	R.CAP.ANTONIO ROSA,376-15o.ANDAR	01443-S.PAULO-SP- BRASIL
219	SERBONCINI,AMAURI	O & K - ORENSTEIN & KOPPEL EQUIP.LTDA.	R.CAP.ANTONIO ROSA,376-15o.ANDAR	01443-S.PAULO-SP- BRASIL
220	KASAI,MOBORU	ONODA BRASILEIRA IND.COM.LTDA.	AV.BERNARDINO DE CAMPOS,98	04004-S.PAULO-SP- BRASIL
221	MORAES,MARIA LUIZA	PETROBRAS - CENPES	CID.UNIVERSITARIA-ILHA DO FUNDAO-B.7	21910-R.JANEIRO-RJ- BRASIL
222	NUNES,NEY VIEIRA	PETROBRAS - CENPES	CID.UNIVERSITARIA-ILHA DO FUNDAO-B.7	21910-R.JANEIRO-RJ- BRASIL
223	PARENTE,FERNANDO	PETROBRAS - CENPES	CID.UNIVERSITARIA-ILHA DO FUNDAO-B.7	21910-R.JANEIRO-RJ- BRASIL
224	SILVA,MARIA DAS GRACAS	PETROBRAS - CENPES	CID.UNIVERSITARIA-ILHA DO FUNDAO-B.7	21910-R.JANEIRO-RJ- BRASIL
225	EFTIMIADES,MARIO	POLYSIUS PROJ.IND.LTDA.	AV.BRIG.FARIA LIMA,1885-14o.ANDAR	01451-S.PAULO-SP- BRASIL

	NAME	COMPANY	ADRESS	ZIP-CITY-STATE-COUNTRY
226	GEIB,HERIBERT	POLYSIUS PROJETOS IND.LTDA	AV.BRIG.FARIA LIMA,1885-14o.ANDAR	01451-S.PAULO-SP- BRASIL
227	GONCALEZ,FRANCISCO	POLYSIUS PROJETOS IND.LTDA	AV.BRIG.FARIA LIMA,1885-14o.ANDAR	01451-S.PAULO-SP- BRASIL
228	GRINFEDER,CLAUDE	POLYSIUS PROJETOS IND.LTDA	AV.BRIG.FARIA LIMA,1885-14o.ANDAR	01451-S.PAULO-SP- BRASIL
229	THIEME,KLAUS	POLYSIUS PROJETOS IND.LTDA	AV.BRIG.FARIA LIMA,1885-14o.ANDAR	01451-S.PAULO-SP- BRASIL
230	BURIGO,ARYOVALDO	POZOLANA IND.E COM.LTDA.	AV.PROF.FRANCISCO MORATO,492	05512-S.PAULO-SP- BRASIL
231	ABREU,MIRIAN ANTONIO	SABESP	AV.DO ESTADO,561	01107-S.PAULO-SP- BRASIL
232	DE OLIVEIRA,ROBERTO	SERRANA S.A.DE MINERACAO	CAIXA POSTAL 5	11940-JACUPIRANGA-SP-BRASIL
233	DJANIKIAN,JOAO GASPAR	SERRANA S.A.DE MINERACAO	AV.MARIA COELHO AGUIAR,215-3o.AND.BL-A	05804-S.PAULO-SP- BRASIL
234	GOMES,DURVAL	SERRANA S.A.DE MINERACAO	ROD.BR-116,KM-488	11950-JACUPIRANGA-SP-BRASIL
235	GUIDA,LIVIO	SERRANA S.A.DE MINERACAO	AV.MARIA COELHO AGUIAR,215-3o.AND.BL-A	05804-S.PAULO-SP- BRASIL
236	MARTINS,JOANIEL MUNHOZ	SERRANA S.A.DE MINERACAO	CAIXA POSTAL 5	11940-JACUPIRANGA-SP-BRASIL
237	FERNANDES FILHO,OSCAR	SIKA S.A.PRODUTOS QUIMICOS	ESTRADA DO TIMBO,52	21061-R.JANEIRO-RJ- BRASIL
238	COUTO,TIAGO	SOEICOM S.A.-SOC.DE EMP.IND.,COM.E MIN.	AV.PORTUGAL,700	33200-VESPASIANO-MG- BRASIL
239	WAISBERG,BENAMI	SOEICOM S.A.-SOC.DE EMP.IND.,COM.E MIN.	AV.PORTUGAL,700	33200-VESPASIANO-MG- BRASIL
240	AURICCHIO,ELCIO	S.A.INDUSTRIAS VOTORANTIM	PRACA RAMOS DE AZEVEDO,254	01037-S.PAULO-SP- BRASIL
241	BENEDETTI,NILDO MAXIMO	S.A.INDUSTRIAS VOTORANTIM	PRACA RAMOS DE AZEVEDO,254	01037-S.PAULO-SP- BRASIL
242	FERREIRA FILHO,FRANCISCO DIAS	S.A.INDUSTRIAS VOTORANTIM	PRACA RAMOS DE AZEVEDO,254	01037-S.PAULO-SP- BRASIL
243	MARTINI,CELSO ANTONIO	S.A.INDUSTRIAS VOTORANTIM	AV.SENADOR JOSE E.DE MORAES	28500-CANTAGALO-RJ- BRASIL
244	MARTINS,OSORIO L.SILVEIRA	S.A.INDUSTRIAS VOTORANTIM	PRACA RAMOS DE AZEVEDO,254	01037-S.PAULO-SP- BRASIL
245	MENDES,ROBERTO PEREIRA	S.A.INDUSTRIAS VOTORANTIM	AV.SENADOR JOSE E.DE MORAES	28500-CANTAGALO-RJ- BRASIL
246	MORAES,JOSE ROBERTO	S.A.INDUSTRIAS VOTORANTIM	PRACA RAMOS DE AZEVEDO,254	01037-S.PAULO-SP- BRASIL
247	RESENDE,MARCOS MARRA	S.A.INDUSTRIAS VOTORANTIM	AV.SENADOR JOSE E.DE MORAES	28500-CANTAGALO-RJ- BRASIL
248	SANCHEZ,ISIDRO L.C.CONTRERAS	S.A.INDUSTRIAS VOTORANTIM	PRACA RAMOS DE AZEVEDO,254	01037-S.PAULO-SP- BRASIL
249	BIRINDELLI,LUCY O.	THEMAG ENGENHARIA LTDA.	R.BELA CINTRA,986-12o.ANDAR	01415-S.PAULO-SP- BRASIL
250	KUPERMAN,SELMO	THEMAG ENGENHARIA LTDA.	R.BELA CINTRA,986-12o.ANDAR	01415-S.PAULO-SP- BRASIL
251	CARVALHO,MOACYR	UNIV.DO ESTADO DO RIO DE JANEIRO	R.SAO FRANCISCO XAVIER,524-5o.ANDAR	20550-R.JANEIRO-RJ- BRASIL
252	CARVALHO FILHO,ARNALDO CARDIM	UNIV.DO EST.DE S.PAULO-ESC.POLITECNICA	AV.PROF.ALMEIDA PRADO-TRAV.2,271	05598-S.PAULO-SP- BRASIL
253	VOLLET,DIMAS ROBERTO	UNIV.DO EST.DE S.PAULO-IBA	FRANCISCO DEGNI,S/N - C.P.174	14800-ARARAQUARA-SP- BRASIL
254	CAMPITELI,VICENTE CONEY	UNIV.ESTADUAL DE PONTA GROSSA	PRACA SANTOS ANDRADE,S/N	84100-P.GROSSA-PR- BRASIL
255	PINHEIRO,ALCINA KOENOW	UNIV.FED.RJ-ESCOLA DE ENGENHARIA	R.MARQUES DO PARANA,128-COB.	22230-R.JANEIRO-RJ- BRASIL
256	ZAKON,ABRAHAM	UNIV.FED.RJ-ESCOLA DE QUIMICA	R.GENERAL CANABARRO,79-203	20271-R.JANEIRO-RJ- BRASIL
257	COSTA,DARY WERNECK	UNIV.FED.MS	CIDADE UNIVERSITARIA - CICET	79100-C.GRANDE-MS- BRASIL
258	PINTO,JOSE ANTONIO	UNIV.FED.SANTA MARIA	R.BENJAMIN CONSTANT,1096-CID.UNIVERS.	97050-S.MARIA-RS- BRASIL
259	OLIVEIRA,MARILDA BARRA	UNIV.FED.UBERLANDIA	AV.UNIVERSITARIA,S/N	38400-UBERLANDIA-MG- BRASIL
260	VOLKOV,VASIL	HIGHER INST.OF CHEMISTRY TECHNOLOGY	8 KLIMENT OHRIDSKI	1156-SOFIA-BULGARIA
261	WALDNER,ERWIN	MIRON INC.	2201 CREMAZIE EAST	H1Z 2C1-MONTREAL-QB- CANADA
262	FELDMAN,ROLF F.	NAT.RES.COUNCIL CANADA-INST.RES.CONST.	M-20 MONTREAL ROAD	K1A OR6-OTTAWA-ON- CANADA
263	LITVAN,GERARD	NAT.RES.COUNCIL CANADA-INST.RES.CONST.	M-20 MONTREAL ROAD	K1A OR6-OTTAWA-ON- CANADA
264	AITCIN,P.-C.	UNIV.DE SHERBROOKE-FAC.APPLIED SCI.	DEPT.CIVIL ENG.	J1K 2R1-SHERBROOKE-QB-CANADA
265	MINDESS,SIDNEY	UNIV.OF BRITISH COLUMBIA	DEPT.CIVIL ENG.	V6T 1W5-VANCOUVER-BC- CANADA
266	MACINNIS,CAMERON	UNIV.OF WINDSOR	401 SUNSET AVENUE	N9B 3P4-WINDSOR-ON- CANADA
267	CORNEJO,EDUARDO	CEMENTO MELON S.A.	PEDRO DE VALDIVIA 98	LA CALERA- CHILE
268	PEREZ,MARCELO UBILLA	CEMENTO POLPAICO S.A.	AMUNATEGUI,178-5o.PISO	SANTIAGO- CHILE
269	CUEVAS,ARNOLDO BUCAREY	CEMENTOS BIOBIO S.A.	AV.GRAN BRETANA,1725-93 C - CONCEPCION	TALCAHUANO-CHILE
270	KITTL,PABLO	UNIV.DE CHILE - IDIEM	CASILLA 1420	SANTIAGO- CHILE
271	MONDACA,JORGE MAURICIO OSSA	UNIV.DE CHILE - IDIEM	PLAZA ERCILLA 883	SANTIAGO- CHILE
272	VALENZUELA,PABLO CARRILLO	UNIV.DE CHILE - IDIEM	PLAZA ERCILLA 883	SANTIAGO- CHILE
273	CHEN,QUANDE	THE CHINESE SILICATE SOCIETY	BAI WAN ZHUANG	BEIJING -CHINA
274	HUANG,SHIYUAN	THE CHINESE SILICATE SOCIETY	BAI WAN ZHUANG	BEIJING -CHINA
275	SU,MUZHEN	THE CHINESE SILICATE SOCIETY	BAI WAN ZHUANG	BEIJING -CHINA
276	SUN,GUOKUANG	THE CHINESE SILICATE SOCIETY	BAI WAN ZHUANG	BEIJING -CHINA
277	TONG,DAMAO	THE CHINESE SILICATE SOCIETY	BAI WAN ZHUANG	BEIJING -CHINA
278	WU,ZHONGWEI	THE CHINESE SILICATE SOCIETY	BAI WAN ZHUANG	BEIJING -CHINA
279	YANG,NANRU	THE CHINESE SILICATE SOCIETY	BAI WAN ZHUANG	BEIJING -CHINA
280	YE,RUILUN	THE CHINESE SILICATE SOCIETY	BAI WAN ZHUANG	BEIJING -CHINA
281	CHEN,ZHI-YUAN	TONGJI UNIVERSITY	SHIPING ROAD,1239	200092-SHANGAI -CHINA
282	PING,LU	TONGJI UNIVERSITY	SHIPING ROAD,1239	200092-SHANGAI -CHINA
283	WEI,SHEN	TONGJI UNIVERSITY	SHIPING ROAD,1239	200092-SHANGAI -CHINA
284	LOU,ZONGHAN	ZHEJIANG UNIVERSITY	DEPT.OF MATERIALS SCI.& ENG.	HANGZHOU-CHINA
285	STAMARIA,FERNANDO ARTURO RODRIGUEZ	CEMENTOS DEL CARIBE S.A	VIA 40 - LAS FLORES	AA 2739-BARRANQUILLA-COLOMBIA
286	SUAZA,JAIME	CEMENTOS RIOCLARO S.A.	CRA 46-No.5611-TORREARGOS-P.14	7421-MEDELLIN- COLOMBIA
287	NOGUERA,JAIME COVILLA	CIA.COLOMBIANA DE CLINKER S.A.	MOMONAL	AA 3344-CARTAGENA- COLOMBIA
288	OROZCO,ORLANDO LAFAURIE	TOLTECEMENTO	APDO.AEREO 292	SINCELEJO-SUCRE- COLOMBIA
289	MAINIERI,ENRIQUE ALBERTO ACOSTA	CEMENTOS DEL PACIFICO S.A.	APDO.6559	SAN JOSE-COSTA RICA
290	ALMEBORG,JORN	AALBORG PORTLAND	RORDA SVEJ 44-P.O.BOX 165	9100-AALMORG-DENMARK
291	CHRISTENSEN,JENS TIM	AALBORG PORTLAND	RORDA SVEJ 44-P.O.BOX 165	9100-AALMORG-DENMARK
292	KNUDSEN,TORBEN	DANISH TECHNICAL UNIVERSITY	ANKER ENGELUNDSSVEJ	2800-LYNGBY-DENMARK
293	ENKEGAARD,TORBEN	F.L.SMIDTH & CO.A/S	77 VIGERSLEV ALLE	2500-VALBY-COPENHAGEN-DENMARK
294	FEDDERSEN,OLE FINN	F.L.SMIDTH & CO.A/S	77 VIGERSLEV ALLE	2500-VALBY-COPENHAGEN-DENMARK
295	JOHANSEN,VAGN	F.L.SMIDTH & CO.A/S	77 VIGERSLEV ALLE	2500-VALBY-COPENHAGEN-DENMARK
296	OSBAECK,BJARNE	F.L.SMIDTH & CO.A/S	77 VIGERSLEV ALLE	2500-VALBY-COPENHAGEN-DENMARK
297	IDORN,GUNNAR	GMIDORN CONSULT A/S	ROEJELSKAER 15	2840-HOLTE-DENMARK
298	POLAK,ELZBIETA	BIRKBECK COLLEGE	MALET STREET	WC1 7HX-LONDON-ENGLAND,U.K.
299	GUNSON,ALAN	BLUE CIRCLE INDUSTRIES PLC.	GROUP RESEARCH-305 LONDON ROAD	DA9 9JQ-GREENHITHE-ENGLAND,U.K.
300	MOIR,GRAEME K.	BLUE CIRCLE INDUSTRIES PLC.	GROUP RESEARCH-305 LONDON ROAD	DA9 9JQ-GREENHITHE-ENGLAND,U.K.

	NAME	COMPANY	ADRESS	ZIP-CITY-STATE-COUNTRY
301	BENSTED,JOHN	BRITISH PETROLEUM,INC.	RESEARCH CENTRE	TW16 7LN-SUNBURY-ENGLAND,U.K.
302	MATTHEWS,JOHN	BUILDING RESEARCH STATION	GARSTON	WD2 7JR-WATFORD-ENGLAND,U.K.
303	LEES,TIMOTHY	CEMENT AND CONCRETE ASSOCIATION	WEXHAM SPRINGS	SL3 6PL-SLOUGH BUCKS-ENGLAND,U.K.
304	POMEROY,CHARLES DUNCAN	CEMENT AND CONCRETE ASSOCIATION	WEXHAM SPRINGS	SL3 6PL-SLOUGH BUCKS-ENGLAND,U.K.
305	BALDIE,KEITH	CESB	CERL,KELVIN AVENUE	KT22 7SE-LEATHERHEAD-ENGLAND,U.K.
306	SCRIVENER,KAREN	IMPERIAL COLLEGE OF SCIENCE AND TECHN.	PRINCE CONSORT ROAD	SW7 EBP-LONDON-ENGLAND,U.K.
307	FORRESTER,JAMES	KING'S COLLEGE LONDON	12 MAYFLOWER WAY	HP9 1JE-BEACONSFIELD-ENGLAND,U.K.
308	RODGER,SALLY	OXFORD UNIVERSITY-DEPT.OF METTALURGY	PARKS ROAD	OX1 3PH-OXFORD-ENGLAND,U.K.
309	MILLS,PETER	PRIVATE INDIVIDUAL	30 SWINBURNE STREET	DERBY-ENGLAND,U.K.
310	JACKSON,PETER	THE RUGBY PORTLAND CEMENT	CENTRAL LABORATORY-PARKFIELD	CV21 1QJ-RUGBY-ENGLAND,U.K.
311	CABRERA,JOSEPH G.	THE UNIVERSITY OF LEEDS	DEPT.OF CIVIL ENGINEERING	LS2 9JT-LEEDS-ENGLAND,U.K.
312	BANFILL,PHILLIP F.G.	THE UNIVERSITY OF LIVERPOOL	DEPT.OF BUILDING ENGINEERING	L69 3BX-LIVERPOOL-ENGLAND,U.K.
313	BAILEY,JOHN	THE UNIVERSITY OF SHEFFIELD	ELMFIELD NORTHUMBERLAND ROAD	S10 2TZ-SHEFFIELD-ENGLAND,U.K.
314	ERIKSSON,BO-ERIK	LOHJA CORPORATION		08700-VIRKKALA-FINLAND
315	PALM,CARL-OLOF	OY PARTEK AB	DEVELOPMENT CENTRE	21600-PARGAS-FINLAND
316	TALLING,BOB	OY PARTEK AB	DEVELOPMENT CENTRE	21600-PARGAS-FINLAND
317	NIEMINEN,PERTTI	TAMPERE UNIVERSITY OF TECHNOLOGY	P.O.BOX 527	33101-TAMPERE-FINLAND
318	COLLIS,HENRY	CEMBUREAU	2 RUE SAINT-CHARLES	75015-PARIS-FRANCE
319	DUTRON,PIERRE	CEMBUREAU	2 RUE SAINT-CHARLES	75015-PARIS-FRANCE
320	SOUKATCHOFF,PASCAL	CENTRE DE RECHERCHES DE PONT	A.MOUSSON-BP 28	54700-PONT A MOUSSON-FRANCE
321	BOMBLED,JEAN-PAUL	CERILH	23 RUE DE CRONSTADT	75015-PARIS-FRANCE
322	FAUVEAU,PIERRE	CERILH	23 RUE DE CRONSTADT	75015-PARIS-FRANCE
323	REGOURD,MICHELINE	CERILH	23 RUE DE CRONSTADT	75015-PARIS-FRANCE
324	LOVICHI,JEAN-PIERRE	CIMENTS LAFARGE FRANCE	30 COURS PIERRE PUGET	13006-MARSEILLE-FRANCE
325	CASTANET,ROBERT	CNRS	3 RUE THIEUX	13008-MARSEILLE-FRANCE
326	BERNAUDAT,FRANCOIS	COMMISSARIAT A L'ENERGIE ATOMIQUE	60-68 AV.DU GENERAL LECLERC-B.P.6	92265-FONTENAY-AUX-ROSES-FRANCE
327	LAMEILLE,JEAN-MICHEL	COMMISSARIAT A L'ENERGIE ATOMIQUE	60-68 AV.DU GENERAL LECLERC-B.P.6	92265-FONTENAY-AUX-ROSES-FRANCE
328	REVERTEGAT,ELIANE	COMMISSARIAT A L'ENERGIE ATOMIQUE	LABO.BETONS-BAT.158-SACLAY	91191-GIF-SUR-IVETTE-FRANCE
329	OBERSTE-PADTBERG,RUDIGER	DOWELL SCHLUMBERGER	B.P.90	42003-SAINT-ETIENNE-FRANCE
330	PARCEVAUX,PHILIPPE	DOWELL SCHLUMBERGER	B.P.90	42003-SAINT-ETIENNE-FRANCE
331	GUILHOT,BERNARD	ECOLE DES MINES	158 COURS FAURIEL	42100-SAINT-ETIENNE-FRANCE
332	SOUSTELLE,MICHEL	ECOLE DES MINES	158 COURS FAURIEL	42023-SAINT-ETIENNE-FRANCE
333	BARRET,PIERRE	FACULTE DES SCIENCES MIRANDE	B.P.138	21004-DIJON-FRANCE
334	AMBROISE,JEAN	INSA	20,RUE ALBERT EINSTEIN	69621-VILLE URBANNE-FRANCE
335	PERRA,JEAN	INSA	20,RUE ALBERT EINSTEIN	69621-VILLE URBANNE-FRANCE
336	GRANDET,JACQUES	INSA-LABORATORIE DE GENIE CICIL	AVENUE DE RANGUEIL	31077-TOULOUSE-FRANCE
337	OLLIVIER,JEAN-PIERRE	INSA-LABORATORIE DE GENIE CICIL	AVENUE DE RANGUEIL	31077-TOULOUSE-FRANCE
338	DRON,ROGER	LABORATORY CENTRAL PONTS & CHAUSSEES	58 BD.LEFEBVRE-CEDEX 15	75732-PARIS-FRANCE
339	RIVES,JEAN	LAFARGE COPPEE	28,RUE EMILE MENIER	75116-PARIS-FRANCE
340	RIVOIRE,CLAUDE	LAFARGE COPPEE	28,RUE EMILE MENIER	75116-PARIS-FRANCE
341	SANTOS,FERNANDO M.OLIVEIRA	LAFARGE COPPEE-DIV.INTERNATIONAL	28,RUE EMILE MENIER	75116-PARIS-FRANCE
342	BARON,JACQUES	LAFARGE COPPEE RECHERCHE	B.P.8	07220-VIVIERS-SUR-RHONE-FRANCE
343	BORREIL,ANDRE	LAFARGE COPPEE RECHERCHE	B.P.8	07220-VIVIERS-SUR-RHONE-FRANCE
344	CHAPPUIS,JACQUES	LAFARGE COPPEE RECHERCHE	B.P.8	07220-VIVIERS-SUR-RHONE-FRANCE
345	SORRENTINO,DANIELLE	LAFARGE COPPEE RECHERCHE	B.P.8	07220-VIVIERS-SUR-RHONE-FRANCE
346	SORRENTINO,FRANCOIS	LAFARGE COPPEE RECHERCHE	B.P.8	07220-VIVIERS-SUR-RHONE-FRANCE
347	HAWTHORN,FRANCK	SOCIETE DES CIMENTS FRANCAIS	TOUR GENERALE 5,PLACE DE LA PYRAMIDE	92088-PARIS LA DEFENSE-FRANCE
348	MARIOT,RENE JEAN	SOCIETE DES CIMENTS FRANCAIS	TOUR GENERALE 5,PLACE DE LA PYRAMIDE	92088-PARIS LA DEFENSE-FRANCE
349	MERIC,JEAN-PAUL	SOCIETE DES CIMENTS FRANCAIS	TOUR GENERALE 5,PLACE DE LA PYRAMIDE	92088-PARIS LA DEFENSE-FRANCE
350	RICHER,FRANCOIS	SOCIETE DES CIMENTS FRANCAIS	CEREG-B.P.01	78930-GUERVILLE-FRANCE
351	VERNET,CHRISTIAN	SOCIETE DES CIMENTS FRANCAIS	CEREG-B.P.01	78930-GUERVILLE-FRANCE
352	VON EDW,MARCEL	SOCIETE DES CIMENTS FRANCAIS	TOUR GENERALE 5,PLACE DE LA PYRAMIDE	92088-PARIS LA DEFENSE-FRANCE
353	FRESSY,MICHEL	VICAT	TOUR GAN - CEDEX 13	92082-PARIS-FRANCE
354	GISAS,KOSTAS	HERACLES G.C.C.	S.VENIZELOU,49-51	14123-ATHENS-GREECE
355	MARINOS,IOANNIS	HERACLES G.C.C.	S.VENIZELOU,49-51	14123-ATHENS-GREECE
356	VASILOUDIS,PASCHALIS	HERACLES G.C.C.	S.VENIZELOU,49-51	14123-ATHENS-GREECE
357	HALSTEAD,PHILIP E.	MATERIALS MEASUREMENT LTD.	GPO BOX 4194	HONG KONG-HONG KONG
358	KOLTAI,IMRE	NIKEX-DEPARTMENT 32	MESZAROS-UTCA 48-54	BUDAFEST-HUNGARY
359	TALABER,JOZSEF	RESEARCH AND DES.INST.SILICATE IND.	BECSI UT 126-128	H-1300-BUDAFEST-HUNGARY
360	TAMAS,FERENC	UNIVERSITY OF VESZPREM	P.O.BOX 158	H-8201-VESZPREM-HUNGARY
361	CHATTERJEE,ANJAN KUMAR	ASSOCIATED CEMENT COMPANIES LTD.	CENTRAL RESEARCH STATION	400604-THANE-SHARTRI MARG-INDIA
362	NARANG,KARTAR CHAND	DALMIA CEMENT(BHARAT)LIMITED	HANSALAYA,15-BHARAKHAMBA RD.-11/12 FLS.	110001-NEW DELHI-INDIA
363	DAS,KESHAB	DEVELOPMENT CONSULTANTS P.LTD.	24 B,PARK STREET	700016-CALCUTTA-INDIA
364	IRANI,DINSHAW BOMANJI	NAT.COUNCIL FOR CEMENT & BUILDING MAT.	M-10 SOUTH EXTENSION PART II	110049-NEW DELHI-INDIA
365	KANURI,HARINADHA BABU	NAT.COUNCIL FOR CEMENT & BUILDING MAT.	M-10 SOUTH EXTENSION PART II	110049-NEW DELHI-INDIA
366	LAXMI,SHOBHAY	NAT.COUNCIL FOR CEMENT & BUILDING MAT.	M-10 SOUTH EXTENSION PART II	110049-NEW DELHI-INDIA
367	RAINA,SHIBAN J.	NAT.COUNCIL FOR CEMENT & BUILDING MAT.	M-10 SOUTH EXTENSION PART II	110049-NEW DELHI-INDIA
368	VIVESVARAYA,MOSAGRAHAR C.	NAT.COUNCIL FOR CEMENT & BUILDING MAT.	M-10 SOUTH EXTENSION PART II	110049-NEW DELHI-INDIA
369	AHSAN,MANZOOR	ORISSA CEMENT LIMITED	B 45/47 CONNAUGHT PLACE-SHIV MAHAL	110001-NEW DELHI-INDIA
370	PANDAKASALA,JACOB ALEXANDER	THE TRAVANCORE CEMENTS LTD.	NATTAKOM KOTTAYAM KERALA	686013-KOTTAYAM-INDIA
371	SOROKA,ITZHAK	TECHNION	TECHNION CITY	32000-HAIFA-ISRAEL
372	AUSTONI,SERGIO	CEMENTI TICINO CETI SPA	VIA BONGIASCA	21020-COMABBIO-ITALY
373	PIAZZA,EUGENIO	CEMENTI VICTORIA	VIA MONTESANTO 13	13039-TRINO VERCELLESE-ITALY
374	FRIGIONE,GIUSEPPE	CEMENTIR	VIA COROGLIO 71	80124-NAPLES-ITALY
375	BUZZI,SANDRO	FRATELLI BUZZI CEMENTI SPA	CORSO GIOVANE ITALIA 39	15033-CASALE MONFERRATO-ITALY

	NAME	COMPANY	ADRESS	ZIP-CITY-STATE-COUNTRY
376	BUCCHI,RENATO	ITALCEMENTI SPA	VIA G.CAMOZZI 124	24100-BERGAMO-ITALY
377	COSTA,UMBERTO	ITALCEMENTI SPA	VIA G.CAMOZZI 124	24100-BERGAMO-ITALY
378	MASSAZZA,FRANCO	ITALCEMENTI SPA	VIA G.CAMOZZI 124	24100-BERGAMO-ITALY
379	ORTOLANI,VITTORIO	ITALCEMENTI SPA	VIA G.CAMOZZI 124	24100-BERGAMO-ITALY
380	TOGNON,GIAMPIETRO	ITALCEMENTI SPA	VIA G.CAMOZZI 124	24100-BERGAMO-ITALY
381	BIAGINI,STEFANO	MAC SPA	VIA VICINALE CORTI 21	31100-TREVISO-ITALY
382	COLLEPARDI,MARIO	MAC SPA	VIA VICINALE CORTI 21	31100-TREVISO-ITALY
383	GUELLA,SILVIO MAURO	MAC SPA	VIA VICINALE CORTI 21	31100-TREVISO-ITALY
384	INDELICATO,FERDINANDO	POLITECNICO DI TORINO-DIP.DI ING.STRUT.	CORSO DUCA DEGLI ABRUZZI 24	10129-TORINO- ITALY
385	LUCCO-BORLERA,MARIA	POLITECNICO DI TORINO-DIP.DI ING.STRUT.	CORSO DUCA DEGLI ABRUZZI 24	10129-TORINO- ITALY
386	CUSSINO,LUCIANO	UNICEM SPA	VIA CARLO MARENCO 25	10126-TORINO- ITALY
387	NEGRO,ALFREDO	UNICEM SPA	VIA CARLO MARENCO 25	10126-TORINO- ITALY
388	AIELLO,ROSARIO	UNIV.DELLA CALABRIA	ARCAVACATA DI RENDE	87030-COSENZA-ITALY
389	MONOSI,SAVERIA	UNIV.DI ANCONA-DIP.SCIENZE DEI MATER.	VIA DELLE BRESCE BIANCHE	60131-ANCONA- ITALY
390	MORICONI,GIACOMO	UNIV.DI ANCONA-DIP.SCIENZE DEI MATER.	VIA DELLE BRESCE BIANCHE	60131-ANCONA- ITALY
391	PAURI,MARCO	UNIV.DI ANCONA-DIP.SCIENZE DEI MATER.	VIA DELLE BRESCE BIANCHE	60131-ANCONA- ITALY
392	AMICARELLI,VINCENZO	UNIV.DI BARI-FACOLTA DI INGEGNERIA	VIA REDAVID 200	70124-BARI- ITALY
393	MASSIDDA,LUIGI	UNIV.DI CAGLIARI	PIAZZA D'ARMI	09100-CAGLIARI-ITALY
394	SANNA,ULRICO	UNIV.DI CAGLIARI	PIAZZA D'ARMI	09100-CAGLIARI-ITALY
395	MARCHESE,BERNARDO	UNIV.DI NAPOLI-DIP.ING.DEI MATERIALI	PIAZZALE TECCHIO	80125-NAPOLI- ITALY
396	MASCOLO,GIUSEPPE	UNIV.DI NAPOLI-DIP.ING.DEI MATERIALI	PIAZZALE TECCHIO	80125-NAPOLI- ITALY
397	SANTORO,LUCIANO	UNIV.DI NAPOLI	VIA MEZZOCANNONE 4	80134-NAPOLI- ITALY
398	SERSALE,RICCARDO	UNIV.DI NAPOLI-DIP.ING.DEI MATERIALI	PIAZZALE TECCHIO	80125-NAPOLI- ITALY
399	VALENTI,GIAN LORENZO	UNIV.DI NAPOLI	PIAZZALE TECCHIO	80125-NAPOLI- ITALY
400	FESTA,DINA	UNIV.DI PADOVA	VIA MARZOLO 9	35100-PADOVA- ITALY
401	SCARINCI,GIOVANNI	UNIV.DI PADOVA	VIA MARZOLO 9	35100-PADOVA- ITALY
402	CIGNA,RANIERI	UNIV.DI ROMA-DIP.ICMMPM	VIA EUDOSSIANA 18	00184-ROMA- ITALY
403	TURRIZIANI,RENATO	UNIV.DI ROMA-DIP.ICMMPM	VIA EUDOSSIANA 18	00184-ROMA- ITALY
404	MCLEOD,MAURICE	CARIBBEAN CEMENT COMPANY	ROCKFORT	KINGSTON-JAMAICA
405	FUKAYA,YASUBUMI	CHICHIBU CEMENT CO.LTD.	2-1-1,TSUKUMI-CHO	360-KUMAGAYA-SHI-JAPAN
406	TAKANO,YUKIO	CHICHIBU CEMENT CO.LTD.	2-1-1,TSUKUMI-CHO	360-KUMAGAYA-SHI-JAPAN
407	KOIBUCHI,KIYOSHI	DAICHI CEMENT CO.LTD.	1-1,ASANO-CHO,KAWASAKI	KAWASAKI-JAPAN
408	NAKAGAWA,KOJI	DENKI KAGAKU KOGYO CO.LTD.	AOMI-CHO,NISHIKUBIKI-GUN	949-03-NIIGATA-JAPAN
409	HARA,NAOMICHI	GOVERNMENT INDUSTRIAL	RESEARCH INSTITUTE,KYUSHU	841-TOSU-SAGA-KEN-JAPAN
410	HASABA,SHIGEMASA	ISHIKAWA TECHNICAL COLLEGE	TUBATA,KANOKU,	920-ISHIKAWA-JAPAN
411	KAWAMURA,MITSUNORI	KANAZAWA UNIVERSITY-FAC.OF ENGINEERING	40-20,KODATSUNO 2 -CHOME	920-KANAZAWA-JAPAN
412	TORII,KAZUYUKI	KANAZAWA UNIVERSITY-FAC.OF ENGINEERING	40-20,KODATSUNO 2 -CHOME	920-KANAZAWA-JAPAN
413	ASAKURA,ETSURO	MITSUBISHI MINING & CEMENT CO.	2270 YOSOKE-CHO,CHICHIBU-GUN	SAITAMA-KEN-JAPAN
414	MAKI,IWAO	NAGOYA INST.OF TECHNOLOGY	GORISO-CHO,SHOWA-KU	466-NAGOYA-JAPAN
415	MITSUDA,TAKESHI	NAGOYA INST.OF TECHNOLOGY-CERAMICS LAB.	ASAHIGAOKA,TAJIMI	507-GIFU-KEN-JAPAN
416	YAMAZAKI,YUKINORI	NIHON CEMENT CO.LTD.	2-23-1,KIYOSUMI,KOTO-KU	TOKYO-JAPAN
417	AOKI,SHIGEKI	NIHON UNIVERSITY	1-8-14,SURUGA-DAI,KANDA	101- TOKYO-JAPAN
418	TSUYUKI,NAOMITSU	NIHON UNIVERSITY	7-24-1,NARASHINODAI	274-FUNABASHI-SHI-JAPAN
419	TSUJIMATSU,HIROSHI	NIPPON KOKAN K.K.	1-1-2,MARUNOUCHI,CHIYODA-KU	TOKYO-JAPAN
420	HANEHARA,SHUNSUKE	ONODA CEMENT CO.LTD.	1-1-7,TOYOSU,KOTO-KU	135- TOKYO-JAPAN
421	TAKEMOTO,KUNIHIRO	ONODA CEMENT CO.LTD.	1-1-7,TOYOSU,KOTO-KU	135- TOKYO-JAPAN
422	UCHIDA,SHUNICHIRO	ONODA CEMENT CO.LTD.	1-1-7,TOYOSU,KOTO-KU	135- TOKYO-JAPAN
423	UCHIKAWA,HIROSHI	ONODA CEMENT CO.LTD.	1-1-7,TOYOSU,KOTO-KU	135- TOKYO-JAPAN
424	KOBAYASHI,SHIGEHIRO	OSAKA CEMENT CO.LTD.	7-1-49,MINAMI OKAJIMA,TAISHO-KU	OSAKA-JAPAN
425	INOKAWA,HISASHI	SUMITOMO CEMENT CO.LTD.	585,TOYOTOMI-CHO,FUNABASHI	CHIBA-JAPAN
426	KATO,OSAMU	THE CEMENT ASSOCIATION OF JAPAN	17-33-4,TOSHIMA,KITA-KU	TOKYO-JAPAN
427	USHIYAMA,HIROTAKA	TOKUYAMA SODA CO.LTD.	1-1,MIKAGE-CHO	TOKUYAMA-JAPAN
428	GOTO,SEICHI	TOKYO INSTITUTE OF TECHNOLOGY	2-12-1,OOKAYAMA-MEGURO	152- TOKYO-JAPAN
429	NISHIMOTO,NOBUYOSHI	UBE INDUSTRIES,LTD.	1-12-32,NISHIHON-MACHI	755- UBE- JAPAN
430	IKEDA,KO	YAMAGUCHI UNIVERSITY	TOKIWADAI 2557	755- UBE- JAPAN
431	IWABUCHI,TOSHITSUGU	YAMASO CHEMICAL CO.LTD.	25-5-2,CHOME HATCHOBORI CHUO-KU	104- TOKYO-JAPAN
432	DOUMET,JOSEPH	CIMENTERIE NATIONALE S.A.L.	B.P.11	5101- BEYROUTH-LIBAN
433	ULIBARRI,RAMON POO	CEMENTOS MEXICANOS	APDO.POSTAL 392	64520- MONTERREY-MEXICO
434	REGGAD,AHMED	CIMENTERIE DE L'ORIENTAL	B.P.44	OUJDA-MOROCCO
435	AHMOUZ,BELKACEM	ASMENT DE TEMARA	AIN ATTIG	TEMARA-MOROCCO
436	VAN KLAVEREN,WILLEM	CEMENTIFABRIEK(CEMIJ)BV	POST BOX 462	1970-AL/IJMUIDEN-NETHERLANDS
437	DE JONG,JAN	ENCI	LAGE KANAALDIJK,115-P.O.BOX 1	6200-AA/MAASTRICHT-NETHERLANDS
438	MELAND,INGER	CEMENT AND CONCRETE INSTITUTE	SINTEF	7034-TRONDHEIM-NORWAY
439	LINDSTAD,JORN	NORCEM A/S	HAAKON 7,GT.2	0114-OSLO 1-NORWAY
440	STOLTENBERG-HANSSON,ERIK	NORCEM A/S		3950-BREVIK-NORWAY
441	GJORV,ODD E.	UNIVERSITY OF TRONDHEIM NTH		7034-TRONDHEIM-NORWAY
442	PITERSON,RAMON ABRAHAM BALID	CEMENTO PANAMA S.A.	P.O.BOX 1755	ZONA 1-PANAMA-PANAMA
443	QUINTERO,GUSTAVO	CEMENTO PANAMA S.A.	P.O.BOX 1755	ZONA 1-PANAMA-PANAMA
444	BAIBE,ISABELINO E.GAMARRA	INDUSTRIA NACIONAL DEL CEMENTO	GENERAL SANTOS-6o.PISO	ASUNCION-PARAGUAY
445	PALACIO,HIGINIO VILLALBA	INDUSTRIA NACIONAL DEL CEMENTO	GENERAL SANTOS-6o.PISO	ASUNCION-PARAGUAY
446	DUARTE,JOSE DOMINGO CARRERAS	ITAIPU BINACIONAL	PARAGUAY-BRASIL	PARAGUAY
447	VERA,CARMELO ACOSTA	ITAIPU BINACIONAL	PARAGUAY-BRASIL	PARAGUAY
448	GONZALES DE LA COTERA,MANUEL ALFONSO	ASOC.DE PRODUCTORES DE CEMENTO	AV.CARLOS VILLARAN,504,STA.CATALINA	LIMA-PERU
449	ARATA,EDUARDO RODRIGUEZ	CEMENTOS LIMA S.A.	LAS BEGONIAS,475-OF.234	LIMA-PERU
450	ARDILES,LUIS ENRIQUE SALINAS	CEMENTOS LIMA S.A.	LAS BEGONIAS,475-OF.234	LIMA-PERU

	NAME	COMPANY	ADRESS	ZIP-CITY-STATE-COUNTRY
451	KURDOWSKI,WIESLAW	AKADEMIA GORNICZO-HUTNICZA	AL.MICKIEWICZA 30	30059-KRAKOW-POLAND
452	GOMES,ALVARO NUNES	CIMPOR-CIMENTOS PORTUGAL EP	R.ALEXANDRE HERCULANO,35	1200-LISBOA-PORTUGAL
453	OLIVEIRA,MARIO MARQUES	CIMPOR-CIMENTOS PORTUGAL EP	R.ALEXANDRE HERCULANO,35	1200-LISBOA-PORTUGAL
454	REIS,MARIA OLINDA BRAGA	LABORATORIO NAC.DE ENGENHARIA CIVIL	AV.BRASIL,101	1799-LISBOA-PORTUGAL
455	AL-NOURY,SOLIMAN	KING ABDULAZIZ UNIVERSITY	P.O.BOX 9027	21413-JEDDAH-SAUDI ARABIA
456	AFSHAR,ALI BEHROOZ	HERIOT-WATT UNIVERSITY	RICCARTON CAMPUS	EH10 4ER-EDINBURGH-SCOTLAND,U.K.
457	MCCARTER,WILLIAM JOHN	HERIOT-WATT UNIVERSITY	RICCARTON CAMPUS	EH10 4ER-EDINBURGH-SCOTLAND,U.K.
458	BARTOS,PETER	PAISLEY COLLEGE	HIGH STREET	PA1 2BE-PAISLEY-SCOTLAND,U.K.
459	GLASSER,FREDRIK PAUL	UNIVERSITY OF ABERDEEN	MESTON WALK	AB9-2UE-OLD ABERDEEN,SCOTLAND,U.K.
460	TAYLOR,HARRY F.W.	UNIVERSITY OF ABERDEEN	DEPT.OF CHEMISTRY,MESTON WALK	AB9-2UE-OLD ABERDEEN,SCOTLAN
461	CREMIEUX,PIERRE	SOCOCIM INDUSTRIES	B.P.29	RUFISQUE-SENEGAL
462	KELLY,R.J.	BLUE CIRCLE LIMITED	P.O.BOX 2484	2000-JOHANNESBURG-SOUTH AFRICA
463	OBERHOLSTER,BERTIE	NATIONAL BUILDING RES.BUILDING	P.O.BOX 395	0001-PRETORIA-SOUTH AFRICA
464	CHOI,SANG-HEUL	HANYIANG UNIVERSITY	17 HAENGDANG-DONG,SUNGDONG-KU	133-SEOUL-SOUTH KOREA
465	HAN,KI-SUNG	INHA UNIVERSITY	253 YONGHYUN-DONG,NAM-KU	160-INCHON-SOUTH KOREA
466	SEO,IL-YOUNG	SSANG-YONG RESEARCH CENTER	YUSEONG-P.O.BOX 12	300-32-DAE-JEON-SOUTH KOREA
467	NAM,KEE DONG	TONG YANG CEMENT CORPORATION	60 DORYOM-DONG CHONGRO-KU	110-SEOUL-SOUTH KOREA
468	GOMA I GINESTA,FERRAN	ASLAND CATALUNIA S.A.	CORSEGA 325	08025-BARCELONA-SPAIN
469	CORONAS,JUAN RAMON BARRAGANO	ASLAND-CIYD	VILLALUENGA DE LA SAGRA	TOLEDO-SPAIN
470	ALONSO,JULIO PEREZ	ASLAND S.A.	ORENSE 81	28020-MADRID-SPAIN
471	REY,PEDRO	ASLAND S.A.	CARRETERA ALMADEN,KM 1	14007-CORDOBA-SPAIN
472	CASTRO,NESTOR	AUXILIAR DE LA CONSTRUCCION	DIAGONAL 534	08006-BARCELONA-SPAIN
473	MURTRA,ISIDORO	AUXILIAR DE LA CONSTRUCCION	DIAGONAL 534	08006-BARCELONA-SPAIN
474	VILA ,VICTORIANO JOSE GONZALEZ	CEMENTOS ATLANTICO S.A.	APARTADO 65	ALCALA DE GUADAIRA-SPAIN
475	FERNANDEZ,MARCOS	CEMENTOS COSMOS S.A.	OURAL	LUGO-SPAIN
476	LONGARELA,ANGEL	CEMENTOS COSMOS S.A.	LUCHANA,23-4o.PISO	28010-MADRID-SPAIN
477	MARTINEZ,ARTURO	CEMENTOS COSMOS S.A.	OURAL	LUGO-SPAIN
478	CEBRIAN,JOSE LUIS	CEMENTOS MONTORIA	VENTA DE BANOS	VALENCIA-SPAIN
479	MONTRAVERA,JUAN PUIG	CEMENTOS MOLINS S.A.	PASEO DE GRACIA,92	BACELONA-SPAIN
480	CARMONA,JOSE MARIA SARDI	CEMENTOS MORATA DE JALON S.A.	PASEO MARI AGUSTIN,4-6	50004-ZARAGOZA-SPAIN
481	HUARTE,GABRIEL	CEMENTOS PORTLAND S.A.	ESTELLA 6,APARTADO 107	31080-PAMPLONA-SPAIN
482	FRADERA,ENRIQUE	CEMENTOS UNILAND S.A.	CORSEGA 299	08008-BARCELONA-SPAIN
483	FERRANDO,JOAQUIM	CIA.VALENCIANA DE CEMENTOS PORTLAND	COLON 6B	46004-VALENCIA-SPAIN
484	CALLEJA,JOSE	IECA-OFICEMEN	VELAZQUEZ,23	28001-MADRID-SPAIN
485	ALONSO,MARIA CRUZ ALONSO	INSTITUTO EDUARDO TORROJA	SERRANO GALVACHE S/N.	28033-MADRID-SPAIN
486	ANDRADE,MARIA DEL CARMEN	INSTITUTO EDUARDO TORROJA	SERRANO GALVACHE S/N.	28033-MADRID-SPAIN
487	BLANCO-VARELA,MARIA TERESA	INSTITUTO EDUARDO TORROJA	SERRANO GALVACHE S/N.	28033-MADRID-SPAIN
488	DE LUXAN,MARIA PILAR	INSTITUTO EDUARDO TORROJA	SERRANO GALVACHE S/N.	28033-MADRID-SPAIN
489	GASPAR-TEBAR,DEMETRIO	INSTITUTO EDUARDO TORROJA	SERRANO GALVACHE S/N.	28033-MADRID-SPAIN
490	SORIA,FRANCISCO	INSTITUTO EDUARDO TORROJA	SERRANO GALVACHE S/N.	28033-MADRID-SPAIN
491	TRIVINO,FERNANDO	INSTITUTO EDUARDO TORROJA	SERRANO GALVACHE S/N.	28033-MADRID-SPAIN
492	VAZQUEZ-MORENO,TOMAS	INSTITUTO EDUARDO TORROJA	SERRANO GALVACHE S/N.	28033-MADRID-SPAIN
493	CORONINA,JORGE	L.A.C. S.A.	APARTADO 56-S.FELIU LLOBREGAT	SARCELONA-SPAIN
494	GIBERT,SANTIAGO	L.A.C. S.A.	APARTADO 56-S.FELIU LLOBREGAT	BARCELONA-SPAIN
495	BRAVO,FRANCISCO	SOCIEDAD FINANCERA Y MINERA	C.TOMAS HEREDIA,27	29001-MALAGA-SPAIN
496	MANCHON,JOSE LUIS MARTINEZ	S.A.E.DE CEMENTOS PORTLAND		45220-YELES(TOLEDO)-SPAIN
497	RUDENIUS,ARNE	ABETONG-SABEMA	BOX 24	VAEXJOE-SWEDEN
498	WARRIS,BIRGER	CEMENTA AB-RESEARCH AND DEVELOPMENT	P.O.BOX 144	S-182 12-DANDERYD-SWEDEN
499	NAREDI,ROBERT	CEMCON	HYLLTORPSGATAN 6	S-216 16-MALMO-SWEDEN
500	CHANDRA,SATISH	CHALMERS UNIVERSITY OF TECHNOLOGY	SVEN HULTINSGATAN 8	S-412 96-GOTHENBURG-SWEDEN
501	NILSSON,LARS-OLOF	CHALMERS UNIVERSITY OF TECHNOLOGY	DIVISION OF BUILDING MATERIALS	S-412 96-GOTHENBURG-SWEDEN
502	HANNAWAYYA,FRANCISA	HANNAWAYYA S.LABORATORY	HUNDHAMRAVAGEN 7-NORSBORY	+ 753 -STOCKOLM-SWEDEN
503	PETERSON,OLOF	LUND INST.OF TECHN.-DIV.OF BUILD.MAT.	P.O.BOX 118	S-221 00-LUND-SWEDEN
504	KLINGSTEDT,GUNNAR	SWEDISH CEMENT & CONCRETE	RESEARCH INSTITUTE	S-100 44-STOCKHOLM-SWEDEN
505	PICCOLI,MARCO BERETTA	CEMENTIA PLANUNGS AG	NUESCHELERSTRSSE 45	CH-8001-ZURICH-SWITZERLAND
506	PETER,GUSTAV	ETH	INSTITUTE BAUSTOFFE	-ZURICH-SWITZERLAND
507	BRAUN,HANS	HOLDERBANK MANAGEMENT & CONSULTING		CH-5113-HOLDERBANK-SWITZERLAND
508	GEBAUER,JURAJ	HOLDERBANK MANAGEMENT & CONSULTING		CH-5113-HOLDERBANK-SWITZERLAND
509	SCHRAEMLI,WERNER	HOLDERBANK MANAGEMENT & CONSULTING		CH-5113-HOLDERBANK-SWITZERLAND
510	KOELLIKER,EMIL	INSTITUTE TECH.RESEARCH	SWISS CEMENT INDUSTRY	CH-5103-WILDEGG-SWITZERLAND
511	LAUBER,JOSEF	PORTLAND CEMENT-WERK	WUERENLINGEN-SIGGENTHAL	CH-5301-ST.SIGGENTHAL-SWITZERLAND
512	BRUNNER,PAUL	VIGIER CEMENT LTD.		CH-4708-LUTERBACH-SWITZERLAND
513	SINGH,RAMJATTAN	TRINIDAD CEMENT LTD.	SOUTHERN MAIN ROAD-CLAXTON BAY	SAN FERNANDO-TRINIDAD & TOBAGO
514	TONAK,TULIN	CEMENT MANUFACT.ASSOC.-CRDC	P.O.BOX 2 - BAKANLIKAR	TR 06582-ANKARA-TURKEY
515	BRUSCHERA,JORGE	ANCAP	C.C.1090	MONTEVIDEO-URUGUAY
516	SUAREZ,JOSE	ANCAP	C.C.1090	MONTEVIDEO-URUGUAY
517	PHILLED,ROBERT	CONSULTING ENGINEER	7420 ANNANWOOD COURT	22003-ANNANDALE-VA-U.S.A.
518	MAC DOWELL,JOHN F.	CORNING GLASS WORKS	SULLIVAN PARK FR-5	14831-CORNING-NY-U.S.A.
519	COOK LONNIE	DAVENPORT CEMENT COMPANY	P.O.BOX 4049	52808-DAVENPORT-IA-U.S.A.
520	PATZIAS,TERRY	DUNDEE CEMENT CO.	P.O.BOX 122	48131-DUNDEE-MI-U.S.A.
521	KOLAN,ANDREW	ENERGY SERVICES,INC.	205 PINE AVENUE	21146-SAVERNA PK-MD-U.S.A.
522	GUITTON,ETIENNE	GENERAL PORTLAND,INC.	NORTH CENTRAL PLAZA III,SUITE 1700	75248-DALLAS-TX-U.S.A.
523	ROWE,WALT	GENERAL PORTLAND,INC.	3333 FORT WORTH AVENUE	75211-DALLAS-TX-U.S.A.
524	GEORGE,CHARLES	LAFARGE FONDU INTERNATIONAL	18 KOGER EXECUTIVE CENTER	23502-NORFOLK-VA-U.S.A.
525	MOORE,CLYDE W.	LONE STAR INDUSTRIES INC.	515 WEST GREENS ROAD	77067-HOUSTON-TX-U.S.A.

	NAME	COMPANY	ADRESS	ZIP-CITY-STATE-COUNTRY
526	WILLIAMS,CRAIG	MASTER BUILDERS	23700 CHAGRIN BLVD.	44022-CLEVELAND-OH-U.S.A.
527	FROHNSDORFF,GEOFFREY	NATIONAL BUREAU OF STANDARDS	BUILDING 226,ROOM B-368	20899-GAITHERSBURG-MD-U.S.A.
528	DAUGHERTHY,KENNETH	NORTH TEXAS STATE UNIVERSITY	DEPT.OF CHEMISTRY	76203-DENTON-TX-U.S.A.
529	BHATTY,MUHAMMAD	PORTLAND CEMENT ASSOCIATION	5420 OLD ORCHARD ROAD	60648-SKOKIE-IL-U.S.A.
530	DIAMOND,SIDNEY	PURDUE UNIVERSITY	SCHOOL OF CIVIL ENGINEERING	47906-WEST LAFAYETTE-LA-U.S.A.
531	KLEMM,WALDEMAR	SOUTHWESTERN PORTLAND CEMENT CO.	P.O.BOX 937	93392-VICTORVILLE-CA-U.S.A.
532	GRUTZECK,MICHAEL	THE PENNSYLVANIA STATE UNIVERSITY	104 MATERIALS RESEARCH LABORATORY	16802-UNIVERSITY PARK-PA-U.S.A.
533	ROY,DELLA M.	THE PENNSYLVANIA STATE UNIVERSITY	217 MATERIALS RESEARCH LABORATORY	16802-UNIVERSITY PARK-PA-U.S.A.
534	SULLIVAN,PATRICK	UNION CARBIDE CORP.	P.O.BOX 8361	25303-SUTH CHARLESTON-U.S.A.
535	MEHTA,POVINDAR K.	UNIV.OF CALIFORNIA-CIVIL ENG.DEPT.	723 DAVIS HALL	94720-BERKELEY-CA-U.S.A.
536	BUCK,ALAN D.	U.S.CORPS OF ENGINEERS	P.O.BOX 631	39180-VICSBORG-MS-U.S.A.
537	TURK,DANICA	USG CORPORATION	700 N.HIGHWAY 45	60048-LIBERTYVILLE-IL-U.S.A.
538	MATHER,BRYANT	WATERWAYS EXPERIMENT STATION	BOX 631-WESSV-Z	39180-VILKSBURG-MS-U.S.A.
539	MATHER,KATHERINE	WATERWAYS EXPERIMENT STATION	BOX 631-WESSV-Z	39180-VILKSBURG-MS-U.S.A.
540	FARKAS,EMERY	W.R.GRACE & CO.	62 WHITTEMORE AVENUE	02140-CAMBRIDGE-MS-U.S.A.
541	HAYDEN,THOMAS D.	W.R.GRACE & CO.	62 WHITTEMORE AVENUE	02140-CAMBRIDGE-MS-U.S.A.
542	ROBERTS,LAWRENCE R.	W.R.GRACE & CO.	62 WHITTEMORE AVENUE	02140-CAMBRIDGE-MS-U.S.A.
543	SKALNY,JAN	W.R.GRACE & CO.	7379 ROUTE 32	21044-COLUMBIA-MD-U.S.A.
544	STERLING,WILLIAM T.	W.R.GRACE & CO.	1114 AVENUE OF THE AMERICAS	10036-NEW YORK-NY-U.S.A.
545	PETRAVITCHUS,LEOPOLDAS	AKMIARCEMENTAS		235464-NOV.AKMIANE-LITUANIA-U.S.S.R.
546	KOUZNETZOVA,TAMARA	INSTITUT CHEMICO-TECHNOLOGIQUE	PLACE MIOUSKAIA,9	125820-MOSCOW-U.S.S.R.
547	BOIKOVA,ALEXANDRA	INSTITUT DE CHIMIE SILIC.	QUAI MAKAROV,2	199164-LENINGRAD-U.S.S.R.
548	NIKIFOROV,YOURIY	INSTITUT GIPROCEMENT	RUE TCHELIEV,13	193224-LENINGRAD-U.S.S.R.
549	AITMOURATOV,ROUSTEM	INSTITUT NIICEMENT	3,ZOUTCHEVOI PROSEK 12	107014-MOSCOW-U.S.S.R.
550	KHLOUSOV,VLADIMIR	INSTITUT NIICEMENT	3,ZOUTCHEVOI PROSEK 12	107014-MOSCOW-U.S.S.R.
551	MTCHEDLOV-PETROSIAN,OTAR	INSTITUT OJGIPROCEMENT	AVENUE PRADVA,10	310022-KHARKOV-U.S.S.R.
552	KOUSCHIDI,VICTOR	MINISTRY OF BUILDING MATERIALS	PLACE NOGINA,2/5	103713-MOSCOW-U.S.S.R.
553	GOMEZ C.,JESUS M.	C.A.FABRICA NACIONAL DE CEMENTOS	TORRE MADELCA-JESUITAS A.MATURIN/1366	1010-CARACAS-VENEZUELA
554	GOUVEA A.,FLAVIO	C.A.FABRICA NACIONAL DE CEMENTOS	TORRE MADELCA-JESUITAS A.MATURIN/1366	1010-CARACAS-VENEZUELA
555	PERZ,CESAR ARBALAEZ	C.A.VENCEMOS LARA	APARTADO 577	BARQUISIMETO-VENEZUELA
556	LOSADA.JOSE FLORENCIO RAMOS	CEMENTO ANDINO S.A.	CALLE RIO DE JANEIRO	VALERA-VENEZUELA
557	SALAZAR B.,RAMON V.	CEMENTOS GUAYANA S.A.	APARTADO DE CORREO 235	PUERTO ORDAZ-BOLIVAR-VENEZUELA
558	AUMUND,FRANZ	AUMUND FOERDERERBAU GMBH	SAALHOFER STRASSE 17-POST 1261	D-4134-RHEINBERG-WEST GERMANY
559	BEUMER,BERNHARD	BEUMER MASCHINENFABRIK KG	DELDER STRASSE 40	D-4720-BECKUM-WEST GERMANY
560	HAEGERMANN.HANS	BUDERUS AG	MUEHLRAIN 12	633-WETZLAR-WEST GERMANY
561	RUDERT,VOLKHART	DYCKERHOFF AG	RHEINGAUSTRASSE 180	D-6501-WIESBADEN-WEST GERMANY
562	BLUNK,GUENTER	FORSCHUNGSGEM.EISENHUETTERSCH.	BLIERSHEIMER STRASSE 62	41 DUISBURG 14-WEST GERMANY
563	LOCHER,FRIEDRICH	FORSCHUNGSINSTITUT D.ZEMENTINDUSTRIE	TANNENSTRASSE 2-PF 301063	D-4000-DUSSELDORF-WEST GERMANY
564	SPRUNG,SIEGBERT	FORSCHUNGSINSTITUT D.ZEMENTINDUSTRIE	TANNENSTRASSE 2-PF 301063	D-4000-DUSSELDORF-WEST GERMANY
565	WISCHERS,GERD	FORSCHUNGSINSTITUT D.ZEMENTINDUSTRIE	TANNENSTRASSE 2-PF 301063	D-4000-DUSSELDORF-WEST GERMANY
566	HASCHKE,WOLFGANG	HAVER & BOECKER	CARL-HAVER PLATZ	D-4740-OELDE-WEST GERMANY
567	HAVER,RUDOLF	HAVER & BOECKER	CARL-HAVER PLATZ	D-4740-OELDE-WEST GERMANY
568	KROBOTH,KARL	HEIDELBERGER ZEMENT AG	BERLINER STRASSE 6	D-6900-HEIDELBERG-WEST GERMANY
569	LIEBER,WERNER	HEIDELBERGER ZEMENT AG	BERLINER STRASSE 6	D-6900-HEIDELBERG-WEST GERMANY
570	LUEHR,HANS-PETER	INSTITUT FUER BAUTECHNIK	REICHPIETSCHUFER 74-76	D-1000-BERLIN 30-WEST GERMANY
571	TEODORU,GEORGE	INSTITUTE OF TROPICAL TECHNOLOGY	P.O.BOX 250171	D-5000-KOLN 1-WEST GERMANY
572	ODLER,IVAN	INST.FUR NICHTMETALLISCHE WORKSTOFFE	ZEHNTNERSTRASSE 2A	D-3302-CLAUSTHAL-WEST GERMANY
573	WOLTER,ALBRECHT H.	KHD HUMBOLDT WEDAG	POSTFACH 910457	D-5000-KOLN 91-WEST GERMANY
574	SCHEUBEL,BERN	KRUPP POLYSIUS AG	GRAFF GALEN STRASSE 17	D 4720-BECKUM-WEST GERMANY
575	WEBER,PAUL	KRUPP POLYSIUS AG	GRAFF GALEN STRASSE 17	D-4720-BECKUM-WEST GERMANY
576	KUZEL,HANS-JURGEN	MINERALOGISCHES INSTITUT-ERLANGEN UNIV.	SCHLOSSGARTEN 5	D-8520-ERLANGEN-WEST GERMANY
577	POELMANN,HERBERT	MINERALOGISCHES INSTITUT-ERLANGEN UNIV.	SCHLOSSGARTEN 5A	D-8520-ERLANGEN-WEST GERMANY
578	PISTERS,HEINZ	READMIX ZEMENTWERKE GMBH R	CO KG,AM KOLLENBACH 27	D-4720-BECKUM-WEST GERMANY
579	DALDRUP,HEINRICH GROSSE	REFRATECNIK GMBH	RUDOLF-WINKEL STRASSE 1-3	D-3400-GOETTINGEN-WEST GERMANY
580	LUDWIG,UDO	RWTH AACHEN		D-5100-AACHEN-WEST GERMANY
581	BILLHARDT,HERMANN-WOLFRAM	SPENNER ZEMENT KG	P.O.BOX 1126	D-4782-ERWITTE-WEST GERMANY
582	BUNDFUSS,KERSTIN	UNIVERSITAET KARLSRUHE	AM FASANENGARTEN	D-7500-KARLSRUHE-WEST GERMANY
583	WIERIG,HANS-JOACHIM	UNIVERSITAT HANNOVER	HINDENBURGALLEE 31A	D3007-GEHRDEN-WEST GERMANY
584	OSEN,ERNST	UNIVERSITY OF KARLSRUHE	KAISERSTRASSE 12	D-7500-KARLSRUHE-WEST GERMANY
585	WEISWEILER,WERNER	UNIVERSITY OF KARLSRUHE	KAISERSTRASSE 12	D-7500-KARLSRUHE-WEST GERMANY
586	MLAKAR-BEC,VIKTORIJA	CEMENTARNA	KOLODVORSKA 5	TRBOVLJE-YUGUSLAVIA
587	POPOVIC,KRESIMIR	CIVIL ENGINEERING INSTITUTE	JANKA RAKUSE,1	41000-ZAGREB-YUGUSLAVIA
588	DRASICEVIC,LJUBINKO	INSTITUT ZA PUTEVA	KUMODRASKA 257	11000-BEOGRAD-YUGUSLAVIA
589	ZIVANOVIC,BRANISLAV	INSTITUTE FOR MATERIALS TESTING	BULEVAR VOJV.ODE MISICA 43	11000-BEOGRAD-YUGUSLAVIA
590	DIMIC,DANIJANA	ZAVOD ZA RAZISKAVO MATERIALA	DIMICEVA 12	61000-LJUBLJANA-YUGUSLAVIA